The Permeabilities of Hydrogen, Sodium and Calcium Ions in Mixed Solvents across Ion-exchange Membranes

By Manabu SENŌ and Takeo YAMABE

(Received July 19, 1963)

The ion-exchange equilibria in mixed solvents exhibit some different behaviors from those in aqueous solutions. For example, the selectivity coefficient, K_H^{Na}, of the ion exchange of sodium for hydrogen ions increases remarkably with the decrease in the dielectric constants of the media.[1,2] On the other hand, it has been revealed that the selective permeability of ions across ion-exchange membranes is primarily ruled by the concentrations and the mobilities of ions in the membrane phase.[3,4] In this paper, the permeabilities of hydrogen, sodium and calcium ions across ion-exchange membranes in mixed solvents will be examined and discussed. The aim of this investigation is to disclose the behavior of ions in mixed solvents and to give some information on the mechanism of the ion transportation across the membranes.

Experimental

The electrodialysis apparatus is a cell with two compartments separated by a cation-selective membrane and equipped with silver-silver chloride electrodes. The solvent systems examined were water-methanol, water-ethanol and water-acetone, from which the sample solutions were prepared by adding nearly the same equivalent quantities of two kinds of chlorides, hydrogen chloride-sodium chloride, sodium chloride-calcium chloride. The total concentration was nearly 0.1 N. The membranes used were heterogeneous, prepared from pulverized ion-exchange resins (Amberlite IR-120), poly(vinyl chloride), dioctyl phthalate and cyclohexanone.

The electrodialyses were carried out for 90, 60 and 30 min. under the current densities of 5, 10 and 30 mA/cm^2, respectively. From the analytical data for sample solutions, the coefficient, T_B^A, of the permselectivity of ion A for ion B are calculated by

$$T_B^A=\left(\frac{m_A}{m_B}\right)\Big/\left(\frac{C_A}{C_B}\right)$$

where m is the quantity of ions transferred across the membrane and C is the mean concentration in the compartment from which ions flow out. In these calculations, the effect of the concentration diffusion has been disregarded, based on the results of the preliminary experiments.

The electric conductivity of the membranes in each ionic form was measured by the use of a universal bridge, Yokogawa BV-Z-103B. The method, each membrane being sandwiched directly between two mercury electrodes, was employed.

Results and Discussion

The experimental results are shown in Figs. 1 and 2. The premselectivity coefficients, T_{Na}^H

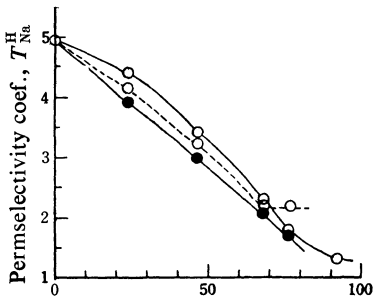


Fig. 1. Relationship between permselectivity coefficient T_{Na}^H and solvent composition.

—○— Water-methanol
--○-- Water-ethanol
—●— Water-acetone

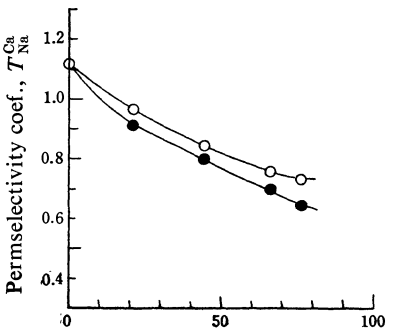


Fig. 2. Relationship between permselectivity coefficient T_{Na}^{Ca} and solvent composition.

—○— Water-methanol
—●— Water-acetone

1) T. Sakaki, This Bulletin, **28**, 217 (1955).
2) T. Yamabe, T. Saito and M. Senō, unpublished.
3) T. Yamabe, M. Senō, T. Tanaka and I. Kamii, This Bulletin, **33**, 1740 (1960).
4) M. Senō and T. Yamabe, *Monthly J. Inst. Ind. Sci. Univ. of Tokyo* (*Seisan Kenkyu*), **13**, 433 (1961).

and T^{Ca}_{Na}, decrease upon the addition of the organic solvents. The decrease is approximately linear with the increasing contents of the organic solvents, but it shows a tendency to converge to a limiting value at higher organic contents, especially in the water-ethanol system.

The increase in the current densities decreases the permselectivity coefficients, T^{H}_{Na} and T^{Ca}_{Na}. The effect is pronounced at the lower current densities. An example is shown in Fig. 3.

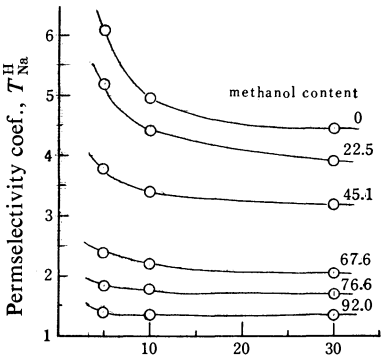


Fig. 3. Dependence of T^{H}_{Na} on current densities.

It is considered that the transport of ions across ion-exchange membranes is effected by both the number of movable ions and the mobility of the ions in the membrane. That is, the coefficient of the permselectivity, T^{A}_{B}, is split into two terms, the mobility terms and the concentration term:

$$T^{A}_{B}=\left(\frac{\bar{u}_A}{\bar{u}_B}\right)\left(\frac{\bar{C}_A}{\bar{C}_B}\Big/\frac{C_A}{C_B}\right)$$

It may readily be shown that, in the limiting region of the lowest current densities, the concentration term approaches the separation factor, S^{A}_{B}, of the ion-exchange equilibria. Moreover, the conductivity ratio, $\kappa_{ACl}/\kappa_{BCl}$, estimated from the electric conductivity of the membranes in each ionic form should be nearly equal to the mobility ratio, if all the ions in the membrane are active in the transportation. The measured values of the separation factor and the conductivity ratio and the product of these values are shown in Tables I and II.

The product, $S^{A}_{B}\cdot\kappa^{A}_{B}$, has characteristics similar to those of T^{A}_{B}. It is considered that the quantitative disagreement between the two values is largely due to the facts that, firstly, the true equilibrium is not attained in the transport process and, secondly, the conductivity ratio estimated from the conductivities of the membranes in each ionic form does not give the true values in the mixture systems. The former results in a concentration ratio nearer to unity, while the latter results in a conductivity ratio nearer to unity, because the slower ions are

TABLE I. CHARACTERISTICS OF HYDROGEN-SODIUM SYSTEM IN MIXED SOLVENTS

Vol. percent of org. solv. %	Separation factor S^{H}_{Na}	Conductivity ratio κ^{H}_{Na} *	Product $S^{H}_{Na}\cdot\kappa^{H}_{Na}$	Coef. of permselectivity T^{H}_{Na}
Water-ethanol				
0	0.82	5.02	4.12	4.95
22.5	0.31	4.53	1.41	4.20
45.1	0.12	4.10	0.49	3.25
67.6	0.025	3.92	0.098	2.25
76.6	0.012	3.68	0.044	2.20
Water-methanol				
0	0.82	5.02	4.12	4.95
22.5	0.38	4.32	1.64	4.50
45.1	0.18	3.50	0.61	3.35
67.6	0.07	3.05	0.21	2.30
76.6	0.051	3.05	0.16	1.72
Water-acetone				
0	0.82	5.02	4.12	4.95
22.5	0.24	4.83	1.16	4.00
45.1	0.093	4.11	0.38	3.20
67.6	0.017	3.60	0.061	2.05
76.6	0.004	3.12	0.013	1.65

* $\kappa^{H}_{Na}=\kappa_{HCl}/\kappa_{NaCl}$

TABLE II. CHARACTERISTICS OF SODIUM-CALCIUM SYSTEM IN MIXED SOLVENTS

Vol. percent of org. solv. %	Separation factor S_{Na}^{Ca}	Conductivity ratio κ_{Na}^{Ca}	Product $S_{Na}^{Ca} \cdot \kappa_{Na}^{Ca}$	Coef. of permselectivity T_{Na}^{Ca}
Water-methanol				
0	14.5	0.51	7.38	1.05
22.5	9.2	0.44	4.05	0.96
45.1	5.3	0.39	2.07	0.83
67.6	2.8	0.36	1.01	0.76
76.6	2.0	0.35	0.75	0.74
Water-acetone				
0	14.5	0.51	7.38	1.05
22.5	8.5	0.46	3.93	0.90
45.1	4.1	0.42	1.74	0.80
67.6	2.0	0.35	0.68	0.71
76.6	1.5	0.34	0.51	0.63

accelerated by the faster ions and vice versa. The effect of partial immobilization pointed out by the present authors[3] is included in the conductivity ratio.

When an ion in the membrane phase has a stronger attractive interaction with the membrane matrix, the concentration of this ion in the membrane phase is higher and its mobility is lower. The concentration and the mobility terms have the opposite effects on the permselectivity.

The decrease in the separation factors, S_{Na}^{H} and S_{Na}^{Ca}, shows that the attractive interaction of hydrogen and calcium ions with the resin matrix becomes smaller than that of sodium ions upon the addition of the organic solvents. This is probably caused by the decrease in the dielectric constant, which results in stronger electrostatic interaction for the smaller hydrated ions. Thus, the permselectivity is in the order $H \gg Ca > Na$ in aqueous solutions, and in the order $H > Na > Ca$ in mixed solvent solutions. This behavior is observed more clearly in solutions with the higher contents of organic solvents or with the solvent of the lower dielectric constant.

The effect of the partial immobilization gives the complicated feature to the conductivity ratio. In the present investigation, the decrease in the conductivity ratio upon the addition of the organic solvents seems to be primarily a result of the partial immobilization. Further investigation is required in this respect.

Under the present experimental conditions, the hydrated state of ions seems not to be affected greatly by the addition of the organic solvents, except for the addition of methanol over 80 percent, where the concentration term changes reversely and the decrease in the permselectivity becomes small.

The Institute of Industrial Science
The University of Tokyo
Azabu, Tokyo

Microwave Spectrum of s-Trioxane

By Takeshi OKA, Katsura TSUCHIYA, Suehiro IWATA and Yonezo MORINO

(Received July 27, 1963)

The microwave spectrum of formaldehyde in the ground vibrational state has been extensively studied.[1,2] In order to analyze the microwave spectrum of formaldehyde in the excited vibrational states, however, it is necessary to observe weak spectral lines. *s*-Trioxane is the cyclic trimer of formaldehyde; microwave investigation of this molecule was first started because it was suspected to exist as an impurity in the sample of formaldehyde evolved by heating paraformaldehyde vapor. After making some measurements, this possibility has been eliminated. No trace of *s*-trioxane line was observed in the formaldehyde sample. However, rather strong spectral lines were observed for pure *s*-trioxane, and the spectroscopy has been continued to determine the molecular structure, the dipole moment and the vibration-rotation constants in the excited vibrational states of this molecule.

A preliminary report on the microwave spectrum of this molecule was published by Amble in 1951,[3] but no other work seems to have been reported. The molecular structure of *s*-trioxane has been examined by electron diffraction.[4] There are also vibrational and dipole moment studies of this molecule.[5] These previous works report that the *s*-trioxane molecule is a chair-form symmetric top both COC and OCO angles nearly tetrahedral.

Experimental

s-Trioxane was prepared by heating paraformaldehyde and dilute sulfuric acid in an oil bath.[6] The product was purified by sublimation. A commercially-available sample was also used. Purified *s*-trioxane is a colorless crystalline compound and is stable. The vapor pressure is large enough to observe the spectral lines at room temperature, but measurement at dry-ice temperature was impossible because of the low vapor pressure of the sample. The spectrograph used was a conventional one, with 100 kc. Stark modulation.

Spectrum

s-Trioxane is an oblate symmetric top, and the R-branch transitions, $J=1\leftarrow0$, $2\leftarrow1$ and $3\leftarrow2$, fall in the centimeter-wave region. Although this molecule is rather heavy and has low frequency vibrations, it gives fairly strong spectral lines because of the large dipole moment and so the spectral lines of ^{13}C isotopic species could be observed in the natural abundance. The dipole moment is directed along the axis with the largest moment of inertia, and c-type transitions are observed for the isotopic species.

TABLE I. OBSERVED FREQUENCIES OF *s*-TRIOXANE (IN Mc./sec.)

Transition	Observed frequency
$(^{12}CH_2{}^{16}O)_3$	
$J=1\leftarrow0$	10546.46 ± 0.05
$J=2\leftarrow1$	21092.97
$J=3\leftarrow2$	31639.36
$(^{12}CH_2{}^{16}O)_2(^{13}CH_2{}^{16}O)$	
$3_{30}\leftarrow2_{20}$	31354.0 ± 0.2
$3_{21}\leftarrow2_{11}$	31203.0 ± 1

The observed frequencies are listed in Table I. The assignment of the $3_{30}-2_{20}$ transition was confirmed by the Stark behavior of the line. The $3_{21}-2_{11}$ transition was measured with rather large uncertainty because of the weakness and the large Stark shift of the line. The $3_{31}-2_{21}$ transition could not be separated from the excited vibrational lines of the normal

TABLE II. ROTATIONAL CONSTANTS OF *s*-TRIOXANE

$(^{12}CH_2{}^{16}O)_3$	
$B=$	5273.23 ± 0.01 Mc./sec.
$(^{12}CH_2{}^{16}O)_2(^{13}CH_2{}^{16}O)$	
$A=$	5270.76 ± 0.4 Mc./sec.
$B=$	5176.68 ± 0.4 Mc./sec.

1) T. Oka, H. Hirakawa and K. Shimoda, *J. Phys. Soc. Japan*, **15**, 2265 (1960); T. Oka, ibid., **15**, 2274 (1960). T. Oka, and Y. Morino, ibid., **16**, 1235 (1961).
2) K. Takagi and T. Oka, ibid., **18**, 1174 (1963).
3) E. Amble, *Phys. Rev.*, **83**, 210A (1951).
4) M. Kimura and K. Aoki, *J. Chem. Soc. Japan, Pure. Chem. Sec.* (*Nippon Kagaku Zassi*), **72**, 169 (1951); W. Shand, *Acta Cryst.*, **3**, 54 (1950); O. Hassel and H. Viervoll, *Acta Chem. Scand.*, **1**, 149 (1947); L. E. Sutton and L. O. Brockway, *J. Am. Chem. Soc.*, **57**, 473 (1935).
5) S. T. Stair, Jr., and J. R. Nielsen, *J. Chem. Phys.*, **27**, 402 (1957); J. C. Decius, W. C. Steele and R. G. Snyder, ibid., **19**, 806 (1951); D. A. Ramsay, *Trans. Faraday Soc.*, **44**, 289 (1948); A. A. Maryott and S. F. Acree, *J. Research Natl. Bur. Standards*, **33**, 71 (1944).
6) J. F. Walker, "Formaldehyde," Reinhold Publishing Corporation, New York (1953).

TABLE III. MOLECULAR STRUCTURE OF *s*-TRIOXANE

	Present work	Amble	Kimura and Aoki	Shand
r(C-O), Å	1.411 ±0.01	1.41	1.42±0.02	1.40±0.02
∠COC	108°10′±1°	109°	110°±2°	112°±3°
∠OCO	111°10′±1°	109°	110°±1°	112°±3°

species. Weak lines with $K=2$ were not observed. The rotational constants have been determined from these frequencies, as Table II shows.

Molecular Structure

If the position of the six hydrogen atoms relative to the carbon atoms and the C_{3v} symmetry are assumed, the molecular structure of *s*-trioxane is expressed by three independent parameters. They have been determined by using the rotational constant, B, of the normal species and A and B of the ^{13}C isotopic species. It was assumed that the hydrogen atoms are attached to the carbon atoms at the tetrahedral angle, with three hydrogen-carbon bonds parallel to the symmetry axis. The carbon-hydrogen distance was assumed to be 1.09±0.005 Å. The coordinate system are taken so that the symmetry axis coincides with the z axis and one carbon atom (C_1) lies in the xz plane (Fig. 1).

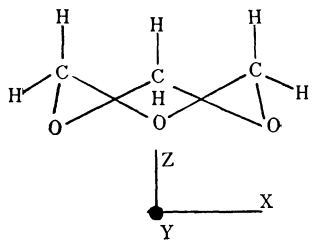


Fig. 1. The *s*-trioxane molecule.

The x and z coordinates of the carbon atom, C_1, have been determined by the substitution method[7] from the formula:

$$z^2_{C_1}=\frac{\Delta I_{aa}}{\mu}\left[1-\frac{\Delta I_{bb}-\Delta I_{aa}}{I_{aa}-I_{cc}}\right]$$

$$x^2_{C_1}=\frac{\Delta I_{bb}-\Delta I_{aa}}{\mu}\left[1+\frac{\Delta I_{aa}}{I_{aa}-I_{cc}}\right] \quad (1)$$

where ΔI_{aa} and ΔI_{bb} are the changes in the moments of inertia due to the isotopic substitution and $\mu=M\Delta C/(M+\Delta C)$, with M the total mass and ΔC the difference between the masses of ^{12}C and ^{13}C. There is no experimental data for I_{cc}, but, since the latter term in the bracket of Eq. 1 is much smaller than one, the value of I_{cc} calculated from a reasonable structure was used.

The z coordinates of the oxygen atoms have been determined from the condition of the center of gravity;

$$m_C z_C+m_O z_O+m_H(2z_C+2/3r)=0 \quad (r=1.09) \quad (2)$$

The x coordinate of the oxygen atom, O_1, is determined from the moment of inertia of the normal species by the formula:

$$I_{bb}=3\,[m_C(x^2_{C_1}/2+z^2_{C_1})+m_O(x^2_{O_1}/2+z^2_{O_1})+m_H(x^2_{C_1}+2\sqrt{2x_{C_1}}r/3+2z^2_{C_1}+4z_{C_1}r/3+14r^2/9)] \quad (3)$$

The molecular structure thus determined is shown in Table III, together with the previous results.

The uncertainty of the molecular structure was estimated from the probable error of the experimental rotational constants and the uncertainty in the assumed hydrogen parameters. Although the uncertainty in the z coordinate is rather large, it is reduced in the C–O bond length and COC and OCO angles. The COC angle is smaller than the OCO angle by about 3 degrees. The C–O distance is shorter than the corresponding distances in trimethylene oxide (1.449±0.002 Å[8]) and methanol (1.434 Å[9]), but it is close to that of dimethyl ether (1.410±0.003 Å[10]).

Excited Vibrational States

In addition to the spectral lines of *s*-trioxane in the ground vibrational state, many vibrational satellites were observed, as shown in Table IV and Fig. 2. They were found to be the rotational lines of molecules in the excited states of four normal vibrations. Two of them were assigned to the degenerate E species, since they clearly showed l-type doubling. The l-type doubling constants, q_l, were determined from the splitting, as is shown in Table V. These two vibrations come from the COC and OCO bending vibrations, with a strong coupling with the torsional motion. They are named $\nu_E(1)$ and $\nu_E(2)$, as shown in Fig. 2. Since the frequency of $\nu_E(1)$ is

7) J. Kraitchman, *Am. J. Phys.*, 21, 17 (1953).
8) S. I. Chan, J. Zinn and W. D. Gwinn, *J. Chem. Phys.*, 34, 1319 (1961).
9) E. V. Ivash and D. M. Dennison, ibid., 21, 1804 (1953).
10) U. Blukis, P. H. Kasai and R. J. Myers, *J. Chem. Phys.*, 38 2753 (1963).

TABLE IV. OBSERVED FREQUENCIES OF *s*-TRIOXANE IN THE EXCTED VIBRATIONAL STATES (IN Mc./sec.)

Vibrational assignment	$J=1\leftarrow0$	$J=2\leftarrow1$	$J=3\leftarrow2$
$v_E(2)=1$	10553.76	21108.28	31699.4* 31661.95 31623.8*
Ground state	10546.46	21092.97	31639.36
$v_E(1)=1$	10536.17	21086.47* 21072.67 21057.47*	31633.1* 31609.4 31582.8*
$v_E(1)=2$	10526.46	21052.97	31579.3
$v_E(1)=3$	10517.21	21033.65	31550.0
$v_A(1)=1$	10520.73	21040.89	31561.0
$v_A(2)=1$		21025.73	31536.8

Experimental errors for the frequencies of the ground state and $v_E(1)=1$ state are 0.1 Mc./sec. For the weaker transitions except l-type doublets, the experimental errors are 0.6 Mc./sec. For the l-type doublets the experimental errors are larger. It is possible that experimental errors are as large as 2 Mc./sec.

* l-Type doublets

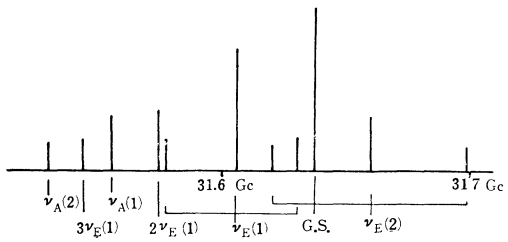


Fig. 2. $J=3\leftarrow2$ transition of *s*-trioxane.

small, the excited states up to $v_E(1)=3$ have been clearly observed. Up to $v_E(1)=3$, there is no indication of the inversion of the ring and the spacings between the satellites are normal.

The other two satellites must be assigned to the totally symmetric A_1 species, since no more low frequency degenerate vibration is expected. One of them, named $\nu_A(1)$, is fairly strong; it is evident that it corresponds to the totally symmetric vibration with the lowest frequency. The other one is rather weak and appears far from the ground state line. It is probable that the line corresponds to another totally symmetric vibration, but we cannot disregard the possibility that this might be due to the $\nu_A(1)+\nu_E(1)$ state. The values of α and q_l for the various vibration are listed in Table V.

TABLE V. MOLECULAR CONSTANTS FOR THE EXCITED STATES (IN Mc./sec.)

Vibrational state	B_v	α_s	q_l
$v_E(2)=1$	5276.95	− 3.72	7.50
$v_E(1)=1$	5268.16	4.95	12.60
$v_E(1)=2$	5263.23		
$v_E(1)=3$	5258.45		
$v_A(1)=1$	5260.25	12.98	
$v_A(2)=1$	5256.28	16.95	

Statistical Spin Weights of the Rotation-vibrational States

The statistical spin weights of the rotational state of symmetric top molecules in the ground vibrational state has been worked out by Wilson.[11] In order to ascertain the statistical spin weights of the rotation-vibrational states of symmetric top molecules, it is necessary to extend his theory.

The rotational subgroup for the molecule with C_{3v} symmetry is C_3, the character table of which is shown in Table VI. Since ^{12}C and ^{16}O are Bose particles with spin zero, the symmetry of the spin-wave function of *s*-trioxane is determined solely from the hydrogen atoms. It can be shown, by directly applying Wilson's method,[11] that the wave function of *s*-trioxane has the symmetry of $24A+20(E_1+E_2)$. The symmetry of the rotational wave function is classified by the value of K as:[11]

TABLE VI. CHARACTER TABLE FOR C_3 SYMMETRY

C_3	E	C_3	C_3^2
A	1	1	1
E_1	1	$e^{2\pi i/3}$	$e^{4\pi i/3}$
E_2	1	$e^{4\pi i/3}$	$e^{2\pi i/3}$

$$K=0 \qquad (2J+1)A$$
$$K=3p\,(p\neq0) \qquad 2(2J+1)A$$
$$K=3p+1 \qquad (2J+1)E_1$$
$$K=3p-1 \qquad (2J+1)E_2$$

In discussing the symmetry of rotation-vibrational states, K is the quantum number for the total angular momentum along the symmetry axis, including the vibrational angular momentum. The symmetry of the vibrational part of the wave function which is multiplied to the rotational wave function can be specified by l, the quantum number of the vibrational angular momentum along the symmetry axis, as follows:[12,13]

$$l=0 \qquad A$$
$$l=3p\,(p\neq0) \qquad 2A$$

11) E. B. Wilson, Jr., *J. Chem. Phys.*, 3, 276 (1935).
12) L. D. Landau and E. M. Lifshitz. "Quantum Mechanics Non-Relativistic Theory," Addison-Wesley Publishing Company, Reading, Massachusetts.
13) J. T. Hougen, *J. Chem. Phys.*, 37, 1433 (1962).

$$l=3p+1 \qquad E_2$$
$$l=3p-1 \qquad E_1$$

The symmetry of the total rotation-vibrational wave function, including spin, can be obtained by taking a direct product of these three parts.

Any operation in the C_3 point group applied to the trioxane molecule corresponds to an even exchange of the nuclei, so the total wave function must be totally symmetric. Thus, the spin weights of the states are derived as shown in Table VII.

Table VII. Spin weight for the rotation-vibrational states of *s*-trioxane

	$K=0$	$K=3p$	$K=3p+1$	$K=3p-1$
$l=0$	24	48*	20	20
$l=3p$	48*	96*	40	40
$l=3p+1$	20	40	24*	20
$l=3p-1$	20	40	25	24*

* These states may show doubling if some terms in the vibration rotation Hamiltonian are large.

Low Frequency Vibrations in *s*-Trioxane

Since the spin weight of each quantum state has been obtained, it is possible to estimate the frequencies of the low frequency vibrations *s*-trioxane from the observed relative intensities of the vibrational satellites. The relative intensities were measured for the three transitions, $J=1\leftarrow0$, $2\leftarrow1$ and $3\leftarrow2$, but the data from $J=1\leftarrow0$ gives the most reliable value because of the simple Stark effect. The frequencies thus obtained are listed in Table VIII, together with the infrared results. Because of the rather large experimental errors in the intensity measurement, the uncertain in the vibrational frequencies are large. However, the assignment is in agreement with the infrared results for the lowest three frequencies. The frequency of $\nu_A(2)$ has not yet been definitely determined.

Table VIII. Low frequency vibrations of *s*-trioxane (in cm^{-1})

	Present work	Stair and Nielsen
$\nu_E(1)$	290 ± 40	307
$\nu_E(2)$	490 ± 30	472
$\nu_A(1)$	470 ± 30	524
$\nu_A(2)$	650 ± 100	748

Thermal Decomposition

In order to test the thermal stability of *s*-trioxane, the absorption cell was heated to about 250°C, but no trace of a formaldehyde line was observed. The observation was accomplished by using the $32_{5,27}\leftarrow32_{5,26}$ transition line of formaldehyde, which comes close to the $J=1\leftarrow0$ line of *s*-trioxane.[1] It can be said, therefore, that *s*-trioxane is stable up to this temperature.

Dipole Moment

The dipole moment of *s*-trioxane has been determined from the second order Stark shift of the $J=3\leftarrow2$ line. This absorption line splits into a triplet when a strong electric field ($\sim$1000 V./cm.) is applied. From the spacings of the triplet, the dipole moment has been determined to be 2.07 ± 0.04 Debye. If tetrahedral angles are assumed between the bonds in *s*-trioxane, the dipole moment of this molecule can be experessed by the bond moment along the C–O axis and that along the C–H axis as

$$\mu = 2(\mu_{CO} + \mu_{CH})$$

The experimental value gives $\mu_{CO}+\mu_{CH}=1.04$ Debye. This value should be compared with that of methanol for which $\mu_{CO}+\mu_{CH}=0.88$ Debye.

The authors wish to express their appreciation to the Fund of the Toyo Rayon Foundation for the Promotion of Science and Technology for the grant which made this research possible.

Department of Chemistry
Faculty of Science
The University of Tokyo
Hongo, Tokyo

Planar Quadri-co-ordinate Complexes of Cobalt(II) with Schiff Bases Derived from Salicylaldehyde

By Hiroaki NISHIKAWA and Shoichiro YAMADA

(Received August 2, 1963)

The chemistry of transition-metal complexes with Schiff bases derived from salicylaldehyde is considered to involve a number of interesting problems of fundamental importance in the field of co-ordination chemistry.[1-3] The copper(II) and nickel(II) compounds of this type have been studied in some detail, but there have been very few systematic studies of cobalt(II)-complexes with *N*-alkylsalicylideneiminate ions. Thus, the configuration of quadri-co-ordinate cobalt(II)-complexes of this kind was in dispute when the present study was started. There are some cobalt(II)-complexes in which the steric requirements alone determine the configuration of the complex, allowing only one of two possibilities, that is, a planar or a tetrahedral co-ordination. As a step to the elucidation of the structure of cobalt(II)-complexes with Schiff bases, the present paper is concerned with those compounds whose structure is necessarily planar because of the steric conditions imposed by the ligands, and with the determination of the main characteristics of their spectroscopic properties. The electronic spectra of the planar cobalt(II)-complexes have never been unanimously characterized; it is thought that their establishment will be useful for the discussion of the structure of, and the chemical bond involved in, cobalt(II)-complexes.

Experimental

Materials. — *Bis(salicylaldehyde)ethylenediiminatocobalt(II)*[4] (Fig. 1, A) was prepared previously[5] by adding an aqueous solution of cobalt(II) acetate to an ethanolic solution of bis(salicylaldehyde)-ethylenediimine under reduced pressure. The crystals of the compound obtained by this method, however, are generally so small that they are very susceptible to oxygenation. In the present work, a different method was devised for preparation of the compound in larger cystals, which were bound to be more inert in the atmosphere. A suspension of bis(salicylaldehyde)cobalt(II) dihydrate (2.0 g.) in methanol (400 ml.) was boiled in a flask. While this was boiling and while the vapor of methanol filled the flask, a theoretical amount of ethylenediamine was added to the orange-colored solution; then the flask was closed tightly. When the mixture was kept at room temperature for a few hours, needle-like crystals first started to separate out; these were soon changed, in the solution in the absence of oxygen, into dark-violet, prism-like crystals, which were finally collected. The nature of the red crystals which separated at first and which then disappeared was not characterized in the present study. The dark-violet crystals obtained according to this method are hardly oxygenated at all, even when filtered in the air. They are slightly soluble in chloroform and benzene.

Found: C, 59.3; H, 4.36; N, 8.90. Calcd. for $C_{16}H_{14}O_2N_2Co$: C, 59.1; H, 4.34; N, 8.61%.

Bis(salicylaldehyde)propylenediiminatocobalt(II) (Fig. 1, B) was prepared as reddish-brown, needle-like crystals by a new method similar to that for "salcomine" which was devised by the present authors. The crystals, which are readily oxygenated in the atmosphere, are slighty soluble in ethanol, chloroform and benzene.

Found: C, 59.4; H, 4.90; N, 8.00. Calcd. for $C_{17}H_{16}O_2N_2Co$: C, 61.2; H, 5.13; N, 7.93%.

Bis(salicylaldehyde)-α, α'-dimethylethylenediiminatocobalt(II) (Fig. 1, C) was previously reported by Diehl.[6] In the present work, a different method was devised. Under reduced pressure, bis(salicylaldehyde)-cobalt(II) dihydrate and a slight excess of α, α'-dimethylethylenediamine were reacted in a water-ethanol mixture for several minutes. Then the solution was evaporated in vacuo to give an orange, crystalline powder. The micro-crystals, which are stable in the atmosphere, are soluble in common organic solvents.

Found: C, 60.5; H, 5.45; N, 7.47. Calcd. for $C_{18}H_{18}O_2N_2Co$: C, 61.2; H, 5.13; N, 7.93%.

Bis(salicylaldehyde)-α, α'-diphenylethylenediiminatocobalt(II) (Fig. 1, D) has not been reported yet. In the present study, this compound was synthesized from bis(salicylaldehyde)cobalt(II) dihydrate and α, α'-diphenylethylenediamine according to a method similar to that used for bis(salicylaldehyde)-α, α'-dimethylethylenediiminatocobalt(II). Recrystallization of the crude product from chloroform yielded pure, red crystals, which are quite stable in the atmosphere. These crystals are soluble in ethanol,

1) H. Nishikawa, S. Yamada and R. Tsuchida, *Z. Naturforsch.*, **17b**, 78 (1962); *Z. anorg. u. allgem. Chem.*, **316**, 278 (1962); H. Nishikawa and S. Yamada, This Bulletin, **35**, 1430 (1962); S. Yamada and H. Nishikawa, ibid., **36**, 755 (1963), etc.

2) B. O. West, *J. Chem. Soc.*, **1962**, 1374; ibid., **1960**, 4944; *Nature*, **173**, 1187 (1954), etc.

3) L. Sacconi, M. Ciampolini, F. Maggio and F. P. Cavasino, *J. Am. Chem. Soc.*, **84**, 3246 (1962); L. Sacconi, P. L. Orioli, P. Paoletti and M. Ciampolini, ibid., **85**, 411 (1963), etc.

4) This compound is abbreviated "salcomine."

5) P. Pfeiffer, E. Breith, L. Lübbe and T. Tsumaki, *Ann.*, **503**, 84 (1933).

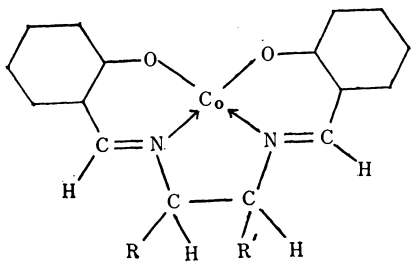


Fig. 1. Bis(salicylaldehyde)ethylenediiminatocobalt(II) and related compounds.
A, R=R'=H; B, R=H, R'=CH_3; C, R=R'=CH_3; D, R=R'=C_6H_5.

chloroform and benzene, and they are stable in solution as well as in the solid state.

Found: C, 71.6; H, 4.99; N, 5.47. Calcd. for $C_{28}H_{22}N_2O_2Co$: C, 70.4; H, 4.64; N, 5.86%.

Bis(salicylaldoximato)cobalt(II) was prepared by a new method, one invented for the present work in order to obtain crystals of a larger size by avoiding undesirable oxygenation during the process. Prior to the synthesis, the fiask was evacuated, and it was eventually filled with ethanol vapor. Cobalt(II) chloride and salicylaldoxime were dissolved in warm ethanol in the molar ratio of 1:2.2, and a methanolic solution of lithium methylate (2.0 mol.) was added drop by drop to the solution. Red-brown crystals separated out immediately, and they were collected. The crystals obtained are slightly soluble in common organic solvents.

Found: C, 50.7; H, 3.59; N, 8.04. Calcd. for $C_{14}H_{12}N_2O_4Co$: C, 50.8; H, 3.65; N, 8.46%.

Bis(salicylaldiminato)cobalt(II) was prepared by the following two methods: (i) Bis(salicylaldehyde)-cobalt(II) dihydrate (2.0 g.) was suspended in 200 ml. of ethanol in a flask at 60~65°C. A concentrated aqueous ammonia (9 ml.) was added to the solution in the flask which was evacuated, and the reaction mixture was kept at this temperature for about one and a half hours to give orange, plate-like crystals. The crystals were filtered, washed with a mixture of a concentrated aqueous ammonia and methanol, and dried in vacuo. (ii) Bis(salicylaldehyde)cobalt(II) dihydrate (2.5 g.), ammonium chloride (2.5 g.) and methanol (100 ml.) were placed in a flask, which was evacuated until the solution in it started boilig.

Then the flask was closed and warmed to 65°C while being stirred, and lithium methylate prepared from lithium metal (0.28 g.) and methanol (20 ml.) was added drop by drop into the flask. Orange, plate-like crystals separated out immediately; they were filtered while hot, washed with a mixture of concentrated aqueous ammonia and methanol, and dried in vacuo.

The crystals are readily soluble in pyridine, but insoluble in other common organic solvents.

Found: C, 56.0; H, 4.05; N, 9.38. Calcd. for $C_{14}H_{12}N_2O_2Co$: C, 56.2; H, 4.04; N, 9.36%.

6) H. Diehl and T. S. Chao, *Iowa State Coll. J. Sc.*, **22**, 126 (1947).

The crystals prepared by the above-described methods are obviously different from those reported previously. Fomerly Endo[7] claimed to have isolated bis(salicylaldiminato)cobalt(II) dihydrate from hydrosalicylamide and cobalt(II) acetate. Our experiments using his procedures yielded a substance with the same properties as those described in the literature. The substance, however, gave an analytical value for nitrogen, an appreciable deviation from the formula of bis(salicylaldiminato)-cobalt(II) or its hydrate. Moreover, observation under a microscope indicates that the product consists of two kinds of crystals. It is likely that a mixture is obtained by this procedure. The most remarkable difference seems to be that the product obtained by the Endo's method was reported to be stable in boiling chloroform, whereas the product obtained by the method reported here was quite sensitive to air.

Measurements.—The electronic absorption spectra of the compounds in solution were determined with a Beckman DU spectrophotometer. Since all the compounds are more or less sensitive to oxygen in the air, the measurements were carried out in a nitrogen atmosphere. Examination was made after every measurement to see whether or not any change occurred in the solution. In general, Beer's law was obeyed in the concentration range of the present measurements, which varied between 10^{-2} and 10^{-5} mol./l.

Results and Discussion

Bis(salicylaldehyde)ethylenediiminatocobalt-(II) and Its Derivatives.—Judging from the steric requirement of the ligand (Fig. 1, A), bis(salicylaldehyde)ethylenediiminatocobalt(II) is considered to have a quadri-co-ordinate, planar complex of the *cis*-$[Co(N)_2(O)_2]$ type. The visible and ultraviolet spectrum of "salcomine" in solution has previously been reported, but the measurement did not cover the whole region of the ligand field bands.[8] In the present study, therefore, the measurements were carried out in the atmosphere of nitrogen and were extended to a much lower frequency region than that previously reported. The results of the measurements are shown in Fig. 2. In the region of the higher frequency, there appear intense absorption bands; these are regarded as resulting mainly from the ligand group in the complex. These absorption bands, however, do not extend beyond $60\times10^{13}sec^{-1}$ (500 mμ), so that a considerable part of the ligand field band region is left uncovered. In the lower frequency region, the main features of the ligand field bands of "salcomine" are definitely different from those of cobalt(II)-complexes with a sexa-co-ordinate octahedral

7) J. Endo, *J. Chem. Soc. Japan (Nippon Kwagaku Kwaisi)*, **65**, 428 (1944).

8) R. Tsuchida and T. Tsumaki, This Bulletin, **13**, 527 (1938).

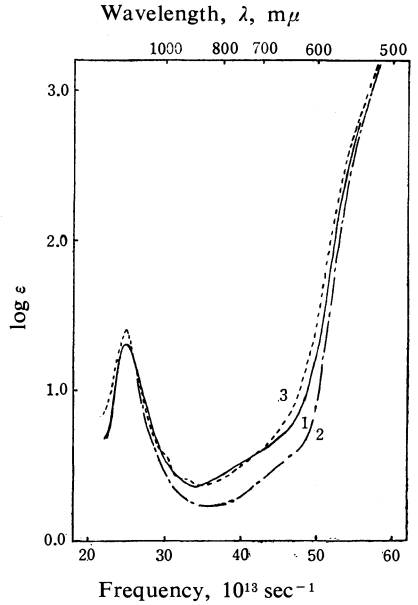


Fig. 2. Visible and near-infrared absorption spectra of "salcomine" and related compounds in chlorofom.
1. $Co(O\cdot C_6H_4\cdot CH:N\cdot CH_2\cdot CH_2\cdot N:CH\cdot C_6H_4\cdot O)$, (salcomine); 2, $Co(O\cdot C_6H_4\cdot CH:N\cdot CH(CH_3)\cdot CH(CH_3)\cdot N:CH\cdot C_6H_4\cdot O)$; 3, $Co(O\cdot C_6H_4\cdot CH:N\cdot CH(C_6H_5)\cdot CH(C_6H_5)\cdot N:CH\cdot C_6H_4\cdot O)$.

or a quadri-co-ordinate tetrahedral configuration. Thus, the spectrum of "salcomine," which has a sharp peak at about 25×10^{13} sec^{-1} (1200 mμ), may be considered to represent the main features characteristic of cobalt(II)-complexes with a planar configuration.

Bis(salicylaldehyde)propylenediiminatocobalt-(II) is regarded, on the basis of the steric condition (Fig. 1), as taking a quadri-co-ordinate, cis-planar configuration. The ligand field bands (Fig. 3) of bis(salicylaldehyde)-propylenediiminatocobalt(II) are quite similar to those of "salcomine," both show a sharp absorption peak at about 25×10^{13} sec^{-1} (1200 mμ).

Bis(salicylaldehyde)-α, α'-disubstituted ethylenediiminatocobalt(II) complexes (Fig. 1) are also considered, on the basis of the steric condition of the ligands, to take a planar co-ordination around the cobalt(II) ion. Thus, compouds C and D (Fig. 1) both show spectra quite similar to that of "salcomine," as is shown in Fig. 2. The sharp peaks in the near-infrared region of the complexes shown in Fig. 1 do not differ much from one another (Table I).

It is of significance that the quadri-co-ordinate cobalt(II)-complexes with a planar configuration, examined in the present study, exhibit characteristic ligand field bands, with

TABLE I. LIGAND FIELD ABSORPTION BANDS OF BIS(SALICYLALDEHYDE)ETHYLENEDIIMINATO-COBALT(II) AND RELATED COMPLEXES WITH A PLANAR CONFIGURATION

Compound	ν	$\Delta\nu$	log ε
Compound I	25.1	3.6	1.31
Compound II	24.9	3.9	1.31
Compound III	25.1	3.3	1.31
Compound IV	24.9	3.2	1.40
Bis(sal. aldoxim.)-cobalt(II)	28.6	4.0	(0.99)
Bis(sal. aldimin.)-cobalt(II)	24.9	1.6	(1.49)

ν: 10^{13} sec^{-1}; $\Delta\nu$: half width, 10^{13} sec^{-1}

a sharp peak at about 25×10^{13} sec^{-1} (1200 mμ). Since this is remarkably different from that which is observed for sexa-co-ordinate octahedral or quadri-co-ordinate tetraherdal complexes of cobalt(II), this difference may be diagnostic in the discussion of the configuration of cobalt(II)-complexes.

It is also characteristic that the oscillator strength of this sharp peak in the near-infrared region is very small. Although an unambiguous assignment of the band is difficult at the time, the quite small oscillator strength of the band seems to indicate that this peak may be ascribed to a spin-forbidden d-d transition. On the basis of the energy level diagram provided by Cotton and Holm,[9] the peak may tentatively be ascribed to an electronic transition from $^2B_{2g}$ to $^4A_{2g}$ or ^4E_g.

The Configuration of Bis(salicylaldoximato)- and Bis(salicylaldiminato)-cobalt(II).—The co-ordination around the cobalt(II) ion in bis-(salicylaldoximato)-cobalt(II) is either planar or tetrahedral. From the magnetic moment of 2.6 B. M. for the compound in the solid state,[10] it was formerly assumed that the compound had a planar configuration.[11] This compound is exceedingly susceptible to oxidation, and a specimen obtained by the conventional method of preparation often contains oxygen molecules absorbed from the atmosphere.[12] It is not quite certain whether or not, in the former studies of the magnetic moment, due care was exercised in this respect; reexamination of the problem, preferably using evidence of another sort, was thought to be desirable. In the present work, the pure specimen of bis(salicylaldoximato)cobalt(II) has been prepared with the utmost care to prevent the undesirable oxygenation, and the

9) F. A. Cotton and R. H. Holm, *J. Am. Chem. Soc.*, **82**, 2979 (1960).
10) D. P. Mellor and D. P. Craig, *J. Proc. Roy. Soc. N. S. W.*, **74**, 475 (1941).
11) B. M. Figgis and R. S. Nyholm, *J. Chem. Soc.*, **1954**, 12.
12) B. O. West, ibid., **1952**, 3120, 3115.

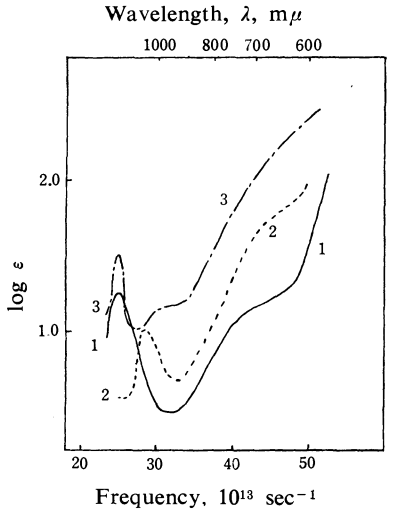


Fig. 3. Visible and near-infrared absorption spectra.
1, $Co(O\cdot C_6H_4\cdot CH:N\cdot CH(CH_3)\cdot CH_2\cdot N:CH\cdot C_6H_4\cdot O)$ in ethanol; 2, $Co(O\cdot C_6H_4\cdot CH:N\cdot OH)_2$ in chloroform; 3, $Co(O\cdot C_6H_4\cdot CH:N\cdot H)_2$ in ethyl methyl ketone.

spectrum of the compound in solution has also been determined in an inert atmosphere. The qualitative spectrum thus determined is shown in Fig. 3. In spite of the great care paid to the determination of the spectrum, a slight oxidation is noticeable in the determined spectrum, which shows an inflation at about 45×10^{13} sec^{-1}. The spectrum, however, is regarded as being accurate enough for the purpose and the nature of the present discussion. The spectrum has a sharp peak, at about 28.4×10^{13} sec^{-1}, which is characteristic of the quadri-co-ordinate square-planar complex of cobalt(II). It may, therefore, be concluded that bis(salicylaldoximato)cobalt(II) has a quadri-co-ordinate planar configuration around the cobalt(II) ion. A comparison of the absorption maximum of the sharp peak in the near-infrared region reveals that the ligand field of the salicylaldoximate ion in the planar cobalt(II)-complex is stronger than that of salicylaldiminate or bis(salicylaldeyde)ethylenediiminate.

It will be shown in forthcoming papers that, with *N*-alkyl- and *N*-aryl-salicylideneimine, most quadri-co-ordinate cobalt(II)-complexes take a tetrahedral configuration, unless the steric condition of the ligands demands a planar co-ordination. It is to be noted that bis(salicylaldoximato)- and bis(salicylideneiminato)-cobalt(II) take a quadri-co-ordinate planar configuration; this is especially noteworthy in view of the fact that these ligands, which are similar in their bonding ability to salicylaldoximate or bis(salicylaldehyde)ethylenediiminate, except for the steric factor, do not necessarily demand a planar configuration for cobalt(II).

One of the necessary conditions for the cobalt(II)-complex to take a planar co-ordination is that the field produced by the ligands in the complex be stronger than a certain threshold value, below which the complex is assumed to take a tetrahedral co-ordination with the ligands. Another cause for the formation of the planar cobalt(II)-complex may be the steric conditions favorable for the square-planar co-ordination of the metal-ion. Thus, if bis(salicylaldoximato)cobalt(II) is assumed to be a planar trans-complex, a strong hydrogen bond of an O—H—O type may be possible. This is probably one of the factors which favor the planar co-ordination of salicylaldoximato-complex of cobalt(II). In this connection, it is of significance that a strong hydrogen bond of an O—H—O type has been reported to exist in bis(salicylaldoximato)nickel(II).[13]

The crystals of bis(salicylaldiminato)cobalt(II) are readily oxidized in the air, and their solubility in solvents is generally low, so that the measurement of the spectrum was not very easy. With precautions to prevent oxidation, the qualitative absorption spectra of the compound in chloroform and in ethyl methyl ketone were determined; the results are given in Fig. 3 and Table I. The spectra in the two different solvents coincide essentially with each other in all important points.

Bis(salicylaldiminato)cobalt(II) in non-co-ordinating solvents has a quadri-co-oridinate, planar configuration; the spectrum of this compound, which shows a sharp peak at about 24.8×10^{13} sec^{-1}, is regarded as characteristic of the quadri-co-ordinate, planar cobalt(II)-complex.

As will be described in a forthcoming paper, bis(*N*-*n*-alkylsalicylideneiminato)cobalt(II) complexes, which are derived by substituting *n*-alkyl groups for the hydrogen atoms of bis(salicylaldiminato)cobalt(II), take a tetrahedral co-ordination around the cobalt(II) ion. This remarkable change in configuration, caused by a change of a substitutent, may be due partly to the fact that the ligand field produced by the salicylideneiminate group is stronger than that produced by the *N*-*n*-alkylsalicylideneiminate group. In addition to this there may be cited the possibility that hydrogen bonding of an N—H—O type would be formed in bis(salicylideneiminato)cobalt(II) when the complex is trans-planar.

In the light of the findings of the present

13) L. L. Merritt, C. Guare and A. E. Lessor, *Acta Cryst.*, **9**, 253 (1956).
14) J. F. Fackler, *Inorg. Chem.*, **2**, 266 (1963).

work, the configuration of bis(acetylacetonato)-cobalt(II) may be discussed. The complex has a magnetic moment correspondig to three unparied electrons, and a planar configuration would be ruled out by the conventional argument of magnetism. The complexes of cobalt(II), whose configurations have been firmly established as planar, are all of a low-spin type, with a magnetic moment corresponding to one unpaired election. On the basis of theoretical consideration, however, Cotton and Holm[6] claimed that bis(acetylacetonato)cobalt-(II) was a rare example of a planar cobalt-(II)-complex of a high-spin type. Its electronic absorption spectra, its ligand field bands in particular, are quite different from the spectra of the typical planar cobalt(II)-complexes studied in the present work. Thus, the square-planar configuration of bis(acetylacetonato)-cobalt(II) is to be rejected; there is no warrant for assuming the existence of planar cobalt(II)-complexes of a high-spin type, none of which have ever been established with reasonable certainty. It has also been pointed out recently that the association of the cobalt-(II)-complexes occurs to some extent, a sexa-co-ordination around the cobalt(II)-ion being thereby completed[14].

Summary

In order to establish the electronic absorption spectra of quadri-co-ordinate, square-planar cobalt(II)-complexes, the absorption spectra of bis(salicylaldehyde)ethylenediiminato- and bis-(salicylaldehyde)propylenediiminato-cobalt(II) in solution have been determined, with the utmost care taken to avoid undesirable oxidation of the complexes. These compounds show characteristic ligand field band, with a comparatively sharp peak in the near-infrared region.

Bis(salicylaldehyde)-α-α'-dimethylethylenediiminato- and bis(salicylaldehyde)-α,α'-diphenylethylenediiminato-cobalt(II) have deen prepared, and their spectra examined. These also show characteristic ligand field bands, with a sharp peak in the near-infrared region.

Bis(salicylaldoximato)- and bis(salicylaldiminato)-cobalt(II) have been prepared, and their spectra examined. On the basis of the results obtained above, it has been concluded that these two complexes take a quadri-co-ordinate, planar configuration.

The authors are very grateful to the late Professor Ryutaro Tsuchida for his interest in this work, and to Professor Yoshiharu Izumi and Dr. Kensaku Morihara of the Institute for Protein Research for their advice on the syntheses of the organic ligands. This work was supported in part by the Ministry of Education.

Department of Chemisty
Faculty of Science
Osaka University
Nakanoshima, Osaka

Syntheses and Structures of Acetylformoin and Its Related Compounds. IV. Solvent Effects on a Tautomerism

By Yo MIYAGI

(Received August 7, 1963)

A condensation of the benzoin type of an α-ketoaldehyde RCOCHO yields a formoin, the most primitive structure of which is RCOCH·(OH)COCOR :

$$2\ \mathrm{RCOCHO} \xrightarrow{\mathrm{CN^-}} \mathrm{RCOCH(OH)COCOR}$$

The formoins which had been synthesized were listed in a previous paper.[1] The conditions of the condensation of methylglyoxal were studied by Görlich,[2] while the products other than the formoin were isolated by Franzen.[3] The possible structures for the formoin are I—V.[4-7]

The present author and his co-workers have

1) Y. Miyagi and R. Goto, This Bulletin, **36**, 650 (1963).
2) B. Görlich, *Ber.*, **89**, 2145 (1963).
3) V. Franzen, ibid., **89**, 2154 (1963).
4) P. W. Abenius and H. G. Söderbaum, ibid., **24**, 3033 (1891); **25**, 3468 (1892); P. W. Abenius, ibid., **27**, 706 (1894).
5) A. H. Blatt, *J. Am. Chem. Soc.*, **57**, 1103 (1935); **58**, 1894 (1936).
6) E. Steinbauer and E. Waldman, *Monat. Chem.*, **89**, 570 (1958).
7) R. Nodzu and S. Kunichika, This Bulletin, **15**, 211 (1940).

studied the structures and the chemical behavior of several formoins. Acetylformoin[8] has been proved to have an enediol structure II ($R=CH_3$) in the solid state and in chloroform solution. Benzoylformoin,[8] neopentoylformoin[1] and isobutyrylformoin[9] are furanones IV ($R=C_6H_5$, $C(CH_3)_3$ and $CH(CH_3)_2$ respectively) in the solid state. Isobutyrylformoin[9] has structure IV in tetrahydrofuran solution and structure II in chloroform solution.

Most of these conclusions have been deduced from infrared spectral data. Structure II is characterized by a broad, weak band of the OH stretching absorption and by an intense band of the C=O stretching absorption at a lower frequency, around 1620 cm^{-1}.[10] On the other hand, in structure IV, a rather broad but distinct band arises in the region of the OH stretching absorption, while the C=O and C=C stretching absorption bands are observed around 1690 and 1600 cm^{-1} respectively. Furthermore, these assignments are supported by some of the chemical behavior of formoins.

Results

The ultraviolet and infrared spectra of isobutyrylformoin was found to depend remarkably on the solvent in which it is measured, suggesting a tautomerism between structures II and IV in solution.[9] An ultraviolet absorption arises at 305 mμ ($\varepsilon=7350$) in tetrahydrofuran, and at 360 mμ, with a great enhancement of the intensity ($\varepsilon=14200$), in chloroform (Fig. 1). It has been concluded that the 305 mμ band is attributable to structure IV and the 360 mμ one to structure II, since the infrared spectra had established structure II for chloroform solution and structure IV for tetrahydrofuran solution.

The ultraviolet spectra of isobutyrylformoin were measured in some other solvents. Since the 305 mμ band arises in ethanol and ether (Fig. 2), structure IV may be considered to predominate in these solvents. A slight but distinct tailing beyond 350 mμ in tetrahydrofuran and ether indicates the existence of a

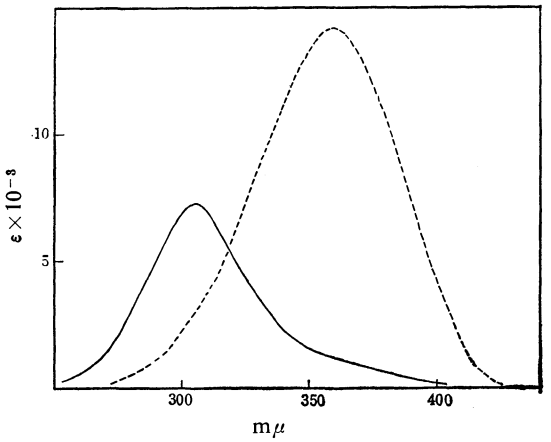


Fig. 1. Ultraviolet spectra of isobutyrylformoin in tetrahydrofuran (——) and chloroform (------).

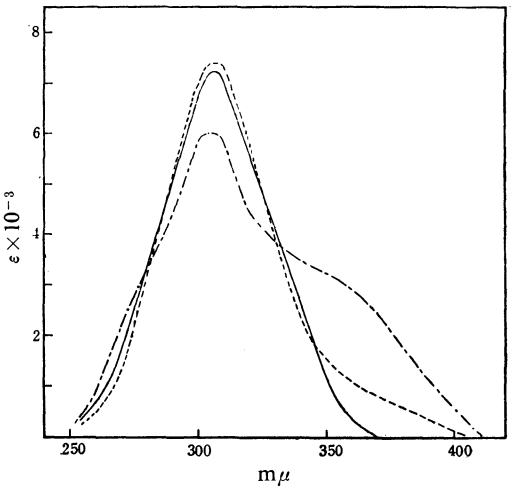


Fig. 2. Ultraviolet spectra of isobutyrylformoin in ethanol (——), acetonitrile (— — —) and ether (------).

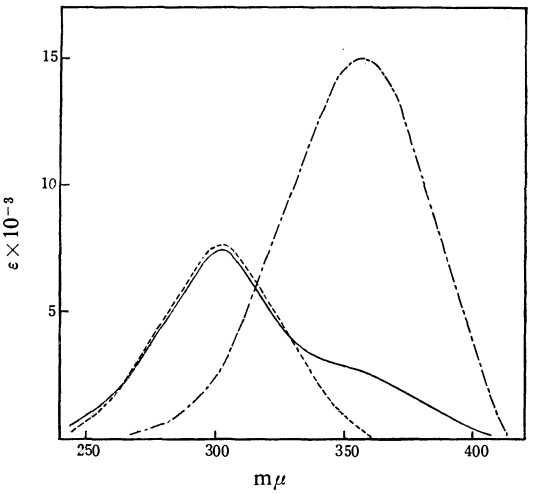


Fig. 3. Ultraviolet spectra of acetylformoin in tetrahydrofuran (——), chloroform (— — —) and ethanol (------).

8) R. Goto, Y. Miyagi and H. Inokawa, This Bulletin, 36, 147 (1963).
9) Y. Miyagi and R. Goto, ibid., 36, 961 (1963).
10) The enol form of a β-diketone, $-C=C(CH)-C(=O)-$, constitutes a conjugate chelation, which gives a broad, weak hydroxyl band and a widely shifted, intense carbonyl band: see, for example, L. J. Bellamy, "Infrared Spectra of Complex Molecules," Methuen, London (1958), pp. 104, 147.

small amount of structure II. In acetonitrile, isobutyrylformoin shows the 305 mμ band with a somewhat decreased intensity (ε=6000) and a shoulder at 360 mμ (ε=2950), suggesting an equilibrium between structures II and IV.

The above findings necessitate a reinvestigation of the structures of other formoins in solution. In the ultraviolet spectrum of acetylformoin in ethanol, the 303 mμ band is dominant (Fig. 3). In tetrahydrofuran there

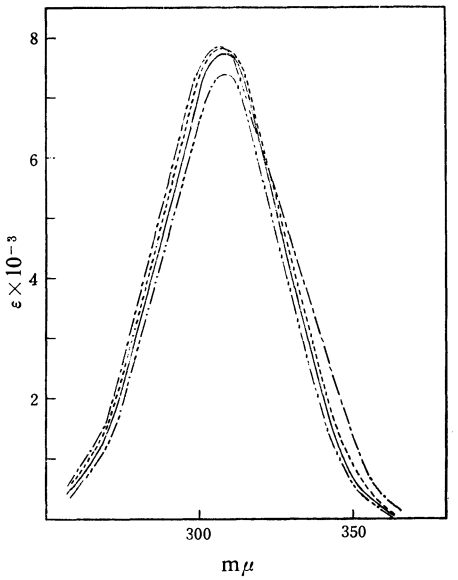


Fig. 4. Ultraviolet spectra of neopentoylformoin in tetrahydrofuran (——), acetonitrile (– – – –), ethanol (— — —) and ether (------).

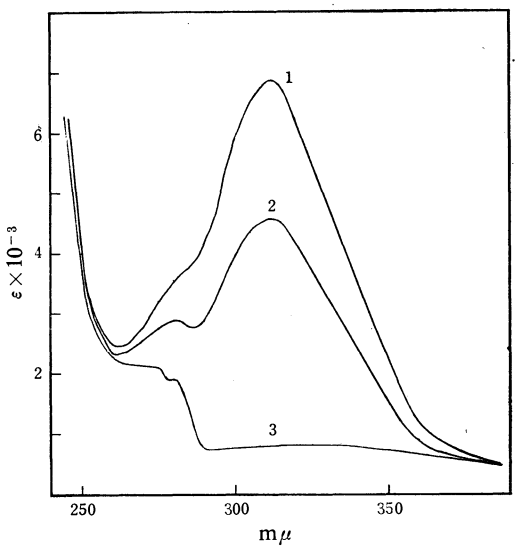


Fig. 5. Ultraviolet spectra of neopentoylformoin in chloroform: 1, in vacuo; 2, 5 hr. after breaking the seal; 3, 1 day after breaking the seal.

is an intense absorption at 303 mμ (ε=7100), with a shoulder around 360 mμ. Thus, in the former solvent, structure IV, and in the latter solvent, an equilibrium between IV and II, may be established. In chloroform an ultraviolet absorption also arises at 355 mμ with an enhancement of the intensity, indicating structure II.

The infrared spectrum of isobutyrylformoin in chloroform (Fig. 8) is very similar to those of acetylformoin in chloroform and in the solid state (Fig. 9). As has been stated in previous papers,[8,9] these spectra are characteristic of structure II: a broad weak band of the OH stretching absorption and an intense one of the C=O stretching absorption at 1620 cm^{-1}. The infrared spectrum of acetylformoin in carbon tetrachloride makes these characteristics more distinct: it becomes more apparent that the OH absorption is broad and weak, because of the disappearance of the C–H stretching absorption of the solvent, which makes the OH band ambiguous. The insolubleness of isobutyrylformoin in this solvent fails to give such a characteristic spectrum as that of acetylformoin in this solvent.

Neopentoylformoin has spectral characteristics consistent with structure IV in ethanol, tetrahydrofuran, ether, acetonitrile and even in chloroform. In the first three solvents, neopentoylformoin shows an ultraviolet absorption at 308 mμ (ε=ca. 7000). In tetrahydrofuran and ether no such tailing beyond 350 mμ is observed as in acetyl- and isobutyrylformoin (Fig. 4). In acetonitrile an absorption arises also at 307 mμ without any shoulder around 360 mμ.

The infrared spectra in ether, tetrahydrofuran and acetonitrile are characteristic of structure IV: the C=O, C=C and OH stretchching absorptions are located at 1705, 1630 and ca. 3300 cm^{-1} respectively (Fig. 10).

Neopentoylformoin is rapidly oxidized in chloroform, so the ultraviolet spectrum in this solvent was measured in a cell sealed in vacuo. There occurs an absorption at 311 mμ with a slight shoulder around 275 mμ; when the sealed cell is opened, the 311 mμ band decreases and the shoulder at 275 mμ can be recognized as an absorption band (Fig. 5). Though the origin of this band has not been found, the dominating 311 mμ band suggests structure IV for neopentoylformoin in chloroform.

The spectra of benzoylformoin indicates structure IV for solution. In tetrahydrofuran it shows an infrared spectrum characteristic of structure IV (Fig. 11); the OH and C=O stretching absorptions arise at 3240 and 1705 cm^{-1} respectively, while the C=C stretching

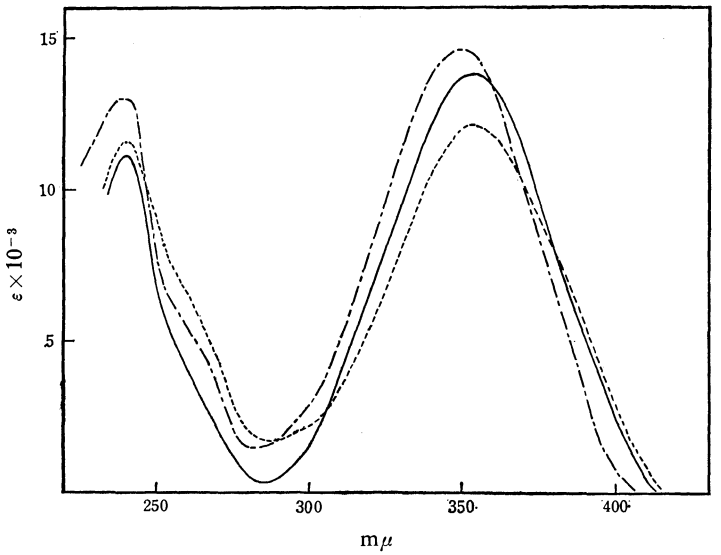


Fig. 6. Ultraviolet spectra of benzoylformoin in tetrahydrofuran (——), ether (— — —) and ethanol (------).

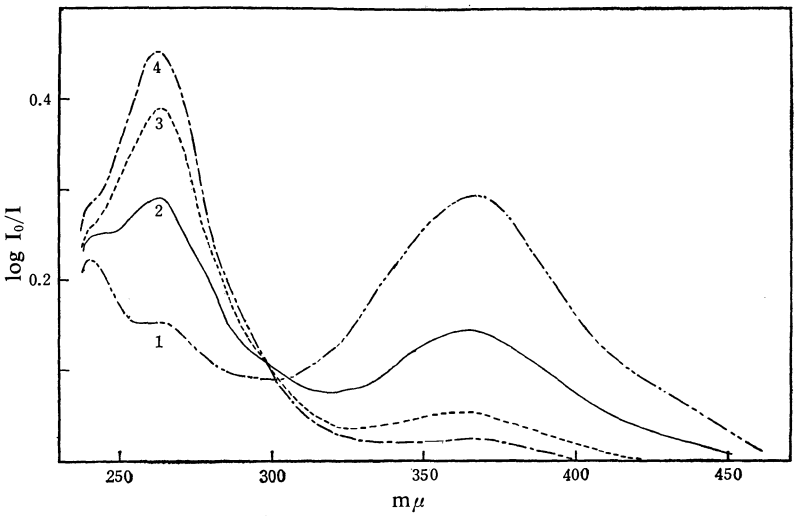


Fig. 7. Ultraviolet spectra of benzoylformoin in chloroform: 1, in vacuo; 2, 2 hr. after breaking the seal; 3, 4 hr. after breaking the seal; 5, 1 day after breaking the seal.

absorptions are located at 1615 and 1595 cm^{-1}. The ultraviolet spectrum of benzoylformoin in tetrahydrofuran is quite identical with those in ether and ethanol (Fig. 6); the absorptions are observed at 354 and 240 mμ. Since structure IV is established for tetrahydrofuran solution by the infrared spectral evidence mentioned above, the two ultraviolet absorptions at 354 and at 240 mμ should be attributed to structure IV. It may be elucidated as follows: the absorption arising from the chromophore, C=C–C=O of IV, is shifted to longer wavelengths by conjugation with a phenyl group.

Benzoylformoin is also rapidly oxidized in chloroform; the ultraviolet spectrum in this solvent was measured in a sealed cell in vacuo. The absorption arises at 370 and at 240 mμ. The lapse of time does not change the spectrum. Opening the sealed cell decreases the 370 and 240 mμ bands. However, Eistert[11] has pointed out a spectral change which might be attributed to a reaction of benzoylformoin with the ethanol present in chloroform as a stabilizer.

11) B. Eistert, private communication.

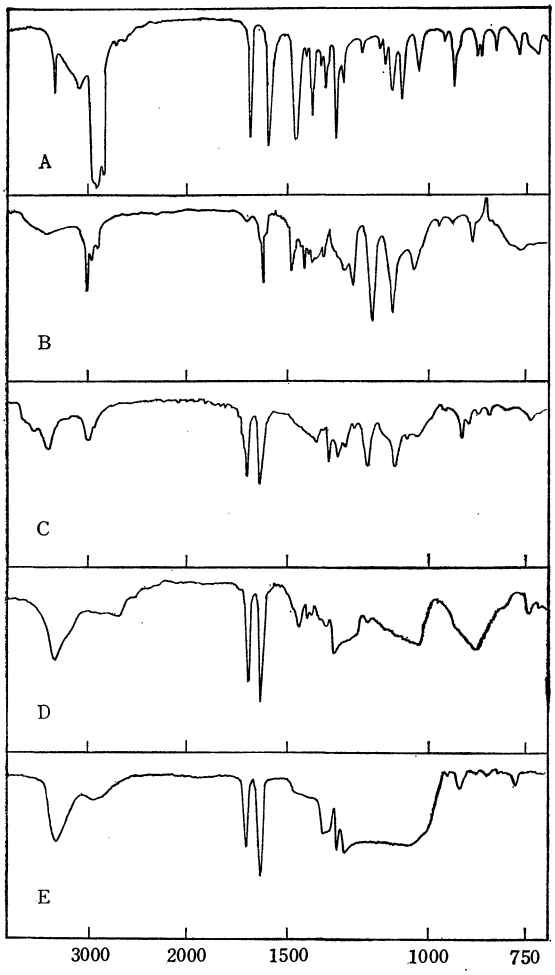


Fig. 8. Infrared spectra of isobutyrylformoin in Nujol (A), chloroform (B), acetonitrile (C), tetrahydrofuran (D) and ether (E).

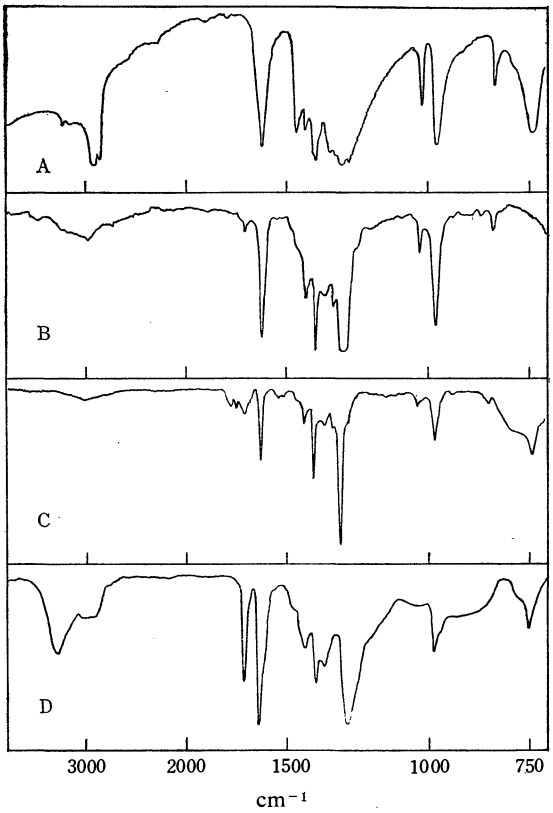


Fig. 9. Infrared spectra of acetylformoin in Nujol (A), chloroform (B), carbon tetrachloride (C) and tetrahydrofuran (D).

Discussion

The above results are summarized in Table III. This tautomerism is apparently affected by two factors: the substituent R and the solvent. Some conclusions may be deduced as follows:

i) In benzoyl- and neopentoyl-formoin, structure IV is dominant in any solvent;

ii) In acetyl- and isobutyryl-formoin, a tautomerism between II and IV occurs in solution; in an A-type solvent,*1 structure IV is dominant, while in a B-type*1 solvent, structure II prodominates;

iii) In the solid state, benzoyl-, neopentoyl- and isobutyryl-formoin have structure IV; only acetylformoin has structure II.

*1 A-type solvent: ethanol, ether and tetrahydrofuran. B-type solvent: chloroform and carbon tetrachloride.

TABLE I. ULTRAVIOLET ABSORPTION BANDS OF FORMOINS

Formoin	Solvent	λ_{max}, mμ	ε_{max}
Acetyl	THF*	303	7300
	EtOH	303	7500
	$CHCl_3$	355	15000
Isobutyryl	EtOH	305	7200
	THF*	305	7350
	Et_2O	305	7400
	CH_3CN	305 360	6000 2950
	$CHCl_3$	360	14200
Neopentoyl	EtOH	308	7350
	THF*	308	7750
	Et_2O	308	7850
	CH_3CN	307	7750
	$CHCl_3$	311	ca. 6330
Benzoyl	EtOH	354 240	12000 10800
	THF*	354 240	13700 11300
	Et_2O	350 240	14600 13000
	$CHCl_3$	367 240	** —

* THF; tetrahydrofuran
** See Experimental.

The discussion of the cause of the tautomerism will be restricted here to the case of solution. It may be reasonable to consider that a tautomer predominating in a solvent is stabililized by a solvation. The most likely explanation is as follows: all A-type solvents have an oxygen atom carrying lone pair electrons, which may be supposed to take part in the formation of hydrogen bondings with the hydroxyl group of formoins, as in Fig. 17, and so the formoins are greatly stabilized. A B-type solvent has no such lone pair electrons with the ability to form a hydrogen bonding and structure IV can not be stabilized by such a solvation as above.*2 Consequently, in chloroform acetyl- and isobutyryl-formoin have more

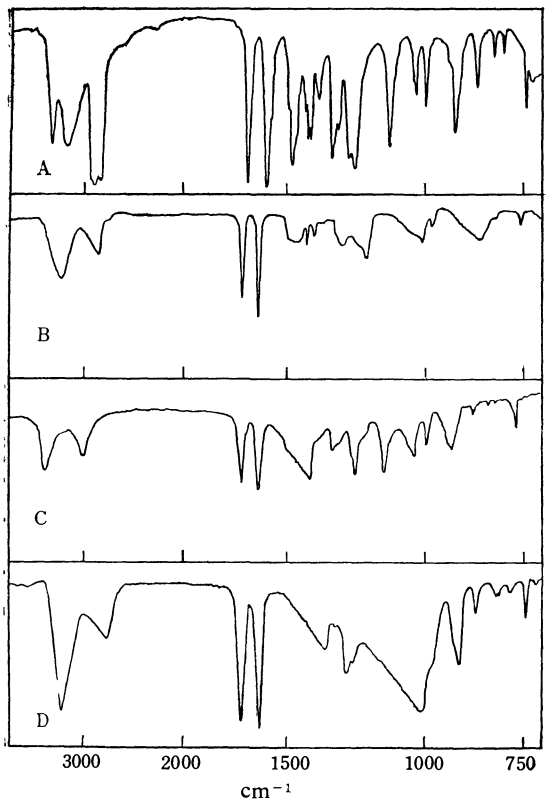


Fig. 10. Infrared spectra of neopentoylformoin in Nujol (A), tetrahydrofuran (B), acetonitrile (C) and ether (D); in ether, a 0.2 mm. cell was used.

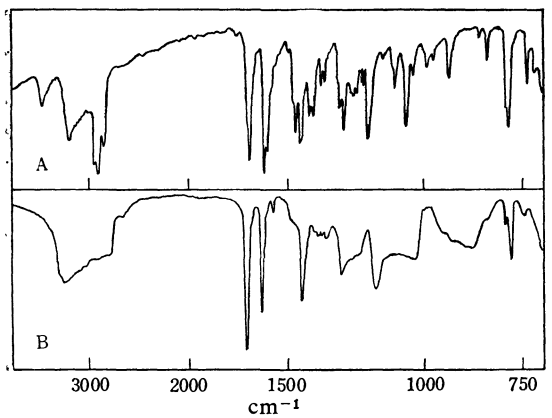


Fig. 11. Infrared spectra of benzoylfomoin in Nujol (A) and tetrahydrofuran (B).

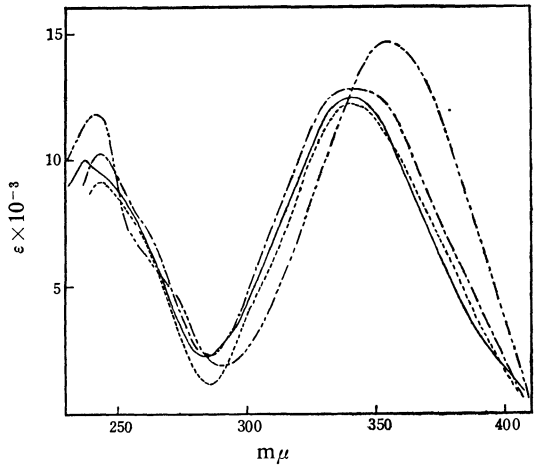


Fig. 12. Ultraviolet spectra of derivatives of benzoylformoin: 1st mono-*O*-methyl benzoylformoin in ethanol (———); di-*O*-methyl benzoylformoin in ethanol (– – –); 2nd mono-*O*-methyl benzoylformoin in tetrahydrofuran (——) and chloroform (------).

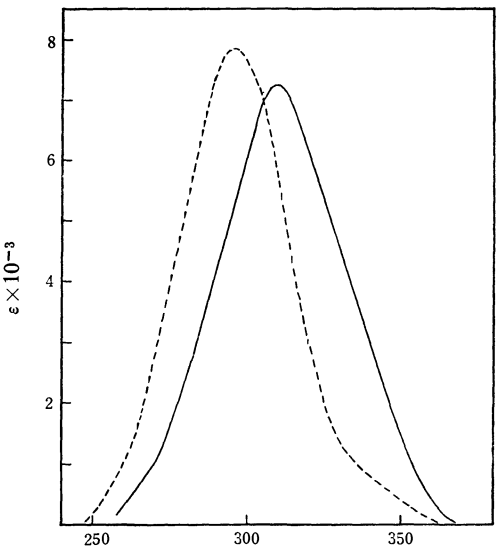


Fig. 13. Ultraviolet spectra of derivatives of neopentoylformoin in ethanol: mono-*O*-methyl neopentoylformoin (——); di-*O*-methyl neopentoylformoin (------).

*2 The B-type solvent may also stabilize formoins by a solvation, but the effect is not so great as in the above-depicted case.

stable tautomer II. In benzoyl- and neopentoylformoin, structure II seems to be unstable, and both formoins have structure IV even in

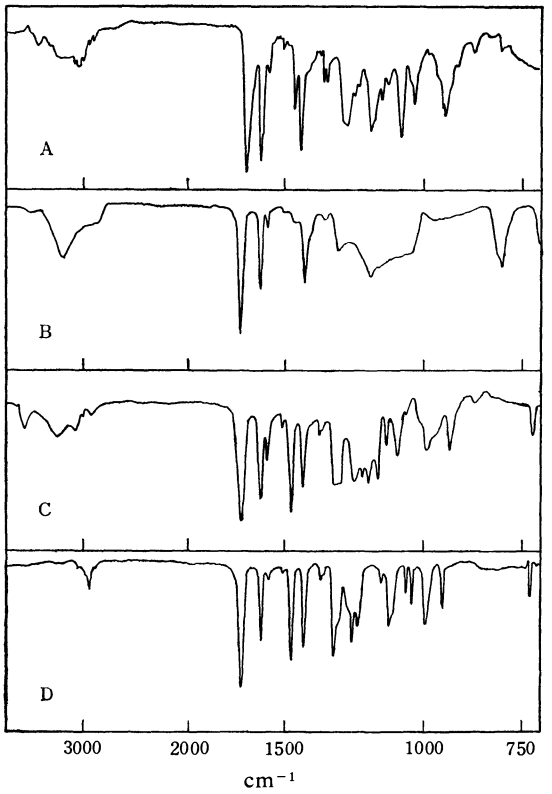


Fig. 14. Infrared spectra of derivatives of benzoylformoin: 1st mono-*O*-methyl benzoylformoin in chloroform (A); 2nd mono-*O*-methyl benzoylformoin in tetrahydrofuran (B) and chloroform (C); di-*O*-methyl benzoylformoin in carbon tetrachloride (D).

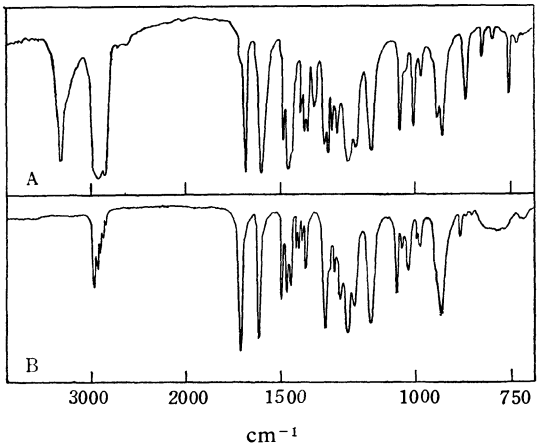


Fig. 15. Infrared spectra of derivatives of neopentoylformoin: mono-*O*-methyl neopentoylformoin in Nujol (A); di-*O*-methyl neopentoylformoin in carbon tetrachloride (B.)

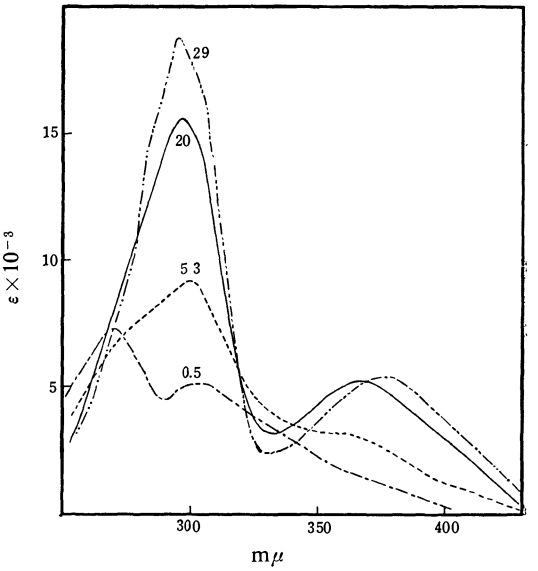


Fig. 16. Ultraviolet spectra of isobutyrylformoin in methanolic hydrogen chloride: numbers are the weight per cent of hydrogen chloride.

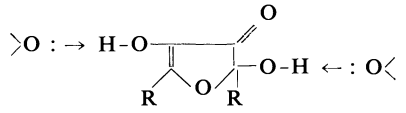


Fig. 17

a B-type solvent, chloroform. However, in this solvent structure IV can not be stabilized so much as in an A-type solvent because of the absence of the solvation,*2 so both formoins are easily oxidized.

The solubility*3 of the formoins seems to have a correlation with their structures. While acetylformoin is very soluble in chloroform and carbon tetrachloride (B-type solvents), the other three formoins are only slightly soluble in chloroform and quite insoluble in carbon tetrachloride. This difference may be explained in terms of the solvation energy and the interaction of molecules in the solid state.*4

All the formoins except acetylformoin show slight but definite discrepancies (about 20 cm^{-1}) in the C=O and C=C stretching absorption bands of structure IV between the solid state and solutions in A-type solvents. On the other hand, the C=O stretching absorption of

*3 This investigation often encounters a difficulty with low solubilities of the formoins in solvents desirable for the spectroscopic measurement (carbon tetrachloride, heptane, cyclohexane; i. e., B-type solvents).

*4 In general, the solubility is proportional to $e^{-\Delta H/RT}$, where ΔH is the energy change in dissolving and is further expressed:

$\Delta H = \Delta H_V - \Delta H_S$

ΔH_V; heat of vaporization

ΔH_S; solvation energy

TABLE II. INFRARED ABSORPTION BANDS OF FORMOINS, cm^{-1}

Formoin	Phase	ν_{OH}	$\nu_{C=O}$	$\nu_{C=C}$	
Acetyl	Nujol	broad and weak	1620		
	$CHCl_3$	broad and weak	1625		
	CCl_4	broad and weak	1630		
	THF*	3280	1705	1640	
Isobutyryl	Nujol	3340 3100	1685	1605	
	$CHCl_3$	broad and weak	1630		
	THF*	3290	1705	1630	
	CH_3CN	3380	1705	1630	
	Et_2O	3320	1710	1635	
Neopentoyl	Nujol	3330 3180	1690	1605	
	THF	3280	1705	1630	
	CH_3CN	3400	1705	1630	
	Et_2O	3240	1703	1627	
Benzoyl	Nujol	3500 3210	1685	1608	1595(shoulder)
	THF*	3240	1705	1615	1595(shoulder)

* THF: Tetrahydrofuran

TABLE III. STRUCTURES OF FORMOINS

Formoin	R	Solid state	Solution	
			A-Type solvent	B-Type solvent
Acetyl	CH_3	II	IV	II
Isobutyryl	$CH(CH_3)_2$	IV	IV	II
Neopentoyl	$C(CH_3)_3$	IV	IV	IV
Benzoyl	C_6H_5	IV	IV	IV

TABLE IV. ULTRAVIOLET AND INFRARED ABSORPTION BANDS OF *O*-METHYL DERIVATIVES OF BENZOYL- AND NEOPENTOYL-FORMOIN

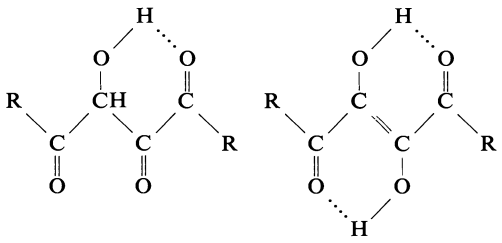
	UV absorption band			IR absorption band, cm^{-1}			
	Solvent	λ_{max}, $m\mu$	ε_{max}	Phase	ν_{OH}	$\nu_{C=O}$	$\nu_{C=C}$
1st mono-*O*-methyl benzoylformoin	EtOH	355 241	14500 11800	$CHCl_3$	3530 3340～3100	1705	1625 1585
Di-*O*-methyl benzoylformoin	EtOH	342 243	12800 10300	CCl_4		1710	1612 1690
2nd mono-*O*-methyl benzoylformoin	EtOH	342 237	12400 10100	THF*	3580～3600 3240	1710	1614
	$CHCl_3$	342 244	12200 9200	$CHCl_3$	3580 3260	1705	1610
Mono-*O*-methyl neopentoylformoin	EtOH	309	7250	Nujol	3310	1690	1610
Di-*O*-methyl neopentoylformoin	EtOH	296	7850	CCl_4		1710	1610

* THF: Tetrahydrofuran

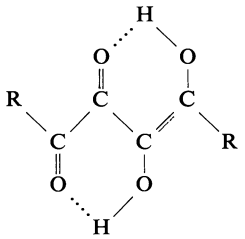
acetylformoin in the solid state (structure II) arises at the same position as that in a B-type solvent. In other words, the positions of the infrared absorptions of structure IV are different in the solid state and in the solution, while that of structure II is identical in both states. It means that the intermolecular bonding in the solid state is strong in structure IV, but not so strong in structure II. This is easily understandable, because the intermolecular chelation is very intense in structure II. A large intermolecular bonding in the solid state suggests a large value of the heat of vaporization (ΔH_v) : the ΔH_v value of structure IV is larger than that of structure II. As has been mentioned previously, the solvation to structure IV is large in an A-type solvent. This means that the ΔH_s value of structure IV

is large in the A-type solvent but small in B-type solvents, while that of structure II in B-type solvents is small.

In spite of its small ΔH_S value, acetylformoin has a large solubility in the B-type solvent because it has structure II in the solid state; in other words, it has a small ΔH_V value. A combination of a large ΔH_V value and a small ΔH_S value results in low solubilities of the other three formoins in B-type solvents.



I II



III



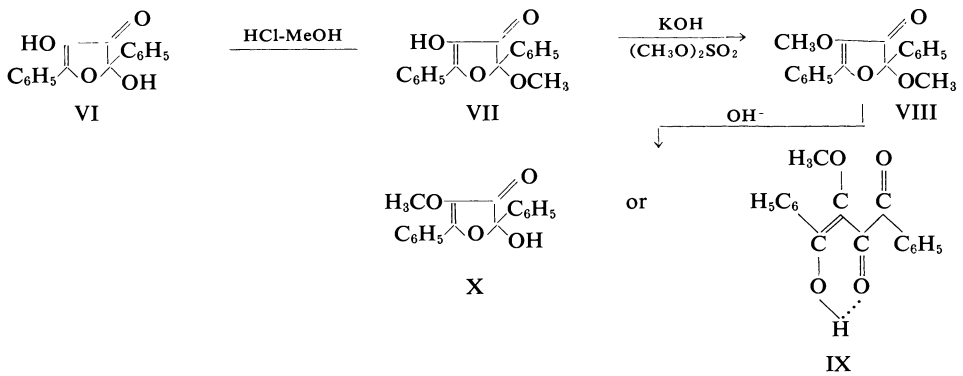
IV V

Further Results

***O*-Alkyl Derivatives of Benzoylformoin.**—Benzoylformoin undergoes a series of reactions as follows: it suffers methanolysis with methanolic hydrogen chloride to give a mono-*O*-methyl benzoylformoin, which is further methylated with dimethyl sulfate to give di-*O*-methyl benzoylformoin. A hydrolysis of the latter compound yields a second mono-*O*-methyl benzoylformoin, which is soluble in chloroform.

Blatt[5a] has stated that second mono-*O*-methyl benzoylformoin was IX. However, structure X may also be possible. A careful study of the ultraviolet and infrared spectra of this compound was undertaken (Figs. 12 and 14). Its ultraviolet spectrum in chloroform is almost identical with that in ethanol and is similar to that of di-*O*-methyl benzoylformoin,*5 the structure of which was established as VIII by chemical evidences. Moreover, there have been found no differences between the infrared spectrum in chloroform (a B-type solvent) and that in tetrahydrofuran (an A-type solvent): the C=O and C=C stretching absorptions arise around 1705 and 1610 cm^{-1} respectively. In structure IX, a partial structure OH·····O constitutes a conjugate $-\overset{|}{C}=C(OCH_3)-\overset{||}{C}-$ chelation. If second mono-*O*-methyl benzoylformoin were IX, it would show a broad weak band of the OH stretching absorption and of the C=O stretching absorption around 1620 cm^{-1} and the ultraviolet absorption at 340 mμ would be shifted to longer wavelengths. For instance, 1-benzoyl-2-α-pyridylethenediol (XII)[12] shows a broad band of the OH stretching absorption, the C=O stretching absorption band at 1603 cm^{-1}, and an ultraviolet absorption at 405 mμ ($\varepsilon = 15940$).

These results indicate that the structure of second mono-*O*-methyl benzoylformoin is X in both types of solvents. Here again a tautomerism between IX and X does not arise.

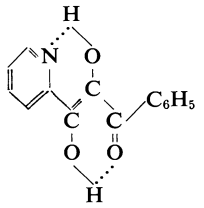


VI VII VIII X or IX

*5 The introduction of a glycosidic ether linkage does not bring about a shift of the ultraviolet absorption. However, that of an enol ether linkage results in a shift of the 354 mμ band to 340 mμ. A similar shift was observed in di-*O*-methyl neopentoylformoin (Fig. 13).

12) B. Eistert and H. Munder, *Ber.*, **91**, 1415 (1958).

Alcoholysis of Isobutyrylformoin.—There is an interesting experimental observation: neo-



XII

pentoylformoin and benzoylformoin undergo methanolysis with methanolic hydrogen chloride to give quantitatively mono-*O*-methyl derivatives. On the other hand, the color of the methanolic hydrogen chloride solutions of isobutyryl- and acetyl-formoin is yellow at first; it turns black while the alcohol and the acid being evaporated under reduced pressure. The residues are black syrups, from which the isolation of mono-*O*-methyl derivatives failed.*6

No differences were observed between the ultraviolet spectrum of neopentoylformoin in ethanol and those in methanolic hydrogen chloride (the concentration of hydrogen chloride, 8 and 17 wt. %), and the latter spectra show no absorptions beyond 350 mμ. On the other hand, the ultraviolet spectra of isobutyrylformoin in methanolic hydrogen chloride (Fig. 16) differ greatly from those of neopentoylformoin. In 0.5% methanolic hydrogen chloride, a band arises at 269 mμ besides the 304 mμ band of a slightly decreased intensity ($\varepsilon=5100$). The absorption band of 7% methanolic hydrogen chloride, arising at 300 mμ, seems to be a overlapping band of the two above bands of a 0.5% solution. In a greatly concentrated solution, the absorption has a remarkably increased intensity. It may be considered that the band located at 269 mμ in 0.5% solution is shifted to longer wavelengths and that its intensity is remarkably enhanced to overlap with the 304 mμ band of 0.5% solution, which may be attributed to the enone chromophore of the formoin.

In methanolic hydrogen chloride solutions of acetyl- and isobutyryl-formoin, it may be considered that some chemical reaction other than etherification occurs, probably a condensation involving C-H bonds of the substituent R. The ultraviolet absorption at 269 mμ arising in the 0.5% methanolic hydrogen chloride solution of isobutyrylformoin may be attributed to this condensation product, the amount of which may increase with the increment in concentration of hydrogen chloride, thus enhancing the intensity of the ultraviolet absorption. Though the attempts to isolate the condensation product have not been successful, the above explanation may be reasonable, because a condensation of a ketone having hydrogen atoms attached to α-carbon atoms occurs under acidic conditions.*7)

Isobutyrylformoin in methanolic hydrogen chloride shows at 360 mμ an additional absorption band, the intensity of which increases also with the increment in the concentration of hydrogen chloride. This band may be ascribed to the condensation product or to the shift of the equilibrium toward structure II upon the decrease in the solvation of methanol: in methanolic hydrogen chloride the proton forms an oxonium ion, $CH_3\text{-}O^+H_2$, to deprive methanol of the ability to solvate.

In an alcoholic solution of an acid, the protonated ketone shows an additional absorption band at a longer wavelength.[13] However, the 360 mμ band arising in a methanolic hydrogen chloride solution of isobutyrylformoin is not attributable to the protonated ketone. If this were the case, neopentoylformoin would show an absorption at 360 mμ in methanolic hydrogen chloride.

Conclusion

When R is methyl or isopropyl (i. e., acetyl- or isobutyryl-formoin), a tautomerism between structures II and IV occurs in solution. When R is phenyl or *t*-butyl (i. e., benzoyl- or neopentoyl-formoin), structure IV predominates in both types of solvents. In a B-type solvent, acetyl- and isobutyryl-formoin have structure II, the more stable tautomer. In an A-type solvent, they have structure IV, a tautomer stabilized by the solvation depicted in Fig. 17.

The above sequence of investigation suggests two assumptions: structure IV is generally more stable than structure II, although when R is methyl or isopropyl, the latter becomes more stable than the former; structure II is, in general, more stable than structure IV, although the former structure becomes unstable when R is phenyl or *t*-butyl. The former assumption is apparently reasonable because γ-

*6 Steinbauer and Waldman[6] isolated mono-*O*-methyl acetylformoin in a 30% yield. The author isolated a trace of a solid product by pouring a methanolic hydrogen chloride solution of isobutyrylformoin into cold water. The product is probably the mono-*O*-methyl derivative because it shows ν_{OH} at 1960, and $\nu_{C=C}$ at 3160, $\nu_{C=O}$ at 1620 cm^{-1} in Nujol.

*7 For example, diacetyl gives a trimer when shaken with concentrated hydrochloric acid at 0°C (R. M. Cresswell, W. R. D. Smith and H. L. S. Wood, *J. Chem. Soc.*, **1961**, 4882). The self-condensation of acetone in the presence of hydrochloric acid gives mesityl oxide, phorone and isophorone (J. B. Conant and N. Tuttle, "Organic Syntheses," Coll. Vol. I, 346 (1948)).

13) See, for example, J. F. Thomas and G. Branch, *J. Am. Chem. Soc.*, **75**, 4793 (1953); M. H. Palmer and D. S. Urch, *J. Chem. Soc.*, **1963**, 174.

and δ-oxy-aldehydes or ketones prefer hemiacetal or hemiketal forms; for example, aldoses and ketoses exist as pyranoses and furanoses. However, structures II and IV involve conjugation, so that the above analogy may not always hold true.

Experimental

Formoins.—All formoins were prepared by the usual method of the benzoin condensation described in previous papers.

Acetylformoin.[8]—Yellow needles, purified by vacuum sublimation; m. p. 82~83°C.

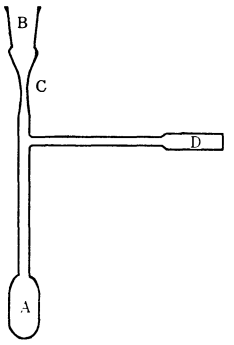


Fig. 18

Isobutyrylformoin.[9]—Colorless needles, recrystallized by adding water to an alcoholic solution; m. p. 87~93°C.

Neopentoylformoin.[1]—Colorless needles, recrystallized from isopropanol; m. p. 170~171°C.

Benzoylformoin.[8]—yellow needles, recrystallized from ethanol; m. p. 186~188°C.

First Mono-*O*-methyl Benzoylformoin (VII).—Benzoylformoin (4 g.) was dissolved in ca. 10% methanolic hydrogen chloride (80 ml.) (slightly warmed). After they had stood overnight, the solvent and the acid were evaporated off under reduced pressure. The residue was washed with cold water and dried in vacuo. The recrystallization was carried out from 50 ml. of ethanol: yellow needles; 3 g.; m. p. 180~182°C.

Found: C, 72.15; H, 4.91. Calcld. for $C_{17}H_{14}O_4$: C, 72.33; H, 5.00%.

By the addition of 10 ml. of water to the mother liquor, 1 g. of the product was collected; m. p. 176~182°C.

Di-*O*-methyl Benzoylformoin (VIII).—First mono-*O*-methyl benzoylformoin (2.5 g.) was dissolved in a solution of 0.7 g. of sodium methoxide in 50 ml. of methanol. After the addition of 15 g. of methyl iodide, the solution was refluxed for 3 hr. After it had stood overnight, the solvent was evaporated off under reduced pressure. Water and ether were added to the residue. The product was obtained as yellow needles by evaporating ether from the ethereal layer and then recrystallized from 2 ml. of methanol: 2.1 g.; m. p. 79.5~80.5°C.

Found: C, 72.85; H, 85.29. Calcd. for $C_{15}H_{16}O_4$: C, 72.96; H, 5.44%.

Second Mono-*O*-methyl Benzoylformoin (X).—This compound was prepared by the method of Blatt:[5a] m. p. 120~124°C.

Found: C, 72.19; H, 5.01. Calcd. for $C_{17}H_{14}O_4$: C, 72.33; H, 5.00%.

Mono-*O*-methyl Neopentoylformoin.[1]—Colorless needles; recrystallized from isopropanol; m. p., 100.5~101°C.

Di-*O*-methyl Neopentoylformoin.[1]—Colorless liquid; b. p., 107~108°C/5 mmHg.

The Ultraviolet Spectra of Neopentoyl- and Benzoyl-formoin in Chloroform.—A definite quantity (3 ml.) of a tetrahydrofuran solution of neopentoylformoin (ca. 5×10^{-5} M) was placed in bottle A, which was then attached to a vacuum line through ground joint B. The solvent was distilled off under 10^{-4} mmHg. Chloroform (3 ml.) was placed in a flask attacthed to the vacuum line, and chloroform was distilled into bottle A which was cooled by liquid air under 10^{-4} mmHg. The thin glass tube C was sealed. After the contents of bottle A reached room temperature, it was poured in cell D and the spectrum was recorded. Consequently, the molecular extinction coefficient was nearly correct. In the case of benzoylformoin, about 0.5 mg. of crystals was placed in bottle A and chloroform was distilled in by the same method as above: the intensity in Fig. 7 is arbitrary.

Spectra.—The infrared spectra were recorded with a Koken model DS-301 and IR-S spectrophotometer. The ultraviolet spectra were recored with a Shimadzu model QR-50 spectrophotometer.

The author wishes to express his thanks to Professor Ryozo Goto of Kyoto University for his kind guidance and encouragement throughout the work, and to Professor Saburo Nagakura of The University of Tokyo and Dr. Yoshiki Matsui of Shionogi & Co. for their discussions.

Department of Chemistry
Faculty of Science
Kyoto University
Sakyo-ku, Kyoto

*The Cationic Copolymerization of Styrene and Isobutene in Liquid Sulfur Dioxide**

By Masashi IINO and Niichiro TOKURA

(Received August 10, 1963)

Recently, there have been published many investigations of the solvent effect on the monomer reactivity ratios as a means of examining the reaction mechanism operating during a cationic polymerization.[1a-g]

A study of the cationic copolymerization of styrene and *p*-bromostyrene presented in a previous paper[3] by the present authors has demonstrated that:

(1) The monomer reactivity ratios in liquid sulfur dioxide are $r_1=0.8$ and $r_2=0.4$ respectively, where r_1 is the ratio of styrene and r_2 is that of *p*-bromostyrene.

(2) In nitrobenzene, $r_1=1.8$ and $r_2=0.3$.

(3) The values of the reactivity ratios in the mixed solvent systems (equivolume) of liquid sulfur dioxide-benzene, liquid sulfur dioxide-nitrobenzene and liquid sulfur dioxide-carbon tetrachloride are almost the same within the range of experimental error as those in liquid sulfur dioxide itself (in case 1).

The absence of any distinct difference in monomer reactivity ratios, *r*'s, among these solvent systems is due perhaps to the similarity of the reactivities of styrene and *p*-bromostyrene. The purpose of the present investigation is to make clearer the behavior of liquid sulfur dioxide in the cationic copolymerization of styrene and isobutene, which are different from each other in monomer structure and in reactivity.

Lately, Higashimura and his coworkers[1g] have reported, of the cationic copolymerizations of styrene-isobutene in various organic solvents, that the isobutene monomer, which is usually more reactive than styrene in cationic polymerization, gets less reactive as the dielectric constants of the systems become lower.

Overberger et al.[1c] have found the same relation between dielectric constant and monomer reactivity ratios in the copolymerization of *p*-chlorostyrene and isobutene.

However, it is doubtful whether the reactivity of the monomer will be explained only by the differences in the dielectric constants of the solvent, since in liquid sulfur dioxide behavior considerably different from that of usual organic solvents have been seen in cationic polymerization.[2a,b]

Experimental

Materials. — The purification of styrene, liquid sulfur dioxide, benzene, nitrobenzene and ethylene dichloride was carried out according to the procedures described in a previous paper.[3] Isobutene used was fractionated after the removal of water with sodium-wire. It was confirmed by gas chromatography that its purity was 99%; it contained about one per cent propane. Stannic chloride was distilled under reduced pressure in a nitrogen stream and sealed into an ampoule. Nitromethane was dehydrated over the phosphorus pentoxide and distilled.

Polymerization. — The charge of isobutene into the reaction tube was carried out according to the same procedure as that employed previously (using a pressure buret), and the other details of the polymerization employed here were the same as those employed in the previous paper[3] with the exception that stannic chloride was used as an

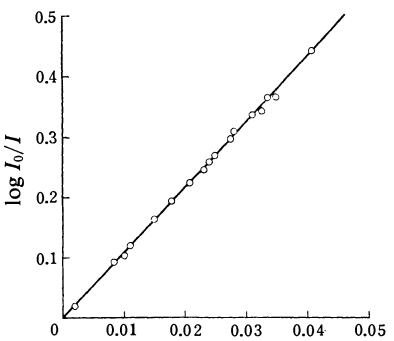


Fig. 1. Relationship between IR-absorbancy and concentration of styrene unit in mixture.

* Polymerization in Liquid Sulfur Dioxide, Part XX.

1) a) C. G. Overberger, L. H. Arond and J. J. Taylor, *J. Am. Chem. Soc.*, **73**, 554 (1951); b) C. G. Overberger, R. J. Ehrig and D. Tanner, ibid., **76**, 772 (1954); c) C. G. Overberger and V. G. Kamath, ibid., **81**, 2910 (1959); d) C. G. Overbegrer and V. G. Kamath, ibid., **85**, 446 (1963); e) C. S. Marvel and J. F. Dunphy, *J. Org. Chem.*, **25**, 2209 (1960); f) R. E. Florin, *J. Am. Chem. Soc.*, **73**, 4468 (1951); g) T. Higashimura, *Kagaku*, Special Issue No. 7, "Syntheses of High Polymers" (1960), p. 46.

2) a) R. Asami and N. Tokura, *J. Polymer Sci.*, **42**, 545 (1960); b) N. Tokura, M. Matsuda and Y. Watanabe, ibid., **62**, 135 (1962).

3) N. Tokura, M. Matsuda and M. Iino, This Bulletin, **35**, 278 (1963).

initiator. Moreover, this polymerization resulted in a heterogeneous system, a polyisobutene or isobutene-rich copolymer being insoluble in liquid sulfur dioxide.

Analyses of Copolymers.—The quantity of styrene in the copolymer was determined on the basis of infrared spectrometry using a Hitachi EPI-S infrared spectrometer, with ν_{max}, 700 cm^{-1}, as the key band. Carbon disulfide was used as the solvent; the thickness of the sodium chloride cell was 0.516 or 0.525 mm. The copolymer used for the measurement was purified by precipitation from carbon disulfide. Beer's law held strictly, as may be seen in Fig. 1.

Results

The r_1 and r_2 Values on Using Liquid Sulfur Dioxide as the Solvent. — The experimental conditions were as follows; total volume of styrene and isobutene, 10.0 ml.; liquid sulfur dioxide, 10.0 ml.; polymerization temperature, −78°C (dry ice-methanol bath); concentration of stannic chloride, 2.1×10^{-3} mol./l.

Figures 2 and 5a show the feed-copolymer composition curve and the results obtained

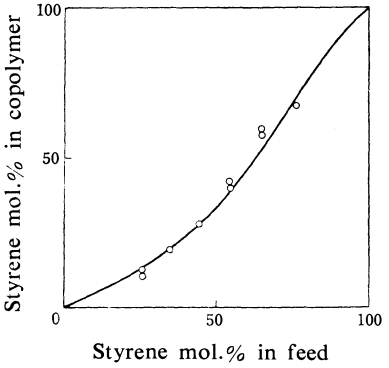


Fig. 2. Copolymerization in liquid sulfur dioxide.

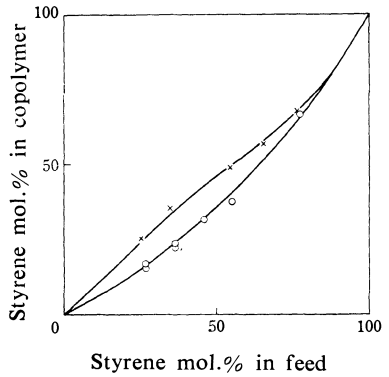


Fig. 3. Copolymerization in liq. SO_2+nitrobenzene and in liq. SO_2+benzene.
× Liq. SO_2+nitrobenzene
○ Liq. SO_2+benzene

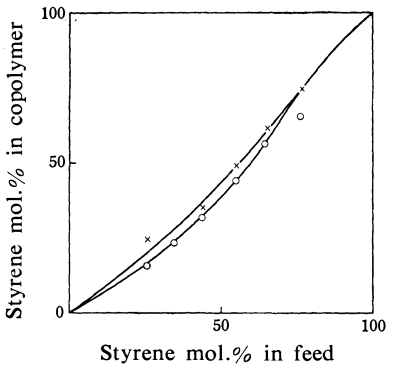


Fig. 4. Copolymerization in liq. SO_2+ethylene dichloride and in liq. SO_2+nitromethane.
× Liq. SO_2+ethylene dichloride
○ Liq. SO_2+nitromethane

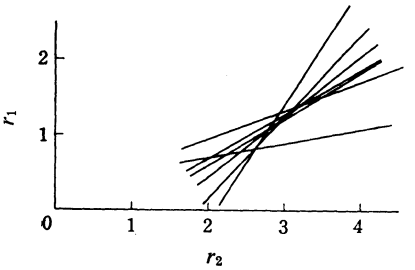


Fig. 5a. MRR of copolymerization in liq. SO_2. r_1, Styrene, r_2, Isobutene

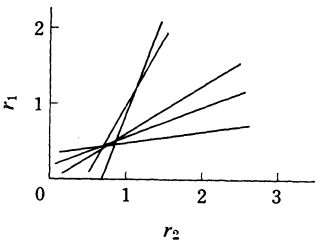


Fig. 5b. MRR of copolymerization in liq. SO_2+nitrobenzene. r_1, Styrene, r_2, Isobutene

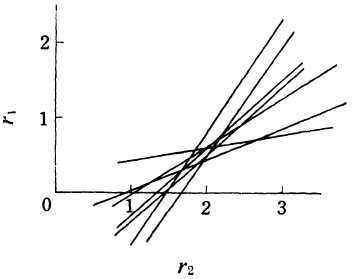


Fig. 5c. MRR of copolymerization in liq. SO_2+benzene. r_1, Styrene, r_2, Isobutene

TABLE I. MONOMER REACTIVITY RATIOS OF THE COPOLYMERIZATION OF STYRENE (M_1) AND ISOBUTENE (M_2) IN LIQUID SULFUR DIOXIDE

Solvent.	r_1	r_2	$r_1 \times r_2$	SO_2 $\times 10$ mol./l.	$SnCl_4$ $\times 10^{-3}$ mol./l.	Poly. temp., °C
Liq.SO_2[a]	1.1	3.1	3.4	1.1	2.1	−78
Liq.SO_2+CH_3NO_2[b]	1.1	2.2	2.4	1.0	4.2	−78
Liq.SO_2+$C_2H_4Cl_2$[b]	1.0	1.5	1.5	1.0	4.2	−78
Liq.SO_2+$C_6H_5NO_2$[b]	0.5	0.8	0.4	1.0	4.2	−78
Liq.SO_2+C_6H_6[b]	0.6	1.9	1.1	1.0	7.4	−78

a) Liq.SO_2, 10.0 ml. styrene+isobutene, 10.0 ml.

b) Liq.SO_2, 11.5 ml. added solvent, 4.0 ml. styrene+isobutene, 10.0 ml.

TABLE II.

Monomer, ml.	Liq. SO_2, ml.	$SnCl_4$ $\times 10^{-3}$ mol./l.	Conversion %	$\bar{P} \times 10^{-2}$	α, %
Styrene 10.0	10.0	1.2	5.3	63	3.2
Isobutene 10.0	10.0	1.2	5.2	5.7	43

α = (Total numbers of polymers/Total numbers of catalysts) $\times 100$

from the intersection method respectively.

The reactivity ratios of $r_1 = 1.1$ and $r_2 = 3.1$, where styrene and isobutene are M_1 and M_2 respectively, were obtained from Fig. 5a.

The r_1 and r_2 Values in the Mixed Solvent Systems of Liquid Sulfur Dioxide-Benzene, Liquid Sulfur Dioxide-Nitrobenzene, Liquid Sulfur Dioxide-Nitromethane and Liquid Sulfur Dioxide-Ethylene Dichloride. — In each solvent system, the composition in feed was as follows: total volume of styrene and isobutene, 10.0 ml.; liquid sulfur dioxide, 11.5 ml.; and the added solvent, 4.0 ml.

Figures 3 and 4 show the composition curve and r_1 and r_2 were obtained by the intersection method respectively. Figure 5 illustrates the results obtained by the intersection method in each solvent system of liquid sulfur dioxide, liquid sulfur dioxide-benzene, and liquid sulfur dioxide-nitrobenzene.

Discussion

The results described above are summarized in Table I.

In liquid sulfur dioxide, the rate of the polymerization of isobutene is far larger than that of styrene. A comparison of the two monomers is shown in Table II.

In the case of styrene polymerization, $\alpha =$ 3.2, and only 3% of the catalyst at the maximum (without transfer) was used, whereas the α value of isobutene is 43%, suggesting that the initiation rate of the latter was very fast in liquid sulfur dioxide when stannic chloride was used as the catalyst.

As has been mentioned before, in the usual cationic copolymerization,[1g] the value of r_2 decreases but r_1 increases as the dielectric constant of the system is reduced, and the product, $r_1 \times r_2$, is approximately unity. A similar tendency was also observed in the cationic copolymerization of *p*-chlorostyrene and isobutene.[1c] On the contrary, as may be seen in Table I, the results obtained here have proved there to be no definite relation between r values and the dielectric constants of the systems, the order of the dielectric constants of the solvents being: liq. SO_2+nitromethane > liq. SO_2+nitrobenzene > liq. SO_2 > liq. SO_2+ethylene dichloride > liq. SO_2+benzene, whereas, r_2 values vary in the order liq. SO_2 > liq. SO_2+nitromethane > liq. SO_2+benzene > liq. SO_2+ethylene dichloride > liq. SO_2+nitrobenzene; r_1 values are classified in two groups, one being $r_1 \fallingdotseq 1$ in liq. SO_2, liq. SO_2+nitromethane and liq. SO_2+ethylene dichloride and the other being $r_1 \fallingdotseq 0.5$ in liq. SO_2+nitrobenzene and liq. SO_2+benzene.

The differences in r_1 values in the two groups may be ascribed to the differences in the monomer reactivities in these two sets of solvent systems. The values of the products, $r_1 \times r_2$ cover a wide range from 0.4 in liquid sulfur dioxide-nitrobenzene to 3.4 in liquid sulfur dioxide.

The r_1 values show no difference in the series of solvent mixtures, liquid sulfur dioxide, liquid sulfur dioxide+nitromethane and liquid sulfur dioxide+ethylene dichloride, wherein $r \fallingdotseq 1$, while r_2 values differ as the solvents are varied. Obviously the differences in reactivities of the carbonium ions derived from the isobutene moiety of the growing end in each solvent may be responsible for these phenomena.

In liquid sulfur dioxide, styrene can give a high molecular weight polymer, whereas isobutene can not. Figure 6 illustrates the correlation between the composition of the feed

and the intrinsic viscosity of the copolymer in the copolymerization. That the η values here can give the measurement of the degrees of polymerization for polymers of styrene, isobutene, and the copolymers of the two on the same basis has been demonstrated elsewhere.[4] Isobutene polymerizes heterogeneously in liquid sulfur dioxide, and the solubility of the polyisobutene is extremely meager.

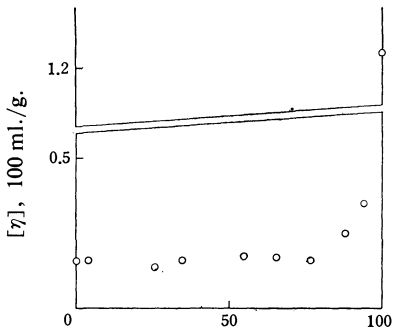


Fig. 6. Relationship between styrene concentration in feed and the intrinsic viscosity* of the copolymer.
* Viscosity was measured in toluene at 30°C.

Though the molar per cent of styrene in feed is about 70%, the η values of the copolymers are as small as in the case of polyisobutene, which suggests that though isobutene is a more reactive monomer than styrene, the growing of the isobutene carbonium ion end is likely to be easily terminated in liquid sulfur dioxide. A controlled polymerization of isobutene in liquid sulfur dioxide (an experiment to be reported on in the near future) also proved the formation of a very low molecular weight polymer. Polyisobutene cannot remain in the solution and separates out on the surface of liquid sulfur dioxide, the polymerization being terminated by keeping away monomers in the solution and eliminating any catalyst fragments. The present authors would like to recall the fact that the classical Edeleanu process for petroleum refining by using liquid sulfur dioxide is based on the scarce solubility of paraffins in liquid sulfur dioxide. At the experimental temperature (−78°C), the higher polymers of isobutene may be insoluble. This means that if the copolymer's propagating end consists of two or more sequences of isobutene units, the copolymer may be separated out and a heterogeneous copolymerization may occur. In mixed solvent systems, the sequence length of isobutene units may also be affected by the added solvents. It should be also noticed that styrene has a stronger solvation than isobutene with liquid sulfur dioxide because the former has a benzene nucleus. However, the present authors have not yet examined precisely the correlation between the reactivities and the solubilities of the monomers and the carbonium ions in each mixed solvent; further study is called for.

4) S. Okamura, T. Higashimura and K. Takeda, *Kobunshi Kagaku*, **18**, 389 (1961).

Summary

The copolymerizations of styrene and isobutene in liquid sulfur dioxide and in mixtures of liquid sulfur dioxide with nitromethane, ethylene dichloride, nitrobenzene and benzene have been carried out at −78°C. The r_1 and r_2 values have been estimated by the intersection method. When M_1 stands for styrene and M_2 for isobutene, r_1 and r_2 are 1.1 and 3.1 in liquid sulfur dioxide. The r_2 values vary, as the added solvent is changed. Two sets of r_1 values, approximately unity and 0.5, have been found. The meager solubility of polyisobutene and isobutene sequence in the copolymer may be responsible for the findings.

The authors are indebted to the Seitetsu Kagaku K. K. for the donation of liquid sulfur dioxide and to the Ministry of Education for a grant-in-aid for this project.

The Chemical Research Institute of Non-Aqueous Solutions
Tohoku University
Katahira-cho, Sendai

The Theory of the Indicator Transition in Chelatometry

By Genkichi NAKAGAWA and Motoharu TANAKA

(Received August 12, 1963)

Though various theories have been proposed for the indicator transition in chelatometry, the discussion seems to have been restricted more or less to particular cases; we find hardly any general treatments applicable to every case of chelatometry.[1-5]

In our preceding paper[1] a formula has been proposed for the indicator transition in the chelatometry of a metal using the NY-HA system as an indicator. In the present investigation the effect of a second metal is considered theoretically, and general equations are proposed for the indicator transition in the chelatometry of a metal in the presence of a second metal using HA or the NY-HA system as an indicator.

Theoretical Consideration

The Derivation of the Expressions of the Indicator Transiton.—*Chelatometry Using HA as an Indicator.*—In order to secure a distinct indicator transition in the vicinity of the equivalence point of the chelatometry of M_I, it is necessary for reaction 1.1 to proceed in favor of the right side and, at the same time, for reaction 1.2 to proceed in favor of the left side.

$$M_I' + A' \rightleftarrows M_IA \qquad (1.1)^{6}$$

$$M_IY + A' \rightleftarrows M_IA + Y' \qquad (1.2)$$

From the constant of the (1.1) equilibrium, i.e., the conditional stability constant of M_IA,

$$[M_I]' = \frac{[M_IA]}{[A]'K_{M_IA'}} \qquad (1.3)$$

The constant of the (1.2) equilibrium, which is equal to $K_{M_IA'}/K_{M_IY'}$, is given by the following:

$$\frac{K_{M_IA'}}{K_{M_IY'}} = \frac{[M_IA][Y]'}{[M_IY][A]'}$$

Hence,

$$[Y]' = \frac{[A]'}{[M_IA]}\frac{[M_IY]K_{M_IA'}}{K_{M_IY'}} \qquad (1.4)$$

Stoicheometric relationships 1.5 through 1.8 hold throughout the titration:

$$C_{M_I} = [M_IY] + [M_IA] + [M_I]' \qquad (1.5)$$

$$C_Y = [M_IY] + [M_{II}Y] + [Y]' \qquad (1.6)$$

$$C_{M_{II}} = [M_{II}Y] + [M_{II}]' \qquad (1.7)$$

$$C_A = [M_IA] + [A]' \qquad (1.8)$$

The side reaction coefficient of the protonation and the formation of $M_{II}Y$, $\alpha_{H,M_{II}(Y)}$, is given by 1.9:

$$\alpha_{H,M_{II}(Y)} = \frac{[M_{II}Y] + [Y]'}{[Y]} \qquad (1.9)^{7}$$

When Eq. 1.9 is substituted into Eq. 1.6,

$$C_Y = [M_IY] + [Y]\ \alpha_{H,M_{II}(Y)} \qquad (1.10)$$

When Eqs. 1.4 and 1.10 are combined,

$$C_Y = [M_IY]\left(1 + \frac{[A]'}{[M_IA]}\frac{K_{M_IA'}\alpha_{H,M_{II}(Y)}}{K_{M_IY}}\right) \qquad (1.11)$$

By substituting Eqs. 1.3 and 1.5 into 1.11, we have

$$C_Y = \left(C_{M_I} - [M_IA] - \frac{[M_IA]}{[A]'}\frac{\beta_{(M_I)}\alpha_{H(A)}}{K_{M_IA}}\right) \times \left(1 + \frac{[A]'}{[M_IA]}\frac{K_{M_IA}\alpha_{H,M_{II}(Y)}}{K_{M_IY}\alpha_{H(A)}}\right) \qquad (1.12)$$

The indicator transition, ϕ, is defined as:

$$\phi = \frac{[A]'}{C_A} \qquad (1.13)$$

Designating $C_Y/C_{M_I} = a$, we obtain Eq. 1.14 from 1.8, 1.12 and 1.13:

$$a = 1 - \frac{1-\phi}{\phi}\frac{\beta_{(M_I)}\alpha_{H(A)}}{C_{M_I}K_{M_IA}} + \frac{\phi}{1-\phi}\frac{K_{M_IA}\alpha_{H,M_{II}(Y)}}{K_{M_IY}\alpha_{H(A)}} - \frac{C_A}{C_{M_I}}\left(1-\phi + \phi\frac{K_{M_IA}\alpha_{H,M_{II}(Y)}}{K_{M_IY}\alpha_{H(A)}}\right) - \frac{\beta_{(M_I)}\alpha_{H,M_{II}(Y)}}{C_{M_I}K_{M_IY}} \qquad (1.14)$$

1) G. Nakagawa and M. Tanaka, *Talanta*, **9**, 917 (1962).
2) J. M. H. Fortuin, P. Karsten and H. L. Kies, *Anal. Chim. Acta*, **10**, 356 (1954).
3) H. Flaschka and S. Khalafalla, *Z. anal. Chem.*, **156**, 401 (1957).
4) C. N. Reilley and R. W. Schmid, *Anal. Chem.*, **31**, 887 (1959).
5) H. Flaschka, *Talanta*, **1**, 60 (1958).
6) A is assumed to form a 1:1 chelate with M_I.
7) From the formation constant of $M_{II}Y$, we have $\alpha_{H,M_{II}(Y)} = K_{M_{II}Y}[M_I^I] + \alpha_{H(Y)}$
For a more detailed discussion of the concept of the ligand buffer, as well as for the calculation of $\alpha_{H,M_{II}(Y)}$, cf. M. Tanaka, *Anal. Chim. Acta*, **29**, 193 (1963).

Equation 1.14 is a quantitative expression of the indicator transition in the chelatometry of M_I in the presence of M_{II}, using HA as an indictor. Under conditions favorable for the titration, the last term of Eq. 1.14 may be neglected, and, when $C_A \ll C_{M_I}$, the fourth term on the right side of Eq. 1.14 may also be neglected. Therefore,

$$a=1-\frac{1-\phi}{\phi}\frac{\beta_{(M_I)}\alpha_{H(A)}}{C_{M_I}K_{M_IA}}+\frac{\phi}{1-\phi}\frac{K_{M_IA}\alpha_{H,M_{II}(Y)}}{K_{M_IY}\alpha_{H(A)}} \quad (1.15)$$

Near the equivalence point $[M_{II}Y]$ is negligibly small compared with $[M_{II}]'$ in Eq. 1.7, so

$$\alpha_{H,M_{II}(Y)}=K_{M_{II}Y}C_{M_{II}}/\beta_{(M_{II})}+\alpha_{H(Y)}$$

When the formation of $M_{II}Y$ is not appreciable, $\alpha_{H,M_{II}(Y)}=\alpha_{H(Y)}$. The substitution of this relationship into Eq. 1.15 gives an equation for the indicator transition in the absence of a second metal, M_{II}.[4,5]

Chelatometry Using the NY-HA System as an Indicator.—The indicator transition of a chelatometry using the NY-HA system as an indicator should be discussed for the following two cases separately:

a) $K_{M_I'Y'}>K_{N'Y'}$, e.g., the titration of calcium with EDTA, using the Mg-EDTA-Erio T system as an indicator, and b) $K_{N'Y'}>K_{M_I'Y'}$, e. g., the titration of aluminum with EDTA using the Cu-EDTA-PAN system as an indicator.

a) $K_{M_I'Y'}>K_{N'Y'}$. — This case corresponds to the so-called partial replacement titration, in which we consider the following two equilibria:

$$N' + A' \rightleftharpoons NA \quad (2.1)$$

$$NY + A' \rightleftharpoons NA + Y' \quad (2.2)$$

From the constants of equilibria 2.1 and 2.2, we have

$$[N]'=\frac{[NA]}{[A]'K_{N'A'}} \quad (2.3)$$

$$[Y]'=\frac{[A]'}{[NA]}\frac{[NY]K_{NA'}}{K_{NY'}} \quad (2.4)$$

Stoicheometric relationships 2.5 through 2.8 hold throughout the titration:

$$C_{M_I}=[M_IY]+[M_I]' \quad (2.5)$$

$$C_Y=[M_IY]+[NY]+[M_{II}Y]+[Y]' \quad (2.6)$$

$$C_N=[NY]+[NA]'+[N]' \quad (2.7)$$

$$C_A=[NA]+[A]' \quad (2.8)$$

N being added as NY, the total concentration of the complexan used as the titrant, C_Y', is given by $C_Y'=C_Y-C_N$. Therefore, from Eqs. 2.5, 2.6 and 2.7, we obtain

$$C_Y'=C_{M_I}-[M_I]'-[N]'+[Y]\alpha_{H,M_{II}(Y)}-[NA] \quad (2.9)$$

From the formation constants of M_IY and NY,

$$\frac{[M_IY]}{[M_I]'K_{M_I'Y}}=\frac{[NY]}{[N]'K_{N'Y}}$$

Therefore,

$$[M_I]'=\frac{C_{M_I}[N]'K_{N'Y}}{K_{M_I'Y}(C_N-[N]')+[N]'K_{N'Y}} \quad (2.10)$$

Substituting Eq. 2.10 into 2.9, we have

$$a=C_Y'/C_{M_I}=1-\frac{[N]'}{C_{M_I}}\times\left(1+\frac{C_{M_I}K_{N'Y}}{K_{M_I'Y}(C_N-[N]')+[N]'K_{N'Y}}\right)+\frac{[Y]\alpha_{H,M_{II}(Y)}}{C_{M_I}}-\frac{[NA]}{C_{M_I}} \quad (2.11)$$

When $K_{M_I'Y'}>K_{N'Y'}$ and $a>1-C_N/C_{M_I}$, we can neglect the second term in the parentheses of the second term on the right side of Eq. 2.11. Therefore, by combining Eqs. 2.3, 2.4 and 2.11, we obtain

$$a=1-\frac{1-\phi}{\phi}\frac{\beta_{(N)}\alpha_{H(A)}}{K_{NA}C_{M_I}}+\frac{\phi}{1-\phi}\frac{K_{NA}\alpha_{H,M_{II}(Y)}C_N}{K_{NY}\alpha_{H(A)}C_{M_I}}-\frac{C_A}{C_{M_I}}\left(1-\phi+\phi\frac{K_{NA}\alpha_{H,M_{II}(Y)}}{K_{NY}\alpha_{H(A)}}\right)-\frac{\beta_{(N)}\alpha_{H,M_{II}(Y)}}{K_{NY}C_{M_I}} \quad (2.12)$$

In a favorable condition for the titration, we can neglect the last term on the right side of Eq. 2.12, and, C_{M_I} being generally much greater than C_A, we can also neglect the fourth term. Therefore, we have

$$a=1-\frac{1-\phi}{\phi}\frac{\beta_{(N)}\alpha_{H(A)}}{K_{NA}C_{M_I}}+\frac{\phi}{1-\phi}\frac{K_{NA}\alpha_{H,M_{II}(Y)}C_N}{K_{NY}\alpha_{H(A)}C_{M_I}} \quad (2.13)$$

In the vicinity of the equivalence point, $\alpha_{H,M_{II}(Y)}=K_{M_{II}Y}C_{M_{II}}/\beta_{(M_{II})}+\alpha_{H(Y)}$ in Eq. 2.13, and when the formation of $M_{II}Y$ is not appreciable, $\alpha_{H,M_{II}(Y)}=\alpha_{H(Y)}$.

It should be remembered that Eq. 2.13 holds for $a>1-C_N/C_{M_I}$. For $a<1-C_N/C_{M_I}$, however, Eq. 2.13 does not hold; we can not neglect the second term in parentheses on the right side of Eq. 2.11. In this case, most Y being combined with M_I, $[N]'\simeq C_N$. Therefore, from Eq. 2.3,

$$1-\phi=\frac{C_NK_{N'A'}}{C_NK_{N'A'}+1}$$

The maximum coloration of the indicator is

determined by this equation. It then follows that, in order to secure a full coloration of NA before the equivalence point, the $C_N K_{N'A'}$ value should be much greater than unity.

b) $K_{N'Y'} > K_{M_I'Y'}$.—We shall consider the following two equilibria, the constants of which are denoted as K_1 and K_2:

$$NY + M_I' + A' \overset{K_1}{\rightleftharpoons} M_IY + NA$$

$$K_1 = \frac{[M_IY]\,[NA]}{[NY]\,[M_I]'\,[A]} = \frac{K_{M_I'Y} K_{NA'}}{K_{NY}} \quad (2.14)$$

$$NY + A' \overset{K_2}{\rightleftharpoons} NA + Y'$$

$$K_2 = \frac{[NA]\,[Y]'}{[NY]\,[A]'} = \frac{K_{NA'}}{K_{NY'}} \quad (2.15)$$

From expressions 2.14 and 2.15, we have

$$[M_I]' = \frac{[M_IY]\,[NA]}{[NY]\,[A]'K_1} \quad (2.16)$$

$$[Y]' = \frac{[A]'\,[NY]K_2}{[NA]} \quad (2.17)$$

The following stoicheometric relationships, 2.18 through 2.22, hold throughout the titration:

$$C_{M_I} = [M_IY] + [M_I]' \quad (2.18)$$

$$C_Y = [M_IY] + [M_{II}Y] + [NY] + [Y]' \quad (2.19)$$

$$C_{M_{II}} = [M_{II}Y] + [M_{II}]' \quad (2.20)$$

$$C_N = [NY] + [NA] + [N]' \quad (2.21)$$

$$C_A = [NA] + [A]' \quad (2.22)$$

N being generally added as NY, the total concentration of the complexan used as the titrant, C_Y', is given by the following:

$$C_Y' = C_Y - C_N \quad (2.23)$$

When N does not form any appreciable complexes other than NY and NA, [N]' can be neglected in Eq. 2.21. Therefore, by combining Eqs. 1.9, 2.19 and 2.23, we have

$$C_Y' = [M_IY] + [Y]\,\alpha_{H,M_{II}(Y)} - [NA] \quad (2.24)$$

Substituting Eq. 2.17 into 2.24,

$$C_Y' = [M_IY] + \frac{[A]'}{[NA]} \frac{[NY]\,K_2 \alpha_{H,M_{II}(Y)}}{\alpha_{H(Y)}} - [NA] \quad (2.25)$$

On the other hand, from Eqs. 2.16 and 2.18,

$$C_{M_I} = [M_IY]\left(1 + \frac{[NA]}{[A]'} \frac{1}{[NY]\,K_1}\right) \quad (2.26)$$

By combining Eqs. 2.25 and 2.26, we have

$$C_{Y'} = C_{M_I} \Big/ \left(1 + \frac{[NA]}{[A]'} \frac{1}{[NY]\,K_1}\right) + \frac{[A]'}{[NA]} \frac{[NY]\,K_2 \alpha_{H,M_{II}(Y)}}{\alpha_{H(Y)}} - [NA] \quad (2.27)$$

Under conditions favorable for titration, $[NA]/[A]'\,[NY]\,K_1$ is much smaller than unity in the vicinity of the equivalence point. Since C_{M_I} is generally much greater than C_A, the fourth term on the right side of Eq. 2.27 can be neglected. Moreover, when C_N is much greater than C_A, [NY] may be regarded as C_N. Therefore,

$$a = 1 - \frac{1-\phi}{\phi} \frac{K_{NY} \beta_{(M_I)} \alpha_{H(A)}}{K_{M_IY} K_{NA} C_N} + \frac{\phi}{1-\phi} \frac{K_{NA} \alpha_{H,M_{II}(Y)} C_N}{K_{NY} \alpha_{H(A)} C_{M_I}} \quad (2.28)$$

In the vicinity of the equivalence point, $\alpha_{H,M_{II}(Y)}$ is given by the following:

$$\alpha_{H,M_{II}(Y)} = K_{M_{II}Y} C_{M_{II}} / \beta_{(M_{II})} + \alpha_{H(Y)}$$

and, when the formation of $M_{II}Y$ is not appreciable, $\alpha_{H,M_{II}(Y)} = \alpha_{H(Y)}$.

A General Discussion of the Indicator Transition in the Vicinity of the Equivalence Point of Chelatometry.—In Eqs.1.15, 2.13 and 2.28, ϕ is a value expressing the indicator transition, and the second term is mainly concerned with the color transition before the equivalence point, while the third is mainly concerned with the color transition after the equivalence point.

Equations 1.15, 2.13 and 2.28 can be rewritten as the following general form:

$$a = 1 - \frac{1-\phi}{\phi} f_1 + \frac{\phi}{1-\phi} f_2$$

Thus the indicator transition near the equivalence point in any chelatometry is determined by a combination of f_1 and f_2 values; the lower the values of f_1 and f_2, the sharper the indicator transition.

Now it should be noted that the value of $f_1 f_2$ is independent of the indicator characteristics and is given by the following:

$$f_1 f_2 = \frac{\alpha_{H,M_{II}(Y)} \beta_{(M_I)}}{K_{M_IY} C_{M_I}}$$

Thus, if $K_{M_{II}'Y'}$ is sufficiently low, a distinct indicator transition will be obtained even for a high value of $C_{M_{II}}/C_{M_I}$. From Eqs. 1.15, 2.13 and 2.28, it can easily be seen that M_{II} hardly affects the indicator transition *before* the equivalence point. However, the higher the value of $\alpha_{H,M_{II}(Y)}$ or $K_{M_{II}'Y'} C_{M_{II}}$, the less distinct the indicator transition *after* the equivalence point. ϕ or $1-\phi$ versus a diagrams drawn for various combinations of f_1 and f_2 values facilitate the establishment of the optimum conditions for a given problem; the computation of f_1 and f_2 values for a given

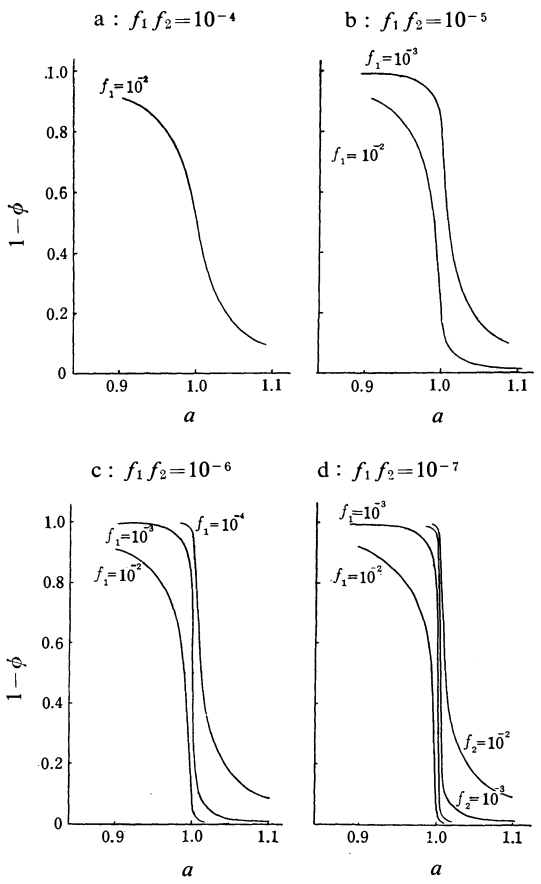


Fig. 1. Theoretical indicator transition for various couples of f_1 and f_2.

system makes possible the prediction of the indicator transition (Fig. 1).

We would like to emphasize that Eqs. 1.15, 2.13 and 2.28 make possible a theoretical consideration of the indicator transition in any type of chelatometry using HA or the NY-HA system as an indicator.

Applicability of the Theory

The above theory has been confirmed experimentally in some familiar examples of the titration of alkaline earths with EDTA, using Erio T as an indicator.

HA as an Indicator.—The titration of magnesium with EDTA, using Erio T as an indicator.

a) In the absence of a second metal.

Condition: $C_{M_I} = C_{Mg} = 10^{-3}$ M; $C_{M_{II}} = 0$; pH $= 10$.[8] Using log $K_{MgY} = 8.69$ and log $K_{MgA'}$ (pH $= 10$) $= 5.44$,[9] f_1 and f_2 are computed thus:

$$f_1 = \frac{1}{K_{MgA'} C_{Mg}} = 10^{-2.44}; \quad f_2 = \frac{K_{MgA'}}{K_{MgY'}} = 10^{-2.80}$$

From these values, a distinct indicator transition is anticipated in the vicinity of the equivalence point (cf. Fig. 1).

b) In the presence of sodium.

When $C_{M_{II}} = C_{Na} = 1$ M, f_1 is the same as in a) and, from log $K_{NaY} = 1.66$,

$$f_2 = \frac{K_{MgA'}}{K_{MgY'}} (K_{NaY'} C_{Na} + 1) = 10^{-1.56}$$

Thus the discoloration of Mg-Erio T after the equivalence point will become somewhat sluggish. However, the visual titration of magnesium in the presence of 1 M sodium is possible.[10]

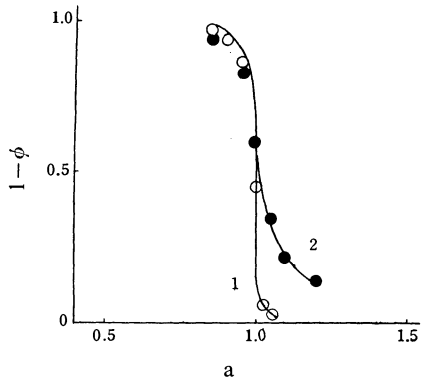


Fig. 2. Indicator transition of the titration of magnesium using Erio T as an indicator.
—— Theoretical indicator transition:
Curve 1: Na=0, Curve 2: Na=1 M
○● Experimental values:
○: Na=0, ●: Na=1 M

Figure 2 shows the results of the photometric titration of magnesium, using Erio T as an indicator, as well as the theoretical indicator transition curve. The experimental results agree well with the theoretical curves after the equivalence point. The discordance between the observed and the theoretical curves before the equivalence point may be attributable to the decomposition of Erio T, which is accelerated in the presence of sodium.[11]

The purity of commercial preparations of Erio T is often very low, and the decomposition of impure Erio T is particularly fast. A method for the purification of Erio T has

8) At a pH value of 10 neither hydrolysis nor the ammine formation of magnesium needs to be taken into consideration.

9) G. Schwarzenbach, "Die komplexometrische Titration," Ferdinand Enke Verlag, Stuttgart (1955). p. 27.

10) Using an indicator such as Erio T, of which the contrast of metallized and unmetallized indicator is sufficiently large, visual titration is possible with values of f_1 and f_2 up to about $10^{-1.5}$.

11) G. Nakagawa and M. Tanaka, unpublished results.

been described[12]; in the present investigation, however, we employed Erio T purified by the following simplified procedure: 20 g. of commercial Erio T (Dojindo Chemical Co., Kumamoto) are washed five times with 50 ml. of 2 N hydrochloric acid. The desalted dye is then air-dried and recrystallized from dimethylformamide. Though the obtained dimethylammonium salt of Erio T is not very pure, it is satisfactory for all practical purposes.

The NY-HA System as an Indicator.—*i) Partial Replacement Titration, $K_{MI'Y'} > K_{N'Y'}$.*—The titration of calcium, with EDTA using the MgY-ErioT system as an indicator.

a) In the absence of a second metal.

Condition: $C_{MI} = C_{Ca} = 10^{-3}$M; $C_{MII} = 0$; pH $=10$. Using the values log $K_{CaY} = 10.70$, K_{MgY} and $K_{MgA'}$ (pH$=10$), f_1 and f_2 in Eq. 2.13 are computed:

$$f_1 = \frac{1}{K_{MgA'} C_{Ca}} = 10^{-2.44}$$

$$f_2 = \frac{K_{MgA'} C_{Mg}}{K_{MgY} C_{Ca}} = 10^{0.20} C_{Mg}$$

f_1, f_2 and $(1-\phi)_{max}$ values for various values of C_{Mg} are given in Table I.

Table I. f_1 and f_2 for various values of C_{Mg} in the chelatometry of calcium using MgY-Erio T system as an indicator

C_{Mg}, M	log f_1	log f_2	$(1-\phi)_{max}$
10^{-3}	−2.44	−2.80	0.996
10^{-4}	−2.44	−3.80	0.965
10^{-5}	−2.44	−4.80	0.734

From Table I it may easily be deduced that about 10^{-4}M of magnesium will give the best results.

b) In the presence of sodium.

The indicator transition is considered for the chelatometry of calcium in the presence of 1M sodium using C_{Mg} of 10^{-4}M, which gives the best indicator transition in the absence of a second metal. f_1 and $(1-\phi)_{max}$ are the same as in i a), and

$$f_2 = \frac{K_{MgA'} C_{Mg}}{K_{MgY'} C_{Ca}} (K_{NaY'} C_{Na} + 1) = 10^{-2.57}$$

It is evident that calcium is successfully titrated in the presence of 1M sodium.

ii) $K_{N'Y'} > K_{MIY'}$.—The titration of barium with EDTA, using the MgY-Erio T system as an indicator.

a) In the absence of a second metal.

Condition: $C_{MI} = C_{Ba} = 10^{-3}$M; $C_{MII} = 0$; pH $=10$. Calculation gives the following values:

$$f_1 = 10^{-4.51}/C_{Mg} \text{ and } f_2 = 10^{0.20} C_{Mg}$$

12) H. Diehl and F. Lindstrom, *Anal. Chem.*, **31**, 414 (1959).

f_1 and f_2 for various values of C_{Mg} are given in Table II. Table II also shows that 5×10^{-3}M of magnesium will give the best indicator

Table II. f_1 and f_2 for various values of C_{Mg} in the chelatometry of barium using MgY-Erio T system as an indicator

C_{Mg}, M	log f_1	log f_2
10^{-2}	−2.51	−1.80
5×10^{-3}	−2.21	−2.10
2×10^{-3}	−1.81	−2.50
10^{-3}	−1.51	−2.80
10^{-5}	−0.51	−3.80

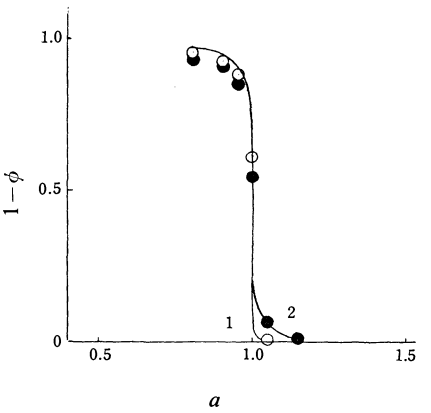


Fig. 3. Indicator transition of the titration of calcium using MgY-Erio T system as an indicator.
—— Theoretical indicator transition:
Curve 1: Na$=0$, Curve 2: Na$=1$ M
○● Experimental values:
○: Na$=0$, ●: Na$=1$ M

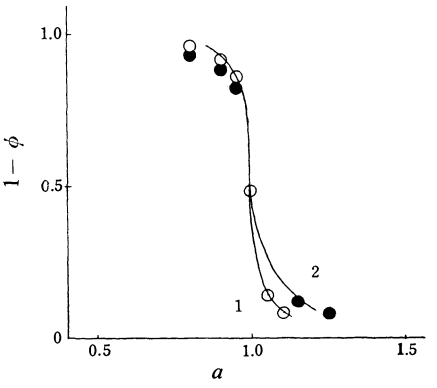


Fig. 4. Indicator transition of the titration of barium using MgY-Erio T system as an indicator.
—— Theoretical indicator transition:
Curve 1: Na$=0$, Curve 2: Na$=1$ M
○● Experimental values:
○: Na$=0$, ●; Na$=1$ M

transition; this is not, however, very satisfactory.

The discussion given under i), agrees well with that of Schwarzenbach.[13]

b) In the presence of sodium.

A similar consideration has been made for $C_{Mg}=5\times10^{-3}$M, $C_{Na}=0.1$ N. The computed values of f_1 and f_2 are as follows:

$$f_1=10^{-2.21} \text{ and } f_2=10^{-1.68}$$

Judging from these values, it is anticipated that the presence of 0.1M sodium may be tolerable in the visual titration of barium, using MgY-Erio T as an indicator. However, a larger amount of sodium will make the indicator transition sluggish.

Figures 3 and 4 show the results obtained for calcium and barium. The experimental results agree well with the theoretical indicator transition after the equivalence point. As has been indicated, the discordance between the observed and the theoretical curves before the equivalence point may be attributable to the decomposition of Erio T.[14]

It is true that the difference in ionic strength or the addition of an organic solvent may modify the constants involved, but in the ordinary range of the usual experimental conditions the modification of the constants rarely exceeds one logarithm unit. Therefore, for most cases, the titration can be predicted on a sound theoretical basis by the proposed equations.

Summary

General equations have been proposed for the indicator transition in the chelatometry of a metal in the presence of other metals, using HA or the NY-HA system as an indicator. The validity of these equations has been confirmed experimentally in several examples of practical importance. If the constants involved are all available, it is possible, by the aid of the proposed equations, to predict the optimum conditions for any type of chelatometry.

List of Symbols

Symbols used are summarized below in the order of appearance in the text. Most of them are of current use in the literature, but in order to avoid confusions they are defined once when appeared for the first time.

- M, N Metal
- Y Complexan
- NY Chelate of metal N with complexan Y
- HA Metallochromic indicator
- M′ Metal M not combined with Y and A
- Y′ Y not combined with M_I
- [M]′, etc. Concentration of M′, etc.
- K_{MY}, etc. Stability constant of MY, etc.
- $\alpha_{H(Y)}$ Side reaction coefficient of protonation of Y.
- $\alpha_{H(A)}$ Side reaction coefficient of protonation of A: $\alpha_{H(A)}=[A]'/[A]$
- $\alpha_{H,M_{II}(Y)}$ Side reaction coefficient of protonation and chelation with M_{II} of Y
- $\beta_{(M)}$ Side reaction coefficient of complex formation of M with auxiliary complexing agents: $\beta_{(M)}=[M]'/[M]$
- $K_{M'Y'}$ etc. Conditional stability constant of MY: $K_{M'Y'}=K_{MY}/\alpha_{H(Y)}\beta_{(M)}$, $K_{M'Y}=K_{MY}/\beta_{(M)}$, $K_{MY'}=K_{MY}/\alpha_{H(Y)}$
- C_M, etc. Total concentration of M, etc.
- $C_{Y'}$ Total concentration of Y used as titrant
- a Fraction titrated: C_Y/C_{MI}
- ϕ Indicator transition: $[A]'/C_A$

Laboratory of Analytical Chemistry
Nagoya Institute of Technology
Showa-ku, Nagoya (G. N.)

Laboratory of Analytical Chemistry
Faculty of Science, Nagoya University
Chikusa-ku, Nagoya (M. T.)

13) Schwarzenbach, op. cit., p. 53.

14) The decomposition of impure Erio T is much more considerable.

A New Method for the Colorimetric Determination of Hypophosphate Ions with the Molybdenum(V)-Molybdenum(VI) Reagent

By Norimasa Yoza and Shigeru Ohashi

(Received August 12, 1963)

This work was undertaken to establish a method for the colorimetric determination of hypophosphate ions in the presence of hypophosphite, phosphite, and orthophosphate ions. No colorimetric methods specific to hypophosphate ions have yet been reported. Hypophosphate ions can be determined indirectly by oxidizing them to orthophosphate ions and then by employing conventional method for the colorimetric determination of orthophosphate ions. However, this procedure can not be employed in the presence of hypophosphite or phosphite ions. In a previous paper[1] it has been mentioned that hypophosphoric acid does not give any colored products when it is treated with ammonium molybdate(VI) in a perchloric acid solution.

Lucena-Conde and Prat[2] have proposed a new reagent for the colorimetric determination of orthophosphate ions. This reagent is an acid solution of a mixture of molybdenym(V) and molybdenum(VI) and reacts with orthophosphoric acid to form a blue complex. In the present paper this reagent is called the molybdenum(V)-molybdenum(VI) reagent. During the course of a series of investigations of lower oxo acids of phosphorus, it was found that hypophosphoric acid reacts with this molybdenum(V)-molybdenum(VI) reagent to form a blue complex and that this reaction can be applied to the colorimetric determination of hypophosphate ions in the presence of hypophosphite, phosphite, and orthophosphate ions. The properties and composition of the blue complex due to hypophosphoric acid were compared with those of the blue complex due to orthophosphoric acid by means of spectrophotometry and the solvent extraction method.

The term "heteropoly blue" has commonly been used for the blue complex of orthophosphoric acid with molybdenum.[3] For the sake of convenience, the present authors employ the term "hypophosphoric heteropoly blue" for the blue complex produced by the reaction of hypophosphoric acid with the molybdenum molybdenum(VI) reagent and the term "orthophosphoric heteropoly blue" for the blue complex due to orthophosphoric acid.

Experimental

Apparatus.—A Shimadzu photoelectric spectrophotometer, QB-50, with 1.00 cm. cells was employed.

Reagents.—Disodium dihydrogen hypophosphate hexahydrate was supplied by Blaser and Worms. Sodium hypophosphite monohydrate, disodium phosphite pentahydrate, potassium dihydrogen orthophosphate, and the other reagents used were commercial reagents of the purest grade. The molybdenum(V)-molybdenum(VI) reagent was prepared by the procedure described by Lucena-Conde and Prat.[2] The concentrations of the constituents of this reagent were 0.08 M for molybdenum(V), 0.12 M for molybdenum(VI), 10 N for sulfuric acid, and 3 N for hydrochloric acid.

The Procedure for the Determination of Hypophosphate.—A suitable amount of an approximately neutral solution of a given sample was placed in a 25 ml. volumetric flask and diluted to about 20 ml. with water. After 2 ml. of the molybdenum(V)-molybdenum(VI) reagent had been added, the solution was shaken well. Then, the volume was adjusted to the mark with water and again the solution was well shaken. After the solution had been kept at room temperature for 30 min., the absorbance at 670 mμ was measured. A reagent blank was used as a reference solution.

The Procedure for the Determination of Molybdenum in Organic Extracts.—The molybdenum contained in "hypophosphoric and orthophosphoric heteropoly blue" extracted in an organic phase was determined by Lueck and Boltz's method.[4] An *n*-butyl alcohol phase which separated from an aqueous phase was washed three times with an equal volume of 1 N sulfuric acid to remove an excess of molybdate in the organic phase. By shaking the organic phase with a buffer solution of 0.5 M aqueous ammonia and 0.5 M ammonium chloride, the molybdate in the organic phase came into the aqueous phase. The absorbance at 230 mμ due to molybdate(VI) ions was measured.

Results and Discussion

Reactions at 95°C.—Lucena-Conde and Prat have investigated the color reaction of ortho-

1) S. Ohashi and N. Yoza, This Bulletin, **36**, 707 (1963).
2) F. Lucena-Conde and L. Prat, *Anal. Chim. Acta*, **16**, 473 (1957).
3) D. F. Boltz, "Colorimetric Determination of Nonmetals," Interscience Publishers, Inc., New York (1958), p. 33.
4) C. H. Lueck and D. F. Boltz, *Anal. Chem.*, **30**, 183 (1958).

phosphoric acid with the molybdenum(V)-molybdenum(VI) reagent and its application to the determination of orthophosphate ions. In this case it is necessary to heat a test solution at 95°C for 1 hr. in order to ensure complete color development. Under the same conditions, the reactions of hypophosphorous, phosphorous, and hypophosphoric acid with the molybdenum(V)-molybdenum(VI) reagent were examined. As is shown in Fig. 1, hypo-

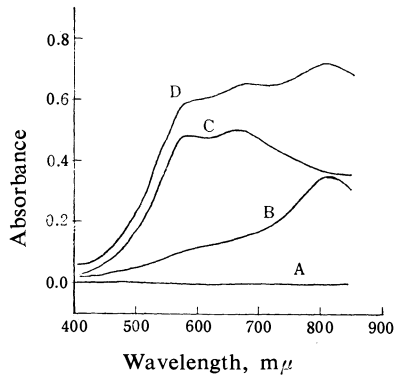


Fig. 1. Absorption spectra of reaction products between oxo acids of phosphorus and the molybdenum(V)-molybdenum(VI) reagent.
A: Hypophosphorous and phosphorous acid, each 62.0 μg. as P in 25 ml.
B: Orthophosphoric acid, 12.4 μg. as P in 25 ml.
C: Hypophosphoric acid, 25.9 μg. as P in 25 ml.
D: A mixture of orthophosphoric acid, 12.4 μg. as P, and hypophosphoric acid, 25.9 μg. as P in 25 ml.
Reaction temp.; 95°C, Reaction time; 1 hr.

phosphorous and phosphorous acid do not give any color reactions, while hypophosphoric acid gives "hypophosphoric heteropoly blue," the absorption spectrum of which has two maximums, at 590 and at 670 mμ. "Orthophosphoric heteropoly blue" gives a spectrum, with a maximum at 820 mμ, which is identical with the spectrum of the well-known blue complex produced by the reduction of molybdophosphoric acid. Curve D in Fig. 1 was obtained for a mixture of orthophosphoric and hypophosphoric acid, the quantities of which are equal to those used in the cases of curves B and C respectively. The sum of the absorbances of curves B and C is quite identical with curve D. It is well known that hypophosphoric acid is hydrolyzed by heating it with mineral acid to form phosphorous and orthophosphoric acid.[5] However, the facts mentioned above indicate that hypophosphoric acid is not hydrolyzed by heating it in an acid solution at 95°C for 1 hr. if the molybdenum(V)-molybdenum(VI) reagent is also present.

Reactions at Room Temperature.—The reactions of hypophosphorous, phosphorous, hypophosphoric, and orthophosphoric acid with the molybdenum(V)-molybdenum(VI) reagent at room temperature were examined. As was to be expected, hypophosphorous and phosphorous acid do not cause any color reactions. Hypophosphoric acid forms "hypophosphoric heteropoly blue." As is shown in Fig. 2, there is no difference among the shapes of absorption spectra of "hypophosphoric heteropoly blue" produced from hypophosphoric acid of various concentrations at room temperature (curves A, C, E, and F) and at 95°C (curves B and D). Therefore, it has been concluded that the species of "hypophosphoric heteropoly blue" produced under the various conditions mentioned above are quite identical with one another. Orthophosphoric acid gives a faint blue color (curve G in Fig. 2), the intensity of which is highly dependent on the reaction temperature.[2]

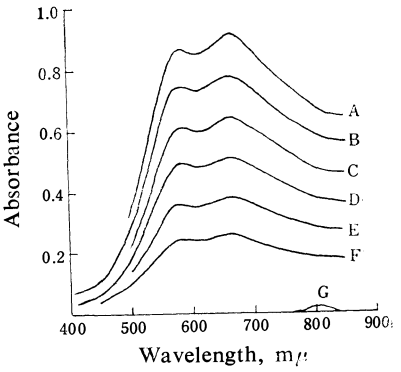


Fig. 2. Absorption spectra of "hypophosphoric heteropoly blue" produced under various conditions and an absorption spectrum of "orthophosphoric heteropoly blue" produced at room temperature.
A, C, E, and F: Hypophosphoric acid, 45.5, 32.5, 19.5, and 13.0 μg. as P in 25 ml., respectively. Reaction temp.; room temp. Reaction time; 30 min.
B, and D: Hypophosphoric acid, 39.0 and 26.0 μg. as P in 25 ml., respectively. Reaction temp.; 95°C, Reaction time; 1 hr.
G: Orthophosphoric acid, 12.4 μg. as P in 25 ml. Reaction temp.; room temp. Reaction time; 30 min.

The Effect of Reagent Concentration.—Varying quantities of the molybdenum(V)-molybdenum(VI) reagent and hypophosphoric acid, 32.4 μg. as phosphorus, were allowed to react at room temperature for 30 min. When the reagent amount was 0.5, 1.0, 2.0 or 4.0 ml., the

5) J. R. Van Wazer "Phosphorus and Its Compounds," Interscience Publishers, Inc., New York (1958), p. 410.

absorbance at 670 mμ was 0.551, 0.620, 0.620, or 0.621 respectively. Hence, 2 ml. of the reagent is sufficient to ensure the color development.

The Effect of Acid Concentration.—If 2 ml. of the molybdenum(V)-molybdenum(VI) reagent is added to an approximately neutral solution of a sample and diluted to 25 ml. with water, the final acidity will be 1.04 N. The reaction of hypophosphoric acid with the reagent at room temperature was studied at various final acidities, which were regulated by the addition of sulfuric acid or sodium hydroxide. When a final acidity is lower than 0.3 N, a reagent blank is blue. On the other hand, the higher a final acidity is, the lower the reaction rate becomes. For instance, when a final acidity is 2.0 N, it took about 2 hr. for the complete color development. When a final acidity lies between 0.6 and 1.4 N, the complete color development is attained within 30 min. The resulting blue color is stable for at least 3 hr.

A recommended procedure for the determination of hypophosphate ions is described in the experimental section. A calibration curve obtained by this procedure follows Beer's law, as Fig. 3 shows. A molar extinction coefficient of "hypophosphoric heteropoly blue" at 670 mμ is 3.04×10^4 on the assumption that a molecule of the blue complex contains a molecule of hypophosphoric acid.

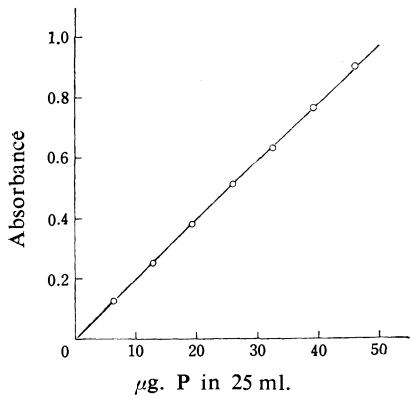


Fig. 3. Calibration curve for hypophosphate ions, at 670 mμ.

Interference.—The effect of several ions on the determination of hypophosphate ions is indicated in Table I. The presence of a large excess of hypophosphite, phosphite, orthoarsenate, and metasilicate ions caused no interference. The presence of orthophosphate ions likewise caused no serious interference if its quantity was less than or comparable with the quantity of hypophosphate ions. Wolframate ions caused a serious interference because they form a blue product by reaction with the reagent.

TABLE I. THE EFFECT OF SEVERAL IONS ON THE DETERMINATION OF HYPOPHOSPHATE IONS

Hypophosphate ions, 30.2 μg. as P in 25 ml.

Coexistent substance			Absorbance	Error
Formula	Amount μg.			%
None	—		0.5884	—
$NaH_2PO_2\cdot H_2O$	350	as P	0.5884	0.00
$Na_2HPO_3\cdot 5H_2O$	335	as P	0.5901	+0.29
KH_2PO_4	6.22	as P	0.5884	0.00
KH_2PO_4	15.6	as P	0.5884	0.00
KH_2PO_4	31.1	as P	0.5918	+0.57
$Na_2WO_4\cdot 2H_2O$	500	as W	0.8153	+38.6
H_3AsO_4	500	as As	0.5867	−0.12
Na_2SiO_3	500	as Si	0.5850	−0.60

The Solvent Extraction of "Hypophosphoric and Orthophosphoric Heteropoly Blue."—"Hypophosphoric and orthophosphoric heteropoly blue can be extracted into *n*-butyl alcohol, isobutyl alcohol, tributyl phosphate, or cyclohexanone. Chloroform, carbon tetrachloride, hexane, benzene, xylene, cyclohexane, *n*-butyl acetate, and ethyl ether are not good extractants for both heteropoly blues. "Orthophosphoric heteropoly blue" produced by the reduction of molybdophosphoric acid shows a similar behavior in the solvent extraction.[6] When aqueous solutions of "hypophosphoric and orthophosphoric heteropoly blue" produced by reaction with the molybdenum(V)-molybdenum(VI) reagent are shaken with an equal volume of *n*-butyl alcohol, the blue complexes are completely extracted into the organic phase. When *n*- or iso-butyl alcohol diluted with benzene is used as an extractant, the difference between the extractability of the two heteropoly blues can be observed as is illustrated in Fig. 4. "Hypophosphoric heteropoly blue" is less extractable than "orthophosphoric heteropoly blue." Absorption spectra of both heteropoly blues in *n*-butyl alcohol are shown in Fig. 5.

Lueck and Boltz[4] have described a method for the determination of the molybdenum(VI) content in an organic extract of molybdophosphoric acid. This method was applied in the present investigation to the determination of molybdenum combined with hypophosphoric acid and orthophosphoric acid in both heteropoly blues. When organic extracts of both heteropoly blues were shaken with a buffer solution of ammonia and ammonium chloride, the blue colors disappeared. It was found that no molybdenum remains in the organic phase after this

6) M. Miyamoto, *Japan Analyst (Bunseki Kagaku)*, **12**, 32 (1963).

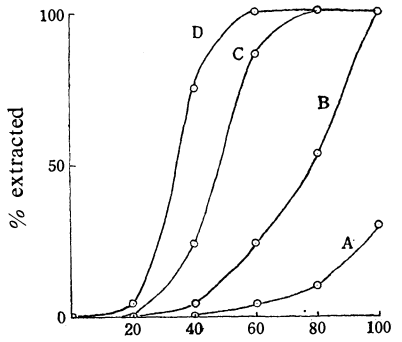


Fig. 4. Extractability of "hypophosphoric and orthophosphoric heteropoly blue."
"Hypophosphoric heteropoly blue"
A; Isobutyl alcohol-benzene
B; *n*-Butyl alcohol-benzene
"Orthophosphoric heteropoly blue"
C; Iso butyl alcohol-benzene
D; *n*-Butyl alcohol-benzene

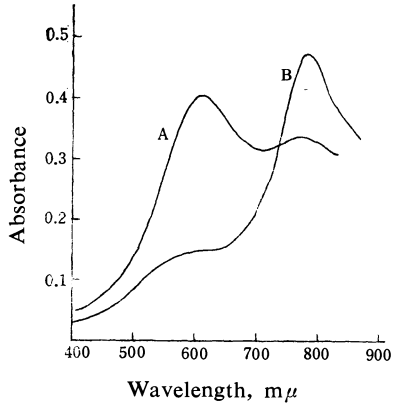


Fig. 5. Absorption spectra of "hypophosphoric and orthophosphoric heteropoly blue" in *n*-butlyl alcohol.
A; "Hypophosphoric heteropoly blue," 24.8 μg. as P in 25 ml.
B; "Orthophosphoric heteropoly blue," 18.7 μg. as P in 25 ml.

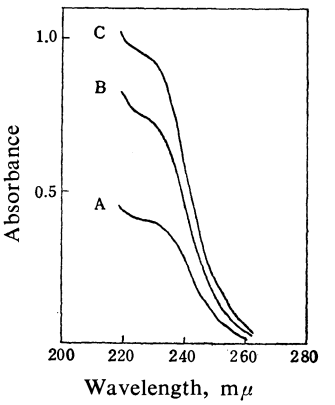


Fig. 6. Absorption spectra of molybdate(VI) ions.
A; Molybdate(VI) ions back extracted from an *n*-butyl alcohol phase containing "hypophosphoric heteropoly blue", 13.0 μg. as P in 25 ml.
B; Ammonium molybdate, 13.4 ppm of molybdenum(VI), as a standard solution
C; Molybdate(VI) ions back-extracted from an *n*-butyl alcohol phase containing "orthophosphoric heteropoly blue", 12.4 μg. as P in 25 ml.

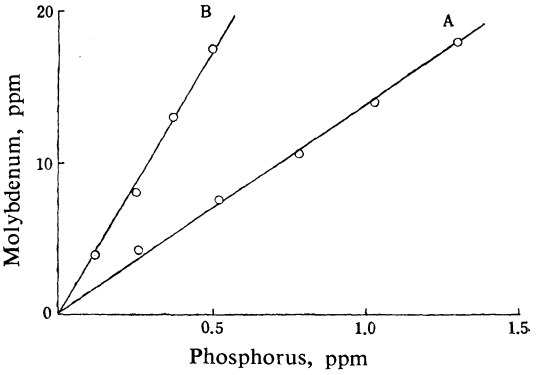


Fig. 7. Relations between contents of molybdenum and phosphorus in "hypophosphoric and orthophosphoric heteropoly blue."
A; "Hypophosphoric heteropoly blue"
B; "Orthophosphoric heteropoly blue"

treatment and that molybdenum(V) is oxidized to molybdenum(VI) by shaking it with the buffer solution in air. The resulting molybdenum(VI) in the aqueous solution can be determined by measuring the absorbance at 230 mμ (Fig. 6). The relations between the contents of molybdenum and phosphorus in both heteropoly blues are shown in Fig. 7. From these data, the mole ratios of molybdenum (a sum of molybdenum(V) and molybdenum(VI)) to hypophosphoric and orthophosphoric acid in both heteropoly blues were calculated to be approximately 9 and 12 respectively.

Summary

It was found that hypophosphoric acid reacts with the molybdenum(V)-molybdenum(VI) reagent at room temperature as well as at 95°C to form a blue complex, the absorption spectrum of which has maximums at 590 and 670 mμ. Although orthophosphoric acid reacts with this reagent at 95°C to form a blue complex, it gives only a faint blue color at room temperature. Hypophosphorous and phosphorous acid do not give any colored products when treated with this reagent. Therefore, the

reaction of hypophosphoric acid with this reagent at room temperature can be applied to the colorimetric determination of hypophosphate ions in the presence of hypophosphite, phosphite, and orthophosphate ions. The differences in the absorption spectra and solvent extraction behavior between the two blue complexes due to hypophosphoric and orthophosphoric acid (" hypophosphoric heteropoly blue " and " orthophosphoric heteropoly blue ") have been described. The mole ratios of molybdenum to hypophosphoric and orthophosphoric acid in the blue complexes were found to be approximately 9 and 12 respectively.

The authors wish to express their hearty thanks to Professor Jun Yoshimura for the kind suggestions made in the course of this work. The authors also wish to thank Dr. Bruno Blaser and Dr. Karl-Heinz Worms for supplying the sodium hypophosphate used in this study.

Department of Chemistry
Faculty of Science
Kyushu University
Hakozaki, Fukuoka

The Reactions of Lower Oxo Acids of Phosphorus with the Molybdenum(V)-Molybdenum(VI) Reagent

By Norimasa YOZA and Shigeru OHASHI

(Received August 14, 1963)

In a previous paper[1] it has been found that hypophosphoric acid reacts with the molybdenum(V)-molybdenum(VI) reagent to form a blue complex, while hypophosphorous and phosphorous acid do not produce any color reactions. Orthophosphoric acid also reacts with this reagent to form a blue complex, as has been pointed out by Lucena-Conde and Prat.[2] The blue complexes due to hypophosphoric and orthophosphoric acid are called "hypophosphoric heteropoly blue" and "orthophosphoric heteropoly blue" respectively.[1] The present investigation deals with the color reactions of various lower oxo acids of phosphorus with this reagent. The data obtained indicate that the mechanism of these reactions are closely related to the structural units of the lower oxo acids of phosphorus and their hydrolysis reactions. The abbreviated notations proposed by Blaser and Worms[3] will be used for the oxo acids of phosphorus in this paper. For instance, hypophosphorous, phosphorous, hypophosphoric, and orthophosphoric acid are represented by the notations, ^{1}P–, ^{3}P–, ^{4}P–^{4}P–, and ^{5}P–acid respectively. The Arabic numerals attached to the phosphorus atoms represent the oxidation numbers of the phosphorus atoms.

Experimental

Reagent. — All the reagents used in this work have been described in previous papers.[1,4]

The Procedure for the Color Reactions. — A suitable aliquot of a neutral solution of a given sample (about 10^{-4} M) was taken in a 25 ml. volumetric flask, diluted to approximately 20 ml. with water, and treated by each of the following three procedures. After the volume of the solution had been adjusted to the mark with water, the absorption spectrum was measured by the use of a Shimadzu photoelectric spectrophotometer, QB-50, with 1 cm. cells.

Procedure I. — The sample solution was allowed to react with 2 ml. of the molybdenum(V)-molybdenum(VI) reagent for 30 min. at room temperature.

Procedure II. — The sample solution was allowed to react with 2 ml. of the molybdenum(V)-molybdenum(VI) reagent for 1 hr. at 95°C.

Procedure III. — The sample solution was allowed to react with a mixture of 1 ml. of 1 M sodium hydrogen sulfite solution and 2 ml. of the molybdenum(V)-molybdenum(VI) reagent for 1 hr. at 95°C.

Results and Discussion

As has been pointed out in a previous

1) N. Yoza and S. Ohashi, This Bulletin, **37**, 33 (1964).
2) F. Lucena-Conde and L. Prat, *Anal. Chim. Acta*, **16**, 473 (1957).
3) B. Blaser and K.-H. Worms. *Z. anorg. u. allgem. Chem.*, **300**, 225 (1959)
4) S. Ohashi and N. Yoza, This Bulletin, **36**, 707 (1963).

paper,[1] $^{4}_{4}$P–P–acid reacts with the molybdenum-(V)-molybdenum(VI) reagent under the conditions of procedures I and II to form hypophosphoric heteropoly blue, the absorption spectrum of which has two maxima, at 590 and 670 mμ, while ^{1}P– and ^{3}P–acid do not give any colored products under the conditions of either procedures I or II. ^{5}P–Acid reacts with this reagent under the conditions of procedure II to form orthophosphoric heteropoly blue, the absorption spectrum of which has a maximum at 820 mμ. Under the conditions of procedure I, the rate of the reaction is so slow that ^{5}P–acid gives only a faint blue color. If the quantity of ^{5}P–acid is comparable to that of $^{4}_{4}$P–P–acid, the absorbance due to orthophosphoric heteropoly blue is negligibly small compared with that due to hypophosphoric heteropoly blue.

In the course of this investigation, it was found that ^{1}P– or ^{3}P–acid is quantitatively oxidized with sodium hydrogen sulfite to ^{5}P–acid when heated in an acid solution at 95°C. The sulfite is reduced to elemental sulfur in the course of this reaction. Therefore, when ^{1}P– or ^{3}P–acid is treated by procedure III, orthophosphoric heteropoly blue is produced quantitatively. Since the elemental sulfur produced coagulates, it does not interfere with the measurement of the absorbance of the blue color.

The reactions of twelve lower oxo acids of phosphorus as well as of ^{5}P–acid with the molybdenum(V)-molybdenum(VI) reagent were carried out by procedures I, II, and III. All the blue products were either orthophosphoric or hypophosphoric heteropoly blue, or a mixture of them. The quantities of both the heteropoly blues were calculated from the absorbances of the spectra. All the results are summarized in Table I. The final acidity of the reaction mixture is approximately 1 N with respect to the sulfuric and hydrochloric acid in all cases.[1] Since the molecular structures of orthophosphoric and hypophosphoric heteropoly blue have not been determined, it is assumed, for the sake of convenience, that one mole of each heteropoly blue contains one mole of ^{5}P– or $^{4}_{4}$P–P– units.

The Reactions with Procedure I. — One mole of ^{3}P–O–$^{4}_{4}$P–P–, (–$^{4}_{4}$P–P–O–)$_2$–ring, $^{4}_{4}$P–P–O–$^{4}_{4}$P–P–, or ^{5}P–O–$^{4}_{4}$P–P–acid, which contains one or two

Table I. The products obtained by the reactions of oxo acids of phosphorus with the molybdenum(V)-molybdenum(VI) reagent

Oxo acid of phosphorus (starting compd.)	Procedure I		Procedure II		Procedure III	
	$^{4}_{4}$P–P–Mo	^{5}P–Mo	$^{4}_{4}$P–P–Mo	^{5}P–Mo	$^{4}_{4}$P–P–Mo	^{5}P–Mo
^{1}P–Acid	0	0	0	0	0	1.04
^{3}P–Acid	0	0	0	0	0	1.01
^{3}P–O–^{3}P–Acid	0	0	0	0	0	1.96
$^{2}_{4}$P–P–Acid	0	0	0	0	<0.2	1.94
(–^{3}P–)$_6$–Ring acid	0.81	0	0.81	0	1.26±0.1	3.28±0.2
^{3}P–O–$^{4}_{4}$P–P–Acid	1.05	0	1.04	0	1.04	1.03
^{4}P–^{3}P–^{4}P–Acid	1.00	0	1.02	0	1.02	0.99
^{3}P–O–^{5}P–Acid	0	0	0	1.03	0	2.01
$^{4}_{4}$P–P–Acid	1.00	0	1.00	0	1.01	0
(–$^{4}_{4}$P–P–O–)$_2$–Ring acid	2.06	0	2.03	0	2.07	0
$^{4}_{4}$P–P–O–$^{4}_{4}$P–P–Acid	1.89	0	1.91	0	1.93	0
^{5}P–O–$^{4}_{4}$P–P–Acid	0.98	0	0.98	0.98	0.98	0.98
^{5}P–Acid	0	0	0	1.01	0	1.00

Mole ratios of the products to the starting compounds are shown.

$^{4}_{4}$P–P–Mo ; Hypophosphoric heteropoly blue

^{5}P–Mo ; Orthophosphoric heteropoly blue

$^{4\ 4}$P–P–units in its structure, produces one or two moles of hypophosphoric heteropoly blue when procedure I is used. These results suggest that all the four oxo acids undergo hydrolysis to form $^{4\ 4}$P–P–acid, which reacts successively with the molybdenum(V)-molybdenum(VI) reagent. One mole of $^{4\ 3\ 4}$P–P–P–acid produces one mole of hypophosphoric heteropoly blue. Therefore, it is evident that $^{4\ 3\ 4}$P–P–P–acid is hydrrolyzed by procedure I according to Eq. 1, not Eq. 2:

$$^{4\ 3\ 4}\text{P–P–P–Acid} \rightarrow {}^{4\ 4}\text{P–P–Acid} + {}^{3}\text{P–Acid} \quad (1)$$

$$^{4\ 3\ 4}\text{P–P–P–Acid} \rightarrow {}^{2\ 4}\text{P–P–Acid} + {}^{5}\text{P–Acid}$$

$$\rightarrow 2\,{}^{3}\text{P–Acid} + {}^{5}\text{P–Acid} \quad (2)$$

As has been discussed in a previous paper,[5] $^{4\ 3\ 4}$P–P–P–acid is hydrolyzed also in a perchloric acid solution according to Eq. 1. One mole of $(-{}^{3}\text{P}-)_6$–ring acid produces approximately 0.8 mol. of hypophosphoric heteropoly blue. Although the reaction mechanism of the hydrolysis of $(-{}^{3}\text{P}-)_6$–ring acid has not been clarified, the data obtained here indicate at least that $^{4\ 4}$P–P–acid is one of the main intermediate products in the hydrolysis of $(-{}^{3}\text{P}-)_6$–ring acid. ^{1}P–, ^{3}P–, $^{3\ 3}$P–O–P–, $^{2\ 4}$P–P–, $^{3\ 5}$P–O–P–, and ^{5}P–acid do not give any colored products when procedure I is used, because of the impossibility of its producing $^{4\ 4}$P–P–acid.

The Reactions Using Procedure II.—The final products in the hydrolysis of ^{3}P–O–P–P–, $^{4\ 3}$P–P–P, $^{4\ 4}$P–P–, $(-{}^{4\ 4}\text{P–P–O}-)_2$–ring, $^{4\ 4}$P–P–O–P–P–, and ^{5}P–O–P–P–acid are ^{3}P– and ^{5}P–acid when they are boiled in mineral acid.[6,7] As for $(-{}^{3}\text{P}-)_6$–ring acid, the final products in the hydrolysis with mineral acid are ^{1}P–, ^{3}P– and ^{5}P-acid.[8] However, when procedure II is used, $(-{}^{3}\text{P}-)_6$–ring, ^{3}P–O–P–P–, $^{4\ 4}$P–P–P–, $(-{}^{4\ 4}\text{P–P–O}-)_2$–ring, and $^{4\ 4}$P–P–O–P–P–acid give hypophosphoric heteropoly blue, the absorption spectra of which are quite identical with those of the blue products obtained from the respective compounds by procedure I. One mole of ^{5}P–O–$^{4\ 4}$P–P–acid produces a mixture of one mole of orthophosphoric heteropoly blue and one mole of hypophosphoric heteropoly blue when procedure II is used. These results indicate that $^{4\ 4}$P–P–acid produced by the hydrolysis of the lower oxo acids of phosphorus mentioned above reacts preferentially with the molybdenum(V)-molybdenum(VI) reagent and that the resulting hypophosphoric heteropoly blue is remarkably stable under the conditions of procedure II.

One mole of ^{3}P–O–^{5}P–acid produces one mole of orthophosphoric heteropoly blue when procedure II is used, because ^{3}P–O–^{5}P–acid is hydrolyzed to form ^{3}P– and ^{5}P–acid. ^{1}P–, ^{3}P–, ^{3}P–O–^{3}P–, and $^{2\ 4}$P–P–acid do not give any colored products when procedure II is used.

The Reaction Using Procedure III.—One mole of ^{3}P–O–^{3}P–acid produces two moles of orthophosphoric heteropoly blue when procedure III is used, because ^{3}P–O–^{3}P–acid is hydrolyzed in the course of procedure III to form ^{3}P–acid. When procedure III is used, $^{4\ 4}$P–P–, $(-{}^{4\ 4}\text{P–P–O}-)_2$–ring, $^{4\ 4}$P–P–O–$^{4\ 4}$P–P–, and ^{5}P–O–$^{4\ 4}$P–P–acid give the same products as in the case of procedure II, because there is no ^{1}P– or ^{3}P–acid in the hydrolysis products of these oxo acids. Since one mole of ^{3}P–O–$^{4\ 4}$P–P– or $^{4\ 3\ 4}$P–P–P–acid is converted into one mole of $^{4\ 4}$P–P–acid and one mole of ^{3}P–acid in the first step of its hydrolysis, the reaction products of ^{3}P–O–$^{4\ 4}$P–P– or $^{4\ 3\ 4}$P–P–P–acid obtained by procedure III exhibit the absorption spectra due to an equimolar mixture of orthophosphoric and hypophosphoric heteropoly blue. One mole of ^{3}P–O–^{5}P–acid produces, of course, two moles of orthophosphoric heteropoly blue when procedure III is used. $^{2\ 4}$P–P–Acid produces orthophosphoric heteropoly blue with a small amount of hypophosphoric heteropoly blue when procedure III is used. Since the hydrolysis product of $^{2\ 4}$P–P–acid in mineral acid is ^{3}P–acid, it is reasonable that the main product obtained by procedure III is orthophosphoric heteropoly blue. The small amount of hypophosphoric heteropoly blue may be due to the redox

5) N. Yoza and S. Ohashi, ibid., **36**, 1485 (1963).
6) J. R. Van Wazer, "Phosphorus and its Compounds," Interscience Publishers, Inc., New York (1958), pp. 345-418.
7) B. Blaser and K.-H. Worms, *Z. anorg. u. allgem. Chem.*, **300**, 250 (1959); **301**, 7 (1959); **311**, 313 (1961).
8) B. Blaser and K.-H. Worms, ibid., **300**, 237 (1959).

reaction between sulfite and $\overset{2\ 4}{\text{P–P}}$–acid, where a part of the $\overset{2\ 4}{\text{P–P}}$–acid is oxidized to $\overset{4\ 4}{\text{P–P}}$–acid. One mole of $(\overset{3}{\text{–P–}})_6$–ring acid produces a mixture of orthophosphoric and hypophosphoric heteropoly blue when procedure III is used. The data indicate that the mechanism of the hydrolysis of $(\overset{3}{\text{–P–}})_6$–ring acid varies with small differences in the reaction conditions. The results obtained for $(\overset{3}{\text{–P–}})_6$–ring acid by using procedures II and III suggest that $\overset{5}{\text{P}}$–acid, as one of the final products in the hydrolysis of $(\overset{3}{\text{–P–}})_6$–ring acid by the action of mineral acid, may be derived from $\overset{4\ 4}{\text{P–P}}$–acid as one of the intermediate products. $(\overset{3}{\text{–P–}})_6$–Ring acid forms a larger quantity of hypophosphoric heteropoly blue when procedure III is used than when procedure III is used. This fact may suggest that certain intermediate products, e. g., $\overset{2\ 4}{\text{P–P–}}$ or $\overset{2\ 3\ 4}{\text{P–P–P}}$–acid (a hypothetical compound), in the process of the hydrolysis of this ring acid, are oxidized with sulfite to $\overset{4\ 4}{\text{P–P}}$–acid or some other compounds that give $\overset{4\ 4}{\text{P–P}}$–acid as the result of hydrolysis.

Summary

The reaction of twelve lower oxo acids of phosphorus and orthophosphoric acid with the molybdenum(V)-molybdenum(VI) reagent have been carried out under the conditions prescribed by three different procedures: (1) the reactions for 30 min. at room temperature, (2) the reactions for 1 hr. at 95°C, and (3) the reactions in the presence of sodium hydrogen sulfite for 1 hr. at 95°C. The absorption spectra of the reaction products have been measured. It has been found that the blue products obtained by these reactions are orthophosphoric heteropoly blue and/or hypophosphoric heteropoly blue in all cases and that mechanisms of these reactions are closely related to the structural units of the lower oxo acids of phosphorus and their hydrolysis reactions.

The authors wish to express their hearty thanks to Professor Jun Yoshimura for the kind suggestions he made in the course of this work. The authors also wish to thank Dr. Bruno Blaser and Dr. Karl-Heinz Worms for supplying the samples used in this study.

Department of Chemistry
Faculty of Science
Kyushu University
Hakozaki, Fukuoka

Some Benzonorbornadiene Derivatives[1)]

By Hiroshi TANIDA, Ryonosuke MUNEYUKI and Teruji TSUJI

(Received August 21, 1963)

Bicyclo [2, 2, 1] heptane and the compounds with this skeleton have received wide attention in the past few years. They have been employed so often as a suitable model for developing modern organic theory because of their special fixed stereochemistry and because of the high strain of the ring system. Of particular interest are the demonstration of anchimeric assistance or homoconjugation in solvolytic displacement reactions,[2)] and that of trans-annular interaction between the double bond and the carbonyl group of dehydronorcamphor.[3)] Along with these developments in the theoretical field, remarkable progress was made in the syntheses of bridged ring compounds. Particularly, the success of the syntheses of norbornane derivatives condensed with an aromatic nucleus have opened a new area of organic chemistry. Norbornadiene I prepared by the Diels-Alder reaction of cyclopentadiene and acetylene[4)] is commercially available now,

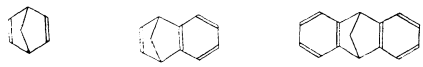
1) Some of the results of this paper have appeared in preliminary form: H. Tanida, *J. Am. Chem. Soc.*, 85, 1703 (1963).

2) S. Winstein and C. Ordronneau, ibid., 82, 2084 (1960) and references therein.

3) R. C. Cookson and N. S. Wariyar, *J. Chem. Soc.*, 1956, 2302.

4) J. Hyman. E. Freireich and R. E. Lidov, U. S. Pat. 2875256; *Chem. Abstr.*, 53, 13082 (1959).

benzonorbornadiene II is easily obtained by the cycloaddition of benzyne to cyclopentadiene,[5] and dibenzobicyclo[2, 2, 1]heptadiene III can be prepared by the condensation of norbornadiene with butadiene, followed by dehydrogenation.[6] They may be likened to a series of benzene, naphthalene and anthracene.



I II III

One of our chief objectives in investigating the chemistry of these systems has been to gain some insight into the nature of the homobenzylic conjugation.[1] Toward this end, we have studied the cycloaddition of substituted benzynes in the preparation of β-substituted benzonorbonadiens. This paper describes a convenient and steady method for the generation of benzynes, which carry several kinds of substituents, by the development of Wittig's procedure.[5] Furthermore, we would like to demonstrate that Wittig's procedure is very often more convenient than the decomposition of the zwitterionic diazonium salts of anthranilic acid derivatives,[7] a method which has recently been advocated, for use in syntheses.

Results and Discussion

One of the conditions necessary for the cycloaddition of benzynes generated via metal aromatics is the fragmentation of suitably ortho-substituted di-halobenzenes under an aprotic solvent. According to the Huisgen addition-elimination mechanism[8] for the formation of benzynes, the Wittig process is assumed to be composed of two steps, the metallation and the subsequent elimination of metal halogenide. Huisgen proposed that the rate-determining step was generally in the metalation reaction and that the rate of the elimination of halogen anions was in the order of iodine >bromine>chlorine≫fluorine. Several kinds of *o*-dihalobenzene have been prepared on the basis of the above discussions.

4-Bromo-3-iodoanisole IV, prepared from 6-bromo-*m*-anisidine V,[9] was proved to be a good source for the generation of 4-methoxybenzyne. Racemic 4'-methoxybenzonorbornadiene VI was obtained in a 40% yield by the reaction of IV with cyclopentadiene and magnesium. 3-Bromo-4-flourotoluene VII was prepared from 2-bromo-*p*-toluidine by the Schiemann reaction, and its cycloaddition to cyclopentadiene was satisfactorily carried out, yielding 4'-methylbenzonorbornadiene VIII in a 54% yield. The benzyne reaction of 2-bromo-4-chloroflourobenzene IX, obtained by the Schiemann reaction of 2-bromo-4-chloroaniline, proceeded successfully with cyclopentadiene by the elimination of bromine and fluorine, giving 4'-4-chlorobenzonorbornadiene X in a 55.6% yield. The position of the substituents on the benzene nucleus of the benzonorbornadienes obtained was unequivocally established by the conversion into the 2-substituted naphthalenes through the route of benzoyloxylation at the 7-position, hydrolysis and the Oppennauer oxidation.[1,10]

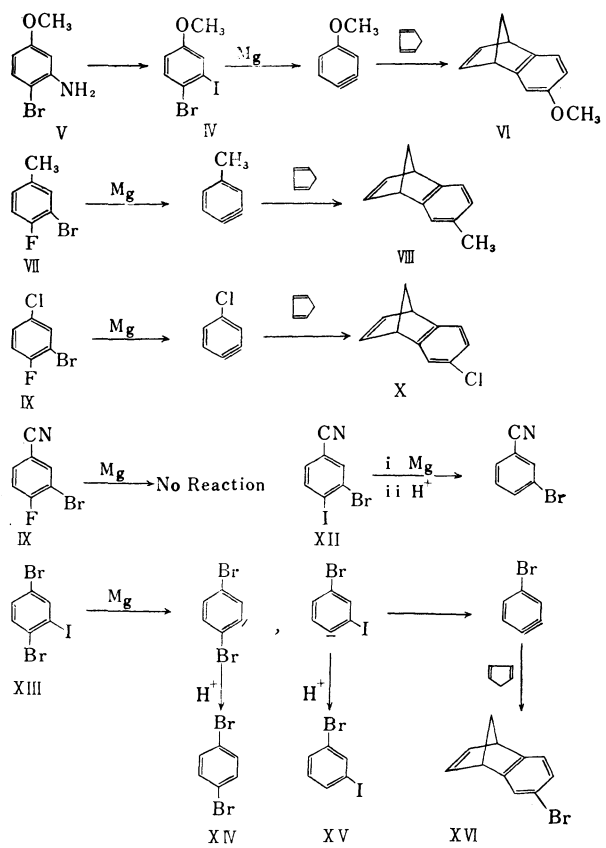


Chart. 1

5) G. Wittig and E. Knauss, *Chem. Ber.*, **91**, 895 (1958).
6) W. R. Vaughan and M. Yoshimine, *J. Org. Chem.*, **22**, 7 (1957).
7) M. Stiles and R. G. Miller, *J. Am. Chem. Soc.*, **82**, 3802 (1960); M. Stiles, R. G. Miller and U. Burckhardt, ibid., **85**, 1792 (1963); R. G. Miller and M. Stiles, ibid., **85**, 1798 (1963); L. Friedman and F. M. Logullo, ibid., **85**, 1549 (1963).
8) R. Huisgen and J. Sauer, *Angew. Chem.*, **72**, 91 (1960); R. Huisgen, in H. Zeiss, "Organometallic Chemistry," Reinhold Publishing Co., New York, N. Y. (1960), p. 36 and references thereon.
9) V was prepared in the following way: *p*-Anisidine—(nitration)→2-nitro-*p*-anisidine—(Sandmeyer)→4-bromo-3-nitroanisole—(Fe+HCl)→6-bromo-*m*-anisidine.
10) H. Tanida and T. Tsuji, *Chem. & Ind.*, **1963**, 211.

Attempts to generate cyanobenzyne, which is interesting in view of the fact that the benzyl has a strongly electronegative group, failed when either 3-bromo-4-fluorobenzonitrile XI or 3-bromo-4-iodobenzonitrile XII was used.[11] Compound XI did not react with magnesium in tetrahydrofuran. The reaction of XII with magnesium afforded 3-bromobenzonitrile as an isolable product, while no reaction with lithium occurred.

Of particular interest was the reaction of 2, 5-dibromo-1-iodobenzene XIII with cyclopentadiene and magnesium. Gas chromatography of the product, which had been distilled under reduced pressure, indicated the existence of seven compounds. The residue not distillated presumably consisted of high molecular substances. The identities of the main four compounds, *p*-dibromobenzene XIV, 3-bromoiodobenzene XV, the desired 4'-bromobenzonorbornadiene XVI and benzonorbornadiene XVII, were confirmed by retention time analysis in gas chromatography. The estimation of their relative yields was carried out on the basis of the peak area, as Table II shows. Furthermore, XIV, XVI and XVII were isolated and identified by mixed melting point determination and by a comparison of the infrared spectra. The formation of XVII is probably due to the further reaction of XVI with magnesium. No evidence of the formation of *o*-bromoiodobenzene was obtained. This fact may imply that the rate of formation of phenyl anion was enhanced by ortho halogen.[12] The percentage of the benzyne formation would be more than the total yield of XVI and XVII because of the polymerization of benzynes.

The formation of considerable amounts of XIV and XV suggests that the metalation reaction took place without the subsequent elimination. The above experiments of XII gave an analogous result. Contrary to Huisgen's popular mechanism, Zieger and Wittig[13] recently reported that, in the case of the reaction of 3-chloro-4-dimethylaminophenylsulfone XVIII with *n*-butyllithium and furan, XVIII was metalated very rapidly and completely at a low temperature such as $-80°C$, but that the elimination of lithium chloride proceeded at a measurable rate, giving a k_1 value of $0.094 \sim 0.064\ min^{-1}$ at 0°C. Therefore, we think that Huisgen's discussions and Wittig's finding are probably valid in terms of their own experiments and, that which step, metalation or elimination, is the rate-determining step depends primarily upon the particular case. The benzyne formation will substantially be a two-step reaction.

The ultraviolet spectra data, listed in Table I, exhibits the transannular interaction of the double bond and the benzene ring in the benzonorbornadiene derivatives prepared here. It is interesting to note the absorption maximum[14] around 230~240 mμ, which may correspond to the π-π^* band of the styrene derivatives. The spectral data and electronic structures of these compounds will be discussed in detail later.

TABLE I. UV SPECTRA OF BENZONORBORNADIENE DERIVATIVES

λ_{max} in mμ, log ε in parentheses, solvent is cyclohexane, except for the 4'-bromo compound in *n*-hexane.

Substituent	λ_{max}				
None	216	231	262	269	277
	(4.00)	(3.06)	(2.66)	(2.76)	(2.72)
4'-CH_3		238	267	273	281
		(3.13)	(2.79)	(2.90)	(2.91)
4'-CH_3O		249		284	290
		(3.35)		(3.26)	(3.23)
4'-Cl	214	241	269	276	284
	(4.23)	(3.28)	(2.83)	(2.92)	(2.90)
4'-Br		242	267	275	284
		(3.38)	(2.86)	(2.89)	(2.82)

Experimental[15]

4-Bromo-3-iodoanisole.—Into a mixture of 20.2 g. (0.10 mol.) of 6-bromo-*m*-anisidine,[16] 47 ml. of concentrated hydrochloric acid and 31 g. of cracked ice, a solution of 7.6 g. (0.11 mol.) of sodium nitrite in 31 ml. of water at 0~3°C was slowly stirred over a ten-minute period. Stirring was kept up for additional fifteen minutes. The deep orange solution which resulted was filtered, slowly stirred at approximately 10°C into a solution of 57 g. (0.344 mol.) of potassium iodide in 187 ml. of water, and left to stand overnight at room temperature. The violet oil which separated was extracted with ether, wahed with 10% aqueous sodium hydroxide, water and 5% aqueous sodium bisulfite, and then dried over anhydrous sodium sulfate. After the removal of the solvent, the residue was distilled at 124~126°C (2 mmHg) to give 15.9 g. of the expected product as a yellow oil, in a 60% yield; n_D^{25} 1.6493.

11) XI (m. p. 57~58°C) was prepared in the following way: VII→3-bromo-4-fluorobenzaldehyde (b. p. 120°C) (21 mmHg), n_D^{24} 1.5795→the oxime (m. p. 104~104.5°C)→XI. XII (m. p. 137~138.5°C) was prepared from 3-amino-4-iodobenzonitrile by the Sandmeyer reaction.

12) Cf. J. Hine and P. B. Langford, *J. Org. Chem.*, **27**, 4149 (1962) and references therein.

13) H. Zieger and G. Wittig, *J. Org. Chem.*, **27**, 3270 (1962).

14) No maximum was observed in benzobicyclo[2, 2, 2]-octadiene, according to a private communication from Dr. K. Kitahonoki. Cf. K. Kitahonoki and Y. Takano, *Tetrahedron Letters*, **24**, 1597 (1963).

15) All melting points and boiling points are uncorrected.

16) H. H. Hodgson and R. J. H. Dyson, *J. Chem. Soc.*, 1935, 946.

Found: C, 27.09; H, 1.99; Br, 25.25. Calcd. for C_7H_6OBrI: C, 26.86; H, 1.93 Br, 25.55%.

3-Bromo-4-fluorotoluene (VII).—B. p. 186°C; n_D^{25} 1.5281. Found: C, 44.70; H, 3.27. Calcd. for C_7H_6BrF: C, 44.47; H. 3.20%.

2-Bromo-4-chlorofluorobenzene (IX).—B. p. 90°C (30 mmHg); n_D^{19} 1.5549. Found: C, 34.51; H, 1.58. Calcd. for C_6H_3BrClF: C, 34.41; H. 1.44%. were prepared from the corresponding amino compounds by the Schiemann procedure of Roe.[17]

4'-Methoxybenzonorbornadiene (VI).—A three-necked flask, equipped with a stirrer, a pressure-compensated dropping funnel, a gas inlet tube, and a reflux condenser with a Drierite tube, was charged with 4.1 g. (0.158 mol.) of magnesium turning and flushed with dry nitrogen for 30 min. to remove the air completely. In the dropping funnel there was then placed a solution of 44 g. (0.141 mol.) of 4-bromo-3-iodoanisole and 9.5 g. (0.143 mol.) of fresh-distilled cyclopentadiene in 240 ml. of anhydrous tetrahydrofuran. A part of the solution from the funnel was dropped to cover the magnesium and heated to boiling. When a vigorous reaction commenced, the stirrer was started and the remaining main part of the solution was added at such a rate that the temperature in the flask was kept at 60~65°C (this took about 50 min.), after which the mixture was refluxed gently for 30 min. After removal of the solvent under slightly reduced pressure, the residue was poured into a mixture of a saturated aqueous solution of ammonium chloride and 300 ml. of ether. The ether layer was separated, washed repeatedly with 5% aqueous sodium bisulfite and water, and dried over sodium sulfate. The ether extracts were distilled under reduced pressure to obtain 9.7 g. (40%) of a colorless oil at b. p. 99~100°C (4 mmHg). The oil contained a small amount of impurity, presumably 4-bromoanisole. Elution chromatography by Florisil, hexane and benzene gave completely pure 4'-methoxybenzonorbornadiene (n_D^{23} 1.5642) after of 4-bromoanisole had been eluted as a forerun. Found: C, 84.03; H, 7.16; O, 9.11. Calcd. for $C_{12}H_{12}O$: C, 83.69; H, 7.02; O, 9.29%.

4'-Methylbenzonorbornadiene (VIII).—By means of the above procedure, 42 g. of VII, 14.7 g. of cyclopentadiene and 6 g. of magnesium turning in 270 ml. of dry tetrahydrofuran, 18.6 g. (53.6%) of VIII as a colorless oil was obtained; b. p. 110~112°C (22mm Hg); n_D^{24} 1.5541.

Found: C, 93.09; H, 6.77, Calcd. for $C_{21}H_{18}$: C, 93.29; H,6.71%.

4'-Chlorobenzonorbornadiene (X)—It was prepared from XI, cyclopentadiene and magnesium in the same manner as the above. It is a colorless oil with a boiling point of 112~112.5°C (10 mmHg); n_D^{21} 1.5763. The yield was 55.6%.

Found: C, 74.44; H, 5.20; Cl, 20.25. Calcd. for $C_{11}H_9Cl$; C, 74.79; H, 5.14; Cl, 20.07%.

The Reaction of 2, 5-Dibromo-1-iodobenzene (XIII) with Magnesium and Cyclopentadiene.—With 75 g. of XIII, 16.5 g. of cyclopentadiene and 6.05 g. of magnesium turning in 300 ml. of tetrahydrofuran, the above procedure was carried out. The ether extracts were distilled up to 132°C (10 mmHg) to obtain 26.4 g. of a mixture of oil and crystals. The composition of the distillate was investigated by gas chromatography. The components and the relative yields are shown in Table II. 4'-Bromobenzonorbornadiene (XVI), fractionated by preparative gas chromatography, has a b. p. of 127 ~129°C (10 mmHg); n_D^{29} 1.5910.

Found: C, 59.96; H. 4.24. Calcd. for $C_{11}H_9Br$: C, 59.76; H, 4.10%.

Table II. The components of the reaction product of 2, 5-dibromo-1-iodobenzene with magnesium and cyclopentadiene

1	Benzonorbornadiene	25.4%
2	*p*-Dibromobenzene	28.6%
3	3-Bromoiodobenzene	6.6%
4	x(unidentified)	1.6%
5	4'-Bromobenzonorbornadiene	21.1%
6	y(unidentified)	4.9%
7	z(unidentified)	11.8%

The authors are grateful to Professor Eiji Ochiai and Dr. Kénichi Takeda for their encouragement and to M. Hiroyuki Ishitobi and Mr. Tadashi Irie for their skillful technical assistance.

Shionogi Research Laboratory
Shionogi & Co., Ltd.
Fukushima-ku, Osaka

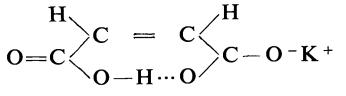
17) A. Roe, "Organic Reactions," Vol. V, John Wiley and Sons, Inc., New York, N. Y. (1949), p. 193.

*The Electron Spin Resonance of an Irradiated Single Crystal of Potassium Hydrogen Maleate**

By Machio IWASAKI and Koichi ITOH

(Received August 22, 1963)

Although the electron spin resonance (ESR) of many irradiated single crystals of organic molecules has been reported on in the past five years, few attempts have been made to examine molecules containing conjugate systems. It has been found by I. Miyagawa** that the ESR spectra of several dicarboxylic acids, such as formic acid, fumaric acid, and maleic acid, were very weak, while very much stronger spectra were obtained from saturated carboxylic acids. The common characteristics of these dicarboxylic acids are that all molecules in a crystal are linked by intermolecular hydrogen bonds and that each molecule has a conjugate system. The odd electrons or holes produced in a crystal by irradiation may easily migrate throughout the entire crystal through the conjugate systems and the intermolecular hydrogen bonds, accompanied by the recombination and disappearance of the odd electrons or holes. In this respect, potassium hydrogen maleate (KHM) is an especially interesting case. In this molecule the intermolecular hydrogen bonds are broken by the substitution with potassium as:



Unlike maleic acid, this molecule gave strong and sharp spectra, supporting the interpretation of the phenomenon mentioned above. This paper will deal with the identification of the radical produced in a single crystal of this interesting molecule.

Experimental Procedure

Single crystals of potassium hydrogen maleate and its deuterium-exchanged compound (KOOCCH=CHCOOD) were grown from aqueous and heavy water solutions respectively by the slow cooling method. The purity of the deuterium-exchanged compound was tested by means of its infrared spectra. The single crystals obtained were typical orthorhombic crystals, the crystal axes of which were identified by taking vibration photographs of the X-ray diffraction. The crystal structure of KHM has been completely analyzed by Darlow and Cochran,[1] giving the orthorhombic space group Pbcm, with four molecules per unit cell and cell dimensions of $a=4.578$Å, $b=7.791$Å and $c=15.953$Å. The results of the ESR will be compared with their crystal analysis in a later paragraph of this paper.

The single crystals were irradiated at room temperature with an X-ray source operating at 30 kV. and 15 mamp. The ESR of irradiated single crystals was measured mainly at 24 kMc./sec. for various orientations of the crystal in the magnetic field at room temperature. As a reference for the spectroscopic splitting factor, the sharp resonance of DPPH was used. The separations of the hyperfine structures were measured by a proton resonance with a side-band technique.

Experimental Results

The ESR spectra first observed at 9 kMc./sec. showed a marked second order effect,[2] making the spectra somewhat complicated, but the

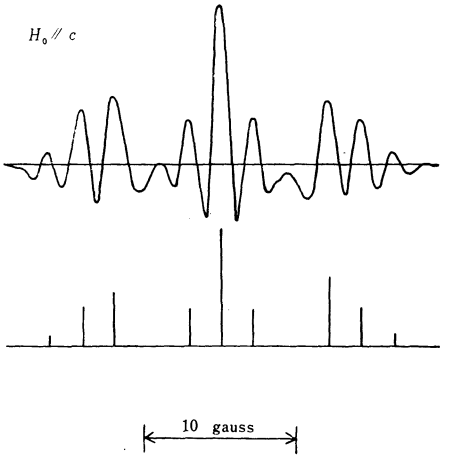


Fig. 1. Electron spin resonance curves at 9 kMc./sec. of an X-irradiated single crystal of potassium hydrogen maleate with the static magnetic field parallel to the c-axis. The vertical lines indicate the theoretical positions and intensities.

* This work was presented at the 16th Annual Meeting of the Chemical Society of Japan, Tokyo, April, 1963.

** Private communication.

1) S. F. Darlow and W. Cochran, *Acta Cryst.*, **14**, 1250 (1961).

2) I. Miyagawa and W. Gordy, *J. Chem. Phys.*, **32**, 255 (1960).

one observed at 24 kMc./sec. showed practically no second order effect, making the spectra simple enough to interpret very easily and accurately. Therefore, the measurements for various orientations of the crystal were mainly carried out at 24 kMc./sec. Figure 1 depicts the ESR spectrum measured at 9 kMc./sec. for the orientation of the crystal in the magnetic field parallel to the crystal c-axis. The hyperfine structure of the spectrum was interpreted on the basis of the theory of the second-order effect[2], giving a good agreement with observed results. The vertical lines under the absorption lines indicate the theoretical spectral positions and their intensities.

The spectra observed at 24 kMc./sec. for orientations of the crystal in the magnetic field parallel to the three crystallographic axes consist of three lines, the relative intensities of which are 1 : 2 : 1. If the crystal is rotated around the a- or b-axis, fixing the magnetic field in the (bc) or (ca) plane of the crystal respectively, the triplet is resolved into a quartet consisting of the pair of doublets expected for two non-equivalent protons with a spin of 1/2 (see Figs. 2 and 3). This suggests that, for these orientations, the unit cell contains only one radical having two chemically-equivalent protons, and that the two protons

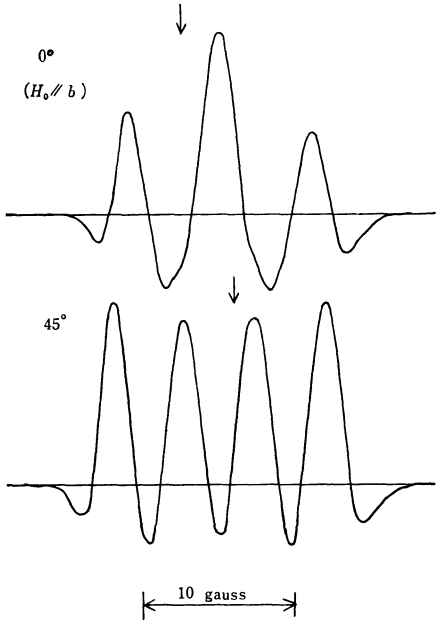


Fig. 2. Electron spin resonance curves at 24 kMc./sec. of an X-irradiated single crystal of potassium hydrogen maleate with the static magnetic field in the (bc) plane. Angles are measured from the b-axis. Arrows show the position for the DPPH resonance.

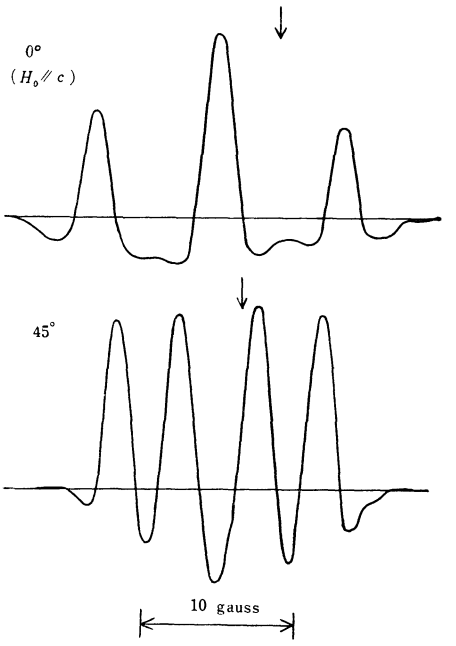


Fig. 3. Electron spin resonance curves at 24 kMc./sec. of an X-irradiated single crystal of potassium hydrogen maleate with the static magnetic field in the (ca) plane. Angles are measured from the c-axis.

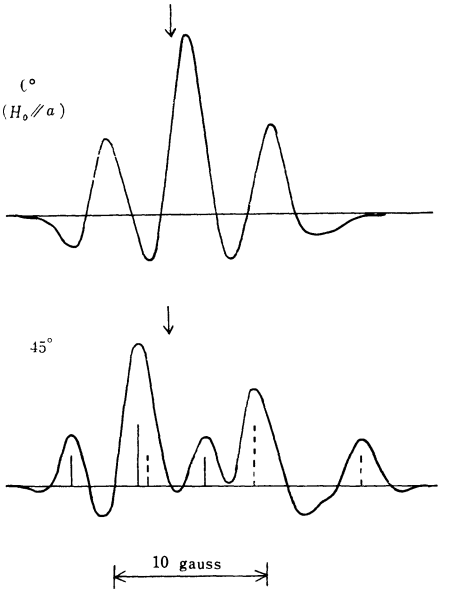


Fig. 4. Electron spin resonance curves at 24 kMc./sec. of an X-irradiated single crystal of potassium hydrogen maleate with the static magnetic field in the (ab) plane. Angles are measured from the a-axis.

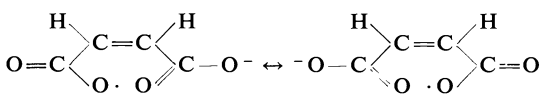
are not magnetically equivalent for the field along the intermediate directions of the crystal axes. However, if the crystal is rotated around the c-axis, fixing the magnetic field in the (ab) plane of the crystal, the single triplet is resolved into a pair of triplets, the *g*-factors of which are different from each other (see Fig. 4). This means that, for this orientation of the crystal, there are two magnetically non-equivalent radicals. In this case, the triplets were not resolved into a quartet as in the case of the rotation around the a- or b-axis. Therefore, two coupling protons in a radical are magnetically equivalent for any orientation produced by the rotation around the c-axis.

From the interpretation of the observed spectra, it is concluded that there are four coupling protons in a unit cell. The principal values and the direction cosines of the hyperfine tensors for these protons determined from the angular dependence of the coupling constants are tabulated in Table I. The principal values and the direction cosines of the *g*-tensors were determined from the angular dependence of the center of the hyperfine patterns and are also listed in Table I.

The ESR of an irradiated single crystal of potassium deuterium maleate (KDM) was also measured in order to get some additional information about the structure of the free radical. The observed spectra, however, was not any different in the coupling values from the one for KHM. The line widths for both compounds were very narrow and in both the distance between maximum slopes was 1—2 gauss. Although slightly sharper lines were observed for KDM, it was shown by a comparison of the spectra for rotations around the a-, b-, and c-axes that the largest difference between the line widths of the two compounds was only 0.5 gauss.

Analysis of the Results and Discussion

These features of the observed spectra suggest that the radical is produced by the removal of OH hydrogen, and that the coupling protons are two vinylene protons which can be chemically equivalent because of the following resonance:



Two vinylene protons are always equivalent for the orientations of the crystal in the magnetic field in the (ab) plane, so the (ab) plane should be perpendicluar to the C=C bond. Furthermore, it is expected from the experimental results that the two kinds of molecules in a unit cell are oriented in such a way that the (ca) or (bc) plane of the crystal makes an equal angle to the two planes of molecules corresponding to the two magnetically-non-equivalent radicals.

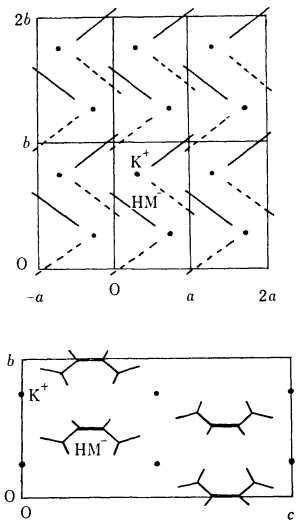


Fig. 5. Projection of the structure of potassium hydrogen maleate to the c- and a-axes.

Shown in Fig. 5 is the arrangement of the four molecules in the unit cell as determined by Darlow and Cochran.[1] It may be seen that the orientations of the molecules expected from the observed ESR spectra are entirely consistent with the crystallographic results. The direction cosines of the C–H bond and the directions perpendicular to it can be calculated from the crystallographic data and compared with those of the principal axes of the hyperfine tensor. As Tables I and II indicate, the direction for the smallest element approximately coincides with the C–H bond direction, while that for the largest coincides with the direction perpendicular to the C–H bond in the molecular plane. This finding indicates that the origin of the hyperfine structure is two vinylene protons, and that the structure of the free radical produced is not very much deformed from the parent molecule as far as the vinylene portion of the molecule is concerned.

The results listed in Table I indicate that the smallest principal element of the *g*-tensor has its axis perpendicular to the molecular plane and that the other two pincipal elements are approximately equal and are directed in the molecular plane. This means that the spin density is in a p-orbital of the carbon,

TABLE I. VALUES OF THE PROTON HYPERFINE AND g-FACTOR TENSORS IN X-IRRADIATED POTASSIUM HYDROGEN MALEATE

Tensor	Principal values gauss obs.	theo.	Direction cosines* with respect to the a-, b- and c-axes			Directions with respect to the molecule
Proton H_2	$(-)2.1_1$	−2.5	∓0.649	±0.560	∓0.515	∥ C_2-H_2**
	$(-)7.0_1$	−6.8	±0.669	±0.743	0.000	⊥molecular plane
	$(-)10.1_3$	−9.9	±0.360	∓0.370	∓0.857	⊥ C_2-H_2 in molecular plane
Proton H_2'	$(-)2.1_1$	−2.5	∓0.649	±0.560	±0.515	∥ $C_2'-H_2'$
	$(-)7.0_1$	−6.8	±0.669	±0.743	0.000	⊥molecular plane
	$(-)10.1_3$	−9.9	∓0.360	±0.370	∓0.857	⊥ $C_2'-H_2'$ in molecular plane
g	2.0024		±0.629	±0.778	0.000	⊥molecular plane
	2.0040		∓0.778	±0.629	0.000	⊥C=C in molecular plane
	2.0045		0.000	0.000	±1.000	∥ C=C

* The uncertainties in the coupling constants, the g-factor, and the directions of the coupling constants are estimated to be 0.3 gauss, 0.0006, and 2°, respectively.

** Determined by X-ray diffraction data.[1]

TABLE II. DIRECTION COSINES OF THE C-H BOND AND ITS PERPENDICULAR IN THE MOLECULAR PLANE OBTAINED FROM THE X-RAY DATA

Direction	Direction cosines with respect to the a-, b-, and c-axes			Angle made with the principal axes of the hyperfine tensor
∥ C_2-H_2	∓0.715	±0.548	∓0.435	6°
⊥ C_2-H_2 in plane	±0.339	∓0.272	∓0.901	6°
∥ $C_2'-H_2'$	∓0.715	∓0.548	∓0.435	6°
⊥ $C_2'-H_2'$ in plane	∓0.339	∓0.272	∓0.901	6°

which has its direction perpendicular to the molecular plane.

The nuclear hyperfine interaction constant, A, of the $\diagdown$·C—H$\diagup$ fragment consists of an isotropic Fermi term, A_f, and an anisotropic dipole-dipole interaction term, A^{μ}. The isotropic term, A_f, is determined from the three principal elements by $(A_1+A_2+A_3)/3$ to be 6.4 gauss for the present free radical. With this value, the spin density on the vinylene carbon atom is found to be 0.26, employing 25 gauss as the A_f value for unit spin density. The anisotropic hyperfine interaction for π-eletron free radicals has been estimated by McConnell and Strathdee,[3] who gave the principal elements the values of 15.4, −1.7, and −13.6 gauss along the C–H bond, along the density axis of the p-orbital, and perpendicular to those two respectively. For the present radical these principal values should be reduced by 74% to 3.9, −0.4, and −3.5 gauss respectively. Since A_f is known to be negative in sign,[4] adding the observed isotropic component, $A_f=-6.4$ gauss, to the theoretical anisotropic components yields −2.5 gauss for the total coupling constant along the C–H bond, −6.8 gauss along the p-orbital, and −9.9 gauss perpendicular to the C–H bond in the molecular plane. These values are in very good agreement with the observed principal elements of the hyperfine tensor shown in Table I. Figure 6 indicates the directions of the principal axes, A_1, and A_3; A_2, which is not indicated, is perpendicular to the molecular plane.

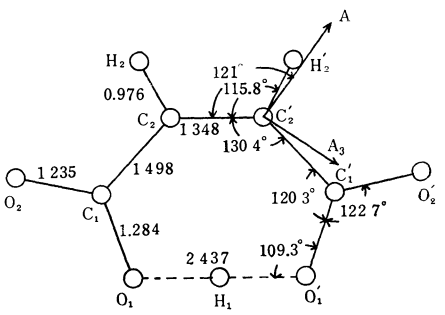


Fig. 6. The molecular structure of the hydrogen maleate ion and the directions of the proton coupling tensor.

The observed narrow line widths and their small change upon deuterium substitution

3) H. M. McConnell and J. Strathdee, *Mol. Phys.*, **2**, 129 (1959)

4) H M. McConnell and D. E. Chesnut, *J. Chem. Phys.*, **28**, 108 (1958); H. M. McConnell, C Heller, T. Cole and R. W. Fessenden, *J. Am. Chem. Soc.*, **82**, 766 (1960).

suggest that no nuclear spin except two vinylene protons exists in the present radical. The difference of line width in both compounds when the OH proton exists in the produced radical was estimated on the basis of the following assumptions: (1) the radical has the same geometrical structure as that of the parent molecule;[1] (2) the spin density in the vinylene carbon atom is +0.26; (3) the remaining spin density, +0.48, is equally assigned to the most distant side oxygen atoms from the OH protons; (4) each spin density is located on the nucleus as a point spin density; (5) the Fermi term of the OH proton-coupling constant is assumed to be −0.1 gauss, which gives the smallest possible total coupling constant; (6) the contributions from the neighboring molecules to the line width are disregarded. As nothing is known about the quantities in assumptions 3 and 5, they are assumed to give the lowest possible value for differences in line widths as far as these quantities are concerned. Thus, the principal elements of the coupling constant for the OH proton were estimated to be +1.5, −1.5, and −0.3 gauss for the direction perpendicular to the C=C bond in the molecular plane, for that perpendicular to the molecular plane, and for that parallel to the C=C bond respectively. When the OH proton is substituted with deuteron, the line widths are expected to be reduced at least by 1.0, 1.0, and 0.2 gauss for the principal directions. A comparison of these calculated values with the observed ones excludes the possibility that the radical which gives the observed absorption has an OH hydrogen atom as does the parent molecule.

It is interesting to note that the discrepancy between the observed direction of the C–H bond in the radical and the calculated direction from the X-ray crystallographic data of the parent molecule may be responsible for the loss of the bridge hydrogen bond. Darlow[5] pointed out that this intramolecular hydrogen bond produces strain in the bond angles of this molecule. The C=C–C angle in unstrained molecules[5] is about 121.5±1.0°, while the same angle in the present molecule[1] is 130.4 ±0.2°, the strain angle being 8.9±1.0°. Therefore, if the strain is removed by the loss of the bridge hydrogen, the C=C–C angle will be closed by about 8.9°, accompanied by a change in the C=C–H angle which will amount to about a half of this strain, that is, to 4.5°. Thus, the C=C–H angle will change from 115.8° (X-ray value) to 120.3° in the unstrained radical. The observed C=C–H angle in the radical, 121°, is in good agreement with the expected value, 120.3°.

It is of interest that simple LCAO calculation shows that the unpaired electron must be a π-electron for the proposed radical produced by the removal of the OH hydrogen during irradiation. It is assumed in the calculations that the Coulomb integral to the ring oxygen is smaller than the side oxygen for the following reasons. (1) According to the X-ray data, the side C–O distance is shorter than the ring C–O in the parent molecule (see Fig. 6). (2) In the radical produced upon the removal of the OH hydrogen, the ring O···O distance becomes so short that the β_{OO} can not be ignored. Instead of including β_{OO}, the contribution from the β_{OO} may be replaced by taking the smaller value of the Coulomb integral for the ring oxygen. With $\alpha_O(\text{ring}) = \alpha_C + 1.8\beta_C$, $\beta_{CO}(\text{ring}) = 0.85\beta_C$, $\alpha_O(\text{sid}) = \alpha_C + 1.2\beta_C$, and $\beta_{CO}(\text{side}) = 0.95\beta_C$, the energy level of the highest-filled π-orbital was found to be higher than that of a pπ lone-pair electron on an oxygen atom by $0.71|\beta_C|$, where α_C is the Coulomb integral and β_C is the resonance integral of a pπ electron in a C=C bond. The unpaired electron which should be formed on the oxygen atom by the removal of the OH hydrogen atom is equivalent to one of the σ lone-pair electrons. The energy level of the latter electron is equal to that of a pπ lone-pair electron on the same atom for a simple LCAO approximation. Thus, to minimize the energy of the radical, an electron in the highest-filled orbital is relocated at the half-filled σ lone-pair orbital, the remaining π electron becoming an unpaired electron. The spin density on the vinylene carbon atom was found to be +0.28, which is in very good agreement with the +0.26 estimated from the proton-coupling constant.

After finishing our work, we found that Heller and Cole[6] had obtained a similar results. However, our results may be more accurate than those of (HC), since their results were derived mainly from measurements at 9 kMc./sec. These two independent measurements are in very good agreement with each other. The discrepancies between the principal values in Table I and those given by (HC) are within 0.2 gauss and 2.5° for the values and directions of the principal elements of the proton-coupling constant respectively, and within 0.0012 and 1° for those of the g-factor respectively.

The authors are greatly indebted to Professor Ichiro Miyagawa of Duke University for his

5) S. P. Darlow, *Acta Cryst.*, **14**, 1257 (1961).

6) H. C. Heller and T. Cole, *J. Am. Chem. Soc.*, **84**, 4448 (1962).

suggestion of this problem and his valuable advice, and to Professor Saburo Nagakura for his kindly supplying the sample. One of the authers (M. I.) wishes to thank the Institute for Solid State Physics, the University of Tokyo for the financial support during his stay.

Government Industrial Research Institute, Nagoya
Kita-ku, Nagoya (M. I.)

Institute for Solid State Physics
The University of Tokyo
Azabu, Tokyo (K. I.)

Electron Paramagnetic Resonance Studies of Titanium(III) Ions with Complexing Compounds

By Shizuo FUJIWARA and Maurice CODELL

(Received August 28, 1963)

The nuclear hyperfine structure of titanium-(III) was first observed by Waters and Maki[1] using titanium(III) complexes formed by the interaction of equimolar quantities of titanium-(III) chloride in methanol and sodium methylate in methanol and slightly more than two equivalents of hydrogen fluoride in methanol to one equivalent of titanium(III) chloride in methanol. The spectra which were obtained in the methanol solution at $-45°C$ consisted of eight lines, which is in accordance with the predictions of Jeffries[2] who determined through nuclear magnetic resonance measurements that ^{47}Ti and ^{49}Ti have spins of 5/2 and 7/2 respectively. The spectrum obtained by Waters and Maki is highly unsymmetrical, with peak intensities decreasing at higher fields.

A symmetrical hyperfine spectrum of titanium(III) was obtained by McGarvey[3] at 77°K using a single crystal of aluminum acetylacetonate containing a small amount of titanium acetylacetonate. A signal for titanium(III) in solution has been observed by Shien and Boss[4] using the $(\pi\text{-}C_5H_5)_2Ti(C_2H_5)$ complex in toluene at 300°K, and by Avvakumov, Garif'yanov and Semenova[5] using supercooled solutions of $TiCl_3\cdot 6H_2O$ and $Ti_2(SO_4)_3\cdot 4H_2O$ in alcohol and glycerine at 200, 77°K, and 300°K. The g values were measured, as were the g values at 200 and 77°K of the solid salts, used in the above solutions[6] (see Table II). The hyperfine spectrum of titanium(III) arises from the interaction of the unpaired 3d electron with the nucleus. The eight lines of the hyperfine pattern are formed by the contributions of the ^{47}Ti and ^{49}Ti isotopes with spins of 5/2 and 7/2 respectively; two of them are overlapped by the large central line from ^{46}Ti, ^{48}Ti, and ^{50}Ti with zero spins.

It was decided to investigate the EPR spectra of other titanium(III) solutions at about 9000 Mc. in order to determine if the hyperfine spectra could be obtained in an aqueous solution and at room temperature. Because of their known ability to form chelate complexes, we chose the complexing agents listed in Table I, which also lists the conditions for preparing the samples.

The spectra obtained in this investigation are the first examples of the hyperfine structure of the complexes of paramagnetic ions to be observed in aqueous solutions.

The features of the simple and hyperfine spectra of several of the chelate compounds were considerably changed by varying the pH values by varying the quantities of complexing agents.

Results and Discussion

The spectra for the titanium(III)-NTA complex is unique in showing practically no change when the pH values are changed from 3 to 10.2. At lower pH values the hyperfine structure diminishes in intensity, until at pH 1.90 very little of the hyperfine structure is discernible. The disappearance of the hyperfine pattern may result from 3d-electron exchange among titanium ions or from the rapid relaxation of titanium nuclear spins.

1) E. L. Waters and A. H. Maki, *Phys. Rev.*, **125**, 233 (1962).
2) C. D. Jeffries, ibid., **92**, 1262 (1953).
3) B. R. McGravey, *J. Chem. Phys.*, **38**, 388 (1963).
4) J. C. W. Chien and C. R. Boss, *J. Am. Chem. Soc.*, **83**, 3767 (1961).
5) V. I. Avvakumov, N. S. Garif'yanov and E. I. Semenova, *Zhur. Eskptl. i. Teoret. Fiz.*, **39**, 1215 (1960).
6) V. I. Avvakumov, N. S. Garif'yanov, S. G. Salikhov and E. I. Semenova, *Fiz. Tverdogo Tele*, **3**, 2111 (1961).

TABLE I. PREPARATION OF SAMPLE SOLUTIONS

Complexing agent	Name	Formula	pK_{a_i} $i=1,2,3,4$	Quantity added per 10 ml.	Control of pH by addition of	Additional reagent
NTA	Nitrilotriacetic acid	$N(CH_2COOH)_3$	1.9, 2.5, 9.7	0.3 g.	NH_4OH	
HEID	Hydroxyethyl-iminodiacetic acid	$N(CH_2COOH)_2 \cdot CH_2CH_2OH$	2.2, 8.7	0.3 g.	NH_4OH	
BHEG	Bis-(2-hydroxyethyl)-glycine	$N(CH_2CH_2OH)_2 CH_2COOH$	8.08	0.3 g.	NH_4OH	(1) Tartaric acid (2) No tartaric acid
TEOHA	Triethanolamine	$N(CH_2CH_2OH)_3$	7.90	—	Complexing agent itself	Tartaric acid
DEA	Diethylamine	$NH(CH_2CH_3)_2$	11.0	—	Complexing agent itself	Tartaric acid
NBA	*N*-Butylamine	$H_2N(C_4H_9)$		—	Complexing agent itself	Tartaric acid
EDTA	Ethylendiamine-tetraacetic acid disodium salt	$C_2H_4 \cdot \{N(CH_2COOH) \cdot (CH_2COONa)\}_2$	2.2, 8.0, 5.2, 10.3	0.3 g.	NH_4OH	(1) Tartaric acid (2) No tratraic acid
AAC	Acetylacetone	$CH_3COCH_2COCH_3$		3 ml. saturated soln.	NH_4OH	
TEA	Triethylamine	$N(CH_2CH_3)_3$	10.8	—	Complexing agent itself	Tartaric acid

The titanium(III)-NTA spectra are unsymmetrical and similar to those obtained by Waters and Maki. The other complexes studied exhibited remarkable changes at higher pH ranges. The stability of this complex probably results from the three carboxyl groups of NTA, which allows the molecule to enter into a three-dimensional system with titanium(III) with little probability of interaction with the nitrogen of NH_4 when an excess of ammonium hydroxide is added. In less stable titanium(III) complexes, titanium-(III) hydroxide tends to precipitate at higher pH values.

The cause of the unsymmetrical hyperfine structure of this spectrum may be deduced from the suggestion made by McConnell[7] and confirmed experimentally by Rogers and Pake[8] regarding the observed broadening of the hyperfine spectrum of VO(III) ions in an aqueous solution. This condition can also exist with the solutions used in this investigation.

$$1/T_2 \approx \lambda_c(\Delta g \beta H_0 + b m_I)^2/h^2$$

where b is $A_{\parallel} - A_{\perp}$; the other symbols possess their usual meanings. The above equation generally predicts a different width contribution for each hyperfine line. The minimum width should occur for the m_I value which causes the bracket to approach a minimum.

The spectra for the titanium(III)-HEID complex show a hyperfine structure which is far less intense than but which has the same unsymmetrical features as the previously-discussed complex. This hyperfine structure is only discernible at pH ranges from about 5.0 to 7.9. At appreciably higher or lower pH values, no hyperfine structure is exhibited by the complex. Since HEID contains only two carboxyl groups, the three-dimensional system which was thought to be obtained with the NTA complex is less likely to be obtained with this complex.

With BHEG, which contains only one carboxyl group, no hyperfine structure is obtained at any pH value. This complex is not as stable as either of the above complexes, and titanium(III) hydroxide begins to precipitate at a pH of approximately 9.0. Upon the addition of tartaric acid, however, the precipitation is prevented and a signal at higher pH values can be obtained.

The spectrum for the titanium(III)-EDTA

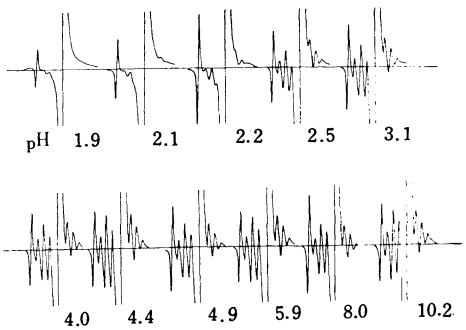


Fig. 1. Spectra for the Ti(III)-NTA complex. The concentration of $TiCl_3$ is 0.11 M. The field increases from left to right. The initial peak is that of DPPH.

7) H. M. McConnell, *J. Chem. Phys.*, 25, 709 (1956).
8) R. N. Rogers and G. E. Pake, ibid., 33, 1107 (1960).

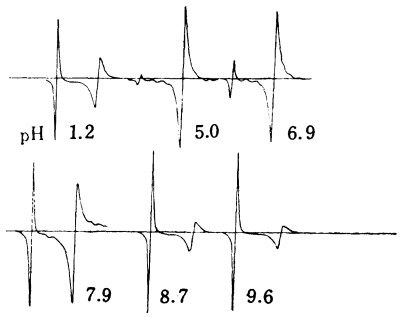


Fig. 2. Spectra for the Ti(III)-HEID complex. The concentration of $TiCl_3$ is 0.11 M. The field increases from left to right. The initial peak is that of DPPH.

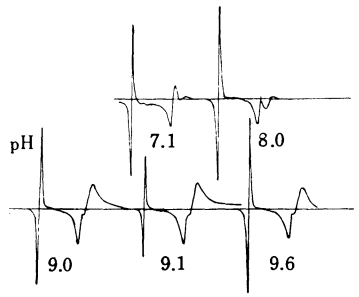


Fig. 3. Spectra for the Ti(III)-EDTA complex. The concentration of $TiCl_3$ is 0.11 M. The field increases from left to right. The initial peak is that of DPPH.

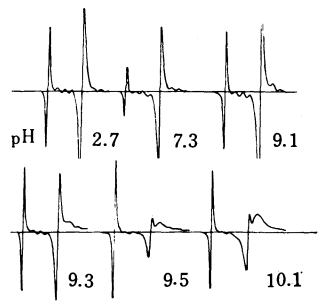


Fig. 4. Spectra for the Ti(III)-EDTA-tartaric acid complex. The concentration of $TiCl_3$ is 0.11 M. The field increases from left to right. The initial peak is that of DPPH.

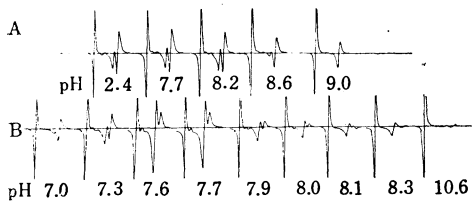


Fig. 5. Spectra for the Ti(III)-TEOHA-tartaric acid complex. The concentration of $TiCl_3$ is (A) 0.044 M. and (B) 0.088 M. The field increases from left to right. The initial peak is that of DPPH.

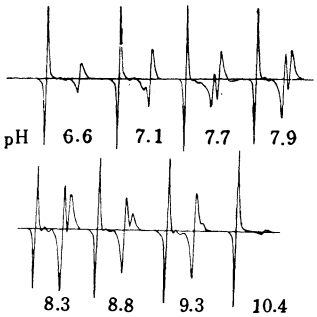


Fig. 6. Spectra for the Ti(III)-TEA-tartaric acid complex. The concentration of $TiCl_3$ is 0.11 M. The field increases from left to right. The initial peak is that of DPPH.

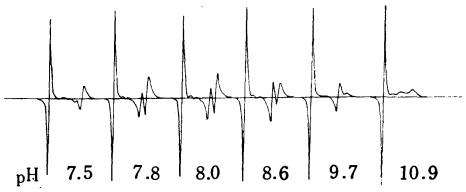


Fig. 7. Spectra for the Ti(III)-DEA-tartaric acid complex. The concentration of $TiCl_3$ is 0.088 M. The field increases from left to right. The initial peak is that of DPPH.

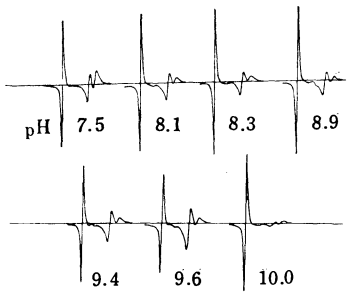


Fig. 8. Spectra for the Ti(III)-NBA-tartaric acid complex. The concentration of $TiCl_3$ is 0.11 M. The field increases from left to right. The initial peak is that of DPPH.

complex is especially interesting because of the different spectra obtained with and without the addition of tartaric acid. With no tartaric acid, the spectra (Fig. 3) shows a less hyperfine structure, but evidence for more than one complex is clearly seen. Two peaks are observed for all pH values but are more pronounced at the pH values of 7 and 8. With the addition of tartaric acid, the spectrum exhibits an observable hyperfine structure in which each component of the hyperfine lines is broadened at higher pH values. At pH 9.5, another peak without a hyperfine structure appears at higher

TABLE II. g Values of Ti(III) complexes

Complexing agent	Concn. of $TiCl_3$ (molarity)	pH	g value$\pm$0.002
Acetylacetone	0.011 and 0.022	1.7 to 2.6	1.946
NTA	0.11	1.9, 8.0, 10.2	1.962
NTA	0.11	2.1, 2.2, 2.5, 3.1, 4.0, 4.4, 4.9, 5.9	1.961
HEID	0.11	1.2	1.952
HEID	0.11	5.0, 7.9	1.953
HEID	0.11	6.9	1.950
HEID	0.11	9.6	1.954
BHEG	0.11	3.3, 3.7, 3.9	1.957
BHEG	0.11	8.9, 9.2	1.954
BHEG	0.11	9.6, 10.1	1.953
EDTA (no tartaric acid)	0.11	1.1, 7.1	1.958
EDTA (no tartaric acid)	0.11	8.0, 9.0, 9.1, 9.6	1.956
EDTA (tartaric acid)	0.11	2.7, 7.3, 9.1, 9.3	1.957
EDTA (tartaric acid)	0.11	9.5, 10.1	1.956

Complexing agent	Concn. of $TiCl_3$ (molarity)	pH	Peak a	Peak b
TEOHA	0.044	7.4, 8.2, 8.6, 8.8, 9.0	1.970	1.964
TEOHA	0.088	7.0, 7.6, 7.7, 7.9, 8.1, 8.3	1.970	1.964
TEA	0.11	6.6	1.969	(1 peak)
TEA	0.11	7.1, 7.7, 7.9, 8.3, 8.8, 9.3	1.970	1.965
TEA	0.11	10.4	1.970	(1 peak)
DEA	0.088	7.5, 7.8, 8.0, 8.6, 9.7	1.970	1.964
NBA	0.088	7.5, 8.1, 8.3, 8.9, 9.4, 9.6, 10.0	1.970	1.964

$(\pi\text{-}C_5H_5)_2Ti(C_2H_5)$ in toluene	1.94 (300°K)[4]
$TiCl_3 \cdot 6H_2O$ (solid salt)	1.91 (77° and 200°K)[6]
$Ti_2(SO_4)_3 \cdot 4H_2O$ (solid salt)	1.91 (77° to 200°K)[6]
$TiCl_3 \cdot 6H_2O$ (ethanol solution)	1.9$\pm$0.1 (Room temp.)[5]
Ti(III) : CH_3OH (methanol solution)	1.9532$\pm$0.0005 (−45°C)[1]
TiF_2^+ (methanol solution)	1.9465$\pm$0.0004 (−45°C)[1]

fields. At pH 10.1, the increase in the intensity of the second peak indicates a change in the equilibrium mixture of the two complexes.

The principles of the complex formation of titanium(III) with TEOHA (Fig. 5), TEA (Fig. 6), DEA (Fig. 7), and NBA (Fig. 8) are similar. A hyperfine structure is seen with all the complexes. The spectra clearly show the presence of two different complexes for each complexing agent. The concentration of one complex with respect to the other depends upon the amount of complexing agent which has been added, rather than upon the pH of the solution. This is shown with the different equilibrium mixtures of complexes obtained using different concentrations of titanium(III) with TEOHA at pH 7.7 (Fig. 5). Since the concentration of titanium(III) in one case is double that of the other, a different complex is dominant. The g values for this group (Table II) are all 1.974$\pm$0.002, which is excellent evidence for the fact that the orbital character of the ground electronic doublet of titanium(III) remains the same with these compounds for all pH values. Similar conditions appear to exist with NTA, HEID, BHEG, and EDTA, as is shown in Table II, where g varies from 1.950 to 1.962. The g value for titanium(III) acetylacetonate is 1.946, which is a fairly sizable shift from that of the other complexes. It is interesting to note that the g values are little changed with different complexing agents and varying pH values. This shows that the contributions of the spin orbit coupling are little changed despite the fact that different colors are obtained.

The titanium(III) used in this investigation was a commercial grade in hydrochloric acid and contained zinc in excess of a 1 : 1 ratio to titanium. Recent work has shown that zinc is necessary in order to obtain spectra with

complexing agents which do not contain carboxyl groups. Somewhat similar spectra can be obtained with a mixture of titanium(III), tartaric acid and zinc.

Summary

The EPR spectra of a number of titanium-(III) complex compounds have been obtained at room temperature and in aqueous solutions; these compounds show either a hyperfine structure alone or a mixture of hyperfine and simple structures. The g values for the various complexes have been determined and compared. This technique should provide a simple method for studying the state in solution of the complexes of several other metals and their isotopes.

The authors acknowledge with gratitude the excellent suggestions made by Dr. Kozo Nagashima and Mr. Yuzuru Fujiwara of this department.

Department of Chemistry
Faculty of Science
The University of Tokyo
Hongo, Tokyo

The Use of NMR Spectroscopy as a Structural Probe in Ferrocene Chemistry[1]

By Yoichiro NAGAI, John HOOZ and Robert A. BENKESER

(Received August 30, 1963)

Electrophilic substitution reactions in the ferrocene systems give rise, in most instances, to complex isomeric mixtures,[2] such that separation and structural characterization often constitute a perplexing problem. Several methods have been employed for structure determination, of which the most generally useful has proved to be infrared spectroscopy. In particular, the "9, 10μ" Rule[3] has been an invaluable aid for distinguishing between homoannularly- and heteroannularly-substituted ferrocene derivatives.

Classic methods of structure proof involving either independent syntheses[2] or degradative (e.g., bromination,[4] forced catalytic hydrogenation[4,5] and chemical reduction[6]) schemes appear to be limited to mono- or symmetrically-substituted ferrocene types. Unequivocal syntheses are hampered by the relative inaccessibility of the appropriately substituted cyclopentadiene (except in the simplest cases),[7] whereas degradative methods frequently bring about mixtures of substituted cyclopentadienes and cyclopentanes, the structures of which are also frequently unestablished.

Relative yield data[8] and arguments based on analogy to the benzenoid analogs[9] have also been offered as evidence in support of structures. Another proposal of practical use has been advanced[10] that the relative adsorbabilities of disubstituted ferrocenes on the alumina column provided to effect their separation constitute a useful primary indication of structure. Thus, it has been found that, for a variety of alkyl- and arylferrocenes, the order of the elution of isomers from an alumina column is $1,2>1,1'>1,3$.

Ultraviolet spectroscopic data have been

1) This research was supported by the United States Air Force through the Air Force Office of Scientific Research of the Air Research and Development Command under Contract No. A. F. 49(638)—297. Reproduction in whole or in part is permitted for any purpose of the United States Government.

2) P. L. Pauson, "Organometallic Chemistry," Ed. by H. Zeiss, Reinhold Publishing Corp., New York, N. Y. (1961).

3) a) M. Rosenblum, *Chem. & Ind.*, **1958**, 953; b) M. Rosenblum and R. B. Woodward, *J. Am. Chem. Soc.*, **80**, 5443 (1958).

4) A. N. Nesmeyanov, E. G. Perevalova and O. A. Nesmeyanova, *Doklady Akad. Nauk. SSSR*, **100**, 1099 (1955).

5) A. N. Nesmeyanov et al., *Izvest. Akad. Nauk. SSSR Otdel. Khim. Nauk.*, 749 (1956).

6) D. S. Trifan and L. Nicholas, *J. Am. Chem. Soc.*, **79**, 2746 (1957).

7) For example, the symmetrical structure of dibenzoylferrocene was confirmed by conversion to dibenzhydrylferrocene (addition of phenyl Grignard reagent followed by reduction of the tertiary carbinol). The properties of the latter were identical to those of the material prepared from benzhydrylcyclopentadiene, cf. B. F. Hallam and P. L. Pauson, *J. Chem. Soc.*, **1956**, 3030.

8) K. L. Rinehart, Jr., K. L. Motz and S. Moon, *J. Am. Chem. Soc.*, **79**, 2749 (1957).

9) C. R. Hauser and J. K. Lindsay, *J. Org. Chem.*, **21**, 382 (1956).

10) M. Rosenblum, *J. Am. Chem. Soc.*, **81**, 4530 (1959).

employed[8,11] to distinguish between homoannular isomers; the absorption for the 2-isomer is more intense, but it appears at a shorter wavelength than that of the 3-isomer.

Recently, it has been suggested that infrared absorptions may serve to define the structures of homoannularly-disubstituted ferrocene derivatives;[12] a 1, 3-structure exhibits two bands in the region between 10.8 and 11.2 μ, whereas the 1, 2-isomer possesses only one band, near 10.9 μ.

It can be seen from Table VIII,[13] however, that it is difficult to distinguish between the 1, 2 and 1, 3-structures of the acylalkyl series by a simple application of this generalization.

Another attempted correlation,[14] in which the infrared absorption at 7.80 μ was said to be characteristic of a 1, 3-disposition of groups, has been questioned recently.[15] It will be noted from Table VIII that the 1, 1' compounds, as well as several of the 1, 2-types, show absorption very near 7.80 μ.

In many cases, a judicious combination of all these methods has been employed.[11] However, relatively little use has been made of NMR spectroscopy to distinguish between various structural types.[16]

It is the purpose of this paper to report that NMR spectroscopy can provide an unequivocal and universal probe for determining the structure of many substituted ferrocenes.

Results and Discussion

In connection with another study[17] we have had occasion to acylate the homologous series of alkylferrocenes. The isomeric acetylmethyl- and acetylethyl-derivatives are known, whereas the isopropyl- and *t*-butyl-derivatives have not yet been reported. Each of these compounds could be conveniently prepared by a modification of the mild acylation procedure described by Hauser and Lindsay.[18] The resulting isomeric acetylalkylferrocenes were separated by column chromatography (Merck neutral alumina). For the methyl, ethyl and isopropyl-derivatives, the course of the separation was conveniently followed by vapor phase chromatographic analysis.[19]

Incomplete resolution of the vapor chromatogram for the mixture of 1, 1'- and 1, 3-acetyl-*t*-butylferrocenes required that a different criterion of purity be employed (cf. Experimental). Interestingly, the order of the increasing retention times (VPC) of isomers within a given set parallels the order of increasing adsorbability on the alumina column initially employed for their separation, i.e., 1, 2-<1, 1'<1, 3-acetylalkylferrocene.

A preliminary determination of the chemical shifts[20] for a variety of monosubstituted ferrocenes revealed that the 2- (or 5-) and 3- (or 4-) protons[21] were shielded only slightly by alkyl substituents (ca. 0.09~0.14 p.p.m. relative to ferrocene), whereas electron-withdrawing substituents (e.g., acetyl, carbomethoxy) displayed a pronounced deshielding effect. These results are analogous to those already described for the benzenoids.[22]

For the homoannular acetylalkylferrocenes, there is one "ortho" proton (relative to the acetyl group) for the 1, 2-isomer, whereas for the 1, 3-structure there are two such positions. It was reasoned qualitatively that if any small shielding effects imposed by alkyl groups were outweighed by the more substantial deshielding effect caused by electronegative functions, NMR spectroscopy should provide a useful probe for elucidating homoannular positional isomers. That this indeed proved to be the case is convincingly demonstrated by the data in Table I. (See also the N.M.R. illustrations.)

All 1-acetyl-1'-alkylferrocenes exhibit similar patterns for the ring protons.[23] When the

11) K. L. Rinehart, Jr., D. E. Bublitz and D. H. Gustafson, ibid., **85**, 970 (1963).

12) M. Rosenblum and W. G. Howells, ibid., **84**, 1167 (1962).

13) This table summarizes all the characteristic infrared absorption bands for the acylalkylferrocenes we have prepared and characterized.

14) A. N. Nesmeyanov, L. A. Kazitsyna, B. V. Lokshin and V. D. Vil'chevskaya, *Doklady Akad. Nauk. SSSR*, **125**, 1037 (1959).

15) Ref. 12 and E. W. Neuse and D. S. Trifan, *J. Am. Chem. Soc.*, **85**, 1952 (1963).

16) K. L. Rinehart et al. (*J. Am. Chem. Soc.*, **82**, 4111 (1960).) made use of this method, as did M. Rosenblum et al. (*J. Am. Chem. Soc.*, **85**, 316 (1963).), to study the conformation of alkyl-bridged ferrocenes. Apparently the only use of NMR to distinguish between homoannularly-substituted isomers is the recent report by Rinehart and his coworkers, which was contemporaneous with our preliminary communication. [R. A. Benkeser, Y. Nagai and J. Hooz, This Bulletin, **36**, 482 (1963).].

17) R. A. Benkeser, Y. Nagai and J. Hooz, *J. Am. Chem. Soc.*, to be prepared.

18) C. R. Hauser and J. K. Lindsay, *J. Org. Chem.*, **22**, 482 (1957).

19) There is relatively little mention in the literature of the use of VPC for ferrocene compounds. Perhaps the reason for such an aversion resides in the fact that ferrocene and many of its derivatives are solids. That such a view is unwarranted is clearly demonstrated by the successful analysis of numerous ferrocene compounds in our laboratory.

20) The nuclear magnetic resonance spectra were determined in a carbon tetrachloride solution employing a Varian A-60 spectrometer. Tetramethylsilane served as an internal standard. Chemical shifts are reported to the estimated center of a singlet or multiplet. Peak areas were determined by electronic integration.

21) The 2- (or 5-) and 3- (or 4-) protons represent the positions "ortho" and "meta" to the substituent. In the discussion of the spectra of acetylalkylferrocenes presented below, the acetyl group is assigned position one.

22) L. M. Jackman, "Applications of Nuclear Magnetic Resonance Spectroscopy in Organic Chemistry," Pergamon Press, New York, N. Y. (1959).

TABLE I. CHEMICAL SHIFTS FOR THE RING PROTONS OF SUBSTITUTED FERROCENES[1,2]

Substituent	*a*[3]	*b*[4]	*c*[5]	*d*[6]
H (ferrocene)	—	—	5.94	—
Me	—	—	6.01(7)	6.06(2)
Et	—	—	5.99(5)	6.03(4)
i-Pr	—	—	5.98(5)	6.04(4)
t-Bu	—	—	5.98(5)	6.08(4)
Ac (acetyl)	5.33(2)	5.64(2)	5.88(5)	—
1-Ac-1'-Me	5.42(2)	5.70(2)	—	6.01(4)
1-Ac-2-Me	5.56(1)	5.72(1); 5.82(1)	5.95(5)	—
1-Ac-3-Me	5.40(2)	5.69(1)	5.92(5)	—
1-Ac-1'-Et	5.41(2)	5.69(2)	—	5.99(4)
1-Ac-2-Et	5.53(1)	5.69(1); 5.79(1)	5.93(5)	—
1-Ac-3-Et	5.37(2)	5.69(1)	5.91(5)	—
1-Ac-1'-*i*-Pr	5.39(2)	5.66(2)	—	5.98(4)
1-Ac-2-*i*-Pr	5.51(1)	5.64(1); 5.76(1)	5.92(5)	—
1-Ac-3-*i*-Pr	5.41(2)	5.71(1)	5.91(5)	—
1-Ac-1'-*t*-Bu	5.32(2)	5.61(2)	—	5.98(4)
1-Ac-2-*t*-Bu	5.46(1)	5.71(1); 5.79(1)	5.85(5)	—
1-Ac-3-*t*-Bu	5.43(2)	5.72(1)	5.90(5)	—

1) The data listed are "tau" values, using tetramethylsilane as an internal standard.
2) The values in parentheses are relative intensities. All measurements were made on a Varian A-60 analytical spectrometer.
3) Column "*a*" values refer to the H in the 2- and 5-position relative to the acetyl group.
4) Column "*b*" values refer to the H in the 3- and 4-position relative to the acetyl group.
5) Column "*c*" values refer to the H on an unsubstituted ring.
6) Column "*d*" values refer to the H on an alkylated ring.

spectrum of acetyl- and the appropriate alkylferrocene is inspected, it may be seen that the only reasonable assignment for the ring protons of 1, 1'-isomers is to ascribe the two low-field resonances (each of an intensity of two) to the acetylated ring. The lower resonance (column a, Table I) is due to 2- and 5-H (relative to the acetyl group), and the higher field triplet, to 3- and 4-H. Within this set, the alkylated ring protons possess chemical shifts that are only slightly different from the alkylated ring protons of the parent alkylferrocene.

Unsubstituted ring protons of all 1-acetyl-2-alkylferrocenes are singlets, exhibiting a deshielding order from methyl (5.95 tau) through *t*-butyl (5.85 tau). Of greater interest to the present investigation, however, was the appearance of the disubstituted ring protons as three complex peaks, indicating three non-equivalent protons. The most deshielded multiplet (column a, Table I) was reasonably assigned to 5-H, by analogy with acetylferrocene itself. The high-field multiplet (column b, Table I, higher entries) was assigned to 3-H by inspection of the alkylated ring protons of the parent alkylferrocene, whereas the mid-field multiplet (the lower of the two tau values in column b, Table I) was assigned to 4-H. The general appearance of three complex peaks of the intensity 1 : 1 : 1[24] was in itself diagnostic of a 1, 2-disubstituted ferrocene, bearing an alkyl and an electronegative moiety.

Furthermore, clinching evidence in support of these assignments is provided by the model have space compound, 1, 2-(α-ketotetramethylene)-ferrocene.[25] Infrared absorptions at 9 and 10 μ eliminate the possibility of the 1, 1'-structure, and a 1, 3-disposition is seemingly impossible on structural grounds. The NMR spectrum showed three peaks[26] on the low-field side of the unsubstituted ring (intensities 1 : 1 : 1); this is in complete agreement with the above assignments for the 1-acetyl-2-alkylferrocenes. In this instance, any structural assignments based upon only infrared generalizations might prove ambiguous, as will be shown later (Table VIII).

The 1, 3-structures presented an entirely different NMR pattern. The spectra of all

23) We are concerned here only with ring proton spectra. The alkyl groups behaved normally, although it should be mentioned that the gem-dimethyl groups of the 1-acetyl-2-isopropylferrocene displayed two nonequivalent methyl groups, each split into a doublet by the methine hydrogen.

24) Alternatively, since the shoulders of the 3-H multiplets were frequenly hidden under the wings of the 4-H multiplet, one may consider the intensities as 1 : 2 (in order of increased shielding). The difference in chemical shifts between 5-H and 4-H was greater than that between 4-H and 3-H (see in particular the 1-acetyl-2-*t*-butyl entry).

25) K. L. Rinehart, Jr., et al., *J. Am. Chem. Soc.*, **84**, 3263 (1962).

26) The tau values obtained in a carbon tetrachloride solution are 5.28 (5-H), 5.60 (4-H), 5.66 (3-H), 5.88 (unsubstituted ring protons), and 7.68 ($-CH_2-$).

1, 3-isomers displayed two peaks on the low field side of the respective unsubstituted ring in the ratio of 2 : 1. (The peak of intensity 2 was in all cases more deshielded than the intensity 1 peak.) Each peak appeared as an unresolved multiplet. In these isomers there are two unsubstituted positions adjacent to an acetyl group, the other position being adjacent only to an alkyl function. There can be little doubt, therefore, that the peaks of intensity 2 correspond to the two protons (2-H and 5-H) adjacent to the acetyl group. The somewhat higher-field peak (intensity 1) is due to 4-H. The latter proton for each 1, 3-isomer possesses a chemical shift not widely different from the 4-H of the corresponding 1, 2-isomer.

These structural assignments receive further support from the trend of the chemical shifts of the α-protons of the alkyl groups attached to the ferrocene ring (see Table II). It may be seen from the table that the frequencies for the α-protons of the 1, 1'-isomers are only slightly different from those of the respective parent hydrocarbons.

TABLE II. CHEMICAL SHIFTS FOR α-PROTONS[1] OF ALKYL GROUPS ON FERROCENE RINGS[2-4]

Substituent	α-H(Me)	α-H(Et)	α-H(*i*-Pr)
R (alkyl)	8.04	7.71	7.41
1-Ac-1'-R	8.09	7.73	7.43
1-Ac-2-R	7.67	7.28	6.59
1-Ac-3-R	7.97	7.62	7.34

1) The α-protons referred to in this table are those located on the carbon atom of the alkyl group which is attached to the ferrocene ring.
2) The data listed are "tau" values, using tetramethylsilane as an internal standard. A Varian A-60 analytical spectrometer was used for all the measurements.
3) Ac in the table refers to the acetyl group.
4) The spectra of all the compounds listed in this table, as well as all those in Table I, were obtained in a solvent of carbon tetrachloride.

For the homoannularly-substituted acetylmethylferrocenes, the α-proton of one isomer is deshielded 0.37 p. p. m., whereas that of the other is deshielded 0.07 p. p. m. (relative to methylferrocene). Consequently, due to the shielding effect on the α-protons induced by their proximity to the acetyl group, the former isomer must possess the 1, 2-, and the latter, the 1, 3-structure.

The same trends are manifest for the homoannularly-substituted acetylethyl- and acetylisopropylferrocenes, the largest deshielding (relative to the corresponding alkylferrocene) occurring for the 1, 2-isomer.

Interestingly enough, it was observed that the chemical shifts for ring protons of those acetylalkylferrocenes could be calculated with a reasonable degree of accuracy (average deviation: 0.04 p. p. m.) employing a simple additivity relationship[27] akin to that developed by Shoolery[28] for acyclic systems.

Shielding constants, measuring the effect of a substituent at a given position (in a given solvent),[29] are tallied relative to the chemical shift for the ring protons of ferrocene itself in Table III.

It is evident from Table I that an acetyl group deshields "ortho" hydrogens by -0.61 p.p.m. and "meta" hydrogens by -0.30 p.p.m. The alkylated ring protons of isopropylferrocene appear as a singlet at 6.04 tau, so that an isopropyl group shields both "ortho" and "meta" hydrogens by $+0.10$ p.p.m. A set of shielding constants calculated in this manner appears in Table III. Using these values, a chemical shift for the ring protons of an acetyl-isopropylferrocene may be calculated. For example, the 5-H resonance of the 1, 3-isomer is obtained from: $5.94+(-0.61+0.10)=5.43$ tau (versus 5.41 tau, observed). Tables IV to VII list predicted and observed tau values for the ring protons in the acetylalkylferrocenes,

TABLE III. SHIELDING CONSTANTS (p.p.m.)

Group	2-Position	3-Position	1'-Position
Me	+0.12	+0.07	+0.07
Et	+0.09	+0.09	+0.05
i-Pr	+0.10	+0.10	+0.04
t-Bu	+0.14	+0.14	+0.04
Ac	−0.61	−0.30	−0.06
CO_2Me[a]	−0.66	−0.21	−0.07

a) Carbomethoxyferrocene absorbs at 5.28 tau (2- and 5-H); 5.73 tau (3- and 4-H) and 5.87 tau (the unsubstituted ring protons).

27) A simple additivity rule was also observed for various alkylcarbomethoxy and alkyldicarbomethoxyferrocenes, the NMR spectra of which will be described later.
28) Ref. 22, p. 59.
29) The simple additivity observed and the conclusions drawn are to be considered limited to carbon tetrachloride solutions. NMR spectra of acetylalkylferrocenes were also determined in benzene solvent, which proved far less satisfactory than carbon tetrachloride. In general, chemical shifts were higher in benzene. The spectra of all the 1, 3-isomers possessed the 2 : 1 intensities of substituted ring protons already noted in carbon tetrachloride. However, the greater differential shielding (in benzene) caused an overlap of 4-H and 5-H for the 1, 2-isomes when R = *i*-Pr and *t*-Bu; consequently, the 1, 2-structure also displayed a 2 : 1 intensity relationship in the region of interest, which could lead to ambiguity. For this reason, carbon tetrachloride is the preferred solvent. Since the proton frequencies are solvent-dependent, no general conclusions regarding the additivity of substituent effects may as yet be drawn. It is not unreasonable, however, to employ shielding constants characteristic of substituents in a given solvent as a first approximation. This approach has been used by Taft et al. (*J. Am. Chem. Soc.*, **85**, 709 (1963).) to determine substituent constants in a study of the NMR spectra of meta-substituted fluorobenzenes.

TABLE IV. COMPARISON OF PREDICTED AND OBSERVED τ-VALUES FOR RING PROTONS OF 1-ACETYL-2- and -3-ALKYLFERROCENES AND 1,1'-DICARBOMETHOXY-2- AND 3-ALKYLFERROCENES

Compound	2-Proton		3-Proton		4-Proton		5-Proton	
	Calcd.	Obs.	Calcd.	Obs.	Calcd.	Obs.	Calcd.	Obs.
1-Ac-2-Me	—	—	5.76	5.82	5.71	5.72	5.40	5.56
1-Ac-3-Me	5.45	5.40	—	—	5.76	5.69	5.40	5.40
1-Ac-2-Et	—	—	5.73	5.79	5.73	5.69	5.42	5.53
1-Ac-3-Et	5.42	5.37	—	—	5.73	5.69	5.42	5.37
1-Ac-2-*i*-Pr	—	—	5.74	5.76	5.74	5.64	5.43	5.51
1-Ac-3-*i*-Pr	5.43	5.41	—	—	5.74	5.71	5.43	5.41
1-Ac-2-*t*-Bu	—	—	5.78	5.79	5.78	5.71	5.47	5.46
1-Ac-3-*t*-Bu	5.47	5.43	—	—	5.78	5.72	5.47	5.43
2-Me-1,1'-DCM[a]	—	—	5.78	5.74	5.73	5.74	5.28	5.35
3-Me-1,1'-DCM[b]	5.33	5.31	—	—	5.78	5.74	5.28	5.31
2-Et-1,1'-DCM	—	—	5.75	5.78	5.75	5.78	5.30	5.33
3-Et-1,1'-DCM	5.30	5.30	—	—	5.75	5.74	5.30	5.30
3-*i*-Pr-1,1'-DCM	5.31	5.35	—	—	5.76	5.76	5.31	5.35
3-*t*-Bu-1,1'-DCM	5.35	5.31	—	—	5.80	5.75	5.35	5.31

a) DCM=dicarbomethoxy

b) Sample calculation: $\tau(2)=5.94+[\sigma(\text{2-CM})+\sigma(\text{2-Me})+\sigma(\text{h-CM})]=5.94+[-0.66+0.12-0.07]=5.94-0.61=5.33$. In all the dicarbomethoxy compounds the effect of the heteroannular carbomethoxy group is taken into account.

TABLE V. PREDICTED AND OBSERVED τ-VALUES FOR HOMOANNULAR-SUBSTITUTED ACETYLALKYLFERROCENES[a]

Compound	1'-Proton	
	Calcd.	Obs.
1-Ac-2-Me	5.95	5.95
1-Ac-3-Me	5.95	5.92
1-Ac-2-Et	5.93	5.93
1-Ac-3-Et	5.93	5.91
1-Ac-2-*i*-Pr	5.92	5.92
1-Ac-3-*i*-Pr	5.92	5.91
1-Ac-2-*t*-Bu	5.92	5.85
1-Ac-3-*t*-Bu	5.92	5.90

a) For these compounds, all protons of the unsubstituted ring appear as a singlet and are simply designated as 1'-.

and in several 1,1'-dicarbomethoxy-2- and 3-alkylferrocenes.[30]

This very simple but valuable method of prediction should serve as a useful guide for the elucidation of many other ferrocene derivatives.

Summary

All of the acetylalkylferrocenes have been synthesized and obtained in a highly pure state. The infrared and NMR spectrum of each of these compounds has been determined, and the results tabulated.

It has been shown that NMR spectroscopy provides a convenient tool in elucidating the structure of substituted ferrocenes. It is particularly useful in distinguishing between 1,2- and 1,3-disubstituted structures, a situation where infrared has its greatest limitations.

A series of shielding constants has been developed for a variety of ferrocene substituents. These enable one to predict with considerable precision the chemical shifts of a variety of protons bonded to the ferrocene nucleus.

Experimental

Alkylferrocenes.—These materials were prepared by procedures described elsewhere.[31]

Acetylferrocene.—This was prepared following the directions of Hauser and Lindsay,[18] with the exception that boron fluoride-etherate was used instead of the boron fluoride-ethyl acetate complex.

Acetylation of Alkylferrocenes.—The acetylation procedure was identical for all alkylferrocenes. A solution of 0.05 mol. of the appropriate alkylferrocene and 10.2 g. (0.1 mol.) of acetic anhydride in 100 ml. of methylene chloride was cooled to 0°C. To this solution was added 21.3 g. (0.15 mol.) of boron fluoride-etherate with stirring. A nitrogen sweep was employed throughout. The mixture was stirred at 0°C for 30 min. and at room temperature for 2 hr. The contents of the flask were decomposed with water and extracted with methylene chloride. The organic layer was dried over calcium chloride. The residue obtained after removal of

30) The observed values for the latter compounds are taken from the Ph. D. thesis of J. L. Bach, Purdue University, June, 1963.

31) R. A. Benkeser and J. L. Bach, *J. Am. Chem. Soc.*, 85 (1963), in press.

32) E. A. Hill and J. H. Richards. ibid., 83, 4216 (1961).

TABLE VI. PREDICTED AND OBSERVED τ-VALUES FOR THE ALKYL- AND ACETYL RINGS OF 1-ACETYL-1'-ALKYLFERROCENES

Compound	Alkyl ring protons		Acetyl ring protons 2=5		3=4	
	Calcd.	Obs.	Calcd.	Obs.	Calcd.	Obs.
1-Ac-1'-Me	6.00[a]	6.01	5.40	5.42	5.71	5.70
1-Ac-1'-Et	5.97	5.99	5.38	5.41	5.69	5.69
1-Ac-1'-*i*-Pr	5.98	5.98	5.37	5.39	5.68	5.66
1-Ac-1'-*t*-Bu	6.02	5.98	5.37	5.32	5.68	5.61

a) The H atoms in the 2-position were used in this calculation.

TABLE VII. PREDICTED AND OBSERVED τ-VALUES FOR 1, 1'-DICARBOMETHOXY-2- AND 3-ALKYLFERROCENES

Compound	2'-Proton		3'-Proton	
	Calcd.	Obs.	Calcd.	Obs.
2-Me-1,1'-DCM[a]	5.28	5.35	5.73	5.74
3-Me-1,1'-DCM	5.28	5.31	5.73	5.74
2-Et-1,1'-DCM	5.26	5.33	5.71	5.78
3-Et-1,1'-DCM	5.26	5.30	5.71	5.74
3-*i*-Pr-1,1'-DCM	5.25	5.35	5.70	5.76
3-*t*-Bu-1,1'-DCM	5.25	5.31	5.70	5.75

a) DCM=dicarbomethoxy

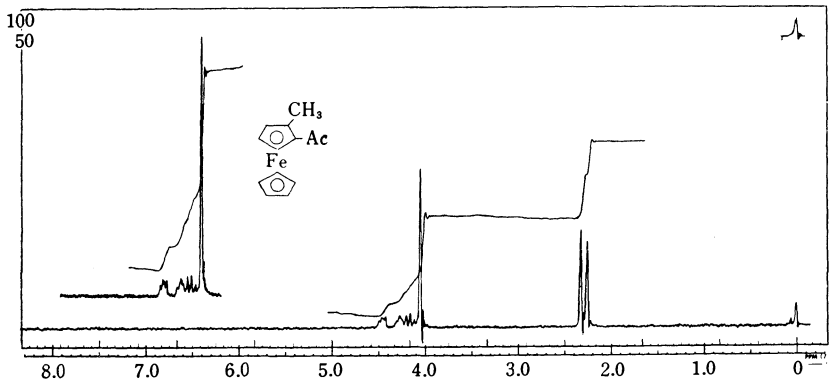


Fig. 1.

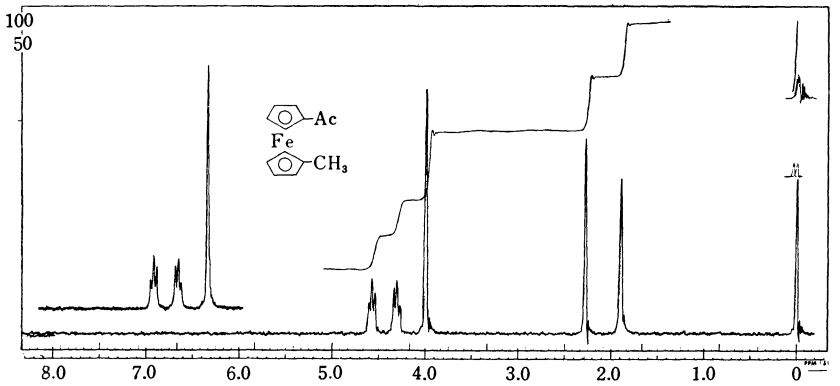


Fig. 2.

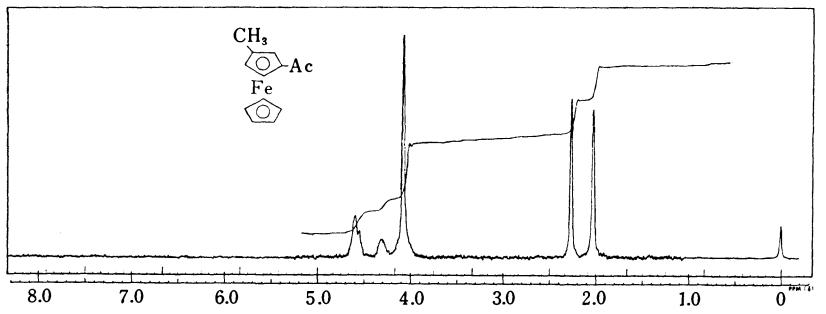


Fig. 3.

TABLE VIII. THE INFRARED SPECTRA OF ACYLFERROCENES (μ)[a,b]

Substituent	Characteristic absorptions[c,d]					
Ac	11.19(s)	—	9.96(s)	9.01(s)	8.98(s)	7.81(s)
1-Ac-1'-Me	11.23(m)	10.85(m)	—	—	8.96(m)	7.82(s)
1-Ac-2-Me	11.17(w)	10.72(s)	9.96(s)	9.05(s)	—	7.85(s)
1-Ac-3-Me	11.05(m)	10.69(w)	9.95(s)	9.05(s)	—	7.70(s)
1-Ac-1'-Et	11.20(m)	11.02(m)	—	—	8.97(s)	7.82(s)
1-Ac-2-Et	11.21(w)	10.80(s)	9.98(s)	9.04(s)	—	7.87(s)
1-Ac-3-Et	11.10(s)	10.88(m)	9.97(s)	9.04(s)	—	7.75(s)
1-Ac-1'-*i*-Pr	11.20(s)	10.86(m)	—	—	8.97(s)	7.82(s)
1-Ac-2-*i*-Pr	—	10.77(s)	9.96(s)	9.02(s)	—	7.90(s)
1-Ac-3-*i*-Pr	11.10(s)	10.70(m)	9.96(s)	9.03(s)	—	7.80(s)
1-Ac-1'-*t*-Bu	11.20(s)	11.00(s)	—	—	8.97(s)	7.85(s)
1-Ac-2-*t*-Bu	11.25(w)	10.83(s)	9.95(s)	9.01(s)	—	8.02(s)
1-Ac-3-*t*-Bu	11.11(s)	10.83(w)	9.95(s)	9.05(s)	—	8.05(s)
1,2-(α-Ketotetramethylene)	11.22(m)	—	9.96(s)	9.02(s)	—	7.80(s)

a) Spectra of crystalline materials were determined as Nujol mulls, those of liquids, as capillary films. A Perkin-Elmer Model 221 spectrophotometer was used.
b) s=strong, m=medium, w=weak
c) Rosenblum's correlations (Ref. 12) hold with a slight modification. Actually, in most cases, both the 1,2- and 1,3-isomers exhibit two bands in the region between 10.7 and 11.25 μ. It may be said, however, that for these bands a stronger absorption appears at a shorter wavelength with the 1,2-structure, while with a 1,3-disposition a more intense peak lies at a higher wavelength. An exceptional case is 1,2-(α-ketotetramethylene)-ferrocene.
d) The "9, 10 μ" rule holds in every case.

the solvent was chromatographed on an alumina (Merck, neutral grade) column.

The development and elution of methylacetyl-isomers were carried out with pentane-ether mixtures (approximately 1 : 1 by volume). A faster moving band was separated from the major band. The first compound eluted was 1-acetyl-2-methylferrocene (1.34 g.) (m. p. 62.5~63.5°C) (lit.[32] 62.2~63.2°C).

Found: C, 64.82; H, 5.77; Fe, 23.39. Calcd. for $C_{13}H_{14}OFe$: C, 64.49; H, 5.83; Fe, 23.07%.

The second isomer eluted from the column was 1-acetyl-1'-methylferrocene (2.74 g.) (m. p. 42~43°C) (lit.[32] 42.7~43.2°C). Found: C, 64.45; H, 5.75; Fe, 23.30%.

The third isomer eluted from the column was 1-acetyl-3-methylferrocene (1.16 g.) (m. p. 61.5°C) (lit.[32] 57.5~61.5°C). Found: C, 64.54; H, 6.00; Fe, 23.30%.

The ethylacetyl-isomers were separated in the same manner as above. The first compound eluted was 1-acetyl-2-ethylferrocene (0.94 g.) (m. p. 44.5°C) (lit.[3b] 42.5~44.5°C).

The second isomer eluted from the column was 1-acetyl-1'-ethylferrocene (1.59 g.) (b. p. 128°C/0.2 mmHg) (lit.[3b] m. p. 12.5~13.2°C).

Found: C, 65.97; H, 6.24; Fe, 21.56. Calcd. for $C_{14}H_{16}OFe$: C, 65.65; H, 6.30; Fe, 21.80%.

The third isomer eluted from the column was 1-acetyl-3-ethylferrocene (0.55 g.) (b. p. 144°C/0.8 mmHg) (lit.[3b] m. p. 11.6~12.6°C). Found: C, 66.13; H, 6.69; Fe, 22.19%.

The separation of the isomeric acetyl-isopropylferrocenes was more laborious than that of the methyl- or ethyl-acetyl analogs. Using a pentane-ether (ca. 9 : 1 by volume) mixture, a faster-moving band could be separated from the major broad band. The first compound eluted was 1-acetyl-2-isopropylferrocene (1.03 g.) (b. p. 145°C/1 mmHg).

Found: C, 67.21; H, 7.00; Fe, 21.10. Calcd. for $C_{15}H_{18}OFe$: C, 66.69; H, 6.71; Fe, 20.67%.

Elution was continued using a pentane-ether mixture, gradually enriching the ether content. The major band became broader than it was at the beginning, but no discrete bands were formed. Thus, ten fractions of ca. 100 ml. each were taken. The separation was conveniently checked by VPC (F and M Model 500 vapor fractometer; DEGS column; 15 feet×1/4 inch; 215°, at a flow rate of helium of 60 ml./min.). From the first two cuts 1-acetyl-1'-isopropylferrocene (2.04 g.) was obtained (b. p. 146°C/1 mmHg.). Found: C, 66.60; H, 6.25; Fe, 20.43%.

From fractions 9 and 10 1-acetyl-3-isopropylferrocene (0.99 g.) was obtained (b. p. 143°C/1 mmHg). Found: C, 66.81; H, 6.61; Fe, 20.90%.

The separation of the *t*-butylacetylferrocenes (1,1'- and 1,3-isomers) was accomplished only with great difficulty. Elution with pentane-ether mixtures (ca. 9 : 1 by volume), gradually enriching the ether content, developed a discrete, faster-moving band, followed by a broad and unresolved major band. The first compound eluted was 1-acetyl-2-*t*-butylferrocene (0.38 g.) (m. p. 99~100°C).

Found: C, 67.83; H, 7.19; Fe, 19.55. Calcd. for $C_{16}H_{20}OFe$: C, 67.62; H, 7.09; Fe, 19.65%.

No discrete separation of the major band could be effected. A total of ten fractions were taken of ca. 100 ml. each. The course of the separation in this instance could not be followed by vapor phase chromatographic analysis, since a wide variety of column materials proved ineffective in separating the 1,1'- and 1,3-isomers. A method based on infrared spectroscopy was employed. Earlier frac-

tions were characteristically devoid of the "9, 10μ" absorption bands. This indicated the presence of 1,1'-disubstituted products. Although these fractions did possess strong absorption bands at 7.85 and 8.97 μ, they had no absorption at 8.0 μ.[33] The first four fractions were combined and rechromatographed in the same manner. From the latter first fraction 1-acetyl-1'-*t*-butylferrocene (1.22 g.) was isolated (b. p. 144°C/3 mmHg). Found: C, 67.15; H, 7.02; Fe, 19.99%.

The middle fractions of the original chromatograph possessed an infrared absorption at 7.85 μ, but a band started appearing at 8.0 μ. The "9, 10 μ" bands also started appearing, with the 9 μ band possessing a shoulder on the low wavelength side. The last fractions taken indicated the total disappearance of the 7.8 μ band, but a strong absorption at 8.05 μ. The "9,10 μ" bands appeared at 9.05 and 9.95 μ respectively. In this manner there was obtained 3.09 g. of 1-acetyl-3-*t*-butylferrocene, melting at 83.5~84.5°C. Found: C, 67.77; H, 7.00; Fe, 19.59%.

1,2-(α-Ketotetramethylene)-ferrocene. — This compound was prepared according to the directions of Rinehart and his coworkers[25] (m. p. 86~87°C) (lit.[25] 87.5~88.5°C).

Department of Chemistry
Purdue University
West Lafayette, Indiana
U. S. A.

33) The correlation of 10.8 and 11.2 μ bands for a 1,3-disposition of substituents[12] could not be employed since the 1,1'-structure absorbs in this region.

Colloid Chemical Studies of Starching Materials. V. Rheological Properties of Concentrated Polyvinyl Alcohol Solutions

By Masayuki NAKAGAKI* and Takako NISHII

(Received September 3, 1963)

In a previous paper,[1] the dynamic viscosity and rigidity of starch solutions measured by a top-drive coaxial rheometer have been reported, and the results have been discussed[2] on the basis of Rouse's theory[3] as modified to take the intermolecular association into account. On the other hand, the structural viscosity of dilute solutions of polyvinyl alcohol has also been reported on previously[4]. These papers have, however, been chiefly interested in the anomalous viscosity due to the intermolecular association.

In the present paper, the viscoelastic behaviour of concentrated solutions of polyvinyl alcohol will be studied by means of a rotation viscometer, together with the rheometer previously used for starch solutions, and the results will be discussed on the basis of Rouse's theory, considering the change in intermolecular association in the solutions.

Experimental

Sample.—The polyvinyl alcohols used in these experiments are the same as those used in a previous paper.[5] They are Gohsenol GH-17 (degree of saponification $S=88.1\%$, average degree of polymerization $P=1700$), GH-23 ($S=87.5\%$, $P=2300$), NH-17 ($S=98.8\%$, $P=1700$), and NH-26 ($S=99.4\%$, $P=2600$).

To prepare aqueous solutions of polyvinyl alcohol, 90 g. of the polymer was put in 600 g. of distilled water, together with 0.18 ml. of Shinetsu Silicone Antifoaming Agent KM-65, and the whole was heated at 95°C for 30 min. (in the case of NH-17 and NH-26) or 1 hr. (in the case of GH-17 and GH-23) while being stirred well with a glass rod. After the solution had cooled to room temperature, the film which had formed on the surface of the solution was removed and kept in a closed vessel. The concentration was determined by measuring the weight of the polymer which remained after a known weight of the solution had been dried.

For the dynamic measurement, a solution put in the rheometer was covered with liquid paraffine and the measurements were made for the same solution 20, 60 and 110 hr. after the preparation of the solution. For the measurement of the steady-flow viscosity, a solution kept in a closed vessel for 20, 60 and 110 hr. was put in the rotation viscometer for each measurement.

Oscillation Rheometer.—A top-drive coaxial rheometer used was the same as has been reported on in a previous paper.[1] All measurements have been made in a thermostat at 30°C.

* Present address: Faculty of Pharmacy, Kyoto University, Sakyo-ku, Kyoto.

1) M. Nakagaki and K. Muragishi, This Bulletin, **34**, 316 (1961).
2) M. Nakagaki, ibid., **35**, 606 (1962).
3) P. E. Rouse, *J. Chem. Phys.*, **21**, 1272 (1953),
4) M. Nakagaki and A. Shimazaki, This Bulletin, **29**, 60 (1956).
5) M. Nakagaki and K. Goto, ibid., **35**, 791 (1962).

Rotation Viscometer.—A coaxial rotation viscometer of the Couette type was newly constructed. An inner cylinder 30 mm. in diameter ($2r_1$), 75 mm. long, and weighing 461.72 g. was hung in an outer cylinder 42 mm. in inner diameter ($2r_2$) and 90 mm. deep with a steel wire 490 mm. long, the torsional constant of which was $k_0=1.036\times10^5$ (dyn. cm.). The sample solution was put into the gap between the inner and outer cylinders, and the inner cylinder was held to dip into the solution by $h=65$ mm. The outer cylinder set in a thermostat at 30°C was rotated. The rate of the rotation, Ω (r. p. m.), was variable between 6 r. p. m. to 190 r. p. m. by means of thirty combinations of gears. The velocity gradient, g (sec^{-1}), was calculated by the following relation:

$$g=\frac{2\pi r_2}{60(r_2-r_1)}\quad \Omega=0.367\,\Omega \tag{1}$$

By measuring the angle of the deflection of the inner cylinder, θ (degree), the steady-flow viscosity of the solution can be calculated by the equation:

$$\eta=\left(\frac{k_0}{24\,\pi\,h}\right)\left(\frac{1}{r_1^2}-\frac{1}{r_2^2}\right)\frac{\theta}{\Omega} \tag{2}$$

All data are given in c. g. s. units.

Theoretical

In a previous paper,[2] the viscoelastic behavior of starch solutions has been discussed on the basis of a modified Rouse equation:

$$\left.\begin{aligned}\eta&=(F/\sqrt{\omega})\alpha\\ G&=G_0+F\sqrt{\omega}\beta\end{aligned}\right\} \tag{3}$$

where ω is the angular frequency, τ is the relaxation time, F is a constant, and α and β are functions depending on $\omega\tau$ only. The values of the functions have been given in that previous paper.[2]

In the case of polyvinyl alcohol solutions, however, the viscoelastic behaviour is different from that of starch solutions, especially in the low frequency region, where the polyvinyl alcohol solutions showed the following features: (1) The dynamic viscosity, η, is almost constant (except for NH-26), and (2) the dynamic rigidity, G, is nearly equal to zero; that is, $G_0\fallingdotseq0$.

Since the α function tends to the following value when $\omega\tau\ll1$,

$$\alpha=(\sqrt{2}\,\pi/3)\sqrt{\omega\tau}=1.48020\sqrt{\omega\tau} \tag{4}$$

the value of η at $\omega\to0$, designated by η_0, is given by:

$$\eta_0=1.48020\,F\sqrt{\tau} \tag{5}$$

Therefore, the following equations can be used for polyvinyl alcohol solutions:

$$\left.\begin{aligned}\eta/\eta_0&=A(\omega\tau)\\ G/\eta_0&=B(\omega\tau)/\tau\end{aligned}\right\} \tag{6}$$

where $G_0=0$ was used. Here, A and B are the functions of $\omega\tau$ only, as defined by the following:

$$\left.\begin{aligned}A&=\alpha/1.48020\sqrt{\omega\tau}\\ B&=\sqrt{\omega\tau}\,\beta/1.48020\end{aligned}\right\} \tag{7}$$

The theoretical relations of $\log(\eta/\eta_0)$ and $\log(G/\eta_0)$ relative to $\log\omega$ can be drawn for various values of τ (sec.), as shown in Fig. 1.

In order to compare the experimental with the theoretical values, the experimentally-obtained values were plotted on $\log\eta$ and $\log G$ vs. a $\log\omega$ chart with the same scale as the theoretically-drawn Fig. 1, and the chart was superposed on Fig. 1 by sliding it along the ordinate. In order to obtain the best fit, attention must be paid to the values of η at low frequencies. The values of η_0 can then be read off from the position of the ordinate at the best fit, and the value of τ (sec.) can

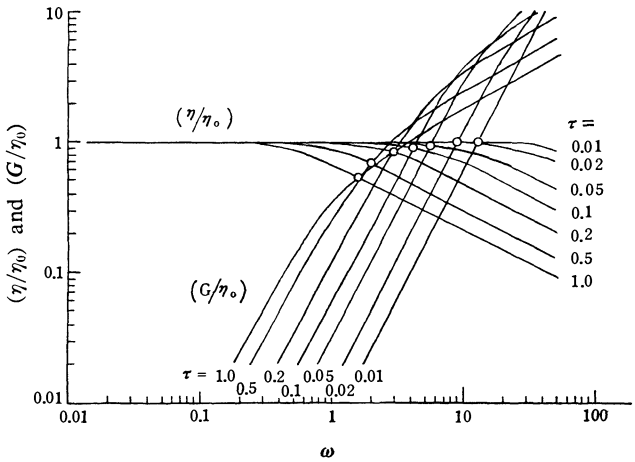


Fig. 1. Theoretical relations calculated for various τ (sec.) values.

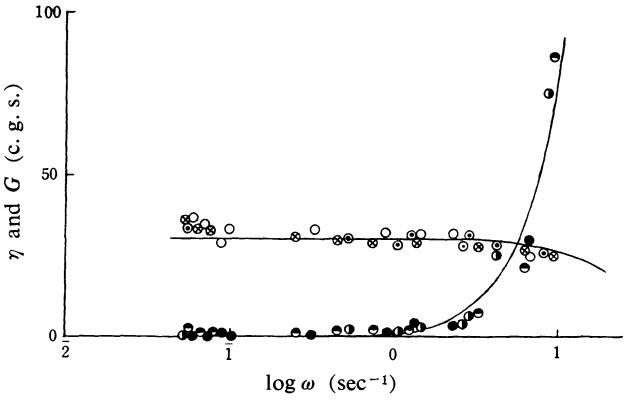


Fig. 2. Dynamic measurements for GH-17. η after 20 hr. (○), 60 hr. (⊗), 110 hr. (⊙), G after 20 hr. (●), 60 hr. (◓) and 110 hr. (◑).

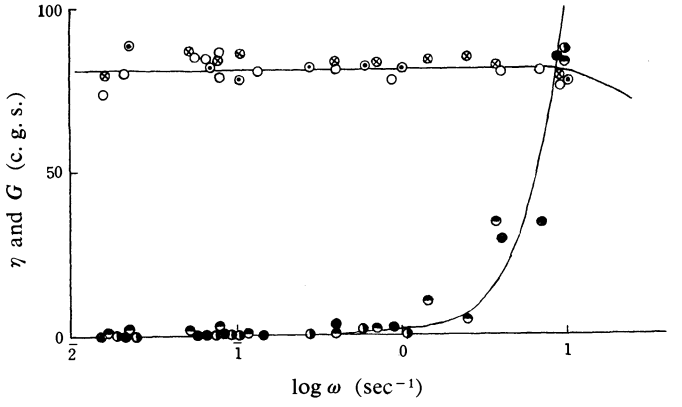


Fig. 3. Dynamic measurements for GH-23. η after 20 hr. (○), 60 hr. (⊗), 110 hr. (⊙), G after 20 hr. (●), 60 hr. (◓) and 110 hr. (◑).

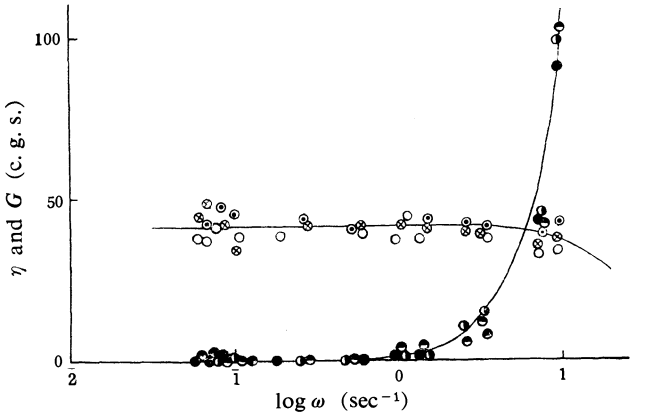


Fig. 4. Dynamic measurements for NH-17. η after 20 hr. (○), 60 hr. (⊗), 110 hr. (⊙), G after 20 hr. (●), 60 hr. (◓) and 110 hr. (◑).

TABLE I. PARAMETER VALUES (in c. g. s. units).

Sample	Dynamic measurement				Steady-flow measurement		
	η_0	τ	F	$\eta_0/P^2\times10^5$	η_N	Time, hr.	G_y
GH-17	30	0.05	91	1.04	28	20	10
						60	60
						110	240
GH-23	81	0.02	387	1.53	87	20	150
						60	740
						110	1310
NH-17	41	0.05	124	1.41	40	20	60
						60	150
						110	190
NH-26	100	0.015	551	1.48	95	20	950
						60	1320
						110	1650

be obtained from the location of the experimental $\log\eta$ and $\log G$ curves, paying attention especially to the point of intersection of these curves, that is, the points marked by open circles in Fig. 1.

Results and Discussion

Dynamic Viscosity and Dynamic Rigidity.— The experimental values of η and G obtained by the oscillation rheometer at 30°C are shown in Fig. 2 for a 11.51% GH-17 solution, in Fig. 3 for a 12.38% GH-23 solution, and Fig. 4 for a 11.09% NH-17 solution. All these correspond well with the theoretical curves drawn by Eq. 6 with the parameter values cited in Table I. The length of time between the preparation of the solutions and the measurement did not make much difference in the η and G values.

The viscoelastic behavior of NH-26 was fairly different from that of other samples. The viscosity changed with the time which elapsed from the preparation of solutions to the measurement. If one pays attention to the frequency value at which the curves of η and G intersect, the values $\eta_0=100$ and $\tau=0.015$ are obtained, as is cited in Table I. The theoretical η and G curves for these parameter values, calculated by Eq. 6 and shown in Fig. 6 by broken lines, do not however, correspond well with the experimental values, especially at the small ω values, where the experimental η values are much greater than the η_0 value, probably because of the association of polymer molecules. If it is assumed that the degree of association is the greater, and the η value is the greater, the smaller the frequency, ω, the fraction of the highly-associated component x_1 could, of course, be calculated for various frequency values by using the method already described in a previous paper.[2] In the present paper, however, it is assumed that, because of the existence of the highly-associated component, the average τ value is the greater, the smaller the ω value. The ω dependency of τ is calculated as follows. It can be shown that the following equation should be used when $\omega\tau\ll1$;

$$\tau\fallingdotseq(\eta/1.48020\,F)^2 \tag{8}$$

where F is a constant which is believed to be independent of ω and τ. The value of $F=551$ is obtained from Eq. 5 on the basis of $\eta_0=100$ and $\tau=0.015$. The frequency dependence of τ obtained by Eq. 8 for NH-26 is shown in Fig. 5. By using the τ values

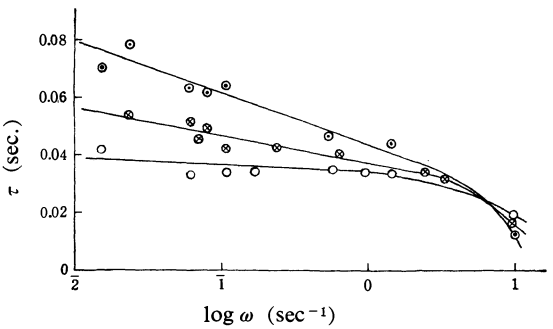


Fig. 5. Apparent relaxation time of NH-26 after 20 hr. (○), 60 hr. (⊗) and 110 hr. (⊙).

corresponding to the solid lines in Fig. 5 drawn by assuming that the $\tau-\log\omega$ relation is linear for $\omega\leqq1$, the values of η and G calculated from Eq. 6, instead of from the approximate Equation 8, are shown in Fig. 6 by solid lines. Thus, it is concluded that the "structure" due to the intermolecular association is developed in the NH-26 solution; that the average relaxation time, τ, and, therefore, the dynamic viscosity, η, are increased with the lapse of time after the preparation of the solution, and that the structure is destroyed and that η is decreased with the increase in the frequency, ω.

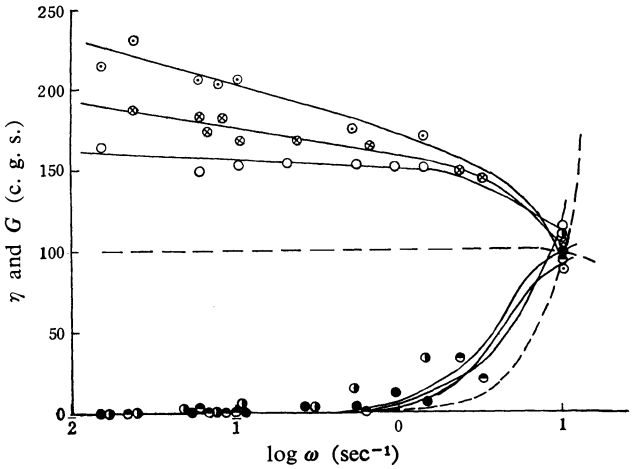


Fig. 6. Dynamic measurements for NH-26. η after 20 hr. (○), 60 hr. (⊗), 110 hr. (⊙), G after 20 hr. (●), 60 hr. (◓) and 110 hr. (◑). Broken curves are for $\eta_0=100$, $\tau=0.015$.

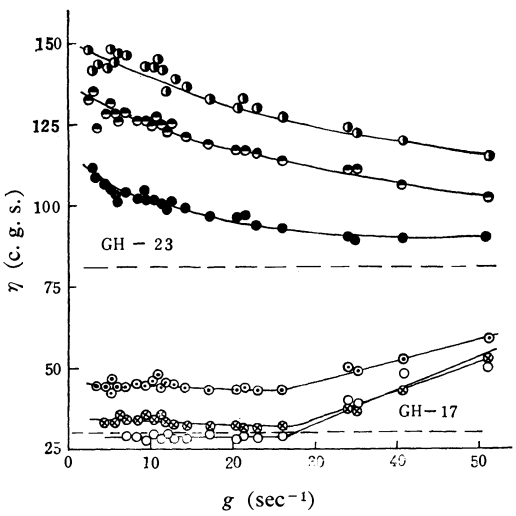


Fig. 7. Steady-flow measurements of GH-17 after 20 hr. (○), 60 hr. (⊗), 110 hr. (⊙) and of GH-23 after 20 hr. (●), 60 hr. (◓), and 110 hr. (◑).

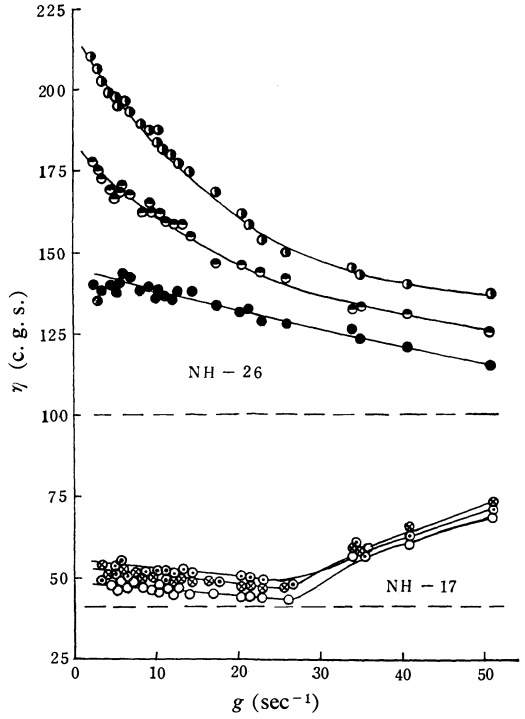


Fig. 8. Steady-flow measurements for NH-17 after 20 hr. (○), 60 hr. (⊗) and 110 hr. (⊙) and for NH-26 after 20 hr. (●), 60 hr. (◓) and 110 hr. (◑).

Steady-flow Viscosity.—The steady-flow viscosities measured by a coaxial rotational viscometer at 30°C are shown in Fig. 7 for GH-17 and GH-23 and in Fig. 8 for NH-17 and NH-26. The order of magnitude of the steady-flow viscosity values agrees with the values of η_0 in Table I obtained dynamically by the oscillation rheometer and shown in Figs. 7 and 8 by horizontal broken lines. There are, however, several important points of disagreement between the dynamic and steady-flow measurements.

The discussions in the present paper are essentially based on Rouse's theory, a theory which is presumed by some people[6] to be applicable to the steady-flow viscosity, too, if one substitutes the frequency, ω, in the dynamic measurement as is in the original Rouse equation with the velocity gradient, g, in the steady-flow measurement. The present authors, however, do not agree with this conventional substitution; they believe that the steady-flow

6) E. g., J. D. Ferry, M. L. Williams and D. M. Stern, *J. Phys. Chem.*, **58**, 987 (1954).

viscosity is equal to η_0. The steady flow viscosity should, therefore, be Newtonian except in the case of NH-26, for which the structural change with ω is observed in the course of dynamic measurement.

The solution of NH-26 showed structural viscosity as expected and as shown in Fig. 8. However, the steady-flow viscosities of GH-17, GH-23 and NH-17 also showed dependencies not only on the velocity gradient but also on the time after the preparation of the solution, as Figs. 7 and 8 show. Neither of these dependencies could be expected on the basis of the dynamic measurements reported in the preceding paragraph.

The steady-flow viscosity of the relatively low molecular weight samples, GH-17 and NH-17, increase with the velocity gradient, g, when the g value exceeds 30 sec^{-1}. In this region of g, the solutions, therefore, behave as if they are dilatant. This dilatant behavior might be due to a certain unexpected factor involved in the method of measurement, although the authors can not think of any fault in the experiment.

As for the structural viscosity of polyvinyl alcohol solutions, it has been reported[4] that the apparent viscosity is linear to the reciprocal of the rate of flow ($1/Q$), and that the limiting value of viscosity, η_N, extrapolated to ($1/Q \rightarrow 0$) is independent of the history of the solution.

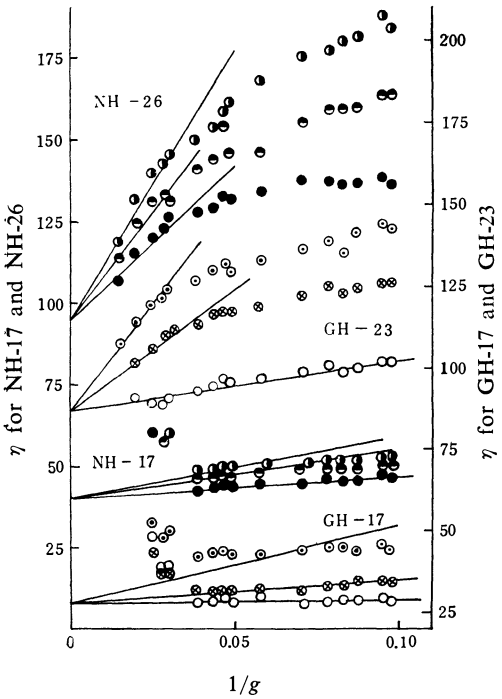


Fig. 9. Relation between η and $1/g$ for the samples after 20 hr. (○, ●), 60 hr. (⊗, ◓) and 110 hr. (⊙, ◑).

The empirical relation translated to the present notation is:

$$\eta = \eta_N + G_y/g \tag{9}$$

For the concentrated solutions discussed here, however, this relation holds not over the whole range of $1/g$, but only in the range of small $1/g$ values, excluding the dilatant behavior of GH-17 and NH-17. The results are shown in Fig. 9, while the values of the parameters, η_N and G_y, are given in Table I. The value of η_N is independent of the time which has elapsed before the measurement and is in good agreement with the dynamically-obtained η_0 value. The G_y has the dimension of rigidity and corresponds to the yield value of Bingham flow, although the behavior of the solution is not Bingham-like because the value of η is smaller than that expected from Eq. 9 in a high ($1/g$) region. The increase in G_y with time suggests the development of structure in the solutions.

An Examination of Parameter Values.—As has been shown in a previous paragraph, the viscoelastic behavior of polyvinyl alcohol solutions may be described fairly well with Eq. 6, which is essentially based on Rouse's theory. On examining the values of parameters, however, it appears that the theory is not very good in explaining all the results. First of all, the value of F calculated by Eq. 5 and given in Table I is a constant throughout the experiments any on one sample, but it is not a constant common to all the samples. The same has been observed in the case of starch solutions reported on before.[2] On the other hand, the theoretical expression of F is, as has already been shown in a previous paper:[2]

$$F = nN\sigma\sqrt{kT}/4\sqrt{3}\sqrt{B} \tag{10}$$

where n is the number of molecules in a unit volume of the solution, N is the number of segments contained in one polymer molecule, σ is the length of the segment, and B is the mobility of the end of a segment. If the polymer molecules aggregate in the solution, and if the average number of molecules to form one aggregate is m, then n and N in Eq. 10 should be replaced by (n/m) and (mN) respectively, but this replacement does not make any difference in Eq. 10 because $(n/m)\cdot(mN)$ is equal to nN. Therefore, F should be a constant independent of the degree of intermolecular association, and it should be a constant for various samples of the polymer composed of the same monomeric unit. Contrary to this theoretical expectation, however, the experimental values of F for various samples do not equal each other. This is

probably due to the change in $\sigma/\sqrt{B}$. However, the situation is supposed to be complicated in concentrated polymer solutions because of various reasons such as are, for example, described below: (1) The manner of the intermolecular aggregation might be different. If the molecules associated head to tail to form a linear aggregate, Rouse's theory may be applied without further modification, but if the molecules associate with intermediate segments to form a "star"-shaped aggregate, the viscoelastic behavior will be different from that expected by Rouse's theory derived for linear molecules. (2) If the possibility of intramolecular interaction can be expected, the interaction will change not only $\sigma/\sqrt{B}$ but also the effective number of segments, N. These changes will, of course, explain the variation in the value of F.

At any rate, it seems to be necessary to presume that the molecular aggregates are formed in the solutions of all samples, and that the aggregation is the cause of the non-Newtonian behavior of the steady-flow viscosity, but that the structural change of the aggregates is not dominant, except for NH-26, within the extent of the range of the frequency used for the dynamic measurement. Although this view still can not explain why the time dependence of η was not observed in the dynamic measurement, one of the reasons might be that the solution kept in the apparatus was used for successive measuments in the case of the dynamic experiment, while a part of a solution kept in a reservoir was placed in the apparatus for each steady-flow experiment.

Although it is not clear whether it is theoretically valuable or not, it may be worthwhile to point out here the entirely empirical fact that the value of η_0/P^2 is fairly constant, as is shown in Table I, where P is the degree of polymerization of the polymers.

Summary

The dynamic viscosity, dynamic rigidity and steady-flow viscosity at 30°C have been measured for 11~12% solutions of four specimens of polyvinyl alcohol, GH-17, GH-23, NH-17 and HN-26, 20, 60 and 110 hr. after the preparation of the solutions.

In the dynamic measurement by a top-drive coaxial oscillation rheometer, the relations of η and G vs. ω did not depend on time and have all been explained by Rouse's theory except for NH-26, the latter showing time and ω dependencies of the structure. In the steady-flow measurement by a coaxial rotation viscometer, the viscosity of all the polymers showed both time and velocity gradient dependencies.

The authors wish to thank Nippon Gosei Kagaku Kogyo Co., Ltd., which kindly provided Gohsenols.

Faculty of Living Science
Osaka City University
Nishi-ku, Osaka

*The Photometric Determination of Traces of Platinum in Electrolyte using Copper Sulfide as a Collector**

By Yûsuke UJIHIRA and Shizo HIRANO**

(Received February 15, 1963)

In recent years, considerable interest has been aroused concerning the behavior of platinum dissolved from platinum anode during electrolysis. Consequently, a simple, sensitive and accurate method for the determination of microgram quantities of platinum is required.

To determine the platinum content in electrolyte, a preliminary separation step is necessary because of the presence of macro amounts of diverse ions and the need to reduce the solution to a small volume.

Several papers have been published for this purpose.

Wölbling[1] reported the adsorption of platinum with activated charcoal, Beamish[2] separated microgram quantities of platinum from

* Presented at the 14th Annual Meeting of the Chemical Society of Japon, Tokyo, April, 1961.

** Present address: Applied Chemistry Department, Faculty of Engineering, Tôyo University, Kawagoe, Saitama.

1) H. Wölbling, *Z. angew. Chem.*, **45**, 1720 (1932).

2) F. E. Beamish and A. G. Marks, *Anal. Chem.*, **30**, 1464 (1958).

macro amounts of iron, nickel and copper by the use of a cation-exchange resin, Salyards[3] concentrated minute quantities of platinum by precipitation with stannous chloride from a hydrochloric acid solution containing 1 mg. of tellurium, Bufatin[4] precipitated platinum sulfide using 10 mg. of copper as a carrier, and Poluektov[5] developed a method for the concentration of platinum with mercury-mercuric chloride.

In this paper, the authors will describe the separation of trace amounts of platinum by the use of carrier precipitation with 1.5 to 3.0 mg. of copper sulfide and subsequent photometric determination by the stannous chloride method.

A photometric stannous chloride method for the determination of platinum in a hydrochloric acid solution has been described by Ayres and Mayer[6,7] and by Maziekien and his coworker,[8] and the nature of the platinostanno-chloro-complex has been studied by Ayres[9] and Mayer.[10]

In order to reduce interference by diverse ions in the photometric step, the authors studied the color development of the platinostanno-chloro-complex in an aqueous solution and in ethyl acetate.

The separation of platinum from the interfering elements by this carrier precipitation method is simple, and traces of platinum are determined photometrically by mean of the stannous chloride ethyl acetate extraction method, which has the sensitivity required.

This method has been developed specifically for the determination of platinum in electrolytes for the electrolysis of sodium chlorate, but it can be applied equally well to most aqueous solution samples.

Experimental

Apparatus. — A Hirama photoelectric filter photometer, model II, was used for all measurements of the absorbancy, matched 1 cm. glass cells also being used.

Materials. — A standard platinum solutions was prepared by dissolving 0.998 g. of pure platinum metal in aqua regia and evaporating it to dryness. Then 5 ml. of concentrated hydrochloric acid and 0.1 g. of sodium chloride were added to the residue, and the resulting solution was evaporated again to dryness. The residue was dissolved in 20 ml. of hydrochloric acid (1 : 1) and diluted to 100 ml. with water.

This solution was diluted with hydrochloric acid (1 : 0) to give a solution containing 9.8 μg.-Pt/ml.

A copper solution was prepared by dissolving 1.964 g. of reagent grade copper sulfate in 500 ml. of water. This solution contained 1 mg. of copper per 1 ml.

An ammonium nitrate solutions was prepared by dissolving 80 g. of analytical reagent grade ammonium nitrate in 1000 ml. of water.

Aqua regia was prepared by mixing one portion of concentrated nitric acid and three portions of concentrated hydrochloric acid.

A stannous chloride solution was prepared by dissolving 23 g. of analytical reagent grade stannous chloride dihydrate in 30 ml. of concentrated hydrochloric acid and diluting it to 100 ml. with water.

The ethyl acetate used was of the analytical reagent grade, as were the hydrochloric acid and nitric acid used.

Method. — To determine the recovery of trace quantities of platinum from hydrochloric acid solutions with copper sulfide, an aliquot of the standard platinum solution was placed in a 100 ml. beaker and diluted to 50 ml. with 0.5 to 3.0 N hydrochloric acid. After the addition of 1 to 2 ml. of the copper sulfate solution, a fairly rapid stream of hydrogen sulfide was passed into the solution for 10 min.

This solution was heated to near the boiling point and kept at this temperature for 10 min.; then the gas was passed again for 10 min. The precipitate was filtered off through a paper filter (Toyo Roshi No. 5C (ϕ 5.5 cm.)) and then washed successively with 10 ml. of hydrochloric acid (1 : 10), 10 ml. of the ammonium nitrate solution and a few milliliters of water.

The precipitate and the filter paper were ignited in a casserole, and the residue was dissolved in 0.4 ml. of aqua regia. This solution was transferred to a 50 ml. Terex beaker, and the same treatment was repeated with another 0.5 ml. of aqua regia. The casserole and rod were then washed several times with a few milliliters of hydrochloric acid (1 : 1), and the washings were drawn into the same beaker.

The solution was evaporated to dryness on a water bath without prolonged heating, the residue was dissolved in 2.0 ml. of hydrochloric acid (1 : 7), and 0.5 ml. of the stannous chloride solution was added. The colored solution was transferred to a glass-stoppered test tube and was shaken for 1 min. with 2.5 ml. of ethyl acetate.

The color intensity of the organic phase was measured at 420 mμ with a photometer.

The investigation of the photometric stannous chloride method and the tests of the effect of diverse ions were made as follows unless otherwise stated.

The desired volume of the standard platinum solution, and, if necessary, of a diverse ion solution was placed in a 50 ml. Terex beaker and

3) L. B. Salyards, Data obtained from Sandell's "Colorimetric Determination of Traces of Metals," Interscience Publ., N. Y. (1959), p. 721.
4) O. I. Bufatin et al., *Zhur Anal. Khim.*, **13**, 116 (1958).
5) N. S. Poluektov and F. G. Spivak, *Zavodskaya Lab.*, **11**, 398 (1945); *Chem. Abstr.*, **40**, 1418 (1946).
6) G. H. Ayes and A. S. Mayer, Jr., *Anal. Chem.*, **23**, 299 (1951).
7) G. H. Ayres and A. S. Mayer, Jr., *J. Am. Chem. Soc.*, **77**, 2671 (1955).
8) I. Maziekien et al., *Anal. Chem.*, **32**, 645 (1960).
9) G. H. Ayres, ibid., **25**, 1622 (1953).
10) A. S. Mayer, Jr., and G. H. Ayres, *J. Am. Chem. Soc.*, **79**, 49 (1957).

evaporated to dryness on a water bath. The residue was dissolved in 4 ml. hydrochloric acid (1 : 7), and 1.0 ml. of the stannous chloride solution was added. One half of the volume of this solution was extracted with an equal volume of ethyl acetate. The intensities of the resulting color in the aqueous solution and in ethyl acetate were measured at 420 mμ.

Results and Discussion

The recovery of platinum from a solution with copper sulfide is shown in Table I. Table I indicates that 1 mg. of copper is sufficient for gathering microgram quantities of platinum from a 3 N hydrochloric acid solution. This amount of copper does not interfere at all with the photometric step.

Though the carrier precipitation with copper sulfide is somewhat lacking in selectivity, a trace amount of platinum is completely collected and separated from macro amounts of salt or other diverse ions (especially chromium).

Filtration of the precipitate by a sintered glass filter is unsuitable because of the difficulty of dissolving copper sulfide completely in nitric or hydrochloric acid.

The decomposition of the precipitate and of the filter paper was attained by burning them in a casserole. Their ashes are easily dissolved in 0.4 ml. of aqua regia.

TABLE I. RECOVERY OF PLATINUM BY CARRIER PRECIPITATION WITH COPPER SULFIDE

Cu added mg.	Acidity of solution HCl, N	Pt added μg.	Pt found μg.
1	1	0	0
1	3	0	0.1
2	3	0	0
1	0.3	4.9	4.8
1	3.0	4.9	5.0
1	3.0	9.8	9.8
2	1.0	9.8	9.9
1	3.0	19.6	20.0
1	0.3	19.6	19.5
2	1.0	19.6	19.8
1	3.0	29.4	30.5

TABLE II. COLOR DEVELOPMENT OF PLATINO-STANNO-CHLORO-COMPLEX WITH VARIOUS AMOUNTS OF PLATINUM

Platinum μg./2.5 ml.	Absorbance	
	In water	In ethyl acetate
0	0.000	0.000
4.9	0.072	0.072
9.8	0.145	0.144
19.6	0.289	0.286
39.2	0.575	0.570

TABLE III. EFFECT OF STANDING TIME ON COLOR DEVELOPMENT
(Platinum 14.7 μg./2.5 ml.)

Time min.	Absorbance	
	In water	In ethyl acetate
1	0.217	0.218
2	0.217	0.218
5	0.216	0.217
10	0.216	0.216
20	0.216	0.216
30	0.216	0.210
40	0.216	0.030

The results of a study of the color development of the platino-stanno-chloro-complex in the aqueous phase and in the ethyl acetate phase, and the effect of the presence of diverse ions (especially chromium) in the photometric step are shown in Tables II, III and IV.

TABLE IV. DETERMINATION OF PLATINUM IN PRESENCE OF OTHER METALS

Diverse ion added	Absorbance	
	In water	In ethyl acetate
Cu 1 mg.	0.142	0.141
Cu 2 mg.	0.143	0.142
Cr 50 μg.	0.145	0.141
Cr 100 μg.	0.151	0.140
Cr 200 μg.	0.164	0.141
Cr 300 μg.	0.174	0.142
Cr 500 μg.	0.190	0.142
Cr 1 mg.	0.219	0.141
Fe 3 mg.	0.150	0.143
Hg 50 μg.	0.120	0.140
Te 1 μg.	0.150	0.149
Au 2 μg.	0.144	0.143
As 10 mg.	0.145	0.143

Table II indicates that the colored substance is almost quantitatively extracted into ethyl acetate, in which it has essentially the same characteristics as in the aqueous solution.

Table III indicates that this colored complex gives a reproducible color that is stable for half an hour.

Table IV indicates that any interference, in the measurement of the color intensity of the platino-stanno-chloro-complex, caused by the presence of chromium is remarkably reduced by ethyl acetate extraction.

The Determination of Platinum in Electrolytes

The methods described in the preceding chapter were applied to the determination of platinum in electrolytes containing large

TABLE V. PLATINUM CONTENT OF ELECTROLYTE FOR THE ELECTROLYSIS OF SODITM CHLORATE

	Constituents of sample solution w/v %		Pt added μg.	Pt found μg.	Content of Pt p.p.m.	Other methods (1)	Other methods (2)
A	NaCl	13	0	0.2			
	$NaClO_3$	46.5	9.8	10.0			
	$Na_2Cr_2O_7$	0.2	9.8	9.9	<0.004	0	0
			19.6	20.2			
B	NaCl	12.2	0	5.6	0.22	0.19	0.23
	$NaClO_3$	53					
	$Na_2Cr_2O_7$	0.2	0	13.2	0.53	0.50	0.50
C	NaCl	7.8	0	4.1	0.16	0.17	0.18
	$NaClO_3$	37.5					
	$Na_2Cr_2O_7$	0.2	0	56.0	2.24	2.16	1.80

(1) Data obtained by amalgamation method. —*a* Clear solution.
(2) Obtained by ion exchange method. —*b* Solution containing mud.

amounts of sodium chloride, sodium chlorate and sodium bichromate.

Twenty-five milliliters of a sample solution was taken in a 200 ml. beaker, then concentrated and hydrochloric acid was carefully added. The quantities and the speed of the addition of the acid were experimentally selected to avoid the spraying of the sample solution by the rapid evolution of chlorine gas.

After evolution had ceased, the solution was warmed to ensure the complete decomposition of the oxidizing substances. Then platinum was isolated by carrier precipitation with copper sulfide and was determined photometrically by the stannous chloride method described previously.

The results of eight determinations of micro amounts of platinum in electrolytes sodium chlorate electrolysis are shown in Table V. The results are in good agreement with those obtained by other methods of analysis. The blank value obtained by running the full procedure corresponded to less than 0.1 μg. of platinum.

Summary

A method of separation has been developed for the photometric determination of trace amounts of platinum in electrolytes for the electrolysis of chlorate by the use of carrier precipitation with copper sulfide.

After a sample solution had been treated with concentrated hydrochloric acid, the preliminary separation of platinum was made by carrier precipitation with copper sulfide, and, following the ignition of the precipitate, the ashes was introduced into a hydrochloric acid solution. The orange-colored substance which was produced by the addition of the stannous chloride solution was extracted into ethyl acetate, and the color intensity of the ethyl acetate phase was measured at 420 mμ.

The recovery of platinum was quantitative, and the removal of macro amounts of salt and divers ions was satisfactory.

Experiments using synthetic sample solutions indicate that trace quantities of platinum in electrolytes for the electrolysis of sodium chlorate could be determined by this method with an accuracy of from 5 to 10% in the range between 0.02 and 0.00 p.p.m.

The authors wish to express their grateful thanks to Dr. Atsushi Mizuike of the University of Tokyo for his continuous interest and encouragement throughout this investigation.

Institute of Techno-Analytical Chemistry
Faculty of Engineering
The University of Tokyo
Hongo, Tokyo

The Direct Spectrophotometric Determination of Iron with Dibenzoylmethane in the Organic Phase

By Yoshimi UMEZAKI

(Received August 21, 1963)

In the preceding paper,[1] the author has described a spectrophotometric determination of uranium with dibenzoylmethane (DBM) in the organic phase. Since DBM reacts with iron(III) to form a colored complex, iron may be determined in a way similar to that used for uranium. Shigematsu and Tabushi[2] have reported a spectrophotometric determination of iron with DBM after forming an iron-DBM complex in an aqueous solution and after extracting the complex into butyl acetate. This method, however, is too greatly subject to interference by diverse ions.

As the extraction of iron(III) with methyl isobutyl ketone (MIBK) in a hydrochloric acid solution is an excellent method for separating iron from interfering ions, this extraction method is, as a preliminary separation, employed in various methods of determination for iron.[3] Recently, Jackson and Phillips[4] have reported a spectrophotometric determination of iron with *o*-phenanthroline after the MIBK extraction. In this case, iron extracted in MIBK is stripped by an aqueous solution and reduced to iron(II), and then the color is developed.

This paper describes a simple, sensitive and selective spectrophotometric determination of iron(III) with DBM in the organic phase after the MIBK extraction.

Experimental

Apparatus.—Absorbance measurements were made with a Hitachi spectrophotometer, Model EPV-2A, using 1-cm. glass cells.

Reagents.—*Standard Iron Solution.*—A stock solution containing 100 μg. of iron(III) per ml. was prepared by dissolving iron(III) chloride in a 0.1 N hydrochloric acid solution. Standardization was made by titration with a 0.01 M EDTA solution.

Dibenzoylmethane Solution.—A 0.5% solution was prepared by dissolving 0.5 g. of dibenzoylmethane in 100 ml. of methanol.

Solutions of Diverse Ions.—Reagents grade salts, usually the chlorides, were used for testing the interference of cations. Anions were tested by the addition of sodium or potassium salts.

Traces of iron involved in the reagents were removed when necessary with an anion exchange resin column.

Procedure.—Transfer 5.0 ml. of a slightly acidic sample solution containing less than 40 μg., preferably 10 to 30 μg., of iron(III) to a 50 ml. separatory funnel. Add 5.0 ml. of concentrated hydrochloric acid and 3.0 ml. of MIBK. Shake vigorously for about 1 min. After the phases have separated, discard the aqueous layer. Run the organic phase through a small plug of filter paper* in the stem of the separatory funnel into a dried small vessel. Transfer 2.0 ml.** of the extract to a 10 ml. volumetric flask. Add 2.0 ml. of a 0.5% DBM solution and 0.5 ml. of pyridine, and dilute with methanol to the mark. Measure the absorbance at 410 mμ (or 425 mμ) against a blank.

Results and Discussion

Absorption Spectra.—The absorption spectra of the blank and the iron complex are shown in Fig. 1, together with those of copper, tin, vanadium and molybdenum. The maximum absorbance of the iron complex is observed at 410 mμ.

The Effect of the Diluent.—Since the iron-DBM complex is insoluble in methyl or ethyl alcohol, MIBK was primarily used as a diluent. In this case, however, an extremely large amount of DBM was necessary in order to ensure full color development, and this induced large blank values. In the study of the color reaction of the complex, it was found that the absorbance of the complex was markedly affected by the choice of diluent, as has been reported by Mann and White[5] for the *in situ* spectrophotometric determination of chromium with diphenylcarbazide. The comparison of some diluents, shown in Fig. 2, revealed that methanol is best for this purpose,

1) Y. Umezaki, This Bulletin, **36**, 769 (1963).
2) T. Shigematsu and M. Tabushi, *J. Chem. Soc. Japan, Pure Chem. Sec.* (*Nippon Kagaku Zasshi*), **81**, 265 (1960).
3) H. Goto and E. Sudo, *Japan Analyst* (*Bunseki Kagaku*), **9**, 213 (1960); N. Tajima and S. Kurobe, ibid., **9**, 399 (1960); N. Tajima and S. Kurobe, ibid., **9**, 798 (1960); N. Tajima and S. Kurobe, ibid., **10**, 528 (1961).
4) H. Jackson and D. S. Phillips, *Analyst*, **87**, 712 (1962); H. Jackson and D. S. Phillips, ibid., **87**, 718 (1962).

* A one-eighth part of 11 cm. filter paper.
** When all the extracts are used for the color development, the effluent is collected directly in the volumetric flask, and the inside of the separatory funnel and the plug are washed with 1 ml. of MIBK.
5) C. K. Mann and J. C. White, *Anal. Chem.*, **30**, 989 (1958).

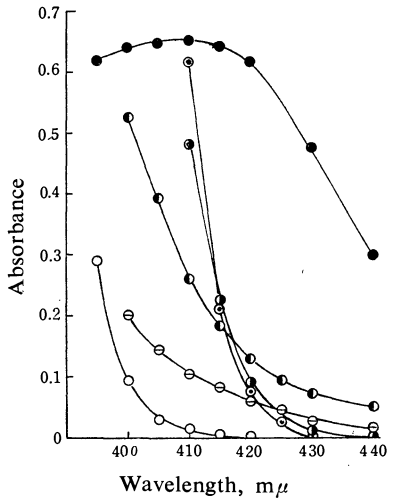


Fig. 1. Absorption spectra.

● Fe(III) 30 μg. ○ Blank, 0.5% DBM×2 ml.
⊖ Cu(II) 10 mg. ⊙ Sn(IV) 10 mg.
◑ Mo(VI) 200 μg. ◐ V(V) 200 μg.

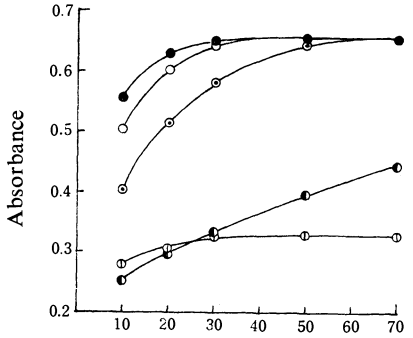


Fig. 2. Effect diluent.
30 μg. of Fe(III) present in aq. soln.

● Methyl alcohol, 0.5% DBM×2 ml., 2 ml. extract was used.
○ Ethyl alcohol, 1% DBM×2 ml., 2 ml. extract was used.
⊙ Ethyl alcohol, 0.5% DBM×2 ml., 2 ml. extract was used.
◐ Acetone, 0.5% DBM×2 ml., 2ml. extract was used.
⦶ Ethyl alcohol, 0.5% DBM×2 ml. 1 ml. extract was used.

while ethanol is barely satisfactory. No precipitation of the complex occurred in this combination of solvents (MIBK : pyridine : methanol=2 : 0.5 : 7.5). The effect of diluents on the color development of the complex apparently parallels the magnitude of the dielectric constants of the solvents. If this assumption is true, water, which has the highest dielectric constant, should be most effective. In fact, the addition of water instead of methanol up to 2 ml. gave a light pink color even before the addition of pyridine, though its use is not adequate for the standard procedure because a large amount of water causes precipitation.

Pyridine Concentration.—Pyridine was chosen as a miscible base in order to neutralize the acid extracted simultaneously into the organic phase and in order to ensure the full color development of the complex. The role of pyridine is not clear; it is not certain whether it only neutralizes the acid or whether it forms some adducts with iron-DBM as in cobalt-TTA and pyridine.[6]

As Fig. 3 shows a very small amount of pyridine is sufficient for full color development; 0.5 ml. was used in practice.

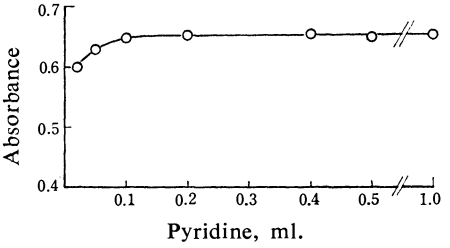


Fig. 3. Effect of pyridine.
30 μg. of Fe(III) present in aq. soln. 0.5% DBM×2 ml.

DBM Concentration.—As Fig. 4 shows, 2 ml. of a 0.5% DBM solution is sufficient in the methanol system.

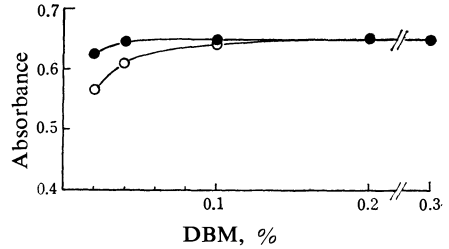


Fig. 4. DBM concentration.
30 μg. of Fe(III) present in aq. soln.; 1 ml. of pyridine was used.

● Methyl alcohol was used as diluent.
○ Ethyl alcohol was used as diluent.

The Effect of the Volume of the Aqueous Solution.—Since MIBK dissolves in water to some extent and vice versa, any change of the volume ratio of the two phases should be avoided as much as possible. In the recommended procedure, 3 ml. of MIBK decreases its volume to 2.1 to 2.2 ml. after passing through the filter paper plug. The effect of the volume of the aqueous solution was ex-

6) J. P. Fackler, *Inorg. Chem.*, 2, 266 (1963).

TABLE I. EFFECT OF VOLUME OF AQUEOUS SOLUTION (20 μg. of iron(III) present)

Volume of aq. soln. ml.	Absorbance
8.0	0.429
9.0	0.436
10.0	0.437
11.0	0.437
12.0	0.441

amined with varying volumes of the sample solution using 3 ml. of MIBK. As Table I shows, a variation of the volume by $\pm$1 ml. for 10 ml. of the sample solution does not yield any appreciable error.

The Effect of the Acidity of the Aqueous Solution.—Since the volume of the extract decreases with the increasing acidity of the aqueous solution, a relatively severe control of the acidity is desired. As is shown in Table II, the range of permissible variation in the acidity is narrow; i. e., about $\pm$0.15 N corresponds to a 1% error.

TABLE II. EFFECT OF ACIDITY OF AQUEOUS SOLUTION (20 μg. of iron(III) present)

Acidity of aq. soln. N	Absorbance	
	2 ml. extract	Whole extract
5.3	0.422	0.524
5.9	0.437	0.523
6.5	0.456	0.527
7.1	—a)	0.511
7.7	—a)	0.487

a) Volume of extract was less than 2 ml.

When the adjustment of the acidity is rather difficult, the use of the entire extract instead of a 2 ml. portion is preferable.

Stability and Sensitivity.—The color develops almost instantaneously on the addition of the reagent and pyridine, and it is stable for a long time provided the container is sealed.

The sensitivity of this reaction is 0.0046 μg. Fe/cm^2 for $-\log T=0.001$ (2 ml. extract) and 0.0038 μg. Fe/cm^2 (whole extract).

Beer's Law.—Beer's law is obeyed up to 40 μg. of iron in an aqueous solution in the recommended procedure, as Fig. 5 shows.

The Mole Ratio.—The mole ratio of the complex was studied by the method of continuous variations; it is clear that, in the lower concentration of DBM, the ratio of iron to the reagent is 1 : 2, as is shown in Fig. 6. How-

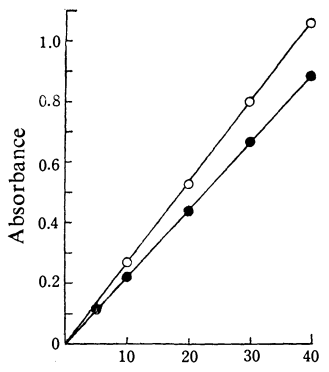


Fig. 5. Calibration curve.
● 2 ml. extract was used.
○ Whole extract was used.

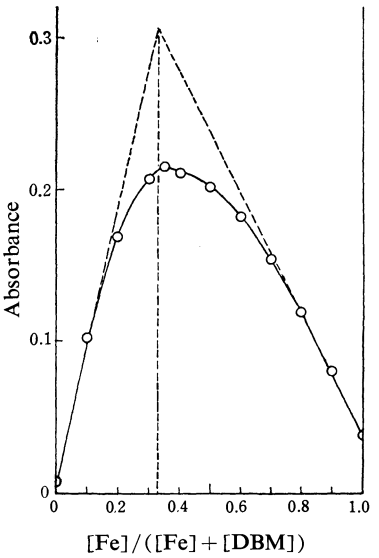


Fig. 6. Continuous variation method.
Wavelength: 410 mμ
[Fe]+[DBM]=8.0×10^{-5} M

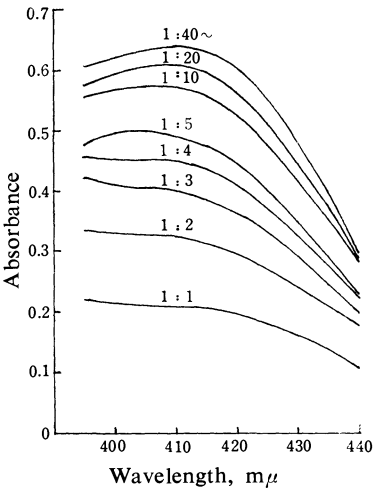


Fig. 7. Absorption spectra of iron-DBM complexes.
[Fe]=4×10^{-5} M
Ratios in the figure indicate [Fe]/[DBM].

ever, the absorption spectrum of this species is slightly different, there being no peak at 410 mμ, from that of the species obtained in a higher concentration of the reagent, which presumably has a mole ratio of 1 : 3, judging from its close resemblance to the absorption spectrum of iron-DBM in butyl acetate reported by Shigematsu and Tabushi.[2] The absorption spectra of these species change gradually with an increasing concentration of DBM; the change is hardly observed when this ratio exceeds 1 : 40, as Fig. 7 shows.

The Effect of Diverse Ions.—The effect of diverse ions on the determination of iron is summarized in Table III.

TABLE III. EFFECT OF DIVERSE IONS
(20 μg. of iron(III) present)

Ion	Added mg.	Fe recovered μg.
As(III)	20	20.5, 20.5
Sb(V)	2	20.4, 20.3
Se(IV)	2	21.2, 21.0
Te(IV)	2	—[a]
	0.2	18.8, 18.5
Ge(IV)	2	20.8, 19.9
Sn(IV)	2	32.2, 33.2
	1	20.8,[b] 20.6[b]
V(V)	0.2	29.9
	0.04	20.8,[b] 21.0[b]
Cr(VI)	0.2	29.4
Cr(III)	20	20.4, 20.7
Mo(VI)	20	—[a]
	0.2	45.3
	0.2	22.2,[b] 22.0[b]
Cu(II)	20	24.2
	1	20.4, 20.5
Co(II)	20	19.7, 20.9
Ni(II)	20	19.7, 20.2
Mn(II)	20	20.4, 19.4
Zn(II)	20	20.7, 20.2
Hg(II)	20	20.5, 20.5
Be(II)	10	19.7, 20.4
Ce(III)	10	19.6, 20.2
Bi(III)	10	20.8, 20.1
Th(IV)	20	19.5, 20.2
Ti(IV)	2	20.2, 20.4
W(VI)	0.2	19.1, 19.4
U(VI)	20	90.7
	0.2	20.0, 20.7
NO_3^-	20	18.4, 18.1
	2	19.8, 20.0
SO_4^{2-}	20	19.0, 19.7
CH_3COO^-	20	19.5, 20.2
F^-	20	17.5, 17.1
PO_4^{3-}	20	19.8, 19.5

a) Precipitate was produced in the organic phase.
b) Measured at 425 mμ.

Goto et al.[7] reported that antimony(III, V), arsenic(III, V), tin(IV), selenium(IV), tellurium(IV), germanium(IV), chromium(VI), vanadium(V) and molybdenum(VI) are also extracted, more or less, with MIBK from a hydrochloric acid solution. Of these ions, arsenic, antimony, selenium and germanium do not interfere with the determination of iron, whereas tellurium, vanadium, chromium, molybdenum and tin do cause interference more or less. However, these interferences are reduced or eliminated by reduction (for chromium, chromium(VI) to chromium(III)) or by the measurement of the absorbance at a longer wavelength, where the absorbances due to these elements decrease rapidly, as Fig. 1 shows.

Among the ions which are not extractable, copper(II), uranium(VI) and tungsten(VI) interfere more or less. However, the interference with these ions is not so serious that the presence of 10- (for uranium and tungsten) to 50-fold (for copper) is permissible. Of the cations tested, the interference with vanadium is the most serious.

Sulfate, acetate and phosphate do not interfere, whereas nitrate interferes, especially in its higher concentration, where both the volume of the MIBK extract and the amount of the co-extracted acid become larger; this spoils the experimental conditions.

Summary

A method has been described for the direct spectrophotometric determination of up to 40 μg. of iron(III) with DBM in the organic phase.

An orange complex, which is formed with the addition of DBM and pyridine to the MIBK extract of iron, has a maximum absorbance at 410 mμ. The effect of the diluent on the color reaction has been studied; methanol has been selected as the best diluent of those tried. The color reaction conforms to Beer's law and has a sensitivity of 0.0046 μg. Fe/cm² for $-\log T = 0.001$. The effects of diverse ions on the determination of iron have been studied; it has been found that this method is simple and is sensitive and selective to iron.

Resources Research Institute
Kawaguchi, Saitama

7) H. Goto, Y. Kakita and K. Furukawa, *J. Chem. Soc. Japan, Pure Chem. Sec.* (*Nippon Kagaku Zassi*), **79**, 1513 (1958).

The Condensation of Acetonitrile with Formaldehyde

By Yoshiro OGATA, Yasuji IZAWA and Yasuo OSUMI

(Received June 3, 1963)

The condensations of nitriles with aldehydes have been reported with both acidic and basic catalysts. Examples of an acid-catalyzed condensation are the formation of methylenebisamides or that of triacyltrihydrotriazines.[1,2] In base-catalyzed condensations, the nitriles with an active methylene group, such as cyanoacetic acid,[3] ethyl cyanoacetate[4,5] and malononitrile[6], can easily be converted to the corresponding α, β-unsaturated nitriles. It has been shown that the reaction of acetonitrile with aldehyde is difficult with ordinary base catalysts, but that it reacts with benzaldehyde or benzophenone, using sodium amide as a catalyst, yielding β-hydroxynitriles, i. e., β-hydroxy-β-diphenylpropionitrile, respectively.[7] However, the aldol-type condensation of acetonitrile with such aliphatic aldehydes as formaldehyde has not yet been reported.

The present paper will describe the aldol-type condensation of acetonitrile with formaldehyde in tetrahydrofurane (THF), using as a base catalyst sodium naphthalene complex, which has been proved to be effective for the alkylation of nitriles with aldehydes.[8] Although the reaction was complicated by side reactions, β-hydroxynitrile (ethylene cyanohydrin) was identified in the reaction product by gas chromatography and spectrography.

$$HCHO + CH_3CN \xrightarrow{Na\cdot C_{10}H_8} \underset{|}{\overset{OH}{HCH}}\text{-}CH_2CN$$

In the reaction product, 2, 4, 6-trimethyltriazine was also detected. A similar reaction using a SiO_2-NaOH catalyst[8a] at 280~300°C was unsuccessful.

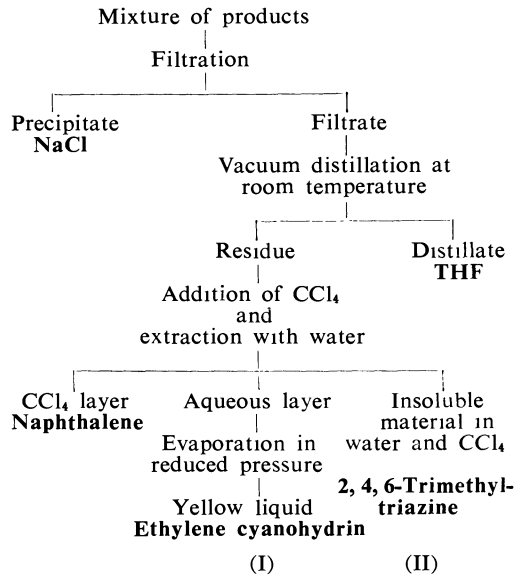
Experimental

Materials.—Acetonitrile (first grade) was dried over anhydrous potassium carbonate and fractionally distilled (b. p. 81~82°C). Naphthalene was of the first grade. THF (first grade) was dried over sodium for a few days and distilled over sodium hydroxide in an all-glass apparatus protected from the moisture in the air by a calcium chloride tube (b. p. 66°C).

Preparation of Sodium Acetonitrile.—Sodium acetonitrile was prepared according to the Horner-Güsten method;[8] 5.0 g. (0.2 mol.) of sodium was added to a solution of 25.6 g. (0.21 mol.) of naphthalene in 200 ml. of THF, and the mixture was stirred at room temperature for about 3 hr. in an atmosphere of nitrogen. The solution was then added slowly to a solution of 25.6 ml. (0.2 mol.) of acetonitrile in 100 ml. of THF at −8 and −10°C.

Reaction of Sodium Acetonitrile with Formaldehyde.—Gaseous formaldehyde was preparaed by dropping liquid paraffin slurry, containing 12 g. of paraformaldehyde, into a preheated flask at 115~140°C. The gaseous formaldehyde was bubbled into the THF solution of sodium acetonitrile for one hour at room temperature and then for an additional 0.5 hr. to ensure the completion of the reaction. The resulting yellow and viscous liquid was carefully neutralized with concentrated hydrochloric acid. Instead of gaseous formaldehyde, paraformaldehyde and trioxane could be used, but the yields were poorer (see Table I).

Ehtylene cyanohydrin in the products was isolated according to the following scheme:



1) E. Hepp, *Ber.*, **9**, 1424 (1876); E. Hepp, ibid., **10**, 1649 (1877).
2) M. W. Pollock and E. Zenner, U. S. Pat. 2493360 (1950); U. S. Pat. 2559835 (1952).
3) J. T. Carrick, *J. prakt. Chem.*, [2] **45**, 500 (1892).
4) S. Patai and Y. Israeli, *J. Chem. Soc.*, **1960**, 2030.
5) G. P. Schiemenz and H. Engelhard, *Chem. Ber.*, **95**, 967 (1962).
6) S. Patai and Y. Israeli, *J. Chem. Soc.*, **1960**, 2020, 2025.
7) H. Lettré, G. Meiners and H. Wichmann, *Naturwiss.*, **33**, 157 (1946).
8) L. Horner and H. Gusten, *Ann.*, **652**, 99 (1962).
8a) M. I. Yakushkin, *Khim. Prom.*, **1959**, 575; *Chem. Abstr.*, **54**, 23701 (1960).

Table I. Reaction of acetonitrile with formaldehyde

Aldehyde	Reaction time hr.	Reaction temp. °C	$HOCH_2CH_2CN$ yield, %
Gaseous formaldehyde	2(1)[a]	0~5	6.0
Gaseous formaldehyde	2(1)[a]	15	6.4
Gaseous formaldehyde	2(1)[a]	20	7.7
Paraformaldehyde	2	30	0
Paraformaldehyde	2	50	1.0
Trioxane	2	50	2.8

a) The figures in the parenthesis are the bubbling time (hr.) of gaseous formaldehyde.

Identification of Ethylene Cyanohydrin.—Both infrared spectrography and gas chromatography showed that the main component in the products (I) was identical with an authentic sample of ethylene cyanohydrin, prepared from ethylene chlorohydrin and sodium cyanide. The wave numbers (cm^{-1}) of the characteristic absorption bands of ethylene cyanohydrin and the product sample are as follows: 3400 (ν_{OH}), 2920 (ν_{CH_2}), 2260 (ν_{CN}), 1410 ($\delta_{CH_2(CN)}$), 1060 (ν_{CO})cm^{-1}.[9]

Figure 1 presents the gas chromatography curves on the authentic and resulting ethylene cyanohydrin; these also support our findings.

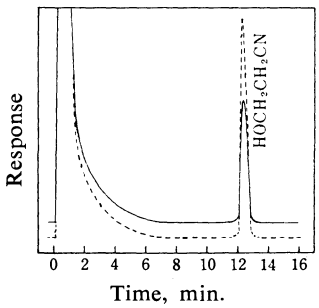


Fig. 1. Gas chromatography curves on ethylene cyanohydrin.
Partition liquid: PEG 4000, 25 wt.%/Celite 545, 80~100 mesh
Column length: 2 m.
Column temp.: 203°C
Carrier gas: He 49 ml./min.
Detection current: 150 mamp.
——: EtOH solution of I
- - -: Addition of pure ethylene cyanohydrin to the above solution.

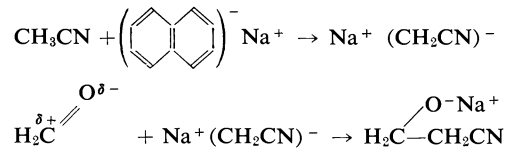
It was found both by a qualitative test of nitrogen (alkali fusion) and by ultraviolet absorption spectrography that the insoluble material (II) in water and carbon tetrachloride contained 2, 4, 6-trimethyltriazine, since it has the characteristic absorption band at 254 mμ (256 mμ[10]) in ethanol.

The yields on the basis of used acetonitrile, together with the reaction conditions, are presented in Table I.

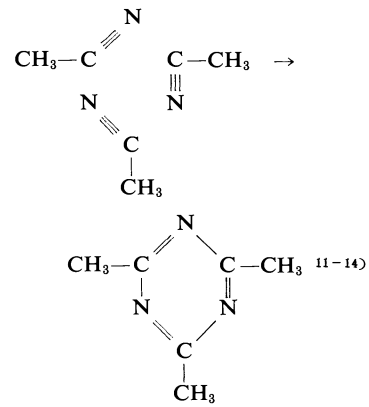
The yields of ethylene cyanohydrin in these experiments were estimated by gas chromatography. The yields, high (6.0~7.7 %) with gaseous formaldehyde, tended to be lower (1.0~2.8%) with paraformaldehyde and trioxane.

Discussion

The present fiindings show that formaldehyde can be reacted with acetonirile through the aldol-type condensation to form ethylene cyanohydrin. The reaction appeares to proceed by way of the attack of the carbanion of acetonitrile on the carbonyl carbon of formaldehyde.



The above reaction was successful with a strong base catalyst such as sodium naphthalene, but it appears that the reaction does not occur with a weaker base because of the difficulty of forming carbanion. The base-catalyzed polymerizations of acetonitrile may also occur—for instance, the trimerization of acetonitrile:



2, 4, 6-Trimethyltriazine

In fact, we could identify 2, 4, 6-trimethyltriazine.

9) E. F. Dupre, A. C. Armstrong, E. Klein and R. T. O'Conner, *Anal. Chem.*, 27, 1878 (1955).
10) T. L. Cairns, A. V. Larchar and B. C. McKusick, *J. Am. Chem. Soc.*, 74, 5633 (1952).

The poor yield of ethylene cyanohydrin may be due to the formation of such polymers of acetonitrile as cyamethine, *N*-(2, 6-dimethyl-*N*-(2, 6-dimethyl-4-pyrimidyl)-acetamidine, and 2, 4, 6-trimethyltriazine, the hydrolysis of acetonitrile and/or the base-catalyzed condensation of formaldehyde.[10] The other aliphatic aldehydes, e. g., acetaldehyde, are easily subject to aldol condensation by themselves; hence, the reaction with acetonitrile was found to be difficult.

11) E. Frankland and J. C. Evans, *J. Chem. Soc.*, **37**, 560 (1880).
12) A. Lettermoser, *J. prakt. Chem.*, **54**, 113 (1896).
13) R. M. Anker and A. H. Cook, *J. Chem. Soc.*, **1941**, 323.
14) F. W. Swamer, G. A. Reynolds and C. R. Hauser, *J. Org. Chem.*, **16**, 43 (1950); G. A. Reynolds, W. J. Humphlett and F. W. Swamer, ibid., **16**, 165 (1950).

Summary

The condensation of acetonitrile with formaldehyde using sodium naphthalene as a base catalyst has been studied. The results showed that formaldehyde reacted with acetonitrile through the aldol-type condensation to form ethylene cyanohydrin (1.0~7.7%). 2, 4, 6-Trimethyltriazine was detected as one of the by-products.

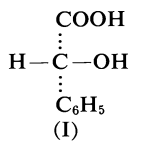
Department of Applied Chemistry
Faculty of Engineering
Nagoya University
Chikusa-ku, Nagoya

The Anomalous Adsorption of Enantiomers of Mandelic Acid and Atrolactic Acid on the Optically-Active Adsorbent

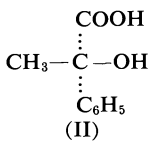
By Masaaki OHARA, Kosuke OHTA and Takao KWAN

(Received July 1, 1963)

The present paper is concerned with the selective adsorption of enantiomers of mandelic acid (I) and atrolactic acid (II) on a starch column.



(I)



(II)

As has been described in a previous paper,[1] the (−) isomer of mandelic acid is eluted from a starch column earlier than the (+) isomer. A similar selectivity in the adsorption was found with the homologues of mandelic acid except with atrolactic acid (II), where the (+) isomer was eluted earlier than the (−) isomer. The apparently anomalous selectivity in the adsorption of these enantiomers will be discussed here.

Experimental and Results

Racemic mandelic acid or atrolactic acid (0.5 g.) in 50% aqueous methanol was adsorbed at room temperature on a starch column 1.6×60 cm. and chromatographed with the same solvent. The optical rotation of the eluted was measured by a Zeiss-Kreis polarimeter. The concentration of the acid in the fraction was determined by absorption at 257 mμ.

In Fig. 1 the specific rotations of mandelic acid as well as of atrolactic acid are plotted against the fraction numbers. The observed angle of rotation, α, and the concentration of the adsorbates, c, in g. per 100 ml. of an aqueous methanol solution are given for some of the fractions.

As shown in the figure with atrolactic acid the (+) isomer is eluted earlier, while with mandelic acid the (−) isomer is eluted earlier, in accordance with the previous observation.[1] Over 90% of the acids were recovered in either case. Judging from the reversal order of the elution of the enantiomers of mandelic acid

TABLE I. THE ELUTION OF SEVERAL HOMOLOGUES OF MANDELIC ACID ON A STARCH COLUMN (15~18°C)

Racemate	The sign of the isomer eluted earlier	The sign of the isomer eluted later
Mandelic acid	(−)	(+)
Atrolactic acid	(+)	(−)
Methyl mandelate	(−)	(+)
Acetyl mandelic acid	(+)	(−)
β-Phenyl lactic acid	(+)	(−)
Tropic acid	(−)	(+)

1) M. Ohara, I. Fujita and T. Kwan, This Bulletin, 35, 2049 (1962).

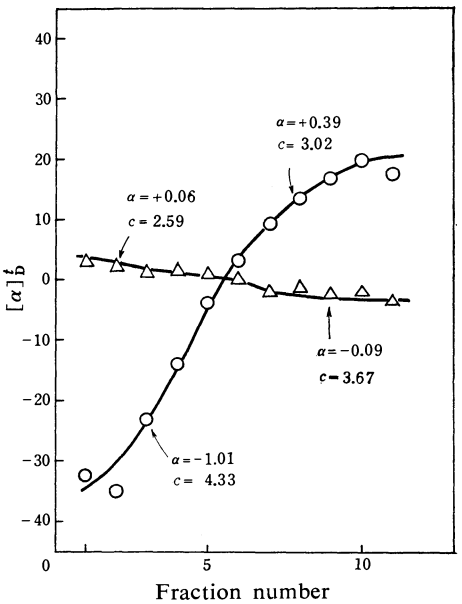


Fig. 1. The specific rotation $[\alpha]_D^t$ of mandelic acid and atrolactic acid against fraction numbers (t, 15~18°C).
○ Mandelic acid
△ Atrolactic acid

and atrolactic acid, it can be considered that the adsorption affinity of mandelic acid and that of atrolactic acid are reversed with respect to their enantiomers.

(+) mandelic acid > (−) mandelic acid

(+) atrolactic acid < (−) atrolactic acid

Several homologues of mandelic acid were investigated in a similar manner. The order of appearance is shown in Table I.

Optical isomers with the same sign can not always be assigned to the same configuration. In Table I it may be seen that atrolactic acid, acetyl mandelic acid and β-phenyl lactic acid are different with respect to the sign of the isomer eluted earlier. The literature shows, however, that the (+) isomers of the latter two have the same configuration as the (−) isomer of mandelic acid.[2,3] On the other hand, optical isomers of mandelic acid and atrolactic acid with the same sign have generally been assigned to the same configuration.[3-6] Therefore, the fact that the (+) isomer of atrolactic acid is eluted earlier may be considered peculiar with regard to the relative adsorption affinity of enantiomers or may raise some question of the configurational interaction between the adsorbate molecule and the surface of starch.

Discussion

The configurational relation of the enantiomers of mandelic acid and its homologues has been established so far by the chemically correlative method. For instance, Brewster[5] clarified the configurational correlation of mandelic acid with atrolactic acid by means of a diastereoisomer, i. e., *threo*-1, 2 diphenyl propanediol. Support for this conclusion was provideded by Cram and his co-workers[6] through a similar stereochemical course. The physical method was also applied in determining the configurational relationship; the change in the molecular rotation of several of their derivatives were investigated,[3] leading to results consistent with the chemical method. Another physical method, the quasi-racemate one, was also tried, but it was found ineffective.[7]

On the other hand, the so-called adsorption affinity method has sometimes been proposed; in this method the adsorbability of one optical isomer in preference to its enantiomer was investigated on a certain optically-active adsorbent. For instance, it was adopted by Beckett and his co-workers[8] in such systems as quinine-quinidine or cinchonine-cinchonidine adsorbed on quinine-pretreated silica gel. They were successful in correlating the configuration of the adsorbent to the strongly-adsorbed epimers. In this case, the adsorbent molecule is similar to the adsorbate molecule in size. Thus the method may resemble the quasi-racemate method.[7]

In contrast, in cases where adsorbents are macromolecules, the adsorption affinity may be conceptually included in the biological method in view of the specificity-like enzyme action. An investigation of the adsorbed configuration of enantiomers along such lines may be found the work of Balandin and his co-workers.[9]

Now, the observed reversal order of elution with mandelic acid and atrolactic acid seems to be incosistent with their *established* configurational correlations; one has to seek an interpretation of the *anomalous* selectivity in the relative configuration of the adsorbate-adsorbent complex. On the other hand, if we assume that the substitution of H for CH_3 with mandelic acid has little effect on the

2) G. W. Clough, *J. Chem. Soc.*, **27**, 2805 (1925).
3) K. Freudenberg, J. Todd and R. Seidler, *Liebig Ann.*, **501**, 199 (1933).
4) V. Prelog, *Helv. Chim. Acta*, **36**, 308 (1953).
5) J. H. Brewster, *J. Am. Chem. Soc.*, **78**, 4061 (1956).
6) D. J. Cram and K. R. Kopecky, ibid., **81**, 2748 (1959); D. J. Cram, K. R. Kopecky, F. Hauck and A. Langemann, ibid., **81**, 5754 (1959).
7) K. Mislow and M. Heffler, ibid., **74**, 3668 (1952).
8) A. H. Beckett and P. Anderson, *Nature*, **179**, 1074 (1957).
9) A. A. Balandin, E. I. Klabunovskii and Yu. I. Petrov, *Doklady Akad. Nauk. S. S. S. R.*, **127**, 557 (1959).

adsorption on starch, then the *established* relation between the sign and the configuration with enantiomers of mandelic acid and atrolactic acid will be false.

Two tentative explanations to this anomaly have been proposed. One is that the true configurational relationship of enantiomers is a reverse one, being consistent with the order of adsorption affinity. Another is associated with the structure-sensitive properties of starch.

When the above-mentioned configuration relationship is admitted as having been established, the relationship between the adsorption affinity and the configuration of the enantiomers is reversed.

In the latter explanation, when a three-point adsorption model, as was mentioned by, for instance, Ogston,[10] is adopted and when the common functional groups (-OH, -COOH, and $-C_6H_5$) are responsible to the adsorption force, it is impossible to expect the reversal effect in the adsorption of the enantiomers of mandelic acid and atrolactic acid. Perhaps a kind of multiple interaction would have to be assumed between the adsorbate and the surface of the starch.

At present it is difficult to determine what kind of interaction is responsible for the specific adsorption of mandelic acid and atrolactic acid.

Division of Physicochemical Technology
Faculty of Pharmaceutical Sciences
The University of Tokyo
Hongo, Tokyo

10) A. G. Ogston, *Nature*, **162**, 963 (1948).

The Rheological Properties of Concentrated Suspensions. III. Dynamic Properties and Their Correlations with Stationary Flow Properties

By Masaharu TAKANO

(Received August 9, 1963)

In a previous paper[1] the construction and principles of a versatile rheometer have been described. The dynamic properties of concentrated suspensions at lower frequencies and stationary flow properties at very low rates of shear may be measured with this apparatus. Preliminary investigations of the dynamic properties of concentrated suspensions have been reported on in another previous paper.[2]

It is the purpose of the present paper to examine the concentration dependence of dynamic properties and their correlations with stationary flow properties and to prove the validity of theoretical considerations based on a network model.[3]

Experimental

Materials.—The fillers used in this work were barium sulfate of a chemical grade and barium sulfate coated with sodium stearate; both of these have very narrow size distributions. The mediums used were linseed oil and polyisobutylene whose number average molecular weight is 858. The characteristics of the materials are listed in Table I.

The Preparation of Suspensions.—The filler was dried at 110°C in a vacuum of 20 mmHg for three hours prior to the preparation of suspensions. Suspensions were prepared by ten "tight" passes of the mixed components through a three-roll paint mill, with a roll 5 cm. in diameter, 10 cm. long and with revolution velocities of 18, 60 and 170.5 r.p.m. The additive was adsorbed to the filler before the preparation of suspensions. Suspensions prepared in such a manner were kept at 30°C for six days before being measured.

Apparatus and Methods.—The apparatus used in this work has been described in detail in a previous paper.[1] The apparatus can be used as a rotational viscometer and as an oscillatory viscoelastometer under the same geometrical conditions. For this work, stationary flow properties at very low rates of shear and dynamic properties at lower frequencies (below 1 c.p.s.) were measured.

In simple shear experiments, the shearing stress, S, and the apparent rate of shear, $\dot{\gamma}$, at the surface of the inner cylinder were given as follows:

$$S=T/2\pi R_i^2 L=k\theta/2\pi R_i^2 L \quad (1)$$

$$\dot{\gamma}=2\omega/\{1-(R_i/R_o)^2\} \quad (2)$$

1) H. Kambe and M. Takano, *Rept. Aeronaut. Res. Inst., Univ. Tokyo*, **28**, 159 (1963).
2) M. Takano and H. Kambe, *J. Japan Soc. Test. Matls. (Zairyô Shiken)*, **10**, 315 (May, 1961).
3) M. Takano, This Bulletin, to be published.

TABLE I. CHARACTERISTICS OF MATERIALS

Material	Viscosity* at 30°C poises	Density at 30°C g./cm³	Particle size μ $(\bar{R})$	$(\bar{R^2})^{1/2}$	$(\bar{R^3})^{1/3}$
Barium sulfate	—	4.50	0.075	0.079	0.082
Linseed oil	59.3	0.960	—	—	—
Polyisobutylene	154.0	0.883	—	—	—

* Measured by a capillary viscometer.

TABLE II. EXPERIMENTAL CONDITIONS

Radius of outer cylinder	R_o	1.400 cm.	
Radius of inner cylinder	R_i	1.250 cm.,	1.000 cm.
Depth of outer cylinder		8.365 cm.	
Length of inner cylinder	L	5.000 cm.,	4.000 cm.
Maximum angular deflection of inner cylinder	θ_o	below 4 degrees	
Region of frequency	ν	from 0 to 1 c. p. s.	
Torsional constant	k	from 0 to 8.55×10^3 dyn.-cm./deg.	
Amplitude of shear strain (at wall of inner cylinder)	γ_{max}	below 0.685,	below 0.285
Amplitude of shear stress (at wall of inner cylinder)	S_{max}	below 11.7 dyn./cm²,	below 55.0 dyn./cm²
Range of revolution velocity of outer cylinder		from 0 to 400 r. p. m.	

where R_i and R_o are the radii of the inner and outer cylinders respectively; L is the length of the inner cylinder; T, the torque; k, the torsional constant of the inner cylinder; θ, the angular deflection of the inner cylinder, and ω, the angular velocity of the outer cylinder.

In dynamic measurements, the basic equation of the motion of the inner oscillatory unit is:[1,4,5]

$$(M+m+C)\mathrm{d}^2\theta/\mathrm{d}t^2+\{(\eta'/A)+B\}\mathrm{d}\theta/\mathrm{d}t+(G'/A)\theta=T \quad (3)$$

$$T=Ki_d-k\theta \quad (4)$$

where M, C, B and K are the instrument constants; m is the moment of inertia of the sample; A the shape factor; i_d, the current through a torque motor which gives torque to the inner cylinder, and η' and G' are the dynamic viscosity and the dynamic modulus of the sample respectively. When the moment of inertia of sample m is negligibly small compared to $(M+C)$ and the current, i_d, changes sinusoidally, the dynamic viscosity and the dynamic modulus are given by the following equations:[1,4,5]

$$\eta'=A[\{K'(f_{d_0}/f_{\theta_0})\sin d\}/\omega-B] \quad (5)$$

$$G'=A[K'(f_{d_0}/f_{\theta_0})\cos d-k+(M+C)\omega^2] \quad (6)$$

where f_{d_0} and f_{θ_0} are the amplitudes of the recorded curves of the current, i_d, and of the deflection, θ, respectively; K' is the instrument constant, and d, the phase lag between the current and the deflection.

The shape factor A and the phase lag d are given as follows:

$$A=(1/4\pi L)\{(1/R_i)^2-(1/R_o)^2\} \quad (7)$$

$$d=\cos^{-1}\{f^2_{\theta_0}+f^2_{d_0}-f^2_{s_0})/2f_{\theta_0}f_{d_0}\} \quad (8)$$

where f_{s_0} is the amplitude of recorded curve of difference between the current and the deflection.[1]

The dimensions of the assemblies of coaxial cylinders and the experimental conditions are listed in Table II. The temperature was maintained at 30 ± 0.2°C during measurements. For Newtonian liquids, the dynamic experiments and the simple shear measurements were made within a range of error of $\pm10\%$.

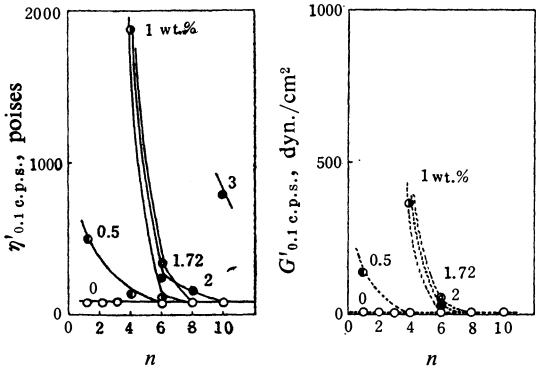
Experimental Results and Discussion

The Influence of the Conditions of Mixing and Resting.—The rheological behavior of a disperse system is closely related to the state of the flocculation of its particles and is influenced by the conditions of preparation and resting.

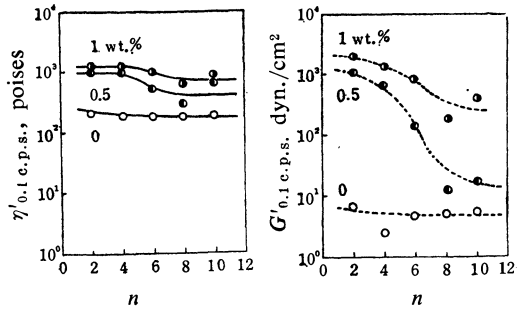
For the study of the influence of mixing conditions, a small quantity of suspension was taken out after each pass through the mill and examined rheometrically. Figure 1 shows the relation between the dynamic properties of suspensions of barium sulfate in linseed oil and in polyisobutylene, with and without water added, and the number of passes through the mill.

In suspensions of barium sulfate in linseed oil with water added, the higher dynamic viscosity and dynamic modulus observed at the earlier stages of milling decrease rapidly with milling to limiting values which are almost independent of the amount of water. Without

4) T. E. Morrisson, L. J. Zapas and T. W. DeWitt, *Rev. Sci. Instr.*, **26**, 357 (1955).
5) R. H, Shoulberg, F. H. Zimmerli and O. C. Kohler, *Trans. Soc. Rheology*, **3**, 27 (1959).



(a) 40 wt. % suspensions of barium sulfate in linseed oil, at 0.1 c.p.s., with or without water added.



(b) 10 wt. % suspensions of barium sulfate in polyisobutylene, at 0.1 c.p.s., with or without water added.

Fig. 1. Influence of the number of passes through the mill on the dynamic properties.

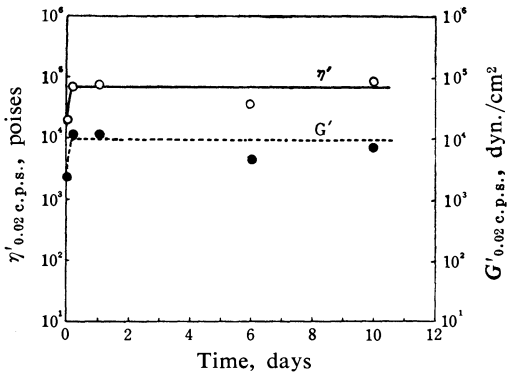


Fig. 2. Change in the dynamic properties with resting time, at 0.02 c.p.s., in 30 wt. % suspension of barium sulfate in polyisobutylene (30°C).

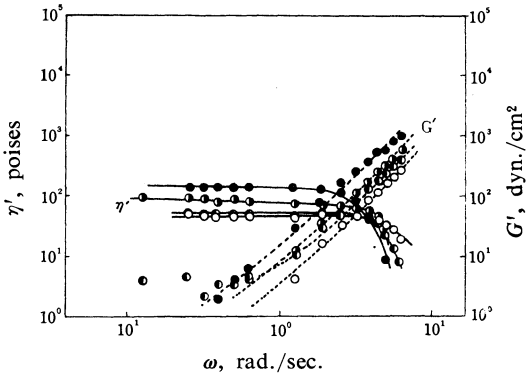


Fig. 3. Dependence of the dynamic properties on the concentration and the frequency in the suspensions of barium sulfate in linseed oil (30°C): ○, 0 wt. %; ◐, 10 wt. %; ◑, 30 wt. %; ● 50 wt. %.

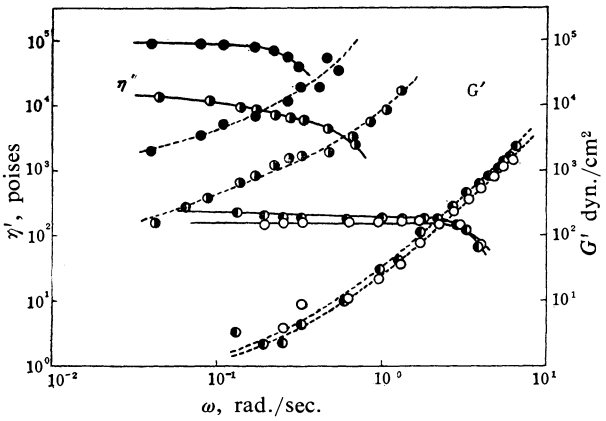


Fig. 4. Dependence of the dynamic properties on the concentration and the frequency in the suspensions of barium sulfate in polyisobutylene (30°C): ○, 0 wt. %; ◐, 10 wt. %; ◑, 20 wt. %; ●, 30 wt. %.

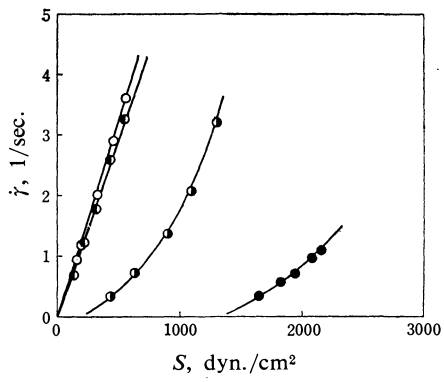


Fig. 5. Flow curves of the suspensions of barium sulfate in polyisobutylene at various concentrations (30°C): ○, 0 wt. %; ◐, 10 wt. %; ◑, 20 wt. %; ●, 30 wt. %.

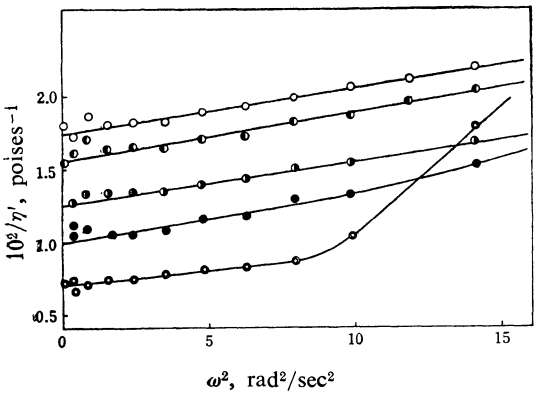


Fig. 6. Dependence of the dynamic viscosity on the concentration and the frequency in the suspensions of barium sulfate in linseed oil, with 0.5 wt. % water added (30°C): ○, 10 wt. %; ◐, 20 wt. %; ◑, 30 wt. %; ●, 40 wt. %; ◎, 50 wt. %.

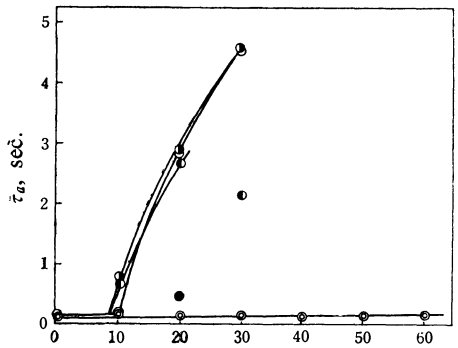
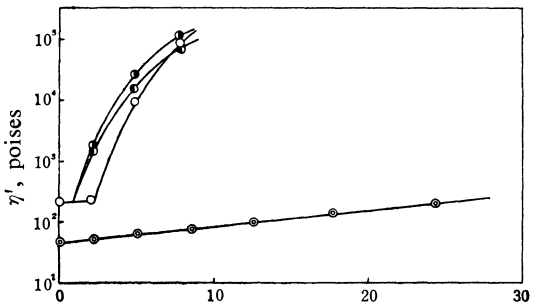


Fig. 7. Dependence of the apparent relaxation time on the concentration in various suspensions: ○, barium sulfate in polyisobutylene; ◐, barium sulfate in polyisobutylene, with 0.5 wt. % water added; ◑, barium sulfate in polyisobutylene, with 1.0 wt. % water added; ●, barium sulfate coated by 1 wt. % sodium stearate in polyisobutylene; ◎, barium sulfate in linseed oil, with or without water added.

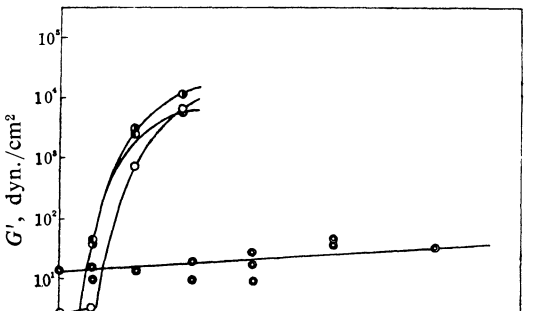
water added, the dynamic properties of suspensions in linseed oil show no changes upon milling.

In suspensions of barium sulfate in polyisobutylene, the dynamic viscosity and dynamic modulus of suspensions are generally decreased by milling at the earlier stages and approach limiting values upon repeated passages through the mill.

Figure 2 shows the increase in the dynamic viscosity and dynamic modulus with resting time in a suspension of barium sulfate in polyisobutylene. The dynamic properties seem to have stationary values after resting for about three hours.



(a) Dynamic viscosity.



(b) Dynamic modulus.

Fig. 8. Concentration dependence of the dynamic properties: ○, barium sulfate in polyisobutylene, at 0.02 c.p.s. ◐, barium sulfate in polyisobutylene, with 0.5 wt. % water added, at 0.02 c.p.s. ◑, barium sulfate in polyisobutylene, with 1.0 wt. % water added, at 0.02 c.p.s. ◎, barium sulfate in linseed oil, with or without water added, at 0.20 c.p.s.

Data for suspensions which have been passed ten times through the mill and rested for three hours will be compared below.

The Concentration Dependence and Frequency Dependence of Dynamic Properties. — The dynamic viscosity and the dynamic modulus of suspensions are shown in Figs. 3 and 4 as functions of the frequency and of the concentration. Stationary flow curves of suspensions in polyisobutylene at various concentrations are illustrated in Fig. 5.

The linseed oil and polyisobutylene used in this work are viscoelastic by themselves. In a previous paper[3] it has been pointed out theoretically that the dynamic properties of concentrated suspensions are given approximately by the sum of the viscoelasticities of the medium and network-structures formed by suspended particles.

Assuming a suspension as a Maxwell body, we can get the apparent relaxation time, τ_a, from the following equation:

$$1/\eta'_s(\omega) = 1/\eta'_s(0) + (\tau_a^2/\eta'_s(0))\omega^2 \quad (9)$$

where $\eta'_s(\omega)$ is the dynamic viscosity of the suspension at the angular frequency ω. Figure 6 shows the relation of $1/\eta'_s(\omega)$ to ω^2 for suspensions of barium sulfate in linseed oil. The apparent relaxation times obtained experimentally for various suspensions are listed in Table III. The apparent relaxation time generally increases with an increase in the concentration, as is shown in Fig. 7. In linseed oil, the apparent relaxation time of the suspension shows a slight change with the concentration. In polyisobutylene, on the other hand, the apparent relaxation time increases abruptly above a critical concentration, at which a network structure is formed by the particles in the medium.

The concentration dependence of dynamic properties at a given frequency is shown in Fig. 8 and in Table IV. In polyisobutylene, the dynamic viscosity and dynamic modulus of a suspension increase abruptly above a critical concentration. The mean free energy of the activation for breaking links between particles, ΔF, and the mean number of links to be broken for the separation of two neighboring particles, σ', can be evaluated from the critical concentration ϕ'_{crit}.[3,6] In suspensions of barium sulfate in polyisobutylene, the energy of interaction, ΔF, has the order of $33 \sim 34\,kT$, while the mean number of links,

TABLE III. APPARENT RELAXATION TIMES OF SUSPENSIONS OF BARIUM SULFATE IN LINSEED OIL AND POLYISOBUTYLENE (30°C)

Concentration wt. %		Na-stearate*	Apparent relaxation time of suspension, sec.	
$BaSO_4$	H_2O*		In linseed oil	In polyisobutylene
0	0	0	0.09	0.21
10	0	0	0.10	0.21
	0.5	0	0.13	0.70
	1.0	0	0.13	0.84
20	0	0	0.12	2.9
	0.5	0	0.15	2.7
	1.0	0	0.16	2.9
	0	1	—	0.48
30	0	0	0.17	4.6
	0.5	0	0.15	2.1
	1.0	0	0.14	4.6
40	0	0	0.18	—
	0.5	0	0.18	—
	1.0	0	0.19	—
	2.0	0	0.09	—
	3.0	0	1.4	—
	0	1	>5.0	—
50	0	0	0.19	—
	0.5	0	0.15	—
	1.0	0	0.21	—
60	0	0	0.18	

* Based on barium sulfate.

TABLE IV. DYNAMIC PROPERTIES OF SUSPENSIONS OF BARIUM SULFATE IN LINSEED OIL AND POLYISOBUTYLENE (30°C)

Concentration		Na-stearate*	G' dyn./cm²	η' poises	G' dyn./cm²	η' poises
$BaSO_4$	H_2O*		In linseed oil, at 0.20 c.p.s.		In polyisobutylene, at 0.02 c.p.s.	
0	0	0	12.8	47.0	2.7	170.0
10	0	0	2.8	45.8	3.1	225.0
	0.5	0	16.2	54.9	43.1	1360.0
	1.0	0	8.7	48.4	36.9	1450.0
20	0	0	12.7	58.2	727.0	9420.0
	0.5	0	12.9	60.6	2180.0	14200.0
	1.0	0	11.3	62.6	2590.0	26300.0
	0	1	—	—	0.0	997.0
30	0	0	0.0	68.9	6180.0	85900.0
	0.5	0	19.3	74.6	10400.0	53100.0
	1.0	0	9.4	73.3	10700.0	106000.0
40	0	0	26.1	89.7	—	—
	0.5	0	16.1	95.9	—	—
	1.0	0	28.4	87.5	—	—
	1.72	0	8.1	81.0	—	—
	2.0	0	19.8	85.7	—	—
	3.0	0	—	—	—	—
	0	1	4030.0	—	—	—
50	0	0	38.0	135.0	—	—
	0.5	0	50.6	135.0	—	—
	1.0	0	42.1	143.0	—	—
60	0	0	32.4	180.0	—	—

* Based on barium sulfate.

TABLE V. CRITICAL CONCENTRATION AND THE INTERACTION PARAMETERS IN SUSPENSIONS OF BARIUM SULFATE IN POLYISOBUTYLENE (30°C)

Concn. of water (wt. % based on barium sulfate)	0	0.5	1.0
ϕ'_{crit} in η' (vol. %)	2.0	0.8	0.8
ϕ'_{crit} in G' (vol. %)	2.0	1.2	1.2
$\Delta F/kT$ in η' ($\sigma'=1$)	33.3	34.2	34.2
$\Delta F/kT$ in G' ($\sigma'=1$)	33.3	33.3	33.8
σ' in η'	1.49_1	1.49_2	1.49_2
σ' in G'	1.49_1	1.49_2	1.49_2
$\Delta F/kT$ in η' ($\sigma'=1.49$)	32.9	33.8	33.8
$\Delta F/kT$ in G' ($\sigma'=1.49$)	32.9	33.4	33.4

σ', is 1.49, as Table V shows. These values coincide well with those evaluated from the stationary flow properties.[6] In suspensions of barium sulfate in linseed oil, the concentration dependence of the dynamic viscosity and the dynamic modulus are given by the following equations (at 0.20 c.p.s.):

$$\eta'_s(0.20) = \eta'_m(0.20)\exp(5.53\,\phi) \qquad (10)$$

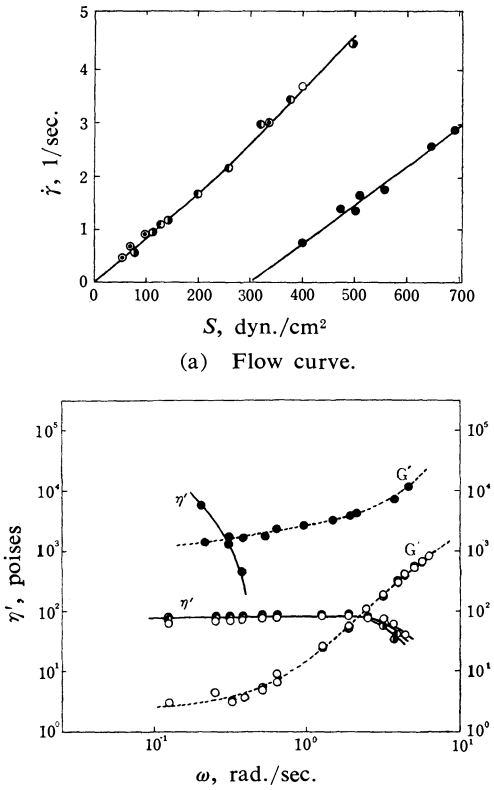
$$G'_s(0.20) = G'_m(0.20)\exp(3.92\,\phi) \qquad (11)$$

where $\eta'_m(0.20)$ and $G'_m(0.20)$ are the dynamic viscosity and the dynamic modulus of an unfilled medium at 0.20 c.p.s. respectively, and where ϕ is the volume fraction of the filler. The increase in the apparent relaxation time with the concentration can be explained qualitatively by the difference in the concentration dependences between the dynamic viscosity and the dynamic modulus.

The Influence of Additions of Water and Sodium Stearate on the Dynamic Properties.— Dynamic properties also change upon the addition of additives which have an influence on the energy of interaction between particles, as is shown in Tables III, IV and V.

In relatively polar linseed oil, the dynamic viscosity and dynamic modulus of a concentrated suspension with water added increase in the earlier stages of milling, as is shown in Fig. 1. However, it is shown in Figs. 1, 8, 9 and Table IV that the dynamic properties decrease to limiting values upon milling, that these properties are slightly influenced by the amount of water, and that they are increased by coating particles with sodium stearate. The apparent relaxation time is also slightly influenced by the addition of water, as is illustrated in Table III.

In non-polar polyisobutylene, the dynamic viscosity and dynamic modulus of a concentrated suspension are increased by the addition of water independently of milling, as is shown in Figs. 1, 8, 10 and Table IV. The apparent relaxation time at lower concentrations also increases upon the addition of water, as Fig. 7 and Table III show. The critical concentration above which the dynamic properties increase appreciably is lowered, and the energy of interaction between particles, is increased by the addition of water, as is shown

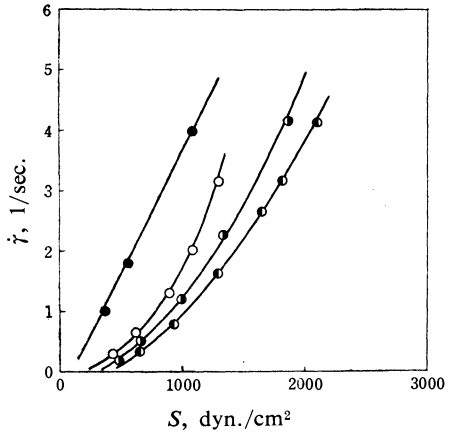


(a) Flow curve.

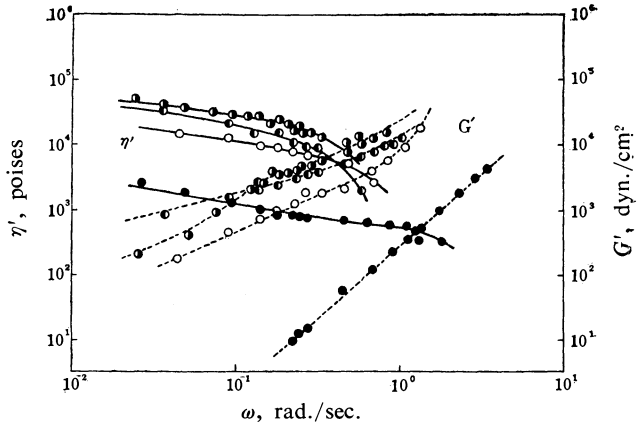
(b) Frequency dependence of the dynamic properties.

Fig. 9. Influence of the addition of water and sodium stearate on rheological properties of 40 wt. % suspensions of barium sulfate in linseed oil: ○, without additive; ◐, with 0.5 wt. % water added; ◑, with 1.0 wt. % water added; ◉, with 2.0 wt. % water added; ●, coated by sodium stearate.

6) M. Takano and H. Kambe, This Bulletin, to be published.



(a) Flow curve.



(b) Frequency dependence of dynamic properties.

Fig. 10. Influence of the addition of water and sodium stearate on rheological properties of 20 wt. % suspensions of barium sulfate in polyisobutylene: ○, without additive; ◐, with 0.5 wt. % water added; ◑, with 1.0 wt. % water added; ●, coated by sodium stearate.

in Fig. 8 and Table V. The dynamic viscosity and dynamic modulus are decreased by coating particles with sodium stearate.

The change in the dynamic properties by additives must be attributed to the influence of the additive on the interactions between particles: van der Waals-London attractions,[7,8] capillary forces due to interfacial tension between additive and medium,[9-11] the repulsion of two electric double layers,[12] the entropic repulsion of adsorbed molecules of the medium on the surfaces of particles,[8,13] contractive forces arising from the elastic property of a medium when the medium is viscoelastic by itself,[14] and others. The diffusion of water into the polar medium must also be taken into account.

In the present experiments, it seems that capillary forces originating from the presence of water do not have a decisive effect on the interaction between particles at a stationary state of dispersion. The interfacial tension between water and linseed oil is larger than that between water and polyisobutylene, as shown in Table VI. Besides, it seems that water is adsorbed on the surfaces of particles

TABLE VI. INTERFACIAL TENSION (26.3°C)

Interface	Interfacial tension* dyn./cm.
Water-Air	71.2
Linseed oil-Air	36.2
Polyisobutylene-Air	32.0
Linseed oil-Water	49.0
Polyisobutylene-Water	39.5

* Measured by Du Noüy's surface tension meter.

without diffusion into the medium. If water adheres to the surfaces of particles, contractive forces originating from the viscoelastic properties of the medium may be decreased by the addition of water. In a previous paper,[3] the following equation has been derived for the frequency dependence of the dynamic viscosity:

$$1/\{\eta'_s(\omega)-\eta'_m(\omega)\}=a+b\omega^2 \qquad (12)$$

where

$$a=\lambda_2^2\pi R_1/\boldsymbol{h}\exp(\Delta F/\boldsymbol{k}T)\,\sigma'(\phi-\phi'_{crit}) \qquad (13)$$

$$b=\boldsymbol{h}\pi R_1\exp(\Delta F/\boldsymbol{k}T)/4g_2^2\lambda_2^2\sigma'(\phi-\phi'_{crit}) \qquad (14)$$

In Eqs. 13 and 14, $\boldsymbol{h}$ and $\boldsymbol{k}$ are the constants of Planck and Boltzmann respectively; R_1 is the diameter of particles; λ_2, the distance by which particle moves whenever the secondary links between particles are broken reversibly; T, the absolute temperature; ΔF, the mean free energy of activation for breaking the links between particles; g_2, the mean stiffness of the secondary links, and σ', the mean number of links to be broken for separating two particles at very small deformations. If there are no

7) H. C. Hamaker, *Physica*, **4**, 1058 (1937).
8) M. J. Vold, *J. Colloid Sci.*, **9**, 451 (1954); ibid., **16**, 1 (1961).
9) G. L. Brown, *J. Polymer Sci.*, **22**, 423 (1956).
10) R. R. Myers, J. C. Miller and A. C. Zettlemoyer, *J. Appl. Phys.*, **27**, 468 (1956).
11) E. K. Fischer, "Colloidal Dispersions," John Wiley & Sons Inc., New York (1953), p. 128.
12) J. Th. G. Overbeek, "Colloid Science," Vol. I, Ed. by H. R. Kruyt, Elsevier Publ. Co., Amsterdam (1952), p. 245.
13) N. Casson, "Rheology of Disperse Systems," Ed. by C. C. Mill, Pergamon Press, London (1959), p. 84.
14) A. M. Bueche, *J. Polymer Sci.*, **15**, 105 (1955); ibid, **25**, 139 (1957).

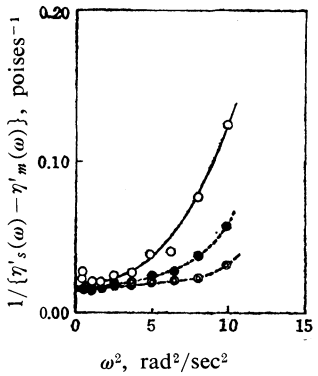


Fig. 11. Influence of the addition of water on the frequency dependence of the dynamic viscosity in 50 wt. % suspensions of barium sulfate in linseed oil: ○, without water; ◎, with 0.5 wt. % water added; ●, with 1.0 wt. % water added.

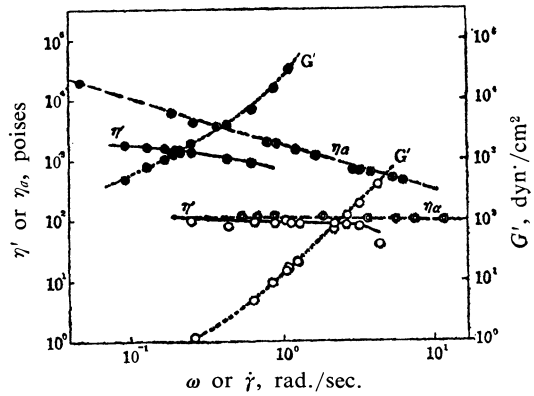


Fig. 12. Correlation between the dynamic properties and the apparent viscosity in 40 wt. % suspensions of barium sulfate in linseed oil: ○◎, with 2.0 wt. % water added (yield value, 0); ●◉, with 3.0 wt. % water added (yield value, 1280 dyn./cm^2).

contractive forces arising from the viscoelastic property of the medium, the values of a and b must be effectively independent of the frequency. Figure 11 shows the relation of $1/\{\eta'_s(\omega)-\eta'_m(\omega)\}$ to ω^2. However, it has been assumed that the dynamic viscosity of a medium involving particles at the volume fraction ϕ is given by the following equation:[15]

$$\eta'_m(\omega)=\eta'_{mo}(\omega)(1+2.5\phi+7.17\phi^2+16.2\phi^3)$$

where $\eta'_{mo}(\omega)$ is the dynamic viscosity of an unfilled medium. The dependence of b on the frequency apparently decreases on the addition of water. Such a tendency is observed both in polar and in non-polar media.

The magnitude of the van der Waals-London attraction between two spherical particles can be approximately evaluated as in a previous paper.[6] The change in dynamic properties by additives can be explained at least qualitatively by considering van der Waals-London attractions between particles.[6] However, other forces must also be taken into account, particularly such forces as the contractive forces of the medium. In a polar medium, the repulsion of two electric double layers may have an influence on the interaction between particles. In a medium with a high molecular weight, the entropic repulsion of adsorbed macromolecules may be considered between particles.

The Correlation between Dynamic Properties and Stationary Flow Properties. — In unfilled media and pseudo-plastic suspensions, the apparent viscosity at lower rates of shear coincides with the dynamic viscosity at lower frequencies. In plastic suspensions, however, the former does not generally coincide with the latter.

In plastic suspensions, the apparent viscosity at lower rates of shear may be higher or lower than the dynamic viscosity at lower frequencies when they are compared with each other on the same time scale. Figures 12 and 13 show the shear-rate dependence of the apparent viscosity, along with the frequency dependence of dynamic viscosity and dynamic modulus. In a series of suspensions of barium sulfate in polyisobutylene, the apparent viscosity in simple shear experiments is lower than the dynamic viscosity on the same time scale. Such a tendency is observed independently of the presence of water. In suspensions of barium sulfate in linseed oil, with a large quantity of water added, the apparent viscosity is higher than the dynamic viscosity on the same time scale.

These correlations between the apparent viscosity and the dynamic viscosity are at least qualitatively explained by the network model described in the previous paper.[3] The dynamic viscosity at very small deformations, $\eta'_s(\omega)$, and the apparent viscosity, η_a, are given by the following equations:

$$\eta'_s(\omega)=\eta'_m(\omega)+(2/\pi R_1)g_2\{\tau_2/(1+\tau^2{}_2\omega^2)\}\sigma'(\phi-\phi'_{crit}) \quad (15)$$

$$\eta_a=S/\dot{\gamma}=\eta_{pl}+S_o/\dot{\gamma} \quad (16)$$

where η_{pl} and S_o are given as follows:

$$\eta_{pl}=\eta_m+(R_1^2/3)(g_1+g_2)\tau_2\{(6/\pi R_1^3)+(3\eta\dot{\gamma}/kT\pi\phi_c)\}\sigma(\phi-\phi_{crit}) \quad (17)$$

$$S_o=(R_1^2/3)g_1\gamma_1\{(6/\pi R_1^3)$$

15) V. Vand, *J. Phys. and Colloid Chem.*, 52, 277, 300 (1949).

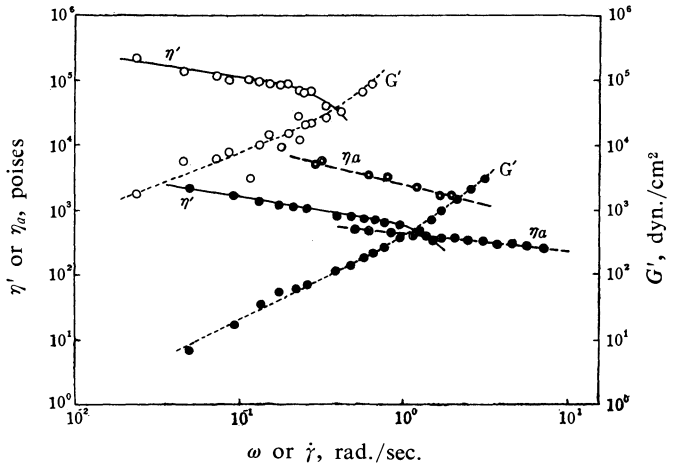


Fig. 13. Correlation between the dynamic properties and the apparent viscosity in suspensions of barium sulfate in polyisobutylene: ●◉, 10 wt. % suspension with 1.0 wt. % water added (yield value, 130 dyn./cm²); ○◎, 30 wt. % suspension with 1.0 wt. % water added (yield value, 1500 dyn./cm²).

$$+(3\eta\dot{\gamma}/\boldsymbol{kT}\pi\phi_c)\}\sigma(\phi-\phi_{crit}) \qquad (18)$$

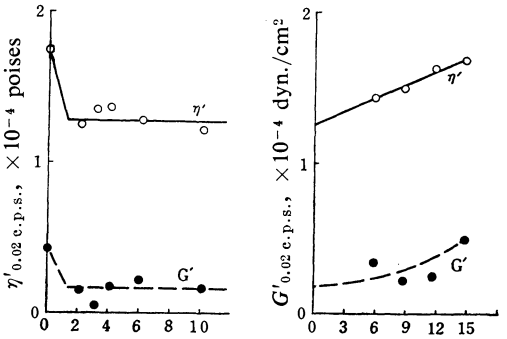
where g_1 is the mean stiffness of the primary links; τ_2, the relaxation time of the secondary links; γ_1, the mean strain of the primary links in the stationary flow; ϕ_c, the mean fraction of the volume occupied by particles in a multiple flocculate, and σ and ϕ_{crit} are the mean number of links to be broken for separating two particles and the critical concentration above which stationary links between particles would appear respectively at the shear-rate of $\dot{\gamma}$.[3] Equations 17 and 18 can be approximated by the following equations at very low rates of shear;[3]

$$\eta_{pl}=\eta_m+(g_1+g_2)\tau_2(2/\pi R_1)\sigma'(\phi-\phi'_{crit}) \qquad (17')$$

$$S_o=(2/\pi R_1)g_1\gamma_1\sigma'(\phi-\phi'_{crit}) \qquad (18')$$

In pseudo-plastic suspensions, the apparent viscosity at a zero rate of shear must be equal to the dynamic viscosity at zero frequency because, in Eqs. 17′ and 18′, γ_1 and g_1 are effectively zero and $\eta'_m(0)$ is generally equal to η_m.

In plastic suspensions, the apparent viscosity must be infinite at a zero rate of shear if a remarkable change in the structure of the network is not effected by shearing forces, whereas the dynamic viscosity has a finite value on the same time scale. Such a case is encountered in suspensions of barium sulfate in linseed oil, with a large quantity of water added. However, if the network is broken appreciably by shearing forces, the apparent viscosity may occasionally be lower than the dynamic viscosity at a finite rate of shear, as in suspensions of barium sulfate in polyisobutylene, since in Eqs. 17 and 18 σ is decreased and ϕ_{crit} is increased by shearing forces.[3] Figure 14 shows the fall of dynamic properties by shearing actions and their restoration by resting the solution in a 20 wt. % suspension of barium sulfate in polyisobutylene. The abscissas represent the number of repeated revolutions at a given rate of shear (3.78 sec^{-1}) and the resting time after 30 revolutions. In this system, it seems that the network is easily broken down by shearing actions and that it takes at least fifteen minutes for the restoration of the broken network-structure. The discrepancy between the apparent viscosity and the dynamic viscosity at lower rates of shear seems to be related to the sensitivity of the network structure to shearing forces and



(a) Structure break down with shearing actions ($\dot{\gamma}=3.78$ sec^{-1}).

(b) Structure restoration after 30 revolutions.

Fig. 14. Change in the dynamic properties with shearing conditions in 20 wt. % suspension of barium sulfate in polyisobutylene.

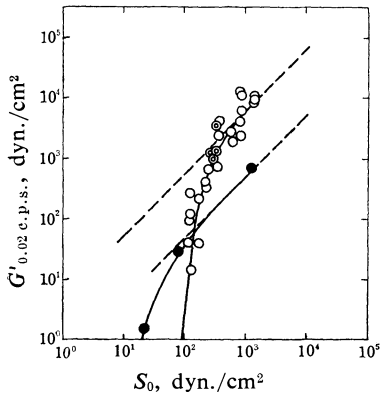


Fig. 15. Correlation between the dynamic modulus and the yield value: ○, suspensions of barium sulfate in polyisobutylene; ●, suspensions of barium sulfate in linseed oil, with water added; ◎, suspensions of barium sulfate coated by sodium stearate in linseed oil.

to the time necessary for the restoration of broken structures. Besides, it is likely that the discrepancy between viscosities is independent of the magnitude of yield value in stationary flow experiments, as is shown in Figs. 12 and 13.

The correlation of the dynamic modulus at a frequency of 0.02 c. p. s. and the yield value obtained by extrapolation to zero shear-rate in stationary flow experiments are shown in Fig. 15. The dynamic modulus apparently increases with an increase in the yield value.

According to theoretical considerations based on a network model,[3] the dynamic modulus, $G'_s(\omega)$, is given by the following equation at very small deformations:

$$G'_s(\omega) = G'_m(\omega) + (2/\pi R_1)\{g_1 + g_2\tau_2^2\omega^2/(1+\tau_2^2\omega^2)\}\sigma'(\phi - \phi'_{crit}) \quad (19)$$

where $G'_m(\omega)$ is the dynamic modulus of a medium involving particles. If the dynamic modulus of the medium is negligibly small compared to that of the network structure formed by particles at lower frequencies and if the network is not changed by shearing forces, the dynamic modulus at lower frequencies must be approximately proportional to the yield value given by Eq. 18′ at very low rates of shear. Consequently, the slope in Fig. 15 must be approximately equal to unity. In the experimental results, the slope seems to approach unity only at higher concentrations, where stronger network structures may be formed by particles. The deviation from the theoretical prediction at lower concentrations seems to be connected with the amplitude dependence of the dynamic modulus. If the network structure is sensitive to shearing forces, it is likely that the network is broken down irreversibly at lower concentrations and that the dynamic modulus decreases with an increase in the amplitude of oscillation, since measurements are made with a constant amplitude of the activating current, i_{d_0}.

In suspensions of barium sulfate in polyisobutylene, the time dependence of the apparent viscosity resembles that of the dynamic viscosity, as is shown in Fig. 13. However, it is dangerous to attribute two behaviors to the same mechanism. As has been described in a previous paper,[3] the dependence of the apparent viscosity on the rate of shear is connected with the structural changes of the network caused by shearing forces, whereas the frequency dependence of the dynamic viscosity originates mainly from the relaxation of the network structures formed by particles in the medium. For the elucidation of the correlation between the dynamic properties and stationary flow properties of concentrated suspensions, further investigation of the amplitude dependence of rheological properties is necessary.

The Amplitude Dependence of Dynamic Properties.—In unfilled media and non-flocculated systems, the dynamic properties fall well within the linear viscoelasticity at smaller amplitudes of oscillation.

In flocculated systems, however, the dynamic viscosity and the dynamic modulus inevitably decrease with an increase in the amplitude of oscillation.[16-18] Figure 16 shows the amplitude dependence of the dynamic properties in a 10 wt. % suspension of barium sulfate in polyisobutylene, with 0.5 wt. % water added. In Fig.

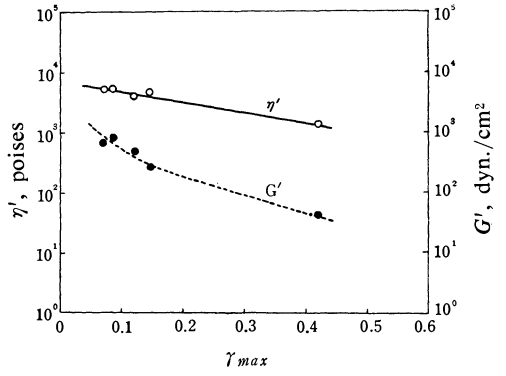


Fig. 16. Amplitude dependence of the dynamic properties in a 10 wt. % suspension of barium sulfate in polyisobutylene, with 0.5 wt. % water added, at 0.02 c.p.s.

16) M. Senō, *J. Chem. Soc. Japan, Pure Chem. Sec.* (*Nippon Kagaku Zassi*), **78**, 66 (1957).
17) R. B. Stambaugh, *Ind. Eng. Chem.*, **34**, 1358 (1942).
18) A. R. Payne, *J. Appl. Polymer Sci.*, **3**, 127 (1960).

16, the maximum shear strain at the wall of the inner cylinder, γ_{max}, is calculated as follows:[19]

$$\gamma_{max,\, r=R_i} = 2\theta_o R_o^2/(R_o^2 - R_i^2) \qquad (20)$$

The amplitude dependence of the dynamic modulus is more remarkable than that of the dynamic viscosity. The amplitude dependence of the dynamic properties in flocculated systems is caused by the structural change in the network formed by particles and by the non-linearly elastic nature of the links between particles. In a previous paper,[3] it has been theoretically pointed out that the dependence of the dynamic viscosity on amplitude mainly originates from the structural change in the network, while that of the dynamic modulus originates from both the structural change and the non-linearly elastic nature of the links between particles. According to theoretical considerations based on a network model,[3] we obtain the following approximation at lower frequencies:

$$\{G'_s(\omega) - G'_m(\omega)\}_{\dot{\gamma},f}/\{G'_s(\omega) - G'_m(\omega)\}_{\dot{\gamma},f\fallingdotseq 0} \fallingdotseq \{(g_1)_{\dot{\gamma},f}/(g_1)_{\dot{\gamma},f\fallingdotseq 0}\}\{\eta'_s(\omega) - \eta'_m(\omega)\}_{\dot{\gamma},f}/\{\eta'_s(\omega) - \eta'_m(\omega)\}_{\dot{\gamma},f\fallingdotseq 0} \qquad (21)$$

where the subscripts s and m represent the values of the suspension and the medium respectively, and $\dot{\gamma}$ and f represent the experimental conditions of the rate of shear and the shearing forces. In flocculated systems, since $G'_m(\omega)$ and $\eta'_m(\omega)$ may be negligibly small compared to $G'_s(\omega)$ and $\eta'_s(\omega)$, we have, approximately:

$$\{G'_s(\omega)\}_{\dot{\gamma},f}/\{G'_s(\omega)\}_{\dot{\gamma},f\fallingdotseq 0} \fallingdotseq \{(g_1)_{\dot{\gamma},f}/(g_1)_{\dot{\gamma},f\fallingdotseq 0}\}\{\eta'_s(\omega)\}_{\dot{\gamma},f}/\{\eta'_s(\omega)\}_{\dot{\gamma},f\fallingdotseq 0} \qquad (22)$$

Consequently, the difference between the amplitude dependences of dynamic properties, as shown in Fig. 16, may be regarded as a measure of the non-linearity of the elastic nature of the links between particles.

The experimental data given in this paper were obtained with a given amplitude of torque acting on the inner cylinder. The amplitude of the deflection of the inner cylinder was consequently decreased with an increase in the frequency. As a result of these features in dynamic properties and dynamic experiments, the apparent relaxation time of suspensions may be slightly shorter than those evaluated in the present experiments. Dynamic properties were measured with as small an amplitude as possible.

19) Th. Schwedoff, *J. de Phys.*, (2), **8**, 341 (1889).

Summary

The dynamic properties and stationary flow properties of suspensions of barium sulfate in polyisobutylene and in linseed oil have been measured by the use of an electrically-recording rotational rheometer.

The concentration dependence, the influence of mixing conditions, the effects of the addition of water and of sodium stearate on the dynamic viscosity and the dynamic modulus, and the correlation of the dynamic properties with stationary flow properties have been examined experimentally.

In suspensions of barium sulfate in linseed oil, the dynamic viscosity and dynamic modulus increase monotonously with an increasing concentration, and no critical concentration is observed up to the highest concentration. The apparent relaxation time shows a slight increase with an increase in the concentration of particles.

In suspensions of barium sulfate in polyisobutylene, the dynamic viscosity and dynamic modulus increase abruptly above a critical concentration. The apparent relaxation time also increases remarkably above the critical concentration. The mean free energy of the activation for breaking links between particles and the mean number of links to be broken for the separation of two neighboring particles have been evaluated as 33~34 kT and 1.49 respectively.

The influence of additives on dynamic properties resembles that on stationary flow properties and can be explained qualitatively by assuming a van der Waals-London attraction between particles. However, in a viscoelastic medium, contractive forces arising from the elastic property of the medium seems to be altered by the addition of additives.

For pseudo-plastic systems, the dynamic viscosity coincides with the apparent viscosity at lower frequencies. However, for plastic systems, the apparent viscosity may be higher or lower than the dynamic viscosity at lower frequencies, depending on the sensitivity of the network structures formed by particles and on the time necessary for the restoration of broken structures. The dynamic modulus at lower frequencies increases with an increase in the yield value, while the former increases proportionally to the latter at higher concentrations also.

The non-linearity of dynamic properties has been observed as a feature of their amplitude dependence. The change in the dynamic modulus is more remarkable than that in the dynamic viscosity.

The experimental results described above at least qualitatively agree with the theoretical predictions based on a network model.

The author wishes to express his cordial thanks to Professor Hirotaro Kambe for his invaluable advice and the encouragement extended to the author. Thanks are also due to the author's colleagues in the Aeronautical Research Institute, the University of Tokyo, for their stimulating discussions.

Aeronautical Research Institute
The University of Tokyo
Meguro-ku, Tokyo

The Rheological Properties of Concentrated Suspensions. IV. The Viscoelastic Properties of Concentrated Dispersions in Molten Polymers

By Masaharu TAKANO and Hirotaro KAMBE

(Received August 9, 1963)

The effects of fillers on the equilibrium modulus of solid polymers and on the viscosity of molten polymers have been studied extensively.[1-4] The viscoelastic properties of filled polymers have also been much investigated.[5-7] However, these investigations have mainly been concerned with properties in the transition region from flexible to glasslike consistency and have not attempted to extend the experiment to the molten state. Very little work has been done on the viscoelastic properties of filled molten polymers.

In the transition region, it has been observed experimentally that if particles are dispersed homogeneously and too apart from each other to be bridged by single polymer molecules, the relaxation spectrum of the polymer is essentially unaffected by the filler on the high frequency side, although it is broadened on the lower frequency side because of the suppression of the molecular motion of the polymer by dispersed particles.[6-8] In suspensions of finer particles, however, the aggregation of the particles may also complicate circumstances. In such a case, when particles approach each other, each particle may be bonded to others by single polymer molecules and the whole system may act as a highly crosslinked polymer.[3,8,9] Furthermore, additional forces, e. g., van der Waals-London attraction, should also be considered between particles. It is evident that the concentration dependence of dynamic properties cannot be described in terms of the volume-filling properties alone in concentrated dispersions of fine particles.[4,8,10]

It is the purpose of this paper to examine experimentally the dependence of the dynamic properties of concentrated dispersions in the molten polymer on the concentration, the particle size and the amplitude of oscillations.

We have studied the dynamic viscosity and the dynamic modulus of disperse systems containing fillers of various particle sizes. In order to eliminate complex chemical crosslinking, we chose an uncrosslinked polyethylene containing non-interacting fillers, that is, small glass spheres, barium sulfate powder and calcium carbonate powder.

Experimental

Materials.—The medium used in this work is a melt of a low density polyethylene, "Sumikathene F-70-6," whose number average molecular weight is 28000, with a melt index of 7, a melting temperature of 109~112°C, and a density of 0.921 g./cm^3 at 23°C.

The fillers used in this work are two kinds of barium sulfate, two kinds of calcium carbonate,

1) E. Guth, *J. Appl. Phys.*, **16**, 20 (1945).
2) H. M. Smallwood, ibid., **15**, 758 (1944).
3) A. M. Bueche, *J. Polymer Sci.*, **15**, 105 (1955); **25**, 139 (1957).
4) J. Furukawa, *Chem. High Polymer, Japan* (*Kôbunshi Kagaku*), **6**, 265 (1949).
5) S. Nohara, ibid., **12**, 527 (1955).
6) R. F. Landel, *Trans. Soc. Rheology*, **2**, 53 (1958).
7) A. R. Payne, "Rheology of Elastomers," Ed. by P. Mason and N. Wookey, Pergamon Press, London (1958).
8) J. D. Ferry, "Viscoelastic Properties of Polymers," John Wiley & Sons Inc., New York (1961).
9) P. J. Flory, *Ind. Eng. Chem.*, **38**, 417 (1946).
10) Y. Satô and J. Furukawa, *Rubber Chem. Technol.*, **35**, 857 (1962); Y. Satô, *High Polymers* (*Kôbunshi*), **7**, 396 (1958); *J. Solid State Phys.* (*Busseiron Kenkyû*), **2**, No. 2, 854, 871 (1957); **2**, No. 3, 1, 12, 274, 294, 404, 422 (1958).

and four kinds of glass spheres with various particle sizes. Calcium carbonate and barium sulfate powders were chosen because of their approximately spherical shapes and the narrow distributions of particle sizes. Besides, their dielectric constants are nearly equal to those of glass spheres and may be regarded as chemically inactive to polyethylene. The particle sizes were determined microscopically or electron-microscopically. Details of the size analyses, expressed on a statistical basis, are listed in Table I. The statistical diameters are defined as follows :[11]

Number average diameter : $d_n = \sum nd / \sum n$

Mean surface diameter : $d_s = (\sum nd^2 / \sum n)^{1/2}$

Mean volume diameter : $d_v = (\sum nd^3 / \sum n)^{1/3}$

Mean volume-surface diameter :

$$d_{vs} = (\sum nd^3 / \sum nd^2)$$

where n is the number of particles contained in a small size range, the mid value of which is d. The mean diameters were determined by measuring one hundred particles.

The Preparation of the Suspensions.—The fillers were dried at 110°C, in a vacuum of 20 mmHg, for three hours. Polyethylene was milled at 105± 2°C for two minutes prior to mixing it with particles through a plastic roll-mill, the roll of which was 3 inches in diameter, 7.5 inches long, and with revolution velocities of 18 and 20 r. p. m. After the filler had been added to the molten polyethylene, the suspension was milled for seven minutes and finished as a sheet about 2 mm. thick. A circular disk 2 cm. in diameter was cut off from the sheet and used as a specimen. The effect of the oxidation and shear degradation of polyethylene during milling on the dynamic properties seemed to be negligibly small compared to the effect of the filler. The dynamic viscosity, η', and the dynamic modulus, G', of milled polyethylene are not altered from those of raw polyethylene after 10 min. milling.

Apparatus and Methods. — The cone-and-plate rheometer used in this work has been described in detail in previous papers.[12-14] The apparatus can be used essentially as a rotationally oscillatory viscoelastometer, at small deformations. A feature of the rheometer is the completely automatic electrically detecting and recording system. The oscillatory torque is supplied to the shaft of the movable cone by a torque motor. The clearance between the cone and the plate is sufficiently large so that the dispersed particles do not interfere with the measurements. The dimensions of the assemblies of cone-and-plate and of coaxial coni-cylinders are as follows :

(a) Cone and plate : the angle between cone and plate is 9°58′, the radius of the cone is 1.002 cm. and the tip of the cone is truncated by 1/100 mm.

(b) Coaxial coni-cylinders : the angle between the conical end of the inner cylinder and the plane bottom of the outer cylinder is 19°58′, the radii of the inner and outer cylinders are 0.501 cm. and 0.951 cm. respectively, the depth of the outer cylinder is 0.683 cm. and the tip of the inner cone is truncated by 1/100 mm.

Since the assemblies are made so small in size, as has been described above, great care must be paid to the accuracy of the distance between cone and plate. The distance between the truncated cone tip and the stationary plate was held at 1/100 mm., within a margin of error of ±2/1000 mm., by using a micrometer unit with an electric contact. The shape factor was determined experimentally. The dynamic viscosity and the dynamic modulus were calculated from the amplitude ratio and the phase lag between the recorded curves of torque and deflection.

Experiments were made at a torsional constant of 2.39×10^4 dyn.-cm./rad. In this case, the moment of inertia of the oscillatory unit was 50± 0.5 dyn.-cm.-sec^2/rad., the amplitude of the angular deflection of the cone was below 4 degrees, and the amplitude of the torque could be varied from 0 to 3×10^3 dyn.-cm. The dynamic viscosity, η', and the dynamic modulus, G', were measured at frequencies from 1/100 to 75/100 c. p. s. The temperature was varied from 155 to 230°C within a margin of error of ±1°C. During the experiments a stream of hot nitrogen gas was supplied to the atmosphere in order to avoid the rapid oxidation of the specimen.

Experimental Results

The Thixotropic Behavior of Filled Systems.—In such a highly viscous medium as molten polyethylene, the state of the dispersion of particles seems to be determined essentially by the mechanical conditions of milling. The dynamic viscosity and the dynamic modulus of filled systems changed almost not at all during measurements in suspensions of glass spheres and in those of calcium carbonate of larger particle sizes. Table II and Fig. 1 show the time dependence of dynamic properties in a suspension of calcium carbonate. In suspensions of barium sulfate of finer particles, however, the dynamic viscosity and the dynamic modulus increased with time under periodic strains. Figure 2 shows the change in dynamic properties with time in such a filled system. Measurements were made with a given amplitude of torque, 1.8×10^3 dyn.-cm., in an atmosphere of nitrogen gas. The increase in the dynamic viscosity and in the modulus is not due to any chemical changes in the specimen but to structural changes in the network formed by the agglomeration of particles in such a highly viscous medium. No gel fraction could be obtained practically

11) G. F. Eveson, *J. Oil and Colour Chem. Assoc.*, **40**, 456 (1957).
12) H. Kambe, *J. Japan Soc. Test. Matls. (Zairyô Sikiken)*, **8**, 354 (1959).
13) H. Kambe and M. Takano, *Rept. Aeronaut. Res. Inst., Univ. Tokyo*, **28**, 159 (Rept. No. 377, 1963).
14) H. Kambe and M. Takano, ibid., **28**, 175 (Rept. No. 378, 1963).

TABLE I. CHARACTERISTICS OF FILLERS

Filler	Glass sphere				$CaCO_3$		$BaSO_4$	
	I	II	III	IV	I	II[a)]	I	II
Number average diameter, μ	91.1	49.5	32.3	24.0	2.28	0.04	0.265	0.075
Mean surface diameter, μ	91.5	51.2	32.9	24.8	2.65	—	0.283	0.079
Mean volume diameter, μ	92.2	52.0	33.8	25.6	2.99	—	0.311	0.082
Mean volume-surface diameter, μ	93.5	53.5	35.6	27.3	3.80	—	0.375	0.088
Density at 25°C g./cm^3	2.36				2.71		4.47	
Dielectric constant e. s. u.	7～10[b)]				8.8[c)]～9.15[d)]		10.2～10.25[e)]	

a) Hakuenka CC (calcium carbonate coated by calcium stearate).
b) F. Keller, *Z. tech. Physik.*, **13**, 237 (1932) ; A. Güntherschulze and F. Keller, *Z. Physik.*, **75**, 78 (1932).
c) F. Wachholtz and A. Franceson, *Kolloid Z.*, **92**, 75 (1940).
d) P. Schupp, *Z. Physik.*, **75**, 84 (1932).

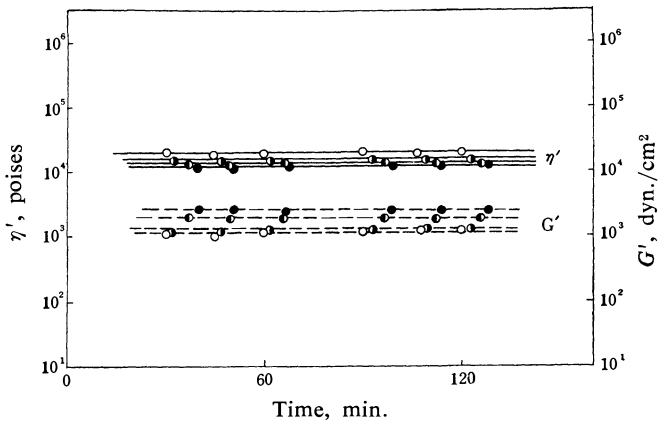


Fig. 1. Change in the viscoelastic properties with time in 28.6 wt.% suspension of calcium carbonate-I in polyethylene (210°C) : ○, 0.02 c. p. s.; ◑, 0.05 c. p. s.; ◐, 0.08 c. p. s.; ●, 0.10 c. p. s.

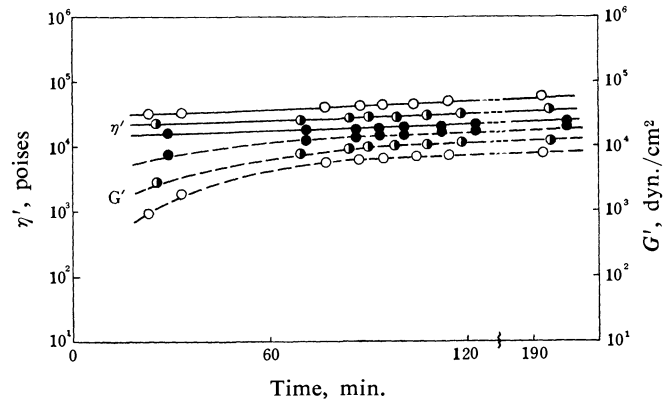


Fig. 2. Change in the viscoelastic properties with time in 28.6 wt.% suspension of barium sulfate-II in polyethylene (210°C) : ○, 0.02 c. p. s.; ◑, 0.05 c. p. s.; ●, 0.10 c. p. s.

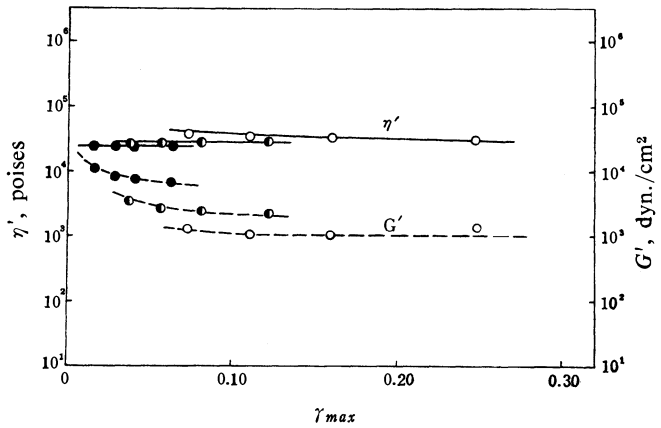


Fig. 3. Amplitude dependence of the viscoelastic properties in 60 wt. % suspension of calcium carbonate-I in polyethylene (210°C) : ○, 0.02 c. p. s.; ◐, 0.05 c. p. s.; ●, 0.10 c. p. s.

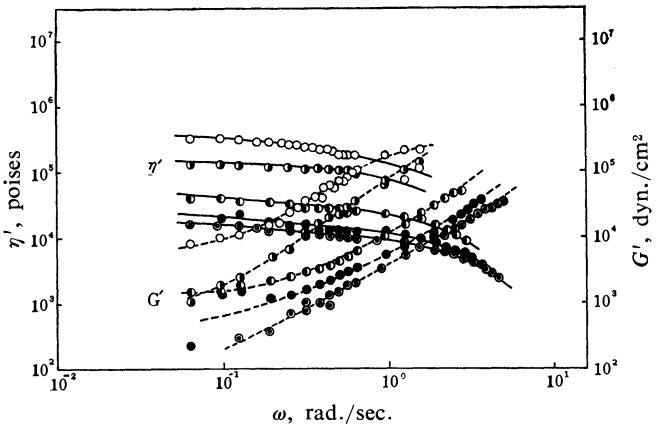


Fig. 4. Dependence of the viscoelastic properties on the concentration and the frequency in suspensions of glass sphere-I in polyethylene (200°C) : ⊙, 0 wt.%; ●, 28.6 wt.%; ◐, 60.0 wt.%; ◑, 75.0 wt.%; ○, 80 wt.%.

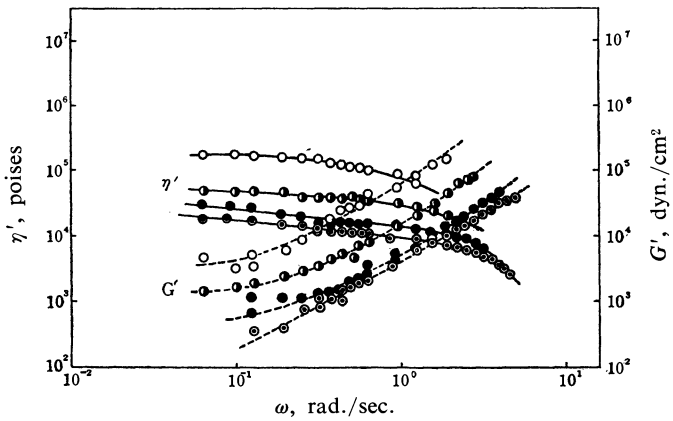


Fig. 5. Dependence of the viscoelastic properties on the concentration and the frequency in suspensions of glass sphere-IV in polyethylene (200°C) : ⊙, 0 wt.%; ●, 28.6 wt.%; ◑, 60.0 wt.%; ○, 75.0 wt.%.

TABLE II. DEPENDENCE OF DYNAMIC PROPERTIES ON TIME

(a) 28.6 wt.% suspension of calcium carbonate-I in polyethylene (210°C)

Frequency, c. p. s.	0.02				0.05		
Time min.	γ_{max}	$G'\times10^{-3}$ dyn./cm^2	$\eta'\times10^{-4}$ poises	Time min.	γ_{max}	$G'\times10^{-3}$ dyn./cm^2	$\eta'\times10^{-4}$ poises
30	0.212	1.02	1.86	32	0.146	1.12	1.41
45	0.233	0.90	1.68	47	0.151	1.13	1.37
60	0.220	1.07	1.82	62	0.153	1.12	1.37
90	0.213	1.11	1.94	93	0.148	1.10	1.42
107	0.214	1.15	1.88	109	0.147	1.17	1.43
120	0.212	1.15	1.89	123	0.155	1.05	1.33
Frequency, c. p. s.	**0.08**				**0.10**		
Time min.	γ_{max}	$G'\times10^{-3}$ dyn./cm^2	$\eta'\times10^{-4}$ poises	Time min.	γ_{max}	$G'\times10^{-3}$ dyn./cm^2	$\eta'\times10^{-4}$ poises
37	0.101	1.99	1.27	39	0.090	2.59	1.18
49	0.109	1.75	1.24	51	0.091	2.42	1.18
67	0.106	1.84	1.25	68	0.091	2.36	1.22
97	0.102	1.82	1.33	99	0.089	2.41	1.23
112	0.107	1.68	1.25	114	0.091	2.36	1.20
126	0.109	1.73	1.23	128	0.093	2.09	1.19

(b) 28.6 wt.% suspension of barium sulfate-II in polyethylene (210°C)

Frequency, c. p. s.	0.02				0.05		
Time min.	γ_{max}	$G'\times10^{-3}$ dyn./cm^2	$\eta'\times10^{-4}$ poises	Time min.	γ_{max}	$G'\times10^{-3}$ dyn./cm^2	$\eta'\times10^{-4}$ poises
23	0.113	0.96	3.04	25	0.063	2.81	2.18
33	0.104	1.81	3.07	69	0.045	7.63	2.30
77	0.065	5.47	3.76	84	0.041	8.35	2.52
87	0.061	5.94	3.80	90	0.040	8.85	2.59
94	0.060	6.02	4.05	98	0.038	9.39	2.49
104	0.054	7.23	4.14	108	0.036	9.88	2.76
114	0.051	7.22	4.83	118	0.034	11.1	2.74
192	0.050	7.10	5.49	195	0.031	10.3	3.83
Frequency, c. p. s.	**0.10**						
Time min.	γ_{max}	$G'\times10^{-3}$ dyn./cm^2	$\eta'\times10^{-4}$ poises				
29	0.036	7.52	1.69				
71	0.030	11.9	1.66				
86	0.028	13.8	1.64				
93	0.026	15.4	1.66				
101	0.026	14.4	1.88				
112	0.024	16.6	1.72				
122	0.022	17.8	1.93				
200	0.020	20.3	2.16				

in hot tetralin. Furthermore, the dependence of dynamic properties on the amplitude was examined, since dynamic properties at lower frequencies are very sensitive to structural change in a network formed by particles.[15-17] Table III shows typical data of the amplitude dependence of dynamic properties in various suspensions. The maximum shear strain, γ_{max}, is defined as follows:[18] in an assembly of cone and plate,

$$\gamma_{max}=\theta_o/\beta$$

and in an assembly of coaxial cylinders,

$$\gamma_{max}=2\theta_o R_o^2/(R_o^2-R_i^2)$$

where θ_o is the amplitude of deflection; β, the angle between cone and plate, and R_i and R_o, the radii of the inner and the outer cylinder respectively.

15) A. R. Payne, *J. Appl. Polymer Sci.*, 3, 127 (1960).
16) M. Senō, *J. Chem. Soc., Japan Pure Chem. Sec.* (*Nippon Kagaku Zassi*), **78**, 66 (1957).
17) M. Takano, This Bulletin, **36**, 1418 (1963).
18) Th. Schwedoff, *J. de Phys.*, (2), **8**, 341 (1889).

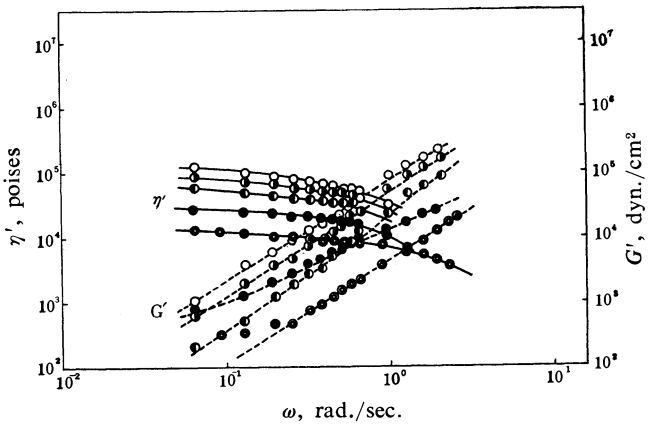


Fig. 6. Dependence of the viscoelastic properties on the concentration and the frequency in suspensions of calcium carbonate-I in polyethylene (210°C) : ◎, 0 wt.%; ●, 16.7 wt.%; ◐, 54.5 wt.%; ◑, 60.0 wt.%; ○, 66.7 wt.%.

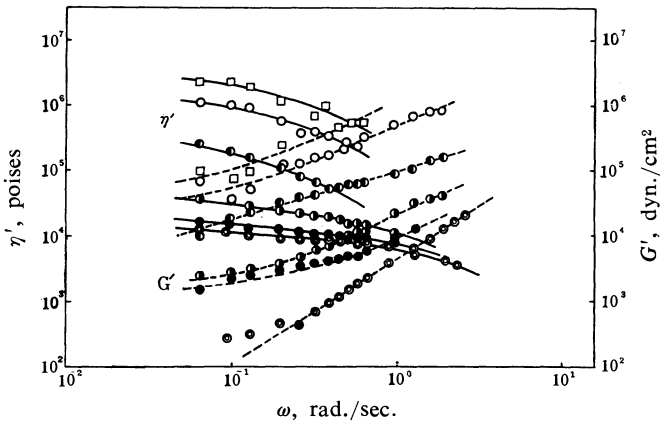


Fig. 7. Dependence of the viscoelastic properties on the concentration and the frequency in suspensions of barium sulfate-II in polyethylene (210°C) : ◎, 0 wt.%; ●, 16.7 wt.%; ◑, 28.6 wt.%; ◐, 37.5 wt.%; ○, 44.4 wt.%; □, 50.0 wt.%.

Whereas in the dynamic properties of suspensions at lower concentrations the linearity of viscoelasticity holds well, the dynamic properties of concentrated suspensions depend on the amplitude, even at very small deformations.[15,19] The dynamic viscosity and modulus seem to fall off with an increase in amplitude beyond a kind of yield strain whose magnitude depends on the concentration and on the particle size of the filler. These phenomena coincide with a common characteristic of thixotropic systems, the breaking of certain linkages strained beyond their elastic limits.

As the viscoelastic properties depend on their mechanical history in such thixotropic systems, great care must be paid to the mechanical conditions of preparation and experimentation. In suspensions of glass spheres and of calcium carbonate of larger particle sizes, the dependence of the dynamic modulus on the amplitude of oscillation is more remarkable than that of the dynamic viscosity, as is shown in Table III and Fig. 3. According to theoretical considerations based on a network model,[17] the decrease in dynamic viscosity is mainly due to structural changes in the network formed by particles, while the decrease in dynamic modulus is due to both the structural change in the network and the nonlinear characteristics of the links between particles.

The Dependence of Dynamic Properties on the Concentration and Frequency.—As has been described above, dynamic properties depend on the amplitude of oscillation as well as on the frequency and concentration of filler, especially

19) R. B. Stambaugh, *Ind. Eng. Chem.*, **34**, 1358 (1942).

TABLE III. DEPENDENCE OF DYNAMIC PROPERTIES ON AMPLITUDE OF OSCILLATION

(a) 75 wt.% suspensions of glass spheres in polyethylene (200°C)

Filler		I			II	
Frequency, c. p. s.		0.02			0.02	
	γ_{max}	$G'\times10^{-3}$ dyn./cm²	$\eta'\times10^{-4}$ poises	γ_{max}	$G'\times10^{-3}$ dyn./cm²	$\eta'\times10^{-4}$ poises
	0.130	2.98	13.8	0.135	3.41	12.3
	0.109	2.00	11.3	0.115	3.12	12.6
	0.107	3.54	14.1	0.110	2.39	11.1
	0.098	2.20	12.6	0.100	3.36	12.3
	0.085	3.46	14.7	0.070	3.54	12.7
	0.058	3.88	14.0	0.044	3.57	11.8
Filler		III			IV	
Frequency, c. p. s.		0.02			0.02	
	γ_{max}	$G'\times10^{-3}$ dyn./cm²	$\eta'\times10^{-4}$ poises	γ_{max}	$G'\times10^{-3}$ dyn./cm²	$\eta'\times10^{-4}$ poises
	0.107	7.82	13.6	0.115	4.67	16.2
	0.092	8.35	13.6	0.101	4.34	15.8
	0.086	6.34	12.8	0.086	4.35	15.7
	0.081	6.82	13.7	0.082	4.63	17.0
	0.059	6.39	13.1	0.056	5.07	17.3
	0.041	6.73	12.8	0.039	5.67	15.4

(b) Suspensions of calcium carbonate-I in polyethylene (210°C)

Concn. of filler wt.%		28.6			60.0	
Frequency, c. p. s.		0.02			0.02	
	γ_{max}	$G'\times10^{-3}$ dyn./cm²	$\eta'\times10^{-4}$ poises	γ_{max}	$G'\times10^{-3}$ dyn./cm²	$\eta'\times10^{-4}$ poises
	0.357	0.343	1.52	0.249	1.39	3.22
	0.234	0.973	1.70	0.160	0.99	3.31
	0.206	0.484	1.52	0.110	1.05	3.43
	0.181	1.02	1.52	0.073	1.30	3.59
	0.135	1.26	1.36			
Concn. of filler wt.%		60.0			60.0	
Frequency, c. p. s.		0.05			0.10	
	γ_{max}	$G'\times10^{-3}$ dyn./cm²	$\eta'\times10^{-4}$ poises	γ_{max}	$G'\times10^{-3}$ dyn./cm²	$\eta'\times10^{-4}$ poises
	0.122	2.22	2.96	0.063	6.74	2.49
	0.081	2.47	2.88	0.040	8.01	2.62
	0.056	2.71	2.93	0.028	8.25	2.53
	0.037	3.34	2.74	0.016	10.4	2.40

(c) Suspensions of barium sulfate-II in polyethylene (210°C)

Concn. of filler wt.%		28.6			60.0	
Frequency, c. p. s.		0.02			0.02	
	γ_{max}	$G'\times10^{-3}$ dyn./cm²	$\eta'\times10^{-4}$ poises	γ_{max}	$G'\times10^{-3}$ dyn./cm²	$\eta'\times10^{-4}$ poises
	0.139	7.60	2.79	0.017	7.59	25.4
	0.104	7.40	3.46	0.008	15.2	46.6
	0.069	8.55	3.01	0.007	21.2	63.1
	0.053	8.57	3.53	0.005	16.0	142.0
	0.038	8.93	3.08	0.004	18.8	121.0
				0.004	14.3	101.0

TABLE IV. DEPENDENCE OF DYNAMIC PROPERTIES ON CONCENTRATION

(a) Suspensions of glass spheres in polyethylene (0.02 c. p. s., 200°C)

Filler	I			II		
Concn. wt.%	γ_{max}	$G' \times 10^{-3}$ dyn./cm²	$\eta' \times 10^{-4}$ poises	γ_{max}	$G' \times 10^{-3}$ dyn./cm²	$\eta' \times 10^{-4}$ poises
0		0.65	1.51			
16.7	0.213	0.75	1.50	0.193	1.49	2.60
28.6	0.178	6.09	3.19	0.200	0.24	2.74
28.6*	0.177	1.66	2.64	0.223	0.28	2.26
44.5	0.176	2.71	2.40	0.199	0.70	3.00
54.5	0.208	0.87	2.63	0.197	1.09	4.40
60.0	0.179	2.13	3.72	0.183	1.60	4.54
61.5	0.176	1.99	3.74	0.184	1.41	4.27
66.7	0.186	0.74	4.07	0.160	1.45	6.04
75.0	0.088	2.20	12.6	0.083	2.39	11.1
80.0	0.054	7.14	28.8	—	—	—

Filler	III			IV		
Concn. wt.%	γ_{max}	$G' \times 10^{-3}$ dyn./cm²	$\eta' \times 10^{-4}$ poises	γ_{max}	$G' \times 10^{-3}$ dyn./cm²	$\eta' \times 10^{-4}$ poises
16.7	0.214	0.57	1.91	0.208	1.15	2.16
28.6	0.210	0.62	3.06	0.206	1.20	2.78
28.6*	0.222	0.42	2.35	0.204	0.72	2.72
44.5	0.231	0.19	2.48	0.195	1.08	3.36
54.5	0.196	0.23	3.57	0.206	0.64	3.78
60.0	0.191	1.12	4.24	0.171	1.74	4.50
61.5	0.192	0.63	4.56	0.190	0.72	4.97
66.7	0.173	0.93	5.73	0.182	1.03	5.36
75.0	0.093	6.34	12.8	0.085	4.35	15.7
80.0	0.056	12.1	25.2	—	—	—

* Prepared under the same condition with the other.

(b) Suspensions of calcium carbonate in polyethylene (0.02 c. p. s., 210°C)

Filler	I		
Concn. wt.%	γ_{max}	$G' \times 10^{-3}$ dyn./cm²	$\eta' \times 10^{-4}$ poises
0		0.55	1.33
16.7	0.229	1.36	2.31
28.6	0.209	1.07	3.05
28.6*	0.153	1.25	3.46
37.5	0.186	1.00	4.04
44.5	0.167	0.55	3.96
44.5*	0.169	1.09	3.85
50.0	0.118	0.46	5.32
54.5	0.196	0.49	4.58
60.0	0.093	2.09	7.11
66.7	0.078	3.87	9.10
66.7*	0.080	7.04	7.56
73.3	0.041	21.3	15.2
	0.037	26.3	22.7
	0.019	30.4	46.7
80.0	0.007	58.3	134.0
	0.005	99.2	164.0

Filler II

Concn. wt.%	γ_{max}	$G' \times 10^{-3}$ dyn./cm²	$\eta' \times 10^{-4}$ poises
18.8	0.272	1.20	1.54
	0.113	0.93	1.41
	0.027	1.32	1.13
31.7	0.014	46.5	42.8
	0.005	29.3	50.2
41.2	0.0044	269.0	154.0
	0.0037	445.0	146.0
48.4	0.0022	550.0	760.0
	0.0018	757.0	453.0
	0.0015	179.0	325.0

* Prepared under the same condition with the other.

(c) Suspensions of barium sulfate in polyethylene (0.02 c. p. s., 210°C)

Filler I

Concn. wt.%	γ_{max}	$G' \times 10^{-3}$ dyn./cm²	$\eta' \times 10^{-4}$ poises
0		0.55	1.33
16.7	0.220	1.17	2.55
27.5	0.227	1.23	2.37
43.2	0.221	1.75	3.09
60.3	0.016	124.0	49.5
69.7	0.004	424.0	398.0

Filler II

Concn. wt.%	γ_{max}	$G' \times 10^{-3}$ dyn./cm²	$\eta' \times 10^{-4}$ poises
16.7	0.152	2.65	1.22
28.6	0.069	8.55	3.01
	0.038	8.93	3.08
37.5	0.030	28.6	13.6
	0.022	27.8	14.1
44.5	0.007	41.7	93.5
	0.006	138.0	86.1
50.0	0.007	81.4	86.3
	0.002	90.2	184.0
54.5	0.003	282.0	252.0
	0.003	258.0	201.0
60.0	0.004	143.0	101.0
	0.003	239.0	278.0
66.7	0.007	134.0	95.2
	0.003	235.0	324.0

in thixotropic systems. In such filled systems, therefore, it is very difficult to obtain the exact frequency dependence of dynamic properties, independent of the amplitude. Figures 4—7 show the frequency dependence of the dynamic viscosity and the dynamic modulus obtained by a given amplitude of torque in the range of $1.6 \sim 2.0 \times 10^3$ dyn.-cm. at various concentrations and in various suspensions.

In suspensions of glass spheres, the amplitude dependence of the dynamic properties may be ignored within the range of experimental error of $\pm 10\%$, as shown in Table III. In suspensions of calcium carbonate and barium sulfate of smaller particle sizes, the dependence of the dynamic properties on the amplitude exceeds the range of experimental error because of their thixotropic nature. In the latter case, therefore, the frequency dependence curve represents only a qualitative tendency.

However, it is evident that the dynamic modulus at lower frequencies increases with an increase in the concentration of filler, and that the superposition of the frequency dependence curves with respect to the concentration

of filler can not be made as simply as was done in polymer solutions by Ferry.[20] Table IV shows the concentration dependence of the dynamic properties of suspensions of glass spheres, calcium carbonate and barium sulfate at a given frequency, 0.02 c. p. s. In order to confirm the reproducibility of these data, some suspensions were prepared twice; the dynamic viscosity and modulus were then measured under nearly the same mechanical conditions. In thixotropic suspensions, it is essentially impossible to obtain the limiting values of dynamic properties independent of the mechanical history. In thixotropic suspensions of calcium carbonate-I, the particles are relatively large and the restoration of the network broken by shearing forces requires a long time; therefore, the dynamic viscosity and modulus of these systems fall off appreciably after large deformations. The data listed in Table IV were obtained with as small a strain as possible. In suspensions of barium sulfate-II, the dynamic viscosity and modulus increase with time, as has been described above; therefore, data were obtained after heating the suspension for about two hours. By conditioning the system in such a way, the scattering of data could be reduced tolerably. Figures 8 and 9 show the dependence of the dynamic viscosity and the dynamic modulus at a given frequency, 0.02 c. p. s., on the volume fraction of the filler. The volume fraction of the filler has been calculated by assuming that the density of molten polyethylene is 0.76 g./cm^3 at 200~210°C;[21,22] the thermal expansion of the filler may be ignored, as the volume expansion of the filler is negligibly small compared to that of the polymer.

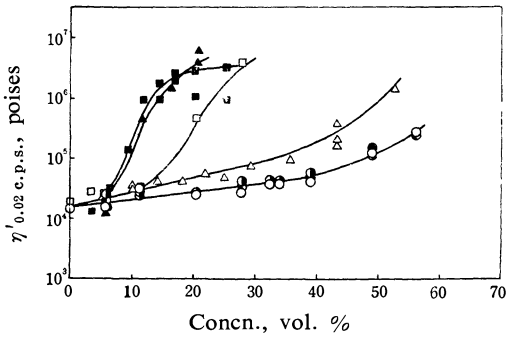


Fig. 8. Dependence of the dynamic viscosity on the concentration, at 0.02 c. p. s., in various suspensions: ○, glass sphere-I; ◑, glass sphere-II; ◐, glass sphere-III; ●, glass sphere-IV; △, calcium carbonate-I; ▲, calcium carbonate-II; □, barium sulfate-I; ■, barium sulfate-II.

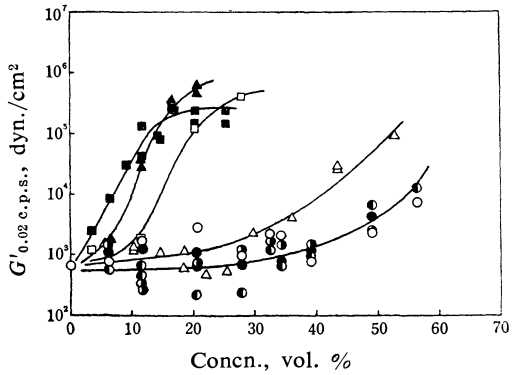


Fig. 9. Dependence of the dynamic modulus on the concentration, at 0.02 c. p. s., in various suspensions: ○, glass sphere-I; ◑, glass sphere-II; ◐, glass sphere-III; ●, glass sphere-IV; △, calcium carbonate-I; ▲, calcium carbonate-II; □, barium sulfate-I; ■, barium sulfate-II.

In suspensions of glass spheres, the concentration dependence of the dynamic viscosity at a frequency of 0.02 c. p. s. closely follows a generalized Robinson formula:[23,24]

$$\ln(\eta'/\eta'_0) = K\phi/(1-S'\phi)$$

where η'_0 is the dynamic viscosity of an unfilled polymer; ϕ, the volume fraction of the filler, and K and S', 2.5 and 1/0.74 respectively. The concentration dependence of the dynamic modulus resembles that of the dynamic viscosity.

In thixotropic suspensions of calcium carbonate and barium sulfate, the concentration dependence of the dynamic viscosity can not be represented by such a simple formula. The dynamic viscosity and the modulus increase more remarkably with an increase in the concentration. In suspensions of finer particles, the dynamic viscosity and the modulus suddenly increase beyond a sort of critical concentration. In suspensions of glass spheres of larger particles, no such critical concentration could be observed up to the highest concentration used in our experiments. In suspensions of calcium carbonate of an intermediate particle size, also, no such critical concentration could be observed. It is evident that the critical concentration depends on the particle size and that the effect of a filler on the dynamic properties of molten polymer can not be described in terms of the volume-filling properties alone. Although the filler used in

20) J. D. Ferry, *J. Am. Chem. Soc.*, **72**, 3746 (1950).

21) I. Sakurada and A. Nakajima, *Chem. High Polymer, Japan* (*Kôbunshi Kagaku*), **3**, 91 (1946).

22) F. C. Hahn, M. L. Macht and D. A. Fletcher, *Ind. Eng. Chem.*, **37**, 526 (1945).

23) J. V. Robinson, *Trans. Soc. Rheology*, **1**, 15 (1957).

24) M. Mooney, *J. Colloid Sci.*, **6**, 162 (1951).

TABLE V. APPARENT COEFFICIENTS OF TEMPERATURE DEPENDENCE OF DYNAMIC VISCOSITY AT 0.02 c. p. s.

(a) Suspensions of glass spheres in polyethylene (200°C)

Filler	I	II	III	IV
Concn. wt.%	ΔH kcal./mol.	ΔH kcal./mol.	ΔH kcal./mol.	ΔH kcal./mol.
0	11(11)			
54.5	10(16)	13(15)	12(16)	13(14)
60.0	12(13)	13(15)	11(14)	13(17)
61.5	14(14)	12(13)	14(16)	13(17)
66.7	14(21)	12(13)	—(16)	13(17)
75.0	15(16)	16(18)	15(14)	13(17)
80.0	16(18)	—	11(14)	—

(b) Suspensions of calcium carbonate and barium sulfate in polyethylene (210°C)

Filler	Calcium carbonate-I	Barium sulfate-II
Concn. wt.%	ΔH kcal./mol.	ΔH kcal./mol.
0	11	
16.7	11	11(15)
28.6	—	18(22)
37.5	—	7(13)
44.5	12	5(13)
54.5	12	—

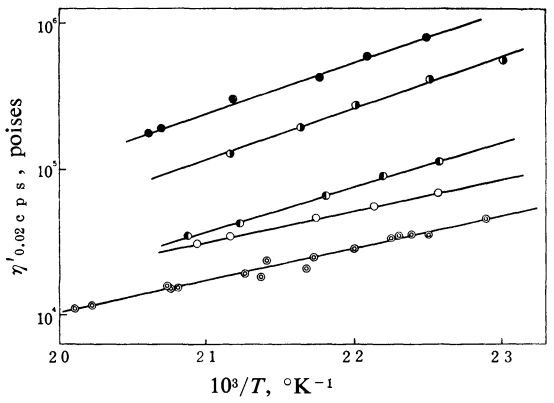


Fig. 10. Temperature dependence of the dynamic viscosity at 0.02 c. p. s. for suspensions of glass sphere-I in polyethylene with various concentrations : ◎, 0 wt.% ; ○, 54.5 wt.% ; ◐, 66.7 wt.% ; ◑, 75.0 wt.% ; ●, 80.0 wt.%.

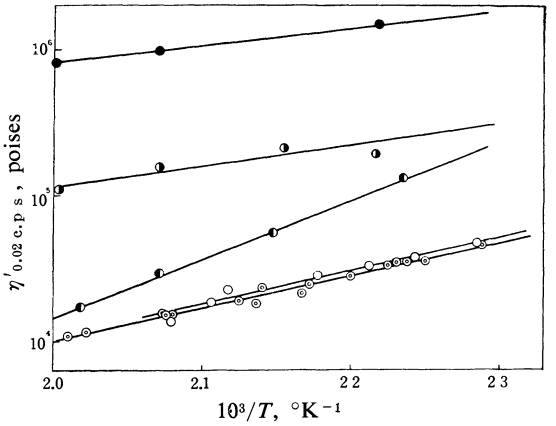


Fig. 11. Temperature dependence of the dynamic viscosity at 0.02 c. p. s. for suspensions of barium sulfate-II in polyethylene with various concentrations : ◎, 0 wt.% ; ○, 16.7 wt.% ; ◐, 28.6 wt.% ; ◑, 37.5 wt.% ; ●, 44.5 wt.%.

the present experiment has a perfectly or approximately spherical shape, the shape of particles also seems to have a great influence on the concentration dependence of dynamic properties, as our other experiments have discovered.

The Dependence of Dynamic Properties on the Temperature. — According to the experimental results described above, it is evident that particles aggregate in concentrated suspensions of finer particles, whether they are covered by polymer molecules or not. An examination of the temperature dependence of dynamic properties will present information on the nature of links between particles. Figures 10 and 11 show the temperature dependence of the dynamic viscosity at a frequency of 0.02 c. p. s. The coefficients of the temperature dependence of the dynamic viscosity calculated from the slopes of the above curves are listed in Table V. However, these values are not the true activation energies

for a viscous flow at zero rate of shear, because the dynamic viscosity depends on the frequency and the temperature. Therefore, they are only approximate values of the activation energies for flow. The values in parentheses have been approximately calculated from the temperature dependence of the shift factor as determined by the frequency dependence curves at 200 or 210°C and by the dynamic properties at a frequency of 0.02 c. p. s. at various temperatures. As Table V shows, the apparent coefficients of the temperature dependence for a viscous flow in various suspensions agree approximately with that of unfilled polyethylene. Consequently, in suspensions of finer particles, it is likely that dispersed particles are covered by polymer molecules and are bridged by single molecules at higher concentrations.

Discussion

As is shown in Figs. 8 and 9, the dynamic properties depend appreciably on the particle size of the filler. The effect of particle size on the melt viscosity and on the elasticity of rubber has been discussed by Furukawa[4] and Bueche[3] in detail. However, according to Furukawa's theory, the logarithmic relative viscosity of filled molten polymer must be proportional to the specific surface area and to the volume ratio of dispersed particles to polymer:

$$\ln(\eta/\eta_0) = (a+b/\boldsymbol{RT})(1+SM/\alpha A\rho)X$$

where η and η_0 are the viscosities of filled and unfilled polymers; a and b are constant; M is the molecular weight of the polymer; ρ, the density of the polymer; α, the surface area occupied by an adsorbed polymer molecule; $\boldsymbol{R}$, the gas constant; A, Avogadro's constant; S, the specific surface area per unit volume, and X, the volume ratio of the filler to the polymer. The dynamic viscosity at lower frequencies may be approximately equal to the melt viscosity. Figure 12 shows the relation of the relative dynamic viscosity at a frequency of 0.02 c. p. s. to the volume ratio of the filler. The linear relation expected by Furukawa's theory can not be observed, even in the suspensions of glass spheres of larger particle sizes. This means that the effect of the filler on the dynamic viscosity at small strains can not be described only in terms of an increase in the volume of particles caused by adsorbed polymer molecules but that it is rather closely connected with the network structure formed by particles bridged by single polymer molecules. Bueche has suggested that the effective number, ν, of polymer segments

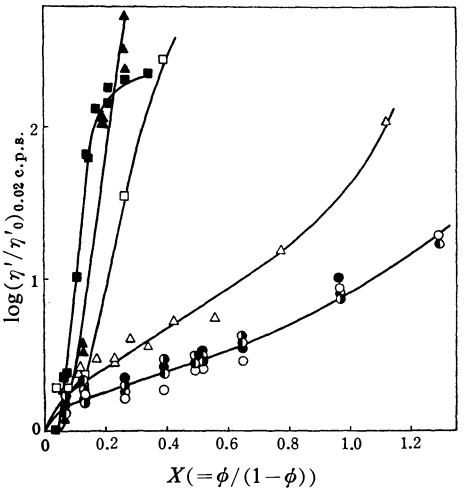


Fig. 12. Relation between the relative dynamic viscosity at 0.02 c.p.s. and the volume ratio of filler to polymer: ○, glass sphere-I; ◑, glass sphere-II; ◐, glass sphere-III; ●, glass sphere-IV; △, calcium carbonate-I; ▲, calcium carbonate-II; □, barium sulfate-I; ■, barium sulfate-II.

which can act as a molecular spring is given by the following equation:

$$\nu = N\{(1-1/N)^n - (1-n/N)\}$$

where N is the number of linear polymer molecules and n, the number of points of adherence. In the case of spherical particles with the radius r, we have:[3]

$$n = 3fv_2/r$$

and

$$N = \rho v_1/m$$

where f is the number of points of adherence per unit area; m, the mass of a polymer molecule, and v_1 and v_2 the volume fractions of the polymer and the filler respectively. Bueche's theory predicts that the first few filler particles will be relatively ineffective and that at higher concentrations the number of molecular springs will approach[3]

$$\nu = n - N = 3fv_2/r - \rho v_1/m$$

The critical volume ratio beyond which dynamic viscosity and modulus increase appreciably is, therefore, given by:

$$X_c = \rho r/3mf = A\rho r/3Mf$$

As $\rho = 0.76$ and $M = 2.8\times10^4$ in the present experiments, we have

$$X_c = 2.73\times10^{18}d/f$$

and

$$1/f = 3.66\times10^{-19}X_c/d$$

where d is the mean volume-surface diameter of the particles.

In suspensions of barium sulfate-II and -I, the values of X_c are 0.06 and 0.12 respectively, as shown in Figs. 8 and 9. Therefore, the surface area necessary for one point of adherence, $1/f$, are 25 Å^2 and 12Å^2 for barium sulfate-II and -I respectively. In suspensions of calcium carbonate-II, X_c is 0.06, and so the value of $1/f$ is 55Å^2. The value of $1/f$ seems to be decreased by a decrease in the particle size. If we assume that the surface area necessary for one point of adherence, $1/f$, is 10Å^2 for particles larger than that of calcium carbonate-I, the critical volume ratio, X_c, is expected to be 0.72 in suspensions of calcium carbonate-I. In suspensions of glass spheres, the critical volume ratio, X_c, is expected to be near to the closest packing.

Furthermore, if particles are covered by polymer molecules and are bridged partially by single molecules, it is expected that the dynamic viscosity and the modulus will increase as the mean distance between the surfaces of the particles approaches the molecular dimension of the polymer. Assuming that the particles of calcium carbonate and barium sulfate have also a perfectly spherical shape, we can calculate the mean distance between the surfaces of particles, δ_m, by the following equation:

$$\delta_m = d\{(\phi_c/\phi)^{1/3} - 1\}$$

where ϕ_c is the volume fraction at the closest packing, 0.7405. Figure 13 shows the relation of the relative dynamic viscosity at a frequency of 0.02 c. p. s. to the mean distance between the surfaces of the particles at the various concentrations, 6.1, 11.4, 20.5 and 27.9 vol. %. The root-mean square end-to-end separation of polyethylene, the number average molecular weight of which is 28000, is 97Å, and the end-to-end separation at maximum extension is 2540 Å.[25] The relative dynamic viscosity apparently increases as the mean distance between the surfaces of particles approaches the molecular dimension of the polymer. Therefore, it may be concluded that the dispersed particles are covered by polymer molecules and that in suspensions of finer particles they are partially bridged by single molecules.

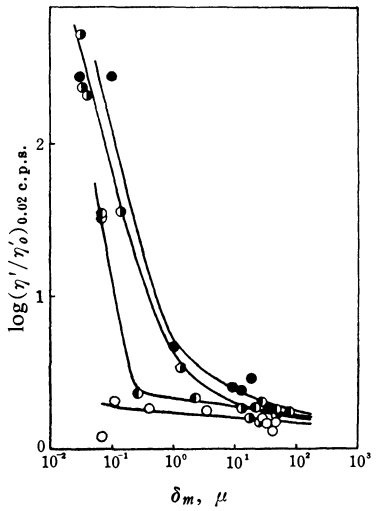


Fig. 13. Relation between the relative dynamic viscosity at 0.02 c. p. s. and the mean distance between surfaces of particles: ○, 6.1 vol.%; ◐, 11.4 vol.%; ◑, 20.5 vol.%; ●, 27.9 vol.%.

If particles sufficiently approach each other, the van der Waals-London attraction may also be considered among neighboring particles. The energy of interaction between two neighboring particles covered by polymer molecules is given by the following equation;[26]

$$\Delta F = (A_m^{1/2} - A_p^{1/2})^2 d/24(\delta + 2\Delta)$$

where A_m and A_p are the Hamaker parameters of the medium and of the particles respectively, Δ is the thickness of the layer of bound polymer molecules, and δ, the distance of the closest approach of the covered surfaces. The magnitudes of the Hamaker parameters A_m and A_p evaluated from the dielectric constants of the polymer and of the particles are approximately 2×10^{-12} and 6×10^{-13} ergs.[27]

Therefore, the energy of interaction due to the van der Waals-London attraction is

$$\Delta F = 1.70\times10^{-14} d/(\delta + 2\Delta)$$

and the additional shear modulus due to the van der Waals-London attraction, ΔG, is

$$\Delta G \fallingdotseq N_a(d+2\Delta)(d^2\Delta F/d\delta^2)/3$$
$$= 1.13\times10^{-14} N_a(d+2\Delta)d/(\delta+2\Delta)^3$$

where N_a is the number of links between particles per unit cross-sectional area which transmit forces from one part of the sample to the other. If all the dispersed particles are involved in a flocculate, N_a is given approximately by $2\phi\sigma(d+2\Delta)/\pi d^3$; thus we have

$$\Delta G \fallingdotseq 7.20\times10^{-15}\phi\sigma(d+2\Delta)^2/d^2(\delta+2\Delta)^3$$

where σ is the parameter depending on the network structure and with values in the range of 1~3.[17] When the thickness of the layer of a bound polymer, Δ, is negligibly small compared to the diameter of the particles, we have approximately:

$$\Delta G \fallingdotseq 7.20\times10^{-15}\phi\sigma/(\delta+2\Delta)^3$$

25) P. J. Flory, "Principles of Polymer Chemistry," Cornell University Press, Ithaca, New York (1953), p. 415.
26) M. J. Vold, *J. Colloid Sci.*, **16**, 1 (1961).
27) M. Takano and H. Kambe, This Bulletin, **36**, 1424 (1963).

In this case, the additional shear modulus due to the van der Waals-London attraction is independent of the particle size, and if particles approach each other within 100Å at a concentration of 10 vol. %, the magnitude of the additional shear modulus, ΔG, may be in the order of $10^2 \sim 10^3$ dyn./cm^2. This order seems to be sufficiently small compared to the observed order of the modulus, $10^4 \sim 10^6$ dyn./cm^2. Therefore, the van der Waals-London attraction seems to be of secondary importance in the forces between particles.

Summary

The dynamic viscoelastic properties of molten polyethylene with various fillers have been measured in nitrogen gas at frequencies from 0.01 to 0.75 c. p. s. The dynamic viscosity and dynamic modulus have been measured at the temperatures of 150~230°C.

Glass spheres, calcium carbonate powder and barium sulfate powder have been used as fillers. The average diameter of the particles covers the range of 0.04~91 μ. The polyethylene used was one of a low density, "Sumikathene F-70-6," whose number average molecular weight is 28000.

The dynamic viscosity and modulus of molten polyethylene are increased by the addition of fillers. The viscoelastic properties at low frequencies depend differently on the concentration in each suspension. In suspensions of glass spheres of the larger particle sizes (particle diameter: 24.0, 32.3, 49.5 and 91.1 μ), the concentration dependence of the dynamic viscosity, η', follows a generalized Robinson's formula:

$$\ln(\eta'/\eta'_0) = K\phi/(1-S'\phi)$$

where η'_0 is the dynamic viscosity of polyethylene; ϕ, the volume fraction of the suspended particles, and K and S', 2.5 and 1/0.74 respectively, regardless of the particle size. In suspensions of calcium carbonate of the intermediate particle size (particle diameter: 2.4 μ), the dependence of the dynamic viscosity on the concentration and on the amplitude of oscillation is observed more remarkably than that in suspensions of glass spheres. In suspensions of calcium carbonate and barium sulfate of the smaller particle sizes (particle diameter: 0.04, 0.08 and 0.27 μ), the dynamic viscosity and modulus increase appreciably above a critical concentration of the filler, a point which depends on the particle size. Beyond this critical concentration, the particles seemed to be linked with each other by single polymer molecules.

The dynamic viscosity and modulus at lower frequencies increase remarkably as the mean distance between the surfaces of particles becomes less than the molecular dimension of the polymer. In suspensions of the larger particles of glass spheres, this critical concentration can not be observed up to the highest concentration.

The temperature dependence of the dynamic viscosity at lower frequencies approximately agrees with that of unfilled polymers.

The dependence of dynamic properties on the time and on the amplitude of oscillations is observed in suspensions of calcium carbonate and in those of barium sulfate of comparatively small particles. In the barium sulfate suspensions of the finest particles, the dynamic viscosity and modulus increase with time under periodic strains and decrease with the increase in the amplitude of oscillations. The amplitude dependence of the dynamic modulus is more remarkable than that of the dynamic viscosity generally. In such thixotropic suspensions, the dynamic properties were measured with as small a strain as possible.

One of the present authors (M. T.) especially wishes to express his gratitude to the Japan Society for the Promotion of Science for its financial support during the work described in the present paper.

Aeronautical Research Institute
The University of Tokyo
Meguro-ku, Tokyo

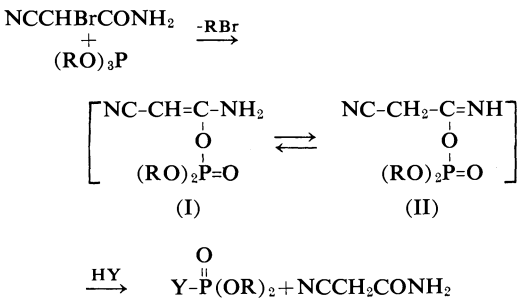
Synthesis of Testosterone Dimethyl Phosphate, Bornyl Phosphate and Adenosine 5'-Phosphate

By Tsujiaki HATA and Teruaki MUKAIYAMA

(Received June 19, 1963)

A previous paper described a useful method for the selective phosphorylation of alcohols and the diesters of phosphoric acid by means of α-bromocyanoacetamides and trialkyl phosphites to yield phosphates and pyrophoshates.[1]

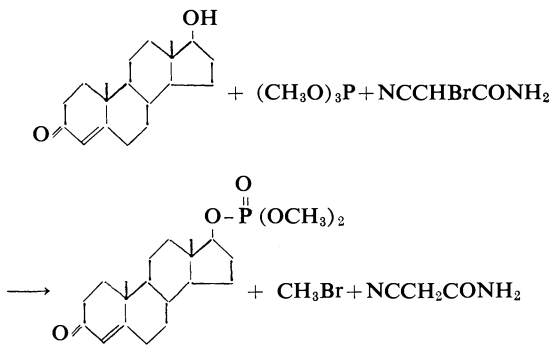
A selective phosphorylation can be effected successfully by this method without isolating the intermediate, enol-phosphate (I) or imidoyl phosphate (II), since it reacts exclusively with nucleophilic reagents, such as alcohols, phenols, diesters of phosphoric acid and amines, under mild conditions.



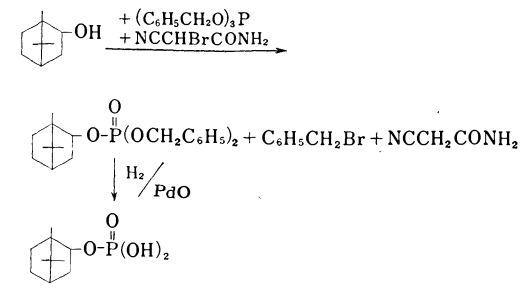
HY: alcohol or diester of phosphoric acid or amine

In the present paper, a successful application of this method to the synthesis of a steroid phosphate, a terpene phosphate and a nucleotide is described.

Müller and his co-workers[2] reported that testosterone dimethyl phosphate was obtained by the oxidation of the dimethyl ester of androst-5-ene-3β, 17β-diol 17-phosphate with chromic acid. It has now been found that testosterone dimethyl phosphate is obtained in a good yield from testosterone and the phosphorylating reagents, i. e., monobromocyanoacetamide and trimethyl phosphite. When trimethyl phosphite was added to a solution of one mole of testosterone and one mole of monobromocyanoacetamide in dry ether at $-40°C$, testosterone dimethyl phosphate was obtained in a 62% yield.

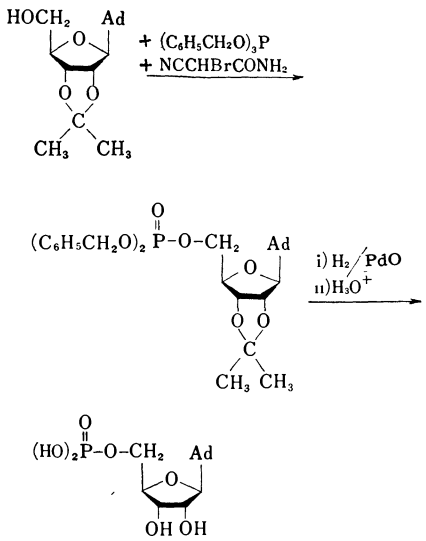


In the next place, a synthesis of bornyl phosphate, which had been reported to be synthesized from borneol and phosphorus oxychloride,[3] by means of the afore-mentioned phosphorylating reagents was tried. It was obtained in a 60% yield by the reaction of borneol with monobromocyanoacetamide and tribenzyl phosphite, followed by hydrogenolysis to remove the benzyl group.



Finally, it was established that adenosine 5'-phosphate[4] was successfully synthesized. Adenosine 5'-phosphate was obtained in a 62% yield when one mole of 2', 3'-isopropylideneadenosine was treated with one mole of monobromocyanoacetamide and one mole of tribenzyl phosphite, followed by hydrogenolysis and hydrolysis.

1) T. Hata and T. Mukaiyama, This Bulletin, **35**, 1106 (1962).
2) E. Müller, A. Langerbeck and W. Riedel, *Z. physiol. Chem.*, **281**, 29 (1944).
3) C. Neuberg, J. Wagner and K. P. Jacobsohn, *Biochem. Z.*, **188**, 227 (1927).
4) J. Baddiley and A. R. Todd, *J. Chem. Soc.*, **1947**, 648.



Ad: Adenine

Experimental

Testosterone Dimethyl Phosphate.—Into a solution of testosterone (0.20 g.) and monobromocyanoacetamide (0.11 g.) in 20 ml. of dry ether, trimethyl phosphite (0.08 g.) in 10 ml. of dry ether was stirred drop by drop at −40°C. A white precipitate, cyanoacetamide, separated. The solution was kept at room temperature overnight and then filtered. After the removal of methyl bromide and ether, testosterone dimethyl phosphate was obtained as a colorless crystalline solid weighing 0.17 g. (62%) and melting at 144~149°C. The crude product was recrystallized from ether (m. p. 152°C).

Bornyl Phosphate.—Into a solution of borneol (1.54 g.) and monobromocyanoacetamide (1.63 g.) in 100 ml. of dry ether, tribenzyl phosphite (3.80 g.; purity 80%) was stirred drop by drop at room temperature. The solution was further stirred for 2 hr. and then left to stand overnight. After removal of the ether, the residual material was dissolved in aqueous alcohol (50 ml. of 50%), and the solution was shaken with hydrogen at atmospheric pressure over an Adams palladium oxide catalyst, the theoretical amount of hydrogen for the removal of two benzyl groups being taken up in 100 min. The catalyst was removed by filtration, the solution was evaporated to dryness at 40°C under reduced pressure, and the crude bornyl phosphate (1.40 g., 60%) was recrystallized from benzene-petroleum ether (m. p. 155~156°C), alone and in admixture with an authentic sample.

Adenosine 5'-Phosphate.—To a solution of 2', 3'-isopropylideneadenosine (0.31 g.) and tribenzyl phosphite (0.44 g.; purity 80%) in 15 ml. of anhydrous dimethylformamide, monobromocyanoacetamide (0.33 g.) in 10 ml. of anhydrous dimethylformamide was added drop by drop with shaking at room temperature. The solution was then kept at room temperature for 3 days and the solvent evaporated at 30~35°C under reduced pressure (3~4 mmHg). The residual syrup was dissolved in aqueous alcohol (30 ml. of 50%), and the solution was shaken with hydrogen at atmospheric pressure over an Adams palladium oxide catalyst. The absorption of the hydrogen was rapid, the theoretical amount for the removal of two benzyl groups being taken up in 60 min. After the catalyst had been removed by filtration, the filtrate was evaporated at 30°C under reduced pressure to a faintly yellow syrup. The syrup was dissolved in dilute sulfuric acid (5 ml. of a 0.1 N solution), and the solution was set aside for 2 days to effect the hydrolysis of the isopropylidene residue, The sulfuric acid was neutralized with a calculated amount of barium hydroxide (5 ml. of a 0.1 N solution). Barium sulfate was removed by centrifugation, aqueous ammonia (0.1 N) was added to pH 10, and then a saturated solution of barium chloride was added. The precipitate was collected by centrifugation and washed with two portions (10 ml.) of water. The crude barium salt of adenosine 5'-phosphate was suspended in a small amount of water, and dilute hydrochloric acid (1 N) was added to pH 2. The adenosine 5'-phosphate did not crystallize instantly, but, on standing overnight at 0°C, it separated as needles (0.23 g., 66%) (m. p. 187~190°C). Recrystallized from water, it melted at 191°C; the R_f value was 0.70.* The melting point was not depressed in admixture with natural adenosine 5'-phosphate (m. p. 191~192°C).

Laboratory of Organic Chemistry
Tokyo Institute of Technology
Meguro-ku, Tokyo

* 5% Na_2HPO_4 aq. solution/isoamyl alcohol: 1.0 cm./0.5 cm.

A Cobalt Complex Catalyst for the Linear Dimerization of Butadiene

By Taro SAITO, Yasuzo UCHIDA and Akira MISONO

(Received April 26, 1963)

We have found that the selective dimerization of 1, 3-butadiene to 3-methyl-hepta-1, 4, 6-triene is carried out by a complex catalyst composed of triethylaluminum and cobalt complexes such as cobalt(III) acetylacetonate, cobalt salicyl aldehyde, a cobalt chloride pyridine complex, and cobalt chloride. Some of the results using cobalt(III) acetylacetonate have been previously reported.[1] The order of mixing cobalt acetylacetonate, butadiene and triethylaluminum had a great effect on the rate of formation of the butadiene dimer; the best results were obtained when cobalt acetylacetonate, butadiene and triethylaluminum were mixed in that order. These results suggest that the coordination of butadiene to cobalt is affected by the mixing order of the monomer and catalyst components and has an important influence on the dimerization of butadiene.

In this paper, an explanation for the formation of an active complex will be attempted by means of the results from infrared spectra, magnetic susceptibility and electron spin resonance spectra.

Experimental

Reagents. — Benzene was purified by washing it with concentrated sulfuric acid and then distilling it with metallic sodium in an atmosphere of nitrogen gas.

Triethylaluminum (made by the Ethyl Corp., U. S. A.) was used in the experiments without further purification.

Cobalt acetylacetonate was synthesized according to the method described in "Inorganic Syntheses."[2]

Infrared Analysis. — The infrared spectra of the samples were found by means of a Nihon-Bunko double-beam spectrometer model 401 G for the sodium chloride region and model 201 for the potassium bromide region.

Known amounts of cobalt acetylacetonate, butadiene (benzene solution) and triethylaluminum (benzene solution) were introduced into a glass tube in an atmosphere of nitrogen gas, and a part of the solution was transfused into a 0.1 mm.-path. length sodium chloride cell with a glass syringe.

TABLE I. THE PREPARATION METHOD OF THE SAMPLES EMPLOYED

1) Infrared analysis

Fig. No.	No.	Molar ratio				Mixing order
		Benzene	C_4H_6	$Co(acac)_3$	$AlEt_3$	
1	1	177	9.5	1	4.2	Bz+Co+BD+Al
	2	183	9.6	1	4.1	Bz+BD+Al+Co
	3	182	9.6	1	4.0	Bz+Co+Al+BD
2	4	75	0	1	0	Bz+Co
	5	65	5.0	0	0	Bz+BD
	6	71	4.8	1	2.5	Bz+Co+BD+Al
	7	69	5.3	1	2.1	Bz+Co+Al+BD

2) Magnetic susceptibility

No.	Weight fraction				Mixing order	χ_g for complex $\times 10^6$	χ_M for cobalt $\times 10^6$	μ_{eff}	n
	Benzene	C_4H_6	$Co(acac)_3$	$AlEt_3$					
8	0.949	0.0300	0.0100	0.0111	Bz+Co+Al+BD	9.74	7320	3.95	3.18
9	0.908	0.0565	0.0185	0.0170	Bz+Co+BD+Al	1.23	867	1.41	0.72

3) Electron spin resonance

Fig. No.	No.	Molar fraction				Mixing order
		Benzene	C_4H_6	$Co(acac)_3$	$AlEt_3$	
3	10	181	6	1	2.4	Bz+Co+Al+BD
	11	181	6	1	2.4	Bz+Co+BD+Al

1) T. Saito, T. Ohno, Y. Uchida and A. Misono, *J. Chem. Soc. Japan, Ind. Chem. Sec.* (*Kogyo Kagaku Zasshi*), **66**, 1099 (1963).

2) J. C. Bailar, Jr., "Inorganic Syntheses," Vol. 5, 188 (1953).

Magnetic Susceptibility. — The Gouy method was adopted for observing the magnetic susceptibility of the compounds placed between the poles of an electric magnet with a value of 25000 gauss; a quartz sample tube was also employed. The measurement were carried out at 10°C. The samples were prepared in the way described in the above section.

Electron Spin Resonance Spectra. — The spectra were recorded in the X-band (9400 Mc.) with 100 kc. modulation by means of a Nihon-Denshi Model JES-3B ESR spectrometer. The method of sample preparation was the same as that described above; the conditions of sample preparation for each experiment are shown in Table I.

Results and Discussion

When triethylaluminum reacts with cobalt acetylacetonate in the presence of butadiene, the resultant solution shows a marked catalytic activity in the linear dimerization of butadiene, whereas the solution prepared by the reaction of cobalt acetylacetonate and triethylaluminum without butadiene is considerably inactive. Thus, the order of mixing the catalyst and butadiene components is very important in obtaining the active catalyst.[1)]

Infrared spectra were recorded for each solution of a different mixing order of the components. In the infrared spectrum in the sodium chloride region, the decrease in the absorptions of the CH- and CH_2-wagging vibrations of butadiene, at 1008 and 908 cm^{-1} respectively, was very marked in the sample prepared by adding triethylaluminum last (Fig. 1-1). This result indicates that butadiene molecules are strongly bound in that case. Triethylaluminum is assumed to play the role of reducing cobalt to the state in which butadiene molecules readily coordinate to cobalt. On the other hand, when triethylaluminum is added before butadiene (Fig. 1-3), a complex is formed to which butadiene molecules hardly coordinate at all. Figure 1-2 displays the intermediate state.

Infrared spectra in the potassium bromide region were recorded to elucidate the bond structure between the transition metal and the oxygen atoms of acetylacetone ligands. Nakamoto[3)] has reported on the infrared spectra in the potassium bromide region of acetylacetonates of trivalent metals. He assigned the 466 and 490 cm^{-1} bands to Co–O and Al–O stretching vibrations respectively. In the present investigation, the reaction mixtures of cobalt acetylacetonate, butadiene and triethylaluminum in both orders of mixing (Figs. 2-6 and 2-7) showed the Al–O band at

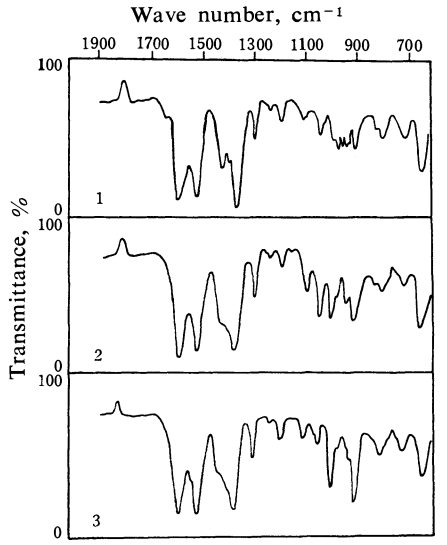


Fig. 1. IR spectra of the solutions prepared by different orders of mixing.

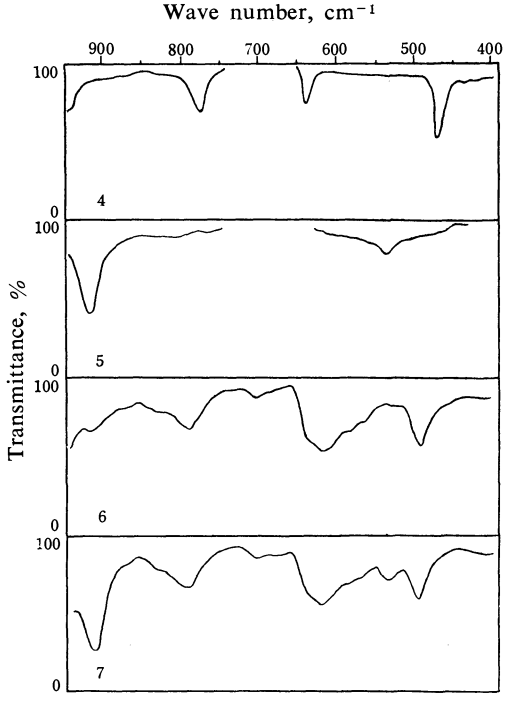


Fig. 2. IR spectra of the solutions prepared by different orders of mixing.

490 cm^{-1} instead of the Co–O band at 466 cm^{-1}, indicating that the acetylacetone ligands of cobalt acetylacetonate come to be coordinated to aluminum as the result of the ligand exchange reaction effected by triethylaluminum.

By evaporating the solvent and low-boiling materials from the reaction solution of cobalt acetylacetonate, butadiene and triethylaluminum in benzene, a catalytically-active solid

3) K. Nakamoto, *J. Am. Chem. Soc.*, **83**, 1066 (1961).

was obtained. By sublimation of the solid, it was confirmed that one sublimate was aluminum acetylacetonate. The sublimation residue was cobalt metal. These results support the theory that the reduction of the cobalt and ligand exchange reaction between cobalt and aluminum take place.

The magnetic susceptibilities of these reaction solutions were measured to determine the number of unpaired electrons of cobalt. Calculations based on the assumption that the sum of $w_i\chi_{gi}$ equals the χ_g value of the solution, where w_i is a weight fraction and χ_{gi} is a gram susceptibility of a component, indicated that the reaction product of cobalt acetylacetonate, butadiene and triethylaluminum mixed in that order is slightly paramagnetic, while, on the other hand, the product prepared by mixing cobalt acetylacetonate, triethylaluminum and butadiene in that order is strongly paramagnetic. Although the calculations are not decisive enough, because of the obscurity of the structure of the complex formed, to determine unequivocally the exact number of unpaired electrons of cobalt the reaction product of cobalt acetylaluminum with triethylaluminum in the presence of butadiene is probably diamagnetic. (The paramagnetism is due to the partial reaction of cobalt acetylacetonate and triethylaluminum without butadiene.) It is considered to be a diamagnetic complex formed by the removal of the acetylacetone ligands of cobalt acetylacetonate by triethylaluminum, with the simultaneous π-bonding of butadienes to cobalt.

The electron spin resonance spectra support the noticeable relation between the paramagnetism and the mixing order of the catalyst and butadiene components. The strong paramagnetism of the sample agrees very well with the results of the magnetic susceptibility measurement.

It may be suggested on the basis of these experimental results that the active catalyst complex for the dimerization is probably a π-complex of cobalt. Triethylaluminum deprives cobalt acetylacetonate of acetylacetone ligands, and simultaneously butadiene molecules coordinate to cobalt to form the active catalyst complex for the dimerization. Butadiene molecules coordinated to cobalt are considered to form a dimer, and the coordination force of the dimer is so much weaker than that of butadiene that the formed dimer is removed from the cobalt by ligand exchange with the butadiene in the solution. Dimerization will proceed until butadiene is consumed by repeated coordination, dimerization and detachment by ligand exchange processes.

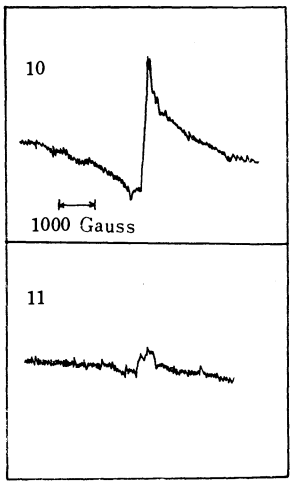


Fig. 3. ESR spectra of the solutions prepared by different orders of mixing.

Summary

In the linear dimerization of butadiene, the mixing order of butadiene and catalyst components, cobalt acetylacetonate and triethylaluminum affects the activity of the catalyst. When cobalt acetylacetonate and triethylaluminum react in the presence of butadiene, the solution possesses marked catalytic activity. In the infrared spectrum of this system, the intensity of the absorption peaks of the CH- ($1008\,cm^{-1}$) and CH_2- ($908\,cm^{-1}$) wagging vibrations of butadiene decrease significantly as compared with the case when butadiene is added last. In both cases, the absorption of Co–O ($466\,cm^{-1}$) disappered and that of Al–O ($490\,cm^{-1}$) was found. These results indicate that triethylaluminum reduces cobalt acetylacetonate and coordinates butadiene to cobalt. When butadiene is absent, triethylaluminum and cobalt acetylacetonate react to form a complex to which butadiene coordinate scarcely at all afterwards. The former solution shows a weak paramagnetism ($\mu_{eff}=1.4$), while the latter shows a strong paramagnetism ($\mu_{eff}=4.0$). From these results, the catalyst of the reaction is considered to be a diamagnetic complex of cobalt coordinated by butadiene.

Department of Industrial Chemistry
Faculty of Engineering
The University of Tokyo
Hongo, Tokyo

Studies of the Photoreduction of Thiazine Dyes in Aqueous Solutions

By Masao KOIZUMI, Hiroshi OBATA and Shigenari HAYASHI

(Received August 14, 1963)

In 1961 Usui, Obata and Koizumi[1] found that methylene blue in suitable buffer solutions, without any reducing agents added, is photoreduced to leuco dye by the visible light. According to them, the quantum yield of photoreduction reaches as much as 10^{-3} in the phosphate buffer, but it is to be noted that the formation of leuco dye is accompanied by some degree of demethylation and a slight decomposition of the dye. Following this paper, Usui and Koizumi[2] attempted a kinetic treatment and found that in the borate buffer solution the reaction proceed approximately as of the first order with respect to the dye, while in the phosphate buffer solution, the reaction is a simple second order one with respect to the dye. It seemed that there is some difference between the reaction mechanisms of these two cases, but this was not conclusive in view of the rather tentative nature of the treatment.

The present paper is concerned with one, examining whether other kinds of dye show a similar photoreduction or not, and two, studying further the kinetic nature of the reaction in question.

The result is that, so far as we have examined, there are no kinds of dye other than thiazine dyes that show such a reaction. It seems that the reaction is specific for thiazine dyes. As to the second question, another example was found which behaves in a manner similar to methylene blue in the phosphate buffer solution. From the present investigation it has become more certain that in suitable cases the photoreduction of thiazine dyes process in a simple second order with regard to the dye.

I. A Search for Other Dyes which Display a Similar Photoreduction.—The following dyes were examined, each in plain aqueous, borate and phosphate buffer solutions.

a) Indophenol dye
  1) 2, 6-Dichlorophenol indophenol (Merck or Wako-junyaku)

b) Thiazine dyes
  2) New methylene blue (Tokyo-kasei)
  3) Methylene green (Tokyo-kasei)
  4) Toluidine blue (Tokyo-kasei)
  5) Thionine

c) Oxazine dyes
  6) Nile blue (Tokyo-kasei)
  7) Capri blue (Tokyo-kasei)

d) Phenazine dye
  8) Neutral red (Merck)

Experimental

Purification.—All the dyes were recrystallized from an ethanol solution several times. Sodium borate, sodium monohydrogen phosphate, and potassium dihydrogen phosphate (all G. R.) were recrystallized 3~4 times from an aqueous solution.

Apparatus and Procedures.—The sample solution in a spherical ampule (2 cm. radius) was evacuated 5~7 times by freezing and thawing and then poured into a reaction cell, which consisted of a spectrophotometer cell (1×1×4 cm.) and the upper part of which was connected to the above ampule by a glass tube. The experiment was performed in a thermostat at 30°C. The light source was a 500W/100V. projection lamp which usually operated at 75V. A suitable combination of filters were used for each system. At various time intervals, the sample cell was taken out and the absorption spectra were measured with a Hitachi spectrophotometer. The pH of the buffer solution was measured with a Hitachi pH-meter.

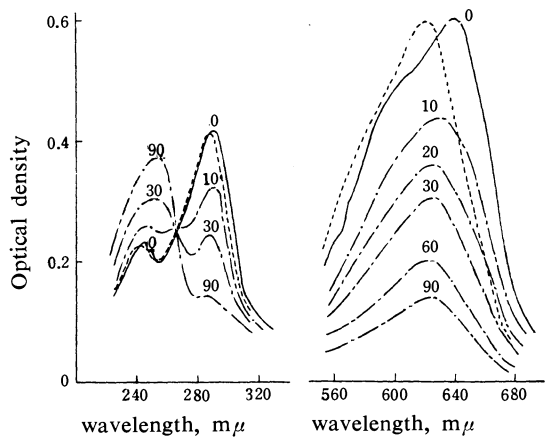


Fig. 1. Spectral change of toluidine blue in the photobleaching; dye conc. 2×10^{-5} M, phosphate buffer 1.0×10^{-2} M, pH 7.7. Numbers denote the time of illumination (min.); dotted line, after the introduction of air into the bleached solution.

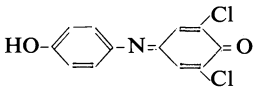
1) Y. Usui, H. Obata and M. Koizumi, This Bulletin, **34**, 1049 (1961).
2) Y. Usui and M. Koizumi, ibid., **34**, 1651 (1961).

The following two tests were employed to decide whether or not the bleaching is due to photoreduction; 1) the measurement of the absorption spectra of the illuminated sample in the visible and ultraviolet regions, and 2) the recovery of color by the introduction of air. For example, when a phosphate buffer solution of toluidine blue is illuminated, the spectra decline in the visible region and a new absorption band appears at 255 mμ with an isosbestic point at 266~7 mμ, this band being just the same as that of the chemically-prepared leuco dye. This is shown in Fig. 1.

Furthermore, when air is introduced after the reaction, the absorption spectra in the visible region increase again, as is shown by a dotted curve. From these facts one can conclude that the photoreduction occurs in the case of toluidine blue. The phenomena described above are not observed in the case of irreversible decomposition.

Results

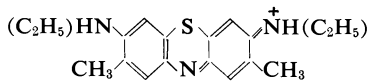
i) 2,6-Dichlorophenol Indophenol (2,6-DPIP)



This dye was studied because it has an oxidation-reduction potential as high as 0.217 V. (at pH=7). Its absorption spectra in the aqueous solution have three peaks, at 270, 310 and 600 mμ, while the reduced dye (prepared chemically) has one peak, at ~265 mμ.

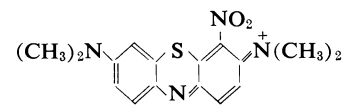
The stock solution must be kept in a refrigerator.[3] The dye was scarcely bleached at all by the visible light in the deaerated condition. Thus, the plain aqueous solution and the borate buffer solution (pH=9.2, 8.0), as well as the phosphate buffer solution (pH=8.9, 5.7), showed no change of absorption spectra even when illuminated as long as 430 min.

ii) New Methylene Blue (NMB)



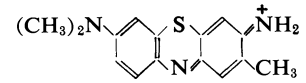
The absorption spectra have two peaks, at 285 and 630 mμ. The dimer peak exists at 585 mμ. The bleaching occurred, but very slowly, without any accompanying shift. The influence of the buffer solution on the rate was rather small. When the air was introduced after the reaction, 40~50% of the dye was restored.

iii) Methylene Green (MG)



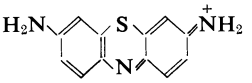
The λ_{max} lies at 275 and 650 mμ. The bleaching was moderately fast, with a shift of the maximum from 650 to 610~620 mμ. A new band appeared at 260 mμ. The rate increased in the order: plain aqueous solution <borate < phosphate. The introduction of air after the reaction restored 50~60% of the dye. The quantum yield of bleaching was ca. 3×10^{-4}.

iv) Toluidine Blue (TB)



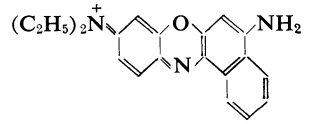
The photobleaching was rather rapid, with a shift of λ_{max} from 640 to 620 mμ. The order of the rate was: water <borate <phosphate. The introduction of air after the reaction recovered about 85% of the dye in case of the borate buffer solution, while in the phosphate buffer practically a 100% recovery was realized.

v) Thionine (Th)



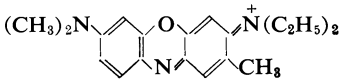
A gradual photoreduction occurred. The details will be described elsewhere.

vi) Nile Blue



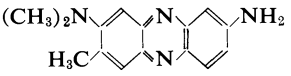
The rate of bleaching was very slow, and there was scarcely any recovery of dye by the introduction of air. It is to be noted that the borate buffer solution, when kept in the dark, showed a remarkable change in the absorption spectra and orange needle-like crystals precipitated.

vii) Capri Blue



The absorption spectra have two peaks, at 260 and 655mμ. The bleaching was very small, even with a 600 min. illumination. There was no effect of buffering on the rate, and no shift of the peak. The air-introduction recovered 20~30% in all cases examined.

viii) Neutral Red



This dye has two peaks, at 275 and 530 mμ. The plain aqueous solution and the phosphate buffer solution, when illuminated, showed a very small change in the absorption spectra. In the case of the borate buffer, the absorp-

3) I. Tachi and T. Tukamoto, *J. Agr. Chem. Soc. Japan*, 25, 340, 386 (1951).

TABLE I

Thiazine dyes				
Methylene blue	(MB)	(0.01)	◎	notable shift of λ_{max}
Toluidine blue	(TB)	(0.03)	◎	
Methylene green	(MG)	(—)	◎	
Thionine	(Th)	(0.06)	○	no shift of λ_{max}
New methylene blue	(NMB)	(−0.02)	○	
Oxazine dyes				
Capri blue		(ca. −0.07)	×	
Nile blue		(−0.12)	×	
Miscellaneous				
2, 6-Dichlorophenol indophenol		(0.22)	×	
Neutral red		(−0.33)	×	

tion spectra changed remarkably immediately after the buffer solution had been added to the dye solution (the resultant pH was 8~9), and in addition, some precipitate was produced. It is to be added that, in the plain aqueous solution (pH≈6), mere evacuation caused a shift of λ_{max} from 530 to 465 mμ, and the introduction of air restored the original absorption spectra. The above absorption spectra in the evacuated solution resembled those of the phosphate buffer solution (pH≈7). These phenomena seem to deserve further study.

ix) Résumé

Table I summarizes the results so far obtained. In this table, the numbers in parentheses denote the oxidation-reduction potential and the signs ◎, ○ and × represent, respectively, that the reaction is prominent, moderate and practically non-existent.

From the above table one can say that the reaction in question is rather specific for thiazine dyes; it is notable that the reaction is especially prominent when there is an accompanying demethylation. The effect of the buffer solution is quite similar to that observed in methylene blue, the rate increasing in the order of plain aqueous solution<borate buffer<phosphate buffer. The magnitude of the reaction cannot be correlated with the oxidation-reduction potential. Generally, the photoreduction is more or less accompanied with the irreversible decomposition of the dye, which prevents the complete recovery of the oxidized form. Toluidine blue, however, is very fortunately an exception, the recovery of this dye in the phosphate buffer solution being practically 100%. This dye is therefore expected to be particularly suitable for quantitative studies, including kinetic studies. These will be described in II. As to toluidine blue in the phosphate and borate buffer solutions, the detection of hydrogen peroxide was undertaken by the method of Meloan, Manck and Huffman,[4] but the sensitivity was not good enough for our purposes.

4) C. E. Meloan, M. Manck and C. Huffman, *Anal. Chem.*, 33, 104 (1961); 32, 791 (1960).

II. Kinetic Studies, Chiefly of Toluidine Blue

The most reliable data obtained from the experiment concern the change of the absorbance at λ_{max}. However, a slight shift of λ_{max}, accompanied by a fall in absorbance, makes it necessary to examine the interrelation between these two quantities.

From the analogy of methylene blue, there is scarcely any doubt that the shift in the present case is due also to demethylation from the side dimethylamino groups. Therefore, the absorption spectra at various times of illumination were analysed by the minimum ratio method of Blaisdell. This gives the absorption spectra of the demethylated dye which is shown in Fig. 2. It is clear that the demethylated product consists only of one species, with a maximum at 620 mμ. In view of the

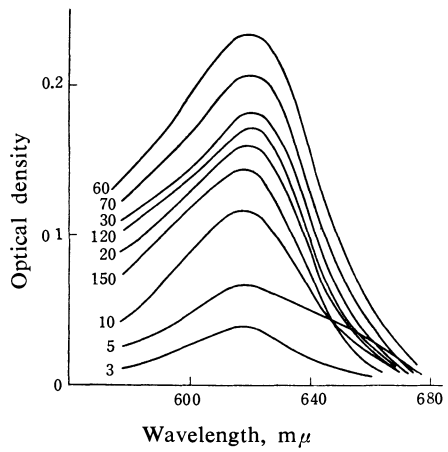
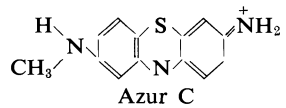


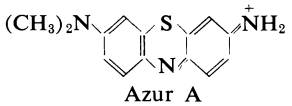
Fig. 2. Absorption spectra of the demethylated product (oxidized form) obtained by the Blaisdell method.

Toluidine blue	2.7×10^{-5} mol./l.
Phosphate buffer	1.7×10^{-2} mol./l.
pH	7.71

fact that the difference of λ_{max} between azur A and azur C is ca. 20 mμ, it is very reasonable



Azur C



Azur A

to consider that only one methyl group is detached in the case of toluidine blue. Table II gives the absorbance of the remaining toluidine blue at various times of illumination, D_0-D_t, and the absorbance of the demethylated product, D'_t.

From the above table one can see that, at an earlier stage of reaction, the ratio of the absorbance of the demethylated product to the total decrease in the absorbance of the original dye is near 0.5 in the case of phosphate, while in the case of borate it is less than 0.3. If one takes into account the fact that the restoration of dye by the introduction of air is almost complete in phosphate,

TABLE II

a) Dye 2.7×10^{-5} M, phosphate buffer 1.0×10^{-2} M, pH=7.71

Time of illumination min.	D_t	D_0-D_t	D_t'
0	0.720	0	0
3	0.638	0.08	0.037
5	0.571	0.15	0.064
10	0.495	0.22	0.12
20	0.366	0.35	0.16
30	0.300	0.42	0.18
60	0.169	0.55	0.24
70	0.121	0.60	0.21
120	0.087	0.63	0.17
150	0.072	0.65	0.14

b) Dye 1.7×10^{-5} M, borate buffer 1.0×10^{-2} M, pH=9.4

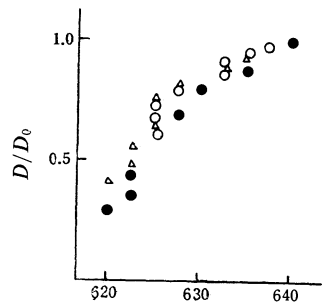
0	0.480	0	0
3	0.413	0.07	0.016
5	0.397	0.08	0.025
11	0.375	0.10	—
20	0.330	0.15	0.045
30	0.309	0.17	—
60	0.255	0.22	0.05
90	0.198	0.28	0.083
120	0.154	0.33	0.10
210	0.144	0.34	0.094

it appears that, in this case, demethylation participates in the photoreduction, probably in the ratio of one to one.

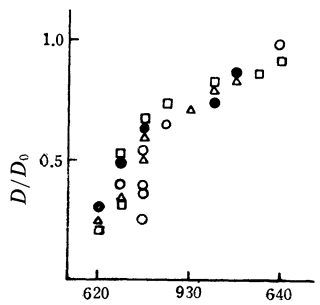
In Figs. 3 a, b and c the values of D/D_0, where D and D_0 are, respectively, the absorbance at the maximum wavelength at time t and at time $t=0$, are plotted against λ_{max} at various times. The figure concerns the phosphate buffer solution. From the results one may say that, in the case of the phosphate buffer, the shift accompanies the decline in almost the same ratio always, irrespective of the concentration of dye, the temperature, or the intensity of the exciting light.

Such a situation does not hold in the case of the borate buffer, where the relation between the shift and the bleaching is different from case to case. The increase in dye concentration and pH seems to favor the shift much more than the bleaching. Some data are shown in Fig. 4. These results, quite similar to those obtained for methylene blue, suggest some differences, between the processes occurring in the phosphate and borate buffer solutions.

On the basis of the above results it seems quite rational to undertake the kinetic treatment for the phosphate buffer based on the



(a)



(b)

Fig. 3. Relation between D_0/D and a shift of λ_{max} in phosphate buffer.
a) Effect of light intensity
● I_0 △ $0.49\,I_0$ ○ $0.13\,I_0$
b) Effect of dye concentration
○ 0.7×10^{-5} mol./l. △ 2.1×10^{-5} mol./l.
● 1.4×10^{-5} mol./l. □ 3.6×10^{-5} mol./l.

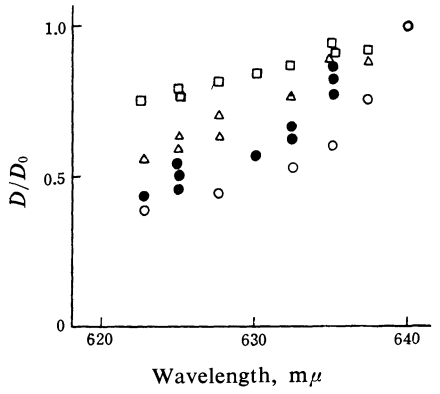


Fig. 4. Relation between D/D_0 and wavelength shift in borate buffer (constant pH).
Dye concn.
○ 0.5×10^{-5} mol./l. △ 1.7×10^{-5} mol./l.
● 1.0×10^{-5} mol./l. □ 2.6×10^{-5} mol./l.

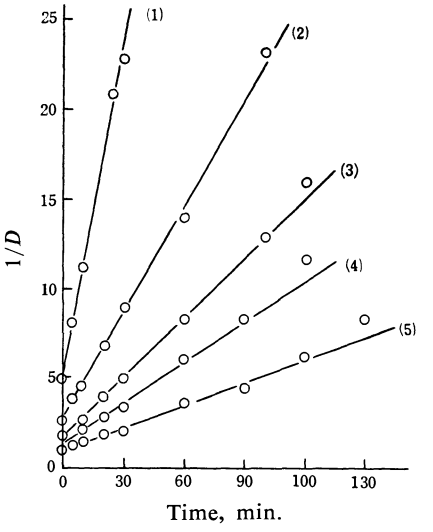


Fig. 5. Application of the second order rate formula. Effect of concentration of dye in phosphate buffer (constant pH).
Dye concn.
(1) 0.7×10^{-5} mol./l. (4) 2.7×10^{-5} mol./l.
(2) 1.4×10^{-5} mol./l. (5) 3.5×10^{-5} mol./l.
(3) 2.1×10^{-5} mol./l.

decline of the absorption spectra of the remaining dye. This treatment, of course, concerns both photoreduction and demethylation, but these two processes, as has been mentioned above, go parallel in the case of toluidine blue in the phosphate buffer, irrespective of the experimental conditions. If demethylation plays an essential role in the photoreduction, as will be suggested later, the present treatment is most satisfactory. It must be added that the inner filter effect of the demethylated product will not cause much error because in a later stage, where the effect is expected to become notable, the concentration of the total dye (oxidized form) becomes much smaller.*

It must be added that the composition of the product consisting of demethylated dye and leuco dye obeys very rapidly the oxidation-reduction equilibrium and that a part of demethylated oxidized dye, after being produced by the reaction, will turn into the leuco form, while the corresponding quantity of leuco toluidine blue goes back to the oxidized form. These phenomena have already been treated to some extent in a previous paper;[1] the present finding that the recovered dye after the introduction of air has exactly the same λ_{max} as that of the remaining dye prior to aeration clearly demonstrates the existence of such an equilibrium as that discussed in the previous paper. In the following treatment, however, the effect of this phenomenon on the reaction rate will be disregarded in favor of a first approximation (see Appendix).

i) The Rate Formula.—A simple second-order rate formula was found to hold for the concentration of the remaining toluidine blue. However, as is shown in Fig. 5, the rate constant decreases as the concentration of dye increases. Some examples of the second order rate constant at various dye concentrations are given in Table III.

TABLE III. KINETIC DATA AND THE CONDITION OF THE SOLUTION

Phosphate buffer, pH=7.71
Na_2HPO_4 9.0×10^{-3} M
KH_2PO_4 1.0×10^{-3} M

Dye concn. $\times10^{-5}$ M	k $\times10^{-2}$ mol^{-1} l. sec^{-1}
0.7	3.07
0.9	2.03
1.4	0.935
1.8	0.735
2.1	0.534
2.7	0.375
3.6	0.238

A plot of $1/k$ against C_0 and a plot of $1/kC_0$ against C_0 are given in Figs. 6 a and b. The latter gives a good linear plot. Therefore, one can write the following equation as an experimental rate formula:

$$-\frac{dc}{dt}=kC^2=\frac{\alpha C^2}{\beta C_0(\gamma C_0+\delta)} \quad (1)$$

or $$\frac{1}{kC_0}=\frac{\beta\gamma}{\alpha}C_0+\frac{\beta\delta}{\alpha} \quad (2)$$

* If the concentration of the two components, C_1 and C_2, are very small, the quantity of light absorption by one component is $\varepsilon_1\times C_1\times I_0$, irrespective of the other components.

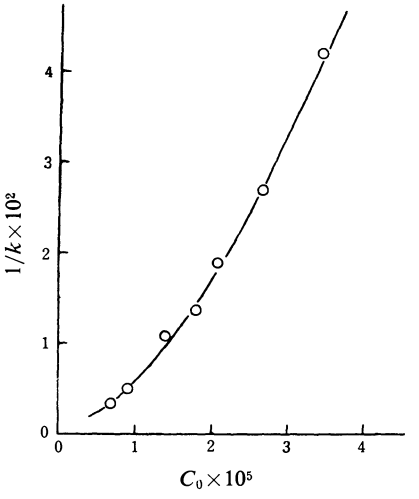


Fig. 6a. Relation of velocity constant to the initial dye concentration in phosphate buffer.

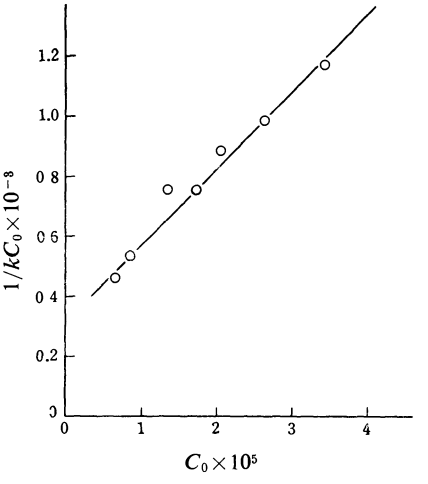


Fig. 6b. Relation of the velocity constant to the initial dye concentration in phosphate buffer.

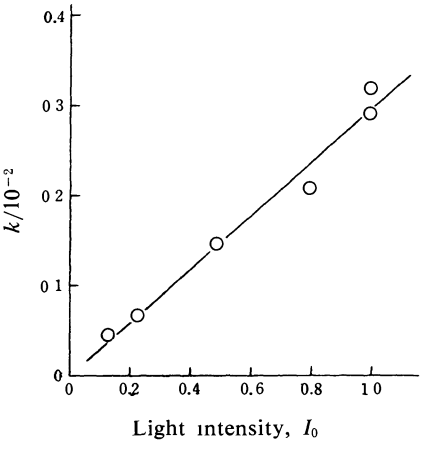


Fig. 7. Effect of incident light intensity on the rate constant in phosphate buffer.

From the above experimental data, one obtains;

$$\beta\gamma/\alpha=2.4\times10^7 \text{ mol. l. sec}^{-1}$$

$$\beta\delta/\alpha=0.3\times10^3 \text{ sec}^{-1}$$

ii) The Effect of Intensity.—The intensity of the illuminating light was varied by means of neutral filters, the transmission of which is 80, 49, 23 and 13%. The results are shown in Table IV and Fig. 7.

TABLE IV

Dye, ca. 2.5×10^{-5} M; Phosphate, 1.0×10^{-2} M

I_0	k $\times10^2$ mol^{-1} l. sec^{-1}
1.0	0.285
1.0	0.320
0.8	0.205
0.8	0.195
0.49	0.142
0.23	0.065
0.13	0.045

iii) The Effect of pH.—This is rather small, as Table V shows:

TABLE V

Dye, 1.8×10^{-5} M

pH	$k\times10^2$ mol^{-1} l. sec^{-1}	log k
9.10	1.18	2.07
7.71	0.735	1.87
7.00	0.595	1.78
5.93	0.239	1.38

iv) Temperature Effect.—Table VI.

TABLE VI

Dye, 2.1×10^{-5} M; pH=7.74

Temp., °C	$k\times10^2$ mol^{-1} l. sec^{-1}
20	0.421
30	0.534
40	0.627

From the above data, the apparent activation energy was evaluated as 4.2 kcal.

v) Quantum Yield (γ).—The following values were obtained. In the phosphate buffer (pH=7.74) and at 1.0×10^{-5} M of dye, $\gamma=6\times10^{-4}$. In the borate buffer (pH=9.40) and at 1.7×10^{-5} M of dye, $\gamma=4.4\times10^{-4}$. (The light quanta absorbed is 4.0×10^{14} sec^{-1} cc^{-1})

vi) Kinetic Results for Other Systems.—In the case of toluidine blue in a borate buffer, a simple second-order rate formula could not reproduce the experimental results. This is natural, since in this case there is an accompanying irreversible reaction and since, moreover, the degree of demethylation depends on

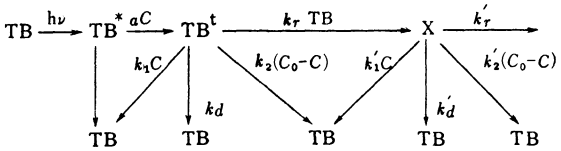
the experimental conditions. Most of the other cases could not be treated by a simple second-order rate formula either. An example for which a simple second-order rate formula holds approximately, however, was methylene green in a phosphate buffer solution.

Discussion

Usui and Koizumi tentatively applied, and with some success, the second-order rate formula to the photoreduction of methylene blue in a phosphate buffer. At that time they supposed that the success was rather fortuitous because the overall reaction, consisting of reversible and irreversible bleaching and, furthermore, of demethylation, was so complicated that the treatment could not be expected to be more than approximate. Now in the case of toluidine blue in a phosphate buffer, for which the second-order rate formula proved to hold satisfactorily again, the situations, though still complicated, are considered to be much better than in the case of methylene blue. Thus, first, the recovery of dye by the introduction of air being almost complete, there is no irreversible decomposition of dye occurring in this case. Second, the shift of λ_{max} is much less than that of methylene blue and corresponds to the elimination of one methyl group. Lastly, the fact that the quantity of demethylation is about half of the total decrease in the original dye, irrespective of the experimental conditions, suggests that demethylation is coupled in some way with the photoreduction. In view of these results, there is scarcely any doubt that a bimolecular process with regard to the dye is taking place in this case. Furthermore, the fact that the rate is proportional to the light intensity indicates that the photoreduction in this case occurs between some excited species and the ground state dye.

It must be added here that, for the simple second-order rate formula to hold, the absorption of light must be proportional to the concentration of dye, and so the concentration of dye must be low enough. Some of the experimental results for cases in which the concentration is rather large do not fulfil the above condition in an early stage of the run, and it seems rather strange that the same rate formula still appears to hold in this region.

Disregarding this point for the moment, however, the scheme will be discussed below on the basis of the experimental rate formula. The following scheme, which is somewhat different from that proposed before,[1] can interpret the present experimental rate formula. Although of course, the scheme is not conclusive, yet the authors believe that, in view of various facts, some of which will be published in a following paper,[5] the scheme is established almost definitely, at least in its essential point, i. e., in the point that it involves a bimolecular process with regard to dye. The success of the following analysis also favors the scheme.



In this scheme, C_0 and C are the concentration of TB at time $t=0$ and t, and aC is the rate of the production of the triplet dye, the absorption of light being assumed to be proportional to the concentration of dye. a can be written alternatively as $I_0 \times \varepsilon \psi_{S-T}$, and where I_0 is the incident light intensity, ε the molar absorbance, and ψ_{S-T}, a probability of intersystem crossing to the triplet state. Further, in the above scheme, the triplet dye is assumed to disappear via the following four processes; spontaneous deactivation k_d, reaction and deactivation with the ground state dye (the rate constant of the former being written k_r and the total sum of the reaction and deactivation, k_1), and, lastly, the deactivation by some reaction product, perhaps leuco dye. The effect of leuco dye was experimentally confirmed as in the case of methylene blue. The reaction between the triplet dye and the ground state dye will produce another transient species, X, which perhaps consists of half-hydrogenated dye and half-oxidized dye. If these two components can separate away or if the half-oxidized state is removed by a suitable (reducing) agent, then a net photoreaction will result. The rate constant connected with this net reaction will be written as k'_r. Most of X in the absence of any reducing agent will, however, return to two ground state dye molecules spontaneously (k'_d) or by interacting with the ground state dye, $k'C$, or with the leuco dye, $k'_2(C_0-C)$.

From the above scheme one can write:

$$-\frac{dc}{dt}=\frac{ak_rk_r'C^2}{\{k_d+k_1C+k_2(C_0-C)\}\times\{k_d'+k_1'C+k_2'(C_0-C)\}} \quad (1)$$

If one assumes here that the deactivation of the triplet dye and X is encounter-rate-determining, one may approximately put:

$$k_1 \approx k_2 \qquad k_1' \approx k_2' \quad (2)$$

If one further assumes that $k_dk_d' \approx 0$, then;

5) S. Kato, M. Morita and M. Koizumi, This Bulletin, 37, 117 (1964).

$$-\frac{dc}{dt}=\frac{ak_r k_r' C^2}{k_2k_2'C_0^2+(k_2k_d'+k_2'k_d)C_0}=kC^2 \quad (3)$$

$$k=\frac{ak_r k_r'}{k_2k_2'C_0^2+(k_2k_d'+k_2'k_d)C_0} \quad (4)$$

These are just the same form as the experimental rate formula.

From 4,

$$\frac{1}{kC_0}=\frac{k_2k_2'}{ak_rk_r'}C_0+\frac{k_2k_d'+k_2'k_d}{ak_rk_r'}$$

Hence, the experimental parameters $\beta\gamma/\alpha$ and $\beta\delta/\alpha$ can be expressed as follows:

$$\frac{\beta\gamma}{\alpha}=\frac{k_2k_2'}{ak_rk_r'} \qquad \frac{\beta\delta}{\alpha}=\frac{k_2k_d'+k_2'k_d}{ak_rk_r'}$$

From the experimental values of $\beta\gamma/\alpha$ and $\beta\delta/\alpha$, one can estimate the rate constants for each elementary reaction as follows. Thus, if one tentatively assumes that $k_2\approx k_2'\approx 10^{10}$ mol^{-1} l. sec^{-1}, then:

$$10^{20}=2.4\times 10^7\, ak_rk_r'$$

$$10^{10}(k_d+k_d')=3.2\times 10^2 ak_rk_r'$$

Hence,

$$k_d+k_d'\approx 1.3\times 10^5\ sec^{-1}$$

$$ak_rk_r'\approx 4\times 10^{12}$$

The values of k_d+k_d' are consistent with the results of the flash experiment, which gives, for methylene blue in the buffer solution, $k_d\approx 10^5\ sec^{-1}$ and about a one order smaller value of k_d'. From the quantity of light absorption, one puts

$$aC=a\times 10^{-5}=\frac{4\times 10^{17}}{6\times 10^{23}}\phi_{S-T}$$

and so a may be approximately $7\times 10^{-2}\phi_{S-T}$ sec^{-1}. Therefore,

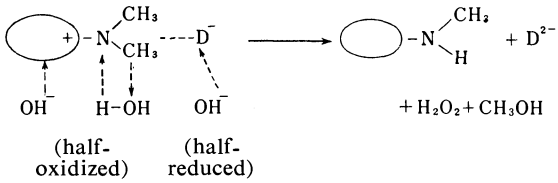
$$\phi_{S-T}k_rk_r'\approx 6\times 10^{13}$$

According to Oster, ϕ_{S-T} is ca. 0.21 for methylene blue; if one uses the same value, k_r and k_r' may be, respectively, of the order 10^{10} mol^{-1} l. and 10^4 sec^{-1}, as is to be expected. Thus, the above scheme, although it involves some processes which must be verified, can lead to the experimental rate formula. The most dubious point to be ascertained is the deactivation of both D^t and X by the ground state dye and by leuco dye, which takes place as an encounter-rate-determining process.

Putting together the above kinetic analysis and the fact that the quantities of demethylation and the photoreduction are about equal, irrespective of the experimental conditions, it seems natural to consider that, in the case of toluidine blue in a phosphate buffer, the triplet dye interacting with the ground state dye produces a transient species which consists perhaps of the half-oxidized and half-reduced form, that a part of the former is demethylated, and that a corresponding quantity of the latter goes to leuco dye. Thus, it may be said that the reduction is promoted by the coupling with demethylation. The scheme will hold more or less for the photoreduction of thiazine dyes in general. The transient electron transfer between the triplet dye and the ground state dye is somewhat similar to that which Lindqvist[6] proposed for the photoreduction of xanthene dyes on the basis of the flash experiments.

It is quite unknown how the formation of leuco dye and demethylation occur. The following is only to show one conceivable scheme.

Writing X as $D^+\cdots C^-$ (D^+ and D^- are, respectively, the half-oxidized and the half-reduced state):



Such a scheme seems to be reasonable since demethylation will afford some quantity of free energy, which will in turn make the decomposition of water energetically feasible; further, this is consistent with the well-known fact that demethylation easily occurs in the oxidative condition. If the transient electron transfer between the triplet dye and the ground state dye occurs generally in thiazine dyes, then one may suppose that some reducing agents, especially weak ones, will selectively attack the half-oxidized form. Therefore, the overall rate formula is expected to be approximately of the second order with regard to dye. From such a point of view, we have reexamined the data of the photoreduction of methylene blue by means of trimethylamine.[7]

It was found that the application of the simple second-order rate formula $-dC/dt=kC^2$ can satisfactorily reproduce most of the experimental results, at least in the initial stage, until 60% or more photoreduction proceeds. The later part deviates in most cases in the concave direction upward; this suggests the participation of the first-order reaction. Some examples are shown in Table VII.

As has been shown above, the second-order

6) L. Lindqvist, *Arkiv. för Kemi*, **16**, 79 (1960).

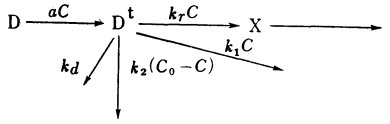
7) H. Obata and M. Koizumi, This Bulletin, **30**, 136, 142 (1957). Details will be reported in the near future.

TABLE VII

Borate buffer pH=9.2
Trimethylamine 5×10^{-4} M

Exciting light	Concn. of MB($\times10^{-5}$)	$k\times10^{-4}$ l. mol^{-1} sec^{-1}	$kC_0\times10^2$ min^{-1}
λ=662 mμ	1.57	0.21	3.3
	1.20	0.38	4.55
	0.57	0.83	4.73
	0.28	1.58	4.43
λ=685 mμ	1.50	0.48	7.2
	1.17	0.63	7.25
	0.55	1.36	7.47
	0.30	2.40	7.2

rate constant in this case is inversely proportional to the initial concentration of dye. If one assumes that trimethylamine attacks the half oxidized component of X very effectively, then the mechanism can be written as follows:



Hence,

$$-\frac{dc}{dt}=\frac{ak_rC^2}{k_1C+k_d+k_2(C_0-C)}$$

If one puts $k_1\approx k_2$ and $k_d\approx0$, then:

$$-\frac{dc}{dt}=\frac{ak_rC_2}{k_2C_0}$$

Thus, the above experimental results have been interpreted. It is to be added that no shift and, hence, no demethylation occurs in this case, and so there is less ambiguity in the kinetic treatment than in the case of toluidine blue in the phosphate buffer. One reason why Obata and Koizumi misinterpreted the results was that the second-order rate formula was very difficult to understand at that time. Of course, some reducing agents will attack D^t directly, and in such cases an overall rate formula will be simply proportional to the absorption of light. Further, it is expected that in some cases the two mechanisms will work simultaneously.

We are now reinvestigating various so-called reducing agents from this point of view. According to our preliminary experiments, EDTA is an example of a reducing agent which directly attacks the triplet dye, while allyl thiourea, ethanol, and trimethylamine belong to the other class.

Summary

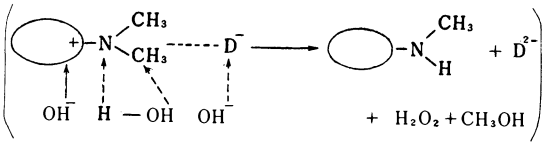
Judging from the experiments performed in our laboratory, the photoreduction of dye without the addition of any reducing agent takes place only in thiazine dyes, and the reaction is particularly prominent when demethylation occurs simultaneously.

The reaction proceeds in the following way:

$$D + h\nu \rightarrow D^*$$

$$D^* \rightarrow D^t$$

$$D^t + D \rightarrow X \quad (X=D^-\cdots\cdots D^+)$$



The part in parentheses is still doubtful. The above conclusion is consistent with the results of the flash experiment which will be described in a following paper. It has been proposed that some reducing agents attack D^t directly, while others attack the half-oxidized state.

Department of Chemistry
Faculty of Science
Tohoku University
Katahira-cho, Sendai

Appendix

When the photoreduction occurs in such a way that a part of half-oxidized state is demethylated and an equal quantity of the half-reduced form is fixed as a leuco dye, then some of the former will turn into leuco dye, while the same quantity of the latter returns to the oxidized dye. Such an interchange will decrease the rate to some extent. If one takes a special case where 1) demethylated dye is not photoreduced at all, and 2) the ratio of the oxidized form to the reduced form is exactly the same for the original dye and the demethylated dye, the rate formula will have to be modified to some extent.

Putting the concentration of the original dye, demethylated dye, as x_1, x_2, and that of each reduced form as y_1, y_2, all at time t, one can write:

$$x_1+x_2+y_1+y_2=C_0 \quad (1)$$

$$x_2=y_1 \quad (2)$$

and

$$\frac{y_1}{x_1}=\frac{y_2}{x_2}=\frac{y_2}{y_1}=K \quad (3)$$

Hence,

$$y_1=Kx_1,\ y_2=Ky_1=K^2x_1,\ x_2=Kx_1 \quad (4)$$

Suppose that the coupled reaction of leuco dye formation and demethylation (process i) obeys the following rate formula:

$$-\frac{dx_1}{dt}=f(x_1) \quad (5)$$

then, due to the oxidation-reduction equilibrium between the original and demethylated dye (process ii), the rate formula observed experimentally will be altered as follows: From 5, x_1 decreases during

Δt by $\Delta x_1 = f(x_1)\Delta t$, while x_2 and y_1 increase by $f(x_1)\Delta t/2$ during the same period. However, by process ii a certain portion of the increase of x_2 (oxidized demethylated) and y_1 (reduced methylated) turns into a reduced demethylated form (y_2) and into an oxidized methylated form (x_1). This quantity, $\Delta' x_1 = |-\Delta' x_2| = |-\Delta' y_1| = \Delta y_2$, can be calculated using relation 3 as follows, because Eq. 3 is considered to hold instantaneously:

$$\frac{x_2 + \frac{f(x_1)}{2}\Delta t - \Delta' x_1}{y_2 + \Delta' x_1} = \frac{x_1 - f(x_1)\Delta t + \Delta' x_1}{y_1 + \frac{f(x_1)}{2}\Delta t - \Delta' x_1}$$

From this, using relation 4,

$$f(x_1)\Delta t\left\{\frac{x_2+y_1}{2} + y_2\right\} = \Delta' x_1\{x_1+y_1+x_2+y_2\}$$

Thus,

$$\Delta' x_1 = \frac{2y_2+x_2+y_1}{2C_0} f(x_1)\Delta t$$

This is the amount which returns to the original dye during Δt due to the equilibration of the oxidized and reduced forms. Hence, the net rate of reaction is written as follows:

$$-\frac{dx_1}{dt} = \left\{1 - \frac{2y_2+x_2+y_1}{2C_0}\right\} f(x_1)$$

This can be rewritten as follows by means of relation 4:

$$-\frac{dx_1}{dt} = \left\{1 - \frac{K(K+1)x_1}{C_0}\right\} f(x_1) \qquad (6)$$

From Eqs. 1 and 4,

$$K = \sqrt{\frac{C_0}{x_1}} - 1$$

Therefore, Eqs. 6 becomes:

$$-\frac{dx_1}{dt} = \sqrt{\frac{x_1}{C_0}} f(x_1) \qquad (7)$$

Thus, in the above ideal case the resultant rate formula has the factor $\sqrt{x_1/C_0}$.

However, the above treatment concerns an ideal case under very specified conditions; in most cases it is believed that demethylated dye will also be photoreduced. It is believed that the correction term involved in Eq. 6 may be neglected and that the original rate formula will still hold approximately.

Studies of the Transient Intermediates in the Photoreduction of Methylene Blue

By Shunji KATO, Masaharu MORITA and Masao KOIZUMI

(Received August 14, 1963)

In the preceeding paper[1] some kinetic work has been reported on the photoreduction of thiazine dyes which proceeds in the absence of any reducing agent in the deaerated buffer solutions, especially in the phosphate buffer.

In connection with these, the photoreduction of methylene blue by means of trimethylamine as a reducing agent has been re-examined.

The most characteristic feature of these reactions is that the essential process in the reaction is the interaction of the excited state dye with the ground state dye, perhaps producing semiquinone and half-oxidized dye; it seems that this is rather more common than it was at first supposed to be.

Further investigations now under way in our laboratory show that the photoreduction of methylene blue by allylthiourea (ATU) and other mild reducing agents often obeys a similar rate formula; the only clear-cut exception that has ever been found is the photoreduction by EDTA, in which the rate formula is satisfactorily of the first order of dye.

In order to get more direct insight into the mechanism of such reactions, studies of the transient intermediates by the flash-technique have been undertaken. The aim of the present paper is to report on the general features and behavior of the transient intermediates observed in an aqueous solution of methylene blue. The transient spectra at various pH values, especially in borate and phosphate buffer and also in the solutions containing various reducing agents, such as trimethyl-amine (TMA), allylthiourea (ATU), EDTA and $K_4 \cdot [Fe(CN)_6]$, have been compared. The decays of the chief transient spectra has also been investigated.

Experimental

Materials. — *Methylene Blue.* — Merck's special grade sample was recrystallized four times from an

1) M. Koizumi, H Obata and S Hayashi, This Bulletin, 36, 108 (1964).

aqueous solution and dried in vacuo. The ε_{max} value in the aqueous solution was 72000. All the inorganic reagents were submitted to recrystallization or repeated distillation.

ATU.—Three recrystallizations from water.

EDTA. — A G. R. reagent was used without further purification.

The Preparation of the Sample Solution.—After it had been evacuated more than five times with freezing and thawing, the solution was poured into a reaction cell and was sealed. The experiments were performed at room temperature. The spectra before and after the flash experiment were taken by a Hitachi autorecording spectrophotometer or a Kotaki spectrophotometer. The concentration of dye was usually 0.5×10^{-5} M$\sim1.0\times10^{-5}$ M.

Apparatus. — Two quartz flash lamps filled with xenon were used for the photolysis. The electrode distance was 10 cm. The input energy was varied from 31.5 to 180J by changing the capacitance 10 μF$\sim$40μF and applied voltage, 2500$\sim$3000 V. Hoya O-54 filters were inserted between the light source and the reaction cell so as to cut off $<$540 mμ. A spectro-flash was worked at 10 μF and 3000 V. The time interval between the photolysis flash and the spectro-flash was controlled by a delay circuit in the range from 20 μsec. to 0.8 sec.

The half-width of the photolysis flash was about 40 μsec.

Transient spectra were taken on Fuji Neopan plates with a Shimadzu QF-60 quartz spectrograph.

In measuring the decays of the transient absorption spectra, the sample was irradiated by a xenon lamp (20 V., 7.2$\sim$8.0 amp.) instead of the spectro-flash used above, and the monitoring light beam at a fixed wavelength was received by a photomultiplier through a slit attached to the spectrograph. The signal was recorded with an Iwasaki synchroscope SS 5151 through a cathode follower.

The reaction cells were of Shibata SB glass tubes, 10 cm. long and 7 mm. in diameter, to both ends of which were cemented plane quartz plates. A shorter cell, 2.5 cm. long, was used in order to measure the transient decrease of the main absorption band of methylene blue.

Results

Transient and Permanent Bleaching by Flash Illumination. — In general, illumination by a flash causes transient bleaching to a large extent, the magnitude depending upon the intensity of the flash, but it produces only a rather small quantity of permanent bleaching unless no suitable reducing agent is present.

First the effect of the flash intensity upon the quantity of the transient bleaching in the plain aqueous solution and in the phosphate buffer solution will be described. The results were quite similar. At 125J the transient bleaching was almost complete, whereas at 31.5J a considerable quantity of the ground state dye remained. Figure 1 shows the results in the plain aqueous solution. In Fig. 1., $\Delta D'$ is the

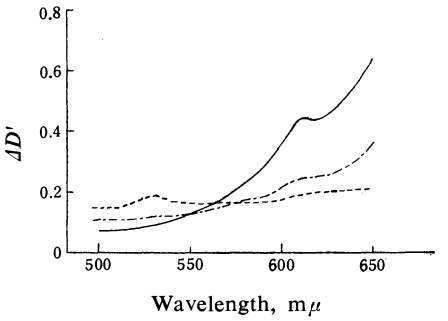


Fig. 1. The transient bleaching of the dye at different input energies.
——: Before flash, —·—·: 31J flash
----: 125J flash

difference in plate blackness between the sample and pure water, a difference which is proportional to the absorbance of the sample.

The quantity of the transient intermediate corresponds quite well to the above results, as is shown in Fig. 2. In this figure, and also in Figs. 3, 4, 5, 6, 7 and 8, ΔD is the difference in the blackness of two plates, one of which was measured at a given time after the photolysis flash and the other, about five minutes later.

This value is proportional to the absorbance of the transient species. The amount of permanent bleaching by one flash of 125J in the phosphate buffer was about 4%, while in the plain aqueous solution it was about 3%, the difference between the two solutions being rather small in comparison with that for the steady illumination. There is no doubt that most of the transient species returns to the ground state dye. About 10% of the dye was permanently bleached by six flashes in the case of the phosphate buffer (pH $\sim$8.12), while the introduction of air restored the color of the dye almost completely. There was no shift of the main peak, in contradiction to the results for the steady illumination.

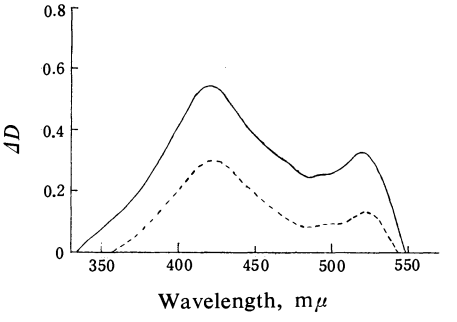


Fig. 2. The absorption spectra of transient species in a plain aqueous solution at different input energies.
——: 125J, ----: 31J

The addition of a 350-fold concentration of TMA (3.53×10^{-3} M) to the dye produced about a 40% permanent bleaching by one flash of 125J, but the quantity of bleaching per flash decreased for successive flashes. Along with the permanent bleaching, a new peak became apparent at 258~260 mμ. The introduction of air after almost complete bleaching led to a 100% recovery of the dye and the disappearance of the absorption in the ultraviolet region.

There was no shift of the main peak. Comparing these results with the ones in the steady illumination, the general features are quite similar, though there are some differences in details.

When the degassed 0.01 N hydrochloric acid solution of methylene blue was mixed with the degassed solution of ATU, the bleaching occurred even in the dark, and only a very little recovery of color was observed upon the introduction of air. The addition of a few drops of a 3% hydrogen peroxide solution and subsequent shaking restored the initial color. The above-mentioned decolorization did not occur appreciably when the solution was not acidic. Further studies by means of the steady illumination seem to be desirable.

By the addition of a 100-fold quantity of EDTA (10^{-3} M) to that of methylene blue, flash illumination brought about remarkable permanent bleaching, as was expected on the basis of the steady illumination results reported by Oster.[2] The quantity of bleaching per flash was larger in the phosphate buffer solution with a high pH than in the plain aqueous solution, the degree of permanent bleaching in the former reaching about 80%. The product with the absorption peak at 258 mμ is considered, without doubt, to be leuco dye, just as in the case of TMA. The introduction of air caused a 100% recovery of the dye. No shift of the main peak was observed in the course of either bleaching or recovery

Although the photoreduction of methylene blue by EDTA, ATU, and other mild reducing agents has been studied extensively by many workers,[3] including Oster,[2] using a steady illumination, the present results by flash illumination seem to require a reinvestigation by the steady illumination; this is now being undertaken in our laboratory from a somewhat different point of view.

Transient Spectra in the Absence of Any Reducing Agent. — All the transient spectra described below are those at 20 μsec. after the main flash and are for the energy input of 125J unless otherwise described.

In an acidic solution of 0.01 N hydrochloric acid the transient absorption spectra spread over 330~540 mμ, peaking at 375 mμ, as is shown in Fig. 3. Its lifetime is so short that it seems to survive only while the photolysis flash is still on; i. e., τ is estimated to be less than 30 μsec. These results agree quite well with those of Parker,[4] and there is scarcely any doubt that this transient species is the triplet dye.

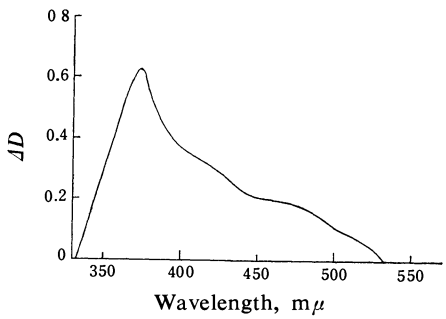


Fig. 3. The absorption spectrum of transient species in a 0.01 N HCl solution.

In the plain aqueous solution, the main absoption spectra spread from 340 to 550 mμ, with rather sharp peaks at 415 and 520 mμ, as is shown by the full line in Fig. 4. Besides, there is a weak transient absorption in ultraviolet, at 260~280 mμ and in the infrared region near 800 mμ. At 100 μsec., however, the shape of the spectra changes to some extent, as is shown by the broken line in Fig. 4. This implies that there are at least two transient species in the region near 415 mμ,

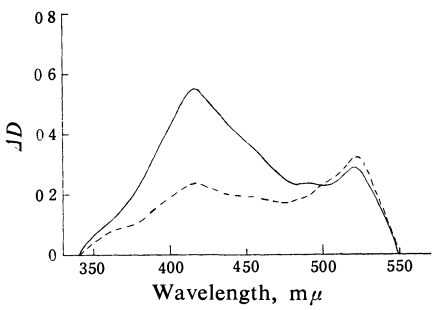


Fig. 4. The absorption spectra of transient species in the plain aqueous solution.
——: 20 μsec. after flashing
----: 100 μsec. after flashing

2) G Oster and N. Wotherspoon, *J. Am. Chem. Soc.*, **79**, 4836 (1957).

3) G. Holst, *Z. physik. Chem.*, **A179**, 172 (1937); **A182**, 231 (1938). M. Pestemer, *Z. Elektrochem.*, **58**, 121 (1954); G. Oster and N. Wotherspoon, *J. Chem. Phys.*, **22**, 157 (1954); R. Havemann and H. Pietsch, *Z. physik. Chem.*, **211**, 257, 267 (1959); S Matsumoto, This Bulletin, **35**, 1861, 1866 (1962).

4) C. A. Parker, *J. Phys. Chem.*, **63**, 26 (1959); C. G. Hatchard and C. A. Parker, *Trans. Faraday Soc.*, **57**, 1093 (1961).

each with a different lifetime. The shorter one will most certainly be a triplet, but it is possible that even at 20 μsec., the spectra are still a superposition of the two. The transient spectra in a borate and in a phosphate buffer solution (pH 8.2) are quite similar to those in the plain aqueous solution, with two peaks at 415 and 520 mμ.

The fact that in a strong acidic solution a peak exists at 375 mμ, while at a higher pH ($\geqq$7) a peak shifts to 415 mμ, irrespective of the presence of buffering substances, strongly suggests the existence of an acid-base change in the transient species, almost certainly a change in the triplet dye. Hence, the systematic study of the dependence of the transient spectra on pH was made from pH=2.2 to 10.2. For lower pH values, sodium acetate-hydrochloric acid or only hydrochloric acid was used, while for higher pH values, the sodium acetate-sodium hydroxide system was used. As had been expected, the variation in the spectra is very regular, with a clear isosbestic point at 400 mμ.

Figure 5 gives the relation between the differences in the plate blackness, differences which are certainly proportional to the absorbance, and the pH at three wavelengths, 415, 375 and 400 mμ. From these results one gets pK=6.7.

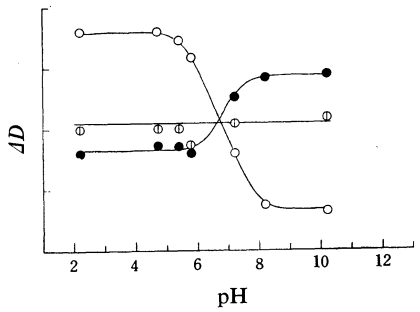


Fig. 5. The acid-base equilibrium of transient species. The change in the difference of plate blackness at various wavelengths, observed 20 μsec. after flashing, as a function of the pH value.
● 415 mμ ◑ 400 mμ ○ 375 mμ

The Transient Spectra in the Presence of Some Reducing Agents.—The transient spectra of the solution containing a 350-fold concentration of TMA compared to that of dye are shown in Fig. 6. Broadly speaking, they are similar to those for the plain aqueous solution or for the buffered solutions, with the absorption in the 250~280 mμ region, with a peak at 260~263 mμ, and in the 340~540 mμ region, with two peaks at 415~420 mμ and at 520 mμ. A slight difference is that the height at 520 mμ is less prominent in comparison with that of a solution containing no amine. The

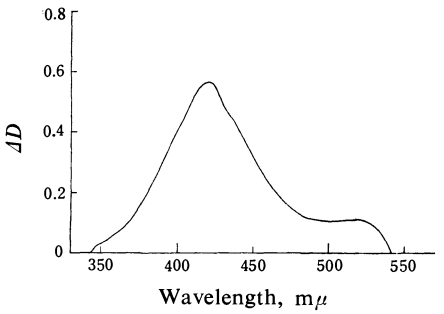


Fig. 6. The absorption spectrum of transient species in the plain aqueous solution containing 3.53×10^{-3} M TMA.

general features are also similar to those in a borate buffer solution (pH=8.2) to which TMA has been added, except that the 520 mμ peak is a little more prominent, all the spectra resembling those of the plain aqueous solution rather more.

The transient spectra of the solution to which ATU has been added are also similar to those of the plain aqueous solution of methylene blue, with two peaks at 415 and 520 mμ.

The addition of a 100-fold quantity of EDTA (1.0×10^{-3} M) to that of methylene blue causes a notable change in the transient spectra as compared with those of the plain aqueous solution. Thus, the peak at 520 mμ becomes less prominent and a shoulder appears near 370~380 mμ, although the other peak still exists at 415~420 mμ (Fig. 7). With 3000 times more EDTA than dye (dye, 1.3×10^{-5} M, EDTA, 4.0×10^{-2} M), the peak near 520 mμ completely disappears and the transient spectra extend from 340 to 475 mμ. Moreover, the shape of the spectra changes appreciably in the course of time, as is shown in Fig. 8. The curve is rather flat in the neighborhood of the maximum at 20 μsec., but at 200 μsec., two maxima, at 375 and 413 mμ, become apparent.

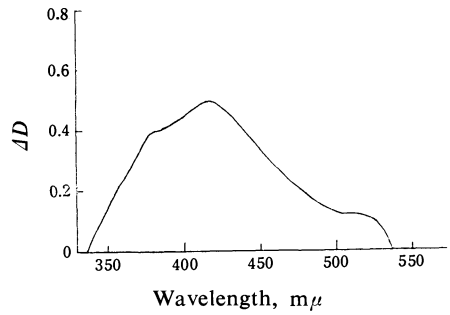


Fig. 7. The absorption spectrum of transient species in the plain aqueous solution containing 1.0×10^{-3} M EDTA.

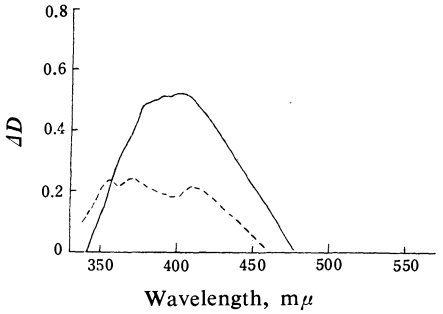


Fig. 8. The absorption spectra of transient species in the phosphate buffer solution (pH 8.1) containing 4.0×10^{-2} M EDTA.
——: 20 μsec. after flashing
----: 200 μsec. after flashing

When a concentration of $K_4[Fe(CN)_6]$ 50 times that of the dye is added to the plain aqueous solution of methylene blue, the transient spectra extend from 340 to 540 mμ, with a peak at 413 mμ. The peak at 520 mμ is completely lacking.

When leuco methylene blue (0.9×10^{-5} M) is added to the solution of methylene blue (1.5×10^{-5} M), the intensity at 415 mμ about doubles and the peak at 520 mμ is completely absent.

Lastly, when various amounts of oxygen are added to the solution, the transient absorption still appears in the 340~540 mμ region at 20 μsec.; on the other hand, at 100 μsec. the peak at 415 mμ declines remarkably, while quite a strong absorption is still existent in the ~520 mμ region.

Table I summarises the peaks of the transient spectra observed 20 μsec. after flashing in the visible region for various systems. s, m and w mean, respectively, that the intensity is strong, moderate and weak.

TABLE I

Solution	Peak
0.01 N HCl	375(s)
Plain aq. solution	415(s) 520(m)
Borate or phosphate	415(s) 520(m)
TMA	420(s)
TMA and phosphate	420(s) 520(w)
ATU	415(s) 520(m)
EDTA	415(s) 520(w or none)
$K_4[Fe(CN)_6]$	415(s)
Leuco methylene blue	415(v. s)
O_2	415(s) 520(m)

The Decay of the Transient Spectra.—In an 0.01 N hydrochloric acid acidic solution, the decay at 375 mμ obeyed the simple first order rate formula, giving a lifetime of about 30 μsec.

For the plain aqueous solution, the decays were examined at 415, 520 and 800 mμ. The initial part of the decay at 415 mμ obeyed the first order law approximately, giving a τ-value of 60~90 μsec. The same was true for the entire decay at 800 mμ, τ being 70~90 μsec. The approximate agreement of τ-values justifies the assignment of these two to the same transient species, most certainly to the triplet state. The latter part of the decay at 415 mμ showed a gradual deviation from the first order plot, but it seemed to fit another first order plot and a rough estimation gave a τ-value of about a few hundred μsec. The latter part of the decay at 520 mμ gave a τ-value of 200~260 μsec., roughly coinciding with the value for 415 mμ. Figure 9 shows a decay at 415 mμ.

It is very remarkable that the decay at 415 mμ for borate and phosphate buffer solution shows a clear hump at the earlier period as shown in Fig. 10. It is very difficult to express this decay curve analytically, but it is quite certain that the transient species survives longer than in the plain aqueous solution. It is to be noted that the above hump in the decay curve disappears when the energy input

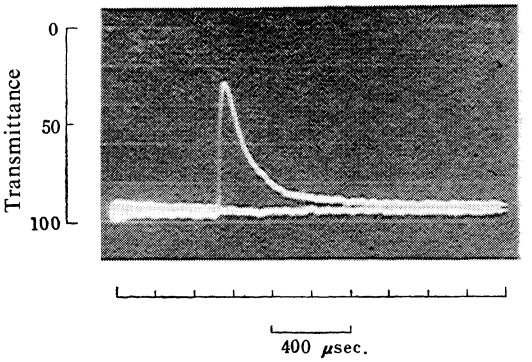


Fig. 9. The change in the transmittance at 415 mμ in the plain aqueous solution of 0.7×10^{-5} M methylene blue (input energy 125J).

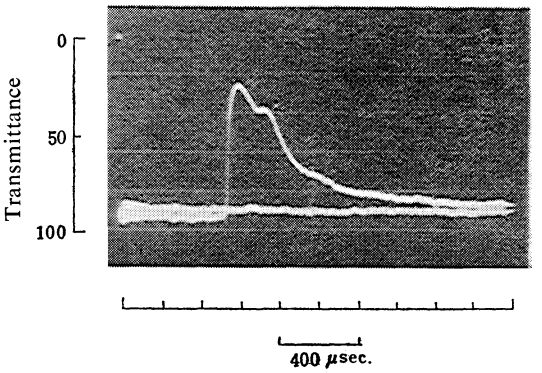


Fig. 10. The change in the transmittance at 415 mμ in the borate buffer solution (pH 8.2) of 0.7×10^{-5} M methylene blue (input energy 125J).

of the main flash is decreased to 31.5J. As has been mentioned before, almost all the dye turns into transient species at 125J, while at 31.5J more than half of the dye remains in the ground state. There is no doubt that the different results are due to these different situations (see Discussion).

The decay curve at 415 mμ when TMA or ATU was added displayed a small hump similar to that in the buffer solution.

Another notable finding is that the decay curve at 415 mμ when EDTA was added was simply monotonous. Although the entire decay curve did not obey the simple first order law, its earlier portion and the later one gave the lifetimes of the respective transient species, as respectively, about 170 μsec. and about 430 μsec.

Summarizing the results of the decay at 415 mμ, one can say that the decay is anomolous, with a hump in the early stage when there are two peaks at 415 and 520 mμ in the transient spectra, the only exception being the plain aqueous solution. On the other hand, the decay in question is simply monotonous when the peak at 520 mμ is low or is not present in the transient spectra.

When various amounts of oxygen were added to the solution, the decay at 520 mμ became slower with the increase in the oxygen concentration.

Discussion

Broadly speaking, the general features of the flash photobleaching correlate well with those of the steady-light photobleaching. Thus, in the evacuated state the bleaching is reversible; i. e., the introduction of air restores the color of the dye, indicating that the product is lecuo dye.

However, there are a few discrepancies which suggest that some different processes are occurring in the flash experiment. For example, n the presence of oxygen the bleaching is rreversible in the steady illumination, while n the case of a flash there is not any slight leaching observed, even by ten successive lashes. Further, the addition of amine to the hosphate buffer solution of methylene blue ncreases the steady-light bleaching more than enfold, while in the flash experiment the uantity of bleaching only doubles that in the bsence of amine, even when a large amount f amine is added.

There is scarcely any doubt that all the ansient spectra observed in the present investigation are due to some intermediates from ye in the photoreduction.

In the acidic solution there is only one intermediate, with a peak at 375 mμ with $\tau \approx$ 30 μsec. As has already been reported by Parker,[4] there is scarecely any doubt that this is due to the triplet state.

In the neutral solution quite different spectra than those of the acidic solution come into existence, and they show a rather complicated behavior. Thus in the plain aqueous solution, for example, the peaks at 415 and 520 mμ do not decline in a parallel way, the former declining a little faster at an early stage while at a later stage it seems that both decline at approximately the same rate. From the earlier part of the decay at 415 mμ, τ is estimated to be several ten μsec., while from the later part it is estimated as a few hundred μsec. Further, the decay curve at 415 mμ displays a notable anomaly in the phosphate and borate buffer and τ becomes a little longer.

From these facts there is no doubt that there are at least two transient species existing in this wavelength region. The one with the shorter τ may be a basic species of the triplet state. The effect of pH value on the transient spectra shown in Fig. 5 strongly supports this view. It seems worth mentioning that the pK-value obtained, pK=6.7, coincides with the sharp change in the rate of photoreduction observed by Oster[2] in steady-light photoreduction by EDTA.

However, it is questionable what kind of molecular change corresponds to this spectra change, because there is no corresponding different species existent in the ground state from pH $\approx$0 to pH $\approx$11. Although the acid-base property in the singlet excited state often differs from that in the ground state so greatly that the pK of the former is several units apart from that of the latter, there is no such difference in the triplet, according to Jackson and Porter.[5] Their results, however, are concerned with rather a limited group of compounds; it is possible that different types of substances behave differently. At any rate, we must in the future decide whether the 375 mμ band belongs to the protonated triplet bivalent cation and the 415 mμ band to the univalent cation, or whether the 375 mμ band is the univalent cation and the 415 mμ band a neutral molecule with OH^- attached, or whether quite a different interpretation must be made. Here, we would like to attribute tentatively the 375 and 415 mμ bands (with shorter τ) to two different species of the triplet. The fact that the transient species in the infrared region has τ=70~90 μsec., which is about equal to that of the earlier stage of

5) G. Jackson and G. Porter, *Proc. Roy. Soc.*, **260**, 13 (1961).

415 mμ absorption, also supports the triplet hypothesis.

As to the transient species which follow the triplet state, it is notable that there are two peaks, at 415 and 520 mμ, and that these transient spectra sometimes behave in a like manner, while in other cases they behave quite differently. Thus, when TMA or ATU is added, two peaks are observed, while when EDTA is added only the 415 mμ band appears; the 520 mμ band then becomes very weak or completely disappears. It is very natural, therfore, to consider that the two are produced by the same process in some cases but that only 415 mμ is produced in other cases and that the 415 mμ band is more intimately connected with the bleaching, because an effective reducing agent such as EDTA produces only this species.

In connection with this finding, it must be recalled that in the case of TMA and ATU, the rate formula for the steady illumination reaction closely approximates the second order law, while in case of EDTA the first order rate law holds.

From the above results it may be inferred that in the former case the excited dye (triplet, D^t), interacting with the ground state dye, D, produces semiquinone and a half-oxidized state, while in the latter case, the excited dye, by reacting with a reducing agent, produces only semiquinone. On this basis, the 415 and 520 mμ bands may be attributed respectively, to semiquinone and a half-oxidized state.

This hypothesis is further supported by the fact that the addition of leuco methylene blue greatly increases the peak at 415 mμ and completely eliminates the peak at 520 mμ. This implies that leuco dye, interacting with the triplet dye, produces semiquinone by the reaction $D^t + DH_2 \rightarrow DH + DH$ and that this occurs quite efficiently. It must be added here that the inhibiting action of leuco dye often referred to in the steady illumination experiment[1] is almost certainly due to such a reaction. The dehavior of the system containing oxygen also supports the above hypothesis. Thus, the finding that the absorbance by the existent oxygen at 415 mμ rapidly decreases while the decay at 520 mμ becomes slower is easy to understand if one considers that the former is a half-reduced form and the latter, a half-oxidized form.

It is well known that an analogous mechanism has been proposed by Lindqvist[6] for fluorescein on the basis of his extensive studies by the flash technique, but there have been no such examples reported since then.

As additional support for the above view, mention may be made of the features of the decay curves. The most conspicuous result is that in some cases a clear hump appears in the early stage of the decay. Such a phenomenon can be explained only if a certain transient species with a certain value of ε changes to another species with a negligible ε and is then transformed again into a third species with a rather large ε. The most plausible process satisfying the above conditions is considered to be the following one; the triplet dye with a certain value of ε goes back to the ground state, and the ground state dye thus produced, interacting with the remaining triplet dye, produces some new species with a larger ε. Thus D^t, at first, will perhaps go to the ground state by $D^t + D^t \rightarrow 2D$ or by a monomolecular process, but as the ground state dye accumulates, the $D^t + D \rightarrow 2D$ process will begin to make a greater contribution; accompanying this, the $D^t + D \rightarrow X(D^+ \cdots D^-)$ reaction will also occur. The later part of the above scheme is just the one proposed for the case when the second order rate formula is applied to the steady illumination experiment. Although exact analysis is very difficult, the conditions needed for the hump to appear may be something like the one described below.

Denoting a loosely-combined pair of semiquinone and a half-oxidized state as X and identifying the concentration of the triplet dye D^t, the ground state dye D, and X by, respectively, $[D^t]$, [D] and [X], the above scheme and the corresponding rate formulas may be written as follows, on the assumption that at $t=0$, $[D^t]_0 = a$, $[D]_0 = 0$, and $[X]_0 = 0$:

$D^t \rightarrow D$ k_1

$D^t + D \rightarrow 2D$ (deactivation) k_2

$D^t + D \rightarrow X$ (reaction) k_3

$X \rightarrow$ leuco dye or ground state dye k_4

$$-\frac{d[D^t]}{dt} = k_1[D^t] + k_2[D^t][D] + k_3[D^t][D]$$

$$\frac{d[D]}{dt} = k_1[D^t] + k_2[D^t][D] - k_3[D^t][D]$$

$$\frac{d[X]}{dt} = k_3[D^t][D] - k_4[X]$$

The absorbance of the system at 415 mμ [Ab] can then be given as follows if the molecular extinction coefficients of D^t, D, and X are, respectively, ε_1, $\varepsilon_2 = 0$ and ε_3:

$$[Ab] = l\{\varepsilon_1[D^t] + \varepsilon_3[X]\}$$

and

6) L. Lindqvist, *Arkiv för Kemi*, **16**, 79 (1960).

$$\frac{d[Ab]}{dt} = l\left\{\varepsilon_1\frac{d[D^t]}{dt} + \varepsilon_3\frac{d[X]}{dt}\right\}$$
$$= l\{-\varepsilon_1 k_1[D^t] - \varepsilon_1 k_2[D^t][D] - \varepsilon_1 k_3[D^t][D] + \varepsilon_3 k_3[D^t][D] - \varepsilon_3 k_4[X]\}$$

where l is the length of the reaction system.

At the earliest stage of the decay, $[D] \approx 0$; hence, $d[Ab]/dt < 0$, as is naturally expected.

For the hump to appear, $d[Ab]/dt > 0$ must hold in some region of the decay curve.

This requires

$$(\varepsilon_3 k_3 - \varepsilon_1 k_2 - \varepsilon_1 k_3)[D^t][D] > \varepsilon_1 k_1[D^t] + \varepsilon_3 k_4[X]$$

When X disappears very fast, a steady state condition may hold with regard to X and it will be possible to put $k_3[D^t][D]$ as approximately equal to $k_4[X]$. In this case the above condition never holds. However, if X is much more stable than D^t, then, by putting approximately $k_4 \approx 0$, the above conditions change as follows:

$$\varepsilon_3 > \varepsilon_1\left(\frac{k_2}{k_3} + \frac{k_1}{k_3[D]} + 1\right) \quad (1)$$

In fact, k_1 is $\sim 10^5\ sec^{-1}$, while k_4 may be put approximately as $\sim 10^3\ sec^{-1}$ from the later part of the decay curve. The situation is considered not to be very different from the above conditions. Provided that $k_1 \approx 10^5$, $k_2 \approx k_3 \approx 10^{10}$, and $[D] \approx 10^{-6}$ M, then (1) requires that $\varepsilon_3/\varepsilon_1 > 10$.

Thus it is expected in general that there are rather few chances for such a hump to appear, but it is not inconceivable. Borate and phosphate buffer solutions and solutions to which TMA or ATU has been added, are supposed to satisfy the above condition when the exciting light intensity is great enough. However, in the plain aqueous solution, in which X has a rather short lifetime, the condition would fail.

Further, when the intensity of the exciting light is small, the deactivation of X by the remaining ground state dye is large, as is expected from the steady illumination results, and so condition 1 can not hold again. In the case of EDTA, for which the rate formula is of the first order, D^t is directly reduced by EDTA, and so it is quite natural that the decay is simply monotonous.

To sum up, the results obtained in the flash experiments can be very satisfactorily correlated with the results obtained in the steady illumination experiments from the view point that the photoreduction of thiazine dyes in a neutral or an alkaline solution proceeds, in some cases, by a bimolecular process, $D^t + D \rightarrow D^- + D^+$ and, in other cases, by a direct electron transfer from the reducing agent to D^t.

It is to be hoped that more quantitative studies on the rate will be made and that the rate constant for each elementary reaction will be evaluated.

Summary

The intermediate species which are produced in the course of the photoreduction of methylene blue have been investigated by flash photolysis in plain aqueous, borate and phosphate buffer solutions with and without reducing agents. In an acidic solution, an absorption band with the lifetime of 30μsec. appears at 375 mμ, while in neutral and basic solutions, two bands appear, at 415 and 520 mμ, with lifetimes of 70~90 μsec. The bands at 375 and 415 mμ are considered to be due, respectively, to the acidic and basic forms of the triplet state, since the transient spectra change with pH, making an isosbestic point.

The band at 415 mμ is overlapped by another one with a lifetime longer by several hundred microseconds; this is presumed to be semiquinone. The intensity of the band at 520 mμ decreases upon the addition of reducing agents and increases upon the introduction of oxygen.

Hence, this band may be due to the half-oxidized form of the dye. These results support the reaction scheme that the excited state of the dye reacts with the ground state, which has been proposed in the investigation of steady light photobleaching.

Department of Chemistry
Faculty of Science
Tohoku University
Katahira-cho, Sendai

*Entropy and Molecular Motion in the Condensed Phases of Tetrahedral Molecules**

By Hideaki CHIHARA and Takako SHINODA

(Received August 29, 1963)

Much attention has been paid to the molecular motion in a class of compounds which were named plastic crystals by Timmermans,[1] who illustrated that crystals composed of molecules more or less spherical in shape have small entropies of fusion (less than 5 e.u.) and exhibit plasticity below their melting point. Evidence has been accumulated by studies of X-ray diffraction, nuclear magnetic resonance, dielectric absorption, etc. to indicate that molecules in the plastic crystals are capable of rotational motion, if not completely free. Since the entropy is a measure of the degree of disorder, it will also give us some clue to the state of molecular motion in solids, a clue which would complement the deductions from other types of experiments.

Plastic crystals usually have a transition accompanying a large entropy change comparable to or greater than the entropy of fusion. The sum of the two entropies is close to what one expects from Walden's rule (13 e.u.).[2] This forms the basis of the interpretation that such crystals melt in two successive processes; the rotational degrees melt at the transition point, while the translational degrees melt at the triple point. However, this is an over-simplified model, as is evident from detailed studies. For example, the X-ray diffraction[3] of Si_2Me_6 indicates that the molecular axis is statistically oriented along one of the body-diagonals of the cubic unit cell; therefore, the disorder is not considered perfect. The nuclear magnetic resonance study of CMe_4 by Gutowsky et al.[4] found the potential barrier hindering molecular reorientation in the plastic phase (called phase I hereafter) to be 1.0 kcal./mol.; it also showed that the molecular rotation is not free. One should then be able to see some consequences of the hindrance of rotation in the thermodynamic quantities.

A comparison of the entropy of fusion of, say, face-centered cubic carbon tetrachloride (2.401 e.u.) with that of an inert gas solid (3.395 e.u. for argon) provides a clue to this problem. The fact that the fusion of argon requires a larger entropy change than does the fusion of carbon tetrachloride is just the contrary to what one would anticipate on the basis of the over-simplified model. The situation may conveniently be visualized in terms of diagrams of the degree of disorder in different phases; such diagrams are drawn in Fig. 1

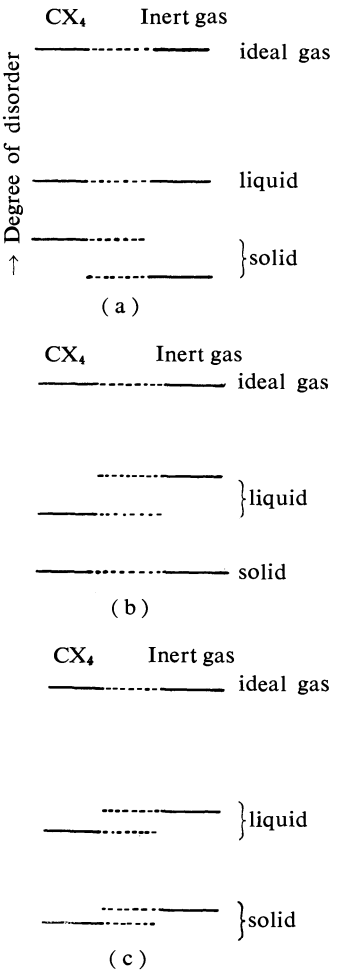


Fig. 1. A schematic representation of the degree of disorder in different phases of CX_4 type molecules and inert gases. (a) and (b) are extremely idealized situation, (c) is the actual situation.

* Presented before the 16th Annual Meeting of the Chemical Society of Japan, Tokyo, April, 1963.

1) J. Timmermans, *J. chim. phys.*, 35, 331 (1938).
2) P. Walden, *Z. Elektrochem.*, 14, 713 (1908).
3) Y. Chatani, unpublished.
4) E. O. Stejskal, D. E. Woessner, T. C. Farrar and H. S. Gutowsky, *J. Chem. Phys.*, 31, 55 (1959).

on the analogy of the more familiar energy-level scheme. The fact that carbon tetrachloride has a smaller entropy of fusion than an average inert gas solid may be accounted for in two extreme ways: (a) carbon tetrachloride molecules would move more freely than argon in the solid state if fusion in general could remove all the positional and orientational constraints in the solid to give any liquid the same degree of disorder (see Fig. 1a), and (b) the motion of carbon tetrachloride molecules would be less free in the liquid if both carbon tetrachloride and argon possess the same degree of disorder in the solid just before they melt (Fig. 1b). Of course, there are other possibilities, such as an intermediate between those two extremes, in which both of the carbon tetrachloride "levels" are displaced with respect to the corresponding argon "levels". In what follows, the actual level scheme will be shown to correspond to the one given in Fig. 1c. It will also be shown that the displacement of the solid levels may be explained by the hindered rotation of carbon tetrachloride molecules in the solid and that the displacement of the liquid levels may be explained by a simple cluster model of the carbon tetrachloride liquid. Effective values of the hindering potential barriers were derived for carbon tetrafluoride, carbon tetrachloride and neopentane in connection with a consideration of the possible orientations of molecules in crystals.

The Entropy of Sublimation and Molecular Motion in Solid. — Let us take the state of ideal gases at the triple points as the state of perfect disorder; neither the solid nor the liquid state is by itself in general a state of a well-defined degree of order. The degree of disorder in a solid at the same temperature will then be quantitatively expressed by its entropy of sublimation at the triple points. Since we are interested in the difference in behavior between inert gas molecules (suffix 1) and tetrahedral molecules (suffix 2), we shall fix our attention upon the difference in the entropies of sublimation:

$$(\Delta S_2-\Delta S_1)^{S\to G}=(T_2{}^G-T_2{}^S+R_2{}^G-R_2{}^S)-(T_1{}^G-T_1{}^S) \quad (1)$$

where T and R are the entropies of the translational (including configurational) and the rotational degrees of freedom respectively, and where the superscripts G and S refer to the ideal gas at atmospheric pressure and at the solid states respectively. Here it has been assumed that the intramolecular contribution to the entropy remains unaltered in the process of the phase change involved. A rearrangement of Eq. 1 gives

$$R_2{}^G-R_2{}^S=(\Delta S_2-\Delta S_1)^{S\to G}+\{(T_1{}^G-T_1{}^S)-(T_2{}^G-T_2{}^S)\} \quad (2)$$

We now assume that the bracketed term on the right hand side may be disregarded if we choose a hypothetical inert gas whose molecular weight is the same as for the particular CX_4; in other words, we assume that the degree of disorder is the same with respect to the configuration and motion of the molecular centers of mass, the molecular masses and the crystal structures being identical.

Table I lists the thermochemical values*1 relevant to the present calculation. A value of $\Delta S_1{}^{S\to G}$ was read off Fig. 2 for an appropriate molecular weight. The $(R_2{}^G-R_2{}^S)$ value thus obtained can be interpreted in various ways. An obvious way is that the rotational motion of CX_4 molecules is restricted in the solid state. The motion could either be a reorientation or a hindered rotation.*2

TABLE I. TRIPLE POINTS AND ENTROPY CHANGES (e.u.) AT THE TRIPLE POINTS

	Triple point, °K	$\Delta S^{S\to L}$	$\Delta S^{L\to G}$	$\Delta S^{S\to G}$	Ref.
Ne	24.57	3.26	16.23	19.49	5
Ar	83.810	3.395	18.15	21.54	6,13
Kr	115.776	3.386	18.38	21.77	7,25
Xe	161.3	3.400	19.216	22.616	8
CH_4	90.66	2.474	18.76	21.23	9
CF_4	89.47	1.87	24.81	26.68	10
CCl_4	250.3	2.401	24.52	26.92	11
CMe_4	256.53	3.03	20.70	23.73	12

*1 The entropies of vaporization at the triple points were computed from literature values of the entropy of vaporization at the boiling point (or at 25°C) and of the heat capacities of liquid and ideal gases. The entropies were corrected for the non-ideality of the gas and for the work of expansion from the triple point pressure to the standard pressure. The value for carbon tetrabromide was not obtained because its liquid heat capacity is not completely known.

*2 It seems that there has been some confusion or an indiscriminate use of the terms, reorientation and hindered rotation; thus it would be appropriate to define the words here, at least for the present purposes. By hindered rotation, it is meant that the molecules can rotate in one or the other direction over potential barriers with an average total energy sufficient to surmount the barrier; the rotational energy level is, therefore, above the top of the hindering barrier, On the other hand, if the average total energy is numerically less than the hindering potential, the molecule will normally oscillate in the potential well, with only occasional go-over when the molecule has acquired greater energy through statistical fluctuation. This we call reorientation. The frequency of the reorientation depends on the temperature and on the height of the potential barrier.

5) F. Rossini, D. D. Wagman, W. H. Evans, S. Levine and I. Jaffe, "Selected Values of Chemical Thermodynamic Properties," NBS Circular 500 (1952), p. 543.
6) K. Clusius and A. Frank, *Z. Electrochem.*, **49**, 308 (1943).
7) K. Clusius, A. Kruis and F. Konnertz, *Ann. Physik*, **33**, 642 (1938).
8) K. Clusius and L. Riccoboni, *Z. physik. Chem.*, **B38**, 81 (1938).
9) A. Frank and K. Clusius, ibid., **B36**, 291 (1937).

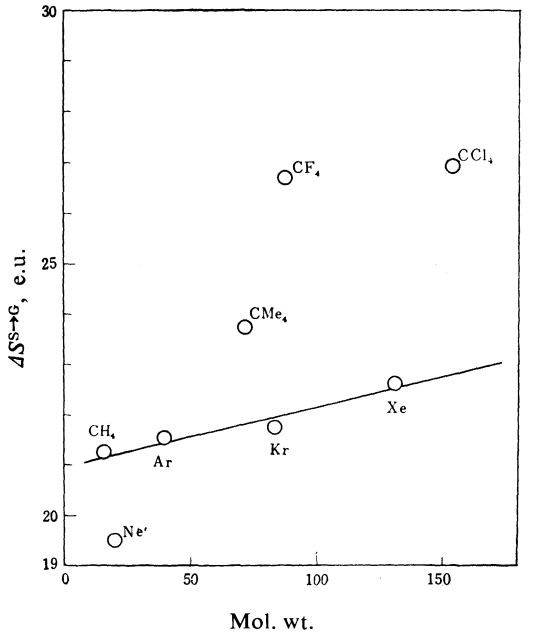


Fig. 2. Entropy of sublimation plotted versus molecular weight. A hypothetical inert gas of the same molecular weight is chosen to compare with a particular CX_4.

Our knowledge of the crystal structures of these compounds is not very complete. Their structure in the plastic phases is all face-centered cubic, at least with regard to the spatial arrangement of the center of gravity of the molecules; the one possible exception is carbon tetrafluoride, the structure of which is not yet known. It is reasonable, however, to assume that carbon tetrafluoride is isomorphous with carbon tetrachloride. The orientation of molecules in the lattice was not determined with certainty. For instance, the X-ray diffraction intensities from carbon tetrachloride[14] in its phase I can not be accounted for by a model of fixed molecular orientations, but they are appropriate to a model of rotating molecules even though the rotation is not perfectly free. For neopentane,[15] the temperature factor of the X-ray diffraction is so large that an almost free rotation of the molecules is suggested. The nuclear magnetic resonance experiments[16] (except carbon tetrachloride) give more direct information as to the mode of molecular motion in phase I (relative to X-ray studies), and it is strongly suggested that molecules are undergoing general rotation or three-dimensional reorientation (no distinction seems possible). Gutowsky[4] was able to derive the barrier height hindering the reorientation of the neopentane molecule as 1.0 kcal./mol. The crystal structure of phase II of these solids is even less well known. Mones and Post[15] reported that neopentane is weakly birefringent below the transition point and that it is probably tetragonal (close to cubic, however, $a_0=11.2$Å, $c_0=11.5$Å). It is generally agreed that methane is very close to cubic at lowest temperatures. Its zero-point configuration was studied by Nagamiya[17] and by James and Keenan[18]; the latter made a careful analysis of the stability of various orientations of molecules. Although James and Keenan's model for the structure of phase II of CD_4 is extremely idealized, their zero-point configuration is much more reliable*3 in the sense that it is the result of the self-consistent calculation of static lattice energy. We shall use this configuration as the basis of the present analysis.

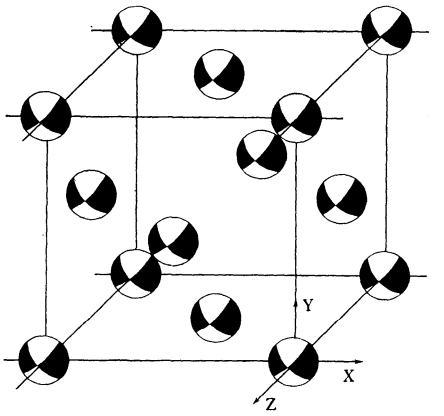


Fig. 3. Zero-point configuration of CD_4 crystal derived by James and Keenan, taken from Fig. 7 of Ref. 16. Black spots represent D atoms.

The James and Keenan structure for the phase III of CD_4 is reproduced from their paper in Fig. 3. We shall assume that this structure represents the features of the molecular orientational arrangement in all CX_4 molecules to be considered in this paper. In

10) A. Eucken and E. Schröder, ibid., B41, 307 (1938).
11) J. F. G. Hicks, J. G. Hooley and C. C. Stephenson, *J. Am. Chem. Soc.*, 66, 1064 (1944).
12) J. G. Aston and G. H. Messerly, ibid., 58, 2354 (1936); J. G. Aston, *Chem. Revs.*, 27, 59 (1940).
13) P. Flubacher. J. Leadbetter and J. A. Morrison, *Proc. Phys. Soc.*, A78, 1449 (1961).
14) B. Post, *Acta Cryst.*, 12, 349 (1959).
15) A. H. Mones and B. Post, *J. Chem. Phys.*, 20, 755 (1952).
16) J. G. Aston, Q. R. Stottlemyer and G. R. Murray, *J. Am. Chem. Soc.*, 82, 1281 (1960).

*3 Recently Savitsky and Hornig[19] cast, on the basis of infrared studies, some doubt on the James and Keenan structure, but their doubt is not considered definite either.
17) T. Nagamiya, *Prog. Theor. Phys.*, 6, 702 (1951).
18) H. M. James and T. A. Keenan, *J. Chem. Phys.*, 31, 12 (1959).
19) G. B. Savitsky and D. F. Hornig, ibid., 36, 2634 (1962).

TABLE II. DERIVED PROPERTIES OF CX_4 MOLECULES

	Rotational entropy in solid R_2^S (e.u.)	Reorientation mechanism		Hindered rotation mechanism
		torsional freq. cm^{-1}	pot. barrier kcal./mol.	pot. barrier kcal./mol.
CH_4	6.67	—	—	—
CF_4	11.67	30.4	3.4	1.0
CCl_4	18.95	24.8	7.7	2.4
CMe_4	18.33	28.3	3.8	1.3

the James and Keenan structure, the centers of the mass of molecules form a face-centerd lattice and one of the molecular C_2 axes is parallel with one of the crystallographic axes, while the others make an angle of 45° with two other crystallographic axes. The structure of the plastic phase is, of course, related to this zero-point configuration, the latter, however, being tetragonal rather than cubic. The structure of Fig. 3 can be rendered as a cubic symmetry, and, at the same time, as a rotational disorder if the plastic phase structure is assumed to be a hybrid of three such configurations in which crystal axes are permuted. As a first approximation, we shall assume that molecular rotation is a superposition of three independent plane rotations; the potential barrier hindering the rotation thus lies at 90° from the orientation of the minimum potential energy in three directions, in an adiabatic approximation in which the orientations of neighboring molecules are fixed. Such tetragonality disappears at the transition point in accordance with the excitation of the molecular rotational degrees of freedom or reorientation. A Similar consideration will apply to other CX_4 molecules.

i) Reorientation Mechanism.—First we will consider a model in which molecules reorient themselves in order that the crystal may possess the cubic symmetry. Molecules are in the state of harmonic libration (torsional oscillation) of frequency in potential minima and occasionally jump over the potential barrier. There are two distinguishable configurations*4 per molecule which contribute to the entropy R_2^S, which now becomes

$$R_2^S = 3R\,[x\exp(-x)/\{1-\exp(-x)\} - \ln\{1-\exp(-x)\}] + R\ln 2 \qquad (3)$$

where $x = h\nu/kT$

The values of ν and their corresponding potential barriers, V_0, were derived from $(R_2^G - R_2^S)$ by the use of Eq. 3 and $V = (1/2)V_0(1-\cos 2\theta)$ and are given in Table II. For methane, the $(R_2^G - R_2^S)$ is very close to zero, and, therefore, the molecules are rotating almost freely in phase I (at the triple point), in agreement with Staveley's analysis of the heat capacity.[20] There are no literature values available to compare with the ν and V_0 values derived here except for the ν of carbon tetrachloride in the low temperature phase, which was estimated to be 36.5~38 cm^{-1} by Gutowsky and McCall[21] from their measurements of chlorine nuclear quadrupole resonance frequencies as a function of temperature. The present value of 24.8 cm^{-1} for carbon tetrachloride is not unreasonable for the high temperature phase.

ii) Hindered Rotation Mechanism. — If one assumes the superposition of three plane rotators of CX_4 molecules in a solid in a potential field of the type

$$V = (1/2)V_0(1-\cos 2\theta) \qquad (4)$$

which is equivalent to assuming the rotation around the two-fold axes of a molecule, its contribution, R_2^S, to the entropy can be calculated by the help of Pitzer's table.[22] The values of the hindering potential, V_0, which correspond to the $(R_2^G - R_2^S)$ values for three degrees of freedom of rotation, are listed in Table II.

For the three compounds, carbon tetrafluoride, carbon tetrachloride and neopentane, the potential barrier in the reorientation mechanism is, as we have seen in Table II, comparable in magnitude with the heat of sublimation (2.4, 6.7 and 6.1 kcal./mol., respectively), and it is larger than the barrier for the hindered rotation mechanism by a factor of about three. Therefore, we consider that mechanism ii), the hindered rotation mechanism, is the more likely one. There is another reason for believing so: a consideration of the nuclear magnetic resonance of carbon tetrafluoride. Aston and others[16] showed that the

*4 Starting with the zero-point configuration, in which two of the diad axes of neighbor molecules make an angle of 45° with, say, the b and c axes of the lattice, a central molecule has two distinguishable orientations. The cubic symmetry of the crystal lattice is then acquired if the neighbor molecules take three different orientations wihch are obtained by the permutation of the crystal axes, a, b, and c. The original zero-point configuration, therefore, appears at the probability of 1/3, and there are three permutations of the crystal axes. The total number of distinguishable configurations will thus be $(2\times 1/3\times 3)^N = 2^N$.

20) L. A. K. Staveley, *J. Phys. Chem. Solids*, **18**, 46 (1961).
21) H. S. Gutowsky and D. W. McCall, *J. Chem. Phys.*, **32**, 548 (1960).
22) K. S. Pitzer, "Quantum Chemistry," Constable and Company, Ltd., London (1953), p. 498.

rigid lattice width of the fluorine resonance absorption in carbon tetrafluoride is about 12 gauss, which narrows in two distinct steps, at 55~65°K and at the transition point. They suggested, on the basis of their calculation of second moments, that carbon tetrafluoride molecules begin to rotate first around their two-fold axis at about 55°K and then rotate about all axes at higher temperatures. Now it is of some interest to examine what consequences in the nuclear resonance may be anticipated if we apply the familiar equation of the absolute reaction rate theory[23]

$$\nu \approx (kT/h) \exp(-V_0/kT) \tag{5}$$

to derive the frequency at which the molecules would jump over the potential barrier, V_0. The substitution of $V_0=3.4$ kcal./mol. and $T=89.47$°K leads to $\nu \doteqdot 9.2\times10^3\ \mathrm{sec}^{-1}$. This value of ν indicates that the motional narrowing will not occur until higher temperatures (97°K) because the rigid lattice width, 12 gauss, corresponds to $4.8\times10^4\ \mathrm{sec}^{-1}$ for the fluorine nucleus[24]. On the other hand, $V_0=1.0$ kcal./mol. gives $\nu \approx 7\times10^{10}\ \mathrm{sec}^{-1}$, which is sufficiently rapid to cause motional narrowing; the narrowing would occur at 30°K if the same potential barrier height persisted at such a temperature.

The fore-going analysis gives support to the view that the rotation of tetrahedral molecules in their plastic phase is not free, except possibly in the case of methane.

A Model for Liquid Carbon Tetrachloride at Its Triple Point

It remains to be examined how the displacement (in Fig. 1c) of the "level" of carbon tetrachloride with respect to the inert gas liquid "level" can be explained. The model we will now present is perhaps one of the simplest, but yet, we hope, it represents the feature of the structure of liquid at the triple point. We shall here consider carbon tetrachloride as an example.

It may be assumed that liquid carbon tetrachloride consists of clusters (embryos of crystallites), each containing n molecules, and that the arrangement and motion of the centers of mass of clusters are in the same degree of disorder as in an inert gas liquid. The molar entropy of liquid carbon tetrachloride will, then, be

$$S_2^{\mathrm{L}} = \frac{1}{n}(T_2+R_2+C_2)_{\mathrm{cluster}} + \frac{1}{n}(3n-6)s_l + R_2^{\mathrm{L}} + I_2 \tag{6}$$

where C_2 is the configurational entropy, s_l is the internal entropy (per degree of freedom) of a mole of clusters, R_2 is the molar entropy of molecular rotation, and I_2 is the intramolecular contribution to the entropy. The rotational modes of clusters related to R_2 (cluster) are nearly equivalent to a mode of intra-cluster vibration at the limit of a long wavelength and may, therefore, be approximated by additional degrees for intra-cluster modes:

$$S_2^{\mathrm{L}} = \frac{1}{n}(T_2+C_2)_{\mathrm{cluster}} + \frac{1}{n}(3n-3)s_l + R_2^{\mathrm{L}} + I_2 \tag{7}$$

The entropy of vaporization at the triple point is given by

$$\Delta S_2^{\mathrm{L}\to\mathrm{G}} = (T_2^{\mathrm{G}}+R_2^{\mathrm{G}}) - \frac{1}{n}(T_2+C_2)_{\mathrm{cluster}} - \frac{1}{n}(3n-3)s_l - R_2^{\mathrm{L}} \tag{8}$$

The corresponding expression for an inert gas is

$$\Delta S_1^{\mathrm{L}\to\mathrm{G}} = T_1^{\mathrm{G}} - (T_1^{\mathrm{L}}+C_1^{\mathrm{L}}) \tag{9}$$

Now, if we adopt the free volume model for the liquid,

$$T_1^{\mathrm{L}}+C_1^{\mathrm{L}} = R\left(-\ln N + \frac{5}{2} + \ln N\omega_1 + \frac{3}{2}\ln(2\pi mk/h^2) + \frac{3}{2}\ln t_1\right) \tag{10}$$

and

$$\frac{1}{n}(T_2+C_2) = \frac{R}{n}\left\{-\ln(N/n) + \frac{5}{2} + \ln(N\omega_2/n) + \frac{3}{2}\ln(2\pi mnk/h^2) + \frac{3}{2}\ln t_2\right\} \tag{11}$$

where a hypothetical inert gas was chosen so that it would have the same molecular mass, m, as carbon tetrachloride. The triple point, t_1, is also a hypothetical temperature for this value of m and was determined from a plot of the triple point temperature vs. the molecular weight. In the absence of a better alternative, an assumption, $n\omega_1=\omega_2$, was made concerning the free volumes, ω_1 and ω_2. Cancelling common terms between Eq. 10 and Eq. 11, we obtain, from Eqs. 8 and 9:

$$\Delta S_2^{\mathrm{L}\to\mathrm{G}} = (T_2^{\mathrm{G}}+R_2^{\mathrm{G}}) - \frac{1}{n}\left[(T_1^{\mathrm{G}} - \Delta S_1^{\mathrm{L}\to\mathrm{G}}) - \frac{3R}{2}\ln t_1 + \frac{3R}{2}\ln t_2 + \frac{5R}{2}\ln n\right] - \frac{1}{n}(3n-3)s_l - R_2^{\mathrm{L}} \tag{12}$$

23) S. Glasstone, K. J. Laidler and H. Eyring, "The Theory of Rate Processes." Princeton University Press (1941), Chapter IV.

24) E. R. Andrew, "Nuclear Magnetic Resonance," Cambridge University Press (1955), p. 167.

The intra-cluster entropy, s_l, may be approximated by the translational lattice entropy of solid T_2^S:

$$3s_l = T_2^S = T_2^G + R_2^G - R_2^S - \Delta S_2^{S\to G} \quad (13)$$

Finally, the estimation of R_2^L was made comparing the potential barriers hindering molecular rotation in a liquid with that in a solid at the triple point. The difference in the potential barrier arises from the difference in the average intermolecular distances (6.0Å in liquid and 5.897Å in solid). A good approximation to that part of intermolecular interaction which depends on the relative spatial orientation of molecules would be to use an effective cube octupole to represent a carbon tetrachloride molecule, thus taking into account the electric charge distribution and, to some extent, the shape of the molecule or the steric effect, because molecular dipole and quadrupole moments vanish by virtue of the tetrahedral symmetry of the molecules. The dispersion energy also depends on the relative molecular orientation and, therefore, contributes to the potential barrier; however, we shall incorporate the non-spherical part of the dispersion interaction into the effective octupole moment. Such interaction leads to the relation:

$$V_0(\text{liquid})/V_0(\text{solid}) = \{r(\text{solid})/r(\text{liquid})\}^7 \quad (14)$$

and the hindering potential barrier in liquid carbon tetrachloride at the triple point is found to be 2.1 kcal./mol. This value of V_0 gives R_2^L through the help of Pitzer's table.

The substitution of numerical values ($t_1 = 180°K$, $T_2^G = 40.13$ e.u., $R_2^G = 23.09$ e.u., $R_2^L = 19.42$ e.u., the other values have been taken from Tables I and II) into Eq. 12 gives, for the calculated entropy of vaporization of carbon tetrachloride at its triple point, t_2:

$$\Delta S_2^{L\to G} = 25.25 \text{ e.u.}$$

if one assesses on n the number 13, the number of nearest neighbor molecules in addition to the one at the center. This value, 25.25 e.u., is in excellent agreement with the observed value, 24.52 e.u.

Discussion

It has been suggested in the preceding sections that the small entropies of fusion of CX_4 molecules are the consequences of two effects combined; i. e. in the solid state the molecules are in the state of hindered rotation, and thus they possess a smaller degree of disorder than in an average inert gas solid, while in the liquid state they have still smaller degree of disorder than inert gas liquids. Thus, Fig. 1c shows what the actual situation looks like: both solid and liquid levels of CX_4 are lower than the corresponding levels of an inert gas in such a manner that the separation between the solid and liquid levels of CX_4 is smaller than that for inert gas. The interpretation that has been put forward in the present paper is based on the use of inert gases as the reference substance with which to compare tetrahedral molecules in regard to their behavior in condensed phases. Such a method of comparison is particularly useful because some of the properties of condensed phases are difficult to calculate from first principles. Thus, a straightforward calculation of the thermodynamic properties of liquids in terms of molecular distribution functions is a formidable task except for monatomic liquids. Also, the configurational entropy of a liquid can be estimated only to a certain limit, even in model theories. In the present treatment, such terms have been crossed out by similar terms for inert gases, and this is considered to be a major reason for the good agreement between the observed and calculated entropies of vaporization of carbon tetrachloride. Although the so-called free volume model was adopted for the liquid, the approximation imposed by the model was largely eliminated by virtue of the nature of the method of comparison. The present model of the liquid carbon tetrachloride is, of course, a statistical one. The clusters are constantly being formed and demolished. The number 13 for n should also be regarded as an average value.

One thing that has not been considered here is the effect of vacancy formation and self-diffusion in the solid at high temperatures. In the cases of argon and krypton, the measurements of heat capacity near the triple point were used to derive the equilibrium concentration of Schottky vacancies in the solid, which amounted to 2~3% at the triple points[25,26]. The contribution of the vacancy formation to the entropy would, however, be small even if there were no lattice relaxation; the difference between an inert gas and CX_4 solids would then be by far smaller. Self-diffusion in the solid will acquire an entropy of R if it is fully excited. The calculation of the entropy of diffusion in the intermediate state is not easy; here again there is a definite merit in the comparison method.

It is interesting to note that the potential barrier height hindering molecular rotation is

25) R. H. Beaumont, H. Chihara and J. A. Morrison, *Proc. Phys. Soc.*, **A78**, 1462 (1961).
26) A. J. E. Foreman and A. B. Lidiard, *Phil. Mag.*, **8**, 97 (1963).

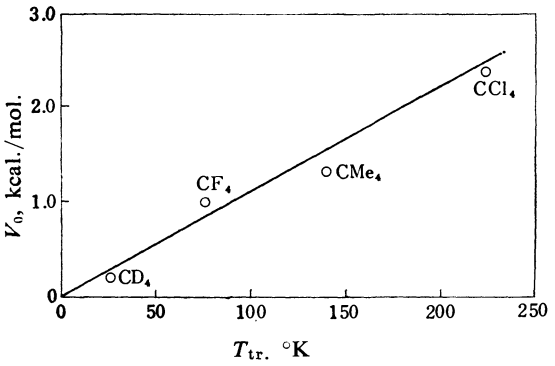


Fig. 4. Relation between the potential barrier hindering molecular rotation and the transition point.

related to the transition temperature in the solid, as is shown in Fig. 4. The point for CD_4 given by James and Keenan is also included in the figure. The points lie on a straight line which passes through the origin. While the entropy of fusion becomes larger in the order CF_4, CCl_4, CD_4 and CMe_4, the transition point becomes higher in the order CD_4, CF_4, CMe_4 and CCl_4, and so does the hindering potential. It is believed that such a linear relation between V_0 and the transition temperature justifies the treatment of a solid developed in the present paper. The apparently irregular order of the entropies of fusion has thus been straightened out.

Summary

By a comparison of the entropies of sublimation at the triple points of carbon tetrafluoride, carbon tetrachloride and neopentane with those of inert gas solids, it has been shown that these molecules are in the state of hindered rotation rather than of reorientation in the solid at the respective triple points, with heights of the potential barrier of 1.0, 2.4 and 1.3 kcal./mol. respectively. The hindering potential has been shown to be proportional to the transition temperatures of these solids.

A simple model for the structure of liquid carbon tetrachloride has been presented to account for its entropy of vaporization; the model consists in assuming nearest neighbor crystallite embryos in the liquid.

The authors are grateful to Professor Isamu Nitta of Kwansei Gakuin University, and to Professor Syûzô Seki and Dr. Hiroshi Suga of Osaka University for discussing the models with us.

Department of Chemistry
Faculty of Science
Osaka University
Nakanoshima, Osaka

SHORT COMMUNICATION

The Polymerization of 1, 1-Dichloro-2-vinylcyclopropane

By Takako TAKAHASHI, Iwao YAMASHITA and Takaharu MIYAKAWA

(Received October 21, 1963)

The ring-opening polymerization of cyclopropane derivatives has attracted keen interest recently. However, only a few reports that the oligomers of cyclopropane[1] and alkyl- or aryl-cyclopropanes[2] have been obtained have appeared. We have studied the polymerization of 1, 1-dichloro-2-vinylcyclopropane (I).

The compound I was prepared by the method of Woodworth and Skell.[3] We carried out bulk or solution polymerization in a nitrogen atmosphere with a sealed tube. I failed to polymerize when such usual ionic catalysts as $BF_3 \cdot (C_2H_5)_2O$, $AlCl_3$, $TiCl_4$, Et_3Al-$TiCl_4$ and Na (in liq. NH_3) were used, although in some

1) L. Harris, A. A. Ashdown and R. T. Armstrong, *J. Am. Chem. Soc.*, **58**, 852 (1936); H. E. Gunning and E. W. R. Steacie, *J. Chem. Phys.*, **17**, 351 (1947); R. J. Scott and H. E. Gunning, *J. Phys. Chem.*, **56**, 156 (1952).

2) H. Pines, W. D. Huntsman and V. N. Ipatieff, *J. Am. Chem. Soc.*, **75**, 2315 (1953); A. D. Ketrey, *Polymer Letter*, **1**, 313 (1963); A. Yamada. M. Yanagita and S. Suzuki, *Rikagaku Kenkyusho Hokoku*, **37**, 429 (1961).

3) R. C. Woodworth and P. S. Skell, *J. Am. Chem. Soc.*, **79**, 2542 (1957).

* Measured by the cryoscopic method in benzene.

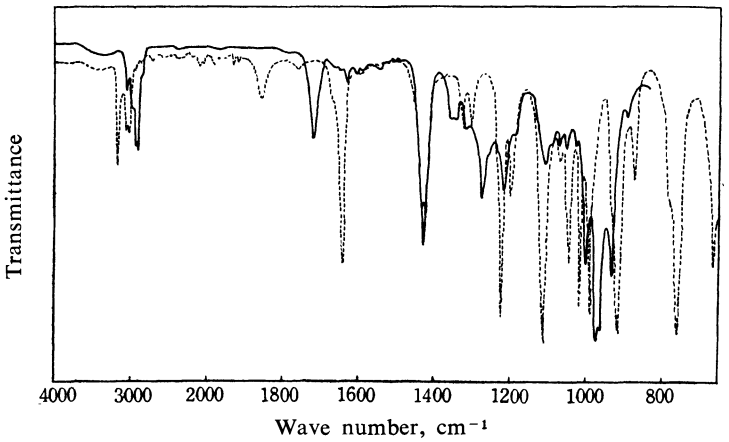


Fig. 1. Infrared spectra: (a) solid line, polymer obtained by benzoyl peroxide in CCl_4 paste; (b) dotted line, 1, 1-dichloro-2-vinylcyclopropane.

cases a trace of a solid product was obtained. When, however, benzoyl peroxide or α, α'-azobisisobutyronitrile was used as a catalyst, a polymeric product was obtained. For instance, when the bulk polymerization of I was carried out by benzoyl peroxide (5% wt.) for 40 hr. at 80°C, a crude polymer (with an average molecular weight* of about 1000) was obtained in a 36% yield. The curde polymer was dissolved in benzene, purified by pouring the solution into a large excess of methanol, and dried in vacuo. The purified polymer was powdery white, it melted at 70°C, its molecular weight* was about 7000, and its reduced viscocity was 0.025 (measured on a solution of 0.037 g. of polymer in 100 ml. of benzene at 30°C).

The chlorine content of the polymer (48.18 %) was found to be comparable with that of the monomer (calcd. 51.76%). Therefore, almost no dehydrochlorination or dechlorination took place in the polymerization process. The near-infrared spectrum of the polymer had no absorption band at 1.63 μ that might be assigned to the 1, 1-dichlorocyclopropane ring. The infrared spectra of I and the polymer obtained by benzoyl peroxide are shown in Fig. 1. In the spectrum of the polymer, the absorption bands of the cyclopropane ring (1020 cm^{-1}) and of the end vinyl group (990 cm^{-1}, 910 cm^{-1}) almost disappeared and that of the trans-double bond (965 cm^{-1}) was observed. Three peaks, 1720 cm^{-1}, 1270 cm^{-1}, and 1110 cm^{-1}, might be due to those of the benzoate group, which is an initiator fragment attached to the polymer's end. The presence of this end group was confirmed by the fact that, in the infrared spectrum of the hydrolysis product of the polymer, these absorption bands were absent. The polymer obtained by the use of α, α'-azobisisobutyronitrile had the absorption band of the immonium group (1800 cm^{-1}) in place of that of the benzoate group.

The infrared spectrum of unreacted monomer was in agreement with that of I.

On the other hand, 1, 1-dichloro-2-ethylcyclopropane gave no polymer when radical catalysts were used.

These facts might suggest that the polymerization of I mainly occurs by opening both the double bond and the cyclopropane ring, as is shown in the following scheme. This scheme is similar to those that have been proposed for the 1, 4-polymerization of conjugated dienes.

$$CH_2{=}CH\text{-}\overset{2}{C}H\text{—}\overset{3}{C}H_2 \rightarrow$$
$$\qquad\qquad\quad \diagdown\overset{1}{C}Cl_2$$
(I)

$$\text{-}[\text{-}CH_2\text{-}\overset{2}{C}H{=}\overset{1}{C}Cl_2\text{-}\overset{3}{C}H_2\text{-}]_n\text{-}$$

or $$\text{-}[\text{-}CH_2\text{-}\overset{2}{C}H{=}\overset{3}{C}H_2\text{-}\overset{1}{C}Cl_2\text{-}]_n\text{-}$$

Further details of such polymerization results and of the polymer structure will soon be published.

Government Industrial Research Institute, Osaka
Oyodo-ku, Osaka

Effect of Solvation on the Menschutkin Reaction in Liquid Sulfur Dioxide[1,2]

By Niichiro TOKURA and Yasuhiko KONDO

(Received July 8, 1963)

When the Menschutkin reaction in liquid sulfur dioxide was recently carried out,[2] it was indicated that the reaction in liquid sulfur dioxide is extremely slow compared to that in such nucleophilic dipolar solvents as dimethylformamide or dimethylsulfoxide. In the light of the facts that liquid sulfur dioxide is one of the best ionizing solvents[3] and that the product is an ion-pair (alkylammonium cation and halide anion), and judging from extensive previously-reported discussions,[4] the Menschutkin reaction should be very fast in liquid sulfur dioxide. The reasons for such a discrepancy perhaps lie both in the strong solvation of the solvent (liquid sulfur dioxide) to amines and the fact that the rate-determining step of the reaction may be the step of attack by the base on the alkyl halide.

In contrast to the cationic polymerization and the Beckmann rearrangement in liquid sulfur dioxide, which are very fast and in which unsolvated carbonium ions are favored,[2] the Menschutkin reaction is one of the reactions in which the unsolvated base (or anion) is favored. In both cases, the unsolvated or *bare* species (ion or substrate) is a predominating factor in carrying out the reactions rapidly. That a borderline case between S_N1 and S_N2 reactions has been observed by Ingold[5] in a substitution in liquid sulfur dioxide which would otherwise be an S_N1 reaction is to be understood as the result of the fact that the rate-determining ionization of alkyl halide is not followed by the fast step of the combination of alkyl carbonium ion with an anion or a base, since the base or the anion is solvated by sulfur dioxide and since the second step is also occasionally a slow step.

The organic reaction in a solution is a reaction of polymolecularity in the sense that the solvent molecule always has some interaction during the course of the reaction, as has already been pointed out by Winstein[6] and Ingold[6b]. In the present paper, the reaction of methyl iodide with *N, N*-dimethylaniline, pyridine, triethylamine, *N, N*-dimethylbenzylamine or their *o*-methyl-substituted derivatives has been undertaken in order to further elucidate the effect of the solvation of liquid sulfur dioxide on the bases as compared with that of nitrobenzene or methanol.

Experimental

Materials. — Methyl iodide was washed with a sodium thiosulfate solution, water, a sodium carbonate solution and water successively, then dried and distilled; b. p. 42.5~43°C. *N, N*-Dimethyl-*o*-toluidine was synthesized from *o*-toluidine-bromohydrate and methanol at 145~150°C,[7] and the twice-distilled product boiling at 181~182°C was used. *N, N*-Dimethylaniline and triethylamine were refluxed with acetic anhydride and distilled respectively. The bases were dried over potassium hydroxide and redistilled; b. p., *N, N*-dimethylaniline; 189°C, and triethylamine; 89.5~90.1°C. Pyridine was dried with potassium hydroxide and barium oxide successively and distilled; b. p. 115.5°C. *N, N*-Dimethylbenzylamine was dried over potassium hydroxide and distilled; b. p. 177~177.5°C. α-Picoline and 2,6-dimethylpyridine were purified as the following; a double salt from the base, hydrochloric acid and mercuric chloride was recrystallized three times from a dilute hydrochloric acid solution and decomposed with a sodium hydroxide solution. The product was extracted with benzene, dried with potassium hydroxide and barium oxide successively, and distilled; α-picoline; b. p. 129~131°C, and 2,6-dimethylpyridine; b. p. 143.0~143.1°C. Liquid sulfur dioxide was dried with phosphorus pentoxide and distilled. Nitrobenzene and methanol were purified by known methods.

Kinetic Procedure. — The method described in a preceding paper[2] was used. A potentiometric titration was used to estimate the amount of iodide anions produced.

1) Substitution in Liquid Sulfur Dioxide, Part III.
2) Part II: N. Tokura and Y. Kondo, This Bulletin, **36**, 200 (1963).
3) S. G. Smith, A. H. Fainberg and S. Winstein, *J. Am. Chem. Soc.*, **83**, 618 (1961).
4) E. A. Moelwyn-Hughes, "Reactions in Solution," 2nd ed., Oxford Univ. Press, London (1947), p. 208; M. S. Newman, "Steric Effects in Organic Chemistry," John Wiley, New York (1956), p. 70, contributed by E. Eliel.
5) M. L. Baird, E. D. Hughes and C. K. Ingold, *J. Chem. Soc.*, **1954**, 634.
6) a) S. Winstein, E. Grunwald and H. W. Jones, *J. Am. Chem. Soc.*, **73**, 2700 (1951); b) C. K. Ingold, "Structure and Mechanism in Organic Chemistry," Cornell Univ. Press, Ithaca (1953).
7) H. Reinhardt and W. Staedel, *Ber.*, **16**, 29 (1883).

Results and Discussion

The Kinetical Order of the Reaction.—Methyl iodide was used as the alkyl halide since it is believed to be ionizable only with difficulty, since the reaction may thus be conveniently carried out by a S_N2 mechanism, and since it has the least steric hindrance to a coupling with the nitrogen atom of the amines. However, as may be seen in Table I, the kinetical order of the reaction (methyl iodide with pyridine) varied from second order to first order as the molar ratio, [base]/[halide], exceeded unity. When the base was used excessively against the halide, the reaction rate followed the first order rate law, the first order in methyl iodide, and the zero-th order in pyridine.

These phenomena are reported to be often encountered in cases wherein a one-to-one intermediate complex is formed reversibly in a reaction course.[8] In the reaction of methyl iodide and pyridine, the intermediate may be,

Pyridine···Me···I

The formation of such an intermediate is consistent with the experimental fact that the

TABLE I. THE RATE CONSTANTS OF THE REACTION BETWEEN METHYL IODIDE AND PYRIDINE IN LIQUID SULFUR DIOXIDE AT 40°C

(a) Methyl iodide: 0.399 mol./l.
Pyridine: 0.820 mol./l.

t min.	I^- $\times10^2$ mol./l.	k_1 $\times10^3$ min^{-1}	k_2 $\times10^2$ l. mol^{-1} min^{-1}
10	4.25	1.13	1.45
20	8.05	1.13	1.52
30	11.45	1.16	1.65
40	14.5	Const. 1.12	1.66
50	17.3	1.13	1.75
65	20.8	1.16	1.90

(b) Methyl iodide: 0.399 mol./l.
Pyridine: 0.615 mol./l.

15	4.75	8.78	1.54
30	8.95	8.20 Const.	1.56
45	12.4	7.71	1.57
60	15.4	7.55	1.64
75	18.0	Const. 7.49	1.72
90	21.0	7.31	1.81

(c) Methyl iodide: 0.399 mol./l.
Pyridine: 0.359 mol./l.

20	3.50	4.85	1.50
40	6.75	4.41	1.51
60	9.47	4.16 Const.	1.58
80	11.82	3.70	1.53
100	13.76	3.50	1.59
120	15.47	3.18	1.56

TABLE II. SECOND ORDER RATE CONSTANTS OF THE REACTIONS. METHYL IODIDE WITH BASES IN LIQUID SULFUR DIOXIDE

Base	Reaction temp., °C	k, l. mol^{-1} sec^{-1}	$\Delta E^{\neq}$, kcal. mol^{-1}	A
N,N-Dimethylaniline[2]	30	1.72×10^{-5}	17.2	5.11×10^{7}
	40	4.77×10^{-5}		
	50	9.93×10^{-5}		
Pyridine[2]	20	3.38×10^{-5}	17.8	6.50×10^{8}
	30	9.00×10^{-5}		
	40	2.47×10^{-4}		
Triethylamine	40	5.69×10^{-5}	22.7	4.03×10^{11}
	50	1.79×10^{-4}		
	60	5.10×10^{-4}		
N,N-Dimethylbenzylamine	45	2.93×10^{-5}	22.6	9.91×10^{10}
	55	8.62×10^{-5}		
	65	2.41×10^{-4}		

TABLE III. A COMPARISON OF THE RELATIVE RATES IN SOLVENTS (40°C)

Base		*N,N*-Dimethyl-aniline	Pyridine	Triethylamine	*N,N*-Dimethyl-benzylamine
K_b, 25°C*		1.15×10^{-9}	2.3×10^{-9}	7.36×10^{-4}	1.86×10^{-4}
Liq. SO_2	$k\times10^5$	4.77[2]	24.70[2]	5.69	1.64
	Relative rate	1	5.18	1.19	0.34
Nitrobenzene	$k\times10^4$	2.10[9]	9.82[10]	708[11]	Very fast
	Relative rate	1	4.68	338	
Methanol	$k\times10^5$	19.4[12]	9.29	221	579
	Relative rate	1	0.48	11.4	29.8

* Landolt-Börnstein Tabellen

8) L. G. Cannel, *J. Am. Chem. Soc.*, 79, 2929 (1957).
9) K. J. Laidler, *J. Chem. Soc.*, **1938**, 1786.
10) H. C. Brown and A. Cahn, *J. Am. Chem. Soc.*, 77, 1715 (1955).
11) H. C. Brown and N. R. Eldred, ibid., 71, 445 (1945).
12) A. G. Evans et al., *J. Chem. Soc.*, **1939**, 1345.

TABLE IV. THE ARRHENIUS PARAMETERS IN THE MENSCHUTKIN REACTION IN SOLVENTS*

Base \ Solvent		Liq. SO_2	Nitrobenzene	Methanol
N, *N*-Dimethylaniline	$\Delta E^{\ddagger}$	17.2	12.8[9]	15.2[12]
	$\Delta S^{\ddagger}$	−25.3	−36.4	−29.0
Pyridine	$\Delta E^{\ddagger}$	17.8	13.6[10]	18.2
	$\Delta S^{\ddagger}$	−20.3	−29.8	−21.0
Triethylamine	$\Delta E^{\ddagger}$	22.7	9.7[11]	16.4
	$\Delta S^{\ddagger}$	− 7.5	−34.7	−20.4
N, *N*-Dimethylbenzylamine	$\Delta E^{\ddagger}$	22.6	—	13.9
	$\Delta S^{\ddagger}$	−10.3	—	−26.5

* $\Delta E^{\ddagger}$, kcal. mol^{-1}, $\Delta S^{\ddagger}$, e. u.

ionizing power of the solvent has little influence on the reaction rate.[2] Therefore, the reaction rates were followed in the range of the molar ratio, in which the second order rate law was dominating, and in the initial stage of the reaction. A typical run with triethylamine is shown in Fig. 1.

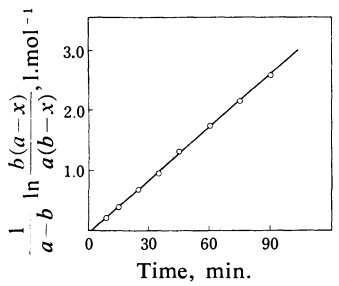


Fig. 1. A typical run in liquid sulfur dioxide. Temp. 60°C, triethylamine: 0.431 mol.l^{-1}, methyl iodide: 0.301 mol.l^{-1}

The Effect of Bases on the Reaction Velocity.—The results are indicated in Tables II and III.

In general, the rate of the Menschutkin reaction is in the order.

nitrobenzene > methanol > liquid sulfur dioxide

in liquid sulfur dioxide, however, the rate is slower than in methanol or in nitrobenzene. In nitrobenzene, the order of the relative rates of the bases is dependent upon the K_b values of the respective bases:

N, *N*-dimethylbenzylamine > triethylamine > pyridine > *N*, *N*-dimethylaniline

and in methanol, the order is:

N, *N*-dimethylbenzylamine > triethylamine > *N*, *N*-dimethylaniline > pyridine

whereas in liquid sulfur dioxide, the order is reversed:

pyridine > triethylamine > *N*, *N*-dimethylaniline > *N*, *N*-dimethylbenzylamine

Moreover, the difference in the relative rates is small (in the range of 0.34~5.18) in liquid sulfur dioxide, whereas in nitrobenzene the relative rates are scattered throughout the 1~338 range and in methanol, the 1~29.8 range. Thus in liquid sulfur dioxide the rate constants are leveling, while in nitrobenzene they are differentiating. A comparison of the Arrhenius parameters is givin in Table IV.

As may be seen in Table IV, both the energy and the entropy of the activation are larger in liquid sulfur dioxide. The entropy of the activation of triethylamine is the largest (−7.5 e. u.). This is very consistent with the very small value of the dissociation constant, (0.007 in benzene[13]) of the triethylamine-sulfur dioxide complex and suggests the effect of sulfur dioxide solvation on the reaction velocity. The release of the solvated sulfur dioxide may be necessary in the reaction sequences. The inverse order of the relative rates in liquid sulfur dioxide may perhaps be ascribed to the following reasons. First, in sulfur dioxide, the stronger the bases, the more will be the solvation by sulfur dioxide molecules; thus, the attacking rate may be modified according to their strength as bases. The dissociation constant of the pyridine-sulfur dioxide complex is as large as 4.0[13] (571 times that of the triethylamine-sulfur dioxide complex), while the K_b values also reflect the above relation. In methanol the hydrogen bonding may be operative, and in nitrobenzene some interaction with the bases may be considered; however, these solvents are less solvating to the bases than is liquid sulfur dioxide.

Effect of *o*-Methyl Substituents.—An intimate relation between the rate and the solvation has been further clarified by study of the ortho-substituent effect. The effect of the *o*-methyl substituent of *N*, *N*-dimethylaniline or pyridine on the reaction rate has been examined in liquid sulfur dioxide and has been compared

13) J. A. Moede and C. Curran, *J. Am. Chem. Soc.*, **71**, 852 (1949).

TABLE V. EFFECT OF *o*-METHYL SUBSTITUENT ON THE RATE CONSTANT AND THE ARRHENIUS PARAMETER

Solvent	Base	Reaction temp., °C	k l. mol^{-1} sec^{-1}	$\Delta E^{\ddagger}$ kcal. mol^{-1}	A
Liquid sulfur dioxid	*N*,*N*-Dimethyl *o*-toluidine	40	1.65×10^{-5}	15.9	2.17×10^{6}
		50	3.62×10^{-5}		
		60	7.81×10^{-5}		
	α-Picoline	30	9.50×10^{-5}	17.4	3.39×10^{8}
		40	2.44×10^{-4}		
		50	5.63×10^{-4}		
	2,6-Dimethyl-pyridine	30	7.95×10^{-5}	14.4	1.93×10^{6}
		40	1.72×10^{-4}		
		50	3.51×10^{-4}		
Methanol	Pyridine	40	9.29×10^{-5}	18.2	4.59×10^{8}
		50	2.26×10^{-4}		
		60	5.35×10^{-4}		
	α-Picoline	40	3.07×10^{-5}	19.2	7.66×10^{8}
		50	7.91×10^{-5}		
		60	1.95×10^{-4}		
	2,6-Dimethyl-pyridine	55	1.25×10^{-5}	22.0	5.3×10^{9}
		65	3.20×10^{-5}		
		75	8.60×10^{-5}		

TABLE VI. COMPARISON OF THE RATE CONSTANTS OF *o*-SUBSTITUTED BASES AT 40°C

Base \ Solvent	Liquid sulfur dioxide		Methanol	
	k	k/k_H	k	k/k_H
N,*N*-Dimethylaniline	4.77×10^{-5} [2]	1	1.19×10^{-3} a)	1
N,*N*-Dimethyl-*o*-toluidine	1.65×10^{-5} [2]	0.346	4.17×10^{-5} a)	0.035
Pyridine	2.47×10^{-4} [2]	1	9.29×10^{-5}	1
α-Picoline	2.44×10^{-4}	0.988	3.07×10^{-5}	0.330
2,6-Dimethylpyridine	1.72×10^{-4}	0.696	2.34×10^{-6} b)	0.0252

a) Ref. 12
b) Calculated from the results in Table V

TABLE VII. COMPARISON OF THE ARRHENIUS PARAMETERS

Base \ Solvent		Liquid sulfur dioxide	$\Delta E^{\ddagger}_{o\text{-Me}}-\Delta E^{\ddagger}_{H}$	Methanol	$\Delta E^{\ddagger}_{o\text{-Me}}-\Delta E^{\ddagger}_{H}$
N,*N*-Dimethylaniline	$\Delta E^{\ddagger}$, kcal. mol^{-1}	17.2		15.2	
	$\Delta S^{\ddagger}$, e. u.	−25.3		−29.0	
N,*N*-Dimethyl-*o*-toluidine	$\Delta E^{\ddagger}$, kcal. mol^{-1}	15.9	−1.3	21.1	+5.9[12]
	$\Delta S^{\ddagger}$, e. u.	−31.6		−18.0	
Pyridine	$\Delta E^{\ddagger}$, kcal. mol^{-1}	17.8		18.2	
	$\Delta S^{\ddagger}$, e. u.	−20.3		−21.0	
α-Picoline	$\Delta E^{\ddagger}$, kcal. mol^{-1}	17.4	−0.4	19.2	+1.0
	$\Delta S^{\ddagger}$, e. u.	−21.6		−20.0	
2,6-Dimethylpyridine	$\Delta E^{\ddagger}$, kcal. mol^{-1}	14.4	−3.4	22.0	+3.8
	$\Delta S^{\ddagger}$, e. u.	−31.9		−16.1	

with that in methanol (cf. Tables V, VI and VII).

A dramatical difference is observed in the ortho-effect between the rates in liquid sulfur dioxide and in methanol. As may be seen in Table VI, $k_{o\text{-Me}}/k_H$ is the ratio of the rate constants of the *o*-methyl-substituted and the unsubstituted bases. In liquid sulfur dioxide, the ratios are 0.346 (*N*, *N*-dimethyl-*o*-toluidine), 0.988 (α-picoline) and 0.696 (2, 6-dimethylpyridine) respectively, while in methanol the ratios are greatly depressed: 0.035 (*N*, *N*-dimethyl-*o*-toluidine), 0.330 (α-picoline) and 0.0252 (2, 6-dimethylpyridine) respectively, a leveling effect being again prevalent in liquid sulfur dioxide.

In methanol, both the activation energy and the entropy of activation increase when the methyl group is introduced in the ortho-position. In liquid sulfur dioxide, both the parameters decrease upon the introduction of the *o*-methyl substituent, as is shown in Table VII. The

above results may also be well interpreted as due to the effect of solvation by liquid sulfur dioxide. The *o*-methyl group in dimethylaniline or in the pyridine ring is expected to lower the basicity of the base, either by hydrogen bonding (chelate formation as in Fig. 2) or by partial inhibition of the resonance by the steric hindrance of the methyl group.[14] In liquid sulfur dioxide, the reduction of

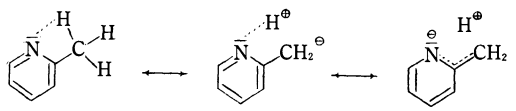


Fig. 2

solvation may compensate for the basicity depression by the *o*-methyl group and thus eliminate the difference or level off the rate constants, as may be seen in Table VI. An alternative explanation is that the solvation of sulfur dioxide to the nitrogen atom of the base is competitive against the chelation or the resonance inhibition. The lack of the linear dependence of the activation energy difference on the heat of the vaporization of the base in liquid sulfur dioxide, as will be described below, seems to support both views.

The Heat of Vaporization and the Difference in the Activation Energy. — If the basicity depression of an *o*-methyl substituted base is to be ascribed to the chelation effect, the reaction rate of the Menschutkin reaction should have some linear dependence on the heat of the vaporization of the base, since it is a well-established fact[15] that the boiling point of *o*-methylaniline is lower than that of *p*-methylaniline because of the same chelation, as Fig. 2 shows. In Fig. 3, the difference, $\Delta E^*_{o\text{-Me}} - \Delta E^*_{H}$, was plotted against the difference of the heat of evaporation of the *p*- and *o*-methyl derivative, $\Delta H_p - \Delta H_o$. In methanol, a linear plot is obtained, where ΔH_p, ΔH_o, $\Delta E^*_{o\text{-Me}}$ and ΔE^*_{H} are the heat of the vaporization of the *p*-methyl derivative, that of the *o*-methyl derivative, the activation energy of *o*-methyl, and that of the unsubstituted bases respectively.

As may be seen in Fig. 3, in liquid sulfur dioxide the plots are scattered, while in methanol a linear dependence between the differences in activation energies and in heats of evaporation is observed.

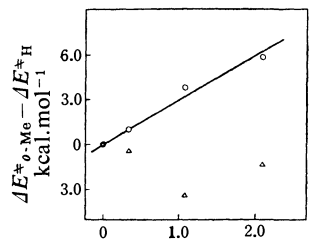


Fig. 3. Dependence of difference of activation energies on difference of heat of evaporation.
○ MeOH △ liq. SO_2

TABLE VIII. THE HEAT OF VAPORIZATION OF *o*- AND *p*-METHYL-SUBSTITUTED BASES

Base	B. p. °C[a]	Heat of evaporation[a] kilojoule/mol.
N,*N*-Dimethylaniline	192.7	44.35
N,*N*-Dimethyl-*o*-toluidine	183.9	39.7
N,*N*-Dimethyl-*p*-toluidine	210.0	48.5[b]
Pyridine	115.2	35.11
α-Picoline	129.4	37.77
γ-Picoline	145.4	39.20
2,6-Dimethylpyridine	144.0	39.52
3,5-Dimethylpyridine	171.9	44.09

a) Landolt-Börnstein Tabellen
b) Calculated from the relationship between vapor pressure and temperature

The Isokinetic Relation. — Although a linear relationship has never been obtained in liquid sulfur dioxide between the activation energy and the heat of vaporization, it seems likely that a similar reaction mechanism is taking place throughout the reaction in liquid sulfur dioxide. The plots of ΔE^* against ΔS^* gave a linear isokinetic relation[16] (Fig. 4), whose slope indicates that the isokinetic temperature is 350°K. The temperature is very close to the experimental condition (30~75°C), again proving the leveling effect of liquid sulfur dioxide.

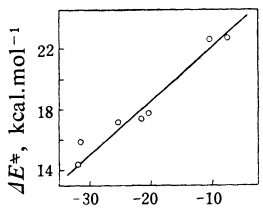


Fig. 4. Isokinetic relationship in liquid sulfur dioxide, methyl iodide with various bases.

Summary

1) The effect of the solvent solvation has been compared in the reaction between methyl

14) J. W. Smith, *J. Chem. Soc.*, **1961**, 31.
15) E. Pimental and A. L. McClellan, "The Hydrogen Bond," W. H. Freeman Co., New York (1960), p. 8.
16) J. E. Leffler, *J. Org. Chem.*, **20**, 1202 (1955).

iodide and various bases in liquid sulfur dioxide, methanol and nitrobenzene. The reaction rate in liquid sulfur dioxide is very much depressed, and the differences in the relative rates among bases are reduced in sulfur dioxide (a leveling effect) as compared to the other two solvents.

2) The order of the relative rates is reversed in liquid sulfur dioxide; pyridine>triethylamine > *N*, *N*-dimethylaniline > *N*, *N*-dimethylbenzylamine, whereas in methanol and in nitrobenzene, *N*, *N*-dimethylbenzylamine is the fastest of the bases. The reasons for this have been discussed.

3) The effect of the *o*-methyl substituent of the bases on the reaction rate has been examined. In liquid sulfur dioxide, the rate ratios $k_{o\text{-Me}}/k_{H}$ are again leveling, while in methanol the ratios are differentiating. The solvation of sulfur dioxide has been considered to be the reason.

4) An isokinetic relation between $\Delta E^{\ddagger}$ and $\Delta S^{\ddagger}$ has been observed, and the isokinetic temperature calculated as 350°K; however, no linear dependence was obtained between $\Delta E^{\ddagger}_{o\text{-Me}} - \Delta E^{\ddagger}_{H}$ and $\Delta H_{p} - \Delta H_{o}$.

The authors are indebted to the Seitetsu Kagaku K. K. for its gift of liquid sulfur dioxide.

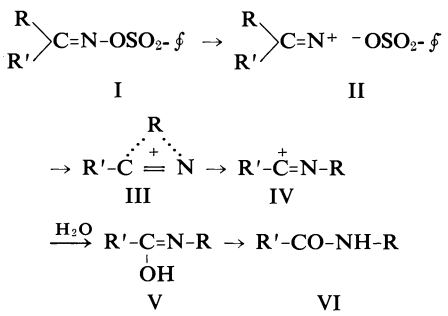
The Chemical Research Institute of Non-Aqueous Solutions
Tohoku University
Katahira-cho, Sendai

Solvent Effect on the Rearrangement of Cyclohexanoneoxime-p-toluenesulfonate. The Ionizing Power of Liquid Sulfur Dioxide[1,2]

By Niichiro TOKURA, Tetsuyo KAWAHARA and Sachio IKEDA

(Received July 20, 1963)

In liquid sulfur dioxide, the Beckmann rearrangement has been reported to take place with unusual rapidnesss,[3] at a low temperature[4] and without any side reaction,[5] giving a product of an extreme purity.[3,4] The Beckmann rearrangement was elucidated first by Kuhara in 1906, when he observed that benzophenoneoxime-benzenesulfonate rearranges spontaneously and that the product formed is hydrolyzed to yield benzanilide.[6,7] He studied this rearrangement under varying conditions, thus finding out that the reaction rate depends both on the acid strength and on the easiness of the cleavage of the N–O bond of the oximeester to an ion-pair, $=N^+ \ ^-O-$. Lately the mechanism of the reaction has been generally accepted as depicted in Chart 1, according mainly to the studies of Chapman,[7] Pearson[8] and Huisgen[9].



In a recent paper, Heldt[10] has found that the first order rate of the rearrangement of cyclohexanoneoxime-*p*-toluenesulfonate depends on the ionizing power of the solvents. The solvents used were acetic acid, chloroform, methanol and ethanol. The present authors have also attempted to study the solvent effect on the rearrangement, paying special attention to the ionizing power of liquid sulfur dioxide.

The results confirm that sulfur dioxide is an excellent solvent for the rearrangement,

1) The Beckmann Rearrangement in Liquid Sulfur Dioxide, Part XII.

2) Part XI: N. Tokura, K. Shiina and T. Terashima, This Bulletin, **35**, 1986 (1962).

3) N. Tokura, R. Asami and R. Tada, *Science Report of Res. Inst., Tohoku University*, A8, 149 (1956).

4) R. Tada, Y. Masubuchi and N. Tokura, This Bulletin, **34**, 209 (1961).

5) N. Tokura and K. Shiina, ibid., **35**, 1779 (1962); N. Tokura, K. Shiina and T. Terashima, ibid., **35**, 1986 (1962).

6) M. Kuhara and T. Kainosho, *Memoirs Coll. Sci. Kyoto*, **1**, 254 (1906).

7) A. W. Chapmann et al., *J. Chem. Soc.*, **1933**, 806; **1935**, 1223; **1936**, 448.

8) D. E. Pearson et al., *J. Org. Chem.*, **14**, 118 (1949); **17**, 1511 (1952); **19**, 957 (1954); **20**, 488 (1955); *J. Am. Chem. Soc.*, **81**, 612 (1959).

9) R. Huisgen et al., *Ann.*, **604**, 191 (1957); **602**, 127 (1957); *Chem. Ber.*, **90**, 1844 (1957).

10) W. Z. Heldt, *J. Org. Chem.*, **26**, 1695 (1961); *J. Am. Chem. Soc.*, **80**, 5972 (1958).

although no distinct solvent effect could be deduced to show the relationship between the rate of rearrangement and the ionizing power of the solvent. The ionizing powers of liquid sulfur dioxide, nitromethane, ethylenedichloride and ethyl methyl ketone have also been estimated according to the method of Kosower.[11]

Experimental

Materials.—Cyclohexanoneoxime was prepared according to the known method; m.p. 90.5~91.0°C. Commercial *p*-toluenesulfonylchloride was dissolved in carbon tetrachloride and then precipitated by petroleum ether. Liquid ammonia was dried with sodium wire and distilled. Liquid sulfur dioxide was dried with phosphorus pentoxide and distilled. Benzene, carbon tetrachloride, petroleum ether (b.p. 30~60°C), acetone and chloroform were purified according to the known methods.

The acetonitrile of the first grade materials was dehydrated with phosphorus pentoxide and distilled; b. p. 82.0°C. Pyridine was dehydrated with potassium hydroxide and then with barium oxide, and distilled over barium oxide; b.p. 115.0°C. Ethylenedichloride was dehydrated with calcium chloride and then with phosphorus pentoxide, and distilled; b.p. 83.0~83.7°C. Ethyl methyl ketone was dried over phosphorus pentoxide and fractionated; b.p. 79.3~79.8°C.

Preparation of Cyclohexanoneoxime-*p*-toluenesulfonate.—The preparative method of Heldt,[10] was modified. Into a cooled, three-necked flask, 200 ml. of liquid ammonia was introduced. 3.26 g. of sodium wire was rapidly stirred in, and then a trace of ferric nitrate was added as a catalyst. The color of the solution changed from blue to dark green in 60 min. The excess ammonia was evaporated, and a solution consisting of 15.7 g. of cyclohexanoneoxime in 70 ml. of dry benzene was added to the mixture while the temperature of the flask was kept below 35°C. After the addition of the oxime, the mixture was stirred for a further 16 hr. at room temperature. Then the precipitate was filtered, washed eight times with dry benzene, and dried under reduced pressure; yield, 16 g.

To a slurry of 16 g. of sodium oximate thus prepared in 30 ml. of benzene, 17 g. of *p*-toluenesulfonyl chloride in 70 ml. of dry benzene was added, and the mixture was stirred for two hours at 25~30°C. The precipitate was filtered, dissolved in dry carbon tetrachloride, treated with active carbon, and again filtered. Petroleum ether was added to the filtrate to cause a white clouding, and the mixture was allowed to stand in an ice box for 24 hr. The precipitate formed was separated and dried under reduced pressure; m.p. 57°C (lit.,[10] m.p. 56.8~58°C).

Found: N, 5.28. Calcd. for $C_{13}H_{17}NO_3S$: N, 5.24%.

Apparatus and Procedure. — *Ionizing Power (Z-Value[11]) of Solvents, Including Liquid Sulfur Dioxide.* —The ultraviolet absorption spectra were measured by an Hitachi Model EPU-2A type spectrophotometer using 1-ethyl-4-carbomethoxypyridiniumiodide (m. p. 111°C) (lit.,[11] 111~112°C) as the reagent. The c-t band was estimated in a quartz cell 10 mm. wide at 25°C. A specially-designed pressure cell with quartz windows (0.36 mm. wide) was used for liquid sulfur dioxide.

Kinetic Procedure.—The change of the concentration of oxime-*p*-toluenesulfonate was followed by the infrared spectrometry of Heldt.[10] An Hitachi Model EPI-S double beam spectrometer was used, with a specially-designed pressure cell (KCl width: 0.077 mm.) for liquid sulfur dioxide and with a cell (NaCl width: 0.1 mm.) for the other solvents. The absorption at 857 cm^{-1} (a frequency due to the N-O stretching vibration of oxime) was used.[10] Beer's law was obeyed throughout the experiment. The base line method was used for the estimation of the absorbancy.

The first order reaction dominated in each solvent, the rate constants of which were obtained from the linear plot of the time, t, vs. $\log a/(a-x)$, where a is the initial concentration of the ester and $(a-x)$ is the concentration at the time, t. The reaction was measured at 21.5°C. An example of the results obtained is shown in Fig. 1. From this plot, k (in acetone) is estimated as 1.92×10^{-5} sec^{-1}. The maxima at 857 cm^{-1} showed little shift when solvents of different natures were used.

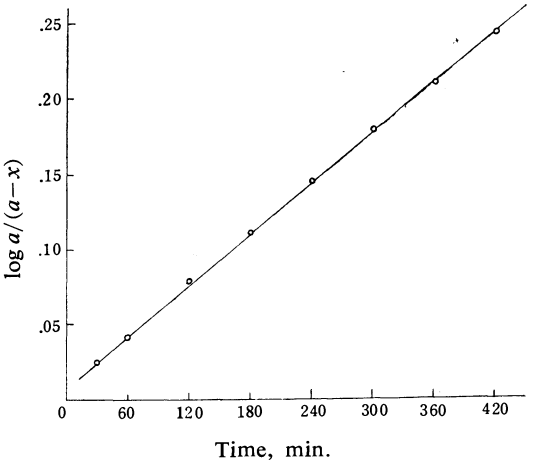


Fig. 1. A typical plot of $\log a/(a-x)$ vs. time. Rearrangement of cyclohexanoneoxime-*p*-toluenesulfonate in acetone at 21.5°C. Oxime-ester, 0.2260 mol./l.

Results and Discussion

The Ionizing Power of Liquid Sulfur Dioxide. —The absorption maximum of the charge-transfer band of 1-ethyl-4-carbomethoxypyridiniumiodide (7.27×10^{-4} mol./l.) in liquid sulfur dioxide was at 3650Å, with an apparent ε value of 2.83×10^{4}. The Z-value of liquid sulfur dioxide was calculated from the E(kcal./mol.) $=2.859\times10^{-3}\times\tilde{\nu}$ equation[11] to be 78.3.

Charge Transfer Bands in Various Mixtures

11) E. M. Kosower, ibid., **80**, 3267 (1958).
12) "Organic Syntheses," Coll. Vol. 2, 76 (1943).

of Liquid Sulfur Dioxide and Acetone.—As is shown in Fig. 2, the λ_{max}'s of the charge-transfer bands of 1-ethyl-4-carbomethoxypyridiniumiodide were estimated in various mixtures of liquid sulfur dioxide in acetone, from 0 (acetone only) to 100% surfur dioxide (21.38 mol./l.). The c−t band in acetone (4354 Å) dropped abruptly upon the addition of a slight amount of liquid sulfur dioxide, a specific solvation by liquid sulfur dioxide being observed.

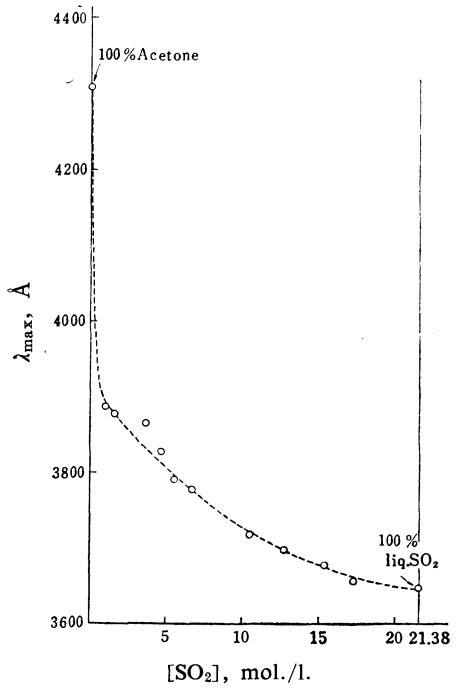


Fig. 2. Maxima of charge transfer band of 1-ethyl-4-carbomethoxypyridiniumiodide in various mixtures of acetone and liquid sulfur dioxide.

TABLE I. THE RATE CONSTANTS OF THE REARRANGEMENT IN MIXTURES OF LIQUID SULFUR DIOXIDE AND ACETONE AT 21.5°C

Concn. of liq. SO_2 mol./l.	k, sec^{-1}
0	1.92×10^{-5}
0.212	4.09×10^{-5}
0.491	4.37×10^{-5}
1.261	5.63×10^{-5}
2.212	8.40×10^{-5}
4.140	1.68×10^{-4}
7.811	5.02×10^{-4}
11.372	1.09×10^{-3}
12.385	1.38×10^{-3}
14.631	2.66×10^{-3}
16.406	3.84×10^{-2}

The Rate Constants in Various Mixtures of Liquid Sulfur Dioxide and Acetone.—The rate constants of the rearrangement of the oxime-ester in various mixtures of liquid sulfur dioxide and acetone, from 0 (acetone only) to

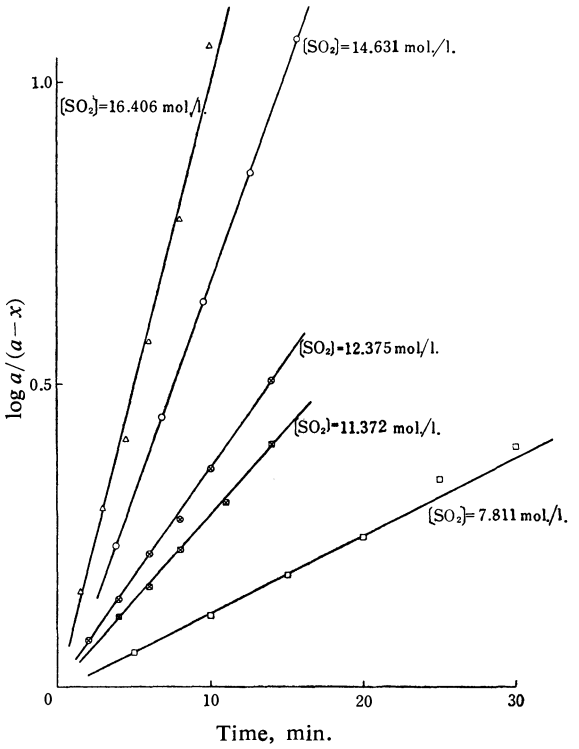


Fig. 3. Some examples of rate-runs in mixtures of acetone and liquid sulfur dioxide. 21.5°C

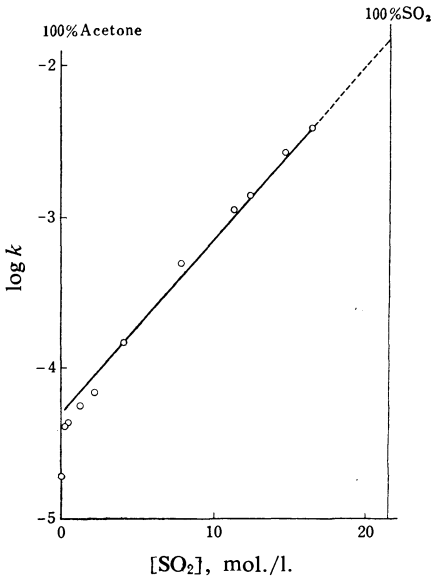


Fig. 4. The plot of log k vs. liquid sulfur dioxide concentration in acetone.

16.406 mol./l. (76.74 mol.%) of liquid sulfur dioxide in acetone are estimated and listed in Table I, some of the $\log a/(a-x)$ vs. t plots being shown in Fig. 3.

A linear plot of the $\log k$ vs. lquid sulfur dioxide concentration in acetone was obtained as in Fig. 4. The rate constant in liquid sulfur dioxide (100%) is obtained, by extrapolation of this plot to 100 % (21.38 mol./l.) liquid sulfur dioxide, as $k=1.6\times10^{-2}$ sec^{-1}.

The *Z*-Values of Nitromethane, Ethylenedichloride and Ethyl Methyl Ketone.—The same method was applied in estimating the *Z*-values of the solvents which were not measured in Kosower's papers. The results are listed in Table II.

TABLE II. *Z*-VALUES OF SOLVENTS

Solvent	λ_{max}, Å	ε_{max}	*Z*-Value
Nitromethane	3750	389	76.2
Ethylenedichloride	4400	703	64.4
Ethyl methyl ketone	4320	825	66.0

The Rate Constants in Various Solvents. The Correlation of the Rates with the Dielectric Constants. — The rearrangements were also carried out in various solvents, such as methanol, acetic acid, nitromethane, ethanol, acetonitrile, pyridine, chloroform, acetone, ethylenedichloride, ethyl methyl ketone and carbon tetrachloride. The rate constants were estimated from linear plots of $\log a/(a-x)$ vs. t, which are depicted in Fig. 5. These results, together with those with liquid sulfur dioxide, are listed in Table III; among them, the values of k at 21.5°C in chloroform, acetic acid, methanol and ethanol are calculated from the results of Heldt.[10] No correlation is found either between $\log k$ and the dielectric constant, D, or between $\log k$ and the dipole moment of

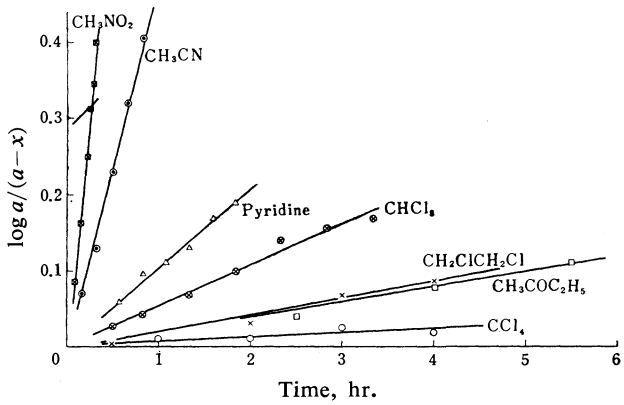


Fig. 5. The rate constants in various solvents. 21.5°C

TABLE III. THE FIRST ORDER RATE CONSTANTS OF THE REARRANGEMENT OF CYCLOHEXANONEOXIME-*p*-TOLUENESULFONATE IN SOLVENTS, 21.5°C

Solvent	*Z*-Value	Dielectric[b] const., 20°C	Dipole[b] moment	k, sec^{-1}	$\log k$	k/k_{CHCl_3}
Liq. SO_2	78.3[a]	12.35	1.61	1.6×10^{-2}	$\bar{2}.20$	480
Methanol	83.6	32.63	1.69	2.0×10^{-3} [c]	$\bar{3}.30$	61
Acetic acid	79.2	6.15	1.73	2.0×10^{-3} [c]	$\bar{3}.30$	61
Nitromethane	76.2	35.87	3.0	7.5×10^{-4}	$\bar{4}.88$	23
Ethanol	79.6	24.30	1.67	5.0×10^{-4} [c]	$\bar{4}.70$	15
Acetonitrile	71.3	37.5	3.2	3.1×10^{-4}	$\bar{4}.49$	9.4
Pyridine	64.0	12.3	2.30	8.5×10^{-5}	$\bar{5}.93$	2.6
Chloroform	63.2	4.80	1.05	3.3×10^{-5} [c]	$\bar{5}.52$	1.0
Acetone	65.7	20.7	2.83	2.0×10^{-5}	$\bar{5}.30$	0.6
Ethylenedichloride	64.4[a]	10.36	1.51	1.5×10^{-5}	$\bar{5}.18$	0.5
Ethyl methyl ketone	66.0[a]	18.51	2.75	1.2×10^{-5}	$\bar{5}.08$	0.4
Carbon tetrachloride		2.24	0	1.0×10^{-6}	6.00	0.03

a) Estimated by the present authors
b) "Organic Solvents, Technique of Organic Chemistry," Ed. by A. Weissberger, Interscience Publishers, New York (1955).
c) Calculated from the values of Heldt (Ref. 10)

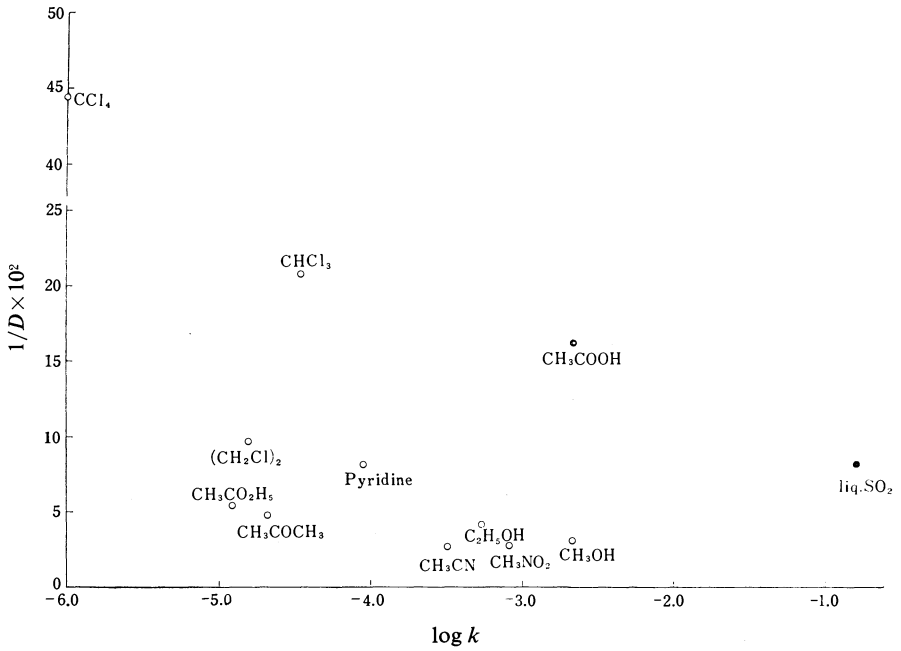


Fig. 6. Correlation of log k vs. $1/D$.

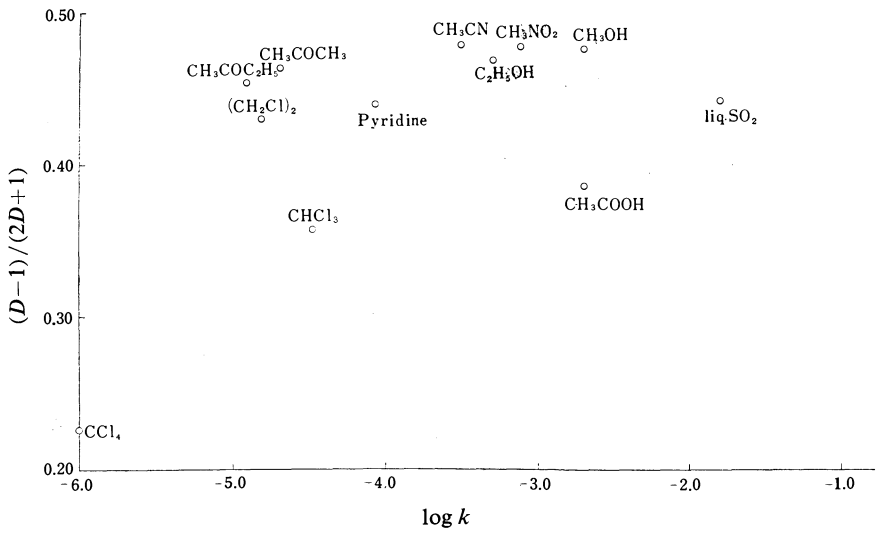


Fig. 7. Correlation of log k vs. $(D-1)/(2D+1)$.

the solvent. Figures 6 and 7 show the plots of log k vs. $1/D$ and log k vs. $(D-1)/(2D+1)$ respectively. The rate constants decrease in the following order: liquid sulfur dioxide> methanol>acetic acid>nitromethane>ethanol > acetonitrile > pyridine>chloroform>acetone >ethylenedichloride > ethyl methyl ketone > carbon tetrachloride. The fastest rate, in liquid sulfur dioxide, is eighty times that in methanol, 480 times that in chloroform and 1.6×10^4 times that in carbon tetrachloride at 21.5°C.

The rate in the mixtures of liquid sulfur dioxide in acetone was dependent on the molarity of liquid sulfur dioxide, as may be seen in Fig. 4, and relation 1 is observed:

$$\log k = \text{const.} \times [SO_2] \qquad (1)$$

which means that the higher the concentration of liquid sulfur dioxide in acetone, the smaller will be the activation free energy of the reaction.

The Ionizing Power of the Solvent. The

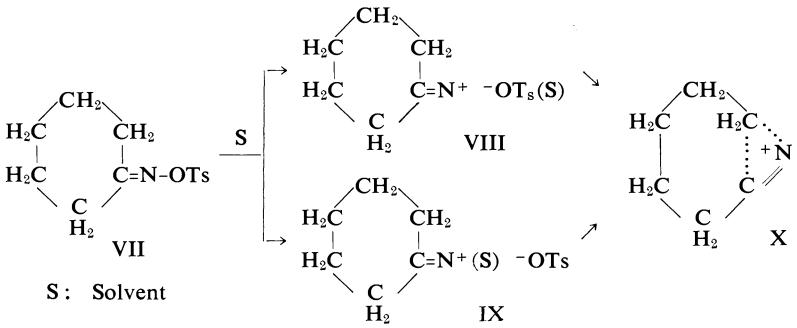


Chart 2

Correlation of *Z*-Values with the Rate Constants of the Rearrangement.—As is visualized in Figs. 6 and 7, no dependency of $\log k$ on $1/D$ or on $(D-1)/(2D+1)$, the latter relation being well-known as Kirkwood's relation,[13] is observed. Although Chapman[14] has revealed that the added solvents accelerated the Beckmann rearrangement in carbon tetrachloride and that the rates were dependent on the dipole moments of the added solvents, no linear correlation is seen between the $\log k$ and the dipole moment of any of the solvents used in this experiment. The relationship of $\log k$ against *Z*-value is also a disappointing one (Fig. 8).

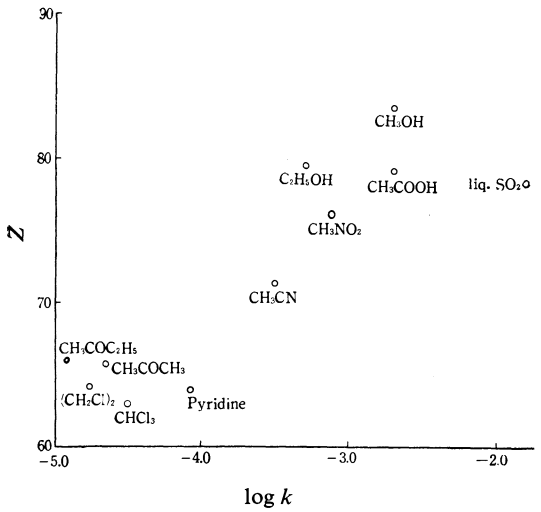


Fig. 8. Correlation of $\log k$ vs. *Z*-value.

The assertion of Heldt[10] that $\log k$ was dependent on the *Z*-value must be amended, for only four solvents were used in his work. An inspection of Fig. 8 will enable us to understand that the $\log k$ vs. *Z* relation is not linear but consists of a broad zigzag band; the explanation of such a result must await further study. For instance, the *Z*-value of ethanol is larger than that of acetonitrile, and that of methanol is larger than the *Z*-value of acetic acid; the $\log k$'s of ethanol and acetonitrile or those of methanol and acetic acid are very close to each other. In chloroform the rate is faster than in acetone, whereas the *Z*-value of acetone is larger than that of chloroform. The comparatively small *Z*-value of liquid sulfur dioxide (78.3) is unexpected in view of the largest rate constant in this solvent.

In a preceding paper[15] by one of the present authors, a proposal has been made regarding the reasons for the unusual rapidness of the Beckmann rearrangement and the cationic polymerization, and for the unexpected dullness of the Menschutkin reaction in liquid sulfur dioxide, in which the presence and the importance of the unsolvated *(bare)* carbonium ion in liquid sulfur dioxide have been emphasized. The rapidness of these reactions is largely a result of the ability of the solvent, (1) to ionize the covalent linkage to an ion-pair and (2) to prevent the harmful attachment (association) of counter anion or nucleophilic species to carbonium ions or cations by the strong solvation of the solvent (liquid sulfur dioxide) on anions or nucleophiles.

It is generally accepted that the formation of an aza-cyclopropenium cation (X) is the intermediate step in the Beckmann rearrangement.[8,9] The fact that the rearragement is always a *trans*- and intramolecular-migration supports this view. Since the results indicated here suggest that the ionizing power of the solvents is important but not the final word in the elucidation of the solvent effect on the rearrangement, another source for such behavior should be sought.

As is illustrated in Chart 2, to attain the intermediate X, two extreme cases of the solvent solvation may be considered. When the solvent is an electrophile, the anion

13) J. G. Kirkwood, *J. Chem. Phys.*, **2**, 351 (1934).
14) A. W. Chapman, *J. Chem. Soc.*, **1934**, 1550.
15) N. Tokura and Y. Kondo, This Bulletin, **36**, 200 (1963).

($^-$OTs anion) may be strongly solvated and the intermediate X may easily be formed concertedly or by ionization via VIII. However, when the solvent used is a nucleophile, the solvation of the cation (=C=N$^+$) by the solvent may be predominant, as is seen in IX, the formation of X being thus retarded or inhibited. If such is the case, the migrating group (α carbon atom) should have enough driving force to push away the nucleophilic solvent to obtain the intermediate X. Acetone, pyridine and acetonitrile are to be classified as nucleophilic solvents, whereas sulfur dioxide is to be considered an electrophilic solvent. However, the ionizing powers of ethanol and methanol are large; these solvents are biphilic (both electrophilic and nucleophilic), and the behavior of these solvents towards the oximeester is of a complicated nature. The effect of the strong ionizing power on the rate of the rearrangement may perhaps be compensated for partly by the nucleophilicity of these hydroxyl solvents. There remain many problems to be solved concerning the ionizing power of solvents. Many suggestions which have intended to classify the solvents by their ionizing powers such as dielectric constants, *Y*-values[16] or *Z*-values are not satisfactory. The consistent relations between such ionizing powers of the solvents and the rate of the reactions in the solvents are only observed among the solvents with similar natures. Meanwhile, the superiority of liquid sulfur dioxide as the solvent in many reactions is probably largely due to its electrophilic and non-nucleophilic nature.

16) S. Winstein, E. Grunwald and H. W. Jones, *J. Am. Chem. Soc.*, 73, 2700 (1951).

Summary

The Beckmann rearragement of cyclohexanoneoxime-*p*-toluenesulfonate has been carried out in various solvents and the results have been discussed. The rate in liquid sulfur dioxide is the fastest among the solvents examined. The plots of the log k vs. ionizing powers of the solvents are not linear. The electrophilic solvation of liquid sulfur dioxide on the *p*-toluenesulfonate anion is important if the reaction is to be carried out rapidly and if an intermediate bridged cation, an azacyclopropenium cation, is to be obtained.

Thanks are due to the Seitetsu Kagaku K.K. for its donation of liquid sulfur dioxide.

The Chemical Research Institute of Non-Aqueous Solutions
Tohoku University
Katahira-cho, Sendai

The Velocity of Ascending Air Bubbles in Aqueous Solutions of a Surface Active Substance and the Life of the Bubble on the Same Solution

By Satiko OKAZAKI*

(Received July 19, 1963)

The surface tension and the adsorption from an aqueous solution of a surface active substance have been studied by many authors with refererence to the problem of surface activity. However, from the practical point of view, the properties of the system in the dynamic state[1-4] are more important than those in equilibrium, as in the cases of emulsification, dispersion, foaming, detergency and wetting. Unfortunately, the studies of such dynamic properties are very few, especially concerning the mechanism of surface activity. In this connection, it is important to study the phenomena of the ascending of air bubbles in an aqueous solution of a surface active substance.

Concerning these phenomena, an empirical formula for the velocity of bubbles ascending in a liquid and various effects upon the velocity, for instance, the effects of the size and the shape of the bubble, of the circulation of gas inside the bubble, of impurities in the solution, and of bubbles rising in succes-

* Present address: Faculty of Science and Technology, Sophia University, 7 Kioicho, Chiyoda-ku, Tokyo, Japan.

1) E. J. Burcik, *Colloid Sci.*, 5, 421 (1950).
2) H. Lange, *Kolloid Z.*, **121**, 131 (1951).
3) D. G. Dervichian, *Z. f. Elektrochem.*, **59**, 290 (1955).
4) K. Schäfer, ibid., **59**, 273 (1955).

sion have been reported.[5-8] However, as to the actual conditions of the system under which the above formula can be applied or the effects appear, the results reported by vavious authors are not concorbant. Garner and Hammerton,[5] for instance, made an experiment with vaseline-contaminated bubbles and confirmed a retarding action of the hydrocarbon film on the bubble surface for the ascending velocity; Stuke[8] also reported an extreme sensitivity of the ascending velocity of bubbles to the presence of a surface active substance in the solution. However, the results and the explanations of these findings differ greatly. The present author has, therefore, made a similar experiment for the aqueous solutions of surface active substances and has also measured the density, the viscosity, the compressibility, the surface tension, and the stability of bubbles for the same solution in order to elucidate the phenomena.[9,10] The present report will discuss these results in detail.

Experimental, Results and Discussion

Materials.—For the study of the surface active substances, sodium dodecyl sulfate (SDS) and isoamyl alcohol were selected as two typical substances for producing stable and unstable aqueous foams respectively. SDS was prepared and purified by the usual method. In order to eliminate any possible error due to aging, the solution of SDS was prepared and kept overnight in a stoppered glass bottle before use. The sample of isoamyl alcohol was purified by the distillation of a commercial product over calcium oxide.

The Ascending Velocity of Bubbles in the Solution of a Surface Active Substance. — The velocity of an air bubble ascending in an aqueous solution of a surface active substance was measured in a glass cylinder (9 cm. in diameter and 50 cm. high) which had been filled with an aqueous solution of SDS or isoamyl alcohol to the depth of 40 cm.[9,10] By means of a capillary tube varying in size, air bubbles were produced at the center of the bottom of the cylinder and were made to ascend through the liquid. Special care was taken to keep the orifice of the capillary clean by drawing it anew in each run. Each bubble was made to ascend separately, allowing a time interval of at least three seconds between successive bubbles, this interval is needed to avoid the error due to the streaming bubble effect,[5] which will be discussed later. The uniform velocity portion of the bubbles was measured for the varying distances from 10 to 40 cm., to the accuracy of 1/10 sec.

Ascending air bubbles were also caught under a watch glass which was held near the surface of the solution, and their radii were measured by a microscope equipped with an ocular scale.

The measurements were mainly conducted at room temperatures ranging from 20 to 25°C. The temperature fluctuation of this range did not obscure the results obtained.

The ascending velocity, V, of the bubble in an aqueous solution of SDS is plotted against its radius, r, in Fig. 1. We can see in this diagram that in the region of $r<0.03$ cm. all of the plots for different concentrations of the SDS solution fall on one straight line, while in the region of $0.03<r<0.07$ cm. they break into separate and nearly straight lines of different inclinations for different concentrations of SDS.

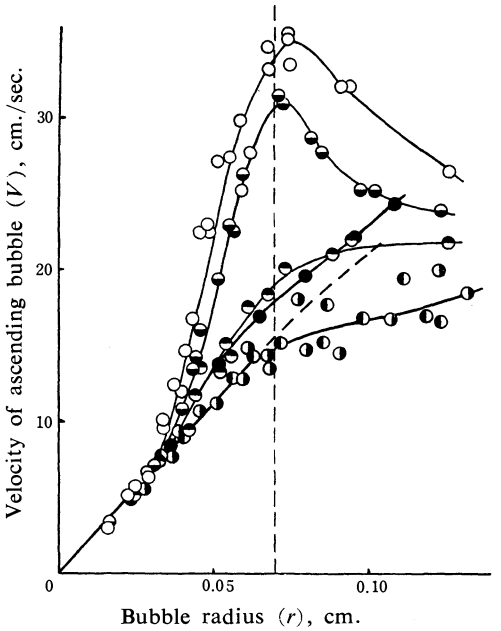


Fig. 1. Velocity of air bubbles ascending in the aqueous solutions of SDS.
○ Distilled water
◒ 1.0×10^{-6} molar aqueous SDS
◓ 1.2×10^{-5} molar aqueous SDS
◑ 1.0×10^{-4} molar aqueous SDS
◐ 1.0×10^{-3} molar aqueous SDS
● Rigid sphere in distilled water by empirical formula
Broken line; distilled water by Garner

5) F. H. Garner and D. Hammerton, *Chem. Eng. Sci.*, 3, 1 (1954).
6) K. L. Sutherland and M. Linton, *2nd International Congress of Surface Activity*, 1, 494 (1957); S. G. Mason and F. D. Rumscheidt, *Colloid Sci.*, 61, 238 (1961); W. L. Harberman and R. K. Molton, *NAVY Department, the David W. Taylor Model Basin Report 802 Sept.* (1953).
7) J. M. Dallavalle, "Micromeritics," 2nd ed., Pitman Publishing Corp., New York (1952), p. 23.
8) B. Stuke, *Z. f. Elektrochem.*, 59, 281 (1955).
9) T. Sasaki, Y. Miyazaki and S. Okazaki, *3rd International Congress of Surface Activity*, 2B, 549 (1960).
10) S. Okazaki, *Kolloid-Z. Z. Polymere*, 185, 154 (1962).

The inclination is largest for pure water, decreases with the increase in the concentration of SDS, and is smallest for 10^{-3} molar and 10^{-4} molar SDS, which give a common straight line without a break point at $r=0.03$ cm. We can further confirm this by the visual observations that above a certain critical radius the bubble fluctuates and that all of the polts deviate from the lineality rather abruptly.* In our experiments this critical radius is about 0.07 cm. for all solutions, independent of their concentrations (as shown by a dotted vertical line in Fig. 1). In Fig. 2 a similar relation

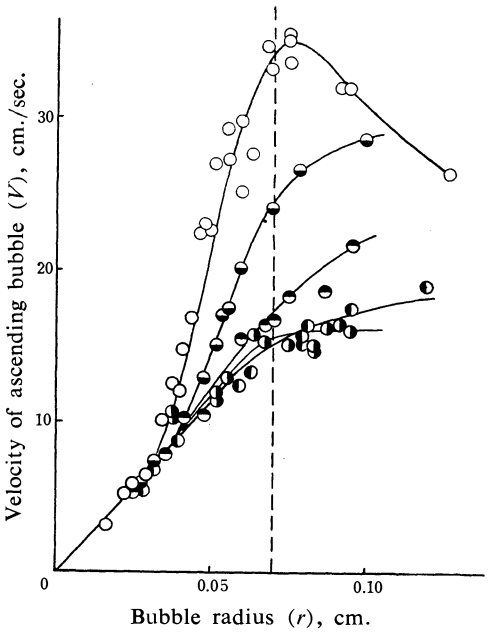


Fig. 2. Velocity of air bubbles ascending in the aqueous solutions of isoamyl alcohol.

- ○ Distilled water
- ◒ 0.5×10^{-3} molar aqueous isoamyl alcohol
- ◓ 1.0×10^{-3} molar aqueous isoamyl alcohol
- ◑ 1.9×10^{-3} molar aqueous isoamyl alcohol
- ◐ 5.0×10^{-3} molar aqueous isoamyl alcohol

between V and r is shown for an isoamyl alcohol solution. All these findings are similar as a whole to what was briefly reported by Stuke,[8] while it differs in some respects from what was reported by Garner and Hammerton.[5]

It can be noticed at once that the ascending velocity of air bubbles in water is retarded by the presence of SDS, even in such a small concentration as 10^{-6} molar. This is rather surprising, considering the physico-chemical properties of the solution of a surface active substance in such a dilution where the properties are not practically different from those of pure water, as will be mentioned later. We can further see in Fig. 1 that a straight line expressing V—r relations up to $r=0.03$ cm. for all concentrations of SDS solution, and up to $r=0.07$ cm. for 10^{-3} and 10^{-4} molar SDS solutions, together with the deviation from this linearity above $r=0.07$ cm. for the latter solutions, show an apparent coincidence with the results obtained by Garner[5] for the ascending bubble contaminated with vaseline, where he insists that the linearity indicates the spherical shape of the rising bubble and that the deviation from the linearity above $r=0.07$ cm. is explained by the deformation of the bubble due, in his case, to the hydrocarbon film on the bubble surface. However, before the results of his experiment are accepted, a marked difference should be pointed out between his results and ours for the rising velocity of air bubbles in distilled water, as is shown in Fig. 1. To check this point, the $V-r$ relation for a rigid spherical bubble will be established independent of these measurements.

The Ascending Velocity of a Rigid Spherical Bubble.—The V—r relation for a rigid spherical bubble is calculated by using an entirely empirical formula[7] and is plotted as solid circles in Fig. 1. This curve coincides with the V—r relation of a 10^{-5} molar SDS solution and is somewhat greater than those of 10^{-3} and 10^{-4} molar SDS. This may predict a possible deformation from a sphere of rising bubble of $r<0.07$ cm. in 10^{-3} and 10^{-4} molar SDS solutions. However, is also probable that the uncertainty is due to the empirical nature of the equation,[7] which has no adjustable constnats relating to the dimensions of the apparatus used. Thus, it was further necessary to make an experiment in our own apparatus to obtain an actual V—r relation of the rising velocity of a rigid spherical bubble which exactly fits our experimental conditions.

For this purpose the present author has measured the falling velocity of rigid glass spheres, the density being 2.37, in water and in the solution under experimental conditions similar to those which held in the measurement of the rising bubble velocity, from which the rising velocity, V, and the radius, r, of an air bubble considered to be a rigid sphere, with the same drag coefficient and Reynolds number, were calculated.[11] The V—r relation thus obtained is plotted with

* The present discussion is mainly concerned with the phenomena occuring in the region of $r<0.07$ cm. in order to avoid the complications coming from the bubble fluctuation. The discussion is also restricted to the bubble radius far greater than about 0.008 cm., a point which corresponds to the upper limit of the Stockes velocity region of this system. Ref. 7, p. 24.

11) Ref. 7, p. 19.

TABLE I. PHYSICAL CONSTANTS OF SDS SOLUTION

	Distilled water	SDS solution 10^{-5} mol./l.	Temp. °C
Density, g./cm³	0.9983	0.9986	20
Compressibility, cm²/dyn.	45.48×10^{-12}	$45.46\times^{-12}$	20
Viscosity, centipoise	0.855	0.855	20
Surface tension, dyn./cm.	73.3	73.3	16

circles and curve 1 in Fig. 3, where the V—r curves for the actual air bubble in the aqueous solution of SDS shown in Fig. 1 are reproduced.

Now in the range of $r<0.07$ cm., the V—r curve for the rigid spherical bubbles obtained from a glass sphere experiment and the curves for the actual air bubbles in concentrated aqueous solutions of 10^{-3} and 10^{-4} molar SDS coincide with each other, while the curve for 10^{-5} molar SDS is somewhat higher.

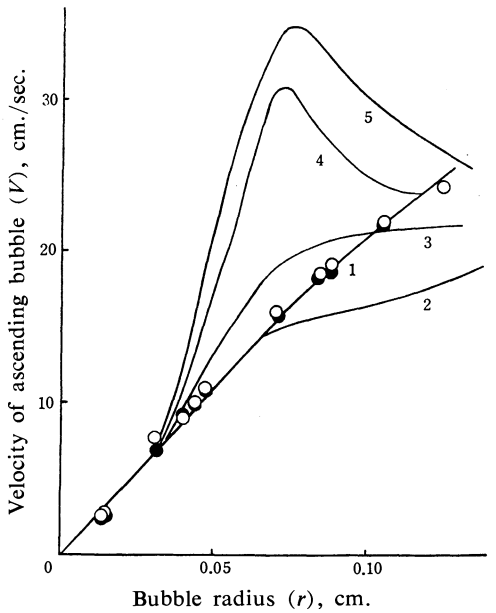


Fig. 3. Velocity of air bubbles ascending in the aqueous solutions of SDS.
(1) Rigid spherical bubble in distilled water (○) and in 1.0×10^{-3} molar SDS solution (●), actual air bubble in aqueous SDS of (2) 1.0×10^{-3} and 1.0×10^{-4} molar, (3) 1.2×10^{-5} molar, (4) 1.0×10^{-6} molar solution and (5) in distilled water.

This shows the rigid spherical nature of the rising bubble in 10^{-3} and 10^{-4} molar SDS. It may also be inferred that, though our V—r curves for 10^{-3} and 10^{-4} molar SDS actually coincide with Garner's curve (shown in Fig. 1), they do not represent the rising velocity in distilled water, as Garner insisted; rather, they correspond to the spherical bubble rigidly covered with the adsorbed film, and the effect of vaseline-contamination is considered to appear already in the region of $r<0.07$ cm. His explanation of the rising velocity of the bubble of $r>0.07$ cm. mentioned above may also be invalid. Since, as has been mentioned above, this critical radius of 0.07 cm. is largely independent of the SDS concentration and is equal to the value in distilled water, such a critical radius and the retardation of the rising velocity of bubbles beyond this radius is likely to be explained mainly by the hydrodynamic effect prevailing even in distilled water. The fairly good coincidence of our critical value with those of Garner[5] and Coppock[12], who used different substances or worked under widely differing conditions, also confirms this.

The Ascending Velocity of Bubbles in a Dilute Solution.—As for the extremely sensitive effect of 10^{-5} and 10^{-6} molar SDS solutions in retarding the ascending velocity of bubbles in the region of $0.03<r<0.07$ cm., the following factors may be pointed out in explanation;

(1) A change in the physical properties of the solution, a change which affects the hydrodynamic properties of the solution.

(2) The streaming bubble effect.

(3) The contamination or adsorbed film on the bubble surface.

As for 1, the density, velocity, compressibility, and surface tension were measured for these solutions and distilled water as shown in Table I. None of the data of this table can, however, in any way explain the retardation of the ascending velocity since there is no difference in the magnitude of these properties between pure water and a SDS solution.

Next we may take account of the streaming bubble effect, that is, the acceleration of an ascending bubble by another one rising just above it.[5] It has been reported that, at the speed of one bubble per second, the rising velocity of bubbles in a series is about three times as large as that of a solitary bubble,[13] and that the apparent increase in the rising velocity due to such an effect is less than 1%

12) P. D. Coppock and G. T. Meikeljohn, *Trans. Inst. Chem. Engrs., London*, **29**, 75 (1951).
13) R. I. Datta and D. G. Napier, ibid., **28**, 14 (1950).

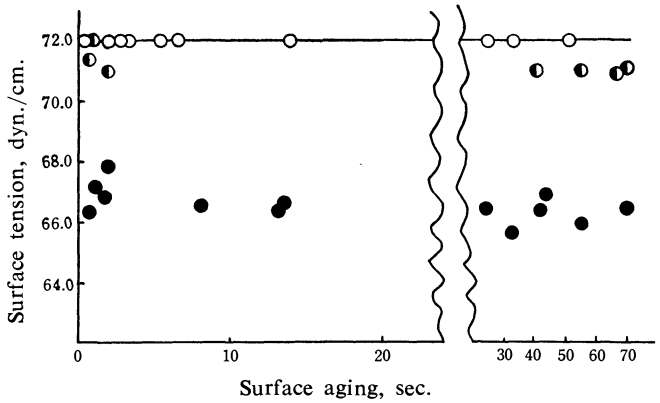


Fig. 4. Dynamic surface tension of the aqueous solutions of SDS.
○ 1.0×10^{-5} molar aqueous SDS
◐ 1.0×10^{-4} molar aqueous SDS
● 1.0×10^{-3} molar aqueous SDS

only when the time interval between two neighboring bubbles exceeds three seconds.[5] In our experiment, however, the time interval of the successive bubbles is longer than three seconds, as has been mentioned above, so the possibility of the streaming bubble effect can be eliminated.

We may, therefore, concentrate on the effect of the third factor. The effect of surface contamination is considered to appear in two ways, namely, by deforming bubbles and by inhibiting both the circulation of gas taking place inside and the liquid flow at the surface of ascending bubbles in pure water.[6] Of these two possibilities, the former seems not to occur in all solutions of the concentration studied, since in 10^{-3} and 10^{-4} molar SDS, the ascending bubble can be treated as a rigid sphere, as has already been mentioned, and deformation from the sphere, if any, should result in a V—r line of the inclination less than this, as in the case of the retardation at $r>0.07$ cm. This is, however, just opposite to what was observed.

Therefore, the inhibition of gas circulation or liquid flow remains as the only possible explanation for the remarkable retardation of the ascending velocity of the bubble. Here, it is interesting to note that our V—r curves between $0.03<r<0.07$ cm. are very similar in shape to what was obtained by Nawab[14] for the effect of the emulsifier film surrounding emulsion droplets upon the emulsion viscosity, where not only the viscosity of the liquid of the external phase but also that of the internal phase, namely, the emulsion droplets, have an influence upon the emulsion viscosity. Both of these phenomena may be similarly explained by the adsorbed film on emulsion droplets or bubbles, which acts to retard or inhibit the circulation or flow inside and at the surface of the droplets or bubbles. In the studies of circulation in sedimenting fluid spheres, the inhibition of the internal circulation by the addition of surface active impurities to the external phase has been confirmed, from which the rigid nature of the adsorbed film surrounding the liquid droplets has been inferred.[15] The movement inside the ascending bubble was reported to start in pure water at a bubble radius as small as 0.02 cm. and to reach a maximum speed at the radius of 0.125 cm.[5] Bond[16] calculated the effect of circulation inside the bubble in increasing the ascending velocity of a spherical bubble from a Stokes law velocity without internal gas circulation. The adsorbed film of a surface active substance is also inferred to dissipate the kinetic energy at the bubble surface through the relaxation effect.[5] A similar explanation for the retardation is possible by introducing the concept of surface transport proposed by Sutherland.[17] Thus, we are of the opinion that the increase in the ascending velocity beyond the velocity of a rigid spherical bubble in pure water at $0.03<r<0.07$ cm. is chiefly aided by the gas circulation inside the bubble, and that the sensitive action of retarding the rising velocity of bubbles in an aqueous SDS solution is to be ascribed to the adsorbed film of the surface active substance, which acts to reduce or inhibit both the movement of liquid at the surface and the circulation of gas inside the bubbles.

14) M. A. Nawab and S. G. Mason, *Trans. Faraday Soc.*, 54, 1712 (1958).

15) F. H. Garner and A. H. P. Skelland, *Chem. Eng. Sci.*, 4, 149 (1955).

16) W. N. Bond, *Phil. Mag.*, (7) 4, 889 (1927).

17) W. E. Ewers and K. L. Sutherland, *Austr. J. Sci. Res.*, A5, 697 (1952).

A similar explanation is possible for the system of an isoamyl alcohol solution, as may be understood from the similar V—r curves in Fig. 2.

Dynamic Surface Tension, Surface Viscosity, and Bubble Life.—As for the remarkable effect of SDS on the ascending velocity of the bubble, it has already been stated that all the static properties of the solution fail to explain the phenomena. Now let us take into account such surface properties as the surface viscosity or the dynamic surface tension, as Bryn and Garner suggested.[5]

The dynamic surface tension was measured by using a stalagmometer.[18] This enabled us to regulate the dropping speed and thus facilitated the detection of the aging of the solution which might occur during the bubble ascension. In order to estimate the surface tension of a relatively fresh surface of a solution, the age of the drop surface was decreased by increasing the dropping speed. Precautions were taken to eliminate the error due to the dropping speed by conducting a similar experiment with pure water. The results obtained are shown in Fig. 4. This figure again shows no difference in surface tension between pure water and 10^{-5} or 10^{-6} molar SDS, at least for the aqueous surface aged more than two seconds, though an apparent slight time effect can be seen for the 10^{-4} molar SDS solution. Concerning the effect of surface viscosity, we did not actually make any measurements, but its order of magnitude may also be very small for the 10^{-6} and 10^{-5} molar SDS solutions; at least this can be expected from the data of McBain.[19] This quantity too, therefore, may not be sensibly different from that of water. Thus, we can find no difference in either the static or the dynamic properties of the system between pure water and 10^{-5} molar SDS to elucidate the phenomena as far as the above measurements are concerned.

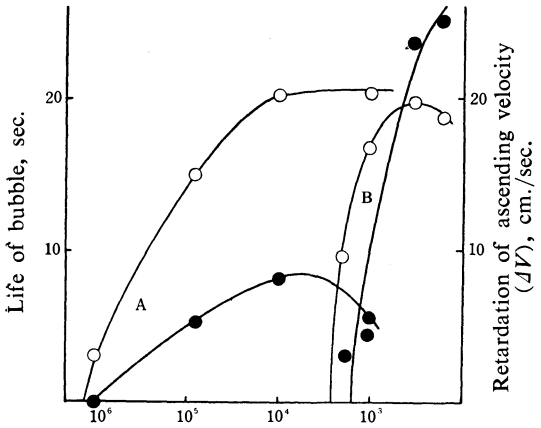


Fig. 5. Bubble life and retardation of the ascending velocity of bubbles.
○ $\Delta V = V_{water} - V_{solution}$ at $r = 0.07$ cm.
● Life of single bubble ($r = 0.07$ cm.) on surface of solution
A SDS solution
B Isoamyl alcohol solution

However, the ascending bubble has been estimated to have a surface zone of considerable thickness in which the viscosity of the liquid is not normal,[20] and there is ample reason to believe that the surface viscosity or flow resistance near the bubble surface, though directly undetectable in magnitude, sensitively affects the ascending velocity of bubbles in water. In this connection it is important to measure the stability or the life of bubbles on the aqueous surface, which has also been known to be sensitively affected by the adsorbed layer of the surface.[21] The life time of bubbles was measured in a glass vessel 10 cm. in diameter. As is shown in Fig. 5, the stability of bubbles at the surface of the SDS solution becomes perceptible and gradually increases when the concentration exceeds 10^{-6} molar, the whole appearance of the stability concentration curve being very similar to the concentration dependence of the retardation of the ascending velocity of the bubble, which is also shown in Fig. 5. It is known that the drainage of liquid in the bubble film is one of the factors determining the life time of bubbles.[22] Particularly in our very dilute solution of SDS, where the surface tension is not sensibly different from that of pure water and where the strength of the bubble film due to the solute adsorption is almost imperceptible, the bubble life is affected chiefly by the rate of drainage, which is in turn influenced by the surface viscosity or the resistance to surface flow.[17] Thus, the surface viscosity affects the rate of drainage and, therefore, the life of sessile bubbles at a liquid surface, just as it affects the velocity of the ascending bubbles. The common cause of resistance to flow and a similar high sensitivity to surface active substances makes the two phenomena very similar, as may be seen in Fig. 5.

The probable mechanism of the resistance to flow may be such that, on the surface of

18) C. G. McGee, in the textbook of J. T. Davies and E. K. Rideal, "Interfacial Phenomena," Academic Press, New York, London (1961), p. 172.

19) A. G. Brown, W. C. Thuman and J. W. McBain, *J. Colloid Sci.*, **8**, 491 (1958).
20) J. C. Henniker, *Rev. Modern Phys.*, **21**, 322 (1949).
21) J. T. Davies, *2nd International Congress of Surface Activity*, **1**, 241 (1957).
22) S. Ross and G. J. Young, *Ind. Eng. Chem.*, **43**, 2520 (1951).

the ascending bubble, there may occur some uneven distribution of the adsorbed solute molecules of the surface active substance arising from the sweeping action of liquid flow around the ascending bubble. Accordingly, during ascension, a surface pressure difference, though slight, is produced on the bubble surface, which sets up the force to oppose the liquid flow near the bubble, as Sutherland pointed out in terms of the surface transport.[17] This may cause a decrease in its ascending velocity.

Here one should further refer to the electrophoretic velocity of a highly purified paraffin oil (Nujol) droplet in water.[23] In has been reported that the mobility of Nujol in water alone is $-4.35\,\mu$/sec./V./cm., but that the addition of as little as 7.5×10^{-5}% of pyridinium salt reduces the mobility to zero. In spite of this marked change in mobility, the lowering of the interfacial tension is appreciable at a concentration below 0.01% of this salt. This suggests the important rôle of the change in a diffuse electrical double layer surrounding the oil droplet. In our case of an ascending bubble, similar conditions may also be considered to exist which act to retard its motion. However, the effect of inorganic ions on the ascending velocity of the bubble is rather opposite in its action in this respect, at least so far as our experiment is concerned.[10] Further detailed studies should be made of this point.

Summary

1) The velocity of an air bubble ascending in water is remarkably retarded by the addition of a minute amount of sodium dodecyl sulfate (SDS) or isoamyl alcohol. With an air bubble with a radius ranging from 0.03 to 0.07 cm., the decrease in velocity is perceptible even in a 10^{-6} molar SDS solution, while it tends to a limiting value in 10^{-3} and 10^{-4} molar SDS solutions, where the rising velocity is about half as large as that in pure water.

2) To elucidate this retardation, the static properties of the solution, such as surface tension, density and compressibility, and the dynamic properties, such as viscosity and the change in surface tension with time, have been measured. However, no difference could be found in these properties between pure water and a 10^{-5} molar SDS solution to account for the retardation phenomena.

3) The rising velocity of a bubble considered to be a rigid sphere calculated by using an empirical formula fails to explain the results, since the formula does not fit our experimental conditions. The rising velocity of a rigid spherical bubble calculated from the observed data of a falling velocity of glass spheres in water in our apparatus is found to be in good agreement with that in 10^{-3} and 10^{-4} molar SDS solutions.

4) It has been concluded that, in all concentrations of the solution studied and for the bubble with a radius less than 0.07 cm., the bubble rises as a sphere and that the air circulation inside the bubble is closely related to the rising velocity of the bubble. The air circulation, which is strongest in the rising bubble in pure water, is hindered in 10^{-5} and 10^{-6} molar SDS solutions by the formation of an adsorbed film of SDS on this bubble, and the rising velocity is also thereby retarded. The circulation is actually suppressed, and the bubble rises as a rigid sphere in 10^{-3} and 10^{-4} molar SDS solutions. The retardation of the rising velocity of bubbles with radii larger than 0.07 cm. is due to the deformation of the bubbles from a sphere.

5) The life time of bubbles on an aqueous solution is affected by the surface active substance as sensitively as in the case of the effect of the same substance on the velocity of the rising bubble. Both phenomena are explained by the common factor of the retardatoin of the flow around the bubble surface.

The author wishes to express her gratitude to Professor Tsunetaka Sasaki for his kind direction and valuable criticism. The cost of this research has been defrayed by a grant of the Ministry of Education given to Professor Sasaki. The author also wishes to thank Mr. Kiyoshi Tamura of our laboratory for his measurements of compressibility and density.

Department of Chemistry
Faculty of Science
Tokyo Metropolitan University
Setagaya-ku, Tokyo

23) J. Powney and L. J. Wood, *Trans. Faraday Soc.*, **37**, 152 (1941).

A Novel Rearrangement of α, β-Unsaturated Ketones[1]

By Sachihiko Isoe and Masao Nakazaki

(Received July 25, 1963)

In the course of studies of Plancher's rearrangement, the smooth conversion of 1b-methyl-5, 6-dihydro-11b-benzo[c]carbazole (I) and spirocyclopentane-1, 3'-pseudo-2'-phenylindole (II) into 6a-methyl-5, 6-dihydro-6a-benzo[a]carbazole (III) and 11-phenyltetrahydrocabazolenine (IV) respectively by heating them with polyphosphoric acid at 150~188°C, have been reported.[2,3] (Fig. 1)

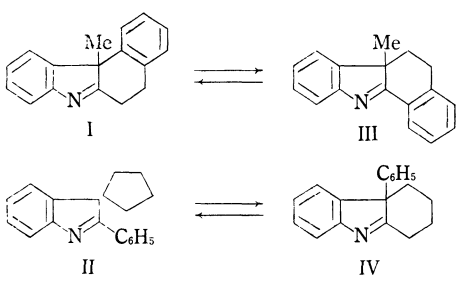


Fig. 1

A twofold Wagner-Meerwein type mechanism has been proposed to explain these facile rearrangements, and an analogous mechanism may be advanced for the well-known rearrangements of various carbonyl compounds, an example of which is illustrated in Fig. 2.[4]

Hitherto, however, the same type of rearrangement has not been demonstrated involving the twofold Wagner-Meerwein shift in more complex systems, e. g., mono-, bi-, and tri-cyclic α, β-unsaturated ketones.

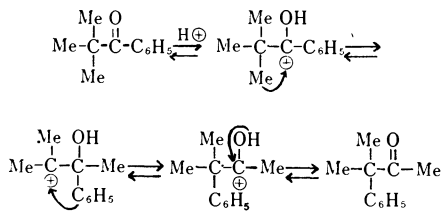


Fig. 2

This contribution is concerned with the syntheses of various α, β-unsaturated ketones which have electronic features analogous to those of the indolenines I and II, and with their interconversions with polyphosphoric acid.

Syntheses of α, β-Unsaturated Ketones.[5]—The α, β-unsaturated ketones (6-phenyl-spiro[4, 5]-dec-6-en-8-one (V), 3-keto-10-phenyl-$\Delta^{4,5}$-octalin (VI), 3-keto-10a-methyl-2, 3, 9, 10, 10a, 1-hexahydrophenanthrene (VIIIa), 3-keto-4, 10a-dimethyl-2, 3, 9, 10, 10a, 1-hexahydrophenanthrene (VIIIb), 4, 4-dimethyl-3-phenylcyclohex-2-enone (Xa) and 2, 4, 4-trimethyl-3-phenylcyclohex-2-enone (Xb)) were synthesized by the usual Robinson annelation method, but the syntheses of the two unsaturated ketones, VIIa and IXa, seem to call for special comment.

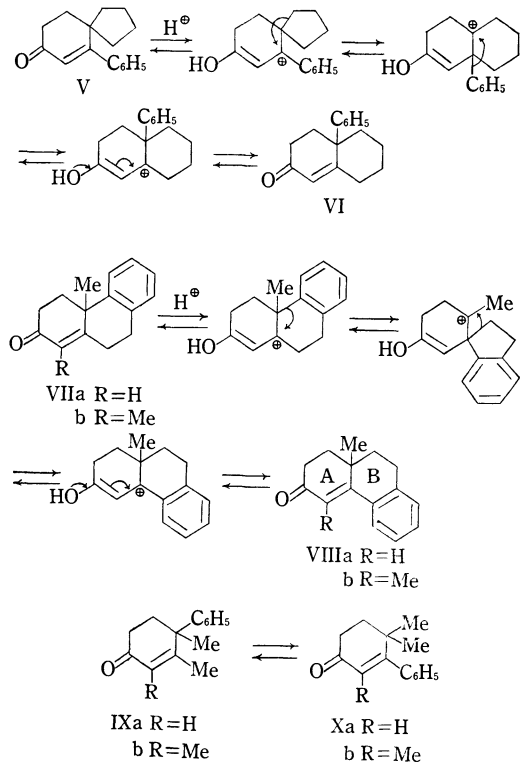


Fig. 3

1) For the preliminary report of this work, see M. Nakazaki and S. Isoe, *Chem. & Ind.*, **1959**, 1574.

2) M. Nakazaki, K. Yamamoto and K. Yamagami, This Bulletin, **33**, 467 (1960).

3) For the analogous twofold Wagner-Meerwein type rearrangements of 2, 3-disubstituted indoles and indolenium compounds, see M. Nakazaki, ibid., **33**, 461, 472 (1960).

4) S. Barton, F. Morton and C. R. Portor, *Nature*, **169**, 373 (1952); *J. Chem. Soc.*, **1956**, 2483.

5) According to the nomenclature of A. M. Paterson and L. T. Capell, "The Ring Index," Reinhold Pub. Corp., New York (1940).

In an attempt to obtain 2-keto-4a-methyl-2, 3, 4, 4a, 9, 10-hexahydrophenanthrene (VIIa), 1-methyl-2-tetralone was condensed with methiodide of 1-diethylaminobutan-3-one in the presence of potassium *t*-butoxide. Although the oily product, (b. p. 152~156°C/1 mmHg) showed a carbonyl absorption band at 1715 cm^{-1} in an infrared spectrum, it also exhibited a peak at 3390 cm^{-1} (hydroxy group). Most simply interpreted, this implies that the product may have the structure XI (Fig. 7)

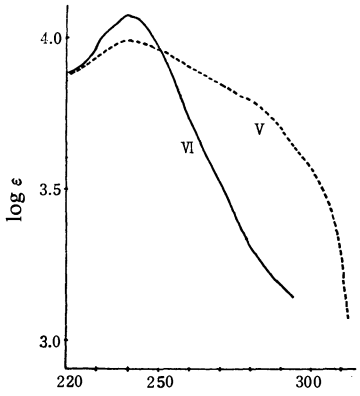


Fig. 4

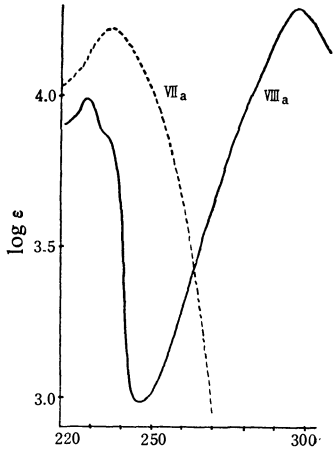


Fig. 5

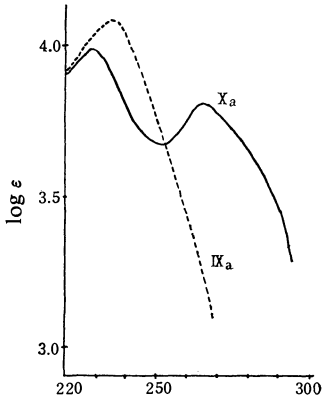


Fig. 6

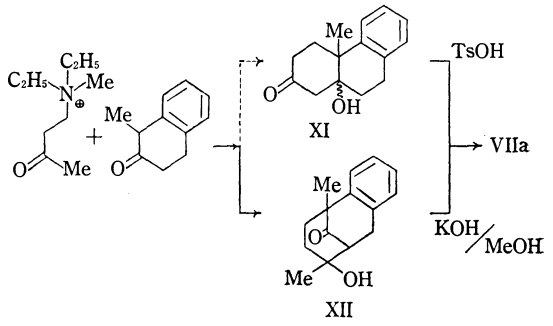


Fig. 7

(4a-methyl-10a-hydroxy-3, 4, 4a, 9, 10, 10a - hexahydrophenanthrene), the cis isomer (m. p. 157~158°C), of which has been synthesized by Wenkert and Stevens[6] via another route. They succeeded in converting *cis*-XI into VIIa (m. p. 89~91°C), by dehydration with toluenesulfonic acid, but our product was found to be recovered unchanged by this procedure. These facts, together with the steric hindrance around the carbonyl group (2, 4-dinitrophenylhydrazone could not be prepared by the usual procedure), suggest the ketol structure XII. This view is supported by the smooth conversion of the oil into VIIa upon heating it with methanolic potassium hydroxide. Recently, Johnson et al.[7] provided ample evidence that a bridge-ring ketol like XII is a common intermediate in Robinson's annelation reaction.

Another perplexing situation arose when

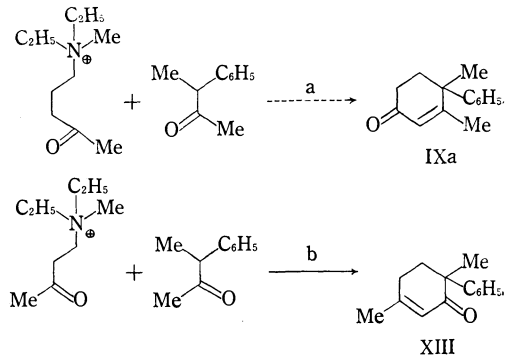


Fig. 8

6) E. Wenkert and T. S. Stevens, *J. Am. Chem. Soc.*, **78**, 238 (1956).
7) W. S. Johnson, J. J. Korst, R. A. Clement and J. Dutt, ibid., **82**, 614 (1960).

2-phenylbutan-3-one and methiodide of 1-diethylaminobutan-3-one were condensed in the presence of sodium amide in an attempt to secure IXa. (Fig. 8). The product, an oil (b. p. 112~116°C/1 mmHg), showed the expected absorption in infrared region (1661 cm^{-1}, for α, β-unsaturated ketone), but the carbonyl group was found very reluctant to give a semicarbazone, indicating that the carbonyl group is sterically hindered. Apparently, the ring closure took place to give the unsaturated ketone XIII (route B in Fig. 8) instead of the expected IXa (route A).[8,9] As an alternative synthetic route to IXa, the *t*-butyl chromate oxidation of 2, 3-dimethyl-3-phenylcyclohexene was attempted, and this process eventually afforded IXa in a fairly good yield. The structure of the ketone IXa thus obtained was supported by the ease with which semicarbazone and 2, 4-dinitrophenylhydrazone were formed, as well as by its ultraviolet absorption, λ_{max} 236 mμ (log ε 4.08), which is very close to the expected value calculated by Woodward's rule.[10]

Table I summarizes the properties of the unsaturated ketones, while Fig. 4, 5 and 6 reproduce the ultraviolet absorption spectra of the V, VI, VIIa, VIIIa, IXa and Xa ketones.

Rearrangements of the α, β-Unsaturated Ketones.—Having secured these α, β-unsaturated ketones, we can proceed to explore their interconversion by acid. The heating of the ketone V with polyphosphoric acid at 150~160°C for 10 min. gave rise to the formation of VI in a 60% yield; identification was established by comparison of an infrared spectrum with synthetic VI and by a mixed melting point determination of their semicarbazones. Under the same conditions, the ketone VIIa rearranged smoothly to the ketone VIIIa, whereas the ketone IXa was recovered unchanged after heating it with polyphosphoric acid at 150~160°C for 4 min. A more vigorous treatment, 170~175°C for 6 min., apparently caused a considerably deep-seated decomposition of IXa, and the ketone recovered exhibited, in addition to the original absorption maximum at 228 mμ, a shoulder at 270 mμ in an ultraviolet spectrum. The detection of the semicarbazone of Xa in the crude semicarbazone (m. p. 205~209°C) derived from the recovered ketone was unsuccessful; we obtained only the semicarbazone (m. p. 215°C) of the starting material, IXa. Attempts to convert VI and VIIIa back to V and VIIa respectively under various conditions (ethanolic hydrochloric acid, zinc chloride in ethanol and polyphosphoric acid at 150°C) failed.

Discussion

The facile rearrangements, V→VI and VIIa → VIIIa, are parallel with the conversions, I→III and II→IV, demonstrated in indolenine compounds, and an analogous mechanism involving a twofold Wagner-Meerwein-type shift can be advanced (Fig. 2). At first sight, the directions of the rearrangements of V and VII seem contradictory; the one leading to the α, β-unsaturated ketone VI with no conjugation with the phenyl group, while the other leading to VIIIa, conjugated with the phenyl goup. However, an inspection of the molecular models of these compounds explained this seeming discrepancy. In the compound V, a considerable steric repulsion between the spiropentan group and the phenyl group forces the phenyl group to pivot around, out of the plain of the α, β-unsaturated ketone group. This can be see from a comparison of the ultraviolet absorption of the compound V and that of VIIIa, which has the phenyl group fully conjugated with the α, β-unsaturated carbonyl group because of the coplanarity of the two groups. (Figs. 4 and 5; Table I). Thus, the tendency to be released from the steric compression would be the driving force of the V→VI rearrangement. The compound VIIa suffers no such non-bonding interaction, and the driving force may simply be a gain in delocalization energy earned by going to the compound VIIIa. As was demonstrated elegantly by the successful optical resolution of 4, 5-disubstituted phenanthrene derivatives,[11] the substitutions at the 4- and 5-positions of the phenanthrene force the plane of the aromatic molecule to twist. In the compound VIIIb which has an extra methyl group at the 4 position of VIIIa, the non-bonding interaction between the methyl group and the hydrogen atom at the position 5 also causes the molecule to twist, and the molecule can no more enjoy the most stable conformation, in which both A and B rings (VIIIb in Fig. 3) have *quasi* chair forms, with the phenyl group coplanar with the plain of the α, β-unsaturated carbonyl system. This effect can account for the observed hypsochromic shift in an ultraviolet spectrum of VIIIb (Table I; compare with the compound VIIIa), and would compensate for the mesomeric stabilization, shifting the equilibrium toward VIIb, in the reverse

8) Cf. G. G. Walker, ibid., **77**, 3664 (1955).

9) Unfortunately, after we submitted our preliminary report,[1] this fact attracted our attention. Consequently, the physical contsants given in the report for the compound IX are actually for the compound XIII.

10) R. B. Woodward, ibid., **63**, 1123 (1941); **64**, 76 (1942).

11) M. S. Newman and A. S. Hussey, ibid., **69**, 3023 (1947), for leading references, see M. S. Newman," Steric Effects in Organic Chemistry," John Wiley and Sons, Inc., New York (1956), p. 476.

Table I. Summary of properties of α,β-unsaturated ketones

Ketone	M. p., °C or (b. p., °C/mmHg)	IR spectra[a] cm^{-1}	UV spectra[b] $m\mu$ (log ε)	Semicarbazone M. p., °C	Semicarbazone UV spectra[b] $m\mu$ (log ε)	2,4-Dinitrophenylhydrazone M. p., °C
V	(151~153/2)	1672	239 (3.99)	228~229[c]	229 (3.97) 281 (4.47)	
VI	(153~156/2)	1678	239 (4.04)	229~230[c]		
VIIa	89~91	1667	237 (4.22)	223[c]	271 (4.57)	200~201
VIIIa	62~63	1656	228.5(3.98) 297 (4.30)	248[c]	239 (4.07) 317 (4.54)	232~233
VIIIb	(160~162/2)	1658	228.5(3.90) 287 (4.13)	220~221	229 (4.01) 300 (4.58)	
IXa	(163~164/10)	1667	236 (4.08)	217~218[c]	269 (4.54)	146~147
Xa	(124~126/2)	1675	228 (3.98) 265 (3.81)	242[c]	228 (3.98) 279 (4.44)	198~199
Xb	(172~175/27)	1678	244.5(4.03)	239~240	271 (4.51)	247~248
XIII	(112~116/1)	1661	239 (4.00)			

a) Taken on a Perkin Elmer model 12C, in a Nujol mull
b) Taken on an EPS-2 Hitachi spectrophotometer, in ethanolic solution, also see Figs. 4, 5 and 6
c) Decomposition point

direction from that of VIIa→VIIIa. Contrary to this expectation, heating VIIb with polyphosphoric acid gave the starting material unchanged.

So far, the direction of the rearrangements is in a line with that established in the corresponding indolenine derivatives. However, the unsaturated ketones, IXa, Xa and Xb, were found recovered unchanged after heating them at 160~170°C with polyphosphoric acid for 6 min., and they decomposed under a more drastic treatment. On the other hand, in the corresponding indolenines,[12] an equilibrium mixture consisting of 70% 2,3-dimethyl-3-phenylindolenine and 30% 3,3-dimethyl-2-phenylindolenine was obtained from both compounds upon heating them with polyphosphoric acid at 150°C.

Special interest arises in the conversion of VIIa→VIIIa, since derivatives of VIIa have frequently been employed as intermediates in the syntheses of various steroids as well as of tricyclic diterpenes.[13]

Experimental*

6-Phenyl-spiro[4, 5]dec-6-en-8-one (V). — Into a solution of potassium *t*-butoxide prepared from 100 cc. of *t*-butanol and 4.0 g. of potassium, 17.4 g. of cyclopentyl phenyl ketone[14] (b. p. 135~137°C/10 mmHg; m. p. of the 2,4-dinitrophenylhydrazone, 142°C) were added; the mixture was then refluxed for 2~3 min. in an atmosphere of nitrogen. After a solution of the quarternary ammonium salt[15] prepared from 14.3 g. of 1-diethylamino-3-butanone and 14.3 g. of methyliodide in 60 cc. of absolute ethanol had been added to the chilled and stirred solution over a one-hour period, the stirring was continued for 10 hr. at room temperature. The solvent and diethylmethylamine were removed, and the residue was diluted with water and then extracted with ether. The ether solution was washed with 3 N hydrochloric acid and dried over anhydrous sodium sulfate. Removal of the solvent gave an oil which was distilled in a vacuum to give 8.5 g. of recovered cyclopentyl phenyl ketone and 5.3 g. of the unsaturated ketone V (b. p. 151~153°C/2 mmHg).

The semicarbazone was recrystallized from ethanol to yield crystals; m. p. 228~229°C (decomp.).

Found: C, 72.34; H, 7.65; N, 14.71. Calcd. for $C_{17}H_{21}ON_3$: C, 72.05; H, 7.47; N, 14.83%.

3-Keto-10-phenyl-$\Delta^{4,5}$-octalin (VI).—VI was prepared from 2-phenylcyclohexanone (b.p. 136~137°C/6 mmHg)[17] following Boekelheide's procedure.[16] B. p. 153~156°C/2 mmHg. The semicarbazone was recrystallized from ethanol to afford crystals (m. p. 229~230°C (decomp.)).

2-Keto-4a-methyl-2, 3, 4, 4a, 9, 10-hexahydrophenanthrene (VIIa).—A solution of 8 g. of 1-methyl-2-tetralone (b. p. 100°C/1 mmHg; the semicarbazone,

12) F. J. Evans, G. G. Lyle, J. Watkins and R. E. Lyle, *J. Org. Chem.*, **27**, 1553 (1962).
13) a) J. W. Cornforth and R. Robinson, *J. Chem. Soc.*, **1946**, 676; **1949**, 1854; b) G. Strok and W. J. Schulenberg, *J. Am. Chem. Soc.*, **78**, 250 (1956); c) P. N. Rao, *Experientia*, **12**, 472 (1956); *Tetrahedron*, **4**, 294 (1958).
* All melting points and boiling points are uncorrected. The infrared and ultraviolet spectra were taken on a Perkin Elmer model 12C spectrophotometer and on an EPS-2 Hitachi spectrophotometer respectively. The elemental analyses were performed in the microanalytical laboratory of the Institute of Polytechnics, Osaka City University. Since spectroscopic data are recorded on Table I, they will not be described in the Experimental section.
14) D. H. Hey and O. C. Musgrave, *J. Chem. Soc.*, **1949**, 3156, reported b. p. 135~136°C/10 mmHg, 2,4-dinitrophenylhydrazone, m. p. 142°C.
15) E. C. Du Feu, F. J. McQuillin and R. Robinson, ibid., **1937**, 53.
16) V. Boekelheide, *J. Am. Chem. Soc.*, **69**, 790 (1947), reported b.p. 136~140°C/0.5 mmHg, semicarbazone, decomp. p. 230~232°C.
17) M. S. Newman and M. D. Farbman, ibid., **69**, 1550 (1944).

m. p. 196~198°C.)[18] was added to a solution of potassium *t*-butoxide prepared from 2.7 g. of potassium and 62 cc. of *t*-butanol, and the reaction mixture was refluxed for 4 min. in an atmosphere of nitrogen. After a solution of the methiodide of 1-diethylamino-3-butanone prepared from 10.8 g. of the amine and 10.8 g. of methyl iodide in 37 cc. of ethanol had been added drop by drop over a 20 min. period, the mixture was stirred for 8 hr. at room temperature and then was allowed to stand for 10 hr. at the same temperature. The mixture was poured into water and extracted with ether. The ether solution was washed with 4 N hydrochloric acid and water, dried over anhydrous sodium sulfate, and freed of the solvent. The residue was distilled in a vacuum to yield 1.0 g. of the recovered 1-methyl-2-tetralone (b. p. 70~76°C/1 mmHg) and 5.6 g. of the ketol XII (b. p. 152~156°C/1 mmHg). An infrared spectrum indicated major peaks at 3390 and 1715 cm^{-1}. To a solution of 12.5 g. of the ketol XII in 30 cc. of methanol, was added 30 cc. of 50% methanolic potassium hydroxide, and the mixture was refluxed for 1 hr. Water was added, and the aqueous mixture was extracted with ether. The ether solution was separated, washed with water, and dried over anhydrous sodium sulfate, and the solvent was evaporated. When the residure was recrystallized from petroleum ether and benzene, colorless crystals separated (m. p. 86~89°C) which weighed 0.7 g. Recrystallization from petroleum ether and ether yielded crystals; m. p. 89~91°C (reported 89~91°C).[6,19]

Found: C, 84.60; H, 7.67. Calcd. for $C_{15}H_{16}O$: C, 84.87; H, 7.60%.

The semicarbazone was recrystallized from ethanol to yield crystals (m. p. 223°C (decomp.)).

Found: C, 71.67; H, 7.30; N, 15.41. Calcd. for $C_{16}H_{19}ON_3$: C, 71.34; H, 7.11; N, 15.60%.

The 2, 4-dinitrophenylhydrazone melted at 200~201°C, after recrystallization from ethyl acetate (reported 203~204°C).[6,19]

Found: C, 64.12; H, 5.27; N, 14.40. Calcd. for $C_{21}H_{20}O_4N_4$: C, 64.27; H, 5.14; N, 14.26%.

3-Keto-10a-methyl-2, 3, 9, 10, 10a, 1-hexahydrophenanthrene (VIIIa).—To a chilled solution of potassium *t*-butoxide prepared from 8.6 g. of potassium and 200 cc. of *t*-butanol, 29.0 g. of 2-methyl-1-tetralone[20] (b. p. 88~90°C/1 mmHg; the semicarbazone, decomp. p. 201°C) were added in an atmosphere of nitrogen. The solution was refluxed for 3 min. and then chilled in an ice bath. A solution of the quarternary ammonium salt prepared from 35 g. of 1-diethylamino-3-butanone and 35 g. of methyl iodie in 120 cc. of ethanol was added to the stirred solution over a one-hour period. The reaction mixture was then allowed to stand at room temperature for 10 hr. After the solvent had been removed, the residue was diluted with water and extracted with ether. The ether solution was washed twice with 3 N hydrochloric acid and then with water and dried over anhydrous sodium sulfate. Removal of the solvent yielded an oil which was distilled to give 4.3 g. of the recovered 2-methyl-1-tetralone (b. p. 150°C/1 mmHg) and 16.3 g. of the unsaturated ketone VIIIa (b. p. 155~156°C/1 mmHg), which crystallized on standing at room temperature. Recrystallization from petroleum ether afforded crystals (m. p. 62~63°C).

Found: C, 85.23, H, 7.68. Calcd. for $C_{15}H_{16}O$: C, 84.87; H, 7.60%.

The semicarbazone which was prepared by the usual procedure decomposed at 248°C after recrystallization from ethanol.

Found: C, 71.16; H, 7.00; N, 15.90. Calcd. for $C_{16}H_{19}ON_3$: C, 71.34; H, 7.11; N, 15.60%.

The 2,4-dinitrophenylhydrazone was recrystallized from ethyl acetate (m. p. 232~233°C).

Found: C, 64.70; H, 5.16; N, 14.75. Calcd. for $C_{21}H_{20}O_4N_4$: C, 64.27; H, 5.14; N, 14.28%.

3-Keto-4, 10a-dimethyl-2, 3, 9, 10, 10a, 1-hexahydrophenanthrene (VIIIb).—To a chilled solution of potassium *t*-butoxide prepared from 5.5 g. of potassium and 125 cc. of *t*-butanol, 17 g. of 2-methyl-1-tetralone were added in an atmosphere of nitrogen. The solution was refluxed for 3 min. and then cooled in an ice bath. A solution of the quaternary ammonium salt prepared from 24 g. of 1-diethylamino-3-pentanone and 22 g. of methyl iodide in 75 cc. of ethanol was added into the solution over a 20 min. period. The temperature was gradually raised to room temperature and kept at this temperature for 2.5 hr. The mixture was refluxed for 1 hr., and the solvent was removed. The residue was diluted with water and extracted with ether. The ether extract was washed with 3 N hydrochloric acid and water, and then dried over anhydrous sodium sulfate. The solvent was removed and the residue distilled to yield two high boiling fractions: (1. b. p. 155~162°C/2 mmHg, 11.5 g.; 2. b. p. 168~182°C/2 mmHg, 4.4 g.), besides a low boiling fraction (b. p. 100~125°C/2 mmHg), which consisted mainly of the recovered 2-methyl-1-tetralone. The combined high boiling fractions were distilled to afford 12.0 g. of the unsaturated ketone VIIIb (b. p. 160~162°C/2 mmHg). The semicarbazone was prepared by the usual procedure and was recrystallized from ethanol (decomp. p. 220~221°C).

Found: C, 72.34; H, 7.42; N, 14.39. Calcd. for $C_{17}H_{21}O_4N_3$: C, 72.08; H, 7.42; N, 14.83%.

The 2, 4-dinitrophenylhydrazone was recrystallized from ethyl acetate to give dark red needles (m. p. 188~189°C).

Found: C, 64.88; H, 5.54; N, 13.95. Calcd. for $C_{22}H_{22}O_4N_4$: C, 65.01; H, 5.40; N, 13.79%.

3, 6-Dimethyl-6-phenylcyclohex-2-enone (XIII).—To a slurry of sodium amide prepared from 4.6 g. of sodium in 150 cc. of ether, a solution of 29.6 g. of 3-phenyl-2-butanone[21] (b. p. 105~107°C/17 mmHg) was added, and the mixture was refluxed for 1 hr. (ammonia gas evolved). To the reaction mixture was added a solution of the quaternary ammonium salt prepared from 15 g. of 1-diethylamino-3-butanone, 15 g. of methyl iodide and 60 cc. of ethanol over a one-hour period., and then the

18) a) H. Hock, S. Lang and G. Knanel, *Chem. Ber.*, **83**, 227 (1950); b) J. English and G. Cauaglieri, *J. Am. Chem. Soc.*, **65**, 1085 (1943).

19) a) K. Zwahlen, W. J. Horton and G. J. Fujimoto, ibid., **79**, 3131 (1957); b) F. H. Howell and D. A. H. Taylor, *J. Chem. Soc.*, **1958**, 1248.

20) W. Hückel and E. Goth, *Ber.*, **57**, 1285 (1924).

21) H. M. Crawford, *J. Am. Chem. Soc.*, **56**, 140 (1934).

mixture was refluxed for 6 hr. with stirring. The mixture was poured into water and extracted with ether. The ether solution was washed with 4 N hydrochloric acid and then with water. Drying and removal of the solvent yielded a residue which was distilled in a vacuum to give 14.5 g. of the recovered 3-phenyl-2-butanone and 5.3 g. of an oil (b. p. 112~116°C/1 mmHg). The semicarbazone could not be prepared by the usual method, but 2, 4-dinitrophenylhydrazone could be obtained with Brady's reagent. Recrystallization from ethanol-ethyl acetate gave orange red needles (m. p. 204~206°C).

Found: C, 63.29; H, 5.27; N, 14.99. Calcd. for $C_{20}H_{20}O_4N_4$: C, 63.15; H, 5.30; N, 14.73%.

2,3-Dimethyl-3-phenylcyclohex-1-ene.—A stream of methyl bromide gas was passed through a stirred suspension of 3 g. of magnesium in 100 cc. of ether until the magnesium disappeared. After a solution of 12 g. of 2-methyl-2-phenylcyclohexanone[17] in 50 cc. of ether had been added over a 30 min. period, the reaction mixture was refluxed for 1 hr. The Grignard complex was decomposed with diluted aqueous hydrochloric acid and extracted with ether. The ether solution was washed with water, dried, and evaporated. To the viscous residue 0.1 g. of iodine was added, and the mixture was heated at 100°C for 30 min. and then distilled to give a dark brown oil (b. p. 124~126°C/13 mmHg). The distillate was diluted with ether, washed with an aqueous sodium hyposulfite solution to remove the iodine, and washed with water. Removal of the solvent and distillation yielded 7.9 g. of oil (b. p. 118~119°C/10 mmHg).

3, 4-Dimethyl-4-phenylcyclohex-2-enone (IXa).—A solution of 7.9 g. of 2, 3-dimethyl-3-phenylcyclohexene in 50 cc. of carbon tetrachloride was stirred at 80°C, and then a mixture of 175 cc. of a *t*-butyl chromate solution[22] (which corresponds to 32 g. of chromic anhydride), 53 cc. of acetic acid, and 21.6 g. of acetic anhydride was added. After having been stirred at this temperature for 8 hr., the solution was cooled and the excess oxidation reagent was decomposed with a solution of 35 g. of oxalic acid in 350 cc. of water. The mixture was then passed through a layer of Hyflo super cells to remove a sludgy material. After having been separated from the carbon tetrachloride layer, the aqueous solution was extracted with carbon tetrachloride three times. The combined carbon tetrachloride solutions were washed with water, 5% aqueous sodium carbonate, 2 N sodium hydroxide and water successively. Drying and removal of the solvent gave a residue, which was distilled to yield 2.1 g. of the recovered hydrocarbon (b. p. 130°C/10 mmHg) and 3.0 g. of the unsaturated ketone IXa (b. p. 163~164°C/10 mmHg). The semicarbazone was recrystallized from ethanol (decomp. p. 217~218°C).

Found: C, 69.87; H, 7.30; N, 16.12. Calcd. for $C_{15}H_{19}ON_3$: C, 70.00; H, 7.44; N, 16.33%.

The 2, 4-dinitrophenylhydrazone was recrystallized from ethyl acetate to afford orange red needles (m. p. 146~147°C).

Found: C, 62.95; H, 5.30; N, 14.82. Calcd. for $C_{20}H_{20}O_4N_4$: C, 63.15; H, 5.30; N, 14.73%.

4, 4-Dimethyl-3-phenylcyclohex-2-enone (Xa).—To a solution of potassium *t*-butoxide prepared from 4.0 g. of potassium and 100 cc. of *t*-butanol, 14.8 g. of isopropyl phenyl ketone (b. p. 97~99°C/13 mmHg, 2, 4-dinitrophenylhydrazone, m. p. 161~162°C) were added, and the solution was refluxed for 3 min. in an atmosphere of nitrogen. A solution of the quarternary ammonium salt prepared from 14.3 g. of 1-diethylamino-3-butanone and 14.3 g. of methyl iodide in 60 cc. of ethanol was added over a period of 35 min., and the reaction mixture was then allowed to stand at room temperature for 11 hr. After having been refluxed for 20 min., the mixture was concentrated and diluted with water. The aqueous solution was extracted with ether, and the ether extracts were washed with 3 N hydrochloric acid and then with water. Drying and removal of the solvent afforded a viscous oil which distilled in a vacuum to yield 10.0 g. of the recovered ketone (b. p. 100°C/13 mmHg) and 2.5 g. of the unsaturated ketone Xa (b. p. 124~126°C/2 mmHg). The semicarbazone was recrystallized from ethanol to give crystals (decomp. p. 242°C).

Found: C, 69.83; H, 7.47; N, 16.24. Calcd. for $C_{15}H_{19}ON_3$: C, 70.00; H, 7.44; N, 16.33%.

The 2, 4-dinitrophenylhydrazone was recrystallized from ethanol-ethyl acetate (m. p. 198~199°C).

Found: C, 63.12; H, 5.43; N, 14.99. Calcd. for $C_{20}H_{20}O_4N_4$: C, 63.15; H, 5.30; N, 14.73%.

2, 4, 4-Trimethyl-3-phenylcyclohex-2-enone (Xb).—To a solution of potassium *t*-butoxide prepared from 5.8 g. of potassium and 120 cc. of *t*-butanol, 17.5 g. of isopropyl phenyl ketone were added, and the mixture was refluxed for 3 min. After a solution of the quarternary salt[23] prepared from 24 g. of 1-diethylamino-3-pentanone and 22 g. of methyl iodide in 70 cc. of ethanol had been added over a period of 45 min., the mixture was cooled in an ice bath for 4 hr. and then refluxed for 1 hr. After the solvent had been removed, the reaction mixture was diluted with water and extracted with ether. The ether solution was washed with 3 N hydrochloric acid and water, and then dried over anhydrous sodium sulfate. The ether was removed and the residual liquid distilled to give 7.2 g. of a colorless liquid (b. p. 172~175°C/27 mmHg). The semicarbazone was recrystallized from ethanol to afford crystals (decomp. p. 239~240°C).

Found: C, 70.73; H, 8.02; N, 15.36. Calcd. for $C_{16}H_{21}ON_3$: C, 70.82; H, 7.80; 15.49%.

The 2, 4-dinitrophenylhydrazone was recrystallized from ethanol-ethyl acetate to yield red needles (m. p. 247~248°C (with decomposition)).

Found: C, 63.99; H, 5.56; N, 14.40. Calcd. for $C_{21}H_{22}O_4N_4$: C, 63.94; H, 5.62; 14.21%.

Interconversion between V and VI.—*a) V→VI.*—To a polyphosphoric acid prepared from 8 cc. of 85% phosphoric acid and 12.5 g. of phosphorous pentoxide, 2.5 g. of the unsaturated ketone V were added, and the mixture was heated at 150~155°C for 10 min. Ice water was added to the reaction mixture, and the turbid solution was extracted with ether. The ether extract was washed with an

22) K. Heusler and A. Wettstein, *Helv. Chim. Acta*, **35**, 284 (1952).

23) P. S. Adamson, F. J. McQuillin and R. Robinson, *J. Chem. Soc.*, **1937**, 1576.

aqueous sodium carbonate solution and then with water. Removal of the solvent gave a liquid which distilled to give 1.0 g. of a liquid (b. p. 149~152°C/2 mmHg). An infrared spectrum of the product and that of VI were indistinguishable. The semicarbazone was prepared to give crystals (m. p. 229°C (with decomposition)). The mixed melting point with the semicarbazone of the starting ketone (decomp. p. 228~229°C) was 215°C (with decomposition), while the mixed melting point with the semicarbazone of VI (decomp. p. 229~230°C) was 228°C (with decomposition).

b) *VI→V.*—A mixture of 2.0 g. of VI and 20 g. of polyphosphoric acid was heated at 100°C for 30 min. and then at 150°C for 5 min. The reaction mixture was poured into ice water and extracted with ether. Evaporation of the solvent and distillation gave 1.5 g. of an oil (b. p. 140~150°C/2 mmHg). Identification of the product with the starting material was established by comparison of their infrared spectra and by a mixed melting point determination of their semicarbazones.

Interconversion between VIIa and VIIIa.—*a*) *VIIa→VIIIa.*—A mixture of 0.7 g. of the ketone VIIa and 20 g. of polyphosphoric acid was heated in an oil bath; the temperature was raised rapidly to 165°C and then kept at this temperature for 3 min. After the reaction mixture had been poured quickly into water, the mixture was extracted with ether. The ether solution was washed with water and with a 5% sodium carbonate solution. Drying and removal of the solvent gave an oil which distilled to afford 0.55 g. of a viscous oil (b. p. 157~163°C/1 mmHg). The product crystallized upon standing at room temperature and was recrystallized from petroleum ether to yield crystals (m. p. 60~61°C), the identification of which with VIIIa was established by a comparison of their infrared spectra and by mixed melting point determination. The identification was further confirmed by the mixed melting point, 248°C (with decomposition) of the semicarbazone of the produt, with the semicarbazone of VIIIa (decomp. p. 248°C).

b) *VIIIa→VIIa.*—A mixture of 2.0 g. of VIIIa and 30 g. of polyphosphoric acid was heated at 160°C for 3 min. and then poured into ice water. The mixture was extracted with ether, and the ether solution was washed with aqueous sodium carbonate and then with water. Drying and removal of the solvent gave a residual oil which distilled to yield 1.9 g. of a liquid (b. p. 165~170°C/1 mmHg). The product which crystallized upon standing at room temperature was recrystallized from petroleum ether to afford crystals, (m. p. 62 63°C). The mixed melting point with the starting material was 62~63°C.

Reaction of VIIIb with Polyphosphoric Acid.—A mixture of 3.0 g. of the ketone VIIIb and 30 g. of polyphosphoric acid was heated at 160°C for 15 min. Upon the usual work-up, 2.5 g. of VIIIb were recovered. Identification was established by an infrared absorption spectrum.

Interconversion between IX and Xa.—*a*) *IX→Xa.*—A mixture of 2.0 g. of the ketone IX and 25 g. of polyphosphoric acid was heated at 150~160°C for 4 min. The reaction mixture was poured into water and extracted with ether. The ether solution was washed with aqueous sodium carbonate and with water. Removal of the solvent and distillation of the residue gave 1.6 g. of an oil (b. p. 160~163°C). Although the infrared spectrum was found indistinguishable with that of the starting material, the ultraviolet spectrum showed a peak at 228 mμ, with a shoulder at 270 mμ. The semicarbazone prepared from the product decomposed at 203~209°C after one recrystallization from ethanol. This was found contaminated with a very small number of needles. Four recrystallizations from ethanol raised the decomposition point to 215°C, which was unchanged upon admixture with the semicarbazone of the starting material.

b) *Xa→IX.*—A mixture of 2.3 g. of Xa and 30 g. of polyphosphoric acid was heated at 150~160°C for 10 min. Upon the usual work-up, 1.5 g. of the starting material was recovered; identification was established by a comparison of the infrared spectrum and the melting point (m. p. 190~193°C) of the 2, 4-dinitrophenylhydrazone.

Reacton of Xb with Polyphosphoric Acid.—A mixture of 3.0 g. of ketone Xb and 35 g. of polyphosphoric acid was heated at 160~170°C for 6 min. From the reaction mixture, 2.5 g. of the starting material (b. p. 115~117°C/2 mmHg) was recovered; identification was established by comparing the infrared spectra and the melting points (decomposed at 240~241°C) of the semicarbazone of the starting material with those of the reaction product.

The authors are very grateful to the Nitto Kasei Co. for its financial support. A part of the cost of this research was also defrayed by a grant-in-aid for fundamental scientific research from the Ministry of Education, to which the authors' thanks are due.

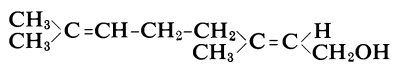
Department of Chemistry
Institute of Polytechnics
Osaka City University
Sumiyoshi-ku, Osaka

Stereoselective Synthesis of Nerol

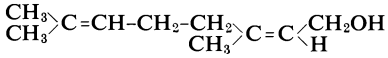
By Yasuhide YUKAWA, Terukiyo HANAFUSA and Kaneko FUJITA

(Received July 27, 1963)

It is well known that geraniol and nerol are the most fundamental acyclic monoterpenoid alcohols and that both are geometric isomers. Their geometric configurations were mainly elucidated by the following chemical and physical evidence. Zeitschel[1] showed in 1906 that when fifty grams each of geraniol, linalool and nerol were cyclized to α-terpineol with dilute sulfuric acid, the yields of the reaction were 0.35 g., 1.75 g. and 2.5 g. respectively. Judging from the ease of cyclization, he assumed that the isohexenyl group and the hydroxymethyl group in geraniol (I) were trans to each other and that these groups in nerol were cis, based upon the ease of the cyclization.



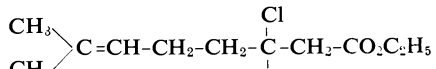
(I)



(II)

Recently Jeffery[2] has established by X-ray crystallographic study that geranyl amine hydrochloride derived from geraniol has a structure which agrees with the chemically-assigned configuration. Thus, geraniol, in which relatively bulky groups are trans, may be thermodynamically more stable than nerol, and this may be correlated to the fact that the melting point of geranyl derivatives is higher than that of neryl compounds.[3,4]

Two synthetic methods of nerol have been reported in the literature. One[5] is the isomerization of geraniol to nerol; this reaction involves the addition of hydrogen iodide to geraniol and the subsequent elimination of the acid with alcoholic sodium hydroxide to give nerol. In the other,[6] nerol is obtained by the lithium aluminum hydride reduction of *cis*-geranic acid, which has been prepared by the elimination of hydrogen chloride with pyridine from the chloroester III. Both routes to form



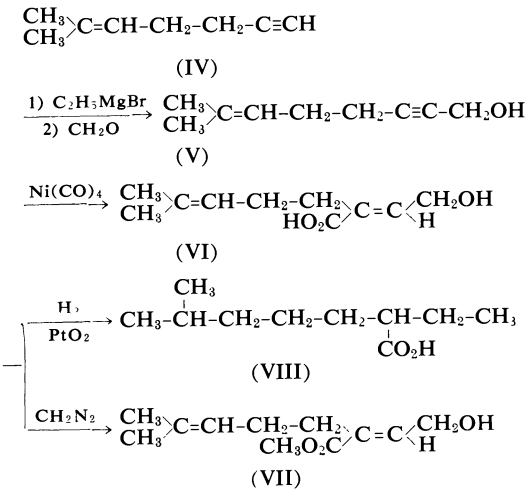
(III)

the double bond concerned are base-catalyzed eliminations; it seems probable that a major product would be a more thermodynamically stable isomer in these reactions. In the syntheses of nerol, thus, an ambiguity still remains.

In this paper we wish to report the stereoselective synthesis of nerol allophanate, starting with an acetylenic compound.

Results and Discussion

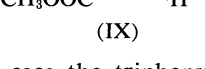
The starting material, 6-methyl-5-hepten-1-yne (IV), was prepared from γ-butyrolactone and acetylene according to Eschenmoser's procedure[7] and was converted into 7-methyl-6-octen-2-yn-1-ol (V) by the reaction of its Grignard compound with paraformaldehyde. The acetylenic alcohol V was reacted with nickel carbonyl in a solvent mixture of alcohol, acetic acid and water at 70°C to give unsaturated hydroxylic acid VI, which did not lactonize on being heated to 120°C for 5 hr. The catalytic hydrogenation of this acid VI over platinum oxide afforded 2-ethyl-6-methylheptanoic acid (VIII), with hydrogenolysis of



1) O. Zeitschel, *Ber.*, **39**, 1782 (1906).
2) G. A. Jefferey, *Proc. Roy. Soc.*, **A183**, 388 (1945).
3) H. von Soden and O. Zeitschel, *Ber.*, **36**, 266 (1903); A. Blumann and O. Zeitschel, ibid, **44**, 2593 (1911).
4) D. Barnard, L. Bateman, A. J Harding, H. P. Koch, N. Sheppard and G. B. B. M. Sutherland, *J. Chem. Soc.*, **1950**, 915.
5) A. Verley, *Bull. soc. chim. France*, **25**, (4) 68 (1919).
6) A. Mondon and G. Teege, *Chem. Ber.*, **91**, 1020 (1958).
7) G. Gamboni, H. Schinz and A. Eschenmoser, *Helv. Chim. Acta*, **37**, 964 (1954).

the allylic hydroxyl group, which was characterized as its anilide (m. p. 66~67°C[8]). If the carboxylation of the acetylenic alcohol V with nickel carbonyl occurred in the β-position of the hydroxyl group, the hydrogenation of this reaction product should give 2, 7-dimethyloctanoic acid, which is an isomer of VIII. However, it is reported that its anilide melted at 93°C.[8] Since it has been established[9,10] that this carboxylation of the acetylenic compound, developed by Jones,[9] results in the formation of α, β-unsaturated carboxylic acid, in which the carboxyl function and the hydrogen atom introduced are on the same side of the double bond, these evidences confirm the correctness of the above formulation.

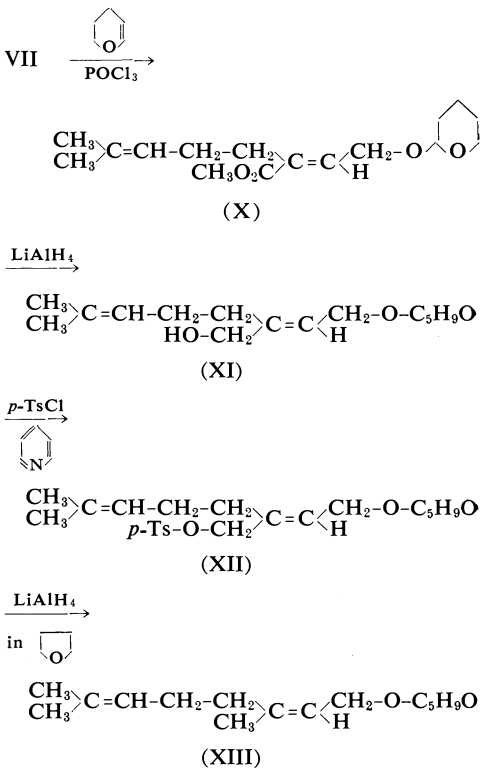
The esterification of the unsaturated hydroxylic acid VI smoothly proceeded using diazomethane to give an unsaturated ester VII. During the subsequent reduction of the ester function to the methyl group it is necessary to protect the hydroxyl function in a form unaffected by reducing agents. In our previous investigation,[10] 4-methoxycarbonyl-3-hexen-1-ol (IX) was converted into triphenylmethyl ether of IX in order to prevent the elimination of the hydroxyl function during hydrolysis and decarboxylation. It was found, however, that



(IX)

in this case the triphenylmethoxy group in the trityl ether of VII was replaced by a hydrogen atom during the course of the reduction of the ester function to the methyl group. Recently we reported[11] that the reaction of dihydropyran with catechol furnished protection to the hydroxyl group in catechol to give the di-(tetrahydropyranyl)ether of catechol, which was stable in basic media and which was readily hydrolyzed with dilute mineral acid. This procedure has also been employed in the study of aliphatic unsaturated hydroxylic compounds.[12]

The ester VII was treated with dihydropyran and a catalytic amount of phosphorous oxychloride to afford tetrahydropyranyl ether X. The ester function of the tetrahydropyranyl derivative X was transformed into the hydroxymethyl group with lithium aluminum hydride in a cold ethereal solution. The reaction of the resulting alcohol XI with *p*-toluenesulfonyl chloride in pyridine gave a sulfonate XII, which was further reduced with lithium aluminum hydride in tetrahydrofuran under reflux. In some reactions of allylic derivatives, allylic rearrangement may occasionally occur. However, it has proved by a study using ^{14}C as a tracer[13] that allylic rearrangement does not occur when the *p*-toluenesulfoxyl group in an allylic situation is replaced with nucleophilic reagents. This procedure has ordinarily been employed in the transformation of the hydroxymethyl group to the methyl group.[14]



(X)

(XI)

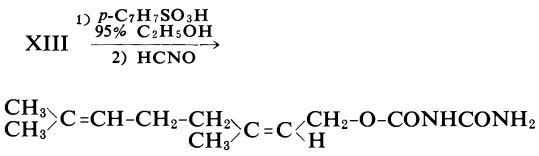
(XII)

(XIII)

The reduction product was purified by alumina chromatography, and the pure tetrahydropyranyl ether XIII was eluted with petroleum ether. It has been reported that the hydrolysis of tetrahydropyranyl ether has been carried out by the action of warm dilute mineral acid, a boiling aqueous oxalic acid solution, 2, 4-dinitrophenylhydrazine in 2 N hydrochloric acid or *p*-toluenesulfonic acid in aqueous alcohol.[15] In this case it was experimentally found that the last of these reagents

8) H. Suzuki, *J. Pharm. Soc. Japan* (*Nippon Yakugaku Zasshi*), **56**, 860 (1936).
9) E. R. H. Jones, T. Y. Shen and M. G. Whiting, *J. Chem. Soc.*, **1951**, 48.
10) Y. Yukawa and T. Hanafusa, *J. Chem. Soc. Japan, Pure Chem. Sec.* (*Nippon Kagaku Zassi*), **76**, 572 (1955).
11) T. Hanafusa and Y. Yukawa, *Chem. Ind.*, **1961**, 23.
12) G. F. Woods and E. L. Anderson, *J. Am. Chem. Soc.*, **69**, 2246 (1947); H. B. Henbest, E. R. H. Jones and I. M. S. Walls, *J. Chem. Soc.*, **1950**, 3648; S. S. Nigam and B. C. L. Weedon, ibid., **1956**, 4050.
13) R. F. Nystrom and J. C. Leak, *J. Am. Chem. Soc.*, **75**, 3039 (1953).
14) W. G. Brown, "Organic Reactions," Vol. VI, 471 (1951).
15) Houben-Weyl, "Methoden der Organischen Chemie," 4 Aufl.. VI, (1), (1954), p. 423.

was the most satisfactory. The tetrahydropyranyl ether XIII was treated with a small amount of *p*-toluenesulfonic acid in 95% ethyl alcohol at 55°C for one-and-a-half hours to give an oil, into which cyanic acid was then introduced at room temperature. The allophanate XIV was obtained as colorless needles after one recrystallization each from benzene and from petroleum ether. It was much more soluble in benzene or petroleum ether than in



XIII $\xrightarrow[2)\ HCNO]{1)\ p\text{-}C_7H_7SO_3H,\ 95\%\ C_2H_5OH}$

$$\begin{matrix} CH_3 \\ CH_3 \end{matrix}\!\!>\!C\!=\!CH\!-\!CH_2\!-\!CH_2\!-\!\underset{CH_3}{\overset{}{>}}\!C\!=\!C\!<\!\begin{matrix} CH_2\!-\!O\!-\!CONHCONH_2 \\ H \end{matrix}$$

(XIV)

geranyl allophanate and melted at 84~86°C. The melting point was not raised by further recrystallization and was not depressed upon admixture with geranyl allophanate (m. p. 110°C).

Other investigators[3,4,16,17] have also recorded that the crystalline derivatives of nerol are much more soluble in ordinary solvents than that of geraniol, that the melting points of neryl derivatives are lower than that of geranyl derivatives, and that they did not depress upon admixture with geranyl compounds. It is evident that the allophanate XIV is neryl allophanate since its behavior agrees with these results.

As has been described above, Mondon[6] has reported obtaing *cis*-geranic acid by the reaction of chloroester III with pyridine and by the hydrolysis of the resulting ester. Its *S*-benzylthiourea adduct recrystallized from dioxane melted at 133°C, while the adduct of *trans*-geranic acid, prepared by the oxidation of geraniol, melted at 141~143°C after recrystallization from dilute alcohol. However, it was found that these two adducts were the same compound. The adduct of *cis*-acid melted at 141~143°C when it was recrystallized from dilute alcohol, and the reduction product of *cis*-acid purified by Mondon's procedure was geraniol, which was characterized as its allophanate (m. p. 107~110°C). These results agree with the generality that the base-catalyzed elimination of hydrogen halide from a halogeno compound gives a more thermodynamically stable isomer at a higher rate.[18]

16) Y. R. Naves and A. V. Grampoloff, *Helv. Chim. Acta*, **25**, 1500 (1942).
17) Y. R. Naves, ibid., **29**, 557 (1946).
18) D. J. Gram, "Steric Effects in Organic Chemistry," Ed. by M. S. Newman, John Wiley & Sons, Inc., New York (1956), p. 339.

Experimental

7-Methyl-6-octen-2-yn-1-ol (V). — 6-Methyl-5-octen-1-yne (IV) (16 g.), prepared according to Eschenmoser's procedure, was added to an ethereal solution of ethylmagnesium bromide prepared from ethyl bromide (22 g.) and magnesium (5 g.) in ether (150 ml.). The reaction mixture was heated under reflux for 2 hr., after which paraformaldehyde (22 g.) was stirred in efficiently at −5°C over a 1 hr. period. After being stirred for 2 hr. at 0°C, the mixture was decomposed with a saturated aqueous ammonium chloride solution. The ether extracts were washed with water and dried over anhydrous magnesium sulfate. This compound (12 g.) was obtained as an oil (b. p. 93~95°C/3 mmHg, n_D^{23} 1.4761). Its phenyl urethane did not solidify.

3-Carboxy-7-methyl-2, 6-octadien-1-ol (VI).—A solution of nickel carbonyl (7.5 ml.) in absolute ethyl alcohol (15 ml.) was added dropwise at 65~70°C with stirring under an inert atmosphere into a solution of the acetylenic alcohol (V) in ethyl alcohol (32 ml.) acetic acid (6.5 ml.), and water (3 ml.). After being heated under reflux for 2 hr., the mixture was treated with 5% sulfuric acid (35 ml.) and ether (100 ml.) at 0~5°C. The water layer was repeatedly extracted with ether. The combined ether was extracted with saturated aqueous sodium hydrogen carbonate until the pH value in an alkaline solution did not change (twelve times). The alkaline layer was acidified with dilute hydrochloric acid. Continuous ether extraction from the acidic solution afforded, after removal of the solvent, this acid VI (6.9 g.) (b. p. 145~147°C).

Found: C, 65.19; H, 8.75. Calcd. for $C_{10}H_{16}O_3$: C, 65.38; H, 8.43%.

The compound was redistilled unchanged under reduced pressure and did not change on being heated at 120°C for 5 hr.

2-Ethyl-6-methylheptanoic Acid (VIII). — The acid VI was hydrogenated in ethyl acetate over platinum oxide under atmospheric pressure. 3.5 equivalents of hydrogen were absorbed over a 6 hr. period. The product was then extracted with a 10% aqueous sodium carbonate solution. After acidification with 2 N hydrochloric acid, the saturated acid VIII was extracted with ether in a 63% yield. This compound was distilled at 105°C/20 mmHg and showed no band in the region of 3000~4000 cm^{-1}.

Found: C, 69.14; H, 11.70. Calcd. for $C_{10}H_{20}O_2$: C, 69.72; H, 11.70%.

The anilide of this acid melted at 66~67°C; this agrees with Suzuki's finding.[8]

3-Methoxycarbonyl-7-methyl-2, 6-octadien-1-ol (VII).—A solution of diazomethane prepared from *N*-nitrosomethylurea (15 g.) in ether (30 ml.) was introduced into a solution of the unsaturated acid (VI) (6.9 g.) in an ice-salt bath. After it had been left standing overnight, the reaction mixture was shaken with 2 N hydrochloric acid, with a saturated aqueous sodium hydrogen carbonate solution, and with water successively. The ester VII (5 g.) was distilled at 128~129°C/3 mmHg; n_D^{28} 1.4737.

Found: C, 66.77; H, 9.59. Calcd. for $C_{11}H_{18}O_3$: C, 66.64; H, 9.15%.

3-Methoxycarbonyl-7-methyl-2,6-octadienyl Tetrahydropyranyl Ether (X). — A few drops of phosphorous oxychloride were added to a mixture of the ester VII (5 g.) and dihydropyran in an ice bath. After it had stood at room temperature for 3 hr., the reaction mixture was added to a 20% aqueous sodium carbonate solution. Ether extraction gave, after removal of the solvent, the ether X (4 g.) (b. p. 120~121°C/0.1 mmHg).

Found: C, 68.20; H, 9.37. Calcd. for $C_{16}H_{26}O_4$: C, 68.05; H, 9.28%.

3-Hydroxymethyl-7-methyl-2, 6-octadienyl Tetrahydropyranyl Ether (XI).—A solution of the above ether X (4 g.) in absolute ether (50 ml.) was stirred, at −10°C, into a solution of lithium aluminum hydride (0.6 g.) in absolute ether (30 ml.). The reaction mixture was heated under reflux for a short time. After ethyl acetate (1 ml.) had been added to the mixture in an ice-salt bath, 2 N hydrochloric acid (30 ml.) was introduced. An ethereal layer was washed with water and dried over anhydrous magnesium sulfate. This compound XI (2.8 g.) was distilled at 130~137°C/0.3 mmHg.

Found: C, 70.25; H, 10.30. Calcd. for $C_{15}H_{26}O_3$: C, 70.83; H, 10.30%.

The Sulfonate of XI (XII).—A solution of XI (2.8 g.) in dry pryridine (30 ml.) was stirred, at −1~−3°C, into a solution of *p*-toluenesulfonyl chloride (4.5 g.) in the solvent. After having been stirred for 3 hr. at room temperature, the mixture was poured into cold dilute hydrochloric acid. Chloroform extraction afforded this compound XII as an viscous oil after evaporation of the solvent under reduced pressure. The sulfonate was easily soluble in chloroform or tetrahydrofuran, only but with difficult in ether, and it was not further purified.

Neryl Tetrahydropyranyl Ether (XIII).—A solution of the above sulfonate XII in tetrahydrofuran (50 ml.) was stirred into a solution of lithium aluminum hydride (1 g.) in tetrahydrofuran (50 ml.) in an ice-salt bath. The reaction mixture was heated under reflux for 10 hr. After having been cooled, the mixture was decomposed with ethyl acetate (4 ml.), water (10 ml.) and 2 N hydrochloric acid (50 ml.) successively. The water layer was extracted with ether. The combined ether solution was then washed with a 20% sodium carbonate solution and an aqueous saturated sodium chloride solution. After removal of the solvent, the residue was purified by alumina column chromatography. Elution with light petroleum (600 ml.) gave neryl tetrahydropyanyl ether XIII (0.4 g.) (b. p, 150°C (bath temp.)/0.3 mmHg). The infrared spectrum of this compound resembled that of the geranyl derivative.

The Allophanate of Nerol (XIV).—A solution of the neryl tetrahydropyranyl ether (XIII) (0.4 g.) and *p*-toluenesulfonic acid (0.05 g.) in 95% ethyl alcohol (8 ml.) was heated to 52~58°C for one and a half hours. The mixture was then extracted with light petroleum after having been added to water. An organic layer was washed with a 10% aqueous sodium carbonate solution and water, and then dried over magnesium sulfate. After removal of the solvent, the cyanic acid generated from the thermal decomposition of cyanuric acid (0.5 g.) was introduced into the residue in an ice bath. The solids thus produced were washed with light petroleum and recrystallized once from benzene and once from light petroleum. The allophanate XIV (0.1 g.) was obtained as needles, which melted at 84~86°C by themselves and which melted at 84~88°C on admixture with the allophanate of geraniol. The melting point was not raised by further recrystallization.

Found: C, 59.03; H, 8.39; N, 11.72. Calcd. for $C_{12}H_{20}O_3N_2$: C, 59.98; H, 8.46; N, 11.66%.

Reduction of the Triphenylmethyl Ether of VII.—A mixture of VII (4 g.), triphenylmethyl chloride (7 g.) and pyridine (3 g.) in benzene (70 ml.) was heated under reflux for 4 hr. After removal of the solvent under reduced pressure, the residue was extracted 4 times with light petroleum (100 ml.). The trityl ether (5.4 g.) was obtained as a viscous oil after having been purified by alumina column chromatography.

A solution of the substance (5 g.) in absolute ether (30 ml.) was ordinarily reduced with lithium aluminum hydride in an ice bath. The reaction products were chromatographed on alumina. 3-Hydroxymethyl-7-methyl-2, 6-octadienyl triphenylmethyl ether (1.8 g.) was eluted, using 30% benzene-light petroleum as a syrup, a syrup which was decomposed on distillation, even under highly reduced pressure.

Found: C, 84.30; H, 7.92. Calcd. for $C_{29}H_{32}O_2$: C, 84.42; H, 7.82%.

The reduction procedure of this compound was analogous to that described in the reduction of XI through its sulfonate XII with lithium aluminum hydride. The products were chromatographed on alumina. An olefin was eluted with light petroleum and seemed to be 2, 6-dimethyl-2, 6-octadiene judging from its boiling point (100~110°C (bath temp.)/20 mmHg), its analytical datum and its infrared spectrum.

Found: C, 87.49; H, 11.63. Calcd. for $C_{10}H_{18}$: C, 86.88; H, 13.12%.

The other product was eluted with 50% benzene-light petroleum as plates; the m. p. was 150~155°C, which was not depressed when the product was admixed with triphenylmethyl alcohol.

Geranyl Tetrahydropyranyl Ether.—This compound (3.5 g.) (b. p. 122~124°C/5 mmHg) was prepared from geraniol (3 g.) and dihydropyrane (3 g.) in a manner similar to that described in the synthesis of X.

Found: C, 76.05; H, 10.70. Calcd. for $C_{15}H_{26}O_2$: C, 75.63; H, 10.92%.

Hydrolysis of Geranyl Tetrahydropyranyl Ether.—1) A mixture of the ether (1 g.) and oxalic acid (0.5 g.) in water (5 ml.) was heated while being stirred at 100°C for 1.5 hr. Steam distillation gave the starting material (0.6 g.) unchanged; this was confirmed by its infrared spectrum.

2) A mixture of the ether (1 g.) in 2 N sulfuric acid (10 ml.) was slowly distilled with steam to give an alcohol, but its allophanate melted at 70~80°C.

3) The ether was shaken with excess 2, 4-dinitrophenylhydrazine in 2 N hydrochloric acid for 7 hr. The ether was recovered unchanged.

The Reduction of *cis*-Geranic Acid.—*cis*-Geranic acid was prepared from III following Mondon's procedure. Its *S*-benzylthiuronium salt melted at 133°C on recrystallization from dioxane and at 141~143°C on recrystallization from dilute alcohol. The purified acid through the *S*-benzylthiuronium salt was reduced with lithium aluminum hydride by Mondon's procedure. The reduction product (b. p. 86~87°C/4 mmHg) was converted into its allophanate, which melted at 107~110°C after having been recrystallized from benzene. The melting point was not depressed when the product was admixed with geranyl allophanate.

Summary

Nerol, acyclic monoterpene alcohol, has been stereoselectively synthesized using as an intermediate the unsaturated hydroxylic acid VI, in which the carboxyl and the hydroxymethyl groups are evidently in the cis-relation.

The authors wish to express their thank to Mr. Tsuguyo Shishido for his microanalysis and to Miss Kayo Kabazawa for her infrared spectroscopy. They are also indebted to the Shiono Koryo Co., Ltd., and to the Hagihara Laboratory for their kind assistance throughout this work.

The Institute of Scientific and Industrial Research
Osaka University
Sakai, Osaka

The Rotatory Dispersion and Stereochemistry of Organic Compounds. V.[1] *On Anomeric Pyranoses with a Xanthate Group*

By Yojiro TSUZUKI, Koko TANABE, Masuo AKAGI and Setsuzo TEJIMA

(Received July 27, 1963)

In a previous paper[1] it was shown that some of the rotatory contribution of the hydroxyl groups in glucose can be studied by means of rotatory dispersion with its derivatives which contain a xanthate group. The present paper will report on similar, comparative studies made of a variety of newly-synthesized xanthates with a pyranose configuration, namely:

2, 3, 4, 6-Tetra-*O*-acetyl-α-D-glucopyranosyl ethylxanthate (compound I),

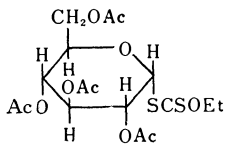
2, 3, 4, 6-Tetra-*O*-acetyl-β-D-glucopyranosyl ethylxanthate (compound II),

2, 3, 4-Tri-*O*-acetyl-β-D-xylopyranosyl ethylxanthate (compound III),

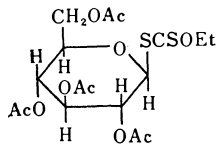
Methyl 2, 3, 4-tri-*O*-acetyl-β-D-glucopyranuronate 1-ethylxanthate (compound IV),

2-Acetamido-2-desoxy-3, 4, 6-tri-*O*-acetyl-β-D-glucopyranosyl ethylxanthate (compound V),

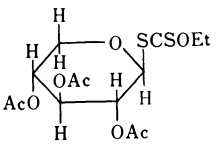
6-Desoxy-6-ethylxanthogen-α-D-glucopyranose tetraacetate (compound VI),



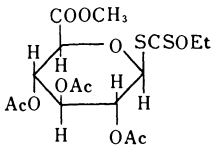
(I) -Et=-C_2H_5
-Ac=-$COCH_3$



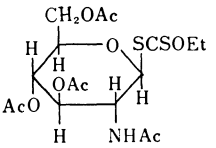
(II)



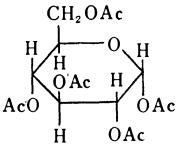
(III)



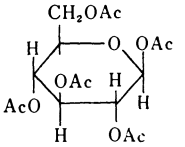
(IV)



(V)



(VI)



(VII)

6-Desoxy-6-ethylxanthogen-β-D-glucopyranose tetraacetate (compound VII).

1) Y. Tsuzuki, K. Tanaka and K. Tanabe, This Bulletin, 35, 1614 (1962).

Results and Discussion

The RD curves of these compounds are shown in Figs. 1, 2 and 3. Figure 1 shows distinctly the difference between α- and β-anomers. The rotatory background of the α-form I is, as expected, more positive, but its Cotton effect is negative in sign, the peak being 380 mμ, whereas the β-form II shows a stronger, positive Cotton effect (the peak being 381 mμ, the trough, 334 mμ).

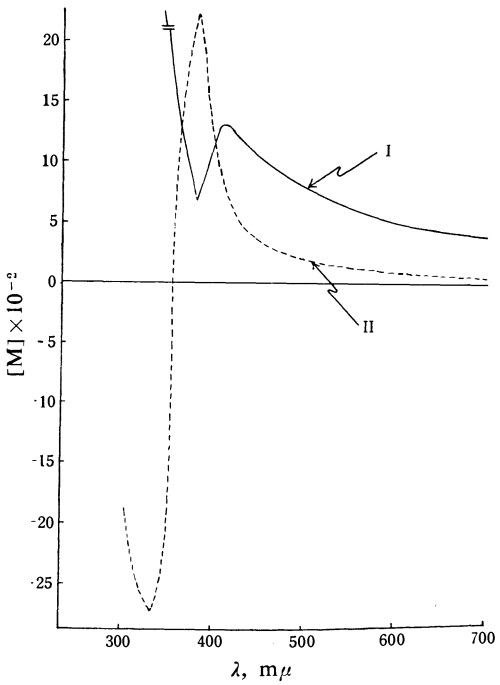


Fig. 1. RD of α- and β-1-xanthogen glucose.

Figure 2 shows the effects of the C_2 and C_5 groups on the rotatory contribution in the β-xanthate series, which exhibit, without exception, obviously positive Cotton effects. Since, in D-glucose and D-xylose and their derivatives, the C_2 group is expected to contribute to the positive rotation, it is possible that the glucosamine derivative V, being a β-configuration, is distinguished from others in high rotation. Its molecular amplitude (the difference of [M] between peak and trough) is also far greater. It is observed that the C_5 effect is insignificantly small when it carries no chromophoric group. The [M] values of these compounds are almost identical above the absorption region, irrespective of the C_5 groups (H, $COOCH_3$, CH_2OCOCH_3); however in molecular amplitude there are little grades of difference which might be of some significance as to the configuration and the group of optically-active absorption, but at present the authors can not consider this point since the sign of the rotatory contribution of the C_5 group has not yet been elucidated. It should, however, be pointed out that all the peaks are situated near 380 mμ, the troughs at 334 mμ, and λ_0, the optically-active absorption maximum, at 360 mμ.

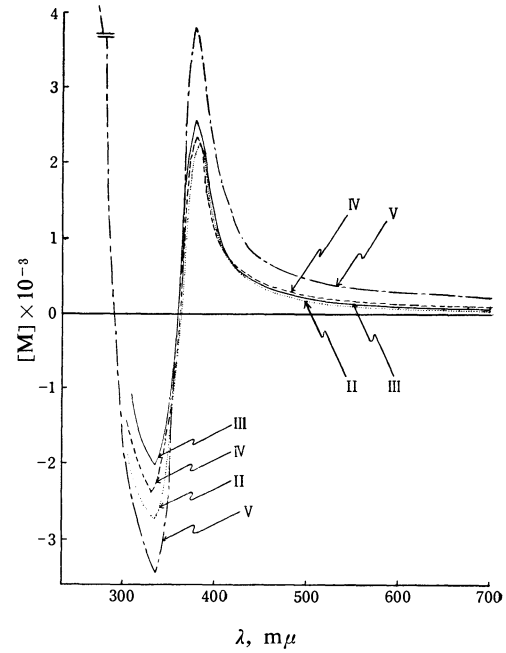


Fig. 2. RD of β-1-xanthates.

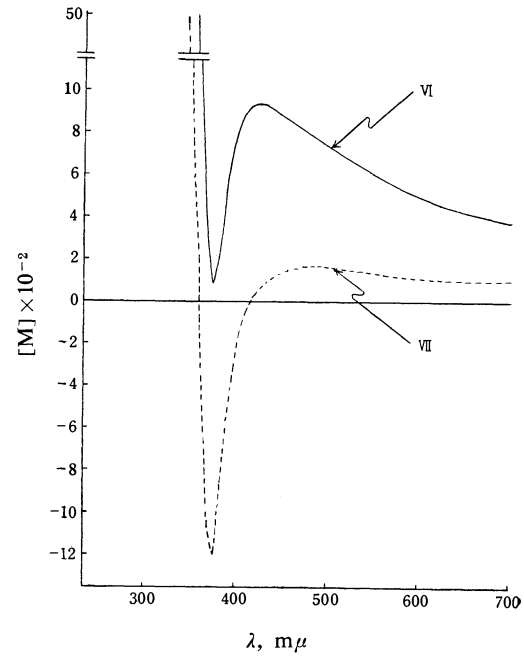


Fig. 3. RD of 6-xanthogen α- and β-acetylglucose.

TABLE I. RD COSTANTS AND UV ABSORPTION MAXIMA

Compound	Rotatory dispersion				Molecular amplitude	Ultraviolet absorption			
	Peak		Trough			R-band		K-band	
	mμ	[M]	mμ	[M]	$\times 10^{-1}$	mμ	ε	mμ	ε
I	380 (negative)	+686°	—	—	—	363	32.0	276	4280
II	381	+2220°	334	−2720°	494°	363	36.4	275	10400
III	378	+2510°	335	−2010°	452°	364	42.5	275	9750
IV	378	+2270°	330	−2320°	459°	360	40.0	274	3330
V	378	+3780°	335	−3340°	712°	360	42.3	276	11400
VI	375 (negative)	+98.7°	—	—	—	356	49.7	279	13100
VII	376 (nagative)	−1190°	—	—	—	356	40.4	279	12900

It can readily be seen from Fig. 3 that the negative Cotton effects are both due to the C_6-xanthate groups, the α-anomer VI showing the RD curve of the greater positive rotation, as expected. The negative peaks are in both cases situated at 375 mμ.

Some characteristic constants of the Cotton effects are collected in Table I, together with those of the ultraviolet absorption, which were measured with a self-recording spectrophotometer of the Hitachi EPU-II type.

The values of λ_0 practically coincide with those of the absorption maximum of the weak band due to the $-\overset{\overset{S}{\|}}{C}-S$ group. The absorption maxima of the strong K-band due to the $>C=S$ moiety are also inserted in the table, although the latter may have no direct relation with the optical activity in these cases.

Expression by the Two-term Drude Equation and the Physical Meaning of the Dispersion Constants

In the expectation that the dispersion data would conform, at least approximately, to the two-term Drude equation:

$$[M] = \frac{A_1}{\lambda^2 - \lambda_1^2} + \frac{A_2}{\lambda^2 - \lambda_2^2}$$

the authors carried out very complicated calculations by means of the least square method using an electronic computer of the Fuji FACOM 201 type. The results are shown in Table II. The agreement between the observed and the calculated values of rotation is tolerably good, the difference between them being mostly only a few per cent outside the absorption region, although in the neighborhood of the absorption center it sometimes rises to even fifty per cent.

TABLE II. DISPERSION CONSTANTS FOR D-GLUCOSE DERIVATIVES (BY THE TWO-TERM DRUDE EQUATION)

Compound	A_1	A_2	λ_1^2	λ_2^2
I	167.77	−6.544	0.211^2	0.370^2
VI	204.39	−29.83	0.202^2	0.353^2
VII	67.13	−19.90	0.209^2	0.366^2

As may be seen in Table II, the values of λ_2 thus calculated from the dispersion data are in the neighborhood of 360 mμ and practically coincide with the corresponding absorption maxima of the R-band shown in Table I; therefore, their physical meaning is self-evident. The strength and sign of the rotatory contribution of the chromophor is embodied in the term of A_2, which is, in these compounds, negative in sign and relatively small as compared to A_1, an important factor in the residual rotation. The negative sign of A_2 is natural, since the negative Cotton effects of compounds VI and VII are obviously to be attributed to their xanthate groups attached to the C_5 conformation of the L-type.[2]

The cotton effect is especially feeble in compound I, the value of A_2 being particularly small, probably because it is overwhelmed by the strong background of the dextrorotatory α-configuration.

On the contrary, all the β-ethylxanthates (compounds II, III, IV, and V) show distinctly positive Cotton effects, although the optically-active xanthate group is situated in the β-configuration. This apparent anomaly may also be accounted for by the idea of the inversion of the sign of rotation, as has been suggested in a previous paper.[1]

With these β-ethylxanthates the dispersion

2) In a previous, preliminary paper (This Bulletin, 35, 1617) the authors (Y. T. and K. T.) provisionally interpreted the apparently positive, feeble Cotton effect of a derivative of D-glucose 6-benzylxanthate in terms of the inversion of the sign of rotation, but it is now realized that the Cotton effect should be judged as negative, considering the position of the negative peak. Reinvestigation of this point, together with recalculation, is being made; the results will be published in due time.

data conform more suitably to the following abbreviated two-term expression of the Drude equation:

$$[M] = \frac{A}{\lambda^2} + \frac{B}{\lambda^2 - \lambda_c^2}$$

The results of calculations are shown in Table III. The agreement with the experimental results is not yet satisfactory, the difference between them often exceeding several percentage points, even outside the absorption region. It may be advisable to study them more fully, but at present the authors think they can preliminarily offer some interesting stereochemical information.

TABLE III. DISPERSION DATA FOR β-ETHYLXANTHATES (BY AN ABBREVIATED TWO-TERM DRUDE EQUATION)

Compound	A	B	λ_c^2
II	−13.68	27.33	0.369^2
III	−2.38	23.28	0.361^2
IV	−3.88	33.43	0.357^2
V	46.23	39.62	0.362^2

As may be seen in Table III, the values of λ_c are again nearly 360 mμ, practically in good accord with the corresponding absorption maxima of the R-band shown in Table I. In contrast to the former cases (Table II), the values of B are positive, showing that the sign of the Cotton effects is definitely positive. The first term, A/λ^2, of the equation is the sum of the rotational contributions from the other optically-active centers. In the first three compounds (II, III, IV), the sign A is negative, presumably because the basically strong levorotation of the β-configuration predominates, while in the last compound V, the acetamino group of the D-configuration is, as has already been mentioned, likely to overwhelm the other, partial rotations.

Experimental

The rotatory dispersion was measured with a Rudolph spectropolarimeter, mostly at 22.5~22.6°C over the wavelength region of 270 to 700 mμ. Under each compound several values of the specific rotation will be described so as to indicate the main features of the RD curve.

As the light source a xenon lamp was used. The length of the layer was 1 dm., but below 380 mμ 0.1 dm.

2,3,4,6-Tetra-*O*-acetyl-α-D-glucopyranosyl Ethylxanthate[3] (Compound I).—Syrup. $[\alpha]_D = +133.2°$ (*c* 1.1, chloroform).[3] The RD was measured at 22.6°C in tetrahydrofuran (T.H.F.) (*c* 1.1934). $[\alpha]_{700}$ 86.06°, $[\alpha]_{600}$ 114.8°, $[\alpha]_{589}$ 119.7°, $[\alpha]_{500}$ 173.5°, $[\alpha]_{412}$ 291.3° (broad extreme), $[\alpha]_{400}$ 256.5°, $[\alpha]_{380}$ 152° (negative peak), $[\alpha]_{315}$ 838°.

2,3,4,6-Tetra-*O*-acetyl-β-D-glucopyranosyl Ethylxanthate (Compound II).[4,5] — M. p. 75~76°C. $[\alpha]_D = +30.0°$ (*c* 1.2, chloroform).[5] The RD was measured at 22.5°C in T.H.F. (*c* 1.0176). $[\alpha]_{700}$ 11.3°, $[\alpha]_{600}$ 17.8°, $[\alpha]_{589}$ 19.5°, $[\alpha]_{500}$ 39.2°, $[\alpha]_{400}$ 247.6°, $[\alpha]_{381}$ 491° (peak), $[\alpha]_{334}$ −601° (trough), $[\alpha]_{305}$ −416°.

2,3,4-Tri-*O*-acetyl-β-D-xylopyranosyl Ethylxanthate (Compound III).[6]—M. p. 105~105.5°C, $[\alpha]_D^{25}$ 17.30° (chloroform). The RD was measured at 22.6°C in T.H.F. (*c* 1.0391). $[\alpha]_{700}$ 15.69°, $[\alpha]_{600}$ 21.80°, $[\alpha]_{589}$ 23.53°, $[\alpha]_{500}$ 62.75°, $[\alpha]_{400}$ 305.1°, $[\alpha]_{378}$ 660° (peak), $[\alpha]_{335}$ −529° (trough), $[\alpha]_{310}$ −292°.

Methyl 2,3,4-Tri-*O*-acetyl-β-D-glucopyranuronate 1-Ethylxanthate (Compound IV).[7]—M. p. 114~115°C, $[\alpha]_D^{16} = 42.0°$ (*c* 1, chloroform).[7] The RD was measured at 23.8°C in T.H.F. (*c* 0.4404). $[\alpha]_{700}$ 20.4°, $[\alpha]_{600}$ 29.1°, $[\alpha]_{589}$ 32.5°, $[\alpha]_{500}$ 56.5°, $[\alpha]_{400}$ 234°, $[\alpha]_{378}$ 518° (peak), $[\alpha]_{330}$ −529° (trough), $[\alpha]_{305}$ −341°.

2-Acetamido-2-desoxy-3,4,6-tri-*O*-acetyl-β-D-glucopyranosyl Ethylxanthate (Compound V).[8]—M. p. 142~143°C, $[\alpha]_D^{15} = +36.1°$ (*c* 1.2, chloroform).[8] The RD was measured at 22.0°C in T.H.F. (*c* 0.1997). $[\alpha]_{700}$ 46.1°, $[\alpha]_{600}$ 60.1°, $[\alpha]_{589}$ 64.6°, $[\alpha]_{500}$ 104.7°, $[\alpha]_{400}$ 461.7°, $[\alpha]_{378}$ 838.8° (peak), $[\alpha]_{335}$ −740° (trough), $[\alpha]_{300}$ −531°, $[\alpha]_{270}$ +3830°.

6-Desoxy-6-ethylxanthogen-α-D-glucopyranose Tetraacetate (Compound VI).[9] — M. p. 129~130.0°C, $[\alpha]_D = +98.9°$ (*c* 0.8, chloroform).[9] The RD was measured at 22.6°C in T.H.F. (*c* 0.8714). $[\alpha]_{700}$ 85.84°, $[\alpha]_{600}$ 110.5°, $[\alpha]_{589}$ 114.3°, $[\alpha]_{500}$ 161.5°, $[\alpha]_{424}$ 206.7° (broad extreme), $[\alpha]_{400}$ 178.0°, $[\alpha]_{375}$ 21.8° (negative peak), $[\alpha]_{320}$ 1230°.

6-Desoxy-6-ethylxanthogen-β-D-glucopyranose Tetraacetate (Compound VII).[9] — M. p. 121~123°C, $[\alpha]_D^{24} = +23.2°$ (*c* 1.1, chloroform).[9] The RD was measured at 22.5°C in T.H.F. (*c* 0.9656). $[\alpha]_{700}$ 21.75°, $[\alpha]_{600}$ 26.20°, $[\alpha]_{589}$ 27.34°, $[\alpha]_{500}$ 34.07°, $[\alpha]_{490}$ 34.9° (broad extreme), $[\alpha]_{400}$ −51.9°, $[\alpha]_{376}$ −263° (negative peak), $[\alpha]_{310}$ +1088°.

Department of Chemistry
Tokyo College of Science
Kagurazaka, Tokyo (Y. T. & K. T.)

Faculty of Pharmaceutical Sciences
School of Medicine
Hokkaido University
Sapporo (M. A. & S. T.)

3) M. Akagi et al., unpublished.

4) W. Schneider, R. Gille and K. Eisfeld, *Ber.*, **61**, 1244 (1928).
5) M. Akagi, S. Tejima and M. Haga, to be published.
6) M. Gehrke and W. Kohler, *Ber.*, **64**, 2696 (1931).
7) M. Akagi, S. Tejima and M. Haga, *Chem. & Pharm. Bull.*, **8**, 1114 (1960).
8) M. Akagi, S. Tejima and M. Haga., ibid., **9**, 360 (1961).
9) M. Akagi et al., ibid., **10**, 562 (1962).

*The Gamma Ray-Induced Addition of Acetaldehyde to Cyclohexene and Normal Hexene**

By Motoyoshi HATADA, Jun'ichi TAKEZAKI and Kozo HIROTA

(Received July 31, 1963)

In the present series of research papers[1] radiation-induced telomerizations have been studied, making gaseous olefins (ethene, propene and isobutene) the taxogens and acetaldehyde, the telogen, respectively; i. e., several methyl-alkyl ketones have been synthesized by the following reaction:

$$RCH{=}CH_2 + CH_3CHO \xrightarrow{\sim} CH_3CO(RC_2H_3)_nH \quad (n=1, 2,.....) \quad (1)$$

However, since these research papers, as well as that published by others,[2] have been mainly interested in finding a new method of synthesizing ketones, the results are not suitable for a detailed discussion of the reaction mechanism. Especially, because of the small solubilities of gaseous olefins in acetaldehyde, the composition of the liquid part of the sample was not exactly the same as that of the gaseous part, resulting in a difficulty of drawing definite conclusions.

Such being the situation, it will be interesting to study the system where a liquid olefin perfectly soluble in acetaldehyde is used as the taxogen. Therefore, normal hexene-1 and/or cyclohexene is adopted as the taxogen in the present research. Thus, the reactivity of olefins other than α-olefins can be investigated at the same time. Second, according to the method of research hitherto published, it was difficult to discuss the point if the initial process 2 could be regarded as a single reaction brought about by irradiation.

$$CH_3CHO \xrightarrow{\sim} CH_3\dot{C}O + H \quad (2)$$

In order to solve this problem, gaseous products are analyzed, as well as liquid products on samples the initial composition of which covers the entire range.

The research carried out along these lines will be reported on with reference to the reaction mechanism of this telomerization in general.

Experimental

Materials.—The acetaldehyde used was prepared from commercial acetaldehyde by the method described in previous reports.[1] Commercial cyclohexene was used after purification by distillation. Commercial *n*-hexene-1 was used without further purification. No impurity was detected in cyclohexene by gas chromatographic analysis, while the total amount of impurities in *n*-hexene-1 was found to be 5%. Mixtures of hexene and acetaldehyde were prepared and charged in vacuo into glass ampoules by a procedure reported on already.[1]

Irradiation.—The mixtures were irradiated at room temperature or at higher temperatures up to 180°C with gamma rays from a cobalt-60 source installed in our laboratory. The dose rate, which was determined by the use of a Frick dosimeter, was varied over the range from 1.4 to 9.7×10^4 r/hr.

The Analysis of the Liquid Products.—The liquid part of the irradiated mixture was subjected to both gas chromatographic and mass spectrometric analyses. The gas chromatograph used was an apparatus (the Shimadzu Model GCIA), the analytical conditions being as follows: column length, 5.25 m.; adsorbent, high vacuum oil; column temperature, 152°C; flow rate of the carrier gas (helium), 150 cm³/min.

The Analysis of the Gaseous Products.—The gaseous product was collected with an automatic töpler pump and was analyzed with a mass spectrometer (Hitachi RMU-5).

Results and Discussion

a) The Identification of the Liquid Products.—Only one new peak appeared in the gas chromatogram of the liquid part in the irradiated samples besides the peaks of acetaldehyde and cyclohexene. The fraction corresponding to this peak was collected and identified as methyl cyclohexyl ketone (McHK) by mass spectrometry. This substance is an addition product or a 1 : 1 telomer of acetaldehyde to cyclohexene. However, Mayo et al.[3] had reported that cyclohexanol was produced as the main product in the ultraviolet-irradiated

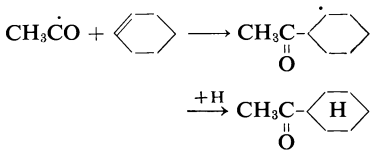
* Chain Telomerization Induced by Radiation. V. (A part of this paper was presented at the 14th Annual Meeting of the Chemical Society of Japan, Kyoto, April, 1961).

1) K. Hirota, M. Hatada et al., a) This Bulletin, **33**, 1682 (1960); b) ibid., **34**, 1644 (1961); c) ibid., **36**, 817 (1963); d) The IV Isotope Symposium (Japan), No. R-7 (1961), Kyoto.

2) C. E. Stoops and C. L. Furrow, *J. Org. Chem.*, **26**, 3264 (1961).

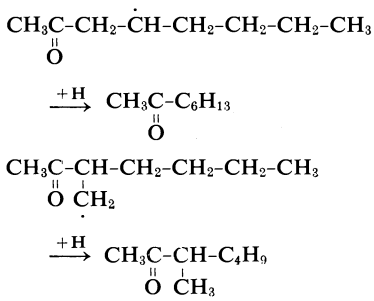
3) P. de Mayo, J. B. Stothers and W. Templeton, *Can. J. Chem.*, **39**, 488 (1961).

mixture of acetaldehyde and cyclohexene, especially when the latter was present in excess. However, no peak was found in the gas chromatogram of the present experiment over the region where the peak of cyclohexanol might be expected to appear. Therefore, the addition of the acetyl radical to cyclohexene will be the main process in the γ-ray irradiated system, as is shown by Eq. 3:



(3)

By a similar process, methyl *n*-hexyl ketone (MnHK) and methyl isohexyl ketone (MiHK) were found to be produced from the irradiated mixture of acetaldehyde and *n*-hexene-1. Both ketones are evidently the addition products of acetaldehyde and *n*-hexene-1. Apparently the mechanism of producing them will be the same as has been explained in the mixtures of aldehyde and lower olefins;[1] e. g., according as the acetyl radical attaches to the carbon-1 or the carbon-2 of *n*-hexene-1, followed by the addition of a hydrogen atom, MnHK or MiHK respectively, may be obtained as is shown below.



(4)

In both reactions, such products, which correspond to the higher telomers, could not be identified, partly because of their high boiling point as well as because of their small quantity caused by the difficulty of reaction. However, assuming the reaction to proceed by the mechanism already proposed, the methyl hexyl ketones mentioned above will be called 1 : 1 telomers hereafter.

b) The *G* Values of the Formation of Telomers.—In Fig. 1, the yield of the McHK produced in the mixture of acetaldehyde and cyclohexene is plotted vs. the irradiation time, keeping the dose rate at 7.4×10^4 r/hr. It is shown that, approximately, the yield increases linearly with the increasing dose. Similar curves could be obtained for the yields of MnHK and MiHK in the mixture of acetaldehyde and normal hexene, the *G* values of each

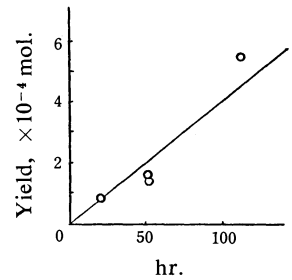


Fig. 1. The amount of McHK formation vs. irradiation time.

telomer were calculated from these curves. Generally speaking, MnHK was always produced most easily. This point will be discussed further in b).

However, it is noteworthy that *G*(MnHK) is larger than the value to be expected from *G*(1 : 1 telomer) of the mixtures of ethene,[4] propene[1] and/or isobutene[5] with aldehyde, because the *G*(1 : 1 telomer) decreases as the carbon number of the taxogens increases. Such a contradictory result may be explained by the possibility that the liquid part of the mixture contains much less olefin than would be estimated from its initial charge in the samples, as has been mentioned in the introduction.

The main components of the gas produced at room temperature by irradiation on the mixture of cyclohexene and acetaldehyde were found to be carbon monoxide, methane and hydrogen, as in the case of propene and acetaldehyde.[1a]

c) The Effect of the Dose Rate on *G*(Telomer)'s.—The *G*(telomer)'s thus obtained are plotted vs. dose rate *I* in logarithmic scales in Fig. 2, where the total dose is kept at 2.25×10^6 r, while the dose rate ranges from 10^4 to 10^5 r/hr. From the inclination of the lines, the *G*(McHK) is shown to increase in inverse proportion to the square root of *I*, while both *G*(MnHK) and *G*(MiHK) increase to the three-fourth power of *I*; i. e., the relation is expressed by a formula:

$$\log G = \text{Const.} - \alpha \log I \qquad (5)$$

where $\alpha=0.5$ for McHK and $\alpha=0.75$ for MnHK and MiHK respectively.

The fact that α has a value somewhat larger than 0.5 in the latter system suggests that a minor part of the reaction chain terminates in a monomolecular mechanism, as may be observed in the ionic mechanism.

4) K. Hirota, S. Iizuka, H. Ochi and M. Hatada, This Bulletin, **36**, 115 (1963).

5) K. Hirota, S. Iizuka and M. Hatada, *Annual Report of the Japanese Association of Radiation Research on Polymers*, **1**, 165 (1959); **2**, 169 (1960); This Bulletin, in press.

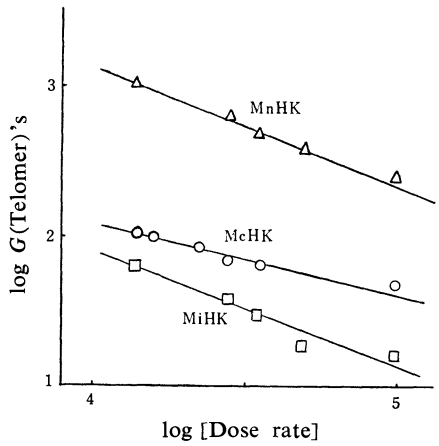


Fig. 2. Log [G(Telomer)'s] vs. log [Dose rate].
Total dose 2.25×10^6 r

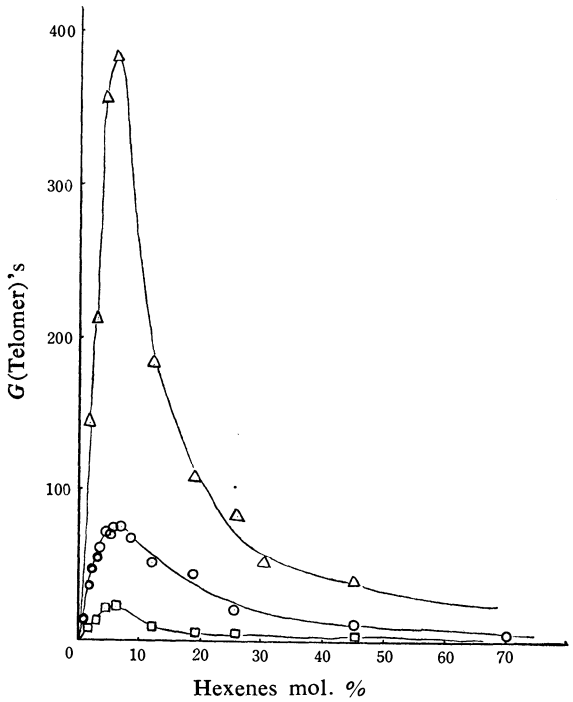


Fig. 3. G(Telomer)'s vs. mol. % of hexenes in the feed.
Dose rate 9.7×10^4 r/hr.
Dose 1×10^7 r
△ MnHK ○ McHK □ MiHK

d) The Effect of the Composition of the Feed on the G(Telomer)'s.—In Fig. 3, the G(1 : 1 telomer)'s obtained at the same dose rate (9.7×10^4 r/hr.) are plotted vs. the mole per cent of olefin in the feed. The curves thus drawn for the three telomers show a similar shape, with a maximum at ca. 5 mol.% of olefin concentration.

These curves may appear in the situation where some part of the acetyl radicals is consumed to form by-products and does not contribute to the production of methyl hexyl ketones.

The G(MnHK)$>$$G$(McHK)$>$$G$(MiHK) relation, mentioned in b), exists over the entire concentration range; i. e., MnHK is produced the most favorably, while MiHK is produced the least. This relation, contrary to Markownikoff's rule, may be an indication that telomerization proceeds by a radical chain mechanism, since the addition of the polar substance to the double bonds is known to follow Markownikoff's rule. Moreover, it will be noted that the G(MnHK)$>$$G$(MiHK) relation is concordant with the fact[2] that 1-olefin is more reactive than 2-olefin to aldehyde.

e) The Temperature Dependency on the G(Telomer).—The G(telomer)'s obtained at various temperatures take maximum values in both systems, e. g., at 70~80°C, as Figs. 4 a and 4 b show. Such maxima have already been observed in other systems where the taxogens were lower olefins,[2-4] but it could not be made clear that this decrease of G(telomer)'s in the high temperature region comes either from the instability of radicals or from the decrease in the solubility of the taxogens. Since hexenes are perfectly soluble in acetaldehyde, the decrease of G at the higher temperature may be ascribed to the decomposition of the acetyl radical because, the decomposition

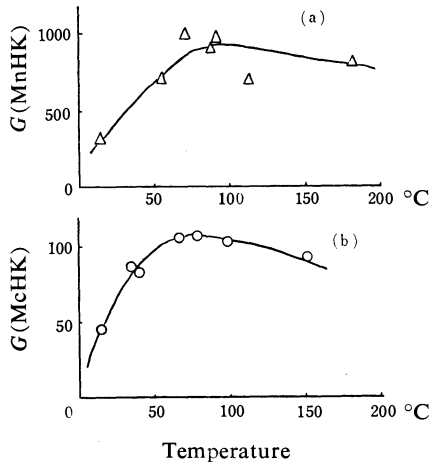


Fig. 4. G(Telomer)'s vs. irradiation temperature.
△ MnHK ○ McHK

$$CH_3\dot{C}O \rightarrow \dot{C}H_3 + CO \qquad (6)$$

with the activation energy of 15 kcal.,[6] proceeds more favorably at the higher temperature. Such an explanation will also be reasonable on the basis of the experimental finding that the shapes of both curves are the same, irrespective of the taxogen.

In order to determine the overall activation energy of formation, the logarithmus of the $G(1:1$ telomer)'s was plotted against $1/T$. The activation energies thus determined in the region of room temperature were 4.3 kcal./mol. for MnHK and 3.7 kcal./mol. for McHK respectively. They practically correspond to the activation energy of the propagation step, if a bimolecular termination of the propagating radical with a negligibly small activation energy is assumed. However, it is noteworthy that the values actually observed are smaller in this system than those in the system where the taxogens were ethene (5.0 kcal.)[4] or isobutene (6.5 kcal.).[5] The values may be ascribed to the decrease in the solubility of lower olefins with the temperature, so that their initial concentration in the liquid part of the samples decreased more than in the feed.

f) Gases Produced by Irradiation on the Mixture of Cyclohexene and Acetaldehyde.—As has already been mentioned, hydrogen, methane and carbon monoxide were the main gaseous products. They were produced in almost equal amounts, as is shown by Fig. 5, by the irradiation of samples rich in acetaldehyde, although the latter two components decrease with an increase in the cyclohexene fraction in the initial mixture. These may be explained easily by the decomposition of acetaldehyde: $CH_3CHO \rightarrow CH_4+CO$, and the primary process may be the one designated by Eq. 6, as well as by the direct scission of the C–C bond.

$$CH_3CHO \rightsquigarrow \dot{C}H_3 + CHO \qquad (7)$$

The slight difference between $G(CH_4)$ and $G(CO)$ may be caused by the recombination of methyl radicals into ethane, whose formation is favorable in the aldehyde-rich region, $G(C_2H_6)$ being, however, experimentally difficult to determine.

The $G(H_2)$~composition curve has a minimum in the middle region. This is because hydrogen is produced as the by-product of the telomerization as well as by the decomposition of cyclohexene, the $G(H_2)$ value of cyclohexene-rich samples was 1.3, which agreed well with that ($G(H_2)=1.2$) obtained by Freeman[7] in the γ-ray irradiation on pure cyclohexene. On the other hand, hydrogen may be produced by the decomposition of acetaldehyde, e.g., $CH_3CHO \rightarrow H_2+CH_2C{=}O$. Since $G(H_2)$ nearly equal to $G(CO)$ in the acetaldehyde-rich region, the $G(H_2)$ produced from acetaldehyde in the middle region may may be given approximately by the value of $G(CO)$. If so, $G(H_2)$-$G(CO)$ as shown by the dotted line α in Fig. 5 can be regarded as the $G(H_2)$ from cyclohexene only.

In short, considering the magnitude of $G(H_2)$, $G(CO)$ and $G(CH_4)$ in Fig. 5, radiation-induced decompositions of aldehyde and cyclohexene may be said to proceed parallel with the telomerization.

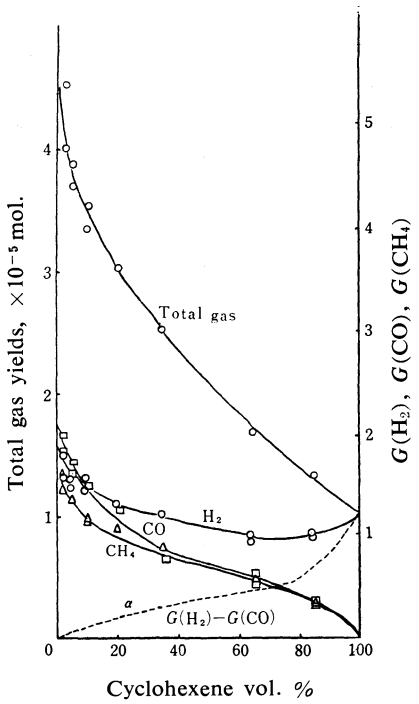


Fig. 5. G(gases) vs. cyclohexene vol. % in the feed.

g) The Effect of Benzene and Cyclohexane Added to the System.—Since benzene is known to act as a scavenger of hydrogen atoms, the dilution of the samples with benzene may give us knowledge of the fate of the hydrogen atoms produced in Eq. 2. The experiment is interesting from the viewpoint of increasing the yield of telomers, because the hydrogen produced in Eq. 2 might be captured, otherwise it would act as a terminating agent.

The experiment was carried out on various mixtures of aldehyde (A), cyclohexene (B) and benzene (C), keeping the amounts of A and B+C respectively constant. As is shown by the full line in Fig. 6, the G(McHK) became, contrary to expectation, slightly smaller upon the addition of benzene over the whole range of composition expressed by the electron fraction than that denoted by the dotted line

6) Cf. E. W. R. Steacie, "Atomic and Free Radical Reactions," 2nd ed., Reinhold Publishing Corp., New York (1954).

which was calculated under the assumption that benzene plays the role of a mere diluent.

It might be possible that the above tendency comes, rather, from an energy transfer to benzene molecules from excited cyclohexene molecules, which can easily react with acetyl radicals. If this be true, the addition of cyclohexane to the feed might increase the G(McHK), because cyclohexene would behave also to some extent as an energy acceptor from the excited cyclohexane. This reasoning may be justified by the fact that cyclohexane is regarded as acting as an energy donor in the cyclohexane-benzene mixture.[7,8] However, as the broken line in Fig. 6 shows, in the systems where cyclohexane was added to the mixture, a curve was obtained which is also concave upward but slightly different in shape from the systems where benzene was added. In order to explain these findings, it is not necessary to assume that the excitation of the cyclohexene molecule is important in the production of methyl hexyl ketones.

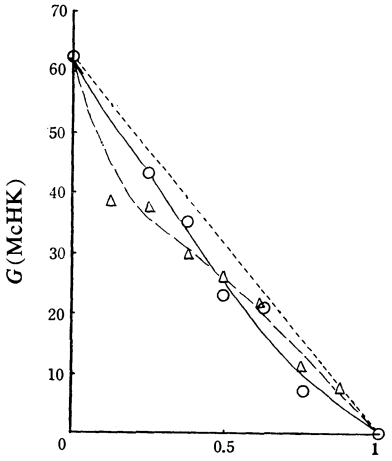


Fig. 6. G(McHK) vs. electron fraction of the additives.

Cyclohexene+Additive : 0.2 ml.
Acetaldehyde : 1.8 ml.

Dose rate 8×10^4 r/hr., dose 5×10^6 r

○ Benzene △ Cyclohexane

In summarizing the conclusions obtained from c) to g), it can be said that the mechanism of the telomerization of the aldehyde-olefin mixture is generally expressed by the radical mechanism hitherto proposed.[1]

Summary

By the radiation-induced telomerization of acetaldehyde-hexene mixtures, McHK has been produced when cyclohexene is used, while MnHK and MiHK have been produced when normal hexene is used. The G(MnHK) at room temperature has been found to be 400 (dose rate $=9.7\times10^4$ r/hr.), which is larger by a factor of ten than the G(MiHK) and the G(McHK). Irrespective of the dose rate, a G(MnHK)$>G$(McHK)$>G$(MiHK) relation always exists.

It has been found that: (i) the G(MnHK) value, as well as the G(MiHK) and the G(McHK) values, increases with the rise in temperature, they all show however, maxima at 70~80°C, because of the thermal decomposition of the acetyl radical, (ii) sharp maxima are shown in the curves of G(telomer) vs. initial composition at 5 mol.% of hexenes, (iii) the analytical data of the gaseous products establish that the radiation-induced decomposition of aldehyde and hexene occurs in parallel with the telomerization, and (iv), upon the addition of benzene or cyclohexane to the system, the G(telomer)'s decrease slightly in both systems, suggesting that they act as diluents rather than as agents of the energy transfer.

A part of the expenses has been defrayed by a grant (1961) given by the Science and Technology Agency, to which the authors' thanks are due.

Osaka Laboratories
Japanese Association for
Radiation Research on Polymers
Neyagawa, Osaka (M. H. & J. T.)

Science Faculty
Osaka University
Nakanoshima, Osaka (K. H.)

7) G. R. Freeman, *Can. J. Chem.*, **38**, 1043 (1960).
8) J. P. Manion and M. Burton, *J. Phys. Chem.*, **56**, 560 (1952).

The Thermal Decomposition of Ammonium Polymolybdates. I

By Eikoh MA

(Received August 6, 1963)

When a normal ammonium molybdate solution is acidified, various polyanions of increasing degrees of condensation are obtained according to different acidifications and other conditions.[1] Gmelin[2] has reported the existence of nine kinds of molybdates with different mole ratios of R_2O: MoO_3. In ammonium polymolybdates of various compositions, the structures of the heptamolybdate (paramolybdate) ion and the octamolybdate (tetramolybdate) ion have been crystallographically investigated by Lindqvist.[3] Little is known about the crystal structures of the rest. The present paper is concerned with four of them, ammonium di-, hepta-, tri- and octa-molybdate; the thermal decomposition of each has also been studied.

The thermal decomposition of ammonium heptamolybdate has previously been studied by several authors, Duval[4] using thermogravimetric analysis and Hegedüs et al.,[5] using X-ray diffraction techniques besides thermogravimetric analysis. Funaki and Segawa[6] reported the thermal decomposition of several kinds of polymolybdates, but they gave no description on the experimental method employed. A differential thermal analysis of the thermal decomposition of ammonium tetra-, para- and normal-molybdate has been reported by Rode and Tverdokhlebov.[7] Rode and Tverdokhlebov, however, adopted for heptamolybdate (paramolybdate) an empirical formula, $5(NH_4)_2O\cdot 12MoO_3\cdot 12H_2O$, which has been proved incorrect; an alternative formula, $3(NH_4)_2O\cdot 7MoO_3\cdot 4H_2O$, had long been supported by crystallographic studies.[8] The tetramolybdate in their paper, $(NH_4)_2O\cdot 4MoO_3\cdot 2H_2O$, is essentially identical with octamolybdate, $(NH_4)_4Mo_8O_{26}\cdot 4H_2O$, the crystal structure of which has been determined by Lindqvist. Previous works of crystallographic significance seem to have been ignored in their paper. The behaviors of ammonium polymolybdates in the thermal decomposition are comparable with those of ammonium polytungstates, since they are both ammonium salts of the polyacid of transition elements in the sixth group of the periodic table. Reference may be made to a previous work on the thermal decomposition of ammonium paratungstate.[9] In the present paper the thermal decomposition of ammonium polymolybdates is treated by means of thermogravimetric analysis, ammonia determination and omegatron mass-spectrometry; in a succeeding paper studies by means of differential thermal analysis and X-ray diffraction techniques will be reported.

Experimental

Chemical Analysis.—Samples of ammonium dimolybdate, heptamolybdate, trimolybdate and octamolybdate were first identified as such by determining their compositions through chemical analysis. The quantity of molybdenum was determined by the gravimetric method, using lead acetate, and that of ammonia, by the Kjeldhal method. The results were found to be in agreement with the empirical formulae, $(NH_4)_2O\cdot 2MoO_3$ for dimolybdate, $3(NH_4)_2O\cdot 7MoO_3\cdot 4H_2O$ for heptamolybdate, $2(NH_4)_2O\cdot 8MoO_3\cdot 2H_2O$ for octamolybdate, and $(NH_4)_2O\cdot 3MoO_3\cdot xH_2O$ for trimolybdate, where x depends upon conditions of preparation.*

X-Ray Analysis.—Samples of ammonium heptamolybdate and octamolybdate, the lattice constants of which had been known,[10] were further identified as such by crystallographic data of single crystals using rotation photographs. The unit cell dimensions for ammonium heptamolybdate are: $a=8.382$ Å $b=36.125$ Å, $c=10.464$ Å and $\beta=116°0'$, while those for octamolybdate are: $a=7.76$ Å, $b=9.75$ Å, $c=9.78$ Å, $\alpha=97°2'$, $\beta=100°5'$ and $\gamma=98°$. X-Ray diffraction patterns were taken by a Guinier focussing camera using Cu$K\alpha$ radiation. The

1) I. Lindqvist, *Nova Acta Reg. Soc. Sci. Upsal. Ser. IV*, 15 (1950), I. Lindqvist, *Acta Chem. Scand.*, **5**, 568 (1951).
2) Gmelin, "Handbuch der Anorganischen Chemie," Nr. 53, Verlag Chemie G. m. b. H., Weinheim (1935), p. 113.
3) I. Lindqvist, *Arkiv Kemi*, **2**, 325, 349 (1950).
4) C. Duval, "Inorganic Thermogravimetric Analysis," Elsevier, Amsterdam (1953), p. 332.
5) A. J. Hegedüs, K. Sasvari and J. Neugebauer, *Z. anorg. u. allgem. Chem.*, **293**, 56 (1957).
6) K. Funaki and T. Segawa, *J. Electrochem. Soc. Japan (Nippon Denkikagaku Zasshi)*, **18**, 152 (1950).
7) E. Ya. Rode and V. N. Tverdokhlebov, *Zhur. Neorg. Khim.*, **3**, 2343 (1958).
8) J. H. Sturdivant, *J. Am. Chem. Soc.*, **59**, 630 (1937), cf. Ref. 3.
9) Y. Ahn, *J. Japan Soc. Powder Metallurgy (Funtai oyobi Funmatsu Yakin)*, **8**, 253 (1961).
* Heptamolybdate and octamolybdate are terms indicating chemical species, while dimolybdate and trimolybdate are terms indicating merely stoichiometry. Chemical formulae based on structural studies, $(NH_4)_6Mo_7O_{24}\cdot 4H_2O$ and $(NH_4)_4Mo_8O_{26}\cdot 4H_2O$, have been given for heptamolybdate and octamolybdate respectively.
10) Cf. Ref. 3.

powder patterns of the starting materials are given in Tables Ia, Ib and Ic. Table Ia is in good agreement with the data described in ASTM 11-71. There has been no description of other ammonium polymolybdates in ASTM.*

TABLE I

(a) Ammonium heptamolybdate		(b) Ammonium dimolybdate		(c) Ammonium octamolybdate	
d Å	I/I_1	d Å	I/I_1	d Å	I/I_1
9.08	100	6.92	11	9.21	34
7.56	33	6.11	100	7.21	100
7.42	30	4.98	3	5.98	12
7.15	40	4.70	4	5.50	5
6.41	13	3.58	5	4.79	29
4.52	17	3.32	9	4.04	12
3.09	14	3.27	9	3.60	38
3.02	37	3.21	21	3.44	23
2.65	14	3.15	8	3.30	23
2.25	9	3.11	8	3.21	12
2.01	7	2.98	3	3.08	12
		2.95	2	2.95	50
		2.24	3	2.59	7
		2.16	14	2.39	23
				2.11	10

The Determination of Evolved Ammonia.—When a sample was heated in a furnace, the ammonia which evolved was carried into 1 N sulfuric acid by a stream of air and of nitrogen at 30 l./hr.; it was determined by titration using methyl orange as an indicator. By continually titrating it during the thermal decomposition, smooth curves of ammonia evolution were obtained, as Fig. 1 shows. The heating rate employed was 3°C/min.

Thermogravimetric Measurement.—Thermogravimetric measurement was performed in air at a heating rate of 3°C/min. by an automatic thermobalance.

Analysis by an Omegatron Mass-spectrometer.—Omegatron mass-spectrometric analysis was performed with about 30 mg. of a sample at 10^{-5} Torr, in the mass range between 1 and 50 and in the temperature range between room temperature and 400°C. The resolution of the omegatron was $M/\Delta M=56.5$ (calcd.) and 56.0 (obs.) at mass 28. It was possible to detect a partial pressure of 10^{-11} Torr by the omegatron. The measurement was performed at about every 50°C of elevation while the sample was being evacuated by oil diffusion pumps with an activated charcoal trap, the temperature being held constant during the measurement. Every time the sample was heated in a furnace, the pressure rose to 10^{-3} Torr at first because of the vigorous decomposition. However, since the omegatron measuremont was favorable at a pressure lower than 10^{-4} Torr, measurement was performed only when the pressure decreased to 10^{-5} Torr and became as constant as possible.

* By X-ray examination, the sample of ammonium trimolybdate was found to have changed into ammonium octamolybdate in about half a year when left undisturbed.

Results

The Evolution of Ammonia.—It is important, in the pyrolysis study of ammonium salts, to determine continuously the ammonia which is liberated during the thermal decomposition. Figure 1 shows the ammonia evolution curves.

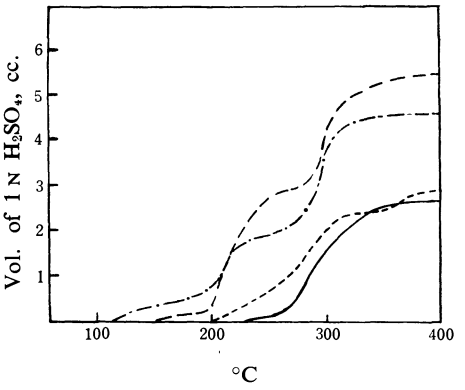


Fig. 1. Ammonia evolution curves.
——— Ammonium dimolybdate
—·—·— Ammonium heptamolybdate
——— Ammonium octamolybdate
-------- Ammonium trimolybdate

Heptamolybdate begins to evolve ammonia at the lowest temperature, about 120°C. Dimolybdate begins to evolve ammonia next, around 150°C; rapid evolution subsequently begins around 200°C. Octamolybdate and trimolybdate begin to evolve ammonia only above 200°C. By contrast, the evolution of ammonia is complete in all at almost the same temperature, 360~375°C. Each of the ammonia evolution curves of heptamolybdate and dimolybdate has three well-defined stages. X-Ray study illustrates that three different structures correspond to the respective stages, as will be discussed later.

Weight-decrease Curves. — Weight-decrease curves drawn by an automatic thermo-balance are shown by the solid lines in Figs. 3, 4, 5 and 6. It is noticeable that heptamolybdate and dimolybdate begin to decompose rapidly at 110 and 200°C respectively, their weight-decrease curves forming sharp inflections. Octamolybdate and trimolybdate, by contrast, decompose gradually at the beginning of heating. The end-points of decomposition are very clearly defined for all the molybdates. Decomposition is complete in all at almost the same temperature of 360~375°C. Heptamolybdate, dimolybdate and trimolybdate decompose in three stages, and octamolybdate in two stages.

Observation by Means of an Omegatron Mass-spectrometer.—Omegatron mass-spectrometer has been found to be effective in the

pyrolysis study in this research.[11] An example of the results obtained by the omegatron is given in Fig. 2. The observed mass numbers and the ionic species corresponding to them are as follows: 2 (H_2^+), 14(N^+, N_2^{2+}, CO^{2+}), 15 (NH^+), 16 (NH_2^+), 17 (NH_3^+, OH^+), 18 (H_2O^+), 19 (H_3O^+), and 28 (N_2^+, CO^+).

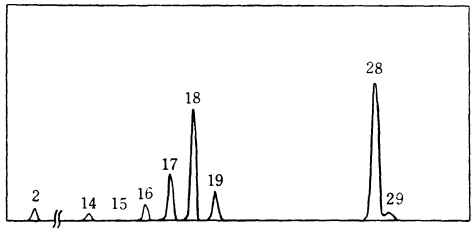


Fig. 2. Mass-spectrum of gases evolved from ammonium heptamolybdate at 395°C. Sensitivity of mass 2 is three times that of other masses.

Mass 29 seems to be a fragment of residual gas, but it is unidentifiable. The mass spectra were treated in the following way:

1) Since the observed intensities of the ionic current are proportional to the square root of the mass numbers, an appropriate adjustment was made.

2) Since one-fifth of H_2O^+(18) is known to appear as OH^+ in the same place as NH_3^+ (17) is observed, it was subtracted from the intensity of NH_3^+.

3) NH^+ and NH_2^+ are considered to be fractions of NH_3^+. These fractions, added to NH_3^+ (17) and then with one-fifth of H_2O^+ (18) subtracted, gave the sum of ammonia.

4) H_3O^+ (19), OH^+ (17) and H_2O^+ (18) gave the sum of water.

5) N^+ (14), N_2^{2+} (14) and N_2^+ (28) gave the sum of nitrogen.*

6) The partial pressure of water, ammonia and nitrogen were calculated for each temperature and, for the sake of comparison, were re-estimated as values at the same total pressure. Thus Fig. 7 was obtained.

The final product obtained in the omegatron at 10^{-6} Torr and at 400°C consisted of purple-black oxides of molybdenum, in which MoO_3, Mo_9O_{26} and Mo_4O_{11} are predominant and Mo_8O_{23} is only auxiliary.

Discussion

Since one molecule of water accompanies every two molecules of ammonia when they are liberated from the salt, the ammonia evolution curves, NH_3 curves, shown in Fig. 1, must be represented as $(NH_4)_2O$ curves. By superimposing the latter on the weight-decrease curves obtained by the automatic thermo-balance, the dotted lines in Figs. 3, 4, 5 and 6 are obtained. With ammonium

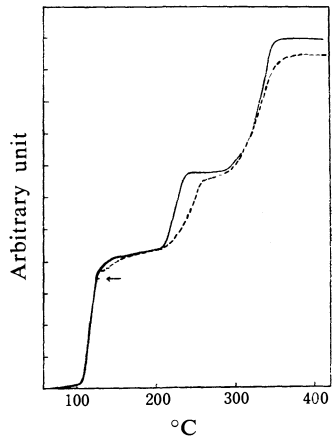


Fig. 3. Weight-decrease curve (solid line) and $(NH_4)_2O$ curve (dotted line) of ammonium heptamolybdate.

heptamolybdate tetrahydrate (Fig. 3), a fairly good coincidence as to the shape and height of the curves between 130 and 360°C is noticeable. The three stages in the $(NH_4)_2O$ curve correspond to those in the weight-decrease curve. Therefore, the weight decrease from 130°C up to 360°C may be correlated with the evolution of ammonia and water accompanying it. Consequently, the weight decrease from room temperature up to 130°C is correlated with the dehydration of crystals. The theoretical value of four molecules of the water of hydration is shown by an arrow mark; it is in good agreement with the observed value. We might conclude that dehydration begins very slowly at room temperature, that around 115°C dehydration becomes rapid, and that it is almost complete at 130°C. The discrepancy between the weight-decrease curve and the $(NH_4)_2O$ curve above 360°C is due to the formation of nitrogen from ammonia, which will be discussed below. Indeed, the observed values of the quantitative determination of ammonia always fall short of the theoretical values.

The four molecules of water of hydration are not included in the crystal structure of the discrete heptamolybdate ion, $Mo_7O_{24}^{6-}$.[12] The crystal structure of heptamolybdate does not break down until 130°C, when most of

11) M. Onchi and E. Ma, *J. Phys. Chem.*, **67**, 2240 (1963).

* CO^+ (28) and CO^{2+} (14) as background are evacuated to negligible amounts, Moreover, the pattern coefficient of the 28 peak justifies its identification as nitrogen.

12) Cf. Ref. 3.

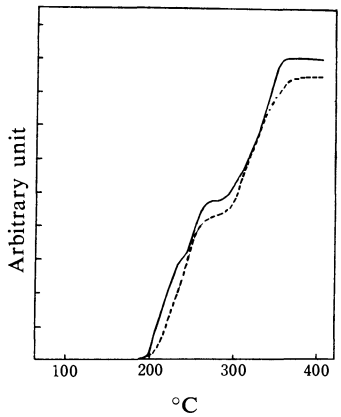


Fig. 4. Weight-decrease curve (solid line) and $(NH_4)_2O$ curve (dotted line) of ammonium dimolybdate.

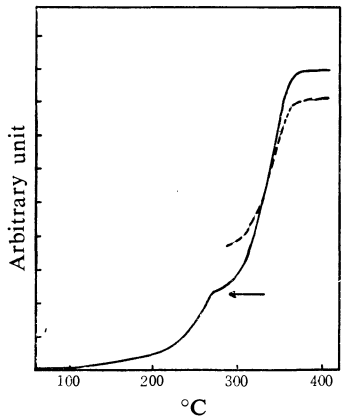


Fig. 5. Weight-decrease curve (solid line) and $(NH_4)_2O$ curve (dotted line) of ammonium octamolybdate.

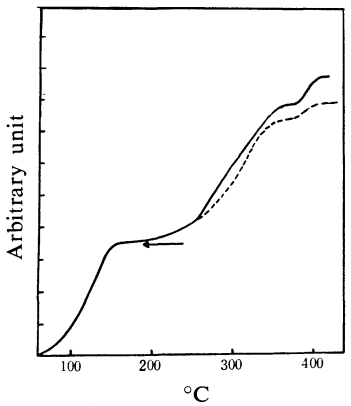


Fig. 6. Weight-decrease curve (solid line) and $(NH_4)_2O$ curve (dotted line) of ammonium trimolybdate.

the water is lost. As the dehydration does not proceed step by step, some part of the water may be regarded as of the zeolitic type.

Since ammonium dimolybdate is not hydrated, the weight-decrease curve is approximately equal to the $(NH_4)_2O$ curve, and the decomposition begins at a temperature higher than that in the case of heptamolybdate. (Fig. 4).

In the case of trimolybdate, dehydration is complete around 150°C, and the crystal structure changes into octamolybdate above 200°C.

In the case of ammonium octamolybdate dihydrate, dehydration is complete around 280°C, and the crystal structure of octamolybdate does not break down until around 360°C. Therefore, some of the water molecules are tenaciously held up to 280°C. Consequently, they must be water molecules of a different type. (Figs. 5 and 6).

The step-by-step decompositions indicate that water and ammonia, presumably as ammonium ions in the crystal, are bonded with the molybdate ions in different strengths, and that there should be a further difference in bonding strength in ammonia. To each stage of the weight-decrease curves, there should be a corresponding crystal structure. Studies of structural change will be reported on in a succeeding paper.

The ultimate discrepancy between the weight-decrease curves and the $(NH_4)_2O$ curves in Figs. 3, 4, 5 and 6 may be assumed to be referrable to the formation of nitrogen from ammonia, as has been mentioned above. In order to confirm this, the process of the thermal decomposition was analyzed by means of omegatron, taking ammonium heptamolybdate as an example.

The most significant information provided by the omegatron was that the existence of nitrogen in the process of thermal decomposition was definitely established. Water, ammonia and nitrogen are plotted on the ordinate of the same arbitrary unit in Fig. 7, which, therefore, provides an estimate of the relative values of these gases. The sudden decrease in

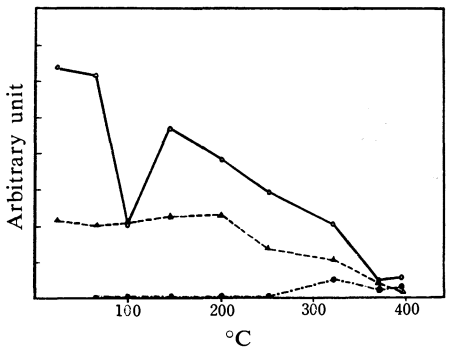


Fig. 7. Partial pressure vs. temperature
—— Water ---- Ammonia
—·—·— Nitrogen

water quantity at 100°C might be due to the end of dehydration. Nitrogen formation began around 250°C and reached a maximum around 320°C. Consequently, it became of interest to determine whether hydrogen also existed. Molecular hydrogen was also successfully detected by the omegatron. The formation of hydrogen goes on in a way quite similar to that of nitrogen, i. e., beginning to form around 250°C and reaching a maximum around 320°C. The hydrogen is not to be considered to come from water. In Fig. 8 the amounts of nitrogen and hydrogen are plotted on ordinates of different arbitrary units. Neither H_2O^+ nor H_3O^+ has a tendency to increase when nitrogen is being yielded.

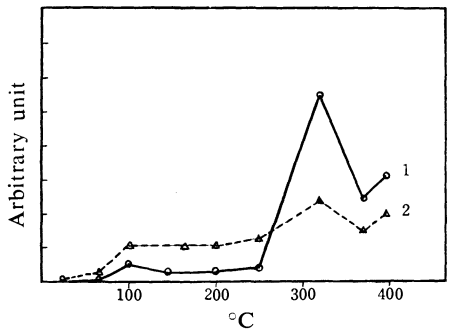


Fig. 8. Partial pressure vs. temperature.
1) Nitrogen 2) Hydrogen

These findings might be interpreted as meaning that ammonia is oxidized to nitrogen by the molybdenum oxide resulting from the thermal decomposition. Thus the molybdenum oxide is reduced to a lower oxide. An alternative interpretation is that ammonia is decomposed into nitrogen and hydrogen at the surface of molybdenum oxide through its catalytic action. The detection of hydrogen by the omegatron may support the latter interpretation. The amount of nitrogen at 320°C is more than ten times the amount at 250°C, while the amount of hydrogen at 320°C is less than ten times that at 250°C. Therefore, a larger amount of nitrogen must be yielded through oxidation than through decomposition. The formation of nitrogen from ammonia was detected in vacuo by the omegatron. Similar considerations apply to the formation of nitrogen from ammonia in air. It takes place even more vigorously if it is yielded through oxidation. Since the precise mole ratios of the nitrogen and hydrogen formed in vacuo have not yet been determined, quantitative argument will be deferred pending further investigation.

Figure 7 shows that water is evolved more abundantly than ammonia throughout the process; this is contrary to the theoretical expectation, and the cause is not certain. One possible explanation is as follows: When the sample was heated in a furnace while being evacuated, it decomposed vigorously at first and the pressure rose to 10^{-3} Torr. The omegatron measurement was performed, however, only when the pressure decreased to 10^{-5} Torr, when the evolution of the gases was almost in equilibrium. Accordingly, the composition of evolving gases might be different from that at 10^{-3} Torr.

Summary

The thermal decomposition of ammonium di-, hepta-, tri- and octa-molybdate has been investigated by means of thermogravimetric analysis, ammonia determination and the use of an omegatron mass-spectrometer. Both weight-decrease curves and ammonia evolution curves exhibit stepwise decomposition, indicating that there should be a difference in bonding strengths of water and of ammonia, presumably as ammonium ions in the crystal, with molybdate ions. Hepta-, di- and trimolybdate decompose in three stages, and octamolybdate in two stages. A certain crystal structure should correspond to each stage. Dehydration precedes deammoniation. Dehydration is complete at about 130, 150 and 280°C with hepta-, tri- and octa-molybdate respectively. Deammoniation is complete in all at the same temperature of 360~375°C. The existence of nitrogen above 250°C in vacuo has been established. Nitrogen is yielded in the process of the thermal decomposition through oxidation as well as through the catalytic decomposition of ammonia. Nitrogen reached a maximum around 320°C. As evidence for the formation of nitrogen through decomposition, hydrogen was also detected above 250°C, and was found to reach a maximum at about 320°C, although in a much smaller quantity.

The author wishes to express his deep gratitude to Professor Kumasaburo Kodera and to Professor Sukeji Kachi of Kyoto University for their continued interest in this investigation and for their valuable suggestions. He is also greatly indebted to Dr. Minoru Ozasa of the Matsushita Electronics Corporation for courtesies extented to him and for fruitful discussions. He wishes to thank Dr. Masaru Onchi of Kyoto University for measurement using the omegatron mass-spectrometer.

Department of Chemistry
Faculty of Science
Kyoto University
Sakyo-ku, Kyoto

*Thermoanalytical Studies of the Thermal Stability of High Polymers. II. The Differential Thermal Analysis and Thermogravimetric Analysis of Some Polyethylenes**

By Shoichi IGARASHI and Hirotaro KAMBE

(Received August 7, 1963)

Previous investigations of the thermal decomposition of high polymers have dealt almost entirely with isothermal experiments using thermobalance[1-5] to record the change in the weight of the sample at elevated temperatures. Recently the melting behavior and thermal changes of high polymers during oxidation or degradation have been investigated by differential thermal analysis,[6-10] and the thermal stability of linear polymers has been studied by thermogravimetric analysis.[11-17]

Although Paulik et al.[12] reported some thermoanalytical results on polyethylenes obtained by using the Derivatograph, the kinetic parameters for the thermal decomposition of polyethylenes were not determined. Anderson and Freeman[11] evaluated the activation energy and order of reaction for the thermal decomposition of a high-pressure polyethyene from the derivative thermogravimetric analysis curve, in which the rate of the weight loss of the sample is plotted against the temperature of a furnace at a constant rate of heating.

In the first paper of this series[18] an automatic recording thermobalance for studying the thermal stability of high polymers was described and a thermoanalytical study of the thermal decomposition of a commercial low-pressure polyethylene was presented.

It is the purpose of this paper to examine the thermal stability of some polyethylenes, when they are heated at a constant rate of 1°C/min., by differential thermal analysis and by thermogravimetric analysis, both in air and in a nitrogen atmosphere.

Experimental

Materials.—The polymers used were the low-pressure polyethylenes Hizex 5000 and 7000, supplied by the Mitsui Chemical Co., and the high-pressure polyethylenes Sumikathene MF-40 and F-70-6, produced by the Sumitomo Chemical Co. The materials were purified by precipitation using xylene as a solvent and methyl alcohol as a precipitant at room temperature and were then dried at about 60°C in vacuo for about 24 hr.

The melting point of the paraffin used is 56.0~56.5°C.

Differential Thermal Analysis.—The apparatus which has been described in the previous paper[19] was used. Concentric cylindrical sample cells of stainless steel were used; they were essentially similar to that described by Vold.[20] The diameter and the depth of the sample cell are 1.5 cm. and 5 cm. respectively. The sample was put into the gap between the external sample holder and the concentric internal cylinder. Within the hollow of the internal cylinder, a two-junction chromel-constantan thermocouple was inserted in order to measure the temperature difference between the sample and the reference substance. The thermoelectric output was amplified and recorded on the chart of an electric recorder.

The temperature of the vertical electric furnace was automatically controlled so as to increase at a constant rate of about 1°C/min., and it was measured by means of another thermocouple of chromel-alumel and recorded on the same chart.

The sample weight used was about 1 g., a calcined alumina was used as the inert reference substance.

Experiments were carried out both in air and in a nitrogen atmosphere.

* Presented partly at the 14th Annual Meeting of the Chemical Society of Japan, Tokyo, April, 1961.

1) N. Grassie, "The Chemistry of High Polymer Degradation Processes," Butterworths, London (1956).
2) H. H. Jellinek, *J. Polymer Sci*, **4**, 13 (1949).
3) S. L. Madorsky and S. Straus, *J. Res. Natl. Bur. Stands.*, **53**, 361 (1954).
4) S. L. Madorsky, ibid., **62**, 219 (1959).
5) L. A. Wall and S. Straus, *J. Polymer Sci.*, **44**, 313 (1960).
6) B. Ke, ibid., **42**, 15 (1960).
7) B. Ke, ibid., **61**, 47 (1962).
8) B. Ke, ibid., **A1**, 1453 (1963).
9) F. Danusso and G. Polizzotti, *Chim. e Ind. (Milan)*, **44**, 241 (1962).
10) A. Rudin, H. P. Schreiber and M. H. Waldman, *Ind. Eng. Chem.*, **53**, 137 (1961).
11) D. A. Anderson and E. S. Freeman, *J. Polymer Sci.*, **54**, 253 (1961).
12) J. Paulik, H. Macskásy, F. Paulik and L. Erdey, *Plaste und Kautschuk*, **8**, 588 (1961).
13) B. Kaesche-Krischer and H. J. Heinrich, *Z. physik. Chem., Neue Folge*, **23**, 292 (1960).
14) J. B. Gilbert, J. J. Kipling, B. McEnancy and J. N. Sherwood, *Polymer*, **3**, 1 (1962).
15) H. Anderson, *Makromolek. Chem.*, **51**, 233 (1962).
16) I. J. Goldfarb, R. J. McHenry and E. C. Penski, *J. Polymer Sci.*, **58**, 1283 (1962).
17) A. R. Shultz, N. Knall and G. A. Morneau, ibid., **62**, 211 (1962).
18) H. Kambe and S. Igarashi, *Report of Aeronaut. Res. Inst., the Univ. of Tokyo*, **28**, No. 376, 145 (1963).
19) H. Kambe, T. Ozawa, M. Onoue and S. Igarashi, This Bulletin, **35**, 81 (1962).
20) M. J. Vold, *Anal. Chem.*, **21**, 683 (1949).

Thermogravimetric Analysis. — An automatic recording thermobalance, which had been designed and constructed in our laboratory[18] using a calibrated phosphor-bronze spring and a linear variable differential transformer, was used to record the change in the weight of the sample, while the furnace temperature was continuously elevated at a constant rate of about 1°C/min., in air and in a nitrogen atmosphere. The temperature of the cylindrical electric furnace was controlled by an electronic program controller.

The temperature of the sample was measured by means of a chromel-alumel thermocouple located near the sample glass crucible; the output of this thermocouple was recorded. The diameter and the depth of the crucible were 1.1 cm. and 1.0 cm. respectively. The sample weight used was about 90 mg.

Results and Discussion

Differential Thermal Analysis.—Typical results of the differential thermal analysis curves for some polyethylenes are shown in Fig. 1. In these curves the differential temperature between the sample and the reference substance is plotted against the reference temperature.

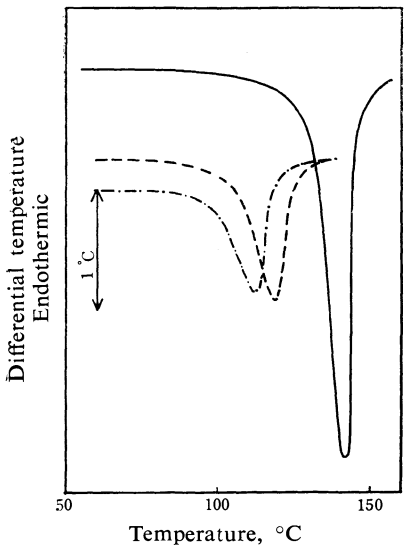


Fig. 1. Differential thermal analysis curves for polyethylenes. Solid line, Hizex 7000; dashed line, Sumikathene MF-40; chain line, Sumikathene F-70-6.

A low-pressure polyethylene, Hizex 7000, displayed a sharp endothermic peak over the range from 120 to 145°C. Two high-pressure polyethylenes, Sumikathene MF-40 and F-70-6, showed a small peak over the ranges from 103 to 118°C and from 103 to 112°C respectively. It is evident that each endothermic peak corresponds to a melting point of the polymer.

The area of a peak in the differential thermal analysis curve is proportional to the amount of the absorbed (or evolved) heat in the sample, and it can be calibrated by a known heat. When the heat of fusion for benzoic acid was used as a standard for calibration, the heats of fusion for these polymers were obtained as follows: 51 cal./g. for Hizex 7000, 42 cal./g. for Hizex 5000, 24 cal./g. for Sumikathene MF-40 and 22 cal./g. for Sumikathene F-70-6. Dividing these values by the heat of fusion for a perfectly crystalline polyethylene (i.e., 66 cal./g.[21]), the crystallinity of each sample was obtained. These values are listed in Table I. It is clear that the

Table I. Differential thermal analysis of polyethylenes

Polymer	M. p. °C	Heat of fusion cal./g.	Crystallinity %	Entropy of fusion e. u./g.
Sumikathene				
F-70-6	103~112	22	33	0.057
MF-40	103~118	24	36	0.062
Hizex				
5000	122~140	42	64	0.102
7000	120~145	51	77	0.123

crystallinity of the branched high-pressure polyethylene is smaller than that of the low-pressure polymer. The results are in agreement with the work of Ke.[6] In Table I the crystallinity of the polymer is shown to be smaller than the reported values of Hizex 5000 and 7000 (e.g., 80~90%). However, according to the theory of differential thermal analysis,[22] the area of a peak depends not only on

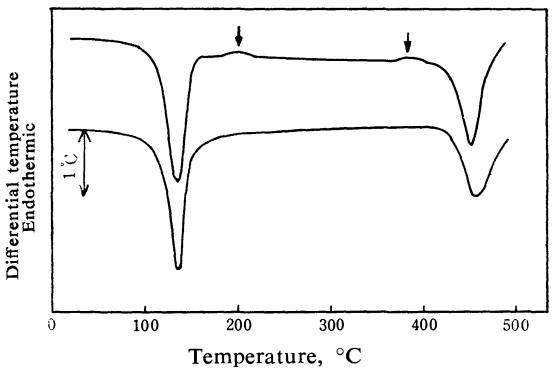


Fig. 2. Differential thermal analysis curves for low-pressure polyethylene Hizex 5000. Upper curve, in air; lower curve, in a nitrogen atmosphere.

21) M. Dole, W. P. Hettinger, Jr., N. R. Larson and J. A. Wethington, Jr., *J. Chem. Phys.*, **20**, 781 (1952); M. Dole and B. Wunderlich, *J. Polymer Sci.*, **24**, 139 (1957).

22) W. J. Smothers, "Differential Thermal Analysis: Theory and Practice," Chemical Publishing Co., Inc., New York (1958), p. 85.

the amount of the absorbed heat, but also on the thermal conductivity of the sample. Since the latter value is not kept constant over the melting range in the polymer, it should be noticed that the latent heat (or crystallinity) obtained from the data of the differential thermal analysis may be the apparent value.

In his earlier work Ke[6] observed that the crystallinity of commercial polyethylene estimated by differential thermal analysis agreed well with the reported one determined by the X-ray method; however, he has recently reported[7] that there was a considerable discrepacy between the two crystallinities of the ethylene copolymers. Therefore, it may be suggested that this discrepancy between the crystallinity evaluated by differential thermal analysis and the reported value may be due to the difference in methods.

Figure 2 shows the differential thermal analysis curves for a low-pressure polyethylene, Hizex 5000, in air and in a nitrogen atomsphere from the ambienat temperature to approximately 500°C. The upper curve in Fig. 2 shows two endothermic peaks at 135 and 457°C. The former peak for the melting of the sample agrees with the literature value of 135°C. The latter peak at 457°C is due to the thermal decomposition of polyethylene, which will be discussed in the following section.

Two small exothermic peaks, indicated by arrows, show the oxidation of polyethylene, because these exothermic peaks are not observed in the lower curve in a nitrogen atmosphere.

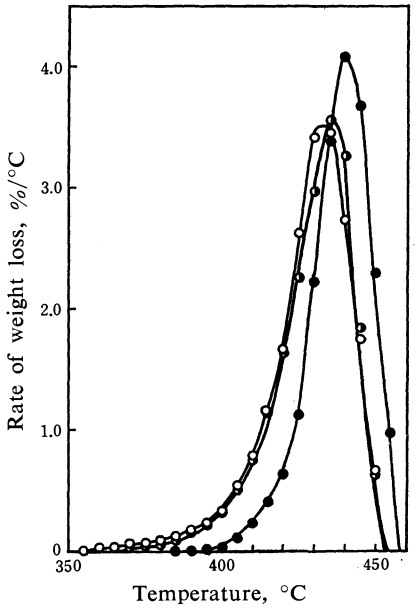


Fig. 3. Thermogravimetric analysis curves for polyethylenes in a nitrogen atmosphere. (●), Hizex 7000; (◑), Sumikathene MF-40; (○), Sumikathene F-70-6.

In the differential thermal analysis curve of low-pressure polyethylene in the presence of air, a small exothermic peak has been observed by Paulik et al.[12] in the range from 190 to 250°C. Danusso et al.[9] have also reported that, after the melting of the polyethylene, an exothermic peak due to oxidation was observed in the differential thermal analysis curve in air.

By a gas-flow-type differential thermal analysis apparatus recently constructed in our laboratory, it has been observed that the crystallinity of polyethylene decreases abruptly in the first exothermic stage (ca. 180°C). The results will be reported elsewhere.

Thermogravimetric Analysis in Nitrogen. — The thermogravimetric analysis curves for Hizex 7000, Sumikathene MF-40 and Sumikathene F-70-6 in a nitrogen atmosphere are shown in Fig. 3. These curves, in which the rate of weight loss (%/°C) is plotted against the temperature, were obtained by a graphical differentiation of the curve of weight loss as a function of the temperature.

From Fig. 3 it is clear that thermal decomposition for each sample takes place in one stage. The weight losses of the two high-pressure polyethylenes, Sumikathene MF-40 and F-70-6, commence at approximately 360°C, and the weight losses for these polymers reach a maximum rate (ca. 3.5%/°C) at about 435°C. However, the thermal decomposition of the low-pressure polyethylene, Hizex 7000, takes place over the range from 380 to about 455°C. The temperature at which the thermal decomposition of high-pressure polyethylene commences is obviously higher by about 20°C

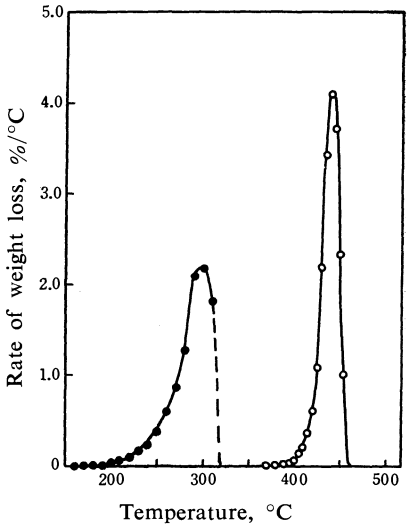


Fig. 4. Thermogravimetric analysis curves for paraffin and Hizex 7000 in a nitrogen atmosphere. (●), paraffin; (○), Hizex 7000.

than that of low-pressure polyethylene.

The above results obtained from the thermogravimetric measurements support the conclusion that a branched polyethylene is thermally more unstable than a linear one in isothermal experiments[5] because thermal decomposition is initiated at the branched point with a tertiary hydrogen atom.

Paulik et al.[12] have reported thermogravimetric studies of polyethylenes including low-pressure, medium-pressure and high-pressure samples in air and in a nitrogen atmosphere. However, they have not described the thermal stability of these polymers in a nitrogen atmosphere. It seems to be impossible in a nitrogen atmosphere for the Derivatograph to clarify the differences in the chemical structure of commercial polyethylenes.

In Fig. 4 the derivative thermogravimetric analysis curves for paraffin (m. p. 56.0~56.5°C) and polyethylene (Hizex 7000) are shown. Figure 4 shows that the weight loss of paraffin begins slowly at about 180°C and that that of polyethylene begins at 380°C. The degradation products were collected into the trap which was set below the sample crucible. The melting points of the trapped products for paraffin and polyethylene were 55.0~55.5°C and 51.0~67.0°C respectively. Since the melting point of the trapped products for paraffin corresponds well with the original one, it is confirmed that the weight loss of paraffin is mainly due to the vaporization of the sample. When the melting point of the trapped paraffin is compared with that of the degradation products for polyethylene, it is also confirmed that the thermal decomposition of polyethylene occurs at the peak appearing in the derivative thermogravimetric analysis curve.

Madorsky et al.,[23] when investigating the degradation products for polyethylene by means of a mass spectrometer, have found that the products contained very little monomer but mainly paraffins and olefins with up to about fifty carbon atoms. As has been mentioned above, the degradation products for Hizex 7000 melts over a wide range in temperature. This means that the products contain a number of hydrocarbon members.

The apparent activation energy and the order of reaction for the thermal decomposition of polymers in a nitrogen atmosphere were evaluated from the derivative thermogravimetric analysis curve by the method of Freeman and Carroll.[24] They derived the following equation:

$$\Delta \log(dW/dT)/\Delta \log W_r = n - (E/2.3R) \times \Delta(1/T)/\Delta \log W_r$$

where dW/dT is the rate of change in weight, n is the order of reaction, E is the apparent activation energy, R is the gas constant, T is the absolute temperature, and W_r is the weight of the reactant at the temperature, T. If we plot $\Delta \log(dW/dT)/\Delta \log W_r$ against $\Delta(1/T)/\Delta \log W_r$, we obtain a linear plot with an intercept, n, on the ordinate and slope equal to $E/2.3R$. This plot for the thermal decomposition of the low-pressure polyethylene Hizex the 7000 is shown in Fig. 5. Thus we found that $E=73.6$ kcal./mol. This agrees with the value of 72 kcal./mol. for the polymethylene of Madorsky.[4] The order of reaction for this stage was not clear. The results are listed in Table II.

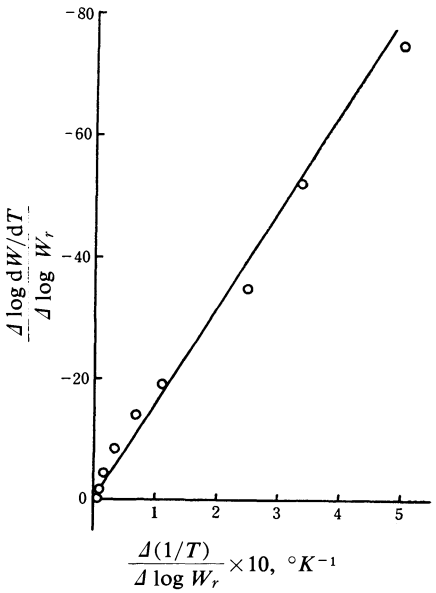


Fig. 5. Freeman's plot for thermal decomposition of low-pressure polyethylene Hizex 7000.

TABLE II. THERMOGRAVIMETRIC ANALYSIS OF POLYETHYLENES IN NITROGEN ATMOSPHERE

Polymer	Decomp. temp. °C	Apparent activation energy kcal./mol.	Residue %
Sumikathene			
F-70-6	360~450	74	0
MF-40	360~450	61	0
Hizex			
7000	380~450	74	0

Anderson and Freeman[11] have studied thermogravimetrically the thermal decomposition of high-pressure polyethylene (DYNH) in vacuo. They have established that the thermal

23) S. L. Madorsky, S. Straus, D. Thompson and W. Williamson, *J. Res. Natl. Bur. Stands.*, **42**, 499 (1949).
24) E. S. Freeman and B. Carroll, *J. Phys. Chem.*, **62**, 394 (1958).

TABLE III. THERMOGRAVIMETRIC ANALYSIS OF POLYETHYLENES IN AIR

Polymer	Decomp. temp. °C	Weight loss at 1st stage %	2nd stage %	3rd stage %	Residue %
Sumikathene					
F-70-6 (purified)	190~440	8.8*	13.2	74.0	4.0
F-70-6 (unpurified)	210~450	4.3	26.8	66.6	2.3
Hizex					
7000	250~450	2.6	21.6	73.0	2.8

* Estimated value

decomposition of the polymer takes place in three stages; the initial, 3% zero-order reaction, the second, 3 to 15% zero-order stage, and the final, first-order reaction, occurring above 35% degradation. The energies of activation for the stages are 48 kcal./mol., 61 kcal./mol. and 67 kcal./mol. respectively.

Thermogravimetric Analysis in Air. — The thermogravimetric analysis curves for Hizex 7000, Sumikathene F-70-6 (unpurified) and Sumikathene F-70-6 (purified) in air are shown in Fig. 6. The curves are different from that obtained in a nitrogen atmosphere (Fig. 3).

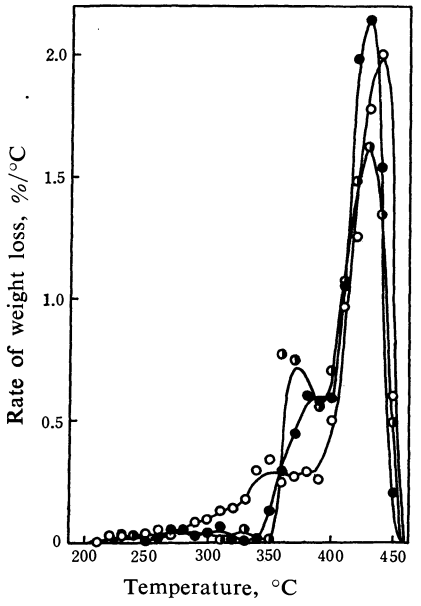


Fig. 6. Thermogravimetric analysis curves for polyethylenes in air. (●), Hizex 7000; (◑), Sumikathene F-70-6 (unpurified); (○),Sumikathene F-70-6 (purified).

The weight loss of Sumikathene F-70-6 commences at about 200°C, and that of Hizex 7000, at 250°C. The maximum rates of weight loss of these polymers occur at about 430°C. In these curves it seems that the oxidative degradation takes place in three stages: the first, up to approximately 350°C, the second from 350 to about 390°C, and the third from 390 to about 455°C.

When the curve for the purified Sumikathene is compared with that for the unpurified one, it is found that the weight loss for the first stage of the latter is smaller than for that of the former. This may indicate the effect on the theraml stability exerted by an antioxidant added to the commercial polymer. In the lower-temperature range the weight loss is mainly due to the degradation at the branching point in the polymer molecule. In accordance with this, the weight loss of the less-branched Hizex 7000 in this stage is smaller than that of Sumikathene. In a previous paper[25] it has also been recognized that the chain branching and the unsaturation have a marked effect on the weight loss at the first stage of the oxidative degradation of the irradiated polyethylene.

Paulik et al.[12] observed from the Derivatograph of the low-pressure polyethylene that the weight gain of the sample took place in the range from 160 to 200°C and that the rapid oxidative weight loss occurred over the range from 320 to about 400°C.

Since the oxidative degradation of the polymer may begin at its surface, the influence of the surface area of the sample on the weight loss in the thermogravimetric analysis was examined. For this purpose the sample crucible, the surface area of which is 1.63 times that of the crucible usually used, was utilized for low-pressure polyethylene. As a result, it was recognized that the weight loss at the low-temperature stage increased to 1.4 times the value obtained with the usual crucible.

Summary

The thermal stability of polyethylenes has been studied by differential thermal analysis and by thermogravimetric analysis in air and in a nitrogen atmosphere.

25) S. Igarashi, I. Mita and H. Kambe. *J. Appl. Polymer Sci.*, in press.

The crystallinities of some polyethylenes have been evaluated from the data of differential thermal analysis. These values are smaller than the reported value. This discrepancy may be due to differences in the methods.

In the differential thermal analysis curve for low-pressure polyethylene Hizex 5000 in air, two small exothermic peaks due to oxidation were observed at about 200 and at about 390°C. The endothermic peaks at 135 and at 457°C correspond to the melting and to the thermal decomposition points of polyethylene.

In thermogravimetric analysis in a nitrogen atmosphere, the thermal decomposition of low-pressure polyethylene takes place over the range from 380 to about 450°C, and that of high-pressure polyethylene, from 360 to about 450°C. In the presence of air, the oxidative degradation of low-pressure and high-pressure polyethylenes occurs in three stages: the first from about 200 to 350°C, the second from about 350 to 390°C, and the third from about 390 to 455°C.

It has been concluded that the thermal stability of high-pressure polyethylene is smaller than that of low-pressure polyethylene. This may be attributed to the difference in branching of commercial polyethylenes.

Polymer Research Division
Aeronautical Research Institute
The University of Tokyo
Meguro-ku, Tokyo

Studies of the Organic Reactions of Metal Carbonyls. I. The Isomerization of Alkyl- and Acylcobalt Carbonyls

By Yoshinobu TAKEGAMI, Chikao YOKOKAWA, Yoshihisa WATANABE and Yasukazu OKUDA

(Received August 9, 1963)

Heck and Breslow[1] obtained two isomeric products by the carbonylation of, for instance, methyl acrylate or 1-pentene with cobalt hydrocarbonyl. This seems to indicate that the addition of the carbonyl group to the olefinic bonds has taken place at both carbon atoms of the C=C double bond. It is possible, however, to assume that the alkyl- and/or acylcobalt carbonyls which are formed in the course of this type of reaction have been isomerized.

In the present program, in order to check the possibility of this isomerization, the reactions of some alkyl (*n*-propyl iodide, ethyl α-bromopropionate) and acyl halides (*n*-butyryl- and iso-butyryl halide) with potassium cobalt tetracarbonyl have been carried out. By means of the results of the structural determination of the products, it has been established that the isomerization mentioned above does indeed take place.

Experimental

The Preparation of Cobalt Hydrocarbonyl. — The aqueous solution of potassium cobalt tetracarbonyl was prepared by Blanchard's method.[2] After the acidification of this solution with hydrochloric acid, cobalt hydrocabonyl was extracted by toluene. Into a 2 l. bottle 250 ml. of an aqueous solution containing 160 g. of potassium hydroxide and 20 g. of potassium cyanide were placed. After the air in the bottle had been replaced with carbon monoxide, the solution containing 50 g. of cobalt(II) chloride hexahydrate and 250 ml. of water was added. The bottle was connected to a reservoir of carbon monoxide and shaken mechanically for 10 to 20 hr. at room temperature under the atmospheric pressure of carbon monoxide. After 17 to 20 l. of the carbon monoxide had been absorbed, a yellow solution of potassium cobalt tetracarbonyl was formed. This solution was stored in a dark and cool place under a carbon monoxide atmosphere. About 250 ml. of this solution and 400 ml. of toluene[3] were then placed in a 1 l. four-necked flask, fitted with a dropping funnel, a stirrer and a rubber stopple, and flashed with carbon monoxide. Seventy to eighty milliliters of concentrated hydrochloric acid were gradually but vigorously stirred in at 0°C. By the use of a hypodermic syringe, the cobalt hydrocarbonyl solution in toluene thus formed was transferred into another bottle, which was then filled with carbon monoxide and kept at −70°C.

1) R. F. Heck and D. S. Breslow, *J. Am. Chem. Soc.*, **83**, 4023 (1961).

2) A. A. Blanchard and P. Gilmont, ibid., **62**, 1192 (1940).

3) In some cases *n*-heptane was used instead of toluene (cf. Tables).

The concentration of this solution was determined by the analytical method proposed by Sternberg,[4] using 20 ml. of the sample. By diluting it with toluene, a 0.09 M solution was prepared and used for the reaction.

The Reaction of Alkyl Halides with Potassium Cobalt Tetracarbonyl. — A 100 ml., four-necked flask, fitted with a 50 ml. dropping funnel, a stirrer and a rubber stopple, was connected with a gas buret, and the air in the system was replaced with carbon monoxide or nitrogen. By the use of a syringe, 50 ml. of the cobalt hydrocarbonyl solution was put into the flask; then the solution was titrated with a 1/2 N alcohol[5] solution of potassium hydroxide in the presence of phenolphthalein. To the potassium cobalt tetracarbonyl thus formed, a desired amount of alkyl halide was introduced, and the reaction mixture was agitated at various temperatures for several hours. In the course of this reaction, the amounts of carbon monoxide absorbed were determined by following the change in the readings of the buret. In the case of the reaction of ethyl α-bromopropionate under a nitrogen atmosphere, gas formation was observed.

The Reaction of Acyl Halides with Potassium Cobalt Tetracarbonyl.—The solution of potassium cobalt tetracarbonyl, obtained by the procedure mentioned above, was evaporated to dryness[6] under reduced pressure at room temperature, and 50 ml. of anhydrous tetrahydrofuran or isopropyl ether were added. The solution[8] thus formed was mixed with 4.5 mmol. (equi-mole of potassium cobalt tetracarbonyl) of *n*-butyryl chloride or isobutyryl bromide, and the reaction was carried out as in the case of alkyl halides. In every case gas formation was observed.

Analytical Procedures.—After a desired reaction time, 30 ml. of a saturated solution of iodine in toluene[9] and 4 ml. of alcohol[10] were vigorously stirred into the reaction mixture at the same temperature as that for the reaction; the agitation was continued until gas ceased to evolve. By this treatment acylcobalt carbonyl was converted into the corresponding ester of carboxylic acid[1]. The solution of this ester was concentrated under reduced pressure (20 to 30 mmHg) and was then gas chromatographed. A column three meters long, filled with dilauryl phthalate on cerite, was used; the column temperature was varied between 100 to 150°C, depending on the boiling point of the sample, and the flow rate of the carrier gas (hydrogen) was set at 75 ml./min. The identification of the materials was made by means of a mixed melting point test with authentic samples.

Other Materials Used. — Methyl iodide, ethyl iodide, isopropyl bromide, *n*-butyl bromide, benzyl bromide, iodobenzene, bromobenzere, ethyl α-bromopropionate, *n*-butyryl chloride and isobutyryl bromide were commercial products, and all of them were proved to be sufficiently pure by gas chromatography. *n*-Propyliodide and isopropyl iodide were synthesized by the iodination of alcohols with iodide and red phosphor.[11]

Results

The Reactivity of Alkyl Halides with Potassium Cobalt Tetracarbonyl.—The reaction of *n*-propyl iodide with potassium cobalt tetracarbonyl is important in determining the isomerization mentioned at the beginning of this paper. No detailed observation had, however, been reported on the reaction of alkyl halide homologs higher than ethyl halide. Therefore, some alkyl or aryl halides have been reacted with potassium cobalt tetracarbonyl, and the amounts of carbon monoxide absorbed have been determined as the measure of their reactivity. It is believed[12] that the carbon monoxide absorption occurs as a result of the following reactions; the alkylcobalt tetracarbonyl ($RCo(CO)_4$), which is formed at the initial stage of the reaction, is converted to acylcobalt tricarbonyl ($RCOCo(CO)_3$), and the latter absorbs carbon monoxide to form acylcobalt tetracarbonyl ($RCOCo(CO)_4$).

The results for the reactions of ethyl iodide and *n*-propyl iodide illustrated in Fig. 1, in which the amounts of carbon monoxide

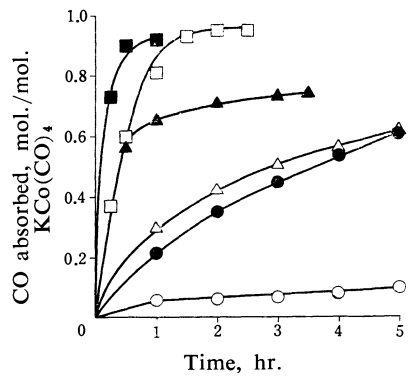


Fig. 1. Carbon monoxide absorption curves of the reaction of some alkyl halides with potassium cobalt tetracarbonyl.

- ○ *n*-Propyl iodide (0°C)
- ● *n*-Propyl iodide (25°C)
- △ Ethyl iodide (0°C)
- ▲ Ethyl iodide (25°C)
- □ Methyl iodide (0°C)
- ■ Benzyl bromide (0°C)

4) H. Sternberg, *Anal. Chem.*, **24**, 174 (1952).
5) Ethyl and *n*-propyl alcohol (cf. Tables).
6) No trace of the alcohol used as a solvent was detected by the xanthate method.[7]
7) F. Feigl, "Spot Tests," Vol. II, Elsvier Publishing Co., Amsterdam (1954), p. 129.
8) Potassium cobalt tetracarbonyl is apparently soluble in tetrahydrofuran, but it is only partly soluble in isopropyl ether.
9) Benzene was used instead of toluene for *n*-propyl esters.
10) *n*-Propyl alcohol was used for acyl halides.
11) L. Gatterman, "Die Praxis des Organischen Chemikers," Walter De Gruyter, Berlin (1958), p. 88.
12) D. S. Breslow and R. F. Heck, *Chem. & Ind.*, **1960**, 467.

Table I. Reactions of *n*-propyl iodide and ethyl α-bromopropionate with potassium cobalt tetracarbonyl

No.	Substrate	Atmosphere	Temp. °C	Time hr.	Mol. Halide / Mol. $KCo(CO)_4$	Solvent	CO Absorbed (Mol. / Mol. $KCo(CO)_4$)	Yield of ester*2 (Mol. / Mol. $KCo(CO)_4$)	Ratio of isomeric esters *n/iso**3
1	*n*-Propyl iodide	CO	25	5.0	20	*n*-Heptane	0.63	0.41	12
2	*n*-Propyl iodide	CO	0	5.0	20	*n*-Heptane	0.10	—	7
3	*n*-Propyl iodide	N_2	25	5.0	20	*n*-Heptane	—	0.18	2
4	*n*-Propyl iodide	N_2	0	5.0	20	*n*-Heptane	—	—	5
5	Ethyl α-bromopropionate	CO	25	4.3	5.0	Toluene	−1.5*1	0.22	2.5
6	Ethyl α-bromopropionate	CO	0	5.3	5.0	Toluene	0.15	0.26	0.4
7	Ethyl α-bromopropionate	CO	−25	4.5	5.0	Toluene	0.23	—	0.0
8	Ethyl α-bromopropionate	N_2	25	4.5	5.0	Toluene	−1.8*1	0.12	3.3
9	Ethyl α-bromopropionate	N_2	0	4.5	5.0	Toluene	−1.5*1	0.12	0.2

*1 Gas was evolved.
*2 The products from *n*-propyl iodide and ethyl α-bromopropionate were identified as *n*-propyl ester and ethyl ester, respectively.
*3 Cf. Footnote 14.

Table II. Reactions of butyryl halides with potassium cobalt tetracarbonyl

No.	Substance	Reaction condition*1			Yield of ester*2 (Mol. / Mol. $KCo(CO)_4$)	Ratio of isomeric ester, *n/iso**3	Amount of gas evolved (Mol. / Mol. $KCo(CO)_4$)
		Atmosphere	Temp., °C	Solvent			
10	*n*-Butyryl chloride	CO	0	Tetrahydrofuran	0.08	∞	0.25
11	*n*-Butyryl chloride	CO	−20	Tetrahydrofuran	0.23	∞	0.17
12	*n*-Butyryl chloride	CO	−40	Tetrahydrofuran	0.27	∞	nil
13	*n*-Butyryl chloride	N_2	0	Tetrahydrofuran	0.15	∞	0.43
14	*n*-Butyryl chloride	N_2	25	Tetrahydrofuran	0.09	∞	0.77
15	*n*-Butyryl chloride	N_2	0	Isopropyl ether	0.49	∞	0.18
16	Isobutyryl bromide	CO	25	Tetrahydrofuran	0.19	4.6	0.40
17	Isobutyryl bromide	CO	0	Tetrahydrofuran	0.10	5.0	0.13
18	Isobutyryl bromide	CO	−20	Tetrahydrofuran	0.13	2.9	0.18
19	Isobutyryl bromide	CO	−40	Tetrahydrofuran	0.03	1.0	0.07
20	Isobutyryl bromide	CO	25	Isopropyl ether	0.32	0.6	0.14
21	Isobutyryl bromide	CO	0	Isopropyl ether	0.38	0.5	nil
22	Isobutyryl bromide	CO	−25	Isopropyl ether	0.37	0.4	0.08
23	Isobutyryl bromide	N_2	25	Tetrahydrofuran	0.27	8.8	0.94
24	Isobutyryl bromide	N_2	0	Tetrahydrofuran	0.13	7.5	0.51

*1 Reaction time: 3 hr., mol. halide/mol. $KCo(CO)_4$ 1.0
*2 The reaction products were identified as *n*-propyl esters.
*3 Cf. Footnote 14.

absorbed are plotted against the reaction time, indicate that these two halides scarcely reacted at 0°C, as it had already been observed,[13] but that they react fairly well at 25°C. For convenience of comparison, the results for methyl iodide and benzyl bromide are also given in Fig. 1.

Besides the halides mentioned above, isopropyl bromide, isopropyl iodide, *n*-butyl bromide, iodobenzene and bromobenzene were subjected to the reaction. It seems that none of them react; there was no absorption of carbon monxide nor any change in the color of the reaction mixtures when five times mole of halides were submitted to the reaction with potassium cobalt tetracarbonyl at 25°C for 2 hr.

The Reaction of *n*-Propyl Iodide and Ethyl α-Bromopropionate with Potassium Cobalt Tetracarbonyl.—*n*-Propyl iodide, which is the simplest compound for the study of the isomerization of alkyl- or acylcobalt carbonyls, and ethyl α-bromopropionate were subjected to react with potassium cobalt tetracarbonyl; the results are summarized in Table I. The latter was chosen as a sample for the secondary halide, because isopropyl iodide did not react with potassium cobalt tetracarbonyl. Methyl α-bromopropionate was submitted to this same type of reaction by Heak and Breslow,[13] but they did not identify the reaction products.

From *n*-propyl iodide only *n*-propyl *n*-butyrate should be produced if no isomerization takes place, but the product contained *n*-propyl isobutyrate besides *n*-butyrate. This formation of the isomeric esters was observed under the atmospheres of both carbon monoxide and nitrogen, but it seems that isobutyrate was formed easily under the nitrogen atmosphere. On the other hand, it was evident that no isomerization of alkyl halide took place in the course of reaction, because no isopropyl iodide was detected in the reaction product, while the amount of *n*-propyl iodide remained unchanged. These findings lead to the conclusion that the isomerization of alkyl- or acylcobalt carbonyls takes place.

In the reaction of ethyl α-bromopropionate, carbon monoxide was absorbed at −25°C and 0°C under a carbon monoxide atmosphere, but, on the contrary, gas evolution was observed at 25°C under a carbon monoxide or nitrogen atmosphere. The reaction at −25°C under a carbon monoxide atmosphere gave only diethyl methylmalonate, but at 0°C and 25°C both isomeric products (diethyl methylmalonate and diethyl succinate) were formed. Diethyl methylmalonate (A) was predominant in the reaction product at 0°C, but diethyl succinate (B) was the main product at 25°C. The ratio of B/A was just reversed at 0°C and at 25°C. These tendencies are also observed in a nitrogen atmosphere. Because no ethyl β-bromopropionate is formed in these reactions, it can be concluded that the isomerization of alkyl- or acylcobalt carbonyls takes place.

The Reaction of *n*-Butyryl Chloride and Isobutyryl Bromide with Potassium Cobalt Tetracarbonyl.—In order to check the possibility of the isomerization of acylcobalt carbonyls, *n*-butyryl chloride and isobutyryl bromide were made to react with potassium cobalt tetracarbonyl; the results are summarized in Table II. It is evident in all the conditions examined, that *n*-butyryl chloride gave only *n*-propyl *n*-butyrate, but that isobutyryl bromide gave *n*-butyrate besides isobutyrate. It is clear also that *n*-butyrate is predominant when the reactions are carried out in tetrahydrofuran, especially under a nitrogen atmosphere.

These findings seem to indicate that isoacylcobalt carbonyl is easily isomerized to form *n*-acylcobalt carbonyl, but that the reverse isomerization, *n*-acylcobalt carbonyl to isoacylcobalt carbonyl, is extremely difficult.

Comparing the findings concerning acyl halides with those concerning alkyl halides and summarizing the characteristic behavior observed in the course of these two types of reaction, in conclusion it may be said that:

Both isoalkyl- and isoacylcobalt carbonyls are isomerized easily to form large amounts of *n*-structural products,[14] and *n*-alkylcobalt carbonyl is also isomerized to result in a relatively small amount of iso-structural products.[14] On the other hand, *n*-acylcobalt carbonyl gives no iso-structural product. These findings appear to be related to the general tendency for the *n*-structural products to increase as the reaction temperature rises.

In all the experiments described here, the yields of the expected products (esters) are not good; this is because the intermediates, i. e., alkyl- or acylcobalt carbonyls, are very reactive and because some side reactions have taken place. Actually, it is clear that some side reactions occur, because in the reactions of ethyl α-bromopropionate in toluene and of acyl halide in tetrahydrofuran, organic crystalline substances were isolated from the concentrated reaction mixtures, and in the case of acyl halides, a relatively large amount of unknown substances was detected in the gas

13) R. F. Heck and D. S. Breslow, *J. Am. Chem. Soc.*, **84**, 2499 (1962).

14) The structures of types A and B are called *n*- and iso-structures respectively:
(A) R-C-C-CO (B) R-C-C
CO

chromatograms.

As has already been described, the reactions studied in this program are complicated, and their details are not yet solved, but the conclusion, that the isomerization of alkyl- or acylcobalt carbonyl takes place, is unquestionable.

Discussion

It has been postulated by Breslow and Heck[12] that the mechanism of the reaction of organohalides with potassium cobalt tetracarbonyl can be represented as follows:

$$RX + KCo(CO)_4 \rightarrow RCo(CO)_4$$
$$\rightleftarrows RCOCo(CO)_3 \xrightarrow[CO]{} RCOCo(CO)_4$$
$$RCOX + KCo(CO)_4 \rightarrow RCOCo(CO)_4$$

They did not consider any possibility of isomerization during the course of the reaction sequences mentioned above.[15] Our experiments, however, have shown clearly that isomerization does occur at some step of the reaction. On the basis of our finding that the isomerization of acylcobalt carbonyl is accelerated under a nitrogen atmosphere and on the basis of the equilibrium established previously,[16] $RCOMn(CO)_5 \underset{CO}{\overset{\Delta}{\rightleftarrows}} RMn(CO)_5 + CO$, it may reasonably be concluded that [the isomerization species is the carbon monoxide-lacking complex in the reaction sequences described above: i. e., alkylcobalt tetracarbonyl and/or acylcobalt tricarbonyl.

Department of Fuel Chemistry
Faculty of Engineering
Kyoto University
Sakyo-ku, Kyoto

15) R. F. Heck, *J. Am. Chem. Soc.*, **85**, 651 (1963).
16) T. H. Coffield, J. Kozikowski and R. D. Closson, *J. Org. Chem.*, **22**, 598 (1957).

Thermally-induced Changes in Poly-α-amino Acids Containing Methyl Sidechains[1]

By Tadao HAYAKAWA

(Received August 9, 1963)

Poly-α-amino acids containing α-methyl sidechains have been synthesized by the Leuchs method. These acids include poly-L-alanine, poly-DL-alanine, poly-α-aminoisobutyric acid, copoly(DL-alanine, L-glutamic acid) and copoly-(α-aminoisobutyric acid, L-glutamic acid). Copolymers have been coagulated in an aqueous solution by heat; other changes in the properties of both polymers and copolymers have been studied by the methods or measurements of specific rotation, specific viscosity, differential thermal analysis and infrared absorption spectra. The effects have been interpreted as being due to changes in the secondary structure. The poly-α-amino acids containing the alanine residue show changes in these properties at about 60°C, while the polymers containing the α-aminoisobutyric acid residue show such changes at about 50°C. The infrared absorption spectra indicate a change from the α to the β form.

It has been reported that poly-ε-aminocaproyl-DL-alanine,[2] poly-ε-aminocaproyl-α-aminoisobutyric acid[3] and poly-ε-aminocaproyl-L-proline[4] are slightly soluble in water and that these solutions are reversibly coagulated by heat; they precipitate from an aqueous solution upon being heated and redissolve upon being cooled. Kurtz et al.[5] observed the same phenomenon with poly-L-proline. Elliott[6] reported the thermal conversion of poly-DL-alanine from the α to the β formin an aqeuous solution. The β-form can be converted into the α-form by treating it with formic acid.[6]

1) Presented at the 10th Annual Meeting of the Society of Polymer Science Japan, Tokyo, May, 1961.

2) J. Noguchi, T. Hayakawa, J. Suzuki and M. Ebata, *J. Chem. Soc. Japan, Pure Chem. Sec.* (*Nippon Kagaku Zassi*), **76**, 648 (1955); J. Noguchi, T. Hayakawa and M. Ebata, *J. Polymer Sci.*, **23**, 843 (1955).

3) J. Noguchi, M. Ebata, T. Hayakawa and T. Saito, *J. Chem. Soc. Japan, Pure Chem. Sec.* (*Nippon Kagaku Zassi*), **77**, 469 (1956).

4) J. Noguchi et al., *Annual Report of the Fiber Research Institute, Japan*, **9**, 118 (1956).

5) J. Kurtz, A. Berger and E. Katchalski "Recent Advances in Gelatin and Glue Research," Ed. by G. Stanish, Pergamon Press, London (1958), p. 131.

6) A. Elliott, *Nature*, **170**, 1066 (1952); C. H. Bamford, L. Brown, A. E. Elliott, W. Hanby and I. F. Trotter, ibid., **173**, 27 (1954).

TABLE I. MOLAR RATIOS OF REACTANTS AND SOLUBILITIES OF POLY-α-AMINO ACIDS

No.	Polymer	Mole ratio	Solubility in water
I	Poly-L-alanine		Insoluble
II	Poly-DL-alanine		Easily soluble
III	Poly-α-aminoisobutyric acid		Insoluble
IV-1	Copoly(DL-alanine, L-glutamic acid)	1 : 1	Insoluble
IV-2	Copoly(DL-alanine, L-glutamic acid)	2 : 1	Insoluble
IV-3	Copoly(DL-alanine, L-glutamic acid)	5 : 1	Slightly soluble
IV-4	Copoly(DL-alanine, L-glutamic acid)	10 : 1	Slightly soluble
IV-5	Copoly(DL-alanine, L-glutamic acid)	20 : 1	Soluble
V-1	Copoly(α-aminoisobutyric acid, L-glutamic acid)	1 : 1	Insoluble
V-2	Copoly(α-aminoisobutyric acid, L-glutamic acid)	2 : 1	Insoluble
V-3	Copoly(α-aminoisobutyric acid, L-glutamic acid)	5 : 1	Slightly soluble
V-4	Copoly(α-aminoisobutyric acid, L-glutamic acid)	10 : 1	Slightly soluble
V-5	Copoly(α-aminoisobutyric acid, L-glutamic acid)	20 : 1	Slightly soluble

Methyl groups of alanine or α-aminoisobutyric residues and tetrahydropyrrole rings of proline residues may contribute to the alteration of the secondary structure of the polypeptide chain upon being heated possibly resulting in the coagulation phenomenon. These groups may also be important in the heat denaturation of protein. This paper reports on the effect of heat upon various properties of poly-α-amino acids containing α-methyl groups. The polymers studied were poly-L-alanine (I), poly-DL-alanine (II), poly-α-aminoisobutyric acid (III), copoly(DL-alanine, L-glutamic acid) (IV), and copoly(α-aminoisobutyric acid, L-glutamic acid) (V). They were prepared by the Leuchs method[7] (Table I), glutamic acid being protected as the γ-benzyl ester during the synthesis.

The properties of the polymers studied, or the methods of studying the reversible heat coagulation, were specific rotation, specific viscosity, differential thermal analysis and infrared absorption spectra.

Experimental

The polymers studied and their solubilities in water are listed in Table I.

Poly-L-alanine (I).—This was prepared by the usual method.[7] The L-alanine was suspended in dry dioxane and treated with dry phosgene, and the resulting Leuchs anhydride was polymerized in benzene at 80°C for 48 hr. The polymer was insoluble in all the solvents tested except dichloroacetic acid. The intrinsic viscosity was measured with an Ostwald viscosimeter in dichloroacetic acid at 30±0.01°C. $[\eta]=[\eta_{sv/c}]_{c\to 0}=0.0216$, ml./g.

Poly-DL-alanine (II).—This was prepared in the same way as was poly-L-alanine. The molecular weight was determined by *N*-terminal analysis by titration with perchloric acid in glacial acetic acid. Mol. wt.=5000.

Poly-α-aminoisobutyric Acid[8] (III).—α-Aminoisobutyric acid (6.0 g.) was suspended in 300 ml. of dry dioxane, and dry phosgene was passed in at 50°C. It was almost completely dissolved after ten hours. Carbon dioxide was then passed in to remove the excess phosgene, and the solvent was removed under reduced pressure. The residual crystals were treated with petroleum ether, filtered and dried. The Leuchs anhydride was recrystallized from ethyl acetate-petroleum ether; yield, 5.0 g. The Leuchs anhydride (5.0 g.) was dissolved in 100 ml. of dry dioxane and polymerized with a sodium methylate initiator at room temperature. After a week, the solvent was removed, and the residue was treated with water, filtered and dried; yield, 2.2 g. (66.7%).

This polymer was insoluble in all the solvents tested except dichloroacetic acid. The intrinsic viscosity was measured in dichloroacetic acid in the same way as was the poly-L-alanine at 30±0.01°C. $[\eta]=[\eta_{sp/c}]_{c\to 0}=0.00187$, ml./g.

Copoly(DL-alanine, L-glutamic acid) (VI).—The method of preparing IV-2, IV-3, IV-4, and IV-5 samples has been reported earlier.[8] The IV-1 sample was prepared in the same way.

Found: N, 14.00; Calcd. for $1C_3H_5ON$-$1C_5H_7O_3N$: N, 14.00%.

The molecular weight was determined by the *N*-terminal titration of the intermediate, copoly(DL-alanine, γ-benzyl-L-glutamate); mol. wt.=19000.

Copoly(α-aminoisobutyric acid, L-glutamic acid) (V).—Mixtures of α-aminoisobutyric acid NCA and γ-benzyl-L-glutamate NCA were each dissolved in dry dioxane in the ratios of 1 : 1, 2 : 1, 5 : 1, 10 : 1 and 20 : 1. Each mixture was polymerized for several

7) H. Leuchs, *Ber.*, **39**, 857 (1906); A. C. Farthing and R. J. W. Reynolds, *Nature*, **165**, 647 (1950).

8) J. Noguchi, *High Polymer Chem., Japan* (*Kobunshi Kagaku Zassi*), **6**, 193 (1949).

TABLE II. COPOLYMERS OF α-AMINOISOBUTYRIC ACID AND γ-BENZYL L-GLUTAMATE

Copolymer	Amino acid Mole ratio	NCA g.	Initiator mg.	Yield g.	Amino acid composition Mole ratio	Mol. wt.	N, % Found	N, % Calcd.
α-Aminoisobutyric acid γ-Benzyl L-glutamate	1 1	3.58 7.30	15.1	7.0	1 1	9700	9.10	9.21
α-Aminoisobutyric acid γ-Benzyl L-glutamate	2 1	5.39 5.50	17.0	5.5	2 1	5500	10.60	10.79
α-Aminoisobutyric acid γ-Benzyl L-glutamate	5 1	8.08 3.30	20.2	5.1	4.9 1	6100	12.85	13.00
α-Aminoisobutyric acid γ-Benzyl L-glutamate	10 1	9.82 2.00	23.0	5.1	9.9 1	5400	14.02	14.20
α-Aminoisobutyric acid γ-Benzyl L-glutamate	20 1	11.4 1.15	25.0	5.6	19 1	4100	14.98	15.27

days at room temperature, using sodium methylate as the initiator. The mixture in each case was then heated on a boiling water bath for one hour, and the solvent was removed under reduced pressure. The residue was treated with much water, filtered, and dried. The molecular weight was determined by endgroup titration. Portions of these copolymers were hydrolyzed with 6 N hydrochloric acid, and the component amino acids were assayed from paper chromatograms after ninhydrin staining by means of the densitometer (Table II).

These copolymer were debenzylated with glacial acetic acid and hydrogen bromide at 50°C in the usual way[10] (Table III).

TABLE III. COPOLYMERS OF α-AMINOISOBUTYRIC ACID AND L-GLUTAMIC ACID

	Mole ratio	N, % Found	N, % Calcd.
α-Aminoisobutyric acid L-Glutamic acid	1 1	12.92	13.08
α-Aminoisobutyric acid L-Glutamic acid	2 1	13.70	14.05
α-Aminoisobutyric acid L-Glutamic acid	5 1	14.84	15.14
α-Aminoisobutyric acid L-Glutamic acid	10 1	15.47	15.72
α-Aminoisobutyric acid L-Glutamic acid	20 1	15.66	16.06

Discussion

Reversible Heat Coagulation.—It was not possible to test the water-insoluble poly-L-alanine (I), poly-α-aminoisobutyric acid (III), copoly(DL-alanine, L-glutamic acid) (IV) (1)–(2) and copoly(α-aminoisobutyric acid, L-glutamic acid) (V) (1)-(2) for reversible coagulation by heat. The water-soluble poly-DL-alanine and copoly(DL-alanine, L-glutamic acid)

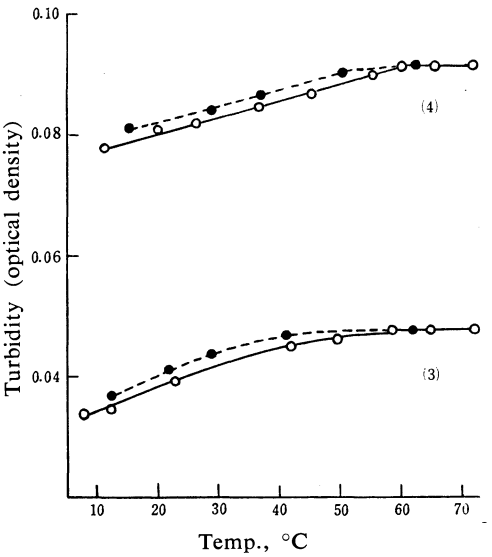


Fig. 1. Turbidity of copoly(DL-ala, L-glu) IV concentration: IV-3 0.45%, IV-4 0.62%.
(Measured after keeping for 15 min. at each temp.)
○—○ Points obtained with rising temp.
●—● Points obtained with falling temp.

(V-5) were also not coagulated by heat, possibly because of their high solubility in water. Other slightly-soluble copolymers, IV-3, IV-4, V-3, V-4 and V-5, were reversibly coagulated by heating and cooling. The relationship between the turbidity and the temperature is shown in Figs. 1 and 2. The turbidity increased with an increase in the temperature, the polymers of group IV, which contains DL-alanine, reaching a constant value at about 60°C, and those of groups V, which contains α-aminoisobutyric acid, reaching one at about 50°C. However, the ascending and descending temperature curves did not coincide. When the glutamic acid residues were converted to sodium salts, the water solubility of these

9) J. Noguchi, T. Saito, T. Hayakawa, H. Tokuyama and T. Harada, *J. Chem. Soc. Japan, Pure Chem. Sec.* (*Nippon Kagaku Zassi*), **82**, 597 (1961).
10) D. Ben-Ishai, *J. Org. Chem.*, **19**, 62 (1954).

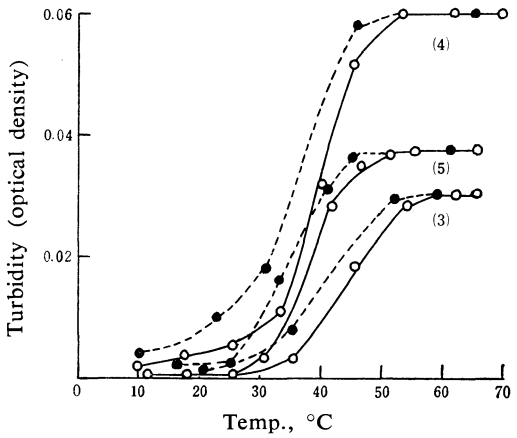


Fig. 2. Turbidity of copoly(α-aminoisobut., L-glu) V concentration: V-3 1.8%, V-4 2.1%, V-5 2.7%.
(Measured after keeping for 15 min. at each temp.)
○—○ Points obtained with rising temp,
●—● Points obtained with falling temp.

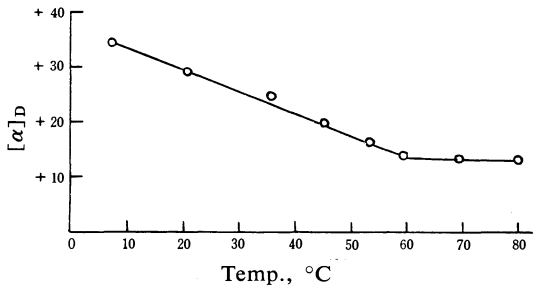


Fig. 3. Optical rotation of poly-L-alanine I (c=1.31, dichloroacetic acid).
(Measured after keeping for 15 min. at each temp.)

samples increased, and they were no longer heat-coagulable.

Specific Rotation.—The effect of the temperature on the optical rotation of these polymers is shown in Figs. 3, 4 and 5. The levorotation of poly-L-alanine (I) (Fig. 3), measured in dichloroacetic acid, decreased with a rise in the temperature, reaching, however, an almost constant value at about 60°C. The sodium salt of copoly IV also exhibited the same critical temperature, as Fig. 4 shows. The sodium salt of copolymer V had a critical temperature of about 50°C, as is shown in Fig. 5. These optical properties are complementary with the reversible heat coagulation phenomena. It is possible that the structure of the polymer chain which has methyl side-chains may be altered by heating, and that this may cause delicate changes in the solubility. The poly-α-amino acids containing the alalyl residue seem to undergo a change (or

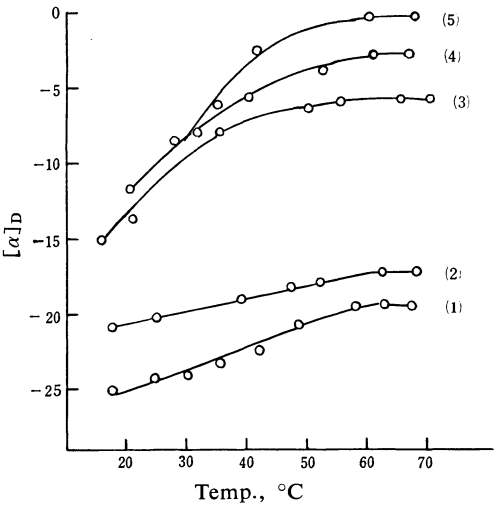


Fig. 4. Optical rotation of copoly(DL-ala, L-glu-Na) IV in water (1) C=5.00, (2) c=5.00, (3) c=5.00, (4) c=3.46, (50) c=1.71.
(Measured after keeping for 15 min. at each temp.)

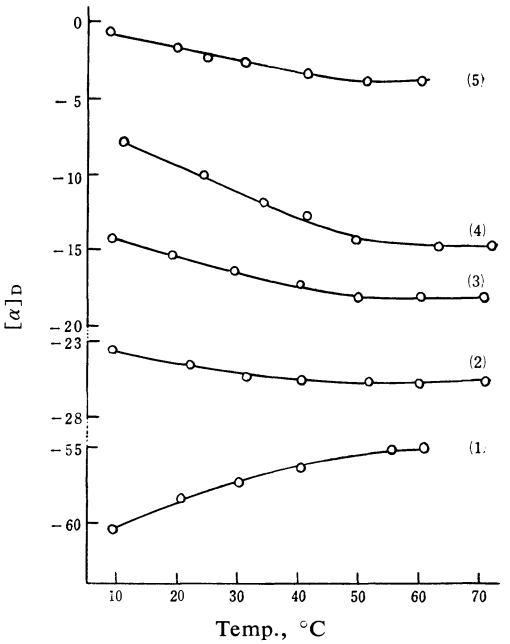


Fig. 5. Optical rotation of copoly(α-aminoisobut, L-glu-Na) V in water (1) c=1.85, (2) c=3.98, (3) c=1.14, (4) c=2.30, (5) c=1.50.
(Measured after keeping for 15 min. at each temp.)

changes) in their secondary structure at about 60°C, while the polymers containing α-aminoisobutyryl residues show their initial response at about 50°C.

In order to verify these phenomena, specific viscosity determinations, differential thermal analyses and infrared spectra were performed on poly-L-alanine (I), poly-DL-alanine (II), and poly-α-aminoisobutyric acid (III).

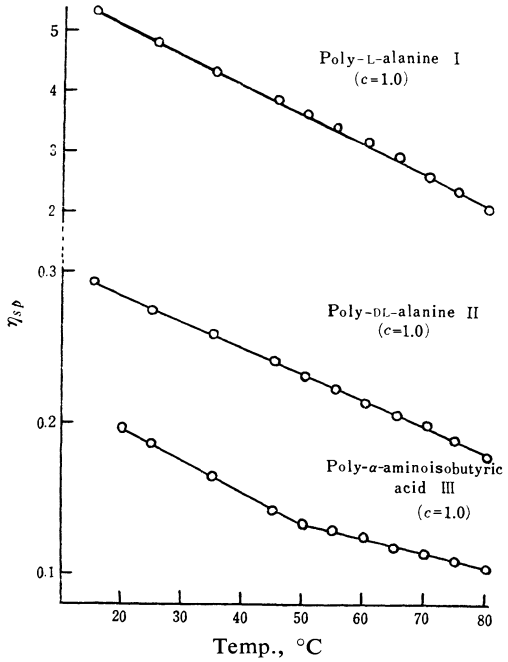


Fig. 6. Specific viscosity in dichloroacetic acid.
(Measured after keeping for 30 min. at each temp.)

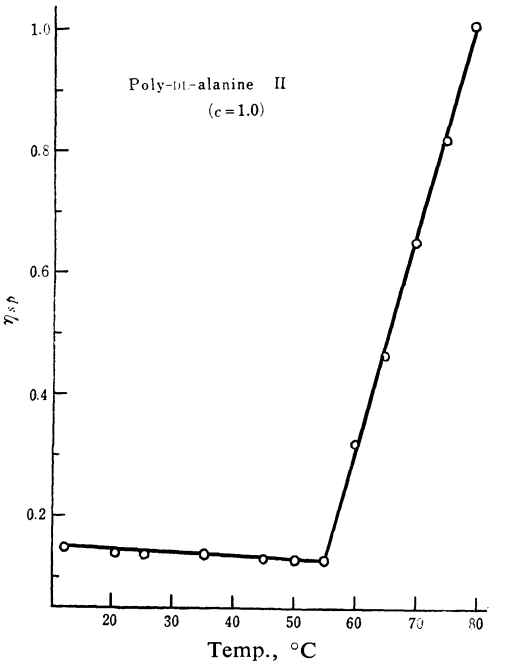


Fig. 7. Specific viscosity in water.
(Measured after keeping for 2 hrs. at each temp.)

Specific Viscosity.—The specific viscosities of I, II and III in 1% dichloroacetic acid solutions were measured in an Ostwald viscosimeter at varying temperatures, as is shown in Fig. 6. The specific viscosity decreased with a rise in the temperature. The viscosity of I and II decreased linearly, while the viscosity of III was observed to have a transition point at 50°C. In a dichloroacetic acid solution, the change in viscosity was not great. II was water-soluble; the specific viscosity in an aqueous solution is shown in Fig 7. The measurements of viscosity were carried out after the substance had stood for two hours at each temperature. In this case, the specific viscosity decreased slightly until the temperature reached 55°C but it increased rapidly when the temperature exceeded 55°C. This finding is consistent with Ebata's report,[11] in which the aqueous solution of poly-ε-aminocapryol-DL-alanine showed a minimum viscosity at about 55°C, with an increase at higher temperatures. This effect may be due to the influence of alanine residues in the polymer. The aqueous solution of II at more than a 4% concentration formed a gel at 60°C or a higher temperature, as has been reported by Elliott.[6]

Differential Thermal Analyses.—The differential thermal analytical data for I, II and III are shown in Fig. 8. With polymer I, an endothermal change was observed from 38 to 120°C, with polymer II, from 60 to 160°C, and with polymer III, from 50 to 120°C. The

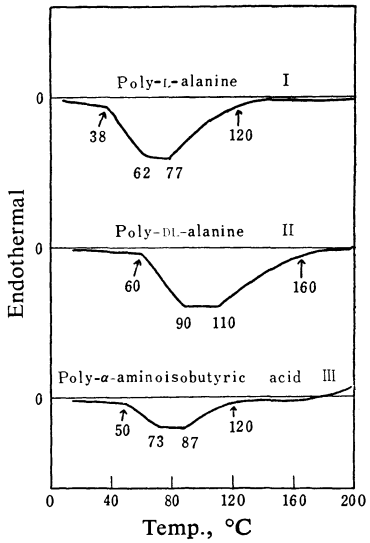


Fig. 8. Differential thermal analyses.

11) M. Ebata, This Bulletin, 33, 899 (1960).

maximum endothermal change was observed from 62 to 77°C, from 90 to 110°C and from 73 to 87°C, respectively, for the polymers I, II and III. The endothermal changes of poly-DL-alanine (II) and poly-α-aminoisobutyric acid (III) started at 60 and 50°C respectively, they are in good agreement with the viscosity and heat coagulation curves.

Infrared Analyses.—The infrared absorption spectra of I, II and III that were measured at room temperature were compared with the spectra that were measured at the maximum endothermal value temperature in the differential thermal analyses, i.e., at 62°C for I, at 100°C for II and at 80°C for III (Fig. 9). The

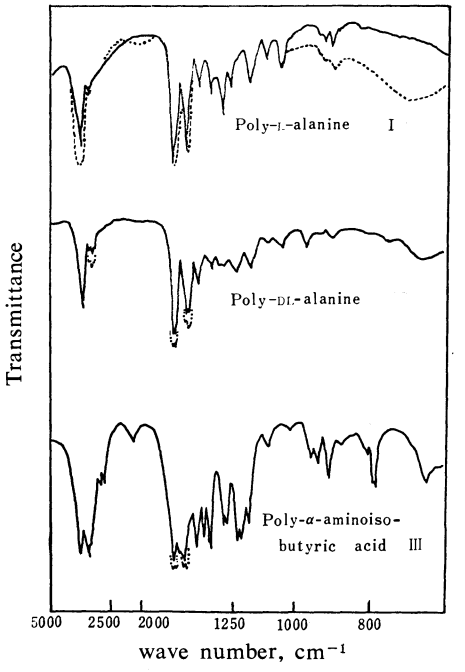


Fig. 9. Infrared absorption spectra.

observations were carried out after two hours at the above-mentioned temperatures. The dotted lines in Fig. 9 depict the spectra observed at higher temperatures, which are different from those measured at room temperature. At high temperatures, poly-L-alanine (I) (film) showed a wider absorption at 3300 cm^{-1}, (νNH) and a broader absorption at about 2070 cm^{-1} than the spectra measured at room temperature. In a region longer than 1000 cm^{-1}, the absorption spectra showed a different pattern, which may be due to the conformational changes in the polymer. These differences observed in the absorption spectra disappeared when the sample was cooled to room temperature. The absorption bands at 1660 cm^{-1} (Amide I) and at 1550 cm^{-1} (Amide II) appeared slightly broader when they were measured at a higher temperature. This effect may be due to the shift from the α to the β form. These phenomena were observed more clearly with poly-DL-alanine (II) (film) and poly-α-aminoisobutyric acid (III) (pellet). The absorption bands at 1630 cm^{-1} and at 1530 cm^{-1} in II were relatively weak at room temperature, but they were significantly stronger at 100°C. This behavior may be explained by the shift from the α to the β conformation of the peptide chain. With III, only the 1660 cm^{-1} and 1550 cm^{-1} bands were exhibited at room temperature. At higher temperatures, however, these bands were split, the former into 1660 cm^{-1} and 1630 cm^{-1} and the latter into 1550 cm^{-1} and 1530 cm^{-1}. This might represent a shift to the β-form from the α-form, as has been postulated above. The absorption due to methyl at 2960 cm^{-1} in I and II was strong at a high temperature, and the absorption with III, at about 3000 cm^{-1} was very strong because of the additional methyl group. Again, a conformational change from the α-form to the β-form is assumed to occur at a high temperature.

Conclusion

Poly-α-amino acids containing alanine and α-aminoisobutyric acid, i.e., containing one and two α-methyl groups respectively, have been synthesized. From the findings of coagulation phenomena, specific rotation, specific viscosity and differential thermal analysis, these poly-α-amino acids containing the alanine residue and the α-aminoisobutyric acid residue may be understood to undergo steric structural changes at about 60°C and 50°C respectively. The difference in critical temperature between the above two polymers can be explained by the presence of one more methyl group per residue in the polymer from α-aminoisobutyric acid. From the infrared results a conformational change at high temperature from the α- to the β-form has been inferred.

The author wishes to express his thanks to Professor Junzo Noguchi of Hokkaido University and to Professor Sidney W. Fox and Dr. Kaoru Harada of Florida State University for their helpful suggestions.

Department of Chemistry
Faculty of Science
Kanazawa University
Kanazawa

Syntheses of α-Amino Acid Menthyl Esters

By Kaoru HARADA and Tadao HAYAKAWA

(Received August 20, 1963)

l-Menthol[1] has been used as an optically-active moiety in many kinds of stereochemical studies.[2] However, few α-amino acid menthyl esters have been prepared[3] because the conventional esterification methods, such as the hydrogen chloride or sulfuric acid methods, fail to give satisfactory results.

In this paper a new method of preparing α-amino acid menthyl esters is described. The method involves a direct esterification of α-amino acids with menthol, using a Dean and Stark distillation tube[4,5] in azeotropic distillation. *p*-Toluenesulfonic acid was used as a catalyst, and benzene or a benzene-toluene mixture was used as the solvent.[5] The α-amino acid menthyl esters thus prepared were isolated as hydrochlorides; they are abbreviated as amino acid M. HCl.

DL-, D- and L-Amino acid M. HCl's were prepared. It was found that the solubility of D-amino acid M. HCl was generally smaller than that of L-amino acid M. HCl. The fractionation of the diastereomers of DL-amino acid M. HCl during the isolation and recrystallization was checked by comparing the $[\alpha]_D$ value of the DL-amino acid M. HCl with those of the synthesized L- and D-amino acid M. HCl's. The $[\alpha]_D$ values of L-phenylalanine M. HCl and D-phenylalanine M. HCl were $-20.8°$ and $-75.1°$ respectively, so the calculated $[\alpha]_D$ value of DL-phenylalanine M. HCl should be $-48.0°$. The $[\alpha]_D$ values of isolated DL-phenylalanine M. HCl were found to be $-51.4°$ and $-55.2°$, before and after recrystallization respectively (Table I). These results showed that the fractionation of diastereomers occurred during the isolation and recrystallization steps. Table I shows that the yield of D-amino acid M. HCl is generally twice as high as that of L-amino acid M. HCl. This means that the rate of the esterification of D-amino acids with menthol is faster than that of L-amino acids. This suggests the possibility of the fractionation of D- and L-amino acid M. HCl's during the synthesis of these esters.

The menthyl esters of D-phenylalanine and D-methionine were resolved by seeding the supersaturated DL-amino acid M. HCl solution with D-phenylalanine M. HCl and D-methionine M. HCl respectively. The 89% optically-active D-phenylalanine M. HCl and the 65% optically-active D-methionine M. HCl were each isolated in one seeding procedure.

Generally, D- and L-amino acid M. HCl's showed sharp melting points, whereas DL-amino acid M. HCl's showed relatively broad melting points because the DL compounds were a mixture of diastereomers. L-Leucine M. HCl and D-leucine M. HCl did not crystallize, so they were converted to *N*-benzoyl derivatives. D-Alanine and L-alanine M. HCl showed similar $[\alpha]_D$ values (L, -67.3; D, -70.9). These compounds were also converted to *N*-benzoyl derivatives (Table II), which also exhibited similar $[\alpha]_D$ values (L, -57.7; D, -43.2). The free α-amino acid menthyl esters were stable and did not form diketopiperazine derivatives after standing a few days at room temperature. It was difficult to apply the esterification method to the hydroxy amino acids (serine, threonine and phenylserine) or to the basic amino acids (arginine and histidine). The reaction conditions, yields, physical properties and elemental analyses are shown in Tables I and II.

These results might be useful in providing standards for the field of stereochemistry or in the asymmetric synthesis of α-amino acid menthyl esters.

Experimental

L-Phenylalanine Menthyl Ester Hydrochloride.—8.26 g. (0.05 mol.) ($[\alpha]_D^{27} = -33.4$, H_2O, *c* 1.50) of L-phenylalanine, 12.0 g. (0.077 mol.) of *l*-menthol ($[\alpha]_D^{27} = -50.0$, abs. EtOH, *c* 3.5), and 12.0 g. 0.063 mol.) of *p*-toluenesulfonic acid monohydrate were mixed with 100 ml. of a benzene-toluene mixture (7 : 3) and refluxed with a Dean and Stark distillation apparatus[4,5] in azeotropic distillation for 24 hr. The nascent water was then removed azeotropically. The insoluble materials (unreacted

1) *l*-Menthol was used throughout in this study; m. p. 42~44°C, $[\alpha]_D^{27} = -50.0°$ (*c* 3.50, in abs. EtOH).

2) A. McKenzie, *J. Chem. Soc.*, **85**, 1249 (1904); A. McKenzie and H. B. P. Humphries, ibid., **95**, 1105 (1909); A. McKenzie and I. A. Smith, *Ber.*, **58**, 899 (1925).

3) A. Shimomura and J. B. Cohen, *J. Chem. Soc.*, **119**, 1816 (1921).

4) J. D. Cipera and R. V. V. Nicholls, *Chem. & Ind.*, **1955**, 16.

5) L. Zervas, M. Winitz and J. P. Greenstein, *J. Org. Chem.*, **22**, 1515 (1957).

TABLE I. α-AMINO ACID MENTHYL ESTER HYDROCHLORIDES, R-CH-COOM
NH₂·HCl

α-Amino acid menthyl ester hydrochloride	Reaction solvent[a]	Reaction time, hr.	Yield %	Recryst. solvent[b]	M. p. °C[c]	After recryst. $-[\alpha]_D^{26\sim27}$ [d]	c	Molecular formula	Calcd., %			Found, %		
									C	H	N	C	H	N
Gly	B	24	88	Et	*253~256	66.9	0.615	$C_{12}H_{24}O_2NCl$	57.70	9.68	5.61	57.10	9.78	5.54
L-Ala	B-T	30	69	A	218	67.3	1.14	$C_{13}H_{26}O_2NCl$	59.18	9.93	5.31	59.41	9.70	5.13
D-Ala	B-T	30	79	A	188~189	70.9	1.08	$C_{13}H_{26}O_2NCl$	59.18	9.93	5.31	59.12	9.93	5.08
DL-Ala	B-T	30	58	A	*166~168	70.2	1.03	$C_{13}H_{26}O_2NCl$	59.18	9.93	5.31	59.19	9.78	5.30
L-Val	B-T	24	11	A	224~225	48.3	0.697	$C_{15}H_{30}O_2NCl$	61.72	10.36	4.80	61.72	10.28	4.72
D-Val	B-T	24	23	A	209~210	78.6	0.701	$C_{15}H_{30}O_2NCl$	61.72	10.36	4.80	61.95	10.24	4.52
DL-Val	B-T	24	17	A	183~185	62.9	0.839	$C_{15}H_{30}O_2NCl$	61.72	10.36	4.80	61.43	10.26	4.67
L-Leu	B-T	24	—	—	Oil	—	—	$C_{16}H_{32}O_2NCl$	62.82	10.55	4.58	—	—	—
D-Leu	B-T	24	—	—	Oil	—	—	$C_{16}H_{32}O_2NCl$	62.82	10.55	4.58	—	—	—
DL-Leu	B-T	24	64	E-PE	*87~ 90	51.9	0.847	$C_{16}H_{32}O_2NCl$	62.82	10.55	4.58	62.96	10.30	4.51
L-α-NH_2-but	B-T	48	33	A	207~208	55.7	0.912	$C_{14}H_{28}O_2NCl$	60.52	10.16	5.04	60.41	10.06	4.90
D-α-NH_2-but	B-T	48	71	A	185~186	74.5	0.768	$C_{14}H_{28}O_2NCl$	60.52	10.16	5.04	60.21	9.80	5.05
DL-α-NH_2-but	B-T	48	76	Et	159~162	67.0	0.735	$C_{14}H_{28}O_2NCl$	60.52	10.16	5.04	60.99	9.90	4.97
L-Phe	B-T	24	32	Et	165~166	20.8	0.774	$C_{19}H_{31}O_2NCl$	66.93	9.16	4.10	66.89	8.90	4.26
D-Phe	B-T	24	75	A	185~186	75.1	1.07	$C_{19}H_{31}O_2NCl$	66.93	9.16	4.10	66.65	8.92	4.16
DL-Phe	B-T	24	66	A	*147~160	55.2	0.743	$C_{19}H_{31}O_2NCl$	66.93	9.16	4.10	67.05	9.15	4.20
L-Met	B-T	24	31	Et	115~116	42.4	1.03	$C_{15}H_{30}O_2NSCl$	55.61	9.33	4.32	55.95	9.19	4.42
D-Met	B-T	24	73	Et	154~156	63.4	1.02	$C_{15}H_{30}O_2NSCl$	55.61	9.33	4.32	55.66	9.34	4.32
DL-Met	B-T	24	41	Et	*115~122	50.8	0.702	$C_{15}H_{30}O_2NSCl$	55.61	9.33	4.32	55.98	9.36	4.37
L-Pro	B	30	64	A	185	87.0	0.975	$C_{15}H_{27}O_2NCl$	62.16	9.74	4.83	62.39	9.55	4.83
DL-Pro	B	30	41	A	*142~166	71.2	0.859	$C_{15}H_{27}O_2NCl$	62.16	9.74	4.83	62.00	9.89	5.01
DL-Phenylgly	B-T	24	52	A	*153~156	63.0	1.15	$C_{18}H_{28}O_2NCl$	66.34	8.66	4.30	66.74	8.53	4.30

a) Solvent: B=benzene; B-T=benzene-toluene mixture (7:3)
b) Recrystallization solvent: A=alcohol and ether; Et=ethyl acetate and ether; E-P=ether and petroleum ether
c) All melting points are uncorrected.
d) Optical rotation: All samples were measured in abs. ethanol at 26~27°C.
All samples exhibited negative rotations.
* Melting points are not sharp.

TABLE II. BENZOYL DERIVATIVES OF AMINO ACID MENTHYL ESTER, BzNH-CH(R)-COOM

Benzoyl-amino acid menthyl ester	Yield %	Recryst. solvent[a]	M. p. °C[b]	After recryst. $-[\alpha]_D^{26\sim27}$[c]	c	Molecular formula	Calcd., % C	H	N	Found, % C	H	N
Bz gly	88	E-PE	105~106	51.0	0.772	$C_{19}H_{27}O_3N$	71.89	8.57	4.41	71.87	8.63	4.37
Bz L-ala	85	E-PE	112~113	57.7	0.852	$C_{20}H_{29}O_3N$	72.47	8.82	4.23	72.71	9.01	4.07
Bz D-ala	63	E-PE	93~ 94	43.2	0.845	$C_{20}H_{29}O_3N$	72.47	8.82	4.23	72.65	9.09	4.10
Bz DL-ala	86	E-PE	104~105	50.9	0.893	$C_{20}H_{29}O_3N$	72.47	8.82	4.23	72.72	8.91	4.08
Bz L-leu	75	E-PE	119~121	60.6	0.824	$C_{23}H_{35}O_3N$	73.95	9.45	3.75	73.90	9.56	3.68
Bz D-leu	76	E-PE	110~112	28.6	0.802	$C_{23}H_{35}O_3N$	73.95	9.45	3.75	74.03	9.28	3.70
Bz DL-leu	81	E-PE	112~114	41.7	0.796	$C_{23}H_{35}O_3N$	73.95	9.45	3.75	74.18	9.56	3.81
p-NO_2Bz gly	55	Et	160~163	43.6	0.982	$C_{19}H_{26}O_5N_2$	62.96	7.23	7.73	63.46	7.09	7.97

a) Recrystallization solvent: E-PE=ether and petroleum ether; Et=ethyl acetate and ether
b) All melting points are uncorrected.
c) All samples were measured in abs. ethanol at 26~27°C. All samples exhibited negative rotations.

L-phenylalanine and its *p*-toluenesulfonate) were removed by filtration, and the solvent was evaporated to about 30 ml. in vacuo. To this was added about 30 ml. of ether, and then the acidic material was extracted with 8% sodium hydrogen carbonate. The organic layer was washed once with water and dried with anhydrous sodium sulfate. To this dried solution, dry hydrogen chloride gas was introduced to precipitate the L-phenylalanine M. HCl. The crystals were filtered and washed with ether and petroleum ether. Yield, 5.45 g. (32%); $[\alpha]_D^{27}=-21.8°$ (*c* 0.623, in abs. EtOH). This was recrystallized from ethyl acetate and ether.

***l*-Menthyl *N*-Benzoyl L-Leucinate.**—3.28 g. (0.025 mol.) ($[\alpha]_D^{27}=+15.3°$, 5 N HCl, *c* 2.01) of L-leucine, 6.0 g. (0.0385 mol.) of menthol, and 6.0 g. (0.0315 mol.) of *p*-toluenesulfonic acid monohydrate were mixed with 50 ml. of a benzene-toluene mixture (7 : 3) and refluxed with the Dean and Stark distillation apparatus[4,5] for 24 hr. The reaction mixture was then filtered and the solvent removed in vacuo to about 20 ml. Then 20 ml. of ether was added to the solution, and this was extracted with 8% sodium hydrogen carbonate three times. The organic layer was dried with anhydrous sodium sulfate. Dry hydrogen chloride was introduced into the free menthyl ester solution. No hydrochloride of the menthyl ester crystallized. The solvent was removed, and the syrupy ester hydrochloride was dissolved in ether. The ether solution was extracted with 8% sodium hydrogen carbonate to make the free ester. The ethereal solution of the free menthyl ester was dried with anhydrous sodium sulfate. A part of the solution was titrated in an aqueous condition with 0.1 N hydrochloric acid, using methyl red as an indicator to determine the free ester content (0.015 mol., 60%). The solution was then strongly agitated, together with a slight excess of benzoyl chloride (2.39 g., 0.017 mol.) and triethylamine (1.82 g., 0.018 mol.) in ice water. The reaction mixture was washed with 5% sodium hydrogen carbonate, 0.5 N hydrochloric acid, and water. The ethereal solution was dried with anhydrous sodium sulfate. To this solution, petroleum ether was added to precipitate the *N*-benzoyl L-leucine menthyl ester. Yield, 3.84 g. (0.0103 mol.); 75% from free ester. $[\alpha]_D^{27}=-61.0°$ (*c* 0.960, in abs. EtOH). This was recrystallized from ether and petroleum ether.

Benzoyl D-, L- and DL-Alanine Menthyl Ester.—The benzoylation of the D-, L- and DL-alanine menthyl esters was carried out by the use of sodium ethoxide and benzoyl chloride in absolute alcohol. The yields of the benzoyl derivatives were 85.2, 63.2 and 86.2% respectively. Physical and analytical data are shown in Table II. The *p*-nitrobenzoyl glycine menthyl ester was also prepared by the use of sodium ethoxide and *p*-nitrobenzoyl chloride in absolute alcohol; yield, 55.0%.

The Fractionation of Diastereomers of the DL-Phenylalanine Menthyl Ester.—Two grams of DL-phenylalanine M. HCl was dissolved in 100 ml. of hot ethyl acetate and filtered. About 3 mg. of powdered D-phenylalanine M. HCl in 5 ml. of absolute ether was then added to the filtrate and kept at room temperature for 3 hr. The D-rich crystals obtained weighed 0.40 g.; $[\alpha]_D^{27}=-72.1°$ (*c* 1.25, in abs. EtOH) (D : 94.5%; L : 5.5%). To the mother liquor 80 ml. of ether was added, and the resulting solution was seeded with D-phenylalanine M. HCl. After standing for 3 hr. at room temperature, an additional 0.52 g. of a D-rich fraction was obtained. $[\alpha]_D^{27}=-64.4°$ (*c* 1.05, in abs. EtOH) (D : 80.3%; L : 19.7%). By use of the seeding procedure, the first D-rich crystals were fractionated and obtained as pure D-phenylalanine M. HCl. 0.22 g. $[\alpha]_D^{27}=-75.6$ (*c* 1.29, in abs. EtOH).

The fractionation of DL-methionine M. HCl (1.0 g.) followed essentially the same pattern. However, crystallization was carried out by lefting it stand in the cold for three days. 0.32 g. of D-rich crystals were obtained. $[\alpha]_D^{27}=-59.7°$ (D : 82.7%; L : 17.3%). From the mother liquor, an additional 0.30 g. of D-rich fraction was obtained by evaporation, $[\alpha]_D^{27}=-54.6°$ (D : 55.6%; L : 44.4%).

This work was supported by National Aeronautics and Space Administration Grant No. NsG-173-62. Contribution No. 18 of the Institute for Space Biosciences. The authors

wish to express their sincere appreciation to Professor Sidney W. Fox of Florida State University for his advice. Thanks are also extended to Mr. David Joseph for his measurements of the optical rotation.

Institute for Space Biosciences and
Department of Chemistry
Florida State University
Tallahassee, Florida, U. S. A.

The Synthesis and Configurational Analysis of 2-Amino-1,3-cyclohexanediol

By Tetsuo SUAMI and Seiichiro OGAWA

(Received August 10, 1963)

Interest in inosamine and inosadiamine has been stimulated by their occurrence in certain antibiotics. The previous studies of 2-amino-cyclohexanol derivatives[1,2] have stimulated our interest in the synthesis of alicyclic compounds which have three neighboring groups. An attempt to prepare 2-amino-1, 3-cyclohexanediol was abandoned by McCasland et al. because of the poor yield of a corresponding nitrodiol.[3] Very recently, however, Lichtenthaler[4] synthesized two diastereomeric 2-amino-1, 3-cyclohexanediols (trans and DL-isomers) through the nitrodiol obtained by the cyclization of glutaraldehyde with nitromethane.

In the present paper, synthetic routes to another diastereomeric 2-amino-1, 3-cyclohexanediol (cis isomer) will be described, and its structure assignment will be made by means of the proton magnetic resonance spectrum of its acetyl derivative.

The cyclization of glutaraldehyde with nitromethane in the presence of sodium carbonate gave 2-nitro-1, 3-cyclohexanediol (IV).[4] Hydrogenation with Raney nickel, T4,[5] gave 2α-amino-1β, 3β-cyclohexanediol (Ia) in a 63% yield. In order to establish the configurational purity of Ia, paper chromatography was employed. The compound, Ia, consumed 1.91 mol. of the periodate in an aqueous solution in 20 hr., showing a single spot (R_f 0.59) in 1-butanol-ethanol-water (2 : 1 : 3), and also a single spot (R_f 0.45) in 1-butanol-acetic acid-water (4 : 1 : 5). These data provide strong, if not conclusive, evidence that Ia is a single isomer.

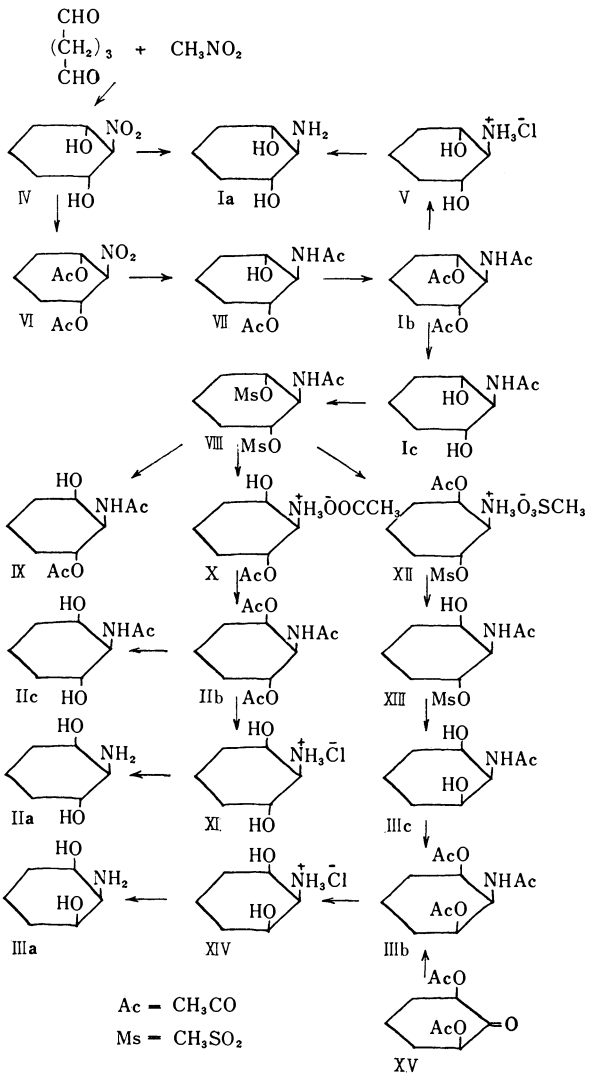
The acetylation of IV with acetic anhydride and a small amount of concentrated sulfuric acid gave di-*O*-acety-2-nitro-1, 3-cyclohexanediol (VI).[4] VI was hydrogenated with Raney nickel, T4,[5] to give 2α-acetamido-*O*-aecty-1β, 3β-cyclohexanediol (VII) in a 75% yield; this might be obtained through the O→N migration of an acetyl group[6] during the course of reduction. VII was further acetylated to give the triacetyl derivative of Ia, Ib, in a 83% yield. Under Kunz's conditions,[7] Ib was selectively deacetylated; this showed the presence of two hydroxyl groups. The *N*-acetyl derivative Ic was recovered from the neutralized solution of Kunz's hydrolysis. Ic did not consume any periodate in an aqueous methanol solution in 50 hr. These data are consistent with a cyclic structure with one acetamido group between two hydroxyl groups.

To obtain the other diastereomers of Ia, an inversion reaction of its mesyl derivative was employed. When a cyclohexane ring containing vicinal mesyloxy and acylamido groups in the trans position was treated with sodium acetate in refluxing aqueous 2-methoxyethanol, the replacement of the mesyloxy group takes place with Walden inversion through an intermediary oxazolinium ion to give *cis*-acylamido alcohol.[8] On the other hand, when vicinal mesyloxy and acylamido groups are in the cis position, the replacement of the mesyloxy group takes place at a considerably slower rate.[9]

1) T. Suami, S. Ogawa and S. Umezawa, This Bulletin, **35**, 474 (1962).
2) T. Suami, S. Ogawa and S. Umezawa, ibid., **36**, 459 (1963).
3) G. E. McCasland, T. J. Matchett and M. Hollander, *J. Am. Chem. Soc.*, **74**, 3429 (1952).
4) F. W. Lichtenthaler, *Chem. Ber.*, **96**, 845 (1963).
5) S. Nishimura, This Bulletin, **32**, 61 (1959).
6) G. Fordor and J. Kiss, *J. Am. Chem. Soc.*, **72**, 3495 (1950).
7) A. Kunz and C. S. Hudson, ibid., **48**, 1982 (1926).
8) S. Winstein and R. E. Buckles, ibid., **64**, 2787 (1942); G. E. McCasland, R. K. Clark, Jr., and H. E. Carter, ibid., **71**, 637 (1949); S. Winstein, L. Goodman and R. Boschan, ibid., **72**, 2311 (1950); T. Taguchi and M. Nakayama, ibid., **73**, 5679 (1951); B. R. Baker and R. E. Schaub, *J. Org. Chem.*, **19**, 646 (1954); B. R. Baker, R. E. Schaub and J. H. Williams, *J. Am. Chem. Soc.*, **77**, 7 (1955); R. W. Jeanloz, ibid., **79**, 2591 (1957); A. C. Richardson and H. O. L. Fischer, ibid., **83**, 1132 (1961).
9) S. Winstein, E. Grunwald, R. E. Buckles and C. Hanson, ibid., **70**, 816 (1948).

The compound, Ic, gave a dimesyl derivative (VIII) by reaction with mesyl chloride in pyridine.[4] The displacement of both mesyloxy groups of VIII gave DL-*O*-acetyl-2α-amino-1α, 3β-cyclohexanediol acetate (X) when the reaction with two moles of sodium acetate was carried out in boiling water for 1 hr. The fact that the replacement of two mesyloxy groups in VIII took place at a considerably higher rate showed that the C-1 and C-3 mesyloxy groups were both situated in the trans position to the C-2 acetamido group.[9] X gave a triacetyl derivative IIb melting at 146°C in a 74% overall yield, after acetylation. Studies of a detailed reaction mechanism in this reaction are in progress.

When IIb was hydrolyzed with 6 N hydrochloric acid, DL-2α-amino-1α,3β-cyclohexanediol hydrochloride (XI) melting at 117°C was obtained. The free base IIa melting at 113°C was recovered from XI with a sodium hydroxide solution. A paper chromatography of IIa showed a single spot (R_f 0.49) in 1-butanol-acetic acid-water (4 : 1 : 5).

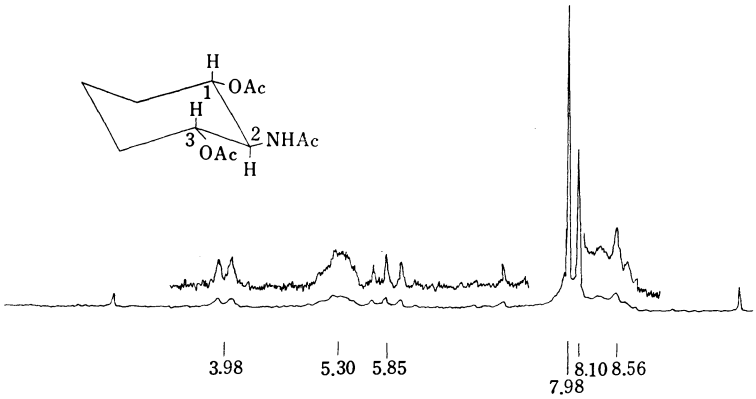


When VIII was refluxed in water for a few minutes, without adding any sodium acetate, DL-*O*-acetyl-*O*-mesyl-2α-amino-1α, 3β-cyclohexanediol methanesulfonate (XII) was produced in a 74% yield. In this reaction, the replacement of the mesyloxy group yielded an oxazolinium ion which was attacked by water to give *cis*-acetamido alcohol as usual. Then the acetyl group could migrate from nitrogen to oxygen in an acidic medium to yield XII, which could not have a further inversion because of the lack of an acetamido group adjacent to the mesyloxy group.

When treated with sodium hydroxide solution, XII gave DL-2α-acetamido-*O*-mesyl-1α, 3β-cyclohexanediol (XIII) in a 73% yield. Accordingly, it must involve the O→N migration of the acetyl group.[6] Since XIII had the mesyloxy group situated in the trans position to the vicinal acetamido group, a further inversion was expected. XIII was refluxed in 95% aqueous 2-methoxyethanol for 5 hr. to yield the *N*-acetyl derivative IIIc melting at 121.5°C with an inversion of the configuration. IIIc was acetylated to give the triacetyl derivative IIIb melting at 179°C.

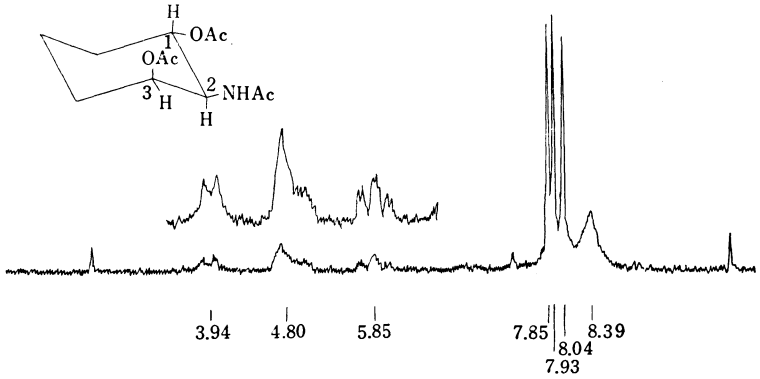
IIIb was also obtained via a different synthetic route starting from *cis*-2, 6-diacetoxycyclohexanone (XV). XV was prepared by the oxidation of cyclohexanone with lead tetraacetate in boiling benzene.[10] The structure and configuration of XV were established by converting it to 1α, 2α, 3α-cyclohexanetriol of a known configuration.[11] Anderson and Lardy[12] found that the primary amine obtained from the phenylhydrazone or oxime of *scyllo*-inosose practically consisted of a single isomer, when glacial acetic acid was used as a solvent and Adams platinum oxide, as a catalyst. Therefore, the reduction of *cis*-2, 6-diacetoxycyclohexanone oxime was carried out using the procedure of Anderson and Lardy.[12] Then the crude reduction product was treated with acetic anhydride in pyridine to obtain the compound, which was identical with IIIb. However, the yield was unexpectedly low. Since the starting material, XV, had a known configuration, the only point requiring to be clarified was the configuration of the newly-introduced amino group. The steric selectivity of the reduction condition employed in this

10) G. W. K. Cavill and D. H. Solomon, *J. Chem. Soc.*, **1955**, 4427.
11) T. Posternak and F. Ravenna, *Helv. Chim. Acta*, **80**, 441 (1947).
12) L. Anderson and H. A. Lardy, *J. Am. Chem. Soc.*, **72**, 3141 (1950).



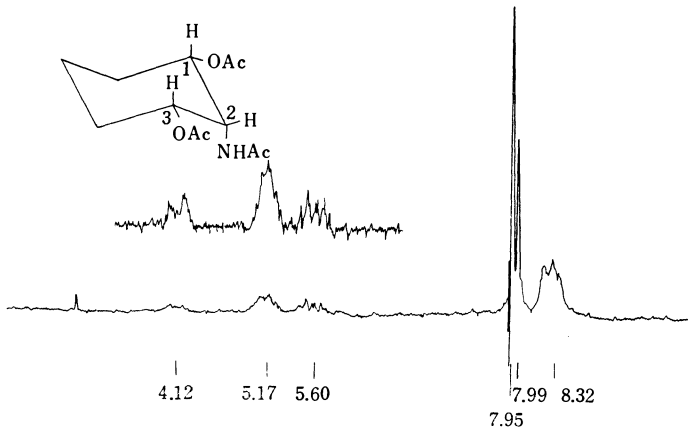
p. p. m., $H \rightarrow$

Fig. 1-A.



p. p. m., $H \rightarrow$

Fig. 1-B.



p. p. m., $H \rightarrow$

Fig. 1-C.

Fig. 1. NMR spectra in deuteriochloroform at 60 Mc.
Peak positions are given in τ-values.

synthesis seemed ample enough to enable us to assign IIIb as all-cis configuration.

IIIb was hydrolyzed with 6 N hydrochloric acid to give 2α-amino-1α, 3α-cyclohexanediol hydrochloride (XIV) melting at 161.5°C. The free base IIIa melting at 128°C was obtained from XIV by an ordinary method. A paper chromatography of IIIa showed a single spot (R_f 0.44) in 1-butanol-acetic acid-water (4 : 1 : 5).

The above consideration of the configuration of IIIb has been fully substantiated by means of its proton magnetic resonance spectra, as will be described below.

The protons of the acetoxy and acetamido groups of Ib and IIb have already been assigned by Lichtenthaler.[4] In the present study, the NMR spectrum of the compound, IIIb, gave two sharp signals of a 2 : 1 relative intensity (cf. Fig. 1-C), as was to be expected from the two equatorial acetoxy groups (τ of 7.95) and the axial acetamido group (τ of 7.99).

Lemieux et al.[13] assigned the configurations of two diastereomeric 2-acetoxy-1, 3-dimethoxycyclohexanes on the basis of the fine structure of an axial proton on C-2 in their NMR spectra. In the present experiments, the axial proton on C-2 of Ib was coupled with the two axial protons on the neighboring carbon atoms (C-1 and C-3) ; the signal for this proton should be a triplet with an intensity of 1 : 2 : 1 (J_{aa}=8~11.5 c.p.s.).[14] As Fig. 1-A shows, Ib was readily recognized as a trans isomer by the triplet centered at 5.85 with a 1 : 2 : 1 relative intensity (observed J=10.5 c.p.s.). In the case of IIb, the proton on C-2 was coupled with an axial proton (C-1 or C-3) and an equatorial proton (C-3 or C-1). Since the coupling between an equatorial proton and an axial proton was considerably weaker than that between two axial protons, the signal for the proton on C-2 could be anticipated to be a quartet. However, the sextuplet at 5.85 in the observed spectrum of IIb shown in Fig. 1-B could not be interpreted without counting the spin-spin coupling between the proton on C-2 and the proton on the nitrogen atom.[15] The spin-spin coupling constant between the proton on C-2 and the proton on the nitrogen atom in the trans orientation was about 9.0 c.p.s. (observed value); this value was close to that of the observed J_{aa}.

Also in the case of IIIb, it could be distinguished from the others by its lack of an axial proton on C-2. In Fig. 1-C, the signal for the proton on C-2 appears in a lower field (centered at 5.60) ; it can be recognized that this proton is in an equatorial position.

The signal of the protons on C-1 and C-3 was not well resolved, but the width of the signal presented some information on the configurations. The spin-spin coupling constant was greater between two axial protons than between axial-equatorial, or two equatorial protons.[16] Therefore, the most narrow peak width observed in Fig. 1-C was consistent with the assigned configuration of IIIb. The peak widths are listed in Table I.

Table I. Chemical shifts expressed in τ-values

Protons (C-1 and C-3)		Peak width c.p.s.
Ib	5.30	30
IIb	4.80	30
IIIb	5.17	17

The other six protons showed a signal at 8.32~8.56, as was expected from the ring protons of cyclohexane in the chair conformation.[17]

As a result of these considerations of the NMR spectra and the chemical evidence, it has been concluded that the compound IIIb (m. p. 179°C) has the cis configuration, and Lichtenthaler's assignmets for the Ib and IIb compounds have been further confirmed. All three predicted diastereomers of 2-amino-1, 3-cyclohexanediol have now been synthesized.

Experimental

All melting points are corrected, and unless noted otherwise, they were measured in a liquid bath. The melting points marked with asterisks were measured on a Mitamura-Riken micro hot stage. The NMR spectra of all the acetyl derivatives were determined at a frequency of 60 Mc. with a Japan Electron Optics instrument JNM-C-60 in deuteriochloroform containing tetramethylsilane as an internal reference. The peak positions are given in τ-values. The infrared spectra were recorded in potassium bromide pellets.

2α-Nitro-1β, 3β-cyclohexanediol (IV). — By the method of Lichtenthaler,[4] the cyclization of glutaraldehyde with nitromethane gave IV in a 59.5% yield ; m. p. 161.5~163.5°C (recrystallized from ethyl acetate). (Reported m. p. 159~161°C).[4] (Found : C, 44.92 ; H, 6.70 ; N, 8.71%).

2α-Amino-1β, 3β-cyclohexanediol (Ia).—A mixture of 5.0 g. of IV and 50 ml. of absolute ethanol was hydrogenated at room temperature under 40 p. s. i. g. of initial hydrogen pressure with a Raney

13) R. U. Lemieux, R. K. Kullnig and R. Y. Moir, ibid., **80**, 2237 (1958).
14) W. F. Trager, F. F. Vincenzi and A. G. Huitric, *J. Org. Chem.*, **27**, 3006 (1962).
15) J. A. Pople, W. G. Schneider and H. J. Bernstein, "High-resolution Nuclear Magnetic Resonance," McGraw-Hill, New York (1959), pp. 366~371 ; L. H. Piette, L. D. Ray and R. A. Ogg, *J. Mol. Spectroscopy*, **2**, 66 (1958).
16) S. Brownstein and R. Miller, *J. Org. Chem.*, **24**, 1886 (1959).
17) F. R. Jensen, D. S. Noyce, C. H. Sederholm and A. J. Berlin, *J. Am. Chem. Soc.*, **84**, 386 (1962).

nickel T4 catalyst,[5] obtained from 7.0 g. of Raney nickel alloy, in a Parr shaker-type hydrogenation apparatus for 1 hr. After the catalyst had been removed by filtration, the filtrate was evaporated under reduced pressure. The residue was recrystallized from absolute ethanol to yield 2.3 g. (56%) of needles melting at 190.5~193.5°C (decomp.). The second crop of the product (0.25 g.) was obtained from the mother liquor. The total yield was 62.5%. Recrystallization from ethanol gave an analytically pure sample melting at 191.5~193.5°C (decomp).

Found: C, 54.77; H, 9.72; N, 10.74. Calcd. for $C_6H_{13}NO_2$: C, 54.94; H, 9.99; N, 10.68%.

Paper Chromatography. — 1-Butanol-ethanol-water (2 : 1 : 3) gave a single spot of R_f 0.59 (R_f of D-glucosamine hydrochloride : 0.33) in ascending development at 23°C. The spot was developed with ninhydrin. Both the pure crystals and the crude product gave a single spot in the same R_f region, and no other spot was observed.

Also, an upper layer of 1-butanol-acetic acid-water (4 : 1 : 5) gave one spot of R_f 0.45 in acending development at 25°C (R_f of D-glucosamine hydrochloride : 0.14).

Periodate Oxidation.—A mixture of 100 mg. of Ia was treated with 100 ml. of a 0.1 M sodium metaperiodate solution at 24°C. Iodometric titrations with sodium arsenite[18] revealed that 1.91 mol. of periodate had heen consumed per mole of Ia in 20 hr.

Di-*O*-acetyl-2α-nitro-1β, 3β-cyclohexanediol (VI).—The acetylation of IV with a mixture of acetic anhydride and a small amount of concentrated sulfuric acid gave a crude product in a 79% yield.[4] (Found: C, 49.02; H, 6.05; N, 5.60%).

***N, O*-Diacetyl-2α-amino-1β, 3β-cyclohexanediol (VII).**—A mixture of 10 g. of VI and 120 ml. of absolute ethanol was hydrogenated, as described in the hydrogenation of IV, to yield 6.6 g. (75.2%) of pale yellow crystals. The crude product was recrystallized from benzene to yield 5.4 g. (61.6%) of colorless needles melting at 126~130°C. An analytical sample was further recystallized from benzene; it melted at 130.5~131.5°C.

Found: C, 55.62; H, 8.24; N, 6.63. Calcd. for $C_{10}H_{17}NO_4$: C, 55.80; H, 7.96; N, 6.51%.

IR: 3420 (OH), 1626, 1566 (amide) and 1745 (ester) cm^{-1}.

Triacetyl-2α-amino-1β, 3β-cyclohexanediol (Ib).—A 2.0 g. portion of the crude product of VII was acetylated with 20 ml. of acetic anhydride and 20 ml. of pyridine at room temperature overnight. The mixture was then evaporated under reduced pressure. The product was recrystallized from ethanol to give 1.98 g. (83.0%) of needles melting at 152~152.5°C.

Found: C, 56.17; H, 7.20; N, 5.56. Calcd. for $C_{12}H_{19}NO_5$: C, 56.02; H, 7.44; N, 5.44%.

The product was identified with the triacetyl derivative[4] on the basis of a mixed melting point determination and infrared spectra.

2α-Acetamido-1β, 3β-cyclohexanediol (Ic). — Ib gave 2.15 mol. of acetic acid on hydrolysis under Kunz's conditions.[7]

18) J. M. Bobbitt, "Advances in Carbohydrate Chem.," Vol. XI, Academic Press, Inc., New York (1956), pp. 1—41.

The neutralized hydrolyzate was evaporated in vacuo and the residue was extracted with acetone. The combined acetone extract was evaporated to yield a crude product of *N*-acetyl derivative Ic. The product was recrystallized from ethanol to yield 48 mg. (28.2%) of crystals melting at 208.5~210°C. (Found: C, 55.60; H. 8.64; N, 8.31%). A mixed melting point determination with an authentic sample[4] was undepressed.

The porduct (200 mg.) did not consume any periodate in 50 hr. in a mixture of 40 ml. of a 0.1 M sodium metaperiodate solution and 10 ml. of methanol at 26°C.

2α-Amino-1β, 3β-cyclohexanediol Hydrochloride (V).—A mixture of 200 mg. of Ib and 10 ml. of 6 N hydrochloric acid was refluxed for 6 hr. The hydrolyzed solution was evaporated under reduced pressure to dryness, the residue was dissolved in 2 ml. of absolute ethanol, and 6 ml. of absolute ether was added. The mixture was stored in a refrigerator to yield 100 mg. (77%) of needles melting at 143.5~145.5°C. The mixed melting point determination with an authentic sample[4] was undepressed.

The free base, Ia, was regenerated from V by dissolving a 374 mg. portion of V in 30 ml. of a 0.5 N sodium hydroxide solution. The mixture was evaporated, and the residue was extracted with absolute ethanol to yield 217 mg. (74%) of crystals melting at 188.5~190.5°C (decomp.)., the melting point being undepressed upon adimxture with Ia.

2α-Acetamido-di-*O*-mesyl-1β, 3β-cyclohexanediol (VIII).—Ic gave VIII by a reaction with mesyl chloride in pyridine[4] in an 80% yield. Recrystallization from 95% ethanol afforded colorless needles melting at *153~154°C (Found: C, 36.86; H 5.96; N, 4.27; S, 19.43%).

DL-*N,O*-Diacetyl-2α-amino-1α, 3β-cyclohexanediol (IX).—VIII was refluxed with sodium acetate and 95% aqueous 2-methoxyethanol for 6 hr. to yield IX in a 36% yield.[4] The crude product was recrystallized from ethanol-ether to yield colorless plates melting at *148~152°C (Found: C, 55.96; H, 7.98; N, 6. 43%).

DL-*O*-Acetyl-2α-amino-1α, 3β-cyclohexanediol Acetate (X).—A mixture of 5.0 g. of VIII, 2.75 g. of anhydrous sodium acetate, and 100 ml. of water was refluxed for 1 hr. Then the mixture was evaporated under reduced pressure to dryness. The residue was extracted with boiling acetone repeatedly. The combined acetone extract was evaporated under reduced pressure to yield a crystalline residue. The residue was washed with a small amount of cold acetone to give 1.3 g. (20%) of colorless needles melting at 104~113°C. Recrystallization from acetone afforded needles melting at 130.5~132°C; these were shown by infrared spectrum and elementary analysis to be DL-*O*-acetyl-2α-amino-1α, 3β-cyclohexanediol acetate.

Found: C, 51.33; H, 8.44; N, 6.14. Calcd. for $C_{10}H_{19}NO_5$: C, 51.49; H, 8.21; N, 6.01%.

IR: 3200 (OH), 1725 (ester), 1638 (NH_3^+), 1547 and 1403 (COO^-) cm^{-1}.

DL-Triacetyl-2α-amino-1α, 3β-cyclohexanediol (IIb).—A mixture of crude X, obtained from 5.0 g. of VIII, 25 ml. of acetic anhydride, and 25 ml.

of pyridine, was left to settle at room temperature overnight and then heated at 80°C for 1 hr. The mixture was evaporated under reduced pressure and the residue was dissolved in 100 ml. of chloroform. The chloroform solution was washed with cold water, dried over anhydrous sodium sulfate, and then evaporated in vacuo to dryness. Crystallization of the residue with a mixture of benzene and petroleum ether gave 2.9 g. (74%) of the product melting at 140.5~143.5°C. Recrystallization from benzene afforded colorless crystals melting at 144.5~146.5°C.

Found: C, 55.81; H, 7.35; N, 5.39. Calcd. for $C_{12}H_{19}NO_5$: C, 56.02; H, 7.44; N, 5.44%.

DL-2α-Acetamido-1α, 3β-cyclohexanediol (IIc).—IIb was treated with methanol saturated by ammonia to give the crude product in a 74% yield.[4] (Found: C, 55.65; H, 8.37; N, 8.46%).

DL-2α-Amino-1α, 3β-cyclohexanediol Hydrochloride (XI).—A mixture of 0.3 g. of IIb and 15 ml. of 6 N hydrochloric acid was refluxed for 7 hr. The mixture was evaporated under reduced pressure to dryness. The residue was dissolved in 4 ml. of absolute ethanol, and absolute ether was added. The mixture was kept in a refrigerator to yield 0.13 g. (67%) of crystals melting at 111~117°C. The product was recrystallized from absolute ethanol-ether to yield needles melting at 115~117°C after sintering at 110°C.

Found: C, 42.89; H, 8.40; N, 8.18; Cl, 21.33. Calcd. for $C_6H_{14}NClO_2$: C, 42.99; H, 8.42; N, 8.36; Cl, 21.15%.

DL-2α-Amino-1α, 3β-cyclohexanediol (IIa).—A 517 mg. portion of XI was treated, as described in the regeneration of Ia from V, to yield 400 mg. (98%) of a crude product which crystallized gradually in a vacuum desiccator. The crude product was recrystallized from absolute ethanol-ether to give hygroscopic crystals melting at *112~113°C.

Found: C, 54.81; H, 10.01; N, 10.89. Calcd. for $C_6H_{13}NO_2$: C, 54.93; H, 9.99; N, 10.68%.

Paper Chromatography.—A nupper layer of 1-butanolacetic acid-water (4 : 1 : 5) gave a single spot of R_f 0.49 in ascending development at 25°C.

DL-*O*-Acetyl-*O*-mesyl-2α-amino-1α, 3β-cyclohexanediol Methanesulfonate (XII).—A mixture of 5.0 g. of VIII and 70 ml. of water was refluxed for a few minutes to give a clear acidic solution (pH 1.0). After standing ovenight, the solution was evaporated under reduced pressure. The residue was recrystallized from ethanol to yield 3.6 g. (68%) of crystals melting at *173~174°C. A second crop of the product (0.3 g.) was obtained from the mother liquor. The total yield of the crude product was 74%. The product was recrystallized from ethanol to yield needles melting at *174.5~175°C.

Found: C, 34.80; H,6.23; N, 3.97; S, 18.11. Calcd. for $C_{10}H_{21}NO_9S_2$: C, 34.57; H, 6.09; N, 4.03; S, 18.46%.

IR: 1740 (ester) 1622 (NH_3^+), 1355, 1170 (mesyloxy), 1200 and 1045 (SO_3^-) cm^{-1}.

DL-2α-Acetamido-*O*-mesyl-1α, 3β-cyclohexanediol (XIII). A 2.0 g. portion of XII was dissolved in 6 ml. of water, and the pH was adjusted with a 10% potassium hydroxide solution to 11. Then the solution was cooled in an ice bath to give a white crystalline precipitate. After cooling at 0°C for 1 hr., the product was collected by filtration, washed with ethanol, and dried to yield 1.05 g. (72.5%) of crystals melting at *118~119°C. A sample was recrystallized from ethanol for analysis; it melted at *118~118.5°C.

Found: C, 43.17; H, 7.07; N, 5.61; S, 12.69. Calcd. for $C_9H_{17}NO_5S$: C, 43.01; H, 6.82; N, 5.58; S, 12.78%.

IR: 3540 (OH), 1643, 1542 (amide), 1340, 1175 (mesyloxy) and 960 (cyclohexane) cm^{-1}.

2α-Acetamido-1α, 3α-cyclohexanediol (IIIc).—a) A mixture of 0.55 g. of XIII, 0.6 g. of anhydrous sodium acetate, 0.5 ml. of water, and 10 ml. of 2-methoxyethanol was refluxed for 5 hr. The mixture was evaporated under reduced pressure to dryness. After drying, the residue was extracted with 10 ml. of boiling acetone five times, and the combined acetone extract was evaporated under reduced pressure to give an oily residue. Trituation of the residue with a mixture of ethanol and ether gave 0.30 g. (79%) of crystals melting at *118~120°C. Two recrystallizations from acetone afforded colorless needles melting at *120~123°C.

Found: C, 55.21; H, 8.97; N, 8.31. Calcd. for $C_9H_{15}NO_3$: C, 55.47; H, 8.73; N, 8.09%.

b) A 203 mg. portion of IIIb was added to 10 ml. of methanol saturated with ammonia. The mixture was kept at room temperature overnight and evaporated under reduced pressure to obtain a crystalline residue. The product was recrystallized from ethanol to yield 117 mg. (85.6%) of crystals melting at 119~123°C. A mixed melting point determination with an authentic sample was undepressed.

Triacetyl-2α-amino-1α, 3α-cyclohexanediol (IIIb).—a) The crude IIIc, obtained from 2.2 g of XIII, was treated with a mixture of 20 ml. of acetic anhydride and 20 ml. of pyridine for 24 hr. The mixture was evaporated in vacuo, and the residue was recrystallized from benzene to give 1.6 g. (71%) of colorless needles melting at 175.5~177.5°C. An analytical sample was obtained by recrystallization from benzene; m. p. 177.5~179°C.

Found: C, 56.23; H, 7.56; N, 5.45. Calcd. for $C_{12}H_{19}NO_5$: C, 56.02; H, 7.44; N, 5.44%.

b) A starting material, *cis*-2, 6-diacetoxycyclohexanone (XV), was prepared by the method of Cavill and Solomon.[10] A mixture of 2.97 g. of XV and 70 ml. of methanol was added to a mixture of 1.49 g. of hydroxylamine hydrochloride, 2.58 g. of sodium hydroxide, and 13 ml. of water under ice cooling. The mixture was kept in a refrigerator overnight and then evaporated. The residue was added to ethanol, and an insoluble salt was removed by filtration. The filtrate was evaporated in vacuo, and the residue was dissolved in 50 ml. of glacial acetic acid. The mixture was shaken with 0.57 g. of an Adams platium catalyst under an atmospheric pressure of hydrogen for 130 min. The crude hydrogenated product was then heated with pyridine and acetic anhydride for 3 hr. at 100°C. The crude product was dissolved in ethanol, and ether was added to give 0.53 g. (14.8%) of crystals melting at 170~176°C. The product was recrystallized twice from ethanol-ether to yield 0.33 g. (9.3%) of needles melting at 176.5~178°C.

A mixed melting point determination with an authentic sample was undepressed. The infrared spectrum of the product was superimposable on that of an authentic sample.

2α-Amino-1α, 3α-cyclohexanediol Hydrochloride (XIV).—A mixture of 2.0 g. of IIIb and 100 ml. of 6 N hydrochloric acid was refluxed for 6 hr. The mixture was then evaporated under reduced pressure to yield 1.21 g. (93%) of crystals melting at 156.5~160°C. The crude product was recrystallized from absolute ethanol-absolute ether to give needles melting at 160.5~161.5°C.

Found: C, 42.67; H, 8.46; N, 8.41; Cl, 21.38. Calcd. for $C_6H_{14}NClO_2$: C, 42.99; H, 8.42; N, 8.36; Cl, 21.15%.

2α-Amino-1α, 3α-cyclohexanediol (IIIa).—A 1.02 g. portion of the crude XIV was treated, as described in the regeneration of Ia from V, to yield 743 mg. (93%) of crystals melting at 78~83°C. The product was recrystallized from absolute ethanol-absolute ether to yield 322 mg. (40.5%) of crystals melting at 126~128°C.

Found: C, 54.65; H, 9.97; N, 10.84. Calcd. for $C_6H_{13}NO_2$: C, 54.93; H,9.99; N, 10.63%.

Paper Chromatography. — An upper layer of l-butanol-acetic acid-water (4 : 1 : 5) gave a single spot of R_f 0.44 in ascending development at 25°C.

The authors are grateful to Pofessor Sumio Umezawa and Professor Herbert E. Carter for their helpful advice and to Mr. Saburo Nakada for his microanalysis. Also, the authors are indebted to Miss Sunao Ohata for her measurement of the infrared spectra, to Miss Sumiko Uchida for her assistance in the analytical experiments, and to the Japan Electron Optics Co., Ltd., for the NMR spectra.

Department of Applied Chemistry
Faculty of Engineering
Keio University
Koganei-shi, Tokyo

Studies of the Synthesis of Peptides Containing C-Terminal Glutamine. II. The Synthesis and Use of α-p-Nitrobenzyl γ-Methyl L-Glutamate

By Yasutsugu SHIMONISHI

(Received August 12, 1963)

In a previous paper,[1] it has been described how the usual synthetic methods of peptides containing *C*-terminal glutamine are attended with many difficulties, and how the introduction of a xanthyl group into the γ-amide nitrogen is effective in reducing these troubles. The present study is concerned with another approach to the same problem using α-*p*-nitrobenzyl γ-methyl glutamate as an intermediate. It is known that the *p*-nitrobenzyl ester derivative of an amino acid[2] is easily crystallizable; morever, its ester bond is quite stable to dry hydrogen bromide in hydrous organic solvents. The cleavage of the *p*-nitrobenzyl ester linkage is effected not only by means of alkaline hydrolysis but also by catalytic hydrogenolysis. Since the methyl ester linkage is stable to hydrogen bromide or hydrogenolysis, glutamine peptide can be prepared from the carbobenzoxy peptide of the glutamate by catalytic hydrogenation, followed by ammonolysis.

The starting material, *N*-carbobenzoxy-(α-*p*-nitrobenzyl, γ-methyl)glutamate (I), was prepared in a good yield from *N*-carbobenzoxy-(γ-methyl)glutamate and *p*-nitrobenzyl bromide in the presence of triethylamine. Substance I was treated with hydrogen bromide in glacial acetic acid to give α-*p*-nitrobenzyl γ-methyl glutamate hydrobromide (II). The hydrobromide II was stable and easily crystallizable. First, carbobenzoxy-glycine was coupled with this compound I to form peptide under several conditions. In the case of a mixed anhydride with isobutyloxycarbonic acid or an active ester with *p*-nitrophenol, the product was not pure, and purification was very difficult. It was finally found that dicyclohexylcarbodiimide was the most effective reagent in this case. The urea-derivative formed and the unreacted starting materials were separated easily, and carbobenzoxy-glycyl-(α-*p*-nitrobenzyl, γ-methyl)-glutamate (III) was obtained as crystals. There was no difficulty in obtaining glycyl-(γ-methyl)-glutamate, which was converted to glycyl-glutamine as expected (Fig. 1). The optical purity of the glycyl-L-glutamine was checked after hydrolysis with 6 N hydrochloric acid, and no difference was observed between the

1) S. Akabori, S. Sakakibara and Y. Shimonishi, This Bulletin, 34, 739 (1961); 35, 1966 (1962).
2) H. Schwarz and K. Arakawa, *J. Am. Chem. Soc.*, 81, 5691 (1959).

optical rotation of the hydrolyzate and that of the artificial mixture of the same components. When this synthetic procedure was applied to several carbobenzoxy amino acids, the following depeptides were synthesized: L-alanyl-L-glutamine, L-valyl-L-glutamine, L-leucyl-L-glutamine, L-prolyl-L-glutamine, and L-phenylalanyl-L-glutamine.

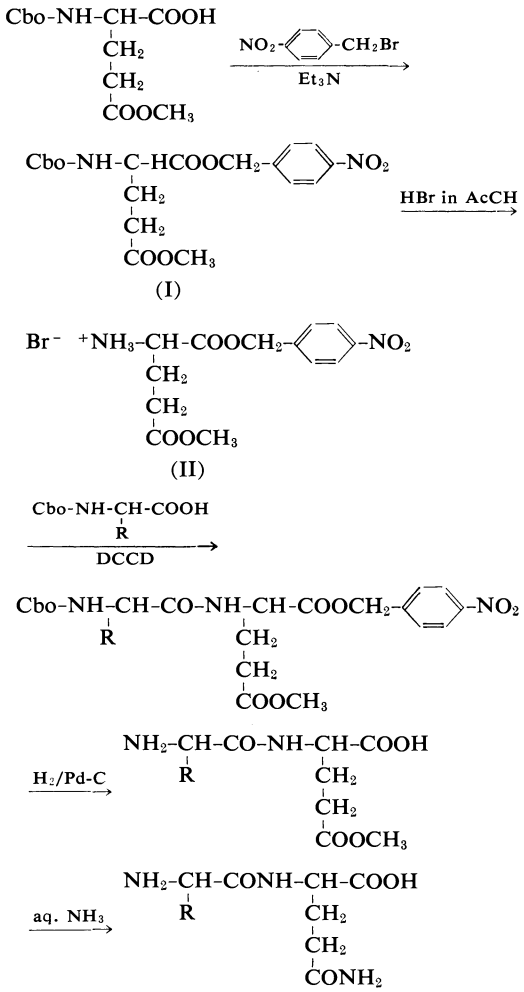


Fig. 1. Synthetic procedure.

Experimental*

***N*-Carbobenzoxy-(*α*-*p*-nitrobenzyl, *γ*-methyl)-L-glutamate (I).**—A mixture of carbobenzoxy-(*γ*-methyl) L-glutamate (59.0 g., 0.2 mol.), *p*-nitrobenzyl bromide (54.0 g., 0.25 mol.) and triethylamine (36.0 ml., 0.25 mol.) in ethyl acetate (800 ml.) was refluxed for 5 hr. The triethylamine hydrobromide which precipitated was removed by filtration, and the filtrate was washed with 0.2 N hydrochloric acid, 5% aqueous sodium bicarbonate, and water, dried over anhydrous magnesium sulfate, and concentrated under reduced pressure to a residue, which was then triturated with petroleum benzine. The crude material (80.0 g.) was recrystallized as needles from ethyl acetate-petroleum benzine; yield, 70 g. (80%); m. p. 67~69°C; $[\alpha]_D^{28}$ −15.2° (*c* 3.21, methanol).

Found: C, 58.51; H, 5.22; N, 6.37. Calcd. for $C_{21}H_{22}O_8N_2$: C, 58.60; H, 5.15; N, 6.51%.

***α*-*p*-Nitrobenzyl *γ*-Methyl L-Glutamate Hydrobromide (II).**—This compound was prepared by Ben-Ishai's method.[3] Compound I (43.0 g., 0.1 mol.) was treated with 33% hydrogen bromide in glacial acetic acid (61.5 g., 0.25 mol.). During the course of the reaction, the hydrobromide of the decarbobenzoxylated product deposited as a crystalline mass. After this mixture had stood for an hour at room temperature, ether (1000 ml.) was added and the precipitates were filtered, washed with a sufficient amount of ether, and dried over sodium hydroxide pellets in vacuo. The crude material (37.0 g.) was recrystallized as fine needles from methanol-ether; yield, 31.0 g. (83%); m. p. 156°C; $[\alpha]_D^{27}$ +9.6° (*c* 5.02, methanol).

Found: C, 41.50; H, 4.59; N, 7.17; Br, 20.86. Calcd. for $C_{13}H_{17}O_6N_2Br$: C, 41.39; H, 4.54; N, 7.43; Br, 21.19%.

Carbobenzoxy-glycyl-(*α*-*p*-nitrobenzyl, *γ*-methyl)-L-glutamate (III).—A solution of II (22.6 g., 0.06 mol.) and triethylamine (8.2 ml., 0.06 mol.) in anhydrous chloroform (100 ml.) was cooled to −15°C. Solutions of carbobenzoxy-glycine (10.5 g., 0.05 mol.) in ethyl acetate (70 ml.) and of dicyclohexylcarbodiimide (10.3 g., 0.05 mol.) in ethyl acetate (30 ml.) were stirred into the above solution at −15°C, and the mixture was allowed to stand overnight at the same temperature. Dicyclohexyl urea and triethylamine hydrobromide were filtered off and washed with ethyl acetate. The combined filtrate and washings were washed with 5% aqueous sodium bicarbonate, 0.5 N hydrochloric acid, and a small amount of water, dried over anhydrous magnesium sulfate, and concentrated to dryness under reduced pressure. A residual oil was crystallized from ethyl acetate-petroleum benzine; wt., 22.5 g.; m. p. 105~106°C. The product was recrystallized from ethyl acetate-petroleum benzine; yield, 21.3 g. (87%); m. p. 106~108°C; $[\alpha]_D^{16}$ −15.1° (*c* 5.11, DMF**).

Found: C, 56.61; H, 5.23; N, 8.58. Calcd. for $C_{23}H_{25}O_9N_3$: C, 56.67; H, 5.17; N, 8.62%.

Carbobenzoxy-L-alanyl-(*α*-*p*-nitrobenzyl, *γ*-methyl) L-glutamate (IV).—To a solution of II (22.6 g., 0.06 mol.) and triethylamine (8.2 ml., 0.06 mol.) in anhydrous chloroform (100 ml.), a solution of carbobenzoxy-L-alanine (11.2 g., 0.05 mol.) in ethyl acetate (70 ml.) was added at −15°C. Then dicyclohexylcarbodiimide (10.3 g., 0.05 mol.) in ethyl acetate (30 ml.), which had been cooled to −15°C, was added with swirling. The mixture was kept overnight at −15°C and then treated as described above. The product was recrystallized from ethyl acetat-petroleum benzine as colorless needles; wt. 21.0 g. (87%); m. p. 132~138°C; $[\alpha]_D^{16}$ −11.9° (*c* 5.48, DMF).

* All melting points are uncorrected.

3) D. Ben-Ishai and A. Berger, *J. Org. Chem.*, **17**, 1564 (1952).

** DMF: dimethylformamide

Found: C, 57.26; H, 5.54; N, 8.25. Calcd. for $C_{24}H_{27}O_9N_3$: C, 57.48; H, 5.43; N, 8.38%.

Carbobenzoxy-L-valyl-(α-*p*-nitrobenzyl, γ-methyl)-L-glutamate (V). — To a solution of II (17.4 g., 0.046 mol.) and triethylamine (6.3 ml., 0.046 mol.) in anhydrous chloroform (120 ml.), which had been cooled to −15°C, carbobenzoxy-L-valine (9.7 g., 0.039 mol.) in ethyl acetate (50 ml.) was added. Then dicyclohexylcarbodiimide (8.0 g., 0.039 mol.) in ethyl acetate (50 ml.), which had been cooled to −15°C, was added. The mixture was kept at the same temperature overnight and then treated as described above. The crude product (17.7 g.; m. p. 133°C) was collected with ethyl acetate-petroleum benzine. Recrystallization of the crude material from ethyl acetate-petroleum benzine gave colorless needles (15.2 g., 75%; m. p. 138~140°); $[\alpha]_D^{16}$ −6.1°C (*c* 6.02, DMF).

Found: C, 59.02; H, 6.09; N, 7.92. Calcd. for $C_{26}H_{31}O_9N_3$; C, 58.97, H, 5.90; N, 7.94%.

Carbobenzoxy-L-leucyl-(α-*p*-nitrobenzyl, γ-methyl) L-Glutamate (VI). — Compound II (22.6 g., 0.06 mol.) and triethylamine (8.2 ml., 0.06 mol.) in an hydrous chloroform (100 ml.), carbobenzoxy-L-leucine (13.3 g., 0.05 mol.) in ethyl acetate (70 ml.), and dicyclohexylcarbodiimide (10.3 g., 0.05 mol.) in ethyl acetate (30 ml.) were treated by the procedure described above. The crude product which had been collected from ethyl acetate-petroleum benzine was recrystallized from ethyl acetate-petroleum benzine as colorless needles; yield 23.0 g. (85%); m. p. 109~113°C; $[\alpha[_D^{18}$ −14.8° (*c* 6.10, DMF).

Found: C, 59.35; H, 6.24; N, 7.97. Calcd. for $C_{27}H_{33}O_9N_3$: C, 59.66; H, 6.12; N, 7.73%.

Carbobenzoxy-L-prolyl-(α-*p*-nitrobenzyl, γ-methyl)L-glutamate (VII). — Carbobenzoxy-L-proline (12.5 g., 0.05 mol.) in ethyl acetate (70 ml.), II (22.6 g., 0.06 mol.) and triethylamine (8.2 ml., 0.06 mol. in anhydrous chloroform (100 ml.), and dicyclohexylcarbodiimide (10.3 g., 0.05 mol.) in ethyl acetate (30 ml.) were mixed at −15°C. The mixture was maintained overnight at the same temperature and treated as above. The crude material (25.0 g.) was collected with ethyl acetate-petroleum benzine and melted at 102~106°C. Recrystalization of the crude product from ethyl acetate-petroleum benzine gave colorles needless; yield 24.0 g. (91%); m. p. 104~107°C; $[\alpha]_D^{18}$ −33.4° (*c* 5.92, DMF).

Found: C, 59.27; H, 5.48; N, 8.15. Calcd. for $C_{26}H_{29}O_9N_3$: C, 59.19; H, 5.54; N, 7.97%.

Carbobenzoxyl-L-phenylalanyl-(α-*p*-nitrobenzyl, γ-methyl)L-glutamate (VIII). — Carbobenzoxy-L-phenylalanine (15.0 g., 0.05 mol.) in ethyl acetate (70 ml.), II (22.6 g., 0.06 mol.) and triethylamine (8.2 ml., 0.06 mol.) in anhydrous chloroform (100 ml.) and dicyclohexylcarbodiimide (10.3 g., 0.05 mol.) in ethyl acetate (30 ml.) were mixed at −15°C. The mixture was allowed to stand overnight at the same temperature. Ethyl acetate (100 ml.) was added to the reaction vessel, and the mixture was heated to boiling. The undissolved materials were removed by filtration and washed with a small amount of hot ethyl acetate. From the filtrate, a crystalline material was filtered and dried in a vacuum desiccator. The crude material (32.0 g., m. p. 147~148.5°C) was recrystallized as colorless fine needles from ethyl acetate; yield 25.9 g. (87%); m. p. 151~152°C; $[\alpha]_D^{18}$ −13.4° (*c* 5.43, DMF).

Found: C, 62.18; H, 5.53; N, 7.47. Calcd. for $C_{30}H_{31}O_9N_3$: C, 62.38; H, 5.41; N, 7.28%.

Carbobenzoxy-(γ-methyl)-L-glutamyl-(α-*p*-nitrobenzyl, γ-methyl)L-glutamate (IX).—To a solution of carbobenzoxy-(γ-methyl)L-glutamate (11.2 g., 0.038 mol.) in ethyl acetate (50 ml.), II (17.2 g., 0.046 mol.) and triethylamine (6.2 ml., 0.046 mol.) in anhydrous chloroform (80 ml.) was added. To the mixture, which had been cooled to −15°C, was added a cooled solution of dicyclohexylcarbodiimide (7.85 g., 0.38 mol.) in ethyl acetate (30 ml.). After the treatment of the reaction mixture in the same manner as descrired in the synthesis of IV, the crude material (19.8 g.) was obtained and recrystallized from ethyl acetate as needles; yield 18.5 g. (85%); m. p. 97~100°C; $[\alpha]_D^{18}$ −9.7° (*c* 6.51, DMF).

Found: C, 56.87; H, 5.58; N, 7.35. Calcd. for $C_{27}H_{31}O_{11}N_3$: C, 56.54; H, 5.45; N, 7.33.

Glycyl-(γ-methyl)L-glutamate (X).—Compound III (15.0 g., 0.031 mol.) was suspended in a mixture of methanol (200 ml.) and water (100 ml.), and then hydrogenated over a 3% palladium-charcoal catalyst (1.5 g.) for 6 hr. The catalyst was then filtered off and washed with water. The filtrate was evaporated to dryness, and the residue was dissolved in a small amount of hot water. The insoluble material was removed by filtration. When acetone was added to the filtrate, a crystalline material (6.0 g.) was obtained. Recrystallization from water-acetone gave colorless needles; yield 5.5 g. (82%); m. p. 178~179°C (decomp.); $[\alpha]_D^{19}$ −3.5° (*c* 5.11, water).

Found: C, 44.14; H, 6.57; N, 12.59. Calcd. for $C_8H_{14}O_5N_2$: C, 44.03; H, 6.47; N, 12.84%.

L-Alanyl-(γ-methyl)L-glutamate (XI). — Compound IV (15.0 g., 0.03 mol.) and 3% palladium-charcoal (1.5 g.) were suspended in a mixture of methanol (200 ml.) and water (100 ml.) and hydrogenated until the evolution of carbon dioxide stopped. The catalyst was then filtered off and washed with a small amount of hot water. The filtrate and washing were combined and concentrated under reduced pressure. A crude product (6.5 g., m. p. 186~187°C (decomp.)) was collected with acetone. Recrystallization of the crude material from water-acetone gave colorless needs; yield 6.2 g. (90%); m. p. 186°C (decomp.); $[\alpha]_D^{20}$ +8.0° (*c* 5.72, water).

Found: C, 46.37; H, 6.95; N, 12.03. Calcd. for $C_9H_{15}O_5N_2$: C, 46.54; H, 6.94; N, 12.06%.

L-Valyl-(γ-methyl)L-glutamate (XII).—Compound V (12.8 g.) and a 3% palladium-charcoal catalyst (1.5 g.) in a mixture of methanol (250 ml.) and water (80 ml.) were treated in the same manner as has been described above. Recrystallization of the crude material from water-acetone gave fine colorless needles; yield 4.3 g. (68%); m. p. 195~195.5°C; $[\alpha]_D^{20}$ +25.9° (*c* 6.07, water). L-Valyl-(γ-methyl)L-glutamate was submitted to elementary analysis after being dried over phosphorus pentoxide in vacuo at 110°C. The results of the analysis

were identical with the calculated values for the ester plus one and half moles of water, as is shown by the analytical data.

Found: C, 46.31; H, 7.99; N, 9.86. Calcd. for $C_{11}H_{20}O_5N_2 \cdot 3/2H_2O$: C, 46.00; H, 8.08; N, 9.76%.

L-Leucyl-(γ-methyl)L-glutamate (XIII). — Compound **VI** (15.0 g., 0.028 mol.) and a 3% palladium-charcoal catalyst (1.5 g.) in a mixture of methanol (200 ml.) and water (100 ml.) were treated in the same way as has been described above. The crude product (6.6 g.) was recrystallized from water-acetone as colorless needles; yield 5.3 g. (70%); m. p. 196~197°C (melted and decomposed with coloring); $[\alpha]_D^{20}$ +27.2° (*c* 5.62, water).

Found: C, 52.45; H, 8.06; N, 10.52. Calcd. for $C_{12}H_{22}O_5N_2$; C, 52.54: H, 8.08; N, 10.21%.

L-Prolyl(γ-methyl)L-glutamate (XIV). — Compound VII (15.0 g., 0.029 mol.) and a 3% palladium-charcoal catalyst (1.5 g.) were suspended in a mixture of methanol (200 ml.) and water (200 ml.) and treated in the same way. The crude product (5.1 g.) was obtained and recrystallized from water as colorless long needles; yield 4.8 g. (66%); m. p. 208°C (decomp.); $[\alpha]_D^{20}$ −38.5° (*c* 6.02, water).

Found: C, 47.82; H, 7.30; N, 10.14. Calcd. for $C_{11}H_{18}O_5N_2 \cdot H_2O$: C, 47.81; H, 7.17; N, 10.29%.

L-Phenylalanyl-(γ-methyl)L-glutamate (XV). — Compound VIII (15.0 g., 0.026 mol.) was suspended in a mixture of methanol (200 ml.) and water (50 ml.) and catalytically hydrogenated in the presence of 3% palladium-charcoal (1.5 g.). The crude material (8.0 g.) was recrystallized from water-acetone as prisms; yield 6.1 g. (77%); m. p. 228~232°C (decomp.); $[\alpha]_D^{20}$ +27.1° (*c* 6.09, water).

Found: C, 57.90; H, 6.72; N, 9.07. Calcd. for $C_{15}H_{20}O_5N_2$: C, 58.43; H, 6.54; N, 9.09%.

γ-Methyl-L-glutamyl-(γ-methyl)L-glutamate (XVI).—Compound IX (11.5 g., 0.02 mol.) and a 3% palladium-charcoal catalyst (1 g.) in a mixture of methanol (130 ml.) and water (60) ml. were treated in the manner described above. The crude product was recrystallized from water-acetone as colorless needles; yield 3.2 g. (53%); m. p. 153~154°C (decomp.); $[\alpha]_D^{20}$ +32.3° (*c* 5.75, water).

Found: C, 47.26; H, 6.51; N, 9.09. Calcd. for $C_{12}H_{20}O_7N_2$: C, 47.36; H, 6.63; N, 9.21%.

L-Glycyl-L-glutamine (XVII). — Compound X (2.0 g., 0.092 mol.) was dissolved in concentrated aqueous ammonia (100 ml.) The solution was then allowed to stand for 24 hr. at room temperature (about 15°C) and then concentrated to a syrup under reduced pressure at room temperature. After being flushed once with a small amount of water, the residue was crystallized from water-ethanol. The crude product (1.8 g.) was recrystallized as color less needles from water-ethanol; yield 1.8 g. (90%); m. p. 203~204°C (decomp.); $[\alpha]_D^{21}$ −1.6° (*c* 3.85, water); $[\alpha]_D^{20}$ −7.0° (*c* 3.29, N HCl).

Found: C, 37.95; H, 6.98; N, 19.52. Calcd. for $C_7H_{13}O_4N_3 \cdot H_2O$: C, 38.00; H, 6.84; N, 19.00%.

L-Alanyl-L-glutamine (XVIII). — Compound XI (3.5 g., 0.015 mol.) was dissolved in concentrated aqueous ammonia (150 ml.) and treated in the manner described above. The crude product (3.0 g.) was collected with water-ethanol and recrystallized from the same solvents as needles; yield 2.6 g. (74%); m. p. 215~216°C (decomp.); $[\alpha]_D^{24}$ −3.0° (*c* 3.31, N HCl). A sample for elementary analysis was dried over phosphorus pentoxide in vacuo for 20 hr. at 110°C.

Found: C, 44.50; H, 7.06; N, 18.85. Calcd. for $C_8H_{15}O_4N_3$: C, 44.23; H, 6.96; N, 19.35%.

L-Valyl-L-glutamine (XIX).—Compound XII (3.6 g., 0.014 mol.) in concentrated aqueous ammonia (140 ml.) was treated in the manner described above. The crude product (2.5 g.) was obtained and crystallized from water as needles; yield 2.2 g. (65%); m. p. 218~219°C (decomp.); $[\alpha]_D^{20}$ +15.8° (*c* 3.08, N HCl).

Found: C, 49.12; H, 7.78; N, 17.20. Calcd. for $C_{10}H_{19}O_4N_3$: C, 48.96; H, 7.81; N, 17.13%.

L-Leucyl-L-glutamine (XX).—Compound XIII (4.1 g., 0.015 mol.) was treated in the same manner described above. The crude product (3.5 g.) was obtained and recrystallized from water as colorless needles; yield 3.2 g. (84%); m. p. 236~237°C (decomp.); $[\alpha]_D^{19}$ +14.2° (*c* 3.57, N HCl).

Found: C, 50.68; H, 8.13; N, 16.10. Calcd. for $C_{11}H_{21}O_4N_3$: C, 50.95; H, 8.16; N, 16.21%.

L-Prolyl-L-glutamine (XXI). — Compound XIV (2.6 g., 0.01 mol.) in concentrated aqueous ammonia (100 ml.) was treated in the manner described above. Recrystallization of the crude product from water gave colorless needles; yield 2.0 g. (77%); m. p. 211~212.5°C (decomp.); $[\alpha]_D^{21}$ −52.2° (*c* 3.91, N HCl).

Found: C, 45.93; H, 7.31; N, 16.19. Calcd. for $C_{10}H_{17}O_4N_3 \cdot H_2O$: C, 45.97; H, 7.33; N, 16.08%.

L-Phenylalanyl-L-glutamine (XXII).—Compound XV (3.1 g., 0.01 mol.) in concentrated aqueous ammonia (100 ml.) was treated in the manner described above. The crude product (2.7 g.) was obtained and recrystallized from water as needles. The first crop of crystallization was 1.8 g. and the second crop was 0.8 g.; yield 2.6 g. (87%); m. p. 213~214°C (decomp.); $[\alpha]_D^{19}$ +17.3° (*c* 3.42, N HCl).

Found: C, 57.04; H, 6.42; N, 14.49. Calcd. for $C_{14}H_{19}O_4N_3$: C, 57.32; H, 6.53; N, 14.33%.

The Hydrolysis of Glycyl-L-glutamine Monohydrate. — Glycyl-L-glutamine monohydrate (104 mg.) was placed in a volumetric flask (3.04 ml.) filled with 6 N hydrochloric acid, and the solution was refluxed for 5 hr. After the hydrolysis, the volume of the solution was adjusted to exactly 3.04 ml. by adding 6 N hydrochloric acid, and the optical rotation of the solution was determined; $[\alpha]_D^{19}$ +31.3°. The optical rotation of a solution containing L-glutamic acid (68.1 mg.), glycine (34.7 mg.) and ammonium chloride (24.7 mg.) gave $[\alpha]_D^{19}$ +31.4°.

The author wishes to express his deep gratitude to Professor Dr. Shiro Akabori and Dr. Shumpei Sakakibara for their kind advice throughout this work. The author is also indebted to Misses Kiku Koike and Masako Kawakita of this Institute for performing elementary microanalyses.

Division of Organic Chemistry
Institute for Protein Research
Osaka University
Kita-ku, Osaka

*The Nitration of Some Derivatives of 1, 3, 5-Tri-t-butylbenzene**

By Setsuo WATARAI

(Received August 15, 1963)

In connection with the interesting problem of the possible existence of derivatives of *sym*-tri-*t*-butylbenzene with two or three functional groups, the nitration of some derivatives of 1, 3, 5-tri-*t*-butylbenzene has been undertaken.

Sym-tri-methyl-, or tri-isopropylbenzenes bearing three functional groups,[1] and *sym*-tri-*t*-butylbenzenes with one functional group[2] have already been known, but derivatives of the latter hydrocarbon bearing two or three functional groups have not yet been prepared. It has recently been suggested[3] that the steric requirements of the bulky *t*-butyl groups cause the distortion of the benzene ring in *o*-di-*t*-butylbenzene or in 1, 2, 4, 5-tetra-*t*-butylbenzene.

The nitration of 2, 4, 6-tri-*t*-butylphenol[4] has been shown to give various unusual nitration products. Among them, there were products in which original *t*-butyl groups were replaced by nitro groups, or, products of quinoid or quinolide structures, depending upon the conditions of nitration. Such a replacement of a *t*-butyl group by a nitro group has frequently been described in the literature[5] and has been found to be the case in the nitration of 2, 4, 6-tri-*t*-butylaniline.[6]

While 2, 4, 6-tri-*t*-butylnitrobenzene (I) can be obtained by a rather mild nitration of the corresponding hydrocarbon, the further nitration of I to a dinitro compound (m. p. 290~292°C) was found to require much more severe conditions using fum. nitric acid in sulfuric acid at 70°C. This dinitro compound II, when analyzed, is found to correspond to the molecular formula $C_{18}H_{28}O_4N_2$ and to have a molecular weight of 336 (Rast method), while still retaining three *t*-butyl groups.

The structure of II has been elucidated on the basis of the evidence given below.

The catalytic hydrogenations of the nitro compound II and the related nitro compounds shown in Fig. 1 were carried out under atmospheric pressure and at room temperature in the presence of the same amount of Raney nickel per each nitro group. II was found to resist hydrogenation very strongly, while all the nitro groups of *m*-dinitrobenzene (IIa) and of other *m*-di-nitro-*t*-butylbenzenes** (IIb and IIc) were readily reduced, absorbing theoretical quantities of hydrogen rapidly. On the other hand, the reduction of the nitro group substituted between the two ortho *t*-butyl groups in I proceeded very slowly, although it gave the expected reduced product. This experiment seems to indicate that both nitro groups in II are highly sterically hindered.

The steric hindrance of the nitro group was further supported by the infrared spectra of

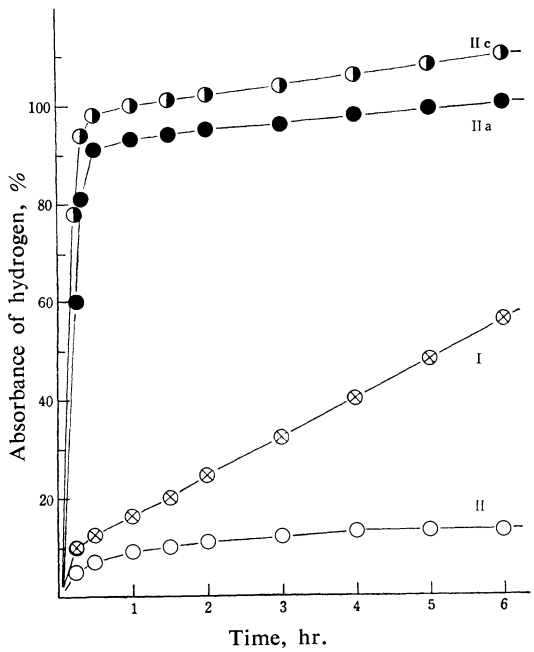


Fig. 1. Hydrogenations of *t*-butyl-*m*-dinitrobenzenes.

* This work was presented at the 16th Annual Meeting of the Chemical Society of Japan, Tokyo, April, 1963.

1) For example: a) trinitromesitylene: Heilbron and Bunbury, "Dictionary of Organic Compounds," Eyre & Spottiswoode, London (1953), Vol. IV, p. 623; b) trinitro-*sym*-tri-isopropylbenzene: A. Newton, *J. Am. Chem. Soc.*, **65**, 2435 (1943).

2) E. E. Betts and L. R. C. Barclay, *Can. J. Chem.*, **33**, 1768 (1955).

3) C. Hoogzand and W. Hübel, *Tetrahedron Letters*, No. 18, 637 (1961).

4) K. Ley and E. Müller, *Chem. Ber.*, **89**, 1402 (1956).

5) P. B. D. de la Mare and J. H. Ridd, "Aromatic Substitution," Butterworths Scientific Publications, London (1959), p. 210; cf. also D. V. Nightingale, *Chem. Revs.*, **40**, 117 (1947).

6) B. M. Wepster et al., *Rec. trav. chim.*, **75**, 1327 (1956).

** The only curve of IIc is shown in Fig. 1, but almost the same one was also obtained in the case of IIb.

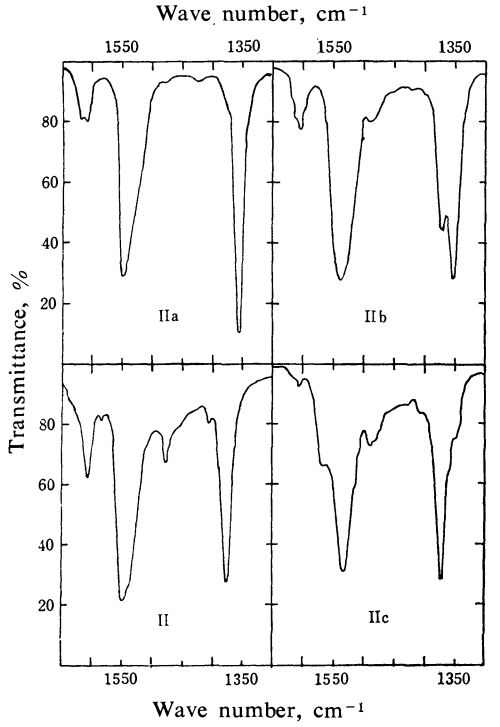


Fig. 2. Infrared spectra of *t*-butyl-*m*-dinitrobenzenes.

TABLE I. NO_2-STRETCHING VIBRATION BANDS OF *m*-DINITROBENZENES

m-Dinitrobenzenes	Band frequency cm^{-1}		Transmittance %	
	ν_a	ν_s	ν_1	ν_s
Unsubstituted, IIa	1545	1352	28.5	10.5
4-*t*-Butyl-, IIb	1537	1372 1354	28.0	44.0 27.5
4,6-Di-*t*-butyl, IIc	1535	1372	31.0	28.0
2,4,6-Tri-*t*-butyl-, II	1548	1375	22.0	28.0

N–O stretching vibrations shown in Fig. 2 and Table I. The most characteristic feature is the change in the N–O symmetric stretching vibration band of the dinitro-*t*-butylbenzenes from that of IIa. The shifts of these bands to higher frequencies, accompanied by the decreases in the apparent intensities relative to their N–O antisymmetric stretching bands, also suggest that the nitro groups in these compounds are sterically hindered.[7] Moreover, the N–O symmetric stretching band of IIb, in which only one nitro group is sterically hindered, splits into a doublet; on the contrary, that of II is a sharp singlet, as are those of IIa and IIc, in which the two nitro groups are indistinguishable.

On the basis of these data, the structure of II is assumed as 2,4,6-tri-*t*-butyl-*m*-dinitrobenzene.

An absolutely negative result for the high pressure catalytic hydrogenation of I over Raney nickel has been reported by other workers.[8] Indeed, we found I to be reduced very slowly in a low pressure and over this catalyst, as is shown in Fig. 1, but at a high pressure and over 50°C it was readily reduced under the same catalyst to afford almost quantitatively the corresponding aniline, 2,4,6-tri-*t*-butylaniline (III).

Nitration in acetic acid and acetic anhydride converted III into a di-*t*-butylnitroaniline (IV) in which a *t*-butyl group was replaced by a nitro group. The m.p. (256°C) of IV was distinctly different from that (89.5°C) of 2,4-di-*t*-butyl-6-nitroaniline,[9] one of the expected products in this dealkylnitration. Therefore, it was shown that the *t*-butyl group at the para-position of the amino group was replaced by the nitro group.

Several attempts to convert IV directly to a known 5-nitro-*m*-di-*t*-butylbenzene[9] by diazotization, under varying conditions, were unsuccessful. However, upon the reduction of the nitro group, the resulting diamine V could be converted, by oxidation with ferric chloride, to the known 2,6-di-*t*-butylbenzoquinone (VI).[10]

This experiment indicates that V is *p*-diamine and that, hence, IV is 2,6-di-*t*-butyl-4-nitroaniline. This result was in accordance with the assignment of the structure for IV made by other workers[6] on the basis of the rate constant of the catalytic deacetylation of the bisacetylamino compound derived from IV.

It is interesting to compare the present nitrations with those of the *sym*-tri-alkylbenzenes and with some of their amino derivatives.

Trinitro-derivatives have been obtained from mesitylene, triisopropylbenzene,[1b] and *t*-butyl-*m*-xylene[11] without any replacement of the alkyl groups; however, the introduction of more than two nitro groups into *m*-di-*t*-butyltoluene[12] has been shown to be unsuccessful. From mesidine, 2,4,6-tri-isopropylaniline,[1b] and 3,5-di-*t*-butyl-*o*-toluidine[12], only the usual nitration products have been reported.

Therefore, the failure to obtain the trinitro-derivative of *sym*-tri-*t*-butylbenzene, even with the application of drastic nitration conditions, may definitely be ascribed to the steric effect of the bulky *t*-butyl groups. The replacement

7) T. Kinugasa and S. Watarai, *J. Chem. Soc. Japan, Pure Chem. Sec.* (*Nippon Kagaku Zasshi*), **83**, 472, 476, (1962).

8) P. D. Bartlett, M. Roha and R. M. Stiles, *J. Am. Chem. Soc.*, **76**, 2349 (1954).

9) T. Kinugasa and S. Watarai, *J. Chem. Soc. Japan, Pure Chem. Sec.* (*Nippon Kagaku Zasshi*), **83**, 333 (1962).

10) G. R. Yohe et al., *J. Org. Chem.*, **21**, 1289 (1956).

11) A. Baur, *Ber.*, **24**, 2841 (1891).

12) B. M. Wepster et al., *Rec. trav. chim.*, **75**, 301 (1956).

of the *p*-*t*-butyl group by the nitro group, in the case of the nitration of IV, also seems to be caused by the steric effect of these groups. Undoubtedly the *t*-butyl group activated by the electron-releasing substiuent, such as the *p*-amino group, is displaced with remarkable ease in the electrophilic substitution.[5]

Experimental

2, 4, 6-Tri-*t*-butylnitrobenzene (I), was prepared from 1, 3, 5-tri-*t*-butylbenzene[13] in the manner described in the literature;[2] 80% of yield, m. p. 200~203°C.

Found: C, 74.37; H, 10.13; N, 5.08. Calcd. for $C_{18}H_{29}O_2N$: C, 74.18; H, 10.13; N, 4.81%.

The Nitration of I: 2, 4, 6-Tri-*t*-butyl-*m*-dinitrobenzene (III).—A finely ground mononitro derivative (7 g. of I) was added in small portions to the stirred mixture of 13 ml. of fuming nitric acid (d=1.50) and 36 ml. of concentrated sulfuric acid at 20°C. The reaction mixture was subsequently heated to 80°C for 5 hr.; the product, when cooled, was then poured onto a large amount of ice. The yellow solid was collected, washed with water, dilute ammonia and water, and then dried. It weighed 6.6 g. and melted at 220~269°C.

Purification by recrystallization from benzene and by chromatography on alumina with benzene-ligroin (b. p. 80~100°C) gave pale yellow needles (m. p. 290~292°C). The molecular weight of this product was determined by the Rast method.

Found: C, 64.27; H, 8.42; N, 8.58%; mol. wt., 324.1. Calcd. for $C_{18}H_{28}O_4N_2$: C, 64.26; H, 8.39; N, 8.33%; mol. wt., 336.4.

The Reduction of I at a High Pressure: 2, 4, 6-Tri-*t*-butylaniline (III).—A suspension of 30 g. of I and a catalyst prepared from 20 g. of Raney-nickel-alloy in 300 ml. of ethanol was reduced with hydrogen (60 kg./cm^2) at 50~80°C for 3.5 hr. in a 500 ml. autoclave. After the catalyst had been filtered off, the solvent was distilled off; 22 g. of practically pure III with a m. p. of 143~145°C was thus obtained. One recrystallization from ethanol gave a sample melting at 145°C.

Found: C, 82.65; H, 11.79; N, 5.61%. Calcd. for $C_{18}H_{31}N$: C, 82.69; H, 11.95; N, 5.36%.

The Nitration of III: 2, 6-Di-*t*-butyl-4-nitroaniline (IV).—This was prepared in essentially the manner described in the literature,[6] except that the reaction was carried out at 40°C, because most of the starting material (about 70%) was recovered at −10~−12°C, as is mentioned in the literature.

To a solution of 5.2 g. of III in a mixture of 40 ml. of acetic anhydride and 20 ml. of glacial acetic acid, 22 ml. of a mixture of 1 vol. of nitric acid (d=1.52) and 19 vol. of glacial acetic acid was added drop by drop at 40°C; hereupon III crystallized out in yellow needles. While the stirring was continued, the crystals of III disappeared and other crystalline material IV was obtained in the reaction mixture. After a total reaction time of 4.5 hr., the product was collected and dried; 1.9 g. Upon treatment with water, the filtrate gave further crops; 0.1 g.

The recrystallization of this product (m. p. 240~247°C) from benzene-ethanol (10:1) gave IV as pale yellow leaf crystals; m. p. 256°C.

Found: C, 66.92; H, 9.00; N, 10.92%. Calcd. for $C_{14}H_{22}N_2O_2$: C, 67.17; H, 8.86; N, 11.69%.

2, 6-Di-*t*-butyl-*p*-diaminobenzene (V).—A suspension of 3.0 g. of IV in 100 ml. of ethanol was shaken with hydrogen at room temperature under atmospheric pressure over Raney nickel for 6 hr. The catalyst was then filtered off under a stream of nitrogen. After the filtrate had been saturated with dry hydrogen chloride, the solvent was distilled off under reduced pressure. The dihydrochloride of V separated in the crystalline state. This salt was collected, washed with dry ether, and dried; yield 3.4 g. (96%). Recrystallization from ethanol saturated with dry hydrogen chloride gave a colorless salt which melted at 204°C (decomp.).

Found: Cl, 23.42%. Calcd. for $C_{14}H_{26}N_2Cl_2$: Cl, 24.17%.

Through a treatment of the salt with a dilute alkali solution, the base was liberated; m. p. 94~95°C.

2, 6-Di-*t*-butyl-*p*-benzoquinone (VI).—A suspension of 1 g. of the above salt in a solution of 15 g. of ferric chloride crystals in a mixture of 7.6 ml. of water and 1 ml. of concentrated hydrochloric acid was stirred overnight at room temperature and was then heated on a water bath for 2 hr. The product was then collected through steam distillation. The yield was 0.6 g. of orange yellow crystals (VI); 80% of yield, m. p. 66.5~68.5°C. Recrystallization from aqueous ethanol gave a sample melting at 67.5°C; this sample showed no depression on admixture with an authentic sample synthesized from 2, 6-di-*t*-butylphenol.[10]

Found: C, 76.48; H, 9.12%. Calcd. for $C_{14}H_{20}O_2$: C, 76.32; H, 9.15%.

The Preparation of Other *m*-Dinitrobenzenes.—IIa, IIb and IIc were prepared by the standard procedures.

IIa, m. p. 90°C; IIb, m. p. 61~63°C; IIc, 165~166°C.

The Reduction of Dinitro Derivatives (Fig. 1).—A mixture of the purified dinitro compound (0.005 mol.) in 50 ml. ethanol was shaken with hydrogen for several hours at room temperature under atmospheric pressure in the presence of a catalyst prepared from 5 g. of Raney-nickel-alloy (5 g. of alloy for 0.01 mol., of I in 100 ml. ethanol) until no more hydrogen was absorbed. About 10~13% more than the stoichiometric quantity of hydrogen for the reduction of nitro groups was absorbed. II resisted hydrogenation very strongly; most of it was recovered.

Infrared Spectra.—The spectra of 0.02 M solutions in chloroform were measured in a 0.511 mm. cell on a Hitachi EPI-2 double-beam prism spectrometer (with a rock salt prism).

The frequencies (in wave numbers) and the transmittance (%) of the symmetric (ν_s) and antisymmetric (ν_a) stretching modes of the nitro-group are summarized in Table I.

13) S. Watarai, This Bulletin, 36, 747 (1963).

The author wishes to express his thanks to Professor Toshio Kinugasa for his kind advice and encouragement throughout this work, and to the members of the Faculty of Science of Osaka University for their elementary analyses and infrared spectra measurements. He is also indebted to Mr. Mitsumasa Taniyama and Miss Setsuko Ikegami for their skillful collaboration.

Department of Chemistry
Faculty of Science
Kobe University
Mikage, Kobe

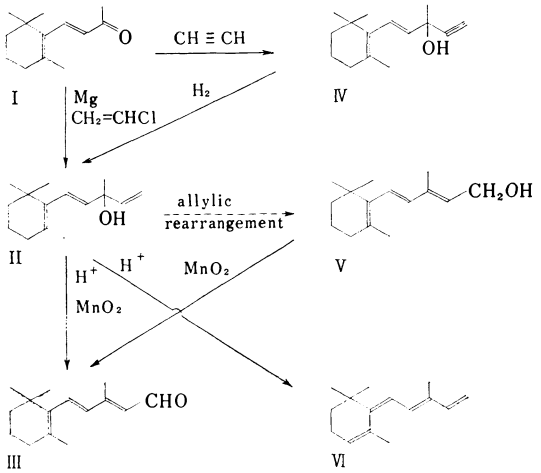
The Synthesis of β-Ionylideneacetaldehyde

By Yozo Ishikawa

(Received August 16, 1963)

This paper will present a simple method to prepare β-ionylideneacetaldehyde, which is an important intermediate in the synthesis of vitamin A or its homologous compounds. *trans*-β-Ionylideneacetaldehyde (III) was obtained by the oxidation of vinyl-β-ionol (II) with manganese dioxide under an acidic condition. II was prepared by means of a Grignard reaction from β-ionone (I) and vinyl chloride.

II has been prepared by the reduction of ethynyl-β-ionol (IV)[1-4] derived from I and acetylene. Another method which utilizes the Grignard reaction of I with vinylmagnesium bromide has been reported,[4] but the yield of II is not so satisfactory (41%). The author obtained II in a 91% yield by means of the Grignard reaction of I with vinylmangnesium chloride.



1) K. Suga, Y. Ishikawa and S. Watanabe, *J. Chem. Soc. Japan, Pure Chem. Sec.* (*Nippon Kagaku Zasshi*), to be published.

The synthesis of vinylmagnesium chloride by means of Normant's method[5] and the continuous preparation of the chloride have been reported by Ramsden et al.[8] and by Reimschuessel[7] respectively. The present author applied Ramsden's method, but vinyl chloride gas was passed into tetrahydrofuran at 15~20°C as the reaction proceeded more rapidly. The Grignard compound of I with vinylmagnesium chloride was allowed to react as usual, and the product distilled to give II.[8]

III may be prepared by the oxidation of β-ionylideneethanol (V), the isomerization product of II. Because of the tendency to give a "*retro*-compound,"[11-14] it is very difficult to obtain V by the allylic rearrangement

2) R. G. Gould, Jr., and A. F. Thompson, Jr., *J. Am. Chem. Soc.*, **57**, 340 (1935).
3) W. Oroshnik, G. Karmas and A. D. Mebane, ibid., **74**, 295 (1952).
4) L. A. Yanovskaya, *Izv. Akad. Nauk SSSR, Otd. Khim. Nauk*, 1435 (1960); *Chem. Abstr.*, **55**, 413e (1961).
5) H. Normant, *Compt. rend.*, **239**, 1510 (1954); **241**, 1946 (1955).
6) H. E. Ramsden, J. R. Leebrick, S. D. Rosenberg, E. H. Miller, J. J. Walburn, A. E. Balint and R. Cserr, *J. Org. Chem.*, **22**, 1602 (1957).
7) H. K. Reimschuessel, ibid., **25**, 2256 (1960).
8) Karrer et al.[9] reported that 1,4-addition may occur in the Grignard reaction of I. On the other hand, Oroshnik et al.[10] described how the 1,2-adducts were the main products of this reaction. In the present experiment the reaction product was proved to be II, and I was found to react normally with the Grignard reagent to give the 1,2-adduct as a major product.
9) P. Karrer, H. Salomon, R. Morf and O. Walker, *Helv. Chim. Acta*, **15**, 878 (1932).
10) W. Oroshnik, G. Karmas and R. A. Mallory, *J. Am. Chem. Soc.*, **76**, 2325 (1954).
11) A. F. Thompson, Jr., N. A. Milas and I. Rovno, ibid., **63**, 752 (1941).
12) H. O. Huisman, A. Smit, S. Vromen and L. G. M. Fisscher, *Rec. trav. chim.*, **71**, 889 (1952).
13) P. H. van Leeuwen and H. O. Huisman, ibid., **80**, 115 (1961).
14) H. Pommer and W. Sarnecki, German Pat. 1059900, (1957).

of II in spite of the easier oxidation of V with manganese dioxide to III ;[1] V has, therefore, usually been prepared by the reduction of β-ionylideneacetates. The author obtained *trans*-III in one step by treating II with manganese dioxide under an acidic condition.

To a solution of II in petroleum ether containing a small quantity of 50% sulfuric acid, manganese dioxide was added with vigorous agitation. The product was chromatographed on a silica-gel column. A hydrocarbon (A) and a carbonyl compound (B) were eluted with petroleum ether and benzene-ether (9 : 1) respectively. The properties of B agreed with the authentic data of *trans*-β-ionylideneacetaldehyde, which will be described later. The mechanism of this reaction is not clear as yet, but we can assume that as soon as II rearranges to V, oxidation occurs simultaneously.

The infrared absorption spectrum of A did not show the presence of either a hydroxyl or a carbonyl group. As the ultraviolet absorption spectrum shows the characteristic "*retro*-ionylidenetetraene" structure (λ_{max} 319 mμ ; ε, 52300), A may be considered to be, for the most part, "*retro*-compound (VI)."

Experimental[15]

β-Ionone (I).—The properties of I used in this experiment were as follows : d_{25}^{25} 0.943 ; n_D^{20} 1.5198 ; Acid value 0.1 ; λ_{max} 296 mμ ; ε, 9900 (lit.,[10] $\lambda_{max}^{96\%\ ethanol}$ 296 mμ ; ε, 10550) ; the 2,4-dinitrophenylhydrazone, m. p. 125°C ; λ_{max} 389 mμ ; ε, 21000.

Found : C, 61.40 ; H, 6.14 ; N, 15.21 ; Calcd. for $C_{19}H_{24}O_4N_4$: C, 61.29 ; H, 6.50 ; N, 15.05%.

Vinyl-β-ionol (II). — In a four-necked flask equipped with a thermometer, a dropping funnel, as gas inlet tube and a reflux condenser, 200 cc. of dry tetrahydrofuran, 13 g. (0.54 mol.) of magnesium, and a few crystals of iodine were placed. To this mixture 3.0 g. (0.03 mol.) of ethyl bromide was added drop by drop. When magnesium had been activated, the mixture was allowed to react with dry gaseous vinyl chloride at 40°C. After 30 min., the mixture was cooled to 15~20°C and vinyl chloride was passed through for an additional 9 hr. The reaction mixture turned dark brown and viscous. After the completion of the reaction, the gas inlet tube was removed, and 60 g. (0.31 mol.) of I in 60 cc. of tetrahydrofuran was stirred into this solution at 5~10°C. After having been stirred for another hour, the solution was heated to 40°C. The reaction mixture was decomposed with an ice-cooled ammonium chloride solution and extracted with ether. The ethereal layer was washed with a 2% aqueous solution of sodium hydrogen carbonate and water, and then dried over anhydrous sodium sulfate. Evaporation under reduced pressure gave 67 g. of a light yellow oil. By fractional distillation 57.4 g. of vinyl-β-ionol (II) was obtained (91.4% yield) : b. p. 113~115°C/2 mmHg (lit., 113~115°C/2 mmHg ;[4] 91~92°C/0.8 mmHg[3]) ; n_D^{20} 1.5045 (lit., n_D^{20} 1.5702 ;[4] 1.5022[3]) ; λ_{max} 237 mμ ; ε, 5700 (lit.,[3] λ_{max} 235 mμ ; 5700).

Found : C, 81.35 ; H, 10.91 ; Calcd. for $C_{15}H_{24}O$: C, 81.76 ; H, 10.98%.

The infrared absorption spectrum showed the characteristic bands of a tertiary hydroxyl group (3400 and 1100 cm^{-1}) and of a vinyl group (920 and 990 cm^{-1}). The infrared and ultraviolet absorption spectra were identical with those of the partial reduction product of ethynyl-β-ionol derived from β-ionone and acetylene.[1]

***trans*-β-Ionylideneacetaldehyde (III).** — To a solution of 5.00 g. (0.023 mol.) of vinyl-β-ionol in 150 cc. of petroleum ether, 1.3 cc. of 50% sulfuric acid and 50 g. of activated manganese dioxide were added under efficient agitation. The mixture was stirred for 72 hr. at room temperature. Upon the product had been worked up, 4.10 g. of a light yellow oil was obtained. This oil was chromatographed on a silica-gel column. From the petroleum ether-eluted fraction, a 0.69 g. of hydrocarbon (A) was obtained, while 1.77 g. (a 35.8% yield) of a carbonyl compound (B) was obtained from the benzene-ether (9 : 1).

The infrared absorption spectrum of B was super-imposable on that of the authentic sample ;[1] 1670 and 965 cm^{-1}. The ultraviolet absorption spectrum : λ_{max} 275, 326 mμ ; ε, 11000, 14000 (lit.,[16] λ_{max} 273, 326 mμ ε, 11800, 15600).

Semicarbazone.—Recrystallized from ethanol : m. p. and mixed m. p. 195°C ; λ_{max} 324 mμ ε, 34700 (lit.,[17] m. p. 195~196°C ; λ_{max} 323 mμ $E_{1cm}^{1\%}$ 1330).

Found : N, 14.85. Calcd. for $C_{16}H_{25}ON_3$: N, 15.26%.

2, 4-Dinitrophenylhydrazone. — Recrystallized from chloroform-ethanol : m. p. and mixed m. p. 198°C ; λ_{max} 410 mμ ; ε, 40000 (lit.,[16] m. p. 198°C ; λ_{max} 408 mμ ε 37000).

Found : C, 62.83 ; H, 6.35 ; N, 14.05. Calcd. for $C_{21}H_{26}O_4N_4$: C, 63.30 ; H, 6.58 ; N, 14.06%.

An attempt to isolate III by means of the addition product with sodium hydrogen sulfite[12] was unsuccessful.

The ultraviolet absorption spectrum of A showed the characteristic "*retro*-ionylidenetetraene" structure at λ_{max} 319 mμ (lit., $\lambda_{max}^{96\%\ ethanol}$ 313 mμ ;[12] $\lambda_{max}^{ethanol}$ 317 mμ[18]), suggesting the formation of a retro-form unsaturated hydrocarbon. The isolated A changed to a gummy substance within a few hours and became insoluble in the usual solvents, so its structure was not identified.

15) The UV absorption spectra were measured in ethanol, chloroform (the semicarbazone and the 2, 4-dinitrophenylhydrazone of (III)) or benzene (VI), and the IR absorption spectra, with liquid film. Elementary analyses were performed at the Institute of Physical and Chemical Research, Tokyo.

16) C. D. Robeson, J. D. Cawley, L. Weisler, M. H. Stern, C. C. Eddinger and A. J. Chechak, *J. Am. Chem. Soc.*, 77, 4111 (1955).

17) N. L. Wendler, H. L. Slates. N. R. Trenner and M. Tishler, ibid., 73, 719 (1951).

18) W. Oroshnik, A. D. Mebane and G. Karmas, ibid., 75, 1050 (1953).

The author is indebted to Professor Kyoichi Suga and Mr. Shoji Watanabe of Chiba University for their cordial guidance throughout this work.

Miyoshi Oil & Fat Co., Ltd.
Katsushika-ku, Tokyo

*The Electronic Effect of the Substituents on the Intramolecular Hydrogen Bonding of o-Aryloxybenzoic Acids**

By Michinori Ōki and Minoru Hirota

(Received August 19, 1963)

As early as 1955, Davies[1,2] reported the intramolecular hydrogen bonding of *o*-methoxybenzoic acid (II: $R=CH_3$); the enthalpy of the hydrogen bonding was then estimated to be 3.3 kcal./mol. It is also known that *o*-alkoxy- and *o*-aryloxybenzoic acids show some anomalous properties which may be attributed to intramolecular interaction.[3-5] In spite of this early discovery, however, systematic studies of this phenomenon are lacking and little is known about its nature. Since the authors are interested in the intramolecular hydrogen bonding of carboxylic acids, this work was undertaken as an extension of their earlier work.

An earlier study disclosed that the intramolecular hydrogen bonding of the alkoxy- and aryloxy-alkanoic acids is observed only when the alkoxyl or aryloxyl group is placed at the α-position of the carboxyl group to form five-membered rings by means of the hydrogen bond (III: $n=1$).[6] Therefore, we have to face a very interesting problem; "Why does the six-membered hydrogen bond system exist very stably in *o*-alkoxybenzoic acid, but not in β-phenoxy- or β-methoxy-propionic acid (III: $n=2$)?" In order to clarify the situation, various effects on the interaction must be studied. Thus, the electronic effect exerted by the substituent in the aryl group of *o*-aryloxybenzoic acid was investigated as a first step, the effect of the configuration being also discussed.

Experimental

The Preparation of Materials. — All the *o*-aryloxybenzoic acids were prepared from *o*-chlorobenzoic acid and the corresponding phenols by modifying Fritzsche's method[7] as described below.

Into a methanol solution (70 ml.) of sodium methoxide prepared from 4.6 g. (0.2 g. atom) of sodium, a mixture of phenol (9.4 g., 0.1 mol.) and *o*-chlorobenzoic acid (15.7 g., 0.1 mol.) was added with efficient stirring. As soon as the addition was over, about 0.5 g. of copper powder was added, and then the solvent was distilled off to dryness by immersing the flask in an oil bath kept at 150°C. The reaction mixture was heated up to 190~220°C in the oil bath, whereupon the abrupt initiation of the condensation was observed. After an hour, the reaction mixture was cooled and the entire mixture dissolved in water. After filtration, the filtrate was acidified to give crude *o*-phenoxybenzoic acid. Recrystallization from xylene-ligroin yielded 18.0 g. (84%) of the pure compound. Similarly, the following compounds were prepared (Table I):

Table I. Analytical data and physical constants of 2-(*p*-substituted phenoxy)-benzoic acids

p-Substituent	Analytical data: Calcd., % C	Calcd., % H	Found, % C	Found, % H	M. p. °C
Acetyl	70.30	4.72	70.34	4.83	182
Chloro	62.70	3.63	62.93	3.78	112
Methoxy	68.84	4.95	68.86	4.96	144

Measurement of the Spectra. — The infrared spectra were recorded with a Perkin Elmer 112G grating infrared spectrophotometer; the spectral slit widths were 1.0 cm^{-1} and 0.6 cm^{-1} for the O-H and C=O stretching regions respectively. The measurement was carried out in a carbon tetrachloride solution with a concentration of less than

* The preceding paper: M. Ōki and M. Hirota, This Bulletin, **36**, 290 (1963).

1) M. Davies and D. M. F. Griffiths, *J. Chem. Soc.*, **1955**, 132.
2) M. Davies, "Hydrogen Bonding—Papers presented at the Symposium on Hydrogen Bonding held at Ljubljana, 29 July—3 August, 1953" (Pergamon Press, 1959). p. 393.
3) C. J. W. Brooks, G. Eglinton and J. E. Morman, *J. Chem. Soc.*, **1961**, 106.
4) D. Peltier and A. Pichevin, *Bull. soc. chim. France*, **1960**. 1141.
5) O. H. Wheeler, *Can. J. Chem.*, **39**, 2603 (1961).
6) M. Ōki and M. Hirota, This Bulletin, **34**, 374 (1961).
7) P. Fritzsche, *J. prakt. Chem. N. F.*, **20**, 269 (1879).

0.002 mol./l. in the ν_{O-H} region and less than 0.0005 mol./l. in the $\nu_{C=O}$ region at 20~25°C. Each absorption curve was assumed to be a Lorentzian curve, and the integrated intensity was calculated from the equantion : [8,9]

$$A=2.30\times\frac{\pi}{2}\cdot\frac{1}{cl}\log\left(\frac{T_0}{T}\right)_{max}\times\Delta\nu_{1/2}$$

Since the spectral measurements were carried out under conditions which gave spectral slit widths less than one-tenth of the half-band width, the application of the equation is permissible.

TABLE II. THE INFRARED ABSORPTION SPECTRA OF *o*-(*p*-SUBSTITUTED PHENOXY)BENZOIC ACIDS (p-$XC_6H_4OC_6H_4COOH$-o)

The ν_{O-H} absorption data

X		ν_{max} cm^{-1}	ε_{max}	$\Delta\nu_{1/2}$	$A\cdot10^{-2}$	A_t/A_c
CH_3O	cis	3528.2	22.9	29.7	2.46	13.7
	trans	3391.0	130	53.2	24.98	
		3350.4	44.0	54.5	8.65	
CH_3	cis	3528.4	33.5	30.9	3.75	8.12
	trans	3393.8	125	54.0	24.38	
		3350.1	30.9	53.6	5.98	
H	cis	3527.8	40.4	29.8	4.35	6.70
	trans	3399.5	120	50.6	21.92	
		3357.9	34.1	58.4	7.20	
Cl	cis	3527.6	59.6	30.1	6.49	2.86
	trans	3411.7	74.7	54.5	14.70	
		3374.8	17.4	61.6	3.86	
CH_3CO	cis	3528.6	66.8	42.2	10.19	0.903
	trans	3421.5	36.1	53.3	6.95	
		3387.6	11.3	55	0.98	

TABLE III

The $\nu_{C=O}$ absorption data

X		ν_{max} cm^{-1}	ε_{max}	$\Delta\nu_{1/2}$	$A\cdot10^{-3}$	A_t/A_c
CH_3O	cis	1730	74.0	15.5	4.14	8.58
	trans	1752.4	863	11.4	35.54	
		1762	73.0	12.3	3.24	
CH_3	cis	1730.7	102	15.9	5.86	6.76
	trans	1750.9	838	13.1	39.65	
		1759	138	10.6	5.28	
H	cis	1731	157	14.8	8.40	3.88
	trans	1752.1	785	11.5	32.59	
		1762	155	10.4	5.82	
Cl	cis	1733	188	18.0	12.21	2.21
	trans	1752.1	646	11.6	27.05	
		1763	135	10.6	5.17	
CH_3CO	cis	1733.9	154	17.2	9.56	1.13
	trans	1752.0	268	11.2	10.84	
		1761	53.5	14.0	2.70	

8) D. A. Ramsay, *J. Am. Chem. Soc.*, **74**, 72 (1952).
9) K. Kuratani et al., *J. Japanese Chem.* (*Kagaku-no-ryōiki*), Suppl. Ed., No. 31, 1 (1958).

Results and Discussion

The O–H stretching and the C=O stretching absorptions were determined with various *o*-(*p*-substituted phenoxy)benzoic acids; the results are summarized in Tables II and III.

Assignment of the Infrared Spectra.—Before the intramolecular hydrogen bonding is discussed, the assignment of the absorption bands should be carried out. The O–H and the C=O stretching absorption spectra of *o*-phenoxybenzoic acid are illustrated in Figs. 1 and 2 respectively. In the O–H stretching region, three absorption bands were found; the one at 3527.8 cm^{-1} is no doubt the absorption

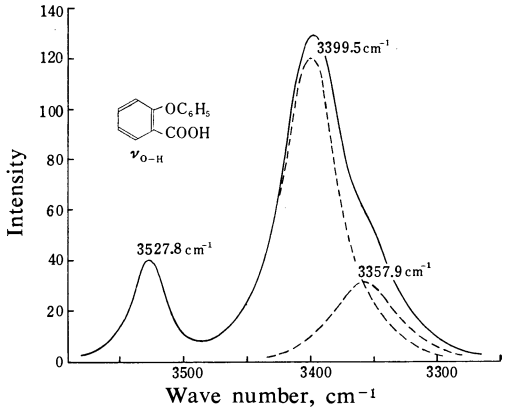


Fig. 1

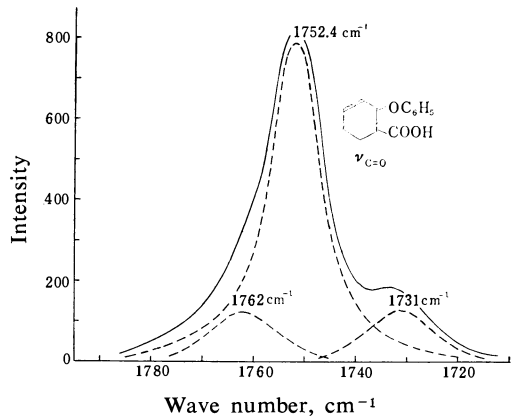
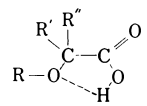


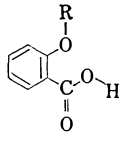
Fig. 2

caused by the monomeric cis-configuration (IIa), while the others may arise from the monomeric trans forms and/or the dimeric forms.

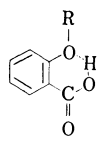


I

R=CH_3, C_2H_5, $CH(CH_3)_2$ or XC_6H_4
R′ and R″=H or CH_3



IIa



IIb

$RO(CH_2)_nCOOH$

III

The results obtained at various concentrations, however, exclude the latter possibility, and so the two absorption bands at 3399.5 cm^{-1} and 3357.9 cm^{-1} are both attributed to the hydrogen-bonded trans-configuration.

Then the measurement was carried out at various temperatures, with both the O–H and the C=O stretching absorptions (Table IV),

TABLE IV. THE TEMPERATURE DEPENDENCE OF THE INTENSITY RATIO (A_t/A_c) OF *o*-PHENOXYBENZOIC ACID

ν_{O-H} Region

T, °K	$1000/T$	Absorption intensity		Intensity ratio
		ε_{cis}	ε_{trans}	$\varepsilon_t/\varepsilon_c$
296.7	3.37	43.0	122	2.83
307.0	3.26	47.2	125	2.65
317.2	3.15	53.5	125	2.32
325.5	3.07	62.8	129	2.09
339.2	2.95	64.4	124	1.93

$\Delta H = 1.89$ kcal./mol.

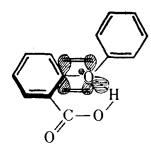
$\nu_{C=O}$ Region

T, °K	$1000/T$	Absorption intensity		Intensity ratio
		ε_{cis}	ε_{trans}	$\varepsilon_t/\varepsilon_c$
296.7	3.37	135	852	6.31
312.7	3.19	149	845	5.77
322.8	3.10	154	792	5.14
336.0	2.98	169	794	4.70
345.2	2.90	208	864	4.16

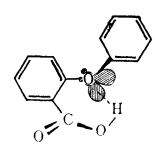
$\Delta H = 1.78$ kcal./mol.

and the enthalpy difference, ΔH, for IIa → IIb was determined to be 1.89 kcal./mol. from the results obtained in the O–H stretching region by assuming the above assignment. Here the 3357.9 cm^{-1} band is disregarded for the sake of simplicity. From the $\nu_{C=O}$ spectrum, the enthalpy difference is determined to be 1.78 kcal./mol. by assigning the band at 1731 cm^{-1} to the cis configuration and the band at 1752.4 cm^{-1} to the trans. The agreement of the two ΔH values supports the above assignment and also the reliabilty of the enthalpy difference value for this equilibrium. The much smaller ΔH value than that of *o*-methoxybenzoic acid indicates a weaker hydrogen bonding; this will be discussed later. The fact that the carbonyl absorption of the trans isomer appears at a higher frequency had already been interpreted as arising from the absence of intramolecular interaction between the hydroxyl and the carbonyl group in the same carboxyl group.[6,10]

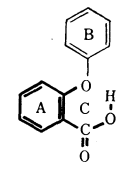
The carbonyl band at 1762 cm^{-1} is assigned to the trans-configuration which causes the 3357.9 cm^{-1} band in the O–H stretching region, from the parallel change in intensity.* On the other hand, the higher C=O stretching band should be assigned to the structure which makes the less contribution to the resonance between the benzene nucleus and the carboxylic C=O group. Thus, the trans ν_{O-H} absorption at the higher frequency and the $\nu_{C=O}$ absorption at the lower frequency are attributed to the system IVa (The thick lines in IVa' indicate the planar conjugated system.), while the trans ν_{O-H} absorption at the lower frequency and the trans $\nu_{C=O}$ absorption at the higher frequency are attributed to the less probable conjugate system, IVb. In the IVa system, the hydrogen bond is formed by the lone pair electrons conjugating with the B ring (in IVa'), and the hydrogen-bonded ring system C is on the same plane with the ring system A, a pseudo-aromatic nature being expected. On the other hand, the hydrogen bond is formed by the participation of the lone pair electrons conjugating with the A ring in the IVb system, and the conjugated six-membered hydrogen bond system existing in IVa is partly destroyed.



IVa



IVb



IVa'

The diphenyl ether system is concluded to be non-planar, and the two stable rotational isomers are assumed by some authors.[11] It is obvious, in accordance with the postulation, that the existence of the two rotational isomers is also probable in this diphenyl ether system, that of *o*-aryloxybenzoic acids.

In the case of *o*-aryloxybenzoic acids, the shift of the ν_{O-H} absorption maxima caused

10) M. Ōki and M. Hirota, *Spectrochim. Acta*, 17, 583 (1961).

* The following may be added as another proof for this assignment. The introduction of a 3-alkyl group to 2-methoxybenzoic acid causes a ν_{O-H} shift to a lower frequency. It is assumed that the steric interference between 3-alkyl and 2-methoxyl groups causes the rotation of the C_{Ph}-O bond, leaving the CH_3O group intact; therefore, the hydrogen bonding may be strengthened because of the richer electron density of the oxygen atom. Therefore, a higher ν_{O-H} absorption corresponds to a more planar structure.

11) One of the latest reports on this problem is that of S. Fujiwara H. Shimizu, and Y. Morimo, *J. Chem. Phys.*, 34, 1467 (1961). See also K. Higashi and S. Uyeo, This Bulletin, 14, 87 (1939).

by the hydrogen bonding ($\Delta\nu_{max}$) is much larger than in the case of 2-aryloxyalkanoic acids, but the assignment established to the latter is qualitatively applicable.

The Substituent Effect on the Absorption Intensity.—The data in Tables II and III show the variation of the ratio (A_t/A_c) of the absorption intensity due to the trans isomer to that due to the cis isomer with the change in the electronic nature of the substituents; this result is illustrated by the $\log(A_t/A_c)$ vs. σ relation presented in Fig. 3. Table V also gives numerical values.

In general, the hydrogen bonding is favorable when the electron density of the hydrogen-accepting atom (the ether oxygen atom in this case) is large; therefore, the larger A_t/A_c ratio

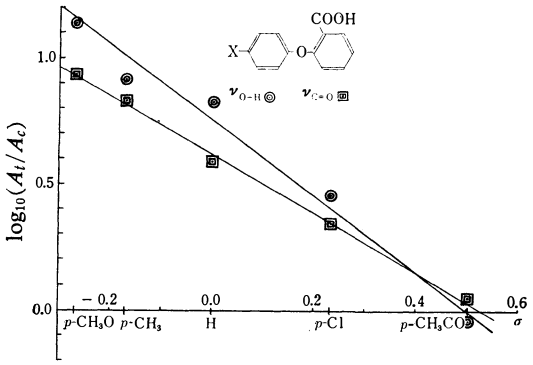


Fig. 3

Table V. The relation between the σ-constant and $\log(A_t/A_c)$ of o-(p-substituted phenoxy)benzoic acids

Substituent	σ-Constant	$\log(A_t/A_c)$ O–H Region	$\log(A_t/A_c)$ C=O Region
CH_3O	−0.268	1.137	0.933
CH_3	−0.170	0.910	0.830
H	0.000	0.826	0.589
Cl	0.227	0.456	0.344
CH_3CO	0.502	−0.044	0.053

is expected for the bases with electron-repelling substituents.

This tendency is observed in many hydrogen bond systems, and the same is observed with the spectra of o-aryloxybenzoic acids, in both the O–H and C=O absorption bands. This finding also supports the assignment of the $\nu_{C=O}$ absorptions, since the opposite inclination of the $\log(A_t/A_c)$ vs. σ plot would be expected from a wrong assignment.

Conclusions on the Nature of the Hydrogen Bonding.—The hydrogen bonding in o-aryloxybenzoic acid causes a much larger ν_{O-H} shift and enthalpy gain, and the hydrogen-bonded species are much more favorable than are α-aryloxyacetic acids and their homologs. This cannot be explained by the steric factor only. The pseudo-aromatic nature of the hydrogen bond system (the C ring in IVa') could explain the unusual stability of this hydrogen bonding. The pseudo-aromatic nature of the hydrogen bond system will be established in the following paper.[12]

Summary

The infrared hydroxyl and carbonyl absorptions of o-aryloxybenzoic acids have been reported and the assignment of each absorption band in these regions made. The higher carbonyl-stretching absorptin at about 1752 cm^{-1} has been attributed to the intramolecular hydrogen-bonded trans isomer from the following reasons: i) The A_t/A_c intensity ratio in the hydroxyl-stretching region increases as the Hammett σ-constant of the substituent decreases, and the same tendency is observed by assigning the carbonyl band at a higher frequency to the trans isomer; ii) From the measurement of the absorption intensity of 2-phenoxybenzoic acid at various temperatures, in both the hydroxyl and carbonyl regions, the authors have obtained nearly equal enthalpy difference values (1.89 and 1.78 kcal./mol. respectively) between the cis and trans isomers by assuming the above assignment.

Department of Chemistry
Faculty of Science
The University of Tokyo
Hongo, Tokyo

12) M. Ōki and M. Hirota, This Bulletin, 37, 213 (1964).

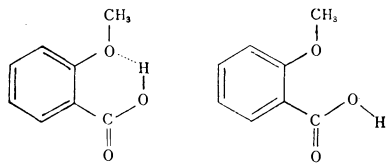
The Steric Requirements and the Nature of the Intramolecular Hydrogen Bonding of o-Methoxybenzoic Acid[*1]

By Michinori Ōki and Minoru Hirota

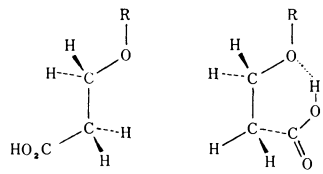
(Received August 19, 1963)

The existence of the six-membered intramolecular hydrogen bonding in *o*-aryloxybenzoic acids[1] and in *o*-methoxybenzoic acid[2] has already been established, but the reason why the six-membered hydrogen bonding is present in *o*-aryloxy- and *o*-alkoxybenzoic acids but not in *β*-phenoxy- and *β*-alkoxybenzoic acids has not yet been explained.

An answer to this question may be given by the entropy difference between the two systems. That is, the intramolecular hydrogen bonding is forced in *o*-alkoxybenzoic acids (such as I), while the rotational isomerism around the C–C single bond reduces the probability of the intramolecular hydrogen bonding in *β*-alkoxypropionic acid, since the most stable rotamer is IIa if there is no stabilization by the hydrogen bond formation.



Ia Ib



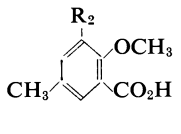
IIa IIb

An alternative answer to this question may be that the intramolecular hydrogen bonding in *o*-alkoxybenzoic acids is stabilized by resonance, since this kind of stabilization is present in many hydrogen bond systems, such as the enol form of acetylacetone and salicylaldehyde. The resonance-stabilized hydrogen bond systems usually have a characteristic electronic spectra in the ultraviolet region. Ultraviolet spectral studies of the intramolecular hydrogen bonding have been carried out with many ortho-substituted phenols by Burrawoy and his co-workers,[3] who concluded that the intramolecular hydrogen bonding causes a remarkable red shift of the so-called B-bands, which have the longitudinal transition moment. On the other hand, the ultraviolet spectral measurement is also a very useful tool for the estimation of the steric hindrance; extensive study in this field has been reported by Braude and his co-workers.[4]

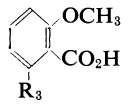
Thus, the ultraviolet spectral technique, as well as the infrared spectral measurement, has been employed in order to study the nature of the intramolecular hydrogen bonding of *o*-alkoxybenzoic acid derivatives, and the spectral data have been interpreted from the stand-point of steric hindrance and that of the characteristic absorption of the conjugated system.

Experimental

Preparation of the Materials. — *Substituted 2-Methoxybenzoic Acids.* — To a solution of 25 g. of 2,4-dimethylanisole in 150 ml. of chloroform, an equi-molecular amount (29.5 g.) of bromine was added at such a rate that the large excess of bromine did not remain unreacted in the reaction mixture. The mixture was left to stand for 10 min. after the addition was over; then the solvent distilled off, and the residual liquid was distilled under reduced pressure. The liquid, which boiled at 130 ~134°C/15 mmHg, was almost pure 6-bromo-2,4-dimethylanisole. Yield: 32 g. (81%).



III $R_2=H$
IV $R_2=CH_3$
V $R_2=C_2H_5$
VI $R_2=CH(CH_3)_2$



VII $R_3=CH_3$
VIII $R_3=C_2H_5$

*1 Presented at the Symposium on Molecular Structure and Spectroscopy, IUPAC, Tokyo, September, 1962. The preceding paper: M. Ōki and M. Hirota, This Bulletin, 37, 209 (1964).

1) M. Ōki and M. Hirota, ibid., 35, 1048 (1962).

2) M. Davies, "Hydrogen Bonding—Papers Presented at the Symposium on Hydrogen Bonding Held at Ljubljana, 29 July—3 Aug., 1957" (Pergamon Press, 1959), p. 393.

3) A. Burawoy, ibid., p. 259, and other publications by the same author, such as A. Burawoy, M. Cais, J. T. Chamberlain, F. Liversedge and A. R. Thompson, *J. Chem. Soc.*, 1955, 3721.

4) E. A. Braude and F. Sondheimer, ibid., 1955, 3754, and other publications by the same authors. See also E. A. Braude and E. S. Waight, "Progress in Stereochemistry," Ed. by Klyne, Butterworth, London (1954), p. 126.

Table I. Substituted 2-methoxybenzoic acids

Substituent	Yield	M. p., °C	Calcd., %		Found, %	
			C	H	C	H
3,5-Dimethyl	64	90	66.65	6.71	66.78	6.73
3-Ethyl-5-methyl	45	135	68.02	7.27	68.13	7.35
3-Isopropyl-5-methyl	70	87.5	69.21	7.74	69.24	7.81
6-Methyl*	75	138	65.21	6.18	65.05	6.07
6-Ethyl	—	110	66.65	6.71	66.57	6.70

* The preparation of this compound had been reported[5] by means of the hydrolysis of the corresponding nitrile. However, the hydrolysis was found to be very slow and the reported melting point did not agree with the present results.

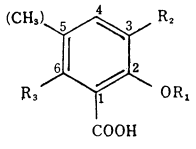
A solution of 32 g. of 6-bromo-2,4-dimethylanisole in 50 ml. of dry ether was added to 3.6 g. of magnesium in 100 ml. of ether, while the flask was externally heated to the boiling point. The heating was continued for 2 hr. after the completion of the addition; then the Grignard reagent was cooled to room temperature and treated with a large excess of solid carbon dioxide until the reaction mixture was saturated with carbon dioxide. The mixture was kept overnight and decomposed with hydrochloric acid. The ether layer was collected and, after washing with water, extracted with an aqueous sodium bicarbonate solution. The solution was heated to remove the ether in the solution and then acidified. The solid was dried and recrystallized from a xylene-petroleum mixture to give 17 g. (64%) of 2-methoxy-3,5-dimethylbenzoic acid (m. p. 90°C).

Other subtituted 2-methoxybenzoic acids were prepared in a similar manner; the results are tabulated in Table I.

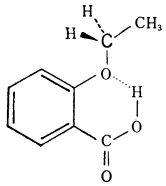
Spectral Measurement.—Ultraviolet spectra were measured with a Beckman model DU spectrophotometer, the samples being dissolved in an appropriate solvent to make up ca. 3×10^{-4} mol./l. solution. The details of the infrared spectral measurement have been reported elsewhere.[6]

Results and Discussion

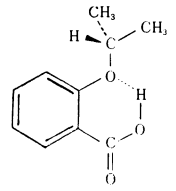
To investigate the steric effect of the intramolecular hydrogen bonding of *o*-methoxybenzoic acid, various alkyl substituents were introduced to the oxygen atom at the 2-position (R_1 in IX), to the 3-position (R_2), and to the 6-position (R_3).*[2]



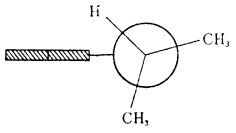
IX



X



XI



XII

The *O*-alkyl group R_1 is introduced to test the effect of the steric interference between the alkyl substituent and the hydrogen atom at the 3-position. The steric interference could be reduced if the alkyl substituent exists as an appropriate rotational isomer, as shown by X and XI. The infrared O–H stretching absorption spectra in the 3 μ region and the near-ultraviolet absorption spectra of 2-methoxy-, 2-ethoxy- and 2-isopropoxy-benzoic acids are shown in Tables II and III.

The results show that these acids apparently have two absorption bands in the O–H stretching region. One absorption at the higher frequency (about 3530 cm^{-1}) was assigned to the

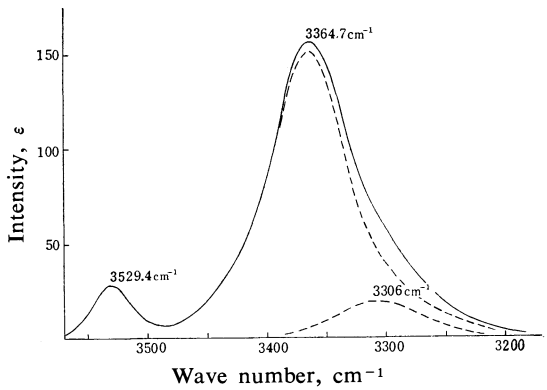


Fig. 1. The infrared ν_{O-H} spectrum of 2-methoxybenzoic acid.

5) G. P. Gibson, *J. Chem. Soc.*, **123**, 1269 (1923).
6) M. Ōki and M. Hirota, *Spectrochim. Acta*, **17**, 583 (1961).
*[2] In this report, 2-methoxybenzoic acid derivatives are always named on the basis that carboxyl and methoxyl groups occupy the 1- and 2-positions respectively (see formula IX).

TABLE II. INFRARED ν_{O-H} ABSORPTION SPECTRA OF SUBSTITUTED 2-ALKOXYBENZOIC ACIDS

Benzoic acid		ν_{max}, cm^{-1}	ε_{max}	$\Delta\nu_{1/2}$	$A \cdot 10^{-3}$	A_t/A_c
2-Methoxy	cis	3529.4	27.8	38.2	3.83	11.02
	trans	3364.7	151	77.6	42.3	
		3305.1	19.4	77.5	5.43	
2-Ethoxy	cis	3530.6	19.6	38.7	2.74	13.82
	trans	3351.4	125	83.8	37.8	
		3275.0	23.5	76.0	6.45	
2-Isopropoxy	cis	3531.1	19.2	38.4	2.66	12.41
	trans	3320.9	104	88.2	33.12	
		3255.0	30.4	80.4	8.82	
2-Methoxy-5-methyl	cis	3528.9	12.2	38.1	1.68	
	trans	3356.8	98.7	76.2	27.2	
		3290.0	13.8	65.6	3.27	
2-Methoxy-3,5-dimethyl	cis	3532.9	28.6	36.6	3.78	8.48
	trans	3275.3	77.0	115.0	31.96	
3-Ethyl-2-methoxy-5-methyl	cis	3533.0	28.7	38.1	3.96	7.90
	trans	3275.0	79.4	108.9	31.22	
2-Isopropyl-2-methoxy-5-methyl	cis	3534.7	33.4	37.0	4.46	6.11
	trans	3273.3	69.5	108.6	27.3	
2-Methoxy-6-methyl	cis	3518.9	72.8	32.0	8.41	—
	trans	3331.8	27.2	*		
2-Methoxy-6-ethyl	cis	3518.6	89.1	30.8	9.91	—
	trans	3320	16.3	**		

* A small maximum in a broad absorption band.
** Shoulder.

TABLE III. ULTRAVIOLET ABSORPTIONS OF SUBSTITUTED 2-METHOXYBENZOIC ACIDS

Acid	Absorption maxima, mμ (extinction coeff.)		
	Heptane	Ethyl ether	Ethanol
2-Methoxybenzoic	286 (2480) 293 (2380)	291 (2970)	294 (3180)
2-Ethoxybenzoic	286.5(2550) 294 (2450)	—	294.5(3190)
2-Isopropoxybenzoic	288 (2760) 295 (2540)	292.5(2770)	296 (2950)
5-Methyl-2-methoxybenzoic (III)	295 (2820) 302 (2540)	300 (3220)	302.5(3180)
3,5-Dimethyl-2-methoxybenzoic (IV)	287 (1860) 297 (2240)	295.5(2230)	296 (2020)
3-Ethyl-5-methyl-2-methoxybenzoic (V)	287 (1900) 295 (2030)	—	294 (1960)
3-Isopropyl-5-methyl-2-methoxybenzoic (VI)	289 (1860) 294.5(1940)	292.5(2140)	291.5(1830)
6-Methyl-2-methoxybenzoic (VII)	282 (1910)	279.5(2030)	280 (2020)
α-Phenoxyisobutyric	264 (1420) 270.5(1720) 276.5(1280)	—	265 (1350) 271 (1680) 277 (1250)
Methyl 2-methoxybenzoate	295.5(3160)	296 (4090)	300 (3530)

cis form, and the other at the lower frequency, ranging from 3364.7 cm^{-1} to 3320.9 cm^{-1}, to the trans form. The infrared ν_{O-H} spectra of 2-methoxybenzoic acid, as illustrated in Fig. 1, show a somewhat asymmetric band at the lower frequency. The band is divided into two absorptions by assuming that it is the overlap of two Lorentzian curves, the treatment being that carried out in the previous paper*1 with *o*-aryloxybenzoic acids. The ν_{O-H} frequencies of the cis forms are nearly constant throughout this series, but the ν_{O-H} frequencies of the trans forms shift to the lower frequency as the substituent becomes bulky, while the A_t/A_c intensity ratio are invariant throughout the series. The integrated intensity (A) of the cis and the trans forms should be proportional to the amount of the energy absorbed by each form of the acid molecule and related to the populations of the molecules existing as the assigned isomeric forms. However, the existence of the dimer, though its proportion to the rest is very small, prevents the exact discussion of the absolute intensity values and of the intensity ratio, which is supposed to be proportional to the population of the cis and the trans forms. The intensity ratio would be more reliable and could be an important element in comparing the relative population ratio existing in the two states of the acid if the effect of the dimer were negligible. However, the invariance of the A_t/A_c ratios indicates that the bulkiness of the *O*-alkyl substituent does not influence the equilibrium constant between the two forms.

Figures 2 and 3 show the ultraviolet spectra of these acids in heptane and ethanol respectively, together with the spectra of 2-methoxy-5-methylbenzoic acid and methyl 2-methoxybenzoate in the same solvents. The ultraviolet spectra of 2-methoxybenzoic acid and its 5-methyl derivative in ether are also shown in Fig. 4. From a comparison of these spectra, it becomes clear that the spectra of these acids in heptane differs from those in other polar solvents which are capable of hydrogen bond formation. The characteristic feature of the absorption curves in heptane is its two-peaked envelope, the maxima of which are located at 286~288 mμ and at 293~295 mμ with 2-alkoxybenzoic acids. The band envelope of the spectrum of methyl 2-methoxybenzoate in heptane is quite different from that of the parent acid, while those in ethanol are similar to each other except for a considerable red shift caused by the esterification.

The peak at the shorter wavelength is attributed to the ordinary B-band of 2-methoxybenzoic acid, and the one at the longer wavelength, to the intramolecular hydrogen-bonded

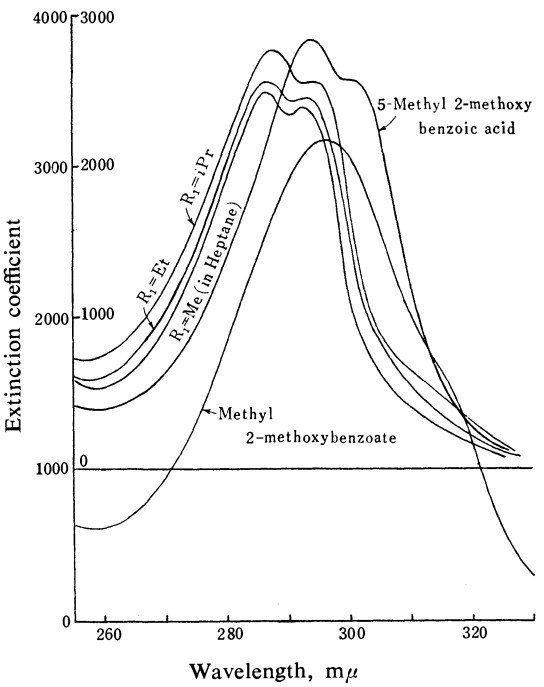


Fig. 2. The ultraviolet spectra of 2-alkoxybenzoic acids and related compounds in heptane.

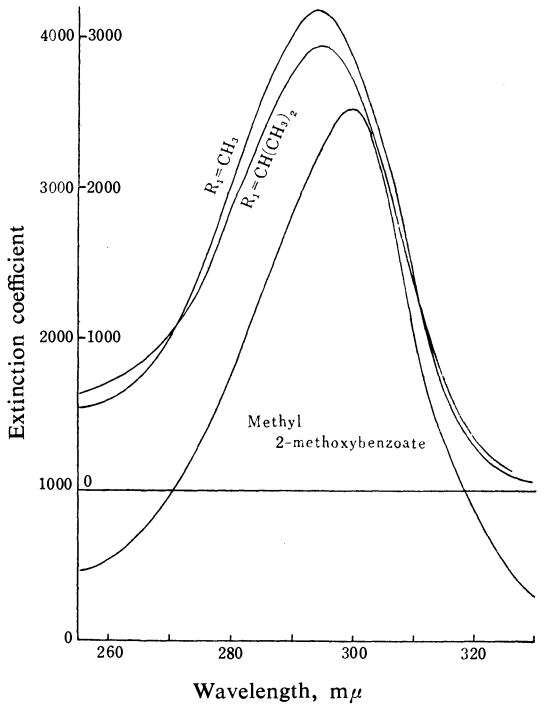


Fig. 3. The ultraviolet spectra of 2-alkoxybenzoic acids and methyl 2-methoxybenzoate in ethanol.

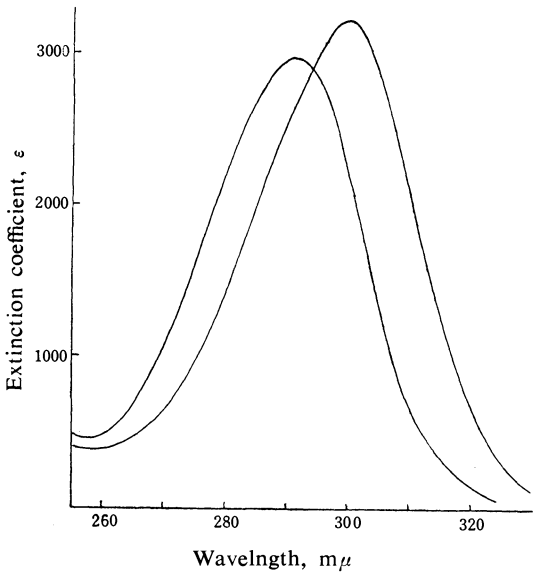
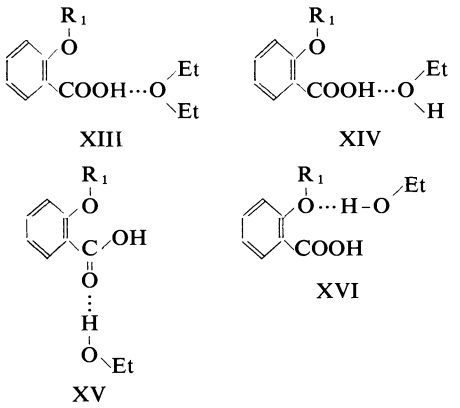


Fig. 4. The ultraviolet spectra of 2-methoxybenzoic acid (λ_{max}: 291 mμ) and its 5-methyl derivative (λ_{max}: 300 mμ) in diethyl ether.

structure (Ia); these assignments will be discussed below. Thus, additional evidence for the intramolecular hydrogen bonding was given from the ultraviolet spectral measurement. This two-peaked absorption pattern disappears in ether and in ethanol; this phenomenon is interpreted as stemming from the destruction of the intramolecular hydrogen bonding.

In ether, the intramolecular hydrogen bonded structure (Ia) is probably destroyed because intermolecular hydrogen bonding with ether is more favored than intramolecular hydrogen bonding. The enthalpy difference value for the intramolecular hydrogen bonding of 2-methoxybenzoic acid and for the association between acetic acid and dibutyl ether have been determined to be 3.3±0.5 kcal./mol.[2] and 4.56±0.3 kcal./mol.[7] respectively. Since the intermolecular hydrogen bonding enthalpy of this acid has not yet been obtained, the exact discussion cannot be given, but the above ΔH value for the intermolecular hydrogen bonding of carboxylic acid with ether and the advantage in entropy term in association (because the hydrogen acceptor is the solvent itselt) suggest the existence of the acid molecules as intermolecularly associated structures XIII.

In ethanol, the acid can associate with the solvent both as a hydrogen donor (XIV) and as a hydrogen acceptor (XV and/or XVI). However it has not been clearly established whether either or both of these types of hydrogen bonding exists in the solution. Ito, Tsukioka and Imanishi[8] determined the ultraviolet spectra of benzoic and *o*-toluic acids in various solvents as functions of the temperature and of the concentration, but they could not reach a decisive conclusion on the type of hydrogen bonding. At any rate, it seems quite natural to conclude that the intramolecularly hydrogen-bonded structure Ia is destroyed in ether and in ethanol. Since the two-peaked absorption pattern disappears in these solvents, the assignment of the absorption to the intramolecularly hydrogen-bonded form is justified. This relation between ultraviolet spectra and intramolecular hydrogen bonding is also observed in other series of acids investigated.



A red shift upon the esterification of *p*-substituted cinnamic acids has been observed by one of the authors[9] and interpreted as arising from the unfavorable effect of the hydroxyl group on the electron-attracting property of the carboxylic carbonyl group; a similar discussion is applicable in this case. The absorption band at ca. 300 mμ of 2-methoxybenzoic acid and its derivatives should be the B(benzenoid)-band according to the Gillam's classification.[10] From Burawoy's theory,[3] the B-band transition involves a charge migration from the terminal methoxyl group into the receiving termial carboxyl or methoxycarbonyl group in 2-methoxybenzoic acid and its methyl ester. In other words, the contribution of the polarized structure XVII plays an important role in this transition, although the electronegative character of the carboxylic hydroxyl group (the contribution of the structure XVIII) in the ground and ex-

7) M. Ōki and M. Hirota, This Bulletin, **36**, 290 (1962).

8) M. Ito, H. Tsukioka and S. Imanishi, *J. Am. Chem. Soc.*, **82**, 1559 (1952).

9) Y. Urushibara and M. Hirota, *J. Chem. Soc. Japan, Pure Chem. Sec.* (*Nippon Kagaku Zasshi*), **82**, 358 (1962).

10) A. E. Gillam and E. S. Stern, "An Introduction to Electronic Absorption Spectroscopy in Organic Chemistry," Edward Arnold Ltd., (1954), pp. 111, 116.

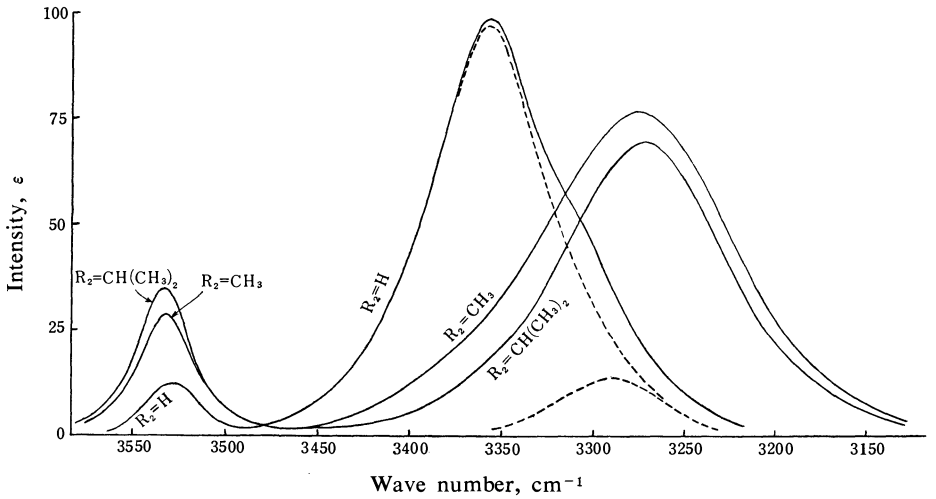
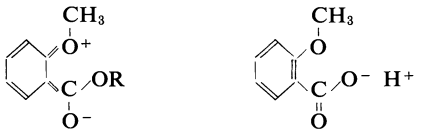


Fig. 5. The infrared ν_{O-H} spectra of 3-Alkyl-2-methoxy-5-methylbenzoic acids.

cited states of the acid does not favor the contribution of the structure XVII.



XVII XVIII

The substituent at the 3-position is then introduced to test the necessity of the coplanarity of the methoxyl group with the benzene nucleus. Phenol and its derivatives are concluded to take the planar structure,[11,12] and the methoxyl group of 2-methoxybenzoic acid should take the S-trans configuration with respect of C_1, which carries the carboxyl group, in the absence of the steric hindrance created by the alkyl group at the 3-position. The slight steric effect on the resonance interaction of the methoxyl group with the 3-hydrogen atom is known[13], but it is estimated to be negligible by means of Braude's method[14] (XIX) for the estimation of the steric hindrance. On the other hand, a considerable steric hindrance is foreseen from the molecular chart (XX) by the introduction of the methyl group to the 3-position. The method uses covalent radii as a measure of the steric hindrance and so has a tendency to underestimate the steric hindrance.

The infrared ν_{O-H} absorption and near-ultraviolet absorption spectra of 2-methoxy-5-methylbenzoic acid (III) and its 3-alkyl(R_2)-derivatives (IV, V and VI) are listed in Tables II and III, together with those of other series of acids. The 5-methyl group is introduced for the convenience of synthesis. The infrared spectra of these compounds and their ultraviolet spectra in heptane are illustrated in Figs. 5 and 6 respectively. As is to be expected from the above consideration of the steric effect, the 3-alkyl group causes a considerable decrease in the A_t/A_c ratio, and it is concluded that an unfavorable effect is exerted by the 3-alkyl substituents. The A_t/A_c intensity ratios of 3-methyl (IV), 3-ethyl (V) and 3-isopropyl (VI) derivatives are 8.48, 7.91 and 6.11 respectively. This shows the gradual decrease in the A_t/A_c ratio as the substituent changes from methyl

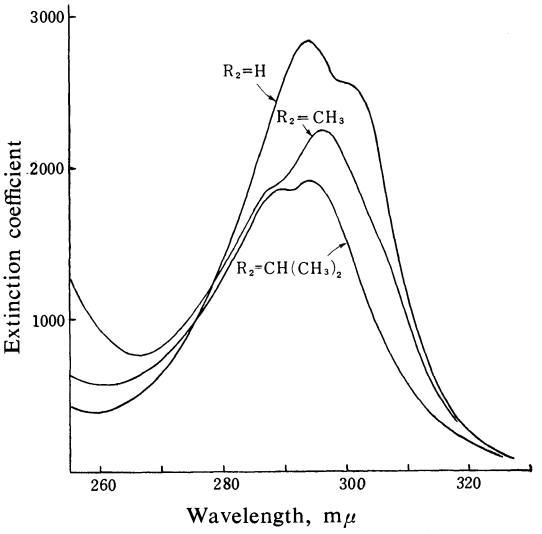
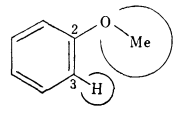


Fig. 6. The ultraviolet spectra of 3-alkyl-2-methoxy-5-methylbenzoic acids in heptane.

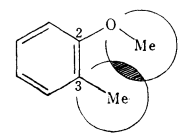
11) L. Pauling, *J. Am. Chem. Soc.*, **58**, 94 (1936).
12) O. R. Wulf, U. Liddel and S. B. Hendricks, ibid., **58**, 2287 (1936).
13) G. Baddely, N. H. P. Smith and M. A. Vickars, *J. Chem. Soc.*, **1956**, 2455.
14) E. A. Braude, E. R. H. Jones, H. P. Koch, R. W. Richarson, F. Sondheimer and J. B. Toogood, ibid., **1949**, 1890.

to isopropyl; therefore, the unfavorable steric effect on a hydrogen-bonded structure like Ia increases in this order. The ultraviolet spectra of these compounds show a gradual decreases in the characteristic absorptions which have two peaks at about 295 mμ when the alkyl group R_3 is changed from hydrogen to isopropyl. This agrees with the infrared results. The introdction of the 3-*t*-butyl group would be very interesting since the very bulky *t*-butyl group would force the methoxyl group to take the S-cis configuration with respect to C_1, which carries the carboxyl group and so prevents the acid from existing as a hydrogen-bonded structure like Ia, but 3-*t*-butyl-2-methoxy-5-methylbenzoic acid has not been obtained in a pure state. Examining the frequency difference data $\Delta\nu(\equiv\nu_{max}^{cis}-\nu_{max}^{trans})$ in the ν_{O-H} region, it is concluded that the increase is caused by the larger bulk of the 3-alkyl substituents. In general, a parallel relation is expected between the $\Delta\nu_{max}$ and A_t/A_c values if the nature and steric conditions of the hydrogen bonding are similar.

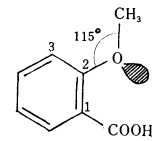
In this case, the 3-alkyl substituent hinders the coplanarity of the methoxyl group with respect to the benzene ring and destroys the conjugation between the p-π electrons of the methoxyl group and the π-electrons of the aromatic ring. The deviation from coplanarity causes, first, the alteration of the direction of the electron orbitals and, second, the localization of the electron on the oxygen atom, which is responsible for the higher electron density. On the other hand, the buttressing effect given by the 3-alkyl group causes the distance between the methoxyl oxygen and the carboxylic O–H group to be shorter than that in 2-methoxybenzoic acid. The C-O-H(C) angles of phenols and their alkyl ethers have been determined to be 115° from the dipole moment investigations[15]; the bond angle indicates that the alkoxyl oxygen takes a hybridized state between sp^2 and sp^3. Assuming that the oxygen atom takes a planar sp^2-like configuration, the four lone-pair electrons fill a p-π orbital which is perpendicular to the molecular plane and conjugate with the aromatic π-electrons and another sp^2-like orbital, the axis of which is planar with the other part of the molecule and divides the C_{Me}–O–C_{Ph} angle into two almost equal parts (XXI). The electron of the latter orbital is available to form a dative bond (hydrogen bond) with the carboxyl group. The steric hindrance is supposed to cause some twisting of the methoxyl group from the plane of the benzene ring without any appreciable change in hybridization. This twisting will reduce the probability of the hydrogen bond formation. The reduced probability of the hydrogen bonding and the shorter O···H–O distance are reflected in the decreased A_t/A_c ratio and in the larger $\Delta\nu_{max}$ values of the O–H stretching absorption bands. Another interpretation of the larger $\Delta\nu_{max}$ may be given by the increased electron density caused by the decreased contribution of the resonance form XXVII, resulting in the larger energy of hydrogen bonding. In any case, the introduction of the 3-akyl groups causes a considerable decrease in the relative population of the hydrogen-bonded species and an increase in $\Delta\nu_{max}$.



XIX



XX*3



XXI

The introduction of the methyl or ethyl group to the 6-position causes the disappearance of the O–H stretching absorption of the hydrogen-bonded trans isomer and of the characterstic ultraviolet absorptions. The infrared and ultraviolet absorption spectra of these acids (VII and VIII) are shown in Figs. 7 and 8.

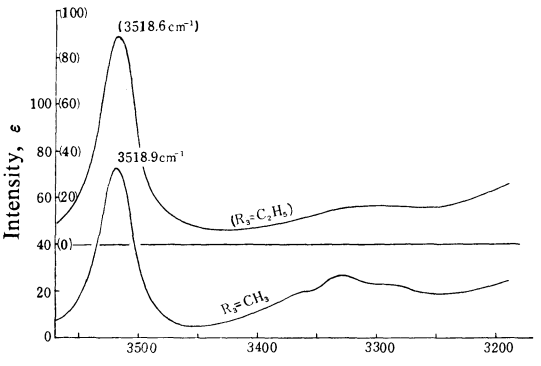


Fig. 7. The infrared ν_{O-H} spectra of 6-alkyl-2-methoxybenzoic acids.

15) C. P. Smyth, "Dielectric Behavior and Structure," McGraw-Hill, New York (1954), p. 319.

*3 These molecular diagrams were drawn according to the method reported by Braude and his co-workers.[14] In these figures, the following dimensions were used: C-C (aromatic) 1.40 Å, C-H 1.98 Å, Me covalent radius 1.39 Å, =O covalent radius 1.10 Å, and C-O-C angle 115°.[15]

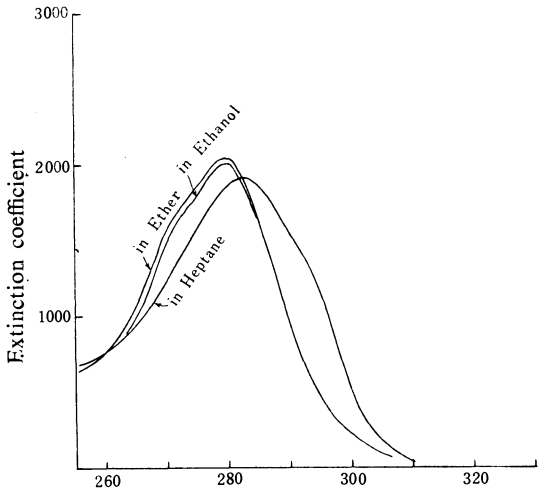
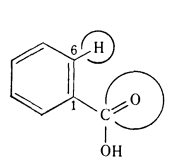


Fig. 8. The ultraviolet spectrum of 6-methyl-2-methoxybenzoic acid in various solvents.

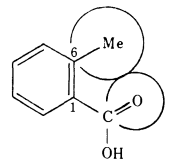
The ultraviolet spectrum of the 6-methyl acid VII in heptane and ether are almost identical, and, though the spectrum in heptane exhibits a small red shift, the band envelopes of the acid in every solvent investigated resemble one other. Consequently, it is concluded that the spectral behavior of 6-alkyl-2-methoxybenzoic acid differs from those of the acids of other series. A comparison of the infrared spectra of the 6-alkyl-2-methoxybenzoic acids indicates the existence of a broad and weak absorption in the hydrogen-bonded O–H stretching region when the alkyl group is methyl, but the characterization of the absorption band was impossible because of the low intensity, the diffuse band envelope and the very high background absorption, which is supposed to be the wing of either the C–H absorption or, less probably, the dimeric O–H absorption.

When the steric hindrance is estimated from the molecular diagram (XXIII) drawn by Braude's method,[14] a much smaller steric interaction is expected between the carbonyl oxygen and the 6-methyl group of 2-methoxy-6-methylbenzoic acid than the steric interference between the methoxyl and methyl groups of 2-methoxy-3-methylbenzoic acid (as is shown by XIX, XX, XXII and XXIII), but the actual steric effect is by far larger in the 6-alkyl acids. This indicates the important role of the planarity of the carboxyl group. In other words, the contribution of the resonance form XXV is much more important than that of the structure XXVII.

The importance of the resonance form XXV should be reflected in the polar C=O bond; the C=O stretching absorptions of these acids



XXII

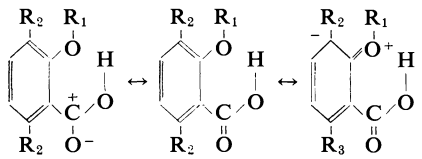


XXIII

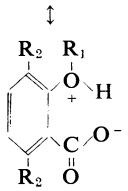
suggest this tendency. The infrared C=O stretching absorption data of some representative acids are tabulated in Table IV. The measurement of the spectra was carried out under almost the same conditions as that of the O–H spectra. The higher frequency of the

TABLE IV. THE INFRARED C=O STRETCHING ABSORPTION SPECTRA OF 2-METHOXYBENZOIC ACID AND RELATED COMPOUNDS

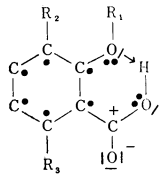
Acid	C=O Stretching bands, cm^{-1}		$\Delta\nu_{max}$ (C=O) cm^{-1}
	cis	trans	
α-Phenoxyisobutyric	1755	1786	31
2-Methoxybenzoic	1742	1750	7
3,5-Dimethyl-2-methoxybenzoic	1739	1752	13
2-Toluic[16]	1740	—	—
Benzoic[16]	1742	—	—



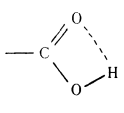
XXV XXIV XXVII



XXVI



XXVIII



XXIX

16) D. Peltier and A. Pichevin, *Bull. soc. chim. France*, **1960**, 1141.

$\nu_{C=O}$ absorption attributable to the trans isomer is explained in terms of the absence of the hydrogen bond-like interaction shown by XXIX.[17] The frequency shift ($\Delta\nu_{max}$) in the $\nu_{C=O}$ region caused by this four-membered ring interaction is as large as 32 cm^{-1} for α-phenoxyisobutyric acid, to which no resonance contribution of the polar C^+-O^- structure is expected on the formation of the intramolecular hydrogen bond as XXIX.[17] On the other hand, the $\Delta\nu_{max}$ (C=O)*4 values for 2-methoxybenzoic and 3, 5-dimethyl-2-methoxybenzoic acids are 7 cm^{-1} and 13 cm^{-1} respectively, values being much smaller than that of α-phenoxyisobutyric acid. This implies the contribution of the polar structure C^+-O^-, even in the trans hydrogen-bonded isomer; as a result, the force constants of their C=O bond become less.

In view of the electronic theory, the results may be interpreted as follows. The structure of 2-methoxybenzoic acid may be expressed as the resonance hybrid of the canonical formulas XXIV, XXV, XXVI and XXVII when it takes the trans structure. The structure XXIV is the only structure without a charge separation, and its contribution is by far the greatest. Formulas XXV, XXVI and XXVII represent the canonical structures with the polarized carbonyl bond, with the charge transfer through the hydrogen bridge, and with the contribution of the electron-repelling property of the methoxyl group respectively. The strong hydrogen bond with a considerable lowering of the O–H stretching frequency is always accompanied by the weakening of the O–H bond to compensate the energy of the hydrogen bond, corresponding to the contribution of the charge transfer structure XXVI. The contribution of the polarized carbonyl structure XXV is concluded to be essential and to play a decisive part in the hydrogen bonding of this type. The importance of the structure XXV suggests that the stability of the planar hydrogen bond system in 2-methoxybenzoic acid is due to its pseudo-aromatic nature, which arises from the 10-π-electron system as illustrated by XXVIII, in which π-electrons are expressed by dots on the atoms to which the electrons originally belong.

The characteristic ultraviolet absorption bands for the intramolecularly hydrogen-bonded acids may be due to the electronic transition caused by this pseudo-aromatic system, but a more detailed investigation is needed before this hypothesis can be proven.

17) M. Ōki and M. Hirota, This Bulletin, 33, 119 (1960).

*4 To distinguish the $\Delta\nu_{max}$ in the O-H region from that of the C=O region, $\Delta\nu_{max}$(C=O) is used for the frequency difference between the absorption maxima of the two $\nu_{C=O}$ absorptions assigned to the cis and the trans structures.

Summary

The infrared and ultraviolet absorption spectra of derivatives of salicylic acid with alkyl substituents at the 2-*O*-, 3- and/or 6-positions have been measured, and much information on the nature of the intramolecular hydrogen bonding has been obtained from these data. The infrared O–H stretching absorption measurement shows that a substituent at the 6-position inhibits the formation of hydrogen bonding and that a substituent at the 3-position has some unfavorable steric effects.

These data imply the importance of the coplanarity of the carboxyl group with the benzene nucleus; moreover, a consideration of these data, together with the infrared C=O streching and ultraviolet spectral data, leads to the conclusion that the structure of the hydrogen-bonded trans isomer Ia may be expresed as a resonance hybrid among XXIV, XXV, XXVI and XXVII, the contribution of XXIV being the most important and that of XXV the next most important.

The authors are indebted to Professor Saburo Nagakura and Dr. Haruo Hosoya for their valuable discussions throughout this work.

Department of Chemistry
Faculty of Science
The University of Tokyo
Hongo, Tokyo

Infrared Spectroscopic Studies of Hexammine- and Pentammine-chromium(III) Complexes

By Nobuyuki TANAKA, Minoru KAMADA, Junnosuke FUJITA* and Eishin KYUNO**

(Received September 23, 1963)

Studies of the infrared spectra of the inorganic coordination compounds offer interesting information concerning the natures of the coordination bond and of the molecular structure. From this point of view, cobalt(III)-ammine complexes have been often investigated.[1-9] Chromium(III)-ammine complexes, on the other hand, have not been studied systematically. Indeed, Nakamoto et al.[9] reported on the effect of the outer ions on the infrared spectra of chromium(III)-ammine complexes. Their discussion, however, was mainly devoted to hexamminechromium(III) complexes.

In the present work, the infrared spectra of twenty-nine samples of hexammine and pentammine complexes of chromium(III) and cobalt(III) have been measured, and the shift of the observed bands with the change in the outer ions has been discussed.

Experimental

Preparation of Chromium(III)-Ammine Complexes. — Hexamminechromium(III) chloride and aquopentamminechromium(III) chloride were obtained, by the procedure given by King,[10] from the nitrates of the corresponding complexes, which had been prepared according to the method of Mori.[11] Bromides, iodides and perchlorates of hexammine- and aquopentamminechromium(III) complexes were prepared from the chlorides by the same method as reported by King.[10]

Halopentamminechromium(III) complexes were obtained by heating aquopentamminechromium(III) halide at 80~120°C for a few hours, and the outer ions of those complexes, if necessary, were converted by procedures similar to those used for hexamminechromium(III) complexes.

Some selected samples were deuterated by dissolving them in heavy water (D_2O). D_2O was subsequently removed by evaporation at reduced pressure, and the samples were dried in vacuo over P_2O_5.

Measurements of Infrared Spectra. — Infrared spectra were measured by using a Hitachi EPI-2G recording infrared spectrophotometer equipped with a potassium bromide foreprism and a grating double monochrometer. The potassium bromide disk method was employed for the measurement in the sodium chloride prism region, and both the potassium bromide disk and the Nujol mull methods, in the potassium bromide prism region. The values obtained by the Nujol mull method, however, were adopted for the determination of the wavelength of absorption peaks, because, in general, the spectra are clearer in the Nujol mull method than in the potassium bromide disk method.

The calibration of the frequencies was made with polystylene film, and with carbon dioxide and water vapor.

Results

Typical infrared spectra of hexammine- and pentamminechromium(III) complexes in the

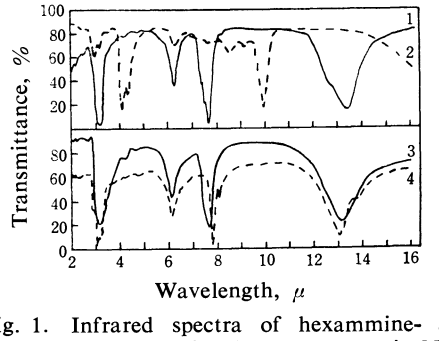


Fig. 1. Infrared spectra of hexammine- and pentamminechromium(III) complexes in NaCl prism region (KBr disk method): 1, $[Cr(NH_3)_6]Cl_3$; 2, deuterated $[Cr(NH_3)_6]Cl_3$; 3, $[Cr(H_2O)(NH_3)_5]Cl_3$; 4, $[CrCl(NH_3)_5]Cl_2$.

* Present address: Department of Chemistry, Faculty of Science, Osaka University, Kita-ku, Osaka.
** Present address: Department of Chemistry, Faculty of Science, Kanazawa University, Kanazawa.

1) R. Duval, C. Duval and J. Lecomte, *Compt. rend.*, **224**, 1632 (1947).
2) D. G. Hill and A. F. Rosenberg, *J. Chem. Phys.*, **22**, 148 (1954).
3) S. Mizushima, I. Nakagawa and J. V. Quagliano, ibid., **23**, 1367 (1955).
4) D. B. Powell and N. Sheppard, *J. Chem. Soc.*, **1956**, 3108.
5) J. Fujita, K. Nakamoto and M. Kobayashi, *J. Am. Chem. Soc.*, **78**, 3295 (1956).
6) G. M. Barrow, R. H. Krueger and F. Basolo, *J. Inorg. Nuclear Chem.*, **2**, 340 (1956).
7) S. Mizushima and I. Nakagawa, *J. Chem. Soc. Japan, Pure Chem. Sec.* (*Nippon Kagaku Zasshi*), **80**, 124 (1959).
8) T. Shimanouchi and I. Nakagawa, *Spectrochim. Acta*, **18**, 89 (1962).
9) K. Nakamoto, Y. Morimoto and J. Fujita, Proceedings, Seventh International Conference on Coordination Chemistry, p. 14 (1962).
10) H. J. S. King, *J. Chem. Soc.*, **127**, 2100(1925).
11) M. Mori, *J. Chem. Soc. Japan, Pure Chem. Sec.* (*Nippon Kagaku Zassi*), **74**, 253 (1953).

sodium chloride prism region are shown in Fig. 1. They, and the spectra of other hexammine- and pentamminechromium(III) complexes, give four main absorption bands. Since these bands shifted to lower frequencies upon the deuteration of ammonia, they were assigned to be N–H stretching, degenerated deformation, symmetric deformation and rocking vibrations.[3] All spectra of $[CrX(NH_3)_5]Y_{2,3}$, where X is NH_3, H_2O and halide ions, and Y, ClO_4^-, NO_3^- and halide ions, shifted to higher frequencies in the N–H stretching vibration and to lower frequencies in the other three deformation vibrations when the outer ions were changed to the order of chloride, bromide and iodide, as Table I shows.

Table I. Shift of absorption bands of hexammine- and pentamminechromium-(III) complexes with varied outer ions (sodium chloride prism region)

Complex	Wave number, cm^{-1}			
$[Cr(NH_3)_6](ClO_4)_3$	3311	1614	1339	743
$[Cr(NH_3)_6](NO_3)_3$	3268	1613	1304	747
$[Cr(NH_3)_6]Cl_3$	3185	1605	1307	748
$[Cr(NH_3)_6]Br_3$	3185	1603	1307	746
$[Cr(NH_3)_6]I_3$	3190	1600	1305	741
$[CrCl(NH_3)_5](ClO_4)_2$	3284	1600	1287	767
$[CrCl(NH_3)_5](NO_3)_2$	3279	1596	1285	765
$[CrCl(NH_3)_5]Cl_2$	3277	1600	1289	774
$[CrCl(NH_3)_5]Br_2$	3283	1595	1286	767
$[CrCl(NH_3)_5]I_2$	3280	1590	1284	755

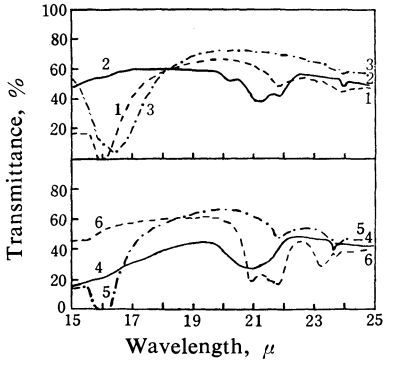


Fig. 2. Infrared spectra of hexammine- and pentamminechromium(III) complexes in KBr prism region (Nujol mull method): 1, $[Cr(NH_3)_6](ClO_4)_3$; 2, $[Cr(NH_3)_6]Cl_3$; 3, deuterated $[Cr(NH_3)_6]Cl_3$; 4, $[Cr(H_2O)(NH_3)_5]Cl_3$; 5, $[CrCl(NH_3)_5](ClO_4)_2$; 6, $[CrBr(NH_3)_5]Cl_2$.

Figure 2 shows the infrared spectra of several complexes in the potassium bromide prism region. From the assignment of the absorption bands of hexamminecobalt(III) ions,[8] the Cr–N stretching vibration is expected to be observed in this frequency region, but at somewhat lower frequencies than those of the corresponding cobalt(III) complex, because the coordination effect of chromium(III) is considered weaker than that of cobalt(III).[12] When the outer ions of hexamminechromium-(III) are halide ions, three bands appear in the potassium bromide prism region. All these bands were assigned to be Cr–N stretching vibrations for the following two reasons. First, as the Cr–N stretching vibration of hexamminechromium(III) complex belongs to the F_{1u} species if the ammonia molecule is taken as a single group, this band splits into three components because of the lowering of symmetry which is caused by the formation of a hydrogen bond between ammonia and halide ion and by the deformation in the crystal state. Second, these bands shifted to lower frequencies upon the deuteration of the coordinating ammonia. The frequency ratio of the band of the undeuterated complex to that of the deuterated complex (ν_{NH_3}/ν_{ND_3}) is 1.09 (Table II),

Table II. Observed frequencies of $[Cr(NH_3)_6]Cl_3$ and $[Cr(ND_3)_6]Cl_3$

Frequencies of $[Cr(NH_3)_6]Cl_3$ ν_{NH_3}, cm^{-1}	Frequencies of $[Cr(ND_3)_6]Cl_3$ ν_{ND_3}, cm^{-1}	ν_{NH_3}/ν_{ND_3}
3257 sh	2415	
3185	2347 sh	
3130	2283	
1630	1171	
1307	1007	
748	603	
495 w	455 vw	1.09
473	435	1.09
456	424	1.08

which is in good agreement with the theoretical value (1.06) calculated from a harmonic oscillator consisting of a chromium(III) atom and ammonia (or deuterated ammonia) group.

In pentamminechromium(III) complexes, $[CrX(NH_3)_5]^{2,3+}$, similar phenomena were observed. A pentammine complex ion has C_{4v} symmetry, if the ammonia molecule is taken as a single group, and A_1- (Cr–X stretching, Cr–N symmetric stretching) and E-species (Cr–N asymmetric stretching) are infrared active. $[CrCl(NH_3)_5](ClO_4)_2$ gives two weak absorption bands, at 457 and 420 cm^{-1} (Fig. 2). When the outer ions were halide ions, three bands were observed in the potassium bromide prism region upon the split of E-species, as is shown in Table III. All these bands shifted to lower frequencies upon the deuteration of ammonia and when the outer ions were changed from

12) M. Kobayashi and J. Fujita, *J. Chem. Phys.*, 23, 1354 (1955).

TABLE III. OBSERVED FREQUENCIES $[Cr(NH_3)_6]Y_3$ AND $[CrX(NH_3)_5]Y_{2,3}$ IN KBr PRISM REGION (cm^{-1})

Complex ion	Outer ion				
	ClO_4^-	NO_3^-	Cl^-	Br^-	I^-
$[Cr(NH_3)_6]^{3+}$	458	467	495 473 456	488 468 453	475 462 449
$[Cr(H_2O)(NH_3)_5]^{3+}$	457	476	478	476	479
$[CrCl(NH_3)_5]^{2+}$	457 420	460	471 458 431	460 448 423	447 440 416
$[CrBr(NH_3)_5]^{2+}$		471^{sh}_{vw} 462	476 459	467 451	452 440
$[CrI(NH_3)_5]^{2+}$		457^{sh}_{vw} 471^{sh}_{vw} 463	429 488 472 462 426	423	460 453 440

chloride to iodide. When the outer ions were nitrate and perchlorate, which do not form a strong hydrogen bond, the splitting of the band was not observed. From this spectral evidence, it was concluded that the absorption bands of $[CrX(NH_3)_5]^{2,3+}$ appearing in the potassium bromide prism region were all due to the Cr–N stretching vibration, not to the Cr–X stretching vibration.

Discussion

Table I shows that the absorption bands of hexammine- and pentamminechromium(III) complexes shift with the change in outer ions. It is well known that the band shifts because of the formation of a hydrogen bond of the X···H–N type,[5] where X indicates halide ions or oxyacids. The strength of the hydrogen bond between the anions and ammonia increases in the order of ClO_4^-, NO_3^-, I^-, Br^- and Cl^-. Table I shows that the N–H stretching band shifts to lower frequencies, while the deformation band shifts to higher frequencies in the order of the strength of the hydrogen bonding. The relation between the rocking vibration frequencies and outer halide ions is shown in Table IV. The differences in frequencies (Δ) between the chloride and the iodide are 7 cm^{-1} in $[Cr(NH_3)_6]^{3+}$ and 13 cm^{-1} in $[Cr(H_2O)(NH_3)_5]^{3+}$, and 26 and 20 cm^{-1}, respectively, in the corresponding cobalt(III) complexes.

The effect of outer ions was remarkable in the potassium bromide prism region, also. As Table III shows, spectra shift to lower frequencies when the outer ions are changed from chloride to iodide. As explanation of this experimental data, it is considered that the M–N stretching vibrations shift to higer frequencies with an increasing strength of hydrogen bond formation because the M–N stretching vibration is apt to couple with the NH_3 rocking vibration.

TABLE IV. EFFECT OF OUTER IONS ON THE FREQUENCIES OF THE ROCKING VIBRATION BAND OF NH_3 (cm^{-1})

Complex ion	Cuter ion			
	Cl^-	Br^-	I^-	Δ
$[Cr(NH_3)_6]^{3+}$	748	746	741	7
$[Co(NH_3)_6]^{3+}$	818	797	792	26
$[Cr(H_2O)(NH_3)_5]^{3+}$	756	752	743	13
$[Co(H_2O)(NH_3)_5]^{3+}$	837	832	817	20
$[CoF(NH_3)_5]^{2+}$	845	820	806	39
$[CrCl(NH_3)_5]^{2+}$	774	767	755	19
$[CrBr(NH_3)_5]^{2+}$	773	765	755	18
$[CrI(NH_3)_5]^{2+}$	768	—	752	16

TABLE V. OBSERVED FREQUENCIES OF SPLIT IN THE Cr–N STRETCHING VIBRATION BANDS OF HEXAMMINE- AND HALOPENTAMMINECHROMIUM-(III) HALIDES

Complex ion	Outer ion			
	Cl	Br^-	I^-	NO_3^-
$[Cr(NH_3)_6]^{3+}$	39	35	26	0
$[CrCl(NH_3)_5]^{2+}$	40	37	31	0
$[CrBr(NH_3)_5]^{2+}$	47	44	—	14
$[CrI(NH_3)_5]^{2+}$	26	—	20	13

The M–N stretching vibration band splits into three components when the outer ions are halide ions. The magnitudes of the split are 39, 35 and 26 cm^{-1} in the chloride, the bromide and the iodide of hexamminechro-

mium(III) respectively. Table V summarizes the magnitude of the split in other complexes. In all cases, the magnitude of the split increases in the order of the iodide, the bromide and the chloride. From the facts that a stronger hydrogen bonding between an ammonia molecule and an outer ion results in a larger split of the M–N stretching vibration and that the M–N stretching vibration does not split in the perchlorate and the nitrate, it is expected that the main cause for the split and the shift of absorption band is the formation of the hydrogen bond.

Halopentamminechromium(III) complexes showed a tendency similar to that of hexamminechromium(III) complexes with regard to the split and the shift of absorption bands. These phenomena may be explained in the same way as were those of the hexamminechromium(III) complexes. Although the M–N stretching vibration did not split in $[Cr(NH_3)_6](NO_3)_3$, it did split to three components in $[CrX(NH_3)_5](NO_3)_2$, where X indicates halide ions. The magnitude of split, however, is smaller than that observed with the corresponding halides (Table V). This experimental result coincides with the view that a nitrate ion forms a weaker hydrogen bond with ammonia than a halide ion does. The differences in the M–N stretching frequencies between the chlorides and the iodides of $[CrX(NH_3)_5]^{2+}$ (X=halide ion) are almost equal; they are 18, 19 and 19 cm^{-1} when X is chloride, bromide and iodide ions respectively. It can be expected, from this fact, that coordinating halide ion has almost the same effect on the hydrogen bonding between the outer ion and the ammonia molecule. When coordinating halide ions were varied with the same outer ion, the M–N stretching bands shifted to slightly higher frequencies in the order of chloro-, bromo- and iodopentamminechromium(III) complexes, that is, 460, 462 and 463 cm^{-1} in the nitrates. This fact that the magnitude of shift is not appreciable may indicate that the effects of coordinating halide ions on the adjacent M–N bond are almost the same.

The spectra of aquopentamminechromium(III) complexes in the potassium bromide prism region were different from those of hexammine- and halopentamminechromium(III) complexes, because only one absorption band was observed, even in the case of the halides. If the ammonia molecule is taken as a single group, an aquopentamminechromium(III) ion has C_{4v} symmetry and, consequently, should give at least two absorption bands.

This discrepancy may be explained as follows: $[Cr(H_2O)(NH_3)_5]^{3+}$ has a similar structure to that of the complex that has O_h symmetry because the mass of the ammonia molecule is almost equal to that of water molecule.[2] Moreover, since the electronegativity of the oxygen atom of water is larger than that of the nitrogen atom of ammonia, water can more easily form a hydrogen bond with an outer ion than ammonia does. The effect of the outer ion on the ammonia of $[Cr(H_2O)(NH_3)_5]^{3+}$ is small, and, consequently, no split of the M–N stretching band occurs. The M–N stretching frequencies of $[Cr(H_2O)(NH_3)_5]^{3+}$ were found to be 478, 476 and 479 cm^{-1} in the chloride, the bromide and the iodide respectively. These experimental results support the above consideration.

Summary

Twenty-nine samples of hexammine and pentammine complexes of chromium(III) and cobalt(III) have been prepared, and their infrared spectra have been measured in the region of 2~25 μ. The absorption peaks of these complexes have been found to shift to higher frequencies in the N–H stretching vibrations, and to lower frequencies in the NH_3 deformation and the Cr–N stretching vibrations in the order of the chlorides, the bromides and the iodides. In a potassium bromide prism region, three absorption bands due to the Cr–N stretching vibrations have been observed in hexammine- and halopentamminechromium(III) halides, but only one in the aquopentamminechromium(III) complexes. The shifts of the absorption bands observed have been discussed from the standpoint of the hydrogen bond formation.

The authors wish to thank the Ministry of Education and the Japan Society for the Promotion of Science for the financial support granted this research.

Department of Chemistry
Faculty of Science
Tohoku University
Katahira-cho, Sendai

Polarographic and Coulometric Studies of cis-Dioxalatodiaquochromate(III)

By Nobuyuki TANAKA, Eiki ITABASHI, Reita TAMAMUSHI and Gen SATÔ*

(Received August 26, 1963)

In a previous paper,[1] the present authors reported on the polarographic behavior of various oxalato complexes of chromium(III) in acidic or neutral aqueous solutions. As for dioxalatodiaquochromate(III), no reduction wave was observed, in acidic solutions, at less negative potentials than the potential of the reduction of hydrogen ions, while a reduction wave was obtained in neutral solutions. In this paper, an extensive study of the reduction of *cis*-dioxalatodiaquochromate(III) in neutral aqueous solutions at the mercury electrode is presented. The mechanism of the reduction process is discussed on the basis of the experimental results obtained by direct current and alternating current polarography, the measurements of Kalousek polarograms and current-time curves, and the controlled potential electrolysis.

Experimental

Materials.—*cis*-Potassium dioxalatodiaquochromate(III) was prepared according to the method of Werner.[2] It was identified as a cis-form, and its chromium and oxalate contents were determined by the procedure given by Palmer.[3]

Found: Cr, 15.18; ox, 53.5. Calcd. for $K[Cr(ox)_2(H_2O)_2]2H_2O$: Cr, 15.33; ox, 51.89%. *cis*-Potassium dioxalatodiaquochromate(III) is stable for a few months in the solid state and for a few hours in solutions, unless it is exposed to light. All the other chemicals used were of a guaranteed reagent grade.

Polarography. — Current-voltage curves were recorded with a pen-recording polarograph, a Yanagimoto Galvarecorder Model PR-2 with an automatic potential scanner. A Yanagimoto Y-GR 2 Galvarecorder was used for recording alternating current (a. c.) polarograms. Kalousek polarograms were recorded with the same circuit as has previously been described.[4] The current-time ($i-t$) curves during the life of a mercury drop were recorded with a Rikadenki ER-J1 recorder equipped with an RLDC-201 preamplifier.

Measurements were made at 25.00±0.05°C unless otherwise stated. The characteristics of the dropping mercury electrode employed in this study are given in Table I. The cell equipment used was the same as has been reported on previously.[5] The potentials were referred to a saturated calomel electrode(SCE). The dissolved oxygen in the solution was removed by bubbling pure nitrogen gas through the solution. The current-potential curves presented in this paper are corrected for the residual current and for the ohmic (iR) drop across the electrolysis cell.

TABLE I. CHARACTERISTICS OF THE DROPPING MERCURY ELECTRODE

	Height of mercury reservoir cm.	Rate of flow of mercury, m mg./sec.	Drop time, t_d sec.
Electrode A*	50	1.499	3.32
Electrode B**	45	1.862	3.25

* Measured in a dearated 1.0 M KNO_3 solution containing 0.005% gelatin.

** Measured in a dearated 1.0 M KCl solution containing 0.005% gelatin.

Coulometry.—Controlled potential electrolysis[6] was carried out with a Yanagimoto automatic potentiostat, Model VE-3. The working electrode was a mercury-pool electrode whose surface area was approximately 20 cm^2. The anode was a platinum spiral electrode which was connected with the electrolytic solution through a salt bridge of potassium chloride. The electrolytic current was recorded with a Yanagimoto pen-recording Galvarecorder, Model GR-103. The electrical circuit of the equipment and the electrolysis cell used were the same as have been described previously by Tanaka et al.[7] The electrolytic solution was stirred by means of a magnetic stirrer and by bubbling pure nitrogen gas through the solution.

Results

The reduction wave of *cis*-dioxalatodiaquochromate(III) in potassium oxalate solutions changed considerably with time and was

* Present address: Department of Chemistry, Faculty of Science and Technology, Sophia University, Chiyoda-ku, Tokyo.

1) N. Tanaka, E. Itabashi and E. Kyuno, This Bulletin, **36**, 917 (1963).

2) A. Werner, W. J. Bowis, A. Hoblik, H. Schwarz and H. Surker, *Ann.*, **406**, 261 (1914).

3) W. G. Palmer, "Experimental Inorganic Chemistry," Cambridge University Press, Cambridge (1954), p. 387.

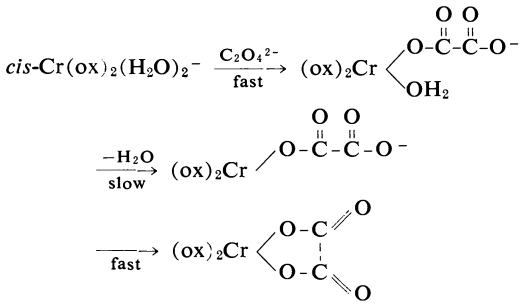
4) N. Tanaka, R. Tamamushi and M. Kodama, This Bulletin, **33**, 14 (1960).

5) N. Tanaka, K. Ebata and G. Satô, ibid., **36**, 912 (1963).

6) J. J. Lingane, "Electroanalytical Chemistry," Interscience Publishers, Inc., New York (1958), pp. 450-481.

7) N. Tanaka, T. Nozoe, T. Takamura and S. Kitahara, This Bulletin, **31**, 827 (1958).

affected by the concentration of potassium oxalate. According to Hamm and Perkins,[8] this is due to the reaction of *cis*-dioxalatodiaquochromate(III) with oxalate ions to form trioxalatochromate(III) :



cis-Dioxalatodiaquochromate(III) gives an ill-defined current-potential curve in potassium nitrate solutions, while a well-defined and reproducible reduction wave is observed in potassium chloride or potassium sulfate solutions (see Fig. 1). Therefore, most of the measurements were carried out in potassium chloride solutions.

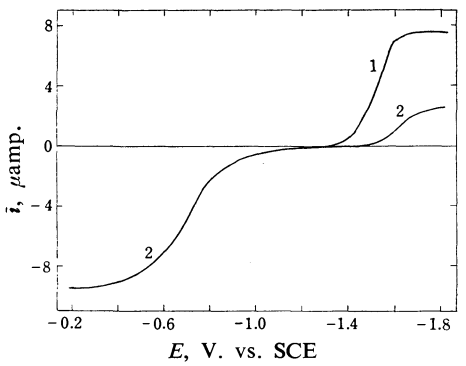


Fig. 1. A direct current polarogram (1) and a Kalousek polarogram (2) of 1.0 mM *cis*-$[Cr(ox)_2(H_2O)_2]^-$ in 0.3 M KCl solutions containing 0.005% gelatin. (Electrode A). For (2), the constant potential was applied at −1.80 V. vs. SCE.

In potassium chloride solutions, the limiting current was proportional to the concentration of the complex up to 2 mM and also to the square root of the effective height of the mercury reservoir. No well-defined wave was obtained in the absence of gelatin. The shape of the reduction wave was affected considerably by the concentration of gelatin. The reduction wave shifted to more negative potentials and its limiting current decreased with an increase in gelatin concentration (Table II).

8) R. E. Hamm and R. H. Perkins, *J. Am. Chem. Soc.*, **77**, 2083 (1955).

Table II. Effect of gelatin on the polarogram of 1.0 mM *cis*-$[Cr(ox)_2(H_2O)_2]^-$ in 0.3 M KCl solutions (electrode B)

Concn. of gelatin %	t_d sec.	$\bar{i}_d$ μamp.	$E_{1/2}$ V. vs. SCE
0	3.25	8.50±0.05	—*
0.001	3.25	8.42	−1.505
0.002	3.24	8.27	−1.509
0.005	3.23	7.89	−1.522
0.01	3.19	7.35	−1.542
0.02	3.15	6.04±0.05	−1.60

* Not determined because of maximum.

Measurements were also made in potassium chloride and potassium sulfate solutions of various ionic strengths. The results obtained are presented in Table III. The effect of the temperature on the reduction wave is shown in Table IV; the temperature coefficient of the limiting current was found to be 1.8%/degree in the range of 0 to 35°C. On the a. c. polarogram a peak was observed at a little more negative potential than the half-wave potential of the corresponding d. c. polarogram. One of the typical Kalousek polarograms of *cis*-dioxalatodiaquochromate(III) in a 0.3 M potassium chloride solution containing 0.005%

Table III. Effect of ionic strength and supporting electrolyte on the polarogram of 1.0 mM *cis*-$[Cr(ox)_2(H_2O)_2]^-$ in solutions containing 0.005% gelatin (electrode A)

Ionic strength	$\bar{i}_d$ μamp.	$E_{1/2}$ V. vs. SCE	Slope of log-plot, mV. Before $E_{1/2}$	After $E_{1/2}$
(A) KCl				
0.08	6.87	-1.54_5	90	90
0.1	7.18	-1.53_4	95	85
0.3	7.33	-1.52_2	103	82
0.6	7.35	-1.51_6	127	80
1.0	7.35	-1.50_9	157	79
(B) K_2SO_4				
0.1	6.15	-1.55_0	88	88
0.3	6.59	-1.52_8	97	86
0.6	6.96	-1.52_2	97	83
1.0	6.99	-1.51_0	105	81

Table IV. Effect of temperature on the polarogram of 1.0 mM *cis*-$[Cr(ox)_2(H_2O)_2]^-$ in 0.3 M KCl solutions containing 0.005% gelatin (electrode A)

Temp. °C	$\bar{i}_d$ μamp.	$E_{1/2}$ V. vs. SCE	Slope of log-plot, mV. Before $E_{1/2}$	After $E_{1/2}$
0.3	4.87	-1.57_0	130	78
5.0	5.37	-1.55_0	123	79
15.0	6.43	-1.54_1	110	80
25.0	7.33	-1.52_2	103	82
34.9	8.21	-1.51_0	95	85

gelatin is reproduced in Fig. 1, where the anodic wave is apparently separated from the cathodic wave. The current-time curves during the life of a mercury drop were recorded at various potentials and at various concentrations of gelatin. Some of the curves are shown in Fig. 2.

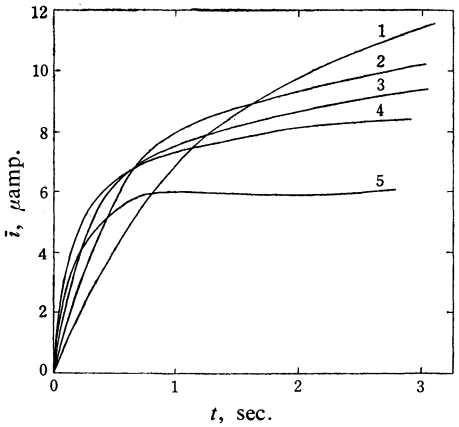


Fig. 2. Current-time curves of 1.0 mM *cis*-$[Cr(ox)_2(H_2O)_2]^-$ measured at −1.75 V. vs. SCE in 0.3 M KCl solutions containing various concentrations of gelatin: (1) 0%; (2) 0.001%; (3) 0.005%; (4) 0.01%; (5) 0.02% gelatin present. (Electrode B).

The number of electrons which are involved in the overall electrode reaction of *cis*-dioxalatodiaquochromate(III) was determined coulometrically by controlled potential electrolysis. The electricity Q (coulombs) required in the controlled potential electrolysis was determined by integrating the recorded current-time curves, with correction being made for the contribution of the residual current. The number of electrons, n, can be calculated from the relation

$$n=\frac{Q}{FN}\times\frac{(\bar{i}_l)_2}{(\bar{i}_l)_1-(\bar{i}_l)_2}$$

where N is the initial amount of *cis*-dioxalatodiaquochromate(III) present in the solution expressed in mole; F, the faraday, and $(\bar{i}_l)_1$ and $(\bar{i}_l)_2$, the limiting currents of the polarograms before and after the electrolysis respectively. The current-voltage curves after the electrolysis were different from those before the electrolysis, as Fig. 3 shows. This seemed due to the increase in the pH of the solution during the course of electrolysis. In the determination of $(\bar{i}_l)_2$, the pH of the solution after the electrolysis was adjusted with hydrochloric acid to be equal to that of the initial solution. The controlled potential electrolysis of *cis*-dioxalatodiaquochromate(III) was also complicated by the evolution of hydrogen gas at the cathode which was observed when the

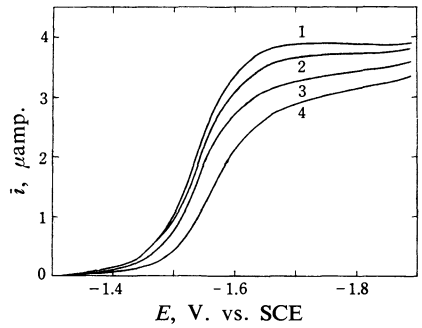


Fig. 3. Current-voltage curves of *cis*-$[Cr(ox)_2(H_2O)_2]^-$ in 0.3 M KCl solutions containing 0.005% gelatin before (1) and after (2-4) the controlled potential electrolysis. (Electrode B). The concentration of the complex and the pH of the initial solution were 0.50 mM and 5.29, respectively. The electrolysis periods and pH of the resulted solutions are: 2, 100 sec. (pH 5.49); 3, 180 sec. (pH 5.50); 4, 300 sec. (pH 5.82).

electrolysis was continued for a longer time. Under these conditions, a shorter period of electrolysis was more favorable for determining the quantity of electricity required for the reduction of *cis*-dioxalatodiaquochromate(III). Therefore, a procedure previously reported[7] was employed to determine the true value of n; the apparent n values obtained from the electrolyses of varied electrolysis periods were plotted against the electrolysis period to estimate the true value of n by the extrapolation of the plot to a zero time (Fig. 4). Fig. 4 indicates that the reduction process of *cis*-dioxalatodiaquochromate(III) at a mercury electrode in potassium chloride solutions is a three-electron process.

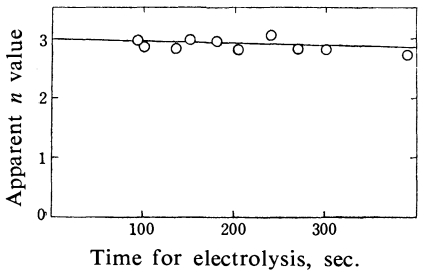


Fig. 4. Plot of apparent number of electrons involved in the reduction of *cis*-$[Cr(ox)_2(H_2O)_2]^-$ as a function of electrolysis period, being measured in 0.3 M KCl solutions containing 0.005% gelatin. The initial concentration of the complex was 0.50 mM. The controlled potential was −1.70 V. vs. SCE.

In order to examine the reduced species of *cis*-dioxalatodiaquochromate(III), current-voltage curves were measured, using a mercury

pool electrode with an area of approximately 1 cm^2 as a working electrode. An apparent anodic wave was observed when the working electrode was polarized at less negative potentials than −0.4 V. vs. SCE immediately after it had been polarized for 5 to 10 min. at the potentials where the reduction of the complex takes place. No anodic current, however, was observed at the DME inserted in the same solution. This result clearly indicated that the reduced substance was contained in the mercury of the electrode. The conventional chemical analysis of the mercury which had been used as the cathode in the electrolysis also showed the presence of chromium.

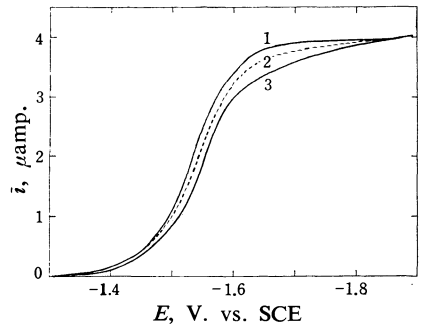


Fig. 5. Current-voltage curves of 0.5 mM *cis*-$[Cr(ox)_2(H_2O)_2]^-$ obtained in 0.3 M KCl solutions of various pH's containing 0.005% gelatin: 1, pH 5.3 (no NaOH added); 2, pH 5.6; 3, pH 5.9. (Electrode B).

Discussion

The experimental results indicate that the limiting current of *cis*-dioxalatodiaquochromate(III) in 0.3 M potassium chloride solutions containing 0.005% gelatin is diffusion-controlled. The diffusion coefficient is calculated to be 6.0×10^{-6} cm^2 sec^{-1} at 25°C by using the Ilkovič equation under the assumption that the number of electrons is equal to three. This value seems reasonable when it is compared with those of analogous complex ions, such as hexamminechromium(III) (8.5×10^{-6} cm^2 sec^{-1})[5] and aqopentamminechromium(III) (8.0×10^{-6} cm^2 sec^{-1}).[9]

The alternating current and the Kalousek polarograms suggest that the reduction process of *cis*-dioxalatodiaquochromate(III) in neutral solutions is totally irreversible in the polarographic sense. The relation between $\log\{\bar{i}/(\bar{i}_d-\bar{i})\}$ and the electrode potential, *E*, however, does not give a straight line. This complication makes the theoretical analysis of the current-potential curve less feasible.

The decrease in the limiting current with the decrease in the ionic strength of potassium chloride solutions is due to the migration effect, because *cis*-dioxalatodiaquochromate(III) is an anion. The potentials of the reduction wave are also dependent on the ionic strength of the solution; the half-wave potential shifts to more negative potentials as the ionic strength decreases (Table III). This can be explained, at least qualitatively, by considering the effect of the diffuse double layer on the irreversible reduction process.

As has been mentioned above, the shape of the reduction wave of *cis*-dioxalatodiaquochromate(III) gradually changes during the course of the controlled potential electrolysis. This is considered due to the increase in the pH of the solution, and is supported by the observation of the change in the reduction wave with the change in the pH of the solution. Figure 5 shows the current-potential curves obtained in 0.3 M potassium chloride solutions containing 0.005% gelatin at three different pH's, the adjustments being made with sodium hydroxide. It has been known that there exist the following equilibria in the aqueous solution of *cis*-dioxalatodiaquochromate(III):[10]

$$cis\text{-}[Cr(ox)_2(H_2O)_2]^- \rightleftharpoons cis\text{-}[Cr(OH)(ox)_2(H_2O)]^{2-} + H^+ \quad (pK=6.4)$$

$$cis\text{-}[Cr(OH)(ox)_2(H_2O)]^{2-} \rightleftharpoons cis\text{-}[Cr(OH)_2(ox)_2]^{3-} + H^+ \quad (pK=8.8)$$

The polarographic reduction wave of *cis*-hydroxodioxalatoaquochromate(III) appears at a potential about 200 mV. more negative than that of *cis*-dioxalatodiaquochromate(III).[1] Therefore, the change in the reduction wave of *cis*-dioxalatodiaquochromate(III) in solutions of pH 5~6 is considered to be due to the contribution of *cis*-hydroxodioxalatoaquochromate(III), whose concentration increases with an increasing pH.

The polarographic reduction wave of *cis*-dioxalatodiaquochromate(III) in potassium chloride solutions resembles the hydrogen wave. However, the appearance of a large anodic wave on the Kalousek polarogram (Fig. 1) eliminates the possibility that the reduction wave of *cis*-dioxalatodiaquochromate(III) is due to the discharge of hydrogen ions; hydrogen ions in potassium chloride solutions were found to give no apparent anodic wave on the Kalousek polarogram. The results obtained by controlled potential electrolysis

9) N. Tanaka, Y. Sato, R. Tamamushi and G. Satô, This Bulletin, **36**, 1059 (1963).

10) D. M. Grant and R. E. Hamm, *J. Am. Chem. Soc.*, **78**, 3006 (1956).

and coulometric analysis suggest that *cis*-dioxalatodiaquochromate(III) is reduced at the mercury electrode to chromium(0), probably to chromium amalgam.

From these results, it can be concluded that the reduction process of *cis*-dioxalatodiaquochromate(III) at the DME in potassium chloride solutions proceeds irreversibly according to this overall reaction;

$$cis\text{-}[Cr(ox)_2(H_2O)_2]^- + 3\ e \rightarrow Cr(0) + 2\ ox^{2-} + 2\ H_2O$$

Summary

The current-voltage curves of *cis*-dioxalatodiaquochromate(III) have been recorded at the dropping mercury electrode in various supporting electrolyte solutions. A well-defined wave with a half-wave potential of -1.52_2 V. vs. SCE was obtained in 0.3 M potassium chloride solutions containing 0.005% gelatin. The limiting current in this case was proved to be diffusion-controlled from its dependence on the effective pressure of mercury on the dropping mercury electrode and from the characteristics of the current-time curve during the life of a mercury drop. The electrode reaction of the complex was found to be irreversible by a study of both the characteristics of the Kalousek polarogram and the relation of $\log\{\bar{i}/(\bar{i}_d-\bar{i})\}$ against E.

The number of electrons involved in the reduction was determined by the controlled-potential coulometric method. The coulometric investigation showed that *cis*-dioxalotodiaquochromate(III) is reduced to the metal at the dropping mercury electrode. This conclusion was also supported by the detection of chromium from the surface of the mercury pool electrode used in the controlled potential electrolysis. The value of the diffusion coefficient of *cis*-dioxalatodiaquochromate(III), calculated for a three-electron reduction, was also reasonable in comparison with those of other chromium(III) complexes.

The authors wish to thank the Ministry of Education for the financial support granted for this research.

Department of Chemistry
Faculty of Science
Tohoku University
Katahira-cho, Sendai

Analytical Studies Using the Convection Electrode. VII. The Use of the Pushed-out Mercury-drop Electrode

By Junsuke SUZUKI and Tokuro OZAKI

(Received August 27, 1963)

The "rotating disk" convection electrode of platinum wire has previously been devised as a new polarographic electrode by one of the present authors, and the current-voltage curves for the oxidation of iodide and the reduction of cadmium and thallum(I) have been studied. However, the platinum wire electrode, like the other solid electrodes, showed a poor reproducibility.[1] Therefore, using a mercury-coated platinum wire, polarographic waves for the reduction of cadmium and thallium(I) have been investigated and well-reproducible waves obtained.[2] In a neutral or almost neutralized medium, good results were achieved, but in a strongly alkaline or acidic medium, coated mercury on the platinum wire is often detached from the wire during the electrolysis and, in this case, the electrode loses its function as a mercury electrode. Consequently, the polarographic applications of this electrode were found to be limited to a narrow range of pH.

In order to correct these weak points, the authors prepared an electro-deposited mercury-drop electrode.[3] It has a small cup-shape vessel at the end of a glass tube and a small mercury drop electro-deposited on the tip of platinum wire sealed at the bottom of the vessel. The electro-deposited mercury-drop is never detached, even in strongly alkaline or acidic solutions. However, this electrode is difficult to construct and to manipulate, and, also, it takes much time to deposit a mercury drop electrolytically. In order to improve these points, the "pushed-out" mercury-drop

1) T. Ozaki and T. Nakayama, *J. Chem. Soc. Japan, Pure Chem. Sec.* (*Nippon Kagaku Zasshi*), **81**, 98 (1960).
2) T. Ozaki and T. Nakayama, ibid., **82**, 46 (1961).
3) T. Ozaki, *Bull. of Educ. Fac. of Shizuoka Univ.*, **11**, 133 (1960).

convection electrode (PMDCE) has recently been invented by the authors as a new polarographic electrode. This is much easier to construct and to manipulate than the electrodes mentioned above.

In the present paper, polarographic studies using this electrode on various depolarizers, i. e., cadmium, thallium(I) and lead, are reported, and the following points, among others, are examined: (1) the reproducibility of limiting currents or half-wave potentials, (2) the relation between the concentration and the wave height, (3) the relation between the stirring rate of the rotated disk and the wave height, and (4) the half-wave potential and its shift. The results are discussed in detail.

Experimental

Apparatus. — A Shimadzu RP-2 type polarograph was employed for the measurement of all the current-voltage curves. The curves were recorded with a chart speed of about 2 cm./min. and a rate of change of applied potential of about 100 mV./min. A rotating apparatus of a Shimadzu "rotated platinum electrode" was also used in all experiments. It can be rotated at 600, 800, 1000 or 1200 r. p. m. by shifting the gears. The rotated disk was fixed to the axis of the rotator. The disk was made of hard polyvinyl chloride resins and pulley shape.

Cell and Electrode. — The cell and the electrode used in this experiment are shown in Fig. 1. The cell was made of hard glass, while the electrode tube is composed of three parts: (A) a small cup-shape glass vessel (0.2 cm. in inside diameter, 0.3 cm. in outside diameter, and 0.4 cm. deep), (B) a glass capillary for inserting mercury, into A, and (C) a glass tube connecting it with the large mercury reservoir.

Small amounts of mercury are pushed-out into vessel A through B by the pressure caused by raising the mercury reservoir. When the reservoir is lowered, the mercury in vessel A is separated from the mercury in C and, accordingly, a mercury drop is formed in the vessel and the mercury remaining in the capillary B moves back to C.

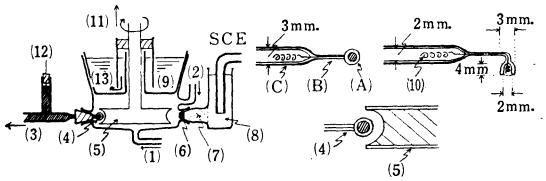


Fig. 1. Polarographic cell and electrode.

(1), (2) Inlet pipe of H_2 gas
(3) To mercury reservoir
(4) Electrode (PMDCE)
(5) Rotating disk (stirrer)
(6) Sintered glass
(7) Agar bridge
(8) Sat. KCl solution
(9) Water
(10) Mercury coated platinum wire
(11) To synchronous motor
(12) Cathode
(13) Outlet of H_2 gas

The electric connection of a mercury drop in vessel A with the mercury in C was made by mercury-plated platinum wire (0.01 cm. in diameter). The platinum wire prevents a mercury drop from falling out of A.

The solution containing the supporting electrolyte has a tendency to penetrate into the vessel. Therefore, the inside of the vessel is coated with silicone film.

The capillary B is constructed so finely as to separate the mercury drop in vessel A from the mercury in C in order to avoid the diffusion of an amalgamated metal from A to C.

The mercury drop prepared as mentioned above does not fall out of the vessel even under such severe experimental conditions as in 1 M sodium hydroxide or 1 M hydrochloric acid or at the rate of rotation of 1200 r. p. m.

Reagents.—Each solution of thallium(I), cadmium and lead was prepared from chemicals of an extra pure reagent grade without further purification. The other chemicals used are all of extra pure reagent grade.

Procedure. — The mercury drop is renewed in each polarographic measurement. The procedure is as follows.

Before the measurement of a current-voltage curve, the mercury reservoir is raised to the height of about 27 cm. A few mercury drops are made to fall out of vessel A because of the pressure created by raising the reservoir. When the last of these drops falls, the reservoir is brought down to the height of about 5 cm. The fall of mercury drops then stops, and, in vessel A, a mercury drop is formed. After that, a polarogram is recorded. The mercury drop can be renewed as the electrode by repeating the above process.

Dissolved oxygen is removed by passing H_2 gas through the solution or by adding small amounts of a sodium sulfite solution.

0.3 ml. of a 1 M sodium sulfite solution freshly prepared is added to 50 ml. of a 0.1 M potassium chloride solution containing thallium(I) or cadmium ions as depolarizers. A reduction wave is measured after 15 min. Also, after 50 ml. of 1 M sodium hydroxide or hydrochloric acid containing a lead depolarizer is poured into the electrolysis cell, a hydrogen gas stream is passed, at the rate of about 4 bubbles per second for about 1 hr., through the solution to remove the dissolved oxygen. These lead sample solutions are electrolyzed by the constant bubbling of hydrogen gas (by using gas-inlet pipe (2) in Fig. 1).

All the measurements were carried out at 16.5± 0.5°C.

Results

The Reproducibility of the Limiting Currents. — A mercury drop is pushed out into the vessel of the electrode before each measurement, so its surface area must always be kept

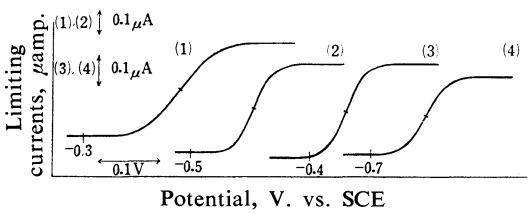


Fig. 2. Typical current-voltage curves of thallium, cadmium and lead (HCl and NaOH).
(1) 5×10^{-6} M Tl^+ in 0.1 M KCl
(2) 5×10^{-6} M Cd^{2+} in 0.1 M KCl
(3) 5×10^{-6} M Pb^{2+} in 1 M HCl
(4) 5×10^{-6} M Pb^{2+} in 1 M NaOH

constant. To test the reproducibility of the area, the limiting currents were measured with various depolarizers. Typical current-potential curves are shown in Fig. 2, while some of these results are given in Table I. The curves oscillated slightly, but this had no effect upon the results.

On the other hand, the limiting currents obtained by the renewal method of the electrode proposed by Marple et al.[4] are shown in Table II (the applied voltage and the time for the renewal were −0.4 V. vs. SCE and 5 min. respectively).

As is shown in Tables I and II, reproducibility with the PMDCE was slightly poor in comparison with the method of Marple et al.,[4] but it is considered that the surface area of the mercury drop can be kept fairly constant, because good reproducibilities of the limiting currents can always be obtained within a range of error of 2%.

The Reproducibility of Half-wave Potentials. — The half-wave potentials of various depolarizers were determined by the ordinary method; the results are listed in Table III. As is shown in Table III, the half-wave potentials have a good reproducibility.

The Relation between the Concentration of Depolarizers and the Limiting Currents. — The

TABLE I. REPRODUCIBILITY OF THE LIMITING CURRENTS (i_l) OBTAINED WITH THE PMDCE (STIRRING RATE: 800 r. p. m.)

	Depolarizer	Cd^{2+}	Tl^+	Pb^{2+}(NaOH)	Pb^{2+}(HCl)
i_l	Average*, μamp.	4.807	4.055	4.762	5.564
	Mean deviation, %	1.07	1.36	0.71	0.57

* Average value of 5~6 data

TABLE II. REPRODUCIBILITY OF THE LIMITING CURRENTS (i_l) OBTAINED BY USING THE METHOD OF MARPLE ET AL.[4] (STIRRING RATE: 800 r. p. m.)

Exp. No.		1	2	3	4	5	Average, μamp.
i_l	Cd^{2+}, 5×10^{-6} M	0.203	0.206	0.203	0.206	0.201	0.203
	Tl^+, 5×10^{-6} M	0.197	0.199	0.198	0.199	0.199	0.199

Mean deviation (%) —— Tl^+: 0.49, Cd^{2+}: 0.59

TABLE III. REPRODUCIBILITY OF HALF-WAVE POTENTIALS ($E_{1/2}$, V. vs. SCE) (STIRRING RATE: 800 r. p. m.)

Depolarizer*		Cd^{2+}(KCl)	Tl^+(KCl)	Pb^{2+}(NaOH)	Pb^{2+}(HCl)
$E_{1/2}$	Average	−0.610	−0.479	−0.784	−0.467
	Mean deviation	0.07	0.21	0.10	0.17

* The concentration of each depolarizer is 1×10^{-4} M.

TABLE IV-1. RELATION BETWEEN CONCENTRATION (C) AND THE LIMITING CURRENTS (i_l) (STIRRING RATE: 800 r. p. m.)

Depolarizer C, mol./l.	Cd^{2+}(KCl)		Tl^+(KCl)	
	i_l, μamp.	$(i_l/C)\times10^{-4}$	i_l, μamp.	$(i_l/C)\times10^{-4}$
1×10^{-4}	4.807	4.81	4.055	4.06
5×10^{-5}	2.276	4.55	1.903	3.81
2×10^{-5}	0.886	4.43	0.851	4.26
5×10^{-6}	0.205	4.10	0.195	3.90
1×10^{-6}	0.044	4.40	—	—
5×10^{-7}	0.021	4·20	—	—

4) T. L. Marple and L. B. Rogers, *Anal. Chem.*, **25**, 1351 (1953).

TABLE IV-2. RELATION BETWEEN CONCENTRATION (C) AND THE LIMITING CURRENTS (i_l) (STIRRING RATE : 800 r. p. m.)

Depolarizer C, mol./l.	Pb^{2+} (NaOH)		Pb^{2+} (HCl)	
	i_l, μamp.	i_l/C, $\times10^{-4}$	i_l, μamp.	i_l/C, $\times10^{-4}$
1×10^{-4}	4.762	4.76	5.564	5.56
5×10^{-5}	—	—	2.865	5.73
2×10^{-5}	0.973	4.87	1.100	5.50
5×10^{-6}	0.243	4.86	0.256	5.12
1×10^{-6}	0.047	4.70	0.051	5.10
5×10^{-7}	0.023	4.60	0.029	5.80

TABLE V. EFFECT OF STIRRING RATE ON HALF-WAVE POTENTIALS (V. vs. SCE)

Depolarizer*	Stirring rate, r. p. m.			
	600	800	1000	1200
Cd^{2+} (KCl)	−0.610	−0.610	−0.610	−0.611
Tl^{+} (KCl)	−0.478	−0.479	−0.481	−0.480
Pb^{2+} (NaOH)	−0.782	−0.784	−0.785	−0.783
Pb^{2+} (HCl)	−0.466	−0.467	−0.468	−0.468

* Each concentration of these depolarizers is 1×10^{-4} M.

TABLE VI. EFFECT OF THE RATE OF POLARIZATION ON THE LIMITING CURRENTS (i_l, μamp.) AND HALF-WAVE POTENTIALS ($E_{1/2}$, V. vs. SCE)

Depolarizer	Rate of polarization, mV./min.					
	$E_{1/2}$	i_l	$E_{1/2}$	i_l	$E_{1/2}$	i_l
Cd^{2+} (KCl)[1]	−0.611	0.870	−0.611	0.886	−0.609	0.938
Tl^{+} (KCl)[2]	−0.488	3.918	−0.479	4.042	−0.463	4.349
Pb^{2+} (NaOH)[3]	—	—	−0.782	1.515	−0.777	1.866
Pb^{2+} (HCl)[4]	−0.458	2.825	−0.460	2.880	−0.463	2.988

Stirring rate : 800 r. p. m.
1) 2×10^{-5} M 2) 1×10^{-4} M 3) 3×10^{-5} M 4) 5×10^{-5} M

relations between the limiting currents and concentration are shown in Table IV. It can be seen from Table IV that a satisfactory proportionality between the limiting currents and concentration is obtained.

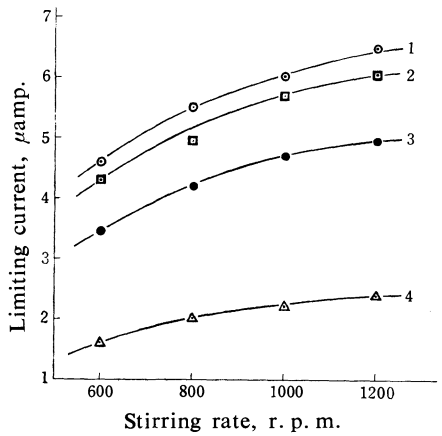


Fig. 3. The effect of stirring rate on limiting currents.
1 : 1×10^{-4} M Pb^{2+} in 1 M HCl
2 : 1×10^{-4} M Cd^{2+} in 0.1 M KCl
3 : 1×10^{-4} M Pb^{2+} in 1 M NaOH
4 : 5×10^{-5} M Tl^{+} in 0.1 M KCl

The Effect of the Stirring Rate on Limiting Currents. — The dependence of the limiting currents on the stirring rate of the rotating disk was investigated by using a cadmium, thallium(I) or lead solution respectively. The results are shown in Fig. 3. It can be seen that no linear relation between the limiting currents and the stirring rate is obtained, although the currents decrease gradually with the increase in the stirring rate.

The Effect of the Stirring Rate on the Half-wave Potentials. — The effect of the stirring rate on the half-wave potentials of cadmium, thallium(I) and lead was investigated; the results are shown in Table V. It can there be seen that the change in the stirring rate of 600～1200 r. p. m. has no effect on the half-wave potentials.

The Effect of the Rate of Polarization. — It was observed with a stationary mercury-plated platinum electrode by Marple et al.[4] that the half-wave potential was shifted toward positive potentials as the rate of polarization was increased from 37 mV. to 222 mV. per minute.

Therefore, the effect of the rate of polarization was investigated with the PMDCE. The results are given in Table VI. It can be seen from Table VI that the limiting currents are increased with the increase in the rate of polarization and that, at the same time, the half-wave potentials are slightly shifted toward positive potentials, as Marple et al.[4] observed, in the cases of thallium(I) and lead (in 1 M sodium hydroxide). However, no change in the half-wave potential is observed on the other ions.

A comparison with the Dropping Mercury Electrode (DME). — The limiting currents obtained with the PMDCE (1200 r. p. m.) for thallium(I), cadmium, and lead (in 1 M hydrochloric acid and in 1 M sodium hydroxide) were, respectively, about eighteen, fifteen, sixteen and fourteen times as large as the corresponding diffusion currents obtained by the DME. The capillary of the DME used had an m value of 0.92 mg./sec. and a drop time of 5.1 sec./drop at −0.8 V. vs. SCE in a 0.1 M potassium chloride solution.

Discussion

Sensitivity. — Table VII lists the values of sensitivity, "S" ($S=i_l/nC$), which derived by Kolthoff and Jordan[5] to characterize the convection electrode, at the PMDCE; the values of $S/D^{2/3}$ (D: diffusion coefficient) are shown in column 4 of this table. If the limiting currents are completely controlled with convection, the S values of these depolarizers should be of the same value, because all measurements were carried out under the same hydrodynamic conditions. As is shown in Table VII, however, at the PMDCE the S values of these depolarizers are not equal, while the $S/D^{2/3}$ values agree well with one other. Therefore, it is found that the limiting currents change proportionally with two-thirds the power of the diffusion coefficient. Apparently both diffusion and convection contribute to the currents; i. e., the limiting currents depend on the diffusion coefficient and, at the same time, on the convection coefficient.[5]

The Relation between the Stirring Rate and the Limiting Currents. — The relation between the limiting currents and the speed of the rotation of the stirrer can generally be expressed by this equation:[6]

$$i_l = pr^a$$

where p is a constant, r is the number of rotations per minute of the stirrer, and a is a constant which is generally comprised between 0.4 and 1 and which depends on the geometric factors of the electrolytic cell, the stirrer and the electrode.

This relation was investigated with the PMDCE in the cases of cadmium, thallium(I) and lead. A logarithm of limiting current was plotted against a logarithm of the stirring rate of the stirrer. These plots are shown in Fig. 4, where the plots of various depolarizers give straight lines. The values of a in the above equation can be determined with the slope of a line in Fig. 4. The value of a

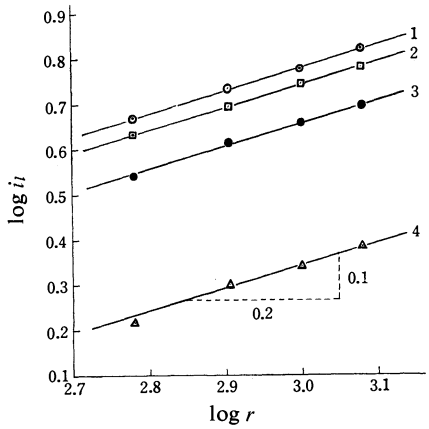


Fig. 4. The relation between logarithm of stirring rate (r) and logarithm of limiting currents (i_l).
1: 1×10^{-4} M Pb^{2+} in 1 M HCl
2: 1×10^{-4} M Cd^{2+} in 0.1 M KCl
3: 1×10^{-4} M Pb^{2+} in 1 M NaOH
4: 5×10^{-5} M Tl^{+} in 0.1 M KCl

TABLE VII. COMPARISON OF S VALUES AND $S/D^{2/3}$ VALUES OF VARIOUS DEPOLARIZERS. (STIRRING RATE: 800 r. p. m.)

Depolarizer	Supporting electrolyte	S*	$S/D^{2/3}$
Cd^{2+}	0.1 M KCl	2.49×10^4	6.7×10^7
Tl^{+}	0.1 M KCl	5.10×10^4	6.9×10^7
Pb^{2+}	1 M NaOH	2.95×10^4	6.5×10^7
Pb^{2+}	1 M HCl	3.08×10^4	6.6×10^7

* μamp./equiv. per liter

5) I. M. Kolthoff and J. Jordan, *J. Am. Chem. Soc.*, 76, 3843 (1954).

6) P. Delahay, "New Instrumental Methods in Electrochemistry," Interscience Publishers, New York (1953), pp. 217-249.

obtained is 0.50. This shows that the limiting currents change in proportion to the square root of the stirring rate.

Accordingly, the limiting currents at the PMDCE change linearly with the square root of the stirring rate and, at the same time, with two-thirds the power of the diffusion coefficient.[3] If it is assumed that the velocity of the stream on the surface of the electrode, which can hardly be measured, is proportional to the rate of the rotation of the disk, it seems that the limiting currents with the PMDCE conform to the equation of the limiting currents for the rotating disk electrode derived by Levich,[7] which is as follows:

$$i_l = knF'ACD^{2/3}\omega^{1/2}\nu^{-1/6}$$

where i_l=limiting currents, C=bulk concentration, ω=angular velocity of electrode, and ν=kinematic viscosity.

The relation between i_l and ν has not yet been investigated experimentally. This result is very similar to that obtained by Galus et al.[8] or by Galus and Adams.[9]

Half-wave Potentials. — Table VIII summarizes the half-wave potentials at the PMDCE and DME. As is shown in Table VIII, the half-wave potentials of various depolarizers at the PMDCE are slightly more negative than the corresponding half-wave potentials of DME. It seems probable that the rate of mass transfer becomes large as compared with the rate of electron transfer, as has been reported by Jordan,[10] or that δ_0, the effective thickness of the diffusion layer, is smaller, as has been pointed out by Delahay,[6] because of the convection effect caused by increasing the stirring rate. Table V shows the effect of the stirring rate on the half-wave potential; the results indicate that the half-wave potential is not affected by the stirring rate. It seems probable that a change in δ_0 can be almost disregarded in the range of a given stirring rate, as the relationship of the half-wave potential to δ_0 is of an exponential function.[3]

The effect of the concentration of reducible material on the half-wave potential is shown in Table IX. For cadmium, the half-wave potential is nearly the same at every concentration, but with the others, the half-wave potentials are shifted slightly toward positive potentials with the decreasing concentration of depolarizers. Such a shift can be found

Table VIII. Comparison of half-wave potentials at DME and PMDCE
(stirring rate: 800 r. p. m.)

Electrode	Depolarizer			
	Cd^{2+}(KCl)	Tl^{+}(KCl)	Pb^{2+}(NaOH)	Pb^{2+}(HCl)
DME, 4×10^{-4} M	−0.60	−0.46	−0.76	−0.44
PMDCE, 1×10^{-4} M	−0.61	−0.48	−0.78	−0.47

Table IX. Effect of depolarizer concentration on half-wave potentials
(stirring rate: 800 r. p. m.)

Depolarizer	Concentration, mol./l.			
	1×10^{-4}	5×10^{-5}	5×10^{-6}	5×10^{-7}
Cd^{2+}(KCl)	−0.611	−0.609	−0.610	−0.613
Tl^{+}(KCl)	−0.479	−0.470	−0.462	—
Pb^{2+}(NaOH)	−0.783	—	−0.780	−0.776
Pb^{2+}(HCl)	−0.467	−0.461	−0.458	−0.456

Table X. Effect of stirring rate on the slope (mV.)

Stirring rate r. p. m.	Depolarizer					
	Cd^{2+}(KCl)		Pb^{2+}(NaOH)		Pb^{2+}(HCl)	
	mV.	n	mV.	n	mV.	n
600	32.3	1.78	29.0	1.98	29.0	1.98
800	33.3	1.72	29.6	1.94	29.7	1.93
1000	33.3	1.72	30.0	1.91	32.3	1.78
1200	35.0	1.64	33.3	1.72	32.4	1.77

7) V. G. Levich, *Acta Physicochim.*, **17**, 257 (1942).
8) Z. Galus, C. Olson, H. Y. Lee, and R. N. Adams, *Anal. Chem.*, **34**, 164 (1962).
9) Z. Galus and R. N. Adams, *J. Am. Chem. Soc.*, **84**, 2061 (1962).
10) J. Jordan, *Anal. Chem.*, **27**, 1708 (1955).

reported also by Arthur et al.[11]

Plot of the Applied Potential against log $i/(i_l-i)$. — The logarithm of quantity (i/i_l-i) was plotted against the applied potential at the PMDCE. These plots for thallium, cadmium and lead how perfectly straight lines. Table X shows both the values of the slope (mV.) and the number of electrons, n calculated from it.

The data given in Table X show that the values of n decrease with an increase in the stirring rate. It is considered that the increase in the mass transfer due to the convection gives the increase in quasi-irreversibility.[10]

11) P. Arthur, J. C. Kamyathy, R. F. Maness and H. W. Vaughan, ibid., **27**, 895 (1955).

Summary

The limiting currents with the PMDCE depend on the factors of both convection and diffusion. The PMDCE is easy to prepare and to manipulate, and it has an excellent sensitivity. It can be used even in a strongly alkaline or acidic medium and can be reused many times with good reproducibility. Therefore, various applications to analytical chemistry can be expected.

The authors wish to express their thanks to the Ministry of Education for the financial support given to this research.

Faculty of Education
Shizuoka University
Ooiwa, Shizuoka

The Synthesis of Oxygenated Organic Compounds from Methanol and Carbon Monoxide-Hydrogen Mixtures in the Presence of a Mixture of Cobalt Acetate and an Iodide Used as the Catalyst

By Tsutomu MIZOROKI and Mikitake NAKAYAMA

(Received August 30, 1963)

The treatment of methanol with carbon monoxide-hydrogen mixtures under the oxo reaction conditions results in the formation of ethanol. This is well known as the homologation of methanol. When cobaltcarbonyl or cobalt salts were used as catalysts in this reaction, small portions of the methanol were converted into ethanol.[1] However, Berty found that the yields of ethanol and other oxygenated compounds (acetaldehyde, methyl or ethyl acetate) were increased by adding a small amount of iodine as an additive for the cobalt acetate catalyst.[2]

In a preceding paper,[3] it was shown that, in a bathwise experimental run using a mixture of cobalt acetate and an iodide (LiI, NaI, KI and CaI_2) as the catalyst, acetic acid was synthesized in a 90% yield from methanol and carbon monoxide in a liquid phase under pressures from 300 to 500 kg./cm^2 and at temperatures from 210 to 240°C. However, when this reaction was carried out in a flow reactor under the same conditions except that the carbon monoxide contained 10% hydrogen, it was found that the amount of hydrogen was strikingly decreased, that this reaction was invariably accompanied by the formation of acetaldehyde and ethanol, and that the extent of methanol conversion into free acetic acid was less than 60%.[4] This led us to investigate the homologate of methanol with the same catalyst.

For acetic acid synthesis with a mixture of cobalt acetate and an iodide at the catalyst, it is necessary to add a considerable amount of water,[3] while for the formation of ethanol and other oxygenated compounds from methanol and carbon monoxide-hydrogen mixtures with the same catalyst, it in unnecessary to add water to methanol. This is very significant.

From a comparison of the effect of an iodide with that of iodine on the extent of methanol conversion into C_2-oxygenated compounds, we found that an iodide serves as an additive for increasing the yield of ethanol and other oxygenated compounds.

The present work was undertaken in order to study in detail the influence of an iodide

1) K. H. Ziesecke, *Brenn. Chem.*, **33**, 385 (1952).
2) J. Berty and L. Marko, *Chem. Tech. (Berlin)*, **8**, 260 (1956).
3) T. Mizoroki, M. Nakayama, Y. Andō and M. Furumi, *J. Chem. Soc. Japan, Ind. Chem. Sec. (Kogyo Kagaku Zasshi)*, **65**, 1049, 1054 (1962).
4) T. Mizoroki, M. Nakayama, Y. Andō and M. Furumi, *Repts. Govt. Chem. Ind. Research Inst. Tokyo (Tokyo Kōgyo Shikensho Hōkoku)*, **58**, 310 (1963).

as an additive for a cobalt acetate catalyst on the reaction of methanol with carbon monoxide-hydrogen mixtures.

Experimental

Apparatus for Carrying out the Reaction.—In all experiments, the reaction was carried out in a titanium-manganese alloy autoclave (185 or 225 ml.). The complete apparatus used was essentially the same as that described in the preceding paper.[3]

When a solution of cobalt acetate and an iodide in methanol is heated without the addition of acetic acid, a precipitate is formed. However, in the presence of acetic acid*1 no precipitate is formed by heating, though the color of the solution changes from pale pink to blue or green. (These observations have been made by heating the solutions in a sealed, thick-walled glass tube.) In the latter case, the reaction between methanol and carbon monoxide-hydrogen takes place without an induction period being exhibited.

The experiments were carried out in the following way. The reaction vessel was heated in a shaking-type electric furnace (60 r. p. m.) after a mixture of methanol and acetic acid containing cobalt acetate and an iodide had been charged. After this solution had been maintained at a reaction temperature (between 160 and 240°C) for about one hour, the synthesis gases were introduced and continuously supplied from the pressure accumulator to keep the pressure (between 250 and 500 kg./cm^2) constant during the reaction. After a predetermined time of reaction, the heating and the addition of gases were stopped, the reaction vessel was allowed to cool to room temperature, and the gases and the liquid product were discharged.

Materials.—The methanol, acetic acid, cobalt acetate and iodides used were obtained from commercial sources. The synthesis gases were mixtures*2 of hydrogen from water electrolysis and carbon monoxide from formic acid decomposition, materials which had been compressed into the pressure accumulator.

Analytical Procedure. — The main components in the liquid product were determined by the gas-chromatographic procedure. A 2.5 meter glass column with carbo-wax 400 on a Johns-Manville C-22 fire brick was used at the temperature of 80°C with a hydrogen carrier at the gas flow rate of 70 ml. per minute. In this way, dimethyl ether, acetaldehyde, methyl acetate, ethyl acetate, methanol, ethanol, crotonaldehyde and water were quantitatively determined using pyridine as an internal standard. Since formic acid, propionic acid and their esters could not be detected in the liquid product, the amount of free acetic acid was determined by titration with an aqueous potassium hydroxide solution. The amount of each of these components as determined by this method was approximately in agreement with that obtained from the fractional distillation (Podbielniak 3500, Heli-Grid column).

Cobaltous ions and iodide ions were determined by EDTA and Volhard's methods respectively in the usual manner, but cobalt-carbonyl complex compounds in the liquid product were too unstable to be investigated.

Carbon monoxide, carbon dioxide, methane and hydrogen in gases were determined by absorption and combustion methods in the usual manner.

Results

A Comparison with Iodine. — In order to compare the effect on the extent of methanol conversion of an iodide as an additive for a cobalt acetate catalyst with the effect of iodine, the reaction was carried out by the use of sodium iodide and iodine under the same conditions. The volume of synthesis gases supplied during the reaction for maintaining the reaction pressure constant is plotted against the time in Fig. 1, while the conversion values of methanol into C_2-oxygenated compounds are presented in Table I.

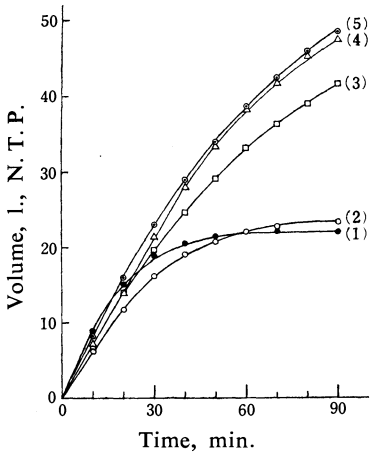


Fig. 1. The effect of iodine or sodium iodide as an additive for a cobalt acetate catalyst when a mixture of MeOH (1.62 mol.), AcOH (0.18 mol.) and $Co(AcO)_2 \cdot 4H_2O$ (9.0 mmol.) is treated for 90 min. under 300 kg./cm^2 and at 200°C. The added amounts of additives are (1) I_2 3.0 mmol., (2) I_2 6.0 mmol., (3) NaI 6.0 mmol., (4) NaI 12.0 mmol. and (5) NaI 18.0 mmol.

When iodine is used as an additive, the gas volume supplied becomes nearly constant after 30~40 min., the reaction ceases, and, as is shown in Table I, a considerable amount of dimethyl ether is formed. However, when sodium iodide is used instead of iodine, the reaction proceeds smoothly, the extent of methanol conversion to C_2-oxygenated compounds is about twice as much as that obtained with the use of iodine, and the amount of

*1 The amount of acetic acid in methanol is 5.0 to 10.0 mol. %.

*2 The amounts of CH_4, CO_2 and N_2 were less than 1.0 vol. %.

TABLE I. MASS BALANCE OF METHANOL

No in Fig. 1	Total AcOH	Total EtOH	Total aldehyde	Residual MeOH	CH_4	CH_3OCH_3	Others	MeOH conversion into C_2
1	11.9	4.3	13.6	40.6	5.5	13.1	10.5	30.3
2	10.0	4.4	11.1	38.2	5.0	21.3	11.0	25.1
3	15.7	25.6	4.8	42.2	5.9	1.9	3.6	46.4
4	16.5	25.3	6.3	37.7	5.6	1.0	7.6	48.1
5	14.6	23.4	8.6	38.4	5.6	1.5	6.7	47.2

Total AcOH=free acetic acid+acetic esters
Total EtOH=ethanol+ethyl acetate
Total aldehyde=acetaldehyde+crotonaldehyde

ethanol in the product is relatively large. From these results, the addition of iodine as an additive for a cobalt acetate catalyst in this reaction is undoubtedly disadvantageous.

The infrared spectra of the high temperature fractions obtained from the fractional distillation of the product showed the presence of *n*-butanol, but its amount was too small to be quantitatively determined. A trace of dimethylacetal, also, was detected.

Lithium iodide, sodium iodide, potassium iodide and calcium iodide were used as additives, there was little difference between their effects on the reaction rates and the extent of methanol conversion into C_2-oxygenated compounds. The results obtained with the use of lithium iodide or sodium iodide will be described later.

The Effect of Pressure, the Composition of Synthesis Gases and Temperature.—The effect of reaction pressure on the extent of methanol conversion was examined by using the synthesis gases of 1-CO : 1-H_2. The results are presented in Fig. 2, in which the conversion values of methanol into aldehyde (acetaldehyde+crotonaldehyde), acetic acid*3 (acetic esters+free acetic acid) and ethanol (ethanol+ethyl acetate) are plotted against the pressure; the volume % of carbon monoxide and hydrogen in the discharged gases after reaction is plotted in the upper part.

The increase in pressure results in an increase in the extent of methanol conversion, but it has little more effect on the ratios of the yield of ethanol, acetaldehyde or acetic acid than that of the other. The amount of hydrogen in the discharged gases is much less than that in synthesis gases in every case. The loss of methanol by the formation of methane and dimethyl ether is less than 5%.

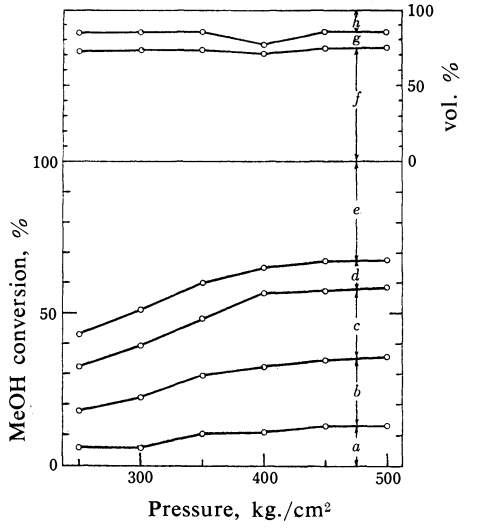


Fig. 2. The effect of pressure when a mixture of MeOH (1.425 mol.), AcOH (0.075 mol.), $Co(AcO)_2 \cdot 4H_2O$ (6.0 mmol.) and LiI (9.0 mmol.) is treated for 90 min. at 200°C.
a : total aldehyde, b : total acetic acid, c : total ethanol, d : methane+dimethyl ether+others, e : residual methanol, f : carbon monoxide, g : hydrogen and h : methane+carbon dioxide+nitrogen.

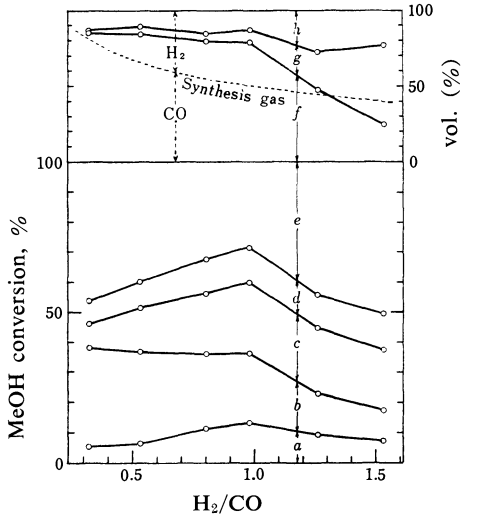


Fig. 3. The effect of the composition of synthesis gases when a mixture of MeOH (1.425 mol.), AcOH (0.075 mol.), $Co(AcO)_2 \cdot 4H_2O$ (6.0 mmol.) and LiI (9.0 mmol.) is treated for 90 min. under 400 kg./cm² and at 200°C.

*3 The amount of acetic acid previously charged in the autoclave was excluded and acetic acid was confirmed not to be hydrogenated under these conditions.

TABLE II. CONVERSION VALUES OF METHANOL OBTAINED AT SUITABLE CATALYST CONCENTRATIONS

The amounts, respectively, of MeOH and AcOH are 1.35 and 0.15 mol., the temperature 200°C and the reaction time 90 min.

Synthesis gases CO : H_2	Catalyst Concn., mol. ratio $Co(AcO)_2 \cdot 4H_2O$: NaI	Press. kg./cm²	Total AcOH	Total EtOH	Total aldehyde	CH_4 and CH_3OCH_3	Others	MeOH conversion into C_2
			%	%	%	%	%	%
1 : 1	0.1 : 2.0	300	16.5	3.0	20.6	3.7	6.9	40.1
1 : 1	0.1 : 2.0	400	20.0	5.3	28.3	3.8	6.3	54.5
1 : 1	0.1 : 2.0	500	21.9	10.1	24.9	3.5	11.4	55.9
1 : 1.26	0.27 : 0.73	400	16.8	20.6	13.3	2.8	8.0	50.8
1 : 1.26	0.27 : 0.73	500	17.8	23.8	14.3	3.3	8.8	55.9
1 : 1.57	0.45 : 0.55	350	10.6	22.3	8.8	3.5	10.3	41.7
1 : 1.57	0.45 : 0.55	400	11.1	26.3	10.1	4.5	8.6	47.7
1 : 1.57	0.45 : 0.55	450	10.0	28.2	14.3	5.5	8.7	52.5

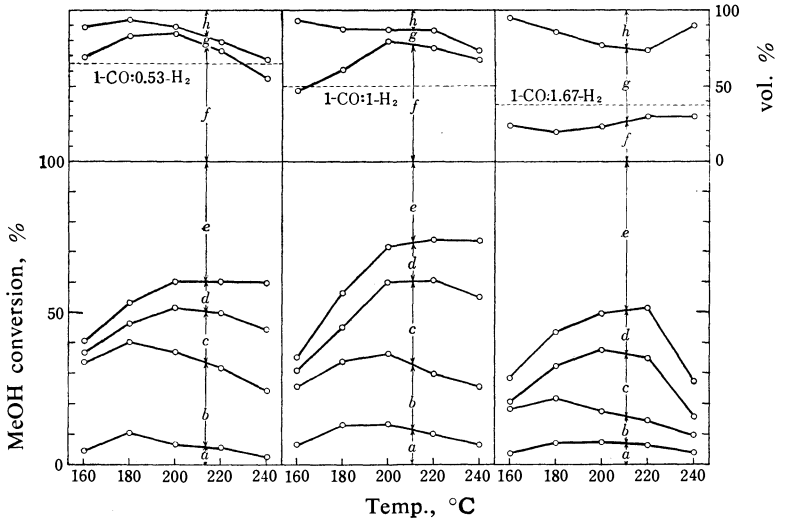


Fig. 4. The effect of temperature when a mixture of MeOH (1.425 mol.), AcOH (0.075 mol.), $Co(AcO)_2 \cdot 4H_2O$ (6.0 mmol.) and LiI (9.0 mmol.) is treated for 90 min. under 400 kg./cm².

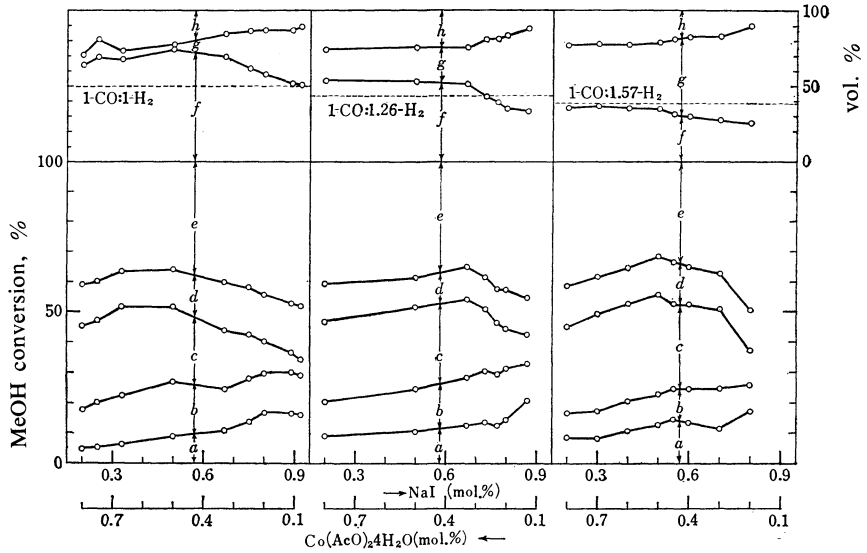


Fig. 5. Effect of the catalyst concentration at 200°C and the reaction time 90 min.

The effect of the composition of synthesis gases is represented in Fig. 3. Since the reaction was carried out at a constant pressure of 400 kg./cm^2, independently of the composition of synthesis gases, the partial pressures of hydrogen and carbon monoxide were different from each other. The evident formation of ethanol is expected to be favored in the presence of a large amount of hydrogen in this reaction, while the yield of ethanol does not increase as much as expected.

The effect of the temperature was examined at the pressure of 400 kg./cm^2 in the use of the synthesis gases of 1-CO : 0.53-H_2, 1-CO : 1-H_2 and 1-C : 1.67-H_2. The experimental results made at temperatures from 160 to 240°C are summarized in Fig. 4. At an elevated temperature, the amount of hydrogen reacting with methanol is more than that of carbon monoxide and the yield of ethanol consequently increases, although at a low temperature, the yield of acetaldehyde is relatively large. However, the increase in temperature beyond 220°C must be avoided, because then the amounts of methane, C_3- and higher oxygenated compounds increase and the methanol conversion decreases. A similar behavior with regard to temperature is observed in the synthesis of aldehydes and alcohols by oxo reactions.[5]

The Influence of the Catalyst Concentration. —For the purpose of obtaining more detailed information on the effect of the catalyst concentration, the variation of the values of the conversion of methanol into C_2-oxygenated compounds was examined by the use of a mixture of methanol (1.62 mol.) and acetic acid (0.18 mol.) over the range of the ratios of cobalt acetate to sodium iodide from 0.1 to 4.0, in which the sum of their concentrations was kept constant (1.0 mol. %). The reaction pressures were 300, 400 and 450 kg./cm^2 with the synthesis gases of 1-CO : 1-H_2, 1-CO : 1.26-H_2 and 1-CO : 1.57-H_2 respectively. The results are summarized in Fig. 5. The yield of ethanol evidently increases with an increase in the ratio of cobalt acetate to sodium iodide, while the yield of acetaldehyde increases with a decrease in it. It is very interesting to note that the composition of the discharged gases becomes approximately equal to that of synthesis gases at a certain ratio of an iodide to cobalt acetate. Such ratios of I^-/Co^{2+} were more than 10, 3 to 4 and 1 to 1.5 with the H_2/CO ratios of synthesis gases of 1.0, 1.3 and 1.6 respectively.

The experimental results made at the suitable catalyst concentration for each synthesis gas considered from the results of Fig. 5 are represented in Table II. They show that the extent of methanol conversion into ethanol and acetaldehyde considerably depends on the catalyst concentration.

Discussion

The possible reactions leading to the formation of acetaldehyde, ethanol and acetic acid can be represented by the following equations. However, the ease of the formation of these compounds considerably depends on the catalyst concentration, as has already been described.

		$-\Delta F°_{(25°C)}$[6] kcal./mol.	$-\Delta F°_{(200°C)}$[*4] kcal./mol.
$CH_3OH+CO+H_2$ $=CH_3CHO+H_2O$	(1)	16.1	9.8
$CH_3OH+CO+2H_2$ $=C_2H_5OH+H_2O$	(2)	25.9	11.0
$CH_3OH+CO=CH_3COOH$	(3)	21.3	11.8
$CH_3CHO+H_2=C_2H_5OH$	(4)	9.8	1.2

On the basis of the experimental results, we can postulate that, in the reaction of methanol with carbon monoxide-hydrogen mixtures, methanol is converted in the first place to acetaldehyde, that subsequently this is hydrogenated to ethanol or dimerized to other oxygenated compounds (2·acetaldehyde → ethyl acetate, 2·acetaldehyde → crotonaldehyde → n-butanol), and that the rates of the formation of methylacetate, acetic acid, C_3- and higher compounds are small, partly because the amounts of free acetic acid, C_3- and higher compounds present in the product are small and partly because the amount of hydrogen reacting with methanol is always larger than that of carbon monoxide.

It is well known that cobaltous salts react with carbon monoxide under high pressures to form dicobalt octacarbonyl, which undergoes a homomolecular disproportionation in methanol and which forms cobalt hydrocarbonyl in the presence of hydrogen[5]. However, only with these cobalt carbonyl catalysts, a small part of the methanol used is converted into C_2-oxygenated compounds under the oxo condition[1,5], although aldehydes are hydrogenated to alcohols or dimerized[7,8].

On the other hand, cobaltous halides form green or blue tetrahedral complex anions[9],

5) P. H. Emett, "Catalysis," Vol. V, Reinhold Press, New York, (1957), p. 73.

*4 Calculated by $d\ln K_p/dt = \Delta H°_{(25°C)}/RT^2$.

6) "Selected Values of Chemical Thermodynamics Properties," Part 1, N. B. S. (1961).

7) I. Wender, R. Levine and M. Orchin, *J. Am. Chem. Soc.*, 72, 4375 (1950).

8) R. W. Gaetz and M. Orchin, *J. Org. Chem.*, 27, 3698 (1962).

9) D. P. Graddon, "An Introduction to Co-ordination Chemistry," Pergamon Press., London, (1961).

such as $CoCl_4^{2-}$, $CoBr_4^{2-}$ and CoI_4^{2-} in an organic solvent[10-12] (nitromethane, *N*, *N*-dimethylformamide or acetone). The same complex ions have been considered to be formed from cobalt acetate and litium or sodium iodide in glacial acetic acid.[13,14] In the experimental section, it was mentioned that cobalt acetate in methanol containing an iodide and acetic acid forms, at an elevated temperature, a greenish compound, which is presumably tetrahedral.

From these facts and experimental results, we can expect the catalytic action of cobalt acetate and an iodide in the reaction of methanol with carbon monoxide-hydrogen mixtures to be as follows: a part of the cobalt acetate forms a complex compound of the $[CoX_4(CO)H]^{2-}$ ($X=I^-$ or CH_3COO^-) type, which is similar in electronic configuration to cobalt hydrocarbonyl $HCo(CO)_4$, hydropentacyano cobaltate anion[15] $[Co(CN)_5H]^{3-}$, carbonyl ferrocyanic anion $[Fe(CN)_5CO]^{3-}$, etc. (Hieber[16] reported that solid cobaltous iodide reacted with pure carbon monoxide to form a dark brown crystalline carbonyl apparently represented by CoI_2CO, in which the cobaltous ion was probably surrounded by more than two iodide ions.) With this complex compound, a methanol reacts with a carbon monoxide and a hydrogen to form an acetaldehyde. The other part of the cobalt acetate froms cobalt hydrocarbonyl, with which the acetaldehyde produced is hydrogenated to ethanol or dimerized to ethyl acetate and other things. When a relatively large amount of an iodide is added, most of cobalt acetate forms $[CoX_4(CO)H]^{2-}$ according to the above expectation and the yield of acetaldehyde therefore increases, while in the presence of a large amount of cobalt acetate, a considerable amount of cobalt hydrocarbonyl is formed simultaneously and the yield of ethanol, therefore, apparently increase.

10) N. S. Gill and R. S. Nyholm, *J. Chem. Soc.*, **1959**, 3397, 3512.
11) S. Buffagni and T. M. Dum, ibid., **1961** 5105.
12) D. A. Fine, *J. Am. Chem. Soc.*, **84**, 1139 (1962).
13) P. J. Proll and L. H. Sutellife, *J. Phys. Chem.*, **65**, 445, 1993 (1961).
14) T. Mizoroki, Y. Andō and M. Furumi, Presented at the 16th Annual Meeting of the Chemical Society of Japan, Tokyo, April, 1963.
15) B. DeVries, *J. Catalysis*, **1**, 489 (1962).
16) W. Hieber, *Z. anorg. u. allgem. Chem.*, **243**, 145 (1939).

Summary

The reaction of methanol with carbon monoxide-hydrogen mixtures has been carried out in the presence of a mixture of cobalt acetate and an iodide as catalyst. The extent of methanol conversion into C_2-oxygenated compounds (acetaldehyde, ethanol and acetic esters) was 40 to 60% when the catalyst concentration ($Co(CH_3COO)_2 \cdot 4H_2O$ + an iodide) range was form 1.0 to 20 mol%; the temperature range was from 180 to 220°C; the pressure range was from 300 to 500 kg./cm^2 (the H_2/CO values in synthesis gases were 1.0 to 1.5), and the reaction time was 90 min. The amount of free acetic acid, C_3- and higher oxygenated compounds in the liquid product was small. The use of iodine instead of an iodide as an additive for the cobalt acetate catalyst is disadvantageous for this reaction. From the detailed investigation of the influence of the catalyst concentration on the extent of the conversion of methanol into C_2-oxygenated compounds, it has been shown that the formation of acetaldehyde is favored in the presence of a relatively large amount of an iodide and that an increase in cobalt acetate results in an increase in the yield of ethanol. It has been postulated that, under these conditions, methanol reacted with carbon monoxide and hydrogen to form acetaldehyde, which subsequently was hydrogenated to ethanol or dimerized to other oxygenated compounds.

The authors wish to express their thanks to Dr. Hiroshi Uchida for his invaluable advice and criticism.

Government Chemical Industrial Research Institute, Tokyo
Meguro-ku, Tokyo

Syntheses and Properties of 2-Oxothiazolidine-4-carboxylic Acid and Its Derivatives[*1]

By Takeo KANEKO, Takeo SHIMOKOBE,[*2] Yoshimoto OTA,[*3] Ekido TOYOKAWA,[*4] Toshishige INUI and Tetsuo SHIBA

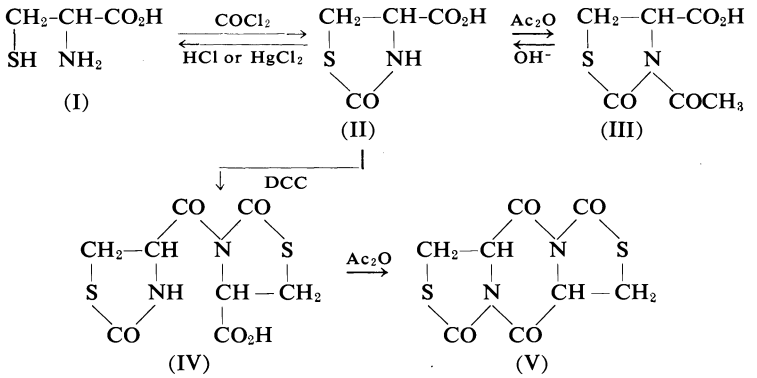
(Received September 9, 1963)

It has been shown that DL- or L-threonine is easily cyclized with phosgene to DL- or L-*trans*-5-methyl-2-oxo-oxazolidine-4-carboxylic acid in an alkaline solution without any configurational change at the either asymmetric center.[1] Cysteine may be similarly cyclized to 2-oxothiazolidine-4-carboxylic acid with phosgene beacause of the expected reactivity of the thiol group. Cook et al. have reported that the penicillamine methyl ester was also cyclized to the corresponding thiazolidone derivative with phosgene in the presence of sodium hydrogen carbonate.[2] This paper deals with the cyclization of L-cysteine with phosgene and with the properties of the cyclization product.

The cyclization of L-cysteine (I) to L-2-oxothiazolidine-4-carboxylic acid (II) with phosgene occured by means of the modified method as carried out in the cyclization of threonine.[1] The cyclized product II melted at 171~172.5°C and gave a strongly acidic aqueous solution. The racemic form of II (m. p. 155°C) was obtained from *S*-benzylthiocarbonyl-DL-cysteine by means of the action of alkali by Crawhall et al.[3] On hydrolysis in 6N hydrochloric acid or treatment with mercuric chloride, the starting L-cysteine (I) was recovered in its pure state. During this cyclization reaction, no configurational change took place.

When II was heated in acetic anhydride, L-3-acetyl-2-oxothiazolidine-4-carboxylic acid (III) and two other by-products were obtained. One of the two by-products, which was also obtained by the dehydration of the other with acetic anhydride, melted at 259~260°C and had the empirical formula $C_4H_3NO_2S$. The other (m. p. 215°C) possessed the empirical formula $C_8H_8N_2O_5S_2$ and was identified with the dehydration product of II by *N*, *N'*-dicyclohexyl carbodiimide (DCC). This second compound is probably 2-oxo-3-(2'-oxothiazolidine-4'-carbonyl-)-thiazolidine-4-carboxylic acid(IV), while the former seems to be the diketopiperazine-type compound, 1, 4, 5, 8-tetraoxo-2, 6-dithia-4a, 8a-diazaperhydro-*s*-indacene (V).

Therefore, if *N*-acetyl-L-cysteine[4] is similarly cyclized with phosgene, III will be obtained directly. The cyclization of *N*-acetyl-L-cysteine, however, was unsuccessful. The *N*-benzoyl-L-cysteine ethyl ester (VII) obtained by the reduction of the *N*, *N'*-dibenzoyl-L-cystine diethyl ester (VI) with zinc and hydro-



*1 Partly presented at the 15th Annual Meeting of the Chemical Society of Japan, Kyoto, April, 1962.

*2 Present address: Osaka Branch, Showa Denko K. K., Higashi-ku, Osaka.

*3 Present address: Institute for Food Chemistry, Kita-ku, Osaka.

*4 Present address: Nippon Paint Co., Ltd., Oyodo-ku, Osaka.

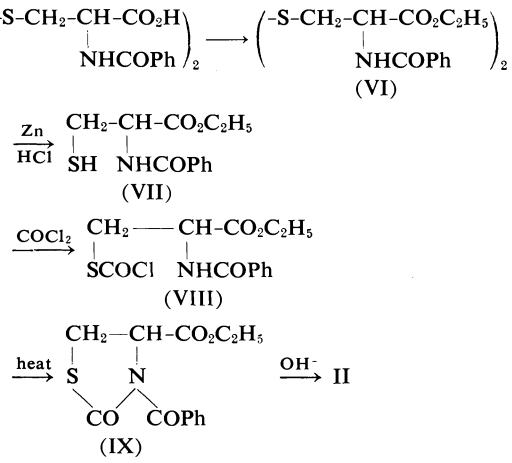
1) T. Kaneko and T. Inui, *J. Chem. Soc. Japan, Pure Chem. Sec.* (*Nippon Kagaku Zasshi*), **82**, 1075 (1961); T. Inui and T. Kaneko, ibid., **82**, 1078 (1961).

2) A. H. Cook, J. A. Elvidge and G. Shaw, *J. Chem. Soc.*, **1949**, 2367.

3) J. C. Crawhall and D. F. Elliott, ibid., **1951**, 2071.

4) N. W. Pirie and T. S. Helo, *Biochem. J.*, **27**, 1716 (1933).

chloric acid was used. According to the method employed in the reaction of the *N*-benzyloxycarbonyl-DL-serine benzyl ester with phosgene by Bergel,[5] VII was treated with phosgene in benzene and thereby an expected *S*-chlorocarbonyl intermediate VIII was obtained. This intermediate was cyclized to 3-benzoyl-4-ethoxycarbonyl-2-oxothiazolidine (IX) when refluxed in xylene for 6 hr. by applying the method of Ben-Ishai.[6]



When III was treated in an aqueous solution with dilute sodium hydroxide, the separation of the acetyl group took place and II was recovered without any racemization. In a similar way, IX yielded II and benzoic acid under the same conditions.

It is expected that these results will be of use in discussing the synthetic and structural problems of cysteine peptides.

Experimental

L-2-Oxothiazolidine-4-carboxylic Acid (II).—To a cold solution of 24.2 g. (0.200 mol.) of L-cysteine ($[\alpha]_D$ +7.9° (1 N hydrochloric acid)) in 350 ml. of water, 50 ml. of 40% potassium hydroxide was added and cooled below −5°C in an ice-salt bath. A solution of 26.0 g. (0.262 mol.) of phosgene in 100 ml. of toluene and 100 ml. of 40% potassium hydroxide were simultaneously vigolously stirred into the solution over a 10~15 min. period. After the solution had been stirred for a half hour, the toluene layer was separated. The aqueous layer was extracted twice with ether and acidified to Congo red with concentrated hydrochloric acid. The acidic solution concentrated to dryness in vacuo, and the residue was extracted three times with 250 ml. of ethanol while hot. The extract was concentrated to dryness in vacuo, and residual oil was dissolved in 10 ml. of hot water. A crude II (23.2 g.) crystallized out after the solution had been left standing for several hours. After two recrystallizations from hot water, the pure substance was obtained. Yield, 14.5 g. (49%); m. p. 171~172.5°C, $[\alpha]_D^{16}$ −57.3° (*c* 2.7, water).

IR (Nujol mull): 3260 (amide), 2600, 1740, 1225 (carboxylic acid), 1625 (cyclic amide) cm^{-1}.

Found: C, 32.91; H, 3.47; N, 9.52; S, 21.40. Calcd. for $C_4H_5NO_3S$: C, 32.64; H, 3.42; N, 9.52; S, 21.79%.

L-3-Acetyl-2-oxothiazolidine-4-carboxylic Acid (III).—Eight and eight-tenth grams (0.06 mol.) of II was heated in 50 ml. of acetic anhydride until the II had been dissolved. After cooling at room temperature, the V which had separated was filtered off (0.55 g.) To a filtrate, 30 ml. of water was added and heated several times in order to effect the decomposition of the excess acetic anhydride. The solution was then concentrated to a half volume in vacuo, and the crystallized IV was filtered (2.4 g.) When the filtrate was again evaporated to dryness in vacuo, III crystallized out. The yield was 5.9 g. (52.1%). It melted at 152~154°C after recrystallization from ethyl acetate and light petroleum, and it gave $[\alpha]_D^{20}$ −136.4° (*c* 1.8, water-acetone (1 : 1)).

IR (Nujol mull): 2600, 1710 (carboxylic acid), 1730 (acetyl), 1650 (cyclic amide) cm^{-1}.

Found: C, 38.30; H, 3.59; N, 7.42. Calcd. for $C_6H_7NO_4S$: C, 38.08; H, 3.74; N, 7.40%.

2-Oxo-3-(2'-oxothiazolidine-4'-carbonyl-)-thiazolidine-4-carboxylic Acid (IV).—To a cold solution of 1.47 g. (0.01 mol.) of II in 40 ml. of *N*,*N*-dimethylformamide, 1.1 g. (0.005 mol.) of DCC was added drop by drop. After the mixture had been left standing overnight, the precipitated *N*,*N'*-dicyclohexyl urea was removed. The filtrate was acidified with 10 ml. of 6 N hydrochloric acid and extracted five times with 50 ml. of ethyl acetate. The extract was concentrated to dryness in vacuo, and when water was added to the residue, IV crystallized out. Yield, 0.9 g. (65%); m. p. 215°C (decomp.).

IR (Nujol mull): 3260 (amide), 2500, 1710 (carboxylic acid), 1625 (cyclic amide) cm^{-1}.

Found: C, 34.98; H, 3.08; N, 10.14. Calcd. for $C_8H_8N_2O_5S_2$: C, 34.77; H, 2.91; N, 10.13%.

1,4,5,8-Tetraoxo-2,6-dithia-4a,8a-diaza-perhydro-*s*-indacene (V).—A solution of 0.10 g. (0.0004 mol.) of IV in 10 ml. of acetic anhydride was heated under reflux for about 3 hr., when V began to appear. When it had then been cooled at room temperature for a few hours, V filtered off. Yield, 0.085 g. (91%); m. p. 259~260°C (decomp.)

IR (Nujol mull): 1747, 1675 (cyclic amide) cm^{-1}.

Found: C, 37.60; H, 2.50; N, 10.81. Cacld. for $C_8H_6N_2O_4S_2$: C, 37.20; H, 2.34; N, 10.84%.

L-Cysteine (I).—*By Hydrolysis with Hydrochloric Acid.*—A solution of 3.0 g. (0.02 mol.) of II in 20 ml. of 6 N hydrochloric acid was heated on steam-bath for 20 hr. I was isolated from the hydrolizate in the usual way. Yield, 1.0 g. (40%). All the properties of this sample were identical with those of an authentic sample.

Treatment with Mercuric Chloride.—To a suspension of 3.0 g. (0.02 mol.) of II in 50 ml. of water, a solution of 10.0 g. (0.037 mol.) of mercuric chloride in 80 ml. of water was added. After it had been shaken at 75°C for 15 min., this mixture was

5) F. Bergel and R. Wade, *J. Chem. Soc.*, **1959**, 941.
6) D. Ben-Ishai, *J. Am. Chem. Soc.*, **78**, 4962 (1956).

allowed to stand at room temperature for 40 hr. A mercaptide which was precipitated was filtered and I was isolated from the mercaptide in the usual way. Yield, 0.8 g. (32%).

***N,N'*-Dibenzoyl-L-cystine Diethyl Ester (VI).**—Thirty grams (0.067 mol.) of *N,N'*-dibenzoyl-L-cystine[7] was esterified with hydrogen chloride in absolute ethanol in the usual way. Yield, 31.3 g. (78%). It melted at 183~185.5°C after recrystallization from absolute ethanol and gave $[\alpha]_D^{30}$ +13.3° (*c* 0.5, 99% ethanol).

Found: C, 56.96; H, 5.50; N, 5.33; S, 12.35. Calcd. for $C_{24}H_{28}N_2O_6S_2$: C, 57.14; H, 5.59; N, 5.55; S, 12.71%.

***N*-Benzoyl-L-cysteine Ethyl Ester (VII).**—To a suspension of 20 g. (0.037 mol.) of VI in 300 ml. of 50% ethanol, 20 g. of zinc dust and 50 ml. of acetic acid were added and heated with occasional shaking at 50~60°C for about 1 hr., or until the VI had been dissolved. After it had stood overnight at room temperature, the solution was evaporated to a small volume in vacuo under an atmosphere of nitrogen and extracted with benzene. The extract was evaporated to dryness in vacuo, and the residue was recrystallized from ethanol. Yield, 15 g. (70%); m. p. 85~89°C, $[\alpha]_D^{30}$ −30.6° (*c* 1.6, 99% ethanol).

Found: C, 56.38; H, 5.86; N, 5.32; S, 12.77. Calcd. for $C_{12}H_{15}NO_3S$: C, 56.91; H, 5.97; N, 5.53; S, 12.66%.

***N*-Benzoyl-*S*-chlorocarbonyl-L-cysteine Ethyl Ester (VIII).**—Phosgene was passed into a stirred suspension of 10 g. (0.036 mol.) of VII in 160 ml. of benzene at 5~10°C for 1 hr. VII was dissolved into a solution by additional stirring at room temperature for 2~3 hr. The next day, carbon dioxide was passed through the solution to remove the excess phosgene and the organic layer was evaporated to dryness in vacuo. The residue obtained was recrystallized from benzene. Yield, 10 g. (80%); m. p. 119~122°C (decomp.)

L-3-Benzoyl-4-ethoxycarbonyl-2-oxothiazolidine (IX). — Five grams (0.016 mol.) of VIII was refluxed in 100 ml. of xylene for about 6 hr., or until no hydrogen chloride had been evolved. After the removal of the solvent, the residue was recrystallized from benzene or xylene. Yield, 3.5 g. (79%); m. p. 130~132°C, $[\alpha]_D^{15}$ +18.0° (*c* 0.5, benzene).

IR (Nujol mull): 1735 (ester), 1710 (benzoyl), 1695 (cyclic amide) cm^{-1}.

Found: C, 55.94; H, 4.91; N, 4.88; S, 11.16. Calcd. for $C_{13}H_{13}NO_4S$: C, 55.91; H, 4.70; N, 5.02; S, 11.48%.

The Treatment of *N*-Acyl-thiazolidone Derivatives with Alkali. — a) To a solution of 0.38 g. (0.002 mol.) of III in 10 ml. of acetone and 10 ml. of water, 5 ml. (0.006 mol) of 1.25 N sodium hydroxide was added. After it had stood (and occationally been shaken) at room temperature for 1 hr., the mixture was acidified with 6 N hydrochloric acid and concentrated to drynes in vacuo. The residue was extracted with ethanol, and II was obtained from this ethanol extract. Yield, 0.24 g., (82%); m. p. 171~172°C (decomp.), $[\alpha]_D^{15}$ −57.8° (*c* 2.1, water). Its infrared absorption spectra were identical with those of the cyclized product of L-cysteine.

b) In a similar way, 3 g. (0.011 mol.) of IX were hydrolyzed with 1.2 g. (0.022 mol.) of potassium hydroxide in 40 ml. of 70% ethanol. After the removal of the benzoic acid, II was obtained. Yield, 0.9 g. (57%); m. p. 171~172.5°C (decomp.), $[\alpha]_D^{19}$ −56° (*c* 3.0, water).

Department of Chemistry
Faculty of Science
Osaka University
Nakanoshima, Osaka

7) E. M. Fry, *J. Org. Chem.*, **15**, 438 (1950).

The Thermal and Radiation Oxidation of Benzene to Phenol in Aqueous Solutions Containing Metal Ions at Elevated Temperatures. IV. The Effect of Impurities in Benzene

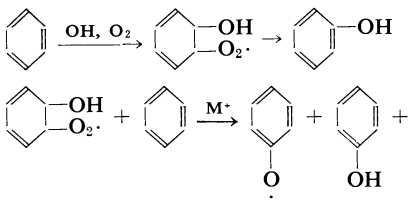
By Nobutake SUZUKI and Hiroshi HOTTA

(Received September 9, 1963)

The oxidation of benzene to phenol catalyzed by metal ions has been studied in aqueous solutions under high oxygen pressure at elevated temperatures.[1,2] In a ferrous sulfate solution, phenol is produced in a good yield either with or without gamma-ray irradiation.[1] In a ferric sulfate solution, phenol is similarly produced by irradiation, but only above 180°C when not irradiated.[1] In a cupric sulfate solution, phenol is produced above 180°C either with or without irradiation.[2]

These facts have been interpreted as follows:[1,2] The chain processes of benzene oxidation are:

1) H. Hotta, A. Terakawa, K. Shimada and N. Suzuki, This Bulletin, **36**, 721 (1963).
2) H. Hotta, N. Suzuki and A. Terakawa, ibid., **36**, 1255 (1963).



(1)

(2)

$$PhO + PhH = PhOH + Ph \quad (3)$$

$$Ph + O_2 = PhO_2 \quad (4)$$

$$PhO_2 + PhH = PhO_2H + Ph \quad (5)$$

$$PhO_2H + M^{2+} = PhO_2 + H^+ + M^+ \quad (6)$$

$$PhO_2H + M^+ = PhO + OH^- + M^{2+} \quad (7)$$

$$2PhO_2 = 2PhO + O_2 \quad (8)$$

where Ph represents the phenyl radical, M^+, the ferrous or cuprous ion, and M^{2+}, the ferric or cupric ion. The OH radicals for the initiation reaction 1 are produced from the reactions:

$$H_2O \rightsquigarrow H, OH, H_2, H_2O_2 \quad (9)$$

$$M^+ + O_2 + H^+ = M^{2+} + HO_2 \quad (10)$$

$$HO_2 \text{ or } H_2O_2 \xrightarrow{M^+} OH \quad (11)$$

However, the phenol production above 180°C in non-irradiated ferric or cupric solutions cannot be interpreted in terms of the above reaction scheme because of a lack of reactions 9, 10 and 11. This fact suggests that there are some additional reactions above 180°C. Later, it has been found, as is shown in the present paper, that the results for carefully purified benzene are quite different from the previous results.[1,2] These observation will be interpreted in the present paper, together with the effect of impurities in benzene.

Experimental

Benzene was purified carefully by several methods, using mercury, sulfuric acid, sodium hydroxide, freezing, and distillation. The concentration of impurities in benzene with and without purification, analyzed by gas chromatography, using TCP-column at 70°C, is shown in Table I. Cyclohexane could not be separated by the present methods.

Benzene, with or without purification, was oxidized in neutral aqueous solutions of ferrous, ferric and cupric sulfates,[3] by means of the following procedure, as in the previous paper:[1] 1 cc. of benzene was put on 15 cc. of the aqueous phase in a hard-glass tube in a 50 cc. stainless-steel reactor under the oxygen pressure of 30 atm. Then this system was heated by a controlled procedure and kept for 30 min. at a given temperature. When it was irradiated, the dose was about 1.3×10^4 r of cobalt-60 gamma-rays for 25 min.

After cooling, it was analyzed by the same methods as in the previous papers.[1,2] A large portion of the iron species was precipitated above 160°C.

3) The initial concentration of metal ions was 0.01 M, except for the experiments shown in Fig. 4 and Table II.

Results and Discussion

The Ferrous Sulfate Solution. — The total amounts of phenol produced in the solution of 0.01 M ferrous, ferric and cupric sulfates[3] with (circle marks) and without (triangle marks) radiation are plotted against the reaction temperature in Figs. 1, 2 and 3 in order to compare purified (solid marks) and unpurified (open marks) benzene.

The yield of phenol from unpurified benzene is larger than that from purified benzene, even in the ferrous solution. This indicates that some peroxides are forced rseadily to initiae the chain process from the impurities in unpurified benzene, which is more readily oxidized than benzene. That is, the reaction

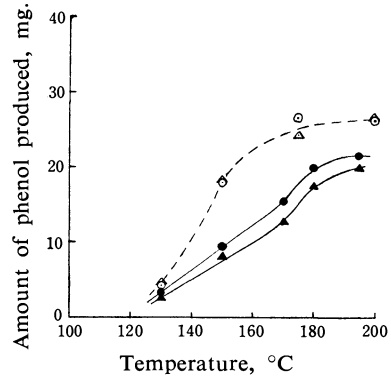


Fig. 1. Amounts of phenol produced in the irradiated (⊙ and ●) and non-irradiated (△ and ▲) neutral 0.01 M ferrous sulfate solutions, from purified (solid marks) and unpurified(open marks) benzene.

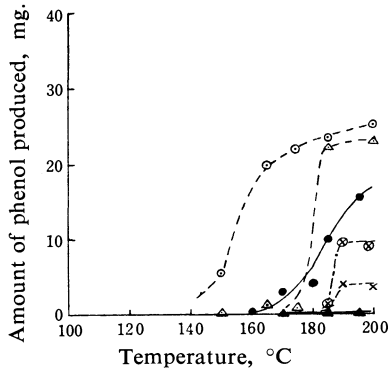


Fig. 2. Amounts of phenol produced in the neutral 0.01 M ferric sulfate solutions; circle and triangle marks are the same as in Fig. 1. The results in the non-irradiated solution for purified benzene containing toluene (3.3×10^{-3} M) and thiophene (4×10^{-4} M) are shown by ⊗ and × respectively.

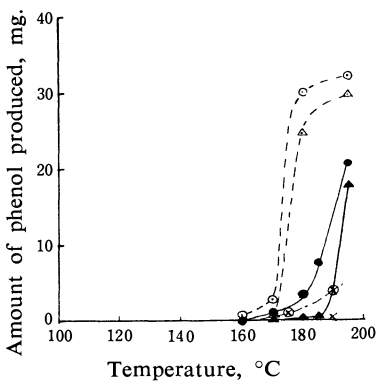


Fig. 3. Amounts of phenol produced in the neutral 0.01 M cupric sulfate solution; circle and triangle marks are the same as in Fig. 1. The results for purified benzene in the 0.01 M cupric sulfate—0.01 M ferric sulfate solution are show by ⊗ and × for the irradiated and non-irradiated cases respectively.

$$RH \xrightarrow{OH,\ O_2} \text{peroxide } (R'O_2) \qquad (12)$$

(RH: impurities in benzene)

should be assummed to be a faster initiation process than reaction 1 for cases of unpurified benzene. R' is not necessarily equal to R. It is known that a small of organic additives promotes the oxidation of benzene to phenol in the gaseous phase.[4]

The results in the ferrous sulfate solution, seen in Fig. 1, can be interpreted by means of the present reaction scheme.

The Irradiated Ferric Sulfate Solution.—The results in the irradiated ferric sulfate solution, shown by open and solid circles in Fig. 2, can also be interpreted by means of reaction 12. The remarkable decrease in the phenol yield upon purification indicates that the initiation process is reaction 12 rather than reaction 1. Even for purified benzene, the chain process might be initiated by the oxidation of cylohexane, which cannot be separated by the purification described previuosly. Accoring to Bach,[5] the yield of radiation oxidation is in the order of *n*-heptane>toluene>cyclohexane> benzene. Therefore, reactions 13—15:

$$R'O_2 + PhH = R'O_2H + Ph \qquad (13)$$

$$R'O_2H + M^{2+} = R'O_2 + H^+ + M^+ \qquad (14)$$

$$R'O_2H + M^+ = R'O + OH^- + M^{2+} \qquad (15)$$

should form the initial process instead of reactions 1 and 2. Phenyl radicals are consumed as in the previous scheme. Hydroxycyclohexadienyl peroxide, detected by Dorfman et al,[6] may not take a major part in the chain process at elevated temperatures; it does only as a precursor to phenol, as is shown in reaction 1. The greater part of the OH radicals from reactions 9, 10 and 11 are consumed by reaction 12 rather than by reaction 1, at least at the initial stage. The rate of the chromic acid oxidation of benzene is very slow in comparison with that of other compounds.[7]

When there are a large number of ferrous ions, as in the ferrous solution, reaction 2 may play some part in the initiation process (see Fig. 1). At any rate, it is certain that ferrous ions are indispensable to the chain process at lower temperatures in either reaction 2 or 12, for scarcely any phenol is produced below 160°C from purified benzene in Fig. 2, even when it is irradiated. It may also be concluded from a comparison of the results of purified benzene in the irradiated ferrous and in the same ferric solutions that the yield of OH radicals by in reaction 10 is much larger than that by reaction 9.

Since almost all of the iron species are ferrous in the solution after oxidation reaction, it is supposed that the rate of reaction 6 is faster than that of reaction 7. As phenyl peroxides are accumulated by reaction 6, they are converted to phenoxy radicals for reaction 3 by reaction 8.

Only a small amount of phenol is produced, even from unpurified benzene, at 200°C in an irradiated aqueous phase containing no metal ions, as is shown in Table I of Part II.[1] This is due to the lack of reactions 14 and 15, which regenerate $R'O_2$ and R'O.

The Non-irradiated Ferric Sulfate Solution.—As shown by open and solid triangles in Fig. 2, in the non-irradiated ferric sulfate solution, phenol is produced in a good yield above 180°C from unpurified benzene in spite of the lack of reactions 9, 10 and 11 to give OH radicals for reaction 12. On the other hand, purified benzene is hardly oxidized to phenol at least up to 200°C. Therefore, the initiation process for this case is attributed to the formation of hydroperoxides by oxygen from the impurities:

$$RH \xrightarrow{O_2} RO_2H \qquad (16)$$

The hydroperoxides are isolated for the oxiation of the compounds listed in Table I.[8,9] Since the hydroperoxides are built up to some

4) W. I. Denton, H. G. Doherty and R. H. Krieble, *Ind. Eng. Chem.*, **42**, 777 (1950).
5) N. Bach, *Proc. Intern. Conf. of Geneva*, **7**, 538 (1956).
6) L. M. Dorfman, I. A. Taub and R. E. Bühler, *J. Chem. Phys.*, **36**, 3051 (1962).
7) F. Mares and J. Rocek, *Collection Czechoslov. Chem. Commun.*, **26**, 2370 (1961).
8) C. Walling, "Free Radicals in Solution," John Wiley & Sons, New York (1957), Chap. 9.
9) A. V. Tobolsky and R. B. Mesrobian, "Organic Peroxides," Interscience Publishers, New York (1954).

TABLE I. IMPURITY CONCENTRATIONS AND THEIR EFFECT

Impurity	Concn., M		Yield of phenol, mg.[a]	
	before purification	after purification	I[b]	II[c]
Carbon disulfide	4×10^{-4}	0	3.6	3.6
n-Hexane	4×10^{-4}	0	1.1	1.1
Cyclohexane	6.7×10^{-3}	6×10^{-3}	0.1	<0.1
Cyclohexene	$<2 \times 10^{-5}$e	0	0.4[d]	2.5
Thiophene	$<6 \times 10^{-4}$e	0	3.1[d]	3.0
Toluene	3.3×10^{-3}	0	9.9	3.4
Xylene	0	0	—	—

Note:

a) The amount of phenol produced at 190°C in the non-irradiated neutral ferric sulfate solution.
b) For benzene containing the same amount of the respective impurity as unpurified benzene.
c) For benzene containing 4×10^{-4} M of the respective impuritiy.
d) For benzene containing the amount of the upper limit before purification, noted by e, as an impurity.

extent above 180°C, they can propagate the chain process, as has been mentioned with regard to reaction 12. The rate of reaction 12 must be larger than that of reaction 16, especially at temperatures lower than 170°C, in view of the difference in unpurified benzene with and without irradiation.

To compare the relative promotive effect of the respective impurities, they were added separately, in portions as large as are present in unpurified benzene, to purified benzene. The amounts of phenol produced from this benzene at 190°C are shown in column I of Table I. The effect of toluene (3.3×10^{-3} M, ⊗) and thiophene (4×10^{-4} M, ×) were examined at other temperatures also, as Fig. 2 shows. Moreover, they are compared by adding an equal amount of 4×10^{-4} M, as is shown also in column II of Table I.

Although cyclohexane seems not, judging from Table I, to promote the production of phenol, its hydroperoxide is also actually isolated.[8] Therefore, a small amount of phenol production for non-irradiated purified benzene, as is seen in Fig. 2, may be attributed not to a trace amount of ferrous ions in the ferric solution, as was assumed in Part II,[1] but to cyclohexane as an impurity.

The Cupric Sulfate Solution.—All the results for the 0.01 M cupric sulfate solution, shown by circles and triangles in Fig. 3, are consistent with the above conclusions.

For the results of unpurified benzene, it is noticeable that the tendency is almost the same in the non-irradiated solution as for ferric sulfate, seemingly supporting reaction 16 as the common process. The lack of the production of phenol below 160°C for the irradiated case is attributed to the lack of cuprous ions because of the fast rate of cuprous oxidation if it is produced, as has been discussed in Part III.[2] On the other hand, phenol is produced in a good yield above 180°C. This is due to the build-up of indispensable cuprous ions over cuprous oxidation with the rise in temperature, which accelerates not only the formation of hydroperoxides but also their thermal decomposition by cupric ions.

Phenol is produced remarkably well at 200°C from purified benzene, even in the non-irradiated solution, in contrast to the case of ferric sulfate. This is due to the difference between the ion concentrations in the solution; that is, hardly any cupric sulfate is precipitated, even at 200°C, but ferric sulfate is almost all precipitated, up to less than 10^{-4} M. In fact, the yield of phenol decreases with a decrease in the cupric concentration, as is shown in Fig. 4, which gives the results of purified benzene in the non-irradiated aqueous

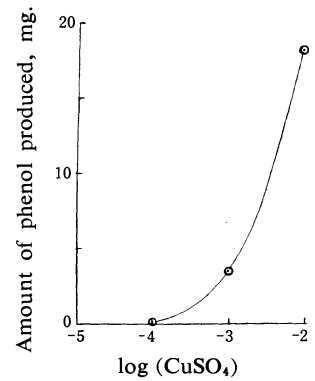


Fig. 4. Amount of phenol produced at 198°C purified benzene in the non-irradiated aqueous solution as a function of the concentration of cupric sulfate in M.

TABLE II. DEPENDENCE OF SULFATE CONCENTRATION

Composition of aq. soln., M				Amount of phenol produced (198°C) mg.	Ferrous concentration after reaction M
$CuSO_4$	$Fe_2(SO_4)_3$	Na_2SO_4	Total SO_4		
0.001	0	0	0.001	3.52	—
0.001	0.00005	0	0.00115	4.08	5.3×10^{-5}
0.001	0.0005	0	0.0025	1.50	5.1×10^{-5}
0.001	0	0.0015	0.0025	1.68	—
0.001	0.005	0	0.016	0.24	6.6×10^{-5}
0.001	0	0.015	0.016	0.50	—

solution of cupric sulfate. Such dependence of the cupric concentration was reported for unpurified benzene by Terakawa et al.[10]

The Cupric-Ferric Sulfate Solution.—As is shown in Fig. 3, the yield of phenol decreases in the irradiated (⊗) and non-irradiated (×) cupric sulfate solutions when 0.01 M ferric sulfate is added. The same fact is also shown for unpurified benzene in Fig. 3 of Part III.[2] For these cases, the concentration of iron species is no mere than 10^{-4} M at elevated temperatures due to precipitation, but the greater part of sulfate groups are still in the solution. On the other hand, the yield of phenol is suppressed in the concentrated sulfuric acid solution, as is seen in Fig. 1 of Part III.[2] This decrease in the yield is supposed to be attributable to the decrease in the cupric ion concentration due to the suppression of the dissociation of cupric sulfate effected by the addition of sulfate groups. To confirm this assumption, purified benzene was oxidized at 198°C without radiation in an aqueous solution of 0.001 M cupric sulfate by adding various amounts of ferric or sodium sulfate so as to give the equivalent sulfate concentration for both cases. The results, shown in Table II, indicate that the amounts of phenol produced are dependent on the total concentration of sulfate, but are independent of the kind of cation apparently supporting the above assumption.

10) A. Terakawa, Y. Hosaka, M. Nitto and T. Hirayama, *J. Chem. Sec. Japan, Ind. Chem. Sec.* (*Kogyo Kagaku Zasshi*), **66**, 1328 (1963).

Summary

The yield of phenol from the oxidation of unpurified benzene catalyzed by metal ions in an aqueous solution is much larger than from that of purified benzene. Phenol is produced in a good yield at temperatures lower than 160°C only in an oxygenated solution, in which OH radicals are produced, either with or without irradiation. Therefore, the autoxidation of impurities in benzene, initiated by OH radicals, is the initiation reaction of the chain oxidation process. On the other hand, phenol is also produce above 180°C even when OH radicals are not produced. Therefore, it is considered that the hydroperoxides of impurities are formed at higher temperatures without the OH radical by means of their autoxidation. Moreover, the yield of phenol in a cupric sulfate solution decreases remarkably with an increase in the sulfate concentration.

Japan Atomic Energy Research Institute
Tokai, Ibaraki

Spectroscopic and Theoretical Studies of Charge-Transfer Type Molecular Complexes between Monoölefins and Metal Ions: Selective Complex Formation Abilities of Copper(I), Silver(I) and Mercury(II) Ions

By Haruo Hosoya and Saburo Nagakura

(Received September 10, 1963)

Since Mulliken[1] developed the quantum-mechanical concept of the electron donor and acceptor with relation to the mechanism of molecular complex formation, both experimental and theoretical studies have been successively and successfully accomplished by many authors.[2] Rather little, however, is known about molecule-ion type complexes, such as the silver cation complexes with olefins and aromatic hydrocarbons; many problems are yet unsolved for this type of molecular complexes. Some of them are as follows:

i) Among the closed shell-type metal ions, why can only the copper(I), silver(I) and mercury(II) ions form stable complexes with monoölefins? [3,4]

ii) To what extent do the d-orbital electrons of these ions play a role in the complex formation,[5] and what kind of role is it?

iii) Do these monoölefin-metal ion complexes really show charge-transfer absorption bands? [6-8]

iv) Counter negative ions of silver salts affect the stability of the monoölefin-silver ion complexes. That is, the stability decreases in the order of $AgClO_4 > AgNO_3 \gg AgCl$, Ag_2SO_4.[7,8] How do we explain the difference in stability?

v) Is there any relation between the olefin-silver ion complex and the olefin-bromonium ion complex, which is known to be a reaction intermediate for the bromine addition reaction? [9]

The aim of the present study is to settle some of these problems as definitely as possible. In order to accomplish this purpose, we undertook to measure the ultraviolet, infrared and Raman spectra of the cyclohexene-silver perchlorate complex under various conditions, and to carry out some theoretical studies of the electronic energy levels of the complex. Furthermore, the stability of monoölefin-metal ion complexes will be discussed in detail in connection with the solvation energies of various metal ions.

Experimental

Materials. — Cyclohexene was distilled from cyclohexanol over a small amount of concentrated sulfuric acid. The distillate was dried with sodium metal and purified by repeating fractional distillation. Silver perchlorate of E. P. grade was used without further purification, since the infrared spectrum showed no marked difference between the cyclohexene complex with silver perchlorate recrystallized from acetone and that with the commercial silver perchlorate. Silver chloride precipitated from the mixture of aqueous silver nitrate and sodium chloride was dried over phosphorus pentoxide in the dark. Anhydrous cadmium perchlorate was synthesized from cadmium carbonate and perchloric acid, followed by dehydration at 100°C in vacuo.[10] Commercial silver nitrate, silver sulfate, potassium perchlorate, sodium perchlorate and magnesium perchlorate were used without further purification.[11]

Methanol, ethanol and tetrahydrofuran used as solvents were purified according to the standard methods.[12,13] Deuterated water (99.8%) was purchased from Asahi Kasei Co.

The cyclohexene-silver perchlorate complex was obtained by mixing the component substances directly and was recrystallized from ethanol.[14]

1) R. S. Mulliken, *J. Chem. Phys.*, **56**, 801 (1952).
2) G. Briegleb, "Elektronen-Donator-Acceptor-Komplexe," Springer-Verlag, Berlin (1961).
3) S. Winstein and H. J. Lucas, *J. Am. Chem. Soc.*, **60**, 836 (1938); H. J. Lucas, F. R. Hepner and S. Winstein, ibid., **61**, 3102 (1939).
4) F. Basolo and R. G. Pearson, "Mechanisms of Inorganic Reactions," John Wiley & Sons Inc., New York (1958), p. 351.
5) M. J. S. Dewar, *Bull. soc. chim. France*, **1951**, C71; *J. Chem. Soc.*, **1946**, 406, 777; *Discussions Faraday Soc.*, **2**, 151 (1947).
6) R. S. Mulliken, *J. Am. Chem. Soc.*, **74**, 811 (1952); *J. Chem. Phys.*, **19**, 514 (1951).
7) G. Salomon, "Cationic Polymerisation and Related Complexes," Ed. by P. H. Plesch, Academic Press, New York (1953), p. 57.
8) L. E. Orgel, *Quart. Revs.*, **8**, 422 (1954).
9) J. W. Kraus and E. W. Stern, *J. Am. Chem. Soc.*, **84**, 2893 (1962).
10) H. Hering and A. Leray, *Bull. soc. chim. France*, **6**, 1034 (1939).
11) Cyclohexene was found immissible with aqueous $KClO_4$, $NaClO_4$, $Mg(ClO_4)_2$ and $Cd(ClO_4)_2$. The white crystals of cyclohexene-silver perchlorate were soluble in methanol, ethanol and tetrahydrofuran, but were insoluble in water, carbon tetrachloride and *n*-heptane. The mixture of cyclohexene with acetonitrile or concentrated sulfuric acid became turbid. The cyclohexene-silver perchlorate complex became yellowish the moment it came in contact with potassium bromide, indicating decomposition into silver bromide.
12) A. Weissberger and E. Proskauer, "Organic Solvents," Oxford University Press, Oxford (1935), pp. 114, 118.
13) A. Ishitani, K. Kuwata, H. Tsubomura and S. Nagakura, This Bulletin, **36**, 1357 (1963).
14) A. E. Comyns and H. J. Lucas, *J. Am. Chem. Soc.*, **79**, 4339 (1957).

The cyclohexene-silver nitrate complex was crystallized from an ethanol solution of cyclohexene and silver nitrate at 0°C.[14]

Measurements of Ultraviolet Absorption Spectra. —A Cary recording spectrophotometer model 14 M was used for measuring ultraviolet spectra, fused quartz cells of 1 mm. light-path length being used. All the measurements were carried out at a constant temperature (20°C). The relatively strong absorption of the silver ion prevents us from measuring the spectra of solutions with concentrations higher than 0.1 N. The spectrum of cyclohexene was measured in aqueous silver perchlorate solutions with various concentrations and in a relatively concentrated aqueous cadmium perchlorate solution.

Measurements of Infrared and Raman Spectra. —A Hitachi EPI-2 infrared spectrophotometer, with a rock salt prism attached, was used for the infrared absorption measurements. Some of the solution spectra in the regions of 6 μ and 14 μ were measured with polyethylene bags. An envelope ca. 20×30 mm^2 was made from two sheets of polyethylene film 0.08 mm. thick, with no adhesive reagent but with moderate heating. The bag was then filled with a liquid sample and held by a commercial cell-window holder more or less tightly in order to avoid the wrinkling of the film and the vaporization of the solvent.

Raman spectra were measured with a Cary recording Raman spectrophotometer model 81 located at the Government Chemical Industrial Research Institute.[15]

Experimental Result for the Cyclohexene-Silver Perchlorate Complex

The Ultraviolet Absorption Spectrum of the Complex. — The absorption spectra measured with the cyclohexene-silver perchlorate-water system are shown in Fig. 1, whose ordinate represents the apparent molar extinction coefficients, ε's, the definition of which will be given later. As may be seen in Fig. 1, the ultraviolet absorption spectrum of cyclohexene in an aqueous silver perchlorate solution gradually but definitely increases its intensity with the increment of the salt concentration; in spite of less accuracy partly because of the relatively strong absorption of silver perchlorate ($\varepsilon=800$ at $\lambda_{max}=210$ mμ). This absorption change clearly shows that a new band appears at 220~230 mμ for the cyclohexene-silver perchlorate-water system. On the other hand, the spectrum of cyclohexene in an aqueous solution of 2 N cadmium perchlorate, like that of free cyclohexene, shows no absorption band above 220 mμ.

From a consideration of the equilibrium

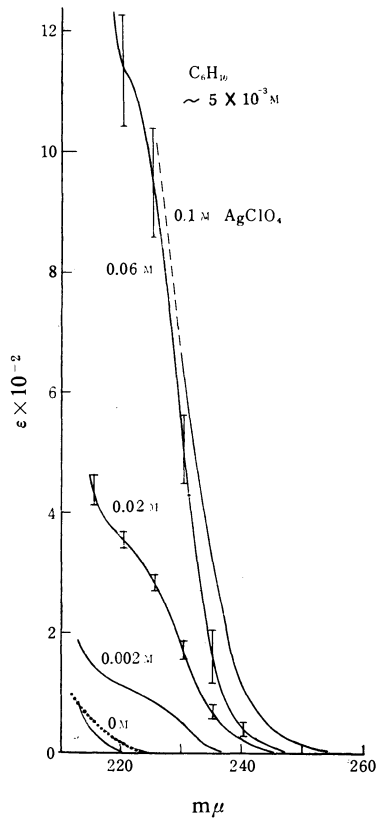


Fig. 1. Ultraviolet absorption spectra of cyclohexene in aqueous solutions of various concentrations of silver perchlorate (——) and of 1 mol./l. cadmium perchlorate (·····). Vertical lines represent the possible errors due to absorption by aqueous silver perchlorate solutions.

constant described below, we can safely conclude that the new band at about 220~230 mμ is due to the one-to-one complex of monoölefin and silver salt. This seems to mean that we could find Mulliken's[6] charge-transfer absorption band, which Salomon[7] and others[8] were unable to find for this system. Further details on the nature of this band will be discussed in a later part of the present paper.

Let us make a rough estimation of the equilibrium constant, K, for the system;

$$C_6H_{10} + AgClO_4 \rightleftharpoons C_6H_{10}\cdots Ag^+ClO_4^-$$

$$d-x \quad a-x \quad x \text{ (in mol./l.)}$$

$$K=x/(a-x)(d-x) \qquad pK=-\log K \qquad (1)$$

The apparent molar extinction coefficient of the complex, ε, can be defined by the following equation:[16]

15) The authors wish to express their hearty thanks to Miss Yuriko Matsubayashi of the Government Chemical Industrial Research Institute, Tokyo, for measuring the Raman spectra.

16) $\varepsilon=(I_T-I_A)/d$, where I_T and I_A are the optical densities of the cyclohexene-silver perchlorate-water system and the aqueous solution of silver perchlorate respectively; they can be represented by the following equations: $I_T=\{x\varepsilon_C+(a-x)\varepsilon_A\}$ (for $\lambda>220$ mμ) and $I_A=a\varepsilon_A$.

$$\varepsilon = x(\varepsilon_C - \varepsilon_A)/d \qquad (2)$$

where ε_C and ε_A are the molar extinction coefficients of the complex and silver perchlorate respectively at a certain wavelength. Setting d as a constant value, ε is dependent on the salt concentration (a), as is shown in Fig. 1, through the unknown parameters K and ε_C. By trial and error calculations, we actually estimated the pK and ε_C values in such a way that the dependence of ε on a can be explained as well as possible. The results are as follows:

$$pK = 0 \sim -2$$

$$\varepsilon_C = 10^3 \sim 10^4 \quad \text{for} \quad 220 \sim 230\ m\mu$$

Although the pK value obtained by the present authors is not accurate because of the superposition of the strong absorption of silver perchlorate, it is consistent with the value (pK = −1.9) obtained by Winstein and Lucas[3] from distribution experiments.

The Infrared and Raman Spectra of the Complexes. — The infrared absorption spectra of the Nujol and hexachlorobutadiene mulls of the solid complex of (cyclohexene)$_2$-$AgClO_4$[14] are shown in Fig. 2,[17] together with that of pure liquid cyclohexene. The former two spectra are in fairly good agreement with each other in the region where both solvents are transparent. The wave numbers of the observed bands of the complex are tabulated in Table I, compared with those of pure cyclohexene. The olefinic C–H out-of-plane bending band at 716 cm^{-1} shifts to a higher frequency, 748 cm^{-1}, in the complex. It is reported that this type of band in monoölefinic steroids also shifts to higher frequencies with the increasing strain in the ring.[18] The 900 and 1350 cm^{-1} bands intensified by the complex formation are assigned to C–H out-of-plane and in-plane bendings respectively. Although the assignment of the broad and weak 1900 cm^{-1} band has not yet been established, it is interesting to note that the frequency shift of +33 cm^{-1} is the same as that of 900 cm^{-1} band (+32 cm^{-1}). The olefinic C–H stretching band at 3020 cm^{-1} of free cyclohexene is weakend to

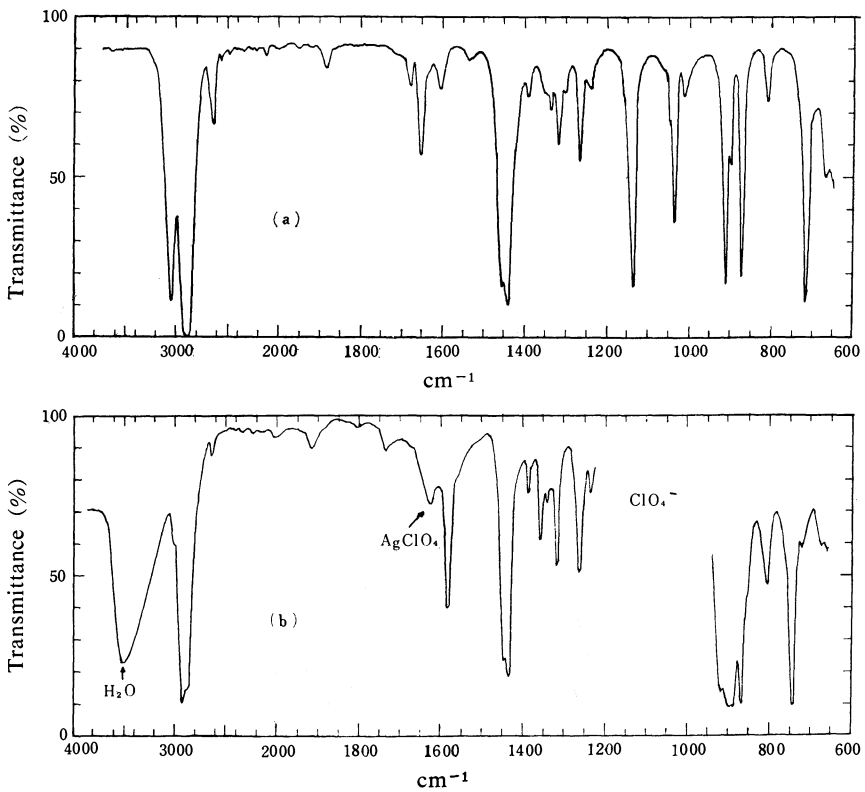


Fig. 2. Infrared absorption spectra of (a) pure cyclohexene and (b) the Nujol and hexachlorobutadiene mulls of the solid complex of $(C_6H_{10})_2 \cdots AgClO_4$.[17]

17) The Spectrum of the complex shown in Fig. 2b was synthesized by a complimentary combination of the spectra in Nujol and hexachlorobutadiene mulls. Accordingly, its absolute intensity is somewhat uncertain.

18) H. B. Henbest, G. D, Meakins and G. W. Wood, *J. Chem. Soc.*, **1954**, 800; H. B. Henbest, G. D. Meakins, B. Nicholls and R. A. L. Wilson, ibid., **1957**, 997.

Table I. Infrared absorption bands (in cm^{-1}) with tentative assignments of pure C_6H_{10} and the solid complex of $(C_6H_{10})_2\cdots AgClO_4$

Liquid C_6H_{10}	Solid $(C_6H_{10})_2\cdots AgClO_4$ In Nujol	Solid $(C_6H_{10})_2\cdots AgClO_4$ In HCBD	
3020 (s)		3000 (vw)	C-H Stretching (olef.)
2925 (vs)		2924 (vs)	C-H Stretching
2850 (vs)		2850 (vs)	C-H Stretching
2643 (m)	2645 (w)	2645 (w)	
2560 (vw)	2570b (vw)	2570b (vw)	
2460 (vw)	2460b (vw)	2460 (vw)	
2350b (vw)			
2245 (vw)	2245 (vw)	2245 (vw)	
2195 (vw)		2195b (vw)	
	2130 (vw)	2130 (vw)	
2100 (w)			
	2015 (w)	2015 (w)	
1950b (vw)			
	1914 (w)	1914 (w)	?
1881 (w)			
1790 (vw)	1795 (vw)	1795 (vw)	
1745b (vw)	1738 (w)	1738 (w)	
1709 (vw)			
1680 (w)			
1653 (m)		*	C=C Stretching (free)
	1625 (w)	*(~1625b)	$AgClO_4$
1605 (w)		*	
	1582 (m)	*(~1580b)	C=C Stretching (bonded)
	1560 (vw)		
1530 (vw)			
1446 (s)	*	1448 (s)	
1439 (s)	*	1434 (s)	
1393 (w)	*	1389 (w)	
1351 (vw)	1350 (m)	1350 (m)	C-H In-plane bending
1340 (w)	1338 (w)	1338 (w)	
1322 (m)	1319 (m)	1319 (m)	
1264 (m)	1264 (m)	1264 (m)	
1241 (w)	1238 (w)	1238 (w)	
1215b (vw)	1213 (w)	1213 (w)	
1137 (s)			
1061 (vw)			
1037 (s)	$\cdots ClO_4^- \cdots$		
1008 (w)			
915 (s)	919 (s)	919 (s)	
903 (m)	895b (vs)	895b (vs)	C-H Out-of-plane bending
876 (s)	869 (s)	869 (s)	
808 (m)	808 (m)	*	
	748 (s)	748 (s)	
716 (s)		720b (vw)	C-H Out-of-plane bending
667 (w)	667 (w)	667 (w)	

* Masked by the solvent absorption.

a considerable extent and shifts to a lower frequency, 3000 cm^{-1}, by the complex formation. The band of the complex is so weak that there may be another possibility of its further shift down into the aliphatic C-H stretching frequency region. This fact suggests that the complex formation causes an increase in the strain or a decrease in the s-character in the carbon valence orbital of the C-H bond.

The change in the C=C stretching band is the most prominent. As may be seen in Fig. 3, where the infrared absorption spectra of the complex measured under various conditions are shown, the 1653 cm^{-1} in free cyclohexene

is lowered to 1582 cm^{-1} by the complex formation. The result was confirmed by the Raman spectrum measured with the complex under various conditions. This is also consistent with the observation by Taufen et al.[19,20] that the frequency of the ν(C=C) Raman band of cyclohexene is 1575 cm^{-1} in a concentrated silver nitrate solution. The weaker broad peak near 1625 cm^{-1} in the infrared absorption of the complex also appears in the spectrum of the Nujol mull of silver perchlorate and can not be attributed to the absorption of the complex.

All of these changed bands of the complex are pertinent to the C=C double bond part. This probably indicates that the silver ion attacks the C=C bond, weakening its double bond character and giving rise to some strain in the olefinic part. Table II summarizes the observed infrared and Raman bands in 6 and 14 μ regions of cyclohexene under various conditions.[21] It is striking that the perturbed C=C stretching frequencies are almost the same in the solid complex (1582 cm^{-1} for $(C_6H_{10})_2\cdots AgClO_4$) and in the complex in solution (1585 cm^{-1} for $C_6H_{10}\cdots AgClO_4$). This seems to suggest that the complex is in a similar state in a solid and in a solution.

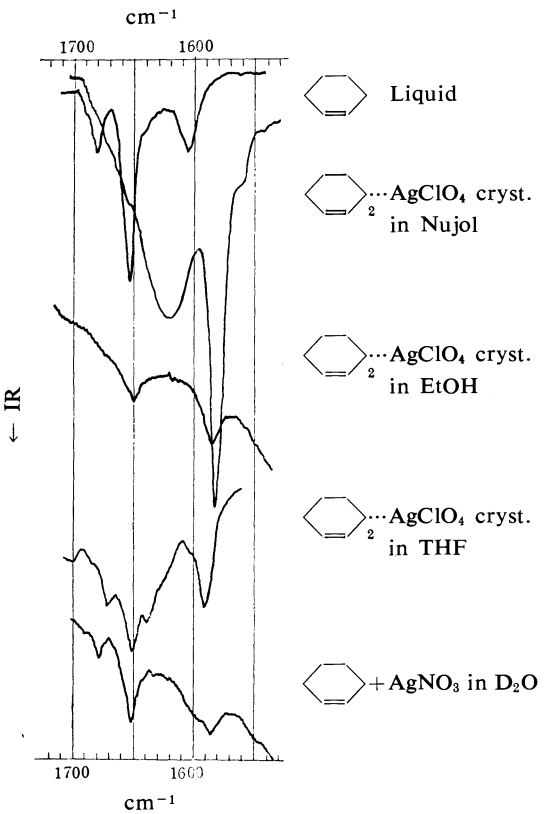


Fig. 3. Infrared absorption spectra of the 6 μ region of cyclohexene under various conditions.

A Theoretical Consideration of the Cyclohexene-Silver Perchlorate Complex

In the present theoretical study, the geometry of the cyclohexene-silver ion complex was assumed to be shown in Fig. 4 by analogy with those of the benzene-silver perchlorate[22a] and cycloöctatetraene-silver nitrate[22b] complexes. The electronic states of the complex were calculated by considering the interaction among the ground configuration and the several excited configurations caused by local excitations within the components and by charge-transfers between them.[23,24]

Component AO's and MO's.—For the olefinic part, besides the $2p\pi$ bonding (φ_1) and $2p\pi^*$ antibonding (φ_2) orbitals, the $3s\sigma$ bonding (φ_3) orbital was taken into account. These molecular orbital wave functions can be represented as follows:

$$\varphi_1=(\chi_1^{2p}+\chi_2^{2p})/\sqrt{2(1-S_{2p\pi})} \quad (3)$$

$$\varphi_2=(\chi_1^{2p}+\chi_2^{2p})/\sqrt{2(1-S_{2p\pi})} \quad (4)$$

$$\varphi_3=(\chi_1^{3s}+\chi_2^{3s})/\sqrt{2(1+S_{3s})} \quad (5)$$

Concerning the silver ion, two of the five 4d orbitals, $4d_{zx}$ (χ_d) and $4d_{z^2}$ (χ_e) and 5s (χ_s) orbitals were considered,[25] the x, y and z axes being taken as shown in Fig. 4. The component orbitals φ_1, φ_3, χ_e and χ_s are symmetric ($S=A_1$), while φ_2 and χ_d are antisymmetric ($A=B_2$) with respect to the σ_v plane. All the atomic orbitals are of the Slater type.

19) H. J. Taufen, M. J. Murray and F. F. Cleveland, *J. Am. Chem. Soc.*, **63**, 3500 (1941).

20) This is the only spectroscopic result reported hitherto about this type of complex.

21) All cyclohexene molecules interact with silver perchlorate in the solid complex, while in alcoholic and tetrahydrofuran solutions the complex and the free components are in equilibrium. The cyclohexene-silver nitrate complex is also in equilibrium with free components in (deuterated) water. Contrary to this, Taufen et al.[18] obtained no Raman band of free cyclohexene in its aqueous silver nitrate solution.

22) a) H. G. Smith and R. E. Rundle, *J. Am. Chem. Soc.*, **72**, 5337 (1950); **80**, 5075 (1958).
b) F. S. Mathews and W. N. Linscomb, *J. Phys. Chem.*, **63**, 845 (1959).

23) H. C. Longuet-Higgins and J. N. Murrell, *Proc. Phys. Soc.*, **A68**, 601 (1955); J. N. Murrell, ibid., **A68**, 969 (1955); J. A. Pople, ibid., **A68**, 81 (1955).

24) J. Tanaka, *J. Chem. Soc. Japan, Pure Chem. Sec. (Nippon Kagaku Zassi)*, **78**, 1636 (1957); **79**, 1373 (1958); S. Nagakura, *Mol. Phys.*, **3**, 105 (1960); H. Hosoya, J. Tanaka and S. Nagakura, This Bulletin, **33**, 850 (1960); H. Hosoya, J. Tanaka and S. Nagakura, *Tetrahedron*, **18**, 859 (1962).

25) The $4d_{x^2-y^2}$ orbital with A_1 symmetry character is excluded from the calculation, because of its smaller overlap with φ_1 or φ_2 (see Figs. 5 and 6 in Ref. 62). The remaining $4d_{xy}$ and $4d_{yz}$ orbitals can not interact with the φ_1, φ_2 and φ_3 MO's of the olefinic part because of their different symmetry properties.

Table II. Infrared and raman spectra of 6 and 14 μ regions of cyclohexene under various conditions (in cm^{-1})

	Added reagent	Solvent[a]	Cell[a]	C=C Stretching				C-H Out-of-plane bending	
				Free			Bonded	Bonded	Free
IR	None	None	NaCl	1680	1653	1605			716
	None	EtOH	NaCl	1682	1653	1606		—[b]	
	$Cd(ClO_4)_2$	THF	PE	1680	1652	1600		—	
	AgCl	Nujol	NaCl		1650			—	
	Ag_2SO_4	Nujol	NaCl	1680	1652	1605		—	
	$AgNO_3$	D_2O	PE	1680	1653		1585[c]	—	
	$AgNO_3$[g]	Nujol	NaCl				d)		
	$AgClO_4$	EtOH	NaCl		1650[e]		1585[c]	—	
	$AgClO_4$	THF	NaCl		1650[e]		1585[c]	740	715
	$AgClO_4$	THF	PE	1680	1650[e]		1585[c]	740	—
	$AgClO_4$[g]	Nujol	NaCl		1625[e]		1582	748	
	$AgClO_4$[g]	HCBD	NaCl		—		1582	748	
	$AgClO_4$[g]	KBr	None				f)		
Raman	None	None	Pyrex		1650				720
	$AgClO_4$	THF	Pyrex		1655[e]		1585[c]	—	
	$AgClO_4$	aqMeOH	Pyrex		1665[e]		1575[c]	—	
	$AgNO_3$	H_2O[h]	Glass				1584		

a) THF: Tetrahydrofuran, HCBD: Hexachlorobutadiene, PE: Polyethylene
b) The dashed line regions are masked by the absorption of the solvent and/or cell material.
c) $\pm 5\ cm^{-1}$
d) Prevented by water deposited on the cooled cell surface.
e) Band due to solid $AgClO_4$.
f) C_6H_{10} was pumped out from the solid mixture of C_6H_{10}-$AgClO_4$ complex and KBr powder, leaving the yellowish color of AgBr on the disk.
g) Solid complex.
h) Ref. 19

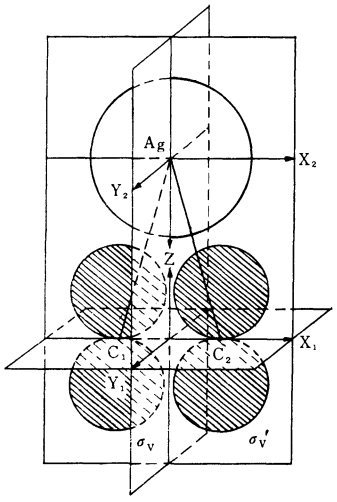


Fig. 4. The geometry of the monoölefin-metal ion complex. For $C_6H_{10}\cdots Ag^+$ the C_1-C_2 and the two Ag-C distances are 1.34 and 2.50Å, respectively.

Configurations and Their Energies.—Five symmetric (ψ_N, ψ_P, ψ_Q, ψ_R and ψ_S) and three antisymmetric (ψ_V, $\psi_{Q'}$ and $\psi_{S'}$) singlet configurations were taken into consideration. These configurations are given in Table III and Fig. 5. Among them, ψ_N, ψ_P and ψ_Q correspond to the no-bond, σ-type charge-transfer and π-type charge-transfer structures[5] respectively. The ψ_S (d-s transition) is the configuration in which one of the 4d orbital electrons of silver ion is excited to the 5s orbital. The importance of ψ_R (corresponding to the Rydberg transition in the olefinic part) has hitherto been overlooked; its inclusion is one of the important characteristics of the present theoretical treatment.[26]

The energy of the no-bond configuration, E_N, being taken as the standard, E_V and E_R can be taken to be equal to the observed transition energies corresponding to the N→V ($\pi\rightarrow\pi^*$ 6.79 eV.) and N→R (Rydberg 5.92 eV.) transitions of cyclohexene respectively.[27] E_S and $E_{S'}$ (5.71 eV.), the so-called singlet d-s separation energy, were obtained from the

26) The important role of the $3s\sigma$ bonding orbital in the charge-transfer process will be explained in a coming paper about the mechanism of "trans-addition."
27) W. J. Potts, Jr., *J. Chem. Phys.*, **23**, 65 (1955).

TABLE III. ELECTRONIC CONFIGURATIONS FOR THE $C_6H_{10}\cdots d^{10}$ TYPE METAL ION COMPLEXES

Symmetric

$\psi_N=(1\bar{1}d\bar{d}e\bar{e})$ [a]	
$\psi_P=1/\sqrt{2}\{(1s\bar{d}de\bar{e})+(s\bar{1}d\bar{d}e\bar{e})\}$	Charge-transfer (σ-type)
$\psi_Q=1/\sqrt{2}\{(1\bar{1}d2e\bar{e})+(1\bar{1}2d\bar{e}e)\}$	Back charge-transfer (π-type)
$\psi_R=1/\sqrt{2}\{(13d\bar{d}e\bar{e})+(3\bar{1}d\bar{d}e\bar{e})\}$	Rydberg
$\psi_S=1/\sqrt{2}\{(1\bar{1}d\bar{d}es)+(1\bar{1}d\bar{d}s\bar{e})\}$	d-s Transition

Antisymmetric

$\psi_V=1/\sqrt{2}\{(12\bar{d}d\bar{e}e)+(2\bar{1}d\bar{d}e\bar{e})\}$	N → V Transition
$\psi_{Q'}=1/\sqrt{2}\{(1\bar{1}d\bar{d}e2)+(1\bar{1}d\bar{d}2\bar{e})\}$	Back charge-transfer (π-type)
$\psi_{S'}=1/\sqrt{2}\{(1\bar{1}ds\bar{e}e)+(1\bar{1}s\bar{d}e\bar{e})\}$	d-s Transition

a) The complete form is expressed as follows:

$$(1\bar{1}d\bar{d}ee)=\frac{1}{\sqrt{6!}}\sum_P(-1)^P P\begin{Bmatrix}\varphi_1(1) & \varphi_1(2) & \chi_d(3) & \chi_d(4) & \chi_e(5) & \chi_e(6)\\ \alpha(1) & \beta(2) & \alpha(3) & \beta(4) & \alpha(5) & \beta(6)\end{Bmatrix}$$

atomic spectral data collected by Moore.[28] The energies of the three charge-transfer configurations were calculated by means of the following equations:

$$E_P=I_{C_6H_{10}}-A_{Ag^+}+0.8\cdot S_{Ag^+}$$
$$=9.00-7.58+4.45=5.87\text{ eV}.$$
$$E_Q=E_{Q'}=I_{Ag^+}-A_{C_6H_{10}}-2e^2/R-0.8\times 3/4S_{Ag^+}$$
$$=21.49+0.10-11.52-3.34=6.73\text{ eV}.$$

where the I's and A's are ionization potentials and electron affinities respectively. $A_{C_6H_{10}}$ was assumed to be -0.10 eV. so as to make the sum $I+A=8.90$ eV. for alternant hydrocarbons.[29] S_{Ag^+}, the hydration energy of the silver ion, was calculated by Oshida and Horiguchi.[30] R is the distance between the silver ion and one of the olefinic carbon atoms, 2.50 Å. A detailed description of the derivation of these equations will be given later in this paper.

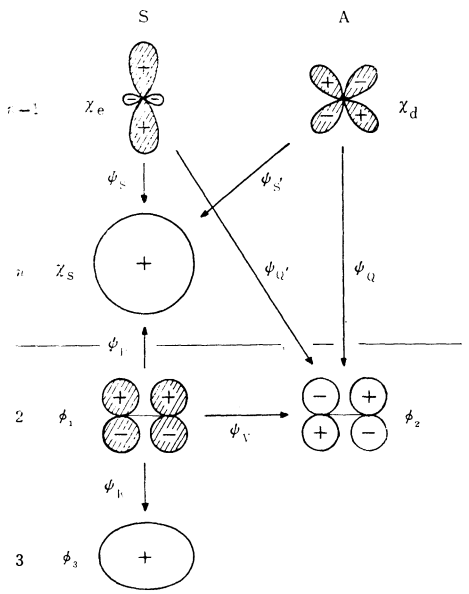


Fig. 5. Schematic representation of the component orbitals and the electron configurations important for the ground and lower excited states of the monoölefin-d^{10} type metal ion complex. These atomic or molecular orbitals are shaded which are doubly occupied in the ground configuration ψ_N. The letters $n-1$ and n for the metal ion and 2 and 3 for the monoölefin indicate the principal quantum numbers of the orbitals in the respective row, while the letters S (symmetric) and A (antisymmetric) represent the symmetry properties, with respect to the σ_V plane, of the orbitals in the respective column. The configurations represented by the vertical arrow have the same symmetry property as the ground configuration does and contribute to lower its energy.

Configurational Interaction.—The off-diagonal matrix elements of the total electronic Hamiltonian were accounted for only by means of the core resonance integral β.[31] For example:

$$H_{NP}=1/\sqrt{2}\int(1\bar{1}d\bar{d}ee)H\{(1s\bar{d}de\bar{e})+(s\bar{1}d\bar{d}e\bar{e})\}d\upsilon$$
$$=\sqrt{2}\int\varphi_1 H^{(1ddee)}\chi_s\,d\upsilon=\sqrt{2}\beta_{1s}^{(1ddee)}$$

28) C. E. Moore, "Atomic Energy Levels," Vols. I, II, III, National Bureau of Standards (1949, 1952, 1958).

29) N. S. Hush and J. A. Pople, *Trans. Faraday Soc.*, **51**, 600 (1955).

30) I. Oshida and D. Horiguchi, *Bull. Kobayashi Inst. Phys. Res.*, **5**, 61 (1955) (in Japanese); *J. Phys. Soc. Japan*, **11**, 330 (1956).

31) Generally speaking, the off-diagonal matrix elements comprise non-zero terms due to two-center Coulomb repulsion integrals. For example, $H_{RS}=(13\mid se)=\int\varphi_1^*(1)\times\varphi_3(1)(e^2/r_{12})\chi_e^*(2)\chi_S(2)d\upsilon$ contains non-zero Coulomb repulsion integral terms. However, this can be disregarded, as is clear from the following consideration. H_{RS} can be represented approximately by $\mu_{13}\cdot\mu_{es}/R$, where $\mu_{13}=e\int\varphi_1 r\varphi_3 d\upsilon$ and $\mu_{es}=e\int\chi_e r\chi_S d\upsilon$. The latter quantity is zero because it corresponds to the transition moment between s and d orbitals within the silver atom. The $H_{VS'}=(12\mid ds)$ value can also be disregarded.

Table IV. Effective charges and ionization energies of electrons for various states of cyclohexene obtained from spectroscopic results

Electronic configuration[a]	Ionizing electron	Slater's μ factor[38]	Ionization energy, eV.	Remark[b]
(11)	1	1.625	9.00	$=I_{C=C}$
(112)	2	1.45	−0.10	$=A_{C=C}$
(12)	2	1.625	2.21	$=I_{C=C}-\Delta E_{N\to V}$
(13)	3	0.483	3.08	$=I_{C=C}-\Delta E_{N\to R}$
(112)	1	1.45	6.69	$=\Delta E_{N\to V}+A_{C=O}$

a) 1, 2 and 3 are the molecular orbitals φ_1, φ_2 and φ_3, respectively.
b) I: Ionization potential;[33,34] A: Electron affinity (assumed); ΔE: Transition energy[27]

where $\beta_{1s}^{(1dd\epsilon e)}$ is the core resonance integral between the φ_1 and χ_s orbitals in the core potential field of $\boldsymbol{H}^{(1ddee)}$, which is the common part in the two configurations, ψ_N and ψ_P. According to Mulliken,[32] this value is approximated as proportional to the product of the overlap integral, $S_{1s}^{(1dd\epsilon e)}$, and the mean ionization potential, $\bar{I}$.

$$\beta_{1s}^{(1dd\epsilon e)}=C\cdot S_{1s}^{(1dd\epsilon e)}\cdot\bar{I}$$
$$=C\cdot S_{1s}^{(1dd\epsilon e)}\{I(11\to1)+I(ddees\to ddee)\}/2 \quad (6)$$

Here C is a constant, and $I(11\to1)$ and $I(ddees\to ddee)$ are the ionization potentials of cyclohexene and of the silver atom respectively.

The first ionization potential of cyclohexene was determined to be 9.00 eV. from the data of Watanabe[33] and others.[34] The values of the ionization energies for the other states of cyclohexene were estimated by combining the first ionization potential value with the spectroscopic data (see Appendix I). These values are summarized in Table IV, while the values for the metal ion part were taken from Moore's table.[28] The overlap integrals were mostly calculated from the published tables[35-37] but partly, where necessary, from our new tables (see Appendix II) by assuming appropriate effective charges for the Slater-type AO's.[38] The formulae for the iterative degradation of overlap integrals between the various types of d-orbitals and the olefinic p-orbitals into simpler forms are listed in Appendix III. The proportional constant, C, was evaluated to be -1.0,[39] by taking into account the following relation for ethylene:

$$\beta=C\cdot S\cdot I_C=-3.125$$
$$=-1.003\times0.270\times11.54 \text{ (eV.)}$$

where β is the value adopted by Pariser and Parr[41] and I_C, the $2p\pi$ valence state ionization potential of a carbon atom.[42] The non-zero off-diagonal elements thus obtained are included in Table IX.

The Stabilization Energy and the CT-R Band of the Cyclohexene-Silver Perchlorate Complex. —The secular equations constructed from the matrix elements evaluated as mentioned above were solved by the aid of an IBM 7090 electronic computer. Among the evaluated energy levels and wave functions, those for the lowest three levels are tabulated in Table V (see also Fig. 6).

According to the present theoretical study, the complex is stabilized by charge-delocalization by about 1.05 eV., with the 7.4 and 6.9 per cent contributions of the ψ_P and ψ_Q charge-transfer configurations respectively. The Rydberg configuration contributes to the ground state by 2.0 per cent. The in-phase mixing of the widely extended $3s\sigma$ orbital with the $2p\pi$ bonding orbital corresponds to the polarization of the latter electronic cloud toward the silver ion, especially in the outer skirts.

32) R. S. Mulliken, *J. Phys. Chem.*, **56**, 295 (1952).
33) K. Watanabe, *J. Chem. Phys.*, **26**, 542 (1957).
34) W. C. Price and W. T. Tutte, *Proc, Roy. Soc.*, **A174**, 207 (1940); J. D. Morrison, *J. Chem. Phys.*, **19**, 1305 (1951); J. Hissel, *Bull. Soc. Roy. Sci. Liège*, **21**, 457 (1952).
35) R. S. Mulliken, C. A. Rieke, D. Orloff and H. Orloff, *J. Chem. Phys.*, **17**, 1248 (1949).
36) D. P. Craig, A. Maccoll, R. S. Nyholm, L. E. Orgel and L. E. Sutton, *J. Chem. Soc.*, **1954**, 332,
37) H. H. Jaffé and G. O. Doak, *J. Chem. Phys.*, **21**, 196 (1953); H. H. Jaffé, ibid., **21**, 258 (1953); J. L. Roberts and H. H. Jaffé, ibid.. **27**, 883 (1957).
38) J. C. Slater, *Phys. Rev.*, **36**, 57 (1930).
39) If Eq. 6 be taken as proven, two problems still remain. One is whether the use of Slater-type wave functions for the silver 4d and 5s orbitals gives correct values for the overlap integrals, S's, which in principle should be calculated with the SCF orbitals. According to the test calculation by Mulliken et al.,[35] there arose no serious dircrepancy between the $S(2p\sigma C, 2p\sigma C)$ values calculated with Slater-type and SCF functions, especially for the bond length region around 2 Å (the S(SCF)/S(Slater) ratio being 1.4~0.7). By the use of numerical tables for metal s-orbitals calculated by Hartree et al.[40] with the SCF method, the $S(2p\sigma C(\text{Slarer}), 4sZn^+(\text{SCF}); 2.06 \text{ Å})$ value was numerically calculated and compared with the $S(2p\sigma C(\text{Slater}), 4sZn^+(\text{Slater}); 2.06 \text{ Å})$ value. The agreement was found unexpectedly well (the ratio being 1.2=0.21/0.17).
The other is whether the semi-empirical parameter, C, is applicable to the intermolecular lateral overlaps. In the present study, we have made calculations for the three cases of $C=-0.6$, -0.8 and -1.0.
40) W. Hartree, D. R. Hartree and M. F. Manning, *Phys. Rev.*, **59**, 299 (1940).
41) R. Pariser and R. G. Parr, *J. Chem. Phys.*, **21**, 466, 767 (1953).
42) H. O. Pritchard and H. A. Skinner, *Chem. Revs.*, **55**, 745 (1955).

TABLE V. WAVE FUNCTIONS AND ENERGIES OF THE LOWER ELECTRONIC STATES OF THE $C_6H_{10}\cdots Ag^+$ COMPLEX

$W_0=-1.052$ eV.	$\Psi_0=0.9125\phi_N+0.2717\phi_P+0.2624\phi_Q+0.1416\phi_R-0.0676\phi_S$
$W_1=2.150$	$\Psi_1=-0.2745\phi_N+0.6489\phi_P-0.1341\phi_Q+0.6257\phi_R-0.3068\phi_S$
$W_2=4.487$	$\Psi_2=0.7024\phi_V-0.7117\phi_{Q'}$
$W_3=5.710$	$\Psi_3=\phi_{S'}$
$W_4=5.747$	$\Psi_4=-0.0025\phi_N+0.0200\phi_P-0.0058\phi_Q+0.4214\phi_R+0.9066\phi_S$

TABLE VI. ENERGY LEVELS OF THE GROUND AND LOWEST EXCITED STATES OF THE $C_6H_{10}\cdots Ag^+$ COMPLEX WITH THEIR PER CENT CONTRIBUTION BY THE SEVERAL CONFIGURATIONS WITH VARYING PARAMETER C

C	$\Delta E=-W_0$ eV.	W_1-W_0 eV.	W_2-W_1 eV.	Ground state				CT-R state			
				ϕ_N	ϕ_P	ϕ_Q	ϕ_R	ϕ_N	ϕ_P	ϕ_Q	ϕ_R
−0.6	0.381	3.933	1.844	94.1	2.2	3.4	0.3	1.9	47.3	40.1	10.4
−0.8	0.675	3.507	2.110	89.4	4.3	5.2	0.8	4.1	45.1	40.0	9.9
−1.0	1.052	3.202	2.337	83.3	7.4	6.9	2.0	7.5	42.1	39.2	9.4

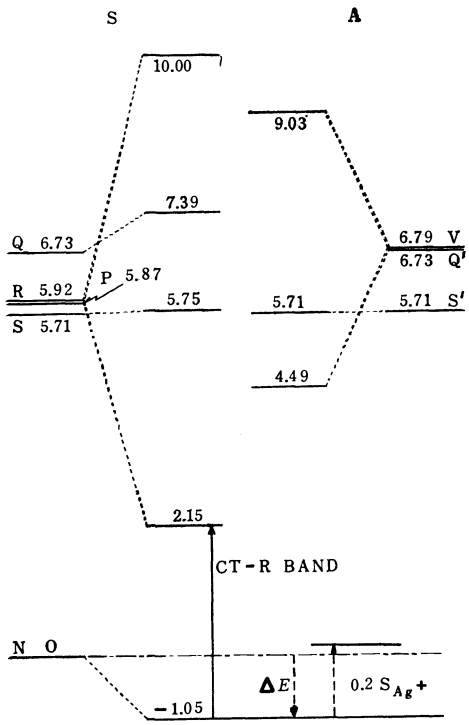


Fig. 6. Energy diagram (in eV.) for the $C_6H_{10}\cdots Ag^+$ complex in water showing configuration interaction, stabilization (ΔE) and destabilization ($0.2\cdot S_{Ag^+}$), and CT-R transition.

The stabilization energy of 1.05 eV. should not be taken literally, since the silver ion is destabilized by the replacement of a portion of the hydrated water molecules by a non-polar olefin molecule. This energy may be estimated to be about two-tenths of the hydration energy of a silver ion, because the solid angle spanning the cyclohexene molecule from the silver ion in this geometry is just two-tenths of the whole angle. Since the hydration energy of the silver ion is 5.56 eV.,[30] the destabilization energy due to the destruction of the water sheath may be estimated to be 1.11 eV. This is consistent with the electrostatic calculation by Eley and Evans[43] that the enegy requirement for removing one water molecule from the hydration sphere of the silver ion is larger than 20 kcal./mol. (=0.87 eV.). The most important point in the present treatment is that the olefinic π-electron stabilization energy (1.05 eV.=24.2 kcal./mol.) is comparable to the lost hydration energy (1.11 eV.=25.6 kcal./mol.).

The lowest excited state, with 42 and 39 per cent contributions by the ϕ_P and ϕ_R configurations respectively, is only 3.2 eV. higher than the ground state. The poor agreement between the observed (~5.4 eV.) and calculated (~3.2 eV.) values may possibly be attributed to the use of the macroscopic hydration energy (see later) obtained from the Born-Haber cycle instead of the structure-dependent microscopic hydration energy, and to the lack of detailed quantitative knowledge about the electronic states of larger atoms with d-electrons and intermolecular interaction energies. However, as is evident in Table VI, for calculation with C values varying from −0.6 to −1.0, the lowest excited state is invariably 2 eV. lower than the next higher excited state (V state) and its character is invariant. Namely, ϕ_P and ϕ_R contribute to the lowest excited state by almost the same amount, 40 per cent. The new band at about 230 mμ for the cyclohexene-silver ion complex is, then, determined to have the mixing character of charge-transfer from the olefin to the silver ion and the Rydberg transition in the olefin part (CT-R band).

43) D. D. Eley and M. G. Evans, *Trans. Faraday Soc.*, **34**, 1093 (1938).

A Theoretical Consideration of the Selective-Complex Formation Abilities of Copper(I), Silver(I) and Mercury(II) Ions[44]

In order to clarify the reason why some of the closed shell (d^{10} and p^6)-type metal ions form stable complexes with olefins, while the others can not, we undertook to calculate the stabilization energy due to the electron delocalization for the systems containing various metal ions and cyclohexene, assuming reasonable geometrical configurations. A hypothetical monoölefin-metal ion complex is assumed to have the C_{2v} symmetry property (for the π-electronic part), with R_{MC} equal to $r_{M^{n+}}+1.32$ Å, where 1.32 Å is a constant determined in such a way that R_{MC} for the case of silver ions is equal to 2.50 Å.[51] The ionic and metallic raddii of silver ions are 1.18 and 1.34 Å, while the covalent radius of carbon atoms and the half thickness of aromatic molecules proposed by Pauling[52] are 0.77 and 1.70 Å respectively. That the sum of the respective mean values is equal to 2.50 Å is indeed a fortuitous coincidence, but it may be the ground for some possible additivity relationship.

Since the energy evaluations of the charge-transfer configurations are important in discussing the stabilities of various monoölefin-metal ion complexes, first of all a detailed description will be given of the evaluation of the charge-transfer configurational energy.

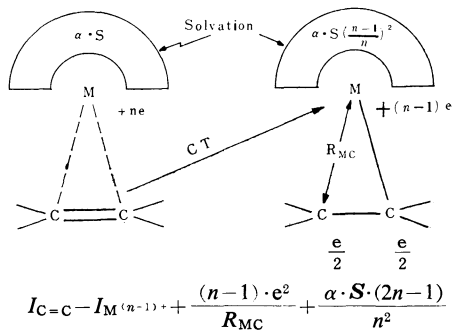
The Estimation of Charge-Transfer Configuration Energies. — The hydration energy of the metal ion may be thought to diminish greatly in the charge-transfer configuration compared with that of the ground configuration. Therefore, in the evaluation of the charge-transfer configuration energy, we must reasonably estimate the magnitude of the change of hydration energy. The solvation energy of a metal ion is known to be roughly proportional to the square of the charge number. If the solvated molecules are assumed not to change their positions during an electron transfer in the solvated cage, the decrease in solvation energy is approximately equal to

$$\alpha\,[n^2-(n-1)^2]/n^2\cdot S_{M^{n+}}=\alpha(2n-1)/n^2\cdot S_{M^{n+}}$$

where $S_{M^{n+}}$ is the solvation energy of a metal ion, M^{n+}, and α is a universal parameter representative of effective solvation by the olefin molecules. The energy necessary for an electron transfer from the olefin to the ion may then be estimated as follows:

$$H_{PP}=I_{C=C}-I_{M^{(n-1)+}}+(n-1)e^2/R_{MC}+\alpha\cdot S_{M^{n+}}\cdot(2n-1)/n^2 \qquad (7)$$

where $I_{C=C}$ and $I_{M^{(n-1)+}}$ indicate the ionization potentials of the olefin and the metal ion (or atom) $M^{(n-1)+}$, the latter quantity being identical to the electron affinity of the ion M^{n+}. The third term is the repulsion energy between charges of the metal and carbon atoms (see Fig. 7). In the above treatment, the change in the solvation energy of the olefinic part is disregarded, since the resulting net charge is divided into two carbon atoms and since, moreover, they are shielded by the other carbon and hydrogen atoms to a considerable extent. Even if it can not completely be disregarded, it may conceivably be included in the unknown parameter, α, the determination of which is the next problem.



$$I_{C=C}-I_{M^{(n-1)+}}+\frac{(n-1)\cdot e^2}{R_{MC}}+\frac{\alpha\cdot S\cdot(2n-1)}{n^2}$$

Fig. 7. Estimation of the charge-transfer configurational energy H_{PP}.

We have plotted the $(2n-1)\cdot S_{M^{n+}}/n^2$ $(=X)$ values for twenty-five d^{10} and p^6-type metal ions and for the halogen cations Br^+ and I^+ against the sum (Y) of the first three terms in Eq. 7 by using the following values: $I_{C=C}=9.00$ eV. for cyclohexene;[33] $I_{M^{(n-1)+}}$, from Moore's table;[28] $R_{MC}=1.32+r_{M^{n+}}$ Å, where the $r_{M^{n+}}$'s were taken from the table of ionic radii by Stockar;[53] the $S_{M^{n+}}$ value was taken from the table of hydration energies by Oshida and Horiguchi[30] (see Table VII). It may easily be shown that, for a fixed α value, the points for the metal ions with the same charge-transfer

44) The complexes considered here differ from such square planar Zeise salts as $K[(C_2H_4)\cdot PtCl_3]$[45], such transition metal carbonyl-olefin complexes as $C_5H_8\cdot Fe(CO)_3$[46] or such mercury ion-olefin addition compounds as $HO\cdot CH_2CH_2\cdot HgCl$,[47] which are shown to have true or nearly covalent metal-carbon bonds by the evidence of X-rays,[48] infrared absorption,[49] NMR spectroscopy[50] and from some other chemical properties.

45) W. C. Zeise, *Pogg. Ann.*, **9**, 632 (1827).

46) M. A. Benett, *Chem. Revs.*, **62**, 611 (1962).

47) J. Chatt, ibid., **48**, 7 (1951).

48) P. R. H. Alderman, P. G. Owston and J. M. Rowe, *Acta Cryst.*, **13**, 149 (1960).

49) J. Chatt and L. A. Duncanson, *J. Chem. Soc.*, **1953**, 2939; J. Chatt and M. L. Searle, "Inorganic Syntheses," **5**, Ed. by Moeller., McGraw-Hill, New York (1957), p. 210.

50) D. B. Powell and N. Sehenert, *J. Chem. Soc.*, **1960**, 2519.

51) R_{MC} and $r_{M^{n+}}$ are, respectively, the carbon-metal distance and the ionic radius of a metal ion, M^{n+}.

52) L. Pauling, "The Nature of the Chemical Bond," Cornell Univ. Press, Ithaca, New York (1960).

53) K. Stockar, *Helv. Chim. Acta*, **33**, 1409 (1950).

TABLE VII. EVALUATION OF H_{PP} VALUES

Ion	Lewest vacant orbital	$I_{M^{(n-1)+}}$ Å	$r_{M^{n+}}$ Å	$S_{M^{n+}}$ eV.	Y[b] eV.	X[a] eV.	$Y+0.8X=H_{PP}$ eV.
Na^+	3s	5.14	0.86	4.61	3.86	4.61	6.55
K^+	4s	4.34	1.22	3.75	4.66	3.75	7.67
Rb^+	5s	4.18	1.40	3.52	4.82	3.52	7.63
Cs^+	6s	3.89	1.61	3.19	5.11	3.19	7.66
Mg^{2+}	3s	15.03	0.65	20.61	1.28	15.46	13.65
Ca^{2+}	4s	11.87	0.99	17.04	3.36	12.78	13.59
Sr^{2+}	5s	11.03	1.15	15.69	3.80	11.77	13.22
Ba^{2+}	6s	10.00	1.37	14.81	4.35	11.11	13.24
Al^{3+}	3s	28.45	0.61	49.46	− 4.53	27.48	17.46
Sc^{3+}	3d	24.76	0.81	43.51	− 2.24	24.17	17.10[c]
Y^{3+}	4d	20.55	0.95	38.82	1.14	21.57	18.40[c]
Ti^{4+}	3d	43.25	0.68	84.69	−12.65	37.05	17.00[c]
Zr^{4+}	4d	34.34	0.80	70.85	− 4.96	31.00	19.84[c]
Cu^+	4s	7.73	0.90	6.47	1.27	6.47	6.45
Ag^+	5s	7.58	1.18	5.56	1.42	5.56	5.87
Au^+	6s	9.23	1.29	6.81	− 0.23	6.81	5.22
Zn^{2+}	4s	17.96	0.74	21.90	− 1.97	16.43	11.17
Cd^{2+}	5s	16.91	0.97	19.41	− 1.62	14.56	10.03
Hg^{2+}	6s	18.76	1.10	19.51	− 3.81	14.63	7.89
Ga^{3+}	4s	30.71	0.62	49.20	− 6.86	27.33	15.00
In^{3+}	5s	28.03	0.81	43.99	− 5.51	24.44	14.04
Tl^{3+}	6s	29.83	0.95	44.34	− 8.14	24.63	11.56
Ge^{4+}	4s	45.71	0.54	91.68	−13.48	40.11	18.61
Sn^{4+}	5s	40.73	0.70	89.28	−10.34	39.06	20.91
Pb^{4+}	6s	42.32	0.84	75.88	−13.32	33.20	13.24
Br^+	4p	11.84	0.71	6±1	− 2.84	6±1	2.0±0.8
I^+	5p	10.46	1.05	5±1	− 1.46	5±1	2.5±0.8

a) $X=S_{M^{(n-1)+}}\cdot(2n-1)/n^2$ (eV.)

b) $Y=9.00-I_{M^{(n-1)+}}+(n-1)\cdot e^2/R_{MC}$ (eV.), $R_{MC}=1.32+r_{M^{n+}}$ (Å)

c) These values are $H_{P''P''}$'s, since $H_{P''P''}$ is smaller than H_{PP} for these ions.

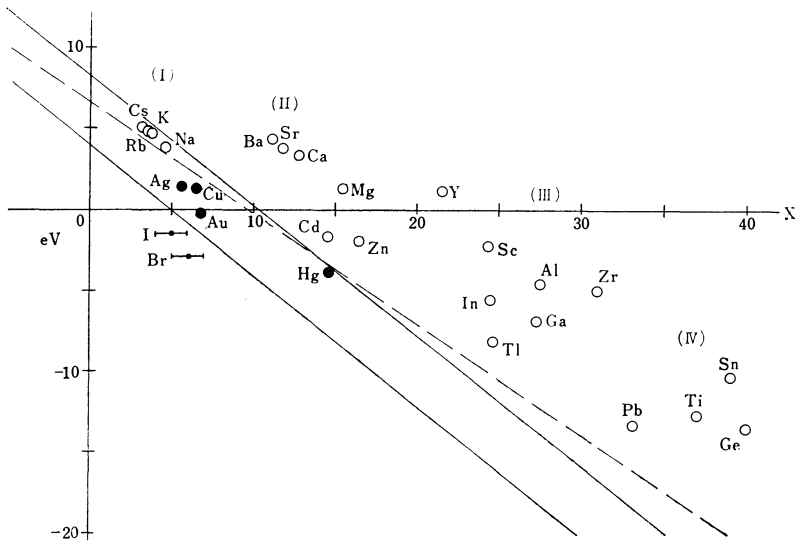


Fig. 8. Determination of α. The two parallel lines have α equal to 0.8, while the broken line 0.7. The Roman numerals indicate the charge numbers of the ions. The ions are classified into three groups:

○ without an ability of complex formation,

● with an ability of complex formation, and

I–•–I with a tendency for further addition reaction.

energy, $H_{PP}=Y+\alpha\cdot X$, lie exactly on a straight line with the slope $-\alpha$ and intercepting the Y axis at $Y=H_{PP}$. The Cu^+, Ag^+, Au^+ and Hg^{2+} ions, together with alkali metal ions, were found distinguishable from the others, since the points for the former ions lie beneath the line with α equal to about 0.8; this indicates that the former ions have lower H_{PP} values than the latter do. In spite of their higher electron affinities the trivalent and tetravalent ions show larger H_{PP} values. This is because the third and fourth terms of Eq. 7, namely, the electrostatic repulsion and solvation energy terms, become larger for these ions and compensate for the smaller value of the $I_{C=C}-I_{M^{(n-1)+}}$ term.

It is interesting to note that the plots for Br^+ and I^+ ions lie in the region for beneath the line, indicating their low H_{PP} values and, accordingly, the possibility of further addition reaction.

Similarly, the energies for the back charge-transfer H_{QQ}'s for twelve d^{10}-type metal ions were evaluated by the following equation:

$$H_{QQ}=I_{M^{n+}}-A_{C=C}-(n+1)e^2/R_{MC}-0.8\cdot S_{M^{n+}}(2n+1)/(n+1)^2 \quad (8)^{54)}$$

where $A_{C=C}$ is the electron affinity of cyclohexene, -0.10 eV. (estimated). Again, Cu^+, Ag^+, Au^+ and Hg^{2+} have much lower H_{QQ} values than do any other metal ions (see Table VIII). This fact is also closely related to the selected abilities of Cu^+, Ag^+ and Hg^{2+} for complex formation with monoölefins.

TABLE VIII. EVALUATION OF H_{QQ} VALUES

Ion	Highest occupied orbital	$I_{M^{n+}}$ eV.	X [a] eV.	Y [b] eV.	$H_{QQ}=Y+0.8X$ eV.
Cu^+	3d	20.29	4.85	7.42	3.54
Ag^+	4d	21.49	4.17	10.07	6.73
Au^+	5d	20.50	5.11	9.57	5.48
Zn^{2+}	3d	39.71	12.17	18.84	9.10
Cd^{2+}	4d	37.48	10.78	18.72	10.10
Hg^{2+}	5d	34.20	10.84	16.45	7.78
Ga^{3+}	3d	64.17	21.53	34.58	17.36
In^{3+}	4d	54.40	19.25	27.46	12.06
Tl^{3+}	5d	50.72	19.40	25.45	9.93
Ge^{4+}	3d	93.45	33.00	54.84	28.44
Sn^{4+}	4d	72.30	32.14	36.76	11.05
Pb^{4+}	5d	68.80	27.32	35.57	13.71

a) $X=S_{M^{n+}}\cdot(2n+1)/(n+1)^2$ (eV.)
b) $Y=I_{M^{n+}}+0.10-(n+1)\cdot e^2/R_{MC}$ (eV.)
$R_{MC}=1.32+r_{M^{n+}}$ (Å)

The Estimation of Stabilization Energies for Various Monoölefin-Metal Ion Complexes.—The stabilization energies were estimated on the basis of charge-transfer configurational energies evaluated by the above-mentioned method.

The component MO's and AO's are the same as those for the silver complex. The effective charges and orbital energies were determined according to the Slater rule,[38] and by the atom ionization potentials and atomic spectral data,[28] respectively.

In this calculation, only the singlet symmetric (with respect to the yz plane), $^1A_1$, configurations are considered, because we are concerned with rough estimations of stabilization energies due to charge delocalization and of the loss in hydration energies. The H_{PP}'s for the d^{10}- and p^6-groups and the H_{QQ}'s for the d^{10}-group were estimated by the method described in the preceding section. H_{RR} is again 5.92 eV. Since, for the p^6-group ions, the energy separations between the ns- and np-orbitals are generally small (a few eV.), another charge-transfer configuration, $\psi_{P'}$ namely, the one caused by the charge-transfer from φ_1 to χ_{npz} (χ_p) was considered. For Sc^{3+}, Y^{3+}, Ti^{4+} and Zr^{4+}, with $(n-1)$d but not ns-orbital as the lowest vacant one, an extra charge-transfer configuration, $\psi_{P''}$, namely, the one caused by the charge-transfer from φ_1 to $\chi_{(n-1)dz^2}$ ($\chi_{e'}$; see Fig. 9) was considered. These configurational energies, $H_{P'P'}$ and $H_{P''P''}$'s, were determined by the algebraic addition of the doublet p-s ($(n-1)p^6\cdot ns\rightarrow(n-1)p^6\cdot np$) and d-s ($(n-1)p^6\cdot ns\rightarrow(n-1)p^6\cdot(n-1)d$) separation energies of $M^{(n-1)+}$ ion (or atom) to the H_{PP} values. The H_{SS}'s for the

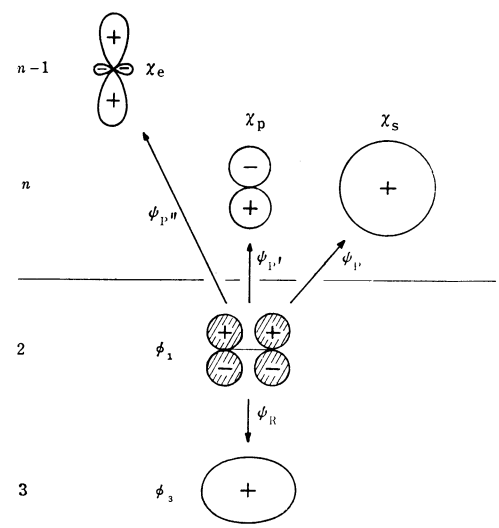


Fig. 9. Schematic representation of the component orbitals and the electron configurations (symmetric) of the hypothetical monoölefin-p^6 type metal ion complex. See the caption of Fig. 5.

54) The choice of $(2n+1)/n^2$ instead of $(2n+1)/(n+1)^2$ for the coefficient of $0.8\cdot S_{M^{n+}}$ in the last term was proved to give abnormally lower energies for H_{QQ}.

TABLE IX. NON-ZERO MATRIX ELEMENTS (IN eV.) FOR THE $C_6H_{10}\cdots d^{10}$ TYPE METAL ION COMPLEXES

	H_{PP}	H_{QQ}	H_{RR}	H_{SS}	H_{NP}	H_{NQ}	H_{PR}	H_{PS}
Cu^+	6.45	3.54	5.92	3.26	−1.774	−1.385	−3.384	0.900
Ag^+ a)	5.87	6.73	5.92	5.71	−1.372	−2.238	−3.635	1.683
Au^+	5.22	5.48	5.92	3.67	−1.173	−2.279	−4.302	1.894
Zn^{2+}	11.17	9.10	5.92	10.35	−4.461	−2.605	−5.334	1.474
Cd^{2+}	10.03	10.10	5.92	11.02	−3.334	−4.150	−5.597	2.622
Hg^{2+}	7.89	7.78	5.92	7.57	−3.082	−4.123	−6.705	2.950
Ga^{3+}	15.00	17.36	5.92	19.32	−8.368	−3.851	−7.214	1.948
In^{3+}	14.04	12.06	5.92	17.20	−6.703	−5.951	−7.498	3.606
Tl^{3+}	11.56	9.93	5.92	11.99	−5.986	−6.192	−8.524	3.888
Ge^{4+}	18.61	28.44	5.92	30.00	−13.192	−13.192	−9.221	2.330
Sn^{4+}	20.91	11.05	5.92	23.96	−10.584	−7.301	−9.375	4.311
Pb^{4+}	13.24	13.71	5.92	16.86	−9.870	−7.335	−10.056	4.773

a) $H_{VQ'}=2.273$ eV. for another secular equation concerning the antisymmetric configurations, ψ_V, $\psi_{Q'}$ and $\psi_{S'}$, with respect to the yz (σ_V) plane.

TABLE X. NON-ZERO MATRIX ELEMENTS (IN eV.) FOR THE $C_6H_{10}\cdots p^6$ TYPE METAL ION COMPLEXES

	H_{PP}	$H_{P'P'}$	$H_{P''P''}$	H_{RR}	H_{NP}	$H_{NP'}$	$H_{NP''}$	H_{RP}	$H_{RP'}$	$H_{RP''}$
Na^+	6.55	8.65		5.92	−1.087	−1.021		−3.045	−0.969	
K^+	7.67	9.28		5.92	−0.227	−0.023		−3.095	−1.041	
Rb^+	7.63	9.19		5.92	0.034	0.217		−3.012	−1.210	
Cs^+	7.66	9.05		5.92	0.568	0.255		−2.959	−1.330	
Mg^{2+}	13.65	18.07		5.92	−4.071	−3.066		−4.793	−0.398	
Ca^{2+}	13.59	16.71		5.92	−1.631	−1.284		−5.343	−1.198	
Sr^{2+}	13.22	16.16		5.92	−1.061	−0.799		−5.483	−1.518	
Ba^{2+}	13.24	15.75		5.92	−0.849	−0.746		−5.142	−1.720	
Al^{3+}	17.46	24.06		5.92	−8.320	−6.804		−6.525	−0.153	
Sc^{3+}	20.27	24.80	17.10	5.92	−4.186	−3.520	−4.372	−6.901	−1.021	0.372
Y^{3+}	19.33	23.53	18.40	5.92	−2.979	−2.560	−1.430	−7.057	−1.453	0.099
Ti^{4+}	26.97	32.86	17.00	5.92	−7.740	−6.013	−9.525	−8.421	−0.552	0.683
Zr^{4+}	24.58	30.00	19.84	5.92	−6.116	−5.461	−4.732	−8.439	−0.994	0.395

d^{10} group were determined as the singlet d-s separation energies ($d^{10}\rightarrow d^9\cdot s$) of M^{n+} ions. The offdiagonal elements were calculated in a manner similar to that used for a silver complex ($C=-1.0$). The non-zero matrix elements thus obtained for many metal ion complexes are tabulated in Tables IX and X. By solving the secular equations constructed from the matrix elements for each metal ion complex, the stabilization energy due to charge delocaliztion, ΔE, was evaluated. The results are shown in Table XI.

A Comparison of the Delocalization Energies Evaluated for Various Metal Ion Complexes.— In Table XI the $|\Delta E|$ values are compared with the $0.2\cdot S_{M^{n+}}$ values corresponding to the loss of hydration energy. As is evident from these results, the copper(I), silver(I), gold(I) and mercury(II) ions are distinguished from other closed shell-type metal ions with very small values of $(0.2\cdot S_{M^{n+}}-|\Delta E|)/0.2\cdot S_{M^{n+}}$ and are correlated with the very selective complex formation abilities except for the case of the gold(I) ion. The reason why the stable monoölefin-Au^+ complex can not exist may be due to the infrequent occurrence of the monovalent ion itself.

The fact that ψ_P and ψ_Q contribute to the ground state of copper(I), silver(I) and mercury(II) complexes by almost the same amounts seems to show the importance of the π-type back charge-transfer mechanism.[5] This may be supported by the fact that the p^6 group metal ions without outer d-electrons can not form stable complexes with monoölefins. The overlap integrals between the olefinic carbon, 2pz AO, and χ_s and χ_d have been shown not to deviate substantially from ion to ion, while the energies of the two charge-transfer configurations seem to correlate well with the complex formaton ability. It is interesting to note that a good correlation is also found with the smaller d-s separation energy (H_{SS}) for copper(I), silver(I) and mercury(II) ions

Table XI. Delocalization and destabilization energies of the hypothetical complexes of the C_6H_{10}···closed shell type metal ions

Ion	Delocalization energy $\lvert\Delta E\rvert$ eV.	Destabilization energy $0.2\cdot S_{M^{n+}}$ eV.	$\frac{0.2\cdot S_{M^{n+}}-\lvert\Delta E\rvert}{0.2\cdot S_{M^{n+}}}$
Na^+	0.36	0.92	0.61
K^+	0.01	0.75	0.99
Rb^+	0.01	0.70	0.99
Cs^+	0.06	0.64	0.91
Mg^{2+}	1.82	4.12	0.56
Ca^{2+}	0.41	3.41	0.88
Sr^{2+}	0.19	3.14	0.94
Ba^{2+}	0.13	2.96	0.96
Al^{3+}	5.26	9.89	0.47
Sc^{3+}	2.48	8.70	0.71
Y^{3+}	1.11	7.76	0.86
Ti^{4+}	6.79	16.94	0.60
Zr^{4+}	3.68	14.17	0.74
Cu^+	0.99	1.29	0.23
Ag^+	1.05	1.11	0.05
Au^+	1.22	1.36	0.10
Zn^{2+}	2.54	4.38	0.42
Cd^{2+}	2.65	3.88	0.32
Hg^{2+}	3.27	3.90	0.16
Ga^{3+}	5.21	9.84	0.47
In^{3+}	5.30	8.80	0.40
Tl^{3+}	5.87	8.87	0.34
Ge^{4+}	8.79	18.34	0.52
Sn^{4+}	7.92	17.86	0.56
Pb^{4+}	9.03	15.18	0.41

(see Table IX). As Orgel[55] has pointed out, the mixing of χ_{dz^2} orbital with a χ_s orbital facilitates the extension of the diagonal valency character.[56] The difficulty polyvalent ions have in forming complexes with olefins can be explained as follows. The destabilization energies ($0.2\cdot S_{M^{n+}}$) of metal ions in the same periodic row are proportional to the square of the charge number (n), whereas the competing delocalization energies (ΔE) were found to be roughly proportional to the three-halves order of the charge number (see Table XI). The reason why, among the divalent ions, mercury(II) ion alone has a selective complex formation ability is not attributed to the difference in its hydration energies or ionic radii but to the instability of its d^{10} state and, hence, its large electron affinity relative to other ions.

Although our calculations appear to be based on some bold assumptions and on arbitrarily numerical parameters, the results obtained here, specifically for the importance of the $3s\sigma$ orbital in the lowest excited state and for the selective complex-formation abilities of copper(I), silver(I) and mercury(II) ions, are invariant. Since both the method of the "composite molecule" and the concepts of charge-transfer and hybridization can be derived as consequeces of a mathematical development describing a true state in terms of quantities with clearer physical meanings, another approach, e.g., the LCAO MO method, to this problem would give similar results.

The Effect of Olefins and Negative Ions upon the Stability of Monoölefin-Metal Ion Complexes. — A similar calculation was made for the ethylene-silver ion complex. The ionization potential (10.52 eV.)[33] and the electron affinity (−1.81 eV.)[29] of the ethylene molecule and therefore, H_{PP} (7.49 eV.) and H_{QQ} (8.44 eV.) are different from those of cyclohexene. H_{VV} and H_{RR} are the observed $N\rightarrow V$ and $N\rightarrow R$ transition energies, 7.65 and 7.11 eV. respectively.[57,58] These four diagonal elements are larger than those for the cyclohexene complex. The other diagonal and all of the off-diagonal elements are just the same as were used for the cyclohexene complex.

With $C=-1.0$, the delocalization energy was evaluated to be 0.841 eV., which is smaller than that of the cyclohexene complex by 0.21 eV. This seems to mean that the silver ion complexes with ethylene and other simple monoölefins with higher ionization potentials may be more unstable than the cyclohexene-silver ion complex.

Although the effect of the anions of silver salts is disregarded in the present treatment, this is not the case experimentally. The cyclohexene-silver nitrate complex is stable only at a low temperature and no cyclohexene complexes have ever been known with silver salts other than the perchlorate and nitrate.[59] The different stabilities of these complexes seem to depend on the strengths of the interaction between the metal ions and the negative ions. Hence, the inability of silver chloride and sulfate to form complexes with cyclohexene may be explained by assuming that these anions have a strong affinity for silver cations.

Summary

The ultraviolet, infrared and Raman spectra of the cyclohexene-silver perchlorate complex

55) L. E. Orgel, "An Introduction to Transition-Metal Chemistry," Methuen & Co., London (1959), p. 67.

56) Winstein and Lucas[3] showed the existence of olefin-silver complexes with a 2:1 ratio in aqueous media. The solid complex also has the same composition ratio.[14] In both cases, a silver ion is supposed to be stacked in between two olefin molecules.[9]

57) P. G. Wilkinson and R. S. Mulliken, *J. Chem. Phys.*, **23**, 1895 (1955); G. Reid, ibid., **18**, 1299 (1950); D. F. Evans, *J. Chem. Soc.*, **1960**, 1735.

58) R. S. Mulliken, *J. Chem. Phys.*, **33**, 1596 (1960).

59) The possible existence of cyclohexene-silver fluoborate is anticipated.

TABLE XII. ELECTRONIC TRANSITION ENERGIES (IN eV.) OF CYCLOHEXENE AND ETHYLENE WITH VIBRATIONAL PROGRESSIONS (IN PARENTHESES, IN cm^{-1})

	V_{peak}	R_{OO}	T_R	T_{peak}
Cyclohexene	6.79	5.92 (1450)	4.9 (900)	3.8 (1200~1300)
Ethylene[27,57,58]	7.65 (850)	7.11 (1375)	6.4 (1400)	4.6 (~1000)
Electronic configration and spin multiplicity of the upper state	$^1(12)$	$^1(13)$	$^3(13)$	$^3(12)$

have been measured under various conditions. A new band has been found in the 220~230 mμ region for the complex in an aqueous solution; it has been found to have the mixing character of the charge-transfer from the olefin to the metal ion and of the Rydberg transition within the olefin molecule. The equilibrium constant (pK) has been evaluated spectrophotometrically as 0~−2 for the equilibrium

$$C_6H_{10} + Ag^+ \rightleftharpoons C_6H_{10}\cdots Ag^+$$

The 1653 cm^{-1} ν(C=C) and 716 cm^{-1} δ(=C–H) bands of pure cyclohexene have been found to shift to about 1585 and 745 cm^{-1} respectively by means of complex formation with silver perchlorate, both in solids and in solutions. This and other facts concerning the vibration spectrum of the complex show that the C=C bond is weakened by the complex formation.

The very selective complex formation ability of Cu^+, Ag^+ and Hg^{2+} toward monoölefins has been explained by the calculation in which we explicitly took into account the charge number, the ionization potential, the electron affinity, the ionic radius, the hydration (solvation) energy, and the various atomic excitation energies of the ions. It has been pointed out that the roles of the d-electrons of the metal ion and the 3sσ-electrons of the olefin molecule are important in the ground state and the lowest excited state respectively, while the effect of the hydration (or lattice) energy is important in both states.

The Institute for Solid State Physics
The University of Tokyo
Azabu, Tokyo

Appendix I

The Various Electronic States of Cyclohexene.—The 209 mμ (5.92 eV.) band of cyclohexene was found, on the longer wavelength side, to have progressions with a vibrational frequency interval of about 1450 cm^{-1}. This band may possibly be assigned to be the Rydberg transition (N→R) on the basis of a comparison with the 7.11 eV. band of ethylene with 1375 cm^{-1} spacing so assigned by Mulliken.[57,58] Potts[27] observed the N→V transition of cyclohexene at 183 mμ (6.79 eV.), but he undertook no vibrational analysis. By measuring the spectrum of pure liquid cyclohexene with 1 cm. and 10 cm. cells, we have observed two different kinds of vibrational progressions in the longer wavelength region, namely, one around 4.9 eV. with 900 cm^{-1} spacings and another around 3.8 eV. with 1200~1300 cm^{-1} spacings. The former and the latter have tentatively been assigned to the Rydberg triplet (T_R) and the $\pi\rightarrow\pi^*$ triplet transition (T) respectively on the basis of the expected parallelism with the ethylene bands. There are doubts, however, about this assignment, because the magnitudes of their spacings are quite the reverse of those for ethylene and cyclohexene. Both triplet bands show the expected O_2-intensification and N_2-weakening, the effect being more pronounced for the longer wavelength one. Table XII lists the observed four transition energies of cyclohexene, along with the assignment for ethylene bands by Mulliken.[58]

Appendix II

Tables of Overlap Integrals.—The overlap integrals of the S(3s, 3s), S(3s, 5s) and S(2pπ, 5pπ) types were calculated according to the standard method.[35-37,60] The results are shown in Table XIII—XV.

TABLE XIII. S(3s, 3s)

p	t=0	t=0.125	t=0.25	t=0.5
0.0	1.000	0.946	0.798	0.365
1.0	0.968	0.918	0.780	0.369
2.0	0.885	0.846	0.734	0.375
2.5	0.832	0.800	0.703	0.377
3.0	0.772	0.746	0.666	0.378
3.5	0.708	0.688	0.624	0.376
4.0	0.641	0.626	0.576	0.370
4.5	0.672	0.563	0.528	0.360
5.0	0.504	0.499	0.475	0.345
5.5	0.438	0.437	0.424	0.330
6.0	0.375	0.376	0.372	0.311
7.0	0.264	0.269	0.277	0.267
8.0	0.177	0.183	0.197	0.221
9.0	0.114	0.119	0.135	0.177
10.0	0.070	0.075	0.089	0.138

Appendix III

The Evaluation of Overlap Integral, Including d- and p-Orbitals with Distorted Conformation.—

60) M. Kotani, A. Amemiya and T. Simose, *Proc. Math. Soc. Japan*, **20**, Extra No. 1, 1 (1938); M. Kotani, A. Amemiya, E. Ishiguro and T. Kimura, "Table of Molecular Integrals," Maruzen Co., Tokyo (1955).

TABLE XIV. $S(3s, 5s)$

p	t						
	−0.5	−0.25	−0.125	0	0.125	0.25	0.5
0.0	0.513	0.933	0.996	0.935	0.775	0.560	0.171
0.5	0.512			0.930			0.173
1.0	0.510	0.910	0.961	0.914	0.759	0.566	0.178
1.5	0.506			0.888			0.186
2.0	0.502	0.850	0.900	0.855	0.730	0.555	0.196
2.5	0.496			0.816			0.208
3.0	0.489	0.767	0.806	0.772	0.681	0.540	0.220
3.5	0.479			0.724			0.231
4.0	0.467	0.670	0.693	0.672	0.610	0.511	0.241
4.5	0.453			0.618			0.249
5.0	0.435	0.565	0.576	0.562	0.527	0.464	0.254
5.5				0.505			
6.0	0.391	0.457	0.456	0.448	0.432	0.401	0.256
6.5				0.393			
7.0	0.340	0.354	0.346	0.340	0.333	0.330	0.246
7.5				0.291			
8.0	0.285	0.262	0.249	0.246	0.252	0.259	0.226
9.0	0.232	0.187	0.173	0.170	0.179	0.195	0.201
10.0	0.183	0.128	0.114	0.112	0.122	0.141	0.172
12.0		0.055	0.045	0.044	0.051	0.066	
14.0		0.021	0.016	0.015	0.019	0.028	
16.0		0.008	0.005	0.005	0.006	0.011	

TABLE XV. $S(2p\pi, 5p\pi)$

p	t						
	−0.5	−0.25	−0.125	0	0.125	0.25	0.5
0.0	0.802	0.973	0.891	0.732	0.539	0.350	0.089
0.5	0.794			0.726			0.090
1.0	0.770	0.931	0.855	0.707	0.525	0.346	0.091
1.5	0.731	0.883		0.677		0.341	0.093
2.0	0.681	0.812	0.755	0.635	0.484	0.330	0.095
2.5	0.622	0.736		0.584		0.316	0.096
3.0	0.559	0.652	0.612	0.526	0.416	0.296	0.097
3.5	0.494	0.569		0.464		0.275	0.096
4.0	0.431	0.483	0.455	0.401	0.330	0.249	0.094
4.5	0.371	0·405		0.341		0.223	0.091
5.0	0.316	0.336	0.316	0.284	0.245	0.196	0.087
5.5	0.266	0.287		0.234		0.170	0.082
6.0	0.223	0.218	0.205	0.189	0.170	0.125	0.076
6.5				0.151			
7.0	0.152	0.135	0.127	0.119	0.113	0.103	0.064
7.5				0.093			
8.0	0.102	0.081	0.075	0.072	0.071	0.069	0.052
8.5				0.055			
9.0	0.067	0.047	0.042	0.041	0.043	0.045	0.041
9.5				0.030			
10.0	0.043	0.026	0.023	0.023	0.025	0.028	0.031

For evaluating the matrix elements, we need to estimate the overlap integrals involving d- and p-orbitals in the assumed geometrical conformation of the complex. Let us consider the case in which the two xz planes of the metal (M) and carbon (C) atoms coincide with each other and in which the line (MC) joining the atoms is inclined at an angle α to the z axis. The overlap integrals for the various combinations shown in Fig. 10 between the d-orbitals of the atom M and the p_z-orbital of the atom C are expressed as linear combinations of $S(\sigma, \sigma)$ and $S(\pi, \pi)$ forms for which published

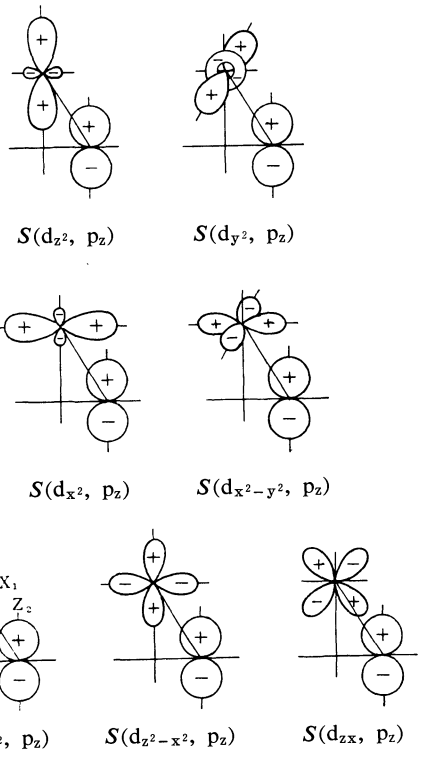


Fig. 10. Various combinations of the d-orbitals of a metal atom and the p_z orbital of a carbon atom.

tables[35-37] are available. The results are as follows:

$$S(d_{x^2}, 2p_z) = -1/4 \cdot \cos\alpha (3\cos 2\alpha - 1) \cdot S(d\sigma, 2p\sigma) - \sqrt{3}/2 \cdot \sin\alpha \cdot \sin 2\alpha \cdot S(d\pi, 2p\pi)$$

$$S(d_{y^2}, 2p_z) = -1/2 \cdot \cos\alpha \cdot S(d\sigma, 2p\sigma)$$

$$S(d_{z^2}, 2p_z) = 1/4 \cdot \cos\alpha (3\cos 2\alpha + 1) \cdot S(d\sigma, 2p\sigma) - \sqrt{3}/2 \cdot \sin\alpha \cdot \sin 2\alpha \cdot S(d\pi, 2p\pi)$$

$$S(d_{x^2-y^2}, 2p_z) = \sqrt{3}/4 \cdot \sin\alpha \cdot \sin 2\alpha \cdot S(d\sigma, 2p\sigma) + 1/2 \cdot \sin\alpha \cdot \sin 2\alpha \cdot S(d\pi, 2p\pi)$$

$$S(d_{y^2-z^2}, 2p_z) = -\sqrt{3}/2 \cdot \cos^3\alpha \cdot S(d\sigma, 2p\sigma) + 1/2 \cdot \sin\alpha \cdot \sin 2\alpha \cdot S(d\pi, 2p\pi)$$

$$S(d_{z^2-x^2}, 2p_z) = \sqrt{3}/2 \cdot \cos\alpha \cdot \cos 2\alpha \cdot S(d\sigma, 2p\sigma) - \sin\alpha \cdot \sin 2\alpha \cdot S(d\pi, 2p\pi)$$

$$S(d_{xy}, 2p_z) = S(d_{yz}, 2p_z) = 0$$

$$S(d_{zx}, 2p_z) = \sqrt{3}/2 \cdot \cos\alpha \cdot \cos 2\alpha \cdot S(d\sigma, 2p\sigma) + \sin\alpha \cdot \cos 2\alpha \cdot S(d\pi, 2p\pi)$$

It should be emphasized here that, unlike the p-orbitals, the d-orbitals are not vectoricaly decomposed into their x, y and z components; some authors[61] have wrongly evaluated the overlap integrals involving d-orbitals with distorted conformations. General formulations, their derivations, and the necessity for using auxiliary d_{x^2}, d_{y^2}, $d_{y^2-z^2}$ and $d_{z^2-x^2}$ functions will be described elsewhere.[62]

61) D. A. Brown, *J. Chem. Phys.*, 33, 1037 (1960).
62) H. Hosoya, *Tech. Rept. ISSP* (The Institute for Solid State Physics, the University of Tokyo), Ser. B, to be published.

Synthetic Studies of the Flavone Derivatives. III.[1] *The Synthesis of 3, 7-Dimethoxy-5, 6 ; 3', 4'-bismethylenedioxyflavone, an Isomer of Meliternatin*

By Kenji FUKUI, Takashi MATSUMOTO and Sachiko MATSUZAKI

(Received September 12, 1963)

In a previous paper,[1] meliternatin (I)' which had been isolated from the bark of *Melicope ternata* by Briggs and Locker,[2] was synthesized. In this case, I was obtained from a ketone which had been prepared with the Hoesch condensation of 3-methoxy-4, 5-methylenedioxyphenol and methoxyacetonitrile. The structure of the ketone was expected to be either 2-hydroxy-6, ω-dimethoxy-4, 5-methylenedioxyacetophenone (II) or 2-hydroxy-4, ω-dimethoxy-5, 6-methylenedioxyacetophenone (III). According to the Allan and Robinson method, a flavone was prepared with piperonylic anhydride from the ketone. If the structure of the ketone is II, the flavone must 3, 5-dimethoxy-6, 7 ; 3', 4'-bismethylenedioxyflavone (I), which has been proposed by Briggs et al[3] as the structure of meliternatin. An unambiguous synthesis of 3, 7-dimethoxy-5, 6 ; 3', 4'-bismethylenedioxyflavone (IV) must be made in order to settle this question. In the present paper, therefore, the synthesis of IV is described.

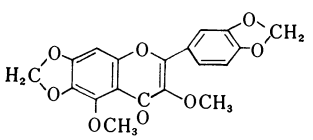
The treatment of 6-hydroxy-3, 5, 7-trimethoxy-3', 4'-methylenedioxyflavone (V)[4] with anhydrous aluminum chloride afforded a demethyl compound, which gave a dark green color ferric

1) K. Fukui and T. Matsumoto. This Bulletin, **36**, 806 (1963).
2) L. H. Briggs and R. H. Locker, *J. Chem. Soc.*, **1949**, 2157.

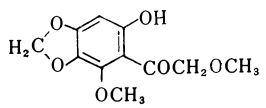
chloride reaction and a diacetate. It is well known that the demethylation of flavonols under the above-mentioned condition occurs at the 5-position[3-7] or occasionally at the 3-position.[3] Therefore, this demethyl compound should be either 5, 6-dihydroxy-3, 7-dimethoxy-3' 4'-methylenedioxyflavone (VI) or 3, 6-dihydroxy-5, 7-dimethoxy-3', 4'-methylenedioxyflavone (VII). As the compound was methylated with diazomethane to yield melisimplin (VIII; 5-hydroxy-3, 6, 7-trimethoxy-3', 4'-methylenedioxyflavone),[4,8,9] it is clear that the demethyl compound has one hydroxy group at the 5-position which is not methylated with diazomethane. On the basis of this result, VI is postulated as its structure.

VI has previously been prepared;[9] our product differs in melting point from that previously reported, but the color reaction with ferric chloride, the elementary analysis and the infrared spectrum (hydroxy bands, 3615 and 3483; carbonyl band, 1659; methylenedioxy band, 926 cm^{-1}) all confirm our assignment of structure to the material. Therefore, the preparation of VI from 2, 5-dihydroxy-4, ω-dimethoxyacetophenone (IX) via the intermediates, 6-hydroxy-3, 7-dimethoxy-3', 4'-methylenedioxyflavone (X) and 5-formyl-6-hydroxy-3, 7-dimethoxy-3', 4'-methylenedioxyflavone (XI), according to the published procedure,[9] was reexamined. The VI obtained was identified with the above demethyl compound by a mixed melting point determination and by an infrared spectral comparison. The melting points of some compounds (VI, X and XI) differed from those previously reported,[9] as is shown in the Experimental section.

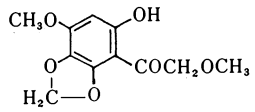
The methylenation of VI with methylene iodide afforded 3, 7-dimethoxy-5, 6; 3', 4'-bismethylenedioxyflavone (IV). IV did not agree



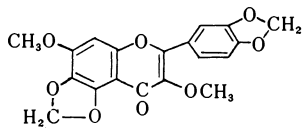
(I)



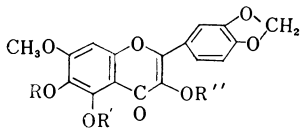
(II)



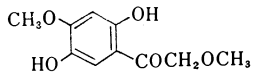
(III)



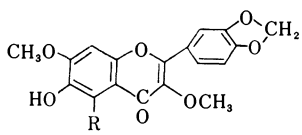
(IV)



(V) R=H R'=R''=CH_3
(VI) R=R'=H R''=CH_3
(VII) R=R''=H R'=CH_3
(VIII) R'=H R=R''=CH_3



(IX)



(X) R=H
(XI) R=CHO

with meliternatin in its properties. The structure of meliternatin has, therefore, been established as 3, 5-dimethoxy-6, 7; 3', 4'bismethylenedioxyflavone (I).[1,2]

Experimental*

2,5-Dihydroxy-4, ω-dimethoxyacetophenone (IX). —This ketone was prepared by a method reported in the literature;[10] m. p. 148~149°C (reported m. p. 145~146°C[10]).

6-Hydroxy-3, 7-dimethoxy-3', 4'-methylenedioxyflavone (X).—From the ketone IX, X was obtained in the form of colorless needles according to a procedure previously reported[9]; m. p. 253~254°C (reported m. p. 213~214°C[9]). X gave a negative ferric chloride reaction in ethanol. IR: 3384(OH), 1624(C=O), 1037(=C-O-C), 929 (O-CH_2-O) cm^{-1}.

Found: C, 62.94; H, 4.14. Calcd. for $C_{15}H_{14}O_7$: C, 63.16; H, 4.12%.

The acetylation of X gave the acetate (m. p. 201~202°C, reported m. p. 202°C[9]) in the form of colorless rectangular plates. IR: 1757(OAc), 1621 (C=O), 1037(=C-O-C), 934 (O-CH_2-O) cm^{-1}.

3) L. H. Briggs and R. H. Locker, ibid., **1951**, 3131.
4) L. H. Briggs and R. H. Locker, ibid., **1950**, 2379.
5) W. Baker, ibid., **1939**, 961.
6) W. Baker, N. C. Brown and J. A. Scott, ibid., **1939**, 1925.
7) W. Baker and W. H. C. Simmonds, ibid., **1940**, 1373.
8) L. H. Briggs and R. H. Locker, ibid., **1950**, 2376.
9) A. C. Jain, T. R. Seshadri and K. R. Sreenivasan, ibid., **1955**, 3908.

* All melting points are uncorrected; the infrared spectra were measured in Nujol.
10) L. R. Row and T. R. Seshadri, *Proc. Indian Acad. Sci.*, **21A**, 155 (1945).

Found: C, 62.57; H, 4.26. Calcd. for $C_{20}H_{16}O_8$: C, 62.50; H, 4.20%.

5-Formyl-6-hydroxy-3, 7-dimethoxy-3', 4'-methylenedioxyflavone (XI).—From the flavone X, XI was obtained in the form of yellow needles according to a procedure previously reported;[9] m. p. 262～263°C(decomp.) (reported m. p. 248～249°C[9]). XI gave a brown ferric chloride reaction in ethanol. IR: 1647, 1619(C=O), 1038(=C-O-C), 929 (O-CH_2-O) cm^{-1}.

Found: C, 61.39; H, 3.99. Calcd. for $C_{19}H_{14}O_8$: C, 61.62; H, 3.81%.

5, 6-Dihydroxy-3, 7-dimethoxy-3', 4'-methylenedioxyflavone (VI).—*a) From 6-Hydroxy-3, 5, 7-trimethoxy-3', 4'-methylenedioxyflavone (V).*—A solution of V[4] (1.0 g.) and anhydrous aluminum chloride (13.5 g.) in anhydrous ether (60 ml.) was refluxed for 10 hr. After the reaction mixture had been poured into ice-water and kept for several hours at room temperature, the precipitate was collected and refluxed with a solution of acetic acid (55 ml.) and concentrated hydrochloric acid (30 ml.) for 20 min. The resulting precipitate was collected and recrystallized from ethanol to give VI in the form of yellow needles (m. p. 187～188°C) (reported m. p. 218～219°C[9]), which gave a dark green ferric chloride reaction in ethanol; yield, 0.4 g. IR: 3615, 3483(OH), 1659(C=O), 1035(=C-O-C), 926 (O-CH_2-O) cm^{-1}.

Found: C, 60.34; H, 4.03. Calcd. for $C_{18}H_{14}O_8$: C, 60.34; H, 3.94.

The acetylation of VI gave the acetate (m. p. 231～233°C) (reported m. p. 226～227°C[9]), which gave a negative ferric chloride reaction in ethanol. IR: 1771(OAc), 1631(C=O), 1032(=C-O-C), 925 (O-CH_2-O) cm^{-1}.

Found: C, 59.76; H, 4.16. Calcd. for $C_{22}H_{18}O_{10}$: C, 59.73; H, 4.10%.

b) From 5-Formyl-6-hydroxy-3, 7-dimethoxy-3', 4'-methylenedioxyflavone (XI).—From the aldehyde XI, VI was prepared in the form of yellow needles (m. p. 187～188°C) according to a procedure previously reported.[9] This substance was identified with a specimen, prepared by the above-mentioned method a), by a mixed melting point determination and by an infrared spectral comparison.

Milisimplin (VIII).—The treatment of VI (60 mg.) in acetone (20 ml.) with an ethereal solution of diazomethane gave VIII as yellow needles (m. p. 233～234°C) (reported m. p. 234～235°C[9] and 235～236°C[4,8]) from ethyl acetate; yield, 20 mg. This substance gave a green ferric chloride reaction in ethanol. IR: 1667(C=O), 1037(=C-O-C), 925 (O-CH_2-O) cm^{-1}.

Found: C, 61.08; H, 4.36. Calcd. for $C_{19}H_{16}O_8$: C, 61.29; H, 4.33%.

3, 7-Dimethoxy-5, 6; 3', 4'-bismethylenedioxyflavone (IV).—A mixture of VI (350 mg.), methylene iodide (1.1 g.) and anhydrous potassium carbonate (4.0 g.) in anhydrous ethyl methyl ketone (50 ml.) was refluxed for 26 hr. on a steam bath. The reaction mixture was filtered from the precipitates, and ethyl acetate (70 ml.) was added to the filtrate. The solution was washed with a 5% aqueous sodium hydroxide solution and then with water. The solvent was distilled off, and the residue was recrystallized from acetone and then from aqueous acetic acid to give IV in the form of pale yellow needles (m. p. 233～234°C), which gave a negative ferric chloride reaction in ethanol: yield, 60 mg. IR: 1650～1643 (C=O), 1041 (=C-O-C), 930 (O-CH_2-O) cm^{-1}.

Found: C, 61.33; H, 3.99. Calcd. for $C_{19}H_{14}O_8$: C, 61.62; H, 3.81%.

The authors are grateful to Professor Tetsuo Mitsui of Kyoto University for his microanalyses. This work was supported in part by a grant-in-aid from the Ministry of Education.

Department of Chemistry
Faculty of Science
Hiroshima University
Higashi-Sendamachi, Hiroshima

Stability Order in Metal Chelate Compounds. II.[1] *5-(p-Sulfophenylazo)-salicylate Complexes**

By Yukito MURAKAMI and Makoto TAKAGI

(Received September 16, 1963)

In accordance with the work reported, up to the present time it is understood that the stability of metal chelate compounds and their stability order with respect to nuclear metal atoms are functions of the geometrical and electronic structures of a ligand molecule and of the character of the resultant coördinate bonds as well.

In continuation of an investigation which may contribute to the clarification of these relationships, 5-(*p*-sulfophenylazo)-salicylic acid has been used as a chelating agent in the present work. Recently, 5-(*p*-sulfophenylazo)-salicylic acid was employed as a reagent to detect the presence of magnesium,[2] aluminum, beryllium,[3] gallium and indium[4] for analytical purposes; nevertheless, no quantitative study of the interaction of this ligand with any metal ion has been reported up to the present time.

Since the stability constants of metal-salicylate and metal-5-sulfosalicylate complexes have been evaluated,[5-7] the substituent effect of the *p*-sulfophenylazo group, which is situated at the 5-position in the parent molecule, on the chelate formation may be compared with those of other substituents among the chelate derivatives.

Experimental

5-(*p*-Sulfophenylazo)-salicylic Acid.—The coupling reaction of the diazotized sulfanilic acid with salicylic acid in equimolar amounts was carried out in alkaline aqueous media. Acidification of the reaction mixture with hydrochloric acid resulted in the formation of a precipitate. This precipitate was then recrystallized several times from water or aqueous ethanol, giving a 90% yield of yellow-orange needles. These fine crystals were found to be the dihydrated monosodium salt of 5-(*p*-sulfophenylazo)-salicylic acid (I), which was dehydrated above 180°C and decomposed above 250°C. The estimated molecular weight was 380.7 by potentiometric titration (calcd. 380.3).

Found: C, 41.06; H, 3.55; N, 7.44. Calcd. for $C_{13}H_{13}N_2O_8SNa$ (dihydrate): C, 41.05; H, 3.44; N, 7.36%.

The dihydrate form I was transformed to the corresponding monohydrate at 110°C under reduced pressure (5 mmHg); it was also identified by reductive cleavage to sulfanilic acid and 5-aminosalicylic acid.

The synthesized material I was used to prepare a stock solution for potentiometric titrations after the establishment of the purity by means of potentiometric titration with a standard base.

Metal Solutions.—The bivalent metal nitrates, $Zn(NO_3)_2 \cdot 6H_2O$, $Cu(NO_3)_2 \cdot 3H_2O$, $Ni(NO_3)_2 \cdot 6H_2O$, $Co(NO_3)_2 \cdot 6H_2O$, $Mg(NO_3)_2 \cdot 6H_2O$, $Ca(NO_3)_2 \cdot 4H_2O$, and manganese sulfate, $MnSO_4 \cdot nH_2O$, of analytical grade were purchased from the Wako Pure Chemical Industries, Ltd. The nona-hydrated ferric nitrate, $Fe(NO_3)_3 \cdot 9H_2O$, was a pure grade reagent of the same company. Aqueous stock solutions of these metal salts were standardized for metal ion concentration by the usual procedures of chelatometric titration.

Potentiometric Measurements.—The apparatus and procedures for potentiometric measurements have been mentioned elsewhere.[8] In the present work, the temperature and ionic strength of a titrating solution were maintained, respectively, at 25.0 $\pm$0.1°C and 0.10 M with potassium nitrate. Since the solubility of the ligand in aqueous media at μ=0.10 M in potassium nitrate was observed to be very low, the ligand concentration for potentiometric measurements had to be maintained in a relatively low range (approximately 2×10^{-3} M or less). The measurement of each metal chelate system was checked by repeated titrations to avoid any significant error which might be caused by the low concentration of the system.

Calculation of Acid Dissociation Constants.—The dissociation constants of the dibasic acid I are defined as follows:

$$K_{H_2L}=\frac{[H^+][HL^{2-}]}{[H_2L^-]}, \qquad K_{HL}=\frac{[H^+][L^{3-}]}{[HL^{2-}]}$$

These constants were evaluated in a manner similar to that mentioned in a previous paper.[1]

* Contribution No. 53 from the Department of Organic Synthesis, Faculty of Engineering, Kyushu University.

1) Part I: Y. Murakami, K. Nakamura and M. Tokunaga, This Bulletin, 36, 669 (1963).

2) I. M. Korenman and E. I. Levina, *Uchenye Zapiski Gor'kovsk. Gosudarst. Univ. im. N. I. Labachevskogo, Ser. Khim.*, **1958**, No. 32, 149; *Chem. Abstr.*, **54**, 5339 (1960).

3) N. Appala Raju and K. Neelakantam, *Current Sci. (India)*, **29**, 52 (1960); *Chem. Abstr.*, **54**, 17152 (1960).

4) M. Z. Yampol'skii, *Trudy Komissii Anal. Khim., Akad. Nauk S. S. S. R., Inst. Geokhim. i Anal Khim.*, **11**, 5 (1960); *Chem. Abstr.*, **55**, 11177 (1961).

5) J. Bjerrum, G. Schwarzenbach and L. G. Sillén, "Stability Constants, Part I, Organic Ligands," The Chemical Society, London (1957).

6) D. D. Perrin, *Nature*, **182**, 741 (1958).

7) C. V. Banks and R. S. Singh, *J. Inorg. Nucl. Chem.*, **15**, 125 (1960).

8) Y. Murakami, This Bulletin, 35, 52 (1962).

TABLE I. ACID DISSOCIATION CONSTANTS OF SALICYLIC ACID AND ITS DERIVATIVES

Ligand	5-(*p*-Sulfophenylazo)-salicylic acid	5-Sulfosalicylic acid[6,7]		Salicylic acid[6]
μ	0.10	0.1	0.15	0.15
t°C	25.0 ±0.1	25	20	20
pK_{H_2L}	2.38±0.02	2.49	2.62	2.98
pK_{HL}	11.04±0.02	12.00	11.95	13.61

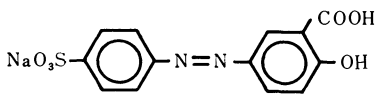
The Calculation of Stability Constants.—Because of the hydrolytic behavior of the chlates of nickel(II), cobalt(II) and manganese(II), only potentiometric data of a limited range were used for the evaluation of the stability constants of these chelate systems. Such ranges were: 6~9.5, 6~9.5 and and 7~9.3 in $-\log[H^+]$; up to 1.35, 1.30 and 0.85 in $\bar{n}$-value* for nickel(II), cobalt(II) and manganese(II) respectively. No such limitations were required for alkaline earth metal chelates, even though an $\bar{n}$-value did not exceed 1.3 over the whole pH range studied. In these regions of $\bar{n}$-value, the main chelate species existing in the system were considered to be the 1 : 1 and 2 : 1 (lignd to metal) chelates. Therefore, the stability constants for each chelate system were evaluated in accordance either of two methods, namely, (1) the intersection method[1,8] or (2) the lineation method.[8] The two stability constants, K_1 and K_2, are defined as follows:

$$K_1=\frac{[ML]}{[M][L]}, \qquad K_2=\frac{[ML_2]}{[ML][L]}$$

On the other hand, the $\bar{n}$-value already exceeded 1.2 at a=0** in the potentiometric titration of the iron(III) chelate system. Thus, the only stability constant evaluated was for the 2 : 1 chelate.

Results and Discussion

Acid Dissociation Constants. — A titration curve of the monosodium salt of 5-(*p*-sulfophenylazo)-salicylic acid (II) is shown in Fig. 3.



II

The titrating solution was pale yellow-orange below a=1 and became reddish in the region beyond a=1, where the reddish color deepened as the pH increased. The first dissociation process is clearly separated from the second; thus the carboxy-proton of the ligand is very acidic in comparison with the phenol-proton. The acid dissociation constants of ligand II evaluated in this work are shown in Table I, together with those of 5-sulfosalicylic acid[6,7] and of salicylic acid.[6] Both K_{H_2L} and K_{HL} values vary in a parallel manner among these ligands, and the acidity increases in the order: salicylic acid<5-sulfosalicylic acid<5-(*p*-sulfophenylazo)salicylic acid. Therefore, a *p*-sulfophenylazo group seems to be a more effective substituent in electron-withdrawing effect than a sulfonate group. Judging from these observations, a phenylazo group may transmit the electron-withdrawing effect of the para sulfonate group through resonance interaction and withdraw an electron from the salicylate group as well.

Interaction of Bivalent Metal Ions with 5-(*p*-Sulfophenylazo)-salicylate. — Titration curves are illustrated in Figs. 1 and 2 for the 5-(*p*-sulfophenylazo)-salicylate chelate systems of manganese(II), cobalt(II), nickel(II), zinc(II), magnesium(II) and calcium(II) for 10 : 1 and 4 : 1 molar ratios of ligand to metal ion.

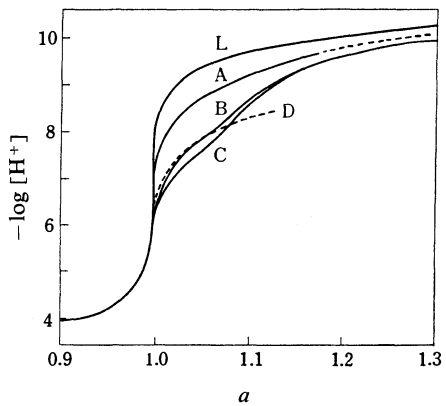


Fig. 1. Potentiometric titration of bivalent metal chelates of 5-(*p*-sulfophenylazo)-salicylate at total ligand concentration of 2.03×10^{-3} M with 10 : 1 molar ratio of ligand to metal ion: A, Mn; B, Co; C, Ni; D, Zn; L, ligand alone; a=moles of base added per mole of ligand; t=25°C; μ=0.10 M (KNO_3). Dotted lines represent non-equilibrated titration.

Since 5-(*p*-sulfophenylazo)-salicylate is considered to be a bidentate ligand, at most three moles of the ligand per mole of metal ion would be enough to satisfy the coördination sites of these bivalent metal ions. However, potentiometric titrations in the present work were carried out with an excess of the ligand

* n is referred to the Bjerrum formation function.
** a stands for the amount of base added per mole of ligand.

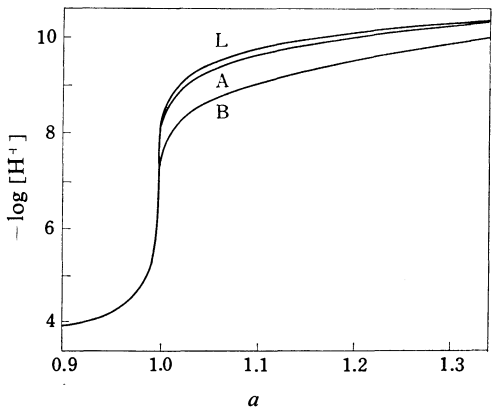


Fig. 2. Potentiometric titration of bivalent metal chelates of 5-(*p*-sulfophenylazo)-salicylate at total ligand concentration of 2.03×10^{-3} M with 4 : 1 molar ratio of ligand to metal ion: A, Ca; B, Mg; L, ligand alone; a=moles of base added per mole of ligand; t=25°C; μ=0.10 M (KNO_3).

in an attempt to avoid as much as possible both disproportionation and hydrolysis of metal chlates in a higher pH region.

Manganese(II), Cobalt(II), Nickel(II) and Zinc(II). — All the titration curves coincide well with that of the ligand alone in the lower buffer region, $a=0\sim1.0$, as is shown in Fig. 1. Thus, the only significant chemical process occurring in this region is the dissociation of a carboxyl-proton.

The depression of titration curves was observed beyond an a-value of 1.0 in comparison with the titration curve of the ligand alone. Such a depression became noticeable at pH 6.0 and above for cobalt(II) and nickel(II), and above pH 7.0 for manganese(II), as may be seen in Fig. 1. It is obvious that ligand II undergoes chelation with these bivalent metal ions in these higher pH regions. A small inflection region, which corresponds to the formation of a 1 : 1 chelate, was observed at $a=1.1$ for the nickel(II) chelate system and less significantly for the cobalt(II). Judging from the extent of the depression of titration curves among these bivalent metal chelate systems, the stability order with respect to metal ions is: manganese(II) < cobalt(II) < nickel(II). Meanwhile, the hydrolytic tendency of these metal chelates was found to be significant beyond $a=1.18$ for manganese(II) and beyond $a=1.3$ for cobalt(II) and nickel(II) in a manner similar to these observed for the salicylate and 5-sufosalicylate chelates of the same bivalent metals.[6,7]

Such hydrolytic behavior was much pronounced for the zinc(II) chelate system, and a pH drifting became significant in the region immediately beyond $a=1.0$. Further addition of a base resulted in the gradual formation of a precipitate. It seems, therefore, that the zinc chelate is much less stable than the corresponding cobalt and nickel chelates, since the hydrolytic tendency of zinc(II) was found to be comparable with these of cobalt(II) and nickel(II) ions.* On the other hand, the greater hydrolytic behavior** of the zinc(II) ion than that of the manganese(II) ion is responsible for the precipitation in the lower pH range, where the manganese chelate system did not form a precipitate.

Copper(II). — Titration of the copper(II) chelate system was carried out at various molar ratios of ligand to metal ion, ranging from 1 : 1 to 10 : 1 under the same experimental conditions as employed for other bivalent metal chelate systems. An appreciable pH-depression was observed, even in the a-range below 1.0. Equilibrium of the system was reached in a short period of time in a limited initial range of titration with a base; nevertheless, equilibrated potentiometric data were not obtained over most of the pH range studied due to the sluggish pH-drifting. Such a drifting tendency became increasingly pronounced as the pH was raised, even though no precipitate was noticed throughout the titration. Since the hydrolysis of copper ion alone is not significant in the lower pH region[9,10] the slow rate of the equilibration of the chelate system is conceivably due to the sluggish formation of chelate species. Because of such complex behavior of the copper chelate system, no quantitative interpretation of the data was possible.

Magnesium(II) and Calcium(II). — Neither drifting of pH nor precipitation was observed throughout the titration. These bivalent metal ions and the ligand undergo chelation in the region beyond $a=1.0$, as may be seen in Fig. 2. Both alkaline earth metal ions form much less stable chelates than the transition metal ions.

Interaction of Iron(III) with 5-(*p*-Sulfophenylazo)-salicylate. — Titration of a solution containing a 4 : 1 molar ratio of ligand to metal ion resulted in a large pH depression over the whole pH range and in two steep inflections, at 1.50 and 1.75, in a-value, as is shown in Fig. 3. No precipitate was observed at any time during the titration. The

* The estimated hydrolysis constants for zinc(II), cobalt(II) and nickel(II) are 8.7, 8.9 and 9.4 respectively in pK unit, at 30°C and μ=0.1 (S. Chaberek, Jr., R. C. Courtney and A. E. Martell, *J. Am. Chem. Soc.*, **74**, 5057 (1952)).

** The thermodynamic hydrolysis constants for zinc(II) and manganese(II) ions were 8.96±0.03 and 10.59±0.04 respectively in pK unit, at 25°C (D. D. Perrin, *J. Chem. Soc.*, **1962**, 2197, 4500).

9) C. Berecki-Biedermann, *Arkiv. Kemi*, **9**, 175 (1956).
10) D. D. Perrin, *J. Chem. Soc.*, **1960**, 3189.

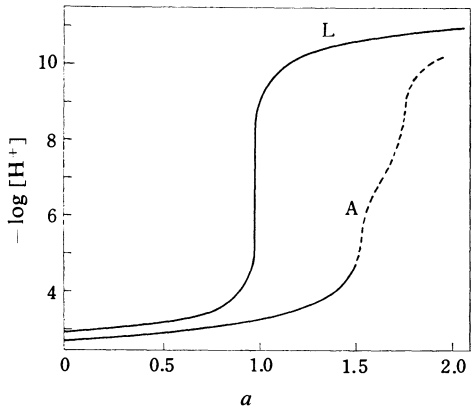


Fig. 3. Potentiometric titration of Fe(III)-5-(*p*-sulfophenylazo)-salicylate chelate system at total ligand concentration of 2.03×10^{-3} M with 4 : 1 molar ratio of ligand to metal ion: A, Fe; L, ligand alone; a=moles of base added per mole of ligand; t=25°C; μ=0.10 M (KNO_3). Dotted curve represents non-equilibrated titration.

former inflection corresponds to the formation of the 2 : 1 chelate, in addition to the liberation of a carboxy-proton of the uncoördinated ligand, while the latter most probably corresponds to the formation of the 3 : 1 chelate. Such a profound pH depression is to be ascribed to the greater stability of iron(III) chelates in comparison with that of other bivalent metal chelates. Similar results were obtained for the salicylate and 5-sulfosalicylate chelates.[6]

On the other hand, the sluggish pH drifting in the region beyond a=1.5 precludes the quantitative analysis of the chelating behavior of the system. Since 5-(*p*-sulfophenylazo)-salicylate demonstrated a strong affinity to ferric ion, the slow rate of the chelate formation would be responsible for such a pH drifting, and neither a hydrolytic reaction nor other complex reactions of the chelates would be the significant account. A similar conclusion was reached concerning the sluggish equilibration of the 4-sulfocatechol-iron(II) chelate system.[11]

The development of the deeper color for the ferric chelate system than for the ligand alone also provides evidence for the strong interaction of ferric ion with the ligand. The titrating solution was dark brownish in the lower buffer region (a<1.0). A reddish color gradually developed in the solution on approaching to the first inflection region, and this was further deepened as the pH was raised. However, the intensity of this reddish color gradually diminished in the second inflection region, and more apparently as the pH increased further. The hydrolysis of the chelate system, which may proceed extensively in this higher pH region, is most probably the cause of this color-fading.

Stability Constants.—The stability constants for the 5-(*p*-sulfophenylazo)-salicylate, as well as for the salicylate and 5-sulfosalicylate chelates, are listed in Table II. The stability order of these chelates in K_1 with respect to the ligands is shown in the increasing order: 5-(*p*-sulfophenylazo)-salicylate < 5-sulfosalicylate < salicylate. The decreased basicity of the donor group of the present ligand is responsible for the lower stability. The slightly greater

Table II. Stability constants of the metal salicylates

Ligand		5-(*p*-Sulfophenylazo)-salicylic acid	5-Sulfosalicylic acid[6,7]		Salicylic acid[6]
μ		0.10	0.1~0.15	0.15	0.15
t°C		25.0±0.1	25	20	20
Mn(II)	$\log K_1$	4.94±0.02	5.24	5.10	5.90
	$\log K_2$	3.5 ±0.1	3.00	2.90	3.9
Fe(II)	$\log K_1$	—	—	5.90	6.55
	$\log K_2$	—	—	<4.0	4.7
Co(II)	$\log K_1$	5.84±0.02	6.13	6.00	6.75
	$\log K_2$	3.93±0.02	3.69	3.60	4.7
Ni(II)	$\log K_1$	6.17±0.02	6.42	6.30	6.95
	$\log K_2$	4.05±0.03	3.82	3.90	4.8
Cu(II)	$\log K_1$	—	9.52	9.50	10.60
	$\log K_2$	—	6.93	6.80	7.85
Zn(II)	$\log K_1$	—	—	6.05	6.85
	$\log K_2$	—	—	<4.6	—
Mg(II)	$\log K_1$	4.45±0.02			
	$\log K_2$	3.04±0.1			
Ca(II)	$\log K_1$	3.10±0.03			
Fe(III)	$\log K_1$	—	—	14.60	16.35
	$\log K_2$	10.70±0.02	—	10.55	11.90

11) Y. Murakami and K. Nakamura, This Bulletin, **36**, 1408 (1963).

values of K_2 for the 5-(*p*-sulfophenylazo)-salicylate chelates than those for the corresponding 5-sulfosalcylate chelates are rather unexpected.

The stability order with respect to the bivalent metal ions in the present work may be put foward in an increasing manner as follows: calcium(II) < magnesium(II) < manganese(II) < (zinc(II)) < cobalt(II) < nickel(II) < (copper(II)). By referring to other analogous metal chelates listed in Table II, the following general stability order with respect to the bivalent transition metals may be afforded: manganese(II) < iron(II) < zinc(II) ~ cobalt(II) < nickel(II) < copper(II). Zinc(II) is placed below nickel(II) in stability, contrary to what was observed for the catechol chelates.

The pronounced color-deepening effect of the iron(III) chelate system indicates a strong electronic interaction among the ligand molecules and the metal atom through the coördinate bonds.

Summary

The interaction of 5-(*p*-sulfophenylazo)-salicylic acid with zinc(II), copper(II), nickel(II), cobalt(II), manganese(II), magnesium(II), calcium(II) and iron(III) has been investigated in aqueous media at 25.0±0.1°C and the ionic strength of 0.10 M. The stability constants for the 1 : 1 and 2 : 1 (ligand to metal) chelates of nickel, cobalt, manganese and magnesium, and for the 1 : 1 calcium chelate, as well as for the 2 : 1 ferric chelate, have been evaluated, and the resulting stability order with respect to the bivalent metals has been found to follow the sequence: calcium(II) < magnesium(II) < manganese(II) < (zinc(II)) < copper(II) < nickel(II) < copper(II). The stability sequence, zinc(II) < nickel(II), is contrary to that observed for the catechol chelates.

A *p*-sulfophenylazo group demonstrated an electron-withdrawing effect, the magnitude of which was slightly greater than that of a sulfonate group. However, the effect of the former group on the chelate-stability has been found to be comparable with that of the latter.

The present salicylate derivative is also a good chelating agent for iron(III) ion, even though the chelate system somehow becomes involved in a higher pH range.

Department of Organic Synthesis
Faculty of Engineering
Kyushu University
Hakozaki, Fukuoka

The Electronic Structures and Spectra of Pentalene and Heptalene

By Takeshi NAKAJIMA, Yoshiko YAGUCHI, Ryoji KAERIYAMA* and Yuzo NEMOTO**

(Received September 25, 1963)

Recently Dauben and Bertelli[1] have reported the synthesis of the bicyclic nonbenzenoid aromatic hydrocarbon, heptalene (II), and discussed its physical and chemical properties. From the viewpoint of the molecular orbital theory, pentalene (I) is closely related to the hydrocarbon; pentalene has, however, so far defied synthesis, although the molecule has long been of interest since it was first postulated as a possible aromatic system by Armit and Robinson.[2] It should be noted that if the bridged bonds are disregarded, both these molecules are very similar to the planar cyclic polyenes with the general formula $C_{4n}H_{4n}$.

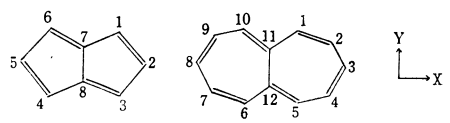


Fig. 1. Carbon skeleton, choice of axes, and numbering of pentalene and heptalene.

Early theoretical investigators,[3] presuming the molecular symmetry D_{2h} and using the simple MO and VB methods, have predicted appreciable π-electron delocalization energies for I and II and, on this basis, have suggested that the molecules may have a more or less

* Present address: Laboratory of Polymer Science, Tokyo Institute of Technology, Meguro-ku, Tokyo.
** Present address: Hitachi Chemical Co., Ltd., Chiyoda-ku, Tokyo.

1) H. J. Dauben, Jr. and D. J. Bertelli, *J. Am. Chem. Soc.*, **83**, 4659 (1961).

2) J. W. Armit and R. Robinson, *J. Chem. Soc.*, **121**, 827 (1922).

3) Reviewed by E. D. Bergmann, "Non-Benzenoid Aromatic Compounds," Ed. by D. Ginsburg, Interscience Publishers, New York (1959), p. 141. See also (a) B. Pullman and A. Pullman, "Les Théories Electroniques de la Chimie Organique," Masson, Paris (1952); and (b) C. A. Coulson and R. Daudel, "Dictionary of Values of Molecular Constants," Vol. III, D. N. R. S., Paris (1955).

pronounced aromatic character. Craig and Maccoll[4] have, on the other hand, pointed out that the two methods are discordant, even as regards such a fundamental property as the symmetry of the ground state, and in a latter paper Craig[5] has classified molecules like I and II as pseudo aromatics. In addition, Longuet-Higgins[6] has suggested that pentalene may tend to be distorted in an asymmetrical (C_{2h}) manner and to undergo, at the limit, spontaneous decomposition to give two molecules of acetylene and one of butadiyne. Boer et al.[7,8] and Snyder,[9] on the basis of a modified MO theory, have recently shown that in I and II an asymmetrical (C_{2h}) structure is more favorable energetically than the symmetrical (D_{2h}) one. A more elaborate treatment, one which explicitly includes electron repulsion, has been proposed by Silvestri et al.,[10] who have examined the ground-state electronic properties of molecules I and II by a semiempirical self-consistent field method. These authors have, however, presumed molecular symmetry D_{2h} and have not been concerned with the electronic spectra.

It is the purpose of this paper to deepen our understanding of the aromatic characteristics of I and II through an attempt to examine the ground-state electronic properties and the electronic spectra in particular by means of a semiempirical SCF method. Calculations have been carried out for the two molecular symmetry models, D_{2h} and C_{2h}, of both I and II.

Method and Procedure

The SCF technique of Roothaan[11] was employed in conjunction with the Pariser-Parr approximations,[12] with slight modifications. In computing interaction terms for adjacent atoms, the internuclear distances at each step of the iterative process are predicted from the π-bond orders, p, with the aid of the formula;[13]

$$r(\text{in Å}) = 1.520 - ap \quad (1)$$

with

$$a = 0.186 \quad (2)$$

Nonneighbor internuclear distances are calculated assuming the rings to be regular, with the bond lengths taken to be 1.397Å. The Coulomb penetration and nonneighbor resonance integrals are all disregarded. The one-center electronic repulsion integral, (pp/pp), given in the Pariser-Parr theory as $I_c - A_c$ was taken to be $11.54 - 0.46 = 11.08$ eV.,[14] while the two-center repulsion integrals, (pp/qq), were determined by the extrapolation procedure of Pariser and Parr.

In addition, the resonance integral $\beta(r)$ is supposed to vary exponentially with r according to the relation:

$$\beta(r) = -2.38 \exp[b(1.397 - r)] \text{ eV.} \quad (3)$$

with

$$b = 2.5802 \text{ Å}^{-1} \quad (4)$$

This value of b is considerably smaller than that, 5.6864 Å^{-1}, obtained by Pariser and Parr. The b value of Pariser and Parr was determined from $\beta(r)$ values so adjusted as to reproduce the experimental spectral data for ethylene and benzene, the bond lengths of which were taken to be 1.35 and 1.39Å respectively. The present b value was obtained by the use of the same spectral data, but using the recently observed value, 1.333Å, for the bond length of ethylene[15] and 1.397Å for that of benzene.

It is perhaps interesting to note in this connection that the applicability of the Pariser-Parr parameterization to the calculation of ground-state electronic properties has not been clearly established. In fact, Pariser-Parr's formulation, with its original parameterization, if applied to benzene in conjunction with the SCF technique, gives the unexpected result that self-consistency is achieved for two symmetry types, D_{6h} and D_{3h}, and there is good reason for believing that in such a case the skew structure (D_{3h}) is more favorable energetically than the symmetrical one (D_{6h}).[16] This absurd result is undoubtedly due to too large a value of b having been assigned by Pariser and Parr. According to the present parameterization, the symmetrical structure turns out to be most stable.

The starting molecular orbitals employed were the Hückel-type ones obtained with $\beta_{single}/\beta_{double} = 1$ for the D_{2h} model and those obtained with $\beta_{single}/\beta_{double} = 0.55$ for the C_{2h} model. In general, some ten iterative procedures were followed to achieve four-place self-consistency.

Results and Discussion

Charge Densities, Bond Orders and Free Valences. — The calculated charge densities,

4) D. P. Craig and A. Maccoll, *J. Chem. Soc.*, **1949**, 964.
5) D. P. Craig, ibid., **1951**, 3175.
6) H. C. Longuet-Higgins, "Theoretical Organic Chemistry; Kekulé Symposium," Butterworths, London (1959), p. 19.
7) P. C. den Boer-Veenendaal and D. H. W. den Boer, *Mol. Phys.*, **4**, 33 (1961).
8) P. C. den Boer-Veenendaal, J. A. Vliegenthart and D. H. W. den Boer, *Tetrahedron*, **18**, 1325 (1962).
9) L. C. Snyder, *J. Phys. Chem.*, **66**, 2299 (1962).
10) A. J. Silvestri, L. Goodman and J. A. Dixon, *J. Chem. Phys.*, **36**, 148 (1962).
11) C. C. J. Roothaan, *Rev. Mod. Phys.*, **23**, 69 (1951).
12) R. Pariser and R. G. Parr, *J. Chem. Phys.*, **21**, 466, 767 (1953).
13) T. Nakajima and S. Katagiri, *Mol. Phys.*, **6**, (1963) in press.
14) H. D. Pritchard, *Chem. Revs.*, **52**, 529 (1955).
15) L. S. Bartell and R. A. Bonham, *J. Chem. Phys.*, **31**, 400 (1959).
16) T. Nakajima and Y. Yaguchi, to be published.

TABLE I. CHARGE DENSITIES, BOND ORDERS AND FREE VALENCES

Molecule	Molecular symmetry	Atom	Charge density	Free valence	Bond	Bond order
Pentalene	D_{2h}	1	0.797	0.558	1— 2	0.657
		2	1.176	0.417	1— 7	0.517
		7	1.230	0.173	7— 8	0.525
	C_{2h}	1	0.975	0.581	1— 2	0.923
		2	1.048	0.506	1— 7	0.229
		3	0.917	0.550	2— 3	0.303
		7	1.060	0.321	3— 8	0.879
					7— 8	0.303
Heptalene	D_{2h}	1	1.158	0.527	1— 2	0.676
		2	0.851	0.435	1—11	0.529
		3	1.153	0.489	2— 3	0.621
		11	0.829	0.186	11—12	0.487
	C_{2h}	1	1.002	0.546	1— 2	0.919
		2	0.983	0.513	1—11	0.267
		3	1.017	0.524	2— 3	0.301
		4	0.979	0.509	3— 4	0.908
		5	1.042	0.540	4— 5	0.315
		11	0.977	0.310	5—12	0.878
					11—12	0.278

bond orders, and free valences for the two molecular symmetry types are summarized in Table I. In both I and II, the charge distributions for the asymmetrical models are remarkably smoothed out as compared with those for the symmetrical models. In contrast to this, the distributions of bond orders for the asymmetrical models are significantly uneven. The predicted bond lengths are 1.35 to 1.36Å for the double bonds and 1.46 to 1.48Å for the single bonds, the extent of bond length alternation being comparable to those in such chain polyenes as butadiene. From the viewpoint of the chemical reactivity, of particular notice is the fact that the free valences of the peripheral (secondary) carbon atoms of I and II, particularly for the asymmetrical models, are considerably larger than those for classical aromatic molecules (e. g., benzene, 0.40). Both of these molecules are thus expected to be highly susceptible to homolytic reactions. This is in agreement with the available experimental facts. Heptalene has been known readly to undergo polymerization by oxygen or mild warming.[1] In addition, the free valence numbers indicate that in I and II the highest reactivity should be expected at the ortho-positions. As regards II, this has also been confirmed experimentally.

The Total Electron Energy. — Now let us enquire which of the symmetrical and asymmetrical models is more favorable energetically. It has been emphasized[17,18] that a conclusion regarding the stability or the equilibrium configuration of a conjugated molecule cannot be based on π-electron calculations only; allowance for the effects of the σ-bond compression must also be made. Obviously the total electron energy should be considered in comparing the energetic stabilities of the two models. Using the assumptions of Longuet-Higgins and Salem,[17] the total binding energy of a conjugated molecule, taken to be the sum of π-bond energy and σ-bond energy, is given by

$$V=E_\pi+E_\sigma=(2/ab)\sum_{p<q}\bar{\beta}_{pq}+\sum_p q_p\bar{\alpha}_p+\text{const.} \tag{5}$$

in which we assume

$$\bar{\beta}(r)=\bar{\beta}_0\exp[\bar{b}(1.397-r)] \tag{6}$$

$$\bar{\alpha}_p=\bar{\alpha}_0+\omega(1-q_p)\bar{\beta}_0 \tag{7}$$

where ω is a proportionality coefficient here taken to be unity. Equation 6 differs from Eq. 3. $\beta(r)$ is the core resonance integral. On the other hand, $\bar{\beta}(r)$ should be interpreted as an effective resonance integral which includes an electron interaction term;* the value 4.5988

17) H. C. Longuet-Higgins and L. Salem, *Proc. Roy. Soc.*, **A251**, 172 (1959).

18) C. A. Coulson and W. T. Dixon, *Tetrahedron*, **17**, 215 (1962).

* Explicitly, β_{pq} may be expressed as $(\beta_{pq}+\beta^F_{pq})/2$, where $\beta^F_{pq}=\beta_{pq}-\frac{1}{2}p_{pq}(pp/qq)$.[16]

TABLE II. PREDICTED AND OBSERVED SINGLET TRANSITIONS

Molecule	Molecular symmetry	Transition type	Excitation energy, eV.		f, c. g. s.	
			Calcd.	Obs.	Theor.*	Obs.
Pentalene	D_{2h}	$B_{1g}\leftarrow A_{1g}$	0.75		Forb.	
		$B_{3u}\leftarrow A_{1g}$	3.73		0.75 (x)	
		$B_{2u}\leftarrow A_{1g}$	4.99		0.52 (y)	
	C_{2h}	$A_g\leftarrow A_g$	2.43		Forb.	
		$B_u\leftarrow A_g$	4.54		0.64	
		$B_u\leftarrow A_g$	5.64		0.51	
Heptalene	D_{2h}	$B_{1g}\leftarrow A_{1g}$	0.67		Forb.	
		$B_{3u}\leftarrow A_{1g}$	3.18		1.29 (x)	
		$B_{2u}\leftarrow A_{1g}$	4.06		0.64 (y)	
	C_{2h}	$A_g\leftarrow A_g$	2.72	Tail	Forb.	Tail
		$B_u\leftarrow A_g$	4.10	3.52	0.76	0.15
		$B_u\leftarrow A_g$	4.93	4.84	0.44	?

* Theoretical f values for pentalene were calculated using the predicted transition energies (in cm^{-1}) for ν in Eq. 8.

$Å^{-1}$ is taken for the parameter, $\bar{b}$.[13] The total energy values thus calculated indicate that in both I and II the asymmetrical structures are more favorable energetically than the symmetrical ones, the deformation energies which favor the structures being, respectively, -0.52 and $-0.58\bar{\beta}_0$, about 10 kcal./mol., if we take $\bar{\beta}_0=-16.5$ kcal./mol.[19] These figures are appreciable, and it is now clear that in I and II there exists a significant bond length distortion, one comparable in extent to those in linear chain polyenes. Such alternating bond lengths, if molecules I and II are treated as slightly perturbed hypothetical planar cyclooctatetraene and cyclodoecahexaene respectively, may be understood to be due to a pseudo Jahn-Teller effect.[20]

Electronic Spectra.—The calculated energies and oscillator strengths, f, for the lower singlet electronic transitions in I and II are summarized in Table II. No configuration interactions were allowed for (see below), and the theoretical f values were all obtained by the use of the well-known formula;

$$f_{th}=1.085\times10^{11}\nu Q^2 \qquad (8)$$

It may be noted that the f_{th} values calculated using Eq. 8 are usually about three times as large as the f_{obs} values.

It may be seen that, in both I and II, in passing from the symmetrical (D_{2h}) to the asymmetrical model (C_{2h}), the transition energies (particularly for the lowest (forbidden) transitions) increase, while the f_{th} values decrease, and in heptalene the C_{2h} model leads to numerical results in good agreement with experimental data. In this molecule the longest wavelength maximum is assigned to an electronic transition, $B_u\leftarrow A_g$, polarized approximately along the long axis (x), whereas the next maximum is assigned to a transition of the same type but with a moment roughly parallel to the short axis (y). The longest wavelength maximum is accompanied by an almost linearly decreasing absorption tail throughout the visible region. Such a tail may arise from a forbidden transition becoming partially allowed by molecular vibrations or twisting, and from transitions which take place according to the Franck-Condon process between a ground and an excited state having potential energy curves appreciably different in shape from each other. It has been shown[19] that in heptalene the potential energy curve for the lowest excited state differs considerably in shape from that for the ground state, the former having a single potential energy minimum, whereas the latter has a double minimum.

Recently hexaphenyl pentalene has been synthesized by Le Goff.[21] The absorption spectrum of this molecule shows a weak maximum at 13900 cm^{-1} (1.72 eV.) with $\log\varepsilon=1.95$ and followed by a long tail. This maximum may perhaps be assigned to the predicted forbidden transition, $A_g\leftarrow A_g$, in pentalene, which is allowed and shifted toward the red by the substitution.

In molecules I and II, if they are distorted in an asymmetrical mannar, a configuration interaction is possible between the ground and the lowest excited state, as the symmetry

19) T. Nakajima, "Molecular Orbitals in Chemistry, Physics and Biology," Ed. by P. O. Löwdin and B. Pullman, Academic Press, New York (1963), in press.
20) C. A. Coulson, *Chem. Soc. (London) Spec. Publ.*, No. 12, 85 (1958).
21) E. Le Goff, *J. Am. Chem. Soc.*, **84**, 3975 (1962).

groups of the two states are both A_g in distorted structures. Insofar as the distortion remains slight, this interaction may be of primary importance, and heavy mixing of the two states will occur, the ground state being substantially depressed in energy (pseudo Jahn-Teller effect).[6] However, in the asymmetrical structures here achieved, the interaction is of little importance, for the two states are well separated in energy from each other. In fact, in heptalene the lowering of the ground state energy caused by the interaction is calculated to be only about 0.1 eV. The SCF technique considerably reduces the effects of the configuration interaction.

Ionization Potentials. — In Roothaan's SCF formulation the ionization potentials are approximated by the orbital energies (Koopmans' theorem). Although this approximation has recently been criticized,[22-24] the orbital energies may still give at least an indication of the relative magnitude of ionization potentials. The orbital energies, $\varepsilon - W_{2p}$ (where W_{2p} is the ionization potential of the $2p\pi$-electron of the carbon atom) for the top occupied orbitals of I and II are calculated to be 1.55 (D_{2h}) and 0.84 (C_{2h}), and 3.20 (D_{2h}) 2.17 eV. (C_{2h}) respectively. It should be noted that, while in general $\varepsilon - W_{2p}$ values are negative for the top occupied orbitals (and for all other occupied orbitals), the values turn out to be positive in I and II. This indicates that the ionization potentials of these molecules are exceptionally small; in this sense they are unstable, the symmetrical structures being less stable than the asymmetrical ones.

22) R. D. Brown and A. Heffernan, *Trans. Faraday Soc.*, **54**, 757 (1958).
23) J. R. Hoyland and L. Goodman, *J. Chem. Phys.*, **33**, 946 (1960).
24) Y. I'Haya, *Mol. Phys.*, **3**, 513 (1960).

Summary and Conclusion

The semiempirical SCF technique has been applied to pentalene and heptalene. Self-consistency has been achieved for the two symmetry types, D_{2h} and C_{2h}, and the total binding energy examination indicates that in both the molecules the asymmetrical structure (C_{2h}) is more favorable energetically than the symmetrical one (D_{2h}). The calculated uneven charge distributions, the high free valence values, and the low ionization potentials supply the reasons for the instability of these molecules. The theoretical spectral calculations for the asymmetrical structures are in good agreement with the available experimental data. It may be concluded that, in these molecules, there exists a remarkable bond length alternation, and that in this sense they cannot be considered aromatic. They show, rather, characteristics of cyclic polyolefins.

The authors would like to thank Professor Yoshio Kitahara and Dr. Shigeyoshi Katagiri for their continued interest and stimulating discussions.

Department of Chemistry
Ibaraki University
Watarai-cho, Mito

Kinetic Studies of Solvolysis. IX.[1] *The S_N1-type Cleavage of t-Butyl p-Substituted-phenyl Ethers and Optically-active α-Phenethyl Phenyl Ether by Hydrogen Halides in a Phenol-Dioxane Solvent**

By Kunio OKAMOTO, Ken-ichi TAKEUCHI and Haruo SHINGU

(Received June 12, 1963)

It has been well established experimentally that the mechanism for the cleavage of primary and secondary alkyl ethers by hydrogen halides is an S_N2-type displacement between a protonated ether (an oxonium ion-pair) and a hydrogen halide.[2] There have been, however, no publications concerning an unambiguous kinetic example of the S_N1-type cleavage for tertiary alkyl ethers, although the existence of such a cleavage has been suggested[3] on the basis of the rate sequence

1) Part VIII: K. Okamoto, K. Takeuchi and H. Shingu, This Bulletin, 35, 525 (1962).

* Presented at the 14th Annual Meeting of the Chemical Society of Japan, Tokyo, April, 1961.

2) For a review see R. L. Burwell, Jr., *Chem. Revs.*, 54, 615 (1954).

3) E. g., R. L. Burwell, Jr., ibid., 54, 626 (1954).

of alkyl ethers.[4] It is anticipated that, unlike the S_N2-type cleavage, which obeys third-order kinetics,[5] the S_N1-type mechanism would display second-order kinetics, for in this mechanism the oxonium ion-pair cleaves unimolecularly.

In this paper typical examples of the S_N1-type cleavage are presented for the cleavages of *t*-butyl *p*-substituted-phenyl ethers and of α-phenethyl phenyl ether by a hydrogen halide in a phenol-dioxane solvent. In addition, the steric course and the mechanism are discussed in detail for the S_N1-type cleavage of optically-active α-phenethyl phenyl ether.

The Molecularity of the Hydrogen Chloride Cleavage of *t*-Butyl Phenyl Ether. — The hydrogen chloride cleavage of *t*-butyl phenyl ether was followed titrimetrically from 20 to 60% of completion in 20 wt. % phenyl-80 wt. % dioxane at 70.0°C. Assuming the S_N1-type mechanism for this cleavage, we calculated the rate constants from the second-order rate equation:

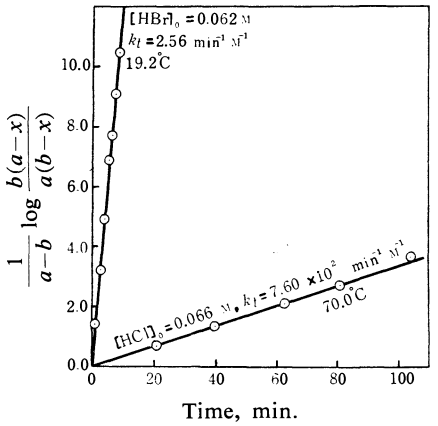


Fig. 1. Cleavage of *t*-butyl phenyl ether with hydrogen halides in 20 wt.% phenyl-dioxane.

TABLE I. SUMMARY OF RATES OF CLEAVAGE OF PHENYL ETHERS WITH HYDROGEN CHLORIDE IN PHENOL-DIOXANE

Compond	wt.% of phenol	Temp. °C	Initial concn. of the ether M	Initial concn. of HCl M	10^2k_t min.$^{-1}$ M^{-1}	10^2k_{tcorr} min.$^{-1}$ M	Conversion % of the ether
t-Butyl	20.0	70.0	0.100	0.102	9.50	10.3	45
phenyl	20.0	70.0	0.100	0.0660	7.60	8.57	40
ether	20.0	70.0	0.100	0.0325	8.42	9.45	20
t-Butyl	20.0	70.0	0.100	0.103	8.40	9.26	55
p-tolyl	20.0	70.0	0.100	0.0650	6.91	7.79	35
ether	20.0	70.0	0.100	0.0309	7.08	7.60	18
t-Butyl	20.0	7.00	0.100	0.0487	2.04	2.26	4.1
p-chlorophenyl ether	20.0	70.0	0.100	0.0251	2.26	2.42	3.9
t-Butyl	20.0	70.0	0.100	0.0601	4.37	5.16	4.2
p-nitrophenyl ether	20.0	70.0	0.100	0.0280	4.15	4.53	4.1
t-Butyl	0.0	70.0	0.100	0.0620	0.93	—	9.0
phenyl ether	10.0	70.0	0.100	0.0593	2.5	—	25
t-Butyl	20.0	70.0	0.100	0.0570	15.8[a]	18.1	36
phenyl	20.0	70.0	0.100	0.0595	14.8[b]	16.5	39
ether	20.0	70.0	0.100	0.0595	12.7[c]	14.5	36
	20.0	70.0	0.100	0.0605	9.37	10.6	39
t-Butyl phenyl ether	20.0	19.2	0.100	0.0620[d]	256	—	53
α-Phenethyl	50.0	30.0	0.200	0.219	—	5.50[e]	60
phenyl ether	50.0	30.0	0.200	0.212	—	4.65	39

a, b and c) In the presence of 0.100, 0.0500, and 0.0250 M of *p*-nitrophenol, respectively
d) Concn. of HBr
e) The value of k_p (see text).

4) B. W. Tronow and L. W. Ladigina, *Ber.*, **62**, 2844 (1929).
5) a) F. R. Mayo, W. B. Hardy and C. G. Shultz, *J. Am. Chem. Soc.*, **63**, 426 (1941); b) A. Y. Drummond and A. M. Eastham, ibid., **79**, 3689 (1957).

$$k_t=\frac{1}{t(a-b)}\ln\frac{b(a-x)}{a(b-x)} \quad (1)$$

where a is the initial concentration of the ether, b is the initial concentration of hydrogen chloride, and x is the concentration decrease in hydrogen chloride after the time lapse, t. Satisfactory second-order behavior was observed for each run; a representative run is illustrated in Fig. 1.

The values of the rate constants did not show any appreciable change between runs in various initial concentrations of hydrogen chloride, except for a slight increase probably due to the ionic strength effect of hydrogen chloride. These values are illustrated in Table I.

An examination of the extent of the completion of the reaction revealed that the consumption of hydrogen chloride did not exceed 91% of the starting ether after ten half-lives reaction time. This indicates that the major reaction is that of the cleavage, but also that there is, to a certain minor extent, a side reaction or a reverse reaction. Since the rate of the reverse reaction, i. e., the phenolysis rate of *t*-butyl chloride, was found to be negligibly small under these cleavage conditions, this incompleteness of hydrogen chloride comsumption may be ascribed to a concurrent side reaction. Although no attempt was made to clarify the characteristics of this side reaction, this seems to be rearrangement of the *t*-butyl group from ether-oxygen to the benzene-nucleus. This type of rearrangement has already been known in the hydrogen chloride cleavage of *t*-butyl phenyl ether in the absence of solvent at 20.0°C.[6]

In view of the fact that both the cleavage and the rearrangement proceed unimolecularly through the protonated ether, the ratio of the concentration decrease of hydrogen chloride to that of the ether at any reaction time should be equal to the ratio, r, of the concentration of the hydrogen chloride consumed by the ether at an infinite reaction time to the initial concentration of the ether. On the basis of this consideration, the ether concentration was expressed as $\{a-(x/r)\}$ instead of $(a-x)$ in Eq. 1, where a represents the initial concentration of the ether, and x represents the concentration decrease in hydrogen chloride after the time lapse, t. Thus, rate expression for the ether consumption:

$$-\mathrm{d}\{a-(x/r)\}/\mathrm{d}t=k_{t\mathrm{corr}}\{a-(x/r)\}(b-x) \quad (2)$$

gave a modified second-order kinetic equation:

$$k_{t\mathrm{corr}}=\frac{1}{(ar-b)}\ln\frac{b(ar-x)}{ar(b-x)} \quad (3)$$

The corrected second-order rate constants also gave good second-order behavior; these values are shown in Table I.

Hence, this cleavage is evidently a typical example of the S_N1-type ether cleavage, where an oxonium ion-pair, rapidly formed from the ether and hydrogen chloride, reacts intramolecularly by way of slow, unimolecular carbon-oxygen ionic fission.

Additional S_N1-type Characteristics of the Cleavage of *t*-Butyl Phenyl Ether.—The titrimetric rate constants (uncorrected), measured at 70.0°C in a series of solvents, i. e., dioxane 10 wt.% and 20 wt.% phenol-dioxane, increased with the phenol concentrations; this is illustrated in Fig. 2.

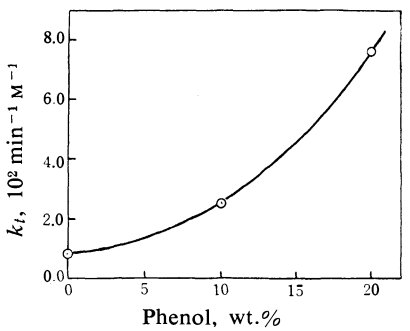


Fig. 2. Solvent effect in hydrogen chloride cleavage of *t*-butyl phenyl ether in phenol-dioxane.
$[\mathrm{ether}]_0=0.100$ M
$[\mathrm{HCl}]_0=0.059\sim0.066$ M, 70.0°C

Although the protonation of the ether might be promoted in the phenolic solvents by the relative decrease in dioxane concentration, it is more probable that the subsequent unimolecular cleavage would be greatly accelerated by an increase in phenol concentration. This kind of acceleration has already been found to be a normal pattern of the S_N1-type reaction in the phenolysis of *t*-butyl chloride.[6]

In addition, it was found that the titrimetric rate constants were markedly enhanced in the presence of added *p*-nitrophenol. This is illustrated in Fig. 3. This kind of phenomena has also been observed in the S_N1-type acetolysis of *t*-butyl bromide in acetic acid-carbon tetrachloride,[7] where it was interpreted as an acceleration of ionization due to hydrogen bonding. It may, therefore, be suggested that the similar acceleration by *p*-nitrophenol is effective in this cleavage.

6) H. Shingu and K. Okamoto, *J. Chem. Soc. Japan, Pure Chem. Sec.* (*Nippon Kagaku Zasshi*), **81**, 111 (1960).

7) K. Okamoto and H. Shigu, This Bulletin, **34**, 1131 (1961).

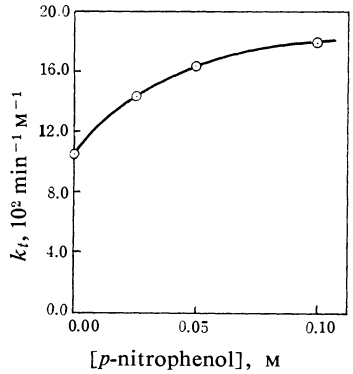


Fig. 3. Plot of k_t vs. [*p*-nitrophenol] for hydrogen chloride cleavage of *t*-butyl phenyl ether.

$[ether]_0=0.100$ M
$[HCl]_0\fallingdotseq0.06$ M, 70.0°C, 20 wt.% phenol

The Substituent Effect for the Hydrogen Chloride Cleavage of *t*-Butyl *p*-Substituted-phenyl Ether.—The cleavage of *p*-tolyl *t*-butyl ether, followed titrimetrically in 20 wt. % phenol-dioxane at 70.0°C, obeyed good second-order kinetics. The titrimetric rate constants for *p*-chlorophenyl and *p*-nitrophenyl *t*-butyl ether, especially for the run with higher concentrations of the *p*-nitrophenol ether, showed a tendency to drift upward in the plot for the second-order rate constant. In view of the acceleration of the cleavage of *t*-butyl phenyl ether by *p*-nitrophenol, this upward drift may probably be ascribed to autocatalytic acceleration by the *p*-chlorophenol or *p*-nitrophenol liberated during the cleavage. The second-order rate constants of these ethers were calculated from the initial rates. The rate constants are shown in Table I.

The percentages for the completion of the hydrogen chloride consumption of the *p*-methyl-, *p*-chloro- and *p*-nitro-phenyl ethers amounted to 92 (at about 40 half-lives), 95.5 (at about 11 half-lives) and 94.3% (at about 10 half-lives) respectively. Using these values for *r*, we calculated the corrected rate constants from Eq. 3; they are shown in Table I.

The plot of the corrected rate constants vs. Hammett's σ-constants shows that there are no linear free-energy relationships involving these constants, as Fig. 4 illustrates. Since the reaction proceeds through an oxonium ion-pair formation, these substituents might display a counter effect for the oxonium ion-pair formation and the subsequent unimolecular cleavage. The para-nitro group may accelerate the cleavave and retard the protonation because of its electron-attracting effect, and the para-methyl group may show converse tendencies in each of the processes. This seems to be

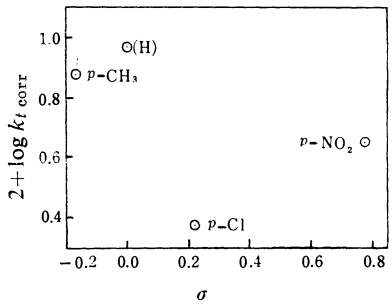


Fig. 4. Plot of $\log k_{t\,corr}$ vs. Hammett's σ constants for hydrogen chloride cleavage of *t*-butyl *p*-substituted-phenyl ether in 20 wt.% phenol-dioxane at 70.0±0.1°C.

the cause of the failure of Hammett's linear free-energy relationship for this reaction.

The Hydrogen Bromide Cleavage of *t*-Butyl Phenyl Ether. — Satisfactory second-order behavior was observed for the hydrogen bromide cleavage of *t*-butyl phenyl ether in 20 wt. % phenol-dioxane at 19.2°C; this is illustrated in Fig. 1. Although no attempt was made to correct to a side reaction, this result indicates that the reaction is of the S_N1-type. The rate constant is definitely higher than that of the hydrogen chloride cleavage. In view of the fact that the protonated ether can exist along with the anion as an oxonium ion-pair, it is unlikely that the enhancement of the rate by hydrogen bromide is due only to the ease of formation of the protonated ether. It is more reasonable to assume that the predominant cause of the enhancement is acceleration by the nucleophilic attack of the bromine ion, for the bromine anion is more nucleophilic than the chlorine ion. From this consideration it follows that the unimolecular cleavage of the oxonium ion-pair is of the "intramolecular" nature and that it is mechanistically similar to the S_Ni-type reaction.

The Hydrogen Chloride Cleavage of Optically-Active α-Phenethyl Phenyl Ether.—To substantiate the intramolecular cleavage of the oxonium ion-pair, the hydrogen chloride cleavage of (+)-α-phenethyl phenyl ether was followed polarimetrically in 50 wt. % phenol-dioxane at 30°C. The optical rotation associated with the disappearance of the (+)-ether decreased, and at the completion of the reaction (at about 14 half-lives) it reached a minus value, having crossed the zero line. Since the (+)-ether has the same configuration as the (−)-chloride,[8a] this result indicates that the configuration of the ether was retained after the cleavage. This is consistent with the previous

8) a) H. Hart and H. S. Eleuterio, *J. Am. Chem. Soc.*, **76**, 518 (1954); a) H. Hart and H. S. Eleuterio, ibid., **76**, 1379 (1954); c) H. Hart and R. J. Elia, ibid., **83**, 985 (1961).

observation that optically-active α-phenethyl phenyl ether is cleaved by hydrogen chloride in benzene,[8b] toluene,[8c] 3-pentanone[8c] and isobutanol;[8c] also, the rotation of the α-phenethyl chloride so formed shows that the process involves retention of the configuration, accompanied by a slight racemization.[8]

The polarimetric rate constant, k_p, was calculated from the rate equation 4:

$$\frac{-\mathrm{d(ether)}}{\mathrm{d}t} = k_p \ \mathrm{(ether)}\ \mathrm{(HCl)} \qquad (4)$$

by ploting d(ether)/dt, graphically calculated, against (ether) (HCl), where (ether) represents the ether concentration calculated from the polarimetric measurement and (HCl) represents the concentration of hydrogen chloride measured at a titrimetric run carried out under the same conditions. This is illustrated in Fig. 5.

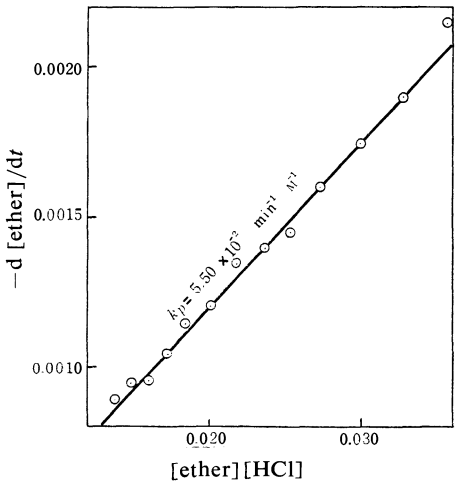


Fig. 5. Plot of −d[ether]/dt vs. [ether][HCl] for hydrogen chloride cleavage of (+)-α-phenethyl chloride in 50 wt.% phenol-dioxane at 30.0±0.1°C.

The titrimetric constant, $k_{t\ \mathrm{corr}}$, for this cleavage was also measured. The hydrogen chloride consumption at the completion of the reaction amounted to 75% of the starting ether. The rate of the reverse reaction was found to be negligibly small (2.3% of conversion at twenty half-lives of the cleavage). Evidently the incompleteness of hydrogen chloride consumption is due to a side reaction, probably a rearrangement of the oxonium ion-pair. Making a consideration analogous to the case of t-butyl phenyl ether, we estimated the concentration of the changed ether to be $x/0.75$, where x represents the concentration of the consumed hydrogen chloride at time t. The titrimetric rate constant was calculated from Eq. 5

$$k_{t\ \mathrm{corr}} = \frac{1}{(0.75a-b)} \ln \frac{b(0.75a-x)}{0.75a(b-x)} \qquad (5)$$

This was derived from the rate expression

$$\frac{-\mathrm{d}\{a-(x/0.75)\}}{\mathrm{d}t} = k_{t\ \mathrm{corr}}\{a-(x/0.75)\}\ (b-x) \qquad (6)$$

where a represents the initial concentration of α-phenethyl phenyl ether and b represents the initial concentration of hydrogen chloride.

A good second-order titrimetric rate constant was obtained by a plot of $(1/0.75a-b)\log b(0.75a-x)/0.75a(b-x)$ vs. t,; this is illustrated in Fig. 6.

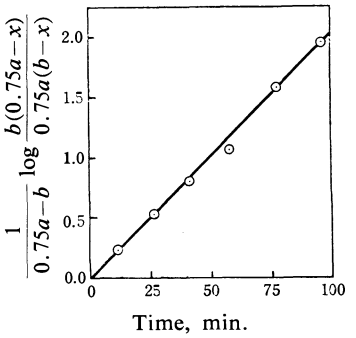


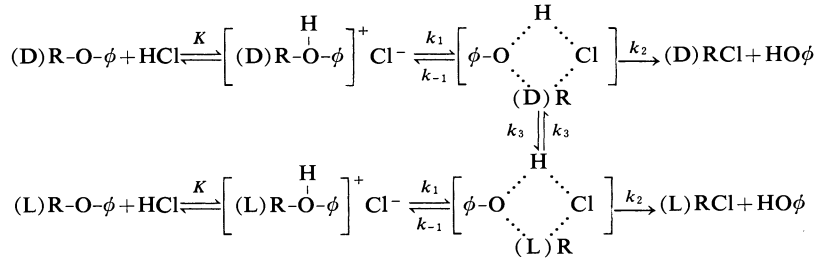
Fig. 6. Cleavage of α-phenethyl phenyl ether with hydrogen chloride in 50 wt.% phenol-dioxane at 30.0±0.1°C.
[ether]$_0$=0.200 M
[HCl]$_0$=0.212 M
$k_{t\ \mathrm{corr}}$=4.65×10^{-2} min^{-1} M^{-1}

As Table I shows, the polarimetric constant exceeds the titrimetric constant. This indicates kinetically that the racemization (or ionization) process of the oxonium ion-pair precedes the product-formation stage.

The Mechanism of the Hydrogen Halide Cleavage of *t*-Butyl and α-Phenethyl Phenyl Ether.—In the preceding sections the S_N1-type characteristics of the protonated ether have been clearly indicated on the basis of the molecularity, the solvent effect, and the acceleration by phenolic compounds for the cleavage reaction.

The intramolecular, S_Ni-like nature for this cleavage has also been suggested from the rate enhancement by hydrogen bromide for the cleavage of t-butyl phenyl ether and from the steric course revealed for the cleavage of optically-active α-phenethyl phenyl ether.

Since the optically-active product was obtained at the cleavage of optically-active α-phenethyl phenyl ether, the intermediate should retain the optical activity. Therefore, we can postulate two "parallel" series of two-stage reactions of the "antipodal," protonated ethers for the simplest expression of the ether



Scheme A

cleavage, as is depicted in Scheme A. The two parallel series of reactions of the antipodal substrates were previously postulated for the mechanism of the phenolysis of the optically-active α-phenethyl chloride.[1] In this mechanism the racemization is caused by way of interconversion between two antipodal intermediates. As a plausible structures for the intermediate; a quadrupolar type with a retained configuration; as has been suggested by Hart and Elia,[8b] may be assumed.

From Scheme A a quantitative explanation for the gap between the k_p and the k_t may be obtained by the following rate expressions:

$$k_p = Kk_1/(1+k_{-1}/(k_2+2k_3)) \qquad (7)$$

$$k_t = Kk_1/(1+k_{-1}/k_2)$$

In Eqs. 7 and 8, K, k_1, k_2 and k_3 represent the equilibrium constant for the protonated ether formation, the rate constant for the intermediate formation, the rate constant for the product formation, and the interconversion rate constant of the antipodal intermediates respectively,

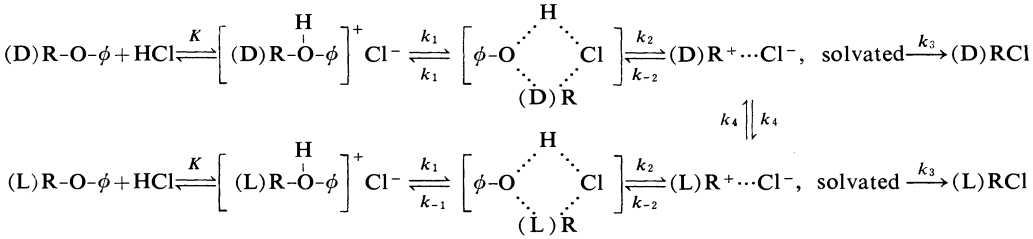
However, it would be possible to explain this cleavage mechanism, especially for the α-phenethyl system, by a more complicated mechanism. Since it was concluded in the previous paper[1] that the phenolysis of α-phenethyl chroride in a phenol-benzene solvent, i.e., the reverse reaction of the ether cleavage, proceeded under a "three-stage" mechanism of the S_N1-type with two kinds of intermediates, there is a possibility that the cleavage in phenol-dioxane goes back through the same "three-stages" as those of the phenolysis in a phenol-benzene solvent, This hypothesis seems reasonable judging from the principle of microscopic reversibility. Thus, the "three-stage" cleavage of the protonated ether is shown in Scheme B. In this mechanism the first intermediates would be a quadrupolar type intermediate consisting of an RCl and a phenol molecule, and the second ones, an ion-pair derived from RCl and surrounded by a solvation shell. If these intermediates are compared with those postulated for the phenolysis,[1] the first group may be considered to be non-racemizable and the second, racemizable (see Part VIII of this series[1]). The overall rate expressions for the k_t and k_p in this scheme are given in Eqs. 9 and 10 respectively:

$$k_p = Kk_1/\left\{1+\frac{k_{-1}}{k_2}\left(1+\frac{k_{-2}}{k_3+2k_4}\right)\right\} \qquad (9)$$

$$k_t = Kk_1/\left\{1+\frac{k_{-1}}{k_2}\left(1+\frac{k_{-2}}{k_3}\right)\right\} \qquad (10)$$

Discrimination between mechanisms A and B seems to be impossible on the basis of the kinetic examination of the trend of the gap between the k_t and the k_p. Namely, the change of solvent composition or the addition of a scavenger for the intermediates may cause an increase in the k_2 in Eqs. 7 to 10 or in the k_3 in Eqs. 9 and 10, but this will lessen the gap between the k_p and the k_t in "both" of Schemes A and B.

Thus, the experimental descrimination between Schemes A and B needs further study, although the principle of microscopic reversibility seems to favor Scheme B, especially for the α-phenethyl system.



Scheme B

Experimental[9]

Materials.—The preparation of *t*-butyl phenyl ether has been described previously[6] (b.p. 89.0°C/35.5 mm Hg, Found: C, 79.80; H, 9.04. Calcd, for $C_{10}H_{14}O$: C, 79.95; H, 9.39). *t*-Butyl *p*-tolyl ether and *t*-butyl *p*-chlorophenyl ether, prepared in the respective phenol by a method similar to that used for *t*-butyl phenyl ether,[6] had b.p.'s of 86~87°C/15.2 mmHg. (Found: C, 80,23; H, 9.71. Calcd. for $C_{11}H_{16}O$: C, 80.44; H, 9.82%) and 84.0~85.5°C/9.0 mmHg respectively.

Found: C, 64.74; H, 6.89. Calcd. for $C_{10}H_{13}OCl$: C, 65.04; H, 7.09%.

t-Butyl *p*-nitrophenyl ether was obtained by means of the addition reaction of *p*-nitrophenol to isobutylene, To a mixture of 5.0 g of *p*-nitrophenol, 50 cc. of methylene chloride, and 0.55 cc. of 96% sulfuric acid, in a 200 cc., three-necked flask equipped with a thermometer, a cooled dropping funnel, and a drying tube, 12.0 g. of liquefied isobutylene were added in one portion at 0°C. After the mixture had stood for 20 hr. at 0~5°C, 40 cc. of 10% aqueous sodium carbonate was added to the reaction mixture to precipitate unchanged *p*-nitrophenol as the sodium salt. To the filtrate was added 10 cc. of ether, and the mixture was extracted with 10% aqueous sodium hydroxide, washed with water, dried and concentrated. The residue was fractionally distilled in vacuo, giving 1.91 g. (27.2% of theory) of *t*-butyl *p*-nitrophenyl ether; b.p. 103~110°C/2 mmHg.

Found: C, 62.02; H, 7.02. Calcd. for $C_{10}H_{13}NO_3$: C, 61,52; H, 6.71%.

(+)-α-Phenethyl phenyl ether was prepared from (+)-α-phenethyl chloride ($[\alpha]_D^{27°}$ 45.3°, homogeneous, 1 dm.) in the manner of Hart and Eleuterio[9a] (b.p. 106~110°/1 mmHg, $[\alpha]_D^{27°}$ 10.11±0.05°, homogeneous, 1 dm.). Aniline, phenol and dioxane (each of reagent grade) were dried and purified by fractional distillation; b.p. 42.0~43.0°C/1 mmHg, 178.5°C and 101.5°C respectively.

Kinetic Measurements.—The sealed ampoule technique was employed. The diminution of hydrogen chloride was followed by titration with standard sodium acetate in acetic acid, using crystal violet as an indicator. The polarimetric run was carried out in a manner similar to that previously described.[1]

Summary

1) Hydrogen chloride cleaves *t*-butyl phenyl ether at 70.0°C in 20 wt.% phenol-dioxane. The reaction is kinetically first-order in each reactant. The second-order rate constants show an increase with increasing phenol concentrations, and *p*-nitrophenol accelerates the reaction.

2) The hydrogen bromide cleavage of *t*-butyl phenyl ether at 19.2°C in 20 wt. % phenol-dioxane gives a second-order rate constant greater than that of hydrogen chloride.

3) The rate sequence of the hydrogen chloride cleavage of *t*-butyl *p*-substituted-phenyl ethers at 70.0°C in 20 wt.% phenol-dioxane is $H > p\text{-}CH_3 > p\text{-}NO_2 > p\text{-}Cl$, and there is no linear relationship between those rate constants and Hammett's σ constants.

4) The hydrogen chloride cleavage of (+)-α-phenethyl phenyl ether at 30.0°C in 50.0 wt.% phenol-dioxane obeys good second-order kinetics for both polarimetric and titrimetric runs. The value of the polarimetric rate constant exceeds that of the titrimetric constant, and from the final reading of the polarimetric run it has been concluded that the α-phenethyl chloride produced in the cleavage partly retained the configuration.

5) It has been concluded that the hydrogen halide cleavage of those phenyl ethers in phenol-dioxane proceeds through the protonated ether produced by a rapid equilibration between hydrogen halide and those ethers, and that the protonated ether reacts by an S_Ni-like mechanism. For the cleavage of the optically-active ethers, a detailed mechanism involving two parallel series of cleavage reactions of antipodal protonated ethers has been suggested wherein the partial racemization of the product is explained as resulting from the interconversion between the antipodal intermediates. For each series of S_Ni-type reactions, the possibility of a two-stage or three-stage mechanism has been discussed.

Department of Fuel Chemistry
Faculty of Engineering
Kyoto University
Sakyo-ku, Kyoto

9) Microanalyses by Microanalytical Center, Kyoto University.

NOTES

Tetrodotoxin. III.[1] *A Revised Molecular Formula for Tetrodotoxin*

By Toshio GOTO, Sho TAKAHASHI, Yoshito KISHI and Yoshimasa HIRATA

(Received August 21, 1963)

The molecular formula of tetrodotoxin, a strongly toxic compound obtained from ovaries of swellfish (*Spheroides rubripes*), was said by Yokoo[2] in 1952 to be $C_{12}H_{17}O_{10}N_3$ on the basis of elementary analyses and the molecular weight determination by means of freezing point depression and the titration of its basic group. In 1953, Tsuda and Kawamura[3] reported on the analytical values of the toxin, but they did not give any definite molecular formula, since the values fluctuated considerably. Several years later, both Kakisawa et al.[4] and Tsuda et al.[5] gave a molecular formula, $C_{12}H_{19}O_9N_3$, based on elementary analyses and a titration equivalents.

Though it has previously been considered very difficult to purify tetrodotoxin (I), we have found that it can be purified through its nicely crystalline picrate II, which can be recrystallized from hot water. Acetylation of the toxin I with acetic anhydride and *p*-toluenesulfonic acid afforded, in a good yield, amorphous tetraacetyltetrodotoxin *p*-toluenesulfonate (III), which was further acetylated with acetic anhydride in the presence of pyridine to pentaacetylanhydrotetrodotoxin *p*-toluenesulfonate (IV).

The equivalent values of the purified toxin I determined by several runs of titration were between 311 and 324. The molecular weight of the crystalline pentaacetate IV was found to be 673±10 by means of the osmometer method[6] in a chloroform solution. These results, coupled with the analytical values of tetrodotoxin (I), the picrate II, and the acetates, III and IV, led to the molecular formula $C_{11}H_{17}O_8N_3$ for tetrodotoxin (I).

Experimental

Tetrodotoxin (I).—This toxin was purified by precipitating it with alcohol from its aqueous acetic acid solution according to the method of Tsuda and Kawamura[3] (samples 1 and 2), or through its crystalline picrate II, which had been treated with aqueous ammonia to precipitate the toxin (sample 3). The toxin I was obtained as microscopic crystals and darkened over 200°C without melting. Analytical samples were dried at 80~100°C for ca. 20 hr. in vacuo.

Found: (Sample 1) C, 40.21, 40.40; H, 5.62, 5.72; N, 12.52, 12.70;[7a] O, 41.43, 41.11, 41.00.[7b] (Sample 2) C, 40.62, 40.61; H, 5.75, 5.66; O, 41.73;[7c] titration equivalent (5 runs) 311 to 324. (Sample 3) C, 40.58, 40.87; H, 5.63, 5.94; N, 12.61, 12.60.[7d] Calcd. for $C_{11}H_{17}O_8N_3 \cdot \frac{1}{2}H_2O$: C, 40.24; H, 5.53; N, 12.80; O, 41.43%; mol. wt., 328.28.

Tetrodotoxin Picrate (II).—After this had been prepared from the toxin I and picric acid in water, it was recrystallized from water to give yellow needles which darkened over 200°C. An analytical sample was dried at 80~100°C for 20 hr. in vacuo.

Found: C, 36.25, 36.52; H, 3.95, 4.03; N, 14.24, 14.40.[7d] Calcd. for $C_{11}H_{17}O_8N_3 \cdot C_6H_3O_7N_3 \cdot H_2O$: C, 36.05; H, 3.92; N, 14.84%.

Tetraacetyltetrodotoxin *p*-Toluenesulfonate (III).—Tetrodotoxin (100 mg.) was suspended on a solution of *p*-toluenesulfonic acid hydrate (100 mg.) in acetic acid (2 ml.); the mixture was then allowed to stand overnight at room temperature. The resultant clear solution was evaporated to dryness under reduced pressure at 55°C (water-bath temp.), and the residue was treated with ice water containing sodium acetate (200 mg.) and then extracted

1) Part II: T. Goto, K. Kishi and Y. Hirata, This Bulletin, **35**, 1244 (1962).
2) A. Yokoo, *Proc. Japan Acad.*, **28**, 200 (1952).
3) K. Tsuda and M. Kawamura, *Pharm. Bull. (Japan)*, **1**, 112 (1953).
4) H. Kakisawa, Y. Okumura and Y. Hirata, *J. Chem. Soc. Japan, Pure Chem. Sec. (Nippon Kagaku Zasshi)*, **80**, 1483 (1959).
5) K. Tsuda, M. Kawamura and R. Hayatsu, *Chem. Pharm. Bull. (Japan)*, **8**, 257 (1960).
6) A Mechrolab. Inc. osmometer, Model 301A, was used. We wish to thank Takeda Chemical Industries, Ltd., for this measurement.
7) The authors are indebted to the following laboratories and companies for the microanalyses: a) Scandinavian Microanalytical Lab. b) Takeda Chemical Ind., Ltd. c) Elementary Analysis Center, Kyoto University. d) Fujisawa Pharmaceutical Co., Ltd. e) Elementary Analysis Lab., Osaka City University.

with chloroform (three times). The combined extracts were washed with water, dried over anhydrous sodium sulfate, and evaporated to dryness. The residue was dissolved in chloroform and precipitated by the addition of petroleum ether. The precipitate (110 mg.) was further purified by dissolving it in benzene and precipitating it with ether. The analytical sample was a white amorphous powder; m. p. 162~164°C.

Found: C, 46.97; H, 5.27; N, 6.44.[7e] Calcd. for $C_{11}H_{13}O_8N_3(CH_3CO)_4 \cdot C_7H_8O_3S$: C, 47.34; H, 5.04; N, 6.37%.

Pentaacetylanhydrotetrodotoxin *p*-Toluenesulfonate (IV). — The tetraacetate III (500 mg.) was dissolved in a mixture of pyridine (2 ml.) and acetic anhydride (2 ml.), and the mixture was allowed to stand overnight at room temperature. The reaction mixture was evaporated at 55°C (bath temp.) under reduced pressure, and the residue was dissolved in chloroform. Ether was added to the solution to precipitate the product, which was then recrystallized from ethanol to give 200 mg. of white needles; m. p. 208~210°C.

Found: C, 48.83; H, 5.20; N, 5.81;[7e] C, 48.53, 48.80, 48.77; H, 4.77, 5.03, 5.40; N, 6.32;[7d] N, 6.13;[7a] O, 35.42;[7e] mol. wt., 673±10 (0.6418% solution in chloroform). Calcd. for $C_{11}H_{10}O_7N_3 \cdot (CH_3CO)_5 \cdot C_7H_8O_3S$: C, 49.19; H, 4.87; N, 6.15; O, 35.11%; mol. wt., 683.62.

The authors wish to thank the Fujisawa Pharmaceutical Co. Ltd., for collecting the ovaries of swellfish and also to express their appreciation to the Public Health Service, National Institute of Health, U. S. A., for its support of this work under Research Grant RG-7969.

Chemical Institute
Faculty of Science
Nagoya University
Chikusa-ku, Nagoya

The Isotopic Composition of Magnesium in Terrestrial Samples

By Makoto SHIMA*

(Received August 27, 1963)

The variation in the isotopic abundance of the stable isotopes of magnesium, one of the most common elements in the earth's crust and in meteorites, has received little detailed study. It has been reported on by Blewett and Jones (1936),[1] and by White and Cameron (1948),[2] using a commercial magnesium reagent. In dolomite samples, Daughtry, Perry and Williams (1962)[3] found a different magnesium 24-magnesium 26 ratio. However, on the whole it has been little studied.

Since some experimental difficulties were experienced in measuring the magnesium isotope ratio, the present study was begun with the hope of resolving these difficulties and with the thought that knowledge of the magnesium isotope ratio in the terrestrial sample might lead to useful geochemical findings.

The magnesium was mainly separated by the classical method of rock analyses. Dilute sulfuric acid and 50% hydrofluoric acid were added to two grams of the sample. After the calcium had been separated by the ordinary ammonium oxalate method, the magnesium was precipitated by oxine. After ignition, it was leached by hydrochloric acid. The ion exchange resin (Dowex 50-X12) was used for the purification of the magnesium of sodium and aluminum, which might disturb mass spectrometric analyses.[4] Magnesium oxide was mounted on the sample filament with phosphoric acid. The isotopic composition was measured in a mass-spectrometer, built by Nuclide Analysis Associates, with a 12-inch radius and a deflection of 60°. The ions, Mg^+, were produced by using a triple filament source made of tungsten ribbons. The beam current was amplified with an electron multiplier. In order to stabilize the ion beam, an advantage was gained by the use of phosphoric acid for mounting the magnesium oxide samples. The peak shape thus obtained is shown in Fig. 1.

There are several possible sources of error in the determination of magnesium isotope composition (Masses 24, 25 and 26) : isotopic fractionation in the sample preparation, mass discrimination in the ion production, instrument drift, and instability. The isotopic fractionation in the sample preparation and also the contamination were avoided by the use of

* Present address: The Institute of Physical and Chemical Research, Kamifujimae, Bunkyo-ku, Tokyo, Japan.

1) J. P. Blewett and E. J. Jones, *Phys. Rev.*, **50**, 464 (1936).

2) J. R. White and A. E. Cameron, ibid., **74**, 991 (1948).

3) A. C. Daughtry, D. Perry and M. Williams, *Geochim. et Cosmochim. Acta*, **26**, 857 (1962).

4) J. Yoshimura and H. Waki, *Anal. Chem. Japan*, **6**. 362 (1957).

TABLE I. THE RESULTS OF MAGNESIUM ISOTOPE RATIO

Sample	25/24×100	26/24×100	Note
G-1	12.748±0.05	13.984±0.03	Standard rock sample
W-1	12.749±0.05	13.965±0.04	Standard rock sample
Sea water*	12.750±0.03	13.965±0.02	Pacific ocean
	12.762±0.03	13.966±0.02	Pacific ocean
Reagent	12.708±0.02	13.987±0.02	Magnesium chloride
	12.704±0.05	13.966±0.04	Magnesium chloride
Table**	12.880	14.141	

* Supplied by Dr. D. Schink.
** F. A. White, T. L. Collins and F. M. Rourke, *Phys. Rev.*, **101**, 1786 (1956).

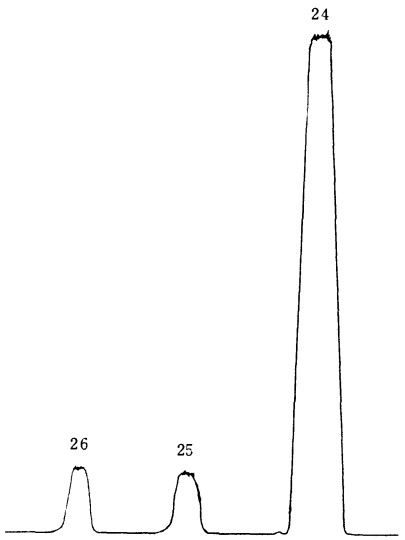


Fig. 1. The obtained peak shape of magnesium isotope.

the same chemical procedure and the same reagents as far as possible. The mass discrimination in the production of ions is not believed to be serious because the mass analyses were always repeated under the same conditions. Moreover, no variation in the isotopic ratio with time was observed during the course of the individual runs. The statistical uncertainty of each run—due principally to the instrumental effect—was usually within 2%. The difference in the average ratio on repeated runs was not significant.

The results of the measurement are shown in Table I. No mass correction factor is necessary for the relative ratio to be compared, because this study was designed to check the terrestrial magnesium samples with existed in the different formulae. On the basis of these preliminary results, no difference in the magnesium isotope composition of standard rocks, of sea water and of chemical reagents could be found. In other words, within the limits of the samples and of analytical error, no difference in the isotopic ratio among the terrestrial magnesium samples has been established. However, nothing decisive can be stated about the secondary dolomite which was reported by Daughtry et al. (1962).[3]

I am grateful to Dr. H. C. Urey for his encouragement throughout this work. I am also indebted to Dr. D. Schink for supplying me with samples.

Department of Chemistry
University of California
La Jolla, California
U. S. A.

The Formation of Methyl Methanethiolsulfonate, an Antibacterial Substance, from Dimethylsulfoxide

By Tsutomu TSUCHIYA, Setsuko IRIYAMA and Sumio UMEZAWA

(Received September 10, 1963)

When dimethylsulfoxide (DMSO) as a solvent is treated with an excess of hydrogen chloride and when the reaction product is subjected to paper bioautography, there is found an antibacterial spot which was presumed to be derived from DMSO; therefore, an attempt has been made to isolate the active substance from the reaction product of DMSO with hydrogen chloride. The purpose of this paper is to establish that the active substance is methyl methanethiolsulfonate.

Sulfoxides (I) are basic, as is indicated by their ability to form salts with strong acids, and it is known that sulfoxides are reduced by hydrogen halides to sulfides[1] (IV) via the diacid salts (III):

$$\underset{\text{(I)}}{R_2SO} \xrightarrow{HX} \underset{\text{(II)}}{R_2SO\cdot HX} \xrightarrow[-H_2O]{HX} \underset{\text{(III)}}{[R_2SX]^+X^-} \xrightarrow[-X_2]{} \underset{\text{(IV)}}{R_2S}$$

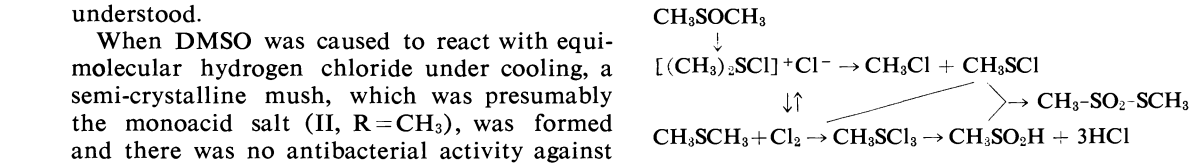
The reaction between DMSO and hydrogen chloride, however, is complicated and not fully understood.

When DMSO was caused to react with equimolecular hydrogen chloride under cooling, a semi-crystalline mush, which was presumably the monoacid salt (II, $R=CH_3$), was formed and there was no antibacterial activity against *Bacillus subtilis*. When DMSO was further treated with an excess of hydrogen chloride, however, a clear solution was obtained, and when the solution was allowed to stand, the temperature of the solution spontaneously rose to about 60°C and a considerable amount of gas was evolved. The low-boiling product collected was found to be mainly composed of hydrogen chloride and a water-insoluble component which was presumably dimethyl sulfide (IV, $R=CH_3$). The resulting solution was neutralized thoroughly with powdered sodium bicarbonate or pyridine and, as described in the experimental section, repeatedly treated with organic solvents to produce a crude product almost free from chlorine. This product was purified by vacuum-distillation to give methyl methanethiolsulfonate (CH_3–SO_2–SCH_3). The product purified gave analyses for methyl methanethiolsulfonate, and the boiling point and infrared absorption bands corresponded well with those reported for the compound prepared by a different method.[2]

Methyl methanethiolsulfonate has been found to have antibacterial and antifungal activities. This suggested that the methanethiolsulfonates have an antimicrobial interest. An antimicrobial test of a variety of methanethiolsulfonates is, therefore, under way.

Discussion

The inter-relationships of the products in the reaction of DMSO with hydrogen chloride may be represented by the accompanying diagram. All the inter-relationships except the formation of methanesulfenyl chloride ($CH_3\cdot SCl$) have been established.



The formation of methylsulfur trichloride (CH_3SCl_3) from methanesulfenyl chloride and chlorine was established by Douglass and coworkers.[3] The formation of methanesulfinic acid (CH_3SO_2H) by the hydrolysis of methylsulfur trichloride was found by Douglass and Farah.[2] The reaction of sulfenyl chloride with sulfinic acid was applied to the preparation of thiolsulfonate esters (R–SO_2–SR) by Stirling.[4] The formation of thiolsulfonate esters from sulfenyl chlorides and sulfinic acids was also concluded by Douglass and Farah[2] in the chlorination of alkyl disulfides.

Any mechanism which would account for the formation of methanesulfenyl chloride must involve the rupture of the sulfur-carbon bond,

1) Recent applications of the reaction to the preparation of sulfides have been described in the following papers: B. Iselin, *Helv. Chim. Acta*, **44**, 61 (1961); E. N. Karaulova and G. D. Gal'pern, *Zhur. Obshchei Khm.*, **29**, 3033 (1959); *Chem. Abstr.*, **54**, 12096 (1960).

2) I. B. Douglass and B. S. Farah, *J. Org. Chem.*, **24**, 973 (1959).

3) K. R. Brower and I. B. Douglass, *J. Am. Chem. Soc.*, **73**, 5787 (1951); I. B. Douglass, K. R. Brower and F. T. Martin, ibid., **74**, 5770 (1952).

4) C. J. M. Stirling, *J. Chem. Soc.*, **1957**, 3597.

and it seems reasonable to suppose that the diacid salt of DMSO decomposes into methanesulfenyl chloride and methyl chloride. This kind of decomposition is rather unusual and the major known product of the decomposition of the diacid salt of DMSO is dimethyl sulfide. Several instances of this kind of decomposition, however, have been found in the literature related to the chlorination of sulfides. An example is the formation[5] of 2-nitro-4-methylbenzenesulfenyl chloride from methyl 2-nitro-4-methylphenyl sulfide and chlorine. Moreover, Bordwell and Pitt[6] described that the presence of colored impurities in several of the products obtained by the chlorination of sulfides suggested contamination by sulfenyl chlorides.

Methanesulfenyl chloride probably was formed by the nucleophilic attack of chloride ions on the carbon in the chlorosulfonium ions.

Experimental

Methyl Methanethiolsulfonate.—DMSO was dried over potassium carbonate or potassium hydroxide and vacuum-distilled (b. p. 51°C/3.5 mmHg). DMSO (100 g.) was placed in a three-neck flask fitted with a sealed stirrer, a thermometer and a gas inlet tube. The flask and its contents were then cooled and a gentle stream of dry hydrogen chloride gas was admitted until about 60 g. hydrogen chloride had been absorbed. The temperature of the contents was not allowed to rise above 40°C. When about half of the hydrogen chloride had been absorbed, the contents crystallized. When the addition of hydrogen chloride was complete, however, a solution was obtained.

While the resulting solution was allowed to stand at room temperature, the temperature of the contents spontaneously rose to about 60°C and a considerable amount of gas evolved. The low-boiling product, collected in a bottle cooled in liquid air, mainly consisted of a water-insoluble liquid (about 15 g.) and hydrogen chloride. The water-insoluble liquid had a b. p. of about 37°C and was presumed to be dimethyl sulfide.

The solution left after the gas evolution was subjected to vacuum-distillation at about 50°C; when the vacuum reached 2 mmHg, the distillation was stopped. The viscous liquid (70 g.) left in the flask was thoroughly neutralized with sodium bicarbonate (about 50 g.) by mixing, and the mixture was allowed to stand at room temperature for 1 hr. The mixture was then extracted four times with 150 ml. portions of ethanol. The extracts were combined and allowed to stand for a while to give a small quantity of precipitate. After removal of the precipitate by filtration, the extract was distilled under reduced pressure to remove the solvent. The oily residue was again extracted with acetone (300 ml.), and the solvent was removed by distillation to give a yellowish, clear liquid (7.0 g.). The product was finally extracted three times with portions of 15 ml. of ether. The ether-insoluble part obtained was a viscous liquid and had a weak antibacterial activity against *Bacillue subtilis*.

The ethereal extract was distilled under reduced pressure to yield a colorless liquid of methyl methanethiolsulfonate, b. p. 82.5~83.5°C (2.5 mmHg)[7] at a bath-temperature of 100~120°C; yield, 3.5 g. The infrared spectrum showed strong absorptions at 1330, 1305, 1135, 958 and 750 cm^{-1}.

Found: C, 19.54; H, 4.99; S, 50.62. MW,* 117. Calcd. for $C_2H_6O_2S_2$: C, 19.04; H, 4.79; S, 50.81%. MW, 126.

The product inhibited the growth of *Trichophyton rubrum*, *Trichopyton asteroides*, *Bacillus subtilis* and *Escherichia coli* in the minimum concentrations of 15.6, 31.2, 125 and 125 mcg./ml. respectively. A detailed report on the antimicrobial spectrum and toxicity will be published elsewhere.

Summary

1) Methyl methanethiolsulfonate has been obtained from the reaction product of dimethyl sulfoxide with hydrogen chloride. Methyl methanethiolsulfonate has been found to have antifungal and antibacterial activities.

2) It has been suggested that methanesulfenyl chloride is formed from the diacid salt of DMSO and that it reacts with methanesulfinic acid to yield methyl methanethiolsulfonate.

The authors are indebted to Mr. Saburo Nakada for the microanalyses and to Mr. Hiroshi Saito for his assistance in the experimental work.

Department of Applied Chemistry
Faculty of Engineering
Keio University
Koganei-shi, Tokyo

5) T. Zincke and H. Röse, *Ann.*, **406**, 127 (1914).
6) F. G. Bordwell and B. M. Pitt, *J. Am. Chem. Soc.*, **77**, 573 (1955).
7) E. J. Baker, *Rec. trav. chim.*, **67**, 897 (1948); reported b. p. 84~85°C/2.5 mmHg.
* By the cryoscopic method with benzene.

SHORT COMMUNICATIONS

The Polarography of Lead(II) Ions in Fused Sodium Fluoride-Potassium Fluoride-Lithium Fluoride Ternary Eutectic

By Makoto SAITŌ and Shin SUZUKI

(Received October 18, 1963)

So far, it has not been possible to carry out the polarography of metal ions in a medium of fused fluoride salts because of the generally high melting points of fluoride salts and because of their strongly corrosive action. However, a good polarogram of a metal ion was obtained by using a eutectic mixture of sodium fluoride-potassium fluoride-lithium fluoride as the fused salt solvent, as proposed by Bergman et al.[1] The advantage of this solvent are its good thermal stability, the wide span of its electrolytic decomposition potential, its high conductivity and fluidity, and the commercial availability of its components as reagent-grade salts. Further, its melting point is the lowest of all the fluorides, and its chemical reactivity is such that a high pure alumina can be utilized as construction material. The properties of the solvent thus permit, in theory, a study of the electrochemistry of a wide variety of solutes with a minimum of interference from solvent effects and with only moderate experimental difficulty as high-temperature work goes.

In the present work, the dipping-type microelectrode, described in a previous report,[2] was modified for the fluoride bath, as is shown in Fig. 1, and the polarogram of the lead(II) ions in this solvent was obtained.

The fused salt was prepared in the following way: Sodium fluoride, potassium fluoride and lithium fluoride were separately dried in a vacuum desiccator at $10^{-2}\sim10^{-3}$ mmHg for 1~2 weeks. A mixture of 11.5 mol. % of sodium fluoride, 42 mol. % of potassium fluoride and 46.5 mol. % of lithium fluoride was placed in an alumina cell and heated in an electric furnace while being evacuated to $10^{-2}\sim10^{-3}$ mmHg. The temperature was raised to fuse the salts and was maintained at 850~900°C for 1.5~3.0 hr. The furnace temperature was then adjusted to 650±2°C.

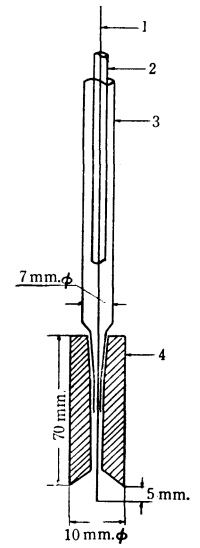


Fig. 1. Dipping type Mo microelectrode for fluoride bath.
1. Mo wire (0.3 mm. ϕ) 3. Quartz glass
2. Borosilicate glass 4. Graphite ring

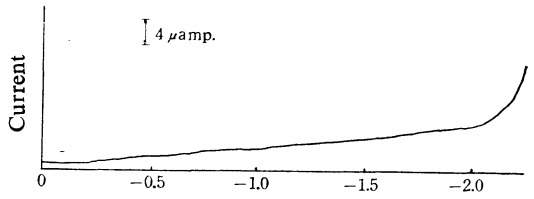


Fig. 2. Residual current curve of fused NaF-KF-LiF eutectic at 650°C.

The residual current curve obtained is shown in Fig. 2. The terminal voltage rise occurred at about −2.1 V. vs. the Mo anode.

1) A. G. Bergman and E. P. Dergnnov, *Compt. rend. acad. sci. U. R. S. S.*, **31**, 754 (1941).
2) H. Gotô, S. Suzuki and M. Saitô, *J. Chem. Soc. Japan, Pure Chem. Sec. (Nippon Kagaku Zasshi)*, **84**, 332 (1963).

A typical polarogram of lead(II) ions is shown in Fig. 3; the wave form is similar to that described in a previous report.[2] The corresponding log plot is shown in Fig. 4. It was found that there is a linear relationship between the applied voltage and $\log(i_d-i)/i$, in spite of the fact that plotting the applied voltage against $\log(i_d-i)$ did not produce a straight line.

The half wave potential was -0.55 V. vs. the Mo anode.

The concentration of lead(II) ions, in the range of 1.95~4.60 mmol./1000 g. fused salt, was found to be directly proportional to the limiting current.

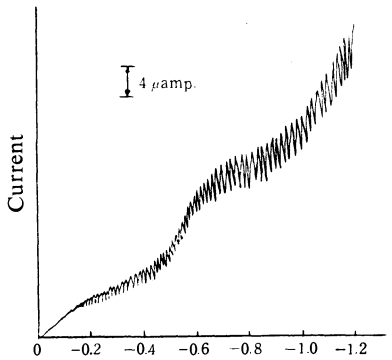


Fig. 3. Polarogram of Pb(II) ion in fused NaF-KF-LiF eutectic at 650°C.

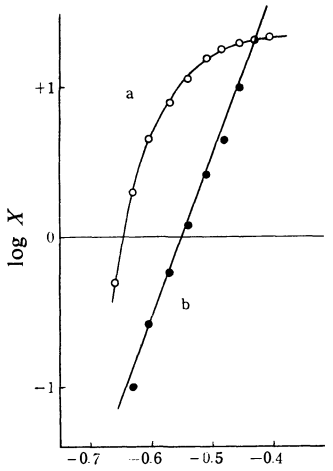


Fig. 4. Log plot of the current-voltage curve of Pb(II) ion.
a: $E\sim\log(i_d-i)$
b: $E\sim\log(i_d-i/i)$

Consequently, it is thought that the procedure described here may be useful for the study of the electrochemical behavior of metal ions in a medium of fused fluoride salt.

The Research Institute for Iron, Steel and Other Metals
Tohoku University
Katahira-cho, Sendai

The Synthesis of an MSH-active Tetrapeptide, L-Histidyl-L-phenylalanyl-L-arginyl-L-tryptophan

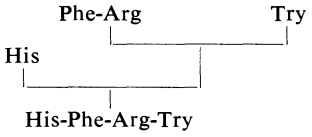
By Hideo OTSUKA and Ken INOUYE

(Received November 7, 1963)

Hofmann and Yajima[1] and Pickering and Li[2] concluded that the key to the melanocyte-stimulating activity resided in the His-Phe-Arg-Try-Gly sequence (positions 6 to 10) in the α-MSH molecule. However, the requirement for the glycine is not yet clear.

We have now synthesized a tetrapeptide, L-histidyl-L-phenylalanyl-L-arginyl-L-tryptophan (I), which exhibits the same level of MSH potency as do the pentapetides, L-histidyl-L-phenylalanyl-L-arginyl-L-tryptophyl-glycine[3] and its D-phenylalanine analog.[4] From this observation it may be concluded that the glycine is not essential for the biological activity, and that the tetrapeptide is the smallest peptide fragment exhibiting MSH activity found so far. The outline of the synthetic route is:

1) K. Hofmann and H. Yajima, *Recent Progress in Hormone Research*, **18**, 41 (1962).
2) B. T. Pickering and C. H. Li, *Biochem. Biophys. Acta*, **62**, 475 (1962).
3) K. Hofmann, M. E. Woolner, H, Yajima, G. Spühler, T. A. Thompson and E. T. Schwarz, *J. Am. Chem. Soc.*, **80**, 6458 (1958); R. Schwyzer and C. H. Li, *Nature*, **182**, 1669 (1958).
4) E. Schnabel and and C. H. Li, *J. Am. Chem. Soc.*, **82**, 4576 (1960).



N^G-Tosyl-L-arginine methyl ester (crystalline free base, m. p. 98~98.5°C, $[\alpha]_D^{25} = +14.8°$ (MeOH)) and *t*-butyloxycarbonyl-L-phenylalanine (prepared from the dicyclohexylamine salt; m. p. 210~212°C decomp., $[\alpha]_D^{25.5} = +28.9°$ (MeOH)) were coupled by the *N*,*N'*-dicyclohexylcarbodiimide (DCCI) method[5] to give *t*-butyloxycarbonyl-L-phenylalanyl-N^G-tosyl-L-arginine methyl ester (II); amorph., $[\alpha]_D^{25} = -5.9°$ (MeOH). Found: C, 56.8; H, 7.0; N, 11.8; S, 5.6. Calcd. for $C_{28}H_{39}O_7N_5S$: C, 57.1; H, 6.7; N, 11.9; S, 5.4%. Compound II was converted into the corresponding acid (III) (amorph., $[\alpha]_D^{24} = +1.0°$ (MeOH). Found: C, 56.0; H, 6.8; N, 11.4; S, 5.8. Calcd. for $C_{27}H_{37}O_7N_5S$: C, 56.3; H, 6.5; N, 12.2; S, 5.6%.) by saponification or into the hydrazide (IV) (crystalline, m. p. 110~114°C, $[\alpha]_D^{24} = -6.3°$ (MeOH)). Found: C, 55.2; H, 7.2; N, 16.6; S, 5.5. Calcd. for $C_{27}H_{39}O_6N_7S$: C, 55.0; H, 6.7; N, 16.6; S, 5.4%. The coupling of the azide (derived from compound IV) with L-tryptophan benzyl ester (m. p. 71°C, $[\alpha]_D^{26.5} = +12.8°$ (MeOH); lit.[6] m. p. 71°C) gave a tripeptide, *t*-butyloxycarbonyl-L-phenylalanyl-N^G-tosyl-L-arginyl-L-tryptophan benzyl ester (V); amorph., purified on a silica gel column, $[\alpha]_D^{24.5} = -6.6°$ (MeOH). Found: C, 63.3; H, 6.4; N, 11.1; S, 3.7. Calcd. for $C_{45}H_{53}O_8N_7S$: C, 63.5; H, 6.3; N, 11.5; S, 3.8%. Compound V was, after the removal of the *t*-butyloxycarbonyl group by trifluoroacetic acid treatment, condensed by the DCCI method with N^α, N^{Im}-dicarbobenzoxy-L-histidine[7] to afford a tetrapeptide derivative, N^α, N^{Im}-dicarbobenzoxy-L-histidyl-L-phenylalanyl-N^G-tosyl-L-arginyl-L-tryptophan benzyl ester (VI); amorph., purified on silica gel, $[\alpha]_D^{24.5} = -10.9°$ (MeOH). Found: C, 64.3; H, 5.9; N, 11.9; S, 3.0 Calcd. for $C_{62}H_{64}O_{11}N_{10}S$: C, 64.4; H, 5.6; N, 12.1; S, 2.8%. The protecting groups of compound VI could be removed by treatment with sodium in liquid ammonia to give peptide I, which was, after purification on a carboxymethyl cellulose column, homogeneous with ninhydrin, Pauly, Ehrlich, and Sakaguchi reagents on paper chromatography ($R_f = 0.55$ in the system of *n*-butanol/acetic acid/water (4/1/2)) and on paper electrophoresis at pH 3.8, 6.6, and 11.1. $\lambda_{max}^{HCl} = 280.5$ mμ (ε, 5100), $[\alpha]_D^{24.5} = -5.4°$ (N HCl). Found: C, 55.3; H, 6.7; N, 18.0. Calcd. for $C_{32}H_{40}O_5N_{10} \cdot CH_3COOH \cdot 2H_2O$: C, 55.1; H, 6.5; N, 18.9%. The amino acid ratios[8] were $His_{1.00}$ $Phe_{1.00}$ $Arg_{1.03}$ ($Try_{0.79}$) (recovery 92.2%) in acid hydrolysate and $His_{1.00}$ $Phe_{1.03}$ $Arg_{0.97}$ $Try_{0.98}$ (recovery 92.5%) in LAP[9] digest. The MSH activity, as estimated by the method of Shizume and Lerner,[10] was 3.6×10^4 units per gram.[11]

The synthesis of compound V is the first instance in which the azide method could be successfully employed in the synthesis of arginyl peptide. When the Arg-Try bond was formed by means of the DCCI method, by the route shown above, the tetrapeptide obtained was contaminated by at least 10 to 15% of the racemate, but it exhibited the same hormonal potency.

Biochemistry Division
Shionogi Research Laboratory
Shionogi & Co., Ltd.
Fukushima-ku, Osaka

5) J. C. Sheehan and G. P. Hess, ibid., **77**, 1067 (1955).
6) M. Brenner and W. Huber, *Helv. Chim. Acta*, **36**, 1109 (1953).
7) K. Inouye and H. Otsuka, *J. Org. Chem.*, **27**, 4236 (1962).
8) D. H. Spackman, W. H. Stein and S. Moore, *Anal. Chem.*, **30**, 1191 (1958).
9) Leucine aminopeptidase, Worthington Biochemical Corporation, lot No. 5930.
10) K. Shizume, A. B. Lerner and T. B. Fitzpatrick, *Endocrinology*, **54**, 553 (1954); A. B. Lerner and M. R. Wright, *Methods of Biochemical Analysis*, **8**, 295 (1960).
11) We wish to express our sincere thanks to Prof. C. H. Li, Hormone Research Laboratory, University of California, for giving us a standard preparation of α-MSH (1×10^9 units per gram).

The Concentration Effect of the Long-range Proton Spin-spin Coupling Constant in Ketones

By Kensuke TAKAHASHI

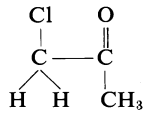
(Received November 11, 1963)

A previous communication[1] has reported that the multiplet structures have been observed in the spectra of the methyl group adjacent to the carbonyl group in ethyl methyl ketone and in isopropyl methyl ketone. Such a coupling has also been investigated in some substituted acetones, CH_3COCH_2X or CH_3COCHX_2 (X=Cl and Br), and it has been pointed out: (1) the more electronegative X is, the less the coupling constant becomes, and (2) this coupling will be dependent upon the dihedral angle between the C–H bond and the π-orbital of the carbon atom in the carbonyl group.[2] Therefore, it is plausible to consider that the coupling will be dependent upon the population of the rotational isomers in each ketone. The four compounds have been examined briefly in the pure liquid and in a 5 mol. % solution in carbon tetrachloride, at 60 Mc. and 22.8±0.5°C. The experimental results are shown in Table I. Although the

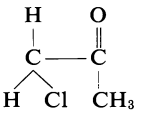
TABLE I. THE LONG-RANGE PROTON-PROTON COUPLING CONSTANTS IN KETONES (IN c. p. s.)

Compound	Pure	in CCl_4
$CH_3COCH(CH_3)_2$	0.45±0.05[1]	0.44±0.03
CH_3COCH_2Br	0.40±0.01	0.37±0.01[2]
CH_3COCH_2Cl	0.33±0.03	0.22±0.03[2]
$CH_3COCHCl_2$	0.24±0.03	0.30±0.01[2]

differences are very small, the variation of the coupling constants is clearly real. This result is acceptable on the basis of the following consideration about the rotational isomers. In chloroacetone, Mizushima[3] and Bellamy[4] suggested two rotational isomers, I and II, on the basis of the infrared and dipole moment studies. The carbonyl-stretching frequencies of this compound were observed at 1752 and 1726



I



II

cm^{-1} in a carbon tetrachloride solution,[4] corresponding to the two rotational isomers, the cis-form (I) and the trans-form (II) with respect to the Cl atom and the CO group, respectively. The former is more polar than the latter, so that a very marked change in the relative intensities of these bands was observed when the compound passed from the pure liquid to the solution in carbon tetrachloride. The contribution of each hydrogen in I and II, depending upon the dihedral angle (ψ), to the long-range coupling in chloroacetone is supposed to be:

$$a \sim P_{\mathrm{I}}[a(30°)+a(30°)]+P_{\mathrm{II}}[a(30°)+a(90°)]$$

$$a(\psi) \propto \cos^2\psi$$

where a corresponds to the hyperfine constant as defined by Karplus[5] and where P_i is the population of the i isomer. Therefore, the contribution of II is half that of I. The decrease in the coupling constant in a carbon tetrachloride solution may be caused by the increase in the population of II as compared with that of I. This kind of variation in the long-range coupling constants has not yet been reported in the literature. Detailed results will be published later in this Bulletin.

The Chemical Research Institute of Non-Aqueous Solutions
Tohoku University
Katahira-cho, Sondai

1) K. Takahashi, This Bulletin, 35, 1046 (1962).
2) K. Takahashi, Paper presented at the Symposium on Molecular Structure, Sendai, October, 1963.
3) S. Mizushima, T. Shimanouchi, T. Miyazawa, I. Ichishima, K. Kuratani, I. Nakagawa and N. Shido, *J. Chem. Phys.*, 21, 815 (1953).
4) L. J. Bellamy and R. L. Williams, *J. Chem. Soc.*, 1957, 4294.
5) M. Karplus, *J. Chem. Phys.*, 33, 1842 (1960).

Tetraphenylallene- and Tetraphenylbutatriene-Iron π-Complexes

By Akira NAKAMURA, Pu-Jun KIM and Nobue HAGIHARA

(Received December 7, 1963)

Although a number of organometallic π-complexes of conjugated 1,3-diene systems have been reported,[1] no report on an example of the π-complexes of cumulene systems has been published as yet. We will now report a preparation which is believed to be the first example of the π-complexes of the cumulene systems.

The reaction of tetraphenylallene with an excess of iron pentacarbonyl in refluxing isooctane under nitrogen for 13 hr. proceeded with the evolution of a gas. After the removal of the solvent from the deep reaction mixture, a red semisolid was obtained. The semisolid crystallized from ethanol to give red crystals (I) (m. p. 102~103°C, decomp. 230°C) in 29% yield. The elemental analysis and molecular weight determination indicated the composition: (tetraphenylallene)$Fe(CO)_3$, (Found: C, 74.00; H, 4.45; mol. wt. (in benzene), 518. Calcd. for $C_{30}H_{20}FeO_3$: C, 74.39; H, 4.16%; mol. wt., 484).

Carbon monoxide (2.6 mol. equiv.) was evolved on the pyrolysis of I under nitrogen. The pyrolysis gave tetraphenylallene and 1,1-diphenyl-3-phenylindene.[2] The infrared spectrum of I showed the presence of terminal iron carbonyl groups (2060, 1999, and 1985 cm^{-1} in carbon tetrachloride) and phenyl groups. In the visible region it showed a maximum at 468 mμ (log ε: 2.91) and had an increasing absorption towards the shorter wavelengths. The compound I was found to be diamagnetic and was quite stable in air. It was soluble in *n*-hexane, benzene and ethanol.

Tetraphenylbutatriene was allowed to react with an excess of iron pentacarbonyl in ethylcyclohexane under nitrogen for 14 hr. at reflux. The evolution of a gas was accompanied by a change in color to deep red. Red crystals mixed with a small number of yellow ones were obtained on cooling. The product was purified by repeated crystallization from a benzene-*n*-hexane mixture. Pure red crystals (II) (decomp. 200°C) were obtained in 26% yield. The product was found to have the composition: (tetraphenylbutatriene)$Fe_2(CO)_5$. (Found: C, 64.90; H, 3.55; mol. wt. (in benzene) 500. Calcd. for $C_{33}H_{20}Fe_2O_5$: C, 65.16; H, 3.31 %; mol. wt., 608).

The amount of carbon monoxide which evolved upon pyrolysis indicated five CO groups present in a molecule of II. The pyrolysis gave tetraphenylbutatriene and 1-diphenylmethylene-3-phenylindene.[2] The infrared spectrum of II showed the presence of terminal iron carbonyl groups (2072, 2035, 1998, and 1988 cm^{-1} in carbon tetrachloride) and phenyl groups. The visible and ultraviolet spectra showed no maxima.[3] An increasing absorption towards shorter wavelengths was observed. This spectral evidence indicates the absence of tetraphenylbutatriene chromophore, which has a strong absorption maximum at 420 mμ. Therefore, the butatriene chromophoric system is destroyed by bonding with the iron carbonyl group. The compound II was diamagnetic and was stable in air. It was soluble in benzene and slightly soluble in *n*-hexane.

It is interesting to discuss how these cumulene systems interact with iron carbonyl groups. The bonding of the iron tricarbonyl group in I through the benzene nucleus is very unlikely since no examples of benzene iron tri- or dicarbonyl type compounds are known. The bonding through one of the double bonds of the allene system and a double bond of the benzene nucleus is also less probable as a possible steric hindrance. Therefore, we are left with the possibility of the bonding through two double bonds of the allene system. We believe that cumulated double bonds in a straight chain are responsible for stable bond formation. By similar reasoning and also from the spectral evidence, we judge that the bonding in II is probably through the butatriene system. The chemical approach to the structure determination seems to be inconclusive to us. It is hoped that structure elucidation by means of X-ray will clarify the nature of the bonding in these compounds.

The Institute of Scientific and Industrial Research
Osaka University
Sakai, Osaka

1) a) R. G. Guy and B. L. Shaw, "Advances in Inorganic Chemistry and Radiochemistry," Vol. IV, Academic Press Inc., New York (1962), p. 78; b) M. A. Bennett, *Chem. Revs.*, **62**, 611 (1962): c) E. O. Fischer and H. Werner, *Angew. Chem.*, **75**, 57 (1963).

2) Identified by a comparison of the infrared spectra of the authentic samples.

3) The visible and ultraviolet spectra were measured, I in ethanol, II in tetrahydrofuran.

*Tensammetric Waves in Oscillographic Square-wave Polarography**

By Koichi OKAMOTO

(Received October 10, 1963)

In previous papers[1-5] the oscillographic square-wave polarographic behavior of some reducible or oxidizable depolarizers has been reported on. Since the oscillographic square-wave polarograph can selectively eliminate the charging current by means of the gating and the positive feed-back techniques, as described in a previous paper,[1] the reduction or the oxidation waves obtained by this method may contain none of the charging current. On the contrary, the changes of the electric double layer at the electrode surface, according to the adsorption or desorption of surface-active substances, can be observed as tensammetric waves by this polarograph. This work will study the possibility of the observation of tensammetric waves by means of this polarograph and will compare the properties of the waves with those obtained by a conventional a. c. polarograph.

There are two experimental methods used in order to obtain the tensammetric waves by this equipment. One of them is the suitable regulation of the amount of the positive feed-back of an electrolytic current. Another method is the removal of the gating circuit from the electric circuit of the polarograph. In the present study the measurements were carried out under the optimum positive feed-back conditions.

In this paper the behavior of such surface-active substances as aliphatic alcohols and several synthesized surface active substances will be presented in relation to their behavior in the pen-recording sine wave a. c. polarograph. Moreover, the measuring method of the critical micelle concentrations of the synthetic surface-active substances will also be presented.

Experimental and Results

Apparatus.—The oscillographic square-wave polarograph reported on in a previous paper[1] was used. A pen-recording a. c. polarograph (Yanagimoto Model PA-102; frequency=50 c. p. s., amplitude=15 mV_{p-p}) was also used. The characteristics of the DME used were $m=0.529$ mg. sec^{-1}, $t=6.26$ sec. (open circuit) in a 1 N sodium sulfate solution.

The measurements were carried out at 25±0.5°C unless otherwise stated, and the potentials were referred to the external SCE, which was connected to the mercury pool anode through a 200 μF condenser. The dissolved air was removed by nitrogen gas. The degree of the positive feed-back of the electrolytic current was fixed at the optimum point for the base solution so as to completely eliminate its charging current, and then the studies with the sample solutions were carried out.

The Behavior of Aliphatic Alcohols.—In the oscillographic square-wave polarograph, the wave which appears at the potentials more positive than zero can not be observed because of the large charging current of the dissolution of the Hg-cathode, so only the waves appearing between 0 and −2 V. vs. SCE were studied.

The Summit Potentials and Currents.—Most of the aliphatic alcohols studied gave clear tensammetric waves, as is shown in Figs. 1—3; their summit potentials and currents are shown in Table I.

Generally speaking, the weakly surface-active alcohols, such as *n*- and isopropyl alcohols and *n*-butyl alcohol, show the broad waves, while the strongly surface-active alcohols, such as *t*-amyl alcohol and *n*-octyl alcohol, show the sharp waves.

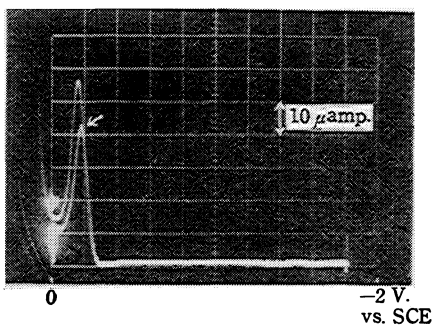


Fig. 1. 1 mol./l. isopropyl alcohol in 1 N Na_2SO_4, air free, 25°C. The wave in the cathodic sweep process is indicated by an arrow.

* Oscillographic Square Wave Polarography. Part VI.

1) Y. Saitō and K. Okamoto, *Rev. Polarography*, **10**, 227 (1962).
2)-4) K. Okamoto, ibid., in press.
5) K. Okamoto, This Bulletin, **36**, 1381 (1963).

TABLE I. THE SUMMIT POTENTIALS AND CURRENTS OF ALIPHATIC ALCOHOLS

Base solution: 1 N Na_2SO_4, 25±0.5°C, air free

Alcohol	Concn.	Oscillographic				Pen-recording	
		$-E_s$, V. vs. SCE		i_s, μamp.		$-E_s$ V. vs. SCE	i_s μamp. r.m.s.
		Cathodic	Anodic	Cathodic	Anodic		
Isopropyl-	1 M	0.138 1.112	0.123 1.112	38.7 5.0	50.4 5.0	1.080	0.30
n-Butyl-	Satd.	1.335	1.317	39.9	43.0	1.334	0.69
t-Butyl-	1 M	0.069 1.456	0.048 1.456	24.8 1.1	42.0 1.1	0.035 1.281	2.25 0.59
n-Amyl-	Satd.	1.247	1.242	7.3	8.4	1.278	1.15
t-Amyl-	Satd.	1.335	1.315	72.0	74.8	1.349	1.11
Isoamyl-	Satd.	1.244	1.236	5.9	7.3	0.052 1.250	1.35 1.16
n-Hexyl-	Satd.	1.234	1.209	14.0	15.6	0.034 1.239	1.26 2.01
s-Hexyl-	Satd.	1.216	1.194	58.6	65.2	1.211	1.76
n-Heptyl-	Satd.	1.194 1.240	1.148 1.231	2.2 23.7	27.9 14.5	1.041 1.193	0.36 0.76
3-Heptyl-	Satd.	1.218	1.198	30.2	36.3	1.217	1.34
4-Heptyl-	Satd.	0.044 1.130	0.017 1.114	18.8 6.0	? 6.6	0.045 1.116	2.25 1.01
n-Octyl-	Satd.	0.053 1.126	0.032 1.116	21.0 99.2	5.0 130.6	1.134	1.19
2-Octyl-	Satd.	1.018	0.110	0.7	5.3	0.040 1.100	1.20 0.13
n-Nonyl-	Satd.	0.035 1.118	0.035 1.089	10.7 37.2	23.9 2.4	0.022 1.110	1.38 0.87
n-Decyl-	Satd.	1.069	0.050 1.060	16.6	25.0 0.9	0.039 1.070	1.60 1.18
n-Undecyl-	Satd.	0.087 0.060	0.063 0.096 1.053	21.6 13.2	29.7 7.6 6.3	0.026 1.073	1.04 0.40
Cyclohexyl-	Satd.	0.119 1.385	0.065 1.369	2.3 35.7	5.1 34.6	1.442 1.650	1.38 1.27

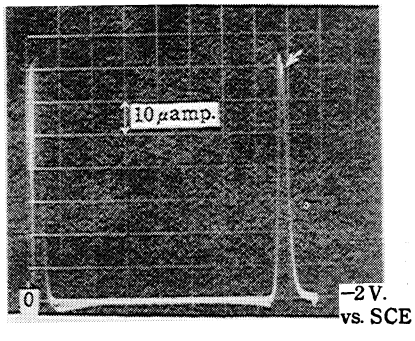


Fig. 2. *t*-Amyl alcohol satd. in 1 N Na_2SO_4, air free, 25°C.

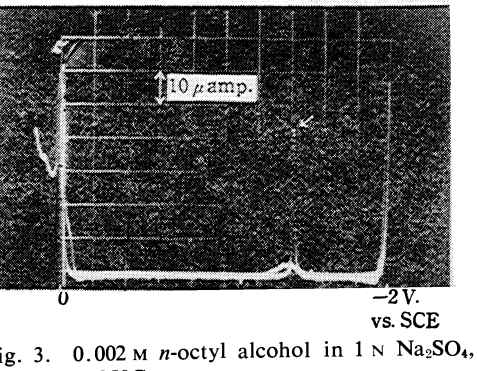


Fig. 3. 0.002 M *n*-octyl alcohol in 1 N Na_2SO_4, air free, 25°C.

With the oscillographic square-wave polarograph, the waves in the cathodic and the anodic sweep processes are very similar to each other, as is shown in Figs. 1 and 2. This is considered to correspond to the a. c. polarographic-reversible property of the adsorption-desorption reactions. Some exceptions were, however, observed, as in the case of *n*-octyl alcohol (Fig. 3). This may indicate an a. c. polarographic-irreversible property.

The Relation of the Concentrations to the Summit Potentials and Currents.—The findings on *t*-amyl alcohol are shown in Figs. 4 and 5. The summit potentials of their positive and negative tensammetric waves tend to approach each other as the concentration decreases, and the relationships between $(E_s^c - E_{ecm})^2$ or $(E_s^a - E_{ecm})^2$ and $\log C$ were linear, where

E_{ecm} is the electro-capillary maximum potential. In the present study, $E_{ecm} = -0.50$ V. vs. SCE was employed according to the electro-capillary curve. The summit currents increased to the limiting values as the concentration increased. However, the relation of $\log C$ to the summit current, i_s^c or i_s^a, was not linear. This relation of $\log C$ to i_s values is not the same as the finding reported by Senda[8] on the a. c. waves of *t*-amyl alcohol obtained by by a pen-recording a. c. polarograph.

Temperature Effects.—As Fig. 6 shows, the summit currents of *t*-amyl alcohol decreased with the rise in temperature, while the summit potential scarcely changed. These results may show the typical properties of the adsorption waves.

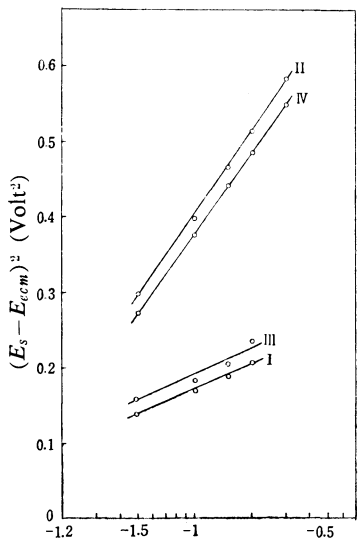


Fig. 4. Relation of $(E_s-E_{ecm})^2$ to $\log C$.
t-Amyl alcohol in 1 N Na_2SO_4, 25°C, air free
I, II: Positive and negative waves in cathodic process respectively
III, IV: Positive and negative waves in anodic process respectively

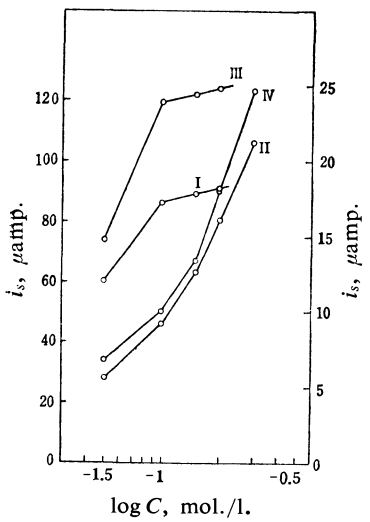


Fig. 5. Relation of i_s to $\log C$.
t-Amyl alcohol in 1 N Na_2SO_4, 25°C, air free
I, II: Positive and negative waves in cathodic process respectively
III, IV: Positive and negative waves in anodic process respectively

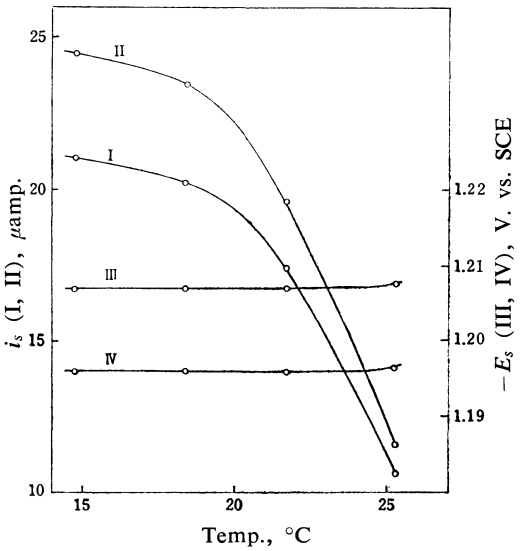


Fig. 6. Relations of i_s and E_s to temperature.
0.15 mol./l. *t*-amyl alcohol in 1 N Na_2SO_4, air free
I, III: Negative wave in cathodic process
II, IV: Positive wave in anodic process

The Behavior of the Mixtures of Alcohols.—When the pen-recording a. c. polarograph is used the solution containing two or more surface-active substances gives the tensammetric wave of only one component which has the strongest surface activity.[6]

The polarographic behavior of the binary mixtures shown in Table II was studied.

The system of isopropyl alcohol - *n*-butyl alcohol showed waves similar to those of *n*-butyl alcohol. No wave of isopropyl alcohol could be observed. The summit potentials, however, of the mixture were slightly more negative than those of *t*-butyl alcohol, and the summit currents were not equal to those of *t*-butyl alcohol. A similar result was also obtained with an isopropyl alcohol - *t*-amyl alcohol system. The mixture of *t*-amyl alcohol and *n*-

6) M. Maruyama et al., *Kagaku-no Ryōiki, Extra Ed.*, **50**, 124 (1962).

TABLE II. THE SUMMIT POTENTIALS AND CURRENTS OF THE MIXTURES OF ALCOHOLS

Base solution: 1 N Na_2SO_4, 25°C, air free

Alcohol	Concn. M	Oscillographic $-E_s$, V. vs. SCE Cathodic	Oscillographic $-E_s$, V. vs. SCE Anodic	Oscillographic i_s, μamp. Cathodic	Oscillographic i_s, μamp. Anodic	Pen-recording $-E_s$ V. vs. SCE	Pen-recording i_s μamp. r.m.s.
Isopropyl-	0.5	0.201 1.112	0.214 1.112	17.8 3.5	30.0 3.5	1.080	0.30
n-Butyl-	0.5	1.337	1.306	19.3	29.4	1.294	0.33
t-Amyl-	0.5	1.337	1.317	29.3	40.9	1.268	0.49
n-Octyl-	0.002	1.152	1.137	44.4	3.5	1.062	0.07
Isopropyl- +*n*-butyl-	0.5 0.5	1.372	1.335	20.5	28.1	1.323	0.53
Isopropyl- +*t*-amyl-	0.5 0.5	1.341	1.335	45.1	69.2	1.239	0.83
n-Butyl- +*t*-amyl-	0.5 0.5	1.275	1.256	20.5	30.5	1.314	0.38
t-Amyl- +*n*-octyl-	0.5 0.002	1.344	1.324	29.4	39.2	1.286	0.17

TABLE III. THE SUMMIT POTENTIALS AND CURRENTS OF SYNTHETIC SURFACE ACTIVE SUBSTANCES

Base solution: 0.5 M KCl, 25°C, air free

Compound	Concn. M	$-E_s$, V. vs. SCE Cathodic	$-E_s$, V. vs. SCE Anodic	i_s, μamp. Cathodic	i_s, μamp. Anodic
CTACl*1	10^{-2}	0.069	—	27.6	—
SLS*2	10^{-3}	1.209	1.168	24.0	1.2
NaCap.*3	10^{-2}	0.074 1.069	0.048 1.069	14.8 2.0	13.7 2.0
SPEG-19*4	$5\cdot10^{-3}$	ca. 0.14 1.757	0.144 1.746	ca. 2 50.1	13.7 23.3
SPEG-30*5	$5\cdot10^{-3}$	ca. 0.12 ca. 1.78	0.111 1.749	ca. 2 55.2	ca. 4 40.0
SPEG-40*6	5.10^{-3}	ca. 0.11 1.784	ca. 1.1 1.753	ca. 2 58.6	ca. 2 51.2
LPEG-8*7	10^{-2}	1.761	1.760	68.8	17.1
OPEG-10*8	10^{-2}	1.784	1.783	66.5	25.6
OPEG-12*9	10^{-2}	1.780	1.773	45.5	31.8
NPPEG-10.5*10	10^{-2}	1.746	1.747	71.0	7.4
NPPEG-12*11	10^{-2}	1.787	1.786	48.9	36.4

*1 Cetyltrimethylammonium chloride
*2 Sodium lauryl sulfate, base solution=0.5 N Na_2SO_4
*3 Sodium caprate
*4 Stearylpolyethyleneglycol ether (n=19)
*5 n=30
*6 n=40
*7 Laurylpolyethyleneglycol ether (n=8)
*8 Oleylpolyethyleneglycol ether (n=10)
*9 n=12
*10 Nonylphenylpolyethyleneglycol ether (n=10.5)
*11 n=12

octyl alcohol showed quite the same waves as those of *t*-amyl alcohol. However, the mixture of *n*-butyl alcohol and *t*-amyl alcohol gave a wave with a more positive summit potential and a higher summit current than those of the individual components.

The tensammetric wave of a mixed alcohol solution may correspond to the wave of the alcohol, the negative tensammetric wave of which appears at more negative potentials than that of the other alcohol. When the summit potentials of the alcohols in a mixture are, however, almost identical, a new wave appears as is observed in a *n*-butyl alcohol - *t*-amyl alcohol mixture.

The Synthetic Surface-active Agents. — A cationic agent (cetyltrimethylammonium chloride (CTACl)), and anionic agents (sodium

caprate (SC) and sodium laurylsulfate (SLS)) of the reagent grade were studied. Non-ionic agents (oleylpolyethyleneglycol ethers ($n=10$ and 12, OPEG), stearylpolyethyleneglycol ethers ($n=19$, 30 and 40, SPEG), laurylpolyethyleneglycol ether ($n=8$, LPEG) and nonylphenylpolyethyleneglycol ethers ($n=10.5$ and 12, NPPEG)) which had been synthesized in this laboratory were also studied.

The Summit Potentials and Currents. — The samples studied, except SLS, gave the waves at the potentials near to 0 and −2 V., as Fig. 7 shows. The numerical data are listed in Table III. The shape of the waves is very sharp, and their heights in the cathodic and the anodic processes were not generally equal.

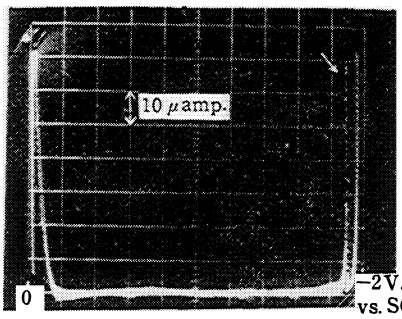


Fig. 7. 10^{-2} mol./l. oleylpolyethyleneglycol ether ($n=10$) in 0.5 M KCl, air free, 25°C.

The Relation of the Concentrations to the Summit Potentials and Currents.—The effect of the concentration change upon the cathodic waves of the non-ionic agent OPEG is shown in Fig. 8. The summit current increases to the limiting value as the concentration increases, and the potentials began to shift to more negative values at concentrations lower than ca. 2×10^{-4} mol./l.

The Influence of the Micelle Formation upon the Polarographic Waves of Some Metallic Ions. —In order to obtain the relation of critical micelle concentration (CMC) to the polarographic data, the values of the CMC of several agents were measured beforehand by the usual spectrophotometric method, using the color change of a dye.[7] The results are listed in Table IV.

The obscure negative shift of the summit potential of OPEG at the concentration of ca. 2×10^{-4} mol./l. (Fig. 8) was thought to correspond nearly to the CMC of OPEG, but the waves at such low concentrations can not be measured well. Therefore, the detection of the CMC from the concentration $-E_s$ or i_s curves is not a suitable method.

7) T. Nakagawa, *Shionogi's Ann. Rep.*, **8**, 31 (1958).

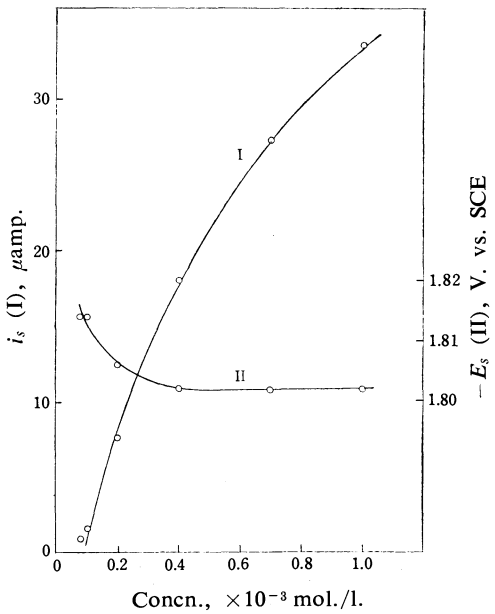


Fig. 8. Relation of i_s and E_s to concentration.
Oleylpolyethyleneglycol ether ($n=10$) in 0.5 N Na_2SO_4, 25°C, air free

The d. c. polarographic wave of a metallic cation is considerably affected by the addition of a surface-active agent, so the CMC of the agent can be detected by the change in the wave height or the half-wave potential of the metallic cation.[7] This change may mean a decrease in the reversibility of the electrode reaction of a metallic cation. The a. c. polarographic method is more sensitive than the d. c. method with respect to the response to the change in the reversibility of the electrode reaction. Therefore, the author's oscillographic method was also considered to be suitable for this purpose. Moreover, with this polarograph, since the cathodic and the anodic waves can be observed continuously, the change of the wave form can be observed more precisely than with the conventional pen-recording method.

The metallic ions used were lead(II) and zinc(II), which give a reversible and a quasi-reversible wave respectively. The surface-active agents used were CTACl, SLS, OPEG and NPPEG. The measurements were carried out in a deoxygenated 0.5 N sodium sulfate aqueous solution containing a constant amount of the metallic ions (2.5×10^{-4} mol./l. in lead(II) or 10^{-3} mol./l. in zinc(II)) and also various amounts of the surface-active agents. The degree of the positive feed-back of the electrolytic current was fixed at the optimum point for the solution of 0.5 N sodium sulfate containing only the metallic ions.

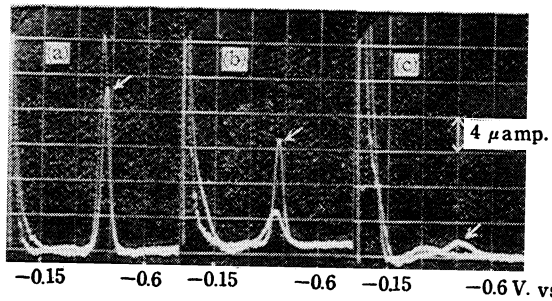


Fig. 9. 0.25×10^{-3} mol./l. Pb(II) + OPEG ($n=10$); (a) 0.01×10^{-3}, (b) 0.10×10^{-3}, (c) 0.20×10^{-3} mol./l., in 0.5 M KCl, air free, 25°C.

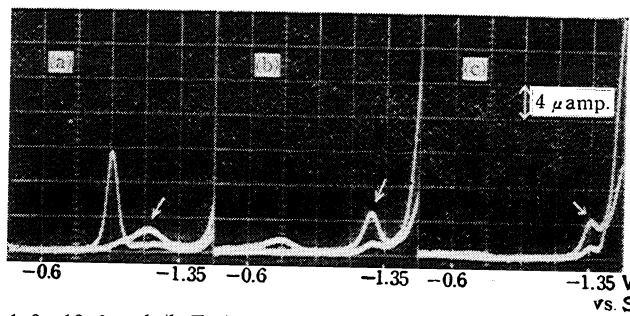


Fig. 10. 1.0×10^{-3} mol./l. Zn(II) + OPEG ($n=10$); (a) 0, (b) 0.10×10^{-3}, (c) 0.40 $\times10^{-3}$ mol./l., in 0.5 N Na_2SO_4, air free, 25°C.

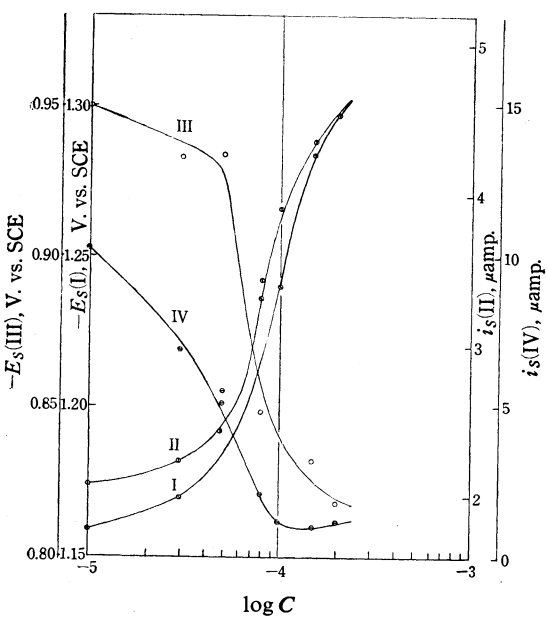


Fig. 11. Relations of i_s and E_s of waves of 1×10^{-3} mol./l. Zn(II) to concentration of CTACl, 25°C, air free, in 0.5 N Na_2SO_4.

I, II: Reduction wave
III, IV: Oxidation wave

Typical changes in the reduction and the oxidation waves of lead(II) and zinc(II) upon the addition of OPEG are shown in Figs. 9 and 10 respectively. In all the cases studied, the remarkable decrease in the summit currents and the shifts in the summit potentials were observed at the concentration near to the CMC. These relations are indicated in Fig. 11 in the case of the zinc(II)-CTACl system.

The nature of these changes can not be explained theoretically, but the inclusion of a metallic ion by the micelles or the increase in the thickness of the adsorption layer on the electrode surface upon the micelle formation may interfere with the electrode reaction of the metallic ions.

The concentration ranges where the summit potentials and currents of the metallic ions changed are summarized in Table IV. It appears that they represent the appoximate CMC values of the surface-active agents.

TABLE IV. THE CMC VALUES

Solvent: 0.5 N Na_2SO_4, 25±0.5°C

Compound	By oscillographic square wave polarograph $\times10^{-4}$ mol./l.	By spectrophotometric method $\times10^{-4}$ mol./l.
CTACl	0.4～1.8	2.0*1
SLS	2.0～5.0	1.5*2
OPEG-10	0.5～1.8	2.5*2
NPPEG-10.5	0.3～1.1	1.5*2

*1 Obtained from the shift of λ^{516}_{max} and ε^{516}_{max} of eosin yellow

*2 Obtained from the shift of λ^{547}_{max} of pinacyanol chloride

Discussion

The tensammetric waves of surface-active substances are said to correspond to the reversible wave in a pen-recording a. c. polarograph. This is also applicable to an oscillographic square-wave polarograph. As has been described in previous sections. the tensammetric wave could be observed very clearly and rapidly by means of the oscillographic method.

The values of the summit potentials of aliphatic alcohols obtained with the oscillographic method were almost always equivalent to those obtained with the pen-recording method as is shown in Table I. The summit current values, on the other hand, were found to be very much higher than those obtained by means of the pen-recording method. This may be mainly due to the difference between the frequencies of the a. c. potentials: the oscillographic method employs 3 kc./sec. and the pen-recording method employs 50 c.p.s. The sensitivity of the oscillographic square wave polarograph for the measurement of the adsorption-desorption wave is superior to that of the pen-recording polarograph.

The relation between the logarithm of the concentrations and the square of the summit potentials of *t*-amyl alcohol showed a linear relation similar to that in a pen-recording polarograph, as Fig. 4 shows.

When the concentration of a surface active substance is comparatively high, and when the concentrations at the electrode surface and in the bulk solution (C_n^0) can be thought to be equal, the relation of the summit potential to the bulk concentration may be expressed as $\ln C_n^0 \propto (E_s - E_{ecm})^2$, as was shown by Senda.[8] This relation seemed to be adaptable to the oscillographic polarographic waves of *t*-amyl alcohol.

The summit currents increased as the concentration increased, but the behavior of the positive tensammetric wave was not equal to that of the negative tensammetric wave (cf. Fig. 5). The relation between the $\log C$ and i_s of the negative wave is near to the linear relation.

The wave height in an anodic sweep process, as was observed on *n*-octyl alcohol (Fig. 3) and also on synthetic surface-active agents (Fig. 7), is not equal to that in a cathodic process. This may indicate the a. c. polarographically-irreversible property of their adsorption-desorption processes.

The critical micelle concentration of synthetic surface-active agents can be measured or detected by means of the measurement of the change, caused by the addition of the surface-active agents, in the summit potentials or the currents of such metallic ions as lead(II) and zinc(II). The mechanisms of the change in the form of the reduction or oxidation waves of the ions may possibly be studied by means of the author's polarograph.

8) M. Senda and I. Tachi, *Rev. Polarography*, **10**, 79 (1962).

Summary

The possibility of observing the tensammetric waves of surface-active agents by an oscillographic square wave polarograph has been investigated. Well-defined tensammetric waves of some aliphatic alcohols, as well as those of some synthetic surface-active agents, can be obtained both in the cathodic and anodic sweep processes. The summit potential values, measured by the oscillographic method and pen-recording method, are almost identical. The relations of the concentrations and temperature to the summit potentials obtained by the two methods are almost equivalent, also. However, the summit current observed by the oscillographic method is higher than that obtained by the pen-recording method, and also the relation of $\log C$ to i_s is not equivalent.

In order to measure the CMC of surface-active agents, the author had made use of the fact that, at the CMC of the agents, the form of the reduction or the oxidation wave of a metallic ion added to the solution of the agent changes remarkably. This method is thought to be superior to the conventional d. c. polarographic method, for the reduction and also the oxidation waves of a metallic ion can be observed, and the response to the change in the reversibility of the electrode reaction is much faster than with the d. c. method.

The author is much indebted to Professor Taichirō Fujinaga (Kyōto University) for his kind instruction and to Dr. Munetoshi Matsui and Dr. Akira Itō (both of this laboratory) for affording facilities for this investigation.

Research Laboratories of
Sankyo Co., Ltd.
Sinagawa-ku, Tokyo

Synthetic Studies of Sesamol Derivatives. IV.[*1] *Preparation and Reaction of 2-Hydroxy-4, 5-methylenedioxyacetophenones*[*2]

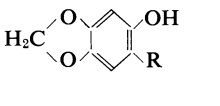
By Kenji FUKUI and Mitsuru NAKAYAMA

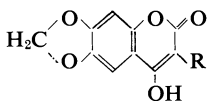
(Received July 30, 1963)

In continuation of a series of studies of sesamol derivatives, the present paper will report on the preparation of 2-hydroxy-4, 5-methylenedioxyacetophenones (I) and the reaction of I to give 4-hydroxycoumarins (II).

2-Hydroxy-4, 5-methylenedioxyacetophenone (Ia)[1] has been obtained by the Fries rearrangement of sesamol acetate in a poor yield (5%). A better result (35%) was obtained by means of the Hoesch reaction of sesamol (III) with acetonitrile. On the other hand, the acetylation of III with acetic acid and boron trifluoride to obtain the ketone Ia was extremely difficult, and it was unsuccessful with polyphosphoric acid. The failure may be due to an attack on the methylenedioxy system by the reagents which is not encountered in the Hoesch reaction. The Friedel-Crafts reaction of the methyl ether[2] of III also gave Ia (36%). By a similar Hoesch reaction employing methoxyacetonitrile and phenylacetonitrile, III was converted into 2-hydroxy-4, 5-methylenedioxy-ω-methoxyacetophenone (Ib)[3] and 2-hydroxy-4, 5-methylenedioxyphenyl benzyl ketone (Ic) respectively. 4-Hydroxyayapin (IIa) was obtained from Ia with ethyl carbonate,[4] but not with ethyl chloroformate.[5] The condensation of Ia with ethyl cyanoacetate[6] also gave IIa. On the other hand, either with ethyl carbonate or with ethyl chloroformate, Ib and Ic were converted into 3-methoxy- (IIb) and 3-phenyl-4-hydroxy-6, 7-methylenedioxycoumarin (IIc) respectively. 7-Benzyloxy-3-(3′, 4′-methylenedioxyphenyl)-4-hydroxycoumarin (IV) was obtained from 4-benzyloxy-2-hydroxyphenyl 3, 4-methylenedioxybenzyl ketone[7] with the former reagent.

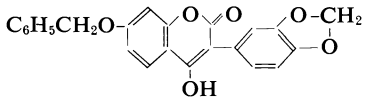
These 4-hydroxycoumarins (II) exhibited fluorescence in alcohol, as did 3-substituted ayapin,[8] and the fluorescence of the acetate and the methyl ether of IIc was especially strong.





Ia R=$COCH_3$
Ib R=$COCH_2OCH_3$
Ic R=$COCH_2C_6H_5$
III R=H

IIa R=H
IIb R=OCH_3
IIc R=C_6H_5



IV

Experimental[*3]

2-Hydroxy-4,5-methylenedioxyacetophenone (Ia).—*The Hoesch Reaction.*—A mixture of III (5.0 g.),[9] acetonitrile (2.0 g.) and anhydrous zinc chloride (2.0 g.) in dry ether (30 ml.) was saturated with dried hydrogen chloride for 3 hr. at 0°C and then allowed to stand overnight. The ethereal solution was decanted from the greenish mass of ketimine hydrochloride which had separated. The residue was washed twice with dry ether (20 ml.) and then heated on a steam bath with water (30 ml.) for 0.5 hr. After cooling and standing, the resulting precipitates were collected and recrystallized from ethanol to give Ia in the form of pale yellow needles; m. p., 113~114°C (reported m. p. 114°C[1]); yield, 2.3 g. (35%). This was identical with an authentic sample[1] and gave a blue color with alcoholic ferric chloride solution. IR: 1634 (C=O); 1023, 918 (O-CH_2-O) cm^{-1}.

Found: C, 59.77; H, 4.53. Calcd. for $C_9H_8O_4$: C, 60.00; H, 4.33%.

The Boron Trifluoride Method.—With good cooling, a solution of III (5.0 g.) in acetic acid (40 ml.) was saturated with dried boron trifluoride for 3 hr., during which time care was taken to prevent the formation of solids. The resulting solution was heated at 80~90°C for 1.5 hr. and poured into a

*1 Part III: K. Fukui and M. Nakayama, *J. Chem. Soc. Japan, Pure Chem. Sec.* (*Nippon Kagaku Zasshi*), **84**, 606 (1963).

*2 Presented in part at the Tokushima Meeting of the Chemical Society of Japan, Tokushima, August, 1962.

1) A. Romeo and G. Gargellini, *Ann. chim.* (*Rome*), **42**, 361 (1952); *Chem. Abstr.*, **47**, 10529 (1953).

2) K. Fukui and M. Nakayama, *J. Chem. Soc. Japan, Pure Chem. Sec.* (*Nippon Kagaku Zasshi*), **84**, 606 (1963).

3) K. Fukui and T. Matsumoto, This Bulletin, **35**, 1931 (1962).

4) J. Boyd and A. Robertson, *J. Chem. Soc.*, **1948**, 174.

5) A. H. Gilbert, A. McGookin and A. Robertson, ibid., **1957**, 3740.

6) A. Sonn, *Ber.*, **50**, 1292 (1917).

7) H. S. Mahal, H. S. Rai and K. Venkataraman, *J. Chem. Soc.*, **1934**, 1769.

8) K. Fukui and M. Nakayama, This Bulletin, **35**, 1321 (1962).

*3 All melting points are uncorrected; the infrared spectra were measured in Nujol, while the ultraviolet spectra were measured in an ethanol solution.

9) K. Fukui and M. Nakayama, *J. Sci. Hiroshima Univ.*, Series A-II, **26**, 131 (1963).

saturated sodium acetate solution (100 ml.). After the solution had been extracted with ether, the ethereal solution was washed with a saturated sodium bicarbonate solution and water. The product was recrystallized from ethanol to give Ia; m. p. 112~113°C; yield, 0.3 g. (5%). It was identical with the above sample.

The Friedel-Crafts Reaction.—To a solution of anhydrous aluminum chloride (5.0 g.) in dry ether (50 ml.), sesamol methyl ether (b.p. 110~114°C/18 mmHg)[2] (3.0 g.) was added. Acetyl chloride (2.0 g.) was well stirred drop by drop into the solution for 0.5 hr., the stirring was continued another 5 hr. at room temperature, and the mixture was allowed to stand overnight. The ethereal solution was decanted from the dark-colored mass. Ice water containing dilute hydrochloric acid was cautiously added to the residue in order to dissolve the aluminum compounds. The crystalline product was collected and recrystallized from ethanol to give Ia (m.p. 112~113°C; 0.9 g.). The aqueous layer was extracted with ethyl acetate. After the extracted solution had been washed with water and saturated sodium bicarbonate solution, the solution was extracted with a 2 N sodium hydroxide solution. The aqueous layer was acidified with 2 N hydrochloric acid. The product was collected and recrystallized from ethanol to give Ia (m.p. 112~113°C; 0.4 g.). Total yield; 1.3 g. (36%). It was identical with the above sample.

The acetate was prepared by the pyridine-acetic anhydride method; m.p. 88~89°C (colorless prisms from ethanol), IR: 1731 (acetate); 1662 (C=O); 1027, 918 (O-CH_2-O) cm^{-1}.

Found: C, 59.35; H, 4.53. Calcd. for $C_{11}H_{10}O_5$: C, 59.46; H, 4.54%.

2-Hydroxy-4, 5-methylenedioxyphenyl Benzyl Ketone (Ic).—By a similar Hoesch reaction, Ic was obtained from III (5.0 g.), phenylacetonitrile (5.0 g.) and anhydrous zinc chloride (3.0 g.) in dry ether (120 ml.); m. p. 130~131°C (pale yellow prisms from ethanol); yield, 2.6 g. (28%). It gave a green color with an alcoholic ferric chloride solution. IR: 1649 (C=O); 1031, 923 (O-CH_2-O) cm^{-1}.

Found: C, 70.30; H, 4.87. Calcd. for $C_{15}H_{12}O_4$: C, 70.30; H, 4.72%.

The acetate; m.p. 124~125°C (colorless needles from methanol). IR: 1768 (acetate); 1692 (C=O); 1031, 923 (O-CH_2-O) cm^{-1}.

Found: C, 68.58; H, 4.97. Calcd. for $C_{17}H_{14}O_5$: C, 68.45; H, 4.73%.

4-Hydroxyayapin (IIa).—*The Ethyl Carbonate Method.*—A mixture of Ia (1.0 g.), ethyl carbonate (35 ml.) and pulverized sodium (1.5 g.) was warmed on a steam bath for 20 min. After the vigorous reaction had ceased, sufficient methanol was added to the cooled mixture to destroy the excess of sodium, and then the residue was added to ether (100 ml.). The extraction of the sodium salt of the product with water (100 ml.) and acidification of it with 2 N hydrochloric acid gave IIa, which formed colorless tiny needles from methanol; m.p. 274~275°C (decomp.); yield, 0.9 g. (79%). This dissolved in a sodium bicarbonate solution with effervescence. It did not give any color with an alcoholic ferric chloride solution. IR: 1706 (C=O); 1043, 934 (O-CH_2-O) cm^{-1}. UV: λ_{max}^{EtOH} mμ (log ε); 230.5(4.40), 254$_I$(3.80), 275(3.81), 285(3.88), 328(4.15).

Found: C, 58.15; H, 3.18. Calcd. for $C_{10}H_6O_5$: C, 58.26; H, 2.93%.

The Ethyl Cyanoacetate Method.—A mixture of III (10.0 g.), ethyl cyanoacetate (4.0 g.) and anhydrous zinc chloride (10.0 g.) in dry ether (120 ml.) was saturated with dried hydrogen chloride for 3 hr. at 0°C and then allowed to stand overnight. The ethereal solution was decanted from the dark-colored oil which had separated. The residue was washed twice with dry ether (20 ml.) and then treated with water (150 ml.). Upon being stirred, the ketimine hydrochloride separated as a dark violet mass (m. p.>300°C). It was hydrolyzed with 50% sulfuric acid (80 ml.) by heating it on a steam bath for 2 hr. The reaction mixture was added to a large quantity of water. The resulting precipitates were collected and recrystallized from methanol to give IIa; m.p. 270~272°C (decomp.); yield, 1.6 g. (11%). This was identical with the above sample.

The methyl ether was prepared by the methyl iodide-potassium carbonate method; m.p. 183~184°C (colorless needles from methanol). IR: 1728 (C=O); 1031, 921 (O-CH_2-O) cm^{-1}.

Found: C, 60.26; H, 3.83. Calcd. for $C_{11}H_8O_5$: C, 60.00; H, 3.66%.

3-Methoxy-4-hydroxy-6, 7-methylenedioxycoumarin (IIb).—*The Ethyl Carbonate Method.*—By a similar reaction, IIb was obtained from Ib (m.p. 136~138°C[3]) (0.5 g.), ethyl carbonate (20 ml.) and sodium (0.5 g.); m.p. 261~262°C (decomp.) (colorless needles from methanol); yield, 0.5 g. (89%). It dissolved in a sodium bicarbonate solution with effervescence. It did not give any color with an alcoholic ferric chloride solution. IR: 1699 (C=O); 1031, 937 (O-CH_2-O) cm^{-1}. UV: λ_{max}^{EtOH} mμ (log ε); 231(4.52), 256$_I$(3.90), 280(4.03), 289(4.11), 330(4.52).

Found: C, 55.72; H, 3.52. Calcd. for $C_{11}H_8O_6$: C, 55.94; H, 3.41%.

The Ethyl Chloroformate Method.—A mixture of Ib (1.0 g.), ethyl chloroformate (2 ml.), anhydrous potassium carbonate (5.0 g.) and acetone (50 ml.) was heated under reflux for 5 hr., poured into water, and acidified with concentrated hydrochloric acid. The resulting precipitates were collected and recrystallized from methanol to give IIb, m.p. 261~262°C (decomp.); yield 0.7 g. (62%). This was identical with the above sample.

The methyl ether; m.p. 161~162°C (colorless needles from methanol). IR: 1706 (C=O); 1031, 933 (O-CH_2-O) cm^{-1}.

Found: C, 57.66; H, 4.16. Calcd. for $C_{12}H_{10}O_6$: C, 57.60; H, 4.03%.

The acetate: m.p. 136~137°C (colorless needles from methanol). It gave a blue fluorescence in alcohol. IR: 1783 (acetate); 1721 (C=O); 1037, 931 (O-CH_2-O) cm^{-1}.

Found: C, 56.16; H, 3.75. Calcd. for $C_{13}H_{10}O_7$: C, 56.12; H, 3.62%.

3-Phenyl-4-hydroxy-6, 7-methylenedioxycoumarin (IIc).—By similar reactions, IIc was obtained from Ic; m. p. 267~268°C (decomp.) (colorless needles

from methanol); yield, 91% (the ethyl carbonate method) and 69% (the ethyl chloroformate method). It dissolved in a sodium bicarbonate solution with effervescence. It did not give any color with an alcoholic ferric chloride solution. IR; 1660 (C=O); 1040, 941 (O-CH_2-O) cm^{-1}. UV: λ_{max}^{EtOH} mμ(log ε); 225(4.41), 288(3.87), 336(4.30).

Found: C, 67.98; H, 3.78. Calcd. for $C_{16}H_{10}O_5$: C, 68.08; H, 3.57%.

The methyl ether; m.p. 189~190°C (colorless needles from methanol). It gave a blue fluorescence in alcohol. IR: 1703 (C=O); 1029, 926 (O-CH_2-O) cm^{-1}.

Found: C, 68.96; H, 4.19. Calcd. for $C_{17}H_{12}O_5$: C, 68.91; H, 4.08%.

The acetate; m.p. 214°C (colorless plates from methanol). It gave a blue fluorescence in alcohol. IR: 1771 (acetate); 1708 (C=O); 1041, 941 (O-CH_2-O) cm^{-1}.

Found: C, 66.53; H, 3.83. Calcd. for $C_{18}H_{12}O_6$: C, 66.67; H, 3.73%.

7-Benzyloxy-3-(3', 4'-methylenedioxyphenyl)-4-hydroxycoumarin (IV). — By the ethyl carbonate method, 2-hydroxy-4-benzyloxyphenyl 3,4-methylenedioxybenzyl ketone (m.p. 94°C[8]) gave IV; m.p. 204~205°C (colorless needles from ethanol); yield, 85%. IR: 1656 (C=O); 1038, 930 (O-CH_2-O) cm^{-1}.

Found: C, 71.12; H, 4.30. Calcd. for $C_{23}H_{16}O_6$: C, 71.63; H, 4.51%.

The methyl ether; m.p. 134~135°C (colorless needles from ethanol). IR: 1708 (C=O); 1038, 921 (O-CH_2-O) cm^{-1}.

Found: C, 71.66; H, 4.58. Calcd. for $C_{24}H_{18}O_6$; C, 71.63; H, 4.51%.

The acetate; m.p. 184~185°C (colorless needles from ethanol). IR: 1778 (acetate); 1721 (C=O): 1038, 921 (O-CH_2-O) cm^{-1}.

Found: C, 69.77; H, 4.31. Calcd. for $C_{25}H_{18}O_7$: C, 69.76; H, 4.22%.

The authors are grateful to Professor Tetsuo Mitsui, Kyoto University, for making the microanalyses. This work was supported in part by a grant-in-aid from the Ministry of Education.

Department of Chemistry
Faculty of Science
Hiroshima University
Higashi-sendamachi, Hiroshima

*The Cationic Polymerization of Acrolein**

By Yoshio Toi and Yoshikazu Hachihama

(Received August 9, 1963)

Generally speaking, the ionic polymerization of acrolein[1,3] gives soluble polymers in organic solvents and the polymers have low molecular weights and melting points. The structures of the polymers are extremely different from those of the polymers obtained by radical polymerization;[1-9] contrary to the case of radical polymerization, which proceeds through the vinyl group, in the case of ionic polymerization the carbonyl group plays a more important role in the polymerization than does the vinyl group. Schulz and Passmann[10] reported on the behavior of acrolein in ionic polymerization in their recent work on anionic polymerization. In the present paper the cationic polymerization of acrolein will be studied. The kinetics of polymerization and the influence of the polymerization temperature on the structure of polymers will be investigated.

Experimental

Material. — Commercial acrolein was distilled, dried over anhydrous cupric sulfate, and distilled again immediately before the polymerization procedure; the distillate at b. p. 52.5~53.5°C was used as the acrolein monomer.

Polymerization Procedure.—The monomer and the solvent were precooled at the desired temperature under nitrogen in a glass tube with a rubber stopper; the initiator, boron trifluoride etherate, was stirred in via the rubber stopper with an injector. The mixture was kept at the desired temperature for the desired length of time. After

* Presented at the 16th Annual Meeting of the Chemical Society of Japan, Tokyo, April, 1963.

1) R. C. Schulz, *Makromol. Chem.*, **17**, 62 (1955).
2) R. C. Schulz and W. Kern, ibid., **18/19**, 4 (1956).
3) R. C. Schulz, H. Fauth and W. Kern, ibid., **20**, 161 (1956).
4) R. C. Schulz, H. Fauth and W. Kern, ibid., **21**, 227 (1956).
5) R. C. Schulz, H. Cherdron and W. Kern, ibid., **24**, 141 (1957).
6) R. C. Schulz, *Kunststoffe*, **48**, 257 (1958).
7) R. C. Schulz, E. Muller and W. Kern, *Makromol. Chem.*, **30**, 39 (1959).
8) R. C. Schulz, S. Suzuki, H. Cherdron and W. Kern, ibid., **53**, 145 (1962).
9) R. C. Schulz, J. Kovacs and W. Kern, ibid., **54**, 140 (1962).
10) R. C. Schulz and W. Passmann, ibid., **60**, 139 (1963).

the polymerization, the resulting mixture was added to a large excess of a water-methanol mixture (3 : 1 vol.), and then the unreacted monomer, the solvent and most of the methanol were removed by distillation under reduced pressure until the polymer was precipitated as a white powder in a transparent aqueous solution. The polymer was filtered, washed with water and dried under reduced pressure at room temperature.

The Treatment of the Polymer. — *Aldehyde Content.*—The method reported by Bryant and Smith[11] was employed. 0.5 g. of polymer was dissolved in 25 ml. of dioxane, to this solution 10 ml. of a 0.5 N hydroxylamine hydrochloride water-methanol solution and 35 ml. of a bromophenol blue ethanol solution containing pyridine were added, and the resulting mixture was warmed at 70°C for three hours. After this treatment, the mixture was titrated with a 0.5 N sodium hydroxide methanol solution. A blank was run under the same conditions without the polymer. The aldehyde content was calculated from the amount of alkali consumed.

The Determination of the Unsaturation Value.—0.5 g. of the polymer was dissolved in 90 ml. of acetic acid and was hydrogenated in the presence of 0.2 g. of platinum black under the atmospheric pressure of hydrogen and at room temperature. The carbon-carbon double bond in the polymer was calculated from the volume of hydrogen gas consumed.

Ozone Degradation.—0.5 g. of the polymer was dissolved in 250 ml. of dry chloroform, and an oxygen-ozone mixture was passed through the solution for a long enough length of time at −50°C. After ozonization, the chloroform was removed from the solution under reduced pressure at room temperature. The ozonide which remained as a white powder was cleaved by treatment with 50 ml. of 3% aqueous hydrogen peroxide at 50°C to yield a transparent solution. The solution was distilled under reduced pressure to separate the volatile organic acid from the other products. The distillate was titrated with alkali, and the acidity was calculated as formic acid. It has been demonstrated by means of paper chromatography[12] that the distillate contains only formic acid. The R_f value of hydroxamate of formic acid was 0.49 when the mixture of 1-butanol, acetic acid and water (4 : 1 : 5 v/v) was used as the development solvent.

Molecular Weight.—For the measurement of the molecular weight of polymers, the cryoscopic method in acetic acid was employed.

Results

The polymerization of acrolein in an ethyl ether solution in the presence of a boron trifluoride etherate was made. Figure 1 shows the relationship between the concentration of the initiator ([C], mol./l.) and the overall rate of polymerization (R_p), which was calculated from the slope of the time-conversion curve shown by a straight line at the early stage of polymerization (<20% of conversion). The relationship between the monomer concentration ([M], mol./l.) and R_p is shown in Fig. 2. It is confirmed by Figs. 1 and 2 that

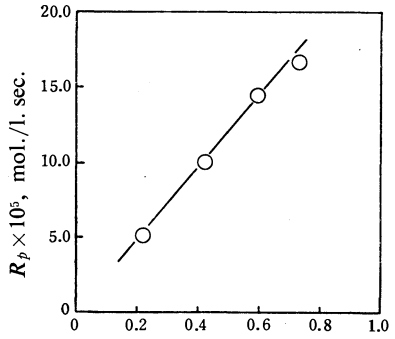


Fig. 1. Relationship between concentration of initiator and overall rate of polymerization.
Reaction temp.: 0°C
Concn. of monomer: 7.00 mol./l.
Solvent: ethyl ether

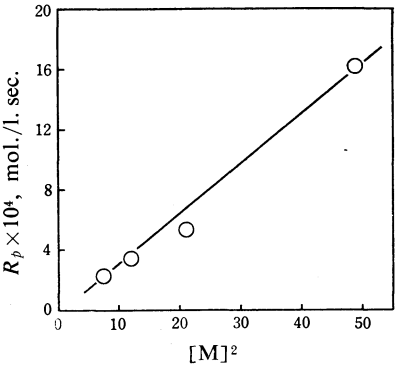


Fig. 2. Relationship between concentration of monomer and overall rate of polymerization.
Reaction temp.: 0°C
Concn. of initiator: 0.74 mol./l.
Solvent: ethyl ether

R_p is proportional to the first order of concentration of the initiator and to the second order of concentration of the monomer. From these results, the equation of the overall rate of polymerization is shown as Eq. 1:

$$R_p = K[C][M]^2 \qquad K: \text{constant} \qquad (1)$$

Equation 1 supports the theory that the initiation and termination reactions are bimolecular and monomolecular respectively. The temperature dependence on R_p is shown in Fig. 3. From R_p calculated from the slope

11) W. M. D. Bryant and D. M. Smith, *J. Am. Chem. Soc.*, 57, 57 (1935).
12) R. J. Blook, E. L. Durrum and G. Aweig, "A Manual of Paper Chromatography and Paper Electrophoresis," Academic Press, New York (1955), p. 163.

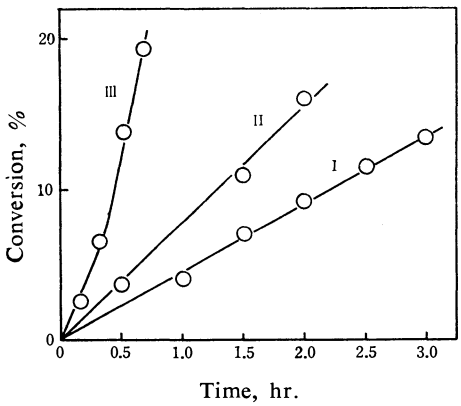


Fig. 3. Conversion curves of the polymerization of acrolein in ethyl ether solution with boron trifluoride etherate at the following temperature.
Curve I: −20°C
Curve II: 0°C
Curve III: 20°C
Concn. of monomer: 7.00 mol./l.
Concn. of initiator: 0.74 mol./l.

Table I. Rate constants at various temperatures

Temp. °C	R_p mol./l. sec.	K
−20	9.030×10^{-5}	2.415×10^{-6}
0	1.572×10^{-4}	5.470×10^{-6}
20	2.823×10^{-4}	8.060×10^{-6}

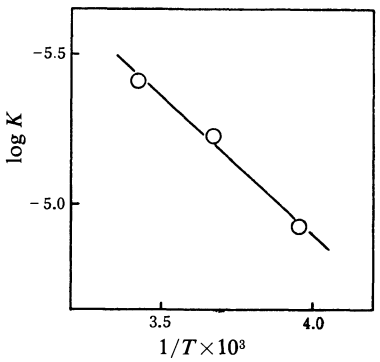


Fig. 4. Arrhenius polt of the rate constant in polymerization of acrolein by boron trifluoride etherate.

Table II. Polymerization by ionic initiators

Initiator	Solvent	Temp. °C	Time hr.	Conv. %	Polymer No.
$BF_3\cdot(C_2H_5)_2O$, 2.65 mol. %[d]		−78	115.0	38.1[a]	I
K_2CO_3, 3.52×10^{-3} mol. %[d]		20	2.0	21.3[b]	II
$(C_6H_5)_3P$, 6.35×10^{-4} mol. %[d]	MeOH ([M]/[S]=0.2)	5	16.7	85.0[c]	III

a) The polymerization was performed as described in the polymerization procedure.
b) The polymerization was performed by the method similar to the one described by Schulz.[1]
c) The polymerization was made in a round bottom flask with stirring under nitrogen, the polymerization in acetonitrile, dichloromethane and benzene solution were also made at 0~10°C, but these polymers were not soluble in common organic solvents without warm formic acid.
d) It is shown in mol. % based on monomer used.

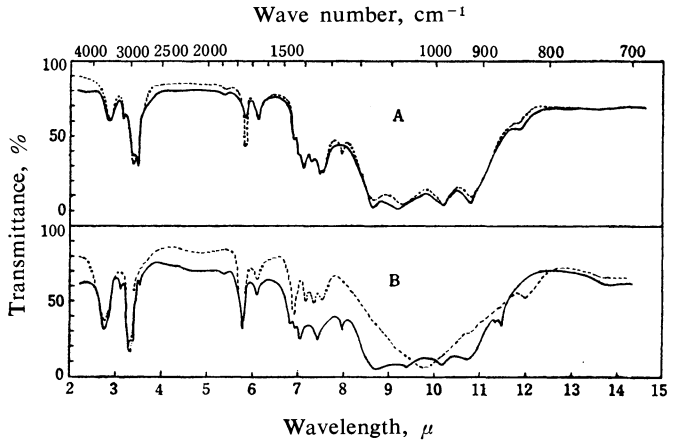


Fig. 5. Infrared spectra of polymers in KBr disk.
A: I (——) and I-7 (------)
B: II (——) and the polymer obtained by gamma-rays-initiated polymerization in bulk at −78°C (------).

of the time-conversion straight line and Eq. 1, the rate constants (K) of the polymerization reaction were calculated as is shown in Table I. 4.5 kcal./mol. was calculated as the activation energy of the reaction from the slope of the straight line of the Arrhenius plot (Fig. 4).

The bulk polymerization in the presence of boron trifluoride etherate at $-78°C$ was made, while anionic polymerizations by potassium carbonate and triphenyl phosphine were also made. These results are shown in Table II. Polymers obtained by polymerizations initiated with these cationic or anionic initiators were soluble in ethyl ether, benzene, dioxane and acetic acid, etc., but were insoluble in water and *n*-hexane. The melting points of the polymers were 65~70°C.

The molecular weight of the polymer obtained by the solution polymerization with boron trifluoride etherate is given in Table III. The molecular weights of I, II and III (cf. Table II) are 643, 430 and 1270 respectively. The results of the elementary analysis of polymers are shown in Table IV. The infrared spectra of I, I-7 and II are shown in Fig. 5 (for reference, the spectrum of the polymer obtained by radical polymerization is shown in the same figure). At 1725 cm^{-1}, the absorption of the carbonyl group is observed. At 3080, 1645, 1410, 985 and 930 cm^{-1}, absorptions of the vinyl group are observed; these absorptions disappear or diminish in the spectra of hydrogenated polymers. In the spectra of II and I-7, a weak absorption of -C=C-O- is observed at 1250 cm^{-1}; this absorption disappears in a hydrogenated polymer. The aldehyde content and the carbon-carbon double bond in polymers were measured; these results are shown in Tables V and VI. Polymer I, which has a maximum double-bond content and a minimum aldehyde content compared with other polymers, was subjected to the ozonolysis. If the polymer has a double bond as vinyl group in a pendant of the polymer (as is shown in B), formic acid is produced as product of the ozone degradation as follows:

$$\begin{array}{l}\text{-CH-O-} \rightarrow \text{-CH-O-} + \text{HCOOH}\\ \quad\text{CH} \qquad\quad \text{COOH}\\ \quad\text{CH}_2\end{array}$$

(B)

On the other hand, if the polymer has a double bond in the main chain of the polymer as is shown in C, the formic ester of glycolic acid is produced as a product of the ozone degradation and this ester is saponified by the formic acid actually present in the mixture of the products, thus yielding a glycolic acid.

$$\text{-CH}_2\text{-CH=CH-O-} \rightarrow \text{O=CH-O-CH}_2\text{-COOH}$$

(C)

$$\rightarrow \text{HCOOH} + \text{HO-CH}_2\text{-COOH}$$

Formic acid was confirmed as the only volatile product by paper chromatography. Its acidity as determined by alkali titration was equivalent to 50% of the theoretical amount based on monomer units; this value is approximately in agreement with the degree of unsaturation as estimated by hydrogenation. In the nonvolatile product, glycolic acid was not identified by paper chromatography. It is confirmed by the above evidence that the

Table III. Molecular weight of the polymer obtained by ethyl ether solution polymerization with boron trifluoride etherate

Monomer mol./l.	Initiator mol./l.	Temp. °C	Conv. %	M. w.	Polymer No.
7.00	0.73	−20	13.4	504	I-1
7.00	0.73	0	16.4	671	I-2
7.00	0.44	0	15.5	516	I-3
7.00	0.22	0	11.9	466	I-4
4.67	0.74	0	14.7	532	I-5
2.80	0.74	0	11.3	525	I-6
7.00	0.73	20	14.0	384	I-7

Table IV. Results of elementary analyses of polymers

Polymer No.	Found		Calcd. for $(C_3H_4O)_n$	
	C, %	H, %	C, %	H, %
I	63.86	7.35	64.27	7.19
I-1	62.63	7.67	64.27	7.19
I-2	62.90	7.63	64.27	7.19
I-7	60.62	7.01	64.27	7.19
II	59.59	7.52	64.27	7.19
III	58.62	7.91	64.27	7.19

Table V. Aldehyde contents of polymers

Polymer No.	Polymer g.	Consumed alkali $\times 10^4$ mol.	Content of aldehyde %
I	0.1426	4.1052	16.12
I-1	0.1372	9.6746	39.50
I-2	0.1552	5.8645	21.16
I-7	0.1537	6.7442	24.57
II	0.1590	7.6239	26.85
III	0.1205	6.6600	30.80

Table VI. Contents of carbon-carbon double bonds in polymers

Polymer No.	Polymer g.	Consumed hydrogen ml.	Content of double bond %
I	0.5629	148.0	62.0
I-1	0.4111	67.0	43.8
I-2	0.4492	50.0	29.8
I-7	0.3952	31.0	21.1
II	0.5455	140.0	61.0
III	0.5203	75.0	34.0

carbon-carbon double bond belongs to vinyl group in a pendant of the polymer; this is also supported by the infrared absorption spectra of the polymer.

Discussion

Understandably, acrolein is polymerized in a different orientation under suitable conditions; the polymers thus obtained contain the following structural units in some ratios:

$$CH_2{=}CH{-}CH{=}O$$

$$\underset{\text{(A)}}{-CH_2{-}\underset{\displaystyle CHO}{\underset{|}{CH}}-} \qquad \underset{\text{(B)}}{-\underset{\displaystyle \overset{\displaystyle CH}{\overset{\|}{CH_2}}}{\underset{|}{CH}}{-}O-} \qquad \underset{\text{(C)}}{-CH_2{-}CH{=}CH{-}O-}$$

Such behavior of acrolein is attributed to the conjugation of a carbonyl group with the vinyl group within its structure. In radical catalytic or gamma-rays-initiated polymerization, the polymers obtained belong to type A. For example, in the polymer obtained by the irradiation of gamma-rays at $-78°C$[13] or by redox polymerization,[5] the aldehyde content is 75~85% of the theoretical amount which is calculated as type A and the content of the carbon-carbon double bond is either not present or present in a negligibly small amount (4% in redox polymer[9]). On the other hand, in the polymer obtained by ionic polymerization, the aldehyde content is much less than that of the polymer given by radical polymerization, and the content of the carbon-carbon double bond increases. According to the recent work by Schulz[10] on anionic polymerization in the presence of sodium naphthalene, the polymer contains 70% of the theoretical amount of double bond and only 2% of the theoretical amount of the aldehyde group, and it is assumed that the polymer consists mainly of type B.

The similar behavior of acrolein upon polymerization is found in the cationic polymerization in the presence of boron trifluoride etherate. The polymer obtained at $-78°C$ has only 16% of the aldehyde group and 60% of the carbon-carbon double bond in the side chain, findings which are supported by the infrared spectrum, the hydrogenation and the ozone degradation of the polymer, so that the polymer consists of type B in magnitude and also contains some A. On the other hand, in the infrared spectra of the polymers obtained at a higher temperature, 0 or 20°C, a weak absorption of -C=C-O- at 1250 cm^{-1} is observed (Fig. 5), and in the polymer, the ratio of the amount of the aldehyde group to the carbon-carbon double bond is increased (Table IV). In the ionic polymerization of acrolein, the carbonyl's double bond plays an important role in the polymerization reaction, one which can be predicted from the fact that, in the acrolein molecule, the position of the maximum and minimum of π-electron density exist on the oxygen and carbon atoms of the carbonyl group respectively. This orientation of the polymerization reaction is more remarkable still at lower temperatures.

13) Y. Toi, T. Fujii and Y. Hachihama, presented at the 16th Annual Meeting of the Chemical Society of Japan, Tokyo, April, 1963.

Summary

The cationic polymerization of acrolein with boron trifluoride etherate at various temperatures has been studied.

(1) The polymerization rate may be given as follows: $R_p = K[C][M]^2$, on the basis of the polymerization in an ethyl ether solution, and the activation energy of reaction is 4.5 kcal./mol.

(2) The structure of polymers depends very much on the polymerization temperature; the polymerization at the lower temperature gives a polymer containing the larger amount of the end vinyl group as a side chain, and the smaller amount of the aldehyde group.

The authors wish to express their thanks to the Nippon Kayaku Co., which supplied acrolein for this study.

Department of Chemical Technology
Faculty of Engineering
Osaka University
Miyakojima-ku, Osaka

Polymerization of Acrolein Initiated by Gamma-rays

By Yoshio Toi, Toshikatsu Fujii and Yoshikazu Hachihama

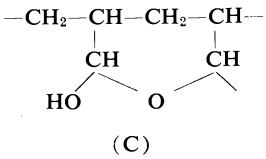
(Received August 10, 1963)

It is known that acrolein is polymerized easily upon standing alone at room temperature, yielding an insoluble product. Moureu and Dufraisse[1] reported that the polymerization is greatly accelerated by heat and light. Scherlin[2] demonstrated the polymerization by Diels-Alder reaction under the action of heat. Thompson and Linnett,[3] and Blacet, Fielding and Roof[4] investigated the photochemical polymerization of acrolein in the vapor phase by irradiation with an ultraviolet light. Schulz, Kern and their co-workers[5-14] published a series of papers on the polymerization of acrolein in the presence of radical and ionic initiators. Under the action of gamma-rays at room temperature, acrolein is polymerized easily, yielding an insoluble polymer in common organic solvents.[15,16]

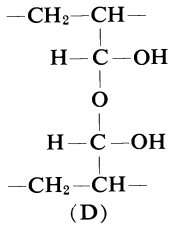
Generally the acrolein-polymer obtained by radical polymerization is assumed to consist of the following structural units, while the insolubility of the polymer is assumed to arise by means of the formation of intermolecular cross-linking as shown by D.



(A) (B)



(C)



(D)

In the present paper, the bulk polymerization at various temperature under irradiation by gamma-rays will be studied, and the influence of the polymerization temperature on the properties of the polymers obtained has been investigated.

Experimental

Material.—Commercial acrolein was distilled, dried over anhydrous cupric sulfate, and distilled again immediately before polymerization; the distillate at b. p. 52.5~53.5°C was used as acrolein monomer.

Polymerization Procedure.—The monomer was sealed under reduced pressure of nitrogen atmosphere in a glass tube after degassification and was kept at the desired temperature and for the desired length of time in the gamma-ray field with a constant dose rate. After irradiation, the resulting reaction mixture was transferred into a large excess of methanol; the polymer obtained as a precipitate was isolated, washed with methanol, and dried under reduced pressure at room temperature.

Analysis of the Polymer.—The measurement of the aldehyde content of the polymer was done as follows: 0.1 g. of the polymer and 0.4 g. of hydroxylamine hydrochloride were dissolved in 20 ml. of pyridine with a small amount of anhydrous sodium carbonate, and the mixture was warmed at 70°C for 3.0 hr. The polyoxime obtained in the reaction mixture was isolated by the precipitation method from water, dried under reduced pressure at room temperature, and subjected to an elementary analysis by nitrogen. The aldehyde content of the polymer was calculated from the nitrogen content of polyoxime.

The determination of the degree of unsaturation of the polymer (I-S-3) was made as follows; 1.0 g. of the polymer was dissolved in 20 ml. of pyridine, and to this solution 10 ml. of an aqueous solution in which 0.5 g. of sodium boron hydride has been dissolved was stirred in. The mixture was kept at room temperature for 20 hr. and was then dialyzed by water. From the dialyzed aqueous solution, the water was removed by distillation

* Presented at the 16th Annual Meeting of the Chemical Society of Japan. Tokyo, April, 1963.

1) C. Moureu and C. Dufraisse, *Compt. rend.*, **169**, 621 (1919).
2) S. M. Scherlin, T. A. Sserebrennikowa and F. E. Rabinowitsch, *Chem. Zentr.*, I, 1971 (1939).
3) H. W. Thompson and J. W. Linnett, *J. Chem. Soc.*, **1935**, 1452.
4) F. E. Blacet, G. H. Fielding and J. G. Roof, *J. Am. Chem. Soc.*, **59**, 2375 (1937).
5) R. C. Schulz, *Makromol. Chem.*, **17**, 62 (1955).
6) R. C. Schulz and W. Kern, ibid., **18/19**, 4 (1956).
7) R. C. Schulz, H. Fauth and W. Kern, ibid., **20**, 161 (1956).
8) R. C. Schulz, H. Cherdron and W. Kern, ibid., **24**, 141 (1957).
9) R. C. Schulz, H. Fauth and W. Kern, ibid., **21**, 227 (1956).
10) R. C. Schulz, *Kunststoffe*, **48**, 257 (1958).
11) R. C. Schulz, E. Muller and W. Kern, *Makromol. Chem.*, **30**, 39 (1959).
12) R. C. Schulz, S. Suzuki, H. Cherdron and W. Kern, ibid., **53**, 145 (1962).
13) R. C. Schulz, J. Kovacs and W. Kern, ibid., **54**, 146 (1962).
14) R. C. Schulz and W. Passmann, ibid., **60**, 139 (1963).
15) A. Henglein, W. Schnabel and R. C. Schulz, ibid., **31**, 181 (1959).
16) Y. Toi and Y. Hachihama, *J. Chem. Soc. Japan, Ind. Chem. Sec.* (*Kogyo kagaku Zassi*), **62**, 1924 (1959).

Table I. Separation of soluble part from I*

Exp. No.	Monomer g.	Dose rads. $\times 10^{-5}$	Polymer g.	Conversion %	I-S g.	I-S %**
1	16.850	2.75	0.238	1.26	0.238(I-S-1)	100.0
2	16.850	5.86	0.542	3.22	0.514(I-S-2)	95.0
3	16.850	8.88	0.905	5.36	0.657(I-S-3)	72.6
4	16.850	14.9	2.992	17.70	1.308(I-S-4)	43.7
5	16.850	25.0	6.138	36.40	1.089(I-S-5)	17.7

* Solvent: pyridine, Temperature: room temperature
** Percentage based on total polymer obtained.

under reduced pressure to isolate the product, and the resultant polyalcohol was dried under reduced pressure at room temperature. 0.5 g. of the polyalcohol obtained was dissolved in 90 ml. of acetic acid, and the experimenters tried to hydrogenate it in the presence of 0.2 g. of platinum black under atmospheric pressure and at room temperature. However, no hydrogenation of the polymer was observed.

Dosimetry. — A ceric solution was used for the dosimetry.

Results

Polymerization.—The conversion curves obtained in the gamma-ray-initiated polymerization of acrolein in bulk at various temperatures are shown in Fig. 1. It appears that the conversion increase proportionally to the irradiated dose in the early stages, but that after this stage the overall rate of polymerization increases acceleratively. This acceleration of the rate might be due to the fact that, in the higher range of conversion, above a ca. 10% precipitation of product in the reaction system appears. This behavior is more remarkable in polymerization at higher temperatures. Figure 2 shows the Arrhenius plot of the

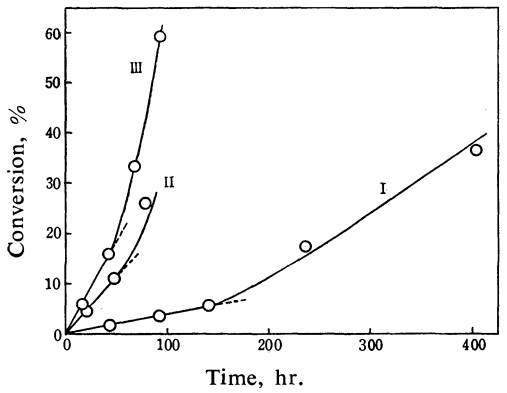


Fig. 1. Conversion curves of bulk polymerization of acrolein.

Curve I : −78°C, 1.76 rads./sec.
Curve II : −20°C, 1.76 rads./sec.
Curve III : 10°C, 1.88 rads./sec.

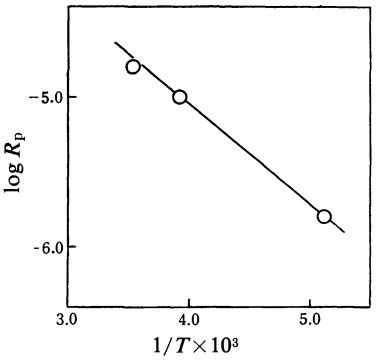


Fig. 2. Arrhenius plot of the rate of bulk polymerization of acrolein.

overall rate of polymerization derived from the slope of the portion of the straight line of the conversion curve in the early stages. The overall activation energy, calculated from the slope of the straight line of Fig. 2, was 3.1 kcal./mol.

Properties of Polymer.—For convenience, the polymers obtained at −78°C, −20°C and 10°C are designated I, II and III respectively. I consists of the soluble part (I-S) and the insoluble part (I-InS) in pyridine at room temperature. The result of the separation of I-S from I by extraction with pyridine is shown in Table I. I-S is a white powder which is soluble in pyridine, dimethylformamide, and

Table II. Aldehyde content and solution viscosity of I-S

Polymer	Nitrogen content* %	Aldehyde content %	$[\eta]$**	k'***
I-S-1	16.11	81.6	0.34	1.1
I-S-2	16.50	83.7	0.34	1.1
I-S-3	16.52	84.0	0.36	1.1
I-S-4	16.58	79.0	1.20	1.1
I-S-5	15.27	77.5	0.32	1.1

* Theoretical value of nitrogen content is 19.72% calculated on $-(-CH_2-\underset{\displaystyle CH=NOH}{\underset{|}{CH}}-)-_n$
** In pyridine at 30°C, c: 0.5 g./dl.
*** Huggins' constant

dimethylsulfoxide at room temperature and is decomposed at about 320°C. The results of both the analysis of the aldehyde content and the measurement of the solution viscosity of I-S are shown in Table II. I-InS, which is insoluble at room temperature, becomes soluble at elevated temperatures, 120~150°C, in pyridine, dimethylformamide and dimethylsulfoxide. However, the polymer recovered from the solution by the reprecipitation method becomes insoluble again in the same solvents. The same behavior was reported in the polymer obtained by redox polymerization.[17] The variation in aldehyde content and solution viscosity induced by heat treatment in pyridine on I-InS was also investigated; the results are presented in Table III. The fact that the solution viscosity decreases with the increase in the duration of heat treatment supports the degradation of intermolecular cross-linking (D). The aldehyde content also decreases slightly as the duration of the heat treatment increases.

Table III. Aldehyde content and solution viscosity of I-InS after heat treatment*

Time min.	Nitrogen content %	Aldehyde content %	Inherent viscosity 0.5 g./dl.
60	17.00	86.4	0.49
100	16.46	83.5	0.44
140	14.67	74.5	0.42
180	15.11	76.6	0.35

* Sample: I-InS obtained in Exp. No. 3 of Table I.
Treatment: 0.25 g. of sample in 50 ml. of pyridine was heated at 150°C in sealed glass tube under nitrogen atmosphere.

Table IV. Fractionation of II and III by solubility in pyridine

Polymer	Conversion %	Soluble part[a] %	Soluble part at elevated temp.[b] %	Insoluble part[c] %
II	11.1	0.7 (85.2)[d]	99.3 (58.8)[d]	—
	25.8	—	77.5	22.5
III	15.8	—	21.6 (47.6)[d]	78.4
	33.4	—	14.5	85.5

a) Soluble in pyridine at room temperature
b) To be soluble in pyridine by treatment at 170°C for 1.0 hr.
c) Quite insoluble resinous compound
d) Aldehyde content (%)

In the case of II, a small amount of a soluble part is observed at a lower conversion, but most of II is soluble in pyridine only at elevated temperatures, 150~170°C, and with an increase in conversion the part of resinous compound which is entirely insoluble is increased. In the case of III, most of it is a resinous compound. The result of the separation of the parts of the polymer on II and III by extraction with pyridine are shown in Table IV.

Discussion

When acrolein is polymerized in bulk at various temperatures, at −78°C, −20°C and 10°C, by irradiation by gamma-rays, the resulting polymer precipitates in the reaction medium at a higher conversion because the polymer is not soluble in its own monomer, and the acceleration of the overall rate of polymerization is observed. However, in the early stage of polymerization, up to approximately 10% conversion, the reaction proceeds without any remarkable precipitation of the polymer and linear conversion curves are observed. The value of the overall activation energy, 3.1 kcal./mol., calculated from Fig. 2 is a reasonable value, one which supports the that theory, in the temperature range from 10°C to −78°C (the melting point of acrolein is −86.95°C), the polymerization of acrolein proceeds by a free radical mechanism. In the case of the radical polymerization of acrolein in dimethylformamide with azobisisobutylonitrile, the overall activation energy is 25.4 kcal./mol.[18] The G-values of the conversion in the early stage at each temperature are presented in Table V. The influence of the reaction temperature is important on the properties of the

Table V. G-value of conversion in bulk polymerization of acrolein

Temp., °C	Dose rate rads./sec.	G (conversion)
−78	1.76	9.85×10^{2}
−20	1.76	5.99×10^{3}
10	1.88	9.55×10^{3}

polymer obtained, especialy on the solubility of the polymer in organic solvents. That is, in the polymerization at −78°C most of the polymer obtained is soluble in pyridine, etc., but with an increase in the reaction temperature the soluble part of the polymer decreases extremely. The formation of intermolecular cross-linking, assumed to be the next reaction

17) R. Hank, *Makromol. Chem.*, **52**, 108 (1962).

18) Presented at the 16th Annual Meeting of the Chemical Society of Japan, Tokyo, April, 1963.

of aldehyde after the polymerization reaction, is disturbed by taking a lower reaction temperature; the mechanism mentioned above is supported by the fact that the aldehyde content of the polymer obtained decreases with an increase in the reaction temperature (Tables II and IV). On the other hand, the monomer or polymer concentration in the polymerization system might be important on such a gel-formation, but not as important as the effect of temperature. Actually the percentage of the soluble part of I decreases greatly above an approximate 15% conversion (Table I). On the other hand, in the solution polymerization of acrolein by gamma irradiation[15,16] or radical catalysts,[8] the resulting polymers are not soluble in organic solvents at room temperature. For example, the polymerization of acrolein at 40~70°C by azobisisobutylonitrile in dimethylformamide, which can dissolve the polymer I-S, gives an insoluble polymer (the aldehyde content is 70~90%). That is, it is suggested that the influence of the polymerization temperature is predominant over other effects on the solubility of the polymer obtained. In the polymerization of acrolein initiated by gamma-rays, the reaction proceeds by a free radical mechanism through a carbon-carbon double bond. This theory is supported by the high aldehyde content and the very small content of the carbon-carbon double bond in the polymer, contrary to the existence of a double bond in the polymer obtained by ionic initiators. For instance, unlike I, which contains 75~85% of aldehyde and no unsaturation group, the polymer obtained by the bulk polymerization in the presence of boron trifluoride etherate at −78°C contains 16% of aldehyde and 62% of carbon-carbon double bond in the side chain.[18] The same behavior of acrolein on anionic polymerization, the predominant role of the carbonyl group on the polymerization reaction, was reported by Schulz and his coworkers.[14]

Summary

The bulk polymerization of acrolein initiated by gamma-rays at various temperatures has been studied. Most of the polymers obtained at −20° and 10°C are insoluble in organic solvents. On the other hand, most of the polymers obtained at −78°C are soluble in pyridine, dimethylformamide, and dimethylsulfoxide at room temperature. The aldehyde content of the soluble polymer is 75~85% of the theoretical amount, and its intrinsic viscosity is 0.32~1.20.

The influence of the polymerization temperature on the solubility of the polymer in organic solvents has been discussed, as has the polymerization mechanism.

The authors wish to express their thanks to the Nippon Kayaku Co., which supplied acrolein to this study.

Department of Chemical Technology
Faculty of Engineering
Osaka University
Miyakojima-ku Osaka

Stereochemical Studies of Monoterpene Compounds. I. The Conformation of (+)-p-Menthane-3, 4-diol Obtained by the Performic Acid Oxidation of (+)-p-Menth-3-ene

By Takayuki SUGA, Tsuyoshi SHISHIBORI and Tamon MATSUURA

(Received August 9, 1963)

The hydroxylation of *p*-menth-3-ene with performic acid in the presence of water has been reported by Naves[1] to afford *p*-menthane-*cis*-3, 4-diol (m. p. 76~77°C) by a comparison of the melting point with that in the literature*1 cited as footnote 13 in Ref. 1. In the ring-opening reaction of *p*-menthane-3, 4-epoxide using dilute mineral acid, Tanaka[2] obtained a 3, 4-diol*2 with the same melting point (75~76°C) as that of the diol obtained by the

1) Y.-R. Naves, *Helv. Chim. Acta*, **42**, 1174 (1959).

*1 G. Wagner (1894) obtained (±)-*p*-menthane-3, 4-diol (m. p. 76.5~77°C) by the potassium permanganate oxidation of *p*-menth-3-ene. J. Böeseken (1923) showed that the hydroxylation of an olefin hydrocarbon by a permanganate reagent proceeds by cis addition. The reports by S. Tanaka (Ref. 2) and by H. Hock and S. Lang (Ref. 3) are also cited.

2) S. Tanaka, *Mem. Coll. Sci. Kyôto Imp. Univ. Series A*, **22**, 97 (1939) (*Chem. Zentr.*, **1940**, I, 688).

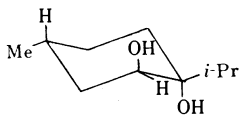
*2 (+)-*p*-Menth-3-ene ($[\alpha]_D$+107.24°) has been used for preparing the 3, 4-epoxide; the 3, 4-diol is presumed to be dextrorotatory.

potassium permanganate oxidation of *p*-menth-3-ene, while Hock and Lang[3] obtained a (±)-diol melting at 95°C from the 3, 4-epoxide and considered it to be trans. However, there has been no experimental evidence with respect to a spatial arrangement of the two hydroxyl groups. Generally, the hydroxylation[4] of an ethylenic compound with performic acid in the presence of water leads to *trans*-α-glycol by means of the ring opening of the epoxide which is the intermediate product. However, a few exceptions to this stereochemical course in this opening reaction are known.[4c,5] Therefore, we have investigated the conformation of *p*-menthane-3, 4-diol prepared by the same manner as in Naves' report,[1] particularly the hydroxyl groups in it.

(+)-*p*-Menth-3-ene (I) used was prepared by the pyrolysis of methyl (−)-menthylxanthate, but it was accompanied by (+)-*p*-menth-2-ene (28%). The hydroxylation of the sample hydrocarbon was carried out by hydrogen peroxide in an aqueous formic acid at 35°C, giving crude glycol in a 66% yield on the basis of the hydrocarbon. The crude glycol was separated into crystalline (+)-*p*-menthane-3, 4-diol (m. p. 76.5~77°C; a 71% yield based on the crude glycol) and oily (+)-*p*-menthane 2, 3-diol (29%) by elution chromatography on a silica-gel column; no other glycol, i. e., no *cis* or *trans*(diequatorial)-glycol, could be isolated in spite of a careful examination. Each of the diols was shown to be homogeneous by gas phase and chromatostrip chromatography.

(+)-*p*-Menthane-*trans*-3, 4-diol (V). — The crystalline diol was dextrorotatory and showed the same melting point as the previously-described 3, 4-diol,[3*] which is certainly optically inactive, because the *p*-menth-3-ene in Naves' report[1] was prepared from dihydro-α-terpineol by sulfuric acid dehydration. Treatment of the above crystalline diol with 10% sulfuric acid resulted in pinacolic dehydration affording a menthone mixture consisting of (−)-menthone (65%) and (+)-isomenthone (35%). Also, oxidation of the diol with *t*-butyl chromate gave (−)-4-hydroxymenthone. Thus it was confirmed that the hydroxyl groups are situated in both C_3- and C_4-positions.

The melting points of the *p*-menthane-3, 4-diol[4*] (m. p. 76.5~77°C) and its mono-3, 5-dinitrobenzoate (m. p. 150~150.5°C) differ from those of (+)-*cis*-4-hydroxymenthol (m. p. 80~81°C)[6a] and its mono-3, 5-dinitrobenzoate (m. p. 124~125°C)[6a,b] respectively. Moreover, the infrared spectrum of the diol in a highly dilute carbon tetrachloride solution, where intermolecular hydrogen bonding is out of the question, did not show any hydroxyl stretching absorption peak due to an intramolecular hydrogen bond, but only a free hydroxyl stretching absorption peak at 3630 cm^{-1}.[7] It has been established[8] that, at an ordinary temperature, the comparatively bulky isopropyl group in cyclohexane derivatives takes an equatorial conformation, because such conformation seems to be more energetically favored than an axial conformation. Accordingly, from the absence of an intramolecular hydrogen bonding in the 3, 4-diol, the two hydroxyl groups at C_3- and C_4-positions in it should be considered to take a diaxial conformation (V). It was thus shown that the predominant conformation of the hydroxyl groups in this crystalline *p*-menthane-3, 4-diol is in the diaxial trans position.



(V)

The methyl group in the sample *p*-menth-3-ene is considered to retain an equatorial orientation since the hydrocarbon was prepared from methyl (−)-menthylxanthate (1e, 3e, 4e)[9] by thermal decomposition proceeding by cis elimination[10] between the C_3-equatorial xanthate group and C_4-axial hydrogen. Moreover, it is generally accepted[4] that in the hydroxylation reaction of an olefin by performic acid in the presence of water, the intermediate epoxide with a cis configuration is immediately subjected to acid-catalyzed opening reaction by the reaction medium (in this case, formic acid), the opening reaction being initiated by protonation. Thus, the structure of protonated intermediate *p*-menthane-3, 4-epoxide is probably the II in Fig. 1. Generally, the acid-catalyzed opening reaction of cyclohexane epoxides containing no

3) H. Hock and S. Lang, *Chem. Ber.*, **75**, 300 (1942).

4) a) D. Swern, "Organic Reactions," Vol. 7, Ed. by R. Adams, John Wiley and Sons, Inc., New York (1953), p. 378; b) E. L. Eliel, "Stereochemistry of Carbon Compounds," McGraw-Hill Book Company, Inc., New York (1962), p. 356; c) R. E. Parker and N. S. Isaacs, *Chem. Revs.*, **59**, 737 (1959).

5) Z. Chaubudziński and H. Kuczyński, *Bull. Acad. Polon. Sci., Ser. Sci. Chim.*, **9**, 519 (1961).

3* There is no description of the optical property.

4* The *trans*-3, 4-diol and its derivatives which are dextrorotatory in optical property have not yet been reported.

6) a) W. Tagaki and T. Mitsui, *J. Org. Chem.*, **25**, 1476 (1960); b) S. A. Kozhin, S. I. Yakimovich and G. V. Pigulecski, *J. Gen. Chem. USSR (Eng. Transl.)*, **32**, 2334 (1962).

7) A. R. H. Cole and P. R. Jefferies, *J. Chem. Soc.*, **1956**, 4391.

8) H. D. Orloff, *Chem. Revs.*, **54**, 347 (1954).

9) Ref. 8, p. 366.

10) a) W. Hückel, W. Tappe and G. Legutke, *Ann.*, **543**, 194 (1940); b) Ref. 4b, p. 232; c) Ref. 8, p. 371.

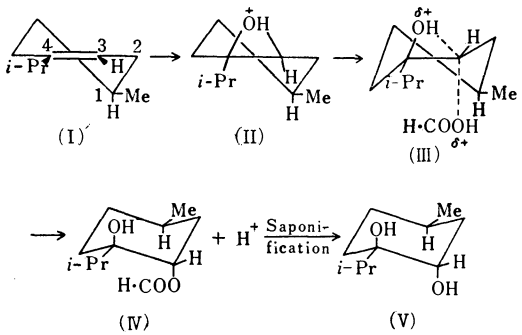
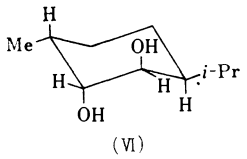


Fig. 1

group capable of exerting any marked polar or conjugative effect proceeds by the S_N2 attack of a reagent molecule from the axial side on the epoxide ring carbon atom, and the direction of the ring opening depends, consequently, on the steric factor.[4c] Therefore, the normal isomer corresponding to the attack of formic acid on the least-substituted carbon atom at the 3-position will be formed for the steric hindrance of the bulky isopropyl group, and the inversion of the configuration at the point of attack (the C_3-position) occurs because of the approach of the acid on the side opposite the displaced oxygen (cf. III). Thus, the opening reaction produces a monoformate of *p*-menthane-diaxial-3, 4-diol (IV), both alkyl groups of which are equatorial. Alkaline saponification of the formate affords only *trans*-diaxial-3, 4-diol (V).

(+)-*p*-Menthane-*trans*-2, 3-diol (VI).—This was isolated as a minor product and was a viscid oil. The infrared spectrum in a highly dilute carbon tetrachloride solution showed only one peak of a free hydroxyl stretching absorption at 3635 cm^{-1}.[11] This indicates the diaxial orientation of the two hydroxyl groups. Furthermore, the diol gave the same dinitrobenzoate as that of (+)-*trans*-2-hydroxyneomenthol.[11] Therefore, the 2, 3-diol was (+)-*trans*-2-hydroxyneomenthol (VI), which resulted certainly from the *trans*-*p*-menth-2-ene which coexisted in the sample of *p*-menth-3-ene.



(VI)

It appears that the hydroxylation of *p*-menth-2-ene takes place by the attack of formic acid on the C_2-position of *p*-menthane-2, 3-epoxide in the same way as with 3, 4-epoxide.

11) P. R. Jefferies and B. Milligan, *J. Chem. Soc.*, **1956**, 2363.

Experimental

Sample.—(+)-*p*-Menth-3-ene (I)[10a,12] (b. p. 168~169°C, n_D^{25} 1.4492, d_4^{25} 0.8080, $[\alpha]_D^{25}$ +114.8°) was prepared from (−)-menthol by the pyrolysis of methyl (−)-menthylxanthate (m. p. 40.5~41°C). According to the racemization procedure with *p*-toluenesulfonic acid,[13] the hydrocarbon was shown to be a mixture of (+)-*p*-menth-3-ene (72%) and (+)-*p*-menth-2-ene (28%). However, the isolation of pure *p*-menth-3-ene was so difficult that the hydrocarbon mixture was employed as the sample, without further purification.

Hydroxylation.—Into a mixture of the sample hydrocarbon (73 g.) and 77% aqueous formic acid (370 g.) 30% hydrogen peroxide (83 g.) was stirred drop by drop over a period of 0.5 hr. at 35°C, and then the mixture was maintained under the same conditions for a further 3 hr. The reaction mixture was treated as in Naves' report.[1] The crude glycol monoformate (84 g.) thus obtained was distilled to afford 63.2 g. of the main fraction boiling at 93~105°C/3 mmHg (reported :[1] b. p. 105°C/3 mmHg for *p*-menthane-3,4-diol monoformate). The infrared spectrum showed the peaks of ν_{OH} 3503, $\nu_{C=O}$ 1726, ν_{C-O-} 1188, and ν_{C-OH} 991 cm^{-1}. Hydrolysis of the formate with 14% ethanolic potassium hydroxide gave 47.8 g. of a crude glycol boiling at 99~110°C/3 mmHg; this was a viscid oil which solidified softly after being kept in a refrigerator. The gas chromatogram (3 m. column, Thermol-1 on quartz (150~200 mesh), 140°C, 50 ml. helium/min.) showed a main peak (t_R=16.3 min.) corresponding to the 3,4-diol and a small peak (t_R=20.2 min.) corresponding to the 2,3-diol. The crude glycol was chromatographed on silica-gel. The column was eluted with a mixture of ethyl acetate and *n*-hexane, and the elutes were separated into two fractions.

(+)-*p*-Menthane-*trans*-3, 4-diol (V).—The first elute gave 33.9 g. of a crystalline mass. Recrystallization of the mass from *n*-hexane gave white crystals with a m. p. of 76.5~77°C ($[\alpha]_D^{25}$ +27.5° (*c* 1, methanol) and +22.3° (*c* 1, chloroform)). The gas phase chromatogram on Thermol-1 packing showed only one peak; moreover, only one spot was observed on the chromatostrip chromatogram[14] (solvent: 20% ethyl acetate in *n*-hexane).

Found: C, 69.81; H, 11.48. Calcd. for $C_{10}H_{20}O_2$: C, 69.72; H, 11.70%.

Mono-3,5-dinitrobenzoate melted at 150~150.5°C (recrystallized from petroleum benzine) and showed $[\alpha]_D^{25}$ +36.8° (*c* 1, chloroform).

Found: N, 7.49. Calcd. for $C_{17}H_{22}O_7N_2$: N, 7.65%.

Pinacolic Dehydration.—A mixture of (+)-*p*-menthane-3,4-diol (0.5 g.) and 10% sulfuric acid (5 ml.) was refluxed for 2 hr. and then steam-distilled. The distillate gave a menthone mixture (0.36 g.). The infrared spectrum corresponded to

12) L. Tschugaeff, *Ber.*, **32**, 3332 (1899).
13) J. P. Wibaut, H. C. Beyerman and H. B. Van Leeuwen, *Rec. trav. chim.*, **71**, 1032 (1952).
14) J. G. Kirchner, J. M. Miller and G. J. Keller, *Anal. Chem.*, **23**, 420 (1951); J. M. Miller and J. G. Kirchner, ibid., **25**, 1107 (1953).

that[15] of a mixture of (−)-menthone and (+)-isomenthone. The composition (mentioned above) of the menthone mixture was calculated from its optical rotation value, $[\alpha]_D^{20}$ +15.2° (*c* 2, methanol), using $[\alpha]_D^{20}$ −25° (*c* 2, methanol) for (−)-menthone and $[\alpha]_D^{20}$ +90° (*c* 2, methanol) for (+)-isomenthone. Only (−)-menthone 2,4-dinitrophenylhydrazone (m. p. and mixed m. p. 145~145.5°C) was prepared.

Oxidation with t-Butyl Chromate (The Formation of 4-Hydroxymenthone).—A *t*-butyl chromate solution[16] was prepared from chromic trioxide (1.75 g.), *t*-butyl alcohol (3.5 g.) and benzene (20 ml.). The 3,4-diol (3.0 g.) in benzene (15 ml.) was oxidized with this oxidant at 25~30°C for 2 hr. Then a neutral reaction mixture (2.7 g.) obtained was fractionated into 1.3 g. of a keto alcohol (n_D^{25} 1.4641; d_4^{25} 0.9906; $[\alpha]_D^{25}$ −96.7°; IR (liq. film): 3493 (OH), 1709 (C=O), 1430 ($-CH_2-CO-$), 1154 (OH) cm^{-1}) and 1.3 g. of unchanged diol by elution chromatography on a silica-gel column using ethyl acetate—*n*-hexane as an eluant.

Treatment of the keto alcohol with 2 N hydrochloric acid solution of 2,4-dinitrophenylhydrazine gave (−)-4-hydroxymenthone 2,4-dinitrophenylhydrazone (m. p. 102.5~103°C; UV: λ_{max}^{alc} 360 mμ, ε=22400; Found: N, 15.73. Calcd. for $C_{16}H_{22}O_5N_4$: N, 15.99%). On the other hand, (±)-*p*-menth-3-en-5-one 2,4-dinitrophenylhydrazone (m. p. and mixed m. p. 147.5~148.5°C) was produced on treating it with an ethanol-sulfuric acid solution of 2,4-dinitrophenylhydrazine.[17]

(+)-*p*-Menthane-*trans*-2,3-diol (VI).—In the elution chromatography of the crude glycol described above, the second elute gave a viscid oil (13.8 g.), which was confirmed to be homogeneous by gas phase and chromatostrip chromatography as in the case of V. The oil showed $[\alpha]_D^{25}$ +37.2° (*c* 1, chloroform) (reported;[11] $[\alpha]_D^{20}$ +40.8°) and gave di-*p*-nitrobenzoate, m. p. 173.5~174°C (reported[11]: m. p. 174°C).

Measurement of the Infrared Spectra in the Hydroxyl Stretching Region.—The infrared spectra were measured by a Hilger H-800 double-beam spectrophotometer under the following conditions. Calcium fluoride prism. The wave number accuracy at 3500 cm^{-1}: ±3 cm^{-1}. Temperature: 20°C. Solvent: carbon tetrachloride. Cell: 20 mm. long. Sample concentration: 0.003 mol.

15) Y.-R. Naves and J. Lecomte, *Bull. soc. chim. France*, **1955**, 792.
16) Cf. T. Suga, *J. Chem. Soc. Japan, Pure Chem. Sec. (Nippon Kagaku Zasshi)*, **80**, 918 (1959); S. M. Linder and F. R. Greenspan, *J. Org. Chem.*, **22**, 949 (1957).
17) P. R. Jefferies and B. Milligan, *J. Chem. Soc.*, **1956**, 4390.

Summary

The conformational analysis of (+)-*p*-menthane-3, 4-diol, which had been obtained by the hydroxylation of (+)-*p*-menth-3-ene with performic acid in the presence of water, has been performed mainly by means of infrared spectra. It has been shown that the two hydroxyl groups at the C_3- and C_4-positions take a diaxial conformation, that they are, accordingly, trans to each other, and that the methyl group presumably holds an equatorial orientation. It has also been found that *p*-menthane-*trans*(diaxial)-2, 3-diol results from the *p*-menth-2-ene coexisting in the sample of *p*-menth-3-ene. A stereochemical course of the hydroxylation reaction has been discussed.

The microanalyses were performed by Mr. Toshiharu Takagi and Mr. Keiichi Kihara of the Tôyô Soda Co., Ltd., and the late Kazuko Iwata of the Faculty of Pharmacy of Kyoto University, to all of whom the authors' thanks are due. The present work was partly supported by a grant-in-aid of the Ministry of Education.

Department of Chemistry
Faculty of Science
Hiroshima University
Hiroshima

The Purification of Silicon Tetrachloride from Traces of Boron with N, N-Diphenylacetamide

By Masanao NAKAGAWA

(Received August 24, 1963)

During the past decade many studies have been made of the purification of silicon for use as a semiconductor and of its raw materials, particularly from traces of boron. The purification of silicon tetrachloride and trichlorosilane,[1,2] the raw materials, from the boron, however, has not been fully studied because of the lack of any appropriate method for chemical analysis, although a report[3] on it has recently been published.

In previous papers[4] it has been shown that the boron in silicon tetrachloride can be decreased by the addition of many Lewis bases, such as nitriles, amides, aniline derivatives and some others, followed by distillation. Among those bases, *N*, *N*-diphenylacetamide appeared to be a particularly effective reagent, because the amide gave a stable addition compound[5,6] with boron trichloride, with an equilibrium constant[7] of more than an order of 10^3, the heating of which up to 100°C evolves no detectable volatile boron compounds, as has also been reported previously.[8]

On the other hand, an analytical method[9] for traces of boron based on the extraction of a boron tetrafluoride ion-methylene blue complex, followed by spectrophotometric determination, appeared to be a useful and convenient method for the present study.

Thus, the present work was undertaken to clarify the effects of *N,N*-diphenylacetamide in the purification from boron (1 p.p.m. or 1 p.p.b. order) by a slight modification of the methylene blue method.

Experimental

Reagents.—Pure silicon tetrachloride was prepared by refluxing its crude chloride with copper powder (3%), followed by fractional distillation. Boron trichloride was obtained as a liquefied gas (a purity of 99.5%) in a steel cylinder from the American Potash and Chemical Corp. Carbon tetrachloride was distilled in the presence of phosphorus pentoxide. Dichloroethane, methylene blue and *N, N*-diphenylacetamide were purified by the normal procedure.

The Procedure for the 1 p. p. m. Order.—The standard solution of boron trichloride in carbon tetrachloride (1.125 M) was prepared by dissolving the vapor from the steel cylinder in the solvent; the concentration of the solution was determined by the titration, with a standard sodium hydroxide solution, of an aqueous solution obtained by hydrolyzing a portion of the solution in carbon tetrachloride.

The standard solution of boron in silicon tetrachloride (1.1 μg./ml.) was also prepared by diluting the standard solution in carbon tetrachloride (1.125 M) with pure silicon tetrachloride. The standard solution (25 ml.) and the amide (1/400 mol.)[10] were taken into a distillation flask (100 ml.), and, after having been stirred or refluxed for a stated number of times, the silicon tetrachloride was completely distilled off at 62~65°C, and dry nitrogen was passed through the flask overnight. The residue was hydrolyzed by stirring in a dilute sodium hydroxide solution (25 ml. of distilled water and 2 ml. of 5% sodium hydroxide) for 1 hr. The solution was filtered from the amide, and the filtrate was concentrated to about 5 ml.

The concentrate was diluted in a volumetric flask (25 ml.), and the solution (10 ml.) was taken into a polyethylene bottle (100 ml.) and acidified with phosphoric acid (1 ml. of a 1 : 10 solution). After the successive addition of hydrofluoric acid (5 ml. of a 5% solution) and distilled water (10 ml.), the bottle was tightly stoppered and kept at room temperature for 2 hr. Then ferrous ammonium sulfate (2 ml. of a 4% solution), distilled water (78 ml.) and methylene blue (2 ml. of a 1/1000 M aqueous solution) were successively added to the bottle, and the solution was vigorously shaken for 2 min. with dichloroethane (25 ml.). After the solution had stood for 30 min. the dichloroethane layer (1 ml.) was pipetted off and diluted with pure dichloroethane (5 ml.).

The dichloroethane solution was taken into a quartz cell (1 cm.), and the absorbance at 660 mμ

1) H. C. Theuerer, *J. Electrochem. Soc.*, **107**, 29 (1960).
2) E.g., G. Rosenberger, German Pat. 955415; *Chem. Zblt.* **128**, 6864 (1957); G. A. Wolf. U. S. Pat. 2857249; *Chem. Abstr.*, **53**, 4673 (1959).
3) M. Miyamoto, *Japan Analyst*, **12**, 233 (1963).
4) M. Nakagawa, *J. Chem. Soc. Japan, Ind. Chem. Sec.* (*Kogyo Kagaku Zasshi*), **63**, 135, 2115 (1960).
5) W. Gerrard, M. F. Lappert and J. W. Wallis, *J. Chem. Soc.*, **1960**, 2141.
6) M. J. Frazer, W. Gerrard and J. K. Patel, ibid., **1960**, 726.
7) M. Nakagawa, *J. Chem. Soc. Japan, Ind. Chem. Sec.* (*Kogyo Kagaku Zasshi*), to be published.
8) M. Nakagawa, ibid., **66**, 168 (1963).
9) L. Pasztor and J. D. Bode, *Anal. Chem.*, **32**, 277 (1960).
10) The amount was favorable in a preliminary test with a standard solution of boron (25 ml. of 0.045 M) in carbon tetrachloride, in silicon tetrachloride or in a mixture of them.

was measured by a Shimadzu QR-50 type photoelectric spectrophotometer. After the reagent blank with pure silicon tetrachloride had been subtracted from the absorbance, the amount of boron taken out with *N*, *N*-diphenylacetamide was obtained by the calibration curve made up with the standard aqueous solution of boron.

The Procedure for the 1 p.p.b. Order.—The standard solution of boron in silicon tetrachloride (0.009 μg./ml.) was prepared as has been described above, and the solution (100 ml.) was taken into a polypropylene beaker (100 ml.). After the addition of *N*, *N*-diphenylacetamide (0.1 g.), the beaker was placed in a vacuum desiccator equipped with two stopcocks, which were connected to a scrubbing bottle with concentrated sulfuric acid, through which dry air could be admitted, and to a vacuum pump via a phosphorus pentoxide column, two scrubbing bottles with a sodium hydroxide solution (1 : 2), and a calcium chloride column.

The vacuum desiccator was evacuated by heating it by two lamps (60 W.) above the desiccator, and the silicon tetrachloride was completely distilled off. The residue was taken out and hydrolyzed with distilled water (10 ml.). After the mixture had stood overnight in order to complete the hydrolysis the aqueous solution was filtered from the amide, and the beaker was washed two times with distilled water (5 ml.). The washing solution was also filtered by the filter paper previously used, and those filtrates were taken into a polyethylene bottle (100 ml.). The aqueous solution was submitted to extraction, followed by the measurement of the absorbance, which was as described previously except for the following points: dichloroethane, 10 ml., the shaking time for the extraction, 10 min., the quartz cell, 3 mm., and the absorbance was measured without the dilution of the extracts.

Results and Discussion

Figure 1 gives the calibration curve for the

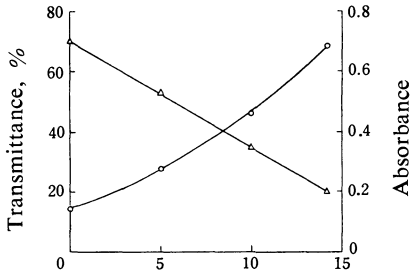


Fig. 1. Calibration curve for 1 p.p.m. order.
△ Transmittance ○ Absorbance

boron of the 1 p.p.m. order, which rather deviates from Beer's law, but which gives a good reproducibility and an accuracy within ±0.3 μg. The deviation observed might be due to certain interference by the amide slightly dissolved in the aqueous solution.

It had been reported[9] that the extraction oculd be well carried out with dichloroethane (25 ml.) and methylene blue (1/1000 M, 10 ml.). In the present study, however, a smaller amount of methylene blue (1/1000 M, 2 ml.) was used to decrease the blank value of the absorbance; the use of more was unfavorable for sensitive analyses.

The effects of the reaction factors on the recovery of boron (1 p.p.m. order) are shown in Fig. 2. The stirring at room temperature

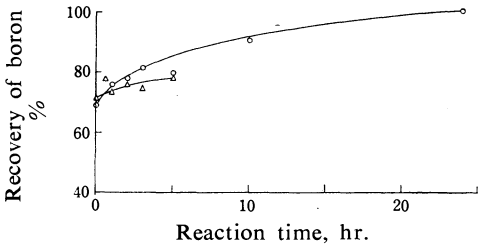


Fig. 2. Effect of the reaction time of the recovery of the boron (1.08 μg./ml.).
○ Stirring △ Refluxing

gave a slightly high recovery, and the stirring for 24 hr. led to a recovery of about 100%, which suggests that the boron contents in the silicon tetrachloride distilled off should be 0.06 μg./ml. or less, as could be estimated from the maximum experimental error involved.

Figure 3 represents the calibration curve for

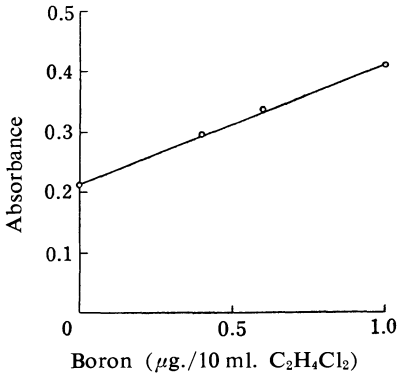


Fig. 3. Calibration curve for 1 p.p.b. order.

the 1 p.p.b. order, which obeys Beer's law. The analytical method herein used was sensitive, but the curve was less reproducible, and all the curves in the repeated experiments slightly varied parallel with one another from day to day. The lesser reproducibility appeared to be due to the slight variation in contamination involved. The respective calibration curve, therefore, was prepared in every experiment.

Table I reports on the recovery of the boron from the standard solution in silicon tetrachloride (100 ml. of 0.009 μg./ml.) by the vacuum

TABLE I. RECOVERY OF THE BORON OF 1 p.p.b. ORDER*

No.	A from pure $SiCl_4$ μg.	B from boron soln. μg.	(A-B) μg.	Recovery %
1	0.08	1.86	1.78	
2	0.14	1.07	0.93	
3	0.05	0.58	0.53	
4	0.17	0.93	0.76	
5	0.25	1.78	1.53	
Mean	0.14	1.2	1.1	1.2×100

* The recovery from the standard silicon tetrachloride soln. (100 ml. of 0.009 μg./ml.) with the amide (0.1 g.).

distillation carried out immediate after the addition of the amide (0.1 g.). Every numerical value given in the table varied, with some error, but the effects of the amide were apparent, and the amount of amide required was less than could be estimated by the equilibrium constant reported previously.[7]

The effects of the reaction factors were also studied, but similar results were obtained within the range of experimental error. For the purification, however, the stirring with amide, followed by the distillation, appeared to be more favorable, as could be expected by analogy with the results obtained with the solution of boron of the 1 p.p.m. order.

Summary

A standard solution of boron in silicon tetrachloride (1 p.p.m. or 1 p.p.b. order) has been distilled in the presence of *N*, *N*-diphenylacetamide. The residue of the distillation has been analyzed for boron by the spectrophotometric measurement of the methylene blue complex of boron tetrafluoride ions. The boron of an order of 1 p.p.m. has been about 100% recovered when the solution in silicon tetrachloride has been distilled after being stirred for 24 hr. with the amide. The recovery of the boron of an order of 1 p.p.b. has also been satisfactory. The silicon tetrachloride distilled off in the presence of the amide, therefore, believed to be almost free of boron.

The author is indebted to Mr. Seiichi Ujiie of this Institute and Mr. Toshio Seto for their experimental work.

Government Chemical Industrial Research Institute, Tokyo
Shibuya-ku, Tokyo

The Solvolysis of Acid Chlorides. A Presentation of the Problem and a Proposal for the Mechanism

By Hiroshi MINATO

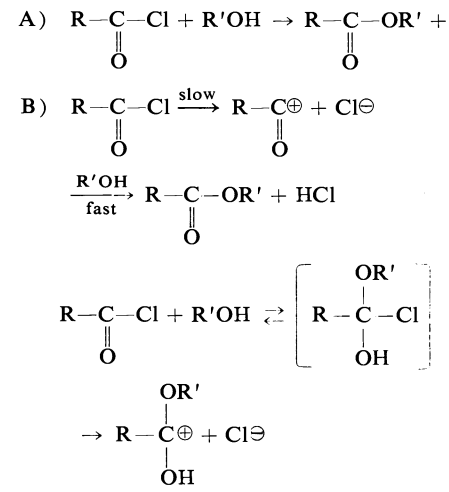
(Received August 28, 1963)

The nucleophilic substitution reactions of derivatives of carboxylic acids, especially the hydrolysis of esters, have been studied very thoroughly, and the mechanism is well understood.[1] However, the investigations of the kinetics of the hydrolysis and alcoholysis of acid chlorides have not led to completely concordant conclusions, and a reasonable explanation for all the data available seems to be lacking. Hudson and his co-workers,[2-10] Gold, Hilton and Jefferson,[11] and Kelly and Watson[12] have suggested that aromatic acid chlorides may be hydrolyzed by either the S_N1 or the S_N2 mechanism, and Newman,[13] Gould[14] and Hine[15] have agreed with them. The two paths they proposed are as follows:

* Present address: International Christian University, Mitaka, Tokyo, Japan.

1) For instance, M. L. Bender, *Chem. Revs.*, **60**, 53 (1960).
2) R. F. Hudson and J. E. Wardill, *J. Chem. Soc.*, **1950**, 1729.
3) B. L. Archer and R. F. Hudson, ibid., **1950**, 3259.
4) D. A. Brown and R. F. Hudson, ibid., **1953**, 883.
5) B. L. Archer, R. F. Hudson and J. E. Wardill, ibid., **1953**, 888.
6) D. A. Brown and R. F. Hudson, ibid., **1953**, 3352.
7) R. F. Hudson and B. Saville, ibid., **1955**, 4121.
8) R. F. Hudson and B. Saville, ibid., **1955**, 4130.
9) E. W. Crundon and R. F. Hudson, ibid., **1956**, 501.
10) C. W. L. Bevan and R. F. Hudson, ibid., **1953**, 2187.
11) V. Gold, J. Hilton and E. G. Jefferson, ibid., **1954**, 2756.
12) M. J. Kelly and G. M. Watson, *J. Phys. Chem.*, **62**, 260 (1958).
13) M. S. Newman in Newman (ed.), "Steric Effects in Organic Chemistry," John Wiley & Sons, Inc., New York (1956), p. 225.
14) E. S. Gould, "Mechanism and Structure in Organic Chemistry," Henry Holt & Co., New York (1959), p. 332.
15) J. Hine, "Physical Organic Chemistry," McGraw-Hill, New York (1956), p. 300.

On the other hand, Bunton et al.[16,17] and Peeling[18] have suggested a two-stage process, excluding path B.



In order to resolve these two divergent views and to find a reasonable mechanism for the hydrolysis of acid chlorides the present investigation was undertaken.

Evaluation of the Two Mechanisms

The mechanism of Hudson et al. differs from the addition-ionization mechanism in that it has a path B in addition to a path A, the latter being essentially similar to the addition-ionization mechanism.

The evidence which has led some workers to propose path B is as follows:

a) The relative rates of the solvolysis of the following *p*-substituted benzoyl chlorides suffer an almost complete reversal in order as the reaction is transferred from 40/60 ethanol-ether (dielectric constant 13) to 50/50 water-acetone (dielectric constant 53),[4] as Table I shows. In 50% water-acetone, the solvolysis of only the *p*-nitro compound appears to have retained its bimolecular character.

Table I. Effect of solvent changes on relative solvolysis rates of *p*-substituted benzoyl chlorides

Medium	D	Relative solvolysis rate				
		p-NO_2	*p*-Br	H	*p*-Me	*p*-MeO
40% EtOH-ether	13	32	2.5	1	0.47	0.25
EtOH	22	22	2.1	1	0.70	0.81
50% H_2O-acetone	52	12	0.92	1	2.9	30

b) When the logarithms of the observed first-order rate constants of benzoyl chloride in water-acetone are plotted against the logarithms of water concentrations the "apparent order" in water varies from about 1.1～1.5 in 5～15% water to near 7 in 50% water.[3,11,12] The apparent order in water of the hydrolysis of 2, 4, 6-trinitrobenzoyl chloride in 10～30% water-90～70% acetone at 0°C is ca. 1. The apparent order in water of the hydrolysis of *p*-methoxybenzoyl chloride in 10～30% water -90～70% acetone at 0°C is ca. 3.5.[6]

c) The alcoholysis or hydrolysis of mesitoyl chloride is very fast, even faster than *p*-nitrobenzoyl chloride,[6,18,19] as Table II shows.

However, the following evidence seems to be against the path B):

a) Boehme[20] measured the hydrolysis of benzoyl chloride in 2～30% water-98～70% dioxane; his findings show that the apparent order in water at 2～5% water-dioxane is ca. 2.9. This cannot be explained by path B, which is considered to take place only at a higher water concentration, or at a higher dielectric constant.

b) Peeling[18] and Bunton et al.[17] found that the solvolysis of mesitoyl chloride is accelerated by the presence of alkali, as is shown in Table II. Although Brown and Hudson[6] reported that the hydrolysis rate of mesitoyl chloride in 5% water-acetone at 0.2°C did not change upon the addition of 0.001 M alkali, Bender and Chen[21] established that hydroxide ions do catalyze the hydrolysis of 4-substituted-2, 6-dimethylbenzoyl chlorides in 99% acetonitrile-water. This means that the solvolysis of mesitoyl chloride proceeds through a tetrahedral complex, at least in the presence of alkali.

Table II. Alcoholysis of substituted benzoyl chlorides in 80% alcoholic acetone at −10.75°C

1) In the absence of alkali

Substituents	H	*p*-NO_2	*p*-Me	2,4,6-Trimethyl
10^6k_1 (sec^{-1})	4.97	212	2.25	521

2) In the presence of alkali (0.2 M ⊖OEt)

	H	*p*-Nitro	2,4,6-Trimethyl
Second order rate constant k_2 ($M^{-1}\,sec^{-1}$)	3	3	0.34

16) C. A. Bunton, T. A. Lewis and D. A. Llewellyn, *Chem. & Ind.*, 73, 1154 (1954).
17) C. A. Bunton and T. A. Lewis, ibid., **1956**, 180.
18) E. R. A. Peeling, *J. Chem. Soc.*, **1959**, 2307.
19) J. F. Norris and V. W. Ware, *J. Am. Chem. Soc.*, **61**, 1418 (1939).
20) H. Boehme and W. Schuelhoff, *Ber.*, **84**, 28 (1951).
21) M. L. Bender and M. C. Chen, *J. Am. Chem. Soc.*, **85**, 30 (1963).

c) In the reaction with diazomethane, benzoyl chloride is reactive, whereas mesitoyl chloride is inert.[22] If acylium ions are formed, mesitoyl chloride should react with diazomethane also.

d) Bunton et al.[17] found that the carbonyl oxygen of mesitoyl chloride suffers exchange with the oxygen of the solvent water. This indicates the existence of a tetrahedral intermediate of a finite life-time.[23] Their results are shown in Table III.

TABLE III. COMPARISON OF RATES OF EXCHANGE (k_e) AND HYDROLYSIS (k_h) OF SUBSTITUTED BENZOYL CHLORIDES AT 25°C

Substituents	% Water in the mixture with dioxane	$10^4 k_h$ sec^{-1}	$10^4 k_e$ sec^{-1}	k_h/k_e
H	5	1.2[20]	0	—
	25	7.57	0.30	25
	33	14.8	0.82	18
p-Me	5	0.346[4]	0	—
	25	6.22	0	—
	33	22.7	0.44	51
2,4,6-TriMe	5	33.5	1.1	31

e) The chlorine exchange between $Li^{36}Cl$ in dry acetone and mesitoyl chloride is much slower than with benzoyl chloride.[17] If acylium ions are formed, exchange should be faster with mesitoyl chloride. The slow exchange of chlorine atoms must be taking place through a tetrahedral intermediate.

f) Although mesitoyl chloride reacts with methanol or ethanol almost instantaneously at room temperature, it reacts with *t*-butyl alcohol or *t*-amyl alcohol much slower, and when mesitoyl chloride was mixed with a great excess of *t*-amyl alcohol at room temperature, about a 1 : 1 mixture of mesitoyl chloride and *t*-amyl mesitoate was observed by the infrared absorption method after 10 min.[24] The formation of *t*-butyl mesitoate from *t*-butyl alcohol and mesitoyl chloride is catalyzed by pyridine.[25] The reaction should not be catalyzed by pyridine if it proceeds via an acylium ion.

g) Although it is known that 2, 4, 6-trimethylbenzyl chloride ionizes in a liquid sulfur dioxide solution to a greater extent than does benzyl chloride,[26] conductance measurements on a solution of mesitoyl chloride in liquid sulfur dioxide indicated no appreciable ionization.[27]

h) The rate of the solvolysis of 2, 4, 6-trimethylbenzyl chloride and mesitoyl chloride are shown in Table IV. Table IV shows that 2, 4, 6-trimethylbenzyl chloride can not be solvolyzed by the S_N1 mechanism in 25% H_2O-acetone. In view of the evidence cited in g), it seems unlikely that mesitoyl chloride is solvolyzed by S_N1 in a poorer ionizing solvent than the solvent in which 2, 4, 6-trimethylbenzyl chloride failed to be solvolyzed by S_N1.

The evidence gathered above seems to indicate that the solvolysis of mesitoyl chloride does not proceed via an acylium ion but via a tetrahedral intermediate. If mesitoyl chloride is not solvolyzed by S_N1, it is reasonable to assume that other benzoyl chlorides are also solvolyzed by way of tetrahedral intermediates. A simple expression of an addition-ionization mechanism through a tetrahedral intermediate

TABLE IV. RATES OF SOLVOLYSIS OF 2,4,6-TRIMETHYLBENZYL AND MESITOYL CHLORIDES

Substance	Solvent	Temp.	Added material	$10^4 k_1$ sec^{-1}	$10^3 k_2$ M^{-1} sec^{-1}	Ref.
Trimethylbenzyl chloride	25%H_2O-acetone*	30	—	0.134	—	6
	25%H_2O-acetone	30	0.027 M$\ominus$OH	—	4.306	6
	50%H_2O-acetone	20.4	—	103.2	—	6
	50%H_2O-acetone	20.4	0.027 M$\ominus$OH	104.1	—	6
Trimethylbenzoyl chloride	5%H_2O-acetone	0.2	—	15.84	—	6
	5%H_2O-dioxane	25	—	33.5	—	17
	5%H_2O-dioxane	25	1 M$\ominus$OH	—	2650	17

* x% A−B means x% A−(100−x)% B, (v/v)

22) W. E. Bachman and J. Sheehan, unpublished results; cited from p. 227 of Ref. 13.

23) In 99% acetonitrile-water, which has a higher dielectric constant and a lower water content, Bender and Chen[10] observed no carbonyl oxygen exchange. The absence of exchange is, however, "not an infallible indication of an acylium ion intermediate," as Bender and Chen state. An explanation for their results is given later in the text.

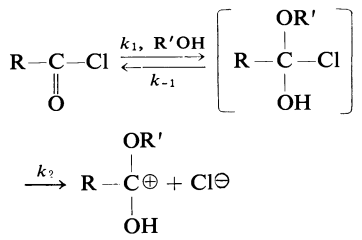
24) Mesitoyl chloride was dissolved in respective alcohols, and the carbonyl absorption of the solution was determined in calcium fluoride cells against the pure alcohols at room temperature. In the cases of methyl and ethyl alcohols, only the ester absorption was observed at 5.77 μ, even immediately after mixing, while in the case of *t*-amyl alcohol, the height of the peaks due to *t*-amyl mesitoate (5.77 μ) and mesitoyl chloride (5.57 μ) was about the same at 10 min. after mixing.

25) S. G. Cohen and A. Schneider, *J. Am. Chem. Soc.*, 63, 3382 (1941).

26) W. T. Nauta and J. W. Dienske, *Rec. trav. chim.*, 55, 1000 (1936).

27) N. N. Lichtin, Boston Univ.; cited from p. 226 of Ref. 13.

is the following:



The rate of solvolysis is expressed by:

$$-\frac{d(RCOCl)}{dt}=\frac{k_1k_2(RCOCl)(R'OH)}{k_2+k_{-1}} \quad (1)$$

However, this simple mechanism fails to explain some of the data available. As is shown in Table III, the hydrolysis rate of *p*-toluyl chloride increases very much as the water concentration increases from 5% to 33%, yet k_h/k_e is very large, i.e., over 51. When k_h/k_e $(=k_2/k_{-1})$ is very large, Eq. 1 becomes

$$-\frac{d(RCOCl)}{dt}=k_1(RCOCl)(R'OH) \quad (2)$$

The observed increase of rate upon the increase in water concentration from 25 to 33% gives a value of 4.4 as an apparent order in water by plotting $\log k_1$ versus $\log(H_2O)$.

$$-\frac{d(RCOCl)}{dt}=k_{obs}(RCOCl)$$

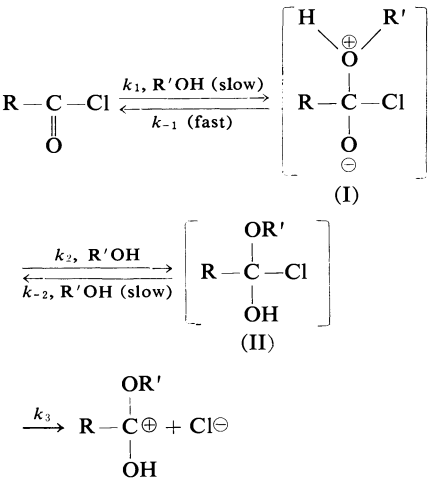
$$=\text{constant}\times(H_2O)^n(RCOCl)$$

$$n=\frac{\Delta(\log k_{obs})}{\Delta(\log(H_2O))}=\text{apparent order in } (H_2O)$$

However, k_1 should not be so much dependent upon the concentration of water. Generally the substituted benzoyl chlorides with electron-releasing groups show a greater dependence upon the concentration of water, and this is incompatible with Eq. 1 or 2.

A Refined Addition-Ionization Mechanism

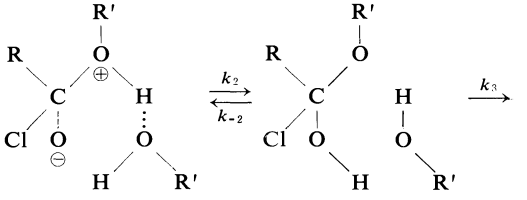
The Solvolysis of Aroyl Chlorides.—Therefore, the following mechanism[28] is proposed in order to explain the available data on the solvolysis of substituted benzoyl chlorides:**



With the usual steady-state assumptions for I and II, the rate of solvolysis is calculated as:

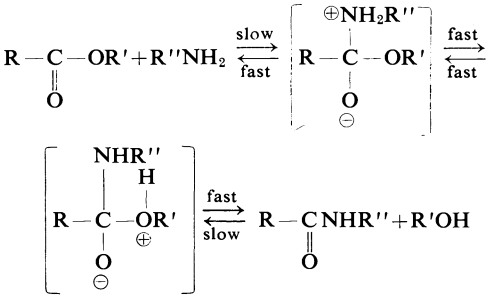
$$-\frac{d(RCOCl)}{dt}=\frac{k_1k_2k_3(RCOCl)(R'OH)^2}{k_{-1}k_3+k_{-1}k_{-2}(R'OH)+k_2k_3(R'OH)} \quad (3)$$

Although k_2 and k_{-2} could be an intramolecular proton transfer, it may be more plausible to go through a six-membered transition state with another solvent, since hydroxylic solvents exist as polymers.



Hudson and Saville[7] found that the alcoholysis of acetyl chloride and *p*-nitrobenzoyl chloride is much faster in ethanol-carbon tetrachloride than in an ethanol-ether mixture at the same ethanol concentration. Their results are shown in Table V. While ethanol exists as a polymer in carbon tetrachloride, it probably exists in ether as a hydrogen-bonded form with ether molecules. In carbon tetrachloride, the attack of ethanol on the acid chloride, is

28) This is somewhat analogous to the aminolysis of esters (Ref. 14, p. 330):



** A difficulty with this mechanism has been pointed out by a referee; that is, the mechanism proposed here may not be compatible with the linear relationship between σ^+ and ρ, or with the rather large negative ρ value observed for the hydrolysis of 4-substituted-2,6-dimethylbenzoyl chlorides.[21] However, the present author is not quite convinced by these results and the interpretations thereof, mainly because of the conditions employed for the kinetic and isotopic studies.

TABLE V. ETHANOLYSIS OF ACID CHLORIDES AT 20°C

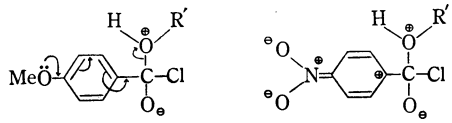
Substance	(EtOH) mol./l.	10^4k_1 (min^{-1}) in CCl_4	in ether	k_{CCl_4}/k_{ether}
Acetyl chloride	0.172	369	4.8	77
	0.345	969	16.85	57.5
	0.69	2290	61.8	37.1
p-Nitrobenzoyl chloride	0.69	139	10.0	13.9

followed by a proton transfer through another ethanol molecule which is hydrogen-bonded to the reacting ethanol molecule. In ether, every ethanol molecule is linked to an ether molecule rather than to another ethanol molecule at low concentrations of ethanol, and thus the formation of intermediate I is not readily followed by a proton transfer; rather, it dissociates back to the starting materials. Since the dielectric constant of ether is even a little larger than that of carbon tetrachloride and since the mole fractions of ethanol in ether and carbon tetrachloride with the same concentration of ethanol are about the same, it is not at all possible to attribute the large difference in rate to the change in the dielectric constant of the medium. The hydrolysis rates of benzoyl chloride in 5% water-dioxane (dielectric constant 3.8) and 5% water-acetone (dielectric constant 22.2) are not very different (7.30×10^{-5} sec^{-1} and 5.45×10^{-5} sec^{-1}, respectively[4]). Thus, the data on the ethanolysis of acid chlorides in ether and in carbon tetrachloride seem to indicate the validity of the proposed intermediates, I and II.

As is shown in Table III, k_h/k_e is very large for benzoyl and *p*-toluyl chloride in 5~33% water-dioxane and for mesitoyl chloride in 5% water-dioxane at 25°C. When k_h/k_e is very large, i.e., $k_3 \gg k_{-2}$[R'OH], Eq. 3 becomes

$$-\frac{d(RCOCl)}{dt}=\frac{k_1k_2(RCOCl)(R'OH)^2}{k_{-1}+k_2(R'OH)} \quad (4)$$

k_{-1} is large in a solvent of low polarity and small in a solvent of high polarity. k_1 is large for *p*-nitrobenzoyl chloride and small for *p*-anisoyl chloride. k_{-1} is small for the former and large for the latter, since an electron-releasing group helps R'OH leave from I and an electron-withdrawing group prevents its departure. When the polarity of the medium



is low and/or an electron-releasing substituent is present, $k_{-1} \gg k_2$ (R'OH) may be realized. Then, Eq. 4 becomes:

$$-\frac{d(RCOCl)}{dt}=\frac{k_1k_2}{k_{-1}}(RCOCl)(R'OH)^2 \quad (5)$$

Although k_1 and k_2 also depend upon the polarity of the medium or on the concentration of water, the dependence of k_{-1} on the polarity of the medium may be far greater. Thus, an apparent order in water of 2 or more may be realized in these cases. We recall that the apparent order in water, *n*, is ca. 2.9 for benzoyl chloride in 2~5% water-dioxane at 25°,[20] and *n* is ca. 3.2 for *p*-anisoyl chloride in 10~30% water-90~70% acetone at 0°C.[6]

When the polarity of the solvent is rather high and electron-withdrawing substituents are present, it is possible that $k_{-1} \ll k_2$ (R'OH) is realized. Then, Eq. 4 becomes

$$-\frac{d(RCOCl)}{dt}=k_1(RCOCl)(R'OH) \quad (6)$$

n is ca. 1.15 for benzoyl chloride in 5~15% water-acetone at 25°C, ca. 0.8 for *p*-nitrobenzoyl chloride in 5~25% water-acetone at 0°C, and ca. 1.06 for 2, 4, 6-trinitrobenzoyl chloride in 10~30% water-acetone at 0°C.[5]

When the concentration of water becomes very large, k_{-2} becomes appreciable; the trend may be seen in Table III. Therefore, we have to consider Eq. 3 rather than 4, 5 or 6. k_3 is an ionization step and highly dependent on the polarity of the medium, and it is probable that the apparent order in water, *n*, is rather great. The *n* for benzoyl chloride in 25~40% water-acetone at 25°C is ca. 2.72 and in 50~75% water-acetone at 0°C is ca. 6.85.[3] The fact that no carbonyl oxygen exchange was observed with mesitoyl chloride in 99% acetonitrile-water[21] can be explained by this mechanism. The conversion of intermediate II to I is helped by water, and at the very low concentration of water, k_{-2} may be inappreciably small; the trend may be seen in Table III. Thus, the findings of Bender and Chen[21] (no oxygen exchange) is understandable, while at the higher concentration of water the exchange of oxygen is expected, and it was really found to take place.[17]

Thus, all the data available on the hydrolysis of aroyl chlorides[29] can be explained very well in terms of intermediates I and II, and Eqs. 3, 4, 5 and 6.

The Solvolysis of Acyl Chlorides and Chloroformates.—It is not certain whether or not acetyl chloride and chloroformates are solvolyzed via a tetrahedral intermediate, and there are no data available on the exchange of the

29) The papers not so far cited include; J. F. Norris and H. H. Young, Jr., *J. Am. Chem. Soc.*, **57**, 1420 (1935); G. E. K. Branch and A. C. Nixon, ibid., **58**, 2499 (1936); C. G. Swain, R. B. Mosley and D. E. Bown, ibid., **77**, 3731 (1955).

TABLE VI. SOLVOLYSES OF VARIOUS ACID CHLORIDES AT 25°C

Substance	Solvent	10^5k_1, sec^{-1}	Ref.
2,4,6-Trimethoxybenzoyl chloride	5% water-dioxane	830	16
2,4,6-Trimethylbenzoyl chloride	5% water-dioxane	335	16
2,6-Dimethoxybenzoyl chloride	5% water-dioxane	330	16
Acetyl chloride	5% water-acetone	668	29
p-Nitrobenzoyl chloride	5% water-acetone	169	3
Benzoyl chloride	5% water-acetone	7.71	3
p-Methoxybenzoyl chloride	5% water-acetone	3.0	3
Ethyl chloroformate	10% water-dioxane	0.39	19

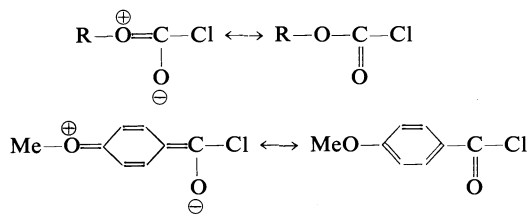
oxygen of these compounds with a solvent. However, it is very probable that these substances are also solvolyzed by a similar mechanism. The rates of the solvolysis of various acid chlorides are compared in Table VI.

There have been several papers reporting on the solvolysis of acyl chlorides[30-35] and chloroformates,[20,36-39] but none of them present clear evidence with which one can decide the mechanism unambiguously.

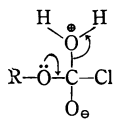
Some workers presuppose, without good evidence, the appearence of an acylium ion during the solvolysis of acyl chlorides and chloroformates. However, the absence of this species may be clearly understood if one compares their rates with the rate of benzoyl chlorides and also the rates of the solvolysis of ethyl chloride, benzyl chloride and methoxymethyl chloride. The rate of the alcoholysis of ethyl chloride at 25°C is extremely slow, that of benzyl chloride is fairly fast, and that of methoxymethyl chloride is extremely fast.[40] Thus, the order is $CH_3CH_2Cl \ll C_6H_5CH_2Cl \ll CH_3OCH_2Cl$. This rate sequence is what is expected for an S_N1 reaction, based on the stability of the carbonium ions formed. On the other hand, the rate sequence for the solvolysis of acetyl chloride, benzoyl chloride and alkyl chloroformates is completely the opposite, that is, $CH_3COCl \gg C_6H_5COCl \gg C_2H_5OCOCl$, as Table VI shows. If an acylium ion is playing any significant role in the solvolysis of acyl chlorides or chloroformates, the rate sequence should be the opposite; that is, the chloroformates capable of forming the most stable acylium ion should be solvolyzed the most quickly and acetyl chloride should be solvolyzed the most slowly because of the unstabilized acetyl cation. Since what was found in various media by various workers is contrary to this, acyl chlorides and chloroformates must be solvolyzed, not via an acylium ion, but by way of the addition-ionization mechanism.

Acetyl chloride is more reactive than benzoyl chloride because of a lack of conjugation with the phenyl ring. If acetyl chloride follows the mechanism proposed for benzoyl chloride, k_1 is very large, k_{-1} is probably very large, and the rate may follow Eq. 5. The apparent order in water, n is found to be 2 in 1~5% water-acetone at 24.8°C,[30] 1.4 in 1~4% ethanol-carbon tetrachloride, and 2.0 in 1~40% ethanol-ether at 20°C.[7]

Chloroformates are less reactive than acetyl chloride because of resonance such as the following, and these compounds are somewhat analogous to *p*-anisoyl chloride.



If chloroformates follow the mechanism proposed for benzoyl chlorides, k_1 is rather small, k_{-1} may be very large, and the rate may follow Eq. 5:



The apparent order in water, n, is found to be 1.6~2.2 for ethyl chloroformate in 10~70%

30) G. Zimmerman and C. Tuan, ibid., **77**, 332 (1955).
31) V. Gold and J. Hilton, *J. Chem. Soc.*, **1955**, 838.
32) C. G. Swain and C. B. Scott, *J. Am. Chem. Soc.*, **75**, 246 (1953).
33) E. J. Cairns and J. M. Prausnitz, *J. Chem. Phys.*, **32**, 169 (1960).
34) M. L. Bender and M. S. Fong, *J. Am. Chem. Soc.*, **82**, 6318 (1960).
35) J. Cason and K. W. Kraus, *J. Org. Chem.*, **26**, 2624 (1961).
36) H. K. Hall, Jr., *J. Am. Chem. Soc.*, **77**, 5993 (1955).
37) M. Green and R. F. Hudson, *Proc. Chem. Soc.*, **1959**, 149.
38) E. W. Crunden and R. F. Hudson, *J. Chem. Soc.*, **1961**, 3748.
39) R. F. Hudson and M. Green, ibid., **1962**, 1055.
40) Extrapolation of the rates of the solvolysis of methoxymethyl chloride in a methanol-dioxane mixture[41] to pure methanol gives $k_1 = 2.2\ sec^{-1}$ at 25°C.[42] On the other hand, the rate constant of α, 2, 4, 6-tetramethylbenzyl chloride in pure ethanol at 25°C is only $3.27 \times 10^{-4}\ sec^{-1}$.[43]
41) P. Salomaa, *Ann. Acad. Turkuensis*, **1953**, A14.
42) P. D. Bartlett and B. T. Storey, *J. Am. Chem. Soc.*, **80**, 1398 (1958).
43) G. Baddeley and J. Chadwick, *J. Chem. Soc.*, **1951**, 368.

water-dioxane at 25°C, and 1.1～1.4 for *t*-butylperoxy chloroformate in 20～100% methanol-carbon tetrachloride.[44] Leimu studied the rate of the methanolysis of chloroformates and found that β-chloroethyl chloroformate is solvolyzed 12.5 times faster than isopropyl chloroformate.[45]

The Solvolysis of Aroyl Chlorides in the Presence of Alkali.—Although the solvolysis of acid chlorides in general is not catalyzed by the presence of acids, [2,31,46] it is much accelerated by the addition of alkali, as Table VII shows.

TABLE VII. EFFECT OF ALKALI ON THE SOLVOLYSES OF ACID CHLORIDES[6,18]

1) 80% alcoholic acetone at −10.75°C

	Benzoyl chloride	*p*-Nitrobenzoyl chloride	Mesitoyl chloride
10^6k_1 (sec^{-1})	4.97	212	521
k_2* ($M^{-1}\,sec^{-1}$)	3	2	0.34
k_2/k_1	6×10^5	6×10^5	650

* $(OEt^{\ominus})=0.02$ M

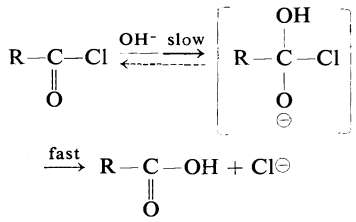
2) 25% water-acetone at 0.2°C

	p-Nitrobenzoyl chloride	*p*-Anisoyl chloride	$\frac{k_{nitro}}{k_{anisoyl}}$
10^4k_1 (sec^{-1})	20.32	2.82	7.2
k_2* ($M^{-1}\,sec^{-1}$)	6.82	0.405	16.8
k_2/k_1	3360	1430	

* 0.003 M $OH^{\ominus}$

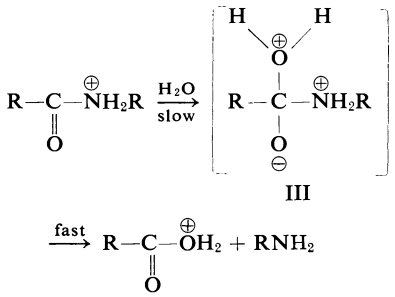
The relatively small increase of the rate on the addition of alkali to mesitoyl chloride is interesting. The slower rate of mesitoyl chloride than benzoyl and *p*-nitrobenzoyl chloride in alkali may be explained by the presence of steric hindrance and electron-releasing substituents.

When alkali is present, a probable mechanism may be the following:



If the alkaline solvolysis proceeds by this scheme, the rate increase upon the addition of alkali should be greater in a solvent of low polarity and greater for an acid chloride with electronegative substituents. Table VII is in agreement with this.

The basic hydrolysis of acid chlorides is somewhat analogous to the acid hydrolysis of amides:



In this case, an inappreciable oxygen exchange between solvent and amide is observed, and cation III seems to be an activated complex rather than an intermediate. There are no experimental data available on the isotope exchange in the alkaline solvolysis of acid chlorides, but the alkaline solvolysis of acid chlorides may possibly proceed through an activated complex, not an intermediate.

Mesitoyl Chloride. — The case of mesitoyl chloride is worthy of further comment. It is well known that mesitoic acid is resistant to esterification under ordinary conditions and that methyl mesitoate is saponified with difficulty.[47-48] However, Bender proved conclusively that the alkaline hydrolysis of methyl mesitoate proceeds through a tetrahedral intermediate, which goes to hydrolyzed acid 6.8 times faster than it goes back to the starting ester.[49] Acetomesitylene gives a 2,4-dinitrophenylhydrazone[50] and reacts with hydroxylamine to give acetomesidide.[51] Although these examples show that it is not impossible to form a tetrahedral intermediate for mesitoic acid derivatives, the very fast solvolysis of mesitoyl chloride[52] is yet to be explained.

From dipole moments,[53-54] ultraviolet absorption[55] or infrared absorption,[56] it is known

44) H. Minato, Ph. D. thesis (Harvard University, 1961), p. 40.
45) R. Leimu, *Ber.*, **70B**, 1040 (1937).
46) The only exception reported is mesitoyl chloride.[21]
47) H. L. Goering, T. Rubin and M. S. Newman, *J. Am. Chem. Soc.*, **76**, 787 (1954). In the alkaline hydrolysis of methyl mesitoate in 60% dioxane −40% water, $k_2=1.40\times10^{-3}\,M^{-1}\,sec^{-1}$ at 126°C.
48) M. L. Bender, R. D. Ginger and J. P. Unik, ibid., **80**, 1044 (1958). In the alkaline hydrolysis of ethyl benzoate at 25°C, $k_2=8.4\times10^{-3}M^{-1}\,sec^{-1}$. By extrapolating the data of Refs. 47 and 48, k_2 (Ethyl benzoat)/k_2(Methyl mesitoate) = 44000 at 25°C and 1530 at 125°C.
49) M. L. Bender and R. S. Dewey, ibid., **78**, 317 (1956).
50) D. E. Pearson and F. Greer, ibid., **77**, 1294 (1955).
51) E. Feith and S. H. Davies, *Ber.*, **24**. 3546 (1891).
52) For the more recent papers on this compound, see Ref. 21 and I. Ugi and F. Beck, *Ber.*, **94**, 1839 (1961).
53) J. B. Bentley, K. B. Everard, R. J. B. Marsden and L. E. Sutton, *J. Chem. Soc.*, **1949**, 2957.
54) H. B. Keevans and J. R. Platt, *J. Am. Chem. Soc.*, **71**, 1741 (1949).
55) E. A. Braude, F. Sondheimer and W. F. Forbes, *Nature*, **173**, 117 (1954).
56) Methyl benzoate 5.80 μ, methyl mesitoate 5.77 μ, methyl acetate 5.73 μ; benzoyl chloride 5.64 μ, mesitoyl chloride 5.57 μ, acetyl chloride 5.55 μ.

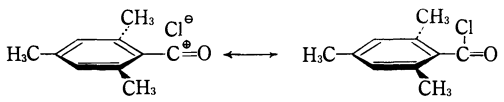
TABLE VIII. RELATIVE RATES OF SOLVOLYSES OF SOME ESTERS AND ACID CHLORIDES

Condition	Ethyl acetate	Ethyl benzoate	Methyl mesitoate	Ref.
Acid[a)]	173	1	too slow	57
Basic[a)]	10	1	2.3×10^{-5}	47,48
Condition	Acetyl chloride	Benzoyl chloride	Mesitoyl chloride	Ref.
Neutral or acid[b)]	86.7	1	43.5	18
Basic[b)]	too fast	more than 925[c)]	1	18

a) Second order rate constants
b) First order rate constants
c) Too fast to measure accurately

that steric hindrance by *o*-substituents can decrease the extent of conjugation between a benzene ring and a carbonyl group by preventing these groups from becoming coplanar. Bunton and Lewis[17] attributed the fast solvolysis rate of mesitoyl chloride to the failure of the carbonyl group to conjugate with the benzene ring. The solvolyses of some esters and acid chlorides are compared in Table VIII. The resistance of mesitoic acid towards esterification or of mesitoate towards hydrolysis is usually explained by the blocking effect of *o*-substituents. If mesitoyl chloride is reactive only because of the lack of conjugation between a carbonyl group and a benzene ring, as Bunton and Lewis maintain, it is difficult to explain why methyl mesitoate is not solvolyzed more easily than benzoate in a weakly acid solution, and why methyl mesitoate is solvolyzed 10^5 times more slowly than ethyl benzoate in an alkaline solution. It seems that the explanation must depend upon a factor peculiar to acid chlorides.

It is conceivable that the structure of mesitoyl chloride differs from those of benzoyl chloride and of mesitoate esters. Although the ortho substituents prevent the chlorocarbonyl group from becoming coplanar with the ring, the carbonyl group may remain colinear with the bonding-ring carbon atom as in the mesitoyl cation. The molecule may then be described by the resonance structures (IV).



IV

The fact that mesitoyl chloride is a non-conductor in sulfur dioxide[27] need not void this hypothesis. An incoming hydroxylic solvent can attack the carbonyl carbon from the direction of the *p*-orbital perpendicular to the ring without steric hindrance. The solvolysis still proceeds not by the direct displacement of chloride but rather by addition-ionization, since the isotope exchange experiment showed the existence of a tetrahedral intermediate. The tetrahedral intermediate formed in the hydrolysis of mesitoate esters, on the other hand, is formed very much more sluggishly because, as we postulate, the alkoxy-carbonyl group does not depart from the usual trigonal structure.

Summary

A mechanism has been proposed which seems to be consistent with all the experimental results obtained by various workers on the solvolyses of acid chlorides.

The author wishes to thank Professor Paul D. Bartlett of Harvard University for his encouragement and valuable advice, the members of Professor Bartlett's research group in 1958—1961 for their stimulating discussions, and the Bell Telephone Laboratories for a research fellowship in 1959—1961.

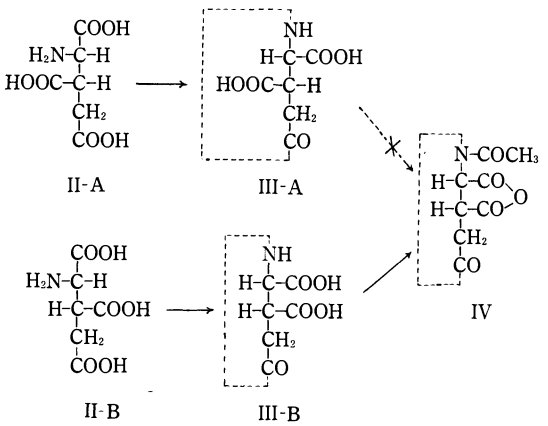
Harvard University
Cambridge 38, Massachusetts
U.S.A.

On the Configurations of α-Aminotricarballylic Acids

By Takeo KANEKO, Yasuo ARIYOSHI, Seiji ANDŌ*1 and Hakuji KATSURA

(Received September 10, 1963)

Greenstein et al.[1] have reported on the configuration of the α-asymmetric carbon atoms of α-aminotricarballylic acids and isocitric acids. Recently, the absolute configurations of isocitric acids have been confirmed wholly and undoubtedly by us[2] and by Patterson et al.[3] As a result, the conclusion suggested by Greenstein et al.[1] has been rectified. In this paper, the absolute configurations of α-aminotricarballylic acids will be characterized by confirming the stereostructures of their pyrrolidone derivatives. α-Aminotricarballylic acid (II) was prepared from ethyl acetamidocyanoacetate and diethyl monobromosuccinate by the method of Greenstein et al.,[4] and from diethyl formylsuccinate (I) by Strecker synthesis. The yields of the diastereoisomeric α-aminotricarballylic acids A*2 (II-A) and B*2 (II-B) were obtained at the rate of three to one in the former method, but at the rate of eleven to one in the latter method. The pyrrolidone derivative (III-B) of II-B afforded



N-acetyl acid anhydride (IV) when heated with acetic anhydride, but from that of II-A (III-A), no acid anhydride was obtained at all. From these results, III-B may be identified as cis, and III-A as trans; therefore, the stereostructures of II-A and II-B may be shown as in the figure. According to Greenstein,[4] (+)- and (−)-alloisocitric lactones were derived from (+)- and (−)-II-A respectively by the action of nitrite, and, similarly, (+)- and (−)-isocitric lactones were derived from)+)- and (−)-II-B. It is evident that the absolute configurations of the β-asymmetric carbon atoms of α-aminotricarballylic acids are identical with those of the correspoding isocitric acids, because there was no effect on the configurations of the β-carbon atoms in the treatment of α-aminotricarballylic acids with nitrite. The determination of the relative configuration between the β- and α-asymmetric carbon atoms of the diastereoisomeric DL-α-aminotricarballylic acids, therefore, is sufficient to clarify the absolute configurations, of the α-asymmetric carbon atoms of the amino acids. Consequently, the absolute configurations of these amino acids II-A and II-B may be shown as in Table I. This table shows that Lutz-Jirgensons' displacement rule[5] is applicable to these amino acids II-A and II-B, and that in the derivations from amino acids II to hydroxy acids III no Walden inversions are observed.

Experimental

Diethyl Formylsuccinate (I).—From diethyl succinate (50 g.) and ethyl formate (30 g.), I (b. p. 92~105°C/3 mmHg: 41~45 g., 70~77%) was prepared by the method described by Wislicenus.[6]

α-Aminotricarballylic Acid A (II-A) and Pyrrolidone Carboxylic Acid B (II-B).—To the addition product prepared from I (60.6 g.) and sodium hydrogen sulfite (37.5 g.), a solution of sodium cyanide (18 g.) in water (145 ml.) was added. Oily cyanohydrine was separated and added to a concentrated aqueous ammonium hydroxide solution (330 ml.). After the mixture had been allowed to react in a pressure bottle for 30 days at room temperature, the reaction mixture was concentrated and the

*1 Present address: Kōa Petroleum & Co., Iwakuni, Yamaguchi.

1) M. Winitz, S. M. Birnbaum and J. P. Greenstein, *J. Am. Chem. Soc.*, **77**, 716 (1955).

2) T. Kaneko, H. Katsura, H. Asano and K. Wakabayashi, *Chem. & Ind.*, **1960**, 1187; T. Kaneko and H. Katsura, ibid., **1960**, 1188; H. Katsura, *J. Chem. Soc. Japan, Pure Chem. Sec.* (*Nippon Kagaku Zasshi*), **82**, 91, 92, 98 (1961).

3) J. P. Glusker, A. L. Patterson, W. E. Lore and M. L. Dornberg, *J. Am. Chem. Soc.*, **80**, 4426 (1958); A. L. Patterson, C. K. Johnson, D. Van der Helm and J. A. Minkin, ibid., **84**, 309 (1962).

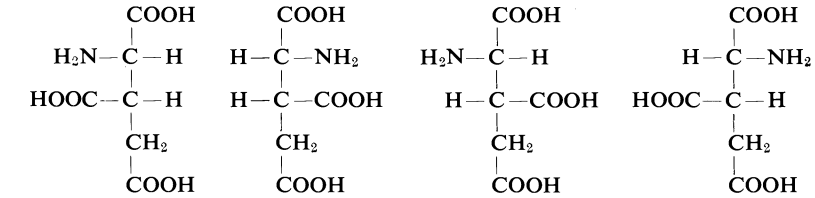
4) J. P. Greenstein, N. Izumiya, M. Winitz and S. M. Birnbaum, ibid., **77**, 707 (1955).

*2 A and B were named by Greenstein.[4]

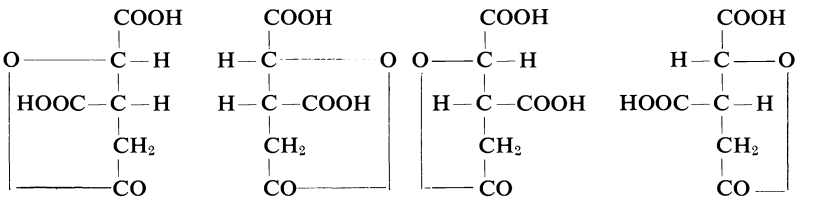
5) O. Lutz and B. Jirgensons, *Ber.*, **63**, 448 (1930); **64**, 1221 (1931); **65**, 784 (1932).

6) W. Wislicenus, E. Boeklen and F. Reute, *Ann.*, **363**, 340 (1908).

TABLE I. THE ABSOLUTE CONFIGURATIONS OF α-AMINOTRICARBALLYLIC ACIDS AND ISOCITRIC ACIDS



		II-A		II-B	
$[\alpha]_D$ in HCl		+36.4°	−36.5°	+48.0°	−48.7°
$[\alpha]_D$ in H_2O		+ 7.5°	− 6.8°	+32.8°	−33.5°
Absolute configuration*	α	S	R	S	R
	β	S	R	R	S



		III-A		III-B	
$[\alpha]_D$ in H_2O		+41.0°	−40.5°	+60.9°	−62.0°
Absolute configuration*	α	S	R	S	R
	β	S	R	R	S

*) This is specified by the (R)-, (S)-system of D. S. Cahn, C. K. Ingold and V. Prelog (*Experientia*, **12**, 81 (1956)).

TABLE II. PAPER CHROMATOGRAM OF α-AMINOTRICARBALLYLIC ACIDS (II-A AND II-B) AND PYRROLIDONE CARBOXYLIC ACIDS (III-A AND III-B)

Solvent	R_f-value			
	II-A	II-B	III-A*	III-B*
n-Butanol : acetic acid : water (4 : 1 : 5(v/v), upper layer)	0.16	0.19	0.45	0.39
Phenol : water : 85% formic acid (3 g. : 1 ml. : 1%)	0.25	0.25	0.59	0.59
Isopropanol : *t*-butanol : benzylalcohol : water : 85% formic acid (1 ml. : 1 ml. : 3 ml. : 1 ml. : 2%)			0.53	0.44
t-Butanol : benzylalcohol : water : 85% formic acid (5 ml. : 15 ml. : 2 ml. : 1%)			0.44	0.36
n-Butanol : benzylalcohol : water : 85% formic acid (5 ml. : 5 ml. : 1 ml. : 1%)			0.40	0.33

* Colored by spraying with brom phenol blue solution

residue was refluxed with 6 N hydrochloric acid (800 ml.) for 7 hr. Inorganic salts were removed by extraction from the hydrolysate with cold ethanol (500 ml.), and chloride ions were removed by the aid of silver carbonate (38 g.); then the solution was treated with hydrogen sulfide. When the purified solution was concentrated and kept at 5°C for 20 hr., II-A (14 g.) deposited as a solid and was recrystallized from water.

Found: C, 37.77; H, 4.99; N, 7.23. Calcd. for $C_6H_9O_6N$: C, 37.70; H, 4.75; N, 7.33%.

Another crop (3 g.) was obtained by the concentration of the above filtrate.

The filtrate separated from II-A crystals was made to pH 5 with an aqueous sodium hydroxide solution, and a solution of copper acetate (65 g.) in hot water (650 ml.) was added to this solution to give blue crystals of copper salt (14 g.), which were collected after standing at room temperature for 20 hr. The copper was removed as copper sulfide, and the solution was refluxed with a large amount of water for 7 hr. When the solution was concentrated and kept at 5°C for 20 hr., III-B (1.5 g.) was obtained and recrystallized from water; m. p. 225°C (decomp.): lit.,[4] m. p. 230°C.

Found: C, 41.29; H, 4.16; N, 8.01. Calcd. for

$C_6H_7O_5N$: C, 41.62; H, 4.08; N, 8.09%.

Pyrrolidone Carboxylic Acid A (III-A).—From II-A (12 g.), III-A (8.5 g.) was obtained by the method described by Greenstein[4] and then recrystallized from water; m. p. 210°C: lit.,[4] 210°C. This sample contains one mole of the water of crystallization.

Found: C, 37.70; H, 4.73; N, 7.42; H_2O, 9.82 (dried at 90~100°C in vacuo for 18 hr.). Calcd. for $C_6H_7O_5N \cdot H_2O$: C, 37.70; H, 4.75; N, 7.33; H_2O, 9.43%.

Acid Anhydride (IV) of *N*-Acetyl-pyrrolidone Carboxylic Acid B.—III-B (2.7 g.) was dissolved in acetic anhydride (400 ml.) by heating it gently over a 30-min. period, and then the solution was heated at 120~140°C for 15 min. After some insoluble materials had been filtered off from the hot reaction mixture, the solution was cooled to room temperature. IV (2.1 g.) thereupon crystallized out, and yet another crop (0.3 g.; total, 2.4 g., 80%) was obtained by the cocentration of the filtrate; m. p. 225°C (decomp.). A sample (1 g.) was recrystallized from acetic anhydride and washed with acetone. The pure substance (0.7 g.) was obtained after drying it over phosphorus oxide in a vacuum desiccator; m. p. 225°C (decomp.).

Found: C, 48.68; H, 3.55; N, 7.11. Calcd. for $C_8H_7O_5N$: C, 48.74; H, 3.58; N, 7.11%.

When this sample (1 g.) was hydrolyzed with 2 N hydrochloric acid (30 ml.), III-B (m. p. 225°C (decomp): 0.4 g.) was recovered.

The R_f values of II-A and II-B, and III-A and III-B are shown in Table II.

Department of Chemistry
Faculty of Science
Osaka University
Nakanoshima, Osaka

Catalysis by Organic Semi-conductors. The Photo-oxidation of Isopropyl Alcohol in the Liquid Phase

By Hiroo INOUE, Shigeki HAYASHI and Eiji IMOTO

(Received September 12, 1963)

Some organic catalytic reactions in biological systems, especially oxidation and reduction, have been explained recently by means of a concept of an organic semi-conductor,[1] though no catalytic reaction of an organic semi-conductor has ever been studied *in vitro*. Zinc oxide, which is a typical n-type semi-conductor, is effective as a catalyzer for the oxidation of isopropyl alcohol to acetone with oxygen under ultraviolet-irradiation.[2] On the other hand, it has been reported by many workers[3] that some photo-oxidations of organic compounds with oxygen under ultraviolet or visible light irradiation are accelerated by various kinds of organic dyes, though there have not been many of the kinds of dye used as the catalyst for these photo-oxidations. Moreover, the property of a dye as an organic semi-conductor, chiefly the kind of charge-carrier, has been studied by Terenin[4] and others[5,6]; some of their results are shown in Table I in the present paper.

TABLE I. SIGN OF THE CHARGE CARRIERS

Dye	Meier[5]	Terenin[4]	Nelson[6]
Crystal violet	n*	n	
Malachite green	n	n	n
Ethyl violet	n		
Methyl green	n		
Brilliant green	n	p	
Pinacyanole	n	n	n
Rhodamine B	n	n	
Auramine	n	p	
Erythrosine	p*		p
Eosine Y	p		
Acridine orange	p		
Rose bengal	p		
Congo red	p		
Kryptocyanine	p		n
Pyocyanine		n	
Floxine		p	
Chlorophylls		p	
Methyl-free phthalocyanine(Co^{2+}, Mn^{2+}, Fe^{2+}, Mg^{2+})		p	

* Sign of n or p means n- or p-type semi-conductor respectively.

Here it is attempted to correlate the natures of organic semi-conductors with the catalytic ability of the dye used as a catalyzer for the

1) M. Calvin, *Rev. Mod. Phys.*, **31**, 147, 157 (1959).
2) G. M. Schwab, *Chem. Ber.*, **93**, 2755 (1960).
3) G. O. Schenck, *Naturwiss.*, **40**, 205, 229 (1953); K. Uchida, S. Kato and M. Koizumi, This Bulletin, **35**, 16 (1962).
4) A. Terenin, *Proc. Chem. Soc.*, **1961**, 321.
5) H. Meier, *Z. Wiss. Phot.*, **53**, 1 (1958).
6) N. Petruzzella and R. C. Nelson, *J. Chem. Phys.*, **37**, 3010 (1962).

photo-oxidation of isopropyl alcohol to acetone with oxygen under ultraviolet or visible light irradiation.

Experimental

Materials.—Isopropyl alcohol was purified by a fractional distillation after dehydration on calcium oxide. The dyestuffs used as the catalyzer, auramine, safranine T, fluorescein, eosine Y, crystal violet, malachite green, rhodamine B and brilliant blue, were of a commercial grade and had been purified by recrystallization or by extraction. Condensed aromatic or aza-aromatic hydrocarbons, such as anthracene, perylene, violanthrone, isoviolanthrone, phenazine, acridine and indanthrene, were also of a commercial grade and had been purified by sublimation or the recrystallization method.

The Measurement of the Reaction Rate.—The rate of the oxidation of isopropyl alcohol with oxygen was determined by measuring the amount of oxygen absorbed. To make a solution with a catalyzer in an appropriate concentration, a weighed amount of a catalyzer was dissolved or dispersed into 10 ml. of isopropyl alcohol which had been placed in a test tube of a common quantity (inner diameter, 15 mm.; thickness of the wall, 0.5 mm.). After oxygen had been bubbled in for 5 min., the test tube was connected with a gas burette, the air space of which had previously been filled with oxygen, and placed in a thermostat at a distance from the light source, which was placed in the same thermostat. The light source used was a 200 W. tungsten lamp or a Toshiba mercury lamp SHEL-100, which irradiates the waves at 2500, 3200, 3600, 4400, 5500 and 5800 Å.

Analysis of the Acetone and Pinacol Produced.—The acetone and the pinacol formed in the reaction mixture, after they had cooled in dry ice, were analyzed with a gas chromatograph, Hitachi KGL-2, in which polyethylene glycol was used as an adsorbent and hydrogen gas as a carrier gas.

Results and Discussion

The Effects of Dyes on the Rate of Oxygen Absorption.—As is shown in Fig. 1, the amount of oxygen absorbed increased linearly with the reaction time after a certain induction period, no matter what kind of dye was chosen as the catalyzer. However, the absorption rates differed from dye to dye. They may be classified into two groups, one group with a large rate, and another group with a small rate. All the catalyzers which afford the large rate are the dyes which were identified as p-type semi-conductors by Terenin, while those which afford the small rate are ones which were identified as n-type semi-conductors by the same author. Although the magnitude of the induction period of each of the oxidations catalyzed by p-type dyes was not the same, all

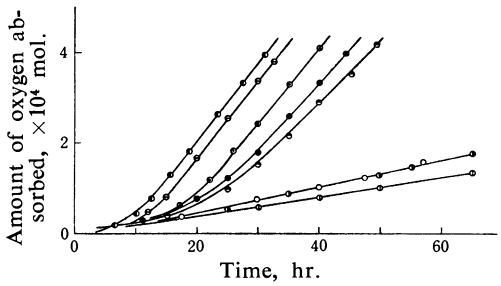


Fig. 1. Effects of dyes on the rate of the oxygen absorption: Light source; 100 W. mercury lamp, irradiated distance; 10 cm., irradiated temp.; 43~44°C, concn.; 5×10^{-4} mol./l. and reaction vessel; Pyrex glass. ◐ Blank, ⊖ eosine Y, ⊙ auramine, ● fluorescein, ◓ safranine T, ◐ rhodamine B, ○ crystal violet, and ⓘ brilliant blue.

Table II. Decoloration of dyes*

Dye	Irradiated time, hr.	Decoloration, %
Fluorescein	30	82.8
Eosine Y	15	68
	24	97.4
Safranine T	19	6.5
	38	15.2
	43	28.6
Auramine	19~20	22.9
Rhodamine B	40	1.6
Crystal violet	40	1.8
Malachite green	27	58.2
	57~60	80.3

* Light source; 100 W. mercury lamp, concentration of dye; 5×10^{-4} mol./l. and irradiated distance; 10 cm.

the inclinations of the straight lines in Fig. 1 are parallel and are also parallel to that of the oxidation which proceeded without a dye. As Table II shows, the p-type dyes were gradually decolorized during the reaction and the decolorized dyes may not be effective in accelerating the production of hydrogen peroxide. Therefore, the curves of the oxygen absorption rate must have the same inclination after the induction period as in an oxidation without a dye. This means that the oxidation is a chain reaction carried out by means of the hydrogen peroxide which is produced by the reaction of dyes, isopropyl alcohol and oxygen, and p-type dyes are effective merely in producing hydrogen peroxide. On the other hand, the n-type dyes must not be effective in producing hydrogen peroxide.

The second remarkable difference between the reaction with an n-type dye and that with a p-type dye is the molar ratio of the acetone formed to the oxygen absorbed. As Table III

TABLE III. RELATION BETWEEN OXYGEN ABSORBED AND ACETONE FORMED (IN THE CASE OF DYE)*1

Exp. No.	Dye	Irradiated distance cm.	Temp. °C	Time hr.	Amount of O_2 absorbed $\times 10^4$ mol.	Amount of acetone formed $\times 10^4$ mol.	Ratio*2
1	Fluorescein	10	42~43	46	3.89	7.74	1.93
2	Safranine*3 T	10	42~43	47.7	4.81	7.84	1.63
3	Eosine Y	10	43	30.4	3.52	5.66	1.61
5	Auramine	10	44	46.8	5.95	7.02	1.17
6	Crystal violet	10	43~44	67.0	2.07	0.10	0.05
7	Crystal violet	5~6	30	21.3	1.1	0.7	0.64
8	Crystal violet*3	10	43~44	94.5	3.23	2.10	0.65
9	Rhodamine B*3	10	43~44	67.6	2.3	0.57	0.25
10	Rhodamine B*3	5~6	30	20.7	1.00	0.79	0.79
11	Malachite green	5~6	30	27.3	0.98	0.55	0.56
12	Brilliant blue	5~6	30	21.4	0.49	0.35	0.72
13	Eosine Y-Rhodamine*4 B	5~6	30	4.9	0.44	0.40	0.90
14	Eosine Y-Rhodamine*4 B	5~6	30	19.5	1.00	1.27	1.27
15	Blank	10	43~44	32.3	4.4	7.15	1.63

*1 Light source; 100 W. mercury lamp, concentration of dye; $5\sim10^{-4}$ mol./l. except Exp. Nos. 2, 8, 9 and 10. Reaction vessel; Pyrex glass tube.
*2 Ratio is the molar ratio of the acetone formed to the oxygen absorbed.
*3 The concentration of dye: Exp. Nos. 2, 8 and 9; 2.5×10^{-4} mol./l., Exp. No. 10; 8×10^{-4} mol./l.
*4 Eosine Y: 5×10^{-4} mol./l., rhodamine B: 5×10^{-4} mol./l.

shows, the p-type dyes afforded a ratio larger than unity, while the n-type dyes afforded a ratio less than unity. Even when the crystal violet of an n-type dye was used as the catalyzer and the reaction system was irradiated at a nearer distance, 5~6 cm., from a light source, the amount of the acetone formed was yet very little.

Furthermore, it was astonishing that the reaction catalysed by a p-type dye produced mainly acetone, while that catalyzed by an n-type dye produced pinacol. The irradiation of isopropyl alcohol in an atmosphere of oxygen in the presence of crystal violet at the distance of 5~6 cm. from the light source for 210 hr. at 40~50°C produced about 7×10^{-4} mol. of pinacol per 10 ml. of isopropyl alcohol. Under the same conditions, eosine Y of a p-type produced only about 1.05×10^{-4} mol. of pinacol per 10 ml. of isopropyl alcohol, even after irradiation for two weeks.

The Effects of the Mixed Dyes on the Oxygen Absorption.—Eosine Y (a p-type dye) and rhodamine B (an p-type dye) were used together as the catalyzers of the oxidation, because it was expected that a combination of a p-type catalyzer and an n-type catalyzer might be effective because synergitic. Since the visible absorption spectrum of these mixed dyes was the sum of the absorption spectra of eosine Y and rhodamine B, it seems that there is no molecular interaction between eosine Y and rhodamin B in isopropyl alcohol.

As is shown in Figs. 2 and 3, the rate of oxygen absorption increased with the increase in the concentration of eosine Y at a constant concentration of rhodamine B; on the other hand, it did not vary with an increase in the concentration of rhodamine B at a constant concentration of eosine Y. This means that, contrary to our expectations, there was no synergitic action, even when two kinds of dyes were mixed. While the oxygen absorbed-reaction time curve rose steeply at the beginning of the reaction, as Fig. 2 shows, the inclination of the curve decreased gradually and at the final stage of the reaction approached

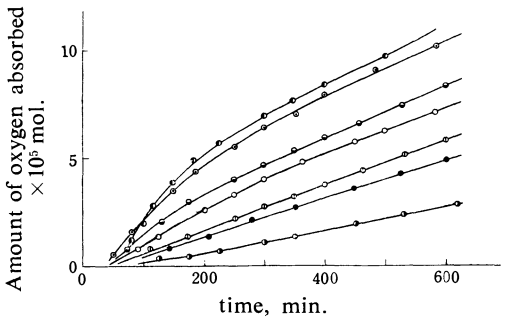


Fig. 2. Effects of the mixed dyes on the oxygen absorption (at the constant concentration of rhodamine B): Irradiated distance; 5~6 cm., irradiated temp.; 30°C, and reaction vessel; Pyrex glass.
Concn. of rhodamine B; ◐ 5×10^{-4} mol./l.
Eosine Y; ◐ 12×10^{-4} mol./l., ⊙ 10×10^{-4} mol./l., ◒ 7×10^{-4} mol./l., ○ 6×10^{-4} mol./l., ① 5×10^{-4} mol./l., ● 3.5×10^{-4} mol./l.

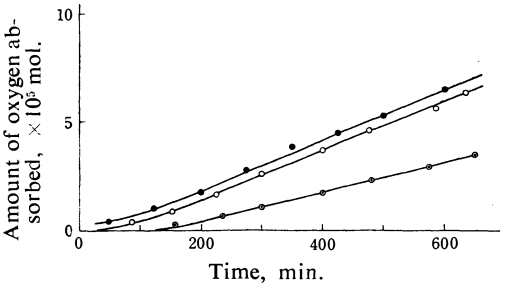


Fig. 3. Effects of the mixed dyes on the oxygen absorption (at the constant concentration of eosine Y): Condition of irradiation was same to Fig. 2.
Eosine Y; 5×10^{-4} mol./l. Rhodamine B; ○ 5×10^{-4} mol./l., ● 10×10^{-4} mol./l. ⊙ Rhodamine B alone; 5×10^{-4}mol./l.

the inclination of that curve obtained with rhodamine B alone. This fact could be explained as follows. When eosine Y was used as the catalyzer together with rhodamine B, eosine Y was also decolorized gradually as much as 67.7% after 450 min. and 79% after 1168 min.; consequently, the oxidation rate was retarded.

The Effects of Dyes on the Rates of the Formation of Acetone.—When isopropyl alcohol was irradiated in an atmosphere of oxygen at 17~18°C for 20 hr. with a 200 W. tungsten lamp placed 15 cm. from the vessel, no acetone was detected. However, when a p-type dye was present in this system, acetone was produced, while, except for rhodamine B, no n-type dyes were effective (Fig. 4). Now, the rate of the formation of acetone was measured under the reaction conditions just cited. As is clear from the results shown in Fig. 5, each dye has its optimum concentration at which the

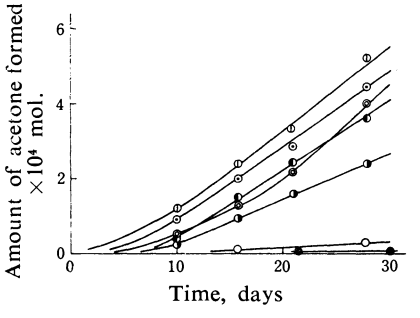


Fig. 4. Catalytic action of dyes: Light source; 200 W. tungsten lamp, irradiated distance; 15 cm., temp.; 17~18°C, and reaction vessel; Pyrex glass.
⊙ Eosine Y; 5×10^{-4} mol./l., ◎ fluorescein; 5×10^{-4} mol./l., ① auramine; 0.1×10^{-4} mol./l., ◑ safranine T; 0.1×10^{-4} mol./l., ◐ rhodamine B; 0.1×10^{-4} mol./l., ● brilliant blue, crystal violet; 5×10^{-4} mol./l. and ○ without dye.

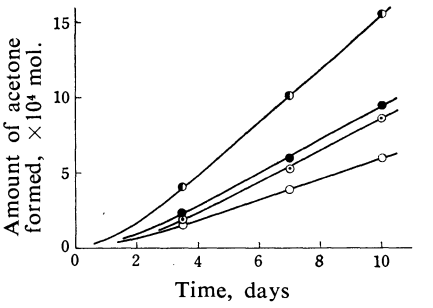


Fig. 5. Effect of the concentration of eosine Y to catalytic action: Irradiated distance; 17 cm., temp.; 39~42°C and light source; 200 W. tungsten lamp.
Concn. of eosine Y; ● 10×10^{-4} mol./l., ◐ 7.5×10^{-4} mol./l., ⊙ 5.0×10^{-4} mol./l., ○ 1.0×10^{-4} mol./l.

maximum rate was exhibited: eosine Y, 8×10^{-4} mol./l.; fluorescein; 7.5×10^{-4}; auramine and safranine T, $0.05\sim0.5\times10^{-4}$ mol./l., and rhodamine B, 0.08×10^{-4} mol./l. The order of the magnitude of these optimum concentrations was the same as that indicated in Fig. 1.

The Effects of Condensed Aromatic and Aza-aromatic Hydrocarbons.—An oxidation catalyzed by a condensed aromatic or aza-aromatic hydrocarbon was carried out in the presence of rhodamine B, which may be effective in suppressing the effects of hydrogen peroxide, and also, if necessary, in the presence of sodium palmitate, with which an insoluble aromatic hydrocarbon could be dispersed. The other experimental conditions were the same as those holding in the cases of dyes. As is clear from the results shown in Fig. 6, the compound

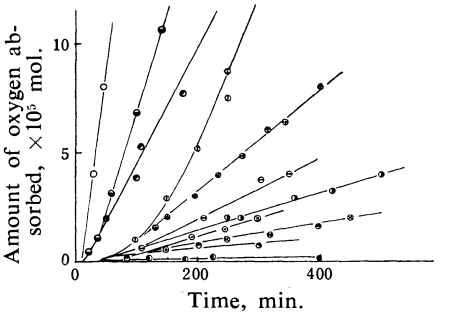


Fig. 6. Effects of aromatic and aza-aromatic hydrocarbons on the rate of the oxygen absorption: Condition of irradiation; same to Table IV. ① Anthracene; 5×10^{-4} mol./l., ⊖ pyrene; 2 mg., ◒ phenazine; 5×10^{-4} mol./l., ○ anthraquinone; 5×10^{-4} mol./l., ◑ perylene; 10^{-3} mol./l., ◐ violathrone; 2.3 mg., ● isoviolanthrone; 2.8 mg., ◓ indanthrene; 2 mg., ⊗ fluoridine; 3.0 mg., ◐ triphenodioxazine; 3 mg., ⊕ rhodamine B alone; 5×10^{-4} mol./l., ⊙ rhodamine B and sodium palmitate; 5×10^{-4} mol./l.

TABLE IV. RELATION BETWEEN OXYGEN ABSORBED AND ACETONE FORMED (IN THE CASE OF CONDENSED AROMATIC AND AZA-AROMATIC HYDROCARBONS)*1

Compound	Irradiated time hr.	Amount of O_2 absorbed $\times 10^4$ mol.	Amount of acetone formed $\times 10^4$ mol.	Ratio
Anthracene	6.05	1.71	2.2	1.29
Acridine	7.21	1.64	—	—
Phenazine	2.9	1.34	1.47	1.09
Anthraquinone	2.53	1.8	3.93	2.18
Pyrene	7.61	0.61	0.4	0.65
Perylene	7.06	0.34	0.41	1.2
Fluoridine*2	5.1	0.67	—	—
Triphenodioxazine*2	5.18	0.07	0	0
Indanthrene*2	5.08	0.43	0.06	0.14
Violanthrone*2	6.73	0	—	—
Isoviolanthrone*2	2.6	0	—	—

*1 Reaction was carried out in the presence of rhodamine B. The concentration of each compound was 5×10^{-4} mol./l., that of rhodamine B being equivalent. Irradiated distance: 5~6 cm. Temperature: 30°C

*2 This compound was dispersed by sodium palmitate.

TABLE V. RELATION BETWEEN THE CATALYTIC ABILITY AND THE CONDUCTIVE PROPERTY OF ORGANIC SEMI-CONDUCTORS

Compound	Catalytic ability*1	Type of conductivity*2	Compound	Catalytic ability	Type of conductivity
Eosine Y	+	p	Anthracene	+	p
Safranine T	+	p	Acridine	+	p
Auramine	+	p	Phenazine	+	p
Fluorescein	+	p	Pyrene	+	p
			Fluoridine	+	p
Crystal violet	−	n	Triphenodioxazine	−	n
Rhodamine B	+	n	Indanthrene	−	n
Malachite green	−	n	Violanthrone	−	n
Brilliant blue	−	n	Isoviolanthrone	−	n

*1 Sign of + means to have cataltic action, and sign of − means not to have it.

*2 B. Rosenberg, *J. Chem. Phys.*, **29**, 1108(1958); ibid., **37**, 1371 (1962); H. Inoue, K. Noda and E. Imoto, This Bulletin, in press; Literature, 4, 5 and 6, described in this paper.

containing a few condensed benzene rings and a heteroatom is rather more effective than a compound containing many condensed benzene rings. It is uncertain whether this is caused by the difference between the dispersed and dissolved states of the catalyzer, or, substantially, by the difference in the excited energies. As Table IV shows, the molar ratio of the acetone produced to the oxygen absorbed was larger than unity. p-Type compounds were effective, but n-type compounds ineffective, similar to the cases of dyes. Furthermore, a compound which can easily take its triplet state seemed to be more effective. For example, phenazine, the density of the triplet of which was 10^3 larger than that of anthracene, was more effective than anthracene.

An Assumed Mechanism of the Sensitized Photo-oxidation of Isopropyl Alcohol.—Electrical conductivity is a property which should be attributed to a solid aggregate of molecules, and the catalytic action of a dye in a solution must result from the property of an isolated molecule. In spite of this inconsistency, the fact that electrical conductivity is very dependent on properties of the molecule itself has allowed us to classify dyes into two groups according to the type of electrical conductivity. As has been described above and as is summarized in Table V, p-type compounds are generally effective as a sensitizer of the photo-oxidation of isopropyl alcohol with oxygen, while n-type compounds are ineffective. Compounds containing a heteroatom are particularly effective. p-Type conductivity has been explained by Rosenberg[7] as the trapping of an excited electron at a triplet state, whereupon the hole formed migrates to an electrode. A hetero-

(7. B Rosenberg, *J. Chem. Phys.*, 37, 1371 (1962).

aromatic compound may be easily excited to its triplet state, as has been found true of quinoline and phenazine. In a heteroaromatic compound excited to a triplet state, an excited electron may be trapped and a hole may migrate to another compound. The migration of a hole from one compound to another compound means an oxidation. Now, the sensitized photo-oxidation of isopropyl alcohol with oxygen to acetone may proceed at first by the migration of a hydrogen atom of isopropyl alcohol to an excited p-type sensitizer. The formation of DH_2 by some reaction, for example, by reaction 3 or 4, involves the decoloration of the dye.

$$D \rightarrow D^* \quad (1)$$

$$(CH_3)_2CHOH + D^* \rightarrow (CH_3)_2\dot{C}OH + HD\cdot \quad (2)$$

$$(CH_3)_2CHOH + HD\cdot \rightarrow (CH_3)_2\dot{C}OH + H_2D \quad (3)$$

$$(CH_3)_2\dot{C}OH + HD\cdot \rightarrow (CH_3)_2CO + H_2D \quad (4)$$

Though the mechanism of the formation of hydrogen peroxide is not certain and is not within the scope of this paper, hydrogen peroxide must be produced from some radicals, such as HD· (5 and 6).

$$HD\cdot + O_2 \rightarrow D + HO_2\cdot \quad (5)$$

$$(CH_3)_2CHOH + HO_2\cdot \rightarrow (CH_3)_2\dot{C}OH + H_2O_2 \quad (6)$$

When a molecule of hydrogen peroxide is produced, it must oxidize a molecule of isopropyl alcohol to acetone by the following chain reactions (7—11), though this mechanism is merely speculative. This must also be the reason why the molar ratio of the acetone produced to the oxygen absorbed was larger than unity.

$$H_2O_2 \rightarrow HO\cdot + \cdot OH \quad (7)$$

$$(CH_3)_2CHOH + \cdot OH \rightarrow (CH_3)_2\dot{C}OH + H_2O \quad (8)$$

$$(CH_3)_2\dot{C}OH + O_2 \rightarrow (CH_3)_2CO + HO_2\cdot \quad (9)$$

$$(CH_3)_2CHOH + HO_2\cdot \rightarrow (CH_3)_2\dot{C}OH + H_2O_2 \quad (10)$$

$$(CH_3)_2\dot{C}OH + \cdot OH \rightarrow (CH_3)_2CO + H_2O \quad (11)$$

$$2(CH_3)_2CHOH + O_2 \rightarrow 2(CH_3)_2CO + 2H_2O$$

On the other hand, since a photo-excited sensitizer of the n-type could not abstract a hydrogen atom from isopropyl alcohol, it was ineffective as the catalyzer. The radical, $(CH_3)_2\dot{C}OH$, which is necessary for the formation of pinacol may be produced directly from isopropyl alcohol and oxygen.

Summary

The natures of organic semi-conductors have been correlated with the catalytic ability for the photo-oxidation of isopropyl alcohol to acetone with oxygen under ultraviolet or visible light irradiation. p-Type compounds are generally effective as sensitizers, but n-type compounds are ineffective. Heteroaromatic compounds are more effective than the parent aromatic compounds among p-type compounds. The molar ratio of the acetone formed to the oxygen absorbed is larger than unity in the case of p-type compounds and less than unity in the case of n-type compounds. Finally, it has been assumed that the migration of a positive hole in a p-type compound can be correlated with the migration of a hydrogen atom of isopropyl alcohol.

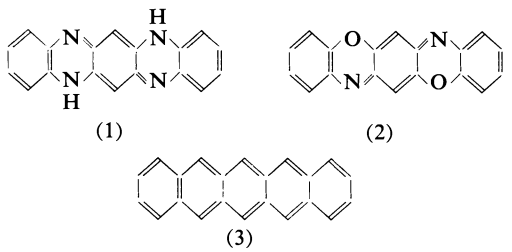
Department of Applied Chemistry
College of Engineering
The University of Osaka Prefecture
Sakai, Osaka

The Electrical Conductivity of Heterocyclic Compounds. Fluoridine and Triphenodioxazine

By Hiroo INOUE, Kazuo NODA and Eiji IMOTO

(Received September 12, 1963)

The electrical conductivity of aza-aromatic hydrocarbons has been studied by Akamatu and Inokuchi[1] and by others.[2] The photoconductivity of phenazine has also been reported on recently by Rosenberg,[3] MacGlynn[4] and others.[3] In this paper, for the purpose of investigating the effect of a heteroatom on the electrical conductivity of a heterocyclic compound, the dark- and photo-conductivities of fluoridine (1) and triphenodioxazine (2) will be compared with those of their parent aromatic compound, pentacene (3), the conductivity of which has been reported by Northrop and Simpson.[6]



(1) (2)

(3)

Experimental

Materials.—Fluoridine and triphenodioxazine were prepared according to the methods reported by Badger[7] and by Fierz-David[8] and were purified three times by sublimation at 200~250°C under a reduced pressure of 0.1 mmHg. Fluoridine purified is violet-green crystals, does not melt until 360°C, and is slightly soluble in organic solvents, but it is easily soluble in concentrated sulfuric acid, where it gives a pink-colored fluorescence, though no fluorescence is found in ethanol. The spectrum shows two absorption maxima, at about 517 and 552 mμ in dimethylformamide, and at about 541 and 579 mμ in ethanol, with red shifts of about 24~27 mμ from the bands in dimethylformamide, as is shown in Fig. 8. Triphenodioxazine is red crystals, does not melt until 360°C, and is a little soluble in xylene, giving a green fluorescence. The spectrum shows two absorption maxima, at about 474 and 508 mμ in dimethylformamide, and at about 479 and 510 mμ in ethanol, with red shifts of about 2~5 mμ from the bands in dimethylformamide, as Fig. 9 shows. That is, the effect of a solvent on the spectrum of triphenodioxazine is less remarkable than that of fluoridine.

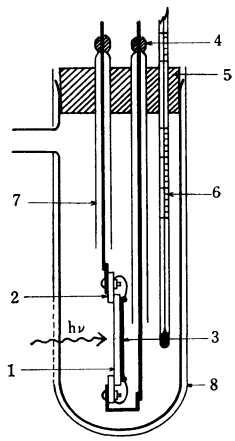


Fig. 1. The chamber used in the measurement of the dark- and photo-conductivity.
1 Glass substrate, 2 terminal electrode, 3 organic thin layer, 4 epoxy-resin seal, 5 rubber stopper, 6 thermometer, 7 quartz tube, 8 copper-film

Apparatus.—The chamber used for the measurement of the electric conductivity is shown in Fig. 1. The resistance of materials, kept in a vacuum of 10^{-2} mmHg or less, was measured with the ultra-megohm meter.

The measurement of the electrical conductivity was performed by using conductivity cells of the following three types.

Surface-type Cell.—This cell was prepared by the sublimation of the sample in a thickness of a few microns on a transparent quartz plate (3×3 cm^2) which has aluminum or silver electrodes of a comb form that are separated from each other by a gap of 0.2 mm. or 0.5 mm., as in Fig. 2.

Sandwich-type Cell.—The sample was deposited by vacuum sublimation in a thickness of from three to eight microns on a quartz plate, which had previously been provided with an aluminum film as one electrode. Another film-electrode was formed by the sublimation of aluminum onto the surface of the specimen film. When Nessa glass was used

1) H. Akamatu and H. Inokuchi, *J. Chem. Phys.*, **18**, 810 (1950).
2) G. C. Martin and A. R. Ubbelohde, *J. Chem. Soc.*, **1961**, 4948.
3) B. Rosenberg, *J. Chem. Phys.*, **37**, 1371 (1962).
4) M. Kleinerman, L. Azarraga and S. P. McGlynn, ibid., **37**, 1825 (1962).
5) G. Aftergut and G. P. Brown, *Nature*, **189**, 827 (1961).
6) D. C. Northrop and O. Simpson, *Proc. Roy. Soc.*, **A234**, 124 (1956).
7) G. M. Badger and R. Pettit, *J. Chem. Soc.*, **1951**, 3211.
8) H. E. Fierz-David, *Helv. Chim. Acta*, **22**, 1348 (1938).

instead of the quartz plate, the initial sublimation of aluminum was omitted.

Bulk Specimen.—The d-c resistivity was measured under a pressure of 100 kg./cm² at an applied electric field of 1000 V./cm. according to the method described in previous papers.[9]

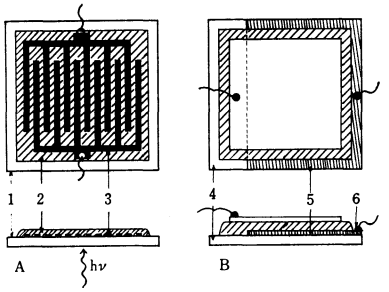


Fig. 2. Conductivity cell.
A Surface type, B sandwich type:
1 Quartz glass, 2 organic film, 3 aluminum film, 4 Pylex glass, 5 Nessa glass, 6 terminal electrode

Results

Dark-conductivities.—*Current/Voltage Relationship.*—The dark-currents of fluoridine and triphenodioxazine measured with sandwich- and surface-type cells were ohmic up to 10^4~10^5 V./cm. The relation between current and voltage is shown in Fig. 3. Even when the electrodes are reversed, identical results were obtained.

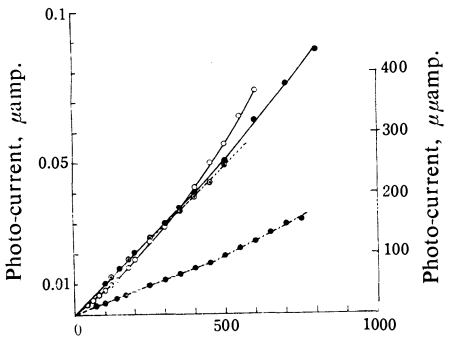


Fig. 3. Current/voltage relationship in the absence of oxygen.
—●— Surface type for fluoridine (μamp.)
---●--- Sandwich type for fluoridine (μμamp.)
—○— Surface type for triphenodioxazine (μμamp.)
---⊙--- Sandwich type for triphenodioxazine (μamp.)

Resistivity/Temperature Relationships.—The resistance of the surface- and sandwich-type cells and of the bulk specimens was measured at a range of 20~140°C under a reduced pressure of 0.1~0.01 mmHg, after the temperature had been kept for about 1/2~1 hr. at 115~120°C for triphenodioxazine and at 130~140°C for fluoridine. The range of the temperature of the measurement was limited because of the high resistances of the samples at temperatures lower than 20°C and because of the easy sublimation at temperatures higher than 140°C. The resistance of triphenodioxazine was too high to measure in bulk.

The electrical resistivity (ρ) at an ascending temperature was identical with that at a descending temperature, and a linear relationship between $\log \rho$ and $1/T$ (reciprocal absolute temperature) was observed, as Fig. 4 shows. Thus, the resistivity of the substances as typical organic semiconductors obeyed the following equation:

$$\rho = \rho_0 \exp(\Delta\varepsilon/2kT)$$

where $\Delta\varepsilon$ is the energy gap and k, the Boltzmann constant. The values of ρ_{20} and $\Delta\varepsilon$ are shown in Table I, in which the values of pentacene are those given by Northrop and Simpson.[6]

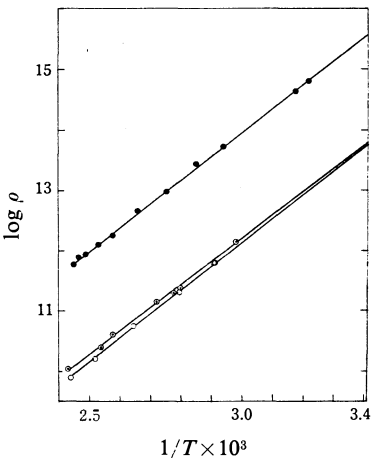


Fig. 4. The relationship between $\log \rho$ and $1/T$ for fluoridine.
● Sandwich type cell
⊙, ○ Surface type cell (descending and ascending temperature)

TABLE I. THE VALUE OF RESISTIVITY AT 20°C (ρ_{20}), $\Delta\varepsilon$ AND ρ_0 OF FLUORIDINE, TRIPHENODIOXAZINE AND PENTACENE

Compound	Cell type	ρ_{20} Ω·cm.	$\Delta\varepsilon$ eV.	ρ_0 Ω·cm.
Fluoridine	Surface	6×10^{13}	1.6	0.6
	Sandwich	4×10^{15}	1.6	60
	Bulk	2.5×10^{13}	1.95	4×10^{-4}
Tripheno-dioxazine	Surface	5×10^{14}	1.65	3
	Sandwich	2×10^{16}	1.7	30
Pentacene	Sandwich	6×10^{13}	1.5	10

9) H. Inoue, T. Takiuchi and E. Imoto, *J. Chem. Soc. Japan, Ind. Chem. Sec.* (*Kogyo Kagaku Zasshi*), **65**, 1291 (1962).

Photo-conductivities.—A tungsten lamp as the light source, and a band-pass filter which allowed the ray to pass between 350 and 700 mμ, were used for the measurement of photo-conductivities. Light intensity was measured by using a standard cadmium sulfide cell. A surface-type cell was used for the measurement, and the back face of a sample was illuminated (Fig. 2). As Fig. 5 shows, the

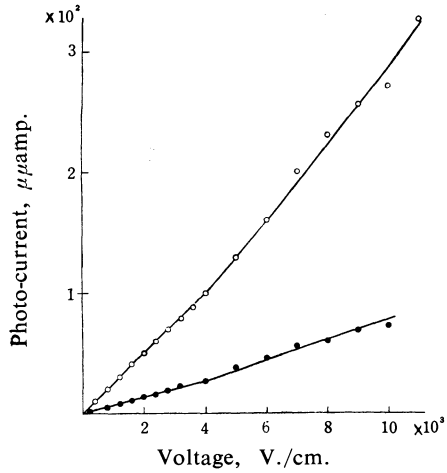


Fig. 5. The variation of the photo-current with the applied voltage: illuminated with tungsten lamp at 6000 lux.
● for fluoridine, ○ for triphenodioxazine

photo-currents of fluoridine and triphenodioxazine approximately obeyed Ohm's law up to 4×10^3 V./cm. The dependence of the steady-state photo-current on the light intensity in the absence of oxygen gas was investigated at a field strength of 2×10^3 V./cm. The rise and the decay of the photo-current of triphenodioxazine and fluoridine were comparably rapid, 5 sec. or less. The photo-current (i_{ph}) was related to the light intensity (L) by the following equation:

$$i_{ph}\propto L^{0.67}$$

Since the photo-current is nearly proportional to half the order of the light intensity, it seemed probable that the generation of a carrier is bimolecular. The ratio of the photo-current to the dark-current at a light intensity of 10^5 lux was about 39 for fluoridine, and about 8100 for triphenodioxazine. The photo-current of triphonodioxazine was about ten times larger than that of fluoridine.

The Effect of Oxygen.—The effect of oxygen on the dark- and photo-conductivity of fluoridine and triphenodioxazine was examined using a surface-type cell. After a cell of fluoridine had been degassed in vacuo, it was heated on P_2O_5 at 150~160°C in the presence of air for 2 hr., then the temperature dependence of the dark-conductivity was investigated. As is shown in Fig. 6, the resistivity and the activation energy became smaller after the air treatment, but recovered to some extent when the oxygen absorbed was pumped out in vacuo. The reason why the initial conductivity in vacuo was not recovered entirely, even after prolonged heating at 100°C, may be explained by the retention of a small amount of oxygen in the film. Moreover, the decrease in the activation energy of the dark-conductivity after the air treatment might allow it to assume the energy level of an oxygen-trapped state, similar to the case of phthalocyanine as reported by Vartanian and Karpovitch.[10] Furthermore, the air treatment of fluoridine increased its photo-current, as Fig. 7 shows, and the photo-current was proportional to the intensity (i_{ph}) of light irradiated, as given by the following equation:

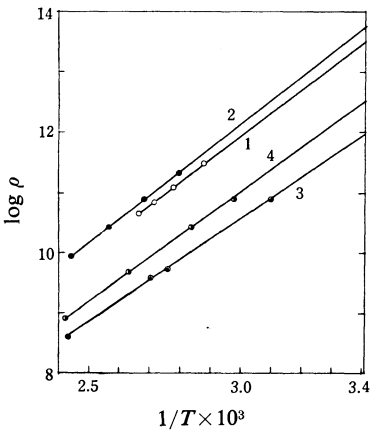


Fig. 6. The effect of oxygen on the surface dark-conductivity of fluoridine: 1, 2 in the absence of oxygen; 3 heated at 150~160°C on P_2O_5 in the presence of air for 2 hr. and measured in vacuo; 4 the oxygen absorbed was pumped out in vacuo.

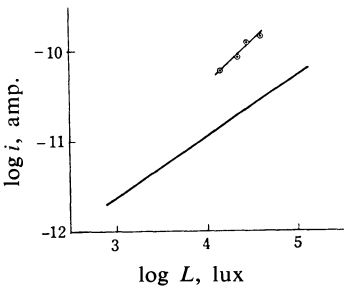


Fig. 7. The effect of oxygen on photo-current of fluoridine: —⊙— kept on P_2O_5 in the presence of oxygen for 1.5 months; — heated at 130°C in vacuo for 4 hr.

10) A. T. Vartanian and I. A. Karpovitch, *Zhur. Fiz. Khim.*, 32, 178, 274, 543 (1958).

$$i_{ph} \propto L$$

On the other hand, the air treatment of triphenodioxazine resulted in a lowering of the dark- and photo-conductivity, but the photocurrent was proportional to the light intensity, similar to the case of fluoridine.

Visible Light Absorption Spectra.—The visible light absorption spectra of fluoridine and triphenodioxazine in dimethylformamide or ethanol, and of their sublimed thin films (0.02～0.03 in thickness), are shown in Figs. 8 and 9

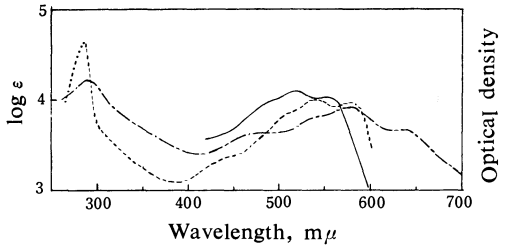


Fig. 8. Absorption spectra of fluoridine:
—— in dimethylformamide, ------ in ethanol,
—·—·— of sublimed thin film.

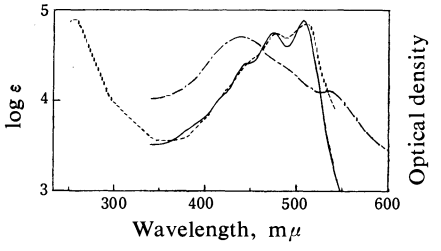


Fig. 9. Absorption spectra of triphenodioxazine:
—— in dimethylformamide, ------ in ethanol,
—·—·— of sublimed thin film

respectively. In these figures, the absorption coefficient was taken for the solution spectra, and the optical density for films. The main absorption bands of fluoridine dissolved in ethanol were in good agreement with those reported by Badger.[7] The main absorption maxima are evident in their visible regions. The absorption curves of sublimed films were broad and seemed to correspond to those in solution, although the absorption densities were altered. Namely, the absorption spectrum of a sublimed film of fluoridine showed two main absorption maxima, at 580 and 640 mμ, which shifted bathochromically from the corresponding band in the solution. On the other hand, the absorption maximum of triphenodioxazine at 479 mμ in solution was shifted to blue, while the one at 510 mμ shifted to red. Also, the spectral shifts of fluoridine were found to be larger than those of triphenodioxazine. The presence of oxygen did not change the spectral curve.

X-Ray Diffraction.—The X-ray diffraction of the transparent films sublimed on a glass was examined by using a Geiger counter X-ray diffractometer. The number of the diffraction lines in sublimed films decreased in both fluoridine and triphenodioxazine compared with that of the powder, whereas the intensity of the diffraction was very small. No remarkable change of X-ray diffraction pattern in fluoridine upon the thermal or air treatment of a sublimed film was found.

Discussion

As Table I shows, the activation energy ($\Delta\varepsilon$) obtained from the dark-conductivity of a sandwich cell was in quite good agreement with that of the surface cell for both fluoridine and triphenodioxazine. However, the resistivity of a surface-type cell was less than that of the sandwich-type cell by a factor of 10～10^2; this indicates an anisotropy of resistivity which may be caused by the mode of the arrangement of crystallites, as has already been mentioned by Akamatu and Inokuchi.[11] The ρ_0 of three compounds decreased in the following order: triphenodioxazine>fluoridine in the surface type, and fluoridine>triphenodioxazine >pentacene in the sandwich type. The ρ_0 of fluoridine along the surface of the film is the smallest in three compounds; particularly, the anisotropy in the surface and sandwich conductivity of fluoridine becomes larger than that in the case of triphenodioxazine. This probably means that the mode of the arrangement of crystallites in fluoridine may become better than that in triphenodioxazine, because of the effects of -NH- groups in fluoridine, for example, the hydrogen bond between adjacent molecules. Thus, the substitution of a heteroatom for a ring carbon atom has a large effect on ρ_0. On the other hand, the relation between the lowest singlet absorption level ($^1E_1$) in a solution and $\Delta\varepsilon$ for fluoridine and triphenodioxazine coincided with that for various aromatic hydrocarbons, as Fig. 10 shows. Thus, the $\Delta\varepsilon$ of triphenodioxazine and fluoridine depends on the $^1E_1$ of the absorption spectrum.

The property of being a charge carrier was investigated by means of the effect of oxygen on the dark- and photo-conductivity. The effects of oxygen on the electrical conductivity of many dye stuffs have been examined by Meier,[12] who has shown that the electrical conductivity of a p-type compound increases in the presence of oxygen, while that of a n-type compound decreases. If Meier's results are applied to the present case, the charge carrier must be posi-

11) H. Inokuchi, H. Kuroda and H. Akamatu, This Bulletin, 34, 749 (1961).
12) H. Meier, *Z. Wiss. Phot.*, 53, 1 (1958).

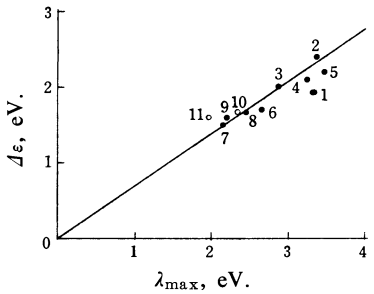


Fig. 10. Relationship between activation energy and the lowest absorption level ($^1E_1$).
1 anthracene, 2 pyrene, 3 perylene, 4 1,2-benzanthracene, 5 chrysene, 6 tetracene, 7 pentacene, 8 triphenodioxazine, 9 fluoridine, 10 triphenodioxazine (film), 11 fluoridine (film)

tive for fluoridine (p-type) and negative for triphenodioxazine (n-type). Moreover, it is found from the report of Vartanian[13] that the photo-current of a p-type compound containing heteroatoms is generally less than that of an n-type compound containing heteroatoms. As has been described above, the characters of the photo-current of fluoridine and triphenodioxazine coincided with Vartanian's results; that is, the photo-current of fluoridine, which is considered to be p-type, is less than that of triphenodioxazine, which is n-type. That is, the mobility of the photo-current is less than that of triphenodioxazine in spite of the large molecular interaction in fluoridine. This implies that the probability of a drift of a hole is small because of the localization of a hole on heteroatoms, as has been shown by Rosenberg[3] in the difference in photo-current in anthracene and phenazine of the p-type.

Summary

The electrical conductivities of fluoridine and triphenodioxazine have been measured, and it has been confirmed that (1) the ρ_0 of three compounds decreased in the following order: triphenodioxazine>fluoridine in the surface-type cell and fluoridine>triphenodioxazine>pentacene in the sandwich-type cell; (2) $\Delta\varepsilon$ depended on the $^1E_1$ of the absorption spectrum; (3) in the presence of oxygen, the dark- and photo-current of fluoridine increased, while those of triphenodioxazine decreased; (4) the photo-current of fluoridine was less than that of triphenodioxazine, and (5) the generation of the charge carrier in both fluoridine and triphenodioxazine was bimolecular in the absence of oxygen.

The authors wish to express their gratitude to Dr. Kosaburo Baba of the Hayakawa Electric Industry Co. for permitting the use of the experimental apparatus and for his helpful advice in this study.

Department of Applied Chemistry
College of Engineering
The University of Osaka Prefecture
Sakai, Osaka

13) A. T. Vartanian and L. D. Rosenstein, *Doklady Akad. Nauk S. S. S. R.*, **124**, 295 (1959).

The Electrical Conductivity of Heterocyclic Compounds. Molecular Complexes of Phenazine

By Hiroo INOUE, Shigeki HAYASHI and Eiji IMOTO

(Received September 12, 1963)

As a part of a series of studies of the electrical conductivity of heterocyclic compounds, some molecular complexes of phenazine (cf. Fig. 1) were prepared, and their electrical conductivities were compared with those of molecular complexes of the quinhydrone-type.

Experimental

Materials.—Phenazine, phenazinium chloride and phenazinium methosulfate were prepared according to the methods described in the literature.[1] Hydroquinone, pyrene and all other materials were of a commercial grade. All the materials were purified by repeated recrystallization and sublimation.

The Preparation of Molecular Complexes.—*Molecular Complexes of the Quinhydrone Type.*—Molecular complexes of the quinhydrone type of phenazine (abbreviated as ph) with *o*-, *m*- and *p*-hydroquinone (abbreviated as Hy), *o*-phenylenediamine (abbreviated as BNH_2), dihydrophenazine (abbreviated as phH_2) or trinitrobenzene (abbreviated

1) A. Wohl and W. Aue, *Ber.*, **34**, 2442 (1901).

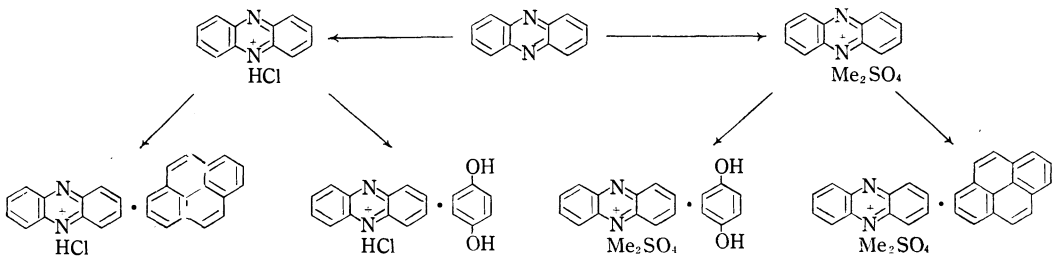


Fig. 1. Molecular complexes of salt type.

TABLE I. THE CONDITIONS OF THE PREPARATIONS FOR MOLECULAR COMPLEXES

Donor and acceptor	Solvent	Yield %	M. p. °C	Color of crystals
py, ph-HCl	HCl-ethanol	90	133 ~135	Black needle
Hy(*p*), ph-HCl	HCl	60	168.5~170	Black-brown plate
py, ph-Me_2SO_4	Ethanol	30~40	156 ~157	Black prism
Hy(*p*), ph-Me_2SO_4	Ethanol	30~40	118 ~119.5	Black prism
py, ph-HCl	Dry ether	0	—	—
Hy(*p*), ph	Ethanol	62	234 ~236	Yellow needle
Hy(*m*), ph	Ethanol	70	213 ~214	Yellow needle
Hy(*o*), ph	Ethanol	74	181 ~182	Yellow needle
BNH_2, ph	Ethanol	70	150 ~151	Red-blown plate
ph, TNB	Ethanol	85	151 ~153	Yellow needle
phH_2, ph	Acetone	50	223 ~225	Blue-violet needle

as TNB) were prepared according to the methods described in the literature,[2-4] these will be abbreviated as ph-Hy(*o*), ph-Hy(*m*), ph-Hy(*p*), ph-BNH_2, ph-phH_2 and ph-TNB in this paper. The conditions of the preparation of these molecular complexes are shown in Table I.

Molecular Complexes of the Salt Type.—a) Phenazinium Chloride and Pyrene (abbreviated as ph-HCl-py).—To a warm solution of 0.9 g. of phenazine in 70 ml. of concentrated hydrochloric acid, 1 g. of pyrene dissolved in 80 ml. of ethanol was added, and the mixture was refluxed for about half an hour. After filtering, the filtrate was left to cool, and 1.8 g. of black needle crystals were obtained. However, no molecular complex was obtained from pyrene and phenazine themselves. When hydrogen chloride was introduced into a solution of pyrene and phenazine in dry ether, no black precipitate was obtained, but red crystals of phenazinium chloride were recovered. However, when ether which had previously been saturated with water was used instead of dry ether as the solvent, black needle crystals of the molecular complex were obtained. Thus, it seems that a little water may be necessary in a reaction system to form a molecular complex of a salt type from phenazinium salt.

b) Phenazinium Chloride and p-Hydroquinone (abbreviated as ph-HCl-Hy(*p*)).—To a solution of 0.3 g. of phenazine in 30 ml. of concentrated hydrochloric acid, 1 g. of *p*-hydroquinone was added at 70~80°C, and the solution was refluxed for half an hour. After it had been treated in a manner similar to that described above, 0.3 g. of black plate crystals was obtained.

c) Phenazinium Methosulfate and Pyrene (abbreviated as ph-Me_2SO_4-py).—Into a solution of about 0.5 g. of phenazine in 25 ml. of nitrobenzene, 0.5 g. of dimethylsulfate was stirred, after which the reaction mixture was heated at 100~110°C for about 15 min. The cooling of the reaction mixture resulted in a precipitation of crystals. After filtering, the filtrate was diluted by 25 ml. of dry ether to precipitate crystals again. Both sets of crystals were recrystallized from ethanol; yield, 0.6 g. (70%); m. p. 151~153°C (decomp.). Six-tenths of a gram of ph-Me_2SO_4 and 0.4 g. of pyrene were dissolved in 4~5 ml. of ethanol and refluxed for about half an hour. About 0.3 g. of black prism crystals precipitated. After filtering, the precipitate was washed with a mixed solvent of benzene and ether and dried on P_2O_5 under the reduced pressure of 10 mmHg for about ten hours; m. p. 156~157°C.

d) Phenazinium Methosulfate and p-Hydroquinone (abbreviated as ph-Me_2SO_4-Hy(*p*)).—A solution of 0.3 g. of ph-Me_2SO_4 and 0.18 g. of *p*-hydroquinone in 1~2 ml. of ethanol was refluxed for about half an hour and then treated in a manner similar to that used in the case of ph-HCl-py. About 0.15 g. of black prism crystals was precipitated. The properties of the molecular complexes obtained above are shown in Table I.

Results

The Properties of Molecular Complexes of the Salt Type.—The constitutions of the molecular complexes obtained were analyzed. Since

2) J. S. Morley, *J. Chem. Soc.*, **1952**, 4008.
3) T. Zerewitinoff, *Ber.*, **44**, 2402 (1911).
4) O. Blum, ibid., **62**, 881 (1929).

ph-HCl-py and ph-HCl-Hy(p), which were dried on calcium chloride at 20°C under the reduced pressure of 10 mmHg for 5 hr., contained more than the expected amounts of excess hydrogen chloride and water, as may be seen in Figs. 2 and 3, they were dried under the same conditions for a prolonged period. During this treatment, the features of the molecular complexes changed, as Table II and Figs. 2 and 3 show.

The color changed from black to yellow, and the shape of the crystals changed from needle to fine amorphous. The melting points decreased gradually. When kept on P_2O_5 at 50~60°C under the reduced pressure of 5~10 mmHg for a long time, the melting points of the molecular complex became near to those of the simple mixture of their constituents.

The content of hydrogen chloride and water, which had been calculated from the analytical results of nitrogen and chlorine shown in Figs.

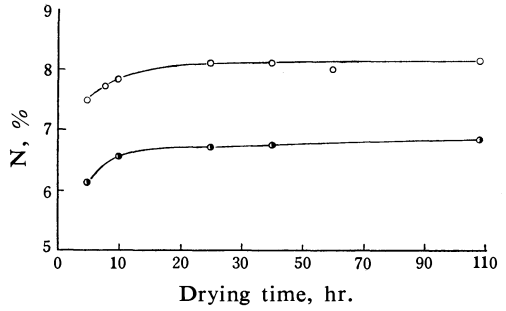


Fig. 2. The variation of nitrogen percentage to drying time: ◑ ph-HCl-py, ○ ph-HCl-Hy(p); Calcd. for ph-HCl-py: N, 6.69%, for ph-HCl-py-H_2O: N, 6.41%, for ph-HCl-Hy(p): N, 8.56%, and for ph-HCl-Hy-H_2O: N, 8.12%.

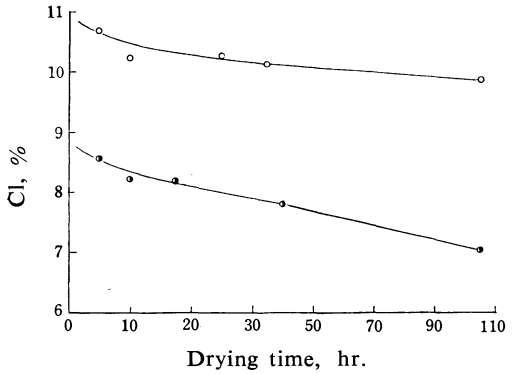


Fig. 3. The variation of chlorine percentage to drying time: ◑ ph-HCl-py, ○ ph-HCl-Hy(p); Calcd. for ph-HCl-py: Cl, 8.46%, for ph-HCl-py-H_2O: Cl, 8.11%, for ph-HCl-Hy(p): Cl, 10.86%, and for ph-HCl-Hy(p)-H_2O: Cl, 10.30%.

TABLE II. THE VARIATION OF MELTING POINT TO DRYING TIME

Melting point of the simple mixture: ph and py; 118~121°C, ph and Hy(p); 167~230°C

Drying time hr.	ph-HCl-py °C	ph-HCl-Hy(p) °C	ph-HCl °C
1	133~135	168.5~170	214~216
3	130~133.5	168 ~170	212~216
10	128~133	162 ~166	205~209
30	123~132	—	—
100	120~130	163 ~167	169~175

2 and 3, decreased gradually with the drying time. The decrease in the quantity of water during the process of drying was confirmed also by the disappearance of the infrared absorption band at 3500 cm^{-1} after the drying. Thus, the water included in the crystals of the molecular complexes may be regarded as one of the constituents of the molecular complex, because a little water in a reaction system is necessary in order to obtain the molecular complexes.

The ultraviolet absorption spectrum of an ethanolic solution of ph-HCl-py was merely the sum of the absorption spectra of ph-HCl and py in ethanol, because ph-HCl-py dissociates thoroughly into each component in ethanol. On the other hand, the ultraviolet absorption spectrum of the same compound obtained by the KBr-method showed a new band at about 620 mμ which must be a charge transfer absorption, as Fig. 4 shows. A charge

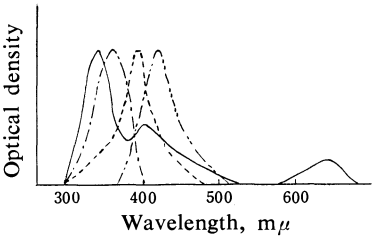


Fig. 4. Absorption spectra of ph-HCl-py, ph-HCl-Hy(p), ph-HCl and ph in KBr: —— ph-HCl-py, ------ ph-HCl-Hy(p), —··— ph-HCl and —·— ph.

transfer absorption for ph-HCl-Hy(p) could not be confirmed by the KBr method. The infrared absorption spectra of ph-HCl-py and ph-HCl-Hy(p) showed out-of-plane deformation bands at 700~1000 cm^{-1} which shifted about 5~30 cm^{-1} to a lower wave number than those of each component. This may imply that there is some molecular interaction in the molecular complex.

The ESR spectra of ph-HCl-py and ph-HCl-Hy(p) which had been kept over calcium chloride at room temperature under the reduced pressure of 10 mmHg for three days are shown in Fig. 5. The spin concentrations and g values which were calculated from the ESR spectra were as follows:

ph-HCl-py; g value 2.0033, spin concentration 5.8×10^{20}

ph-HCl-Hy(p); g value 2.0022, spin concentration 3.9×10^{20}

Though the curves of the ESR spectra were comparably broad, they showed three fine structures. Hence, it may be considered that an unpaired electron is localized on the nitrogen atom of phenazine. Also, the infrared spectra showed that the intensities of the peaks at 1917 and 2380 cm^{-1} assigned to $=\overset{+}{N}H-$ for py-HCl-ph and ph-HCl-Hy(p) decreased as compared with those of ph-HCl. From these results, the following structural formula may be assigned to the structure of molecular complexes:

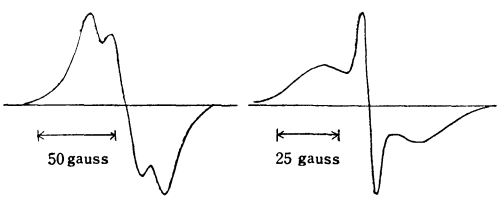
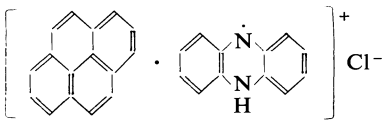


Fig. 5. ESR spectra of ph-HCl-py and ph-HCl-Hy(p).



The properties of molecular complexes of a methosulfate type were similar to those of a hydrogen-chloride type.

Electrical Conductivities.—The d.c. resistivity was measured under the pressure of 100 kg./cm^2 in vacuo according to the methods described in previous papers.[5] Since the dark current of all samples obeyed Ohm's law up to $10^3\sim10^4$ V./cm., all d.c. resistivities in this paper were measured at an applied electric field in the range of 2000$\sim$4000 V./cm.

The electrical resistivity (ρ_{20}) of ph-HCl-py, ph-HCl-Hy(p) and ph-HCl, which had been dried under the conditions shown in Figs. 2 and 3, was measured at 20°C for various periods, as is shown in Fig. 6. Each resistivity increased with the drying time, but each then became nearly constant after about 20 hr. Also, the resistivity of the compounds which had been dried for 20 hr. or more did not change when kept under the applied field of about 10^4 V./cm. for eight days. Judging from these results, it seems probable that the electrical conductivities of the compounds dried for over 20 hr. are electronic.

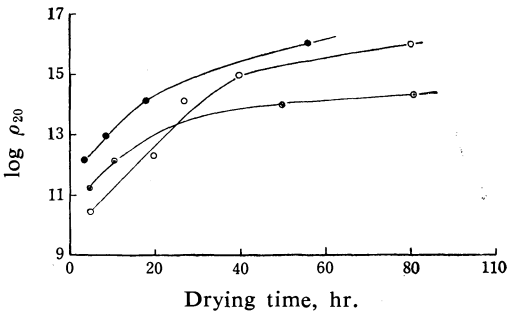


Fig. 6. The variation of log ρ_{20} of salt type compounds to drying time: ● ph-HCl, ⊙ ph-HCl-Hy(p), ○ ph-HCl-py.

The dependencies of the d.c. resistivities on the measuring temperature are shown in Fig. 7. The resistivity as an ascending temperature coincides with that at a descending temperature for all samples, except ph-phH_2, ph-HCl-Hy(p) and ph-Me_2SO_4-Hy(p), and a linear relationship between log ρ and $1/T$ was confirmed. $\Delta\varepsilon$ was calculated by the following equation:

$$\rho=\rho_0\exp(\Delta\varepsilon/2kT)$$

where $\Delta\varepsilon$ is an appearent energy gap, k is the Boltzman constant, and ρ is a specific electrical resistivity. The values of ρ_{20} and $\Delta\varepsilon$ are given in Table III.

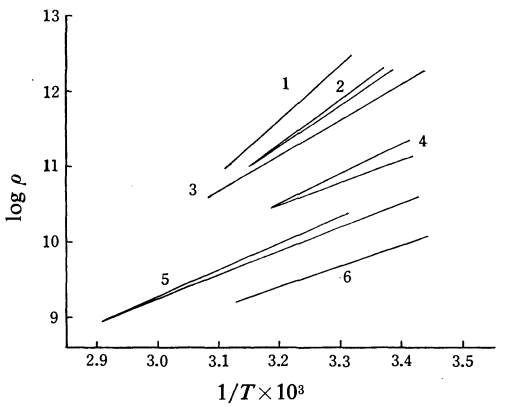


Fig. 7. The relationship between log ρ and $1/T$: 1 ph-Me_2SO_4-py, 2 ph-Me_2SO_4-Hy(p), 3 ph-HCl, 4 ph-HCl-Hy(p), 5 ph-phH_2, 6 ph-HCl-py.

5) H. Inoue, T. Takiuchi and E. Imoto, *J. Chem. Soc. Japan, Ind. Chem. Sec.* (*Kogyo Kagaku Zasshi*), 65, 1291 (1962).

TABLE III. THE VALUE OF RESISTIVITY AT 20°C (ρ_{20}) AND $\Delta\varepsilon$ OF MOLECULAR COMPLEXES

Molecular complex	ρ_{20} Ω·cm.	$\Delta\varepsilon$ eV.
ph-HCl-py*	6×10^{10}	1.2
ph-HCl-Hy(*p*)*	3×10^{11}	1.1~1.5
ph-Me_2SO_4-py	1.5×10^{13}	2.8
ph-Me_2SO_4-Hy(*p*)	2.9×10^{12}	3.7
ph-Hy(*p*)	3×10^{15}	—
ph-Hy(*m*)	1×10^{16}	—
ph-Hy(*o*)	7×10^{12}	0.5
ph-TNB	1×10^{15}	—
ph-BNH_2	3×10^{13}	—
ph-phH_2	3.7×10^{10}	1.3~1.5

* This sample was dried on P_2O_5 under the ordinary pressure at room temperature for a week.

Discussion

The ρ_{20} values of salt-like molecular complexes are smaller than those of molecular complexes of the quinhydrone type. This means that the effect of the intermolecular charge-transfer on the ρ_{20} of the former is larger than that on ρ_{20} of the latter. Also, the resistivities of molecular complexes of the methosulfate type were larger than those of molecular complexes of the hydrogen-chloride type. These results seem to show that the resistivity is affected by the compactness of molecular arrangement, because it seemed that the molecular arrangement of the methosulfate-type complex was less compact than that of the hydrogen chloride-type complex because of the steric effect of the CH_3-group.

The ρ_{20} of ph-phH_2 was the lowest among those of the molecular complexes of the quinhydrone type. This may be caused by the fact that the molecular arrangement of ph-phH_2 is more favorable than that of the others because of the good symmetry in the dimensions of the donor and acceptor molecules.

The resistivities of the salt-like molecular complexes described above possess a much higher value than those of the aromatic hydrocarbon-halogen complexes, which have been reported on by Akamatu and Inokuchi.[6] That is, it seems that these results may be attributed to the following causes; (1) the crystal of the molecular complex was contaminated with phenazine and pyrene or *p*-hydroquinone, because a part of the molecular complex dissociates to these compounds when water was removed; (2) an unpaired electron was localized on nitrogen atoms of phenazine, and (3) the molecular arrangement is incomplete, as may be presumed from the broadness of the ESR spectrum.

Summary

Some molecular complexes of the salt type have been prepared from phenazinium chloride or methosulfate and pyrene or *p*-hydroquinone. It has been confirmed that (1) the constitution, the color and the melting point of the molecular complexes varied with the drying conditions; (2) the ultraviolet absorption spectrum of ph-HCl-py by KBr shows a new band at about 620 mμ; (3) an unpaired electron is localized on the nitrogen atom of phenazine, and (4) the electrical conductivities of molecular complexes of the salt type are better than those of the quinhydrone type of phenazine.

Department of Applied Chemistry
College of Engineering
The University of Osaka Prefecture
Sakai, Osaka

6) H. Akamatu, H. Inokuchi and Y. Matsunaga, This Bulletin, **29**, 213 (1956).

The Reaction of Carbon Monoxide with Organometallic Compounds. VIII. The Synthesis of Aromatic Aldehydes by the Reaction of Iron Pentacarbonyl with Aryllithiums*

By Membo RYANG, Ilsong RHEE and Shigeru TSUTSUMI

(Received October 3, 1963)

In a previous paper[1] of this series, it was reported that carbon monoxide reacted with organolithium compounds in an ether solution at $-70°C$ to give the corresponding symmetrical ketones in good yields. In these reactions, it was assumed that carbon monoxide attacked organolithium compounds and abstracted the lithium as lithium carbonyl, producing symmetrical ketones (Eq. 1).

$$2\ R\text{-}Li + 3\ CO \rightarrow R\text{-}\underset{\underset{O}{\|}}{C}\text{-}R + 2\ LiCO \qquad (1)$$

On the other hand, iron pentacarbonyl reacted with organolithium compounds in an ethereal solution at $-50°C$, giving various reaction products.[2] For example, the aryllithium yielded the corresponding aromatic aldehydes, benzhydrol derivatives and benzoin derivatives by the reaction with iron pentacarbonyl, but the alkyllithium and *p*-tolyllithium yielded symmetrical ketones. The formation of aldehydes, benzhydrol derivatives and benzoin derivatives can be interpreted in terms of an ionic reaction sequence judging from the results of the reaction of carbon monoxide with organomagnesium halides[3]. Therefore, the following reaction scheme was assumed: the addition of aryllithium to the carbonyl double bond of iron pentacarbonyl resulted in the fission of the iron-carbon bond of iron pentacarbonyl, producing the unstable intermediate I (aroyllithium). (Fig. 1)

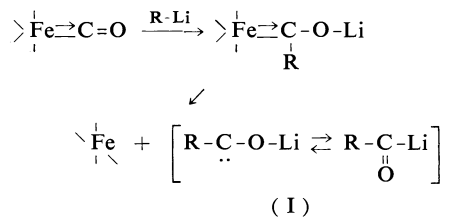


Fig. 1

This intermediate I is assumed to give aldehydes by hydrolysis (Eq. 2), benzoin derivatives by dimerization (Eq. 3), and benzhydrol derivatives by further reaction with aryllithium (Eq. 4).

$$I \xrightarrow{H^+} RCHO \qquad (2)$$

$$I + R\text{-}\underset{\underset{O}{\|}}{C}\text{-}Li \longrightarrow R\text{-}\underset{\underset{O}{\|}}{\overset{\overset{Li}{|}}{C}}\text{-}R \xrightarrow{H^+} R\text{-}\underset{\underset{O}{\|}}{\overset{\overset{H}{|}}{C}}\text{-}R \qquad (3)$$
$$\qquad\qquad\qquad

TABLE I

Starting material	Aromatic aldehyde	Yield,* %
2, 6-Dimethylbromobenzene	2, 6-Dimethylbenzaldehyde	36.4
2, 4-Dimethylbromobenzene	2, 4-Dimethylbenzaldehyde	65.4
p-Bromo-*t*-butylbenzene	*p*-*t*-Butylbenzaldehyde	47.0
o-Bromo-*t*-butylbenzene	*o*-*t*-Butylbenzaldehyde	54.3
p-Bromoanisole	*p*-Methoxybenzaldehyde	24.2
Bromomesitylene	2, 4, 6-Trimethylbenzaldehyde	60.5

* The calculations of yields are based on the number of organic halides used.

methods: elementary analysis, mixed melting point measurements of their semicarbazone derivatives, and infrared absorption spectra measurements.

Thus various aromatic aldehydes were synthesized in a good yield, and we have found that this new method is simple and can be extended to the synthesis of other aromatic aldehydes, the preparation of which by earlier methods was not satisfactory in yield and involved complicated starting materials. Of course, the exclusive formation of aldehydes in good yields in these reactions, even though various products were obtained from the reaction in the previous report,[2] is not due only to the reaction conditions (dilution with the solvent and the rapid addition of iron pentacarbonyl). It also seemed to be connected with the structural factor of organolithium compounds; for example, *m*-tolylaldehyde was isolated as a main product from the reaction of *m*-tolyllithium with iron pentacarbonyl under the conditions described in our previous report.

Details of the studies of the mechanism of the above reactions will be published elsewhere in the near future.

Experimental

Materials. — Several bromobenzene derivatives were prepared by the Sandmeyer reaction of the corresponding aniline derivatives: 2, 6-dimethylbromobenzene (b. p. 97°C/26 mmHg, $n_D^{15.5}$ 1.5573), 2, 4-dimethylbromobenzene (b. p. 95~97°C/22 mmHg), *o*-*t*-butylbromobenzene (b. p. 115°C/22 mmHg, n_D^{15} 1.5285), and *p*-*t*-butylbromobenzene (b. p. 114°C/20 mmHg, n_D^{15} 1.5377).

p-Methoxybromobenzene.—Commercial *p*-methoxybromobenzene was purified by fractional distillation; b. p. 95°C/15 mmHg, n_D^{15} 1.5641. Bromomesitylene was prepared by the action of bromine on mesitylene:[6] b.p. 105~107°C/17 mmHg. Iron pentacarbonyl was prepared by the reaction of fine iron poweder with carbon monoxide at 200°C under 300 CO atm. and was purified by distillation; b. p. 102°C, n_D^{15} 1.5202.

n-Butyllithium.—A commercial heptane solution of *n*-butyllithium (21.4 wt.%) was used.

The Synthesis of Aromatic Aldehydes.—*2, 6-Dimethylbenzaldehyde.*—Into a 500 ml., four-necked flask equipped with a mechanical stirrer, a low temperature thermometer, a reflux condenser protected from moisture, a gas bubbler and a dropping funnel, 40 ml. of anhydrous ether (dried over sodium) were placed and, after sweeping the apparatus with dry oxygen-free nitrogen, 1.4 g. (0.2 g. atom.) of lithium in the form of small pieces of thin coil. A solution of 14.8 g. (0.08 mol.) of 2, 6-dimethylbromobenzene in 20 ml. of anhydrous ether was stirred in via the dropping funnel over a period of 2 hr., while the internal temperature was maintained at 35°C.

After the addition had been completed, the stirring was continued for a further 2 hr., after which the reaction mixture was cooled to −60°C with a dry ice-methanol bath kept at −65°C. 3.2 g. (0.016 g. atom) of iron pentacarbonyl in 40 ml. anhydrous ether were next introduced via the dropping funnel over a period of 2 min. Then, with the internal temperature maintained at −50°C, the stirring was continued for a further 2 hr. The reaction mixture was decomposed with 20 ml. of 95% ethanol and, further, with 40 ml. of 4 N hydrochloric acid. The separated organic layer was treated with three succesive 50 ml. portions of saturated aqueous potassium carbonate and then with three succesive 50 ml. portions of aqueous sodium hydroxide and divided into (1) the organic layer, (2) a potassium carbonate solution and (3) a sodium hydroxide solution. The organic layer containing neutral compounds was washed with water and dried over sodium sulfate. The brownish residual oil obtained after removal of the solvent was distilled under reduced pressure to give the following fractions: (1) b. p. 30~40°C/18 mmHg (0.8 g.), (2) b. p. 40~60°C/18 mmHg (1.1 g.), (3) b. p. 100~110°C/18 mmHg (3.9 g.), and a dark orange residue. Fraction 3 was identified as 2, 6-dimethylbenzaldehyde from the results of infrared absorption spectra measurement and a mixed melting point test of its semicarbazone (m. p. 176~177°C, recrystallized from benzene). Also, the results of gas chromatographic analysis showed that fraction 3 was mainly 2, 6-dimethylbenzaldehyde (theoretical yield: 36.4 %).

Found: C, 62.76; H, 6.92. Calcd. for $C_{10}H_{13}ON_3$: C, 62.80; H, 6.85%.

The other fractions have not yet been examined. The acidic and phenolic compounds which were involved in the potassium carbonate solution and the sodium hydroxide solution respectively were confirmed to be the same as those of a previous report.[1]

6) "Organic Syntheses," Coll. Vol. II (1948), p. 95.

2, 4-Dimethylbenzaldehde. — The procedure employed here was identical with that described above. 3.92 g. of iron pentacarbonyl were added to the ethereal solution of 2,4-dimethylphenyllithium, which had been prepared by using 18.5 g. of 2, 4-dimethylbromobenzene and 1.75 g. of lithium. The neutral part was distilled under reduced pressure to give the following fractions: (1) b. p. 110~137°C/13 mmHg (8.7 g.), and (2) b. p. 160~163°C/4 mmHg (0.3 g.). Fraction 1 gave a positive result with the Brady's reagent and was identified as 2, 4-dimethylbenzaldehyde by the elementary analysis of its semicarbazone derivative (m. p. 222°C, recrystallized from ethanol) (theoretical yield: 65.4 %).

Found: C, 62.50; H, 6.93. Calcd. for $C_{10}H_{13}ON_3$: C, 62.82; H, 6.85%.

Fraction 2 was recrystallized from petroleum ether to give yellow crystals (m. p. 137°C). The infrared spectrum of this crystal showed the presence of the conjugated carbonyl group (1650 cm^{-1}), and the elementary analysis of the above crystal is correct for $C_{18}H_{18}O_2$. From the above results, fraction 2 was confirmed to be 2, 2', 4, 4'-tetramethylbenzil.

Found: C, 81.08; H, 6.93. Calcd. for $C_{18}H_{18}O_2$: C, 81.20; H, 6.78%.

p-t-Butylbenzaldehyde.—2.5 g. of pure iron pentacarbonyl were allowed to react with *p-t*-butylphenyllithium prepared from 10.7 g. of *p-t*-butylbromobenzene and 1 g. of lithium. The neutral part was distilled under reduced pressure to give the following fractions: (1) b. p. 100~115°C/11 mmHg (2.8 g.), (2) b. p. 130~133°C/3 mmHg (0.3 g.), and (3) b. p. 160~185°C/3mmHg. (2.3 g).

The infrared spectrum of fraction 1 showed the presences of a carbonyl group conjugated with an aromatic ring (1680 cm^{-1}) and a 1, 4-disubstituted aromatic ring (820 cm^{-1}, 1210 cm^{-1}, 1090 cm^{-1} and 1070 cm^{-1}). Fraction 1 was confirmed to be *p-t*-butylbenzaldehyde from the results of the mixed melting point measurement of its semicarbazone derivative. Fraction 3 was recystallized from ethanol to give colorless crystals (m.p. 131°C). This compound was assumed to be 1, 4-disubstituted aromatic hydrocarbon from the results of the infrared spectrum and was confirmed to be *p, p'*-di-*t*-butyl-diphenyl.

Found: C, 89.50; H, 10.06. Calcd. for $C_{20}H_{26}$: C, 90.16; H, 9.84%.

o-t-Butylbenzaldehyde.—2.5 g. of iron pentacarbonyl were added to an ether solution of *o-t*-butylphenyllithium prepared by using 10.7 g. of *o*-bromo-*t*-butylbenzene and 1.0 g. of lithium. The distillation of the neutral part gave the following fractions: (1) b. p. 50~55°C/10 mmHg (0.6 g.), (2) b. p. 80~90°C/3 mmHg (4.4 g.), and (3) b. p. 100 ~160°C/3 mmHg (0.3 g.). Fraction 2 gave a positive result to Brady's reagent and was identified as *o-t*-butylbenzaldehyde by the mixed melting point measurement of its 2, 4-dinitrophenylhydrazone (m. p. 256°C, recrystallized from ethylacetate) and of its semicarbazone (m. p. 210~211°C, recrystallized from ethanol) (theoretical yield: 54.3%). The elementary analysis of semicarbazone is correct for $C_{12}H_{18}ON_3$:

Found: C, 65.68; H, 7.93. Calcd. for $C_{12}H_{18}ON_3$: C, 65.72; H, 7.81%.

p-Methoxybenzaldehyde.—A solution of 18.7 g. of *p*-bromoanisol in 40 ml. of anhydrous ether was stirred in via the dropping funnel, over a period of 2 hr., to 30 g. of a solution of *n*-butyllithium (*n*-heptane solution, 21.4 wt. %), while the internal temperature was maintained at −10°C. After the addition had been completed, the stirring was continued for a further 8 hr., after which the reaction mixture was cooled to −65°C and allowed to react with 5 g. of iron pentacarbonyl. The neutral part was distilled under reduced pressure to give the following fractions: (1) b. p. 20~27°C/22 mmHg (2.4 g.), (2) b. p. 80~118°C/15 mmHg (3.3 g.), and (3) b. p. 105~140°C/5 mmHg (1.6 g.). Fraction 2 gave a positive result to Brady's reagent and was confirmed to be *p*-methoxybenzaldehyde from the results of the elemental analysis of its semicarbazone (m. p. 211~212°C, recrystallized from ethanol) (theoretical yield: 24.2%).

Found: C, 56.19; H, 5.80. Calcd. for $C_9H_{11}O_2N_3$: C, 55.95; H, 5.69%.

Fraction 3 was recrystallized from ethanol to give colorless crystals (m. p. 185°C), which were assumed to be *p, p'*-dimethoxy-diphenyl.

2, 4, 6-Trimethylbenzaldehyde.—2.5 g. of iron pentacarbonyl were added to a solution, cooled to −65°C, of 2, 3, 6-trimethylphenyllithium prepared from 10 g. of bromomesitylene and 15 g. of a heptane solution of *n*-buthyllithinum (21.4 wt. %). The neutral part was distilled under reduced pressure to give the following: (1) b. p. ~115°C/10 mmHg (2.3 g.), (2) b. p. 105~110°C/10mmHg (5.0 g.), and (3) b. p. 160~170°C/2.5 mmHg (1.4 g.).

Fraction 2 gave a positive result to Brady's reagent and was assumed to be 2, 4, 6-trimethylbenzaldehyde (theoretical yield: 60.5%), and its 2, 4-dinitrophenylhydrazone was recrystallized from ethylacetate to give reddish-yellow crystals (m. p. 227~228°C).

Summary

The reaction of iron pentacarbonyl with aryllithiums at −50~−60°C has yielded the corresponding aromatic aldehydes in good yields. 2, 6-Dimethylbenzaldehyde (36.4%), 2, 4-dimethylbenzaldehyde (65.4%), *p-t*-butylbenzaldehyde (47.0%), *o-t*-butylbenzaldehyde (54.3%), *p*-methoxybenzaldehyde (24.2%) and 2, 4, 6-trimethylbenzaldehyde (60.5%) have been prepared by this method.

A reaction process for this reaction has been discussed.

Department of Chemical Technology
Faculty of Engineering
Osaka University
Miyakojima-ku, Osaka

Nuclear Magnetic Resonance Spectra of Amino Acids and Their Derivatives. III

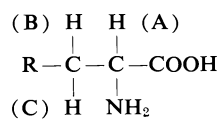
By Shizuo FUJIWARA and Yoji ARATA

(Received September 27, 1963)

The proton magnetic resonance of NH and CH groups of amino acids has been studied by a number of workers.[1-5] Takeda and Jardetzky[1] measured the resonance positions of NH protons in strongly acidic solutions and those of CH protons of such simple amino acids as alanine and glycine. O. and C. D. Jardetzky[2] published additional measurements of the chemical shifts of CH and NH groups, but they did not include any information concerning the spin coupling constants. Bovey and Tiers[3] obtained the spectra of amino acids in trifluoroacetic acid, where the NH signal is observable. They also presented the spectra with a fine structure due to spin coupling and reported the values of several spin coupling constants obtained by first order analyses.

Generally, the NH proton signal cannot be observed in aqueous solutions because of rapid proton exchange with the solvent. However, it was found that the 2, 4-dinitrophenyl (DNP) derivatives of amino acids dissolved in dry dioxane exhibit signals due to NH protons and that their resonance positions are useful for the identification of molecules.[4]

The CH protons give spectra which are more complex than those due to NH protons. For example, the spectra due to the three protons of the type:



where "R" has no protons interacting with those under investigation, were measured and analyzed. Some of these results have been previously reported.[5] In many cases the three protons, A, B, and C, are non-equivalent to each other. However, in the case of amino acids with small R groups, such as cysteine dissolved in an acid medium, H_B and H_C are equivalent.

The three non-equivalent protons show spectra of the ABC type.[6] This type of spectra has been investigated by a number of groups of workers.[7-13] Iterative methods have commonly been used for the analyses of these spectra. The method of least-squares proposed by Shimizu and the present authors[13] has been successfully applied to acrylic acid and its related compounds[13] and to amino acids.[5] This paper will present the results of the application of this method to L-cystine, L-cysteine, L-serine, L-phenylalanine, and L-aspartic acid.

A chief drawback of the iterative method is that it is always accompanied by ambiguities, whether the molecular constants (chemical shifts and spin coupling constants) obtained by analyses are unique or not. In fact, it has been found that, in analyzing the spectra of acrylic acid and ethyl acrylate, two sets of molecular constants were obtained which gave exactly the same line positions, fitting the observed data satisfactorily.[13] These ambiguities can be avoided when the relative intensities are used as a criterion. A correct set of constants may be obtained by a careful comparison of the relative intensities of the calculated spectra with those observed. The results may be further confirmed by measuring the spectra at different spectrometer frequencies; the correct molecular constants must explain the observed spectra at different frequencies.

The relative signs of spin coupling constants can also be determined conventionally by the iterative method outlined above, utilizing

1) M. Takeda and O. Jardetzky, *J. Chem. Phys.*, **26**, 1346 (1957).
2) O. Jardetzky and C. D. Jardetzky, *J. Biol. Chem.*, **233**, 383 (1958).
3) F. A. Bovey and G. V. D. Tiers, *J. Am. Chem. Soc.*, **81**, 2780 (1958).
4) S. Fujiwara, Y. Arata, N. Hayakawa and H. Momoi, This Bulletin, **35**, 1658 (1962).
5) S. Fujiwara and Y. Arata, ibid., **36**, 578 (1963).
6) H. J. Bernstein, J. A. Pople and W. G. Schneider, *Can. J. Chem.*, **35**, 65 (1957).
7) R. A. Hoffman and S. Gronowitz, *Arkiv Kemi*, **15**, 45 (1957); R. A. Hoffman, *J. Chem. Phys.*, **33**, 1256 (1960).
8) C. A. Reilly and J. D. Swalen, ibid., **32**, 1378 (1960); **33**, 1257 (1960); **34**, 980 (1961).
9) S. Alexander, ibid., **32**, 1700 (1960).
10) E. O. Bishop and R. E. Richards, *Mol. Phys.*, **3**, 114 (1960).
11) W. Brugel, T. Ankel and F. Kruckenberg, *Z. Elektrochem.*, **64**, 1121 (1960).
12) S. Castellano and J. S. Waugh, *J. Chem. Phys.*, **34**, 295 (1961); **35**, 1900 (1961).
13) Y. Arata, H. Shimizu and S. Fujiwara, *J. Chem. Phys.*, **36**, 1951 (1962).

various sets of spin coupling constants with different relative signs. As is well known, the determination of the relative sign can best be accomplished by using the double resonance technique.

Experimental

Materials.—The amino acids studied were L-cysteine, L-cystine, L-phenylalanine, L-aspartic acid, and L-serine, all commercial materials (Ajinomoto Co.). They were dissolved in heavy water of various acidities. The acidity was adjusted by adding concentrated hydrochloric acid or powdered sodium peroxide to heavy water. One-molar solutions were used for all measurements. Heavy water was purchased from the Showa Denko Co. and had a purity of 99.5 mol.%.

Spectrometer.—A Varian DP-60 NMR spectrometer operating at 60.00 Mc./sec. was employed for all measurements.

Calibration of the Spectra.—Measurements were performed at about 28°C. The frequency separations were determined by the usual side-band technique. Numerical data for the line positions used for the analyses were obtained by averaging the results of ten determinations. The numerical data for line positions are listed in Table I.

Numerical Calculations

Analyses were carried out through the use of the Parametron digital computer PC-2 of the Physics Department of the University of Tokyo. The flow diagram of the computation is given in Fig. 1. If molecular constants are adequately assumed, after four or five iterations, within one minute, the refined molecular constants and the corresponding spectrum are printed out.

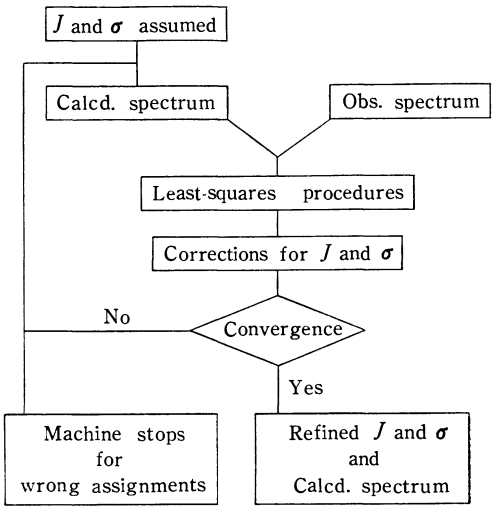


Fig. 1. The flow diagram of computation.

Results

Analyses of the Spectra and the Relative Sign of the Spin Coupling Constants.—As an

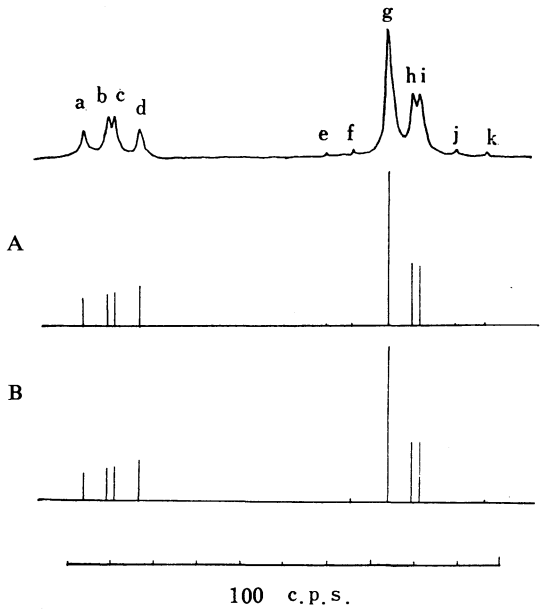


Fig. 2a. The observed and calculated spectra of phenylalanine in 2 N HCl at 60 Mc./sec. A and B were calculated from the molecular constants given in Table II. The magnetic field increases from left to right.

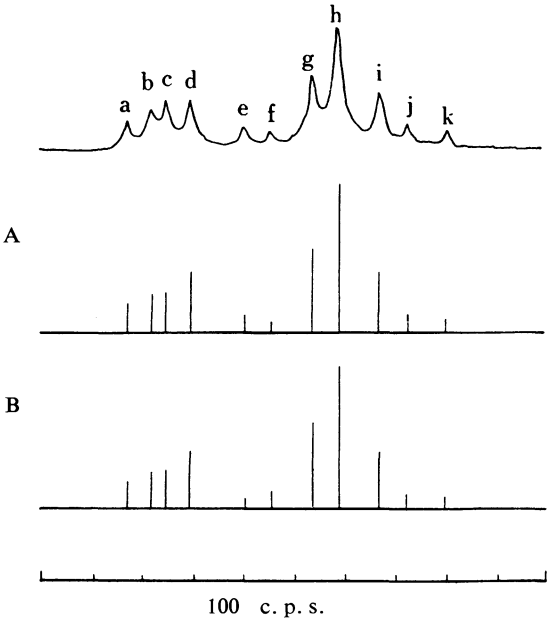


Fig. 2b. The observed and calculated spectra of phenylalanine in 2N NaOD at 60 Mc./sec. A and B were calculated from the molecular constants given in Table II. The magnetic field increases from left to right.

TABLE I. OBSERVED AND CALCULATED SPECTRA OF AMINO ACIDS AT 60.00 Mc./sec.

The line positions are given in c. p. s. and the relative intensities are normalized to unity.
O: observed, A and B: calculated from the molecular constants given in Table II.

(1) L-Phenylalanine in 2 N HCl

	Line position			Relative intensity		
	O	A	B	O	A	B
a	50.7	50.7	50.7	0.064	0.068	0.068
b	44.6	44.8	44.8	0.092	0.080	0.077
c	43.5	43.4	43.4	0.092	0.084	0.079
d	37.5	37.5	37.5	0.070	0.101	0.101
e	− 4.0	− 4.0	− 4.0	0.013	0.003	0.000$_0$
f	−10.0	−10.0	−10.0	0.020	0.006	0.011
g	−18.8	−18.6	−18.6	0.315	0.179	0.184
		−18.9	−18.9		0.182	0.183
h	−24.4	−24.6	−24.6	0.148	0.146	0.142
i	−26.2	−26.1	−26.1	0.158	0.143	0.140
j	−33.5	−33.5	−33.5	0.015	0.003	0.000$_0$
k	−40.8	−40.7	−40.7	0.014	0.005	0.006

(2) L-Phenylalanine in 2 N NaOD

	Line position			Relative intensity		
	O	A	B	O	A	B
a	30.2	30.2	30.2	0.057	0.057	0.058
b	25.1	25.2	25.2	0.081	0.076	0.077
c	22.5	22.4	22.4	0.101	0.081	0.079
d	17.5	17.4	17.4	0.102	0.118	0.117
e	7.3	7.3	7.3	0.043	0.031	0.022
f	2.4	2.3	2.3	0.034	0.022	0.033
g	− 6.1	− 6.1	− 6.1	0.148	0.164	0.174
h	−11.2	−11.1	−11.1	0.242	0.117	0.107
		−11.3	−11.3		0.170	0.171
i	−19.3	−19.1	−19.1	0.108	0.110	0.109
j	−24.7	−24.7	−24.7	0.047	0.029	0.026
k	−32.6	−32.6	−32.6	0.036	0.023	0.026

(3) L-Cystine in 2 N HCl

	Line position			Relative intensity		
	O	A	B	O	A	B
a	50.3	50.4	50.4	0.078	0.069	0.070
b	45.4	45.5	45.4	0.081	0.078	0.075
c	43.6	43.5	43.5	0.078	0.083	0.079
d	38.6	38.5	38.5	0.077	0.099	0.099
e	− 4.2	− 4.1	− 4.1	0.013	0.001	0.000$_0$
f	− 9.1	− 9.1	− 9.1	0.020	0.010	0.013
g	−19.2	−19.2	−19.2	0.347	0.178	0.182
		−19.3	−19.3		0.181	0.181
h	−24.1	−24.2	−24.1	0.143	0.146	0.144
i	−26.3	−26.3	−26.3	0.130	0.142	0.140
j	−34.4	−34.4	−34.4	0.016	0.002	0.000$_0$
k	−41.4	−41.3	−41.3	0.017	0.007	0.008

(4) L-Aspartic acid in 2 N NaOD

	Line position		Relative intensity	
	O	A	O	A
a	50.2	50.2	0.052	0.068
b	45.6	45.7	0.066	0.078
c	41.2	41.2	0.079	0.086
d	36.8	36.7	0.080	0.101
e	0.4	0.4	0.028	0.027
f	− 4.2	− 4.1	0.034	0.032
g	−15.1	−15.1	0.153	0.153
h	−19.5	−19.6	0.160	0.122
i	−21.5	−21.6	0.172	0.158
j	−30.7	−30.6	0.114	0.117
k	−37.0	−37.1	0.034	0.030
l	−46.1	−46.1	0.028	0.029

(5) L-Cysteine in 2 N NaOD

	Line position		Relative intensity	
	O	A	O	A
a	28.5	28.5	0.052	0.058
b	24.0	24.0	0.088	0.076
c	21.1	21.1	0.120	0.083
d	16.4	16.6	0.116	0.117
e	7.0	6.9	0.020	0.026
f	2.3	2.4	0.030	0.021
g	− 6.4	− 6.2	0.146	0.166
h	−10.6	−10.4	0.261	0.174
		−10.7		0.119
i	−17.7	−17.8	0.107	0.112
j	−23.4	−23.5	0.024	0.026
k	−30.7	−30.8	0.013	0.022

example of spectra of the ABC type, the observed spectra of phenylalanine in 2 N hydrochloric acid and 2 N sodium deuteroxide are shown in Fig. 2. The numerical data of the observed line positions and relative intensities are listed in Table I. In the table the observed data of other amino acids exhibiting spectra of the ABC type are also included.

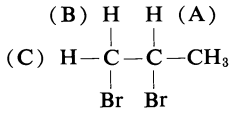
When spin coupling constants are initially assumed to have the same relative sign, one obtains the refined constants shown in Table II, a portion of which has already been reported.[5] These results seem quite satisfactory with regard to the positions of the spectral lines. Calculated spectra obtained from these constants are compared with the observed ones in Table I and in Fig. 2, which show good coincidence. A careful comparison of the relative intensities of the observed spectra with those calculated shows that these constants are unsatisfactory. For instance, in the calculated spectra of phenylalanine the "e" and "f" lines are reversed in the ratio of intensities (in an alkaline solution) and the "e" and "j" lines

TABLE II. THE RESULTS OF ANALYSES IN C. P. S. AT 60.00 Mc./sec.

			δ_{AC}	δ_{BC}	J_{AB}	J_{BC}	J_{CA}
Phenylalanine	2 N HCl	A	68.1	4.9	5.5	−14.6	7.7
		B	67.4	3.7	3.2	14.6	10.0
	2 N NaOD	A	42.1	14.6	5.1	−13.5	7.9
		B	42.1	14.5	4.0	13.4	8.9
Cystine	2 N HCl	A	68.9	5.3	3.7	−15.1	8.2
		B	68.3	4.3	2.0	15.1	9.8
Aspartic acid	2 N HCl		76.4	0	5.3	—	5.3
	2 N NaOD	A	73.8	18.4	4.1	−15.5	9.4
Cysteine	2 N HCl		74.2	0	5.0	—	5.0
	D_2O		55.5	0	4.9	—	4.9
	2 N NaOD	A	39.5	13.0	4.5	−13.2	7.5

are too weak to be observed (in a hydrochloric acid solution). The situation is almost the same with other amino acids.

Because of the above findings, it seemed advisable to seek another means of choosing a set of spin coupling constants with different relative signs. When J_{BC} was initially assumed to have a sign opposite J_{CA} and J_{AB}, a different set of molecular constants was obtained, which gave quite a satisfactory fit between the observed and calculated spectra with respect not only to the line positions but also to the relative intensities. The molecular constants obtained are shown in Table II, while the spectra calculated by using these constants are presented in Fig. 2. The results on the relative sign of spin coupling constants are consistent with those of Freeman and Bhacca,[14] who showed by using the double resonance technique that in 1, 2-dibromopropane,



J_{BC} has a sign opposite J_{AB} and J_{CA}.

To confirm the results obtained, spectra were measured at 40 Mc./sec. and were compared with the spectra calculated by using two sets of constants with different relative signs. For example, the observed and calculated spectra of cystine in 2 N hydrochloric acid are shown in Fig. 3. Unfortunately, as can been seen from this figure, the calculated spectra were very similar to each other. In addition to this, the signal-to-noise ratio was not satisfactory. Therefore, it was difficult to eliminate a wrong set and to determine the relative sign by this procedure.

14) R. Freeman and N. S. Bhacca, *J. Chem. Phys.*, **38**, 1088 (1963).

TABLE III. THE CHEMICAL SHIFTS AND SPIN COUPLING CONSTANTS IN C. P. S. OF L-SERINE AT 60.00 Mc./sec.

		$\nu_A - \nu_B$	J
2 N HCl		11.1	4.2
pH	2	− 5.2	4.6
	5	− 6.9	4.8
	9	−10.6	4.9

The Spectra of Serine and Their pH Dependence.—The molecular constants and, hence, the patterns of the spectra are sensitively influenced by the acidity of the solutions. An example of this is the case of L-valine, which was previously reported on.[5] Another example will now be presented. The spectra of serine in heavy water with various acidities are given in Fig. 4. The a through d spectra are of the AB_2 type[6] and can easily be analyzed to furnish the molecular constants. They are shown in Table III. Serine dissolved in a 2 N sodium deuteroxide solution gives a different type of a spectrum. At first sight it seems to be of the AB_2 type. However, it does not give a satisfactory fit to the observed spectrum when J_{AB} and J_{CA}, and δ_{AB} and δ_{CA}, are assumed to be identical. This suggests that the B and C protons are no longer equivalent.

Concluding Remarks

The values obtained above for chemical shifts and spin coupling constants are actually averages over rotational isomers. The appearance of the spectra is governed by the factors, including the relative energies of the rotational isomers, the potential barriers to internal rotation about the C–C bond, and the chemical shifts and spin coupling

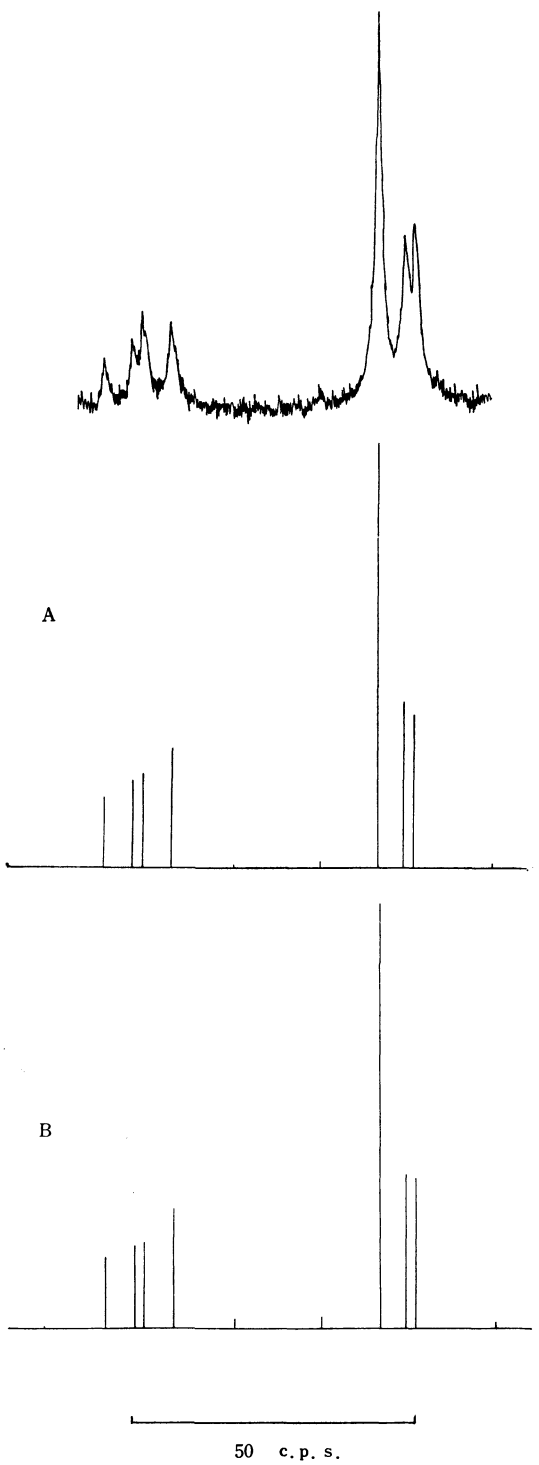


Fig. 3. The observed and calculated spectra of cystine in 2 N HCl at 40 Mc./sec.
A and B were calculated from the molecular constants given in Table II. The magnetic field increases from left to right.

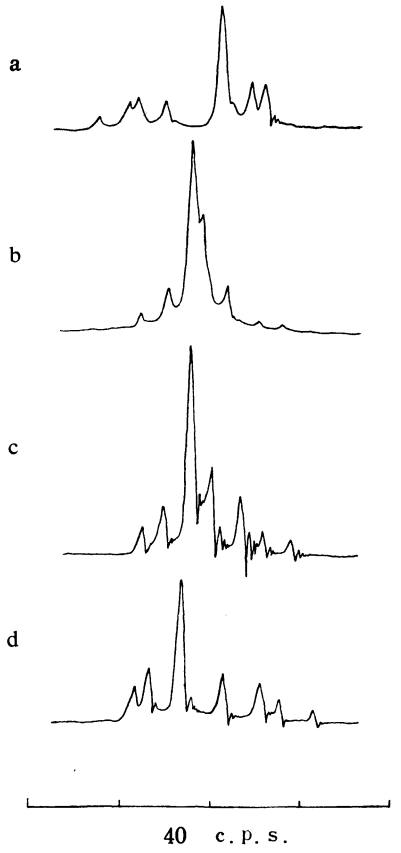


Fig. 4. The observed spectra at 60 Mc./sec. of serine in heavy water of various acidities (a: 2 N HCl, b: pH 2, c: pH 5, d: pH 9). The magnetic field increases from left to right.

constants, characteristic of each isomer.[15,16] Several groups of workers have tried to obtain these quantities by analyzing spectra at various temperatures.[17-19] Gutowsky, Belford, and McMahon[19] studied the temperature dependence of the spectra of polysubstituted ethanes and developed a method including the least-squares procedure. When the spectra of the amino acids studied here show an appreciable dependence upon the temperature, it may be possible to obtain the above quantities utilizing this method.

15) J. A. Pople, W. G. Schneider and H. S. Bernstein, "High Resolution Nuclear Magnetic Resonance," McGraw-Hill Book Company, Inc., New York (1959).
16) H. S. Gutowsky, "Technique of Organic Chemistry," Ed. by A. Weissberger, Interscience Publishers, Inc., New York (1960).
17) R. W. Fessenden and J. S. Waugh, *J. Chem. Phys.*, **37**, 1466 (1962).
18) D. S. Thompson, R. A. Newmark and C. H. Sederholm, ibid., **37**, 411 (1962).
19) H. S. Gutowsky, G. G. Belford and P. E. McMahon, ibid., **36**, 3353 (1962).

The authors are indebted to Mr. Osamu Yamamoto of the Government Industrial Research Institute of Tokyo for letting them use the NMR spectrometer and to Mr. Shoichi Hayashi of the Institute of Physical and Chemical Research in Tokyo for measuring the NMR spectra at 40 Mc./sec. Thanks are also due to Mr. Takeo Yamamoto of the University of Tokyo for his assistance in writing a program for the digital computer.

Department of Chemistry
The University of Tokyo
Hongo, Tokyo (S. F.)
University of Electro-communications
Chofu, Tokyo (Y. A.)

The Normal Vibrations of Diketopiperazine and Its N-Deuterated Compound

By Kunio FUKUSHIMA, Yoshiko IDEGUCHI and Tatsuo MIYAZAWA

(Received October 21, 1963)

The infrared absorption bands of the *trans*-CONH group have been extensively studied.[1] On the other hand, the characteristic vibrations of the *cis*-CONH group have not been established. Newman and Badger[2] and Shimanouchi et al.[3] measured the infrared dichroism of single crystals of diketopiperazine in the region above 700 cm^{-1} and assigned the observed bands to the A_1 or B_u fundamental vibrations. Miyazawa, measuring the infrared spectra of diketopiperazine and its *N*-deuterated compound, assigned that absorption bands with reference to the isotope shifts and to the normal vibration calculation for the planar cis form of *N*-methylacetamide.[4]

In the present study the normal vibrations (B_u) of diketopiperazine and its *N*-deuterated compound are treated, and the origin of the infrared bands is studied. The nature of the characteristic vibrations of the *cis*-CONH group will also be elucidated.

Normal Coordinate Treatment

According to the X-ray diffraction study by Corey,[5] the molecule of diketopiperazine is planar (except for the hydrogen atoms of the methylene groups) with the point group, C_{2h}. On the basis of this model, we have calculated the normal vibrations of diketopiperazine and its *N*-deuterated compound as a ten-body problem, treating the methylene groups as mass points. Wilson's $\boldsymbol{GF}$ matrix method[6] was used for the calculation. The internal coordinates are as shown in Table I, while the molecular parameters used are the same as those of polyglycine I.[7] The inverse kinetic energy matrix, $\boldsymbol{G}(B_u)$, for the B_u vibrations was constructed in terms of the symmetry coordinates:

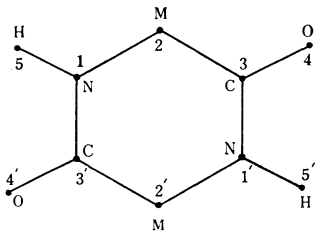


Fig. 1. Molecular conformation and indices of atoms of diketopiperazine.

$$S_j=(R_i-R_i')/2^{1/2} \quad (i=1, 2,\cdots\cdots, 10) \qquad (1)$$

The two redundant coordinates were removed by the numerical diagonalization of the $\boldsymbol{G}$ matrix. The potential energy matrix, $\boldsymbol{F}(B_u)$, was derived from the Urey-Bradley potential function,[8] and the potential constants were taken to be the same as those of polyglycine I.[7] The numerical computations were made with an NEAC 2101 electronic computer. The calculated frequencies, the diagonal terms of the potential energy distributions, and the atomic displacements are shown in Tables II and III, and Figs. 2 and 3, respectively.

1) T. Miyazawa, *Kagaku to Kogyo*, **15**, 137 (1962); "Polyamino-acids, Polypeptides, and Proteins," Ed. by M. Stahmann, University of Wisconsin Press, Madison (1962), p. 201.
2) R. Newman and R. M. Badger, *J. Chem. Phys.*, **19**, 1147 (1951).
3) T. Shimanouchi, K. Kuratani and S. Mizushima, ibid., **19**, 1479 (1951).
4) T. Miyazawa, *J. Mol. Spectr.*, **4**, 155 (1960).
5) R. B. Corey, *J. Am. Chem. Soc.*, **60**, 1598 (1938).
6) E. B. Wilson, Jr., *J. Chem. Phys.*, **7**, 1047 (1939); **9**, 76, (1941).
7) K. Fukushima, Y. Ideguchi and T. Miyazawa, This Bulletin, **36**, 1301 (1963).
8) T. Shimanouchi, *J. Chem. Phys.*, **17**, 245 (1949).

TABLE I. INTERNAL COORDINATES

R_1	Δr_{15}	$R_{1'}$	$\Delta r_{1'5'}$
R_2	$\Delta(2\alpha_{3'12}-\alpha_{513'}-\alpha_{215})/6^{1/2}$	$R_{2'}$	$\Delta(2\alpha_{31'2'}-\alpha_{5'1'3}-\alpha_{2'1'5'})/6^{1/2}$
R_3	$\Delta(\alpha_{513'}-\alpha_{215})/2^{1/2}$	$R_{3'}$	$\Delta(\alpha_{5'1'3}-\alpha_{2'1'5'})/2^{1/2}$
R_4	Δr_{12}	$R_{4'}$	$\Delta r_{1'2'}$
R_5	$\Delta\alpha_{123}$	$R_{5'}$	$\Delta\alpha_{1'2'3'}$
R_6	Δr_{23}	$R_{6'}$	$\Delta r_{2'3'}$
R_7	Δr_{34}	$R_{7'}$	$\Delta r_{3'4'}$
R_8	$\Delta(2\alpha_{231'}-\alpha_{432}-\alpha_{1'34})/6^{1/2}$	$R_{8'}$	$\Delta(2\alpha_{2'3'1}-\alpha_{4'3'2'}-\alpha_{13'4'})/6^{1/2}$
R_9	$\Delta(\alpha_{432}-\alpha_{1'34})/2^{1/2}$	$R_{9'}$	$\Delta(\alpha_{4'3'2'}-\alpha_{13'4'})/2^{1/2}$
R_{10}	$\Delta r_{31'}$	$R_{10'}$	$\Delta r_{3'1}$

TABLE II. THE DIAGONAL TERMS OF POTENTIAL ENERGY DISTRIBUTIONS (IN %)

$(-CH_2CONH-)_2$

ν_c	S_1	S_2	S_3	S_4	S_5	S_6	S_7	S_8	S_9	S_{10}
3339	101	0	0	0	0	0	0	0	0	0
1657	0	1	16	1	0	3	70	9	0	18
1450	0	0	80	3	1	0	18	0	1	0
1383	0	2	0	6	0	25	4	0	13	72
1056	0	9	2	68	0	2	0	1	17	2
892	0	4	3	0	7	61	2	0	10	10
728	0	22	1	7	19	0	9	40	0	1
403	0	2	0	15	1	11	1	1	65	1

$(-CH_2COND-)_2$

ν_c	S_1	S_2	S_3	S_4	S_5	S_6	S_7	S_8	S_9	S_{10}
2437	101	0	0	0	0	0	0	0	0	0
1639	0	1	4	0	1	3	81	9	0	19
1381	0	2	2	9	0	23	7	0	11	70
1195	0	1	54	20	1	8	5	1	15	0
1010	0	9	12	47	0	17	2	0	5	6
812	0	3	25	4	8	38	0	0	11	6
720	0	21	5	5	16	1	9	40	0	1
401	0	2	0	16	1	11	1	2	64	1

TABLE III. OBSERVED (ν_o) AND CALCULATED (ν_c) FREQUENCIES (IN cm^{-1}) OF DIKETOPIPERAZINE AND ITS *N*-DEUTERATED COMPOUND AND THEIR ASSIGNMENTS

$(-CH_2CONH-)_2$		$(-CH_2COND-)_2$		Assignment
ν_o	ν_c	ν_o	ν_c	
1690	1657	1675	1639	C=O stretch.
1443	1450			N-H in-plane bend.
1340	1383	1349	1381	C-N stretch., C-CH_2 stretch.
		1232	1195	N-D in-plane bend., N-CH_2 stretch.
1075	1056			N-CH_2 stretch., C=O in-plane bend.
		970	1010	N-CH_2 stretch., C-CH_2 stretch., N-D in-plane bend.
910	892			C-CH_2 stretch., C-N stretch., C=O in-plane bend.
		887	812	C-CH_2 stretch., N-D in-plane bend.
806	728	780	720	CH_2-C-N deform., C-N-CH_2 deform.
449	403	446	401	C=O in-plane bend., N-CH_2 stretch.

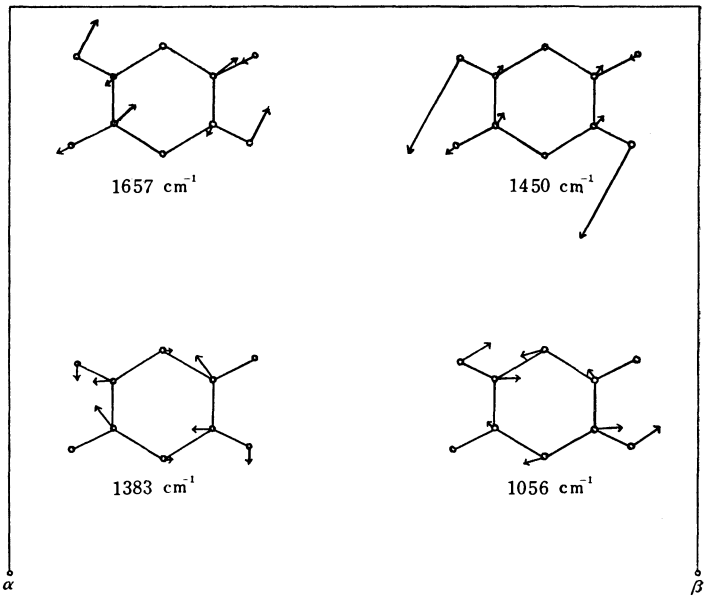


Fig. 2a.

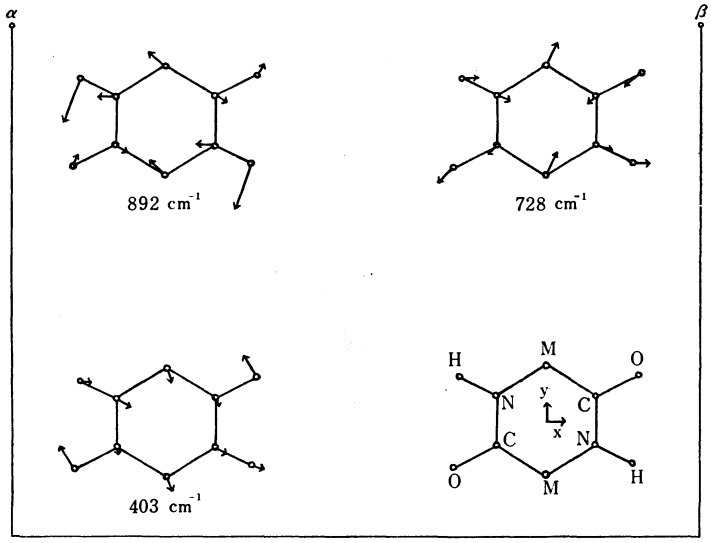


Fig. 2b.

Fig. 2. Schematic representation of the vibrational modes of diketopiperazine.

Assignments

With reference to the calculated frequencies and the potential energy distributions, the observed infrared bands[4] may be assigned as shown in Table III. The present assignment agrees with the previous assignments except for the few cases described below (the abbreviations DP and DP-d represent diketopiperazine and *N*-deuterated diketopiperazine respectively). The band of DP at 806 cm^{-1} has been established as due to B_u vibrations.[2,3] In a previous study[4] this band has been assigned to the C=O in-plane bending mode. However, since the observed frequency corresponds most closely with the calculated frequency at 728 cm^{-1}, this band is now assigned to the ring deformation vibration. The dichroism of the bands at 449 cm^{-1} (DP) and at 446 cm^{-1} (DP-d) have not been determined experimentally. These bands correspond to the B_u frequency calculated at 403 cm^{-1} (DP) and at 401 cm^{-1} (DP-d) respectively, and are now assigned to the C=O in-plane bending mode as coupled slightly with the $N-CH_2$ stretching mode.

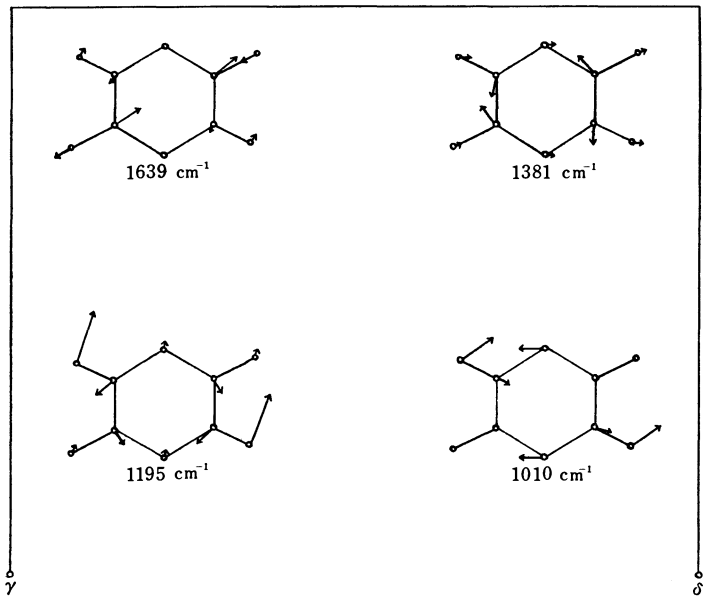


Fig. 3a.

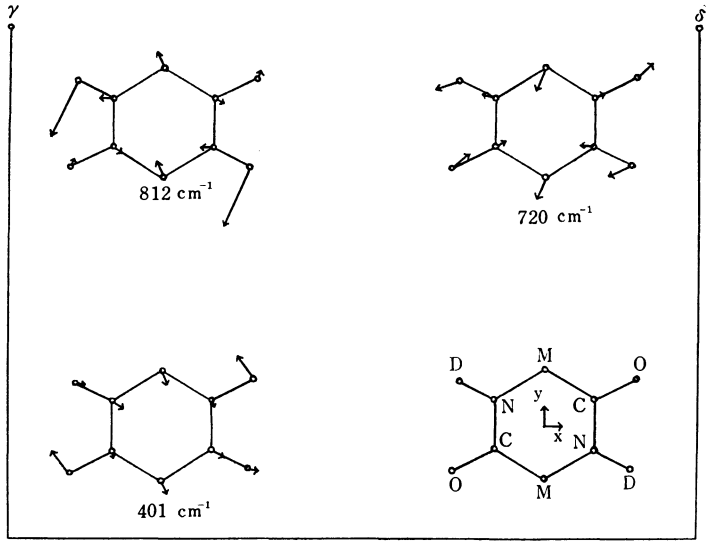


Fig. 3b.

Fig. 3. Schematic representation of the vibrational modes of *N*-deuterated diketopiperazine.

The Characteristic Vibrations of the *cis*-CONH Group

The *cis*-Amide I Band (C=O Stretching Vibration).—For this vibration at 1690 cm^{-1}, 70% of the potential energy is associated with the C=O stretching mode. However, the energy distributions at the C–N stretching (18%) and the N–H bending modes (16%) are not quite negligible.

The *cis*-Amide II Band (N–H In-plane Bending Vibration). — For this vibration at 1443 cm^{-1}, 80% of the potential energy is associated with the N–H in-plane bending mode, while 20% of the energy is associated with the C=O stretching mode.

The *cis*-Amide III Band (C–N Stretching Vibration).—For this vibration at 1340 cm^{-1}, 70% of the potential energy is associated with the C–N stretching mode, and 25% of the energy is associated with the C–CH_2 stretching mode.

The *cis*-Amide IV Band (C=O In-plane Bending Mode).—For this vibration at 449 cm^{-1}, 65% of the potential energy is associated with

the C=O in-plane bending mode, while 26% of the energy is associated with the N-CH_2-C symmetric streching mode. This vibration is not localized in the CONH group as highly as are the *cis*-amide I, II, or III vibrations.

The *N*-Deuterated *cis*-Amide Group.—On *N*-deuteration, the frequencies and the potential energy distributions of the *cis*-amide I, III, or IV vibrations do not change appreciably (Tables II and III). The *cis*-amide II vibration is shifted to a much lower frequency, and then the N–D in-plane bending mode is strongly coupled with the C–N and C–C stretching modes (see Table III for the nature of the vibrations at 1195 cm^{-1} and 812 cm^{-1}).

Summary

The normal vibrations of diketopiperazine and its *N*-deuterated compound have been calculated, with the metylene groups treated as mass points. An assignment of the infrared absorption bands has been made on the basis of the calculated frequencies and potential energy distributions, and the nature of the characteristic vibrations of the *cis*-amide group has been discussed.

Institute for Protein Research
Osaka University
Kita-ku, Osaka

*The Formation of Sulfur Compounds in the Radiolysis of a Toluene Solution of Sulfur**

By Wataru ANDO, Ken'ichi SUGIMOTO and Shigeru OAE

(Received September 9, 1963)

In a previous investigation of the radiolysis of a benzene solution of sulfur,[1] the formations of mercaptan, disulfide and a few minor products have been observed, and it has been suggested that the reaction passes through the initial formation of a phenyl radial, which eventually reacts with sulfur to give the final products.

The treatment of hydrocarbon with ionizing radiation usually results in the formation of a variety of fragmentation products.[2] These radicals attack the S–S bond of elemental sulfur, thus:

$$RH \overset{I}{\sim\!\sim\!\sim\!\sim}\!\!\rightarrow R + H$$

$$R + S_8 \rightarrow RS_8 \rightarrow RS$$

Consistent with this view, the reaction of sulfur with cyclohexane under the ionizing radiation with gamma rays has also been shown by Barzynski and Hummel[3] to proceed via the initial formation of a cyclohexyl radical which cleaves the S–S bond of sulfur in the following step.

However, in the case of toluene, the free radical that formed initially would be benzyl which is remarkably more stable than the phenyl or cyclohexyl radical, and which hence might show somewhat different reaction patterns. In fact, the formation of dimerization products is the main path for the thermal reaction of toluene with sulfur,[4] while the similar reaction of cyclohexane undergoes dehydrogenation to benzene[5] and that of benzene leads to the formation of benzenethiol and its derivatives.

Thus, the study of the radiolysis of a toluene solution of sulfur would provide further insight into the nature of the radiolysis process of hydrocarbons in the presence of sulfur.

In the radiolysis of a toluene solution of sulfur, benzyl mercaptan was found to be formed by the cleavage of the S–S bond with the benzyl radical. Hydrogen and hydrogen sulfide were observed to evolve during the runs. This paper will describe a detailed study of the mechanism of the radiation-induced reaction of toluene with sulfur.

Experimental

Reagents.—Toluene was purified by fractional distillation just before use. The sulfur used in this

* The Study of the Radiation Chemistry of Organic Sulfur Compounds, II.

1) W. Ando, K. Sugimoto and S. Oae, This Bulletin, **36**, 893 (1963).

2) A. J. Swallow, "Radiation Chemistry of Organic Compounds," Pergamon Press, Oxford (1960).

3) H. Barzynski and D. Hummels, *Z. physik. Chem. N. F.*, **33**, 352 (1962).

4) A. W. Horton, *J. Org. Chem.*, **14**, 761 (1949).

5) A. S. Brown and B. V. Ioffee, *Nauk. Byull. Leningrod. Gosudarst Univ.*, **20**, 11 (1948); *Chem. Abstr.*, **43**, 5376e (1949).

work was of an exceptionally high purity, as in the previous experiment.[1]

The preparation of the samples and the techniques of irradiation by cobalt-60 gamma rays have been described in a previous paper.[1]

Product Handling and Analysis.—After irradiation, the ampoules were broken in an evacuated system. All the volatile products formed were vacuum-transferred into a trap cooled with liquid nitrogen and carefully degassed by repeated warming and cooling. Then, non-condensable gases were vacuum-transferred to another trap by pumping.

The major portion of the non-condensable gases at the temperature of liquid nitrogen, e.g., hydrogen and methane, were pumped into calibrated glass tubing with a Töpeler pump, and the pressure was measured. From this pressure measurement, *G*-values for the hydrogen gases were calculated.

The procedures for the determination of the mercaptan and hydrogen sulfide were almost identical with those described in the previous paper.[1]

Results and Discussion

Effects on Radiation on the Toluene-Sulfur System.—The irradiation of toluene with sulfur at room temperature gave benzyl mercaptan, hydrogen and hydrogen sulfide as the main products. The results of several illustrative runs are shown in Table I. In the experimental results, the following features are observed; 1) The *G*-value of the formation of the mercaptan depends on the concentration of sulfur. 2) The *G*-value for the formation of hydrogen is almost identical with that of hydrogen formation in the radiolysis of toluene alone, increasing slightly with the increase in sulfur concentration.

TABLE I. IRRADIATION OF TOLUENE WITH SULFUR

Sulur concn.	*G*-Value of product		
g./100 ml.	$C_6H_5CH_2SH$	H_2	H_2S
0.25	0.068	0.14	0.008
0.5	0.088	0.15	0.011
1.0	0.107	0.17	0.014
1.5	0.123	0.18	0.017

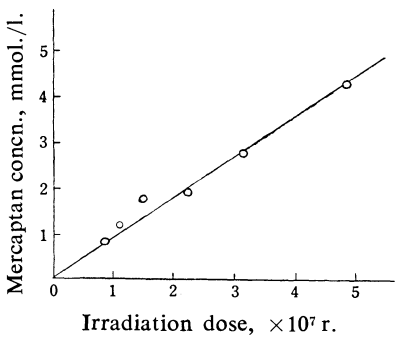


Fig. 1. Formation of benzyl mercaptan in radiolysis of toluene with sulfur (1.0 g. sulfur per 100 ml. of toluene).

Figure 1 shows that the amount of mercaptan formed increases linearly with the increase of the dose.

The increasing formation of the mercaptan appears to suggest that the reaction proceeds through the initial opening of the S_8 ring by γ-ray irradiation to form an open-chain sulfur radical which subsequently abstracts the hydrogen of the methyl group of toluene, producing the benzyl radical and the HS_x radical:

$$S_8 \overset{\gamma}{\rightsquigarrow} S_x$$

$$C_6H_5CH_3 + S_x \rightarrow C_6H_5CH_2 + HS_x$$

$$C_6H_5CH_2 + S_x \rightarrow C_6H_5CH_2S_x \rightarrow C_6H_5CH_2S$$

However, the fact that the *G*-value of the hydrogen formation in this reaction system is nearly identical with that of the radiolysis of toluene alone[6] seems to suggest that the first step of this reaction is the radiolysis of toluene, forming hydrogen and the benzyl radical, which then opens the S_8 ring to form the mercaptan.

The radiolysis of toluene can be represented by the equation:

$$C_6H_5CH_3 \overset{\gamma}{\rightsquigarrow} C_6H_5CH_2 + H \qquad (1)$$

The benzyl radical thus formed can react by any one of the following paths:

$$C_6H_5CH_2 + H \rightarrow C_6H_5CH_3 \qquad (2)$$

$$2C_6H_5CH_2 \rightarrow C_6H_5CH_2CH_2C_6H_5 \qquad (3)$$

$$C_6H_5CH_2 + S_8 \rightarrow C_6H_5CH_2S_8 \rightarrow C_6H_5CH_2S \qquad (4)$$

The formation of the mercaptan can be considered to result from reaction 4, and the mercapto radical thus formed would abstract hydrogen from the methyl group of toluene:

$$C_6H_5CH_2S + C_6H_5CH_3 \rightarrow C_6H_5CH_2SH + C_6H_5CH_2 \qquad (5)$$

while the hydrogen atom formed in the initial radiolysis of toluene is expected to react as in the following scheme:

$$H + C_6H_5CH_3 \rightarrow H_2 + C_6H_5CH_2 \qquad (6)$$

$$H + S_8 \rightarrow HS_8 \rightarrow HS \qquad (7)$$

The benzyl-hydrogen atom is undoubtedly more readily abstracted than phenyl hydrogen.

As can be seen from Table I, the *G*-values of hydrogen formation are considerably larger than those of hydrogen sulfide but are not much

6) L. H. Gale, B. E. Gordon, G. Steiberg and C. D. Wagner, *J. Phys. Chem.*, 66, 1538 (1962).

larger than that of toluene alone ($G_{H_2}=0.13$). The hydrogen atom, once formed, will react either with toluene to give a hydrogen molecule or with sulfur to form hydrogen sulfide, and the results suggest that the former reaction is more favorable. The increasing G-values of hydrogen formation with the increasing sulfur concentration could be interpreted as resulting from the additional formation of hydrogen in the secondary reaction of the decomposition of mercaptan to form the disulfide and the hydrogen molecule.

The G-value of the formation of hydrogen sulfide varies remarkably when the hydrocarbon in the reaction system is changed.

The relative ratios of the G-values of hydrogen and of hydrogen sulfide for the benzene system are far less than those for the toluene system.

The Toluene-Sulfur-Carbon Disulfide System.—In order to clarify the nature of the radiolysis of toluene and sulfur, radiolysis was studied for a mixed solution of carbon disulfide and toluene, with a constant concentration of sulfur dissolved in it. In this mixture, the fate of the radical or atom formed could be altered by the presence of the other component. However, if the initial step of the reaction process is the cleavage of the sulfur ring, the formation of the sulfur biradical must depend on the irradiation dose, and the G-value of formation of mercaptan is constant when the irradiation was applied to solutions containing enough toluene and a constant concentration of sulfur, because the formation of mercaptan depends on the number of sulfur biradicals formed—toluene is merely a hydrogen donor in such a reaction process.

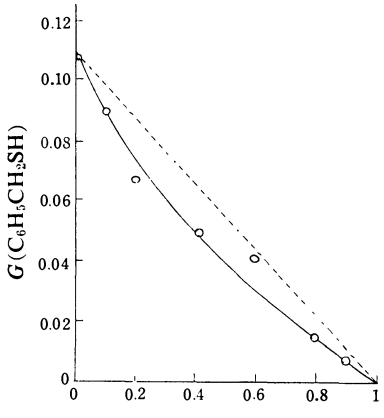


Fig. 2. Variation of G-value of mercaptan with electron fraction of carbon disulfide for toluene-carbon disulfide-sulfur system. (2.0 g. sulfur per 100 ml. of solution, irradiation dose was 4.8×10^7 r.).

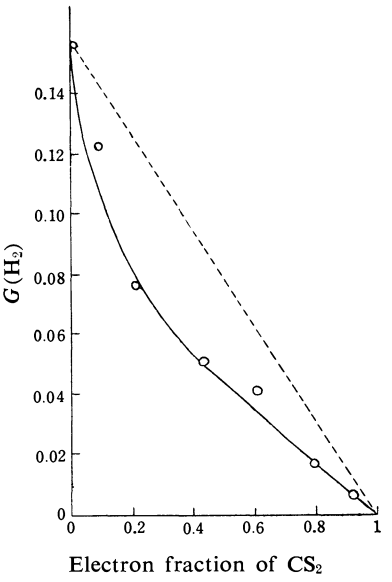


Fig. 3. Variation of G-value of hydrogen with electron fraction of carbon disulfide for toluene-carbon disulfide-sulfur system: (2.0 g. of sulfur per 100 ml. of solution, irradiation dose was 4.8×10^7).

Figures 2 and 3 give the G-values for the formation of benzyl mercaptan and hydrogen as a function of the electron fraction of a toluene-carbon disulfide mixture. The G-values of the formation of mercaptan and hydrogen are proportional to the electron fraction of toluene. The actual curves obtained show a substantial departure from the dotted lines, which represent the yields that are expected in an average absorption of energy into the system.

The results could, therefore, be explained on the basis of an energy transfer mechanism in which the initial step is the decomposition of the toluene molecule. Here again, the formation of hydrogen and mercaptan should result from the initial radiolysis of toluene.

The Interaction of Hydrogen Atom and Elemental Sulfur.—It has been shown in a previous paper[1] that the hydrogen atom formed by the radiolysis of benzene could be used for the formation of hydrogen sulfide by reacting it with sulfur and that this reaction between hydrogen and the sulfur molecule takes place more readily than the reaction between hydrogen and benzene. In the radiolysis of a toluene solution of sulfur, however, the G-value of the formation of hydrogen is higher than that of hydrogen sulfide. In order to compare the reactivity of various types of hydrocarbons, the radiolysis of a toluene-cyclohexane mixture dissolving sulfur of a definite concentration were carried out. Data on the hydrogen and

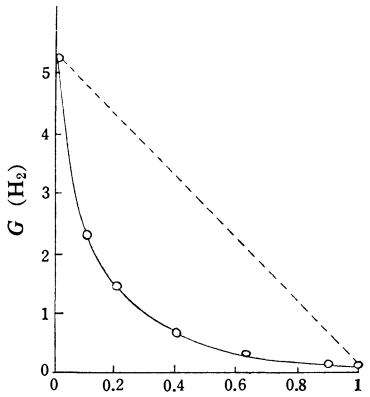


Fig. 4. Variation of G-value of hydrogen with electron fraction of toluene for cyclohexane-toluene-sulfur system (0.2 g. sulfur per 100 ml. of solution).

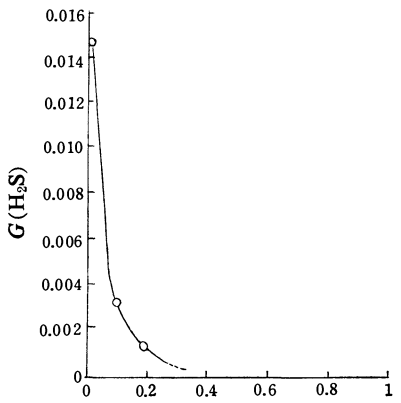


Fig. 5. Formation of hydrogen sulfide with electron fraction of mixture for toluene-cyclohexane-sulfur system (0.2 g. sulfur per 100 ml. of solution).

hydrogen sulfide yields are shown in Figs. 4 and 5.

The G-value of the formation of hydrogen sulfide which may be formed from the initial reaction of the hydrogen atom with sulfur clearly depends on the concentration of toluene. At a high concentration of cyclohexane, hydrogen is the major product, and the reaction between sulfur and the hydrogen atom is apparently of minor importance. Therefore, the hydrogen atom, once formed, seems to abstract hydrogen from cyclohexane preferentially, to form a hydrogen molecule rather than to react with sulfur.

A General Scheme for the Radiolysis of Hydrocarbon Solutions of Elemental Sulfur.—In a series of the related reactions of hydrocarbons with sulfur, the primary reaction involving C–H bond rupture may be schematically written as:

$$RH \overset{r}{\sim\!\sim\!\sim\!\longrightarrow} R + H$$

Here, the reaction undoubtedly depends on the bond energy of the C–H bond from which the hydrogen atom is cleaved in the reaction. Hydrocarbon-free radicals which escape the recombination reaction will react with sulfur to form mercapto radicals, which eventually give rise to mercaptan or disulfide.

$$R + S_8 \rightarrow RS_8 \rightarrow RS$$

In benzene or cyclohexane, the formation of orgnic sulfur compounds does not depend on the concentration of sulfur, but it does on that of toluene, probably because the benzyl radical is cosiderably stabilized by the resonance, and the reaction of sulfur with the benzyl radical apppears to be the product-determining step.

In the case of toluene and cyclohexane mixtures, the hydrogen atom probably abstracts hydrogen from the hydrocarbons a little faster than it reacts with sulfur to form hydrogen sulfide, thus lowering the yield of hydrogen sulfide. Only in benzene would the reaction of the hydrogen atom with sulfur be favored, and thus the yield of hydrogen sulfide is more than that of hydrogen molecules.

A General Examination of the Energy Transfer of the Radiolysis of the Toluene Solution System.—The formations of both the hydrogen molecule and the mercaptan are initiated by the prior decomposition of toluene. In the mixture of toluene and carbon disulfide, carbon disulfide is considered to behave only as an energy-absorbing solvent which absorbs the radiation energy of gamma rays and transfers the energy to reacting molecules to form excited molecules, since carbon disulfide does not seem to react to give the related products.

The deviation from linearity in Figs. 2 and 3 can be considered to be derived from the energy transfer from toluene to carbon disulfide. Probably the contribution of the ionization transfer mechanism is unimportant, for the ionization potential of toluene is lower than that of carbon disulfide. Consequently, the overall reaction may proceed via energy transfer only through excitation. As has been stated by Inokuti,[7] it might be that carbon disulfide has a large cross section value for the excitation of electrons, and that it is easily excited to lower excited levels. The energy stored in the lower excited levels of carbon disulfide is then transferred to toluene molecules, which eventually undergo a series of radiolysis reactions.

7) M. Inokuti, *Isotope and Radiation*, 1, 82 (1958).

The Cyclohexane-Toluene System. — As has been stated by Manion and Burton, the formation of hydrogen in Fig. 4 clearly shows that energy transfer is taking place from cyclohexane to toluene; this is consistent with the interpretation that toluene protects cyclohexane because it has both lower ionization and lower excitation potentials.

Summary

The radiolysis of a toluene solution of sulfur has been investigated. The formations of benzyl mercaptan, hydrogen, and hydrogen sulfide have been observed, and their amounts determined under various considerations. The amounts of mercaptan formed increase linearly with the concentration of sulfur, and the reactions seem to proceed through the initial decomposition of toluene to form the benzyl radical, which then opens the S_8 ring molecule to form the mercaptan. The *G*-value of hydrogen formation is considerably larger than that of hydrogen sulfide. Similar studies were made of the systems of toluene - cyclohexane - sulfur and of toluene - carbon disulfide - surfur in order to clarify the nature of the radiolysis of toluene and sulfur.

Department of Chemistry
Radiation Center of Osaka Prefecture
Sakai, Osaka (W. A. & K. S.)

Department of Applied Chemistry
Faculty of Engineering
Osaka City University
Kita-ku, Osaka (S. O.)

*Decomposition and Energy Transfer in the Radiolysis of Sulfur Compounds in Toluene**

By Wataru ANDO, Ken'ichi SUGIMOTO and Shigeru OAE

(Received September 9, 1963)

One of the most interesting problems in the radiation chemistry of organic compounds is that of energy transfer from excited solvent molecules to reacting solute molecules. Energy transfer has been used to explain the non-linear dependence of product yields upon the electron fraction of a two-componet system. In the typical example of the cyclohexane-benzene system,[1] the yield of the hydrogen formed was found to be always less than that to be expected from the decomposition of two components.

Much evidence on the energy transfer has been obtained recently. For example, unusually high *G*-values have been found for the nitrate decomposition in alkali halide,[2] and for the radical formation in a benzene solution of organic disulfide.[3] Gusynin and Tal'roze[4] have found that, for terphenyl in dioxane, the quenching cross section for an alcohol is proportional to the number of carbon atoms in the alcohol, suggesting that energy can be transferred readily along the $-CH_2-$ chain to the OH group. The compounds, 1, 1-dicyclohexyldodecane, 1, 1-diphenyldodecane, 1-phenyl-1-cyclohexyldodecane, cyclohexane, and benzene, were irradiated while frozen at $-120°C$, and their radical yields and ESR spectra were measured.[5] The results have suggested a possible intramolecular transfer of energy to the benzene ring. Intermolecular transfer also occurs, but with a lower efficiency.

The recent study of energy transfer in the benzene - thiophenol system[6] has shown that most of the energy of the excited benzene molecule is transferred to thiophenol. Furthermore, in the toluene - sulfur - cyclohexane or the toluene - sulfur - carbon disulfide system,[7] hydrogen formation is consistent with the interpretation that toluene is protected by carbon disulfide because the latter compound has a lower excitation, or that cyclohexane is protected by toluene because the latter has lower excitation and ionization potentials.

* The Study of the Radiation Chemistry of Organic Sulfur Compounds, III.

1) J. P. Manion and M. Burton. *J. Phys. Chem.*, **56**, 560 (1952).

2) A. B. Jones, *J. Chem. Phys.*, **35**, 751 (1961).

3) V. A. Krongauz and Kh. S. Bagdasaryan, *Doklady. Akad. Nauk. S.S.S.R.*, **132**, 1136 (1960).

4) V. I. Gusynin and V. L. Tal'roze, ibid., **135**, 1160 (1960).

5) Yu. N. Molin, I. I. Chkheidze, Al. A. Petrovo, V. V. Voevodskii and N. Ya. Buben, *Doklady. Akad. Nauk. SSSR*, **131**, 125 (1960).

6) W. Ando. K. Sugimoto and S. Oae, This Bulletin, **36**, 893 (1963).

7) W. Ando, K. Sugimoto and S. Oae, ibid., **37**, 353 (1964).

The present investigation was undertaken in order to obtain some direct information about the energy transfer in the free radical formation from a toluene solution of sulfur compounds under irradiation.

Experimental

Material.—Toluene was purified by the usual fractional distillation, and its purity was checked by gas chromatography. All the disulfides were purchased from Tokyo Kasei and were used after recrystallization from 96% ethanol. Purified products with a melting point range of less than 1.0 deg. were used. Diphenyl sulfide was obtained by the reaction of benzene with sulfur in the presence of aluminum chloride, and it was purified by vacuum distillation[8] (b. p. 126°C at 3 mmHg.).

Procedure.—The free radical yields in the decomposition of the sulfur compounds were determined by scavenging the radicals with diphenyl picryl hydrazyl (DPPH). The disappearance of the scavenger was followed by measuring the decrease in the optical density at 530 mμ with the absorption coefficient of 1.2×10^{4} mol^{-1} l. cm^{-1}, where the absorption of the yellow scavenged product is insignificant.

The concentration of DPPH in toluene was kept constant within the range of 1×10^{-3} and 4×10^{-4} mol./l. during the run. The observed optical densities were corrected against the relaltive background absorption of the solution of DPPH in toluene without sulfur compounds which would be formed during the irradiation. The solution of DPPH in pure toluene was irradiated under the same conditions as those used for the solution ncotaining the sulfur compound, and the differenec between the absorbances of DPPH in the two solutions was taken as the consumption of DPPH reacting with radicals derived from the sulfur compounds.

All the samples were thoroughly degassed by twice freezing and thrawing them in a vacuum. Irradiation was carried out with a 1000-curie Co-60 source at room temperature, and the dose rate was 1.6×10^{4} r.

Results and Discussion

The irradiation of the sulfur compounds in toluene at room temperature produced a significant change in the optical density of DPPH, presumably by means of the formation of radicals from the decomposition of the sulfur compounds. The overall reaction of DPPH with free radicals is complicated by secondary reactions.[9,10] However, it may safely be assumed that the free radicals formed by the decomposition of the sulfur compounds in the primary step react with two DPPH molecules to form inactive products, and that, therefore, the amount of the decomposition of a sulfur compound is just a half of that of the disappearance of DPPH.

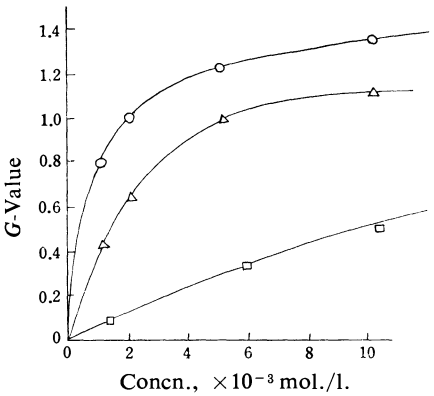


Fig. 1. Comparison of *G*-value on the decomposition of benzyl sulfur compounds in toluene solution.
○ Benzyl mercaptan
△ Benzyl disulfide
□ Benzyl sulfide

From Fig. 1, it is quite obvious that the amount of the decomposition of a sulfur compound depends on the initial concentration of the sulfur compounds. Assuming that the ionizing radiation directly effects the decomposition of the sulfur compound, the apparently higher *G*-values can be calculated on the basis of the direct effect; thus, the *G*-values are calculated to be nearly 700 for the disulfide, 200 for the sulfide, and 25000 for the mercaptan.

When one considers their bond dissociation energies, these *G*-values are much higher than the maximum *G*-values to be expected from the complete consumption of the direct energy absorbed. A better interpretation would be that the excited toluene formed by the irradiation transfers energy relatively easily to the sulfur compounds, resulting in dissociation into free radicals. Figure 2 shows the linearity of the relationship of the benzyl disulfide decomposition against the irradiation dose.

Now, let us assume that most of the energy is absorbed by toluene and that the amount of energy absorbed directly by the small amount of a sulfur compound is presumably small enough to be disregarded, since the absorption of energy is essentially independent of the nature of the component.

$$C_6H_5CH_3 \overset{I}{\sim\!\sim\!\sim\!\rightarrow} C_6H_5CH_3^* \qquad (1)$$

Therefore, excited toluene molecules in the system would usually lose their energy by the

8) G. Dougherty and P. D. Hammond, *J. Am. Chem. Soc.*, **57**, 117 (1935).
9) C. Walling. "Free Radicals in Solution," John Wiley & Sons, Inc., N. Y. (1957), p. 320.
10) J. Russel, *J. Phys. Chem.*, **58**, 437 (1954).

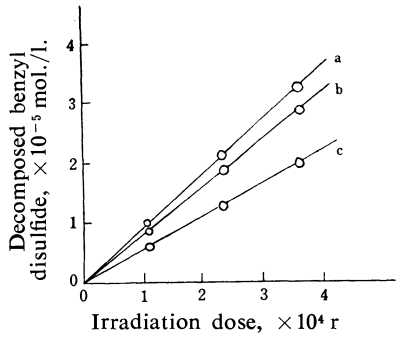


Fig. 2. Decomposition of benzyl disulfide in toluene solution under irradiation.
a 10 mmol./l. b 5 mmol./l. c 2 mmol./l.

following two processes:

Deactivation $C_6H_5CH_3^* \xrightarrow{k_1} C_6H_5CH_3$ (2)

Transfer of energy

$C_6H_5CH_3^* + \text{Sulfur compd.} \xrightarrow{k_2} C_6H_5CH_3 + \text{Sulfur compd.}^*$ (3)

Each sulfur compound, when sufficiently excited, produces at leasts two radicals by the decomposition. A part of the excited sulfur compound may lose its energy by collision without decomposition.

Decomposition

$$\text{Sulfur compd.}^* \xrightarrow{k_3} 2\ \text{Radicals} \quad (4)$$

Deactivation

$$\text{Sulfur compd.}^* \xrightarrow{k_4} \text{Sulfur compd.} \quad (5)$$

Recombination

$$2\ \text{Radicals} \xrightarrow{k_5} \text{Sulfur compd.} \quad (6)$$

Radicals formed according to Eq. 4 will be trapped by DPPH, which is present in a high concentration.

$$\text{Product Radical} + \text{DPPH} \xrightarrow{k_6} \text{Product} \quad (7)$$

Using the steady state equation, the G-value of the decomposition of a sulfur compound is obtained from this expression, which is based on a relatively small value of k_2:

$$G = -\frac{k_3 \cdot k_2 \cdot I \cdot C}{(k_3 + k_4)(k_1 + k_2 \cdot C)}$$

In the above equation I represents the number of molecules excited by 100 eV. of gamma rays, where C is the concentration of the sulfur compound. The above relation may be rewritten in the following convenient form, since k_3 would be much larger than k_4:

$$\frac{1}{G} = \frac{1}{I}\left(1 + \frac{k_1}{k_2 \cdot C}\right)$$

The relations of $1/G$ and $1/C$ for the benzyl sulfur compounds are shown in Fig. 3.

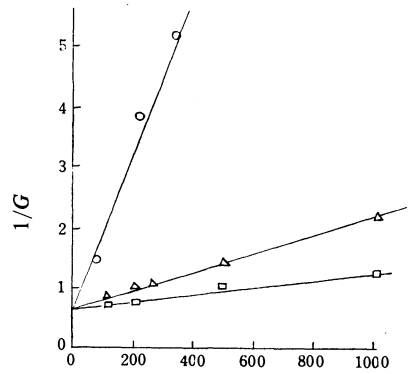


Fig. 3. Relation of $1/G$ and $1/C$ of sulfur compounds.
□ Benzyl mercaptan
△ Benzyl disulfide
○ Benzyl sulfide

The intercept of a straight line in Fig. 3 presumably gives the value of $1/I$, in which I represents the number of excited toluene molecules formed by 100 eV. of gamma rays. From the slope of the lines, one can get the relation of k_1 and k_2, which may represent the efficiency of the energy transfer from excited toluene to the sulfur compounds. Table I shows the relative energy transfer and the G-value at 5 mmol. of the sulfur compounds.

Table I. Radiolysis of sulfur compounds in toluene

Compound	I	k_2/k_1	G-Value at 5 mmol./l.
Benzyl mercaptan	1.4	1160	1.22
Benzyl disulfide	1.4	470	1.0
Benzyl sulfide	1.4	45	0.26
Diphenyl disulfide	1.4	660	1.1
p-Tolyl disulfide	1.4	660	1.1
Diphenyl sulfide	1.4	3.5	0.01
p-Tolyl sulfide	1.4	1.4	0.025

The largest energy transfer from toluene was observed in the decomposition of benzyl mercaptan. The lower value of decomposition for the disulfides shows that the disulfides can absorb energy from the excited toluene less than half as effectively as does the mercaptan.

As compared to the mercaptans or the disulfides, benzyl sulfide is less effective in energy absorption. This means that the C–S bond is relatively insensitive to radiation compared to the –S–H or –S–S– bond. However, the C–S bond in dibenzyl sulfide is relatively

more sensitive to the radiation than that in diphenyl sulfide.

In dibenzyl sulfide, not only the cleavage of C–S bond but also that of the C–H bond of methylene linkage could take place, since the latter cleavage would be facilitated by the stabilization through the following electron-sharing 3d-orbital resonance with a sulfur atom :[11,12]

$$\mathrm{Ph{-}\overset{\cdot}{\underset{\mathrm{H}}{\overset{\cdot\cdot}{\underset{|}{C}}}}{-}\overset{\cdot\cdot}{S}{-}CH_2{-}Ph} \leftrightarrow \mathrm{Ph{-}\overset{\cdot}{\underset{\mathrm{H}}{\underset{|}{C}}}{=}\overset{\cdot}{\underset{\cdot\cdot}{S}}{-}CH_2Ph}$$

Particularly important are the findings that the S–H bond is very effective in energy absorption from the solvent and that the S–S bond is similarly quite effective in energy absorption from the solvent.

An interesting implication from these data is that a similar process may be involved in the radiation protection in the biological system by such mercapto compounds as cystein or cysteamine.[13-15] Here, too, mercaptans are more effective in protecting radiation than disulfides, which in turn are better radiation-protecting compounds than sulfides.

11) C. C. Price and S. Oae, "Sulfur Bonding," Ronald Press, New York, N. Y. (1962), Chapter 2.
12) S. Oae, "3d-Orbital Resonance Involving the Sulfur Atom in Organic Sulfide," in "Organic Sulfur Compounds," Ed. by N. Kharasch, Pergamon Presss, N. Y. (in press).
13) B. Shapiro and L. Eldjarn, *Radiation Research*, **3**, 255, 393 (1955).
14) S. L. Whitcher, M. Rotheran and N. Todd, *Nucleonics*, **11**, No. 8, 30 (1953).
15) A. J. Swallow, *J. Chem. Soc.*, **1952**, 1334.

Summary

The decomposition yields of organosulfur compounds in toluene have been studied using DPPH as a radical scavenger. The effect of the concentration of sulfur compound is quite marked, and the irradiation energy absorbed in the solution of toluene seemed to be transferred to the sulfur compound. The largest energy transfer from toluene has been observed in the decompostion of benzyl mercaptan, while the disulfide has been shown to absorb the energy from the excited toluene less than half as effectively as does the mercaptan. As compared to the mercaptan or the disulfide, benzyl sulfide is far less effective in energy absorption.

Department of Chemistry
Radiation Center of Osaka Prefecture
Sakai, Osaka. (W. A. & K. S.)

Department of Applied Chemistry
Faculty of Engineering
Osaka City University
Kita-ku, Osaka (S. O.)

*The Radiation-induced Reaction of Benzyl Mercaptan and p-Tolyl Mercaptan in Various Organic Solvents**

By Wataru ANDO, Ken'ichi SUGIMOTO and Shigeru OAE

(Received September 9, 1963)

The radiation chemistry of hydrocarbon has been widely investigated. However, the effect of a minute amount of solute in the radiolysis of hydrocarbon has to date received very little attention.[1,2] When a solute is dissolved in a large excess of hydrocarbon, the direct effect of irradiation on the solute is rather unimportant. However, when the solute is involved in the reaction, additional effects occur; the solute is attacked by active species formed from the hydrocarbon, or excited energy is transferred to it from the hydrocarbon. Williams and Hamill[3] have previously shown that the irradiation of cyclohexane containing methyl iodide at the concentration of 1 mol.% results in a considerable dissociation of the methyl iodide. The effect has been ascribed to the dissociative capture of free electrons by methyl iodide. Furthermore, Hughes[4] has pointed out, in the radiolysis of iodine cyanide as a scavenger in liquid benzene, that energy from benzene is transferred, leading to the dissociation of the iodine cyanide, which in turn results in the production of iodine.

* The Study of the Radiation Chemistry of Organic Sulfur Compounds, IV.

1) R. H. Schuler, *J. Phys. Chem.*, **61**, 1472 (1957).

2) M. Burton and S. Lipsky, ibid., **61**, 1461 (1957).

3) R. R. Williams and W. H. Hamill, *Radiation Research*, **1**, 158 (1954).

4) G. Hughes, *J. Phys. Chem.*, **65**, 2160 (1961).

It has been observed in previous investigations[5,6] the radiolysis of hydrocarbon solutions of sulfur compounds that they are all appreciably reactive and that the efficiency of energy absorption from hydrocarbon is usually very high.[7,8] The effect of thiophenol in the radiolysis of benzene has already been investigated.[5]

It is the purpose of the present investigation to extend these studies to other organic solvents. It is well known that six electrons of the aromatic molecule are loosely coupled to form a π-bond and that these π-electrons are non-localized and are thus free to move around in the molecule. Therefore, a π-electron system is expected to possess many excited levels, with lower excited energies. When an electron collides with a hydrocarbon which has a π-electron system, the non-localized electrons are expected to interact with the incident electron rather strongly, either dissociating themselves to form two active species or absorbing the energy. Meanwhile, the yields of free radicals from hydrocarbons have been shown to be related to the sensitivities of the hydrocarbons to radiation.[9]

In this work, the effects of the solvents on the decomposition of benzyl mercaptn and *p*-tolyl mercaptan will be investigated using a wider variety of solvents.

The solvents are divided into radiation-sensitive and -insensitive molecules from the magnitudes of the *G*-values of the radical formations, as is shown below :[10]

RELATIVELY RADIATION-INSENSITIVE MOLECULES

Solvent	*G*-value for radical yield
Carbon disulfide	0.85
Benzene	1.8
Toluene	3.1
Nitrobenzene	4.5

RELATIVELY RADIATION-SENSITIVE MOLECULES

Solvent	*G*-value for radical yield
Hexane	7.6
Cyclohexane	14.3
Acetone	50.0
Methanol	24.0
Dioxane	20.0

This paper will also discuss the reaction mechanism on the basis of a good set of experimental data on the effect of solvents.

5) W. Ando, K. Sugimoto and S. Oae, This Bulletin, **36**, 893 (1963).
6) W. Ando, K. Sugimoto and S. Oae, ibid., **37**, 353 (1964).
7) W. Ando, K. Sugimoto and S. Oae, ibid,, **37**, 357 (1964).
8) V. A. Krongang. and Kh. S. Bagadasaryan, *Doklady. Akad. Nauk. S.S.S.R.*, **132**, 1136 (1960).
9) M. Inokuti, *Isotope and Radiation*, **1**, 82 (1958).
10) A. Prevost-Bernas, *Discussions Faraday Soc.*, **12**, 88 (1958).

Experimental

Experimental details are similar to those outlined in an earlier paper.[5] All the solvents used were purified by ordinary distillations. Benzyl mercaptan and *p*-tolyl mercaptan were purchased from Tokyo Kasei and were distilled in a vacuum under a nitrogen atmosphere before use. A solution of mercaptan was made by weighing, and also the concentration was checked by potentiometric titration with silver nitrate. Each sample was composed of a 20 ml. solution and was degassed in a vacuum line by repeating a cycle of freezing, pumping and melting at least three times. The degassed samples were sealed in irradiation tubes 200 mm. long and 20 mm. in diameter and irradiated.

After irradiation the samples were placed in a beaker, and the amount of mercaptan present was determined by potentiometric titration with silver nitrate. Irradiations were carried out at room temperature with a 5000 curie Co-60 source at a dose rate of 2×10^5 r/hr. The relative values for the decompositions were expressed by the difference between the mercaptan concentrations before and after the irradiation of 100 eV. absorbed into the solution.

Results

The Decomposition of Benzyl Mercaptan in Relatively Radiation-sensitive Solvents.—The radiolysis of benzyl mercaptan in the solvents which are relatively sensitive to the irradiation leads the mercaptan to the disulfide quite readily. The results obtained in cyclohexane, dioxane, methanol, acetone and hexane solutions are shown in Table I. The results indicate that in all the runs high degrees of the decomposition of the mercaptan (over 50~80% at 9.0×10^6 r) were observed.

TABLE I. THE DECOMPOSITION OF BENZYL MERCAPTAN IN THE SOLVENTS

Solvent	% Decomposition of 0.047 mol./l. of solvent at 9.0×10^6 r
Hexane	79
Acetone	64
Methanol	63
Cyclohexane	57
Dioxane	56

Although the initial mercaptan concentration varied from about 10 to 50 mmol./l., the *G*-values apparently depend on the concentration of the mercaptan.

The kinetics of the decomposition of the mercaptan are summarized in Fig. 1.

The decomposition of the mercaptan appears to be of the first order with respect to its concentration at the beginning, but it then rapidly levels off as soon as an equilibrium is

TABLE II. THE EFFECT OF CONCENTRATION ON THE DECOMPOSITION OF BENZYL MERCAPTAN IN SOLVENTS

Solvent	Initial concentration mol./l.	*G*-Value of decomposition of mercaptan at 9.0×10^6 r
Hexane	0.047	6.1
	0.035	4.5
	0.024	3.0
	0.0096	1.0
Acetone	0.047	4.1
	0.035	2.8
	0.024	2.5
	0.0096	0.8
Methanol	0.048	4.2
	0.036	3.3
	0.024	2.5
	0.0096	0.64
Cyclohexane	0.042	3.4
	0.031	3.1
	0.024	2.2
	0.0084	1.0
Dioxane	0.043	3.3
	0.032	2.7
	0.024	2.3
	0.0084	0.75

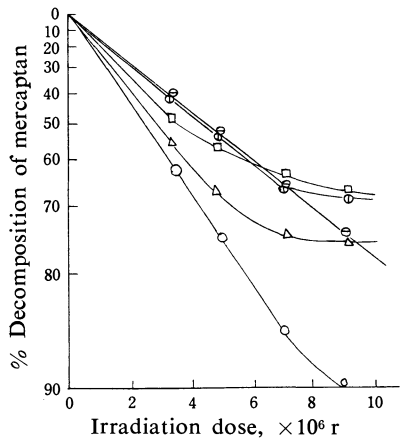


Fig. 1. The decomposition of benzyl mercaptan in various solvents at room temperature.
△ hexane ◑ cyclohexane ○ dioxane
⊖ acetone □ methanol

attained by the reversal hydrogen-abstraction reaction of the mercapto radical from the solvents.

The Decomposition of *p*-Tolyl Mercaptan in Relatively Radiation-sensitive Solvents. — The radiolysis of *p*-tolyl mercaptan in hexane, cyclohexane, dioxane, methanol and acetone follows a course very similar to that of benzyl mercaptan in relatively radiation-sensitive solvents; the conversion of the mercaptan with radiation dose was nearly of the first order with

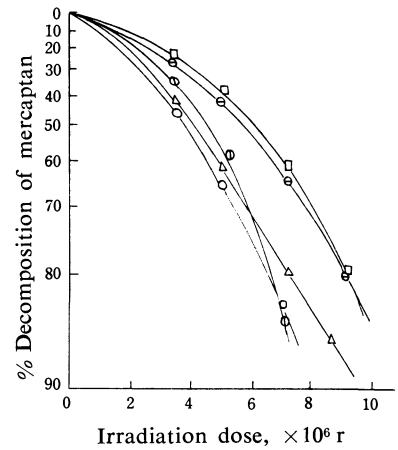


Fig. 2. The decomposition of *p*-tolyl mercaptan in various solvents at room temperature.
△ hexane ○ cyclohexane ◑ dioxane
□ acetone ⊖ methanol

respect to its concentration, but it is gradually accelerated as the decomposition of the mercaptan proceeds further. Table III and Fig. 2 show the results of these experiments.

TABLE III. THE EFFECT OF CONCENTRATION ON THE DECOMPOSITION OF *p*-TOLYL MERCAPTAN IN SOLVENTS

Solvent	*G*-Value of the decomposition of the mercaptan at 9.0×10^6 r Initial concn., mol./l.			
	0.048	0.036	0.024	0.010
Hexane	4.6	4.4	3.5	1.5
Acetone	3.7	3.2	2.5	1.2
Methanol	2.7	2.7	2.6	1.1
Cyclohexane	4.2	3.8	3.3	1.4
Dioxane	2.2	2.1	2.3	0.6

This evidence leads to the following conclusion. The mercapto radical formed in the radiolysis of the mercaptan may usually abstract hydrogen from hydrocarbon, as was discussed in the previous section. However, the mercapto radical formed by the decomposition of *p*-tolyl mercaptan would be substantially resonance-stabilized, and hydrogen abstraction by this mercapto radical is not favored. In this case, probably some radicals formed by the dissociation of solvent molecules leads the decomposition of *p*-tolyl mercaptan.

The Decomposition of Benzyl Mercaptan and *p*-Tolyl Mercaptan in Relatively Radiation-insensitive Solvents.—Carbon disulfide, benzene, toluene and nitrobenzene were investigated as solvents for the decomposition of benzyl mercaptan and *p*-tolyl mercaptan (Tables IV and V). It was found that the amount of the decomposition of the mercaptans in these

solvents was much less than that in radiation-sensitive solvents, and that the *G*-values of the decomposition of the mercaptans were of the same order of magnitude in all four cases.

TABLE IV. THE EFFECT OF THE CONCENTRATION ON THE DECOMPOSITION OF BENZYL MERCAPTAN IN RELATIVELY RADIATION-INSENSITIVE SOLVENTS

Solvent	The *G*-value of decomposed mercaptan at 9.0×10^6 r Initial concn., mol./l.			
	0.048	0.036	0.024	0.0096
Carbon disulfide	0.78	—	0.58	0.35
Benzene	1.9	1.7	1.5	0.8
Toluene	2.1	1.8	1.7	0.8
Nitrobenzene	1.3	1.1	0.9	0.36

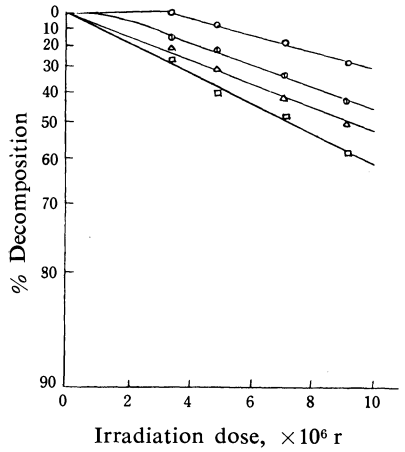


Fig. 3. The decomposition of benzyl mercaptan in aromatic hydrocarbon at room temperature.
○ carbon disulfide △ benzene □ toluene
① nitrobenzene

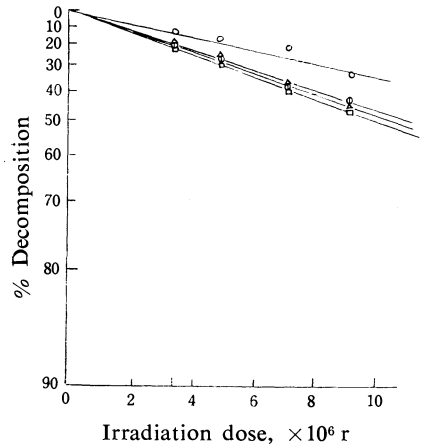


Fig. 4. The decomposition of *p*-tolyl mercaptan in aromatic hydrocarbon at room temperature.
○ carbon disulfide △ benzene ① toluene
□ nitrobenzene

TABLE V. THE EFFECT OF THE CONCENTRATION ON THE DECOMPOSITION OF *p*-TOLYL MERCAPTAN IN RELATIVELY RADIATION-INSENSITIVE SOLVENTS

Solvent	The *G*-value of Decomposition of mercaptan at 9.0×10^6 r Initial concn., mol./l.			
	0.048	0.036	0.024	0.0096
Carbon disulfide	0.96	0.76	0.65	0.33
Benzene	1.7	1.5	1.3	0.5
Toluene	1.9	1.7	1.1	0.5
Nitrobenzene	1.1	1.1	1.0	0.5

Figures 3 and 4 indicate that the decomposition of both benzyl mercaptan and *p*-tolyl mercaptan is of the first order with respect to the mercaptans and that there is no deviation from the first order kinetics, unlike in radiation-sensitive solvents.

The results indicate that either the mercapto radicals formed by the decomposition of the mercaptans do not abstract hydrogen from these solvents, or the induced decomposition of the mercaptans by the solvent radicals is much less than that in radiation-sensitive solvents.

Discussion

A General Examination of the Reaction Mechanism for the Decomposition of Mercaptan. —Our original intention was to estimate the extent of the radiation-induced decomposition of mercaptan. For this purpose it is, however, necessary to identify the liquid decomposition products. Even so, a few suggestions can be made on the basis of our previous observations and of the present findings on the decomposition of the mercaptans.

Haines, Cook and Ball,[11] in studying the photochemical decomposition of sulfur compounds, have indicated that the decomposition of mercaptan involves primarily the cleavage of RS-H linkage, as can be formulated in the following equations:

$$RSH \rightarrow RS + H \quad (1)$$

$$H + RSH \rightarrow RS + H_2 \quad (2)$$

$$2RS \rightarrow RS\text{-}SR \quad (3)$$

This mechanism can be adopted similarly for the interpretation of the observation made in the radiolytic decomposition of benzyl mercaptan. In order to get a clear picture of the decomposition of the mercaptan in the solvents, it is desirable to obtain the *G*-values of the decomposition of the mercaptan alone without solvents.

The results obtained are shown in Table VI.

11) W. E. Haines, G. L. Cook and J. S. Ball, *J. Am. Chem. Soc.*, **78**, 5213 (1956).

TABLE VI. BENZYL MERCAPTAN DECOMPOSITION UNDER GAMMA-RAY IRRADIATION

Irradiation	1.8×10^{7} r
Sample	5.290 g.
$G(H_2)$	0.95
$G(-C_6H_5CH_2SH)$	1.9, assuming $G(-SH)=2G(H_2)$

Now that the G-value of the mercaptan decomposition can be compared with those in solvents, one can draw the following conclusions concerning the general nature of the decomposition processes of mercaptan. (1) The reaction presumably proceeds through the process of transferring energy from the solvents to mercaptan. (2) The intermediate radicals from solvents are hydrogen acceptors of mercaptan.

It may be seen from the data in radiation-insensitive solvents that the concentration of mercaptan appears to effect the decomposition of mercaptan, and that the G-value of mercaptan decomposition is nearly identical with that of mercaptan alone. One can, therefore, assume that the radiation energy from the gamma rays effects the mercaptan decomposition either by a direct or an indirect process.

First the energy of irradiation is absorbed by then solvent; then it forms some radicals so formed attack the S–H bond of the mercaptan as illustrated below:

$$S \rightsquigarrow S^* \quad (4)$$

$$S^* \rightarrow S\cdot \quad (5)$$

$$S\cdot + RSH \rightarrow SH + RS\cdot \quad (6)$$

where S is the solvent.

The mercapto radicals formed will then lead to reaction 3. However, the kinetic data which follow the first order with respect to the mercaptan are not in accord with this process. The other possibility is that the radiation energy initially absorbed by the solvent is transferred very rapidly to the mercaptan. Such a direct transfer of radiation-excited energy is well known in liquid solutions.[12] It is possible that this process of energy transfer is responsible for the decomposition of mercaptan. In addition to the excitation process of the solvent in reaction 4, the energy transfer to the mercaptan can be represented by:

$$S^* + RSH \rightarrow S + RSH^* \quad (7)$$

Excited mercaptan would then be led to dissociation into two radicals according to reaction 1. The decomposition of the mercaptan can thus be correlated with the experimental observations, especially in the case of the decomposition in radiation-insensitive solvents.

However, since mercaptan is quite sensitive to radical attack, one cannot be absolutely certain that this process alone is responsible for the decomposition of mercaptan. The results obtained in this work to indicate, however, that energy can be absorbed readily into the solvent and that the process of energy transfer to the solute (reaction 7) is in competition with the process of forming their own radicals from the excited solvent molecules (reaction 5).

Evidence of Solvent-Mercaptan Interaction.—As can be seen in Figs. 1 and 2, the two different mercaptans follow different courses in the decompositions in relatively radiation-sensitive solvents. The decomposition of benzyl mercaptan initially increases linearly with the increase in the radiation dose, then it rapidly levels off from the linear relationship. This could be interpreted as being caused by the equilibration, arising from the hydrogen abstraction by the mercapto radicals in order to reverse the reaction, since the solvents are generally thought to function as hydrogen donors.[13]

$$RS\cdot + RH \rightleftarrows RSH + R\cdot \quad (8)$$

However, the results for the decomposition of the mercaptan in radiation-insensitive solvents indicate that it is difficult for the above process to occur, as can be seen in Figs. 3 and 4, since the bond energy of the C–H linkage of the radiation-insensitive solvents is much higher than that of the sensitive solvents; hence, the radiation-insensitive solvents can not be good hydrogen donors. Meanwhile, the decomposition of *p*-tolyl mercaptan in radiation-sensitive solvents initially shows a linear relationship with the dose; it is rapidly accelerated as the decomposition proceeds, thus suggesting that the reaction is promoted by some process as the decomposition of the mercaptan proceeds further.

This is not surprising, since the mercapto radical from *p*-tolyl mercaptan is substantially resonance-stabilized; thus the radicals, formed by the radiolysis of solvents, may easily abstract hydrogen from *p*-tolyl mercaptan, accelerating the decomposition of the mercaptan as the reaction proceeds.

The Solvent Effect on the Decomposition of Mercaptan.—The results of the decomposition of mercaptan in various solvents may be summarized thus. (1) The radiation-sensitive solvents are easily attacked by the benzyl mercapto

12) J. P. Manion and M. Burton, *J. Phys. Chem.*, **56**, 560 (1952).

13) C. Walling and R. Rabinowitch, *J. Am. Chem. Soc.*, **81**, 1137 (1959).

radical and function as hydrogen donors. (2) When the resulting mercapto radicals are fairly stabilized by resonance such as that of the tolyl mercapto radical obtained from tolyl mercaptan, solvent radicals from the radiolysis of solvents will abstract hydrogen from mercaptan. This will cause the additional decomposition of mercaptan which is seen in *p*-tolyl mercaptan in solvents. (3) The decomposition of the mercaptan in radiation-insensitive solvents show relatively lower *G*-values than those in radiation-sensitive solvents. When a radiation-insensitive solvent has an aromatic π-electron system, the radiation energy absorbed will be dissipated quite readily through the electronic excitation to lower levels of the solvent molecules; therefore, the proportion of energy transferred to the solute became very small, thus reducing the decomposition of the mercaptan.

Summary

The decomposition of benzyl mercaptan and *p*-tolyl mercaptan in various organic solvents has been studied, and the following conclusions have been obtained. 1) A radiation-sensitive solvent such as hexane is readily attacked by the benzyl mercapto radical. 2) When the resulting mercapto radicals are stabilized substantially by resonance, solvent radicals from the radiolysis of solvents will abstract hydrogen from the mercaptan. 3) The *G*-values of mercaptan decomposition in such solvents as hexane, cyclohexane, acetone, methanol and dioxane are relatively higher than those in carbon disulfide, benzene, toluene and nitrobenzene. The reaction presumably proceeds through the energy transfer process from solvent to mercaptan. When an aromatic π-electron system is present in any solvent, the radiation energy absorbed will be dissipated quite readily through electronic excitation to lower-energy levels of the solvent molecule.

Department of Chemistry
Radiation Center of Osaka Prefecture
Sakai, Osaka, (W. A. & K. S.)

Department of Applied Chemistry
Faculty of Engineering
Osaka City University
Kita-ku, Osaka (S. O.)

*The Radiation-induced Addition of Hydrogen Sulfide to Propylene**

By Ken'ichi SUGIMOTO, Wataru ANDO and Shigeru OAE

(Received September 20, 1963)

The free-radical addition of thiols to olefinic compounds has been studied extensively during the past twenty-five years,[1] but the addition of hydrogen sulfide to olefinic compounds has received rather scanty attention. The photochemical addition of hydrogen sulfide to olefinic bonds has, however, at least been shown to give mixtures of the corresponding mercaptans and the sulfides.[2] This paper will present the results of a study of the gamma-ray initiated free radical addition of hydrogen sulfide to propylene.

The radiation-induced addition of hydrogen sulfide to propylene took place very readily, giving mainly *n*-propylmercaptan and di-*n*-propylsulfide, and was completed at room temperature with a relatively small radiation dose. The *G*-values of this reaction were found to be more than ten thousand. The addition followed a non-Markownikoff rule, as in the case of the change of mercaptan to olefins.[3] Apparently the reaction proceeds through a free radical chain process, where the sulfhydryl radicals formed in the initial step of the radiolysis of hydrogen sulfide undergo a radical addition to the olefin in the following chain-propagating step.

During the preparation of this paper, a report[4] on the X-ray initiated addition of hydrogen sulfide to fluoroethylenes appeared. Although the *G*-values for these reactions were somewhat smaller than those of the present work, the nature of the addition appears to be similar.

* Presented at the 16th Annual Meeting of the Chemical Society of Japan, Tokyo, March, 1963.

1) C. Walling, "Free Radicals in Solution," John Wiley and Sons, New York, N. Y. (1957), p. 313.

2) W. E. Vaughan and F. F. Rust, *J. Org. Chem.*, 7, 472 (1942).

3) Posner, *Ber.*, 38, 646 (1905).

4) J. F. Harris, Jr. and F. W. Stacey, *J. Am. Chem. Soc.*, 85, 749 (1963).

TABLE I. THE RESULTS OF THE RADIATION-INDUCED ADDITION OF HYDROGEN SULFIDE TO PROPYLENE

Dose rate r/hr.	Product	Net G-value	Amount of product, mmol. Irradiation time 24 hr.	Irradiation time 48 hr.		
					Apparent yield	Net yield
2.8×10^4	C_3H_7SH	2.5×10^4	1.30	1.48	20%	83%
	$(C_3H_7)_2S$	1.1×10^4	1.93	2.34	63%	63%
1.1×10^4	C_3H_7SH	3.6×10^4	1.50	1.40	19%	71%
	$(C_3H_7)_2S$	1.7×10^4	1.31	1.96	52%	52%
5.7×10^3	C_3H_7SH	5.6×10^4	1.08	1.43	19%	62%
	$(C_3H_7)_2S$	2.6×10^4	1.12	1.59	43%	43%

Sample C_3H_6 1160 mmHg 7.48 mmol.
H_2S 660 mmHg 4.27 mmol.

TABLE II. THE AMOUNTS OF PRODUCTS AND THE YIELD FOR INITIAL AMOUNT OF PROPYLENE

Component	Product	24 hr.	48 hr.	96 hr.
7.48 mmol. C_3H_6	C_3H_7SH	2.12 mmol. (28%)	2.04 mmol. (27%)	
6.41 mmol. H_2S	$(C_3H_7)_2S$	1.49 mmol. (40%)	2.41 mmol. (64%)	
7.48 mmol. C_3H_6	C_3H_7SH	1.50 mmol. (20%)	1.40 mmol. (19%)	0.88 mmol. (12%)
4.27 mmol. H_2S	$(C_3H_7)_2S$	1.31 mmol. (35%)	1.96 mmol. (52%)	2.67 mmol. (71%)
7.48 mmol. C_3H_6	C_3H_7SH	0.73 mmol. (10%)	0.86 mmol. (11%)	
2.59 mmol. H_2S	$(C_3H_7)_2S$	0.72 mmol. (19%)	1.08 mmol. (29%)	

Irradiation dose rate 1.1×10^4 r/hr.

Experimental

Irradiations.—The gamma radiation was provided by a 1000 curie cobalt-60 source.[5] The dose rates were obtained by means of a Fricke ferrous sulfate dosimeter, taking G as 15.6.[6] Samples were irradiated at three fixed positions, at which the dose rates were 2.8×10^4, 1.1×10^4, and 5.7×10^3 r/hr. respectively. The G-values were calculated from the relation of the products formed and the absorption energy of the gaseous sample. The absorption energies of propylene and hydrogen sulfide were based on the absorption energy of air, 88 erg./g./r. All the irradiations were carried out at room temperature.

Reaction Vessel.—The irradiation vessel used for this gaseous reaction was a Pyrex tube 25 mm. in outside diameter and 25 cm. long, and equipped with a breakoff seal.

Materials.—Propylene was purchased from the Takachiho Chemicals Co., Tokyo, and hydrogen sulfide, from the Seitetsu Chemicals Co., Kakogawa; both were purified by vacuum distillation. The impurities in both the propylene and the hydrogen sulfide used were found to be less than 0.5% by gas-chromatographic analysis.

Analyses.—Conventional high-vacuum techniques were employed throughout the investigation. All the analyses of the irradiated samples were carried out by a combination of fractional distillation and gas-chromatographic separation. The irradiated sample was passed first through a series of dry-ice acetone-cooled traps and then through liquid nitrogen-cooled traps.

The fraction condensed in dry-ice acetone cooled traps was analyzed by gas-chromatography (Hitachi Type KGL-2A) using a 2 m. column packed with celite 545, impregnated with 30% silicon DC 550 and operated at 80°C with an H_2 carrier at 40 ml./min.; it was found to be a mixture of *n*-propylmercaptan and di-*n*-propylsulfide. The amount of *n*-propylmercaptan was also determined by potentiometric titration with silver nitrate in isopropyl alcohol;[7] the end point was found to be between approximately −200 and −50 mV. vs. SCE. On the other hand, the amount of di-*n*-propylsulfide was calculated by subtracting that of the *n*-propylmercaptan formed from the amounts of hydrogen sulfide and propylene reacted. The gas which condensed at the liquid-nitrogen temperature through a series of dry-ice acetone traps was identified as unreacted hydrogen sulfide and propylene. This portion was measured by a manometer.

5) T. Azuma et al., *Ann. Rept. Rad. Center, Osaka Pref.*, 2, 56 (1961).
6) C. J. Hochanadel and J. A. Ghormley, *J. Chem. Phys.*, 21, 880 (1953).
7) M. W. Tamele and L. B. Ryland, *Ind. Eng. Chem., Anal. Ed.*, 8, 16 (1936).

Results and Discussion

Various amounts of hydrogen sulfide were mixed with propylene, and these mixtures were irradiated at several radiation doses in a static system. The results of the radiation-induced addition of hydrogen sulfide to propylene are shown in Tables I and II.

In Table I, the apparent yield of products means the amount of the final products formed against the initial amount of propylene, while the net yield is the total amount of *n*-propylmercaptan formed during the reaction, that is, the actual amount of the mercaptan plus the sulfide formed, because the *n*-propylmercaptan is gradually converted to the di-*n*-propylsulfide by the further reaction of *n*-propylmercaptan with propylene.

The Effects of the Dose Rate on the *G*-Value.—The effects of dose rate *I* on the yield are shown in Figs. 1 and 2. The *G*-values were estimated from the initial inclination of the curves in Fig. 1, while the logarithms of the *G*-values are plotted against the logarithms of *I* in Fig. 2. From these plots, it is clearly shown that *n*-propylmercaptan and di-*n*-propylsulfide are produced in proportion to the -0.52 and -0.54 powers of *I*. These values are slightly smaller than -0.50 which would be derived under the assumption of a bimolecular termination of all the propagating radicals. This finding also seems to indicate a radical chain mechanism[8] for this radiation-induced reaction.

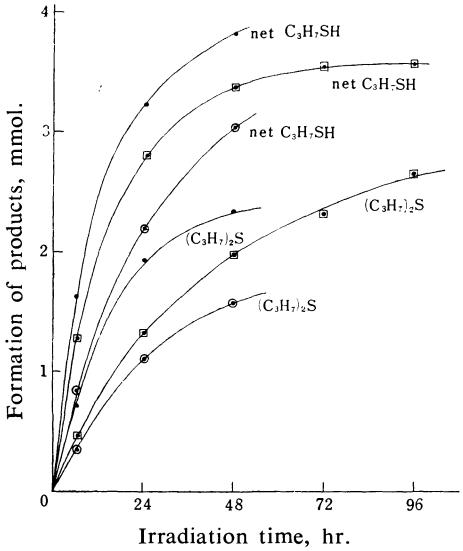


Fig. 1. The formations of *n*-propylmercaptan and di-*n*-propylsulfide.
• 2.8×10^4 r/hr. ◙ 1.1×10^4 r/hr.
⊙ 5.7×10^3 r/hr.
Sample C_3H_6 7.48 mmol.
H_2S 4.27 mmol.

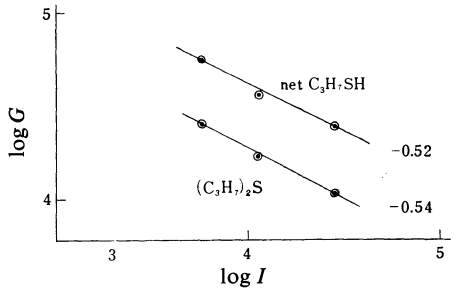


Fig. 2. The relation of log *G* and log *I*.

The Effect of the Molar Ratio of the Hydrogen Sulfide in the Sample.—It is shown in Fig. 3 that the yield increases with the increasing molar ratio of hydrogen sulfide, while the inclination of the curve gradually decreases. It would be interesting to see whether or not the yield will keep increasing at a higher molar per cent of hydrogen sulfide. Further work in this connection is in progress in our laboratory.

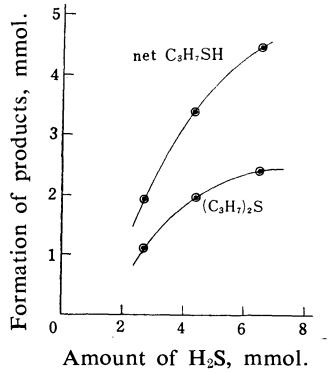


Fig. 3. Effect of molar ratio of hydrogen sulfide in the sample.
Dose rate 1.1×10^4 r/hr.
Irradiation time 48 hr.
C_3H_6 7.48 mmol.

When one makes *n*-propylmercaptan, it is desirable to employ a large molar ratio of hydrogen sulfide initially, or to separate the mercaptan at an early period of the radiation-induced reaction, as shown in Table II. When the reaction is completed, the product is found to be mainly di-*n*-propylsulfide; also, the radiolysis of propylene with a smaller amount of hydrogen sulfide preferentially leads to the formation of di-*n*-propylsulfide rather than to that of *n*-propylmercaptan. Therefore, this reaction can be used for the preparation of

8) S. Iizuka, M. Hatada and K. Hirota, This Bulletin, 36, 817 (1963).

n-propylmercaptan or of di-*n*-propylsulfide if one properly adjusts the reaction conditions.

The Reaction Mechanism. — Both *n*-propylmercaptan and di-*n*-propylsulfide were found to be produced in the irradiation of the sample. *n*-Propylmercaptan is undoubtedly the free-radical addition product of hydrogen sulfide to propylene, while di-*n*-propylsulfide is the secondary addition product of *n*-propylmercaptan to propylene.

$$CH_2{=}CH{-}CH_3 + H_2S \rightarrow HSCH_2{-}CH_2{-}CH_3 \quad (1)$$

$$CH_2{=}CH{-}CH_3 + HSCH_2{-}CH_2{-}CH_3 \rightarrow (CH_3{-}CH_2{-}CH_2)_2S \quad (2)$$

Both yields increased with an increase in the irradiation time, as is shown in Fig. 1. Besides, a small amount of hydrogen was found, probably produced by the following termination reaction.

$$H\cdot + H_2S \rightarrow H_2 + HS\cdot \quad (3)$$

The hydrogen atom in Eq. 3 might be produced by the radiolysis of hydrogen sulfide:[9]

$$H_2S \rightsquigarrow H\cdot + HS\cdot \quad (4)$$

A small amount of air was found to reduce the production of *n*-propylmercaptan and di-*n*-propylsulfide. Air apparently acts as a free radical scavenger to retard this chain reaction.

As has been discussed above, the reaction in all the cases is undoubtedly a free-radical chain reaction. The *G*-values calculated for the gamma ray-initiated experiments indicate that, in most cases, the kinetic chain is quite long.

Hydrogen sulfide is known to decompose the H atom and the HS radical.[9] These radicals can initiate a chain reaction in the following manner. As well as the reaction started by the radiolytically-generated HS radical in process 4, the HS radicals generated in the processes 6 and 3 would also lead to the chain propagation,

$$H_2S \rightsquigarrow HS\cdot + H\cdot \quad (4)$$

$$H\cdot + H_2C{=}CH{-}CH_3 \rightarrow H_3C{-}\dot{C}H{-}CH_3 \quad (5)$$

$$H_3C{-}\dot{C}H_3 + H_2S \rightarrow H_3C{-}CH_3{-}CH_3 + HS\cdot \quad (6)$$

$$H\cdot + H_2S \rightarrow H_2 + HS\cdot \quad (3)$$

$$HS\cdot + H_2C{=}CH{-}CH_3 \rightarrow HSCH_2{-}\dot{C}H{-}CH_3 \quad (7)$$

$$HSCH_2{-}\dot{C}H{-}CH_3 + H_2S \rightarrow HSCH_2{-}CH_2{-}CH_3 + HS\cdot \quad (8)$$

The reaction proceeds according to the chain mechanism shown by Eqs. 7 and 8, regenerating the sulfhydryl radical during these chain-propagating steps. Such a free radical chain mechanism is in good accord with the inhibiting effect of air. The great length of the chains precludes the ready detection of the saturated hydrocarbon or hydrogen formed in 6 and 3. Steps 7 and 8 are the chain-carrying steps, their length depending upon the processes of radical termination, which may occur either at walls or by recombination in the system.

n-Propylmercaptan, once formed, undergoes further reaction with propylene to give di-*n*-propylsulfide. The free radical addition of thiols to olefins, which has been studied extensively,[10] is considered to involve the following chain-propagating steps:

$$C_3H_7SH \rightsquigarrow H\cdot + C_3H_7S\cdot \quad (9)$$

$$C_3H_7S\cdot + CH_2{=}CH{-}CH_3 \rightarrow C_3H_7SCH_2{-}\dot{C}H{-}CH_3 \quad (10)$$

$$C_3H_7SCH_2{-}\dot{C}H{-}CH_3 + C_3H_7SH \rightarrow C_3H_7SCH_2{-}CH_2{-}CH_3 + C_3H_7S\cdot \quad (11)$$

Summary

The radiation-induced free radical addition of hydrogen sulfide to propylene to give *n*-propylmercaptan and di-*n*-propylsulfide has been studied. The direction of the addition to propylene is consistent with that of the radical addition to such olefins previously studied, suggesting that the SH is both the adding and chain-carrying species. The addition of the thiol to propylene has been found to undergo a free radical chain reaction, readily yielding di-*n*-propylsulfide in the succeeding step.

Department of Chemistry
Radiation Center of Osaka Prefecture
Sakai, Osaka (K. S. & W. A.)

Department of Applied Chemistry
Faculty of Engineering
Osaka City University
Kita-ku, Osaka (S. O.)

9) E. C. Truesdale and S. C. Lind, *J. Am. Chem. Soc.*, **54**, 516 (1932).

10) A. Fontijn and J. W. T. Spinks, *Can. J. Chem.*, **35**, 1384, 1397, 1410 (1957); K. Araki, T. Hoshino, S. Shida and K. Yamagishi, *Proceedings of the Second Symposium on Atomic Energy of Japan*, **4**, 158 (1958).

The Polymerization and Polymers of Itaconic Acid Derivatives. VI.[1] *The Polymerization and Copolymerization of Itaconic Anhydride*[2]

By Susumu NAGAI

(Received September 11, 1963)

Previous work reported in this series of papers has shown that[3] the rate constants of the polymerization of dialkyl itaconates decrease in the order of di-2-ethylhexyl> di-*n*-butyl>di-*n*-propyl≃diethyl>dimethyl, and that[4] the monomer reactivity ratios in the copolymerization with vinyl chloride are as follows: $r_1=0.053\sim0.06$ (M_1: vinyl chloride) and $r_2=5.1\sim7.0$ (M_2: dialkyl itaconates).

The purpose of the present investigation is to clarify the polymerization and copolymerization characteristics of itaconic anhydride compared with those of itaconic esters.

While many reactions of itaconic anhydride are described in the literature, its polymerization has not yet been reported* except for a few patents[5] including copolymers with styrene.

Experimental

Materials.—Itaconic anhydride (produced by the Tokyo Kasei Co.) was recrystallized from ethyl ether. M. P. 67~68°C. Dimethyl itaconate and di-2-ethylhexyl itaconate were prepared by the method described before.[4] Vinyl chloride, supplied by the Kanegafuchi Kagaku Co., was used as a comonomer. Butyl acetate and tetrahydrofuran were distilled and used as solvents in the copolymerization.

Copolymerization.—The copolymerization of itaconic anhydride with vinyl chloride was carried out, first in butyl acetate and then in tetrahydrofuran, in both cases in a sealed glass tube at 50°C. In both cases, copolymers were found to precipitate after copolymerization. The precipitates were filtered and washed with ethyl ether before being dried. The compositions of the copolymers were determined by the analysis of their chlorine contents.

The Rate of Polymerization.—The rates of the bulk polymerization of itaconic anhydride, dimethyl itaconate and di-2-ethylhexyl itaconate were measured in a dilatometer at 75°C. It is difficult to feed a monomer as crystal or powder through the capillary tubing into the bulb of the commonly-used dilatometer. In the present study a special dilatometer, shown in Fig. 1, was used. In this

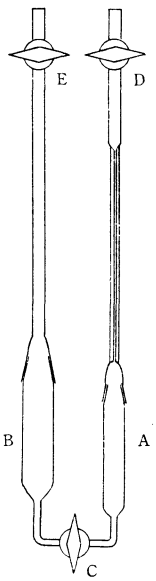


Fig. 1. The dilatometer used in the present study.

apparatus the capillary tubing and the bulb were connected by ground glass joints in order to facilitate the feeding of the monomer. The height of the meniscus of the melted monomer could be controlled by means of a movable bottom of mercury, which will be described below. There are two chambers, A and B, separated by a glass stopper, C. First, with C opened, several milliliters of clean mercury was charged into the bottoms of both A and B. Then C was closed. Monomer was charged into A on the mercury, and then the initiator was charged. Assembled with the tubings, the dilatometer was attached to the vacuum line. The content of the dilatometer was degassed and flushed with nitrogen alternatively. Then the dilatometer was immersed in a thermostat set at 75°C. As soon as the monomer melted, the dilatometer was picked up quickly and inclined, with the stopper C, and D and E opened, so that the mercury in B moved over to A, sending the liquid monomer

1) Part V of this series; S. Nagai, This Bulletin, **36**, 1459 (1963).
2) Presented at the Local Meeting of the Chemical Society of Japan, Fukuoka, October, 1961,
3) S. Nagai and K. Yoshida, *Chem. High Polymers, Japan*, **17**, 79 (1960).
4) S. Nagai and K. Yoshida, ibid., **17**, 77 (1960).
* After this paper was presented,[2] two other reports[6,7] appeared.
5) U. S. Pat. 2625471 (1952); 2625529 (1953); etc.
6) J. Drougas and R. L. Guile, *J. Polymer Sci.*, **55**, 297 (1961).
7) S. Ishida and S. Saito, *J. Japan Soc. of Color Material*, **35**, 377 (1962).

TABLE I. THE COPOLYMERIZATION OF ITACONIC ANHYDRIDE AND VINYL CHLORIDE

Monomers in feed g.				Solvent cc.		Time hr.	Conversion wt. %	Mol. % of ItAnh	
VC	ItAnh	AIBN	BPO	BuAc	THF			in Monomers	in Copolymer
7.207	0.112	0.0828		15		3	1.5	0.86	26.9
7.120	0.111		0.1395		5	6	21	0.86	—
7.204	0.224	0.0835		15		5	1.4	1.7	47.7
6.918	0.560	0.0863		15		5	0.3	4.32	—
7.306	0.560	0.0860		15		8.25	1.9	4.10	58.3
6.258	0.562	0.0855		15		9.5	2.2	4.77	53.8
6.941	0.561		0.1395		5	6	4.8	4.31	54.6
6.055	1.125	0.0911		15		17.5	2.6	9.39	61.5
5.803	1.125		0.1294		5	12	8.5	9.75	66.2
7.541	2.245	0.0993		25		17.5	1.9	14.24	62.7
7.142	2.243		0.1694		5	6	7.2	14.8	73.3

TABLE II. RATE OF POLYMERIZATION OF ITACONIC ANHYDRIDE IN COMPARISON WITH THOSE OF ITACONIC ESTERS*

Monomer	ItAnh		DMI	DEHI
Wt. of monomer, g.	3.1798	3.1129	4.1224	3.6837
Wt. of initiator, g.	0.0173	0.0325	0.0349	0.0113
Polymerization time, min.	92	73	61	65
Yield of polymer, g.	0.9146	1.3318	0.5677	0.8557
Conversion, %	28.6	42.4	13.3	23.2
Initial volume of the system, cc.	2.55	2.51	3.95	4.10
Mol. of monomer, $\times 10^2$	2.84	2.78	2.67	1.04
[M], mol./l.	11.1	11.1	6.76	2.53
Mol. of initiator, $\times 10^4$	0.72	1.34	1.44	0.47
[I]/[M], mol. ratio	1/397	1/208	1/185	1/223
[I], mol./l. $\times 10^2$	2.80	5.34	3.65	1.14
R_p,** mol./l./min. $\times 10^2$	4.63	6.53	1.63	0.90
k_o,** $l^{1/2}/mol^{1/2}/min.$ $\times 10^2$	2.49	2.54	1.26	3.34
$[\eta]_{acetone}$, 100 cc./g.	0.132	0.195	0.128	—

* Polymerization temperature was 75.1°C and the initiator used was benzoyl peroxide.

** R_p was calculated from the initial slope of the curve shown in each Fig. and the rate constant k_o was calculated assuming $R_p = k_o[M][I]^{1/2}$.

on the mercury up until the meniscus rose to a sufficient level of the capillary. Then, with all the stoppers closed, the dilatometer was again immersed into the bath. It took less than 7 min. from the first immersion to the final setting. The polymerization time was counted from this final setting, and the rate of the shrinkage of the monomer was measured with a cathetometer. After it had been polymerized for 1~2 hr., the dilatometer was taken off the bath and cooled. Polyitaconic anhydride was precipitated by pouring an acetone solution of the reaction mixture into a large excess of ethyl ether; it was then washed with fresh ether and dried in a vacuum oven at 40~50°C. for several hours. For polydimethyl itaconate and polydi-2-ethylhexyl itaconate, benzene was used as the solvent and methanol was used as the precipitant.

Viscosity Measurement.—The viscosity of the polymer solution was measured by a Ubbelohde-type viscometer at 30°C, using acetone as the solvent.

Hydrolysis.—Polyitaconic anhydride (54.1 mg.) was dissolved in 50 ml. of water at room temperature. After it had been stirred for 5 min., the pH of the solution showed 3.1; it changed no more, even after 24 hr.

Results and Discussion

Copolymerization.—The results of the copolymerization of itaconic anhydride and vinyl chloride are presented in Table I and Figs. 2 and 3.

From these results it can be seen that, when copolymerized with vinyl chloride, the anhydride always produced copolymers with considerably higher ratios of anhydride than in the feed. This tendency is quite analogous to the case of itaconic esters and vinyl chloride, as Fig. 2 shows.

The monomer reactivity ratios are approximately 5~10 for r_2 (M_2: ItAnh) and 0.01 for r_1. However, it is rather difficult to determine their definite values for each solvent system,

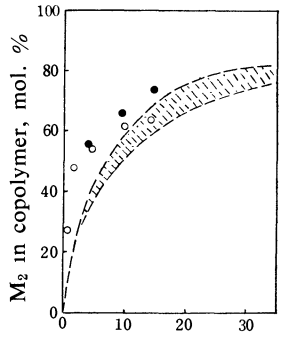


Fig. 2. Relationship between monomer compositions and copolymer compositions in the copolymerization of vinyl chloride (M_1) and itaconic derivatives (M_2).
○ M_2: ItAnh (in BuAc), ● M_2: ItAnh (in THF), dotted line zone: M_2: DMI, DEI, DiPI and DEHI (bulk)

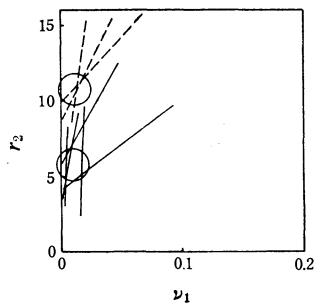


Fig. 3. Diagram of calculation for r_1 and r_2.
---- VC-ItAnh (in THF)
—— VC-ItAnh (in BuAc)

since a large difference exists between r_1 and r_2 values; on the other hand, in the case of itaconic anhydride and styrene Drougas and Guile[6] determined somewhat different values for r_1 and r_2 depending on the different solvent systems.

The Rate of Polymerization.—The copolymerization data obtained above suggest that itaconic anhydride homopolymerizes quite readily. For the preliminary test the bulk polymerization in a sealed glass tube was carried out at 75°C, using 5 wt. % benzoyl peroxide as the initiator. After the polymerization had continued for 140 min., the conversion of the monomer to the polymer was about 76%.

Detailed results of the dilatometry are shown in Figs. 4 and 5 and in Table II.

It is of interest to note that the rate constant of the polymerization (k_o) of itaconic anhydride is larger than that of dimethyl itaconate but smaller than that of di-2-ethylhexyl itaconate. As for the viscosity data, although the intrinsic viscosity of the polyitaconic anhydride

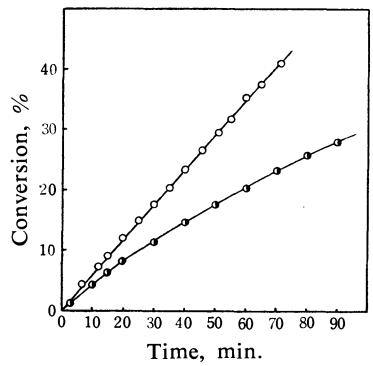


Fig. 4. Relationship between time and conversion in the bulk polymerization of ItAnh, at 75°C, by dilatometry.
—○— [I] $=5.34\times10^{-2}$ mol./l.
—◑— [I] $=2.80\times10^{-2}$ mol./l.

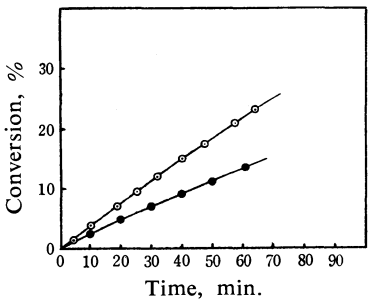


Fig. 5. Relationship between time and conversion in the bulk polymerization of itaconic esters, at 75°C, by dilatometry.
—⊙— DEHI, [M] $=2.53$ mol./l.
[I] $=1.14\times10^{-2}$ mol./l.
—●— DMI, [M] $=6.76$ mol./l.
[I] $=3.65\times10^{-2}$ mol./l.

obtained was somewhat larger than that of polydimethyl itaconate, these small values of both polymers, at any rate, represent very low $\bar{P}$ values.

The above facts might be partly explained qualitatively by considering the propagation reactivity as well as the chain transfer reactivity of the anhydride in comparison with those of dialkyl itaconates.[3] It is thought that the double bond of itaconic anhydride is in the most free state from the steric effect, if any, of the adjacent carboxylate groups among the double bonds of itaconic derivatives. This advantage might serve somewhat to increase k_o. On the contrary, it is also considered that the anhydride has the most exposed active methylene among the itaconic derivatives. This might increase the anhydride's susceptibility to the chain transfer reaction and, hence, decrease k_o to some degree. Perhaps the observed rate of polymerization can be determined from a balance of these factors. Of course,

however, it is not possible at present to come to any definite conclusion.

Infrared Spectra.—Infrared absorption spectra of the monomer and polymer are presented in Fig. 6. The bands near 1665 cm^{-1} (CH_2=C< stretching), 1408 cm^{-1} (CH_2=C< in plane deformation) and 925 cm^{-1} (CH_2=C< out plane deformation) in the monomer disappeared in the polymer, while the bands near 1850 and 1760 cm^{-1} (C=O stretching) and 1220 cm^{-1} (C–O–C stretching) in the monomer remained, slightly shifting to 1860, 1775 and 1225 cm^{-1} respectively after polymerization.

Solubility Test.—Ten milligrams of itaconic anhydride did not dissolve in 4 cc. portions of petroleum ether, ligroin, *n*-hexane, cyclohexane, benzene, toluene or carbon tetrachloride at

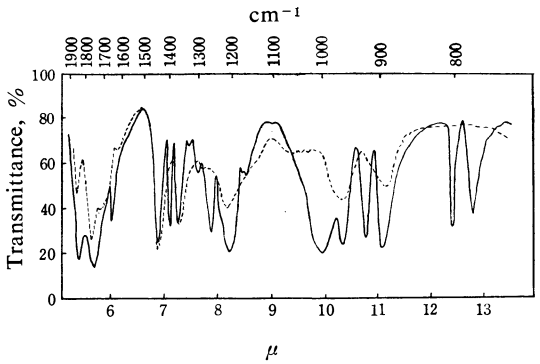


Fig. 6. Infrared spectra of monomer (——) and polymer (----). (Nujol).

room temperature. The monomer dissolved in ethyl ether and chloroform, but the polymer did not dissolve. The solvents for both the monomer and the polymer so far tested are acetone, cyclohexanone, ethyl methyl ketone, dioxane, glacial acetic acid, tetrahydrofuran and ethyl ether. Water, alcohols, dimethyl sulfoxide, dimethyl formamide, and pyridine may be classified as reactive solvents. The anhydride dissolved rapidly in methyl alcohol, but it did so slowly in ethyl and propyl alcohols. It is considered that the corresponding monoesters were partly formed. When the anhydride was dissolved in dimethyl sulfoxide, dimethyl formamide and pyridine respectively, a yellow or brownish yellow color appeared, and this became deeper with time. Perhaps some complex was formed, but this has not yet been confirmed. In the case of the polymer solution, the color was slight and did not become deeper with heating.

The Hydrolysis of the Polymer.—The hydrolysis of polyitaconic anhydride was carried out with ease, yielding polyitaconic acid or its copolymer structure with the unreacted anhydride, if any. The viscosity measurement of

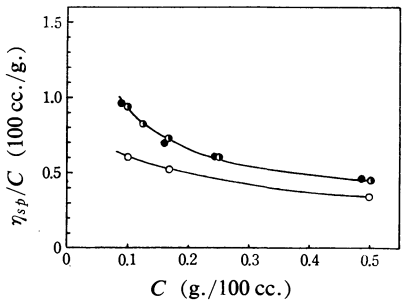


Fig. 7. Viscosity of aqueous solution of polyitaconic anhydride polymerized in bulk with [I]=2.80×10^{-2} mol./l. (◑) and [I]=5.34×10^{-2} mol./l. (○) at 75°C compared with that of polyitaconic acid obtained previously by polymerization of itaconic acid with [M]=1.5, [I]=1.0×10^{-2} mol./l. at 50°C (●).

the aqueous solution of polyitaconic anhydride showed a concentration-viscosity curve similar to that of polyitaconic acid, as Fig. 7 shows.

It is of much interest that polyitaconic acid is easily obtained (in the form of an aqueous solution) in the course of the polymerization of itaconic anhydride, followed by a simple isolation process and further hydrolysis,* while the direct polymerization of itaconic acid itself has been stated to occur only rarely in bulk, in acetone and methyl alcohol, but chiefly in water.**

Summary

The copolymerization of itaconic anhydride and vinyl chloride has yielded copolymers with itaconic anhydride much richer than that in the feed. The rate of the homopolymerization of itaconic anhydride has been compared with the rates of itaconic esters, obtaining the following order: di-2-ethylhexyl ester>anhydride>dimethyl ester. The infrared spectra and solubility character of the polymer have been shown in comparison with those of the monomer. Further, polyitaconic acid has been obtained by the hydrolysis of polyitaconic anhydride with some ease.

The author wishes to thank Dr. Keinosuke Yoshida and Dr. Taizo Uno for their direction, Dr. Kazuhiro Shimizu for his kind advice regarding infrared spectroscopy, Mr. Yoshihiro

* Although the preparation of polyitaconic acid by means of the hydrolysis of polyitaconic anhydride might easily follow from the knowledge of the reactivity of anhydride, the homopolymerization of itaconic anhydride itself had been an untouched problem before the beginning of the present study.

** It was rather tedious to isolate the polymer from the solution of the reaction mixture in this case (Ref. S. Nagai and K. Yoshida, *Chem. High Polymers, Japan*, 17, 748 (1960)).

Hidaka for his help in the dilatometry, and Mr. Yasushi Yoshinaga for his cooperation throughout this experiment.

The Osaka Municipal Technical Research Institute
Kita-ku, Osaka

The Preparation of Dimer Aldehydes and Dimer Alcohols in an Oxo Reactor. II. The Initial Rate of the Hydroformylation of Propylene in the Presence of Magnesium Methylate as a Modifier

By Hiroshi UCHIDA and Akio MATSUDA

(Received October 10, 1963)

The preceding paper[1] of this study reported that the addition of magnesium methylate to the starting material for propylene hydroformylation produced C-8 aldehydes in a good yield, without causing any reduction in the initial rate at 150°C. These results alone, however, were not enough to enable us to understand well the effect of magnesium methylate addition upon the initial rate. This paper will, therefore, present more accurate and comprehensive data on the initial rates in a certain range of temperatures which are prevalent in practical hydroformylation runs. The discussion of the results obtained will suggest other catalysts for hydroformylation in the presence of magnesium methylate besides that of cobalt carbonyl.

Experimental

The hydroformylation run was conducted, by use of the same 300 cc. autoclave, in essentially the same way as in the preceding paper,[1] except that the addition of dicobalt octacarbonyl was modified in such a manner that a more accurate determination of the initial rate was possible: Before the autoclave was covered up, an amount of dicobalt octacarbonyl crystals was placed in a small saucer (0.5 cc.) of stainless steel held on a wing of a stirring mechanism. Having been charged with a *n*-butyraldehyde solution of magnesium methylate besides the carbonyl in the saucer, the autoclave was flushed with a synthesis gas of 1 : 1 H_2-CO, some propylene was introduced, and then the autoclave was pressured with the synthesis gas from a pressure storage, to which the autoclave was connected by way of a needle valve, to about 140 kg./cm^2 at room temperature. The autoclave was heated to the reaction temperature, and then a small amount of the synthesis gas was added from the pressure storage to raise the total pressure to 200 kg./cm^2. The instant the stirring mechanism was started, the saucer was allowed to fall down from the wing to dissolve the dicobalt octacarbonyl in the solution, whereupon the hydroformylation reaction set in. During the run, the synthesis gas was continuously supplied through the needle valve from the pressure storage into the autoclave in order to maintain the total pressure at 200 kg./cm^2. The accompanying pressure drops in the pressure storage with time were recorded. The recorded data might serve as a measure of the initial rate provided that the data could be interpreted in terms of a reasonable evaluation of the amount of synthesis gas consumed by the hydroformylation itself.

After the reaction period of an hour, the autoclave was cooled in running water. The gaseous material was purged, metered, and analyzed for the unchanged propylene in order to obtain the propylene conversion rate. The analysis of propylene as well as that of constituents in the liquid product was made in the way described in the preceding paper.[1] The raw materials used in this study were obtained from the same sources as those in the preceding study.[1]

In order to obtain a picture of the catalyst in the simultaneous presence of cobalt carbonyl and magnesium methylate, both the ratio of combined carbon monoxide (mole) to the total cobalt (atom) (hereafter denoted by CO_c/Co) and the ratio of cobalt (atom) existing as a carbonyl anion to the total cobalt (atom) (hereafter denoted by Co_{an}/Co) were determined, together with an infrared spectrum, on the liquid samples at the earlier stages of runs with and without magnesium methylate. The runs for this purpose were made by means of another autoclave (100 cc. in volume) of the same construction but lined with titanium over the whole inner surface lest the liquid samples should be contaminated with metal carbonyls from the autoclave material. From the beginning a few samples of a small portion (ca. 5 cc.) of the liquid product were sucked at five-minute intervals into a titanium dip-tube withdrawn out of the autoclave by passing them through a stainless steel tube cooled in ice, and subjected to immediate determination. The

1) H. Uchida and A. Matsuda, This Bulletin, **36**, 1351 (1963).

combined carbon monoxide was determined according to the method of Sternberg et al.[2] who measured the volume of the carbon monoxide liberated by the addition of excess iodine, and the carbonyl anion according to the method of Iwanaga,[3] who titrated the sample with an acetic acid-toluene solution of methyleneblue. The infrared spectrum was determined by means of a rock salt prism using *n*-butyraldehyde as the reference solution.

Results and Discussion

The Rate of Hydroformylation. — In the preceding paper,[1] the initial rate constant, k, for the batchwise run of propylene hydroformylation was represented by the following formula:

$$k=(1/t)\ln(c_0/c_t)=(1/t)\ln[c_0/(c_0-V/2)] \quad (1)$$

where t (min.) was the reaction time, c_0 (mol.) was the initial amount of propylene, c_t (mol.) was the amount of propylene at reaction time t, and V (mol.) was the amount of synthesis gas introduced from the pressure storage into the autoclave at reaction time t. The formula, however, was rather a conventional one because V, as measured by the drop in pressure of the pressure storage, was simply put as equal to $2(c_0-c_t)$ (mol.). In fact, however, V consisted of two portions of the synthesis gas, one (V_r, mol.) that consumed by the hydroformylation reaction itself and the other (V_0, mol.) that necessary to compensate for the fall in propylene partial pressure as the reaction proceeded. V_r, in place of V, should have been identical with $2(c_0-c_t)$. In this connection, Eq. 1 will be improved to give a more accurate expression of k.

Under the assumption that the propylene partial pressure, p, is proportional to the total propylene content,[4] the drop in propylene partial pressure (p_0-p) is written as:

$$p_0-p=p_0(c_0-c_t)/c_0 \quad (2)$$

where p_0 is the initial propylene partial pressure under the reaction conditions. Taking Eq. 2 into consideration, V_0 is given by Eq. 3:

$$V_0=a(p_0-p)=ap_0(c_0-c_t)/c_0 \quad (3)$$

In the above equation, a is a coefficient whose value is dependent on the reaction temperature. Since $V=V_r+V_0$, V is then expressed as follows:

$$V=2(c_0-c_t)+ap_0(c_0-ct)/c_0 \quad (4)$$

The substitution of the c_t obtainable from Eq. 4 into Eq. 1 results in the following expression of k:

$$k=(1/t)\ln\{c_0/[c_0-V(2+ap_0/c_0)]\} \quad (5)$$

To calculate Eq. 5 for k, ap_0 (mol.) at the present reaction conditions should be determined first. The determination, including some experimental measurements, has resulted in the respective values of 0.140, 0.155, 0.178, and 0.191 mol. at 130, 140, 150, and 160°C, provided that the initial charges of propylene and *n*-butyraldehyde in the autoclave are 0.22 and 0.068 mole respectively and the total pressure is 200 kg./cm^2.

Meanwhile, let us explain the procedure for calculating ap_0. The Benedict-Webb-Rubin equation of state[5] can give p_0 if the initial propylene density, d_0, in the autoclave at the reaction conditions is known. To obtain d_0, the initial propylene mole fraction, s_0, in the gas phase at the reaction conditions has only to be determined experimentally, since d_0 (g. mol./l.) is expressed by the formula:

$$d_0=n_0/V=s_0P/zRT \quad (6)$$

where n_0 is the initial propylene content (g. mol.) in the gas phase under the reaction conditions, V (l.) is the volume of the gas phase in the autoclave, P (atm.) is the total pressure, and z is the compressibility factor of the gaseous mixture under the reaction conditions. The determination of s_0 was made on four samples withdrawn from the gas phase at the temperatures of 130, 140, 150, and 160°C in the autoclave; the initial charges of the samples were 0.22 mol. propylene and 0.068 mol. *n*-butyraldehyde, with neither cobalt carbonyl nor magnesium methylate, and they were subsequently added with the synthesis gas to 200 kg./cm^2. Once s_0 is obtained, z is evaluated as ca. 1.02 at 200 kg./cm^2 over the 130 to 160°C temperature range; consequently, d_0 is determined by the aid of Eq. 6. The substitution of the values of d_0 into the Benedict-Webb-Rubin equation results in the corresponding values of p_0, which are 18.7, 21.2, 25.0 and 27.5 atm. at 130, 140, 150 and 160°C respectively. The determination of ap_0 is then possible by a simple calculation.

Findings on the initial rates of hydroformylation over a temperature range from 130 to 160°C are exemplified in Figs. 1 and 2 as plots of $\ln[c_0/\{c_0-V/(2+ap_0/c_0)\}]$ vs. t. Throughout the runs, the initial charges of *n*-butyraldehyde,

2) H. W. Sternberg, I. Wender and M. Orchin, *Anal. Chem.*, **24**, 174 (1952).

3) R. Iwanaga, This Bulletin, **35**, 247 (1962).

4) At the earlier stages of the present experiment, a major part of the propylene exists in the gaseous phase.

5) $p_0=RTd_0+(B_0RT-A_0-C_0/T^2)d_0^2+(bRT-a)d_0^3+a\alpha d_0^6+[cd_0^3(1+\gamma d_0^2)\exp(-\gamma d_0^2)]/T^2$ (cf. 6)).
where R is the gas constant, T is the temperature (°K), and B_0, A_0, C_0, b, a, c, α, and γ are constants whose values with respect to propylene are available from the literature.[7]

6) E. D. Comings, "High Pressure Technology," McGraw-Hill Book Co. N. Y. (1956), p. 251.

7) Ibid., p. 485.

propylene, and dicobalt octacarbonyl were kept constant at the respective amounts of 0.068, 0.22 mol., and 0.4 mmol., but magnesium methylate was varied in amount at 0.8 mmol. intervals between 0 and 3.2 mmol. In each run the plot is linear, and the initial rate constant, k, is readily evaluated from the slope of the plot. For each series of runs with a fixed amount of magnesium methylate, an Arrhenius plot is drawn, as shown in Fig. 3. In the figure the plots intersect with one another at A, where $1/T$ is 423°K. This plainly indicates that the initial rate constant, and thus the initial rate at 150°C, remains unchanged, independent of the amounts of magnesium methylate added, but that within the amount of about 2.4 mmol. the initial rates at the reaction temperatures below 150°C

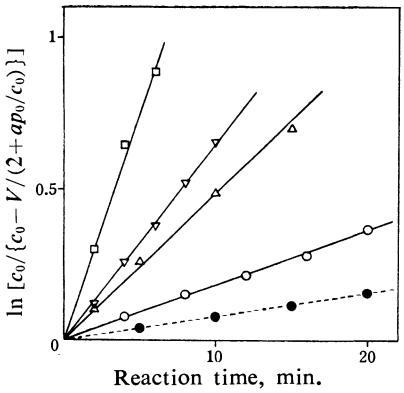


Fig. 1. Initial rate of propylene hydroformylation without magnesium methylate.
—○— Reaction temperature, 130°C, $k=1.8\times10^{-2}$ min^{-1}
—△— 140°C, 4.8×10^{-2} min^{-1}
—▽— 150°C, 6.5×10^{-2} min^{-1}
—□— 160°C, 15.0×10^{-2} min^{-1}
···●··· 140°C, 0.8×10^{-2} min^{-1}
The dotted line indicates the initial rate in the presence of an amount of 2-ethylhexenal.

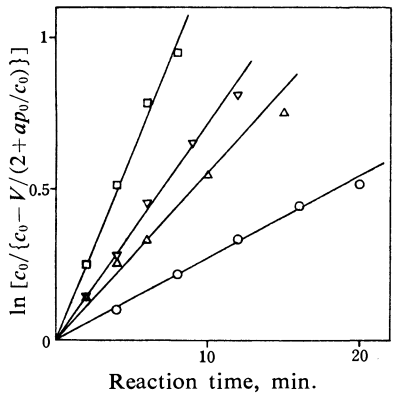


Fig. 2. Initial rate of propylene hydroformylation with magnesium methylate (0.8 mmol.).
—○— Reaction temperature, 130°C, $k=2.7\times10^{-2}$ min^{-1}
—△— 140°C, 5.6×10^{-2} min^{-1}
—▽— 150°C, 7.2×10^{-2} min^{-1}
—□— 160°C, 12.4×10^{-2} min^{-1}

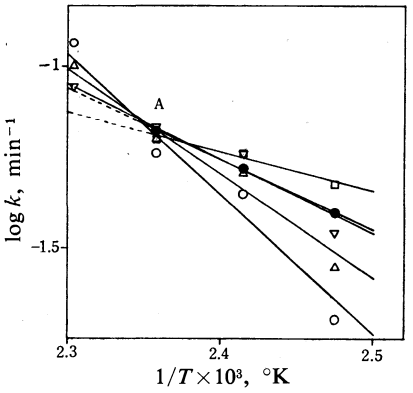


Fig. 3. Arrhenius plot of initial rate constant.
—○—: Magnesium methylate (mmol.), 0
—△—: 0.8 —△—: 1.6
—□—: 2.4 —●—: 3.2

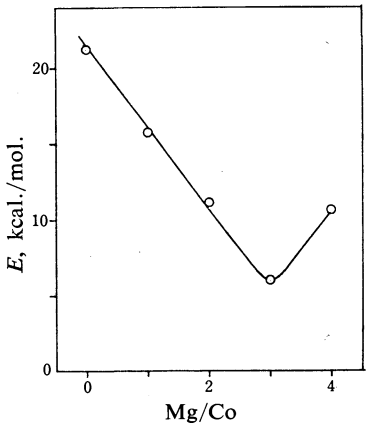


Fig. 4. Activation energy of propylene hydroformylation as function of Mg/Co (atom).

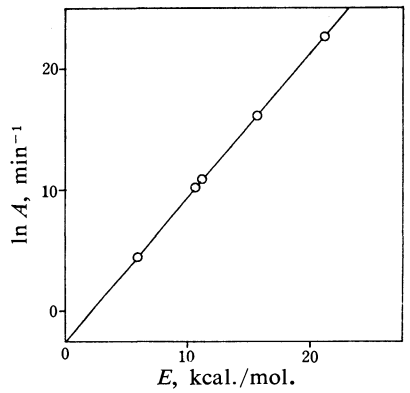


Fig. 5. Plot of logarithm of frequency factor against activation energy.

increase more markedly as the amount of magnesium methylate is increased, whereas the situation is reversed above 150°C.

On the basis of the plots in Fig. 3, the activation energies, E, as well as the frequency factors, A, of hydroformylation reactions with varying amounts of magnesium methylate can be calculated. A plot of E vs. Mg/Co (atom ratio) in the raw material, as illustrated in Fig. 4, indicates that E diminishes with Mg/Co at first, passes through a minimum at Mg/Co=3 and then rises. Moreover, a plot of $\ln A$ against E appears to be linear, as is shown in Fig. 5. The linear relationship is represented by the following equation:

$$\ln A = E/R\Theta + \ln A' \qquad (7)$$

where Θ is a constant of the proportionality with the dimension of temperature and A' is another constant, their respective values being calculated as 423°K (150°C) and 0.074 min^{-1}. This relationship indicates that a compensation effect appears in a particular manner that obeys the "Theta Rule."[8]

The compensation effect has been reported in a number of liquid-phase reactions, such as hydrolysis and esterification in the presence of inorganic acid, where a series of differently substituted compounds or of different kinds of solvents was used (cf. 9) and 10)). Nevertheless, no paper, so far as we are aware, has ever dealt with the compensation effect taking place in a series of liquid-phase reactions with different catalyst compositions. On the other hand, there are many examples of gas-solid heterogeneous catalysis where the compensation effect appears as the catalyst compositions are changed. According to Cremer[11] the effect on the heterogeneous catalysis can be ascribed to the simultaneous presence of two or more kinds of active sites participating in the reaction, with different activation energies and frequency factors. Extending the view of Cremer to the present liquid-phase reaction, the compensation effect can be interpreted as coming from the presence of two kinds of catalysts, presumably one being the carbonyl of cobalt and the other being the compound into which the carbonyl and magnesium methylate have been combined. At first sight, one may be apt to consider the latter catalyst as consisting of three moles of magnesium methylate and one mole of the carbonyl (cf. Fig. 4), but a detailed examination of the chemistry of the catalyst itself reveals that this is not necessarily the case, as will be mentioned in the next section.

Catalysts in the Presence of Magnesium Methylate.—The CO_c/Co and Co_{an}/Co ratios were determined for the samples at earlier stages of the runs using 0.136 mol. of *n*-butyraldehyde, 0.1 mol. of propylene, and 0.6 mmol. of dicobalt octacarbonyl, either without or with 3.6 mmol. of magnesium methylate (Mg/Co=3). The runs were conducted at 150°C at 200 kg./cm^2. The results are cited in Table I. In accordance with the results of

Table I. Ratios of combined carbon monoxide and cobalt as carbonyl anion to total cobalt

Reaction time min.	With $Mg(OCH_3)_2$[a]		Without $Mg(OCH_3)_2$	
	CO_c/Co	Co_{an}/Co	CO_c/Co	Co_{an}/Co
ca. 1	2.7	0.19	2.9	0
5	3.0	0.34	—	—
10	2.9	0.22	2.9	0.05

a) Magnesium methylate was added in the amount corresponding to Mg/Co (atom ratio) of 3.

Heck and Breslow,[12] the value of CO_c/Co is always about three, independent of whether magnesium methylate was added or not. In constrast to this, Co_{an}/Co is zero or an extremely low value in the absence of magnesium methylate, while in its presence it attains to such higher values as 0.2 to 0.34. The carbonyl anion, as is well known,[13] would not be detected in the reaction medium at the earlier stage of the usual hydroformylation where a considerable amount of olefin remains. Accordingly, the carbonyl anion thus detectable in the present runs can be ascribed to that of a mixed metal carbonyl of $[Co(CO)_4]_2Mg$ produced in a way similar to that in which the carbonyl of $[Co(CO)_4]_2Zn$[14] is produced. The mixed metal carbonyl $[Co(CO)_4]_2Mg$, as well as $[Co(CO_4]_2Zn$, can act as the catalyst for aldehyde dimerization, but it can not be the catalyst for hydroformylation. Moreover, it should be emphasized that only one-third to one-fifth of the cobalt, not all of the cobalt, participates in producing the mixed metal carbonyl, even though magnesium methylate is added in the great excess of Mg/Co=3. This may be the reason why magnesium methylate produced dimer aldehydes in a good yield, without exercising an

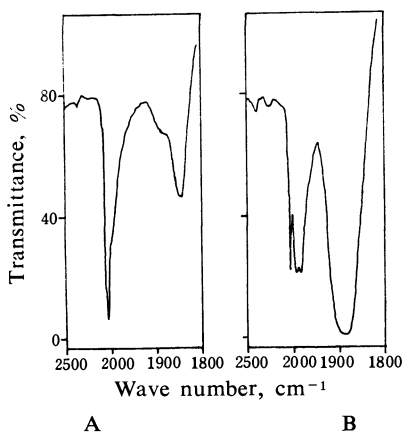
8) M. Boudart, *Chem. Eng. Prog.*, **57**, No. 8, 33 (1961).
9) J. E. Leffler, *J. Org. Chem.*, **20**, 1202 (1955).
10) R. F. Brown, ibid., **27**, 3015 (1962).
11) E. Cremer, "Advances in Catalysis," VIII, Academic Press, N. Y. (1955), p. 85.
12) R. F. Heck and D. S. Breslow, *J. Am. Chem. Soc.*, **83**, 4023 (1961).
13) M. Orchin, L. Kirch and I. Goldfarb, ibid., **78**, 5450 (1956).
14) H. Hieber and H. Schulten, *Z. anorg. u. allgem. Chem.* **243**, 145 (1929).

TABLE II. PROPYLENE CONVERSION AND COMPOSITION OF HYDROFORMYLATION PRODUCT

Expt. No.	Reaction temp., °C	$Mg(OCH_3)_2$ mmol.	Propylene conversion %	Product composition wt. %						
				n-C_3H_7CHO	*i*-C_3H_7CHO	*n*-C_4H_9OH	*i*-C_4H_9OH	$C_7H_{13}CHO$	$C_7H_{15}CHO$	Residue
1	130	none	94.6	56.7	20.1	2.0	0.3	0	2.1	18.8
2	140	none	99.4	51.2	21.9	2.2	1.2	0	3.9	19.6
3	150	none	99.5	53.4	21.0	2.6	1.0	0	4.7	17.3
4	160	none	—	41.6	21.0	5.5	2.5	0	7.3	22.1
5	130	0.8	93.4	45.3	20.7	2.5	0.9	4.8	9.3	16.5
6	140	0.8	98.6	41.4	22.7	2.8	1.3	4.0	14.8	13.0
7	150	0.8	99.7	34.7	22.7	4.0	3.0	0	21.0	14.6
8	160	0.8	—	29.7	21.1	5.9	3.2	0	21.8	18.3
9	130	1.6	91.4	38.5	20.0	2.3	1.0	8.5	17.5	12.2
10	140	1.6	97.7	33.8	22.6	3.0	2.1	5.0	20.8	12.7
11	150	1.6	99.2	30.7	22.6	4.2	3.0	1.1	24.3	14.1
12	160	1.6	—	26.9	22.4	6.4	4.6	0	22.9	16.8
13	130	2.4	90.9	33.0	21.1	2.3	0.8	11.1	18.0	13.7
14	140	2.4	96.9	29.8	22.3	3.4	1.2	5.8	24.3	13.2
15	150	2.4	98.9	25.4	23.2	4.4	1.6	1.5	31.6	12.3
16	130	3.2	87.3	28.6	19.3	2.3	1.0	12.7	18.0	18.1
17	140	3.2	94.5	23.6	23.2	4.2	1.2	7.2	28.0	12.6
18	150	3.2	98.4	23.1	22.6	4.3	1.6	2.0	33.2	13.2

unfavorable effect on the initial rate of hydroformylation.

So far as the afore-mentioned results are concerned, it remains undetermined whether the remaining portions of cobalt carbonyl and of magnesium methylate exist separately or as a complex compound into which they have combined. In this connection, a possible interpretation of the compensation effect has suggested a kind of catalyst for hydroformylation besides cobalt carbonyl. The suggestion is supported by the following results on the infrared spectrum measurement: The infrared spectrum of the reaction product (e. g., the product at 10 min. interval from beginning)



Figs. 6 and 7. Infrared spectra of reaction products starting with raw materials (A) without and (B) with magnesium methylate respectively.

without magnesium methylate is similar to, though not identical with, that of dicobalt octacarbonyl (cf. 15)), but the spectrum of the reaction product with magnesium methylate differs markedly from that described just (compare Fig. 6 with Fig. 7[16]). The latter spectrum contains characteristic peaks at 1991 and 1974 cm^{-1} and a band at 1891 cm^{-1} which is assignable to the carbonyl anion of the mixed metal carbonyl,[17] besides a band at 2030 cm^{-1} which also appears in the former spectrum but is much reduced in intensity. The marked difference thus observed between the two spectra indicates a bonding taking place between cobalt carbonyl and magnesium methylate. However, nothing more decisive can be said about the composition of the compound, or of the catalyst, because the data on the equilibrium, such as $1/2 \cdot Co_2(CO)_6 + xMg(OCH_3)_2 \rightleftarrows [Co(CO)_3]^{-\delta}[Mg(OCH_3)_2]_x^{+\delta}$, are not yet available.

Propylene Conversion and Product Composition.—Table II summarizes the propylene conversion and the product composition after an hour's reaction period. The rate of conversion tends to lower with Mg/Co, and this tendency appears more clearly at the lower reaction temperatures, where the content of unsaturated C-8 aldehyde is larger. It is to be expected that the conversion should be low

15) R. A. Friedel, I. Wender, S. L. Shuffer and H. W. Sternberg, *J. Am. Chem. Soc.*, 77, 3951 (1955).

16) Magnesium methylate alone does not give any absorption band in the region under investigation. The band at 1841 cm^{-1} in the spectrum of Fig. 6 may be assingnable to a bridge carbonyl of $Co_2(CO)_6$ (cf. 15)).

17) O. Vohler, *Chem. Ber.*, 91, 1161 (1958).

TABLE III. COMPOSITION OF PRODUCT AFTER HYDROGENATION

Expt. No.	Product composition, wt.%							
	n-C_3H_7CHO	*i*-C_3H_7CHO	*n*-C_4H_9OH	*i*-C_4H_9OH	$C_3H_7COOC_4H_9$	C-8[a] alcohol(1)	C-8[a] alcohol(2)	Residue
1	1.5	0.8	53.8	16.2	1.8	0	8.7	17.2
3	0.4	0.1	52.4	19.4	1.1	0	7.8	18.1
5	0.6	0.5	40.4	15.8	2.5	0.6	25.5	14.1
7	0.5	0.2	31.5	17.3	2.1	2.5	27.8	18.1
9	0.7	0.3	37.0	15.3	1.8	1.4	29.4	14.1
11	0.4	0.2	27.3	18.5	3.2	2.4	29.5	18.5
13	0.6	0.3	32.6	15.9	1.9	1.5	32.7	14.5
15	0.5	0.3	25.9	18.4	1.2	3.0	32.1	18.6
16	0.7	0.2	30.0	15.9	1.8	1.7	35.6	14.1
18	0.6	0.3	24.1	18.6	1.3	2.6	33.7	18.8

a) C-8 alcohol(1) and C-8 alcohol(2) stand for 2-ethyl-4-methylpentanol and 2-ethylhexanol respectively.

in the presence of the unsaturated aldehyde because cobalt carbonyl and the unsaturated aldehyde combine into a catalytically inactive compound. This was confirmed with an experimental run starting with a raw material containing a some considerable amount of 2-ethyl-hexenal (0.05 mol.). The results, as shown by the dotted line in Fig. 1, reveal that the unsaturated aldehyde not only lowers the propylene conversion but also retards the initial rate of hydroformylation. However, it should be noticed that the retarding effect on the initial rate need not be considered with respect to the present data, since the amount of unsaturated aldehyde at the earlier stage might be too small to have any effect on the initial rate. In fact, the effect in the low temperature range is of a kind opposite to what one might expect.

Within the Mg/Co range of the present study, the dimer aldehydes content increases with the ratio. The residue in the table stands for the sum of the matter not identified as yet; it may mainly consist of compounds whose distillation temperatures are above those of C-8 aldehydes. Table III gives the compositions of some final products after the hydrogenation of the products in Table II in the usual manner, using a Raney cobalt catalyst.

Summary

The effect of magnesium methylate addition upon the initial rate of propylene hydroformylation has been explained in terms of Arrhenius plots of the initial rate constants, and in terms of the activation energy as a function of Mg/Co. Moreover, the plot of the logarithm of the frequency factor vs. the activation energy appears to be linear, which indicates that a compensation takes place with respect to the initial rate in the presence of magnesium methylate. The extension of Cremer's view about the compensation effect in heterogeneous catalysis into this kind of liquid-phase reaction leads one to expect another catalyst besides that of cobalt carbonyl.

The determination of the cobalt carbonyl anion in the reaction product obtained from raw material either with no or with a large excess of magnesium methylate (Mg/Co=3) indicates that in the former product scarcely no cobalt is detectable as the carbonyl anion, whereas in the latter product a part of the cobalt exists as such. The anion is to be ascribed to that of a mixed metal carbonyl of $[Co(CO)_4]_2Mg$, which facilitates the production of dimer aldehydes. Further, the infrared spectrum of the latter product differs markedly from that of the former product. This may afford evidence for the other catalyst expected.

In addition, this paper has presented data on the propylene conversion and the compositions of reaction products before and after hydrogenation, data obtained with raw materials containing varying amounts of magnesium methylate.

Government Chemical Industrial Research Institute, Tokyo
Shibuya-ku, Tokyo

The Oxo Reaction of Unconjugated α, ω-Diolefin

By Masanobu MORIKAWA

(Received October 15, 1963)

The reaction of olefin with carbon monoxide and hydrogen to form aldehyde is well known as the oxo reaction or hydroformylation.[1] In this reaction, it is not only desirable but also interesting to study whether it is possible to prepare dialdehyde from diolefin.

It has, however, been reported that a conjugated diolefin, such as butadiene and 1, 3-pentadiene, yields not dialdehyde, but saturated monoaldehyde under oxo conditions.[2] Also, it has been reported that an unconjugated cyclic diolefin, such as 4-vinylcyclohexene and dicyclopentadiene, gives a mixture of mono- and dialdehydes in a low selectivity.[3] On the other hand, the reaction of an unconjugated α, ω-diolefin has not been thoroughly studied. From this standpoint, we have been interested in the reaction with 1, 4-pentadiene and 1, 5-hexadiene in order to synthesize dialdehydes and have found that the dialdehydes can be obtained as a main product from the unconjugated α, ω-diolefins under suitable conditions.

It was found essential to carry out the reaction at a lower temperature (below 100°C), in a dilute alcoholic solution and in the presence of a rhodium catalyst instead of the cobalt catalyst usually used in the oxo reaction. The use of a cobalt catalyst or of other solvents resulted in a lower yield of dialdehyde.

After the reaction had been carried out under the conditions cited above, the reaction mixture was catalytically hydrogenated, because it is easier to isolate the reaction products as saturated aldehydes when unsaturated ones are also present. Then the reaction products were identified by converting them into 2, 4-dinitrophenylhydrazones and other derivatives of the corresponding saturated aldehydes.

From 1, 4-pentadiene pimelaldehyde was obtained as a main product in addition to monoaldehydes and other aldehydes in the presence of a rhodium oxide catalyst, but cyclohexanecarboxaldehyde was obtained in the presence of a rhodium chloride catalyst, which generates hydrogen chloride in the course of the reaction. Cyclohexanecarboxaldehyde is formed by an intramolecular aldol condensation of the dialdehyde. As supporting evidence, cyclohexene-1-carboxaldehyde was isolated as the hydrazone in another run. Pimelaldehyde was converted by reduction with lithium aluminum hydride to 1, 7-heptanediol, which was identified as diacetate by comparing the NMR- and infrared-spectra and retention time of its gas chromatograph with those of an authentic sample.

2-Methylheptanedial was obtained from 1, 5-hexadiene as a main product. The dialdehyde was converted by permanganate oxidation to the corresponding diacid and was identified as its dimethylester.

Interestingly, it has already been reported that monoölefin forms mainly branched-chain aldehyde,[4] but in our experiments pimelaldehyde and 2-methylheptanedial were obtained from 1, 4-pentadiene and 1, 5-hexadiene respectively. This suggests that these diolefins form the complexes with the rhodium carbonyl suitable for the 1, 5-insertion of carbon monoxide and that the migration of the double bond[1] into the conjugated position does not take place.

Even under these conditions, butadiene and 1, 3-pentadiene did not give dialdehyde, but only monoaldehyde.

Experimental[5]

The Reaction of 1, 4-Pentadiene.—1, 4-Pentadiene (1.36 g.) prepared from 1, 5-pentanediol diacetate by pyrolysis,[6] rhodium oxide (0.5 g.) and ethanol (50 ml.) were charged in a 200 ml. stainless steel pressure reactor. Air was removed, and a carbon monoxide-hydrogen mixture (1 : 1) was introduced up to the pressure of 150 kg./cm^2. The reaction was carried out at 60~100°C for 15 min., during which time a pressure drop of 15 kg./cm^2 was observed. The gas mixture was released, the carbonyl catalyst was decomposed, and the reaction mixture was hydrogenated at room temperature

1) I. Wender and H. W. Sternberg, "Catalysis," Vol. V, Ed. by P. H. Emmett, Reinhold, New York (1957), p. 73.
2) H. Adkins and J. L. R. Williams, *J. Org. Chem.*, **17**, 980 (1952).
3) U. S. Pat. 2810748 (1957); Brit. Pat. 808124 (1959); Brit. Pat. 750144 (1956).
4) Brit. Pat. 801734 (1958); German Pat. 953605 (1956).
5) All melting points and boiling points are uncorrected. The microanalyses were performed by analytical division in the Laboratories. IR- and NMR-spectra were obtained using a Shimadzu Model IR-27 and a Varian Model HR-60, respectively. Materials were obtained from commercial sources.
6) "Organic Syntheses," Vol. **38**, 78 (1958).

under atmospheric pressure over a platinum catalyst. Then, the reaction mixture was treated with 2, 4-dinitrophenylhydrazine in an acidic ethanol solution, giving 5 g. of a hydrazone mixture.

The portion of the hydrazone more soluble in benzene was separated and purified by neutral alumina column chromatography and was recrystallized from ethanol, giving 0.7 g. of yellow crystals, a mixture of the hydrazones of monoaldehydes (m. p. 95~98°C).

Found: C, 51.54; H, 5.71. Calcd. for $C_{12}H_{16}N_4O_4$; C, 51.42; H, 5.75%.

The portion less soluble in benzene was the hydrazone of cyclohexanecarboxaldehyde (0.5 g., m. p. 169~170°C), and no depression of melting point was observed with an authentic sample prepared by the hydroformylation of cyclohexene.

Found: C, 53.28; H, 5.49. Calcd. for $C_{13}H_{16}N_4O_4$: C, 53.42; H, 5.52%.

When rhodium chloride was used as a catalyst instead of rhodium oxide, cyclohexanecarboxaldehyde was a main product and the hydrazone of 1-cyclohexene-1-carboxaldehyde was isolated on treating the reaction mixture with 2, 4-dinitrophenylhydrazine without hydrogenation (red crystals of m. p. 214°C decomp., (lit.[7] 215°C decomp.)).

Found: C, 53.56; H, 4.87. Calcd. for $C_{13}H_{14}N_4O_4$: C, 53.79; H, 4.86%.

The portion insoluble in benzene was further fractionated by recrystallization from dimethylformamide. The portion less soluble was considered to be the hydrazone of branched-chain dialdehyde (0.8 g., m. p. 214~216°C).

Found: C, 47.20; H, 4.16. Calcd. for $C_{19}H_{20}N_8O_8$: C, 46.72; H, 4.13%.

The portion more soluble was a main product identified with the hydrazone of pimelaldehyde (1.6 g., m. p. 177~179°C (lit.[8] 180~181°C), and no depression of melting point was observed with an authentic sample prepared by the Rosenmund reduction of pimeloyl chloride.

Found: C, 46.81; H, 4.10. Calcd. for $C_{19}H_{20}N_8O_8$: C, 46.72; H, 4.13%.

In another run, the reaction mixture was poured into water and extracted with ether. The ether layer was dried, the extact was reduced with lithium aluminum hydride, and the dialcohol boiling between 140 and 150°C at 8 mmHg was collected (0.5 g. from 1.36 g. of diolefine). The dialcohol was converted into the diacetate and purified by "Megachrom." The identity of the product with an authentic sample of 1, 7-heptanediol diacetate was confirmed by comparing the retention time of their gas chromatographs and the NMR- and infrared-spectra. NMR-spectra: CH_2O, 6.10 τ and 6.58 τ; CH_3CO, 8.07 τ; CH_2, 8.62 τ.

An authentic sample of 2, 4-dinitrophenylhydrazone of pimelaldehyde was synthesized in the following way. Pimelic acid (8 g.) was converted into acyl chloride by treatment with oxalyl chloride in benzene. The acyl chloride was reduced in xylene (35 ml.) in the presence of 5% palladium on barium sulfate (1 g.) and "Quinoline-S" (0.1 ml.) at 150~160°C by bulbbling a hydrogen stream until no more hydrogen chloride was evolved. The catalyst was then removed, and the reaction mixture was treated with 2, 4-dinitrophenylhydrazine. The hydrazones obtained (1.2 g.) were separated into the red hydrazone of cyclohexene-1-carboxaldehyde (0.6 g., m. p. 218°C (decomp.)) and the yellow hydrazone of pimelaldehyde (0.5 g., m. p. 177~178°C).

The Reaction of 1, 5-Hexadiene.—The reaction of 1, 5-hexadiene (1.65 g.) prepared from allyl magnesium bromide[9] was carried out for 20 min. at 60~100°C in the same way as with 1, 4-pentadiene. The reaction mixture was hydrogenated and treated with 2, 4-dinitrophenylhydrazine. 3.6 g. of hydrazones were obtained. The hydrazones were fractionated and recrystallized to give the following products; the hydrazones of monoaldehydes (0.8 g.; m. p. 96~100°C. Found: C, 53.20; H, 5.98. Calcd. for $C_{13}H_{18}N_4O_4$: C, 53.05; H, 6.16%), the hydrazone of suberaldehyde (0.6 g., melting point and mixed melting point with an authentic sample prepared by ozonolysis of cyclooctene 177°C (lit. 175°C,[10] 167~169°C[8]). Found: C, 47.30; H, 4.46. Calcd. for $C_{20}H_{22}N_8O_8$: C, 47.77; H, 4.41%), and the hydrazone of 2-methylheptanedial (1.3 g. obtained at a main product; m. p. 185°C (unreported). Found: C, 47.81; H, 4.38. Calcd. for $C_{20}H_{22}N_8O_8$: C, 47.77; H, 4.41%).

In another run, the reaction mixture was poured into water and extracted with ether, and then the ether was replaced by acetone. The acetone solution was oxidized with an aqueous permanganate solution to give the dicarboxylic acid. After esterification, 0.6 g. of pure dimethyl 2-methylheptanediate (b. p. 90~92°C/5 mmHg) was obtained from 1.67 g. of diene and was identified by comparing the infrared- and NMR-spectra and the retention time in its gas chromatography with those of an authentic sample, which had in turn been prepared from dimethyl pimelate and methyl iodide in the presence of sodium alcoholate.[11] The NMR-spectra ($CHCl_3$); OCH_2, 6.34 τ; CH_2CO and CHCO, 7.75 τ; CH_3, 8.50 τ; CH_3, 8.85 τ.

Summary

Pimelaldehyde and 2-methylheptanedial have been obtained from 1, 4-pentadiene and 1, 5-hexadiene respectively by carrying out the oxo reaction in alcohol at a lower temperature (below 100°C) using a rhodium catalyst.

The author wishes to express his thanks to Dr. Toshio Hoshino for his guidance throughout this work.

Basic Research Laboratories
Toyo Rayon Co., Ltd.
Kamakura, Kanagawa

7) D. T. C. Gillespie, P. R. Jeffevies, A. K. Macbeth and M. J. Thompson, *J. Chem. Soc.*, **1955**, 665.
8) W. Treib and R. Helbig, *Chem. Ber.*, **92**, 1559 (1959).
9) "Organic Syntheses," Coll. Vol., 3, 121 (1955).
10) H. J. Bestmann and H. Schulz, *Chem. Ber.*, **92**, 530 (1959).
11) W. Dieckman, ibid., 33, 2683 (1900).

The Complex Formation of Boron Fluoride with Lower Olefins at Low Temperatures. II. Isotope Effects and Absorption Spectra of Boron Fluoride-Butene Systems

By Ryohei NAKANE, Tsunao WATANABE and Toshiyuki ŌYAMA

(Received July 5, 1963)

By measuring the isotope effects and absorption spectra of boron fluoride-ethylene and -propyrene systems, the authors predicted in a preceding paper[1] that only polar mono-olefins would form σ-complexes with boron fluoride at low temperatures. In the present report similar measurements for boron fluoride-1-butene, -*cis*-2-butene and -*trans*-2-butene systems will be reported and the prediction confirmed. The relation between the values of the equilibrium constant of isotopic exchange and the catalytic ability of boron fluoride complexes will also be discussed.

Experimental

Except for a low temperature bath prepared by the use of the melting point of $-95°C$ of toluene, the experimental methods were exactly the same as those used in the preceding work.

Results and Discussion

Isotope Effects. — Findings concerning the isotope effect are shown in Table I. The values

TABLE I. EQUILIBRIUM CONSTANT OF BORON ISOTOPE EXCHANGE FOR BORON FLUORIDE-BUTENE SYSTEMS AT LOW TEMPERATURE

System	Equilibrium constant $[^{10}B/^{11}B]_{liq}/[^{10}B/^{11}B]_{gas}$	
	$-95°C$	$-112°C$
BF_3-1-C_4H_8	1.012 ± 0.002	1.017 ± 0.002
BF_3-*cis*-2-C_4H_8	1.015 ± 0.002	1.020 ± 0.002
BF_3-*trans*-2-C_4H_8	1.006 ± 0.002	1.011 ± 0.002

of the equilibrium constants of isotopic exchange with polar mono-olefins, 1-butene and *cis*-2-butene, were found to be appreciably larger than 1.011 while that with a non-polar *trans*-2-butene was 1.011 at $-112°C$.

These findings indicate again that boron fluoride can form σ-complexes with polar mono-olefins at low temperatures, but not with non-polar mono-olefins. Thus, the conclusion drawn in the preceding work was confirmed to be correct.

The values of the equilibrium constants of isotopic exchange between boron fluoride gas and many liquid boron fluoride complexes at various temperatures are summarized in Table II, and the values for very strong complexes with an *n*-donor, such as methyl ether, are compared with the values for weak complexes found by us. The equilibrium constants for systems of boron fluoride-*n*-donor complexes or of tetrafluoborate ions are the largest, while those for systems of liquid boron fluoride or of solutions of boron fluoride in non-polar mono-olefins are the smallest. The equilibrium constant for the system of tetrafluoborate ions, the structure of which is completely tetrahedral, is 1.028 ± 0.008 at temperatures from 20 to 30°C.[2] The equilibrium constant for the boron fluoride-methyl ether complex system is also 1.028 ± 0.002 at 25°C,[3] and the value calculated from the experimental equation given by Palko et al.[3] is 1.082 at $-112°C$. In the boron fluoride-methyl ether complex, every boron atom is situated at the top of the pyramidal structure.[4] On the other hand, the equilibrium constant for the system of liquid boron fluoride, the molecule of which has a structure of a planar form, is 1.011 ± 0.002 at $-112°C$.[1] The methyl fluoride-boron fluoride complex has been considered to be a weak complex, $^{\delta+}CH_3\cdot F \rightarrow {}^{\delta-}BF_3$, for its conductivity is poor.[5] The equilibrium constant for the methyl fluoride-boron fluoride complex system is 1.020 ± 0.002 at $-95°C$,[6] appreciably smaller than that for the boron fluoride-methyl ether complex system and larger than that for the liquid boron fluoride system. Though the boron fluoride-sulfur dioxide complex has been considered to be a weak complex because of the shape of its

1) R. Nakane, T. Watanabe, O. Kurihara and T. Ōyama, This Bulletin, **36**, 1376 (1963).

2) B. Kiselev, "Kernenergie," 4 Jahrgang, 421 (1961).

3) A. Palko, G. Begun and L. Landau, *J. Chem. Phys.*, **37**, 552 (1962).

4) S. Bauer, G. Finlay and A. Laubengeyer, *J. Am. Chem. Soc.*, **65**, 889 (1943).

5) G. Olah, S. Kuhn and J. Olah, *J. Chem. Soc.*, **1957**, 2174.

6) R. Nakane and O. Kurihara, unpublished.

TABLE II. EQUILIBRIUM CONSTANT OF BORON ISOTOPE EXCHANGE BETWEEN BORON FLUORIDE GAS AND LIQUID BORON FLUORIDE COMPLEXES

Liquid complex	Equilibrium constant, $[^{10}B/^{11}B]_{liq}/[^{10}B/^{11}B]_{gas}$				Ref.
	+25°C	−95°C	−96.5°C	−112°C	
BF_3-CH_3OCH_3	1.028	(1.071)[a,b]		(1.082)[a,b]	3
BF_4^-	1.028	—[a]		—[a]	2
BF_3-$C_6H_5OCH_3$	1.032	—[a]		—[a]	9
BF_3-$(C_4H_9)_2S$	1.033	—[a]		—[a]	9
BF_3-C_6H_5OH	1.027	—[a]		—[a]	9
BF_3-$(C_2H_5)_3N$	1.023	—[a]		—[a]	10
BF_3-C_4H_8O	1.036	—[a]		—[a]	10
BF_3-SO_2			1.022	—[a]	8
BF_3-CH_3F		1.020			6
BF_3-CH_3Cl			1.016	1.021	8
BF_3-*cis*-2-C_4H_8		1.015		1.020	present report
BF_3-C_3H_6		1.013[c]		1.018	1
BF_3-1-C_4H_8		1.012		1.017	present report
BF_3-$CHClF_2$			1.011	1.017	8
BF_3, C_2H_4				1.011	1
BF_3, *trans*-2-C_4H_8		1.006		1.011	present report
BF_3		(1.006)[d]		1.011	1

a) solid; b) calculated from experimental equation; c) measured newly; d) estimated

fusion curve,[7] its equilibrium constant is nearly equal to that for the boron fluoride-methyl chloride complex system.[8] These results show that the value of the equilibrium constant is proportional to the stability of the complex.

Now, when the following isotopic exchange occurs betwen gaseous boron fluoride and the liquid boron fluoride complex which is formed with the donor molecule YA,

$$^{10}BF_{3(gas)} + {}^{11}BF_3\cdot YA_{(liq)} \overset{k}{\rightleftharpoons} {}^{11}BF_{3(gas)} + {}^{10}BF_3\cdot YA_{(liq)} \quad (1)$$

the equilibrium constant is given by

$$K=\frac{[Q_{^{10}BF_3\cdot YA\,(liq)}]}{[Q_{^{11}BF_3\cdot YA\,(liq)}]}\Big/\frac{[Q_{^{10}BF_3\,(gas)}]}{[Q_{^{11}BF_3\,(gas)}]} \quad (2)$$

Here, the ratio between the partition functions of isotopic molecules is

$$\frac{Q_2}{Q_1}=\frac{\sigma_1}{\sigma_2}\prod_i \frac{u_{2i}\exp(-u_{2i}/2)\,[1-\exp(-u_{1i})]}{u_{1i}\exp(-u_{1i}/2)\,[1-\exp(-u_{2i})]} \quad (3)$$

where 1 and 2 refer to the different isotopic molecules, σ_1 and σ_2 are the symmetric numbers, $u_i=hc\omega_i/kT$, and ω_i is the ith normal vibrational frequency.[9] Thus, when the normal vibrational frequencies of gaseous boronfluoride and liquid boron fluoride complexes are obtained, the equilibrium constants can be calculated from Eqs. 2 and 3.

In the isotopic exchange between boron fluoride gas and the boron fluoride-methyl ether complex, Palko et al.[3] compared the observed equilibrium constants with the values calculated by Eqs. 2 and 3 from infra and Raman spectra data and found that, when the transformation of boron fluoride from planar to pyramidal resulted in an increase in the B—F distance and a weakening of the B—F force constant, the isotope effect caused by the B—F bond was so marked that it overbalanced the formation of the B—O bond, which had the opposite effect upon the partition function ratio. This suggests the possibility that the equilibrium constants of the isotopic exchange between gaseous boron fluoride and all boron fluoride complexes may depend mostly on the B—F force contants and scarcely at all on the force constant of the bond formed between boron and donor atoms. This possibility is supported by the observation of many strong boron fluoride complexes other than the boron fluoride-methyl ether complex, for example, boron fluoride-anisole,[10] -thioether,[10] -phenole,[10] -triethyl amine[11] and -furan[11] complexes. That is, the equilibrium constants between gaseous boron fluoride and these complexes, in which every boron atom will be situated at the top of the pyramidal structure and the vacant orbital of the boron atom will

7) H. Booth and D. Martin, *J. Am. Chem. Soc.*, **64**, 2198 (1942).
8) R. Nakane and O. Kurihara, *Papers Inst. Phys. Chem. Research (Tokyo)*, **56**, 161 (1962).
9) H. Urey, *J. Chem. Soc.*, **1947**, 562.
10) R. Healy and A. Palko, *J. Chem. Phys.*, **28**, 211 (1958).
11) S. Ribnikar and G. Bootsma, *Bull. Inst. Nucl. Sci.*, "Boris Kidrich," **9**, 91 (1959).

be completely filled with electrons from donor atoms, as in the cases of the boron fluoride-methyl ether complex and tetra-fluoborate ions, are also approximately 1.03 at room temperature, as is shown in Table II.

Therefore, the equilibrium constants for these strong complex systems may always be expected to be approximately 1.08 at $-112°C$, for the value calculated for the boron fluoride-methyl ether system is 1.082 at $-112°C$.

Liquid boron fluoride, the equilibrium constant of which is 1.011 at $-112°C$, has the planar structure and vacant orbitals of the boron atom. The weak complexes which have intermediate values between 1.011 and 1.08 at $-112°C$ have slightly-dissociated polar covalent bonds such as are found in $^{\delta+}CH_3 \cdot F \rightarrow {}^{\delta-}BF_3$, but the boron fluoride in these complexes has not yet been completely transformed to a pyramidal structure and only small parts of the electrons from donor atoms may be located on the vacant orbitals of boron atoms.

Thus, it seems very likely that the equilibrium constants of isotopic exchange for boron fluoride complex systems depend mostly on the density of electrons coming from donor atoms and locating on the vacant orbitals of boron atoms, or on the B—F force constant, which becomes weaker in proportion to the transformation of boron fluoride from planar to pyramadial; the equilibrium constants seem to depend scarcely at all on the force constant of the bond formed between boron and donor atoms. Accordingly, they indicate the possibility of complex formation and the degree of the transformation of boron fluoride. Therefore, the larger the equilibrium constant, the larger the degree of deformation, and, hence, the more stable the complex.

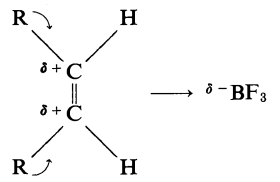
If, in the complex, the pyramidal form is the dative structure and the planar form is the no-bond structure, the equilibrium constant of isotopic exchange may be assumed to represent the abundance ratio of both structures in the complex, as does the dipole moment.

When the structure of complex is completely dative, the equilibrium constant will be approximately 1.08 at $-112°C$, as in the case of the boron fluoride-methyl ether complex system, while when it is completely no-bond, the constant will be 1.011 at $-112°C$, as in the case of the liquid boron fluoride system. In a complex in which the constant has intermediate values, the ratio of dative to no-bond structures will have values between one and zero.

Thus, it seems certain, from the observed values of the equilibrium constants, that boron fluoride can form weak σ-complexes with polar mono-olefins only at low temperatures, but that boron fluoride dissolved in liquid non-polar mono-olefins has the same planar structure as liquid boron fluoride molecule and that, therefore, no σ-bond can be formed between boron and carbon atoms, even at low temperatures.

In boron fluoride-polar mono-olefin-σ-complexes, the dative structure may be ($R-{}^{+}CH-CH_2-{}^{-}BF_3$), in which π-electrons of the double bond are transferred completely to vacant orbitals of the boron atoms and the boron fluoride molecule becomes deformed completely to the pyramidal structure, while the no-bond structure remains ($R-CH=CH_2$, BF_3). The ratio of dative to no-bond structures may be far smaller than one, for the equilibrium constants observed at $-112°C$ are far smaller than 1.08. Hence, it seems clear that σ-complexes have not the ultimate structure of $R-{}^{+}CH-CH_2-{}^{-}BF_3$, as was formerly believed of intermediate products in the polymerization of olefins by a boron fluoride catalyst.[12]

As has been shown in the preceding work and as will also be shown in the next section, V←N absorption bands, indicating the presence of a double bond, were still observed in the measurements of the absorption spectra of boron fluoride-mono-olefin complexes. Therefore, it seems very likely that the σ-complexes are $R-{}^{\delta+}CH=CH_2 \rightarrow {}^{\delta-}BF_3$ or



It is also interesting to consider the relation between the equilibrium constants and the dipole moments of mono-olefins. The following values of the dipole moments of gaseous mono-olefins are known: 0.35 D,[13] 0.37 D[14] or 0.35 ± 0.01 D[15] for propylene; 0.30 D[16] or 0.37 D[17] for 1-butene; 0.00 D[16] for *trans*-2-butene, and 0.33 D[18] for *cis*-2-butene. The values for liquid mono-olefins at low temperatures are not known, but they may not be very different from the above values.

12) C. Price and J. Ciskowski, *J. Am. Chem. Soc.*, **60**, 2499 (1938).
13) K. McAlpine and C. Smith, ibid., **55**, 459 (1933).
14) H. Watson, G. Rao and K. Ramaswamy, *Proc. Roy. Soc.*, **A143**, 582 (1934).
15) A. Mariott and F. Buckley, "Table of Dielectric Constants and Dipole Moments of Substances in the Gaseous State," Natl. Bur. Stand. Circ., No. 537, Washington, D. C. (1953).
16) H. Watson and K. Ramaswamy, *Proc. Roy. Soc.*, **A156**, 142 (1936).
17) C. Smith and C. Zahn, *J. Am. Chem. Soc.*, **47**, 2501 (1925).
18) J. Boggs, C. Crain and J. Whiteford, *J. Phys. Chem.*, **61**, 482 (1957).

Propylene and 1-butene are both mono-substituted terminal mono-olefins, although their electron-releasing substituents are different. *cis*-2-Butene is a di-substituted internal mono-olefin. Now, mono-olefin must polarize in order to form σ-complexes with boron fluoride. When polar, the larger the dipole moment of mono-olefin, the larger the deformation of boron fluoride, and therefore, the larger will the equilibrium constant be expected to become. To infer from the values of the dipole moments of gaseous propylene and 1-butene, liquid propylene and 1-butene may be expected to have nearly the same dipole moment value. Therefore, it is no wonder that boron fluoride-propylene and boron fluoride-1-butene systems have nearly the same equilibrium constant of the isotope. However exchange the equilibrium constant for boron fluoride-*cis*-2-butene system is larger than that for the boron fluoride-propylene and -1-butene systems even though the value of the dipole moment of liquid *cis*-2-butene is supposed to be nearly the same or a little smaller than that of propylene or 1-butene. This may be attributed to the fact that there are two electron-releasing groups in one molecule of *cis*-2-butene, while there is only one electron-releasing group in one molecule of propylene or 1-butene. Thus, it seems certain that equilibrium constant relates not only to the dipole moment but also to the steric structure of mono-olefin or the number of electron-releasing groups existing in a molecule of mono-olefin.

The boron fluoride-methyl ether complex is a very active catalyst. The methyl fluoride-boron fluoride complex, which is a less reactive catalyst, can alkylate benzene readily, since alkylation needs the presence of only such incipient carbonium as is found in the $^{\delta+}CH_3 \cdot F \rightarrow {}^{\delta-}BF_3$ complex, for example; such free carbonium ions as CH_3^+ are not required.[19] Polar mono-olefin-boron fluoride complexes do exist at low temperatures, but they do not partake in the polymerization of mono-olefin, and methyl chloride or mono-chlorodifluoro methane-boron fluoride complexes have no catalytic ability. Therefore, there should also be the following relation between the equilibrium constant and the catalytic ability of a Friedel-Crafts catalyst: the larger the former, the more active will the latter become.

Absorption Spectra.—No $T_R \leftarrow N$ absorption band of 1-butene, *cis*- and *trans*-2-butenes could be observed at the temperatures of their melting points, for the band was obscured by the long-wavelength tail of strong $V \leftarrow N$ absorption bands. Therefore, the effects of boron fluoride upon the $T_R \leftarrow N$ bands of 1-butene, *cis*- and *trans*-2-butene have been left unexamined.

In the present work, the effects of boron fluoride upon the fine structure of the long-wavelength tail of $V \leftarrow N$ bands have been examined, because the band peaks that lie in the region of wavelengths shorter than 190 mμ could not be traced by the Type 14 M Cary recording spectrophotometer used. The fine structure of the $V \leftarrow N$ bands of 1-butene dissolved in a large amount of methane at a temperature near the freezing point of the solution (approximately -170°C) is shown in Fig. 1. Since the fine structure of the V←N bands of *trans*-2-butene was indistinct, a measurement similar to the above was made on ethylene instead; the results are shown in Fig. 2.

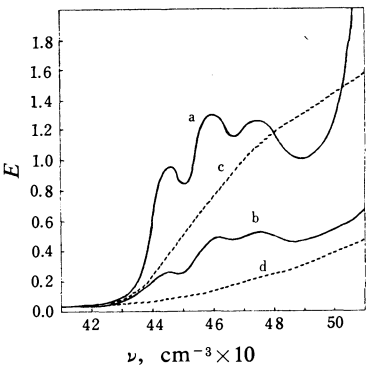


Fig. 1. Absorption spectra of 1-butene in liquid methane and boron fluoride.
Solvent: —— methane ---- boron fluoride
mole fraction of 1-butene in solution: (a) 0.33×10^{-2} (b) 0.2×10^{-2}, (c) $<1.89\times10^{-2}$ (d) $<0.13\times10^{-2}$

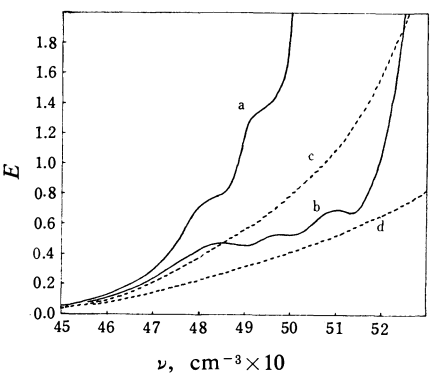
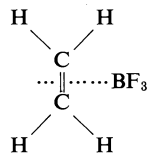


Fig. 2. Absorption spectra of ethylene in liquid methane and boron fluoride.
Solvent: —— methane, ---- boron fluoride
mole fraction of ethylene in solution: (a) 10.0×10^{-2}, (b) 0.72×10^{-2} (c) 7.7×10^{-2} (d) 3.8×10^{-2}

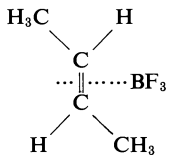
19) H. Brown, H. Pearsall, L. Eddy, W. Wallace, M. Grayson and K. Nelson, *Ind. Eng. Chem.*, 45, 1462 (1953).

Similar measurements were also made on the absorption spectra of 1-butene and ethylene in large amounts of boron fluoride at temperatures near the freezing points of the solutions (approximately $-130°C$); these results are also shown in Figs. 1 and 2. Although the $V \leftarrow N$ bands were still observed in both cases, two points are noticeable. First, in order to obtain the same values of intensity for $V \leftarrow N$ bands at the same wavelengths, the concentration of mono-olefin must be larger in a boron fluoride solution than in a methane solution. Second, the fine structures of $V \leftarrow N$ bands, which were observed in a methane solution, disappeared in a boron fluoride solution. As for the first point, it cannot yet be determined whether the intensity of $V \leftarrow N$ bands really decreases or whether the peaks of these bands shift towards shorter wavelengths, for these peaks were not measured. At any rate, the fact is that boron fluoride influenced. the intensity or the wave number of $V \leftarrow N$ bands. As for the second point, it must be remembered that the fine structures of the absorption bands in benzene at 267 mμ disappeared when benzene formed a π-complex with hydrogen fluoride.[20] Therefore, the above two points seem to suggest the complex formation of boron fluoride with 1-butene and ethylene.

However, in the preceding work, experiments on isotope effects showed that ethylene cannot form a σ-complex with boron fluoride. Hence, the complex formed with ethylene is concluded to be an unstable π-complex:



trans-2-Butene may also form a π-complex:



On the other hand, 1-butene, and perhaps propylene and *cis*-2-butene too, may form both σ-complexes and π-complexes.

In the polymerization isomerization and other reaction of olefins by boron fluoride catalysts, the σ-complexes found by us are not the intermediate products, and the σ-complex formation proceeds parallel with these reactions, as has been explained in the preceding work. No doubt these reactions occur through the actual transfer of protons to mono-olefins to form such ions as $R-{}^{+}CH-CH_3$, and the rates of the reactions are proportional to the stability of the ion. No doubt, it can be taken for granted that these reactions proceed through π-complexes, yet needless to say, the rate-determining step in these reactions does not involve the initial formation of π-complexes as is in the case of aromatic substitution.[21]

Summary

The equilibrium constants of isotopic exchange between boron fluoride gas and boron fluoride in 1-butene and *cis*-2-butene solutions have been found to be 1.017 ± 0.002 and 1.020 ± 0.002 at $-112°C$, and 1.012 ± 0.002 and 1.015 ± 0.002 at $-95°C$. In boron fluoride-*trans*-2-butene system, the equilibrium constant is 1.011 ± 0.002 at $-112°C$ and 1.006 ± 0.002 at $-95°C$.

When 1-butene and ethylene are dissolved in liquid boron fluoride, the intensity or the wave number of the $V \leftarrow N$ absorption bands in mono-olefins is changed and the fine structure of these bands disappear.

Thus, the following conclusion, more decisive than that of the preceding work, has been obtained:

Boron fluoride can form liquid σ-complexes with polar mono-olefins with electron-releasing substituents. On the other hand, with non-polar mono-olefins it cannot form σ-complexes but only unstable π-complexes. Although σ-complexes are not the intermediate products in reactions by boron fluoride catalysts, it is possible that these reactions proceed through π-complexs. However, the rate-determining step does not involve the initial formation of π-complexes.

It has also been suggeted that the equilibrium constant may be proportional to the ratio of dative to no-bond structure in the complex, and it has been found that the larger the equilibrium constant, the higher become the stability and the catalytic activity of the complexes.

The Institute of Physical and Chemical Research
Bunkyo-ku, Tokyo

20) M. Kilpatrick and H. Hyman, *J. Am. Chem. Soc.*, **80**, 77 (1958).

21) H. Brown and J. Brady, ibid., **74**, 3570 (1952).

The Electrokinetic Potential of Sparingly Soluble Salts

By Tetsuo MORIMOTO

(Received August 16, 1963)

Investigations concerning the dispersion of particles have been made in this laboratory by measuring the sedimentation volume of sparingly soluble salts in electrolyte solutions.[1] Actually the sedimentation volume of precipitated salts changes widely upon the addition of ions to water in which the particles are suspended. This fact suggests that the preferential adsorption of ions on the solid-liquid interface may result in the variation of charge density on it. The electrical charge on solid particles is the only cause of the repulsive force between them,[2] having been also the essential factor for interpreting the stability of hydrophobic colloids. The origin of the surface charge is, however, still obscure. In order to clarify, therefore, the surface charge or the electrokinetic potential and the origin of ionogenic substances, the present work has been carried out for barium sulfate, barium chromate, lead sulfate and lead chromate. For these purposes, two different samples of each salt were prepared, in each of which one of the two component ions of the precipitated salts were used in excess.

Also, the effects of the lattice ions and some non-lattice ions on the electrokinetic potential of the precipitated salts have been examined. Experiments have been carried out along lines analogous to this study by Reyerson et al.[3] and Buchanan and Heymann,[4] who investigated principally the charge of barium sulfate. Reyerson et al. report a negative charge on barium sulfate in water, while the result of Buchanan and Heymann is the reverse. It is, however, found in the present work that most of the precipitated salts tested may represent either a positive or negative charge in water according to the method of preparing the sample. Furthermore, a few measurements were carried out on the electrokinetic potential of the crystal surfaces in a solution containing two electrolytes, giving some information about the preferential adsorption of ions. It is also noticeable that some phosphates have a serious effect on the charge of the solid surface, as a citrate does.

Experimental

Materials.—All the materials used in this experiment were prepared by means of precipitation reaction; e. g., barium sulfate was prepared by allowing 1M barium chloride and 1M sodium sulfate to mix while being vigorously stirred in water heated at 80°C. The other materials were precipitated in the same manner except for different temperatures: barium chromate was prepared from barium chloride and potassium chromate at 60°C, lead sulfate from lead nitrate and sodium sulfate at 30°C, and lead chromate from lead nitrate and potassium chromate at 30°C. The precipitated salts were washed with water by repeating the decantation and filtration for a few months, until the electrical conductivity of the supernatant liquid attained a lower limiting value. Finally, the salts were washed with pure ethanol and dried at 110°C for several hours. Two different samples of each salt were provided in which either component ion was used in a 5% excess over the other when the salts were prepared.

Electrokinetic Measurements.—To determine the electrokinetic potential, the streaming potential method was used. The cells for the streaming potential measurement were almost the same as those described by Gortner[5] and by Reyerson et al.[3] In order to prevent the polarization of electrodes, the perforated platinum electrodes were substituted for by a reversible electrode, Ag-AgCl.[6] This device made it possible to develop the stable streaming potential between the electrodes. The precipitates were packed directly between the electrodes.

To develop a streaming potential, the solution was forced to flow through the diaphragm under a given pressure from one reservoir to the other. The nitrogen was used to maintain the pressure needed for the streaming potential measurement. The streaming potentials developed were measured by the vacuum-tube potentiometer with a highly sensitive galvanometer attached. Besides the measurement of the streaming potential, it was necessary to measure the specific conductance of the solution in the pores of the diaphragm. A sensitive conductance bridge was used satisfactorily for this purpose, and the cell constant was determined in each packed diaphragm by using a 0.01M

1) T. Morimoto, *J. Chem. Soc. Japan, Pure Chem. Sec.* (*Nippon Kagaku Zasshi*), **81**, 236 (1960).
2) E. J. W. Verwey, *Kolloid-Z.*, **13**, 46 (1954).
3) L. H. Reyerson, I. M. Kolthoff and K. Coad, *J. Phys. & Colloid Chem.*, **51**, 321 (1947).
4) A. S. Buchanan and E. Heymann, *J. Colloid Sci.*, **4**, 137 (1949).
5) R. A. Gortner, *Trans. Faraday Soc.*, **36**, 63 (1940).
6) A. S. Brown, *J. Am. Chem. Soc.*, **56**, 646 (1934).

potassium chloride solution. From the measurement of the streaming potential developed, the specific conductance of the liquid in the diaphragm, and the pressure applied to force the liquid to flow, it was possible to calculate the electrokinetic potential (ζ-potential) from Helmholtz-Smoluchowski's equation:

$$\zeta=\frac{4\pi\eta\kappa E}{DP} \quad (1)$$

where E is the streaming potential; κ, the specific conductance of a liquid in the diaphragm; P, the pressure driving the liquid; η, the viscosity of the streaming liquid, and D, the dielectric constant of the liquid. In any given run the linear relationship between E and P was checked, because the leakage of precipitated substances from a diaphragm might cause a deviation from linearity. Practically, the gradient of the straight line obtained by plotting E against P, was used for calculating the electrokinetic potential. It is shown by Eq. 1 that the greater the specific conductance of a solution, the less the streaming potential develops and, accordingly, the greater the experimental error, in a system consisting of one solid and one liquid. At a higher concentration of an electrolyte, therefore, the streaming potential measurement is difficult. In the present work the upper limit of the electrolyte concentration capable of the measurement was about 0.02N.

Results and Discussion

Electrokinetic Potentials in Water.—The ζ-potentials obtained on sparingly soluble salts in water are presented in Table I. Most samples studied have a charge of the same sign as that of the lattice ions used in excess when the sample was prepared; e. g., the ζ-potential of barium sulfate prepared from excess barium ions is 11.2 mV., while that of the sample prepared from excess sulfate ions is −6.10 mV. It is often described how the ζ-potential of such ionogenic substances as silver iodide is greatly affected by the adsorption of ions, especially that of lattice ions.[7] Accordingly, it is plausible that, if the one component ions of the substance are present in excess when the substance is formed, the surface lattice points occupied by the ions will be increased in number compared to those occupied by the other component ions. The present results not only prove the above statement to be valid, but also establish the great persistence of the ions against washing. Therefore, we may generally conclude that the surface of an ionogenic substance has a charge of the same sign as that of the ions used in excess on its preparation.

Table I. ζ-Potentials of sparingly soluble salts in water

Substance	Reactant used in excess	mV.
$BaSO_4$	$BaCl_2$	+11.2
	Na_2SO_4	− 6.10
$BaCrO_4$	$BaCl_2$	+10.2
	K_2CrO_4	− 7.75
$PbSO_4$	$Pb(NO_3)_2$	+16.0
	Na_2SO_4	+ 7.00
$PbCrO_4$	$Pb(NO_3)_2$	+25.7
	K_2CrO_4	−15.1

Lead sulfate is an exception. In the case of lead sulfate, the two samples have a positive charge irrespective of the method of preparing them; the ζ-potential is 16.0 mV. on the sample prepared from excess lead ions and 7.00 mV. on the sample prepared from excess sulfate ions. According to the experiments carried out in more detail in our laboratory,[8] the charge of lead sulfate appears to be always positive in water, regardless of such conditions of preparation as the kind of reagents and the pH value of the reacting solutions.

In Table II the solubilities of all the samples studied in this experiment are presented.[9] The solubility of lead sulfate is the greatest of those of the four salts, while that of lead chromate is the least. Because of this relatively larger solubility of lead sulfate and the extremely small solubility of lead hydroxide,[10] it is conceivable that the surface of lead sulfate crystals is hydrolyzed partially in water to produce lead hydroxide. Considering the fact that most metal hydroxides have a positive charge in water,[11] one can understand the fact that the surface of lead sulfate crystals has a positive charge. This, however, does not occur on the surface of a lead salt with so small a solubility as lead chromate.

Table II. Solubilities of sparingly soluble salts in water (25°C)[9]

Substance	$BaSO_4$	$BaCrO_4$	$PbSO_4$	$PbCrO_4$*
Solubility (mol./l.)	1.25×10^{-5}	1.64×10^{-5}	14.8×10^{-5}	0.053×10^{-5}

* The value obtained at 20°C.

The Electrokinetic Potential in an Electrolyte Solution.—As has been described above, it is seen that the lattice component ions which were used in excess on preparation have a pronounced effect on the surface of ionogenic

7) A. E. Alexander and P. Johnson, "Colloid Science," Clarendon Press, Oxford (1949).

8) To be published.

9) Y. Seidell, "Solubilities of Inorganic and Metal Organic Compounds," Van Nostrand, New York (1940).

10) P. Deschamps and B. Charreton, *Compt. rend.*, **232**, 162 (1951).

11) J. Sameshima, "Koshitsugaku," Shokabo, Tokyo (1949).

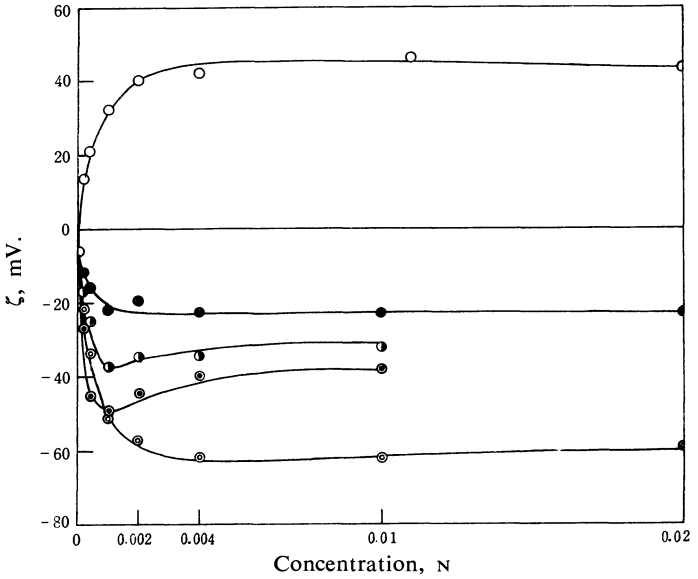


Fig. 1. ζ-Potentials of $BaSO_4$ in solutions of electrolytes.
○ $Ba(NO_3)_2$ ● Na_2SO_4 ⊙ Na_2SO_4 and sodium citrate
◎ Sodium citrate ◑ $Ba(NO_3)_2$ and sodium citrate.

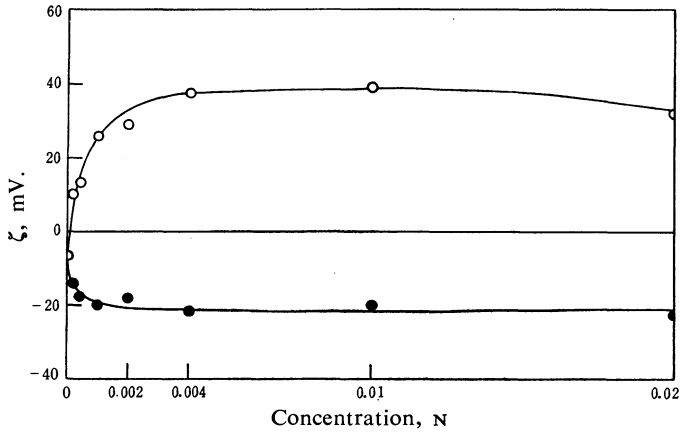


Fig. 2. ζ-Potentials of $BaCrO_4$ in solutions of lattice ions.
○ $Ba(NO_3)_2$ ● K_2CrO_4

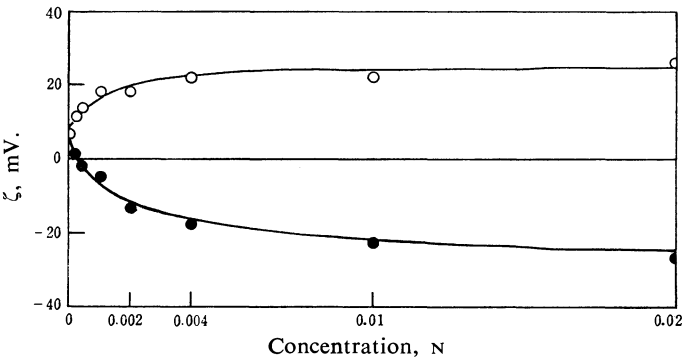


Fig. 3. ζ-Potentials of $PbSO_4$ in solutions of lattice ions.
○ $Pb(NO_3)_2$ ● Na_2SO_4

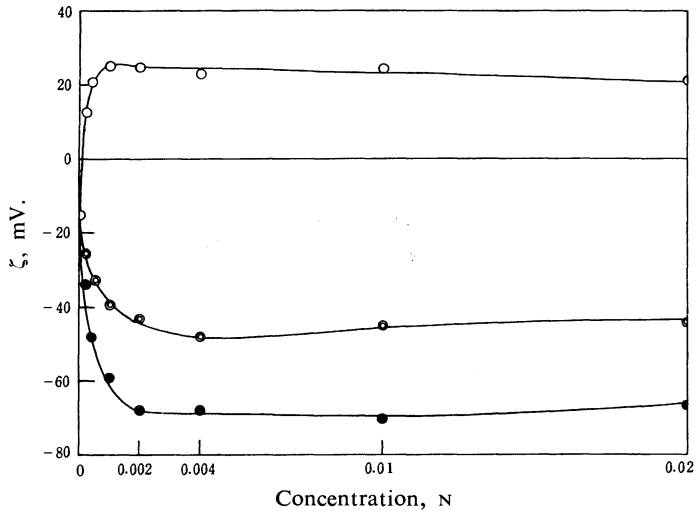


Fig. 4. ζ-Potentials of $PbCrO_4$ in solutions of electrolytes.
○ $Pb(NO_3)_2$ ● K_2CrO_4 ◎ Sodium citrate

substances. Similarly, it is expected that when the lattice ions are added to the water with which the surface of the salt crystals comes in contact, they will have a great influence on the surface charge. In the preliminary experiments, by using samples charged both positively and negatively in water, the effect of barium ions on the ζ-potential of barium sulfate was tested. It was thus found that the ζ-potential curves were nearly parallel to each other, independently of their initial ζ-values. This was the case also with the effect of sulfate ions. Hence, in this series of experiments, one kind of sample for each material was chosen. The results obtained are shown in Figs. 1—4. As expected, it is seen that the lattice ions have a great effect on the surface charge of the precipitated salts. The barium ions, even at an extremely small concentration, charge barium sulfate, which originally has a negative charge, positively. After that the ζ-value increases with the increasing concentration of barium nitrate to a limiting value of 45 mV. Sodium sulfate increases the negative charge of barium sulfate, but the change in ζ-potential caused by sulfate ions is much less than that caused by barium ions.

The results obtained in this work agree well with those of Reyerson et al.[3] and Buchanan and Heymann[4] in that barium ions affect barium sulfate more pronouncedly than sulfate ions, irrespective of the ζ-value in water. Furthermore, Reyerson et al. concluded that barium ions act peptizingly and sulfate ions coagulatingly on barium sulfate. In our laboratory it has been found that the sedimentation volume of barium sulfate decreased steeply in the presence of barium ions, whereas no great changes occurred in the solution of sulfate ions.[1] These phenomena may be explained in terms of the change in ζ-potential.

The behaviors of barium ions and chromate ions for barium chromate are quite similar to those of barium ions and sulfate ions respectively for barium sulfate. On lead sulfate, however, both lead ions and sulfate ions have a very weak effect compared to that of barium ions on barium sulfate. It is, therefore, characteristic that the initial part of ζ-potential curves increases or decreases slowly. Also, the limiting ζ-values are only +20 mV. and −20 mV. respectively. On the contrary, the change in the ζ-potential of lead chromate by lead ions and chromate ions is very large; the ζ-value increases from −15 mV. to +25 mV. in the presence of lead ions and decreases from −15 mV. to −70 mV. in the presence of chromate ions. In this case, the effect of chromate ions is nearly equal to or slightly greater than that of lead ions. The only previous finding concerning the ζ-potential of lead chromate, obtained by Reyerson et al.,[3] shows fairly good agreement with the present finding. Certainly the fact that the sedimentation volume of lead chromate is more decreased in the presence of chromate ions than in the presence of lead ions, must be related closely to the ζ-potential change.

It is strange that, on barium sulfate and barium chromate, the lattice cations, barium ions, have a more serious effect than the anions, while on lead chromate the lattice anions, chromate ions, have the more serious effect. Generally, the adsorbability of ions on a polar solid surface from a solution depends largely upon their hydrating tendency

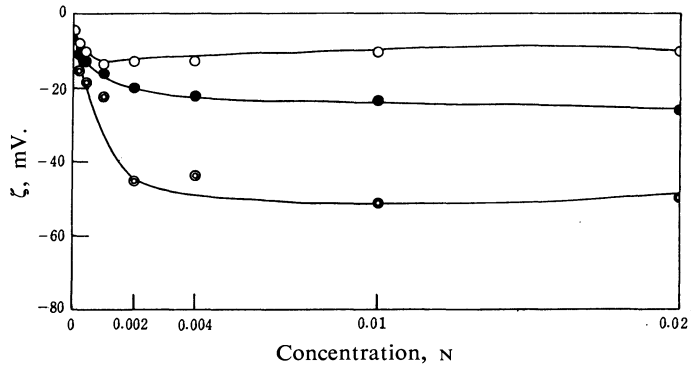


Fig. 5. ζ-Potentials of $BaSO_4$ in Solutions of phosphates and KOH.
○ KOH ● Na_2HPO_4 ◎ $Na_5P_3O_{10}$

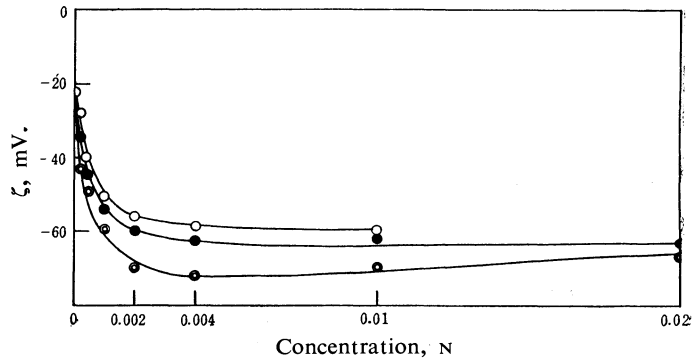


Fig. 6. ζ-Potentials of $PbCrO_4$ in solutions of phosphates and KOH.
○ KOH ● Na_2HPO_4 ◎ $Na_5P_3O_{10}$

and on their valency; the stronger the tendency, the less the adsorbability. However, the solids have also their own problems. As is shown in Table II, there are large differences in solubility among the materials used. The solubility decreases in the order: lead sulfate > barium chromate, barium sulfate > lead chromate. The variation of the potential is, however, just the reverse. Buchanan and Heymann[4] reported a similar tendency when strontium sulfate, lead sulfate and barium sulfate are used. Thus we may conclude that the smaller the solubility of the ionic crystal, the greater the effect of lattice ions on its surface. Really the variation in the ζ-potentials of lead chromate upon the addition of lead or chromate ions amounts to 50 mV., whereas that of lead sulfate upon the addition of lead or sulfate ions is only 20 mV.

At the surface of a crystal having a smaller solubility, the electrical double layer is possibly constructed more definitely than at the surface of a crystal having a larger solubility. When the solubility of a solid is large, the lattice ions will be diffused in large quantities across the electrical double layer, bringing about the agitation of the double layer; therefore, the fixation of ions on the "fixed layer" occurs only with difficulty. Of course, on such a solid surface the adsorption of indifferent ions also becomes difficult.

The interactions of a salt with its lattice ions, should be considered to cause partially the incorporation of the ions with the solid surface simultaneously with their adsorption on the fixed layer. Lead chromate shows well-defined prism-shaped crystals under an electron microscope.[1] The surface of well-defined crystals will be favorable for producing the streaming potential corresponding to the charge in the diffused layer of an electrical double layer as compared with an irregular surface, because little turbulences occur. The large change in the ζ-value of lead chromate may be partially due to this reason.

The Effect of Foreign Ions.—Sodium citrate has a remarkable effect on the ζ-potential of barium sulfate and lead chromate, as Figs. 1 and 4 show, in accordance with the results of Reyerson et al.[3] Apparently, on barium sulfate the effect of sodium citrate is much greater than that of sodium sulfate, whereas

on lead chromate it is less than that of potassium chromate. Because of the possibility of forming a complex of citrate ions with barium ions,[12] citrate ions will be adsorbed strongly onto the surface of barium sulfate.

By using sodium citrate and the lattice ions of barium sulfate, the effect of mixed electrolytes on the ζ-potential of barium sulfate was investigated, as is shown in Fig. 1. In these cases, the concentration indicated in abscissa should be read as that of each electrolyte present, so that the equal equivalents of the two electrolytes were dissolved in a solution. The ζ-potential curves of barium sulfate in these two solutions represent an almost identical development over all the range of concentration examined. As has been described above, the effect of sodium citrate on the ζ-potential of the barium sulfate crystal is greater than that of sodium sulfate. In the solution containing these two electrolytes together, the ζ-potential curve of barium sulfate initially goes parallel with the curve obtained in the presence of sodium citrate only, arriving at a limiting value. After that it rises, differing substantially from the effect of sodium citrate only. This means that, because of the stronger adsorption of citrate ions, it excels the adsorption of sulfate ions at smaller concentrations, but at increased concentrations sulfate ions also take part in the adsorption on the fixed layer, together with citrate ions, causing a considerable decrease in the negative ζ-potential of barium sulfate. Even when we use barium nitrate and sodium citrate as mixed electrolytes, the results are almost the same. The resultant ζ-potential rises more steeply after the attainment of the minimum than in the former case, but it does not exceed the isoelectric point. In any case, it is characteristic of the adsorption of ions from a mixed electrolyte solution that the preferential adsorption of the ion affecting more strongly occurs at lower concentrations. The sedimentation volume of barium sulfate measured in these mixed electrolyte solutions decreases initially, attains a minimum, and then rises, corresponding to the change in the ζ-potential.[13] In a solution of sodium citrate only, however, the sedimentation volume of barium sulfate remains almost constant after attaining a limiting value, corresponding to the change in the ζ-potential. This fact is positive evidence that the ζ-potential is responsible for the change in the sedimentation volume of powders. Although one can expect a similar conclusion concerning the ζ-potential of lead chromate in mixed electrolyte solutions, it was impossible to observe this because the extremely small solubility of lead citrate does not permit both lead ions and citrate ions to coexist at the concentrations used here.

Recently studies of the properties of various phosphates which differ in degree of polymerization have been carried out. If they are used on surface phenomena, it may be expected that they will behave as polyelectrolytes. In the present work, phosphates of a lower degree of polymerization were used, along with potassium hydroxide, to investigate the effect on the surface charge of barium sulfate and lead chromate. As shown in Fig. 6, triphosphate, orthophosphate and hydroxyl ions all seriously decrease the ζ-potential of lead chromate. It is peculiar that hydroxyl ions have a large effect in this case, probably because of their greater adsorbability arising from the extremely small solubility of lead hydroxide. For barium sulfate, three kinds of ions affect it differently: the effect of triphosphate is the greatest, as it is for lead chromate, while that of orthophosphate is moderate and that of hydroxyl ions, very small as is shown in Fig. 5. It appears that there are differences between the adsorbabilities of various phosphates corresponding to their polymerization degrees, and that the higher the polymerization degree, the stronger the adsorbability. The detailed observation of the effect of such a series of phosphates on surface properties is a problem for future study.

Summary

1) The ζ-potentials of such sparingly soluble salts as barium sulfate, barium chromate, lead(II) sulfate and lead(II) chromate have been measured in water by means of the streaming potential method. Most samples prepared by using either lattice ion in excess have a charge of the same sign as that of the ion. This suggests that the lattice ions occupy many more lattice points on the surface than do other ones, and that it is difficult to remove them by washing. One exception is lead(II) sulfate, in which the ζ-potentials of the two samples are positive. This seems to depend on the surface hydrolysis of lead(II) sulfate.

2) The ζ-potentials vary widely also when the lattice ions are added to water. The effect of both lattice ions are the greatest on lead(II) chromate and the least on lead(II) sulfate.

12) J. Schubert and J. W. Richter, *J. Am. Chem. Soc.*, **70**, 4259 (1948).

13) T. Morimoto, *J. Chem. Soc. Japan, Pure Chem. Sec. (Nippon Kagaku Zasshi)*, **81**, 74 (1960).

14) The solubility of lead citrate is 0.05344 g./100g. (25°C), cf. Ref. 9.

The solubility of the solids is an important factor affecting the variation of ζ-potentials when the lattice ions are added.

3) In order to investigate the effect of the mixed electrolyte solution on the ζ-potential of barium sulfate, sodium citrate, which has a remarkable effect by itself, has been mixed with sodium sulfate or barium nitrate. The resultant ζ-potential curves show a definite minimum, which demonstrates that, although the adsorption of citrate ions excels that of sulfate or barium ions at smaller concentrations, the latter become comparable to the former at larger concentrations.

4) The surface chemical action of triphosphate and orthophosphate ions has been tested. As expected, the higher the polymerization degree of phosphates, the larger the effect on the charge of solid surfaces.

The author wishes to express his deep appreciation to Professor Masaji Miura of Hiroshima University for his valuable advice and encouragement, and to Mr. Masashi Sakamoto for his assistance in this work.

Department of Chemistry
Faculty of Science
Okayama University
Tsushima, Okayama

The Heat of Immersion of Aluminum Oxide in Water

By Tetsuo MORIMOTO, Koichi SHIOMI and Hiroshi TANAKA

(Received December 6, 1963)

It has been reported by several authors[1-4] that various silicas show a maximum in the temperature range of 200 to 300°C in the curve of the heat of immersion in water vs. the outgassing temperature. Two theories have been proposed to explain this phenomenon. According to one theory, the hydroxyl groups on the surface of silica samples form hydrogen bonds with water molecules upon immersion. Most of the heat evolved upon immersion is thus due to the hydrogen bonding energy; the highest concentration of surface hydroxyl groups brings the maximum in the heat of immersion. At temperatures higher than 300°C condensation of the surface hydroxyl groups occurs, converting silanol groups to siloxanes, which are not rehydrated easily on immersion in water; consequently, the heat of immersion decreases. On the other hand, at lower temperatures the surface hydroxyl groups are partly covered by some amount of water molecules adsorbed physically, so that the heat becomes less.[1,2]

According to another theory, the condensation of surface hydroxyl groups proceeds with heat treatment, forming a siloxane surface which, on immersion in water, reproduces the hydroxyl groups by a reverse reaction. The immersion heat increases as the dehydration proceeds with the heat treatment. When the temperature of the treatment rises further, the siloxane surface formed is stabilized and becomes difficult to be rehydrated; therefore, the heat of immersion decreases.[3,4]

In these two explanations it may be seen that the existence and behavior of surface hydroxyl groups play an important role. Also, from the viewpoint of catalytic action, the behavior of the surface hydroxyl groups on metal oxide is important. The present investigation will deal with the behavior of the surface hydroxyl groups on alumina by measuring the heat of immersion in order to compare it with that of those groups on silica samples and to test the validity of the two explanations mentioned above in the case of alumina samples.

Experimental

Samples.—The samples studied were α- and γ-alumina. The former, made by the Showa Denko Co., was washed with 4 N hydrochloric acid and then with water until the value of the electrical conductance of the mother liquor became that of water, while the latter was prepared by calcining, at 550°C in air, gibbsite, which was supplied by

1) A. C. Makrides and N. Hackerman, *J. Phys. Chem.*, **63**, 594 (1959).
2) M. M. Egorov, V. F. Kiselev, K. G. Krasilnikov and V. V. Murina, *J. Phys. Chem.* (*U. S. S. R.*), **33**, 65 (1959).
3) G. J. Young and T. P. Bursh, *J. Colloid Sci.*, **15**, 361 (1960).
4) J. W. Whalen, "Solid Surfaces and the Gas-Solid Interface," Ed. by L. E. Copeland et al., Am. Chem. Soc., Washington, D. C. (1961). p. 281.

the Showa Denko Co., and then washing it with water in a way similar to that used for the former. X-Ray investigations showed that the latter is amorphous, while the former gives the α-form. Just prior to the immersion measurement, the sample was outgassed in a glass ampoule for 4 hr. at a given temperature in a vacuum of 10^{-4} mmHg, and then sealed off. When the pretreatment was carried out above 500°C, silica ampoules were used.

Immersion Measurement. — The heat evolved upon the immersion of the sample in water was measured by a precision calorimeter equipped with a thermistor as a temperature-sensing element.[5,6] The galvanometer reading was calibrated by supplying a given electrical energy through a constantan wire of about 50 Ω. In the course of the measurements of the immersion heat, the slow heat evolution described by Guderjahn et al.[7] has never been detected; rather, the evolution of heat was extinguished in just a few minutes. All the measurements were carried out at 25±0.01°C.

Surface Area Measurement.—The B. E. T. surface areas were measured by nitrogen adsorption. The surface area of α-alumina was constant (1.91 m^2/g.), independent of the outgassing temperatures employed here, while the area of γ-alumina was almost constant to 600°C and then decreased with the further rise in the outgassing temperature above 600°C, as Fig. 1 shows.

Water Content. — The water content of the samples was determined as follows: the water vapor generated by the heat treatment of the

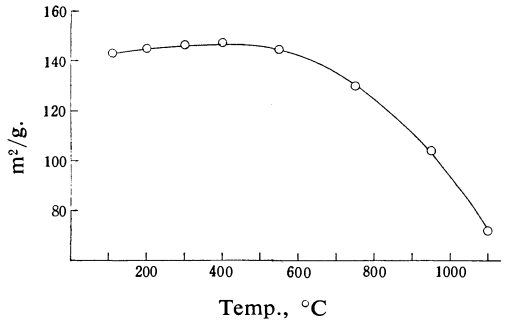


Fig. 1. Temperature variation of the specific area of γ-Al_2O_3.

samples in an evacuated apparatus was gathered in a trap cooled at the boiling point of nitrogen, and then the volume of the vapor reevaporated at room temperature was measured volumetrically. In order to raise the sensitivity of the pressure reading, an oil manometer was used. The measurements were carried out at 100°C temperature intervals from 300 to 1100°C, keeping the sample at each temperature for 4 hr.

5) A. C. Zettlemoyer, G. J. Young, J. J. Chessick and F. H. Healey, *J. Phys. Chem.*, **57**, 649 (1953).
6) T. Morimoto, M. Yamaguchi. T. Matsumoto and K. Juna, *Rep. Res. Lab. Surface Science, Okayama Univ.*, **2**, 65 (1962).
7) C. A. Guderjahn, D. A. Paynter, P. E. Berghausen and R. J. Good, *J. Phys. Chem.*, **63**, 2066 (1959).

Results and Discussion

The findings on the immersion heat of alumina in water are shown in Fig. 2. The heat of immersion of α-alumina, like that

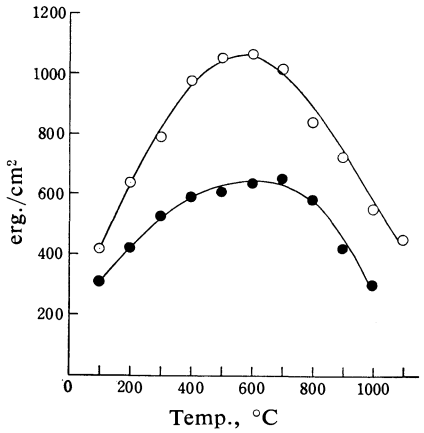


Fig. 2. Immersion heat vs. outgassing temperature curve of Al_2O_3.
○ α-Al_2O_3 ● γ-Al_2O_3

of γ-alumina, increases to a maximum value and then decreases as the outgassing temperature is raised. This phenomenon was also found in the case of silica, as has been mentioned above. It may be seen, however, that there are two remarkable differences between the immersion heat curve of silica and that of alumina. First, the absolute values of the heat of alumina are much greater than those

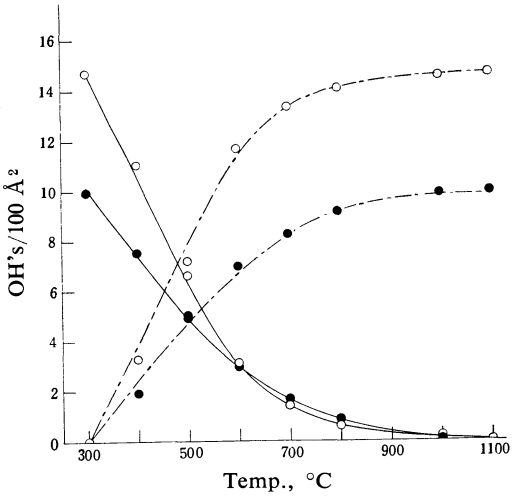


Fig. 3. Temperature variation of the dehydration amount and the water content of Al_2O_3.
○ α-Al_2O_3 ● γ-Al_2O_3
------ dehydration amount
—— water content

of silica, and, second, the outgassing temperature at which the heat of immersion of alumina showed a maximum is 600 to 650°C, much higher than that (200~300°C) in the case of silica. This latter fact suggests that the bonding energy of aluminol is remarkably large. Wade and Hackerman[8] could not find such a maximum on alumina since they treated alumina only to 450°C.

The amounts of dehydration and the water contents of alumina are given in Fig. 3. Since the degassed amounts of both α- and γ-alumina from 1000 to 1100°C were negligible, the water contents at various temperatures were calculated by assuming the value at 1100°C to be zero. Furthermore, assuming that the dehydrated water arises from the condensation of surface hydroxyl groups, the numerical value of these amounts was expressed in OH's/100Å^2. It may be seen from these curves that the water contents of alumina decrease steeply from 300 to 600°C, followed by a slow dehydration up to 1100°C.

Crystallographic data show that the surface layer of α-alumina consisting of the closest packing of oxygen ions contains 19 O^{2-}/100Å^2, as was calculated by Wade and Hackerman.[8] If all the oxide ions are hydrated normally, the same number of hydroxyl groups will be formed; this can be compared to 8 OH's/100Å^2 for the silica surface.[9] All the figures obtained as the water contents of alumina above 300°C are less than this value. Moreover, it is known that physically-adsorbed water molecules on solid surfaces can be removed by heating them up to 200~250°C.[1,10] In view of these circumstances, it is plausible to consider that the water vapor which was generated above 300°C had been bound chemically on the surface, forming surface hydroxyl groups. The water content of samples decreases linearly from 300 to 600°C, while, on the other hand, the immersion heat of the same samples increases linearly in the same temperature range. It may be considered from these observations that, on the samples treated in such a temperature range, the rehydration of dehydrated sites on the surface occurs easily on immersion in water, accompanied by the evolution of hydration energy. The appropriateness of this consideration seems to be supported by the following fact: in such a temperature range the increase in the immersion heat of α-alumina, in which the decrease in water content is more marked, is steeper than in the case of γ-alumina, in which the decrease in water content is less. In this range of outgassing temperature, surface hydroxyl groups, aluminoles, will be regenerated reversibly from dehydrated sites on immersion in water. Therefore, one can calculate the heat of hydration from the amount of dehydration and the immersion heat. Figure 4 shows the relation between the immersion heat and water

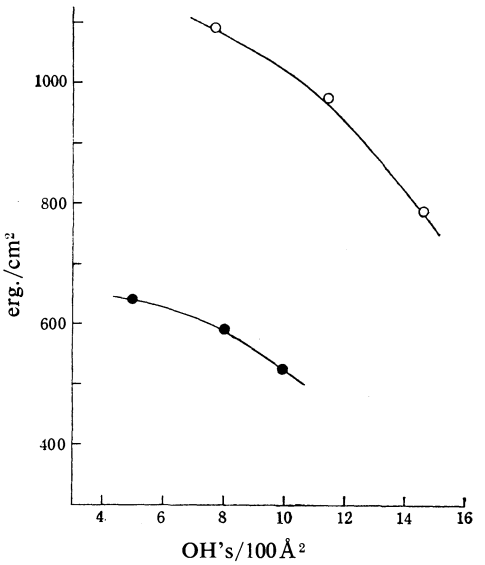


Fig. 4. Immersion heat vs. water content curve of Al_2O_3.
○ α-Al_2O_3 ● γ-Al_2O_3

contents in this temperature range. Regarding each of these curves as straight near the end, the heats of hydration on the surfaces of α- and γ-alumina can be calculated as 15.8 and 9.60 kcal./mol. water respectively. These values are several times greater than those obtained on the surface of silica samples[4] and are a little greater than the values known as the energy of hydrogen bonds.

When the outgassing temperature exceeds 600°C, the immersion heat begins to decrease, probably because of the stabilization of the dehydrated product, aluminoxane, produced on the surface. It may be seen from these discussions that the immersion phenomenon of alumina in water can be explained by the theory of rehydration, which is the second one of the two mentioned above. However, it is surprising that the immersion heats of the samples treated at 1100°C, on the surface of which the water contents are regarded as zero, are fairly large compared with those on silica samples.[1-4]

This fact seems to suggest that the wetting

8) W. H. Wade and N. Hackerman, *J. Phys. Chem.*, **64**, 1196 (1960).
9) R. K. Iler, "The Colloid Chemistry of Silica and Silicates," Clornell University Press, Ithaca, N. Y. (1955).
10) W. H. Wade and N. Hackerman, *J. Phys. Chem.*, **63**, 1639 (1959).

of the surface of aluminoxane should be considered significant. In order to solve the problem of the wetting degree of the aluminoxane surface or, in other words, the problem whether or not the rehydration of the aluminoxane surface is significant in the sample treated at 1100°C, the kinetic study of the hydration is needed for alumina samples. The heats of immersion of α-alumina are considerably greater than those of γ-alumina. Some authors have pointed out that the immersion heats of the amorphous silica in water are less than those of crystalline silica.[1,11] The reason for this phenomenon remains unclear. The strength of the bonding force of surface radicals with water molecules is, however, probably an important factor, in addition to the concentration of the surface radicals.

11) W. H. Wade, R. L. Every and N. Hackerman, ibid., **64**, 355 (1960).

Summary

1) The surface properties of two kinds of alumina have been studied by measuring the immersion heats and the water contents. The heat of immersion of alumina showed a maximum at about 600~650°C, which is considerably higher than the 200~300°C of silica, and the heat values were much greater than those of silica.

2) It has been concluded that the rehydration process of dehydrated sites plays an important role in the case of the immersion of alumina in water. The heats of hydration calculated from the immersion heats of α- and γ-alumina were 15.8 and 9.60 kcal./mol. water respectively.

Department of Chemistry
Faculty of Science
Okayama University
Tsushima, Okayama

The Diamagnetic Study of the Nature of Association in Acetic Acid

By S. Sriraman and V. Shanmugasundaram

(Received September 25, 1963)

A great deal of work has been done on the magnetic study of liquid mixtures, but comparatively very little work has been done on the influence of the hydrogen bond on the diamagnetism. The earliest report on this subject was by Angus and Hill,[1] who studied substances capable of forming a hydrogen bond in order to ascertain whether the formation of such bonds could be detected by magnetic methods. They confined their investigations to very dilute solutions. Their results showed that the formation of hydrogen bonds involving a ring closure decreases the susceptibility value. Ananthakrishnan and Varadachari,[2] on the basis of a critical analysis of the results on the subject, concluded that the formation of hydrogen bonds in certain cases where multiple linkages are involved should increase the susceptibility value. When Venkataramiah[3] studied the susceptibility of alcohohols in various solvents, his results indicated an increase in diamagnetism when the hydrogen bond is ruptured. However, the investigations of some organic compounds by Rumpf and Seguin[4] seem to show that no appreciable change occurs in the formation of hydrogen bonds. Later Venkateswarlu and Sriraman[5] studied the changes of susceptibility when benzoic, cinnamic, salicylic, and acetic acids are dissolved in a number of solvents with widely different proton-coordinating powers. Their results are in accordance with those of Angus and Hill.[1] Recently Deshpande and Pathki[6] studied magnetically acetic acid dissolved in pyridine at different concentrations. From their results they concluded that the maximum departures from the additive value at certain concentrations are due to the formation of complexes at those concentrations and that the formation or rupture of a hydrogen

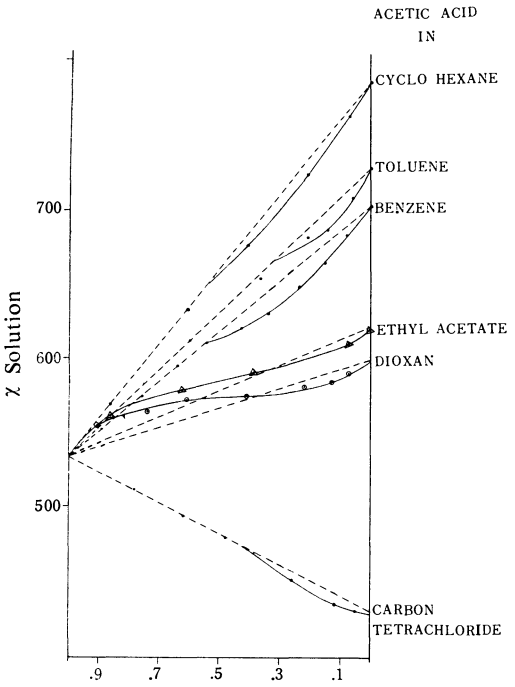
1) W. R. Angus and W. K. Hill, *Trans. Faraday Soc.*, **36**, 923 (1940).
2) S. V. Ananthakrishnan and P. S. Varadachari, *Proc. Indian Acad. Sci.*, **20A**, 128 (1944).
3) H. S. Venketaramiah, *J. Mysore Univer., Sec. B*, Contrib. in Physics, 19, Pt. 4, 3, 1942.
4) P. Rumpf and M. Seguin, *Bull. soc. chim. France*, **1950**, 542; ibid., **1950**, 177.
5) K. Venkateswarlu and S. Sriraman, *Trans. Faraday Soc.*, **53**, 433 (1957).
6) V. T. Deshpande and K. G. Pathki, ibid., **58**, 2134 (1962).

bond does not by itself appreciably affect the susceptibility value. In view of these divergent conclusions by different workers, it was considered desirable to study in detail some compounds in which the hydrogen bond is known to exist predominantly. Acetic acid, one such typical substance, has been chosen for study in the pure and dissolved states.

Experimental

The purification of the acid and the solvents was generally based upon the methods given by Vogel[7] and was continued until the acid and the solvents gave physical constants in good agreement with previously recorded values.

The susceptibility measurements were made by the Gouy method, using a large Pye magnet. The field strength had a range from 12 to 14 k. gauss for the different field currents used. For every measurement, observations were made with two experimental tubes of different cross-sections for the three field currents. Assuming the influence of the vapour to be negligible, the susceptibility values have been corrected for residual air in the space above the liquid by the manner described by Rao and Narayanaswami.[8] The densities of the liquids were found with a special type of stoppered, specific-gravity bottle assuming the density of water to be 0.9951 g. cm^{-3} at 32°C.



←Wt. fraction of CH_3COOH

Fig. 1.

7) A. I. Vogel, "Textbook of Practical Organic Chemistry," Longmans, London (1948).

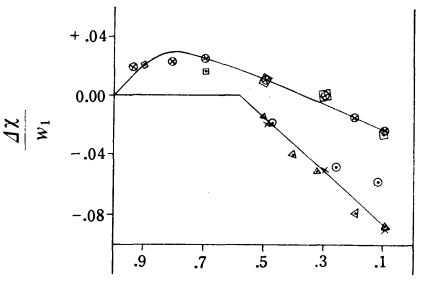
8) S. R. Rao and A. S. Narayanaswami, *Proc. Indian Acad. Sci.*, 9A, 35 (1939).

Results

The specific susceptibility values of the pure liquids and mixtures studied at different concentrations are given in the table with an experimental accuracy of ±0.5%. For mixtures, the χ values, calculated on the basis of the additive law, are also given. The values of χ are plotted against the weight fraction in Fig. 1. If χ_1 and χ_1' are the specific susceptibility values of the acetic acid in its pure and dissolved states respectively, and w_1, its weight fraction, then, according to Angus and Tilston ;[9]

$$\chi_1' - \chi_1 = \frac{\chi_{(observed)} - \chi_{(additive)}}{w_1} = \frac{\Delta\chi}{w_1}$$

These values are calculated and plotted against the mole fraction in Fig. 2.



←Mol. Fraction of CH_3COOH

Fig. 2.

△ Benzene
⊙ Carbon tetrachloride
× Cyclohexane
⊗ Dioxan
▣ Ethyl acetate

Discussion

It has been generally assumed by earlier workers[5,10] that acetic acid in the pure liquid state exists in a cyclic hydrogen-bonded dimer. However, the existence of a non-zero dipolemoment indicates that a portion of the dimeric units should be non-cyclic. Pohl et al.,[11] on the basis of their studies of electric polarisation, concluded that chains of molecules are also present. Recent studies relating to the mechanism of association in acetic acid by the Raman effect,[12] the dipole moment,[13] and proton magnetic resonance[14] reveal that the

9) W. R. Angus and D. V. Tilston, *Trans. Faraday Soc.*, 43, 221 (1947).

10) G. V. L. Murthi and T. R. Seshadri, *Proc. Indian Acad. Sci.*, 16A, 51 (1942).

11) H. A. Pohl, M. E. Hobbs and P. M. Cross, *J. Chem. Phys.*, 9, 408 (1941).

12) M. I. Batuev, *Doklady Akad. Nauk S. S. S. R.*, 59, 1170 (1948).

13) M. Blinc and R. Blinc, *J. Polymer Sci.*, 32, 506 (1958).

14) L. W. Reeves and W. G. Schneider, *Trans. Faraday Soc.*, 54, 314 (1958).

TABLE I.

Solvent	Mol. frac.	Wt. %	Density ρ_4^{32}	χ* Solution Calcd.	χ* Solution Obs.	$\frac{\Delta\chi}{w_1}$
Benzene	1.00	—	1.043	—	0.533	—
	0.91	89.00	1.019	0.551	0.550	—
	0.80	75.84	0.991	0.574	0.574	—
	0.70	64.13	0.968	0.594	0.593	—
	0.61	54.50	0.948	0.610	0.610	—
	0.50	43.70	0.929	0.628	0.621	−0.017
	0.40	34.03	0.914	0.644	0.631	−0.039
	0.32	24.13	0.899	0.661	0.649	−0.051
	0.19	15.17	0.888	0.676	0.665	−0.075
	0.10	7.86	0.877	0.689	0.682	−0.088
	0	—	0.876	—	0.702	Taken as standard
Cyclohexane	0.89	85.88	0.985	0.569	0.568	—
	0.69	61.16	0.903	0.633	0.632	—
	0.49	40.64	0.847	0.685	0.677	−0.019
	0.30	21.10	0.808	0.735	0.725	−0.047
	0.10	6.80	0.780	0.772	0.766	−0.088
	0	—	0.772	—	0.790	
Toluene	0.70	60.34	0.970	0.610	0.611	—
	0.50	37.24	0.908	0.655	0.655	—
	0.30	20.90	0.882	0.687	0.683	−0.019
	0.20	12.37	0.870	0.704	0.700	−0.024
	0.10	5.98	0.864	0.716	0.714	−0.033
	0	—	0.860	—	0.728	
Carbon tetrachloride	0.90	77.93	1.132	0.510	0.511	—
	0.80	61.70	1.191	0.493	0.493	—
	0.70	47.94	1.251	0.479	0.480	—
	0.48	26.18	1.374	0.457	0.452	−0.019
	0.26	12.15	1.472	0.442	0.436	−0.049
	0.12	5.15	1.534	0.435	0.432	−0.058
	0	—	1.581	—	0.430	—
Ethyl acetate	0.90	86.14	1.018	0.545	0.562	+0.019
	0.70	61.69	0.979	0.566	0.575	+0.016
	0.50	39.34	0.947	0.585	0.590	+0.012
	0.30	22.23	0.933	0.600	0.600	0.000
	0.10	7.53	0.902	0.612	0.610	−0.026
	0	—	0.892	—	0.619	
Dioxan	0.94	91.96	1.045	0.538	0.556	+0.019
	0.81	74.18	1.044	0.549	0.565	+0.021
	0.70	61.05	1.040	0.557	0.572	+0.024
	0.50	40.94	1.035	0.570	0.575	+0.012
	0.30	21.90	1.030	0.582	0.582	0.000
	0.20	12.91	1.028	0.588	0.586	−0.015
	0.10	6.66	1.023	0.592	0.590	−0.030
	0	—	1.028	—	0.596	

* All the susceptibility values in this paper are expressed in 10^{-6} c.g.s. units.

association is a mixture of non-polar dimer association and polar chain association.

When acetic acid is diluted with non-interacting solvents, such as benzene, toluene, cyclohexane, and carbon tetrachloride, there is no possibility of the formation of hydrogen bonds between the solute and solvent molecules; any deviation from the additive law should arise only from the change in the mechanism of association of the acetic acid molecules. The results obtained for these mixtures in Fig. 1 show that the χ values of

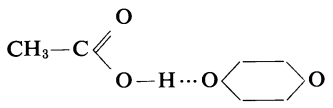
mixtures are strictly additive up to nearly equimolecular proportions; then a regular diminution of χ values occurs on further dilution.

The formation of hydrogen bonds between the hydrogen and carbonyl groups can be considered to be due to an electrostatic force, and the presence of such a force can be considered as equivalent to an electric field between the two groups and its contribution to the diamagnetism, to be paramagnetic. Therefore, the rupture of the hydrogen bond should give an increased χ value of the molecule. It is clear that the monomeric form of the acetic acid molecule should have a higher susceptibility value than the associated form.

The decrease in $\Delta\chi/w_1$ values at dilutions beyond equimolecular proportions can be explained in terms of polymer-dimer equilibria. The hydrogen bonds in the polar chain polymers are weaker than those in closed dimers. The effect of dilution is to break the polymers into monomers. The monomers are strongly polar and could not have stability as such. Hence, they probably combine to form closed dimers. The progressive diminution of $\Delta\chi/w_1$ in Fig. 2 at a higher dilution evidently indicates the progressive formation of ring dimers since such a formation of closed rings should result in a decrease in χ value.[1,5,15] The studies of the dilution shift of the proton resonance signal of the -OH group of acetic acid by Reeves and Schneider[14] indicate a shift to the low field up to a 0.1 mol. fraction of the acid and explains it as arising from the formation of dimers. The higher value of χ obtained by Deshpande and Pathki[6] for all the concentrations in an acetic acid-pyridine mixture has been explained as arising from the stabilization of monomers, even at a higher concentration. However, our results indicate positively that monomerization does not take place, even up to a 0.1 mol. fraction in solutions of non-interacting solvents.

Dioxan and ethyl acetate, both with powerful anionoid centres, are capable of breaking down the molecular aggregates of acetic acid.[5,10] When acetic acid is diluted with these solvents, there is a marked increase in χ at the initial dilutions but a regular decrease (Fig. 1) on further dilution. In these solutions the competition of the solvent molecule as a hydrogen-bonding base causes the dissociation of acetic acid dimers also. Therefore, even at a very low dilution the formation of a strong hydrogen bond of the hetero-molecular type is highly probable. This breaking of the non-polar dimeric units of acetic acid by donor solvents like acetone has been suggested by Huggins et al.[16] from the proton magnetic resonance study of these mixtures. The replacement of the -OH doublet of the cyclic dimer by a diffuse band in the Raman spectra of an acetic acid-dioxan mixture has been explained by Batuev[12] as being due to the breaking of ring dimers and to the formation of hydrogen-bonded chain complexes between acetic acid and dioxan. The contribution of this type of complex formation to the magnetic susceptibility may be in two forms: (1) an increased diamagnetism brought about by the release of constraints upon the breaking of the dimers, or (2) a paramagnetic contribution arising from the formation of a strong hydrogen bond with the solvent molecule. The observed increased value of χ on the initial dilution of the acid by dioxan and ethyl acetate may be the net effect of these two contributions.

The $\Delta\chi/w_1$ value of these mixtures at a high dilution causes a negative deviation (Fig. 2). The results are best explained in these cases with the predominant occurrence of a strong hydrogen-bonded addition compound of donor solvents with a monomeric acid molecule, as is shown below:



Batuev's report[17] of the complete disappearance of the lines at 1668 and 1710 cm^{-1} characteristic of C=O in ring dimers and coordinated C=O respectively, lines which appeared in the Raman spectrum of pure acid, and of the exclusive appearance of the line (1740 cm^{-1}), which is characteristic of the C=O free from a hydrogen bond, with an increased intensity in weak dioxan solutions lends support to the above argument.

Summary

The magnetic susceptibilities of acetic acid in the pure and dissolved states have been investigated, and the results obtained have been attributed to the changes that take place in the association of acetic acid molecules.

Department of Physics
Annamalai University
Madras State, S. India

15) J. Farquharson, ibid., **32**, 219 (1935).

16) C. M. Huggins and G. C. Pimental, *J. Phys. Chem.*, **60**, 1314 (1956).

17) M. I. Batuev, *Comp. rend. acad. Sci., U. R. S. S.*, **53**, 507 (1946).

Electron Microscopic Study of the Dehydration of Brucite and the Recrystallization of Periclase upon Further Heating

By Goro YAMAGUCHI and Toshio TOKUDA

(Received August 2, 1963)

A number of investigators have studied the transformation of brucite to periclase through dehydration. Büssem and Köberich[1] showed that the periclase crystallites produced from brucite by dehydration were oriented in such a way that (111) of the periclase is parallel with (0001) of the brucite. Goodman[2] investigated the transformation process with an electron microscope. He decomposed the brucite crystals by electron bombardment and took sets of an electron micrograph and a corresponding diffraction photograph at various stages of the bombardment. He concluded that, in the decomposition process, the small shrinkage in the basal plane of the brucite took place first, and then the collapse of the planes downward to the original [0001]. Ball and Taylor[3] proposed the existence of a spinel-like intermediate phase, $Mg_3(OH)_2O_2$, between brucite and periclase after an X-ray analysis of natural brucite. In order to explain the spinel-formation process, he suggested an inhomogeneous dehydration, instead of a homogeneous dehydration. Recently Anderson and Horlock[4] investigated the dehydration process of natural brucite and found that the dehydration proceeded from the edge of the crystal toward the center, that no spinel-like intermediate was found, and that similar lattices of magnesium hydroxide and magnesium oxide-like intermediate, with only slightly different sizes, could be recognized.

In the present work the brucite crystals obtained by the hydrothermal treatment of chemically-pure magnesium hydroxide will be used to get rid of as much effect of impurities as possible.

Experimental

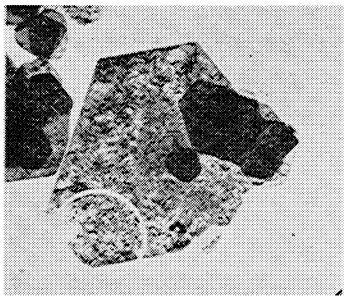
The Preparation of the Brucite Crystals. — In order to take an electron diffraction photograph of a single crystal, the brucite crystals must be thin enough to transmit electrons but be at least 0.5 μ across so as to be separated from one another. Brucite crystals satisfying the requirements and still free from impurities were obtained by the following procedures. Chemically-pure magnesium hydroxide was put in an autoclave with water and kept at an appropriate temperature (with reference to the magnesium oxide water phase equilibrium[5]) for several hours. Different amounts of water and of magnesium hydroxide and various treating temperatures and heating periods were employed. Properly-crystallized brucite was obtained by treating 2 g. of chemically-pure magnesium hydroxide in a 30 cc. autoclave with 15 cc. water at 350°C for 24 hr.

Heating and Examination Methods.—The brucite crystals were heated in the following two different methods and were examined with an electron microscope operated at 80 kV.

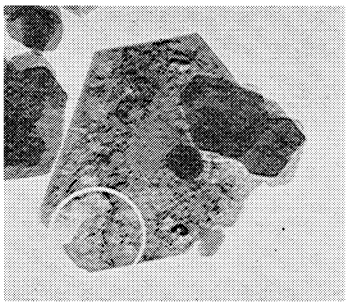
Heating in the Electron Microscope with a Specimen-heating Attachment.—The crystals were first laid on a Pt-mesh and heated at the heating rate of about 10°C per min. up to 400°C with a heating attachment in the electron microscope. Choosing one crystal, a series of electron micrographs and corresponding diffraction photographs were taken at various stages of heating in order to pursue the crystal transformation through the dehydration. Next the crystals were heated further at a heating rate of about 30°C per min. up to 900°C, and the graphs were also taken at various stages of heating in order to observe any change after the dehydration. More than ten crystals were examined by these procedures.

Heating by Electron Bombardment. — The crystals were heated by electron bombardment in the electron microscope. The beam intensity was gradually increased, and at successive stages of bombardment, pairs of electron micrographs and corresponding diffraction photographs were taken. The maximum temperature rise as a result of the extensive electron bombardment was checked by the behavior of metal powder particles of various kinds (aluminum, copper, manganese, nickel, iron and chromium) in the bombardment. Only chromium particles remained undecomposed. From the standpoint of the melting points, the maximum temperature was estimated to be somewhere between 1453°C and 1535°C. In a high vacuum condition, however, the evaporation of metals cannot be disregarded so the temperature might be lower.

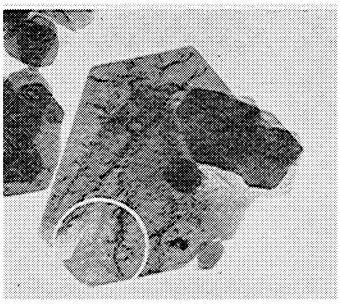
1) W. Büssem and F.Köberich, *Z. physik. Chem.*, **B, 17**, 310 (1932).
2) J. F. Goodman, *Proc. Roy. Soc.*, A247, 346 (1958).
3) M. C. Ball and H. F. W. Taylor, *Miner. Mag.*, 32, 754 (1961).
4) P. J. Anderson and R. F. Horlock, *Trans. Faraday Soc.*, **58**, 1993 (1962).
5) D. M. Roy, R. Roy and E. F. Osborn, *Am. J. Sci.*, **251**, 337 (1953).



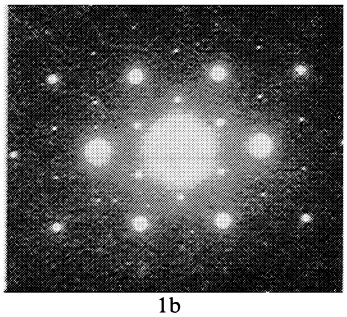
1a



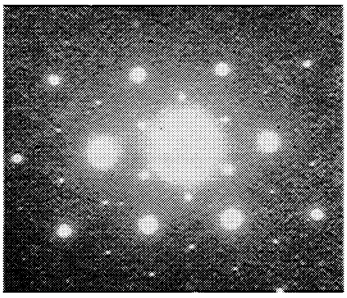
2a



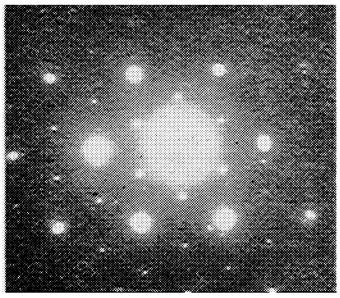
3a



1b

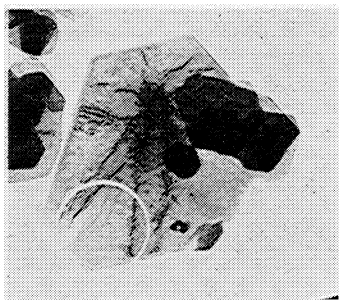


2b

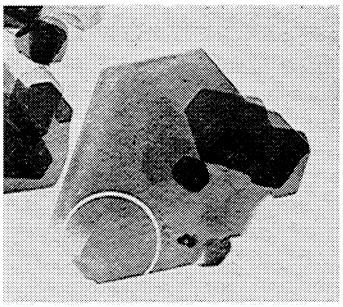


3b

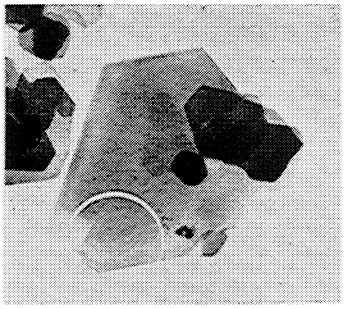
Fig. 1a. Brucite crystal before heating (×30000).
Fig. 1b. Diffraction pattern from the area in a circle in Fig. 1a.
Fig. 2a. Brucite crystal heated 10°C per minute up to 250°C with a heating attachment (×30000).
Fig. 2b. Diffraction pattern from the area in a circle in Fig. 2a.
Fig. 3a. Brucite crystal heated 10°C per minute up to 270°C with a heating attachment (×30000).
Fig. 3b. Diffraction pattern from the area in a circle in Fig. 3a.



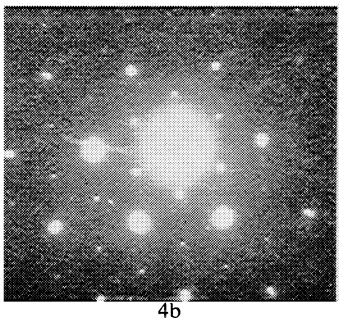
4a



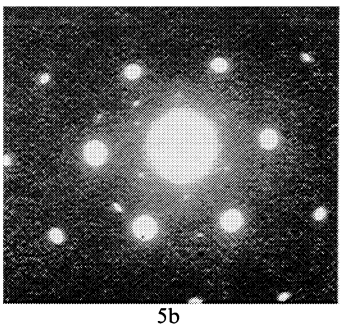
5a



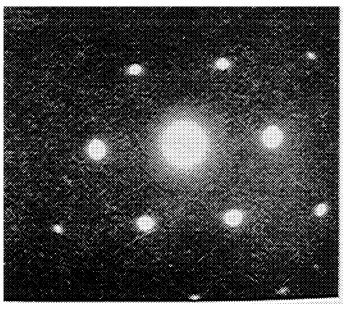
6a



4b

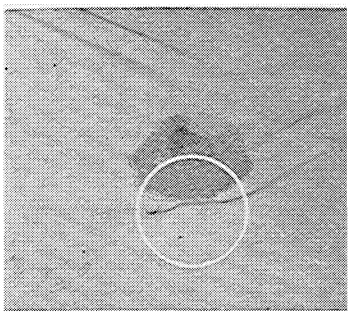


5b

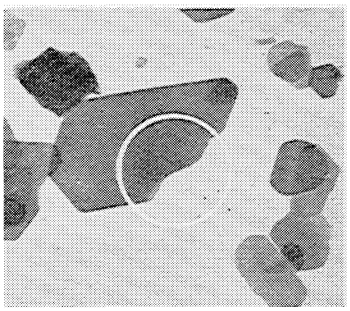


6b

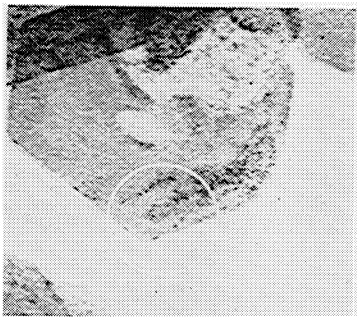
Fig. 4a. Brucite crystal heated 10°C per minute up to 290°C with a heating attachment (×30000).
Fig. 4b. Diffraction pattern from the area in a circle in Fig. 4a.
Fig. 5a. Brucite crystal heated 10°C per minute up to 310°C with a heating attachment (×30000).
Fig. 5b. Diffraction pattern from the area in a circle in Fig. 5a.
Fig. 6a. Brucite crystal heated 10°C per minute up to 330°C with a heating attachment (×30000).
Fig. 6b. Diffraction pattern from the area in a circle in Fig. 6a.



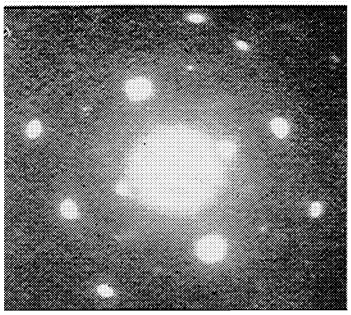
7a



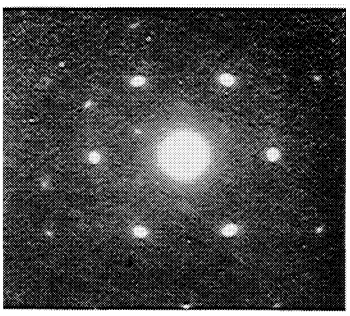
8a



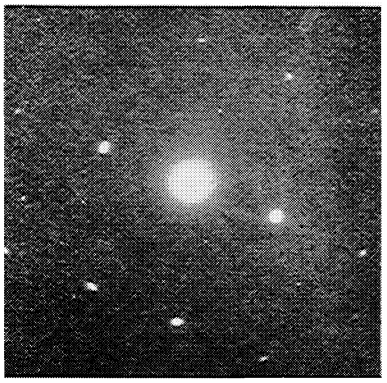
9a



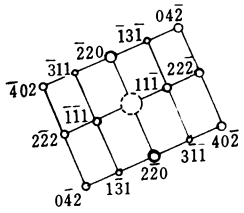
7b



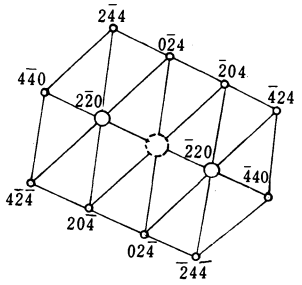
8b



9b

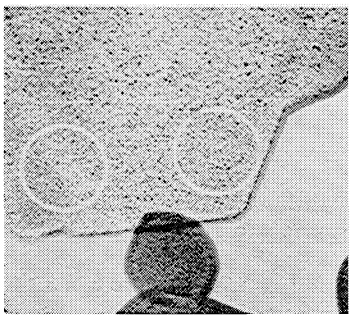


7c

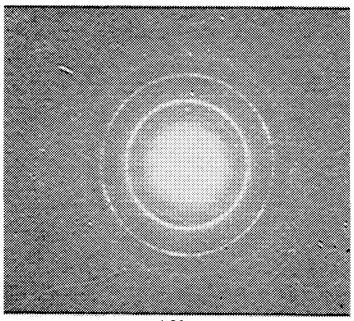


9c

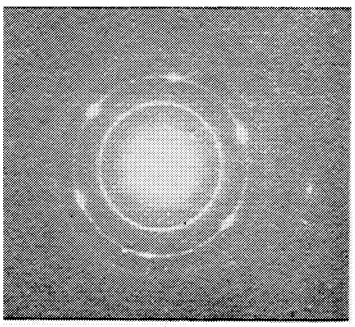
Fig. 7a. Brucite crystal heavily bombarded by electrons (×15000).
Fig. 7b. Diffraction pattern from the area in a circle in Fig. 7a.
Fig. 7c. An indexing of the diffraction pattern shown in Fig. 7b.
Fig. 8a. Brucite crystal heated 10°C per minute up to 600°C with a heating attachment (×15000).
Fig. 8b. Diffraction pattern from the area in a circle in Fig. 8a.
Fig. 9a. Brucite crystal heavily bombarded by electrons (×30000).
Fig. 9b. Diffraction pattern from the area in a circle in Fig. 9a.
Fig. 9c. An indexing of the diffraction pattern shown in Fig. 9b.



10a



10b



10b′

Fig. 10a. Brucite crystal heavily bombarded by electrons (×30000).
Fig. 10b. Diffraction pattern from the area in the left circle in Fig. 10a.
Fig. 10b′. Diffraction pattern from the area in the right circle in Fig. 10a.

TABLE I. RELATIONS OF THE ORIENTATIONS BETWEEN THE PERICLASE AFTER FURTHER HEATING AND THE ORIGINAL BRUCITE

Type	Corresponding faces in orientation		Occurrence	Heating method	Fig. No.
	Periclase	Original brucite			
1	(111) (220)	(0001) (11$\bar{2}$0)	almost always	A, B	same as 6a, 6b
2	(112) (220)	(0001) (11$\bar{2}$0)	rarely	A, B	7a, 7b, 7c
2′	(112) (220)	(0001) {(11$\bar{2}$0), (1$\bar{2}$10), ($\bar{2}$110) in three directions	rarely	A	8a, 8b
3	(221) (220)	(0001) (11$\bar{2}$0)	rarely	A, B	9a, 9b, 9c
4	Random orientation		rarely	B	10b

Heating methods: A, heating attachment B, electron bombardment

Results

Crystal Changes upon Dehydration. — The brucite crystals were laid flat on carbon film, which was put on a Pt-mesh by spattering, since (0001) was perpendicular to the electron beam. Like the natural brucite crystals used by Goodman, the present ones had complex patches on the surface (Fig. 1a) which might come from the internal-disordered structures, as Goodman suggested. The changes in the diffraction patterns through the dehydration were the same in the two different ways of heating. The crystals were heated in a heating attachment at the heating rate of about 10°C per min., and electron micrographs and corresponding diffraction photographs of one crystal of each of them were taken at 250°C, 270°C, 290°C, 310°C and 330°C. These graphs are shown in Figs. 1a, 1b, 2a, 2b, 3a, 3b, 4a, 4b, 5a, 5b, 6a and 6b. The original reflections of the brucite first diffused outward, and then the reflections of the periclase appeared. In Figs. 2b and 3b, it can be observed that the original reflections have diffused outward. In the dehydrating stage, a_0 of the brucite is calculated to cover a range from 3.11 Å to 3.03 Å in Fig. 2b, and from 3.11 Å to 3.01 Å in Fig. 3b, while the a_0 of the original brucite is 3.11 Å. In Fig. 4b reflections from the periclase have appeared distinctly apart from the diffused ones. In Fig. 5b, all the reflections belong to the periclase except the six patterns nearest the center. These six reflections belong to a hexagonal lattice. Other corresponding reflections cannot be detected, perhaps because they are too vague and too near those of the periclase. From these six reflections, a_0 is calculated to be 2.99 Å. This fact shows that a_0 of the brucite shrinks to 2.99 Å through the dehydration. In Fig. 6b the dehydration has been completed. Figure 6b shows that (111) of the periclase is parallel with (0001) of the original brucite and that (220) of the periclase is parallel with (11$\bar{2}$0) of the original brucite.

Crystal Changes upon Further Heating after Complete Dehydration.—The changes in diffraction patterns caused by further heating after complete dehydration were also almost identical in the two methods of heating. Upon further heating, the patterns of many crystals remained as they were. In a few crystals, however, the patterns were changed into several other types, as Table I shows; type 1 was sometimes mixed slightly into the other types.

Discussion

Dehydration Process. — Although Goodman has observed only one intermediate shrinked lattice (a_0=2.99 Å), the results in the present work show that the brucite lattice shrinks gradually as the water molecules are expelled. No information could be obtained about the dimension of the C-axis. Judging from the crystal structure of the brucite, however, the shrinkage will be more extensive in the C direction. Each region where the shrinkage takes place is supposed to be 40~50 Å across, because the periclase crystallites produced from the brucite at 300°C are known to be about this size.[6] Water molecules possibly escape at the sites where defects exist and then through the cracks caused by the lattice shrinkage. Through the shrinkage, slight slips between oxygen layers are required to produce the periclase, because oxygens are hexagonal-closed packing in the brucite, whereas in the periclase they are cubic-closed packing. Thus the dehydration seems to take place in two steps. The gradual shrinkages of the lattice

6) W. R. Eubank, *J. Am. Cer. Soc.*, **34**, 225 (1951).

with the escape of the water molecules first take place, and then the slips between oxygen layers or the crystallizations take place.

The Changes in the Diffraction Patterns Caused by Further Heating After Complete Dehydration.—Goodman noticed a change in the diffraction patterns after the complete dehydration by extensive bombardment. The patterns partially became rings, which shows random orientation. He referred this to a bulk movement of the solids under the influence of the thermal stress. In the present work, the changes in the orientation upon further heating took place in the several ways shown in Table I. It seems that the structure immediately after complete dehydration is so defective that the recrystallization upon further heating sometimes takes place with a slight movement of the orienting direction, and also in rare cases with an extensive movement of the structure, which causes the random orientation. A strict interpretation of the mechanism of this phenomenon, however, has not yet been established.

Summary

1) The hexagonal plate crystals of the brucite, about 1 μ across, have been obtained by the hydrothermal treatment of chemically-pure magnesium hydroxide.

2) The brucite crystals transformed themselves upon dehydration into aggregates of the minute periclase crystallites oriented in such a way that (111) is parallel with (0001) of the original brucite crystal and (220) is parallel with $(11\bar{2}0)$.

3) The dehydration seems to take place in two steps. The escape of water molecules and the gradual shrinkage of the lattice take place at the first step of the dehydration. The slip of the oxygen layers and the crystallization take place at the second step.

4) Upon further heating after complete dehydration, the orientation of the crystallites remained unchanged in many crystals. In a few crystals, however, the orientation changed in the several ways shown in Table I. This phenomenon is a kind of sintering in the grain.

The present authors are greatly indebted to the Nippon Denshi Co. Ltd., for its co-operation.

Department of Applied Chemistry
Faculty of Engineering
The University of Tokyo
Hongo, Tokyo

The Viscometric Properties of Polyesters. II. Viscosity in the Range of Low Temperatures near the Glass Transition Point

By Ryuzo NAKATSUKA

(Received July 9, 1963)

The glass transition temperature (T_g) is one of the most important properties of liquid state polymers.[1-3]

Although T_g values vary with individual polymers, the properties at a given temperature share common features; that is, (1) the apparent activation energy for viscous flow[1] ($E^{\ddagger}$), (2) the free volume fraction[1] (f), (3) the viscosity[2] (η), and (4) the thermal expansion coefficient of the free volume fraction[6,7] (α_f) show similar values irrespective of the nature of the polymers.

Hirai et al.[6] derived a theoretical expression on viscosity near the glass transition point from such empirical formulas as the WLF type,[7] the Fox-Flory type[8] and the Tobolsky-Catsiff type[10] equations, by means of the free volume theory for viscous flow.[5]

The object of the present paper is (1) to represent the viscometric property in the aspect of free volume, (2) to obtain more exact information about the "transition area" for the

1) T. G. Fox and P. J. Flory, *J. Appl. Phys.*, **21**, 581 (1950).
2) R. F. Boyer and R. S. Spencr, ibid., **16**, 594 (1945).
3) R. F. Boyer, ibid., **25**, 825 (1954).
4) R. Kawai, *Kobunshi*, **6**, 348 (1957).
5) A. K. Doolittle, *J. Appl. Phys.*, **22**, 1471 (1951); ibid., **23**, 236 (1952).
6) N. Hirai, *Kobunshi Kagaku*, **19**, 191 (1962); ibid., **19**, 528 (1962).
7) M. L. Williams, R. E. Landel and J. D. Ferry, *J. Am. Chem. Soc.*, **77**, 3701 (1955).
8) T. G. Fox and P. J. Flory, *J. Appl. Phys.*, **21**, 581 (1950).
9) P. J. Flory, *J. Am. Chem. Soc.*, **62**, 11057 (1940).
10) A. V. Tobolsky and E. Catsiff, ibid., **76**, 4204 (1954).

TABLE I. RELATIONSHIP BETWEEN CHEMICAL STRUCTURE AND VISCOMETRIC PROPERTIES

	T_s °C	η_s poise	E_c^* kcal./mol.	δ	C. E. D. cal./cc.
DE-Su	− 2	7000	32	0	98
Ad	−23	20000	23	0	86
Az	—	—	—	—	74
Se	—	—	—	—	72
TE-Su	− 8	7000	30	0	92
Ad	−24	13000	23	0	83
Az	−31.5	7000	18	0	74
Se	—	—	—	—	71
DP-Su	5	9000	34	−0.69	85
Ad	−22	20000	25	0	77
Az	−36.5	7000	19	−0.34	68
Se	−37.5	6000	19	+0.22	66
Bu-Su	4	10000	23	−0.34	96
Ad	−28	50000	21	−1.00	85
Az	−39	150000	18	−0.69	75
Se	−39	100000	18	−0.47	73

Note

(1) Chemical

	(Conventional)	(IUPC)
Su:	Succinic acid	Butanedioic acid
Ad:	Adipic acid	Hexanedioic acid
Az:	Azeraic acid	Nonanedioic acid
Se:	Sebacic acid	Decandioic acid
DE:	Diethylene glycol	2,2'-Dihydroxydiethyl ether
TE:	Triethylene glycol	1,2-Ethanediol bis(2-hydroxyethylether)
DP:	Dipropylene glycol	2,2'-Dihydroxydipropyl ether
Bu:	—	1,3-Butanediol

(2) Physical

T_s, η_s: Constants in the WLF equation

$$\ln \eta/\eta_s = -[8.86(T-T_s)]/[101.6+T-T_s]$$

E_c^*: Average activation energy in the range of temperature −30∼5°C

δ: Corrected value in Eq. 2' or 8'

$$f(\eta)_{cal} = 1/(2.3 \log \eta + 10.1 + \delta) \quad (2')$$

$$E_{A\,cal}^* = 2.0T(2.3 \log \eta + 10.1 + \delta) \quad (8')$$

C. E. D.: Cohesive energy density calculated by Kawai's method[4]

viscous flow mentioned in Part I, and (3) to consider how the viscosity is affected by the difference of a few degrees in chemical structure.

The actual observation of viscosity indicates that (1) linear relationships are obtained in curves of f vs. T, (2) the "transition area" for viscous flow is an intermediate region between the WLF and the Andrade liquid, and (3) some viscometric properties are proportional to the intermolecular force within polyesters of the same glycol series.

Experimental

The Preparation of the Polyesters.—*The Reaction of Long-chain Polyesters* (cf. Part I).

The Fractionation of Polyesters. — Samples were treated at 130°C to remove volatile contaminants and were fractionated under high vacuum (ca. 10^{-4} mmHg) by being distillated two or three times. The distillates at 160°C contained a crystalline substance, while the distillates at 200°C did not.

The Measurement of Viscosity.—A Brookfield-type rotational viscometer was used for the range of 10^{-1}∼10^{3} poises, while a Couette-type viscometer was used for the higher range (10∼10^{6} poises).

Rotational viscometer (Couette-type):

Range 1×10∼5×10^{6} poise (accuracy ±2%)

Number of revolutions 0.8∼83 r. p. m. (14-stage change)

Rate of shear 63∼0.06 sec^{-1}

Radius of outer cylinder 1.4 cm.

Radii of inner cylinders 1.2, 1.1, and 0.6 cm.

Length of inner cylinders 5.5 cm.

The sample was put in a dry ice-methanol bath and kept for 35∼40 min. until the temperature equilibrium was attained. The viscosity was measured at temperature intervals of 3∼5°C in the ragne from −60 to 30°C.

11) J. D. Ferry, "Die Physik der Hoch Polymeren," Ed. by H. A. Stuart, Springer-Verlag, Berlin, Bd 4 (1956), p. 392.

On the basis of this measurement of viscosity, every sample could be regarded as a Newtonian liquid over the whole range of viscosity as had been expected,[8,12] but over 10^3 poises it was difficult to measure the viscocity at a constant temperature except in the case of an extremely low shear rate, because of the great generation of heat by friction during the measurement, and it was also difficult to ascertain the effect of the shear rate on the viscosity.

Results and Discussion

The Temperature Dependence of the Viscosity near the Glass Transition Point. — The amorphous polyesters used in this experiment are listed in Table I. As has been stated in Part I, diethylene azelate, diethylene sebacate and triethylene sebacate were all crystalline, and therefore, their viscosities could not be measured at a low temperature.

In any case, the experimental values fit the WLF equation only within the range of 10^2~10^8 poises; the difference between the experimental and the calculated values becomes evident from the viscosity of 10~10^2 poises.

$$\log \eta/\eta_s = -8.86(T-T_s)/(101.6+T-T_s) \qquad \text{WLF eq.}$$

The "transition area" mentioned in Part I corresponds to the range of viscosity where experimental results begin to deviate from the WLF equation.

By applying the experimental values to the WLF equation, the corresponding T_s and η_s are obtained as shown in Table I.

The Temperature Dependence of the Apparent Activation Energy for Viscous Flow (E^*) in the WLF Liquid State. — The relations of $\log \eta$ vs. $1/T$ and E^* vs. $1/T$ are shown in Figs. 1 and 2. From these relations, it can be observed that the temperature dependence of E^* behaves peculiarly; over a viscosity range higher than 10^2 poises and within the region of −30~5°C, most polyesters have a region in which the apparent activation energy for viscous flow becomes nearly constant. In the case of the succinic acid polyester series, however, this region deviates a little towards the high temperature side. The average value of activation energy in this region (E_c^*) is shown in Fig. 2 and Table I.

For the purpose of elucidating this phenomenon, the same investigation was carried out on several samples of triethylene adipate with different molecular weights (690~3600), as is shown in Figs. 3 and 4.

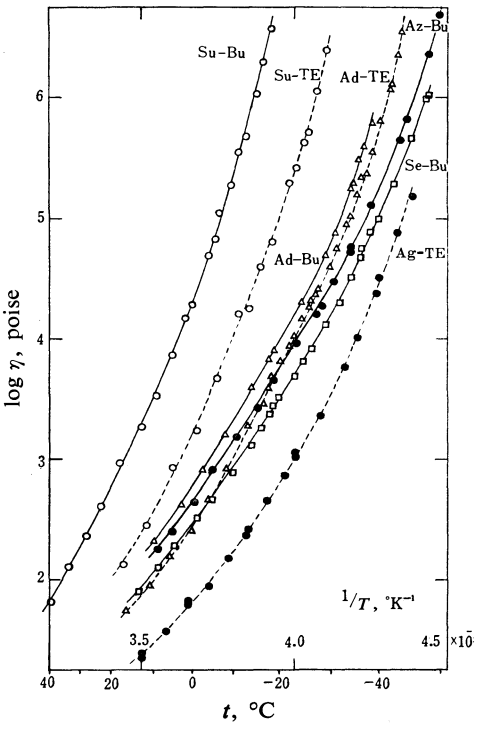


Fig. 1. Relationship between viscosity and temperature.
(1,3-Butanediol series and triethylene glycol series)
—— Bu series, ····· TE series

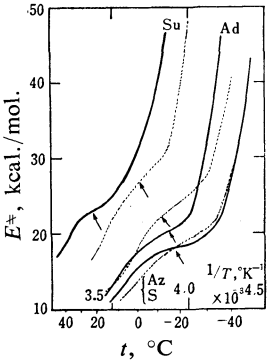


Fig. 2. Apparent activation energy for viscous flow.
(1,3-Butanediol series and triethylene glycol series)
—— Bu series, ····· TE series, ↑ E_c^*

Samples 1—3 and 4 were obtained by the conventional method and by molecular distillation at 200°C respectively.

Although polyesters have considerably different molecular weights, they show a similar tendency regarding this peculiarity of E^*: the region where E^* is considered to be constant is observed in the range of −30~5°C

12) M. Takayanagi and S. Kuriyama, *J. Chem. Soc. Japan, Ind. Chem. Sec.* (*Kōgyō Kagaku Zassi*), 57, 873 (1954); ibid., 57, 876 (1954); ibid., 59, 49 (1956).

for all samples, and yet the average values of $E^{\ddagger}$ in this region are equal except for sample 4.

Generally such a special type of curve for the temperature dependence of $E^{\ddagger}$ has not been observed[8,12] except in the example of a rubber-like polymer.[11]

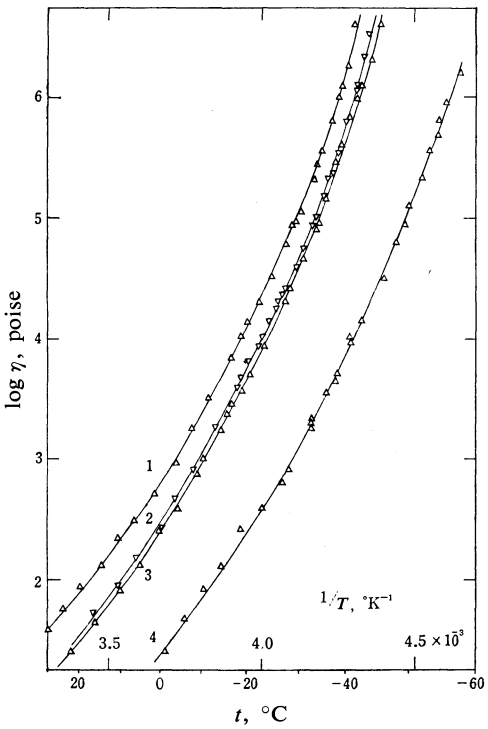


Fig. 3. Effect of molecular weight. (Triethylene adipate)

Sample	$\overline{M}_n$	Sample	$\overline{M}_n$
1	3600	2	1900
3	1200	4	680

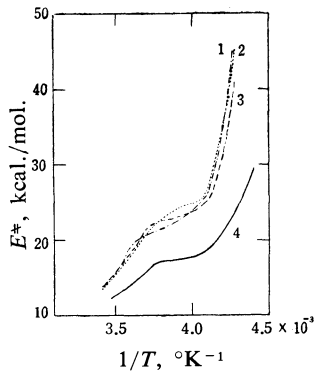


Fig. 4. Effect of molecular weight on activation energy. (Triethylene adipate)

Sample	$\overline{M}_n$	Sample	$\overline{M}_n$
1	3600	2	1900
3	1200	4	680

Even in this region each polyester behaves not as a non-Newtonian body but as a Newtonian liquid, and its molecular weight is too small to cause the so-called intermolecular entanglement; the general properties of the polyesters used in this experiment are very different from those of a rubber-like polymer.

Though it is impossible at present to explain this special phenomenon regarding the temperature dependence of $E^{\ddagger}$, the author wishes to point out two problems. One is the question whether this is one of the phenomena corresponding to the discontinuous change in the temperature dependence of the thermal expansion coefficient of the free volume fraction of the polyester, and the other is the question whether this depends on the time scale of measurement, for it takes a great deal of time to reach the equilibrium liquid state near the glass transition point. For the moment it can only be said with certainty that this phenomenon has something to do with the "transition area" for viscous flow.

Estimation of the Free Volume Fraction. — The Doolittle equation is generally applicable to the actual liquid, especially in the non-Andrade liquid state:

$$\ln \eta/\eta_g = B(1/f - 1/f_g) \tag{1}$$

The relationship between the free volume fraction (f) and the temperature (T) can be calculated from the results of the temperature dependence of the viscosity:

$$f = B/(\ln \eta/\eta_g + B/f_g) \tag{2}$$

The WLF equation and its function of the free volume fraction, $f(T)$, are deduced[7] from Eq. 1.

$$\ln \eta/\eta_g = [(T - T_g)/f_g]/[T - T_g + f_g/\alpha_{fg}] \tag{3}$$

$$f(T)_{\mathrm{WLF}} = f_g + \alpha_{fg}(T - T_g) \tag{4}$$

The functions of $f(T)_A$ and $E_A^{\ddagger}$ in the Andrade equation have been shown to be as follows by Hirai et al.:[6]

$$\ln \eta/\eta_g = (E_A^{\ddagger}/R)(1/T - 1/T_g) \tag{5}$$

$$f(T)_A = \alpha_l T \tag{6}$$

$$E_A^{\ddagger} = BR/\alpha_l \tag{7}$$

$$E_A^{\ddagger} = RT(\ln \eta/\eta_g + 1/f_g) \tag{8}$$

Equations for calculating the free volume fraction, $f(\eta)_{\mathrm{cal}}$ and $E_{A\,\mathrm{cal}}^{\ddagger}$ are obtained by substituting the following empirical values in Eqs. 2 and 8; a correction term δ is also added at the same time in order to assure the validity of this mathematical treatment.

$$f(\eta)_{\mathrm{cal}} = 1/(2.3 \log \eta + 10.1 + \delta) \tag{2'}$$

$$E_{A\,\mathrm{cal}}^{\ddagger} = 2.0T(2.3 \log \eta + 10.1 + \delta) \tag{8'}$$

In Eq. 1—8, the constants are termed as follows:

R: gas constant 1.987 cal./mol. deg.
η_g: viscosity at glass transition point (T_g) about 10^{13} poises[2]
B: a constant about 1[5,6]
f_g: Doolittle's free volume fraction at T_g about 0.025[7]
α_{fg}: thermal expansion coefficient of f at T_g about 4.8×10^{-4} ($°K^{-1}$)[7]
α_l: thermal expansion coefficient of f in Andrade liquid
E_A^*: activation energy for viscous flow in Andrade liquid

The correction term δ can be obtained from Eq. 8' by comparing the calculated value of the activation energy with the observed value, because the latter value for every polyester is almost constant (about 7.3 kcal./mol.) in the range between 370 and 420°K, as has already been shown in Part I.

The correction term δ is listed in Table I; this value depends on the molecular weight and the chemical structure of the polyester. In this table, all the δ values of the diethylene or triethylene glycol polyester series are zero.

In this manner, it is possible to discuss the temperature dependence of the f of amorphous polyesters as shown in Figs. 5—6.

The curve virtually consists of three straight-line part.

A typical pattern of the relation between f and T is represented in Fig. 7. We can divide the viscous flow state into three parts; (1) the Andrade liquid state ($T_1<T$; $f_1<f$), (2) the "transition area" for viscous flow ($T_2<T<T_1$; $f_2<f<f_1$), and (3) the WLF liquid state ($T_g<T<T_2$; $f_g<f<f_2$).

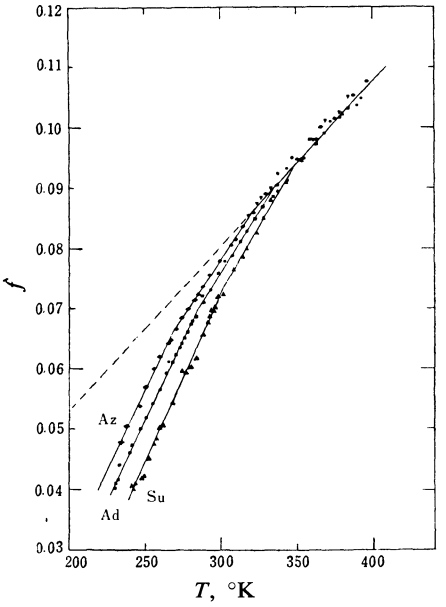


Fig. 5. Relationship between free volume fraction and temperature.
(Triethylene glycol series)

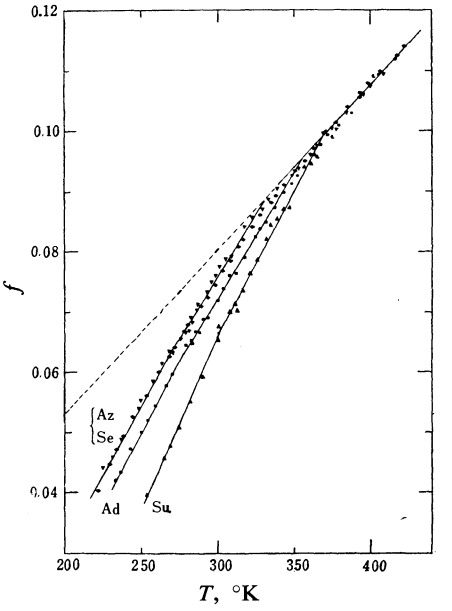


Fig. 6. Relationship between free volume fraction and temperature.
(1,3-Butanediol series)

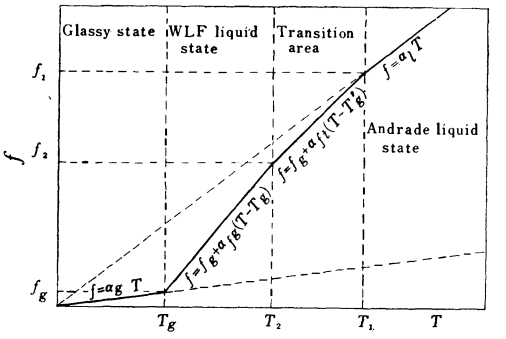


Fig. 7. Relationship between free volume fraction and viscous flow state.
(Schematic)

In the Andrade and the WLF liquid states, the values of f estimated from η are in good agreement with Eqs. 6 and 4 respectively, and the constants of these equations can be estimated for every polyester (cf. Table II).

The experimental values of f_1, f_2, α_l and α_g are approximately 0.10, 0.07, 2.69×10^{-4} and 4.8×10^{-4} respectively, independent of the type of polyester.

In the "transition area" ($0.10>f>0.07$), the relationship between f and T can be represented by Eq. 4', the form of which is similar to Eq. 4:

TABLE II. RELATIONSHIP BETWEEN CHEMICAL STRUCTURE AND TEMPERATURE DEPENDENCE OF FREE VOLUME FRACTION

	T_g' °K	T_g °K	α_{ft} $\times10^{-4}$ °K^{-1}	α_{fg} $\times10^{-4}$ K°$^{-1}$	T_1 °K	T_2 °K	f_1	f_2
DE-Su	191	221.5	4.03	5.62	386	303	0.108	0.071
Ad	175	205	3.94	5.27	346	293	0.093	0.072
Az	159	—	3.71	—	329	(280)	0.088	(0.070)
Se	159	—	3.71	—	329	(308)	0.088	(0.080)
TE-Su	193	216	4.31	5.63	347	303	0.094	0.074
Ad	174	203	4.01	5.63	335	288	0.090	0.072
Az	166	193	3.94	5.93	321	269	0.099	0.071
Se	166	—	3.94	—	321	(318)	0.099	(0.085)
DP-Su	213	228.5	4.58	5.53	374	319	0.101	0.075
Ad	148	203.5	3.45	5.17	367	313	0.099	0.085
Az	148	189	3.45	4.57	367	298	0.099	0.075
Se	148	189	3.45	5.22	367	298	0.099	0.075
Bu-Su	214	226.5	4.77	5.70	372	305	0.101	0.068
Ad	115	196.5	4.14	5.77	359	276	0.097	0.063
Az	172	191.5	3.95	4.60	342	267	0.092	0.063
Se	172	188.5	3.95	4.94	342	268	0.092	0.063

Note

T_g, α_{fg}: Constants in the WLF liquid state
$f(\eta)_{cal}=f_g+\alpha_{fg}(T-T_g)$

T_g', α_{fg}: Constants in the "transition area"
$f(\eta)_{cal}=f_g+\alpha_{ft}(T-T_g')$

T_1, f_1: Boundary between the Andrade liquid state and the "transition area"

T_2, f_2: Boundary between the WLF liquid state and the "transition area"

$$f=f_g+\alpha_{ft}(T-T'_g) \qquad (4')$$

This shows that the WLF-type equation is also applicable to the "transition area," but that the estimated value of the glass transition point in this area is different from that in the WLF liquid state.

Nevertheless, even in crystalline polyesters with structures similar to those of amorphous polyesters, f at the melting point exists in the range of about 0.07~0.10 and this range of f corresponds to the "transition area" for viscous flow in amorphous polyesters.

The range corresponding to the "transition area" for viscous flow has been observed near the respective melting points of several *n*-paraffines by Miller.[13]

Moreover, even though the estimated value of f only in the range of high temperature changes considerably as a result of a little change in α_l or E_A^*, the relation between f and T would not be significantly changed.

Influences of Chemical Structure on Viscometric Properties.—The influences of chemical structure can be elucidated more clearly by comparing the cohesive energy density,[4] calculated from the structural unit of polyesters, with such viscometric properties as f, E_c^* or T_g.

It follows from these results that there is a linear relation between the cohesive energy density and the viscometric properties in a certain kind of glycol polyester series; i.e., the plots of these straight lines are those

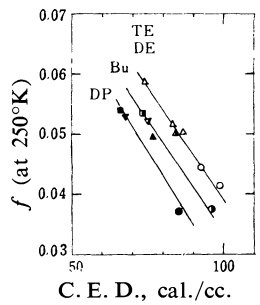


Fig. 8. Relationship between cohesive energy density and free volume fraction.

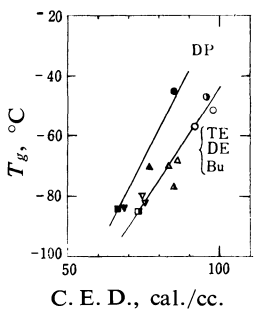


Fig. 9. Relationship between cohesive energy density and glass transition temperature.

13) A. A. Miller, *J. Chem. Phys.*, **67**, 1031 (1963).

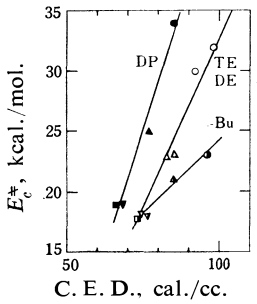


Fig. 10. Relationship between cohesive energy density and average activation energy for viscous flow (cf. Fig. 2).

from the following series respectively;

(1) Ether-type polyesters without side chains (TE and DE series)

(2) Ether-type polyesters with side chains (DP series)

(3) Ordinary-type polyesters with side chains (Bu series).

It seems probable that the viscometric properties are not perfectly represented by only the intermolecular forces because these tendencies are different according to the kinds of gylcol; a similar relation for many polymers has been obtained by Kawai.[4]

It is observed that, with an increasing intermolecular force, the free volume fraction (f) decreases, while the activation energy for viscous flow (E_c^*) in a peculiar region (cf. Fig. 2) and the glass transition point (T_g) increase.

As Figs. 8—10 show, in the series of dipropylene glycol (with the side chains) the above tendencies between the cohesive energy density and the viscometric properties are more strongly recognized than the expected tendencies from the series of diethylene- and triethylene glycols (without side chains); therefore, this shows that the intramolecular rotation in the liquid state was remarkably disturbed by the existence of side chains. In contrast with the dipropylene glycol series, the 1,3-butanediol polyester series (without ether bond) show a different pattern of viscometric properties.

Since the tendencies of the 1,3-butanediol polyester series are too complex to be explained clearly, at present it can be said with certainty only that the ether- and the methylene-bond in the main chain of polyesters behave remarkably differently in terms of viscosity.

Summary

The viscosities of amorphous long-chain polyesters have been measured in the range of $10\sim10^6$ poises and between -60 and 30°C, and the following results have been obtained (cf. also Part I).

(1) Within the limit of $10^2\sim10^6$ poises, all the polyesters are consistent with the WLF equation. At the "transition area" which was described in Part I, the observed viscosity begins to deviate from the WLF equation.

(2) The apparent activation energy for the viscous flow (E^*) is nearly constant within the range of $-30\sim5$°C, and over the range of viscosity beyond 10^2 poises for all the polyesters.

(3) The estimated curve of the temperature dependence of the free volume fraction (f) can be divided into three straight-line parts, corresponding to the WLF liquid state, the "transition area" for viscous flow, and the Andrade liquid state respectively.

(4) The relationship between the chemical structure and the viscosity can be represented in connection with intermolecular force, intramolecular rotation and so on.

The author is indebted to Professor Hiromu Murata of Faculty of Science of Hiroshima University for his helpful discussion and encouragement throughout the work, and to Dr. Keiji Oshima, Director of the Osaka Municipal Technical Institute, for his advice and encouragement. He also wishes to express his gratitude to Mr. Tadao Nakao, Senior Managing Director of Sumitomo Bakelite Co., Ltd., and Director of the Central Research Laboratory of the company, for permission to publish this paper, and to Mr. Kyosuke Miki and Mr. Shozo Yoshizumi of this Laboratory for their valuable assistance.

Central Research Laboratory
Sumitomo Bakelite Co., Ltd.
Totsuka-ku, Yokohama

The Electrolytic Formation of an Oxide Layer on Platinum in a Sulfuric Acid Solution

By Shigeo SHIBATA

(Received October 7, 1963)

Although the electrolytic formation of oxide films on the surface of platinum electrodes has been extensively studied,[1-28] there are still remain quite a few questions concerning the actual electrode reaction and its mechanism.

Wakkad and Emara[9] found two plateaus in the oxygen region of a slow anodic charging curve (the variation of potential with the passage of electricity) and suggested that these were to be attributed to definite oxides of platinum(II) oxide and platinum(IV) oxide, on the basis of the fact that the potential of these plateaus were equal to the thermodynamic standard potentials of the platinum-platinum(II) oxide and platinum-platinum(IV) oxide couples respectively.

The construction of the oxide formed on the platinum surface was estimated by chemical analysis[16] to be a mixture of platinum(II) oxide and platinum(IV) oxide in a molar ratio close to 6:1. Laitinen[23] pointed out that one must be certain that during the chemical attack in this analysis the oxidation state of the platinum has not been changed. Giner[20] has examined the question of whether or not the definite oxides are formed on platinum by anodic polarization and has concluded that definite oxides don't exist, only chemisorbed oxygen.

A comparison of the anodic and the cathodic charging curves also shows that more electricity is used to form the oxide than to remove it. Vetter and Berndt[19] attributed the difference in the amounts of electricity to the possibility that some of the oxide or oxygen layer is reduced to hydrogen peroxide, which requires less electricity than the formation of the layer. Laitinen and Enke[23] stressed another possibility, that on the loss of oxygen atoms from the surface oxygen tends to diffuse into the grain boundaries of the platinum.

This study was undertaken in order to obtain further information on the behavior of deposited oxygen and on the oxide-film formation on smooth platinum electrodes by measuring the potential behavior, the electrode capacity and the attack on the electrode surface by the alternating anodic and cathodic polarizations.

The results of the present investigation indicate that the anodic film formation reaction proceeds through two steps: an adsorption step of deposited oxygen, and a step of the formation of a definite oxide film.

Experimental

The electrolyte used was a 1 N sulfuric acid solution. Sulfuric acid was distilled twice under reduced pressure, and laboratory-distilled water was further purified by redistillation with alkaline permanganate, followed by double distillations in a quartz still. The electrolyte was pre-electrolyzed with a current of 100 mamp. for at least 23 hr. using platinum electrodes. Unless otherwise stated, the solution was continuously swept with purified nitrogen gas in order to keep it free from dissolved

1) F. P. Bowden, *Proc. Roy. Soc.*, **A125**, 446 (1929).
2) J. A. V. Butler and G. Armstrong, ibid., **A137**, 605 (1932).
3) J. A. V. Butler and G. Armstrong, *J. Chem. Soc.*, **1934**, 743.
4) A. L. Ferguson and M. B. Towns, *Trans. Electrochem. Soc.*, **83**, 271, 285 (1943).
5) A. Hickling, *Trans. Faraday Soc.*, **41**, 333 (1945).
6) B. V. Ershler, *Discussions Faraday Soc.*, **1**, 269 (1947).
7) A. Hickling and W. H. Wilson, *J. Electrochem. Soc.*, **98**, 425 (1951).
8) Ts. I. Zalkind and B. V. Ershler, *Zhur. Fiz. Khim.*, **25**, 565 (1951).
9) S. E. S. Wakkad and S. H. Emara, *J. Chem. Soc.*, **1951**, 461.
10) I. M. Kolthoff and T. Tanaka, *Anal. Chem.*, **26**, 623 (1954).
11) M. Breiter, C. A. Knorr and W. Wolkl, *Z. Elektrochem.*, **59**, 681 (1955).
12) M. Becker and M. Breiter, ibid., **60**, 1080 (1956).
13) K. I. Rosenthal and V. I. Veselowskii, *Doklady Akad. Nauk S. S. S. R.*, **111**, 637 (1956).
14) J. W. Ross and I. Shain, *Anal. Chem.*, **28**, 548 (1956).
15) F. C. Anson and J. J. Lingane, *J. Am. Chem. Soc.*, **79**, 1015 (1957).
16) F. C. Anson and J. J. Lingane, ibid., **79**, 4901 (1957).
17) J. K. Lee, R. N. Adams and C. E. Briker, *Anal. Chim. Acta*, **17**, 321 (1957).
18) G. Radlein, *Z. Elektrochem.*, **61**, 727 (1957).
19) K. J. Vetter and D. Berndt, ibid., **62**, 378 (1958).
20) J. Giner, ibid., **63**, 386 (1959).
21) B. B. Baker and W. H. Macnevin, *Zhur. Fiz. Khim.*, **75**, 1476 (1959).
22) J. Giner, *Z. Elektrochem.*, **64**, 491 (1960).
23) H. A. Laitinen and C. G. Enke, *J. Electrochem. Soc.*, **107**, 773 (1960).
24) F. G. Will and C. A. Knorr, *Z. Eletrochem.*, **64**, 258 (1960).
25) W. Bold and M. Breiter, *Electrochimica Acta*, **5**, 145 (1961).
26) A. Kozawa, This, Bulletin, **35**, 1051 (1962).
27) A. Kozawa, *J. Electrochem. Soc. Japan (Denki Kagaku)*, **30**, 720 (1962); **31**, 183, 315, 618 (1963).
28) S. W. Feldberg, C. G. Enke and C. E. Briker, *J. Electrochem. Soc.*, **110**, 826 (1963).

oxygen and hydrogen. The presence of oxygen or hydrogen is undesirable; oxygen acts as a depolarizer when the electrode is treated cathodically, while hydrogen reacts chemically with the oxygen on the platinum electrode surface and acts as a depolarizer for anodic electrode treatment.

The test electrodes were cleaned by treating them successively with hot concentrated hydrochloric acid, hot concentrated nitric acid and hot chromic acid, and finally by washing them with distilled water.

As the reference electrode, a saturated calomel electrode was used throughout. The values of the potentials described in this paper are on the standard hydrogen scale. All measurements were made at a constant temperature of 25 ± 0.1°C.

The Charging Curves.—Both the test electrode and the counter electrode were smooth platinum plates 2.0 cm^2 in apparent area, counting both sides. The electrolytic cell was constructed entirely of Pyrex glass, with the two compartments of the test electrode and of the counter electrode separated from one another by a sintered glass disk; each was equipped with a gas inlet tube. The compartment of the test electrode was fitted with a water jacket, through which water regulated at 25°C was circulated.

The circuit for the measurement was of the usual type, equipped with two large B-type batteries of 67.5 V. in series to power the electrolysis circuit. A potentiometer recorder with a high impedance input pre-amplifier (50 MΩ) was used to record the charging curves.

Electrode Capacity. — The test electrode was formed of wire 0.5 mm. in diameter and 5 mm. long; the end of the electrode was covered with a small glass ball to prevent an edge effect of the discharge. The counter electrode of platinum gauze in the shape of a cylinder 20 mm. high and 25 mm. in diameter was placed around the test electrode. The set of these electrodes was placed in a double walled glass vessel, between which two walls there flowed water of a constant temperature. This cell was also used for the measurement of the square-wave alternating-current electrolysis to be described in the next section.

The behavior of the differential capacity of the electrical double layer during forced anodic polarization with a constant current was measured by a fast single-current pulse method. This technique is nearly the same as that described by Schmid and Hackerman.[29] The method consists of calculating the capacity from the initial slope of the potential-time curve produced by the pulse under the assumption that the slope of the potential-time curve just before the onset of the pulse is zero. Though this is not true in a strict sense, the slope before the onset of the pulse, not exceeding the order of 10^{-2} V./sec., can be ignored in comparison with the slope produced by the pulse of the order of 10^2 V./sec.

A block diagram of the electronic apparatus is given in Fig. 1. The potential of the electrode

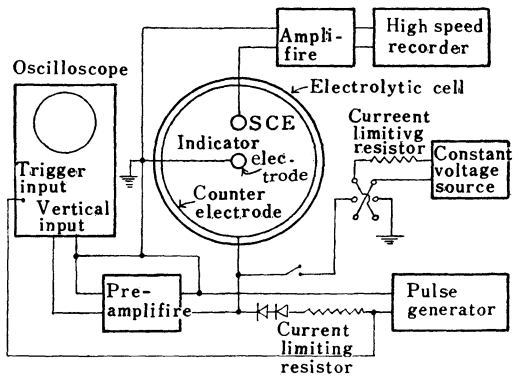


Fig. 1. Circuit diagram.

was measured against the reference electrode through a Luggin capillary by feeding the output of this cell into the recorder. In addition to the steady current, the cathodic pulses were delivered from a generator at the regular rate of 1 pulse every 2.0 sec. The pulses from the generator were passed first through a current-limiting resistor and then through a series of two diodes in order to eliminate a residual direct current from the genarator. The pulse-rise time was 0.2 μsec., and the duration was 8 μsec. The ratio of the current to the slope of the potential-time curve, $\Delta E/\Delta t$, gives the double-layer capacity. In practice, the current was so adjusted that ΔE was 1~4 mV. at a Δt of 8 μsec. Since Presbery and Schuldiner[30] showed that practically all of the applied current goes to the charging of the double layer in the first 10 μsec., the Faradaic effect is probably negligible. The potential changes of the test electrode caused by these pulses were photographed from the screen of a carefully calibrated cathode-ray oscilloscope (Iwasaki synchroscope, Model SS-5151) equipped with an input pre-amplifier (1 mV./cm.). The beam of the oscilloscope was triggered by the pulse itself, and the curves of the potential change caused by the pulse were successively photographed by means of winding a roll film a little every pulse, the shutter of the camera being kept open.

Square-wave Alternating-current Electrolysis.—This experiment was undertaken to study the effect of the repeated alternate anodic formation and cathodic dissolution of the oxide film on the electrode surface.

The test electrodes for this experiment were platinum wire 0.5 mm. in diameter and 6~4 mm. long; a new one was used for every run of the measurement. The frequency of the square wave was 78 or 40 c. p. s., the rise time was 1 μsec., and the voltage, 100 V.

The electrolysis was carried out in a hydrogen-saturated solution for a given time under the conditions of a constant shape and a constant amplitude of a charging curve resulting from the square-wave current electrolysis. When any change was found on the curve during the electrolysis, which was watched closely with the oscilloscope,

29) G. M. Schmid and N. Hackerman, *J. Electrochem. Soc.*, **109**, 1096 (1962).

30) C. H. Presbery and S. Schuldiner, ibid., **108**, 985 (1961).

the current was increased or decreased slightly so as to restore the curve to its original state. The degree of the attack of the surface may be estimated by measuring the increase in true area per apparent unit area, i. e., the increase in roughness factor, because the surface is coarsened by the electrolytic attack ; the increase in the true surface area can be approximated to the degree of the attack, unless the surface suffers too much corrosion. Since the value of the electricity Q_a (coulombs/apparent unit area) required to form the oxide film, which can be measured from the anodic charging curve, is proportionate to the true area of the electrode, the degree of the attack is estimated by the ratio of the Q_a' for the electrode already electrolyzed to the Q_a for that not yet electrolyzed. For this purpose, the charging curves were photographed with the oscilloscope.

Results and Discussion

The Possibility of the Existence of Adsorbed Hydrogen Which is Removed in the Oxygen-deposition Region.—Typical charging curves for an oxygen-hydrogen-free solution with a small current density are shown in Fig. 2. The initial rise of the potential (region α_a) is attributed to the ionization of adsorbed hydrogen. The second rapid linear rise (region β_a) is ascribed to the charging of the double layer, and a final slow linear change (region γ_a), to the deposition of oxygen, which forms a monolayer of oxygen atoms on the surface

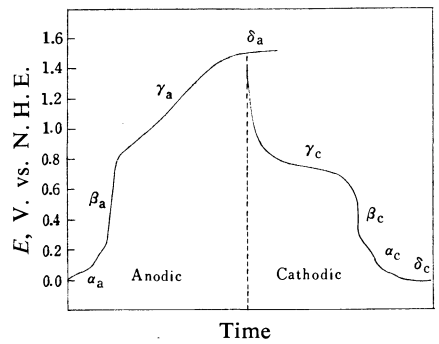


Fig. 2. Charging curves with small current density.

prior to the evolution of gas (region δ_a). When the current is reversed and the anodized electrode is made cathodic, the potential falls very rapidly to a plateau (region γ_c) which corresponds to the reduction of the oxide film formed during the γ_a region of the anodization. When all of the oxide has been reduced, the potential falls again through β_c and the hydrogen deposition (region α_c) prior to the final evolution of gas (region δ_c).

One of possible presumptions we can make as to the cause of the fact that the quantity of the electricity, Q_c, required to remove the oxide is smaller than that, Q_a, required to form the same substance would be that, in the anodic polarization, some of hydrogen atoms not removed in the α_a region are oxidized at the initial stage of γ_a.[31] If this is the case, Q_a, the sum of the quantity of electricity consumed to remove the hydrogen and to form the oxide film, should be larger than Q_c, the quantity required only to remove the oxide, and there should be a difference in the shape of the charging curve for the γ_a stage or in the quantity of electricity consumed for this stage in the anodic polarization between the bare electrode and that one covered with adsorbed hydrogen. The BCDEF curve in Fig. 3 is for the electrode polarized

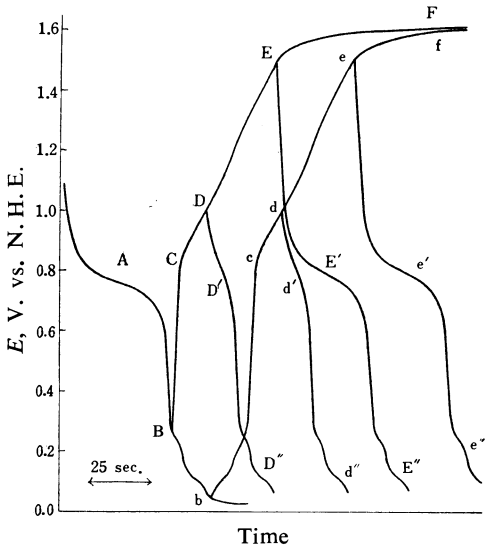


Fig. 3. Anodic and cathodic curves from various initial potentials.
$i_a = i_k = 20$ μamp./cm^2

from the potential B, where its surface is bare, while the bcdef curve is for the one polarized from the potential b, where its surface is completely covered with adsorbed hydrogen atoms. Between these curves no difference can be found. Moreover, it should be expected that the transition time of γ_c for the DD'D'' curve obtained when the current is reversed immediately at the D potential on the ABCD curve is larger than that for the dd'd'' curve reversed at the d potential on the abcd curve, but in practice these two curves, like also EE'E'' and ee'e'', were identical. For these reasons, we cannot accept the above assumption under the conditions of the experiment carried out in this work.

31) T. C. Franklin and S. L. Cooke, ibid., **107**, 556 (1960).

The Detection of Hydrogen Peroxide.—If the presumption of Vetter and Berndt[19] is true as to the cause of inequality between Q_a and Q_c, it should be possible to detect hydrogen peroxide near the electrode during cathodization.

A differential spectrophotometric method using 1,10-phenanthroline[32] was used for the determination of a trace of hydrogen peroxide. This method enables us to detect 0.1 to 2.5 p. p. m. of hydrogen peroxide with satisfactory precision and accuracy.

As the test electrode, a platinum wire 0.1 mm. in diameter and 10 m. long wound on a glass frame was used. According to the above presumption, 0.203×10^{-6} mol. hydrogen peroxide must be produced in the electrolyte during cathodization, because the value of Q_c for this electrode was measured as 4.032×10^{-2} coulombs. Since the volume of the electrolyte used for the measurement was 15 cc., the concentration of the hydrogen peroxide is expected to be 0.474 p. p. m.

Although the analysis was carried out very cautiously several times, the hydrogen peroxide could not be detected in a stationary solution, in an agitated solution, or on a rotated electrode. Consequently, the suggestion of Vetter and Berndt must be rejected.

The Loss of the Oxygen Deposited on the Surface.—In order to study the behavior of the oxygen deposited on the platinum electrode, the anodic and cathodic charging curves were taken under various conditions.

When the anodic current was reversed immediately at a potential, E_a, during the γ_a process, the charging curves shown in Fig. 4 were obtained. The ratios of q_a, the quantity of electricity required for the process from the initial potential of γ_a to E_a on the anodic curve, to q_c, that used for the plateau of γ_c on the cathodic curve taken subsequently, were plotted against E_a, as is shown by curve A in Fig. 5. For E_a exceeding 1.20 V. ($=E_a^\circ$), the ratio, q_c/q_a, has a constant value, but it decreases below this value.

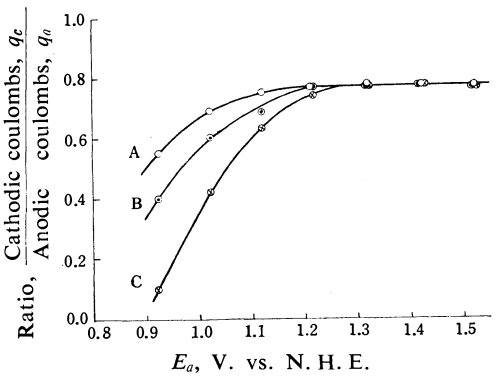


Fig. 5. Cathodic and anodic coulomb ratio as a function of potential, E_a, where the current was reversed.
-○- immediately reversed
-⊙- allowded to remain at open circuit for 2 min. in stationary solution
-⊗- allowed to remain at open circuit for 2 min. in agitated solution

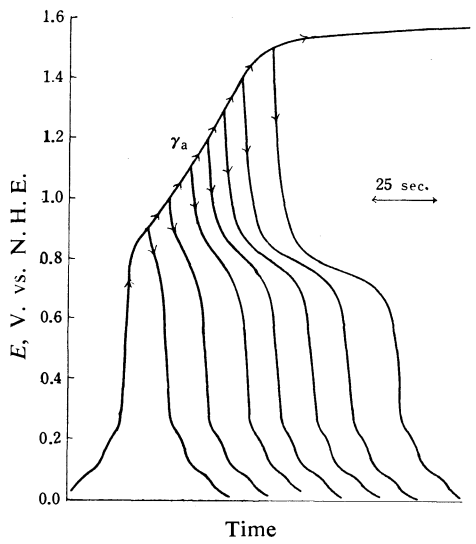


Fig. 4. Alternating anodic-cathodic charging curves when the current was reversed at various potential, E_a.
$i_a=i_k=20$ μamp./cm^2

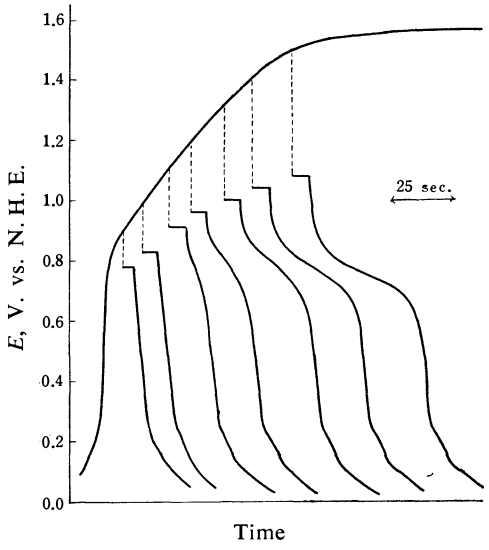


Fig. 6. Cathodic charging curves in stationary solution after anodic polarization till a various potential, E_a, and allowing to remain at open circuit for 2 min. in continuously agitated solution.
$i_a=i_k=20$ μamp./cm^2

32) R. Bailey and D. F. Boltz, *Anal. Chem.*, 31, 117 (1959).

When the solution was agitated vigorously by passing bubbling nitrogen gas through, the value of Q_a increases to 1.4 times that obtained under the stationary solution, whereas the value of Q_c suffers little effect from the agitation. For this reason, it may be presumed that a part of the oxygen deposited in the process of γ_a is very unstable and may be easily removed from the surface. After it is polarized to a given potential, E_a, of the γ_a region with a constant anodic current, the electrode was allowed to remain at an open circuit for 2 min.; then it is polarized cathodically with the same current density. The variation of the ratio, q_c/q_a, thus obtained against E_a is shown by curve B in Fig. 5. If the solution was agitated while the electrode was allowed to stand in this experiment, curve C in Fig. 5 was obtained. When the solution was continuously agitated throughout the anodic polarization and the standing, the curves shown in Fig. 6 were obtained. The plateau, γ_c, of the cathodic curve for the electrode anodized to the potential E_a below 1.05 V. vanished completely, and the potential fell rapidly and immediately reached the hydrogen deposition region.

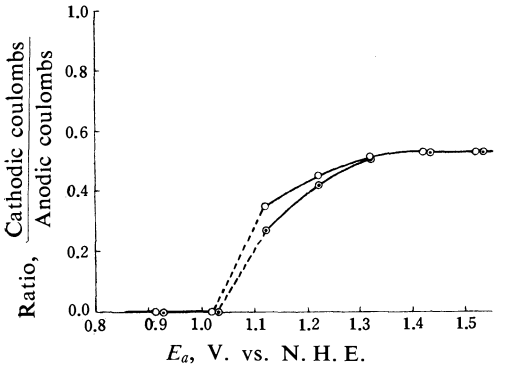


Fig. 7. Cathodic to anodic coulomb ratio as a function of anodically polarized potential, E_a.
$i_a = i_k = 20$ μamp./cm^2
-○- for anodic process in agitated solution and cathodic process in stationary solution after standing for 2 min. in stationary solution.
-⊙- for anodic process in agitated solution and cathodic process in stationary solution after standing for 2 min. in agitated solution.

The data shown in Figs. 5 and 7 suggest strongly that oxygen deposited in the first half of the γ_a region is attached loosely on the surface and is easily removed spontaneously during the standing or by the agitation of the solution.

The inequality between Q_a and Q_c may be caused by such a loss of the deposited oxygen from the surface in the initial stage of γ_a.

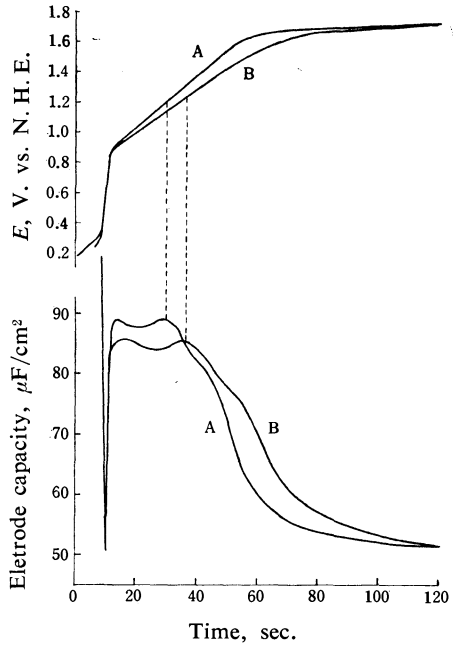


Fig. 8. Electrode potential and double layer capacitance during anodization at 25 μamp./cm^2 as a function of time.
A in stationary solution
B in agitated solution

The Capacity Change in the Course of the Anodic Process.—The potential-time and the capacity-time curves were measured simultaneously during the anodic polarization in the stationary solution, the results being shown in Fig. 8. The capacity-time curve may be divided into three portions: (a) the first portion, which starts with the oxygen deposition potential, where the capacity has a maximum value of approximately 90 μF/cm^2; (b) the second portion, characterized by a fall of the double layer capacity with time, beginning from 1.15 V. ($=E_w^\circ$), and (c) the third portion, with a stationary capacity value of 50 μF/cm^2, which is very close to the value found by Laitinen and Enke[23] for an oxidized surface. The result obtained with an agitated solution is shown by curve B in Fig. 8. The maximum value of the capacity is 4~5 μF/cm^2, which is smaller than that for the stationary solution, but the potential at which the capacity value begins to fall coincides with that for the stationary solution.

According to Llopis and Colum,[33] the increase of the electrode capacity of a

33) J. Llopis and F. Colum, Proceedings of the International Committee on Electrochemical Thermodynamics and Kinetics, Eighth Meeting, 1958, Butterworths, London, pp. 414-427.

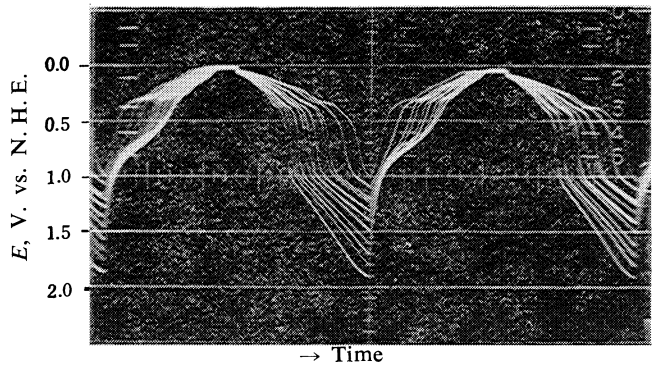


Fig. 9. Oscilloscope traces of electrode potential in square wave current electrolysis of frequency 78 c. p. s. at various c. d.

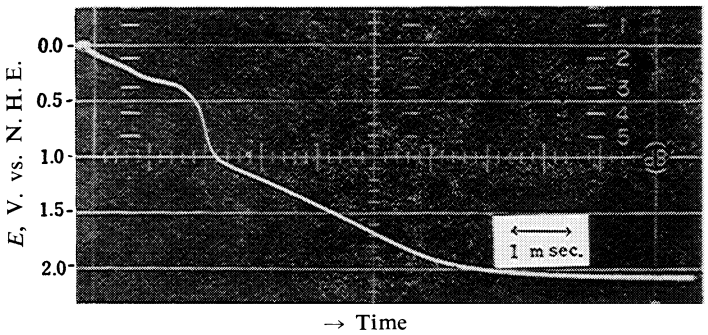


Fig. 10. Typical oscilloscope trace of anodic charging curve. i_a=190 mamp./cm²

platinum electrode at the beginning of the surface oxide formation is due to the presence of a dipole such as Pt···O at the electrode-solution interface. On the basis of this explanation, it is possible to account for the capacity vs. surface charge curve. Highly polar groups, which might be represented by $Pt^+\cdots O^-$, $Pt^+\cdots OH^-$ or $Pt\cdots OH_2$, may exist at the metal-solution interface on which the initial stage of oxygen deposition is proceeding. These dipoles replace the water molecules and ions which had formed the electrical double layer at the reduced electrode surface. The decrease in electrode capacity that was observed at the potential above E_w° may be caused by the decrease in the number of highly polar groups, or by their conversion to non-polar ones, probably to definite oxide molecules.

The Attack by Square-wave Alternating-current Electrolysis.—The mechanism of the change in the structure of a platinum electrode surface caused by repeated alternate anodic and cathodic polarizations calls for our intensive attention. The oscillogram of Fig. 9 shows the charging curves of the test electrode observed when the square-wave current of various current densities were passed through the cell containing a hydrogen-saturated solution. The amplitude of its oscillation increased with the increase in current density. A square-wave current was so adjusted that the maximum value of the oscillating potential was the desired value, E_s; the lowest potential, on the other hand, was equal to the hydrogen-evolution potential, which should be slightly increased by the hydrogen overpotential when the current density increases. The oscillogram shown in Fig. 10 is typical of the anodic charging curves photographed in order to determine the increase in true surface area caused by the electrolysis. The degree of the attack resulting from the electrolysis is shown in Fig. 11. It may be found from this figure that the surface of the electrode was not attacked at all as long as the potential did not exceed 1.15 V. ($=E_s^\circ$), regardless of the electrolysing duration or the frequency, whereas if the potential exceeded E_s°, the ratio Q_a'/Q_a rose rapidly, the bright surface becoming cloudy. The rate of the attack is faster at a frequency of 78 c. p. s. than at one of 40 c. p. s. and the surface is attacked more deeply when the electrolysis is prolonged at a given fre-

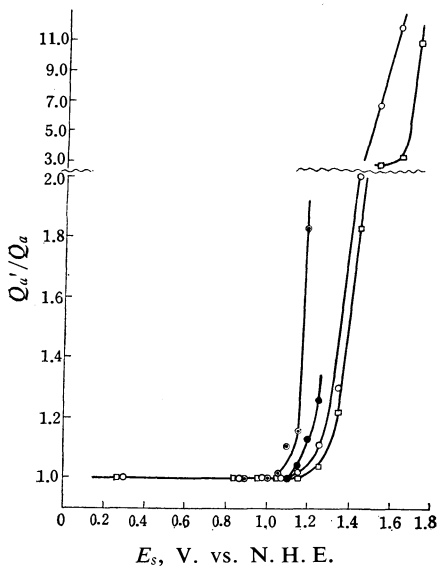


Fig. 11. Relation for maximum value, E_s, of oscillated potential and attack of electrode surface in square wave current electrolysis.

	Frequency c.p.s.	Electrolysing time hr.
-□-	40	1.0
-○-	78	1.0
-●-	78	3.0
-⊙-	78	6.0

quency. As has been pointed out in previous papers[34,35] on the sine-wave alternating-current electrolysis, it is clear that the attack of the electrode is not due to the alternate anodic dissolution and cathodic redeposition of platinum itself. Rather, the attack may be attributed to the repetition of the alternate formation and reduction of the oxide film, in which an oxygen atom forms a chemical bond with a surface platinum atom so that the bonds between the oxidized platinum atom and atoms adjoining it are either weakened or ruptured, according to the circumstances. The accumulation of these bond changes due to the repetition of the formation and reduction of the oxide rearranges the platinum atoms to make a recrystallization of platinum on the surface. The fact that surface did not suffer any attack at all the potential below E_s° suggests that the oxygen atoms deposited on the surface under that condition are only at a state of the adsorption in which they are not able to effect a serious change in the Pt–Pt bonds.

During the electrolysis at a potential below E_s° with a constant current density, the shape of the charging curve did not change for a long time. The activity of the electrode, however, was lost gradually as the electrolysis was prolonged. At a potential above E_s°, the current density had to be increased slowly with time in order to hold the wave shape invariable, because the roughness factor of the surface was increased by the beginning of the attack. In this case, the activity suffered no decay at all for the long period of the electrolysis.

The activation of the platinum surface by the pretreatment of anodic and subsequent cathodic polarization may be attributed to the light platinization due to the formation and reduction of oxide films.[36] On the other hand, the loss of the activity with time may be attributed to the settling down of the active platinum atoms on the surface into a stable state[37,38] as well as to poisoning by the impurities. Consequently, whether or not the activity decays during the alternating-current electrolysis should depend on whether the deposited oxygen is only adsorbed on the surface or whether it forms the oxide with platinum.

When platinum electrodes which have been aged in a hydrogen atmosphere for a long period of time are anodically polarized with a small constant current in a solution containing hydrogen, periodic oscillations of the electrode potential are often observed.[39,40] This potential-time curve for an acidic solutions shows a transition to a potential ca. +1.0 V., at which the deactivated electrode is reactivated, and then it sweeps down to near the reversible hydrogen potential. The noteworthy fact is found in this experiment that the electrode is not activated at the starting potential of the oxygen deposition process, γ_a, but at the potential nearly, corresponding to E_s°. This behavior of the electrode may also be interpreted reasonably by the mechanism described above.

Conclusion

The process of the deposition of the oxygen at the anodization has been observed only as a monotonous increase in the potential on the charging curve. However, it has been found that the γ_a region may properly be divided into two portions at the potential 1.15 V.

34) S. Shibata, *J. Chem. Soc. Japan, Pure Chem. Sec.* (*Nippon Kagaku Zassi*), **79**, 239 (1958).
35) S. Shibata, ibid., **80**, 453 (1959).
36) F. C. Anson and D. M. King, *Anal. Chem.*, **34**, 362 (1962).
37) L. P. Hammett and A. E. Lorch, *J. Am. Chem. Soc.*, **55**, 70 (1933).
38) S. Shibata, This Bulletin, **36**, 525 (1963).
39) G. Armstrong and J. A. V. Butler, *Discussions Faraday Soc.*, **1**, 122 (1947).
40) D. T. Sawyer and E. T. Seo, *J. Electroanal. Chem.*, **5**, 23 (1963).

($=E_a^\circ=E_w^\circ=E_s^\circ$), the reaction taking place in different ways in the respective portions.

According to the observed anodic behavior of the electrode, the mechanism of the surface oxidation may be proposed as follows, partly in identical terms with the proposal of Laitinen and Enke.[23]

On the first half portion of γ_a,

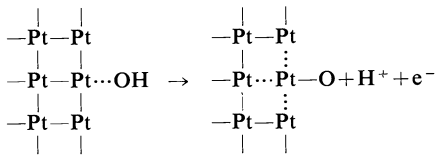
$$Pt + H_2O \rightarrow Pt\cdots OH + H^+ + e^- \quad (1a)$$

some of the $\cdots$OH intermediates thus adsorbed weakly on surface platinum atoms can further behave in either of two ways. First, they may be desorbed naturally from the surface, and, secondly, an oxygen evolution reaction may remove the surface hydroxyl, forming a bare platinum site as follows:

$$Pt\cdots OH + H_2O \rightarrow Pt\cdots OOH + 2H^+ + 2e^- \quad (1b)$$

$$Pt\cdots OOH \rightarrow Pt + O_2 + H^+ + e^- \quad (1c)$$

On the latter half of γ_a, the surface hydroxyl is converted to a surface oxygen atom which is so firmly bound, producing the definite oxide of platinum, that the bond between the oxidized platinum atom and atoms adjoining it is weakened.



(2)

Department of Chemistry
Faculty of Liberal Arts and Science
Yamagata University
Koshirakawa-cho, Yamagata

Vacuum Ultraviolet Absorption Spectra of Saturated Organic Compounds with Non-bonding Electrons

By Hiroshi TSUBOMURA,* Katsumi KIMURA,* Koji KAYA, Jiro TANAKA and Saburo NAGAKURA

(Received November 7, 1963)

The electronic spectra of aliphatic compounds have received relatively little attention from organic chemists because they lie mostly in the vacuum ultraviolet region. Saturated compounds containing non-bonding electron pairs like alcohols, ethers, amines, and halides show characteristic absorption bands in the region between 1600 and 2000 Å, the investigation of which seems to be important for a theoretical understanding of the electronic structures of these compounds. These bands may be important also for the chemical analysis of these compounds.

Most of the spectral measurements in the vacuum ultraviolet region have been made with the photographic method. About ten years ago, Klevens and Platt[1] measured the spectra of various aliphatic and aromatic compounds in the vacuum ultraviolet region up to 1750 Å. A group at Mount Holyoke College has also measured the vacuum ultraviolet absorption spectra of many aliphatic compounds, including olefins, aliphatic amines and alcohols.[2,3]

Photoelectric measurements of the vacuum ultraviolet spectra have been carried out by Watanabe and others.[4] Most of their work, however, has been on very simple molecules. Recently, some automatic recording spectrophotometers have become commercially available with which the measurements can be extended down to 1850 or even 1750 Å. Kaye[5] has done work by a commercially-available instrument on some alcohols and has found that their spectra shift to the blue as a result of the hydrogen bonding. Under these circumstances, the present authors undertook to construct a recording spectrophotometer suitable

* Present address: Department of Chemistry, Faculty of Engineering Science, Osaka University, Toyonaka, Osaka.

1) H. B. Klevens and J. R. Platt, "Technical Report of Laboratory of Molecular Structure and Spectra, Dept. Phys., University of Chicago," (1953-1954).

2) J. T. Gary and L. W. Pickett, *J. Chem. Phys.*, **22**, 599, 1226 (1954).

3) E. Tannenbaum, E. M. Coffin and A. J. Harrison, *J. Chem. Phys.*, **21**, 311 (1953).

4) K. Watanabe, M. Zelikoff and E. C. Y. Inn, Geophysics Research Papers 21. AFCRC Technical Report No. 53-23, Geophysics Research Directorate, Air Force Cambridge Research Center, 1953.

5) W. B. Kaye and R. E. Poulson, *Nature*, **193**, 675 (1962); also 13th Pittsburgh Conference on Anal. Chem. and Applied Spectroscopy., 1962.

for the accurate measurement of absorption intensity in the vacuum ultraviolet region from 1450 to 2200 Å, and to measure the vacuum ultraviolet absorption spectra of some saturated organic compounds with non-bonding electrons, such as alcohols, ether, amines and chlorides.

Mulliken was the first to give a theoretical explanation of the spectra of aliphatic alcohols, amines and halides. In his early-published paper,[6a] he explained that the near vacuum ultraviolet absorption bands of these compounds may be attributed to the Rydberg-type transition from the lone pair np atomic orbital to the vacant $(n+1)$s atomic orbital. Later, he pointed out that these bands are more likely to be of the $n \rightarrow \sigma^*$ type, because of the transition from the non-bonding atomic orbital (abbreviated hereafter to AO) to the vacant σ-antibonding molecular orbital (abbreviated hereafter to MO), although the possibility of the Rydberg nature of these bands can not be entirely excluded.[6b] The present authors intend to give a more detailed theoretical interpretation of the nature of these bands.

Experimental

The near ultraviolet absorption spectra ($\lambda > 1900$ Å) were measured with a Cary model 14M spectrophotometer, while the spectra in the region of wavelengths shorter than 2200 Å were measured by a vacuum ultraviolet spectrophotometer constructed in our laboratory. The instrument, shown diagramatically in Fig. 1, is more or less similar to the one constructed by Watanabe and Inn.[7]

The spectrophotometer uses a Bausch & Lomb concave grating (catalog No. 33-52-25-41; concave radius 995.4 mm., ruled area 56 mm. × 96 mm., 600 grooves/mm., blazed at 1500 Å, blaze angle 2°35′). The center of the grating and the two slits S_1 and S_2 are on the Rowland circle (with the diameter equal to the concave radius), so the light from the entrance slit, S_1, is always focused at the exit slit, S_2. The grating holder is fixed on a steel ball at the center of the circle and has two small rollers under the grating. It also has a vertical lever which is pushed by a micrometer head for scanning. The micrometer has a pitch of 0.5 mm. and is rotated by a synchronous motor through a gear set at speeds of 2, 4 and 8 rotations per minutes. The wavelength changes by about 45 Å per each rotation.

Hydrogen-discharge lamps from Hitachi, Ltd. and the Asahidenko Co. were used as light sources. They are hot-cathode type lamps with working voltages of 60 to 100 V. and a current of about 1 amp. Each of these lamps has a specially-designed power supply; further, a voltage stabilizer was used. The lamp has an optically-flat fused silica window which is pushed against the lithium fluoride window (also optically-flat) in front of the entrance slit of the monochrometer so as to minimize the air gap between them.

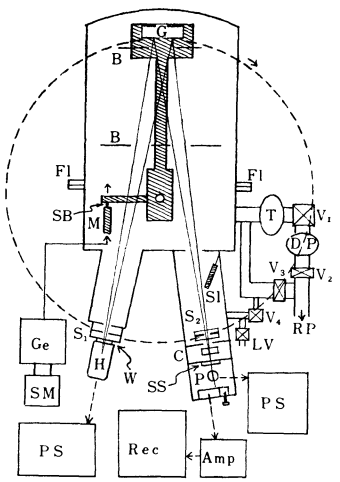


Fig. 1. Block diagram of the vacuum ultraviolet spectrophotometer. G, Grating; B, Baffle; Fl, Flange; SB, Steel ball; M, Micrometer; Sl, Shutter; S_1, S_2, Slits; H, Hydrogen disharge lamp; W, Lithium fluoride window; C, Cell; SS, A glass plate coated with sodium salicylate; P, Photomultiplier; Z, Zero adjuster; PS, Power supply; Amp, Amplifier; Rec, Recorder; SM, Synchronous motor; Ge, Gear set; LV, Leak valve; V_1, $\sim V_4$, Valves; T, Cold trap; Dp, Diffusion pump; RP, Rotary pump

The shutter designated by Sl in Fig. 1 can be operated from outside and serves both as a light shutter and a vacuum valve to insulate the cell compartment from the main body of the monochrometer. Each of the cells is cemented with Araldite to the cover plate, which is fixed in position at the flange of the cell compartment when it is in use (see Fig. 2). Such cell assemblies can be exchanged for various purposes after filling the cell compartment with air by operating the shutter, Sl, the valves LV, and other parts.

The light passing through the cell finally hits a glass window cemented on the outer surface of the cell compartment. The inner surface of the glass is covered with a thin layer of sodium salicylate, and the fluorescence caused by the vacuum ultraviolet light is received by a RCA 1P28 photomultiplier tube. The output is amplified by a DC micromicroammeter of the Ohkura Electric Co. and recorded by a Brown recorder. A zero adjuster consisting of a battery and a variable resistance is also connected.

The monochrometer tank consists of two parts, which are joined together with volts and nuts at the flanges. The rear part of the tank has rollers under it and can be moved along the rail when service is needed for the inside of the monochrometer.

6) a) R. S. Mulliken, *Phys. Rev.*, **47**, 413 (1935); b) R. S. Mulliken, *J. Chem. Phys.*, **8**, 382 (1940); *Phys. Rev.*, **61**, 277 (1942).

7) K. Watanabe and E. C. Y. Inn, *J. Opt. Soc. Am.*, **43**, 32 (1953).

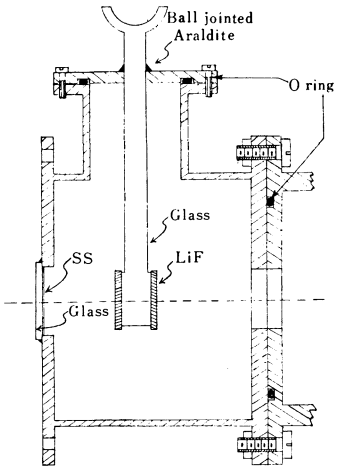


Fig. 2. The cell compartment and the vapor cell.

Figure 2 shows one of the cells for vapor measurement; they are made of glass and have two lithium fluoride windows cemented with Araldite. The inner thickness of the cell ranges from 7 to 30 mm. Each of the cells is connected with a vacuum line with a ball joint and is evacuated. The hydrogen lamp emission intensity is recorded under these conditions for use as reference. The sample vapor is then introduced, and the pressure is measured with a mercury manometer with an inner diameter of 20 mm. The mercury level is read with a measuring microscope. The sensitivity of the pressure reading is about 0.01 mm. The emission intensity is recorded for the sample. In Fig. 3, the measured curve for ethanol is given as a typical example of vapor measurements. Curve A is for the reference, curve B for the sample, and curve C for the molar extinction calculated from the two former curves. The short vertical lines on curves A and B are wavelength marker, given by the short-circuiting of the recorder input voltage at each rotation of the wavelength-drive micrometer. This is actually done by a microswitch in contact with the micrometer drum, which has a small cut at the periphery. The calibration of the wavelength has been done by comparing the marker readings recorded on the chart and the peak wavelengths of the absorption spectra of a certain number of compounds, for instance, acetone, whose peak wavelengths have been given in an earlier work.

As shown in the figure, the intensity of the emission of the hydrogen lamp decreases gradually in the vacuum ultraviolet region, reaching a minimum at about 1700 Å. Then it rises because of the atomic emission, falls very steeply because of the absorption of fused silica, and becomes almost flat below 1500 Å. In the flat region the intensity of the monochromatized light must be zero; hence, it gives the intensity of the stray light. We therefore call it the stray level. The final falling of the curve corresponds to the shutting off of the shutter, Sl. From the flatness of the stray level below 1500 Å, one may assume that the intensity of the

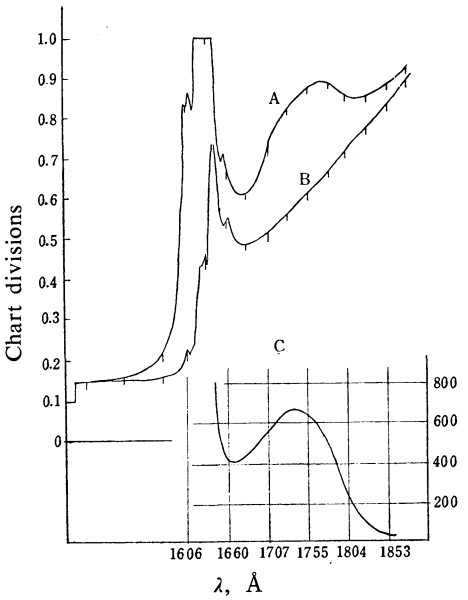


Fig. 3. Recorded curves for ethanol. A, Reference recording; B, Sample recording; C, The curve calculated from A and B (See text).

stray light is nearly constant in the wavelength range we are interested in. Therefore, by taking the "stray level" appearing in the curve to be the zero line, we can calculate the absorbance, $\log_{10}(I_0/I)$, from the curves for the reference and the sample. The effect of stray light can thus be reduced to less than a few percent. The extinction coefficients at about 2000 Å measured with this instrument agree well with those measured with the Cary 14 M spectrophotometer, the differences being in most cases less than 10%.

For solution measurements, fused silica cells, an example of which is depicted in Fig. 4, (made by the Nihon Sekiei Co.) were used. The inner thickness is about 0.1 mm. This seems to be the technically available lower limit for the precise

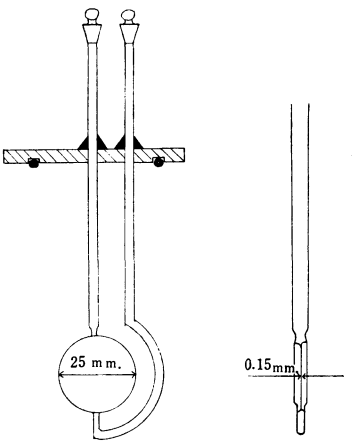


Fig. 4. The solution cell.

TABLE I. THE OBSERVED CHARACTERISTICS OF THE ULTRAVIOLET BANDS

Compound	λ_{max}, Å	ε_{max}, l./mol. cm.	$\Delta\nu_{1/2}$, cm^{-1}	f
a) Oxygen compound				
Water	1670	2120	9100	0.084
Methanol	1742	356	3400	0.0052
Ethanol	1740	670	4400	0.013
Ethyl ether	1885	2820	3400	0.041
b) Amine				
Triethylamine	2120	6100	8400	0.22
c) Chloride				
Methyl chloride	1690	370	6500	0.010
Dichloromethane	1790	510	—	—
Chloroform	1755	950	6400	0.026
Carbon tetrachloride	1740	2370	6200	0.063

construction of such cells. The thickness was calibrated by measurements of the absorption spectrum of a *n*-heptane solution of chlorobenzene with the Cary spectrophotometer. Even with such thin cells, the absorption by the solvents is enormous, and purified *n*-heptane has turned out to be the only solvent which can be used in this range, though some other homologues can probably be so used also.

Results and Discussion

Water, Alcohol and Ether.—Figures 5 and 6 and Table Ia give the results for the spectra of water, alcohols and ether. The spectral shapes obtained are in good agreement with those of Harrison et al.[8,9] and with those of Watanabe and Zelikoff,[10] although our molar extinction values are 1.5 times to twice as large as theirs. The reason for this discrepancy is not clear.

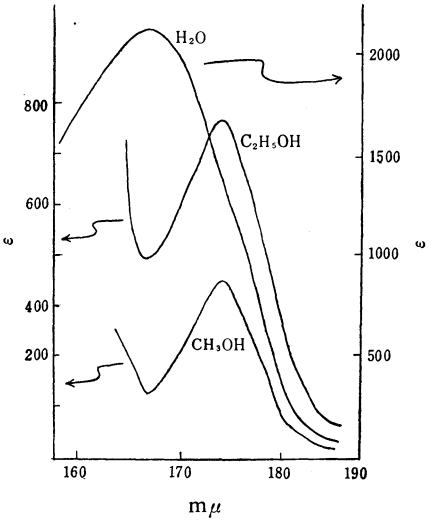


Fig. 5. The absorption spectra for water, methanol and ethanol.

The experimental results seem to be explained reasonably by the following assumption (see Fig. 7): 1) These bands are essentially of the $n\rightarrow\sigma^*$ type, where n means the 2p AO of the oxygen atom directed along the line perpendicular to the molecular plane; 2) the σ^* orbital for the C-O bond, σ^*(CO), has an orbital energy appreciably lower than that for the σ^*(OH) orbital (the reason for this will be given later), and 3) the matrix elements of the Hamiltonian between two σ^* orbitals in a molecule are small (see the Appendix). Therefore, the two upper configurations, $n\rightarrow\sigma^*$(OH) and $n\rightarrow\sigma^*$(CO), in alcohols interact slightly, while the two $n\rightarrow\sigma^*$ configurations of water and ether interact strongly with each other, because they are degenerate. If the

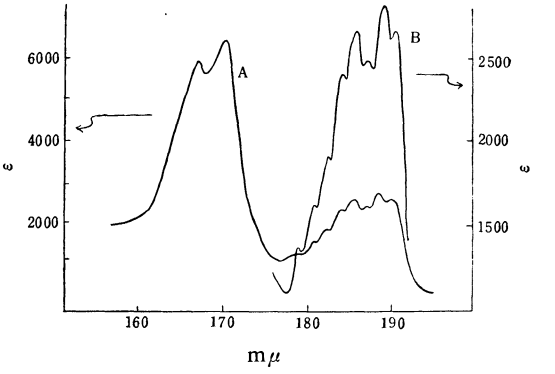


Fig. 6. The spectrum for ether. Curve B is for an expanded scale.

8) A. J. Harrison, B. J. Cederholm and M. A. Terwillinger, *J. Chem. Phys.*, **30**, 355 (1959).
9) A. J. Harrison and D. R. W. Price, ibid., **30**, 357 (1959).
10) K. Watanabe and M. Zelikoff, *J. Opt. Soc. Am.*, **43**, 753 (1953).

* It may be expected that the electron affinity of a molecule generally gets larger as the molecule becomes larger, because the extra charge is more or less stabilized by the polarization of other electrons in the molecules. Therefore, the transition energy may conceivably be affected by the electron affinity, too, but its effect may be smaller than the effect of the ionization potential.

energy levels of the molecular states are approximated by the relevant orbital energies, the lower levels shown in Fig. 7 correspond to the orbital energies of the oxygen non-bonding orbitals, which are taken to be equal to the ionization potentials for these molecules (with the sign reversed). The upper levels correspond to the orbital energies of the σ^* (antibonding) molecular orbitals. The differences in energies between the two levels are taken to be equal to the observed transition energies.

From Fig. 7 it may be seen that the transition energy increases in the order of $(C_2H_5)_2O < C_2H_5OH < H_2O$. The transition energy corresponds roughly to $(I-A-Q)$, where I is the ionization potential of the molecule, A is the electron affinity associated with the σ^* orbital, and Q is the electrostatic energy due to the charge unbalance in the upper state. Moreover, the ionization potential value undoubtedly increases in the following order; $(C_2H_5)_2O<C_2H_5OH<H_2O$. Thus, we can explain the fact the $n\rightarrow\sigma^*$ band shifts toward shorter wavelengths in the order of ether, alcohol and water.* The reason why ether absorbs at longer wavelengths than alcohol may be partly attributed to the splitting of the antibonding σ^* orbital in the former.

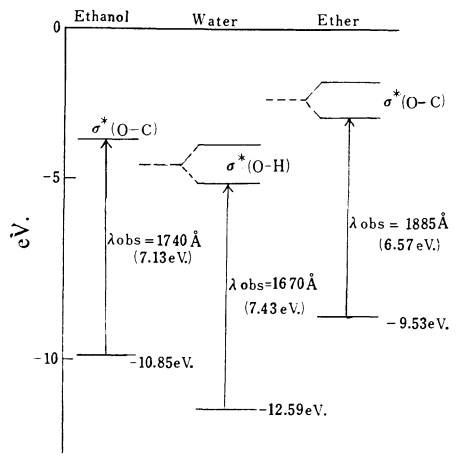


Fig. 7. The energy levels of ethanol, water and ether.

The oscillator strength of a transition, f, is related to the transition moment, μ (in Debye units), by the following equation;

$$f=8\pi^2\nu_{max}\boldsymbol{m}\mu^2/3\boldsymbol{he}^2=4.704\times10^{-7}\nu_{max}\mu^2 \quad (1)$$

where ν_{max} (in cm^{-1}) is the wave number at the maximum, $\boldsymbol{m}$ and $\boldsymbol{e}$ are the mass and the charge of an electron, and $\boldsymbol{h}$ is Planck's constant. The transition moment for the $n\rightarrow\sigma^*$ (CO) transition can be expressed by the present scheme as follows:

$$\mu=\int\psi(n)(\boldsymbol{ex})\psi^*(\sigma)dv=\int\psi_{2px_0}\times(\boldsymbol{ex})(a\psi_{2pz_0}-b\psi_c)dv=b\int\psi_{2px_0}(\boldsymbol{ex})\psi_c dv \quad (2)$$

where a and b are normalized coefficients for the σ^* MO, z is directed along the bond, and x is vertical to the molecular plane. ψ_c is an sp^3-hybridized AO directing the bond. Calculation by the use of the Slater AO's leads to $\mu=0.74b$ in Debye units. If one assumes that $a=b$, f is calculated to be of the order of 0.011, a value which is in good agreement with the experimental value for alcohols. On the other hand, if the upper MO is assumed to be $\sigma^*(OH)=a'\psi_{2pz_0}-b'\psi_{1s_H}$, the transition moment is given by $\mu'=b'\int\psi_{2px_0}(\boldsymbol{ex})\psi_{1s_H}dv$. The result is $\mu=3.0$ D and $f=0.24$. The f value obtained is 20 times larger than the observed f values for alcohols. Therefore, it can be concluded that the upper MO for the case of alcohols is more likely to be σ^*(CO).

In the water and ether molecules, the two σ^* orbitals interact with each other, resulting in two MO's;

$$\psi_1=2^{-1/2}\{\sigma^*(OX_1)+\sigma^*(OX_2)\}$$
$$\psi_2=2^{-1/2}\{\sigma^*(OX_1)-\sigma^*(OX_2)\} \quad (3)$$

The symmetric combination ψ_1 will have the lower energy. By inspection one can easily see that ψ_1 is equivalent to the first vacant SCF MO of water as calculated by Ellison Shull.[11] The transition moment in this case is then given by

$$\mu_{n\psi_1}=2^{-1/2}\left\{\int\psi(n)(\boldsymbol{ex})\sigma^*(OX_1)dv+\int\psi(n)(\boldsymbol{ex})\sigma^*(OX_2)dv\right\} \quad (4)$$

The two terms in the brackets have directions parallel to each other, and their magnitudes are same. Hence,

$$\mu_{n\psi_1}=2^{1/2}\int\psi(n)(\boldsymbol{ex})\sigma^*(OX_1)dv \quad (5)$$

Therefore, the $n\rightarrow\psi_1$ transition has a probability twice as large as that of the $n\rightarrow\sigma^*$ transition in alcohols, and that of $n\rightarrow\psi_2$ is impossible.

In this way we can explain the experimental result that the symmetric molecule (ether) has stronger absorption bands than asymmetric molecules (alcohols). Also, the larger calculated f value for the $n\rightarrow\sigma^*$(OH) transition may explain the experimental f value for water larger than that for ether. Thus, it can be seen that the transition scheme prosposed above explains the qualitative characteristics of observed bands, although a more quantitative agreement between theory and observed

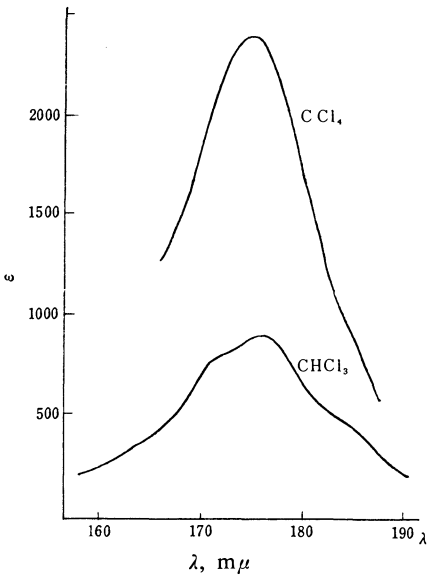
results can not be expected from such a simple treatment.

According to the above treatment, $\mu_{n\psi_2}$ becomes zero. The second absorption band of ether observed by us and also by Harrison and Price at about 1700Å has an intensity larger than that of the first band. It is, therefore, concluded to be due to another transition, and the $n\rightarrow\psi_2$ band may be hidden in it.

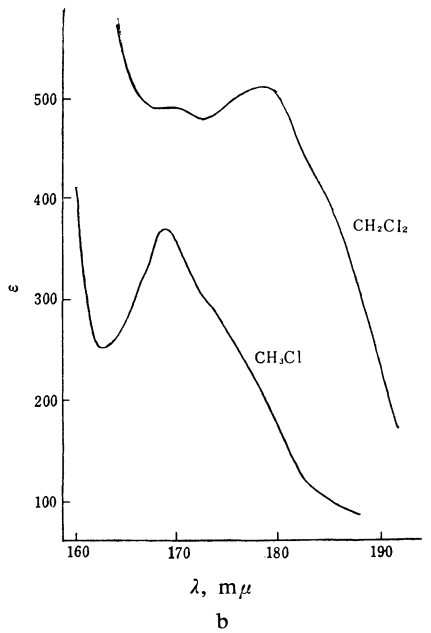
Amine.—The lone pair AO of the nitrogen atom in alkyl amines and ammonia is thought to be the (s, p)-hybridized AO, directed along the symmetry axis or pseudo-symmetry axis of the pyramidal molecules. Therefore, it can easily be seen that the $n\rightarrow\sigma^*$ transition has a fairly strong intensity, since the transition moment integral contains not only the two center terms, such as appear in Eq. 2, but also the one center terms, like

$\int \psi_{2p_xN}(ex)\psi_{2sN}dv$, which is quite large.

Our experimental result on the vapor spectrum of triethylamine has shown that its f value is indeed of an order of magnitude higher than that for alcohols (see Table I).



a



b

Fig. 8. Spectra for the chlorides of methane.

Chlorides.—Figure 8 and Table Ic show the experimental results obtained for the four chlorides of methane. The ε and f values for methyl chloride are of an order of magnitude equal to those for alcohols, and to those for bromides and iodides measured by Kimura and Nagakura.[12] Hence, it seems reasonable to assume that the transition is $n\rightarrow\sigma^*$, where n is the 3px AO of chlorine and σ^* is the antibonding MO for the C–Cl bond.

In polychlorides, there are a number of n and σ^* orbitals. Theoretically, these orbitals should not interact strongly with each other. Hence, the absorption intensities, or f values, for polychlorides must be approximately proportional to the number of chlorine atoms when the axes of the n AO's of the Cl atoms are assumed to be all parallel. The experimental results show that the f values increase approximately at the predicted rate.

The observed spectra of polychlorides show rather complicated features, suggesting that these spectra consist of a certain number of divided bands, as was observed in the case of bromides and iodides.[12] However, the splitting in the present case appears to be much smaller, indicating that the interactions between orbitals belonging to different C–X bonds are smaller in this case.

Comment on the Rydberg Nature of the Transitions. — It is clear that the vacuum ultraviolet bands discussed above are more or less of a *molecular* nature, because they are rather sensitive to the atoms or groups of atoms to which the central atom is bonded. In this sense, it is definitely errorneous to conclude simply that these bands are due to transitions from AO's np to $(n+1)$s, with the energies of these AO's independent of the other components of the molecules.

Kimura and Nagakura[12] calculated the

11) F. O. Ellison and H. Shull, *J. Chem. Phys.*, **23**, 2348 (1955).

12) K. Kimura and S. Nagakura, *Spectrochim. Acta*, **17**, 166 (1961).

oscillator strengths of the $np \rightarrow (n+1)s$ transitions for bromides and iodides and showed that the calculated values were much higher than the observed values. For this reason the bands were concluded to be of the $n \rightarrow \sigma^*$ nature.

The calculated oscillator strength for the $np \rightarrow (n+1)s$ transition generally gets smaller as n becomes smaller. For the $2p \rightarrow 3s$ transition of the oxygen atom, the calculation leads to $f=0.01$, which coincides with the observed value for ethanol. Therefore, we can not apply the same reasoning for the determination of nature of the transition in the present case.

It has been suggested by Mulliken that the σ^* MO of these molecules (especially those of a higher symmetry, for emample, NH_3 or H_2O) may resemble very closely the 3s AO of the central atom, and that they are both appropriate orbitals for describing the first molecular Rydberg states.[13] It also seems probable that the two orbitals will interact with each other and form a mixed MO. The electronic transition to this MO will perhaps describe these upper states the most correctly insofar as the one-electron approximation is concerned. In fact, the $(n+1)s$ AO is so large that it must interact very strongly with the AO's of other atoms in the same molecules. What we want to point out in this paper is that the various charateristics of these bands can be explained well, at least in part, by the $n \rightarrow \sigma^*$ type transition.

13) Personal discussion of H. Tsubomura with Professor Mulliken, 1962.

The Institute for Solid State Physics
The University of Tokyo
Azabu, Tokyo

Appendix

For molecules of the X_1OX_2 type, the σ^* orbitals for the OX_1 bond and the OX_2 bond are given by the following LCAO MO:

$$\sigma^*(OX_1) = a\psi_{\sigma_1} + b\psi_{X_1}$$

$$\sigma^*(OX_2) = a\psi_{\sigma_2} - b\psi_{X_2}$$

where ψ_{σ_1} and and ψ_{σ_2} are the valence AO's directed along the two bonds and where ψ_{X_1} and ψ_{X_2} are the two valence AO's of X_1 and X_2. The interaction between these two orbitals depends on the difference between their orbital energies and the interaction matrix element;

$$\beta = (\sigma^*(OX_1) \mid H \mid \sigma^*(OX_2)).$$

Inserting the explicit form, we have:

$$\beta = a^2 H_{\sigma_1\sigma_2} - b^2 H_{X_1X_2} - ab(H_{\sigma_1X_2} - H_{\sigma_2X_1})$$

All the terms contained in the equation except for $H_{\sigma_1\sigma_2}$ are between the AO's of atoms long distances apart and, hence, small. $H_{\sigma_1\sigma_2}$ is between AO's which belong to the same atom but which are orthogonal to each other with respect to the core potential. Therefore, we can see that all the terms in this equation must be small in absolute magnitude.

NOTES

The Radiolysis of Squalane ($C_{30}H_{62}$) from −196°C to 350°C

By Kiyoshi FURUKAWA,* Shigeyoshi ARAI, Hideo YAMAZAKI** and Shoji SHIDA

(Received July 30, 1963)

The radiolysis of squalane at room temperature has been already studied by Yamazaki and Shida.[1] The present note will describe a study of the influence of the temperature on the γ-radiolysis of squalane. This substance is favorable for studying the effect of the temperature on radiolysis because of its characteristic nature of being liquid over a sufficiently wide range of temperature, i. e., −78.5 to 350°C or more. It was irradiated in vacuo at 350, 300, 250, 200, 150, 100, 0, −78.5 and −196°C by γ-rays with the total doses of 1.5×10^7 and 2.13×10^7 r.

Non-condensable gases at the temperature of liquid nitrogen, hydrogen plus methane, were collected in a micro gas burette mounted directly above a toepler pump until the sample tube was evacuated to 10^{-3} mmHg. The total volume of non-condensable gases was next measured, after which hydrogen was removed by a liquid nitrogen trap through a tube of cupric oxide heated to 270°C, at which temperature no methane was decomposed. The mass-spectrometric analysis of the residual non-condensable gas on several occasions showed it to consist of almost pure methane. The condensable gases were analyzed by gas chromatography. Each product was identified by using a mass-spectrometer. The *G*-values*[1] obtained are given in Table I. In this table, it may be seen that the *G*-values of hydrogen production are nearly constant at 3.8 from −196°C to 100°C, but that they increase to 7.0 at 350°C. For the other products of hydrocarbon, the increases in *G*-values in the region from 150°C to 300°C are larger than those at lower temperatures.

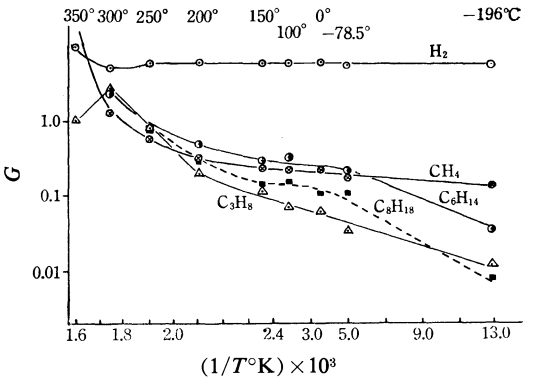
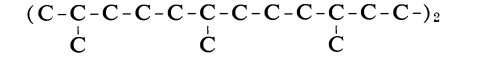


Fig. 1. Plots of log *G* against $1/T$°K.

The skeleton of squalane is as follows:



In this figure, the relation between the logarithmic *G*-values and $1/T$°K is plotted. It appears preferable to divide the temperature range into two parts, below and above 150°C.

Below 150°C.—In this region of temperature, the viscosity of squalane is so high that the molecular motion may be reduced, and the so-called cage effect seems to take place. The diffusion of radicals produced by γ-irradiation, therefore, must be greatly diminished. Under these circumstances, the radical reactions, which are expected to be abstraction, recombination and disproportionation, will be very much affected. Radicals that have diffused out of the cage are converted into products by abstracting hydrogen atoms from squalane molecules. On the other hand, those held in cages may react with each other, undergoing recombination and disproportionation to form original molecules and products consisting of aliphatic

* Present address: Takasaki Laboratory, Japan Atomic Energy Research Institute, Tokai, Ibaraki.
** Present address: National Institute of Radiology, Chiba.

1) H. Yamazaki and S. Shida, *J. Chem. Phys.*, 32, 950 (1960).

*1 The *G*-value is defined as the number of species of a given kind reacting or produced per 100 eV. of radiation energy absorbed.

TABLE I. *G* VALUES OF EACH PRODUCT

°C	H_2	CH_4	C_3H_8	C_3H_6	i-C_4H_{10}	i-C_5H_{12}	C_6H_{12}	C_6H_{14}	C_8H_{18}
−196	3.4	0.12	0.01	0.006			0.03		0.007
− 78.5	3.4	0.16	0.03	0.022			0.2		0.1
0	3.7	0.2	0.055	0.053			0.2		0.1
100	3.7	0.21	0.063	0.02			0.3		0.14
150	4.22	0.28	0.14	0.015	0.025	0.036	0.44	0.27	0.22
200	4.07	0.35	0.17	0.013	0.037	0.088	0.043	0.29	0.26
250	4.07	0.55	0.79	0.045	0.118	0.63	0.82	0.43	0.93
300	3.61	1.21	2.66	—	0.44	2.88	2.15	0.34	—
350	7.0	12.0	1.0	—	0.7	2.4	—	—	—

or olefin. Therefore, the reactions in cages are thought to proceed in a relatively short time, before radicals diffuse out of the cages, i. e., to occur in a spur.[2] The products due to this instantaneous disproportionation reaction may be formed as soon as the C–C bonds are separated by γ-irradation. It should be, therefore, interpreted that a reaction like the so-called molecular detachment takes place in a liquid of high viscosity at a low temperature.[3] In this figure, it may be seen that the curve becomes steeper with the increasing molecular weight of the product. This may be due to the fact that the activation energy for diffusion becomes larger with the increasing molecular weight of the fragment. It may also be noted that near 150°C the slopes tend to be flat. These inflexion points of the curve may indicate some difference between the liquid states below and above 150°C. The pursuit of the discontinuity of this curve will be one of the objects of our later work.

Above 150°C.—Since no thermal cracking of free radicals takes place about 150°C,[4] the activation energies for each product were obtained from the curve above 150°C; they were estimated to be 15±1 kcal./mol. Large radicals, such as that of squalane, presumably, need lower activation energies for thermal cracking.

The rapid increase observed in this region may come simply from the cracking of free radicals produced by the γ-irradiation. It is necessary also to mention that the rupture of the C–C bonds of a radical by thermal cracking occurs at the β-position of free valence.[5] Since the *G*-values of hydrogen production are the largest of all, a lot of squalane radicals may be produded. Among them, the tertiary radicals will be predominant, and the products of their thermal cracking are expected to be C_4, C_5 and C_9. Actually the C_4 and C_5 were produced abundantly. Contrary to the expectation, however, the C_9 product was not observed. It seems, therefore, that the inner C–H bonds of a long molecule have less reactivity. This observation suggests that the "*intramolecular energy transfer*"[6] may take place in a long molecule. Thus, prior to the rupture of C–H bonds, the energy absorbed in a molecule is transferred to the end parts of the molecule and makes their reactivity large enough to separate the hydrogen atoms from the original molecule.

This experiment owes much to Dr. Hirofumi Danno, who offered us a ^{60}Co-γ source in the Japan Atomic Energy Research Institute.

Laboratory of Physical Chemistry
Tokyo Institute of Technology
Meguro-ku, Tokyo

2) I. A. Taub and L. M. Dorfman, *J. Am. Chem. Soc.*, **84**, 4053 (1962).
3) T. J. Hardwick, *J. Phys. Chem.*, **64**, 1623 (1960).
4) A. F. Trotman-Dickenson, "Gas Kinetics," Butterworths Scientific Rublications, London (1955).
5) A. Kossiakoff. and F. O. Rice, *J. Am. Chem. Soc.*, **65**, 590 (1943).
6) H. Sponer, *Radiation Research*, Supplement **1**, 558 (1959).

Spectrophotometric Determination of the Acid Dissociation Constants of Plasmocorinth B

By Haruo MIYATA

(Received Septemper 12, 1963)

Plasmocorinth B (2-(1-hydroxy-4-chloro-2-phenylazo)-1, 8-dihydroxynaphthalene-3, 6-disulfonic acid disodium salt) was proposed as a colorimetric reagent for calcium in serum by Yanagisawa,[1] and it was studied then by Brush;[2] more recently this reagent has been utilized as an indicator of the chelometric titration[3] of calcium in the presence of magnesium.

This paper will report on a more detailed study of the absorption spectra and the acid dissociation constants of this reagent by the spectrophotometric method.

Experimental

Reagents.—A reagent obtained from the Sumitomo Dye Co. (SPB*) and the Dôjin Pharmaceutical Co. (DPB**), with the trade name Plasmocorinth B, was used for the studies without any further purification. It was dried at 60°C in a vacuum, cooled in a phosphorus pentoxide desiccator, and weighed. A solution (3×10^{-4} mol./l.) was prepared and stored in the dark.

Buffer Solution and Sodium Perchlorate Solution.—The method of preparation has been described earlier.[4]

Procedure and Apparatus.—The measurements of the absorption spectra at various pH values were made as follows: Five milliliters of a 3×10^{-4} mol./l. reagent solution was placed in a 50 ml. volumetric flask, and an adequate volume of 1 M perchloric acid, 1 M sodium hydroxide or a buffer solution (acetic acid-sodium acetate, ammonium acetate-ammonia or ammonia-ammonium chloride) was added in order to adjust the pH value. 0.1 ml. of a 0.01 M EDTA solution was added to mask trace amouts of calcium or magnesium contained in sodium hydroxide or ammonia, because the definite isosbestic points can not be obtained in the absence of EDTA, especially at a higher pH. Then, a 1 M sodium perchlorate solution was added to maintain the ionic strength at 0.1, and the volume was made up to 50 ml. with water. The absorbance was then measured with a Shimadzu spectrophotometer QR-50 type, and a Hitachi automatic recording spectrophotometer EPS-2 type, with 1 cm. cells, using water as a reference, while the pH value was measured with a Tôa-Denpa glass electrode pH meter, Model HM-8A.

All the measurements were made at 25°C.

Results and Discussion

Spectral Properties of the Reagent. — The absorption spectra of the reagent solution (3×10^{-5} M) are shown in Fig. 1 over various pH values.

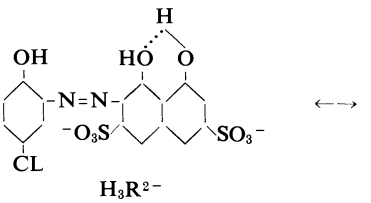
Below pH 4, the reagent gives an absorption spectrum with one absorption maximum at 530 mμ; when the pH of the solution is increased to 8.8, the maximum shifts to 610 mμ. Between pH 1 and 8.8, four isosbestic points exist, at 367, 413, 456 and 573 mμ.

Above pH 9.3, an absorption maximum appears at 576 mμ, and between pH 9.3 and 13, the two isosbestic points are at 467 and 612 mμ.

Between pH 8.8 and 9.3, there are no isosbestic points, so that the curves pass neither the point at 573 mμ nor that at 612 mμ.

Since the reagent faded gradually at a higher pH, the effect of *l*-ascorbic acid and hydroxylamine on the absorbance at the maxium (576 mμ) was studied at pH 13.0. The effect of neither reagent is good, but in the presence of 1.5×10^{-6} M *l*-ascorbic acid the absorbance is constant for ten minutes.

The Acid Dissociation Constant of the Reagent. —Judging from the presence of the isosbestic point, the structures H_3R^{2-} and H_2R^{3-} between pH 1 and 8.8 and the structures H_2R^{3-} and HR^{4-} between pH 9.3 and 13.0 are expected:



H_3R^{2-}

1) F. Yanagisawa, *J. Biochem. (Japan)*, **42**, 3 (1955).
2) J. S. Brush, *Anal. Chem.*, **33**, 789 (1961).
3) G. S. Kovacs and K. E. Tarnoky, *Anal. Chim. Acta*, **21**, 297 (1959).
* Anal. Found: N, 5.40 Calcd. for $C_{16}H_9O_9N_2S_2Na_2Cl$: N, 5.51%.
** Anal. Found: N, 4.91
4) H. Miyata, This Bulletin, **36**, 382, 386 (1963).

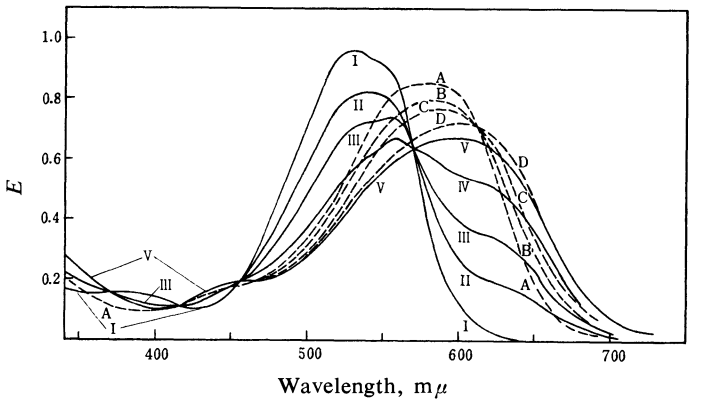
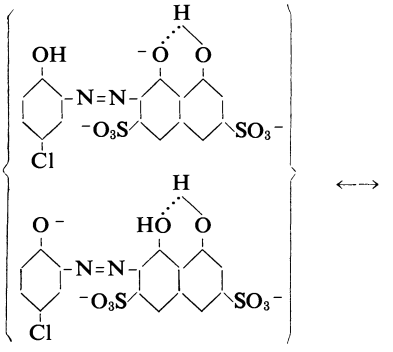


Fig. 1. Absorption spectra of Plasmocorinth B (SPB).
I, pH ~3.86; II, pH 6.64; III, pH 7.25; IV, pH 7.73; V, pH 8.47.
A, pH 13.01; B, pH 10.93; C, pH 10.52; D, pH 9.33



The dissociation constants, K_1 and K_2, can be calculated by the following equations:

$$H_3R \rightleftarrows H_2R + H \quad (1)$$

$$K_1 = [H]\,(E_{H_3R} - E)/(E - E_{H_2R}) \quad (2)$$

$$H_2R \rightleftarrows HR + H \quad (3)$$

$$K_2 = [H]\,(E'_{H_2R} - E')/(E' - E'_{HR}) \quad (4)$$

where E_{H_3R}*, E_{H_2R} and E represent, respectively, the absorbances of H_3R, H_2R and the mixture of H_3R and H_2R at 600 mμ, and E'_{H_2R}, E'_{HR}** and E' represent, respectively, the absorbances of H_2R, HR and their mixture at 640 mμ.

E_{H_3R}* and E'_{HR}** are equal to the absorbances at pH 1~4 and pH 12.4~13 respectively; E_{H_2R} and E'_{H_2R} are, however, not obtainable directly from the experimental absorbances, because the difference between pK_1 and pK_2 is small and the species H_2R always exists together with H_3R or HR, even under the most favorable conditions. Thus, at pH 8.8~9.3 the absorption curves have no isosbestic points, although H_2R is predominant.

Consequently, E_{H_2R} and E'_{H_2R} must be calculated by the following equations reported by Yoshioka et al.:[5]

$$E_{H_2R} = (a_1E_2 - a_2E_1)/(a_1 - a_2)$$

$$a_1 = [H_1]\,(E_{H_2R} - E_1)$$

$$a_2 = [H_2]\,(E_{H_3R} - E_2)$$

$$E'_{H_2R} = (b_1E'_1 - b_2E'_2)/(b_1 - b_2)$$

$$b_1 = [H'_1]/(E'_1 - E'_{HR})$$

$$b_2 = [H'_2]/(E'_2 - E'_{HR})$$

In the equations, E_1 (or E'_1) and E_2 (or E'_2) represent the absorbances at the hydrogen ion concentrations $[H_1]$ (or $[H'_1]$) and $[H_2]$ (or $[H'_2]$) respectively.

On the basis of these calculations, the acid dissociation constants of the reagent have been estimated and compared with the values of Brush:[2]

		pK_1	pK_2	pK_3
Brush[2]		8.0	10.5	11.9
The author	SPB	7.1_5	10.4_8	—
	DPB	7.1_6	10.4_8	—

The value of pK_3 could not be found from the absoption spectra of highly alkaline solutions; however, judging from the pK_2 values of chromotropic acid (15.6)[6] and

* E_{H_3R} = 0.090 for SPB; 0.075 for DPB.
** E'_{HR} = 0.250; 0.223.

5) M. Yoshioka et al., *J. Chem. Soc. Japan, Pure Chem. Sec.* (*Nippon Kagaku Zasshi*), **83**, 229 (1962).
6) J. Heller and G. Schwarzenbach, *Helv. Chim. Acta*, **34**, 1876 (1951).

phenylazo chromotropic acid (14.64)[7], (pK_2 corresponding to the pK_3 of this reagent) and from the absorption spectra of some azo compounds coupled with chromotropic acid,[4,8] Brush's pK_3 value (11.9) seems to be doubtful.

The author wishes to express his hearty thanks to Dr. Kyoji Tôei for his guidance in the course of this experiment. Thanks are also due to Mr. Sachiaki Kiguchi, who joined in this work in its early stages.

Department of Chemistry
Faculty of Science
Okayama University
Tsushima, Okayama

7) J. Bjerrum et al., "Stability Constants, Part I: Organic Ligands," The Chemical Soc., London (1957), p. 95.

8) Unpublished work of H. Miyata.

Anomalies in the Temperature Dependences of the ESR Absorption and Electrical Conductivity of an Anion Radical Salt, $[(C_6H_5)_3PCH_3]^+(TCNQ)_2^-$

By Yôichi IIDA, Minoru KINOSHITA, Mizuka SANO and Hideo AKAMATU

(Received October 9, 1963)

In recent years the anion radical salts of tetracyanoquinodimethane (TCNQ) have aroused much interest because of their prominent electronic properties. In particular, the magnetic property of the salts at low temperature range has been explained in full by Chesnut et al.[1,2] in terms of the singlet-triplet equilibrium resulting from the spin correlation between two anion radicals of TCNQ. Chesnut et al. have referred to the existence of a discontinuity in the magnetic susceptibility of the TCNQ salt of methyltriphenylphosphonium, $[(C_6H_5)_3PCH_3]^+(TCNQ)_2^-$, at 315°K.[1,3] In this report we will present the temperature dependences of the ESR absorption and electrical conductivity of the salt in the temperature range including 315°K.

Single crystals of the phosphonium salt were prepared in the manner described by Melby et al.,[4] and all the measurements were performed with these single crystals. The crystal showed the same ESR fine structures at about 130°K arising from the magnetic dipole interaction as has been examined by Chesnut and Phillips.[1] At a higher temperature range, where the fine structures coalesced, the ESR absorption intensity and the line width varied with the temperature, as shown in Figs. 1 and 2, respectively.

The intensity increased with the rising temperature until about 310°K, in accordance with the following equation:

$$\text{Intensity} \propto [kT(3+e^{J/kT})]^{-1} \quad (J=0.08\text{eV.}) \quad (1)$$

A discontinuity in the intensity occurred at 310~315°K, and then the intensity seemed to obey Curie's law above 315°K. This means

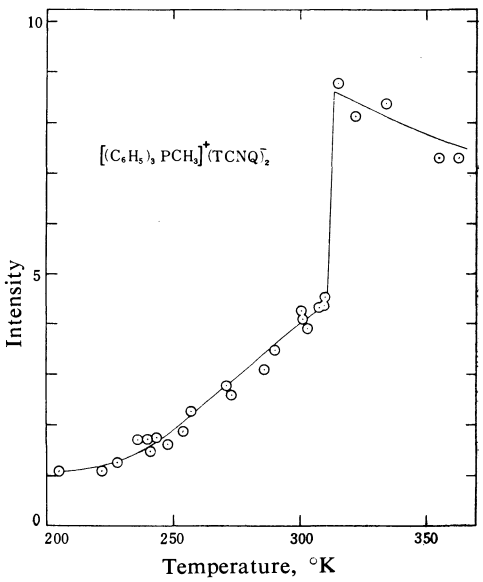


Fig. 1. The temperature dependence of the ESR absorption intensity for the single crystal of $[(C_6H_5)_3PCH_3]^+(TCNQ)_2^-$.

1) D. B. Chesnut and W. D. Phillips, *J. Chem. Phys.*, **35**, 1002 (1961).
2) D. B. Chesnut and P. Arthur, Jr., ibid., **36**, 2969 (1962).
3) M. T. Jones and D. B. Chesnut, ibid., **38**, 1311 (1963).
4) L. R. Melby, R. J. Harder, W. R. Hertler, W. Mahler, R. E. Benson and W. E. Mochel, *J. Am. Chem. Soc.*, **84**, 3374 (1962).

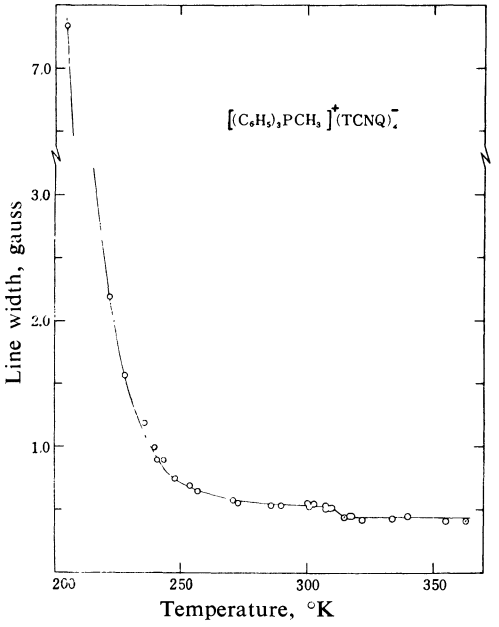


Fig. 2. The temperature dependence of the ESR absorption width (between the inflection points) for an arbitrary oriented single crystal of $[(C_6H_5)_3PCH_3]^+(TCNQ)_2^-$.

that the reduction of J in Eq. 1 should take place in the higher temperature range. The line width became slightly sharper above 315°K. These changes were found to be reversible. It is worthwhile noting that a similar anomaly has been found in the magnetic susceptibility of Würster's blue perchlorate at 186°K.[5]

A similar discontinuity was found in the electrical conductivity, which was measured by the d. c. method. This is shown in Fig. 3. The crystal was a rectangular prism about 2×1×0.5 mm. The conductivity was measured in three directions, which were chosen arbitrarily so that (a) was along the long axis, (b) was normal to the largest plane, and (c) was perpendicular to (a) and (b). In all directions the conductivity varied abruptly by a factor of about 3.5 at about 310°K, and this change was reversible. The current varied with the applied voltage in good acordance with Ohm's law below the electric field of 100 V./cm., and it was found to be constant with time. Hence, the electronic conduction mechanism must be plausible for this salt. although in some salts, for example, $Li^+(TCNQ)^-$, the current was found to change with time; this may be attributable to a partial contribution from the ionic conduction. The activation energy E in the equation $\sigma=\sigma_0 \exp(-E/kT)$ was found to be almost isotropic, and its magnitude changed at the temperature where the anomaly occurred. These values were (a) 0.32 eV., (b)

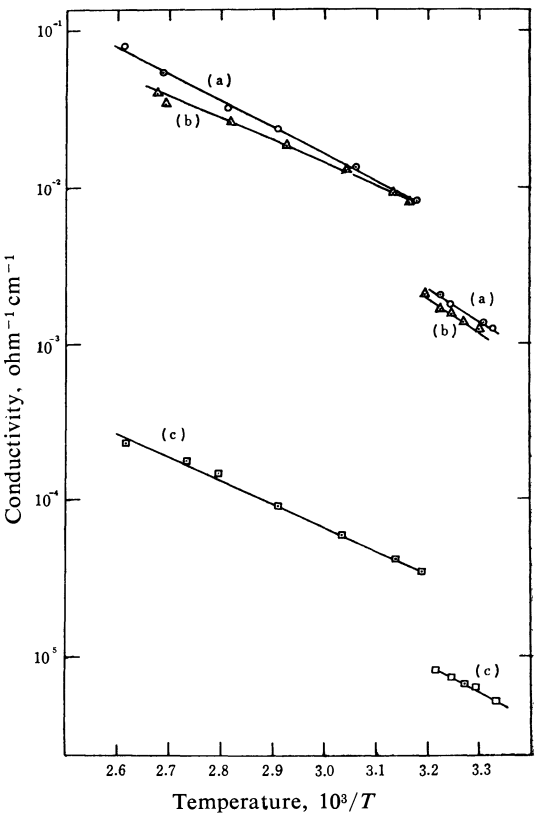


Fig. 3. The temperature dependence of the electrical conductivity of the single crystal of $[(C_6H_5)_3PCH_3]^+(TCNQ)_2^-$, for three directions arbitrarily chosen (a), (b) and (c).

0.29 eV. and (c) 0.30 eV. above 310°K, but a 0.42 eV., (b) 0.42 eV. and (c) 0.38 eV. below 310°K. On the other hand, the conductivity was not isotropic. This might be ascribed to anisotropy in the mobility of the charge carriers.

The reproducibility of our magnetical and electrical observations is good within the range of experimental error, and the values obtained did not depend on the specimens used. Hence, the discontinuity observed for the $[(C_6H_5)_3PCH_3]^+(TCNQ)_2^-$ crystal might be attributed to a phase transition, which is of the same type as has been suggested by McConnell and Lynden-Bell[6] for the case of the Würster's blue perchlorate crystal. Preliminary investigation by the X-ray diffraction method showed that there was a slight, but clear difference in the crystal lattices between those observed at temperatures below and above 310°K.

Department of Chemistry
Faculty of Science
The University of Tokyo
Hongo, Tokyo

5) W. Duffy, Jr., *J. Chem. Phys.*, **36**, 490 (1962).

6) H. M. McConnell and R. Lynden-Bell, ibid., **36**, 2393 (1962).

The Effect of Thiols on the Oxo Reaction

By Masanobu MORIKAWA

(Received October 15, 1963)

The reaction of olefins with carbon monoxide and hydrogen to form saturated aldehydes is well known as the oxo reaction or hydroformylation.[1] In general, this reaction is carried out at an elevated temperature and under a high pressure in the presence of the salts or oxides of cobalt. In this case the reaction products are composed of a mixture of isomeric aldehydes, accompanied by other by-products formed by the secondary reaction of the aldehydes.

In this sense, a high selectivity of the reaction is very desirable. For this purpose, the reaction is carried out at a relatively low temperature. In addition, aliphatic acids,[2] organic bases[3] or noble metals[4] have been proposed as promoters of the lower temperature reaction.

In the course of our studies of the effect of organic ligands co-ordinating with cobalt on the oxo reaction products and conditions, we have found that the reaction is most accelerated by the addition of a small amount of an organic sulfur-compound such as thiol, because of the weak ability of such compounds to co-ordinate.

This accelerating effect of thiols has been investigated; the results of the experiments with cyclohexene are shown in Table I. The results clearly indicate that the reaction can proceed at a lower temperature with a short induction period and with a rapid reaction rate in the presence of a limited amount of thiol. The activation energy of the reaction of cyclohexene was found to be reduced, by the addition of thiophenol, to 13 kcal./mol. from the about 30 kcal./mol. reported without the addition.[5]

The lower temperature-reaction of propylene upon the addition of thiophenol resulted in the selective formation of a straight chain aldehyde. Thus, *n*-butyraldehyde was obtained in a 83% yield at 120°C, as compared to 57% at 160°C without the addition.

It seems likely that thiol has an accelerating effect not only on the reaction catalyzed by the salts or oxides of cobalt, but also on the reaction catalyzed by cobalt calbonyl. Although the raction usually takes place at a lower temperature in the presence of cobalt carbonyl, it has a lengthy induction period under a pressure lower than 110 kg./cm^2. Upon the additon of thiol, the reaction proceeds with a short induction period, as is shown in Table II.

Experimental[6]

The experimental results listed in the tables were obtained in the following way.

In a 100 ml. stainless steel perssure reactor, 0.05 mol. of olefin and 20 ml. of toluene were charged with a cobalt catalyst and additives in the amounts specified in the tables. The air was purged, and a carbon monoxide-hydrogen mixture (1 : 1) was

TABLE I. EFFCT OF THIOLS ON OXO REACTION WITH CYCLOHEXENE*

Additive	10^3 mol.	Temp. °C	Ind. period min.	Sp. rate 10^2k, min^{-1}	Yield %
None	0	120	85	0.9	80
EtSH	3	120	22	1.9	81
EtSH	2	100	100	0.3	72
EtSH	2	160	0	7.3	87
PhSH	3	80	17	3.3	70
PhSH	2	150	0	4.5	81
EtSH	20	120	3	2.2	74

* Cyclohexene=0.05 mol., toluene=20 ml., cobalt oxide=0.02 mol., initial pressure of 200 kg./cm^2 of hydrogen and carbon monoxide mixture (1 : 1).

1) I. Wender and H. W. Sternberg, "Catalysis," Vol. V, Ed. by P. H. Emmett, Reinhold, New York (1957), p. 73.
2) Japanese Pat. 6319 (1958).
3) R. Iwanaga, This Bulletin, 35, 865 (1962).
4) Japanese Pat. 14608 (1961).
5) G. Natta and R. Ercoli, *Chim., ind.* (*Milano*), **34**, 503 (1952).
6) Materials were obtained from commercial sources.

TABLE II. EFFECT OF THIOPHENOL ON OXO REACTION WITH PROPYLENE CATALYZED BY COBALT CARBONYL*

10^3 mol. of thiophenol	Max. press. kg./cm^2	Ind. period min.	Sp. rate $10^2 k$, min^{-1}	Yield** %	Selec.*** %
0	185	3	3	81	78
1	195	0	6	70	79
0	104	160	0.5	85	68
1	103	5	1.3	81	72
10	108	3	1.0	66	65
0	70	$\geqslant$7400	—	—	—
2	75	35	0.4	66	55

* Propylene=0.05 mol., toluene containing cobalt carbonyl (10 g./l.)=20 ml., at 120°C.
** Total yield of aldehyde.
*** % of selective formation of *n*-butyraldehyde.

introduced up to the pressure of 200 kg./cm^2. As soon as the reactor was heated to a specified reaction temperature, agitation was started.

The induction period of the reaction was defined as the time taken for the reaction to start after the beginning of agitation.

The reaction rate deteremined by the rate of gas absorption, while the rate constant was calculated on the basis of the linear relationship between the rate and the olefin concentration.[5]

The reaction was continued until no further pressure drop was observed. The yield of aldehydes and the ratio of the straight chain aldehyde to the branched aldehyde were determined by gas chromatography using an internal standard carried out with a 2 m. "Silicone DC-550" column operated at 120°C or 180°C and with the flow rate of 50 ml./min. of helium gas.

The products was identified by comparing the retention time of the gas chromatograph, the infrared spectra and the melting points of the 2, 4-dinitrophenylhydrazones of the aldehydes with those of authentic samples.

The author would like to thank Dr. Toshio Hoshino, the director of the Laboratories, for his guidance throughout this work.

Basic Research Laboratories
Toyo Rayon Co., Ltd.
Kamakura, Kanagawa

SHORT COMMUNICATIONS

Stereochemistry Related to the Diels-Alder Adducts of 4-Methyl-1, 3-pentadienes[1]

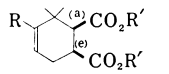
By Iwao ICHIKIZAKI and Atsuaki ARAI

(Received November 6, 1963)

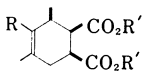
It has been obscure why the conclusions reported by several authors about the behaviour of 3, 4-dimethyl-1, 3-pentadiene (I)[2-4] and 4-methyl-1, 3-pentadiene (II)[5-8] in the Diels-Alder reaction did not agree with each other. We can, however, now reasonably surmise that, during the course of the Diels-Alder reaction with less reactive dienophiles, these dienes are mostly isomerized to more stable ones,[3] while with more reactive dienophiles the reaction smoothly proceeds to give the normal adducts.[8] A recent publication[9] discussing the formation of the normal adducts in the reaction of the dienes I and II with maleic anhydride has prompted us to report our independent studies of the formation and structure of the same adducts and some derivatives.

The diene I reacted easily with maleic anhydride in benzene at a temperature range of 70~120°C in a nitrogen atmosphere to afford an inhomogeneous adduct which gave, on hydrolysis with boiling water, a high yield of the diacid (IIIa) as colorless needles (m.p. 153~153.5°C (lit. m. p. 150~151°C[9]) ; dimethyl ester (IIIb), b. p. 106~107°C/0.4 mmHg, n_D^{15} 1.4781 (lit. b. p. 90~92°C/0.05 mmHg, n_D^{25} 1.4742[9]), ν_{max}^{film} 1735 cm^{-1}, NMR (in CCl_4) : 8.98, 8.86 (gem-Me_2), 8.34 (Me at $C_{(4)}$), 6.45, 6.37 (ester Me) and 4.66 τ (olefinic H)), and the diacid (Va) (m. p. 173~174°C (lit. m. p. 167°C[2]) ; dimethyl ester (Vb), b.p. 149°C/0.7 mmHg, n_D^{15} 1.4816, ν_{max}^{film} 1735 cm^{-1}). It should be emphasized here that the formation of the adduct corresponding to Va tends to be promoted when air remains in the reaction vessel.

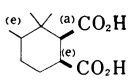
The diacid IIIa was hydrogenated over an Adams catalyst in ethanol or ethyl acetate to afford the saturated diacid (VIIa) (89%), (m.p. 191~192°C, ν_{max}^{KBr} 1706 cm^{-1}). When heated at 220~230°C with concentrated hydrochloric acid, the diacid gave the epimer (VIIb) (80%) (m. p. 202~202.5°C, ν_{max}^{KBr} 1706 cm^{-1}), which returned, after refluxing with acetic anhydride and succeeding hydrolysis, to the starting diacid VIIa. The diacid IIIa was readily lactonized, in the presence of a catalytic amount of hydrochloric acid, to a γ-lactonic acid (VIIIa) (90%) (m. p. 196~197°C, ν_{max}^{KBr} 1772, 1704 cm^{-1}; methyl ester (VIIIb), m.p. 112°C, ν_{max}^{KBr} 1775, 1741 cm^{-1}, NMR (in $CDCl_3$) : 8.89 (gem-Me_2), 8.71 (Me–C(–O)–) and 6.27 τ (ester Me)). Considering the facile formation of VIIIa in addition to the non-bonded 1, 3-diaxial interaction, the present authors confirmed the conformation for the normal product as IIIa.



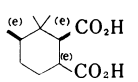
(IIIa) R=Me, R'=H
(IIIb) R=R'=Me
(IVa) R=R'=H



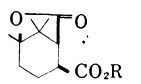
(Va) R=Me, R'=H
(Vb) R=R'=Me
(VIa) R=R'=H



(VIIa)



(VIIb)



(VIIIa) R=H
(VIIIb) R=Me

The infrared spectrum of IIIa in a KBr pellet or Nujol mull indicated bands at 1734 and 1709 cm^{-1} which can be ascribed to two

1) Presented before at the 16th Annual Meeting of the Chemical Society of Japan, Tokyo, April, 1963.
2) I. N. Nazarov and M. V. Mavrov, *Zhur. Obshchei Khim.*, **29**, 1158 (1959).
3) A. Arai and I. Ichikizaki, This Bulletin, **35**, 45 (1962).
4) T. Nishida, A. Arai and I. Ichikizaki, ibid., **35**, 572 (1962).
5) G. B. Bachman and C. G. Goebel, *J. Am. Chem. Soc.*, **64**, 787 (1942).
6) I. N. Nazarov and M. V. Mavrov, *Zhur. Obshchei Khim.*, **28**, 3061 (1958).
7) Y. M. Slobodin, V. I. Grigoreva and Y. E. Schmulyakovskii, ibid., **23**, 1873 (1953).
8) C. A. Stewart, Jr., *J. Am. Chem. Soc.*, **84**, 117 (1963).
9) N. L. Goldman, *Chem. & Ind.*, **1963**, 1036.

different $\nu_{C=O}$ bands and a considerably intense band at 1625 cm^{-1} assignable to $\nu_{C=O}$, while that in a solution ($CHCl_3$) showed only a single absorption, due to $\nu_{C=O}$, at 1709 cm^{-1}. Such spectral characteristics were also observed in a diacid (IVa) described below, but not in several other Δ^4-cyclohexene-1, 2-diacids, including 3, 3, 5-trimethyl-4-cyclohexene-1, *cis*-2-dicarboxylic acid (IX). The lactonization of IX gave δ-lactonic acid, 1, 8, 8-trimethyl-3-oxo-2-oxabicyclo [2, 2, 2]octane-exo-5-carboxylic acid (m.p. 166°C, ν_{max}^{KBr} 1741, 1706 cm^{-1}; methyl ester, (b.p. 131~132°C/0.8 mmHg, n_D^{20} 1.4755, ν_{max}^{film} ~1750 cm^{-1} (broad)).

The diene II produced the diacid IVa as colorless needles (m. p. 172~173°C (lit. m. p. 172~173°C[9]), ν_{max}^{KBr} 1730, 1709 (sh), 1624, 705 cm^{-1}), along with the diacid (VIa) (m. p. 154°C (lit. m. p. 154°C[5])) and *cis*-3, 5-dimethyl-5(a)-hydroxycyclohexane-1, *cis*-2-dicarboxylic acid (m. p. 208~209°C, ν_{max}^{KBr} 3400, 1707, 1698 (sh), 1112 cm^{-1}); the latter two were converted into 1, 8-dimethyl-3-oxo-2-oxabicyclo [2, 2, 2] octane-exo-5-carboxylic acid (m. p. 147~148°C, ν_{max}^{KBr} 1748, 1709 cm^{-1}; methyl ester, b.p. 147~148°C/1.8 mmHg, $n_D^{18.5}$ 1.4752, ν_{max}^{film} ~1743 cm^{-1} (broad)).

Satisfactory analyses were obtained for all compounds.

Laboratory of Organic Chemistry
Kobayasi Institute of Physical Research
Kokubunji, Tokyo

A New Method for the Protection of the Sulfhydryl Group during Peptide Synthesis

By Shiro AKABORI, Shumpei SAKAKIBARA, Yasutsugu SHIMONISHI and Yoshifumi NOBUHARA

(Received November 27, 1963)

The protection of the thiol group in the cysteine residue is of great importance in the field of peptide synthesis. Glutathione, oxytocin and vasopressin have been synthesized by many investigators, and the *S*-benzyl group has generally been used to protect the thiol during the procedures. Recently, however, in connection with the synthesis of insulin, several new *S*-protecting groups have been developed. Some of them, however, were too stable to be split from the final products without causing partial destruction of the peptide, and some of them were too labile to allow preparation of the peptide in a good yield.

In the present investigation, the *p*-methoxybenzyl (anisyl) group was found to be valuable for masking the thiol; that is, the *S*-*p*-methoxybenzyl group was easily cleaved by treatment with boiling trifluoroacetic acid, although it was not affected by hydrogen bromide, as is shown below. Moreover, the synthesis of *S*-*p*-methoxybenzyl-L-cysteine (I) was as easy as that of the *S*-benzyl derivative. Freshly-prepared L-cysteine was treated with *p*-methoxybenzyl chloride in liquid ammonia to form I, which was recrystallized from water; colorless plates were obtained in a 78% yield; m. p. 198~199°C (decomp.), $[\alpha]_D^{25}$ +22.6° (*c* 1.02, N NaOH). Found: C, 54.50; H, 6.33; N, 5.89; S, 13.05. Calcd. for $C_{11}H_{15}O_3NS$: C, 54.75; H, 6.26; N, 5.81; S, 13.29%. After the treatment of I with anhydrous trifluoroacetic acid containing phenol or anisol, followed by oxidation with iodine solution, L-cystine was recovered in a 84% yield; it had the same optical activity as the starting L-cystine. Compound I was submitted to reaction with carbobenzoxy chloride in a basic condition to give *N*-carbobenzoxy-*S*-*p*-methoxybenzyl-L-cysteine (II), which was recrystallized from toluene as colorless needles; yield, 76%; m.p. 66~67°C, $[\alpha]_D^{24}$ −42.1° (*c* 2.0, acetone). Found: C, 60.73; H, 5.80; N, 3.55, S, 8.46. Calcd. for $C_{19}H_{21}O_5NS$: C, 60.78; H, 5.64; N, 3.73; S, 8.54%. The dicyclohexylamine salt of II was recrystallized from ethanolether as fine colorless needles; m. p. 148~149°C, $[\alpha]_D^{27}$ −8.4° (*c* 2.22, EtOH). Found: C, 66.85; H, 7.90; N, 4.94; S, 5.60. Calcd. for $C_{31}H_{44}O_5N_2S$: C, 66.87; H, 7.97; N, 5.03; S, 5.76%. When II was treated with hydrogen bromide in acetic acid, *S*-*p*-methoxybenzyl-L-cysteine was recovered in a 77% yield; this had the same melting point as I and gave one spot on a paper chromatogram.

Compound II was coupled with glycine ethyl ester in the presence of dicyclohexylcarbodiimide in anhydrous acetonirile. Carbobenzoxy-*S*-*p*-methoxybenzyl-L-cysteinyl-glycine

ethyl ester (III) was obtained as fine colorless needles after recrystallization from ethyl acetate-petroleum benzine (81%); m.p. 87.5~89.5°C, $[\alpha]_D^{27}$ −31.1° (*c* 3.15, EtOH). Found: C, 59.89; H, 6.20; N, 5.95; S, 7.07. Calcd. for $C_{23}H_{28}O_6N_2S$: C, 59.98; H, 6.13; N, 6.08; S, 6.96%. Substance III was hydrolyzed in dioxane, using N sodium hydroxide, to give carbobenzoxy-*S*-*p*-methoxybenzyl-L-cysteinyl-glycine (IV), which was recrystallized from ethyl acetate-petroleum benzine as fine colorless needles (69%); m. p. 132~133.5°C, $[\alpha]_D^{24}$ −35.0° (*c* 3.14, EtOH). Found: C, 58.57; H, 5.42; N, 6.34; S, 7.35. Calcd. for $C_{21}H_{24}O_6N_2S$: C, 58.32; H, 5.59; N, 6.48; S, 7.41%. The treatment of IV with hydrogen bromide, followed by neutralization with aqueous sodium acetate, gave *S*-*p*-methoxybenzyl-L-cysteinyl-glycine (V) in a 83% yield; m.p. 164~164.5°C, (decomp.), $[\alpha]_D^{25}$ +29.3° (*c* 2.00, N NaOH). Found: C, 52.52; H, 6.02; N, 9.35; S, 10.47. Calcd. for $C_{13}H_{18}O_4N_2S$: C, 52.33; H, 6.08; N, 9.39; S, 10.75%. Compound V was refluxed with anhydrous trifluoroacetic acid containing phenol. The cysteinyl-glycine thus formed was oxidized by an iodine solution to L-cystinyl-diglycine (VI), which was purified by the procedure descrived by Weygand.[1] Yield, 48%; $[\alpha]_D^{28}$ −68.9° (*c* 0.944, water), reported[2] $[\alpha]_D^{27}$ −67.5° (*c* 1, water). Found: C, 33.91; H, 5.37; N, 16.10; S, 17.59. Calcd. for $C_{10}H_{18}O_6N_4S_2$: C, 33.89; H, 5.12; N, 15.81; S, 18.10%. Detailed results and the application of the procedure will be published elsewhere.

Division of Organic Chemistry
Institute for Protein Research
Osaka University
Osaka

1) F. Weygand and W. Steglich, *Naturforsch.*, **14b**, 472 (1959).

2) H. S. Loring and V. du Vigneaud, *J. Biol. Chem.*, 111, 385 (1935).

A New Colorimetric Determination of Iodide Ions by Solvent Extraction with the 1, 10-Phenanthroline-Iron(II) Complex

By Yuroku YAMAMOTO and Seiichiro KINUWAKI

(Received December 7, 1963)

This study presents a new method for the determination of iodide ions by solvent extraction. We have found that a colored 1, 10-phenanthroline-iron(II) chelate cation was extractable into nitrobenzene from aqueous solution when a small amount of iodide was present. Figure 1 shows the absorption spectra of the extracts against nitrobenzene used as a reference. The extractions were carried out from aqueous solutions containing the phenanthroline-iron(II) complex in an acetate buffer (pH 4.5). Curve 1 is a spectrum of the extract with iodide ions, while curve 2 is that of the extract when iodide is absent. It is shown that when the concentration of acetate ion is quite high, the chelate cation is also extractable into nitrobenzene, but when a small amount of iodide is present, the chelate cation is much more extractable into the organic layer. The results suggest that it is possible to determine the quantity of iodide ions by solvent extraction with the chelate cation, using the reagent blank solution as a reference.

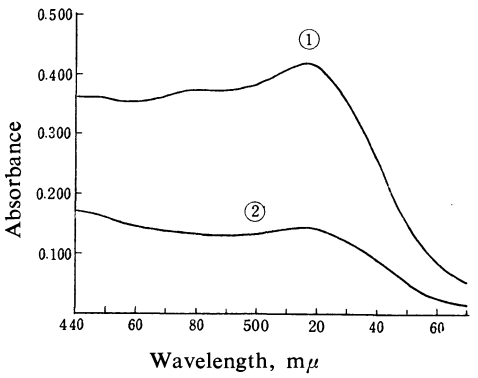


Fig. 1. Absorption spectra.

Water phase	Phenanthroline	8×10^{-4}M
	Fe^{2+}	2×10^{-4}M
	Acetate	0.24M
	I^-	1.7×10^{-5}M
	pH	4.5

① Extracts by nitrobenzene with iodide ion.
② Extracts by nitrobenzene without iodide ion.
Reference: Nitrobenzene

The absorbance maximum of the chelate cation in the organic layer is 516 mμ. The maximum of the chelate cation in an aqueous solution is 510 mμ, which coincides with the

value of the literature.[1] This red shift of the spectrum in the organic layer may be due to the effect of the association between the chelate cations and iodide ions in such a polar solvent as nitobenzene.

The percentage of the extraction of iodide ions was about 90%. This was determined by the radiochemical technique using radioisotope I-131 (NaI) as a tracer. From the above findings, it may be presumed that the chemical form of the extracted species is $[Fe(phen)_3]^{2+} \cdot (I^-)_2$.

Besides nitrobenzene, various organic solvents, such as chloroform, 1, 2-dichloroethane, cyclohexanone, chlorobenzene, and benzene, were tested for the extraction. However, the associated species between the phenanthroline-iron(II) complex and iodide ions was not extractable into such a solvent.

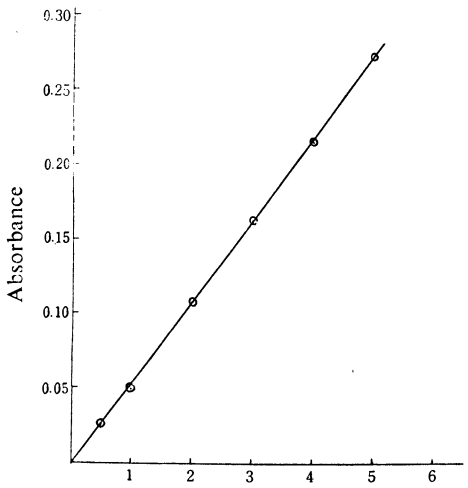


Fig. 2. Calibration curve at 516 mμ.

Water phase	Phenanthroline	8×10^{-4}M
	Fe^{2+}	2×10^{-4}M
	Acetate	0.24M
	I^-	$3.4\times10^{-6}\times x$
	pH	4.5
	Reference	Reagent blank

To obtain an optimum conditions for the determination of iodide ions, various factors were studied: the effects of the concentration of iron(II) ions (as ferrous ammonium sulfate), phenanthroline, the pH of the solution, the stability of the color, the shaking time, and the presence of diverse ions. The recommended procedure for the calibration curve (Fig. 2) is as follows:

Two milliliters of the 1, 10-phenanthroline solution (1×10^{-2}M), 1.0 ml. of the ferrous ammonium sulfate solution (5×10^{-3}M), 2 ml. of the sodium acetate buffer solution (3M, pH 4.5) and varying amounts of the standard sodium iodide solution (8.5×10^{-5}M; 0.5~5.0 ml.) are mixed and diluted to 25 ml. with distilled water. Then 10.0 ml. of purified nitrobenzene is added. After the mixture has been shaken for 20 min., and after the organic layer has been transferred to a glass flask containing 1 g. of anhydrous sodium sulfate, the transparent solution is transferred into a 10.0 mm. cell through folded filter paper. The absorbance of the solution is measured at 516 mμ using the reagent blank solution as a reference. As is shown in Fig. 2, Beer's law is followed in the range of 1×10^{-6} ~5×10^{-5} M of iodide ions.

When a considerable amount of chloride (about 100 times that of iodide) is present, the determination of iodide is not interfered with, but the presence of the same amounts of perchlorate or thiocyanate as iodide gives a considerable positive error.

Department of Chemistry
Faculty of Science
Hiroshima University
Hiroshima

1) M. L. Moss and M. G. Mellon, *Ind. Eng. Chem., Anal. Ed.*, **14**, 825, 931 (1942).

The Condensation of 9-Ethylacridine and p-Nitosodimethylaniline[1]

By Otohiko TSUGE, Minoru NISHINOHARA and Kunio SADANO

(Received December 24, 1963)

It has previously been reported[2] that the condensation of the 9-methylacridine derivative and the aromatic nitroso compound in the presence of a catalytic amount of hydrochloric acid affords the condensation products, an anil and a nitrone, in a fairly good yield compared with the yield when a basic catalyst is used.

From this result, it may be concluded that hydrochloric acid can noticeably activate the active methyl group at the 9-position of the acridine ring in the reaction with the aromatic nitroso compound.

Accordingly, it appeared of interest to investigate whether 9-ethylacridine (I) can be condensed with the aromatic nitroso compound in the presence of hydrochloric acid.

The reaction of I with *p*-nitrosodimethylaniline (II) did not take place in the presence of potassium carbonate, and *p,p'*-bis(dimethylamino)azoxybenzene (III) (m. p. 240~241°C (reported, 241~242°C[3])) was formed in only a small amount. In the presence of hydrochloric acid, however, I reacted with II to give the condensation products. For example, when a solution of 1.0 g. of I, 1.4 g. of II and 0.20 ml. of concentrated hydrochloric acid in 25 ml. of ethanol was refluxed for 5 hrs., 1.29 g. of reddish brown crystals (IV) (m. p. 261~263°C (decomp.)) was obtained. Found: C, 77.51, 77.74; H, 6.04, 6.10; N, 14.11, 14.36%.

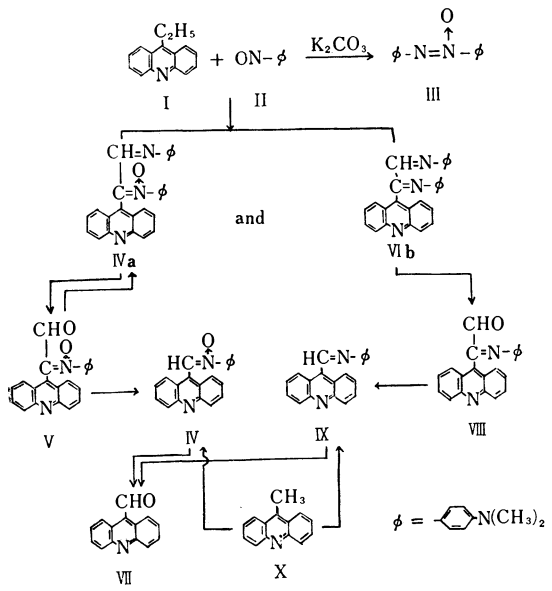


Chart 1.

The hydrolysis of 1.0 g. of IV with 10 ml. of 12% aqueous hydrochloric acid afforded 0.30 g. of acridine-9-carboxaldehyde (VII) (m.p. 147°C (reported, 147°C[4])). The treatment of 0.5 g. of IV with 10 ml. of cold 10% aqueous sulfuric acid gave the α-nitrone-β-formyl compound (V) as orange prisms (m. p. 208°C (decomp.)). Found: C, 74.85; H, 5.18; N, 11.13. Calcd. for $C_{23}H_{19}O_2N_3$: C, 74.78; H, 5.18; N, 11.37%. IR (Nujol): 1662 cm^{-1} (C=O).

From the condensation of V and *p*-aminodimethylaniline, the α-nitrone-β-anil compound (IVa) was obtained as reddish brown prisms (m. p. 265°C (decomp.)). Found: C, 76.67; H, 6.24; N, 14.10. Calcd. for $C_{31}H_{29}ON_5$: C, 76.36; H, 6.00; N, 14.36%. The infrared spectrum of IVa showed the characteristic bands at 1212, 1119, 818 and 758 cm^{-1}. Furthermore, 0.26 g. of V was oxidized with silver oxide to give 0.10 g. of the nitrone (VI), which was prepared by the condensation of 9-methylacridine (X) and II and which was easily hydrolyzed to VII. V was also easily hydrolyzed with dilute hydrochloric acid to afford VII.

On the other hand, the dianil compound (IVb) was obtained as red prisms (m.p. 283°C (decomp.)) by several fractional recrystallizations of IV from pyridine. Found: C, 78.87; H, 6.19; N, 14.65. Calcd. for $C_{31}H_{29}N_5$: C, 78.95; H, 6.20; N, 14.85%. Its infrared spectrum exhibited the distinctive bands at 1228, 1158, 819 and 742 cm^{-1}.

From the results of the infrared spectrum of IV, which revealed all the distinctive bands of IVa and IVb, and from the results of the elemental analysis, IV seems to be a mixture of the two compounds. However, the ratio of these two compounds in IV has not been established.

1) Presented at the General Meeting of the Kyushu, Chugoku and Shikoku Districts of the Chemical Society of Japan, Kagoshima, December, 1963.

2) O. Tsuge, M. Nishinohara and M. Tashiro, This Bulletin, 36, 1477 (1963).

3) H. von Pechmann and W. Schmitz, *Ber.*, 31, 295 (1898).

4) L. Chardonnens and P. Heinrich, *Helv. Chim. Acta*, 32, 635 (1949).

The compounds VIII and IX could not be separated, but it seems most reasonable to conclude from the above results that the hydrolysis of IV to VII proceeds successively through the course depicted in Chart 1.

Further investigation is in progress; details of this work will be published in the near future.

The Research Istitute of Science and Industry
Kyushu University
Hakozaki, Fukuoka

The Crystal Structure of Spermine Phosphate Hexahydrate

By Yōichi IITAKA and Yukiko HUSE

(Received January 9, 1964)

Recently, many interesting findings have been reported concerning the effect of spermine on various enzyme activities and on the relationship of this amine to nucleic acids and to problems of membrane stability.[1] Much of the evidence is indirect, but the data definitely indicate that spermine and nucleic acids have a strong affinity for each other.[2-4] The analysis of the crystal structure of spermine phosphate hexahydrate was, therefore, undertaken to provide information on the binding relation of this amine to phosphoric acid and water.

The unit cell dimensions were found to be: $a=7.95_5$, $b=23.21_6$, $c=6.87_0$ Å, and $\beta=113°39'$. The space group is $P2_1/a$. Density measurements indicated that two units of $C_{10}H_{26}N_4 \cdot 2H_3PO_4 \cdot 6H_2O$ are contained in a cell. The structure was solved by analysis of a three-dimensional sharpened Patterson function and was refined by the Fourier and least-squares methods. The final reliability factor for the 1747 non zero (*hkl*) data was 0.127.

From a consideration of the arrangement of hydrogen bonds and the bond lengths of the phosphate group, it has been concluded that the chemical formula of this compound can be written as $NH_3^+(CH_2)_3NH_2^+(CH_2)_4NH_2^+ \cdot (CH_2)_3NH_3^+ \cdot 2HPO_4^{2-} \cdot 6H_2O$. Two views of the structure, along the b- and c-axes, are shown in Figs. 1 and 2 respectively. The structure consists of parallel sheets of spermine molecules separated by a sheet of phosphate ions and water molecules. These two kinds of sheets are stacked alternatively parallel to the (001) plane and are held together by N–H···O hydrogen bonds. The latter sheet has the composition $HPO_4^{2-} \cdot 3H_2O$, containing hydrogen-bonded chains of phosphate ions, $\cdots O_2\text{–}P\text{–}O_4\text{–}H\cdots O_2\text{–}P\text{–}O_4\text{–}H\cdots$, running along the a-axis. As Fig. 2 shows, adjoining chains in the sheet are arranged antiparallel and are sparated by the distance $b/2=11.6$ Å. The water molecules form a hexagonal network of hydrogen bonds and fill up the spaces between the chains. In the molecular sheets of spermine, the molecules are tilted at about 33° from the a-axis and are arranged in parallel, keeping van der Waals distances, with adjacent molecules in the a-direction. Adjacent molecules in the b-direction are oppositely inclined and form a planar herring-bone arrangement with the spermine molecules. Along the backbones run the phosphate chains. Because of this tilting, the amino and imino nitrogen atoms on one side of a molecule are linked to the same phosphate chain. It is to be noted that of the ten such N–H···O hydrogen bonds, only two are those to the water molecules. All of the rest link the molecule strongly to the phosphate ions.

As for the arrangement of phosphate groups, we noticed a certain similarity between that found in crystalline DNA and that in spermine phosphate. Langridge et al.[5] have shown the arrangement of phosphate groups along the polynucleotide helices in the B-form of LiDNA (Figs. 13 and 14 in their paper). In this structure, two oxygen atoms O2 and O3 of a phosphate group which share one negative formal charge turned outwards and are readily available for interaction with proteins, water, etc. The distance between the O3 oxygen atoms of the successive phosphate groups along the helix is about 7.3 Å, which may be compared

1) H. Tabor, C. W. Tabor and S. M. Rosenthal, *Ann. Rev. Biochem.*, **30**, 579 (1961).
2) S. Razin and R. Rozansky, *Arch. Biochem. Biophys.*, **81**, 36 (1959).
3) H. Tabor, *Biochemistry*, **1**, 496 (1962).
4) D. Kaiser, H. Tabor and C. W. Tabor, *J. Mol. Biol.*, **6**, 141 (1963).
5) R. Langridge, D. A. Marvin, W. E. Seeds, H. R. Wilson, C. W. Hooper, M. H. F. Wilkins and L. D. Hamilton, ibid., **2**, 38 (1960).

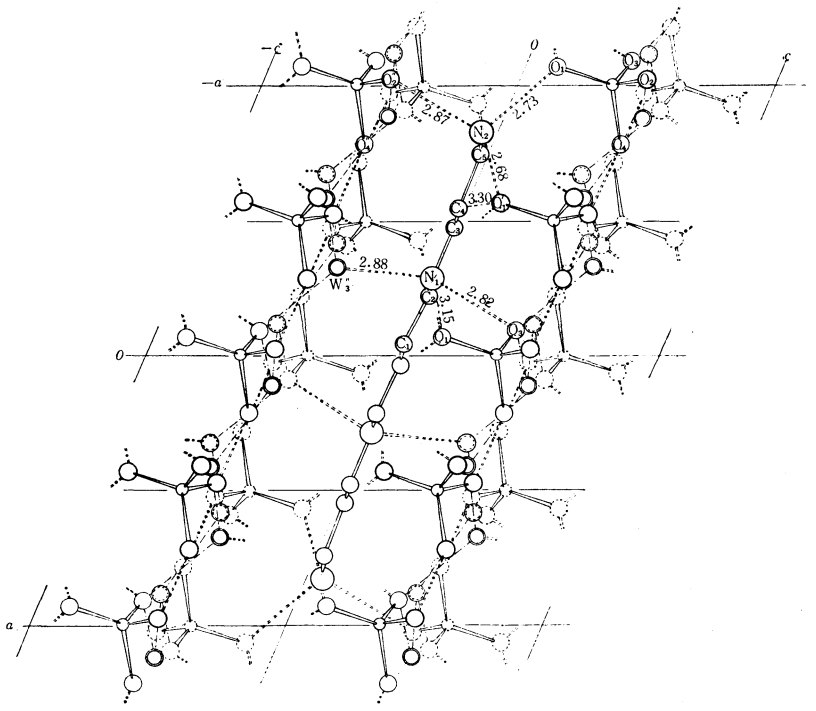


Fig. 1. Projection of the structure along the b-axis. Hydrogen bonds are indicated by double broken lines and by single chain lines. The water oxygen atoms are indicated by double circles. The atoms of the lower phosphate chains are indicated by broken circles. Only one spermine molecule is shown.

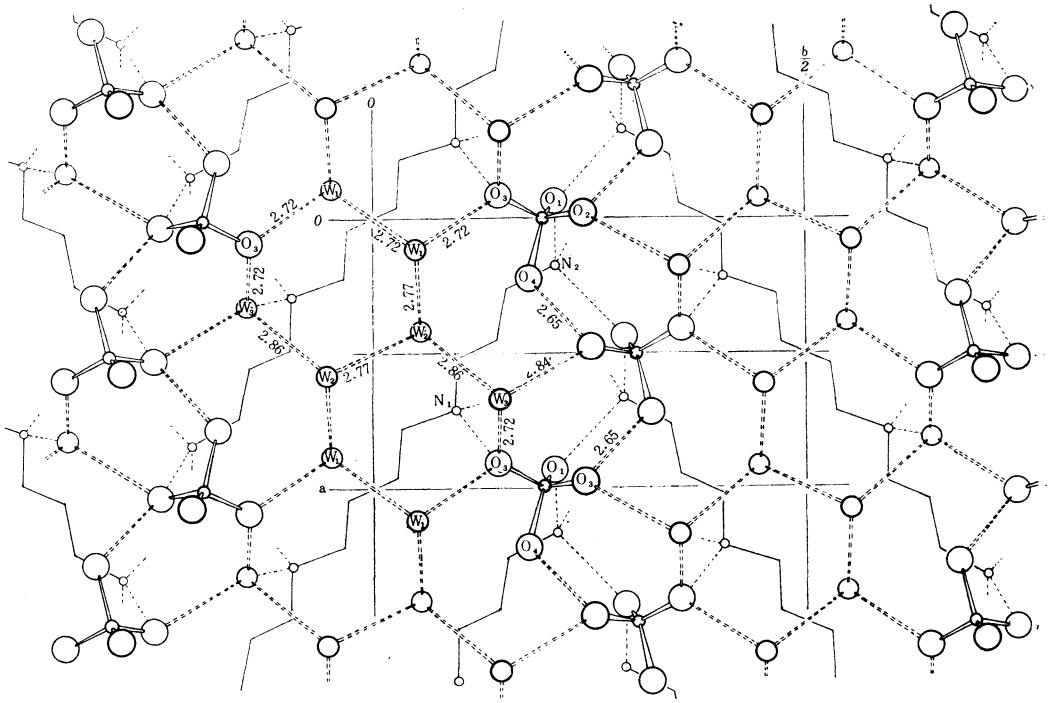


Fig. 2. Projection of the structure along the c-axis. The networks of hydrogen bonding within the phosphate-water sheet are shown. Hydrogen bonds from the spermine molecules are indicated by single broken lines.

with the a-translation period of 7.96 Å along the phosphate chains in spermine phosphate. The perpendicular distance between two nucleotide chains (chains A and B of the same molecule, measured across the shallow) in LiDNA is about 13 Å, while in the latter structure the separation of the phosphate chains within the same sheet is found to be about 11.6 Å.

Full details will be published later.

Faculty of Pharmaceutical Sciences
The University of Tokyo
Hongo, Tokyo (Y. I.)

School of Pharmacy
The University of Chiba
Yahagi, Chiba (Y. H.)

The Isolation, Structure and Properties of a New π-Diene-Iron Tricarbonyl Complex Formed from Methyl Linolate and Iron Pentacarbonyl

By Ikuei OGATA and Akira MISONO

(Received January 10, 1964)

A π-diene-iron tricarbonyl complex, the formation of which in the process of the hydrogenation of cotton seed oil with the iron pentacarbonyl catalyst was reported on in a previous paper,[1] has now been prepared for the first time and isolated by the following procedure: A mixture of fatty acid methyl ester of dehydrated castor oil (30 g.) and iron pentacarbonyl (13.7 ml.) was heated repeatedly under nitrogen at 180°C in a stainless-steel bomb until the evolution of carbon monoxide ceased. The ether solution of the reaction mixture was then washed with aqueous hydrochloric acid (1 : 1) and with water. After the solvent had been removed, a few drops of low-boiling materials were distilled off at 0.1 mmHg below 205°C, the temperature of the bath. The remaining liquid was distilled in a magnetic-stirred pot-type molecular distillation still; as a last fraction, about 8 g. of a yellow-orange oil was obtained. B. p. 79~90°C/10^{-4} mmHg; d_4^{28} 1.092; n_D^{26} 1.5158; mol. wt. (ebullioscopic in MEK), 414; Found: C, 62.2; H, 8.1; Fe, 12.8. Calcd. for $C_{22}H_{34}O_5Fe$: C, 60.8; H, 7.9; Fe, 12.9%.

An attempt to isolate the compound by chromatography over alumina (Woelm, grade II.) with petroleum benzine was unsuccessful.

The infrared spectrum taken in carbon disulfide shows characteristic M–C≡O bands at 2045 and 1975 cm^{-1} ($E_{cm}^{\%}=93$ at $I/I_0=0.5$), and these bands agree closely with those of cyclo-

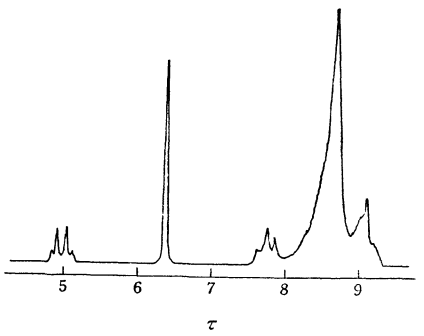


Fig. 1.

octadiene-iron tricarbonyl.[2]

The ultraviolet spectrum taken in cyclohexane shows an absorption maximum at 210(?)~220 mμ (log ε=4.37). The value reported in the literature[3] for butadiene-iron tricarbonyl is 211 mμ (log ε=4.36).

The high resolution NMR-spectrum (Fig. 1) taken in carbon tetrachloride at 60 Mc. indicates the following signals (range in τ-value, relative intensity, structure and/or assignment): 4.8~5.2, 2, double-triplet, coordinated olefinic protons; 6.3~6.5, 3, $-OCH_3$; 7.5~7.9, 2, $-CH_2-CO-$; 7.9~9.4, 27, two overlapped, unsymmetrical bands, aliphatic protons. By analogy from the spectra of the iron tricarbonyl complexes of butadiene, 1, 3-cyclohexadiene, and

1) A. Misono, I. Ogata and F. Funami, *J. Japan Oil Chem. Soc.* (*Yukagaku*), **13**, 21 (1964).

2) K. Noack, *Helv. Chim. Acta*, **45**, 1847 (1962).

3) B. F. Hallam and P. L. Pauson, *J. Chem. Soc.*, **1958**, 643.

1, 3-cycloheptadiene,[4] the lowest-field band may be assigned to the "central" protons of a coordinated conjugate system.

Ligand-exchange reaction with triphenylphosphine in liquid paraffin in a tube at 150°C for 24 hr. afforded yellow crystals, the infrared spectrum of which is identical with that of bis(triphenylphosphine)-iron tricarbonyl.[5] From the infrared spectrum and from the gas-liquid chromatography, the remaining liquid proved mainly to be one of the stereoisomers of methyl-C_{18}-conjugated-diene-carboxylate.

These results indicate that this compound is the iron tricarbonyl complex of methyl-C_{18}-conjugated-diene-carboxylate formed from methyl linolate by isomerization reaction.

The complex is reasonably stable in the condensed state, but it is readily decomposed in solution, even under nitrogen in a dark, cold place, and gives brown or black precipitates. When treated above its decomposition temperature (ca. 225°C), a mixture of this complex and diene-carboxylic acid ester polymerized mainly to the dimer of the acid ester. By hydrocracking at 200°C (100 atm. in a stainless-steel bomb), the complex was converted mainly to methyl stearate.

Faculty of Engineering
The University of Tokyo
Hongo, Tokyo

4) M. L. H. Green, L. Pratt and G. Wilkinson, ibid., **1959**, 3753; R. Burton, L. Pratt and G. Wilkinson, ibid., **1961**, 594.

5) T. A. Manuel and F. G. A. Stone, *J. Am. Chem. Soc.*, **82**, 366 (1960).

The Reduction of Zinc Oxide by Hydrogen. III. The Effect of Nitrogen on the Reduction

By Tatsuya IMOTO, Yoshio HARANO, Yasuhide NISHI and Satoru MASUDA

(Received May 16, 1963)

The following results were obtained in the previous study of the reduction of zinc oxide by hydrogen.[1,2] The reaction proceeds independently of the hydrogen pressure. Additionally, in the presence of a large amount of zinc oxide (case 1), the reduction is not affected by the amount of zinc oxide, and the relationship between the pressure and the reaction time is linear. In the presence of a small amount (case 2), however, the relation is not linear. In the latter case, the data well satisfied Eq. 1, deduced from the assumption that the reaction rate is proportional to the surface area.

$$(p_0-p_\infty)^{1/3}-(p-p_\infty)^{1/3}=k_2(t-t_0) \qquad (1)$$

Here p_0 and p_∞ are the hydrogen pressures when the reaction starts to obey Eq. 1 and when zinc oxide is completely used up respectively. As a result, the reduction of zinc oxide was suggested to be not a surface reaction, but a consecutive one consisting of two processes, the sublimation-decomposition of zinc oxide to zinc vapor and oxygen and the subsequent reaction of oxygen and hydrogen. Further, the former process is the rate-determining step in case 2.

The thermal decomposition of zinc oxide has been known to be influenced by the third gas, i.e., nitrogen or zinc vapor.[3,4] Hence, one can expect the variation of the reaction modes, in case 2, in the presence of these gases. With this expectation the present work was carried out, using nitrogen as the third gas.

Experimental

The apparatus used for this work was the same as that used in the previous paper.[1,5] Just before the reaction started, the reaction tube was evacuated for five minutes, and then nitrogen and, finally, hydrogen were admitted at a given pressure and composition. The rate of the reduction was measured in the temperature range 690~738°C, with the amount of zinc oxide, 40.0 mg., and the pressure range of nitrogen, 0~2 cmHg. The analysis of data was made by applying Eq. 1 as in the previous work.[2] The initial pressure of hydrogen was 6.0~6.4 cmHg. Nitrogen was prepared by purifying the commercial gas in a bomb by passing it through the reduced copper heated at 500°C, through concentrated sulfuric acid and finally through magnesium perchlorate.

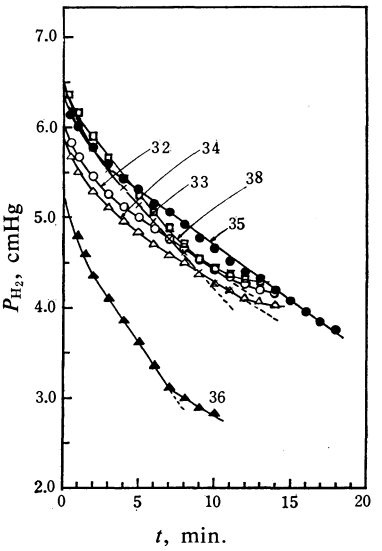


Fig. 1. The relation between residual H_2 and reaction time. Runs are shown in Table I.

Results and Discussion

The results obtained at 670°C are shown in Fig. 1. The initial amount of zinc oxide in all experiments was 40.0 mg., except for the 300 mg. in No. 35, which was done under the same conditions as No. 32. As has been mentioned above, when a large amount of zinc oxide is present, only the linear part appears in the relation between the hydrogen pressure and the reaction time.[1,2] Hence, the slope of a straight line in No. 32 can be estimated by comparing No. 32 with No. 35. From Fig. 1 and by applying Eq. 1, the specific reaction rates, k_1 and k_2, are as shown in Table I; k_1

1) T. Imoto, Y. Harano and Y. Nishi, *J. Chem. Soc. Japan, Pure Chem. Sec.* (*Nippon Kagaku Zassi*), **84**, 115 (1963).
2) T. Imoto, Y. Harano, Y. Nishi and S. Masuda, ibid., **85**, 106 (1964).
3) E. A. Secco, *Can. J. Chem.*, **38**, 596 (1960).
4) W. J. Moore and E. L. Williams, *J. Chem. Phys.*, **63**, 1516 (1959).
5) T. Imoto, Y. Harano and A. Morishima, "The Reduction of Zinc Oxide by Carbon Monoxide. II," submitted to This Bulletin.

TABLE I. THE EFFECT OF NITROGEN ON k_1 AND k_2 AT 690°C

No.	P_{N_2} cmHg	ZnO mg.	k_1 cmHg/min.	k_2 cmHg$^{1/3}$/min.
38	0.000	40.0	0.224	0.107
36	0.340	40.0	—	0.067
33	0.526	40.0	0.184	0.056
32	0.982	40.0	0.120	0.047
35	1.040	300.0	0.120	—
34	1.470	40.0	0.105	0.029

and k_2 correspond to the reactions revealed as a straight line and a curve respectively in Fig. 1 (see also Fig. 2 in the previous report[2]). No. 38 at the zero nitrogen pressure obtained in the previous work[2] was also tabulated for the sake of comparison.

As may be seen in Table I, both k_1 and k_2 decrease with the nitrogen pressure. Moore et al.,[4] who studied the thermal decomposition of zinc oxide, found that the amount of zinc oxide decomposed in the stream of nitrogen is smaller than that in oxygen, and that it is, moreover, much smaller than would be expected from the thermodynamics by 10^{-2}. They made no reference to the reason for this. Assume that some substance retarding the sublimation-decomposition of zinc oxide is produced in the presence of nitrogen, and that the surface area of zinc oxide poisoned by the retarding substance is θ, by taking $\theta=0$ for the surface in the absence of nitrogen. Since k_2 is the specific decomposition rate of zinc oxide per unit surface area, θ at various nitrogen pressures will be given Eq. 2:

$$\theta = 1 - \frac{(k_2)_{P_{N_2}}}{(k_2)_{P_{N_2}=0}} \qquad (2)$$

Let us assume additionally that the retarding substance is produced on the whole surface with the same probability by molecular nitrogen. Thus, at equilibrium, θ will expressed by a form similar to the Langmuir-type adsorption isotherm,[6] Eq. 3:

$$\theta = \frac{aP_{N_2}}{1+aP_{N_2}} \qquad (3)$$

$$\frac{1}{\theta} = 1 + \frac{1}{aP_{N_2}} \qquad (4)$$

TABLE II. THE RELATION BETWEEN P_{N_2} AND θ

No.	P_{N_2} cmHg	$1/P_{N_2}$ cmHg^{-1}	$\frac{(k_2)_{P_{N_2}}}{(k_2)_{P_{N_2}=0}}$	θ
38	0.000	0.00	1.000	0.000
36	0.340	2.94	0.626	0.374
33	0.526	1.90	0.523	0.477
32	0.982	1.02	0.439	0.561
34	1.470	0.68	0.271	0.729

6) I. Langmuir, *J. Am. Chem. Soc.*, **40**, 1361 (1918).

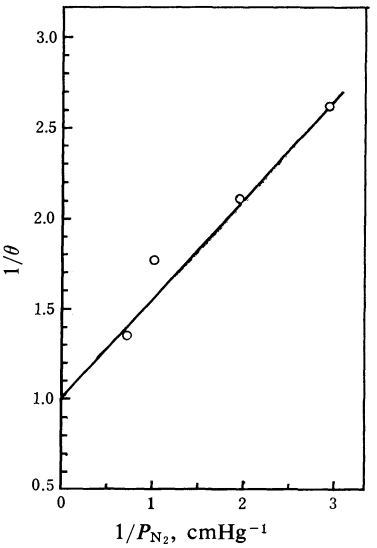


Fig. 2. $1/\theta \sim 1/P_{N_2}$ at 690°C.

θ values calculated from k_2 in Table I according to Eq. 2 are shown in Table II.

In Fig. 2, $1/\theta$ is plotted against $1/P_{N_2}$. Figure 2 shows that every value gives a good straight line, and that Eqs. 2—4, based on the above assumptions, are satisfied. $1/a$ is estimated to be 1.73 from the slope of the line in Fig. 2.

As a result, it is considered that the effect of the nitrogen molecule can be evaluated by the magnitude of a. There is another method of estimating a, even when no data of $(k_2)_{P_{N_2}=0}$ is obtained. As $(k_2)_{P_{N_2}=0}$ will be constant at a constant temperature and a constant state of the surface, the following relations are obtained from Eqs. 2 and 3:

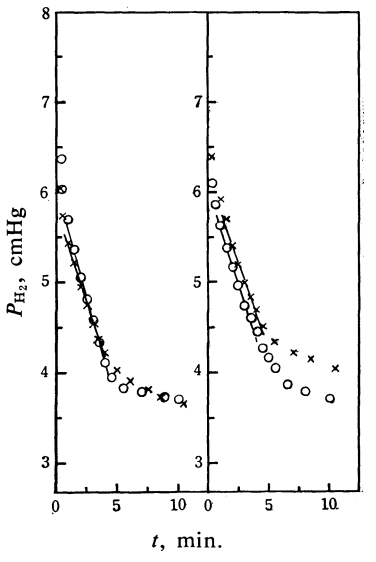


Fig. 3. $P_{H_2} \sim t$, at 714°C; P_{N_2} (cmHg) left: ○ 0.538, × 0.916; right ○ 1.480, × 1.974

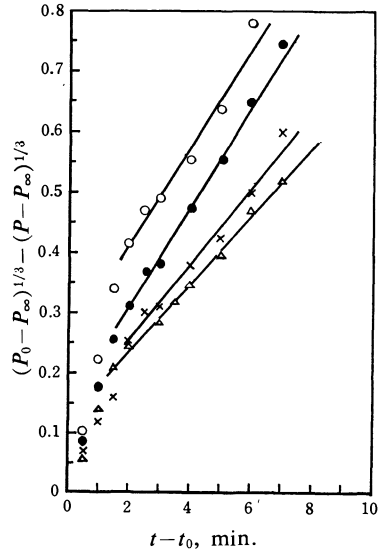


Fig. 4. Plots according to Eq. 1, at 714°C. P_{N_2} (cmHg) ○ 0.538, ● 0.916, × 1.480, △ 1.968

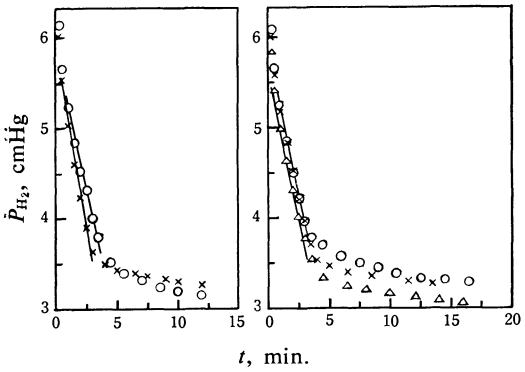


Fig. 5. $P_{H_2}\sim t$, at 738°C.
P_{N_2} (cmHg): left ○ 0.000, × 0.512; right ○ 1.000, × 1.500, △ 2.000

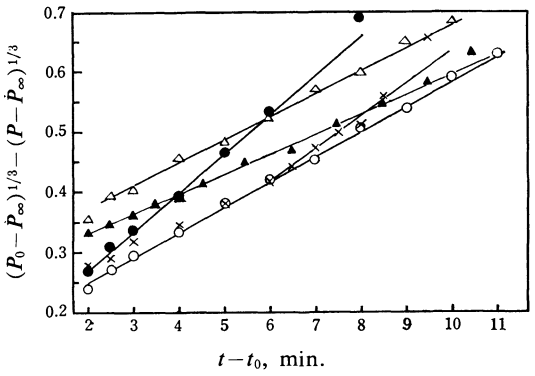


Fig. 6. Plots according to Eq. 1, at 738°C. P_{N_2} (cmHg) ● 0.000, × 0.512, ○ 1.000, △ 1.500, ▲ 2.000

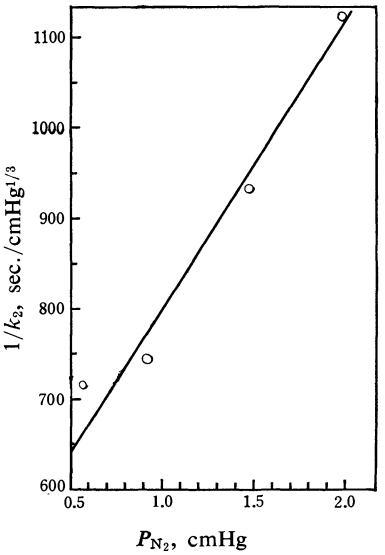


Fig. 7. Plot according to Eq. 4', at 714°C.

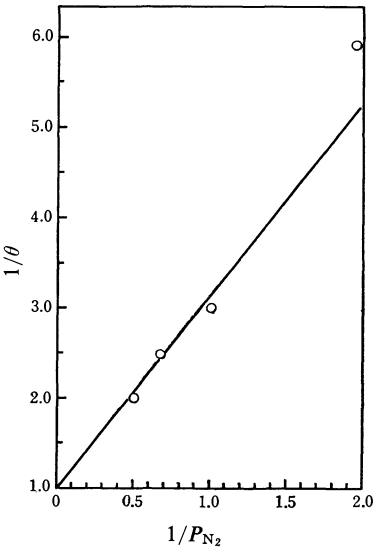


Fig. 8. Plots according Eq. 4, at 738°C.

$$1-\frac{(k_2)_{P_{N_2}}}{A}=1-\frac{1}{1+aP_{N_2}}$$

$$\frac{1}{(k_2)_{P_{N_2}}}=\frac{1}{A}-\frac{a}{A}P_{N_2} \qquad (4')$$

where A is $(k_2)_{P_{N_2}=0}$.

According to Eq. 4', a can also be determined from the linear relation between $1/(K_2)_{P_{N_2}}$.

Results at 714 and 738°C are shown in Figs. 3—8 and Tables III and IV. Figure 7 shows the plotting according to Eq. 4', and Fig. 8, according to Eq. 4. All values give good straight lines; from them a at 714°C and 738°C are evaluated to be 0.500 and 0.400 respectively.

TABLE III. RESULTS AT 714°C

P_{N_2} cmHg	k_2 cmHg$^{1/3}$/min.	$1/k_2$	$1/P_{N_2}$	a
0.538	0.084	11.9	1.86	0.500
0.916	0.081	12.3	1.09	
1.480	0.064	15.6	0.68	
1.968	0.053	18.9	0.51	

TABLE IV. RESULTS AT 738°C

P_{N_2} cmHg	k_2 cmHg$^{1/3}$/min.	θ	$1/P_{N_2}$	a
0	0.064	0	—	
0.512	0.053	0.17	1.95	0.400
1.000	0.043	0.33	1.00	
1.500	0.038	0.41	0.67	
2.000	0.032	0.50	0.50	

As has been mentioned above, it was found that a indicates the degree of the influence of nitrogen, and that a decreases with the temperature. It is comprehensible from the deriving principle of Eq. 3 that a corresponds to an equilibrium constant of the attraction between the substance retarding the decomposition of zinc oxide and the nitrogen in the gas phase. Therefore, the relation between $1/a$ and $1/T$ (°K^{-1}) was obtaining as shown in Fig. 9. The linearity in Fig. 9 supports the above considerations. The slope of the line gives the enthalpy of the reaction, which produces retarding substances by interaction between the surface of zinc oxide and the nitrogen molecule, as -11.5 kcal./mol.

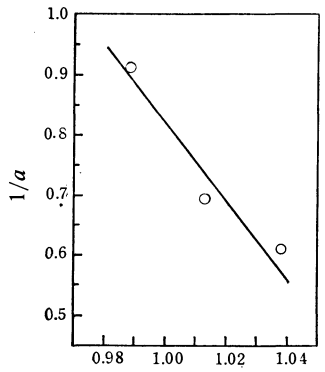


Fig. 9. $1/a$ vs. $1/T$.

As a result, it was found that nitrogen retards the reaction, the rate of which is proportional to the surface area of zinc oxide, and that the degree of the influence of nitrogen is evaluated by means of the constant, a in Eq. 3, which may be considered to reveal the equilibrium constant if the above presumption is valid. It has been reported that zinc nitride is produced by exposing the heated zinc powder in a stream of nitrogen.[7] The most probable retarding factor is the Langmuir-type chemisorption on the surface of zinc oxide —in this case, 11.5 kcal./mol. will represent the heat of chemisorption. The chemisorption of nitrogen, however, occurs only with difficulty on the normal surface of zinc oxide. The effect of nitrogen on the reduction will, however, require further studies from the point of view of the chemisortion and the surface compounds, because, as is well known,[3,4] the surface of zinc oxide submerged in the reducing gas at a high temperature has an excess of zinc, and hence its thermodynamical behavior is abnormal.

It was found that k_1 also decreases with the increase in the pressure of nitrogen (cf. from Table I). Since k_1 is the specific rate of the reaction of hydrogen and oxygen, the depressing effect of such an inert gas as nitrogen is unlikely. As has been previously reported, however, the reduction of zinc oxide is a consecutive reaction involving the decomposition of zinc oxide and the reaction of hydrogen with oxygen. Consequently, the equilibrium constant k is expected to be involved in observable k_1 generally. At present, the authors have not obtained the true rates of the reaction between hydrogen and oxygen and of the formation of zinc oxide from zinc vapor and oxygen (the specific rates are k_1° and k_{-2} respectively) under these experimental conditions; hence, the quantitative relation between k_1 and K $(=k_2/k_{-2})$ is known. At any rate, k_1 may be expressed by a function, $f(k, k_1^\circ)=f(k_2/k_{-2}, k_1^\circ)$. Therefore, k_1 would be affected by nitrogen, since k_2 is affected by nitrogen, as has been mentioned already.

Department of Applied Chemistry
Faculty of Engineering
Osaka City University
Kita-ku, Osaka

7) S. Matsuura, "Aen," Maruzen (1962), p. 553.

Adsorption of Congo Red and Fuchsine Base by Hydrous Beryllium Oxide Aged for Different Periods

By Rup DUTTA

(Received July 4, 1963)

It is well known that hydrous oxides like those of iron, chromium and aluminum are well known to possess a high adsorptive capacity. Mokuskin and Esin, White, Gorden and Porter studied the association of several dyes[1] by these hydrous oxides. Weiser[2] and Sen[3] also made a comparative study of adsorption capacity of the hydrous oxides of chromium, aluminum and iron for different inorganic ions. They are of the opinion that the adsorption process depends on valency of ion, pH of the medium, chemical activity and reactivity of the adsorbent, etc. The aging of hydrated oxides of aluminum, iron, nickel and cobalt has been studied by Lottermoser[4] who performed sedimentation experiments and X-ray studies, and ascribed the changes to be due to (a) the rate of growth of the secondary particles and (b) the rate of orientation of the structural units of the secondary particles. Similar observations were also made by Tewari, Dey and Ghosh[5] who discussed the mechanism of aging of the hydrous oxides of iron, aluminum and chromium.

It has been shown from these laboratories that aging of hydrous oxide has a marked effect on the role of adsorption. But, it can clearly be mentioned here that very little work appears to have been done on the subject, specially on the adsorption of dyes and ions on hydrous beryllium oxide of different characters, aged for different lengths of periods. Hence, in this paper the adsorption of Congo red and fuchsine base by hydrous beryllium oxide aged for different lengths of periods, have been studied and the results are represented in the following tables.

Experimental

Three samples of hydrous beryllium oxide were prepared by adding different quantities of 0.2 N sodium hydroxide solution to a fixed volume of 0.2 N beryllium sulfate solution as follows:

Sample A: precipitated with equivalent sodium hydroxide

Sample B: precipitated with 10% deficient sodium hydroxide

Sample C: precipitated with 10% excess sodium hydroxide.

These samples were then washed thoroughly with distilled water by decantation and allowed to age progressively by standing as a suspension at 30°C.

Adsorption Experiment.—In several 25 ml. jena flasks, containing 5 ml. of 0.001 g. of beryllium oxide and 5 ml. of (0.55 M : 0.1 M) boric acid-borax buffer solution of pH 8.5, varying amounts of the prepared dye solutions of known concentrations were added and the volume of the solutions was raised upto the mark in each case. The dyes used for adsorption were all B. D. H. AnalaR grade and purity was 98% and above. Each sample of the aged hydrous oxid was then kept in contact with the dye solution for 24 hr. at 30°C to attain equilibrium. An aliquot portion was then centrifuged and a measured volume was diluted as required for the estimation.

The residual concentration of the dye solution in the supernatant liquid was estimated by using Klett-Summerson photo-electric colorimeter. Filter number 54 (transmission 520~580 mμ) was found to be suitable for the dye. Before using colorimeter the applicability of Beer's law was tested in the range of pH maintained by the buffer. It was observed that Beer's law only holds good in low concentrations of the dye solution as far as 1×10^{-6}. Therefore, for the purpose of estimation, the dye solution present in the supernatant liquid was diluted to the requisite concentration, where Beer's law holds good, for its estimation.

The concentration of the residual dye solution was calculated by comparing with that of the same concentration, so that:

$$\text{Concn. of unknown dye soln.} = \frac{\left(\begin{array}{c}\text{Colorimetric}\\ \text{reading of}\\ \text{unknown dye}\\ \text{solution}\end{array}\right)\times\left(\begin{array}{c}\text{Concn. of}\\ \text{standard dye}\\ \text{solution}\end{array}\right)}{\text{Colorimetric reading of standard dye solution}}$$

In the following tables the results are recorded in gram moles of the dye adsorbed by the different samples, containing the same hydrous oxide in the system, where x is the amount of adsorbed dye in gram mole, and m is the amount of adsorbent in gram.

Discussions

The results for the adsorption of Congo red and fuchsine base by three samples of hydrous

1) Marker and Gorden, *Ind. Eng. Chem.*, **16**, 1186 (1924); C. E. White and Gorden, *J. Phys. Chem.*, **31**, 1764 (1927).
2) H. B. Weiser, ibid., **26**, 401 (1922).
3) K. C. Sen, ibid., **31**, 1840 (1927).
4) A. Lottermoser, *Kolloid. Beih.*, **38**, 1 (1933).
5) S. N. Tewari, A. K. Dey and S. Ghosh, *Z. anorg. u. allgem. Chem.*, **271**, 150 (1952).

Table I. Adsorption of Congo red by hydrous beryllium oxide at 30°C

Age of the hydrous oxide	Initial concn. $\times 10^6$ mol.	Amount adsorbed $x/m \times 10^3$ Sample A	Sample B	Sample C
5 days	75.2	35.36	47.00	18.97
	56.4	24.82	41.96	15.23
	37.6	19.50	28.60	10.15
	18.8	16.92	18.61	4.51
10 days	75.2	20.10	24.80	4.70
	56.4	16.30	22.55	4.51
	37.6	16.92	20.90	3.94
	18.8	2.28	17.57	3.76
20 days	75.2	14.30		2.26
	56.4	13.10	—	2.82
	37.6	10.15		1.68
	18.8	10.04		0.75
30 days	75.2	11.30	19.70	1.89
	56.4	8.27	19.00	2.06
	37.6	7.30	17.80	2.00
	18.8	7.80	17.87	0.81

Table II. Adsorption of fuchsine base by hydrous berllium oxide at 30°C

Age of the hydrous oxide	Initial concn. $\times 10^7$ mol.	Amount adsorbed $x/m \times 10^4$ Sample A	Sample B	Sample C
5 days	34.4	20.29	7.57	23.50
	25.8	12.92	5.94	17.80
	17.2	8.70	4.13	11.53
	8.6	4.30	2.07	5.85
10 days	34.4	12.40	5.16	21.70
	25.8	8.55	3.56	16.27
	17.2	6.36	1.94	10.84
	8.6	2.95	1.64	5.35
20 days	34.4	8.94	4.47	12.50
	25.8	4.81	2.10	15.70
	17.2	3.27	1.70	10.33
	8.6	2.15	1.30	4.87
30 days	34.4	4.76	3.79	20.64
	25.8	3.86	1.90	14.45
	17.2	2.41	0.80	9.46
	8.6	1.12	0.60	4.64

beryllium oxide are given in Tables I and II, and the amounts adsorbed have been plotted (not shown here) against the end concentrations of the adsorbate. It would be seen that most of the curves are convex to the concentration axis as in the case of Freundlich's adsorption isotherm and, therefore, similar to those obtained for the adsorption of bromine (at 79°C) or iodine by a silica gel.

The adsorption data for different dye-stuffs reveal that the three samples possess different adsorptive capacities. Thus, for the adsorption of Congo red it is maximum for the sample B but in the case of fuchsine base it is maximum for sample C, obtained by adding excess of an alkali for precipitation. These results are quite in good agreement with the view of Ghosh and co-workers. According to them the hydrous oxides, specially of amphoteric nature, should develop a large adsorptive capacity for anions, when precipitated with deficient quantity of an alkali and the adsoption of cation should be more marked for the precipitate obtained by the addition of an excess of an alkali.

It will be further seen that the same sample of hydrous beryllium oxide, aged for different period, have decreasing adsorptive capacity for dye-stuffs. The decrease in the adsorptive capacity with aging, may be due to the following two reasons.

(i) Hydrous beryllium oxide when freshly prepared, shows a high adsorptive capacity for ions and dye-stuffs from the solution due to the size of the particles of the hydrous oxide, which on aging tend to grow larger in size, causing a diminution in the total surface area of the particles and consequently the adsorptive capacity is decreased.

(ii) Adsorptive capacity also decreases, with aging, due to the formation of an inert substance, produced by the internal neutralization of the acidic and basic character of the amphoteric hydroxide, as given below:

$$Be(OH)_2 \rightleftarrows Be(OH)^+ + OH^-$$

$$Be(OH)_2 \rightleftarrows Be\cdot O\cdot (OH)^- + H^+$$

$$Be\cdot O\cdot (OH)^- \cdot Be(OH)^+ \rightarrow 2BeO + H_2O$$

$$H^+ + OH^- \rightarrow H_2O$$

Summary

Three samples of hydrous beryllium oxide, of different character, were prepared by adding different quantities of an alkali to a fixed volume of beryllium sulfate solution for precipitation. These samples were allowed to age progressively and there adsorptive capacities for dye-stuffs were studied. It has been found that the adsorptive capacity of the samples decreases with aging of the hydroxide and the adsorption data dye-stuffs reveal that the three samples possess different adsorptive capacities.

The author is deeply grateful to Professor S. Ghosh and Dr. A. K. Dey for their painstaking and critical review of the work. The author also wish to thank to Council of Scientific and Industrial Research to have had the financial support during this investigation.

Chemical Laboratories
University of Allahabad
Allahabad, India

*Kinetic and Spectrophotometric Studies of the Homogeneous Catalytic Activity of Iron(III) Complexes upon the Decomposition of Hydrogen Peroxide in Aqueous Solution**

By Goro WADA, Tadayoshi NAKAMURA, Kunio TERAUCHI and Toru NAKAI

(Received September 9, 1963)

The mechanism of the homogeneous catalytic decomposition of hydrogen peroxide by ferric or ferrous ions was first presented by Haber and Weiss,[1] who described how the reaction proceeds through a chain mechanism, with the HO_2 radical or the HO_2^- ion as chain carriers and accompanied by repeated redox cycles, Fe(III) $\rightleftarrows$ Fe(II), at the same time. This idea was examined carefully by Barb and others.[2-4] The existence of the free HO_2 radical as an intermediate was confirmed chemically employing 2, 6-di-*t*-butyl-4-methyl phenol in the reaction system[5] and also physically from the ESR spectrum in the case of the cerric ion catalyst.[6] After all, Wang and Jarnagin[7-9] and Kremer and Stein[10,11] proposed a transient occurrence of complex ions between the catalytic ions and the reaction intermediates. Wang and Jarnagin investigated the influence of ligands which occupy coordination sites other than those occupied by HO_2 in a ferric complex ion and found that triethylenetetramineiron(III) ions are most catalytically active in the decomposition of hydrogen peroxide in an alkaline solution, because this ligand is tetradentate and HO_2 is probably bidentate.[9] The study was ultimately intended for the elucidation of the reaction mechanism of catalase, a large coordination compound of the ferric ion, which exhibits the greatest catalytic ability for the decomposition of hydrogen peroxide.[7,12]

In the present paper, it will be made clear how the varieties and the numbers of the coordinating ligands affect, in connection with the energy of coordinate bonds, the catalytic activity of the ferric ion.

Experimental

Materials.—The pure hydrogen peroxide used was obtained by the vacuum distillation of 30% commercial hydrogen peroxide at 30 mmHg, after removing the contained stabilizers by means of adsorption on stannic acid. The concentration of hydrogen peroxide was determined by titration with potassium permanganate. Iron(III) and iron(II) salts were recrystallized from sulfuric acid solutions of $Fe_2(SO_4)_3 \cdot 9H_2O$ and $FeSO_4 \cdot 7H_2O$ respectively. The ligands employed as complexing reagents were monoethylamine (ea), ethylenediamine (en), diethylenetriamine (dien), triethylenetetramine (trien), tetraethylenepentamine (tetraen), *o*-phenanthroline (phen) and α, α'-dipyridyl (dip), which were used without further purification. Iron(III) complexes were prepared by merely mixing the two solutions of the Fe^{3+} ion and a ligand in an appropriate proportion. The pH of the solution was adjusted by adding perchloric acid and was assayed by a pH-meter. The effect of the ionic strength was negligible in every case, because the concentrations of all ionic components in the solution were extremely low.

Kinetic Measurements.—The reaction was regarded as starting at the moment when a solution of the iron(III) complex ion was quickly poured into a reaction vessel containing a hydrogen peroxide solution in a thermostat. The rate of the reaction was determined by measuring the volume of evolved oxygen with a gas buret.

The Determination of Stability Constants.—The stability constants of several iron(III)-complex ions were measured by the pH method, using a Hitachi-Horiba pH-Meter Model P, with an accuracy of pH ± 0.01. Bjerrum's formation function, $\bar{n}$, is thereby defined as follows:

* Presented at the 13th Symposium on Catalysts, Sapporo, September, 1963. The preprint appears in *Shokubai (Catalyst)*, **5**, 199 (1963).

1) F. Haber and J. Weiss, *Proc. Roy. Soc. London*, **A147**, 332 (1934).
2) W. G. Barb, J. H. Baxendale, P. George and K. R. Hargrave, *Trans. Faraday Soc.*, **47**, 462 (1951).
3) W. G. Barb, J. H. Baxendale, P. George and K. R. Hargrave, ibid., **47**, 591 (1951).
4) W. G. Barb, J. H. Baxendale, P. George and K. R. Hargrave, ibid., **51**, 935 (1955).
5) G. M. Coppinger, *J. Am. Chem. Soc.*, **79**, 2758 (1957).
6) B. H. J. Bielski and E. Saito, *J. Phys. Chem.*, **66**, 2266 (1962).
7) J. H. Wang, *J. Am. Chem. Soc.*, **77**, 4715 (1955).
8) R. C. Jarnagin and J. H. Wang, ibid., **80**, 786 (1958).
9) R. C. Jarnagin and J. H. Wang, ibid., **80**, 6477 (1958).
10) M. L. Kremer and G. Stein, *Trans. Faraday Soc.*, **55**, 959 (1959).
11) M. L. Kremer, ibid., **58**, 702 (1962).
12) P. George, *Biochem. J.*, **43**, 287 (1948); ibid., **44**, 197 (1949); P. Jones and W. F. K. Wyne-Jones, *Trans. Faraday Soc.*, **58**, 1148 (1962).

$$\bar{n}=\frac{\sum_{i=1}^{m} iK_1K_2\cdots K_i[L^*]^i}{1+\sum_{i=1}^{m} K_1K_2\cdots K_i[L^*]^i} \quad (1)$$

$$=\frac{C_L-(C_H-[H^+])/p^+}{C_M} \quad (2)$$

where K_i is the i-th stepwise stability constant; [L*] and [H$^+$], the concentrations of the free ligand (coordinating with neither the metal ion nor the hydrogen ion) and of the hydrogen ion respectively; m, the coordination number of the central metal ion; C_M, C_L and C_H, the total concentrations of the Fe^{3+} ion, the ligand and perchloric acid respectively added to the solution, and $\bar{p}$, the ratio between the number of ionizable hydrogen atoms attached to the ligand and the total number of ligand molecules which are not coordinated with the metal ion; namely,

$$\bar{p}=\frac{\sum_{i=1}^{p} \frac{i[H^+]^i}{K_{HL^+}\cdot K_{H_2L^{2+}}\cdots K_{H_iL^{i+}}}}{1+\sum_{i=1}^{p} \frac{[H^+]^i}{K_{HL^+}\cdot K_{H_2L^{2+}}\cdots K_{H_iL^{i+}}}}$$

where $K_{H_iL^{i+}}$ indicates the acid dissociation constant of H_iL^{i+}. By putting this relation into Eq. 2, $\bar{n}$ can be calculated, if the $K_{H_iL^{i+}}$'s are known. According to the difinition, [L*] is also expressed as

$$[L^*]=\frac{C_H-[H^+]}{\sum_{i=1}^{p} \frac{i[H^+]^i}{K_{HL^+}\cdot K_{H_2L^{2+}}\cdots K_{H_iL^{i+}}}}$$

Therefore, by means of titrating a mixed solution of the Fe^{3+} ion and the ligand with perchloric acid and by measuring its pH, one can plot the relation between $\bar{n}$ and $-\log[L^*]$, from which the stability constants are obtained, as is clear from Eq. 1. K_i's are known at the value $\bar{n}=i-0.5$ according to Bjerrum's approximation.

Spectrophotometry.—The individual absorption spectra of aqueous solutions of the Fe^{3+} ion, the Fe^{2+} ion and their complex ions and hydrogen peroxide were observed separately in advance. Then the variations of the spectra of the solution under reaction with the lapse of time were observed as the catalytically-working state of complex ions. For the observation, a Hitachi recording spectrophotometer type EPS-2 was used at the 220~900 mμ wevelength range. A tungsten lamp and a hydrogen discharge tube were employed as light sources for the visible and the ultraviolet regions respectively. The cell was one made of quartz and had an optical length of 1 cm.

Results and Discussion

Velocity Curves and Their pH Dependence.—The reaction rates of hydrogen peroxide decomposition catalyzed by the Fe-aq^{3+} ion are generally of the S-type, as Fig. 1 shows. The reaction proceeds nearly linearly, something like a zeroth-order reaction, after the continuance of some induction period, and then

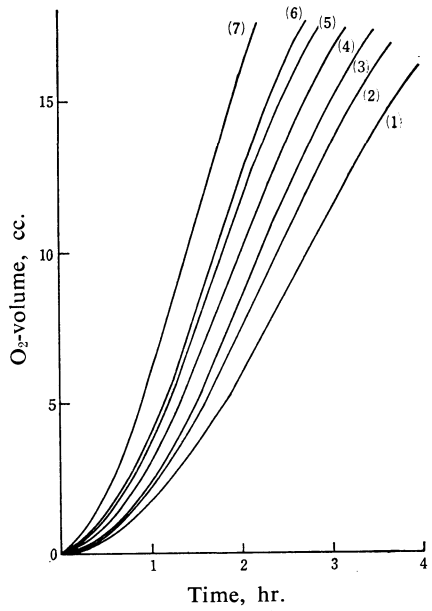


Fig. 1. The pH dependence of the reaction rate at 45°C.
[Fe-aq^{3+}]$=1.013\times10^{-4}$ mol./l., [H_2O_2]$_0=1.010\times10^{-2}$ mol./l. (1) pH 2.65; (2) 2.80; (3) 2.90; (4) 3.01; (5) 3.10; (6) 3.20; (7) 3.40

it falls off gradually.*1

On the average, it takes as long as a few minutes for an Fe^{3+} ion to decompose only one hydrogen peroxide molecule, judging from the slope of the linear part of the reaction in such cases as in Fig. 1. Considering this fact, together with the stability constant of Fe^{3+}-HO_2^-, $\log K_1=9.31$,[13] the rate of the reaction may probably be controlled either by an activated collision between the Fe^{3+} ion and HO_2^- (or HO_2) or by the self-decomposition of the complex. For this reason, the reaction appears as of the zeroth-order. Hereafter, the rate constant, k, will be expressed by the slope of the linear part of the reaction in mol.-H_2O_2/l. hr. The values of k are dependent on the pH of the solution, as is shown in Table I, where the reaction is found to be accelerated as the pH value is raised. However, on account of the restriction arising from the solubility of the iron-complex salts, the pH of the solutions will be generally fixed at

*1 As soon as hydrogen peroxide is supplemented up to a concentration equal to that of the initial state when the reaction has almost completely finished, the reaction comes back immediately to the linear part at the same velocity as that of the previous time, without exhibiting the induction phenomenon again.

13) "Stability Constants of Metal-ion Complexes," Part II, Compiled by J. Bjerrum et al., Chem. Soc., London (1958), p. 68; M. G. Evans, P. George and N. Uri, *Trans. Faraday Soc.*, **45**, 230 (1949).

3.00 in the following sections, unless otherwise specified.

Variations in the Reaction Rate with Concentration and Temperature.—Table II shows the variations in the reaction rate with the concentrations of the Fe^{3+} ion, hydrogen peroxide and the ligand and with the temperature of the reaction system. The ratios of the concentration of the ligand to that of Fe^{3+} in solutions are expressed by $[L]/[Fe^{3+}]$. The apparent activation energies, E_a, are also obtained from the relation between $\log k$ and $1/T$. It can easily be seen from the table that k diminishes with an increase in $[L]/[Fe^{3+}]$ as long as both $[Fe^{3+}]$ and $[H_2O_2]_0$ are kept constant and that k increases approximately in proportion to $[Fe^{3+}]$ and to the 1.5th power of $[H_2O_2]_0$.

Only when phen is employed as a ligand, is the reaction not of the S-type but appears

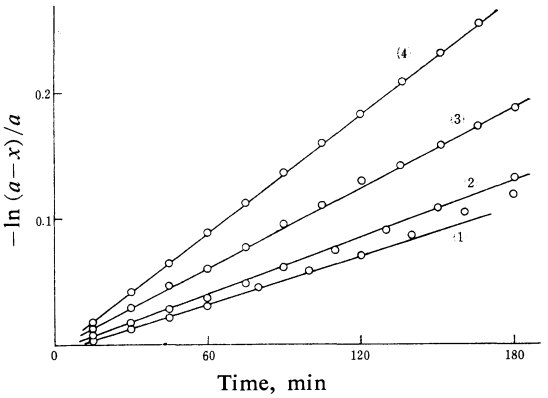


Fig. 2. The reaction rate catalyzed by the Fe(III)-phen complex ion at pH 3.
$[Fe^{3+}]=1.013\times10^{-4}$ mol./l., $[phen]/[Fe^{3+}]=1$, $[H_2O_2]_0=1.010\times10^{-2}$ mol./l. (1) 30°C; (2) 35°C; (3) 40°C; (4) 50°C

Table I. The effect of pH on the reaction rate at 45°C

$[Fe\text{-}aq^{3+}]=1.013\times10^{-4}$ mol./l., $[H_2O_2]_0=1.010\times10^{-2}$ mol./l.

pH	2.65	2.80	2.90	3.01	3.10	3.20	3.40
$k\times10^3$ mol.-H_2O_2/l. hr.	1.31	1.47	1.64	1.79	1.88	2.12	2.51

Table II. The variations of k with concentrations and temperatures, and the apparent activation energies, E_a, at pH 3

Ligand	$[Fe^{3+}]\times10^4$ mol./l.	$[L]/[Fe^{3+}]$	$[H_2O_2]_0\times10^2$ mol./l.	k, $\times10^4$ mol.-H_2O_2/l. hr. 30°C	35°C	40°C	45°C	50°C	E_a kcal./mol.
none(aq)	1.013	—	1.008	6.3	9.1	12.8	17.9	25.4	14.7
	3.336	—	1.611	—	28.6	46.4	74.2	117	18.0
ea	1.013	1	1.010	3.7	7.1	9.8	13.0	18.2	16.5
	1.013	2	1.010	3.1	4.5	8.1	11.5	15.8	16.0
	1.013	3	1.010	2.2	4.1	6.1	10.1	14.0	14.9
	1.013	4	1.010	—	3.5	5.5	9.2	11.9	14.7
	1.013	5	1.010	—	3.6	5.4	7.8	11.5	14.3
	1.013	6	1.010	—	3.1	4.6	7.4	10.7	14.6
	1.013	100	1.010	—	0	0	0	0	—
en	1.013[a]	1	1.010	6.3	10.3	16.5	25.4	—	18.0
	1.013[a]	1	3.391	37.4	59.7	94.0	144	—	17.2
	1.013	2	1.010	6.4	9.9	13.8	22.4	—	16.1
	1.013	3	1.010	5.7	9.3	13.3	19.8	—	15.7
	1.013	3	3.391	33.7	55.4	89.1	168	—	20.8
	1.013	4	1.010	—	9.9	14.7	21.3	31.2	15.1
	1.013	100	1.010	—	2.8	4.3	6.5	9.8	16.6
dien	1.013	1	1.010	—	4.8	8.7	15.4	27.2	22.7
	1.013	2	1.010	—	3.6	6.2	10.9	18.9	21.8
	1.013	100	1.010	—	0	0	0	0	—
trien	1.013[b]	1	1.010	2.3	4.1	7.5	13.2	—	22.5
	2.026	2	1.010	—	2.4	4.3	8.3	15.2	24.5
	1.013	100	1.010	—	0	0	0	0	—
tetraen	1.013	1	1.010	—	2.8	4.9	8.2	13.9	20.8
	2.026	2	1.010	—	1.8	2.4	5.0	8.2	19.9
	1.013	100	1.010	—	0	0	0	0	—

a) pH 3.1
b) pH 2.9

as a first-order reaction with respect to the concentration of hydrogen peroxide, since $\ln[(a-x)/a]$ is linear against time, where x and a are the volumes of oxygen evolved at t and the infinite time respectively, as is pictured in Fig. 2. The rate constants at various temperatures and the apparent activation energies are listed in Table III.

Inspection of Tables II and III reveals that the catalytic activities of iron(III) complexes depend upon the sort of ligands, decreasing in the order:

$$\text{en} > \text{dien} \sim (H_2O) \sim \text{ea} > \text{trien} > \text{tetraen} \sim \text{dip} \sim \text{phen} \quad (3)$$

where H_2O indicates the simple iron(III)-aquo ion without any other ligand in the solution.

On the other hand, the apparent activation energies, E_a, of the reaction catalyzed by various complexes generally show peaks near the concentration ratio of $[L]/[Fe^{3+}]=1$, except for the cases of trien and phen, where the former increases and the latter decreases monotonously with the increasing concentration ratio, as is pictured in Fig. 3. Therefore, the order of E_a with respect to ligands is as follows at their low concentration:

$$\text{dien} \sim \text{trien} > \text{tetraen} > \text{en} > \text{ea} > (H_2O) > \text{phen} \quad (4)$$

All the ligands except phen make E_a larger than that for the case of the simple Fe-aq^{3+}, so long as their concentration is low. Wang[9] said that trien showed the highest catalytic activity in an alkaline solution because of the steric advantage arising from its tetradentate nature. We, however, have found this ligand to be merely a poor catalyst at pH 3, contradictory to Wang's description. In the case of en and dien, since their complexes are more active than Fe-aq^{3+} in spite of the larger E_a, they must make the reaction much easier sterically, overcoming the energetic disadvantage.

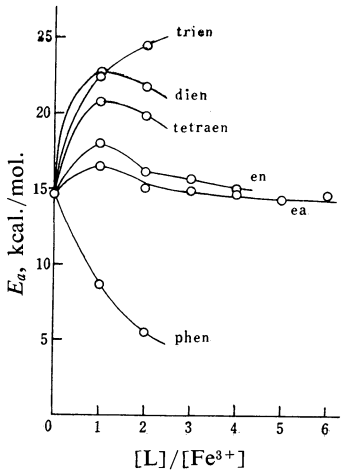


Fig. 3. The variations of the apparent activation energies, E_a, with $[L]/[Fe^{3+}]$ at pH 3. $[Fe^{3+}]=1.013\times10^{-4}$ mol./l., $[H_2O_2]_0=1.010\times10^{-2}$ mol./l.

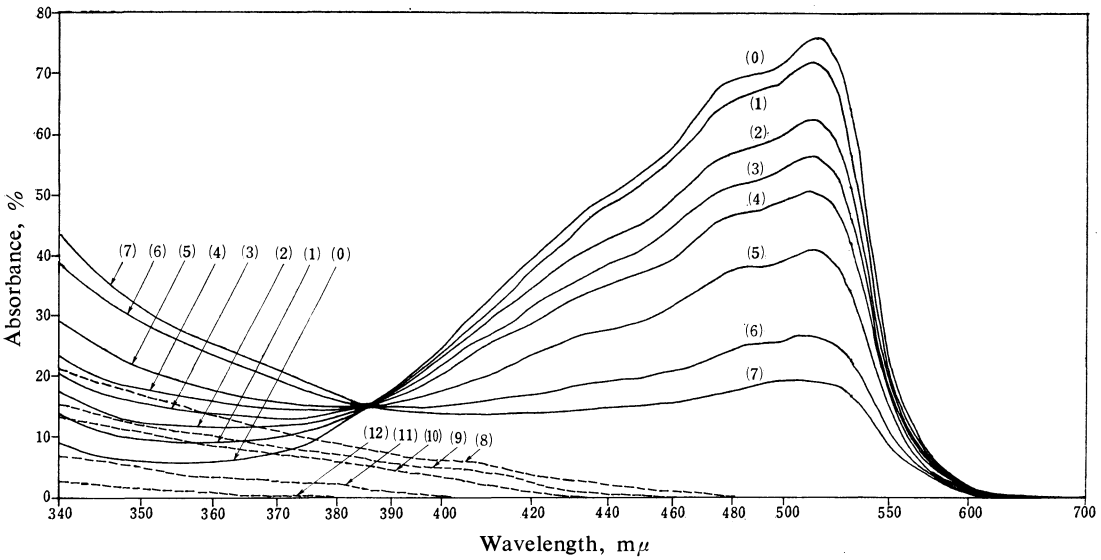


Fig. 4. Time variation of visible absorption spectra of Fe-phen$_3^{2+}$ under a catalytically working state at room temperature.
[Fe-phen$_3^{2+}$]$=1.013\times10^{-4}$ mol./l., $[H_2O_2]_0=1.010\times10^{-2}$ mol./l. (0) $t=0$; (1) 5 min.; (2) 15 min.; (3) 30 min.; (4) 50 min.; (5) 80 min.; (6) 140 min.; (7) 200 min.; (8) 300 min.; (9) 400 min.; (10) 1 day; (11) 7 days; (12) 8 days

TABLE III. THE RATE CONSTANT, k (hr^{-1}), AND THE APPARENT ACTIVATION ENERGY, E_a, OF THE REACTION CATALYZED BY THE Fe(III)-phen COMPLEX ION AT pH 3
$[Fe^{3+}]=1.013\times10^{-4}$ mol./l., $[H_2O_2]_0=1.010\times10^{-2}$ mol./l.

[phen]/[Fe^{3+}]	30°C	35°C	40°C	45°C	50°C	E_a kcal./mol.
1	0.041	0.048	0.066	—	0.098	8.7
2	—	0.041	0.046	0.054	0.061	5.5

TABLE IV. STABILITY CONSTANTS OF VARIOUS IRON(III) COMPLEXES AT 30° AND 45°C AND PERCENTAGES OF THE COORDINATED IRON AT THE CONCENTRATION
$[Fe^{3+}]=[L]=1.013\times10^{-4}$ mol./l. AT 30°C

Ligand	Temp. °C	Dissociation constant*				Stability constant						α %
		$-\log K_{HL^+}$	$-\log K_{H_2L^{2+}}$	$-\log K_{H_3L^{3+}}$	$-\log K_{H_4L^{4+}}$	$\log K_1$	$\log K_2$	$\log K_3$	$\log K_4$	$\log K_5$	$\log K_6$	
ea	30	10.61				11.36	11.25	11.19	10.94	10.73	10.25	<59.5
	45	9.95				11.07	10.93	10.86	10.52	10.10	9.54	
en	30	9.93	7.26			14.77	14.07	8.90				57.6
	45	9.52	6.79			14.18	13.21	8.12				
dien	30	9.94	9.23	4.78		19.37	17.90					79.1
	45	9.55	8.80	4.40		18.56	16.93					
trien	30	9.99	9.36	7.01	3.89	23.54						92.7
	45	9.64	9.03	6.68	3.70	22.79						

* "Stability Constants of Metal-ion Complexes," Part I, Compiled by J. Bjerrum et al., Chem. Soc., London (1957).

TABLE V. THE TRUE VALUES OF RATE CONSTANTS, ACTIVATION ENERGIES AND ACTIVATION ENTROPIES OF THE REACTION CATALYZED BY FeL^{3+} ION WHEN $[H_2O_2]_0=1.010\times10^{-2}$ mol./l. AND $[FeL^{3+}]=1.013\times10^{-4}$ mol./l.

Ligand	k, $\times10^4$ mol.-H_2O_2/l. hr					E_a kcal./mol.	E kcal./mol.	$\Delta(\Delta S)$ cal./deg. mol.
	30°C	35°C	40°C	45°C	50°C			
aq	6.3	9.1	12.8	17.9	25.4	14.7	14.7	Standard
ea	(2.0)	5.7	7.8	9.6	13.5	16.5	12.2	−9.2
en	6.3	11.1	19.3	31.1	—	18.0	22.3	26.0
dien	—	3.7	7.6	14.8	27.8	22.7	27.2	38.9
trien	1.9	3.7	7.1	12.8	—	22.5	25.9	34.5
tetraen	—	—	—	—	—	20.8	—	—

TABLE VI. THE WAVELENGTHS, λ_{max}, AND THE EXTINCTION COEFFICIENTS, ε, AT PRINCIPAL ABSORPTION MAXIMA OF VARIOUS SUBSTANCES IN AQUEOUS SOLUTIONS IN THE 220~900 mμ RANGE AT pH 3
( ): shoulder, [ ]; broad or plateau

phen	λ_{max}	324	(310)	(289)	265	229	(225)	
	log ε	3.12	3.20	3.85	4.29	4.40	4.39	
H_2O_2	Gradual end absorption at $\lambda<300$ mμ							
Fe-aq^{3+}	λ_{max}		298					
	log ε		3.86					
Fe-aq^{2+}	λ_{max}	[370]			(246)			
	log ε	0.45			1.17			
Fe-$phen_3^{3+}$	λ_{max}	(350)	326	(289)	266	[230~225]		
	log ε	3.41	3.66	4.25	4.75	4.95		
Fe-$phen_3^{2+}$	λ_{max}	515	(480)	(420)	(320)	(289)	267	226
	log ε	4.11	3.90	3.60	3.32	4.27	4.92	4.82

TABLE VII. THE d-ORBITAL ENERGY LEVELS IN Dq UNIT IN THE LIGAND FIELD

Coordination number	Structure	$d_{x^2-y^2}$	d_{z^2}	d_{xy}	d_{xz}	d_{yz}
5	Trigonal bipyramid	−0.82	7.07	−0.82	−2.72	−2.72
5	Square pyramid	9.14	0.86	−0.86	−4.57	−4.57
6	Octahedron	6.00	6.00	−4.00	−4.00	−4.00
7	Pentagonal bipyramid	2.82	4.93	2.82	−5.28	−5.28

The Stability Constants of Several Complexes.—The stability constants of iron(III) complexes with ea, en, dien and trien at 30 and 45°C are listed in Table IV. Using the data of the stability constants, the percentages of the coordinated iron in the total iron at $[Fe^{3+}] = 1.013 \times 10^{-4}$ mol./l. are calculated as α, shown in the last column of the table.

The various values of k and E_a as shown in Table II are, of course, those which are averaged with respect to the hydrated iron(III) (non-coordinated by ligands, Fe-aq^{3+}) and the coordinated iron (III) (FeL_i^{3+}) in accordance with their percentages of occurrence. The true values, purely due to the catalytic activity of the coordinated complexes calibrated by α, are shown in Table V. Since K_1 does not vary with the temperature in comparison with the experimental errors, α's at 30°C were used withought alteration in the calculation for other temperatures. In the case of $[L]/[Fe^{3+}] = 1$, $[FeL_2^{3+}]$ and higher complexes are negligibly rare.

According to Table V, the true activation energies, E, are generally greater than E_a, with the exception of the case of ea. Hence, the activation entropy increments putting the activation entropy of the aquo ion as the standard, $\Delta(\Delta S)$, have been calculated and been found to be positive in the cases of en, dien and trien and negative in the case of ea. The parallelism between E and $\Delta(\Delta S)$ is fairly good (the compensation effect). Judging from the large positiveness of $\Delta(\Delta S)$ in the cases of several iron(III)-*N*-multidentate complexes, the activated states of these complexes are supposed to be looser than the pre-activated states; they may be less coordinated than six. This supposition will be proved later.

The Absorption Spectra of Catalytically-Active Complexes in the Working State.—Table VI shows the positions of the peaks, λ_{max}, and the extinction coefficients, ε, in the absorption spectra of phen, hydrogen peroxide, Fe-aq^{3+}, Fe-aq^{2+}, Fe-phen$_3^{3+}$ and Fe-phen$_3^{2+}$ in aqueous solutions. Hydrogen peroxide, Fe-aq^{3+} and Fe-aq^{2+} exhibit no remarkable characteristic absorptions except their end absorption in the region of very short wavelengths. The observed values of λ_{max} and ε of iron-phen complexes agree with the values in the literature rather well.[14] The reason why the phen-complexes are used here is merely the convenience of the spectrophotometric observation, even though they have a disadvantage that the phen molecules themselves are liable to decompose during the reaction.

The visible spectra of Fe-phen$_3^{2+}$ in the catalytically-working state during the decomposition of hydrogen peroxide are shown in Fig. 4, where the absorption at 515 mμ characteristic of Fe-phen$_3^{2+}$ decreases with time, while that at 350 mμ characteristic of Fe-phen$_3^{3+}$ increases. This means that the iron(II)→iron(III) oxidation is occurring. However, with a longer lapse of time, the absorption at 350 mμ begins to decrease after attaining a maximum, while the absorption band at 515 mμ is never recovered again; the solution becomes almost colorless, and at last the spectrum coincides with that of Fe-aq^{2+}. This is due to the consecutive reduction, iron(III)→iron(II), after the preceding oxidation,[15] as well as to the simultaneous decomposition of phen itself. A similar conclusion can be derived from the observed results in the ultraviolet region.

In the same way, the visible absorption curves of the reaction system containing Fe-phen$_3^{3+}$ and hydrogen peroxide show that, although the height of the comparatively low peak at 350 mμ hardly varies at all, another new peak appears at 515 mμ, changing the color of the solution from yellow to reddish. This indicates the occurrence of the iron(III)→iron(II) reduction. However, after more than three hours, the peak at 515 mμ disappears and the solution again becomes yellow, indicating a recovery of iron(II)→iron(III). After that, the curve gradually approaches the characteristic weak curve of Fe-aq^{3+} on account of the decomposition of phen, just as in the case of Fe-phen$_3^{2+}$.

Figures 5 and 6 show the time variations of the ultraviolet absorption spectra in reaction systems containing Fe-phen$_3^{2+}$ and hydrogen peroxide, and Fe-phen$_3^{3+}$ and hydrogen peroxide respectively. Since Fe-phen$_3^{2+}$, Fe-phen$_3^{3+}$ and phen exhibit their individual peaks at 265~267 mμ with nearly the same extinction coefficients, the fact that the absorption at this wavelength region diminishes monotonously with time indicates that the decomposition of phen has begun even at the initial stage of the reaction. In the 300~320 mμ region, on the other hand, the absorption grows stronger with time in Fig. 5, while it does not vary so much in Fig. 6*[2] because of the difference in ε between Fe-phen$_3^{2+}$ and Fe-phen$_3^{3+}$ in this wavelength region. The electron transfer between iron(II) and iron(III) is, therefore,

14) D. H. Busch and J. C. Bailar, Jr., *J. Am. Chem. Soc.*, **78**, 1137 (1956).

15) In reactions between cumene hydroperoxide and the ferrous iron, such as aquo-ferrous ion, ferrous versenate and ferrous pyrophosphate, the formation of ferric iron has also been observed. W. L. Reynolds and I. M. Kolthoff, *J. Phys. Chem.*, **60**, 969, 996 (1956).

*2 The accuracy of Fig. 6 was worse than that of Fig. 5.

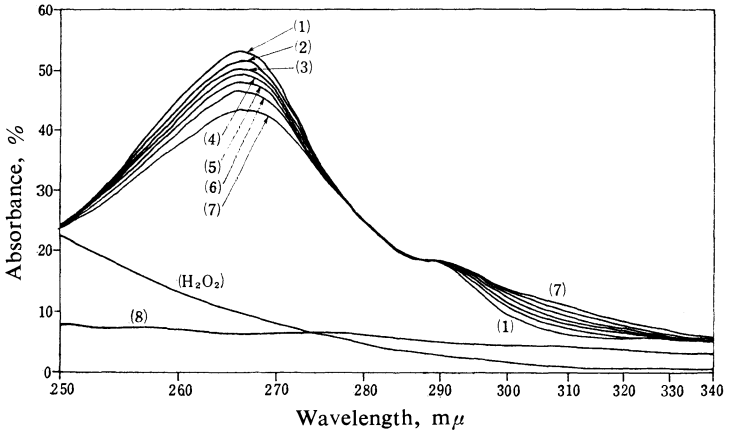


Fig. 5. Time variation of ultraviolet absorption spectra of Fe-phen$_3^{2+}$ under a catalytically working state at room temperature.
[Fe-phen$_3^{2+}$]$=1.013\times10^{-4}$ mol./l., [H_2O_2]$_0=1.010\times10^{-2}$ mol./l. The original solutions were diluted about 13 times when determined. (1) $t=5$ min.; (2) 20 min.; (3) 55 min.; (4) 100 min.; (5) 180 min.; (6) 290 min.; (7) 430 min.; (8) 24 hr.; (H_2O_2) H_2O_2 only at 9.56×10^{-4} mol./l.

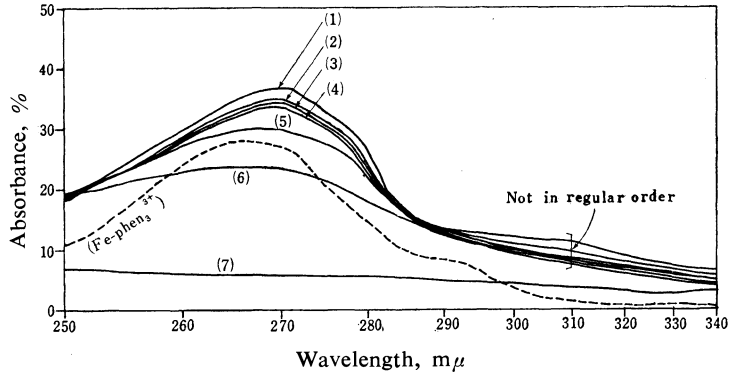


Fig. 6. Time variation of ultraviolet absorption spectra of Fe-phen$_3^{3+}$ under a catalytically working state at room temperature.
[Fe-phen$_3^{3+}$]$=1.013\times10^{-4}$ mol./l., [H_2O_2]$_0=1.010\times10^{-2}$ mol./l. The original solutions were diluted about 25 times when determined. (1) $t=5$ min.; (2) 15 min.; (3) 30 min.; (4) 60 min.; (5) 120 min.; (6) 210 min.; (7) 20 hr.; (Fe-phen$_3^{3+}$) Fe-phen$_3^{3+}$ only

proved.*3

Considering that the absorbance of hydrogen peroxide gradually increases towards shorter wavelengths, as Fig. 5 shows, the characteristic peaks of Fe-phen$_3^{2+}$ at 267 mμ and Fe-phen$_3^{3+}$ at 266 mμ should shift in appearence towards shorter wavelength because of a simple overlapping with hydrogen peroxide, if these complexes do not interact with hydrogen peroxide. In fact, however, according to Figs. 5 and 6, they clearly shift towards rather longer wavelengths as far as 1~4 mμ. This indicates changes in the strength of chemical bondings in both complexes, probably due to the formation of the coordination of HO_2 to iron. Generally speaking, the absorption bands of any complex are determined by the total influence of all the coordinated ligands, and their wavelengths shift continuously with the exchange of the ligands with others one by one. A red shift means the loosening of the coordinate bondings as the resut of the substitution for one ligand of another. HO_2 may be a ligand that makes the coordinate bonds slightly looser.

The Relation Between the Reaction Mechanisms and the Stabilization Energies of the Ligand Fields.—Concerning the central metal ions with the coordination number of six, the order of the ligand field stabilization energy

*3 The rate constant of the Fe-phen$_3^{2+}$→Fe-phen$_3^{3+}$ electron transfer was found to be $k>1\times10^5$ mol^{-1}·sec^{-1} by the N. M. R. method. M. W. Dietrich and A. C. Wahl, *J. Chem. Phys.*, **38**, 1591 (1963).

TABLE VIII. DIFFERENCES IN LIGAND-FIELD STABILIZATION ENERGIES IN Dq, ΔE, THROUGH S_N1- AND S_N2-MECHANISMS BY Fe(II)- AND Fe(III)-COMPLEXES

d^n	Ligand field	Octahedron d^2sp^3	S_N1 Trigonal bipyramid dsp^3	ΔE	S_N1 Squre pyramid d^2sp^2	ΔE	S_N2 Pentagonal bipyramid d^3sp^3	ΔE
Fe(III)-d^5	Strong	20.00	8.98	11.02	19.14	0.86	18.30*	1.70
	Weak	0	0	0	0	0	0	0
Fe(II)-d^6	Strong	24.00	11.72	12.28	20.00	4.00	15.48*	8.52
	Weak	4.00	2.72	1.28	4.57	−0.57	5.28	−1.28

* Among the strong field complexes of ions having d^5 or d^6 electrons, those with the configuration of pentagonal bipyramid are theoretically impossible, because the inner d-orbitals can be completely occupied only by four electrons.

decided from the absorption spectra is known as Fajans-Tsuchida's spectrochemical series:[16]

$$CN^- > phen > dip > trien \sim dien \sim en > NH_3 \sim py > H_2O > OH^- \quad (5)$$

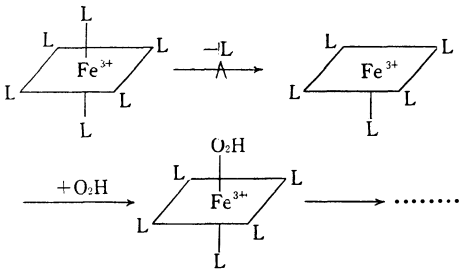
Although this series is not absolutely applicable for iron(III),[17] one can easily find, by comparing the two series, 4 and 5, that the first ligand of the 4 series, dien, is in the middle of the 5 series and that the succeeding ones in the 4 series are situated before and behind dien in the 5 series, regularly going farther away from the middle.

Since the 5 series generally indicates the order of the strength of the coordinate bonds between the central metal ion and the ligand, the following theory seems reasonable. The stability of iron complexes coordinated by HO_2 is quite decisive on the reaction rate, and their stability depends upon the ligand molecules occupying sites other than that occupied by HO_2. Dien, therefore, is the most suitable ligand for the reaction in this point. Ligands of neither higher nor lower ranking positions than dien in the 5 reries are favorable for the reaction, on account of their too strong or too weak coordinate bondings.

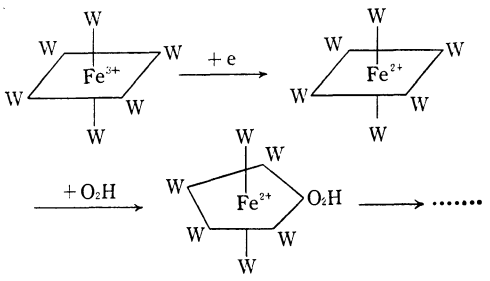
Iron(III) and iron(II) ions have the electron configurations of d^5 and d^6 respectively and ordinarily form complexes with a coordination number of six. According to whether the reaction proceeds through an S_N1 mechanism or through an S_N2 mechanism, there appears an intermediate complex with a coordination number of five or seven respectively. As a complex with the coordination number of five, we must take into account a complex of a trigonal bipyramid with a dsp^3 hybridization orbital and that of a square pyramid with a d^2sp^2 hybridization orbital, and as a complex with the coordination number of seven, that of a pentagonal bipyramid with a d^3sp^3 hybridization orbital. On the basis of the ligand field theory, the energy levels of these d-orbitals can be calculated as shown in Table VII.[18] Accordingly, the ligand field stabilization energies of these complexes and the energy losses, ΔE, of ligand field stabilization on the occasion of the transition from an octahedron to one of other intermediate structures are listed in Table VIII. Since a larger ΔE corresponds to a more difficult transition, the S_N1 mechanism via a square pyramid at the iron(III) state is the most probable in the strong ligand field and the S_N2 mechanism via a pentagonal bipyramid at the iron(II) state in the weak field. Judging from the values of the activation energies and the activation entropies in Table V, the ligands can be divided into two groups: (a) water and ea, which are monodentate ligands with low E and $\Delta(\Delta S)$, and (b) en, dien and trien, which are multidentate ligands with comparatively high E and $\Delta(\Delta S)$. The group a may form weak field complexes with the iron(III) ion (in the case of the Fe-aq^{3+} ion, this is already known from the magnetic and optical data) and make the reaction proceed through the S_N2 mechanism after the complex ion has undergone the acceptance of an electron from the surroundings, while the group b may form strong field complexes, driving the reaction through the S_N1 mechanism. These considerations can be justified as quite plausible from miscellaneous aspects of the activation energies, the activation entropies, the spectrochemical series, the molecular shapes and structures of ligands (whether they are monodentate or multidentate), the ligand field theory, and so forth. The paths of the S_N1 and S_N2 mechanisms may be shown schematically as follows:

16) C. K. Jørgensen, "Absorption Spectra and Chemical Bonding in Complexes," Pergamon Press, Oxford (1962), p. 109.
17) R. J. P. Williams, *J. Chem. Soc.*, **1956**, 8.
18) F. Basolo and R. G. Pearson, "Mechanisms of Inorganic Reactions," John Wiley, New York (1960), p. 55.

S_N1 mechanism (strong field) :



S_N2 mechanism (weak field) :*4



It is especially noteworthy that, since the CN^- ion stands first in the 5 series, the reaction was somewhat suppressed by its stronger coordinate bonding and, therefore, by its greater stabilization in the case of $[Fe^{3+}]$: [en] : $[CN^-] = 1:1:1$,*5 with the result that the reaction rate was lowered as much as 10% and the apparent activation energy was raised as high as 2 kcal./mol. This fact is also consistent with the above explanation. The well-known retardation by the CN^- ions of the coordination of oxygen to hemoglobin in blood might occur in a similar way.

Summary

Hydrogen peroxide is catalytically decomposed by the Fe^{3+} ion, the activity of which is remarkably affected by the kind and the number of ligands coordinated to it. In this paper, the effects of ligands have been kinetically and spectrophotometrically determined and discussed from the view-point of the ligand field theory.

(1) The reaction generally proceeds linearly with time after a certain induction period, and the rate depends upon the pH of the solution.

(2) The reaction rate varies with the kind of the ligand and with its concentration. When $[L]/[Fe^{3+}]$ is equal to unity, the rate decreases in the order: en>dien~(H_2O)~ea >trien>tetraen~dip~phen.

(3) The apparent activation energy of the reaction exhibits a maximum, except in the cases of trien and phen, at the concentration ratio $[L]/[Fe^{3+}] = 1$, and the values of the activation energy at this concentration ratio are in the order: dien~trien>tetraen>en>ea >(H_2O)>phen.

(4) The true activation energy of the reaction catalyzed by the pure iron-complex is calculated from the observation of the stability constants to be in the order: dien>trien>en >(H_2O)>ea, which completely coincides with the order of the activation entropy.

(5) The visible and ultraviolet absorption spectra of Fe-$phen_3^{2+}$ and Fe-$phen_3^{3+}$ as catalysts in the working state were observed, and it was found that there takes place a redox cycle, $Fe^{3+} \rightleftarrows Fe^{2+}$, during the reaction and that phen molecules are gradually decomposed at the same time.

(6) In the course of the reaction, the peaks of the ultraviolet absorption of Fe-$phen_3^{2+}$ and Fe-$phen_3^{3+}$ bring about a slight red shift, which is caused by the coordination of HO_2 to the iron ion.

(7) Judging from a comparison between the activation energy of the reaction and the spectrochemical series of ligands and from the calculation of the stabilization energy due to the ligand field theory, the reaction proceeds through an S_N1 mechanism under the iron(III) oxidation state in the case of strong field complexes and through an S_N2 mechanism under the iron(II) state in the case of weak field complexes.

(8) The reaction is retarded and the activation energy is raised by the addition of the CN^- ion, which strongly coordinates with iron and forms a very strong field complex.

The authors wish to thank President Taro Kaneko and Professor Kiyoshi Tsukida of Kobe Women's College of Pharmacy for allowing them to use a recording spectrophotometer.

Department of Chemistry
Faculty of Science
Kobe University
Nada-ku, Kobe

*4 W means weak ligands, such as water.
*5 The stability constant of the complex containing the CN^- ion is not yet known.

Studies on the Polymerization of Bifunctional Monomers. IV.[*1] *The Intramolecular-Intermolecular Polymerization of 3-Substituted Glutaraldehydes*[*2]

By Chuji Aso and Yuzo AITO

(Received September 17, 1963)

Previously, the present authors found that the concept of intramolecular-intermolecular polymerization, which had been proposed in the polymerization of non-conjugated divinyl compounds,[1] might be applied to the addition polymerization of glutaraldehyde.[2,3]

The polymerization of glutaraldehyde[*3] was also studied by Overberger et al.,[4] Meyersen et al.,[5] and Moyer et al.[6] at almost the same time as by the present authors. These workers, as well as the authors, came to the conclusion that the polymer contained a tetrahydropyran ring as a main structure, although there were a few differences in the polymerization conditions, etc.

Meyersen et al. also described how 3-methylglutaraldehyde and 3-phenylglutaraldehyde were polymerized without a catalyst.[5] However, the catalytic polymerization of these dialdehydes was not reported. The present authors, independently, studied the polymerization of these 3-substituted glutaraldehydes in the absence of a catalyst. Moreover, 3-methyl- and 3-phenylglutaraldehyde were polymerized with a catalytic system of triethylaluminum-water, in order to clarify whether these dialdehydes would yield polymers containing a ring structure similar to that of poly(glutaraldehyde). The influences of substituents and of several additives to the reaction rate were also investigated.

Experimental

3-Methylglutaraldehyde and 3-phenylglutaraldehyde were prepared by hydrolysis of the corresponding 4-substituted 2-ethoxy-3, 4-dihydropyrans.[8] 3-Methylglutaraldehyde: b. p. 87.0 ~ 88.0°C/21.0 mmHg, n_D^{25}, 1.4365. Found: C, 62.51; H, 8.84. Calcd. for $C_6H_{10}O_2$: C, 63.13; H, 8.83%. 3-Phenylglutaraldehyde: b. p. 129.0~131.5°C/4.5 mmHg, n_D^{14}, 1.5355. Found: C, 74.48; H, 7.19. Calcd. for $C_{11}H_{12}O_2$: C, 74.97; H, 6.87%.

The catalyst, solvents and polymerization procedures have been previously described.[3] The viscosities of the soluble polymers were determined in benzene at 30°C, using a modified Ubbelohde viscometer. Molecular weights were measured by Rast's method (solvent: camphene), and the infrared spectra, with a Nippon Koken model 301 spectrophotometer.

The pendant aldehyde content in the polymers was determined by the aid of infrared spectroscopy at the 1730 cm^{-1} band, which is characteristic of the carbonyl group.[3]

Results and Discussion

3-Substituted glutaraldehyde was polymerized at a low temperature to a white solid by using a triethylaluminum-water system as the catalyst. Some of these results are listed in Table I. Polymers in general consist of soluble as well as of insoluble fractions in benzene. The properties of the soluble polymers are shown in Table II.

The infrared spectra of the soluble and the insoluble fractions of poly(3-substituted glutaraldehydes) were quite similar. The infrared spectra of the soluble fraction of 3-methyl- and 3-phenylglutaraldehyde polymers are shown in Figs. 1 and 2 respectively. A very weak band was still observed at 1730 cm^{-1} (C=O band). However, quantitative comparison of the carbonyl bands of these soluble polymers with those of monomers and some monoaldehydes suggests that the pendant aldehyde content of the polymers is very low. Moreover, the absorption bands of these polymers in the

*1 Contribution No. 51 from the Department of Organic Synthesis, Faculty of Engineering, Kyushu University, Fukuoka, Japan.

*2 Partly presented at the 16th Annual Meeting of the Chemical Society of Japan, Tokyo, April, 1963.

1) G. B. Butler and R. J. Angelo, *J. Am. Chem. Soc.*, **79**, 3128 (1957); C. S. Marvel and R. D. Vest, ibid., **79**, 5771 (1957); etc.

2) C. Aso and Y. Aito, This Bulletin, **35**, 1426 (1962).

3) C. Aso and Y. Aito, *Makromol. Chem.*, **58**, 195 (1962).

*3 Recently, Yokota et al. reported the polymerization of glutaraldehyde and 3-methylglutaraldehyde through the Tischenko reaction by using the aluminum alkoxide as a catalyst.[7]

4) C. G. Overberger, S. Ishida and H. Ringsdorf, *J. Polymer Sci.*, **62**, s1 (1962).

5) K. Meyersen, R. C. Schulz and W. Kern, *Makromol. Chem.*, **58**, 204 (1962).

6) W. W. Moyer, Jr., and D. A. Grew, *J. Polymer Sci., Polymer Letters*, **1**, 29 (1963).

7) K. Yokota, Y. Ito and Y. Ishii, *J. Chem. Soc. Japan, Ind. Chem. Sec. (Kogyo Kagaku Zasshi)*, **66**, 1112 (1963).

8) R. I. Longley, Jr., and W. S. Emerson, *J. Am. Chem. Soc.*, **72**, 3079 (1950); R. I. Longley, Jr., W. S. Emerson and T. C. Shafer, ibid., **74**, 2012 (1952).

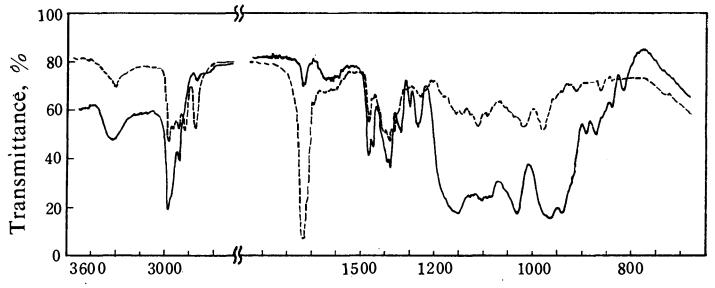
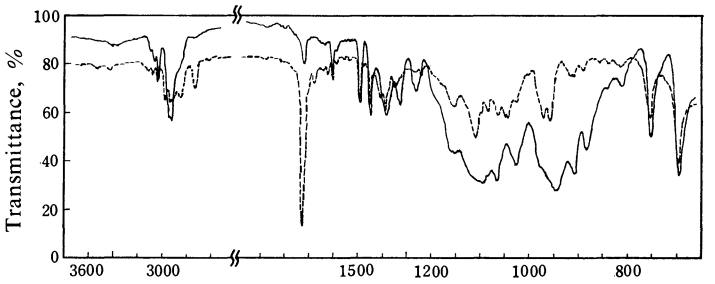


Fig. 1. Infrared spectra of 3-methylglutaraldehyde (in liquid film; - - -) and poly(3-methylglutaraldehyde) (in KBr disk; ——).



Fig, 2. Infrared spectra of 3-phenylglutaraldehyde (in liquid film; - - -) and poly(3-phenylglutaraldehyde) (in KBr disk; ——).

TABLE I. POLYMERIZATION OF 3-METHYLGLUTARALDEHYDE AND 3-PHENYLGLUTARALDEHYDE WITH TRIETHYLALUMINUM-WATER CATALYST (−78°C, IN TOLUENE)

No.[a]	Monomer concn. g./ml.	Catalyst concn. mol.% to monomer	Time hr.	Total conversion %	Soluble fraction[b] %
M-1	0.050	5.60	44.0	9.2	30.5
M-2	0.083	5.87	39.5	14.9	29.6
M-24	0.100	5.02	26.0	13.3	32.2
Ph-12	0.100	5.03	21.0	54.5	80.0
Ph-13	0.050	4.95	25.0	40.2	99.0

a) M: Poly(3-methylglutaraldehyde) Ph: Poly(3-phenylglutaraldehyde)
b) Fraction of the polymer, soluble in benzene.

TABLE II. PROPERTIES OF SOLUBLE POLYMERS OBTAINED BY CATALYST SYSTEM OF TRIETHYLALUMINUM-WATER

No.	M. p. °C	η_{sp}/C[a]	[CHO][b] %	Molecular weight
M-1a	35～ 44	—	11.0	1900～2500
M-2a	35～ 40	—	15.8	1000～1200
M-24a	115～120	0.18	18.3	—
Ph-12a	93～ 97	0.07	6.1	—
Ph-13a	87～ 96	0.06	23.3	—

a) η_{sp}/C (C=0.150 g./dl. in benzene, 30°C)
b) Pendant aldehyde content determined by the infrared spectroscopy.

1000～800 cm^{-1} region resemble those of the 4-substituted 2-ethoxytetrahydropyrans chosen as model compounds. These facts suggest that the polymer formed by the triethylaluminum-water catalyst consists also of recurring tetrahydropyran rings, as Meyersen et al. indicated in the case of spontaneous polymerization.[5]

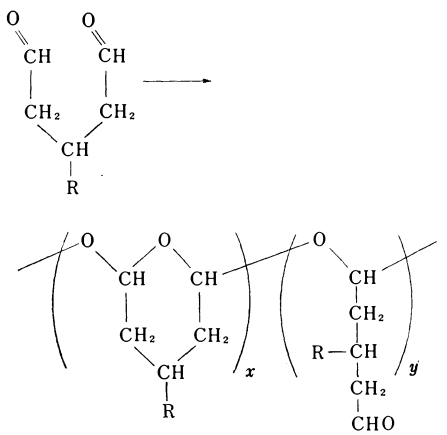
3-Substituted glutaraldehydes changed spontaneously to glassy materials at room temperature or in an ice-box. After repeated reprecipitations, white, solid polymers were obtained. Some properties of these polymers are shown in Table III.

TABLE III. SOME PROPERTIES OF SPONTANEOUS POLYMERS OF 3-METHYLGLUTARALDEHYDE AND 3-PHENYLGLUTARALDEHYDE

No.	M. p. °C	$[\eta]$ dl./g.	[CHO] %	Molecular weight
M-4	56～67	—	8.7	700～800
M-5	62～67	0.03	8.1	—
Ph-2	83～86	—	16.3	～700
Ph-3	79～82	0.03	17.6	—

Since the infrared spectra of the polymers obtained spontaneously are almost in accordance with those of the polymers obtained with a catalyst, the structure of the former is considered to be substantially the same as that of the latter.

As mentioned above, the solubility, the fusibility, the low pendant aldehyde group content and the resemblance of the infrared spectrum of the polymer to those of the model compounds suggest that the ring formation occurs in the course of the polymerization of 3-substituted glutaraldehyde and that the polymer mainly consists of the tetrahydropyran ring. Therefore, polyglutaraldehydes obtained by the polymerization, with or without a catalyst, are probably polyethers with the following structures:



where R is H, CH_3, or C_6H_5. As the content of the ring unit in the polymer is high, the polymerization is considered to proceed mainly through alternative intramolecular cyclization and intermolecular propagation reactions. Succinaldehyde seems also to polymerize through this mechanism.[9]

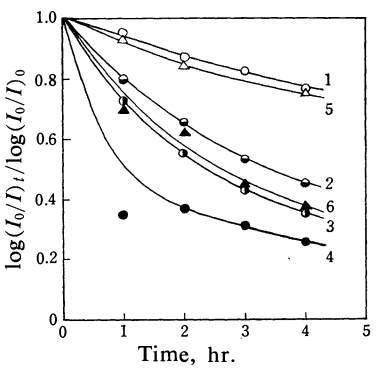


Fig. 3. Influence of additives in polymerization system.
1: Glutaraldehyde (non-additives)
2: Glutaraldehyde (5% of phenol was added)
3: Glutaraldehyde (5% of benzyl alcohol was added)
4: Glutaraldehyde (10% of water was added)
5: 3-Methylglutaraldehyde (non-additives)
6: 3-Methylglutaraldehyde (5% of ethanol was added)

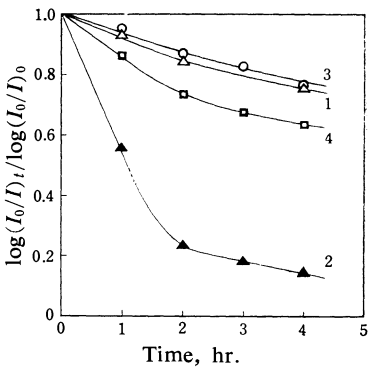


Fig. 4. Influence of polymerization temperature and substituents.
1: 3-Methylglutaraldehyde, at 25°C
2: 3-Methylglutaraldehyde, at 59°C
3: Glutaraldehyde, at 25°C
4: 3-Phenylglutaraldehyde, at 25°C

The infrared absorption intensity due to the carbonyl group of aldehyde was measured during the spontaneous polymerization under given conditions. The ratio of the intensity at time t to that at $t=0$ was plotted against the time.

The rate of consumption of the aldehyde group was markedly accelerated by the addition of a small quantity of water, ethanol or benzyl alcohol, as shown in Fig. 3. The infrared spectrum of the polymer formed spontaneously in the presence of benzyl alcohol shows the presence of a benzyl group in the polymer chain. Thus, these added substances seem to influence the initiation of the polymerization. The polymerization temperature and the substituent at the β-position to the aldehyde group also influenced the rate of aldehyde consumption (Fig. 4). The polymerization mechanism, however, is now being investigated; the details will be reported in the future.

The authors wish to express their gratitude to the Asahi Glass Technical Aid Association for providing the funds for this investigation and also to the Mitsui Petrochemicals Co., Ltd., for the supply of triethylaluminum.

Department of Organic Synthesis
Faculty of Engineering
Kyushu University
Fukuoka

9) C. Aso, Y. Aito and A. Furuta, presented at the 12th Annual Meeting of the High Polymer Chemical Society of Japan, Tokyo, May, 1963.

The Absolute Configuration at C_7 of α- and β-Desmotroposantonin[1]

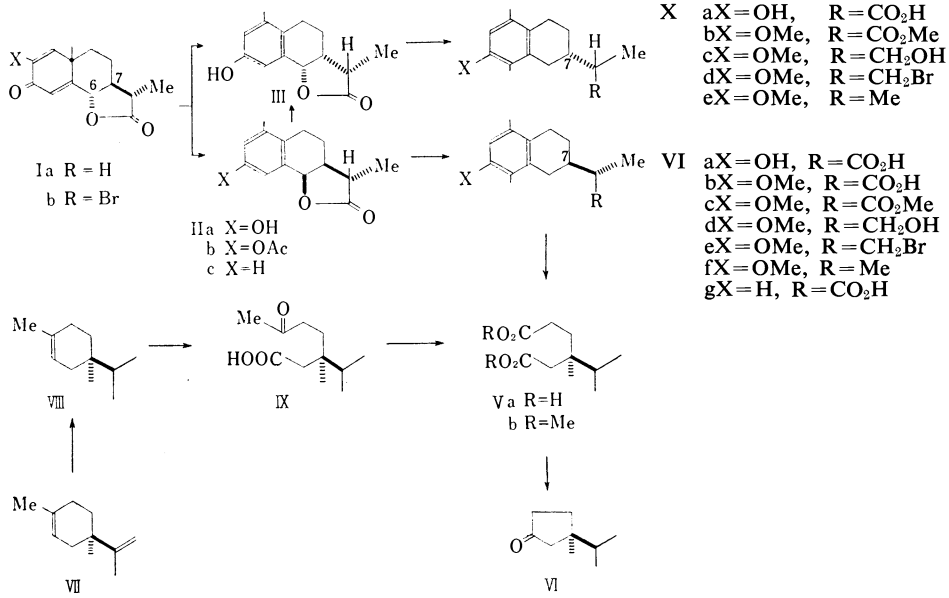
By Masao NAKAZAKI and Kiyoshi IKEMATSU

(Received September 21, 1963)

Although the bulk of evidence,[2] mainly deduced from the stereochemistry of α- (IIa) and β-desmotroposantonin (III), strongly favors the (R)-configuration at position 11 of (−)-α-santonin (Ia), recent publications[3,4] have confirmed Abe's assignment[5] of the (s)-configuration at this center.

Not only to settle this discrepancy, but also in order fully to understand the mechanism of the well-known peculiar cycle of rearrangements in the desmotroposantonin series,[6] the determination of the absolute configuration of α- and β-desmotroposantonin, which have not been established on a firm ground, seems imperative.

Acetyl (−)-α-desmotroposantonin (IIb) prepared from (−)-α-santonin following Huang-Minlon's procedure[7] was first hydrolyzed to (−)-α-desmotroposantonin (IIa), which was then reduced with zinc powder in acetic acid to afford (+)-α-desmotroposantonous acid (IVa).[8] After methylation with dimethyl sulfate, the methyl ether IVb which resulted was esterified with diazomethane to the methyl ester IVc. The methyl ester of (+)-α-desmotroposantonous acid methyl ether was reduced with lithium aluminum hydride to the alcohol IVd, which was converted with phosphorus tribromide/pyridine to the bromide IVe. The bromide was refluxed with lithium aluminum hydride to afford the methyl ether IVf; b. p. 145~155°C/3 mmHg, n_D^{29} 1.5328, $[\alpha]_D^{25}$ +60.0° (in ethanol). Exhaustive ozonolysis of the methyl ether IVf, followed by



1) A preliminary commncication has appeared in this Bulletin, **35**, 1904 (1962).

2) Cf. inter alia. W. Cocker and T. B. H. McMurry, *Tetrahedron*, **8**, 181 (1960), and the literatures cited in our preceding paper on the absolute configuration of (−)-α-santonin.

3) D. H. R. Barton, T. Miki, J. T. Rinhey and R. J. Wells, *Proc. Chem. Soc.*, **1962**, 112; J. D. Asher and G. A. Sim, ibid., **1962**, 111.

4) M. Nakazaki and H. Arakawa, ibid., **1962**, 152.

5) Y. Abe, T. Miki, M. Sumi and T. Toga, *Chem. & Ind.*, **1956**, 953; T. Miki, *J. Pharm. Soc. Japan* (*Yakugaku Zasshi*), **75**, 416 (1955).

6) J. Simonsen and D. H. R. Barton, "The Terpenes," II Ed., Vol. III, Cambridge Univ. Press (1955), p. 263.

7) Huang-Minlon et al., *J. Am. Chem. Soc.*, **65**, 1780 (1943).

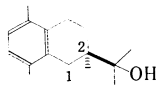
8) Elsevier's "Encyclopedia of Organic Chemistry," Series III, Vol. 12B, Elsevier Pub. Co. Inc., New York-Amsterdam (1948), pp. 3471, 3478.

peracetic acid oxidation, gave crude β-isopropyladipic acid (Va),[9] which was purified via dimethyl ester Vb. Heating the acid with barium hydroxide at 280~300°C following the procedure of Burger and Macbeth[10] gave 3-isopropylcyclopentan-1-one (VI), which was directly converted into the semicarbazone; m. p. 181~183°C, $[\alpha]_D^{31}$ +43.8° (in ethanol). Its identity with (R)-(+)-3-isopropylcyclopentan-1-one semicarbazone (m. p. 186~187°C, $[\alpha]_D^{26}$ +65.2° (in ethanol)) prepared from (R)-(+)-limonene (VII)[11] (via (+)-dihydrolimonene (VIII) and (+)-3-isopropylheptan-6-onic acid (IX)) was established by a mixed melting point comparison (181~183°C) and by a comparison of their infrared absorption spectra (in chloroform).

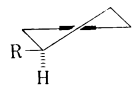
This correlation established the (R)-configuration at position 7. The fact that (+)-β-desmotroposantonin (III) has the opposite configuration from (−)-α-desmotroposantonin (IIa) at C_7 was confirmed by the conversion of the former, through the same sequence of conversions described in the α-series, into the enantiomer Xe (b. p. 110~120°C/0.1 mmHg, n_D^{29} 1.5322, $[\alpha]_D^{28}$ −65.2° (in ethanol)), which showed an infrared spectrum superimposable on that of the methyl ether IVf from (−)-α-desmotroposantonin (IIa).

It is of interest to note here that the compounds derived from (+)-α-desmotroposantonous acid (IVa) as well as from hyposantonous acid (IVg) and occidol (XII),[15] all of which have the same (R)-configuration at C_7, show dextrorotation, whereas the compounds Xa, Xb, Xc, Xd and Xe from the (−)-β-desmotroposantonous acid series all exhibit the opposite rotation (see the Experimental section).

Mill's rule[12] and Brewster's[13] model of optical activity extended to endocyclic compounds show that the cyclohexene derivative with a configuration similar to that of (+)-limonene (VII) exhibits dextrorotation. It is apparent from our experimental results that their rules can be extended to the tetralin series: *2-(R) substituted tetralin XII is dextrorotatory provided that the optical rotatory power of the conformational asymmetry XII is not exceeded by that of the side chain.*

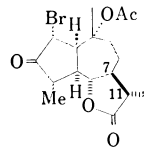


XI



XII

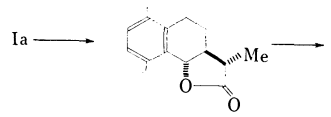
Thus having had established the absolute configuration of the C_7 asymmetric centers of α- and β-desmotroposantonin, our attention was next directed to correlating these centers of asymmetry with that of C_7 of (−)-α-santonin. The C_7 asymmetric center in (−)-α-santonin has been assigned the (R)-configuration[2] by correlating it with (+)-dihydrocarvon via carrison through a long series of degradations and synthetic works involving at least 20 compounds, among them artemisin, ψ-santonin, β-selinene, α- and β-eudesmol and costol. Since these natural compounds related to (−)-α-santonin are important relay substances in the stereochemistry of eudesmane-type sesquiterpene, it seems not superfluous to add other evidence to support the (R)-configuration at the asymmetric center C_7 of (−)-α-santonin. Especially is this so when it is reflected that the absolute configuration of C_{11} of bromoiso-α-photosantonic lactone acetate (XIII)[14] (and consequently that of santonin) has been assigned by X-ray crystal analysis with reference to this C_7 asymmetric center.



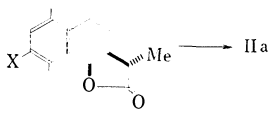
XIII

Hyposantonin (XIV)[15] derived from (−)-α-santonin under very mild conditions, which possesses the original asymmetric configurations of C_6, C_7 and C_{11} of santonin intact, appears a convenient intermediate with which to link (−)-α-santonin and α-desmotroposantonin. During the course of their study of hyposantonylquinol, Asahina and Momose[16] nitrated hyposantonin to obtain a mononitro derivative which they named 2-nitrohyposantonin. Since the same compound could be prepared from isohyposantonin (XVa), which has a cis lactone ring, it is evident that the epimerization at C_6, reminiscent of the process from santonin to α-desmotroposantonin, intervenes during the nitration, implying that the proper name should be 2-nitroisohyposantonin (XVb). The diazotization of 2-amino-isohyposantonin (XVc) prepared from the nitro compound XVb afforded (−)-α-desmotroposantonin (IIa). Thus, this sequence of reactions seems to provide evidence that (−)-α-desmotroposantonin (IIa) and isohyposantonin (XVa) have the same absolute configuration at C_7 and C_{11}.

9) J. v. Braun and G. Werner, *Ber.*, **62**, 1050 (1929).
10) G. Burger and K. Macbeth, *J. Chem. Soc.*, **1946**, 145.
11) A. J. Birch, *Ann. Reports*, **47**, 191 (1950).
12) J. A. Mills, *J. Chem. Soc.*, **1952**, 4975.
13) J. H. Brewster, *J. Am. Chem. Soc.*, **81**, 5493 (1959).
14) J. D. M. Asher and G. A. Sim, *Proc. Chem. Soc.*, **1926**, 111.
15) Ref. 8, p. 3456 and M. Nakazaki, This Bulletin, **35**, 1387 (1962).
16) Y. Asahina and T. Momose, *Ber.*, **71**, 1421 (1938).



XIV



XVa R=H
b R=NO_2
c R=NH_2

However, since Asahina and Momose used rather severe conditions (concentrated nitric acid and concentrated sulfuric acid in acetic acid) in the nitration reaction, during the nitration a rearrangement similar to (−)-α-desmotroposantonin (IIa)→(+)-β-desmotroposantonin (III) may intervene simultaneously. To clarify this point, 2-aminoisohyposantonin (XVc) was diazotized; the deamination of the diazonium compound with hypophosphorous acid[17] gave back the starting compound, isohyposantonin (XVa) implying that no such inversion occured. Thus, the configuration of (−)-α-santonin at C_7 can be related with that of (−)-α-desmotroposantonin; this (R)-configuration at C_7 of (−)-α-santonin is completely in accord with the results obtained from the X-ray crystal analysis of 2-bromosantonin (Ib) by the Glasgow group.[18]

Experimental*

A) The α-Desmotroposantonin Series

Acetyl (−)-α-Desmotroposantonin (IIb).[7]—Twenty grams of (−)-α-santonin was slowly stirred into a mixture of 120 cc. of acetic anhydride and 2 cc. of concentrated sulfuric acid at room temperature. After the solution had been kept at room temperature overnight, the crystals which precipitated were filtered and washed with water. The mother liquor was added to 500 cc. of ice water, and the crystals which deposited were filtered and washed with water. Recrystallization of the combined crystals from ethanol gave 20 g. of IIb (m. p. 155～156°C (lit.[7] m. p. 156～157°C)).

(−)-α-Desmotroposantonin (IIa).[7]—To 20 g. of acetyl-(−)-α-desmotroposantonin (IIb), a mixture of 20 g. of potassium hydroxide, 50 cc. of water and 200 cc. of methanol was added. The mixture was refluxed for 5 hr, and the methanl was distilled off. The residue was dissolved in 200 cc. of water, and the solution was made acidic with concentrated hydrochloric acid. After the crystals had been filtered and washed with water, they were recrystallized from ethanol to give 12 g. of IIa (m. p. 190～192°C). The mother liquor was concentrated to yield the second crop of crystals (m. p. 186～190°C (lit.[7] m. p. 194°C)).

(+)-α-Desmotroposantonous Acid (IVa).[19]—Into a mixture of 50 g. of (−)-α-desmotroposantonin (IIa), 1.2 l. of acetic acid and 100 cc. of water, 300 g. of zinc powder were vigorously stirred (Vibro-Mischer). After the solution had been refluxed and stirred for 16 hr., the excess zinc powder was filtered, and the zinc power was washed with hot acetic acid on a Buchner funnel. The combined filtrate and washing were concentrated under reduced pressure. The crystals which were precipitated by adding water to the residue were collected and washed with water. Recrystallization from ethanol yielded 44 g. of (+)-α-desmotroposantonous acid (IVa) (m. p. 176～178°C). Further recrystallization from 75% acetic acid yielded needles (39 g.) melting at 177～179°C; $[\alpha]_D^{25}$+77.6° (*c* 1.81 in ethanol), (lit.[8] m. p. 182～183°C, $[\alpha]_D$+75° (in ethanol)).

(+)-α-Desmotroposantonous Acid Methyl Ether (IVb).—In an atmosphere of nitrogen, 21 g. of (+)-desmotroposantonous acid (IVa) was dissolved in 127 cc. of 6.5% aqueous sodium hydroxide. When 3.4 g. of dimethyl sulfate was added to the stirred solution, a solid deposited which was then dissolved by adding 70 cc. of water and heating the solution at 50°C. In a period of 1 hr., 10.2 g. of dimethyl sulfate was added; the reaction mixture was then stirred at 80°C for 2 hr. After 20 cc. of 6.5% of aqueous sodium hydroxide was added, the reaction mixture was made acidic with concentrated hydrochloric acid and kept in a refrigerator overnight. The crystals which were deposited were filtered and washed with water. The product weighed 22 g. and melted at 114～117°C after recrystallization from 70% acetic acid; $[\alpha]_D^{25}$+69.5° (*c* 1.21 in ethanol) (lit.[8] m. p. 116～117°C, $[\alpha]_D^{26}$+72.2° (in ethanol)).

Methyl Ester of (+)-α-Desmotroposantonous Acid Methyl Ether (IVc).—A solution of 34 g. of (+)-α-desmotroposantonous acid methyl ether in 60 cc. of methanol was added into a chilled solution of diazomethane in ether prepared from 42 g. of nitrosomethylurea, and the mixture was kept in a refrigerator overnight. The excess diazomethane was decomposed with a small amount of acetic acid. After the reaction mixture had been washed with saturated aqueous sodium chloride to remove the methanol, it was dried over calcium chloride and freed from the solvent. The residue was distilled to yield 33.5 g. of an oil, b. p. 128～140°C/10^{-2} mmHg, n_D^{27} 1.5293, $[\alpha]_D^{27}$+82.0° (*c* 1.82 in ethanol).

Found; C, 73.62; H, 8.82. Calcd. for $C_{17}H_{24}O_3$: C, 73.88; H, 8.75%.

The Alcohol IVd.—In a stream of nitrogen, a solution of 33.5 g. of methyl ester IVc in 40 cc. of ether was stirred into suspension of 3.7 g. of lithium aluminum hydride in 350 cc. of anhydrous ether at room temperature. After the reaction mixture had been gently refluxed for 1.5 hr., the excess lithium

17) N. Kornblum, "Organic Reactions," Vol. 2, 262 (1948).

18) J. D. Asher and G. A. Sim, *Proc. Chem. Soc.*, **1962**, 335.

* All melting and boiling points are uncorrected. The analyses were performed in the Microanalytical Laboratory of the Shionogi Pharm. Co. through the courtesy of Dr. Kenichi Takeda, which is gratefully acknowledged.

19) Following the procedure of G. R. Clemo, *J. Chem. Soc.*, **1934**, 1343.

aluminum hydride was decomposed with 5 cc. of ethyl acetate. Water was added until the aluminum hydroxide deposite in an easily filterable state (about 50 cc. of water was required). The aluminum hydroxide was then filtered and washed with ether thrice. The combined ether solution was washed with saturated aqueous sodium chloride, dried over anhydrous magnesium sulfate, and freed from the solvent. When the residue was distilled, 28.1 g. of a viscous colorless liquid (b. p. 160~180°C/10^{-2} mmHg) was collected in a 94% yield. $[\alpha]_D^{27}$+60.8° (*c* 2.90 in ethanol).

Found; C, 77.0; H, 9.7. Calcd. for $C_{16}H_{24}O_2$: C, 77.37; H, 9.74%.

Phenylurethane. — The recrystallization of the phenylurethane, prepared by the usual method, from ethanol gave prismatic crystals; m. p. 125~126°C, $[\alpha]_D^{27}$+47.3° (*c* 0.65 in ethanol).

Found: C, 75.2; H, 8.2. Calcd. for $C_{23}H_{29}O_3N$: C, 75.17; H, 7.95%.

The Bromide IVe.—Into a chilled (−5~10°C) mixture of 12.0 g. of phosphorus tribromide, 1.7 g. of pyridine and 8 cc. of benzene, a mixture of 28.1 g. of the alcohol IVd, 30 cc. of benzene and 0.6 g. of pyridine was stirred over 4 hr., during which time the temperature was kept constant. After being stirred at this temperature for 2 hr., the reaction mixture was warmed on a water bath (40~50°C) for 2 hr. and then poured on 200 g. of crashed ice and extracted with ether. The ether extract was washed with aqueous sodium hydrogen carbonate, water and saturated sodium chloride solution successively, and then dried over calcium chloride. Removal of the solvent gave a residue which was distilled to yield 18.4 g. (51% yield) of a liquid (b. p. 150~160°C/10^{-2} mmHg, n_D^{29} 1.5638, $[\alpha]_D^{28}$+66.4° (*c* 2.24 in ethanol)).

Found: Br, 22.8. Calcd. for $C_{16}H_{23}OBr$: Br, 22.49%.

The Methyl Ether IVf.—Into a slurry of 2.9 g. of lithium aluminum hydride in 30 cc. of anhydrous tetrahydrofuran, a solution of 18 g. of the bromide in 20 cc. of tetrahydrofuran was stirred over a 1/2 hr. period. The exothermic reaction was observed, and the reaction mixture was gently refluxed for another 2 hr. The cold mixture was diluted with 180 cc. of ether, and the excess reducing reagent was decomposed with a small amount of ethyl acetate. The mixture was decomposed by a dropwise addition of water until aluminum hydroxide was deposited in an easily filterable state. The ether solution was filtered, and the collected aluminum hydroxide was washed with ether three times. The ether filtrate and washings were combined and washed with water and with a saturated sodium chloride solution. After being dried over calcium chloride, the solution was concentrated to afford the residue, which was distilled to give 12.0 g. of a liquid (92.4% yield) (b. p. 145~155°C/3 mmHg, n_D^{29} 1.5328, $[\alpha]_D^{25}$+60.0° (*c* 2.52 in ethanol)).

Found: C, 83.0; H, 10.4. Calcd. for $C_{16}H_{24}O$: C, 82.70; H, 10.41%.

The Exhaustive Ozonolysis of the Methyl Ether IVf.—A stream of ozone (about 2%) was passed into a solution of 6.0 g. of the methyl ether IVf in 70 cc. of acetic acid for 30 hr. at room temperature (28~29°C). To this reaction mixture, 5 cc. of 30% hydrogen peroxide was added, and the mixture was allowed to stand at room temperature overnight. After the mixture had been warmed on a water bath for 2 hr., a small amount of palladium on a carbon catalyst was added to decompose the excess peracetic acid. The mixture was heated on a water bath for 2 hr. and freed from the catalyst. Concentration under reduced pressure gave a sirup which was dissolved in 50 cc. of water and again concentrated at reduced pressure. This process of evaporation was repeated twice in order to remove the acetic acid. The brown, viscous sirup was dissolved in 30 cc. of methanol and treated with 150 cc. of a cold ether solution of diazomethane prepared from 13 g. of nitrosomethylurea. After being kept in a refrigerator overnight, the solution was washed with water and a saturated aqueous calcium chloride solution and dried over calcium chloride. Removal of the solvent gave a viscous brown liquid which was distilled to afford 1.9 g. of the ester Vb (b. p. 100~105°C/5 mmHg (bath temp. 140~150°C), n_D^{30} 1.4493). The ester Vb was saponified by heating it with 2 g. of potassium hydroxide in 20 cc. of methanol containing 0.5 cc. of water for 3 hr. After the methanl had been removed, water was added and the mixture was made strongly acidic with concentrated hydrochloric acid. The solution was saturated with sodium chloride and continuously extracted with ether for 10 hr. When the solvent was removed and the residue was heated with 0.1 g. of barium hydroxide (at 160~180°C for 1 hr., at 180~280°C for 2 hr. and at 280~300°C for 1 hr.), 0.8 g. of a pale yellow liquid with a pleasant smell was obtained. To this oil was added a mixture of 0.7 g. of semicarbazide hydrochloride and 0.8 g. of sodium acetate with a small amount of water; drops of alcohol were also added to remove any turbidity. The crystalline product which separated was recrystallized from ethanol twice and finally from water to give 0.05 g. of fine needles (m. p. 181~183°C, $[\alpha]_D^{31}$+43.8° (*c* 0.48 in ethanol)). A mixed melting point determination with (R)-(+)-3-isopropylcyclopentan-1-one semicarbazone (m. p. 186~187°C, $[\alpha]_D^{26}$+65.2° prepared from (R)-(+)-limonene (vide infra)) was 181~183°C. The infrared spectra of the two compounds in chloroform were indistinguishable.

Found: C, 59.2; H, 8.9; N, 22.7. Calcd. for $C_8H_{17}ON_3$: C, 58.98; H, 9.35; N, 22.93%.

B) β-Desmotroposantonin Series

(+)-β-Desmotroposantonin (III).[20]—A solution of 30 g. of (−)-α-santonin in 180 cc. of fuming concentrated hydrochloric acid, prepared by saturating concentrated hydrochloric acid with dried hydrogen chloride gas at 0~5°C, was sealed in a pressure bottle and kept at 36°C for 2 days, during which time a crystalline solid was deposited. After 1 l. of water had been added to the reaction mixture, the cream-colored crystalline solid was broken up, washed with water, and dried. The product, which weighed 29 g., was recrystallized from about 1 l. of ethanol to yield 20 g. crystals (m. p. 237°C (decomp.)).

20) Following the procedure of G. R. Clemo, *J. Chem. Soc.*, **1930**, 1110, 1114.

Concentration of the mother liquor gave 1.1 g. of the second crop (m. p. 230°C (decomp.), $[\alpha]_D^{26}$ +108° (*c* 0.39 in ethanol)). (lit.[8] decomp. p. 260°C, $[\alpha]_D$ +112.1°)).

(−)-β-Desmotroposantonous Acid (Xa).—Into a refluxing mixture of 31 g. of (+)-β-desmotroposantonin (III) in 950 cc. of acetic acid and 60 cc. of water, 190 g. of zinc powder was vigorously stirred with a Vibro-Mischer. Following the procedure described for the prepartion of IVa, 23 g. of needles (m. p. 174~175°C) were obtained after recrystallization from 70% acetic acid. Concentration of the mother liquor gave the second crop; 2.3 g., m. p. 170~174°C. $[\alpha]_D^{25}$ −56.9° (*c* 1.87 in ethanol) (lit.[21] m. p. 175°C, $[\alpha]_D$ −53.3° (in ethanol)).

Methyl Ester Xb of (−)-β-Desmotroposantonous Acid Methyl Ether.—Twenty grams of sodium hydroxide was dissolved in 400 cc. of water, 280 cc. of which was then added to 25 g. of (−)-β-desmotroposantonous acid (Xa) in an atomosphere of nitrogen. Twenty grams of dimethyl sulfate was stirred into the solution over a 1~1/4 hr. period at room temperature, and the reaction mixture was heated at 70~80°C on a water bath for 2 hr. After the rest of the sodium hydroxide solution had been added, the reaction mixture was refluxed for 1 hr. After it had been acidified with concentrated hydrochloric acid, the viscous semisolid product which deposited was collected and dissolved in ether. The ether solution was washed with water and saturated sodium chloride solution, and dried over anhydrous magnesium sulfate. Removal of the solvent gave a viscous oil which was dissolved in 20 cc. of methanol and treated with 300 cc. of an ether solution of diazomethane prepared from 31 g. of nitrosomethylurea. After being allowed to stand in a refrigerator 1 for 2 days, the excess diazomethane was decomposed with 1 cc. of acetic acid. The solution was washed with saturated aqueous calcium chloride, and dried over calcium chloride. The ether was removed and the residue distilled to give 21.0 g. of a liquid (b. p. 128~135°C/10^{-2} mmHg, n_D^{27} 1.5319, $[\alpha]_D^{27}$ −37.2° (*c* 2.13 in ethanol)).

Found: C, 73.6; H, 8.6. Calcd. for $C_{17}H_{24}O_3$: C, 73.88; H, 8.75%.

The Alcohol Xc.—The reduction of 21.0 g. of the methyl ester Xb with 2.4 g. of lithium aluminum hydride, as described in the preparation of the alcohol IVd, yielded 18 g. (95% yield) of the alcohol Xc (b. p. 160~180°C/10^{-2} mmHg, $[\alpha]_D^{27}$ −74.4° (*c* 3.12 in ethanol)).

Found: C, 76.8; H, 9.7. Calcd. for $C_{16}H_{24}O_2$: C, 77.37; H, 9.74%.

Phenylurethane.—The phenylurethane prepared following the usual method was recrystallized from ethanol to give silky needles (m. p. 106~108°C, $[\alpha]_D^{28}$ −60.2° (*c* 0.93 in ethanol)).

Found: C, 74.9; H, 8.0. Calcd. for $C_{23}H_{29}O_3N$: C, 75.17; H, 7.95%.

The Bromide Xd.—Following the procedure described for the preparation of the bromide IVe, 17 g. of the alcohol Xc was converted into the bromide Xd (12.4 g., 57% yield) (b. p. 197~200°C/3 mmHg, n_D^{27} 1.5640, $[\alpha]_D^{27}$ −41.3° (*c* 1.58 in ethanol)).

Found; Br, 23.42. Calcd. for $C_{16}H_{23}OBr$: Br, 22.49%.

The Methy Ether Xe.—The reaction of 12.0 g. of the bromide Xd with 1.7 g. of lithium aluminum hydride in tetrahydrofuran, as described for the preparation of the methyl ether IVf, gave 8.0 g. of the methyl ether Xe, a colorless liquid (93% yield) (b. p. 110~119°C/0.1 mmHg, n_D^{29} 1.5322, $[\alpha]_D^{28}$ −65.1° (*c* 1.51 in etanol)). The infrared absorption spectra of the methyl ether IVf of the α-desmotroposantonin series and the methyl ether Xe of the β-desmotroposantonin series were indistinguishable.

Found: C, 82.6; H, 10.2. Calcd. for $C_{16}H_{24}O$: C, 82.70; H, 10.4%.

Isohyposantonin (XVa)[22].—To a solution of 3 g. of barium hedroxide hydrate in 30 cc. of water 0.5 g. of hyposantonin XIV was added; the mixture was warmed on a water bath to gave a clear solution. The solution was made acidic with concentrated hydrochloric acid to precipitate isohyposantonin. The crystalline isohyposantonin which separated was recrystallized from ethanol to yield prismatic crystals (m. p. 168~171°C, $[\alpha]_D^{32}$ −76.6° (*c* 0.51 in benene) (lit.[22] m. p. 167.5~168.5°C, $[\alpha]_D$ −73.7° (in benzene)).

2-Nitroisohyposantoin (XVb).[16]—The nitration of 1.5 g. of hyposantonin in 5 cc. of acetic acid with a mixture of 6 g. of concentrated sulfuric acid and 3 g. of concentrated nitric acid at 20~30°C gave 0.85 g. of needles after recystallization from ethanol (m. p. 174~176°C (lit.[16] m. p. 183°C)).

2-Aminoisohyposantonin (XVc).[16]—The reduction of XVb (0.85 g.) with 5 g. of zinc powder and 0.6 g. of ammonium chloride in ethanol afforded 0.7 g. of crystals after washing and drying. Recrystallization from benzene yielded 0.65 g. of a pale yellow powderlike crystalline material (m. p. 188~191°C, $[\alpha]_D^{31}$ −168° (*c* 0.60 in benzene) (lit.[16] m. p. 193°C, $[\alpha]_D^{24}$ −165.7° (in chloroform)).

The Deamination of 2-Aminoisohyposantonin (XVc) to Isohyposantonin (XVa).—Into a chilled solution of 0.40 g. of 2-aminoisohyposantonin (XVc) in 15 cc. of 1 N hydrochloric acid, a solution of 0.12 g. of sodium nitrite in 2 cc. water was stirred. The reaction mixture was chilled at −5~0°C, and 8 cc. of 40% hypophosphorous acid was added over a 1 hr. period. After the solution had been allowed to stand in a refrigerator for 24 hr., the crystalline product was filtered, washed with water, and dried. Recrystallization from ethanol gave 0.20 g. of crystals (m. p. 168~169°C). A mixed melting point with isohyposantonin (m. p. 168~171°C) was 168~170°C. The infrared spectra in chloroform of the product and isohyposantonin were indistinguishable. $[\alpha]_D^{31}$ −73.6° (*c* 0.65 in benzene).

Found: C, 77.9; H, 7.8. Calcd. for $C_{15}H_{18}O_2$: C, 78.23; H, 7.88%.

(+)-3-Isopropylheptan-6-onic Acid (IX).—A stream of ozone (2%) was passed into a mixture of 80 cc. of acetic acid and 19.0 g. of (+)-dihydrolimonene (VIII) (b. p. 64~65°C/20 mmHg. $n_D^{21.5}$ 1.4555, $[\alpha]_D^{21.5}$ +100.8° (neat)) for 4 hr. at room temperature. The reaction mixture was diluted

21) Ref. 8, p. 3478.
22) Ref. 8, p. 3458.

with 10 cc. of water and oxidized by dropwise addition of a solution of 33 g. potassium permanganate in 500 cc. of water at 70°C with stirring. The oxidation mixture was filtered, and the manganese dioxide was washed with hot water. The washing was combined with the fiiltrate and was made acidic with concentrated hydrochloric acid and then extracted with ether. The ether extract was freed of the solvent and the residue was distilled to give 95 g. of a liquid (b. p. 132~137°C/0.8 mmHg, n_D^{22} 1.4557).

(+)-**3-Isopropylcyclopentan-1-one (VI) Semicarbazone.**[10]—A solution of 2.0 g. of the ketocarboxylic acid IX in 20 cc. of 5% sodium hydroxide was added to a chilled hypobromite solution prepared from 9 g. of bromine, 6 g. of sodium hydroxide and 100 cc. of water. After having been stirred for 4 hr., the reaction mixture was washed with ether and was then made acidic with concentrated hydrochloric acid. The mixture was continuously extracted with ether for 30 hr., and the extract was dried over anhydrous sodium sulfate. Removal of the solvent gave an oil which was distilled to give 0.4 g. of a liquid (b. p. 162~175°C/0.6 mmHg). A mixture of this crude β-isopropyladipic acid (Va) and 0.05 g. of barium hydroxide hydrate was heated in a salt bath. When the mixture was heated at 200~260°C for 1/2 hr. and then at 260~300°C for 2 hr., a pale yellow liquid was collected which was directly converted into the semicarbazone with 0.24 g. of semicarbazide hydrochloride, 0.29 g. of sodium acetate and a small amount of water. The crystals which deposited were collected and recrystallized from ethanol to give fine needles (m. p. 186~187°C, $[\alpha]_D^{26}$ +65.2° (*c* 0.62 in ethanol)).

Found: C, 58.8; H, 9.2; N, 22.8. Calcd. for $C_9H_{17}ON$: C, 58.98; H, 9.35; N, 22.93%.

The authors are very grateful to Mr. Eiichi Togashi, Shiono Koryo Kaisha, for his generous gift of (+)-limonene, and to the Nitto Kasei Co. for its financial support.

This work was partilally supported by a grant-in-aid for fundamental scientific research from the Ministry of Education, to which the authors' thanks are due.

Department of Chemistry
Faculty of Engineering Science
Osaka University
Shibahara, Toyonaka

The Absolute Configuration at C_{11} of Santonin[1]

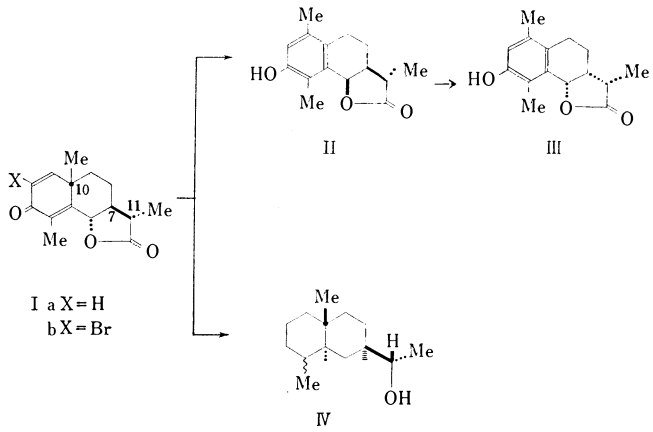
By Masao NAKAZAKI and Hisao ARAKAWA

(Received September 21, 1963)

Although the syntheses of (−)-α-santonin (Ia) and all its possible stereoisomer have been accomplished[2] and although the absolute configurations of the asymmetric centers of C_{10}[3] and C_7[4] have been established unambiguously, that of C_{11} is still in dispute.[4] Deducing mainly from the relative stability of epimeric α- (II) and β-desmotroposantonin (III),[5] Woodward and Yates,[6] Corey[7] and Cocker et al.[4] assigned the (R)-configuration to the C_{11} asymmetric center. The same conclusion was reached by Mitsuhashi[8] after a consideration of the molecular models of santonin and its derivatives as well as of their relative rates of hydrolyses.

Assuming that the stereochemistry of the lactone ring of santonin and the D ring of steroid are isosteric, Miki[9] reached the opposite conclusion, that in santonin the methyl group at C_{11} must have a quasi-equatorial conformation (i.e., the (R)-configuration) and the less stable β-santonin (the C_{11} epimer of Ia) the (S)-configuration. Prelog's atrolactic acid method[10] applied to the alcohol IV derived from santonin added conclusive evidence to support this view.[11] However, the opinions[4] of Cocker et al. have appeared to tend to favor the (R)-configuration at this asymmetic

1) For a preliminary account of this work, see M. Nakazaki and H. Arakawa, *Proc. Chem. Soc.*, **1962**, 151.
2) Y. Abe, T. Harukawa, H. Ishikawa, T. Miki, M. Sumi and T. Toga, *Proc. Japan Acad.*, **28**, 427 (1952); **29**, 113 (1953); **30**, 116, 119 (1954), *J. Am. Chem. Soc.*, **75**, 2567 (1953); **78**, 1416, 1422 (1956).
3) H. Bruderer, D. Arigoni and O. Jeger, *Helv. Chim. Acta*, **39**, 858 (1954); B. Riniker, J. Kalvoda, D. Arigoni, A. Fürst, O. Jeger, A. M. Gold and R. B. Woodward, *J. Am. Chem. Soc.*, **76**, 313 (1954)).
4) For a relevant review, see W. Cocker and T. B. H. McMurry, *Tetrahedron*, **8**, 181 (1960).
5) The correlation of desmotroposantonin series and (−)-α-santonin has not been necessarily established, and this point was discussed in a short communication, M. Nakazaki, This Bulletin, **35**, 1904 (1962).
6) R. B. Woodward and P. Yates, *Chem. & Ind.*, **1954**, 1391.
7) E. J. Corey, *J. Am. Chem. Soc.*, **77**, 1044 (1955).
8) H. Mitsuhashi, *J. Pharm. Soc. Japan* (*Yakugaku Zasshi*), **71**, 1115 (1951).
9) T. Miki, ibid., **75**, 416 (1955).
10) V. Prelog, *Helv. Chim. Acta*, **36**, 308 (1953).
11) Y. Abe, T. Miki, M. Sumi and T. Toga, *Chem. & Ind.*, **1956**, 953.

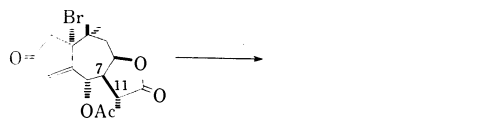


I a X=H
b X=Br

II III IV

center. Moreover, Bose and Chatterjee,[12] formulating a generalized rule permitting the prediction of the absolute configuration of an asymmetric center, have shown that the lactones of the santonin series possess the configuration assigned previously on the basis of thermodynamical studies.

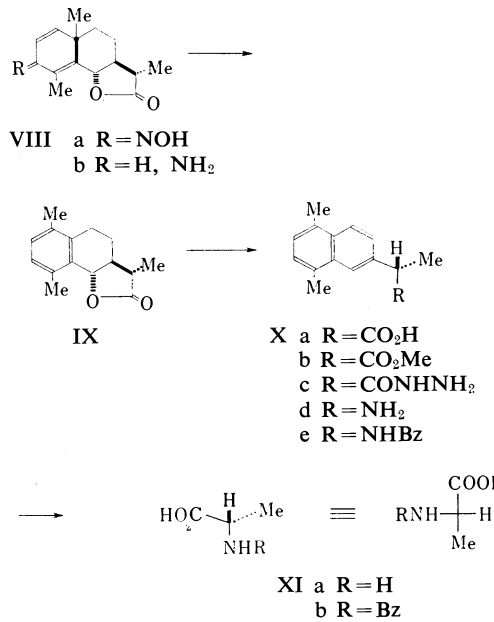
The crystal structure of acetylbromogeigerin (V) determined by the Glasgow group[13] also point to this (R)-configuration when their results are combined with the chemical correlation (via anhydrogeigerin (VI)) between acetylbromogeigerin and artemisin (VII), the relative configuration of which to santonin has been elegantly established by Sumi.[11]



V VI VII

In this communication we will report findings which prove the (s)-configration around this center.

Hyposantonin (IX),[14,15] prepared from santonin oxime (VIIIa) through the dienamine VIIIb by dienamine-benzene rearrangement, was refluxed with iodine in an acetic acid solution for 3 hr., giving santinic acid (Xa),[16] which, after chromatography on silica gel, had an m.p. of 125~127°C ($[\alpha]_D$ +57.3° (in ethanol)).



VIII a R=NOH
b R=H, NH_2

IX

X a R=CO_2H
b R=CO_2Me
c R=$CONHNH_2$
d R=NH_2
e R=NHBz

XI a R=H
b R=Bz

Santinic acid with diazomethane gave the methyl ester Xb, which was converted into the hydrazide Xc. The amine Xd, obtained from this hydrazide by the Curtius rearangement

12) A. K. Bose and B. G. Chatterjee, *J. Org. Chem.*, **23**, 1425 (1958); A. K. Bose. Abstracts of XVth International Congress of Pure and Applied Chemistry, Paris 1957, p. 141. W. G. Dauben, W. K. Hayes, J. S. P. Schwarz and J. W. Farland. *J. Am. Chem. Soc.*, **82**, 2232 (1960) applied this method to ϕ-santonin which has the same configuration around C_{11} as artemisin (VII) and santonin (M. Sumi, *J. Am. Chem. Soc.*, **80**, 4869 (1958); M. Sumi, W. G. Dauben and W. K. Hayes, ibid., **80**, 5704 (1958)) and assigned the (R)-configuraton to this asymmetric center,

13) J. A. Hamilton, A. T. McPhail and G. A. Sim, *Proc. Chem. Soc.*, **1960**, 278. For the chemical correlation between artemisin and geigerin, see D. H. R. Barton and J. T. Pinhey, *Proc. Chem. Soc.*, **1960**, 279.

14) M. Nakazaki, This Bulletin, **35**, 1387 (1962); *Chem. & Ind.*, **1962**, 413. D. Gucci, *Gazz. chim. ital.*, **19**, 367 (1889) (*Chem. Zentr.*, **1889**, II, 595); G. Grassi-Cristaldi, ibid., **19**, 382 (1889) (*Chem. Zentr.*, **1889**, II, 597).

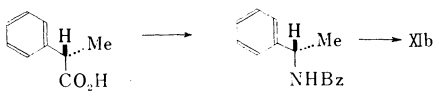
15) Elsevier's "Encyclopedia of Organic Chemistry," Series III, Vol. 12B, Elsevier Pub. Co. Inc., New York-Amsterdam (1948), pp. 3326, 3456.

16) D. Gucci and G. Grassi-Cristaldi, *Gazz. chim. ital.*, **22**, I 35 (1892); J. Simonsen and D. H. R. Barton, "The Terpenes," II Ed., Vol. III, Cambridge Univ. Press (1952), p. 253.

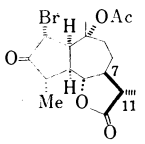
(retention of configuration)[17] was directly benzoylated to the amide Xe (m. p. 172~174°C, $[\alpha]_D$ −12.7° (in chloroform)), which was dissolved in chloroform and exhaustively ozonized for 9 hr. Acetic acid (90%) was added to the remaining solution, and ozonolysis was continued for an additional 12 hr. After oxidation with peracetic acid and concentration, the reaction mixture was hydrolyzed by hot 20% hydrochloric acid and the chloride ion was removed by Amberite IR-4B resin, giving a solution which showed the presence of alanine (XIa) on paper chromatography. The alanine was then converted into (+)-benzoyl-L-alanine (XIb), which showed, after recrystallization from benzene, an m. p. of 148~151°C ($[\alpha]_D$ +7.4° (±4°) (in N potassium hydroxide)) and an infrared spectrum (in dioxane) superimposable on that of an authentic sample.

These facts show that (+)-α-santinic acid (Xa) has the (s)-configuration. Further, since, from a mechanistic standpoint, epimerization at position 11 is inconceivable during the conversion of santonin into the acid, (−)-α-santonin must also have the (s)-configuration at this center, thus confirming the assignment made by Abe et al.[11]

It is of interest to note that during their studies of the stereochemistry of pinacolic deamination, Bernstein and Whitmore[18] converted (+)-hydratropic acid[19] (XII), a phenyl analog of stantinic acid, into (−)-benzoyl-α-phenyl-α-phenylethylamine (XIII), the absolute configration of which was established by the conversion into (+)-benzoyl-L-alanine (XIb) through a sequence of degradations.[20] Eventually, the (s)-configuration was given to (+)-hydratropic acid by this correlation, and the



XII XIII



XIV

observed parallel shift of the optical rotations between these two series of compounds (Xa→Xe and XII→XIII) also confirms the (s)-configuration of santinic acid.[21] The X-ray crystal analysis of bromodihydroiso-α-photosantonic lactone acetate (XIV) by Asher and Sim[22] demonstrated that (−)-α-santonin has the stereo-chemistry Ia with reference to that of the asymmetric carbon atom 7, the absolute configuration of which has been established by a long series of inter-correlations.[4]

The seemingly inconsistent result of Barton et al.[13] (vide supra) could be interpreted by assuming the feasible inversion at C_{11} demonstrated clearly in their synthetic studies of deoxygerin from 8-epiartemisin.[23]

Finally the whole problem was settled by the X-ray analysis of 2-bromo-α-santonin[24] (Ib), which defined its constitution and relative stereochemistry as Ib. Since the absolute configuration at the asymmetric center C_{10} has been firmly established,[3] this result indicates that (−)-α-santonin has the (s)-configuration at C_{11}, confirming the results obtained by chemical methods.[1,11]

Experimental*

(+)-Santinic Acid (Xa).—A solution of 3 g. of hyposantonin (IX)[14,15] and 6 g. of iodine in 55 cc. of acetic acid was refluxed for 3 hr. After 50 cc. of water had been added, the reaction mixture was concentrated under reduced pressure to remove the excess iodine; this process was repeated twice. The residue was dissolved in 200 cc. of ether and washed with water, aqueous sodium thiosulfate and saturated aqueous sodium chloride, and then dried over anhydrous magnesium sulfate. The removal of the solvent gave a viscous oil, which was sublimed at 3 mmHg. The sublimate began to condense at 160°C (bath temperature), and the main fraction came over at 180~220°C. The condensate (2.6 g.) was dissolved in chloroform and chromatographed on a column of 70 g. of silica gel. Elution with chloroform and the removal of the solvent gave 1.5 g. of crystals (m. p. 120~125°C). Recrystallization from aqueous ethanol raised the m. p. to 125~127°C $[\alpha]_D^{20}$ +57.3° (*c* 1.22 in ethanol). (Lit.[16]: m. p. 132~132.5°C, $[\alpha]_D^{16}$ +64.37° (in ethanol)).

(+) Methyl Santinate (Xb).—To an ether solution of diazomethane prepared from 25 g. of nitrosomethylurea, 6.1 g. of (+)-santinic acid were added, and the reaction mixture was allowed to stand overnight. The usual work-up gave 6.1 g. of

17) P. A. S. Smith, "Organic Reactions," Vol. III, 337 (1946); C. K. Ingold, "Structure and Mechanism in Organic Chemistry," Cornell Univ. Press, Ithaca, New York (1953), p. 495; D. J. Cram, "Intramolecular Rearrangements," in M. S. Newman, "Steric Effects in Organic Chemistry," John-Wiley and Sons, Inc., New York (1955), p. 253.

18) H. I. Bernstein and F. C. Whitmore, *J. Am. Chem. Soc.*, **61**, 1325 (1939).

19) On the absolute configuration of hydratropic acid, see W. Klyne, "Progress in Stereochemistry," Vol. I., Butterworth Scientific Pub., London (1954), pp. 187, 195 196.

20) W. Leithe, *Ber.*, **64**, 2827 (1931).

21) This can be predicted also by employing Brewster's model of optical activity, J. H. Brewster, *J. Am. Chem. Soc.*, **81**, 5478 (1959).

22) J. D. M. Asher and G. A. Sim, *Proc. Chem. Soc.*, **1962**, 111.

23) D. H. R. Barton, T. Miki, J. T. Pinhey and R. J. Wells, ibid., **1962**, 112.

24) J. D. Asher and G. A. Sim, ibid., **1962**, 335.

* All melting and boiling points are uncorrected. The analyses were performed in the Microanalytical Laboratory of the Institute of Polytechnics, Osaka City University.

methyl santinate (b. p. 155~157°C/2 mmHg, $[\alpha]_D^{20}$ +70.1° (*c* 1.49 in ethanol)).

Found: C, 78.9; H, 7.6. Calcd. for $C_{16}H_{18}O_2$: C, 79.39; H, 7.49%

The Hydrazide (Xc) of (+)-Santinic Acid.—Six grams of the methyl santinate was stirred into 2.5 g. of hydrazine hydrate (b. p. 117~119°C) at 80°C over a period of 1/2 hr. After a mixture of absolute ethanol and 2 cc. of hydrazine had been added, the reaction mixture was allowed to stand in a refrigerator overnight. The crystals which deposited were filtered and washed with ethanol to yield 1.8 g. of the hydrazide Xc. The filtrate and washing were combined and were refluxed on a water bath for 6 hr. Upon the mixture had cooled in an ice-salt bath, 3.2 g. of crystals were obtained. Recrystallization of the combined crude products from ethanol afforded 4.0 g. of partiallly-racemized hydrazide, which melted at 136°C after sintering at 127~130°C. $[\alpha]_D^{18}$ +25.5° (*c* 1.45 in 95% ethanol).

Found: C, 74.4; H, 7.5; N, 11.8. Calcd. for $C_{15}H_{18}ON_2$: C, 74.35; H, 7.49; N, 11.56%.

Concentration of the mother liquor gave the second crop which was seemingly optically pure and which weighed 0.4 g. (m. p. 151~152°C, $[\alpha]_D^{18}$ +73.2° (*c* 1.01 in ethanol)).

Found: C, 74.4; H, 7.5; N, 11.7. Calcd. for $C_{15}H_{18}ON_2$: C, 74.35; H, 7.49; N, 11.56%.

(−)-*N*-Benzoyl-α-(5, 8-dimethyl-2-naphthyl)ethylamine (Xe).—A mixture of 3.5 g. of the hydrazide Xc ($[\alpha]_D^{18}$ +25.5°), 25 cc. of acetic acid and 50 cc. of benzene was chilled (2~4°C) in an ice bath, and then a solution of 1.2 g. of sodium nitrite in 15 cc. of water was stirred in over a 10 min. period. After water was added, the benzene layer was separated and the aqueous layer was extracted with benzene. The combined benzene extracts were washed with water, aqueous sodium hydrogen carbonate and water successively. After drying over calcium chloride, the benzene solution was heated on a water bath to decompose the acyl azide. Nitrogen was observed to begin to evolve at 50°C, and a vigorous reaction occurred at 60~75°C. After the mixture was refluxed for 15 min., 18 cc. of concentrated hydrochloric acid was added and the mixture was refluxed for 2.5 hr. The crystalline product which deposited was filtered, washed with water and ether, and dried to give 2.1 g. of the hydrochloride of the amine Xd. The hydrochloride of the amine (2.1 g.) was benzoylated with 40 cc. of 10% aqueous sodium hydroxide and 5 cc. of benzoyl chloride. The crude crystalline product was recrystallized from ethanol to afford 2.3 g. of crystals (m. p. 166~172°C). A portion of the benzoyl derivative, after recrystallization from 95% ethanol, melted at 172~174°C, $[\alpha]_D^{19}$ −12.7° (*c* 1.02 in chloroform).

Found: C, 83.0; H, 7.2; N, 4.9. Calcd. for $C_{21}H_{21}ON$: C, 83.13; H, 6.98; N, 4.62%.

The Exhaustive Ozonolysis of the Benzoyl Derivative (Xe).—A stream of ozone was passed into a solution of 2.5 g. of the benzoyl derivative Xe in 60 cc. of chloroform at room temperature. After 9 hr., the solvent evaporated, leaving a residue which was dissolved in 50 cc. of 90% acetic acid; the ozonolysis was then resumed for 13 hr. To the mixture was added 8 cc. of 30% hydrogen peroxide, and the solution was allowed to stand at room temperature for 20 hr. After 50 cc. of water was added, the excess hydrogen peroxide was decomposed by heating it with a small amount of palladium on a carbon catalyst on a water bath for 4.5 hr. After the catalyst had been filtered, the filtrate was freed from the solvent under reduced pressure. The syrup was dissolved in 50 cc. of water and concentrated under reduced pressure; this process was repeated four times. The syrup was dissolved in 20 cc. of water, and an insoluble, brown, viscous material was filtered off. The filtrate was concentrated again under reduced pressure to give a viscous residue which was then dried in a vacuum dessicator over concentrated sulfuric acid overnight. The residue (2.0 g.) was dissolved in 10 cc. of 20% hydrochloric acid and refluxed for 5 hr. The solution was filtered through a layer of Hyflo super cell and treated with Norit. The filtrate was freed from chloride ions with Amberite IR-4B until its pH became about 7. Upon concentration under reduced pressure, a crystalline material deposited which was dissolved in 15 cc. of water and filtered through a layer of Hyflo super cell. A paper chromatogram (acetic acid: butanol: water) exhibited only a single spot corresponding to alanine. After 5 g. of sodium hydrogen carbonate had been added to the aqueous solution, 3.2 g. of benzoyl chloride was added drop by drop over 2 hr. with vigorous shaking at room temperature The turbid reaction mixture was filtered through a layer of Hyflo super cell and made acidic with concentrated hydrochloric acid, and then the mixture was continuously extracted with ether. The removal of the solvent gave a crystalline solid which was dried in a vacuum dessicator. The solid was extracted with four portions of 5 cc. of boiling ligroin to remove the benzoic acid. The insoluble material left in the flask was dissolved in 12 cc. of benzene. Cooling and scratching induced crystallization to afford 10 mg. of (+)-benzoyl-L-alanine (m. p. 148~151°C, $[\alpha]_D^{24}$ +7.4° (±4°) (*c* 0.597 in N potassium hydroxide)). The infrared spectra of this compound and an authentic (+) benzoyl-L-alanine[25] (m. p. 144~146°C, $[\alpha]_D^{15}$ +23.2° (*c* 1.01 in N potassium hydroxide) (Lit.:[25] m. p. 146~148°C, $[\alpha]_D^{20}$ +33.0° (in N potassium hydroxide))) were indistinguishable.

Found: C, 61.9; H, 6.0; N, 7.3. Calcd. for $C_{10}H_{11}NO_3$: C, 62.16; H, 5.74; N, 7.25%.

The authors wish to thanks Drs. Kenichi Takeda and Kaoru Kuriyama, Shinogi Pharm. Co., for their measurement of optical rotation on a Rudolph spectropolarimeter model 200. This work was partially supported by a grant-in-aid for fundamental scientific research from the Ministry of Education, to which the authors' thanks are due.

Department of Chemistry
Facutly of Engineering Science
Osaka University
Shibahara, Toyonaka

25) E. Fischer, *Ber.*, **32**, 2451 (1899).

Studies on Amino-hexoses. VII. The N-Deacetylation of Methyl N-Acetyl α-D-Glucosaminide

By Mamoru FUJINAGA and Yoshio MATSUSHIMA

(Received September 30, 1963)

One of the present authors previously presented a method which might be of use for elucidating aminopolysaccharide structures.[1] The method consisted basically of two procedures, the deacetylation of the *N*-acetyl group in *N*-acetyl aminosugar components and the deamination by nitrous acid of the free amino group thus formed. Anhydrous hydrazine, when used as a deacetylating reagent, had a minimum influence on glycosidic linkages but gave not very satisfactory results. As was shown in the original report,[1] hydrazine treatment of chondroitin sulfate caused considerable degradation of the molecule, and only about 10% of the starting material was recovered as a 90% *N*-deacetylated non-dialysable specimen. Wolfrom and Juliano[2] reported the recovery of a 59~68% *N*-deacetylated specimen in about a 50% yield. Yosizawa and Sato[3-5] observed the formation of 2, 5-anhydrohexose and pentose beside the extensive degradation of the molecule in the hydrazine treatment of the blood group aminopolysaccharide.

The above-mentioned results, obtained in several laboratories, show that more fundamental research into a method is desirable; the present authors chose methyl *N*-acetyl α-D-glucosaminide as the simplest model compound. This compound was treated both with anhydrous and hydrated hydrazine. The deacetylation yield was assayed by Van Slyke nitrogen determination, and the starting compound which remained was assayed by isolation. The results are shown in Table I.

The resultant methyl α-D-glucosaminide showed a marked stability against these reagents in the thin layer chromatography of the reaction mixture, which revealed no spots other than those of the starting compound and the deacetylated product. Refluxing with barium hydroxide for several hours did not give even a trace of any colored substance, though it did give crystalline methyl α-D-glucosaminide in a good yield. Since a convenient method for separating methyl *N*-acetyl-D-glucosaminide anomers has been established,[6] these deacetylation methods afford a conveniet

TABLE I. HYDRAZINOLYSIS OF METHYL *N*-ACETYL α-D-GLUCOSAMINIDE

Reaction time	Reagent	Starting compound[a] mg.	Yield of the deacetylated product, %	Recovery of the starting compound				Total recovery %
				mg.	%	$[\alpha]_D$	m. p., C°	
10 hr.	Hydrazine hydrate (90%)	490.9	70.1	99.5	20.3	+134.8°[b]	189~190	90.4
	Anhydrous hydrazine	512.3	54.2	206.1	40.2	+135.2°[c]	184~186	94.4
20 hr.	Hydrazine hydrate (90%)	498.4	93.2	7.6	1.5	—[e]	—[e]	94.7
	Anhydrous hydrazine	500.1	86.1	60.9	12.2	+134.3°[d]	185~186	98.3

a) The specimen had $[\alpha]_D^{29}$ +136.9° (*c* 1.45, in water) and melted at 188~189°C.
b) *c*=0.920 in water at 28°C.
c) *c*=1.03 in water at 28°C.
d) *c*=0.752 in water at 27°C.
e) Identified by thin layer chromatography.

1) Y. Matsushima and N. Fujii, This Bulletin, **30**, 48 (1957).
2) M. L. Wolfrom and B. O. Juliano, *J. Am. Chem. Soc.*, **82**, 2588 (1960).
3) Z. Yosizawa and T. Sato, *Biochim. Biophys. Acta*, **52**, 591 (1961).
4) Z. Yosizawa and T. Sato, *J. Biochem.*, **51**, 155 (1962).
5) Z. Yosizawa and T. Sato, *Tohoku J. Exp. Med.*, **76**, 100 (1962).
6) Y. Matsushima, T. Miyazaki and J. T. Park, *J. Biochem.*, **54**, 109 (1963).

way to obtain anomerically-pure methyl D-glucosaminides.

Experimental

Hydrazine Treatment and Assay of the Reaction Mixture.—About 500 mg. of methyl *N*-acetyl α-D-glucosaminide and 1.5 ml. of hydrazine were kept in a sealed tube at 100°C for 10 or 20 hr. The reaction mixture was then evaporated in vacuo, and the residue was dissolved in 25 ml. of methanol. In order to remove the acethydrazide which had formed, 8 ml. of benzaldehyde was added and the mixture was refluxed for 15 min. and evaporated in vacuo. Twenty milliliters of water was added to the residue, and the mixture was, after having been washed twice each with petroleum ether and ethyl ether, subjected to Van Slyke nitrogen determination.

The hydrazine treated specimen was, after the removal of the excess hydrazine described above, dissolved in water and passed through a column of Dowex 50 (2×10 cm., H^+ form) and a column of Dowex 1 (2×5 cm., OH^- form). About 200 ml. of the solution thus obtained was evaporated in vacuo to dryness. The crystalline residue was weighed. The methyl *N*-acetyl α-D-glucosaminide thus recovered was identified by melting point determination, specific rotation measurement and thin layer chromatography. The results are shown in Table I and in Fig. 1. A thin layer chromatogram of the recovered substance gave only one spot identical with that of a standard sample of methyl *N*-acetyl α-D-glucosaminide in every run.

The Preparation of Methyl α-D-Glucosaminide and Its Hydrochloride.—*With Hydrazine Hydrate.*—One gram of methyl *N*-acetyl-α-D-glucosaminide and 3 ml. of hydrazine hydrate (90%) were kept in a sealed tube at 100°C for 10 hr. After hydrazine had been removed in vacuo, and after a large amount of chloroform had been added to the residue, the mixture was refluxed for an hour. The chloroform solution was concentrated to a small volume in vacuo and kept in a refrigerator. The jelly product thus obtained was filtered and dried in a desiccator. The yield was 0.54 g. (65.9%). The colorless crystals obtained from absolute ethanol melted at 154~160°C $[\alpha]_D^{30}$ +158.5° (*c* 1.06, in water).

Found: C, 43.69; H, 7.96; N, 7.20. Calcd. for $C_7H_{15}O_5N$: C, 43.51; H, 7.83; N, 7.25%.

The compound was dissolved in water, and the pH of the solution was adjusted to 4.4 with 1 N hydrochloric acid. Evaporation in vacuo gave the hydrochloride as a colorless crystalline powder $[\alpha]_D^{29}$ +131.6° (*c* 1.14, in water).

Found: C, 37.56; H, 6.96; N, 6.88; Cl, 13.97. Calcd. for $C_7H_{16}O_5NCl$: C, 36.61; H, 7.02; N, 6.10; Cl, 15.44%.

With Barium Hydroxide.—The mixture of methyl *N*-acetyl-α-D-glucosaminide (1.0 g.), barium hydroxide (2.5 g., octahydrate) and 18 ml. of water was refluxed for an hour. The mixture was then filtered and saturated with carbon dioxide. After filtration from barium carbonate, the pH of the filtrate was adjusted to 4 by 1 N sulfuric acid. The filtrate free from barium sulfate was passed through a column of Dowex 1 (OH^- form) and the solution was concentrated to dryness in vacuo. The crystalline residue was dissolved in a small volume of hot ethanol and then kept in a refrigerator. The colorless crystals obtained melted at 155~157°C ($[\alpha]_D^{22}$ +157.5°; (*c* 0.838, in water).

Found: C, 43.94; H, 7.98; N, 7.17 (6.94 (Van Slyke)). Calcd. for $C_7H_{15}O_5N$: C, 43.51; H, 7.83; N, 7.25%.

Colorless crystalline hydrochloride ($[\alpha]_{30}^{D}$ +129.2°) (*c* 1.32, in water) was obtained.

Found: C, 36.51; H, 6.99; N, 6.28; Cl, 15.37. Calcd. for $C_7H_{16}O_5NCl$: C, 36.61; H, 7.02; N, 6.10; Cl, 15.44%.

The Identification of the Hydrazinolyzed Product.—As has been described above, the hydrochloride of the deacetylated product gave optical rotation data which were in good agreement with the results obtained by Neuberger and Rivers,[7] who prepared the compound via *N*-carbobenzyloxy-D-glucosamine and gave $[\alpha]_D$ +127°. The melting

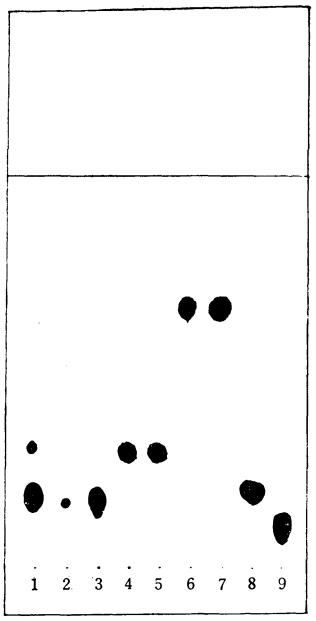


Fig. 1. Thin layer chromatogram of products and authentic specimen.
Moving phase: *n*-BuOH-EtOH-H_2O-NH_4OH (40 : 10 : 49 : 1)
Spray: 5%H_2SO_4
1: Hydrazinolysate freed from acethydrazide
2: Authentic methyl α-D-glucosaminide·HCl[7]
3: Hydrochloride prepared by $Ba(OH)_2$-deacetylation
4: Authentic starting compound
5: Starting compound recovered
6: *N*-Carbobenzyloxy derivative prepared from hydrazinolysate
7: Authentic *N*-carbobenzyloxy compound[7]
8: *N*-Acetyl D-glucosamine
9: D-Glucosamine·HCl

7) A. Neuberger and R. P. Rivers, *J. Chem. Soc.*, 1939, 122.

point determination of our hydrochloride was difficult because of its hygroscopic nature. While thin layer chromatography (Fig. 1) identified our compounds well, a crystalline *N*-carbobenzyloxy derivative was prepared and compared with an authentic specimen synthesized by the Neuberger and Rivers method.

The syrup obtained by treating methyl *N*-acetyl α-D-glucosaminide with hydrazine hydrate was washed repeatedly with hot chloroform until free from acethydrazide. 0.36 g. of the syrup was then dissolved in 15 ml. of water. 0.5 ml. of carbobenzyloxy chloride and 0.36 g. of sodium bicarbonate were mechanically stirred into the solution, and the stirring was then continued for an hour. After having passed through a column of Dowex 50 (H^+ form), the solution was dried up and the residue was crystallized from water as colorless needles which melted at 159~161°C alone or at 157~160°C when mixed with an authentic specimen. The yield was 0.22 g. (36.1%) $[\alpha]_D^{28}$ +100.0° (*c* 0.84, in pyridine).

Found: C, 54.62; H, 6.60; N, 4.23. Calcd. for $C_{16}H_{21}O_7N$; C, 55.04; H, 6.47; N, 4.28%.

Summary

Methyl *N*-acetyl-α-D-glucosaminide has been found to be well *N*-deacetylated by hydrazine treatment. The methyl α-D-glucosaminide thus produced shows so much stability with regarded to hydrazine and to barium hydroxide that these reagents provide a convenient means of preparing anomerically-pure methyl D-glucosaminide and its hydrochloride. The free base of methyl α-D-glucosaminide has been obtained crystalline for the first time.

This investigation was supported by U. S. Public Health Service Grant No. AI-04586-02.

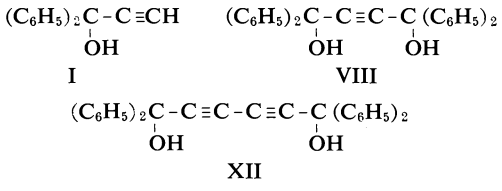
Department of Chemistry
Osaka University
College of Science
Nakanoshima, Osaka

Reactions of Tertiary Acetylenic Alcohols with Phosphorus Tribromide in Acetic Acid

By Hisaya TANI and Fumio TODA

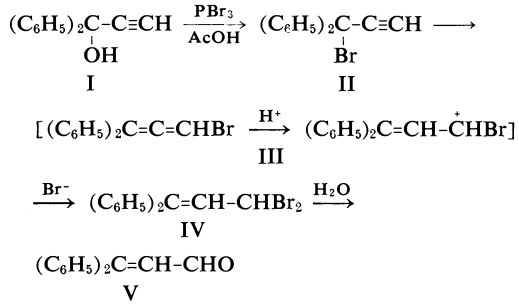
(Received October 3, 1963)

It has been well known that the reaction of acetylenic alcohols with phosphorus tribromide in the presence of pyridine gives corresponding tertiary acetylenic bromides. Some unexpected reactions, however, have been found during the course of studies of the bromination of acetylenic alcohols with phosphorus tribromide in acidic media. The present paper deals with the reaction of some aromatic tertiary acetylenic alcohols, I, VIII, and XII, with phosphorus tribromide in acetic acid.



1, 1-Diphenylprop-2-yn-1-ol (I) reacted with phosphorus tribromide in acetic acid to give 1, 1-diphenyl-3, 3-dibromoprop-1-ene (IV) in a yield of 45%. The structure of the *gem*-bromide IV was determined by the experiments to be described below in addition to elementary analysis and a study of the infrared spectrum. The ultraviolet spectrum of IV shows the presence of a conjugated system corresponding to 1, 1-diphenylethylene, and the NMR spectrum shows the presence of three kinds of hydrogen, i. e., aromatic, vinyl and aliphatic.

The behavior of IV as a representative *gem*-dihalide gave further evidence for the structure.[1] For example, the heating of II in water afforded 1, 1-diphenylprop-1-en-3-al (V) quantitatively; this was also obtained by the treatment of IV with acid, base, or silver nitrate.

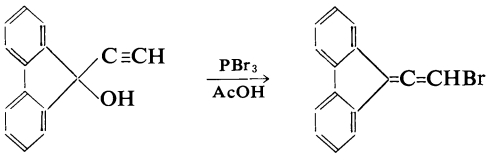


Scheme 1

1) H. Tani and F. Toda, *Chem. & Ind.*, **1963**, 1083.

The reaction can be explained by the successive addition of a proton and a bromide anion to the bromoallene intermediate III produced by the Meyer-Schuster rearrangement of the tertiary acetylenic bromide II initially produced, as is shown in Scheme 1. A proof for the initial production of the tertiary acetylenic bromide II in this reaction was given by the experimental evidence that the action of phosphorus tribromide or hydrogen bromide on the bromide II, prepared by the usual method,[2] in acetic acid yielded the *gem*-dibromide IV in a good yield.

The assumption that the above reaction proceeds through a bromoallene intermediate III was indirectly proved by the reaction of 9-ethynylfluoren-9-ol (VI) under the same conditions as those employed for I.



VI VII

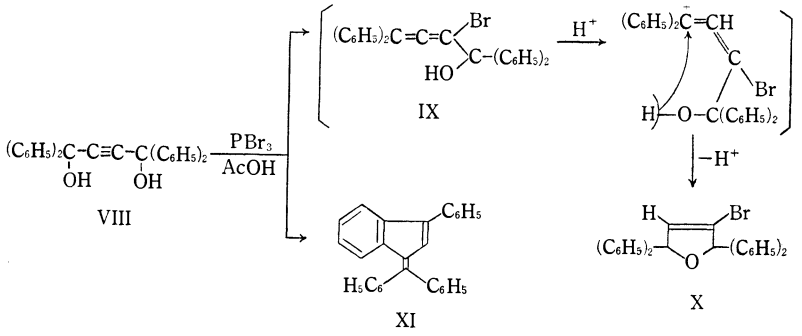
In this case, 9-(bromovinylidene)fluorene (VII) was isolated in a 75% yield as stable yellow leaflets, the structure of which was confirmed by the presence of allenic bands at 1950 and 1915 cm^{-1} in the infrared region and by comparing its ultraviolet spectrum with that of 9-(chlorovinylidene)fluorene.[3] The stability of the allenic bromide VII is attributable to the resonance stabilization arising from the planarity of the fluorene ring. After this investigation had been completed, Landor and Landor[4] reported that the reaction of 1, 1, 3-triphenylprop-2-yn-1-ol with thionyl chloride proceeds through a chloroallene intermediate corresponding to III or VII, resulting in 1, 1, 3-triphenylprop-1-en-3-one and a cyclic dimer.

In contrast with the reaction of terminal acetylenic alcohols, disubstituted acetylenic alcohols reacted with phosphorus tribromide in acetic acid to yield cyclic compounds.

The treatment of 1, 1, 4, 4-tetraphenylprop-2-yne-1, 4-diol (VIII) with phosphorus tribromide in acetic acid gave 1, 10, 10-triphenylbenzofulvene (XI)[5] and 2, 2, 5, 5-tetraphenyl-3-bromodihydrofuran (X) in yields of 30 and 16% respectively.

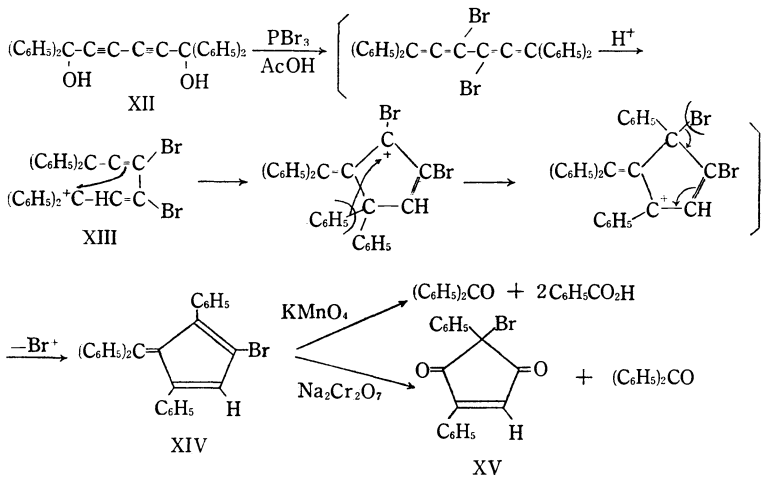
The structure of the dihydrofuran (X) was confirmed by a study of its ultraviolet spectrum, which showed an absence of conjugation between the benzene ring and the double bond, and by a study of its infrared spectrum, which showed the presence of trisubstituted ethylene, vinyl ether and monosubstituted benzene groups. The formation of X may be explained by the protonation and then the cyclization of the allenic intermediate IX produced by the Meyer-Schuster rearrangement of the monobromide of VIII, as is shown in Scheme 2. On the other hand, the formation of the benzofulvene XI may well be explained by the acid-catalyzed reaction of X through the transitory formation of tetraphenylbutatriene, because it has been reported[5] that the action of hydrogen iodide on an iodo-analog of X gives the benzofulvene XI.

The action of phosphorus tribromide on 1, 1, 6, 6-tetraphenylbuta-2, 4-diyne-1, 6-diol (XII) resulted in reddish brown needles. The structure of this compound, $C_{30}H_{21}Br$, was confirmed to be 2, 5, 6, 6-tetraphenyl-3-bromofulvene (XIV) on the basis of the following data: (i) the NMR spectrum of XIV showed the presence of one vinyl hydrogen and twenty aromatic hydrogens. (ii) The bromine atom of XIV reacted with neither sodium ethoxide nor with sodium amide in liquid ammonia. (iii) XIV



Scheme 2

2) A. Kirrmann, *Bull. soc. chim. France*, **39**, 698 (1926).
3) G. F. Hennion and B. Fleck, *J. Am. Chem. Soc.*, **77**, 3253 (1955).
4) P. D. Landor and S. R. Landor, *J. Chem. Soc.*, **1963**, 2707.
5) J. Salkind and A. Kruglow, *Ber.*, **61**, 2306 (1928).



Scheme 3

gave a characteristic fulvene absorption spectrum in the visible region. (iv) The oxidation of XIV by potassium permanganate in acetone gave one part of benzophenone and two parts of benzoic acid. (v) The sodium bichromate oxidation of XIV in acetic acid gave 2, 5-diphenyl-2-bromocyclopent-4-ene-1, 3-dione (XV) and benzophenone, in addition to a small amount of benzoic acid, which was supposed to be produced by the further degradation of the former XV.

The structure of the cyclopentenedione XV was confirmed by elementary analysis and by a study of its infrared, ultraviolet and NMR spectra; the last named indicated the presence of one vinyl hydrogen against ten aromatic hydrogens.

Additional evidence for the structure of the fulvene XIV was given by its infrared spectrum. Two bands of the fulvene XIV appeared at 1310 (weak) and 1265 (strong) cm^{-1}, corresponding to those of 6, 6-diphenyl-2, 3, 4, 5-tetrabromofulvene which appeared at 1315 (medium) and 1230 (strong) cm^{-1}.[6] Moreover, the presence of one nuclear ring hydrogen of the fulvene (XIV) was established by the absorption at 820 cm^{-1}.

The reaction may be interpreted in terms of the cyclization and the phenyl migration of the dibromo cation intermediate XIII produced by the Meyer-Schuster rearrangement and then the protonation of the dibromide of XII, as is shown in Scheme 3.

Experimental*

1, 1-Diphenyl-3, 3-dibromoprop-1-ene (IV).—Into an ice-chilled solution of 1, 1-diphenylprop-2-yn-1-ol (I, 10.5 g., 0.050 mol.) in acetic acid (25 ml.)-carbon tetrachloride (5 ml.), phosphorus tribromide (7.3 g., 0.027 mol.) was stirred drop by drop over a period of 15 min. under a nitrogen atmosphere; the stirring was then continued for an additional hour. The crude crystals which formed were collected by filtration and washed with cold methanol (20 ml.), resulting in IV in the form of colorless rhombic plates (8.5 g. (45%); m. p. 82°C (decomp.)); this was pure enough without further purification to carry out the following experiments. Two recrystallizations of the crystals from petroleum ether (b. p. 60~70°C) did not raise the melting point. IR: KBr disk, 882 (trisubstituted ethylene) and 768, 700 cm^{-1} (monosubstituted benzene). UV: $\lambda_{max}^{Dioxane}$, 242 mμ (ε, 10200), 266 (14700), 273 (16500). NMR: in carbon tetrachloride, 2.75 τ (singlet, aromatic), 3.60 τ (quartet, vinyl) and 7.90 τ (siglet, aliphatic).

Found: C, 51.22; H, 3.41; Br, 45.45. Calcd. for $C_{15}H_{12}Br_2$: C, 51.14; H, 3.41; Br, 45.65%.

The Formation of the *gem*-Bromide (IV) from 1, 1-Diphenyl-1-bromoprop-1-yne (II).—When phosphorus tribromide (or gaseous hydrogen bromide) was added to a solution of II in acetic acid under cooling with ice, colorless rhombic plates IV (m. p. 82°C (decomp.)) were formed almost quantitatively; these did not show any depression of the melting point when mixed with the authentic sample described above.

1, 1-Diphenylprop-1-en-3-al (V).—A solution of 1, 1-diphenyl-3, 3-dibromoprop-1-ene (IV, 1.0 g., 0.0028 mol.) in alcoholic potassium hydroxide (prepared from 30 ml. of ethanol and 0.5 g. of potassium hydroxide) was refluxed for 1 hr. After cooling, the reaction mixture was poured into water and extracted with ether. The crude crystals obtained by the evaporation of the solvent were

6) J. C. Wood, R. M. Elofson and D. M. Saunders, *Anal. Chem.*, 30, 1339 (1958).

* All melting points are uncorrected. The NMR spectra were obtained in a carbon tetrachloride solution with a Varian model A-60 spectrometer, using tetramethylsilane as an internal standard. The molecular weight was determined in a benzene solution using a Mechrolab vapor pressure osmometer model 301 A.

recrystallized from petroleum ether (b. p. 40～50°C) to give colorless needles (m. p. 43°C, 0.5 g. (90%) (lit.,[7] m. p. 44.5～45.5°C)). For this aldehyde, consistent infrared and ultraviolet spectra were obtained. The 2, 4-dinitrophenylhydrazone of the aldehyde melted at 195°C (lit.,[7] m. p. 198°C).

By treating the *gem*-bromide IV with water, aqueous acid or alcoholic silver nitrate in the manner described above, the aldehyde IV was also obtained quantitatively.

9-(Bromovinylidene)fluorene (VII).—To a stirred solution of 9-ethynylfluoren-9-ol (VI, 6.2 g., 0.03 mol.) in acetic acid (20 ml.), phosphorus tribromide (4.4 g., 0.017 mol.) was added under cooling with ice over a period of 30 min. The crude crystals which formed were collected by filtration and washed with methanol, water and methanol successively. The dried crystals were recrystallized from ethyl acetate ethanol to give yellow plates (VII) (6.0 g. (75%); m. p. 220°C (decomp.)). IR: in chloroform, 1950 and 1915 cm^{-1} (allene). UV: $\lambda_{max}^{Dioxane}$, 266 mμ (ε, 23400), 274(25700), 380 (16400).

2, 2, 5, 5-Tetraphenyl-3-bromodehydrofuran (X) and 1, 10, 10-Triphenylbenzofulvene (XI).—To a stirred solution of 1, 1, 4, 4-tetraphenylbut-2-yne-1, 4-diol (VIII, 0.7 g., 0.002 mol.) in a mixture of acetic acid (10 ml.) and carbon tetrachloride (20 ml.), phosphorus tribromide (1.35 g., 0.005 mol.) was added in one portion under cooling with ice; the reaction mixture was then stirred for a further 30 min. After it had been kept standing at room temperature for 1 hr., the reaction mixture was poured into ice-water. The carbon tetrachloride layer was separated, washed with water and dried over sodium sulfate. The evaporation of the solvent yielded a mixture of two kinds of crystals (yellow and colorless), which were then separated mechanically. The recrystallization of the yellow crystals from ethyl acetate resulted in pure bright yellow prisms (XI) (200 mg. (30%); m. p. 204°C (decomp.) (lit.,[5] m. p. 204～205°C)). UV: $\lambda_{max}^{Dioxane}$ 235 mμ (ε, 34200), 254 (32300), 297 (12500), 350 (15900), 410 (shoulder) (5200). NMR: in carbon tetrachloride, 2.62 τ (doublet, aromatic) and 3.35 τ (singlet, fulvene).

Found: C, 93.91; H, 5.69. Calcd. for $C_{25}H_{20}$: C, 94.34; H, 5.66%.

The recrystallization of the colorless crystals from ethyl acetate resulted in colorless prisms (X) (150 mg. (16%); m. p. 175°C). IR: KBr disk, 1657 (double bond), 1013 (ether), 833, 807 (trisubstituted ethylene) and 753, 700 cm^{-1} (monosubstituted benzene). UV: $\lambda_{max}^{Dioxane}$: 233 mμ (ε, 700), 247 (800), 252 (800), 259 (760).

Found: C, 74.21; H, 4.69; Br, 17.82. Calcd. for $C_{25}H_{21}BrO$: C, 74.17; H, 4.63; Br, 17.66%.

2, 5, 6, 6-Tetraphenyl-3-bromofulvene (XIV).—Phosphorus tribromide (2.2 g., 0.008 mol.) was stirred into an ice-cooled solution of 1, 1, 6, 6-tetraphenylbut-2, 4-diyne-1, 6-diol (XII, 4.2 g., 0.01 mol.) in acetic acid (30 ml.) over a period of 5 min. After stirring had been continued for a further 30 min. the crystals which had formed were filtered and washed with water and a small amount of methanol successively. Two recrystallizations of the dried crystals from ethyl acetate afforded reddish brown needles (2.1 g. (43%); m. p. 215°C (decomp.)). IR: KBr disk, 1310, 1265 (fulvene), 805 (hydrogen of fulvene ring) and 770, 723, 695 cm^{-1} (monosubstituted benzene). UV: $\lambda_{max}^{Dioxane}$, 254 mμ (ε, 21300), 358 (23200), 490 (shoulder) (500). NMR: in carbon tetrachloride, 2.63, 2.90, 3.13 and 3.36 τ (aromatic, all the areas are almost equal), 3.62 τ (hydrogen on fulvene ring).

Found: C, 77.81; H, 4.55; Br, 16.95. Mol. wt. 464 (vapor pressure osmometer*). Calcd. for $C_{30}H_{21}Br$: C, 78.10; H, 4.56; Br, 17.34%. Mol. wt. 461.

The Oxidation of XIV by Potassium Permanganate.—To a stirred solution of XIV (0.3 g., 0.00065 mol.) in acetone (20 ml.), potassium permanganate (1.0 g., 0.0063 mol.) was added; the mixture was then stirred at 30～40°C for 2 hr. After the mixture had been kept standing overnight at room temperature, the excess potassium permanganate in the reaction mixture was decomposed with a small amount of ethanol. The acetone solution obtained by the removal of the manganese dioxide by filtration was evaporated to dryness. The residue was mixed with water and extracted with ether. The ether extract was washed with aqueous sodium bicarbonate. The alkaline solution was acidified and then saturated with ammonium chloride. The crude crystals thus obtained were recrystallized from petroleum ether (b. p. 60～70°C), resulting in benzoic acid in the form of colorless plates (100 mg. (60%); m. p. 121°C), which did not show any depression of the melting point when mixed with an authentic sample (m. p. 121°C).

The recrystallization of the crude crystals obtained by the removal of the solvent from the dried ether layer from petroleum ether (b. p. 40～50°C) afforded benzophenone (60 mg. (50%); m. p. 47～48°C), which was identified by a mixed melting point determination with an authentic specimen and by a study of its infrared spectrum.

The Oxidation of XIV by Sodium Bichromate.—A mixture of XIV (0.5 g., 0.001 mol.), sodium bichromate dihydrate (1.5 g., 0.005 mol.) and acetic acid (30 ml.) was refluxed for 1.5 hr. After it had cooled, the reaction mixture was poured into dilute hydrochloric acid and extracted with ether. The ether layer was washed with aqueous potassium carbonate. From the acidified alkaline solution, a small amount of benzoic acid was isolated in the form of colorless plates. The evaporation of the solvent from the dried ether layer yielded a mixture of yellow needles and an oily material. After the mixture had been washed with methanol (5 ml.), insoluble crystals were recrystallized from ethyl acetate to give XV in the form of pale yellow needles (0.1 g. (30%); m. p. 205～206°C). IR: KBr disk, 1670, 1665 (carbonyl) and 830 cm^{-1} (trisubstituted ethylene). UV: $\lambda_{max}^{Dioxane}$, 237 mμ (ε, 19800), 248 (17800), 298 (shoulder) (7300), 332 (3900). NMR: in carbon tetrachloride, 2.10, 2.55, 2.90 τ (aromatic) and 3.53 τ (vinyl).

Found: C, 62.78; H, 3.53; Br, 27.41. Calcd. for $C_{17}H_{11}BrO_2$: C, 62.38; H, 3.36; Br, 24.46%.

7) H. Lorenz and R. Wizinger, *Helv. Chim. Acta*, **28**, 600 (1945).

The recrystallization from petroleum ether (b. p. 40~50°C) of the crude crystals obtained by the removal of the solvent from the methanol layer yielded benzophenone in the form of colorless needles (90 mg. (50%) ; m. p. 48°C), the identification of which was made by a mixed melting point determination with an authentic sample and by a study of its infrared spectrum.

The authors wish to express their thanks to Professor Yasuhide Yukawa of the Institute for Scientific and Industrial Research, Osaka University, for his helpful discussions. They also indebted to Mr. Masakazu Okumiya for the microanalyses.

Department of Polymer Science
Faculty of Science
Osaka University
Nakanoshima, Osaka

Sesquiterpene Constituents of the Essential Oil of Hinoki (Chamaecyparis Obtusa (Sieb. et Zucc.) Endl.)

By Schûichi HAYASHI, Katsumi YANO and Tamon MATSUURA

(Received October 7, 1963)

The sesquiterpene constituents of the essential oil of Hinoki (*Chamaecyparis Obtusa* (Sieb. et Zucc.) Endl.) have been investigated by several workers,[1-3] and two compounds, *l*-[1] or *d*-cadinene[2-3] and cadinol,[3] have been reported. Recently, β-, γ-, δ- and ε-cadinene[4] were identified as isomeric members of cadinene, and α- and δ-cadinol[5] as isomers of cadinol. The present work, along with a forthcoming investigation of the monoterpene constituents[6], was undertaken to clarify the sesquiterpene constituents.

Results

The essential oil from the leaves and twigs of the Hinoki (*Chamaecyparis Obtusa* (Sieb. et Zucc.) Endl.) growing in Kôchi Prefecture, Japan, was investigated. The residual oil, from which the monoterpene fractions were distilled off, was repeatedly fractionated through a packing distillation column to divide it into several sesquiterpene fractions. The physical properties of the fractions are illustrated in Fig. 1.

In the present work, *d*-longifolene and calamenene were newly identified, and cadinene and cadinol, which had formerly been reported, were confirmed to be *d*-γ-cadinene and *l*-α-cadinol respectively. On the basis of the results of both fractionation and gas chromatography, it was assumed that the sesquiterpene fractions of Hinoki oil consisted of approximately 72% *d*-longifolene, 19% *d*-γ-cadinene, 1% calamenene and 8% *l*-α-cadinol. The sesquiterpene fraction amounted to 43.2% of the total essential oil.

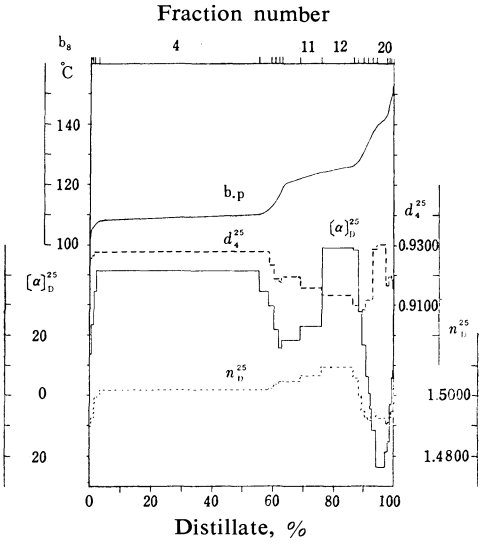


Fig. 1. Fractional distillation of sesquiterpene oil.

***d*-Longifolene.**—Fraction 4 gave a gas chromatogram which mainly showed one peak (retention time; 15.5 min.), and an infrared spectrum (1763, 1661, 1474, 1454, 1376, 1364,

1) R. Kondô, *J. Pharm. Soc. Japan* (*Yakugaku Zasshi*), **29**, 1297 (1909).
2) S. Uchida, *J. Soc. Chem. Ind. Japan* (*Kôgyô Kwagaku Zasshi*), **28**, 1440 (1925); **31**, 650 (1928).
3) N. Hirao, *J. Chem. Soc. Japan* (*Nippon Kwagaku Kwaishi*), **58**, 222 (1937).
4) V. Herout and V. Sýkora, *Tetrahedron*, **4**, 246 (1958).
5) O. Motl, V. Sýkora, V. Herout and F. Šorm, *Collection Czechoslov. Chem. Commun.*, **23**, 1297 (1958).
6) To be published in this Bulletin.

1207, 1175, 873 cm^{-1}) which coincided entirely with that of longifolene.[7]

From this fraction longifolene hydrochloride (m. p. 59~60°C[8]) was prepared. Also, a nuclear magnetic resonance spectrum (τ; 9.116, 9.072, 9.049, 8.475, 8.000, 7.500, 5.630, 5.375) of this fraction agreed with that of longifolene.[9] Accordingly, it is confirmed that longifolene is a main component of fraction 4.

***d*-γ-Cadinene.** — From fraction 12 cadinene dihydrochloride (m. p. 116~117°C[10]) was prepared. However, a gas chromatogram of this fraction contained some weak peaks, together with the main peak (retention time; 30.4 min.), and so this fraction was eluted through a silica gel column, using petroleum ether to divide it into some fractions. The main fraction from the chromatography showed an infrared absorption spectrum (1649, 1454, 1389, 1369, 883, 835 cm^{-1}) which agreed with that of γ-cadinene.[11]

Calamenene.—Another small fraction from the above elution chromatography of fraction 12 gave a gas chromatogram which showed only one peak (retention time; 40.2 min.) and an infrared absorption spectrum (1642, 1613, 1550, 1500, 1464, 1385, 1369, 881, 815 cm^{-1}) which agreed with that of calamenene.[12] The ultraviolet absorption spectrum of this small fraction is shown in Fig. 2, for the ultraviolet spectrum of calamenene seems not to be found in the literature.

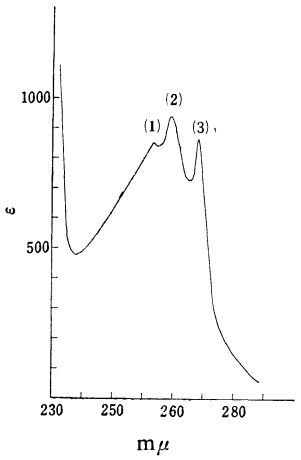


Fig. 2. The ultraviolet absorption spectrum of calamenene.
(1) λ_{max}^{EtOH} 263 mμ (ε 850)
(2) λ_{max}^{EtOH} 269 mμ (ε 940)
(3) λ_{max}^{EtOH} 278 mμ (ε 860)

In addition to *d*-γ-cadinene and calamenene, fraction 12 contained a component which showed an absorption band of λ_{max}^{EtOH} 246 mμ ($E_{1cm}^{1\%}$ 65.2) in its ultraviolet spectrum. This band suggests the presence of the isocadinene named by Gillam.[13] Thus, it is certain that fraction 12 consists of large quantity of *d*-γ-cadinene and small quantities of calamenene and other elements.

***l*-α-Cadinol.** — Cadinene dihydrochloride[5] (m. p. 115.0~116.5°C) and α-cadinol *p*-nitrobenzoate[5,14] (m. p. 134~135°C) were prepared from fraction 20. After being purified by elution chromatography on alumina (activity IV[15]) using petroleum ether, fraction 20 ($[\alpha]_D^{25}$ −32.3°, 0.1066 g./cc., ethanol) gave an infrared absorption spectrum (1656, 1450, 1380, 1370, 1119, 815 cm^{-1}) which agreed with that of α-cadinol.[5] Accordingly, it is certain that fraction 20 consists mainly of *l*-α-cadinol.

Experimental

In the present work, the residual oil (b. p. above 126°C/20 mmHg, 7.14 kg.) from which the monoterpene fractions were distilled off as described in the forthcoming work,[6] was used.

***d*-Longifolene.** — One-half gram of fraction 4 (Found: C, 88.32; H, 11.63%) was dissolved in ether and saturated with dry hydrogen chloride under cooling at −15°C. After the reaction mixture had stood for two hours, needle crystals (0.31 g.) were obtained; these, after being recrystallized from petroleum ether, melted at 59~60°C ($[\alpha]_D^{25}$ +7.5°, 0.2221 g./cc., chloroform). This melting point agrees with that of longifolene hydrochloride.[8]

***d*-γ-Cadinene.**—Seven hundred and twenty milligrams of fraction 12 was treated with dry hydrogen chloride as in the case of longifolene to give needle crystals (0.24 g.) which, after being recrystallized from ethanol, melted at 116~117°C ($[\alpha]_D^{25}$ −36.2°, 0.0486 g./cc. chloroform). This melting point agrees with that of cadinene dihydrochloride.[10] For further purification, 1.46 g. of fraction 12 was chromatographed on silica gel (100~200 mesh, 150 g.) which had been packed in a glass tube (inside diameter, 1.8 cm.) using petroleum ether. The eluate was divided into several fractions by testing its refractive index.

***l*-α-Cadinol.**—When one-half gram. of fraction 20 was treated with dry hydrogen chloride, needle crystals (0.04 g.) were obtained. The needles, after being recrystallized from ethanol, showed a melting

7) G. Dupont, R. Dulou, P. Naffa and G. Ourisson, *Bull. soc. chim. France*, **1954**, 1075.
8) R. H. Moffet and D. Rogers, *Chem. & Ind.*, **1953**, 916.
9) S. Dev, *Tetrahedron*, **9**, 1 (1960).
10) G. G. Henderson and A. Robertson, *J. Chem. Soc.*, **1924**, 1992.
11) V. Sýkora and V. Herout, *Collection Czechoslov. Chem. Commun.*, **24**, 1732 (1959).
12) F. Šorm, K. Vereš and V. Herout, ibid., **18**, 106 (1953).
13) A. E. Gillam, D. G. Moss and T. F. West, *J. Chem. Soc.*, **1948**' 1306.
14) Pl. A. Plattner and R. Márkus, *Helv. Chim. Acta*, **25**, 1674 (1942).
15) H. Brockmann and H. Schodder, *Chem. Ber.*, **74**, 73 (1941).

point of 115.0~116.5°C ($[\alpha]_D^{25}$ −35.15°, 0.0382 g./cc., chloroform), which was confirmed by admixture with cadinene dihydrochloride (m. p. 116~117°C). One gram of fraction 20 was acylated with *p*-nitrobenzoyl chloride, and the crystalline mass (0.03 g.) was prepared. The mass, after being recrystallized from ethanol, showed a melting point of 134~135°C, which agrees with that of *p*-nitrobenzoate of α-cadinol.[5,14]

Gas Chromatography.—A gas chromatogram was made by a Shimadzu GC-2 apparatus equipped with a thermal conductivity cell using a copper spiral column (inside diameter, 4 mm.; length, 3 m.). For hydrocarbon analysis, Shimalite (24~48 mesh) coated with polyethylene glycol-6000 (20%) was used at 140°C, while for oxygen-containing compound analysis, quartz powder (150~200 mesh) coated with Thermol-1 (5%) was used at 170°C.

Summary

d-Longifolene and calamenene have been newly identified from the essential oil of Hinoki. Cadinene and cadinol, which had been formerly reported, have been confirmed to be *d*-γ-cadinene and *l*-α-cadinol respectively.

Department of Chemistry
Faculty of Science
Hiroshima University
Higashi-Sendamachi, Hiroshima

Stability Constants of Palladium, Copper, Nickel, Zinc and Manganese Complexes of 3-Hydroxy-3-phenyl-1-p-chlorophenyltriazene

BY D. N. PUROHIT and N. C. SOGANI

(Received October 8, 1963)

In recent years Sogani et al.[1-5] have reported hydroxytriazenes as a very useful class of chelating reagents. They possess common functional grouping -N(OH)-N=N-. The parent compoud of the series, 3-hydroxy-1, 3-diphenyltriazene, is a highly selective reagent for palladium[1] and copper[2]. Substitution of different groups at different positions of the aryl nuclei of the present compound influenced the stabilities of resulting metal chelates. The present investigation deals with determination of stabilities of bivalent metal chelates of para chloro substituted hydroxytriazene, namely, 3-hydroxy-3-phenyl-1-*p*-chlorophenyltriazene, in 70% v/v dioxan-water mixture, by employing Bjerrum-Calvin pH titration technique.[6] Titrations were carried out in duplicate using 40 : 1 ratio of chelating agent to metal ion concentration.

Experimental

Chelating Agent Solution.—3-Hydroxy-3-phenyl-1-*p*-chlorophenyltriazene was prepared by employing the method given by Sogani et al.[3] Weighed amount of this compound was dissolved in 70% v/v dioxan-water mixture and diluted to give 0.04 M solution.

Standard Palladium, Copper, Nickel, Zinc, and Manganese Solutions.—Analytical grade reagents of palladium chloride, copper chloride, nickel sulphate, zinc oxide, and manganese sulphate were used for preparing standard solutions. After standardizing these solutions by usual classical methods, these were diluted to 0.002 M solution.

Sodium Hydroxide. — Approximately 0.1 M carbonate free sodium hydroxide was prepared and standardized with analytical grade potassium hydrogen phthalate. It was diluted to give 0.02 M solution.

Dioxan. — The B.D.H. dioxan was purified by Weissberger's method.[7]

Potentiometric Titrations.—The pH-titrations of the chelating agents with standard alkali solution in absence and in the presence of different metal ions were carried out by using Cambridge bench-type pH-meter which gave values accurate to 0.01 pH unit. The pH-meter was standardized before, and checked after, each titration with buffer solutions of pH 4.0 and 9.2. Electrode system consisted of glass electrode (pH range 1~13) and saturated calomel-electrode as reference.

Ten milliliters of 0.04 M chelating agent solution in 70% v/v dioxan-water mixture was pipetted in a titration vessel. Sufficient amount of 0.02 M nitric acid was added to it to lower the pH to about

1) N. C. Sogani and S. C. Bhattacharya, *Anal. Chem.*, **28**, 81 (1956).
2) N. C. Sogani and S. C. Bhattacharya, ibid., **28**, 1616 (1956).
3) N. C. Sogani and S. C. Bhattacharya, *J. Indian Chem. Soc.*, **36**, 563 (1959).
4) T. C. Jain, H. K. L. Gupta and N. C. Sogani, ibid., **37**, 531 (1960).
5) H. K. L. Gupta and N. C. Sogani, ibid., **38**, 771 (1961).
6) M. Calvin and N. C. Melchior, *J. Am. Chem. Soc.*, **70**, 3270 (1948).
7) A. Weissberger and E. S. Proskauer, "Organic Solvents," Oxford (1935), p. 139.

2. Final ionic concentration was maintained at 0.1 M by adding 2.5 ml. of 2 M potassium chloride. When titrating in presence of metal ions, 5 ml. of 2×10^{-3} M metal solution were added at this stage. The total volume of the contents was made to 50 ml. by adding varying amounts of dioxan and distilled water in such proportions that it finally became 70% v/v dioxane-water mixture. It was titrated against 0.02 M sodium hydroxide. The temperature of the solution throughout the titration was maintained at 25±0.5°C. The pH-meter readings obtained at a given alkali addition in duplicate titrations were reproducible with a maximum variation of ±0.01 pH unit. The titration curves are given in Figs. 1 and 2.

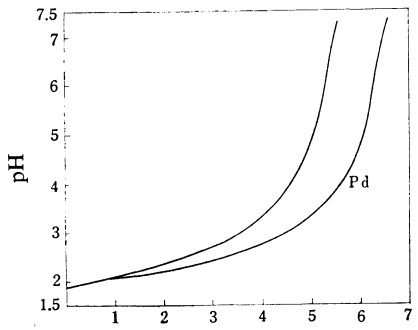
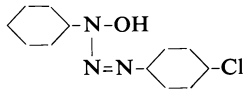


Fig. 1. Titration curve for



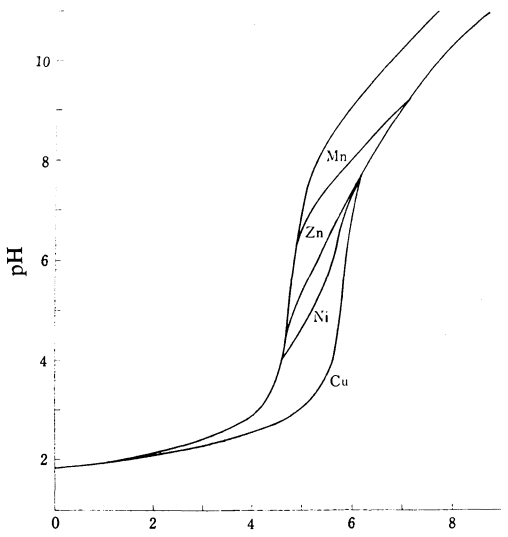
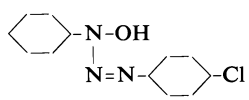


Fig. 2. Titration curve for



Calculations. — The horizontal distance between the reference titration curve and the curve obtained in presence of a metal ion gives the concentration of metal bound chelating agent. This value divided by the total concentration of metal ion gives the value for $\bar{n}$. In this way the values of $\bar{n}$ at different pH values were calculated.

At any pH, the value of free chelating ion concentration, $[T^-]$, was calculated from the total concentration of the chelation agent, and its dissociation quotient. This is based on the assumption that the amount of chelating agent over metal ion is so great that the removal of HT by chelation does not cause any significant change in the equilibrium: $HT \rightleftarrows H^+ + T^-$. The pK_a value of 3-hydroxy-3-phenyl-1-*p*-chlorophenyltriazene has been determined spectrophotometricaly[8] as 10.72.

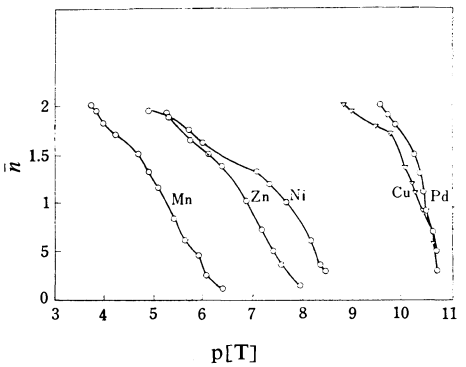
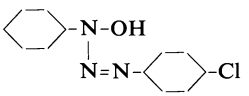


Fig. 3. Formation curves for metal chelates of



In calculating the values for $\bar{n}$ and $[T^-]$, the concentrations were corrected for changes in volume, produced by addition of alkali during titrations. In this way, a series of values for $\bar{n}$ and $[T^-]$, corresponding to different pH values, was obtained. The formation curves for metal chelates of 3-hydroxy-3-phenyl-1-*p*-chlorophenyltriazene are shown in Fig. 3. The values for stepwise stability constants and average stability constant i.e., $\log k_1$, $\log k_2$, and $\log K_{av}$ $(1/2\log K)$ for different metal chelates were

TABLE I. STABILITY CONSTANTS OF METAL CHELATE OF 3-HYDROXY-3-PHENYL-1-*p*-CHLOROPHENYL-TRIAZENE

Metal ion	$\log k_1$	$\log k_2$	$\log K_{av}$	$\log k_1k_2$
Palladium	10.70	10.25	10.47	20.95
Copper	10.67	9.98	10.35	20.65
Nickel	8.25	6.33	7.66	14.58
Zinc	7.41	6.12	6.84	13.53
Manganese	5.83	4.67	5.25	10.50

8) D. N. Purohit, Ph. D. Thesis, University of Rajasthan, Jaipur (India), 1963.

read directly from the formation curves and are given in Table I. K is the overall stability constant.

Discussion

The consumption of alkali during the course of titration may be due to the chelating agent, the hydrolysis of metal ion, and the protons of the chelating agent liberated in complex formation.

The chelating agent under study is a very weak acid ($pK_a = 10.72$) Thus, the proton of the chelating agent as such is not in a titrable form. Hydrolyses of these metal ions have been studied in 70% v/v dioxan-water mixture.[8] The pH for $\bar{n} = 1.5$ in all the cases is lower than the pH at which the hydrolysis of these metal ions start. Hence, hydrolyses of these metal ions do not interfere in the stability measurements. Moreover, there was no precipitation during chelation titrations, ruling out the possibility of appreciable hydrolyses of these metal ions in the presence of large excess of the chelating agent.

Thus, the consumption of an excess of alkali in chelation titration over the simple chelating agent titration is due to protons of the chelating agent liberated during the complex formation. This may be represented as:

$$M^{2+} + HT + OH^- \rightleftharpoons MT^+ + H_2O \quad (1)$$

$$MT^+ + HT + OH^- \rightleftharpoons MT_2 + H_2O \quad (2)$$

The order of stability of hydroxytriazene metal chelates has been found as palladium > copper > nickel > zinc > manganese.

Summary

Stabilities of palladium, copper, nickel, zinc, and manganese chelates of 3-hydroxy-3-phenyl-1-*p*-chlorophenyltriazene have been determined in 70% v/v dioxan-water mixturre by employing Bjerrum-Calvin pH titration technique. The titration medium was maintained at a constant ionic strength (0.1 M, potassium chloride) and at a temperature, 25±0.5°C. Log K, palladium 20.95, copper 20.65, nickel 14.58, zinc 13.53, and manganese 10.50.

The authors express their gratitude to Professor R. C. Mehrotra for providing facilities in the department. They are also grateful to the University Grants Commission for granting a research scholarship to one of them (D. N. Purohit).

Chemistry Department
University of Rajasthan
Jaipur, India

*The Radiolysis of Biphenyl by Gamma-rays**

By Hiroaki KŌYAMA,** Gen-ichi TSUCHIHASHI and Akibumi DANNO

(Received October 21, 1963)

Polyphenyls are the most promising materials for use as organic moderators and coolants. Studies have been developed on the radiolytic and pyrolytic decomposition of these materials. Most of the papers published have, however, concerned the determination of the amount of gaseous products and of the residue with a high boiling point, or gross changes in the physical properties of such materials from engineering points of view.[1-3] Little work has been done on the mechanism of the radiolytic decomposition of polyphenyls.

For the radiolysis of benzene, Patrick and Burton[4] reported that the $G(C_6H_6 \rightarrow \text{polymer})$ value equals 0.75 and that the average polymer contains five molecules of a benzene ring. Gordon et al.[5] studied the reaction further; they identified biphenyl and several types of its partially hydrogenated compounds from the products by means of vapor phase chromatography and mass-spectrometric analysis.

For the identification of radiolytic products of biphenyl, Hellman et al.[6] and West[7]

* Presented partly at the 4th Japan Conference on Radioisotopes, Kyoto, October, 1962 and partly at the 1st Annual Meeting of the Atomic Energy Society of Japan, Tokyo, April 1963.

** Present Address: Central Research Instiute of Electric Power Industry, Komae-cho, Kitatama-gun, Tokyo.

1) R. O. Bolt, J. G. Carroll, R. Harrington and R. C. Gilberson, "Proceedings of the Second United Nations International Conference on the Peaceful Uses of Atomic Energy," **29**, 276 (1958).

2) C. A. Trilling, ibid., **9**, 468 (1958).

3) D. R. de Halas, *HW-56769* (1958).

4) W. N. Patrick and M. Burton, *J. Am. Chem. Soc.*, **76**, 2626 (1954).

5) S. Gordon, A. R. Van Dyken and T. F. Doumani, *J. Phys. Chem.*, **62**, 20 (1958).

6) M. Hellman, R. L. Alexander and C. F. Coyle, *Anal. Chem.*, **30**, 1206 (1958).

7) W. W. West, *AECU-4699* (1960).

adopted a technique of liquid chromatography, while Boxter and Keen[8] developed high temperature gas chromatography. Hall and Elder[9] and Keen et al.[10] determined mass-spectrometrically the yields of the products with a high molecular weight from the radiolysis of biphenyl, which include terphenyl, quaterphenyl, hexaphenyl and quinquephenyl. Meanwhile, Burr and Scarborough[11] and Rayroux and Baertschi[12] investigated the isotope effect on the radiolysis of biphenyl by using deuterated biphenyl.

From these previous investigations, it is clear that the non-volatile products from the radiolytic decomposition mainly consist of polyphenyls, partially-hydrogenated polyphenyls and condensed polynuclear aromatic compounds. Among these polyphenyls appear to be the major products, but few papers have been published on accurate *G*-values for them. Therefore, the present work will aim to obtain precise information concerning the radiolytic mechanism for biphenyl by determining the *G*-values of the non-volatile products. Here, reverse isotope dilution analysis by using a ^{14}C-labeled compound was applied to determine the isomer yields of the terphenyls and quaterphenyls produced by the radiolysis of biphenyl.

On the basis of the results, the mechanism for the present reaction will be discussed.

An abstract was published previously.[13]

Experimental

Preparation of Materials. — *Biphenyl and Terphenyls.*—Commercial products were recrystallized several times from alcohol or benzene until they reached the melting point indicated in the literature.[14]

o, o'-Quaterphenyl.—This substance was synthesized, starting from *o*-aminobiphenyl, by successive diazotization, Sandmeyer decomposition and Ullmann condensation. To improve the yields, slightly modified procedures were employed.

A sodium nitrite (9 g.) solution was vigorously stirred into a mixture of *o*-aminobiphenyl (22 g.) and 6.5% aqueous hydrochloric acid solution in an ice-bath. Then a potassium iodide (50 g.) solution was added to the mixture, the temperature being kept below 10°C. The reaction product was extracted with ether (150 ml.). The ether extract was washed with water and then with a 10% sodium bisulfite solution, and dried over calcium chloride. After the removal of the solvent, 2-iodobiphenyl (46.0 g.) was distilled at 177~178°C under 18 mmHg. Found: C, 51.35; H, 3.53; I, 45.34. Calcd. for $C_{12}H_9I$: C, 51.45; H, 3.24; I, 45.31%.

In a small test tube, 2-iodobiphenyl was mixed with copper powder and placed in an oil-bath at 260°C for 20 min. The reaction mixture was extracted with benzene. Removal of the benzene, chromatography of the residue on activated aluminia with petroleum ether, and three recrystallizations from ethanol gave *o, o'*-quaterphenyl (3.9 g., 17.5% yield, m. p. 119.1~119.6°C). Found: C, 93.96; H, 5.89. Calcd. for $C_{24}H_{18}$: C, 94.08; H, 5.92%.

m, m'-Quaterphenyl.—The product was obtained, starting from *m*-aminobiphenyl, by a procedure similar to that used for *o, o'*-quaterphenyl (4.3 g., 16.3% yield, m. p. 86.6~87.2°C). Found: C, 94.25; H, 6.08. Calcd. for $C_{24}H_{18}$: C, 94.08; H, 5.92%.

p, p'-Quaterphenyl. — A product of the Pilot Chemical Co. Inc. was recrystallized, first from anisole and then from benzene (m. p. 320.0°C).

Triphenylene.—A product of the Aldrich Chemical Co. Inc. was recrystallized from ethanol (m. p. 200.4°C).

Biphenyl-(phenyl-^{14}C). — The synthesis has been described in previous papers.[15,16]

Procedure. — *Irradiation.* — Biphenyl-(phenyl-^{14}C) (33.2 mc./mol., 30~50 mg.) was placed in an irradiation tube of Hario glass (Fig. 1a) and degassed under 10^{-4}~10^{-5} mmHg in a dry ice-ethanol bath. After the sealing of the tube at the position of the dotted line (Fig. 1a), the glass tube, protected with an aluminum capsule, was heated with an electric furnace, the temperature being kept at 100±5°C. The irradiation was carried out by a Co-60 gamma-facility installed at the Japan Atomic

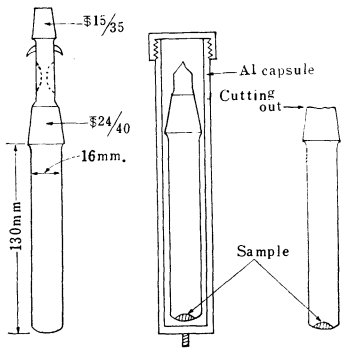


Fig. 1. Irrradiation tube.
(a) Irradiation tube
(b) Irradiation in aluminum capsule after degassing
(c) After irradiation

8) R. A. Boxter and R. T. Keen, *NAA-SR-3154* (1959).
9) K. L. Hall and F. A. Elder, *J. Chem. Phys.*, **31**, 1420 (1959).
10) R. T. Keen, R. A. Boxter, R. H. J. Gercke and W. L. Orr, *NAA-SR-4355* (1962).
11) J. G. Burr and J. M. Scarborough, *J. Phys. Chem.*, **64**, 1367 (1960).
12) J. M. Rayroux and P. Baertschi, *Helv. Chim. Acta.*, **43**, 484 (1960).
13) H. Kōyama, G. Tsuchihashi and A. Danno, This Bulletin, **35**, 696 (1962).
14) I. Heilbron and H. M. Bumbury, "Dictionary of Organic Compounds," Eyre & Spottiswoode, London (1953).
15) H. Kōyama, N. Morikawa, T. Migita, R. Itō and G. Tsuchihashi, *Radioisotopes*, **9**, 112 (1960).
16) H. Kōyama, N. Morikawa and G. Tsuchihashi, ibid., **11**, 107 (1962).

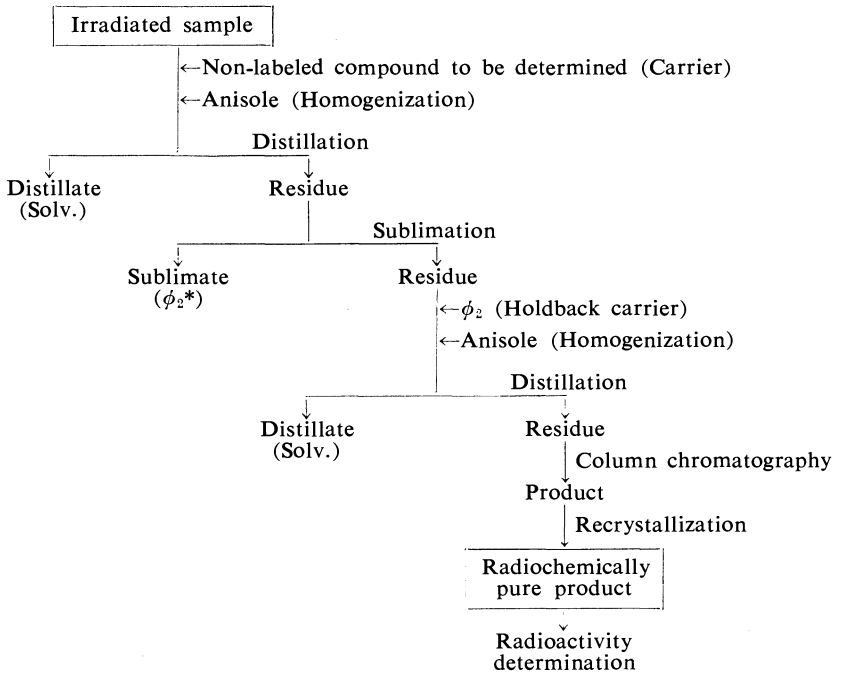


Fig. 2. Isolation process of the radiolytic product.

TABLE I. CHROMATOGRAPHIC CONDITION IN THE ISOLATION OF THE RADIOLYTIC PRODUCTS OF BIPHENYL

Product	Chromato. column*		In maximum eluting power		Solvent for recryst.
	Diameter mm.	Length cm.	Solvent composition (Ratio of vol.)	Temp.	
o-Terphenyl	25	25~26	Pet. ether - benzene (9 : 1)	Room temp.	Methanol
m-Terphenyl	25	25~26	Pet. ether - benzene (4 : 1)	Room temp.	Ethanol
p-Terphenyl	20	25~26	Pet. ether - benzene (1 : 9)	Room temp.	Benzene
o,o'-Quaterphenyl	25	25~26	Pet. ether - benzene (3 : 2)	Room temp.	Ethanol
m,m'-Quaterphenyl	25	25~26	Pet. ether - benzene (2 : 3)	Room temp.	Ethanol
p,p'-Quaterphenyl	20	25~26	Chloroform	50°C	Benzene
Triphenylene	20	25~26	Pet. ether - benzene (1 : 1)	Room temp.	Ethanol

* Absorbent is activated alumina.

Energy Research Institute.[17] The absorbed dose was measured by means of a Fricke dosimeter using a *G*-value of 15.5.

Isolation. — After the irradiation, the radiolytic product to be determined was isolated according to the process diagrammed in Fig. 2. The technique employed here has been described in a previous report.[18] The composition of the eluting solvent in chromatography on activated alumina was gradually varied from petrolum ether to a benzene-rich solvent (Table I). For the isolation of *p,p'*-quaterphenyl, high-temperature chromatography was adopted. Namely, the column was equipped with a jacket and heated by circulating hot water. The recrystallization of the product was repeated to reach a constant specific activity. The radioactivities of all samples except *p,p'*-quaterphenyl were determined by using a Tri-Carb liquid scintillation spectrometer with a correction for the quenching effect. In the case of *p,p'*-quaterphenyl, the sample was oxidized to carbon dioxide by the Van Slyke-Folch method,[19] and the resulting carbon dioxide was charged into an ionization chamber (Applied Physics Co.). Then the radioactivity was determined by the rate-of-charge method[20] with a vibrating-reed electrometer (Cary Model 31).

17) A. Danno, M. Omura, H. Hotta, H. Hirakawa, G. Tsuchihashi and I. Yamaguchi, The 7th Hot Laboratories and Equipent Conference, Cleveland (1959), p. 349.

18) A. Danno, G. Tsuchihashi and H. Kōyama, *JAERI-1040* Report of Japan Atomic Energy Research Institute (1963).

19) D. D. Van Slyke and Folch, *J. Biol. Chem.*, **136**, 509 (1940).

20) B. M. Tolbert, *UCRL-3499* (1956).

TABLE II. *G*-VALUES FOR THE PRODUCTS FROM THE RADIOLYSIS OF BIPHENYL

Product	Number of recryst.	Specific activity μc./mol.	*G*-Value	Ratio of *G*-value
o-Terphenyl	5	1.62	0.0063	7.6
	6	1.58		
m-Terphenyl	7	0.109	0.0012	1.4
	8	0.108		
p-Terphenyl	4	0.0194	0.00083	1.0
	5	0.0200		
o,o'-Quaterphenyl	4	0.348	0.0049	5.9
	5	0.350		
m,m'-Quaterphenyl	4	0.576	0.0051	6.1
	5	0.576		
p,p'-Quaterphenyl	4	1.30	0.0104	12.5
	5	1.60		
Triphenylene	4	0.00	0.0000	—
	5	0.00		

TABLE III. *G*-VALUES OF *o,o'*-QUATERPHENYL PRODUCED FROM THE RADIOLYSIS OF BIPHENYL UNDER VARIOUS CONDITIONS

Temp., °C	Dose rate eV./g. min.	Time hr.	Absorbed dose eV./g.	*G*-Value
100	0.00	150	0.00	0.0000
Room temp.	2.25×10^{17}	168	2.27×10^{21}	0.0004
100	2.54×10^{17}	150	2.29×10^{21}	0.0049
100	2.54×10^{17}	452	6.89×10^{21}	0.0042
100	2.54×10^{17}	602	9.20×10^{21}	0.0048

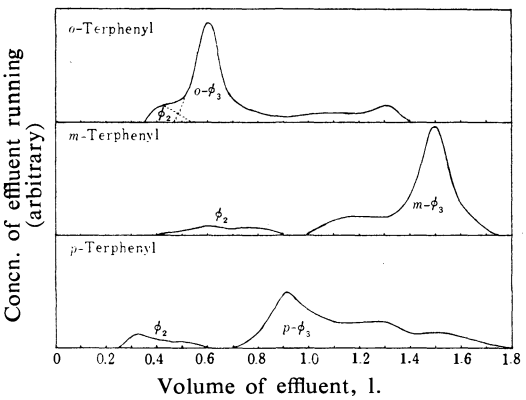


Fig. 3. Isolation of radiolytic terphenyls of biphenyl by liquid chromatography.

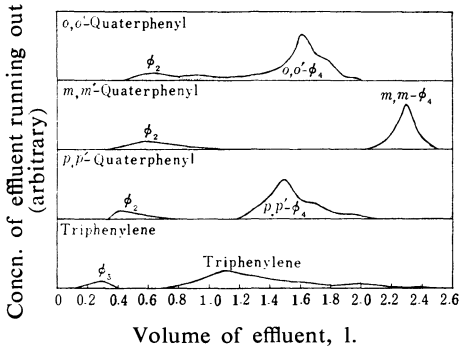


Fig. 4. Isolation of radiolytic quaterphenyls and triphenylene of biphenyl by liquid chromatography.

Results and Discussion

***G*-Values.**—Figures 3 and 4 show the isolation of the radiolytic products of biphenyl by liquid chromatography. The *G*-values of these products are tabulated in Table II. Table III illustrates the *G*-values for the *o,o'*-quaterphenyl produced from the radiolysis of biphenyl under various conditions. The following conclusions may be drawn from Table III; (1) the pyrolysis of biphenyl does not take place under such conditions (2) different reaction patterns were observed between the liquid and solid states, and (3) *G*-values are independent of the total absorbed dose in the range of our experiments.

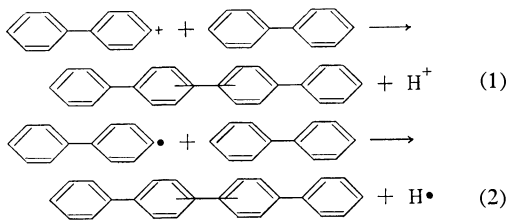
Free Radical Substitution. — The primary process of radiation chemistry is conceived of as the ionization and excitation of molecules. In radiation chemistry of the liquid phase, the reactive entities which bring about most chemical changes are possibly free radicals, since the neutralization of the ions produced by the impact of secondary electrons will often enough to make very probable the production of highly-excited molecules.[21]

Deuterium isotope effects are reported from two different groups.[11,12] Rayroux and Baertschi studied the pile-irradiation of biphenyl and concluded that the deuterated

21) A. J. Swallow, "Radiation Chemistry of Organic Compounds," Pergamon Press, Oxford (1960), p. 15.

compound decomposes more slowly than the ordinary biphenyl by a factor of two. Burr and Scarborough studied the mechanism of hydrogen gas formation in the radiolysis of biphenyl by gamma-rays. They found an isotope effect of 3.00 in the formation of radiolytic hydrogen and deuterium from the ordinary and from the deuterated biphenyls. These large isotope effects clearly indicate that the cleavage of the C–H bond in biphenyl plays an important role in the radiation decomposition, since the probability for the ionization or excitation of ordinary biphenyl should not differ greatly from that of deuterated biphenyl, according to the Frank-Condon principle.[22] Accordingly, the observed isotope effects must be for those of the fragmentation of the ion or the excited molecule. The isotope effect on the fragmentation reaction may be satisfactorily explained in terms of the Frank-Condon principle.[23] The explanation for the isotope effect should be applicable to the molecules which possess large π-electron systems, for example, benzene or biphenyl. For ionization or excitation, the structure change in these molecules will be little, since the promotion of an electron from the π-electron system will have little effect on the whole electronic structure. Therefore, the internuclear distance for the potential minimum point of the upper state will be close to that of the ground state.

Now, on the basis of the isotope-effect studies, the rupture of the C–H bond should take place at the first step in the radiolysis of biphenyl. The intermediate formed as a result may be a biphenylyl cation or radical and a hydrogen atom. The former two species are capable of reacting with a biphenyl molecule to produce the quaterphenyls which are identified as major products in the present work.



(1)

(2)

Equation 1 is a nucleophilic substitution, and Eq. 2 is a so-called homolytic aromatic substitution. The distribution of quaterphenyl isomers should be quite different in the two mechanisms. In order to establish the orientation of the reaction, it is necessary to determine the amount of all the isomers of quaterphenyls. However, it is impossible to derive the origin of quaterphenyls from these yields. For example, from the *G*-value of *o*, *p*'-quaterphenyl, it is impossible to know whether a *o*-biphenylyl radical is substituting the para-position of the biphenyl molecule or whether a *p*-biphenylyl radical is substituting the ortho-position of the biphenyl molecule.

If we assume (1) that the chemical selectivity for the cleavage of the C–H bond by radiation is so small that *o*-, *m*- and *p*-biphenylyl radicals will be produced with equal probability and (2) that the reactivities of the attacking radical are nearly equal, the product ratio for symmetrical quaterphenyls will represent the orientation of the substitution reaction. From our observed values, the ratio of the partial rate factors for ortho-, meta- and para-substitution reactions in the radiolysis of biphenyl are reduced to 1.0 : 1.0 : 8.4.

The partial rate factors for a typical nucleophilic reaction, nitration, were reported by Simamura and Mizuno as 41 and 38 for the ortho- and para-positions respectively.[24] Other types of nucleophilic substitution reactions, such as bromination, chlorination or detritiation reactions, have been tabulated in a reviewing article.[25] These experimental results indicate that biphenyl is a strongly ortho-, para-orienting substrate with relation to nucleophilic substitutions. Our present reaction seems to be different from the nucleophilic substitution mechanism, since the yield for the meta-isomer is rather larger.

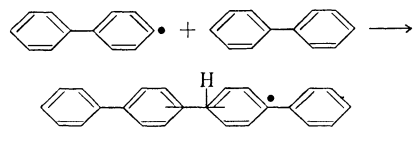
As an alternative mechanism, the possibility of free radical substitution remains. Hey and his co-workers published the ratio of *o*-, *m*- and *p*-terphenyls from the free radical phenylation of biphenyl as 48.5 : 23.0 : 28.5.[26] (The ratio of partial rate factors is 2.1 : 1.0 : 2.5.) Although there remains some doubt about the mechanism of homolytic aromatic substitution by the decomposition of benzoyl peroxide,[27] the above value could be used to indicate the characteristic behavior of biphenyl toward radical substitution reactions. In Hey's experiment, phenyl is the attacking radical, whereas in the present work, the biphenylyl radical is proposed as the substituting entity. The formation of *o*, *o*'-quaterphenyl is the result of the ortho-substitution of the

22) F. H. Field and J. L. Franklin, "Electron Impact Phenomena," Academic Press Inc., New York (1957), p. 57.
23) Ref. 22, p. 204.
24) O. Simamura and Y. Mizuno, This Bulletin, **30**, 196, (1957).
25) V. Gold (editor), "Advances in Physical Organic Chemistry," Vol. I, Academic Press Inc., London (1963), p. 67.
26) J. I. G. Cadogan, D. H. Hey and G. H. Williams, *J. Chem. Soc.*, **1954**, 794.
27) D. F. DeTar and R. A. J. Long, *J. Am. Chem. Soc.*, **80**, 4742, (1958).

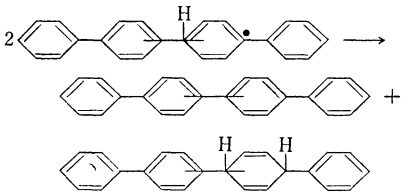
o-biphenylyl radical; hence, considerable steric hindrance of the substitution is to be expected. If the differences in the reactivities of substituting radicals by the steric hindrance are taken into account, we may conclude that the orientation of the reaction roughly agrees with that of the free radical mechanism.

The same examination for the product ratio of terphenyls leads to the conclusion that the phenyl cation should not be the intermediate, but the phenyl radical is likely to give terphenyl by substituting biphenyl molecule.

The formation of polyphenyls by the free radical mechanism probably proceeds according to DeTar's mechanism.[27]



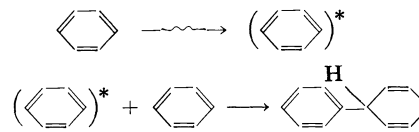
(3)



(4)

Equation 4 is a disproportionation reaction of radicals. The plausibility of this mechanism has been discussed in the summary by Walling, together with other possible mechanisms.[28] DeTar and Long actually obtained 1, 4-dihydrobiphenyl from the reaction of the phenyl radical with benzene; the amount nearly equals that of biphenyl.

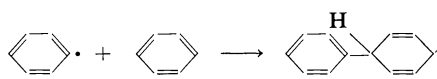
Gordon, Van Dyken and Doumani carried out the gamma-irradiation of benzene and found a mixture of phenyl cyclohexene and phenyl cyclohexadiene in the C_{12} fraction, together with biphenyl.[5] They proposed a molecular-mechanism to account for the formation of these partially-hydrogenated biphenyls:



(5)

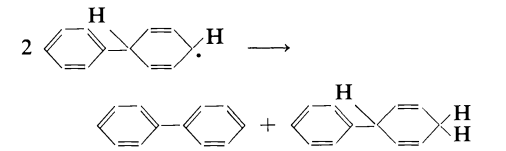
(6)

However, the formation of phenylhexadiene is alternatively explained by the free radical mechanism:



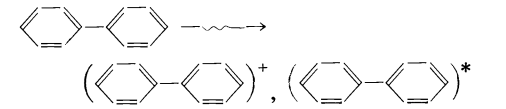
(7)

28) C. Walling, "Free Radicals in Solution," John Wiley & Sons, Inc., New York (1957), p. 482.

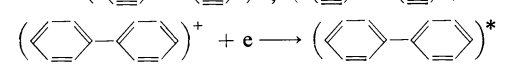


(8)

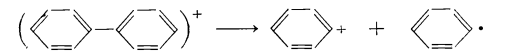
A Comparison of the Formation of Terphenyls and Quaterphenyls.—The production of phenyl and biphenylyl radicals as the intermediates which bring about the formation of polyphenyls may be presented by the following equations:



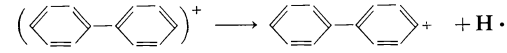
(9)



(10)



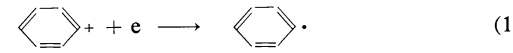
(11)



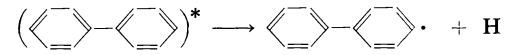
(12)



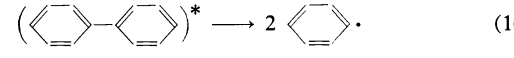
(13)



(14)

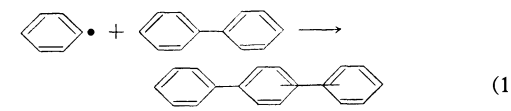


(15)

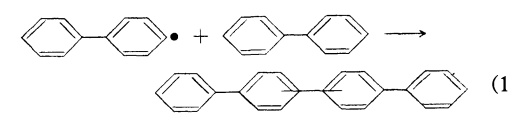


(16)

where $\left(\text{C}_6\text{H}_5\text{-C}_6\text{H}_5\right)^*$ and $\left(\text{C}_6\text{H}_5\text{-C}_6\text{H}_5\right)^+$ represent an excited biphenyl molecule and a biphenyl cation. $\text{C}_6\text{H}_5\text{-C}_6\text{H}_5\cdot$ and $\text{C}_6\text{H}_5\text{-C}_6\text{H}_5^+$ are, respectively, one of three isomeric biphenylyl radicals and cations.



(17)



(18)

Each molecule of terphenyl or quaterphenyl is presumed to be formed by the attack of a phenyl radical or a biphenylyl radical respectively on the biphenyl molecule, while radicals are undoubtedly produced directly in the primary process of the irradiation. Although we did not determine *G*-values for the formation of the three remaining unsymmetrical

quaterphenyls, they would probably be of the same magnitude as those for the symmetrical quaterphenyls. Therefore, the G-value of the unsymmetrical quaterphenyl could be calculated as an arithmetical average of the symmetrical ones; for example, the G-value of m,p'-quaterphenyl is 0.0078. The sums of the G-values for terphenyls and quaterphenyls are 0.0083 and 0.041 respectively; the latter is about five times as large as the former. This relation is different from Hall's report.[9]

The authors are grateful to Dr. Tsutomu Watanabe, the University of Tokyo, for his valuable discussions. They also wish to express their thanks to Dr. Yoshihiko Kashida of the National Institute of Radiological Science for permitting the use of a liquid scintillation spectrometer.

Division of Radiation Applications
Japan Atomic Energy Research Institute
Tokai, Ibaraki-ken

Fundamental Conditions and Reaction Mechanisms in Formation of Phosphomolybdenum Blue

By Hiroshi NAMIKI

(Received September 9, 1963)

Fundamental studies of the color development of phosphomolybdenum blue are essential for establishing the method for determining micro amounts of phosphate. Strickland[1] has extensively studied the condition of the formation and reduction of silicomolybdate, which is similar to phosphomolybdate. Only a few studies, however, have been made of the reduction mechanism of phosphomolybdate. Bolz et al.[2] tried a polarographic study and found two reduction stages in the reduction process of phosphomolybdate, but the half-wave potential for each stage was not clearly given.

The studies described in this paper were undertaken in order to establish the optimum conditions for the determination of phosphate and to explain the mechanism of phosphomolybdenum blue formation.

The effect of acidity and the concentration of molybdate, which affect the formation of phosphomolybdate remarkably, have been extensively studied; the results obtained will be graphically shown. Many photometric methods proposed for the determination of phosphate by the formation of phosphomolybdate are explained by the graph obtained.

The reduction products obtained in the process of phosphomolybdenum blue development have been studied photometrically by measurements of its absorption spectra. Useful information concerning the chemical properties of the development of phosphomolybdenum blue has thus been obtained.

1) J. D. H. Strickland, *J. Am. Chem. Soc.*, **74**, 862, 868 (1952).
2) D. F. Boltz, T. De Vries and M. G. Mellon, *Anal. Chem.*, **21**, 563 (1949).

Conditions for the Formation of Phosphomolybdenum Blue

Acidity and Molybdate Concentration. — The acidity and concentration of molybdate, which remarkably affect the formation of phosphomolybdenum blue, were examined in detail. To a solution containing 50 μg. of phosphate, different amounts of 10 N sulfuric acid and a 2.5% ammonium molybdate solution were added. After the solution had been diluted to about 40 ml., 0.25 ml. of a 2% stannous chloride solution in hydrochloric acid (1+9) was added, and then the solution adjusted to 50 ml. with water. The absorbance of the solution was measured at 10 min. after the addition of the reagents. The measurement was made by use of a Kotaki, AKA-type photoelectric photometer, with a 10-mm. cell and a 660 mμ filter. The temperature of the solution was kept at 25°C throughout the experiment. The results are given in Fig. 1.

The effect of the acidity, with reference to curves 4 and 4' in Fig. 1, for example, the final concentration of 0.15% ammonium molybdate, may be summarized as follows:

(1) When the acidity is lower than 0.5 N, the excess molybdate reagent is also reduced to form a blue color.

(2) With acidity from 0.5 to 0.8 N, a nearly identical intensity of the blue color is always obtained.

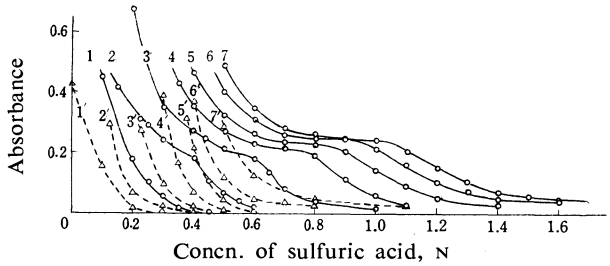


Fig. 1. Effect of concentration of sulfuric acid and ammonium molybdate
PO_4 (1)—(7), 1.0 p.p.m.; (1')—(7'), 0
Ammonium molybdate
1,1'; 0.025% 2,2'; 0.05% 3,3'; 0.10% 4,4'; 0.15% 5,5'; 0.20% 6,6'; 0.25% 7,7'; 0.30%

(3) With acidity more than 0.8, but lower than 1.1 N, the intensity of the blue color is affected by a slight change in acidity.

(4) When the acidity is higher than 1.1 N, no blue color is develops.

Therefore, the suitable acidity for the determination is considered to be in a range of 0.5 to 0.8 N, with 0.15% of ammonium molybdate.

With another concentration of ammonium molybdate, the effect of acidity upon color formation on the curves in Fig. 1 was also examined. Figure 2 indicates the relationship, showing domains, divided by curves, which the author calls "phosphomolybdenum blue color fields." The conditions shown by field 1 in Fig. 2 have been further investigated in order to establish the optimum conditions, and 0.65 N sulfuric acid and 0.15% ammonium molybdate were selected. A mixed solution of sulfuric acid (6.5 N)-ammonium molybdate (1.5%) was then prepared for practical use.[3]

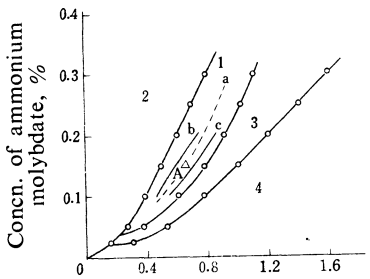


Fig. 2. Phosphomolybdenum blue color field.
1 : Suitable condition for determination
2 : Not applicable condition for determination, blue color formed in the absence of phosphate
3 : Unsuitable condition, color intensity affected by slight change in acidity
4 : Not usable, no color formed
Point A : Optimum condition proposed by author
Line a : Good condition
Line b : Absorbance 0.235 with 1 p.p.m. PO_4 in this study
Line c : Absorbance 0.215 with 1 p.p.m. PO_4 in this study

An Interpretation of the Phosphomolybdenum Blue Color Field.—When blue color is developed under the conditions given by fields 1 and 2 in Fig. 2, approximately the same absorbance values, after correction for blank values, are obtained. This fact indicates that under these conditions all the phosphate is converted to phosphomolybdate and all of the latter is reduced to phosphomolybdenum blue. Therefore, phosphomolybdenum blue color fields may be explained as follows.

Fields 1 and 2: All the phosphate is converted to phosphomolybdate and then reduced to phosphomolybdenum blue. Under the conditions given by field 2, however, molybdate added in excess is also reduced to a blue color.

Field 3: A part of the phosphate is converted to phosphomolybdate, which is reduced to phosphomolybdenum blue.

Field 4: No phosphomolybdate is formed.

These fields are obtained in 10 min. of reaction time at 25°C. The acceleration of the reaction at an elevated temperature would probably result in the complete formation of phosphomolybdate and then phosphomolybdenum blue, even in field 3.

An Examination of Methods for the Photometric Determination of Phosphate by the Formation of Phosphomolybdate.—The photometric determination of phosphate by the formation of phosphomolybdate is carried out by the following different methods:

1) Phosphate in an aqueous solution is converted to phosphomolybdate.

2) The color of phosphomolybdenum blue is developed in an aqueous solution.

3) Phosphomolybdate is extracted by some organic solvents and, after the extraction, the color of phosphomolybdenum blue is developed.

4) Phosphomolybdenum blue is extracted by

3) F. Kawamura and H. Namiki, *Japan Analyst (Bunseki Kagaku)*, **7**, 238 (1958).

some organic solvents.

The acidity and ammonium molybdate concentrations proposed by many authors[4-21] for these procedures are plotted in a phosphomolybdenum blue color field in Fig. 4. Other molybdate is calculated to an equivalent amount of ammonium molybdate. Many conditions have been proposed, as may be seen in Fig. 3; however, a reasonable interrelation between the concentrations of acid and ammonium molybdate in the above methods can easily be obtained from the interpretation of the phosphomolybdenum blue color field.

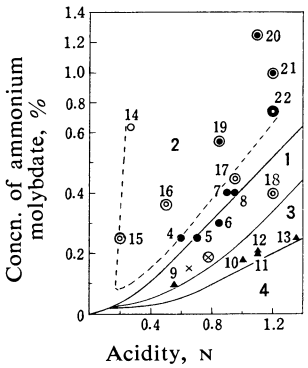


Fig. 3. Color developing conditions for photometric method by formation of phosphomolybdate and phosphomolybdenum blue.

- ● Phosphomolybdenum blue (room temperature)
- ▲ Phosphomolybdenum blue (heating)
- ○ Phosphomolybdate
- ◎ Extraction of phosphomolybdate
- ◉ Reduction of extracted phosphomolybdate
- O Dissolution of extracted phosphomolybdate
- × Phosphomolybdenum blue by author
- ⊗ Extraction of phosphomolybdenum blue by author

Area in dotted line shows good condition reported by Ishibashi and Tabushi for extraction of phosphomolybdate. Number in Figure shows the number of literatures.

The Phosphomolybdate Method, The Phosphomolybdate Extraction Method and The Method of Reducing Extracted Phosphomolybdate to a Blue Color.—All these methods depend on the complete conversion of phosphate to phosphomolybdate. The condition given by fields 1 and 2 in Fig. 3 are, therefore, suitable. Under the conditions given by field 1, however, standing for 10 min. or warming is required in order to complete the reaction. No. 18 in Fig. 3 corresponds to field 1. In this case extraction is made after accelerating the reaction by warming the solution. The conditions reported by many authors correspond to field 2, however. Extensive work by Ishibashi and Tabushi[16] on the extraction of phosphomolybdate also show a good agreement with this explanation.

The Phosphomolybdenum Blue Method and Its Extraction Method.—As has been discussed field 1 is suitable for these methods when the reactions take place at room temperature. If the color is developed by heating, the conditions shown by field 3 are also applicable. The conditions plotted in Fig. 3 show good agreement with this explanation.

The Reducing Agent.—In old works, various reducing agents were proposed in an attempt to effect the selective reduction of phosphomolybdate only. However, the control of acidity and of the concentration of molybdate is more important for this purpose. When these concentrations meet field 1 conditions, an excess of the molybdate reagent does not form a blue complex. (The details will be given in the next section.) The use of weak reducing agent sometimes limits the reduction of the molybdate reagent, even under the conditions in field 2.[4,5,8] Nevertheless, in this case only a part of the phosphomolybdate formed is often reduced to a blue color. The intensity of the resultant color, therefore, is liable to be affected by time and by temperature.

There is a procedure using weak reducing agents for determining more than 10 p.p.m. of phosphate by the phosphomolybdenum blue method.[8,23] With this procedure, only a part of the phosphate may be converted to phosphomolybdenum blue; therefore, the results are considered to be affected by the time, the temperature and other factors. The stannous chloride solution used as the reducing agent

4) P. S. Chen, Jr., T. Y. Toribara and H. Warner, *Anal. Chem.*, **28**, 1756 (1956).
5) K. D. Fleischer, B. C. Southworth, T. H. Hodecker and M. M. Tuckerman, ibid., **30**, 152 (1958).
6) S. R. Dickman and R. H. Bray, *Ind. Eng. Chem., Anal. Ed.*, **12**, 665 (1940).
7) P. Goodloe, ibid., **9**, 527 (1937).
8) M. S. Scherman, ibid., **14**, 182 (1942).
9) F. F. Hoffman, L. C. Jones, Jr., O. B. Robbins, Jr., and F. R. Alsberg, ibid., **30**, 1334 (1958).
10) D. F. Boltz and M. G. Mellon, *Anal. Chem.*, **19**, 873 (1947).
11) O. R. Gates, *Ind. Eng. Chem., Anal. Ed.*, **26**, 730 (1954).
12) W. J. Boyer, *Proc. Am. Soc. Testing Materials*, **44**, 774 (1944).
13) H. L. Katz and K. L. Proctor, *Ind. Eng. Chem., Anal. Ed.*, **19**, 612 (1942).
14) D. F. Boltz and M. G. Mellon, *Anal. Chem.*, **20**, 749 (1948).
15) M. A. De Sesa and L. B. Rogers, ibid., **26**, 1381 (1954); **26**, 1278 (1954).
16) M. Ishibashi and M. Tabushi, *Japan Analyst (Bunseki Kagaku)*, **8**, 588 (1959).
17) C. Wadelin and M. G. Mellon, *Anal. Chem.*, **25**, 1668 (1958).
18) M. Ura, *Japan Analyst (Bunseki Kagaku)*, **7**, 420 (1958).
19) S. Yokosuka, ibid., **5**, 395 (1956).
20) W. A. Pons, Jr., and J. D. Guthrie, *Ind. Eng. Chem., Anal. Ed.*, **18**, 184 (1946).
21) C. H. Lueck and D. F. Boltz, *Anal. Chem.*, **28**, 1168 (1956).
22) C. H. Lueck and D. F. Boltz, ibid., **30**, 183 (1958).
23) L. S. Stoloff, *Ind. Eng. Chem., Anal. Ed.*, **14**, 636 (1942).

for the procedure recommended by the author is superior in that even considerable deviations from the specified amount do not affect the color intensity and in that it can be used for a long time.

The Reaction Mechanism for the Development of Phosphomolybdenum Blue

The Valency of Molybdenum in a Phosphomolybdenum Blue Complex.—Phosphate solutions containing 1, 2, 3, 4 and 6 p. p. m. (0.105×10^{-4}, 0.211×10^{-4}, 0.316×10^{-4}, 0.421×10^{-4} and 0.632×10^{-4} M respectively) were reduced to molybdenum blue by the use of various amounts of a diluted stannous chloride solution, in the optimum concentration of sulfuric acid and ammonium molybdate as described in a previous section. The absorbance of a colored solution at 700 mμ was measured with a Shimadzu photoelectric spectrophotometer, type QB-50, using a 10-mm. cell and water as a reference. The results obtained are shown in Fig. 4. Each of the five curves shows good linearity and has a sharp deflection point, indicating the quantitative reaction of phosphomolybdate with stannous chloride under such conditions. The equivalent mole of stannous

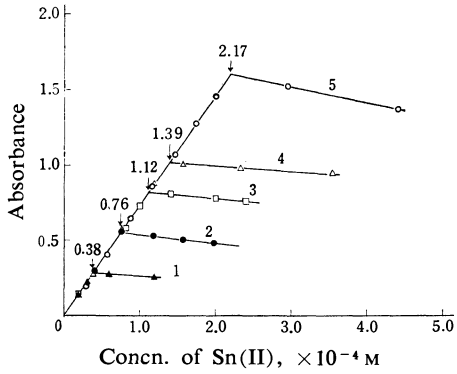


Fig. 4. Intensity of phosphomolybdenum blue vs. Sn(II) concentration.

1: PO_4 1.0 p.p.m. (0.105×10^{-4} M)
2: PO_4 2.0 p.p.m. (0.211×10^{-4} M)
3: PO_4 3.0 p.p.m. (0.316×10^{-4} M)
4: PO_4 4.0 p.p.m. (0.421×10^{-4} M)
5: PO_4 6.0 p.p.m. (0.632×10^{-4} M)

chloride can be found by each deflection point to be 3.62, 3.60, 3.18, 3.30 and 3.43 mol. for each curve, to 1 mol. of phosphate. It has already been reported that, under these conditions, the total amount of phosphate in the solution is completely converted to phosphomolybdate. It is also generally known[24,25] that one molecule of phosphomolybdate contains one atom of phosphorus and 12 atoms of molybdenum. Therefore, according to the reaction ratio described above, it is presumed that in this first step of the reduction seven of the molybdenum atoms in phosphomolybdate are reduced from molybdenum(VI) to molybdenum(V).

The Reduction by Stannous Chloride in Excess Amounts.—A phosphate solution of 2 p. p. m. was reduced to blue with varying amounts of stannous chloride solution in excess. The absorbance of the colored solutions at 700 mμ is given in Fig. 5, while the absorption spectra of these solutions are shown in Figs. 6 and 7. The curve in Fig. 5 shows a horizontal line between the concentration of stannous chloride from 0.74×10^{-4} M (equivalent mole to phosphate) to 3×10^{-4} M. It seems that the same blue product of the first stage of the reduction of phosphomolybdate is always formed in this range of stannous chloride concentration. The blue product obtained within this concentration

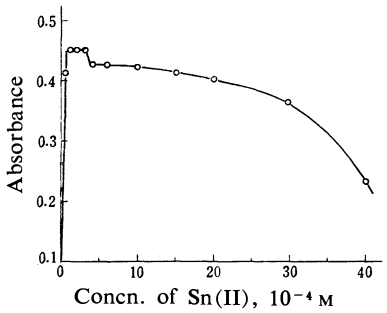


Fig. 5. Intensity of phosphomolybdenum blue v.s. Sn(II) concentration (by filter type photometer).
PO_4: 2.0 p.p.m. (0.211×10^{-4} M)

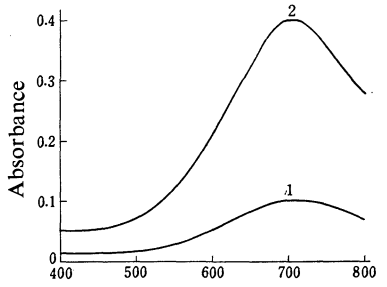


Fig. 6. Change in absorption spectra of phosphomolybdenum blue with different concentration of Sn(II).
PO_4: 2.0 p. p. m. (0.211×10^{-4} M)
Concn. of Sn(II)
1: 0.15×10^{-4} M, 2: 0.55×10^{-4} M

24) H. Remy, "Lehrbuch der Anorganischen Chemie," II, John Wiley and Sons Inc., New York (1952), p. 183.

25) H. J. Emeleus and J. S. Anderson, "Modern Aspects of Inorganic Chemistry," George Routledge and Sons, London (1940), p. 181.

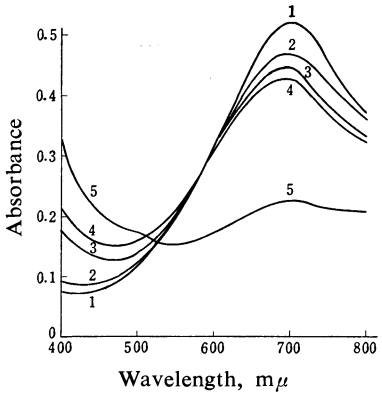


Fig. 7. Change in absorption spectra of phosphomolybdenum blue with different concentration of Sn(II).
PO_4: 2.0 p.p.m. (0.211×10^{-4} M)
Concn. of Sn(II)
1: 1.5×10^{-4} M 2: 5.0×10^{-4} M
3: 20×10^{-4} M 4: 30×10^{-4} M
5: 40×10^{-4} M

range of stannous chloride is hereafter called "normal phosphomolybdenum blue" in this paper. The absorption spectra of the normal phosphomolybdenum blue are given by curves 1 and 2 in Fig. 6 and also by curve 1 in Fig. 7, the characteristics of all of which show good agreement.

To return to Fig. 5, the absorbance falls slightly and sharply between the concentration of stannous chloride of 3×10^{-4} M and that of 4×10^{-4} M. This seems to indicate the occurrence of a second-step reduction. More exact research is required into this interesting phenomenon; the present author has not studied it further since the decrease in absorbance is slight and does not seriously affect his studies in analytical chemistry. The absorption spectra of the blue solution obtained with 5×10^{-4} M of stannous chloride closely resemble that obtained for normal phosphomolybdenum blue, shown by curve 2 in Fig. 7. Therefore, it is also thought to be normal phosphomolybdenum blue in this paper.

The absorbance at 700 mμ decreases gradually with very high concentrations of stannous chloride. This phenomenon is considered to indicate that the third step of the reduction takes place slowly in these solutions and that a part of normal phosphomolybdenum blue is reduced further to a lower valency. Curves 3—5 in Fig. 7 indicate the absorption spectra of these solutions; these spectra differ considerably from the curve for normal phosphomolybdenum blue. Such solutions usually appear green.

The absorbance decrease at 700 mμ is regarded as due to the third step of the reduction; however, the absorbance increase at 400 mμ is not considered due to the same reason. The quantity of phosphomolybdate at the third step of the reduction is considered too small to cause the large change in the absorbanc at 400 mμ shown by curves 3—5 in Fig. 7. The absorbance increase at 400 mμ is regarded by the author as being caused by a reduction of the molybdate reagent added in excess. This consideration is confirmed by the experiments described below.

Examination by the Extraction of Phosphomolybdenum Blue. — It has been generally known[26] that in an acid solution molybdenum is reduced from molybdenum(VI) to molybdenum(V) at the first step of the reduction and from molybdenum(V) to molybdenum(III) at the second step. Some observers think that only a few of the molybdenum atoms constituting the molybdate ion are reduced to molybdenum(V) at the first step of the reduction. The two solutions containing molybdenum(V) and molybdenum(III) are said to show blue and reddish brown, respectively. As was seen in the previous section, the reduction of the molybdate reagent with a blue color development has been observed at low acidity or at a high molybdate concentration. This phenomenon can be prevented when the concentration of reagents is adjusted to proper values. In the presence of strong reducing agents or a large amount of stannous chloride, the molybdate solution is reduced directly to a final reddish-brown solution, showing no intermediate blue stage. Figure 8 gives the absorption spectra of two solutions, containing 0 and 2 p. p. m. phosphate respectively, reduced by shaking them with a 2% zinc-mercury amalgam for a proper length of time. In this case a part of the molybdate reagent has been reduced. The same operation is applicable to the volumetric determination of molybdenum, and molybdenum is known to be reduced to

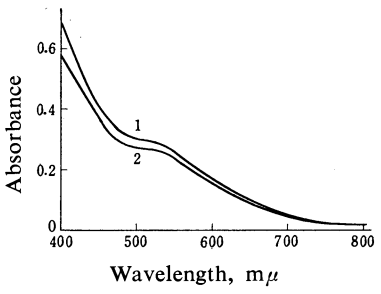


Fig. 8. Absorption spectra for low valency molybdenum reduced with Zn-Hg amalgam.
1: PO_4 2.0 p.p.m. 2: PO_4 0

26) W. M. Latimer "The Oxidation States of the Elements and their Potentials in Aqueous Solution," 2nd Ed., Prentice Hall, Englewood Cliffs, N. J. (1959), p. 251.

TABLE I. CONCENTRATION OF Sn(II) CONSUMED FOR FORMATION OF LOW VALENCY MOLYBDENUM

Concn. of phosphate $\times 10^{-4}$ M	Concn. of Sn(II), $\times 10^{-4}$ M			
	Initial	After color developing	Consumed for reduction	Consumed for reduction to low valency Mo
0[a]	20	20	0	0
0	10	7.3	2.7	2.7
0	40	24.3	15.7	15.7
0.211[b]	10	5.2	4.8	4.1
0.211	20	8.4	11.6	10.9
0.211	30	14.8	15.2	14.5
0.211	40	16.5	23.5	22.8

a) Sulfuric acid only was added, no ammonium molybdate used.
b) Sn(II) equivalent to 0.211×10^{-4}M of phosphate is 0.74×10^{-4} M.

molybdenum(III) in this process. The author has studied these reduction process by the use of various amounts of stannous chloride in excess. The blue color complex obtained was extracted by shaking it with an equal volume of *n*-butyl alcohol for 5 to 10 sec.* The absorption spectra of the solvent and aqueous phase, and also of the original solution are given in Figs. 9 and 10.

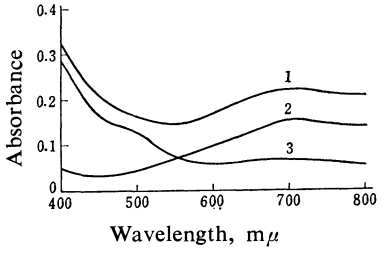


Fig. 9. Absorption spectra of colored complexes in various phases.
10 ml. of colored solution was extracted with 10 ml. of *n*-butyl alcohol
PO_4: 2.0 p.p.m. (0.211×10^{-4} M)
Sn(II): 40×10^{-4} M
1: Original solution
2: *n*-Butyl alcohol phase
3: Aqueous phase

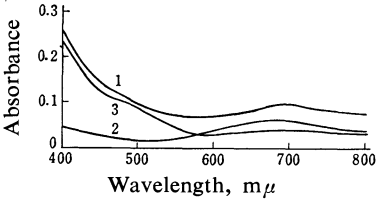


Fig. 10. Absorption spectra of colored complexes in various phases.
10 ml. of colored solution was extracted with 10 ml. of *n*-butyl alcohol
PO_4: 0, Sn(II): 40×10^{-4} M
1: Original solution
2: *n*-Butyl alcohol phase
3: Aqueous phase

* Prolonged shaking resulted in a blank color development, and also in an alteration of the absorption spectra.

The accurate comparison of the absorption curves in these figures was difficult because of the slight volume change which took place in the course of the extraction, the incomplete extraction, and the effect of the solvent on the absorption spectra. Nevertheless, curve 3 in both Figs. 9 and 10 is similiar to that in Fig. 8 at a shorter wavelength range. It is also notable that curve 2 in Fig. 9 is similar to that for normal phosphomolybdenum blue. Therefore, it has been concluded that the complex remaining in the aqueous phase consists of molybdenum reduced to a lower valency, probably molybdenum(III), and that the complex extracted with *n*-butyl alcohol is phosphomolybdenum blue. The appearance of a green color in a solution reduced with a large amount of stannous chloride is considered to be due to the co-existence of these two complexes.

Examination by the Titration of the Stannous Chloride Remaining Unreacted.—The amounts of stannous chloride remaining unreacted in the aqueous phase after the solvent extraction described above can be determined iodometrically with starch as an indicator, and this titration can be carried out without being affected by molybdenum of a lower valency. The data of determination are given in Table I. The top line in Table I is a blank test conducted without the addition of molybdate reagent. It is confirmed that stannous chloride is not lost during this operation, either with air oxidation or with dissolution into the solvent.

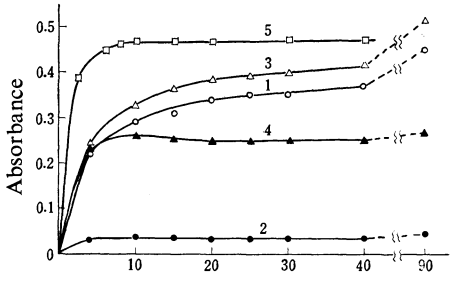
The amounts of stannous chloride consumed by reduction to low valency molybdenum are calculated from the amounts of stannous chloride initially added and equivalent to the existing phosphate. As Table I shows, considerable amounts of stannous chloride, approximately half of the amounts originally

added, are consumed in the formation of low valency molybdenum. In other words, a very large amount of low valency molybdenum is formed. In spite of the fact described above, the fading of the blue color is not as prominent as in Fig. 7. This indicates that the reduction of molybdate reagent to form a low valency of molybdenum takes place more easily than the reduction of normal phosphomolybdenum blue to color fading. Earlier in this paper, it was described that reduction with stannous chloride in an amount less than a mole equivalent to phosphate results in the reduction of phosphomolybdate only.

In the presence of excess stannous chloride, therefore, reduction takes place in the following order:

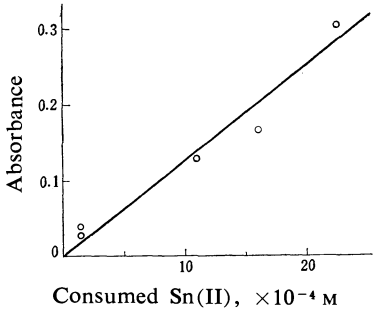
(1) Phosphomolybdate → Normal phosphomolybdenum blue
(2) Molybdate reagent → Low valency of molybdenum
(3) Normal phosphomolybdenum blue→Low valency of phosphomolybdenum blue

The reactions do not always proceed in this sequence, however. With an excess of stannous chloride, reaction 3 proceeds partially via reactions 1 and 2, resulting in a decrease in the intensity of blue. However, with a slight excess of stannous chloride, reaction 3 is negligible because excess stannous chloride is quickly diminished by reaction 2.



Time after addition of reagents, min.

Fig. 11. Reduction rate for phosphomolybdate and molybdate with excess Sn(II).
1 PO_4 0, Sn(II) 40×10^{-4} M, 400 mμ
2 PO_4 0, Sn(II) 40×10^{-4} M, 700 mμ
3 PO_4 2.0 p.p.m., Sn(II) 40×10^{-4} M, 400 mμ
4 PO_4 2.0 p.p.m., Sn(II) 40×10^{-4} M, 700 mμ
5 PO_4 2.0 p.p.m., Sn(II) 5×10^{-4} M, 700 mμ



Consumed Sn(II), $\times10^{-4}$ M

Fig. 12. Absorbance of low valency molybdenum compound v.s. Sn(II) consumed (Measured 10 min. after addition of reagents).

This view will be explained further by the following experiments. Figure 11 shows changes in the absorbance with time at 400 mμ and 700 mμ measured on solutions, containing 0 and 2 p. p. m. of phosphate; these solutions were treated in the same way as in the experiments for Figs. 9 and 10. Figure 12 shows the relation between the absorbance at 400 mμ of low valency molybdenum and the amounts of stannous chloride consumed for its formation. The relation was obtained from data in Table I and Figs. 6, 7, 9 and 10. The consumption of stannous chloride with time shown in Fig. 11 is obtained from the absorbance at 400 mμ and Fig. 12. The amounts of unreacted stannous chloride can be obtained by subtracting the amount consumed from the amounts added initially. For example, by means of curves 1 and 3 in Fig. 11* the amounts of unreacted stannous chloride are found to be 20×10^{-4}, 17×10^{-4}, 16×10^{-4} and 10×10^{-4} M after 5, 7.5, 15 and 30 min. respectively. Stannous chloride in an amount less than $10\sim15\times10^{-4}$ M does not cause the remarkable fading of phosphomolybdenum blue shown in Fig. 5. Thus, the reaction which takes place in Fig. 11 is explained as follows: Through the range of reaction, in the first 10 min. after the addition of the reagent, reactions 1, 2 and 3 progress simultaneously. All the phosphomolybdate is reduced in this period, and then some part of it is further reduced to that of a lower valency with less color intensity than normal phosphomolybdenum blue. After 10 min., the amount of stannous chloride decreases to approximately 16×10^{-4} M, where reaction 3 ceases and the blue color becomes stable.

Summary

The effects of acidity and molybdate concentration on the development of phosphomolybdenum blue have been studied in detail and the relationships among these three factors shown by a graph, called a "phosphomolybdenum blue color field" by the author. A further investigation was undertaken in order to explain the mechanisms of color development and the fundamental properties of reaction products under the optimum conditions established by the author for the determination

* The difference between curves 1 and 3 is due to the absorbance of phosphomolybdenum blue at 400 mμ.

of phosphate. The acidity and molybdate concentration in the graph was divided into 4 fields, the fields denoting the concentration conditions given below.

Field 1: All phosphate forms phosphomolybdate, and then forms phosphomolybdenum blue. No blue color due to the reagent blank is obtained. This field is suitable for the phosphomolybdenum blue method.

Field 2: All phosphate forms phosphomolybdate, and then forms phosphomolybdenum blue. However, the reagent blank also becomes blue. This field is suitable for the phosphomolybdate method.

Field 3: Only a part of the phosphate forms phosphomolybdate and then phosphomolybdenum blue. Heating promotes the reaction, making it suitable for the phosphomolybdenum blue method.

Field 4: No phosphomolybdate is formed. This field is not applicable for determinations.

When the reaction of phosphomolybdenum blue development is carried out in a solution containing 0.65 N sulfuric acid and 0.15% ammonium molybdate, which is optimum for the determination of phosphate, phosphate is completely converted to phosphomolybdate, which in turn is quantitatively reduced by stannous chloride to form phosphomolybdenum blue. At the first stage of the reduction, one phosphomolybdenum blue molecule is regarded as possessing seven molybdenum atoms that have been reduced to molybdenum(V). Reduction by the use of excess amounts of stannous chloride proceeds in the following order:

(1) Phosphomolybdate → Phosphomolybdenum blue
(2) Molybdate reagent → Molybdenum of low valency
(3) Phosphomolybdenum blue → Phosphomolybdenum blue of a low valency

The reduction product in reaction 2 is probably a molybdenum(III) compound. A large excess of stannous chloride fades the blue color of the solution by means of reaction 3. Reaction 3 is negligible compared with reactions 1 and 2 in solutions containing a slight excess of stannous chloride. Under the conditions established by the author for color development, no blue product is formed as a results of the reduction of the molybdate reagent. Molybdate is considered to have been reduced directly to reddish brown molybdenum(III).

The knowledge obtained from these experiments is thought to be enough for the performance of the phosphomolybdenum blue method, although it is still insufficient for a complete explanation of the properties of the reactions and the reaction products.

The author is much indebted to Professor Iwaji Iwasaki of the Tokyo Institute of Technology, Professor Isao Kayama of Hokkaido University of Liberal Arts, and Professor Fumikazu Kawamura of Yokohama National University for their invaluable advice and discussions throughout his work.

Department of Analytical Chemistry
Faculty of Engineering
Yokohama National University
Minami-ku, Yokohama

Flash Photolysis of Methylene Blue. I. Reversible Photolysis in the Absence of a Reducing Agent and in the Presence of Certain Kinds of Reducing Agents

By Shiro MATSUMOTO

(Received September 19, 1963)

It was shown in a previous paper[1] on the photoreduction of methylene blue by *N*-phenylglycines that kinetic data and some other properties of the system indicate a mechanism via a long-lived excited state (presumably the lowest triplet state) of the dye. As it was desired to detect such an intermediate in a more direct way and, simultaneously, to get more information on the mechanism of the photoreduction, a flash photolytic investigation was undertaken. Parker[2] has applied this method to methylene blue in an acid medium

1) S. Matsumoto, This Bulletin, 35, 1860, 1866 (1962).

2) C. A. Parker, *J. Phys. Chem.*, 63, 26 (1959).

with ferrous ions as reductants. He observed two transients of different lifetimes and assigned them to the triplet state and to the semiquinone of the dye. He investigated the reaction, however, only in a 0.1 N sulfuric acid solution. Details of the absorption curves were not given.

For the present work the flash photolysis of methylene blue was carried out in solvents of various pH values, both in the absence and in the presence of a reductant. In Part I, only those cases are treated in which the solution recovers its original absorption and little or no permanent spectral change is observed after a flash illumination. In this case, ferrous sulfate, *p*-phenylenediamine or benzohydroquinone is used as the reductant. When *N*-phenylglycines were used as reductants, or when organic solvents were used, flash photolysis resulted in a more or less apparent permanent spectral change of the solution. Such cases will be treated in Part II of this paper.

Experimental

The exciting flash lamp was made of a quartz tube (1 cm. in external diameter) wound in a helix (3.4 cm. in inner diameter and 6 cm. long). It was filled with xenon to 150 mmHg. To recored the transient absorption spectra, an argon-filled (200 mmHg) linear flash lamp was used. The condensers for these lamps were 20 and 10 μF respectively, and they were charged up to 4000 V. in most cases. The reaction cell was also made of quartz (2.2 cm. in external diameter and 7 cm. long). It was covered with an ordinary-glass tube (wall thickness, 1 mm.), which served as a filter for the short-wavelength part of the exciting flash. The interval between the firings of the two flashes could be varied, by means of an electronic delay circuit, from 3 to 5000 μsec. The spectra were photographed with a Shimadzu Quartz spectrograph QF-60. In ordinary cases, a "Fuji Processpan Plate for Spectrograph" was used, but in some cases a "Fuji Neopan Plate" or a "Fuji Neopan Sheet Film SSS" was preferable. Near-infrared spectra were recorded on a "Fuji Infrared Plate 820" or on "Kodak Infrared Sheet Film." The densities on the plates were traced with a Nalumi recording microphotometer NLM-VII. For a preliminary study of tracing the change in absorption at certain wavelengths, the spectro-flash lamp was replaced by a 40 W./12 V. incandiscent lamp operated by a floating-charged battery. The light was made parallel by a lens, went through the reaction cell and an interference filter, and fell on the photo-cathode of a photomultiplier. Ordinary precautions to minimize the effect of scattered light, namely the use of baffles[3] and the use of a compensating circuit,[4] were adopted, but the relatively long duration of the exciting flash interfered with a detailed kinetic study of the early stage of the photoreaction. Such kinetic study requires a much improved exciting lamp.[3]

Oxygen was removed from solutions by flushing them with pure nitrogen as in previous studies.[1] Although this method of deaeration is imperfect for the complete removal of oxygen, the results were reasonably reproducible and may be compared with the results of the previous experiments[1] performed under the same conditions.

The methylene blue was a G. R. reagent from the Koso Chem. Co.; $\varepsilon_{max}=8.15\times10^4$. The other reagents were also of G. R. grade from the same company and were used without further purification.

Results

Flash Photolysis in the Absence of a Reductant.—*A Transient in an Acid Medium.*—The transient spectrum which appears in a 0.1 N sulfuric acid solution is shown in Fig. 1. It may be seen that in this case the reaction is simple and that only one transient is formed. It has an absorption peak near 375 mμ and decays, in agreement with Parker's statement, almost in parallel with the exciting flash. This must be the triplet state of the dye. A weak second peak is present near 280 mμ. The spectrum is the same in 1 N sulfuric acid. In a more concentrated acid, the region of the absorption seems to remain the same, but its shape is obscured by an increase in the absorption of the ground state of the dye in this region.

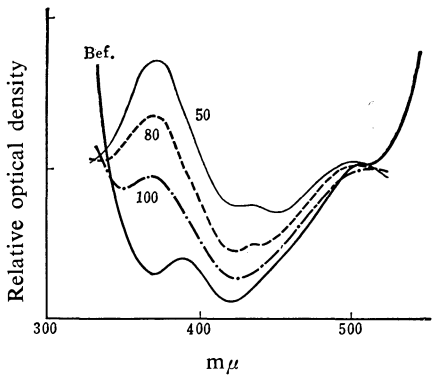


Fig. 1. Transient spectra in 0.1 N H_2SO_4 in the absence of reductant. M. B. 10^{-5} M. Figures beside curves indicate delay time Δt in μsec.

A Transient in Plain Water.—In this case, the transient spectrum is quite distinct from that in an acid medium (Figs. 2, 3 Plate 3). The absorption persists longer and shows peaks near 282 mμ, 420 mμ, and 520 mμ. It also extends to near-infrared region, where no absorption is observed in an acid medium.

3) H. Linschitz and K. Sarkanen, *J. Am. Chem. Soc.*, **80**, 4826 (1958).
4) S. Claesson and L. Lindqvist, *Arkiv Kemi.*, **11**, 535 (1957).

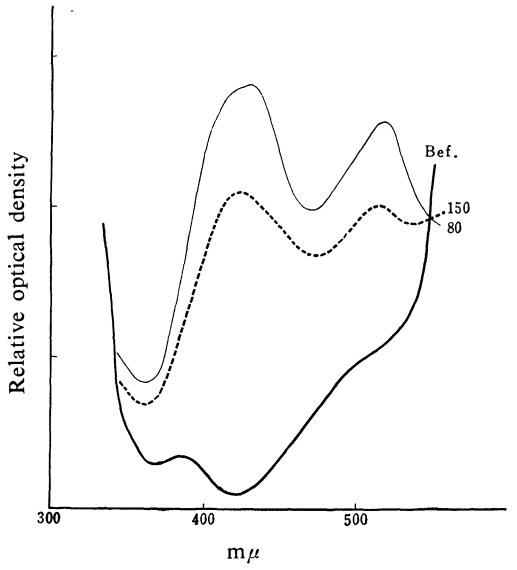


Fig. 2. Transient spectra in water in the absence of reductant. M. B. 10^{-5} M

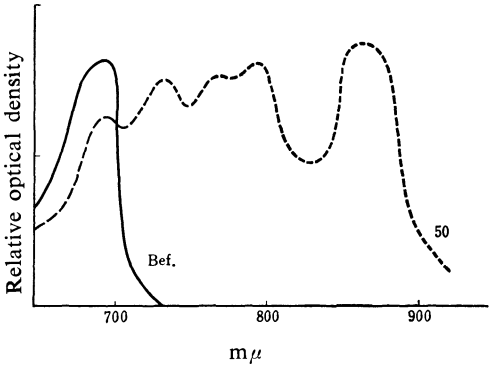


Fig. 3. The same as in Fig. 2. Near-infrared region.

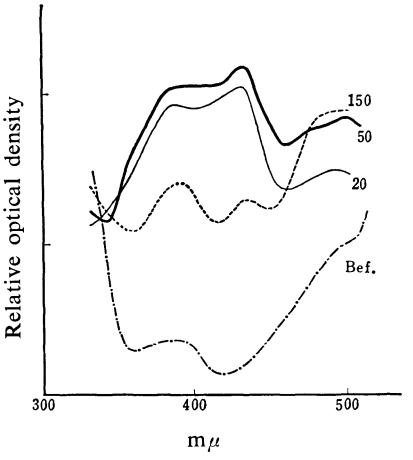


Fig. 4. Transient spectra in the absence of reductant. Solv.: buff. pH 6.8; M. B. 10^{-5} M

Another difference and complication is that the absorption around 520 mμ grows a little more slowly than that in the other region of the spectrum (Plate 1). This shows the superposition of at least two transient spectra, but their separation is difficult at present because the duration of the flash is not sufficiently short compared with the transient lifetimes. Preliminary experimentation shows the decay at 414 mμ to be unimolecular with a half-life of about 130 μsec.

A Transient in Buffer Solutions of Different pH Values.—The spectra at earlier stages of photolysis (e. g. when $\Delta t = 20$ μ sec., Δt is the time interval between the firings of the exciting flash and the spectro-flash) vary regularly according to the pH value of the solvent. Below a pH value of 6.0, only the one found in 0.1 N sulfuric acid (acid form) appears, while above 7.4 only the one found in water (neutral form) appears. At intermediate pH values the two forms appear superposed, and at a pH value near 6.8 both forms seem to appear in equal amounts (Fig. 4). It seems, therefore, that the spectrum which appears initially in the photolysis of methylene blue in water[5] corresponds to the same species as that appearing in an acid medium, only with different protonation. Its pK_A value is approximately 6.8. No other protonation type of the species is found in the pH range from 1 to 12. It may also be seen from Fig. 4 that the increase in the absorption around 500 mμ at the later stage of the flash photolysis is much more pronounced in buffer solutions than in plain water.

A Transient in Dilute Acid Solutions.—When the photolysis was carried out in dilute sulfuric acid solutions, a queer result was obtained. The spectrum in 5×10^{-5} N sulfuric acid resembles that in a buffer solution of pH 6.8 rather than that in pH 4.3. The use of hydrochloric acid in place of sulfuric acid gives the same result. In accord with these results, near-infrared absorption appears in the photolysis in sulfuric or hydrochloric acid when the acid is more dilute than about 10^{-4} N, whereas it appears in buffer solutions only when the pH value is higher than about 6.2. This descrepancy may be explained most simply by the assumption that the neutral form of the triplet is first formed in the course of the photolysis and that in a very dilute acid solution the speed of the protonation producing the acid form of the triplet is so slow that the equilibrium between the two forms is not attained during the short lifetimes of the

5) The transient spectrum in a buffer solution of pH 7.0 contains some acid form. This discrepancy may be related to the facts described in the next sub-section.

transients. In buffer solutions, rather concentrated buffer agents may catalyze the acid-base equilibrium of the triplet. It was found that, in a dilute acid solution, the ratio of the absorption at 370 mμ to that at 420 mμ somewhat increases when $\Delta t = 20 \sim 80$ μ sec.

Flash Photolysis in the Presence of Reductants.—*A Transient in an Acid Medium in the Presene of Ferrous Ions.* — The photolysis in 0.1 N sulfuric acid has been investigated by Parker[2]; in agreement with his result, the transient spectrum in the presence of this reductant is very similar to the triplet spectrum in this medium, only with a much longer lifetime. The broad band has a maximum around 375 mμ (Fig. 5). An experiment at this wavelength shows the disappearance to be roughly bimolecular (Fig. 6). This transient must be the semiquinone of methylene blue, as stated by Parker. The semiquinone also shows absorption from ca. 450 mμ down to the near-infrared region, just as with the transient observed in water in the absence of a reductant, whereas in an acid medium no absorption is observed in the absence of a reductant. Plate 2 shows that at a certain period of the photolysis the absorption in the visible region is weak, although in time the absorption of the original dye is restored. This suggests that some part of the methylene blue is trapped in a rather stable form, with no absorption in the visible region. This may be the leuco form of the dye. This supposition is supported by the appearance of an absorption around 255 mμ[6] (Plate 4). Figure 5 shows that the peak of the semiquinone absorption is displaced towards 390 mμ in media of pH > 3. Here, a less protonated form of the semiquinone must be present. No further change is observed in buffer solutions with pH values lower than 5.3 where the ferrous salt could be used without the trouble of hydrolysis. In 10 N or more concentrated sulfuric acid, a second change in the transient spectrum is observed. The peak of the absorption seems to be moved a little to a longer wavelength (ca. 390 mμ), and the absorption at wavelengths longer than 500 mμ observed in 0.1 N sulfuric acid is lacking. Another feature is that the the absorption appears delayed after the flash and persists much longer than in a 0.1 N acid solution. In an intermediate acid solution, e. g., in 3 N sulfuric acid, an intermediary situation is observed.

Transients in the Presence of p-Phenylenediamine or Benzohydroquinone. — The photolysis in the presence of *p*-phenylenediamine is simple. The spectrum and its change with time in a buffer solution of pH 7.0 is shown in Plate 7. This general apperance does not change in the pH range from 5 to 8. It shows peaks at 390 mμ and 460 mμ and one below 330 mμ. The first coincides with that of the semiquinone of methylene blue, while the latter two probably belong to the semiquinone of the diamine.[7] Absortion also appears in the near-infrared region. As the pH of the solvent is lowered below 5, the transient becomes progressively faint and appears somewhat delayed after the appearance of an absorption due to the triplet. This result is in harmony with the facts that the diamine shows acid-base equilibria[8] of pK_A 6.0 and 2.5 and that only the neutral diamine molecule seems to have a strong deactivating effect on the dye triplet.[9] The absorption near 280 mμ given in Plate 5 shows a close resemblance to that of the triplet, but

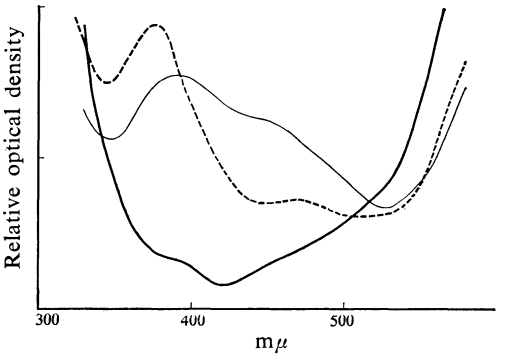


Fig. 5. Transient spectra in the presence of Fe^{2+} in acid medium. M. B. 10^{-5} M; $FeSO_4$ 0.01 M; $\Delta t = 50$ μsec.
—— Before flash
- - - In 0.1 N H_2SO_4
—— In a buff. pH 5.3

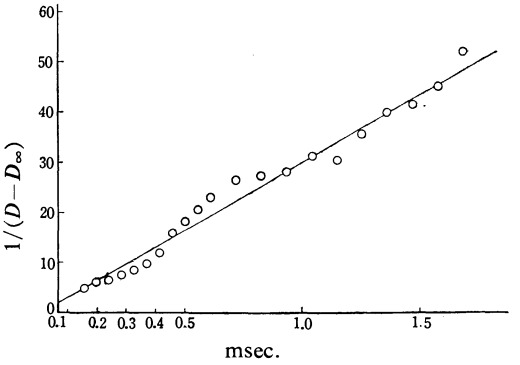


Fig. 6. Bimolecular decay of the transient absorption at 380 mμ.

6) Y. Usui, H. Obata and M. Koizumi, This Bulletin, 34, 1049 (1961).

7) L. Lindqvist, *Arkiv Kemi.*, **16**, 79 (1960).

8) N. A. Lange, "Handbook of Chemistry," 8th Ed., Handbook Publishers, Inc., Sandusky, Ohio (1952), p. 1235.

9) S. Matsumoto, unpublished.

no definite distinction is possible. In Plate 5 it may also be seen that, in this case, the recovery of the ground state of the dye occurs directly from the semiquinone and that little leuco dye is formed, in contrast to the case with ferrous ions and the case with hydroquinones described below. In media with pH values higher than 8.8, the transient spectrum is different (Fig. 7). The absorption maximum at 390 mμ is displaced to a wavelength near 430 mμ, and the absorption at wavelengths longer than 500 mμ is stronger than in solvents with lower pH values.

The result is more complex when hydroquinone is used as the reductant. Figure 8 shows a transient increase in absorption around 490 mμ and at wavelengths longer than 530 mμ preceding the growth of a strong and persistent absortion around 430 mμ in a buffer solution of pH 7.4. The latter may be mainly due to

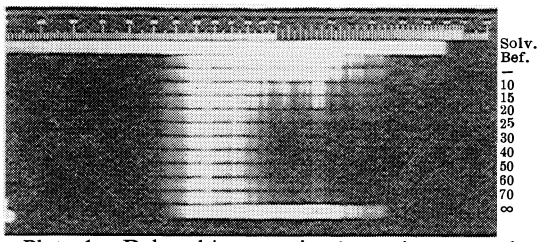


Plate 1. Delayed increase in absorption around 520 mμ in water in the absence of reductant.
M. B. 3×10^{-5} M

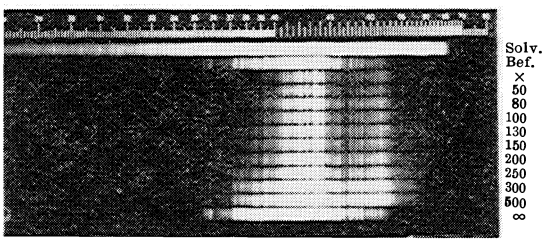


Plate 2. Transient spectra in the presence of $FeSO_4$ (0.1 M) in 0.1 N H_2SO_4.
M. B. 2.5×10^{-5} M

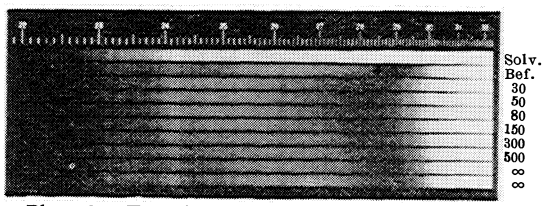


Plate 3. Transient absorption in the range 220 ~320 mμ in the absence of reductant.
Solv. H_2O; M. B. 5×10^{-6} M

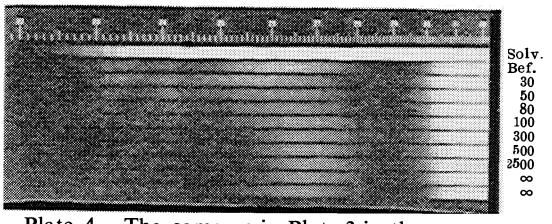


Plate 4. The same as in Plate 3 in the presence of $FeSO_4$, 0.002 M.
Solv. 0.1 N H_2SO_4; M. B. 10^{-5} M

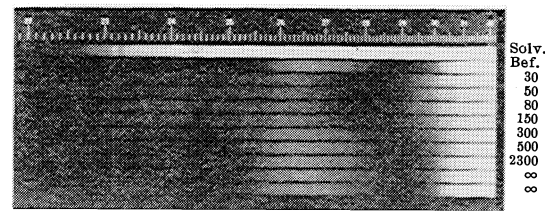
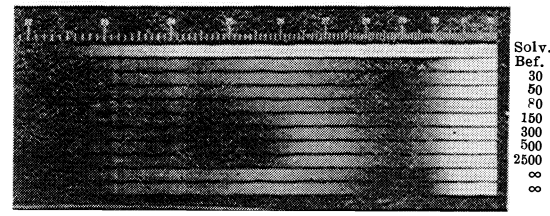
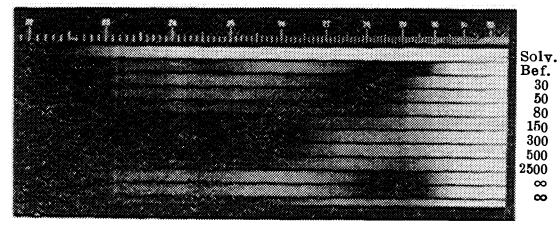


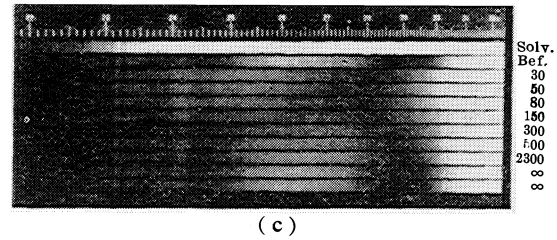
Plate 5. The same as in Plate 3 in the presence of PPD, 10^{-5} M.
Solv. buff. pH 7.4; M. B. 10^{-5} M



(a)



(b)



(c)

Plate 6. The same as in Plate 3 in the presence of HQ, 10^{-5} M.
M. B. 10^{-5} M; Solv.: (a) 0.1 N H_2SO_4 (b) Buff. pH 7.4 (c) Buff. pH 9.2

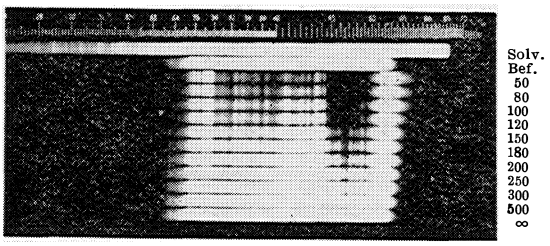
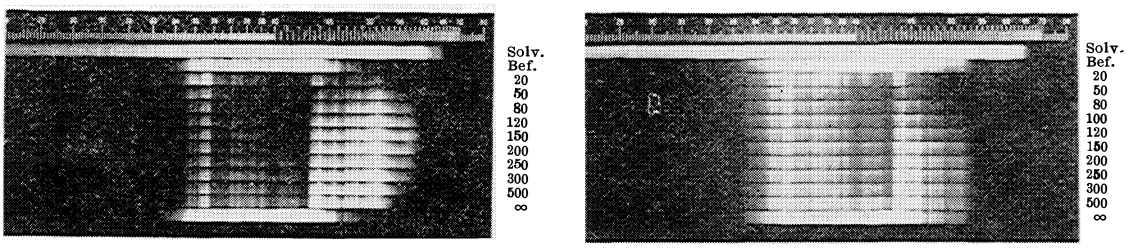


Plate 7. Transient spectra in the presence of PPD (5×10^{-5} M). Solv. buff. pH 7.0; M. B. 2.5×10^{-5} M



(a) (b)

Plate 8. Transient spectra in the presence of HQ (10^{-4} M). M. B. 3×10^{-5} M; Solv.: (a) Buff. pH 7.4 (b) Buff. pH 9.2

the semiquinone produced from hydroquinone,[10] probably superposed by the absorption of methylene blue semiquinone. In the earliest stage, the peak at 400 mμ is more marked than that at 430 mμ. The order is upset at later stages. This may indicate the more rapid deformation of the dye semiquinone than that of the benzosemiquinone. The reaction may be a dismutation of the semiquinone or its reduction by other molecules of hydroquinone. Probably the latter predominates, as will be seen below (Plate 6b). At some stage the absorption in the region of methylene blue absorption reaches its minimum and then increases. This stage is analogous to a later stage of the photolysis with ferrous ions, when semiquinone has been converted into leuco methylene blue (cf. Plates 2 and 8a). The general pattern is the same in the pH range 5~8. Figure 9 shows transient spectra at various pH values. The difference between the spectra at pH 6.5 and 9.2 is remarkable (cf. also Plates 8a and 8b). The spectral shift is similar to the case with *p*-phenylenediamine, but the increase in absorption at wavelengths longer than 500 mμ is more pronounced at an early period than in the latter case. It is also seen that, at pH 9.2, there is no period when methylene blue and its semiquinone disappear simultaneously. At pH values higher than 9.2, the general features of the spectrum and its change with time remain the same, but in an extremely alkaline solution, e. g., a 0.01 N sodium hydroxide solution, an irreversible bleaching of the dye becomes noticeable. In acid media (pH< 5), transient spectra and their change with time

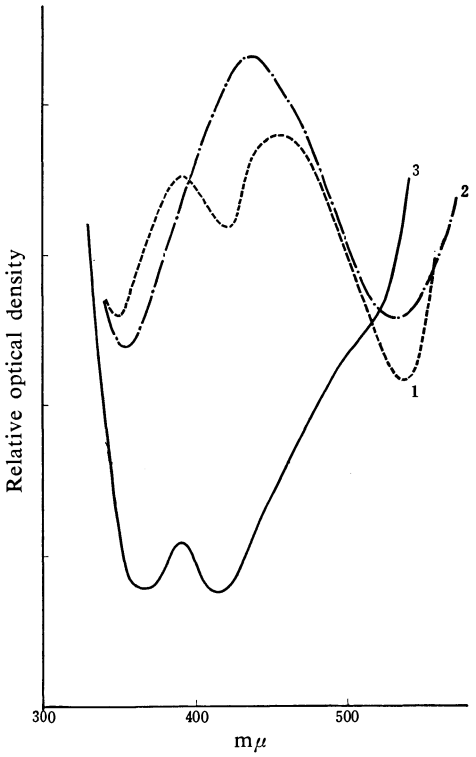


Fig. 7. Shift in transient absorption at a pH near 8, *p*-phenylenediamine being added as reductant, 10^{-4} M. M. B. 3×10^{-5} M; Δt=50 μsec. Curve 1: pH 7.0. Curve 2: pH 9.2. Curve 3 shows spectrum before flash.

10) H. Linschitz, J. Rennert and T. M. Korn, *J. Am. Chem. Soc.*, **76**, 5839 (1954).

are quite similar to those observed when ferrous ions were used, except for an absorption around 400 mμ due to benzosemiquinone. The spectrum at pH 3.2 is red-shifted compared with that at pH 1, parallel with the results obtained in the case of ferrous ions. In view of the results obtained in the cases of ferrous ions and *p*-phenylenediamine, the changes observed at other pH values must be due to the characteristics of the hydroquinone component. In a buffer solution of pH 3.8, the semiquinone of benzoquinone seems to have an absorption around 400 mμ, one which is shifted to 430 mμ in a buffer solution of pH 5.3. Plates 6a—6c show the transient spectra in the wavelength region from 220 mμ to 320 mμ at various pH values. It may be seen that, below a pH value of 8.4, leuco methylene blue is formed in a process of reversible photoreaction. At a pH value of 9.2, however, the recovery of the original dye occurs without the formation of leuco methylene blue. At a pH value of 8.4, an intermediary situation is observed. This pH dependence parallels that of the spectrum of methylene blue semiquinone at longer wavelengths. It may also be seen that, although at pH values higher than 9 little formation of leuco methylene blue is observed, the formation of

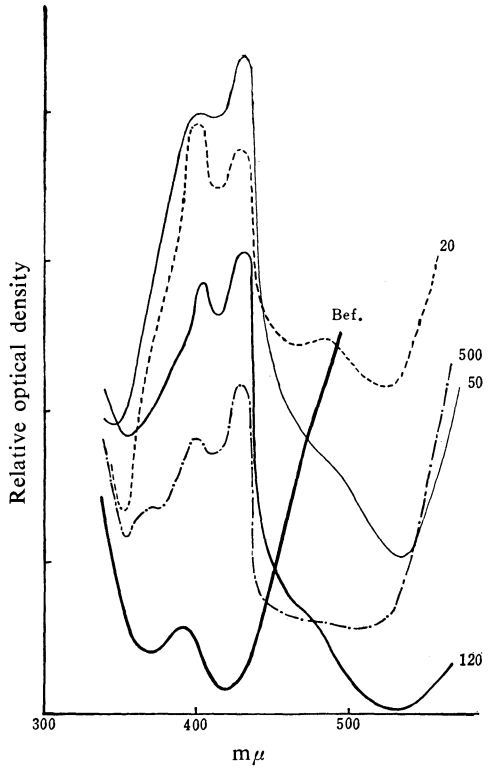


Fig. 8 Transient spectra in the presence of hydroquinone in a buffer of pH 6.5.
M. B. 3×10^{-5} M; HQ 10^{-4} M

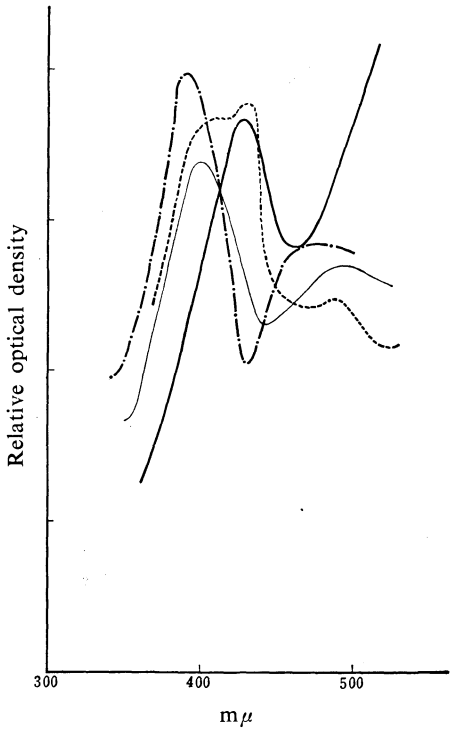


Fig. 9. Transient absorption in the presence of hydroquinone at various pH values.
M. B. 3×10^{-5} M; HQ 10^{-4} M; $\Delta t=50$ μsec.
— pH 9.2 --- pH 6.5
—— pH 3.8 -·- In 0.1 N H_2SO_4

an intermediate (presumably the semiquinone of the dye) is a clear-cut process and the yield of the intermediate is good. On the contrary, the conversion in an acid medium seems to be less perfect.

Discussion

The results just described seem to be related to the fact that the quantum yield of the photoreduction of methylene blue by *N*-phenylglycines reaches a maximum at a pH near 7.8. As was seen above, the transient spectrum that appears after a flash illumination of methylene blue in a neutral or alkaline medium persists longer than the spectrum in an acid medium. Whether this means a longer lifetime of the neutral form triplet itself compared with that of the acid form, or whether it can be accounted for solely by a superposition of another intermediate with a long life, it can not be decided at present. Evidently the delayed increase in the absorption around 530 mμ indicates such a second transient, but the clear-cut separation of the spectra is difficult because of the long duration of the exciting flash. This requires a detailed kinetic study with an improved flash apparatus. At

any rate, the neutral-form triplet must have a different (probably an increased) reactivity or reaction probability towards reductants compared with that of the acid form. For this reason, the velocity of photoreduction increases with the pH value in the range below about 7.8. At still higher pH values, the semiquinone of methylene blue loses a proton to change into its conjugate base. The latter has a very slight tendency to be reduced further and returns smoothly to the original dye cation (Plate 6c). This would explain the sharp decrease in the rate of photoreduction at the higher side of the pH region. If the methylene blue cation is denoted by D^+, the neutral and acid forms of the triplet may be denoted by D^{+t} and DH^{++t} respectively. In the same way, various forms of semiquinone, which appears in solvents of different acidities, may be designated D, DH^+, DH_2^{2+}, and DH_3^{3+}. Only DH^+ and DH_2^{2+} were seen to be reduced or to dismutate rapidly to form the leuco dye, and D would have to be protonated before it is reduced further if it were the first reduction product.

The assignment of the absorption at 520 mμ (in plain water), of those at 490 mμ and at longer wavelengths than 530 mμ (Fig. 8), and of that one at longer wavelengths than 500 mμ (Plate 8b) can be only speculative at present. The first may be assigned to a labile complex between a pair of half-oxidized and half-reduced methylene blue ions produced by a redox-reaction between an excited ion and a normal one stabilized by some negative ions,[11] or to a sort of charge-transfer complex between an excited dye ion and a normal one. The second and the third absorption may also be assigned to the same species or to a similar charge-transfer type of complexes between excited dye ions and reductant molecules.

Summary

Transient spectra which appear in the flash photolysis of methylene blue in aqueous solvents of various pH values have been surveyed both in the absence and in the presence of a reductant. In the absence of a reductant, the triplet state of the dye has been observed to appear in two forms, with different degrees of protonation. The form found in neutral water seems to be formed directly from the excited singlet state of the dye. The pK_A value of the acid-base equilibrium has been found to be approximately 6.8. A second transient has been found to be produced in water and in buffer solutions of a moderate pH value at a later stage of the photolysis. Its formation is more marked in buffer solutions, and it may be supposed to be a sort of charge-transfer complex between an excited dye ion and another dye component. The photolysis in the presence of ferrous ions, *p*-phenylenediamine or benzohydroquinone is nearly reversible, and the absorption of the original dye is restored after the illumination except in an extremely alkaline solution. The transitory formation of leuco methylene blue has been observed when ferrous sulfate or hydroquinone was used as the reductant below a pH value of 8.4, while that was not the case with *p*-phenylenediamine. The formation of leuco methylene blue from semiquinone has been found to be a bimolecular dismutation process in an acid medium when ferrous ions are the reductant, but when hydroquinone is used as the reductant at moderate pH values, it also reduces the methylene blue semiquinone. When hydroquinone is used as the reductant in a neutral or alkaline solvent, an increase in absorption is often observed at some longer wavelengths; this has tentatively been attributed to a complex between excited dye ions and reductant molecules. A comparison of the transient spectra obtained in various conditions has shown that the semiquinone of methylene blue exists in variously protonated forms in the following ranges: pH>9, pH=3~8, in 0.1~1 N sulfuric acid, and in very concentrated sulfuric acid. The pH dependence of the quantum yield of the photoreduction obtained earlier has been tentatively related to the change in the degree of protonation of the triplet state and the semiquinone.

The author is indebted to Professor Noboru Ando and Professor Ikuzo Tanaka of the Tokyo Institute of Tehcnology for their permission to use the laboratory facilities that made this work possible and also for their helpful suggestions. Thanks are also due to Professor Masao Koizumi of Tohoku University and Dr. Yuji Mori of the Tokyo Institute of Technology for their valuable discussions.

Faculty of Agriculture
Kagawa University
Kita-gun, Kagawa

11) Suggested by Professor Masao Koizumi.

Flash Photolysis of Methylene Blue. II. Photolysis in an Aqueous Solvent in the Presence of N-Phenylglycines and Photolysis in Organic Solvents

By Shiro MATSUMOTO

(Received September 19, 1963)

In Part I[1] of this paper the flash-photolytic reduction of methylene blue in aqueous solvents in the presence of several reducing agents was surveyed. Now it is desirable to investigate in this connection the reaction in the presence of *N*-phenylglycines, and to compare the results with those obtained by continuous illumination.[2] In this case an irreversible bleaching of the dye remains after flash illumination. This requires renewed preparation of a degassed solution after every flash to get a series of spectra corresponding to various delay times.

Photolysis in common organic solvents was also found to result in an irreversible bleaching. Preliminary results of photolysis in these solvents will be given also.

Experimental

The apparatus and procedure are the same as those described in Part I. The preparation of *N*-phenylglycines has been described in an earlier paper.[2] The organic solvents were G. R. reagents from the Koso Chem. Co., and were used without further purification.

Results and Discussion

Photolysis in Aqueous Solvents in the Presence of *N*-Phenylglycines.—*1) Resemblance to the Reversible Photolysis.*—Plates 1a and 1b give spectra in which the concentration of the reductant (*N*-*p*-chlorophenylglycine) is varied. It is seen that the spectrum changes from the type observed in pure water to the one observed when *p*-phenylenediamine[1] is used as the reductant. The absorption shows a peak around 410 mμ at the earliest stage of photolysis and somewhat blue-shifts later. This absorption may be mainly that of methylene blue semiquinone superposed by that of the triplet dye. This assumption is substantiated by the fact that the absorption red-shifts to 425 mμ at a pH value where the same change was observed with *p*-phenylenediamine[1] (Fig. 1).

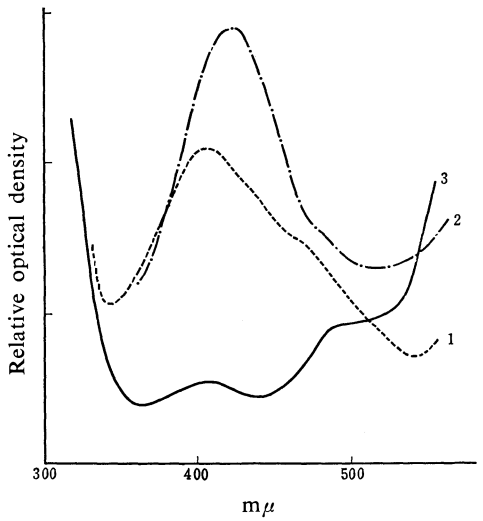
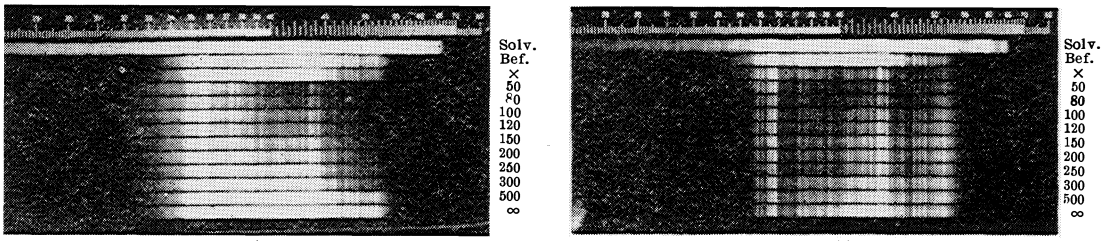


Fig. 1. Shift in transient absorption at a pH near 8, *p*-Cl-ϕ·G being added as reductant, 10^{-4} M. M. B. 10^{-5} M; delay time Δt=50 μsec. Curve 1: pH 7.4; Curve 2: pH 9.2. Curve 3 shows spectrum before flash exctn.

In this case the absorption corresponding to the oxidation product of the reductant is uncertain. The spectrum in the 220~320 mμ region resembles the spectra in the reversible reduction in Part I. The spectrum obtained with *N*-phenylglycine (Plate 2) has features intermediate between those with *p*-phenylenediamine and those with benzohydroquinone (cf. Plates 5 and 6b in Part I). Some part of the semiquinone is going to leuco methylene blue, while the other part is coming back to the original form of the dye. The spectrum with *N*-*p*-methoxyphenylglycine (Plate 3a) resembles that with *p*-phenylenediamine. In this case the photolysis is reversible, in accordance with the results described in a previous paper,[2] where the resemblance of the two reductants was stressed.

2) Relations between the Transient Spectra and the Structure of the Reductant.—Plates 3b—3g show the spectra obtained with typical derivatives of *N*-phenylglycine. The spectrum with *N*-phenylglycine is similar to that with

1) S. Matsumoto, This Bulletin, 37, 491 (1964).
2) S. Matsumoto, ibid., 35, 1860, 1866 (1962).



(a) (b)

Plate 1. Transient spectra in the presence of *p*-Cl·ϕ·G. Solv. buff. pH 7.0; M. B. 2.5×10^{-5} M; concn. of *p*-Cl·ϕ·G: (a) 10^{-6} M (b) 10^{-4} M.

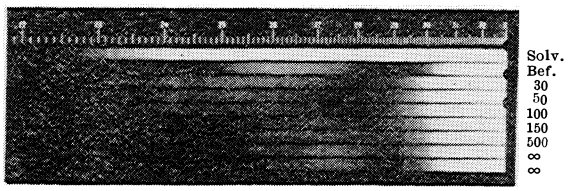


Plate 2. Transient absorption in the 220~320 mμ in the presence of ϕ·G 10^{-5} M. Solv. buff. pH 7.4; M. B. 10^{-5} M.

N-*p*-chlorophenylglycine. In the case of *N*-*p*-bromophenylglycine, the transient absorption is faint. This must be due to the strong deactivating influence of the heavy atom-containing reductant on the triplet state of the dye. In the case *N*-*m*-bromophenylglycine, the formation of methylene blue semiquinone is more apparent, but the yield is still not as good as in the case of *N*-phenylglycine, to judge from the degree of the disappearance of methylene blue absorption. The situation is similar in the case of *N*-*p*-acetylphenylglycine.

The result with α-methyl-*N*-phenylalanine is characteristic. It is seen that the dye ion is converted into its colorless form almost invariably once it is excited by the flash. The relatively faint transient absorption in this case may indicate a low stationary concentration of the intermediate that is brought about by a strong reactivity of the reductant with the intermediate semiquinone. The absorption near 330 mμ may be due to the leuco methylene blue.[3] The spectrum in the 220~320 mμ range (Plate 4) is in accord with these results. The above results, together with the results with *N*-*p*-methoxyphenylglycine described in section 1), support the general idea obtained earlier[2] about the reactivity of various derivatives of *N*-phenylglycine. One point to be modified concerns the mechanism of the deactivation of excited dye ions by some reductant. The excited state seems to be deactivated almost catalytically by *N*-phenylglycines containing heavy atoms at the ortho- or para-position of the benzene ring, while with *N*-phenylglycine having a methoxy substituent in either of these positions, a relatively long-lived intermediate (presumably the semiquinone of the dye) is formed which, in this case, is converted effectively into the ground state of the dye. The net result is an effective deactivation of the excited state. The mechanism of the strong inhibitory action of *p*-phenylenediamine also belongs to the latter category. This difference may, however, be superficial. Dye ions in their excited state may form a sort of charge-transfer complex, however short-lived, with reductant molecules before they are deactivated, as suggested by the effect of the substituent position.[2] In the case of *N*-phenyl-β-alanine, the disappearance of the methylene blue absorption and the increase in the semiquinone absorption is remarkable at first, but the recovery of the original absorption is rapid and complete compared with *N*-phenylglycine; the net quantum yield of the reduction of methylene blue is poor, in accordance with the previous results.[2] This observation stimulates a speculation as to the good quantum yield of photoreduction by *N*-phenylglycines. The half-oxidized form of *N*-phenylglycine may, for some reason, be liable to irreversible decomposition and may so become unable to reoxidize the semiquinone or the leuco base of dye, whereas the half-oxidized *N*-phenyl-β-alanine, with one more methylene unit between the amino- and the carboxyl-groups, may have a different stability and may remain efficient enough to reoxidize the semiquinone.

Photolysis in Organic Solvents.—The solvents used were methanol, ethanol, 1-propanol, 2-propanol, glycerol, acetone, pyridine and

3) A. T. Vartanyan, *Zhr. Fiz. Khimi.*, **29**, 1304 (1955).

acetic acid. The solubility of the dye is slight in 1, 1-dimethylethanol and in less polar solvents. In these solvents flash illumination resulted in a more or less irreversible fading of the dye. The degree of fading observed visually after a same number of flashes was approximately in the order: 2-propanol < 1-propanol < acetic acid, glycerol < ethanol < methanol, pyridine <acetone. There seems to be no relation between the ease with which the solvent molecule is dehydrogenated by an ordinary oxidant and the above series. Probably the net quantum yield of photoreduction depends also on the succeeding reactions, by which the first oxidation product of the solvent is removed from the reacting system;

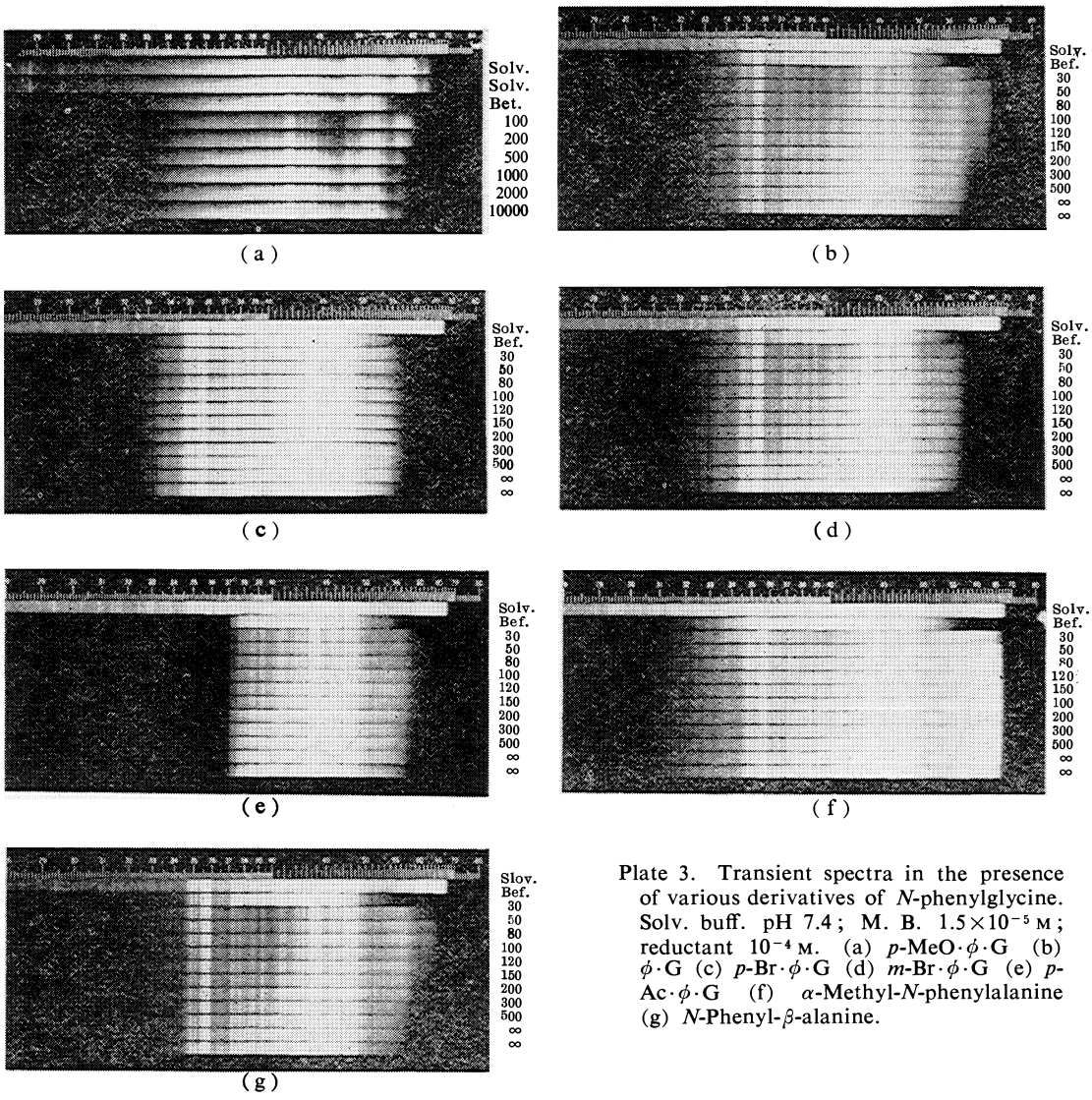


Plate 3. Transient spectra in the presence of various derivatives of *N*-phenylglycine. Solv. buff. pH 7.4; M. B. 1.5×10^{-5} M; reductant 10^{-4} M. (a) *p*-MeO·ϕ·G (b) ϕ·G (c) *p*-Br·ϕ·G (d) *m*-Br·ϕ·G (e) *p*-Ac·ϕ·G (f) α-Methyl-*N*-phenylalanine (g) *N*-Phenyl-β-alanine.

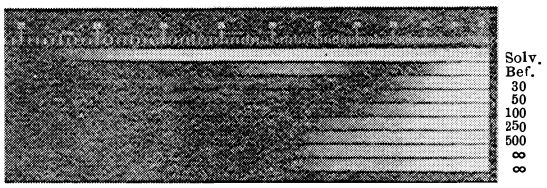
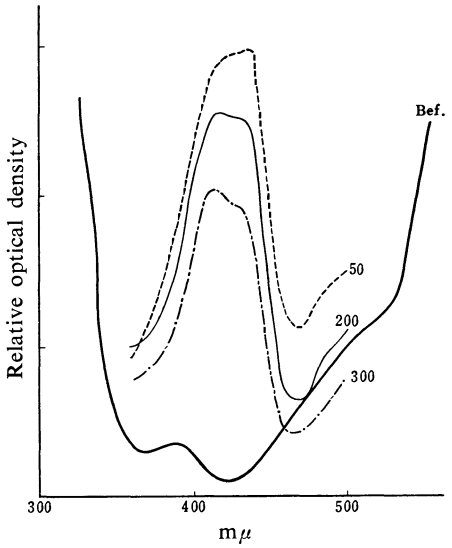
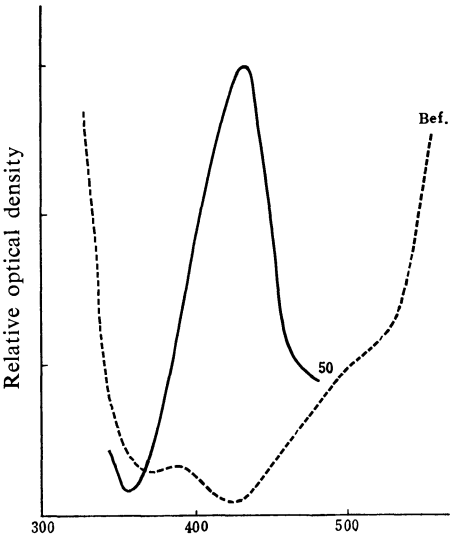


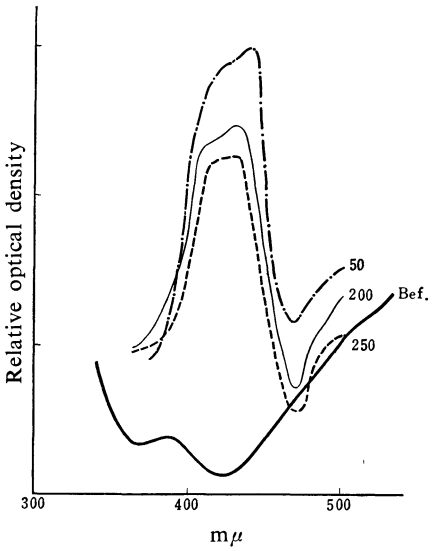
Plate 4. Transient absorption in the region 220~320 mμ in the presence of α-methyl-*N*-phenylalanine 1.5×10^{-5} M. Solv. buff. pH 7.4; M. B. 10^{-5} M



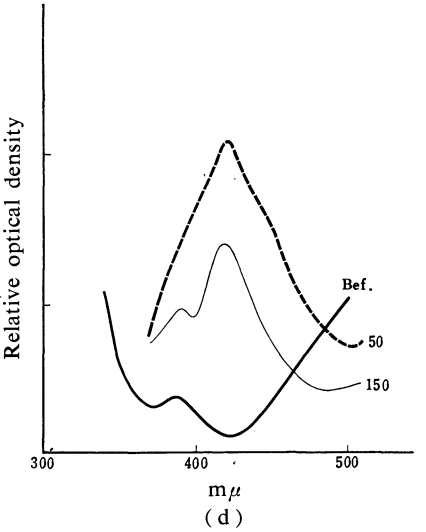
(a)



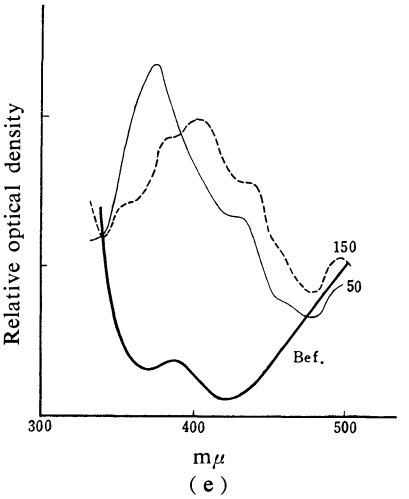
(c)



(b)



(d)



(e)

Fig. 2. Transient spectra in organic solvents. Figures beside curves indicate delay times in μsec.
(a) 1-Propanol (b) 2-Propanol (c) Acetone (d) Glycerol (e) Acetic acid

the intermediary oxidation product will re-oxidize the reduced dye back to the original form. The transient spectra appearing in these solvents are shown in Figs. 2a—2e. Except in acetic acid, the region of strong absorption is in the 400 mμ~430 mμ range. There is also a second peak around 515 mμ; a near-infrared absorption is also observed. As may be seen in the above figures, the absorption persists longer than that observed in plain water.

In the cases of 1- and 2-propanol, two absorptions seem to be superposed. The one which has a peak at a shorter wavelength appears later and persists longer. In these solvents and in glycerol there is a period during the reaction when the absorption in the visible range of the spectrum almost disappears. In time the methylene blue absorption is restored. This phenomenon is quite analogous to that observed in an aqueous medium when ferrous sulfate or hydroquinone is used as the reductant, and it must be attributed to the transitory formation of leuco methylene blue. All these observations suggest that the absorption around 400 mμ at a later stage of the reaction is mainly due to the semiquinone of the dye, although its peak is red-shifted compared with that in an aqueous medium. The spectrum in 1- or 2-propanol at early stages of photolysis may be nearly that of the triplet state. The spectrum observed in acetic acid shows reasonable shifts due to the acidity of the solvent (cf. Part I). Another difference between the transient absorption in an organic solvent and in an aqueous solvent is that, in the latter, a peculiar increase around 520 mμ at a later stage of photolysis is observed, while it is lacking in the former.

Summary

The flash photolysis of methylene blue in an aqueous medium with added *N*-phenylglycines or photolysis in organic solvents results in a more or less apparent bleaching of the dye. In the former case, the general features of the transient spectra are similar to those in the reversible photolysis treated in Part I. An absorption peak at 400 mμ in a solvent with a pH of 8.0 shifts to 430 mμ in a solvent with a pH of 8.8; it is to be attributed to the semiquinone of methylene blue. The absorption around 255 mμ increases at a later stage of the reaction, indicating the formation of leuco methylene blue. The photolysis seems to proceed in a way similar to that of the reversible cases. The results of flash photolysis with several derivatives of *N*-phenylglycine support the general idea of their reactivity obtained in a study with continuous illumination. There is a difference between the ways in which *N*-*p*-bromophenylglycine and *N*-*p*-methoxyphenylglycine retard the photoreduction, although this may be superficial. In the former case, some early intermediate (probably the triplet state of the dye) is deactivated almost catalyticaly, while in the latter case the deactivation takes place at the stage of a long-lived semiquinone-like intermediate. Peculiar features of photolysis with α-methyl-*N*-phenylalanine and *N*-phenyl-β-alanine have also been noted.

The degree of irreversible bleaching in an organic solvent has no regular relation to the ease with which the solvent molecule is dehydrogenated by an ordinary oxidant. The main part of the transient absorption in organic solvents is attributed to the semiquinone of the dye. The peak has somewhat red-shifted compared with that in water. Triplet absorption seems also to appear at an early stage of photolysis. The photolysis in 1- or 2-propanol reveals the reversible feature observed when ferrous ions were used as reductants.

The author is indebted to Professor Noboru Ando and Professor Ikuzo Tanaka of the Tokyo Institute of Technology, who kindly permitted him to use their laboratory facilities and gave him much helpful advice. He also wishes to express his thanks to Professor Masao Koizumi of Tohoku University and to Dr. Yuji Mori of the Tokyo Institute of Technology for their valuable discussions.

Faculty of Agriculture
Kagawa University
Kita-gun, Kagawa

The Spectrophotometric Determination of Cadmium with Xylenol Orange[1]

By Makoto Otomo

(Received September 26, 1963)

The most sensitive spectrophotometric method for the determination of traces of cadmium has been found to be the extraction procedure employing dithizone.[2-4] In this method, however, different amounts of dithizone must be used, depending on the amount of cadmium to be determined, indicating that the method is unfavorable for the determination of cadmium over a wide concentration range. A rapid, sensitive and accurate method which is applicable over a wide concentration range of cadmium is, therefore, desirable. A spectrophotometric method with xylenol orange was formulated for this purpose by the present author, and a suitable method was developed. This method is based on the formation of the cadmium-xylenol orange complex in a solution buffered with hexamethylenetetramine and nitric acid. The complex has an absorption maximum at 575 mμ and a molar extinction coefficient of 18000. By this method, 20 to 120 μg. of cadmium can be determined rapidly within the range of experimental error. In a study of the complex formation, it has been found that xylenol orange forms a 1 to 1 complex with cadmium and that the complex has an apparent formation constant of 6.1×10^3 at a pH value of 5.5.

Experimental

Reagents.—*Standard Cadmium Solution.*—A stock solution of cadmium (about 0.01 M) was prepared by dissolving a reagent-grade cadmium chloride in distilled water. This solution was standardized against a standard EDTA solution, using xylenol orange as the indicator.[5] A working standard solution was prepared by diluting the stock solution with water.

Buffer Solution.—Except where otherwise indicated, solutions of hexamethylenetetramine in conjunction with potassium nitrate and nitric acid were used for pH adjustments.

Xylenol Orange Solution.—A 1×10^{-3} M solution of xylenol orange was prepared by dissolving a Dotite XO reagent (Dôjindô & Co., Kumamoto) in distilled water.

All the other solutions were prepared from reagent-grade chemicals.

Apparatus.—A Hitachi spectrophotometer, Model EPV-2, was used for all absorbance measurements, using 1-cm. glass cells. A Hitachi glass-electrode pH meter, Model EHP-1, was used for all pH determinations.

All experiments were carried out at 25±0.5°C.

Results and Discussion

Absorption Spectra.—The absorption spectra of xylenol orange and its cadmium complex are shown in Fig. 1. When the absorbance measurements were made against a reagent blank, an absorption maximum was found at

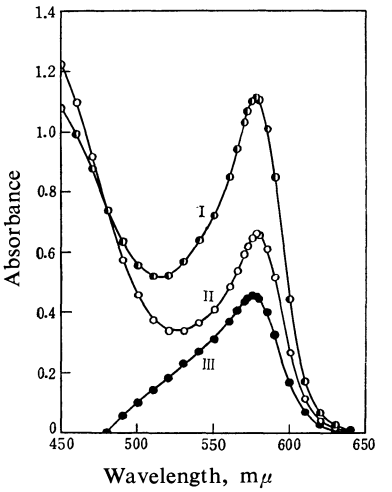


Fig. 1. Absorption spectra of xylenol orange and its cadmium complex at pH 6.3.
Cd : 67.4 μg., XO : 1.114×10^{-4} M, KNO_3 : 0.30 M
I : Cd-XO vs. water
II : XO vs. water
III : Cd-XO vs. a reagent blank

575 mμ. As the considerable absorbance by the blank is evident around the absorption maximum of the complex, all absorbance measurements were made using a reagent blank. The order of the addition of the reagents has no effect on the absorbance values.

Choice of Buffer and the Effect of pH.—A preliminary test showed that xylenol orange

1) A part of this work was presented at the 16th Annual Meeting of the Chemical Society of Japan, Tokyo, April, 1963.
2) F. W. Church, *J. Ind. Hygiene Toxicol.*, **29**, 34 (1947).
3) H. Fischer and G. Leopoldi, *Mikrochim. Acta*, **1**, 30 (1937).
4) B. E. Saltzman, *Anal. Chem.*, **25**, 493 (1953).
5) K. Ueno, "Kireto Tekitei (Chelatometric Titration)" (in Japanese), Nankodo, Tokyo (1960), p. 241.

reacts with cadmium only in a slightly acidic or a neutral solution, giving a red color. Therefore, two buffers are found to be useful: sodium acetate - acetic acid and hexamethylenetetramine - mineral acid. The former has a great buffering capacity in the pH range from 3.5 to 5.6 and has widely been used for many purposes. However, acetate ions form certain acetato-complexes with cadmium[6-8] to inhibit the color formation between cadmium and xylenol orange. The latter, with a great buffering capacity in the pH range from 4.5 to 6.5, has occasionally been used in complexometric titrations. It has no complexing action for cadmium ions. At the same pH values, the cadmium - xylenol orange complex always gave higher absorbances in solutions buffered with the latter than with the former. A hexamethylenetetramine - nitric acid - potassium nitrate buffer was, therefore, adopted throughout the investigation. Potassium nitrate was always used to reduce the error caused by the indicator salt effect.

The variation in the absorbances of the reagent blank and of the cadmium complex with a change in pH value was then studied; the results are shown in Fig. 2. The optimum pH range is fairly narrow, the maximum color development for the complex being found to occur in the pH range from 6.2 to 6.4.

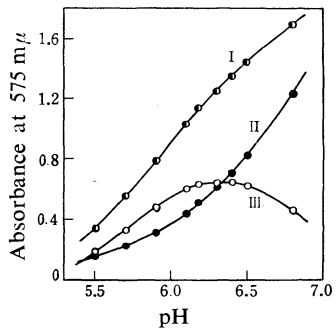


Fig. 2. Effect of pH on color development.
Cd: 112 μg., XO: 1.114×10^{-4} M
KNO_3: 0.20 M, Hexamethylenetetramine: 20% soln. 4 ml.
I: Cd-XO vs. water
II: XO vs. water
III: Cd-XO vs. a reagent blank

The Effect of the Amount of Buffer.—In order to investigate the effect of the amount of the buffer on the absorbances of the reagent and complex, experiments were made with solutions containing 90 μg. of cadmium, 2.8 ml. of a 1 $\times10^{-3}$ M solution of xylenol orange, and varying amounts of a 20% hexamethylenetetramine solution which had been titrated with nitric acid to give a pH value of 6.3. The results showed that, both for the solution containing no potassium nitrate and for the solution containing potassium nitrate (0.35 M at a final concentration), the intensity of the absorbances of xylenol orange and of the complex is greatly affected by the amount of the buffer; larger amounts of the buffer must be added to obtain higher absorbances. However, 10 ml. of a 20% hexamethylenetetramine - nitric acid solution was used for further investigation. The addition of 10 ml. of the buffer to the system gave a reproducible absorbance.

The Effect of the Potassium Nitrate Concentration.—The absorbance of a solution containing a fixed amount of cadmium was found to be dependent also upon the concentration of potassium nitrate. This effect was studied by varying the concentration of potassium nitrate. The pH value of the solution was held constant at 6.3 by the addition of the buffer. The results are shown in Fig. 3. Both xylenol orange and the complex give the maximum absorbance at the potassium nitrate concentration of 0.30 to 0.35 M in a final volume. In further experiments, therefore, 5 ml. of a 1.5 M solution of potassium nitrate was used. This gives 0.30 M at a final concentration.

The Effect of the Amount of Xylenol Orange.—In measuring the effect of the amount of xylenol orange on color development, the amount of a 1×10^{-3} M solution of xylenol orange was varied from 0.7 to 4.5 ml., keeping

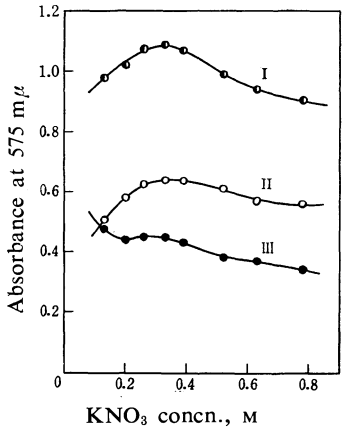


Fig. 3. Effect of KNO_3 concentration.
Cd: 67.4 μg., XO: 1.114×10^{-4} M, pH: 6.3
Hexamethylenetetramine: 20% soln. 10 ml.
I: Cd-XO vs. water
II: XO vs. water
III: Cd-XO vs. a reagent blank

6) A. Jacques, *Trans. Faraday Soc.*, 5, 225 (1910).
7) E. Ferrell, J. M. Ridgion and H. L. Riley, *J. Chem. Soc.*, 1934, 1440.
8) N. Tanaka, M. Kamada, H. Osawa and G. Sato, This Bulletin, 33, 1412 (1960).

other variables constant. As can be seen from Fig. 4, the maximum color formation is obtained when 2.2 to 3.8 ml. of the reagent solution is used. Therefore, 2.8 ml. was chosen as the working volume of the reagent.

The Stability of the Color.—The absorbances of a solution, prepared under the optimum condition, were measured as a function of time following the preparation of the solution. There was no change of absorbance over a period of 3 hr.

Adherence to Beer's Law.—To ascertain the adherence of the system to Beer's law, a calibration curve was prepared in the following manner: To a series of 25 ml. volumetric flasks were added varying quantities of cadmium, 10 ml. of the buffer and 2.8 ml. of a 1×10^{-3} M solution of xylenol orange; the solutions were then diluted to the mark with water. After about 15 min., the absorbance of each solution was measured at 575 mμ against a reagent blank which had been treated in a similar manner. The data showed a linear relationship between concentration and absorbance over the 20 to 120 μg. range of cadmium.

Sensitivity.—According to the notation of Sandell,[9] the sensitivity of the reaction is 0.006 μg. of cadmium per cm^2. The molar extinction coefficient was calculated from the calibration curve to be 18000 at 575 mμ.

Effect of Diverse Ions.—The data concerning the effect of diverse ions were obtained on solutions containing 67.4 μg. of cadmium and the diverse ions added individually. Alkali metal salts of the anions were used. Diverse cations were added as the chloride, nitrate or sulfate salts.

Of the anions tested, the following did not interfere under the described conditions: chloride and sulfate up to 500 μmol., thiocyanate up to 100 μmol., and fluoride and phosphate up to 50μmol. NTA and EDTA, especially the latter, bleach the color of the complex, even when only trace amounts are present.

Because all of the metal cations tested, with the exception of alkaline earth metals, interfere seriously, attempts were made to eliminate the interfering cations with some masking agents; the addition of 60 μmol. of fluoride was effective for rare earths up to 0.5 μmol. and for thorium and zirconium up to 0.05 μmol., while the addition of 50 μmol. of thiocyanate was effective for mercury(II) up to 0.5 μmol.

A Comparison with Other Methods.—Except for dithizone, of the previously-proposed reagents for the spectrophotometric determination of cadmium, di-β-naphthylthiocarbazone[10] and 1-(2-pyridylazo)-2-naphthol (PAN)[11] are perhaps the most sensitive. These reagents can be used even for the determination of a few micrograms of cadmium. Diethyldithiocarbamate[12] has also been reported to be sensitive for cadmium and has been widely utilized for the determination of 50 to 300 μg. of cadmium. All the above reagents, however, form water-insoluble complexes with cadmium. Therefore, these cadmium complexes must be extracted into a suitable organic solvent; this complicates the process of the determination.

Other reagents which have been utilized successfully for the determination of cadmium are 4-hydroxy-3-nitrophenylarsonic acid,[13] chrome dark blue[14] and cadion IREA.[15] These reagents can form water-soluble complexes with cadmium but are far less sensitive than xylenol orange. The colloidal cadmium sulfide formed with cadmium and thiosinamine is unstable,[16] indicating that the absorbance measurements must be made in the presence of a stabilizing agent. An indirect method, based on the interaction of cadmium and the zinc-complex of α-β-γ-δ-tetraphenylporphine,[17] has been proposed for the determination of cadmium, but it is not capable of determining traces of cadmium.

Therefore, it may be concluded that, of the reagents which can form water-soluble cadmium complexes, xylenol orange is the most preeminent colorimetric reagent for cadmium. The proposed method, which is rapid, sensitive and accurate, seems to be applicable for the determination of traces of cadmium in many samples, when cadmium is preliminarily separated from the interfering ions by an ion-exchange or a precipitation method.

Complex Formation.—*Continuous Variations.*—A very rapid and excellent method for determining the composition of the main complex formed in a given concentration range of the reactants is Job's method[18] of continuous variations as extended by Vosburgh and Cooper.[19]

9) E. B. Sandell, "Colorimetric Determination of Traces of Metals," 2nd Ed., Interscience Publishers Co. Inc., New York (1950), p. 49.

10) J. Cholach and D. M. Hubbard, *Ind. Eng. Chem., Anal. Ed.*, **16**, 333 (1944).

11) M. Ishibashi, T. Shigematsu, M. Tabushi, Y. Nishikawa and J. Goda, *J. Chem. Soc. Japan, Pure Chem. Sec. (Nippon Kagaku Zasshi)*, **83**, 295 (1962).

12) E. Sudo, ibid., **73**, 693 (1952).

13) W. Nielsch and G. Böltz, *Chem. Ztg.*, **79**, 364 (1955).

14) G. G. Lomakina and V. N. Tolmacheva, *Zavodskaya Lab.*, **26**, 62 (1960).

15) A. M. Lukin, G. G. Karanovich and G. S. Petvova, *Trudy Vsesoyuz. Nauch. -Issledovatel. Inst. Khim. Reaktivov*, **1959**, No. 23, 55; *Chem. Abstr.*, **54**, 24117 (1960).

16) F. Sabon and H. Grigon, *Bull. soc. pharm. Bordeaux*, **94**, 47 (1955).

17) C. V. Banks and R. E. Bisque, *Anal. Chem.*, **29**, 522 (1957).

18) P. Job, *Ann. Chim.*, **9**, 113 (1928); **6**, 97 (1936).

19) W. C. Vosburgh and G. R. Cooper, *J. Am. Chem. Soc.*, **63**, 437 (1941).

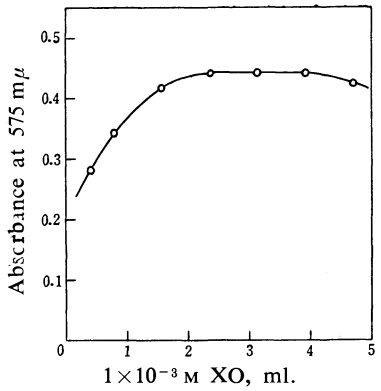


Fig. 4. Effect of amount of xylenol orange.
Cd : 67.4 μg., pH : 6.3
Hexamethylenetetramine : 20% soln. 10 ml.
KNO_3 : 0.30 M

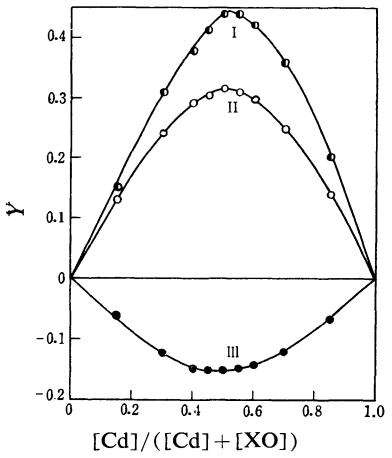


Fig. 5. Method of continuous variations.
[Cd]+[XO]=3.2×10⁻⁵ M
pH : 6.3, KNO_3 : 0.30 M
Hexamethylenetetramine : 20% soln., 10ml.
I : 580 mμ
II : 560 mμ
III : 440 mμ
Reference : water

Figure 5 shows, for three wavelengths, the absorbances, Y, that exceed the absorbances expected for no reaction in various mixtures of equimolar solutions of cadmium and xylenol orange. The pH value was held constant at 6.3 and the potassium nitrate concentration, at 0.3 M. The total concentration of cadmium and xylenol orange was 3.2×10^{-5} M throughout. The curves in Fig. 5 clearly indicate that only one complex, 1 to 1, is formed in solutions containing cadmium and xylenol orange.

The Absorption Spectra of the Complex at Various Concentrations of Cadmium.—Prior to the calculation of the apparent formation constant, the absorption spectra of solutions with a constant concentration of xylenol

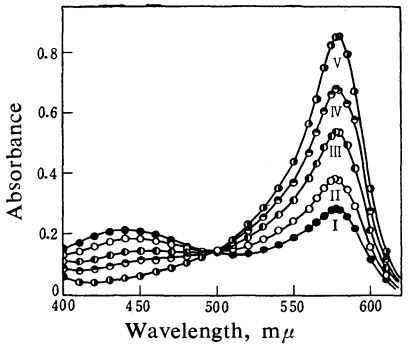


Fig. 6. Absorption spectra of cadmium-xylenol orange complex at pH 6.3.
XO : 2.4×10⁻⁵ M, KNO_3 : 0.30 M
Cd concn.: I, 0.8×10⁻⁵ M ; II, 1.6×10⁻⁵ M ; III, 3.2×10⁻⁵ M ; IV, 6.0×10⁻⁵ M ; V, 3.3×10⁻⁴ M
Reference : water

orange, 2.4×10^{-5} M, and potassium nitrate, 0.30 M, but with various concentrations of cadmium, were studied. The location of the absorption maximum was constant at 578±2 mμ for the range of cadmium concentration investigated. The results are shown in Fig. 6, indicating the existence of only one form of the complex.

The Apparent Formation Constant.—Using as a guide the results of the experiments reported on the previous sections, the calculation of the apparent formation constant of the cadmium - xylenol orange complex was attempted. A method described by Newman and Hume[20] was employed.

Since only a 1 to 1 complex is formed, the equilibrium constant, K, can be expressed as:

$$K=[\mathrm{Cd(XO)}]\,[\mathrm{H^+}]^x/[\mathrm{Cd^{2+}}]\,[\mathrm{XO}] \quad (1)$$

where XO and Cd(XO) represent the total unbound xylenol orange and the total cadmium-xylenol orange complex respectively, and x is the number of hydrogen ion liberated from one molecule of xylenol orange by the chelation. Assuming that two species, the complex and xylenol orange, absorb at the wavelengths under investigation, the apparent formation constant, $K'=K/[\mathrm{H^+}]^x$, may be given by:

$$\log\,(D-D_{\mathrm{XO}})/(D_{\mathrm{C}}-D)=\log K'+\log\{[\mathrm{Cd^{2+}}]_t-(D-D_{\mathrm{XO}})/(\varepsilon_{\mathrm{C}}-\varepsilon_{\mathrm{XO}})\} \quad (2)$$

where ε_{C} and $\varepsilon_{\mathrm{XO}}$ are the molar extinction coefficients of the complex and xylenol orange respectively; D is the absorbance of the solution containing a mixture of cadmium and xylenol orange, and D_{XO} and D_{C} are the absorbances of a solution containing only xylenol orange or a large excess of cadmium ions added to a known amount of xylenol

20) L. Newman and D. N. Hume, ibid., 79, 4571 (1957).

orange respectively. When $\log(D-D_{XO})/(D_C-D)$ is plotted against $\log\{[Cd^{2+}]_t-(D-D_{XO})/(\varepsilon_C-\varepsilon_{XO})\}$, a straight line with a unit slope and intercept $\log K'$ is obtained.

In the work performed in this section, each solution was 2.0×10^{-5} M in xylenol orange, the concentration of cadmium was varied from 1.0×10^{-4} to 4.58×10^{-3} M, the pH value of each solution was adjusted to 5.5 with hexamethylenetetramine-nitric acid, and the concentration of potassium nitrate was maintained constant at 0.3 M. Table I shows the results of the Newman-Hume plots, all of which give good straight lines with a unit slope.

TABLE I. DETERMINATION OF THE APPARENT FORMATION CONSTANT

Wavelength, mμ	Slope	K'
570	1.05	5.1×10^3
575	1.04	5.4×10^3
578	1.06	5.9×10^3
580	1.09	7.1×10^3
585	1.09	7.1×10^3

Av.: Slope=1.07; $K'=6.1\times10^3$

Summary

The red cadmium-xylenol orange complex has been studied spectrophotometrically to establish the optimum conditions for determining traces of cadmium. The absorption spectrum of the colored complex showed a maximum absorption at 575 mμ when measured against a reagent blank. The reaction was carried out in a buffered solution at a pH value of 6.3. Beer's law is obeyed over the 20 to 120 μg. range of cadmium. The sensitivity of the reaction was 0.006 μg. cadmium per cm^2. Job's method of continuous variations and the method of Newman and Hume have been applied to determine the composition of the complex. Both methods showed the existence of only one form of the complex, 1 to 1. The apparent formation constant was calculated to be 6.1×10^3 at a pH value of 5.5.

The author wishes to express his gratitude to Professor Kôichi Tonosaki for his kind guidance and encouragement throughout the course of this study. The author is also indebted to Professor Toshiyasu Kiba of Kanazawa University for his interest and valuable advice concerning this work.

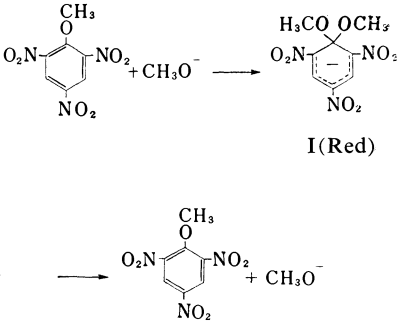
Department of Chemistry
Faculty of Literature and Science
Hirosaki University
Hirosaki, Aomori

*The Spectra of Intermediates and the Mechanism of Their Formation in the Color Reactions of Polynitroanisoles with the Methoxide Ion**

By Takehiro ABE

(Received October 23, 1963)

It has been reported that 2, 4, 6-trinitroanisole and 2, 4-dinitroanisole react with the methoxide (or ethoxide) ion as follows:[1-8]

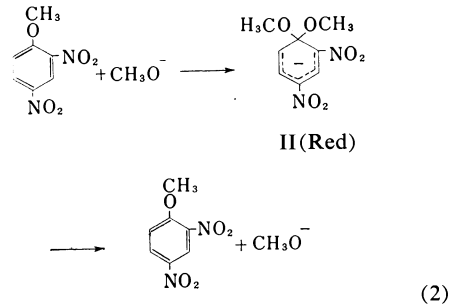


I(Red)

(1)

* Presented at the 16th Annual Meeting of the Chemical Society of Japan, Tokyo, March, 1963.

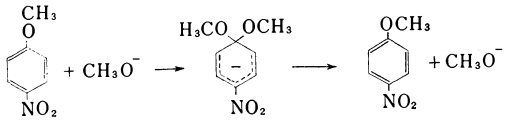
1) T. L. Davis, "The Chemistry of Powder and Explosives," John Wiley and Sons, New York (1953), p. 171.
2) R. C. Farmer, *J. Chem. Soc.*, **1959**, 3425, 3430.
3) R. Foster and D. LL. Hammick, ibid., **1954**, 2153.
4) R. Foster, *Nature*, **176**, 746 (1955); **183**, 1042 (1959).
5) S. Nagakura, S. Oosawa and H. Tsubomura, presented at the Symposium on the Electronic State of Molecules, Kyoto, October, 1958.
6) S. Nagakura and S. Oosawa, presented at the Symposium on Molecular Structure, Sapporo, August, 1960.
7) L. K. Dyall, *J. Chem. Soc.*, **1960**, 5160.
8) S. Nagakura and S. Oosawa, presented at the 13th Annual Meeting of the Chemical Society of Japan, Kyoto, April, 1960.



II(Red)

(2)

The colored species I is more stable than II.[8] On the other hand, it has never been found that *p*-nitroanisole gives the colored intermediate III.



III (3)

The formation of Meisenheimer's intermediates I and II has been confirmed by Nagakura and Oosawa[5,8] and by Dyall[7] on the basis of the infrared spectra of these colored complexes. They indicate that the carbon atom at the seat of substitution has sp^3-hybridization. Recently the constitution of Meisenheimer's type has been widely accepted for many colored complexes of polynitrobenzene derivatives with alkalies.*

In order to interpret the formation of the above intermediates, Bunnett et al.,[9] Nagakura et al.[5,6] and Parker et al.[10,11] presented the two-stage mechanism shown in Fig. 1, for the color reactions.

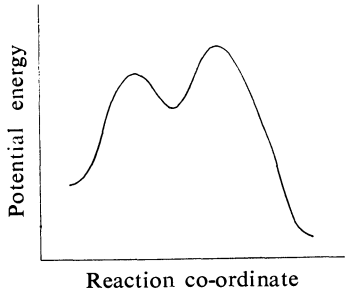


Fig. 1. The energy profile for two-stage mechanism.

From the energy level diagrams for reagents and aromatic molecules,[12] and from the above findings regarding the infrared spectra, Nagakura[13] proposed the following mechanism for the formation of an intermediate in the process of aromatic substitution:

1) A charge transfer occurs between a reagent and an aromatic compound.

2) A π-electron is localized on the carbon atom at the seat of substitution, and the atom is consequently removed from conjugation.

3) The carbon atom undergoes a change in hybridization from sp^2 to sp^3.

Recently, from the concept of Meisenheimer's intermediate complex, Miller[14] made energy calculations for the aromatic nucleophilic substitutions, utililizing bond energies, electron affinities and solvation energies.

In the present work, by means of the simple LCAO MO method, qualitative attempts will be made to account for the visible absorption spectra of Meisenheimer's intermediates I and II and for the fact that the intermediate I is more stable than II, while the intermediate III can not be observed, and to examine the possibility of the appearance of potential-energy minima on the potential energy curves for the substitutions (1)—(3).

Experimental

The Red Complex of 2, 4, 6-Trinitroanisole with Methoxide.—When a methanolic solution of sodium methoxide is added to a methanolic solution of trinitroanisole, a red solution is produced. When the resulting solution is allowed to stand at room temperature, reddish orange crystals precipitate. The spectrum of the orange methanolic solution of the crystals collected was measured as that of Meisenheimer's intermediate I. The orange solution was decolorized soon after, giving an absorption curve similar to that for 2, 4, 6-trinitroanisole.

The Red Complex of 2, 4-Dinitroanisole with Methoxide.—When dinitroanisole in methanol is treated with sodium methoxide, a red solution is formed. The spectrum of the colored solution was measured as that of Meisenheimer's intermediate II, since red-colored crystals did not precipitate from the solution. It is known that the red complex is rapidly converted, mainly into 2, 4-dinitroanisole, in methanol.[8]

The Complex of *p*-Nitroanisole with Methoxide.—When nitroanisole in methanol was treated with sodium methoxide, no colored solution was formed.

Spectra.—The spectra of the solutions were measured using a Hitachi EPU-2 spectrophotometer at room temperature.

* For example: See Ref. 28 below; R. Foster and R. K. Mackie, *Tetrahedron*, **18**, 119, 161 (1961); **18**, 1131 (1962); *Trans. Faraday Soc.*, **58**, 860 (1962).

9) J. F. Bunnett, E. W. Garbisch and K. M. Pruitt, *J. Am. Chem. Soc.*, **79**, 385 (1957).

10) R. E. Parker and T. O. Read, *J. Chem. Soc.*, **1962**, 9, 2314.

11) D. H. D. Elias and R. E. Parker, ibid., **1962**, 2616.

12) S. Nagakura and J. Tanaka, This Bulletin, **32**, 734 (1959).

13) S. Nagakura, *Chem. and Chem. Ind. (Japan)*, **15**, 617 (1962).

14) J. Miller, *J. Am. Chem. Soc.*, **85**, 1628 (1963).

Results of the Measurements

The spectra measured are indicated in Fig. 2. From the above reports,[1-8] Absorption curves 1 and 2 in Fig. 2 can be considered to be due to the Meisenheimer intermediates I and II respectively. The intermediate I has two absorption maxima, at ca. 485 and 415 mμ, while the intermediate II has a maximum at ca. 495 mμ.

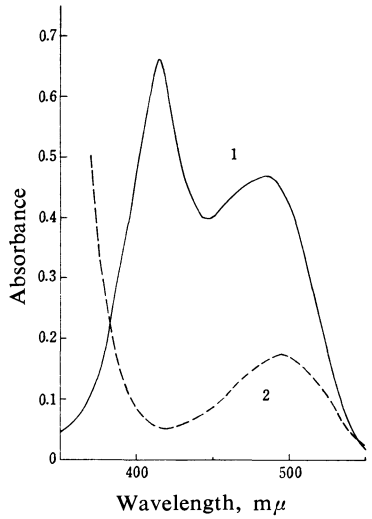


Fig. 2. Absorption spectra of Meisenheimer's intermediates in methanol (at room temperature).
1 [Trinitroanisole·CH_3O]$^-$
2 [Dinitroanisole·CH_3O]$^-$

Method of Calculation

In order to indicate the degree of proceeding of the substitution, the author has introduced the reaction parameter t, which takes continuous values from 1 through zero to -1. Let t change the values of the resonance integrals in the process of the substitution in order to represent the initial and final states at $t=1$ and -1 respectively, and in order to form Meisenheimer's intermediate at $t=0$. As Fukui et al.[15] found, the change in the electronic structure of each activated complex is assumed to be divided into two parts, a σ- and a π-part.

The resonance integrals β' and β for the σ- and π-parts respectively are assumed to be expressed as follows:

In the case of $t=1\rightarrow 0$:

σ-part, $\beta'_{C'O2}=(1-t)b'_{C'O2}\beta'_{CC}$

π-part, $\beta_{C'O1}=tb_{C'O1}\beta_{CC}$

$\beta_{C'C}=t\beta_{CC}$

In the case of $t=0\rightarrow -1$:

σ-part, $\beta'_{C'O1}=(1+t)b'_{C'O1}\beta'_{CC}$

π-part, $\beta_{C'O2}=-tb_{C'O2}\beta_{CC}$

$\beta_{C'C}=-t\beta_{CC}$

Here the suffix C′ denotes the carbon atom at the seat of substitution, while the symbols O1 and O2 indicate the oxygen atoms of the outgoing and ingoing CH_3O-groups respectively.

Coulomb and Resonance Parameters.—The Coulomb integrals are represented by α' and α for the σ- and π-parts respectively.

σ-Part,

for CH_3O (for which the parameters for OH[16] are used directly):

$$\alpha'_O=\alpha'_C+0.5\beta'_{CC}$$
$$b'_{C'O1}=b'_{C'O2}=0.5$$

π-Part,

for CH_3O:[17-19]

$$\alpha_O=\alpha_C+2\beta_{CC}$$
$$b_{C'O1}=b_{C'O2}=0.6$$

for NO_2:[20]

$$\alpha_N=\alpha_O=\alpha_C+\beta_{CC}$$
$$\beta_{CN}=\beta_{NO}=\beta_{CC}$$

In the present calculation the following approximations have been made for convenience:

1) The change in energy due to the change in hybridization from sp^2 to sp^3 has not been considered. This energy will be small. For instance, Coulson[21] estimated the bond energies of the CH bonds of sp^2 and sp^3 as 106 and 103 kcal./mol. respectively.

2) Hyperconjugation has been ignored.

3) The symmetry of C_{2v} has been assumed to hold for the reaction processes of *p*-nitroanisole and 2, 4, 6-trinitroanisole.

On the basis of the above assumptions, the energy levels of the molecular orbitals of the σ- and π-parts in the three activated complexes at $t=1\rightarrow 0\rightarrow -1$ were calculated by means of the simple LCAO MO approximation. In each complex, the molecular orbital of the σ-part was represented as a linear combination of a pseudo-π-atomic orbital of the methoxy group and one of π-atomic orbitals of the polynitroanisole, and the orbital of the π-part was

15) K. Fukui, T. Yonezawa and C. Nagata, This Bulletin, 27, 423 (1954); *J. Chem. Phys.*, 27, 1247 (1957).

16) K. Fukui, H. Kato and T. Yonezawa, This Bulletin, 33, 1197 (1960).

17) L. E. Orgel, T. L. Cottrell, W. Dick and L. E. Sutton, *Trans. Faraday Soc.*, 47, 113 (1951).

18) S. Nagakura and T. Hosoya, This Bulletin, 25, 179 (1952).

19) B. Pullman and A. Pullman, *Revs. Modern Phys.*, 32, 428 (1960).

20) J. I. A. Alonso, *Compt. rend.*, 233, 403 (1951).

21) C. A. Coulson, "Valence," Oxford University Press, Oxford (1953), p. 200.

represented as a combination of all the π-orbitals. A bonding molecular orbital of each σ-part is occupied by two electrons. The bonding molecular orbitals of the π-parts for *p*-nitroanisole, 2, 4-dinitroanisole and 2, 4, 6-trinitroanisole are occupied by 12, 16 and 20 electrons respectively.

For example, in the case of *p*-nitroanisole at $t=1\rightarrow0$, the x'_{ti} energy levels (in units of $(\varepsilon'_{ti}-\alpha'_C)/\beta'_{CC}$) of the molecular orbitals of the σ-part and the x_{ti} levels (in units of $(\varepsilon_{ti}-\alpha_C)/\beta_{CC}$) of the A_1-molecular orbitals of the π-part are obtained from the following secular equations, 4 and 5, respectively:

For the σ-part:

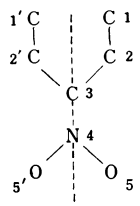
$$0=\begin{vmatrix} -x'_{ti} & 0.5(1-t) \\ 0.5(1-t) & -x'_{ti}+0.5 \end{vmatrix} \qquad (4)$$

and for A_1-orbitals of the π-part:

$$0=\begin{vmatrix} -x_{ti}+2 & 0.6t & 0 & 0 & 0 & 0 & 0 \\ 0.6t & -x_{ti} & 2t & 0 & 0 & 0 & 0 \\ 0 & t & -x_{ti} & 1 & 0 & 0 & 0 \\ 0 & 0 & 1 & -x_{ti} & 1 & 0 & 0 \\ 0 & 0 & 0 & 2 & -x_{ti} & 1 & 0 \\ 0 & 0 & 0 & 0 & 1 & -x_{ti}+1 & 2 \\ 0 & 0 & 0 & 0 & 0 & 1 & -x_{ti}+1 \end{vmatrix}$$

$$=x_{ti}(x_{ti}-2)D_0(x_{ti})-0.6^2t^2D_0(x_{ti})+t(x_{ti}-2)D_{11}(x_{ti}) \qquad (5)$$

Here $D_0(x_{ti})$ and $D_{11}(x_{ti})$ are the secular determinants of the conjugated system IV and the minor of its 11th element respectively.



IV

The energy levels for $t=0\rightarrow-1$ are symmetric to those for $t=1\rightarrow0$ with respect to $t=0$, because the reagent and the group to be substituted are the same.

Results of Calculation

The Energy Levels of Meisenheimer's Intermediates.—The energy levels of the molecular orbitals in Meisenheimer's intermediates are obtained, as indicated in Fig. 3, by calculating the energy levels for the π-parts at $t=0$. Figure 3 shows that the excitation energies are greater in the order of 2, 4-dinitroanisole, 2, 4, 6-trinitroanisole and *p*-nitroanisole. The excitation energy for the intermediate III is considerably greater in comparison with the others. Accordingly, even if the intermediate III should be formed, its longer absorption would not appear in the visible region. It can be expected that the two absorption bands of the intermediate I will appear at the longer wave lengths, because the second lowest vacant orbital lies close to the lowest one. The above predictions qualitatively agree with the experimental results.

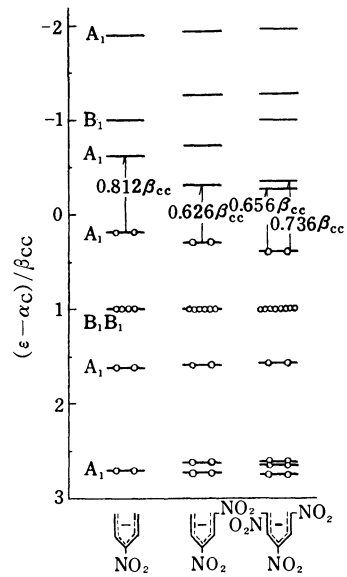


Fig. 3. The energy levels and transitions of π-electrons in Meisenheimer's intermediates.

The Change in the Occupied Orbital Energy of the σ-Part.—The occupied orbital energy ε'_t of the σ-part is obtained from the secular Eq. 4. If the value of ε'_t at $t=1$ is represented as ε'_1, the change in the energy of the σ-part at t can be obtained from:

$$(\varepsilon'_t-\varepsilon'_1)=(x'_t-x'_1)\beta'_{CC} \qquad (6)$$

Figure 4 is drawn by calculating according to

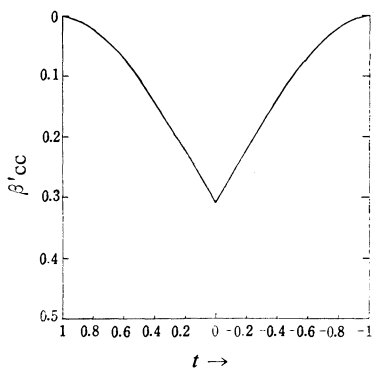


Fig. 4. The change in the occupied orbital energy of each σ-part.

Eq. 6. Of course, the energy of the σ-part is the lowest at $t=0$, because the reagent CH_3O^- is covelently bound to the nucleus of each polynitroanisole.

The Changes in the Occupied Orbital Energies of the π-Parts.—The ε_{ti} energies of the occupied molecular orbitals in the activated complex of each polynitroanisole are indicated in Figs. 5—7. As may easily be seen in these figures, the change in the orbital energy with t is the greatest in the highest occupied orbital. The second greatest change is found for the orbital with the energy value of 2 at $t=0$. These orbitals are to be ascribed to the methoxy groups to be substituted.

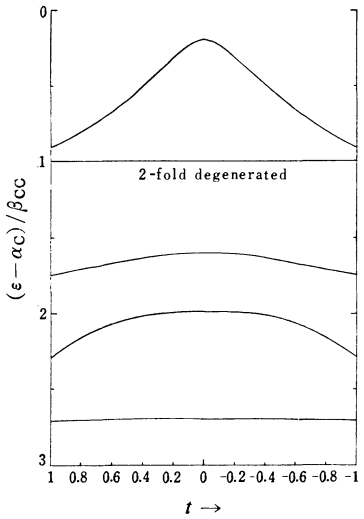


Fig. 5. The change in the occupied orbital energy levels of the π-part for nitroanisole.

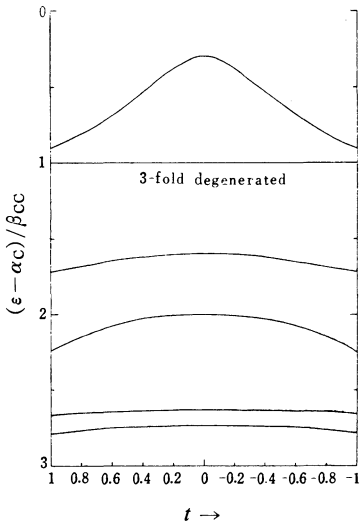


Fig. 6. The change in the occupied orbital energy levels of the π-part for dinitroanisole.

If ε_{1i} denotes the value of ε_{ti} at $t=1$, the change in the electronic energy of the π-part of each polynitroanisole can be given as:

$$\sum_{i}^{occu}(\varepsilon_{ti}-\varepsilon_{1i})=\sum_{i}^{occu}(x_{ti}-x_{1i})\beta_{CC} \qquad (7)$$

The results calculated are shown in Fig. 8. It is reasonable that the change in the electronic energy of each π-part is at its maximum at $t=0$, because the conjugated system is at its minimum at $t=0$. It follows from Fig. 8 that the changes in the energies of the π-parts are

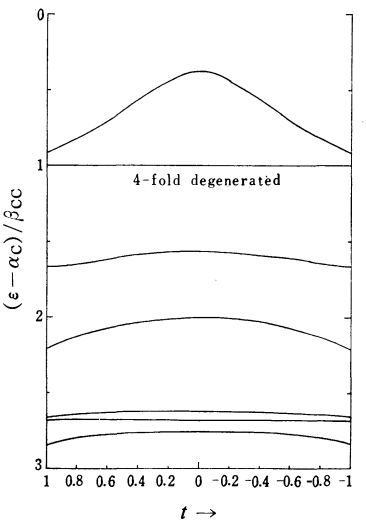


Fig. 7. The change in the occupied orbital energy levels of the π-part for trinitroanisole.

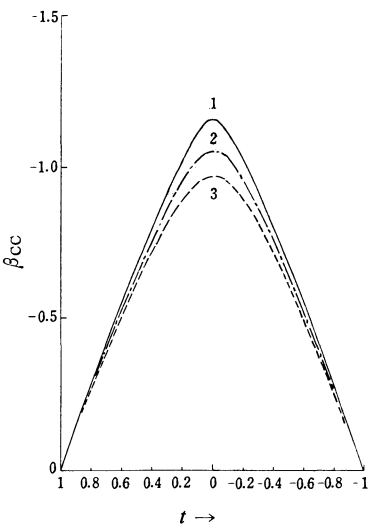


Fig. 8. The changes in electronic energies of the π-parts.
1 Nitroanisole
2 Dinitroanisole
3 Trinitroanisole

smaller with the increasing numbers of nitro groups.

The Total Changes in Electronic Energies.— By adding Eq. 6 to Eq. 7, the total change in the electronic energy of the activated complex of each polynitroanisole at t is given as

$$(\varepsilon'_t-\varepsilon'_1)+\sum_i^{occu}(\varepsilon_{ti}-\varepsilon_{1i})=(x'_t-x'_1)\beta'_{CC}+\sum_i^{occu}(x_{ti}-x_{1i})\beta_{CC} \quad (8)$$

By using $\beta'_{CC}=-6.364$ eV.[22] and $\beta_{CC}=-3$ eV.,* one can find the total changes in electronic energies according to Eq. 8, as is indicated in Fig. 9. It can be seen from Fig. 9 that the activation energies for the formation of the intermediates become smaller as the numbers of nitro groups increase, and that the stabilization energies at $t=0$ are similarly greater. These lead to the expectation that, in the color reactions of the polynitroanisoles with the methoxide ion, the colored intermediates are more easily formed and more stable as the numbers of nitro groups increase. In fact, it has been observed that the intermediates are stable in the order of the increasing numbers of nitro groups. It may also be expected from Fig. 9 that Meisenheimer's intermediate III of *p*-nitroanisole with the methoxide ion is the hardest to form because the energy of activation is the greatest and the stabilization energy at $t=0$ is the smallest in the case of *p*-nitroanisole.

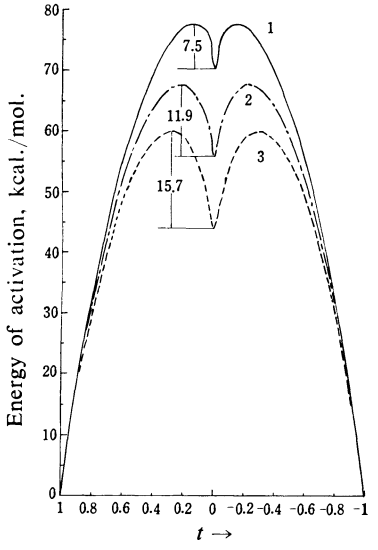


Fig. 9. The total changes in electronic energies.
1 Nitroanisole 2 Dinitroanisole
3 Trinitroanisole

Discussion

As has been mentioned above, the results of the calculation show that the energies of activation for the formation of Meisenheimer's intermediates becomes smaller with the increasing numbers of nitro groups. This is in accordance with the experimental results[23-26] for the similar reactions of polynitrobenzene derivatives.

The fact that the intermediate II is more labile than I can be ascribed to the low stabilization energy of II. Because of the low energy, the intermediate II is more easily converted into 2, 4-dinitroanisole than is I, although the energy of activation for the formation of II is higher than that for I.

Nagakura, Oosawa and Tsubomura[5] reported that the energy of activation for the decomposition of Meisenheimer's complex of 2, 4-dinitroanisole with hydroxyl ions to 2, 4-dinitroanisole is 15.0 kcal./mol. The corresponding energy for 2, 4-dinitroanisole is calculated as 11.9 kcal./mol. in the present work.

The changes in π-electronic energies in the polynitroanisoles at $t=0$, calculated according to Eq. 7, are equal to the localization energies presented by Wheland.[27] Accordingly, the energies of activation for the formation of the three activated complexes are governed by the localization energies, since the changes in energy for the three 6-parts are the same in the calculation. These energies of activation are mainly dependent on the greatest changes of the highest-occupied orbital energies for the π-parts, as is indicated in Figs. 5—7.

The present calculation is too rough to predict the observed values. The following points must be considered in order to calculate them more precisely:

1) It is better to represent the molecular orbital of each activated complex as a combination of all the $2p\pi$-orbitals of each polynitroanisole and the atomic orbital of the reagent.

2) The change in hybridization, $sp^2 \rightarrow sp^3 \rightarrow sp^2$, in the carbon atom at the seat of substitution must be considered.[13]

3) A calculation including hyperconjugation might possibly afford a somewhat smaller

22) K. Fukui, H. Kato and T. Yonezawa, This Bulletin, 33, 1197 (1960).

* This value has often been used in the simple LCAO MO approach.

23) J. Miller, *J. Chem. Soc.*, **1952**, 3550.
24) R. E. Parker and T. O. Read, ibid., **1962**, 9, 3149.
25) D. H. D. Elias and R. E. Parker, ibid., **1962**, 2616.
26) L. F. Fieser and M. Fieser, "Textbook of Organic Chemistry," Maruzen, Tokyo (1952), p. 458.
27) G. W. Wheland, *J. Am. Chem. Soc.*, **64**, 900 (1942).

change in the energy of each π-part.

4) It is necessary to examine the parameters of the coulomb and resonance integrals used.

According to the energy level diagrams of Nagakura and Tanaka,[12] the highest-occupied orbital energy in the methoxy ion CH_3O^- is higher than the lowest vacant one for each polynitroanisole. The parameter of the coulomb integral for the methoxy group used in the present calculation is one for the methoxy radical $CH_3O\cdot$. Miller[14] estimated the loss of the electron affinity of $-O^-$ as -61 kcal. It is necessary to change the coulomb parameter for the methoxy group from CH_3O^- to $CH_3O\cdot$ with t.

5) If configuration interaction is included, the difference between the two excitation energies for the intermediate I will be calculated as somewhat greater.

6) The solvent effect can not be neglected, because the effect on the spectra and life-times of Meisenheimer's intermediates are considerable.[28] According to Miller's calculation, the solvation energy for these intermediates was estimated as 54 kcal. He calculated the activation energies as 14, 19.5 and 25.5 kcal. for reactions 1—3 respectively. In comparison with these values, the corresponding values in the present calculation are much greater. This is possibly due to the neglect of the solvent effect in the calculation.

7) Steric hindrance must be considered.

28) T. Abe, This Bulletin, **34**, 21, 1776 (1961).

Summary

By the simple LCAO MO treatment, introducing the reaction parameter, the following expectations have been obtained for the color reactions of polynitroanisoles with the methoxide ion: 1) Meisenheimer's intermediates are more easily formed and are more stable as the numbers of nitro groups increase. 2) The energies of activation for the formation of the intermediates become smaller as the numbers of nitro groups increase. These expectations are in agreement with the experimental results.

The author is particularly indebted to Professor Hiroshi Azumi, Professor Yoshito Amako and Dr. Shigeyoshi Katagiri for his discussions with them.

The College of Kawauchi
Tohoku University
Kawauchi, Sendai

The Kinetics of the Reaction of Formaldehyde with Ammonia

By Yoshiro OGATA and Atsushi KAWASAKI

(Received November 6, 1963)

It is well known that formaldehyde reacts with ammonia to form hexamethylenetetramine or hexamine (VI) in a good yield.[1] Although kinetic studies have been reported,[2-4] no decisive evidence has been presented about the dependency of the rate on the concentration of each reactant. Richmond, Myers and Wright[5] suggested a mechanism not on the basis of the kinetics but on that of the isolated derivatives of intermediates.

The present report summarizes the results of our kinetic study of the reaction of formaldehyde with ammonia, especially the relation between the pH of the solution and the rate, which implies a probable mechanism of the reaction.

Results and Discussion

Rate Equation.—The stoichiometric equation for the formation of hexamine from formaldehyde and ammonia has been expressed as

$$4NH_3 + 6CH_2O \rightarrow N_4(CH_2)_6 + 6H_2O \quad (1)$$

Although the analysis of ammonia and formaldehyde in the reaction mixture indicated that the molar ratio of consumed ammonia vs. formaldehyde was 2 : 3 throughout the reaction, the consumption of formaldehyde estimated by analysis is due not

1) P. Duden and M. Scharf, *Ann.*, **288**, 218 (1895).
2) M. L. Boyd and C. A. Winkler, *Can. J. Research*, **25B**, 387 (1947); J. R. Polley, C. A. Winkler and R. V. V. Nicholls, ibid., **25B**, 525 (1947).
3) E. Baur and W. Rüetschi, *Helv. Chim. Acta*, **24**, 754 (1941).
4) S. Bose, *J. Ind. Chem. Soc.*, **34**, 663 (1957).
5) H. H. Richmond, G. S. Myers and G. F. Wright, *J. Am. Chem. Soc.*, **70**, 3659 (1949).

only to the formed hexamine but also to some intermediates, because the consumed formaldehyde may exist as some intermediates besides hexamine. If the reaction mixture was acidified with dilute acetic acid before analysis, the analytical value of formaldehyde became higher. Since hexamine did not decompose under these conditions, the higher value may be due to the decomposition of the intermediates to formaldehyde and ammonia. In alkaline solutions held at 0～5°C for the analysis of formaldehyde, however, the decomposition of the intermediates was slow and negligible. The presence of methanol did not affect this analysis.

The rate of the consumption of formaldehyde, v, may be expressed as the third-order equation:

$$v=\frac{dx}{dt}=k\left(a-\frac{2}{3}x\right)(f-x)^2 \qquad (2)$$

where a and f are the initial concentrations (mol. l^{-1}) of ammonia and formaldehyde respectively, x is the concentration of consumed formaldehyde after t seconds, and k, the third-order rate constant. If $a=2/3\ f$, Eq. 2 gives:

$$k=\frac{3}{2}\frac{1}{2t}\left\{\frac{1}{(f-x)^2}-\frac{1}{f^2}\right\}$$

If $a\neq 2/3\ f$,

$$k=\frac{3}{2}\frac{1}{t}\left\{\frac{2.303}{((3/2)a-f)^2}\log\frac{(3/2)a(f-x)}{f((3/2)a-x)}+\frac{1}{(3/2)a-f}\cdot\frac{x}{f(f-x)}\right\} \qquad (3)$$

The values of k, as calculated by Eq. 3 from the data in an unbuffered solution up to 70% conversion, are shown in Table I. Although the change in the pH of the solution was small, even in these unbuffered solutions, and although the effect of the pH on the rate was very small within the 10.2～10.5 pH range, most of our experiments were made on buffered solutions. The kinetics except at pH 9～10 follow the above rate equation with a precision similar to that of the example in Table I. The rate constant at pH 9～10 tended to decrease slightly as the reaction proceeded. The rapid titration of ammonia with hydrochloric acid, using rosolic acid as an indicator to estimate the unreacted ammonia alone, also gave the same third-order constants. While these k values show a good constancy, those values obtained by means of the other third-order or the second-order equations do not. Consequently, it may be concluded that the reaction is first-order with ammonia and second-order with formaldehyde.

Table I. Typical rate data for the reaction of formaldehyde with ammonia in unbuffered solution at 20°C

Initial concn.: ammonia, 0.0264 M; formaldehyde; 0.0532 M
Change of pH: 10.5～10.2

Time sec.	Concn. of unreacted formaldehyde M	Conversion %	k $M^{-2}\,sec^{-1}$
310	0.0443	22.6	0.535
610	0.0384	37.5	0.579
910	0.0340	48.5	0.633
1145	0.0320	53.1	0.615
1815	0.0291	61.0	0.552
2700	0.0254	70.4	0.584
		Av.	0.584±0.051

The Variation of the Rate with the pH of the Solution.—The rate constants with the varying pH of the solution are listed in Table II. The rate increased sharply with an increasing pH to a maximum at pH 9～10, and then it decreased gradually. An analogous relation has

Table II. The variation of rate constants with pH of the solution at 20°C

pH	Buffer concn., M		Initial concn., M		$k\times10^2$, $M^{-2}\,sec^{-1}$
	KH_2PO_4	$Na_2B_4O_7$	Ammonia	Formaldehyde	
6.3	0.351	0.025	0.0265	0.0549	3.81
6.7	0.315	0.022	0.1050	0.0551	14.0
7.1	0.249	0.075	0.0530	0.0525	25.1
7.9	0.178	0.102	0.0265	0.0525	234
7.9[a)]	0.178	0.102	0.0265	0.0525	213
8.5	0.034	0.020	0.0265	0.0523	916
8.9	0.070	0.165	0.0265	0.0525	2040
	NaOH	$Na_2B_4O_7$			
9.8	0.097	0.122	0.0265	0.0265	2520
10.2	0.243[b)]	0.075	0.0265	0.0265	1560
11.0	0.136	0.072	0.0530	0.0530	1280
11.9	0.147	0.066	0.0530	0.0530	348

a) 0.28 M KCl was added.
b) Na_2CO_3 was used instead of NaOH.

been reported for the reaction of amine or phenol with carbonyl compounds.[6] No appreciable acid catalysis was detected, at least in these alkaline solutions. The maximum is not due to general acid catalysis, but to preliminary equilibria of ammonia and formaldehyde (Eqs. 4 and 6). No appreciable salt effect was observed with the run at pH 7.9. These results suggest the following mechanism, involving an attack of ammonia[2] on free formaldehyde, at least under these conditions:

$$NH_3 + H_2O \rightleftharpoons NH_4^+ + OH^- \quad \text{(fast)} \quad (4)$$

$$CH_2O + H_2O \rightleftharpoons CH_2(OH)_2 \quad \text{(fast)} \quad (5)$$

$$CH_2(OH)_2 + OH^- \rightleftharpoons CH_2(OH)O^- + H_2O \quad \text{(fast)} \quad (6)$$

$$NH_3 + CH_2O \rightleftharpoons \underset{\text{(I)}}{NH_2CH_2OH} \quad \text{(fast)} \quad (7)$$

$$NH_2CH_2OH + CH_2O \rightleftharpoons \underset{\text{(II)}}{NH(CH_2OH)_2} \quad \text{(slow)} \quad (8)$$

The mechanism requires that the rate of the consumption of formaldehyde should be expressed as;

$$v = k_8 [NH_2CH_2OH] [CH_2O] = k_8 K_7 [NH_3] [CH_2O]^2$$

Here, k and K are the rate and equilibrium constants of the subscripted steps respectively. The estimation of formaldehyde by Nessler reagent iodometry[7,8] gives only the concentration of the unreacted formaldehyde, but not those from methylolamine and other formaldehyde derivatives. The experiments were carried out in a dilute aqueous solution; hence,

$$a-(2/3)x = [NH_3] + [NH_4^+] = [NH_3]\left\{1+\frac{K_4[H_2O][H^+]}{K_w}\right\}$$

$$f-x = [CH_2O] + [CH_2(OH)_2] + [CH_2(OH)O^-] = [CH_2O]\left(1+K_5[H_2O]+\frac{K_5K_6K_w}{[H^+]}\right)$$

Hence,

$$v = k_8K_7\frac{1}{1+(K_4[H_2O][H^+]/K_w)}\times\left[\frac{1}{1+K_5[H_2O]+(K_5K_6K_w/[H^+])}\right]^2 \times\left(a-\frac{2}{3}x\right)(f-x)^2 \quad (9)$$

Here, K_w is the ionic product of water. At 20°C, $K_4[H_2O] = K_b$[9] $= 1.75\times10^{-5}$, $K_5[H_2O] = K_f$[10] $= 10^4$, $K_6K_w/[H_2O] = K_s$[11] $= 1.62\times10^{-13}$, and $K_w = 0.681\times10^{-14}$.

Therefore, comparing Eq. 9 with Eq. 2,

$$k = \frac{k_8K_7}{K_f^2}\frac{1}{1+[H^+](K_b/K_w)}\left[\frac{1}{1+(K_s/[H^+])}\right]^2 \quad (10)$$

or

$$\log k = \log\frac{k_8K_7}{K_f^2} + \log\frac{1}{1+[H^+](K_b/K_w)} \times\left[\frac{1}{1+(K_s/[H^+])}\right]^2 \quad (11)$$

The differentiation of Eq. 10 with respect to $[H^+]$ gives the pH value of the maximum rate, where the values of K_b, K_w and K_s were corrected for the ionic strength of 0.35 by means of the Debye-Hückel limiting law.

$$[H^+] = \sqrt{\frac{2K_wK_s}{K_b}} = 2.27\times10^{-11} \text{ or } pH = 10.64$$

The plots of the calculated values of $\log[1/\{1+[H^+](K_b/K_w)\}][1/(1+K_s/[H^+])]^2$ and the observed value of $\log k$ against pH are shown in Fig. 1. The observed values show a little deviation from the calculated ones in acidic solutions. In alkaline solutions (pH>10), the observed rate deviates more from the calculated ones.[12]

The difference in height of 0.80 $M^{-2}\,sec^{-1}$ in both linear parts with the slope of ca. 1.0 gives the value of $\log(k_8K_7/K_f^2)$, which leads to 6.3×10^8 for the value of k_8K_7. However, most of formaldehyde is hydrated—i. e., the concentration of free formaldehyde is very small; hence, the concentration of I is negligible except at the initial stages of reaction. Although step 8 is also reversible, the rate of the reverse reaction may be almost negligible at a higher pH.

The reaction product, hexamine, did not appreciably decompose in dilute aqueous acetic acid, at least in an hour's time, but there were intermediates which decomposed completely to ammonia and formaldehyde in

6) J. B. Conant and P. D. Bartlett, *J. Am. Chem. Soc.*, **54**, 2893 (1932); E. H. Cordes and W. P. Jencks, ibid., **84**, 832 (1962); T. Minami and T. Ando, *J. Chem. Soc. Japan, Ind. Chem. Sec. (Kogyo Kagaku Zassi)*, **60**, 1078 (1957).

7) J. F. Walker, "Formaldehyde," 2nd Ed., Reinhold Publ. Corp., New York, N. Y. (1953), p. 387.

8) S. Bose, *J. Ind. Chem. Soc.*, **34**, 497 (1957).

9) T. S. Moore and T. F. Winmill, *J. Chem. Soc.*, **101**, 1635 (1912).

10) R. Bieber and G. Trümpler, *Helv. Chim. Acta*, **30**, 1860 (1947).

11) M. Wadano, C. Trogus and K. Hess, *Ber.*, **67**, 174, 191 (1934).

12) This fact may be due to the change of the rate-determining step to the following step:

$$NH(CH_2OH)_2 + H^+ \underset{\text{(slow)}}{\rightleftharpoons} HOCH_2NHCH_2^+ + H_2O$$

The dependence of the rate constant on the acidity at pH 9~10 seems to support this assumption, but there is little further evidence.

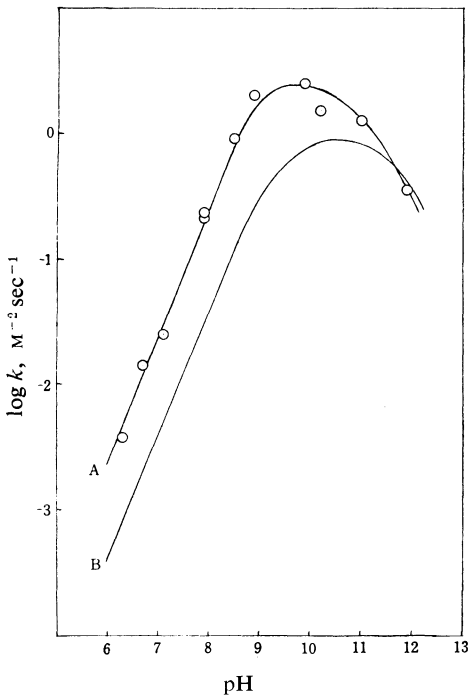


Fig. 1. Plots of logarithm of the observed rate constants (A) and calculated values of $[1/\{1+(K_b/K_w)[H^+]\}][1/\{1+(K_s/[H^+])\}]$ (B) against pH for the reaction of formaldehyde with ammonia.

30 min. under similar conditions. The concentrations of ammonia and formaldehyde produced from the intermediates were observed to be 0.0030 M and 0.0060 M at 15.5 min., 0.0044 and 0.0088 (30 min.), 0.0045 and 0.0094 (60 min.) respectively. Therefore, the molar composition ratio of formaldehyde and ammonia in intermediates should be 2.0, although Bose[4] suggested the value of 1.0 for this ratio. The unstable intermediates may include mono-, di-, and trimethylolamine and other cyclic compounds. Dimethylolamine II rather than *N*-methylolmethylenimine CH_2=N-CH_2OH may be present, since the reaction mixture had no absorption maximum in the range of 210~240 mμ corresponding to a C=N bond,[13] only a maximum at 191~210 mμ (by nitrogen purging), which suggests the presence of amines. Di- and triethanolamine also had absorption maxima in this region. Another probable intermediate, methylenediamine III, the existence of which has been suggested by Richmond et al.,[5] should be more stable than dimethylolamine II and would not decompose, because N-C-N bonds in hexamine VI and 1, 3-diaza-adamantane VIII are stable in aqueous acetic and mineral acids,[14] respectively, and methylenediamine sulfate is isolable in a strongly acidic solution.[5] Nitroso or benzoyl derivatives of cyclotrimethylenetriamine IV and 1, 5-endomethylene-1, 3, 5, 7-tetrazacycloöctane V have been obtained from the reaction mixture.[1,5] When formaldehyde was added to an excess of ammonia and then to benzoyl chloride, methylenedibenzamide (8.4%) was obtained exclusively. On the other hand, both tribenzoylcyclotrimethylenetriamine (7.1%) and methylenedibenzamide (2.6%) were obtained when ammonia was added to an excess of formaldehyde. These facts seem to suggest that the formation of III is faster than that of IV, and that a large ratio of CH_2O vs. NH_3 is favorable for the formation of IV. The following scheme may explain the facts described above.

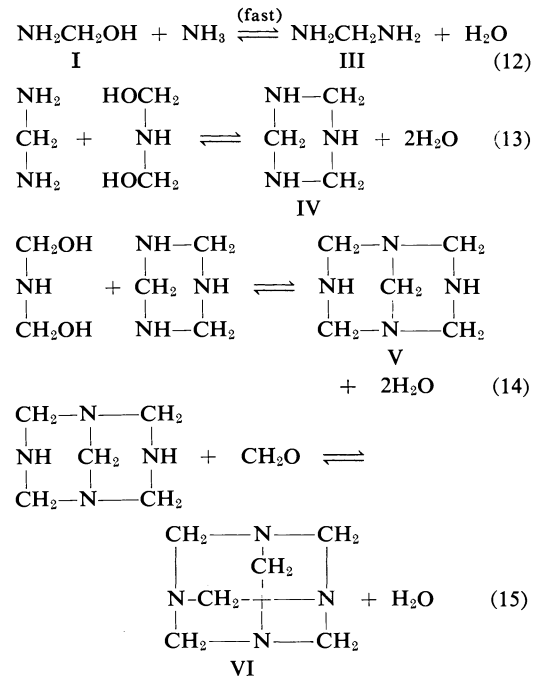


Table III. The molar ratio of formaldehyde vs. ammonia produced from unstable intermediate using 0.0265 M formaldehyde at 23°C after 1 hr.

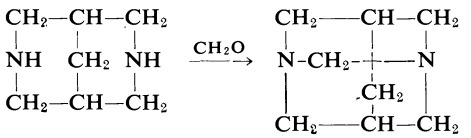
Run	Increase in concn., M		Molar ratio
	Ammonia	Formaldehyde	
1[a]	0.0044	0.0090	2.0
2	0.0019	0.0044	2.3
3	0.0029	0.0054	1.9
4	0.0014	0.0023	1.7
5	0.0018	0.0041	2.3
			Av. 2.0

a) 0.0530 M formaldehyde was used.

13) R. P. Linstead and M. Whalley, *J. Chem. Soc.*, **1955**, 3530; G. E. Ficken and R. P. Linstead, ibid., **1955**, 3525; A. Maccoll, *Quart. Revs.*, **1**, 28 (1947).
14) H. Stetter, *Angew. Chem.*, **74**, 361 (1962).

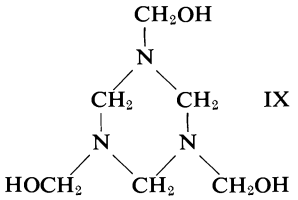
We followed the reaction by estimating the remaining formaldehyde alone; thus, steps 13, 14 and 15 may not be very fast. Therefore, it is not surprising that the derivatives of IV and V were isolated as stable intermediates.

Analogous reactions to steps 13 and 14 have been observed in the reaction between dimethylolnitramide and methylenediamine sulfate to form 1, 5-endomethylene-3, 7-dinitro-1, 3, 5, 7-tetrazacycloöctane.[5] In support of step 15, it has been known that bispidines VII with a structure similar to V react readily with formaldehyde to form 1, 3-diaza-adamantane VIII;[14] for example,



VII VIII

Another mechanism,[3,5] by which hexamine is formed through trimethylolcyclotrimethylenetriamine IX, requires that all three methylol groups should be in cis-configuration.[15] Moreover, the reaction of the trimethylols with



IX

ammonia would be more difficult, since 1-aza-adamantane has been prepared, not directly by the reaction of *cis*-1, 3, 5-tris-methylolcyclohexane with ammonia, but by that of its bromoderivative or methanesulfonate and ammonia in a low yield.[14,16]

Experimental

Materials.—The ammonia and formaldehyde used were of G. R. grade. Small amounts of formic acid and methanol in the formaldehyde had no effect on the rate.

Buffer solutions were prepared from 0.4 M monopotassium phosphate and 0.2 M borax solutions for pH 6~9 and from 0.2 M borax and 0.1 N sodium hydroxide solutions for pH 9.8~12. No Cannizzaro reaction of formaldehyde using this buffer solution with a pH of 11 was observed.

Rate Measurements.—A solution of 0.1 M aqueous fomaldehyde (50 ml.) and a solution of 0.05 M aqueous ammonia (50 ml.), maintained previously at 20°C were mixed in a flask and thermostated at 20±0.1°C. At known intervals of time, an aliquot (5 ml.) was pipetted out into an ice-cooled Nessler solution[7,8] (6.5 ml.) containing mercuric chloride (3 g.) and potassium iodide (40 g.) in distilled water (100 ml.). An aqueous solution of 0.1 N iodine (10 ml.) and then 2 N aqueous sodium hydroxide (5 ml.) were added to the solution, and it was kept standing for 30 min. at 0~5°C. The solution was then acidified with 2 N hydrochloric acid (10 ml.), the excess iodine being titrated with 0.1 N sodium thiosulfate. The amount of unreacted formaldehyde was determined by a blank test. A crystalline precipitate of hexamine (84%), (m. p. 295°C (decomp.)) was obtained at the end of these rate measurements.

Intermediates.—*Methylolamines and Related Intermediates.*—0.1 M aqueous formaldehyde (50 ml.) and 0.05 M aqueous ammonia (50 ml.) were mixed in a flask and thermostated at 20°C. After 15~20 min. the reaction mixture was added to 0.1 M aqueous acetic acid (100 ml.) which had been previously cooled with ice-water. Two aliquots (10 ml. or 20 ml. each) were immediately pipetted out; one was employed to determine the concentration of formaldehyde by Nessler reagent iodometry, and the other, to determine that of ammonia by titrating excess acetic acid with 0.1 N sodium hydroxide using phenolphthalein. The solution was kept standing at 20°C for one hour to complete the decomposition, as above. Then the concentrations of ammonia and formaldehyde was again determined; they indicated the composition of the unstable intermediates—i. e., it was found to be composed of $NH_3 : CH_2O = 1 : 2$.

Methylenedibenzamide and Tribenzoylcyclotrimethylenetriamine. — Aqueous formaldehyde (0.1 mol.) was added to aqueous ammonia (0.2 mol.) cooled by ice for over a 10 min. period. The solution was treated with benzoyl chloride (0.13 mol.) as described by Richmond.[5] Methylenedibenzamide (2.14 g., 8.4%) (m. p. 223°C) was obtained. The freezing point method, using dimethylsulfoxide as a solvent, gave a molecular weight of 227; calcd. for $C_{15}H_{14}O_2N_2$: 254. IR spectrum: ν cm^{-1} 3370 (-NH-); 1640, 1535, 1290 (*s*-amide). A trace of tribenzoylcyclotrimethylenetriamine was obtained.

On the other hand, aqueous ammonia (0.1 mol.) was added to a cold solution of formaldehyde (0.2 mol.), and then the solution was treated with benzoyl chloride. The chloroform extract gave tribenzoylcyclotrimethylenetriamine (1.88 g., 7.1%) (m. p. 219~220°C). IR spectum: ν cm^{-1} 1655 (*t*-amide) (Found: C, 72.3; H, 5.26; N, 10.9. Calcd. for $C_{24}H_{21}O_3N_3$: C, 72.2; H, 5.26; N, 10.5%.). Futhermore, methylenedibenzamide (0.324 g., 2.6%) was obtained from the ethanolic extract.

The change in pH measured by a Hitachi M4 pH meter during the reaction is shown in Table IV. The ultraviolet absorption spectra were measured by a Shimadzu SV50A spectrophotometer in the ranges of 210~300 mμ and 190~210 mμ by nitrogen purging.

Summary

The kinetics of the reaction of formaldehyde with ammonia to form hexamethylenetetramine

15) H. Stetter, ibid., **66**, 217 (1954).
16) M. S. Newman and H. S. Lowrie, *J. Am. Chem. Soc.*, **48**, 861 (1951).

TABLE IV. THE VARIATION OF pH IN UNBUFFERED SOLUTION AT 23°C
Initial concn.: Ammonia, 0.0265 M (with pH of 10.94)
Formaldehyde, 0.0530 M

Reaction time, min.	0	3	7	10	15	25	35	55	80	285
pH	10.57	10.47	10.40	10.36	10.32	10.26	10.17	10.03	9.88	9.64

has been investigated in dilute aqueous solutions at 20°C in the pH range between 6.3 and 11.9. The reaction was first-order with respect to ammonia and second-order with respect to formaldehyde. The rate increased sharply with the increasing pH to a maximum between 9 and 10, and then it decreased gradually. These results may be explained by a mechanism involving a rate-determining attack of methylolamine on free formaldehyde to form dimethylolamine, followed by the formation of hexamine through cyclotrimethylenetriamine and 1, 5-endomethylene-1, 3, 5, 7-tetrazacycloöctane.

Department of Applied Chemistry
Faculty of Engineering
Nagoya University
Chikusa-ku, Nagoya

*Electronic Spectra of Substituted Aromatic Hydrocarbons. IV. Anthramines**

By Satoshi SUZUKI and Hiroaki BABA

(Received November 6, 1963)

In this series of papers,[1-3] the effect of substitution on the electronic transitions of aromatic hydrocarbons, benzene, naphthalene and anthracene has been discussed in terms of the perturbation by the substituent group concerned. Along the same lines, the absorption and fluorescence spectra of α- and β-anthramines have been examined in the present study.

Theoretical calculations[4-6] predicted that the $^1A_g \rightarrow {}^1B_{3u}^-$ ($^1A \rightarrow {}^1L_b$ in Platt's notation[6]) transition of anthracene is hidden under the stronger $^1A_g \rightarrow {}^1B_{2u}$ ($^1A \rightarrow {}^1L_a$) transition. The present authors reported in a preceding paper[3] that the ^1L_b band emerged in the absorption spectrum of β-anthrol on the lower frequency side of the ^1L_a band. This shows that the ^1L_b band increases in intensity and undergoes a characteristic frequency shift as a result of the introduction of an electron-donating group at the β-position. As is well known, an amino group is of a more electron-donating nature than a hydroxyl group, so that one may naturally expect that the separation of the ^1L_b band from the ^1L_a band should be pronounced in the spectrum of β-anthramine. In this paper, special attention will be paid to this point. Furthermore, it will be shown that in the low-frequency region α-anthramine has two absorption bands which seem to correspond to the ^1L_a and ^1L_b transitions.

Experimental

Materials.—α-Anthramine was prepared from α-aminoanthraquinone by refluxing it with zinc dust in an aqueous solution of sodium hydroxide.[7] The product was purified by column chromatography, and finally it was subjected to vacuum sublimation; m. p. 117~119°C in a sealed tube (lit.,[7] 121.5~122.5°C). β-Anthramine was prepared from β-aminoanthraquinone by the same procedure.[8] The product was sublimed in vacuo after crystallization from benzene; m. p. 237~238.5°C (lit.,[8] 238°C). Dioxane was purified by the method described in a previous paper.[9] Triethylamine was fractionally distilled, dried with alumina, and then distilled in vacuo.

* Presented in part at the 14th Annual Meeting of the Chemical Society of Japan, Tokyo, April, 1961.

1) H. Baba, This Bulletin, **34**, 76 (1961).
2) H. Baba and S. Suzuki, ibid., **34**, 82 (1961).
3) H. Baba and S. Suzuki, ibid., **35**, 683 (1962).
4) H. B. Klevens and J. R. Platt, *J. Chem. Phys.*, **17**, 470 (1949).
5) R. Pariser, ibid., **24**, 250 (1956).
6) J. R. Platt, ibid., **17**, 484 (1949).
7) H. E. Fierz-David, L. Blangey and H. Streiff, *Helv. Chim. Acta*, **29**, 1718 (1946).
8) P. Ruggli and E. Henri, ibid., **13**, 409 (1930).
9) H. Baba and S. Suzuki, *J. Chem. Phys.*, **35**, 1118 (1961).

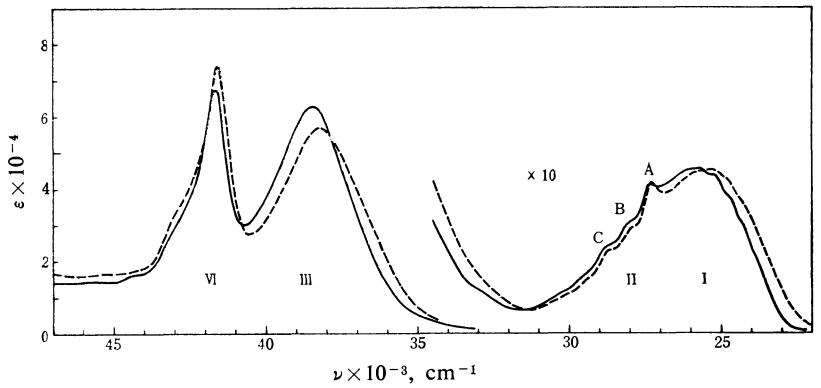


Fig. 1. Absorption spectrum of α-anthramine in isooctane at 20°C and the effect of hydrogen bonding. Solid curve, free molecule; dashed curve, spectrum in the presence of dioxane the concentration of which is 1.0 mol./l.

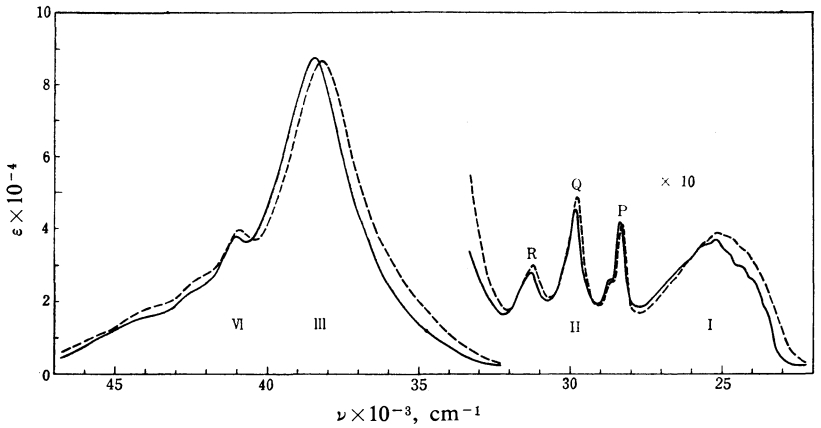


Fig. 2. Absorption spectrum of β-anthramine in isooctane at 20°C and the effect of hydrogen bonding. Solid curve, free molecule; dashed curve, spectrum in the presence of dioxane the concentration of which is 1.0 mol./l.

Apparatus and Procedures.—Absorption spectra at an ordinary temperature were measured with a Hitachi model EPU-2A photoelectric spectrophotometer at the controlled temperature of 20°C. Fluorescence spectra were observed at room temperature by attaching a fluorescence accessory of the L-3 type to the spectrophotometer. Samples were excited with the 365 mμ line of mercury. The slit was kept 0.2 mm. wide for all the fluorescence measurements. The observed spectra were corrected to quantum fluorescence spectra by the procedure described in a preceding paper.[3] All the absorption and fluorescence spectra at ordinary temperature were observed in an isooctane solution.

Absorption spectra at the liquid-nitrogen temperature were obtained using as a solvent the 6 : 1 isopentane—methylcyclohexane mixture which was recommended by Potts[10] as a glass-forming solvent. Measurements of the low-temperature spectra were performed by combining a Hitachi model EPS-2 recording spectrophotometer with a specially-designed low-temperature absorption apparatus. The latter is an all-glass Dewar vessel which has four parallel-plane glass windows transparent down to 250 mμ. Datails about the absorption apparatus and the procedures have been published elsewhere.[11]

Results

Figures 1 and 2 illustrate the absorption spectra of α- and β-anthramines in isooctane at 20°C and the changes in them caused by the addition of dioxane as a proton acceptor. The solid curves depict the spectra of anthramines free from hydrogen bonding. The dashed curves represent the spectra of solutions containing dioxane at a concentration of 1.0 mol./l.

The fluorescence spectra of α- and β-anthramines in isooctane at room temperature are shown in Figs. 3 and 4. In the figures, absorption spectra are given with dashed curves for easy reference.

10) W. J. Potts, ibid., **21**, 191 (1953).

11) H. Baba, S. Suzuki and S. Miura, *Bull. Research Inst. Appl. Electricity*, Hokkaido Univ., **14**, 59 (1962).

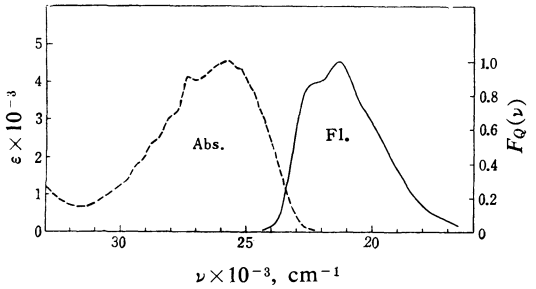


Fig. 3. Fluorescence and absorption spectra of α-anthramine in isooctane. Solute concentration for fluorescence: 8.90×10^{-5} mol./l.

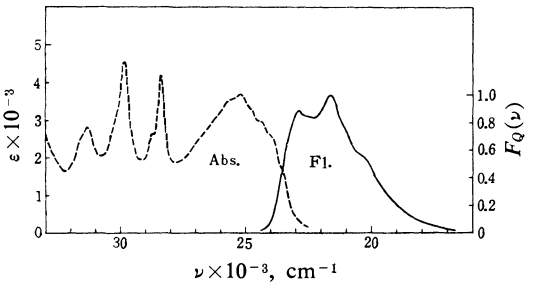


Fig. 4. Fluorescence and absorption spectra of β-anthramine in isooctane. Solute concentration for fluorescence: 3.20×10^{-5} mol./l.

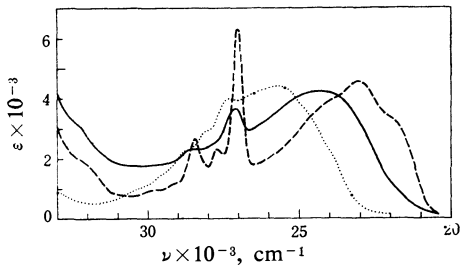


Fig. 5. Absorption spectra of α-anthramine at liquid-nitrogen temperature in 6 : 1 isopentane —methylcyclohexane mixture. Solid curve, free molecule; dashed curve, spectrum in the presence of triethylamine the concentration of which is 0.2 mol./l.; dotted curve, free molecule at room temperature.

The absorption spectra of α-anthramine at the liquid-nitrogen temperature may be seen in Fig. 5. The solid curve is the spectrum of α-anthramine, while the dashed curve is the spectrum in the presence of triethylamine at a concentration of 0.2 mol./l. In the same figure, the absorption spectrum of α-anthramine at room temperature in the same solvent is cited with a dotted line for the purpose of comparison. The absorption spectra at the liquid-nitrogen temperature have been corrected for the solvent contraction.

Discussion

Jones[12] discussed the effect of substitution on the electronic absorption spectrum of anthracene in terms of the resonance theory. From a consideration along his lines, one may predict whether or not the ^1L_b band will appear in some anthracene derivatives. A substituent group introduced at the β-position lies nearly along the long axis of the molecule. The ^1L_b transition of anthracene has a transition moment along the long axis of the molecule, whereas the ^1L_a has a moment along the short axis. Therefore, the ^1L_b transition is subjected to a greater influence than is the ^1L_a transition by the introduction of the substituent group at the β-position. In fact, the authors have reported that in β-anthrol the ^1L_b band emerged on the lower frequency side of the ^1L_a band.[3,13] In the case of β-anthramine, which has a more electron-donating substituent than does β-anthrol, it is expected that the separation of these two bands will become more distinct. On the other hand, upon substitution in the α-position, the ^1L_a transition is expected to show a large frequency shift as compared with the ^1L_b transition, since the α-substitution seems mainly to perturb transitions along the short axis of the molecule. Consequently, when an amino group is introduced in the α-position of anthracene, the ^1L_a band may probably be displaced to the red, leaving the ^1L_b band in its original position. If this is the case, the ^1L_b band will appear on the higher frequency side of the ^1L_a band. Indeed, the ^1L_b band can be detected in the spectrum of α-anthramine.

When a molecule forms a hydrogen bond, characteristic changes are effected in the positions and intensities of its absorption bands. Thus the authors suggested that the observation of this spectral behavior in hydrogen bonding would be useful for distinguishing and assigning the electronic transitions of a given molecule. The hydrogen-bonding effects on the absorption spectra of the anthramines support the band assignments presented here.

Bands in the Low-Frequency Region. — The absorption spectrum of β-anthramine in the low-frequency region (below 35000 cm^{-1}) consists of an absorption band, II, which has three sharp vibrational components, P, Q and R, with almost equal spacings (ν_{max} : 28370, 29830, 31300 cm^{-1}), and a broad band, I (see Fig. 2). (I, II, etc. refer to the absorption bands in the order of increasing frequency.) Such a spectral constitution suggests that there are two kinds

12) R. N. Jones, *Chem. Revs.*, **41**, 353 (1947).
13) S. Suzuki and H. Baba, *J. Chem. Phys.*, **38**, 349 (1963).

of electronic transitions in this region. This is supported by the following two facts. First, due to the formation of a hydrogen bond, the two absorption bands behave differently in their frequency shift; the shifts of the components, P, Q and R, are quite small compared with the shift of the I band. Second, the mirror image relation between fluorescence and absorption spectra favors the view that there are two transitions in the low-frequency region; the fluorescence spectrum of β-anthramine can be interpreted as corresponding to the I absorption band alone. It has therefore been concluded that in this region β-anthramine has two different electronic absorption bands, namely, the I and II bands.

By reference to the band assignment for the related compound, β-anthrol,[3,13] the I band at the longer wavelengths can safely be assigned to the $^1A \rightarrow {}^1L_b$ transition and the II band, to the $^1A \rightarrow {}^1L_a$. Döller et al.[14] and Förster and Renner[15] have made the same assignment without any comments. In agreement with the expectation from the foregoing qualitative argument, the separation of these two bands is considerably larger in β-anthramine than in β-anthrol. It may be noted that there is a close resemblance in the spectral shapes of β-anthramine and β-anthrol anion.[3]

The low-frequency spectrum of α-anthramine appears to involve only a single electronic transition, but on closer inspection it is found that there are also weak vibrational components, A, B and C, at the shorter wavelength side. As may be seen in Fig, 1, the components, A, B and C, are little shifted by the formation of a hydrogen bond; on the other hand, the band with a maximum at 25910 cm^{-1}, I, is considerably shifted toward the red. From these facts one may assume that there are two different electronic transitions in this frequency region. One is the I transition, and the other is the transition to which the vibrational components, A, B and C, belong, the latter being referred to hereafter as the II transition. Although the observed fluorescence spectrum gives no reliable evidence in support of the above statement, it does not conflict with the assumption of two transitions.

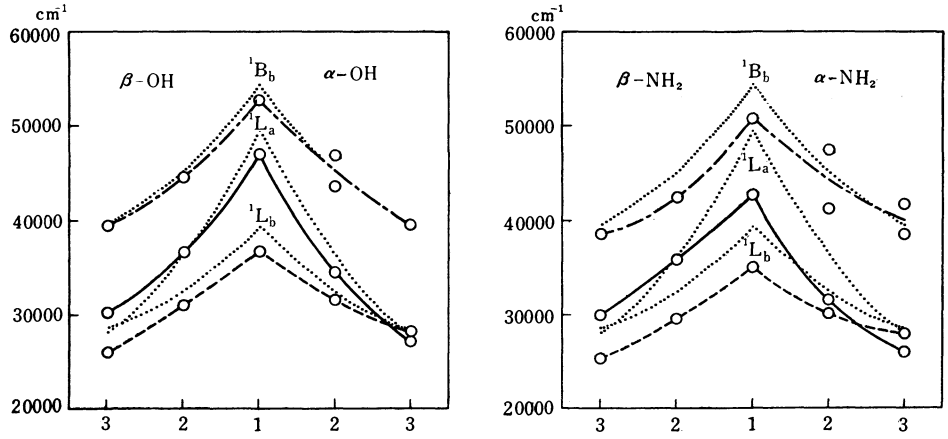
In order to confirm the existence of two different transitions in the frequency region concerned, absorption spectra at the lipuid-nitrogen temperature have been observed (Fig. 5). In general, a lowering of the temperature will be accompanied by a contraction of the solvent and, hence, by an increase in its refractive index. Accordingly, the solvent effect on absorption spectra will be enhanced by the change from room temperature to the liquid-nitrogen temperature. In Fig. 5 it may be seen that the spectrum of α-anthramine, free from hydrogen bonding, is as a whole displaced to the red by lowering the temperature, but the shift of the I band is much larger than that of the vibrational peaks, A, B and C. This indicates that the solvent has different effects on the I and II transitions. When α-anthramine forms a hydrogen bond with triethylamine at room temperature, the I band exhibits a large red shift, whereas the A, B and C peaks show almost no shift in their frequencies. This tendency becomes more pronounced at a low temperature. Thus, as may be seen in Fig. 5, upon the formation of the hydrogen bond with triethylamine at the liquid-nitrogen temperature, the I band is markedly shifted to the red, and, consequently, a clear minimum appears between the I and II bands. The occurrence of such a large separation of the two transitions, I and II, can be interpreted as due to the co-operative effects of hydrogen bonding and the solvent. The absorption spectra of aryl alkali amides have been observed by Döller et al.[14] and Förster and Renner.[15] By referring to their experimental results, one will find that at the liquid-nitrogen temperature α-anthramine does not seem to dissociate a proton, even in the presence of triethylamine.

All of the results of the low-temperature experiments mentioned above show that in the α-anthramine spectrum the vibrational components, A, B and C, belong to an electronic transition which is entirely different in origin from the I transition. As was stated at the beginning of this section, the I band of α-anthramine can reasonably be assigned to the $^1A \rightarrow {}^1L_a$ transition and the II band, to the $^1A \rightarrow {}^1L_b$.

Bands in the High-Frequency Region.—α-Anthramine has two absorption maxima with comparable intensity in this region (above 35000 cm^{-1}). It is evident from their behavior in the hydrogen bond formation that these two bands originate in different kinds of transitions. The one at the lower frequencies shifts toward the red and decreases in intensity, but the other at the higher frequencies shows only a little shift with a slight increase in intensity.

As may be seen in Fig. 2, β-anthramine possesses one intense band, with a weak one on the higher frequency side. The spectral changes caused by hydrogen bonding indicate that the latter belongs to a transition distinct from the former.

14) E. Döller, Th. Förster and H. Renner, *Z. physik. Chem. Neue Folge*, **15**, 34 (1958).
15) Th. Förster and H. Renner, *Z. Electrochem.*, **61**, 340 (1957).



(a) Hydroxyl derivatives (b) Amino derivatives

Fig. 6. Energy correlation diagrams of substituted aromatic hydrocarbons. Circles represent the experimental electronic energies. (Dotted curve refers to parent hydrocarbons.) --○--: ^1B_b, —○—: ^1L_a, --○--: ^1L_b.

In this region anthracene gives an intense absorption band which is assigned to the $^1A_g \rightarrow {}^1B_{3u}^+$ ($^1A \rightarrow {}^1B_b$) transition.[4-6] The intense band of β-anthramine is considered to correspond to the ^1B_b transition of anthracene. The appearance of two intense bands in α-anthramine is interpreted as follows: In anthracene there are symmetry-forbidden or low-intensity transitions in the vicinity of the ^1B_b transition. The introduction of a substituent into the anthracene molecule leads to the destruction of the symmetry of the molecule; therefore, in α-anthramine the ^1B_b transition may happen to be mixed with a neighboring transition to give two mixed transitions of a high intensity. The situation is similar to the case of high-frequency transition in some α-derivatives of naphthalene.[2]

The Correlation of Energy Levels for Derivatives of Aromatic Hydrocarbons from Benzene to Anthracene.—The papers of this series have revealed the origins of the electronic bands of hydroxyl- or amino-substituted aromatic hydrocarbons. The results are summarized in Fig. 6. In the figure, observed electronic energies are plotted against the number of rings separately for α- and for β-derivatives. A diagram of this kind was previously presented by Klevens and Platt for the polyacene series.[4] Adopting the assignment or classification of the electronic bands proposed by the present authors for the derivatives, one will see that the plots give smooth curves, as in the case of the parent hydrocarbons. Regarding the ^1B_b states of α-derivatives, the average energies of two transitions with comparable intensities fall on smooth curves. (In order to facilitate comparison, curves for the parent hydrocarbons are depicted with dotted lines in the same figure.) An inspection of these curves will show that the substitution effect can be interpreted in terms of the perturbation by the substituent.

From the figure one may find several similarities in behavior of the transitions which belong to the same class. In α-derivatives, the curve for the ^1L_b state declines more gently than in the parent hydrocarbons with an increasing number of rings, while the curve for the ^1L_a state of the same derivatives runs almost parallel with that of the hydrocarbons. Consequently, the curves for the ^1L_a and ^1L_b states cross at a smaller number of rings in both hydroxyl and amino derivatives than in the unsubstituted hydrocarbons. On the other hand, the ^1L_a state of β-derivatives moves downward more slowly than does the ^1L_a state of the parent hydrocarbons with an increasing number of rings, but the curve for the ^1L_b state is nearly parallel with the curve for the same state of the parent hydrocarbons, the former curve being located at lower energies. Thus the interval between the ^1L_a and ^1L_b state increases so that, in the β-derivatives of anthracene, the ^1L_b band is clearly separated from the ^1L_a band, as has already been stated. The behavior of the ^1B_b state of β-derivatives resembles that of the same state of the parent hydrocarbons. In α-derivatives the correlation of the high-frequency bands is somewhat complicated, but their average energies lie on smooth lines. This, in turn, suggests that the ^1B_b state is split into two states by substitution because of mixing with one of the neighboring

states. It should be noted here that the state of aniline at 42700 cm^{-1} falls on the intersecting point of the two curves extrapolated from α- and β-amino-derivatives of naphthalene and anthracene. In view of this fact, there is no reason to believe that the corresponding absorption band of aniline should be assigned to a band characteristic of the substitution product, e. g., to a charge-transfer band.

The ^1L_a bands of β-derivatives have a sharp, fine structure, with equally-spaced vibrational peaks.

There are some resemblances in the band shifts produced by the hydrogen bond formation. Thus, in α-derivatives the magnitudes of the frequency shifts of the ^1L_b bands are smaller than those of the ^1L_a bands. On the contrary, the ^1L_a bands of β-derivatives are little shifted, but the ^1L_b bands are noticeably shifted to the red by the formation of hydrogen bonds.[9,13]

Summary

Absorption and fluorescence spectra of α- and β-anthramines have been observed. The $^1A \rightarrow {}^1L_b$ transition, which is masked by the $^1A \rightarrow {}^1L_a$ in anthracene, emerges in both α- and β-anthramines because of the perturbation by the substituent. In β-anthramine, the ^1L_b band is clearly separated from the ^1L_a band. In α-derivatives, the ^1L_b band exists on the higher frequency side of the ^1L_a band. These results may be confirmed by observing the effects of hydrogen bonding on the spectra. At the liquid-nitrogen temperature remarkable changes in the absorption spectrum of α-anthramine occur in the presence of triethylamine; these changes have been interpreted as due to the co-operative effects of hydrogen bonding and the solvent. By using the band assignments proposed in this series of papers, reasonable correlation diagrams of the electronic energy levels have been presented for substituted aromatic hydrocarbons, from benzene to anthracene.

Research Institute of Applied Electricity
Hokkaido University, Sapporo

The Anisotropy of the ESR Spectrum of Irradiated Poly(β-propiolactone)

By Shun-ichi OHNISHI,* Shun-ichi SUGIMOTO, Koichiro HAYASHI and Isamu NITTA

(Received November 6, 1963)

Many works have reported on the electron spin resonance (ESR) of irradiated polymes. Most of these studies, however, have been made with unoriented specimens. They have usually been amorphous polymers, or, even when they have been highly-crystalline, the crystallites are oriented randomly in the specimens. Recently, however, a few studies[1-6] have appeared using some oriented polymers as the samples. Analysis of the anisotropy in the ESR spectra obtained from such oriented specimens would inform us of the structure as well as of orientation of the free radicals in the specimens, as is evident from studies of single crystals of low-molecular-weight compounds. Using stretched polyethylene, Kiselev et al.[1] and Libby and Ormerod[2] have made definite the previous identification of the alkyl-type radical while Ohnishi et al.[3] have given a conclusive choice on the identification of the allyl-type radical. Kashiwagi[4] has discussed molecular orientation in polyethylene on the basis of the doublet splitting in the double-quintet spectrum of the alkyl-type radical.

In the present paper we have measured the angular variation of the ESR spectrum of irradiated poly(β-propiolactone). The polymer was obtained by radiation-induced solid-state polymerization of a single crystal of the

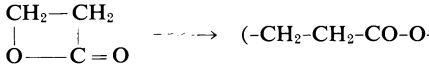
* Present address: Department of Chemistry, Faculty of Science, Kyoto University, Kyoto.

1) A. G. Kiselev, M. A. Mokul'sky and Yu. S. Lazurkin, *Vysokomolekularnye Soedineniya*, **2**, 1678 (1960).
2) D. Libby and M. G. Ormerod, *J. Phys. Chem. Solids*, **18**, 316 (1961).
3) S. Ohnishi, S. Sugimoto and I. Nitta, *J. Chem. Phys.*, **37**, 1283 (1962).
4) M. Kashiwagi, ibid., **36**, 575 (1962).
5) H. Fischer and K.-H. Hellwege, *J. Polymer Sci.*, **56**, 33 (1962).
6) D. W. Ovenall, *J. Chem. Phys.*, **38**, 2448 (1963).

monomer at low temperatures. The sample thus obtained was known to be a highly-oriented crystalline polymer.[7] From an analysis of the anisotropy of the spectra, we have made a definite identification of the radical produced, and we have also discussed molecular orientation in the specimen through the α-proton hyperfine-coupling tensor.

Experimental

Material. — The monomer (Celanese Co. Ltd.) was distilled twice in a nitrogen stream. The single crystal was obtained as a thin plate (~2.5×1.5×0.2 mm^3) by keeping the monomer at −35°C. The polymer was obtained by irradiating the single crystal of the monomer with γ-rays from a cobalt-60 source at −78°C to a dose of 2 Mrad. After



polymerization, the unreacted monomer was removed by washing it several times with methanol, and then the polymer was dried in a vacuum at 50°C. The polymer sample thus obtained had a shape quite similar to the thin plate of the monomer crystal, although the polymerization yield never exceeded 15%. A sketch of the sample and the orthogonal coordinate system xyz used in the present investigation are shown in Fig. 1. X-Ray photographs taken perpendicular to the xy and yz planes showed a fiber structure, while the photograph perpendicular to the xz plane gave only a halo. Okamura et al.[7] suggested that the molecular conformation is a planar zigzag chain pointed in the z direction.

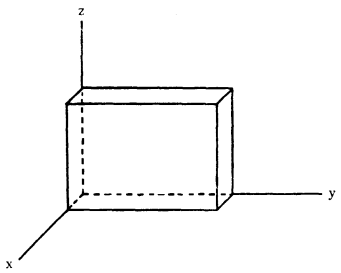


Fig. 1. A sketch of the polymer sample and the xyz coordinate system.

ESR Measurement. — The polymer was irradiated in a vacuum at −196°C with an electron beam from a Van de Graaff accelerator to a dose of 30 Mrad. The ESR spectra of the radical produced were measured at −196°C with a Varian Model V4500 spectrometer (operating frequency: 9160 Mc.). The angular variation of the spectra was measured at 15° intervals in the three planes. Hyperfine splitting values were estimated on the derivative tracing, based on the splitting value of Mn^{2+} resonance.

7) S. Okamura, K. Hayashi and Y. Kitanishi, *J. Polymer Sci.*, **58**, 925 (1962).

Results and Discussion

Angular Dependence of the Spectrum. — The spectrum showed anisotropy in the yz and zx planes, while in the xy plane it was nearly the same at all angular positions. The change of the spectrum in the zx plane is shown in Fig. 2. The main four-line spectrum at an angle $\phi=0°$ changes to a six-line one at $\phi=90°$. Here ϕ is the rotation angle measured from the z axis. The feature of the spectral change suggests that this is a double-triplet spectrum and that the doublet splitting changes with the angle, while the triplet remains almost unchanged. The free radical showing this spectrum, therefore, should have an α proton and two β protons. The angular variation of the spectrum in the yz plane is similar to that in the zx plane. At a magnetic field parallel to the z axis, the spectrum is the same one as that observed at $\phi=0°$ in Fig. 2, and, as the field direction changes, it is gradually converted to the six-line spectrum. The spectrum in the xy plane does not change appreciably with the angle, and it is a six-line spectrum similar to the one shown in Fig. 2(4) at all field orientations.

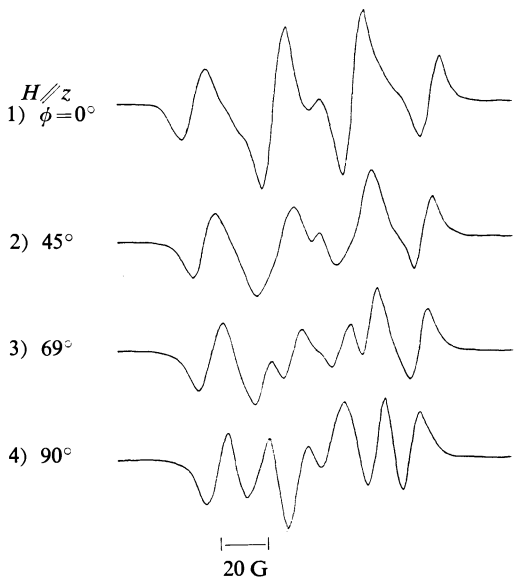


Fig. 2. Angular variation in the zx plane of the ESR spectrum of the irradiated polymer.

The doublet splitting of the α proton, A_α, was read from the separation between the first and the second peaks of the derivative curve; it is plotted against the rotation angle in Fig. 3. The curves in the yz and zx planes approximately obey the $(3\cos^2\phi-1)$ rule, as expected for the dipolar interaction. The triplet splitting value of the β proton, A_β,

was estimated by using the relation:

$$A_\beta = (\Delta H_{overall} - A_\alpha)/2 \quad (1)$$

Here $\Delta H_{overall}$ means the distance between the outermost peaks.

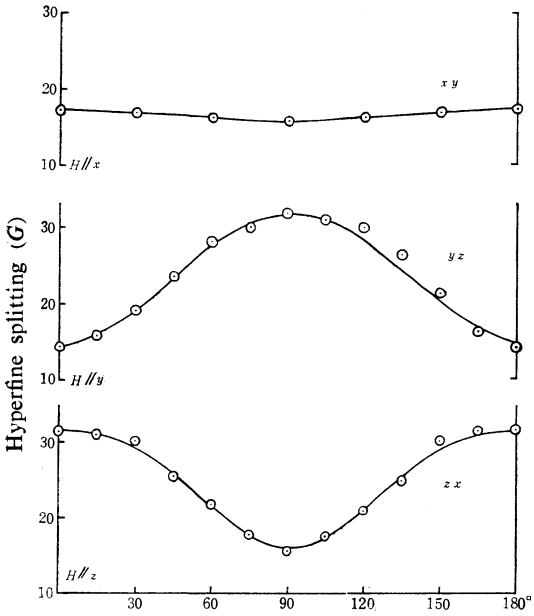


Fig. 3. Angular dependence of the hyperfine splitting of the α proton in the three basic planes.

The triplet splitting was almost isotropic, changing, for example in the yz plane, from 31.2 to 32.5 gauss.

These results indicate that the radical showing the spectrum can be attributed to $-CH_2-\dot{C}H-CO-O-$ or $-CH_2-\dot{C}H-O-CO-$, and also that the orientation of the radical is almost at random in the xy plane, although in the other planes the radicals are highly oriented. Of the two radical species proposed, the former one seems to be more probable because of the resonance stabilization.

Hyperfine-Coupling Tensor.—From the above data, the hyperfine-coupling tensor can be obtained. The spin Hamiltonian for the hf interaction with one proton may be written as[8]

$$\mathscr{H} = \beta\vec{S}\tilde{g}\vec{H} + \vec{S}\tilde{T}\vec{I} - g_N\beta_N\vec{I}\vec{H} \quad (2)$$

where β is the Bohr magneton, β_N the nuclear magneton, g_N the nuclear g-factor, $\tilde{g}$ the g-tensor, $\tilde{T}$ the hf-coupling tensor, $\vec{H}$ the external field, and $\vec{S}$ and $\vec{I}$ the electron spin and nuclear spin operators respectively. Since the electron g-factor showed only a slight anisotropy and since its value was nearly the free-spin value, the g-tensor is taken to be isotropic for the present radical. Moreover, the strong-field approximation is assumed to be as usual; i. e., $\vec{S}$ is replaced by $M_S\vec{Z}$, where $\vec{Z} = \vec{H}/|H|$. Then the spin Hamiltonian becomes:

$$\mathscr{H} = \beta g M_S H + M_S\vec{Z}\tilde{T}\vec{I} - g_N\beta_N\vec{I}\vec{H} \quad (3)$$

From the eigen value of the Hamiltonian, the doublet splitting of the α proton is given as:

$$\begin{aligned} A_\alpha = {} & [l^2(1/2A - \nu_H)^2 + m^2(1/2B - \nu_H)^2 \\ & + n^2(1/2C - \nu_H)^2]^{1/2} \\ & + [l^2(1/2A + \nu_H)^2 + m^2(1/2B + \nu_H)^2 \\ & + n^2(1/2C + \nu_H)^2]^{1/2} \end{aligned} \quad (4)$$

Here ν_H is the nuclear resonance frequency, A, B and C are the principal values of the hf coupling tensor, and l, m, and n are the direction cosines of the field direction with respect to the three principal axes, a, b and c. When evaluating the tensor component from the experimental data, the further assumption was made that the nucleus is also aligned along the field direction.[9] In this case the doublet splitting can be given by a simple formula:

$$\begin{aligned} A_\alpha = \vec{Z}\tilde{T}\vec{Z} = {} & l^2T_{xx} + m^2T_{yy} + n^2T_{zz} \\ & + 2(lmT_{xy} + lnT_{xz} + mnT_{yz}) \end{aligned} \quad (5)$$

Making use of Eq. 5, the tensor components were evaluated and the principal values, as well as the principal directions were calculated (cf. Table I).

As for the hf coupling tensor of the β-proton, only the isotropic component was evaluated as the average of the diagonal components. Its value was found to be 31.9 gauss.

The Orientation of the Free Radical. — The anisotropic hf couping of the α proton in organic radicals has been extensively studied, and the principal axes as well as the principal values of the tensor have been determined for many radicals.[10] For the HOOCCHCOOH radical in malonic acid, for example, the principal values, A, B and C, are reported to be -61, -29 and -91 Mc./sec, with the principal axes parallel to the unpaired π-axis,

8) B. Bleaney and K. W. H. Stevens, *Reports on Progress in Physics*, **16**, 108 (1953).

9) D. K. Ghosh and D. H. Whiffen, *Mol. Phys.*, **2**, 285 (1959).

10) D. H. Whiffen, "Free Radicals in Biological Systems," Ed. by M. S. Blois, Jr., et al., Academic Press, New York and London (1961), pp. 227—238.

TABLE I. HYPERFINE COUPLING TENSOR OF THE α PROTON

Tensor			Principal value	Principal axis		
				l	*m*	*n*
−16.3 (−45.6)	− 0.18 (− 0.52)	− 2.52 (− 7.06)	−15.9 (−44.5)	0.983,	0.092,	−0.160
− 0.18 (− 0.52)	−15.1 (−42.2)	− 0.65 (− 1.83)	−15.0 (−42.1)	−0.097,	0.995,	−0.026
− 2.52 (− 7.06)	− 0.65 (− 1.83)	−31.7 (−88.8)	−32.1 (−90.0)	0.160,	0.039,	0.986

Isotropic component: −21.0 (−58.9)

Values are shown in gauss. Those given in parentheses are in Mc./sec.

to the C–H_α bond, and to the direction perpendicular to both a and b axes respectively.[11] Comparing the values with those obtained for the present radical, the value *C*, −91 Mc., agrees fairly well with one of the observed values, −90.0 Mc. whose axis is almost parallel to the z axis (l=0.160, m=0.039, n=0.986). This suggests that the carbon zigzag chain of the polymer points in the z direction. On the other hand, the other principal values, −44.5 and −42.1 Mc., deviate from the reported values, −61 and −29 Mc., for malonic acid and take some averaged. values. This is a consequence of the almost axially-random orientation of the radical- or zigzag-plane. We may formally evaluate the degree of orientation of the radical in the xy plane from the observed principal values. Suppose that the magnetic field is set along the a axis and that θ measures the angle of the deviation of the π-axis of a radical from the field direction. Making use of Eq. 4 and putting A_α=−44.5 Mc., n=0 and ν_H=13.9 Mc. into the equation, $\langle l^2=\cos^2\theta\rangle$=0.337 was obtained. If we use the following relationship[12] to define the degree of orientation, f becomes 0.02 for the present case.

$$f = (3\langle\cos^2\theta\rangle - 1)/2 \qquad (6)$$

11) H. M. McConnell, C. Heller, T. Cole and R. W. Fessenden, *J. Am. Chem. Soc.*, **82**, 766 (1960).
12) P. H. Hermans and P. Platzek, *Kolloid Z.*, **88**, 68 (1939).

Conclusion

Some conclusions can be drawn from the present ESR study. The produced radical in irradiated poly(β-propiolactone) can be assigned to -CH_2-$\dot{C}$H-CO-O-. The zigzag chain of the radical almost points in the z direction of the sample. In the x and y directions, however, the orientation of the C–H_α and the unpaired π-axis (i.e., the zigzag plane) is almost at random. These resuts are consistent with the reported X-ray result.[7] However, some slight orientation of the zigzag plane is evident from the present study; the principal values, *A* and *B*, are not the same but are slightly different. The average orientation of the π-axis, although almost random, is nearly parallel to the x axis (l=0.983, m=0.092, n=−0.160).

The authors would like to express their thanks to Professor Seizo Okamura of Kyoto University for his helpful discussions and also to Mr. Masanobu Nishii of this Association for his kindness in the sample preparation.

Osaka Laboratories
Japanese Association for
Radiation Research on Polymers
Neyagawa, Osaka

*Infrared Spectra of Metal Chelate Compounds. X. A Normal Coordinate Analysis of Dithiooxalato Complexes**

By Junnosuke FUJITA and Kazuo NAKAMOTO

(Received November 16, 1963)

In general, the infrared spectra of metal chelate compounds are markedly different from those of the pure ligands in the low frequency region. This is mainly due to the difference in vibrational coupling, which in turn is a result of differences in steric configuration and electronic structure.

In order to assign the low frequency bands of metal chelate compounds, it is essential to carry out normal coordinate analysis on the metal chelate ring, including the coordinate bonds. Such attempts have already been carried out on acetylacetonato,[1] oxalato,[2] and carbonato[3] complexes, and the results have proved to be highly important in estimating the strength of the metal-oxygen bonds[4] and in elucidating the electronic structure of the chelate ring.[5] It is, therefore, desirable to extend this work to metal chelate compounds containing other coordinate bonds.

Infrared studies on metal chelate compounds containing metal sulfur bonds are very few. Chatt et al.[6] have, however, reported the infrared spectra of *N*-alkyl, *N*, *N*-dialkyl dithiocarbamato, and xanthato complexes in the NaCl region, and we have carried out a normal coordinate analysis of dithiocarbamato complexes.[7] In view of the scarcity of work on metal chelate compounds containing metal-sulfur bonds, we decided to undertake a similar study on dithiooxalato complexes. Accordingly, we prepared the dithiooxalato complexes of four metals, and obtained their infrared spectra over the wide range of frequency between 4000 and 280 cm^{-1}. We also carried out a normal coordinate analysis of the platinum(II) dithiooxalato complex in order to estimate the force constants as well as to make complete theoretical band assignments.

Experimental

Preparation of Compounds.—Bis(dithiooxalato)-nickel(II), palladium, and platinum(II),[8] and tris-(dithiooxalato)-cobalt(III)[9] were prepared according to the methods described in the literature and were recrystallized several times from an aqueous solution.

Spectral Measurements.—Infrared spectra were obtained on a Perkin-Elmer Model 21 infrared spectrophotometer equipped with NaCl and CsBr optics. The KBr disk method was used for the spectra in the NaCl region, whereas the Nujol mull technique was employed for the spectra in the CsBr region. Frequency calibrations were made with polystyrene film (NaCl region), with 1,2,4-trichlorobenzene (CsBr region), and with water vapor (both regions).

Procedure and Calculations

Figure 1 shows the 1 : 1 (metal/ligand) model of the dithiooxalato complex used for normal

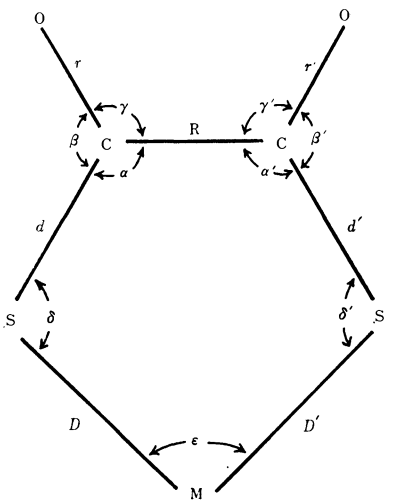


Fig. 1. Molecular model of the 1 : 1 Pt(II) dithiooxalato complex.

* This work was partly supported by the U. S. Army Research Office (Durham) and the National Institute of General Medical Sciences, Public Health Service. Presented at the International Symposium on Molecular Structure and Spectroscopy, Tokyo, Japan, September, 1962.

1) K. Nakamoto and A. E. Martell, *J. Chem. Phys.*, **32**, 588 (1960).
2) J. Fujita, A. E. Martell and K. Nakamoto, ibid., **36**, 324, 331 (1962).
3) J. Fujita, A. E. Martell and K. Nakamoto, ibid., **36**, 339 (1962).
4) K. Nakamoto, P. J. McCarthy, A. Ruby and A. E. Martell, *J. Am. Chem. Soc.*, **83**, 1066 (1961).
5) K. Nakamoto, P. J. McCarthy and A. E. Martell, ibid, **83**, 1066 (1961).
6) J. Chatt, L. A. Duncanson and L. M. Venanzi, *Suomen Kemi.*, **B29**, 75 (1956).
7) K. Nakamoto, J. Fujita, R. A. Condrate and Y. Morimoto, *J. Chem. Phys.*, **39**, 423 (1963).
8) C. S. Robinson and H. O. Jones, *J. Chem. Soc.*, **1912**, 62.
9) F. A. Dwyer and A. M. Sargeson, *J. Am. Chem. Soc.*, **81**, 2335 (1959).

TABLE I. SYMMETRY COORDINATES FOR IN-PLANE VIBRATIONS

A_1 species	$S_1=(1/\sqrt{2})(\Delta r+\Delta r')$	ν(C=O)
	$S_2=(1/\sqrt{2})(\Delta d+\Delta d')$	ν(C-S)
	$S_3=(1/\sqrt{2})(\Delta D+\Delta D')$	ν(M-S)
	$S_4=\Delta R$	ν(C-C)
	S_5*$=(1/\sqrt{2})(\Delta\beta-\Delta\gamma+\Delta\beta'-\Delta\gamma')$	δ(CO)
	$S_6=(1/\sqrt{20})(-\Delta\alpha-\Delta\alpha'-\Delta\delta-\Delta\delta'+4\Delta\varepsilon)$	ring def.
	$S_7=(1/2)(\Delta\alpha+\Delta\alpha'-\Delta\delta-\Delta\delta')$	ring def.
B_2 species	$S_8=(1/\sqrt{2})(\Delta r-\Delta r')$	ν(C=O)
	$S_9=(1/\sqrt{2})(\Delta d-\Delta d')$	ν(C-S)
	$S_{10}=(1/\sqrt{2})(\Delta D-\Delta D')$	ν(M-S)
	S_{11}*$=(1/\sqrt{2})(\Delta\beta-\Delta\gamma-\Delta\beta'+\Delta\gamma')$	δ(CO)
	$S_{12}=(1/2)(\Delta\alpha-\Delta\alpha'+\Delta\delta-\Delta\delta')$	ring def.
	$S_{13}=(1/2)(\Delta\alpha-\Delta\alpha'-\Delta\delta+\Delta\delta')$	ring def.

* Not normalized (see Ref. 1)
ν, stretching mode; δ, bending mode

TABLE II. FORCE CONSTANTS OF THE Pt(II) DITHIOOXALATO COMPLEX (10^5 dyn./cm.)

Stretching	Bending	Repulsive
K_1(C=O) =8.85	H_1(S-C-C) =0.30	F_1(C·····O) =0.30
K_2(C-S) =3.30	H_2(O-C-S) =0.40	F_2(O·····S) =0.40
K_3(Pt-S) =2.30	H_3(Q-C-C) =0.35	F_3(C·····S) =0.10
K_4(C-C) =2.60	H_4(Pt-S-C) =0.05	F_4(C·····Pt) =0.05
	H_5(S-Pt-S) =0.05	F_5(S·····S) =0.35

coordinate analysis. Since the symmetry of this model is C_{2v}, the fifteen normal vibrations are grouped into four species. The in-plane vibrations ($6A_1+5B_2$) can be separated from the out-of-plane vibrations ($2A_2+2B_1$) because they do not interact with each other. Thus, only the eleven in-plane vibrations are calculated in this paper. Most of the out-of-plane vibrations are expected to appear beyond our observable region, since the dithiooxalato complex consists of relatively heavy atoms. The symmetry coordinates used for the calculation are shown in Table I. The $\boldsymbol{G}$ and $\boldsymbol{F}$ matrices are similar to those previously reported for the oxalato complex.[2] In evaluating the $\boldsymbol{G}$ matrix elements of the platinum(II) complex, the following molecular parameters were used: $r=r'=1.28$ Å, $R=1.47$ Å, $d=d'=1.80'$ Å, $D=D'=2.32$ Å, $\alpha=\alpha'=\beta=\beta'=\gamma=\gamma'=120°$, $\delta=\delta'=105°$, and $\varepsilon=90°$. Both the A_1 and B_2 species involve one redundant condition which is a complicated function of the bond distances and angles. It is not necessary, however, to eliminate these redundancies from the calculation since they give "zero frequencies" in the final result. Thus, one seventh-order (A_1) and one sixth-order (B_2) secular equation of the form, $|\boldsymbol{GF}-E\lambda|=0$, were solved using an IBM 709 computer.

The Urey-Bradley force field[10] was used to express the potential energy. Except for those relating to the Pt-S bonds, force constants were transferred from molecules with similar structures[11] and were adjusted so as to obtain the best fit with the observed spectrum. Table II lists the best set of force constants thus obtained. Table III compares the observed frequencies with those calculated with this set of force constants. In order to make theoretical band assignments, the potential energy distribution[12] in each normal vibration was

TABLE III. COMPARISON OF CALCULATED AND OBSERVED FREQUENCIES FOR THE Pt(II) DITHIOOXALATO COMPLEX (cm^{-1})

		Obs.	Calcd.
A_1	λ_1	1594	1568
	λ_2	1083	1102
	λ_3	573	557
	λ_4	436 422	420
	λ_5	322	324
	λ_6	—	170
B_2	λ_7	1594	1629
	λ_8	939	960
	λ_9	515	533
	λ_{10}	398	380
	λ_{11}	322	322

10) T. Shimanouchi, *J. Chem. Phys.*, **17**, 245, 734, 848 (1949).
11) S. Mizushima and T. Shimanouchi, "Infrared Absorption and the Raman Effect," Kyoritsu, Tokyo (1959).
12) Y. Morino and K. Kuchitsu, *J. Chem. Phys.*, **20**, 1809 (1952).

TABLE IV. THE POTENTIAL ENERGY DISTRIBUTION IN EACH NORMAL VIBRATION

		Symmetry coordinate							Assignment
A_1		S_1	S_2	S_3	S_4	S_5	S_6	S_7	
	λ_1	**1.00**	0.02	0.00	0.10	0.01	0.00	0.02	ν(C=O)
	λ_2	0.07	**0.76**	0.00	**1.00**	0.45	0.00	0.04	ν(C-C)+ν(C-S)
	λ_3	0.10	**1.00**	0.25	0.16	0.16	0.06	0.06	ν(C-S)
	λ_4	0.01	0.13	**1.00**	0.26	0.06	0.03	0.11	ν(Pt-S)
	λ_5	0.00	0.00	0.17	0.20	**1.00**	0.00	0.12	δ(CO)
	λ_6	0.00	0.01	0.37	0.02	0.00	**1.00**	**1.00**	ring def.
B_2		S_8	S_9	S_{10}	S_{11}	S_{12}	S_{13}		
	λ_7	**1.00**	0.07	0.00	0.03	0.03	0.09		ν(C=O)
	λ_8	0.19	**0.94**	0.00	**1.00**	0.07	0.00		δ(CO)+ν(C-S)
	λ_9	0.18	0.25	**0.80**	**1.00**	0.06	**0.86**		δ(CO)+ring def.+ν(Pt-S)
	λ_{10}	0.08	**0.97**	0.02	0.41	0.03	**1.00**		ring def.+ν(C-S)
	λ_{11}	0.01	0.05	**1.00**	0.11	0.09	0.00		ν(Pt-S)

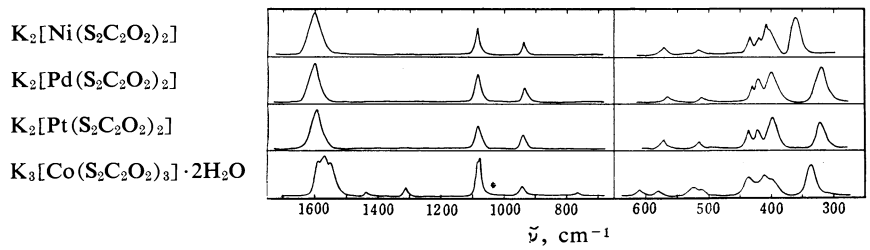


Fig. 2. Infrared spectra of dithiooxalato complexes of various metals.

calculated with respect to each symmetry coordinate. The results are shown in Table IV, along with numbers indicating the relative contribution from each symmetry coordinate.

Results and Discussion

Figure 2 shows the infrared spectra of 1 : 2 and 1 : 3 dithiooxalato complexes with various metals. It is noted immediately that the spectra of the various divalent metal complexes are very similar to one another. Thus, the band assignments obtained for the platinum(II) complex are in the main applicable to the other divalent metal complexes. Although the calculation was carried out using the 1 : 1 complex model, it has already been demonstrated that errors due to this approximation are fairly small.[2]

According to the results shown in Tables III and IV, the strong bands observed near 1600 cm^{-1} (λ_1, λ_7) are assigned to the C=O stretching modes. In the platinum(II) complex, this band appears at 1594 cm^{-1}, and the corresponding force constant is calculated to be 8.85×10^5 dyn./cm. In the $[Pt(ox)_2]^{2-}$ ion, however, the stretching bands due to the uncoordinated C=O bonds were observed at 1674 cm^{-1}, and the corresponding force constant was estimated to be 9.30×10^5 dyn./cm. This comparison seems to suggest that the C=O bonds in dithiooxalato complexes are weaker than those in oxalato complexes.

As is seen in Fig. 2, all the compounds exhibit two bands at about 1080 (λ_2) and 940 cm^{-1} (λ_8). Table IV indicates that the former is a coupled vibration between C–C and C–S stretching modes, whereas the latter is a coupled vibration between C–S stretching and CO bending modes. A similar pattern of vibrational coupling occurs in the oxalato complex,[2] where the bands near 1400 and 900 cm^{-1} are assigned to the coupled vibrations between C–C and C–O stretching, and between C–O stretching and CO bending modes, respectively.

The bands near 570 cm^{-1} (λ_3) are due to an almost pure C–S stretching mode, and the corresponding force constant is calculated to be 3.30×10^5 dyn./cm. This value is similar to that obtained for thiourea (3.20×10^5 dyn./cm.),[13] but it is larger than that of diethylthioether (2.50×10^5 dyn./cm.),[11] which has pure C–S single bonds. The strengthening of the C–S bonds can be accounted for if it is assumed that electron migration occcurs from C=O to C–S bonds in dithiooxalato complexes. It is also interesting to compare the C–S stretching bands in the dithiooxalato and dithiocarbamato platinum(II) complexes.[6] The C–S stretching

13) A. Yamaguchi, S. Mizushima, T. J. Lane, C. Curran and J. V. Quagliano, *J. Am. Chem. Soc.*, **80**, 527 (1958).

force constant of the former is larger than that of the latter (3.00×10^5 dyn./cm.), whereas the C–S stretching frequency of the former is lower than that of the latter (622 cm^{-1}). This result clearly demonstrates the structural dependence of the vibrational frequency.

According to the results shown in Table IV, the weak bands at ca. 515 cm^{-1} (λ_9) are due to a coupling mode between the CO bending, ring deformation and Pt–S stretching vibrations. The bands at 398 (λ_{10}) and 322 (λ_5) cm^{-1} are the ring deformation coupled with the C–S stretching mode and with the CO bending mode respectively.

The Pt–S stretching vibrations are assigned to the bands observed at 436 and 422 (λ_4) and 322 (λ_{11}) cm^{-1}. These frequencies are higher than those observed for the dithiocarbamato platinum(II) complex (375 and 288 cm^{-1}), mainly because the Pt–S stretching force constant of the dithiooxalato platinum(II) complex (2.30×10^5 dyn./cm.) is greater than that of the dithiocarbamato platinum(II) complex (2.10×10^5 dyn./cm.) This seems to suggest that the Pt–S bond of the dithiooxalato complex is slightly stronger than that of the dithiocarbamato complex. These values for the Pt–S stretching force constant would be reduced slightly if the calculation were made on the actual 1 : 2 model instead of the present 1 : 1 approximate model. In the case of the oxalato platinum(II) complex, however, the Pt–O stretching force constant obtained from the 1 : 2 model was only about 6% smaller than that calculated on the 1 : 1 approximate model.[2]

It has been recognized that such sulfur-containing ligands as thioethers and thiols form strong coordinate bonds with platinum(II).[14] The Pt–S bonds may be strengthened in the dithiocarbamato and dithiooxalato complexes, since they presumably involve pertial $d\pi$-$p\pi$ or $d\pi$-$d\pi$ bonding. Therefore, the relatively large Pt–S force constants obtained here are not surprising. This is also in good accord with the chemical observation that the $[Pt\cdot(C_2O_2S_2)_2]^{2-}$ ion is formed immediately after a solution of $K_2(C_2O_2S_2)$ is added to that of $K_2[PtCl_4]$ (The Pt–Cl stretching force constant is estimated to be 1.50×10^5 dyn./cm.[15])

Figure 2 indicates that, except for the lowest frequency band (λ_{11}), the spectra of the dithiooxalato complexes are little sensitive to the nature of the metal. This result is rather unusual, since all the metal chelate compounds studied so far exhibit several metal-sensitive bands in the low-frequency region. The origin of this anomaly can only be understood through normal coordinate analyses of individual complexes; this remains a problem to be solved in the future.

Summary

The infrared spectra of dithiooxalato complexes of platinum(II), palladium(II), nickel(II) and cobalt(III) have been obtained in the range between 4000 and 280 cm^{-1}. A normal coordinate analysis has been carried out for the 1 : 1 (metal/ligand) model of the dithiooxalato platinum(II) complex. The results indicate that the Pt–S stretching bands are at ca. 430 and 320 cm^{-1} and that the corresponding force constant is 2.30×10^5 dyn./cm.

Department of Chemistry
Osaka University
Nakanoshima Osaka (J. F.)

Department of Chemistry
Illinois Institute of Technology
Technology Center
Chicago, U.S.A. (K. N.)

14) For example, see "The Chemistry of the Coordination Compounds," Ed. by J. C. Bailar, Jr., Reinhold, New York (1956), p. 49.

15) J. Hiraishi, I. Nakagawa and T. Shimanouchi, the 16th Annual Meeting of the Chemical Society of Japan, Tokyo, 1963.

Photolyses of Isobornyl and Bornyl Nitrites

By Masao NAKAZAKI and Koichiro NAEMURA

(Received November 18, 1963)

Barton et al.[1] scrutinized the photolysis of alkyl nitrite[2] and demonstrated its usefulness to synthetic organic chemistry, especially in introducing functional groups into an otherwise inert, angular methyl group of steroids by means of a dramatic three-step synthesis of aldosterone acetate from corticosterone acetate.[1a]

They also pointed out that the NO group migrates to the methyl group located at the 1, 3-diaxial position. An inspection of the molecular model of isobornyl nitrite (Ia)[3] reveals that one of the gem-methyl groups and the NO group are in a quasi 1, 3-diaxial relation, fulfiling the conformational requirement of this photochemical migration; therefore, the photochemical product of Ia can be expected to be *cis*-π-oxoisoborneol oxime (IIa). In contrast to the readily-available trans-π-substituted camphor derivatives,[4] *cis*-isoketopinic acid (IIIa) and *cis*-π-hydroxycamphor (IIIb) are the only known examples of cis-π-substituted camphor derivatives. Since we have been interested in the studies of the reactivity of *cis*-π-oxocamphor (IIIc), we hoped that this expected photochemical synthesis would turn out to be the most convenient process to IIIc, as well as a general synthetic route to a cis-π-substituted camphor series of compounds which has been obtained through multistep routes.[4]

When a solution of isobornyl nitrite (Ia) in benzene was irradiated with an ultraviolet lamp for 1 hr., needles (m. p. 214~215°C, $[\alpha]_D$ −71.1° (in ethanol) were obtained. Although this compound's molecular formula was $C_{10}H_{17}O_2N$, isomeric with the starting material, and although its color reaction with ferric chloride was purple, indicating the oxime structure IIa, it soon became evident that this compound has no oxime group. The heating of the compound with acetic anhydride and sodium acetate gave only the monoacetate (m.p. 80~82°C), instead of the expected nitrile. Barton et al. observed the photochemical cleavage of the 5-membered D ring of the nitrite of a 17-ol steroid[1d] (e. g. 5α-androstane-3α, 17β-diol 3α-acetate 17β-nitrite), affording a 6-membered hydroxamic acid derivative. We suspected that the photolysis of Ia did not follow the expected schema (Fig. 1) and that the strained 5-membered ring of Ia was cleaved to the hydroxamic acid derivative, VIIIa. This was confirmed by the reduction of VIIIa with zinc powder in acetic acid to give the lactam IXa (m. p. 156~160°C, $[\alpha]_D$ −51.3° (in ethanol)), which was further converted into the imine IXb with lithium aluminum hydride. Although two alternative direction of the photochemical cleavage reaction seem possible, the one between the carbon atom carrying the nitrite group and the neighboring methylene is inconceivable by analogy with the results established by Barton et al, (*vide supra*) on the nitrite of a 17-ol steroid. This is further supported by the fact that the lactam IXa and the imine IXb were found to be not identical with α-camphidone[5] and camphidine[5] respectively. The oily reaction product freed from the hydroxamic acid VIIIa was chromatographed on an alumina column to give isoborneol (IVb) and an oil which distilled to yield a yellow liquid (b. p. 65~70°C/4 mmHg), the infrared spectrum and NMR spectrum of which showed the presence of an aldehyde group. Although the aldehyde could be converted to α-campholenic acid amide (XIIb) (m. p. 127~128°C) via α-campholenic acid (XIIa) and although its 2, 4-dinitrophenylhydrazone and semicarbazone melted rather sharply (124~126°C and 142~143°C respectively), its vapor phase chromatogram exhibited two peaks with almost equal intensities, indicating that the aldehyde is unhomogeneous. The infrared spectrum of this mixture had

1) a) D. H. R. Barton, J. M. Beaton, L. E. Geller and M. M. Pechet, *J. Am. Chem. Soc.*, **82**, 2640 (1960); **83**, 4076 (1961); b) D. H. R. Barton and J. M. Beaton, ibid., **82**, 2641 (1960); **83**, 4083 (1961); c) A. L. Nussbaum, F. E. Carlon, E. P. Oliveto, E. Townley, P. Kabasakalian and D. H. R. Barton, ibid., **82**, 2973 (1960); d) C. H. Robinson, O. Gnoj, A. Mitchell, R. Wayne, E. Townley, P. Kabasakalian, E. P. Oliveto and D. H. R. Barton, ibid., **82**, 17771 (1961); e) D. H. R. Barton and J. M. Beaton, ibid., **83**, 750 (1961); **84**, 199 (1962); f) D. H. R. Barton, R. P. Budhiraja and J. F. McGhie, *Proc. Chem. Soc.*, **1963**, 170.

2) For a relevant review, see L. Nussbaum and C. H. Robinson, *Tetrahedron*, **17**, 35 (1962).

3) For the absolute configuration of isoborneol, see A. J. Birch, *Ann. Reports*, **47**, 191 (1950).

4) E. J. Corey, M. Ohno, S. W. Chow and R. A. Scherer, *J. Am. Chem. Soc.*, **81**, 6305 (1962).

5) J. Tafel and K. Eckstein, *Ber.*, **34**, 3274 (1901).

6) R. E. Partch, *J. Org. Chem.*, **28**, 276 (1963).

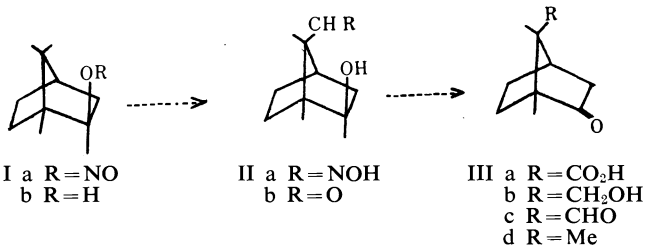


Fig. 1

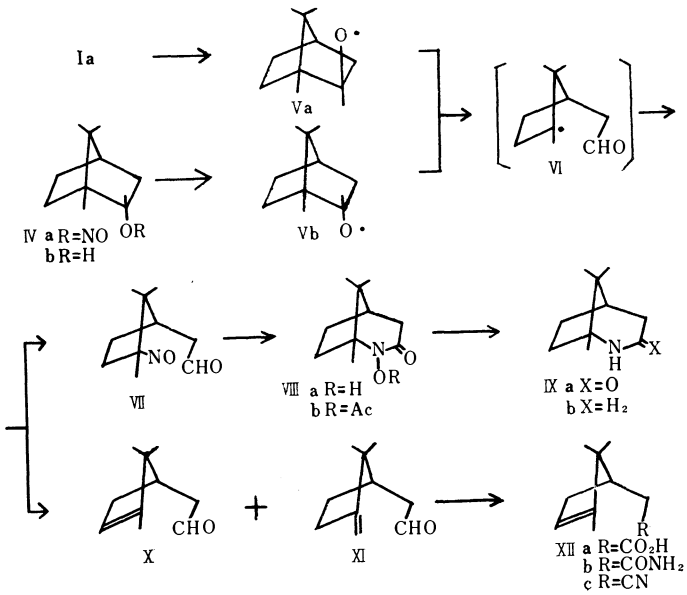


Fig. 2

TABLE I.[6] PHOTOLYSIS OF ISOBORNYL NITRITE

	5.46 mmol./100 cc. benzene			5.46 mmol./14 cc. benzene		
	Retention time min.	Yield mmol.	Molar ratio	Retention time min.	Yield mmol.	Molar ratio
VIIIa	—	1.45	2.63	—	0.16	0.22
X	54.8	0.59	1.07	54.8	0.74	1.09
XI	59.8	0.55	1	59.6	0.68	1
IIIa	—	0.00	0.00	62.6	0.07	0.11
Ib	73.8	0.21	0.38	74.6	1.33	1.95

TABLE II.[6] PHOTOLYSIS OF BORNYL NITRITE

	5.46 mmol./100 cc. benzene			5.46 mmol./14 cc. benzene		
	Retention time min.	Yield mmol.	Molar ratio	Retention time min.	Yield mmol.	Molar ratio
VIIIa	—	1.36	2.40	—	0.12	0.19
X	54.6	0.63	1.10	54.5	0.77	1.19
XI	59.5	0.57	1	59.4	0.65	1
IIId	—	0.00	0.00	62.2	0.05	0.07
IVb	79.6	0.31	0.54	82.2	1.13	1.74

peaks at 880 and 800 cm^{-1}, suggesting the presence of $>C=CH_2$ and $-CH=C<$; this was further supported by the NMR spectrum (4.80 and 5.24 τ*). These results imply that the aldehyde fraction consists of α-campholenic aldehyde (X) and iso-α-campholenic aldehyde (XI); the latter was first detected in the reaction mixture of the lead tetraacetate oxidation of isoborneol (Ib),[6] not in the photolysis of camphor (see the Experimental section). The relative molar amounts of these products together with their retention times in the vapor phase chromatograph, are summarized in Table I.[7] It is noteworthy that, in the photolysis of isobornyl nitrite (Ia) at a much higher concentration, camphor (IIId) was detected in the reaction mixture, which also contained the unsaturated aldehydes X and XI, isoborneol (Ib) and the hydroxamic acid VIIIa; however, the ratio of VIIIa to Ib, in this case, was found to be just the reverse of that observed in the low concentration experiment. The photolyses of bornyl nitrite (IVa) at low and high concentrations were carried out to give analogous results (Table II)[7] in spite of the different stereochemistry of the starting materials.

These facts suggested that these photolyses would be nonstereospecific, and that an intermediate such as VI might be common in both cases. The disproportionation of the intermediate radicals Va and Vb would be enhanced at a higher concentration, thus accounting for the relatively high yields of borneol, isoborneol and camphor in the photolyses performed in higher concentrations, but it does not seem possible to advance, without further study, a plausible mechanism to explain the rather interesting predominant formation of the hydroxamic acid (VIIIa) in the low concentration experiments.

Since Professor Barton[8] has announced that Dr. Kabasakalian of his laboratory has carried out extensive studies of the photolyses of aliphatic nitrites, including bornyl and isobornyl nitrite, we will refrain from further investigation of this problem.

Experimental*

Isobornyl Nitrite (Ia).—Into a chilled solution of 63.0 g. of isoborneol (Ib) (m. p. 211~213°C, $[\alpha]_D^{22}$ −23.5° (*c* 0.845 in ethanol)) in 450 cc. of pyridine, 38.0 g. of nitrosyl chloride[9] gas was passed in a period of 3 hr. After being stirred for 1.5 hr. at room temperature, the reaction mixture was poured into ice water and extracted with ether. The extract was washed with 2% hydrochloric acid and dried over anhydrous sodium sulfate. Removal of the solvent yielded an oil which distilled to afford 66.2 g. of yellow liquid (89% yield) (b. p. 175~176°C/9 mmHg). An infrared spectrum exhibited peaks at 1645 and 1605 cm^{-1} (-NO).

The Photolysis of Isobornyl Nitrite (Ia). — A solution of 6.0 g. of Ia in 600 cc. of benzene was cooled with running water and irradiated with a Toshiba SHL-100UV mercury lamp for 1 hr. in an atmosphere of nitrogen. The crystals which precipitated were collected and recrystallized from benzene-petroleum ether to afford 1.6 g. of the hydroxamic acid VIIIa (m. p. 214~215°C, $[\alpha]_D^{22}$ −71.1° (*c* 0.562 in ethanol)), which gave a red color with a ferric chloride solution. Infrared spectrum in Nujol mull: peaks at 3100, 1640, 1400, 1370 cm^{-1}.

Found: C, 65.70; H, 9.27; N, 7.32. Calcd. for $C_{10}H_{17}O_2N$: C, 65.54; H, 9.35; N, 7.64%.

The reaction mixture freed from the hydroxamic acid VIIIa was concentrated and chromatographed through a column of alumina to give isoborneol (Ib) (m. p. 209~210°C), identified by an infrared spectrum. The second fraction of the chromatographic separation was distilled to afford a liquid (b. p. 65~70°C/4 mmHg); an infrared spectrum in Nujol mull showed peaks at 2740, 1725, 1655, 880 and 800 cm^{-1}, and a NMR spectrum exhibited peaks at 0.26, 4.80, 5.24, 7.62 and 8.40 τ which correspond to $\underline{CHO}$, $>C=\underline{CH}-$, $>C=\underline{CH_2}$, $\underline{CH_2}CHO$, and $-HC=CH\cdot\underline{CH_3}$ respectively.

The 2, 4-dinitrophenylhydrazone was recrystallized from ethanol; m. p. 124~126°C.

Found: C, 57.91; H, 6.11; N, 16.63. Calcd. for $C_{16}H_{20}O_4N_4$: C, 57.82; H, 6.07; N, 16.86%.

The semicarbazone was recrystallized from ethanol; m. p. 142~143°C (lit.[6,10] m. p. 141~142.5°C).

Found: C, 63.12; H, 9.15; H, 20.08. Calcd. for $C_{11}H_{19}ON_3$: C, 63.07; H, 9.00; N, 19.86%.

The quantitative analyses of these products, except that of the hydroxamic acid VIIIa, were performed by means of vapor phase chromatography; they are summarized in Table I.

The Acetate VIIIb of the Hydroxamic Acid VIIIa.—A mixture of 0.5 g. of the hydroxamic acid VIIIa, 27.5 cc. of acetic anhydride and 5.5 cc. of pyridine was heated at 90~100°C for 1/2 hr. After the mixture had been concentrated at reduced pressure, the residue was recrystallized from petroleum ether to yield 0.55 g. of the acetate VIIIb.

Found: C, 64.27; H, 8.42; N, 6.51. Calcd. for $C_{12}H_{19}O_3N$: C, 63.97; H, 8.50; N, 6.22%.

The Lactam IXa.—A mixture of 0.95 g. of the hydroxamic acid VIIIa, 8.0 g. of zinc powder and 60 cc. of acetic acid was refluxed for 6 hr. After

* NMR spectra were measured at 60 Mc. in carbon tetrachloride, using tetramethylsilane as an internal reference.

7) Use was made a 5 m. column of 30% dioctyl phthalate on Cellite 545 (80~100 mesh) at 150°C, and a helium flow rate 80 cc./min. on Yanagimoto Gas Chromatograph GCG-3D type.

8) D. H. R. Barton, "On Some New Photochemical Reactions," in H. Ohtsuka, editor, "Collection of Lectures Commemorating the Inauguration of the New Shionogi Research Laboratory Building," 1963, p. 275.

* The analyses were performed in the Microanalytical Laboratory of the Institute of Polytechnics, Osaka City University.

9) J. R. Morton and H. W. Wilcok, "Inorganic Syntheses," Vol. 4, 48 (1953).

10) R. Srinivasan, *J. Am. Chem. Soc.*, **81**, 2604 (1959).

being freed from the excess zinc powder, the solution was concentrated at reduced pressure. The residue was made basic with aqueous sodium hydroxide and extracted with ether. After being washed with water and dried over anhydrous sodium sulfate, the solution was concentrated to give needles which were recrystallized from petroleum ether to afford 0.50 g. of needles (m. p. 156~160°C, $[\alpha]_D^{22}$ −51.2° (*c* 0.516 in ethanol)).

Found: C, 72.01; H, 10.39; N, 8.07. Calcd. for $C_{10}H_{17}ON$: C, 71.81; H, 10.25; N, 8.38%.

The Imine IXb.—To a stirred mixture of 0.4 g. of lithium aluminum hydride and 50 cc. of dioxane, a solution of 0.30 g. of the lactam IXa in 70 cc. of dioxane was added in a period of 15 min. The mixture was refluxed for 28 hr. and decomposed with water. After the alumina deposited had been filtered, the filtrate was concentrated and made basic with aqueous ammonia. The aqueous mixture was extracted with ether, and removal of the solvent left a residue which resisted crystallization. This was then converted directly into the picrate, yellow needles (decomp. p. 250°C).

Found: C, 49.84; H, 5.78; N, 14.73. Calcd. for $C_{16}H_{22}O_7N_4$: C, 50.26; H, 5.80; N, 14.65%.

α-Campholenic Acid Amide (XIIb).—The aldehyde fraction (1.0 g.) obtained from the photolysis of isobornyl nitrite (Ia) was added to a solution of 2.4 g. of silver nitrate in 10 cc. of water. To the stirred mixture, 1.2 g. of sodium hydroxide were added, and the stirring was continued for 30 min. After being freed from the deposit, the mixture was washed with ether. The aqueous solution was made acidic with hydrochloric acid and extracted with ether. After washing with water, the solvent was removed, yielding 0.75 g. of a viscous liquid; 0.3 g. of this was converted into the acid chloride with thionyl chloride (1.5 cc.). The acide chloride was added to concentrated aqueous ammonia, and the acid amide XIIb deposited was recrystallized from aqueous ethanol (m. p. 127~128°C (lit.[11] 130.5°C)), which was identified as α-campholenic acid amide by comparing it with an authentic specimen prepared from α-campholenic nitrile[11] (XIIc) by alkaline hydrolysis.

Found: C, 71.65; H, 10.28; N, 8.35. Calcd. for $C_{10}H_{17}ON$: C, 71.81; H, 10.25; N, 8.38%

Bornyl Nitrite (IVa).—A chilled solution of 22.3 g. of borneol (IVb) in 200 cc. of pyridine was saturated with nitrosyl chloride gas, and the solution was allowed to stand at room temperature for 30 min. After the usual work up (*vide supra*), 17.9 g. of yellow liquid (b. p. 72~74°C/6 mmHg) was obtained.

The Photolysis of Camphor (IIId).—A solution of 2.0 g. of camphor (IIId) in 200 cc. of benzene was irradiated as was isobornyl nitrite for 1 hr. The product was analyzed by vapor phase chromatography,[7] which indicated the presence of 0.31 g. of α-campholenic aldehyde (X) and 1.26 g. of camphor, but no trace of iso-α-campholenic aldehyde (XI).

Department of Chemistry
Faculty of Engineering Science
Osaka University
Shibahara, Toyonaka

11) F. W. Tiemann, *Ber.*, **28**, 2168 (1895).

*The Isotopic Hydrogen Exchange between Propene and Deuterium Oxide Catalyzed by Nickel Powder**

By Kozo HIROTA and Yoshie HIRONAKA

(Received November 19, 1963)

The catalyzed, isotopic hydrogen exchange of olefins and related compounds with hydrogen gas has been investigated by many workers for thirty years[1] in connection with the mechanism for the catalytic hydrogenation of double bonds.[2] Similar exchange reactions with water have not been reported so much, though it is simpler to clarify their mechanisms because of the lack of simultaneous hydrogenation. One of us (K. H.) studied the exchange reaction of paraxylene with deuterium oxide and found that only the exchange of methyl hydrogen could be recognized at 100°C in the presence of nickel powder.[3] Similar characteristic catalytic activity was recently reported by Crawford and Kemball[4] on nickel films in the exchange of alkylbenzenes; however, they used deuterium gas instead of deuterium oxide.

On the other hand, rhodium, palladium and

* Preliminary reports: "Shokubai" (Tokyo), **4**, 41, 371 (1962).

1) A. Farkas and L. Farkas, *Nature*, **132**, 894 (1933); J. Horiuti and M. Polanyi, *Trans. Faraday Soc.*, **30**, 1164 (1934).

2) Cf. D. D. Eley, "Catalysis" (Ed. by P. H. Emmett), **3**, 49 (1955); T. I. Taylor, ibid., **5**, 257 (1957).

3) K. Hirota, T. Ueda, et al., a) *J. Chem. Soc. Japan, Pure Chem. Sec. (Nippon Kagaku Zasshi)*, **81**, 362 (1960); b) This Bulletin, **33**, 423 (1960); c) **35**, 228 (1962).

4) E. Crawford and C. Kemball, *Trans. Faraday Soc.*, **58**, 2452 (1962).

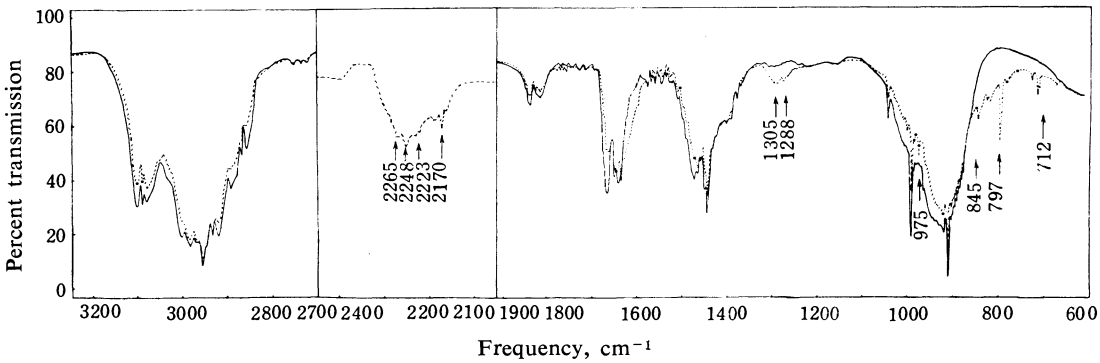


Fig. 1a. IR spectra of propene and the product of deuterium exchange (No. A-4).
—— Propene ---- Reaction product on Ni

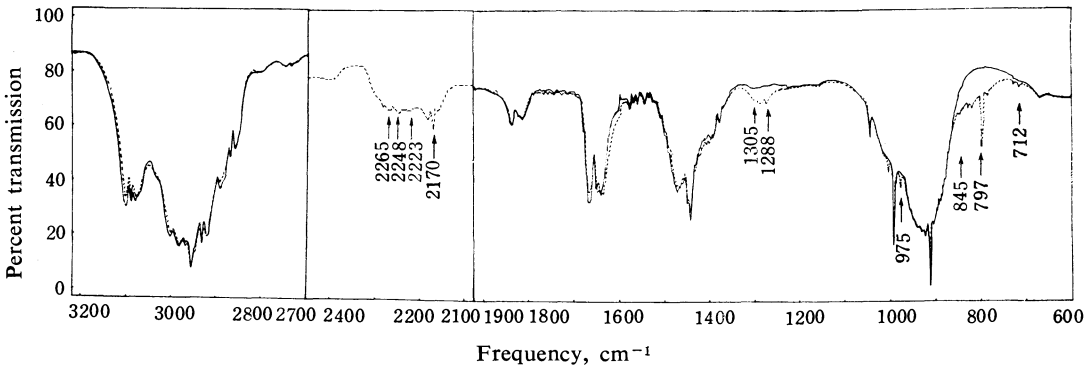


Fig. 1b. IR spectra of propene and the product of the deuterium exchange (No A-9).
—— Propene ---- Reaction product on $Ni\text{-}Al_2O_3$

platinum—the metals also with a face-centered cubic lattice—were found to exchange ring hydrogen to the same order of magnitude under the same experimental conditions.[3c]

Such difference in reaction would seem of interest in order to understand the nature of selectivity on catalytic hydrogenation, so the study has been extended to other olefinic compounds with methyl groups. The exchange reaction of propene with deuterium oxide by the use of nickel catalysts, supported and unsupported, will be described in the present report.

Experimental

Materials. — Commercial pure isopropanol was dehydrated with activated alumina. The propene thus obtained was purified by distillation in vacuo. The deuterium oxide (99.7%) obtained from Showa Denko K. K. was used without any further purification. The other materials were commercial grade pure reagents.

The nickel catalyst was prepared by decomposing commercial nickel formate (Mitsuwa Yakuhin Kogyo K. K.) at 270°C and then degassing it at the same temperature for about 20 hr. A nickel catalyst supported on alumina in the ratio 1 : 1 was prepared by the thermal decomposition of nickel formate supported on activated gamma-alumina (Wako Junyaku K. K.). The nickel formate was prepared as follows:—Nickel carbonate was obtained by the addition of ammonium carbonate into a nickel nitrate solution; the precipitate was washed until the filtrate did not show any alkaline reaction. The dried nickel carbonate and activated alumina (Al_2O_3: Ni=1 : 1 in weight) were mixed well, and then water was added to the mixture until it became a a jelly substance. This jellified mixture was turned into nickel formate by treating it with formic acid. In order to precipitate the formate on alumina completely, acetone was added finally; then the precipitate was dried for 24 hr. at 80°C.

Procedure.—The reaction was always carried out in a glass ampoule into which propene and deuterium oxide had been charged in vacuo. The detailed procedure was nearly the same as that already reported by one of the present authors.[3]

For the quantitative analysis of the deuterated products, both mass-spectrometry (Hitachi RMU-5 installed at the Osaka Laboratory, Japanese Association for Radiation Research on Polymers) and NMR spectrometry (Varian A-60) were adopted.

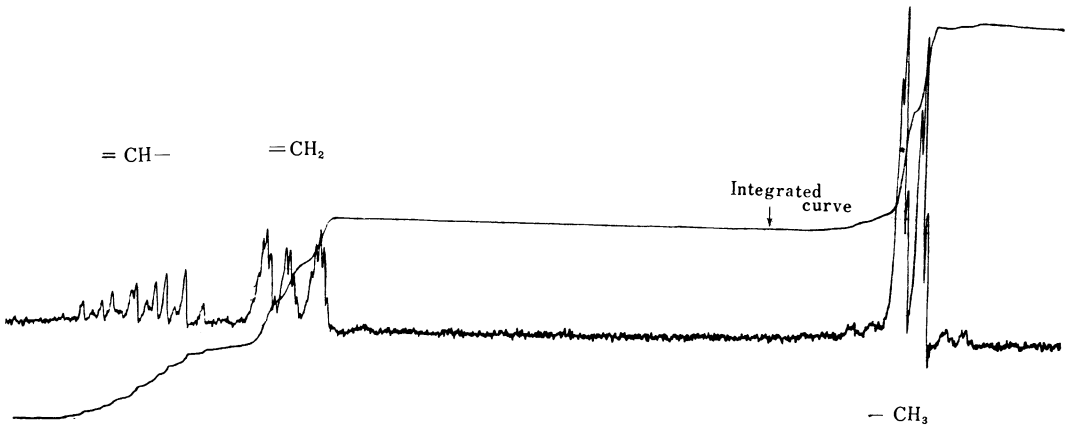


Fig. 2a. NMR spectrum of propene.

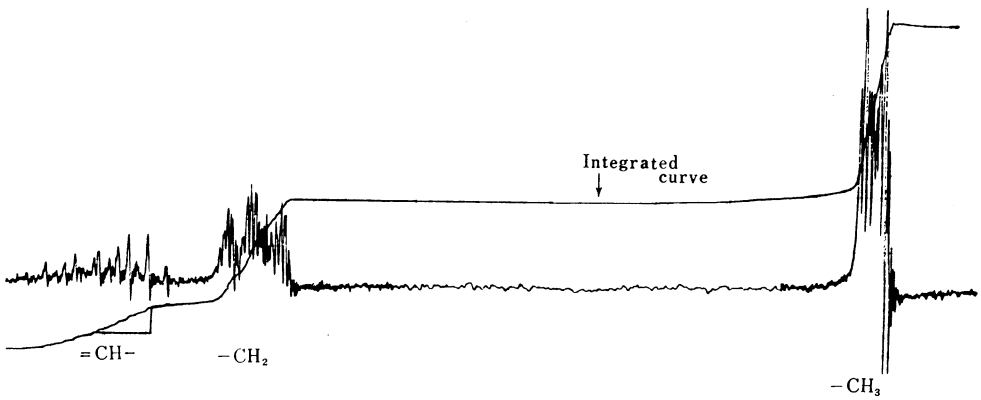


Fig. 2b. NMR spectrum of No. A-4.

For the qualitative analysis, however, infrared-spectrometry (Hitachi EPI-2 and DS 402G of Japan Spectroscopy Co.) was adopted.

Results

Deuterium Distribution.—Table I shows the deuterium distribution in the products which were produced under the experimental conditions described, with $C_3H_{6-i}D_i$ denoted by d_i. Generally speaking, propene exchanged more easily than *p*-xylene with D_2O, because the reaction is measurable even at room temperature.* Secondly, the data on nickel seem to show that the exchange proceeded as a successive reaction, judging from the deuterium distribution in the products. The Datum of No. K1-*i* is a part of those of No. K1 shown in Table II, which gives another indication of the successive production of d_2 via d_1, because the d_1% vs. time curve reaches a maximum value at 5 hr.

* However, so far as the exchange of methyl hydrogen is concerned, the rates may not be so different, as will be found.

The Identification of the Deuterated Groups.—Before entering into a detailed discussion, let us investigate the deuterated groups in the products on No. A4, which was obtained without any carrier, by comparing the infrared spectra (dotted line in Fig. 1a) with that of propene (solid line in Fig. 1a). The infrared data of deuteropropenes obtained by various researchers[5-8] seem to show that the deuterium exchange occurs more easily at the vinyl group rather than at the methyl group in the 2100~2300 cm^{-1} region; because the C–D stretching bands of the vinyl group appearing at 2248 and 2265 cm^{-1} in Fig. 1a show stronger intensities than the bands of $-CH_2D$. appearing at 2161, 2170 and 2183 cm^{-1} [8]

5) B. S. Rabinovitch and F. S. Looney, *J. Am. Chem. Soc.*, **75**, 2652 (1953) and a private communication.
6) a) R. C. Lord and P. Venkateswarlu, *J. Opt. Soc. Am.*, **43**, 1079 (1953); b) M. Farina and M. Peraldo, *Gazz. Chim. Ital.*, **90**, 973 (1960).
7) G. Zerbi, M. Peraldo and E. Mantica, Symposium of Molecular Structure and Spectroscopy, Tokyo, C 213 (1962).
8) Private Communication from Murahashi Lab. of Osaka University.

TABLE I. DEUTERIUM DISTRIBUTION IN THE PRODUCTS

No.	Catalyst, g.		Sample, mol.×10³ C_3H_6	Sample, mol.×10³ D_2O	Reaction temp., °C	Time hr.	Products, % d_0	d_1	d_2	d_3	d_4	d_5
A4	Ni	5	6.96	21.7	11.5	ca. 240	42.5	40.6	13.3	2.1	—	—
A5	Ni	5	7.58	21.5	38.1	17	57.8	32.4	6.9	2.9	—	—
K1-i*	Ni	5	4.14	15.8	38.1	44.0	6.5	19.1	29.4	27.0	14.6	3.4
A6	Ni-Al_2O_3	3.7	7.32	23.6	38.1	44	72.2	23.9	4.9	—	—	—
A7	Ni-Kieselguhr	10	5.95	51.5	38.1	107	23.8	38.1	28.6	9.5	—	—
A8	Ni-Kieselguhr	10	5.95	16.3	38.1	48	47.6	35.2	17.6	—	—	—
A9	Ni-Al_2O_3	5	6.00	18.1	18.6	354	63.6	29.8	5.9	—	—	—
B19-a	Ni	1.65	2.18	10.7	25.0	25	51.6	36.8	10.1	1.5	—	—
B19-b	Ni	1.65	2.18	11.0	25.0	50	39.7	40.5	15.5	3.6	0.7	—
B19-c	Ni	1.65	2.18	10.7	25.0	100	26.8	40.1	23.8	7.8	1.5	—

* The progress of the change of deuterium distributions in K1 is shown in Table II.

TABLE II. KINETICS OF ISOTOPIC HYDROGEN EXCHANGE BETWEEN D_2O AND C_3H_6 ON Ni CATALYST (No. K-1)

	Reaction time min.	Percent distribution of deuterated propenes d_0	d_1	d_2	d_3	d_4	d_5	$\phi = \sum i d_i$	k_ϕ min^{-1}	k_0 min^{-1}
a	0	97.0	3.0	—	—	—	—	3.0		
b	34	90.1	8.8	1.1	—	—	—	11.0	0.32_9	0.21_0
c	72	84.1	13.8	2.1	—	—	—	18.0	0.25_7	0.19_2
d	126	75.1	22.8	2.1	—	—	—	27.0	0.22_3	0.19_6
e	180	65.5	28.6	4.7	1.2	—	—	41.6	0.24_6	0.21_1
f	240	60.6	31.2	6.6	1.6	—	—	49.2	0.22_1	0.19_0
g	300	50.5	37.4	10.3	1.8	—	—	63.4	0.23_4	0.21_0
h	1076	13.9	28.7	30.3	18.9	6.6	1.6	180.4	0.24_1	0.17_6
i	2624	6.5	19.1	29.4	27.0	14.6	3.4	234.3	0.15_3	0.09_8

TABLE III. ASSIGNMENT OF THE IR BANDS OF THE PRODUCTS

Normal propene				No. 4A			
Frequency cm^{-1}	Intensity		Assignment	Frequency cm^{-1}	Intensity		Assignment
3100	s	R	CH_2 stretching	3100	*		
3090	s	Q		3090	*		
3080	s	P		3080	*		
3000	s	R	CH_2 stretching (sym.)	3000	*		
2990	s	Q		2990	*		
2984	vs	P		2984	*		
2967	s	R	CH_3 stretching (anti.)	2967	*		
2955	s	Q		2955	*		
2948	s	R	CH_3 stretching (anti.)	2948	*		
2933	s	Q		2933	*		
2920	s	P		2920	*		
2890	m	R	CH_3 stretching (anti.)	2890	*		
2870	m	Q		2870	*		
2858	w	P		2858	*		
				2294	w		
				2281	w		
				2265	w		*t*-1-d_1
				2248	w		*c*-1-d_1, 2-d_1
				2223	w		1,1-d_2(3-d_2)
				2183	w	(R)	3-d_1
				2170	w	(Q)	
				2161	w	(P)	
1838	w	R	CH_2 bending ($2\times\nu_{912}$)	1838	*		
1824	w	Q		1824	*		
1815	w	P		1815	*		
1665	s	R	C=C stretching	1665	*		
1650	m	Q		1645	m		*t*-1-d_1, 2-d_1
1640	s	P		1634	m		*t*-1-d_1
				1628	m		*c*-1-d_1, 1,1-d_2
				1613	m		1,1-d_2, 2-d_1
1472	m		CH_3 bending (anti.)	1472	**		
1465	m			1465	**		
1460	s			1460	**		
1448	m	R	CH_3 bending (anti.)	1448	**		
1443	s	Q		1443	*		
1400	m	R	CH_3 bending (sym.)	1400	*		
1375		Q		1375	*		
				1305	vw		3-d_x
				1288	vw		3-d_x
1043	w	Q	CH_3 bending	1043	*vw		
				1000	vw		
990	s	Q	CH bending	990	*		
985	vw	Q	CH bending	985	*		
				975	vw		*t*-1-d_1
963	vw		?	963	*		
918	w	Q	C-C stretching	918	*		
912	vs	Q	CH_2 bending	912	*		
				845	w		2-d_1
				830	w		3-d_1
				823	w		*t*-1-d_1
				815	w		
				797	m		c-1-d_1
				782	w		
				728	vw		1,1-d_2
				712	w		1,1-d_2

* The intensity decreased.
** Shapes of the bands changed and their intensities decreased.

in the products. This finding is interesting if compared with the fact that the exchange occurred overwhelmingly at the methyl hydrogen in the case of *p*-xylene.*

* The exchange degree at the ring hydrogen was estimated to be less than 5%, if it occurred at all.[3a]

In order to confirm such an unexpected result, the NMR spectrum of the products of No. A4 was measured in the liquid state. As Fig. 2 shows, the above tendency was also observed. The signal of the methyl protons was complicated by the pertial deuteration of both

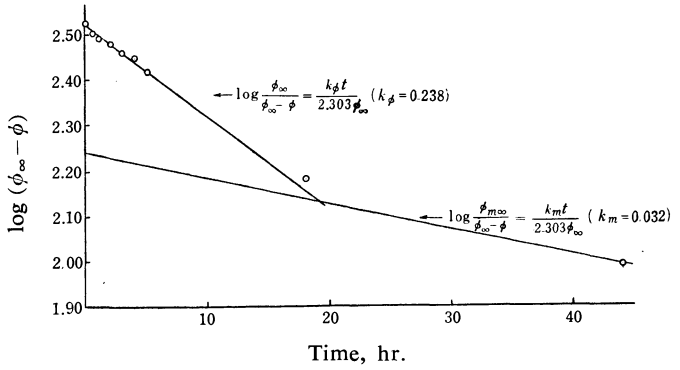
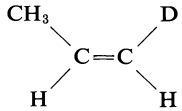


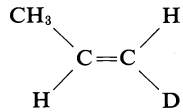
Fig. 3. Plots of log $(\phi_\infty - \phi)$ vs. time.

hydrogens of the methin and methen groups.

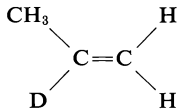
To summarize the above conclusion, all the bands of No. A4 can be assigned as shown in Table III, where the nomenclature used for deutero-propenes deuterated at the vinyl groups is as follows:



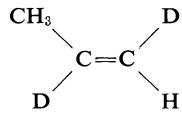
cis-propene-1-d_1 (*c*-1-d_1)



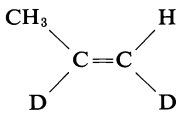
trans-propene-1-d_1 (*t*-1-d_1)



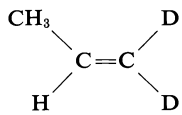
propene-2-d_1 (2-d_1)



trans-propene-1,2-d_2 (*t*-1,2-d_2)



cis-propene-1,2-d_2 (*c*-1,2-d_2)



propene-1,1-d_2 (1,1-d_2)

Table III shows further that the bands of medium intensity at 1613, 1628, 1643 and 1645 cm^{-1}, as well as other bands at shorter wavelengths, support the above conclusion. However, even if the exchange at both hydrogens of the methin and methen groups is found, the exchange degree is hard to determine quantitatively on the basis of the infrared data alone. According to the NMR measurement which is now in progress, the exchange at the methin hydrogen appears to be easier.

Kinetics of the Reactions. — In order to investigate the progress of the exchange reaction, the kinetic data of No. K1 (Table II) were analyzed by plotting log $(\phi_\infty - \phi)$ against t. As curve a in Fig. 3 indicates, a straight line was obtained at the initial stage, suggesting that the reaction is of the first order, when only d_1, d_2 and d_3 were the products. This result is concordant with the fact that the exchange proceeds mostly at the hydrogen atoms of the reactive vinyl hydrogen. The failure of linearity at the later stage, when propene-d_4 was produced, may, however, be ascribed to the fact that the less reactive methyl hydrogen began to play the main role in the exchange as the exchange equilibrium of the vinyl hydrogen was gradually attained. Therefore, by the method given by Kemball and Crawford,[4] the ratio of the rate constant of methyl hydrogen, k_m, to that of vinyl hydrogen, k_v, was calculated, assuming the initial rate constant to be 0.23$_8$. The solid line in Fig. 3 was drawn by using the $k_v/k_m = 6.4$ thus obtained.

The explanation assuming the reactivity of different hydrogens can be justified by the deuterated products of Nos. B19-a, -b and -c (Table I), in which the long reaction times of 25, 50 and 100 hr. respectively at 25°C were adopted. In this series, the curve plotting log d_0 vs. time is not linear, as in the case of No. K-1 (cf. Fig. 2), suggesting the presence of at least two kinds of hydrogen atoms with different reactivities. Besides, as Fig. 4 shows, the infrared spectra of Nos. 19 indicate the successive production of propenes deuterated at both the vinyl (2265 and 2248 cm^{-1}) and methyl (2183 cm^{-1}) groups with time, and shows parallel with the increase of propene-d_2 (cf. the bands at 2223 cm^{-1} as well as at 712 cm^{-1} which are not shown). The ratio of d(methyl)/d(vinyl) was preliminarily estimated on the basis of the infrared bands in Fig. 4 to be 3, if the amount of propene-d_1 is proportional to the absorbance of the bands at 2248 cm^{-1} and 2265 cm^{-1} for vinyl and at 2183 cm^{-1} for methyl C–D stretching respectively, and if their absorption coefficients are equal. The numerical value 3 above mentioned coincides with that of 3.4 determined by the

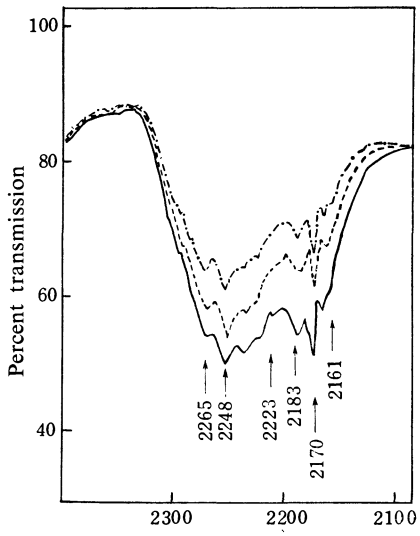


Fig. 4. IR spectra of Nos. B19-a, B19-b and B19-c.

—·— B19-a ---- B19-b —— B19-c

NMR data,* within the range of experimental error.

Effect of Carriers. — As has already been reported,[3] both methyl and ring hydrogen of *p*-xylene were exchangeable if nickel was supported on alumina.[3] Some change in selectivity was also found in the present reaction by the comparison of infrared data of Nos. A5, 6, 7, 8 and 9 with each other, although the change occurred in the direction opposite to that of paraxylene. For example, in the spectrum of No. A-9 shown in Fig. 1b, the band at 2183 cm^{-1} is stronger than those at 2248 and 2265 cm^{-1}. Thus the exchange rate of methyl hydrogen became comparable with or larger than that of vinyl hydrogen as a result of the use of this carrier.

Another point to be mentioned is the absolute decrease in the catalytic activity of carried catalysts. As Table I shows, the exchange degree of Nos. A6, A7, A8 and A9 became similar to that of No. A5 when the reaction time or the amount of the catalyst was increased, while in the case of paraxylene, the activity was always increased by the use of carriers.

Discussion

Propene was found to exchange its three kinds of hydrogen with deuterium oxide. Such a simultaneous exchange of different kinds of hydrogen has already been reported by Twigg[9] on the system when propene and deuterium gas came in contact with the nickel catalyst. Since his results were obtained indirectly by the determination of the total isotopic concentration, it may be said that his conclusion was first confirmed without ambiguity by the present report. It has been found, moreover, that the exchange of methyl hydrogen is more difficult than that of vinyl hydrogen. This finding is to be explained as follows.

As has already been mentioned, the scission of the methyl hydrogen of paraxylene is easier than that of ring hydrogen from the thermochemical viewpoint, because $D(C_6H_5CH_2\text{–}H)$ is 77.5 kcal./mol. and $D(C_6H_5\text{–}H)$ is 104 kcal./mol., according to Szwarc's data.[10] These numerals are favorable for use in the explanation of the experimental results of the exchange reaction carried out on a nickel catalyst. However, the same argument cannot be applied in the present case. Since $D(CH_2 : CH\cdot CH_2\text{–}H)$ is 76.5 kcal./mol. and $D(CH_2CH\text{–}H)$ is 104 kcal./mol., the scission of vinyl hydrogen would be more difficult than that of methyl hydrogen, unlike the present exchange data. The above contradiction may not be very serious, however, because no attention was paid in the argument to the existence of a catalyst on which olefins may be adsorbed at their double bond. Moreover, it must be remembered that the two absolute rates of the exchange of methyl hydrogen are not so different as those which occur in the double bonds.

On the exchange reaction of ethene and heavy water, ethene is often regarded, since Horiuti-Polanyi's work,[1] as forming bonds with metals opening its double bond as follows:

$$C_2H_4 \rightarrow \underset{*\ *}{H_2C\text{–}CH_2} \rightarrow \underset{*}{H_2C\text{–}CH_3}$$

where the star * denotes the bonding thereby produced. From such an adsorbed state of the associated type, a half-hydrogenated state, $CH_2\text{–}CH_3$, is produced if a sufficient amount of $\overset{*}{H}$ exists on the surface. These presumed $\overset{*}{}$ species were recently concluded to be present in ethene and higher olefins by the application of the infrared method[11] so far as silica-supported nickel was concerned. It is natural to adopt the same line of argument in the present exchange reaction, assuming the following scheme:

$$\underset{(I)}{CH_3\text{–}C_2H_3} \rightarrow \underset{(II)}{CH_3\text{–}\underset{*}{CH}\text{–}\underset{*}{CH_2}} + \underset{*}{D}$$

* Details will be published in the future.

9) G. H. Twigg, *Trans. Faraday Soc.*, 35, 934 (1939).

10) M. Szwarc et al., *Proc. Roy. Soc.*, **A207**, 5 (1951).

11) W. A. Pliskin and P. P. Eischens, *J. Chem. Phys.*, **24**, 482 (1956).

$$\begin{cases} \xrightarrow{\alpha} CH_3CHCH_2D \xrightarrow{-H} CH_3\overset{*}{C}HCHD \\ \xrightarrow[\beta]{} CH_3CHDCH_2 \xrightarrow{-H} CH_3\overset{*}{C}DCH_2 \end{cases}$$

(III)

However, propanes would not be produced due to the low surface concentration of $\overset{*}{D}$ in equilibrium with D_2O. The degree of deuterium substitution at the methin or methen group in propene-d_1 may be determined by the relative rate of steps α and β.

The assumption of the adsorbed state II, according to which the most stable valency angle, θ, of carbons would be near to the tetrahedral valency angle of 109°28', may be allowed for geometrical reasons, as has been shown by Twigg and Rideal.[12] Using recent data,* the angle θ is estimated to be 105° if the distance of closest packing is assumed to be 2.47Å, instead of the lattice constant of nickel. This angle is an allowable magnitude for propene to be chemisorbed. On the other hand, the intermediate II, if produced, may not be so stable in the case of paraxylene because of the break in the resonating benzenoid structure. This is the reason why the exchange rate of the ring hydrogen was so small as not to be measured at 100°C in the presence of nickel, while it could be measured in the presence of platinum the angle θ of which was calculated to be 108°17'.

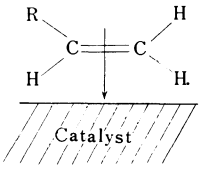
Besides the above adsorbed state, some other state must be assumed to explain the exchangeability of methyl hydrogen. Considering the magnitude of bond-energy mentioned above, an intermediate with the structure of $\overset{*}{C}H_2$–$CH{=}CH_2$ may be produced easily on nickel. The deuterium exchange would proceed by the interconversion of species IV and V:

$$\underset{*}{CH_2CH{=}CH_2} + \overset{*}{D} \rightleftharpoons DCH_2CH{=}CH_2$$

(IV) (V)

where $\underset{*}{CH_2CH{=}CH_2}$ may be expressed by $\dot{C}H_2$–$CH{=}CH_2$, considering the stability of this allyl radical. However, there remains a possibility that the adsorbed species IV may be formed by the isomerization of II. By this process the exchange may occur.*

It must be added that a π-complex intermediate may be formed as an adsorbed state, VI, of ethane and its derivatives, as has been proposed by Crawford and Kemball in the exchange of xylenes with deuterium[4] as well as in some heterogeneous catalyses generally. However, in order to make the exchange proceed, an assumption that the state III is in equilibrium with the state VI is necessary. For sake of simplicity, the traditional state II, allowable from the energetic viewpoint, was adopted in the above discussion.



(VI)

There remains one point to be discussed, i. e., whether the intermediates II—IV mentioned above are charged or not, through they have been treated as if uncharged. This problem will be discussed in a future report.

Summary

Deuterium exchange between propene and deuterium oxide has been found to occur at room temperature successively on a nickel catalyst, but about six times more easily at the vinyl hydrogen than at the methyl hydrogen at room temperature, although this finding is not concordant with the expectation derived from the scission energy of the bonds concerned and although it is also different from the easier exchangeability of the methyl hydrogen in the similar exchange reaction of paraxylene.

The discrepancy has been explained by assuming the classical chemisorbed species of propene as an intermediate, i. e., a state of propene which forms bonds between nickel atoms and the C=C group, besides the formation of adsorbed allyl type species on nickel.

The authors wish to express their thanks to Mr. Motoyoshi Hatada of the Osaka Laboratories of the Japanese Association for Radiation Research on Polymers for his help in the mass-spectrometric measurement, and also to Drs. B. S. Rabinovitch and G. Zerbi for their information on infrared spectra.

Department of Chemistry
Science Faculty
Osaka University
Nakanoshima, Osaka

12) G. H. Twigg and E. K. Rideal, *Trans. Faraday Soc.*, **36**, 533 (1940).

* C-C 1.53Å, C-Ni 1.82Å, and Ni-Ni 2.47Å (cf. L. Pauling, "Nature of the Chemical Bonds," 2nd ed. (1962)).

* We wish to express our sincere thanks to Professors Tadao Shiba and Atsumu Ozaki, Tokyo Institute of Technology, for their suggestion of the possibility of isomerization.

The Mercury-photosensitized Decomposition of Neopentane at High Temperatures

By Shin SATO and Shigeru TSUNASHIMA

(Received November 22, 1963)

The investigation of mercury-photosensitized reactions has been restricted mainly to simple hydrocarbons. Recent developments in gas chromatographic techniques have, however, made the study of the reactions of complex hydrocarbons feasible.

Darwent and Steacie[1] have studied the mercury photosensitization of neopentane and have found that the main products at room temperature were hydrogen and dineopentyl. Methane was a minor product, and its formation was assumed to be due to atomic cracking. One of the characteristic features observed in their study of neopentane was that the quantum yield of hydrogen was extremely low and fairly temperature-dependent, the apparent activation energy being 4.3 kcal. The mercury photosensitization of methane also gives low quantum yields of hydrogen.[2] It is possible that there is some correlation between the low quantum yield of hydrogen and the symmetry of the methane and neopentane molecules. Recently Back and van der Auwera[3] have discussed the various possibilities in an attempt to explain this abnormality.

The mercury-photosensitized decomposition of most alkane molecules proceeds initially by the scission of the C–H bond. The radicals thus produced may combine together or may disproportionate at room temperature, while at high temperatures they decompose to smaller radicals and olefin molecules.[4-6] Neopentyl radicals may be expected to behave similarly, with a rather low activation energy.

Experimental

Neopentane (supplied by Takachiho-Shoji Co.) was purified by bulb-to-bulb distillation, and the middle third was used for the photochemical studies. No impurities were detected by gas chromatographic analysis, indicating that the impurity content is at most below 0.1 %.

The quartz reaction cell (5 cm. wide internally, 8 cm. long) was placed in a furnace, the temperature of which was controlled by a thermister within ± 1°C below 200°C and ± 5°C above 250°C. A spiral mercury resonance lamp (filled with 4 mm. neon) illuminated the reaction cell through a quartz window of the furnace. The reaction cell was connected to the rest of the apparatus through a mercury cut-off.

After each run, the products were transferred to a trap at the liquid nitrogen temperature. The non-condensable gases (hydrogen and methane) were collected by a Toepler pump and the amount measured by a gas buret. The gas was passed over cuprous oxide at 250°C to remove hydrogen, and the amount of gas remaining was measured as methane. The condensable fraction was analyzed by gas chromatography. The column for the analysis of C_3 hydrocarbons and greater was packed with a Celite-dimethylsulpholane mixture (17 m. long) supplied by Shimadzu Co., and the column for the separation of ethane and ethylene was packed with a silica-squalane mixture (1 m. long).

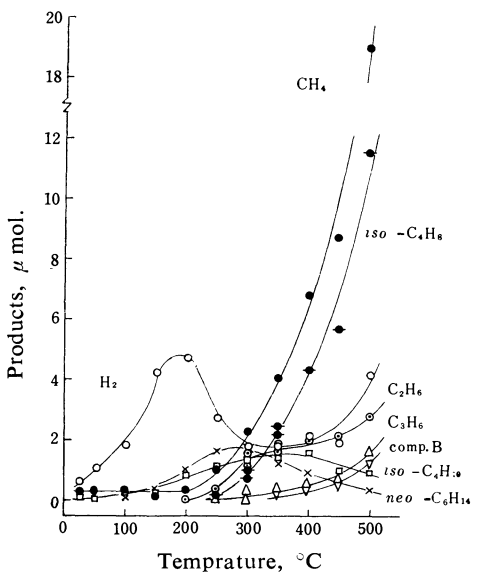


Fig. 1. Temperature dependence of the photosensitized reactions; Comp. B is unknown product, probably C_6.

1) B. deB. Darwent and E. W. R. Steacie, *Can. J. Research*, **27**, 181 (1949).
2) K. Morikawa, W. S. Benedict and H. S. Taylor, *J. Chem. Phys.*, **5**, 212 (1937).
3) R. A. Back and D. van der Auwera, *Can. J. Chem.*, **40**, 2339 (1962).
4) J. A. Kerr and A. F. Trotman-Dickenson, "Progress in Reaction Kinetics," Pergamon Press, London (1961), p. 105.
5) S. Arai, S. Sato and S. Shida, *J. Chem. Phys.*, **33**, 1277 (1960).
6) S. Arai and S. Shida, *J. Chem. Soc. Japan, Ind. Chem. Sec.* (*Kogyo Kagaku Zasshi*), **64**, 454 (1961).

TABLE I. PRESSURE DEPENDENCE OF THE FORMATION OF HYDROGEN AND METHANE*

Temperature ; 50°C						
Initial pressure, mmHg	12.2	22.0	36.4	51.2	81.4	164.2
Hydrogen, μmol.	0.52	0.78	1.20	1.40	2.30	2.79
Methane, μmol.	0.92	0.98	0.81	0.76	0.48	0.52
Temperature ; 100°C						
Initial pressure, mmHg	17.2	21.0	25.6	28.8	55.6	90.2
Hydrogen, μmol.	1.36**	1.85	2.12	2.22	3.30	4.81
Methane, μmol.		0.38	0.40	0.19	0.70	0.12
Temperature ; 150°C						
Initial pressure, mmHg	11.4	23.4	38.4	58.4	87.0	174.0
Hydrogen, μmol.	3.23	6.35	9.42	11.96	17.23	18.92
Methane, μmol.	0.65	0.52	0.41	0.38	0.28	0.34
Isobutane, μmol.	0.60	0.64	0.69			0.55
Neohexane, μmol.	0.56	0.47	0.48	0.56		0.23

* Reaction time ; 5 min.
** Mixture of hydrogen and methane

Results and Discussion

The Temperature Dependence of the Photosensitized Reaction.—In Fig. 1 the amounts of analyzed products from the mercury-photosensitized decomposition of neopentane are plotted as a function of the temperature. The initial neopentane pressure is 30 mmHg and the irradiation time is 5 min. in all cases. Below 250°C, the main products were hydrogen, isobutane, neohexane and methane, while propane was a minor product in all runs. The apparent activation energies for the rate of the formation of hydrogen (25°C to 150°C) and of isobutane and neohexane (25°C to 250°C) were calculated as 4.2 kcal. This value agrees with the activation energy of hydrogen formation obtained by Darwent and Steacie.[1]

Above 250°C, the amounts of methane, isobutene, ethane and propylene markedly increase with the increasing temperature. These products may arise from the decomposition of the neopentyl radicals produced initially. The apparent activation energies for the rates of the formation of methane, isobutene and propylene were 9 kcal. The amounts of isobutane and neohexane decreased with the increasing temperature above 250°C, possibly corresponding to the decomposition of neopentyl radicals. The curve for hydrogen is obviously abnormal. This will be discussed later.

Initial Process.—Table I shows the amounts of the main products from the mercury-photosensitized decomposition of neopentane at various initial pressures and at the temperatures of 50, 100 and 150°C. The ratios of the amounts of methane to those of hydrogen are plotted against the initial pressures in Fig. 2.

To explain these results, the following

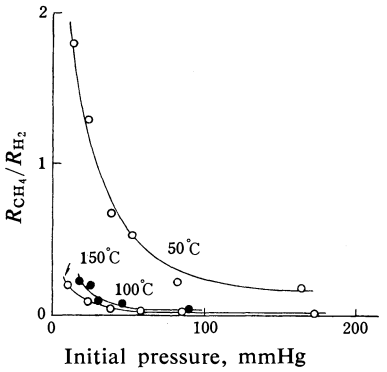


Fig. 2. Pressure dependence of the formations of hydrogen and methane.

mechanism is proposed for the formation of hydrogen and methane:

$$Hg + h\nu \rightarrow Hg^* \ (^3P_1)$$

$$Hg^* \rightarrow Hg + h\nu \quad (1)$$

$$Hg^* + neo\text{-}C_5H_{12} \rightarrow Hg + neo\text{-}C_5H_{12} \quad (2)$$

$$Hg^* + neo\text{-}C_5H_{12} \rightarrow Hg + neo\text{-}C_5H_{11} + H \quad (3)$$

$$H + neo\text{-}C_5H_{12} \rightarrow H_2 + neo\text{-}C_5H_{11} \quad (4)$$

$$H + neo\text{-}C_5H_{11} \rightarrow CH_3 + t\text{-}C_4H_9 \quad (5)$$

$$CH_3 + neo\text{-}C_5H_{12} \rightarrow CH_4 + neo\text{-}C_5H_{11} \quad (6)$$

Here, reaction 2 refers to the physical quenching of the excited mercury atom by the neopentane molecule. This reaction is considered to take part in the mechanism because the quantum yield of hydrogen is known to be extremely low in the mercury-photosensitized reaction of neopentane.[1] Reaction 5 is atomic cracking of neopentyl radicals by hydrogen atoms.[7] The steady-state treatment of

7) E. W. R. Steacie, "Atomic and Free Radical Reaction," Reinhold Publishing Co., New York (1946).

the above mechanism gives the following relation:

$$\frac{I}{R_{non}}=\frac{k_2+k_3}{k_3}\left\{1+\frac{k_1}{(k_2+k_3)\,[C_5H_{12}]}\right\} \qquad (I)$$

where I is the intensity of light, R_{non} is the rate of the formation of non-condensables, and k_1 is the reciprocal of the life-time of the excited mercury atom ($\tau=1.08\times10^{-7}$ sec.). Using the data from Table I, a linear correlation between the reciprocal of the rate of the

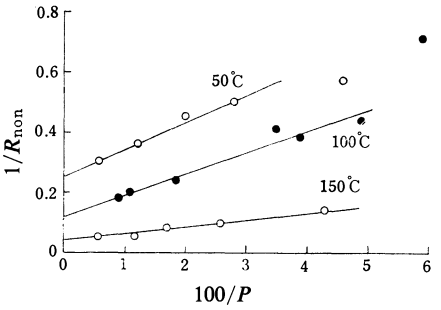


Fig. 3. Reciprocal of the rate of formation of non-condensables as a function of reciprocal of the initial pressure.

formation of non-condensables and the reciprocal of the initial neopentane pressure is obtained (see Fig. 3). The values of k_2+k_3 calculated from the slope and intercept are given in Table II. In Fig. 3, data obtained at low

TABLE II. QUENCHING CROSS SECTIONS OF THE NEOPENTANE MOLECULE

	50°C	100°C	150°C
k_2+k_3 (l. mol^{-1} sec^{-1})	4.3×10^9	4.4×10^9	5.3×10^9
$\sigma_{C_5H_{12}}$ (Å^2)	0.63	0.60	0.68

pressures are scattered, probably due to the importance of the recombination of methyl radicals and wall effects. Therefore, the scattered data have not been used for the calculations of k_2+k_3 in Table II.

The calculated values of k_2+k_3 are almost temperature independent. From these values, the mean quenching cross section of neopentane for excited mercury atoms is calculated as 0.64Å^2, which is smaller than one-half of the value obtained photometrically by Darwent.[8] In the previous section, 4.2 kcal. was obtained for the apparent activation energy of hydrogen formation. This can be explained from Eq. I if $k_2 \gg k_3$ and $E_3 \simeq 4$ kcal. However, the reason for the high activation energy of reaction 3 cannot be explained from the findings of the present work. The same problem has been encountered by Back and van der Auwera for methane.[3]

Atomic Cracking. — Most of the neopentyl radicals produced may combine with each other to give dineopentyl at low temperatures, i. e.,

$$2\ C_5H_{11} \rightarrow C_{10}H_{22} \qquad (7)$$

When neopentane pressure is high, R_4 would be much greater than R_5 and, thus, the steady state treatment would give the following equation:

$$R_{CH_4}{}^2/R_{H_2}{}^3=k_5{}^2/k_4{}^2k_7\,[C_5H_{12}]^2 \qquad (II)$$

where R_{CH_4} and R_{H_2} are the rates of the formation of methane and hydrogen respectively. If it is assumed that reactions 5 and 7 have no or very little activation energy and that reaction 4 has an activation energy of several killocalories,[4] the values of R_{CH_4}/R_{H_2} at high pressures are consistent with Eq. II (see Fig. 2).

Below 150°C, small amounts of propane have always been found by gas chromatography and may arise from the atomic cracking of the tert-butyl radicals produced by reaction 5:

$$H + t\text{-}C_4H_9 \rightarrow CH_3 + C_3H_7 \qquad (8)$$

$$C_3H_7 + C_5H_{12} \rightarrow C_3H_8 + C_5H_{11} \qquad (9)$$

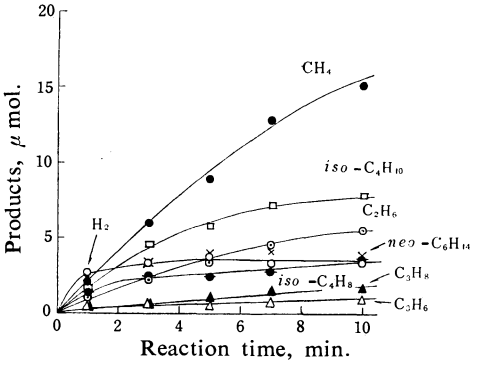


Fig. 4. Time dependence of the photosensitized reaction at 350°C.

The Decomposition of Free Radicals. — As Fig. 1 shows, above 200°C the rates of the formation of methane and isobutene increase with the increasing temperature because of the following reaction occurring at high temperatures:

$$neo\text{-}C_5H_{11} \rightarrow CH_3 + i\text{-}C_4H_8 \qquad (10)$$

The methyl radicals produced in reaction 10 may abstract hydrogen atoms from neopentane molecules and give neopentyl radicals, which may again undergo reaction 10, so that metane and isobutene are produced by a chain mechanism.

Table III and Fig. 4 show the time dependence on the reaction products. The amounts of hydrogen and isobutene are not linear with the irradiation time up to one minute below

8) B. deB. Darwent, *J. Chem. Phys.*, **18**, 1532 (1950).

TABLE III. TIME DEPENDENCE OF THE PHOTOCHEMICAL REACTION AT HIGHER TEMPERATURES

Temp. °C	Initial pressure mmHg	Reaction time min.	Products, μ mol. H_2	CH_4	C_2H_6	C_3H_8	C_3H_6	i-C_4H_{10}	i-C_4H_8	neo-C_6H_{14}
250	32.0	1	3.40	0.36						
	30.8	1	3.10	0.36				0.55		0.94
300	32.4	1/2	1.26	0.67	0.18	0.16	0.09	0.51	0.28	0.80
	30.0	1	2.23	1.52	0.46	0.14	0.05	1.70	0.92	1.08
	30.0	3/2	2.41	2.28	0.69	0.18	0.08	1.75	0.46	2.02
400	30.2	1/2	1.40	1.26	0.87	0.07	0.10	2.08	1.94	0.68
	30.8	1	1.55	2.68	1.47*		0.23	1.56	3.08	1.68
465	30.4	1/4	0.79	1.84	0.78		0.16	0.23	3.29	0.32
500	31.0	35 dark	(0.91)						0.37	
	31.6	1/6	0.94	2.12	0.76		0.01	0.18	4.41	0.24
	30.4	1/2	1.85	3.97	1.47	0.09	0.32	0.50	5.61	0.28
	30.4	1	2.41	5.78	2.32**	0.21	0.62	1.06	6.05	0.54

* C_2H_6 1.33 μ mol., C_2H_4 0.14 μ mol.
** C_2H_6 2.11 μ mol., C_2H_4 0.21 μ mol.

300°C, while methane increases linearly even at 400°C. This may be explained by the combination of two effects; hydrogen has a much larger quenching cross section for the excited mercury atom than does methane ($\delta_{H_2}=8.60$ Å^2, $\sigma_{CH_4}=0.085$ Å^2)[9], and isobutene is reactive to radicals; for example:

$$H + i\text{-}C_4H_8 \rightarrow t\text{-}C_4H_9 \qquad (11)$$

On the basis of these discussions, the abnormality of the curve for hydrogen in Fig. 1 may be understood. In fact, the initial rates of the formation of hydrogen do not show any abnormality (see Table III). At 500°C, however, the amount of hydrogen increases markedly. A possible explanation is that the scission of the C–H of radicals is occurring at higher temperatures,[4] for example,

$$t\text{-}C_4H_9 \rightarrow i\text{-}C_4H_8 + H \qquad (12)$$

Figure 5 shows the relationship between the logarithm of the initial rates of the formation

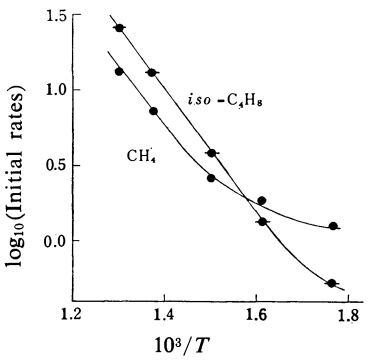


Fig. 5. Logarithm of initial rate of formation as a function of reciprocal of temperature.

9) K. J. Laidler, "The Chemical Kinetics of Excited States," Clarendon Press., London (1955), p. 107.

of methane and isobutene and the reciprocal of the temperature. Values for the logarithm of the initial rate of methane formation are not linear at low temperatures, since small amounts of methane produced by atomic cracking. At high temperatures, the amout of methane is a little less than that of isobutene, probably because methane is not an only product from the methyl radical.

These results may reasonably be explained by the following mechanism:

$$H + C_5H_{12} \rightarrow H_2 + C_5H_{11} \qquad (4)$$

$$C_5H_{11} \rightarrow CH_3 + i\text{-}C_4H_8 \qquad (10)$$

$$CH_3 + C_5H_{12} \rightarrow CH_4 + C_5H_{11} \qquad (6)$$

$$C_5H_{11} + C_5H_{11} \rightarrow C_{10}H_{22} \qquad (7)$$

$$CH_3 + C_5H_{11} \rightarrow C_6H_{14} \qquad (13)$$

$$CH_3 + CH_3 \rightarrow C_2H_6 \qquad (14)$$

When the temperature is not too high, it may be assumed that $R_7 \gg R_{13}$, because the concetration of the methyl radical is much lower than that of the neopentyl radical. Therefore the steady-state treatment gives the following relation:

$$R_{CH_4}/\sqrt{R_{H_2}} \simeq R_{C_4H_8}/\sqrt{R_{H_2}} = k_{10}/\sqrt{k_7} \qquad (III)$$

$R_{C_4H_8}$ and R_{H_2} are calculated from Table III using the data at short irradiation times. Figure 6 shows the straight relationship between the logarithm of $R_{C_4H_8}/\sqrt{R_{H_2}}$ and the reciprocal of the temperature. From the slope of this line,

$$E_{10} - 1/2E_7 = 15.0 \text{ kcal.}$$

Since the activation energy of reaction 7 can be assumed to be about zero to 4 kcal., 17 $\pm$2 kcal. is obtained for the activation energy of reaction 10. This value is reasonable when compared to the activation energy of hydrocarbon radical decomposition.[4]

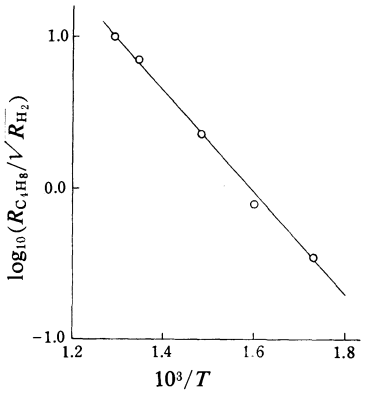


Fig. 6. Activation energy of decomposition of neopentyl radical.

The propylene observed at higher temperatures may be due to the decomposition of the butyl radical, as follows:

$$t\text{-}C_4H_9 \rightarrow i\text{-}C_4H_9 \rightarrow CH_3 + C_3H_6 \qquad (15)$$

However, no quantitative treatment has been attempted, because the amount of propylene produced is small and many speculations have to be made for the isomerization of radicals, although much information has recently been accumulated.[10]

10) J. R. McNesby and W. M. Jackson, *J. Chem. Phys.*, **38**, 692 (1963).

Summary

The mercury-photosensitized decomposition of neopentane has been investigated over the temperature range 25°C to 500°C. If the quenching of excited mercury atoms by neopentane molecules is assumed to occur both physically and chemically, as follows:

$$Hg^{*+}(^3P_1) + neo\text{-}C_5H_{12} \begin{cases} \rightarrow Hg + neo\text{-}C_5H_{12} & (2) \\ \rightarrow Hg + C_5H_{11} + H & (3) \end{cases}$$

it has been shown that $k_2 \gg k_3$ and that the quenching cross section of reaction is about 0.6 Å^2, which is almost temperature independent, and $E_3 \simeq 4$ kcal. Above 250°C, neopentyl radicals decompose to methyl radicals and isobutene molecules with an activation energy of 17 ± 2 kcal.

The authors wish to express their deep thanks to Professor Shoji Shida for his continued encouragement of this work. They are also indebted to Dr. John M. S. Jarvie, Gulf Research & Development Co., Pittsburgh, U.S.A., for his kind advice regarding this manuscript.

Department of Applied Physics
Tokyo Institute of Technology
Meguro-ku, Tokyo

A Convenient Method for the Monobromination of Active Methylene Compounds

By Tsujiaki HATA

(Received November 26, 1963)

A general procedure for the conversion of active methylene compounds to the corresponding monobromoderivatives consists in treating the active methylene compounds with bromine. Numerous examples, however, show that a mixture of dibromo- and monobromo-derivatives is yielded even by the equimolar reaction of the active methylene compounds and bromine.

Although dibromocyanoacetamide was prepared by Hesse[1] as early as 1896, the monobromoderivative was not prepared until 1922 by Gupta and Thorpe.[2] They prepared monobromocyanoacetamide in a 55% yield by the partial debromination of dibromocyanoacetamide with dimethylaniline. Later, Wideqvist[3] reported that monobromocyanoacetamide was obtained in a high yield when an equimolar amount of cyanoacetamide and dibromocyanoacetamide was heated in an aqueous solution. In a previous paper,[4] it was shown that

1) B. C. Hesse, *Am. Chem. J.*, **18**, 723 (1896).

2) B. M. Gupta and J. F. Thorpe, *J. Chem. Soc.*, **121**, 1896 (1922).

3) S. Wideqvist, *Acta. Chem. Scand.*, **7**, 696 (1953).

4) T. Hata and T. Mukaiyama, This Bulletin, **35**, 1108 (1962).

monobromocyanoacetamide was also obtained in a high yield by the reaction of cyanoacetamide and dibromocyanoacetamide in 95% ethanol.

In the present experiment, the proportionation procedure was extended to the preparation of *N*-ethyl monobromocyanoacetamide and *N*-cyclohexyl monobromocyanoacetamide, which were obtained in 84% and 90% yields respectively, according to the following equation:

$$NCCH_2CONHR + NCCBr_2CONHR \rightarrow 2\ NCCHBrCONHR$$

R: C_2H_5 or C_6H_{11}

Similarly, monobromomalonitrile was obtained in a 60% yield by the proportionation reaction of malonitrile and dibromomalonitrile in the presence of a catalytic amount of boron trifluoride.

$$CH_2(CN)_2 + CBr_2(CN)_2 \xrightarrow{BF_3} 2\ CHBr(CN)_2$$

Next, the monobromination of various active methylene compounds by the use of dibromomalonitrile was tried, since it was found that the bromine atoms of dibromomalonitrile are much more active than those of the other dibromoamides.

When two moles of malonamide were treated with one mole of dibromomalonitrile, monobromomalonamide was obtained in a 75% yield, along with malonitrile, as is shown in the following equation:

$$2\ CH_2(CONH_2)_2 + CBr_2(CN)_2 \rightarrow 2\ CHBr(CONH_2)_2 + CH_2(CN)_2$$

Similarly, monobromocyanoacetamide, *N*-cyclohexyl monobromocyanoacetamide, ethyl bromocyanoacetate and ethyl bromomalonate were obtained in high yields by the reaction of dibromomalonitrile with two moles of the corresponding active methylene compounds (see Table I).

On the other hand, it has been reported[5] that the bromination of malonanilide with bromine gives a mixture of several brominated products because the anilide has six replaceable hydrogen atoms in the para- and ortho-positions in each phenyl group, and two hydrogen atoms in the malonyl group.

It was established by the present experiment that the bromination of malonanilide by means of dibromomalonitrile resulted in the exclusive formation of α-monobromomalonanilide in a 85% yield.

$$2\ CH_2(CONHC_6H_5)_2 + CBr_2(CN)_2 \rightarrow 2\ CHBr(CONHC_6H_5)_2 + CH_2(CN)_2$$

5) J. V. Backes, R. W. West and M. A. Whiteley, *J. Chem. Soc.*, **119**, 362 (1921).

Certain mono-bromoderivatives of anilides and *N*-benzylamides were prepared by this method from the corresponding amides (see Table II).

It can be said that the method of monobromination by means of dibromomalonitrile proved remarkably effective for the synthesis of α-monobromo-derivatives of active methylene compounds containing a phenyl group.

Experimental

Reagents.—Cyanoacetamide,[6] dibromocyanoacetamide,[7] malonitrile,[8] dibromomalonitrile,[9] malonamide,[10] malonanilide,[11] cyanoacetanilide,[12] *N*-benzyl cyanoacetamide,[12] acetacetanilide[13] and *N*-benzyl acetacetamide[14] were prepared by the literature procedures.

Ethyl malonate and ethyl cyanoacetate were obtained from a commercial source and were purified by distillation.

***N*-Ethyl Monobromocyanoacetamide and *N*-Cyclohexyl Monobromocyanoacetamide.**—A solution of *N*-ethyl cyanoacetamide (1.12 g., 0.01 mol.) and *N*-ethyl dibromocyanoacetamide (2.70 g., 0.01 mol.) in 100 ml. of 95% ethanol was refluxed for 2 hr. After the ethanol had been removed, a large amount of a white solid was separated, washed with benzene, and recrystallized from 50% ethanol. *N*-Ethyl monobromocyanoacetamide (3.21 g., 84%, m. p. 79~81°C) was obtained.

In a similar fashion, *N*-cyclohexyl monobromocyanoacetamide (90%, m. p. 138~141°C) was obtained.

TABLE I. BROMINATION OF ACTIVE METHYLENE COMPOUNDS BY MEANS OF DIBROMOMALONITRILE*

Monobromo-derivatives (Products)	Yield %	M. p. (°C) or b. p. (°C/mmHg)
$CHBr(CN)_2$	60	63~64, 90/16
$CHBr(CONH_2)_2$	75	175~179
$NCCHBrCONH_2$	57	117~119
$NCCHBrCONHC_6H_{11}$	59	138~141
$CHBr(COOC_2H_5)_2$	52	128~130/30
$CH_3COCHBrCOOC_2H_5$	43	122/25

* Monobromo-derivatives of acetylacetone or benzoylacetone could not be obtained by this method.

6) B. B. Corson, R. W. Scott and C. E. Vose, "Organic Syntheses," Col. Vol. I, 179 (1948).
7) B. C. Hesse, *Am. Chem. J.*, **18**, 725 (1896).
8) A. R. Surrey, "Organic Syntheses," Col. Vol. III, 535 (1955).
9) E. Otto and B. Löpmann, *Ber.*, **55**, 1259 (1922).
10) M. Freund, Inaug Dissertat 18., August, 1884, Berlin; *Zent. Blatt.*, **15**, 920 (1884).
11) F. D. Chattaway and J. M. D. Olmsted, *J. Chem. Soc.*, **97**, 939 (1910).
12) K. G. Naik and Y. N. Baht, *J. Indian Chem. Soc.*, **4**, 547 (1927); *Chem. Abstr.*, **22**, 2353 (1928).
13) J. W. Williams and J. A. Krynitsky, "Organic Syntheses," Col. Vol. III, 10 (1955).
14) The procedure was modified from the method of Williams and Krynitsky in "Organic Syntheses" (cf. 13 above) for the preparation of acetanilide.

TABLE II. BROMINATION OF ACTIVE METHYLENE COMPOUNDS BY MEANS OF DIBROMOMALONITRILE

Monobromo-derivatives (Products)	Yield %	M. p. °C	N, % Calcd.	Found
$CHBr(CONHC_6H_5)_2$	85	184~185	8.42	8.14
$NCCHBrCONHC_6H_5$	79	131~133	11.72	12.26
$NCCHBrCONHCH_2C_6H_5$	79	114~115	11.07	11.30
$CH_3COCHBrCONHC_6H_5$	92	143~144	5.47	5.65
$CH_3COCHBrCONHCH_2C_6H_5$	78	95~96	5.18	5.36

Monobromomalonitrile.—A solution of 0.01 mol. of malonitrile and 0.01 mol. of dibromomalonitrile in 70 ml. of 95% ethanol was refluxed for 15 min. in the presence of a catalytic amount of boron trifluoride. After the ethanol had been removed under reduced pressure, the brownish-yellow residue was distilled in vacuo to give 1.74 g. (a 60% yield) of the yellow liquid (b. p. 90°C/16 mmHg), which solidified at room temperature and melted at 63~64°C.

General Procedure of the Monobromination by Means of Dibromomalonitrile.—A solution of 0.02 mol. of an active methylene compound and 0.01 mol. of dibromomalonitrile in 70 ml. of 95% ethanol was refluxed for 15 min. in the presence of a catalytic amount of boron trifluoride. After the ethanol had been removed under reduced pressure, the precipitates were filtered and washed with ether and recrystallized from 95% ethanol. The yields and the physical constants are listed in Table I.

In a similar fashion, mono-bromoderivatives of anilides and *N*-benzyl amides were prepared. The yields and the physical constants are listed in Table II.

Summary

The monobromination of the active methylene compounds by means of the proportionation procedure between the active methylene compound and its dibromo-derivative has been investigated.

Next, the monobromination of various active methylene compounds by the use of dibromomalonitrile has been tried. The method proved remarkably effective for the synthesis of α-mono-bromoderivatives of active methylene compounds containing a phenyl group.

The author wishes to express his hearty thanks to Professor Dr. Teruaki Mukaiyama for his encouragement and for his kind advice, to Mr. Koa Tasaka for his help during the course of this experiment, and to Miss Toshiko Aoyagi for the microanalysis.

Labroatory of Organic Chemistry
Tokyo Institute of Technology
Meguro-ku, Tokyo

The Absorption Spectra of Chromium(II) Acetate and Copper(II) Acetate

By Sigeo KIDA, Yoshiaki NAKASHIMA, Yukiyoshi MORIMOTO, Kiyoshi NIIMI and Shoichiro YAMADA

(Received December 3, 1963)

Copper(II) acetate and chromium(II) acetate have the same binuclear structure, as Fig. 1 shows.[1,2] The two compounds show a magnetic susceptibilities much lower than those of usual monomeric copper(II) and chromium-(II) complexes (1.39 B. M.[3] for copper(II) acetate and nearly zero for chromium(II) acetate[4] at room temperature). Some direct interaction, therefore, has been assumed between two metal ions at a distance of 2.64 Å.

Yamada et al.[5] have reported the electronic spectra of copper(II) acetate and other cupric alkanoates[6] in solution and in the crystalline state; they have pointed out that the band observed at 27.3 kK. is characteristic of the binuclear structure.

1) J. N. van Niekerk and F. R. L. Schoening, *Acta. Cryst.*, **6**, 227 (1953).
2) J. N. van Niekerk, F. R. L. Schoening and J. F. deWet, ibid., **6**, 501 (1953).
3) B. N. Figgis and R. L. Martin, *J. Chem. Soc.*, **1957**, 3837.
4) W. R. King and C. S. Garner, *J. Chem. Phys.*, **18**, 689 (1950).
5) S. Yamada, H. Nakamura and R. Tsuchida, This Bulletin, **30**, 953 (1957).
6) S. Yamada, H. Nakamura and R. Tsuchida, ibid., **31**, 303 (1958).

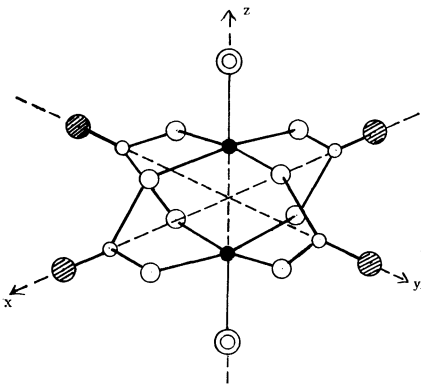


Fig. 1. Molecular structure of chromium-(or copper)(II) acetate.
● Cr or Cu, ○ O, ◦ C, ▨ CH_3
◎ H_2O

The spectrum of chromium(II) acetate in the visible region has been measured by Furlani,[7] but he has not reported the spectrum of the shorter wavelength region, where one may expect a band corresponding to the band observed at 27.3 kK. in copper(II) acetate.

In this investigation the absorption measurements have been carried out on chromium(II) acetate in solution and in Nujol mull from the visible to the near-ultraviolet region, and the dichroism of the single crystal has been determined.

Experimental

Chromium(II) acetate hydrate, $Cr_2(C_2H_3O_2)_4 \cdot 2H_2O$, was prepared by the method described in "Inorganic Syntheses."[8] The material was dissolved in 99% ethanol or water which had been distilled in a nitrogen atmosphere, and it was used for absorption measurements. The absorption measurements were carried out with a Shimadzu spectrophotometer model QR-50 using 1 cm. quartz cells. All these procedures were carried out in a nitrogen atmosphere using the apparatus devised for this purpose; the apparatus is shown in Fig. 2. The concentrations of the solutions used for the measurements were determined by the spectrophotometric analysis of chromium[9] after converting it into chromate ions.

Chromium(II) acetate anhydrate, $Cr_2(C_2H_3O_2)_4$, was prepared from the hydrate, $Cr_2(C_2H_3O_2)_4 \cdot 2H_2O$, by keeping it at 78°C in vaccuo for 8 hr. in an Abderhalden desiccator. The chromium(II) acetate anhydrate thus obtained showed dark orange color in the powder state. The Nujol mulls of these compounds were prepared in a box filled with nitrogen gas; they were used for the absorption measurements.

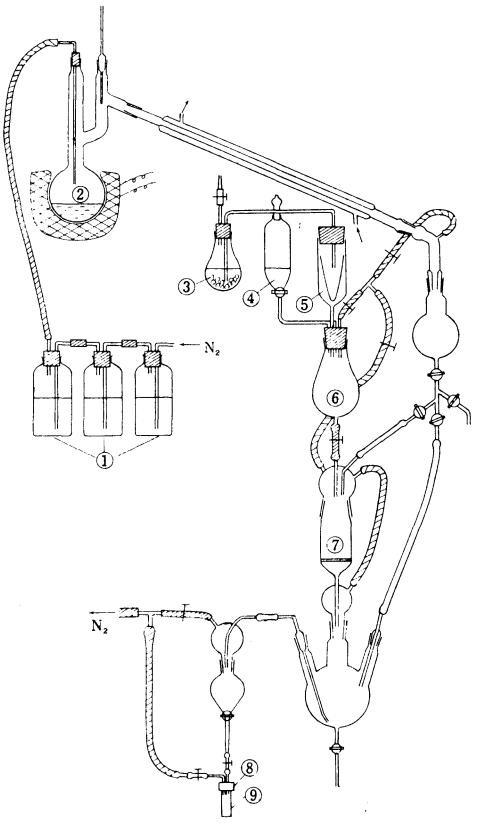


Fig. 2

Quantitative dichroism measurement was made at room temperature by the microscopic method.[10] The measurement was carried out on the (110) face, using the light polarized along the c-axis and the light polarized perpendicular to it. On the basis of crystal structure analysis, the ratio of K_z to K_{xy} is calculated to be about 1/4.5 for the first band and 4 for the second band, where K represents the molar absorption coefficient, and z refers to the Cr-Cr direction in the molecule.

Results and Discussion

The results of the absorption measurements are shown in Figs. 3 and 4 and in Table I. The alcoholic solution shows the same red color as the crystal and obeys Beer's law. On the other hand, the aqueous solution does not obey Beer's law, and the absorption intensity is much lower than that of the alcoholic solution relative to its chromium concentration. This fact implies that the compound considerably hydrolyzes in an aqueous solution.

7) C. Furlani, *Gazz. Chim. Ital.*, **87**, 876 (1957).
8) "Inorganic Syntheses," Vol. I, McGraw-Hill, New York (1939), p. 122.
9) E. B. Sandell, "Colorimetric Determination of Traces of Metals," Interscience Pub. Inc., New York (1950), pp. 258—260.
10) S. Yamada, *J. Am. Chem. Soc.*, **73**, 1182 (1951); R. Tsuchida and M. Kobayashi, "The Color and the Structure of Metallic Compounds," Zōshindo, Osaka (1944), p. 180 (in Japanese).

However, since the peaks in the two absorption curves are nearly identical, it is obvious that the binuclear molecules still exist in considerable concentration in an aqueous solution. This fact contrasts with the fact that the concentration of the binuclear molecule was observed to be much less in an aqueous solution of copper(II) acetate. The absorption in the visible region agrees with Furlani's result.[7] In addition to this absorption ($\nu_{max}=20.58$ kK., $\log\varepsilon=1.80$), another absorption ($\nu_{max}=30.77$ kK., $\log\varepsilon=2.22$ with a shoulder at 29 kK.) was newly observed in this experiment. This absorption, which is tentatively named the "second band," seems to correspond with the "second band" observed at 27.3 kK. in copper(II) acetate. The dichroism of chromium(II) acetate is similar to that of copper(II) acetate,[5] as may be seen in Fig. 4. Thus, the first absorption is more intense in x and y than in z polarization, and vice versa in the case of the second absorption.

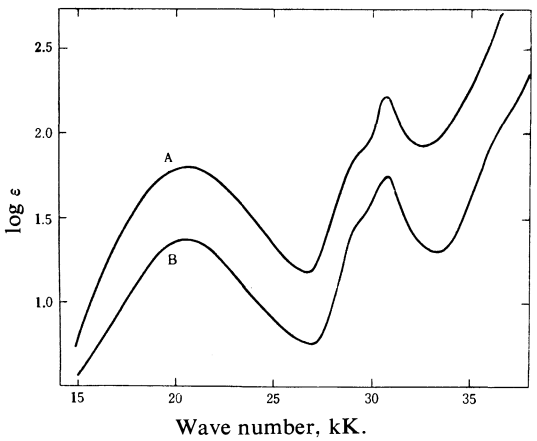


Fig. 3. Absorption spectra of $Cr_2(C_2H_3O_2)_4\cdot 2H_2O$ in solution: A, in 99% ethanol and B, in water. The extinction coefficient is based on the monomeric formula.

TABLE I. ABSORPTION MAXIMA OF CHROMIUM(II) ACETATE (in kK.)

	I	II
(1) $Cr_2(C_2H_3O_2)_4 2H_2O$ (Ethanol solution)	20.58	30.77
(2) $Cr_2(C_2H_3O_2)_4 2H_2O$ (Nujol mull)	20.7	30.7
(3) $Cr_2(C_2H_3O_2)_4$ (Nujol mull)	22.0	30.9
(3)—(2)	1.3	0.2

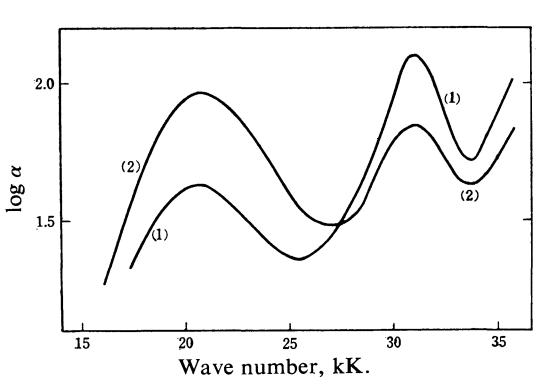


Fig. 4. Absorption spectra of $Cr_2(C_2H_3O_2)_4\cdot 2H_2O$ in the crystalline state: (1) pale-red polarization and (2) red polarization on the (110) face.

From the frequency and the intensity, the first band of chromium(II) acetate and copper(II) acetate in the visible region can undoubtedly be attributed to the d-d transitions. For the second band of copper(II) acetate, Ross[11] has suggested the possibility of a triplet-triplet transition. However, there is no such possibility in the case of chromium(II) acetate, since it is diamagnetic at room temperature. Forster and Ballhausen[12] attributed both the first and the second band to the d-d transitions on the basis of a molecular orbital scheme. However, the molecular orbital method may not give a good approximation in this case, as will be discussed below, and their conclusions were only tentative. Therefor, the origin of the two bands of both compounds will be the subject of the following discussion.

For this type of compounds, the d-d transitions may be devided into two origins; 1) interatomic transitions such as transitions from a bonding to an anti-bonding orbital, or charge transfers from one ion to another, and 2) transitions in a single ion, which correspond to the origin of a usual ligand field band.

Interatomic d-d Transitions.—Since the interatomic distance between two metal ions is relatively large, the interaction should be weak; Forster and Ballhausen[12] estimated the overlap integrals of Cu–Cu interaction to be $S(d_{z^2}, d_{z^2})=0.019$, $S(d_{x^2-y^2}, d_{x^2-y^2})=0.002$ and $S(d_{xz}, d_{yz})=0.012$, which are of the magnitude of about $10^{-1}\sim10^{-2}$ of the usual C–C bond. Therefore, the bonding system between two metal ions is best approximated by the valence bond method rather than by the molecular orbital method.*,[13]

According to the valence bond theory, the wave functions of the valence orbitals in a diatomic unit are expressed as;

$$\Psi=(1-\lambda^2)^{-1/2}[2^{-1/2}\{a(1)b(2)+b(1)a(2)\}+2^{-1/2}\lambda\{a(1)a(2)+b(1)b(2)\}] \quad (1)$$

11) I. G. Ross, *Trans. Faraday Soc.*, **55**, 1057 (1959).
12) L. S. Forster and C. J. Ballhausen, *Acta. Chem. Scand.*, **16**, 1385 (1962).
13) C. A. Coulson, "Valence," Oxford Univ. Press., London (1953), pp. 147—148.
* Discussion was also made of copper(II) acetate on the basis of a similar concept. Cf. M. L. Tonnet, S. Yamada and I. G. Ross, to be published shortly.

for the ground state, where a and b denote atomic wave functions of the different atoms respectively, and λ is a constant which determines the contribution of the ionic term.

In the case of a large interatomic distance, we may neglect the ionic term.

$$\Psi = 2^{-1/2}\{a(1)b(2)+b(1)a(2)\} \quad (2)$$

Similarly, the next higher singlet state may be expressed as:

$$\Psi' = 2^{-1/2}\{a(1)b(2)-b(1)b(2)\}$$

or

$$2^{-1/2}\{a(1)a(2)+b(1)b(2)\} \quad (3)$$

The electronic repulsion energies of the two states are calculated from (2) and (3):

$$E(\Psi) = J(ab)+K(ab)$$

$$E(\Psi') = J(aa)-K(ab) \quad \text{or} \quad J(aa)+K(ab)$$

Since we are dealing with the system of large interatomic distance, $J(ab)$ and $K(ab)$ should be much smaller than $J(aa)$.

$$E(\Psi')-E(\Psi) \fallingdotseq J(aa)$$

This result indicates that the energy of the first spin-allowed transition from the ground state is of the magnitude of $J(aa)$,* which must be larger than 100 kK., as may be roughly estimated from the ionization potentials of the chromium ion.[14]

For the other type of transitions, such as charge transfer from one ion to another, we also have to assign a very high energy to this system, since any charge transfer transition in this system will give rise to a great increase in inter-electronic repulsions, in addition to the energy of the charge separation.

Therefore, the present observed bands are not due to the interatomic d-d transitions.

d-d Transitions in a Single Ion.—To judge from the absorption intensities, the bands under discussion are undoubtedly due to spin-allowed transitions. Therefore, we consider spin-allowed transitions only in this discussion, and, accordingly, the d^4 and the d^9 system can be treated like a d^1 system. In an octahedral field five degenerate d-orbitals are split into triply-degenerate $d\varepsilon$ and doubly-degenerate $d\gamma$ orbitals. In this case only one transition is possible for a d^1-system. As the symmetry goes down from O_h to D_{4h} or C_{4v}, the $d\varepsilon$ and the $d\gamma$ orbital are split, as is shown in Fig. 5: if the tetragonal distortion is considerably large, one can observe two or more separate

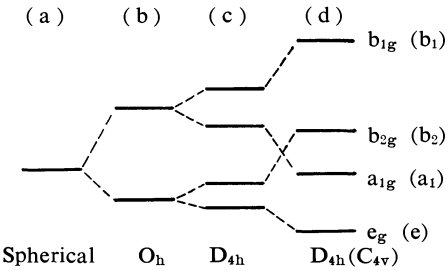


Fig. 5. Energy levels of the d-orbitals.
(c) Weak tetragonal distortion
(d) Strong tetragonal distortion

peaks. However, only one broad band was observed in this region in usual copper(II) and chromium(II) (high spin type) complexes, though these complexes are more or less tetragonally distorted by the Jahn-Teller effect.[15] This fact implies that the tetragonal distortions of these complexes are not large enough to separate the absorption into two distinct peaks. Even if one would assume the larger tetragonal distortion in chromium(II) acetate and copper(II) acetate, the observed value, 8~10 kK., seems to be too large for the splitting due to the tetragonal distortion.

As Table I shows, the first band of chromium(II) acetate anhydrate shows a remarkable blue shift relative to that of the hydrate. On the other hand, very little blue shift was observed in the second band. This implies that the second band is not as sensitive to the change in the tetragonality of the ligand field as the first band is. Therefore, the second band is not likely to be one of the ligand field bands, since if the band were split and shifted by the effect of the tetragonal distortion, it would show a considerable shift upon the change in the tetragonality.

The result of the dichroism measurements also support the above conclusion. If both the observed bands in the visible and near-ultraviolet region were due to the d-d transitions, the most probable assignment should be b_1-a_1 and b_1-e transitions for the first and the second band respectively, as may be seen in Fig. 5. Since the electric vectors transform like E(x, y) and $A_1(z)$ in the symmetry of C_{4v}, the second band, which has been attributed to the b_1-e transition, would be more intense in x and y than in z polarization. However, the experiments show that the second absorption is z-polarized in both compounds, as is shown in Fig. 4 and Ref. 5. Therefore, it is reasonable to assign the b_1-e transition to

* In this system the differences in the nuclear attractions and kinetic energies of the two states are negligibly small relative to $J(aa)$. The Coulomb integral, $J(aa)$, corresponds to the difference between the first and the second ionization energy of the ion.

14) "Atomic Energy Levels," Natl. Bur. Standards, Circ. 467, Vol. 2 (1952), p. 14.

15) T. M. Dunn, "The Visible and Ultra-violet Spectra of Complex Compounds," in J. Lewis and R. G. Wilkins, ed., "Modern Coordination Chemistry," Interscience Pub. Inc., New York (1960), pp. 253—261 and references therein.

the first absorption (x, y-polarized) rather than to the second. On this assumption, one can elucidate the fact that the first absorption band of chromium(II) acetate and copper(II) acetate are considerably more intense than the ligand field bands of usual monomeric chromium(II) (high spin type) and copper(II) complexes. Since the b_1-e transition is allowed in the x, y-plane in C_{4v} symmetry, whereas all the d-d transitions in D_{4h} symmetry are forbidden, one can expect a higher absorption in the former case than in the latter. The above discussion may be regarded as essentially correct, even though in these compounds the deviation from D_{4h} is not very large and the vibronic origin is not negligible.

For the origin of the second band, no definite conclusion can be drawn at present. However, since the second band is characteristic of this type of binuclear configuration, some orbitals, which are characteristic of this configuration, must be responsible for the origin of this band. For instance, the ligand and the metal atoms constitute planar 8-membered rings in this molecule, and some electronic transitions among the molecular orbitals of π-orbital systems on these rings may possibly be one of the origin of the second band. In this connection, however, it seems worth mentioning that cupric formate tetrahydrate and cupric benzoate trihydrate, which contain infinite chains, each consisting of alternate cupric ions and formate[6] or benzoate ions[16], show no absorption band corresponding to band II.

Summary

The electronic absorption spectra of chromium(II) acetate have been determined in ethanol and Nujol mull in the region between 10 and 40 kK. Dichroism in that region has also been determined with a single crystal of the compound. A new absorption band, which has not previously been observed, has been found at about 30.77 kK. ($\log \varepsilon$ 2.22), in addition to a band at about 20.58 kK.

The origins of these bands have been discussed in relation to the absorption bands of copper(II) acetate.

Department of Chemistry
Wakayama University
Masago-cho, Wakayama
(S. K., Y. N., Y. M. & K. N.)

Department of Chemistry
Faculty of Science
Osaka University
Nakanoshima, Osaka (S. Y.)

16) S. Yamada, H. Nishikawa and S. Miki, to be submitted.

Studies of the Metal Ketyls of Phenanthraquinone and Its Derivatives

By Kazuhiro MARUYAMA*1

(Received October 7, 1963)

The electron-spin resonance (ESR) spectra of the potassium ketyl of phenanthraquinone and of the zinc ketyl of phenanthraquinone have been studied by Kazakoba et al.[1] and Adams et al.[2] respectively. They obtained rather broad ESR signals. Recently a more precise study of the ketyl, produced electrolytically in an *N*, *N*-dimethylformamide solution with tetra-*n*-butylammonium perchlorate as a supporting electrolyte, has been reported by Dehl and Fraenkel.[3] The present author has been interested in how the free spin distribution varies with the introduction of a substituent into the aromatic nucleus. It is well known that the introduction of a substituent such as a chlorine atom and a nitro group into the aromatic nucleus of triphenylmethyl does not change its free spin distribution essentially.[4] However, the electron-spin resonance spectra of monosubstituted benzene mononegative anions are very sensitive to the nature of the substituent; small changes in the substituent can lead to drastic changes in the appearance of the spectrum.[5] Therefore,

*1 Present address: Department of Chemistry, Faculty of Science, Kyoto University, Kyoto.

1) V. M. Kazakoba et al., *Zhur. Strukt. Khim.*, 3, 536 (1962).

2) M. Adams, M. S. Blois, Jr., and R. H. Sands, *J. Chem. Phys.*, 28, 774 (1958).

3) D. Dehl and G. K. Fraenkel, ibid., 39, 1793 (1963).

4) M. T. Johns, ibid., 35, 1146 (1961). K. Maruyama, unpublished work.

5) J. A. Bedford, J. R. Bolton, A. Carrington and R. H. Prince, *Trans. Faraday Soc.*, 59, 53 (1963).

lithium-, sodium-, potassium-, cesium-, magnesium-, calcium and barium-ketyl of phenanthraquinone and the potassium-ketyls of 2-nitro-, 2, 7-dinitro-, 2, 7-dibromo- and 2, 7-diamino-phenanthraquinone are examined in the present study. Furthermore, the influence of metal species as a reducing agent upon the splitting constant and dimerization reaction of these ketyls is examined for the metal ketyls of phenanthraquinone in tetrahydrofuran.

Results and Discussion

Materials. — *Phenanthraquinone.*—Commercial phenanthraquinone was recrystallized from acetic acid; m. p. 207°C.

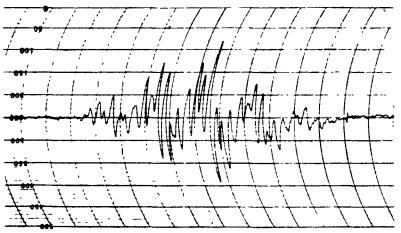


Fig. 1-1. Free ion radical, produced by reduction with potassium metal (liq. NH_3), overall width 7.8 gauss.

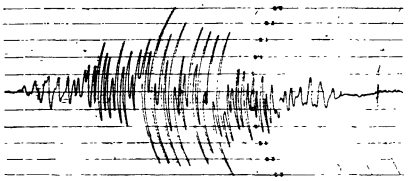


Fig. 1-2. Li-ketyl (THF), overall width 8.9 gauss.

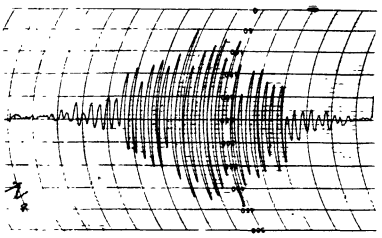


Fig. 1-3. Na-ketyl (THF), overall width 9.4 gauss.

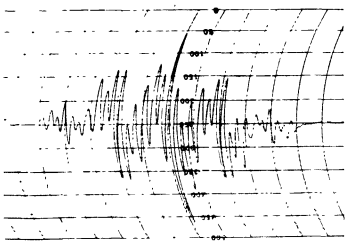


Fig. 1-4. K-ketyl (THF), overall width 8.0 gauss.

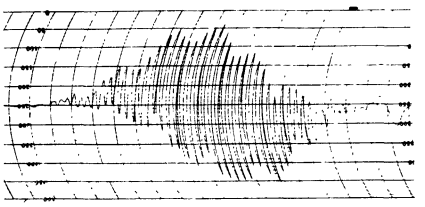


Fig. 1-5. Cs-ketyl (THF), overall width 9.85 gauss.

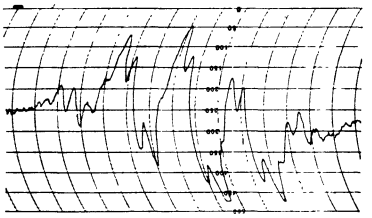


Fig. 1-6. Mg-ketyl (THF), overall width 9.6 gauss.

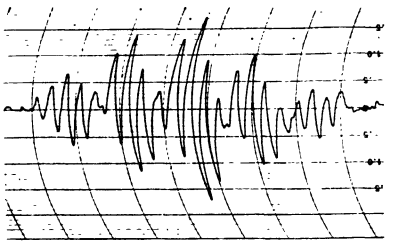


Fig. 1-7. Ca-ketyl (THF), overall width 9.6 gauss.

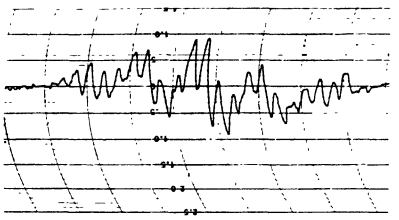


Fig. 1-8. Sr-ketyl (THF), overall width 9.1 gauss.

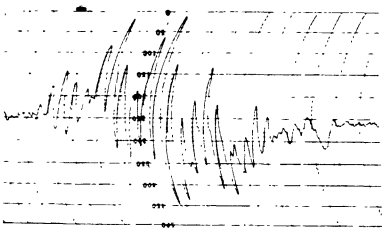


Fig. 1-9. Ba-ketyl (THF), overall width 9.5 gauss.

Fig. 1. ESR spectra of metal ketyls of phenanthraquinone.

TABLE I. SPLITTING CONSTANTS OF THE FREE ION RADICAL OF PHENANTHRAQUINONE IN LIQUID AMMONIA

		1st splitting	2nd splitting	3rd splitting
Equiv. hydrogen atoms		4H	2H	2H
Intensity ratio		1 : 4 : 6 : 4 : 1	1 : 2 : 1	1 : 2 : 1
Splitting constant (gauss)		1.56	0.44	0.36
Calculated free spin density	I[9]	0.0429 0.0399	0.0109	0.0077
	II[3]	0.068 0.056	−0.018	−0.006

Equiv.: equivalent

2-Nitrophenanthraquinone. — Commercial phenanthraquinone was treated with nitric acid (sp. gr. 1.4). The crude crystals were recrystallized from acetic acid; m. p. 257°C.

2,7-Dinitrophenanthraquinone. — Commercial phenanthraquinone was treated with a mixture of nitric acid (sp. gr. 1.5) and conc. sulfuric acid. The crude crystal was recrystallized from acetic acid; m. p. 302~303°C.

2,7-Dibromophenanthraquinone. — Commercial phenanthraquinone was treated with bromine in a sealed tube at 160°C. The crude crystal mass was recrystallized from acetic acid several times; m. p. 323°C.

2,7-Diaminophenanthraquinone. — 2,7-Dinitrophenanthraquinone was reduced by tin and hydrochloric acid. Recrystallization was performed from alcohol. The crystals were deep violet needles and did not melt even above 300°C.

Measurement. — *Metal Ketyl of Phenanthraquinone.*—The electron-spin resonance measurement was performed by using a spectrometer with an X-band, and 100 kc. modulation. The low temperature runs were made by allowing cool nitrogen gas evaporated from liquid nitrogen to flow through.

The electron-spin resonance spectra of metal ketyls of phenanthraquinone produced by reduction with different metals are shown in Fig. 1. It is well known that mononegative anions produced by reduction with an alkali or an alkali earth metal form ion pairs.[6,7] Therefore, the observed additional hyperfine structure from the metal cation attached to the radical may be taken to indicate the ion pair formation. The term "ion pair" is used to represent the associated counter ions which weakly perturb each other. As the metal ketyls form ion pairs in a usual solvent, such as tetrahydrofuran and dimethoxyethane, the details of each spectra are different because of the different nuclear-spin quantum numbers of the metals used as reducing agents. However, the largest splitting consists of the five lines (intensity ratio; 1 : 4 : 6 : 4 : 1) due to four equivalent hydrogen atoms on the phenanthraquinone ring. On the other hand, it has been reported that benzophenone and other ketyls do not show any metal splittings in liquid ammonia;[8] these ketyls do not form ion pairs in liquid ammonia but exist as completely dissociated mononegative anions. A mononegative anion in this state is designated by the term "free ion radical" in this article. From the examination of the spectrum of the free ion radical produced by the reduction of phenanthraquinone by potassium metal in liquid ammonia, it was found that the spectrum can be analysed into the following splitting pattern (Fig. 1-1, Table I).

Although the ESR spectra of metal ketyls of phenanthraquinone are more complicated than that of a free ion radical as the result of ion pair formation, their ESR spectra can be analyzed by means of a comparison of the spectrum with that of a free ion radical. Thus, the splitting constants of the first splitting due to the four equivalent hydrogen atoms of metal ketyls, which were in the ion-pair state in tetrahydrofuran, could be determined. These results are shown in Table II. It is interesting that the value of the splitting constant of the first splitting due to the four equivalent hydrogen atoms is affected by the species of metal. The cause of these changes in the splitting constants with the difference of metal is not clear. The same phenomena are found also in the case of the anion radical of nitrobenzophenone and others.[10]

6) N. M. Atherton and S. I. Weissman, *J. Am. Chem. Soc.*, **88**, 1330 (1961).
7) R. L. Ward, *J. Chem. Phys.*, **32**, 410 (1960); *J. Am. Chem. Soc.*, **83**, 1296 (1961).
8) N. Hirota, Thesis, Washington University, St. Louis 30, Mo., U. S. A. (1963).
9) A. Streitwiesser, Jr., "Molecular Orbital Theory for Organic Chemists," John Wiley & Sons, New York (1961), p. 156.
10) Reported at the 2nd ESR symposium, Kyoto (1963).

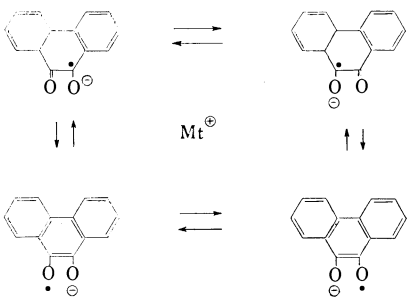
TABLE II. VARIATION OF SPLITTING CONSTANT BY CHANGING THE METAL IN THF

Metal	Overall width of spectrum (gauss)	Color of soln.	Splitting const. of the four equiv. hydrogen atoms (gauss)
Li	10.8	green*2	2.2
Na	9.4	green-red*2	1.7
K	8.0	red	1.5
Cs	9.8	red	—
Mg	9.6	green	1.7
Ca	9.6	green	1.7
Sr	9.1	green	1.6
Ba	9.5	green	1.6

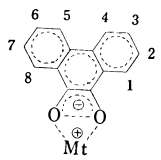
THF: tetrahydrofuran

The ESR spectra of metal ketyls of phenanthraquinone have a narrower overall width (the largest splitting constant due to the four equivalent hydrogen atoms is 1.56 gauss) than the metal ketyl of benzophenone (the largest splitting constant due to para hydrogen atoms is 3.4 gauss.[8]) This means that most of the free spin is accummulated around two carbonyl groups.

The structure of ketyl of phenanthraquinone may be represented by the next resonance formula (structure I), or it may be expressed more conveniently by structure II. The results shown in Table I can be satisfactorily explained by considering the structure proposed and the results of calculations.[3,9] That



Structure I Mt: metal



Structure II Mt: metal

is, H_1, H_3, H_6 and H_8 are responsible for the first splitting, and H_4 and H_5 are responsible for the second splitting for a reason which will be described later; therefore, H_2 and H_7 are responsible for the third splitting.

The Metal Ketyl of Phenanthraquinone Derivatives. — The spectra obtained are shown in Fig. 2. From a comparision of the spectra of 2,7-dibromophenanthraquinone potassium ketyl (Fig. 2-3) and of the free ion radical phenanthraquinone (Fig. 1-1), it can be concluded that the second splitting is caused by the two equivalent hydrogen atoms H_4 and H_5, because

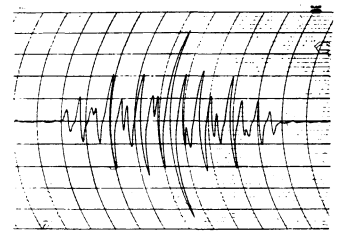


Fig. 2-1. K-ketyl of 2-nitrophenanthraquinone (THF), overall width 7.3 gauss.

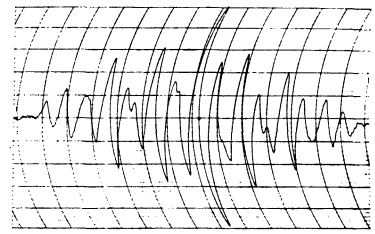


Fig. 2-2. K-ketyl of 2,7-dinitrophenanthraquinone (THF), overall width 7.1 gauss.

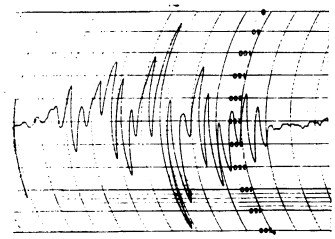


Fig. 2-3. K-ketyl of 2,7-dibromophenanthraquinone (THF), overall width 7.5 gauss.

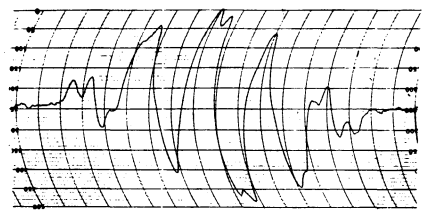


Fig. 2-4. K-ketyl of 2,7-diaminophenanthraquinone (THF), overall width 8.0 gauss.

Fig. 2. Metal ketyls of phenanthraquinone derivatives.

*2 The red substance is paramagnetic. The green substance is diamagnetic and this becomes a red substance in an extremely dilute state. The red substance becomes yellow if it is in contact with a metallic surface; furthermore, this yellow substance is diamagnetic, This yellow substance becomes a red paramagnetic solution when it is mixed with a solution in which unreduced phenanthraquinone remains. Therefore, the yellow substance is a dinegative anion.

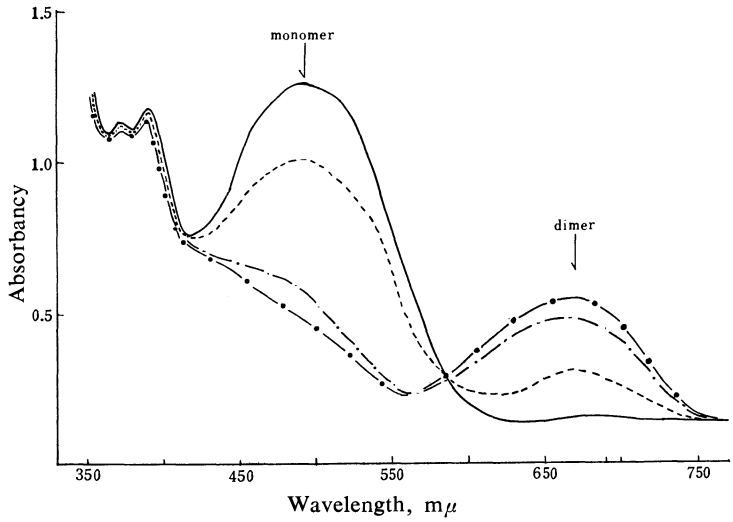


Fig. 3. Absorption spectra of Na-ketyl of phenanthraquinone at different temperatures.
——— 23°C ------ −30°C —·—· −70°C —•—• −85°C

the bromine atom, in general, does not show ESR splitting. This experimental result coincides with calculations based on the molecular orbital theory.[3,9],*3 With regard to the effect of the introduction of substituents into the aromatic nucleus upon free spin distribution, it seems reasonable to deduce that the introduction of bromine and amino groups does not change the intensity ratio (1 : 4 : 6 : 4 : 1) of the five line groups due to the four equivalent hydrogen atoms, but that the introduction of a nitro group does change the appearance of the spectrum. That is, i) in the K-ketyl of 2-nitrophenanthraquinone, the number of apparent line groups in the spectrum is seven and the intensity ratio is nearly 1 : 3 : 3 : 6 : 3 : 3 : 1, and ii) in the K-ketyl of 2, 7-dinitrophenanthraquinone, the number of the apparent line groups is seven and the intensity ratio is nearly 1 : 2.5 : 3.5 : 6 : 3.5 : 2.5 : 1. However, the obtained spectra were too broad to obtain a quantitative estimation of the effect.

Equilibrium between Paramagnetic Monomers and Diamagnetic Dimers. — The existence of an equilibrium between the metal ketyl monomer and the dimer was examined by means of a study of absorption spectra in the visible region and by an absolute free spin determination by an overmodulated ESR technique.[11] The results of the examination of the absorption of metal ketyls of phenanthraquinone in the visible region at different temperatures and with different reducing alkali metals are shown in Table III and Fig. 3.

Table III. Absorption spectra of metal ketyls of phenanthraquinone at different temperatures

Metal	Temp. °C	Paramagnetic monomer mμ	Diamagnetic dimer mμ
Li	23	484 v.s.	646 w.
	−50	484 w.	646 s.
	−70	—	646 v.s.
Na	23	494 v.s.	670 v.w.
	−30	494 s.	670 w.
	−85		670 v.s.
K	23	507 v.s.	
	−60	507 v.w.	641 s.
	−85	507 v.w.	641 v.s.
Mg	23	508 w.	646 w.
	−80	—	646 s.
Ca	23	—	670 v.s.
	−80	—	670 v.s.
Sr	23	—	670 v.s.
Ba	23	—	687 v.s.

Solvent : THF

v.w. : very weak
v.s. : very strong
w. : weak
s. : strong

It is interresting to note that the diamagnetic dimer shows an absorption band at longer wavelength region than does the paramagnetic monomer.

*3 The splitting constant changes with the solvent and with the metal species used as a reducing agent. This coincidence with the results of molecular orbital calculations is, therefore, only a rough estimate.

11) a) K. Halbach, *Phys. Rev.*, **119**, 1230 (1960); b) J. E. Hyde and H. W. Brown, *J. Chem. Phys.*, **37**, 368 (1962).

On the other hand, the decrease of paramagnetic species with a decrease in temperature, was examined with the aid of an overmodulated ESR technique. This results are shown in Fig. 4. This process was found to be completely reversible by a temperature change. The tendency to dimerization is especially strong when a divalent metal such as magnesium, calcium, strontium or barium was used as the reducing agent. Almost all the metal ketyls produced from these reducing agents (in tetrahydrofuran and dimethoxyethane) dimerize in an equilibrium state at room temperature (color: green) except when they were extremely dilute (color: red). Even if the metal ketyl solutions were made by the reduction of phenanthraquinone with lithium, sodium and potassium, they became green when at a high concentration. Only the metal ketyl solution produced by reduction with cesium was strongly red even if it was at a high concentration at room temperature. These results accord with absorption spectrum examinations and with ESR measurements.

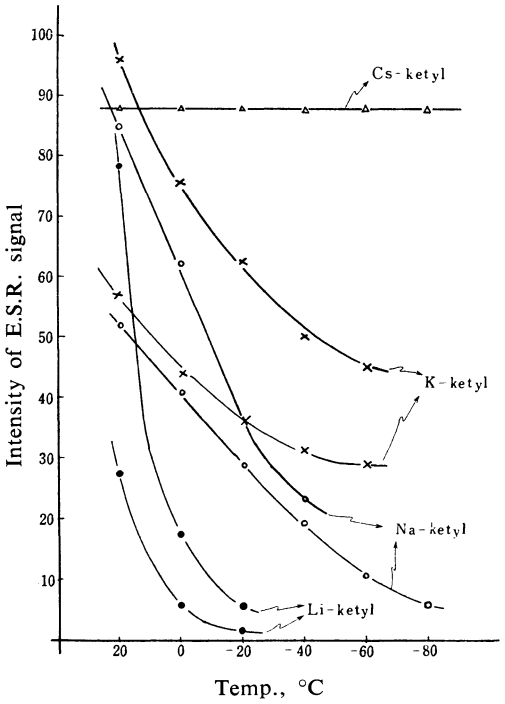


Fig. 4. Change of paramagnetic species with temperature.

To summarize the facts mentioned above:

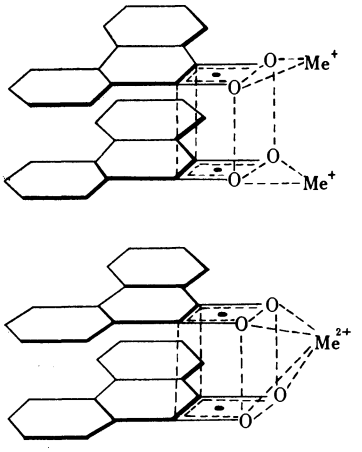
i) The dimer shows absorption at a longer wavelength region (~650 mμ) than the paramagnetic monomer (~500 mμ);

ii) The dimerization reaction is completely reversible with temperature and with concentration, and the dimer is diamagnetic;

iii) The tendency to form dimers is more remarkable in the metal ketyls produced by reduction with metals of smaller atomic size than in the metal ketyls produced by reduction with monovalent metals of larger atomic size. The metal ketyl produced by reduction with cesium metal does not appreciably dimerize even at −80°C.

iv) Metal ketyls produced by reduction with divalent metals show a strong tendency to dimerize.

Considering these results, the following structure, III, seems to be the most favorable for the diamagnetic dimer:



Structure III

The author wishes to express his gratitude to Professor S. I. Weissman for his helpful discussions and encouragement.

Department of Chemistry
Washington University
St. Louis 30, Missouri, U. S. A.

*The Ultrasonic Velocity and Absorption of Aqueous Solutions of Polyvinyl Alcohol**

By Kiyoshi ARAKAWA, Nobuo TAKENAKA, Mineo WATASE and Kazunari KUBOTA**

(Received December 4, 1963)

A number of rheological studies of polymer solutions have been made by various authors. However, for the aqueous solution of polyvinyl alcohol we do not have much information concerning the rheological properties of the solution except for those obtained by the method of stationary flow viscosity. At audio frequencies an extensive study of the dynamic mechanical properties of the solution has been made recently by Onogi and his co-workers.[1] At ultrasonic frequencies several studies by means of ultrasonic interferometers have been made,[2] but with limited success.

Recently, an ultrasonic pulse technique has been developed as the most convenient and standard means for the study of the rheological properties of liquids and solutions at ultrasonic frequencies.[3] In the present experiment we measure the velocity and absorption of the longitudinal sound wave which propagate through an aqueous solution of polyvinyl alcohol.

The oscillational displacement, ξ, at a distance, x, from a source of a sound wave is:

$$\xi=\xi_0 \exp(-\alpha x) \exp\{i\omega(t-x/c)\} \qquad (1)$$

where c is the sound velocity, ω the angular frequency, ξ_0 the amplitude of oscillation, α the absorption coefficient, and t time.

The complex longitudinal wave modulus, M^*, in an infinitely spread medium is:

$$M^*=M_1+iM_2=K^*+(4/3)G^* \qquad (2)$$

where K^* is the complex bulk modulus and G^* is the complex shear modulus.

The real part, M_1, and the imaginary part, M_2, of the complex modulus, M^*, are respectively, expressed as follows;

$$M_1=K_1+\frac{4}{3}G_1=\rho c_l^2 \frac{1-\left(\frac{\alpha_l c_l}{\omega}\right)^2}{\left\{1+\left(\frac{\alpha_l c_l}{\omega}\right)^2\right\}^2} \qquad (3)$$

$$M_2=K_2+\frac{4}{3}G_2=\rho c_l^2 \frac{2\left(\frac{\alpha_l c_l}{\omega}\right)}{\left\{1+\left(\frac{\alpha_l c_l}{\omega}\right)^2\right\}^2} \qquad (4)$$

where ρ is the density and where the suffix l refers to a longitudinal wave.

According to Eqs. 3 and 4 described above, we can obtain the dynamic elastic modulus, M_1, and the loss modulus, M_2, from the values of c_l and α_l.

Experimental

Apparatus and Procedure.—The apparatus used in this experiment for the measurement of the velocity and absorption of a longitudinal ultrasonic wave, is basically similar to that reported previously by Pinkerton and others.[3] A block diagram of it is shown in Fig. 1.

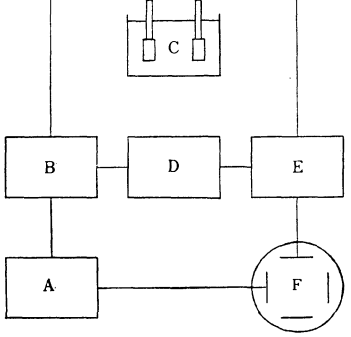


Fig. 1. Block diagram of the apparatus.
A: Pulse generator B: Oscillator
C: Cell D: Attenuator
E: Amplifier F: Synchroscope

A pulse generator supplies an electric pulse of about 10 μ sec. duration and with a repetition rate of 2~5 kc./sec. into a high-frequency oscillator, which operates as an oscillator only during the loading period of the pulse. The pulse-modulated high frequency voltage from the oscillator is led

* Presented in part at the 11th Annual Rheology Symposium, Osaka, October, 1962.

** Present address: Fuji Electric Mfg. Co., Ltd., Matsumoto, Nagano.

1) S. Onogi, I. Hamana and H. Hirai, *J. Appl. Phys.*, **29** 1503 (1958).

2) T. Soeya and R. Kono, *J. Phys. Soc. Japan*, **12**, 950 (1957); H. Shiio and H. Yoshihashi, *J. Phys. Chem.*, **60**, 1049 (1956); T. Yasunaga, K. Iwata and M. Miura, The 7th Annual Symposium of Sound Chemistry, Hiroshima, 1962.

3) J. M. M. Pinkerton, *Proc. Phys. Soc. (London)*, **B62**, 86 (1949); L. Melchor and A. A. Petrauskas, *Ind. Eng. Chem.*, **44**, 716 (1952); D. G. Ivey, B. A. Mrowca and E. Guth, *J. Appl. Phys.*, **20**, 486 (1949).

to a transmitter quartz crystal in a cell which contains a sample solution and is there transduced into an ultrasonic pulse. At the same time, the electric pulse is led also to an attenuator. An ultrasonic pulse which has propagated through the solution is again transduced into a pulse-modulated high frequency voltage by a receiver quartz crystal. The two pulses from the receiver quartz and the attenuator are amplified and, thereafter, supplied into the vertical axis of a synchroscope.

The velocity of the sound wave in a solution is obtained from the amount of the shift of the pulse which has propagated through the solution on the synchroscope screen when the separation of two quartz crystals is varied by the rotation of a micrometer screw.

The absorption coefficient α is obtained by comparing the pulse which has passed through the solution with that which has passed through the attenuator on the synchroscope screen. That is, α is obtained from the tangent of the linear plot of the attenuator reading against the distance between two quartz transducers, when the ultrasonic path is varied and when the height of the two pulses is kept equal by adjusting the attenuator. The separation of two quartz transducers is designed to be always within the Fresnel region.[3]

Samples.—Two commercial samples of polyvinyl alcohol were used. The specification of each sample is given in Table I.

TABLE I. SAMPLES

Sample	Intrisic viscosity $[\eta]_{30°C}$ (100 cc./g.)	Residual acetate groups (mol. %)
A	0.91	<0.7
B	1.00	12.2

The intrinsic viscosity of each aqueous solution at 30°C, $[\eta]_{30}$ was obtained by mean of an Ostwald-type viscometer. The amounts of residual acetate groups were determined by the titration method. The viscosity average molecular weight of sample A, $\overline{M}_V$, was found to be 8×10^4 from the value of $[\eta]_{30°C}$ according to the following formula reported by Nakajima and Furutate:[4]

$$[\eta]_{30°C}=6.66\times10^{-4}\,\overline{M}_V^{0.64} \qquad (5)$$

The integral molecular weight distribution function of sample A was determined by using Spencer's method according to the procedure reported by M. Matsumoto.[5] The integral distribution curve thus obtained is given in Fig. 2.

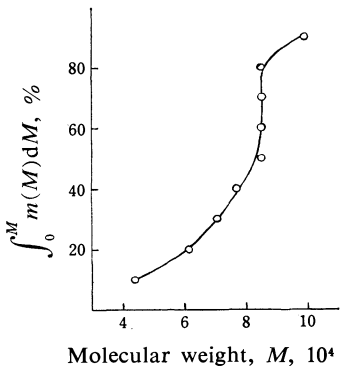


Fig. 2. Integral molecular weight distribution function for sample A obtained from the solution component by Spencer's method.

From the curve it may be seen that the distribution function, $m(M)$, has a sharp peak at 8.5×10^4.

Aqueous solutions of polyvinyl alcohol were prepared as follows. The aqueous solutions were prepared by heating a mixture of a powder sample and a calculated quantity of water, (where the quantity of adsorbed water in a powder sample as determined by the dessication method was taken into account) on a boiling water bath for more than two hours. The solution was poured into a cell which was held in a temperature bath directly after the sample had been completely dissolved, and then the measurement was begun as soon as the thermal equilibrium in the cell was reached.

Measurement. — In this experiment the sound velocity and the absorption were measured for solutions of sample A in which the range of concentration was over 5~15% by weight and also for solutions of sample B in which the range of concentration was 5 and 10% by weight. The temperature was varied within the range of 3~70°C at 10°C intervals. The temperature in the cell was controlled to an accuracy of ±0.1°C for lower temperatures and ±0.2°C for higher temperatures. The frequency of the ultrasound was 1.42 Mc./sec. for all measurements throughout this experiment.

Results and Discussions

Data of Sound Velocity and Absorption.—In

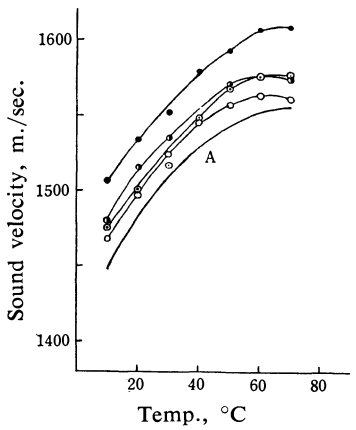


Fig. 3. Sound velocity of the aqueous solutions of sample A.
Concn., wt.%
○ : 5.0, ⊙ : 7.5, ◑ : 10.0, ● : 15.0
(A) Pure water

4) A. Nakajima and K. Furutate, *Chem. High Polymers (Kobunshi Kagaku)*, **6**, 460 (1949).
5) M. Matsumoto, ibid., **9**, 137 (1952).

Fig. 3 the sound velocity obtained for solutions of sample A is plotted against the temperature, while the velocity for solutions of sample B is similarly treated in Fig. 4. The velocity versus temperature curve for pure water reported by Greenspan and Tschiegg[6] is also shown in Figs. 3 and 4 for the sake of comparison. Figures 5 and 6 give, respectively, data of sound absorption for solutions of samples A and B.

The values of M_1 and M_2 were calculated according to Eqs. 3 and 4 for all the solutions used in this experiment. Two examples of M_1 and M_2 versus T curves are given in Figs. 7 and 8, where values of M_2/ω are plotted in place of those of M_2 for the convenience of further discussions.

It is well known that the sound velocity versus temperature curve for pure water at ultrasonic frequencies has a peak at 74°C, and that the maximum value of velocity is 1555.5

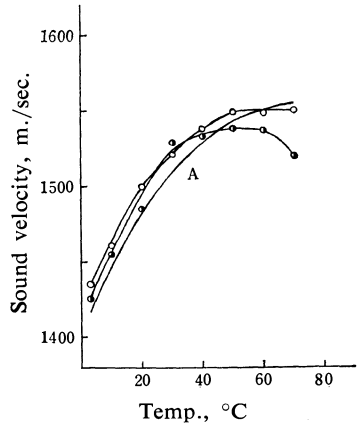


Fig. 4. Sound velocity of aqueous solutions of sample B.
Concn., wt.%
○ : 5.0, ◑ : 10.0
(A) Pure water

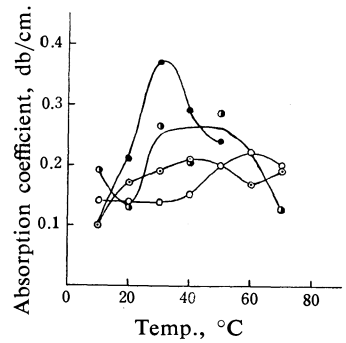


Fig. 5. Sound absorption of the aqueous solutions of sample A.
Concn., wt.%
○ : 5.0, ⊙ : 7.5, ◑ : 10.0, ● : 15.0

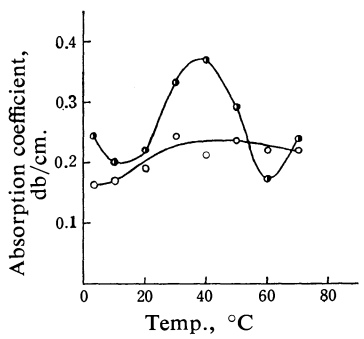


Fig. 6. Sound absorption of the aqueous solutions of sample B.
Concn., wt.%
○ : 5.0, ◑ : 10.0

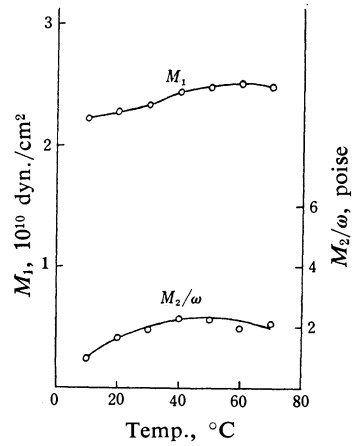


Fig. 7. M_1 and M_2/ω versus T curves of the aqueous solution of sample A.
(7.5 wt.%)

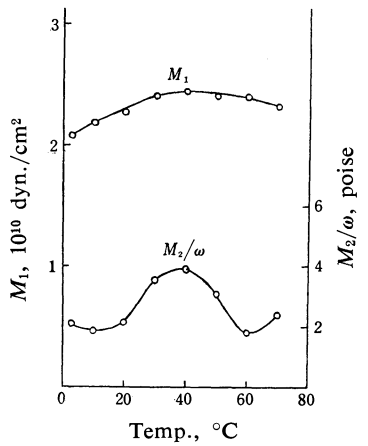


Fig. 8. M_1 and M_2/ω versus T curves of the aqueous solution of sample B.
(10 wt.%)

6) M. Greenspan and C. E. Tschiegg, *J. Res. Nat. Bur. Standards*, **59**, 249 (1957); *J. Acoust. Soc. Am.*, **31**, 75 (1959).

m./sec.[6-7] Concerning the temperature dependence of the sound velocity, the curves given in Fig. 3 for solutions of sample A, which is completely saponified polyvinyl alcohol, are found to have, on the whole, characteristics similar to the curve for pure water, though the peaks of the curves of sample A seem to shift to a little lower temperature side than in those of the latter. For solutions of sample B which contain acetate groups and hydroxyl groups in a mole ratio of about one to eight, the situation appears quite different, as may be seen in Fig. 4.

The peak of velocity versus temperature curve becomes broader and shifts towards a lower temperature region than do the curves for solutions of sample A and for pure water.

Concerning the concentration dependence of the sound velocity, each curve shown in Fig. 3 may be clearly seen to ascend upon an increase in the concentration. In this respect also, the circumstances for solutions of sample B appear to differ considerably from those for sample A, as may be seen in Fig. 4. In the lower temperature region the concentration dependence of the sound velocity for solutions of sample B does not seem to differ much from that for solutions of sample A, but when temperature is raised above about 50°C, the concentration dependence is found to have a reverse tendency; that is to say, the sound velocity becomes smaller with an increase in the concentration for solutions of sample B. This fact suggests that the configuration of high polymers in aqueous solutions of sample B differs considerably from that in solutions of sample A, and that this different behavior may safely be attributed to the presence of acetate groups in the proportion of about one to eight by mole ratio.

The absorption of ultrasound is found to increase with the concentration for both groups of solutions, as may clearly be seen in Table II from the values of the absorption coefficient α_m averaged over the temperature range used in the present experiment. In Table II the values of $(M_2/\omega)_m$ which are averaged over the temperature range are also given, together with the values of the temperature, T_{max}, where the M_2/ω versus T curve has a peak.

TABLE II. DATA OF SOUND ABSORPTION

Sample	Concn., c wt.%	α_m db/cm.	$(M_2/\omega)_m$ poise	T_{max} °C
A	5.0	0.17	1.8	60
	7.5	0.18	1.9	50
	10.0	0.21	2.3	50
	15.0	0.24	2.8	35
B	5.0	0.21	2.1	50
	10.0	0.26	2.6	40

The values of $(M_2/\omega)_m$ are nearly all within the range of 2~3 poises. According to the results reported by Onogi and his co-workers,[1] the values of (G_2/ω) are found to approach the value of about 10 poises or so for 15% solutions at audio frequencies, for example, as may be seen in Fig. 15 of their paper. Our values at the ultrasonic frequency may tentatively be said to be compatible with those of Onogi et al. at audio frequencyies, although our data with respect to M_2/ω, of course, include the contribution from the imaginary part of the bulk modulus, K^*.

The Compressibility of Polymer Molecules in Solutions.—Concerning the compressibility of polymer molecules in solutions, Miyahara, Shiio and others have made several studies by means of ultrasonic interferometers.[8]

We calculate the compressibility of polymer molecules in solutions as follows.

The volume of an aqueous solution V is

$$V = V_1 + V_2 + V_3 \tag{6}$$

where V_1 is the volume of free water, V_2 the volume of bound water, and V_3 the volume of polymer molecules in the solution.

Therefore, the adiabatic compressibility, κ, of the solution may be represented as follows:

$$\kappa = (V_1/V)\kappa_1 + (V_2/V)\kappa_2 + (V_3/V)\kappa_3 \tag{7}$$

where κ_1 is the adiabatic compressibility of free water, κ_2 the adiabatic compressibility of bound water, and κ_3 the adiabatic compressibility of polymer molecules in solutions.

We can obtain values of κ from the data of the sound velocity described above, ignoring the contribution from the shear elasticity, which is supposed to be much smaller than that from the bulk elasticity.[8-9] The values of κ_1 are calculated from the data for pure water reported by Greespan et al.[6] For the values of the compressibility of bound water, κ_2, the value 18×10^{-12} (c.g.s.) is substituted, following Hall and others;[8,10] this is assumed to be the value for the ice structure in water. As has previously been pointed out by Shiio;[11] bound water, which is attracted to solute molecules by a hydrogen bond, is supposed to be in a different state from ordinary water,

7) M. Greenspan, C. E. Tschiegg and F. Breckenridge, *J. Acoust. Soc. Am.*, **28**, 500 (1956).

8) Y. Miyahara and Y. Masuda, *Science (Kagaku)*, **30**, 588 (1960); *J. Chem. Soc. Japan, Pure Chem. Sec. (Nippon Kagaku Zasshi)*, **81**, 692 (1960); Y. Masuda, T. Hasegawa and Y. Miyahara, ibid., **82**, 1131 (1961); Y. Masuda and Y. Miyahara, ibid., **83**, 878 (1962); H. Shiio and H. Yoshihashi, *J. Phys. Chem.*, **60**, 1049 (1956); H. Shiio, T. Ogawa and H. Yoshihashi, *J. Am. Chem. Soc.*, **77**, 4980 (1955).

9) E. Rouse and L. Sittel, *J. Appl. Phys.*, **24**, 690 (1953).

10) L. Hall, *Phys. Rev.*, **73**, 775 (1948).

assumed, that is to say, to be already in a kind of "solid state" at ordinary temperatures. Therefore, it may be reasonable to assign the same value as that of the compressibility of ice to the value of the compressibility of bound water, κ_2. The value of V_2 is estimated from the amount of bound water, for which the value of 0.45 cc. per gram solute is assigned, as reported by Shiio et al.*,[2] The value of V_3 is calculated from the value of concentration by weight in solutions without much error, where the density of solute molecules is assumed to be 1.3 g./cc., which is the value of the density of polyvinyl alcohol in the solid state. The value of V_1 is calculated from the values of V_2 and V_3 according to Eq. 6. The values of κ_3 for solutions of sample A may now calculated from Eq. 7 as in Table III.

Table III. Values of κ_3 at 25°C

Concn., wt.%	5.0	7.5	10.0	15.0	Mean value
κ_3, 10^{-12} c.g.s.	29.5	28.7	23.7	24.0	26.5

In Table III the values of κ_3 may be seen to decrease gradually with the increase in concentration. On the other hand the tendency to decrease is small, and we will not discuss it here. Rather, the fact that the values of κ_3 are nearly equal in spite of a fairly large difference in concentration has been noted; this finding may be said to support the adequacy of employing the concept, "compressibility of solute molecules in a polymer solution," as proposed by Masuda, Hasegawa and Miyahara.[8] In the present case where polymer molecules are supposed to be spread throughout a solution, a polymer solution is regarded as a hypothetical mixture of segments of polymer molecules and solvent molecules, and the compressibility, κ_3, which we discuss here may be regarded as that of the segments in the solution. It may be said that the term "segment" employed here is not always identical with "segment" in the ordinary sense. The values of κ_3 we obtained here are larger than that reported by Shiio et al.[2] However, the discrepancy does not matter at present considering the difference in the procedure for the determination of κ_3.

* Yasunaga et al. have recently reported that the amount of bound water is 0.46 cc./g.[2]

11) H. Shiio, *Kagaku no Ryoiki*, **11**, 440 (1957).

Summary and Conclusions

An ultrasonic pulse technique has been applied to measure the velocity and absorption of the longitudinal sound wave in aqueous solutions of polyvinyl alcohol at ultrasonic frequencies. Two samples of polyvinyl alcohol have been used: sample A, completely saponified polyvinyl alcohol, and, sample B, partially saponified Polyvinyl alcohol (including residual acetate groups by 12.2 mol.%). The following results have been obtained.

1) Ultrasonic velocity and absorption have been measured over the temperature range of 3~70°C in the concentration range of 5~15% by weight.

2) For sample A the temperature dependence of velocity is similar to that for pure water, but for sample B the velocity vs. temperature curves have been found to have a broader peak.

3) Concerning the concentration dependence of the velocity, in sample A the sound velocity increases with the increase in the concentration, but in sample B a reverse dependence of velocity on concentration has been found at higher temperatures.

4) The value of M_2/ω amounts to about 2~3 poises on the average for both samples.

5) The compressibility of polymer molecules in solutions has been calculated to be 26.5×10^{-12} c.g.s.u. on the average for completely saponified polyvinyl alcohol.

The authors wish to thank Mr. Yoshihisa Nagashima and Mr. Keiichi Kasuga for their cooperation in performing this experiment.

Research Institute of Applied Electricity
Hokkaido University
Sapporo (K. A. & N. T.)

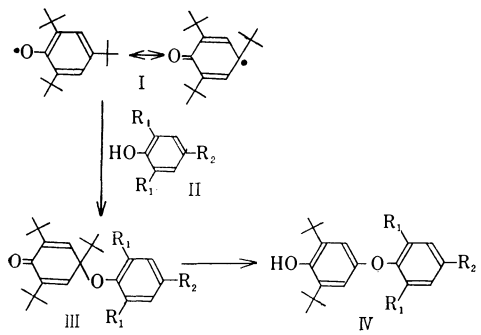
Faculty of Engineering
Shizuoka University
Hamamatsu (M. W. & K. K.)

The Photochemical Transformation of Some p-Quinol Ethers[1]

By Teruo MATSUURA[2]

(Received December 5, 1963)

In our previous reports on the biosynthetic mechanism of thyroxine formation, several quinol ethers III were synthesized by the tri-*t*-butylphenoxy radical I with analogs II of diiodotyrosine.[3,4] Some of these quinol ethers were also converted into analogs IV of thyroxine by reaction with acid or by pyrolsis. This sequenece of reactions represents a complete model for the mechanism by which, according to Johnson and Tewkesbury,[5] thyroxine is synthesized from two molecules of diiodotyrosine *in vivo*. On the basis of the assumption that quinol ethers of type III may be converted into analogs of thyroxine by ultraviolet irradiation, we initiated the photochemical reactions of these quinol ethers. A preliminary investigation of the photoreaction of the quinol ether (III: $R_1=H$, $R_2=(CH_2)_2$-COOEt) gave quite complex results.



R_1=H ; Br ; I
R_2=$(CH_2)_2COOC_2H_5$; $CH_2CH(NH_2)COOH$, etc.

Therefore, the quinol ether V[6] was chosen as the first compound to be studied in the systematic investigation of the photochemical behavior of such quinol ethers.

The irradiation of the quinol ether V[6] in methanol under bubbling nitrogen gave a photoketone $C_{19}H_{32}O_2$ (VI), isomeric to V, in an 11% yield and tri-*t*-butylphenol (VII) in a 3% yield. The photoketone VI was characterized as a conjugated enone from its ultraviolet spectrum (λ_{max} 248 and 282 mμ) and its infrared spectrum (1650 and 1630 cm^{-1}). The structure of VI was indicated by its NMR spectrum (Table I), which consists of four groups of peaks, and by considering the analogous transformation of 2, 5-cyclohexadienones into "photoketones" with bicyclo[3, 1, 0]hex-2-ene-1-one structures.[7,8] Three peaks, at τ=9.07, 8.81 and 8.75, and a singlet at τ=6.40 are readily assigned to the three *t*-butyl groups and a methoxyl group respectively. Two other doublets, at τ=7.03 and 3.67, are attributed to an allylic proton on a cyclopropane ring conjugated with a double bond[9] and to a proton of a double bond. The spin-spin coupling constant (J= 6 c.p.s.) of these doublets suggests that these two protons may be adjacent to each other.

On the other hand, the irradiation of V in ether gave a crytalline photophenol $C_{15}H_{24}O_2$ (VIII) in a 10% yield, in addition to a small amount of VI. The dealkylation of this phenol with aluminum chloride in hot benzene yielded pyrocatechol. The NMR spectrum of VIII shows the presence of two adjacent protons on a benzene ring (AB type quartet, centering at τ=3.27; J=8.5 c.p.s.). The infrared spectrum (815 cm^{-1}) also indicates two adjacent hydrogen atoms on a benzene ring. Therefore, it follows that the structure of the photophenol is represented by the formula VIII, VIIIa, or VIIIb. Among these three formulae, the structure VIII is assigned to the photophenol by considering that the minimum rearrangement has occurred, and by reasoning on the basis of a pre-considered mechanism.

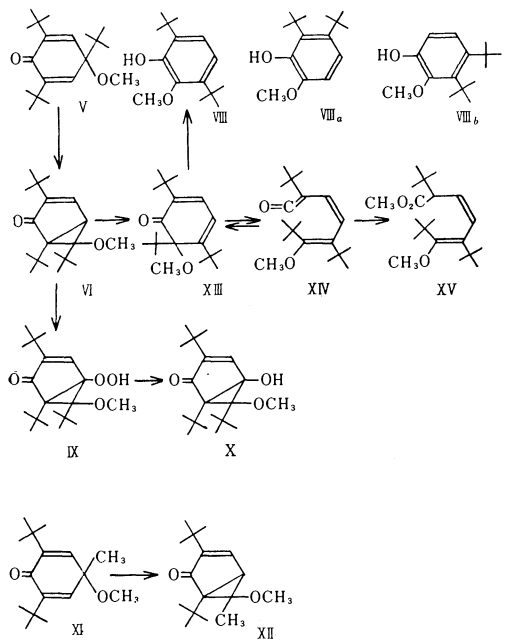
In the presence of oxygen, the irradiation of V in ether gave the photophenol VIII and a crystalline product (IX) $C_{19}H_{32}O_4$ in an 11% yield. The hydroperoxyl nature of IX was

1) This work was presented at the 16th Annual Meeting of the Chemical Society of Japan, April, 1963.
2) The author's present address: Department of Synthetic Chemistry, Faculty of Engineering, Kyoto University, Yoshida, Kyoto.
3) T. Matsuura and H. J. Cahnmann, *J. Am. Chem. Soc.*, **82**, 2055 (1960).
4) T. Matsuura and A. Nishinaga, *J. Org. Chem.*, **27**, 3072 (1962).
5) T. B. Johnson and L. B. Tewkesbury, Jr., *Proc. Natl. Acad. Sci. U. S.*, **28**, 73 (1942).
6) E. Müller, K. Ley and W. Kiedaisch, *Chem. Ber.*, **87** 1605 (1954).
7) a) D. H. R. Barton, P. de Mayo and M. Shafiq, *J. Chem. Soc.*, **1958**, 140; b) D. Arigoni, H. Bosshard, H. Bruderer, G. Büchi, O. Jeger and L. J. Krebaum, *Helv. Chim. Acta*, **40**, 1732 (1957).
8) H. E. Zimmerman and D. I. Schuster, ibid., **83**, 4486 (1961); **84**, 4527 (1962).
9) R. Huisgen and G. Juppe, *Chem. Ber.*, **94**, 2332 (1961).

TABLE I. CHEMICAL SHIFTS AND SPIN-SPIN COULING CONRTANTS*

Compound	Chemical shifts[a] of protons				
	t-Butyl	Methoxyl	Vinyl	Cyclopropyl	Others
V[b]	9.08 s (9) 8.77 s (18)	6.88 s (3)	3.55 s (3)	—	—
VI[b]	9.07 s (9) 8.81 s (9) 8.75 s (9)	6.40 s (3)	3.67 d (1) (J=6 c.p.s.)	7.03 d (1) (J=6 c.p.s.)	—
VIII[b]	8.62 s (18)	6.21 s (3)	3.27 q (2)[d] (J=8.5 c.p.s.)	—	4.45 s (1)[e]
IX[c]	9.01 s (9) 8.75 s (9) 8.67 s (9)	6.00 s (3)	3.58 s (1)	—	2.03 s (1)[f]
X[c]	9.03 s (9) 8.77 s (9) 8.67 s (9)	6.15 s (3)	3.70 s (1)	—	7.93 s (1)[e]
XII[b]	8.92 s (9) 8.88 s (9)	6.96 s (3)	3.17 d (1) (J=3.5 c.p.s.)	8.02 d (1) (J=3.5 c.p.s.)	8.45 s (3)[g]
XI[b]	8.78 s (18)	6.97 s (3)	3.70 s (1)	—	8.70 s (3)[g]

* The NMR spectra were taken in a Varian A-60. a) τ-values: internal TMS reference. s, singlet; d, doublet; q, quartet. Proton numbers in parentheses. b) Taken in carbon tetrachloride (ca. 5% solution). c) Taken in deuteriochloroform (ca. 5% solution). d) Aromatic protons. e) Hydroxyl proton. f) Hydroperoxyl proton. g) Methyl protons.

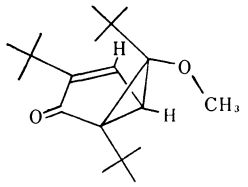


confirmed by the reaction with potassium iodide to yied two equivalents of iodine and a hydroxyl compound (X), $C_{19}H_{32}O_3$. The ultraviolet spectra of IX (λ_{max} 237 and 285 mμ) and of X (λ_{max} 237 and 256.5 mμ; λ_{infl} 290 mμ) and the infrared spectra of IX (1665 and 1625 cm^{-1}) and of X (1660 and 1630 cm^{-1}) indicate the presence of a conjugated enone. The NMR spectrum of IX shows no peak corresponding to a cyclopropane proton conjugated with the double bond, but it does show a singlet at τ=2.03, which is assigned to a hydroperoxyl proton. In this case, the peak attributed to the double bond proton (τ=3.58) is not split. We can thus formulate the hydroperoxide and the hydroxy compound as IX and X respectively. The formation of the hydroperoxide can be explained the photo-induced allylic oxidation[10] of the photoketone VI.

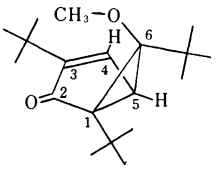
The irradiation of the quinol ether XI[11] in ether gave a crystalline photoketone XII in an 11% yield, whereas irradiation in methanol did not give crystalline products. The structure is assigned to the formula XII by the interpretation of its NMR spectrum, which is similar to that of VI (Table I). The photoketone is unstable, and, on standing for several weeks, it liquefied to form a unidentified product.

Recently Zimmerman and Schuster proposed a mechanism for the photochemical rearrangement of 4, 4-diphenylcyclohexa-2, 5-dienone.[8] This mechanism involves the $n\rightarrow\pi^*$ excitation of the cyclohexadienone system as the initiating step, and it can also account for the formation of VI, VIII and XII. The fact that the phenol VIII is not formed on the irradiation of V in methanol may be due to the conversion of XIII, under these conditions, into the ester XV via the ketene XIV.[12]

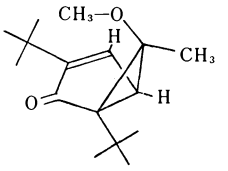
10) E. H. Farmer and D. A. Sutton, *J. Chem. Soc.*, **1943**, 120.
11) G. M. Coppinger and T. W. Campbell, *J. Am. Chem. Soc.*, **75**, 734 (1953).
12) D. H. R. Barton and G. Quinkert, *J. Chem. Soc.*, **1960**, 1.



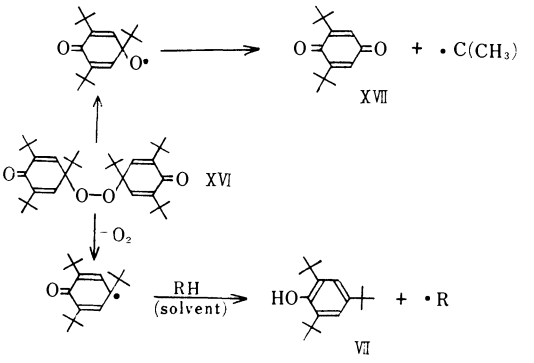
VIa



VIb



XIIa



We wish also to discuss the stereochemistry of the photoketone VI. Of two possible stereochemical structures, VIa and VIb,[13] VIa with an *exo*-methoxyl group was tentatively assigned to the photoproduct for the following reasons: i) A stereomodel for VIb demonstrates that the two *cis*-*t*-butyl groups of the cyclopropane ring strongly hinder each other, whereas the trans arrangement of the *t*-butyl groups in VIa is sterically more favored. ii) The NMR peak of the methoxyl protons of the starting dienone V ($\tau=6.88$) and also of XI ($\tau=6.97$) is located at a higher magnetic field than is usual for methoxyl protons. This shows that these protons must be shielded by the dienone system. It seems, therefore, very likely that this shielding is cancelled in the *exo*-configuration of the methoxyl group ($\tau=6.40$) of VIa. iii) The unusual downward shift ($\tau=6.15$) of the methoxyl peak of the hydroxy compound X suggest that the methoxyl group is sterically close to the hydroxyl group,[14] that, namely, both groups are cis. This argument is also applicable to the hydroperoxide IX (methoxyl protons, $\tau=6.00$), whose precursor is considered to be VI.

On the other hand, the methoxyl protons ($\tau=6.96$) of XII are apparently much shielded by the enone system. This shows that XII may have the stereochemical structure XIIa,[13] with an *endo*-methoxyl group.

The irradiation of the peroxide XVI[15] in petroleum ether gave two crystalline products; one was identified as tri-*t*-butylphenol (VII) (13% yield), and the other as 2,6-di-*t*-butyl-*p*-benzoquinone (XVII) (48% yield). The formation of these products can be formulated as follows:

13) Each one enantiomeric structure was given for VIa, VIb and XIIa.

14) Y. Kawazoe, Y. Sato, N. Natsume, H. Hasegawa, T. Okamoto and K. Tsuda, *Chem. Pharm. Bull. (Japan)*, **10**, 338 (1962).

15) C. D. Cook and R. C. Woodworth, *J. Am. Chem. Soc.*, **75**, 6242 (1953).

Experimental[16]

Photolysis was carried out in a cylindrical vessel, into which a 60 W. low-pressure mercury lamp (spiral type) had been inserted; during irradiation, a nitrogen stream was bubbled through a sintered glass disk jointed at the bottom of the vessel.

The Photolysis of 2, 4, 6-Tri-*t*-butyl-4-methoxycyclohexa-2, 5-dienone (V).—*In Methanol.*—A solution of 4.0 g. of the quinol ether V[6,17] in 160 ml. of absolute methanol was irradiated at 35~40°C under bubbling nitrogen for 7 hr. The progress of the reaction was followed by the decrease of an ultraviolet absorption maximum at 248 mμ and by the appearance of a new maximum at about 280 mμ. The mixture was evaporated under reduced pressure. The residual liquid was dissolved in petroleum ether and chromatographed on a containing 100 g. of neutralized alumina (activity 1). Elution with 100 ml. of petroleum ether yielded 1.43 g. of a pale yellow liquid (A) which deposited 0.44 g. (11%) of crystals. Recrystallization from methanol gave 0.31 g. (7.8%) of the photoketone VI as colorless plates (m. p. 87~87.5°C). IR spectrum (Nujol): 1650, 1630, 1595 cm^{-1}. λ_{max}^{EtOH} 248 mμ (ε, 7780) and 282 mμ (ε, 3070).

Found: C, 78.00; H, 11.01. Calcd. for $C_{19}H_{32}O$: C, 78.03 H, 11.03%.

The fractional recrystallization of the residue from the mother liquor yielded 0.09 g. (3%) of colorless prisms (m. p. 129~130°C), which were identified as 2, 4, 6-tri-*t*-butylphenol (VII) (mixture melting point and infrared spectrum). The other products were not obtained in a pure form.

In Ether.—A solution of 4.0 g. of the quinol ether V in 100 ml. of absolute ether was irradiated at 36°C under bubbling nitrogen for 29 hr. The solvent was removed under reduced pressure, and the residual liquid was dissolved in petroleum ether and chromatographed through a column containing 80 g. of neutralized alumina. Elution with 150 ml.

16) Melting points were determined in capillary tubes and are uncorrected. The infrared spectra were measured with a Nippon Bunko recording spectrophotometer, Model IR-S. The ultraviolet spectra were measured with a Hitachi recording spectrophotometer, Model EPS-2. The microanalyses were made by Mr. J. Goda and his associates of this Faculty.

17) The starting materials, 2, 4, 6-tri-*t*-butylphenol and 2, 6-di-*t*-butyl-*p*-cresol, for the preparation of V, XI and XVI, were kindly supplied by the Koppers Co., Inc.

of petroleum ether yielded 3 g. of a yellow liquid (A). Elution with petroleum ether and then with benzene yielded 0.98 g. of a liquid which crystallized on standing. Recrystallization from petroleum ether at −70°C gave 0.33 g. of the photophenol VII as needles (m. p. 86.5~87.5°C). These crystals were further purified by sublimation at 75~80°C/5 mmHg to give colorless plates (m. p. 87~88°C). IR spectrum (Nujol): 3350, 1610, 815 cm^{-1}. λ_{max}^{EtOH} 209 mμ (ε, 16900) and 278 mμ (ε, 2360).

Found: C, 76.42; H, 10.33. Calcd. for $C_{15}H_{24}O_2$: C, 76.22; H, 10.24%.

This substance gave a positive phenol reaction with a ferric chloride-ferricyanide reagent.[18] The yellow liquid (A) was distilled at 115~118°C/1 mmHg to give a yellow liquid (n_D^{21} 1.4925). The chromatography of the liquid on an alumina column yielded a few milligrams of plates (m. p. 87~87.5°C), which were identified as the bicyclic enone VI by a comparison of the infrared spectra.

In Ether in the Presence of Air.—A solution of 1.50 g. of the quinol ether V in 100 ml. of absolute ether was irradiated at 36°C under bubbling air for 4 hr. The reaction mixture was evaporated under reduced pressure. The residue was dissolved in petroleum ether and chromatographed on a column containing 40 g. of neutralized alumina. Elution with 80 ml. of petroleum ether yielded 0.78 g. of a liquid containing crystals. The hydroperoxide IX, insoluble to petroleum ether, was collected by filtration. It had a m. p. of 145 °C decomp.; yield, 0.175 g. (10.5%). Recrytallization from ether and petroleum ether gave colorless prisms (m. p. 146°C, decomp.). IR spectrum (Nujol): 3350, 1665, 1625, 1595 cm^{-1}. λ_{max}^{EtOH} 237 mμ (ε, 6680), and λ_{infl}^{EtOH} 285 mμ (ε, 2630).

Found: C, 70.52; H. 10.03. Calcd. for $C_{19}H_{32}O_4$: C, 70.33; H, 9.94%.

This substance turned yellow under diffused light.

Elution with benzene and then with methanol yielded 0.40 g. of a liquid which crystallized on standing. Recrystallization from petroleum ether gave 20 mg. (2%) of colorless needles (m. p. 87~88°C), which were identical with an authentic sample of the photophenol VIII (mixture melting point).

In another run, the hydroperoxide IX and the phenol VIII were isolated in 7.5% and 13% yields respectively.

The Dealkylation of the Photophenol VIII.—A solution of 60 mg. of the photophenol VIII in 10 ml. of dry benzene was heated under reflux with 1 g. of powdered anhydrous aluminum chloride. The mixture was then treated with ice-water and extracted with ether. The ethereal layer was washed with water, dried over anhydrous sodium sulfate, and evaporated. Recrystallization of the residue from benzene gave 10 mg. (36%) of plates (m. p. 103~105°C), which were identical with catechol (mixture meeting point and infrared spectrum).

The Reduction of the Hydroperoxide IX to X.—A solution of 64 mg. of the hydroperoxide in 4 ml. of acetic acid was mixed with a solution of 300 mg. of sodium iodide in 3 ml. of acetic acid. The mixture was then warmed at 50°C for 5 min. After dilution with water, the iodine which had been liberated was titrated with 3.50 ml. (corresponding to 0.89 atom oxygen) of a 0.101 N sodium thiosulfate solution. The separated solid was collected by filtration, dried (52 mg.), and recrystallized from ether and petroleum ether to give 38 mg. of the hydroxy compound X as colorless plates (m. p. 147~148.5°C). IR spectrum (Nujol): 3510 (with 3600 infl.), 1660, 1630, 1585 cm^{-1}. λ_{max}^{EtOH} 237 mμ (ε, 5480) and 256.5 mμ (ε, 4780), $\lambda_{infl.}^{EtOH}$ 290 mμ (ε, 2290).

The Photolysis of 2, 6-Di-*t*-butyl-4-methoxy-4-methylcyclohexa-2, 5-dienone (XI).[10,17] — *A) In Ether.*—A solution of 4.0 g. of the quinol ether XI in 160 ml. of absolute ether was irradiated at 36°C under bubbling nitrogen for 6 hr. The solvent was then removed under reduced pressure. The residue was dissolved in petroleum ether and chromatographed on a column containing 100 g. of neutralized alumina. Elution with 300 ml. of petroleum ether yielded 2.0 g. of a yellow liquid which did not crystallize. Elution with petroleum ether, benzene, and then ether yielded 1.13 g. of a yellow liquid which partly crystallized on standing.

After digestion with a small amount of petroleum ether, crystals (0.43 g.; 11%) were collected by filtration and recrystallized from petroleum ether at −70°C to give XII as colorless prisms, m. p. 69~70°C. IR spectrum (Nujol): 1695, 1612 cm^{-1}. λ_{max}^{EtOH} 278 mμ (ε, 2860) and λ_{infl}^{EtOH} 235 mμ (ε, 2550).

Found: C, 76.55; H, 10.27. Calcd. for $C_{16}H_{26}O_2$: C, 76.75; H, 10.47%.

This substance, on standing for several weeks, decomposed to give a yellow liquid whose infrared spectrum showed a broad band centering 1700 cm^{-1} and a broad hydroxyl band near 3200 cm^{-1}.

B) In Methanol.—A solution of 4 g. of the quinol ether XI in 160 ml. of absolute methanol was irradiated under bubbling nitrogen and cooling with tap water for 9 hr. The mixture was treated as described in A). Elution of the chromatogram with 200 ml. of petroleum ether yielded 0.89 g. of an orange liquid which crystallized on standing. Recrystallization from methanol gave 0.28 g. of colorless prisms (m. p. 68~70°C) which were identical with an authentic sample of 2, 6-di-*t*-butyl-*p*-cresol (infrared spectrum). Further elution yielded an orange liquid which did not crystallize.

The Photolysis of Bis(1, 3, 5-tri-*t*-butyl-2, 5-cyclohexadien-4-one) Peroxide (XVI).[15,17]—A solution of 4.0 g. of the peroxide XVI in 160 ml. of petroleum ether was irradiated under bubbling nitrogen and cooling with tap water for 12 hr. The solution showed a greenish yellow color during irradiation. The solvent was removed under reduced pressure. The residue, on treatment with 10 ml. of methanol, deposited some crystals which were collected by filtration. Yield, 0.64 g. (16% recovered); m. p. 139~142°C. The melting point was not depressed on admixture with the starting peroxide XVI. The filtrate was evaporated under reduced pressure, and the residue was dissolved in petroleum ether and chromatographed on a column

18) G. M. Barton, R. S. Evans and J. A. F. Gardner, *Nature*, **170**, 249 (1952).

containing 40 g. of neutral alumina. Elution with 450 ml. of petroleum ether yielded 0.40 g. (13%) of colorless crystals (m. p. 129~131°C), which were identified as 2, 4, 6-tri-*t*-butylphenol (VII) (infrared spetrum).

Elution with 50 ml. of a mixture of petroleum ether and benzene (1 : 1) yielded 0.9 g. of a yellow liquid which did not crystallize. Further elution with the same solvent mixture and then with benzene yielded 1.22 g. (48%) of orange crystals (m. p. 67~68°C), the infrared spectrum of which was identitcal with that of 2, 6-di-*t*-butylbenzoquinone (XVII).[19]

Summary

The ultraviolet irradiation of 2, 4, 6-tri-*t*-butyl-4-methoxycyclohexa-2, 5-dienone (V) in methanol and in ether has yielded a photoketone VI and 3, 6-di-*t*-butylguaiacol (VIII) respectively. The irradiation of V in the presence of oxygen in ether has yielded VIII and the hydroperoxide of VI. Other related *p*-quinol ethers have also been subjected to photolysis.

This work was supported by Grant AM-3706 from the National Institutes of Health, the U. S. Public Health Service. The author wishes to thank Professor T. Kubota for his interest in this work and also Dr. K. Tori, Shionogi Research Labortory, and Dr. Y. Asashi, Takeda Pharm. Co., Ltd., for their NMR spectra measurements.

Faculty of Science
Osaka City University
Sumiyoshi-ku, Osaka

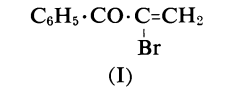
19) E. Müller and K. Ley, *Chem. Ber.*, **88**, 601 (1955).

The Reaction Mechanism of α-Bromo-α,β-unsaturated Ketones with Amines

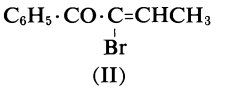
By Hiromi INOKAWA

(Received October 19, 1963)

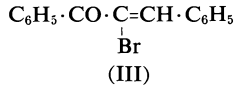
In previous papers,[1] the reaction products of α-bromo-α, β-unsaturated ketones, such as 2-bromo-1-phenyl-2-propen-1-one (I), 2-bromo-1-phenyl-2-buten-1-one (II), 2-bromo-1, 3-diphenyl-2-propen-1-one (III), and 3-bromo-4-phenyl-3-buten-2-one (IV), with methylamine and dimethylamine, were described.



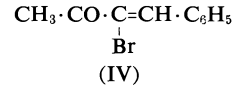
(I)



(II)

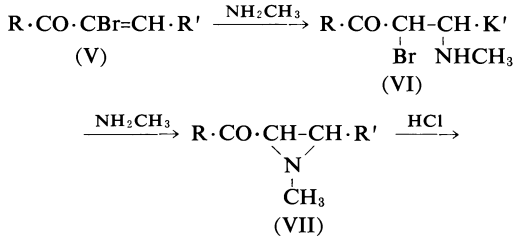


(III)

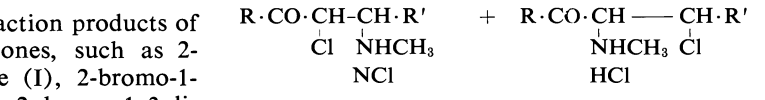


(IV)

The general course of the reactions of α-bromo-α, β-unsaturated ketones with methylamine has been schematized as follows:



(V) (VI) (VII)



(VIII) (IX)

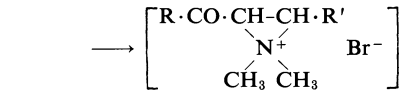
The first step consists of the addition of methylamine to the β-carbon atom of the unsaturated ketones V, followed by the formation of α, β-ethylenimine ketones VII with the excess methylamine. The α, β-ethylenimine ketones VII are converted into α-chloro-β-methylamino ketone hydrochlorides (VIII) and β-chloro-α-methylamino ketone hydrochlorides (IX) by the action of hydrogen choride. However, when R′ is H, only α-chloro-β-methylamino ketone hydrochloride (VIII) is obtained.

The reaction steps of α-bromo-α, β-unsaturated ketones with dimethylamine may be represented as follows:



(V) (X)

1) H. Inokawa, *J. Chem. Soc. Japan, Pure Chem. Sec.* (*Nippon Kagaku Zasshi*), 84, 932, 988 (1963).



(R'=H or CH_3)

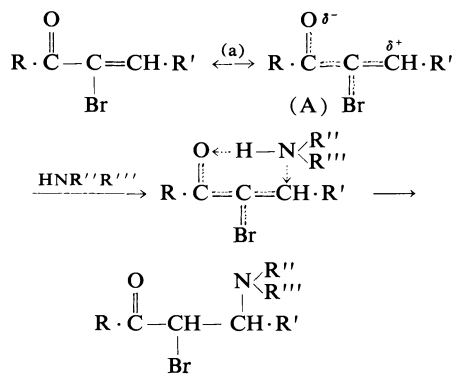
(XI)

The first step is the addition of dimethylamine to the β-carbon atom of the unsaturated ketones. When R' is H or CH_3, the resulting α-bromo-β-dimethylamino ketones (X) give 1, 1-dimethylaziridinium bromides (XI). When R' is C_6H_5, however, the α-bromo-β-dimethylamino ketones (X) remain unchanged.

The products and their yields in these reactions are summarized in Table I.

The facts summarized in Table I led the author to conclude (1) that the addition reactions of amines to the β-carbon atom of α-bromo-α, β-unsaturated ketones become difficult in the order of I<II<III<IV, and (2) that the values of the VIII/IX ratio, in which VIII and IX are produced by the ring-opening reactions of α, β-ethylenimine ketones with hydrogen chloride, decrease in the order of I > II > III > IV.

The former conclusion will be discussed first in relation to the reaction mechanism. The first step of the reactions of α-bromo-α, β-unsaturated ketones with amines may be formulated as the following scheme 1:



Scheme 1

When R is C_6H_5 and R' is turned into H, CH_3, or C_6H_5, the fractional positive charge of the β-carbon atom should decrease as a result of the delocalization caused by the hyperconjugation with a methyl group or by the resonance with a phenyl group. The effect of a phenyl group on the delocalization is larger than that of a methyl group.[2] Consequently, the positive charge of the β-carbon atom should decrease in the order of I > II > III. Comparing III with IV, the formula A in the resonance (a) should contribute more when R is C_6H_5 than CH_3, and thus the addition of amines to the β-carbon atom of III takes place more easily than that of IV. Therefore, the addition of amines becomes difficult in the order of I<II<III<IV.

This conclusion seems to be in agreement with the experimental results obtained by Kohler,[3] who showed that the yields of 1, 4-addition products of phenyl magnesium bromide to 1-phenyl-2-propen-1-one, 1-phenyl-2-buten-1-one, 1, 3-diphenyl-2-propen-1-one, and 4-phenyl-3-buten-2-one are 100, 100, 94, and 12% respectively.

The second conclusion as to the ring-opening reactions of ethylenimine ketones will be discussed in terms of the reaction mechanism. In the reactions of ethylenimine ketones with hydrogen chloride, the intermediate VII' must be produced first* by the addition of a proton, the resulting positive charge facilitates the fission of an ethylenimine ring. Therefore, the reaction proceeds according to two paths, b and c, in Scheme 2.

In the path b, the fractional positive charge on the α-carbon atom is important. The fractional positive charge is caused by the strong electron-attracting force of –CO– and facilitates the attack of Cl^- on the α-carbon atom. The electron-attracting force of a benzoyl group is larger than that of an acethyl group. Accordingly, the path b proceeds more easily when R is C_6H_5 (in VII') than when it is CH_3. In the path c, on the other hand, the stability of

Table I. Yields of Reaction Products

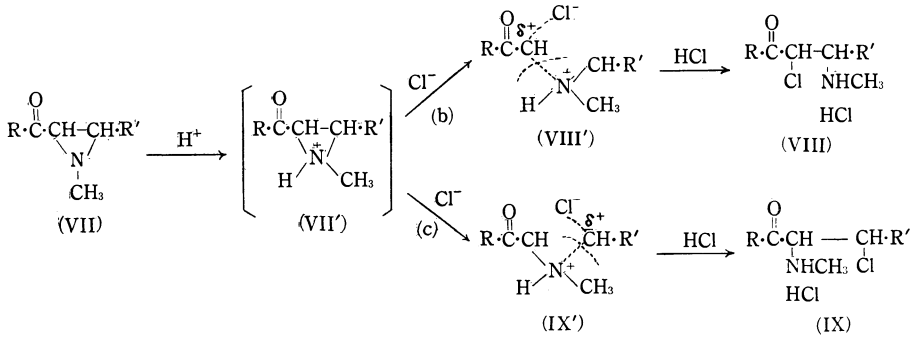
No.	V: R	V: R'	With methylamine: VII %	With methylamine: VIII X	With methylamine: IX %	VIII/IX	With dimethylamine: X %	With dimethylamine: XI %
I	C_6H_5	H	30*	30	0	∞	75	42
II	C_6H_5	CH_3	68	48	20	2.4	73	24
III	C_6H_5	C_6H_5	57	19	38	0.5	56	—
IV	CH_3	C_6H_5	36	6	30	0.2	11	—

* A by-product, $C_{19}H_{18}O_2NBr$, was formed in a 35% yield by the addition of 1 mol. methylamine to 2 mol. of I.

2) W. R. R. Parl and G. F. Wright, *J. Am. Chem. Soc.*, 76, 3036 (1954).

3) E. P. Kohler, *Am. Chem. J.*, 38, 511 (1907).

* The ionization constants (k_b) of the ethylenimines much are greater than 3.8×10^{-10}. H. C. Brown and M. Gerstein, *J. Am. Chem. Soc.*, 72, 2926 (1950).



Scheme 2

the transition state IX′ seems to be of importance. As has been mentioned in the discussion of the addition reaction, the delocalization of the fractional positive charge on the β-carbon atom is caused by the resonance with a methyl or phenyl group, and the stability of IX′ increases by the delocalization energy in the order of I<II<III, the reactions through the path c becoming easier in the order of I<II<III. Consequently, the values of VIII/IX become smaller in the order of I>II>III>IV.

Summary

It has been considered that, in the reaction of α-bromo-α, β-unsaturated ketones with amines, α-bromo-β-amino ketones are produced first by the 1, 4-addition of amines and converted to ethylenimine ketones in the presence of excess amines. The ethylenimine ketones react with hydrogen chloride to give α-chloro-β-amino and β-chloro-α-amino ketones, the yields of these ketones depending on the variation of the fractional positive charge at the α-carbon atom and on the delocalization energy on the β-carbon atom by R′.

The author wishes to express her hearty thanks to Professor Ryozo Goto of kyoto University for his invaluable advice and encouragement throughout this work.

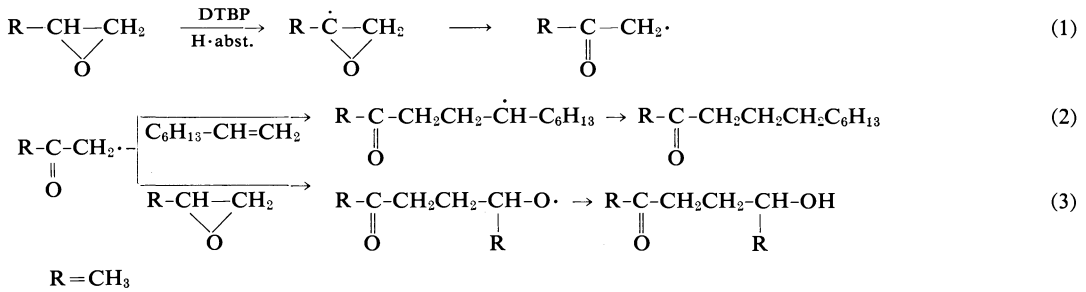
Department of Chemistry
Faculty of Science
Kyoto University
Sakyo-ku, Kyoto

The Peroxide-induced Polymerization of Epoxides

By Akira OKU, Masaya OKANO and Ryohei ODA

(Received December 5, 1963)

Free radical reactions of epoxides have been studied by some workers and classified into two types, one involving the abstraction of a hydrogen atom at the ring carbon and the other involving ring-opening by a radical attack. The observation by Gritter and



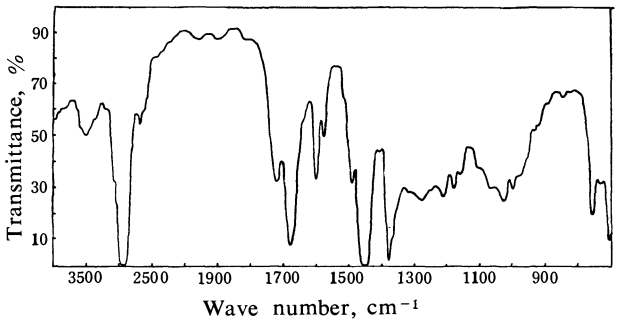


Fig. 1. Infrared spectrum of the SO polymer (Nujol).

Wallace[1] that 5-oxy-2-hexanone and 2-undecanone were formed by two competing reactions, Eqs. 2 and 3, in the di-*t*-butyl peroxide-induced addition of propylene oxide to 1-octene, has been of great interest to us.

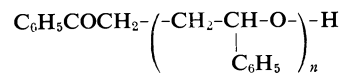
If reaction 3 occurs successively to any appreciable extent, the formation of a polyether having acyl and hydroxyl end groups is to be expected. Indeed, Gritter and Wallace recently pointed out a slight formation of telomers when propylene oxide was treated with peroxides,[2] but no additional information on the polymer was given. Conant and Peterson[3] also observed that, in the presence of a benzoyl peroxide catalyst, cyclohexene oxide was polymerized to a viscous liquid with difficulty, even under severe conditions. On the contrary, Hopff and Zahner[4] reported that styrene oxide could not be polymerized using peroxides and an aliphatic azo compound as initiators.

In order to check the radical polymerization of epoxides and to characterize the resulting polymers, we have now examined the reaction of styrene oxide (SO) and phenyl glycidyl ether (PGE) with some radical initiators. To facilitate the isolation of the polymer, high boiling aromatic or aliphatic epoxides which might be expected to yield a solid polymer have been selected.

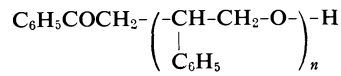
Results and Discussion

The Polymerization of SO with Di-*t*-butyl Peroxide (DTBP).—Some of the results are shown in Table I. Acetophenone was the only low molecular-weight product isolated. This clearly indicates the formation of phenacyl radical which corresponds to acetonyl radical in Eq. 1. By fractional precipitation, a polymeric residue was separated into two fractions, i. e., ethanol-insoluble and ligroin-insoluble fractions. Since their infrared spectra were almost identical, the former was investigated in detail. In addition, control experiments in which SO was heated alone, with *t*-butanol or acetone, gave no polymer.

The polymer was insoluble in aliphatic alcohols and parafinic hydrocarbons, but it was soluble in other solvents. It was tensile when molten, but it was too brittle to be of practical use. Analytical data showed fairly good agreement with the calculated value of $(SO)_n$. The average molecular weight was found to be ca. 1500~2000. An estimation of the epoxy value by the hydrochloric acid-dioxane method showed no evidence for the existence of an epoxide ring. The infrared spectrum exhibited a characteristic absorption at 3500 (hydroxyl), at 1720 and 1680 (carbonyl), and at 1030~1100 cm^{-1} (ether) (see Fig. 1). It seems that these data do not conflict with the tentative structures, I and/or II, for the polymer which are deduced from Eq. 3.



(I)



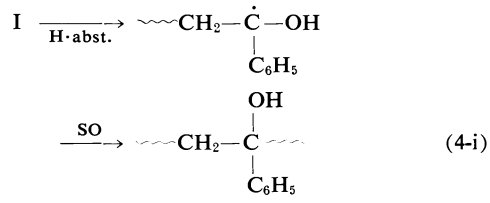
(II)

However, the following additional data indicate that the polymer structure should be represented in somewhat modiffed forms.

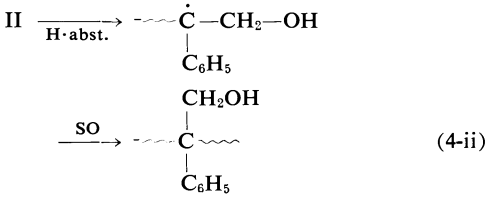
First, the hydroxyl number, as estimated by both acetic anhydride and phenyl isocyanate methods, was 1.8~2.0 per molecule. This result seems to imply that a terminated polymer (initially formed)[5] is revived by hydrogen atom abstraction with any radical at the α-carbon of the phenyl or hydroxyl groups and that then a branching involving a repeated

1) R. J. Gritter and T. J. Wallace, *J. Org. Chem*, **26**, 282 (1961).
2) T. J. Wallace and R. J. Gritter, *Tetrahedron*, **19**, 657 (1963).
3) J. B. Conant and W. R. Peterson, *J. Am. Chem. Soc.*, **54**, 628 (1932).
4) H. Hopff and H. Zahner, *Angew. Chem.*, **72**, 117 (1960).
5) The average degree of polymerization of this polymer is estimated to be nearly 6~7 on the basis of both hydroxyl number and carbonyl number (see below).

attack on the epoxide occurs (see Eqs. 4-i, ii). Here, the facile abstraction of an α-hydrogen atom of alcohols and benzyl compounds is a well-known type of reaction.



(4-i)

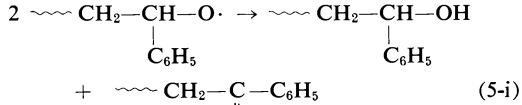


(4-ii)

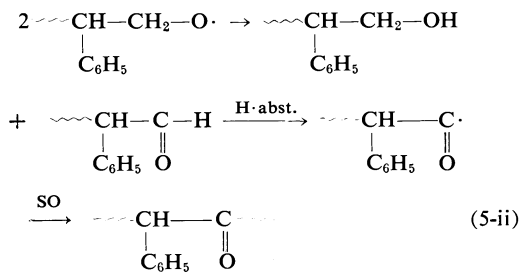
A clear demonstration of a hydroxyl group in the product indicates that, in the propagation step, a preferential attack occurs on the ring carbon atom rather than on the oxygen atom of epoxide. On the other hand, an attack on the ring oxygen would not lead to the appearance of a hydroxyl end group. It is noteworthy that propagation proceeds in a form different from that in the cationic polymerization of epoxides. In connection with the above radical polymerization, the formation of an alternating polymer[6] from ethylene oxide and perfluoropropene under photo- or radical-initiation is of interest; it seems to involve a somewhat similar propagation step ($C\cdot \rightarrow O\cdot \rightarrow C\cdot \rightarrow O\cdot \rightarrow \cdots$). It has also been reported that the copolymerization of trifluoronitrosomethane and perfluoroolefins[7] yielded alternating polymers by a similar mechanism.

There remains the problem of which α-carbon the attack of radicals occurs in. As has been described above, Gritter and Wallace[1] observed a predominant formation of a secondary ketoalcohol in a similar reaction; however, a minor attack on the secondary ring carbon, which seems to be energetically favorable,[8] although sterically unfavorable, may also be considered (see below).

Second, the content of the carbonyl group as determined by the 2, 4-dinitrophenylhydrazine method was, unexpectedly, 1.5~1.6 units per molecule. By this treatment, two carbonyl bands (1720 and 1680 cm^{-1}) which were found in the original polymer completely disappeared. One carbonyl group is clearly due to the phenacyl end group; and the other one would be produced by disproportionation between two alkoxy radicals (see Eqs. 5-i, ii). In the latter case, a revival of the initially-terminated polymer with an aldehyde end group by means of hydrogen transfer may also be considered.



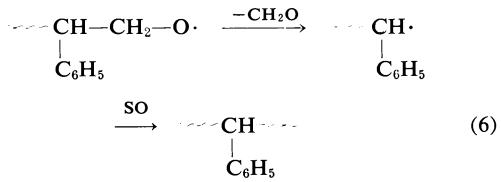
(5-i)



(5-ii)

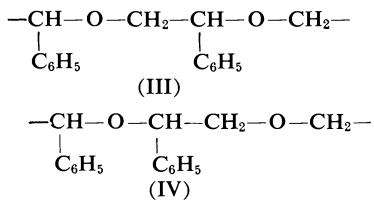
The 1680 cm^{-1} band may be assigned to the carbonyl absorption of phenacyl end groups (cf. Eq. 5-i), and the 1720 cm^{-1} band, to that of the aldehyde and/or the ketone in Eq. 5-ii. The possibility of the radical attack on the secondary ring carbon of the epoxide cannot be excluded because of the appearance of the latter (1720 cm^{-1}) band.

The elimination of formaldehyde, which is a well-known reaction of primary alkoxy radicals,[8] may also be considered (see Eq. 6). However, this was not confirmed experimentally.

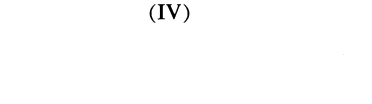


(6)

In addition, the absorption in the 1030~1100 cm^{-1} region, corresponding to ether, exhibited a medium but broad band with two peaks, although ether absorption is known to be considerably strong. Perhaps this is to be ascribed to the separate contributions of two different ether units, III and IV, in which the latter is produced by a competitive attack on another ring carbon of the epoxide during the propagation.



(III)



(IV)

6) M. Hauptshein and J. M. Lesser, *J. Am. Chem. Soc.*, **78**, 676 (1956).
7) G. H. Crawford, D. E. Rice and B. F. Landrum, *J. Polymer Sci.*, A-1, 565 (1963).
8) P. Gray and A. Williams, *Chem. Revs.*, **59**, 239 (1959).

The Polymerization of PGE with DTBP.— The results are presented in Table II. In this reaction, no appreciable amount of the ketone derived from phenoxyacetonyl radical, $C_6H_5OCH_2COCH_2\cdot$, could be isolated. The polymer obtained from PGE was soluble in ethanol, but it could be fractionally precipitated with isobutanol. Its elementary analysis was in good agreement with the expected value, and the average molecular weight was 1200. The polymer had strong absorption bands at 3500 (hydroxyl), 1720 (carbonyl) and 1030~1100 cm^{-1} (ether). Besides, the hydroxyl and carbonyl groups in the polymer were both

Table I. Reaction of SO with DTBP

Run	SO g. (mol.)	DTBP g. (mol.)	Reaction temp. & time[a] °C, hr.	SO recovered %	Acetophenone %[b]	Polymer g. (%)[c]	Remarks on ethanol-insol. fraction: g.	M. p. °C	M.w.[d]	[η][e]	OH group units/molecule	CO group[h]
1	60 (0.50)	7.3 (0.05)	120~130; 10(6)	95		3.5 (5.8)	0.5	100~105				
2	90 (0.75)	14.5 (0.10)	130~135; 7(3)	90	8.8	5.8 (6.5)	1.5	135~140	1300			
3	60 (0.50)	29 (0.20)	140~145; 6(3)	75	5.0	12.5 (21)	9.0	160~165	2000	0.07	1.8[f]; 2.0[g]	1.5
4	240 (2.00)	29 (0.20)	135~143; 5(0)	90		23 (9.6)	6.5	145~150	1800	0.05	2.0[f]; 2.0[g]	1.6

a) Figures in parentheses represent the time required for the addition of the peroxide. b) Based on DTBP. (Determined by 2, 4-D method). c) Total yield of ligroin-insol. and ethanol-insol. fractions. Based on SO. d) By cryoscopic method in benzene. e) In benzene, at 25°C. f) By acetic anhydride method. g) By phenyl isocyanate method. h) By 2, 4-D method.

Table II. Reaction of PGE with DTBP

PGE g. (mol.)	DTBP g. (mol.)	Reaction temp. & time[a] °C, hr.	PGE recovered %	Polymeric residue g. (%)[i]	Remarks on isobutanol-insol. fraction: g.	M. p. °C	M.w.[d]	OH group[g] units/molecule	CO group
194 (1.30)	19 (0.13)	145~155; 4(0)	93	15 (7.7)	3	105~110	1200	1.8	1.0

a), d), g) See footnote in Table I. i) Based on PGE.

Table III. Reaction of SO with BPO

SO g. (mol.)	BPO g. (mol.)	Reaction temp. & time[a] °C, hr.	SO recovered %	Acetophenone %[j]	Polymeric residue g. (%)[k]	Remarks on ethanol-insol. fraction: g.	M. p. °C	M.w.[d]	OH group[f] units/molecule	CO group
180 (1.50)	36.5 (0.15)	80~81; 5.5(1.0)	69	13	38 (21)	4.6	115~120	1300	1.0	0.85

a), d), f) See footnote in Table I. j) Based on BPO. (Determined by 2, 4-D method). k) Based on SO.

Table IV. Reaction of SO with BA

SO g. (mol.)	BA g. (mol.)	Reaction temp. & time °C, hr.	Products: 1 : 1 Adduct[l] g.	2 : 1 Adduct[m] g.	Residue[n] g.
30 (0.25)	6.1 (0.05)	80~81; 4.5	7.5	6.0	trace
30 (0.25)	1.2 (0.01)	80~81; 4.5	0.9	0.7	trace

l) Anal. Found: C, 74.41; H, 6.04. Calcd. for $C_{15}H_{14}O_3$: C, 74.36; H, 5.83%. m) Anal. Found: C, 76.20; H, 6.29. Calcd. for $C_{23}H_{22}O_4$: C, 76.22; H, 6.12%. n) Easily soluble in ethanol or ligroin.

estimated to be 1.8 units per molecule.[9] These data seem to predict the contribution of abnormal structures as in the case of the SO polymer.

A comparison of the polymerizing ability of SO and PGE seems to reflect the difference in their reactivities in radical ring-opening. As to the concentration of initiator radicals (acylmethyl radicals), the phenacyl radical would be superior to the phenoxyacetonyl radical. In fact, Wallace and Gritter[2] have recently found that SO was much more reactive than propylene oxide in a hydrogen atom abstraction by *t*-butoxyl radical, and that in the addition of the resulting keto radical to 1-octene, the yield of adduct from SO was higher than that from propylene oxide. If the ring-opening of SO and of PGE is equally facile, it may then be expected that SO will yield a polymer with a lower degree of polymerization but in a higher yield than in the case of PGE. However, the observed degree of polymerization of SO was about twice as large as that of PGE (see Footnotes 5 and 9), and the yield of SO polymer and PGE polymer in similar conditions were 9.6% and 7.7% respectively. Therefore, it may safely be deduced that the polymerizing ability of epoxides is largely dependent upon the ease of their ring-opening.

The Polymerization of SO with Benzoyl Peroxide (BPO).—Initially, a control experiment was conducted with SO and benzoic acid in order to ascertain the possibility of cationic polymerization with the acid (probably present in the reaction mixture). There was, however, no formation of a polyether, and considerable amounts of 1 : 1 and 2 : 1 adducts were isolated (see Experimental). Hence, it is obvious that the polymer from SO using a BPO catalyst would be formed by a radical mechanism. The results are presented in Table III. The ethanol-insoluble fraction of the polymer showed good analytical data. Its average molecular weight was found to be ca. 1300. This value nearly corresponds with that from the hydroxyl number in the DTBP-induced polymer. Its infrared spectrum showed a characteristic absorptin at 3500 (hydroxyl), 1720 and 1680 (carbonyl), and 1030～1100 cm^{-1} (ether). In this polymerization, the ring-opening of SO by an attack of benzoyloxy radical (formed by the decomposition of BPO) as well as by that of phenacyl radical may be expected. In fact, when the polymer was treated with aqueous sodium hydroxide in dioxane, a marked disappearance of the 1720 cm^{-1} band and an increase in the intensity of the hydroxyl band were observed. The determination of hydroxyl and carbonyl groups in the original polymer gave values of 1.0 and 0.75 units per molecule respectively. These results clearly indicate that both benzoyloxy and phenacyl radicals are used to initiate the polymerization and that the polymer has the normal polyether structure, in contrast with the DTBP-induced polymer. The low molecular weight and straight-chain structure of this polymer may result from the low reaction temperature.

The Reaction of SO with α, α'-Azo-bis-isobutyronitrile (AIBN).—An attempt to polymerize SO using an AIBN catalyst was unsuccessful. The reaction resulted in a complete recovery of SO and the quantitative isolation of tetramethylsuccinonitrile derived from AIBN, without any formation of acetophenone or any polymeric product. This would seem to arise from the poor ability of AIBN in hydrogen atom abstraction.

Conclusion

From these results, it can be concluded that the preparation of high molecular weight polyethers from epoxides by peroxide-induced polymerization is practically impossible. The reasons for this may be summed up as follows. The chain propagation reaction involving the ring-opening seems to be energetically somewhat unfavorable, as compared to the initiation reaction containing an α-hydrogen abstraction from epoxide and successive rearrangement to acylmethyl radical. In addition, the facile hydrogen abstraction and disproportionation reactions of the growing alkoxy radical, especially at high temperatures, promote the short-chain termination and cause the branching.

Experimental

The DTBP-induced Polymerization of SO.—In a four-neck flask flushed with purified nitrogen, 240 g. (2.0 mol.) of SO and 29 g. (0.20 mol.) of DTBP were mixed. Under a nitrogen stream, the mixture was gradually heated and refluxed while being stirred at 135～143°C for 5 hr. All volatile fractions (up to 230°C/2 mmHg), such as acetone, *t*-butanol, acetophenone and unreacted SO etc., were removed, and 23 g. of a resinous polymeric residue was obtained. This was fractionated by precipitation from benzene with ethanol or ligroin into two fractions. Anal. of the ethanol-insoluble fraction. Found: C, 81.65; H, 6.71. Calcd. for $(C_8H_8O)_n$: C, 79.97; H, 6.56%.

The Determination of Hydroxyl and Carbonyl Groups.—The determination of hydroxyl and carbonyl contents in the polymer was carried out according to the following well-known methods.

9) On the basis of these data, the average degree of polymerization (i.e., that of propagation) is estimated to be about 3.

To obtain reliable data in these estimations, both original and reacted polymers were submitted to treatment in pulverized form.

Acetic Anhydride Method.[10]—The polymer (1.0 g.) was acetylated with a mixture of acetic anhydride (1.0 ml.) and pyridine (3.0 ml.) at 75°C for 2 hr. In the estimation of unreacted anhydride, it was necessary to wash thoroughly with water the polymer which separated from the reaction mixture upon the addition of water.

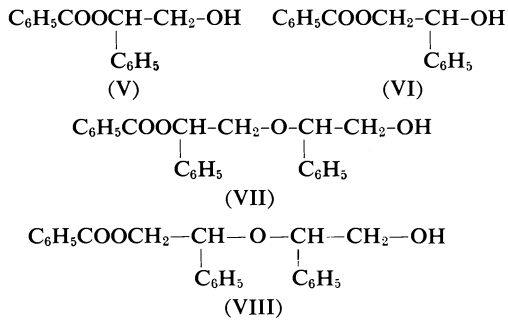
Phenyl Isocyanate Method.—The polymer (0.5 g.) was treated with phenyl isocyanate (0.3 g.) in the presence of pyridine (0.2 g.) in benzene (7 ml.) at 80°C for 2 hr. After the evaporation of low-boiling fractions, the residue was extracted with benzene several times to remove benzene-insoluble by-products (diphenylurea and isocyanate dimer). The dissolved polymer was precipitated with ethanol, and the hydroxyl number was calculated from its nitrogen content.

2, 4-Dinitrophenylhydrazine (2, 4-D) Method.[11]—The polymer (0.5 g.) was added to a dioxane solution (15 ml.) of 2, 4-D (0.4 g.) containing concd. hydrochloric acid (1.0 g.) ; the mixture was refluxed for 1 hr. (when tetrahydrofuran was used as a solvent, the heating was continued for 2 hr.). After evaporation to dryness, the benzene-soluble portion in the residue was collected and repeatedly washed with a mixture of ethanol and hydrochloric acid. Then the polymer was redissolved in benzene and reprecipitated with aqueous ethanol containing hydrochloric acid.

The DTBP-induced Polymerization of PGE.—The procedure was similar to that used in the case of SO. The polymer obtained was a colored viscous oil, and it was fractionated by precipitation from benzene with isobutanol. Anal. of the isobutanol-insoluble fraction. Found: C, 72.72; H, 5.89. Calcd. for $(C_9H_{10}O_2)_n$: C, 71.98; H, 6.71%.

The BPO-induced Polymerization of SO.—To SO in a flask flushed with nitrogen, BPO was added in small portions, and the mixture was stirred at 80~82°C. After dilution of the cooled reaction mixture with ether, the solution was washed four times each with aqueous sodium carbonate, with aqueous sodium thiosulfate and with water, and dried over anhydrous calcium chloride. By the removal of ether and of all volatile fractions (up to 230°C/2 mmHg), a resinous polymeric product was obtained; this was reprecipitated from ether with ethanol. Anal. of the ethanol-insoluble fraction. Found: C, 81.34; H, 6.14. Calcd. for $(C_8H_8O)_n$: C, 79.97; H, 6.71%.

The Reaction of SO with Benzoic Acid (BA).—As a control experiment for the BPO-induced polymerization, a mixture of SO and BA was heated under the same conditions. The distillation of the reaction mixture afforded considerable amounts of 1 : 1 and 2 : 1 (SO : BA) adducts (b. p. 167~172°C/2.5 mmHg and 220~225°C/3 mmHg respectively) and a trace of an ethanol-soluble residue, as Table IV shows. On referring to an authentic material of VI (m. p. 62°C) obtained by an independent method, it was ascertained that the former adduct was a mixture of two structural isomers, V and VI. In view of the facile rearrangement of V to VI, as in the case of the corresponding acetate,[12] the determination of its composition was not carried out. A rough gas-chromatographic analysis of the latter adduct indicated that it was a 2 : 1 mixture of two isomers. Judging from the orientation of the ring-opening of the epoxide, these isomers would correspond to VII and VIII among the four possible isomers:



The Reaction of SO with AIBN.—To 120 g. (1.0 mol.) of SO in a flask flushed with nitrogen, 16.5 g. (0.1 mol.) of AIBN was added over a 1 hr. period at 79~80°C and then stirred for 2 hr. each at 80 and at 90°C. In addition to the complete recovery of SO, a nearly quantitative amount of tetramethylsuccinonitrile and a trace of poly(α-methyl acrylonitrile) were isolated.

Department of Synthetic Chemistry
Faculty of Engineering
Kyoto University
Sakyo-ku, Kyoto (A. O. & R. O.)

Institute for Chemical Research
Kyoto University
Takatsuki, Osaka (M. O.)

10) C. L. Ogg, W. L. Porter and C. O. Willits, *Ind. Eng. Chem., Anal. Ed.*, **17**, 394 (1945).
11) H. A. Iddles and C. E. Jackson, ibid., **6**, 454 (1934).
12) T. Cohen, M. Dughi, V. A. Notaro and G. Pinkus, *J. Org. Chem.*, 27, 814 (1962).

Spectrochemical Study of Microscopic Crystals. XXIV.[1] *The Structure and Light Absorption of Copper(II) Complexes of Benzoic and Substituted Benzoic Acids*

By Shoichiro YAMADA, Hiroaki NISHIKAWA and Seiko MIKI

(Received December 10, 1963)

In previous reports about the molecular structure of copper(II) complexes of fatty acids[2] and halogenoacetic acids[3] in the crystalline state and in solution, it was found that the acid dissociation constant of the carboxylic acid seemed to be related in one way or another to the tendency of their copper(II) complexes to form binuclear complexes. It seemed that it would be interesting to examine, in more detail, the conditions for the formation of the binuclear cupric carboxylates of this type, in relation to the dissociation constant of the ligand carboxylic acids and to the copper-to-oxygen bond in their cupric complexes. In the present paper, copper(II) complexes of benzoic and substituted benzoic acids were examined, mostly on the basis of their electronic absorption spectra.

Experimental

Materials. — Cupric benzoate was prepared by conventional methods,[4] either from cupric carbonate or hydroxide and benzoic acid, or from cupric sulfate and sodium benzoate. Recrystallization of the product from hot water yielded pale-blue needle-like crystals of $Cu(benz)_2 \cdot 3H_2O$, where "benz" denotes a benzoate ion. Recrystallization of the same product from ethanol yielded blue-green prismatic crystals of $Cu(benz)_2 \cdot C_2H_5OH$, as reported by Inoue, Kishita and Kubo.[5] Recrystallization from methanol containing benzoic acid yielded blue-green crystals of $Cu(benz)_2(benzH) \cdot 0.5H_2O$.

Other cupric complexes of substituted benzoic acids were prepared in a way similar to that used for cupric benzoate and were purified by repeated recrystallization. The recrystallization was carried out using dioxan, dioxan-water, dioxan-methanol or dioxan-ethanol. The isolation of the crystals of all the possible forms with a substituted benzoic acid was not attempted in the present work, but one typical form of the cupric complex for each substituted benzoic acid was isolated as crystals by some of the normal procedures and was used for the spectral examination. The different forms of cupric benzoates and substituted benzoate were found to show identical electronic absorption spectra in dioxan. Some of them were also examined in the crystalline state.

The compounds in Table I were prepared according to the methods already reported, and their elemental analyses agreed with the formulae previously given. The main characteristics and elemental analyses of the other compounds are shown in Table II.

Measurements. — Dichroism was determined in the visible and near-ultraviolet regions by Tsuchida and Kobayashi's microscopic method[6] with crystals of cupric benzoate, *o*-methylbenzoate, *o*-chlorobenzoate, *o*-nitrobenzoate, *m*-hydroxybenzoate and *p*-hydroxybenzoate.

The electronic absorption spectra of the compounds in non-donor organic solvents, such as methanol, ethanol and dioxan, were determined with a Beckman DU spectrophotometer, insofar as the solubility allowed. Beer's law was generally obeyed in the concentration range between 10^{-2} and 10^{-5} F, but deviation from the law was sometimes observed in more dilute solutions.

The reflection spectra in the same frequency region were determined with a Hitachi EPU-2A spectrophotometer.

The notations are the same as those in the former papers of this series. Extinction coefficients are based on the monomeric formulae.

Results and Discussion

Cupric Benzoate in Solution and in the Crystalline State.—The electronic absorption spectra of cupric benzoate and substituted benzoates were determined in non-donor organic solvents. The solubility of these compounds in common solvents was generally low, except for dioxan. The results with dioxan as a solvent will be described extensively in the present paper.

1) Part XXIII of this series: S. Yamada and S. Miki, This Bulletin, **36**, 680 (1963).

2) R. Tsuchida and S. Yamada, *Nature*, **176**, 1171 (1955); R. Tsuchida, S. Yamada and H. Nakamura, ibid., **178**, 1192 (1956); S. Yamada, H. Nakamura and R. Tsuchida, This Bulletin, **30**, 953 (1959); ibid., **31**, 303 (1958).

3) R. Tsuchida and S. Yamada, *Nature*, **182**, 1230 (1958); Proceedings of the Symposium on the Chemistry of Coordination Compounds, Agra, India, Part II (1959), p. 35; S. Yamada, H. Nishikawa and R. Tsuchida, This Bulletin, **33**, 1278 (1960).

4) F. Ephraim and A. Pfister, *Helv. Chim. Acta*, **8**, 369 (1925); F. Ephraim and E. Bolle, *Ber.*, **48**, 1770 (1915); etc.

5) M. Inoue, M. Kishita and M. Kubo, *J. Chem. Soc. Japan, Pure Chem. Sec.* (*Nippon Kagaku Zasshi*), **84**, 759 (1963).

6) R. Tsuchida and M. Kobayashi, "The Color and the Structure of Metallic Compounds" (Kinzokukagōbutsu no Iro to Kōzō), Zōshindo, Osaka (1944), p. 180.

TABLE I. BENZOATE AND SUBSTITUTED BENZOATES OF COPPER(II) WHICH WERE PREPARED AS DESCRIBED PREVIOUSLY

Compound	Appearance	Method
$Cu(benz)_2 \cdot 3H_2O$	Blue crystals	Ref. 4
$Cu(benz)_2 \cdot C_2H_5OH$	Blue-green crystals	Ref. 5
$Cu(benz)_2(benzH) \cdot 0.5H_2O$	Blue-green crystals	Ref. 4
$Cu(o\text{-}NO_2\text{-}benz)_2$	Blue-green plates	a
$Cu(m\text{-}NO_2\text{-}benz)_2 \cdot H_2O$	Blue powder	b
$Cu(p\text{-}NO_2\text{-}benz)_2 \cdot H_2O$	Blue needles	a
$Cu(m\text{-}OH\text{-}benz)_2 \cdot H_2O$	Blue-green needles	c
$Cu(p\text{-}OH\text{-}benz)_2 \cdot 6H_2O$	Blue needles	Ref. 4

a) C. Schall, *Z. Electrochem.*, **19**, 830 (1913); H. J. S. King, *J. Chem. Soc.*, **1930**, 2307.
b) G. J. Mulder, *Lieb. Ann.*, **34**, 297 (1840).
c) H. Ley and O. Erler, *Z. anorg. Chem.*, **56**, 401 (1908).

TABLE II. MAIN CHARACTERISTICS AND ELEMENTAL ANALYSES OF SUBSTITUTED BENZOATES OF COPPER(II)

Compound	Appearance	Analyses			
		Found, %		Calcd., %	
		C	H	C	H
$Cu(o\text{-}CH_3\text{-}benz)_2$	Blue-green crystals	56.9	4.98	57.5	4.20
$Cu(m\text{-}CH_3\text{-}benz)_2$	Blue powder	56.8	5.02	57.5	4.20
$Cu(p\text{-}CH_3\text{-}benz)_2 \cdot H_2O$	Green-blue powder	54.7	5.02	54.6	5.11
$Cu(o\text{-}Cl\text{-}benz)_2 \cdot 2H_2O$	Blue-green crystals	40.2	3.34	40.9	2.95
$Cu(m\text{-}Cl\text{-}benz)_2$	Blue powder	45.2	2.35	44.9	2.15
$Cu(p\text{-}Cl\text{-}benz)_2$	Blue-green crystals	44.1	3.02	44.9	2.15
$Cu(o\text{-}OCH_3\text{-}benz)_2$	Blue-green crystals*	53.0	3.75	52.5	3.86
$Cu(p\text{-}OCH_3\text{-}benz)_2$	Blue-green crystals	51.8	4.31	52.5	3.86

* Analyzed after dehydration.

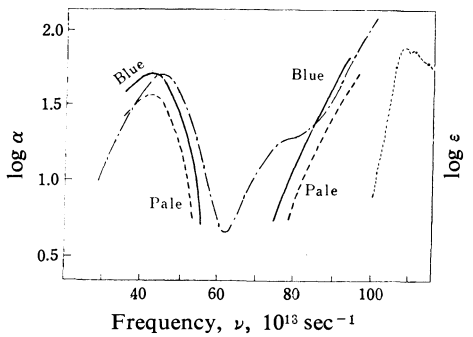


Fig. 1. Absorption spectra of $Cu(benz)_2 \cdot 3H_2O$ in dioxan containing benzoic acid in 1/50 F (—·—) and in the crystalline state (——). The notation "blue" and "pale" represent the absorption spectra along the blue polarization direction and along the pale-blue polarization direction, respectively. The absorption spectrum of benzoic acid in ether (----) is taken from H. Dannenberg, *Z. Naturforsch.*, **4b**, 327 (1949).

Cupric benzoate in dioxan shows an absorption band at about 80×10^{13} sec^{-1} (Band II) in addition to a band at about 44×10^{13} sec^{-1} (Band I), as may be seen in Fig. 1. It is found that Band I of cupric benzoate in dioxan is about ten times more intense than the intensity of the ligand field band of typical cupric complexes with no specific metal-to-metal bond, and that the intensity of Band II of cupric benzoate is considerably lower than the intensity of Band I of the same compound. These relations, which are quite similar to those of cupric alkanoates with the binuclear configuration,[2] seem to show that cupric benzoate in dioxan consists of binuclear molecules similar to those of cupric alkanoates with the copper-to-copper bond.

At least two types of crystals of cupric benzoate were obtained, one being green-blue crystals of $Cu(benz)_2 \cdot C_2H_5OH$ or $Cu(benz)_2 \cdot (benzH) \cdot 0 \cdot 5H_2O$ (Form A) and the other, pale-blue crystals of $Cu \cdot (benz)_2 \cdot 3H_2O$ (Form B). The absorption spectrum of the pale-blue crystal (Fig. 1) was determined on the (010) face with light polarized along the two extinction directions of the crystal. Cupric benzoate trihydrate in the crystalline state exhibits one ligand field band in the low frequency region (about 42×10^{13} sec^{-1}), but no absorption band at 80×10^{13} sec^{-1} until an intense absorption

band, due mainly to the ligands, appears in the region of about 90×10^{13} sec^{-1} to a higher frequency. The band at 42×10^{13} sec^{-1} may be assigned to spin-allowed *d-d* transition. According to the crystal structure analysis,[7] the crystal consists of octahedra of [CuO_6], which share two water molecules in such a way that a column extending along the c-axis is formed. The crystal structure analysis also indicates that the z-axis of one component of [CuO_6] is inclined to the c-axis of the crystal at an angle of about 37° and to the a-axis at an angle of 53°. The estimate using the data of the crystal analysis shows that the ratio of K_{xy} to K_z is approximately 9 for the ligand field band at about 42×10^{13} sec^{-1}. The ratio derived above shows clearly that the xy-absorption is much more intense than the z-absorption, in agreement with the results of the former studies of cupric complexes of an ordinary kind with no specific copper-to-copper bond.[1,8] Thus the crystal spectrum of cupric benzoate trihydrate at room temperature is quite different from that expected for the binuclear complex with the copper-to-copper bond. It is concluded that, in the crystal of cupric benzoate trihydrate at room temperature, there is no copper-to-copper bond similar to the case of cupric acetate monohydrate, although the nearest copper-copper distance is comparatively short (3.15Å). This result is in agreement with the magnetic measurement.[5] This, however, does not completely exclude the possibility that the copper-to-copper bond formation may occur at a lower temperature.

On the contrary, the green-blue crystal of $Cu(benz)_2\cdot C_2H_5OH$ (Form A), which usually grows in the form of hexagonal prisms, exhibits absorption bands at about 79 and 44×10^{13} sec^{-1}, the polarization of the former band being the reverse of that latter. The absorption at about 79×10^{13} sec^{-1} is far more intense along the needle-axis of the crystal than along the direction perpendicular to the needle-axis. The absorption at about 44×10^{13} sec^{-1} is slightly (1/1.5 times) weaker along the needle-axis. This type of dichroism is quite similar to the dichroism reported for a number of cupric carboxylates with the copper-to-copper bond.[2,3] Although the crystal structure analysis of this form is not available, it may safely be concluded from the dichroism that the blue-green form of $Cu(benz)_2\cdot C_2H_5OH$ consists of binuclear molecules of the cupric-acetate type, with the copper-to-copper bond within the molecule. This result agrees with that of magnetic study.[5] An essentially similar relation was obtained for $Cu(benz)_2\cdot(benzH)\cdot 0.5H_2O$ through the dichroism measurement.

The assignment of the absorption bands of the binuclear cupric complex with the metal-to-metal bond has not been finally settled, but it certainly is similar to cupric acetate and alkanoates.[9] A detailed discussion will be presented elsewhere.[10]

Forms A and B were found to give quite identical absorption curves in dioxan; it is therefore concluded that both of them consist of binuclear molecules of the acetate type in dioxan. It is also found, for substituted benzoates of copper(II), that different forms exhibit identical electronic absorption spectra in solution.

Cupric Complexes of Substituted Benzoic Acids.—As Fig. 2 shows, cupric complexes of *o*-, *m*- and *p*-methylbenzoic acids in dioxan all show an absorption band at about 43~45 $\times10^{13}$ sec^{-1} (Band I). In addition, the compounds show a band at about 80×10^{13} sec^{-1} (Band II) the intensity of which is considerably lower than the intensity of band I. Another intense absorption band, which rises sharply from about 90×10^{13} sec^{-1} towards a higher frequency, may be due to the charge-transfer-absorption system of the binuclear cupric complex, superposed over the absorption band due mainly to the methylbenzoate ion, since the methylbenzoate ions alone are found to show absorption bands in this frequency region. The intensity of Band I is several times higher than the ligand field band of cupric complexes of an ordinary type. On the same grounds as in the case of cupric

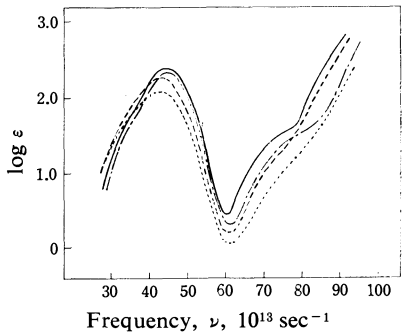


Fig. 2. Absorption spectra of cupric *o*-methylbenzoate in dioxan (——), and in methanol (----), and of cupric *m*-methylbenzoate in dioxan (—·—) and in methanol (·····). Each solution contains *o*- or *m*-methylbenzoic acid in 1/50 F.

7) H. Koizumi, K. Osaki and T. Watanabe, *J. Phys. Soc. Japan*, **18**, 117 (1963).
8) S. Yamada and R. Tsuchida, This Bulletin, **29**, 289, 694 (1956).
9) L. S. Forster and C. J. Ballhausen, *Acta Chem. Scand.*, **16**, 1385 (1962); I. G. Ross, *Trans. Faraday Soc.*, **55**, 1058 (1959).
10) M. L. Tonnet, S. Yamada and I. G. Ross, to be published.

alkanoates, it has been concluded that *o*-, *m*- and *p*-methylbenzoates of copper(II) in dioxan consist of the binuclear molecules of the acetate type.

The *o*-, *m*- and *p*-chlorobenzoates of copper-(II) in dioxan also show absorption spectra which are similar, in both the band maxima and the intensity relation, to one another and to the spectra of the methylbenzoates (Fig. 3).

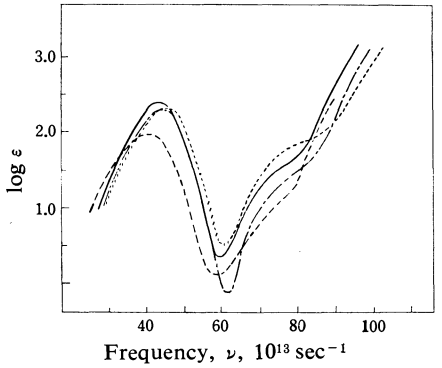


Fig. 3. Absorption spectra of cupric *o*-chlorobenzoate in dioxan (——) and in methanol (----), cupric *p*-chlorobenzoate (—·—), and cupric *p*-hydroxybenzoate (·····) in dioxan. The solutions all contain the corresponding substituted benzoic acid in 1/50 F.

It has been similarly concluded that *o*-, *m*- and *p*-chlorobenzoates of copper(II) in dioxan consist of binuclear molecules of the acetate type with a direct type of linkage between the two copper ions.

The electronic absorption spectra of *o*- and *p*-methoxybenzoates of copper(II) have been determined in dioxan. Since the two complexes show quite similar spectra, only one of them is shown in Fig. 4. For the same reason, only cupric *o*-nitrobenzoate is shown in the figure. It has been concluded, in the same way as has been described above, that cupric complexes of *o*- and *p*-methoxybenzoates in dioxan consist of binuclear molecules of the acetate-type.

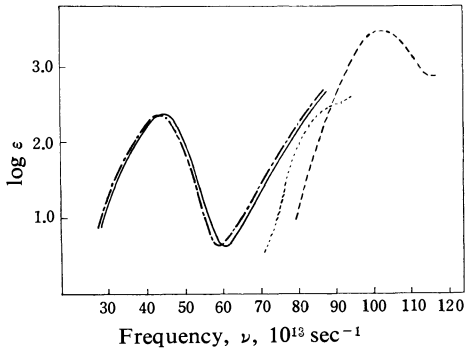


Fig. 4. Absorption spectra of *o*-nitrobenzoic acid (·····), cupric *o*-nitrobenzoate (—·—) and *o*-methoxybenzoate (——) in dioxan. The latter two solutions contain the corresponding substituted benzoic acid in 1/50 F. The absorption curve of *o*-methoxybenzoic in dioxan (----) is taken from E. D. Bergmann, Y. Hirshberg and S. Pinchas, *J. Chem. Soc.*, **1950**, 2351.

The *m*- and *p*-hydroxybenzoate ions in the cupric complexes reported in this paper are considered to be co-ordinated with the cupric ion through their carboxylate group. The *o*-hydroxybenzoate is different from the *m*- and *p*-homologues in their way of co-ordination to the metallic ion, since it can be co-ordinated to the cupric ion through the oxygen atoms of both the phenolate and the carboxylate groups. The *o*-hydroxybenzoate of copper (II) is, therefore, omitted in the present paper.

Cupric *m*- and *p*-hydroxybenzoates show absorption bands at about 45×10^{13} sec^{-1}, but the band at about 80×10^{13} sec^{-1} is obscured to some extent by a much stronger specific absorption bands due mainly to the ligand ion (Fig. 3). A more precise inspection of the curves, however, clearly reveals the presence of the band at about 80×10^{13} sec^{-1}, which corresponds to Band II. It is concluded, therefore, that cupric *m*- and *p*-hydroxybenzoates consist of binuclear molecules similar to those of cupric alkanoates with copper-to-copper linkage within the molecules.

As may be seen in Fig. 4, cupric *o*-, *m*- and *p*-nitrobenzoates in dioxan all show their ligand field band at about 43 to 44×10^{13} sec^{-1}, in the frequency region slightly lower than that of cupric benzoate, but still in the region expected for the binuclear copper(II) carboxylates. Moreover, the intensity of Band I is several times higher than that of ligand field bands of ordinary cupric complexes. The quite high intensity of Band I and the frequency of the band maximum are in agreement with the assumption that the nitrobenzoates of copper-(II) in dioxan consist of binuclear molecules similar to the molecules of cupric alkanoates. The band at about 80×10^{13} sec^{-1}, which is observed with the chloro- and methylbenzoates of copper(II), is not observed with cupric nitrobenzoates. This failure to be observed is, however, regarded as due to the much stronger absorption of the ligand, which is superposed over Band II. An analysis of the absorption curve, which involves the subtraction of the absorption expected for the ligand, reveals the presence of the band at about 80×10^{13} sec^{-1}, the intensity of the band being much lower than that of Band I. This agrees with the binuclear model for the cupric nitrobenzoates in dioxan.

The electronic absorption spectra of cupric chlorobenzoates and methylbenzoates were determined in methanol containing the corresponding substituted benzoic acids in 1/50 F (Figs. 2 and 3). The intensity of the absorption band at about 80×10^{13} sec^{-1} is greatly lowered, and Band I is displaced toward a lower frequency compared with the dioxan solution. This shows that the cupric carboxylates are more liable to form the binuclear complex of the acetate type in dioxan than in methanol, the dissociation of the binuclear complex most probably taking place to an appreciable extent in the latter solvent. This conclusion agrees with the findings about many other cupric carboxylates.[3]

Crystal absorption spectra were examined with some of these cupric complexes (Table III). Since, however, the crystal structure of none of these complexes has been determined, a detailed analysis of the crystal spectra is not possible at the moment. The following points, however, have been definitely confirmed for the cupric *o*-methyl-, *o*-chloro-, *o*-nitro- and *m*-hydroxybenzoates. (1) The blue-green crystals of these complexes show absorption bands at about 43~45 and 80×10^{13} sec^{-1}, the former being several times more intense than the latter. (2) The polarization of the former band is the reverse of the latter. It has been safely concluded that these cupric carboxylates consist of binuclear molecules with the copper-to-copper bond.

Table III. Absorption maxima of cupric benzoate and substituted benzoates in the solid state*

Cmpound	ν(Band I)	ν(Band II)
$Cu(benz)_2\cdot3H_2O$	41.5	None
$Cu(benz)_2\cdot C_2H_5OH$	44.5	79.5
$Cu(benz)_2\cdot(benzH)\cdot0.5H_2O$	44.3 43.8**	ca. 80 ca. 80**
$Cu(o\text{-}CH_3\text{-}benz)_2$	45.0	ca. 80
$Cu(o\text{-}Cl\text{-}benz)_2\cdot2H_2O$	44.0	ca. 79
$Cu(m\text{-}OH\text{-}benz)_2\cdot H_2O$	45.0	ca. 79
$Cu(p\text{-}OH\text{-}benz)_2\cdot6H_2O$	41.5	None
$Cu(m\text{-}NO_2\text{-}benz)_2\cdot H_2O$**	45.0	Covered
$Cu(o\text{-}NO_2\text{-}benz)_2$	44.5	Covered

ν: 10^{13} sec^{-1}
* Unless otherwise indicated, the value is based upon the crystal spectrum.
** Reflection spectrum of the powder.

On the contrary, $Cu(p\text{-}OH\text{-}benz)_2\cdot6H_2O$ in the crystalline state shows an absorption band at about 41.5×10^{13} sec^{-1}, but no band at about 80×10^{13} sec^{-1}, so the crystal contains no binuclear complex of the acetate type.

General Discussion. — Regarding the same substituent, an inspection of Table IV reveals that the absorption maximum of Band I of cupric complexes is parallel with the acid dissociation constant of the substituted benzoic acids. Since the frequency of Band I is regarded as representing approximately the magnitude of the crystal field splitting of the copper(II) ion, the above relation may readily be understood if it is assumed that copper-to-ligand bond becomes stronger as the acid dissociation constant of the parent acid of the ligand decreases. This agrees qualitatively with the previous results about cupric complexes.[11,12] It was also pointed out formerly[3] that the larger acid dissociation constant of the ligand carboxylic acid does not favor the formation of the binuclear molecule with the copper-to-copper bond.

Table IV. Absorption maxima of band I of cupric substituted benzoates and dissociation constants K of the substituted benzoic acids*

R		*o*-	*m*-	*p*-
NO_2	ν	43.4	43.7	43.5
	log ε	2.37	2.34	2.22
	10^5K	671	32.1	37.6
Cl	ν	44.0	44.1	44.4
	log ε	2.40	2.38	2.40
	10^5K	114	14.8	10.5
CH_3	ν	44.6	44.6	44.7
	log ε	2.39	2.33	2.37
	10^5K	12.3	5.35	4.24
OH	ν	—	44.5	45.1
	log ε	—	2.25	2.33
	10^5K	—	8.3	2.9
OCH_3	ν	44.7	—	44.9
	log ε	2.38	—	2.38
	10^5K	8.06	—	3.38
H	ν(log ε)		44.7	(2.42)
	10^5K		6.27	

* The values of K are taken from A. E. Remick, "Electronic Interpretations of Organic Chemistry," John Wiley & Sons, Inc., New York (1950), p. 65.

On closer examination of the data, however, deviation from the parallelism may be recognized in connection with the compounds of the *o*-series. Thus, it may be seen in Fig. 5 that, among *m*- and *p*-substituted benzoates of copper(II) with various substituents, there is a linear proportionality between the pK values of the carboxylic acids and the maxima

11) B. R. James, M. Parris and R. J. P. Williams, *J. Chem. Soc.*, **1961**, 4630.
12) R. May and M. M. Jones, *J. Inorg. Nucl. Chem.*, **24**, 511 (1962).

of the ligand field bands (Band I) of their cupric compounds. The *o*-derivatives, however, show an appreciable deviation from the straight line of the *m*- and *p*-derivatives, although there seems to be a linear relation among the derivatives of the *o*-series alone. This behavior of the *o*-substituted benzoates seems to be related with the so-called "ortho-effect" which is often observed, for example, in the reactions of aromatic compounds, including the substituted benzoic acids.[13] The apparent anomaly of the cupric complexes of *o*-substituted

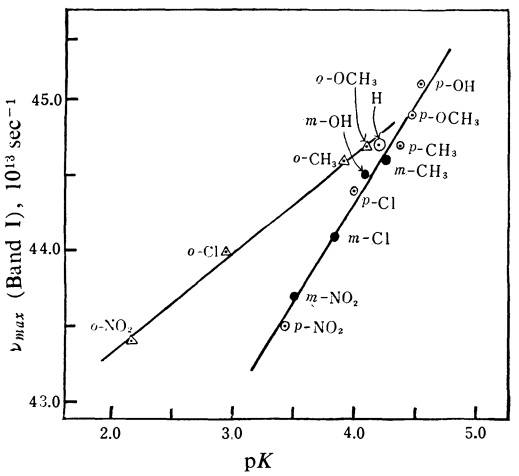


Fig. 5. Plots of absorption maxima (ν) of Band I of cupric substituted benzoates vs. pK of the substituted benzoic acids.

benzoates, as observed in the present work, seems to show that the ortho-effect may be operative in the case of cupric complexes, but in a different way from that of the substituted benzoic acids themselves. The ortho-effect in the dissociation constant of the substituted benzoic acids may be interpreted as mostly due to a twisting of the carboxyl-group from the benzene plane.[13] If this mechanism is assumed to be correct, the observed deviation of the *o*-substituted complexes seems to indicate that the twisting of the carboxyl-group from the benzene plane may be different in the cupric complexes from the twisting in the nucomplexed ion of the substituted benzoates.

On the other hand, Band II is obscured more or less significantly by much stronger absorption bands of other origins, so that it is difficult to determine the exact maximum for most complexes. No discussion similar to that above was, therefore, attempted on the basis of Band II.

13) C. K. Ingold, "Structure and Mechanism in Organic Chemistry," Cornell University Press, Ithaca, New York (1953), p. 140, etc.

Summary

Cupric complexes of benzoic and substituted benzoic acids have been prepared, and their configurations in the solid state and in dioxan examined. The substituents have included methyl, chloro, methoxy, nitro and hydroxy groups.

These cupric complexes in dioxan all consist of binuclear cupric complexes with the copper-to-copper bond. Crystal absorption spectra show that $Cu(benz)_2 \cdot C_2H_5OH$ and $Cu(benz)_2 \cdot (benzH) \cdot 0.5H_2O$ in the crystalline state consist of the binuclear complexes, whereas $Cu \cdot (benz)_2 \cdot 3H_2O$ has no such complexes with the copper-to-copper bond. The absorption spectra of several substituted benzoates of copper(II) in the solid state have also been determined, and the structure of the complexes discussed.

It has been found that the maxima of Band I of substituted benzoates of copper(II) in dioxan are linearly dependent upon the pK values of the substituted benzoic acids themselves.

The authors wish to record their gratitude to the late Professor Ryutaro Tsuchida for his interest in the present work, to Dr. Kenji Osaki of the Physics Department for information about the crystal structure of cupric benzoate trihydrate, and to the Ministry of Education for financial support.

Department of Chemistry
Faculty of Science
Osaka University
Nakanoshima, Osaka

NOTES

*The Radiation-induced Reaction of Sulfur in Various Solvents**

By Wataru ANDO, Ken'ichi SUGIMOTO and Shigeru OAE

(Received September 9, 1963)

Previous papers have described studies of the radiolysis of both benzene and toluene solutions of sulfur.[1-2] The reaction products reported have included such substances as mercaptan, disulfide, sulfide, hydrogen sulfide, hydrogen and other hydrocarbons. Among these products, quantitative determination is possible for mercaptan, hydrogen and hydrogen sulfide.

The radiolysis of solvent hydrocarbon produces free radicals which attack sulfur at room temperature; mercaptan is then formed in this manner:

$$RH \xrightarrow{I} R + H \quad (1)$$

$$R + S_8 \rightarrow RS_8 \rightarrow RS \quad (2)$$

The formation of mercaptan depends mainly on the bond dissociation energy of C–H in the solvent, because the formation of mercaptan through Eq. 3

$$RS + H \rightarrow RSH \quad (3)$$

$$RS + RH \rightarrow RSH + R \quad (4)$$

is rare, even though the reaction in benzene shows very little tendency to undergo radical displacement (reaction 4).

In the reaction with toluene, the benzyl mercapto radical would abstract hydrogen from the methyl group of toluene since its C–H bond is known to be quite weak.

In this investigation, *G*-values for the formation of various mercaptans and hydrogen in the radiolysis of various hydrocarbon solutions of sulfur will be determined, and the *G*-value of hydrogen formation will be compared with these of the corresponding hydrocarbons with the hope of obtaining some direct infomation on the effect of hydrocarbons as solvents on the radiolysis of hydrocarbon solutions of sulfur.

Experimental

The experimental details are similar to those outlined in an earlier paper.[1] The sulfur used in this work was a portion of an exceptionally pure sample previously employed. The solvents were purified by conventional fractional distillations. A solution of sulfur in a solvent was made by weighing and then degassing it by freezing, pumping and thrawing in vacuo. After irradiation, each ampoule was attached to a vacuum line in order to analyze the hydrogen formation. The amount of mercaptan was determined by a potentiometric titration with silver nitrate.[3]

Results and Discussion

The data in Table I on the radiolysis of sulfur in various hydrocarbons indicates that the *G*-values of the formations of mercaptans were of similar magnitudes, with only a little difference caused by the differences in the stabilities of the mercaptans formed.

TABLE I. THE FORMATION OF MERCAPTANS IN THE RADIOLYSIS OF SULFUR WITH HYDROCARBONS AS SOLVENTS (THE CONCENTRATION OF SULFUR IS 0.2 g. PER 50 ml. OF SOLVENT)

Solvent	*G*-value for the mercaptan formation
Hexane	0.06
Cyclohexane	0.07
Mesitylene	0.06
Ethylbenzene	0.06
p-Xylene	0.05
Toluene	0.09
Diphenylmethane	0.013

The interesting feature of Table I is that the radicals formed in the radiolysis of these hydrocarbons as solvents showed similar reactivities toward sulfur. The formation mercaptan is considered to depend on the concentration of sulfur and on the stability of the

* The Study of the Radiation Chemistry of Organic Sulfur Compounds. Part V.

1) W. Ando, K. Sugimoto and S. Oae, This Bulletin, 36, 893 (1963).

2) W. Ando, K. Sugimoto and S. Oae, ibid., in press.

3) M. W. Tamele and L. B. Ryland, *Ind. Eng. Chem. Anal. Ed.*, 8, 16 (1936).

radical formed.

In a diphenylmethane solution of sulfur, the *G*-value for the mercaptan formation is about one-fifth that of the other solvents. Probably the radical, formed in the radiolysis of diphenyl methane, is substantially resonance-stabilized and is, therefore, not reactive enough to open the sulfur ring as do the other solvents.

The Effects of Sulfur on the Formation of Hydrogen from Solvents. — The *G*-value of hydrogen formation observed for various solvent solutions of sulfur are given in Table II, together with those from hydrocarbons without sulfur.

The *G*-values of hydrogen formation in both hexane and cyclohexane solutions of sulfur are appreciably decreased by the presence of sulfur. A similar decrease in hydrogen formation has been reported in other cyclohexane solutions with other solutes dissolved in them.[7] Therefore, these decreases do not seem to be due to any specific chemical nature of the added solute but merely to the introduction of some new physical impurities into the system. The *G*-values of hydrogen formation for mesitylene, ethylbenzene, *p*-xylene and toluene do not change regardless of the presence or absence of sulfur in the hydrocarbons. Here the formation of hydrogen is mainly due to the following reaction:

$$H + RH \rightarrow H_2 + R$$

It is, therefore, not affected by the presence of sulfur. A similar observation on the lack of the effect of the hydrogen atom in the formation of hydrogen sulfide has been reported previously in the system of toluene and sulfur.

TABLE II. THE *G*-VALUE OF HYDROGEN FORMATION IN THE RADIOLYSIS OF HYDROCARBONS

Solvent	In the presence of sulfur	Without sulfur
Hexane	1.6	5.0
Cyclohexane	3.05	5.85[4]
Mesitylene	0.25	0.24[5]
Ethylbenzene	0.19	0.18[6]
p-Xylene	0.17	0.22
Toluene	0.12	0.13[6]
Diphenylmethane	0.026	0.027

4) M. Burton, J. Chang, S. Lipsky and M. P. Reddy, *Rad. Res.*, **8**, 203 (1958).
5) R. R. Hentzad and M. Burton, *J. Am. Chem. Soc.*, **73**, 532 (1951).
6) T. J. Sworski and M. Burton, ibid., **73**, 3970 (1951).
7) R. H. Schuler, *J. Phys. Chem.*, **61**, 1474 (1957).

Department of Chemisty
Radiation Center of Osaka Prefecture
Sakai, Osaka (W. A. & K. S.)

Department of Applied Chemistry
Faculty of Engineering
Osaka City University
Kita-ku, Osaka (S. O.)

Synthesis of Fluoro-aryloxy Fatty Acids and Their Mono-mercurated Derivatives

By K. C. SRIVASTAVA

(Received September 17, 1963)

A considerable amount of work has been done in recent years on pest control chemicals, but comparatively very little work has been done on aromatic fluorine compounds which may act as potential pest control chemicals. The synthesis of several fluoro-aryloxy fatty acids and their mercury derivatives has been reported earlier.[1] Some of these compounds have been investigated for their toxicity against "Alternaria solani" with encouraging results.[2] The present investigation deals with the synthesis of some flourine substituted aryloxy fatty acids and their mercury derivatives as possible antifungal agents.

The condensation of 2-chloro-4-fluorophenol and 2-bromo-4-fluorophenol with halogenated fatty acids in sodium hydroxide solution[3] provides a good method for preparation of fluorine substituted aryloxy fatty acids. The fluoroaryloxy fatty acids have been mercurated

1) K. C. Joshi and S. C. Bahel, *J. Ind. Chem. Soc.*, **37**, 365 (1960).

2) K. C. Joshi et al., *J. Sci. Ind. Res.*, **21c**, 315 (1962).

3) N. V. Hayes and G. E. K. Branch, *J. Am. Chem. Soc.*, **65**, 1555 (1943).

TABLE I

Sample No.	α-Fluoro-aryloxy fatty acid	B. p. °C/mmHg	Yield %	Neut. equiv. Found	Neut. equiv. Calcd.	C, % Found	C, % Calcd.	H, % Found	H, % Calcd.
1	2-Chloro-4-FP propionic acid	144/0.2	60	218.0	218.5	49.00	49.40	3.60	3.66
2	2-Chloro-4-FP butyric acid	154/1	64	232.1	232.5	51.20	51.60	4.25	4.30
3	2-Chloro-4-FP valeric acid	143.5/0.1	48.5	246.0	246.5	53.00	53.54	4.80	4.86
4	2-Chloro-4-FP caproic acid	150.5/1	52	260.8	260.5	54.80	55.27	5.30	5.37
5	2-Chloro-4-FP caprylic acid	169/0.1	48	288.1	288.5	57.60	58.20	6.20	6.23
6	2-Chloro-4-FP capric acid	175/0.05	55	315.9	316.5	60.20	60.66	6.88	6.95
7	2-Bromo-4-FP propionic acid	141/0.05	60	262.4	263.0	40.80	41.06	2.95	3.04
8	2-Bromo-4-FP butyric acid	170/3	56.5	276.5	277.0	43.10	43.32	3.54	3.61
9	2-Bromo-4-FP valeric acid	166/1	56	290.9	291.0	44.90	45.30	4.10	4.12
10	2-Bromo-4-FP caproic acid	180/4	52.5	304.2	305.0	47.00	47.21	4.55	4.59
11	2-Bromo-4-FP caprylic acid	197/1	51	332.4	333.0	50.40	50.48	5.35	5.40
12	2-Bromo-4-FP capric acid	208/1	52	360.2	361.0	52.90	53.18	5.96	6.09

FP Fluorophenoxy

TABLE II

Sample No.	Mercury derivative $XFC_6H_2(OCHR\cdot CO_2)Hg$ X	R	M. p.	Hg, % Found	Hg, % Calcd.	C, % Found	C, % Calcd.	H, % Found	H, % Calcd.
1	Cl	CH_3	—	47.6	48.0	25.7	25.9	1.4	1.44
2	Cl	C_2H_5	—	46.0	46.45	27.4	27.8	2.0	2.03
3	Cl	C_3H_7	—	44.5	45.0	29.2	29.6	2.2	2.24
4	Cl	C_4H_9	—	43.8	43.4	30.9	31.3	2.54	2.61
5	Cl	C_6H_{13}	224°C	40.6	40.11	34.25	34.46	3.25	3.28
6	Cl	C_8H_{17}	—	39.2	38.91	37.0	37.26	3.85	3.88
7	Br	CH_3	250°C (+)	42.9	43.4	23.20	23.39	1.28	1.30
8	Br	C_2H_5	—	41.9	42.1	25.10	25.23	1.65	1.68
9	Br	C_3H_7	—	41.6	41.0	26.8	26.98	2.00	2.04
10	Br	C_4H_9	302°C	39.9	39.80	28.35	28.59	2.35	2.38
11	Br	C_6H_{13}	—	37.3	37.73	31.45	31.60	2.98	3.00
12	Br	C_8H_{17}	—	35.55	35.84	34.0	34.31	3.55	3.57

— Solid did not melt. (+) decomposed.

by the mtehod of Joshi.[1]

Further work on these compounds, viz. their suitability as fungicides against a wide range of fungi, is in progress.

Experimental

2-Chloro-4-fluorophenol was conveniently prepared by passing chlorine gas (40 g.) into *p*-fluorophenol (135 g.) in presence of iron fillings at room temperature for 7~8 hr., b. p. 60.5~61.5°C/0.1~1 mmHg. Finger et al.[4] reported b. p. 88°C/40 mmHg (Mol. wt., Found : 148.8. Calcd. : 146.55). 2-Bromo-4-fluorophenol was prepared by treating *p*-fluorophenol (50 g.) with bromine (72 g.) in carbon disulphide, b. p. 58~60°C/0.5 mmHg. Finger etal.[4] reported b. p. 89°C/1 mmHg. (Mol. wt., Found : 192.5. Calcd. : 191.01).

α-Fluoro-aryloxy fatty acids were prepared by the method of Joshi et al.[1] The compounds were characterized by the determination of their neutralization equivalents and are listed in Table I.

Preparation of Mercury Derivatives.—The α-fluoro-aryloxy fatty acids were mercurated by the method of Joshi.[1] A mixture of equimolecular quantities of fluoro-aryloxy fatty acids in ethyl alcohol and yellow mercuric oxide in acetic acid was treated for 4 to 6 hr., till a sandy powder separated. The powder was washed with hot water, hot dilute acetic acid and hot ethyl alcohol. The results of elementary analyses are recorded in Table II. It is evident that mono-mercurated derivatives are formed.

Department of Chemistry
Birla College of Engineering
Pilani (Rajasthan), India

4) G. C. Finger et al., ibid., **81**, 94, (1959).

Hydrogenation and Hydrogenolysis. VIII.[1] *The Ruthenium-catalyzed Hydrogenation of Aromatic Compounds Containing C–O Linkage to be Easily Hydrogenolyzed*

By Yuzuru TAKAGI, Takatoshi NAITO and Shigeo NISHIMURA

(Received October 23, 1963)

In a series of papers[1,2] it has been shown that (3 : 1) or (7 : 3) rhodium-platinum oxide of Adams' type is a very effective catalyst for selective hydrogenation where one desires to avoid the hydrogenolysis of the C–O linkage. Similar results have also been reported in hydrogenation with 5% rhodium-on-alumina as the catalyst.[3-6]

Only a few examples of the use of ruthenium catalysts in the selective hydrogenation of this kind seem to have been described in the literature. Fairly good yields have been obtained in the hydrogenation of some phenyl-substituted α, ω-glycols,[7] *p*-aminoacetophenone[8] and benzaldehyde[9] to the corresponding saturated glycols or alcohols.

This paper will describe the general applicability of ruthenium dioxide catalyst to the selective hydrogenation of aromatic compounds containing C–O linkage to be easily hydrogenolyzed. This catalyst was also compared with rhodium or (7 : 3) rhodium-platinum oxide in some hydrogenations.

The ruthenium-catalyzed hydrogenation of the aromatic compounds listed in Table I was carried out at 95 to 100°C and under 80 to 100 kg./cm^2 of hydrogen pressure. Usually the use of a solvent was unnecessary, although a small amount of acetic acid was added to neutralize a trace of alkaline substances remaining in the catalyst. Under these conditions most hydrogenations proceed rather rapidly, and good yields of the corresponding saturated alcohols or ethers are obtained. For the successful hydrogenation of benzyl alcohol and benzaldehyde, it was necessary to use ethanol or water as the solvent; otherwise the rate decreased markedly during the hydrogenation. It should be noted that the hydrogenation of these compounds with rhodium or (7 : 3) rhodium-platinum oxide was unsuccessful, even in the presence of alcohol or water.[10] Platinum oxide gives a good yield of cyclohexylcarbinol in the hydrogenation of benzyl alcohol in ethanol containing a small amount of acetic acid,[11] but the rate of the hydrogenation is slow, even under high pressure.

The proportion of hydrogenolysis was somewhat greater with ruthenium dioxide than with rhodium or (7 : 3) rhodium-platinum oxide in the hydrogenation of phenyl ether, hydroquinone dimethyl ether and ethyl *p*-hydroxybenzoate. The probable cause of the higher selectivity of rhodium and (7 : 3) rhodium-platinum oxides over ruthenium dioxide is their use at lower temperature, the former catalysts being sufficiently active at that temperature. It may be explained on the basis of the same reasons that a somewhat larger quantity of *trans*-1, 4-dimethoxycyclohexane and ethyl *trans*-4-hydroxycyclohexane-1-carboxylate was obtained with ruthenium dioxide than with rhodium or (7 : 3) rhodium-platinum oxide.

Benzyl acetate, where the most extensive hydrogenolysis occurred among the compounds investigated, gave a 30% yield of hexahydrobenzyl acetate with ruthenium dioxide. This yield was better than those obtained with rhodium or (7 : 3) rhodium-platinum oxide, though the reaction temperature was higher for the ruthenium catalyst.

Experimental

Catalysts—Ruthenium dioxide was prepared according to the method of Pichler and Buffleb.[12]

Rhodium oxide and (7 : 3) rhodium-platinum

1) Part VII of this series: S. Nishimura and H. Taguchi, This Bulletin, **36**, 353 (1963).
2) S. Nishimura et al., ibid., **33**, 566, 1356 (1960); **34**, 32, 1544 (1961); **36**, 318 (1963).
3) H. A. Smith and R. G. Thompson, "Advances in Catalysis," Vol. IX, Academic Press Inc., New York (1957), p. 727.
4) H. A. Smith and B. L. Stump, *J. Am. Chem. Soc.*, **83**, 2379 (1961).
5) J. H. Stocker, *J. Org. Chem.*, **27**, 2288 (1962).
6) I. A. Kage and R. S. Matthews, ibid., **28**, 325 (1963).
7) H. W. Arnold, U. S. Pat. 2555912 (1951) [*Chem. Abstr.*, **46**, 3074f (1952)].
8) M. Freifelder and G. R. Stone, *J. Org. Chem.*, **27**, 3568 (1962).
9) Y. Takagi, *Sci. Papers Inst. Phys. Chem. Research (Tokyo)*, **57**, 105 (1973).
10) Cf. S. Nishimura, This Bulletin, **34**, 32 (1961); J. H. Stocker, Ref. 5.
11) S. Nishimura, This Bulletin, **32**, 1155 (1959).
12) H. Pichler and H. Buffleb, *Brennstoff-Chem.*, **21**, 257 (1940).

TABLE I. HYDROGENATION OF AROMATIC COMPOUNDS CONTAINING C-O LINKAGE TO BE EASILY HYDROGENOLYZED WITH RUTHENIUM, RHODIUM, AND (7 : 3) RHODIUM-PLATINUM CATALYSTS*

Compound	Catalyst	Solvent or additive, ml.	Temp. °C	Time for hydrogenation min.	% Product
Anisole	Ru oxide	10%AcOH, 0.5	80～82	10	89 Cyclohexyl methyl ether[a]
Hydroquinone dimethyl ether	Ru oxide	10%AcOH, 0.5	95～100	200	74 1, 4-Dimethoxycyclohexane[b] (81% cis, 19% trans)[c] 13 Cyclohexyl methyl ether
Hydroquinone dimethyl ether	Rh oxide	AcOH, 0.05	50～55	65	91 1, 4-Dimethoxycyclohexane[c] (77% cis, 23% trans) 9 Cyclohexy methyl ether[c] Cyclohexane (trace)[c]
Hydroquinone dimethyl ether	Rh oxide**	AcOH, 15	30～32	30	91 1, 4-Dimethoxycyclohexane[c] (85% cis, 15% trans) 9 Cyclohexyl methyl ether[c] Cyclohexane(trace)[c]
Hydroquinone dimethyl ether	(7 : 3)Rh-Pt oxide	AcOH, 15	30～33	15	92 1, 4-Dimethoxycyclohexane[c] (83% cis, 17% trans) 8 Cyclohexyl methyl ether[c] Cyclohexane(trace)[c]
Phenyl ether	Ru oxide	10%AcOH, 0.5	95～100	38	66 Cyclohexyl ether[d] 25 Cyclohexanol[e] (+Cyclohexane)
Phenyl ether	Rh oxide**	AcOH, ca. 2	35～37	85	84 Cyclohexyl ether[c] 16 Cyclohexanol[c] (+Cyclohexane)
Phenyl ether	(7 : 3)Rh-Pt oxide	AcOH, 0.05	35～40	55	87 Cyclohexyl ether[f] 8 Cyclohexanol[f] (+Cylohexane)
Ethyl *p*-hydroxybenzoate	Ru oxide	EtOH, 30 + 10%AcOH, 0.5	95～100	75	96 Ethyl 4-hydroxycyclohexane-1-carboxylate[c,g] (84% cis, 16% trans) 4 Ethyl cyclohexanecarboxylate[c]
Ethyl *p*-hydroxybenzoate	Rh oxide	EtOH, 15 + AcOH, 0.05	50～65	30	98 Ethyl 4-hydroxycyclohexane-1-carboxylate[c] (87% cis, 13% trans) 2 Ethyl cyclohexanecarboxylate[c]
Benzyl alcohol	Ru oxide	EtOH, 30 + 10%AcOH, 0.5	95～100	80	81 Cyclohexylcarbinol[h]
Benzaldehyde	Ru oxide	H_2O, 30 + 10%AcOH, 0.5	95～100	54	72 Cyclohexylcarbinol
Benzyl acetate	Ru oxide	10%AcOH, 0.5	95～100	44	30 Hexahydrobenzyl acetate[i] (+Methylcyclohexane)
Benzyl acetate	Rh oxide**	AcOH, ca. 2	30～32	80	18 Hexahydrobenzyl acetate[c] 82 Methylcyclohexane[c]
Benzyl acetate	(7 : 3)Rh-Pt oxide	AcOH, 0.05	30～35	50	20 Hexahydrobenzyl acetate[c] 80 Methylcyclohexane[c]
Benzyl ether	Ru oxide	10%AcOH, 0.5	95～100	125	85 Hexahydrobenzyl ether[j] 6 Cyclohexylcarbinol (+Methylcyclohexane)
Acetophenone	Ru oxide	10%AcOH, 0.5	95～100	7	90 1-Cyclohexylethanol[k]
Benzophenone	Ru oxide	10%AcOH, 0.5	95～100	22	Dicyclohexylcarbinol

* The substrate (0.1 mol.) was hydrogenated with 0.1 g. (as oxide) of the catalyst at 80 to 100 kg./cm² pressure of hydrogen.

** The oxide was pre-reduced for about one and a half hours in acetic acid at 40 to 45°C under the atmospheric pressure of hydrogen.

a) B. p. 131°C ; n_D^{20} 1.4342 b) B. p. 76～80°C/23 mmHg c) Analyzed by gas chromatography d) B. p. 122～123°C/23 mmHg ; n_D^{20} 1.4691 e) B. p. 73～74°C/23 mmHg ; n_D^{22} 1.4632 f) The yields obtained by distillation. Gas chromatography shows 90% of cyclohexyl ether and 9% of cyclohexanol. g) Ethyl 4-hydroxycyclohexane-1-carboxylate, b. p. 152～153°C/23 mmHg, n_D^{25} 1.4645, was obtained in 91% yield by distillation. h) B. p. 95～95.5°C/28 mmHg ; n_D^{25} 1.4615 i) B. p. 89°C/22mmHg ; n_D^{20} 1.4428 j) B. p. 153～154°C/23 mmHg ; n_D^{20} 1.4693 k) B. p. 96～97°C/30 mmHg ; n_D^{25} 1.4637 l) B. p. 167～168°C/30 mmHg ; m. p. 62～63°C.

oxide were prepared according to the procedure described previously.[13]

Hydrogenations. — All the hydrogenations were carried out in a 100 ml. bomb of an electro-magnetically-stirring type.

13) S. Nishimura, This Bulletin, **34**, 1544 (1961).

The authors are indebted to the Mitsubishi Chemical Industries Co. for its support of this work.

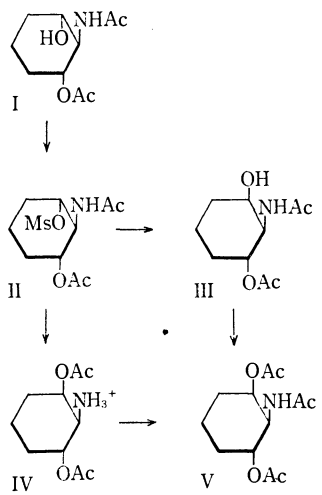
The Institute of Physical and Chemical Research
Bunkyo-ku, Tokyo

Aminocyclitols. II. Stereochemical Studies of 2-Amino-1,3-cyclohexanediol

By Tetsuo SUAMI and Seiichiro OGAWA

(Received November 1, 1963)

In connection with the previous studies of 2-amino-1, 3-cyclohexanediols,[1] an inversion reaction of *trans-O*-acetyl-*O*-mesyl-2-acetamido-1, 3-cyclohexanediol (II) has been studied. II is prepared by the mesylation of *trans-O*-acetyl-2-acetamido-1, 3-cyclohexanediol (I)[1] with mesyl chloride and pyridine. The displacement of the mesyloxy group of II gives DL-*O*-acetyl-2-acetamido-1, 3-cyclohexanediol (III) when the reaction is carried out with sodium acetate in aqueous 2-methoxyethanol. III is identical with an authentic sample[2] which is prepared from *trans-O*-dimesyl-2-acetamido-1, 3-cyclohexanediol. The demesylation of II takes place in boiling water without sodium acetate, and the product is identified as DL-isomer by converting it to the triacetyl derivative (V).[1,2] Moreover, V is obtained by the acetylation of III with acetic anhydride and pyridine.[2] Since there is only one mesyloxy group in II, the product III should have suffered from Walden inversion only at the place where the mesyloxy group had been linked. Thus, the previously-reported DL-configuration of III[1,2] is further confirmed by the present experiments.



Experimental*

***trans*-*O*-Acetyl-*O*-mesyl-2-acetamido-1, 3-cyclohexanediol (II).**—To a stirred solution of 1.1 g. of I in 15 ml. of pyridine, 0.8 ml. of methanesulfonyl chloride was added under ice cooling. After it had been stirred for 4 hr. at room temperature, the mixture was poured into ice and water. The solution was evaporated untile the precipitate appeared. The precipitate was collected by filtation. The second crop of the product was obtained by the further evaporation of the filtrate; the total yield was 1.05 g. (70%); m. p. 125~128°C. The product was recrystallized twice from acetone to give colorless needles; m. p. 137~139°C.

Found: C, 45.12; H, 6.61; N, 4.84; S, 10.83. Calcd. for $C_{11}H_{19}NO_6S$: C, 45.04; H, 6.53; N, 4.78; S, 10.93%.

DL-*O*-Acetyl-2-acetamido-1, 3-cyclohexanediol (III).—A mixture of 1.0 g. of II, 1.0 g. of anhydrous sodium acetate and 20 ml. of 95% 2-methoxyethanol was refluxed for 10 hr. The mixture was evaporated in vacuo to dryness, and the residue was extracted with boiling acetone. The acetone extract was evaporated, and the residue was recrystallized from ethanol-ether to give 0.28 g. (38%) of crystals (m. p. 151~152°C). The product was found identical with an authentic sample[2] on the basis of its mixed melting point and infrared spectra.

DL-Triacetyl-2-amino-1, 3-cyclohexanediol (V).—A mixture of 0.3 g. of II and 5 ml. of water was refluxed for 5 hr. The mixture was evaporated to

1) T. Suami and S. Ogawa, This Bulletin, 37, 194 (1964).
2) F. W. Lichtenthaler, *Chem. Ber.*, 96, 845 (1963).

* All melting points have been corrected.

give an acidic sirup, probably a methanesulfonate (IV), which showed a characteristic infrared absoption at 1200 cm^{-1}. The solvolysis might involve the N→O migration of the acetyl group in an acidic medium.[1] The sirup was treated with acetic anhydride and pyridine, and then evaporated in vacuo. The product was recrystallized from ether-petroleum ether to give 78 mg. (30%) of needles (m. p. 146°C). The product was found identical with an authentic sample[1,2] on the basis of its mixed melting point and infrared spectra.

The authors are grateful to Professor Sumio Umezawa for his helpful advice and to Mr. Saburo Nakada for his microanalysis. This work has been supported in part by a reseach grant from the Ministry of Education.

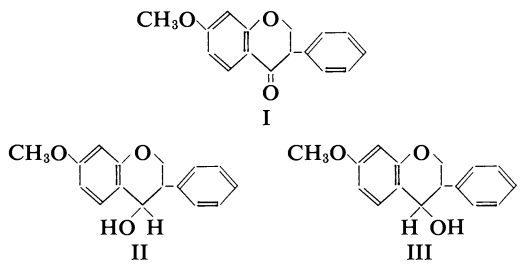
Department of Applied Chemistry
Faculty of Engineering
Keio University
Koganei, Tokyo

The Synthesis of 7-Methoxyisoflavan-4α-ol[1]

By Naoto INOUE, Shozo YAMAGUCHI and Shizuko FUJIWARA

(Received November 11, 1963)

In a previous paper[2] it was reported that the reduction of 7-methoxyisoflavanone[3] (I) with sodium borohydride gave 7-methoxyisoflavan-4α-ol (II) as a minor product and 7-methoxyisoflavan-4β-ol (III) as the main product. Trans configuration was tentatively assigned to the alcohol II and cis configuration to the alcohol III, mainly on the basis of the reduction mechanism:



I

II

III

The following experiments were undertaken to find a synthetic method which affords only II in a good yield. A solution of 7-methoxyisoflavan[2] (0.25 g.) and lead tetraacetate (0.76 g.) in dry benzene (16.8 g.) was refluxed for 6 hr.; The reaction was run until an iodine-starch test for unreacted lead tetraacetate became negative. From this reaction there was obtained II-acetate (45 mg.), but no III-acetate. Acetic acid was not used as a solvent in this reaction, since the acetate of III had been found to be converted into the acetate of II by mild treatment with acetic acid.[2] 7-Methoxy-4-aminoisoflavan acetate (IV), m. p. 145°C (Found: C, 68.73; H, 6.63; N, 4.27. Calcd. for $C_{18}H_{21}O_4N$: C, 68.55; H, 6.71; N, 4.44%) was prepared from the oxime of I[3] by catalytic hydrogenation over a palladium charcoal catalyst in acetic acid. Hydrochloride (V), m. p. 220°C (Found: C, 65.98; H, 6.12; N, 4.47. Calcd. for $C_{16}H_{18}O_2NCl$: C, 65.86; H, 6.22; N, 4.83%). 7-Methoxy-4-aminoisoflavan, m. p. 111°C (Found: C, 75.38; H, 6.63; N, 5.25. Calcd. for $C_{16}H_{17}O_2N$: C, 75.27; H, 6.71; N, 5.49%). A solution of sodium nitrite (0.24 g. in 10 ml. water) was added, over a 30 min. period, to a stirred solution of V (0.49 g.) in 50% acetic acid (30 ml.) at 0°C. The mixture was then stirred for a further 30 min. at room temperature. After the usual treatment, II (70 mg.) was obtained and III was not.[5] With a view of obtaining II as the result of equilibration, III (300 mg.) was treated with aluminum isopropoxide (300 mg., molar ratio to III : 1.3) in a mixture of isopropyl alcohol (10 ml.) and acetone (0.1 ml.) at 95~100°C for 96 hr. The reaction mixture was poured into ice-water (300 ml.) containing concentrated hydrochloric acid (1 ml.). The precipitates were collected, dried and recrystallized from ethyl alcohol. Needles with an m. p. of 111°C were obtained, and II was not found. The product with an m. p. of 111°C did not show a depression of melting point on admixture with the 4-isopropoxy-7-methoxyisoflavan which had been

1) Part VII of Studies of Synthetic Isoflavanones. Presented at the 16th Annual Meeting of the Chemical Society of Japan, Tokyo, April, 1963.

2) Submitted for publication to this Bulletin.

3) N. Inoue, *J. Chem. Soc. Japan, Pure Chem. Sec.* (*Nippon Kagaku Zasshi*), **79**, 218 (1958); N. Inoue, *Science Repts. Tohoku Univ.*, First Ser., XLV, 68 (1961).

4) Cf. M. M. Bokadia, R. B. Brown and W. Cummings, *J. Chem. Soc.*, **1960**, 3380.

5) Cf. R. Bognár, M. Rákosi, H. Fletcher, D. Kehoe, E. M. Philibin and T. S. Wheeler, *Tetrahedron*, **18**, 135 (1962).

obtained as a by-product in the Meerwein-Ponndorf reduction of I.[2] When the molar ratio of aluminum isopropoxide to III was 1 : 1, III was recovered unchanged.

College of Arts and Sciences
Tohoku University
Kawauchi, Sendai

The Rate of Vaporization from the Surface of Molten Germanium Dioxide

By Taneki TOKUDA and W. D. KINGERY

(Received November 30, 1963)

Following the measurement of the oxygen diffusion rate in the solid germanium dioxide,[1] the same experiment was tried on the melt. As it was noticed that the vaporization from the melt was much faster than that from the crystal, and as the movement of the boundary surface could not be ignored, the rate of the vaporization, or the movement of the boundary between the melt and the vapor, was measured. In order that the results could be employed for diffusion measurements, the measurements were made under an oxygen pressure of about 150 mmHg, which corresponds to the partial pressure of oxygen in air. The results obtained seem reasonable compared to those for relative substances.

As a starting material, electronic grade germanium dioxide powder made by the Baker & Adamson Co. was employed. The melting points of the substance are 1116°C for the hexagonal, and 1086°C for the tetragonal crystal respectively.[2] The former form is the high temperature stable phase, and the latter, the low temperature stable phase. When the powder is melted down in the air by an electric furnace, it forms a white translucent glass including a lot of air. To expel the bubbles from the glass, it was heated for one hour each at 1150, 1350, 1400, 1480, 1496 and 1560 °C. The best condition was found experimentally to be 1500±10°C. At higher temperatures than this, much of the substance is lost by evaporation. The transparent bubble-free glass thus obtained was used as a sample.

The rate of boundary movement was calculated from the weight decrease of the sample kept in a platinum dish (Fig. 1) during heating by a high frequency furnace working at 10,000 cycles per second. The temperature of the sample was measured by a potentiometer-type optical pyrometer* made by the Leeds & Northrop Co. (Catalog No. 8622c). Absorption by the window made by a pyrex glass plate was corrected employing the experimental curve (Fig. 2). To avoid the condensation of germania and platinum on the surface of the observation glass window, it was protected by a sheet of iron plate held by a magnet outside, and the iron plate was slid aside only during the temperature observation. When this step was taken, no change in the correction curve was observed before or after the run. The other parts of glass, which had not been protected, changed their absorptivity after the run.

The results of the experiment are shown in Table I. The weight loss of the platinum dish was smaller than the experimental error. The relations between the reciprocal of the absolute temperature ($1/T$°K) and the logarithm of

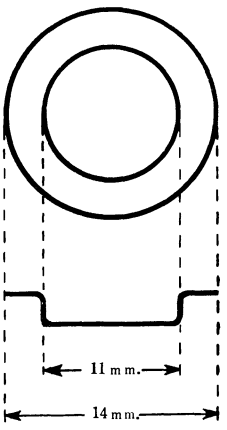


Fig. 1. Size and form of the platinum evaporation vessel.

1) T. Tokuda and W. D. Kingery, *J. Appl. Phys.*, **34**, 2104 (1963).

2) Gmelin, "Handbuch d. Anorg. Chemie, Germanium," Erg. Bd., 498; A. W. Laubengayer and D. S. Morton, *J. Am. Chem. Soc.*, **54**, 2303, 2309 (1932).

* It is more accurate and reliable than the amperemeter-type optical pyrometer.

TABLE I. RATE OF VAPORIZATION FROM THE SURFACE OF MOLTEN GeO_2

Run No.	No. 206	No. 201	No. 207	No. 204	No. 203
Initial weight, g.	0.2519	0.1620	0.2244	0.2540	0.3624
Weight loss observed, mg./hr.	0.663	6.75	32.0	50.7	242.
Vaporization rate, mol./sec. cm^2	1.852×10^{-9}	1.884×10^{-8}	8.940×10^{-8}	1.410×10^{-7}	6.787×10^{-7}
Decrease in thickness, cm./hr.	0.0002329	0.002368	0.011224	0.01778	0.08492
Temperature observed, °C	1140±13	1240±13	1294±4	1360±10	1439±20
Temperature corrected, °C	1171	1262	1320	1390	1478

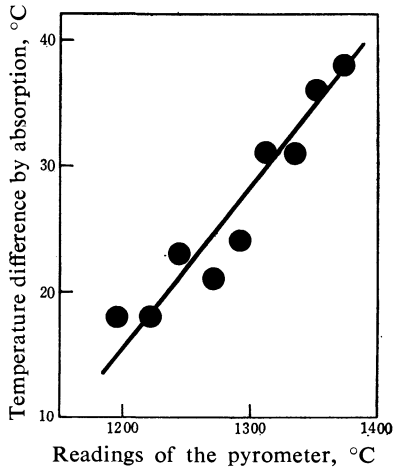


Fig. 2. Correction curve for pyrex glass absorption.

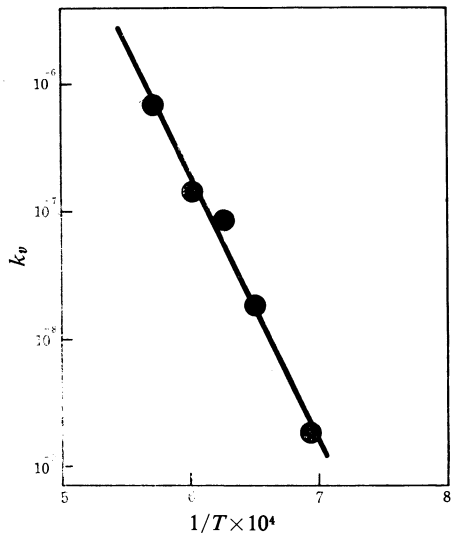


Fig. 3. Rate contstant of evaporation vs. $1/T$.

the rate of vaporization are shown in Fig. 3. The rate constant for the vaporization can be expressed by the following formula;

$$k_v = 4.07\times10^6 \exp(-96{,}000/\boldsymbol{R}T)$$

According to Condon,[3] the activation energies of vaporization for the one oxygen atom in both silicon oxide and boron oxide are 22 kcal. The one in germanium(IV) oxide which we obtained is 96/4=24 kcal. The value we obtained here seems quite reasonable. Assuming that Eyring's equation

$$k_v = (1/6)e\lambda^2(\boldsymbol{k}T/\boldsymbol{h}) \exp(\Delta S^{\neq}/\boldsymbol{R})$$

is applicable in this case, where $\boldsymbol{k}$ is the Boltzmann constant, $\boldsymbol{h}$ is the Planck constant, and $\boldsymbol{R}$ is the gas constant, and where the jump distance, λ, is about 2.7Å, the entropy of vaporization, $\Delta S^{\neq}$, can be calculated. Around the melting point (1116°C), it is calculated as follows; $\Delta S^{\neq} = 39.6$ cal. mol^{-1} deg^{-1}.

3) E. U. Condon, *Am. J. Phys.*, **22**, 132 (1954).

Institute of Scientific and Industrial Research
Osaka University
Sakai, Osaka (T. T.)

Massachusetts Iinstitute Technology
Ceramics Division
Cambridge, Mass., U. S. A. (W. D. K.)

Sorboses. III. The Acetonization of L-Sorbose by Ketal Interchange[1]

By Kanji TOKUYAMA and Etsuko HONDA

(Received December 5, 1963)

In a previous paper,[1] the reaction mechanism of the acid-catalyzed acetonization of L-sorbose (I) with acetone was reported. The acetonized derivatives proved to be useful materials for the production of L-ascorbic acid. However, when the most important derivative, 2, 3 : 4, 6-di-*O*-isopropylidene-α-L-sorbofuranose (II),[2] is formed from I with acetone, it is desirable to remove the water formed during the reaction in order to move the equilibrium toward the favorable side. As azeotropic procedures and the use of various dehydrating agents brought no improvement, we turned to a ketal interchange reaction,[3] that is, to a reaction with a ketal of acetone in the presence of an acid, because no water was formed.

The reaction of I with 2, 2-diethoxypropane[4] (acetone diethyl ketal) in the presence of *p*-toluenesulfonic acid gave a crystalline sirup, whose gas chromatogram exhibited three major components (A, B, and C). L-Sorbose (I), 1, 2-*O*-isopropylidene-α-L-sorbopyranose (III)[1] and 2, 3-*O*-isopropylidene-α-L-sorbofuranose (IV)[1] were detected only as minor spots on thin layer chromatography. The major products, A, B, and C, were separated in pure states by fractional gas chromatography. The infrared absorption spectra showed that all the products had a furanose ring[5] and that the product B was identical wih the desired II.

The product A had a hydroxyl group, which was not considered to be primary because it did not react with trityl chloride. On the basis of these facts and the optical rotation, the structure of the product A was determined to be 1, 2 : 4, 6-di-*O*-isopropylidene-α-L-sorbofuranose (V). The product C had one ethoxy and no hydroxyl group, and it was converted into II by partial hydrolysis. Therefore, the structure of the product C was determined to be 1-*O*-1'-ethoxyisopropyl-2, 3 : 4, 6-di-*O*-isopropylidene-α-L-sorbofuranose (VI).

No change in ultraviolet absorption spectra was observed throughout the course of the reaction.[1] The interchange was also achieved from IV,[6] but not from III, which is a key intermediate in the acetonization with acetone in which only II was obtained as a major product. Consequently, we would like to suggest that the acetonization of I with ketal proceeds on the path, I → IV — II → VI, which is quite different from the process of the acetonization with acetone, I → III → II ⇄ IV.

Experimental[7]

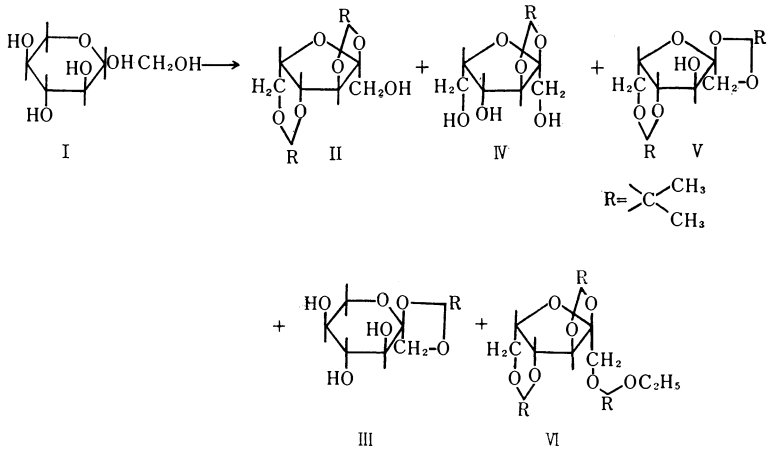
The Ketal Interchange of L-Sorbose (I) with 2, 2-Diethoxy-propane. — Dry, powdered L-sorbose (I) (19.5 g.) was added to a solution of *p*-toluenesulfonic acid (0.5 g.) in 2, 2-diethoxypropane (100 ml.). The dissolution of I was completed after stirring it for 4 hr. at room temperature.[8] The solution was neutralized with ethanolic sodium ethylate, the solvent was removed in vacuo, and the residue was distilled to give a pale yellow sirup (12.7 g.) (b. p. 120~160°C/2 mmHg), which crystallized on cooling. The sirup was fractionated by gas chromatography under the following conditions :[9] Column — silicone 550 (HCl-treated). Flow rate—hydrogen, 200 ml./min. Temperature — 200°C. Sample used : 30~33 mg. (5 times). Yields : V, 18 mg., II, 69 mg., and VI, 43 mg. Retention times : V, 14 min., II, 18 min. and VI, 22.5 min. Ratio of area : V, 19 : II, 67 : VI, 44.

V :[10] colorless rods, m. p. 72~73°C (recrystallized from *n*-hexane), $[\alpha]_D^{23}$ −23.9 (*c* 1.059, acetone). Found : C, 55.32 ; H, 7.63. Calcd. for $C_{12}H_{20}O_6$ (260) : C, 55.39 ; H, 7.79%.

VI :[11] colorless needles, m. p. 99~100°C (recrystallized from *n*-hexane), $[\alpha]_D^{25}$ +1.3 (*c* 1.109, acetone). Found : C, 58.25 ; H, 8.73 ; OC_2H_5, 12.97. Calcd. for $C_{17}H_{30}O_7$ (346) : C, 58.94 ; H, 8.73 ; OC_2H_5, 13.00%.

Partial Hydrolysis of VI. — The mixture of VI (170 mg.) and 60% acetic acid (2 ml.) was warmed at 80°C for 40 min. After cooling, the solution was made alkaline with sodium carbonate, the

1) K. Tokuyama, E. Honda and N. Hōki, *J. Org. Chem.*, **29**, 133 (1964).
2) T. Reichstein, *Helv. Chim. Acta*, **17**, 311 (1934).
3) J. Angyal and R. M. Hoskinson, *J. Chem. Soc.*, **1962**, 2985.
4) C. D. Hurd and M. A. Pollack, *J. Am. Chem. Soc.*, **60**, 1905 (1938).
5) K. Tokuyama, M. Kiyokawa and N. Hōki, This Bulletin, **36**, 1392 (1963).
6) In this case, scarcely any V was detected.
7) All melting points are uncorrected.
8) The higher the reaction temperature, the shorter the reaction time.
9) The fractionation was carried out by Dr. S. Sumimoto and his co-workers.
10) As temperature rose, the yields of V became lower.
11) Since VI was insoluble in water, it was easily isolated by washing the sirup with water. From the aqueous solution, II was extracted with chloroform with no accompanying V, because V was immediately decomposed to I by water.



solvent was removed in vacuo, the residue was extracted with acetone and the acetone was distilled off to obtain a sirup. Recrystallization of the sirup from *n*-hexane gave 100 mg. of II (m. p. 87°C).

The authors to express their gratitude to Dr. Ken'ichi Takeda, Director of this laboratory, and to Dr. Kaname Hamamoto, Assistant Director of this Laboratory, for their encouragement. They are also indebted to Dr. Shinzaburo Sumimoto, Mr. Ichiro Ishizuka and Mr. Katsuhito Okuno for their gas chromatography.

Shionogi Research Laboratory
Shionogi & Co., Ltd.
Fukushima-ku, Osaka

SHORT COMMUNICATIONS

*Stable Radicals of a High Molecular Weight Produced by Oxidizing Diphenylamine with Vanadium Pentoxide**

By Kozo HIROTA and Yoichi KAGEYAMA

(Received November 19, 1963)

In a previous report[1] we reported obtaining an absorbed radical very stable, even in air, by oxidizing diphenylamine at 150°C with vanadium pentoxide; we considered this radical to be $(C_6H_5)_2NO\cdot$, because the ESR signal measured at $g=2.0$ showed a hyperfine structure consisting of a triplet.

The absorbates extracted with carbon disulfide and/or benzene were brown and also showed an ESR signal at $g=2.0$, which had a hyperfine structure consisting of a quintet and splitting equally (5 gauss). However, as Fig. 1 shows, this spectrum is different from that of DPPH in solution, although is very similar to the spectra of DPPH in semifluid Duco cement[2]; moreover, the coupling constant of the nitrogen atom is smaller than that of DPPH and diphenyl nitric oxide. These findings suggest the production of a large radical, whose anisotropic hyperfine interaction with two nitrogen nuclei is involved. Therefore, some reaction seems to have occurred in or after the process of dissolution between the radicals adsorbed on the surface.

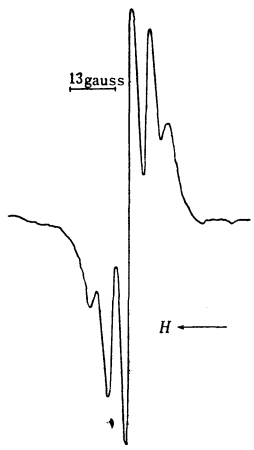


Fig. 1. The ESR spectrum of the products in carbon disulfide solution.

After purification, the solvent was evaporated. A dark brown powder then precipitated which also showed a sharp signal of the Lorentzian type ($\Delta H_{msl}=8$ gauss) at $g=2.0$; its intensity ($10^{19\sim20}$ spins/g.) did not change, even after heat treatment in air at 100°C for more than 300 hr. The cryoscopy in benzene showed the molecular weight to be between 600 and 3000. If the powder was left alone in the solution at 100°C, its molecular weight increased and it became insoluble in solvents. The elemental analysis of a sample (molecular weight: 600~700) showed the composition to be: C, 85.04; H, 5.66; N, 8.36% (total, 99.06%); calculated for $C_{48}H_{38}N_4$: C, 85.92; H, 5.71; N, 8.35%. Therefore, this substance has a composition which corresponds approximately to a condensed product of four diphenylamine molecules. Moreover, the ESR measurements show that one-tenth~one-hundredth of its total molecules are free radicals. The insoluble substance did not melt at 150°C, but slightly sintered at 200°C. It was semiconductive, because its specific resistance was 2.5×10^9 and 8×10^7 ohm·cm. at 20°C and 100°C respectively. The product showed infrared bands at 1270,** 820 and 3420 cm^{-1}, corresponding to ν_{C-N} of a tertiary nitrogen, δ_{C-H} of the hydrogen of a paradisubstituted benzene ring, and ν_{N-H} of the terminal hydrogen respectively.

* A part of this paper was presented at the ESR Meeting, Kyoto, November, 1963.

1) K. Hirota, Y. Kageyama and K. Kuwata, This Bulletin, **36**, 875 (1963).

2) N. W. Lord and S. M. Blinder, *J. Chem. Phys.*, **34**, 1963 (1961).

** In our measurements, triphenylamine showed a strong band at 1270 cm^{-1} which did not appear in the spectrum of diphenylamine.

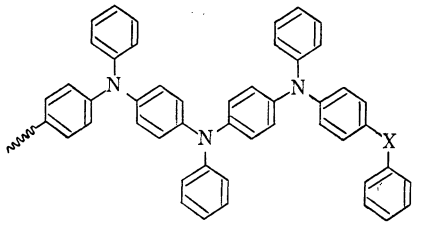


Fig. 2.

In short, the product includes stable radicals of a high molecular weight. Judging from the above discussion, the non-radical and radical structures of the product may be considered to be as shown in Fig. 2, N–H and N· respectively. However, as the radical species, another structure (X=NO·) is possible, for this structure is considered to be more stable.

Chemistry Department
Faculty of Science
Osaka University
Nakanoshima, Osaka

A Spectrophotometric Determination of Mercury(II) or Cadmium(II) by Solvent Extraction with 2, 2'-Dipyridyl Iron(II) Chelate

By Yuroku YAMAMOTO and Keiya KOTSUJI

(Received December 23, 1963)

The present paper will report on a continuation of our study concerning the solvent extraction of an anion with a metal chelate cation and its application to a spectrophotometric determination of the anion. Diamond et al.[1] and Kuznetsov[2] have described in their reviews that a large anion can be extracted into a polar solvent such as nitrobenzene with a large cation of onium or metal chelate. However, there seems to have been no mention of the solvent extraction of the anionic complex of a metal with a metal chelate cation. In our study, it is found that mercury (or cadmium) can be extracted into 1, 2-dichloroethane with 2, 2'-dipyridyl iron(II) chelate if the aqueous solution contains a large excess of iodide ions. Figure 1 shows the absorption spectra in the organic phase. Curve 1 (or 2) is a spectrum of the extract when mercury(II) (or cadminm) is absent in the aqueous solution. Curve 3 (or 4) is that of the extract when a small amount of mercury (or cadmium) is present. It may be observed that the presence of mercury(II) or cadmium ions leads to a considerable increase in the extraction. The absorbance maximum of the chelate cation in the organic phase is at 526 mμ. The maximum of the chelate cation in the aqueous solution was at

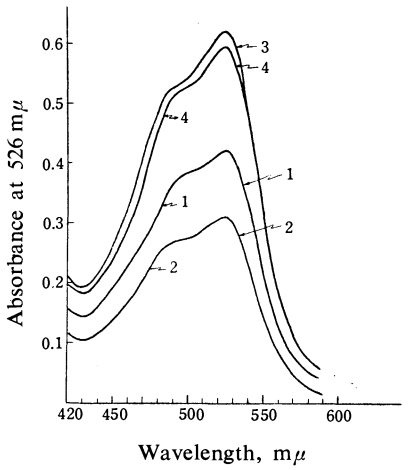


Fig. 1. Absorption spectra.
Reference : dichloroethane, pH : 6.5
Curve 1 : Spectrum of organic phase extracted from the aqueous solution (25 ml.) contained dip. (9.6×10^{-4} M), Fe(II) (2.4×10^{-4} M), NaAc (0.24 M) and KI (8.4×10^{-2} M) but Hg is absent.
Curve 3 : Spectrum of organic phase extracted from the aqueous solution (25 ml.) contained the same component as that of curve 1 and Hg (2 p.p.m.).
Curve 2 : Spectrum of organic phase extracted from the aqueous solution (25 ml.) contains dip. (6.4×10^{-4} M), Fe(II) (1.6×10^{-4} M), NaAc (0.24 M), KI (8.4×10^{-2} M) but Cd is absent.
Curve 4: Spectrum of organic phase extracted from the aqueous solution (25 ml.) contained the same component as that of curve 2 and Cd (1.6 p.p.m.).

1) D. M. Diamond and D. G. Tuck, "Progress in Inorganic Chemistry," Vol. 2, Interscience publishers, Inc., New York (1960), pp. 139—150.
2) B. I. Kuznetsov, "The Chemical Basis for the Photometric Method by Solvent Extraction in Analytical Chemistry," State Printing Office of USSR, Moscow (1963), p. 11.

522 mμ, which coincides with the reported value.[3] This red shift of the spectrum may be attributed to the effect of the association of the cation and the anion in the organic layer. Feigl[4] has shown that 2,2'-dipyridyl iron(II) chelate can be precipitated as a red crystal with a divalent complex anion, such as tetra-iodo-mercury(II) or cadmium. From these facts, it is quite likely that a chemical form of the extracted species is $Fe(dip)_3 \cdot HgI_4$ or $Fe(dip)_3 \cdot CdI_4$. To obtain optimum conditions for the determination of mercury(II) or cadmium, various factors were studied: the effect of the concentration of iron(II) ions and dipyridyl, the pH of the solution, the stability of the color, the shaking time, and the presence of diverse ions. The recommended procedure for the calibration curve is as follows:

1) For Cd: 2.0 ml. of the 2,2'-dipyridyl solution (8×10^{-3} M), 2.0 ml. of the ferrous ammonium sulfate solution (2×10^{-3} M), 2.0 ml. of the sodium acetate solution (3 M), 7.0 ml. of the potassium iodide solution (0.3 M), and varying amounts (1~7 ml.) of the standard cadmium solution (10 p. p. m.), were mixed, and the pH of the solution was adjusted to 6.5. After it had been diluted to 25 ml. with distilled water, the solution was shaken for 4 min. with 10.0 ml. of dichloroethane. The organic layer was then transferred to a flask containing 1 g. of anhydrous sodium sulfate, and the absorbance of the solution was measured at 526 mμ using the reagent blank as a reference. Beer's law is followed in the range of 0.4~2.8 p. p. m. (Fig, 2).

2) For Hg: 3.0 ml. of the 2,2'-dipyridyl solution (8×10^{-3} M), 3.0 ml. of the ferrous ammonium sulfate solution (2×10^{-3} M), 2.0 ml. of the sodium acetate solution (3 M), 7.0 ml. of the potassium iodide solution (0.3 M) and varying amounts of the standard mercury(II) solution (10 p. p. m.) were mixed, and the pH of the solution was adjusted to 6.5. After it had been diluted to 25 ml. with distilled water, the solution was shaken for 6 min. with 10.0 ml. of the organic solvent. Then it was treated as in the procedure for cadmium. Beer's law is followed in the range from 0.4 to 2.4 p. p. m. Although several methods for the determination of mercury or cadmium are presented in the literature,[5] the proposed method is based on a new principle.

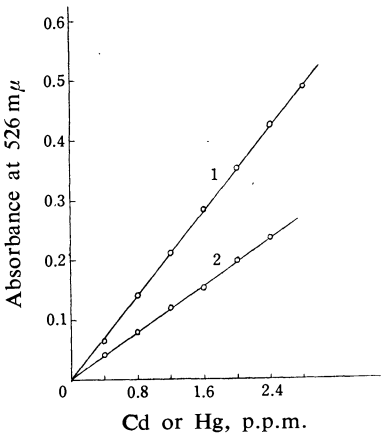


Fig. 2. Calibration curve.
Reference: Reagent blank, pH: 6.5
Curve 1: Dip. 6.4×10^{-4} M, Fe(II) 1.6×10^{-4} M, NaAc 0.24 M, KI 8.4×10^{-2} M, Cd<2.8 p.p.m.
Curve 2: Dip. 9.6×10^{-4} M, Fe(II) 2.4×10^{-4} M, NaAc 0.24 M, KI 8.4×10^{-2} M, Hg<2.4 p.p.m.

Department of Chemistry
Faculty of Science
Hiroshima University
Higashisenda, Hiroshima

3) M. L. Moss and M. G. Mellon, *Ind. Eng. Chem., Anal. Ed.*, **14**, 826 (1942).
4) F. Feigl, "Spot Test, Part I, Inorganic Application," Elsevier Publishing Company (1954), p. 90.
5) For instance, E. B. Sandell, "Colorimetric Determination of Traces of Metals," Interscience publishers, Inc., New York (1959).

The Direct Introduction of Cyano and Ethoxycarbonyl Radicals into Cyclohexane by a Photochemical Reaction

By Tamotsu TOMINAGA, Yoshinobu ODAIRA and Shigeru TSUTSUMI

(Received February 28, 1964)

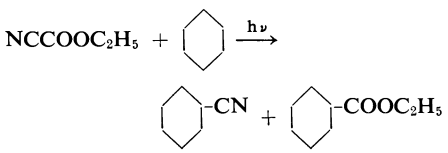
Since the cyanation of cyclohexane by a cyano radical generated photochemically from cyanogen chloride was first attempted by Müller,[1] increasing interest has, from the standpoint of organic synthesis, been shown in the study of the new direct method of introducing the important functional groups (such as cyano and alkoxycarbonyl) by radical reaction.

The present investigation was undertaken to examine the possibility of the direct and concurrent introduction of cyano and ethoxycarbonyl radicals into hydrocarbon by means of photochemical reaction.

For this purpose, ethyl cyanoformate was selected as a source of the above radicals. It has been shown by previous investigations[2,3] that the primary steps occurring in the photolyses of various alkyl esters are as follows:

$$\begin{aligned} RCOOR' + h\nu &\rightarrow RCO\cdot + \cdot OR' \\ &\rightarrow R\cdot + \cdot COOR' \\ &\rightarrow RCOOH + \cdot R'' \end{aligned}$$

Since the above steps may be applicable in the decomposition of ethyl cyanoformate in the presence of cyclohexane, both cyano and ethoxycarbonyl derivatives may be expected to be produced by recombinations between the cyano or ethoxycarbonyl radicals that were generated by the above processes and the cyclohexyl radical formed by hydrogen abstraction from cyclohexane.



The irradiation of a solution of ethyl cyanoformate (99 g.) in cyclohexane (252 g.) with a 600 W. high pressure mercury arc lamp was carried out under nitrogen for 48 hr. at room temperature. During the irradiation, the continuous evolution of gas was observed, and at the end of the reaction, 4000 ml. of gas, consisting of carbon dioxide, carbon monoxide and methane, in the ratio of 30 : 8 : 1 was collected and analyzed, by gas chromatography.

Moreover, the 0.56 g. of hydrogen cyanide produced was determined quantitatively as a cyanide ion by volumetric analysis using silver nitrate. The conversion percentage of the reaction was 38.4% and, as the liquid products a cyanide (1.8 g.) and an ester (3.5 g.) were obtained, accompanied by propionitrile (4.2 g.), ethanol (3.4 g.), ethylcyclohexane (2.5 g.) and bicyclohexyl (0.5 g.). The above cyanide and ester were identified as cyclohexyl cyanide and ethyl cyclohexanecarboxylate respectively by gas chromatographic and infrared analyses and by the mixed melting point tests using an authentic cyclohexanecarboxamide (m. p. 184~186°C) with the amides derived separately from the above compounds.

Although no quantitative interpretation of the results has been given because of the complexity due to the many different radicals generated in the primary steps, the direct introduction of cyano and ethoxycarbonyl radicals has been successful.

In this connection, it would be interesting to study the direct-introducing reaction of the α-keto ester radical, which should be more stable than the ester radical.

Department of Applied Chemistry
Osaka University
Miyakojima-ku, Osaka

1) E. Müller, *Chem. Ber.*, **96**, 670 (1963).
2) R. Brokowski et al., *J. Am. Chem. Soc.*, **83**, 1053 (1961).
3) M. Wijnen, ibid., **82**, 1847 (1960).

The Sensitivity of Radioactivation Analysis by a Low Level Neutron Source

By Yuzuru KUSAKA, Haruo TSUJI and Takayoshi ADACHI

(Received February 5, 1963)

General discussions of the sensitivities attainable with the thermal neutron activation analysis of various elements have been undertaken in several reports.[1-7] Most of their sensitivity estimations have, however, been made for reactor irradiation, based on theoretical computation and expressed with the radioactivities at the end of the irradiation. Although these data are very useful for rough estimations of the sensitivities of each element, even in a low-level neutron flux, they often do not coincide exactly with the experimental values because of the decay effect in the short-lived nuclides to be measured, because of the differences in the kind of detector used, and so on. Moreover, in some reports long-time irradiations such as those for one week or even one month have been adopted. These durations are too long for routine analysis.

The use of a low level neutron source is suited to a " non-destructive " assay of a macro amount of elements possessing high-neutron cross section. In such cases, gamma ray measurement, for example, the use of a well-type sodium iodide scintillator, is a useful counting method. Moreover, the induced radioactivity, in general, is so weak that the counting period must be longer than in the case of a high neutron flux.

In such practical work using a low-level neutron source, therefore, the sensitivity values previously reported must be re-evaluated experimentally. This paper will describe some experimental findings on the sensitivities obtained by irradiation and measurement procedures which are designed to be suitable for a routine analysis of all the elements under consideration. The results of thermal neutron flux determination are also included.

Experimental

Neutron Source. — The source consisted of a mixture of 84.2 mg. radium bromide (49.3 mg. as a radium element) with beryllium, which was sealed in a platinum tube (length ; 40 mm.; diameter, 5 mm.; thickness, 0.5 mm.) with a polyethylene outer tube (length, 85 mm.; diameter, 16 mm.).

Neutron Irradiation.—The geometry of the paraffin moderator block used in this work was the same as that in Ref. 8. The irradiation periods for all the samples under consideration were 10.0 min., 1.0 hr. and 17.0 hr.

Radioactivity Measurement. — The radioactivity induced in the sample was measured by a well-type sodium iodide scintillation detector (Harshaw, 4.45 cm.ϕ×5.08 cm. h ; hole, 1.91 cm.ϕ, 3.81 cm. deep) with a No. 6097F E.M.I. photomultiplier tube. After a 20.0 sec. interval after the end of irradiation, the measurement was started and the gross gamma ray counting was done for 3.0 min., 10.0 min. and 30.0 min.

The measurement of the absolute disintegration rates for the determination of thermal neutron flux was made with a 4π gas flow counter (Kobe Kogyo GM-917) using Q gas.

Irradiation Sample.—A definite amount of the sample was put in a polyethylene capsule (inner diameter, 16 mm.; length, 86 mm.; thickness, 1 mm.) and irradiated. The chemical forms of the samples were as follows: silver, aluminum, gold, bismuth, calcium, cadmium, cerium, cobalt, chromium, copper, iron, germanium, hafnium, iodine, indium, iridium, lithium, magnesium, manganese, molybdenum, nickel, phosphorus, platinum, rhodium, ruthenium, sulfur, antimony, selenium, silicon, tin, tantalum, tellurium, thallium, tungsten, zinc and zirconium as the elements; arsenic, dysprosium, europium, gallium, mercury, lanthanum, niobium, lead, praseodymium, samarium, titanium, vanadium and yttrium as the oxides, cesium, potassium, sodium and rubidium as the carbonates; barium and strontium as the acetates; bromine as the dibromobenzene; chlorine as the hydrogen chloride; fluorine as the calcium fluoride; nitrogen as the ammonium nitrate, and oxygen as the water. All the samples were chemically pure.

Results

Thermal Neutron Flux Determination.—Using indium and gold foils 1.3 cm. in diameter and

1) G. W. Leddicotte and S. A. Reynolds, U. S. Atomic Energy Comm., AECD-3489 (1953).
2) E. N. Jenkins and A. A. Smales, *Quart. Rev.* **10**, 83 (1956).
3) H. Hamaguchi and H. Natsume, "Jikken Kagaku Koza," Ed. by Chem. Soc. Japan, Vol. 12, Maruzen Company Ltd., Tokyo (1956), p. 447.
4) U. Schindewolf, *Angew. Chem.*, **70**, No. 7, 181 (1958).
5) W. W. Meinke, *Anal. Chem.*, **31**, 792 (1959).
6) M. Okada, *J. Chem. Soc. Japan, Pure Chem. Sec. (Nippon Kagaku Zasshi)*, **80**, 1 (1959).
7) O. U. Anders, *Nucleonics*, **18**, No. 11, 178 (1960).
8) H. Tsuji, Y. Kusaka and Y. Namikawa, This Bulletin, **35**, 2045 (1962).

of various thicknesses as the neutron monitors, the thermal neutron flux in the inside bottom of the polyethylene sample capsule in the paraffin block was determined.

For the determination of the absolute disintegration rates, a conventional 4π counting method[9] was applied. In the observed counting rates, some decreasing effects based on a self-absorption effect for soft beta rays and a self-shielding effect for thermal neutrons were recognized in the relatively thick foils. To correct them, an extrapolation to zero thickness was applied, and the extrapolated value was used in the calculation of the neutron flux. The extrapolations in the case of the indium and gold foils are shown in Figs. 1 and 2.

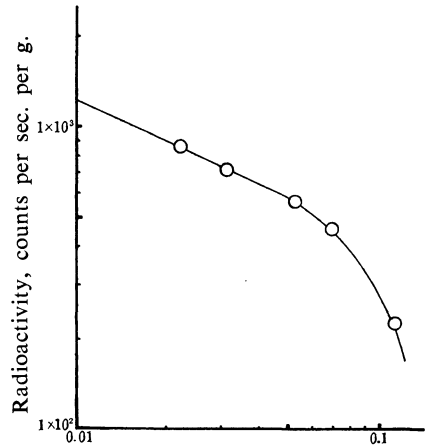


Fig. 1. 4π counting of gold foil.
(Saturation factor in irradiation is 1.0.)

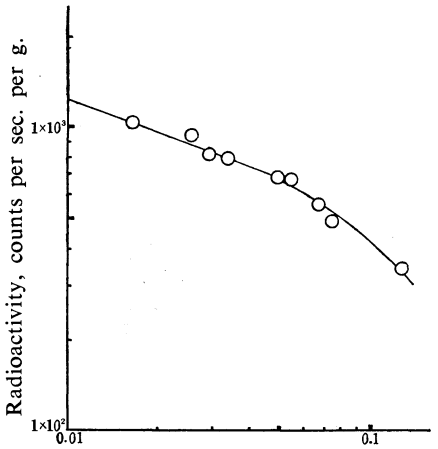


Fig. 2. 4π counting of indium foil.
(Saturation factor in irradiation is 0.5.)

9) G. Friedlander and J. W. Kennedy, "Nuclear and Radiochemistry," John Wiley & Sons, Inc., New York (1955), p. 293.

In obtaining the results, the thermal neutron fluxes were calculated as 4.1×10^3 neutrons per cm^2 per sec. in the indium foil experiment and 4.8×10^3 in the gold foil one. On the basis of these data, 4.5×10^3 was adopted as the probable neutron flux.

The Radioactivation Degree of the Elements. — All the experimental results are shown in Figs. 3, 4 and 5, in the lump. In these figures, the counting rates obtained by 3.0 min., 10.0 min. and 30.0 min. measurments for each element are plotted against the half-life of the induced radioactivity. However, when plural radioactive nuclides are produced in an element, the half-life is represented with that of the radioactivity, which is strongest at the end of the irradiation. No ambiguous radioactivities of less than 100 counts in the measurments are plotted in the figures.

TABLE I. DETECTION LIMIT IN 10 min. IRRADIATION

Detection limit	Element
1～ 10 mg.	In, Dy, Rh, V
10～ 100 mg.	Ag, Eu, Mn, I, Br, Co
100～1000 mg.	Cu, Al, Hf, Ir, Ga, Au, Sm, Cl, Si, Se, As, W
More than 1 g.	H, Li, Be, B, C, N, O, F, Na, Mg, P, S, K, Ca, Ti, Cr, Fe, Ni, Zn, Ge, Rb, Sr, Y, Zr, Nb, Mo, Ru, Cd, Sn, Sb, Te, Cs, Ba, La, Ce, Pr, Ta, Pt, Hg, Tl, Pb, Bi

TABLE II. DETECTION LIMIT IN 1 hr. IRRADIATION

Detection limit	Element
0.1～ 10 mg.	In, Dy, Eu, Rh, Mn, V
10～ 100 mg.	Ag, I, Br, Co, Ir, Au, Sm, Ga, Cu
100～1000 mg.	As, Al, Hf, W, Na, Cl, Pr, La, Cs, Te, Mo, Se, Rb, Ba, Sr, Si, Sn, Sb, Pt, Cd
More than 1 g.	H, Li, Be, B, C, O, F, Mg, P, S, K, Ca, Ti, Cr, Fe, Ni, Zn, Ge, Y, Zr, Nb, Ru, Ce, Ta, Hg, Tl, Pb, Bi

TABLE III. DETECTION LIMIT IN 17 hr. IRRADIATION

Detection limit	Element
0.1～ 1 mg.	In, Eu, Dy
1～ 10 mg.	Mn, Ir, Au, Rh, Br, V, La, I
10～ 100 mg.	As, Ga, Ag, W, Pr, Cu, Na, Co, Cs, Sm, Sb
100～1000 mg.	Rb, Al, Hf, Cl, Ru, Y, Ba, Sr, Mo, K, Te, Hg, Si, Se, Ge, Cd, Pt, Ta, P, Zn, Mg, Sn
More than 1 g.	H, Li, Be, B, C, N, O, F, S, Ca, Ti, Cr, Fe, Ni, Zr, Nb, Ce, Tl, Pb, Bi

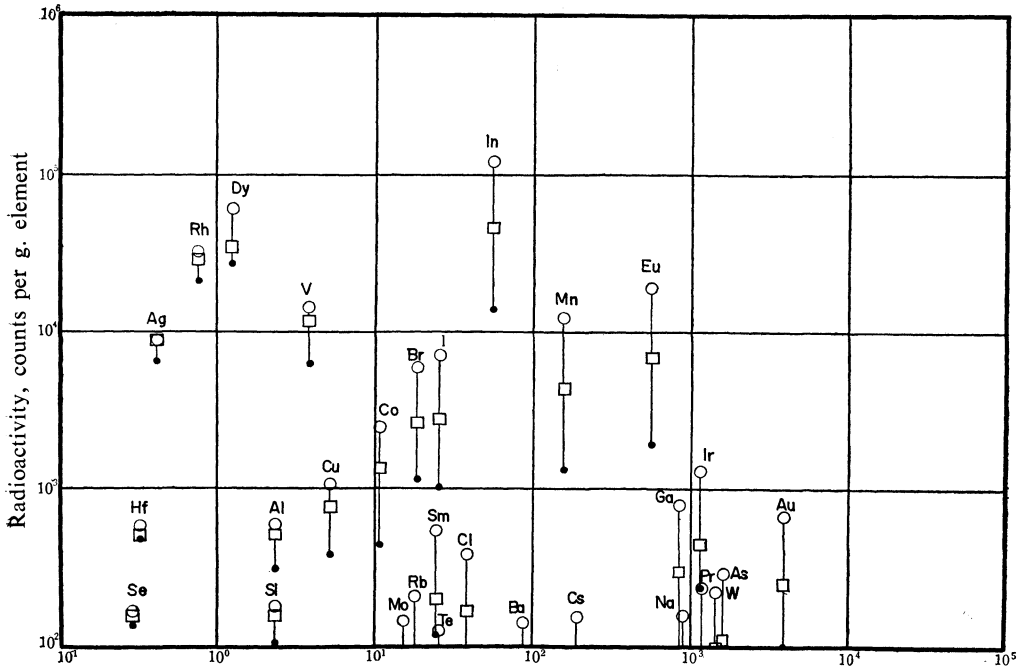


Fig. 3. Radioactivation degree in 10 min. irradiation.
• 3 min. measurement, □ 10 min. measurement, ○ 30 min. measurement

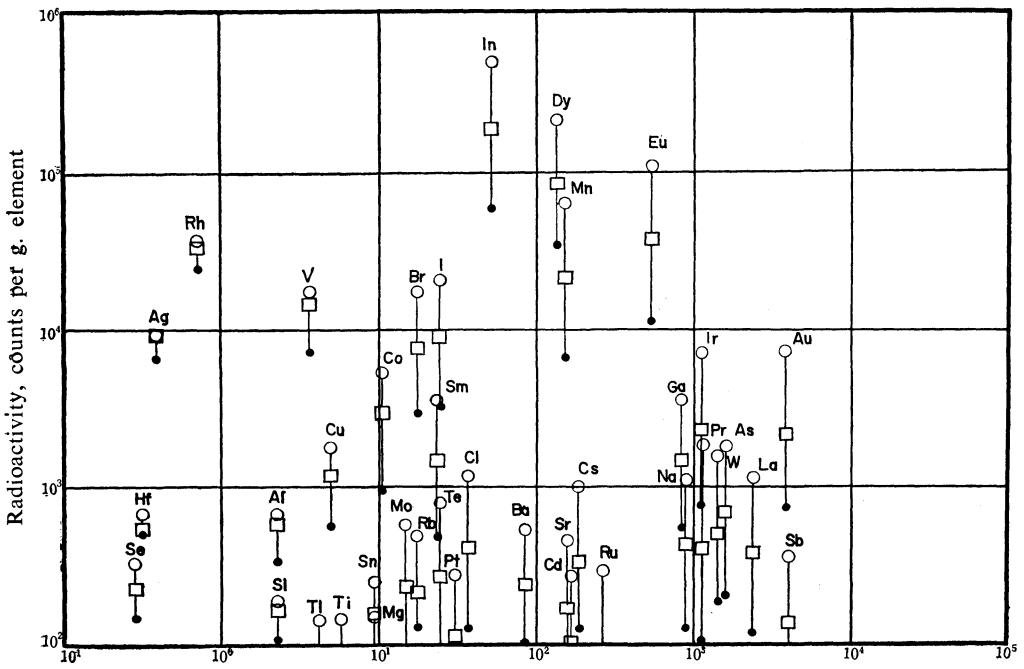


Fig. 4. Radioactivation degree in 1 hr. irradiation.
• 3 min. measurment, □ 10 min. measurment, ○ 30 min. measurement

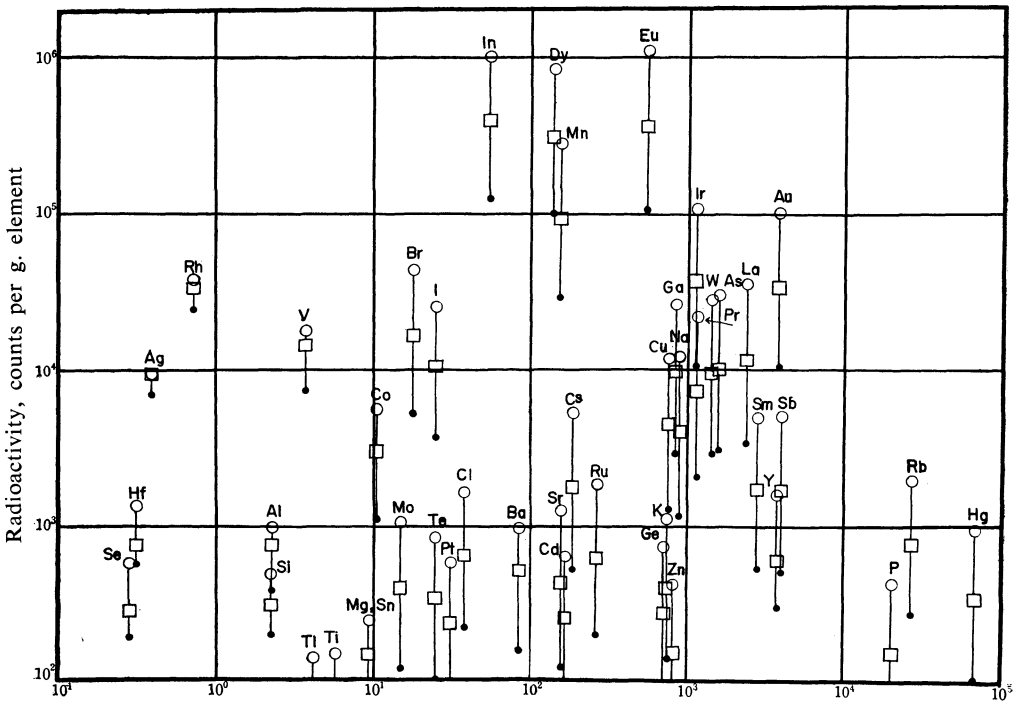


Fig. 5. Radioactivation degree in 17 hr. irradiation.
• 3 min. measurement, □ 10 min. measurement, ○ 30 min. measurement

If the detection limit in the radioactivation analysis is assumed to be the number of grams of an element required to give about 100 counts in 10 min., the detection limits summarized in Tables I, II and III can be obtained. In the tables, the elements listed in each group of detection limits are arranged in the order of decreasing sensitivity, except for "more than 1 g."

Discussion

Because of the sodium iodide scintillation-counting method, such pure beta emitters as Tl-206 and such soft gamma emitters with a high internal conversion efficiency as Co-60m and Ir-192m were measured with a low counting efficiency. For such elements a beta-ray counting method using a Geiger counter would be more suitable.

The self-shielding effect for thermal neutrons, although important in certain cases, was not considered in the treatment of the sensitivity data.

Furthermore, in a practical application, one must remember that an appropriate cooling time after the irradiation allows one to discriminate the nuclides with different half-lives; gamma ray spectrometry is also useful for the discrimination of each species.

It is possible to improve the sensitivities by using more sensitive gamma ray detectors or higher neutron fluxes. However, even then the relative sensitivity value should not change from the data reported here. Therefore, this data should be useful in general radioactivation analysis using a low-level neutron source.

The cost of this research was partly defrayed by the Scientific Research Expenditure Fund of the Ministry of Education, to which the authors' thanks are due.

Department of Chemistry
Faculty of Science
Konan University
Higashinada-ku, Kobe

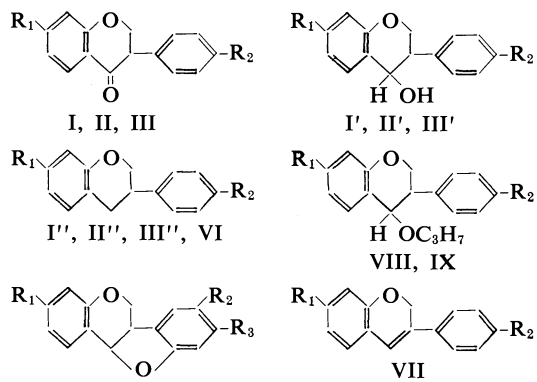
Studies of Synthetic Isoflavanones. V. The Reduction of Isoflavanones[1]

By Naoto INOUE

(Received June 5, 1963)

In the preceding papers of this series, synthetic methods,[2,3] alkaline degradation,[4] and dehydrogenation with *N*-bromosuccimide[5] of isoflavanones have been reported. The present study was undertaken to examine the reduction of isoflavanones. Of the isoflavonoid group, isoflavan-4-ol is one level lower in oxidation state than isoflavanone, and pterocarpin (IV) and homopterocarpin[6,7] (V) are regarded as the derivatives of isoflavan-4-ol. The substance with the lowest oxidation level in this group is isoflavan, and its 7, 4'-dihydroxy derivative (VI) was found in the urine of a mare by Anderson and Marrian.[8] Therefore, the reduction of isoflavanones is of interest not only for organic chemists but also for biochemists.

White and Bradbury[9] carried out the hydrogenation of 7, 4'dimethoxyisoflavanone (III) over platinum oxide in acetic acid and obtained 7, 4'-dimethoxyisoflav-3-en (VII), but they did not isolate 7, 4'-dimethoxyisoflavan-4-ol (III'). In their work, 2-methyl-7-acetoxy-4'-methoxyisoflavone and 2-methyl-7, 4'-diacetoxyisoflavone were hydrogenated to the corresponding isoflavan-4-ols by the same method, and 2-methyl-7, 4'-dimethoxyisoflavone, to the corresponding isoflav-3-en, which was also formed by the reduction of the same isoflavone with lithium aluminum hydride. Prillinger and Wessly[10] obtained 7-hydroxy-4'-methoxyisoflavan, 7, 4'-dihydroxyisoflavan, and 7, 4'-dimethoxyisoflavan (III'') by the catalytic hydrogenation of the corresponding isoflavones over a palladium-charcoal catalyst in acetic acid. The Clemmensen reduction of isoflavanones was carried out by Marrian and Anderson[8] and by King et al.[11] They obtained 7, 4'-dimethoxyisoflavan and 5, 6, 7, 4'-tetramethoxyisoflavan respectively. Adkins and Mozingo[12] hydrogenated 2-methyl-7-hydroxyisoflavone to 2-methyl-7-hydroxyisoflavan at high pressure with a copper chromite catalyst. Suginome and Iwadare[13] reduced 2'-hydroxyisoflavone with lithium aluminum hydride or sodium borohydride and obtained a substance with the skeletal structure of pterocarpin. Since carbon atoms at the 3- and 4- positions of isoflavan-4-ol are asymmetric carbons, there must be cis and trans isomers with reference to the phenyl group at C_3 and the hydroxyl group at C_4. In the reduction of flavanone, either one or the other of the stereoisomers of flavan-4-ol is obtained by changing the method of reduction; it has, therefore, been assumed that different kinds of stereoisomeric isoflavan-4-ols might be obtained by changing the reduction method, as in the case of flavanone. Therefore, isoflavanone (I), 7-methoxyisoflavanone (II), and 7, 4'dimethoxyisoflavanone (III) were reduced by various methods.



I, I', I'' $R_1=R_2=H$; II, II', II'', VIII $R_1=OCH_3$, $R_2=H$; III, III', III'', VII, IX $R_1=R_2=OCH_3$; IV $R_1=OCH_3$, $R_2, R_3=-OCH_2O-$; V $R_1=R_3=OCH_3$, $R_2=H$; VI $R_1=R_2=OH$

1) Presented at the Local Meeting of the Chemical Society of Japan, Morioka, September, 1958, and at the 13th Annual Meeting of the Society, Tokyo, April, 1960.

2) N. Inoue, *J. Chem. Soc. Japan, Pure Chem. Sec. (Nippon Kagaku Zassi)*, **79**, 112, 215, 1124 (1958); *Sci. Repts. Tohoku Univ., First Ser.*, **XLV**, 63 (1961).

3) N. Inoue, *J. Chem. Soc. Japan, Pure Chem. Sec. (Nippon Kagaku Zassi)*, **79**, 218 (1958); *Sci. Repts. Tohoku Univ., First Ser.*, **XLV**, 68 (1961).

4) N. Inoue, *J. Chem. Soc. Japan, Pure Chem. Sec. (Nippon Kagaku Zassi)*, **79**, 1124 (1958); *Sci. Repts. Tohoku Univ., First Ser.*, **XLV**, 73 (1961).

5) N. Inoue, *J. Chem. Soc. Japan, Pure Chem. Sec. (Nippon Kagaku Zasshi)*, **79**, 1537 (1958); *Sci. Repts. Tohoku Univ., First Ser.*, **XLV**, 79 (1961).

6) A. Mcgookin, A. Robertson and W. B. Whalley, *J. Chem. Soc.*, **1940**, 787.

7) E. Späth and J. Schläger, *Ber.*, **73B**, 1 (1940).

8) E. L. Anderson and G. F. Marrian, *J. Biol. Chem.*, **1935**, 649.

9) R. B. Bradbury and D. E. White, *J. Chem. Soc.*, **1953**, 871.

10) F. Wessly and F. Prillinger, *Monatsh.*, **72**, 197 (1939).

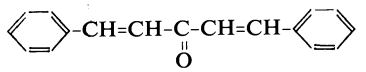
11) F. E. King, T. J. King and A. J. Warwick, *J. Chem. Soc.*, **1952**, 96.

12) R. Mozingo and H. Adkins, *J. Am. Chem. Soc.*, **60**, 669 (1938).

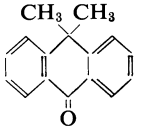
13) H. Suginome and T. Iwadare, This Bulletin, **33**, 568 (1960).

The catalytic hydrogenation of isoflavanone (I) over Raney nickel gave a compound with a m. p. of 75°C. Catalytic hydrogenation with platinum oxide in acetic acid, Meerwein-Ponndorf reduction, or reduction with sodium borohydride gave the same product, and the other stereoisomeric isoflavan-4-ol was not obtained. This reduction product was characterized as isoflavan-4-ol (I') on the basis of its infrared spectrum and the analytical results. The catalytic hydrogenation of I over palladized charcoal in ethanol gave a substance with a m. p. of 54°C, which indicated no stretching vibration band of the hydroxyl group in its infrared spectrum and which was found to be isoflavan (I''), which was also obtained by the Clemmensen reduction of I.

7-Methoxyisoflavanone (II) was hydrogenated over Raney nickel, at ordinary temperature and pressure, to 7-methoxyisoflavan-4-ol (II') with a m. p. of 144°C, which was characterized on the basis of its infrared spectrum and from the analytical results. Meerwein-Ponndorf reduction gave the same product. However, when a larger quantity of II was used and when the reaction time was prolonged, needles with a m. p. of 111°C, besides the main product of II', separated from the mother liquor of the recrystallization of the reduction product. The infrared spectrum of this substance indicated the absence of the hydroxyl group, and its analytical results were consistent with 4-isopropoxy-7-methoxyisoflavan (VIII). The formation of isopropyl ether was reported in the Meerwein-Ponndorf reduction of dibenzalacetone (X) and 9, 9-dimethylanthrone-10 (XI).[14]



X



XI

The reduction of II with sodium borohydride in ethanol gave an alcohol (II') with a m. p. of 144°C along with a minor product of needles with a m. p. of 131°C. The infrared spectrum of this reduction product with a lower melting point demonstrated the presence of a hydroxyl group and the absence of a carbonyl group, and its analytical results agreed with those of II'. The mixed melting point of the two reduction products was depressed more than 10 degrees. Stretching vibrations of the hydroxyl group in these two reduction products exist at different frequencies in KBr and at the same frequencies in chloroform or carbon tetrachloride, as is shown in Table I.

TABLE I. OH STRETCHING VIBRATION OF 7-METHOXYISOFLAVAN-4-OLS

	m. p. 144°C	m. p. 131°C
νOH (KBr)	3570, 3450 cm^{-1}	3310, 3240 cm^{-1}
νOH (CCl_4)	3550, 3450 cm^{-1}	3550, 3450 cm^{-1}

These two reduction products gave different infrared absorption curves in a finger-print region in KBr and in carbon tetrachloride but similar ultraviolet spectra with an absorption maximum at 280 mμ. On the basis of this evidence, the compounds with melting points of 144°C and 131°C were considered to be stereoisomers of 7-methoxyisoflavan-4-ol, and the product with a m. p. of 144°C was designated as the β-compound and that with a m. p. of 131°C, as the α-compound. The acetylation of the β- and α-compounds with acetic anhydride in the presence of pyridine gave acetates with melting points of 121°C and 111°C respectively. The mixed melting point of the two acetates depressed more than 10 degrees. The catalytic hydrogenation of II over a palladium-charcoal catalyst in ethanol afforded 7-methoxyisoflavan (II'') with a m. p. of 111°C, which was also obtained by the Clemmensen reduction of II.

The catalytic hydrogenation of 7, 4'-dimethoxyisoflavanone (III) over Raney nickel yielded a compound with a m. p. of 143°C, which was identified from its infrared spectrum and analytical results as 7, 4'-dimethoxyisoflavan-4-ol (III'). III' was also obtained by the reduction of III with sodium borohydride in ethanol, but the other stereoisomer of III' has not been obtained to date. The Meerwein-Ponndorf reduction of III afforded III'. When a larger quantity of III was used for this reduction and when more time was required for the disappearance of a positive acetone test, a product with a m. p. of 75.5°C was obtained which was identified as 4-isopropoxy-7, 4'-dimethoxyisoflavan (IX) on the basis of its infrared spectrum and analytical results.

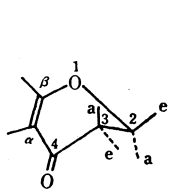
Further, a very small quantity of 7, 4'-dimethoxyisoflav-3-en (VII) separated from the mother liquor of recrystallization. Both II and III afforded a large quantity of unchanged starting material when hydrogenated over platinum oxide in acetic acid even after the absorption of one mole of hydrogen. This phenomenon may perhaps be ascribed to the hydrogenation of the benzene ring at an early stage of the reduction. In the case of the

14) A. L. Wild in "The Organic Reactions," Ed. by R. Adams, Vol. II, John Wiley & Sons, New York (1944), p. 190.

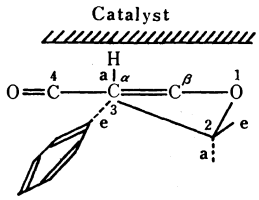
hydrogenation of I over platinum oxide in acetic acid, the starting material was not recovered and isoflavan-4-ol was obtained in about a 70% yield.

Isoflavanone is considered to have the conformation shown in XIIa and XIIb, a conformation which is in accordance with that of flavanone proposed by Phillibin and Wheeler[15] and by Mitsui and Kasahara.[16] The two hydrogen atoms at C_2 are equatorial and axial, and five atoms, O_1, C_3, C_4, C_α and C_β, are coplanar; only C_2 is out of the plane. The conformation of the phenyl group in the 3-position of isoflavanone is assumed to be equatorial, as usual.

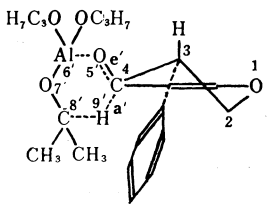
According to Mitsui and Kasahara[16], the Meerwein-Ponndorf reduction of flavanone gave flavan-4α-ol exclusively, contrary to the results of catalytic hydrogenation or of reduction with complex metal hydrides. However, in the case of isoflavanone, the Meerwein-Ponndorf reduction yielded the same isoflavan-4-ol as the product of catalytic hydrogenation with Raney nickel or that of reduction with complex metal hydride. This difference in the results of reduction between flavanone and isoflavanone may be caused by the difference in the positions of the phenyl group in these compounds. In the case of isoflavanone, the steric effect of the phenyl group at C_3 on C_4 carbonyl carbon must be considered. For example, 2, 4-dinitrophenylhydrazine reacts with isoflavanones much slower than with flavanones[2], and the Girard P reagent does not react with isoflavanone,* although it does react with flavanone.



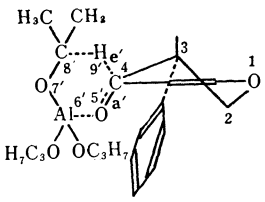
XIIa



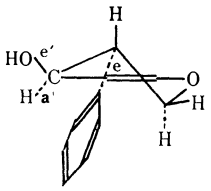
XIIb



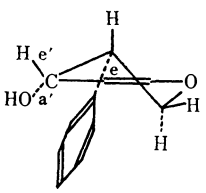
XIIc



XIId



trans
XIIe



cis
XIIf

The transition state of the Meerwein-Ponndorf reduction is regarded as a six-membered ring consisting of a carbonyl group, aluminum, and one of the three isopropoxy groups shown in XIIc and XIId.[17] The isopropyl group which transfers its hydrogen ($H_{9'}$) to carbonyl carbon (C_4) is half fixed and exists nearer to the pyran ring than the other two isopropyl groups, which can move relatively freely. As XIIc shows, when the C_4–$O_{5'}$ bond in the cyclic transition state is quasi-equatorial (e'), two methyl groups on carbon atom 8' are close to the phenyl group in the 3-position and steric interference occurs between these groups. Because of this steric hindrance, the transition state shown in XIIc would have a higher potential energy and may be less stable. On the other hand, in the transition state shown by XIId, which would form a product with a quasi-axial hydroxyl group (XIIf), the two methyl groups on the carbon atom 8' are distant from the phenyl group in the 3-position and there is no steric interference between these groups; the compound XIId is, therefore, more stable than XIIc. For this reason the isoflavan-4-ols which are formed by the Meerwein-Ponndorf reduction of isoflavanones are likely to be cis compounds with a quasi-axial C_4 hydroxyl group, and 7-methoxyisoflavan-4α-ol, which cannot be obtained by the Meerwein-Ponndorf method, would be a trans isomer with a quasi-equatorial hydroxyl group (XIIe).

As has been indicated in Table I, the stretching vibrations of 7-methoxyisoflavan-4α-ol exist at lower frequencies than that of 4β-ol in the KBr disk, but they are in equal posi-

15) E. M. Phillibin and T. S. Wheeler, *Proc. Chem. Soc.*, **1958**, 167.
16) S. Mitsui and A. Kasahara, *J. Chem. Soc. Japan, Pure Chem. Sec. (Nippon Kagaku Zassi)*, **79**, 1382 (1958).

* Unpublished work.
17) L. M. Jackman, A. K. Macbeth and J. T. Mills, *J. Chem., Soc.*, **1949**, 2641.

tions in carbon tetrachloride. This phenomenon indicates that 7-methoxyisoflavan-4α-ol is associated intermolecularly by hydrogen bonding in the KBr disk, but that the β-alcohol is not associated. Since 7-methoxyisoflavan-4β-ol has a cis C_3 phenyl group, the intermolecular association of the C_4 hydroxyl group by hydrogen bonding would be difficult. However, it would not be difficult for the hydroxyl group of *trans*-isoflavan-4-ol to associate intermolecularly by hydrogen bonding, since the phenyl group in the 3-position would not interfere with the trans C_4 hydroxyl group.

The results of the catalytic hydrogenation of isoflavanone can be explained well by the theory proposed by Mitsui and his co-workers.[16,18] As XIIb shows, isoflavanone is adsorbed by a catalyst on the side opposite that where the axial hydrogen in the 2-position projects. According to Mitsui and Imaizumi[18] the first step in the catalytic hydrogenation is the addition of one proton and two electrons, released from the catalyst surface, to the carbonyl carbon atom. In the case of isoflavanone, the conformation of the thereby-formed C–H bond at C_4 would be quasi-equatorial, and the subsequently-formed C–O bond at C_4 would project in the quasi-axial orientation (XIIb, XIIf), away from the catalyst surface. The phenyl group in the 3-position is equatorial and would be cis to the quasi-axial hydroxyl group in the 4-position. Consequently, the isoflavan-4-ol formed by the catalytic hydrogenation of isoflavanone would be the cis isomer. The experimental determination of the cis and trans configurations of 7-methoxyisoflavan-4α-ol and -4β-ol is in progress.

Experimental*

Isoflavan-4-ol.—*1) The Catalytic Hydrogenation of Isoflavanone*[2] *over Raney Nickel.*—When a solution of isoflavanone (0.5 g.) in ethanol (100 ml.) was shaken with hydrogen at atmospheric pressure and at 28°C in the presence of Raney nickel (0.5 g.) for 80 min., 55 ml. (1 equiv.) of hydrogen was absorbed. After the separation of the catalyst, the solution was concentrated to a small volume and diluted with water. The precipitate was collected by filtration, dried, and recrystallized from petroleum ether to prisms (m. p. 75°C). Yield, 0.38 g.

Found: C, 79.81; H, 6.30. Calcd. for $C_{15}H_{14}O_2$: C, 79.62; H, 6.24%.

A mixture of this alcohol (0.2 g.), acetic anhydride (2 ml.), and dry pyridine (1 ml.) was set aside for 20 hr. at room temperature. The solution was then diluted with water (100 ml.), and the precipitate was recrystallized from petroleum benzine. 4-Acetoxyisoflavan of m. p. 93°C was obtained almost quantitatively.

Found: C, 75.83; H, 5.92. Calcd. for $C_{17}H_{16}O_3$: C, 76.10; H, 6.01%.

2) Over Platinum Oxide.—Isoflavanone (1.0 g.) in acetic acid (40 ml.) over platinum oxide (0.2 g.) absorbed 230 ml. of hydrogen in 28 min. at 28°C. The evaporation of acetic acid from the filtered solution under reduced pressure gave a residue which was crystallized from petroleum benzine as needles with a m. p. of 75°C. Yield. 0.7 g.

3) Meerwein-Ponndorf Reduction.—A mixture of isoflavanone (1.0 g.), aluminum isopropoxide (3.7 g.), and dry isopropanol (30 ml.) was heated in a boiling water bath under a Hahn partial condenser. After one hour, another 10 ml. of isopropanol was added and heating was continued for a further 30 min. After the removal of isopropanol in vacuum and the addition of a small amount of water, the syrup was acidified with dilute sulfuric acid and extracted with ether. From the ether solution, isoflavan-4-ol with a m. p. of 75°C (0.8 g.) was obtained after the usual treatment.

Isoflavan. — *1) The Catalytic Hydrogenation of Isoflavanone over a Palladium-charcoal Catalyst.* — Isoflavanone (1.0 g.), palladium-charcoal (10%, 0.3 g.), and ethanol (100 ml.) were shaken with hydrogen at atmospheric pressure until 50 ml. had absorbed. After the removal of the catalyst and ethanol, isoflavan (0.75 g.) was obtained as needles (m. p. 55°C).

Found: C, 85.79; H, 6.78. Calcd. for $C_{15}H_{14}O$: C, 85.68; H, 6.71%.

2) Clemmensen Reduction.—Concentrated hydrochloric acid (5 ml.) was added to a cooled mixture of isoflavanone (0.3 g.), amalgamated zinc dust (0.5 g.), and acetic acid (20 ml.) over a 5 min. period. The mixture was left for 24 hr. at room temperature and poured into water (100 ml.). Isoflavan with a m. p. of 54°C was crystallized from ethanol. Yield, 0.22 g.

7-Methoxyisoflavan-4-ol.—*1) The Catalytic Hydrogenation of 7-Methoxyisoflavanone*[2,3] *over Raney Nickel.* — When 7-Methoxyisoflavanone (1.0 g.), Raney nickel (1.2 g.) and ethanol (60 ml.) were shaken with hydrogen at 28°C in atmospheric pressure for 4 hr., 139 ml. (1.43 mol.) of hydrogen was absorbed. When this was worked up in the usual way and crystallized from ethanol, 7-methoxyisoflavan-4β-ol of m. p. 144°C (0.4 g.) separated.

Found: C, 75.14; H, 6.44. Calcd. for $C_{16}H_{16}O_3$: C, 74.98; H, 6.29%.

The acetylation of this alcohol with acetic anhydride in the presence of pyridine at room temperature gave 7-methoxy-4-acetoxyisoflavan (m. p. 121°C) (from ethanol).

Found: C, 72.75; H, 6.12. Calcd. for $C_{18}H_{18}O_4$: C, 72.46; H, 6.08%.

2) Meerwein-Ponndorf Reduction.—A solution of 7-methoxyisoflavanone (1.0 g.) and aluminum isopropoxide (2.5 g.) in anhydrous isopropanol (30 ml.) was heated under a Hahn partial condenser in a boiling water bath. About 20 ml. of isopropanol distilled out in one hour, and an acetone test with 2, 4-dinitrophenylhydrazine was negative. Most of

18) S. Mitsui and S. Imaizumi, *J. Chem. Soc. Japan, Pure Chem. Sec.* (*Nippon kagaku Zassi*), **77**, 1516 (1956).

* All melting points are uncorrected.

the excess isopropanol was removed under reduced pressure. The cooled residue was hydrolyzed with dilute sulfuric acid. The separated crystals were collected, dried, and recrystallized from ethanol. 7-Methoxyisoflavan-4β-ol (m.p. 144°C) was obtained. Yield, 0.65 g.

3) Novel Meerwein-Ponndorf Reduction.—A solution of 7-methoxyisoflavanone (1.5 g.) and aluminum isopropoxide (3.0 g.) in anhydrous isopropanol (50 ml.) was heated under a Hahn condenser as described above. In 3.5 hr., 38 ml. of isopropanol distilled out and an acetone test was negative. After the addition of another 15 ml. of isopropanol, 7 ml. of liquid distilled out in one hour. The usual treatment gave crystals with a m. p. of 143.5°C (0.9 g.); those were undepressed by admixture with the 7-methoxyisoflavan-4β-ol obtained in 1) and 2). From the mother liquid, needles (m. p. 111°C, 0.2 g.) were obtained which were characterized as 4-isopropyl ether of 7-methoxyisoflavan-4-ol.

UV $\lambda_{max}^{C_2H_5OH}$ 280 mμ (log ε 3.45).

Found: C, 76.44; H, 7.56. Calcd. for $C_{19}H_{22}O_3$: C, 76.48; H, 7.43%.

4) Reduction with Sodium Borohydride.—A solution of 7-methoxyisoflavanone (10.0 g.) and sodium borohydride (1.2 g.) in ethanol (600 ml.) was stirred for 2 days at 36°C. The ethanol was then distilled off under reduced pressure, and the residue was decomposed with acetic acid. The precipitate was fractionally recrystallized from ethanol to give prisms (m. p. 144°C, 4.5 g.) which were undepressed on admixture with the 7-methoxyisoflavan-4β-ol obtained in the experiments described above.

The residual liquor furnished more soluble needles (m. p. 131°C, 2.2 g.), which were identified as 7-methoxyisoflavan-4α-ol.

Found: C, 75.14; H, 6.10. Calcd. for $C_{16}H_{16}O_3$: C, 74.98; 6.29%.

The mixed melting point of 7-methoxyisoflavan-4α- and -4β-ol was 114~116°C.

7-Methoxyisoflavan-4α-ol was acetylated with acetic anhydride and pyridine at room temperature. Recrystallization from ethanol gave plates with a m. p. of 111°C.

Found: C, 72.67; H, 5.98. Calcd. for $C_{18}H_{18}O_4$: C, 72.46; H, 6.08%.

The mixed melting point of the acetyl derivatives of 7-methoxyisoflavan-4α- and -4β-ol was 95~100°C.

7-Methoxyisoflavan. — *1) The Catalytic Hydrogenation of 7-Methoxyisoflavanone.*—When a mixture of 7-methoxyisoflavanone (0.5 g.) and palladized charcoal (10%, 0.3 g.) in acetic acid (40 ml.) was shaken with hydrogen at 24°C, 72.4 ml. (0.93 mol.) of hydrogen was absorbed in 37 min. After the usual treatment, crystals with a m. p. of 95~97°C were obtained. The recrystallization of this product gave needles (m. p. 105~106.5°C). Yield, 0.25 g.

Found: C, 80.17; H, 6.87. Calcd. for $C_{16}H_{16}O_2$: C, 79.97; H, 6.71%.

2) Clemmensen Reduction.—To a mixture of 7-methoxyisoflavan (0.5 g.), acetic acid (30 ml.), and amalgamated zinc (10 g.), concentrated hydrochloric acid (10 ml.) was added over a 20 min. period. After standing at room temperature for 24 hr., the mixture was poured into water (200 ml.) and the precipitate formed was recrystallized from ethanol to crystals with a m. p. of 106°C (0.3 g.). This was identified by mixed melting point with the compound prepared in 1).

7, 4'-Dimethoxyisoflavan-4-ol.—*1) The Catalytic Hydrogenation of 7, 4'-Dimethoxyisoflavanone over Raney Nickel.*—7, 4'-Dimethoxyisoflavanone (0.5 g.) over Raney nickel (from 2.0 g. alloy) in ethanol (200 ml.) absorbed 59 ml. of hydrogen (1.41 mol.) at 19°C in one hour. The removal of ethanol from the filtered solution under reduced pressure gave a solid which was crystallized from ethanol as prisms with a m. p. of 143°C. Yield, 0.31 g.

Found: C, 71.04; H, 6.20. Calcd. for $C_{17}H_{18}O_4$: C, 71.31; H, 6.34%.

2) Reduction with Sodium Borohydride.—A solution of 7, 4'-dimethoxyisoflavanone (1.0 g.) and sodium borohydride (0.1 g.) in ethanol (450 ml.) was kept at 15°C for 2 days. After the usual treatment crystals with a m. p. of 143°C (0.5 g.) were obtained and identified as identical with the compound prepared in 1).

3) Meerwein-Ponndorf Reduction.—A solution of 7, 4'-dimethoxyisoflavanone (1.0 g.) and aluminum isopropoxide (0.7 g.) in anhydrous isopropanol (40 ml.) was heated under a Hahn partial condenser in a boiling water bath. About 32 ml. of isopropanol distilled out in one hour, and an acetone test with 2, 4-dinitrophenylhydrazine was negative. The residual isopropanol was removed under reduced pressure, and dilute hydrochloric acid was added. The recrystallization of the separated solid gave prisms with a m. p. of 142.5°C which were identified as identical with the compound in 1). Yield. 0.6 g.

4) Novel Meerwein-Ponndorf Reduction.—A solution of 7, 4'-dimethoxyisoflavanone (2.0 g.) and aluminum isopropoxide (2.0 g.) in anhydrous isopropanol (120 ml.) was treated as above. A total of 120 ml. of isopropanol was added in 5 portions, and the solution was heated for 10 hr. After the usual treatment, crystals (m. p. 75.5°C, 1.2 g. from ethanol) were obtained. The product, which could not be acetylated with acetic anhydride in the presence of pyridine, was characterized as 7, 4'-dimethoxy-4-isopropoxyisoflavan.

Found: C, 73.12; H, 7.14. Calcd. for $C_{20}H_{24}O_4$: C, 73.14; H, 7.37%.

The recrystallization of the solid which separated from the ethanolic mother liquid with petroleum benzine gave plates with a m. p. of 161°C (50 mg.) which were identified as 7, 4'-dimethoxyisoflav-3-en.

UV $\lambda_{max}^{C_2H_5OH}$ mμ (log ε): 250 (4.22), 335 (4.38).

Found: C, 75.87; H, 6.09. Calcd. for $C_{17}H_{16}O_3$: C, 76.10; H, 6.01%.

The author is grateful to Professor Sekio Mitsui of Tohoku University for his valuable suggestions on the catalytic hydrogenation of isoflavanones. A part of the experiments were carried out by Mannosuke Arai, to whom the author's thanks are also due.

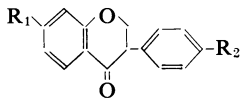
College of General Education
Tohoku University
Kawauchi, Sendai

Studies of Synthetic Isoflavanones. VI. The Reaction of Isoflavan-4-ols with Acetic Acid[1]

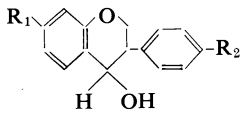
By Naoto INOUE

(Received June 11, 1963)

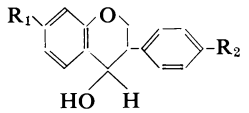
Bradbury and White[2] carried out the hydrogenation reaction of 7, 4'-dimethoxyisoflavanone (II) with platinum oxide in acetic acid to the corresponding isoflav-3-en (XI), but they did not isolate 7, 4'-dimethoxyisoflavan-4-ol (IX) and it is not clear whether or not 7, 4'-dimethoxyisoflavan was produced in their experiment. They hydrogenated 2-methyl-7, 4'-dimethoxyisoflavone by the method similar to the one used for the corresponding isoflavanone and obtained 2-methyl-7, 4'-dimethoxyisoflav-3-en, which was also obtained by the reduction of the same isoflavone with lithium aluminum hydride.



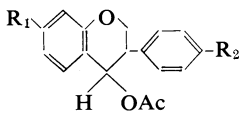
I, II, XIII



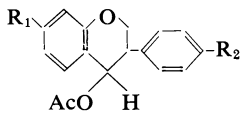
III, IX, XIV



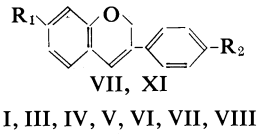
IV



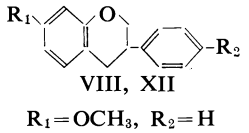
V, X



VI



VII, XI



VIII, XII

I, III, IV, V, VI, VII, VIII $R_1=OCH_3$, $R_2=H$
II, IX, X, XI, XII $R_1=R_2=OCH_3$
XIII, XIV $R_1=R_2=H$

It has been assumed that the isoflav-3-ens obtained in White's experiments were derived from the reduction products, isoflavan-4-ols, by dehydration with acetic acid. With a view to confirming this assumption, several experiments on isoflavan-4-ols were carried out. In the preceding paper of this series,[1] the author reported that 7-methoxyisoflavanone (I) was converted into 7-methoxyisoflavan-4β-ol (III, m.p. 144°C) by catalytic hydrogenation over Raney nickel or by the Meerwein-Ponndorf reduction and that 7-methoxyisoflavan-4α-ol (IV, m. p. 131°C) was obtained as a minor product, along with III, by the reduction of I with sodium borohydride. In order to obtain 7-methoxyisoflav-3-en (VII), III was heated on a water bath with dilute sulfuric acid, phosphoric acid, phosphoric anhydride in benzene, or formic acid. Treatment with all these reagents yielded an amorphous substance which was insoluble in ethanol. The treatment of III with concentrated sulfuric acid at room temperature gave the same result. However, when boiled with acetic acid III was converted into plate crystals (m. p. 108°C) whose ultraviolet absorption spectrum was similar to that of stilbene with absorption maxima at 335 mμ ($\log \varepsilon = 4.31$) and 245 mμ ($\log \varepsilon = 4.28$), as is shown in Fig. 1. The analytical values of this compound conformed with those of the anhydride of III. The product was hydrogenated over palladized charcoal to 7-methoxyisoflavan (VIII), which was also obtained by the Clemmensen reduction of I.[1] These results indicate that the compound with a m. p. of 108°C

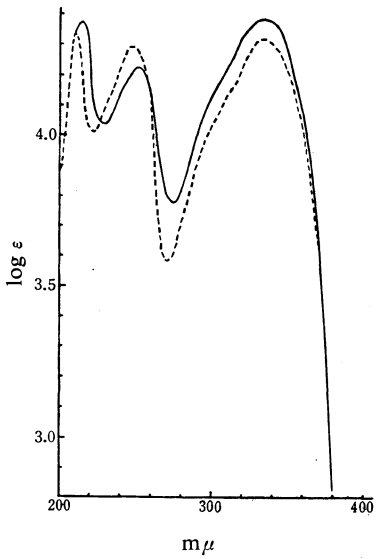


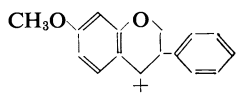
Fig. 1. Ultraviolet spectra of VII (——) and XI (·····) in ethanol.

1) Presented at the 13th and 14th Annual Meetings of the Chemical Society of Japan, Tokyo, April, 1960 and 1961. Part V of this series: N. Inoue, This Bulletin, 37, 601 (1964).

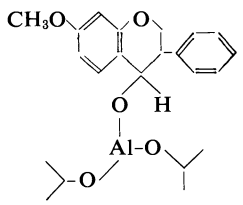
2) R. B. Bradbury and D. E. White, *J. Chem. Soc.*, **1953**, 871.

has the stilbene-type structure VII and that heating it with acetic acid did not cause any migration of the C_3 phenyl group.

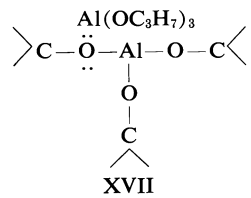
Considering the result of White's experiments, it was presumed that the dehydration of III might occur under milder conditions; therefore, III was treated with acetic acid at 50°C for one hour, by which method a compound with a m.p. of 111°C was obtained. The infrared spectrum of this substance indicated the absence of hydroxyl group and the presence of a carbonyl group ($\nu_{C=O}$ 1732 cm^{-1} in KBr), and its analytical results conformed with that of the acetate of 7-methoxyisoflavan-4-ol. Mixed melting point determination showed the product to be 4α-acetoxy-7-methoxyisoflavan (VI, m.p. 111°C). It is interesting that α-acetate was obtained by the treatment of the β-alcohol (III) with acetic acid. When III was allowed to stand overnight in acetic acid at room temperature, the starting material was recovered unchanged. 7-Methxyisoflavan-4α-ol (IV) was converted into VII on treatment with boiling acetic acid, and into VI on that with acetic acid at 50°C. In the preceding paper[1] it was reported that III and IV were acetylated with acetic anhydride and pyridine to 4β-acetoxy-7-methoxyisoflavan (V, m.p. 121°C) and 4α-acetoxy-7-methoxyisoflavan (VI, m.p. 111°C) respectively. Treatment with sodium methoxide in methanol gave III from V and IV from VI. Both V and VI were converted into VII by being boiled with acetic acid. These experimental results suggest that VI might be an intermediate product in the dehydration of III, IV, and V with boiling acetic acid.



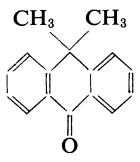
XV



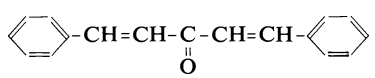
XVI



XVII

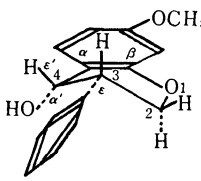


XVIII

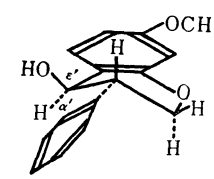


XIX

In the conversion of III to the epimeric acetate VI by treatment with the acetic acid, a proton from acetic acid is thought to be added to the C_4 hydroxyl group, followed by the elimination of water from the oxonium ion to give the carbonium ion (XV), which then reacts with acetic acid to yield the epimeric acetate VI. This is a solvolysis reaction of the S_N1 type in acetic acid. In a previous paper, the author assigned trans configuration to 7-methoxyisoflavan-4α-ol (IV) and a cis to 4β-ol (III) on the basis of the stereochemistry of the transition state of the Meerwein-Ponndorf reduction[3] and Mitsui's theory for catalytic hydrogenation.[4,5] As III' and IV' show, the perferred conformation of the C_3 phenyl group of 7-methoxyisoflavan-4-ol is equatorial and that of C_3 hydrogen atom, axial. The C_4 hydroxyl group could be either quasi-axial (a') or quasi-equatorial (e'), and the C–H bond and C–O bond projected from C_4 are inclined at the same angle to the plane in which C_α, C_β, O_1, and C_4 exist. The catalytic hydrogenation and Meerwein-Ponndorf reduction of I gave III with a quasi-axial C_4 hydroxyl group which is cis to the C_3 equatorial phenyl group (III'). On the other hand, the IV formed as a minor product by the reduction of I with sodium borohydride is a trans compound with a quasi-equatorial C_4 hydroxyl group (IV').



cis
III'



trans
IV'

Because of its quasi-equatorial conformation and trans configuration, the α-compound IV is considered to be more stable than the β-compound III. Therefore, the reactions which proceed through the planar sp^2 form of the C_4 of isoflavan would give the trans or α-type compound. As has been described above, the reaction between III and acetic acid thus proceeds via the C_4 carbonium ion, with sp^2 hybridization, to give a more stable α-acetate. This conclusion suggests that when the carbonium ion XV reacts with water instead of acetic acid, the stereoisomeric alcohol IV will be produced. Therefore, III was dissolved in a dioxane-water mixture with one drop of concentrated sulfuric acid or hydrochloric acid

3) L. M. Jackman, A. K. Macbeth and J. A. Mills, ibid., **1953**, 871.
4) S. Mitsui and K. Kasahara, *J. Chem. Soc. Japan, Pure Chem. Sec.* (*Nippon Kagaku Zassi*), **79**, 1382 (1958); **81**, 1583 (1960).
5) S. Mitsui and S. Imaizumi, ibid., **77**, 1516 (1956).

and the solution was set aside overnight. The desired alcohol IV was obtained as expected. When pure dioxane was used as the solvent instead of a dioxane-water mixture, an amorphous compound was obtained.

7, 4'-Dimethoxyisoflavan-4-ol (IX), which had been obtained by the hydrogenation of 7, 4'-dimethoxyisoflavanone (II) over Raney nickel or by its reduction with aluminum isopropoxide or with sodium borohydride, was treated with acetic acid at 50°C and was converted into 7, 4'-dimethoxyisoflav-3-en (XI) in one experiment and into 4-acetoxy-7,4'-dimethoxyisoflavan with a m. p. of 123°C in another. As has been reported in the preceding paper, the acetylation of IX with acetic anhydride and pyridine gave the acetate (X) with a m. p. of 128°C, which was different from the acetate (m. p. 123°C) obtained above (mixed melting point determination).

Bradbury and White[2] hydrogenated II with platinum oxide in acetic acid to 7, 4'-dimethoxyisoflav-3-en (XI). It was assumed that XI would be derived from the primary reduction product, IX, through reaction with acetic acid. The experimental results mentioned above support this assumption. The reaction of IX with boiling acetic acid gave isoflav-3-en XI, which was then converted into 7, 4'-dimethoxyisoflavan (XII) by catalytic hydrogenation over palladized charcoal. XII was prepared from II by the Clemmensen reduction.

Unlike III and IX, the isoflavan-4-ol (XIV) obtained by the reduction of isoflavanone (XIII) was not converted into 4-acetoxyisoflavan with acetic acid at 50°C, but was recovered unchanged. As has been mentioned above, the conversion of isoflavan-4-ols to 4-acetoxyisoflavans could go through the transition state in which C_4 is a carbonium ion. The resonance stabilization of the carbonium ion might affect the rate of this reaction. A methoxyl group in the 7-position will facilitate the formation of this transition state, and, consequently, the acetylation of the 4-hydroxyl with acetic acid will proceed smoothly. The lack of a electron-releasing substituent in this position makes the transformation of the starting substance into this transition state difficult; in the case of unsubstituted isoflavan-4-ol, acetylation with acetic acid does not occur.

As reported in the previous paper,[1] the Meerwein-Ponndorf reduction of I and II gave isopropyl ethers of the corresponding isoflavan-4-ols. This fact can be explained by the carbonium ion-intermediate theory as follows. The aluminum atom of excess aluminum isopropoxide would combine with the oxygen atom of the intermediate aluminum compound of I or II (XVI) as Lewis acid (XVII), and the oxygen atom in C_4 is likely to be eliminated from C_4, thus forming the carbonium ion XV. Then the carbonium ion would react with isopropanol to give the isopropyl ether of the isoflavan-4-ol. The carbonyl carbons of all the compounds which have been reported to give isopropyl ethers by the Meerwein-Ponndorf reduction[6] have a stable structure when they form carbonium ions (XVIII, XIX). As has been shown above, I and II have the structure which can produce a stable carbonium ion and give isopropyl ether in the Meerwein-Ponndorf reduction.

Experimental*

The Reaction of 7-Methoxyisoflavan-4β-ol (III) with Acetic Acid. — *1) In the Boiling State.* — A solution of III (500 mg.) in acetic acid (10 ml.) was refluxed for one hour. After the acetic acid had been removed under reduced pressure, water (30 ml.) was added to the residue and the mixture was allowed to stand for several hours. The precipitate formed was collected and recrystallized from ethanol in the form of plates (VII) (m. p. 108°C). Yield, 300 mg.

UV: λ_{max}^{EtOH} mμ (log ε): 335 (4.31), 245 (4.28).
Found: C, 80.55; H, 6.09. Calcd. for $C_{16}H_{14}O_2$: C, 80.64; H, 5.92%.

2) At 50°C. — A solution of III (100 mg.) in acetic acid (10 ml.) was heated at 50°C for one hour. After the acetic acid had been removed below 50°C under reduced pressure, water (30 ml.) was added to the residue and the mixture was set aside for several hours. The product formed was collected and recrysallized from ethanol, giving plates with a m. p. of 111°C (70 mg.) which showed no depression of melting point when admixed with 4α-acetoxy-7-methoxyisoflavan (VI).

The Reactions of 7-Methoxyisoflavan-4α-ol (IV) with Acetic Acid.—*1) In the Boiling State.*—A solution of IV (50 mg.) in acetic acid (5 ml.) was refluxed for one hour. The reaction mixture, when worked up as described for III, gave VII (55 mg., m. p. and mixed m. p. 108°C).

2) At 50°C. — A solution of IV (100 mg.) in acetic acid was heated at 50°C for one hour. After the acetic acid had been removed under reduced pressure, the residue was recrystallized from ethanol in the form of plates with a m. p. of 111°C, either alone or mixed with 4α-acetoxy-7-methoxyisoflavan (VI).

The Reactions of 4β-Acetoxy-7-methoxyisoflavan (V) with Acetic Acid.—*1) In the Boiling State.*—A solution of V (100 mg.) in acetic acid (10 ml.) was refluxed for one hour. The reaction mixture, when worked up as described for III, gave VII (m. p. and mixed m. p. 106°C).

2) At 50°C.—A solution of V (100 mg.) in acetic acid (10 ml.) was heated at 50°C for one hour.

6) A. L. Wild in "The Organic Reactions," Ed. by R. Adams, Vol. II, John Wiley & Sons, New York (1944), p. 190.

* All melting points are uncorrected.

The reaction mixture, when worked up as described for III, gave VI (55 mg., m. p. and mixed m. p. 108°C).

The Reaction of 4α-Acetoxy-7-methoxyisoflavan (IV) with Boiling Acetic Acid.—A solution of VI (100 mg.) in acetic acid (10 ml.) was refluxed for one hour. When the reaction mixture was worked up as described for III, it gave VII (70 mg., m. p. and mixed m. p. 108°C).

The Hydrolysis of 4β-Acetoxy-7-methoxyisoflavan (V).—A mixture of V (100 mg.), N/2 methanolic sodium methoxide (1.0 ml.), and methanol (20 ml.) allowed to stand for 24 hr. at room temperature. After dilution with water (100 ml.), the precipitate formed was separated, dried, and recrystallized from ethanol to III (60 mg., m. p. and mixed m. p. 143°C).

The Hydrolysis of 4α-Acetoxy-7-methoxyisoflavan (VI).—A mixture of VI (50 mg.), N/2 methanolic sodium methoxide (0.5 ml.), and methanol (20 ml.) was allowed to stand for 12 hr. at room temperature. On treatment as described above, IV (28 mg.) was obtained (m. p. and mixed m. p. 130°C).

The Reactions of 7-Methoxyisoflavan-4β-ol (III) with Mineral Acid.—Two drops of concentrated sulfuric acid or hydrochloric acid were added to a solution of III (50 mg.) in hydrous dioxane (1 : 1, 40 ml.). The solution was then allowed to stand for 48 hr. at room temperature. After dilution with water (200 ml.), the precipitate formed was recrystallized from ethanol to IV (20 mg., m. p. and mixed m. p. 129°C).

The Reaction of Isoflavan-4-ol (XIV) with Acetic Acid.—A solution of XIV (50 mg.) in acetic acid (10 ml.) was heated at 50°C for one hour. The usual after-treatment of the mixture gave XIV unchanged.

The Reactions of 7, 4'-Dimethoxyisoflavan-4-ol (IX) with Acetic Acid.—*1) At 50°C.*—A solution of IX (50 mg.) in acetic acid (10 ml.) was heated at 50°C for one hour. The reaction mixture, when worked up as described for III, gave 7, 4'-dimethoxyisoflav-3-en (XI) (m. p. 161°C). Yield, 20 mg.

UV: λ_{max}^{EtOH} mμ (log ε): 335 (4.38), 250 (4.22). (Found: C, 75.87; H, 6.09%.)

2) At 50°C.—A solution of IX (100 m.) in acetic acid (10 ml.) was heated at 50°C for one hour. The usual after-treatment gave crystals with a m. p. of 123°C. Yield, 30 mg.

Found: C, 69.63; H, 6.15. Calcd. for $C_{19}H_{20}O_5$: C, 69.50; H, 6.14%.

IR (KBr): 1728 cm^{-1}.

3) In the Boiling State.—A solution of IX (100 mg.) in acetic acid (20 ml.) was refluxed for one hour. The usual treatment of the reaction mixture gave XI (60 mg., m. p. and mixed m. p. 161°C).

7-Methoxyisoflavan.—*The Catalytic Hydrogenation of the VII Obtained by the Reaction of III with Boiling Acetic Acid.*—A mixture of VII (500 mg.) in acetic acid (140 ml.) and palladized charcoal (20%, 500 mg.) was shaken with hydrogen at 30°C until the absorption of hydrogen stopped. One mole of hydrogen had been absorbed. The catalyst was then filtered off, and the filtrate was concentrated under reduced pressure. The residue was recrystallized from ethanol in the form of plates with a m. p. of 106°C (300 mg.). The product was identified, by mixed melting point determination, to be the same compound prepared by the Clemmensen reduction of I[1].

7, 4'-Dimethoxyisoflavan (XII).—*1) The Catalytic Haydrogenation of the XI Obtained by the Reaction of IX with Acetic Acid.*—A mixture of XI (500 mg.) in acetic acid (150 ml.) and palladized charcoal (5%, 1.0 g.) was shaken with hydrogen at 20°C until the absorption of hydrogen stopped. One mole of hydrogen (46 ml.) had been absorbed. Upon working up the product in the usual manner, XII (200 mg., m. p. 113°C (from ethanol)) was obtaind. (Found: C, 75.69; H, 6.78%.)

2) The Clemmensen Reduction of II.—A mixture of II (250 mg.), amalgamated zinc dust (3.6 g.), concentrated hydrochloric acid (5 ml.), and acetic acid (30 ml.) was allowed to stand for 24 hr. at room temperature. The mixture was then poured into water (200 ml.). The recrystallization of the precipitate from ethanol gave a product with a m. p. 114°C (150 mg.) which showed no depression of the melting point when admixed with XII prepaped as above.

College of General Education
Tohoku University
Kawauchi, Sendai

Aromatization of Some 4-Substituted 2, 6-Dimethyl-3, 5-diethoxycarbonyl-1, 4-dihydropyridines to Pyridines

By Ahmad KAMAL, Mansoor AHMAD, Nazar MOHD and Abdul Majid HAMID

(Received June 19, 1963)

Following the preparation of a series of dihydropyridine compounds[1] it was considered interesting to investigate the possibility of preparing the corresponding piperidines through "hydrogen-transfer." When 2,6-dimethyl-3,5-diethoxycarbonyl-4-phenyl-1,4-dihydropyridine was refluxed in cyclohexene in the presence of 5% palladium/charcoal catalyst with a catalytic amount of glacial acetic acid added to it, the product that was obtained was not the corresponding piperidine, instead 2,6-dimethyl-3,5-diethoxycarbonyl-4-phenylpyridine was obtained in 90% yield. The identity of this product was confirmed by comparison with the authentic sample prepared through oxidation of the corresponding dihydropyridine with nitrous oxide.[2]

Accordingly, all the dihydropyridine compounds reported earlier[1] were subjected to this reaction. Since cyclohexene did not play any part, this reaction was carried out by boiling the dihydropyridines in toluene or benzene, containing a catalytic amount of glacial acetic acid and 5% palladium-charcoal catalyst. In the absence of acetic acid, however, no aromatization could be achieved. It was also interesting to observe that in this reaction aromatization did not proceed at all, if the substituent in the fourth position happened to be a phenol. As for instance 2,6-dimethyl-3,5-diethoxycarbonyl-4-(3-hydroxyphenyl)-1,4-dihydropyridine, 2,6-dimethyl-3,5-diethoxycarbonyl-4-(3-methoxy-4-hydroxyphenyl)-1,4-dihydropyridine and 2,6-dimethyl-3,5-diethoxycarbonyl-4-(4-hydroxyphenyl)-1,4-dihydropyridine failed to give the corresponding pyridine derivatives. However, on methylation of phenolic OH the aromatization with palladium/charcoal proceeded as usual.

Reference to literature reveals that Knoevenagel and Fuchs prepared 2,6-dimethyl-3,5-diethoxycarbonylpyridine by heating 2,6-dimethyl-3,5-diethoxycarbonyl-1,4-dihydropyridine with palladium-black at 200~265°C,[3] and also by heating with concentrated hydrochloric acid when the corresponding pyridine derivative was obtained in 5% yield only.

Since oxidation with nitrous oxide gave invariably poor yields of the corresponding pyridine derivatives, oxidation with potassium permanganate in glacial acetic acid was also tried when the pyridine derivatives were obtained in comparatively high yields. Oxidation in acetone however, failed, the dihydropyridines being recovered unchanged.

Experimental

All melting points are corrected. Ultraviolet absorption spectra were determined with a Beckman spectrophotometer model DB in 95% ethanol.

General Method.—*A) Aromatization of the Dihydropyridine Ring with 5% Palladium/Charcoal-Acetic Acid.*—A dihydropyridine (0.002 mol.) dissolved in toluene (25 ml.) containing palladium-on-charcoal catalyst (5%; 50 mg.) and glacial acetic acid (5 ml.) was refluxed (42 hr.) on a sand bath, filtered and filtrate washed thrice with water and then with aqueous sodium hydrogen carbonate (10%; 2 ml.) followed by water. Drying and removal of the solvent gave the corresponding pyridine.

B) Aromatization of Dihydropyridine Ring through Oxidation with Potassium Permanganate.—A dihydropyridine (0.01 mol.) was dissolved in glacial acetic acid (50 ml.) and powdered potassium permanganate (1 g., 0.006 mol.) added. The mixture was heated on a water bath (about 5 hr.) till almost whole of the permanganate was consumed. The very slight excess of the permanganate was destroyed by heating with a little ethyl alcohol and the solvent was removed in vacuo. Water (25 ml.) was added to the residue and the product was isolated with ethyl acetate and worked up.

The pyridine compounds are generally soluble in acetone, benzene, chloroform, dioxane, ethyl acetate, ethyl and methyl alcohols, sparingly soluble in ether, carbon tetrachloride, light-petroleum (60~80°C) and insoluble in water.

West Regional Laboratories
P.C.S.I.R., Lahore
Pakistan

1) A. Kamal and A. A. Qureshi, *Pak. J. Sci. Res.*, **15** (1), 35 (1963).
2) R. Schiff and J. Puliti, *Ber.*, **16**, 1607 (1883).
3) E. Knoevenagel and J. Fuchs, ibid., **35**, 1788 (1902); **36**, 2848 (1903).
4) A. Hantzsch, *Ann.*, **215**, 22 (1882).
5) A. Jaeckle, ibid., **246**, 32 (1888).
6) W. Epstein, ibid., **231**, 7 (1885).
7) B. Emmert, E. Diefenbach and R. Eck, *Ber.*, **60**, 2216 (1927).
8) E. Grischkenwitsch-Trochimowski and I. Pawloskaja, Beilstein, **22**, I, 538.
9) L. E. Hinkel, E. E. Ayling and W. H. Morgan, *J. Chem. Soc.*, **1931**, 1835.
10) R. Lepetit, *Ber.*, **20**, 1338 (1887).
11) L. E. Hinkel and W. R. Madel, *J. Chem. Soc.*, **1929**, 750.
12) F. Heiber, *Ber.*, **25**, 2405 (1892).

TABLE I. YIELDS AND PROPERTIES OF 4-SUBSTITUTED 2,6-DIMETHYL-3,5-DIETHOXYCARBONYLPYRIDINES

4-Substituent	Solvents for crystallization. Shape and color of crystals	Yield, % Method A	Yield, % Method B	M.p. or b.p.	Analysis Found	Analysis Calcd. for	UV Absorption λ_{max}(log ε)
H	Light-petroleum* Colorless needles	43.0	49.0	72°C Lit.[3] 72～73°C		$C_{13}H_{17}O_4N$	265(4.02) 206(4.55)
					C, 62.24 H, 6.72 O, 25.51 N, 5.52	62.14 6.82 25.47 5.57	
Methyl-	Golden yellow oil	27.0	64.0	222°C/2 mmHg Lit. b.p. 308～310°C[4]		$C_{14}H_{19}O_4N$	270(3.32) 208(3.92)
					C, 63.30 H, 6.56 O, 24.38 N, 5.66	63.38 7.22 24.12 5.28	
Propyl-	Brown oil n_D^{22} 1.498	63.0	51.5	132°C/0.5 mmHg Lit. 308°C/714 mmHg[5]		$C_{16}H_{23}O_4N$	270(3.45) 208(4.37)
					C, 65.07 H, 7.65 O, 21.81 N, 4.91	65.51 7.90 21.82 4.78	
Hexyl-	Yellow oil	67.4	74.5	200°C/1.5 mmHg $(C_{19}H_{29}NO_4)_2H_2PtCl_6$ m.p. 140°C Lit.[5] 141°C		$C_{19}H_{29}O_4N$	232(4.16) 208(4.37)
					C, 67.73 H, 8.45 O, 19.41 N, 4.90	68.03** 8.71 19.08 4.18	
Styryl-	Benzene-light petroleum* Long colorless needles	49.7	—	39°C Lit.[6] 39°C		$C_{21}H_{23}O_4N$	287(4.30) 208(4.26)
					C, 71.42 H, 6.26 O, 17.98 N, 3.72	71.37 6.56 18.11 3.96	
Phenyl-	Benzene-light petroleum* Microscopic hexagonal plates	90.0	68.8	65°C Lit.[2] 66～67°C		$C_{19}H_{21}O_4N$	267(3.90) 206(4.50)
					C, 69.32 H, 6.40 O, 19.49 N, 4.49	69.70 6.47 19.55 4.28	
4-Methoxyphenyl-	Benzene Microscopic colorless plates	42.8	64.8	52°C Lit.[7] 51～53°C		$C_{20}H_{23}O_5N$	272(4.06) 206(4.54)
					C, 67.20 H, 6.48 O, 22.43 N, 4.05	67.21 6.49 22.38 3.92	

TABLE I. (Continued)

4-Substituent	Solvents for crystallization. Shape and color of crystals	Yield, % Method A	Yield, % Method B	M.p. or b.p.	Analysis Found	Analysis Calcd. for	UV Absorption λ_{max} (log ε)
3,4-Dimethoxyphenyl-	Benzene Microscopic colorless needles	41.5	35.4	98°C		$C_{21}H_{25}O_6N$	
					C, 65.12	65.10	272(4.11)
					H, 6.53	6.50	204(4.66)
					O, 24.19	24.78	
					N, 4.05	3.62	
Propenyl-	Red oil	65.2	—	230°C/1.5 mmHg Hydroiodide m.p. 140°C (decomp.) Lit.[8] 137～140°C (decomp.)		$C_{16}H_{21}O_4N$**	
					C, 64.14	65.95	208(4.16)
					H, 7.10	7.27	203(4.12)
					O, 21.25	21.97	
					N, 4.81	4.81	
2-Nitrophenyl-	Ether-ligroin Microscopic needles	76.0	47.7	73°C Lit.[9] 75°C		$C_{19}H_{20}O_6N_2$	
					C, 61.32	61.28	268(3.72)
					H, 5.52	5.41	205(4.49)
					O, 25.45	25.78	
					N, 7.36	7.52	
3-Nitrophenyl-	Benzene-ligroin Microscopic prisms	60.4	58.0	60～61°C Lit.[10] 65°C		$C_{19}H_{20}O_6N_2$	
					C, 61.06	61.28	256(4.19)
					H, 5.63	5.41	206(4.65)
					O, 25.97	25.78	
					N, 7.54	7.52	
4-Nitrophenyl-	Ether-light petroleum* Microscopic needles	83.0	56.4	115°C Lit.[7] 117°C		$C_{19}H_{20}O_6N_2$	
					C, 61.21	61.28	270(4.21)
					H, 5.30	5.41	205(4.56)
					O, 25.60	25.78	
					N, 7.61	7.52	
2-Chlorophenyl-	Yellow oil	80.3	34.6	62°C 225°C/1.5 mmHg Lit.[11] 62°C		$C_{19}H_{20}O_4NCl$	
					C, 62.18	62.80	272(3.51)
					H, 5.79	5.54	210(4.30)
					O, 17.65	17.74	
					N, 4.26	3.97	
α-Furyl-	Oil n_D^{22} 1.532	66.0	45.0	40～41°C 180°C/1.5 mmHg Lit.[12] 40～41°C		$C_{17}H_{19}O_5N$	
					C, 63.60	64.34	281(4.13)
					H, 5.79	6.04	212(4.22)
					O, 26.02	25.21	
					N, 4.62	4.41	

* Light petroleum b.p. 60～80°C ** Requires

Confirmation of 5-Pyrophosphomevalonate as an Intermediate in the Enzymatic Synthesis of Bacterial Phytoene from Mevalonate

By Ginzaburo SUZUE

(Received June 25, 1963)

It is well known that MVA is a precursor of isoprenoid compounds, such as carotenoids and steroids, which are found universally in the biological world. In the course of their biosynthesis, MVA is believed to react with ATP by specific kinases to form phosphorylated compounds.[1] Though several phosphorylated intermediates have been confirmed in the case of the biosynthesis of steroids,[2-4] 5-P-MVA is the only intermediate which has been reported in carotenogenesis.[5]

The present paper is concerned with the confirmation of 5-PP-MVA as an intermediary product formed during the biosynthesis of phytoene from MVA or 5-P-MVA, and with its enzymatic conversion into phytoene.

As 5-P-MVA and 5-PP-MVA are formed from MVA by means of reactions with ATP catalyzed by enzymes extracted from a phytoene-accumulating mutant of *Staphylococcus*,[6] the pathway of the phytoene biosynthesis by means of this microorganism may be written as follows:

MVA→5-P-MVA→5-PP-MVA

→(Isopentenylpyrophosphate)→Phytoene

Experimental and Results

Chemicals and Instruments.[5,8] — The ATP used was equally labeled with ^{32}P at β and γ positions.[7] The prostatic phosphomonoesterase used was the generous gift of Professor Tomoji Suzuki of Kyoto University.

Radioactivity was measured by the instruments and techniques previously described.[5]

Preparation of Enzymes.—For the extraction of the cell-free enzymes from a phytoene-accumulating mutant of *Staphylococcus*, the method described previously was applied.[8] After the adjustment of the protein concentration of the crude extract to 10 mg./ml., a 2% solution of protamine was stirred into the diluted enzyme extract to give a final concentration of 0.1% protamine. The resulting supernatant solution was fractionated with ammonium sulfate. Mevalonic kinase was precipitated at 45~60%, phosphomevalonic kinase at 40~55%, and pyrophosphomevalonic decarboxylase, at 60~75% saturation. For the synthesis of 5-PP-MVA from MVA, the precipitate of the 40~60% ammonium sulfate-saturated fraction (tentatively named enzyme I) was employed, while with that of 5-PP-MVA from 5-P-MVA the 40~55% fraction (tentatively named enzyme II) was employed as the method of enzyme preparation.

A 0.1 M Tris buffer (pH 8.0) solution of the proteins precipitated from the crude extract at 0~90% saturation with ammonium sulfate was used for the synthesis of phytoene from MVA or 5-PP-MVA, as has been reported previously.[8]

Isolation and Identification of 5-Pyrophosphomevalonic Acid. — In the previous paper,[5] it was reported that an undetermined substance Y was found in an earlier stage of the enzymatic conversion of MVA to phytoene but that it disappeared in a later stage. Hence, it is quite reasonable to postulate that compound Y is one of the intermediates in the biosynthesis of phytoene from MVA. The enzymatic formation of compound Y from MVA or 5-P-MVA was established in the following experiment.

A reaction system which contained MVA and enzyme I, or 5-P-MVA and enzyme II, and ATP was incubated as shown in Table I. The incubation was carried out at 30°C for 30 min., and then the enzyme action was stopped by heating the reaction vessel at 100°C for 30 sec. After the denatured proteins had been removed by centrifugation, the

TABLE I. INCUBATION SYSTEMS FOR ENZYMATIC SYNTHESIS OF Y (5-PP-MVA) FROM MVA OR 5-P-MVA

Substrate	DL-MVA	5-P-MVA
	900 mμmol.	500 mμmol.
$MgSO_4$ (or $MnSO_4$)	40 μmol.	40 μmol.
ATP	80 μmol.	80 μmol.
Tris buffer (pH 7.5)	100 μmol.	100 μmol.
Enzyme	Enzyme I 0.5 ml.	Enzyme II 0.3 ml.
Protein concn.	7.5 mg./ml.	6.0 mg./ml.
Total volume	1.2 ml.	1.0 ml.
Incubation	30°C, 30 min.	30°C, 30 min.

* Abbreviations: MVA, Mevalonic acid; 5-P-MVA, 5-Phosphomevalonic acid; 5-PP-MVA, 5-Pyrophosphomevalonic acid.

1) G. Popják and J. W. Cornforth, *Advances in Enzymol.*, 22, 281 (1960).
2) S. Chaykin, J. Law, A. H. Philips, T. T. Tchen and K. Bloch, *Proc. Natl. Acad. Sci. U. S.*, 44, 998 (1958).
3) U. Henning, E. M. Möslein and F. Lynen, *Arch. Biochem. Biophys.*, 83, 259 (1959).
4) A. de Waard and G. Popják, *Biochem. J.*, 73, 410 (1959).
5) S. Ohnoki, G. Suzue and S. Tanaka, *J. Biochem.*, 52, 423 (1962).
6) G. Suzue, *Arch. Biochem. Biophys.*, 88, 180 (1960).
7) J. G. Moffatt and H. G. Khorana, *J. Am. Chem. Soc.*, 83, 649 (1961).
8) G. Suzue, *J. Biochem.*, 51, 246 (1962).

TABLE II. R_f VALUES OF COMPOUND Y (5-PP-MVA)

Solvent system	R_f
A	0.03～0.08
B	0.23～0.33
C	0.29～0.36
D	0.06～0.11

Pure compound Y (5-PP-MVA) enzymatically synthesized from 2-^{14}C-MVA was paper chromatographed (ascending) by the following four solvent systems. The component of each system: A, *n*-butanol - formic acid - water (77 : 10 : 13, by volume); B, isobutyric acid - concd. ammonia - water (66 : 3 : 30); C, *t*-butanol - formic acid - water (40 : 10 : 16); D, *t*-amyl alcohol - acetic acid - water (4 : 1 : 2).

supernatants were analyzed by column chromatography or paper chromatography.

By paper chromatographic techniques, using four solvent systems, it was found that the compound Y formed from 2-^{14}C-MVA gave the R_f values shown in Table II. These R_f values are identical with those of 5-PP-MVA previously reported.[3,4,9,10]

When the supernatant (1.1～0.9 ml., incubation scale: Table I) of the enzymatically-synthesized sample is paper chromatographed (paper Toyo-roshi No. 50, size 20 cm.×40 cm.) without prior purification, the observed R_f value of Y is 0.42～0.51 in the methanol - concentrated ammonia - water system. When, however, after the isolation of the material with R_f 0.42～0.51, it was rechromatographed with the same solvent, an R_f value of Y of 0.03～0.08 was observed, corresponding to that of purified 5-PP-MVA. This behavior during the initial chromatography may be attributed to the presence of a large amount of nucleotides.

After purification by paper chromatography using two solvent systems (methanol - concentrated ammonia - water 'R_f 0.42～0.51' and isobutyric acid - concentrated ammonia - water 'R_f 0.23～0.33'), compound Y was further identified using column chromatography on a Dowex 1 - formate column (0.7 cm.×10 cm.). By this technique, too (Fig. 1), compound Y was identified with 5-PP-MVA.[11]

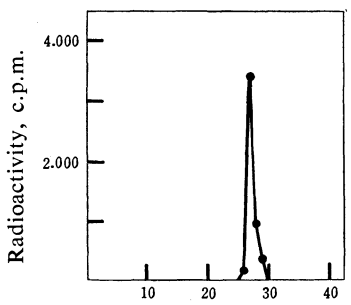


Fig. 1. Chromatographic analysis of compound Y on Dowex 1-formate column (1.7 cm.× 10 cm.).
Sample applied: 5000 c. p. m. (4.5 mμmol.).
Solution used for elution: Fractions 1—16, water; 17—26, 4 N formic acid; 27—31, 0.4 M ammonium formate in 4 N formic acid; 32—35, 0.8 M ammonium formate in 4 N formic acid.

High-voltage paper electrophoresis was performed under the following conditions: buffer solution, pyridine - acetate (pH 6.2); 41 V./cm., 65 mamp.; 120 min.; paper: Toyo-roshi, No. 2. Here compound Y, 5-P-MVA and MVA migrated 21.8 cm., 21.6 cm. and 16.8 cm. respectively. The results also indicate that compound Y is 5-PP-MVA.[3]

Further confirmation was undertaken as follows. The ^{14}C, ^{32}P double-labeled compound Y was enzymatically synthesized from DL-2-^{14}C-MVA, AT^{32}P (β,γ position labeled) and the enzyme preparation described in Table I. The compound Y thus formed was purified at least three times by paper chromatography using the methanol - concentrated ammonia - water or isobutyric acid - concentrated ammonia - water solvent systems. The results are shown in Table III. From the ratio of ^{32}P to ^{14}C in the purified compound Y, it consists of MVA and phosphate in the molar ratio of 1 : 2.

The results of the analysis of the incubation products are summarized in Table IV, where it is shown that these incubation systems are suitable for the preparation of 5-PP-MVA.

TABLE III. RATIO OF ^{32}P TO ^{14}C OF DOUBLY LABELED Y

^{14}C c. p. m.	^{32}P c. p. m.	^{14}C mμ atom	^{32}P mμ atom	^{14}C : ^{32}P
3200	4872	32.0	60.9	1.0 : 1.9

AT^{32}P (80 μmol., specific activity: 8.0×10^4 c. p. m./μmol. in terminal P atom), $MgSO_4$ (40 μmol.), enzyme I (0.5 ml.; protein concentration: 7.5 mg./ml.), Tris buffer (pH 7.5, 100 μmol.) and DL-2-^{14}C-MVA (900 mμmol.; specific activity: 1.0×10^5 c. p. m./μmol.) in a volume of 1.2 ml. were incubated at 30°C for 30 min. The product obtained was purified by the method described in the text and radioactivity was measured in a gas-flow counter with and without aluminum window.

TABLE IV. ANALYSIS OF PRODUCTS AFTER INCUBATION (CF. TABLE I)

	Substrate DL-MVA %	Substrate 5-P-MVA %
MVA	50	—
5-P-MVA	1	1
Compound Y (5-PP-MVA)	49	99

Enzymatic Hydrolysis of Compound Y. — ^{14}C-Labeled compound Y (4000 c. p. m., 3.6 mμmol. equiv.) and 5-P-MVA (4000 c. p. m., 3.6 mμmol. equiv.) were incubated separately for 30 min. at 37°C in a system which consisted of acetate buffer (pH 5.3, 2 μmol.), magnesium sulfate (1 μmol.),

9) K. Bloch, S. Chaykin, A. H. Philips and A. de Waard, *J. Biol. Chem.*, **234**, 2595 (1959).
10) T. T. Tchen, *Methods in Enzymol.*, **5**, 489 (1962).
11) T. N. R. Varma and C. O. Chichester, *Arch. Biochem. Biophys.*, **96**, 265 (1962).

and purified prostatic phosphomonoesterase (0.01 ml.; protein concentration; 0.45 mg./ml.) in a volume of 0.1 ml. After the reaction had been stopped by dipping the vessel in boiling water for 30 sec., the incubation mixture was spotted on paper and developed with isobutyric acid - concentrated ammonia - water (66 : 3 : 30) and *t*-butanol - formic acid - water (40 : 10 : 16) systems. The results of analysis by actigraphy are summarized in Table V. The regeneration of 5-P-MVA and MVA by enzymatic hydrolysis was confirmed by paper chromatography.[5]

TABLE V. ENZYMATIC HYDROLYSIS OF COMPOUND Y (5-PP-MVA) AND 5-P-MVA

	Substrate			
	5-P-MVA		Y	
Time of incubation	10	30 min.	10	30 min.
Y	—	—	80	71%
5-P-MVA	2	1%	2	7
MVA	98	99	18	22

Radioactive 5-P-MVA and compound Y (4000 c. p. m., 3.6 mμmol., respectively) were hydrolyzed by prostatic phosphomonoesterase (0.01 ml.; protein concentration: 0.45 mg./ml.) with acetate buffer (pH 5.3, 2 μmol.) and $MgSO_4$ (1 μmol.) in a volume of 0.1 ml. Products were separated and analyzed by actigraphic method after paper chromatography with isobutyric aicd - concentrated ammonia - water and *t*-butanol - formic acid - water systems.

Enzymatic Synthesis of Bacterial Phytoene from 2-^{14}C-5-PP-MVA. — 2-^{14}C-5-PP-MVA (4000 c. p. m., 3.6 mμmol.) or DL-2-^{14}C-MVA (13000 c. p. m., 12 mμmol.) was incubated at 37°C for 3 hr. while being gently shaken with NADP (0.5 mg.), 6-phosphogluconate (2 μmol.), nicotinamide (50 μmol.), ATP (10 μmol.), FAD (0.05 mg.), a Tris buffer (pH 8.0, 40 μmol.), manganese sulfate (10 μmol.), magnesium sulfate (5 μmol.), Tween 20 (final concentration: 0.17%), KF (10 μmol.) and a 0.1 M Tris buffer (pH 8.0) solution of enzyme preparation precipitated at 90% saturation with ammonium sulfate (0.3 ml.; protein concentration: 42 mg./ml.) in a volume of 0.6 ml. The enzymatic reactions were stopped by the addition of 2 ml. of a 10% ethanolic sodium hydroxide solution to the mixture. *p*-Hydroquinone (10 mg.) and a petroleum benzine solution (1.00 ml.) of pure bacterial phytoene (absorbancy: 8.42 at 286 mμ) were added to the mixture simultaneously. After saponification, the unsaponifiable fraction was washed with water three times, and the aliquots were dried on aluminum planchets and their radioactivity counted as infinitely thin samples. The separation of the phytoene in the unsaponifiable fraction was carried out by chromatography on an activated-alumina column. The fractions containing purified phytoene were dried on aluminum planchets, and their radioactivities were measured. The results obtained are summarized in Table VI. The conversion of 5-PP-MVA or MVA to phytoene is evident.

TABLE VI. BIOSYNTHESIS OF PHYTOENE FROM MVA AND 5-PP-MVA

Substrate	Unsaponifiable fraction c. p. m.	Phytoene c. p. m.
DL-MVA (13000 c.p.m.; 12 mμmol.)	2550	1109
5-PP-MVA (4000 c.p.m.; 3.6 mμmol.)	3320	2625

Each system was consisted of NADP (0.5 mg.), 6-phosphogluconate (2 μmol.), nicotinamide (50 μmol.), ATP (10 μmol.), FAD (0.05 mg.), Tris buffer (pH 8.0, 40 μmol.), $MnSO_4$ (10 μmol.), $MgSO_4$ (5 μmol.), Tween 20 (final concentration: 0.17%), KF (10 μmol.), enzyme (0.3 ml., protein concentration: 42 mg./ml.) and the substrates indicated, in a volume of 0.6 ml. Incubation, in nitrogen (99.9%) for 3 hr. at 37°C.

Discussion

Compound Y is detected in an early stage of the biosynthesis of phytoene from MVA and 5-P-MVA. The behavior of this compound has now been shown to be identical with that of 5-PP-MVA, judging from paper chromatographic, column chromatographic, and paper electrophoretic criteria. It contains two atoms of phosphorus per molecule of mevalonic acid. One phosphorus atom has been shown to be located at the 5-position of MVA, as 5-P-MVA is regenerated by the hydrolytic action of prostatic phosphomonoesterase. The liberation of the first phosphorus moiety from compound Y is slow with this enzyme, as has been previously shown using 5-PP-MVA and other phosphomonoesterases.[9] The rapid regeneration of MVA is readily explicable, as the liberation of the second phosphorus is quite rapid, as in Table V shows. Thus, it seems reasonable to conclude that compound Y has one pyrophosphate linkage and that, after one phosphorus atom is liberated, the 5-P-MVA thus formed is readily susceptible to phosphomonoesterase action with the generation of MVA. On the basis of those facts compound Y has been concluded to be 5-PP-MVA, a substance which has been previously found in the pathway of squalene and cholesterol biosynthesis.[1-4]

5-PP-MVA was incorporated into phytoene with more than twice the efficiency of the DL-MVA, thus showing that 5-PP-MVA is also in the biosynthetic pathway of phytoene from MVA or 5-P-MVA.

Summary

In phytoene biosynthesis from mevalonic acid and 5-phosphomevalonic acid by the

enzyme preparation from the mutant of *Staphylococcus aureus*, a phosphorus-containing substance has been isolated as an intermediate compound. After purification by paper chromatography, column chromatography and paper electrophoresis, this substance has been shown to contain phosphorus and mevalonic acid in the molar ratio of 2 : 1. From its behavior with regard to prostatic phosphomonoesterase, together with the above-mentioned results, this substance has been concluded to be 5-pyrophosphomevalonic acid.

Department of Chemistry
Faculty of Science
Kyoto University
Sakyo-ku, Kyoto

*The Polarography of Terephthalaldehydic Acid**

By Masataka NISHIYAMA, Masao MARUYAMA and Hiroshi HAMAGUCHI

(Received June 29, 1963)

Holleck and Marsen[1] were the first to study the d. c. polarography of terephthalaldehydic acid. Their purpose was to investigate the effect of a substituted group on the polarographic behavior of benzaldehyde for eleven substituted benzaldehydes. Terephthalaldehydic acid has been investigated only qualitatively as one of these substituents.

In a previous paper[2] the present authors investigated the polarographic behavior of terephthalaldehydic acid in a sodium hydroxide solution; they reported a polarographic method for the rapid determination of a small amount of this acid in terephthalic acid, because terephthalic acid was well dissolved only in an alkaline solution.

In this paper, the authors will study in detail the d. c. and a. c. polarography of terephthalaldehydic acid in buffered solutions not containing ethanol over the pH region from 1 to 13.

The experimental results give some new information with respect to the polarographic reduction of terephthalaldehydic acid. The acid recombination and dissociation rate constants for this compound will be calculated, and a reduction scheme will be proposed.

Experimental

Apparatus.—A Yanagimoto AC/DC polarograph, model PA 102, was used for recording d. c. and a. c. polarograms. For the pH measurements, a Toa Dempa pH meter, model HM-5, was adopted. The dropping mercury electrode used had the following characteristics; $m=2.01$ mg./sec., $h=65$ cm., and $t=4.65$ sec. at an open circuit. The polarographic cells were of a modified H-type; the electrolytic compartment contained a mercury pool. When the a. c. polarograms were recorded, a "pool-condenser" of a 100 μF capacity was connected between the saturated calomel electrode and the mercury pool anode.[3]

All polarographic measurements were made at 25±0.5°C in a thermostat. Purified nitrogen gas was bubbled through the test solution for 10 min. to remove any dissolved oxygen.

Reagents. — The terephthalaldehydic acid* and other reagents used were of a guaranteed reagent grade.

Buffers and Test Solutions.—The Britton-Robinson buffers were mainly used to cover the pH range from 1 to 13. The other buffer systems used were as follows; 0.2 N potassium chloride - 0.2 N hydrochloric acid (pH 1.0~2.2), 0.2 N potassium biphthalate - 0.2 N hydrochloric acid (pH 2.2~3.8), 0.2 N potassium phosphate - 0.2 N sodium hydroxide (pH 4.0~6.2), 0.2 M potassium phosphate (monobasic) - 0.2 N sodium hydroxide (pH 6~8), 0.2 M boric acid - 0.1 N sodium hydroxide (pH 8~10), 0.1 M sodium citrate - 0.1 N hydrochloric acid (pH 1.1~5.8) and 0.2 N borax - 0.1 N sodium hydroxide (pH 9.5~12.0).

The test solution was prepared by taking 20 ml. of the buffer of the desired pH value and a given volume of a terephthalaldehydic acid standard solution[2] in a 25 ml. volumetric flask, adjusting the ionic strength to $\mu=0.13$ with 1.0 M potassium chloride, and then filling the flask up to the mark with water. No surface active substances were used. The pH value of the solution was again measured after the preparation of the test solution.

---

* A summary of this work was presented at the 9th Symposium on Polarography held at Kyoto, October, 1962.

1) L. Holleck and H. Marsen, *Z. Elektrochem.*, **57**, 944 (1953).

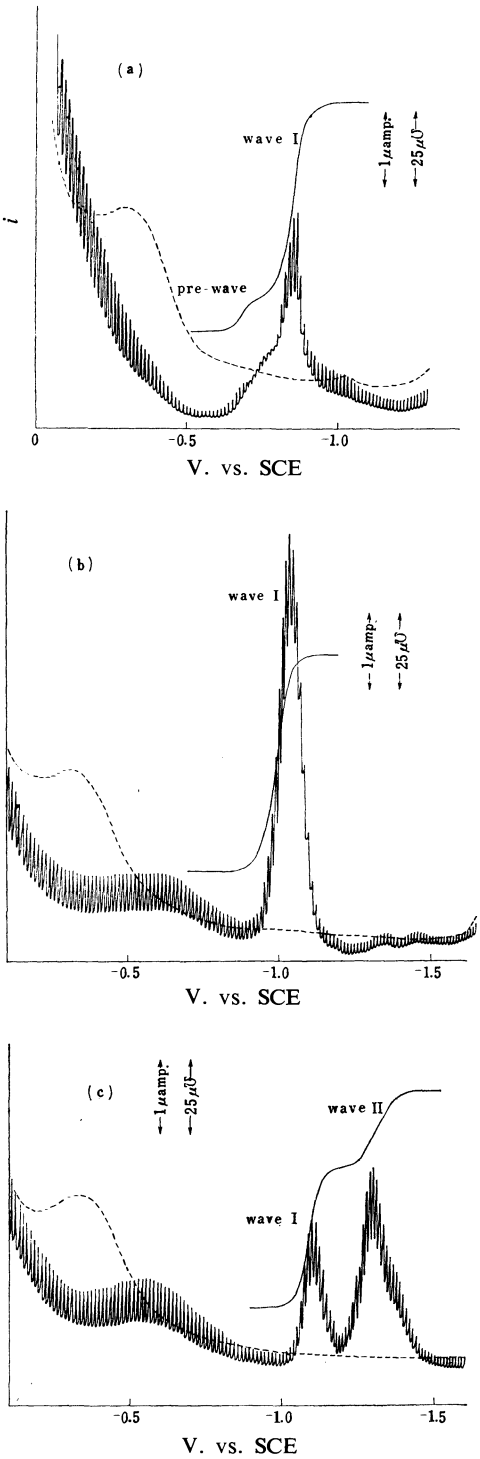
2) M. Nishiyama, M. Maruyama and H. Hamaguchi, *Japan Analyst* (*Bunseki Kagaku*), **12**, 150 (1963).

3) B. Breyer, F. Gutmann and S. Hacobian, *Australian J. Sci. Research*, **A4**, 595 (1951).

* Terephthalaldehydic acid was obtained from the Tokyo Kasei Co.; the analysis data gave a purity of 100±2% from the determination of the carboxyl group of this compound. The melting point was 257°C.

Results and Discussion

D. C. Polarography.—Figure 1 shows some typical d. c. and a. c. polarograms of 0.4 mM terephthalaldehydic acid in Britton-Robinson buffers over the pH range studied.



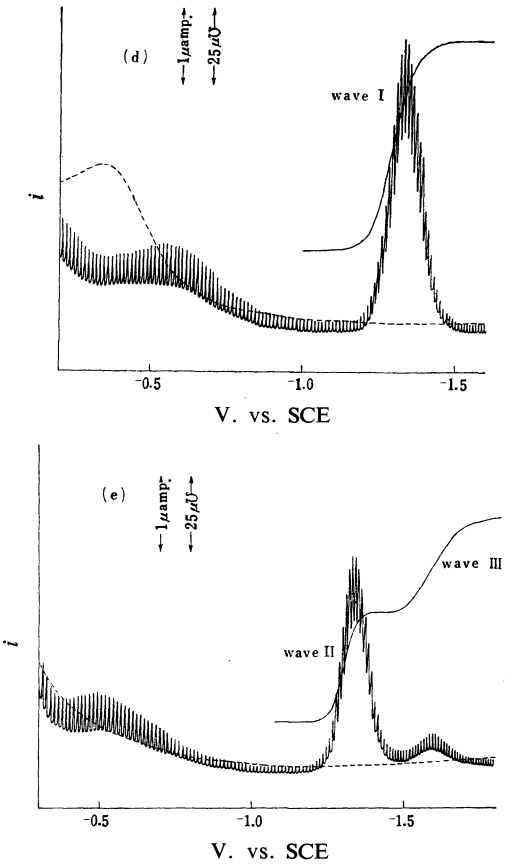


Fig. 1. D. c. and a. c. polarograms of 0.4 mM terephthalaldehydic acid in the Britton-Robinson buffers.
(a) pH 2.1, (b) pH 5.1, (c) pH 6.5, (d) pH 8.0, (e) pH 13.2
——: d. c. polarogram (μamp.)
------: a. c. maximum base current (μ℧)
Oscillated curve: a. c. polarogram (μ℧)

The Effect of pH.—The variations in the wave height and the half-wave potential with variation in the pH are illustrated in Figs. 2 and 3 respectively. The reduction wave of terephthalaldehydic acid at a pH below 4.4 was accompanied by a pre-wave (Fig. 1-a). This pre-wave was not reported in the earlier investigation.[1] The behavior of terephthalaldehydic acid waves above pH 4.4 accorded approximately with the results of Holleck and Marsen; in the pH range from 4.4 to 5.5, a single wave (designated as wave I) was observed (Fig. 1-b); in the pH range from 5.5 to 7.5, two waves appeared—the height of the first wave, a positive one corresponding to wave I, decreased, and that of the second one, designated as wave II, increased with the increasing pH (Fig. 1-c). In the vicinity of pH 8, wave II alone was observed (Fig. 1-d), and as the pH increased from 8.2 to 11.5 the

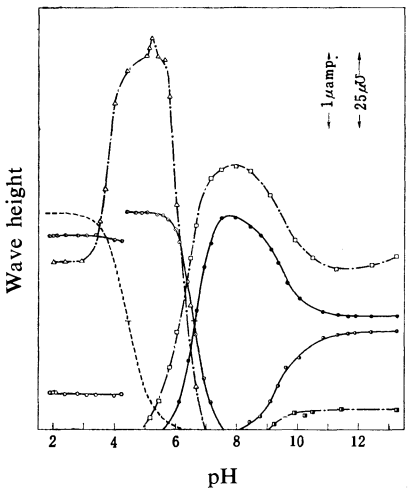


Fig. 2. Variation of the wave heights with pH.
At 0.4 mM terephthalaldehydic acid
——— d.c. waves (○ pre-, ⊙ I, ● II ◑ III)
— • — a.c. waves (△ I, □ II, ◨ III)
-------- theoretical dissociation curve

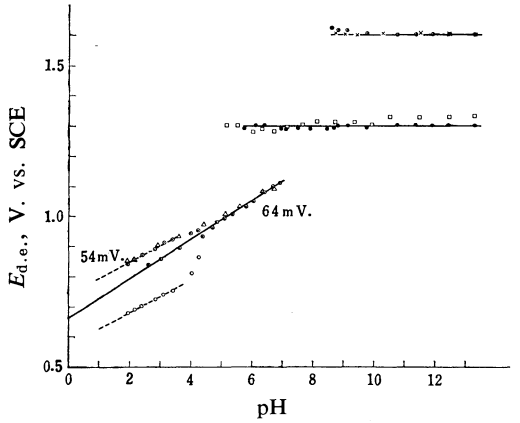


Fig. 3. The pH dependence of the half-wave and peak potentials.
At 0.4 mM terephthalaldehydic acid
——, ------: d.c. waves (○ pre-, ⊙ I, ● II, ◑: III, ◑ I in biphthalate buffers)
a.c. wave (△ I, □ II × III)

height of wave II decreased while a third wave (wave III) appeared at a more negative potential, increasing with the ascending pH, both approaching about half of the sum of the wave heights (Fig. 1-e). The sum of the wave heights was kept approximately constant over the pH range from 4.4 to 13.2, but it increased slightly in the acidic pH region below 4.4 because of the occurrence of the pre-wave. The half-wave potential of wave I depended on the pH. In the pH range from 4.4 to 7.5 where the pre-wave disappeared, the plots of $E_{1/2}$ against pH gave a straight line with a slope of 64 mV./pH, and $E^0_{1/2}$, the half-wave potential extrapolated to pH 0, was −0.69 V. vs. SCE. The $E_{1/2}$-pH plot of wave I in the acidic pH range below 4.4 deviated from the $E_{1/2}$-pH relation line in the pH range from 4.4 to 7.5 and gave a slope of 54 mV./pH. It is an interesting fact, however, that in the biphthalate buffer the height of the pre-wave increased slightly and the $E_{1/2}$-pH plot of wave I, even in the pH range below 4.4, fitted on that straight line with a slope of 64 mV./pH (Figs. 2 and 3). The half-wave potentials for waves II and III under the conditions studied were about −1.30 and −1.60 V. vs. SCE respectively, and neither showed any pH-dependence.

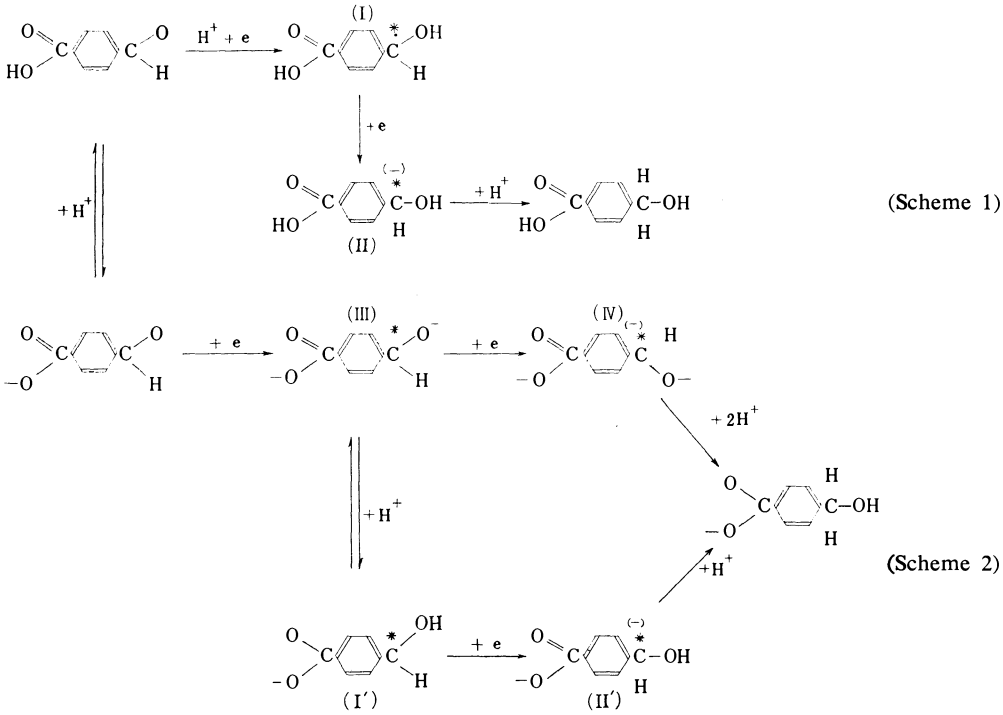
The occurrence of the two waves* in the pH range from 5.5 to 7.5 and their pH-dependence can be explained reasonably by the acid dissociation-recombination mechanism; wave I is due to the reduction of the carbonyl group of the undissociated terephthalaldehydic acid, and wave II, to that of its anion. The pK_a of terephthalaldehydic acid, determined by the acid-base titration method, was 4.47±0.03 at 25°C**. On the other hand, pK'_a, which was obtained from the limiting current against the pH curve of wave I, was 6.60 at 25°C (Fig. 2). This result suggests the existence of an acid recombination kinetic current, as was pointed out by Holleck and Marsen[1]. Furthermore, the second occurrence of two-step waves, weves II and III, above pH 8.2 may be understood by applying the carbinolate-free radical dissociation theory.[4,5] The "pK" for this dissociation equilibrium was about 9.5, which is the pH value corresponding to the increase in the height of wave III to one-fourth of the sum of the wave heights.

The Effect of the Ionic Strength on the Half-wave Potentials.—An investigation of the effect of the ionic strength on the half-wave potentials for waves I, II and III indicated the results given in Fig. 4. Figure 4 reveals that the half-wave potential of wave III is markedly affected by the ionic strength of the test solution. At pH 13.2 wave III was shifted to more positive potentials with the increasing ionic strength. Since wave II scarcely changed, the two waves were inclined to make a single wave. Similar phenomena were observed in

* The methyl ester of terephthalaldehydic acid gave a single wave over the pH range from 1 to 12.[6]

** The dissociation constant of *o*-phthalaldehydic acid has been reported to be 3.6×10^{-5}.[1]

4) L. Holleck and H. Marsen, *Z. Elektrochem.*, **57**, 301 (1953).
5) P. J. Elving and J. T. Leone, *J. Am. Chem. Soc.*, **80**, 1020 (1958).
6) S. Ono and J. Nakaya, *J. Chem. Soc. Japan, Pure Chem. Sec.* (*Nippon Kagaku Zassi*), **74**, 907 (1953).



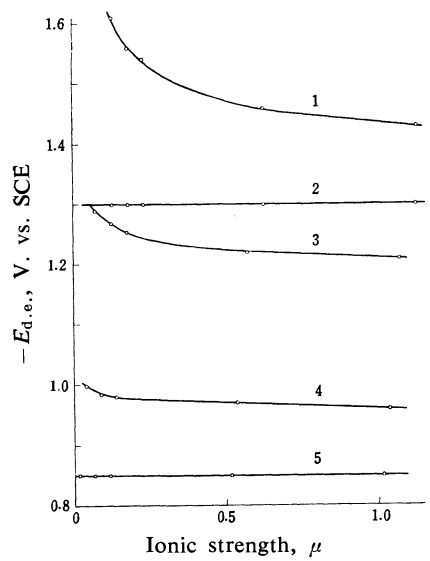


Fig. 4. Effect of the ionic strength on the half-wave potentials.
At 0.4 mM terephthalaldehydic acid
1) wave I at pH 2.1, 2) wave I at pH 5.1, 3) wave II at pH 7.9, 4) wave II at pH 13.2, 5) wave III at pH 13.2

the case of the increasing concentration of such a supporting electrolyte as sodium hydroxide.[2] The positive shift of the half-wave potential of wave III is considered to be a key for elucidating the reduction mechanism for wave III.

The Dependence of the Limiting Current on the Mercury Pressure and the Temperature.—With respect to the mercury pressure-dependence, the plots of i_l against $h^{1/2}$ gave a straight line of a general expression, $i_l = ah^{1/2}+b$. If i_l is controlled exclusively by the diffusion, b should be equal to zero; if it is controlled completely by the reaction rate, a may be expected to be zero. On the other hand, the adsorption current is proportional to the mercury pressure. Table I shows the experimental data of the parameters a and b, and of the temperature coefficients at a proper pH value in five representative pH ranges. Table I reveals that wave I at pH 6.8 and the wave III at pH 13.2 are obviously of a kinetic nature, although both showed temperature coefficients of less than 1%. It is noticable that the temperature coefficient for wave I at pH 6.8 was practically zero.

The pre-wave appears to be the adsorption current, i_a, submitting to a general equation, $i_a = a'h$, where a' is a proportional constant (Table I). The single waves at pH 5.1 and 7.9, waves I and II respectively, seem to be controlled by the diffusion.

The Concentration-dependence and the Diffusion Current Constant.—Linear relationships between the sum of the wave heights and the concentration of terephthalaldehydic acid in the range from 1 to 0.04 mM were obtained over the pH range studied. The diffusion current constants for the single waves were calculated

TABLE I. THE MERCURY PRESSURE-DEPENDENCE AND THE TEMPERATURE COEFFICIENT (d. c. WAVES)

0.4 mM terephthalaldehydic acid in the Britton-Robinson buffers

pH	Wave	$i_l = ah^{1/2*} + b$		Temp. coeff. (20~30°C), %/deg.
		a	b	
2.1	Pre-wave	0.072**		Different
	I	0.28	+0.42	1.41
	Sum	0.39	0	1.36
5.1	I	0.36	0	1.48
6.8	I	0.05	+0.98	0
	II	0.31	−0.98	2.53
	Sum	0.36	0	1.32
7.9	II	0.33	+0.11	1.50
13.2	II	0.27	−0.65	1.49
	III	0.07	+0.65	1.00
	Sum	0.34	0	1.25

* $h = h_{exp} - h_{back}$

** The value was calculated as a', applying equation; $i_a = a'h$.

by Ilković equation as 3.48±0.04 for wave I at pH 5.2 and 3.36±0.07 for wave II at pH 7.9. For wave II and the sum of the two waves at pH 13.2, 1.82±0.03 and 3.38±0.03 were obtained respectively.

The number of electrons, n, involved in the electrode process can be calculated by the equation, $I_D = 607\, n\, D^{1/2}$, where I_D is the diffusion current constant and D is the diffusion coefficient. If the diffusion coefficient for terephthalaldehydic acid is assumed to be 7.35×10^{-6} cm^2 sec^{-1}, that is, the value of the diffusion coefficient for phthalic acid as calculated by the Stokes-Einstein equation, $n = 2.12$, 2.04 and 2.05 are obtained for wave I at pH 5.2, for wave II at pH 7.9, and for the sum of the waves at pH 13.2 respectively. These values indicate that the sum of the wave heights for terephthalaldehydic acid, over the pH range studied, corresponds to a two-electron reduction of the carbonyl group.

Relationships between the heights of the pre-wave and of wave I at pH 2.1 and the concentration over the range from 0 to 0.4 mM of terephthalaldehydic acid are shown in Fig. 5. The height of the pre-wave reached a limiting value with the increasing concentration, substantiating the conclusion that the pre-wave is due to the adsorption of an organic substance, possibly the reduced form of undissociated terephthalaldehydic acid, at the dropping mercury electrode. Wave I at pH 2.1 could be distinguished, down to 0.08 mM of terephthalaldehydic acid, from the pre-wave (Fig. 5). Using the pK value of terephthalaldehydic acid, the bulk concentration of undissociated molecules at pH 2.1 is calculated as approximately equal to that of terephthalaldehydic acid, and at pH 5.16 the bulk concentration of undissociated molecules is calculated as 0.08 mM, when the analytical

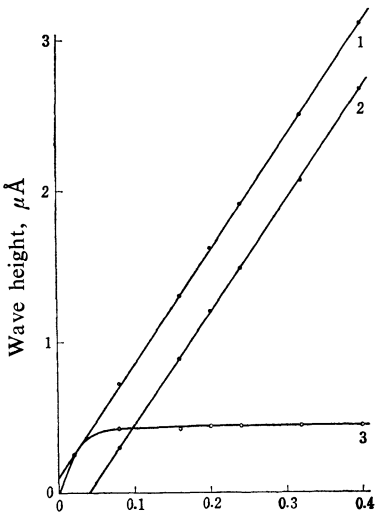


Fig. 5. Relationship between the terephthalaldehydic acid concentration and the d. c. wave heights at pH 2.1.
1) sum of wave heights, 2) wave I, 3) pre-wave

concentration of terephthalaldehydic acid is 0.4 mM. The pre-wave is still expected, therefore, to appear at pH 5.16, but experimentally it was observed at a pH lower than 4.4. To elucidate this fact, the effect of concentration of terephthalaldehydic acid on the half-wave potentials of the pre-wave and wave I at pH 4.0 was investigated (Table II). It was found that the pre-wave was shifted to a more negative potential with the decreasing concentration; on the other hand, the main wave I shifted to more positive potentials. At 0.2 mM terephthalaldehydic acid, the pre-wave marged into wave I, and the half-wave potential for the coalesced wave remained unchanged with

the decreasing concentration. It may be concluded that, since the equilibrium concentration of undissociated molecules in the bulk solution decreases visibly when the pH increases from 3 to 6, the difference in half-wave potentials between the pre-wave and wave I decreases, and the two waves coalesce.

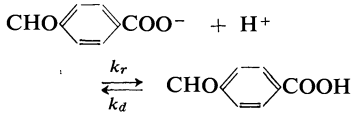
Table II. The effect of terephthalaldehydic acid concentration on the half-wave potentials at pH 4.0

Concn. of terephthalaldehydic acid, mM	$-E_{1/2}$, V. vs. SCE		Difference between two half-wave potentials, V.
	Pre-wave	Wave I	
2.0	0.77	0.99	0.22
1.0	0.80	0.96	0.16
0.4	0.81	0.92	0.11
0.2		0.89	—
0.08		0.90	—
0.04		0.90	—

Log Plot.—For the study of the slopes and shapes of the terephthalaldehydic acid waves, the term $\log i/(i_d-i)$ was plotted against E, at 0.4 mM terephthalaldehydic acid. Wave I at pH 2.0 and 5.6 gave a linear log plot with a slope of about 43 mV., considerably greater than the theoretical value for the reversible two-electron reduction. In other media, the slopes of the log plot for wave I were in the range from 48 to 52 mV. Because wave II in the vicinity of pH 8 tended to show a maximum if a maximum suppresser such as gelatine was not added to the electrolytic solution, the log plot for wave II was slightly curved, even in 0.4 mM terephthalaldehydic acid, and the slopes were in the range from 62 to 78 mV. However, waves II and III at pH 13.2, the heights of which corresponded to a one-electron reduction, gave linear log plots with slopes of 43 and 98 mV. respectively. It seems that the abnormally large value of the slope for wave III indicates the irreversible nature of the electrode process involved.

Recombination and Dissociation Rate Constants.—The reduction current of terephthalaldehydic acid in the pH range from 5.5 to 7.5 well fits the theory of the kinetic recombination currents.[7]

The mechanism of the electrode process is given by;



$$\xrightarrow{2e+2H^+} \quad CH_2OH\text{-}C_6H_4\text{-}COOH \qquad (1)$$

where k_r and k_d are the recombination and dissociation rate constants respectively. The recombination rate constant can be calculated by the following equation;[8]

$$\log K_r = 2pK'_a - pk_a - 2\log 0.886 - \log t \qquad (2)$$

where t is the drop time. t was 4.48 sec. at -1.0 V. vs. SCE in the electrolytic solution studied. The k_r and k_d were calculated as follows; $k_r = 1.5\times10^8$ 1. (mol. sec.)$^{-1}$, and $k_d = 5.2\times10^3$ sec^{-1}.

A. C. Polarography.—*The Behavior of A. C. Waves.*—A. C. polarograms in buffered solutions of various pH values are shown in Fig. 1. As compared with the d. c. wave heights, a. c. wave heights were greatly influenced by the change in the pH (Fig. 2). The peak potential for each a. c. wave agreed approximately with the half-wave potential for the corresponding d. c. waves (Fig. 3). In the acidic pH range below 4, a small "kink" was observed on the positive side of the a. c. first wave (a. c. wave I), where the pre-wave appeared on the d. c. polarogram. This "kink" is considered to be caused by the adsorption of the reduced form of undissociated molecules at the dropping mercury electrode. However, this "kink" differs from the adsorption peak of dyes;[9] riboflavin,[10] methylene blue,[11] flavinmononucleotide[12] and others[9] are known to give a d. c. pre-wave and a sharp, well-defined corresponding a. c. peak as a result of the adsorption of the reduced form in acidic solutions.

The height of a. c. wave I was strongly depressed in the pH range from 1 to 3. In the case of terephthalaldehydic acid, it seems that a strong adsorption of undissociated molecules was present in the potential region where the pre-wave and wave I were observed, resulting in the depression of the a. c. wave heights. (See the discussion of base current effects.) Although the concentration of undissociated terephthalaldehydic acid in equilibrium is considered to decrease rapidly when the pH is increased from 3 to 6, the height of a. c. wave I increased up to a maximum at pH 5.2, where the d. c. pre-wave merges into a

7) For review, R. Brdicka, *Collection Czechoslv. Chem. Communs.*, **19**, Suppl. 2, 41 (1954); R. Bridicka, *Z. Elektrochem.*, **64**, 16 (1960); M. Senda, *Rev. of Polarography*, **6**, 95 (1958).

8) M. Takagi, ibid., **9**, 53 (1961).

9) H. Hamaguchi. M. Maruyama and M. Nishiyama, unpublished. A summary of the work, however, was presented at the 14th Annual Meeting of the Chemical Society of Japan (1961).

10) B. Breyer and T. Biegler, *Collection Czechoslv. Chem. Communs.*, **25**, 3348 (1960); *J. Electroanal. Chem.*, 1, 453 (1960).

11) S. L. Gupta and S. K. D. Agawal, *Kolloid-Z.*, **163**, 136 (1959).

12) M. Senda, M. Senda and I. Tachi, *Rev. Polarography*, **10**, 142 (1962).

coalesced wave. It seems that the decreasing concentration of adsorbable species in the bulk solution weakens the depression of the a. c. wave height. However, the abnormal rise of the height of a. c. wave I in the pH range from 5.1 to 5.5 implies that the a. c. wave formation process in that pH range involves both the reduction of undissociated molecules and the adsorption of the reduced form. Furthermore, the deviation of the wave height against the pH curve of a. c. wave I from the theoretical dissociation curve reveals that it is necessary to take into account the a. c. kinetic current for the formation of a. c. waves. The pH values of the disappearance of a. c. wave I and of the appearance of a. c. wave II were shifted to a pH range more acidic by 0.5 pH unit than in the d. c. polarography (Fig. 2). It is considered that in this case the a. c. current is less affected by the kinetic reaction than are the d. c. kinetic currents.

The a. c. wave height-pH curve for a. c. wave II was found to have a shape analogous to that for d. c. wave II. On the other hand, a. c. wave III was ill-defined, and at pH 13.2 its height was as small as a tenth of the height of a. c. wave II (in the d. c. polarography, the ratio of the height of wave II to III was about unity). The reduction process for wave III is irreversible.

Base Current Effects.—In the pH region below 3, the base current was depressed on both the positive and the negative sides of a. c. wave I, indicating that the undissociated terephthalaldehydic acid and the reduced form were strongly adsorbed at the surface of the dropping mercury electrode (Fig. 1-a). As has been described above, this strong adsorption affects the a. c. pre-wave and wave I so as to depress the heights of these waves. As the pH increased from 3 to 5, the lowering of the base current was decreased, and the depression of a. c. wave I was weakened.

In the pH range from 5.1 to 5.5, where the abnormal rise of the height of a. c. wave I occurred, the base current between a. c. waves I and II was lowered.

Simultaneously, a new and small peak was observed on the negative side a. c. wave II, although there was no corresponding d. c. wave at this potential. This peak was shifted to more positive potentials with the increasing pH, and then it was merged into a. c. wave II. This fact suggests that the new peak is a kind of tensammetric one, because of the desorption of the reduced form of undissociated terephthalaldehydic acid. Further, above pH 5, a "hump" was observed at about —0.5 V. vs. SCE, probably due to the weak adsorption-desorption process for the dissociated terephthalaldehydic acid.

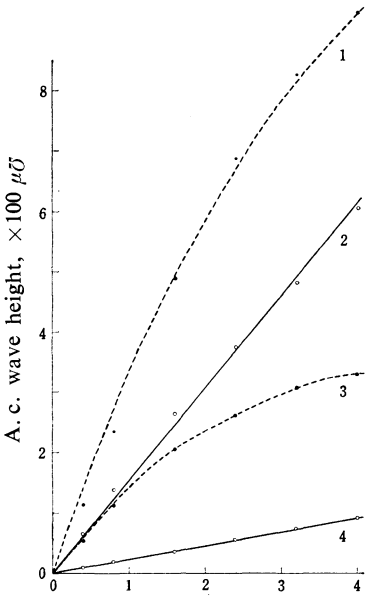


Fig. 6. Relationship between the terephthalaldehydic acid concentration and the a. c. wave heights.
1) wave I at pH 5.1, 2) wave II at pH 13.2, 3) wave I at pH 2.9, 4) wave III at pH 13.2
○, ●: experimental point
------: calculated curve

The Relation between A. C. Wave Height and the Concentration of Terephthalaldehydic Acid.—The plot of the a. c. wave heights at pH 2.1, 5.1 and 13.2 against the concentration of terephthalaldehydic acid are shown in Fig. 6. The plot for a. c. wave I at pH 2.1 and 5.1 were non-linear and fit the equation of the Langmiur adsorption isotherm, $i_p = abC/(1+bC)$, where i_p is the a. c. wave height, C is the molar concentration of terephthalaldehydic acid in the bulk solution, and a and b are the parameters with the following values; a= 669.1 l./mol., b=254.0 μU at pH 2.1 and a= 2364.0, b=163.0 at pH 5.1. In strongly alkaline solutions, a. c. waves II and III each gave a straight line. These results may also substantiate the conclusion that the reduction of undissociated terephthalaldehydic acid includes the adsorption process, at least in the pH range below 5.1.

The Dependence of A. C. Wave Heights on the Mercury Pressure and the Temperature.—The a. c. wave heights of terephthalaldehydic acid change with the mercury pressure, as Table III shows, indicating that the d. c. polarographic electrode process in the reduction of terephthalaldehydic acid is irreversible.[13] The

13) M. Senda, *Kagaku no Ryoiki*, Suppl., No. 50, "Polarography I," p. 28 (1962).

temperature coefficients for a. c. waves gave considerably greater values than those usually observed for a. c. waves.

Table III. The mercury pressure-dependence and the temperature coefficient (a. c. wave)

0.4 mM terephthalaldehydic acid in Britton-Robinson buffers
A. c. wave height (μC)

h, cm.	Wave I			Wave II	Wave III
	pH 2.0	pH 5.1	pH 7.9	pH 13.2	
78.5	53.4	131.0	93.3	77.0	7.6
68.5	55.5	128.5	90.0	73.5	7.2
58.5	52.6	125.0	86.0	65.8	6.8
48.5	48.7	119.0	79.6	58.6	6.0
Temp. coeff., %/deg.					
	2.48	1.28	2.20	0.65	1.50

Reduction Mechanism.—From the d. c. and a. c. polarographic results and the discussion above, and from the similarity between the reduction of the carbonyl group of terephthalaldehydic acid and that of benzaldehyde,[14,15] the following mechanism is proposed; wave I is ascribed to the two-electron reduction of the carbonyl group of undissociated molecules following the adsorption at the electrode surface, and *p*-carboxyl benzyl alcohol is formed. Applying the reduction mechanism for benzaldehyde proposed first by Holleck and Marsen,[4] the process is written as Scheme 1. In this case, the electrode reaction via the intermediate carbinolate-free radical (I) and its radical ion (II) proceeds successively. The electrode reaction product, *p*-carboxyl benzyl alcohol, is adsorbed at the electrode surface, at least in the pH range below 4.4. Wave II is due to the reduction of anions; in the pH range below 8 the anion is reduced first to its radical ion (III), which combines rapidly with a proton, and then the electrode reaction proceeds successively to the formation of dissociated *p*-carboxyl benzyl alcohol. The whole reaction is a two-electron reduction (Scheme 2).

In the pH range from 5.5 to 7.5, the two waves, I and II, form a system of kinetic recombination currents in which the electrode process is given by Eq. 1. In view of the a. c. polarographic behavior in this pH range, it may be concluded the molecules of the undissociated terephthalaldehydic acid formed by the recombination in the reaction layer are first adsorbed at the electrode surface and then reduced. In the treatment of the acid-recombination kinetics of terephthalaldehydic acid, however, the adsorption was not taken into consideration.

The fact that the temperature coefficient of d. c. wave I at pH 6.8 was zero indicates that the dissociation equilibrium is shifted in favor of the anions with an increase in the temperature.

On the basis of their analysis of current-time curves in a drop life of the dropping mercury electrode, Kasening and Holleck[15] recently rejected the carbinolate-free radical dissociation theory for the reduction of benzaldehyde; instead, they proposed a new reduction scheme, in which a dissociation equilibrium of benzaldehyde was antecedent to the competitive reduction processes of the free molecule and the cation.

In the case of terephthalaldehydic acid, however, the polarographic behavior above pH 8.2 cannot be explained by the new theory, but only by the carbinolate-free radical dissociation theory. A dissociation equilibrium between radical ion III and radical I′ is established in the electrode reaction. Radical I′ is reduced at the same potential as the dissociated molecule, while radical ion III is reduced at more negative potentials than wave II, resulting in the appearance of wave III. In a strongly alkaline solution, wave II is due to the reduction to radical ion III, and wave III, to that from radical ion III to *p*-carboxyl benzyl alcohol, both corresponding to a one-electron reduction. The positive shift of the half-wave potential of wave III with the ionic strength or concentration of a supporting electrolyte is attributed to the unstability of radical ion III.

Summary

The d. c. and a. c. polarography of terephthalaldehydic acid has been investigated in buffered solutions containing no ethanol over the pH range from 1 to 13.

D.C. Polarography.—Terephthalaldehydic acid gives a pre-wave and three reduction waves. The pre-wave, which is due to the adsorption of the reduced form of undissociated molecules, is followed by wave I below pH 4.4. Our results above pH 4.4 accord approximately with Holleck and Marsen's. The half-wave potential for the wave I is pH-dependent, and the $E^0_{1/2}$ is -0.69 V. vs. SCE. The half-wave potentials of waves II and III, both pH-independent, are -1.30 and -1.60 V. vs. SCE under the conditions studied. The sum of the wave heights has been kept constant in

14) For review, Y. Nagata, *Rev. Polarography*, **7**, 12 (1959).
15) B. Kasening and L. Holleck, *Z. Elektrochem.*, **63**, 166 (1959).

the pH range from 4.4 to 13.2, and it corresponds to the two-electron reduction of the carbonyl group. The two-step waves, in which wave I is due to the reduction of the undissociated molecule and wave II, to that of its anion, in the pH range from 5.5 to 7.5 form a system of kinetic recombination currents. The recombination and dissociation rate constants have been calculated as $k_r = 1.5 \times 10^8$ l. (mol. sec.)$^{-1}$ and $k_d = 5.2 \times 10^3$ sec^{-1}. The double waves above pH 8.2 have been explained by the carbinolate-free radical dissociation theory.

A. C. Polarography.—A. c. waves have been obtained to corresponding to the d. c. waves. The heights of the a. c. pre-wave and wave I are depressed below pH 5. This depression has been attributed to the strong adsorption of undissociated molecules at the dropping mercury electrode. The relationship between the a. c. wave height and concentration below pH 5 is non-linear. It has been noted that the a. c. kinetic current should be taken into account for the a. c. wave formation.

The electrode process for wave III is irreversible, and a. c. wave III is ill-defined.

A reduction mechanism over the pH range studied has been proposed.

Department of Chemistry
Faculty of Science
Tokyo Kyoiku University
Koishikawa, Tokyo (M. N. & H. H.)

Department of Chemistry
Faculty of Science and Engineering
Chuo University
Koishikawa, Tokyo (M. M.)

*A New Rearrangement Reaction of β-Hydroxy-α-amino Acid N-Carboxy Anhydrides to 2-Oxazolidone Derivatives**

By Tomoo SAITO

(Received August 15, 1963)

An α-amino acid *N*-carboxy anhydride polymerizes into poly-α-amino acid, which is a model substance of protein. The synthesis of β-hydroxyl-containing poly-α-amino acids is of interest, because the polymers provide models of water-soluble proteins.

Polymers containing protected β-hydroxyl groups, viz., poly-*O*-acetyl-DL-serine,[1] poly-*O*-acetyl-L-serine,[2,3] and poly-*O*-acetyl-L-threonine,[3] have been prepared by the polymerization of the corresponding *N*-carboxy anhydrides by using a trace amount of a suitable amine, e. g., triethylamine. The subsequent complete deacetylation of the resultant protected polymers was, however, accompanied by many difficulties. An attempt to polymerize DL- and L-serine *N*-carboxy anhydrides with a free β-hydroxyl group was unsuccessful in obtaining poly-DL- and L-serine, as has been reported by Fasman and Blout.[2]

The present paper will describe a rearrangement of the *N*-carboxy anhydrides of several α-amino acids with free β-hydroxyl groups to 2-oxazolidone derivatives.

Two cyclic compounds, *N*-carboxy anhydride (III) and 2-oxazolidone derivative (VII), are supposed to be produced by the reaction of β-hydroxyl-α-amino acid (I) with phosgene, in which reaction *N*-chlorocarbonyl-β-hydroxy-α-amino acid (II) is a possible intermediate (Scheme A).

The reaction of L-serine, DL-threonine, L-threonine, and DL-β-phenylserine with phosgene

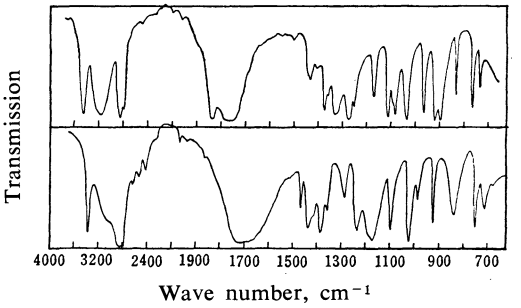


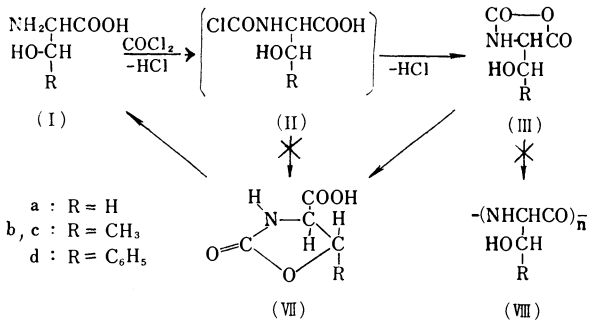
Fig. 1. The infrared spectra of L-serine-*N*-carboxy anhydride (IIIa) (upper) and L-2-oxazolidone-4-carboxylic acid (VIIa) (lower).

* This work was partly repoted in short communication on *J. Chem. Soc. Japan, Pure Chem. Sec.* (*Nippon Kagaku Zasshi*), **84**, 441 (1963).

1) M. Frankel, M. Breuer and S. Cardova, *Experientia*, **8**, 299 (1952); M. Frankel, S. Cardova and M. Breuer, *J. Chem. Soc.*, **1953**, 1991.

2) G. D. Fasman and E. R. Blout, *J. Am. Chem. Soc.*, **82**, 2262 (1960).

3) J. Noguchi and T. Saito, will be published.



Scheme A

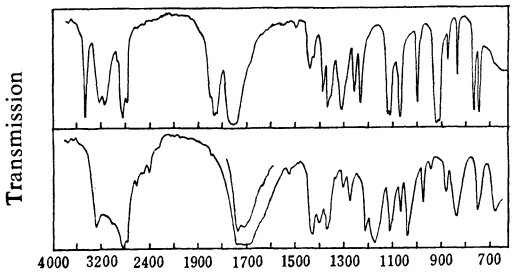


Fig. 2. The infrared spectra of DL-threonine *N*-carboxy anhydride (IIIb) (upper) and DL-*trans*-5-methyl-2-oxazolidone-4-carboxylic acid (VIIb) (lower).

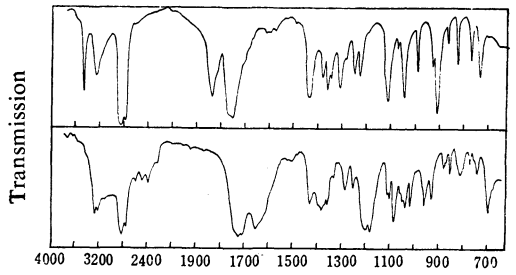


Fig. 3. The infrared spectra of L-threonine *N*-carboxy anhydride (IIIc) (upper) and L-*trans*-5-methyl-2-oxazolidone-4-carboxylic acid (VIIc) (lower).

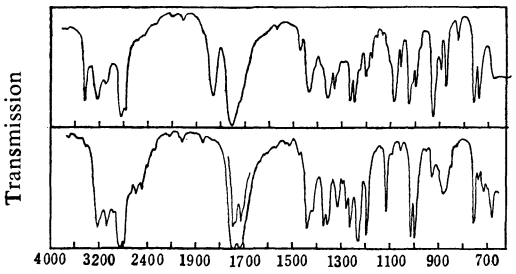
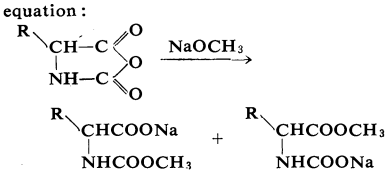


Fig. 4. The infrared spectra of DL-β-phenylserine *N*-carboxy anhydride (IIId) (upper) and DL-*trans*-5-phenyl-2-oxazolidone-4-carboxylic acid (VIId) (lower).

in anhydrous dioxane at 50°C afforded exclusively products corresponding to III. The structure III of these substances was inferred from the following data. The equivalent weights determined for the substances III, by anhydrous sodium methylate titration using thymol blue as an indicator,[4] agreed with those of the corresponding *N*-carboxy anhydrides (III) (Table I), and the ready elimination of carbon dioxide by the action of dilute hydrochloric acid under mild conditions was observed for the substance III, while the use of this reaction in the qualitative identification for *N*-carboxy anhydrides is well known. The infrared absorption spectra showed two typical carbonyl-stretching absorption bands[5] for the cyclic acid anhydride, at 1860~1850 cm^{-1} and at 1780 cm^{-1}, and a hydroxyl-stretching absorption band at 3540 cm^{-1} (Figs. 1—4).

III did not polymerize into polyamino acids under the conditions suitable for the polymerization of *N*-carboxy anhydrides of general amino acids; rather, it was rearranged into a 2-oxazolidone derivative (VII). The evidence is as follows. Some physical constants (Table II) for the products derived from III attracted our special attention and led us to suggest a rearranged product, VII. Confirmatory support was given to the suggested structure VII by the infrared absorption spectra (Figs. 1—4), which indicated two carbonyl-stretching vibration bands at 1770~1650 cm^{-1} assignable to vibrations of cyclic lactone[5] and the free carboxyl group[5] and to the lack of the hydroxyl vibration at 3540 cm^{-1}.

4) A. Berger, M. Sela and E. Katchalski, *Anal. Chem.*, **25**, 1554 (1953). They reported that *N*-carboxy anhydride could be titrated with sodium methylate in non-aqueous solvent, and the reaction proceeds according to the following equation:



5) N. B. Colthup, *J. Opt. Soc. Am.*, **40**, 397 (1950); L. J. Bellamy, "The Infra-red Spectra of Complex Molecules," Methuen & Co., Ltd., London (1958), pp. 95, 125.

TABLE I

β-Hydroxy-α-amino acid *N*-carboxy anhydrides

III	R		Yield %	M. p. °C		Equiv. wt. ($NaOCH_3$ tit.) Found	Calcd.
a	-H	(L)	72	115 [115	(decomp.) (decomp.)][2]	127	131.1
b	$-CH_3$	(DL)	41	117	(decomp.)	141	145.1
c	$-CH_3$	(L)	82	111~112	(decomp.)	147	145.1
d	$-C_6H_5$	(DL)	98	195	(decomp.)	200	207.2

TABLE II

2-Oxazolidone-4-carboxylic acid 5-derivatives

VII	R		Yield %	M. p. °C	Equiv. wt. ($NaOCH_3$ tit.) Found	Calcd.	$[\alpha]_D$	Hydrolysis by 6 N HCl
a	-H	(L)	36	118	134	131.1	−10.95°	L-Serine
b	$-CH_3$	(DL)	78	128~129 (127~128)[6,10]	143	145.1		DL-Threonine
c	$-CH_3$	(L)	90	139 (139)[7]	146	145.1	+41.0° (+41.7°)[7]	L-Threonine
d	$-C_6H_5$	(DL)	96	204 (decomp.) [206~207 (decomp.)][6]	208	207.2		DL-β-Phenyl-serine

Thus, rearranged products VII, viz., L-2-oxazolidone-4-carboxylic acid (VIIa), DL- and L-*trans*-5-methyl-2-oxazolidone-4-carboxylic acid (VIIb and VIIc), and DL-trans-5-phenyl-2-oxazolidone-4-carboxylic acid (VIId), were derived from the corresponding *N*-carboxy anhydrides (III) under the influence of the basic reagent.

Incidentally, Kaneko and Inui[6] have reported the preparation of DL-*trans*-5-methyl-2-oxazolidone-4-carboxylic acid (m. p. 127~128°C) in the different way, from DL-threonine, and they have also obtained its optically active form (m. p. 138.5~139.5°C) by resolution of the DL-compound.[7] VIIb and VIIc, respectively, were also identified with these two oxazolidones by melting point and infrared absorption spectra.

All of the compounds VII are all easily soluble in water, with the exception of the 5-phenyl derivative (VIId), which is slightly soluble, without decomposition, and their aqueous solutions indicate a strong acidity.

Hydrolysis by heating with 6 N hydrochloric acid converted VII into the starting β-hydroxy-α-amino acid (I). Optically-active VIIa and VIIc[7] gave optically-pure L-serine[8] and L-threonine[8] respectively.

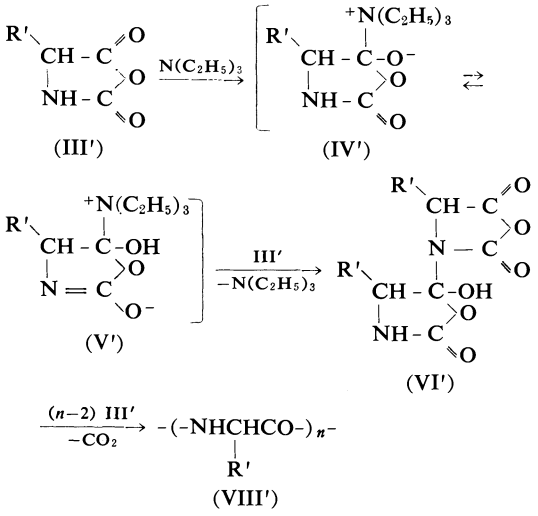
Therefore, during the rearrangement, the configurations at both asymmetric centers remain unchanged. This rearrangement resulted in the formation of VIIb, VIIc, and VIId from the corresponding structures, IIIb, IIIc, and IIId, the rearrangement was especially smooth in the last two cases. However, L-serine *N*-carboxy anhydride (IIIa) gave a considerable amount of amorphous polymeric material, which showed a positive Biuret reaction. This material was characterized as *O*-acyl-polyamino acid by its infrared absorption spectra, but this polymer was not investigated further.

The rearrangement never proceeds exclusively without a side reaction affording a polymer, and the facility of the latter reaction depends on the β-substituted group within the anhydride molecule III. The order of such an effect of decreasing the yield of 2-oxazolidones was as follows:

$$C_6H_5\text{-(DL-)} < CH_3\text{-(L-)} < CH_3\text{-(DL-)} \ll H\text{-(L-)}$$

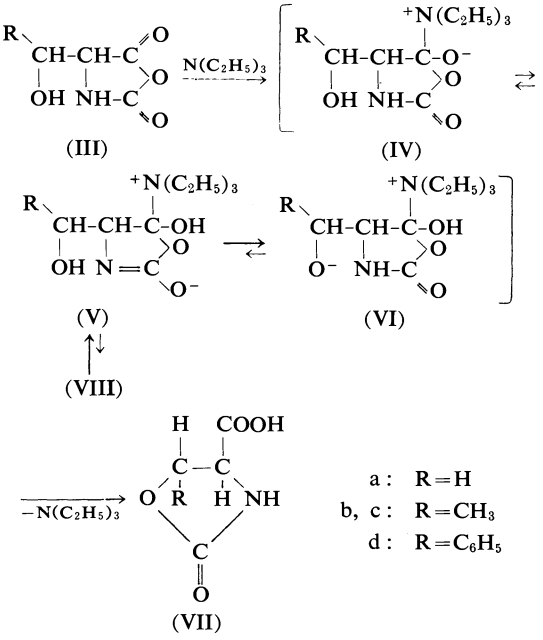
The mechanism of the rearrangement from III to VII is not certain, but the following hypothesis may be proposed. In the initial stages of the polymerization of general α-amino acid *N*-carboxy anhydrides by using a trace amount of amine (cf. Scheme B), the first step is the reversible formation of a complex IV' by the addition of the base to carbonyl-5; this complex may coexist with its tautomeric form V'. The reaction of the latter with an *N*-carboxy anhydride molecule is supposed to lead to the dimer VI' with a scission of the tertiary base molecule. The subsequent addition of

6) T. Kaneko and T. Inui, *J. Chem. Soc. Japan, Pure Chem. Sec.* (*Nippon Kagaku Zasshi*), **82**, 1075 (1961).
7) T. Inui and T. Kaneko, ibid., **82**, 1078 (1961).
8) L-Serine: $[\alpha]_D^{25} = +14.5°$ (in 1N hydrochloric acid), L-Threonine: $[\alpha]_D^{26} = -28.3°$ (in water). S. Akabori and S. Mizushima (Eds.), "Protein Chemistry" (Tanpakushitu Kagaku), Vol. 1, Kyoritsu Shuppan K. K., Tokyo (1952), p. 112.



Scheme B

N-carboxy anhydrides to the dimer VI' leads to a polyamino acid VIII'.[9] However, in the case of an N-carboxy anhydride which possesses a free β-hydroxy group (cf. Scheme C), the tautomer of a complex V corresponding to V' in Scheme B transfers rapidly with the proton migration to another tautomeric form, VI.



Scheme C

This migration rate is supposed to be greater than that which affords polyamino acid (VIII) and which is caused by the addition of N-carboxy anhydride to V. Then the rearrangement may proceed smoothly with the elimination of a tertiary base molecule from VI to VII as a stable form. In the case of IIIa it seems probable that the same intermediate Va in Scheme C affords VIIa through VIa, and VIII by two competing paths.

Experimental

All melting points are uncorrected.

Infrared Measurements. — All infrared spectra were recorded in Nujol mulls with a Koken DS 301-type double-beam spectrometer using a sodium chloride prism.

L-Serine N-Carboxy Anhydride (IIIa).[2]—Phosgene was bubbled into a suspension of L-serine (Ia) (10 g.) in dry dioxane (200 ml.) for three hours, while the temperature was maintained at 50°C. Then carbon dioxide was passed through the solution until it was phosgene-free. After filtration, the solvent was evaporated under reduced pressure, with the temperature kept below 40°C. The resultant oil solidified on rapeated trituration with petroleum ether. The solid was collected, dried, and recrystallized from ethyl acetate and petroleum ether; yield, 4.5 g. (72%); m. p. 115°C (decomp.). Found: N, 10.53; equiv. wt. 127 (determined by anhydrous sodium methylate titration). Calcd. for $C_4H_5O_4N$: N, 10.69%; equiv. wt. 131.1.

DL-Threonine N-Carboxy Anhydride (IIIb), L-Threonine N-Carboxy Anhydride (IIIc), and DL-β-Phenylserine N-Carboxy Anhydride (IIId). — IIIb, IIIc, and IIId were produced, by minor alterations of the method used in the preparation of IIIa, from DL- and L-threonine, and DL-β-phenylserine (m. p. 190°C (decomp.))[11,12] respectively. IIIb: yield, 41%; m. p. 117°C (decomp.). Found: N, 9.70; equiv. wt. 141. Calcd. for $C_5H_7O_4N$: N, 9.65%; equiv. wt. 145.1. IIIc: yield, 82%; m. p. 111~112°C (decomp.). Found: N, 9.61; equiv. wt. 147. Calcd. for $C_5H_7O_4N$: N, 9.65%; equiv. wt. 145.1. IIId: yield, 98%; m. p. 195°C (decomp.). Found: N, 6.68; equiv. wt. 200. Calcd. for $C_{10}H_9O_4N$: N, 6.76%; equiv. wt. 207.2.

L-2-Oxazolidone-4-carboxylic Acid (VIIa).—To a solution of IIIa (2.0 g.) in anhydrous dioxane (20 ml.), triethylamine (0.015 ml.) was added, and the mixture was stirred at room temperature for three days. Some polymeric precipitate was filtered off; this substance gave a positive Biuret reaction and showed not only amide I and II absorption spectra at 1625 cm^{-1} and 1545 cm^{-1} respectively, but also a carbonyl band at 1750 cm^{-1} which may be assignable to the ester. The solvent was evaporated under reduced pressure below 35°C. The resultant crystals were recrystallized from ethyl acetate and petroleum ether; yield, 0.72 g. (36%); m. p. 118°C, $[\alpha]_D^{15} = -10.95°$ (c 4.20, water). Found: C, 36.60; H, 3.91; N, 10.59; equiv. wt. 134 (determined by

9) C. H. Bamford, A. Elliott and W. E. Hanby, "Synthetic Polypeptides," Academic Press Inc., New York (1956), p. 86; E. Katchalski and M. Sela, "Advances in Protein Chemistry," Vol. 13, Academic Press Inc., New York (1958), p. 244.

10) F. Bergel and R. Wade, *J. Chem Soc.*, **1959**, 941.

11) E. Erlenmeyer, Jr., *Ber.*, **25**, 3445 (1892); E. Erlenmeyer, Jr., and E. Früstück, *Ann.*, **284**, 36 (1894); M. O. Forster and K. A. N. Rao, *J. Chem. Soc.*, **1926**, 1943.

12) K. N. F. Shaw and S. W. Fox, *J. Am. Chem. Soc.*, **75**, 3417 (1953).

anhydrous sodium methylate titration). Calcd. for $C_4H_5O_4N$: C, 36.65; H, 3.85; N, 10.69%; equiv. wt. 131.1.

DL-*trans*-5-Methyl-2-oxazolidone-4-carboxylic Acid (VIIb), L-*trans*-5-Methyl-2-oxazolidone-4-carboxylic Acid (VIIc), and DL-*trans*-5-Phenyl-2-oxazolidone-4-carboxylic Acid (VIId).—VIIb, VIIc, and VIId were obtained from IIIb, IIIc, and IIId respectively in the same way as VIIa, but in the case of the preparation of VIIc and VIId, no polymeric materials were produced. VIIb: yield, 78%; m. p. 128~129°C.[6,10] Found: C, 41.40; H, 4.92; N, 9.69; equiv. wt. 143. Calcd. for $C_5H_7O_4N$: C, 41.38; H, 4.86; N, 9.65%; equiv. wt. 145.1. VIIc: yield, 90%; m. p. 139°C, $[\alpha]_D^{15}=+41.0°$ (*c* 3.97, water).[7] Found: C, 41.42; H, 4.92; N, 9.68; equiv. wt. 146. Calcd. for $C_5H_7O_4N$: C, 41.38; H, 4.86; N, 9.65%; equiv. wt. 145.1. VIId: yield, 96%; m. p. 204°C (decomp.).[6] Found: C, 58.01; H, 4.41; N, 6.73%; equiv. wt. 208. Calcd. for $C_{10}H_9O_4N$: C, 57.97; H, 4.38; N, 6.76%; equiv. wt. 207.2.

The Hydrolysis of 2-Oxazolidone Derivatives (VII) by Hydrochloric Acid. — VII (1.0 g.) was dissolved in 6 N hydrochloric acid (20 ml.), and the solution was heated on a boiling water bath. After three hours, the solution was decolorized with active charcoal and concentrated to dryness. The residue was dissolved in absolute alcohol, and the addition of a suitable amount of pyridine to this solution gave crystalline products in an almost theoretical yield. The recrystallization of them was carried out from water and alcohol. The products were identified by comparison with respective authentic samples in all their characteristics. Ia from VIIa: m. p. 220°C (decomp.), $[\alpha]_D^{18}=+14.4°$ (*c* 2.3, 1 N hydrochloric acid);[8] Ib from VIIb: m. p. 233°C (decomp.); Ic from VIIc: m. p. 254°C (decomp.), $[\alpha]_D^{18}=-28.0°$ (*c* 2.6, water);[8] Id from VIId: m. p. 202°C (decomp.).

The author wishes to thank Professor Hiroshi Kotake for his helpful discussions in the course of this study. He also wishes to express his sincere thanks to the Ajinomoto Co., Ltd., for its kind donation of L-serine, DL-threonine, and L-threonine.

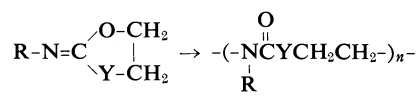
Department of Chemistry
Faculty of Science
Kanazawa University
Kanazawa, Ishikawa

The Ring-opening Addition Reactions of Exo-imino Cyclic Compounds with Carboxylic Acids

By Teruaki MUKAIYAMA, Yorikazu TAMURA and Tamotsu FUJISAWA

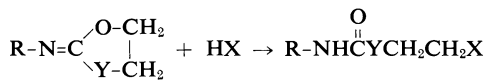
(Received October 10, 1963)

Preceding papers[1-5] have reported that the 1, 4-addition type ring-opening polymerization of exo-imino cyclic compounds, such as ethylene iminocarbonates, 2-iminooxazolidines and 2-iminotetrahydrofurans, in the presence of cationic catalysts, such as Lewis acids or protonic acids, affords polyurethanes, polyureas and polyamides respectively, as is shown in the following equation:



where Y is an oxygen atom, a substituted imino or a methylene group.

Further, it has been shown there that the exo-imino cyclic compounds react with acidic substances, such as carboxylic acids or phenols, to give the corresponding addition compounds by a ring-opening 1, 4-addition reaction:



In the present investigation, the rate constants, the activation energies and the entropies of the activation of the reactions of the exo-imino cyclic compounds with carboxylic acids in various solvents were determined in order to study the mechanism of the reactions.

The results lead to the conclusion that the ring-opening addition reactions involve two stages, namely, the initial formation of the salt from the exo-imino cyclic compound and the acid, followed by the reaction of the salt with another molecule of the acid to yield the addition compounds.

1) T. Mukaiyama, T. Fujisawa and T. Hyugaji, This Bulletin, 35, 687 (1962).
2) T. Mukaiyama, T. Fujisawa, H. Nohira and T. Hyugaji, *J. Org. Chem.*, 27, 3337 (1962).
3) T. Mukaiyama and K. Sato, This Bulletin, 36, 99 (1963).
4) T. Fujisawa, Y. Tamura and T. Mukaiyama, ibid., in press.
5) H. Nohira, Y. Nishikawa and T. Mukaiyama, ibid., in press.

Experimental

Materials. — Ethylene *N*-phenyliminocarbonate was prepared from phenylimidophosgene and sodium ethylene glycolate.[1]

2-Phenylimino-3-methyloxazolidine was prepared by the treatment of 1-(2-chloroethyl)-1-methyl-3-phenylurea with hot water.[5]

The *N*-substituted 2-iminotetrahydrofurans were prepared from 2,2-diethoxytetrahydrofuran and the corresponding amines.[8]

The carboxylic acids were obtained from a commercial source and were purified by recrystallization. The melting points and the pK_a values for these carboxylic acids are listed in Table I.

Table I. The melting points and pK_a values of carboxylic acids used

Acid	M. p., °C	$pK_a^{25°C}$
C_6H_5-	121.7	4.17
o-CH_3O-C_6H_4-	101.5	4.09
p-CH_3O-C_6H_4-	184.0	4.49
o-Cl-C_6H_4-	141.0	2.89
m-Cl-C_6H_4-	154.5	3.82
p-Cl-C_6H_4-	234.0	3.98
m-CN-C_6H_4-	139.0	3.50
p-CN-C_6H_4-	219.0	3.51
o-NO_2-C_6H_4-	148.0	2.21
p-NO_2-C_6H_4-	240.0	3.40
o-Br-C_6H_4-	149.0	2.82
3,5-$(NO_2)_2C_6H_3$-	205.0	2.80
$ClCH_2$-	63.0	2.81

Solvent.—Dioxane (b. p. 101.0°C), toluene (b. p. 111°C), xylene (b. p. 138~140°C) and benzene (b. p. 78°C) were distilled and dried over metallic sodium wire, and chlorobenzene (b. p. 132°C) was purified by distillation.

General Kinetic Method. — An equimolar solution of ethylene *N*-phenyliminocarbonate and carboxylic acid in various solvents in a 50 ml. reaction tube was maintained at a desired, constant temperature by immersion into a thermostat. The temperature control of the thermostat was accurate to ±0.03~0.07°C within the temperature ranges between 20~90°C. Five milliliter aliquots of this solution were withdrawn from time to time by means of a pipet and were put into 15 ml. of dioxane in a 50 ml. Erlenmeyer flask in order to make the titration mixture homogeneous. The unreacted carboxylic acid was titrated with a standard 0.5 N sodium hydroxide solution, using phenolphthalein as an indicator. In the case of the reaction with *m*-cyano-, *p*-cyano- and 3,5-dinitro-benzoic acids, thymolcresolgreen was used as an indicator.

Similarly, the percentage reaction of 2-phenylimino-3-methyloxazolidine or *N*-substituted 2-iminotetrahydrofurans with carboxylic acids was measured by this method.

Results and Discussion

The Reaction of Ethylene *N*-Phenyliminocarbonate with Carboxylic Acids. — Figure 1

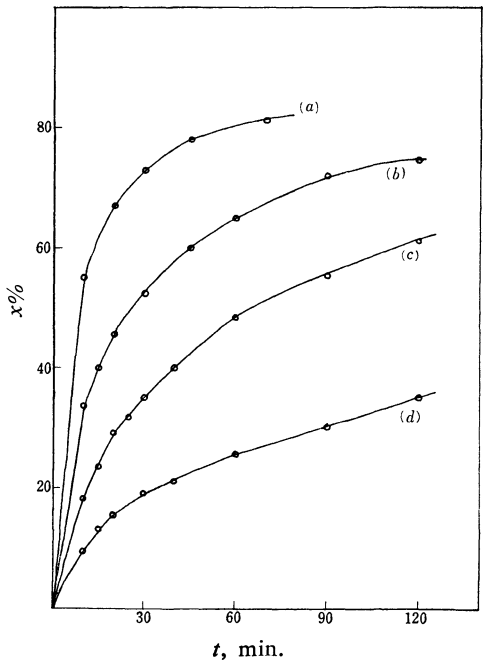


Fig. 1. The reactions of ethylene *N*-phenyliminocarbonate with benzoic acid in xylene. The plots of percentage reaction against time at various temperatures.
a) 60°C (0.50 mol./l.) b) 52°C (0.33 mol./l.)
c) 43.5°C (0.33 mol./l.) d) 30°C (0.33 mol./l.)

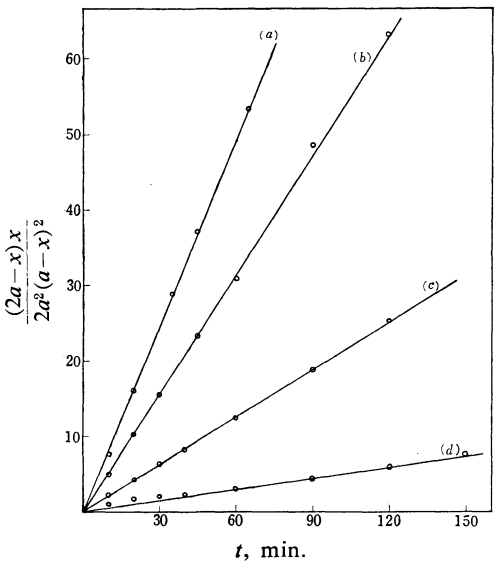
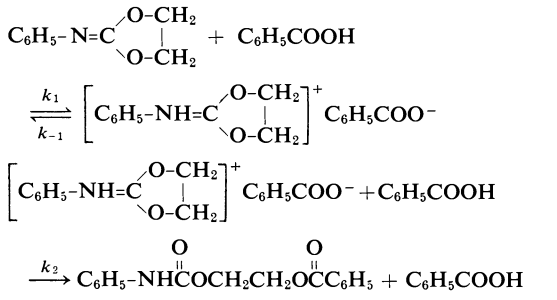


Fig. 2. The reactions of ethylene *N*-phenyliminocarbonate with benzoic acid in xylene at various temperatures.
The plots of the third order function against time.
a) 60°C b) 52°C c) 43.5°C d) 30°C
a: Initial concentration
x: Concentration of addition compound

shows plots of the percentage reaction against time (min.) for the reaction of ethylene *N*-phenyliminocarbonate (0.33 mol./l.) and benzoic acid (0.33 mol./l.) in xylene at various temperatures. As Fig. 2 shows, the third-order plots show sufficiently straight lines, from which the overall reaction order of ethylene *N*-phenyliminocarbonate with benzoic acid is shown to be third from a 20% to 90% completion of the reaction, without any noticeable side reaction.

On the basis of the experimental results mentioned above, the mechanism of the reaction can be considered to proceed via two stages, namely, the initial formation of the salt from the iminocarbonate and the acid, followed by the reaction of the salt with the other acid to yield β-benzoyloxyethyl *N*-phenylcarbamate.



For the first stage, the rate of the formation of the salt may be expressed as:

$$d[\text{salt}]/dt = k_1\left[C_6H_5\text{-}N{=}C\begin{matrix}O\text{-}CH_2\\ |\\ O\text{-}CH_2\end{matrix}\right][C_6H_5COOH] - k_{-1}[\text{salt}] - k_2[\text{salt}][C_6H_5COOH]$$

For the second stage, the rate of formation of the product may be given by:

$$d[\text{product}]/dt = k_2[\text{salt}][C_6H_5COOH]$$

where k_1, k_{-1} and k_2 are the rate constants of these stages.

When the rate of the formation of the salt is zero at the steady state, the overall kinetic equation is expressed as:

$$d[\text{product}]/dt = k_1 \cdot k_2\left[C_6H_5\text{-}N{=}C\begin{matrix}O\text{-}CH_2\\ |\\ O\text{-}CH_2\end{matrix}\right] \times [C_6H_5\text{-}COOH]^2/(k_{-1}+k_2[C_6H_5COOH])$$

If k_{-1} is much larger than $k_2[C_6H_5COOH]$, when, namely, the second stage is the rate-determining step, the rate of the reaction can be expressed as follows:

$$d[\text{product}]/dt = K\left[C_6H_5\text{-}N{=}C\begin{matrix}O\text{-}CH_2\\ |\\ O\text{-}CH_2\end{matrix}\right][C_6H_5COOH]^2$$

The plots of the logarithm of the rate constants vs. the reciprocal absolute temperatures gave a satisfactorily straight line (Fig. 3); the activation energy of the reaction was thus found to be 20.4 kcal./mol.

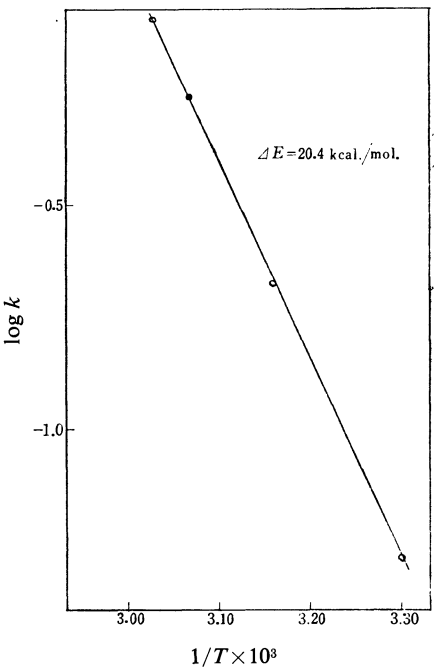


Fig. 3. The reactions of ethylene *N*-phenyliminocarbonate with benzoic acid in xylene. The plots of the rogarithm of the rate constants against the reciprocal absolute temperature.

Moreover, the reaction order changes to the second from the third, when the equimolar reaction of ethylene *N*-phenyliminocarbonate with benzoic acid (pK_a=4.17) was carried out in the presence of a stronger acid, e. g., diphenyl phosphate (pK_a=ca. 1.9), in xylene, as is shown in Fig. 4. The rates of the second-order reaction increase as the concentration of diphenyl phosphate increases. These results show that the reaction is a general acid-catalyzed reaction.

Furthermore, the reactions of ethylene *N*-phenyliminocarbonate with various substituted benzoic acids or chloroacetic acid in dioxane show that the rate increases as the acidity of carboxylic acid increases, as Table II shows. The effect of substituents in meta- and para-substituted benzoic acids follows the Hammett equation. As is shown in Fig. 5, $\log(k/k_0)$ is a linear function of the substituent constant σ given by Hammett,[6] and the gradient of the plots gave a value for the reaction constant ρ of +1.74 for the reaction. In ortho-substituted benzoic acids, the reactions are

6) L. P. Hammett, "Physical Organic Chemistry," McGraw-Hill Book Co., Inc., New York (1941), p. 188.

TABLE II. THE RATE CONSTANTS, THE ACTIVATION ENERGIES AND THE ENTROPIES OF ACTIVATION OF THE REACTIONS OF ETHYLENE *N*-PHENYLIMINOCARBONATE WITH CARBOXYLIC ACIDS IN DIOXANE

Carboxylic acid	k, $l^2\,mol^{-2}\,min^{-1}$							ΔE kcal.	$-\Delta S^{\neq}$ e. u.
	80°C	70°C	60°C	50°C	40°C	30°C	20°C		
C_6H_5-	0.709	0.245	0.111	0.0875	0.0225			19.6	3.34
p-CH_3O-C_6H_4-	0.241	0.113	0.0466	0.0267				15.7	13.90
o-CH_3O-C_6H_4-	0.247	0.112	0.0516	0.0400				15.7	17.30
p-CN-C_6H_4-		4.36	1.97	0.600	0.376			17.5	5.94
m-CN-C_6H_4-		4.42	2.00	0.700	0.379			17.8	3.77
o-Cl-C_6H_4-		2.54	1.25	0.750	0.271			16.6	7.13
p-Cl-C_6H_4-	1.65	0.680	0.367	0.194	0.0866			16.7	10.20
m-Cl-C_6H_4-	3.71	0.985	0.447	0.250	0.139			16.4	11.10
o-NO_2-C_6H_4-				11.5	3.50	2.04	0.710	17.7	3.24
p-NO_2-C_6H_4-			2.56	1.42	0.486	0.145		21.2	−7.40
3,5-$(NO_2)_2C_6H_3$-				21.5	10.0	3.88	1.08	16.7	0.75
o-Br-C_6H_4-				0.955					
$ClCH_2$-							1.30		

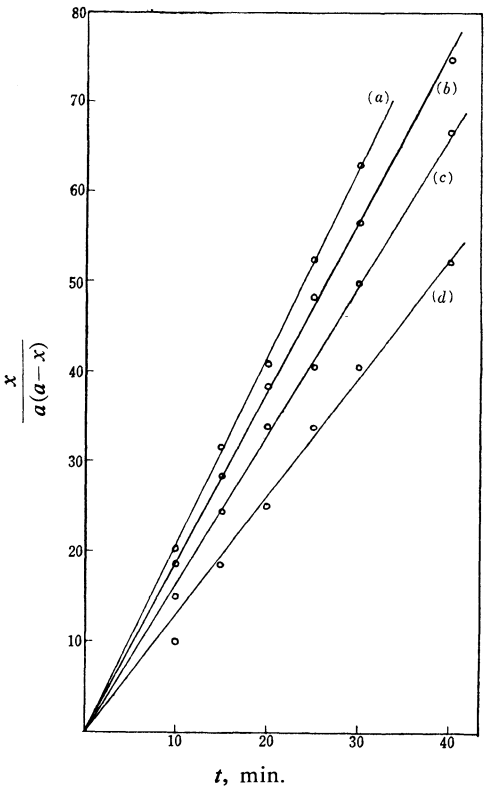


Fig. 4. The reactions of ethylene *N*-phenyliminocarbonate with benzoic acid in the presence of a catalytic amount of diphenyl phosphate in xylene at 70°C.
The plots of the second order function against time.
Concentration of diphenyl phosphate.
a) 5.75×10^{-3} b) 3.84×10^{-3} c) 1.92×10^{-3}
d) 3.20×10^{-4} (mol./benzoic acid mol.)

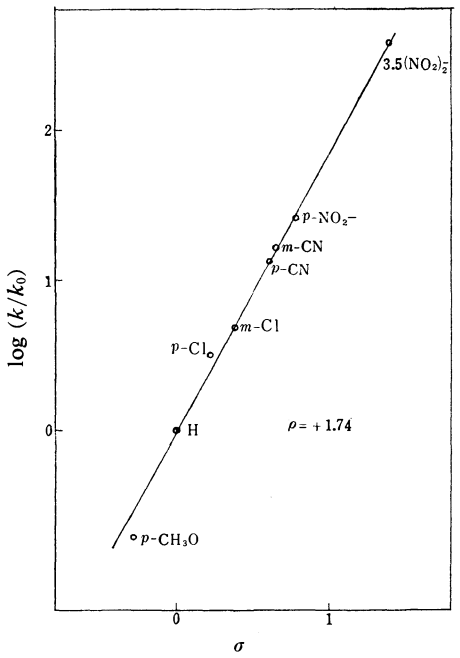


Fig. 5. The reactions of ethylene *N*-phenyliminocarbonate with meta and para substituted benzoic acids in dioxane at 50°C.
The plots of $\log(k/k_0)$ against the Hammett σ-values.

not so fast as might be expected from their acidities; this may be attributed to the steric hindrance of the ortho substituents.

In addition, the rates of this reaction are slightly influenced by the polarity of the solvents used. The results listed in Table III show that the reactions in xylene are about 8~9 faster times than those in dioxane. The slower rate in dioxane than in xylene may result from the possible formation of a complex from a carboxylic acid and dioxane, a complex which prevents the formation of the above-mentioned salt of ethylene *N*-phenyliminocarbonate by the carboxylic acid. It

TABLE III. THE RATE CONSTANTS, THE ACTIVATION ENERGIES AND THE ENTROPIES OF ACTIVATION OF THE REACTIONS OF ETHYLENE *N*-PHENYLIMINOCARBONATE WITH BENZOIC ACID IN VARIOUS SOLVENTS

Solvent	k, $l^2 mol^{-2} min^{-1}$						ΔE kcal.	$-\Delta S^{\neq}$ e. u.
	80°C	70°C	60°C	50°C	40°C	30°C		
Xylene			0.833	0.533	0.211	0.0522	20.4	−2.81
Toluene		2.17	0.790	0.303	0.150		19.2	0.11
Benzene		1.50	0.644	0.255	0.110		19.0	1.92
Chlorobenzene	4.90	2.25	1.03				19.0	2.10
Dioxane	0.709	0.245	0.111	0.0875	0.0225		19.6	3.34
Dioxane 1 : Xylene 1	1.07	0.430	0.198	0.094			17.8	7.87
Dioxane 1 : Xylene 3		0.797	0.408	0.156	0.072		17.5	8.17

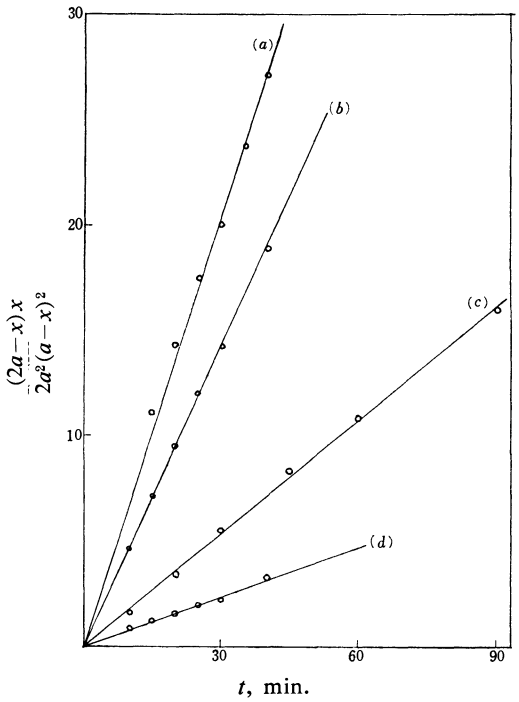


Fig. 6. The reaction of 2-phenylimino-3-methyloxazolidine with benzoic acid in xylene at various temperatures.
The plots of the third order function against time.
a) 90°C (0.25 mol./l.) b) 80°C (0.125 mol./l.)
c) 70°C (0.25 mol./l.) d) 60°C (0.50 mol./l.)

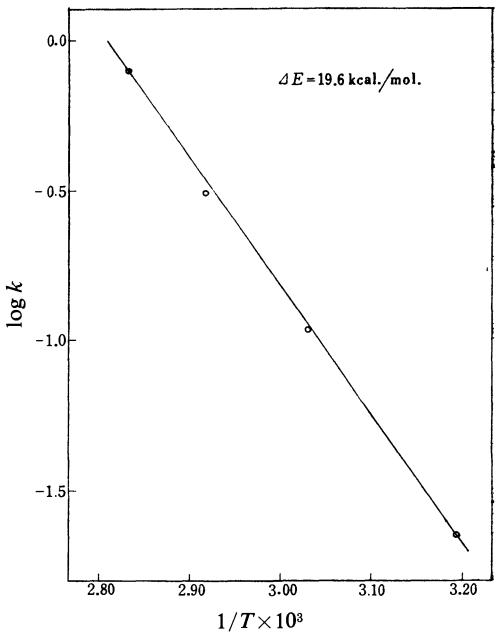
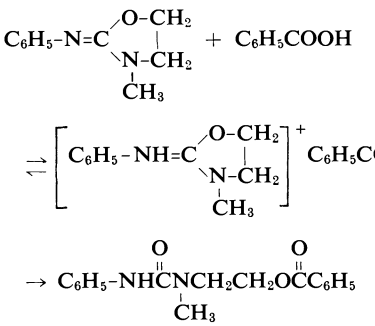


Fig. 7. The reactions of 2-phenylimino-3-methyloxazolidine with benzoic acid in xylene.
The plots of the logarithm of the rate constants against the reciprocal absolute temperature.



was also observed that the addition of dioxane to a toluene solution retards the reaction considerably.

The Reaction of 2-Phenylimino-3-methyloxazolidine with Carboxylic Acids. — Figure 6 shows that the reaction of 2-phenylimino-3-methyloxazolidine with benzoic acid in xylene satisfied the requirement for the third-order reaction kinetics. Analogous to the case of ethylene *N*-phenyliminocarbonate, the reaction can also be considered to proceed via two stages to give 1-(2-benzoyloxyethyl)-1-methyl-3-phenylurea.

The activation energy of this reaction was determined to be 19.6 kcal./mol. (see Fig. 7).

It was also confirmed that the rates of the reactions of 2-phenylimino-3-methyloxazolidine

TABLE IV. THE RATE CONSTANTS OF THE REACTIONS OF 2-PHENYLIMINO-3-METHYL-OXAZOLIDINE WITH CARBOXYLIC ACIDS IN DIOXANE

Carboxylic acid	k, $l^2\,mol^{-2}\,min^{-1}$			
	90°C	80°C	70°C	60°C
C_6H_5-	0.0814	0.0373		
p-Cl-C_6H_4-	0.179	0.0925	0.0614	
p-NO_2-C_6H_4-	1.17	0.785	0.323	
p-CN-C_6H_4-		0.416		
m-CN-C_6H_4-	1.05	0.415		
3,5-$(NO_2)_2C_6H_3$-		9.70	5.65	

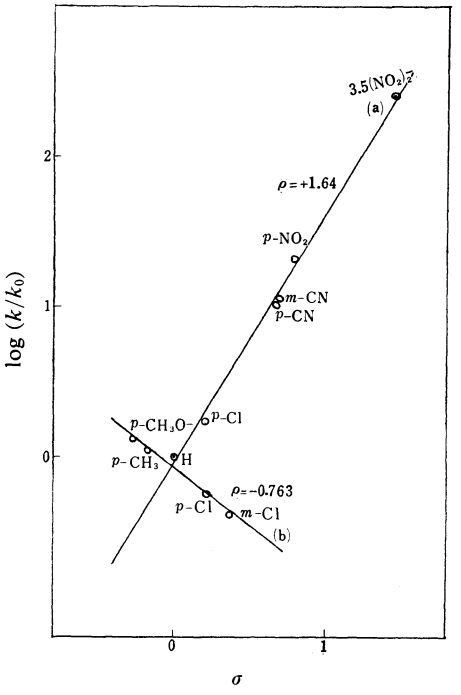


Fig. 8. a) The reactions of 2-phenylimino-3-methyloxazolidine with meta and para substituted benzoic acids in dioxane at 80°C.
b) The reactions of *N*-substituted phenyliminotetrahydrofurans with chloroacetic acid in xylene at 80°C.
The plots of $\log(k/k_0)$ against the Hammett σ-values.

with various substituted benzoic acids in dioxane increase as the acidities of the acids increase (see Table IV). The gradient of the plot $\log(k/k_0)$ against the substituent constant σ shown in Fig. 8 gave a value for the reaction constant ρ of +1.64, which was nearly equal to the case of ethylene *N*-phenyliminocarbonate mentioned above.

The Reaction of *N*-Substituted 2-Iminotetrahydrofurans with Chloroacetic Acid.—2-Phenyliminotetrahydrofuran reacts so very slowly

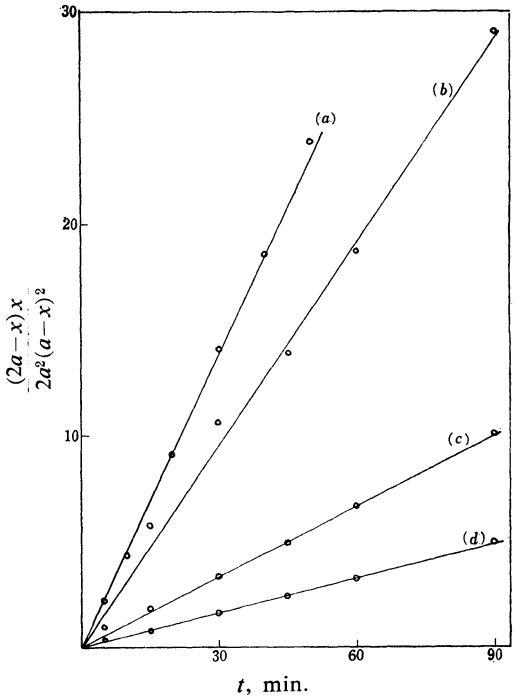
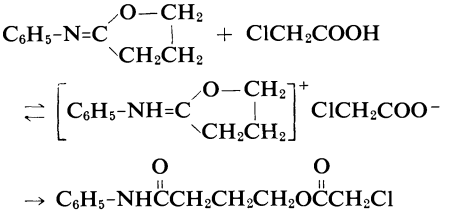


Fig. 9. The reactions of 2-phenyliminotetrahydrofuran with chloroacetic acid in xylene at various temperatures.
The plots of the third order function against time.
a) 90°C (0.25 mol./l.) b) 80°C (0.25 mol./l.)
c) 70°C (0.25 mol./l.) d) 60°C (0.50 mol./l.)

with benzoic acid in xylene that the rate of the reaction cannot be measured. Since it was found by the above experiment that the rate increases as the acidity of carboxylic acid increases, the rates of the reaction of 2-phenyliminotetrahydrofuran were determined by using chloroacetic acid. As Fig. 9 shows, the third-order plots have sufficiently straight lines, suggesting that the reaction also proceeds via two stages to give γ-chloroacetoxybutyranilide, as in the case of ethylene *N*-phenyliminocarbonate.



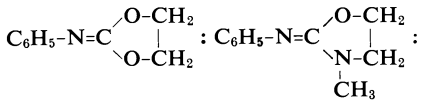
On the other hand, the effect of *N*-substituents on the reactions of *N*-substituted 2-iminotetrahydrofurans with chloroacetic acid indicated that the *N*-aliphatic derivatives react faster than *N*-aromatic ones and that the rates

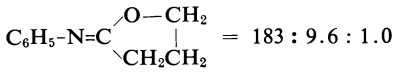
TABLE V. THE RATE CONSTANTS OF THE REACTIONS OF *N*-SUBSTITUTED 2-IMINOTETRAHYDROFURANS WITH CHLOROACETIC ACID IN XYLENE

R-	k, $l^2\,mol^{-2}\,min^{-1}$			
	90°C	80°C	70°C	60°C
C_6H_5-	0.695	0.472	0.181	0.0796
o-CH_3-C_6H_4-		0.311		
p-CH_3-C_6H_4-		0.519		
p-CH_3O-C_6H_4-		0.605		
o-CH_3O-C_6H_4-		0.700		
p-Cl-C_6H_4-		0.282		
o-Cl-C_6H_4-		0.150		
m-Cl-C_6H_4-		0.190		
n-C_6H_{13}-		0.445		
		1.75		

of the reactions of *N*-substituted phenyliminotetrahydrofurans decrease when the electron-attractive groups, such as *o*-chloro, *p*-chloro- or *m*-chlorophenyl groups, are introduced, as is shown in Table V. The gradient of the Hammett plots in Fig. 8 gave a value for the reaction constant ρ of -0.763. This evidence shows that the rate of the reaction increases as the electron density of the imino group increases.

Finally, the relative rate of the reactions of the three exo-imino cyclic compounds, e.g., ethylene *N*-phenyliminocarbonate, 2-phenylimino-3-methyloxazolidine and 2-phenyliminotetrahydrofuran, with carboxylic acids has been determined as:





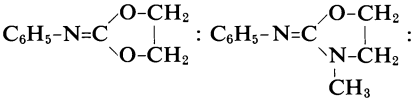
In conclusion, it can be said that the rates of the reactions of the exo-imino cyclic compounds with carboxylic acids depend both on the basicity of the cyclic compounds, which affects the initial formation of the neccessary intermediate salt, and on the number of the oxygen-carbon bond to be cleaved in the ring opening.

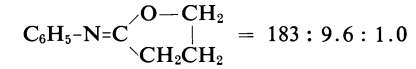
Summary

The rate constants, the activation energies and the entropies of the activation of the ring-opening addition reactions of exo-imino cyclic compounds, such as ethylene *N*-phenyliminocarbonate, 2-phenylimino-3-methyloxazolidine and *N*-substituted 2-iminotetrahydrofurans, with carboxylic acids in various solvents have been determined in order to study the mechanism of these reactions.

The rate of the reactions increases as the acidity of carboxylic acids increases, and the linear Hammett relation is observed in the reactions of ethylene *N*-phenyliminocarbonate or 2-phenylimino-3-methyloxazolidine with meta- and para-substituted benzoic acids.

The relative rate of the reactions of the three exo-imino cyclic compounds, ethylene *N*-phenyliminocarbonate, 2-phenylimino-3-methyloxazolidine and 2-phenyliminotetrahydrofuran, with carboxylic acids is as follows:





These results show that the ring-opening addition reaction involves two stages, namely, the initial formation of the intermediate salt from the exo-imino cyclic compound with carboxylic acid, followed by the reaction of the salt with the other acid to give the ring-opening addition compound.

Laboratory of Organic Chemistry
Tokyo Institute of Technology
Meguro-ku, Tokyo

Studies of Isocyanide. II. The Reaction of Isocyanide with Some Radical Sources

By Tatsuya SHONO, Masatoshi KIMURA, Yoshihiko ITO, Kiyoto NISHIDA and Ryohei ODA

(Received March 24, 1964)

The first paper[1] of this series reported that the reactions of some electrophiles, such as *t*-butyl hypochlorite, *N*-bromosuccinimide and hydroxylamine, with isocyanide produce urethanes and ureas. On the other hand, the reactions of compounds with a lone pair on the nitrogen[2] or phosphorus[3] atom with some radical sources, for example, the reaction of dimethylaniline with benzoyl peroxide, are well known. Since the isocyanide also has a lone electron-pair on its terminal carbon atom, the reactions of isocyanide with radical sources seem interesting.

When cyclohexyl isocyanide was treated with perbenzoic acid, cyclohexyl isocyanate was obtained in a 61% yield, along with *N*-cyclohexyl benzamide. A reasonable path for this reaction would be the electrophilic attack of perbenzoic acid on the lone electron-pair of the isocyanide to form an adduct, which in turn decomposes to give cyclohexyl-isocyanate and benzoic acid:

$$C_6H_{11}N{\rightleftharpoons}C + C_6H_5CO_3H \rightarrow \left[C_6H_{11}N{=}\overset{+}{C}\text{-}OH \quad {}^{-}OOC\text{-}C_6H_5\right]$$
$$\rightarrow C_6H_{11}NCO + C_6H_5CO_2H$$

The reaction of the isocyanide with benzoyl peroxide gave three major products, I, II and III, and one minor product, IV:

$C_6H_{11}NHCOC_6H_5$ (I) $\quad C_6H_{11}N{=}CHOOCC_6H_5$ (II)

$C_6H_{11}N{=}C(C_6H_5)OOCC_6H_5$ (III) $\quad C_6H_{11}NHCONHC_6H_{11}$ (IV)

A preliminary test indicated that the isocyanide did not contribute kinetically to the decomposition of benzoyl peroxide. Thus, the decomposition of benzoyl peroxide must be spontaneous thermal decomposition according to the free radical mechanism. The formation of II and III is rationalized by the following reaction scheme:

$$C_6H_{11}N{\rightleftharpoons}C + C_6H_5COO\cdot \rightarrow C_6H_{11}N{=}\dot{C}OOCC_6H_5$$
$$\xrightarrow{H\cdot} C_6H_{11}N{=}CHOOCC_6H_5 \quad \text{II}$$
$$\xrightarrow{C_6H_5\cdot} C_6H_{11}N{=}C(C_6H_5)OOCC_6H_5 \quad \text{III}$$

An analogous reaction of isocyanide with *t*-butyl perbenzoate yielded similar products, such as I, II and IV, and also unexpected new minor products, V and VI:

$C_6H_{11}NH_3OOCC_6H_5$ (V) $\quad C_6H_{11}NHCHO$ (VI)

In the reaction of isocyanide with *N*-nitroso-acetanilide, two major products, VII and VIII, attributed to the reaction of isocyanide with acetoxy radical, were obtained as expected, along with two minor products, IV and VI:

$C_6H_{11}N{=}CHOOCCH_3$ (VII) $\quad C_6H_{11}NHCOCH_3$ (VIII)

The formation of VII is analogous to the formation of II, but the formation of VIII and other minor products still remains to be explained.

It seems that the isocyanide reacts predominantly with acyloxy radicals: therefore in the reactions with benzoyl peroxide, *t*-butyl perbenzoate or *N*-nitroso-acetanilide, no other products in which the acyloxy radicals are not involved can be obtained.

In order to obtain the product involved with the phenyl radical, the reaction of isocyanide with potassium phenylazoformate was tried, it was verified to yield one major product, IX, and one minor product, IV:

$C_6H_{11}N{=}CHC_6H_5$ (IX)

The formation of IX is rationalized by the following free radical reaction scheme:

$$C_6H_{11}N{\rightleftharpoons}C + C_6H_5\cdot \rightarrow C_6H_{11}N{=}\dot{C}\cdot C_6H_5$$
$$\rightarrow C_6H_{11}N{=}CHC_6H_5$$

Finally, the reaction of isocyanide with di-*t*-butyl peroxide was carried out in order to obtain the product involved with the methyl radical: however, only a resinous product and two minor products, X and IV, were obtained.

1) M. Okano, Y. Ito, T. Shono and R. Oda, This Bulletin, **36**, 1314 (1963).
2) L. Horner and K. Scherf, *Ann.*, **573**, 35 (1951).
3) M. A. Greenbaum, D. E. Denney and A. K. Hoffmann, *J. Am. Chem. Soc.*, **78**, 2563 (1956).

This resinous product may result from the polymerization of the azomethine compound which is formed by the reaction of the isocyanide with the methyl radical:

$$C_6H_{11}NHCOCONHC_6H_{11}$$
X

Experimental

The Reaction of Cyclohexyl Isocyanide with Perbenzoic Acid. — Into a solution of 12.75 g. (0.117 mol.) of cyclohexyl isocyanide in dry chloroform, a solution of 16.21 g. (0.117 mol.) of freshly-prepared perbenzoic acid in 300 ml. of dry chloroform was added drop by drop with stirring at such a rate that the reaction temperature was below 0°C.

After the reaction mixture had been allowed to stand overnight at 0°C, the solvent was removed and the residue was distilled in vacuo to yield 8.9 g. (61%) of cyclohexyl isocyanate (b.p. 39°C/2 mmHg). The distillation residue consisted of 4.6 g. of *N*-cyclohexylbenzamide and 16 g. of benzoic acid.

The Reaction of Cyclohexyl Isocyanide with Benzoyl Peroxide.—Under a nitrogen atmosphere, a solution of 8 g. (0.033 mol.) of benzoyl peroxide in 73 g. of cyclohexyl isocyanide was heated while being stirred at 80~90°C for 5 hr. The reaction mixture was washed with aqueous sodium carbonate and then dried and distilled in vacuo to yield 5.5 g. of an oily product (b. p. 120~135°C/3 mmHg) and 2 g. of a resinous product. The oily product was crystallized on standing and separated into four parts. The part which was easily soluble in ligroin was II (2 g., m. p. 65~67°C), and the hardly soluble part was IV (0.1 g., m. p. 217~220°C). The moderately ligroin-soluble part consisted of two parts; one was III (1 g. recrystallized from acetone, m. p. 129~130.5°C), while the other was I (1 g., recrystallized from ligroin, m. p. 148~150°C). The resinous product afforded 0.6 g. of I after recrystallization from ligroin. The products I and IV were identified by a mixed melting point determinations with the respective authentic samples. The structures of the products II and III were inferred on the basis of their infrared spectra and results of analysis and of hydrolysis. When the II or III was hydrolyzed, benzoic acid and cyclohexylamine were obtained.

The two spectra resembled closely each other. They showed the existence of an ester group (1715 cm^{-1}, 1270 cm^{-1}, 1120 cm^{-1} in III; 1750 cm^{-1}, 1270 cm^{-1}, 1120 cm^{-1} in II), a double bond between nitrogen and carbon (1675 cm^{-1} in II; 1660 cm^{-1} in III), and a monosubstituted phenyl group (735 cm^{-1}, 700 cm^{-1} in II; 725 cm^{-1}, 700 cm^{-1} in III), but exhibited neither a secondary amide group nor a hydroxy group. The results of the analysis of these products were as follows:

Found (for I): C, 76.86; H, 8.41; N, 6.79.
Calcd. for $C_{13}H_{17}NO$: C, 76.81; H, 8.43; N, 6.89%.
Found (for II): C, 73.00; H, 7.49; N, 6.07.
Calcd. for $C_{14}H_{17}NO_2$: C, 72.72; H, 7.36; N, 6.06%.
Found (for III): C, 78.55; H, 7.10; N, 4.60.
Calcd. for $C_{20}H_{21}NO_2$: C, 78.14; H, 6.88; N, 4.55%.
Found (for IV): C, 69.92; H, 10.73; N, 12.23.
Calcd. for $C_{13}H_{24}N_2O$: C, 69.59; H, 10.78; N, 12.48%.

The Reaction of Cyclohexyl Isocyanide with *t*-Butyl Perbenzoate. — The procedure and conditions employed were similar to that used for the above reaction, except that the radical source was divided into ten parts and added at intervals of one hour. 54.5 g. (0.5 mol.) of the isocyanide and 9.7 g. (0.05 mol.) of the perbenzoate were allowed to react. Working-up of the reaction mixture, as described above, gave I (2.1 g.), II (1.6 g.) and IV (0.1 g.) and two new minor products, V (0.2 g.) (recrystallized from acetone, m. p. 179~181°C) and oil (1.4 g.) presumed to be VI on the basis of its infrared spectrum (b. p. 107°C/2 mmHg).

The product V showed no depression in melting point when mixed with an authentic material.

Found (for V): C, 70.72; H, 8.61; N, 6.14.
Calcd. for $C_{13}H_{19}NO_2$: C, 70.55; H, 8.65; N, 6.32%.

The Reaction of Cyclohexyl Isocyanide with *N*-Nitroso Acetanilide.—By the method and conditions described above, the reaction of 136 g. (1.245 mol.) of cyclohexyl isocyanide with 22.8 g. (0.143 mol.) of *N*-nitrosoacetanilide was carried out. The reaction mixture was distilled in vacuo to yield 11.5 g. of an oily product (b. p. 98~125°C/3 mmHg). This was dissolved in ether and washed successively with 5% cold aqueous hydrochloric acid, aqueous sodium carbonate, and finally water. After the oil had been dried, the ether was evaporated off and the residual oil was distilled in vacuo to give 4 g. of VII (b. p. 98~99°C/3 mmHg). The 5% aqueous hydrochloric acid layer was alkalified with sodium carbonate, and the oil which separated was extracted with ether. The ethereal solution was evaporated and distilled in vacuo to yield 2.8 g. of an oily product (b. p. 103~105°C/3 mmHg), which consisted of two parts; one was VIII (1 g., melting at 100~101°C after recrystallization from ligroin), and other was an oil (1.7 g.), presumed on the basis of its infrared spectrum to be VI. The structure of product VII was also presumed on the basis of its infrared spectrum and analytical data.

The spectrum had the absorption resulting from the ester group (1740 cm^{-1}, 1220 cm^{-1}) and double bond between carbon and nitrogen (1675 cm^{-1}) but showed no absorption originating in hydroxy group and secondary amide group. The melting point of the product VIII was undepressed on admixture with an authentic sample.

Found (for VII): C, 64.61; H, 9.23; N, 7.98.
Calcd. for $C_9H_{15}NO_2$: C, 63.88; H, 8.94; N, 8.28%.

The Reaction of Cyclohexyl Isocyanide with Potassium Phenylazoformate.[4]—In a similar way 43.7 g. (0.4 mol.) of cyclohexyl isocyanide and 7.5 g. (0.04 mol.) of potassium phenylazoformate were allowed to react. After the removal of the unreacted isocyanide, the residue was distilled under reduced pressure to afford an oily product (1.4 g., b. p. 92°C/2 mmHg) and IV (0.1 g.).

The oily product had the same infrared spectrum as the authentic sample of IX, and it reacted

4) A Nagasaka and R. Oda, *J. Chem. Soc. Japan, Ind. Chem. Sec.* (*Kogyo Kagaku Zassi*), **58**, 48 (1955).

with 2,4-dinitrophenylhydrazine to give benzaldehyde 2,4-dinitrophenylhydrazone in the theoretical yield. These facts clearly indicate that the oily product is IX.

The Reaction of Cyclohexyl Isocyanide with Di-*t*-butyl Peroxide. — The reaction of 35.5 g. (0.325 mol.) of cyclohexyl isocyanide with 14.6 g. (0.1 mol.) of di-*t*-butyl peroxide was performed in a similar manner described above.

The reaction mixture was distilled to remove the unchanged isocyanide and peroxide. The resulting resinous product (4.8 g.) was dissolved in ethanol, and IV (0.1 g.) and X (0.15 g., m. p. 270~271.5°C, recrystallized from dioxane) were separated from the ethanol solution. The product X showed no depression in melting point when mixed with an authentic sample prepared from cyclohexylamine and oxalyl chloride.

Found (for X): C, 66.05; H, 9.46; N, 11.29. Calcd. for $C_{14}H_{24}N_2O_2$: C, 66.63; H, 9.59; N, 11.10%.

Summary

The reactions of cyclohexyl isocyanide with some radical sources, such as perbenzoic acid, benzoyl peroxide, *t*-butyl perbenzoate, *N*-nitrosoacetanilide, potassium phenylazoformate and di-*t*-butyl peroxide, have been studied. The isocyanide does not contribute kinetically to the mechanism of the decomposition of benzoyl peroxide, but the lone pair electrons existing on the carbon atom of isocyanide react very easily with free radicals, especially with acyloxy radicals.

In the reaction with benzoyl peroxide, *t*-butyl perbenzoate or the *N*-nitrosoacetanilide acyloxy radical chiefly contributes to the reaction. With potassium phenylazoformate, the phenyl radical is the main reacting species. However, in the case of perbenzoic acid, the reaction is heterolytic, and the main product is cyclohexyl isocyanate.

Department of Synthetic Chemistry
Faculty of Engineering
Kyoto University
Sakyo-ku, Kyoto

*Dihydropyridine Derivatives. I. The Reaction of 1,4-Diphenyl-3,5-diacetylpyridinium Salts with Inorganic Bases**

By Noboru SUGIYAMA, Kimie KUBOTA, Goro INOUYE** and Takasi KUBOTA***

(Received December 6, 1963)

During the structural studies of 1, 4-dihydro-1, 4-diphenyl-3, 5-diacetylpyridine (I), a chromium-containing compound was isolated by Inouye[1] from a reaction mixture of I with chromium trioxide in acetic acid, although its structure has not yet been determined. In the present investigation, this compound was found to be 1, 4-diphenyl-3, 5-diacetylpyridinium bichromate (II) on the basis of its analysis, its infrared spectrum and its reaction with inorganic bases. In addition, some new pyridinium salts have been prepared and their reactions with inorganic bases studied.

Mumm[2] and Borsche[3] reported that 1, 4-dihydropyridine derivatives were oxidized to pyridine derivatives with chromium trioxide. However, the isolation of bichromates of pyridine or its derivatives has not been reported. In the present investigation, I was oxidized to II with chromium trioxide in acetic acid. It was found that II is stable even when heated in water, but in organic solvents such as acetic acid, alcohols or acetone, it was decomposed by long heating. A characteristic blue fluorescence was observed with I, but not with II, either in the solid state or in solution. The infrared spectrum of I has an absorption band at 1645 cm^{-1} ($\nu_{C=O}$) which is attributed to a vinylogous amide gruop,[4] while that of II has a band at 1700 cm^{-1} ($\nu_{C=O}$). These facts indicate that the dihydropyridine ring of I was oxidized to a pyridinium ring. The elementary analysis of II also supports the pyridinium salt structure.

* Presented at the 14th Annual Meeting of the Chemical Society of Japan, April, 1961.

** Present address: The Technical Research Laboratory, Asahi Chemical Industry Co., Ltd., Itabashi-ku Tokyo.

*** Present address: Basic Research Laboratories, Toyo Rayon Co., Ltd., Kamakura.

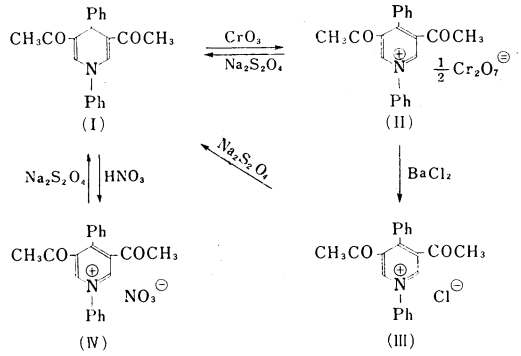
1) G. Inouye, *J. Chem. Soc. Japan, Pure Chem. Sec.* (*Nippon Kagaku Zassi*), **79**, 1243 (1958).

2) O. Mumm and W. Beth, *Ber.*, **54**, 1591 (1921).

3) W. Borsche and H. Hahn, *Ann.*, **537**, 219 (1939).

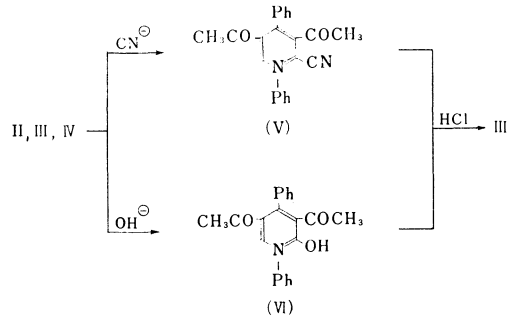
4) A. G. Anderson and G. Berkelhammer, *J. Am. Chem. Soc.*, **80**, 992 (1958).

By treatment with barium chloride, II was converted to 1, 4-diphenyl-3, 5-diacetylpyridinium chloride (III). By oxidation with nitric acid, I gave 1, 4-diphenyl-3, 5-diacetylpyridinium nitrate (IV). Infrared spectra of III and IV, like those of II, show their carbonyl band at 1700 cm^{-1}. Also, they did not show fluorescence, as was expected from the pyridinium structure.

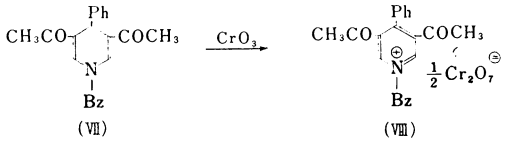


The reaction of II, III and IV with sodium dithionite gave a yellow crystalline compound (m. p. 181°C), which was identified with I by a study of their infrared spectra and by a mixed melting point determination. It has been known that the reduction of a pyridinium derivative with sodium dithionite affords a 1, 4-dihydropyridine derivative.[5]

Mumm[2] reported the formation of an addition compound of the cyano group by the treatment of pyridinium derivatives with potassium cyanide. II, III and IV were converted to 2-cyano-1, 2-dihydro-1, 4-diphenyl-3, 5-diacetylpyridine (V) by reaction with potassium cyanide. The infrared spectrum of V exhibits split carbonyl bands at 1672 cm^{-1} and 1646 cm^{-1} instead of a single band at 1645 cm^{-1} this can be attributed to two acetyl groups at the 3 and 5 positions. The shift to the higher frequency (1672 cm^{-1}) seems to be due to the decrease in the conjugation of the acetyl group with the dihydropyridine ring. It is reasonable that this decrease may be caused by the interaction of the bulky phenyl group and the cyano group.[6] The reaction of II, III and IV with such bases as sodium hydroxide, potassium carbonate or sodium acetate afforded 2-hydroxy-1,2-dihydro-1,4-diphenyl-3,5-diacetylpyridine (VI). No compound analogous to VI has yet been isolated by the reaction of pyridinium salt, similar to the cases of II, III or IV with hydroxide ions. VI is unstable and can be recrystallized only from ethylene dichloride. The infrared spectrum of VI shows bands at 1660 and 1608 cm^{-1} ($\nu_{C=O}$); the latter band is attributed to the 3-acetyl group hydrogen-bonded with the 2-hydroxy group. V and VI show a bluish-green fluorescence in the solid state as well as in solution. They were decomposed by being heated in organic solvents for a long time. After acidifying an ethanolic solution of V and VI with hydrochloric acid, the solvent was removed under reduced pressure to give colorless crystals. These were identified with III by mixed melting point determination and by a study of the infrared spectrum.



In the same way, 1-benzyl-4-phenyl-1, 4-dihydro-3, 5-diacetylpyridine (VII) was also oxidized to 1-benzyl-4-phenyl-3, 5-diacetylpyridinium bichromate with chromium trioxide.



Experimental

1, 4-Diphenyl-3, 5-diacetylpyridinium Bichromate (II).—A solution of 1 g. of chromium trioxide in 1 ml. of water and 2 ml. of acetic acid was added gradually to a solution of 0.5 g. of 1, 4-dihydro-1, 4-diphenyl-3, 5-diacetylpyridine (I) in 10 ml. of acetic acid. The resulting solution immediately became yellowish brown and cloudy, and then an oily product separated. The mixture was heated at 50°C for ten minutes, and 10 ml. of water was added. After standing at room temperature, 0.42 g. of orange crystals were obtained. Recrystallization from water gave 1, 4-diphenyl-3, 5-diacetylpyridinium bichromate (II) as orange-yellow plates; these did not show a definite decomposition point, but gradually turned black above 150°C.

Found: C, 59.44; H, 4.33; N, 3.27. Calcd. for $C_{21}H_{18}O_{21}N \cdot 1/2(Cr_2O_7)$: C, 59.43; H, 4.24; N, 3.30%.

1, 4-Diphenyl-3, 5-diacetylpyridinium Chloride (III).—To a solution of 0.5 g. of II in 100 ml. of hot water, 0.1 g. of barium chloride in 10 ml. of

5) D. Mauzerall and F. H. Westheimer, ibid., 77, 2261 (1958); R. F. Hutton and F. H. Westheimer, *Tetrahedron*, 3, 73 (1958).

6) Curiously the infrared spectrum of V has not a band due to C≡N bond stretching. Reasonable explanation can not be given at present.

water was added in one portion. The solution immediately became yellowish and cloudy. The mixture was heated in a water bath for 1 hr. After the solution had cooled, the precipitate was filtered off and the filtrate was concentrated to dryness under reduced pressure. Ethanol (10 ml.) was added to the residue, the insoluble substance was filtered off, and the filtrate was concentrated to dryness under reduced pressure. The same procedures were repeated several times. The final residue was recrystallized from ethanol-ethyl acetate to give 1, 4-diphenyl-3, 5-diacetylpyridinium chloride (III) (0.35 g.) as colorless needles (m. p. 245~247°C (decomp.)).

Found: N, 3.99. Calcd. for $C_{21}H_{18}O_2NCl$: N, 3.96%.

1, 4-Diphenyl-3,5-diacetylpyridinium Nitrate (IV). I (0.5 g.) was dissolved in 30 ml. of methanol, and 0.5 ml. of concentrated nitric acid was added. The mixture was allowed to stand at room temperature overnight. The solvent was distilled off under reduced pressure, and the residue was recrystallized from ethanol-ethyl acetate. 1, 4-Diphenyl-3, 5-diacetylpyridinium nitrate (IV) (0.32 g.) was obtained as pale brownish needles (m. p. 177~178°C (decomp.)).

Found: N, 7.17. Calcd. for $C_{21}H_{18}O_5N_2$: N, 7.40%.

The Reduction of III with Sodium Dithionite.—To a solution of 0.1 g. of III in 10 ml. of water, 0.5 g. of sodium dithionite was added. The solution became yellowish and exhibited a blue fluorescence. After standing at room temperature for 3 hr., the separated precipitate was collected by filtration. Recrystallization from ethanol gave greenish yellow prisms (0.07 g., m. p. 181°C). No depression of melting point was observed on admixture with an authentic sample of I.

The Reduction of II and IV with Sodium Dithionite.—When the reduction of II and IV with sodium dithionite was carried out as described above for III, I was obtained in both cases.

2-Cyano-1, 2-dihydro-1, 4-diphenyl-3, 5-diacetylpyridine (V).—(i) To a solution of 0.4 g. of II in 100 ml. of water, 1.5 g. of potassium cyanide in 5 ml. of water was added. The solution became yellowish and cloudy. After the solution had stood overnight in an ice box, the yellowish crystals were collected by filtration. Recrystallization from ethanol-water gave 2-cyano-1, 2-dihydro-1, 4-diphenyl-3, 5-diacetylpyridine (V) (0.28 g.) as yellowish green needles (m. p. 154~155°C).

Found: C, 77.35; H, 5.10; N, 7.87. Calcd. for $C_{22}H_{18}O_2N_2$: C, 77.19; H, 5.26; N, 8.18%.

(ii) The similar reaction of III or IV with potassium cyanide afforded the same compound V.

The Reaction of V with Hydrochloric Acid.—To a solution of 0.2 g. of V in 5 ml. of ethanol, 0.1 ml. of concentrated hydrochloric acid was added. The solution turned from yellowish to colorless. After ten minutes, the solvent was distilled off under reduced pressure and the residue was recrystallized from ethanol-ethyl acetate to give colorless needles (0.12 g.) (m. p. 245~247°C). No depression of melting point was observed on admixture with an authentic sample of III.

2-Hydroxy-1, 2-dihydro-1, 4-diphenyl-3, 5-diacetylpyridine (VI).—To a solution of 0.3 g. of III in 5 ml. of water, 0.2 g. of potassium carbonate in 4 ml. of water was added. The solution immediately became yellowish and cloudy. After a few minutes, the yellow precipitates which had separated out were collected by filtration and the crude product was dissolved in ethylene dichloride at 20~30°C. The solution was cooled in an ice box, and 2-hydroxy-1, 2-dihydro-1, 4-diphenyl-3, 5-diacetylpyridine (VI) (0.2 g.) was obtained as yellowish prisms (m. p. 145~147°C (decomp.)).

Found: N, 4.14. Calcd. for $C_{21}H_{19}O_3N$: N, 4.20%.

II and IV also afforded VI by similar procedures. VI was also obtained by the treatment of II, III or IV with sodium hydroxide or sodium acetate instead of potassium carbonate.

1-Benzyl-4-phenyl-3, 5-diacetylpyridinium Bichromate (VIII).—A solution of 0.2 g. of chromium trioxide in 1 ml. of water and 3 ml. of acetic acid was added to a solution of 0.06 g. of 1, 4-dihydro-1-benzyl-4-phenyl-3, 5-diacetylpyridine (VII) in 3 ml. of acetic acid. The mixture was heated at 40°C for ten minutes, and 10 ml. of water was added. After cooling, 0.04 g. of orange crystals were obtained by filtration. Recrystallization from water gave orange yellow plates which decomposed at 350°C.

Found: C, 60.10; H, 4.57; N, 3.25. Calcd. for $C_{22}H_{20}O_2N \cdot 1/2Cr_2O_7$: C, 60.27; H, 4.60; N, 3.19%.

Department of Chemistry
Faculty of Science
Tokyo University of Education
Bunkyo-ku, Tokyo

Infrared Spectroscopic Studies of Acido-pentammine Cobalt(III) Complexes. Sulfato, Nitrito, Nitrato and Carbonato Complexes

By Nobuyuki TANAKA, Haruko SUGI and Junnosuke FUJITA

(Received December 6, 1963)

Several infrared spectroscopic studies of cobalt(III) complexes co-ordinated with oxyanions, such as sulfate, nitrate, carbonate and nitrite, have been reported.[1-4] The spectra of these co-ordinated oxyanions have been found to differ from those of the free anions, because the co-ordination usually causes a change in the symmetry and structure of the ligands. For the nitrato, carbonato and nitrito complexes, empirical assignments of the observed absorption bands have been carried out, but not for the sulfato complexes.

In this investigation, the assignment of the observed frequencies of sulfato and other acido pentammine complexes has been made on the basis of a normal co-ordinate treatment. The effect of co-ordination on the structure of these oxyanions and the applicability of the Urey-Bradley type potential field have been discussed.

Experimental

Preparation.—The $[Co(SO_4)(NH_3)_5]^+$, $[Co(NO_3)(NH_3)_5]^{2+}$ and $[(NH_3)_4Co\langle^{NH_2}_{SO_4}\rangle Co(NH_3)_4]^{3+}$ complexes were prepared according to the methods of Jörgensen,[5] Benrath[6] and Werner[7] respectively, and they were recrystallized more than three times. Since all the compounds studied were typical metallic complexes, their purity was checked by comparing the visible and ultraviolet spectra with the published data.[8,9]

Measurements.—The infrared spectra in the NaCl and the KBr prism region (5000~400 cm^{-1}) were obtained by using a Hitachi EPI-2G infrared spectrophotometer, while those in the CsBr prism region (400~250 cm^{-1}) were obtained by using a Nihonbunko 402-G infrared spectrophotometer. The wavelength calibration was made with the polystyrene, water vapor and carbon dioxide in the air. Spectra were measured by the KBr disk and the Nujol mull methods.

Calculation and Discussion

The vibrations of metal complexes can be divided into two types, one the vibration of ligands, and the other, that of metal-ligand bonding. The former generally appears in the rock salt region, while the latter appears in the longer wavelength region. The infrared absorption spectra of sulfato and nitrato complexes and their deuterated complexes show only two bands, near 330 and 270 cm^{-1}, in the range from 400 to 250 cm^{-1}.

In the calculation, the ligand vibrations were treated separately, without considering the coupling between the ligand vibrations and the metal-ligand vibrations, which has been found to be fairly small in carbonato-pentamminecobalt(III) complexes.[10] The secular equations were set up according to Wilson's procedure,[11] and the Urey-Bradley potential field[12] was used. Internal co-ordinates and symmetry co-ordinates for the

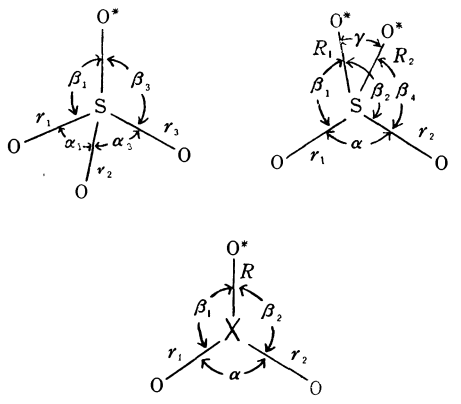


Fig. 1. Internal co-ordinates for SO_4 and XO_3. X means C and N, and O*, the co-ordinated oxygen atom.

1) K. Nakamoto, J. Fujita, S. Tanaka and M. Kobayashi, *J. Am. Chem. Soc.*, **79**, 4904 (1957).
2) E. P. Bertin, R. B. Penland, S. Mizushima, C. Curran and J. V. Quagliano, *J. Am. Chem. Soc.*, **81**, 3818 (1959).
3) B. M. Gatehouse, S. E. Livingstone and R. S. Nyholm, *J. Chem. Soc.*, **1957**, 4222; **1958**, 3137.
4) K. Nakamoto, J. Fujita and H. Murata, *J. Am. Chem. Soc.*, **80**, 4817 (1958).
5) S. M. Jörgensen, *J. prakt. Chem.*, [2] **31**, 269 (1885).
6) A. Benrath and K. Miens, *Z. anorg. Chem.*, **117**, 289 (1929).
7) A. Werner, *Ber.*, **40**, 4610 (1907).
8) Y. Shimura and R. Tsuchida, This Bulletin, **29**, 311 (1956).
9) R. Tsuchida, ibid., **13**, 388, 436 (1938).
10) J. Fujita, A. E. Martell and K. Nakamoto, *J. Chem. Phys.*, **36**, 339 (1962).
11) E. B. Wilson, ibid., **7**, 1047 (1939); **9**, 76 (1941).
12) T. Shimanouchi, ibid., **17**, 245, 734, 848 (1949).

Table I. Symmetry co-ordinates for the C_{3v} and the C_{2v} co-ordinated sulfate

The C_{3v} co-ordinated sulfate

A_1 $S_1=\Delta/\sqrt{3}$ $(r_1+r_2+r_3)$
$S_2=\Delta R$
$S_3=\Delta/\sqrt{6}$ $(\beta_1+\beta_2+\beta_3-\alpha_1-\alpha_2-\alpha_3)$

E $S_4=\Delta/\sqrt{6}$ $(2r_1-r_2-r_3)$
$S_5=\Delta/\sqrt{6}$ $(2\alpha_3-\alpha_1-\alpha_2)$
$S_6=\Delta/\sqrt{6}$ $(2\beta_1-\beta_2-\beta_3)$

The C_{2v} co-ordinated sulfate

A_1 $S_1=\Delta/\sqrt{2}$ (r_1+r_2)
$S_2=\Delta/\sqrt{2}$ (R_1+R_2)
$S_3=\Delta/\sqrt{12}$ $(2\gamma-\beta_1-\beta_2-\beta_3-\beta_4+2\alpha)$
$S_4=\Delta/\sqrt{2}$ $(\gamma-\alpha)$

B_1 $S_5=\Delta/\sqrt{2}$ (R_1-R_2)
$S_6=\Delta/2$ $(\beta_1+\beta_2-\beta_3-\beta_4)$

B_2 $S_7=\Delta/\sqrt{2}$ (r_1-r_2)
$S_8=\Delta/2$ $(\beta_1-\beta_2+\beta_3-\beta_4)$

Table II. Symmetry co-ordinates for the C_{2v} co-ordinated nitrate and carbonate

A_1 $S_1=\Delta/\sqrt{2}$ (r_1+r_2)
$S_2=\Delta R$
$S_3=\Delta/\sqrt{6}$ $(2\alpha-\beta_1-\beta_2)$

B_2 $S_4=\Delta/\sqrt{2}$ (r_1-r_2)
$S_5=\Delta/\sqrt{2}$ $(\beta_1-\beta_2)$

oxyanions investigated are given in Fig. 1 and in Tables I and II respectively.

(1) Sulfato Complexes.—The symmetry of a free SO_4^{2-} ion belongs to the point group T_d, and only two triply-degenerate vibrations of the four fundamentals are infrared active. When this ion is co-ordinated to a metal as a unidentate ligand, its symmetry is lowered to the point group C_{3v} and the triply-degenerate vibration splits into a doubly-degenerate vibratoin (E) and a totally symmetric vibration

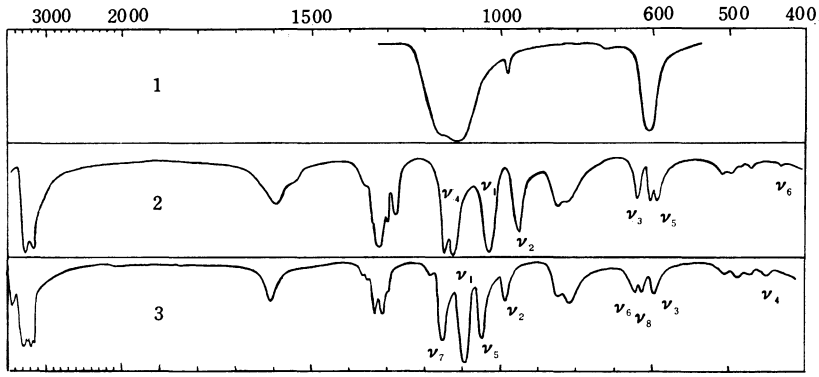


Fig. 2. Observed spectra of K_2SO_4 (1); $[Co(SO_4)(NH_3)_5]I$ (2); $[(NH_3)_4Co\langle^{NH_2}_{SO_4}\rangle Co(NH_3)_4]Br_3$ (3).

Table III. Observed and calculated frequencies and force constants of $[Co(SO_4)(NH_3)_5]^+$

		ν_1	ν_2	ν_3	ν_4	ν_5	ν_6
Calculated frequencies, cm^{-1}	(a)	1072	961	618	1126	613	445
	(b)	1043	963	621	1142	617	452
Assignment		ν(S-O)+ν(S-O*)	ν(S-O*)+ν(S-O)	$\delta(SO_4)$	ν(S-O)	$\delta(SO_3)$+$\rho(SO_3)$	$\rho(SO_3)$+$\delta(SO_3)$
Observed frequencies, cm^{-1}	$[Co(SO_4)(NH_3)_5]Cl$	1044	974	646	1135	614 603	446
	$[Co(SO_4)(ND_3)_5]Cl$	1047	973	645	1136	608	445
	$[Co(SO_4)(NH_3)_5]Br$	1050 1037	974	647	1148 1126	612 600	438
	$[Co(SO_4)(NH_3)_5]I$	1033	958	645	1152 1127	610 595	440
	$[Co(SO_4)(ND_3)_5]I$	1036	959	640	1130	617 596	440
	$[Co(SO_4)(NH_3)_5]NO_3$	1054 1036	974	647	1147 1126	613 598	440

		K_{SO}*	K_{SO}	F_{OO}*	F_{OO}	H_{OSO}*	H_{OSO}	ρ_{SOSO}*	ρ_{SOSO}
Force constant, mdyn./Å	(a)	5.1	6.3	0.7	0.8	0.40	0.45	0	0
	(b)	5.1	6.3	0.7	0.8	0.45	0.45	0.1	−0.2

$\kappa=0.6$ mdyn.Å

TABLE IV. OBSERVED AND CALCULATED FREQUENCIES AND FORCE CONSTANTS OF $\left[(NH_3)_4Co\langle^{NH_2}_{SO_4}\rangle Co(NH_3)_4\right]^{3+}$

	ν_1	ν_2	ν_3	ν_4	ν_5	ν_6	ν_7	ν_8
Calculated frequencies, cm^{-1}	1109	958	590	472	1068	630	1146	620
Assignment	ν(S-O)	ν(S-O*)	$\delta(SO_4)$	$\delta(SO_4)$	ν(S-O*)	$\delta(SO_4)$	ν(S-O)	$\delta(SO_4)$
Observed frequencies, cm^{-1}	$\left[(NH_3)_4Co\langle^{NH_2}_{SO_4}\rangle Co(NH_3)_4\right](NO_3)_3$							
	1109	997	613	454	1064	653	1171	641
	$\left[(NH_3)_4Co\langle^{NH_2}_{SO_4}\rangle Co(NH_3)_4\right]Br_3$							
	1101	991	605	455	1056	649	1155	637
	The deuterated complex							
	1096	988	602		1054	668	1166 1140	658
Force constant, mdyn./Å	K_{SO^*}	K_{SO}	$F_{O^*O^*}$	F_{OO^*}	F_{OO}	$H_{O^*SO^*}$	H_{OSO^*}	H_{OSO}
	5.7	6.8	0.65	0.70	0.80	0.40	0.50	0.45
	κ=0.6 mdyn.Å							

(A_1), and all vibrations become infrared-active. On the other hand, in the case of the binuclear complex, in which the SO_4^{2-} ion is co-ordinated as a bidentate, its symmetry becomes C_{2v} and all degeneracies split.[1] This correlation is apparent from the observed spectra shown in Fig. 2 and from the results of the normal co-ordinate calculation.

The vibrational frequencies were calculated with the force constant values listed in Tables III and IV ((a) in Table III) using the Urey-Bradley potential field. Those force constants were determined on the basis of the values of the free ions.[13] The bond angles were regarded as tetrahedral, while the bond lengths, r_{SO^*}=1.53 and r_{SO}=1.47 Å, were assumed from the value of the free SO_4^{2-} ion (r_{SO}=1.50 Å[14]). The asterisk indicates the co-ordinated oxygen atom. The values of F', the linear terms of the interaction between non-bonded atoms, were determined from the relation, $F'=-1/10\,F$.[15] The results are given in Tables III and IV ((a) in Table III).

Since the calculated frequencies were not in satisfactory agreement with the observed ones, especially for the stretching vibrations, the calculation was also made, in the case of the sulfatopentamminecobalt(III) complex, using a modified Urey-Bradley potential function[16] expressed as:

13) S. Mizushima and T. Shimanouchi, "Infrared Absorption Spectra and Raman Effect," Kyoritsu, Tokyo (1958).
14) L. Pauling, "The Nature of the Chemical Bond," Cornell University Press, Ithaca, N. Y. (1960).
15) T. Shimanouchi, *J. Chem. Soc. Japan, Pure Chem. Sec. (Nippon Kagaku Zassi)*, **74**, 266 (1953).
16) I. Nakagawa and T. Shimanouchi, *Spectrochim. Acta*, **18**, 101 (1962).

TABLE V. POTENTIAL ENERGY DISTRIBUTION OF THE C_{3v} AND THE C_{2v} CO-ORDINATED SULFATE

The C_{3v} co-ordinated sulfate

	ν_1	ν_2	ν_3
Calculated frequencies, cm^{-1}	1072	961	618
S_1	1.00	0.57	0.01
S_2	0.62	1.00	0.06
S_3	0.19	0.06	1.00
	ν_4	ν_5	ν_6
Calculated frequencies, cm^{-1}	1126	613	446
S_4	1.00	0.08	0.00
S_5	0.09	1.00	0.72
S_6	0.07	0.60	1.00

The C_{2v} co-ordinated sulfate

	ν_1	ν_2	ν_3	ν_4
Calculated frequencies, cm^{-1}	1109	958	590	472
S_1	1.00	0.28	0.00	0.01
S_2	0.37	1.00	0.00	0.02
S_3	0.00	0.00	1.00	0.06
S_4	0.12	0.02	0.04	1.00
	ν_5	ν_6		
Calculated frequencies, cm^{-1}	1068	630		
S_5	1.00	0.08		
S_6	0.18	1.00		
	ν_7	ν_8		
Calculated frequencies, cm^{-1}	1146	620		
S_7	1.00	0.15		
S_8	0.14	1.00		

$$V=(1/2)\sum_i K_i(\Delta r_i)^2+(1/2)\sum_{i<j} H_{ij}(r_{ij}\Delta\alpha_{ij})^2 + (1/2)\sum_{i<j} F_{ij}(\Delta q_{ij})^2+(\text{linear terms}) + \sum_{i<j}\rho_{ij}(\Delta r_i)(\Delta r_j) \quad (1)$$

where ρ represents the bond-bond interaction constant. The calculated frequencies which were obtained with Eq. 1 using the force constants of (b) in Table III are given in Table III(b).

The potential energy distribution was calculated, and the band assignments were made. These are given in Table V and Fig. 2 respectively.

The use of the Urey-Bradley potential field failed to give a satisfactory agreement between the calculated and the observed frequencies in the C_{2v} calculation (Table II) also. This, however, seems partly due to the neglect of the effect of the ring vibration, which should have been taken into account for the metal chelate complexes.[10]

Nevertheless, it may be concluded, from the force constants obtained, that a SO_4^{2-} ion combines with cobalt(III) more strongly as a unidentate than as a bidentate.

(2) Nitrito Complex.—In the nitrito complex, ONO* belongs to the point group C_s, and the three A_1 vibrations are all infrared-active. Table VI shows the calculated and the observed frequencies of the nitritopentammine-cobalt(III) complex. The molecular dimensions given in Table VI were assumed from the structures of $NaNO_2$[17] and CH_3ONO.[18] Table VI shows that the effect of the bond angle on the calculated values is not significant. The force constants in Table VI indicate a marked difference in bond orders between the NO and NO* bonds. This suggests that the co-ordination effect is fairly large.

TABLE VI. OBSERVED AND CALCULATED FREQUENCIES AND OBTAINED FORCE CONSTANTS OF $[Co(ONO)(NH_3)_5]Cl_2$

Calculated frequencies,*1 cm^{-1}	(a)*2	1463	1063	824
	(b)*2	1466	1064	835
Observed frequencies, cm^{-1} [14]		1468	1065	825
Assignment		ν(N-O)	ν(N-O*)	δ(ONO*)

Force constant, mdyn./Å	K_{NO^*}	K_{NO}	F_{OO^*}	H_{ONO^*}
	4.2	8.7	2.0	0.90

1 R(N-O)=1.30 Å r(N-O)=1.20 Å,
*2 (a) ∠ONO=120°, (b) ∠ONO=115°

(3) Nitrato and Carbonato Complexes.—Both NO_3^- and CO_3^{2-} in the state of free ions belong to the point group D_{3h}, and two degenerate and one out-of-plane vibrations of the four fundamentals are infrared-active. When these anions are co-ordinated as unidentate ligands, the symmetry lowers to C_{2v} and the irreducible representation, E, splits into A_1 and B_2. Tables VII and VIII present the observed and the calculated frequencies. The latter was obtained with the force constants given in these tables. The bond angles of the nitrato and the carbonato complexes are assumed to be 120° ((a) and (b) in Tables VII and VIII), but in the case of the nitrato complex the calculation was made also with the bond angles, $\alpha=130°$ and $\beta=115°$ ((c) in Table VII). The bond lengths of these complexes are considered to be $r_{XO^*}=1.30$ and $r_{XO}=1.25$ Å. The potential energy distributions of the co-ordinated nitrate and carbonate as unidentate ligands are given in Table IX.

The results of the calculation show that the usual Urey-Bradley force field does not apply well in these molecules. The following four points, therefore, will be discussed:

(i) The effects of the coupling with oxygen-cobalt bond vibrations;

(ii) The effect of hydrogen-bond formation;

(iii) The effect of the molecular dimension and

(iv) The applicability of the Urey-Bradley type force field to the molecules that have unlocalized π-electrons.

In order to investigate the effects of the coupling with oxygen-cobalt bond vibrations, the spectra in the CsBr prism region were obtained. The observed frequencies are given in Table X. The bands of some 330 cm^{-1} shift to lower frequencies by 30 cm^{-1} upon deuteration, while those of some 27 cm^{-1} do not. Although the assignments of these bands are not clear at present, the calculation was made with the value, $K_{Co-O^*}=2$ mdyn./Å[10] and the C_{2v} point symmetry. The results suggested that the effect of the coupling with oxygen-cobalt bond vibrations is insignificant.

As to the molecular dimensions, the effects of the bond length and the bond angle were taken into consideration. It was found that the former is negligibly small, as Table XI shows, whereas the latter is considerably large, as may be seen from the calculated frequencies given in Table VII.

According to the electron diffraction studies of nitric acid in the solid state,[19] the bond angle of ONO is 134° and that of HO–NO, 113°, indicating that the HO–N bond is a

17) G. B. Carpenter, *Acta Cryst.*, **8**, 852 (1955).
18) F. Rogowski, *Ber.*, **75**, 244 (1942).
19) V. Luzzati, *Acta Cryst.*, **4**, 120 (1951).

TABLE VII. OBSERVED AND CALCULATED FREQUENCIES AND FORCE CONSTANTS OF $[Co(NO_3)(NH_3)_5]^{2+}$

		ν_1	ν_2	ν_3	ν_4	ν_5
Calculated frequencies, cm^{-1}	(a)	1341	1018	735	1467	696
	(b)	1290	1026	736	1484	711
	(c)	1305	1019	730	1481	699
Assignment		ν(N-O)+ ν(N-O*)	ν(N-O*)+ ν(N-O)	$\delta(NO_3)$	ν(N-O)	$\rho(NO_2)$
Observed frequencies, cm^{-1}	$[Co(NO_3)(NH_3)_5]Cl_2$	1280	1017	754	1481	724
	$[Co(NO_3)(NH_3)_5](NO_3)_2$	1266	1016	745	1481	716
	$[Co(NO_3)(ND_3)_5](NO_3)_2$	1287	1018		1484	

Force constant, mdyn./Å	K_{NO}*	K_{NO}	F_{OO}*	F_{OO}	H_{ONO}*	H_{ONO}	ρ_{NONO}*	ρ_{NONO}
(a)	3.9	6.5	1.5	1.7	0.50	0.60	0	0
(b)	4.0	6.1	1.5	1.7	0.55	0.60	0.2	−0.5
(c)	4.1	6.25	1.5	1.7	0.50	0.60	0	0

TABLE VIII. OBSERVED AND CALCULATED FREQUENCIES AND FORCE CONSTANTS OF $[Co(CO_3)(NH_3)_5]^+$

		ν_1	ν_2	ν_3	ν_4	ν_5
Calculated frequencies, cm^{-1}	(a)	1414	1051	729	1468	668
	(b)	1366	1054	728	1468	668
Assignment		ν(C-O)+ ν(C-O*)	ν(C-O)*+ ν(C-O)	$\delta(CO_3)$	ν(C-O)	$\rho(CO_2)$
Observed frequencies, cm^{-1} [10]	$[Co(CO_3)(NH_3)_5]Br$	1373	1070	756	1453	678
	$[Co(CO_3)(ND_3)_5]Br$	1369	1072	751	1471	687
	$[Co(CO_3)(NH_3)_5]I$	1366	1065	776	1449	679
	$[Co(CO_3)(ND_3)_5]I$	1360	1063	742	1467	687

Force constant, mdyn./Å	K_{CO}*	K_{CO}	F_{OO}*	F_{OO}	H_{OCO}*	H_{OCO}	ρ_{COCO}*	ρ_{COCO}
(a)	4.7	5.9	1.5	2.0	0.40	0.50	0	0
(b)	4.7	5.7	1.5	2.0	0.40	0.50	0.2	−0.2

TABLE IX. POTENTIAL ENERGY DISTRIBUTION OF THE C_{2v} CO-ORDINATED NITRATE AND CARBONATE

The C_{2v} co-ordinated nitrate

	ν_1	ν_2	ν_3		ν_4	ν_5
Calculated frequencies, cm^{-1}	1341	1018	735	Calculated frequencies, cm^{-1}	1467	690
S_1	1.00	0.55	0.04	S_4	1.00	0.07
S_2	0.56	1.00	0.23	S_5	0.21	1.00
S_3	0.38	0.17	1.00			

The C_{2v} co-ordinated carbonate

	ν_1	ν_2	ν_3		ν_4	ν_5
Calculated frequencies, cm^{-1}	1414	1051	729	Calculated frequencies, cm^{-1}	1468	668
S_1	1.00	1.25	0.01	S_4	1.00	0.07
S_2	0.99	1.00	0.14	S_5	0.21	1.00
S_3	0.47	0.08	1.00			

Table X. Observed frequencies in cm^{-1} obtained in the KBr and the CsBr prism region

$[Co(SO_4)(NH_3)_5]I$	511	501	(486)	469		326	259
$[Co(SO_4)(ND_3)_5]I$		489				296	257
$[Co(SO_4)(NH_3)_5]Br$	515	499				332	264
$\left[(NH_3)_4Co\langle^{NH_2}_{SO_4}\rangle Co(NH_3)_4\right]Br_3$	510	499	476			323	290
The deuterated complex		493				291	259
$\left[(NH_3)_4Co\langle^{NH_2}_{SO_4}\rangle Co(NH_3)_4\right](NO_3)_3$	507			460		323	277
$[Co(NO_3)(NH_3)_5](NO_3)_2$		510	498	475		335	278
$[Co(NO_3)(ND_3)_5](NO_3)_2$						307	271
$[Co(NO_3)(NH_3)_5]Cl_2$		507		460	345	330	284
$[Co(CO_3)(NH_3)_5]NO_3$		505		468	358	333	310
$[Co(CO_3)(NH_3)_5]Cl$	510	495		470	358	330	290

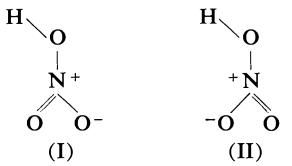
Table XI. Effect of bond length on the calculated frequencies of ONO_2 compound

Bond length, Å						
		ν_1	ν_2	ν_3	ν_4	ν_5
R	*r*					
1.30	1.25	1341	1018	735	1467	696
1.30	1.20	1336	1017	732	1466	692
1.35	1.25	1336	1017	732	1466	692

Table XII. Comparison of the value of F_{OO}[20]

Ion	Atomic distance between non-bonded atoms, Å	F_{OO} (UBFF)	F_{OO} (Ne···Ne)
NO_3^-	2.11	1.59	1.41
CO_3^{2-}	2.27	1.74	0.53
SO_4^{2-}	2.47	0.76	0.15

single bond and that, as a result of the resonance of structures I and II, the N–O bonds come to have a more double-bond character.



(I) (II)

From this fact and from the results of the calculation shown in Table VII, it may be concluded that the complex formation distorts the bond angles of a NO_3^- ion in a way similar to that it does nitric acid. The magnitude of this deformation, however, could not be estimated from these calculations.

The effect of hydrogen bond formation has not been considered in the present investigation, although there must be some influence, because in the case of these pentammine complexes, hydrogen atoms are located close around oxygen atoms.

Recently, several papers have reported on the potential field that can be applied to the compounds with unlocalized π-electrons. These compounds give larger repulsive force constants than the values that would be expected from the interatomic repulsive forces between the iso-electronic inert gas atoms. For example, the *F* constants for NO_3^-, CO_3^{2-} and SO_4^{2-} are much larger than those calculated from the Lennard-Jones equation[20] (Eq. 2), as Table XII shows.

$$F=(12\varepsilon^*/q^2)\ [13(r^*/q)^{12}-7(r^*/q)^6] \qquad (2)$$

were $\varepsilon^*=4.89\times10^{15}$ erg, $r^*=3.08$ Å

In the treatment of such compounds, the interaction terms are generally introduced as additional terms. In this study the bond-bond interaction terms were added to the usual Urey-Bradley function. The calculation of the potential energy distribution, however, requires no change in the assignment.

The negative sign of all the ρ_{XOXO} interaction terms could be interpreted by considering the localization of π-electrons in the X–O bonds.

It may be concluded from the normal coordinate treatment that the co-ordination effects in the sulfato-, nitrito-, nitrato- and carbonato-pentamminecobalt(III) complexes

20) T. Shimanouchi, "Force Constants of Small Molecules," Tokyo University, Tokyo (1962).

are fairly large. Upon co-ordination, the bond orders of X–O and X–O* become considerably different. Consequently, the bond length of X–O decreases and that of X–O* increases. At the same time, the bond angle of O–X–O increases and that of O–X–O* decreases. It may also be concluded from this investigation that the bond character between cobalt and oxygen is considerably covalent; if it is ionic, such a large difference would not appear among the X–O bonds of the co-ordinated oxyanions.

Summary

The infrared spectra of twelve acido-pentammine cobalt(III) complexes have been obtained in the range between 5000 and 250 cm^{-1}, and the vibrational frequencies of the co-ordinated oxyanions have been assigned from the normal co-ordinate treatment based on Wilson's method and on the Urey-Bradley potential field. The results of the calculation show that the co-ordination effects on these oxyanions are fairly large and that the bonds between cobalt and oxygen atoms have a considerably covalent character.

The authors wish to thank the Ministry of Education and the Japan Society for the Promotion of Science for the financial support granted to this research. They are also grateful to Dr. Tsutomu Takamura, Tokyo Shibaura Electric Company, for the measurement of the infrared spectra in the cesium bromide prism region.

Department of Chemistry
Faculty of Science
Tohoku University
Katahira-cho, Sendai

Synthetic Studies Starting from β-Cyanopropionaldehyde. I. The Synthesis of Adipic Dialdehyde

By Shinichi MOTOKI, Sadayoshi SATSUMABAYASHI and Isao TAJIMA

(Received December 9, 1963)

β-Cyanopropionaldehyde (I) is an interesting compound which has two reactive functional groups. Although several procedures for the synthesis of this compound have hitherto been available, all of them are rather cumbersome as methods of preparation. In recent years, however, an improved technique for the oxo reaction of acrylonitrile to form I in a high yield has been developed by the members of the Ajinomoto Co., Ltd.,[1,2] and this cyanoaldehyde is now being used as an intermediate in the manufacturing of glutamic acid.

The purpose of our work is to extend synthetic studies, starting with β-cyanopropionaldehyde. In this paper the synthesis of adipic dialdehyde by Kolbe's electrolytic reaction is presented.

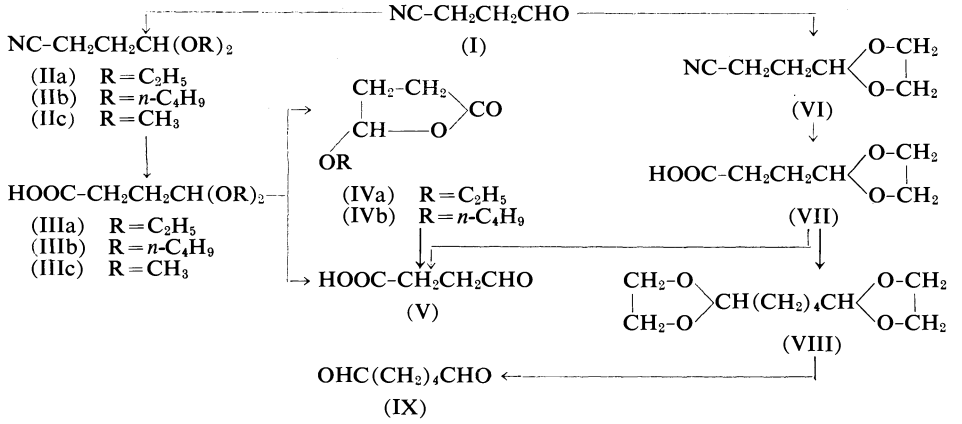
It is expected that the hydrolysis of the nitrile group will lead to β-formylpropionic acid (V), to which Kolbe's reaction is applicable. Although the procedure proposed has already been investigated with diethyl acetal of I (IIa) by Wohl,[3] little attention has been paid to the yield of each step of the reaction and to the isolation of the intermediate, β-formylpropionic acid diethyl acetal (IIIa). Therefore, our experiments will be described in detail in the present communication.

First the authors reinvestigated Wohl's procedure and purified the crude oily product (IIIa) by distillation under reduced pressure. A colorless liquid was obtained in a fairly good yield, but its analytical values were different from those of IIIa. It was a neutral substance, which was insoluble in water and which was hydrolyzed with dilute acid to V. Analytical values were very close to those of 5-ethoxy-γ-butyrolactone (IVa), and the infrared spectrum exhibited characteristic strong peaks at 1790 cm^{-1}, corresponding to that of the γ-lacton linkage. On the basis of these data, it has been concluded that the product is IVa formed by the loss of one molecule of ethanol from IIIa. In addition, it was also found that β-formylpropionic acid dibutyl acetal

1) J. Kato, H. Wakamatsu, R. Iwanaga and T. Yoshida, *J. Chem. Soc. Japan, Ind. Chem. Sec.* (*Kogyo Kagaku Zasshi*), **64**, 2139 (1961).

2) J. Kato, H. Wakamatsu, R. Iwanaga and T. Yoshida, ibid., **64**, 2142 (1961).

3) A. Wohl and H. Schweizer, *Ber.*, **39**, 890 (1906).



(IIIb) was decomposed in a fashion similar to 5-butoxy-γ-butyrolactone (IVb) by distillation, whereas methyl acetal (IIIc) was readily hydrolyzed to V during the course of the isolation.

As an attempt to isolate the acetal acid III of monohydric alcohol was unsuccessful, hydrolysis with the more stable cyclic ethylene acetal VI was examined. In this case, the reaction product was an acidic viscous liquid which was hydrolyzed with dilute acid to V. The analytical values and neutralization equivalent were in harmony with those of the expected acetal acid VII. Therefore, it was identified as β-formylpropionic acid ethylene acetal (VII).

The electrolysis of VII proceeded as usual, and the diethylene acetal of adipic dialdehyde (VIII) was obtained in about a 40%, yield with a small amount of by-product.

Experimental

Material. — β-Cyanopropionaldehyde (β-C.P.A.) (I) was obtained by the hydrolysis of its methyl acetal, supplied by the Ajinomoto Co., Ltd. It was used at once after distillation; b. p. 85°C/3 mmHg.

β-C.P.A.diethyl (IIa) and Dibutyl Acetals (IIb). —These acetals are prepared directly by the oxo reaction of acrylonitrile in the corresponding alcohols.[2] In our experiment, these were obtained by the acetalization of β-C.P.A. with the corresponding alcohols in the presence of hydrochloric acid as a catalyst; diethyl acetal, b. p. 84°C/5 mmHg; dibutyl acetal, b. p. 122°C/3 mmHg.

5-Ethoxy-γ-butyrolactone (IVa). — According to Wohl's method,[3] a crude potassium salt of β-formylpropionic acid diethyl acetal (IIIa) was obtained by the alkaline hydrolysis of β-C.P.A. diethyl acetal (IIa). This potassium salt was dissolved in as little water as possible, and the solution was acidified with dilute hydrochloric acid. Then the acetal acid was separated as a brown oil, which was extracted with ether and dried with anhydrous sodium sulfate. Distillation gave 14.1 g. of 5-ethoxy-γ-butyrolactone (b. p. 85°C/6 mmHg) from 31.4 g. of β-C.P.A. diethyl acetal. It was a neutral substance, insoluble in water, and its infrared spectra exhibited a strong absorption peak at 1790 cm^{-1} (characteristic of γ-lactone). Analysis gave the following results:

Found: C, 55.06; H, 8.01. Calcd. for $C_6H_{10}O_3$: C, 55.36; H, 7.75%.

To 5 g. of 5-ethoxy-γ-butyrolactone, 5 g. of 3% hydrochloric acid were added, and the mixture was refluxed for one hour. After cooling to room temperature, the resulting product was extracted with ether and dried with anhydrous sodium sulfate. Distillation gave 2.1 g. of β-formylpropionic acid (V) (b. p. 130~135°C/14 mmHg) forming a 2,4-dinitrophenylhydrazone, (m. p. 199°C), which showed no depression on admixture with an authentic specimen.

5-Butoxy-γ-butyrolactone (IVb).—Similarly, the hydrolysis of β-C.P.A. dibutyl acetal (IIb) gave 5-butoxy-γ-butyrolactone (b. p. 107°C/6 mmHg).

Found: C, 60.48; H, 9.08. Calcd. for $C_8H_{14}O_3$: C, 60.74; H, 8.92%.

β-Formylpropionic Acid (V). — A Similar treatment of β-C.P.A. dimethyl acetal (IIc) gave β-formylpropionic acid (V), identified as its 2,4-dinitrophenylhydrazone. In this case, no oil was separated after the acidification of the aqueous solution of the potassium salt of IIIc.

β-C.P.A.ethylene Acetal (VI). — A mixture of 1 mol. of β-C.P.A.dimethyl acetal, 1.5 mol. of ethylene glycol and 0.5 g. of *p*-toluenesulfonic acid was heated at 100~130°C in a distillation flask. The methanol formed in the reaction was immediately distilled off. The residue was poured into water, and the oil was extracted with ether. The fractional distillation of the extract gave 92.4 g. of β-C.P.A.ethylene acetal; b. p. 82°C/3 mmHg, yield 72.7%.

Found: N, 11.18. Calcd. for $C_6H_9O_2N$: N, 11.02%.

β-Formylpropionic Acid Ethylene Acetal (VII). —β-C.P.A. ethylene acetal (VI) was hydrolyzed by a method similar to Wohl's procedure. The aqueous solution of the potassium salt of VII was acidified to pH 3 with dilute hydrochloric acid. Since no oil was separated, the solution was extracted with ether repeatedly. The extract was then distilled, and the fraction boiling at 124~126°C/3 mmHg was collected. When this fraction was distilled two more times, 39.1 g. of pure β-formylpropionic acid ethylene acetal was given from 127 g.

of β-C.P.A.ethylene acetal (b. p. 114°C/1 mmHg). The yield was 26.8% of the theoretical amount. The acetal acid was a hygroscopic colorless liquid which solidified on standing at room temperature; m. p. 36°C.

Found: C, 49.07; H, 7.16. Calcd. for $C_6H_{10}O_4$: C, 49.31; H, 6.90%.

Neutralization equivalent. Found: 143.62. Calcd.: 146.14.

Adipic Dialdehyde Diethylene Acetal (VIII).—Forty-five grams (0.31 mol.) of β-formylpropionic acid ethylene acetal (VII) was electrolyzed in 130 ml. of methanol to which 1.7 g. (0.031 mol.) of potassium hydroxide had been added to neutralize about 10% of the total amount of acid used. The solution was placed in a cell consisting of a tall, flat-bottomed cylindrical, glass vessel fitted with a spiral-tube condenser, thermometer, and two parallel electrodes (platinum plate) (4×2.5 cm.), placed about 1~2 mm. apart. The cell was cooled by immersion in an ice-bath (internal temperature of cell, about 25~30°C), and a current of 5 amp. was passed through until the electrolyte became slightly alkaline. This usually required about 20% longer than the calculated time. At the end of the electrolysis, the solvent was removed and the residue diluted with 50 g. of water; the product was separated as an oil, which was extracted with ether and dried with anhydrous sodium sulfate. Distillation gave 12.1 g. of adipic dialdehyde diethylene acetal (b. p. 101~103°C/3 mmHg, yield 38.4%), which solidified upon being cooled in an refrigerator. Plates, m. p. 25~25.5°C.

Found: C, 59.11; H, 9.17. Calcd. for $C_{10}H_{18}O_4$: C, 59.39; H, 8.97%.

Besides, 4.1 g. of a colorless liquid was obtained as an unidentified by-product; b. p. 58~67°C/3 mmHg. VIII was mixed with the same amount of 3% hydrochloric acid and refluxed for one hour. After hydrolysis, the organic layer was extracted with ether and dried with anhydrous sodium sulfate. By distillation, adipic dialdehyde (IX) was obtained at a b. p. of 92~94°C/9 mmHg; yield ca. 95%. Bis-2,4-dinitrophenylhydrazone: m. p. 172~172.5°C (lit. m. p. 170°C).

Summary

A detailed study has been made of the synthesis of adipic dialdehyde starting from β-cyanopropionaldehyde. The hydrolysis of the acetal of this cyanoaldehyde gave β-formylpropionic acid acetal, to which Kolbe's electrolytic reaction was applied. The intermediate acetal acid has been successfully isolated in the case of ethylene acetal, whereas ethyl or butyl acetal decomposed by distillation into ethoxy- or butoxy-γ-butyrolactone, the structure of which has been established by analysis, infrared spectra and conversion to β-formylpropionic acid. Methyl acetal was also readily hydrolyzed to free aldehydic acid during the course of the isolation. Electrolysis of the ethylene acetal of β-formylpropionic acid in methanol gave adipic dialdehyde as its diethylene acetal.

The authors wish the thank Professor Yojiro Tsuzuki for his helpful advice and encouragement. Acknowledgment is also made to the Ajinomoto Co., Ltd., for a grant and for a supply of raw materials.

Department of Chemistry
Faculty of Science
Tokyo College of Science
Shinjuku-ku, Tokyo

The Thermal Decomposition of Ammonium Polymolybdates. II

By Eikoh MA

(Received December 11, 1963)

It was reported in a foregoing paper[1] that the weight-decrease curves and the ammonia evolution curves of ammonium dimolybdate, ammonium heptamolybdate, ammonium octamolybdate and ammonium trimolybdate are step-like. A certain crystal structure should correspond to each stage of these curves. The present paper, therefore, deals with the structural change in the process of thermal decomposition.

1) E. Ma, This Bulletin, 37, 171 (1964).

Experimental

Chemical Analysis.—The starting materials and their decomposition products were chemically analyzed; the quantity of molybdenum was determined by gravimetric analysis, using lead acetate, and that of ammonia, by the Kjeldhal method. The starting materials were found to be in agreement with these empirical formulae: $(NH_4)_2O \cdot 2MoO_3$ for dimolybdate, $3(NH_4)_2O \cdot 7MoO_3 \cdot 4H_2O$ for heptamolybdate, $2(NH_4)_2O \cdot 8MoO_3 \cdot 2H_2O$ for octamolybdate, and $(NH_4)_2O \cdot 3MoO_3 \cdot xH_2O$ for trimolybdate,

where x depends upon the condition of preparation.

Differential Thermal Analysis.—The differential thermal analysis was performed in air at a heating rate of 7~10°C/min. The reference junction of the differential couple was embedded in inert fused quartz. Fifty milligrams of the sample was sandwiched between two layers of about 300 mg. of the fused quartz in a platinum cell. The thermo-couple employed was alumel-chromel.

X-Ray Analysis.—The X-ray diffraction powder patterns were taken by a Guinier focussing camera using Cu$K\alpha$ radiation. The powder patterns of the starting materials were reported on in the foregoing paper.

Results and Discussion

As is usual with differential thermal analysis, the peaks indicate the temperature at which reaction actually ends. The beginning of the reaction corresponds to a cross-point of the straight-line parts of the base line and the relevant peak. Thermograms of ammonium hepta-, di-, octa- and trimolybdates are given in Fig. 1 for purposes of comparison. They give characteristic thermograms and exhibit good reproducibility. Three endothermic peaks are observed for ammonium heptamolybdate tetrahydrate, at 130, 245, and 355°C. Also, three endothermic peaks are observed for ammonium dimolybdate, at 225, 255 and 355°C. Two endothermic peaks are observed for ammonium octamolybdate dihydrate, at 287 and 377°C. Five endothermic peaks are observed for ammonium trimolybdate, at 98, 145, 200, 358, and 375°C. Two exothermic peaks are observed for the trimolybdate, at 255 and 425°C.

Ammonium Heptamolybdate Tetrahydrate.—The X-ray diffraction pattern of ammonium heptamolybdate tetrahydrate, Fig. 2a, does not change until 130°C, the first endothermic peak. At 130°C the crystal lattice of the heptamolybdate collapses, and a new, previously unknown structure appears (Fig. 2b). This structure, which will be called pattern A hereafter, is obtained in the temperature range from 130 to 245°C. The decomposition product corresponding to pattern A was identified as $2(NH_4)_2 \cdot O \cdot 5MoO_3$ through chemical analysis. At 245°C, the second endothermic peak, pattern A changes into another pattern which is identical with the pattern of octamolybdate (Fig. 2c). The octamolybdate is obtained in the temperature range from 245 to 355°C, and it is followed by the pattern of molybdenum trioxide above 355°C (Fig. 2d), which corresponds to the last endothermic peak.

A correlation of the differential thermal analysis curve, the weight decrease curve, and the deammoniation curve in the case of ammonium heptamolybdate tetrahydrate is shown in Fig. 3. The three endothermic peaks in the differential thermal analysis curve correspond to the stages in the weight decrease curve

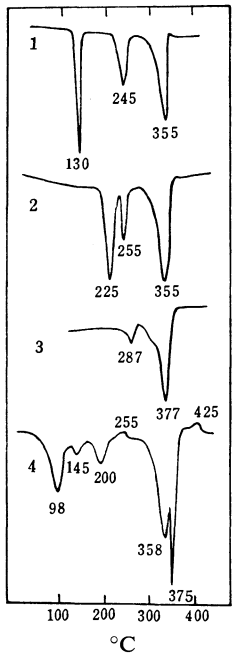


Fig. 1. Differential thermal analysis curves.
1) Ammonium heptamolybdate tetrahydrate
2) Ammonium dimolybdate
3) Ammonium octamolybdate dihydrate
4) Ammonium trimolybdate tetrahydrate

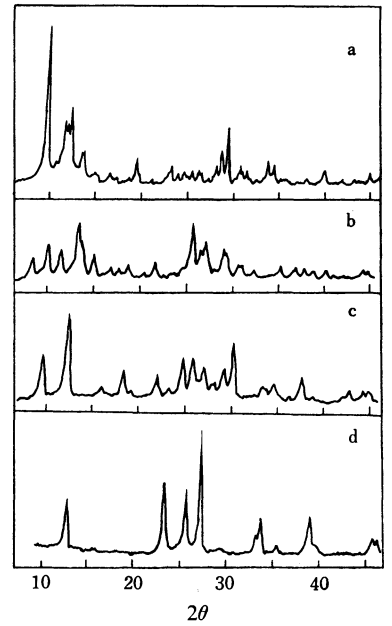


Fig. 2. X-Ray powder patterns.
a) Ammonium heptamolybdate tetrahydrate
b) Pattern A
c) Octamolybdate
d) Molybdenum trioxde

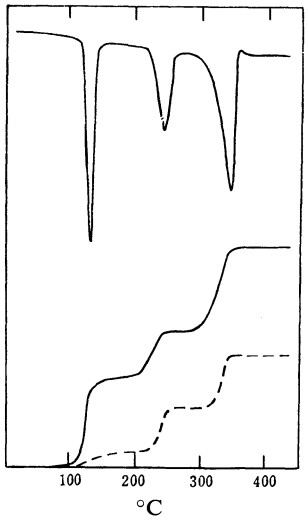


Fig. 3. Ammonium heptamolybdate tetrahydrate.

and in the deammoniation curve, and they are in good agreement. The endotherm at 130°C is referred principally to dehydration, which results in the structural change from ammonium heptamolybdate tetrahydrate to pattern A. Since dehydration does not proceed step-by-step in this case, and since most of the water is lost without resulting in any structural change, they may be regarded as of the zeolitic type. When, however, dehydration proceeds to completion, structural change does occur. The rest of the water, in consequence, must have an important role in constructing the crystal structure. The endotherm at 255°C corresponds to the deammoniation which results in the structural change from pattern A to octamolybdate. The endotherm at 355°C corresponds to the change from octamolybdate to molybdenum trioxide through further deammoniation.

Thus, ammonium heptamolybdate tetrahydrate changes upon heating in the following manner;

$$3(NH_4)_2O\cdot 7MoO_3\cdot 4H_2O \xrightarrow[115\sim130°C]{} 2(NH_4)_2O\cdot 5MoO_3 \xrightarrow[225\sim245°C]{} 2(NH_4)_2O\cdot 8MoO_3 \xrightarrow[320\sim355°C]{} MoO_3$$

The results obtained by previous authors are given below for the purpose of comparison:

Funaki:[2] $3(NH_4)_2O\cdot 7MoO_3\cdot 4H_2O \xrightarrow[110°C]{} 3(NH_4)_2O\cdot 7MoO_3 \xrightarrow[200°C]{} (NH_4)_2O\cdot 4MoO_3 \xrightarrow[280°C]{} MoO_3$

Duval:[3] $3(NH_4)_2O\cdot 7MoO_3\cdot 4H_2O \xrightarrow[50\sim90°C]{} 2(NH_4)_2O\cdot 5MoO_3 \xrightarrow[140\sim200°C]{} (NH_4)_2O\cdot 4MoO_3 \xrightarrow[270\sim340°C]{} MoO_3$

Hegedüs:[4] $3(NH_4)_2O\cdot 7MoO_3\cdot 4H_2O \xrightarrow[110\sim150°C]{} 2(NH_4)_2O\cdot 5MoO_3 \xrightarrow[210\sim255°C]{} (NH_4)_2O\cdot 4MoO_3 \xrightarrow[350\sim400°C]{} MoO_3$

Rode:[5] $5(NH_4)_2O\cdot 12MoO_3\cdot 12H_2O \xrightarrow[125°C]{} 5(NH_4)_2O\cdot 12MoO_3 \xrightarrow[220°C]{} 2(NH_4)_2O\cdot 5MoO_3 \xrightarrow[250\sim265°C]{} (NH_4)_2O\cdot 4MoO_3 \xrightarrow[320\sim370°C]{} MoO_3$

Ammonium Dimolybdate. — In the case of ammonium dimolybdate, the room temperature pattern, Fig. 4a, is preserved until 225°C, the first endothermic peak, and is transformed into a previously unknown structure which has a narrow stability range of 225~255°C. The powder pattern of the structure will be called pattern B. At 225°C, the second endothermic peak, another structure begins to appear; this structure is crystallographically identical with the octamolybdate, Fig. 4c. The pattern of

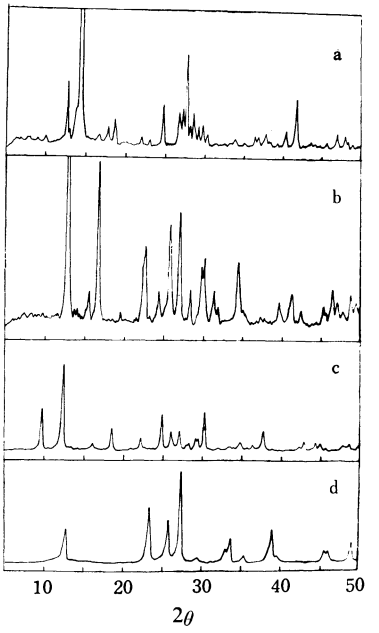


Fig. 4. X-Ray powder patterns.
a) Ammonium dimolybdate
b) Pattern B
c) Octamolybdate
d) Molybdenum trioxide

2) K. Funaki and T. Segawa, *J. Electrochem. Soc. Japan (Nippon Denkikagaku Zasshi)*, **18**, 152 (1950).
3) C. Duval, "Inorganic Thermogravimetric Analysis," Elsevier, Amsterdam (1953), p. 332.
4) A. J. Hegedüs, K. Sasvari and J. Neugebauer, *Z. anorg. u. allgem. Chem.*, **293**, 56 (1957).
5) E. Ya. Rode and V. N. Tverdokhlebov, *Zhur. Neorg. Khim.*, **3**, 2343 (1958).

the octamolybdate is observed in the temperature range from 255 to 335°C and is followed by the pattern of molybdenum trioxide above 355°C, the last endothermic peak (Fig. 4d).

A correlation of the differential thermal analysis curve, the weight decrease curve and the deammoniation curve is shown in Fig. 5. The inflection around 225°C in the weight decrease curve is indicative of a decomposition product with a narrow stability range. Deammoniation until the inflection gives rise to the first endothermic peak at 225°C. The second endothermic peak is, therefore, due to deammoniation from the inflection to the plateau. The plateau in the weight decrease curve between 250 and 320°C corresponds to the octamolybdate. The endotherm at 355°C corresponds to further deammoniation, which results in the change from the octamolybdate to molybdenum trioxide.

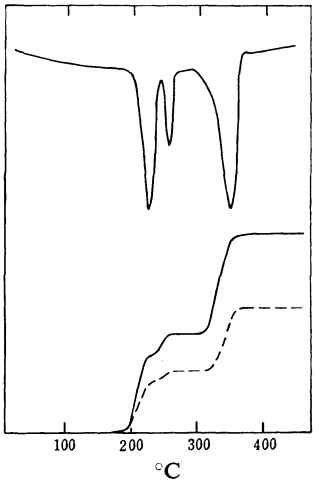


Fig. 5. Ammonium dimolybdate.

Ammonium Octamolybdate. — Figure 6 shows thermograms of three sorts of ammonium octamolybdates of different origins. Figure 6a is octamolybdate dihydrate from an aqueous solution, Fig. 6b is anhydrous ammonium octamolybdate prepared through the calcination of ammonium heptamolybdate tetrahydrate, and Fig. 6c is one prepared through the calcination of ammonium trimolybdate. These three octamolybdates, notwithstanding their non-coincidence in thermogram, give the same X-ray powder pattern as well as the same mole ratio of $(NH_4)_2O : MoO_3 = 1 : 4$ upon chemical analysis. All the octamolybdates change into molybdenum trioxide around 370°C, at the strong endothermic peak. A correlation of the differential thermal analysis curve, the weight decrease curve and the deammoniation

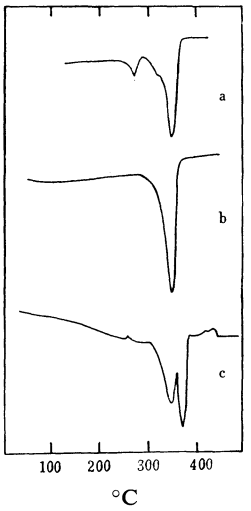


Fig. 6. Differential thermal analysis curves of ammonium octamolybdates.

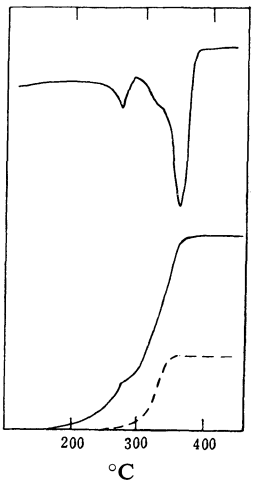


Fig. 7. Ammonium octamolybdate dihydrate.

curve of ammonium octamolybdate dihydrate is shown in Fig. 7. The endotherm at 287°C is referred mainly to dehydration, which results in no structural change. It is an outstanding feature of the octamolybdate that no endotherm which can be referred to dehydration appears around 100°C. Accordingly, the water of crystallization in this case must be of a different character from that in the case of heptamolybdate. As one of five water molecules of copper sulfate pentahydrate is held up to 250°C, so the water molecules in the case of the octamolybdate must be tenaciously held through the hydrogen bond.

Ammonium Trimolybdate.—The existence of the trimolybdate as a chemical species has not yet been confirmed. Lindqvist has suggested

the possibility that the trimolybdate is actually double-salts of hepta- and octamolybdates.[6] The X-ray examination of a sample with the chemical composition of trimolybdate illustrates that octamolybdate is predominant and that a previously unidentified pattern exists as an auxiliary part instead of the heptamolybdate. The trimolybdate has been found to change into an intermediate molybdate, $(NH_4)_2O \cdot 3.5MoO_3$, after two months of standing still and into the octamolybdate after another half-year. The auxiliary part in the powder pattern also definitely diminished in strength after two months, finally disappearing in half a year. Therefore, the starting material might have included some volatile ammonium molybdate, the normal ammonium molybdate, for instance. The first and second endothermic peaks, at 99°C and 146°C are due to dehydration. The powder pattern of the trimolybdate does not change until 200°C, the third endothermic peak, above which the pattern becomes exclusively that of the octamolybdate. The exothermic peak at 255°C is due to the crystallization of the octamolybdate. The last endothermic peak is resolved into two maxima. Above 358°C, the first maximum, molybdenum trioxide is produced, while the octamolybdate is still predominant. Above 375°C, the second maximum, the molybdenum trioxide becomes predominant and the octamolybdate, auxiliary. Above 425°C, the exothermic peak which corresponds to the crystallization of the molybdenum trioxide, the formation of the molybdenum trioxide is complete. A correlation of the differential thermal analysis curve, the weight decrease curve and the deammoniation curve of the ammonium trimolybdate is shown in Fig. 8.

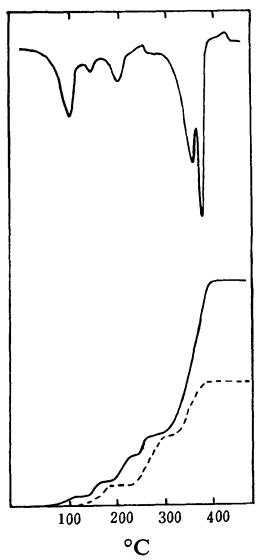


Fig. 8. Ammonium trimolybdate.

Change of Color.—The color of the final decomposition product obtained in air is yellow above 350°C and pale grey-green when cooled to room temperature, while that of the final product in vacuo is purple-black, and this does not change when the product is cooled to room temperature. In respect to the color change during the thermal decomposition, there is little difference among various kinds of polymolybdates. The X-ray investigation revealed that the purple-black oxide is a mixture of MoO_3, Mo_8O_{23}, Mo_9O_{26}, and Mo_4O_{11}, as has been reported in the foregoing paper.[7] The purple-black color may be referred to an oxygen deficiency. When the purple-black oxide, the decomposition product in vacuo, was heated again in air, it became yellow above 350°C, and a slight increase in weight was observed. The change of color in air and in vacuo is given in Tables I and II.

Table I. Change of color in air

100°C	200°C	300°C	400°C	500°C
White	Light grey-green	Yellow green	Yellow	Golden yellow

Table II. Change of color in vacuo

20°C	70°C	100°C	200°C	250°
White	Light green	Yellow green	Dark yellow-green	Purple-black

Summary

The thermal decomposition of ammonium di-, hepta-, tri- and octamolybdates has been investigated by means of differential thermal analysis, chemical analysis, and X-ray diffraction techniques. The steps of the decomposition may be described as follows:

Heptamolybdate

$$3(NH_4)_2O \cdot 7MoO_3 \cdot 4H_2O \xrightarrow[130°C]{} 2(NH_4)_2O \cdot 5MoO_3 \xrightarrow[245°C]{} 2(NH_4)_2O \cdot 8MoO_3 \xrightarrow[360°C]{} MoO_3$$

Dimolybdate

$$(NH_4)_2O \cdot 2MoO_3 \xrightarrow[226°C]{} (NH_4)_2O \cdot 3MoO_3 \xrightarrow[225°C]{} 2(NH_4)_2O \cdot 8MoO_3 \xrightarrow[360°C]{} MoO_3$$

Octamolybdate

$$2(NH_4)_2O \cdot 8MoO_3 \cdot 2H_2O \xrightarrow[287°C]{} 2(NH_4)_2O \cdot 8MoO_3 \xrightarrow[370°C]{} MoO_3$$

6) I. Lindqvist, *Nova Acta Reg. Soc. Sci. Upsal., Ser. IV*, 15, 7 (1950).

7) Cf. Ref. 1.

Trimolybdate

$$(NH_4)_2O \cdot 3MoO_3 \cdot xH_2O \xrightarrow{200°C} 2(NH_4)_2O \cdot 8MoO_3 \xrightarrow{370°C} MoO_3$$

The author wishes to express his deep gratitude to Professor Kumasaburo Kodera and to Professor Sukeji Kachi of Kyoto University for their continued interest in this investigation and for their valuable suggestions. He is also greatly indebted to Dr. Minoru Ozasa of the Matsushita Electronics Corporation for courtesies extended to him and for fruitful discussions.

Department of Chemistry
Faculty of Science
Kyoto University
Sakyo-ku, Kyoto

Synthetic Ammonia Iron Catalysts Containing Magnesia as Its Principal Promoter. I. The Catalysts' Performances[1]

By Hiroshi UCHIDA, Iwao TERAO[2] and Kiyoshi OGAWA

(Received December 12, 1963)

Although the literature contains a few descriptions[3-6] of the synthetic ammonia iron catalysts of the magnesia-promoted type, nothing decisive has ever been reported about the catalysts' performances in relation to the promoter compositions. The present investigation has been undertaken in an attempt to ascertain the kinds and amounts of promoters which are most effective in producing a practicable catalyst of this type. The experimental results here obtained will be able to shed some light on the roles played by the individual promoters.

Experimental

The synthesis gas of $3H_2$-$1N_2$ was compressed into a gas storage vessel (40 l.) and then introduced into another, smaller one (2.5 l.) in which the pressure was automatically controlled at about 110 kg./cm^2 gauge. It was then led, through a needle valve and a high pressure gas flowmeter, into a gas purification train at the fixed pressure of 100 kg./cm^2 gauge. The purification train consisted of a hot nickel-on-kieselguhr plus palladium asbestos deoxidizer, a water cooler, a condenser, and an activated-alumina tower. The gas feed from the train was conducted into a reactor for the ammonia synthesis.

Figure 1 is a simplified diagram of the reactor and its internal parts. The reactor was somewhat different in design from the one which had been used in our previous works (e.g.[7]). An amount (3 cc. in volume, 7.46~7.54 g. depending upon the kinds of catalyst samples) of a granular catalyst was packed into the annular space between the

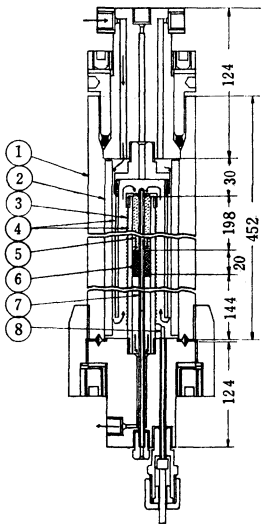


Fig. 1. Reactor for ammonia synthesis.

1 Outer shell 88 mm. O. D. 60 mm. I. D.
2 Quartz tube
3 Heating wire
4 Copper tubes
5 Copper chips
6 Catalyst bed
7 Thermocouple protection tube
8 Lead for heater

1) This paper is the 15th in a series of articles dealing with the synthetic ammonia iron catalysts.
2) Present address: Japan Gas Chemical Co., Enokicho, Niigata.
3) "Ullmanns Encyklopaedie der technischen Chemie," Bd. III, Urban & Schwarzenberg, Muenchen-Berlin (1953), p. 588.
4) W. K. Hall, H. Tarn and R. B. Anderson, *J. Am. Chem. Soc.*, **72**, 5436 (1950).
5) C. Bokhoven, C. van Heerden, R. Westrik and P. Zwieterung, "Catalysis," Vol. III, Reinhold Publ. Corp., N. Y. (1955), p. 265.
6) D. G. Ivanov and N. D. Anastav, *Chem. Tech.*, **15**, 229 (1963).
7) H. Uchida and M. Kuraishi, This Bulletin, **28**, 106 (1955).

inner wall of a copper tube and the outer wall of a thermocouple protection tube to form a bed (14.4 mm. O. D. and 4 mm. I. D. by 20 mm. high) which was supported on a perforated stainless steel plate. Caution was paid to decrease the axial temperature gradient along the bed. An electric heating wire was wound more closely near the top and the bottom of copper tube, and the whole space above the bed in the tube was filled with copper chips to preheat the synthesis gas to a temperature as close to the bed temperature as possible. The axial temperature profile was measured by means of moving a thermocouple in the protection tube (4 mm. O. D. and 2 mm. I. D.). Throughout all the synthesis runs, the axial temperature difference remained within 2°C. The arrows in the figure indicate the movements of the gas flow in the reactor. The synthesis runs were conducted at several temperatures in the range between 300 and 500°C at a fixed pressure of 100 kg./cm^2 gauge and at a fixed gas flow rate of 5000 ± 50 hr^{-1} in terms of space velocity measured on the basis of the exit gas from the reactor. The exit gas was analyzed for ammonia in the same way as has been stated previously[7] and was metered. Plots of the ammonia concentration in the exit gas vs. the reaction temperature for individual catalysts give their relative activities for the ammonia synthesis.

The catalysts were prepared by a fusion process in a manner which has been reported elsewhere,[8] starting with a mixture of powders of electrolytic iron supplied by the Showa Denko Co. and promoter materials of the E. P. grade. Lumps of the finished catalysts were crushed, and granules 1.0~1.5 mm. in size were used. The bed of granular catalysts was reduced at 440°C in a current of the synthesis gas at 100 kg./cm^2 gauge at gas flow rates ranging from 1×10^4 to 2×10^4 hr^{-1}. The reduction was continued until no more increase in the ammonia concentration was observed at the temperature of 425°C and at the gas flow rate of 5000 hr^{-1} after successive six-hour periods of reduction.

After the afore-mentioned synthesis runs had been finished, the catalysts were heated at 650°C for five hours in a current of the synthesis gas at atmospheric pressure, and then the synthesis runs were repeated in the same way as before. The change in the ammonia concentration before and after the heat treatment gives a measure of the thermal stabilities of the catalysts.

With a view to calculating the specific activity constant, which corresponds to the specific activity per unit of the catalyst surface area, from the results of the activity measurement, the bed density and the specific surface area of the catalyst sample after the run were determined. The bed density was determined by weighing the catalyst sample, for the bed volume is not changed by the synthesis run. The specific surface area was determined by applying the BET equation to the nitrogen adsorption isotherm at −196°C. It should be noticed that, in general, the surface area determination was made on the catalyst samples after runs at temperatures below 500°C, but that in some special cases where the activity was increased by the heat treatment of the reduced catalyst at 650°C, the determination was made on the catalyst samples after the thermal stability test.

The catalysts in the present investigation seemed more likely to be reduced easily than the catalysts of the alumina-promoted type. In this connection, the increase in the ammonia concentration with the time of reduction was examined in catalysts of particular interest. The catalyst was heated up to 440°C in four hours according to a predetermined schedule at the pressure and at the gas flow rate of the synthesis conditions; it was then kept at this condition until the ammonia concentration in the exit gas became constant.

Results

Catalytic Activity and Thermal Stability.— The activity measurements made on the individual catalysts of different promoter compositions are illustrated in Figs. 2, 3 and 4 as plots of the ammonia concentration in the exit gas vs. the reaction temperature. The promoter compositions, which are summarized in Table I, are expressed in the weight percentages of promoters in the oxide catalysts, on the basis of the exact oxidation of iron to Fe_3O_4. The expression is a conventional one, for the oxidation does not always proceed to, or stop at, the Fe_3O_4 stage, and the ratios between ferrous and ferric irons of the oxide preparations usually show deviations from the 0.5 that corresponds to Fe_3O_4, as the table shows. On the other hand, the expression is rather convenient for defining the promoter composition from the point of view of practical catalyst-manufacturing. To express the promoter composition in the strict sense of the word, the numerals in the table can be corrected by taking the respective ratios into

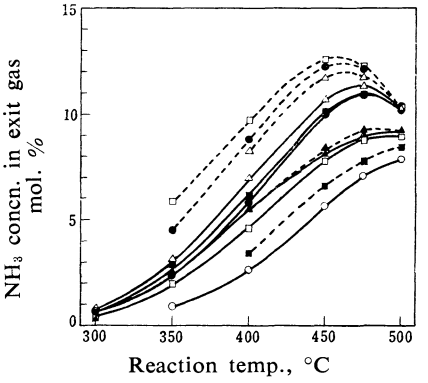


Fig. 2. Activity measurement. I.

Full line, the activity after reduction at 440°C.
Dotted line, the activity after treatment at 650°C for 5 hr.
○ Cat. M-0 ● Cat. M-1 △ Cat. M-2
▲ Cat. M-3 □ Cat. M-5 ■ Cat. M-6

8) G. Shima and H. Uchida, *Rpt. Gov't. Chem. Ind. Research Inst. Tokyo*, **45**, 369 (1950).

TABLE I. PROMOTER COMPOSITION, RATIO OF Fe^{II}/Fe^{III}, BED DENSITY, AND SPECIFIC SURFACE AREA

Catalyst	Promoter composition wt. %	Fe^{II}/Fe^{III}	Bed density g./cc.	Specific surface area $m^2/g.$
M-0	Unpromoted	0.419	1.91	1.15
M-1	2MgO	0.710	1.89	3.02
M-2	5MgO	0.646	1.90	5.57
M-3	5MgO, $1K_2O$	0.545	1.93	1.05
M-4	4MgO, 1CaO	0.611	1.96	4.63
M-5	4MgO, $1SiO_2$	0.674	1.84	12.00
M-7	2MgO, $1SiO_2$, $1K_2O$	0.535	1.95	4.67
M-8	4MgO, $1SiO_2$, $1K_2O$	0.568	1.86	9.37
M-9	4MgO, $1SiO_2$, $0.5K_2O$	0.547	1.96	8.61
M-10	4MgO, $2SiO_2$, $1K_2O$	0.538	1.94	9.12
M-11	4MgO, $0.5SiO_2$, $1K_2O$	0.509	1.91	5.88
M-12	4MgO, $1SiO_2$, $2K_2O$	0.502	1.90	4.44
M-14	2MgO, $1SiO_2$, $1Al_2O_3$, $1K_2O$	0.537	1.89	7.88
A-102	$2Al_2O_3$, 1CaO, $1K_2O$	0.405	1.87	6.76

The bed density and specific surface area refer to the catalyst samples after use in the synthesis runs.

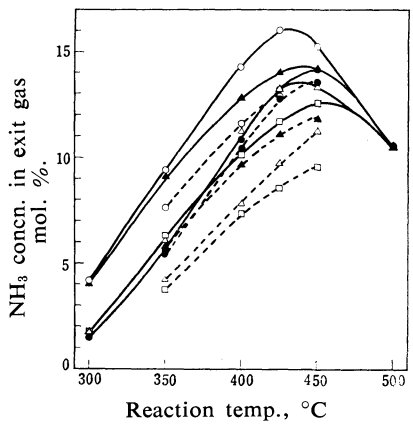


Fig. 3. Activity measurement. II.

Full line, the activity after reduction at 440°C.
Dotted line, the activity after treatment at 650°C for 5 hr.

○ Cat. M-8 ● Cat. M-9 △ Cat. M-10
▲ Cat. M-11 □ Cat. M-12

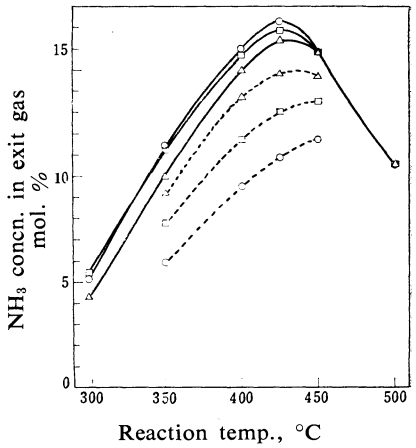


Fig. 4. Activity measurement. III.

Full line, the activity after reduction at 440°C.
Dotted line, the activity after treatment at 650°C for 5 hr.

○ Cat. M-7 △ Cat. M-14 □ Cat. A-102

account. The figures include the thermal stability measurements for the individual catalysts also.

Figure 2 indicates the results on the catalysts, including an unpromoted one (cat. M-0), a couple of magnesia-promoted ones (cats. M-1 and -2), and three doubly-promoted ones, containing potash, lime, and silica (cats. M-3, -4 and -5 respectively) as the second promoter. After reduction, the magnesia-promoted catalysts give essentially the same activity as an alumina-promoted catalyst.[9] A remarkable difference between the above two catalysts, however, appears in their activities after heat treatment at 650°C; the activities of the magnesia-promoted catalyst becomes greater after the heat treatment, whereas that of the alumina-promoted catalyst decreases somewhat (cf.[10]). The increased activity after the heat treatment of the former catalyst stays at the same level, even after prolonged heat treatment for the succeeding five hours, thus demonstrating its excellent thermal stability. Both potash and lime act not as promoters but as moderately effective inactivators (cf. the results on cats. M-3 and -4) insofar as the activities

9) H. Uchida and N. Todo, *J. Chem. Soc. Japan, Ind. Chem. Sec.* (*Kogyo Kagaku Zassi*), **60**, 1235 (1957).

10) H. Uchida, *Rpt. Gov't. Chem. Ind. Research Inst. Tokyo*, **46**, 1 (1951).

after reduction are concerned. Of the above two catalysts, only the one containing lime as the second promoter shows an increase in the activity after the heat treatment at 650°C to such a high level as to be comparable with that after the reduction of a catalyst doubly-promoted by alumina and potash.[9] No such phenomenon was observed in the case of the corresponding catalyst of the alumina-promoted type. Silica added as the second promoter has an unfavorable effect on the thermal stability but has little effect on the activity after reduction.

Figure 3 shows the results on a series of triply-promoted catalysts containing varying amounts of silica and potash with a fixed amount of magnesia (4%). The activities of the triply-promoted catalysts can be much higher than those of the doubly-promoted ones, provided that the added amounts of silica and potash are appropriate. Among the three catalysts (cats. M-8, -10, and -11) with the same magnesia (4%) and potash (1%) content, the catalyst with 1% silica (cat. M-8) exhibits a higher activity than any of the catalysts with 0.5% (cat. M-11) and 2% silica (cat. M-10). Moreover, the activity of the catalyst M-10 with a greater silica content, or with a higher ratio of potash to silica, is apt to descend more rapidly with the lowering of the reaction temperature than do the activities of the catalysts with smaller contents, or with lower ratios. This is also the case for the two catalysts with the same magnesia and silica content but with different amounts of potash (cf. cats. M-9 and -12). Of all the triply-promoted catalysts under investigation, a catalyst (cat. M-7) with a minor magnesia content (2%) and with the same content of silica and potash as that of cat. M-8 gives the highest activity, as is shown in a separate figure of Fig. 4. Unfortunately, the highly active catalysts here obtained have poor thermal stability, the catalyst of the highest activity being the poorest.

Triply-promoted catalysts containing alumina, potash, and lime are in current use in industrial ammonia synthesis. One such catalyst (cat. A-102) is compared with one of the present triply-promoted catalysts (e.g. cat. M-7) for activity and for thermal stability in Fig. 4. The former catalyst exhibits a little more activity than does the latter one, with nearly the same thermal stability. The poor thermal stability of cat. M-7 can be improved by the further addition of a small amount of alumina, accompanying a small decrease in the activity (cf. the plot of cat. M-14).

Bed Density and Specific Surface Area.—The results are summarized in Table I. The bed densities are in a narrow range from 1.84 to 1.96 (g./cc.). As regards the present catalysts, the bed densities may be considered to be of a constant value without bringing about any serious errors in the discussion of the promoters' effects on the catalyst performances. A brief outline of the promoters' effects on the change in the specific surface area of the iron catalysts can be obtained from the data in the table. A detailed description will, however, be made in the next chapter in connection with their contributions to the activities of the individual catalysts.

Reduction of the Catalysts.—The results concerning the five kinds of catalysts, an unpromoted catalyst (cat. M-0), a magnesia-promoted catalyst (cat. M-1), two triply-promoted catalysts of different principal promoters (cats. M-7 and A-102), and a quadruply-promoted catalyst containing magnesia, alumina, potash, and silica (cat. M-14), are illustrated in Fig. 5 as the

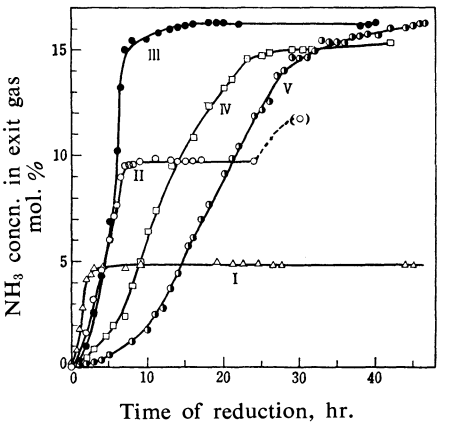


Fig. 5. Increase in ammonia concentration with time of reduction.
Reduction temp., 440°C. ○ in parenthesis indicates the activity after treatment at 650°C for 5 hr.
△ Cat. M-0 (I) ○ Cat. M-1 (II)
● Cat. M-7 (III) □ Cat. M-14 (IV)
◑ Cat. A-102 (V)

plots of the ammonia concentration in the exit gas vs. the reduction time. It is almost certain that the increase in the ammonia concentration runs parallel to the extent of reduction except for the final stage, where the removal of the last traces of oxygen causes a considerable increase in the activity.

The results disclose that the addition of magnesia serves to retard the reduction rate of a magnetite only to a very small extent (compare curve I with curve II), whereas the reduction rate is greatly reduced in the presence of alumina (compare curves IV and V with curve II). Potash and silica, when simultaneously added in addition to magnesia,

seemingly have no effect on the rduction rate at the earlier stage, but they have the effect of enabling the resulting catalyst to be reduced more easily toward the end of the reduction (compare curve II with curve III[11]).

Discussion

Rate Constant and Specific Activity Constant. —A quantitative comparison of the catalyst activities at a fixed temperature can be made in terms of the rate constant, k, of the ammonia synthesis reaction. In this paper, k is calculated by the aid of the expression derived from the Temkin-Pyzhev rate equation:

$$k=\left(\frac{\nu_{H_2}{}^{3/2}}{\nu_{NH_3}}\right)P^{1/2}\cdot SV_0\int_0^z \frac{z(1-z)^{3/2}\,dz}{(1+z)^2\{L^2(1-z)^4-z^2\}} \quad (1)$$

where

$$k=273(3/4)^{-3/2}k_2 \quad (2)$$

and

$$L^2=z_{eq}/(1-z_{eq}) \quad (3)$$

In the above equations, ν is the fugacity coefficient, P (atm. abs.) is the total pressure, SV_0 (hr^{-1}) is the space velocity based on the inlet gas,[12] R (atm. m^3/mol. °K) is the gas constant, and k_2 is the rate constant of the reverse reaction. It should be noticed that k ($atm^{0.5}\,hr^{-1}$) is based on the unit bed volume. Table II lists the values of k at 400°C with the various individual catalysts. Unless otherwise stated, k in this paper will hereafter denote the rate constant at this temperature. On the assumption that the entire catalyst surface is available to the catalytic reaction, the specific rate constant, k', ($atm^{0.5}$ cc./hr. m^2) at 400°C is then calculable from the relation of

$$k=k'\rho S \quad (4)$$

where ρ (g./cc.) is the bed density[13] and where S(m^2/g.) is the specific surface area of the catalyst after use in the synthesis run. In view of the findings of Bokhoven et al.,[14] who calculated the effectiveness factor, i. e., the ratio of the experimental rate constant in the absence of retardation due to diffusion effects in pores of the catalyst, and in view of previous activity measurements by other investigators, the assumption seems to be reasonably applicable to the present results at 400°C. The values of k' thus calculated are summarized in Table II. On the basis of the data available on the k' as well as on the S values of the individual catalysts, a better insight into the promoter effects on the activity or k can be obtained.

Magnesia as a promoter contributes to the increase in k' as well as to the establishment and stabilization of a large S. The smaller amount of 2 wt. % in the oxide catalyst is preferred because the greater amount of 5 wt. % accompanies such a considerable decrease in k' as to result in the smaller k, even though S becomes larger to a small extent. Potash, as the second promoter, increases k' to a certain degree, but it reduces S to so extremely small a value that its effect on k is rather unfavorable. As it is, the effect of potash addition on k appears to be of the opposite kind to that with the catalyst of the alumina-promoted type. Lime as the second promoter has little effect on S, but it contributes to the increase in k', and, as a result, the higher k is established. Silica as the second promoter behaves in a peculiar way; while it is remarkably effective in producing a large S, it reduces k' to such a low level as to be below that of a pure iron catalyst.

In view of the information just obtained on the promoting action of potash and silica, an attempt will be made to interpret the high activity that appears with a few of the present triply-promoted catalysts. Figure 6 gives plots of k, S and k' as a function of the ratio of K_2O/SiO_2, with respect to the series of catalysts containing different amounts of potash

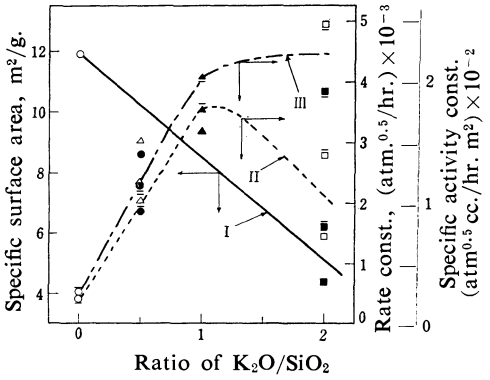


Fig. 6. Specific surface area (I), rate constant (II), and specific activity constant (III) as function of ratio between contents of potash and silica in weight percentage.
Upper barred mark, rate constant: Under barred mark, specific activity constant.
○ Cat. M-5 ▲ Cat. M-8 ● Cat. M-9
△ Cat. M-10 □ Cat. M-11 ■ Cat. M-12

11) The final activity was a little low as compared with the activity in the synthesis run. This catalyst of particularly poor thermal stability may have exhibited lower activity because of the lower gas flow rate during the reduction process.
12) SV_0 is given by $SV_0=SV_z(1+z)$, where SV_z is the space velocity based on the exit gas.
13) In the present discussion, ρ requires little consideration, since it remains almost constant for all the catalysts.
14) C. Bokhoven and W. van Raayen, *J. Phys. Chem.*, **48**, 471 (1954).

TABLE II. RATE CONSTANT (k), SPECIFIC RATE CONSTANT (k') AT 400°C, ACTIVATION ENERGY FOR AMMONIA DECOMPOSITION (E), FREQUENCY FACTOR (A), AND FREQUENCY FACTOR PER UNIT OF CATALYST SURFACE AREA (A')

Catalyst	k $atm^{0.5}/hr.$	k' $atm^{0.5}$ cc./hr. m^2	E kcal./mol.	A $atm^{0.5}/hr.$	A' $atm^{0.5}$ cc./hr.m^2
M-0	9.18×10	0.42×10^2	56	1.2×10^{20}	5.5×10^{19}
M-1	1.15×10^3	2.01×10^2	45	5.9×10^{17}	1.0×10^{17}
M-2	1.05×10^3	0.99×10^2	44	1.4×10^{17}	1.3×10^{16}
M-3	4.25×10^2	2.10×10^2	44	5.7×10^{16}	2.8×10^{16}
M-4	1.54×10^3	1.70×10^2	42	5.1×10^{16}	5.6×10^{15}
M-5	5.38×10^2	0.24×10^2	48	1.5×10^{18}	7.0×10^{16}
M-7	4.71×10^2	5.18×10^2	41	7.7×10^{16}	8.5×10^{15}
M-8	3.57×10^3	2.05×10^2	44	4.8×10^{17}	2.7×10^{16}
M-9	1.91×10^3	1.15×10^2	46	1.4×10^{18}	8.4×10^{16}
M-10	2.08×10^3	1.18×10^2	45	7.3×10^{17}	4.1×10^{16}
M-11	2.78×10^3	2.48×10^2	39	1.2×10^{16}	1.1×10^{15}
M-12	1.62×10^3	1.92×10^2	41	3.9×10^{16}	4.6×10^{15}
M-14	4.01×10^3	2.69×10^2	41	9.6×10^{16}	6.4×10^{15}
A-102	4.57×10^3	3.61×10^2	39	2.8×10^{16}	2.2×10^{15}

and silica, besides a fixed amount of magnesia. In the figure, k' rises rapidly with the ratio at first but much more slowly beyond a ratio of ca. 1, whereas S descends almost linearly as the ratio rises. Accordingly, the high activity, or the high value of k, in the intermediate range of the ratio may be ascribed to a sufficiently high k' and a moderately large S.

Activation Energy and Frequency Factor. — The substitution of Arrhenius equation with reference to k' into Eq. 4 results in the following expression of k:

$$k=k'\rho S=A'\exp(-E/RT)\rho S \qquad (5)$$

where E (kcal./mol.) as defined by Eq. 2 stands for the activation energy of ammonia decomposition, and A' ($atm^{0.5}$ cc./hr. m^2) is the frequency factor per unit of the catalyst surface area, namely, $A'=A/\rho S$. Accordingly, the catalyst activity at a reaction temperature of T (°K) is expressed as a function of A', E, ρ, and S, which are parameters independent of the reaction temperature, T. and E and A' were determined from the Arrhenius plot of k' between 300 and 425°C. The results are summarized in Table II. A rough examination of the table shows that both E and A' change in the same direction as the promoter compositions are changed, both of them being highest with the unpromoted catalyst and lowest with one of the triply-promoted catalysts (cat. M-11).

Since the activity measurements were made mainly on the catalysts promoted doubly and triply, the effects of individual promoters on the change of E and A' can not be clarified separately. However, within certain limits, it is possible to say that magnesia, potash, and lime act similarly to reduce E and A', whereas the situation is the reverse with silica. The differences in effects on E and A' between potash and silica can be seen in a more concrete way from the findings available on the series of triply-promoted catalysts containing varying amounts of potash and silica besides a fixed amount of magnesia. In this connection, Fig. 7 shows the plots of E and A' as a

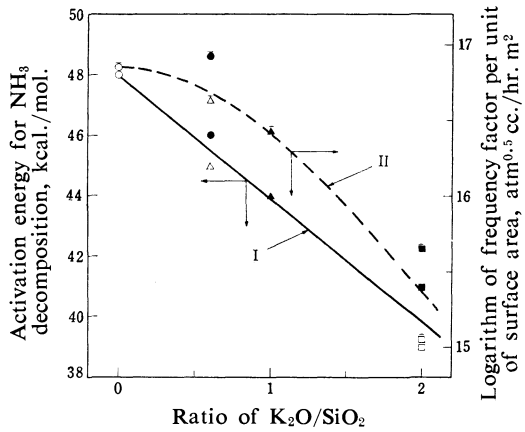


Fig. 7. Activation energy (I) and logarithm of frequency factor per unit of surface area (II) as function of ratio between contents of potash and silica in weight percentage.
Symbol with bar to the top: Frequency factor per unit of surface area.
◑ Cat. M-5 ▲ Cat. M-8 ● Cat. M-9
△ Cat. M-10 □ Cat. M-11 ■ Cat. M-12

function of the ratio of K_2O/SiO_2. Both E and A' tend to diminish almost linearly with the ratio. Further, the highest value of k' is found at the highest ratio, at which E and A' are lowest (cf. the plot III in the figure). This, however, does not necessarily mean that silica is useless as a promoter, for the large S that contributes to the establishment of a high k does not develop until the catalyst contains

some silica.

Reduction Rate and Catalyst Activity. — Kobosev[15] stated that magnesia added as a promoter to a ferrous oxide had rather an accelerating effect on the reduction rate and that it was not at all effective in increasing the catalyst activity. The above statement differs from the present results; the addition to a magnetite does retard the reduction rate, even though to a very small extent, and between the two series that of catalysts containing magnesia as the principal promoter and that of catalysts containing alumina as the principal promoter, no essential differences appear in their activities notwithstanding the fact that their reduction rates differ greatly. A triply-promoted catalyst belonging to either one of the two series can, similarly, be highly active provided appropriate kinds and amounts of promoters are added. Moreover, nothing remarkably different between the two series is recognizable with respect to the factors of S, k', E and A'. Accordingly, the generally accepted opinion (cf.[5]) that oxides which greatly retard the reduction rate are good promoters can not always be true.

Summary

A catalyst promoted singly by magnesia can be as active as one promoted singly by alumina. The activity of the former catalyst is increased by a succeeding reduction at 650°C to a higher level; the increased level is preserved even after the prolonged heating at this temperature. Potash, lime, and silica added as second promoters behave in their respective peculiar manners. Among the catalysts under investigation, a triply-promoted catalyst performs in nearly the same way as one of the catalysts of the alumina-promoted type in current use in industrial ammonia synthesis, provided the amounts of such kinds of promoters as magnesia, potash, and silica are appropriate.

The activity or the rate constant is expressed as a function of the temperature-independent parameters, which are the bed density, the specific surface area, activation energy, the frequency factor per unit of the catalyst surface area, and the reaction temperature. The effects of individual promoters have been discussed in view of the changes in magnitude of each parameter which result from their additions.

The catalysts of the magnesia-promoted type can be reduced much more easily than the catalysts of the alumina-promoted, type, but the reduction rate is only a little below that of the unpromoted catalyst.

Government Chemical Industrial Research Institute, Tokyo
Shibuya-ku, Tokyo

15) N. I. Kobosev, *Acta. Physicochim. U.R.S.S.*, **4**, 829 (1936).

A Note on the Solid Chemisty of the NiO-Li_2O Solid Solution

By Yoshio IIDA and Naoyoshi HAYASHI

(Received December 19, 1963)

Verwey[1] found that an oxide contains a higher or lower valency in its crystal when foreign atoms with, respectively, a lower or a higher valence than the cation of oxide are dissolved in the oxide. From a consideration of the formation of a higher or lower valency of the cations, he successfully explained the electrical conductivity of oxides incorporating foreign atoms with a different valence in terms of the cation of the oxide. This finding is known as the valency control principle. According to the principle, nickel oxide should have x atoms of Ni^{3+} ions to satisfy the electrical neutrality of the crystal when x atoms of Li^+ are dissolved in nickel oxide. The high electrical conductivity of the NiO-Li_2O solution is attributed to the formation of Ni^{3+}. Accordingly, the molecular formula of nickel oxide containing lithium oxide may be expressed by $Ni_{1-2x}{}^{2+}\ Li_x{}^+\ Ni_x{}^{3+}\ O$. However, it seems to be questionable that the number of Ni^{3+} ions is the same as that of Li^+ ions dissolved. Johnston and Heikes[2] did not refer to Mn^{3+} in their report on the

1) E. J. W. Verwey, P, W. Haayman, F. G. Romeyn and G. W. Van Oosterhout, *Philips Res. Rep.*, 5, 173 (1950).

2) W. D. Johnston and R. R. Heikes, *J. Am. Chem. Soc.*, **78**, 3255 (1956).

MnO-Li_2O system. There has also been no report dealing with the relation between Li^+ and Ni^{3+} in the NiO-Li_2O solid solution.

The present study has been undertaken to clarify the question and to measure the solubility limit of lithium oxide in nickel oxide. In addition, from these data the ionic radius of Ni^{3+} has been determined.

Experimental

Nickel oxide was prepared by heating high purity nickel sulfate at 800°C. Mixtures of nickel oxide and lithium carbonate were pressed into tablets heated at various temperatures in air. To prevent the loss of lithium oxide by evaporation, the tablets in a platinum boat were covered by a powdered mixture of lithium carbonate and nickel oxide during the heating.

Free lithium oxide and dissolved lithium oxide were determined by a flame photometer in the way described in a previous paper.[3] The chemical analysis of Ni^{3+} was made according to the directions of Verwey.[1] The X-ray powder diffraction patterns were recorded by a diffractometer with a copper target. The lattice parameter of nickel oxide was determined as a function of dissolved lithium oxide by measuring the spacings of the (420) and (422) peaks.

Results and Discussion

It is not yet known how much lithium can be dissolved in nickel oxide when a mixture of lithium carbonate and nickel oxide is heated in air at high temperatures. To determine the temperature dependency of the solubility of lithium oxide in nickel oxide, a mixture of 90 at.% of nickel oxide and 10 at.% of lithium carbonate was heated in air for 3 hr. Figure 1 shows that the amount of lithium oxide dissolved in nickel oxide decreases with an increase in the heating temperature above 800°C. This decrease is attributed to the extensive evaporation of lithium oxide from the NiO-Li_2O solid solution[4] and to the evaporation of the unreacted lithium oxide. Accordingly, it is found that the temperature of 800°C is most suitable for lithium oxide to dissolve in nickel oxide. It has been reported[3] that the amount of lithium oxide dissolved in nickel oxide becomes essentially constant in a heating period of 3 hr. Mixtures of various ratios of lithium carbonate and nickel oxide were heated in air at 800°C for 3 hr. and then air-quenched.

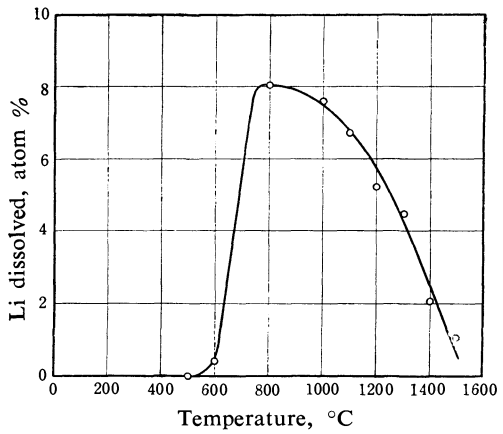


Fig. 1. Relation between the amount of dissolved lithium and heating temperatures.

It may be seen from Fig. 2 that the amount of lithium oxide dissolved in nickel oxide is always lower by a constant ratio than that of additive lithium oxide. Figure 2 shows that the amount of lithium oxide dissolved is constant above 25 at.%. It has, therefore, been concluded that the solubility of lithium oxide in nickel oxide is 25 at.% at 800°C.

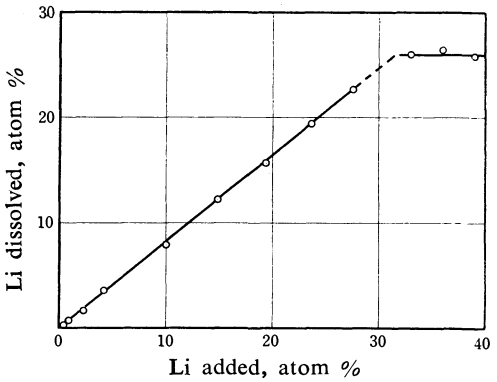


Fig. 2. Relation between the dissolved lithium and added lithium when NiO-Li_2O mixture is heated at 800°C for 3 hr.

The relation between the amount of lithium oxide dissolved and the Ni^{3+} formed in nickel oxide is shown in Fig. 3. The amount of Ni^{3+} ions is essentially the same as that of the dissolved lithium oxide within the solubility of lithium oxide. It is certified that the valency control principle established by Verwey[1] is applicable for the case of the NiO-Li_2O solid solution. Accordingly, the NiO-Li_2O solid solution can reasonably be expressed by the chemical formula of $Ni_{1-2x}^{2+} \cdot Li_x^{+}\ Ni_x^{3+}\ O$. The X-ray pattern of the NiO-Li_2O solid solution exhibits a broad peak as is shown in Fig. 4, as the amount of lithium oxide dissolved increases. The broad peak results from the deformation of the crystal of the NiO-Li_2O solid solution or from

3) Y. Iida, *J. Am. Ceram. Soc.*, **43**, 117 (1960).

4) Y. Iida, ibid., **43**, 171 (1960).

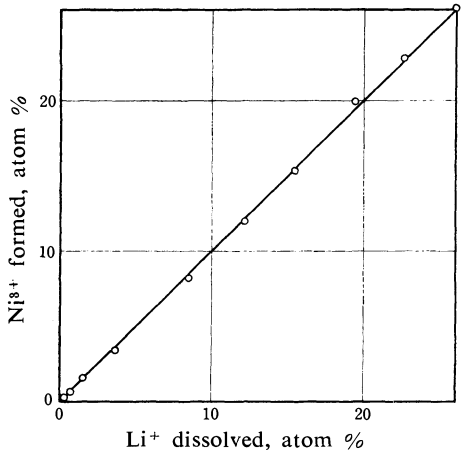


Fig. 3. Relation between the dissolved Li^+ and Ni^{3+} formed in NiO-Li_2O solid solution.

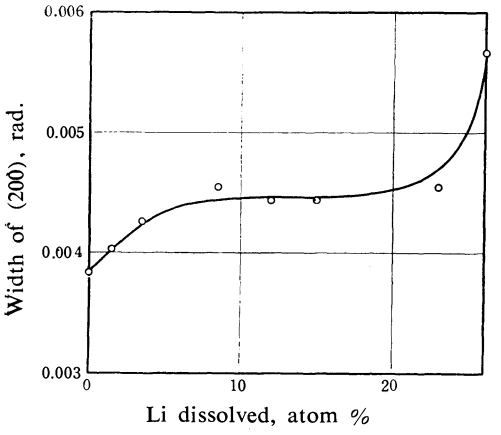


Fig. 4. Width of (200) X-ray peak of NiO-Li_2O solid solution as a function of lithium dissolved.

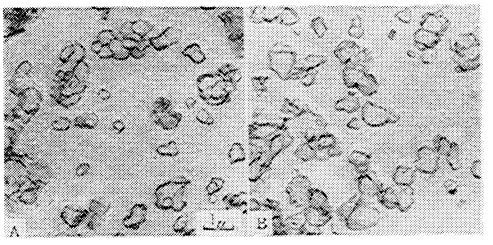


Fig. 5. Electron micrographs of pure NiO (A) and NiO-Li_2O (25 atom %) solid solution (B).

a decrease in its crystal size. The electron microscope photographs shown in Fig. 5 show that the particle size of the NiO-Li_2O solid solution does not vary with an increase in the amount of dissolved Li^+. Therefore, it is reasonable to assume that the crystal lattice of the original NiO is somewhat deformed when the nickel is replaced by lithium in the lattice.

Fensham[5] reported the lattice parameter of the NiO-Li_2O solid solution as a function of the Li^+ ions added. However, the amount of Li^+ ions dissolved is smaller than that of Li^+ ions added, as Fig. 2 shows. It is necessary to plot the Li^{1+} ions dissolved against the lattice parameter of the NiO-Li_2O solid solution. Figure 6 shows that the lattice parameter of nickel(II) oxide decreases linearly with an increase in the amount of lithium oxide dissolved. As the amount of Ni^{3+} ions

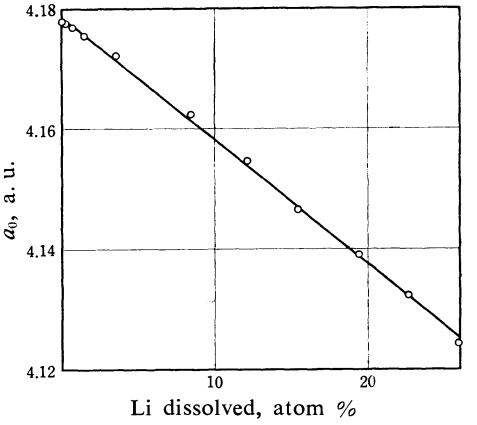


Fig. 6. Lattice parameter of NiO as a function of lithium dissolved.

is the same as that of Li^+ ions dissolved, the variation in lattice parameter can be expressed by Vegard's law as follows:

$$\Delta a_0 = 2(\Delta r_1 + \Delta r_2) \cdot x$$

where Δa_0 is the change in the lattice parameter,
Δr_1 is the difference between the ionic radii of Ni^{2+} and Ni^{3+},
Δr_2 is the difference between the ionic radii of Ni^{2+} and Li^+, and
x is the atomic % of the Li^+ ions dissolved.

There is no literature about the ionic radius of Ni^{3+}. The ionic radius of Ni^{3+} can, however, be calculated by the above equation. According to Ahrens,[6] the ionic radii of Ni^{2+} and Li^+ are 0.69 and 0.68 a. u. respectively. Therefore, the ionic radius of Ni^{3+} is found to be 0.60 a. u., which is quite reasonable in view of the fact that the ionic radius decreases with an increase in its positive valency.

Summary

In the NiO-Li_2O solid solution, it has been certified by a chemical analysis that the

5) P. J. Fensham, *J. Am. Chem. Soc.*, **76**, 969 (1954).
6) L. H. Ahrens, *Geochim. et Cosmochim. Acta*, **2**, 155 (1952).

amount of Ni^{3+} formed in the solid solution was the same as that of Li^{+} dissolved. The $NiO\text{-}Li_2O$ solution can be expressed by a molecular formula, $Ni_{1-2x}^{2+}\ Li_x^{+}\ Ni_x^{3+}\ O$. The solubility limit of lithium to nickel oxide is 25 atomic per cent at 800°C, which is an optimum temperature for the formation of the solid solution.

The lattice parameter of nickel oxide decreases with the increase in the amount of lithium dissolved. From Vegard's law, the ionic radius of Ni^{3+} has been calculated to be 0.60 a. u.

Government Industrial Research Institute
Kita-ku, Nagoya

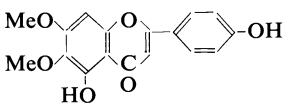
Synthetic Studies of the Flavone Derivatives. IV. The Synthesis of Cirsimaritin*

By Kenji FUKUI, Takashi MATSUMOTO and Takashi KINOSHITA

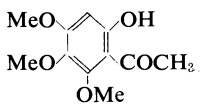
(Received December 20, 1963)

Cirsimarin, an almost colorless glycoside, has been isolated from *Cirsium martimum* MAKINO (Compositae) by Morita and Shimizu.[1] Their hydrolysis of this glycoside with hydrochloric acid has afforded cirsimaritin, a slightly yellow aglycone. They established the latter constitution as 4', 5-dihydroxy-6, 7-dimethoxyflavone (I) on the basis of analytical, spectroscopic and degradative studies. The substitution pattern belongs to the 5, 6, 7-hydroxy or methoxy type as found in scutellarein[2] and pectolinarigenin.[3] However, the new flavone has a unique structure in that it contains two methoxyl groups in the 6, 7-positions. The present report will describe the synthesis of the flavone I.

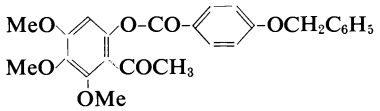
The esterification of 6-hydroxy-2, 3, 4-trimethoxyacetophenone (II)[4] with *p*-benzyloxybenzoyl chloride in the presence of dry pyridine gave the benzoate III. III was subjected to the Baker-Venkataraman rearrangement with pyridine-potassium hydroxide. The resulting diketone IV was converted into 4'-benzyloxy-5, 6, 7-trimethoxyflavone (V) by heating it with acetic acid and sodium acetate. The debenzylation of V with hydrogen afforded 4'-hydroxy-5, 6, 7-trimethoxyflavone (VI), which was demethylated with aluminum chloride in the 5-position to the flavone I. The synthetic product was identical with the natural cirsimaritin in melting point, color reactions and spectral characteristics (Figs. 1 and 2). I was partially methylated with diazomethane in the 4'-position to 5-hydroxy-4', 6, 7-trimethoxyflavone (scutellarein 4', 6, 7-trimethyl ether) (VII). The permethylation of VI or VII gave the same 4', 5, 6, 7-tetramethoxyflavone (scutellarein tetramethyl ether) (VIII).



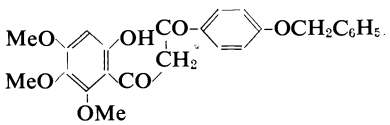
I



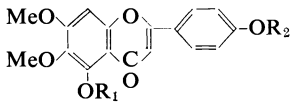
II



III



IV



V R_1=Me R_2=$CH_2C_6H_5$
VI R_1=Me R_2=H
VII R_1=H R_2=Me
VIII R_1=R_2=Me

* Part III: K. Fukui, T. Matsumoto and S. Matsuzaki, This Bulletin, 37, 265 (1964).

1) N. Morita and M. Shimizu, *J. Pharm. Soc. Japan* (*Yakugaku Zasshi*), 83, 615 (1963).

2) G. Goldschmiedt et al,, *Monatsh*, 22, 679 (1901); 31, 439 (1910).

3) K. W. Merz and Y. H. Wu, *Arch. Pharm.*, 274, 126 (1936); *Chem. Abstr.*, 30, 4166 (1936).

4) V. D. N. Sastri and T. R. Seshadri, *Proc. Indian Acad. Sci.*, 23A, 262 (1946).

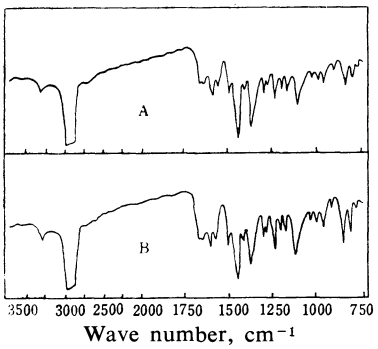


Fig. 1. Infrared absorption spectra of synthetic (A) and natural cirsimaritin (B) in Nujol.

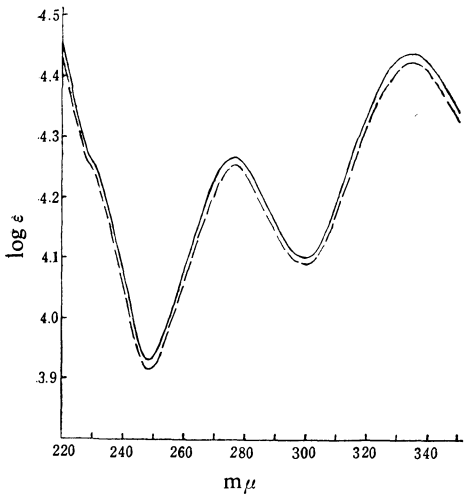


Fig. 2. Ultraviolet absorption spectra of natural (----) and synthetic cirsimaritin (——) in ethanol.

Experimental*

6-(*p*-Benzyloxy)benzoyloxy-2, 3, 4-trimethoxyacetophenone (III).—A mixture of *p*-benzyloxybenzoic acid (1.0 g.) and thionyl chloride (10 ml.) was gently refluxed for 30 min. The acid chloride, obtained by the removal of the excess thionyl chloride under reduced pressure, was added to the solution of 6-hydroxy-2, 3, 4-trimethoxyacetophenone[4] (II, 1.0 g) in dry pyridine (10 ml.). The mixture was refluxed in an oil bath for 30 min. After it had cooled, the reaction mixture was poured into ice-cold dilute hydrochloric acid. The precipitate was collected, washed with water and recrystallized from methanol to give III as colorless needles (m. p. 113~115°C; yield 0.8 g.).

Found: C, 68.67; H, 5.67. Calcd. for $C_{25}H_{24}O_7$: C, 68.80; H, 5.54%.

α-(*p*-Benzyloxy)benzoyl-6-hydroxy-2, 3, 4-trimethoxyacetophenone (IV).—A mixture of the benzoate III (13.2 g.), powdered potassium hydroxide (2.6 g.) and dry pyridine (40 ml.) was heated at 45~50°C for 1 hr. while being stirred; then it was poured into ice-cold dilute hydrochloric acid, and the precipitate was collected, washed with water and crystallized from ethanol to give IV as yellow needles (m. p. 113~114°C), which gave a green ferric reaction in ethanol; yield 8.0 g.

Found: C, 69.07; H, 5.59. Calcd. for $C_{25}H_{24}O_7$: C, 68.80; H, 5.54%.

4'-Benzyloxy-5, 6, 7-trimethoxyflavone (V).—The above diketone IV (0.8 g.) was refluxed with acetic acid (10 ml.) and fused sodium acetate (2.0 g.) for 4 hr., and then the solvent was removed under reduced pressure. The residue was washed with water and recrystallized from methanol to give V as colorless plates (m. p. 156~157°C), which gave a yellow solution with concentrated sulfuric acid; yield 0.6 g. UV λ_{max}^{EtOH} mμ (log ε); 268 (4.27) 322 (4.54).

Found: C, 71.67; H, 5.17. Calcd. for $C_{25}H_{22}O_6$: C, 71.76; H, 5.30%.

4'-Hydroxy-5, 6, 7-trimethoxyflavone (VI).—A solution of the above benzyloxyflavone V (1.0 g.) in ethanol (130 ml.) was shaken with hydrogen in the presence of palladized charcoal (10%; 1.5 g.) until the absorption of hydrogen ceased. The filtered solution was evaporated under reduced pressure, leaving an almost colorless residue. The residue was recrystallized from aqueous methanol to give VI as colorless needles (m. p. 230~231°C (reported m. p. 228°C[1]); yield 0.7 g.). This substance gave a yellow solution with concentrated sulfuric acid. UV λ_{max}^{EtOH} mμ (log ε); 266 (4.17) 325 (4.45).

Found: C, 65.52; H, 4.93. Calcd. for $C_{18}H_{16}O_6$: C, 65.85; H, 4.91%.

It formed an acetate (by the use of acetic anhydride-pyridine), which was crystallized as colorless needles (from aqueous methanol) (m. p. 139~140°C). UV λ_{max}^{EtOH} mμ (log ε); 266.5 (4.38) 309 (4.39).

Found: C, 64.64; H, 4.83. Calcd. for $C_{20}H_{18}O_7$: C, 64.86; H, 4.90%.

Cirsimaritin (4', 5-Dihydroxy-6, 7-dimethoxyflavone) (I).—A mixture of the hydroxyflavone VI (1.0 g) and anhydrous aluminum chloride (10.0 g.) in dry ether (150 ml.) was refluxed for 10 hr. After it had cooled, the reaction mixture was poured into ice-water. The yellow precipitate was collected, then refluxed with a mixture of concentrated hydrochloric acid (40 ml.) and acetic acid (60 ml.) for 30 min., and the reaction mixture was diluted with water. The yellow precipitate was collected, washed with water and recrystallized from methanol to give I as yellow needles (m. p. 257~258°C (reported m. p. 257°C[1])), alone or mixed with natural cirsimaritin; yield 385 mg. It shows all the color reactions of the natural cirsimaritin. IR 3273 (OH), 1665 (C=O), 1029 cm^{-1} (=C-O-C) (Nujol). UV λ_{max}^{EtOH} mμ (log ε); 277 (4.27) 336 (4.44).

Found: C, 64.70; H, 4.34. Calcd. for $C_{17}H_{14}O_6$: C, 64.96; H, 4.49%.

5-Hydroxy-4', 6, 7-trimethoxyflavone (VII).—The flavone I was partially methylated with diazomethane according to the method of Morita and Shimizu.[1] Recrystallization from ethanol gave VII as yellow needles (m. p. 187~188°C (reported m. p.

* All melting points are uncorrected.

183,[1] 188,[3] 189~190°C[5])). UV λ_{max}^{EtOH} mμ (log ε); 278.5 (4.31) 331 (4.45).

Found: C, 65.83; H, 4.62. Calcd. for $C_{18}H_{16}O_6$: C, 65.85; H, 4.91%.

4', 5, 6, 7-Tetramethoxyflavone (VIII).—*From VI.*—The treatment of VI (200 mg.) in acetone (50 ml.) with an ethereal solution of diazomethane for a day at room temperature gave VIII as colorless plates (from methanol) (m. p. 161~162°C (reported m. p. 158~159,[1] 161°C[6])), which in turn gave a yellow solution with concentrated sulfuric acid; yield 130 mg. UV λ_{max}^{EtOH} mμ (log ε); 267.5 (4.23) 321 (4.49).

Found: C, 66.54; H, 5.08. Calcd. for $C_{19}H_{18}O_6$: C, 66.66; H, 5.30%.

From VII.—To a solution of VII (90 mg.) and dimethyl sulfate (0.1 ml.) in acetone (50 ml.), potassium carbonate (2.0 g) was added; the mixture was then refluxed for 48 hr. The product was recrystallized from methanol to give VIII (m. p. and mixed m. p, 161~162°C); yield, 40 mg.

5) V. V. S. Murti, K. V. Rao and T. R. Seshadri, *Proc. Indian Acad. Sci.*, **26A**, 186 (1947).
6) R. Robinson and G. Schwarzenbach, *J. Chem. Soc.*, **1930**, 829.

The authors are grateful to Professor Naokata Morita, Faculty of Pharmacy, Toyama University, for a gift of natural cirsimaritin. Grateful acknowledgment is also made to the members of the Microanalytical Laboratory, Faculty of Pharmacy, Nagasaki University, for the microanalyses. This work was supported in part by a grant-in-aid from the Ministry of Education.

Department of Chemistry
Faculty of Science
Hiroshima University
Higashi-Sendamachi, Hiroshima

Further Studies of the Neutron Shielding of Metals in Thermal Neutron Activation

By Yuichiro KAMEMOTO and Shigeru YAMAGISHI

(Received December 24, 1963)

In thermal-neutron activation analysis, it is desirable to use samples which are smaller than those in which self-shielding effects are observed. Therefore, the permissible size in neutron irradiation in nuclear reactors is limited by the self-shielding in the sample. For elements with very large neutron absorption cross sections, this effect of shielding occurs when even small amounts of the sample are present; this may sometimes cause an error in the determination of such elements by neutron activation. In order to eliminate this error, the weight of a sample which has an appreciable self-shielding effect must be determined experimentally.

The authors have studied this problem in an attempt to ascertain the relationship between the neutron absorption cross section and the weight of each element which brings about an appreciable self-shielding effect, hoping thus to simplify the experimental process.

As a part of the results obtained, a rough relationship has been reported[1] for silver, gold, antimony, chromium and mercury metals. If this relationship is applicable to numerous other elements, it will be useful in estimating the most suitable amounts of sample to be used in neutron activation analysis.

Further studies will be reported on in this report in order to determine the applicability of this relationship to several other elements. In this investigation, the authors measured the self-shielding effects of gold, silver, copper, cobalt, indium, gallium, antimony, chromium, selenium and tin metals.

Experimental

Samples.—Samples were prepared from commercially-available G. R. metal particles or blocks as follows.

Selenium and Copper.—The method of preparing these samples consists of fusing particles of the metal, solidifying different amounts of fused metal on a quartz plate, making the product spherical with emery paper, and washing the surface in order to decontaminate it.

Indium, Silver, Cobalt, Tin, Gold, Gallium, Antimony and Chromium.—These samples were prepared by cutting them into smaller blocks from the original block, making them spherical with emery paper, and washing the surface in order to decontaminate them.

Each sample was wrapped with a parchment paper and sealed in a polyethylene pouch. As the

1) Y. Kamemoto and Y. Onoda, *J. Chem. Soc. Japan, Pure Chem. Sec.* (*Nippon Kagaku Zasshi*), **83**, 1164 (1962).

TABLE I. ACTIVATION AND MEASUREMENT OF SAMPLES

Sample	Irradiation period, hr.	Counted nuclide half life	γ-Ray energy MeV.	Time for calculation of specific activity hr. after irradiation
Se	2	^{81m}Se (57 min.) ^{75}Se (119.9 d)	0.103 0.269, 0.138, 0.077	6
In	0.5	^{116m}In (54.0 min.)	0.137, 0.406	6
Ag	2	^{110m}Ag (253 d)	0.676, 0.885, 1.389	53
Cu	2	^{64}Cu (12.8 h)	0.51	6
Co	2	^{60}Co (5.2 y)	1.173, 1.332	38
Sn	2	^{117m}Sn (14 d)	0.159, 0.162	32
Au	2	^{198}Au (2.72 d)	0.4118	28
Ga	2	^{72}Ga (14.2 h)	0.603, 0.834, 2.203, 2.508	7
Sb	2	^{112}Sb (2.75 d) ^{124}Sb (60 d)	0.57 0.603, 1.71, 2.11	25
Cr	2	^{51}Cr (27.8 d)	0.32	32

standard sample in which self-shielding does not occur, about 20 μg. of a sample was infiltrated into a filter paper (Toyo Roshi No. 5C) 2 cm. in diameter and sealed in a polyethylene pouch. The pouch containing the same element was packed in a capsule with soft paper and irradiated in the reactor.

Neutron Irradiation.—Samples were irradiated in the experimental hole No. 16 (pneumatic tube) of JRR-1 for 30 min.~2 hr. The thermal neutron flux was about 3×10^{11} n/cm^2/sec., and the cadmium ratio was 3~3.7.[2)]

Counting.—The irradiated sample was dissolved in mineral acid and diluted with water. A part of the resultant solution was pipetted into a polyethylene tube and diluted to 5 ml. with water. This sample for counting was mounted on a 3×3 inch NaI crystal attached to the RCL-256 channel pulse height analyzer, and the γ-ray spectrum was measured. By determining the γ-ray energy and the decay time of photopeaks of the γ-ray spectrum, the radiochemical purity of each sample was verified. Thereafter, the relative specific activity of each sample was calculated from the peak height of the γ-ray spectrum.

In the measurement of the γ-ray spectrum, the amount of sample pipetted is abjusted so that the counting rate is similar in each sample, thus reducing error from the difference in counting efficiency between the samples.

The experimental conditions adapted are shown in Table I.

2) T. Kurusu, Y. Saruta and T. Aburai, private communication.

Results and Discussion

The specific activity calculated from the peak height of photopeaks is plotted against the weight of sample. The curves thus obtained are shown in Figs. 1—10.

In the previous report, the weight of a sample (W g.) which has a specific activity 10 per cent smaller than that of "Zero" weight was determined graphically. This weight, W g., was assumed to represent the sample weight at which the self-shielding effect becomes appreciable. As a result of the above assumption, the following rough relationship between W and the neutron absorption cross section of the element (σ_{abs} barn) was found in the case of silver, gold, antimony, chromium and mercury metals. $W\times\sigma_{abs}$/atomic weight of sample = 0.02~0.04.

For the present report, the authors calculated the values of $\sigma_{abs}\times w$/atomic weight of sample (E), where w is the weight of a sample particle and σ_{abs} is the neutron absorption cross section of the sample (the ratio is hereafter shown as E). The relative specific activities were then plotted against E. When E is small, the specific activity is independent of E. Therefore, it is possible to normalize all the curves by bringing together their constant parts. If the neutron absorption cross section is large and if the independent part is not observed, the curves

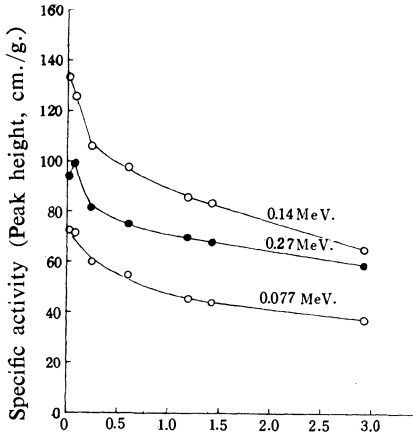


Fig. 1. Neutron shielding of selenium.

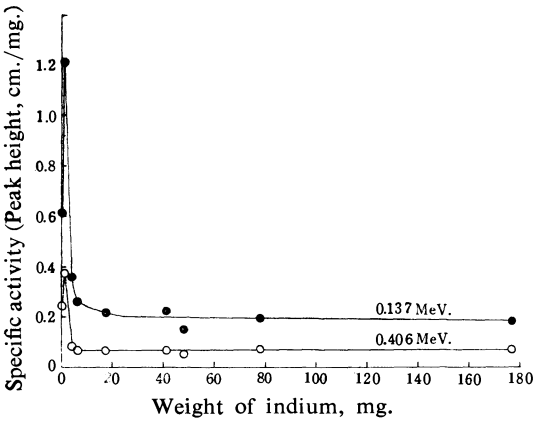


Fig. 2. Neutron shielding of indium.

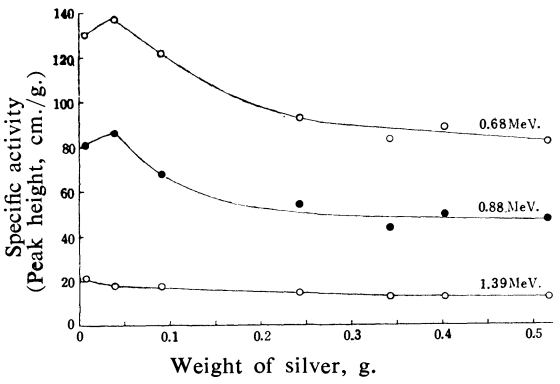


Fig. 3. Neutron shielding of silver.

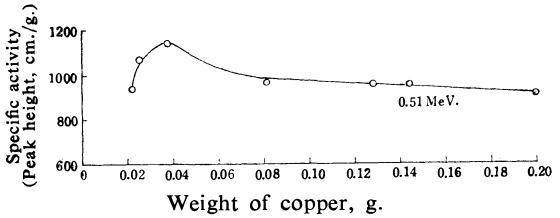


Fig. 4. Neutron shielding of copper.

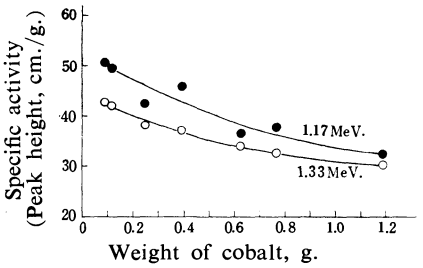


Fig. 5. Neutron shielding of cobalt.

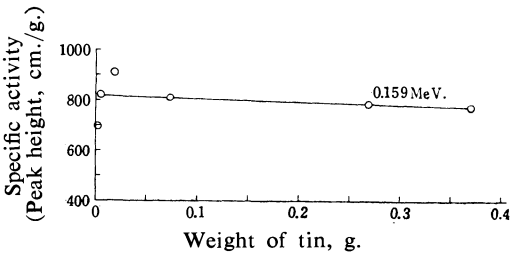


Fig. 6. Neutron shielding of tin.

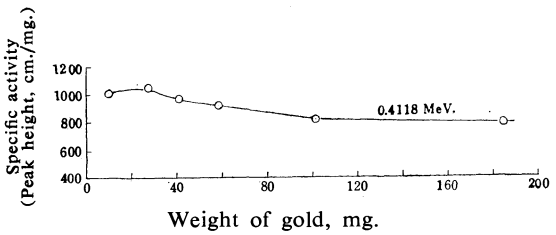


Fig. 7. Neutron shielding of gold.

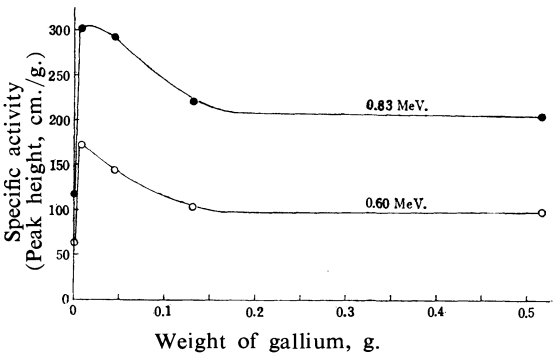


Fig. 8. Neutron shielding of gallium.

are normalized by using the specific activity of the standard samples, which are 20 μg. of the same element, assuming that no self-shieldind effect occurs in the standard. The normalized plots thus obtained are shown in Fig. 11, together with the optimum curve for the combined data.

From Fig. 11 the following relationship is obtained between the neutron absorption cross section in barns, σ_{abs}, and the weight in grams of a element corresponding to a 10 per cent self-shielding effect, W:

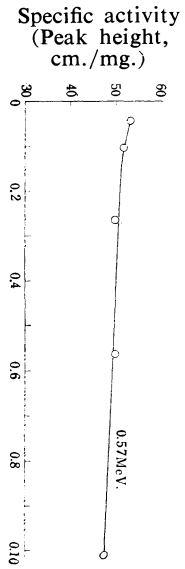


Fig. 9. Neutron shielding of antimony.

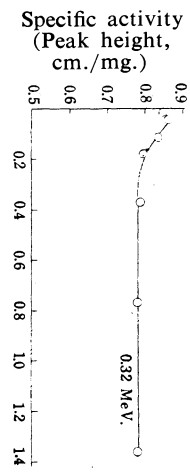


Fig. 10. Neutron shielding of chromium.

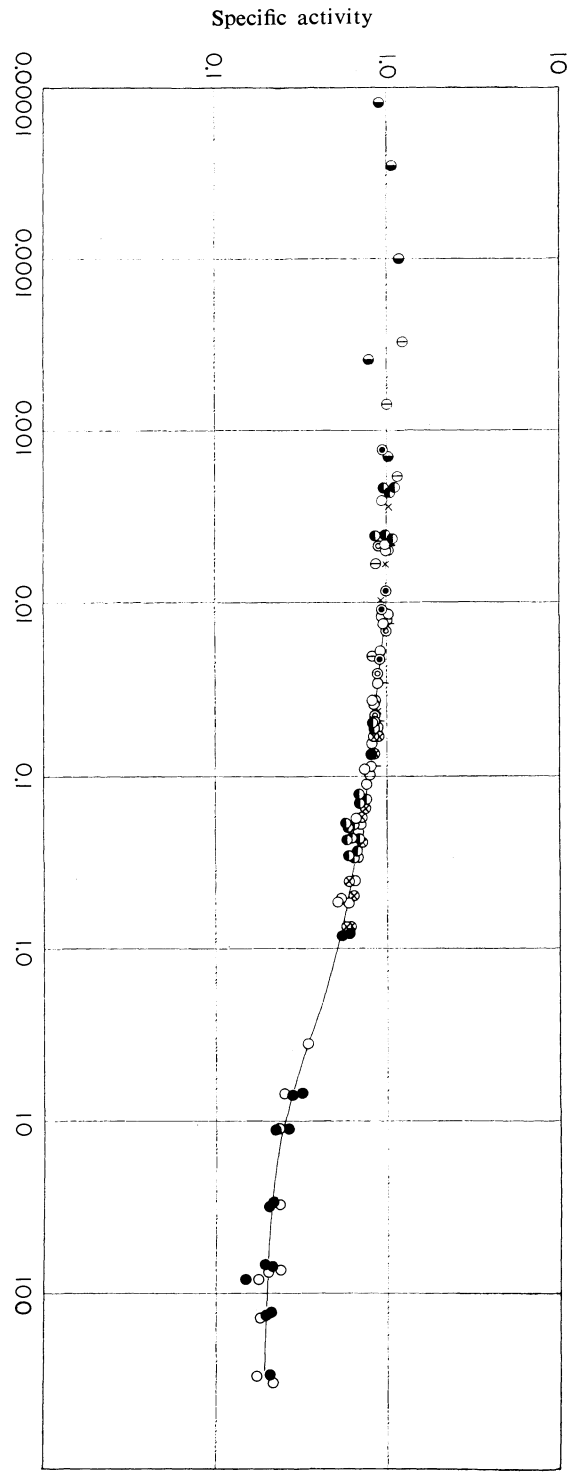


Fig. 11. Normalized plots of specific activity vs. $\sigma_{abs} \times w$/atomic weight.
○ Se ◐ Ag ⊗ Co ⏀ Ga ◎ Sb ● In ⊙ Cu ◑ Sn ◇ Au ×Cr

$$\frac{\sigma_{abs} \times W}{\text{Atomic weight of sample}} \simeq 0.03^{3)} \quad (1)$$

In a similar experiment using indium metal, Okada reported the value of 0.06.[4] However, it was found from our experiments that Eq. 1 was applicable to numerous elements, including indium.

The weight of stainless steel corresponding to a 10 per cent self-shielding effect has been calculated. This value agrees with the value obtained experimentally using an in-pile loop plug in a JRR-3 reactor. The results obtained appear to confirm that this equation is useful in estimating the most suitable amounts of a sample to be used in neutron activation analysis.

Division of Nuclear Engineering
Japan Atomic Energy Research Institute
Tokai, Ibaraki

3) Y. Kamemoto, *Inst. J. appl. Rad. Isotopes, in press.*
4) M. Okada, ibid., **13**, 53 (1962).

On the Electrolytic Rectification Effect in Ion-exchange Membranes

By Manabu SENŌ and Takeo YAMABE

(Received January 25, 1964)

The rectification effect has been observed with many biological membranes.[1] In these systems, a mechanism based on the strength of the contributions of the ionic conduction has been frequently considered. Recently, Lovreček and his co-workers[2] observed the rectification effect in the polyelectrolyte systems. These investigations suggest the possibilty that electric circuits might be constructed with ions as charge carriers. The ions are inferior in their low mobility, but are superior in their various species, to electrons as a charge carrier. This report is our first paper to treat this problem. An experimental and a theoretical treatment of the rectification system of ion-exchange membranes will be given.

Experimental

The ion-exchange membranes used were heterogeneous and were prepared from poly(vinyl chloride) and pulverized ion-exchange resins (commercially-available, Amberlite IR-120 and IRA-400). The membranes were thoroughly washed with hydrogen chloride and sodium hydroxide solutions and then with deionized water. The cation-exchange membrane was made up into the hydrogen form, and the anion-exchange membrane, into the hydroxide form. These membranes were pressed face to face into a double membrane and sandwiched between the two stainless-steel electrodes. Each membrane was 1 cm^2 in area and 0.3 mm. thick. The water content of the membranes, 56% by weight, was maintained through the measurement period by enclosing them in a sealed box.

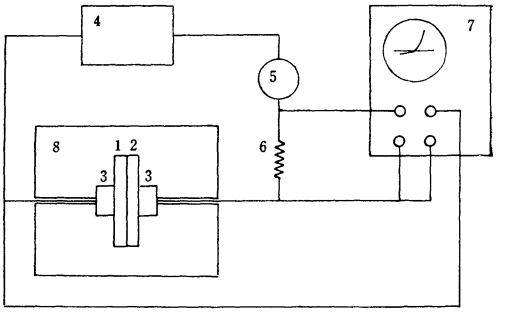


Fig. 1. Apparatus.

1. Cation-selective membrane
3. Anion-selective membrane
3. Electrodes (stainless steel)
4. Voltage source
5. Ammeter
6. Resistance (10 kΩ)
7. Oscilloscope
8. Constant-moisture chamber

The measuring apparatus is shown in Fig. 1. A constant voltage was supplied by a battery, and an alternating voltage, by test-oscillators, Toa-Dempa CR-1E (10^{-2}~10^{3} c. p. s.) and National RC-5A (25~10^{5} c. p. s.). The electric current was measured with a micro-ammeter and an oscilloscope.

Results and Discussion

Constant Voltage - Current Characteristics.— The system in which the positive electrode is connected to the cation-selective membrane and the negative electrode to the anion-selective membrane is highly resistant to the

1) W. F. Floyd, "Modern Aspects of Electrochemistry," Ed. by J. O'M. Bockris, Butterworths Sci. Publ., London (1954), p. 277.

2) B. Lovreček, A. Despic and J. O'M. Bockris, *J. Phys. Chem.*, 63, 730 (1960).

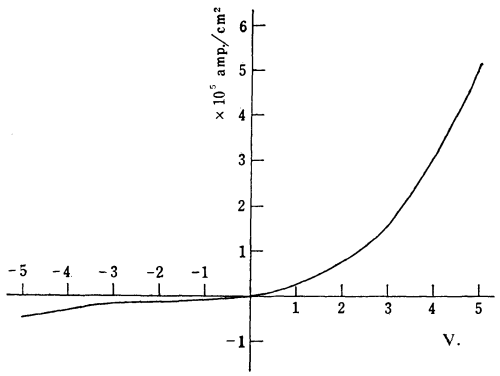


Fig. 2. Current plots versus constant voltages.

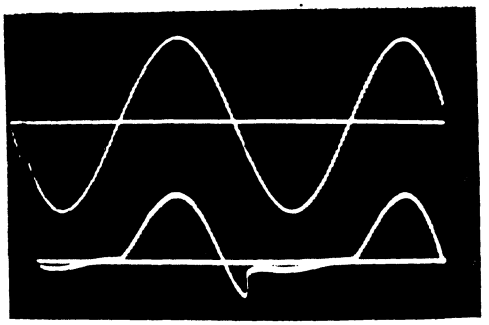


Fig. 3. Rectification of alternating sine-wave current.
Upper curve, input; Lower curve, output

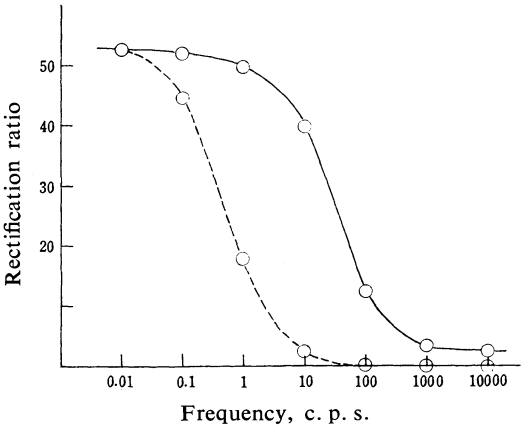


Fig. 4. Dependence of rectification ratio on frequency. (Rectification ratio stands for the current ratio of the forward against the inverse direction.)
Steady line, inverse → forward direction
Dotted line, forward → inverse direction

direct current in comparison with the case where the reverse polarity is applied. The current ratio of the forward direction to the reverse one attains 100 or more. A diagram of the current versus the voltage is shown in Fig. 2. The electric current in the forward direction is stable against the passage of time, while in the reverse direction it has a trend to increase with the lapse of time. The values given in Fig. 2 were read at 30 sec. after the application of a voltage. An increase in the applied volage in the reverse direction results in a gradual increase in the current after an initial trend to saturation.

The relationship between the electric current, i, and the applied voltage, V, is represented by Eq. 1;

$$i = i_0 \ (e^{\alpha V} - 1) \qquad (1)$$

where the experimental parameters, i_0 and α, have the following values in the present experiment;

$$i_0 = 5.0 \times 10^{-1} \text{ amp./cm}^2$$

$$\alpha = 0.49$$

This relation will be discussed in the following section.

Alternating Voltage-Current Characteristics.— The rectification effects are very effective when alternating voltages with very low frequencies (lower than 1 c. p. s.) are applied to the system. An example is shown in Fig. 3. However, it must be pointed out that a clear inflection point appears where the polarity changes from the reverse direction to the forward one, while, when the applied voltage in the forward direction is decreased, no current is observed at a finite value of the applied voltage and then the reversed current becomes to be running. A further decrease in the forward voltage and then an increase in the reverse voltage result in an initial increase in the reverse current, followed by an abrupt decrease, and then the reverse current attains a saturation value. There is observed a hysteresis with a negative resistance in the current-voltage diagram. This is found as a spike current in a current wave. This may be caused by a membrane potential and a capacitance of a liquid film adjacent to the membrane.

When an alternating voltage with frequencies higher than 1 c. p. s. is applied, the rectification effect becomes poorer. One of the observed result is shown in Fig. 4. The primary cause would be a contribution by the capacitance current, based on the capacitance of the membrane system. Assuming an R-C parallel circuit as the simplest equivalent circuit of the system, the following values are measured; $R = 5 \times 10^3$ ohm and $C = 7 \times 10^{-6}$ F. It is estimated from this that the contribution of the capacitance current is major at frequencies higher than $f = 1/2\pi CR = 4.54$ c. p. s. A contribution of the relaxation effect of the

ionic atmosphere[3] will appear at very much higher frequencies, probably 10^7 or higher.

Theoretical Considerations.—The charge carriers in this system will be ions; hydrogen ions (protons) and hydroxide ions in this case. Hydrogen ions are rich in the cation-selective membrane, and hydroxide ions are rich in the anion-selective membrane. The distribution of these carriers is ruled by Boltzmann's law in an equilibrium state. The density, n, of protons is given by:

$$n_x = n_0 \exp(-e\varphi_x/kT) \tag{2}$$

where e the elementary charge, k the Boltzmann constant, and T, the absolute temperatures. The potential, φ, of protons is low in the cation-selective membrane phase (I) and high in the anion-selective membrane phase (II); it is schematicaly shown in Fig. 5.

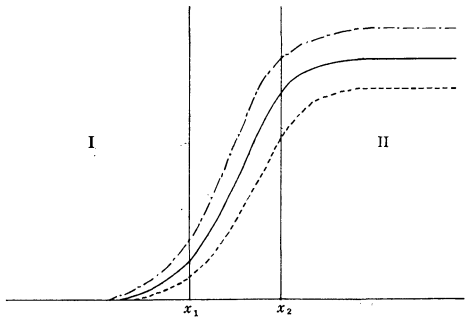


Fig. 5. Potential curve for protons.
I, cation-selective membrane
II, anion-selective membrane
Intermediate, transition region
Steady line, no applied voltage
Dotted line, forward bias voltage
Chain line, inverse bias voltage

The total protonic current is given by adding an driving current to a diffusion current; that is,

$$i_x = eu_n n_x \frac{d\varphi_x}{dx} - eD_n \frac{dn_x}{dx} = en_x \frac{d\varphi_x}{dx}\left(u_n - \frac{e}{kT} D_n\right) \tag{3}$$

In the absence of a bias valtage, Einstein's relation holds true between the mobility, u_n, and the diffusion constant, D_n, of protons; that is,

$$u_n = (e/kT) D_n \tag{4}$$

therefore, the total current does not run.

When a forward voltage is applied, the electric potential difference becomes small in the transient region, as is shown by a dotted line in Fig. 5. As a result, a diffusion current surpasses a driving current and protons flow from the transient region into the region II by diffusion. Then the density of protons in the region II becomes

$$n_x = n_{II} + \Delta n_x \tag{5}$$

according to the principle of electroneutrality, hydroxide ions increase by the same quantity, Δn_x, in this region. At the same time, the excess protons disappear in the formation of water molecules with hydroxide ions. The rate of this recombination reaction, R, is:

$$\begin{aligned} R(x) &= rn_x m_x = r(n_{II} + \Delta n_x)(m_{II} + \Delta n_x) \\ &= rn_{II} m_{II} + rm_{II} \Delta n_x \\ &= g + (1/\tau_n)\Delta n_x \end{aligned} \tag{6}$$

where m is the density of hydroxide ions, $g = rn_{II} m_{II}$ is the rate of the thermal decomposition of water molecules, and $\tau_n = 1/rm_{II}$ is the mean life-time of protons in the region II.

Under such circumstances, the diffusional flow of protons is expressed by:

$$D_n \frac{dn(x+dx)}{dx} - D_n \frac{dn(x)}{dx} = (R(x) - g)dx \tag{7}$$

or

$$D_n \frac{d^2 n}{dx^2} = R(x) - g \tag{8}$$

The boundary condition that, if $x \to \infty$, $n(x)$ equals n_{II}, must be satisfied. The solution of Eq. 8 is at the boundary $x = x_2$:

$$n(x_2) - n_{II} = C \exp\{-(x - x_2)/L_n\} \tag{9}$$

where $L_n = \sqrt{\tau_n D_n}$ is the mean distance which protons proceed in the region II until their disappearance.

Therefore, the current carried by the protonic diffusion is given by:

$$\begin{aligned} i_n(x_2) &= -eD_n\left(\frac{dn(x)}{dx}\right)_{x=x_2} \\ &= \frac{eD_n}{L_n}\{n(x_2) - n_{II}\} \end{aligned} \tag{10}$$

From Boltzmann's law,

$$n(x_2) = n_{II} \exp(eV/kT) \tag{11}$$

These relations lead to the final expression:

$$i_n(x_2) = \frac{eD_n}{L_n} n_{II}(\exp(eV/kT) - 1) \tag{12}$$

Exactly the same relation holds true for hydroxide ions. Therefore, the total current is expressed by:

$$i = e\left(\frac{D_n n_{II}}{L_n} - \frac{D_m m_{II}}{L_m}\right)(\exp(eV/kT) - 1) \tag{13}$$

where the subscript n refers to protons and the subscript m, to hydroxide ions.

3) H. S. Harned and B. B. Owen, "The Physical Chemistry of Electrolytic Solutions," Reinhold Pub. Corp., New York (1950) p. 211.

TABLE I. PARAMETERS OF CHARGE-CARRIERS

	Hydrogen ion	Hydroxide ion
Density in cation-selective membrane, cm^{-3}	$n_I=4.17\times10^{17}$	$m_I=8.67\times10^{9}$
Density in anion-selective membrane, cm^{-3}	$n_{II}=4.41\times10^{9}$	$m_{II}=8.18\times10^{17}$
Mobility, $cm^2/V.\,sec.$	$u_n=3.0\times10^{-3}$	$u_m=1.7\times10^{-3}$
Diffusion constant, $cm^2/sec.$	$D_n=7.8\times10^{-5}$	$D_m=4.4\times10^{-5}$
Mean life-time, sec.	$\tau_n=6.6\times10^{-12}$	$\tau_m=1.3\times10^{-11}$
Mean invation-distance, cm.	$L_n=2.25\times10^{-8}$	$L_m=2.4\times10^{-8}$
Thermal generation rate, $cm^{-3}/sec.$	$g=6.7\times10^{20}$	

When a reverse bias voltage is applied, the density of protons at $x=x_2$ decreases by a ratio of $\exp(-e|V|/\boldsymbol{kT})$. As a result, protons flow out from the region II by diffusion. However, this current is small and soon attains saturation because of the low density of protons in this region.

These considerations explain the observed results well. Using the values of the parameters in Eq. 1 and those of the specific resistance of each membrane, 5×10^3 ohm·cm. for the cation-selective membrane and 4.5×10^3 ohm·cm. for the anion-selective membrane, and assuming $r_n=r_m$, we can estimate the parameters in the above equations. The results are given in Table I.

Although most of the values estimated above seem to be reasonable, there are many discrepancies. That is, the theoretical value of α in Eq. 1 is 38.6, while the observed value is 0.49. The rate of the dissociation of water into hydrogen and hydroxide ions has been observed to be $2.6\times10^{-5}\,sec^{-1}$,[4] from which the rate of the thermal generation has been calculated as $1.56\times10^{16}\,cm^{-3}\,sec^{-1}$, while the present value is $6.7\times10^{20}\,cm^{-3}\,sec^{-1}$. Moreover, the rate of the recombination of hydrogen and hydroxide ions into water has been observed as $1.3\times10^{11}\,l.\,mol^{-1}\,sec^{-1}$,[3] from which the mean-life time has been calculated to be 5.65×10^{-9} sec. for protons and 1.11×10^{-8} sec. for hydroxide ions, while the estimated values are 6.6×10^{-12} and 1.3×10^{-11} sec. respectively.

However, these disagreements are caused not by wrong treatments, but by the roughness of the model and unexpected errors in the experiments.

The final Eq. 13 is the same as Shockley's equation[5] for the p-n junction diode of semiconductors. This means that the same rectification mechanism holds true for the present system, with ionic charge-carriers, as for the semiconductor diode with electronic charge-carriers. Accordingly, the cation-selective membrane corresponds to the n-type semiconductor and the anion-selective membrane, to the p-type semiconductor. Moreover, it may be very instructive to consider hydrogen and hydroxide ions as protons and proton-defects respectively. By this analogy, most of the properties of the charge-carriers in the present ionic system might be understood by the methods used in the solid state physics, where the electron and its defect play an important role.

Summary

The electrolytic rectification effect has been observed in a double-membrane system. The static and dynamic current-voltage characteristics have been measured, and it has been demonstrated that the mechanism of the rectification similar to that of the p-n semiconductor junction holds true for this system. Reasonable values have been estimated for the characteristic parameters, although there are many discrepancies requiring further examination.

The Institute of Industrial Science
The University of Tokyo
Azabu, Tokyo

4) M. Eigen and L. De Mayer, *Z. Elektrochem.*, 59, 986 (1955).

5) W. Shockley, "Electrons and Holes in Semiconductors," D. Van Nostrand Co., New York (1950), p. 309.

Studies of the Organic Reactions of Metal Carbonyl. II. The Reaction of Olefin Oxide with Cobalt Hydrocarbonyl*

By Yoshinobu TAKEGAMI, Chikao YOKOKAWA, Yoshihisa WATANABE and Hiromitsu MASADA

(Received September 2, 1963)

In connection with the Oxo reaction, the reaction of olefins with cobalt hydrocarbonyl and carbon monoxide has been studied by several workers.[1-5] It has been established[5,6] that alkyl- and acylcobalt carbonyl are formed in this reaction.

Recent papers[7-11] have reported that hydroxy-acids, their derivatives or rearranged carbonyl products are formed in the reaction of olefin oxides with carbon monoxide and water or alcohols using a cobalt salt or cobalt carbonyl as catalyst. With regard to these facts, Heck[13] has established, by isolating β-hydroxyacyl-cobalt tricarbonyl triphenylphosphine, that β-hydroxyacylcobalt tetracarbonyl is formed in the reaction of olefin oxide with cobalt hydrocarbonyl.

In the present paper, this type of reaction has been studied with an emphasis on the following two points: a) the effect of the reaction conditions on the nature of this reaction and the structure of the products, and b) the relation between the reactivity of olefin oxides and their structures.

Experimental

Reaction Procedures.—The reactions were carried out as described in the previous paper,[14] using 50 ml. of 0.09 M cobalt hydrocarbonyl solution in toluene.

Analytical Procedures.—The solution of crude products was treated with iodine and ethyl alcohol as described previously,[14] and the excess of iodine was reduced with crystalline sodium thiosulfate. After concentration, the reaction products were gas-chromatographed on a column, three meters in length and 3 mm. in diameter, filled with dilauryl phthalate or silicon DC 550 on cerite, at 140~160°C, and at the flow rate of carrier gas (hydrogen) of 50 ml./min. The identification of ethyl β-hydroxy-propionate, ethyl β-hydroxy-*n*-butyrate, β-hydroxy-*n*-butyraldehyde, α- and β-phenylethyl alcohol was made by mixing them with authentic samples in gas chromatography. The infrared spectra of the solution of reaction products in toluene were recorded by a Shimadzu model IR-27 infrared spectrophotometer, after removing iodohydrin* by treating the crude solution with potassium hydroxide.

Materials.—Ethylene oxide, propylene oxide, styrene oxide, epichlorohydrin and pentene-1 were commercial products. Cyclohexene oxide was synthesized by the oxidation of cyclohexene with perbenzoic acid.[15] All of these compounds were proved to be sufficiently pure by gas chromatography. The cobalt hydrocarbonyl solution in toluene was prepared by a method described previously.[14]

Results and Discussion

Propylene Oxide.—A recent paper reported[13] that olefin oxide reacts readily with cobalt hydrocarbonyl, but the effects of the reaction conditions on the reaction and on the products are unknown. The authors found that the reactions of some olefins with cobalt hydrocarbonyl are remarkably influenced by the reaction conditions (temperature, atmosphere, etc.).*

In this study, the reaction of propylene oxide with cobalt hydrocarbonyl has been

* Presented in part at the 7th Annual Meeting of the Fuel Society of Japan (Kwansai Section), Osaka, November, 1962. Presented at the 16th Annual Meeting of the Chemical Society of Japan, Tokyo, April, 1963

1) I. Wender, H. W. Sternberg and M. Orchin, *J. Am. Chem. Soc.*, 75, 3041 (1953).
2) P. Pino, R. Ercoli and F. Calderazzo, *Chim. e Ind. (Milan)*, 37, 783 (1955).
3) L. Kirch and M. Orchin, *J. Am. Chem. Soc.*, 80, 4428 (1958); 81, 3597 (1959).
4) R. F. Heck and D. S. Breslow, *Chem. & Ind.*, 1960, 467.
5) R. F. Heck and D. S. Breslow, *J. Am. Chem. Soc.*, 83, 4023 (1961).
6) R. F. Heck and D. S. Breslow, ibid., 82, 4438 (1960).
7) M. Seon and J. Leleu, U. S. Pat. 2782226 (1957).
8) H. Nienburg and G. Elschnigg, German Pat. 1066572 (1959).
9) J. L. Eisenmann, R. L. Yamartino and J. F. Howard, Jr., *J. Org. Chem.*, 26, 2102 (1961).
10) W. A. McRae and J. L. Eisenmann, U. S. Pat. 3024275 (1962).
11) J. L. Eisenmann, *J. Org. Chem.*, 27, 2706 (1962).
12) Y. Takegami, C. Yokokawa and Y. Watanabe, The 16th Annual Meeting of the Chemical Society of Japan, Tokyo, April, 1963.
13) R. F. Heck, *J. Am. Chem. Soc.*, 85, 1460 (1963).
14) Y. Takegami, C. Yokokawa, Y. Watanabe and Y. Okuda, This Bulletin, 37, 181 (1964).
15) Gilman and Blatt, "Organic Syntheses," Coll. Vol. I, 494 (1958).

* Believed to have been formed as follows: $RCOCo(CO)_4 \xrightarrow{R'OH+I_2} HI + RCOOR'$, olefin oxide + HI → iodohydrin.

* Presented in part at the 16th Annual Meeting of the Chemical Society of Japan, Tokyo, April, 1963; to be published.

TABLE Ia. THE REACTION OF PROPYLENE OXIDE WITH COBALT HYDROCARBONYL

Exp. No.	Reaction Conditions: Atmosphere	Temp. °C	Mole Ratio*3	Time min.	CO Absorbed (mol./mol.-$HCo(CO)_4$)	Product: Ester*1 (mol./mol.-$HCo(CO)_4$)	Product: Aldehyde*2 (mol./mol.-$HCo(CO)_4$)
1	CO	0	1.4	180	0.15	0.13	—
2	CO	0	2.7	330	0.57	0.30	—
3	CO	0	4.0	220	0.82	0.44	0.09
4	CO	0	6.2	140	0.90	0.60	—
5	CO	25	4.0	120	0.52	0.15	0.10
6	CO	−30	6.2	200	0.78	0.56	—
7	CO	−45	6.2	180	0.85	0.49	—
8	N_2	0	2.7	30	—	0.14	—
9	N_2	0	2.7	60	—	0.15	—
10	N_2	0	2.7	150	—	0.10	0.05
11	N_2	0	6.2	15	—	0.20	0.04
12	N_2	0	6.2	140	—	0.24	—
13	N_2	0	6.2	330	—	0.18	—
14	N_2	−45	6.2	180	—	0.27	—

TABLE 1b

15	N_2-CO*4	0	6.2	15, 60	0.20	0.17	0.1
16	N_2-CO	−30	1.2	15, 210	0.71	0.61	0.05
17	CO-N_2*5	0	6.2	70, 240	0.80	0.35	—
18	CO-N_2-CO	0	6.2	18, 15, 70	0.36, 0.16	0.33	—

*1 Ethyl β-hydroxy-*n*-butyrate.
*2 β-Hydroxy-*n*-butyraldehyde.
*3 Mole of propylene oxide per mole of cobalt hydrocarbonyl used.
*4 At first under nitrogen atmosphere and then under carbon monoxide.
*5 At first under carbon monoxide and then under nitrogen.

examined in detail. Two skeletal isomeric products are possible in this case, but the composition of the reaction products has not been studied.[13]

As is shown in Table I, the major product independent of the atmosphere (one atmosphere of carbon monoxide or nitrogen), temperature (25～−45°C) and mole ratio* of propylene oxide (1.4～13.5), was ethyl β-hydroxy-*n*-butyrate,** which was evidently derived from β-hydroxy-*n*-butyrylcobalt carbonyl by cleavage with iodine and ethyl alcohol. Besides this ester, a small amount of β-hydroxy-*n*-butyraldehyde was formed, but there was no indication of the presence of ethyl α-methyl-β-hydroxypropionate under the reaction conditions used. The yields of the ester tended to decrease as the reaction temperature rose; i.e., the total yields of the ester and the aldehyde in the reactions at 25, 0, and −30°C were about 30, 55, and 80% respectively, on the basis of the amount of carbon monoxide absorbed. Under nitrogen, the yields of the ester were much less than those under carbon monoxide; at 0°C, in the case of a 2.7 or 6.2 mol. ratio, only about 0.15 or 0.25 mol. of the ester, independent of the reaction time (15～330 min.), was formed.

The gas absorption curves shown in Fig. 1., in which the amount of carbon monoxide absorbed is plotted against the reaction time, indicate that, at 0°C and under one atmosphere of carbon monoxide, the rate of the gas absorption at the early stage of the reaction is roughly proportional to the square of the mole ratio. The gas absorption at 25, −30

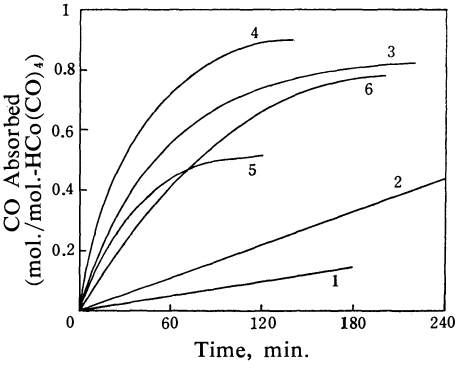


Fig. 1. CO Absorption vs. time plots for the reaction of propylene oxide.
Number: Exp. No.

* Mole of propylene oxide per mole of cobalt hydrocarbonyl used.
** Identified by gas chromatography and by the infrared spectrum of the solution of products in toluene, which had bands at 3630 cm^{-1} and 1735 cm^{-1} corresponding to hydroxy and carbonyl groups.

TABLE II. THE REACTION OF ETHYLENE OXIDE WITH COBALT HYDROCARBONYL

Exp. No.	Reaction Conditions*1		CO Absorbed	β-Hydroxyester*3
	Mole Ratio*2	Time min.	(mol./mol. $HCo(CO)_4$)	(mol./mol. $HCo(CO)_4$)
19	1~2	240	0.16	0.08
20	~4	220	0.80	0.50
21	~5	155	0.96	—

*1 Other reaction conditions: at 0°C and one atmosphere of carbon monoxide.
*2 Mole of ethylene oxide per mole of cobalt hydrocarbonyl used.
*3 Ethyl β-hydroxypropionate.

(and −45°C) occurred more slowly than at 0°C. The amount of gas absorbed at 25°C was less than that at 0°C.

In connection with the fact that the reactions under nitrogen gave the ester with a low yield, the reaction was carried out in two stages, the first stage under nitrogen for 15 min. and, then the second stage under carbon monoxide. At 0°C, only 0.2 mol. of the gas was absorbed in the second stage (Exp. 15 and curve 15). This value obviously corresponds with that of the yield of the ester in the corresponding reaction under nitrogen (Exp. 11). This fact seems to indicate that, under nitrogen, some side reaction other than the carbonylation reaction occurred rapidly to consume a large part of the cobalt hydrocarbonyl used. At −30°C, however, in the second stage, the gas was absorbed in the usual manner (Exp. 16 and curve 16). The reaction was carried out in two or three stages: at first under carbon monoxide, at the second stage under nitrogen, and then under carbon monoxide. The nitrogen atmosphere had no effect on the reaction when the gas absorption had completely occurred at the first stage (Exp. 17). When, however, the gas absorption was only half-completed at the first stage, the nitrogen atmosphere had the effect on the reaction of decreasing the amount of gas absorbed at the third stage (Exp. 18).

According to Heck and Breslow's suggestion[5] that the formation of acylcobalt carbonyl in this type of reaction of olefin is accelerated under nitrogen, it would be expected that the above-mentioned pretreatment under nitrogen would promote the carbonylation reaction of propylene oxide. In reality, however, the amount of gas absorbed and the yields of the ester and the aldehyde were not good, as is demonstrated by Exp. 15; in other words, the nitrogen atmosphere highly promoted some side reaction and then the formation of carbonylated products (ester and aldehyde) was prevented.

In order to compare the reactivity of olefin oxide with that of olefin, the reaction of pentene-1 with cobalt hydrocarbonyl was carried out. The results, shown in Fig. 2(A), indicate that pentene-1 is obviously less reactive than propylene oxide. In general, olefin oxide seems to be more reactive than olefin in this type of reaction. This fact is supported by the authors' observation[12] that propylene oxide undergoes the hydroformylation reaction at a lower temperature (80~90°C) than the usual Oxo reaction temperature.

Ethylene Oxide.—Ethylene oxide undergoes this type of reaction in the same manner as propylene oxide. The results are shown in Table II. As the major product, ethyl β-hydroxypropionate was given. In a recent study, Heck[13] isolated β-hydroxypropionylcobalt tricarbonyl triphenylphosphine from this reaction.

Cyclohexene Oxide.—Cyclohexene oxide, an internal olefin oxide, reacts readily with cobalt hydrocarbonyl. The results are summarized in Table III. The major product is believed to be ethyl 2-hydroxycyclohexanecarboxylate.* As may be seen from the appearance of the gas absorption, cyclohexene

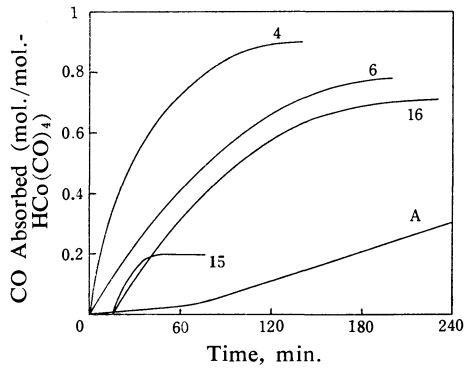


Fig. 2. CO Absorption vs. time plots for the reaction of propylene oxide.
Number: Exp. No.
A: pentene-1 (at 0°C, 10 mole ratio)

* The infrared spectrum of the reaction products in toluene had bands at 3600 cm^{-1} and 1735 cm^{-1}. As further evidence, the retention time of the major product in gas chromatography increased as the molecular weight of the alcohol used in the cleavage of the crude products increased, and the retention time of the product (ethyl ester) was longer than that of ethyl cyclohexanecarboxylate, so this compound seemed to have some additional functional group.

TABLE III. THE REACTION OF CYCLOHEXENE OXIDE WITH COBALT HYDROCARBONYL

Exp. No.	Reaction Conditions* Temp. °C	Mole Ratio	Time min.	CO Absorbed (mol./mol. $HCo(CO)_4$)	Product Ester** (mol./mol. $HCo(CO)_4$)
22	0	2.7	155	0.79	0.58
23	0	4.5	95	0.80	0.57
24	25	2.7	60	0.42	0.1
25	−30	2.7	260	0.72	0.63

* Other reaction condition: under one atmosphere of carbon monoxide.
** Ethyl 2-hydroxycyclohexanecarboxylate.

TABLE IV. THE REACTION OF STYRENE OXIDE WITH COBALT HYDROCARBONYL

Exp. No.	Reaction Conditions Atmosphere	Temp. °C	Mole Ratio	Time min.	CO Absorbed (mol./mol.-$HCo(CO)_4$)	Product α* (mol./mol. $HCo(CO)_4$)	Product β** (mol./mol. $HCo(CO)_4$)
26	CO	0	1.0	190	0.20	0.17	0.10
27	CO	25	1.0	80	0.20	0.19	0.12
28	CO	0	2.0	180	0.32	0.19	0.09
29	CO	0	4.0	80	0.49	—	—
30	CO	0	6.0	60	0.52	—	—

* α-Phenylethyl alcohol.
** β-Phenylethyl alcohol.

TABLE V. THE REACTION OF EPICHLOROHYDRIN WITH COBALT HYDROCARBONYL

Exp. No.	Reaction Conditions Atmosphere	Temp. °C	Mole Ratio	Time min.	CO Absorbed (mol./mol.-$HCo(CO)_4$)	Product Ester* (mol./mol. $HCo(CO)_4$)
31	CO	0	5	270	0	0
32	CO	25	5	240	0	0.15
33	CO	0	30	300	0.60	0.4
34	CO	0	45	330	0.55	0.5

* Ethyl γ-chloro-β-hydroxypropionate.

oxide is obviously more reactive than propylene oxide; for instance, in the case of a 2.7 mol. ratio, cyclohexene oxide absorbs 0.8 mol. of carbon monoxide in 150 min., while propylene oxide absorbs only 0.4 mol. of the gas in 240 min.

The rate of the gas absorption at the early stage of the reaction for cyclohexene oxide is about five times that for propylene oxide. This relation between the reactivity and the chemical structure of two kinds of olefin oxide is the reverse of that for olefins; i.e., in general, the order of the reactivity for olefins is terminal>internal>cyclic.[3]

Styrene Oxide.—In the reaction of styrene oxide, a conjugated olefin oxide, with cobalt hydrocarbonyl, exceptional behavior was observed. The mole ratio of styrene oxide had a significant effect on the nature of the reaction. As Table IV shows, when the mole ratio was relatively small (1 and 2) the major products were α- and β-phenylethyl alcohol and the amount of gas absorbed was small. This indicates that the reduction of styrene oxide with cobalt hydrocarbonyl occurred mainly at these mole ratios. As the mole ratio increased (4 and 6), the amount of gas absorbed increased, but it did not exceed 0.6 mol. In these cases, the identification of the products was impossible since a black tarry material was formed in the course of the analysis, but it seemed, mainly because of the relatively large absorption of the gas, that the carbonylation reaction took place. The tarry material may reasonably be attributed to the polymerization of the excess styrene oxide.

Epichlorohydrin.—Epichlorohydrin seems to react with cobalt hydrocarbonyl only with difficulty under the conditions, at 0°C and in a 5 mol. ratio, under which propylene oxide reacts readily; there was, at any rate, no absorption of the gas, as Table V shows. When, however, the mole ratio of epichlorohydrin was increased to 30 and 45, about 0.6 mol. of the gas was absorbed in 5 hr. Therefore, epichlorohydrin is much less reactive than propylene oxide, but it is believed to

give ethyl γ-chloro-β-hydroxy-*n*-butyrate,* the structure of which corresponds with that of the products propylene oxide gives.

As may be seen from the appearance of the gas absorption, epichlorohydrin seems to react with cobalt hydrocarbonyl about many times more slowly than propylene oxide. In contrast with this fact, the relative reactivities of these olefin oxides with ammonia and perchloric acid are represented as follows:[16] with ammonia epichlorohydrin 4>propylene oxide 1; with perchloric acid, epichlorohydrin 1< propylene oxide 70 (with cobalt hydrocarbonyl epichlorohydrin 1<propylen oxide 20~40).

Thus, the order of the reactivity of these olefin oxides with cobalt hydrocarbonyl corresponds to that with perchloric acid. This fact seems to support Heck's suggestion,[13] which has been drawn from other evidence, that cobalt hydrocarbonyl reacts as an acid.

Summary

The reactions of olefin oxides with cobalt hydrocarbonyl have been studied.

The effect of the reaction conditions on the nature of the reaction, especially that of propylene oxide, has been examined in detail. Propylene oxide gave only the products with β-hydroxy-*n*-butyryl structure under these reaction conditions: temperature, 25~−45°C; atmosphere; nitrogen or carbon monoxide; and mole ratio of propylene oxide, 1.4~6.2. The inhibitory effect of a nitrogen atmosphere on the formation of carbonylated products (ester and aldehyde) has been observed; under nitrogen, some side reaction was highly promoted, and the formation of carbonylated products was thereby prevented.

The reactions of ethylene oxide, cyclohexene oxide, styrene oxide and epichlorohydrin have also been studied. In the reactions of styrene oxide, the mole ratio of styrene oxide had a significant effect on the nature of the reaction; at a relatively small mole ratio, the reduction gave, mainly two isomeric alcohols, but as the mole ratio increased, the carboxylation reaction seemed to increase. Epichlorohydrin gave a product with a γ-chloro-β-hydroxy-*n*-butyryl structure, which corresponds to that which propylene oxide gave.

The order of the reactivity of these olefin oxides is as follows: cyclohexene oxide (about 5) and styrene oxide>propylene oxide (1)>ethylene oxide≫epichlorohydrin (1/20~40); (the numbers indicate the relative reactivities).

This fact seems to indicate that, in general, internal (and conjugated) olefin oxides are more reactive than terminal olefin oxides. By analogy with the relative reactivity of propylene oxide and epichlorohydrin with cobalt hydrocarbonyl, perchloric acid and ammonia, it may reasonably be considered that cobalt hydrocarbonyl reacts as an acid.

Pentene-1 appeared to be less reactive than propylene oxide.

Department of Fuel Chemistry
Faculty of Engineering
Kyoto University
Sakyo-ku, Kyoto

* The infrared spectrum of the product solution in toluene had a band at 1740 cm^{-1}. Further evidence: about 0.5 ml. of the sample solution and about 0.2 g. of potassium hydroxide were placed in a test tube. After the test tube had been shaken, the upper layer was gas-chromatographed. The largest peak of the original gas chromatogram, which is supposed to belong to the ester, vanished, and a new peak, with a comparable area, appeared before the position of the original peak. This fact indicates that the ester has a chlorohydrin structure (γ-chloro-β-hydroxy structure).

16) R. E. Parker and N. S. Isaacs, *Chem. Revs.*, **59**, 737 (1959).

*Studies of the Organic Reactions of Metal Carbonyl. III. The Hydroformylation of Olefin Oxides**

By Chikao YOKOKAWA, Yoshihisa WATANABE and Yoshinobu TAKEGAMI

(Received September 19, 1963)

Recent papers[1,2] have reported that an olefin oxide reacts with cobalt hydrocarbonyl and carbon monoxide to give acylcobalt carbonyl-type compounds, which are considered to be intermediates of the hydroformylation reactions.[3,4]

The reaction of ethylene oxide with water gas was carried out under the conditions of the ordinary Oxo-type reaction by Hamada, Baba and Hagihara,[5] who concluded that the hydroformylation of ethylene oxide did not take place. Lenel[6] concluded that olefin oxides, except ethylene oxide, undergoes the hydroformylation reaction, but he did not mention about the composition of the products. On the other hand, Seon and Leleu[7] obtained 2-hydroxyethyl hydracrylate from ethylene oxide by reaction with water and carbon monoxide in the presence of dicobalt octacarbonyl. Eisenmann, Yamartino and Howard[8] reported that the reaction product of propylene oxide with carbon monoxide and methanol in the presence of dicobalt octacarbonyl was methyl β-hydroxybutyrate.

Thus, the possibility of the hydroformylation of olefin oxide has been suggested, but no definite characteristics of this reaction are known. In this paper it will clearly be demonstrated that propylene oxide undergoes the hydroformylation reaction at a relatively low temperature (80°C) to give β-hydroxy-*n*-butyraldehyde as the major product.

Experimental

Reaction Procedures.—An autoclave of a 300 ml. capacity, made of 18—8 nickel-chrom-iron steel and equipped with a magnetic stirrer, was used. Ninety milliliters of toluene, 10 ml. of dicobalt octacarbonyl solution in toluene (containing 0.22 to 0.24 g. of cobalt by calculation from the content of the carbonyl), and 10 g. of olefin oxide were put into the autoclave. After replacing the air in the autoclave with hydrogen, hydrogen and carbon monoxide were introduced to 150 to 160 atm. using a compressor. The autoclave was kept at the desired temperature by electrical heating, but the heating was turned off when the gauge pressure ceased to decline.

Preparation and Standardization of the Dicobalt Octacarbonyl Solution in Toluene.—Ten grams of cobalt carbonate and 100 ml. of toluene were placed in the autoclave, and water gas was introduced to 160 atm. The autoclave was heated at about 150°C for 4 hr. The dicobalt octacarbonyl solution in toluene was then transferred into a flask by decantation and stored therein under a carbon monoxide atmosphere. An aliquot portion (10 ml.) of this solution was put into a gasometric apparatus by the use of a syringe, and the excess amount of iodine in toluene was added. The cobalt content of this solution was calculated from the amount of carbon monoxide evolved, with the assumption that all of the cobalt exsisted as dicobalt octacarbonyl or cobalt hydrocarbonyl.

Analysis of the Products.—In almost every case, an oily or resinous material which was insoluble in toluene was formed. After the separation of this material by the decantation of the toluene phase, the products in the toluene solution were identified and determined by gas chromatography. The products with boiling points lower than that of toluene were determined from the crude toluene solution, and other products, from the concentrated solution (the crude solution was concentrated under the reduced pressure of about 30 mmHg). The identification of the products was made by mixed gas chromatography with authentic samples. A column three meters long and 3 mm. in diameter, and filled with dilauryl phthalate on cerite, was used. The column temperature was 50 to 80°C for the analysis of the low-boiling-point products and 130°C for the high-boiling-point products. The rate of flow of the carrier gas (hydrogen) was 60 ml. per min.

The infrared adsorption spectrum was obtained in the toluene solution by the use of a Shimadzu Model IR—27 spectrophotometer.

Materials Used.—Ethylene oxide, propylene oxide and toluene were commercial products which were proved to be sufficiently pure by gas chromatography. As authentic samples, the following commercial chemicals were used: acetaldehyde, acrolein,

* Presented at the 16th Annual Meeting of the Chemical Society of Japan, Tokyo, April, 1963.

1) R. F. Heck *J. Am. Chem. Soc.*, **85**, 1460 (1963).
2) Y. Takegami, C. Yokokawa, Y. Watanabe and H. Masada, This Bulletin, **37**, 672 (1964).
3) L. Kirch and M. Orchin, *J. Am. Chem. Soc.*, **80**. 4428 (1958).
4) D. S. Breslow and R. F. Heck, *Chem. & Ind.*, **1960**, 467.
5) K. Hamada, K. Baba and N. Hagihara, *Memoirs Inst. Sci. Ind. Research, Osaka Univ.*, **14**, 207 (1957).
6) P. O. Lenel, *Proc. Chem. Soc.*, **1958**, 50.
7) M. Seon and J. Leleu, U. S. Pat. 2782226, Feb. 19 (1957).
8) J. L. Eisenmann, R. L. Yamartino and J. F. Howard Jr., *J. Org. Chem.*, **26**, 2102 (1961).

TABLE I. HYDROFORMYLATION OF PROPYLENE OXIDE

No.		1	2*1	3	4	5	6*2	7*3
Reaction temp., °C		115~120	105~110	90~95	85~90	80~85	110~115	110~115
H_2/CO		1.0	1.4	1.0	1.0	1.0	2.0	2.0
Reaction time, hr.		2.5	1.0	3.0	3.0	2.0	0.7	1.0
Yield of products (mol. per 100 mol. of propylene oxide used)	Acetone	51	21	6.4	15	4.6	24	6.4
	Isobutyraldehyde	5.1	4.9	1.2	0.5	trace	3.4	nil
	Metacrolein	trace	0.8	0.8	trace	trace	trace	2.1
	n-Butyraldehyde	16.4	8.5	1.4	0.7	0.6	9.3	trace
	Isobutyl alcohol	1.5	0.6	trace	nil	nil	0.2	nil
	Crotonaldehyde	trace	1.2	5.4	0.9	1.2	3.8	15
	n-Butyl alcohol	2.3	trace	trace	nil	nil	trace	nil
	β-hydroxy-isobutyraldehyde	trace	7.5	nil	trace	trace	nil	trace
	β-hydroxy-*n*-butyraldehyde	3.3	24	56	32	42	18	20
Character of polymer		oily	oily	oily	oily	oily	resinous	resinous

*1 The compounds with the relative retention time of 313 and 450 were formed in 0.6 and 1.7 mol. per 100 mol. of propylene oxide, respectively.

*2 Two mol. of pyridine were added per mol. of dicobalt octacarbonyl.

*3 Four mol. of pyridine were added per mol. of dicobalt octacarbonyl. About 20 percent of propylene oxide were recovered unreacted.

metacrolein, acetone, isobutyraldehyde, *n*-butyraldehyde, isobutyl alcohol, *n*-butyl alcohol, crotonaldehyde and β-hydroxy-*n*-butyraldehyde (aldol).

Results

The Interpretation of a Typical Gas Chromatogram.—In order to facilitate further considerations, the gas chromatogram for the products obtained from propylene oxide by the reaction at 115 to 120°C (Exp. 1) will be discussed in detail. This chromatogram illustrates 20 peaks, 10 of which were identified by mixed chromatography with authentic samples. These compounds were propylene oxide (9.9), acetone (12.4), isobutyraldehyde (19.1), metacrolein (21.5), *n*-butyraldehyde (25.3), isobutyl alcohol (45.4), crotonaldehyde (53.0), *n*-butyl alcohol (72.6), toluene (100) and β-hydroxy-*n*-butyraldehyde* (194). (The numbers in ( ) denotes the relative retention time.) The peak with the relative retention time of 163 was believed to correspond with that for β-hydroxyisobutyraldehyde, though an authentic sample was not available, because metacrolein** and isobutyraldehyde, which are considered to have been derived from β-hydroxy-isobutyraldehyde, existed in the same sample and because the retention time of this product is a little smaller than that of β-hydroxy-*n*-butyraldehyde. There were 9 peaks of by-products, whose retention times were larger than that of β-hydroxy-*n*-butyraldehyde, in this gas chromatogram. They were not identified, but all of them diminished to negligible amounts when the reactions were carried out at temperatures below 100°C.

The Hydroformylation of Propylene Oxide.—The hydroformylation reaction of propylene oxide seems to take place at temperatures above 80°C; at any rate, the gauge pressure begins to decrease at this temperature.

The composition of the reaction products is listed in Table I, in which the yield of products is given in the number of mol. per 100 mol. of propylene oxide used. These values were obtained by calculations on the basis of the area of each peak in a gas chromatogram after the usual calibration using authentic samples. In the calculation of β-hydroxy-*n*-butyraldehyde, the amount of crotonaldehyde which is considered to be formed from the former in the course of the gas chromatographic analysis was accounted as before.

It is evident that the major product of the reaction at the temperature of the ordinary hydroformylation reaction of olefins, i.e., 110 to 120°C, is acetone, and so it has been concluded that the isomerization reaction predominates in this reaction condition. The hydroformylation reaction also takes place, giving β-hydroxybutyraldehydes, but these products are converted into isobutyraldehyde, metacrolein, *n*-butyraldehyde, isobutyl alcohol, crotonaldehyde and *n*-butyl alcohol by succeeding dehydration and hydrogenation reactions.

* β-Hydroxy-*n*-butyraldehyde is the major product of this reaction. This compound could be isolated by fractional distillation under reduced pressure in a sufficiently pure state. The infrared spectrum of this product showed strong absorptions at 1720 cm^{-1} and 3350 cm^{-1}. 2, 4-Dinitrophenyl hydrazone was formed, but this hydrazone seemed impure because it is known that β-hydroxy-*n*-butyraldehyde is easily dehydrated to form crotonaldehyde under the conditions of hydrazone formation. It was concluded that this product was β-hydroxy-*n*-butyraldehyde on the basis of the facts mentioned above and because this product showed a peak which corresponded to that of crotonaldehyde when gas chromatographed at 130°C.

** Metacrolein was identified in the crude solution. In the concentrated solution it was not observed but after the solution had been refluxed for 1hr. at the boiling point of toluene, it appeared clearly.

Table II. Hydroformylation of ethylene oxide

No.	Reaction temp. °C	H_2/CO	Reaction time hr.	Yield of products (mol. per 100 mol. of ethylene oxide used)		amount of gas absorbed (mol./mol. of ethylene oxide)
				Acetaldehyde	Acrolein	
8	90~100	1.0	0.8	16	2.8	1.3
9	85~ 86	1.0	1.3	28	1.0	1.2
10	80~ 82	1.5	3.0	26	0.9	0.8
11*	80~ 85	1.7	2.0	30	1.8	0.9
12**	85~ 90	4.0	2.0	8	0.9	—

* Two mol. of pyridine were added per mol. of cobalt.
** Four mol. of pyridine were added per mol. of cobalt.

Moreover, various kinds of high-boiling-point products are formed.

By lowering the reaction temperature for about 10°C (Exp. 2), the yields of the hydroformylation products, i. e., β-hydroxy-*n*-butyraldehyde and β-hydroxy-isobutyraldehyde, increased, and those of the by-products decreased, but still more than 20% of the propylene oxide charged were converted into acetone and various kinds of compounds were formed.

At the reaction temperature below 95°C, β-hydroxy-*n*-butyraldehyde is formed as the major product, as Exps. 3, 4 and 5 show, and so it has been concluded that the hydroformylation of propylene oxide proceeds relatively selectively under these controlled conditions.

The addition of pyridine has evident effects on the character of this reaction. As Exps. 6 and 7 show, the addition of this compound seems to prevent not only the isomerization but also the hydroformylation reaction; the amount of acetone decreases, and relatively large amounts of unreacted propylene oxide and resinous material are recovered.

The isomerization of propylene oxide to acetone in the presence of dicobalt octacarbonyl was studied by Eisenmann[9] in several kinds of solvents. He concluded that this isomerization takes place during a reversible exchange between the solvent molecule and propylene oxides serving as a coördinating molecule to cobalt, and that pyridine retards this isomerization reaction because of its strong coördinating effect. It is believed that the present object is to control the two competitive reactions, i. e., hydroformylation and isomerization, but it seems impossible to attain this purpose by the addition of pyridine.

The Hydroformylation of Ethylene Oxide.— The results of the reaction of ethylene oxide are summarized in Table II. Ethylene oxide produces acetaldehyde and a viscous, oily material as the major products, plus a small amount of acrolein. Thus, ethylene oxide seems to undergo isomerization and polymerization under the conditions which are effective for the hydroformylation of propylene oxide. On the other hand, an appreciable amount of gas is absorbed at temperatures above 80°C, as is indicated by the decrease in the gauge pressure, and acrolein is identified as a minor product. This evidence seems to indicate that the hydroformylation has taken to an appreciable extent. It is reasonably considered that the hydroformylation product of ethylene oxide, β-hydroxypropionaldehyde, would be formed, that this compound would be converted into acrolein by succesive dehydration reaction, and that the latter would polymerize to form the oily or resinous product.

9) J. L. Eisenmann, *J. Org. Chem.*, 27, 2706 (1962).

Summary

The hydroformylation reactions of ethylene oxide and propylene oxide have been carried out; the character of this type of reaction may be summarized as follows:

1) Propylene oxide reacts with water gas, in the presence of dicobalt octacarbonyl serving as a catalyst, to give β-hydroxy-*n*-butyraldehyde as the major product, but it is important to keep the reaction temperature between 80 to 100°C in order to hold the high selectivity of this reaction.

2) At temperatures below 80°C, the reaction does not take place; on the other hand, at temperatures above 100°C, the isomerization of propylene oxide to acetone predominates, and the other side-reactions, such as the dehydration of the hydroformylation products, hydrogenation, condensation and polymerization, take place simultaneously.

3) Ethylene oxide seems to undergo hydroformylation under the same conditions as those used for the propylene oxide, but only a small amount of acrolein is obtained as the hydroformylation product. The expected product, i. e., β-hydroxypropionaldehyde, is formed, but this compound is easily converted into acrolein and the latter seems to polymerize to give a large amount of a resinous or oily material.

Department of Fuel Chemistry
Faculty of Engineering
Kyoto University
Sakyo-hu, Kyoto

The Monoterpene Constituents of the Essential Oil of Hinoki (Chamaecyparis Obtusa (Sieb. et Zucc.) Endl.)

By Shûichi HAYASHI, Katsumi YANO and Tamon MATSUURA

(Received October 7, 1963)

There have been some investigations of the monoterpene constituents of the essential oil of Hinoki (*Chamaecyparis Obtusa* (Sieb. et Zucc.) Endl.). A root oil of Hinoki has been investigated by Hirao,[1] who detected *d*-α-pinene, camphene, *d*-limonene, dipentene, camphor, borneol and α-terpinol. A leaf oil has been investigated by Uchida,[2] Kumagai[3] and Moroe;[4] they have reported the presence of α-pinene, *d*-limonene, borneol, bornyl acetate, bornyl pelargonate and α-terpinyl acetate. In the present work an attempt will be made to obtain a satisfactory confirmation for the monoterpene constituents of the essential oil by means of gas chromatography and ultraviolet and infrared absorption spectroscopies.

Results and Discussion

The essential oil obtained from leaves and twigs of Hinoki which grew in Kôchi Prefecture in Japan, after acids and phenols had been taken off, was repeatedly fractionated through a packing distillation column. The physical properties of the fractions are shown in Fig. 1. From these fractions, *d*-α-pinene, β-pinene, myrcene, *d*-limonene, β-phellandrene, *p*-cymene, 1, 8-cineole, camphor, *l*-α-terpineol, α-terpinyl acetate and bornyl acetate were identified in ways described below, while camphene, linalool and borneol were confirmed by gas chromatography. Among these constituents, β-pinene, myrcene, β-phellandrene, 1, 8-cineole, and *p*-cymene were found out for the first time in the essential oil of Hinoki.

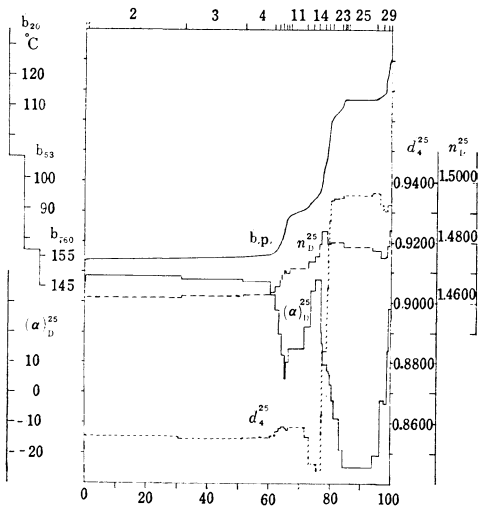


Fig. 1. Fractional distillation of Hinoki oil.

d-α-Pinene.—Each infrared spectrum of fractions 2 to 4 coincides with that of α-pinene,[5] and each gas chromatogram of these fractions shows the main peak corresponding to α-pinene. From fraction 2, *d*-α-pinene hydrochloride[6], (m. p. 131.5~132.0°C) was prepared.

Camphene.—A gas chromatogram of fraction 3 exhibits a small peak corresponding to camphene, besides a main α-pinene peak.

β-Pinene.—A gas chromatogram of fraction 11 shows a strong peak associated with β-pinene, together with other peaks associated with α-pinene, myrcene, limonene, β-phellandrene and

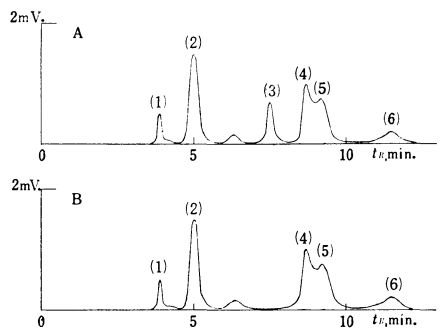


Fig. 2. Gas chromatogram of fraction 11.

A Before the maleic anhydride treatment.
B After the maleic anhydride treatment.
(1) α-pinene (2) β-pinene
(3) myrcene (4) limonene
(5) β-phellandrene (6) *p*-cymene

1) N. Hirao. *J. Chem. Soc. Japan* (*Nippon Kwagaku Kwaishi*), **58**, 222 (1937).
2) S. Uchida, *J. Soc. Chem. Ind. Japan* (*Kōgyō Kwagaku Zasshi*), **31**, 650 (1928).
3) H. Kumagai, *J. Chem. Soc. Japan* (*Nippon Kwagaku Kwaishi*), **63**, 328 (1942).
4) T. Moroe and S. Hara, *J. Pharm. Soc. Japan* (*Yakugaku Zasshi*), **71**, 503 (1951).
5) R. T. O'Conner and L. A. Goldblatt, *Anal. Chem.*, **26**, 1726 (1954).
6) F. H. Thurber and R. C. Thielke, *J. Am. Chem. Soc.*, **53**, 1030 (1931).

p-cymene, as may be seen in Fig. 2-A. From this fraction a thioglycollic acid adduct of β-pinene was prepared; it was identified by preparing its *S*-benzylthiuronium salt.[7]

Myrcene.—The ultraviolet absorption spectrum of fraction 11 has two absorption maxima: λ_{max}^{EtOH} 224 mμ (ε 4380) corresponding to myrcene,[5] and 230 mμ corresponding to β-phellandrene.[8] When fraction 11 was treated with maleic anhydride in ether[9] at room temperature, both the absorption maximum and the peak of gas chromatogram associated with myrcene disappeared (cf. Fig. 2-B).

Limonene and Dipentene.—The gas chromatogram of fraction 14 shows three peaks associated with limonene, β-phellandrene and *p*-cymene, together with some weak peaks (cf. Fig. 3). On the bromination of this fraction, dipentene tetrabromide[10] (m. p. 123~124°C) and *d*-limonene tetrabromide[10] (m. p. 101~102°C) were obtained.

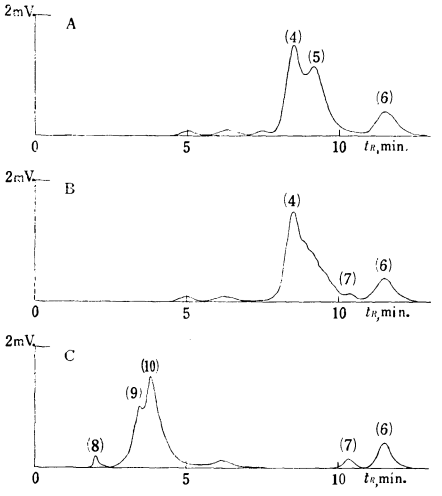


Fig. 3. Gas chromatogram of fraction 14.
A Before the maleic anhydride treatment.
B After the maleic anhydride treatment.
C After hydrogenation.
(4) limonene or dipentene
(5) β-phellandrene
(6) *p*-cymene
(7) 1,8-cineole
(8) hexahydromyrcene
(9) *cis*-*p*-menthane
(10) *trans*-*p*-menthane

β-Phellandrene.—The ultraviolet spectrum of fraction 14 shows an absorption band (λ_{max}^{EtOH} 230 mμ, ε 3590) corresponding to β-phellandrene.[8] When maleic anhydride reacted upon fraction 14, the absorption band and the peak of gas chromatogram associated with β-phellandrene disappeared (cf. Fig. 3-B). From fraction 14, β-phellandrene-β-nitrosite[11] (m. p. 96~97°C) was obtained.

***p*-Cymene.**—The ultraviolet spectrum of fraction 14 has another weak absorption band (λ_{max}^{EtOH} 273.5 mμ) characteristic of *p*-cymene,[5] in addition to the band of β-phellandrene. When fraction 14 was hydrogenated with a nickel catalyst, β-phellandrene and limonene vanished, but the peak associated with *p*-cymene in a gas chromatogram of the hydrogenation product remained, as is shown in Fig. 3-C.

1, 8-Cineole.—The peak of 1, 8-cineole was not observed in the gas chromatogram of any fraction. The peak, however, could be observed after the removal of β-phellandrene from fraction 14 by maleic anhydride-treatment or by hydrogenation, as Figs. 3-B and 3-C show.

Camphor, Linalool, Borneol and *l*-α-Terpineol.—The chromatogram of fraction 23 exhibits four peaks associated with linalool, camphor, borneol and α-terpineol (cf. Fig. 4).

The peak associated with camphor disappeared almost completely upon treatment with a 2, 4-dinitrophenyl hydrazine solution, thereby comfirming the existence of camphor.

l-α-Terpineol was identified by preparing *l*-α-terpinyl phenylurethane (m. p. 109~110°C[12]) from fraction 23.

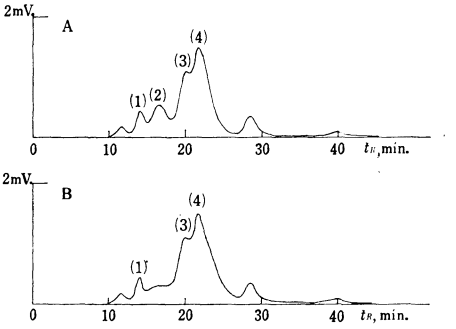


Fig. 4. Gas chromatogram of fraction 23.
A Before the 2,4-dinitrophenylhydrazine treatment.
B After the 2,4-dinitrophenylhydrazine treatment.
(1) linalool (2) camphor
(3) borneol (4) α-terpineol

Bornyl Acetate and α-Terpinyl Acetate.—The gas chromatogram of fraction 29 shows three peaks associated with α-terpineol, bornyl

7) M. D. Sutherland and J. W. Wells, *J. Org. Chem.*, **21**, 1272 (1956).
8) A. K. Macbeth, G. E. Smith and T. F. West, *J. Chem. Soc.*, **1938**, 119.
9) G. A. Rudakov and M. M. Shestaeva, *Zhr. Priklad. Khom.*, **28**, 1199 (1955).
10) O. Wallach, *Liebigs Ann.*, **225**, 304, 318 (1884).
11) T. K. Gaponenkov, *J. Gen. Chem. U. S. S. R.*, **5**, 1485 (1935).
12) O. Wallach, *Liebigs Ann.*, **230**, 268 (1885); **275**, 104 (1893).

acetate and α-terpinyl acetate (cf. Fig. 5). This fraction was then saponified. In a gas chromatogram of the saponification product, the two peaks associated with bornyl acetate and with α-terpinyl acetate both disappeared completely, while a new peak of borneol was found; furthermore, a peak of α-terpineol grew up, as may be seen in Fig. 5-B. On the other hand, from the aqueous layer of the saponification product, acetic acid was detected by paper chromatography as its hydroxamic acid.[13]

The Constitution of the Monoterpene Fractions.—The contents of the above components were calculated in the total monoterpene fractions from the results of fractionation and gas chromatography, as Table I shows. The essential oil of Hinoki was composed of 47.5% monoter penes, 43.2% sesquiterpenes, 7.1% residue and 2.2% acids and phenols.

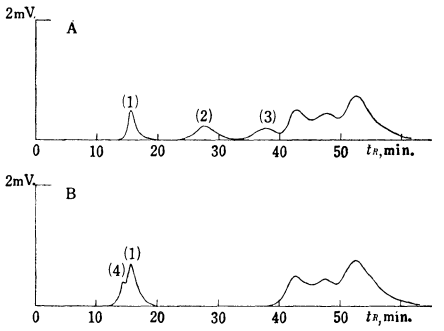


Fig. 5. Gas chromatogram of fraction 29.
A Before saponification.
B After saponification.
(1) α-terpineol (2) bornyl acetate
(3) α-terpinyl acetate (4) borneol

TABLE I. THE CONSTITUTION OF THE MONOTERPENE FRACTION OF HINOKI OIL

Compound	Content, %
d-α-Pinene	66.3
Camphene	0.2
β-Pinene	0.8
Myrcene	0.6
d-Limonene (dipentene)	1.3
β-Phellandrene	1.5
p-Cymene	1.9
1,8-Cineole	trace
Camphor	0.6
Linalool	0.4
Borneol	0.6
l-α-Terpineol	10.1
Bornyl acetate	2.3
α-Terpinyl acetate	0.8
Others	12.4

13) K. Inoue and M. Noda, *J. Agr. Chem. Soc. Japan (Nôgei Kagaku Kwaishi)*, **23**, 294 (1950); **24**, 291 (1951).

Experimental

The sample was the essential oil* (n_D^{25} 1.4832, d_4^{25} 0.8877, $[\alpha]_D^{25}$ +22.76, ester value 0.5) obtained from leaves and twigs of Hinoki by steam distillation. The oil (13.9 kg.) was shaken with a 3% aqueous solution of sodium carbonate and then a 3% aqueous solution of sodium hydroxide to take off acids and phenols. The neutral oil thus obtained (13.6 kg.) was washed with water, dried over anhydrous sodium sulfate, and repeatedly fractionated through a packing distillation column under reduced pressure.

***d*-α-Pinene.**—Dry hydrogen chloride gas was reacted upon fraction 3 under cooling at −10 to −15°C. The crystals thus obtained, after being recrystallized from methyl alcohol, showed a melting point of 131.5~132.0°C, which agrees with that of *d*-α-pinene hydrochloride.[6]

β-Pinene.—From one milliliter of fraction 11, a thioglycollic acid adduct of β-pinene was prepared and converted into *S*-benzyl thiuronium salt according to the procedure of Sutherland and Wells.[7] The white crystalline solid, after being recrystallized from an acetone-methanol (2 : 1) mixture, showed a melting point of 155~157°C, which did not depress when the solid was admixed with an authentic sample (m. p. 156~157°C).

***d*-Limonene and Dipentene.**—Bromine was added to a portion of fraction 14 under ice-cooling, using ether as a solvent. The crystalline mass obtained was fractionally recrystallized from ethyl acetate to give dipentene tetrabromide (m. p. 123~124°C) and limonene tetrabromide (m. p. 101~102°C). Each tetrabromide was identified by admixing it with an authentic sample.

β-Phellandrene.—Four grams of fraction 14 were treated with acetic acid and a saturated aqueous solution of sodium nitrite. The white crystals obtained, after being recrystallized from ethanol, showed a melting point of 96~97°C, which did not depress on admixture with β-phellandrene-β-nitrosite (m. p. 96~97°C).

1, 8-Cineole.—Eight hundred milligrams of fraction 14 were hydrogenated in an autoclave using nickel catalyst and ethanol (initial pressue of hydrogen, 112 kg./cm²; reaction temperature, 155°C; reaction period, 2 hr.). The gas chromatogram of the hydrogenation product was then examined (Fig. 4).

***l*-α-Terpineol.**—Phenylisocyanate was added to 0.5 g. of fraction 25. The phenylurethane obtained showed a melting point of 109~110°C, which agrees with that of the phenylurethane of *l*-α-terpineol.

Gas Chromatography.—A Shimadzu GC-2 apparatus equipped with a thermal conductivity detector and a copper spiral packing column (inside diameter, 4 mm.; length, 3 m.) was used. For hydrocarbon analysis, Shimalite (24~48 mesh) coated with polyethylene glycol (20%) was used at 80°C as a stationary phase; for an oxygen-containing compound analysis, quartz powder (150~200 mesh) coated with Thermol-1 (5%) was used at 140°C.

* Supplied by the Soda Kôryo Co., Ltd., Tokyo, Japan.

Helium was flowed as a carrier gas at the rate of 60 ml./min.

Summary

d-α-Pinene, β-pinene, myrcene, *d*-limonene, dipentene, β-phellandrene, *p*-cymene, 1, 8-cineole, camphor, *l*-α-terpineol, α-terpinyl acetate and bornyl acetate have been identified, and camphene, linalool and borneol have been gas-chromatographically confirmed. Of these compounds, β-pinene, myrcene, β-phellandrene, 1, 8-cineole and *p*-cymene have been found for the first time in this work. The main constituents of the monoterpene fraction are *d*-α-pinene and *l*-α-terpineol; the former amounts to 66.3%, and the latter to 10.1%, the remaining constituents being within a few %.

Department of Chemistry
Faculty of Science
Hiroshima University
Higashi-sendamachi
Hiroshima

Studies of Tritium-labeled Compounds. VII.[1] *The Platinum-catalyzed Exposure Reaction*

By Teruhiko MESHI and Yoshishige SATO

(Received July 4, 1963)

In the gas exposure technique developed by Wilzbach[2] only a small part of the tritium gas used is actually incorporated into organic compounds, and relatively large quantities of tritium gas and prolonged exposure are required to supply sufficient energy to the system. In a previous work,[1] it was found that the platinum catalyst was the most effective in the promotion of labeling, and it was suggested, on the basis of the large increase in the ratio of nonlabile tritium to labile tritium in salicylic acid in the platinum-catalyzed labeling, that this catalytic action probably is due to the catalytic exchange of hydrogen atoms rather than to the increased absorption of the decay energy in the system. It is evident that tritium gas is adsorbed on the surface of the platinum catalyst, but the question remains of whether or not a similar adsorption of solid organic compounds occurs on the catalyst surface. The fact[1] that the aromatic compounds are usually more efficiently labeled than the aliphatic compounds may be accounted for by assuming that the former is more readily chemisorbed on the catalyst surface through such an interaction as the π-complex formation. In order to elucidate the nature of the chemisorption and to obtain some information on possible reaction paths, it seems useful to investigate the effects of the substituents upon the hydrogen-tritium exchange of the aromatic ring and the tritium distributions within aromatic compounds labeled by different methods. Salicylic acid and benzoic acid were chosen as suitable materials for the determination of tritium distribution. The relative amounts of ring tritiation at the *o*-, *m*- and *p*-positions of salicylic acid were determined by the bromination of the recovered salicylic acid, while those of benzoic acid were determined by first converting it into aniline, which was then brominated to give bromination products, whose tritium activities were determined.

Benzoylvaline was used to determine the relative exchange rates of labile, semilabile and nonlabile hydrogen atoms.

Experimental

Samples. — All the chemicals used were of analytical reagent grade and were not subjected to any further purification. Platinum black was prepared by the hydrogenation of Adams platinum oxide. The tritium gas was purchased from the Radiochemical Centre, Amersham.

Exposures. — Exposures were carried out by the same procedure as was described in the previous paper.[1] Since it was found that the highest specific activity was obtainable when the exposure time was less than one hour, all the reactions were performed for one hour at room temperature.

Purifications. — Radiochemical purifications of benzoic acid and salicylic acid have been described in the previous paper. *p*-Aminobenzoic acid and *p*-aminosalicylic acid were purified according to

1) Part VI: T. Meshi and T. Takahashi. This Bulletin, 35, 1510 (1962).
2) K. E. Wilzbach, *J. Am. Chem. Soc.*, **79**, 1013 (1957).

the solvent extraction procedure of Rydberg and Hanngren.[3] Phthalic acid, naphthalene and benzoylvaline were diluted with their respective untritiated compounds and recrystallized from a mixture of ethanol and water until constant specific activities were obtained. Benzene was converted into *m*-dinitrobenzene, which was then purified by repeated recrystallization from ethanol to a constant specific activity. Dimethylaniline was converted into its picrate.

Degradations. — The successive reaction steps used for the determination of tritium distributions of salicylic acid and benzoic acid are as follows:

Salicylic acid $\xrightarrow{Br_2}$ 5-Bromosalicylic acid $\xrightarrow{Br_2}$ 3,5-Dibromosalicylic acid

Benzoic acid $\xrightarrow{SOCl_2}$ Benzoyl chloride $\xrightarrow{NH_4OH}$ Benzamide $\xrightarrow{NaOBr}$

Aniline $\xrightarrow{(CH_3CO)_2O}$ Acetanilide $\xrightarrow{Br_2}$ *p*-Bromoacetanilide

Aniline $\xrightarrow{Br_2}$ Tribromoaniline

The scheme used for benzoic acid was used earlier by Bonner[4] in the determination of the distribution of deuterium.

Benzoylvaline, the labile tritium of which had been removed by treating it with a mixture of water and ethanol, was treated with an alkaline solution to remove the semilabile tritium incorporated at the amide group; then it was hydrolyzed into benzoic acid and L-valine by refluxing it with 6 N-hydrochloric acid.

Tritium Assay. — The tritium activity of each compound was assayed by liquid scintillation counting. An aliquot of a suitable concentration of a compound in ethanol was added to toluene containing 2,5-diphenyloxazole (4 g./l.) and 1,4-bis-2-(5-phenyloxazolyl)-benzene (100 mg./l.), and the solution was counted with a Pachard Tri-Carb liquid scintillation spectrometer cooled to $-10°C$. The efficiency of counting was usually about 13% if the sample was nonquenching. An internal standard consisting of 0.1 ml. of benzene-^3H (2.3×10^5 d. p. m.) was used to correct for the quenching loss and to estimate the efficiency of counting.

Results and Discussion

The data in Table I show the effect of the substituents on the tritium labeling of the aromatic compounds. It may be seen that the amount of nonlabile tritium attached to carbon atoms varies considerably with the nature of the substituents and that the amount of tritium incorporated into the aromatic nucleus is usually small in the substituted compounds, except for salicylic acid. When one compares the amount of tritium incorporation in phthalic acid and phthalic anhydride, one finds that not only the substituents but also the presence of labile hydrogen atoms attached to oxygen or nitrogen substantially lower the amount of tritium incorporation into the aromatic nucleus. If one assumes that the catalytic activity of the platinum catalyst is a consequence of its unfilled d-orbitals and that the chemisorption of the aromatic compounds on a platinum catalyst occurs through the transfer of the π-electrons of the aromatic compounds into the empty d-orbitals of the catalyst, one would expect that the substituents which have higher electron densities than the aromatic rings would monopolize the active centers of the catalyst and that, consequently, the chemisorption of the aromatic ring on the platinum catalyst would be decreased, thus lowering the amount of tritium incorporation into the rings. However, it can not be explained why only the hydroxyl group promotes the isotope exchange of the aromatic ring, as is shown in an experiment carried out with salicylic acid. Garnett et al.[5] studied the catalytic exchange of hydrogen atom using deuterium oxide and concluded that the stronger the chemisorption, the greater the tendency for a compound to poison the catalyst and, consequently, for the exchange to be less efficient.

The competitive incorporation of tritium was performed with a mixture of benzene with another aromatic compounds, using the amount of the tritium incorporation in benzene as the standard. When one compares the specific activities in Table I and Table II, one finds that the tritium incorporation of benzene decreases greatly in the presence of dinitrobenzene, phthalic anhydride, salicylic acid and dimethylaniline, and that of these compounds, except for dimethylaniline, also does in the presence of benzene. These results are in direct contrast to those obtained with the mixture of benzene and cyclohexane, which has only a very small retarding effect on the tritium incorporation of benzene. (Incidentally, the platinum-catalyzed tritium incorporation of cyclohexane is relatively low.)

It is evident from these results that the bond strength of the chemisorption and the π-complex formation are important factors in the determination of the extent of isotope exchange. It may be considered that the amino group and the nitro group are so strongly chemisorbed on the catalyst surface that the specificity of the catalyst is lost, while the hydroxyl group is relatively weakly chemisorbed so as to cause a more facile chemisorption of the aromatic

3) J. Rydberg and A. Hanngren, *Acta Chem. Scand.*, **12**, 332 (1958).
4) W. A. Bonner, *J. Am. Chem. Soc.*, **79**, 2469 (1957).
5) J. L. Garnett, L. J. Henderson and W. A. Sollich, "Symposium on the Detection and Use of Tritium in the Physical and Biological Sciences," Vienna (1961).

TABLE I. EFFECT OF SUBSTITUENTS ON TRITIUM LABELING OF AROMATIC COMPOUNDS*

Compound	Time hr.	Catalyst mg.	Labile tritium A μc./μM	Nonlabile tritium B μc./μM	Increase of[a] specific activity	Ratio of B to A %
Benzene	1	50		15.8	298.0	
Naphthalene	1	50		4.9	76.2	
Dimethylaniline	1	50		1.34		
Dinitrobenzene	1	50		0.59	8.1	
Phthalic anhydride	1	50		9.7	212.0	
Phthalic acid	1	50	50.2	1.27		2.6
Benzoic acid	1	50	44.3	2.31	40.3	5.2
p-Aminobenzoic acid	2	100	71.0	0.21		0.30
Salicylic acid	1	50	95.0	14.1	596.0	14.8
p-Aminosalicylic acid	2	100	63.5	0.07		0.10
5-Bromosalicylic acid	2	100	77.6	0.04		0.06

* One hundred milligrams of each sample was exposed to about 100 mc. of tritium gas.
a) An increase in specific activity compared with gas exposure experiment.

TABLE II. RETARDATION EFFECT OF CATALYST POISONS UPON THE H-T EXCHANGE OF BENZENE*

Reaction mixture	Catalyst mg.	Tritium gas mc.	Quantity mmol.	Specific activity μc./μM	Comparison[a] of specific activities %
Benzene	50	100	1.30	1.36	8.6
Dinitrobenzene			0.65	0.08	14.0
Benzene	50	100	1.30	3.52	22.2
Dimethylaniline			0.65	1.33	99.2
Benzene	50	100	1.30	6.10	38.4
Phthalic anhydride			0.65	0.22	2.28
Benzene	50	100	1.30	1.50	9.5
Salicylic acid			0.65	0.02[b]	0.14
Benzene	100	200	2.60	14.50	91.5
Cyclohexane			2.60	0.26[c]	—

* All reactions were performed at room temperature for one hour.
a) The values in this column represent the ratio of the specific activities in Table II to those in Table I.
b) This value is the amount of the nonlabile tritium attached to carbon atoms but that of the labile tritium is 70.8 μc./μM.
c) This value was obtained when cyclohexane alone was exposed to the tritium gas in the presence of the catalyst.

nucleus by increasing the electronic density of the aromatic ring. The unexpectedly large decrease in the incorporation of tritium into salicylic acid in the presence of benzene can be explained on the basis of the increased probability of the hydroxyl group of the salicylic acid dissolved in benzene being chemisorbed, which would result in the decreased chemisorption of the nucleus of salicylic acid and the predominant exchange of the labile hydrogen attached to oxygen by the tritium present in the adsorption layer, for the amount of the labile tritium incorporated into salicylic acid is as large as 70.8 μc./μM.

The tritium distribution in benzoic acid in salicylic acid treated with tritium gas was determined by measuring the specific activities of the products derived from their acids; they are shown in Table III and Table IV. It may be seen that, in the gas-exposure experiments, i. e., in the absence of platinum black, the ortho hydrogens exchange at a faster rate than do those of the meta and para positions since salicylic acid has two hydrogens at the meta position but only one at the ortho position.

This is in agreement with the result obtained with benzoic acid,[6] toluene,[7] chlorobenzene[8] and nitrobenzene.[8] It may be of interest that, in the gas-exposure technique, the ortho position is always favored. On the other hand, the tritium distribution in benzoic acid and in salicylic acid labeled by the catalyzed exposure method indicates that the predominant exchange occurs at the meta positions of benzoic acid and at the para position to the

6) K. E. Wilzbach, "Proceedings of the Symposium on Tritium in Tracer Applications" (1957), p. 3.
7) H. J. Ache. W. Herr and A. Thiemann, "Symposium on the Detection and Use of Tritium in the Physical and Biological Sciences," Vienna (1961).
8) F. Cacace, *Int. J. Appl. Rad. Isotopes*, **8**, 82 (1960).

TABLE III. THE DISTRIBUTION OF TRITIUM IN BENZOIC ACID

Method	Labile tritium μc./mg.	Nonlabile tritium μc./mg.	Ortho %	Meta %	Para %
Gas exposure	62.5	0.47	58.3	21.3	20.4
Catalyzed exposure	382.3	18.90	5.0	72.5	22.5

One hundred milligrams of benzoic acid was exposed to 100 mc. of the tritium gas for one hour in the presence of 50 mg. of platinum black.

TABLE IV. THE DISTRIBUTION OF TRITIUM IN SALICYLIC ACID

Method	Labile tritium μc./mg.	Nonlabile tritium μc./mg.	Ortho to OH %	Meta to OH %	Para to OH %
Gas exposure	115.6	0.17	39.0	48.4	13.6
Catalyzed exposure	792.0	102.0	16.9	31.7	51.4

One hundred milligrams of salicylic acid was exposed to 100 mc. of the tritium gas for one hour in the presence of 50 mg. of platinum black.

TABLE V. THE AMOUNT OF TRITIUM IN VARIOUS POSITIONS IN BENZOYLVALINE LABELED BY THE DIFFERENT METHODS*

Method	Time hr.	Labile tritium μc./mg.	Semilabile tritium μc./mg.	Nonlabile tritium μc./mg.	Tritium in ring %	Tritium in side-chain %
Gas exposure	1	77.835	0.015	0.15	92.5	7.5
Catalyzed exposure	1	286.26	8.47	0.27	60.2	39.8

* One hundred milligrams of benzoylvaline was exposed to 100 mc. of the tritium gas for one hour in the presence or in the absence of 100 mg. of platinum black.

hydroxyl group of salicylic acid. From the observed tendency in the tritium distributions, it may well be assumed that, in the catalyzed exposure, the hydrogen-tritium exchange in the aromatic ring may follow the substitution rule for electrophilic aromatic exchange. In the gas exposure method, the reactive tritium species are the energetic tritium ions produced by the radioactive decay of the tritium and by the beta radiation,[9] while in the catalyzed exposure it seems to be a tritium ion or atom formed by the dissociation of the tritium molecule on the catalyst surface. Therefore, it would be natural to expect that the tritium arrangements in benzoic acid and salicylic acid would be different between the gas exposure and the catalyzed exposure, and that, in the catalyzed exposure, just as in the chemical substitution reaction, the reactive tritium ion would be directed in this order: meta>para>ortho in benzoic acid and para>ortho>meta in salicylic acid.

The distribution of tritium in benzoylvaline labeled by both the methods is shown in Table V. It is noticeable that the amount of the semilabile tritium incorporated into the amide group varies remarkably with the different methods. In the catalyzed exposure experiment, the amount of the semilabile tritium becomes much larger than that of the nonlabile tritium, although in the gas exposure experiment the amount of the semilable tritium is less than that of the nonlabile tritium. This also seems to suggest that the chemisorption of the benzoylvaline molecule on the platinum catalyst predominates at the amide group.

As Table V shows, the amount of tritium exchange is the largest for labile hydrogen, intermediate for semilabile hydrogen, and the smallest for nonlabile hydrogen. In other words, the more readily a hydrogen dissociates, the more rapidly it undergoes the exchange with tritium.

9) T. H. Pratt and R. Wolfgang, *J. Am. Chem. Soc.*, 83, 10 (1961).

Summary

In order to elucidate the nature of the chemisorption in the platinum-catalyzed exposure reaction with tritium, the effects of the substituents upon the hydrogen-tritium exchange of the aromatic ring and upon the tritium distribution in benzoic acid, salicylic acid and benzoylvaline have been investigated. All the substituents except the hydroxyl group decrease the hydrogen-tritium exchange of the aromatic ring, and the compounds carrying those substituents poison the catalyst for the tritium incorporation of benzene. This retardation effect of the substituents upon the

hydrogen-tritium exchange of the aromatic nucleus may perhaps be attributed to the preferential adsorption of the substituents on the catalyst surface. The tritium distribution in benzoic acid and salicylic acid suggests that the hydrogen-tritium exchange in the aromatic ring may follow the substitution rule for electrophilic aromatic exchange. The relative hydrogen-tritium exchange rates of benzoylvaline show that the more readily a hydrogen dissociates, the more rapidly it undergoes the exchange.

The authors wish to thank Professor Shigeru Oae of Osaka City University for his helpful discussions.

Osaka Research Laboratory
Tanabe Seiyaku Co., Ltd.
Higashiyodogawa-ku, Osaka

Reactions of Methylene Radicals with Benzene and Toluene in the Gas Phase[1)]

By Terumi TERAO* and Shoji SHIDA

(Received May 6, 1963)

Many investigations have been made of the reactions of methylene radicals with a variety of organic substances, concerning the electronic state of methylene radicals during the course of the reactions,[2,3)] the reactivity of the radical,[4,5)] and the unimolecular decomposition and isomerization of energetic addition intermediates of the radical and the parent reactants.[6,7)]

A benzene solution of diazomathane was photo-irradiated to give C_7H_8, and its chemistry was formulated equally well as cycloheptatriene or norcaradiene.[8)] Meerwein et al.[9)] reported that cycloheptatriene and norcaradiene were produced under similar conditions. However, they never obtained toluene.

This paper concerns the reactions of methylene radicals resulting from a photolysis of ketene with benzene and with toluene in the gas phase; it is a part of the study of the reactions of methylene radicals.

Experimental

Ketene was prepared by the pyrolysis of acetic anhydride[10)] at 500°C in vacuo; it was distilled from a trap at −120°C to a trap at −196°C three times and then stored in a sample tube kept at −196°C. Its gas chromatograms (columns, benzyl-ether and squalane) showed no impurity.

Benzene and toluene (G. R. grade reagents supplied by the Tokyo Kasei Kogyo Co.) were repeatedly degassed to 10^{-4} mmHg at −196°C and stored in sample tubes kept at −78°C. Nitrogen, Oxygen and nitric oxide (purity, 99.99, 99.98 and 99.5% respectively; supplied by the Takachiho Shoji Co.) were used without further purification. Carbon dioxide was obtained by evaporation from dry ice at −78°C. All of the above chemicals were shown by gas chromatography to have no impurity affecting the results.

The light source was a high-pressure mercury arc lamp (type I-9, supplied by the Wako Denki Co.) operated at 2.5 amp. and 200 V. Cylindrical irradiation cells were made of pyrex glass (transparent down to 2900 Å) or of quartz, their diameters and lengths being 50 mm. and 10∼50 mm. respectively. In some experiments a UV-25 filter (supplied by the Mitsubishi Denki Co.) was used, one which was transparent down to 2300 Å. Although all the spectral region of the light emitted from the lamp was used to irradiate the cell, the most effective radiation in the present study, where rather high pressures were adopted, is considered to be the light around 3130 Å, since the quantum yield of carbon monoxide formation in the photolysis of pure ketene

* Present Address: Laboratory of Applied Physics, Tokyo Institute of Technology, Ookayama, Meguro-ku, Tokyo.

1) A part of this paper was read at the 15th Annual Meeting of the Chemical Society of Japan, Kyoto, April, 1962.

2) H. M. Frey, *J. Am. Chem. Soc.*, **82**, 5947 (1960).

3) K. R. Kopecky, G. S. Hammond and P. A Leermakers, ibid., **83**, 2397 (1961).

4) J. N. Butler and G. B. Kistiakowsky, ibid., **82**, 759 (1960).

5) J. N. Bradley and A. Ledwith, *J. Chem. Soc.*, **1961**, 1495.

6) H. M. Frey, *Trans. Faraday Soc.*, **58**, 516 (1961).

7) B. Grzybowska, J. H. Knox and A. F. Trotman-Dickenson, *J. Chem. Soc.*, **1961**, 4402.

8) W. von Doering and L. H. Knox, *J. Am. Chem. Soc.*, **72**, 2305 (1950).

9) H. Meerwein, H. Disselnkötter, F. Rappen, H. V. Rintelen and H. van de Vloed, *Ann.*, **604**, 151 (1957).

10) G. J. Fisher, A. F. McLean and A. W. Schizer, *J. Org. Chem.*, **18**, 1055 (1953).

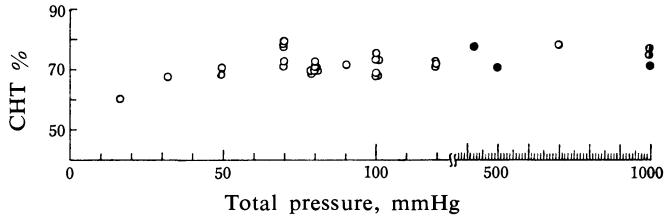


Fig. 1. Percentage yield of CHT plotted against total pressure.
Pyrex irradiation cell.
Ketene pressure: 4~60 mmHg,
Benzene pressure: 12~60 mmHg.
○: Ketene and benzene, ◑: CO_2 added, ●: N_2 added.

has been shown by Strachan and Noyes[11] to be 2 and pressure independent at 3130Å or shorter and to be very much smaller and remarkably reduced by raising the pressure at longer wave lengths (around 3660 Å).

Reactants at suitable pressures were introduced successively into the irradiation cell with a breakable seal and then sealed off. After irradiation the cell was attached to the analysis system, and the breakable seal was broken by a steel breaker. The gasses not condensable at −196°C were analyzed by micro-gas analysis. Hydrocarbons which evaporated at −120°C (C_2~C_4) were analyzed by gas chromatography under reduced pressure. The columns used were packed with benzylether and squalane. The ethane and ethylene which emerged from the former column at the same retention time were recovered by a trap kept at −196°C and were subjected to the latter column in order to separate them. Substances which did not evaporate at −120°C were analyzed with a gas chromatograph (type GC-1A, supplied by the Shimadzu Seisakusho Co.). The separation columns used were Silicone DC550 for the reaction products with benzene and 7, 8-benzoquinoline for the products with toluene.

Results

The Reaction of Methylene with Benzene.— The products detected were carbon monoxide, ethylene, cycloheptatriene (designated afterwards as CHT), toluene (T) and small amounts of acetylene, ethane, propylene and propane. All the products, except CHT and T, were produced from the photolysis of ketene.

When the pyrex irradiation cell was used, the percentage yield of CHT (CHT%, CHT×100/(CHT+T)) was found to be 70±7% at any pressure in the cell raised by added nitrogen or carbon dioxide, as Fig. 1 shows.

When the quartz irradiation cell was used, on the other hand, the percentage yield of CHT decreased with an increase in the irradiation period, but it seemed to move to about 70% at no irradiation (see Fig. 2). A small amount of [3.2.0]-bicyclohepta-2, 5-diene (<5% of CHT+T) was also detected. This time dependence of CHT% and the production of the bicycloheptadiene in the quartz cell can be understood in terms of the secondary photochemical isomerization of CHT, which was at first produced by the reaction of methylene with benzene. The photochemical isomerization of CHT in the gas phase has been reported by Srinivasan[12] to yield toluene and a small amount of the bicycloheptadiene.

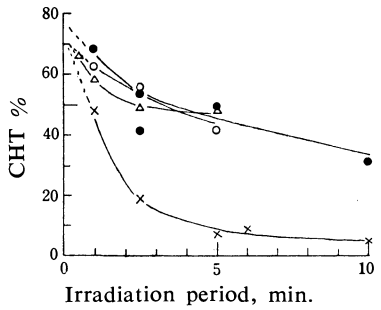


Fig. 2. Percentage yield of CHT plotted against irradiation period.
Quartz irradiation cell.
Ketene pressure: 20 mmHg,
Benzene pressure: 60 mmHg.
○: N_2 500 mmHg, filter, ○: filter,
△: CO_2 500 mmHg, filter, ×: none.

The material balance, $\{2(C_2H_4+C_2H_2+C_2H_6)+3(C_3H_6+C_3H_8)+(CHT+T)\}/CO$, was 0.67±0.1, definitely smaller than unity even at the initial stage of the reaction. This poverty in the material balance shows that there existed some products which could not be detected, since the material balance in the photolysis of pure ketene was good at least at the initial stage of the reaction.

The Reaction of Methylene with Toluene.— The results are summarized in Table I. When the pyrex irradiation cell was used, ethylbenzene (EB), *m*- and *p*-xylenes (*m*-Xy, *p*-Xy) and an unidentified compound (X) were the major products other than those resulting from

11) A. N. Strachan and W. A. Noyes, Jr., *J. Am. Chem. Soc.*, **76**, 3258 (1954).

12) R. Srinivasan, ibid., **84**, 3432 (1962).

TABLE I. REACTION OF METHYLENE WITH TOLUENE

Ketene	Toluene	O_2	Irradiation period	Product				
				X	*o*-Xy	*m*-Xy	*p*-Xy	EB
	mmHg		min.			μmol. (%)		
10	25	0	30	0.12 (8)	0	0.58 (42)	0.35 (25)	0.34 (25)
10	25	0	40	0.36 (10)	trace	1.42 (39)	0.97 (27)	0.90 (25)
10	20	0	30	0	0		0.78[b]	
10	20	0	45	0.19 (11)	0		1.49[b] (89)	
10	20	0	60	0.40 (18)	trace		1.85[b] (82)	
10	20	0	23	0.05 (6)	0		0.79[b] (94)	
20	18	0	30	0.60 (9)	0.28 (4)	2.42 (37)	1.59 (23)	1.61 (25)
20	18	18	ca. 25	0.11 (7)	trace	0.59 (40)	0.38 (26)	0.40 (27)
10[a]	25	0	5	0.26 (6)	0.69 (17)	1.53 (36)	0.83 (20)	0.98 (23)

a) Reaction in the quartz cell. Others are in the pyrex cell.
b) Amount of *m*-Xy+*p*-Xy+EB.

TABLE II. EFFECTS OF OXYGEN AND NITRIC OXIDE ON CHT% (IN THE PYREX CELL)

Ketene	Benzene	O_2, NO	Irradiation period	Product		CHT %
				T	CHT	
	mmHg		min.	μmol.		%
20	60	O_2 20	30	0.93	1.60	63
20	60	O_2 1	30	0.91	2.17	70
20	60	0	30	1.02	2.45	71
20	60	O_2 1	30	0.91	1.99	69
20	60	0	30	0.78	2.11	73
20	60	O_2 10	30	0.61	1.15	66
20	30	NO 15	15	0.82	1.89	70
20	60	0	15	1.01	2.14	68

the photolysis of ketene. The amount of *o*-xylene (*o*-Xy) was too small to be measured quantitatively. When the quartz irradiation cell was used, however, there was much more *o*-xylene. About a five-fold increase in the yield of ethane was observed over that from the photolysis of ketene or that in the reaction of methylene with benzene.

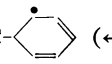
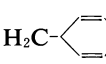
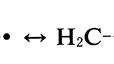
The Effects of Oxygen and Nitric Oxide.— The results are summarized in Tables I and II. The addition of oxygen or nitric oxide did not affect the relative yield among the products which were produced by the reaction of methylene with benzene or toluene.

Discussion

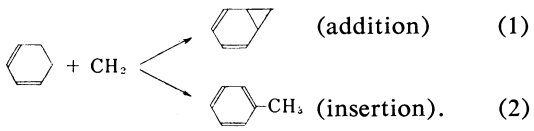
The Reaction of Methylene with Benzene.— The most striking difference between our results and those of Doering and Knox[8] and of Meerwein and his co-workers[9] lies in the fact that we have obtained a considerable amount of toluene, while they did not. This difference must have been caused not by the difference in the source of methylene radicals, *i.e.*, of the photolysis of diazomethane employed by them and that of ketene used by us, but by the difference in the phase of the system, the liquid phase in their experiments and the gas phase in ours; there should be no essential difference in the mode of the reactions of methylene radicals whether they are produced by the photolysis of diazomethane or by that of ketene.[6,7,13]

It is almost certain that the methylene produced by the photolysis of diazomethane is at first in a singlet state and that, in the presence of a large amount of inert gas, the singlet-state methylene is collisionally deactivated to a triplet state.[6,14] Although there is no such positive evidence for the methylene produced by the photolysis of ketene, it would also be in a singlet state if the spin conservation rule is applied. Triplet methylene may

13) H. M. Frey, *Trans. Faraday Soc.*, **57**, 951 (1961).
14) G. Herzberg, *Proc. Royal Soc.*, **A262**, 291 (1961).

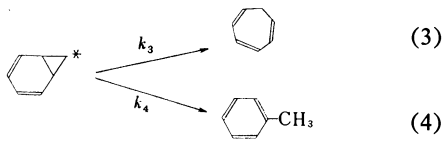
be added to benzene to give a biradical such as H_2C-  ($\leftrightarrow H_2C$-  $\bullet \leftrightarrow H_2C$- ), which may be easily scavenged by oxygen or nitric oxide. The fact that the addition of oxygen or nitric oxide did not alter the CHT%, together with the above discussion, seems to indicate that CHT and T are produced by the singlet methylene and benzene.

As is suggested by the reactions of methylene with olefins, the reaction with benzene may be expected to occur in two parallel ways, namely, the addition to a carbon-carbon double bond and the insertion into a carbon-hydrogen single bond, giving norcaradiene and toluene:


(addition) (1)

(insertion). (2)

The fact that the photolysis of a benzene solution of diazomethane did not give toluene,[8,9] however, seems to obviate the possibility of inserting methylene into the carbon-hydrogen bond in benzene, and the toluene obtained in the gas phase may be produced not by reaction 2 but by the isomerization of the norcaradiene produced in reaction 1. Unsubstituted norcaradiene has not yet been synthesized,[15] and it must be extremely unstable. The norcaradiene formed in reaction 1 would easily isomerize into CHT and T almost instantaneously.

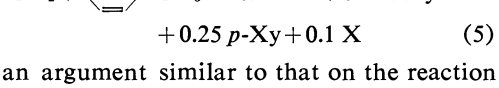

(3)

(4)

The almost constant value of CHT% (70%) indicates that the rate constant ratio, k_3/k_4, is about 7/3 in the gas phase.

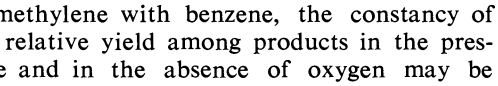
The relative yield of ethane to ethylene did not vary in the photolysis of pure ketene and in the reaction of methylene with benzene. This fact may indicate that the hydrogen atom abstraction from benzene by methylene does not play any important role in the reaction.

The Reaction of Methylene with Toluene.—The overall reaction can be written as follows:


(5)

By an argument similar to that on the reaction of methylene with benzene, the constancy of the relative yield among products in the presence and in the absence of oxygen may be taken as indicating that they are also produced by singlet methylene and toluene. Ethylbenzene can be produced by the insertion of methylene into a carbon-hydrogen single bond of methyl on the benzene ring. The scarcity of *o*-xylene among the products indicates that the steric hindrance caused by the substituted methyl acts strongly in this case.

The approximate five-fold increase in the yield of ethane can be explained by the abstraction of a hydrogen atom by methylene from the substituted methyl in toluene,


(6)

followed by a recombination of the methyl radicals thus formed to give ethane. The complete elimination of ethane by oxygen suggests that ethane is formed by such a radical mechanism.

The formation of *o*-xylene in the quartz cell may be due to the secondary photoisomerization of methylcycloheptatrienes, which might have possibly been produced.

The Reactivity of Methylene Radicals.—The photolysis of pure ketene is accepted as taking place in the following way:

$$CH_2CO + h\nu \rightarrow CH_2 + CO \quad (7)$$

$$CH_2 + CH_2CO \xrightarrow{k_8} C_2H_4 + CO \quad (8)$$

$$\searrow^{k_9} \text{other products.} \quad (9)$$

In the presence of another reactant, R, the methylene produced in reaction 7 reacts with R to give products, P_i's, as follows:

$$CH_2 + R \xrightarrow{k_{10R}} \sum c_i P_i \quad (10)$$

The steady state treatment requires the following relation:

$$\frac{R_{CO}}{R_{C_2H_4}} = 2 + \frac{k_9}{k_8} + \frac{k_{10R}}{k_8}\frac{[R]}{[K]} \quad (I)$$

where [K] refers to the concentration of ketene and k_{10R}, to the rate constant of reaction 10 for a particular reactant, R. The value of k_9/k_8 can be estimated as 0.2 by applying Equation (I) to the photolysis of pure ketene, in which $[R]=0$ and $R_{CO}/R_{C_2H_4}$ is about 2.2.[11] Plotting CO/C_2H_4 against $[R]/[K]$, one can obtain k_{10R}/k_8, the value of which shows the reactivity of methylene with reactant R relative to that with ketene to give ethylene and carbon monoxide.

15) It is highly probable that the product in the liquid-phase reaction of methylene with benzene, which was identified by Meerwein et al.[9] as norcaradiene from the fact that it absorbed two molecules of hydrogen per molecule, was actually [3. 2. 0]-bicyclohepta-2, 5-diene. which is the major product of the photoisomerization of CHT in the liquid phase.[16]

16) W. G. Dauben and R. L. Cargil, *Tetrahedron*, **12**, 186 (1961).

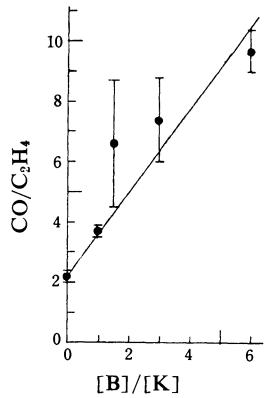


Fig. 3. CO/C_2H_4 plotted against benzene to ketene ratio.

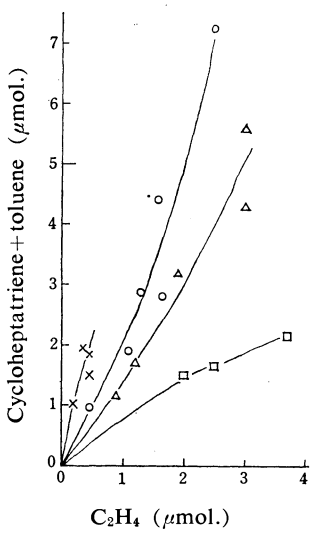


Fig. 4. Amount of cycloheptatriene+toluene plotted against ethylene.
Benzene to ketene ratio,
□: 1, △: 1.5, ○: 3, ×: 6.

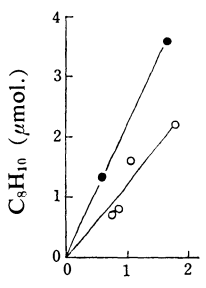


Fig. 5. Amount of C_8H_{10} products plotted against ethylene.
Toluene to ketene ratio,
○: 2, ●: 2.5.

By comparing Reactions (8) and (10), k_{10R}/k_8 can also be obtained from the following equation:

$$\frac{R_{\sum c_i P_i}}{R_{C_2H_4}} = \frac{k_{10R}}{k_8}\frac{[R]}{[K]} \qquad \text{(II)}$$

For benzene, relations I ard II are shown in Figs. 3 and 4, giving 1.4 and 0.7 respectively, for the value of k_{10B}/k_8 where B stands for benzene. The disagreement between the values thus obtained by the two methods implies that, along with CHT and T, some other products which could not be detected are present, possibly a polymer. The poverty of the material balance in the reaction of methylene with benzene supports this idea.

Table III. Rate constant ratios of reactions of methylene with various substances

$$CH_2+CH_2CO \xrightarrow{k_8} C_2H_4+CO$$

$$CH_2+R \xrightarrow{k_{10R}} \sum c_i P_i$$

R	k_{10R}/k_8	Reference
C_6H_6	1.4, >0.7[a]	Present result[b]
$C_6H_5CH_3$	>0.75[a]	Present result
C_2H_2	1.1	Reference 18.
C_2H_4	~1[c]	Reference 17.
CO	2.7, 1.25	Reference 19.[b]
CO_2	~0.02[c]	Reference 20.

a) The sign > means the minimum value.
b) Two different values have been obtained.
c) The sign ~ means the approximate value.

For toluene, relation II is shown in Fig. 5, the initial slopes of which give 0.75 for the value of k_{10T}/k_8. Since we may not have detected all the products for toluene, this value should be considered as the lower limit of k_{10T}/k_8.

The values of k_{10R}/k_8 for various reactants are summarized in Table III. The value of k_8 was estimated by Kistiakowsky and Rosenberg[17] to be 10^{-16} cc./molec./sec., and reaction 8 is generally accepted to be a very fast one. From the table one can see that the reactivity of methylene radicals is very high with ethylene, acetylene and aromatics also, not only confined with ketene.

Summary

The reactions of methylene radicals produced by the photolysis of ketene with benzene and with toluene in the gas phase have been

17) G. B. Kistiakowsky and N. W. Rosenberg, *J. Am. Chem. Soc.*, **72**, 321 (1950).
18) T. Terao, N. Sakai and S. Shida, ibid., **85**, 3919 (1963).
19) T. B. Wilson and G. B. Kistiakowsky, ibid., **80**, 2934 (1958).
20) G. B. Kistiakowsky and K. Sauer, ibid., **80**, 1066 (1958).

studied. The reaction of methylene with benzene gave cycloheptatriene and toluene in a ratio 7 to 3. The ratio varied neither with the pressure raised by the added nitrogen or carbon dioxide nor with the wave lengths of the incident radiation.

The products obtained in the reaction of methylene with toluene were ethylbenzene, *m*-xylene, *p*-xylene and an unidentified product, their percentages being 25, 40, 25 and 10% respectively. About a five-fold increase in the amount of ethane has been observed over that observed in the reaction with benzene or in the photolysis of pure ketene. This fact indicates that the abstraction of the hydrogen atom by methylene from the methyl in toluene does occur, but that that from the benzene ring does not. Oxygen did not alter the relative yield among the products in the reactions of methylene with either benzene or with toluene. This suggests that the products are formed by the reactions of singlet methylene with benzene and toluene via norcaradiene-type intermediates.

It has quantitatively been shown that the reactivity of methylene redicals is very high with aromatics, ethylene and acetylene, as with ketene.

Laboratory of Physical Chemistry
Tokyo Institute of Technology
Meguro-ku, Tokyo

The Formation Constant of Chromium(III)-Ethylenediamine Complexes

By Mitsuo OHTA, Hiroharu MATSUKAWA and Ryokichi TSUCHIYA

(Received October 10, 1963)

Many reports have been published on the formation constants of complexes since Bjerrem's theory[1] was presented. Most of them, however, have the concerned complexes formed by divalent metal cations. The formation constants of complexes containing ethylenediamine already reported concern the divalent metals, such as cadmium(II),[2] cobalt(II),[1] iron(II),[1] magnese(II),[1] nickel(II),[2] copper(II),[3] zinc(II)[4] and mercury(II).[5]

As for the formation constants of complexes of the tervalent metals, only the data concerning cobalt(III)[1] and the rare earths are known. As for chromium(III), there has been no formation constant data about either the ethylenediamine complex or complexes with any other ligand.

The divalent metals, in general, form labile complexes, and the velocity of the formation or aquation of the complexes is so large that the conventional pH titration method can be employed to find the formation constants, whereas the tervalent metals such as chromium(III) show a tendency to form substitution-inert complexes because of the smallness of the radius and because the reaction velocity is too small for the pH titration method to be employed. Therefore, the determination of the formation constant of chromium(III)-ethylenediamine complexes has been carried out by means of the photometric method.

Theoretical

Tris(ethylenediamine)chromium(III) perchlorate is thought to be aquated in the aqueous solution according to the three steps expressed by the following equations:

$$[Cr\,en_3]^{3+} + 2H_2O \rightleftarrows [Cr(H_2O)_2en_2]^{3+} + en \quad (1)$$

$$[Cr(H_2O)_2en_2]^{3+} + 2H_2O \rightleftarrows [Cr(H_2O)_4en]^{3+} + en \quad (2)$$

$$[Cr(H_2O)_4en]^{3+} + 2H_2O \rightleftarrows [Cr(H_2O)_6]^{3+} + en \quad (3)$$

The measurements of the velocity of these

---

* Presented at the 16th Annual Meeting of the Chemical Society of Japan, Tokyo, April, 1963.

1) J. Bjerrum, "Metal Ammine Formation in Aqueous Solution," P. Haase, Copenhagen (1941).

2) C. R. Bertsch, W. C. Fernelius and B. P. Block, *J. Phys. Chem.*, 62, 444 (1958).

3) J. Bjerrum and E. J. Nielsen, *Acta Chem. Scand.*, 2, 297 (1948).

4) C. J. Nyman, E. W. Murbach and G. B. Millard, *J. Am. Chem. Soc.*, 77, 4194 (1955).

5) C.J . Nyman, D. K. Roe and D. B. Masson, ibid., 77, 4191 (1955).

reactions have already been made by Schläfer et al.[6]

In these reactions, when the total concentration of the metal ions is expressed by C_{Cr} and the concentrations of the complex species, hexaaquochromium(III), tetraaquoethylenediaminechromium(III), diaquobis(ethylenediamine)chromium(III) and tris(ethylenediamine)-chromium(III), in the solution at equilibrium, by $[Cr(H_2O)_6^{3+}]$, $[Cr(H_2O)_4en^{3+}]$, $[Cr(H_2O)_2 \cdot en_2^{3+}]$ and $[Cr\ en_3^{3+}]$ respectively, the total concentration, C_{Cr}, is given as:

$$C_{Cr} = [Cr(H_2O)_6^{3+}] + [Cr(H_2O)_4en^{3+}] + [Cr(H_2O)_2en_2^{3+}] + [Cr\ en_3^{3+}] \quad (4)$$

If the molar extinction coefficients of the above four complex species are expressed by ε_1, ε_2, ε_3 and ε_4, and the absorbancy of the solution at equilibrium, by ε, the following relation exists:

$$[Cr(H_2O)_6^{3+}]\varepsilon_1 + [Cr(H_2O)_4en^{3+}]\varepsilon_2 + [Cr(H_2O)_2en_2^{3+}]\varepsilon_3 + [Cr\ en_3^{3+}]\varepsilon_4 = C_{Cr}\varepsilon \quad (5)$$

The acid hydrolyses of ethylenediamine are presumed to be expressed by;

$$H_2en^{2+} \rightleftarrows H^+ + Hen^+ \quad (6)$$

$$Hen^+ \rightleftarrows H^+ + en \quad (7)$$

If the concentration of H_2en^{2+}, Hen^+ and en are expressed by $[H_2en^{2+}]$, $[Hen^+]$ and [en] respectively, the acid dissociation constants of reactions 6 and 7 are given as:

$$k_1 = [H^+][Hen^+]/[H_2en^{2+}] \quad (8)$$

$$k_2 = [H^+][en]/[Hen^+] \quad (9)$$

respectively, where $[H^+]$ is the hydrogen ion concentration.

The concentration of the total of ligand materials, including those involved in the complex formation, C_{en}, is given as:

$$C_{en} = [H_2en^{2+}] + [Hen^+] + [en] + [Cr(H_2O)_4 \cdot en^{3+}] + 2[Cr(H_2O)_2en_2^{3+}] + 3[Cren_3^{3+}] \quad (10)$$

By eliminating $[H_2en^{2+}]$ and $[Hen^+]$ from Eqs. 8, 9 and 10, the following relationship is obtained:

$$[en] = k_1k_2(C_{en} - [Cr(H_2O)_4en^{3+}] - 2[Cr \cdot (H_2O)_2en_2^{3+}] - 3[Cr\ en_3^{3+}])/(k_1k_2 + k_1[H^+] + [H^+]^2) \quad (11)$$

In order to find the molar extinction coefficients of the tris(ethylenediamine)chromium-(III) and aquoethylenediaminechromium(III) complexes, which are formed by the aquation

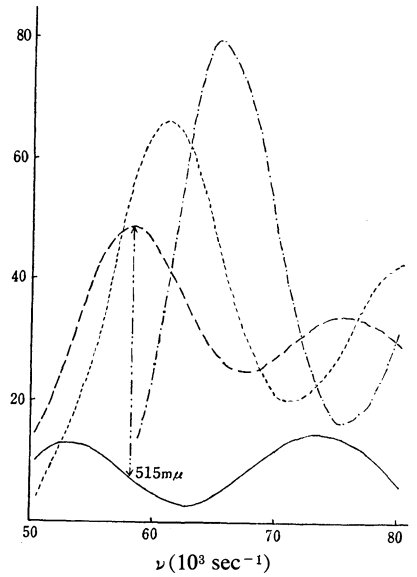


Fig. 1. The absorption spectra of chromium-(III)-ethylenediamine complexes.
Hexaaquochromium(III) complex
Tetraaquoethylenediaminechromium(III) complex
Diaquodiethylenediaminechromium(III) complex
Tris-ethylenediaminechromium(III) complex

of the former, their absorption spectra must be measured; they are shown in Fig. 1. The absorption spectra of the tris(ethylenediamine)-chromium(III) and hexaaquochromium(III) complexes were directly measured, while that of the diaquobis(ethylenediamine)chromium-(III) complex was obtained by tracing the aquation of bromoaquobis(ethylenediamine)-chromium(III) bromide, which is in good agreement with that reported by Schläfer et al.[6] The spectra of the tetraaquoethylenediaminechromium(III) complex was obtained by tracing the aquation of the diaquobis-(ethylenediamine)chromium(III) complex.

From the absorbancy measured at equilibrium in the prepared solution in order to find the formation constant, the following facts could be inferred: The equilibrium state under the conditions selected by the authors is expressed by Eq. 3; that is to say, the equilibrium mixture consists of the tetraaquoethylenediaminechromium(III) and hexaaquochromium(III) complexes. Even though the solution at equilibrium was contaminated with the diaquobis(ethylenediamine)chromium(III) complex, the impurity is no more than 1% of the two main complexes above, the tetraaquoethylenediamine- and hexaaquochromium(III) complexes.

On the assumption that the equilibrium in solution is accurately expressed by Eq. 3, the

6) H. L. Schläfer and O. Kling, *Z. phys. Chem.* **16**, 14 (1958).

formation constant was calculated as is shown below.

In this study, it seems reasonable to consider such condition with regard to the concentration of the complex species as:

$$[Cr(H_2O)_2en_2^{3+}] \text{ and } [Cr\ en_3^{3+}] \ll [Cr(H_2O)_6^{3+}] \text{ and } [Cr(H_2O)_4en^{3+}].$$

Taking into account these conditions, Eqs. 4, 5 and 11 are transformed to the following:

$$C_{Cr} = [Cr(H_2O)_6^{3+}] + [Cr(H_2O)_4en^{3+}] \quad (12)$$

$$[Cr(H_2O)_6^{3+}]\varepsilon_1 + [Cr(H_2O)_4en^{3+}]\varepsilon_2 = C_{Cr}\varepsilon \quad (13)$$

$$[en] = k_1k_2(C_{en} - C_{Cr})/(k_1k_2 + k_1[H^+] + [H^+]^2) \quad (14)$$

By solving Eqs. 12 and 13 with respect to $[Cr(H_2O)_6^{3+}]$ and $[Cr(H_2O)_4en^{3+}]$, the following equations are obtained:

$$[Cr(H_2O)_6^{3+}] = C_{Cr}(\varepsilon_2 - \varepsilon)/(\varepsilon_2 - \varepsilon_1) \quad (15)$$

$$[Cr(H_2O)_4en^{3+}] = C_{Cr}(\varepsilon - \varepsilon_1)/(\varepsilon_2 - \varepsilon_1) \quad (16)$$

By substituting for k_1 and k_2 the values given in the literature[4] and by estimating the range of the hydrogen ion concentration measured, the following orders of magnitude are obtained:

$$k_1k_2 \cong 10^{-8},\ k_1[H^+] = 10^{-12} \sim 10^{-10},\ [H^+] \cong 10^{-6} \sim 10^{-4}$$

Therefore, it is reasonable to express the denominator of Eq. 14 by $[H^+]^2$, neglecting the first and second terms.

By substituting Eq. 16 into Eq. 14 after considering the above approximation, the following equation is obtained as the concentration of the free ligand uncomplexing:

$$[en] = k_1k_2\{C_{en} - C_{Cr}(\varepsilon - \varepsilon_1)/(\varepsilon_2 - \varepsilon_1)\}/[H^+]^2 \quad (17)$$

The equilibrium constant of the reaction

$$[Cr(H_2O)_6]^{3+} + en \rightleftarrows [Cr(H_2O)_4en]^{3+} + 2H_2O, \quad (18)$$

which is the reverse of reaction 3, that is to say, the first formation constant, K_1, of the aquoethylenediaminechromium(III) complexes, is given as:

$$K_1 = [Cr(H_2O)_4en^{3+}]/[Cr(H_2O)_6^{3+}][en] \quad (19)$$

This formation constant may be calculated by substituting Eqs. 15, 16 and 17 into Eq. 19.

The ionic strengths of the solutions at equilibrium, the absorbancies of which were measured, can be calculated by the following equation;

$$\mu = 1/2\{12C_{Cr} + 4[H_2en^{2+}] + [HClO_4] + [H^+]\} \quad (20)$$

where $[HClO_4]$ is the concentration of perchloric acid added in order to control the hydroxo-change of the complex. The concentration of ethylenediamine affecting the ionic strength was thought to be only $[H_2en^{2+}]$, for it was found that the concentrations of $[Hen^+]$ and [en] were negligibly small compared with $[H_2en^{2+}]$ when they were estimated by using the first and second acid dissociation constants and the hydrogen ion concentration.

Experimental

Tris(ethylenediamine)chromium(III) Perchlorate.—When chromium(III) chloride hydrate (green) and ethylenediamine were mixed stoichiometrically, the reaction started with a violent evolution of heat. After the mixture had been kept upon an oil bath for three or four hours in order to complete the reaction and the dehydration, a yellowish-brown residue was obtained. When the product was extracted by water, crystalline tris(ethylendiamine)chromium(III) chloride was obtained and purified by recrystallization.

The perchlorate was obtained by adding perchloric acid to the saturated solution of the chloride and by coolin it with ice. It has no water of crystallization. Analytical values: Cr 9.96% (found), 9.80% (calcd.); C 13.87% (found), 13.58% (calcd.); H 4.53% (found), 4.56% (calcd.)

Procedure.—In order to obtain the equilibrium system, a mixed solution of hexaaquochromium-(III) salt with ethylenediamine was at first used as the starting material, but the reaction did not proceed. Therefore, the equilibrium state was obtained by aquating the tris(ethylenediamine)-chromium(III) salt prepared above.

The procedure by the latter way as follows. The aqueous solutions of various concentrations of tris(ethylenediamine)chromium(III) perchlorate, to which some quantities of free ethylenediamine had been added to prevent complete aquation and to which an excess amount of perchloric acid had been added to protect the chromium(III) aquo-complexes produced in consequence of the reaction from their hydroxo change, were maintained at 25°C in a thermostat for one or two months. The solutions were always kept in brown flasks to avoid photodecomposition.

The absorbancy of the solution was then measured by means of Hitachi EPS-2 type automatic recording and EPU-2 type spectrophotometers after the equilibrium had been attained. Since it was necessary to find the hydrogen ion concentration of the solution at equilibrium in order to calculate the formation constant, the pH was also measured by means of a Horiba HRL model M pH meter. All the measurements were carried out at 25°C.

Results

The measurement of the absorbancy, ε, of the solution at equilibrium was carried out

Table I. The results of measurements and calculation at 25°C

$C_{Cr}\times10^3$ mol./l.	$C_{en}\times10^3$ mol./l.	ε	$[Cr(H_2O)_4en^{3+}]/[Cr(H_2O)_6^{3+}]$	pH	log K_1	$\sqrt{\mu}$
1.986	6.892	32.97	1.726	2.01	16.18	0.2336
2.019	8.393	31.69	1.520	2.05	15.94	0.2395
2.436	8.242	33.86	1.897	2.09	15.99	0.2415
2.019	10.73	31.20	1.449	2.31	16.27	0.2442
3.830	13.83	36.16	2.423	1.85	16.37	0.2817
3.770	12.24	35.28	2.199	1.67	16.74	0.2835
3.790	16.04	36.15	2.425	1.82	16.35	0.2901
5.081	19.91	34.76	2.064	1.80	16.23	0.3126
4.785	18.91	41.59	5.074	1.72	16.81	0.3537
4.293	12.88	31.09	1.434	1.20	17.48	0.3689
4.206	21.96	36.98	2.667	1.29	17.28	0.3805
4.236	31.39	33.64	1.848	1.42	16.71	0.3963

at the wave length of 515 mμ, where the difference in absorbancy between hexaaquochromium(III) and tetraaquoethylenediaminechromium(III) complex is the greatest, as may be seen in Fig. 1. As the molar extinction coefficients of these two complexes in the solution at this wave length, log $\varepsilon_1=5.97$ and log $\varepsilon_2=48.59$ were used respectively.

As the acid dissociation constants of the first and second steps of ethylenediamine, $pk_1=7.42$ and $pk_2=10.14$[4] were employed respectively.

In order to calculate the value of [en] by inserting into Eq. 17 the measured absorbancy, ε, the acid dissociation constants pk_1 and pk_2 given above, and the total concentrations of chromium(III) salts and ethylenediamine, it is necessary to known the hydrogen ion concentration, $[H^+]$. What is obtained by pH measurement is not $[H^+]$, but the activity. Therefore, [en] was first calculated by inserting the value of the activity instead of the value of hydrogen ion concentration into $[H^+]$ in Eq. 17; then the equilibrium constant, K_1, was obtained by applying the value of [en] to Eqs. 15, 16 and 19. The ionic strength was calculated at the same time by means of Eq. 20.

Subsequently, the activity coefficient of the hydrogen ions at each ionic strength calculated as above was obtained from Kielland's table.[7] After the hydrogen ion concentration, $[H^+]$, had been obtained by dividing the activity by its activity coefficient, the equilibrium constant, K_1, was recalculated by inserting the hydrogen ion concentration into Eq. 17 and by computing the value of Eq. 19.

The values obtained by these measurements and those calculated from them are listed in Table I.

The logarithm of the equilibrium constant, K_1, is plotted against the square root of the ionic strength in Fig. 2.

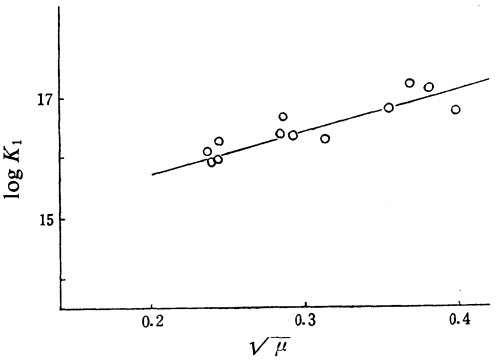


Fig. 2. The relationship between the logarithm of the equilibrium constant and the square root of ionic strength.

The formation constant of the second step of aquoethylenediaminechromium(III) complexes could not be determined spectrophotometrically. The exact formation constants could not be obtained by pH measurements alone, because the error in calculation was too large at low pH values, while decomposition easily occurred at high pH values; consequently, the pH range which gave exact values of formation constants was too restricted. As the rough value of the formation constant of the second step at the ionic strength of $\mu=0.1$, log $K_2<14$ was obtained.

Discussion

It may be seen in Fig. 2 that the formation constants of the first step of aquo-ethylenediaminechromium(III) complexes at the ionic strength of $\mu=0.05$, 0.10 and 0.15 are given by log $K_1=15.9$, 16.5 and 17.0 respectively. As may be seen from these values, the equilibrium constant, K_1, does not depend much on the ionic strength of the solution.

This may be explained by the fact that the hexaaquochromium(III) and tetraaquoethylenediamine chromium(III) complexes, which give

7) J. Kielland, *J. Am. Chem. Soc.*, **59**, 1675 (1937).

TABLE II. FORMATION CONSTANTS OF ETHYLENDIAMINE COMPLEXES OF TERVALENT CHROMIUM OR COBALT AND DIVALENT CHROMIUM AND COBALT

	log K_1	log K_2	log K_3	Condition	
Cr(III)	16.5	<14	—	μ=0.1,	25°C
Co(III)	18.7	16.2	13.8	μ=1.0,	30°C[9]
Cr(II)	5.145	4.035	—	μ=1.4,	25°C[10]
Co(II)	5.93	4.73	3.30	μ=1.0,	25°C[11]

the respective concentrations, $[Cr(H_2O)_6^{3+}]$ and $[Cr(H_2O)_4en^{3+}]$, in the numerator and denominator of Eq. 19 respectively, are both tervalent cations and by the assumption that the ionic radii of these complex cations are approximately equal.

The formation constants of the aquo-ethylenediaminechromium(III) complexes obtained are listed in Table II, together with those of the corresponding cobalt(III) complexes and the ethylenediamine complexes of divalent chromium and cobalt.

Table II shows, in the first place, that the formation constants of the aquo-ethylenediamine complexes of tervalent chromium and cobalt are far larger than those of the corresponding divalent metal complexes. This must be due to the fact that the covalency of the coordinated bond of the ligand with tervalent metal ions is much stronger than that with divalent ions because of the smaller radii of the former ions.

The Table also shows that the formation constants of the aquo-ethylenediaminechromium(III) complexes are a little smaller than those of the corresponding cobalt(III) complexes. On the other hand, it has already been found[8] that the crystal-field stabilization energy of the tris(ethylenediamine)chromium-(III) complex is much smaller than that of the tris(ethylenediamine)cobalt(III) complex. This means that the formation constants of these two complexes can not be determined only by means of the crystal field stabilization energy. In addition, in order to explain the difference in stability between these chromium(III) and cobalt(III) complexes, the following concept is effective: The cobalt complexes are instabilized by the mutual repulsion of the six 3d electrons paired in the bonding orbitals more than the corresponding chromium(III) complexes which have unpaired three electrons; that is to say, the contribution of Racah's electrostatic parameter upon the crystal-field stabilization is greater in the cobalt(III) complex than in the chromium(III) complex.

8) C. K. Jørgensen, "Energy Levels of Complexes and Gaseous Ions," Jul. Gjellerups Forlag, Copenhagen (1957).
9) J. Bjerrum and S. E. Rasmussen, *Acta Chem. Scand*,. **6**, 1265 (1952).
10) R. L. Pecsok and J. Bjerrum, ibid., **11**, 1419 (1957).
11) L. J. Edwards, Diss., Univ. Michigan, 1950.

Summary

1) The formation constants of chromium (III) complexes with ethylenediamine, the simplest bidentate ligand material coordinated by two nitrogen atoms, have been spectrophotometrically determined.

2) It has been shown that the dependence of the formation constant of the first step upon the ionic strength is small.

3) The formation constants of the chromium-(III) complexes with ethylenediamine have been found to be remarkably higher than those of the corresponding chromium(II) complexes and a little lower than those of the corresponding cobalt(III) complexes.

4) The difference between the formation constants of the chromium(III) and cobalt-(III) ethylenediamine complexes has been qualitatively explained with reference to the crystal-field stabilization energy and to Racah's electrostatic repulsive parameter.

Department of Chemistry
Faculty of Science
Kanazawa University
Kanazawa

Relative Sensitivities of Elements in a Spark-Source Mass Spectrograph[*1]

By Hiroyuki KAWANO[*2]

(Received October 23, 1963)

For the quantitative analysis of solids by spark-source mass spectrography, at least two fundamental problems must be studied. One of them concerns a calibration method to obtain the relative ion intensity from the densities of mass lines recorded on a photographic plate. The other concerns the relative sensitivities of elements in a mass spectrograph with a pulsed radio-frequency spark ion source, which has been generally used as the most suitable ion source for the trace analysis of solids since it was first applied to mass spectroscopy by Dempster.[1,2] The sensitivity is a function of both the darkening rate of a photographic plate and the ion production rate from a solid by a spark discharge between two sample electrodes. Therefore, the sensitivity is not only necessary as an analytical constant in quantitative mass spectrography but also very important for the study of the mechanism of ion production by spark discharges in a vacuum. However, relatively little work has been done on the sensitivity,[3,4] and no study has previously been made of the ion production rate using photographic detection.

Thus, a study of the calibration method has been made in this laboratory, and the findings partly published in a preceding paper.[5] For the present work, five kinds of calibration methods have been investigated by applying them to isotopic analyses of magnesium, copper and zinc. The relative sensitivities have been determined for eleven elements contained in several standard samples using the calibration methods mentioned above, and the constancy of the sensitivity to changes in bulk concentration of the element has been examined. The relative ion production rates have also been determined from the above sensitivities with a correction for the darkening rate. In addition, the reproducibility of the relative ion intensities detected with several plates in many exposure stages has been studied for many pairs of isotopes and pairs of different elements, in order to examine whether the relative ion yields obtained from the spark ion source are always constant for all elements contained in the sample electrodes. Finally, a discussion will be given on the general applicability of the sensitivity as the analytical constant.

Apparatus

The Mattauch-Herzog-type double-focusing mass spectrograph used in this work was constructed in this laboratory in collaboration with the Mitsubishi Elec. Mfg. Co. Since details of the instrument have been reported elsewhere,[6] only an outline and the operating conditions employed will be given here. The ion source used was a Dempster-type vacuum spark ion source; the spark voltage applied between two sample electrodes, each about 1 mm. in diameter and 1 cm. in length, was approximately 30 kV., supplied from a 1 Mc./sec. radio-frequency oscillator with pulses about 200 μsec. long at a repetition rate of 60 c./sec. Ions produced under a vacuum of about 5×10^{-6} Torr were accelerated with 15 kV. through the slit system, inclusive of a 0.21 mm. defining slit. Of the ions passing through the energy selector with a mean radius of 150 mm., about 42 per cent enter the magnetic field, and the rest are collected by the beam-monitor electrode which is situated directly behind a selector slit and which is shielded from the field of the radio-frequency used for the spark source.

Individual ions resolved by the mass analyzer were detected by a 3 cm. $\times$ 15 cm. Ilford Q2 plate, which covers a mass range of 10 : 1 in a single exposure. Moreover, eleven exposures can be recorded on the plate without loss of vacuum. The amount of each exposure was determined by the total ion current arriving at the beam-monitor during the exposure. For this purpose, a vibrating-reed electrometer manufactured by the Electronic Instrument Ltd. was used in combination with a 500 pF polystyrene condenser. The exposed plate was developed by an Ilford ID-19 developer continuously agitated by hand at temperatures 20 ± 1°C for exactly 5 min., then it was fixed by Fujifix for about 3 min., washed, and dried. For the purpose

*1 A preliminary report of this work was presented at the 15th Annual Meeting of the Chemical Society of Japan, Kyoto, April, 1962, and at the 1st Annual Meeting of the Society of Mass Spectroscopy (Japan), Tokyo, May, 1962.

*2 Present address: Research Institute for Scientific Measurements, Tohoku University, 5 Gojyo-Dori, Sendai.

1) A. J. Dempster, *Nature*, **135**, 542 (1935).
2) A. J. Dempster, *Rev. Sci. Instr.*, **7**, 46 (1936).
3) A. J. Dempster, MDDC-370, United States Atomic Energy Commission, Oak Ridge (1946).
4) R. D. Craig, G. A. Errock and J. D. Waldron, "Advances in Mass Spectrometry," Ed. by J. D. Waldron, Pergamon Press, London (1959), p. 136.
5) K. Kodera, T. Makita, J. Kai, S. Fukuda and H. Kawano, *Mass Spectroscopy (Shitsuryô Bunseki)*, **9**, 105 (1961).
6) M. Goto and J. Kai, *Mitsubishi Denki Laboratory Reports*, **1**, 51 (1960).

of determining the optical densities of the mass lines, about 2 mm. long and about 0.2 to 0.8 mm. wide on a photographic plate, each spectrum, magnified about 9 times, was scanned through a 0.20 mm. × 3 mm. slit and was registered by a microphotometer with a recorder manufactured by the Rigaku-Denki Co., Ltd.

Experimental Method

Calibration Curve.—*Expression of Density.*— For quantitative analysis by photometry, it is necessary to make a calibration curve which shows the relation between the density of each mass line and its corresponding exposure. It is desirable that the curve has a linear portion over a wider range of exposure. Thus, various methods have been studied to get useful calibration curves from a series of the mass lines of a certain ion recorded by different exposures on the same plate. Among the methods studied, five have been employed here to express the "density" of each mass line:

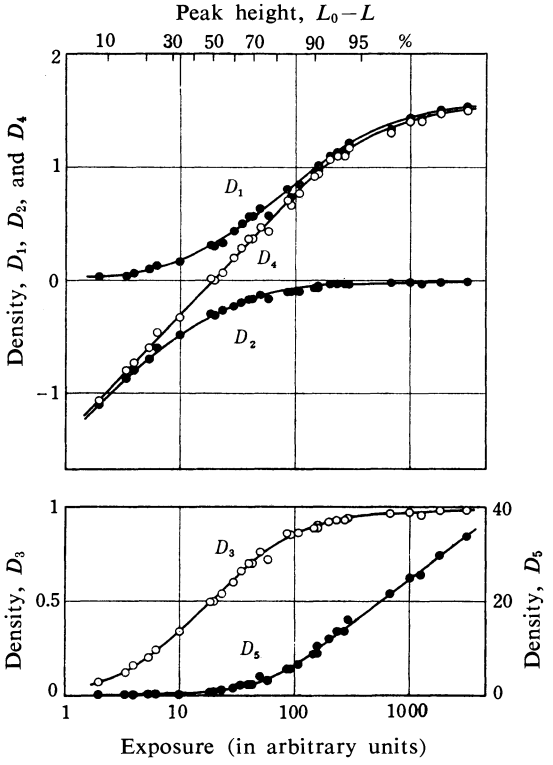


Fig. 1. Examples of the five kinds of calibration curves obtained for zinc isotopes recorded on an Ilford Q2 plate using the different expressions of density. In order to utilize many data points, $r \times Q$ instead of Q was employed as the "exposure", where r and Q are the known relative abundance of each isotope of zinc and the measured value of the integrated monitor current in each exposure stage, respectively.

$$D_1 = \log L_0/L$$
$$D_2 = \log(L_0-L)/L_0$$
$$D_3 = (L_0-L)/L_0$$
$$D_4 = \log(L_0-L)/L$$
$$D_5 = (L_0-L)/L$$

where L_0 and L are the intensities of the incident and the transmitted light in arbitrary units respectively. Examples of the calibration curves using these density expressions are shown in Fig. 1, at the top of which the peak height, L_0-L (i. e., the intensity of the absorbed light) is plotted in per cent of L_0 in order to show the range which corresponds to the linear portion of each calibration curve.

The D_1 expression is the equation of Lambert-Beer's law; it is generally used as an expression of density in mass spectrography. However, in the calibration curve where D_1 is plotted against the logarithm of exposure, more than one-half of the series of mass lines obtained for a certain ion in several exposures are, on the average, unavailable for the calibration only because they are out of the linear portion of the density curve, as may be seen in Fig. 1. For this reason, the usable D_1-curves for all ionic species under investigation can not always be obtained from an exposure range covered by up to eleven exposures. In the other curves, however, using D_2, D_3, D_4, or D_5, it is possible to utilize even those mass lines which are unavailable for the calibration in the D_1-curve because they are too intense or too weak to fall in the linear part. Especially in the D_2- or D_4-curve, any weakline is available so long as it exceeds the noise level around it to a certain degree. Therefore, short exposures less than one-tenth of those necessary in the D_1-curve are sufficient here to get useful curves. Thus, employing the D_2- or D_4-expression is more advantageous when long exposures are undesirable or have produced only weak lines for some of the ions to be studied. Some examples of the D_4-curves obtained from a single Q2 plate, subjected to ten short exposures graded with a factor of about 2 between adjacent stages, is shown in Fig. 2. In the examples no useful curve can be obtained for zinc and manganese if the D_1- or D_5-expression is employed. In the D_5-curve, on the other hand, only intense lines are usable, so this curve is available for the determination of those major elements which from nearly saturated lines. The D_3-curve is appropriate to some of the lines that are unavailable in the D_1- or D_2-curve because they are too weak or too intense respectively. The characteristics of the different expressions of density described above are listed briefly in Table I.

TABLE I. CHARACTERISTICS OF EACH CALIBRATION CURVE, D_n VS. log *Exposure*, OBTAINED FOR AN ILFORD Q2 PLATE (EMULSION NUMBER : S 3399)

The "asymptote" indicates the maximum or the minimum density level to which a calibration curve approaches asymptotically, as the amount of exposure increases or decreases respectively. The "useful range" means (A) the range of peak height in per cent of L_0 or (B) that of the density value which corresponds to the linear part of the curve (cf. Fig. 1). Of the values shown in the second and the third columns, only those with an asterisk are dependent on the characteristics of a photographic plate and on the conditions of development employed.

Density expression	Asymptote	Useful range	Remarks
D_1	$D\approx 1.6$*	(A) 50* ~ 90*%	Useless for low peaks.
	$D=0$	(B) 0.3* ~ 1.0*	Long exposure is necessary.
D_2	$D=0$	(A) 0 ~ 40*%	Applicable to low peaks only.
		(B) $-\infty$ ~ -0.4*	The shortest exposure among the five is sufficient.
D_3	$D=1.0$	(A) 20* ~ 80*%	Applicable to intermediate peaks.
	$D=0$	(B) 0.2* ~ 0.8*	
D_4	$D\approx 1.6$*	(A) 0 ~ 90*%	Applicable from low to high peaks.
		(B) $-\infty$ ~ 1.0*	The linear part is the longest among the five.
D_5	$D=0$	(A) 80* ~ 100%	Applicable to high peaks only.
		(B) 4* ~ ∞	The longest exposure among the five is necessary.

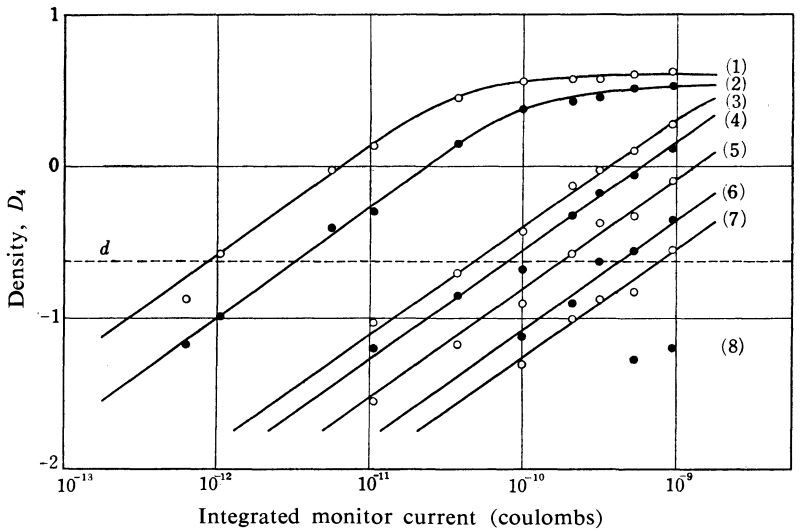


Fig. 2. An example of the calibration graph obtained for the samele S-3 from a Q2 plate using the D_4-expression in ordinate. The integrated monitor current of 10^{-9} coulombs corresponded to an exposure of about 3 min.

(1) : $^{26}Mg^+$ (2) : $^{27}Al^+$ (3) : $^{64}Zn^+$ (4) : $^{66}Zn^+$
(5) : $^{68}Zn^+$ (6) : $^{55}Mn^+$ (7) : $^{67}Zn^+$ (8) : $^{70}Zn^+$

Determination of Exposure. — In order to determine the amount of the "exposure" as a measure of the relative ion intensity corresponding to each line density, several methods have been utilized. One of them is Mattauch-Ewald's method, which uses as internal standards the known relative abundances of the isotopes of an element.[7-10] Therefore, its application is generally confined to those samples which contain in a moderate concentration such an element as has several isotopes with a suitable distribution of the relative abundance. As another method, the exposure time is employed.[11,12] However, in many cases the true amount of exposure can not be obtained from the exposure time without making an appropriate correction,[12] because it

7) J. Mattauch and H. Ewald, *Naturwiss.*, **31**, 487 (1943).
8) J. Mattauch and H. Ewald, *Z. Phys.*, **122**, 314 (1944).
9) H. Ewald, ibid., **122**, 487 (1944).
10) J. Mattauch and H. Scheld, *Z. Naturforsch.*, **3a**, 105 (1948).
11) N. B. Hannay and A. J. Ahearn, *Anal. Chem.*, **26**, 1056 (1954).
12) N. Sasaki and J. Kai, *Mass Spectroscopy (Shitsuryô Bunseki)*, **7**, 64 (1959).

TABLE II. ABUNDANCE RATIO OF COPPER ISOTOPES MEASURED BY THE FIVE KINDS OF CALIBRATION CURVES (D_n vs. $\log Q$), AND COMPARISON OF THE PRESENT MEASUREMENTS WITH PUBLISHED ONES OBTAINED BY PHOTOMETRY OR ELECTROMETRY USING SEVERAL IONIZATION METHODS

In square brackets are given the values corrected by Hess, et al.[15]

Present work		
Expression of density	Number of measurements	$^{63}Cu/^{65}Cu$
D_1	(A) 19	2.27±0.31
	(B) 4	2.14±0.07
D_2	(A) 13	2.16±0.26
	(B) 6	2.21±0.20
D_3	(A) 14	2.20±0.18
	(B) 7	2.25±0.26
D_4	(A) 14	2.22±0.26
	(B) 8	2.13±0.23
D_5	(A) 16	2.18±0.24
	(B) *1	

Reference		
Methods of detection and ionization	Workers	$^{63}Cu/^{65}Cu$
Photometry*2 R. F. Spark	Ewald 9)	2.330±0.032 [2.163]
Photometry*2 R. F. Spark	Duckworth, Hogg 16)	2.277±0.017 [2.092]
Electrometry R. F. Spark	Dempster 17)*3	2.230±0.030
Electrometry Electron impact	White, Cameron 18)	2.220±0.020
Electrometry R. F. Spark	Sommer, Hipple 19)	2.220±0.027
Electrometry Ion impact	White, Sheffield, Rourke 20)	2.25±0.02

*1 Of the Cu^+ peaks obtained from eight plates using the sample B, none was available for the D_5-curve.
*2 Mattauch-Ewald's method was employed.
*3 Cited from Ref. 18.

is very difficult to keep spark discharges constant throughout all the exposures given to a plate, and much more so from plate to plate or from sample to sample. On the other hand, a monitor-current integration method[4,5,13] is free from the disadvantages mentioned above; i. e., no internal standard is necessary for making a calibration curve, and the error due to fluctuations of the total ion amount produced per sec. by spark discharges is avoidable because the integrated monitor current, Q, can be regarded as always proportional to any individual ion amount focused on a plate in any exposure. Therefore, this monitor method was employed, although the disturbance from the field of the R. F. current for spark discharges had to be shielded.

Isotopic Analysis for Testing the Methods.— For testing the usefulness of each D_n-curve for mass-spectrographic measurements, some isotopic analyses were tried using several samples. Each abundance ratio of the isotopes was calculated from the following equation:

$$r_i/r_j = (q_j/q_i)(m_i/m_j)^{1/2} \quad (1)$$

where r_i and r_i are the abundances of the isotopes i and j respectively, q_i and q_j are the integrated monitor currents required for the line densities of i and j respectively to be at the same value, d, which is chosen so as to be on the linear part of the curves, as is shown in Fig. 2, and m_i and m_j are the masses of the isotopes i and j respectively. $(m_i/m_j)^{1/2}$ is the correction factor for the line widths,[14] needed because they vary in proportion to the square root of the mass in the Mattauch-Herzog arrangement.

The results obtained for copper are listed in Table II, where the ions studied are monatomic positive ions originating from two different samples, A and B, which contain about 90 and 1 weight per cent of copper respectively. As Table II shows, the mean values obtained by means of these calibration methods agree with one another rather well, and they also compare favorably with others referred to there. Therefore, the density expressions, D_2, D_3, D_4 and D_5, can be regarded as reliable as D_1. On the other hand, the standard deviations of the values measured with the five methods are about 10 times as large as those by Ewald[9] and Duckworth and Hogg.[16] This seems mainly due to the difference in calibration method. As the abscissa component of a calibration graph, the known relative abundance of the isotopes of a suitable element (zinc, for instance) has been taken, so that every value in the abscissa is free from erratic fluctuations.

The results obtained for magnesium and zinc are also in fair agreement with the referred values, as is shown in Tables III and IV respectively, where they have been calculated from those individually measured values which

13) J. G. Gorman, E. J. Jones and J. A. Hipple, *Anal. Chem.*, **23**, 438 (1951).
14) H. Lichtblau and J. Mattauch, *Z. Phys.*, **117**, 502 (1941).
15) D. C. Hess, Jr., M. G. Inghram and R. J. Hayden, *Phys. Rev.*, **74**, 1531 (1948).
16) H. E. Duckworth and B. G. Hogg, ibid., **71**, 212 (1947).
17) A. J. Dempster, Report for February, CP-3445 (1946).
18) J. R. White and A. E. Cameron, *Phys. Rev.*, **74**, 991 (1948).
19) H. Sommer and J. A. Hipple, ibid., **83**, 229 (1951).
20) F. A. White, J. C. Sheffield and F. M. Rourke, *J. Appl. Phys.*, **33**, 2915 (1962).

TABLE III. ISOTOPIC ANALYSIS OF MAGNESIUM

The author's data have been obtained from 6 measurements.

Detection method	Mass number 24	25	26	Reference
Photometry	79.9±1.5%	9.1±0.5	11.0±0.9	Present work
Electrometry	77.4	11.5	11.1	Dempster 21)
Electrometry	78.60±0.13	10.11±0.05	11.29±0.08	White, Cameron 18)
Electrometry	78.8±0.2	10.15±0.1	11.06±0.1	White, Collins, Rourke 22)

TABLE IV. RELATIVE ABUNDANCE OF ZINC ISOTOPES OBTAINED FROM TWO DIFFERENT SAMPLES, AND COMPARISON WITH PUBLISHED VALUES

In the works A and B, zinc is contained about 2 and 95 weight per cent in the samples used, and the numbers of measurements are 21 and 20 respectively.

Detection method	Mass number 64	66	67	68	70	Reference
Photometry	47.9% ±5.2	28.0 ±3.4	4.3 ±1.1	19.0 ±3.8	0.8 ±0.2	Present work (A)
Photometry	48.3 ±3.4	27.8 ±2.2	4.9 ±1.7	18.3 ±2.3	0.7 ±0.3	Present work (B)
Photometry	50.4	27.2	4.2	17.8	0.4	Aston 23)
Electrometry	50.9	27.3	3.9	17.4	0.5	Nier 24)
Electrometry	48.89	27.81	4.11	18.56	0.62	Hess, Inghram, Hayden 25)*
Electrometry	48.89	27.81	4.07	18.61	0.620	Leland, Nier 26)
Electrometry	48.89 48.90	27.82 27.82	4.14 4.17	18.54 18.48	0.617 0.623	Hess, Inghram, Hayden 15)
Electrometry	49.77	27.19	4.09	18.54	0.41	Okamoto et al. 27)

* Cited from Ref. 28.

were obtained by using the most suitable calibration method among the five according to the densities of the isotopic lines to be studied. In the magnesium analysis, the sample used contains more than 90 weight per cent of magnesium, so that the intensities of the C_2^+, C_2H^+ and $C_2H_2^+$ ions, even if they exist, may be negligibly small compared with those of the magnesium ions.

From these results it seems reasonable to conclude that a mean value of the measurements obtained by any of the five calibration methods is as accurate as that by the electrometry, although good reproducibility has not yet been obtained in the present work.

The Determination of Relative Sensitivity.— If the ion intensity, I_X, of an element, X, which forms a line with a density, d, on a plate is expressed in arbitrary units by the following equation:

$$I_X = m_i^{1/2}/q_i \times r_i \qquad (2)$$

where i is one of the isotopes of X and where every isotope is assumed, in a manner similar to that in Eq. 1, to have the same effect on photographic darkening, the relative sensitivity, S_X, of X will be given as:

$$S_X = S_R(\bar{I}_X/C_X)/(\bar{I}_R/C_R) \qquad (3)$$

where S_R is that of the element, R, adopted as a reference, $\bar{I}$ is the arithmetic average of the I's obtained for all or some isotopes of the element, C is the atomic concentration of each element contained in a sample of known chemical composition, and S is assumed to be independent of C. The samples used are listed in Table V, where each relative atomic concentration for S-1 — S-6 was calculated from data by the ASTM,[29] taking C as 100 for the major element. For the purpose of eliminating surface contaminants from the samples, preparative sparking was carried out before a

21) A. J. Dempster, *Phys. Rev.*, **18**, 415 (1921).
22) F. A. White, T. L. Collins and F. M. Rourke, ibid., **101**, 1786 (1956).
23) F. W. Aston, "Mass Spectra and Isotopes," 2nd Ed., Edward Arnold & Co., London (1942), p. 153.
24) A. O. Nier, *Phys. Rev.*, **50**, 1041 (1936).
25) D. C. Hess, Jr., M. G. Inghram and R. J. Hayden, Plutonium Project Report, ANL-4082 (1947), p. 5.
26) W. T. Leland and A. O. Nier, *Phys. Rev.*, **73**, 1206 (1948).
27) J. Okamoto, M. Kakuta, N. Morito, Y. Nakajima, H. Tsuyama and H. Onuki, *Japan Analyst (Bunseki Kagaku)*, **8**, 445 (1959).
28) L. Kerwin, D. E. McElcheran and M. Cottin, *Can. J. Phys.*, **35**, 783 (1957).
29) R. E. Michaelis, "Report on Standard Samples and Related Materials for Spectrochemical Analysis," American Society for Testing Materials, Philadelphia (1955), pp. 40, 46, 50.

TABLE V. RELATIVE ATOMIC CONCENTRATIONS OF THE ELEMENTS STUDIED FOR THE DETERMINATION OF THE SENSITIVITIES

The samples of copper and zinc, magnesium, and iron were prepared by the National Bureau of Standards, the Dow Chemical Company, and the Sumitomo Metal Industries, Ltd., respectively.

Element	S-1 (Cu-158)	S-2 (Zn-94b)	S-3 (Mg-66482)	S-4 (Mg-66484)	S-5 (Mg-66493)	S-6 (Mg-66851)	S-7 (Fe)
Mg		0.12	100	100	100	100	
Al	1.4	10.4	5.96	6.81	3.46		
Si	6.77		0.15	0.041			
Ca					0.102		
Cr							1.49
Mn	1.67	0.018	0.13	0.073	0.25		
Fe	1.85	0.021					100
Ni							1.36
Cu	100	1.10					
Zn	2.21	100	1.30	1.07	0.500	0.434	
Sn	0.57						

TABLE VI. CONSTANCY OF THE RELATIVE SENSITIVITY OBTAINED FROM DIFFERENT STANDARD SAMPLES

The "No." and the "Mean" indicate the number of S_X/S_R measurements and the mean weighted by the "No." for each sample, respectively.

Sample	Zn	Mg		Al		Mn	
	S_R	S_X	No.	S_X	No.	S_X	No.
S-1	1.00			1.69±0.55	23	1.28±0.35	23
S-2	1.00	2.45±0.61	21	1.66±0.81	22	1.69±0.46	12
S-3	1.00	2.06±0.13	4	1.14±0.17	3	0.66±0.04	3
S-4	1.00	1.63±0.34	7	1.23±0.34	6	1.15±0.08	4
S-5	1.00	2.75±0.10	4	1.70±0.20	3	1.18±0.17	3
S-6	1.00	2.18±0.16	5				
Mean	1.00	2.27±0.54	41	1.60±0.64	57	1.33±0.45	45

plate was first exposed. Each value of r_i used in Eq. 2 was taken from data compiled by Moeller.[30]

In this work the monatomic singly-charged positive ion, the yield of which is generally larger than that of any other ion produced by a spark, such as multiply-charged or polyatomic ions, has been studied for the eleven elements shown in Table V. S_R is taken as unity for zinc, because this element is found in moderate concentrations in all the samples except for S-7 and has five isotopes, so that up to five curves can be utilized in a single calibration graph as a reference to measure the ion intensity ratio, I_X/I_R, as may be seen in Fig. 2. Strictly speaking, I_X/I_R is the "apparent" ion intensity ratio of X to R at the line density, d, because ions of different elements can not have the same darkening rate of a plate unless their mass ratio is very close to unity, as will be described later. Therefore, the sensitivity defined by Eq. 3 contains a factor of the darkening rate of a plate in addition to that of the ion production rate by spark discharges.

30) T. Moeller, "Inorganic Chemistry," 4th Ed., John Wiley & Sons, Inc., New York (1955), p. 911.

Results

Relative Sensitivity.—In Eq. 3, S is assumed to be independent of variations in bulk concentration. To certify this assumption, the constancy of S was studied using several samples. The results obtained for magnesium, aluminum and manganese are shown in Table VI and Fig. 3, where the average for each sample has been calculated by the same procedure as that used in the isotopic analyses of magnesium and zinc. The relative sensitivities obtained for the eleven elements contained in some of the samples used are shown in the second column of Table VII. For comparison with results obtained for the "sensitivity/area-factor" by several workers, the relative sensitivities divided by the square root of the corresponding mass ratio, i. e., $S_X/(m_X/m_R)^{1/2}$, are shown for some elements, taking as unity that for iron in Table VIII. Every value in the fourth column of the table was calculated

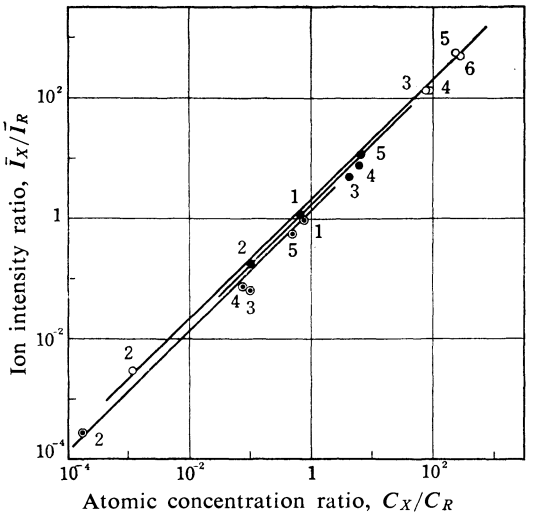


Fig. 3. Linearity of relative ion intensity versus relative atomic concentration. A figure written beside each data point indicates the number of the sample used.
○: Mg ●: Al ◉: Mn

TABLE VII. RELATIVE SENSITIVITIES AND RELATIVE ION PRODUCTION RATES OF ELEMENTS OBTAINED FOR MONATOMIC SINGLY-CHARGED POSITIVE IONS PRODUCED BY A DEMPSTER TYPE VACUUM SPARK ION SOURCE

Element	Relative sensitivity	Relative ion production rate	Number of measurements	Number of samples
Mg	2.3±0.5	1.4±0.3	41	5
Al	1.6±0.6	1.0±0.4	57	5
Si	1.2±0.5	0.8±0.3	31	3
Ca	2.8±0.3	2.2±0.3	3	1
Cr	2.2±1.4	2.0±1.2	17	1
Mn	1.3±0.5	1.2±0.4	45	5
Fe	1.4±0.6	1.3±0.5	37	2
Ni	1.2±0.6	1.2±0.6	8	1
Cu	0.8±0.2	0.8±0.2	24	2
Zn	1.0	1.0		
Sn	0.7±0.2	1.0±0.3	20	1

from the data for the "analysis of copper standards" shown in Ref. 34.

Relative Ion Production Rate.—According to reports by Burlefinger and Ewald,[31] Owens,[32] and Owens and Giardino,[33] the relative darkening rate is approximately proportional to the reciprocal of the square root of the mass. On the basis of their results, it may be deduced that the number of ions necessary for the line density to achieve a certain value, d, is proportional to the square root of the mass.* Thus, applying this correction to Eq. 2, the relative ion production rate, P_X, can be obtained from the following equation:

$$P_X = P_R(S_X/S_R)(m_X/m_R)^{1/2} \quad (4)$$

As is shown in the third column of Table VII, the range of the relative ion production rates obtained is narrower than that of the relative sensitivities. In Table IX the present

TABLE VIII. COMPARISON OF THE "SENSITIVITY/AREA-FACTOR" OBTAINED BY SEVERAL WORKERS TAKING UNITY FOR IRON

Element	Present work	Craig, Errock, Waldron[4]	Elliott, Craig, Errock[34]	Kai[35]
Mg	2.3±1.4	>3		14
Si	1.2±0.9	1.6	0.7	1.8
Ti		1.1		1.6
Cr	1.5±0.4	1—3	1.2	1.5
Mn	0.9±0.6	1.8	1.3	1.8
Fe	1.0	1.0	1.0	1.0
Ni	0.8±0.1	0.9	1.2	0.6
Cu	0.5±0.3	0.8		1.1
Zn	0.6±0.2	5.5	1.0	3.0
Sn	0.3±0.2	>3	2.8	
Matrix element	Mg, Fe, Cu or Zn	Al	Cu	Al or Cu

TABLE IX. RELATIVE ION PRODUCTION RATES OBTAINED WITH PHOTOMETRY AND COMPARISON WITH VALUES WITH ELECTROMETRY

	Photometry	Electrometry	
Element	Present work	Chakravarty, Venkatasubramanian, Duckworth[36]	Gorman, Jones, Hipple[13]
Mg	1.0±0.6	2.4	
Al	0.8±0.5	0.9	
Cr	1.4±0.4	1.4	1.50
Mn	0.9±0.6	2.1	
Fe	1.0	1.0	1.00
Ni	0.9±0.1	0.8	0.89
Cu	0.6±0.4	1.0	
Zn	0.7±0.3	1.9	
Matrix element	Mg, Fe, Cu or Zn	Al, Fe, Ni or Cu	Fe

31) E. Burlefinger and H. Ewald, *Z. Naturforsch.*, **16a**, 430 (1961).
32) E. B. Owens, *Appl. Spectr.*, **16**, 148 (1962).
33) E. B. Owens and N. A. Giardino, a preprint entitled "Quantitative Mass Spectrography of Solids."

* In order to accertain this rule by isotopic analysis using the equation $r_i/r_j=(q_j/q_i)(m_i/m_j)$ instead of Eq. 1, it is necessary to choose those isotopes which are moderate in both mass ratio and abundance ratio. Perhaps ^{6}Li and ^{7}Li are the most suitable isotopes for this purpose. However, the difference in the darkening rate between them is calculated to be no more than 8 per cent. Therefore, the difference in the mass effect among the isotopes of an element of a larger atomic number, such as copper, is negligibly small compared with the erratic fluctuations in the photometry. This is the reason why no correction for the darkening rate is made for any of the isotopes in Eqs. 1 and 2.

data are compared with values determined by the electrometry, taking P_R as unity for iron.

The Constancy of the Relative Ion Yields for Elements.—As may be seen in Fig. 2, the data points for every ion do not exactly fall on a smooth curve. This is presumably due to fluctuations in the relative ion yields for different elements in each exposure, to the non-uniformity of the emulsion of the photographic plate and, to errors in the measurements of both the monitor current and the photometry of the plate. From this point of view, the reproducibility of the relative ion intensities measured for various ions has been studied in every exposure stage using a modified Mattauch-Ewald method. This method employs D_n and $\log r$ as the two components of a calibration graph, while Mattauch-Ewald's method employs $(L_0-L)/L_0$ and r. The former has such advantages over the latter as follows:

(1) A calibration curve with a linear part is always obtainable for the isotopic ions to be used as internal standards only if the most suitable expression of density among the five is employed.

(2) Extrapolation is applicable to the curve according to each "useful range" shown in Table I.

For the purpose of determining the relative intensities of ions detected in the "same" exposure stage, the present method is more suitable than the monitor method, because all the r_i, r_j,..... values in the abscissa are free from erratic fluctuations.

The results are shown in Table X, where the singly-charged ions of the isotopes of zinc contained as one of the impurity elements in S-1 are employed as the internal standards for calibration, and no value in the second column is corrected for the darkening rate.

TABLE X. REPRODUCIBILITY OF RELATIVE ION INTENSITIES MEASURED FOR ISOTOPES AND DIFFERENT ELEMENTS USING THE SAMPLE S-1

Ions	Ion intensity ratio	Number of measurements	Precision %
$^{56}Fe^+/^{54}Fe^+$	14.9 ± 1.4*1	22	± 9
$^{120}Sn^+/^{118}Sn^+$	1.38 ± 0.13*2	20	± 9
$^{66}Zn^{2+}/^{68}Zn^{2+}$	1.55 ± 0.13*3	26	± 8
$^{120}Sn^{2+}/^{118}Sn^{2+}$	1.41 ± 0.12*2	24	± 9
$^{27}Al^+/Zn^+$	0.913 ± 0.357	38	±39
$^{55}Mn^+/Zn^+$	0.882 ± 0.524	43	±59
$^{56}Fe^+/Zn^+$	1.02 ± 0.52	42	±51
$^{120}Sn^+/Zn^+$	0.0577 ± 0.0180	29	±31
$^{27}Al^+/^{56}Fe^+$	1.03 ± 0.49	38	±48
$^{55}Mn^+/^{56}Fe^+$	0.980 ± 0.260	42	±27
$^{120}Sn^+/^{56}Fe^+$	0.0829 ± 0.0445	17	±54
$^{27}Al^+/^{120}Sn^+$	13.7 ± 7.1	14	±52
$^{55}Mn^+/^{120}Sn^+$	14.6 ± 5.7	17	±39
$^{27}Al^+/^{55}Mn^+$	1.01 ± 0.30	38	±30
$^{27}Al^{2+}/^{66}Zn^{2+}$	1.91 ± 1.02	10	±53
$^{55}Mn^{2+}/^{66}Zn^{2+}$	2.92 ± 1.46	29	±50
$^{120}Sn^{2+}/^{66}Zn^{2+}$	0.402 ± 0.247	16	±61
$^{55}Mn^{2+}/^{120}Sn^{2+}$	10.3 ± 5.4	13	±52
$^{27}Al^{2+}/^{55}Mn^{2+}$	0.583 ± 0.186	13	±32
$^{27}Al^{2+}/Zn^+$	0.167 ± 0.098	18	±59
$^{55}Mn^{2+}/Zn^+$	0.257 ± 0.097	37	±38
$^{66}Zn^{2+}/Zn^+$	0.110 ± 0.059	33	±54
$^{120}Sn^{2+}/Zn^+$	0.0330 ± 0.0115	28	±35
$^{27}Al^{2+}/^{27}Al^+$	0.138 ± 0.047	14	±34
$^{55}Mn^{2+}/^{55}Mn^+$	0.334 ± 0.124	35	±37
$^{120}Sn^{2+}/^{120}Sn^+$	0.613 ± 0.144	23	±23

*1–*3 These are in good agreement with values determined by electrometry as shown below:

Fe:	15.77 ± 0.03	(Ref. 18)
Sn:	1.377 ± 0.007	(Ref. 18)
Zn:	1.501 or 1.505	(Ref. 15)

Discussion

It will be found in Table X that the results obtained from repeated measurements of many pairs of different elements are less reproducible by several times than those for isotopes. It is the same with those of four pairs of the same element with single and double charges. The results may suggest that the spark source does not always possess a constant ionization efficiency for all the elements contained in the sample electrodes and/or the relative ion transmission rates from the source to a plate are not always constant for all the ion species produced, probably due to the fluctuations of spark conditions during the exposures, rather than the sample used is not mass-spectroscopically homogeneous in chemical composition. It is possible, with a spark ion source, that on spark spots the chemical composition of the sample electrodes, even if they are originally homogeneous, may be varied during spark discharges because of fractional evaporation, selective sputtering, preferential diffusion, etc. The precision for each pair of iron, zinc and tin isotopes shown in Table X can be considered approximately to indicate the errors attributed to the non-uniformity of photographic emulsion and development in the present work.

Although it may be necessary to study further the elements using many samples different in concentration, Fig. 3 is believed to establish that the relative sensitivity of each element is constant, independent of changes in the bulk concentration of the element to within an uncertainty factor of 1.5 on the average; this compares favorably with the results obtained by Hannay and Ahearn using several samples of both silicon and germanium, including

boron and antimony as impurity elements respectively.[11] Table VII indicates that the relative sensitivities are of the same order of magnitude for all the elements studied in spite of large differences in physical and chemical properties among them, and it is also so with the relative ion production rates. This approximate equality is generally accepted for the Dempster-type vacuum-spark ion source.[3, 4, 34, 36-38]

Owens and Giardino discovered that the relative sensitivity of gallium with respect to arsenic increased considerably in value after prolonged sparking.[33] This discrimination effect was also observed with magnesium and zinc by Duckworth et al.[36] using several alloys, and accepted with zinc by Waldron, who has stated (cf. Ref. 36) that the sensitivity ratio of zinc to iron was found to get much lower values than 5.5 (cf. Table VIII) in subsequent measurements. In the present work, ions produced during the early stage of sparking were studied. As Table VIII shows, the values obtained by the four groups of workers have a large discrepancy among them for magnesium, zinc and tin, although they do not differ for the other elements by more than a factor of 2. This is possibly due to either the above discrimination effect in sparking, to matrix effects, or to both; Craig has found that the relative sensitivity of zinc with respect to iron is about 1 for some matrices, e. g., copper and gallium, but about 6 for other matrices, e. g., aluminum and iron.[39] It may be seen from Table IX that the ion production rates for each element agree also to within a factor of 2 among the three works in spite of the essential differences in detection methods.

On the basis of these considerations, it might be concluded that:

(1) The relative ion yields from a spark source are not always constant for all the elements contained in the sample electrodes even if the operating conditions of the instrument are kept constant throughout the exposures.

(2) This can cause variations in the relative sensitivities by up to several tens of per cent.

(3) Under different experimental conditions, the relative sensitivities are apt to change remarkably for some elements, such as magnesium, zinc and tin although they seem to change rather slightly for others, such as chromium, manganese and nickel.

(4) Since they are subject to changes of value according as various conditions, perhaps they can not be generally applicable as the analytical constant without uncertainty factors, such as about 2 for non-volatile elements and more for volatile ones.

However, much more work must be done to obtain precise informations on the sensitivity.

Summary

The relative sensitivities of eleven elements in a spark-source mass spectrograph have been determined for monatomic singly-charged positive ions detected with Ilford Q2 plates. The results show that the elements have approximately the same sensitivities to within a factor of 3 in spite of large differences in both physical and chemical properties among them, and that the sensitivity of each element is constant in value within an uncertainty factor of 1.5, independent of changes in the bulk concentration of the element. Relative ion production rates have also been determined from the above sensitivities; they are in reasonable agreement with published values determined by electrical detection. From repeated measurements of the relative intensities of various ions, it has been suggested that relative ion yields from a spark ion source are not always constant for different elements. On the basis of these investigations, a discussion has been made of the general applicability of the sensitivity as the analytical constant in the quantitative mass spectrography of solids. Five different formulas have been used to express the "density" of mass lines, and exposures have been determined with an integrated monitor current. By trying several isotopic analyses, the calibration methods have been shown to be useful for mass spectrography.

The author would like to express his hearty thanks to Professor Emeritus Nobuji Sasaki of Kyoto University for his valuable suggestions on the calibration methods, to Professor Kumasaburo Kodera of Kyoto University for his guidance throughout the course of the work, and to Assistant Professor Hokotomo Inouye of Tohoku University for his helpful criticism. He would also like to thank Dr. Tsutomu Makita of the Laboratory and Dr. Junjiro Kai of the Mitsubishi Elec. Mfg. Co.

34) R. M. Elliott, R. D. Craig and G. A. Errock, "Instruments and Measurements," Vol. I, Ed. by H. Koch and G. Ljungberg, Academic Press, New York (1961), p. 271.
35) J. Kai, private communication.
36) B. Chakravarty, V. S. Venkatasubramanian and H. E. Duckworth, "Advances in Mass Spectrometry," Vol. II, Ed. by R. M. Elliott, Pergamon Press, London (1963), p. 128.
37) M. G. Inghram, "Trace Analysis," Ed. by J. H. Yoe and H. J. Koch, Jr., John Wiley & Sons, Inc., New York (1957), p. 437.
38) R. Brown, R. D. Craig and R. M. Elliott, "Advances in Mass Spectrometry," Vol. II, Ed. by R. M. Elliott, Pergamon Press, London (1962), p. 141.
39) R. D. Craig, private communication.

for their helpful advice on the instrument. He is also grateful to Dr. Lorenzo Sturkey of the Dow Metal products Co. for his kindness in offering the magnesium standard samples.

Department of Chemistry
Faculty of Science
Kyoto University
Sakyo-ku, Kyoto

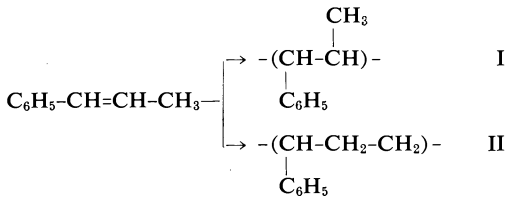
*The Rearrangement Polymerization of Propenylbenzene**

By Shunsuke MURAHASHI, Shun'ichi NOZAKURA,
Kazuhiko TSUBOSHIMA and Yahide KOTAKE

(Received October 21, 1963)

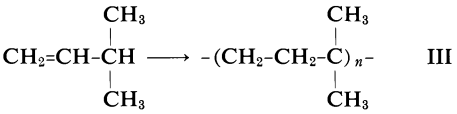
Propenylbenzene belongs to a family of 1, 2-disubstituted ethylenes which are generally reluctant to homopolymerize by means of a radical mechanism.[1] Little information has been reported on the cationic polymerization of the monomer.

In 1935 Staudinger and Dreher observed the cationic polymerization of propenylbenzene when boron trifluoride was used as an initiator.[2] Their close examination of the polymeric product by thermal degradation and viscometric measurements led them to conclude that the chemical structure of the polymer is not the expected one I but structure II.



The occurrance of structure II would, however, involve, in the intermediate stage, an intramolecular hydrogen shift from the primary carbon to the secondary one, a phenomenon which is surprising and contrary to the usual observation on the isomerization of a cation.[3] Although a similar unusual rearrangement during polymerization was reported, without detailed proof, to occur in the polymerization of isobutylene by a Ziegler-type catalyst,[4] it has recently been disproved by Bacskai and Lapporte.[5]

More recently, 3-methylbutene-1 was polymerized by Kennedy and Thomas at a low temperature with a cationic catalyst to give a rearranged polymer III, which involves a normal hydrogen shift from the tertiary to the secondary carbon.[6]



Thus, Staudinger's result presents an example of a rather peculiar type of polymerization reaction, and it seemed worthwhile to reinvestigate it in detail. The present paper will study the chemical structure of polypropenylbenzene by infrared spectroscopy and will also study the effect of reaction conditions on the polymer structure.

Experimental

Monomers. — Propenylbenzene was prepared by the method of Overberger and Tanner[7] through the thermal decomposition of α-ethylbenzyl acetate (b. p. 56.5~63°C 10 mmHg, n_D^{25} 1.5473). The propenylbenzene was found by gas chromatography to consist of 74% trans-isomer and 26% cis-isomer; it was used for polymerization without separation.

Allylbenzene was prepared according to the method of Hershberg from allyl bromide and

* Paper I in a series on "The Polymerization of Internal Olefins."

1) T. Alfrey, Jr., J. J. Bohrer and H. Mark, "Copolymerization," Interscience Publishers, New York (1952), p. 49.

2) H. Staudinger and E. Dreher, *Ann.*, 517, 73 (1935).

3) E. S. Gould, "Mechanism and Structures in Organic Chemistry," Holt, Rinehart and Winston, Inc., New York (1959), p. 449.

4) A. V. Topchiev et al., *Doklady Akad. Nauk S. S. S. R.*, 111, 121 (1956).

5) R. Bacskai and S. J. Lapporte, *J. Polymer Sci.*, Part A, 1, 2225 (1963).

6) J. P. Kennedy and R. M. Thomas, *Makromol. Chem.*, 53, 28 (1962).

7) C. G. Overberger and D. Tanner, *J. Am. Chem. Soc.*, 77, 369 (1955).

phenylmagnesium bromide.[8] B. p. 67.5~69.5°C/35 mmHg.

Catalysts.—Boron trifluoride was prepared when required by the thermal decomposition of phenyldiazonium borofluoride, and it was freed from fluorobenzene by passing it through a dry ice-acetone trap.

Boron trifluoride complexes were prepared by passing a calculated amount of boron trifluoride gas through an appropriate amount of a donor compound, after which it was subjected to vacuum distillation. $BF_3 \cdot 2H_2O$, b. p. 29.0°C/0.33 mmHg; $BF_3 \cdot 2CH_3COOH$, b. p. 138~139°C; $BF_3 \cdot 2CH_3OH$, b. p. 34.0~34.8°C/1.5 mmHg; $BF_3 \cdot (CH_3)_2O$, b. p. 126~127°C.

The other metal halides were commercial products and were used without further purification.

Solvents.—All the solvents used were purified according to the usual method[9] and were stored over a molecular sieve.

The Polymerization of Propenylbenzene.—Polymerization was carried out in a 50 ml. flask under a slight positive pressure of dry nitrogen, with occasional gentle shaking. Solvent and monomer were placed in the flask, which was then flushed with a stream of nitrogen, and the catalyst was injected through a rubber cap using a hypodermic syringe. The fluctuation of temperature of bath was kept at ±1°C. Polymerization was stopped by adding a mixture of concentrated aqueous ammonia and methanol, and the contents of the flask were poured into a large excess of methanol (250 ml.). The precipitated polymer was separated from the mother liquor by filtration through a sintered glass filter of medium porosity, and was weighed after drying as the methanol-insoluble part of the polymer. An aliquot of the filtrate was iodometrically titrated for unreacted monomer using a standard bromate-bromide solution. The remainder of the filtrate was evaporated in vacuo and dissolved in benzene. The benzene solution was washed with dilute aqueous hydrochloric acid and then water, dried with calcium chloride, and evaporated again in vacuo to give the methanol-soluble part of the polymer.

The Polymerization of Allylbenzene.—Allylbenzene (2 g.) was polymerized at 50°C for 48 hr. in a sealed tube using a Ziegler catalyst, which was composed of 6 ml. of heptane, $TiCl_4$ (monomer/Ti=10) and $Al(i\text{-}C_4H_9)_3$ (Al/Ti=1.2).[10] The catalyst was prepared under the refluxing of *n*-heptane.[11] The yield of the polymer was 24%. The polymer was extracted with hot benzene, using a modified Soxhlet apparatus for 15 hr., 32.5% of the total polymer being insoluble (softening pt. 170~210°C).

Molecular Weight. — The molecular weight of the polymers was determined cryoscopically in benzene.

Infrared Spectra.—The infrared spectra of the polymers were obtained in the state of polymer films when possible, in KBr disks, or sometimes in thin liquid films, using a Nihon Bunko DS 402G grating spectrophotometer.

Results and Discussion

The Infrared Spectra of Polypropenylbenzene.—There are two structural possibilities for polypropenylbenzene. One is structure I, resulting from the normal opening of the double bond, and the other is the rearranged structure, II, as has been suggested by Staudinger. In fact, the infrared spectra of polypropenylbenzene obtained show considerable differences in the 2850~2960 cm^{-1} region and in the 1450~1500 cm^{-1} region according to the polymerization conditions.

Figure 1 shows the infrared spectra of the methanol-insoluble part of two polymers obtained by using borontrifluoride as the catalyst at room temperature in toluene and borontrifluoride etherate, at 0°C in toluene. The latter have a very weak absorption of the CH_3 degenerated stretching mode at 2960 cm^{-1} and of the CH_3 symmetric stretching mode at 2870 cm^{-1}, showing a very small methyl-group content. On the other hand, the former BF_3-polymer showed much more intensive absorptions at these two wave numbers, indicating a higher methyl-group content. These differences in spectra correspond to the structural

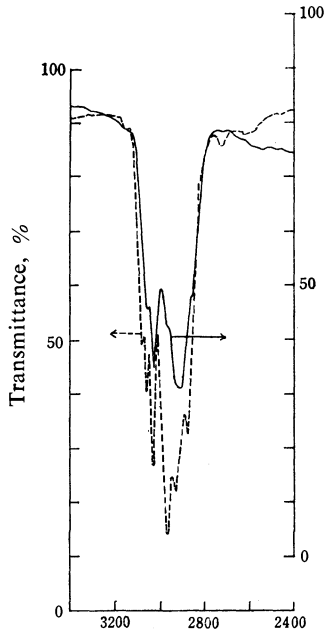


Fig. 1. IR-Spectra of polypropenylbenzene.
—— Polymerized with BF_3Et_2O at 0°C
---- Polymerized with BF_3 at −78°C

8) E. B. Hershberg, *Helv. Chim. Acta*, **17**, 351 (1934).
9) A. Weissberger et al., "Organic Solvents," 2nd. Ed., Interscience Publisher Inc., New York (1955).
10) G. F. D'Alelio, *J. Polymer Sci.*, **45**, 83 (1960); G. Pregaglia and M. Binaghi, ibid., **51**, s61 (1961).
11) S. Murahashi, S. Nozakura, M. Sumi and K. Hatada, This Bulletin, **32**, 1094 (1958).

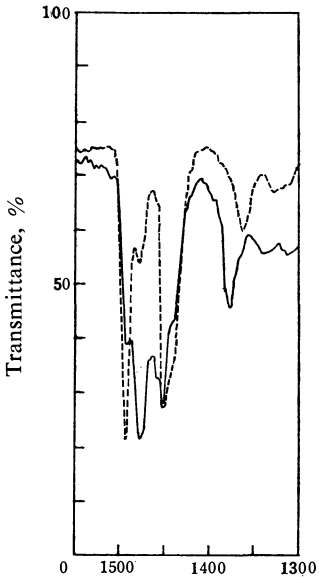
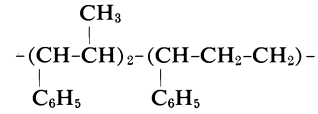


Fig. 2. Comparison of IR spectra of polypropenylbenzene and polyallylbenzene.
—— Polypropenylbenzene prepared with $BF_3 \cdot Et_2O$ at 0°C
---- Polyallylbenzene prepared with Ziegler catalyst

change from I to II, and it was concluded that the BF_3-polymer is relatively rich in structure I and that the $BF_3 \cdot Et_2O$-polymer is rich in structure II. Thus, the authors hereafter will use the ratio of optical densities at 2960 and 2925 cm^{-1}, $D(CH_3/CH_2)$, as a measure of the methyl to the methylene ratio and, hence, of the ratio of structual units I to II in the polymer.* A definite numerical correlation between the values of $D(CH_3/CH_2)$ and the ratio of the structural units, I/II, has not yet been established. Also, we do not have a standard polymer specimen which has either the pure structural unit I or the pure II. However, there is one example which suggests the correspondence between these two values. Poly-α-methylstyrene of high molecular weight has one methyl group and one methylene group, the ratio of methyl and methylene being unity, and the observed value of $D(CH_3/CH_2)$ was 0.7. In the case of polypropenylbenzene, the value, unity, of the methyl/methylene ratio corresponds to the following structural ratio:



Thus, polypropenylbenzene with the $D(CH_3/CH_2)$ value of 0.7 would correspond to a polymer having a 1/3 rearranged structure II and 2/3 normal structure I, as has been indicated above.

There is one more possible structure of the polymer, the structural unit of which is that of polyallylbenzene. This possibility can not be excluded since the existence of an isomerization equilibrium has been reported between allylbenzene and propenylbenzene under some favorable conditions.[13] A comparison was made between the infrared spectra of the BF_3 etherate polymer and polyallylbenzene, which had been prepared with a Ziegler catalyst (Fig. 2). The spectra showed little difference in the CH stretching region, but there was a remarkable difference in the 1450~1495 cm^{-1} region. The band at 1495 cm^{-1} characteristic of polyallylbenzene is absent in the rearranged polymer. In addition, the residual propenylbenzene after the polymerization was found by gas chromatography to contain no detectable amount of allylbenzene. Therefore, the possibility of the existence of the polyallylbenzene structural unit in the present polymers could be excluded.

It should be noted that, when using $D(CH_3/CH_2)$ as a measure of the polymer structure, we did not take account of the structure of the polymer ends, which would have contributed considerably to the $D(CH_3/CH_2)$ values when the molecular weight was very low. Accordingly, the $D(CH_3/CH_2)$ of the methanol-soluble parts (oligomers) of the polymers is not listed in the present data.

A Comparison of Various Catalysts. — Two groups of catalysts were tested. One group is metal halides, which are considered to need water as a co-catalyst (Table I). The other group is boron trifluoride complexes with definite chemical compositions (Table II). Higher yields of total polymer were obtained with metal halide catalysts, especially with such strong Friedel-Crafts-type catalysts as boron fluoride, aluminum bromide and titanium tetrachloride, than with boronfluoride complexes. Boron fluoride complexes exhibited moderate catalytic action. Some metal halides gave higher yields of polymer at −78°C than at 0°C, while all the boronfluoride complexes showed a better yield at 0°C than at −78°C.

Fractions of the methanol-isoluble part are

* The ratio of optical densities at 2960/2850 cm^{-1} is usually used to estimate the ratio of methyl and methylene groups.[12] In our cases, however, the absorption at 2850 cm^{-1} is invariably very weak and is considered unsuitable for the measurement.

12) For example, H. V. Drushell and F. A. Iddings, *Anal. Chem.*, 35, 28 (1963).

13) L. Bateman, *J. Chem. Soc.*, 1951, 2283.

TABLE I. POLYMERIZATION OF PROPENYLBENZENE WITH METAL HALIDE CATALYSTS

Monomer (trans 74%) 1 ml.; solvent 4 ml.;
Catalyst/monomer mole ratio=1/20; 4 hr.

Catalyst	Solvent	Polymer yield, %[b]	Methanol-insoluble part			
			Yield, %	$D(CH_3/CH_2)$	Soft. pt., °C	Mol. wt.
0°C						
BF_3[a]	Toluene	73.3	12.1	0.57	143~154	1100
BF_3[a]	*n*-Heptane	20.1	9.6	1.31	113~121	670
$AlBr_3$[c]	Toluene	72.1	3.5	1.41	135~145	980
$TiCl_4$[c]	Toluene	32.1	3.6	0.29	160~170	710
$FeCl_3$	Toluene	22.2	4.8	0.29	156~165	—
Et_2AlCl	Toluene	(3.4)	—	—	—	—
$SnCl_4$	Toluene	(0.9)	trace	—	—	—
VCl_4	Toluene	(2.0)	0	—	—	—
−78°C						
BF_3[a]	Toluene	31.2	21.2	1.50	127~134	850
BF_3[a]	*n*-Heptane	(8.9)	5.4	0.15	188~197	2900
$AlBr_3$[c]	Toluene	83.4	11.1	1.75	135~145	710
$TiCl_4$[c]	Toluene	55.6	13.3	0.50	160~175	1200
$FeCl_3$	Toluene	(10.3)	5.8	0.18	170~177	2700
Et_2AlCl	Toluene	(8.6)	—	—	—	—
$SnCl_4$	Toluene	(6.4)	2.1	0.27	182~188	—
VCl_4	Toluene	(4.7)	trace	—	—	—

a) BF_3 gas was saturated.
b) Yields in parenthes are values obtained by bromate-bromide titration of the residual monomer.
c) Monomer contains 78% of the trans-isomer.

TABLE II. POLYMERIZATION OF PROPENYLBENZENE WITH BF_3 COMPLEXES

Monomer (trans 74%) 1 ml.; solvent toluene 4 ml.;
catalyst/monomer mole ratio=1/20; 4 hr.

Catalyst	Polymer yield, %[a]	Methanol-insoluble part				
		Yield, %	$D(CH_3/CH_2)$	Soft. pt. °C	Mol. wt.	Unusual IR
0°C						
$BF_3 \cdot 2CH_3OH$	(16.1)	9.6	0.51	150~160	2000	1095 cm^{-1}, ether
$BF_3 \cdot 2CH_3COOH$	(13.5)	10.4	0.37	153~164	2400	1230, 1740 cm^{-1}, ester
$BF_3 \cdot 2H_2O$	(10.8)	trace	—	—	—	
$BF_3 \cdot (CH_3)_2O$	(9.6)	8.6	0.23	168~175	2100	1090 cm^{-1}, ether
$BF_3 \cdot (C_2H_5)_2O$	9.9	8.1	0.17	155~166	1600	1090 cm^{-1}, ether
−78°C						
$BF_3 \cdot 2CH_3OH$	(8.1)	3.6	0.30	172~186	—	1095 cm^{-1}, ether
$BF_3 \cdot 2CH_3COOH$	—	trace	—	—	—	
$BF_3 \cdot 2H_2O$	(4.9)	0	—	—	—	
$BF_3 \cdot (CH_3)_2$	—	trace	—	—	—	
$BF_3 \cdot (C_2H_5)_2O$	1.2	0.7	0.17	102~113	—	1090 cm^{-1}, ether

a) Yields in parenthes are values obtained by bromate-bromide titration of the residual monomer.

generally smaller in amount with BF_3 complexes than with metal halides. There is a sharp contrast between the two groups of catalysts in the effect of the polymerization temperature on the molecular weights of the resulting polymers. Metal halides yielded a higher fraction of the insoluble polymer at −78°C than at 0°C, while the BF_3-complexes showed reverse results.

Among all the catalysts tested, the milder catalysts generally gave polymers with the smaller value of (CH_3/CH_2) and, hence, the larger proportion of rearrangement during polymerization.

It is interesting to note here that there were observed some unusual absorptions in the infrared spectra of the polymers obtained with the borontrifluoride complexes (Table II, the last column). These absorptions are considered to come from the terminal groups of the polymer, probably being incorporated into the polymers by a termination reaction with

TABLE III. EFFECT OF TEMPERATURE ON THE POLYMERIZATION OF PROPENYLBENZENE WITH BF_3 ETHERATE

Monomer (trans 74%) 1 ml.; solvent, toluene 4 ml.; catalyst/monomer mole ratio=1/20; 4 hr.; temperature ±1°C

Temp., °C	Polymer yield, %	Methanol-insoluble part			
		Yield, %	$D(CH_3/CH_2)$	Soft. pt., °C	Mol. wt.
−78	1.2	0.7	0.17	102∼113	−
−60	2.4	1.7	0.11	118∼137	−
−40	6.6	4.5	0.14	155∼165	1600
0	9.9	8.1	0.17	155∼166	1600
20	9.8	6.3	0.12	152∼165	1600
40	12.5	3.6	0.13	145∼154	—

"gegen" ions or initiator molecules.* Another unusual infrared band to be noted is the one observed around 800 cm^{-1} (which is not shown here) in polymers obtained with borontrifluoride in *n*-heptane at 0°C as well as at −78°C. This band may possibly be assigned to the occurrence of *p*-disubstituted benzene which originates from the *p*-substitution of the benzene ring by the growing cation in a termination reaction or during the propagation step. This assignment needs further experimental verification, however.

The Effect of the Polymerization Temperature. —The polymerization ofp ropenylbenzene with BF_3 etherate was carried out in toluene at temperatures from −78 to 40°C (Table III and Fig. 3). The total yields polymer increased with a rise in the temperature. However, the methanol-insoluble part showed a maximum at about 0°C and rapidly decreased thereafter while at the same time the yield of the methanol-soluble low polymer fractions

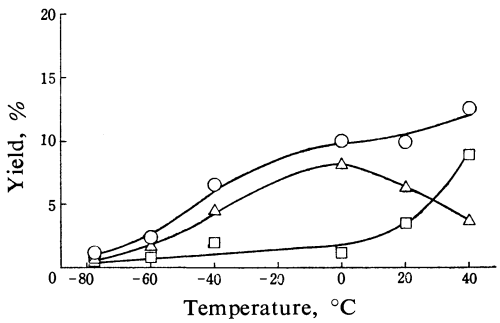


Fig. 3. Effect of temperature on polymerization of propenylbenzene with BF_3 etherate.
○ Total polymer
△ The methanol-insoluble part
□ The methanol-soluble part

* In a preliminary experiment, there was observed less than a first-order dependence of the polymerization rate on the initiator concentration, especially at high initiator concentrations. In addition, the molecular weight was found to decrease with increasing initiator concentrations. These facts appear to suggest qualitatively the existence of a termination or a transfer reaction with initiator molecules.

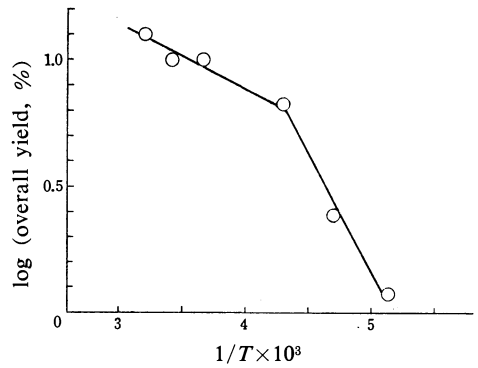


Fig. 4. Effect of polymerization temperature on overall yield of polypropenylbenzene (BF_3Et_2O catalyst).

increased rapidly above 0°C. Correspondingly, the Arrhenius plot of the total yield (Fig. 4) showed a break, giving an activation energy of 1.2 kcal./mol. at the high temperature region and 4.3 kcal./mol. at the low temperature region. The phenomenon seems to indicate that there is some change in the mechanisms of polymerization processes between below and above 0°C.

Although the temperature of the polymerization had a marked effect on the rate of polymerization as well as on the molecular weight, it had no appreciable effect on $D(CH_3/CH_2)$ (Fig. 5). Hence, it is suggested that the activation energy of the normal propagation is nearly equal to that of the rearrangement propagation.

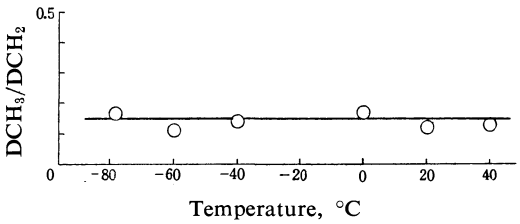


Fig. 5. Effect of polymerization temperature on the chemical structure of polypropenylbenzene (BF_3Et_2O catalyst).

TABLE IV. EFFECT OF DIELECTRIC CONSTANTS OF SOLVENTS ON THE POLYMERIZATION OF PROPENYLBENZENE WITH BF_3 ETHERATE

Monomer (trans 74%) 1 ml.; solvent 4 ml.;
catalyst/monomer mole ratio=1/20; 4 hr. at 0°C

Solvent	Dielectric constant	Yield, %	Methanol-insoluble part			
			Yield, %	$D(CH_3/CH_2)$	Soft. pt., °C	Mol. wt.
CCl_4	2.3	11.5	6.1	0.36	159~167	—
$C_6H_5CH_3$	2.4	9.9	8.1	0.17	155~166	1600
$CHCl_3$	5.2	9.2	5.2	0.33	167~177	2100
CH_2Cl_2	9.9	12.7	8.7	0.52	160~168	1900
$(CH_2Cl)_2$	10.7	13.6	8.4	0.66	153~164	1600

The Effect of the Solvents. — The influence of the dielectric constants of the solvents was studied at 0°C using BF_3-etherate as a catalyst, as is shown in Table IV. The total yields of polymer and those of the methanol-insoluble part were observed to increase slightly with the increasing polarity of the solvents (Fig. 6). The $D(CH_3/CH_2)$ value increased remarkably, showing that the rearrangement in the propagation became unfavorable with the increasing polarity of the solvent (Fig. 7).

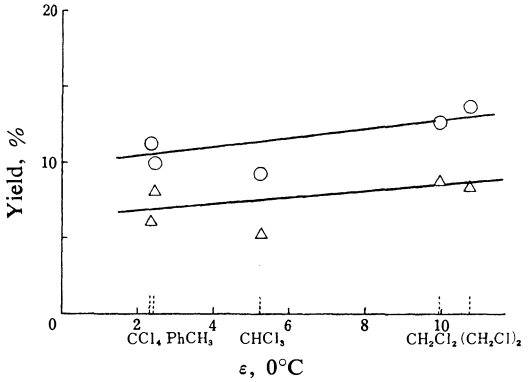


Fig. 6. Effect of dielectric constants of solvents on overall yield of polypropenylbenzene (BF_3Et_2O catalyst).
○ Total polymer
△ The methanol-soluble part

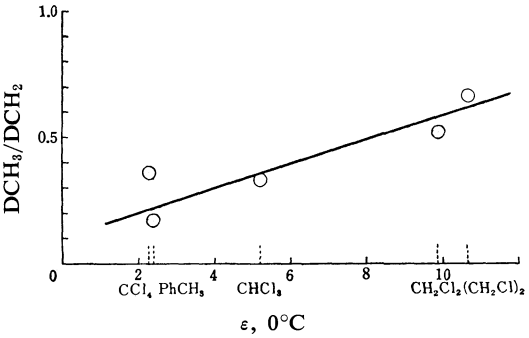


Fig. 7. Effect of dielectric constants of solvents on chemical structure of polypropenylbenzene (BF_3Et_2O catalyst).

The molecular weight of the resulting polymer, on the other hand, appears to decrease with the increasing dielectric constants of the solvents, except for the case of the toluene solvent, where a molecular termination on the aromatic ring may play some role. The decrease of the molecular weight with the increasing polarity of the solvent may be explained as due to a termination reaction which is favored by the polar medium.

Discussion of the Reaction Mechanism.—It has clearly been shown that a variety of "gegen" ions influenced the polymerization of propenylbenzene, i.e., the structure of the resulting polymer as well as the overall rate and the molecular weight. The facts may, as a whole, be interpreted in terms of ion pairs of growing ends. The rearrangement polymerization was found to be favored by mild initiators. Among the catalysts examined, BF_3-etherate showed the better results for the rearrangement polymerization.

Propagation.—The characteristic features of a propagation reaction using BF_3-etherate as a catalyst may be summarized as follows: (i) $D(CH_3/CH_2)$ does not change with a change in the temperature of polymerization, indicating that the activation energy for the usual propagation is nearly equal to that of the rearrangement. (ii) $D(CH_3/CH_2)$ increased markedly with an increase in the dielectric constants of the solvents; in other words, the rearrangement propagation is favored in a less-ionizing medium. This suggests that the growing species may be more intimate ion pairs in the rearrangement propagation than in the usual propagation. Propagation with the usual opening of double bonds (I) will proceed according to Scheme 1, the resonance stabilization of the α-alkylbenzyl cation being the determining factor for the attacking position of the growing cation. This reaction does not seem to need the strong cooperation of "gegen" ions and, hence, will be favored by highly-ionizing solvents. On the other hand, for the rearrangement polymerization two alternative mechanisms, 2 and 3, have to

be considered. Mechanism 2 involves two unfavorable steps, i. e., the prevalent formation of the more unstable secondary carbonium ion instead of the more stable α-alkylbenzyl cation, and the subsequent hydrogen transfer from primary to secondary carbon, which is also energetically unfavorable. Mechanism 3 seems more plausible for the rearrangement propagation. The methyl hydrogen of propenylbenzene would have an acidic nature. The "gegen" ion of the growing ion pair will assist in loosening the proton from the methyl group, and at the same time the growing carbonium ion will make an electrophillic attack on the methyl carbon. The proton will then be transfered to the adjacent

$$P^{\oplus} + C_6H_5\text{-}CH{=}CH\text{-}CH_3 \rightarrow P\text{-}\underset{\displaystyle Ph}{\underset{|}{\overset{\displaystyle CH_3}{\overset{|}{CH}}}}\text{-}CH^{\oplus}$$

$$\rightarrow \text{Propagation} \qquad (1)$$

$$P^{\oplus} + C_6H_5\text{-}CH{=}CH\text{-}CH_3 \rightarrow P\text{-}\underset{\displaystyle Ph}{\underset{|}{CH}}\text{-}CH^{\oplus}\text{-}CH_3$$

$$\rightarrow P\text{-}\underset{\displaystyle Ph}{\underset{|}{CH}}\text{-}CH_2\text{-}CH_2^{\oplus} \rightarrow \text{Propagation} \qquad (2)$$

$$C_6H_5\text{-}CH{=}CH\text{-}CH_3 + P^{\oplus}G^{\ominus} \rightarrow \begin{array}{c} G^{\ominus} \quad P^{\oplus} \\ \diagdown\ \ \downarrow \quad \diagup \\ H \quad CH_2 \\ \downarrow \quad \diagup \\ C_6H_5\text{-}CH{=}CH \end{array}$$

$$\rightarrow C_6H_5\text{-}\underset{\displaystyle G^{\ominus}}{\overset{\displaystyle \oplus}{CH}}\text{-}CH_2\text{-}CH_2\text{-}P \rightarrow \text{Propagation} \qquad (3)$$

double bond. Thus, the growing ion pair cooperates in the push-pull mechanism, and so highly-ionizing solvents will retard the reaction, making the contribution of the rearrangement propagation relatively smaller than the usual propagation in polar media.

Termination.—In the polymers obtained using boron trifluoride complexes as catalysts, some infrared absorption bands characteristic of the initiator fragments have been observed (Table II). This appears to indicate that the termination reaction with "gegen" ions (4) (self termination) or with an initiator (5) seems to play an important role.

$$P\sim\underset{\displaystyle Ph}{\underset{|}{CH^{\oplus}}}\ BF_3\cdot OEt^{\ominus} \rightarrow P\sim\underset{\displaystyle Ph}{\underset{|}{CH}}\text{-}OEt + BF_3 \qquad (4)$$

$$P\sim\underset{\displaystyle Ph}{\underset{|}{CH^{\oplus}}}\ BF_3\cdot OEt^{\ominus} + BF_3\cdot OEt_2$$

$$\rightarrow \text{dead polymer}-OC_2H_5 \qquad (5)$$

Reaction 5 may actually be considered to be a reaction between the growing ion pair and the ionized initiator molecule $BF_3\cdot OEt^{\ominus}$ $Et^{\oplus}$. The concentrations of the ion pairs are usually fairly small compared to the concentration of total initiators and will increase in polar media. Thus, reaction 5 might be accelerated in a polar solvent, resulting in a decrease in the molecular weight of the polymer (Table IV.) Self-termination reaction 4 is a reaction between opposite-charged ions leading to neutral compounds, and so will be accelerated in non-polar media. The Arrhenius plot, as we have observed, of the polymerization of propenylbenzene by boron-trifluoride etherate (Fig. 4) is composed of two straight lines, with a break at about 0°C. The activation energy above 0°C is lower (1.2 kcal./mol.) than that below 0°C (4.3 kcal./mol.). On the other hand, the activation energies for two kinds of propagation reactions (usual and rearrangement) are shown to be nearly equal over the temperature range examined (Fig. 5). Therefore, if we assume only one kind of initiation reaction, we would have to consider at least two kinds of termination reaction, with different activation energies. The termination reaction with a higher activation energy should be predominant at higher temperatures, thus resulting in a smaller overall activation energy at higher temperatures. The authors do not have any evidence at present to show whether these two kinds of termination reactions correspond to the termination schema 4, 5 and/or to others. At any rate, this termination reaction may be at least partly responsible for the existence of a maximum in the yield of the methanol-insoluble polymer, that is, a rapid decrease in the molecular weight of the total polymer at high temperatures (above 0°C). Chain transfer processes are also to be considered in interpreting the decrease in the molecular weight in polymerizations at high temperatures. Kinetic studies are being undertaken in this respect.

Summary

1) Propenylbenzene has been found to polymerize by a cationic mechanism in two ways. Both the structure $-(CHPh\text{-}CH(CH_3))_n-$ (I) resulting from the usual opening of the double bond and the structure $-(CHPh\text{-}CH_2\text{-}CH_2)-$ (II) resulting from the rearrangement along the backbone chain of the resultant polymer occur.

2) The relative ratio of structures I/II has been pursued using the ratio of infrared absorptions, CH_3/CH_2, as a measure.

3) The rearrangement polymerization is generally preferred by mild catalysts, such as BF_3-etherate, while the polymerization to I has been found to predominate in polymerization with BF_3.

4) On the basis of the observed effect of reaction variables on the rate of polymerization and on the I/II ratio, a propagation mechanism has been proposed which includes the "gegen" ion attack on the methyl hydrogen of propenylbenzene.

5) Termination reaction by a "gegen" ion or an initiator has been shown to be important in polymerization catalyzed by BF_3-complexes.

Department of Polymer Science
Faculty of Science
Osaka University
Nakanoshima, Osaka

Added in Proof

During further experiments, the authors have found that the propenylbenzene used in the experiments contains about 5% unknown impurity. They can not at present exclude the possibility that the rearrangement under consideration would have been more or less modified by the existence of this impurity. Experiments for the clarification of this point is in progress.

On the Synthesis of a Hemopeptide

By Sumiko INOUYE, Shumpei SAKAKIBARA and Shiro AKABORI

(Received December 7, 1963)

Cytochrome c is an enzyme which contains one mole of heme as a prosthetic group. The protein part is joined to the heme by two thioether linkages,[1] involving the sulfur of two cysteine residues, as is shown in Fig. 1. The imidazolyl group of the histidine residue is also linked to the iron of heme to form a hemochromogen.[2-4] The heme-containing fragment (hemopeptide) of horse-heart cytochrome c was first isolated by Tsou,[5,6] while

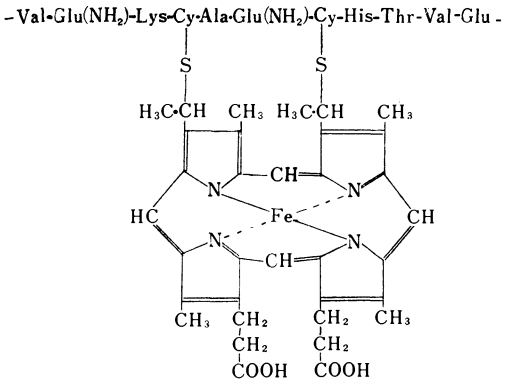


Fig. 1. Hemopeptide obtained from bovine heart cytochrome c by peptic digestion.

the structure shown in Fig. 1 was determined by Tuppy et al.[7-9] After the complete hydrolysis of cytochrome c, there remains a kind of porphyrin which is the so-called "porphyrin c" and which has been considered to be an addition compound of protoporphyrin with two cysteines, as in the case of cytochrome c. More recently, the amino acid sequences of many different hemopeptides which have been isolated from the cytochrome c's of members of various species have been elucidated (Table I). Although the amino acid sequences of those hemopeptides are usually different from one another, they are represented by the general structure -CyS-X-Y-CyS-His-, where X and Y represent two other amino acid residues. It is very interesting that the hemopeptide obtained from beef-heart cytohrome c possesses a much stronger peroxidase-like activity than that of the parent enzyme.[10]

The present work, which adopts a synthetic approach, is on the relationship between the structure and the function of the hemopeptide. Two simplified peptides, cysteinyl-glycyl-glycyl-cysteine and cysteinyl-glycyl-glycyl-cysteinyl-histidine, were selected as the peptide moieties for the synthesis of model hemopeptide.

1) H. Theorell, *Biochem. Z.*, **298**, 242 (1928).
2) H. Theorell and A. Akesson, *J. Am. Chem. Soc.*, **63**, 1804 (1941).
3) K. G. Paul, *Acta Chem. Scand.*, **5**, 389 (1951).
4) A. Ehrenberg and H. Theorell, ibid., **9**, 1193 (1955).
5) C. L. Tsou, *Biochem. J.*, **49**, 362 (1951).
6) C. L. Tsou, ibid., **49**, 367 (1951).
7) H. Tuppy and G. Bode, *Monatsh.*, **85**, 1024 (1954).
8) H. Tuppy and G. Bode, ibid., 85, 1182 (1954).
9) H. Tuppy and S. Paléus, *Acta Chem. Scand.*, **9**, 353 (1955).
10) S. Paléus, A. Ehrenberg and H. Tuppy, ibid., **9**, 365 (1955).

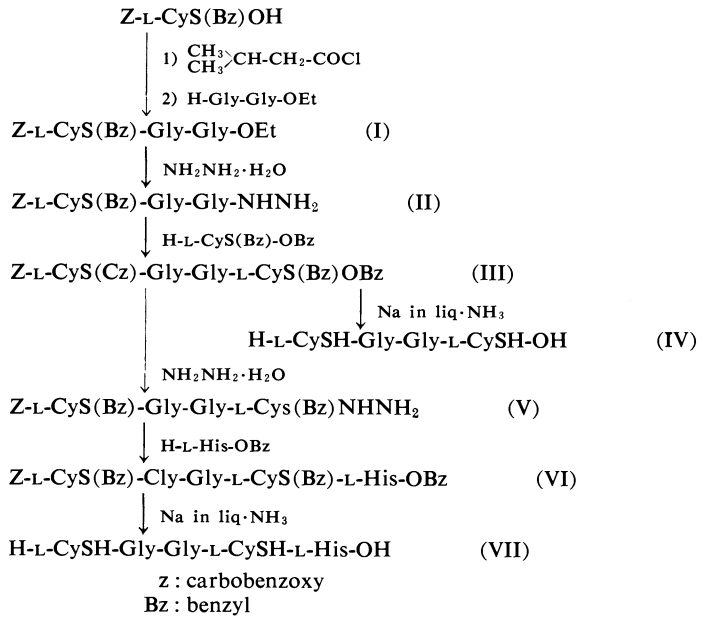


Fig. 2. Syntheses of H-L-CySH-Gly-Gly-L-CySH-OH and H-L-CySH-Gly-Gly-L-CySH-L-His-OH.

TABLE I. AMINO ACID SEQUENCES OF HEMOPEPTIDES OBTAINED FROM CYTOCHROME C

Species	Amino acid sequences
Horse[a]	-Lys-CyS-Ala-Glu(NH_2)-CyS-His-Thr-Val-Glu-
Pig[a]	
Bovine[b]	
Salmon[b]	
Human[c]	-Lys-CyS-Ser-Glu(NH_2)-CyS-His-Thr-Val-Glu-
Chicken[b]	-Lys-CyS-Ser-Glu(NH_2)-CyS-His-Thr-Val-Glu-
Silk Worm[d]	-Arg-CyS-Ala-Glu(NH_2)-CyS-His-Thr-Val-Glu-
Yeast[e]	-Arg-CyS-Glu-Leu-CyS-His-Thr-Val-Glu-
Pseudomonas fluorescens[f]	-Gly-CyS-Val-Ala-CyS-His-Ala-Ileu-Asp-
Rhodospillirum rubrum[g]	-Lys-CyS-Leu-Ala-CyS-His-Thr-Phe-Asp-

a) H. Tuppy and G. Bodo, *Monatsh.*, **85**, 1024, 1182 (1954).
b) H. Tuppy and S. Paléus, *Acta Chem. Scand.*, **9**, 353 (1955).
c) H. Matsubara and E. L. Smith, *J. Biol. Chem.*, **237**, 3575 (1963).
d) H. Tuppy, *Z. Naturforsh.*, **12B**, 784 (1957).
e) H. Tuppy and K. Dus, *Monatsh.*, **89**, 407 (1958).
f) R. P. Ambler, *Biochem. J.*, **82**, 309 (1962).
g) K. Levin, *Acta Chem. Scand.*, **15**, 1739 (1961).

The Synthesis of Peptide.—Carbobenzoxy-*S*-benzyl-L-cysteinyl-glycyl-glycyl-*S*-benzyl-L-cysteinyl-L-histidine benzylester (V) was synthesized as shown in Fig. 2. First, carbobenzoxy-*S*-benzyl-L-cysteinyl-glycyl-glycine ethylester was prepared according to the procedure of Hooper et al.[11] Although, in their paper, ethyl chloroformate was used for the preparation as a mixed anhydride-reagent, it has been found that the use of isovaleroyl chloride, instead of ethyl chloroformate, afforded a product with a higher melting point and a larger optical rotation than that which they reported. The improved procedure favored the succeeding reaction steps, and it was confirmed that the final melting point and the optical rotation of product III were much higher than those previously reported. The carbobenzoxy-tetrapeptide was successfully coupled with histidine benzyl ester by the azide procedure. Then, the carbobenzoxy-tetra- and penta-peptide benzylesters (III and VI respectively) were converted to free peptides (IV and VII) by treatment with sodium in liquid ammonia; they were then uesd in the preparation of the two hemopeptides.

The Preparation of Hemopeptide. — Theorell first demonstrated[1] that when protoporphyrin IX and cysteine were heated in mineral acid, a porphyrinc like compound was formed. Later, Zeile and Meyer[12] developed a practical way of preparing the same compound using hydrobrominated protoporphyrin as an intermediate. This was fused with excess cysteine hydrochloride without any solvent. Recently, Neilands and Tuppy[13] have published an improved method for the purification

11) K. C. Hooper, H. N. Rydon, J. A. Schofield and G. S. Heaton, *J. Chem. Soc.*, **1956**, 3148.
12) K. Zeile and H. Meyer, *Z. Physiol. Chem.*, **262** 178 (1939/40).
13) J. B. Neilands and H. Tuppy, *Biochim. Biophys. Acta*, **38**, 351 (1960).

of the product, producing a crystallizable porphyrin c.

No good procedure has as yet been published for the condensation of porphyrin with peptide, which contains two cysteine residues in the molecule. For the present work, the procedures reported for porphyrin c formation could not be used, because they require excess peptide at a high temperature, and this condition may cause a partial decomposition of the peptides. For the addition reaction of free cysteinyl peptide with hydrobrominated protoporphyrin, various alkaline conditions were tested at room temperature. Aqueous solutions of sodium hydroxide, carbonate or bicarbonate caused a partial decomposistion of sulfhydryl groups before the addition reaction was complete. Liquid ammonia, in which the free peptides were generated by sodium hydrogenolysis, was also not suitable for the reaction, because aminolysis by the bromide was faster than the formation of thioether linkages. Finally, the direct addition of protoheme to free cysteinyl peptide in liquid ammonia was tested, whereupon some kind of addition product was obtained. Although the mode of the formation of the complex between peptide and heme is still unknown, only the histidine containing pentapeptide afforded a reasonable amount of product.*

The crude product synthesized from peptide VII was dialyzed against deionized water to remove the unreacted peptide, and then it was subjected to counter-current distribution in a mixture of chloroform, methanol and 0.1 N hydrochloric acid (2 : 2 : 1). This procedure gave two brown fractions, as is shown in Fig. 3. The distribution coefficient of band I, shown in Fig. 3, agreed with that of hemin, and no amino acid was detected by the paper chromatography of a hydrolyzate of this fraction. On the other hand, glycine, histidine and a small amount of cystine were detected in a hydrolyzate of band II.

When the apparent molecular weight of the synthetic hemopeptide was calculated separately from the iron and glycine contents, values of 1030 and 1120 were obtained respectively. Theses values are in good agreement with the theoretical value of 1127.

No sulfhydryl group was detected by the Folin method[14] in the purified hemopeptide. Disulfide bonds were estimated by polarography, using the diffusion current at the half-wave potential in a range proportional to the concentration of cystine (Fig. 4), and it was concluded that the hemopeptide still contained three per cent of the total cysteine residues as disulfide bonds.

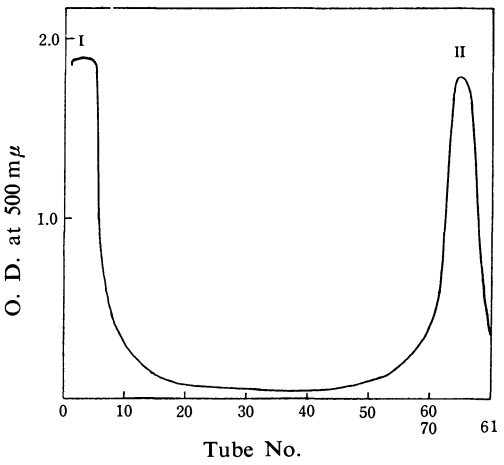


Fig. 3. Counter current distribution pattern of the crude product.
I; Hemin. II; Hemopeptide.
System; methanol : chloroform : 0.1N hydrochloric acid (2 : 2 : 1).

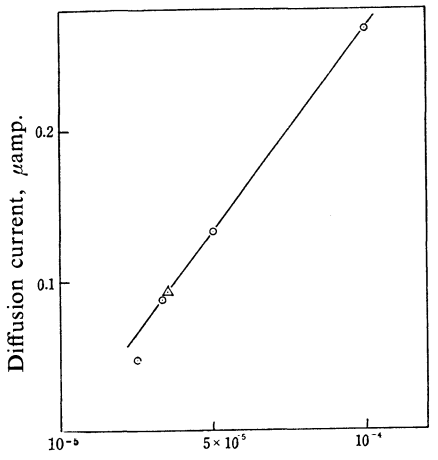


Fig. 4. Rotation between intensity of diffusion current at half-wave potential and concentration of cystine in 0.1 M ammonia buffer, pH 9.
⊙ Standard curve of mixture of cystine and hemin (1 : 1).
△ Intensity of diffusion current at half-wave potential of 9.2×10^{-4} M synthetic hemopeptide.

The Properties of Hemopeptide.—The synthetic hemopeptide was soluble in a water-methanol or water-acetone mixture (1 : 2 v/v), and in water at alkaline pH values. It was insoluble in chloroform, ether and water at neutrality. Although the infrared spectrum

* The authors wish to thank to Dr. Junzo Noguchi of Hokkaido University for his helpful discussion and advice concerning the coupling method.

14) B. Kassell and E. Brand, *J. Biol. Chem.*, **125**, 115 (1938).

resembled that of natural hemopeptide from beef-heart cytochrome c by peptic degradation[15] (abbreviated in this paper as hemopeptide N), the visible absorption spectrum of the synthetic compound was rather more similar to that of hemin than to that of hemopeptide N, as Figs. 5 and 6 show.

The peroxidative activities of hemopeptide N, synthetic hemopeptide, hemin and ferric chloride were compared by Shibata's method, using leuco malachite green as a hydrogen doner. As is shown in Fig. 7, the color of malachite green appeared after the induction period. In the case of ferric ion, no development of color was observed, even after 15 hr. This indicates that the catalytic activity of the synthetic hemopeptide was about 100 times as strong as that of hemin, but it was still inferior to that of natural hemopeptide N (Table II). This could be attributed to differences in the amino acid sequences and/or in the modes of the combination of the peptide and hemin.

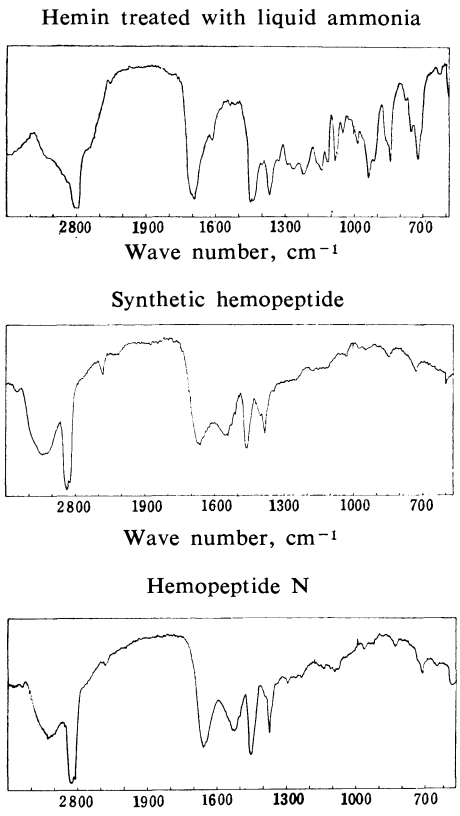


Fig. 5. Infrared absorption spectra recorded on a Shimadzu IR spectrophotometer in Nujol suspension.

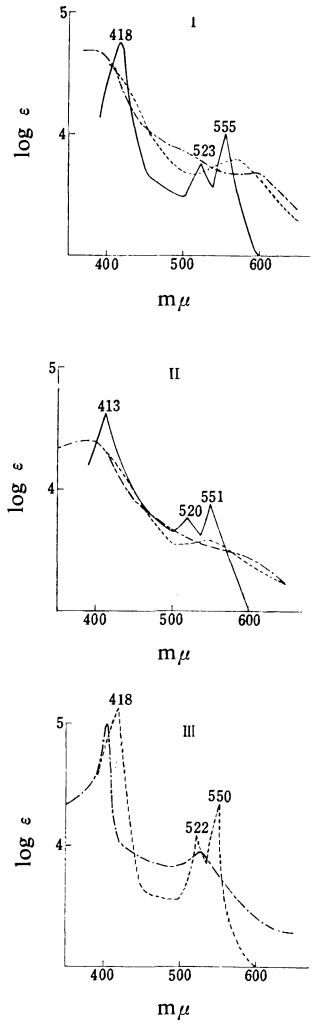


Fig. 6. Visible absorption spectra recorded on Cary model 14 recording spectrophotometer. I; Hemin II; Synthetic hemopeptide III; Hemopeptide N in 1/15 M phosphate buffer, pH 8.
——— No addition
- - - - Reduced by sodium hydrosulfite
——— Pyridine hemochlomogen

After most of this work had been done, Sano[16,17] reported the interesting fact that freshly-prepared protoporphyrinogen combines with various sulfhydryl compounds more readily under mild conditions, and it was demonstrated that a porphyrin c-like compound is readily prepared in this manner by combination with cysteine. This procedure should be quite superior to any previous methods so far published for hemopeptide formation. Studies along these lines are in progress.

15) E. Margoliash. N, Frahwirt and E. Wiener, *Biochem. J.*, **71**, 559 (1958).

16) S. Sano, *Acta Haem. Japan*, **24**, 621 (1961).
17) S. Sano and S. Granick, *J. Biol. Chem.*, **236**, 1173 (1961).

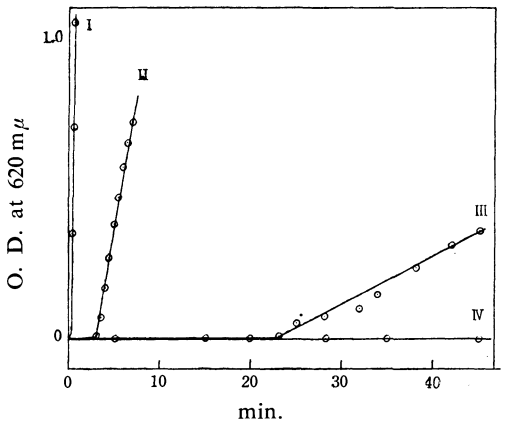


Fig. 7. Peroxidative activity by Shibata's method.
I; Hemopeptide N II; Synthetic hemopeptide III; Hemin IV; Ferric chloride

TABLE II. REACTION VELOCITIES AND INDUCTION PERIODS OF HEMIN, FERRIC ION AND HEMOPEPTIDES

Material	K*	Induction period, min.
Hemopeptide N	23.9	0.25
Synthetic hemopeptide	1.1	3
Hemin	0.009	23
Ferric ion	—	—

* Moles of malachite grean per mole of sample per min. These values were calculated after the respective induction periods.

Experimental*

Carbobenzoxy-*S*-benzyl-L-cysteinyl-glycyl-glycine Ethyl Ester (I).—Isovaleroyl chloride (6 g.; 0.05 mol.) was slowly stirred into a solution of *S*-benzyl-*N*-carbobenzoxy-L-cysteine (17.3 g.; 0.05 mol.) and triethylamine (6.9 ml.) in chloroform (175 ml.) at −5°C. After 1.5 hr., a mixture of glycyl-glycine ethyl ester hydrochloride (11.8 g.; 0.06 mol) and triethylamine (8.2 ml.) in chloroform (125 ml.) was stirred into the reaction mixture at −5°, and then the mixture was stored overnight in a refrigerator. The solution was washed successively with dilute hydrochloric acid, water, a sodium bicarbonate solution, and water, and then dried over anhydrous sodium sulfate. The solvent was removed under reduced pressure, and the residual oil was redissolved in ethyl acetate (90 ml.). The slow addition of ethyl ether (150 ml.) to this solution resulted in the precipitation of a crystalline product (21 g.). The recrystallization of this material from ethyl acetate gave long needles; m. p. 118°C, yield 74% (18 g.). Hooper et al.[11] reported a m. p. of 114~115°C.

Carbobenzoxy-*S*-benzyl-L-cysteinyl-glycyl-glycine Hydrazide (II).—Hydrazine hydrate (7 ml.; 0.11 mol.) was added to a solution of I (17.5 g.; 0.036 mol.) in ethanol (250 ml.), and the solution was kept overnight at room temperature. The precipitate which formed was collected by filtration. The product was recrystallized from ethanol (200 ml.) and water (50 ml.) as needles; m. p. 173°C, yield 92% (15.7 g.). Hooper et al. reported a m. p. of 164°C.

Carbobenzoxy-*S*-benzyl-L-cysteinyl-glycyl-glycyl-*S*-benzyl-L-cysteine Benzyl Ester (III).—Triethylamine (7 ml.) was added to a suspension of *S*-benzyl-L-cysteine benzyl ester *p*-toluenesulfonate (23.7 g:, 0.05 mol.) in a mixture of ethyl ether (250 ml.) and water (40 ml.). The free benzyl ester which formed was extracted thoroughly with ethyl ether, and the ether extract was dried over anhydrous sodium sulfate. A solution of II (23.7 g.; 0.05 mol.) in a mixture of acetic acid (220 ml.), 2N hydrochloric acid (17 ml.) and water (220 ml.) was treated with sodium nitrite (3.5 g.; 0.05 mol.) at −5°C. The azide formed was extracted three times with cold ethyl ether (total: 600 ml.). The combined ethyl ether layer was washed with cold water 100 ml. and dried over anhydrous sodium sulfate at −5°C. The dry ether solution was added to the solution of *S*-benzyl-cysteine benzyl ester prepared as described above, and the mixture was stored overnight in a refrigerator (0~5°C). The precipitate which formed was collected by filtration and recrystallized from ethanol (500 ml.) as needles; yield 83% (3.17 g.); m. p. 178~179°C; $[\alpha]_D^{15}$ −40.7° (*c* 2.73 in pyridine). Hooper et al.[11] reported a m. p. of 175°C and $[\alpha]_D^{20}$ −29.6° in pyridine.

Found: C, 62.81; H, 5.74; N, 7.57; S, 8.40. Calcd. for $C_{39}H_{42}O_7N_4S_2$ C, 63.05; H, 5.70; N, 7.54; S, 8.63%.

Carbobenzoxy-*S*-benzyl-L-cysteinyl-glycyl-glycyl-*S*-benzyl-L-cysteine Hydrazide (V).—A solution of III (10 g.; 13.5 mol.) in a mixture of dioxan (150 ml.) and ethanol (50 ml.) was treated with hydrazine hydrate (30 ml.; 0.5 mol.). After 24hr. at room temperature, the solvent was removed at 30°C under reduced pressure, and the residue was crystallized by adding ethanol (160 ml.). The product was recrystallized from ethanol (160 ml.) and water (40 ml.) as needles; yield 77% (7.1 g.); m. p. 162°C.

Found: C, 57.28; H, 5.82; N, 12.21. Calcd. for $C_{32}H_{38}O_6N_6S_2$ C, 57.64; H, 5.74; N, 12.60%.

Carbobenzoxy-*S*-benzyl-L-cysteinyl-glycyl-glycyl-*S*-benzyl-L-cysteinyl-L-histidine Benzyl Ester (VI).—Substance V (5 g.; 7.5 mmol.) was dissolved in a mixture of acetic acid (40 ml.) and water (40 ml.), and then 2N hydrochloric acid (7.5 ml.) was added to the solution. The mixture was carefully treated with sodium nitrite (0.52 g.; 7.5 mmol.) at −5°C, and the azide which formed was extracted with cold chloroform total: 300 ml.). The azide solution was washed with ice water, and then dried over sodium sulfate at −5°C. The dry chloroform solution was added to a cold solution of L-histidine benzyl ester di-*p*-toluenesulfonate (6.7 g.; 8.8 mmol.) and triethylamine (3.1 ml.) in chloroform (50 ml.), and the reaction mixture was allowed to stand overnight in a refrigarator. It was then washed with water and a sodium bicarbonate solution. During this procedure, some products appeared as

* The melting points given here are uncorrected.

crystals. Petroleum ether (b. p. 60~80°C) was added to the mixture to complete the precipiation, and the preduct was collected by filtration and recryllized from ethanol (24 ml.) and water (6 ml.); yield 60% (4 g.); m. p. 178°C; $[\alpha]_D^{16}$ −54.3° (*c* 0.98 in dioxan).

Found: C, 61.25; H, 5.59; N, 10.96; S, 7.65. Calcd. for $C_{45}H_{49}O_8N_7S_2$ C, 61.41; H, 5.61; N, 11.14; S, 7.29%.

Hemopeptide.—A solution of substance VI (880 mg.; 1 mmol.) in liquid ammonia (500 ml.) was treated wtih approximately 200 mg. of sodium, in portions, until a permanent blue color appeared in the solution. Then 70 mg. more sodium and protohemin (652 mg.; 1 mmol.) were vigorously stirred into the reaction mixture. After the addition of a small amount of ammonium chloride to neutralize the excess sodium, the reaction mixture was stirred for 4hr. and then stored overnight in a dry ice bath. After the evaporation of the solvent, the product was dried under reduced pressure over sulfuric acid in a desiccaior. The residue was dissolved in water (50 ml.), and the aqueous solution was then dialyzed against running deionized water for 3 days. The lyophilization of the solution gave the sodium salt of the crude product as a brown-red prowder (yield, 930 mg.). The product (400 mg.). was subjected to counter-current distribution in a solvent system of chloroform, methanol and 0.1 N hydrochloric acid (2 : 2 : 1) (Fig. 3.). Band II (tubes 61~70) was concentrated to about 50 ml. at 40°C under reduced pressure. The residual solution was adjusted to pH 9 with a dilute aqueous solution of sodium hydroxide and then dialyzed through cellophane tubing against running deionized water. The final solution was lyophilized to yield the sodium salt of the hemopeptide; yield 163 mg.; m. p. above 260°C. For analysis, the hemopeptide (30 mg.) was dissolved in deionized water, and the solution was acidified with dilute hydrochloric acid to about pH 2. The solution was dialyzed against running deionized water, and the precipitates which formed were collected by centrifugation and dried in vacuo at 80°C.

Found: C, 49.91; H, 4.97; N, 13.66; S+Cl, 9.54; Fe, 5.42. Calcd. for $C_{50}H_{56}O_{10}N_{11}S_2Fe \cdot 2HCl$: C, 51.59; H, 5.02; N, 13.24; S+Cl, 11.60; Fe, 4.80%. Mol. wt. Found: 1030*; 1160**. Calcd.: 1164.

Peroxidative Activity.—The peroxidative activities of the synthetic hemopeptide and other substances were assayed, using leuco malachite green as a hydrogen donor, by the method of Shibata[19] as follows: The reaction system was composed of 2.0 ml. of a 0.2 M phosphate-hydrochloric acid buffer (pH 3.1), 8.82×10^{-2} mol. hydrogen peroxide, 6.77×10^{-3} mol. leuco malachite green and 1.485×10^{-5} mol. synthetic hemopeptide or other substances in a total volume of 3.5 ml. of water. The reaction was started by adding the hydrogenperoxide, and incubation was carried out at 15°C. The activity was estimated spectrophotometrically by measuring the increase in optical density at 620 mμ due to the oxidation of leuco malachite green to malachite green. The activity was expressed as the amount of malachite green formed per minute after the induction period.

Summary

Carbobenzoxy-*S*-benzyl-L-cysteinyl-glycyl-glycyl-*S*-benzyl-L-cysteinyl-L-histidine benzylester has been synthesized, and then it has been hydrogenated to the free peptide by treatment with sodium in liquid ammonia. The free peptide has been coupled with protohemin in the liquid ammonia to form a hemopeptide, which has then been purified by counter-current distribution. The visible and infrared absorption spectra of the product have been compared with those of natural hemopeptide, which was obtained from beef-heart cytochrome c by peptic degradation. The peroxidative activity of the synthetic hemopeptide is about 100 times as strong as that of hemin, but it is inferior to that of natural hemopeptide.

Division of Organic Chemistry
Institute for Protein Research
Osaka University
Kita-ku, Osaka

* Calculated from the iron content.

** Calculated from the glycine content in a hydrolyzate by the improved method of Levy.[18]

18) A. L. Levy, *Nature*, **174**, 126 (1954).

19) Y. Nakamura, T. Samejima, K. Kurihara, M. Tohjo and K. Shibata, *J. Biochem.*, **48**, 862 (1960).

The Electrokinetic Potential of Titanium Dioxide

By Tetsuo MORIMOTO and Masashi SAKAMOTO

(Received December 12, 1963)

Recently attention has been drawn by many investigators to the behavior of hydroxyl groups on the surface of insoluble metal oxides, especially from the viewpoints of the adsorption and the catalytic center of the solid surface.

The existence of hydroxyl groups on the surface of insoluble oxides has been demonstrated by the determination of the water content of powders,[1] by studies of wetting heat[2] and, more directly, by the measurement of infrared absorption spectra.[3-5] It has also been reported that a solid retains a small amount of water even after it has been evacuated at a high temperature.[6]

If an insoluble metal oxide is equilibrated with water, a good many hydroxyl groups will be produced on the solid surface; this formation has a serious effect on the physico-chemical properties of the surface. For this reason, it is of special interest to ascertain the dissociation property of surface hydroxyl groups. In the present work, therefore, the dependences of the electrokinetic potential of titanium dioxide in water on the temperature of the pretreatment and on the concentration of added electrolyte in water have been investigated, in connection with the behavior of surface hydroxyl groups on the solid.

Since the surface properties of a solid, such as the surface charge, are usually affected by the presence of impurities, the effect of sulfate groups contaminating the sample on the electrokinetic potential has also been investigated in detail.

Experimental

Materials.—Titanium dioxide was prepared by the hydrolysis of titanium sulfate*. The raw material thus obtained was contaminated with sulfate groups, the amount of which was 54 mg. SO_4/g. of the sample. X-Ray tests showed the raw material to be anatase in form. The sulfate contained in the raw material was removed by treatment with a definite amount of ammonia water. The conditions of the treatment and the amount of sulfate remaining are shown in Table I. After the raw material had been treated with ammonia water for two hours at 70°C, the sample was thoroughly washed with water. Three kinds of samples thus prepared were dried and calcined in a platinum crucible placed in an electric oven held at a given temperature.

TABLE I. CONDITIONS FOR PREPARING SAMPLES AND THE RESULTS OF THEIR ANALYSIS

	Amouut of ammonia water used	Sulfate remained (mg./g. TiO_2)
TiO_2-0	0	54
TiO_2-1.1	1.1 equivalent of sulfate	12
TiO_2-18	18 equivalent of sulfate	0

Electrokinetic Measurement. — The streaming potential method was used for the determination of the electrokinetic potential (ζ-potential). Both the techniques of the measurement of the streaming potential and the method of calculation used to obtain the ζ-potential were the same as have been reported previously.[7]

Results and Discussion

The Electrokinetic Potential of Titanium Dioxide in Water.—The ζ-potentials of titanium dioxide in water are shown in Fig. 1. The ζ-potential vs. the pretreatment temperature curves of three samples agree almost entirely with one another. In the cases of the samples TiO_2-0 and TiO_2-1.1, especially, when treated at 300°C and 500°C, the streaming potentials showed fairly high values at the beginning of the measurement, but thereafter they decreased continuously for many hours, accompanied with a decrease in the electrical conductance. On the other hand, the potential measured on the TiO_2-18, sample which contains no sulfate, remained constant for many hours. Consequently, the decreases in the streaming potentical and electrical conductance in the case of the samples contaminated with sulfate are possibly due to the decontamination of the samples in the course of the streaming operation.

1) M. M. Egorov and V. F. Kiselev, *J. Phys. Chem. (U. S. S. R.)*, **36**, 318 (1962).
2) W. H. Wade and N. Hackerman, *J. Phys. Chem.*, **64**, 1196 (1960).
3) J. B. Peri and R. B. Hannan, ibid., 64, 1526 (1960).
4) R. S. McDonald, *J. Am. Chem. Soc.*, **79**, 850 (1957).
5) M. R. Basila, *J. Chem. Phys.*, **35**, 1151 (1961).
6) G. J. Young, *J. Colloid Sci.*, **13**, 67 (1958).
* This sample was prepared in the laboratory of Teikoku Kakô Co.
7) T. Morimoto, This Bulletin, **37**, 386 (1964).

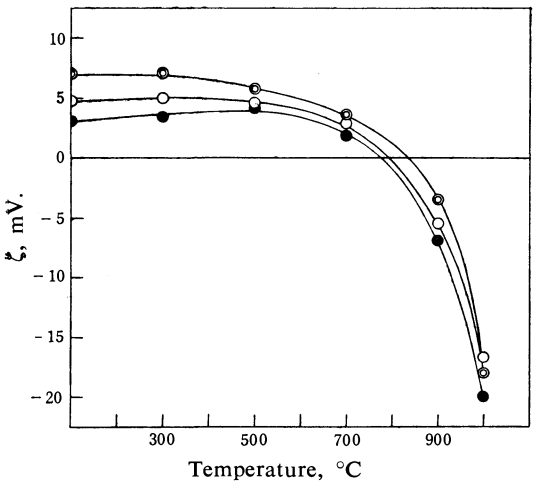


Fig. 1. Dependence of the ζ-potential of TiO_2 on the pretreatment on temperature.
◎ TiO_2-0, ○ TiO_2-1.1, ● TiO_2-18

The results shown in Fig. 1 were obtained after the streaming operation had continued for a long time. It is, therefore, obvious that the values of the streaming potentials on contaminated samples approach those of pure samples when washed with streaming water. Thus, the dependence of the ζ-potential of the TiO_2-18 sample on the pretreatment temperature is considered to be characteristic of titanium dioxide. It may, therefore, be seen from Fig. 1 that titanium dioxide is positively charged in water when it is treated at lower temperatures, whereas it is negatively charged when treated at 1000°C. The inversion of the sign of the surface charge occurs when the sample is treated at about 800°C, a figure which corresponds to the temperature of the transition of anatase to rutile. X-Ray tests on these samples showed that the samples heated at temperatures lower than 700°C are anatase in form, whereas those heated at 1000°C are rutile in form. In order to verify these results, the ζ-potential of rutile powder obtained by the pulverization of the single crystal was measured in water and found to be −36 mV. These results convinced us that the charge of anatase is positive and that of rutile is negative. Although several authors have studied the dependence of the ζ-potential of metal oxides upon their pretreatment temperature,[8-10] no such clearly-established relation has ever been found between the signs of the ζ-potential and the crystal modifications.

When the oxide surface is equilibrated with water, the surface hydroxyl groups will be formed by surface hydration. Further, these hydroxyl groups may be dissociated in two ways:

$$\equiv TiOH \rightarrow \equiv Ti^+ + OH^- \quad (1)$$

$$\equiv TiOH \rightarrow \equiv TiO^- + H^+ \quad (2)$$

If the dissociation of the surface hydroxyl groups occurs according to Eq. 1, it will make the surface positive and basic at the same time. On the contrary, if the dissociation proceeds as in Eq. 2, the surface will become negative and acidic. In our previous study,[11] the surface acidity was observed on the sample of TiO_2-18, which contains no sulfate. Methyl red used as a dyestuff was dissolved in isooctane, a nonpolar solvent. After the dye solution had been shaken with titanium dioxide, the color of the adsorbed dye molecules was observed. When the treatment temperature rises, the color changes from yellow to orange and finally to red, indicating that the surface acidity changes from a basic to an acidic property with an increase in the pretreatment temperature. This proves that the surface hydroxyl groups on titanium dioxide are dissociated following either Eq. 1 or Eq. 2, according to the modifications of the substrate crystal of titanium dioxide.

The crystallographic data of anatase and rutile[12] show that in both crystal forms one titanium atom is surrounded by six oxygen atoms, which are situated on the tops of an octahedron. The bond distances of Ti–O and O–O in anatase and rutile are listed in Table II.[13] It has been reported that the distances

Table II. Bond distances in TiO_2, Å

	Anatase	Rutile
4 Ti–O	1.937	1.946
2 Ti–O	1.964	1.984
O–O	2.802	2.779
O–O	2.446	2.526
O–O	3.040	

of O–O bonds in basic metal hydroxide crystals are longer than about 3.00Å, while in acidic crystals they are less than 2.70 Å.[14] If we assume that the O–O distances remain almost unchanged when the surface of titanium dioxide is hydrated to form surface hydroxyl

8) D. J. O'Connor and A. S. Buchanan, *Austr. J. Chem.*, 6, 278 (1953).
9) D. J. O'Connor, P. G. Johansen and A. S. Buchanan, *Trans. Faraday Soc.*, 52, 229 (1956).
10) D. J. O'Connor and A. S. Buchanan, ibid., 52, 397 (1956).
11) T. Morimoto and M. Sakamoto, This Bulletin, 36, 1369 (1963).
12) R. W. G. Wyckoff, "Crystal Structure," Interscience Pub. Inc., New York, N. Y. (1948).
13) D. T. Cromer and K. Herrington, *J. Am. Chem. Soc.*, 77, 4708 (1954).
14) R. Kiriyama, "Kôzô Muki-Kagaku," Kyôritsu, Tokyo (1955).

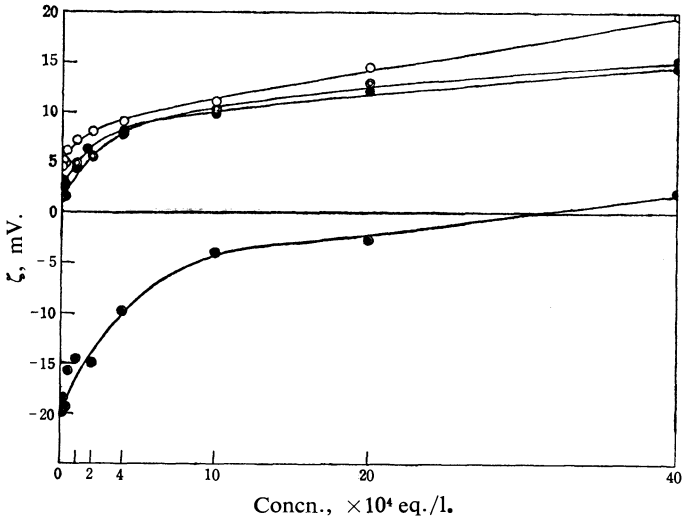


Fig. 2. Effect of barium chloride on the ζ-potential of TiO_2 treated at ● 300°C, ○ 500°C, ◎ 700°C, ◉ 1000°C.

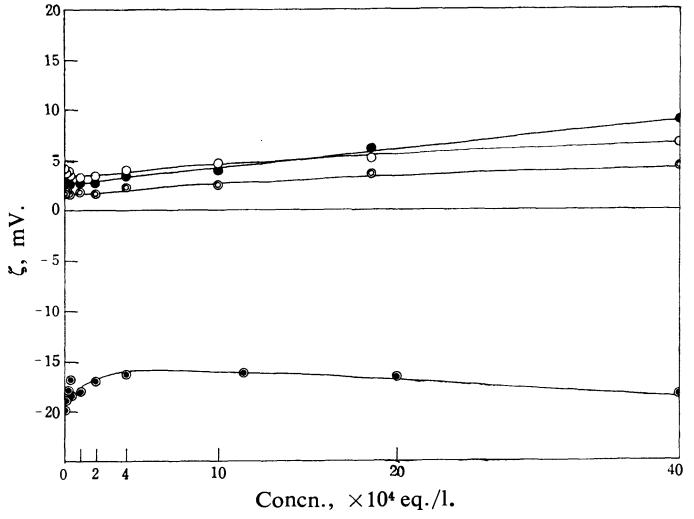


Fig. 3. Effect of potassium chloride on the ζ-potential of TiO_2 treated at ● 300°C, ○ 500°C, ◎ 700°C, ◉ 1000°C.

groups, it may be expected that the surface of rutile is acidic and that of anatase is basic. From this point of view, the present results lead us to postulate that, among the three kinds of O–O bonds of anatase, the longer ones are exposed on its surface to a larger extent.

Electrokinetic Potential in an Electrolyte Solution.—The effect of elctrolytes on the ζ-potential of titanium dioxide has been investigated on the TiO_2-18 sample, which contains no sulfate. The results obtained are shown in Figs. 2—6. Barium chloride seriously affects the ζ-potential of the samples treated at various temperatures (Fig. 2). In this case, the ζ-potential increases with the increasing concentration of barium chloride, independently of the signs of the surface charge of titanium dioxide in water. This indicates that the effect of barium ions is more pronounced than that of chloride ions. The effect of barium ions is greater on the negatively-charged surface than on the positivery-charged surface, and the inversion of the negative charge occurs at a higher concentration. On the other hand, the effect of potassium chloride is much less than that of barium chloride, indicating that the adsorption forces of potassium ions and chloride ions are comparable (Fig. 3). Although at lower concentrations of potassium chloride, the oppositely-charged ions adsorb on the surface of titanium dioxide, at higher

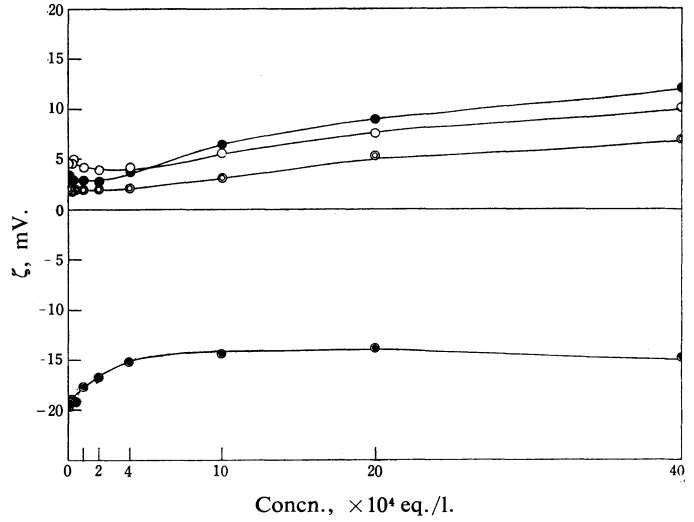


Fig. 4. Effect of hydrochloric acid on the ζ-potential of TiO_2 treated at ● 300°C, ○ 500°C, ◎ 700°C, ◉ 1000°C.

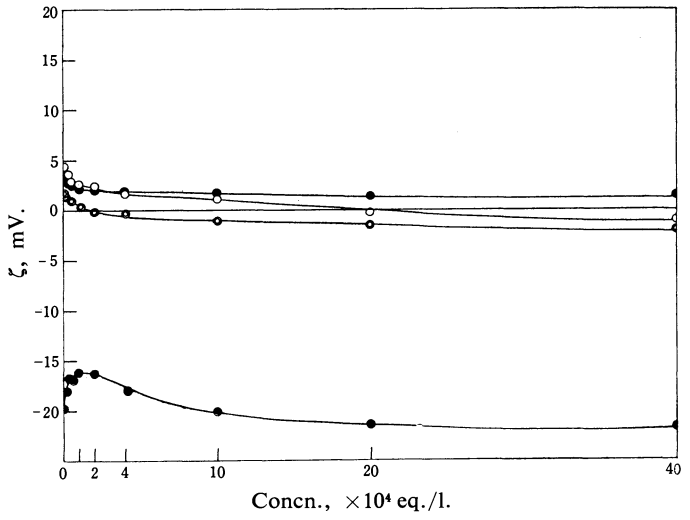


Fig. 5. Effect of potassium hydroxide on the ζ-potential of TiO_2 treated at ● 300°C, ○ 500°C, ◎ 700°C, ◉ 1000°C.

concentrations the counter ions seem to cooperate. The change in ζ-potential in the presence of hydrochloric acid is almost identical with that in the presence of potassium chloride, except that hydrogen ions act more strongly on the solid surface than do potassium ions (Fig. 4). The effect of potassium hydroxide is fairly remarkable, especially in the case of samples treated at moderate temperatures, where the inversion of charge is observed. In the case of a sample treated at 1000°C, the negative potential decreases at first and then increases with the increasing concentration of potassium hydroxide (Fig. 5). In this latter case, the following surface reaction may be considered to take place:

$$\equiv TiOH + KOH \rightarrow \equiv TiOK + H_2O \quad (3)$$

This reaction will promote the dissociation to form the negatively-charged surface, resulting in the increase in the negative potential.

Sodium triphosphate has an extraordinary influence on the ζ-potential of titanium dioxide (Fig. 6) ; the positively-charged surfaces in water are all inverted by the addition of triphosphate, and the negatively-charged rutile surface becomes more negative, even at an extremely low concentration of triphosphate. This is obviously caused by the strong adsorption force of triphosphate, suggesting the formation of a complex compound on the surface of titanium dioxide.

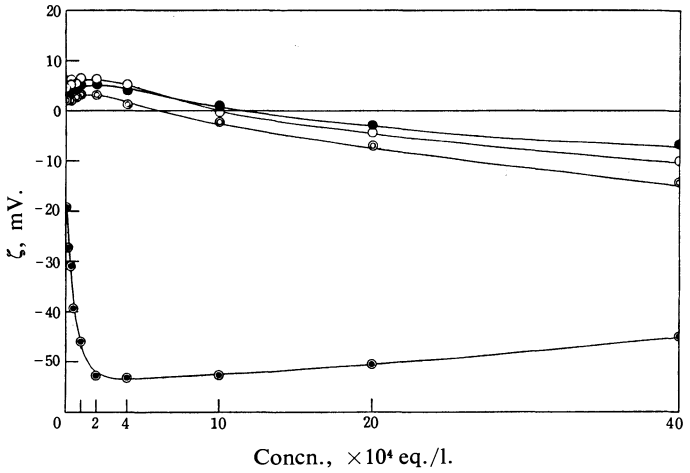


Fig. 6. Effect of sodium triphosphate on the ζ-potential of TiO_2 treated at
● 300°C, ○ 500°C, ◎ 700°C, ◉ 1000°C.

Summary

1) The surface property of titanium dioxide has been investigated by measuring the ζ-potential. The ζ-potential of titanium dioxide in water depends on the temperature of the pretreatment, and its sign changes from positive to negative at about 800°C. This fact has been interpreted in terms of the way of the dissociation of hydroxyl groups on the surface of titanium dioxide, the ways of which depend on its modifications. This phenomenon seems to be supported by crystallographic data.

2) The effects of electrolytes on the ζ-potential of titanium dioxide have been studied. Barium has a chloride greater influence on the ζ-potential of titanium dioxide than does potassium chloride or hydrochloric acid. Hydroxide ions have a fairly great influence on the surface of the solid. The effect of sodium triphosphate is extraordinarily great; by the addition of the electrolyte, the positive potentials of titanium dioxide are inverted to negative potentials and the negatively-charged rutile surface becomes more negative, and this development suggests the formation of a complex compound on the surface of titanium dioxide.

Department of Chemistry
Faculty of Science
Okayama University
Tsushima, Okayama

The Electrolytic Preparation of Vanadium(II) Developers

By Kenichi HONDA

(Received December 24, 1963)

Since photographic development is essentially the reduction of silver ions, the ability of a developing agent can be estimated by the degree of its reducing power, by, that is, the redox potential. According to Reinders,[1] when the redox potential of a developer is more negative than +0.120 V. with respect to the standard hydrogen electrode, a silver bromide particle containing a latent image can be reduced.

Vanadium can take the ionic state in the aqueous solution from +5 to +2 valencies, among which range the vanadous ion (V^{2+}) shows a strong reducing power and the redox potential of the system V^{2+}-V^{3+} is:

$$E^\circ = -0.25_5 \text{ V. } (25^\circ\text{C})$$ [2]

1) W. Reinders, *J. Phys. Chem.*, **38**, 783 (1934); *Sci. Ind. Phot.*, **5**, 284 (1934); **6**, 297 (1935).

2) G. Jones and J. Colvin, *J. Am. Chem. Soc.*, **66**, 1573 (1944).

This value seems suitable for photographic development. Further, in order for such a polyvalent ion to be suitable for the development, both the reductant (V^{2+}) and the oxidant (V^{3+}) before and after the development should be soluble in water, and vanadous ion satisfies this requirement also. The developing reaction may be shown in the following equation:

$$Ag^{+} + V^{2+} \rightarrow Ag + V^{3+}$$

Lumiére[3] reported the first use of vanadium salt as a developing agent at the end of the 19th century. After that, no studies were reported on it until 1952 when Roman[4] carried out the fundamental studies for a rapid developing process using V^{2+} salt. Rasch and Crabtree and their co-workers[5-7] also studied this process and especially its application to the development of motion picture positive films, while Fortmiller and James[8] discussed the rate process of this development. In Japan, this process was taken up by the Institute of Industrial Science of the University of Tokyo and by the NHK Technical Research Laboratories. The former constructed a developing machine for reversal and positive films,[9] and the latter gained experience in developing positive films for television use.[10] The processing using the vanadium developer was summarized by Kikuchi.[11]

The characteristics of the vanadium developer are very superior according to the above-mentioned studies, but in actual automatic processing, it is difficult to obtain a good reproducibility due to the different composition of the developer solution, the contamination of the developer, and the unstability of the vanadous ion. It is, therefore, important to prepare a developing solution of a fixed composition. The vanadium developer can also be regenerated electrolytically during development by circulating the solution, so it is necessary to establish the electrolytic conditions. From these standpoints, the preparation of the vanadium developer, including the electrolytic process, will be studied in detail in the present paper.

As the vanadium pentoxide (V_2O_5) is the most easily available commercially-produced vanadium compound, it is adopted as the starting material. A method for obtaining the vanadous ion electrolytically from metallic vanadium has been reported,[12] but it seems to the author not to be practical. Although ammonium metavanadate is also available, it is not used in the present study.

In starting with vanadium pentoxide, it is necessary to reduce V^{5+} to the V^{2+} state. This reduction process consists of the following two steps:

$V^{5+} \rightarrow V^{4+}$, chemical reduction process

$V^{4+} \rightarrow V^{3+} \rightarrow V^{2+}$, electrolytic reduction process

The present paper is, therefore, divided into two parts.

Chemical Reduction Process

As has been mentioned above, this process is the reduction from V^{5+} to V^{4+}, but V^{4+} usually exists in the form of VO^{2+} salt (vanadyl salt) in an aqueous solution. Accordingly, this process is a preparation of vanadyl salt. Three methods are known for preparing vanadyl salt from vanadium pentoxide, (i) the sulfur dioxide process, (ii) the hydrobromic acid process, and (iii) the oxalic acid process.

The preliminary experiences with these three processes have shown that all of them gave a good yield of vanadyl salt, but in process i, excess sulfur dioxide remained in the reaction solution, which was apt to form hydrogen sulfide during the succeeding process of electrolytic reduction and so cause fog. In process ii, the evolution of bromine during the reaction led to considerable difficulty in manipulation. Finally, process iii was adopted as the best one to obtain the pure vanadyl salt. Another advantage of process iii is that the vanadyl ion can be obtained coupled with an optional anion, depending upon the kind of acid used. For example, when sulfuric acid is used, vanadyl sulfate ($VOSO_4$) is obtained, while in case of the hydrochloric acid, vanadyl chloride ($VOCl_2$) is formed. In this study, the syntheses of vanadyl sulfate, vanadyl chloride and vanadyl nitrate are examined.

Experimental

Material. — The vanadium pentoxide used is yellowish-brown, amorphous and of an extra-pure grade. Extra-pure-grade oxalic acid dihydrate and sulfuric acid, hydrochloric acid and nitric acid of various concentrations are used.

3) A. and L. Lumiére, *Bull. Soc. Fr. Phot.*, **10**, 108 (1894).
4) P. Roman, *Sci. Ind. Phot.*, **23**, 417 (1952).
5) C. Ives, H. Russell and J. Crabtree, *J. Phot. Sci.*, **2**, 7 (1954).
6) A. Rasch and J. Crabtree, PSA technical quarterly, May, 59 (1954).
7) A. Rasch and J. Crabtree, *J.S.M.P.T.E.*, **62**, 1 (1954).
8) L. Fortmiller and T. James, Roy. Phot. Soc. Centenary Conference, Sept., 161 (1953).
9) S. Kikuchi, C. Yoshinaga, W. Fujita, K. Tanimura and K. Akaike, *J. Soc. Sci. Phot. Japan*, **19**, 40 (1956).
10) T. Kitagawa, K. Akaike and K. Hiwatari, ibid., **20**, 62 (1957).
11) S. Kikuchi, *Denki-kagaku*, **24**, 59 (1956).
12) J. Brierley, *J. Chem. Soc.*, **49**, 822 (1886); A. Piccini, *Z. anorg. Chem.*, **19**, 204 (1899); A. Piccini and L. Marino ibid., **32**, 55, 71 (1902).

Procedure. — A calculated weight of vanadium pentoxide is added to the sulfuric acid. As vanadium pentoxide is not easily soluble in sulfuric acid, most of it is suspended as a brownish color. When vigorously stirred, the oxalic acid dihydrate is added slowly into the solution while it is being heated. The reducing reaction proceeds during a vigorous evolution of carbon dioxide. When the added oxalic acid is completely consumed, the evolution of gas stops and the addition of oxalic acid is again continued. As the reaction proceeds, the solution becomes blue-green, the reaction is considered to be over when the yellowish-brown particles of vanadium pentoxide completely disappear.

Results

The Synthesis of Vanadyl Sulfate. — The vanadyl sulfate solution can be directly used for electrolysis, but in order to use the pure vanadyl sulfate for it and to ascertain the yield of this process, the vanadyl sulfate was isolated. The reaction solution was filtered to remove the unreacted vanadium pentoxide and condensed on a water bath. When the solution was left to cool for about 24 hr., blue crystals of vanadyl sulfate, which were somewhat hygroscopic, were obtained. From the weight of crystals, a crude yield is given.

As this crystal is considered to contain sulfuric acid and water, further purification was carried out. This was achieved by means of repeated washing in ethanol and water, utilizing the good solubility of sulfuric acid in water and the difference in the solubility of vanadyl sulfate between that in water and that in ethanol (it is more easily soluble in water). The crystals were then filtered and dried to obtain pale blue, powdery crystals. From the weight of the crystals thus obtained, the yield of purification is given. The loss caused by purification sometimes reaches a 40% maximum. The purified crystals were considered to have the constitution of $VOSO_4 \cdot xH_2O$, so the VO^{2+} ion content in the crystal was determined in order to decide x by means of oxidation titration with ceric sulfate. The results showed the content of 31%. Hence, x is equal to 3. In other words, it is clear that vanadyl sulfate crystal contains 3 molecules of the water of crystallization. This crystal is not hygroscopic and is sufficiently stable in the open air. The final results are shown in Table I.

The Synthesis of Vanadyl Chloride. — The synthesizing procedure and the reaction process are almost the same as those in the synthesis of vanadyl sulfate, where the sulfuric acid is only replaced by the hydrochloric acid. The reacting solution gradually changes in color from brown to the thick blue characteristic of the vanadyl ion. After the reaction, the solution was filtered and condensed, and the isolation of vanadyl chloride was attempted but in vain. It is, hence, believed that vanadyl chloride itself might be uncrystalline or very easily soluble at an ordinary temperature. Accordingly, the vanadyl ion was determined by the oxidation titration described before and the synthetic yield was calculated from the titration. The results are shown in Table II.

Table I. Synthetic conditions of vanadyl sulfate

Material		No. 1	No. 2	No. 3
V_2O_5,	g.	10	40	50
H_2SO_4 (95%),	ml.	20	40	50
H_2O,	ml.	20	60	100
$H_2C_2O_4 \cdot 2H_2O$,	g.	8	33	40
Vanadyl sulfate g. (%)	Crude	13 (55)	114.3 (120)	—
	Purified	4.6 (20)	91 (95.5)	116.8 (98)

Table II. Synthetic conditions of vanadyl chloride

Material		No. 1	No. 2
V_2O_5,	g.	10	50
HCl,	ml.	150 (ca. 5.6 N)	600 (ca. 4.9 N)
$H_2C_2O_4 \cdot 2H_2O$,	g.	8	40
Yield of $VOCl_2$,	%	100	100

The Synthesis of Vanadyl Nitrate.—Vanadyl nitrate seems not to have been isolated; at any rate, its existence has not yet been recognized according to the literature. Although it is impossible to isolate vanadyl nitrate, if the vanadyl ion is synthesized in a solution in which the NO_3^- ion is the sole anion, it can be simply taken as a state in which vanadyl nitrate is dissolved and electrolytically dissociated. This solution can then be used as a starting solution for the electrolysis. By analogy with the syntheses of vanadyl sulfate and vanadyl chloride, the reaction equation is assumed to be:

$$V_2O_5 + H_2C_2O_4 + 4HNO_3 \rightarrow 2VO(NO_3)_2 + 2CO_2 + 3H_2O$$

At 80~90°C, the reaction was carried out in the same way as the synthesis of vanadyl sulfate or vanadyl chloride. During the reaction, the evolution of a red-brown gas was observed and a considerable quantity of unreacted vanadium pentoxide still remained, even when the theoretical weight of oxalic acid was consumed. The reaction was stopped at this point, and the vanadium pentoxide was

filtered out. The filtrate showed a thick blue color, indicating the formation of VO^{2+}. The concentration of vanadyl ions was determined by oxidation titrations with potassium permanganate or ceric sulfate, resulting in a good coincidence for the two methods. When vanadium pentoxide (20 g.) in nitric acid (ca. 2.9 N, 300 ml.) was reacted with $C_2H_2O_4 \cdot 2H_2O$ (14.3 g.), the yield of vanadyl nitrate calculated from the above results was as follows:

$VO(NO_3)_2$	Found	16 g.
	Calculated	42 g.
	Yield	38%
Unreacted V_2O_5		11 g.

Discussion

Vanadyl Sulfate.—(a) The concentration of sulfuric acid may be diluted down to 20 N as long as the reducing power of oxalic acid is not affected.

(b) It is desirable that the quantity of sulfuric acid be kept at a minimum provided that vanadium pentoxide is kept in the state of suspension.

(c) It is best to add a small excess of oxalic acid (1.2 times of the thoretical weight).

(d) It is desirable that the quantity of water be such that the reaction product is easily crystallized when the solution is condensed and dried (about 95°C) after the reaction.

(e) As for the reaction temperature, it is clear that the threshold temperature for the reduction with oxalic acid is about 70°C. No evolution of carbon dioxide is observed below this temperature, but above 100°C the foaming is very much intensified.

(f) It is naturally desirable to stir the solution as vigorously as possible.

(g) The vanadyl sulfate obtained is stable even at temperatures above 100°C.

Vanadyl Chloride.—(a) The reaction proceeds nearly theoretically.

(b) The reaction does not proceed at temperatures below 60°C. The concentration of hydrochloric acid does not affect the yield if it is in the range of 2 N and above.

(d) As it is difficult to isolate vanadyl chloride, the reaction solution should be directly used for the electrolysis.

Vanadyl Nitrate.—The red-brown gas evolving in the course of the reaction is believed to be nitrogen dioxide or nitrogen sesquioxide resulting from the decomposition of nitric acid. Probably the oxalic acid is partly consumed in decomposing the nitric acid, resulting in the poor yield of vanadyl nitrate.

Electrolytic Reduction Process

As has been described before, in this process the vanadyl salt is cathodically reduced to the V^{2+} state. In this case, VO^{+2} is considered to be reduced first to V^{3+} and then to V^{2+}.

$$VO^{2+} + 2H^+ + e \rightarrow V^{3+} + H_2O\,;\quad V^{3+} + e \rightarrow V^{2+}$$

The theoretical electric quantity necessary for the above reduction is two faradays. The redox potential of the former system is:

$$E^\circ_{VO^{2+}/V^{3+}} = +0.337\ \text{V.}^{13)} \quad (25°C)$$

That of the latter has previously been described.

The solution of vanadous salt can also be prepared by chemical reduction using a reducing agent such as zinc amalgam.[14] In the case of photographic use, the electrolytic method is preferable in order to avoid contamination and in order to carry out the continuous regeneration of the developer. It has been reported[4,5] that vanadyl salts, vanadyl sulfate and vanadyl bromide, were electrolyzed with a lead cathode. Schwarzenbach and Sandera[15] also prepared vanadium dichloride using a mercury cathode, and Jones and Colvin[2] obtained vanadium(II) sulfate with a mercury cathode. However, there has been no systematic study of the electrolytic preparation of vanadous salt from the standpoint of electrolytic conditions. Therefore, in the present paper, the influence of various factors, such as (i) the kinds of electrodes, (ii) the kinds of starting compounds and electrolytes, (iii) the current density, and (iv) the acid concentration of catholyte, upon the yield will be described.

Experimental

Materials.—*Vanadyl Sulfate.*—Blue crystals containing 3 molecules of water ($VOSO_4 \cdot 3H_2O$) prepared as described above were used. Their purity was determined by cerimetry to be more than 98%.

Vanadyl Chloride.—The compound prepared as described before was used. As it was not crystallized, the solution in hydrochloric acid was directly used for the electrolysis. Its concentration was determined by cerimetry.

Vanadyl Nitrate.—A solution of the compound in nitric acid was used for the electrolysis, and its concentration was determined in the same way as before.

Cathode.—Mercury, lead, copper or stainless steel (hereunder abbreviated as S. S.) was used as a cathode. Except for those of mercury, the electrodes were cylindrical plates provided with a number of

13) G. Jones and J. Colvin, *J. Am. Chem. Soc.*, **66**, 1563 (1944).
14) L. Meites, *J. Chem. Educ.*, **27**, 458 (1950).
15) G. Schwarzenbach and J. Sandera, *Helv. Chim. Acta*, **36**, 1089 (1953).

small holes (1 cm.ϕ) to help the flow of the electrolyte solution. The circumference, height and area were 21 cm., 6.8 cm. and 121.8 cm^2 respectively. In the case of mercury, the mercury pool at the bottom of the electrolytic cell served as a cathode.

Anode.—As the anode must be acid-proof, lead peroxide and platinum were tested. The surface layer of lead peroxide peeled in the course of a long run, resulting in the contamination of the anolyte, so the platinum anode was finally adopted. The size of the electrode is not directly related to the results of the cathodic reduction, so it is adequate to choose it according to the dimensions of the anode chamber.

Diaphragm.—A cylindrical porous diaphragm was used. In order to avoid the dissolution of the components of the diaphragm, it was first soaked in acid and alkaline solutions and then the weight change of it and its porosity were measured. The diaphragm was treated in the following order: weighing → washing by water → soaking in hydrochloric acid 5% for 24 hr.→washing by water→ soaking in sodium hydroxide 1% for 24 hr.→washing by water→resoaking in hydrochloric acid 5% for 24 hr.→washing by water→drying→weighing. The hydrochloric acid soaking solution was colored somewhat yellow, clearly showing the dissolution of iron. The ratios of the weight change of two tested diaphragms, a and b, before and after the treatment were as follows;

$$a\ -0.33\%;\ b\ -0.35\%$$

The porosity was measured according to the following formula:

$$\text{Porosity} = \frac{\text{Weight(saturated with water)} - \text{Weight(dry)}}{\text{Total volume}}$$

The results obtained from several samples were 25~35% of porosity.

When these diaphragms were used for electrolysis, the following results were obtained.

(a) There is scarcely any dissolution of diaphragm components.

(b) The separation of the catholyte is perfect, and there is no transference of vanadium ions into the anode chamber.

(c) A part of the anolyte moves into the cathode chamber, and the difference between the levels of the anolyte and of the catholyte becomes 2~3 cm. However, as the same kind of acid is used for both anolyte and catholyte, no unfavorable effect of this movement is observed except for the change in the concentration of the acid.

Electrolytic Cell.—A 500 cc. beaker was used for the electrolytic cell, as Fig. 1 shows. The diaphragm was placed at the center of the cell for the anode chamber, and the outside part of it constituted a cathode chamber. The cathode chamber was closed with a rubber stopper to protect the V^{2+} ion from air oxidation. The stopper was provided with several small holes for measuring the cathode potential, for a thermometer, for the passage of nitrogen, and for removing the evolved hydrogen.

Electrolytic DC Power Supply.—AC power was selenium-rectified to be used as the DC electrolytic power source. The voltage was adjusted by a slidac on the AC side and by a sliding resistance on the DC side.

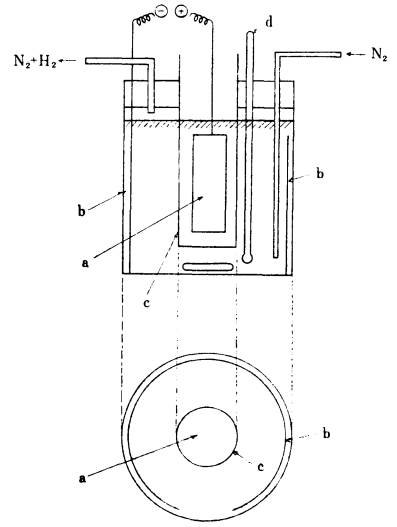


Fig. 1. Electrolytic cell. a, Anode; b, Cathode; c, Diaphragm; d, Thermometer.

Electrolyte.—The three following solutions, (a) a hydrochloric or sulfuric acid solution of vanadyl sulfate, (b) a hydrochloric acid solution of vanadyl chloride, and (c) a nitric acid solution of vanadyl nitrate, served as catholytes, and the same acid was used for the catholyte as for the anolyte.

The acid concentrations of both catholyte and anolyte were kept equal.

When hydrochloric acid or nitric acid was used as an anolyte, stimulative gas evolved; this was removed by an aspirator.

The Possibility of Using V^{3+} Salt as a Starting Material.—If a V^{3+} salt solution exists, there is no need of chemical synthesis and the preparation of developer will be very much simplified. Vanadium trioxide (V_2O_3) is the only V^{3+} compound available on the market. Vanadium trioxide is stable and is almost insoluble in every kind of acid, and the slightly-dissolved components seem to be in a V^{4+} state, judging from the color. On the other hand, V^{3+} precipitates in alkaline solution in the form of vanadium(III) hydroxide. Thus, vanadium trioxide is considered not to be suitable for the starting material in preparing the vanadium developer.

Electrolytic Procedure. — The electrolysis was carried out under strong agitation by a magnetic stirrer. During electrolysis the applied voltage was adjusted so that the current density could be kept constant. The temperature rose with the electrolysis, but it was kept below 30°C by cooling with ice. When vanadyl sulfate or vanadyl chloride was electrolyzed, the catholyte changed its color from blue to green, showing the existence of V^{3+}, and then to the violet of V^{2+}. The hydrogen began to evolve vigorously when the theoretical electric quantity was consumed. When the electric quantity reached twice the theoretical quantity, the electrolysis was stopped and the catholyte was removed

into a stoppered flask. The yield was determined by the simultaneous potentiometric titration of V^{2+} and V^{3+}.[16] During electrolysis, the evolved hydrogen protected V^{2+} from air oxidation, so there was no need for nitrogen passage; otherwise, all the procedures should be carried out in a nitrogen atmosphere.

The electrolysis of vanadyl nitrate will be described later.

Results and Discussion

The Influence of the Kind of Electrodes.—The influence of the kind of electrode upon the electrolytic yield was examined in the case of the catholyte of the vanadyl chloride-hydrochloric acid system. The electrolytic conditions were;

$VOCl_2$ 0.2~0.6 M/1., HCl 1~3 N, cathode current density, D_k=1.64 amp./dm^2. The results are shown in the following table.

Electrode	Yield, %
Pb	82
Cu	62
S. S	25

For the electrolyte of the vanadyl sulfate-sulfuric acid system, the electrolytic conditions were;

$VOSO_4$ 0.1 M/1., H_2SO_4 1 N, and

D_k=1.6~2.0 amp./dm^2

Those results are as follows:

Electrode	Yield, %
Hg	100
Pb	69

The results show that the mercury cathode gives the highest yield, followed by lead and copper, while the stainless steel gives the lowest. In the latter case, a slight corrosion is observed on the surface of the electrode after the electrolysis; the poor yield may be attributed to the fact that a part of the electrolytic current is consumed for the hydrogen evolution due to the corrosion. Furthermore, taking into account the contamination of the electrolyte, the stainless steel electrode is not preferable in the present electrolysis.

The Influence of the Constitution of the Electrolyte.—From the above results, it was clear that the lead electrode was of practical use, so the influence of the constitution of the electrolyte, namely, the relation between the yield and the kind of acids and electrolyzed materials, was studied in the case of the lead electrode. The results are shown in the following table.

Combination of electrolytes	Yield, %
$VOSO_4$ - H_2SO_4	94
$VOSO_4$ - HCl	72
$VOCl_2$ - HCl	82

The other electrolytic conditions were kept constant as follows:

D_k=0.82 amp./dm^2,
acid concentration=1~2 N,
concentration of vanadyl salt=0.1 M/l.

As is clear from the results, the combination of vanadyl sulfate and sulfuric acid gives the highest yield, followed by the combination of vanadyl chloride, hydrochloric acid and vanadyl sulfate - hydrochloric acid. It is concluded that the combination of vanadyl salt and acid gives a higher yield when they possess a common anion.

The Influence of Cathode Current Density (D_k).—The influence of the cathode current density upon the yield, using the lead cathode and the vanadyl sulfate - sulfuric acid electrolyte, the optimum condition so far achieved, was also studied.

The electrolytic conditions were as follows:

Cathode—Pb,		Anode—Pt
Catholyte	$VOSO_4$	0.1 M/l.
	H_2SO_4	1 N
Anolyte	H_2SO_4	1 N

The results are shown in Fig. 2 and in the following table.

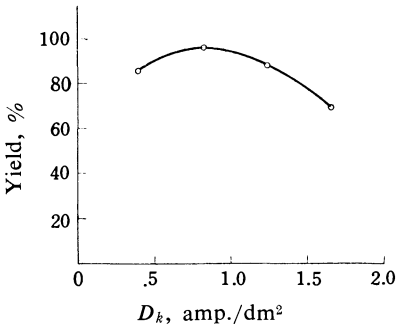


Fig. 2. Relation between the cathode current density (D_k) and the yield.

Current density, amp./dm^2	Yield, %
0.41	85
0.82	94
1.23	87
1.64	69

From the table, it can be seen that the highest yield, 94%, is reached when D_k is about 0.82 amp./dm^2. In general, with the increase of the cathodic current density, the hydrogen over-voltage increases, while the reducing power of the cathode is argumented. However, the results show that, if the current

16) Presented at the 13th Annual Meeting of the Chemical Society of Japan, Tokyo, April, 1960.

density rises, the yield decreases. This is supposed to be due to the fact that the evolution of the hydrogen in a very acidic solution like the present electrolyte competes with the reduction of vanadium.

The Influence of the Concentration of Sulfuric Acid as Catholyte.—The influence of the concentration of sulfuric acid upon the yield was then studied under the optimum conditions hitherto mentioned, with the lead cathode, the vanadyl sulfate - sulfuric acid electrolyte, and $D_k = 0.82$ amp./dm^2.

The electrolytic conditions were as follows:

	Cathode—Pb	Anode—Pt
Catholyte	$VOSO_4$	0.1 M/l.
	H_2SO_4	0.1～8 N

Anolyte—H_2SO_4, the concentration being the same as that of the catholyte.

The results are shown in Fig. 3 and in the following table.

Concn. of H_2SO_4, N	Yield, %
0.1	89
1.0	94
8.0	87

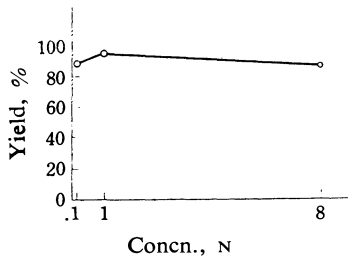


Fig. 3. Relation between the concentration of sulfuric acid as catholyte and the yield.

From the results, it was seen that the concentration of the sulfuric acid in the range of 0.1～8 N does not exert an important influence upon the yield, the variation of the yield being less than 7%.

Therefore, the influence of the concentration of the sulfuric acid may be taken into account in relation with the stability of the V^{2+} ions dissolved and with their reducing power or developing ability.

According to Charlot,[17] the redox potential of the V^{3+}-V^{2+} system becomes more negative with the increase of pH, so its electrochemical reducing power must argument with the decrease in acidity. Furthermore, according to Jones and Colvin,[2] in a strong acid solution, V^{2+} reduces the hydrogen ion, evolving the hydrogen, and V^{2+} itself is oxidized to V^{3+}.

From the above standpoint, it is best if the acid concentration of the catholyte is low as long as the yield of V^{2+} is not affected.

The Electrolysis of Vanadyl Nitrate.—The electrolysis of the solution of vanadyl nitrate mentioned before was attempted under the same conditions as in the case of electrolysis of vanadyl sulfate or vanadyl chloride.

The electrolytic conditions were as follows:

	Cathode—Pb	Anode—Pt
Catholyte	$VO(NO_3)_2$	0.1 M/l.
	HNO_3	ca. 1.3 N
Anolyte	HNO_3	ca. 1.3 N

$D_k = 0.82$ amp./dm^2

The consumption of electricity was three times the theoretical value.

In spite of the excessive consumption of electricity, the color of the electrolyte solution remained blue, a color characteristic of VO^{2+} ions, not showing the violet color of V^{2+}. The potentiometric titration of the electrolyzed solution showed a one-step curve corresponding to the redox potential of VO^{2+}/V^{5+}, undoubtedly indicating that there was no formation of V^{2+} or V^{3+}. Accordingly, it seems impossible to prepare V^{2+} electrolytically from vanadyl nitrate.

The reason why the electrolysis of vanadyl nitrate does not proceed is supposed to be due to the fact that cathodically-formed V^{2+} or V^{3+} reacts with the nitric acid, reduces it, and itself returns to the VO^{2+} state.

Conclusion

The Chemical Reduction Process.—(i) The synthesis of vanadyl sulfate by the oxalic acid method proceeds theoretically, obtaining blue crystals containing 3 molecules of the water of crystallization ($VOSO_4 \cdot 3H_2O$). The crude yield attains 100%, and the purified one, 98%. (ii) The synthesis of vanadyl chloride also proceeds theoretically, and the yield attains 100%. It is, however, impossible to isolate the vanadyl chloride of the crystalline state. (iii) The synthesis of vanadyl nitrate by the oxalic acid method dose not give satisfactory results, showing a yield as poor as 38%. However, the unreacted V_2O_5 can be recovered up to 90%. (iv) None of the synthesizing reactions mentioned above proceed at all at temperatures below 70°C.

The Electrolytic Reduction Process.—(i) The electrolytic preparation of V^{2+} salt from vanadyl sulfate gives the highest yield, 100%. (ii) When the vanadyl chloride is electrolyzed, the maximum yield obtained is 82%. (iii) In both cases, the conditions required for obtaining the maximum yield are:

Cathode—Lead or mercury
Catholyte—All acids contained the same

17) G. Charlot, "L'analyse qualitative et les réactions en solution," Massonet Cie, Paris (1957).

anion as that of vanadyl salt to be electrolyzed.

Concentration of acid—0.1～8 N

Temperature—Room temperature

Cathodic current density—0.82 amp./dm^2

(iv) Vanadyl nitrate is not reduced electrolytically, and it is impossible to obtain V^{2+} salt from it.

Summary

A systematic study of the preparation of a V^{2+} developer for use in the continuous automatic processing machine has been carried out.

At first the vanadyl salts, such as vanadyl sulfate and vanadyl chloride, were chemically synthesized from vanadium pentoxide with a yield of nearly 100%, while vanadyl nitrate was obtained with a yield of only 38%. The synthesizing method using oxalic acid was considered to be the most advantageous from the standpoint of the succeeding electrolytic process.

Concerning the electrolytic reduction process to obtain V^{2+} salt from vanadyl salt, the influence of the kind of electrodes, the combination and concentration of electrolytes, and the cathodic current density upon the yield has been studied. On the basis of these studies, the optimum conditions for the electrolysis have been established except for vanadyl nitrate.

Technical Research Laboratories
Japan Broadcasting Corporation
Setagaya-ku, Tokyo

The Rotatory Dispersion and Stereochemistry of Organic Compounds. VI.[1] *Some Observations on the Sign of Partial Rotations in the Derivatives of Xylofuranose and Mannopyranose*

By Yojiro TSUZUKI, Katsumi TANAKA, Koko TANABE, Masuo AKAGI and Setsuzo TEJIMA

(Received December 24, 1963)

In previous papers[1,2] the rotatory dispersion (RD) of some derivatives of glucose as well as of several anomeric pyranoses has been reported and discussed with relationship to the configuration. In the present paper similar studies will be made on some other monosaccharides, particularly with respect to the sign of the Cotton effect and to the configuration of the functional group, and the results will be compared with the derivatives of glucose. The following compounds will be investigated:

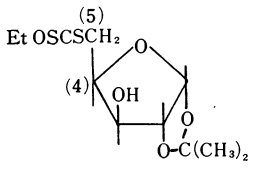
1, 2-*O*-isopropylidene-D-xylofuranose 5-ethylxanthate (compound I),

1, 2-5, 6-*O*-diisopropylidene-D-glucofuranose (compound II),[2]

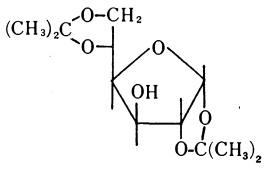
1, 2-5, 6-*O*-diisopropylidene-D-glucofuranose-3-(*S*-methyl)-xanthate (compound III),[2]

2, 3, 4, 6-tetra-*O*-acetyl-β-D-glucofuranosyl ethylxanthate (compound IV),[1]

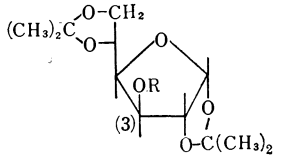
2, 3, 4, 6-tetra-*O*-acetyl-β-D-mannopyranosyl-ethylxanthate (compound V).



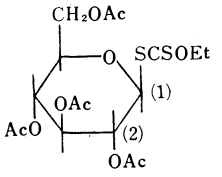
(I)



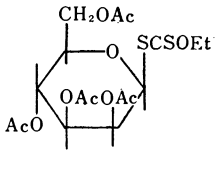
(II)



(III) R= -C-SCH
S



(IV)



(V)

1) Part V: Y. Tsuzuki, K. Tanabe, M. Akagi and S. Tejima, This Bulletin, 37, 162 (1964).

2) Y. Tsuzuki, K. Tanaka and K. Tanabe, ibid., 35, 1614 (1962).

Results and Discussion

The RD curve of compound I shows a positive Cotton effect in the region from 300 to 380 mμ (Fig. 1-I). It is interesting to compare this anomalous curve with those of diisopropylidene-D-glucofuranose (compound II) and its 3-methylxanthate (compound III) of a similar configuration.

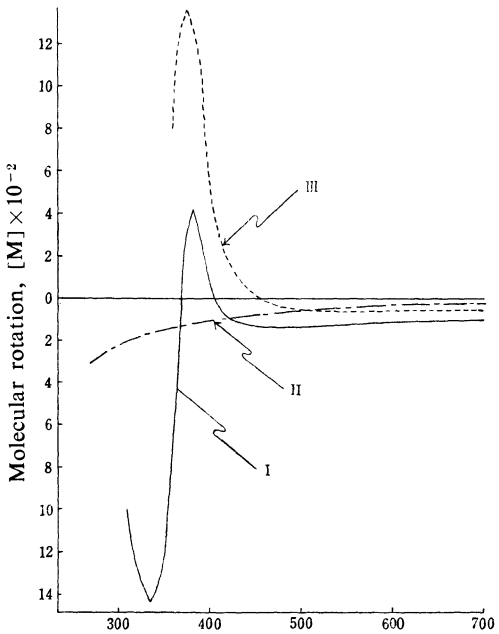


Fig. 1. RD of D-xylofuranose 5-ethylxanthate (I) compared with those of glucofuranose of derivatives (II and III) of similar configuration.

The positive Cotton effect of compound I is due to the $-S-\overset{\overset{S}{\|}}{C}-OC_2H_5$ group attached to the C_4-asymmetric center through the C_5-methylene group. This fact may easily be understood by considering that the compound II, carrying no chromophore, does not show any Cotton effect. In compound III a stronger, positive Cotton effect is observed; this is undoubtedly to be attributed to the $C_3-O-\overset{\overset{S}{\|}}{C}-S-CH_3$ group.[2] In these three compounds the background rotation is always negative, for which the C_3-OH group with an L-configuration may be responsible,[3] although this statement requires further investigation before it can be definitely established.

3) See Y. Tsuzuki, K. Tanaka and K. Tanabe, ibid., 35, 1615 (1962).

The structural difference between compounds IV and V lies in the configuration of the C_2-group, which is reflected in the RD curves seen in Fig. 2. The weaker, positive Cotton effect naturally originates in the $\beta-C_1-S-\overset{\overset{S}{\|}}{C}-OC_2H_5$ group, the amplitude of which is strikingly smaller than that of its epimer (IV).[1]

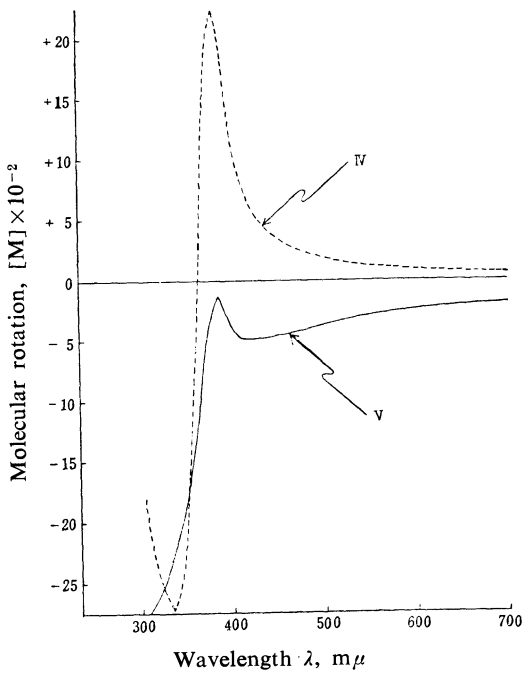


Fig. 2. RD of tetraacetyl β-D-mannopyranosyl 1-ethylxanthate (compound V) compared with its epimer (compound IV).

That the mannofuranose (V) is generally less levo-rotatory than its epimer (IV) is because the C_2-acetoxy group of the former has a configuration of the L-type, suggesting that its partial rotation due to this group is negative in sign. This statement becomes more evident upon analysis of the dispersion data obtained by means of the Drude equation, which will be described later.

The rotatory dispersion constants and the ultraviolet absorption maxima of compounds I and V are tabulated in Table I. The optically-active absorption maximum, λ_0, of compound I lies near 360 mμ, in good agreement with the λ_{max} of its R-band (357 mμ). Although no trough could be observed, the value of λ_0 is presumably not far from the λ_{max} of its R-band (360 mμ), as the amplitude is small.

The data of the RD measurements were calculated according to an abbreviated two-term expression of the Drude equation:

TABLE I. RD CONSTANTS AND UV ABSORPTION MAXIMA

Compound	Rotatory dispersion				Ultraviolet absorption			
	Peak		Trough		R-band		K-band	
	λ, mμ	[M]	λ, mμ	[M]	λ_{max}, mμ	ε	λ_{max}, mμ	ε
I	382	+411°	335	−1420°	357	34.0	280	11800
V	385	−147°	—	—	360	36.7	274	8510

$$[M] = \frac{A}{\lambda^2} + \frac{B}{\lambda^2 - \lambda_c^2}$$

The results are shown in Table II, together with some previous data (III,[2] IV[1]) for the sake of comparison.

TABLE II. DISPERSION CONSTANTS FOR SUGAR DERIVATIVES

Compound	A	B	λ_c^2
I	−61.12	11.79	$(0.361)^2$
III	−37.82	4.54	$(0.380)^2$
IV	−13.68	27.33	$(0.369)^2$
V	−97.29	2.14	$(0.369)^2$

The agreement of the observed and the calculated values of rotation is tolerable over the range from 310 to 700 mμ, the difference between them being mostly only a few percent outside the absorption region.

The values of λ_c are from 361 to 380 mμ, in good accord with the corresponding absorption maxima of the R-band shown in Table I and in previous papers. Among these the λ_c value (0.380 μ) of compound III is particularly high. Here it should be pointed out that the chromophore of III is of the C–O–C(=S)–S–R type, unlike those of the others, which are all of the C–S–C(=S)–OR type.

The rotational strength B due to the chromophore (the xanthyl group) is in all cases positive in sign, but the configuration of the functional group is always of the L-type. This fact is in harmony with the information that the xanthates of L-hydroxylic acids show positive Cotton effects[4] even through the functional group (OH) is expected to contribute to the levo partial rotation, as was pointed out in a previous paper.[2]

The value of B is the largest in β-glucopyranosyl xanthate (IV), but incomparably smaller in the corresponding derivative of mannose (V). Here the chromophore is cis to the adjacent acetoxy group, C_2-OAc (1L-*e*, 2L-*a*), while in the glucose derivative (IV) the conformation (1L-*e*, 2D-*e*) is trans. As there might be some steric disturbance between these two groups, especially in the cis configuration, giving rise to this remarkable difference in B between the epimers (IV and V), the authors have observed the influence of the temperature on RD with V; they expected some change in optical rotation due to thermal agitation, but in reality the RD curve was almost independent of the temperature below 60°C.

The residual rotational strength of A is in all cases negative in sign, and it is greater than that of the main partial rotational strength B except in glucopyranosyl xanthate (IV).

As the RD curve II typically shows, the background rotation of these compounds is negative in sign (Fig. 1). The strong positive rotation near the absorption region of III is, as has already been pointed out, due to the C_3–O–C(=S)–S–CH_3 group.

It is noteworthy that A is negative in compound IV, although the rotation is positive. (Fig. 2-IV) This fact can be interpreted thus: the β-form of the C_1-ligand should contribute potentially to a negative rotation, which is embodied in the negative rotational strength of A, but this negative partial rotation is now canceled by the positive, rotational contribution due to both the C_2 group of D-configuration and the C_1-xanthyl group. That the value of A is unusually large in the mannopyranosyl xanthate (V) may be due to the L-type C_2-acetoxy group, which is evidenced in another expression of RD by the two-term equation of Drude. The RD of compound V is rather better expressed by the following equation, where the calculated values of the molecular rotation are in good agreement with the observed values, with an accuracy of more than 95% over the spectral region from 305 to 700 mμ except in the absorption region:

$$[M] = \frac{-99.35}{\lambda^2 - (0.233)^2} + \frac{13.02}{\lambda^2 - (0.363)^2}$$

In the above equation the first negative term is inferred as expressing mainly the partial rotation due to the C_2-acetoxy group of the L-type; in reality the value of λ_1 (0.233 mμ) nearly coincides with the ultraviolet absorption of the acetoxy group.

4) B. Sjöberg, A. Fredga and C. Djerassi, *J. Am. Chem. Soc.*, **81**, 5002 (1959).

Experimental

The rotatory dispersion was measured in tetrahydrofuran at room temperature over the wavelength region from 300 to 700 mμ with a Rudolph photometric spectropolarimeter. The ultraviolet absorption was measured in the same solvent with a self-recording spectrophotmeter of the Hitachi type. The calculation from the data of RD was made by means of the least-squares method with an electronic computer of the Fuji FACOM 201 type.

The method of preparation and the other properties of the following compounds will be described elsewhere by Akagi and his collaborators.

1, 2-*O*-Isopropylidene-D-xylofuranose 5-Ethylxanthate. (Compound I).—Was prepared from its corresponding iodo compound.[5] Colorless crystals. M. p. 126°C. $[\alpha]_{700}^{16.5} = -33.0°$, $[\alpha]_{589} = -39.9°$, $[\alpha]_{382} = +140°$ (peak), $[\alpha]_{335} = -483°$ (trough), $[\alpha]_{310} = -341°$ (*c* 0.2936, tetrahydrofuran).

2,3,4,6-Tetra-*O*-acetyl-β-D-mannopyranosyl 1-Ethylxanthate (Compound V).—Colorless crystals. M. p. 127~128°C. $[\alpha]_{700}^{17} = -43.4°$, $[\alpha]_{589} = -58.1°$, $[\alpha]_{420} = -110°$ (broad extreme), $[\alpha]_{385} = -32.4°$ (peak), $[\alpha]_{305} = -602°$, (*c*, 0.4362, tetrahydrofuran).

5) P. A. Levene and J. Compton, *J. Biol. Chem.*, **111**, 325 (1935).

Department of Chemistry
Tokyo College of Science
Kagurasaka, Tokyo
(Y. T., K. T. & K. T.)

Faculty of Pharmacy
School of Medicine
Hokkaido University
Sapporo (M. A. & S. T.)

The Synthesis and Configurational Analysis of 2,3-Diaminocyclohexanol

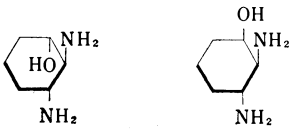
By Tetsuo SUAMI and Seiichiro OGAWA

(Received December 28, 1963)

The previous studies on 2-amino-1,3-cyclohexanediol[1] have stimulated our interest in the synthesis of an alicyclic compound with two amino groups and one hydroxyl group. In the present paper, the synthesis of 2,3-diaminocyclohexanol is described, and its structure is established by means of the proton magnetic resonance spectra of the acetyl derivatives. Di-*O*-mesyl-*trans*-2-acetamido-1,3-cyclohexanediol (I)[2] is used as a starting material for this preparation. By treating compound I with sodium azide in boiling aqueous 2-methoxyethanol, DL-2-acetamido-3-azidocyclohexanol (II) is obtained. This compound is hydrogenated by Raney nickel in a hydrogen stream to give DL-2-acetamido-3-aminocyclohexanol (III) in 48.8% yield from compound I. Compound III is treated with acetic anhydride and pyridine, giving the triacetyl derivative (IV), melting at 206.5°C, in 77.0% yield. Compound IV is selectively deacetylated by methanol saturated with dry ammonia to give 2,3-diacetamidocyclohexanol (V). Also compound III or compound IV is hydrolyzed by 6 N hydrochloric acid, giving 2,3-diaminocyclohexanol dihydrochloride (VI). The picrate is prepared from compound VI.

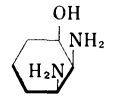
1) T. Suami and S. Ogawa, This Bulletin, **37**, 194 (1964).
2) F. W. Lichtenthaler *Chem. Ber.*, **96**, 845 (1963).

There are four predicted diastereomers of 2,3-diaminocyclohexanol (IX, X, XI and XII), but they are wholly unknown:

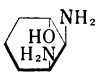


IX

X



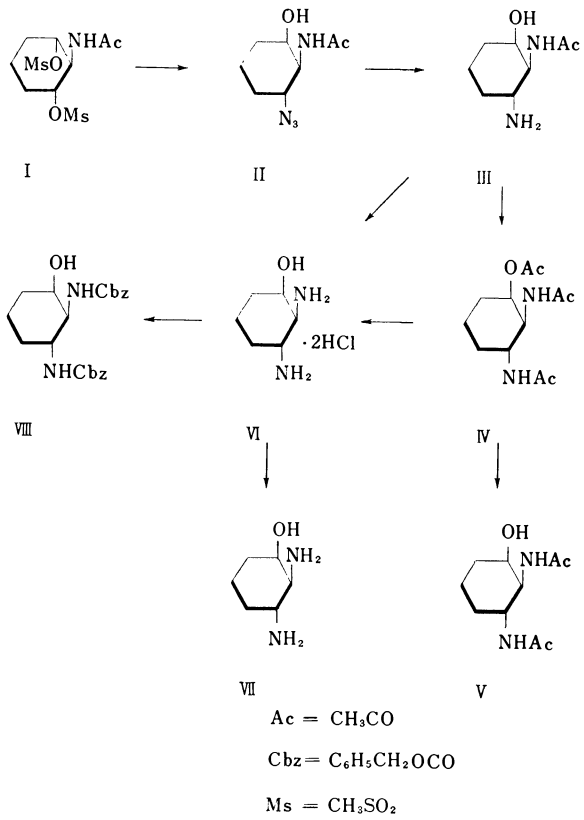
XI



XII

None of them has a plane of symmetry; hence, they are racemic forms.

In the present experiment, the starting material I has the trans configuration.[1,2] The loss of both the mesyloxy groups takes place when compound I is treated with sodium azide in boiling aqueous 2-methoxyethanol, but azido alcohol II is obtained instead of the diazido derivative. An analogous phenomenon has been described in the solvolysis of compound I with sodium acetate.[2] This fact might be explained as follows: the displacement of



Ac = CH_3CO

Cbz = $C_6H_5CH_2OCO$

Ms = CH_3SO_2

mesyloxy group occurs with formation of oxazolinium ions,[3] which are attacked by water to give the *cis*-acetamido alcohol. Then the displacement of another mesyloxy group would take place via an anchimeric reaction or a direct S_N2 mechanism.

Recently the displacement of a secondary sulphonate group in sugar derivatives with sodium azide has been described by several authors,[4] but that in alicyclic compounds has never been described.

In the present experiment, if an attack by an azide ion occurs at C-3 (or C-1), with a retention of the configuration, the product should have the structure X, but if it occurs with an inversion, the product should have the structure XI.

The NMR spectrum of the triacetyl derivative, IV, gives an equivocal answer on this point. An acetoxy group produces a signal at a different field than does an acetamido group; moreover, an axial acetamido group gives a signal at a lower field than does an equatorial acetamido group in cyclohexane derivatives[1,5]. Therefore, the structure could be assigned on the basis of this point. The NMR spectrum of compound IV, as is shown in Fig. 1-A, reveals two sharp signals of a 1 : 2 relative intensity, as is to be expected from one axial acetoxy group (τ of 7.89)[5] and two equatorial acetamido groups (τ of 8.07). The doublet produced by the proton on a nitrogen atom in the acetamido group with a coupling constant of 10 c. p. s. (τ of 3.76) corresponds to two protons and gives further evidence that the two acetamido groups may be expected to have an identical conformation, since inosadiamine hexaacetate with one axial and one equatorial acetamido groups reveals two doublets.[6] The ring protons show a peak at 4.88 τ, as is to be expected from one equatorial proton at C-1, and a peak at 6.08 τ, as is to be expected from two axial protons at C-2 and C-3.

The NMR spectrum of compound V, shown in Fig. 1-B, shows only one sharp signal at 7.97 τ, as is to be expected from two acetamido

3) S. Winstein, E. Grunwald, R. E. Buckles and C. Hanson, *J. Am. Chem. Soc.*, **70**, 816 (1948).

4) E. J. Reist, R. R. Spencer, B. R. Baker and L. Goodman, *Chem. & Ind.*, **1962**, 1794; B.R. Baker and A.H. Haines, *J. Org. Chem.*, **28**, 442 (1963); C. L. Stevens, P. Blumbergs and F. A. Daniher, *J. Am. Chem. Soc.*, **85**, 1552 (1963); C. L. Stevens, P. Blumbergs, F. A. Daniher, R. W. Wheat, A. Kujomoto and E. L. Rollins, ibid., **85**, 3061 (1963).

5) F. W. Lichtenthaler, *Chem. Ber.*, **96**, 2047 (1963).

6) M. Nakajima, A. Hasegawa and F. W. Lichtenthaler, *Ann.*, **669**, 75 (1963).

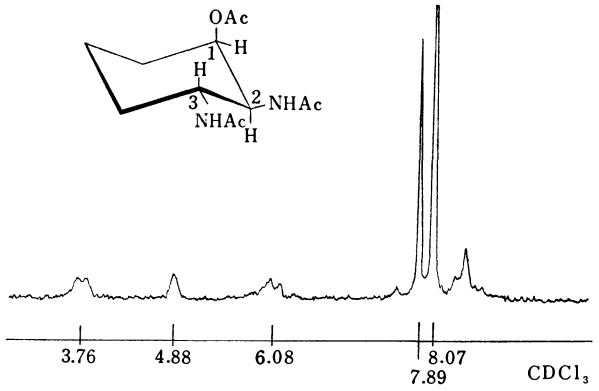


Fig. 1-A

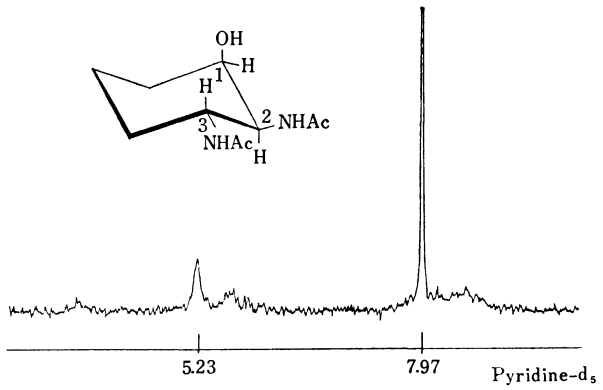


Fig. 1-B

groups; this means that the two acetamido groups are equivalent.

As a result of the consideration of the NMR spectra, it might be concluded that compound IV may be assigned as $2\alpha, 3\beta$-diacetamido-1α-cyclohexyl acetate and that, accordingly, the attack of azide ions occurs anchimerically, with a retention of the configuration.

Experimental

All melting points have been corrected. The NMR spectrum was determined at a frequency of 60 Mc. p. s. with a Varian Associates A-60 spectrometer. Tetramethylsilane was used as an internal reference in the samples. The peak position are given in τ-values.

DL-2α-Acetamido-3β-amino-1α-cyclohexanol (III). — A mixture of 4.0 g. of di-*O*-mesyl-*trans*-2-acetamido-1,3-cyclohexanediol (I), 3.3 g. of sodium azide and 100 ml. of 75% aqueous 2-methoxyethanol was heated under reflux for 2 hr. The mixture was then evaporated to dryness under reduced pressure. The residue was repeatedly extracted with hot acetone. The combined acetone extract was evaporated to give a brownish sirup, which showed infrared absorptions at 3300 (broad) (OH), 2090 (N_3) and 1653, 1544 cm^{-1} (amide).

A solution of the sirup in 40 ml. of ethanol was hydrogenated with Raney nickel T4,[7] obtained from 10 g. of Raney nickel alloy, in a hydrogen stream of an initial pressure of 50 p. s. i. g. for 4 hr. Then the mixture was filtered to remove the catalyst, and the filtrate was evaporated in vacuo. The crystalline residue was recrystallized from ethanol-ether to yield 0.79 g. of compound III, m. p. 174~177°C. The second crop of the product (0.26 g.) was obtained from the mother liquor. The total yield was 48.8% from compound I. The product was recrystallized from the same solvent to give an analytical sample in the form of colorless needles, m. p. 182.5~184°C.

Found: C, 55.63; H, 9.21; N, 16.47. Calcd. for $C_8H_{16}N_2O_2$: C, 55.79; H, 9.36; N, 16.27%.

The infrared spectrum of the product (KBr disk) showed the expected absorptions at 3150 (broad (OH and NH_2), 3290, 1550 (amide) and 1585 cm^{-1} (NH_2.)

DL-2α, 3β-Diacetamido-1α-cyclohexyl Acetate (IV).—A mixture of 1.0 g. of compound III, 50 ml.

7) S. Nishimura, This Bulletin, 32, 61 (1959).

of pyridine and 50 ml. of acetic anhydride was heated at 80°C for 1 hr. and then allowed to stand overnight at room temperature. The mixture was evaporated under reduced pressure. The crystalline residue was recrystallized from ethanol-ether to yield 1.15 g. (77%) of plates, m. p. 203~206.5°C. A sample recrystallized from ethanol-ether (m. p. 205~206.5°C) was subjected to elemental analysis.

Found: C, 56.38; H, 7.78; N, 10.87. Calcd for $C_{12}H_{20}N_2O_4$: C, 56.23; H, 7.87; N, 10.93%.

DL-2α, 3β-Diacetamido-1α-cyclohexanol (V). — A solution of 0.21 g. of compound IV in 20 ml. of methanol previously saturated with ammonia at 5°C was allowed to stand at room temperature overnight. The solution was then evaporated in vacuo. The residue was crystallized from ethanol-ether to yield 0.14 g. (82%) of compound V, m. p. 237~241°C (with decomposition). The sample for analysis obtained from ethanol-ether had an m. p. of 258~259°C (with decomposition).

Found: C, 56.33; H, 8.60; N, 13.09. Calcd. for $C_{10}H_{18}N_2O_3$: C, 56.05; H, 8.47; N, 13.08%.

DL-2α, 3β-Diamino-1α-cyclohexanol Dihydrochloride (VI). — a) A mixture of 0.5 g. of compound IV and 30 ml. of 6 N hydrochloric acid was refluxed for 6 hr. and then evaporated under reduced pressure to dryness, giving 0.31 g. (84.5%) of white crystals, m. p. 289~293°C (with decomposition). The analytical sample was obtained from methanol-ether as colorless plates, which started turning brown at 280°C and which melted at 301~303°C with decomposition.

Found: C, 35.62; H, 7.61; N, 14.26; Cl, 35.45. Calcd. for $C_6H_{14}N_2O \cdot 2HCl$: C, 35.48; H, 7.94; N, 13.79; Cl, 34.91%.

Paper Chromatography. — An upper layer of 1-butanol-acetic acid-water (4 : 1 : 5) gave a single spot of R_f 0.18 in ascending development at 17°C (R_f of glucosamine hydrochloride, 0.15).

b) A mixture of 0.60 g. of compound III and 60 ml. of 6 N hydrochloric acid was treated as described in a) to obtain 0.58 g. (82%) of the product, m. p. 290~293°C (with decomposition.)

DL-2α, 3β-Diamino-1α-cyclohexanol (VII). — A 8 ml. portion of a 0.5 N sodium hydroxide solution was added to a mixture of 406 mg. of compound VI and 20 ml. of methanol. The mixture was evaporated in vacuo, and the residue was extracted with absolute ethanol. The ethanol extract was evaporated to yield 260 mg. of an oily product.

The picrate was obtained by an ordinary method as yellow crystals, m. p. 255°C (with decomposition).

Found: C, 37.06; H, 3.62; N, 19.22. Calcd. for $C_6H_{14}N_2O \cdot 2C_6H_3N_3O_7$: C, 36.74; H, 3.43; N, 19.04%.

Di-*N*-carbobenzoxy-DL-2α, 3β-diamino-1α-cyclohexanol (VIII). — A 0.3 ml. portion of carbobenzoxy chloride in toluene (85% solution) was added to a mixture of 100 mg. of compound VI, 340 mg. of sodium bicarbonate and 3 ml. of water under agitation. After the mixture had been stirred for 6 hr., 157 mg. (79%) of the crude product was obtained as a white powder, m. p. 161.5~164.5°C. The analytical sample was obtained from ethanol as needles, m. p. 163.5~164.5°C.

Found: C, 66.48; H, 6.55: N, 7.07. Calcd. for $C_{22}H_{26}N_2O_5$: C, 66.31; H, 6.58; N, 7.03%.

The authors are indebted to Professor Sumio Umezawa for his helpful advice, to Dr. Frieder W. Lichtenthaler (Technische Hochschule Darmstadt, Germany) for measurements of the NMR spectra and his stimulating discussions on the NMR spectra, and to Mr. Saburo Nakada for his microanalysis. This research has been supported in part by a grant from the Ministry of Education, to which the authors' thanks are due.

Department of Applied Chemistry
Faculty of Engineering
Keio University
Koganei, Tokyo

*The Solid State Polymerization of Trioxane by the Simultaneous Sublimation of the Monomer and Iodine**

By Hajime MIYAMA and Mikiharu KAMACHI

(Received July 12, 1963)

Recently, Kargin et al.[1] published an interesting method of polymerization by the simultaneous condensation of the vapors of monomers and inorganic substances on a strongly cooled surface. The present authors have now applied Kargin's method to the system of trioxane and iodine, both of which can be easily sublimed, and have thereby obtained polyoxymethylene of a high degree of polymerization in a good yield.

Although many reports[2-10] about the solid state polymerization of trioxane have been published, the method of polymerization catalyzed by iodine in the solid state has not been reported as far as the authors know. Also, the present method of polymerization is very different from other methods. Therefore, it seems worthwhile to report the details of our experimental results.

Experimental

The experimental method is as follows. Commercial trioxane (Eastman Kodak and American Celanese) is purified by several sublimations in a high vacuum and then introduced, at the pressure of $10^{-4}\sim10^{-5}$ mmHg, into an ampoule cooled by liquid nitrogen. At the same time, the desired quantity of iodine, which has also been purified by several vacuum sublimations, is introduced into the ampoule. This ampoule, containing the mixture produced by the simultaneous sublimation of trioxane and iodine, is sealed off and placed into a thermostat of a definite temperature. After being left for the definite time, the ampoule is opened. Then monomer and iodine are removed by benzene, and the undissolved polymer is washed two times with benzene.

The ESR spectra of the polymerization system are measured with a Varian V-4500 spectrometer. Also, the temperature-rise of the system during the polymerization is followed by a thermistor inserted into the reaction ampoule.

The inherent viscosity of the polymer obtained is measured in a *p*-chlorophenol solution (0.1 g./100 ml.) containing 2% of α-pinene by using an Ostwald viscometer at 60°C. The softening temperature is measured by a Kofler's Micro-Hot-Stage. Also, the X-ray diffraction of the polymer is measured by using a Rigaku Denki D-5C diffractometer.

Results

In order to conduct the polymerization, it is necessary to keep the pressure as low as possible. The existence of air, oxygen and other radical scavengers inhibits this reaction. Therefore, all measurements are conducted at the pressure of $10^{-4}\sim10^{-5}$ mmHg. The results obtained are shown in Table I and Figs. 1—4. As Figs. 1 and 2 show, the polymerization yield increases with time, but it reaches a limit only after a few ten minutes. Also, the yield increases with the increase in the temperature and in the iodine concentration. Although the inherent viscosity does not change with the polymerization time regularly, it decreases with the increase in the temperature and in the iodine concentration, as is shown in Figs. 3 and 4, where inherent viscosity is measured for the polymers obtained

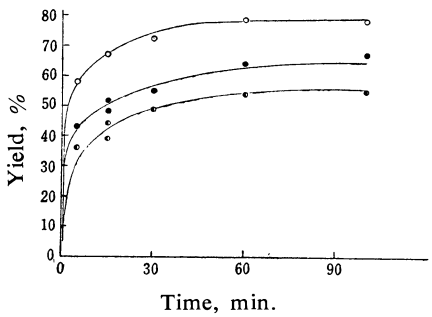


Fig. 1. Change of yield with time at various temperatures. Weight % of iodine is 0.67%.
○ 42.2°C ● 34.2°C ◐ 26.7°C

* An outline of this paper was presented at the 16th Annual Meeting of the Chemical Society of Japan, Tokyo, April, 1963 and will be published as a letter in *Journal of Polymer Science*.

1) V. A. Kargin, V. A. Kabanov, V. P. Zubov and I. M. Pupisov, *Polymer Sci.* U. S. S. R., **3**, 136 (1962).
2) W. Kern, H. Cherdron and V. Jaacks. *Angew. Chem.*, **73**, 177 (1961).
3) W. Kern and V. Jaacks, *J. Polymer Sci.*, **48**, 399 (1960).
4) V. Jaacks and W. Kern, *Makromol. Chem.*, **52**, 37 (1962).
5) S. Okamura, K. Hayashi and Y. Kitanishi, *J. Polymer Sci.*, **58**, 925 (1962).
6) S. Okamura, T. Higashimura and K. Takeda, *Makromol. Chem.*, **51**, 217 (1962).
7) K. Hayashi and S. Okamura, ibid., **47**, 230 (1961).
8) K. Hayashi, Y. Kitanishi, M. Nishii and S. Okamura, ibid., **47**, 237 (1961).
9) W. Wilson and H. May, *Chem. & Ind.* **1962**, p. 412.
10) O. L. Hammick and A. R. Boeree, *J. Chem. Soc.*, **121**, 2738 (1922).

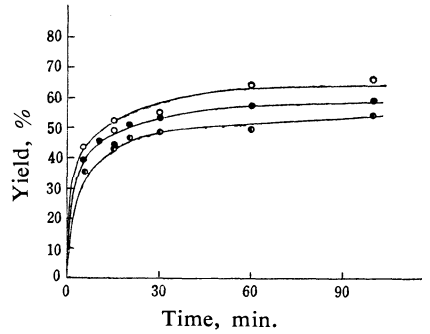


Fig. 2. Change of yield with time at various iodine concentrations at the reaction temperature of 34.2°C.
○ I_2: 0.67 wt. %
● I_2: 0.33 wt. %
◐ I_2: 0.13 wt. %

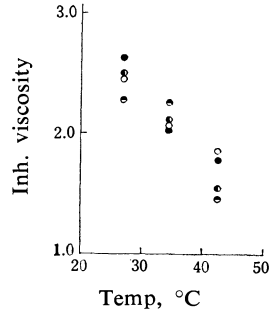


Fig. 3. Change of inherent viscosity with temperatures. Weight % of iodine is 0.67%.
○ Polym. time 5 min.
◐ Polym. time 15 min.
◓ Polym. time 60 min.
● Polym. time 120 min.

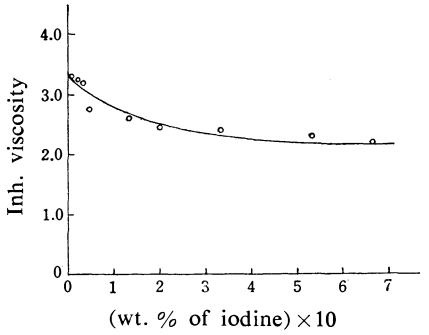


Fig. 4. Change of inherent viscosity with weight % of iodine. Reaction temperature is 34.2°C.

TABLE I

Iodine conc. wt. %	Polym. time min.	Polym. temp. °C	Yield %	η_{inh}	Softening temp. °C
0.67	5	42.2	57.6	1.85	184~186
0.67	10	42.2	64.2	1.57	183~186
0.67	15	42.2	66.9	1.43	184~186
0.67	30	42.2	72.3	1.44	184~186
0.67	60	42.2	78.2	1.78	184~186
0.67	100	42.2	78.6	1.48	184~186
0.67	5	34.2	43.0	2.02	184~187
0.67	15	34.2	48.4	2.05	184~187
0.67	15	34.2	51.1	2.11	184~187
0.67	30	34.2	55.0	2.12	184~187
0.67	60	34.2	63.8	2.26	184~187
0.67	100	34.2	66.9	2.56	184~187
0.67	5	26.7	35.5	2.44	184~187
0.67	15	26.7	39.2	2.20	185~187
0.67	15	26.7	44.3	2.27	184~187
0.67	30	26.7	39.0	2.44	184~187
0.67	60	26.7	54.1	2.29	184~187
0.67	100	26.7	54.2	2.61	184~187
0.33	5	34.2	39.8	2.43	184~187
0.33	10	34.2	44.8	2.51	184~187
0.33	15	34.2	44.9	2.39	184~187
0.33	20	34.2	50.5	2.44	184~187
0.33	30	34.2	52.8	2.39	184~187
0.33	60	34.2	56.5	2.47	184~187
0.33	100	34.2	59.0	2.52	184~187
0.33	5	26.7	34.2	2.47	184~187
0.33	10	26.7	39.2	3.28	186~188
0.33	15	26.7	40.1	3.49	185~188
0.33	20	26.7	41.4	3.23	185~188
0.33	30	26.7	43.3	3.53	184~188
0.33	60	26.7	46.7	3.50	184~188
0.33	100	26.7	48.2	3.79	186~189
0.13	5	26.7	35.8	2.74	184~183
0.13	15	26.7	42.6	2.72	184~186
0.13	20	26.7	46.2	3.08	184~186
0.13	30	26.7	48.6	2.57	184~188
0.13	60	26.7	49.2	2.97	184~186
0.13	100	26.7	53.7	2.71	184~186
0.67	30	34.2	55.6	2.22	184~186
0.53	30	34.2	54.1	2.31	184~186
0.33	30	34.2	52.8	2.39	184~186
0.20	30	34.2	48.3	2.44	184~186
0.13	30	34.2	43.3	2.57	184~186
0.046	30	34.2	41.4	2.72	184~186
0.033	30	34.2	40.1	3.19	184~186
0.020	30	34.2	38.7	3.23	184~186
0.007	30	34.2	36.8	3.31	184~186

by the 30-minute reaction.

The temperature-rise of the reaction system measured by a thermister placed into the ampoule with an internal diameter of 1.8 cm. and a height of 4.0 cm. is shown in Fig. 5. The temperature of the reaction system is not constant during the polymerization, rather, it reaches a constant temperature within 3~4 min. after the ampoule is placed into the thermostat.

By ESR measurements of the reaction system at room temperature, the spectra shown in Fig. 6 are obtained. After opening the ampoule, the intensity of the spectra decreases with time.

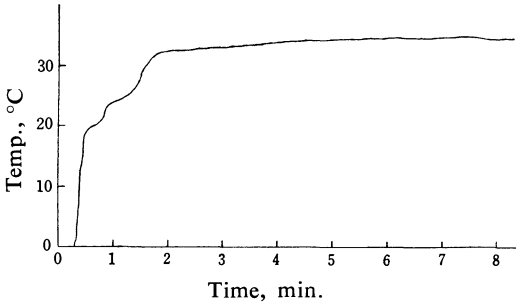


Fig. 5. Temperature change of the reaction system with time.
Reaction temperature; 34.2°C

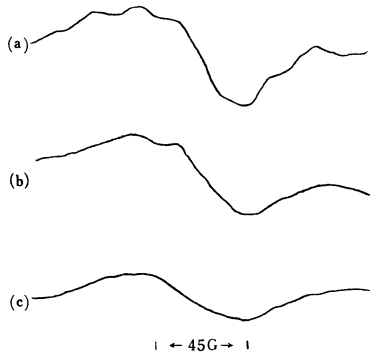


Fig. 6. ESR spectra of reaction mixture.
a) during the polymerization,
b) 10 minutes after the ampoule is opend,
c) 2 days after the ampoule is opend.

Although the ampoule is usually cooled with liquid nitrogen (−196°C) when both trioxane and iodine are sublimed into the ampoule, a higher condensation temperature may be obtained by using other freezing mixtures. As Table II shows, a small quantity of polymer is obtained even at 0°C, but the polymerization yield decreases as the condensation temperature increases. Therefore, all measurements are conducted at the condensation temperature of −196°C.

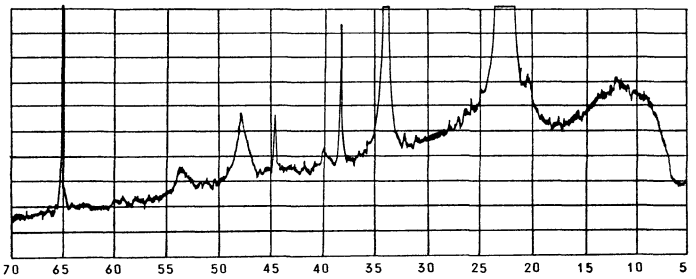


Fig. 7a. X-ray diffraction patterns of polymer obtained by the present method.

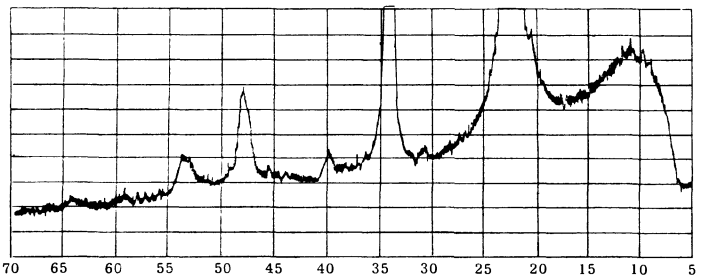


Fig. 7b. X-ray diffraction pattern of polymer made without using iodine.

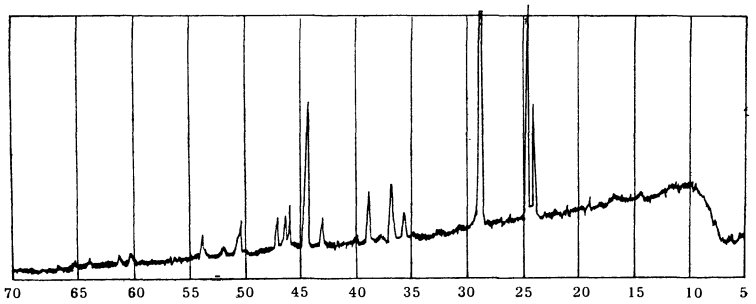


Fig. 7c. X-ray diffraction patterns of iodine.

TABLE II. POLYMERIZATION YIELDS AT VARIOUS CONDENSATION TEMPERATURES

Condensation temp., °C	Yield, %
−196	53.0
− 66	27.7
− 52	25.5
− 31	11.4
− 18	5.0
0	2.5

Here, the iodine concentration is 0.067 weight %, the polymerization time is 30 min., and the polymerization temperature is 42.2°C.

On the other hand, concerning the polymerization temperature (i. e., the temperature of the thermostat), the results shown in Table III are obtained.

TABLE III. POLYMERIZATION YIELDS AT VARIOUS POLYMERIZATION TEMPERATURES

Polymerization temp., °C	Yield
0	none
10	trace
15	26.8
20	32.6
23	42.8
26.7	49.0

Here, the iodine concentration is 0.67 weight %, and the reaction time is 30 minutes. From this result, it is obvious that the polymerization starts in the neighbourhood of 10°C.

No polymerization occurs in the liquid phase when 0.1 g. of iodine and 1.5 g. of trioxane are dissolved into 10 cc. of a solvent such as benzene or ethylene dichloride and heated to 40°C.

In order to confirm that the simultaneous sublimation is absolutely necessary, trioxane is placed into the ampoule first, without sublimation, and then iodine is sublimed into the ampoule. Table IV compares two methods where the iodine concentration is 0.67 weight %, the reaction time is 15 min., and the reaction temperature is 34.2°C.

TABLE IV. A COMPARISON OF TWO METHODS, WITH AND WITHOUT THE SIMULTANEOUS SUBLIMATION OF TRIOXANE

Method	Yield
Simultaneous sublimation	49.2%
Without sublimation of trioxane	trace

Also, in order to confirm whether the initiation of the polymerization occurs in the gas phase or in the solid phase, the alternating sublimations, wherein iodine vapor is removed during the sublimation of trioxane and trioxane vapor is removed during the sublimation of iodine, are compared with simultaneous sublimation in Table V. Here, the iodine concentration is 0.67 weight %, the reaction temperature is 34.2°C, and the reaction time is 30 minutes.

TABLE V. A COMPARISON OF ALTERNATING SUBLIMATION WITH SIMULTANEOUS SUBLIMATION

Method	No. of alterating repetitions	Yield
Alternating sublimation	2	49.4%
	6	52.0
Simultaneous sublimation	—	52.3

From this table, it is obvious that the polymerization does not start in the gas phase.

The inherent viscosity and softening temperature are also shown in Table I. The inherent viscosity is much higher than that (usually 1∼2) of polyoxymethylene obtained by conventional methods. Also, the X-ray diffraction patterns of the polymer obtained by the present method, of the polymer made without using iodine, and of the iodine are shown in Fig. 7. Obviously, a new peak is observed at the diffraction angle of 65°.

Discussion

Since the temperature of the polymerization system reaches the constant temperature after 3∼4 min., as Fig. 5 shows, the polymerization rates have been obtained from the slope of the curves after 4 minutes in Figs. 1 and 2, and the dependence of these rates upon the concentrations of monomer, iodine and polymer has been examined. Thus, it is found that the polymerization rate, V, is proportional to $[C]^{0.25}[M]^2/[P]^2$, as is shown in Fig. 8, where [M], [C] and [P] are weight percentages of the monomer, iodine and the polymer respectively. From the slope of the straight lines

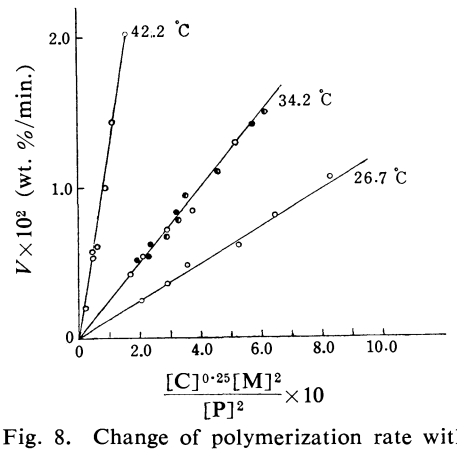


Fig. 8. Change of polymerization rate with $[C]^{0.25}[M]^2/[P]^2$.
○ I_2: 0.67 wt. %
● I_2: 0.33 wt. %
◐ I_2: 0.13 wt. %

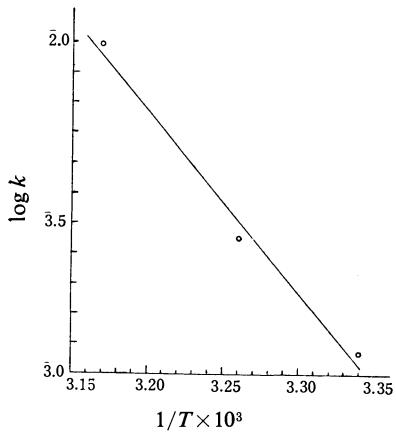


Fig. 9. Arrhenius' plot of $\log k$ via $1/T$.

in Fig. 8, the rate constants at various temperatures are obtained by means of the following equation;

$$V=k[C]^{0.25}[M]^2/[P]^2$$

From the Arrhenius' plot of $\log K$ via $1/T$ shown in Fig, 9, the activation energy is found to be ca. 29 kcal./mol.

According to Kargin et al.,[1] the initiation takes place in the gas phase for the monomer-metal system, but in the solid phase for the monomer-salt and monomer-oxide systems. In our experiment, initiation occurs obviously in the solid phase. This may be due to some crystal defects or dislocations, as has been suggested by Kargin et al.,[1] Bamford et al.[11] and Semenov.[12] As Table II shows, the polymerization yield decreases as the condensation temperature increases. This result may be explained as follows by using their hypothesis. Since the rate of sublimation decreases as the condensation temperature increases, it is expected that number of crystal defects or dislocations produced by simultaneous sublimation will become smaller at a higher condensation temperature and that, therefore, the rate of polymerization will decrease.

The fact that the polymerization system must be heated up to 10°C for the reaction to occur suggests that the favorable orientation of the monomer is necessary for the chain propagation. According to the NMR measurements of Okamura et al.,[13] the movement of the trioxane monomer becomes active about 20°C. Therefore, there is a possibility that this kind of movement causes the orientation favorable to the polymerization. The obtained activation energy of 29 kcal./mol. is large compared with the activation energy of 5 kcal./mol.[14] in the in-source radiation polymerization of trioxane, but it is small compared with the 40 kcal./mol.[15] in the post radiation polymerization. Morawetz[16] obtained the activation energy of 25 kcal./mol. for the post-irradiation polymerization of acrylamide and considered this value to be the activation energy of the propagation step. Taking these results into account, our activation energy might correspond to that of the propagation step.

The ESR spectra shown in Fig. 6 are very close to those obtained by the radiolysis of commercial polyoxymethylene.[17] On the other hand, the results of X-ray diffraction suggest the existence of some interaction between iodine and the polymer. Therefore, it is very difficult to find whether active species of the initiating polymerization are produced from trioxane or from iodine, and no conclusive mechanism can be obtained from the above-described results. The existence of a free radical proved by ESR measurement and the inhibition of polymerization by air, oxygen and other radical scavengers do not support the radical mechanism conclusively. For this purpose, a quantitative agreement between kinetical data and ESR data is necessary. At present, the authors prefer to explain this reaction by assuming that the initiation of the polymerization takes place in association with crystal dislocations or defects caused by the simultaneous sublimation and that the propagation step starts somewhere between 0°C and 15°C.

Summary

It has been found that the polymerization of trioxane occurs in the solid state by subliming the monomers and iodine simultaneously on a cooled surface and raising the temperature over 10°C. This method gives a polymer of a high degree of polymerization in a good yield. As a result of chemical kinetic treatments, the polymerization rate has been found to be proportional to $[C]^{0.25}[M]^2/[P]^2$, where [C], [M] and [P] are the concentrations of iodine, the monomer and the polymer respectively. The reaction mechanism has been discussed in

11) C. H. Bamford, G. C. Eastmond and J. C. Ward, *Proc. Roy. Soc.*, **271**, 357 (1963).
12) N. N. Semenov, *J. Polymer Sci.*, **55**, 563 (1961).
13) K. Hayashi, K. Kamata, H. Yoshida, M. Nishii, Y. Nakase, K. Hayashi and S. Okamura, The 11th Symposium of the High Polymer Society of Japan, Osaka, Nov., 1962.
14) K. Hayashi and S. Okamura, The International Symposium on Radiation-Induced Polymerization and Graft-copolymerization, Columbus, Ohio, Nov., 1962.
15) K. Hayashi, Y. Nakase, H. Ochi, M. Nishii and S. Okamura, The 15th Annual Meeting of the Chemical Society of Japan. Kyoto, April, 1962.
16) F. A. Fadner and H. Morawetz, *J. Polymer Sci.*, **45**, 475 (1960).
17) M. Kashiwagi, unpublished work.

connection with the results of ESR and X-ray measurements.

The authors wish to express their thanks to Dr. Y. Kurita and Mr. Heisaburo Iguchi for their help in the ESR measurements to Dr. Yukio Kinoshita and Messrs. Toshio Mizushima and Masamichi Nakamura for their help in the X-ray diffraction measurements, and to Mr. Atsushi Takeda for his help in the experiment.

Basic Research Laboratories
Toyo Rayon Co., Ltd.
Tebiro, Kamakura

Monolayer Studies of the Interactions between Histidyl Polypeptides and Metal Ions. I. The Effect of Cupric Ions on the Monolayer Properties of Histidyl Polypeptides

By Takuya YAMASHITA* and Toshizo ISEMURA

(Received September 11, 1963)

The histidyl residue in protein is a very important binding site for metal ions because of the reactivity of its imidazole group.[1] It was found in our laboratory that bacterial-α-amylase interacts strongly with metal ions such as copper, zinc and mercury, and that the interaction of cobalt ions with this enzyme is rather weaker.[2] The combination of metal ions has been studied with imidazole[3,4] and with 4-methylimidazole[5] as model substances of the histidyl residue. Patchornik et al.[6] synthesized poly-L-histidine and found that it forms insoluble complexes with various heavy metals.

Monolayer technique appears to be a useful way to investigate the interaction of protein with metal ions, as has been shown by the monolayer studies of the mineral tanning of proteins.[7,8] Schulman and Dogan[7] have found that copper ions do not react with the carboxyl group but with imidazole in the protein monolayer. We have attempted, by using a monolayer technique, to study the interaction of poly-L-histidine with cupric and other biologically-important metal ions in order to investigate the metal binding property of the histidyl residue in protein. Poly-L-histidine, however, could not be spread as a monolayer, even on a subphase containing 40% ammonium sulfate or on subsolutions containing cupric sulfate at various concentrations, probably because of the strong hydrophility of its side chains. Thus, poly-1-benzyl-L-histidine was chosen as a model substance in the present experiments for studying the interaction of metal ions with the histidyl group, as it could form stable films at the air/water interface. The monolayer of copoly-2:2:2:1-(glycine, *O*-benzyl-DL-serine, β-benzyl-L-aspartate, 1-benzyl-L-histidine) were also studied.

Experimental

Poly-1-benzyl-L-histidine and copoly-2 : 2 : 2 : 1-(glycine, *O*-benzyl-DL-serine, β-benzyl-L-aspartate, 1-benzyl-L-histidine), which were synthesized by the polymerization of the *N*-carboxyanhydrides of their corresponding amino acids, were supplied by Professor Junzo Noguchi of Hokkaido University. The spreading solutions were made by dissolving the former in 0.05 N hydrochloric acid and the latter in a mixture of dichloroacetic acid and benzene (1 : 4, v/v). The concentration of these polymers in solutions was about 0.25 mg./ml.

The Wilhelmy hanging-plate method was found inadequate for the present experiments because the surface of the glass plate became remarkably water-repellent, probably because of the adsorption of poly-1-benzyl-L-histidine onto the plate. Therefore, the surface pressure was measured using a float-type surface balance. In order to avoid the contamination by metal ions in the trough, a trough

* Present address: Department of Chemistry, Faculty of Science, Osaka University, Kita-ku, Osaka.

1) F. R. N. Gurd and P. B. Wilcox, "Advance in Protein Chemistry," Vol. 11, Academic Press, New York (1956), p. 311.
2) K. Kakiuchi, S. Kato and T. Isemura, unpublished results.
3) J. T. Edsall, G. Felsenfeld, D. S. Goodman and F. R. N. Gurd, *J. Am. Chem. Soc.*, **76**, 3054 (1954).
4) R. B. Martin and J. T. Edsall, ibid., **80**, 5053 (1958).
5) Y. Nozaki, F. R. N. Gurd, R. F. Chen and J. T. Edsall, ibid., **79**, 2123 (1957).
6) A. Patchornik, A. Berger and E. Katchalski, ibid., **79**, 5227 (1957).
7) J. H. Schulman and M. Z. Dogan, *Discussions Faraday Soc.*, **16**, 158 (1954).
8) K. G. A. Pankhurst, "Surface Phenomena in Chemistry and Biology," Pergamon Press, London and New York (1958), p. 100.

made of poly(methyl methacrylate) was used, the rim of which was coated with purified paraffin.

The surface viscosity was measured by the rotatory oscillation of a disk on the surface of the liquid; it was calculated by the following formula;[9]

$$\eta_s = \Delta\lambda_{10} \frac{2.303I}{2\pi P}\left(\frac{1}{a^2}-\frac{1}{b^2}\right)$$

where I is the moment of inertia of the disk; P, the period of oscillation; $\Delta\lambda_{10}$, the difference between the logarithm decrements of the oscillation in the presence of film and in its absence; a, the radius of the disk, and b, the radius of the film surrounding the oscillation disk. In the apparatus used in the present experiments, I was 31.0 g. cm., P was 13.18 sec., a was 1.00 cm., and b was 3.01 cm.

The surface potential was measured by the vibrating-electrode method. The surface moment, μ, was calculated from the surface potential, ΔV, utilizing the Helmholtz formula, $\mu = \Delta V A/4\pi$, where A is the area.

The compression of the film was started 20 min. after the polypeptides had been spread. All the experiments were carried out at room temperature. The fluctuation of the temperature, however, never exceeded one degree during the course of the experiments. The pH of the subsolution was measured by a Horiba M-3 glass electrode pH-meter.

An acetate buffer consisting of 0.1 M sodium acetate and 0.1 M acetic acid in an appropriate ratio was used as the subsolution in some cases.

Results

The effects of potassium chloride, sodium sulfate and sodium acetate (0.1 M acetate buffer, pH 5.6) on the surface pressure-area (Π-A) relationship of the monolayer of poly-1-benzyl-L-histidine are shown in Fig. 1.

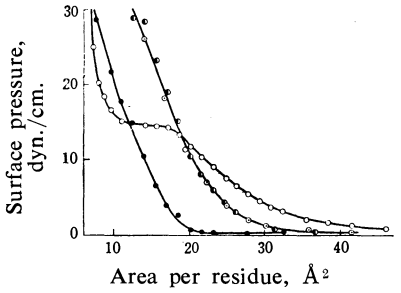


Fig. 1. Surface pressure-area curves of poly-1-benzyl-L-histidine on distilled water (●), 0.1 M potassium chloride (◐), 0.01 M sodium sulfate (⊙) and 0.1 M acetate buffer (pH 5.6, ○): 20°C.

Potassium sulfate (0.01 M, not shown in the figure) gave a Π-A curve identical with that on 0.01 M sodium sulfate. The limiting area per residue, which was determined from the minimum compressibility of the film, was found to be 16.0 Å² for the film on distilled water, a value similar to those for such nonionic polypeptides as poly-DL-phenylalanine (15.6 Å²).[10] The presence of salts in the subsolution resulted in the expansion of the film, which suggests a more horizontal orientation of the side chains. The effect of the acetate ion is very specific. The film expands on the acetate subsolution more than on other salts, such as potassium chloride and sodium sulfate. There appears a plateau region between 12 and 18 Å² per residue in the Π-A curve. The addition of 0.1 M potassium chloride (not shown in Fig. 1) to a 0.1 M acetate buffer had no influence upon the Π-A relationship on the 0.1 M buffer solution.

The effect of cupric sulfate on the poly-1-benzyl-L-histidine monolayer is shown in Fig. 2, together with those of potassium chloride and sodium sulfate. On 0.01 M cupric sulfate, the area per residue is much larger than on 0.1 M potassium chloride, though the film is somewhat more condensed than on 0.01 M cupric sulfate.

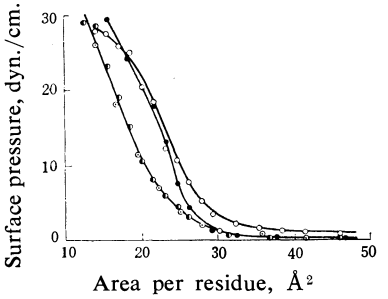


Fig. 2. Effect of cupric sulfate on poly-1-benzyl-L-histidine monolayer at 20°C: ○, 0.01 M cupric sulfate; ●, 0.1 M potassium chloride containing 0.01 M cupric sulfate; ◐, 0.1 M potassium chloride; ⊙, 0.01 M sodium sulfate.

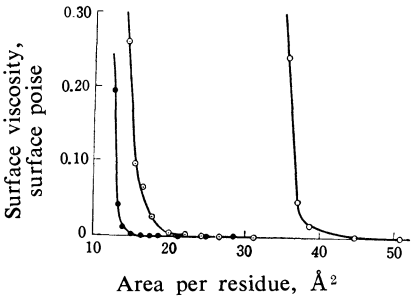


Fig. 3. Surface viscosity-area curves of poly-1-benzyl-L-histidine on distilled water (●), 0.01 M potassium sulfate (⊙) and 0.01 M potassium sulfate containing 0.01 M cupric sulfate (○): 16°C.

9) L. G. Feurt and W. D. Harkins, *J. Phys. Chem.*, **42**, 897 (1938).

10) T. Yamashita and T. Isemura, This Bulletin, **35**, 929 (1962).

Figure 3 shows the surface viscosity-area (η_s-A) curves of this polypeptide on distilled water, on 0.01 M potassium sulfate and on 0.01 M cupric sulfate containing 0.01 M potassium sulfate. The influence of cupric sulfate is markedly different from that of potassium sulfate. The area where the surface viscosity appears is quite large compared with those on distilled water and potassium sulfate. The results shown in Figs. 2 and 3 suggest that the influence of cupric ions on the monolayer properties of poly-1-benzyl-L-histidine differs from that of alkali salts.

The Π-A curves of poly-1-benzyl-L-histidine on the subsolutions at various concentrations of cupric sulfate, in the absence and in the presence of acetate ions, are shown in Figs. 4 and 5 respectively. In both cases, the Π-A relations are affected markedly by a change in the concentration. The plateau of the Π-A curve found on the acetate buffer disappeared upon the addition of cupric ions. The maximum effect of cupric ions was found to be at the concentration of 0.01 M, whether acetate ions are present or not.

The effect of the concentration of cupric

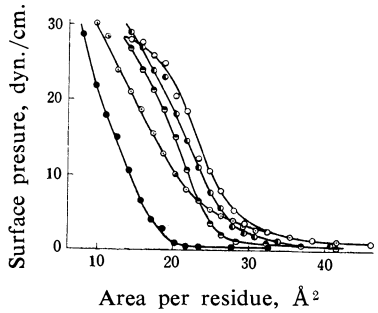


Fig. 4. Effect of the concentration of cupric sulfate on the surfrace pressure-area relation of poly-1-benzyl-L-histidine at 20°C: ●, distilled water; ◓, 0.0001 M; ◐, 0.001 M; ○, 0.01 M; ⊙, 0.05 M.

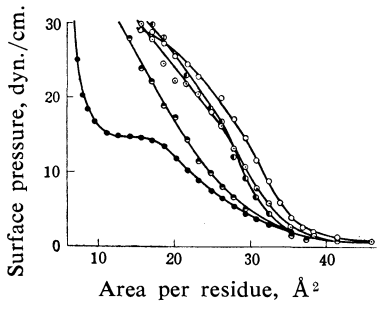


Fig. 5. Effect of the concentration of cupric sulfate dissolved in 0.1 M acetate buffer (pH 5.6) on the surface pressure-area relation of poly-1-benzyl-L-histidine at 20°C: ●, 0 M (control); ◓, 0.0001 M; ◐, 0.001 M; ○, 0.01 M; ⊙, 0.05 M.

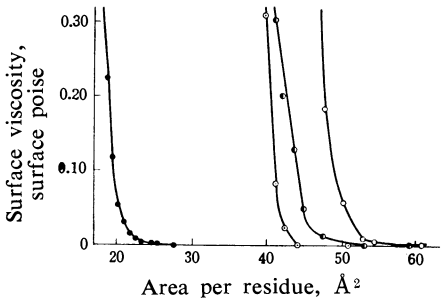


Fig. 6. Effect of the concentration of cupric sulfate dissolved in 0.1 M acetate buffer (pH 5.6) on the surface viscosity-area relation of poly-1-benzyl-L-histidine at 13.5°C: ●, 0 M (control); ◐, 0.001 M; ○, 0.01 M; ⊙, 0.05 M.

sulfate in the subphase of the 0.1 M acetate buffer (pH 5.6) on the η_s-A relation of the poly-1-benzyl-L-histidine monolayer is represented in Fig. 6. The surface viscosity was detected over a much larger area where the surface pressure is considerably lower than in the absence of the cupric ion. The maximum effect of cupric sulfate was found at the concentration of 0.01 M, just as in the case of the Π-A relation.

The surface potential-area (ΔV-A) and the surface moment-area (μ-A) curves of poly-1-benzyl-L-histidine on a 0.1 M acetate buffer (pH 5.6) containing 0.01 M cupric sulfate are compared with those on a copper-free subsolution in Fig. 7.

In the presence of the cupric ion, the surface potential and the surface moment increased more than in its absence in the larger-area region. The surface moment of the film on the subsolution containing the copper ion was higher by about 50 mD in the horizontal portion of the μ-A curve than that on the acetate buffer without the cupric ion.

The effect of the cupric ion on the film properties of this polypeptide is summarized in Table I. It is evident that the interaction

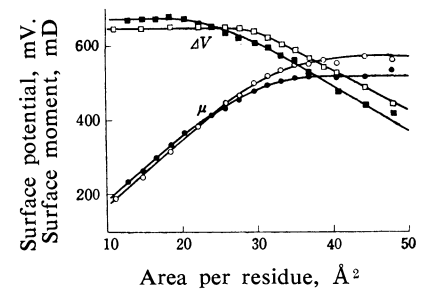


Fig. 7. Surface potential-area and surface moment-area curves of poly-1-benzyl-L-histidine on 0.1 M acetate buffer (pH 5.6; ■, ●) and on 0.1 M acetate buffer containing 0.01 M cupric sulfate (pH 5.6; □, ○): 12°C.

TABLE I. THE EFFECT OF THE CUPRIC ION ON THE SURFACE VISCOSITY, THE SURFACE POTENTIAL AND THE SURFACE MOMENT OF POLY-1-BENZYL-L-HISTIDINE

Subphase	Area at 0.05 surface poise Å²/res.	Π at 0.05 surface poise dyn./cm.	ΔV 35Å²/res. mV.	ΔV 45Å²/res. mV.	μ** mD
Distilled water	13.0	13.6			
0.01 M K_2SO_4	16.6	26.1			
0.01 M $CuSO_4$ in 0.01 M K_2SO_4	37.0				
0.1 M acetate (pH 5.6)	20.4	12.0	546	428	516
$CuSO_4$* 0.001 M	45.0	0.85			
$CuSO_4$* 0.01 M	50.6	0.86	580	484	568
$CuSO_4$* 0.05 M	41.9	1.0			

* Dissolved in 0.1 M acetate buffer (pH 5.6).
** Values at the linear portion of Π-A curves.

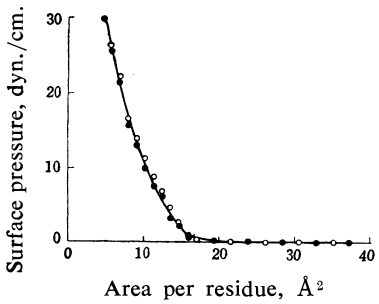


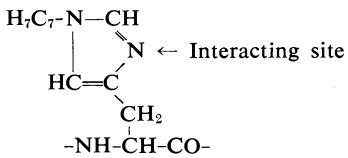
Fig. 8. Surface pressure-area curves of copoly-2 : 2 : 2 : 1-(glycine, *O*-benzyl-DL-serine, β-benzyl-L-aspartate, 1-benzyl-L-histidine) on distilled water (○) and on 0.01 M cupric sulfate (●) at 16°C.

of cupric sulfate with poly-1-benzyl-L-histidine differs from that of alkali salts.

The Π-A curves of copoly-2 : 2 : 2 : 1-(glycine, *O*-benzyl-DL-serine, β-benzyl-L-aspartate, 1-benzyl-L-histidine) on distilled water and on 0.01 M cupric sulfate are shown in Fig. 8. No effects were found with cupric sulfate. 0.05 M potassium chloride and 0.01 N hydrochloric acid also did not affect the Π-A relation of this copolypeptide.

Discussion

As has been described in the preceeding section, cupric sulfate and univalent alkali salts differ significantly in the nature of their interaction with a histidine-containing polypeptide, poly-1-benzyl-L-histidine, although in both cases the interacting site is at the nitrogen atom in the 3-position of the benzylimidazole group,



When cupric sulfate is present in the subsolution, the film expands much more than in the presence of alkali salts. The difference between the effects of alkali salts and cupric sulfate is pronounced in the surface viscosity-area relations. If the cupric ion is present in the subsolution, surface viscosities appear over larger areas and, accordingly, at lower surface pressures than in their absence. Therefore, there might be two types of interaction between poly-1-benzyl-L-histidine and salts: (1) interaction with alkali salts, and (2) interaction with divalent metal salts.

Interaction with Alkali Salts.—On the basis of his study of the properties of long chain amines on aqueous solutions at different pH values, Adam[11] pointed out that the pH's of the subsolution seem to be of little importance in the acid subsolution, and that the films were very much affected by anions in buffer solutions. He concluded that the amines form salts with anions. A similar conclusion was also reached by Hoffman et al.[12]

Patchornik et al.[6] found that a dilute aqueous solution of poly-1-benzyl-L-histidine containing hydrochloric acid gave precipitates of polyvalent salts with various alkali salts. This fact suggests a probable combination of the poly-1-benzyl-L-histidine monolayer with the chloride, sulfate and acetate ions, as in the case of long chain amine monolayers. The salts would be formed between positively-charged benzylimidazolium groups of this polypeptide and anions. Consequently, the film expands on the alkali salt subsolutions more than on distilled water, because the side chains probably take a more horizontal orientation because of the decrease in their hydrophility.

The effect of acetate ions is anomalous.

11) N. K. Adam, *Proc. Roy. Soc.*, **A 126**, 526 (1930).
12) E. J. Hoffman, G. E. Boyd and A. W. Ralston, *J. Am. Chem. Soc.*, **64**, 498 (1942).

Adam[11] found that the monolayer of long chain amine acetate has much less lateral adhesion than that of amine chloride. The monolayer of the salt of poly-1-benzyl-L-histidine with the acetate ion might have much less lateral adhesion than that with chloride or sulfate, which causes a greater expansion and a reorientation of its side chains resulting in the plateau in the Π-A curve.

Interaction with Divalent Metal Salts. — The pronounced effect of the cupric ion on the film properties of poly-1-benzyl-L-histidine can hardly be interpreted in terms of mere interaction between film and anion. A strong interaction exists between the monolayer and the cupric ion. It has been found that the zinc, cobaltous and calcium ions also interact with the poly-1-benzyl-L-histidine monolayer. The results will be reported on in a subsequent paper.

Schulman and Dogan[7] have found a stronger interaction of the copper ion with methemoglobin than with serum albumin in the monolayer, the former having more histidyl groups in its molecule. Patchornik et al.[6] reported that poly-L-histidine forms insoluble complexes with copper, silver, magnesium, mercury, zinc and cobalt. It thus seems reasonable to assume a formation of complexes of poly-1-benzyl-L-histidine with the cupric ions through the nitrogen atoms in the 3-position of benzylimidazole groups. The assumption could possibly be supported by the fact that the surface viscosity of the film appears over a much larger area and at a lower surface pressure in the presence of the cupric ion than in its absence.

It has been found in the mineral or vegetable tanning of protein monolayers that the cross-linkage structure is formed between molecules at the surface, accompanying a remarkable increase in surface viscosity.[13] A similar structure can be considered between poly-1-benzyl-L-histidine molecules as a result of complex formation, which is responsible for the large area over which surface viscosity is first detected. The formation of cross-linkage has been reported also for a protein monolayer reacting with silicic acid.[14][15]

The fact that the surface potential and the surface moment increase more in the presence of the cupric ion than in its absence seems to be another evidence for the formation of complexes. The cationic groups are revealed in the interaction of cupric ions with the poly-1-benzyl-L-histidine monolayer. A similar fact is found to be true in a gelatin monolayer tanned with basic chromium sulfate.[13]

The maximum effect of the cupric ion was found at 0.01 M, above which the area of the monolayer decreased whether acetate ions were present or not, as Figs. 4 and 5 show. It has been found that the coordination ratio of imidazole[3] or 4-methylimidazole[5] to copper decreases from the maximum (4 : 1) with an increasing concentration of the cupric ion. By analogy with this, the number of benzylimidazole groups which associate with a copper ion in subsolution seems to be four at its maximum value and to decrease with an increase in the ion concentration. The decrease may result in the weakening of the cross-linkage structure and may account for the decreases in the areas in Π-A and η_s-A relations.

In contrast with poly-1-benzyl-L-histidine, the monolayer of copoly-2 : 2 : 2 : 1-(glycine, *O*-benzyl-DL-serine, β-benzyl-L-aspartate, 1-benzyl-L-histidine) is not affected by the presence of cupric sulfate in the subsolution. This copolymer contains only 14% of a benzylhistidyl residue, so the polynuclear complexes with copper can be formed only with difficulty.

Summary

The effects of salts on the monolayer properties of poly-1-benzyl-L-histidine and copoly-2 : 2 : 2 : 1-(glycine, *O*-benzyl-DL-serine, β-benzyl-L-aspartate, 1-benzyl-L-histidine) have been investigated.

In the presence of potassium chloride, sodium sulfate, and sodium acetate (pH 5.6), the film expansion has been observed; this has been interpreted in terms of the salt formation between side chains and anions. The addition of cupric sulfate to a subsolution causes the film to expand to increase in surface viscosity and potential, for which cross linkage by complex formation between side chains and metal ions might be responsible.

On the other hand, the monolayer of the copolymer is not affected by the presence of cupric sulfate because of the smaller content of histidyl residue.

The authors wish to express their hearty thanks to Professor Junzo Noguchi of Hokkaido University for supplying them with valuable samples.

Institute for Protein Research
Osaka University
Kita-ku, Osaka

13) S. C. Ellis and K. G. A. Pankhurst, *Discussions Faraday Soc.*, **16**, 170 (1954).
14) S. G. Clark, P. F. Holt and C. W. Went *Trans. Faraday Soc.*, **53**, 1500 (1957).
15) S. G. Clark and P. F. Holt, ibid., **53**, 1509 (1957).

*Flammulin, an Antitumor Substance**

By Yumi WATANABE, Koji NAKANISHI, Nobuhiko KOMATSU, Tomohei SAKABE and Hirofumi TERAKAWA

(Received September 16, 1963)

From the aqueous extract of fruit bodies of *Flammulina velutipes*, an edible mushroom, a high molecular weight substance with antitumor qualities against the Ehrlich ascites tumor was isolated by Komatsu et al.[1] and designated "flammulin."

The present paper deals with a procedure for flammulin's purification, some of its physical and chemical properties, and its amino acid composition.

Although the separation of the active component from the material is rendered very difficult by its unstable properties, considerable purification was achieved by the combination of ammonium sulfate fractionation and ethanol fractionation in the cold. Preliminary experiments showed that the precipitates obtained at 66% ammonium sulfate saturation and 75% ethanol were active, while the precipitates, obtained at 50% ethanol were inactive. Further purification was carried out by ion exchange chromatography using DEAE-Sephadex and CM-Sephadex columns. The active component was not bound to DEAE-Sephadex equilibrated with 0.02 M phosphate buffer at pH 7.0. The active fraction, purified on a DEAE-Sephadex column, seemed to be still contaminated with a small amount of colored impurities, and zone electrophoresis on starch showed that it consisted of two or more components, as Fig. 1 shows. Therefore, it was chromatographed on a CM-Sephadex column equilibrated with a 0.005 M acetate buffer at pH 5.6 eluted step by step with 0.01 M, 0.05 M, 0.1 M, and 0.2 M acetate buffers, and separated into two fractions, active and inactive, as is shown in Fig. 2. The active fraction was subjected to rechromatography on a CM-Sephadex column under gradient elution from a 0.005 M to a 0.1 M acetate buffer and then eluted with about a 0.08 M concentration, as Fig. 3 shows. The purified flammulin by chromatography was dialysed against cold tap water and lyophilized. The lyophilization often caused a slight denaturation, but lyophilized flammulin was obtained in an almost colorless state in an average yield of about 120 mg. from 2 kg. of dried fruit bodies. The final fractionation scheme for 2 kg. of the material is given in Scheme 1.

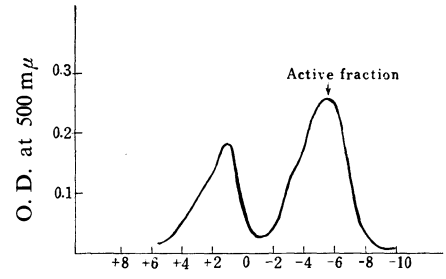


Fig. 1. Zone electrophoresis of partially purified flammulin.
(pH 8.6, μ=0.05, Veronal buffer)

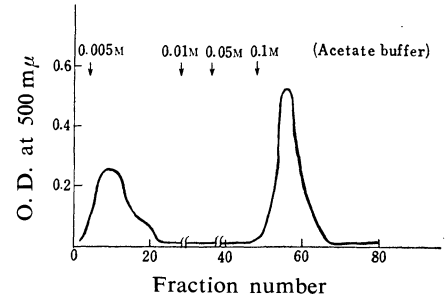


Fig. 2. Chromatogram of partially purified flammulin on CM-Sephadex.

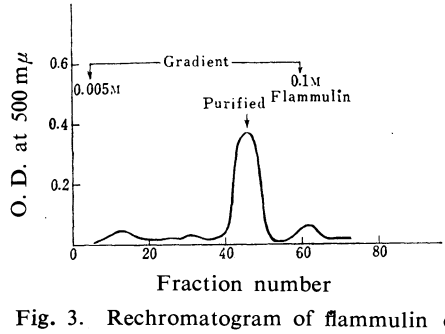


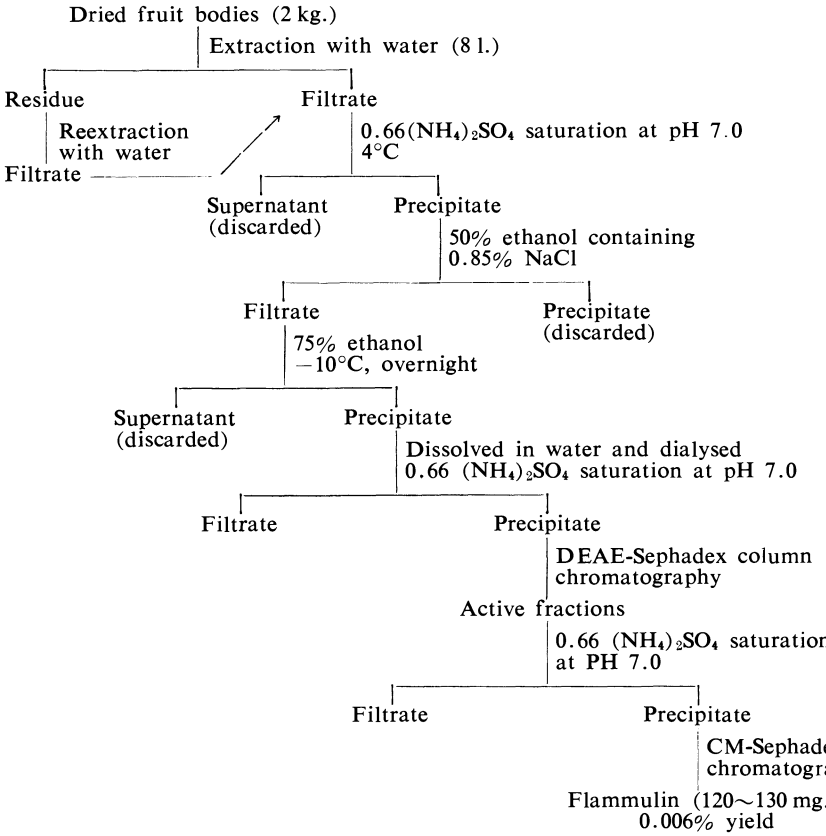
Fig. 3. Rechromatogram of flammulin on CM-Sephadex.

Flammulin purified as above works against the Ehrlichascites tumor when administered at the daily dose of 2.5 γ per mouse.

The purity of lyophilized flammulin was determined by moving boundary electrophoresis, paper electrophoresis, and sedimentation, it was found to be homogeneous in all

* Reported at the 16th Annual Meeting of the Chemical Society of Japan, Tokyo, April, 1963.

1) N. Komatsu, H. Terakawa, K. Nakanishi and Y. Watanabe, *J. Antibiotics, Ser. A.* **16** (3), 139 (1963).



Scheme 1. Purification procedure of flammulin.

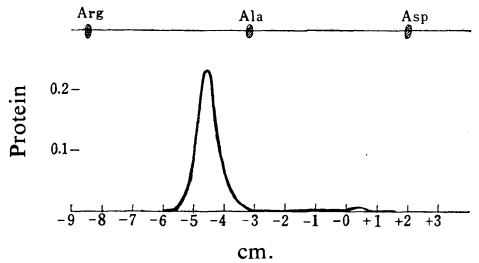


Fig. 4. Paper electrophoresis of flammulin.

these analyses. On the moving boundary electrophoresis, flammulin yielded a single homogeneous peak with a descending mobility of 0.87×10^{-5} cm^2/sec. V. Upon paper electrophoresis at pH 7.0, flammulin moved toward the cathode and showed a single symmetrical peak, as is shown in Fig. 4. The same single bands were obtained on paper electrophoresis over the range from pH 4.6 to 12, and the relative position to the standard amino acids seemed to be unchanged. The sedimentation pattern of flammulin showed only a single symmetrical boundary, indicating that it was homogeneous. The calculated values of the sedimentation and diffusion coefficients were found to be $s_{20w}=2.5$s and $D_{20w}=9.93\times10^{-7}$ cm^2/sec. respectively, figures of which indicate a molecular weight of 24000. The aqueous solution of flammulin shows a typical protein ultraviolet absorption, with the maximum at 277 mμ and the minimum at 251~252 mμ. The nitrogen content of 16.2%, as determined by the micro-Dumas method, is a general value for proteins. Some physical properties are summarized in Table I.

Amino acid analyses of the acid hydrolysates of flammulin were performed on paper chromatography and with an automatic amino acid analyzer; the average results of three separate analyses for the relative stable amino acids are summarized in Table II. The analytical results show that an almost complete liberation of the constituent amino acids was obtained during the first 24-hr. hydrolysis. Since a partial decomposition with an increase in the time of hydrolysis occured with aspartic acid, threonine, serine and proline, the values for these amino acids were corrected for the losses by linear extrapolation to zero time. Similarly, ammonia was found to increase with an increase in the time of hydrolysis, so the value was corrected in the same way as above. As is clear in Table II, flammulin

TABLE I. SOME PROPERTIES OF FLAMMULIN

Electrophoretic mobility ($\mu=0.1$, descending)	0.87×10^{-5} cm²/sec. V. (pH 7.7)
Sedimentation coefficient	$S_{20w}=2.5$ s
Diffusion coefficient	$D_{20w}=9.93\times10^{-7}$ cm²/sec.
Molecular weight	24000
Nitrogen content	16.2%
UV-absorption	$\lambda_{max}=277$ mμ
	$\lambda_{min}=251\sim252$ mμ

TABLE II. AMINO ACID COMPOSITION

Amino acid	Amino acid residue per 100 g. protein g.	Amino acid per 100 g. protein g.	N as % of total N	Calcd. No. of residue for mol. wt. 24000	No. of residue to nearest integer
Lys	2.42	2.76	3.27	4.54	5
His	2.73	3.09	5.16	4.78	5
Arg	9.08	10.13	20.12	13.97	14
Asp	17.60	20.35	13.70	36.72	37
Thr	8.30	9.78	7.10	19.72	20
Ser	4.35	5.25	4.32	12.00	12
Glu	9.50	10.83	6.36	17.68	18
Pro	7.60	9.01	6.76	18.80	19
Gly	5.20	6.84	7.88	21.89	22
Ala	10.17	12.75	12.37	34.38	34
Half-cys	1.28	1.51	1.08	3.02	3
Val	2.12	2.51	1.85	5.14	5
Met	0	0	0	0	0
isoLeu	2.86	3.32	2.18	6.08	6
Leu	4.21	4.88	3.22	8.94	9
alloisoLeu	0.33	0.38	0.25	0.70	1
Tyr	2.50	2.78	1.32	3.69	4
Phe	5.14	5.77	3.02	8.39	8
Try	0.62	0.68	0.28	0.82	1
Amide NH_3	1.80*	1.80*	9.16	25.41	25*
Total	97.48	112.24	99.71	—	222

* Omitted from the total.

contained all of the common amino acids except methionine, and no new amino acid composition; this indicates that flammulin is a simple protein composed of only common amino acids. *N*-Terminal amino acid analysis was carried out according to the procedure of Sanger.[2] In chromatography only a single spot of DNP-amino acid was obtained at the position corresponding to DNP-valine. Flammulin is characterized by its high content of aspartic acid and alanine, but the basic properties of flammulin suggest that the carboxyl groups of aspartic acids are masked in the form of amide as well as peptide linkages.

Experimental

The Determination of Antitumor Activity and Protein. — The activity of all the fractions in the purification procedure were assayed by in vivo experiments, using Ehrlich ascites tumor of mice, while the protein contents were determined by the Folin reaction,[3] using the absorption at 500 mμ.

The Extraction of the Active Substance. — Fruit bodies of *Flammulina velutipes* were air-dried and extracted with water (8 l. for 2 kg.) three times in the cold, and aqueous extracts were fractionated.

Fractionation with Ammonium Sulfate and Ethanol. — All fractionations were carried out in the cold to avoid denaturation; ethanol fractionations, especially, were done below −5°C. Ammonium sulfate fractionation was performed by adding solid ammonium sulfate to the aqueous solution while stirring it in the cold.

Chromatographic Purification. — The preparation of DEAE-Sephadex and CM-Sephadex columns and the chromatographic procedure were carried out according to the general method of Sober et al.[4] About one gram of DEAE-Sephadex A-50 was used for the extract from 2 kg. of dried fruit bodies. To the dialysed flammulin solution, a one-tenth volume of 0.2 M phosphate buffer was added at pH 7.0. The effluent was collected in 2 ml. fractions with an automatic fraction collector, and the

2) F. Sanger, *Biochem. J. (London)*, **39**, 507 (1945).

3) O. H. Lowry, N. J. Rosenbrough, A. L. Farr and R. J. Randall, *J. Biol. Chem.*, **193**, 265 (1951).

4) H. A. Sober, F. G. Gutter, M. M. Wyckoff and E. A. Perterson, *J. Am. Chem. Soc.*, **78**, 756 (1956).

activity and the protein were measured as has been described above. The active fractions were collected, dialysed, and adsorbed on a CM-Sephadex C-50 column equilibrated with 0.005 M acetate buffer at pH 5.6; the concentration of buffer was changed step by step. The effluent was treated in the same way as above. The crude flammulin preparation obtained in the above chromatography was subjected to rechromatography, using a gradient elution system—one chamber filled with 125 ml. of a 0.005 M, and the other, with 125 ml. of a 0.3 M acetate buffer. The other procedures were the same as have been described above. The purified flammulin was then dialysed and lyophilized.

Electrophoresis. — Moving-boundary electrophoresis was carried out at 8°C for two hours in a phosphate buffer (μ=0.1, pH 7.7) using the Tiselius electrophoresis apparatus. Paper electrophoresis was carried out over the range from pH 4.6 to 12 under the following conditions:

Buffer system: 1/10 M-phosphate or 1/10 M-Veronal-Na-HCl, 1/10 M-Veronal-Na-NaOH.
Filter paper: Toyo-Roshi No. 51, 14.5×35 cm.
Voltage: 300 V./35 cm. (5 mamp.)
Temperature and time: 20°C, 3 hr.

After electrophoresis, the paper was colored with a B. P. B. solution. The excess dye was thoroughly washed out, and the paper was dried and cut off in 0.5 cm. widths. These were then eluted with 3 ml. of a 0.01 N sodium hydroxide aqueous solution, and the protein content was determined from the optical density at 590 mμ. Some amino acids were run under the same conditions, and the positions were detected with ninhydrin.

Sedimentation. — The lyophilized sample of flammulin was dissolved in a phosphate buffer of pH 7.2, μ=0.1, and this solution was subjected to sedimentation. Sedimentation experiments were conducted in a Spinco model E ultracentrifuge at 59780 r.p.m., and the observed sedimentation coefficient was corrected to the value in water at 20°C (s_{20w}) in the conventional manner.

Diffusion. — The diffusion measurements were made with a 0.25% solution in a 1/10 M sodium bicarbonate-carbonate buffer solution (pH 9.75) at 20°C with a Spinco model H diffusion apparatus. The diffusion coefficient was also determined by applying the gel diffusion method of Allison.[5]

Amino Acid Analyses. — The Acid Hydrolysis of Flammulin. — Flammulin (10 mg.) was hydrolysed with 1 ml. of 6 N hydrochloric acid or 0.5 ml. of 12 N hydrochloric acid in a sealed tube at 110°C for 10 to 45 hr. At the end of the hydrolysis period, the hydrolysate was concentrated to dryness on a steam-bath, to remove the excess hydrochloric acid, and finally dried over sodium hydroxide in vacuo.

Amino Acid Composition — The amino acid analyses of the hydrolysated flammulin were performed by two-dimensional paper chromatography (*n*-butanol - acetic acid - water, phenol - water) and with a Beckman-Spinco model 120 automatic amino acid analyser.

Analyses of Tryptophane.[6,7] — To 3 to 5 mg. of flammulin in 1 ml. of water, 30 mg. of dimethylaminobenzaldehyde in 9 ml. of 21.4 N sulfuric acid were added. The solution was allowed to stand at 25°C for 12 hr. in the dark and treated with 0.1 ml. of a freshly-prepared 0.4% sodium nitrite aqueous solution; then, after it had been kept standing for another 30 min. in the dark, the optical density at 580 mμ was measured. The tryptophane content was determined from the standard curve after correction for the blank value.

N-Terminal Amino Acid. — Lyophilized flammulin (10 mg.) was dinitrophenylated in 66% ethanol (3 ml.) containing 8 mg. of 2,4-dinitrofluorobenzene and 10 mg. of sodium bicarbonate at room temperature for 10 hr. The acid hydrolysis of DNP-flammulin was carried out in 1 ml. of 6 N hydrochloric acid at 105°C for 12 hr. The ether-soluble DNP-amino acids were subjected to two-dimensional paper chromatography using *n*-butanol saturated with 2 N ammonium hydroxide as the first solvent and a 1.5 M phosphate buffer as the second solvent. DNP-alanine was used as the standard.

Summary

(1) Flammulin, an antitumor substance of *Flammulina velutipes*, has been demonstrated to be a basic simple protein with a molecular weight of about 24000 and to be homogeneous in electrophoresis and sedimentation.

Analyses of amino acids indicated the following composition:

Lys_5, His_5, Arg_{14}, Asp_{37}, Thr_{20}, Ser_{12}, Glu_{18}, Pro_{19}, Gly_{22}, Ala_{34}, Half-cys_3, Val_5, Met_0, $isoLeu_6$, Leu_9, alloisoLeu$_1$, Tyr_4, phe_8, Try_1, $(CONH_2)_{25}$.

The authors wish to express their thanks to Dr. Nobuhiko Kasai of the Institute for Infectious Dieseases, the University of Tokyo, for the Tiselius electrophoresis analyses, to Dr. Susumu Yamamoto for the sedimentation analyses, and to Takeda Pharmaceutical Industries for the collection of the material. We also wish to acknowledge a grant from the Waksman Foundation.

Department of Chemistry
Tokyo Kyoiku University
Otsuka, Tokyo (*Y. W.*)

Department of Chemistry
Tohoku University
Katahira-cho, Sendai (*K. N*)

The Institute for Infectious Diseases
The University of Tokyo
Minato-ku, Tokyo (*N. K.*)

Department of Chemistry
Nagoya University
Chikusa-ku, Nagoya (*T. S.*)

Biological Institute
Tokyo Medical and Dental University
Bunkyo-ku, Tokyo (*H. T.*)

5) A. C. Allison and J. H. Humphrey, *Immunology*, 3, 95 (1960).

6) J. R. Spies and D. C. Chamber, *Anal. Chem.*, 20, 30 (1948).

7) J. R. Spies and D. C. Chamber, ibid., 21 1249 (1949).

NOTES

New Routes for the Preparation of 5, 6-Epoxy-6-methylcholestan-3β-ols

By Michio SHIOTA, Misako NOHIRA* and Misako KAWAMOTO**

(Received September 30, 1963)

The reaction of 3β-acetoxy-6-methylcholest-5-ene with monoperphthalic acid has been shown to afford 5α, 6α-epoxide and 5β, 6β-epoxide.[1,2] The present paper will describe new routes to these epoxides.

The acetylation of 3β-acetoxy-6-methyl-5α-cholestan-5, 6β-diol[1] with acetic anhydride and *p*-toluenesulfonic acid at room temperature gave a diacetate (I), which in turn afforded 5, 6α-epoxy-6-methyl-5α-cholestan-3β-ol when refluxed with alcoholic potassium hydroxide. This reaction is analogous to the formation of 5β, 6β-epoxides from 3β, 5, 6β-triacetoxy-5α-steroids,[3] and it has been inferred that the diacetate I is 3β, 6β-diacetoxy-6-methyl-5α-cholestan-5-ol, because the configuration at C_5 is retained in the course of the epoxide formation.

3β-Acetoxy-5-fluoro-5α-cholestan-6-one[4] reacted with methylmagnesium iodide to give 5, 6β-epoxy-6-methyl-5β-cholestan-3β-ol. 3β-Acetoxy-5-chloro-5α-cholestan-6-one[5] also gave 6-methyl-5β, 6β-epoxide, but the reaction of 3β-acetoxy-5-bromo-5α-cholestan-6-one[6] with methylmagnesium iodide afforded 3β-hydroxy-5α-cholestan-6-one[7].

Experimental***

3β, 6β-Diacetoxy-6-methyl-5α-cholestan-5-ol (I).—A solution of 43.1 mg. of *p*-toluenesulfonic acid monohydrate in 6.5 ml. of acetic anhydride was warmed on a water-bath at 90°C for 10 min. and then cooled to room temperature. 3β-Acetoxy-6-methyl-5α-cholestane-5,6β-diol (113.0 mg.) was added to the solution, and the resultant suspension was stirred at room temperature to give a clear reaction mixture in 1 hr. Stirring was continued for another hour, and then the solution was allowed to stand at room temperature overnight. The reaction mixture was treated with water, and the crystalline material which precipitated was collected by filtration. Recrystallization from methanol gave 63.7 mg. of the product (m. p. 137.5~138°C). Additional recrystallization from methanol raised the melting point to 138.5~139°C. $[\alpha]_D$ −26° (*c* 1.03, chloroform). The product gave no yellow color with tetranitromethane and showed hydroxyl absorption in its infrared spectrum. Analysis produced results which agreed with the formula of a diacetate.

Found: C, 73.93; H, 10.60. Calcd. for $C_{32}H_{54}O_5$: C, 74.09; H, 10.49%.

3β-Acetoxy-5, 6α-epoxy-6-methyl-5α-cholestane.—A solution of 41.6 mg. of I and 60 mg. of potassium hydroxide in 2 ml. of absolute ethanol was heated under reflux for 2 hr. The solvent was removed under reduced pressure, and the product was extracted with ether. When the ethereal solution was washed with water a neutral reaction occurred. The removal of the solvent from the dried solution (sodium sulfate) afforded a jelly residue, which was acetylated with acetic anhydride and pyridine at room temperature to give 32.7 mg. of a crystalline, acetylated product (m. p. ca. 142~143°C). Recrystallization from methanol gave 20.7 mg. of 3β-acetoxy-5, 6α-epoxy-6-methyl-5α-cholestane as needles (m. p. 139.5~140°C and 150.5~151°C (double melting points)). The epoxide was identified by the mixed melting point test with an authentic sample. (Found: C, 78.77; H, 11.02%).

3β-Acetoxy-5, 6β-epoxy-6-methyl-5β-cholestane (II).—To a solution of methylmagnesium iodide prepared from 700 mg. of methyl iodide, 116 mg. of magnesium and 11 ml. of absolute ether, 360 mg. of 3β-acetoxy-5-fluoro-5α-cholestan-6-one was added in 9 ml. of absolute ether at 0°C. The reaction mixture was heated under reflux for 2 hr. The solution was treated with an ammonium chloride solution, and the ethereal solution was worked up in the usual way. An oily residue (277 mg.) was

* Present address: Tokyo Institute of Technology, Meguro-ku, Tokyo.

** Present address: Dainippon Celluloid Co. Ltd., Central Research Laboratory, Oi-mura, Iruma-gun, Saitama-ken.

1) M. Shiota, *J. Chem. Soc. Japan, Pure Chem. Sec.* (*Nippon Kagaku Zassi*), **75**, 1217 (1954).

2) M. Davis and G. H. R. Summers, *J. Chem. Soc.*, **1960**, 4707.

3) M. Davis and V. Petrow, ibid., **1949**, 2536; L. F. Fieser and M. Fieser, "Steroids," Reinhold Publishing Corporation, New York (1959), p. 198.

4) H. B. Henbest and T. I. Wrigley, *J. Chem. Soc.*, **1957**, 4765.

*** All melting points are uncorrected.

5) S. Mori, *J. Chem. Soc. Japan* (*Nippon Kwagaku Kwaisi*), **64**, 981 (1943).

6) D. R. James and C. W. Shoppee, *J. Chem. Soc.*, **1954**, 4224).

7) Cf. M. S. Kharasch and O. Reinmuth, "Grignard Reactions of Nonmetallic Substances," Prentice-Hall, Inc., New York (1954), p. 189.

acetylated with acetic anhydride and pyridine at room temperature to afford 280 mg. of a crystalline, acetylated product (m. p. 75~82°C). Filtration through alumina, followed by recrystallization from methanol, gave 196 mg. of 3β-acetoxy-5, 6β-epoxy-6-methyl-5β-cholestane (m. p. 93.5~94.5°C), $[\alpha]_D$ 0° (*c* 1.60, chloroform). (lit.,[2] m. p. 95~95.5°C, $[\alpha]_D$ −2° (*c* 0.94, chloroform)).

Found: C, 78.26; H, 10.72. Calcd. for $C_{30}H_{50}O_3$: C, 78.55; H, 10.99%.

In the attempted reaction carried out at −70°C[8] to obtain 5α-fluoro-6-methyl-6-ol, the starting material was recovered almost quantitatively.

The hydrolysis of II with alkali afforded a free alcohol (m. p. 131~131.5°C) (lit.,[2] m. p. 133~135°C).

Reactions of the Epoxide II.—The reduction of 50 mg. of II with 50 mg. of lithium aluminum hydride in 15 ml. of absolute ether at the boiling point of the reaction mixture afforded 13.4 mg. of 6-methyl-5α-cholestan-3β, 6β-diol[9] (m. p. 191°C).

The hydrolytic cleavage of 49 mg. of II with a 5% solution of phosphomolybdic acid in acetone[10] gave 48 mg. of crude 3β-acetoxy-6-methyl-5α-cholestan-5, 6β-diol (m. p. ca. 185°C). Recrystallization from methanol raised the melting point to 191.5~192.5°C.

These reactions confirm that the epoxide II is 6-methyl-5β, 6β-epoxide.

3β-Acetoxy-5α-cholestan-6-one from 3β- Acetoxy-5-bromo-5α-cholestan-6-one. — 3β-Acetoxy-5-bromo-5α-cholestan-6-one (144 mg.) in 9 ml. of absolute ether was allowed to react with a Grignard reagent prepared from 240 mg. of methyl iodide, 44 mg. of magnesium and 5 ml. of absolute ether for one hour at the boiling point of the reaction mixture. The solution was then worked up in the usual way to give 113 mg. of a semicrystalline residue. The residue was acetylated with acetic anhydride and pyridine at room temperature, and the resultant oily product was crystallized from methanol. The crystalline product (54.8 mg., m. p. ca. 108°C) was recrystallized from methanol to give 25.6 mg. of 3β-acetoxy-5α-cholestan-6-one[11] (m. p. 127.5~128°C). The product was identified by the mixed melting point test and its infrared spectrum.

The authors wish to express their thanks to the Ministry of Education for its grant-in-aid for Fundamental Scientific Research.

Chemical Laboratory
Ochanomizu University
Bunkyo-ku, Tokyo

8) Cf. J. W. Cornforth, R. H. Cornforth and K. K. Mathew, *J. Chem. Soc.*, **1959**, 112.

9) L. F. Fieser and J. Rigaudy, *J. Am. Chem. Soc.*, **73**, 4660 (1951).

10) M. Sawai, Presented at the 10th Annual Meeting of the Chemical Society of Japan, Tokyo, April, 1957.

11) A. Windaus, *Ber.*, **36**, 3754 (1903).

A New Alumina Hydrate, "Tohdite" ($5Al_2O_3 \cdot H_2O$)

By Goro YAMAGUCHI, Hiroaki YANAGIDA and Shuitiro ONO

(Received November, 15, 1963)

A new crystal of alumina hydrate has been found by the present authors during an investigation into the hydrothermal reactions of the system aluminum oxide-water.[1] This crystal has been studied by various methods, such as X-ray diffraction, electron diffraction, differential thermal analysis, infrared absorption and polarizing microscopy, and has been proved to be a new alumina hydrate. The formula obtained is $5Al_2O_3 \cdot H_2O$. The species Tohdite is named for the Tokyo Daigaku (The University of Tokyo), where the present investigation was carried out.

Method of Preparation

An appropriate amount of aluminum hydroxide, boehmite AlOOH or gibbsite $Al(OH)_3$, was weighed in a silver capsule of the Morey-type autoclave, and a dilute aqueous solution of aluminum fluoride was added to fill about 80% of the reaction vessel. The autoclave was heated at 450~500°C in an electric furnace for 20~100 hr. The reaction was completed under these experimental conditions. Corundum was found to be useful as the seed crystals, and the new formed hydrate to be useful for the same purpose in the subsequent runs. Aluminum fluoride or titanium (IV) sulfate was effective as the mineralizer.

Properties

Crystallographic Forms and Optical Properties.—The new hydrate, Tohdite, occurs as thin hexagonal plates up to a few microns in thickness when aluminum fluoride is used as the mineralizer (Fig. 1). The crystal form is changed into needles when titanium sulfate is

1) G. Yamaguchi, H. Yanagida, S. Ono, S. Koyanagi and S. Wada, Presented at the 16th Annual Meeting of the Chemical Society of Japan, Paper No 1F08 (Tokyo, April, 1963).

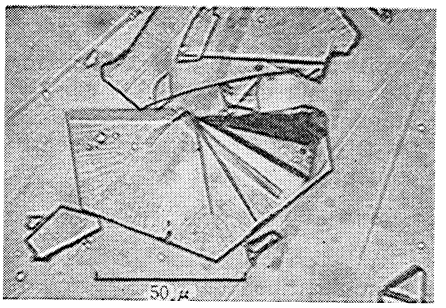


Fig. 1 The new alumina hydrate crystals.

added. Tohdite is uniaxial negative with $\omega=1.738\sim1.748$, $\omega-\varepsilon<0.01$, the c-axis being perpendicular to the plate.

Density.—The density was determined to be 3.72 ± 0.02 g./cm^3.

Thermal Analysis. — Differential thermal analysis was performed up to 1000°C. An endothermic peak was observed between 800 and 900°C, corresponding to the dehydration of Tohdite. The dehydrated form was identified with κ-alumina by X-ray diffraction. The water content, as determined from the weight loss, was about 3.6%. The value calculated for $5Al_2O_3\cdot H_2O$ is 3.42%.

Infrared Absorption Spectra.—The existence of crystalline water was confirmed by the infrared absorption spectra. The absorption band found at 3240 cm^{-1} can be assigned to the stretching frequency for OH groups.

X-Ray Investigations. — The X-ray powder pattern shown in Fig. 2 was recorded on a diffractometer using filtered CuK_α radiation. On the basis of the resemblance of the pattern to that of κ-alumina, this pattern was unmistakably indexed on the hexagonal unit cell with

$$a=5.576\text{Å} \text{ and } c=8.768\text{Å}.$$

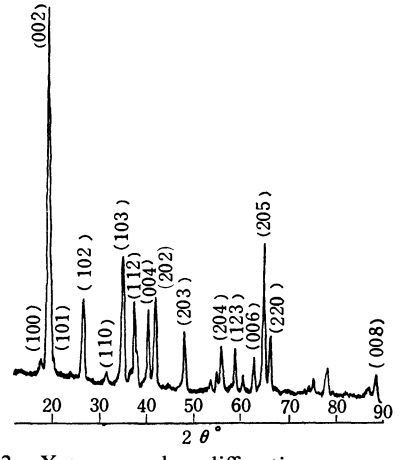


Fig. 2. X-ray powder diffraction pattern of the new hydrate using CuK_α radiation.

TABLE I. X-RAY DIFFRACTION DATA

hkl	d-observed	d-calculated
100	4.85	4.8286
002	4.38	4.3840
101	4.23	4.2296
102	3.246	3.2458
110	2.788	2.7878
103	2.500	2.5003
200	2.416	2.4143
112	2.352	2.3524
201	2.329	2.3277
004	2.192	2.1920
202	2.1146	2.1148
203	1.8614	1.8614
122	1.6854	1.6849
105	1.6482	1.6482
204	1.6232	1.6229
123	1.5479	1.5480
302	1.5105	1.5105
006	1.4609	1.4613
205	1.4190	1.4188
220	1.3939	1.3939
222	1.3283	1.3278
132	1.2809	1.2808
125	1.2650	1.2645
206	1.2499	1.2502
133	1.2173	1.2175
107	1.2124	1.2124
401	1.1966	1.1959
402	1.1639	1.1638
403	1.1158	1.1158
207	1.1121	1.1118
008	1.0960	1.0960

The diffraction data are listed in Table I.

Electron Diffraction. — The $\{hk0\}$ spots of the (0001) orientation can be seen in Fig. 3. The incident beam is perpendicular to the hexagonal plate of the crystal. The inner spots gave a d-spacing of 4.8 Å, corresponding to the (100) in Table I. The other diffraction pattern in Fig. 4 represents the periodicity along the c-axis. The beam is perpendicular to the direction of the elongated needle-like crystal, and the observed d-spacing was 4.4 Å, corresponding to the (002) in

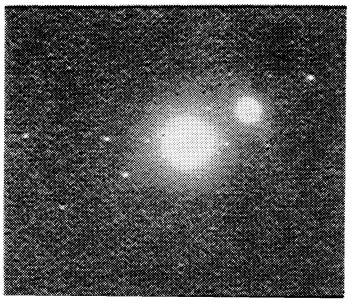


Fig. 3. N-pattern of the new hydrate (electron beam ∥ c-axis).

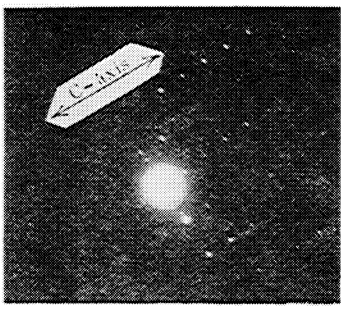


Fig. 4. N-pattern of the new hydrate (electron beam⊥c-axis).

Table I. These results may justify the hexagonal unit cell derived from the powder pattern.

Conclusion

The unit cell dimensions, taken together with the measured values of density and water content, indicate that the unit cell contains $5Al_2O_3 \cdot H_2O$. The calculated density and water content are as follows:

Density	3.71 g./cm^3
Water content	3.42%

The afore-described data seem to establish the existence of a new alumina hydrate, $5Al_2O_3 \cdot H_2O$.

Department of Industrial Chemistry
Faculty of Engineering
The University of Tokyo
Hongo, Tokyo

A Note on the Characterization of the Network Structure of the Ion-exchange Resin

By Manabu SENŌ and Takeo YAMABE

(Received December 14, 1963)

The ion-exchange resin is a crosslinked polyelectrolyte,* and the degree of crosslinking is usually designated in terms of the nominal content (weight percent) of divinylbenzene in the monomer mixture. It may be very desirable to describe the degree of crosslinking by a well-defined parameter based on the structural analysis, because it is one of the most important factors in determining the ion-exchange behavior of the resin. It is the purpose of this paper to propose a parameter, M_c, the mean molecular weight per crosslinked unit, for the characterization of the network structure of the ion-exchange resin, and to provide some information on the pore size of the resin.

The degree of crosslinking has a most remarkable effect on the swelling behavior of the resin. Unfortunately, the theory of the swelling of the network of the polyelectrolyte is not established, in spite of great efforts.[1] On the other hand, the theory of the swelling of the neutral crosslinked polymer has been demonstrated by Flory[2] and many experimental investigations have proved its validity. The final expression is:

$$-[\ln(1-v_{2m})+v_{2m}+\chi_1 v_{2m}^2] = (v_1/\bar{v}M_c)(1-2M_c/M)(v_{2m}^{1/3}-v_{2m}/2)$$

where v_{2m}, the volume fraction of the solute at the swelling equilibrium; χ_1, a parameter expressing the first-neighbor-interaction free energy, divided by kT, for the solvent with a polymer; v_1 the molar volume of the solvent; $\bar{v}$, the specific volume of polymer, and M, the molecular weight of a structural unit. The volume ratio of swelling, q_v, is defined by;

$$q_v = 1/v_{2m}$$
$$= (\text{swollen volume})/(\text{unswollen volume})$$
$$= 1+\frac{\rho_2}{\rho_1}q_w-\frac{\rho_2}{\rho_1}$$

where ρ_1 is the density of the pure solvent, ρ_2. is the density of the polymer in a solution**, and q_w is the weight ratio of the swelling.

Therefore, a characteristic parameter, M_c, of the polymer network can be obtained by the

* Most of the ion-exchange resin available commercially is prepared by the sulfonation or by the chloromethylation, followed by the amination, of the base resin of poly(styrene-divinylbenzene).

1) A. Katchalsky and I. Michaell, *J. Polymer Sci.*, **15**, 69 (1955).

2) P. J. Flory, "Principles of Polymer Chemistry," Cornell Univ. Press, New York (1953), p. 576.

** This is calculated from the density, ρ_{12}, of a polymer solution by:

$$\rho_2 = (1/q_w\rho_1\rho_{12})/\{\rho_1-\rho_{12}(1-1/q_w)\}$$

TABLE I. STRUCTURAL CHARACTERIZATION OF MATRICES OF ION-EXCHANGE RESINS

DVB nominal wt.%	Weight ratio of swelling q_w	Volume ratio of swelling q_v	M_c	n	d, Å
0.05	13.9	15.5	81800	786	6460
0.1	8.8	9.7	35500	341	1070
0.5	4.9	5.37	10200	98	315
1.0	4.1	4.36	5000	48.4	160
2.0	3.05	3.30	2630	25.3	89
4.0	2.25	2.45	1350	13.1	51.3
6.0	1.84	1.93	722	6.96	32.2
8.0	1.70	1.79	432	4.15	23.5
10.0	1.58	1.65	324	3.11	20.3
15.0	1.42	1.47	210	2.02	16.9
20.0	1.34	1.38	165	1.57	15.5

measurement of the swelling ratio of the uncharged matrix of the resin. This is a useful parameter for the theoretical consideration of the ion-exchange behavior, if the introduction of the ion-exchange groups into the resin matrix does not have any appreciable effect on the crosslinked structure of the resin.

The experimental procedure is as follows. The copolymer of styrene and divinylbenzene was prepared with benzoyl peroxide as a catalyst, by the block polymerization in the closed tubes. After purification by means of complete drying in vacuo, the polymer was cut into cylindrical rods, about 5 mm. high and 8 mm. in diameter. The weight ratio of the swelling in toluene was measured by weighing of the rods in dry and swelling-equilibrium states.

The results are shown in Table I. This value agrees well with that cited by Kressman and Millar.[3] From this, the volume ratio of the swelling and the mean molecular weight per crosslinked unit are obtained by the use of the above equations. For this, the following figures are used:

$$\rho_1=0.8716, \quad \rho_2=0.978 \ (20°C)$$

$$\bar{v}=0.952, \quad v_1=105.6, \quad \chi_1=0.38^{4)}$$

The results obtained are shown in Table I. In the same table, the mean number of styrene units per crosslinked unit, n, and the mean (maximum) pore diameter in a full-expanded state, $d=\sqrt{2}\,(2.2n+7.5)$, are also given. The latter value is in accord with Grubhofer's estimation[5] by means of a structural model consideration.

The commercial ion-exchange resins of the nominal 8% divinylbenzene are considered to have the mean available pore size of 30 Å.[6] This value is larger than the present value of 24 Å. This disagreement is probable due to the fact that the usually accepted value is based on the observations of large-ion exchange, dye adsorption and so on; therefore, the larger pores are overcounted than the smaller ones.

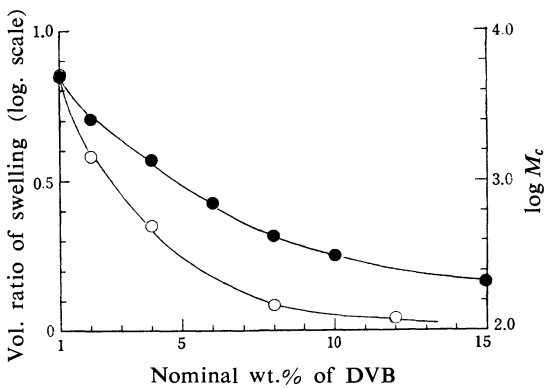


Fig. 1. The volume ratio of the swelling of ion-exchange resins (Dowex 50W, Na-form) in pure water and log M_c–DVB nominal content diagram.
-○- q_v of Dowex 50W, 20°C
-●- log M_c–DVB content

In Fig. 1, the volume ratio of the swelling of the commercially available ion-exchange resin (Dowex 50W, Na-form) in pure water[7] is shown. The ion-exchange resin with a completely dissociated counterion is in a fairly extended state. The details of this will be discussed in a separate paper.

The Institute of Industrial Science
The University of Tokyo
Azabu, Tokyo

3) T. R. E. Kressman and J. R. Millar, *Chem. & Ind.*, **1961**, 1833.
4) C. E. H. Bawn, R. F. J. Freeman and A. R. Kamaliddin, *Trans. Faraday Soc.*, **46**, 677 (1950).
5) N. Grubhofer, *Makromol. Chem.*, **30**, 96 (1959).
6) F. Helfferich, "Ion Exchange," McGraw-Hill Book Co., New York (1962), p. 132.
7) M. Senō and T. Yamabe, unpublished; C. Calmon, *Anal. Chem.*, **24**, 1456 (1952); **25**, 490 (1953).

The Formation of Formic Anhydride with N, N'-Dicyclohexylcarbodiimide

By Ichiro MURAMATSU, Michio ITOI, Masaru TSUJI and Akira HAGITANI

(Received December 14, 1964)

It has been reported that various acid anhydrides can be obtained from acids by treatment with *N, N'*-dicyclohexylcarbodiimide (DCC)[1-3] under mild conditions. This suggests the possibility of a successful dehydration of formic acid to yield formic anhydride, when DCC is used as a dehydrating reagent in an inert solvent at low temperature. Formic anhydride is unstable and has not yet been prepared by the usual method. In the present investigation, the dehydration reaction of formic acid with DCC was studied in order to ascertain the formation of formic anhydride.

When formic acid was treated with DCC in ether at room temperature, the evolution of a gas took place rapidly and the precipitate of *N, N'*-dicyclohexylurea was formed in a good yield (Eqs. 1 and 2). When the reaction was carried out below $-5°C$ in the molar ratio according to Eq. 1, no evolution of gas was observed, but the urea was formed in nearly the theoretical yield. Therefore, it was suspected that formic anhydride was formed without decomposition by this reaction.

$$2\ HCOOH + C_6H_{11}\text{-}N{=}C{=}N\text{-}C_6H_{11} \rightarrow HCO\text{-}O\text{-}COH + C_6H_{11}\text{-}NHCONH\text{-}C_6H_{11} \quad (1)$$

$$HCO\text{-}O\text{-}COH \rightarrow HCOOH + CO \quad (2)$$

To confirm the existence of formic anhydride, a part of the solvent was removed from the filtrate under reduced pressure, and the remaining liquid was added into a solution of L-leucine in formic acid or of *p*-nitrophenol in ether; *N*-formyl-L-leucine and *p*-nitrophenyl formate respectively were obtained in good yields. On the other hand, the reactions of formic acid and L-leucine or *p*-nitrophenol in the absence of DCC did not give the formyl compounds. It was concluded from these results that formic anhydride can be obtained from formic acid with DCC at a low temperature, though it has not yet been isolated.

Experimental

***N*-Formyl-L-leucine.**—Into 3.8 ml. (100 mmol.) of formic acid dissolved in 20 ml. of ether, 10.3 g. (50 mmol.) of DCC in 38 ml. of ether was added with stirring in such a way that the temperature did not exceed $-5°C$. After the stirring had been continued for 3 hr., *N, N'*-dicyclohexylurea (10.57 g., 94%) was filtered off. Most of the ether in the filtrate was removed at water-pump pressure. During these procedures the temperature of the mixture was held below $-5°C$. The residual liquid was added into a solution of 1.31 g. (10 mmol.) of L-leucine in 3 ml. of formic acid. After it had been stirred for 2.5 hr. at 0°C, the mixture was concentrated under reduced pressure. The oily residue was recrystallized from ethyl acetate. Yield, 1.27 g. (80%). M. p. 138~139°C. It was identified by comparison with *N*-formyl-L-leucine[4] [m. p. 139~141°C, $[\alpha]_D^{20}$ $-17.7°$ (*c* 4.97, ethanol)], which was obtained with formic acetic anhydride. When 1.31 g. of L-leucine was treated with 8 ml. of formic acid in the same manner without DCC, no formyl compound was yielded.

***p*-Nitrophenyl Formate.**—Nineteen grams (0.41 mol.) of formic acid was treated with 41.2 g. (0.2 mol.) of DCC in 300 ml. of ether as above. *N, N'*-Dicyclohexylurea (43.1 g., 0.192 mol.) was filtered off, and the filtrate was concentrated in an ice-salt bath under reduced pressure to a volume of 170 ml. The resulting solution was added to 9.73 g. (70 mmol.) of *p*-nitrophenol in 20 ml. of ether. Stirring was continued for 2.5 hr. at -10~0°C. After it had stood overnight at room temperature, the mixture was concentrated under reduced pressure to a syrup. Recrystallization of the residue from tetrahydrofuran gave 6.99 g. (41.8 mmol., 60%) of *p*-nitrophenyl formate; m. p. 73~74°C[5]; IR spectrum (in carbon tetrachloride): 1750, 1200, 1090 cm^{-1} (ester). The same run in the absence of DCC did not give the formate, but the *p*-nitrophenol was recovered.

Department of Chemistry
Faculty of Science
St. Paul's University
(Rikkyo University)
Toshima-ku, Tokyo

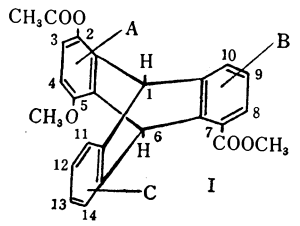
1) M. Smith, J. G. Moffat and H. G. Khorana, *J. Am. Chem. Soc.*, **80**, 6204 (1958).
2) I. Muramatsu and A. Hagitani, *J. Chem. Soc. Japan, Pure Chem. Sec. (Nippon Kagaku Zasshi)*, **80**, 1497 (1959); I. Muramatsu, ibid., **82**, 83 (1961).
3) H. Shüssler and H. Zahn, *Chem. Ber.*, **95**, 1076 (1962).
4) I. Muramatsu, M. Murakami, T. Yoneda and A. Hagitani, unpublished.
5) K. Okawa and S. Hase, This Bulletin, **36**, 754 (1963).

Confirmation of the Structures of 2-Acetoxy-5-methoxy- and 5-Acetoxy-2-methoxy-7-methoxycarbonyl-triptycenes by Means of Electric Dipole Moments

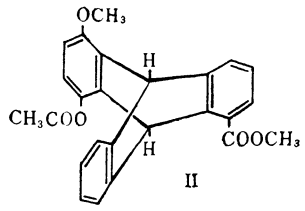
By Fumio OGURA, Yoshio TOSHIYASU,* Ko KIMURA,* Ryoichi FUJISHIRO,* and Masazumi NAKAGAWA

(Received January 24, 1964)

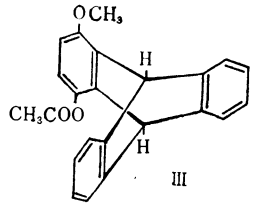
The monomethylation, followed by the acetylation, of 2, 5-dihydroxy-7-methoxycarbonyltriptycene, which was derived from 2, 5-diacetoxy-7-methoxycarbonyltriptycene,[1] afforded two isomers, I (m. p. 269~270°C) and II (m. p. 279~280°C). The deacetylation of I and II yielded the corresponding hydroxymethyl ethers. Only the hydroxy-methyl ether derived from II shows a weak infrared absorption due to an intra-molecular hydrogen bond, indicating the proximate spatial positions of the hydroxyl and methoxycarbonyl groups. On the basis of this evidence, the structures shown below have tentatively been assigned to these compounds.[2]



I



II



III

In order to confirm the structures of I and II, the present authors have measured the electric dipole moments of I and II in *p*-dioxane at 25°C, together with that of 2-acetoxy-5-methoxy-triptycene (III, m. p. 274~275°C) as a reference substance.

The polarization data of these compounds are summarized in Table I. The notations ε, v, n, ω, $p_{2\infty}$, P_2, R_D, and μ represent the dielectric constant, the specific volume, the refractive index, the weight fraction of the solute, the specific polarization, the molecular polarization, the molecular refraction for the sodium D line, and the dipole moment respectively. The dielectric data were analyzed according to the Halverstadt-Kumuler's method, and the dipole moments were obtained on the assumption that distortion polarizations are equal to $1.05\times R_D$.[3]

The estimation of the molecular dipole moments of I, II, and III was carried out on the basis of the following fundamental assumptions: 1) the additivity of the vectors of the group moments,[4] and 2) the D_{3h} symmetry of the triptycene skeleton. The values and directions of the group moments used in the calculation are given in Table II. With regard to the substituents at the 2- and 5-positions, the following three possible configurations (a, b, and c) were taken into consideration: a) both the methoxyl and acetoxyl groups lie in the same plane as that of the aromatic ring A, and the substituent groups take the cis-configuration because of the steric hindrance of the hydrogen atoms at the 1- and 6-positions;[5] b) both the methoxyl and the acetoxyl groups lie on a plane perpendicular to the plane of the aromatic ring A, and the substiuent groups take the cis- or trans-configuration; and c) the methoxyl group takes a coplanar position

* Present address: Department of Chemistry, Faculty of Science, Osaka City University, Sumiyoshi-ku, Osaka.

1) A. Sonoda, F. Ogura, and M. Nakagawa, This Bulletin, 35, 853 (1961).

2) F. Ogura and M. Nakagawa, unpublished work. The details of the synthesis, the spectral properties and the optical rotatory dispersion of these compounds will be reported elsewhere.

3) R. J. W. LeFèvre, "Dipole Moments," Methuen and Co., London (1948), p. 17.

4) C. P. Smyth, "Dielectric Behavior and Structure," McGraw Hill, New York (1955), p. 253.

5) E. A. Braude and F. C. Nachod, "Determination of Organic Structures by Physical Methods," Academic Press Inc., New York (1955), p. 408.

Table I. Polarization data in dioxane at 25°C

	I	II	III
ε	$2.2120+2.95\omega$	$2.2053+1.95\omega$	$2.2053+2.08\omega$
v	$0.97274-0.181\omega$	$0.97277-0.210\omega$	$0.97277-0.175\omega$
n^2	$2.01642+0.436\omega$	$2.01642+0.468\omega$	$2.01642+0.482\omega$
$p_{2\infty}$	0.7034 cc.	0.5402	0.5749
P_2	281.7 cc.	216.3	196.8
R_D	111.8 cc.	111.2	99.0
μ	2.84 ± 0.14D	2.21 ± 0.13	2.13 ± 0.11

Table II. Values and directions of group moments

Group	Moment (D)	Direction
Methoxycarbonyl (CH_3-O-C(=O)-)	1.83	70° with the bond between the carbon of 7-position and the carbonyl carbon.
Methoxyl (CH_3--O-)	1.25	55° with the bond between the carbon of 5- or 2-position and the oxygen atom.
Acetoxyl (CH_3-C(=O)-O-)	1.52	129° with the bond between the carbon of 2- or 5-position and the oxygen atom.

with the aromatic ring A, whereas the acetoxyl group lies on the plane perpendicular to the latter plane. Concerning the methoxycarbonyl group on carbon 7, it was assumed that the group takes a coplanar configuration with the aromatic ring B to attain the maximum mesomeric effect. Since two conformations seem to be possible, i. e., the conformation with the closest distance between the carbonyl oxygen and the hydrogen atom at the 6-position and that with the greatest distance between the above-mentioned two atoms, the notations bearing asterisk (a*, b*, c*) are employed to indicate the latter conformation. The calculated results are given in Table III. The values of the dipole moments based on the configuration b and b* are the root mean square values of the four possible configurations and turn out to be identical. The values based on c and c* are those of the two possible configurations.

Table III. Calculated dipole moments (D)

Configuration	I	II	III
a	2.92	2.09	1.68
a*	2.83	1.95	1.68
b, b*	3.27	2.55	2.29
c	2.98	2.18	2.29
c*	3.53	2.87	2.29

These calculations lead to the conclusion that the dipole moments of I are always greater than those of II for all probable configurations and that discrimination between I and II is, therefore, possible. The most satisfactory agreement with the observed values is obtained in the case of the configuration c which is supported also by the electronic spectral information on I and II.[2)]

Department of Chemistry
Faculty of Science
Osaka University
Nakanoshima, Osaka

The Influence of Heat Treatment on the Solidification Time of the Reversible Sol-Gel Transformation of Gelatin

By Hitoo KAKIYAMA and Tominosuke KATSURAI

(Received January 27, 1964)

In a previous paper it was mentioned that the solidification time of the reversible sol-gel transformation of the sols of silicic acid, of agar-agar and of gelatin is noticeably shortened by heat treatment.[1] The characteristic feature of this phenomenon can be expressed by the formula:

$$T_1 > T_2 \qquad (1)$$

where T_1=the thixotropic solidificatcn time, and
T_2=the solidification time under heat treatment.*

The term "thermopexy," on the model of rheopexy, has been suggested for this phenomenon, indicating that the gelation tendency of thixotropic sol is accelerated by heat treatment.

Lately, however, we have realized that neither the qualification nor the method of preparing the gelatin in the previous experiment was adequate and that the conclusion obtained needed to be corrected. From a comparison of the results of the reinvestigation of gelatin with the data on silicic acid and agar-agar, we came to the following conclusion on the influence of heat treatment: there are two modes in thermopexy, positive and negative, the former being the case with silicic acid and agar-agar, and the latter with gelatin.

Experimental and Discussion

The characteristics of the gelatin used in the experiment are as follows: Water content, 17% wt.; isoionic point, 4.85; viscosity, 5.7 centipoise (measured for 4.2% sol at 35°C by using an Ostwald viscosimeter); rigidity, 4.1×10^5 dyn./cm^2 (measured for the 4.2% gel obtained by keeping the sol 8 hr. at 0~1°C).

The experiments are carried out as follows. Six grams of the gelatin is put into a beaker with 400 ml. of water and is left to stand 2 hr. at room temperature. Swelling takes place. The beaker is then kept at 50°C for 30 min. The swollen gelatin turns out to be a homogeneous sol. The total weight of the sol is then made 500 g. by adding water. Thus we get the gelatin sol of the concentration 1%, i.e., 1 g. gelatin per 100 g. of the sol. Ten milliliters of the sol is put into each of the 20 test tubes, each with a radius 13.5~14 mm. The test tubes are then left to stand at room temperature (10~15°C). The sol changes into a gel which does not flow out, even when the test tube is placed upside down. All of the test tubes are shaken by hand, and the gel in them is brought into sol. The test tubes are then divided into two groups. (a) 10 test tubes are left to stand at room temperature and are used for the study of the thixotropic solidification time, T_1. (b) The other 10 test tubes are used for the study of T_2. They are put into a water bath of 50°C for 2 min. and then left to stand at room temperature; the resulting change is observed. The temperature of 50°C was chosen in order to avoid the denaturation of gelatin. The test tubes (a) and (b) are tilted one after another at certain time intervals, and the resulting decrease in fluidity is observed. The time at which the sol ceases to flow is taken as the solidification time. The average values of T_1 and also of T_2 are taken.

The influence of foreign substances was also studied. Urea and KSCN were chosen as the substances which destroy the hydrogen bond, and $KAl(SO_4)_2$ as the substance which forms bridges between gelatin molecules. The results are summarized in the following table.

Foreign substance	Concn. of the foreign substance mol./1000 g. sol	T_1 min.	T_2 min.	Concn. of sol g./100 g. sol
None	—	25	140	1
$CO(NH_2)_2$	0.1	30	170	1
	0.5	50	225	1
KSCN	0.1	25	140	1
	0	95	220	0.8
$KAl(SO_4)_2$	0.005	80	190	0.8
	0.01	50	180	0.8
	0.02	35	150	0.8

We see that in all cases

$$T_1 < T_2 \qquad (2)$$

1) T. Katsurai and K. Inouye, *Kolloid-Z.*, **142**, 162 (1955).

* For the sake of convenience T_1 is taken as the standard in this article; the change of T_2 is discussed relative to T_1.

This is just the opposite of (1). This means that the influence of heat treatment on the solidification time in the case of gelatin appears in the reverse (or negative) direction as compared with the case of silicic acid and that of agar-agar. Repeated experiments with the same sample gave the same result. Although both T_1 and T_2 increase with the rise in room temperature, relation 2 is still satisfied.

The presence of urea in the sol increases T_1 and T_2. If the concentration of urea exceeds 1 M per 1000 g., the sol does not set into a gel and it becomes impossible to carry out the experiment. In the case of KSCN, the experiment becomes difficult when the concentration exceeds 0.5 M per 1000 g. because of the enormous increase in solidification time. The presence of $KAl(SO_4)_2$ in the sol greatly decreases T_1 and T_2. Thus the experiment was carried out with a sol of a smaller concentration and a small amount of the salt.

The 7th Division
Government Chemical and Industrial Research Institute
Hiratsuka, Kanagawa (H. K.)

Pilot Laboratory
Hiratsuka, Kanagawa (T. K.)

SHORT COMMUNICATIONS

The Polarography of 3, 6-Anhydro-galactose

By Teruko FUJIWARA, Kensaku MORIHARA and Choji ARAKI

(Received September 16, 1963)

As 3, 6-anhydro-galactose is so unstable in acid that it decomposes readily to 5-hydroxymethyl furfural and then to levulic acid and formic acid, it is difficult to obtain this sugar by the methods usually used for the hydrolysis of polysaccharides. Using methanolysis, Araki and Hirase[1,2] first isolated the dimethyl acetal of this sugar and thus confirmed the natural occurrence of anhydro-sugars. Later O'Neil and Stewart[3] developed an indirect procedure for the detection of anhydro-sugars in polysaccharides. This procedure was based on the fact that, when polysaccharide is treated with N/50 sulfuric acid, only anhydro-sugar is converted to 5-hydroxymethyl furfural, and the latter can be determined photometrically. Because the pyranose ring of 3, 6-anhydro-sugar tends to open, giving aldehyde much more easily than do any other hexoses, the authors applied a polarographic method in studies of this sugar. In polarographic studies of various monosaccharides, Cantor and Peniston[4] reported that reduction waves could be detected with ketoses, even in 10^{-3} M in a phosphate buffer. On the other hand, under the same conditions as aldoses, these could only be at much higher concentrations, such as 10^{-1} M. Our studies of 3, 6-anhydro-L-galactose (AG)* and agarobiose (AGB)**, 4-D-galactopyranosyl-anhydro-L-galactose, showed that these compounds showed perceptible waves in the neutral and basic range, even in 10^{-3} M. (Fig. 1); this character was different from that of other aldoses. AG showed triplet and AGB, double waves; in each case, only the last wave changed in height with a change in pH value, (Fig. 2). To judge from the results of

1) C. Araki, *J. Chem. Soc. Japan (Nippon Kwagaku Kwaisi)*, **65**, 725 (1944).
2) C. Araki and S. Hirase This Bulletin, **26**, 463 (1944); **27**, 109 (1954).
3) A. N. O'Neil and D. K. R. Stewart, *Can. J. Chem.*, **34**, 1700 (1956).
4) S. M. Cantor and Q. P. Peniston. *J. Am. Chem. Soc.*, **62**, 2113 (1940).

* Hydrolyzate of 3, 6-anhydro-L-galactose dimethylacetal with N/50 H_2SO_4 at 100°C for 1hr. Concentration: 1.87×10^{-3} M. The 3, 6-Anhydro-L-galactose dimethylacetal (b. p. 158~160°C/0.023 mmHg $[\alpha]_D^{15}$ −28.7 (H_2O) used was prepared from agarobiose dimethylacetal by Araki (1).

** Hydrolyzate of agarobiose dimethylacetal (m. p. 165~166°C $[\alpha]_D^{15}=-29.3$, H_2O) with N/50 H_2SO_4 at 100°C for 1hr.). Concentration: 1.36×10^{-3} M.

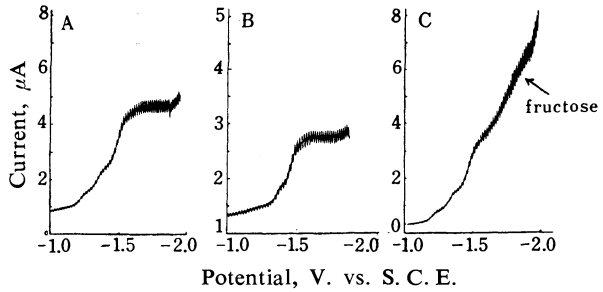


Fig. 1. Polarograms of anhydro-sugars at pH 9.0 (0.2 M NH_3-NH_4Cl buffer).

A) 3,6-Anhydro-L-galactose, 5.3×10^{-3} M, 3rd wave: $E_{1/2}=-1.42$ V, $i_d=1.77$ μA.
B) Agarobiose, 1.36×10^{-3} M, 2nd wave: $E_{1/2}=-1.38$ V, $i_d=0.66$ μA.
C) A mixture of 3,6-anhydro-L-galactose (4.8×10^{-3} M) and D-fructose (4.1×10^{-3} M), 3rd wave: $E_{1/2}=-1.42$ V, $i_d=1.44$ μA.

The procedures were carried out at 20~25°C using a Shimadzu RP-2 type polarograph. The capillary had an *m*-value of 1.227 mg./sec. and the drop time was 5.6 sec. in 0.2 N potassium chloride at a potential of 0.0 V. vs. S. C. E. with a mercury head of 58 cm.

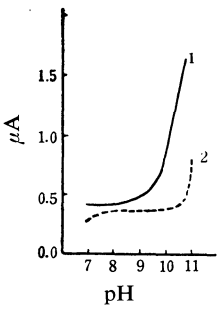


Fig. 2. Relation of wave height and pH for 10^{-3} M. 3,6-anhydro-L-galactose and agarobiose.

1: 3rd wave of 3,6-anhydro-L-galactose
2: 2nd wave of agarobiose

Cantor and Peniston, these waves may be presumed to be reduction waves of the aldehyde of the sugar. The height of the last wave was proportional to the concentration of AG in around 1×10^{-3} M in a Michaelis buffer (0.2 M NH_3-NH_4Cl) at pH 9.0, in which the most typical wave pattern was observed. The half-wave potentials of both sugars were about −1.4 V. vs. S. C. E. respectively (Table I) this value is smaller than those of any other sugars, but larger than that of 5-hydroxymethyl furfural (−1.3 V. vs. S.C.E.), as judged from our preliminary tests. It was also found that 3,6-anhydro-sugars are detectable by polarograpy, even in the presence of fructose (Fig. 1-c). In this case the figure of the wave was partially changed, but the potential of the waves remained unchanged. In conclusion, it may be said that as little 3,6-anhydro-sugar as about 3×10^{-3} M can be determined easily and rapidly by polarography.

TABLE I. HALF-WAVE POTENTIALS OF 3,6-ANHYDRO-L-GALACTOSE AND AGAROBIOSE (V. vs. S. C. E.)

pH	3,6-Anhydro-L galactose[1] 3rd wave	Agarobiose[2] 2nd wave
8.0	−1.41	−1.37
9.0	−1.42	−1.38
10.1	−1.42	−1.40
10.9	−1.46	−1.42

1) Concn. 1.87×10^{-3} M
2) Concn. 1.36×10^{-3} M

Kobe Yamate Women's College
Ikuta-ku, Kobe (T. F.)

Institute for Protein Research
Osaka University
Kita-ku, Osaka (K. M.)

Institute of Chemistry
Faculty of Industrial Arts
Kyoto Technical University
Matsugasaki, Kyoto (C. A.)

The Cation Effect on the Polarographic Reduction of Trioxalatochromate(III) Ions

By Nobuyuki TANAKA, Eiki ITABASHI and Reita TAMAMUSHI

(Received January 13, 1964)

Recently, Pamfilov, Lopushans'ka and Zueva reported that trioxalatochromate(III) ($[Cr(ox)_3]^{3-}$) ions gave two irreversible polarographic waves, with half-wave potentials of -1.315 and -1.450 V. vs. NHE, in a 1.0 N potassium chloride solution.[1] This seemed to contradict our previous statement that $[Cr(ox)_3]^{3-}$ ions gave no reduction wave in a 0.1 M solution of tetramethylammonium bromide.[2] Therefore, the reduction of $[Cr(ox)_3]^{3-}$ ions has been investigated again; a marked cation effect on the half-wave potential and the limiting current of the wave has thus been revealed.

Typical one-step irreversible waves were obtained in various supporting electrolyte solutions. The limitting current was found to be diffusion-controlled and proportional to the concentration of the complex ions. The overall electrode process was considered to be of a three-electron reduction of chromium(III) to chromium(0), (cf. the reduction wave of cis-$[Cr(ox)_2(H_2O)_2]^-$).[3] The half-wave potentials obtained are given in Table I; they clearly indicate that the reduction potentials of $[Cr(ox)_3]^{3-}$ ions depend on the nature and the concentration of the cations present. The half-wave potentials shift to less negative potentials with the increasing ionic charge of the cation and, at the constant ionic charge, with the decreasing radius of the hydrated ion and the increasing concentration of the cations present. The diffusion current constants were also found to be dependent on the nature and the concentration of the cations present.

TABLE I. THE HALF-WAVE POTENTIALS OF THE POLAROGRAPHIC WAVES OF $[Cr(ox)_3]^{3-}$ IONS OBTAINED IN VARIOUS SUPPORTING ELECTROLYTE SOLUTIONS AT 25°C

Electrolyte soln.	$E_{1/2}$ V. vs. SCE
0.1 M $(CH_3)_4NBr$	—
1.0 M LiCl	−1.76
1.0 M NaCl	−1.70
0.1 M KCl	−1.83
0.3 M KCl	−1.76
1.0 M KCl	-1.68_5
3.0 M KCl	−1.64
1.0 M $MgCl_2$	−1.56
1.0 M $SrCl_2$	-1.51_5
1.0 M $BaCl_2$	−1.51

These facts may be explained by taking into account both the double-layer effect and the formation of ion-pairs.[4,5] The $[Cr(ox)_3]^{3-}$ ions are reduced at the negative side of the electrocapillary maximum. If the potential difference across the diffuse double layer decreases with the increasing concentration of electrolytes or by changing the nature of the cation of electrolyte in the solution, the electrostatic hindrance between the electrode and the $[Cr(ox)_3]^{3-}$ ions decreases and, consequently, the surface concentration of the complex anions increases. This and an increase in the effective potential difference in the Helmholtz layer accelerate the reduction of $[Cr(ox)_3]^{3-}$ ions, which therefore takes place at less negative potentials. The formation of ion-pairs, which is to be expected from the change in the diffusion current constant, lessens the total ionic charge of electroactive species and, consequently, facilitates the approach of $[Cr(ox)_3]^{3-}$ anions to the electrode surface.

These results lead to the conclusion that the $[Cr(ox)_3]^{3-}$ ions are reduced to give a one-step polarographic wave provided the electrostatic hindrance between the electrode and the complex ions is decreased by the change in the structure of the double layer and by the formation of the ion-pairs.

Department of Chemistry
Faculty of Science
Tohoku University
Katahira-cho, Sendai

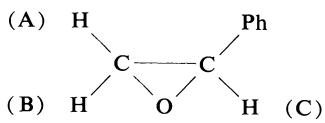
1) A. V. Pamfilov, O. I. Lopushans'ka and T. S. Zueva, *Ukr. Khim. Zh.*, **29**, 299 (1963); *Chem. Abstr.*, **59**, 3543 (1963).
2) N. Tanaka, E. Itabashi and E. Kyuno, This Bulletin, **36**, 917 (1963).
3) N. Tanaka, E. Itabashi, R. Tamamushi and G. Satô, ibid., **37**, 226 (1964).
4) A. N. Frumkin and Nikolaeva-Fedrovich, "Progress in Polarography," Vol. I, by P. Zuman and I. M. Kolthoff, Interscience Publishers, N. Y. (1962), p. 223.
5) P. Delahay and A. Aramata, *J. Phys. Chem.*, **66**, 1194 (1962).

The Relative Signs of the ^1H–^1H Coupling Constants of Styrene Oxide

By Hiroshi SHIMIZU and Yoshifumi HAMA

(Received February 4, 1964)

The NMR spectrum of styrene oxide has analyzed by Railly and Swalen[1] at 60 Mc. They reported that, though the position of the lines could be accounted for by two different nonequivalent assignments, J_{AC} and J_{BC}, with the same signs or different signs, the intensities were much more in agreement when J_{AC} and J_{BC} had the same sign, and that equivalent assignments could be obtained by positive or negative J_{AB} with positive (or negative) J_{AC} respectively. They arbitrarily chose both to be positive: $J_{AB}=+5.65$, $J_{AC}=+2.49$, and $J_{BC}=+4.04$ c.p.s.



On the other hand, the relative signs of the geminal and vicinal ^1H–^1H coupling constants are different in many organic compounds,[2] inconsistent with the prediction from the valence bond theory.[3] This suggests that the set of the coupling constants $-J_{AB}$, $+J_{AC}$, and $+J_{BC}$ (or $+$, $-$, $-$) would be correct, whereas the set of $+$, $+$, and $+$ (or $-$, $-$, $-$) would be wrong. In this communication, the result of our analysis, by means of which the correct set can be chosen, will be reported.

Since our calculations showed that the both sets could be practically distinguished from one another at frequencies below 20 Mc., the NMR spectrum of this compound was observed and recorded at 15 Mc. with a Varian 4300C spectrometer. It was found that the observed line-positions could be accounted for by the set of the coupling constants $+J_{AB}$, $+J_{AC}$, $+J_{BC}$ (or $-$, $-$, $-$) as shown in Fig. 1. This rather unexpected result may be ascribed to the specific structure of the three-membered ring of styrene oxide; it suggests that the signs of ^1H–^1H coupling constants are not definite for one type of a coupling of protons, as has been believed generally, but that they change depending on the chemical structure, for example, those in epoxides.

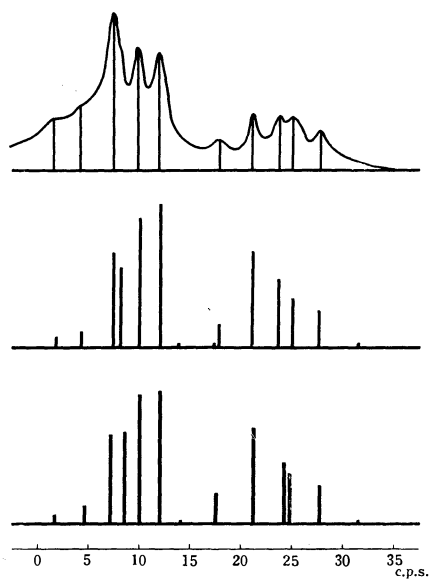


Fig. 1. The observed and calculated spectra of the ABC system of styrene oxide at 15 Mc.: the uppermost one is the observed spectrum and the middle and the lowest ones are the spectra calculated by using the sets $+J_{AB}$, $+J_{AC}$, $+J_{BC}$, and $-J_{AB}$, $+_{AC}$, $+J_{BC}$, respectively. The intensities of the observed lines are inaccurate because the spectrum was not recorded under the optimum conditions.

It is an interesting problem to determine whether the absolute signs of these coupling constants are positive or negative. Our conclusion on this point, as well as more detailed results of our analysis of the NMR spectrum of this compound, will be published elsewhere.

The authors wish to thank Dr. Ichiro Yamaguchi of the Japan Atomic Energy Research Institute for his kindness in measuring the 15 Mc. spectrum.

Department of Chemistry
College of Arts and Sciences
Chiba University
Chiba

1) C. A. Reilly and J. D. Swalen, *J. Chem. Phys.*, **32**, 1378 (1960).
2) C. A. Reilly and J. D. Swalen, ibid., **35**, 1522 (1961); F. Kaplan and J. D. Roberts, *J. Am. Chem. Soc.*, **83**, 4668 (1961).
3) M. Karplus, *J. Chem. Phys.*, **30**, 11 (1959); H. S. Gutowsky, M. Karplus and D. M. Grant, ibid., **31**, 1278 (1959).

On the Thermal Analysis of the Phase Transition of $[(C_6H_5)_3PCH_3]^+(TCNQ)_2^-$

By Yôichi IIDA, Minoru KINOSHITA, Asako KAWAMORI and Keisuke SUZUKI

(Received February 22, 1964)

In a previous paper,[1] we presented the temperature dependences of the electrical conductivity and ESR absorption of the TCNQ anion radical salt of triphenylmethylphosphonium, $[(C_6H_5)_3PCH_3]^+(TCNQ)_2^-$. The magnetic behavior of this salt has been known to show a singlet-triplet nature in the lower temperature range.[2,3] However, the ESR absorption intensity increased abruptly at about 40°C with an increase in the temperature. The discontinuity was also found in the electrical conductivity at 40°C. It was suggested that this discontinuity might be ascribed to a phase transition of the crystal.[1] Our preliminary X-ray study showed that there was a slight but clear difference between the crystal structures above and below 40°C. In this paper we will present other evidence on the phase transition obtained by the method of a differential thermal analysis.

The measurements were performed by means of a Shimadzu DT-10 differential thermal analysis apparatus, using powdered fused silica as a standard substance. One of the thermograms of $[(C_6H_5)_3PCH_3]^+(TCNQ)_2^-$ is shown in Fig. 1, in which the rates of raising and lowering the temperature were 3.0°C/min. and 2.8°C/min. respectively. Evidently the endothermic phase transition occurs at 40.4±0.25°C with an increase in the temperature. In order to determine the heat associated with this phase transition, the area of the signal line of $[(C_6H_5)_3PCH_3]^+(TCNQ)_2^-$ was compared with that of hexachloroethane. The phase transition of hexachloroethane, C_2Cl_6, occurs at 318.1°K with $\Delta H=0.613$ kcal./mol.[4] By using the molecular weight (686) of $[(C_6H_5)_3PCH_3]^+\cdot(TCNQ)_2^-$, the heat of transition, ΔH, was calculated as 0.558 kcal./mol., and the associated entropy change was estimated as $\Delta S=1.78$ e. u. These small values indicate that the phase transition observed is slight in its nature, which is quite in accordance with our preliminary X-ray study. It is interesting to see that this slight change in the crystal structure results in a fairly large change in its physical properties, such as electrical conductivity and magnetic susceptibility.

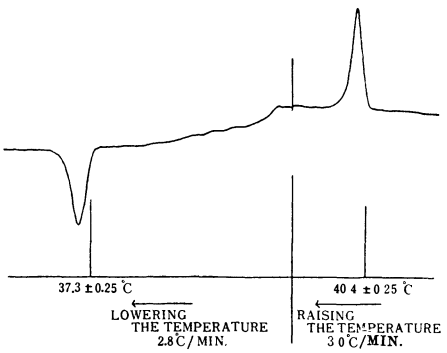


Fig. 1. One of the thermograms of $[(C_6H_5)_3\cdot PCH_3]^+(TCNQ)_2^-$.

On the other hand, a similar result of thermal analysis has been already obtained with Wurster's blue perchlorate crystals by two of the present authors (A. K. and K. S.).[5] McConnell et al.[6] have shown recently that the discontinuity observed in the temperature dependence of the paramagnetic susceptibility of Wurster's blue perchlorate is due to the formation of the dimeric structure below 187°K as a result of the change in the crystal structure. These phenomena appear to be quite analogous to our results.

Department of Chemistry
Faculty of Science
The University of Tokyo
Hongo, Tokyo (Y. I. & M. K.)

Faculty of Science
Kwansei Gakuin University
Nishinomiya (A. K. & K. S.)

1) Y. Iida, M. Kinoshita, M. Sano and H. Akamatu, This Bulletin, 37, 428 (1964),
2) D. B. Chesnut and W. D. Phillips, *J. Chem. Phys.*, 35, 1002 (1961).
3) R. G. Kepler, ibid., 39, 3528 (1963).
4) Landort-Börnstein, "Zahlenwerte und Funkutionen aus Physik, Chemie, Astronomie, Geophysik, Tchnik," II Band, 4 Teil, 6 Auflage, Springer-Verlag, Berlin·Göttingen·Heidelberg (1961); Nippon Kagaku-kai, "Kagaku Benran," Maruzen, Tokyo (1958).
5) H. Suzuki, H. Mitsudo and A. Kawamori, The 16th Annual Meeting of the Chemical Society of Japan, Tokyo, April, 1963.
6) D. D. Thomas, H. Keller and H. M. McConnell, *J. Chem. Phys.*, 39, 2321 (1963).

The Polarography of Ethylenediaminetetraacetato-Cobaltate(III) and Cobaltate(II) Complexes

By Nobufumi MAKI

(Received February 24, 1964)

For analytical purposes the EDTA salts, Na_2H_2 edta·$2H_2O$ and Na_4 edta·1/2 H_2O, have often been used as a masking or a complexing reagent in polarography.[1] However, there have been few reports on the relationship between the structure of EDTA complexes and their polarographic behavior in the absence of an excess $edta^{4-}$ ions.[2]

The present communication dealts mainly with the polarography of EDTA cobalt(III) complexes of the $[Co^{III}$ edta X] type in the absence of an excess $edta^{4-}$ ion, where the unidentate ligand, X, denotes the ion, Cl^-, Br^-, NO_2^-, OH^- or OH_2.

The complex, K $[Co^{III}$ edta] ·$2H_2O$, was found to give rise to only one wave, corresponding to an acceptance of one electron, in a 0.5 F sodium sulfate solution at the dropping mercury electrode (DME). The wave was present in the positive region of the potential. The limiting current of the wave was proportional to the concentration of the complex in the range of 10^{-2}~10^{-4} F and was diffusion-controlled.

The process of the electrode reaction was concluded to be as follows:

$$[Co^{III}\,edta]^- + e^- \rightarrow [Co^{II}\,edta]^{2-}$$

The cobalt(II) complex, $Na_2[Co^{II}$ edta] ·$3/2H_2O$, gave no reduction wave at all in a 0.5 F sodium sulfate solution without an excess $edta^{4-}$ ion.

The hexaquocobalt(II) chloride, $[Co^{II}(OH_2)_6]$·Cl_2, also gave no reduction wave in the presence of 1/4 F sodium ethylenediaminetetraacetate at the DME.

The chloro-, bromo-, nitro- and hydroxo-ethylenediaminetetraacetato-cobaltate(III) complexes, $K_2[Co^{III}$ edta·Cl] ·$3H_2O$, $Na_2[Co^{III}$ edta·Br] ·$4H_2O$, $Na[Co^{III}$ edta$(NO_2)]$ ·$3H_2O$, and $Na_2[Co^{III}$ edta(OH)] ·$3H_2O$,[3] were found to be irreversibly reduced in two steps to the metal through cobalt(II) complexes in a 0.5 F sodium sulfate solution at the DME.

The ratio of the height of the first wave to that of the second was roughly 1 : 2 for all the complexes. All the first waves existed in the positive region of potential except the hydroxo-complex. The limiting current of each wave was proportional to the concentration of the complex in the range between 10^{-4} and 8×10^{-3} F and was diffussion-controlled.

The nitro-EDTA cobalt(III) ion, [Co edta·$(NO_2)]^{2-}$, was found to be reduced up to the cobalt(II) state in a 1 F potassium nitrite solution, not reduced to the metal. Therefore, the second wave obtained in a 0.5 F sodium sulfate solution is due to the reduction of the

TABLE I. HALF-WAVE POTENTIALS OF THE WAVES FOR THE EDTA COBALT(III) AND COBALT(II) COMPLEXES

Compound	$E_{1/2}$ of the 1st wave Co(III) → Co(II)	$E_{1/2}$ of the 2nd wave Co(II) → Co(0)	Supporting electrolyte
$Na_2[Co^{II}$ edta]·$3/2H_2O$	——	No reduction	0.5 F Na_2SO_4 (25°C)
$K[Co^{III}$ edta]·$3H_2O$	+	No reduction	0.5 F Na_2SO_4
K_2[Co edta·Cl]·$3H_2O$	+	ca. −1.6	0.5 F Na_2SO_4
Na_2[Co edta·Br]·$4H_2O$	+	−1.62	0.5 F Na_2SO_4, 0.0058% Triton X 100
Na_2[Co edta $(NO_2)]$·$3H_2O$	+	-1.05_6	0.5 F Na_2SO_4
	+	No reduction	1 F $NaNO_2$
Na_2[Co edta (OH)]·$3H_2O$	-0.10_3	-1.05_5	0.5 F Na_2SO_4 (0°C)*
$[Co^{II}(OH_2)_6]Cl_2$	——	No reduction	1/4 F Na_4 edta (25*C)

Voltage unit: V. vs. SCE. Concentration of the complex: 5×10^{-3} F

* The ion, $[Co\,edta\,(OH)]^{2-}$, is unstable in solution and tends to become the ion, [Co edta·$(OH_2)]^-$ in neutral unbuffered solution.

1) edta = $(OCOCH_3)_2N\cdot CH_2CH_2\cdot N(CH_3COO)_2^{4-}$

2) More exactly, the ions, $edtaH_3^-$, $edtaH_2^{2-}$, etc., are usually present together in solutions.

3) I. A. Shimi and W. C. E. Higginson, *J. Chem. Soc.*, **1958**, 260.

aquated species of this complex.

Table I shows the half-wave potentials of the waves for these complexes. All the waves were irreversible.

The following processes of the electrode reaction are considered to be most plausible:

$$[Co^{III}\,edta\cdot X]^{2-} \xrightarrow{e^-} [Co^{II}\,edta\cdot X]^{3-} \xrightarrow{2e^-} Co\ (metal)\quad X=Cl,\ Br,\ OH$$

$$[Co^{III}\,edta(OH_2)]^{-} \xrightarrow{e^-} [Co^{II}\,edta(OH_2)]^{2-} \xrightarrow{2e^-} \quad \text{in } 0.5\ \text{F } Na_2SO_4$$

$$[Co^{III}\,edta(NO_2)]^{2-} \xrightarrow{e^-} [Co^{II}\,edta(NO_2)]^{3-}$$

in 1 F KNO_2

From these results it can be said that the EDTA-cobalt(II) ion in solution usually contains the $edta^{4-}$ ion as a hexadentate ligand in its coordination sphere.

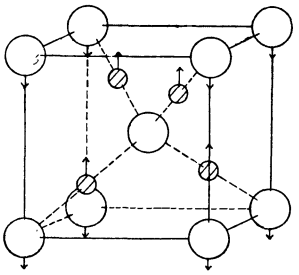
Radiation Center of Osaka Prefecture
Sakai, Osaka

The Infrared Absorption Spectrum of Cuprous Oxide

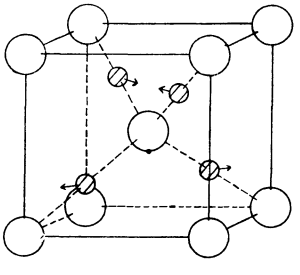
By Minoru TERADA

(Received February 24, 1964)

Cuprous oxide Cu_2O is a well-known crystal whose bond character is considerably covalent. It has a crystal structure belonging to the space group O_h^4. The unit cell contains four copper atoms and two oxygen atoms. A group theoretical consideration shows that this crystal has two F_{1u} optically-active lattice vibrations. Their vibrational modes are shown in Fig. 1. The a mode in Fig. 1 is considered to cause the relatively higher frequency band, and the b mode, the lower one.



Mode a



Mode b

Fig. 1. Infrared active vibrational modes of Cu_2O.

◍ Copper ○ Oxygen

In order to examine the bond character of cuprous oxide, the present writer made an infrared absorption measurement of cuprous oxide in the KBr pellet and in a polyethylene film.[1] The spectrum obtained is shown in Fig. 2. Absorption measurements in the rock-salt, potassium bromide and cesium bromide regions were made by the use of a Perkin-Elmer model-221 spectrometer, and those in the far infrared region, by the use of a grating spectrometer built by Yoshinaga et al.[2]

In the spectral region examined, two strong absorption bands, were found at 617 cm^{-1} and 147.5 cm^{-1}. These are evidently attributable, respectively, to the optically-active lattice

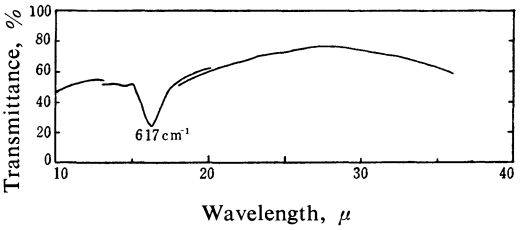


Fig. 2a. Infrared absorption spectrum of Cu_2O in KBr disc.

1) H. Yoshinaga and R. A. Oetjen, *J. Opt. Soc. Am.*, **45**, 1085 (1955).
2) H. Yoshinaga, S. Hujita, S. Minami, A. Mitsuishi, R. A. Oetjen and Y. Yamada, ibid., **28**, 315 (1958).

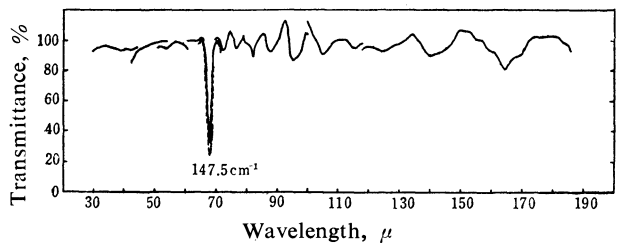


Fig. 2b. Infrared absorption spectrum of Cu_2O in polyethylene film.
(——) 50 mg./2 g. polyethylene
(------) 100 mg./2 g. polyethylene

vibrations a and b mentioned above. Of these two strong bands, the one at 617 cm^{-1} had already been found by O'Keeffe[3] and had been assigned by him to one (a) of the two expected infrared active vibrations. However, it has been a question where the other band (b) is situated. O'Keeffe assigned a band at 1122 cm^{-1} to one (b) of the two infrared-active lattice vibrations. On the other hand, Huang[4] predicted that it would be at 120 μ (83.3 cm^{-1}) on the basis of his calculation of the lattice frequencies of this crystal.

The problem is now settled by the present experiment. It has been found that the b band is situated at 147.5 cm^{-1}, at much lower frequency than that assigned by O'Keeffe but at a cosiderably higher frequency than that predicted by Huang. Huang assumed in his calculation an ionic character of the Cu-O bond in cuprous oxide. The fact that the actually obserwed frequency (147.5 cm^{-1}) is somewhat higher than that predicted (83.3 cm^{-1}) is considered to indicate that the bond is more covalent than he assumed.

Engineering & Research Laboratory
Itami-Branch, Mitsubishi Atomic
Power Industries, Inc.
Amagasaki, Hyogo

3) M. O'Keeffe, *J. Chem. Phys.*, **39**, 1789 (1963).
4) K. Huang, *Z. Physik*, **171**, 213 (1963).

The Isolation of Terephthaldinitrile N-Oxide

By Yoshio IWAKURA, Masayasu AKIYAMA and Kuniharu NAGAKUBO

(Received February 24, 1964)

We wish to report the isolation and characterization of terephthaldinitrile *N*-oxide (I) as a stable compound. Although the chemistry of nitrile *N*-oxides has extensively been studied by several groups of workers in recent years,[1-3] few nitrile *N*-oxides[4-6] have been isolated in a pure state because of the ease of their dimerization to furoxans.[3,6,7]

Terephthaldihydroxamic chloride (II), the starting material in this work, has been used by several previous investigators, but no dinitrile *N*-oxide has been isolated.[7-9]

To a solution of 0.233 g. of II[8] (m. p. 185°C) in 20 ml. of methanol, an equivalent amount of triethylamine in 20 ml. of methanol was added at room temperature. I was soon precipitated out of the mixture as colorless needles. It was filtered and washed thoroughly with methanol (a 70% yield). When the sample was heated gradually, it showed a definite m. p. at 241~243°C (decomp.). On the other hand, when it was put in a bath heated at 150°C, it decomposed instantly.

Found: C, 59.79; H, 2.66; N, 17.77. Calcd.

1) a) R. Huisgen, *Proc. Chem. Soc.*, **1961**, 357; b) R. Huisgen, *Angew. Chem.*, **75**, 604 (1963); c) R. Huisgen, ibid., **75**, 742 (1963).
2) a) N. Barbulescu and P. Grünanger, *Gazz. chim. ital.*, **92**, 138 (1962); b) N. Barbulescu and A. Quilico, *Gazz. chim. ital.*, **91**, 326 (1961), and many previous papers.
3) C. Grundmann, *Angew. Chem.*, **75**, 450 (1963).
4) H. Wieland, *Ber.*, **40**, 1667 (1907).
5) S. Califano, R. Scarpati and G. Speroni, *Atti accad. nazl. Lincei Rend., Classe sci. fis. mat. e nat.*, **23**, 263 (1958); *Chem. Abstr.*, **52**, 12557 (1958).
6) S. Califano, R. Moccia, R. Scarpati and G. Speroni, *J. Chem. Phys.*, **26**, 1777 (1957).
7) R. H. Wiley and B. J. Wakefield, *J. Org. Chem.*, **25**, 546 (1960).
8) M. S. Chang and A. J. Matuszko. ibid., **28**, 2260 (1963).
9) A. Ricca, *Gazz. chim. ital.*, **91**, 83 (1961).

for $C_8H_4N_2O_2$: C, 60.00; H, 2.52; 2.52; N, 17.50.

Infrared spectra were obtained on Nujol mulls and a KBr disc: 841(m), 1025(w), 1100 (s), 1284(w), 1350(s), 1405(w) and 2330(s) cm^{-1}. Absorptions at 1350 and 2330 cm^{-1} have been reported to be characteristic of arylnitrile *N*-oxides.[7] No bands corresponding to furoxans[10] were detected. I is soluble or slightly soluble in dioxane, acetonitrile, chloroform, ethylene dichloride, *o*-dichlorobenzene and *m*-cresol, but insoluble in benzene, diethyl ether, ligroin and carbon tetrachloride.

By the addition reaction of 50 mg. of I with methyl methacrylate at room temperature, 40 mg. of 1, 4-bis(5'-methyl-5'-methoxycarbonyl-3'-$\Delta^{2'}$-isoxazolinyl)benzene[11] was separated as a crystalline compound from the reaction mixture; m. p. 172~173°C (from methanol).

Found: C, 60.16; H, 5.48; N, 8.03. Calcd. for $C_{18}H_{20}N_2O_6$: C, 59.99; H, 5.59; N, 7.77.

$\nu_{C=O}$, 1728(s) cm^{-1} (Nujol).

By treating I with allyl alcohol in tetrahydrofuran, 1, 4-bis(5'-hydroxymethyl-3'-$\Delta^{2'}$-isoxazolinyl)benzene[12] was obtained; m. p. 214~216°C(decomp.) (from ethanol).

Found[13]: C, 61.16; H, 5.98; N, 10.33. Calcd. for $C_{14}H_{16}N_2O_4$: C, 60.86; H, 5.84; N, 10.14.

Infrared absorptions: 3150~3400 cm^{-1} region and 1046, 1055 cm^{-1} doublet (primary alcohol).

Further studies are in progress on addition reactions of I with various mono- and difunctional unsaturated compounds.

Research Laboratory of Resources Utilization
Tokyo Institute of Technology
Meguro-ku, Tokyo

10) N. E. Boyer, G. M. Czerniak, H. S. Gutowsky and H. R. Snyder, *J. Am. Chem. Soc.*, **77**, 4238 (1955).

11) A. Quilico, G. S. D'Alcontres and P. Grünanger, *Gazz. chim. ital.*, **80**, 479 (1950); *Chem. Abstr.*, **45**, 3836 (1951). In this report, methyl 3-phenyl-5-methyl-2-isoxazoline-5-carboxylate is described.

12) G. S. D'Alcontres and P. Grünanger, *Gazz. chim. ital.*, **80**, 741 (1950); *Chem. Abstr.*, **46**, 971 (1952). Here 3-phenyl-5-hydroxymethyl-2-isoxazoline is described.

13) The authors are indebted for the microanalyses to the staff of the Analytical section of the Department of Organic Chemistry, Tokyo Institute of Technology.

Long-range Proton Spin-Spin Interactions in Thianaphthenes

By Kensuke TAKAHASHI, Tatsuo KANDA and Yasuo MATSUKI

(Received March 2, 1964)

The long-range coupling between the protons in different aromatic rings has been observed recently by several authors in quinoline,[1] in *N*-benzylthieno [3, 2-b] -pyrrole,[2] in indene,[3,4] in benzofuran[4] and in acridine.[5] In this report we will present the results observed in the long-range coupling between the 3- and 7-hydrogens in some thianaphthenes. In the spectrum of thianaphthene itself, this coupling is difficult to obtain directly from the signals in a carbon tetrachloride, cyclohexane or acetone solution because of the overlapping of the signals, but in the spectra of some methylthianaphthenes it may be observed directly and with certainty. In the spectrum of 2-methylthianaphthene in a carbon tetrachloride solution, the signal of the 3-hydrogen appears at 5.40 p. p. m. with reference to cyclohexane and shows a quintet-like structure. This means that the 3-hydrogen is coupled to the 2-methyl hydrogens and to one of the other hydrogens. In the spectrum of 3-methylthianaphthene, the signal of the 2-hydrogen appears at 5.51 p. p. m. and shows a quartet-like structure, showing the expected coupling with the 3-methyl hydrogens only. In the spectrum of 5- or 6-methylthianaphthene, the signals of the 2- and 3-hydrogens appear as a doublet and as a double doublet respectively. A typical spectrum in the aromatic region of 5-methylthianaphthene is shown in Fig. 1. In the spectrum of 4-methylthianaphthene, the signals of the 2- and the 3-hydrogens look like a singlet in a carbon tetrachloride or cyclehexane solution because of nearly the same chemical shift between the two hydrogens, whereas those in an acetone solution appear as a doublet and as a double doublet, like those observed in 5- or 6-methylthianaphthene.

1) F. A. L. Anet, *J. Chem. Phys.*, 32, 1274 (1960).
2) H. S. Gutowsky and A. L. Porte, ibid., 35, 839 (1961).
3) D. D. Elleman and S. L. Manatt, ibid., 36, 2346 (1962).
4) J. A. Elvidge and R. G. Foster, *J. Chem. Soc.*, 1963, 580.
5) J. P. Kokko and J. H. Goldstein, *Spectrochimica Acta*, 19, 1119 (1963).

TABLE I. PMR DATA OF METHYLTHIANAPHENES, REFERRED TO CYCLOHEXANE AT 60 Mc./sec.

Substituent	Chemical Shift, p. p. m.							Coupling, c. p. s.
	CH_3	2-H	3-H	4-H	5-H	6-H	7-H	J_{37}
2-CH_3	1.09	—	5.40	~6.1	~5.7	~5.7	~6.1	1.0~0.5
3-CH_3	0.96	5.51	—	~6.2	~5.8	~5.8	~6.2	—
4-CH_3	1.14	5.86	5.86	—	5.59	5.73	6.19	0.7$_5$
5-CH_3	0.99	5.83	5.67	6.04	—	5.60	6.20	0.7$_5$
6-CH_3	1.00	5.78	5.73	6.16	5.63	—	6.14	0.7$_5$
7-CH_3	1.10	5.85*	5.80*	6.12	5.75	5.57	—	—

* Assignment uncertain

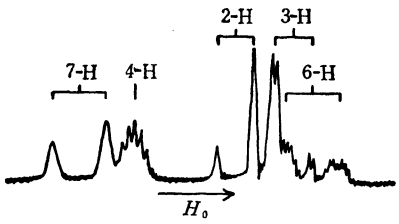


Fig. 1. The ring proton spectrum of 5-methylthianaphthene, in the 5 mole % solution in cyclohexane at 60 Mc./sec.

In the spectrum of 7-methylthianaphthene, the signals of the 2- and 3-hydrogens in a carbon tetrachloride or cyclehexane solution look like a singlet, but those in an acetone solution appear as two doublets, showing no resolved second-order splitting. These facts clearly show that the 3-hydrogen is coupled to the 7-hydrogen in thianaphthenes. The observed second-order splitting gives J_{37}~0.7 c. p. s. in each case.

Another fact of interest has been also observed in the spectrum of 7-methylthianaphthene in an acetone solution. Two doublets originating from the 2- and 3-hydrogens in this compound have different line widths. The one at the lower field is somewhat broader than the other. This suggests the presence of another long-range coupling in this system, for example, one between the 2- and 4-hydrogens, but the assignment is still in question at present.

Table I lists the observed PMR data of our first-order analyses. The chemical shifts were measured in about 0.1 g./cc. solutions in carbon tetrachloride containing 0.5 wt. % cyclohexane as an internal reference.

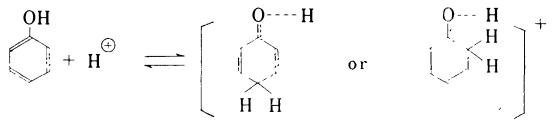
The Chemical Research Institute of Non-Aqueous Solutions
Tohoku University
Katahira-cho, Sendai

The Nucleophilic Substitution of a Phenolic Hydroxy Group in Acidic Media

By Shigeru OAE and Reiko KIRITANI

(Received March 19, 1964)

During our study of the acid-catalyzed hydrolysis of phenyl benzenesulfonate with concentrated hydrochloric acid in ^{18}O-enriched water, we have found that the phenol recovered was always incorporated with an excess of ^{18}O and also, that the amount of ^{18}O incorporation increased with prolonged heating.[1] We then suggested that, in a strong acidic medium, phenol readily accepts a proton at either the para- or ortho-position to form a quasi-stable incipient carbonium ion intermediate, A, in which the original hydroxyl function acquires more of a carbonyl character and hence facilitates the oxygen exchange with ^{18}O-enriched water.



A

We have now extended this remarkable oxygen exchange reaction to a number of phenolic compounds. The conditions used for this reaction were: temperature, 180°C; medium, 10 N hydrochloric acid in $H_2{}^{18}O$, enriched with 0.77 atom % ^{18}O; time, 6 hr. and 24 hr. Resorcinol, and both α- and β-naphthols, which are known to have some carbonyl character, were found to exchange their oxygen atoms substantially in 6 hr. and completely in 24 hr.; the oxygen exchange occured substantially with the ease of ^{18}O incorporation, falling in the order of phenol, *p*-nitrophenol, *p*-cresol, *m*-aminophenol, and *p*-bromophenol, while with tri-substituted phenols, such as 2, 4, 6-trimethylphenol and 2, 4, 6-tribromophenol, very little oxygen exchange took place, even under heating for 24 hr. In order for phenol to get a successful oxygen exchange, perhaps the incipient intermediate A should have a substantially long life. The substitution of electronegative groups at either the ortho- or para-position or at both will discourage the electrophilic addition of proton to form a quasi-stable intermediate A, while the substitutions at both ortho- and para-positions, even with electron-releasing alkyl groups such as in 2, 4, 6-trimethylphenol, will give an unstable unsymmetrical intermediate which may not have a life sufficiently long enough to exchange its oxygen.

Other alternative pathways would be aromatic nucleophilic substitution and that involving incipient aromatic carbonium ions. Aromatic nucleophilic substitution is known to be facilitated by substituting electron-withdrawing groups at either ortho- or para-positions or at both. In this case, however, the substitution of an electron-withdrawing group failed to increase the ^{18}O exchange. Meanwhile, the formation of aromatic carbonium ions would be facilitated by electron-donating substituents at ortho- and/or para-positions, but this trend was not observed in this ^{18}O exchange.

As an extension of this ^{18}O exchange experiment, it was expected that the phenolic hydroxyl group would be replaced by more nucleophilic reagents, such as alcohols and mercaptans. Indeed, when about five equivalent moles of ethanol was added in the reaction mixture of phenol and hydrochloric acid used for the ^{18}O exchange experiment and the mixture was heated in an ampoule at 180°C for two days, phenetole was obtained in a yield exceeding 60%. Naphthols and *p*-cresol also gave the corresponding ethyl ethers in good yields in the same procedures. When *n*-butylmercaptan was used instead of ethanol, phenolic oxygen was replaced by an *n*-butylmercapto group under the same reaction conditions. Thus, from phenol, *p*-cresol and both α- and β-naphthols, the corresponding *n*-butylsulfides of phenyl, *p*-tolyl and α- and β-naphthyl were obtained in good yields, recovering some unreacted starting materials.

Although β-naphthol has been known to react with nucleophilic reagents such as sulfurous acid[2] and thioglycolic acid[3] replacing the phenolic hydroxyl group forming β-naphthyl sulfonic acid and thioglycolic acid, our

1) S. Oae, T. Fukumoto and R. Kiritani, This Bulletin, 346 (1963).

2) See Bucherer Reaction in "Organic Reaction," Vol. I, John Wiley & Sons, Inc., New York. p. 105.

3) F. M. Furman, J. H. Thelin, D. W. Hein and W. B. Hardy, *J. Am. Chem. Soc.*, 82, 1450 (1960).

results are the first general examples in which the phenolic hydroxyl group is replaced by nucleophilic reagents. We believe that this procedure will serve as a general method of substituting the phenolic hydroxyl group with other nucleophilic reagents; further work is in progress here.

Department of Applied Chemistry
Faculty of Engineering
Osaka City University
Kita-ku, Osaka (S. O.)

Department of Chemistry
Radiation Center of Osaka Prefecture
Sakai, Osaka (R. K.)

Reactivity of Chemisorbed Nitrogen on an Ammonia Synthesis Catalyst

By Kenzi TAMARU*

(Received March 24, 1964)

The ammonia synthesis on an ammonia synthesis catalyst has been treated by means of a new approach, studying the nitrogen chemisorption and the reaction between the chemisorbed nitrogen and hydrogen separately under the reaction conditions. The experimental apparatus and procedures were approximately the same as those previously reported.[1] The catalyst (198 g. with aluminum oxide 5% and potassium oxide 1% before the reduction) was reduced with hydrogen at 500°C for about three thousand hours in a closed circulating system with a liquid nitrogen trap.

The rate of hydrogenation of the chemisorbed nitrogen to form ammonia was proportional to the partial pressure of hydrogen at approximately the same amount of nitrogen chemisorbed, as is shown in Fig. 1, the ammonia produced being always trapped out of the circulating system. The adsorption of hydrogen during the reaction approximately reaches the saturation point at higher pressure, as has been reported previously.[1] Consequently, the rate of the reaction is apparently correlated not with the amount of hydrogen chemisorbed, but with the pressure of hydrogen.

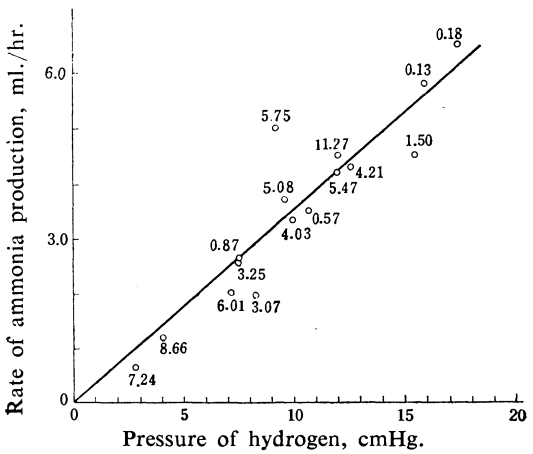


Fig. 1. Dependence of the reaction rate upon hydrogen pressure at 250°C. (N(a)=33~37 ml.(stp)) The numbers designate the pressure of nitrogen in cmHg.

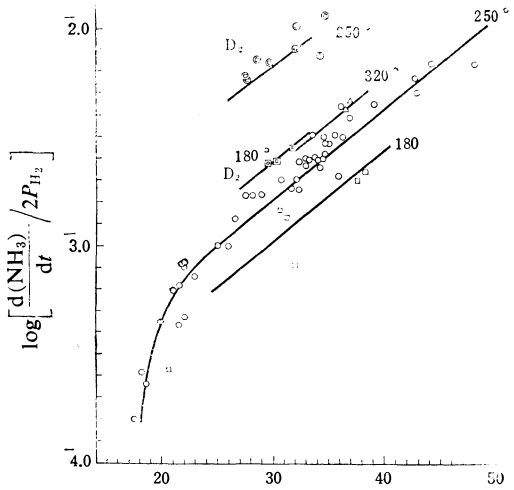


Fig. 2. The rate of hydrogenation of chemisorbed nitrogen to form ammonia as a function of nitrogen adsorption.

* Present Address: Department of Chemistry, Faculty of Science, The University of Tokyo, Hongo, Tokyo.

1) K. Tamaru, Proc. 2nd Intern. Congr. on Catalysis, 1960, p. 325. Technip, Paris, 1961.

The reaction rate was similarly studied in connection with the amount of nitrogen chemisorbed, as Fig. 2 shows. The rate of the reaction was nearly independent of the circulation rate of the reacting gas under the experimental conditions employed.

As Figs. 1 and 2 show, the rate of ammonia formation from the chemisorbed nitrogen and hydrogen, when a negligible amount of ammonia is present, conforms to the following equation except for smaller amounts of nitrogen chemisorbed : $d(NH_3)/dt = CP_{H_2}\exp(\gamma N(a))$ where P_{H_2} is the pressure of hydrogen in the ambient gas, $N(a)$ is the amount of nitrogen chemisorbed, and C and γ are constant. This equation suggests that the Eley-Rideal mechanism is involved.

It is also interesting to note that the reaction of the chemisorbed nitrogen with deuterium proceeds much faster than with hydrogen, as Fig. 2. The author previously found no isotopic effect of hydrogen in the simultaneous adsorption of nitrogen and hydrogen on the catalyst surface.[2] The isotopic effect in the overall reaction, which has been observed by Ozaki, Boudart and Taylor,[3] should, accordingly, be attributed to the effect in the reaction between chemisorbed nitrogen and hydrogen.

Department of Chemistry
Yokohama National University
Minami-ku, Yokohama

2) K. Tamaru, *Trans. Faraday Soc.*, **59**, 979 (1963).
3) A. Ozaki, M. Boudart and H. Taylor, *Proc. Roy. Soc.*, **A258** 47 (1960).

Mixed Chelate Compounds of Titanium(III) as Studied by Electron Paramagnetic Resonance and Spectrophotometry

By Shizuo FUJIWARA, Kozo NAGASHIMA and Maurice CODELL*

(Received November 16, 1963)

Titanium(III) possesses low-spin-orbit coupling, and it was recently demonstrated[1] that, when chelated with ethylenediaminetetraacetic acid (EDTA), nitrilotriacetic acid (NTA), and several other chelating reagents, titanium(III) gives strong EPR signals in an aqueous solution at room temperature. This phenomenon suggests that ions of low-spin-orbit coupling produce EPR signals when strongly coordinated. It was, therefore, decided to investigate several aspects of correlation of complex formation with the EPR signal intensities. An increase in the signal intensity of the titanium(III)-EDTA complex was observed upon the addition of certain organic acids. Complex formation was confirmed for the systems titanium(III)-EDTA with oxalate, tartrate, citrate, and lactate. EPR signals are not exhibited by the titanium(III)-EDTA complex at pH values appreciably lower than 5.7. However, in the presence of any of the above acids, signals are exhibited by the complex at pH 2.5. No signals have been obtained for the titanium(III)-organic acid systems for any of the organic acids tested.

It was noted that complexes formed by titanium(III)-EDTA with three of the above acids show optical absorbance maxima at 720 mμ. No absorbance maximum is shown by titanium-(III)-EDTA alone at any pH value.

The aqueous system of metal ion, EDTA, and an organic acid such as tartaric acid has long been utilized in analytical chemistry for chelatometric titrations. The usual understanding of the system has been that the metal-organic acid complex is less stable than the metal-EDTA complex, and that, consequently, when EDTA is added to a solution containing a metal ion and organic acid, the organic acid is displaced to form the more stable EDTA complex. However, the present study gives counter evidence to this interpretation showing that the organic acid is an integral component of the complex.

Experimental

Apparatus and Reagents.—*Electron Paramagnetic Resonance Spectrometer.* — Model JES-118, Japan Electron Optics Company.

Recording Spectrophotometer.—Cary Model 11.

Spectrophotometer.—Hitachi EPU-2 spectrophotometer.

Titanium(III) Chloride Solution.—A pure grade of titanium sponge (courtesy of the Osaka Titanium Corporation, Amagasaki, Japan) was dissolved in hot 6 N hydrochloric acid. An excess of titanium sponge was added to the hydrochloric acid, and additional acid was added as the reaction progressed to prevent the acid concentration from falling to the point where hydrolysis could occur. The solution was decanted from the metal while the vigorous reaction was proceeding in order to prevent the formation of any appreciable quantity of titanium-(IV). The solution was maintained in an atmosphere of nitrogen. The final concentration of titanium(III) ion was determined volumetrically by titration with a ceric sulfate solution.

Electron Paramagnetic Resonance Spectrometric Procedure.—Intensity measurements were carried out using the same capillary tube for all determinations. A tube containing DPPH (diphenylpycrylhydrazyl) was taped to the capillary tube as an external standard of signal intensity, and the capillary tube was placed in the same position in the cavity for all determinations. It was found, however, that a comparison of the signal obtained for the sample with that of the DPPH was not a reliable process for determining absolute signal intensities because a slight change in position caused large deviations between the signals of the sample and of the DPPH. Signal intenstity measurements were, therefore, made comparing the peak heights of the signals obtained, which were found to be reasonably reproducible.

Spectrophotometric Procedure. — Solutions of titanium(III) chloride, EDTA, and organic acids were mixed in volumetic flasks, and the pH was adjusted to various values by the addition of ammonium hydroxide. The absorbances were measured using a Hitachi spectrophotometer, and spectrophotometric curves covering the range from 350 to 800 mμ were made using a recording spectrophotometer.

Results and Discussion

Table I lists the conditions used to obtain the EPR spectra and the signal intensity

* Present address: The Pitman-Dunn Institute for Research, Philadelphia 37, Pa., U. S. A.

1) S. Fujiwara and M. Codell, This Bulletin, 37, 49 (1964).

Table I. EPR Signal intensities of mixed titanium chelate compounds

Ti(III) molarity	pH	EDTA ratio	Organic acid ratio	Relative peak height
			Oxalic	
0.1	2.5	1	1	6.2
0.1	3.7	1	1	33.0
0.1	4.3	1	1	51.0
0.1	5.7	1	1	64.0
0.1	5.7	1	0.5	35
0.1	5.7	1	2	65
0.1	5.7	1	3	67
0.1	5.7	0.5	1	19
0.1	5.7	2	1	64
0.1	7.5	1	1	55
0.1	8.4	1	1	57
0.2	9.4	1	1	64
0.2	10.2	1	1	31
			Tartaric*	
0.1	5.7	1	1	6.8
0.1	5.7	1	2	12.8
0.1	5.7	1	3	19
0.1	5.7	1	4	24
0.1	5.7	1	5	27
0.1	5.7	3	1	6.1
0.2	3.5	1	1	5.4
0.2	6.4	1	1	9.9
0.2	9.4	1	1	55
			Citric	
0.2	5.7	1	0.8	3.7
0.2	5.7	1	1	4.2
0.2	5.7	1	2.5	7.5
			Lactic	
0.1	3.2	1	1	0.4
0.1	5.7	1	1	3.5
0.1	5.7	1	2	4.0
0.1	5.7	1	3	4.5
			No addition of organic acid	
0.2	4.3	1		No signal
0.2	5.7	1		0.4
0.2	6.3	1		0.5
0.2	7.4	1		1.5
0.2	12.2**	1		6.0

* At pH 9.6 another signal appears and the signal intensity cannot be accurately measured.

** Adjusted with NaOH.

measurements of complexes.

The Titanium(III)-EDTA System.—Curves 2, 3, and 4 of Fig. 1 show the absorption spectra obtained for the titanium(III)-EDTA complex at various pH values, where the concentration of titanium(III) chloride was maintained constant at a titanium(III) to EDTA ratio of 1 to 1.2. Curve 1 shows the absorbance of titanium(III) chloride in an acid solution. From pH 2.5 to pH 8, distinct maxima at 550 mμ are observed for the titanium(III)-EDTA complex. At pH 8 the curve is considerably changed, but it still shows a maximum absorbance at 550 mμ, and a distinct shoulder can be seen at 600 mμ. At pH 9.1 a maximum absorbance at 580~600 mμ is observed. These curves suggest that another complex forms at higher pH values and that it absorbs from 580 to 600 mμ. From Fig. 2 it can be seen that the EPR spectra correspond with this assumption, since an increased intensity is seen for the second peak at higher pH values. The EPR spectrum shown for pH 12.2 was obtained for a solution adjusted with sodium hydroxide; a different piece of DPPH was used for this spectrum than for the other spectra shown in Fig. 2. It is seen that, at this pH, only the second peak is obtained. At pH 13, the complex begins to decompose, and the signal intensity is considerably decreased within a short period. At a pH of about 7, a second peak appears which increases in intensity at higher pH values. This phenomenon is observed whether ammonium hydroxide or sodium hydroxide is used to adjust the pH. The g value for the peak obtained at pH 12.2 is 1.956±0.002. The g value for the first peak is 1.960±0.002, which is in agreement with those of other titanium chelate compounds.[1]

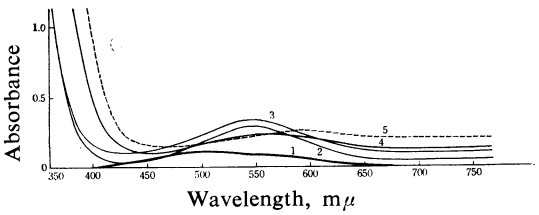


Fig. 1. Absorbance spectra of Ti(III), and Ti-(III)-EDTA at varying pH values.
Curve (1): $TiCl_3$ in 1:10 HCl
Curves (2), (3), (4), and (5): Ti(III)-EDTA (1:1.2 ratio)
Curve (2): pH 2.5, Curve (3): pH 5.0,
Curve (4): pH 8.0, Curve (5): pH 9.1
Ti(III) concentration for all curves: 0.03M

From the above discussion it is apparent that two species of titanium(III)-EDTA complexes exist in neutral and basic solutions, and from the following considerations, we must assume the existence of another titanium(III)-EDTA complex in an acid solution which does not give an EPR signal.

An infrared study[2] has recently shown the presence of five species of EDTA in an aqueous solution, and the existence of acid complexes of metal ions and EDTA has been demonstrated in many instances. From the results of

2) D. T. Sawyer and J. E. Tackett, *J. Am. Chem. Soc.*, 85, 314 (1963).

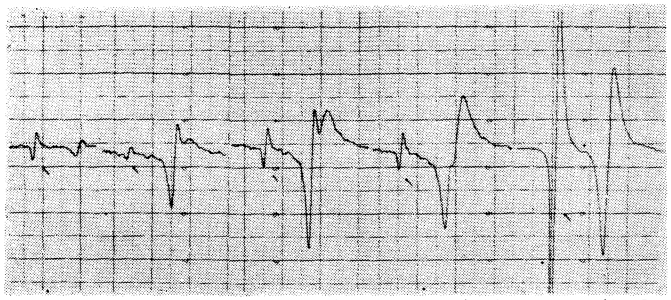


Fig. 2. EPR spectra for the Ti(III)-EDTA complex.
Spectra 1, 3 and 4 were obtained at twice the sensitivity setting of spectra 2 and 5.
Ti(III) concentration for all spectra: 0.02 M. Arrows designate DPPH.

TABLE II. Ti(III)-EDTA SPECIES IN SOLUTION

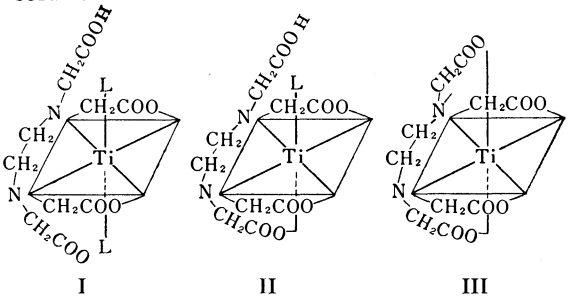
Formula	Formation in	Absorbance maxima	Remark
(Ti(III)-EDTAH_2 L_2)	(I) acid solution	550 mμ	No EPR signal
(Ti(III)-EDTAH L)	(II) neutral solution	550 mμ	EPR signal g=1.960
(Ti(III)-EDTA)	(III) basic solution	580 to 600 mμ	EPR signal g=1.956

previous investigations[2-5] and from our own experimental results, the three species listed in Table II are proposed to represent the complexes which exist in the solutions studied.

In Table II, EDTAH_2, EDTAH and EDTA represent ions where two, three, and four hydrogen ions are removed from the EDTA molecule containing four acid groups. L represents ligands other than EDTA, such as H_2O, Cl^-, and NH_3.

From the EPR spectra (Fig. 2), it appears that, at the approximate range pH 5 to 7, equilibrium mixtures of I and II exist, because the first peak becomes smaller with the decreasing pH and disappears at a pH of about 5, but the existence of a chelate is well established by the reasons given below. At pH 7 to 10, equilibrium mixtures of II and III exist. The same mixtures indicated above by the EPR spectra may be deduced from the spectrophotometric curves (Fig. 1), if we assume that the II complex shows a maximum absorbance at 550 mμ and the III complex, at 580 ~600 mμ, and that the shape of the curves for the I and II complexes are similar to that of the I complex in exhibiting lower absorbance. At lower pH values, a complex forms in solution which gives no EPR signal under the experimental conditions used. It was shown spectrophotometrically at pH 2.5 that a high concentration of this complex exists. It was also experimentally demonstrated that a complex of titanium(III)-EDTA forms in an acidic solution. This was accomplished by first forming the complex of titanium(III) with nitrilotriacetic acid (NTA) at pH 3.5. An intense EPR signal is obtained from this complex at this pH. An identical solution was then prepared, to which EDTA of a molar concentration twice that of titanium was added; the solution adjusted to pH 2.5. No signal was exhibited by this solution. The solution of titanium(III)-NTA was green, while that containing EDTA was purple, which is the color of pure titanium(III)-EDTA solutions at this pH. At pH values of 1 or 2, the color of solutions containing titanium(III) and EDTA, or titanium(III), EDTA, and NTA are the same, while the color of solutions containing titanium(III)-NTA are blue. It was also noticed that a solution containing the intensely-colored titanium(III)-acetylacetonate complex is decolorized upon the addition of EDTA. These phenomena appear to offer good evidence that the titanium(III)-EDTA complex is more stable than the titanium(III)-NTA or the titanium(III)-acetylacetonate complexes.

The following structures are proposed to represent the compounds which exist in the solutions studied:



3) G. Schwarzenbach and W. Biedermann, *Helv. Chim. Acta*, **31**, 459 (1948).
4) K. Saito and H. Terrey, *J. Chem. Soc.*, **1956**, 4701.
5) D. C. Olson and D. W. Margerum, *J. Am. Chem. Soc.*, **82**, 5602 (1960).

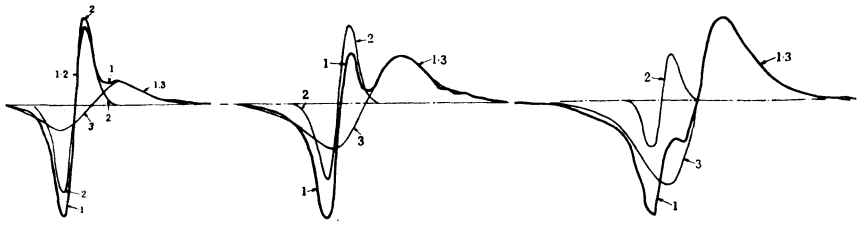


Fig. 3. Procedure for the analysis of signals with two peaks.
Curve 1 is the original spectrum.
Curves 2 and 3 are the reconstructed curve.

Structure I shows the possible complex where EDTA acts a tetradentate. Structure II, in which EDTA acts as a pentadentate, is proposed for the species which exists in neutral solution giving an EPR signal, but the absorbance seen in Fig. 1 is similar to that obtained in acid solutions. The proposed structure III, in which EDTA is a hexadentate, is obtained in a low concentration at pH values above 7, although at pH 10, it appeaes to be the only species in the solution. At pH 7 to 10, a mixture of the two complexes represented by structures II and III appear to be present in the solution.

An analysis was made of the signal of the two peaks obtained for the complex titanium(III)-EDTA at pH 7 to 9, were the concentration of titanium is 0.094 M and the ratio of titanium to EDTA is 1 to 2. The process used in this analysis is shown in Fig. 3; the peaks were first separated into two signals, assuming a normal Maxwell-Boltzmann distribution curve. Each curve was integrated, and the areas under the curves were calculated. The assumption was made that the ratio of the areas represent the ratio of the II and III complexes. Table III lists the results of this analysis. From the information obtained in this analysis, the equilibrium constant can be calculated for the following reaction:

TABLE III. RELATIVE AREAS OF RECONSTRUCTED CURVES AND CALCULATED EQUILIBRIUM CONSTANT FOR THE SYSTEM Ti(III)-EDTA (II AND III IN TABLE II)

pH	Relative areas of separated and integrated curves	*Ke* (mol./l.), calculated
6.9	1 : 1.8	2.07×10^{-7}
7.7	1 : 6.8	1.35×10^{-7}
8.2	1 : 24	1.49×10^{-7}
8.6	1 : 30	0.72×10^{-7}

$$\text{Ti(III)-EDTAH} \rightleftharpoons \text{Ti(III)-EDTA}^- + \text{H}^+$$

$$K_e = \frac{(\text{Ti(III)-EDTA}^-)\ (\text{H}^+)}{(\text{Ti(III)-EDTAH})}$$

The temperature and salt concentrations were not maintained constant for the data obtained for Table III. Although the calculated K_e values shown in Table III are not in excellent agreement, the effect of the temperature and such foreign salts as ammonium chloride and sodium chloride, which usually affect the stability of chelates, must be taken into consideration. The values obtained are of the same order, which strongly indicates that this method of analyzing signals is valid and that the assumed chelate species, II and III, exist in fact.

The Titanium(III)-EDTA-Oxalate System.— The EPR signal intensity and the spectrophotometric absorbance at 720 mμ for the titanium(III)-EDTA system are considerably increased upon the addition of certain organic acids. These effects were studied, and the formation of mixed chelate species was proved.

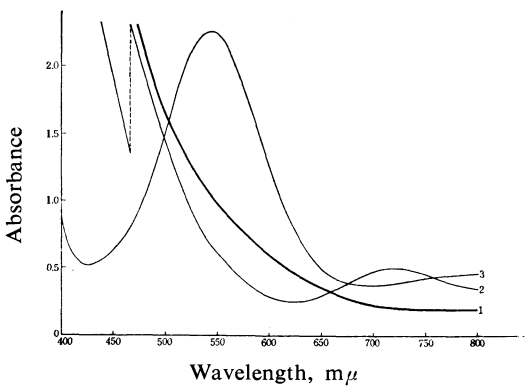
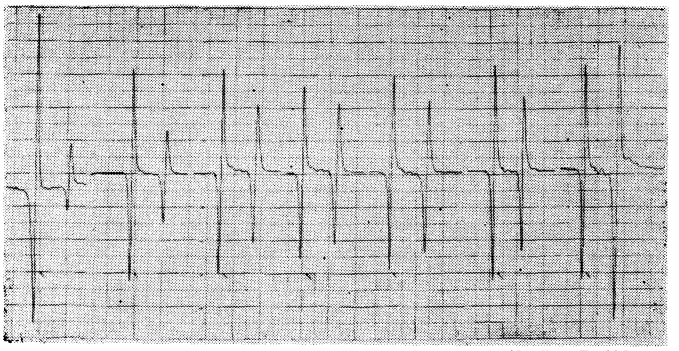


Fig. 4. Spectrophotometric curves for the Ti(III)-EDTA-oxalate system at pH 5.7.
Curve (1) Ti(III)-oxalate (1 : 3 ratio), Ti(III) concentration : 0.03M
Curve (2) Ti(III)-EDTA-oxalte (1 : 1 : 1 ratio), Ti(III) concentration : 0.6M
Curve (3) Ti(III)-EDTA (1 : 1 ratio), Ti(III) concentration 0.16 M

Three curves are shown in Fig. 4. Curve 1 is for the absorbance exhibited by the yellow-brown product formed between titanium(III)



No. (pH) 1 (2.5) 2 (3.7) 3(4.3) 4 (5.7) 5 (7.5) 6 (8.4) 7 (12.2)

Fig. 5. EPR spectra for the Ti(III)-EDTA-oxalate complex.
Spectrum 1 was obtained at three times the sensitivity and spectrum 7 was obtained at four times the sensitivity settings of the other spectra shown in this figure. Ti(III) concentration for spectrum 7 : 0.02 M. The Ti(III) concentration for all other spectra : 0.01M. Arrows designate DPPH.

and oxalic acid. The molar ratio of titanium(III) to oxalic acid is 1 to 3. No EPR signal is given by this complex at any pH value. The optical absorbance of this compound continues to increase with a decrease in the wavelength. Curve 2 is that of an equal molar ratio of titanium(III) and EDTA ; the maximum absorbance is seen at 550 mμ. Curve 3 is that of the amber-colored product of an equal molar ratio of titanium(III), EDTA, and oxalic acid, where the concentration of titanium(III) and EDTA is the same as for curve 2. No absorbance maximum at 550 mμ, such as is characteristic of the titanium(III)-EDTA complex, is observed. These curves undoubtedly prove the formation of a compound of three components; could not be a mixture of two complexes, such as the titanium(III)-EDTA and titanium(III)-oxalate complexes.

In Table I it may be seen that the EPR signal intensity of the titanium(III)-EDTA-oxalate complex increases with an increase in the pH value. The fact that a second peak does not appear at higher pH values (Fig. 5), as occurs with the titanium(III)-EDTA system, the titanium(III)-EDTA-tartrate system and the titanium(III)-EDTA-citrate system, is evidence for the presence of only a single complex. Evidence for the stability of the complex is seen in the fact that quantities of oxalic acid in excess of a 1 to 1 molar ratio have no such apparent effect on the signal intensity as is experienced with tartaric, citric and lactic acids (Table I and Fig. 9).

Figure 6 shows the spectrophotometric establishment of the composition of each component of complexes. A plot of the absorbance versus molar ratio of EDTA to titanium(III) is shown for all points. The pH values of these solutions were adjusted to 5.7 with ammonium hydroxide. A sharp break in the

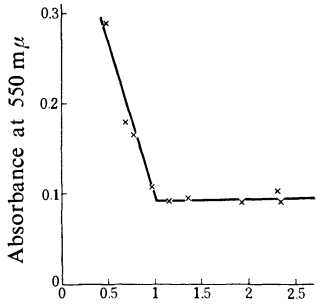


Fig. 6. Molecular ratio method for the determination of the ratio of EDTA in the Ti(III)-EDTA-oxalate complex at pH 5.7. Concentration of Ti(III) : 0.06 M. Concentration of oxalic acid : 0.18 M.

absorbance curve at 550 mμ is seen when the molar ratio of titanium(III) to EDTA reaches unity. The same experimental procedure was carried out at pH 2.5, and the same molar ratio for the complexes was found. The less intense EPR signals obtained at lower pH values probably result from the presence of a higher concentration of a complex of the same composition but possessing a different structure, one which does not give an EPR signal.

The determination of the ratio of oxalate in the titanium(III)-EDTA-oxalate complex is shown in Fig. 7. The ratio of titanium(III) to EDTA was maintained constant, varying amounts of oxalic acid were added, and the pH was adjusted to 4.5. A break in the curve at 550 mμ may be seen when the molar concentration of each component of the complex is approximately equal. At 720 mμ the break in the curve, which is not very pronounced, is seen at approximately the same molar concentration.

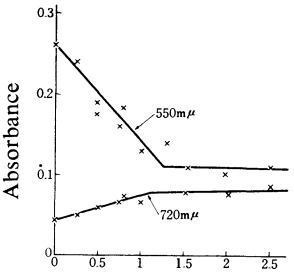


Fig. 7. Molecular ratio method for the determination of the ratio of oxalic acid in the Ti(III)-EDTA-oxalate complex at pH 4.5. Concentration of Ti(III) and EDTA : 0.06 M.

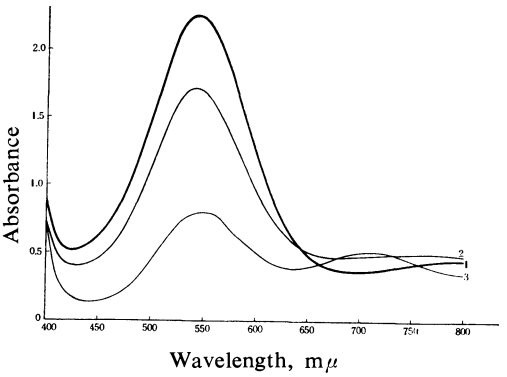


Fig. 8. Spectrophotometric curves for the Ti(III)-EDTA-tartrate system at pH 5.7. Concentration of Ti(III) : 0.16 M
Curve (1) Ti(III)-EDTA (1 : 1 ratio)
Curve (2) Ti(III)-EDTA-tartrate (1 : 1 : 1 ratio)
Curve (3) Ti(III)-EDTA-tartrate (1 : 1 : 3 ratio)

Formula IV is proposed for the main species of the titanium(III)-EDTA-oxalate complex present in solution :

$$(Ti^{3+}EDTAH_2^{2-}(COO)_2^{2-})$$
IV

The Titanium(III)-EDTA-Taratrte, -Citrate, and -Lactate Sytems.—As with oxalic acid, tartaric, citric, and lactic acids also affect the titanium(III)-EDTA complex by increasing the EPR signal intensity and permitting the EPR signal to be obtained at lower pH values. The EPR spectra and spectrophotometric curves are shown in Figs. 8 and 9.

It may be seen in Table I and Fig. 9 that the titanium(III)-EDTA-tartrate EPR signal intensity increases up to a molar ratio of tartaric acid to titanium(III) of at least 50 to 1 under the experimental conditions employed. However, no quantitative measurement of this effect could be made because of the insolubility of some tartrate salts at the ratio of tartaric acid to titanium(III) of 3 to 1.

Upon the addition of tartaric acid to the titanium(III)-EDTA complex, the EPR signal intensity continues to increase. It is shown

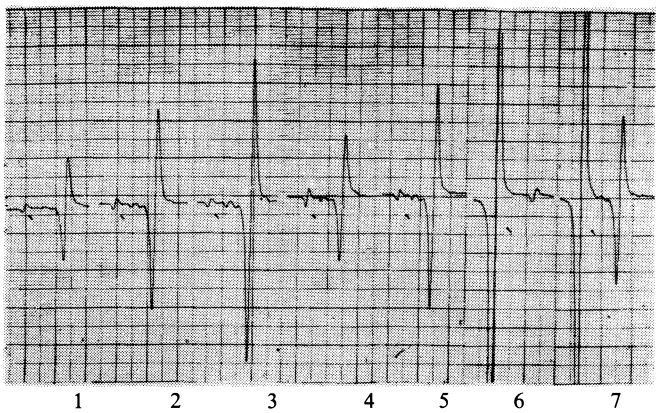


Fig. 9. EPR spectra for the Ti(III)-EDTA-tartrate, -citrate, and -lactate complexes. The sensitivity setting used for spectra 4, 5, 6 and 7 was twice that used for spectra 1, 2 and 3. Arrows designate DPPH.

Spectrum No.	Acid	Ti(III) : EDTA : Acid	Molar Concn. of Ti(III)	pH
1	Tartaric	1 : 1 : 1	0.1	5.7
2	Tartaric	1 : 1 : 2	0.1	5.7
3	Tartaric	1 : 1 : 3	0.1	5.7
4	Citric	1 : 1 : 1	0.2	5.7
5	Citric	1 : 1 : 2.5	0.2	5.7
6	Lactic	1 : 1 : 1	0.2	3.2
7	Lactic	1 : 1 : 3	0.1	5.7

spectrophotometrically in Fig. 8 that, when tartrate ions are present in a 3 to 1 ratio to titanium(III) and EDTA, the concentration of the complex as exhibited by the absorbance at 720 mμ is the same as that shown for the oxalate complex. It may be noted that the EPR signal intensity never reaches half the intensity of the signal obtained for the oxalate complex. The unexpectedly high absorbance which occurs for this complex at 720 mμ may be due to a greater absorbance of the tartrate complex over that of the oxalate complex.

The continuous increase of the EPR signal and in the optical absorbance at 720 mμ with the increase in tartrate ion concentration indicates a lower stability for the three-component complex containing tartrate, but no definite ratio of the complex can be established by these techniques. In this three-component system, the complex obviously exists in pH-dependent and organic acid concentration-dependent equilibria.

With succinic and acetic acids, no maxima are exhibited at 720 mμ, and the absorbance for the entire curve is the same as for the titanium(III)-EDTA complex alone. No EPR signals are obtained for the titanium(III)-EDTA complex in the presence of these acids at low pH values, which appears to show that these acids do not form complexes similar to the titanium(III)-EDTA-oxalate complex.

The spectrophotometric curve for lactic acid falls between curves 1 and 2 in Fig. 8, which indicates that this acid forms a less stable complex than tartaric and citric acids, and we were unable to observe any increase in absorbance at 720 mμ. An EPR signal with lactic acid is obtained at pH 3.2, where the complex with EDTA alone does not give a signal. These spectrophotometric results correspond well with those obtained by EPR.

With the complex formed with citric acid, a spectrophotometric curve is obtained which is very close to curve 1 in Fig. 8. Moreover, the EPR signal obtained for the citrate complex at pH 5.7 is much more intense than that obtained for the titanium(III)-EDTA complex at this pH. These indicate a behavior of citrate similar to that of tartrate with the titanium(III)-EDTA system. At a pH of about 9, a second peak appers for the titanium(III)-EDTA-citrate complex, and at a pH of about 10, a second peak appears for the titanium-(III)-EDTA-tartrate complex. A study of the latter system has been reported on in a previous paper.[1]

Summary

An electron-paramagenetic resonance and spectrophotometric study has been made of the composition of mixed chelate compounds of titanium(III)-ethylenediaminetetraacetic acid (EDTA) and organic acids. The existence of three titanium(III)-EDTA complexes in solution has been established. The complex formation of titanium(III)-EDTA with oxalate, tartrate, citrate and lactate has been confirmed, and the ratio of the oxalate has been established. Structures for the complexes have been proposed, probable equilibrium mixtures of complexes at various pH values have been discussed and new procedures have been proposed for the detection of chelate compounds in solution.

The assistance of Miss Tokuko Seki with the calculations of the equilibrium constans of the complexes is gratefully acknowledged.

Department of Chemistry
Faculty of Science
The University of Tokyo
Hongo, Tokyo

*The Volumetric Determination of Manganese in Ores**

By Kozo NAGASHIMA, Maurice CODELL** and Shizuo FUJIWARA

(Received December 20, 1963)

An improved method has been needed for the determination of moderate amounts of manganese in minerals, ores, and metals. Many methods which are applicable to small amounts of manganese cannot be accurately applied to substances containing high concentrations of manganese.

Of the many methods which have been published concerning the determination of manganese, few exist which do not have serious shortcomings. The method where manganese is oxidized to permanganate with sodium bismuthate[1,2] is time-consuming and requires filtration through a substance which does not reduce permangante, and the danger exists that the solution will come into contact with reducing substances. This method is generally applied to low concentrations of manganese. Cerium and cobalt are known to interfere, and chromium requires special attention. The method in which manganese is oxidized to permanganate with peroxysulfate and titrated with arsenite[3] often gives trouble with the end-point detection because of the reoxidation of manganese by the residual peroxysulfate. As with the bismuthate method, this method is generally applied to small amounts of manganese. The direct Volhard titration method with permanganate[1] is attended with great difficulty since manganese(IV) oxide precipitates and imparts a brown color to the solution which partially obscures the end point. The chelatometric titration of manganese with a solution of ethylenediaminetetraacetic acid (EDTA)[4] is non-specific and requires the presence of masking agents and a careful control of the pH values.

Schroder[5] found that manganese is quantitatively converted to manganese(III) from any valence state by heating solutions containing manganese to fumes with a mixture of perchloric and phosphoric acids; he applied this process to the determination of manganese in ferromanganese, steel, and brass by titrating the manganese(III) with a ferrous solution. He also applied the method to the photometric determination of manganese in aluminum alloys,[6] by measuring the intensity of the redish color of the manganese(III) ion. The process was applied by Nagato[7] to the photometric determination of manganese in ferrite. When possible reagents were investigated by Kitakawa and Shibata[8] for the quantitative conversion of manganese to manganese(III), they reported that a mixture of phosphoric acid and sodium bismuthate was also effective for this purpose. Kimura, Tanino, and Kitahara[9] treated various samples containing manganese(IV) oxide with a mixture of phosphoric and sulfuric acids and titrated the resulting manganese(III) with a ferrous solution; however, this process is applicable only to samples containing manganese chiefly as manganese(IV) oxide.

Several methods which appeared to offer the greatest probability of successful application were tested in this laboratory. The method whereby manganese is oxidized to manganese(III) using the phosphoric acid-perchloric acid system seemed attractive because of its simplicity. The applicability of this method to large amounts of manganese is evident since the reduction of manganese(III) to manganese (II) involves a valence change of one, whereas methods in which manganese is oxidized to permanganate and reduced to the manganous ion involves a valence change of five.

It was found that manganese(III) can be kept in the concentrated acid mixture for several days without any noticeable reduction, but if the solution is diluted, titration should follow within a few hours.

The only interference encountered with the method was titanium in excess of 30 mg. It was found that titanium in excess of this amount precipitated as an insoluble phosphate

* A part of this paper has been published in Japanese. *Japan Analyst*, **13**, 261 (1964).

** Present address: The Pitman-Dunn Institute for Research, Philadelphia 37, Pa., U. S. A.

1) "Japanese Industrial Standards," M8236 (1953), M8236 (1958).

2) "Methods For The Chemical Analysis of Metals," A. S. T. M. 1950, pp., 80, 82, 150.

3) "Methods For The Chemical Analysis of Metals," A. S. T. M., 1950, p. 150.

4) K. Watanuki and S. Tomura, *Japan Analyst*, **10**, 1027 (1961); see also H. Flaschka, *Chemist-Analyst*, **42**, 56 (1958).

5) H. Schroder, *Metall*, 8, 542 (1954).

6) Idem., ibid., **9**, 100 (1955).

7) H. Nagato, *Japan Analyst*, **10**, 985, 991 (1961); **11**, 1291 (1962).

8) K. Kitakawa and N. Shibata, *Japan Analyst*, **9**, 597 (1960).

9) K. Kimura, K. Tanino and S. Kitahara, *Rikagaku Kenkyusho Hokoku*, 229 (1959).

TABLE I. DETERMINATION OF MANGANESE IN VARIOUS MIXTURES

	Sample	Mn added mg.	Mn recovered mg.
1) a)	100 mg. of Mn-oxide ore+100 mg. of pyrite	55.00	55.12
b)	100 mg. of Mn-oxide ore+100 mg. quartz	55.00	55.09
c)	100 mg. of Mn-oxide ore+100 mg. zinc blend	55.00	55.31
2) a)	$KMnO_4$ solution+200 mg. Chromium	54.90	55.55
b)	$KMnO_4$ solution+200 mg. Chromium	54.90	55.23
c)	$KMnO_4$ solution+200 mg. Vanadium	54.90	55.11
3) a)	$KMnO_4$ solution+5 ml. H_2SO_4	54.90	54.95
b)	$KMnO_4$ solution+3 g. Na_2SO_4	54.90	55.22
c)	$KMnO_4$ solution+10 g. K_2SO_4	54.90	—

(1) Manganese oxide ore is the mixture shown in annotation (2) of Table II, average of two determinations.
(2) a) Chromium added as $(NH_4)_2CrO_4$, (2) b) Chromium added as $Cr_2(SO_4)_3$, (2) c) Vanadium added as $VOCl_2$.
(3) c) Upon dilution with water, a considerable amount of K_3PO_4 precipitated and some manganese was retained by the precipitate.

TABLE II. RESULTS OF ANALYSIS

	Sample	Weight of sample, mg.	Mn found %	Mn by other methods, %
(1)	Ferromanganese	100	75.11	75.3*
		200	74.98	
(2)	Mn-oxide ore	100	55.09	55.08
		200	54.91	
(3)	Mn-carbonate ore	100	36.33	36.45
		200	36.41	
(4)	Mn-silicate ore (a)	200	27.03	27.06
		500	27.06	
	(b)	200	31.55	31.78
		300	31.76	
	(c)	200	49.88	49.35
		200	49.03	

(1) Recommended value*: Japanese Standard ferromanganese sample No. 13A.
(2) Mixture of pyrochroite $Mn(OH)_2$ and Hydrohausmannite $(Mn^{2+}, Mn^{3+})(OH,O)_2$ from Noda-Tamagawa mine, Iwate Prefecture, Japan.
(3) Calcian rhodochrosite $(Mn, Ca)CO_3$ from Teine mine, Hokkaido, Japan.
(4) (a) Bustamite $(Mn, Ca)SiO_3$ from Kanoiri mine, Tochigi Prefecture, Japan.
(b) Pyroxmangite $(Mn, Fe)SiO_3$ from Kaso mine, Tochigi Prefecture, Japan.
(c) Tephroite Mn_2SiO_4 from Kanoiri mine, Tochigi Prefecture, Japan

and co-precipitated some manganese. The separation of 25 mg. of manganese from 200 mg. of titanium was carried out by means of the addition of sodium peroxide to a nearly neutral solution, followed by the filtration of the precipitated manganese dioxide.[10] Quantities of manganese in excess of 25 mg. interfered by causing a rapid decomposition of the peroxide, which resulted in the precipitation of a considerable quantity of titanium.

Manganese ores often contain sulfide minerals such as pyrite (FeS_2). It was found that these minerals dissolve readily in the acid mixture used in the procedure and cause no interference. Up to 5 ml. of sulfuric acid in the acid mixture is without effect, and the presence of up to 3 g. of potassium sulfate causes no interference, but more than 5 g. of potassium sulfate caused bad results because of the precipitation of potassium phosphate upon dilution, which co-precipitated some manganese. The presence of 5 g. of sodium sulfate caused difficulty with some samples because of the insolubility of the mixture, which solidifies upon cooling.

The effects of chromium and vanadium upon the determination were investigated. Chromium imparts a color to the solution which makes the end point difficult to detect. The addition of a ferrous *o*-phenanthroline indicator effectively eliminates any interference from

10) M. Codell, "Analytical Chemistry of Titanium Metals and Compounds," Interscience-Wiley, New York (1959), p. 172.

this source, however. Vanadium is converted to vanadium(V) upon fuming with the acid mixture and consumes the ferrous solution upon titration. In the presence of vanadium, it is, therefore, necessary to add an excess of ferrous solution and back-titrate with a permanganate solution. Vanadium(V) is reduced to vanadium(IV) by the ferrous solution and oxidized to vanadium(V) by the permanganate solution; the net result is the same.

Table I shows the recovery of manganese from various ores to which known amounts of manganese have been added, and from solutions of permanganate to which substances have been added to determine their possible interference with the quantitative recovery of manganese.

Table II gives an analysis, by the proposed method, of ferromanganese and ores which have been previously analyzed for manganese content by other methods.

The following procedure and the two modified procedures should provide a means of analyzing most substances containing moderate amounts of manganese which are likely to be encountered.

Experimental

A Procedure for Samples Other than Silicate Ores and Containing Less than 30 mg. of Titanium.—Transfer a sample to a 300 ml. conical beaker. Add 5 ml. of water to moisten the sample, and, if the presence of organic matter is suspected, add 5 ml. of concentrated nitric acid. Add 10 ml. of phosphoric acid and 10 ml. of perchloric acid. Warm gently on a hot plate. If the sample does not dissolve, add 5 ml. of hydrochloric acid and heat gently. If the sample still remains undissolved, remove from heat and add 5 ml. of 10% hydrogen peroxide. Heat strongly until fumes of perchloric acid issue freely from the top of the beaker. Remove from the hot plate and allow to cool. Add 200 ml. of water and titrate with a 0.1 N ferrous ammonium sulfate solution until the red color disappears.

For samples containing chromium in quantities sufficient to cause a deep color, add 4 drops of a ferrous *o*-phenanthroline indicator to enable the end point to be detected.

For samples containing vanadium, add an excess of a ferrous ammonium sulfate solution and 4 drops of a ferrous *o*-phenanthroline indicator and back-titrate with a 0.1 N potassium permanganate solution.

Procedure for Silicate Ores.—Place the sample in a platinum dish, moisten with water, and 10 ml. of perchloric acid and 10 ml. of concentrated hydrofluoric acid. Evaporate to strong fumes of perchloric acid. Cool, transfer the solution to a conical beaker, and proceed as directed above.

Procedure for Samples Containing up to 200 mg. of Titanium and not more than 25 mg. of Manganese.—Dissolve the sample with hydrochloric acid, with a mixture of hydrochloric and hydrofluoric acids, or by fusion with 3 g. of sodium bisulfate with a few drops of sulfuric acid. If alkali fusion has been used, render the solution slightly acid with hydrochloric acid. To the acidic solution of the sample, add 20% sodium hydroxide until the first permanent precipitate forms; then add 3 g. of sodium peroxide and heat gently until it boils. Allow to cool to about 60°C and, if some titanium appears to have precipitated, add 5 ml. of 10% hydrogen peroxide. Filter through a rapid paper and wash the precipitate with a 1% solution of sodium carbonate containing 1% hydrogen peroxide. Discard the precipitate.

To the filtrate add 10 ml. of phosphoric acid and 10 ml. of perchloric acid and proceed as directed under the first procedure.

Department of Chemistry
Faculty of Science
The University of Tokyo
Hongo, Tokyo

The Photometric Determination of Titanium with Acetylacetone

By Shizuo FUJIWARA, Kozo NAGASHIMA and Maurice CODELL*

(Received December 20, 1963)

Many methods have been published concerning the determination of titanium in various substances.[1] The most widely-used method is that based on the yellow complex formed upon the addition of hydrogen peroxide to acidic solutions of titanium. Several factors can affect the results obtained by this procedure; these factors include the quantity of salts present in the solution, the quantity of peroxide used, and the temperature of the solution to which peroxide is added. The method is also subject to much interference, including that of niobium, which forms a red color with peroxide. Niobium frequently accompanies titanium in minerals.

One of the most sensitive and selective methods for the determination of titanium is based upon the measurement of the absorbance of the titanium thiocyanate complex at 432 mμ. after extraction from a hydrochloric or sulfuric acid solution by tri-*n*-octylphosphine oxide dissolved in cyclohexane.[2] The extracted complex follows Beer's law up to at least 1.7 μg. Ti/ml. Niobium and molybdenum are also known to interfere.

Acetylacetone has been of interest in analytical chemistry for many years because of its great ability to form complexes with many metals. Its use in complex formation for the solvent extraction of metals was given an excellent treatment in a monograph on the subject of metal solvent extractions,[3] in which the solvent extraction procedure utilizing acetylacetone was applied to titanium(IV). Acetylacetone forms a complex with titanium-(III) which is intensely red in an acidic solution and blue in neutral and basic solutions. The color and absorbances of titanium(III) acetylacetonate containing 2.0 mg. of titanium in 50 ml. of solution at varying pH values are shown in Table I. The absorbances were measured with a Hirama Filter Photometer using 1 cm. cells. This reagent seemed very desirable for use as an analytical reagent for titanium because of its apparent ease of application, and because of the few ions which may be expected to interfere. Early attempts in this laboratory to utilize this complex for the quantitative determination of titanium were unsuccessful because of the instability of the color, which faded to a considerable extent within a few minutes after the addition of the reagent. This fading was somewhat delayed by the addition of stannous chloride, and a further delay in the fading process was accomplished by adjusting the pH to the range 1.5 to 2.5. Even with these innovations, however, the stability of the color was insufficient for use as an analytical procedure. It was then found that the addition of a few granules of zinc metal to the final solution delayed the fading sufficiently to allow the method to be generally applied.

TABLE I

pH	Lower than 1.5	1.5~2.5	Higher than 2.5
Color	red	red	Becomes more bluish with increasing pH values
Absorbance at 517 mμ	0.20 (at pH 0.5)	0.29	0.28 (at pH 4)

A spectrophotometric curve covering the visible region for titanium(III) acetylacetonate containing 1 mg. of titanium in 50 ml. of solution is shown in Fig. 1. The molar extinction index calculated for the maximum at 500~510 mμ is 350.

Complexing acids were investigated for the purpose of maintaining in solution titanium-(III), tin(II), and other ions likely to be encountered in an analysis. The most desirable reagent for this purpose was found to be citric acid. The pH most suited to color development could be obtained by the addition of citric acid only; there was no necessity of adding any additional reagents to adjust the pH.

It was found that additions of EDTA, ascorbic acid, and thioglycollic acid as a means of eliminating interferences were unsuccessful because the intensity of the color of the titanium(III)-acetylacetonate complex was lower in their presence.

* Present Address: The Pitman-Dunn Institute for Research, Philadelphia 37, Pa., U.S.A.

1) M. Codell, "Analytical Chemistry of Titanium Metals and Compounds," Interscience-Wiley, New York (1959), p. 87.

2) J. P. Young and J. C. White, *Anal. Chem.*, 31, 393 (1959).

3) G. H. Morrison and H. Freiser, "Solvent Extraction in Analytical Chmistry," Wiley, New York (1957), p. 158.

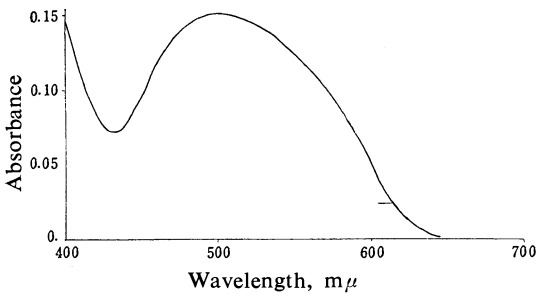


Fig. 1. Absorbance curve of titanium(III)-acetylacetonate.

The Procedure for Silicate Minerals.—Transfer a sample containing 0.2 to 20 mg. of titanium to a platinum dish, and add 10 ml. of sulfuric acid (1 to 1) and 5 ml. of concentrated hydrofluoric acid. Evaporate to fumes of sulfuric acid. Wash the sides of the dish with a small amount of water and again heat to fumes. Repeat the washing and fuming once more to insure the expulsion of all the fluoride. Transfer to a 100 ml. volumetric flask and dilute to 50 ml. Filter, ignite the residue, and fuse with about 2 g. of potassium bisulfate. Dissolve the melt in 10 ml. of sulfuric acid (1 to 10). Transfer the solution to the filtrate. If the titanium content is more than 7 mg. and dilute to a definite volume; then take an aliquot containing 1 to 5 mg. of titanium and add sulfuric acid sufficient to make the total content about 5 ml. of concentrated acid. Adjust the volume to 20 ml. If no aliquot has been taken, evaporate the solution to 20 ml. To the solution in a 100 ml. Ehrlenmeyer flask, add 1 g. of zinc (20 mesh). Let stand for about 10 min. In the presence of more than 20 mg. of iron, allow the solution to stand for 20 min. Add 5 ml. of a stannous chloride solution (5%). Add ammonium hydroxide (1 to 1) until the first faint permanent precipitate forms. Add 10 ml. of a 20% citric acid solution and 5 ml. of a 10% acetylacetone solution, and transfer the solution to a 50 ml. volumetric flask. Add several garnules of zinc metal (approximately 0.1 g.) and dilute to the mark with water. Within 45 min., measure the absorbance of the solution at 510 mμ, and estimate the titanium content by comparison with a calibration curve prepared by the absorbance measurement of a series of standard solutions containing known amounts of titanium, solutions prepared by adding 10 ml. of sulfuric acid (1 to 1) to aliquots of the stock solution contained in a 100 ml. Ehrlenmeyer flask and following the procedure for silicate rocks from the point where 1 g. of zinc is added. A stock standard solution of titanium containing 1 mg./ml. is prepared by heating titanium dioxide with a mixture of sulfuric acid and ammonium sulfate over an open flame and diluting the mixture with 1 : 10 sulfuric acid. A calibration curve prepared in this manner is shown in Fig 2. The results of the titanium analysis of two rock samples are shown in Table II.

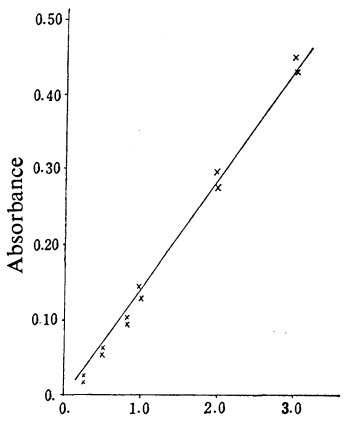


Fig. 2. Calibration curve.

TABLE II. ANALYSIS OF ROCK SAMPLES

Rock	Ti % found	Rock	Ti % found
	0.315		0.465
Granite	0.305	Silica ore	0.443
(2% Fe)	0.300	(0.8% Fe)	0.437
	0.299		0.415
	0.288		
	0.31 (by the H_2O_2 method)		0.45 (by the H_2O_2 method)

The Procedure in the Presence of Niobium Oxide.—Transfer a sample not exceeding 40 mg. of niobium to a platinum crucible. Fuse with 2 g. of potassium bisulfate and dissolve the melt in 10 ml. of sulfuric acid (1 to 1). Transfer the solution to a 100 ml. Ehrlenmeyer flask and dilute to 20 ml. Add 1 g. of zinc and proceed as directed above. The results of the analysis of titanium in titanium-niobium mixtures are shown in Table III.

TABLE III. DETERMINATION OF Ti IN THE PRESENCE OF 30 mg. Nb

Ti added, mg.	Ti recovered, mg.
3.0	3.2, 3.1, 3.0
2.0	2.1, 2.1

The Procedure in the Presence of Chromium, Vanadium and More than 25 mg. of Iron.—Dissolve the sample as directed in either of the above procedures. Transfer to an electrolytic beaker, dilute to 100 ml., adjust the sulfuric acid concentration to 5%, and electrolyze the solution at a mercury cathode for 15 min., using a current of 5 amp. Remove the solution, evaporate to 20 ml., add 1 g. of zinc, and proceed as directed under the

TABLE IV. DETERMINATION OF Ti AFTER TREATMENT WITH A MERCURY CATHODE

Ti presence, mg.	Ions added, mg.	Ti recovered, mg.
3.00	Fe 100	2.87
3.00	Fe 50	3.02
3.00	Cr 30	2.92
3.00	V 30	2.86

first procedure. The results of the analysis of titanium after treatment with a mercury cathode are shown in Table IV.

Summary

A new method has been proposed for the determination of small amounts of titanium in various substances. Acetylacetone forms an intensely-colored red complex in an acid solution with titanium(III), but this complex had not previously been used for the photometric estimation of titanium, probably because of the great instability of its color. A process has now been proposed for stabilizing the color. Up to 30 mg. of niobium and 30 mg. of iron do not interfere. Interference is encountered from chromium and vanadium, and in their presence, or in the presence of more than 30 g. of iron, a mercury cathode separation must be made. The method has been applied to quantities of titanium as small as 0.2 mg. in 50 ml. of solution.

The assistance of Mr. Toshikatu Sugiura in the performance of many of the analyses reported in this paper is gratefully acknowledged.

Department of Chemistry
Faculty of Science
The University of Tokyo
Hongo, Tokyo

The Spectrophotometric Determination of Anions by Solvent Extraction with Metal Chelate Cations. I. A New Method for the Determinetion of Perchlorate Ions*

By Yuroku YAMAMOTO and Keiya KOTSUJI

(Received November 22, 1963)

Although there have been no experimental investigations of the extraction for tris-2, 2'-dipyridyl-iron(II)-perchlorate, theoretically the same behavior of the compound as the phenanthroline chelate may be expected.[1,2] In our investigation, it is confirmed that the perchlorate of the dipyridyl-iron(II) chelate can be extracted into nitrobenzene. However, the following differences exist between the dipyridyl and the phenanthroline chelate. If the perchlorate ion is absent in the 0.2 M acetate buffer solution, the dipyridyl chelate can not be extracted into nitrobenzene (this can be confirmed by the colorlessness of the organic layer) ; on the other hand, the phenanthroline chelate can be extracted moderately well. The behavior of iodide ions is more complicated. In the acetate buffer solution (0.2 M), iodide ions can be extracted with the phenenthroline chelate, but not with the dipyridyl chelate. However, the iodide ions are also extracted with the dipyridyl chelate if a small amount of perchlorate is present. Moreover, an anionic complex such as tetra-iodo-cadmium(II) or mercury(II) can be extracted into 1, 2-dichloroethane with the dipyridyl chelate, but not into nitrobenzene. In the case of the phenanthroline chelate, the extraction of the anionic complex is hindered by a large amount of iodide. For other cationic chelates such as cuproine,*1 Kuznetsov[2] has pointed out that chloride ions are extractable into alcohols with cuproine.*1 It is also confirmed by radioactive tracer in this work that a trace amount of chloride ions is extracted into hexylalcohol when bathocuproine*2 is in the organic phase and when copper(I) ions are in the aqueous phase.

These facts suggest that it may be possible to establish a selective and sensitive method for the determination of simple anions or oxygenated anions, and or the anionic complex ions of some metals. The method is thus based upon the estimation of the absorbance belonging to the chelate cations in the organic phase.

The present work is the first of a series of papers on the photometric determination of anions by solvent extraction with a metal chelate. This paper is concerned with the determination of perchlorate with tris-2, 2'-dipyridyl-iron(II) chelate. In that part of the

* Presented at the 12th Annual Meeting of the Japan Society for Analytical Chemistry, Kanazawa, October, 1963.

1) R. M. Diamond and D. G. Tuck, "Progress in Inorganic Chemistry," 2, (1960), 139-150.

2) B. I. Kuznetsov, "The Chemical Basis for Photometric Method by Solvent Extraction in Analytical Chemistry," Moscow (1963), pp. 11-12.

*1 Biquinolyl.

*2 4, 7-Diphenyl-2, 9-dimethyl-1, 10-phenanthroline.

second paper which has been published as a short communication,[3] a colorimetric determination of iodide is treated in the similar way. The third paper[4] is concerned with mercury(II) and cadmium(II).

Experimental

Apparatus. — The spectrophotometric measurements were made with a Hitachi Model EPU-2 spectrophotometer with 10.0 mm. cells.

The shaking was done with a Iwaki Model KM shaker.

The pH measurements were made with a Horiba M-3 pH meter.

The separation of the organic layer from the aqueous layer was carried out with a separatory funnel of about 120 ml.

Materials.—*Ferrous Ammonium Sulfate Solution.* Guaranteed ferrous ammonium sulfate hexahydrate was dissolved in a small volume of water containing 5 ml. of 1 N sulfuric acid; then the mixture was diluted to 500 ml. with water to make a 3.0×10^{-3} M solution. It was standardized with a standard potassium permanganate solution.

2, 2'-Dipyridyl Solution.—Guaranteed 2, 2'-dipyridyl was dissolved in distilled water containing 1 ml. of 1 M hydrochloric acid, and then the mixture was diluted to 300 ml. with water to make a 1.2×10^{-2} M solution.

Standard Perchlorate Solution.—A standard solution containing 1 mg. of perchlorate ions per millilter was prepared by dissolving guaranteed potassium perchlorate (dried at 100°C) in distilled water. This standard solution was diluted to the concentration required for the experiments.

Nitrobenzene was purified by vacuum distillation at 23~25 mmHg.

Anhydrous sodium sulfate, guaranteed reagent.

All other reagents used were of analytical grade without further purification.

Procedure.—Mix 2, 2'-dipyridyl, ferrous ammonium sulfate, 3 M sodium acetate, and the standard perchlorate solution in the proper concentration. Adjust the pH of the solution to the required value with dilute sulfuric acid or a dilute sodium hydroxide solution and dilute to 25 ml. with distilled water, Add 10.0 ml. of nitrobenzene. Shake for 20 min. After the solution has stood for 30 min., transfer the organic layer into a glass flask containing 1 g. of anhydrous sodium sulfate and shake vigorously to make the solution transparent. Then transfer it through a folded filter paper into a 10.0 mm. cell. Measure the absorbance of the solution at 524 mμ using a reagent blank solution or nitrobenzene as a reference. Measure the pH of the aqueous layer after the separation.

Results and Discussion

Absorption Spectrum.—The spectral absorbance curves are shown in Fig. 1. They were measured for a nitrobenzene solution obtained by extraction from an aqueous solution which contained perchlorate and one which did not. The absorbance maximum is at 524 mμ in the organic layer. The absorbance maximum of the chelate cation in the aqueous solution was at 522 mμ, a value which coincides with that found in literature.[5] This slight red shift in the organic layer may be attributed to the effect of the association between cations and anions in such a polar solvent as nitrobenzene. Therefore, the chemical formula of the extracted species may be $[Fe(II)(dip.)_3]\cdot(ClO_4)_2$.

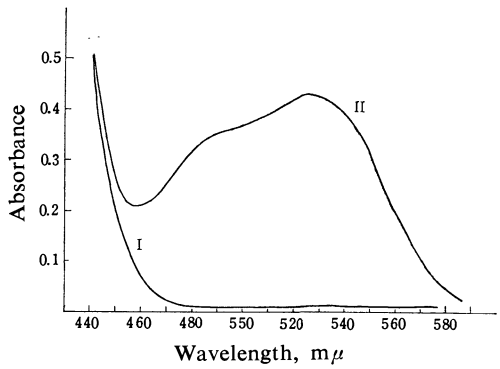


Fig. 1. Absorption spectra.

Curve I Spectrum of nitrobenzen solution extracted from aqueous solution containing Fe(II) 4.8×10^{-4} M, Dip. 2×10^{-3} M, NaAcO 0.24 M, pH 6.5, but ClO_4 absent, reference: water

Curve II Spectrum of nitrobenzene solutions extracted from aqueous solution containing Fe(II) 4.8×10^{-4} M; dip. 2×10^{-3} M, NaAcO 0.24 M, and ClO_4 4×10^{-5} M, pH 6.5; reference: water

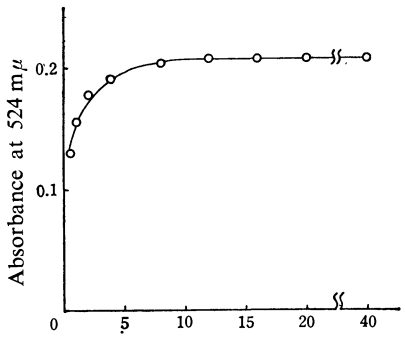


Fig. 2. Effect of concentration of iron(II).

Concn. of Perchlorate: 2.0×10^{-5} M
Mole ratio of dip. to iron: 4
pH: 6.5 Time of shaking: 20 min.
Reference: Reagent blank.

3) Y. Yamamoto and S. Kinuwaki, This Bulletin 37, 434 (1964).

4) Y. Yamamoto and K. Kotsuji, ibid., 37, 594 (1964).

5) M. L. Moss and M. G. Mellon, *Ind. Eng. Chem., Anal. Ed.*, 14, 826 (1942).

The Effect of the Reagent.—The extraction of perchlorate ions into nitrobenzene may be governed by the concentration of ferrous ammonium sulfate, 2, 2'-dipyridyl, and sodium acetate. The effect of changing the amounts of their reagents has to be considered.

A) The Effect of the Ferrouso Ammonium Sulfate Concentration.—To a constant amount of perchlorate ions (2.0 p.p.m.), various amounts of ferrous ammonium sulfate and 2, 2'-dipyridyl, in which the mole ratio of dipyridyl to ferrous iron was kept constant, were added. The mole ratio was kept at 4 to 1 because a slight excess of the dipyridyl may be needed for the stoichiometric formation of the chelate cation. The pH of the solutions was kept at 6.5, and the procedure was carried out for the solution. Figure 2 shows the effect of the concentration of ferrous ions on the extraction of perchlorate ions. It is found that the mole ratio of iron(II) to perchlorate ions has to be held at more than 10 to 1. This mole ratio, therefore, was made 12 to 1 in this work.

B) The Effect of the 2, 2'-Dipyridyl Concentration.—The amount of perchlorate ions and the mole ratio of iron(II) to perchlorate ions were kept at the constants of 2.0 p.p.m. and 12 to 1 respectively. A different amount of the dipyridyl was added, and the extraction was carried out according to the procedure described above. Figure 3 shows that the mole ratio of the dipyridyl to iron(II) has to be held at more than 3 to 1. This mole ratio was kept at 4 to 1 in this work.

C) The Effect of the Sodium Acetate Concentration.—If the concentration of sodium acetate is low in the aqueous phase, it is time-consuming to separate the two phases because of the formation of an emulsion. It was found that the formation of an emulsion could be prevented by the presence of sodium acetate in a concentration of 0.2~0.3 M. The salt was also useful as a buffering agent. The concentration of the acetate was kept at 0.24 M in this work.

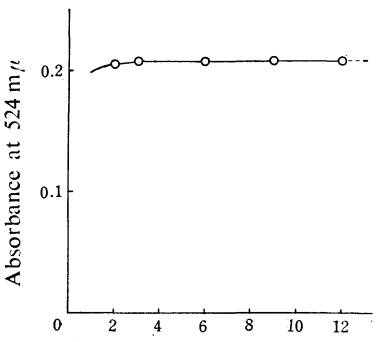


Fig. 3. Effect of mole ratio of dip. to iron(II)
Perchlorate: 2.0×10^{-5} M
Mole ratio of iron(II) to perchlorate: 12
NaAcO: 0.24 M
pH: 6.5
Shaking time: 20 min.

The Effect of the Shaking Time.—The shaking time in the extraction was varied from 5 to 30 min., while the other variables were kept constant. The shaking time had a slight effect on the extraction, and it was enough to shake it for more than 20 min.

The Effect of the pH Value.—It has been stated in the literature,[3] and also confirmed in this work, that the optimum pH for the formation of tris-dipyridyl iron chelate ions is in the range of 3~9 in an aqueous phase. In order to study the effect of pH on the extraction, a series of solutions adjusted to various pH values was preparaed and treated as in the procedure described above. It was found that there is a maximum and constant absorbance in the organic phase over the pH range from 3.5 to 8.5. Therefore, the solution was adjusted at pH 6.5 in this work.

The Stability of the Color.—Color developed immediately at room temperature and was independent of the temperature at 10~20°C. The color of the organic phase was stable, even after 24 hr.

The Choice of an Organic Solvent.—Besides nitrobenzene, various other solvents were tested for the extraction. They are chloroform, 1, 2-dichloroethane, isoamylalcohol, isopropyl ether, butyl acetate, cyclohexanone, chlorobenzene, and benzene. It was found that the perchlorate of the chelate cation was completely non-extractable into these solvents. Moreover, when a mixed solvent, such as nitrobenzene and benzene (1 : 1) or chloroform (1 : 1) was used, the absorbance of the organic layer was remarkably reduced. The reason may be the reducing of the dielectric nature in the mixed solvent. Therefore, benzene-free nitrobenzene has to be used.

The Effect of the Times of Extraction and of the Percentages of Extraction.—The effect of the times of extraction are shown in Fig. 4. The extraction yield using one 10 ml. portion of nitrobenzene is about 90%. The determination of the percentage of extraction was then attempted as follows. By shaking an aliquot of the extract with 1 N sulfuric acid, the perchlorate was transferred again into an aqueous phase. For this aqueous solution, after the reagents had been added and the pH, adjusted the extraction was performed once more. The absorbance value was about 90% of the first extract. It is, therefore, presumed that the percentage of extraction may be about 90%,

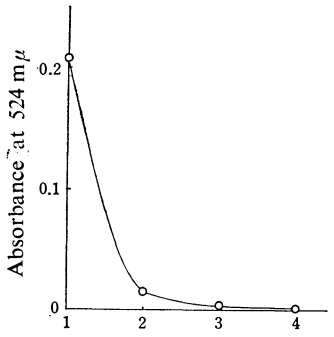


Fig. 4. Effect of times of extraction.
Perchlorate: 2 p.p.m.
(Other valiables were the same as the standard procedure, and the absorbance was measured for the nitrobenzene solution obtained by the extraction)

because Beer's law is followed for the perchlorate, as will be described below.

Calibration Curve.—Four milliliters of the 2, 2'-dipyridyl solution, 4 ml. of the ferrous ammonium sulfate solution, 2 ml. of a 3 M sodium acetate solution, and varying amounts of the standard solution (1~10 ml.) containing 10 μg. per ml. of perchlorate ions were mixed and diluted to 25 ml. with distilled water. Then 10.0 ml. of nitrobenzene was added, and the mixture was treated according to the procedure. The absorbance for each set was measured at 524 mμ against the reagent blank solution. As is shown in Fig. 5, Beer's law is followed in the 0.4~4 p. p. m. range of perchlorate ions.

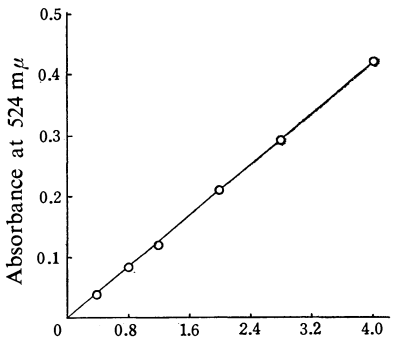


Fig. 5. Calibration curve.
Dip.: 2.0×10^{-3} M
Fe(II): 4.8×10^{-4} M
NaAc: 0.24 M
pH: 6.5
Reference: Reagent blank

The Effect of Diverse Ions.—Table I shows the absorbances of a series of extracts which have been treated according to the procedure. Measurement was done at 524 mμ using a reagent blank. Each solution contains 2.0 p. p. m. of perchlorate and various amounts of diverse ions. The absorbance of 2.0 p. p. m. of perchlorate is 0.209. It is shown that the determination of perchlorate is not interferred with, or is given a positive error of a few percentage points, by the presence of a considerable amount of halogen or oxygenated halogen ions other than iodide and periodate. The reason for the positive error of a small amount of iodide is not clear, because the iodide in a considerable concentration could not be extracted when the perchlorate is absent. This behavior of iodide is very interesting in a system of these extractions, as has been described above. A small amount of periodate give a negative error, presumably because of the oxidizing action with regard to ferrous iron. The proposed method may be useful for the determination of a small amount of perchlorate contained in such a salt as chloride, bromide, chlorate, bromate, iodate, and sulfate.

TABLE I. EFFECT OF DIVERSE IONS ADDED TO 2 p.p.m. OF ClO^-_4 (Abs. 0.209)

Ion	Added as	Concn. p. p. m.	Absorbance at 524 mμ
None	—	—	0.209
ClO_3^-	$NaClO_3$	8	0.209
ClO_3^-	$NaClO_3$	42	0.243
BrO_3^-	$KBrO_3$	60	0.209
BrO_3^-	$KBrO_3$	120	0.211
IO_3^-	KIO_3	1700	0.209
Cl^-	NaCl	350	0.209
Cl^-	NaCl	3500	0.214
Br^-	KBr	60	0.207
Br^-	KBr	2000	0.214
I^-	KI	0.5	0.209
I^-	KI	1	0.213
IO_4^-	KIO_4	4	0.206
SO_4^{2-}	Na_2SO_4	4000	0.209
NO_3^-	$NaNO_3$	6	0.208
NO_3^-	$NaNO_3$	30	0.223

pH of aqueous layer: 6.5, other variables were the same as that of the calibration curve.

Department of Chemistry
Faculty of Science
Hiroshima University
Higashisenda, Hiroshima

Analytical Studies Using the Convection Electrode. VIII. A. C. Polarography with the Pushed-out Mercury Drop Convection Electrode

By Junsuke SUZUKI and Tokuro OZAKI

(Received November 25, 1963)

A series of investigations[1] using the rotating-disk convection electrode as an electrode of d. c. polarography has been carried out by the authors. In a previous paper[2] it was reported that the pushed-out mercury drop convection electrode (PMDCE) has a sensitivity about twenty times larger than the dropping mercury electrode (DME) and, also, that it could be used even in a strongly alkaline or an acidic medium and could be reused many times with a good reproducibility.

On the other hand, it is already known that the sensitivity of the a. c. polarographic method is better than that of the d. c. polarographic method for the reversible reaction, and, also, that in a buffer or an acidic medium it is not necessary to remove dissolved oxygen.[3] Therefore, the application of the convection electrode to the a. c. polarographic method can be expected to obtain a much higher sensitivity.

In the present paper, the results of a. c. polarographic studies using cadmium(II) as a depolarizer are reported. The relations between the concentration of the depolarizer and the summit current, and between the stirring rate of the rotating disk and the summit current or the summit potential are discussed in especial detail.

Experimental

Apparatus.—The electrolytic cell, the electrode and the rotating apparatus are the same as have been described in the previous paper,[2] but the position in which the electrode is set is different.

The Shimadzu model RP-2BF polarograph is employed for the measurements of d. c. and a. c. polarograms.

Reagents.—A cadmium solution is prepared from chemicals of reagent grade, extra pure, without further purification. Also, a hydrochloric acid solution is of reagent grade, extra pure.

Procedure.—About 30 ml. of the solution of cadmium in 1 M hydrochloric acid are poured into the electrolytic cell.

While dissolved oxygen remains in the solution, the a. c. polarogram is recorded immediately after the solution is poured into the cell.

As dissolved oxygen is removed from the solution, a hydrogen gas stream is passed constantly through the solution at the rate of about 4 bubbles per second for 1 hr., and then the a. c. polarogram is recorded.

The procedure for each polarographic measurement, i. e., the renewal of the mercury drop as the electrode, is the same as has been described in the previous paper.[2]

The polarograms are recorded with a chart speed of about 2 cm./min., a rate of change of applied potential of about 100 mV./min., and a superposed alternating voltage of 20 mV.

All the measurements are performed at 15± 0.5°C.

Results

The Reproducibility of the Summit Current.—Typical current-voltage curves for cadmium are shown in Fig. 1. The reproducibility of

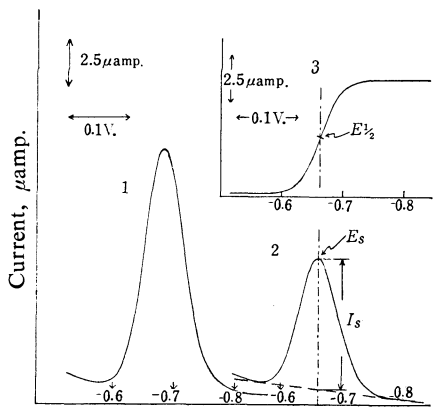


Fig. 1. Current-voltage curves of 1×10^{-4} M cadmium in 1 M HCl.
1 A. C. polarogram at the PMDCE in the presence of dissolved oxygen
2 A. C. polarogram at the PMDCE in the absence of dissolved oxygen
3 D. C. polarogram at the PMDCE

1) T. Ozaki and T. Nakayama, *J. Chem. Soc. Japan, Pure Chem. Sec.* (*Nippon Kagaku Zasshi*), **81**, 98 (1960); T. Ozaki and T. Nakayama, ibid., **82**, 46 (1961).
2) J. Suzuki and T. Ozaki, This Bulletin, **37**, 230 (1964).
3) H. Shirai, *Japan Analyst*, **8**, 331 (1959); K. Itsuki and F. Suzuki, ibid., **8**, 91 (1959); K. Itsuki and T. Kaji, ibid., **8**, 568 (1959); K. Itsuki and M. Nagao, ibid., **8**, 800 (1959).
3) K. Itsuki and M. Nagao, ibid., **8**, 825 (1959); K. Itsuki and M. Nagao, ibid., **9**, 836 (1960).

TABLE I. REPRODUCIBILITY OF THE SUMMIT CURRENT i_s (μamp.)
(Stirring rate: 800 r. p. m.)

Concn. C, mol./l.	Oxygen dissolved		Oxygen removed	
	Average values of i_s	Average deviation %	Average values of i_s	Average deviation %
1×10^{-4}	13.175	0.76	7.067	1.41
5×10^{-5}	6.660	1.08	3.514	1.22
1.5×10^{-5}	2.085	1.68	—	—
7×10^{-6}	0.905	1.50	—	—
2×10^{-6}	0.254	1.66	—	—

TABLE II. REPRODUCIBILITY OF THE SUMMIT POTENTIAL E_s (V. vs. SCE)
(Stirring rate: 800 r. p. m.)

Concn. C, mol./l.	Oxygen dissolved		Oxygen removed	
	Average values of E_s, V. vs. SCE	Average deviation, %	Average values of E_s, V. vs. SCE	Average deviation, %
1×10^{-4}	−0.684	0.17	−0.661	0.18
5×10^{-5}	−0.683	0.09	−0.661	0.13
1.5×10^{-5}	−0.687	0.14	—	—
7×10^{-6}	−0.685	0.12	—	—
2×10^{-6}	−0.680	0	—	—

the summit current for the various concentrations of cadmium was investigated; the results are listed in Table I. As the table shows, the summit current has a good reproducibility. The summit current in the presence of dissolved oxygen in the electrolytic solution is larger than the corresponding current in the absence of dissolved oxygen.

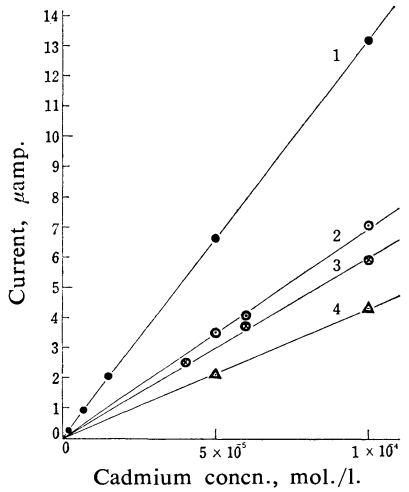


Fig. 2. Relations between the current and Cd^{2+} concentration.
1 At the PMDCE (in the presence of dissolved oxygen, a. c. polarographic method)
2 At the PMDCE (in the absence of dissolved oxygen, a.c. polarographic mothod)
3 At the PMDCE (d. c. polarographic method)
4 At the DME (in the presence of dissolved oxygen, a. c. polarographic method)

The Reproducibility of the Summit Potential.—The summit potential of each concentration was determined by the ordinary method; the results are shown in Table II. As the table shows, the good reproducibility of the summit potential can always be obtained within a mean error of 0.2%. Also, it can be seen that the summit potential in the presence of dissolved oxygen is slightly shifted to a more negative position than the corresponding potential in the absence of dissolved oxygen and that in both cases (in the presence or absence of dissolved oxygen) the potential is not affected by the concentration of cadmium.

The Relation between the Concentration of Cadmium and the Summit Current.—The relation between the concentration and the current is shown in Fig. 2. It can be seen

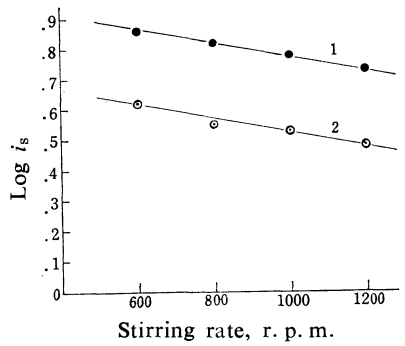


Fig. 3. Relations between the stirring rate and the summit current of 5×10^{-5} M Cd^{2+} in 1 M HCl.
1 In the presence of dissolved oxygen
2 In the absence of dissolved oxygen

Table III. Relation between the stirring rate r (r. p. m.) of the rotating disk and the summit potential E_s V. vs. SCE)

r	600	800	1000	1200	Remark
E_s	−0.679	−0.683	−0.687	−0.687	Oxygen dissolved
	−0.658	−0.661	−0.658	−0.660	Oxygen removed

Table IV. Relation between the superposed alternating voltage ΔE (mV.) and the summit potential E_s (V. vs. SCE). (Stirring rate: 800 r. p. m.)

ΔE	10	20	30	Remark
E_s	−0.683	−0.683	−0.684	Oxygen dissolved
	−0.662	−0.661	−0.660	Oxygen removed

Table V. Influence of the rate of polarization P (mV./min.) on the summit current i_s (μamp.) and the summit potential E_s (V. vs. SCE) (Stirring rate: 800 r. p. m.)

C mol./l. \ P	100		200		Remark
i_s, E_s	E_s	i_s	E_s	i_s	
1.5×10^{-5}	−0.687	2.100	−0.687	2.906	Oxygen dissolved
5×10^{-5}	−0.661	3.514	−0.663	4.285	Oxygen removed

from the figure that a linear relation is obtained between the concentration and the current.

The Effect of the Stirring Rate on the Summit Current.—The effect of the stirring rate of the rotating disk on the summit current was investigated; the results are shown in Fig. 3. From the figure, it can be seen that the current decreases exponentially with the increase in the stirring rate.

The Effect of the Stirring Rate on the Summit Potential.—The dependence of the summit potential on the stirring rate was investigated. The results are listed in Table III. In the oxygen-dissolved solution, the potential is slightly shifted toward a negative position with the increase in the stirring rate (600~1200 r. p. m.), but in the case of the oxygen-free solution, the stirring rate has no effect on the summit potential.

The Relation between the Superposed Alternating Voltage and the Summit Current or the Summit Potential.—The relations between the superposed alternating voltage and the current or potential were investigated. The results are given in Fig. 4 and Table IV respectively. As the figure and the table show, the current is proportional to the superposed alternating voltage, but the potential is not affected.

The Effect of the Rate of Polarization.—The effect of the rate of polarization on the summit current or the summit potential was investigated; the results are listed in Table V.

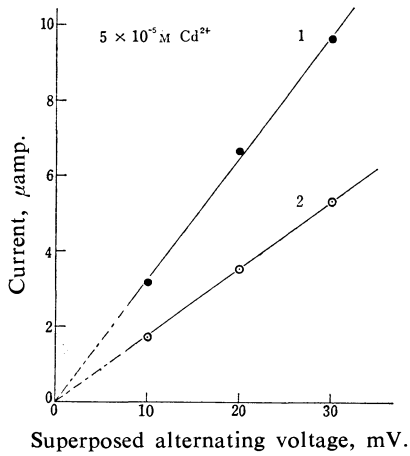


Fig. 4. Relations between the superposed alternating voltage and the summit current.
1 In the presence of dissolved oxygen
2 In the absence of dissolved oxygen

The change of the rate of polarization has no effect on the potential, but the current increases with the increase in the rate of polarization.

A Comparison with the DME.—The summit current obtained with the PMDCE (in the presenceof dissolved oxygen at the stirring rate of 600 r. p. m.) for 1×10^{-4} M cadmium is about thirty times as large as the corresponding diffusion current obtained with the DME using the d. c. polarographic method; moreover, it is about three times as large as the summit current

TABLE VI. COMPARISON OF E_s OR $E_{1/2}$ VALUES WITH THE DME AND THE PMDCE

Electrode \ $E_{1/2}$, E_s	$E_{1/2}$	E_s	
	Oxygen removed	Oxygen dissolved	Oxygen removed
DME	−0.653	−0.655	−0.656
PMDCE*	−0.662	−0.683	−0.661

* Stirring rate of the rotating disk : 800 r. p. m.

obtained with the DME using the a. c. polarographic method.

The capillary of the DME used has an m value of 0.93 mg./sec. and a drop time of 4.9 sec. in a 1 M hydrochloric acid solution at −0.80 V. vs. SCE.

Discussion

Half-wave Potential and Summit Potential.—In order to compare the half-wave potential and the summit potential with the PMDCE or with the DME, a series of investigations was performed; the results are shown in Table VI. When these values of the half-wave potential and of the summit potential are compared, it can be seen that they agree well each other, except for the summit potential with the PMDCE in the presence of dissolved oxygen. In the absence of dissolved oxygen, both the half-wave potential and the summit potential with the PMDCE are slightly shifted to a more negative position than the corresponding half-wave potential and summit potential with the DME. This effect is considered to be due to the fact that the rate of mass transfer becomes larger than the rate of electron transfer because of the convection. This agrees with the results of Jordan.[4]

The Stirring Rate and the Summit Current.—As is shown in Fig. 3, the summit currents decrease with the increase in the stirring rate in the presence or absence of dissolved oxygen.

As has been pointed out by Jordan,[4] Kolthoff and Jordan,[5] and Delahay,[6] at the convection electrode the rate of mass transfer becomes larger than the rate of electron transfer because of the effect; i. e., the effective thickness of the diffusion layer becomes smaller with the increase in the velocity of convection, which depends on the stirring rate. Therefore, the electrode reaction becomes quasi-reversible.[4] Namely, it is considered that the decrease in the summit current with an increase in the stirring rate is caused by the decrease in the reversibility.

The Influence of Dissolved Oxygen.—It is commonly known in the case of an acidic or a buffer medium that the summit current is not affected by dissolved oxygen. In the present investigation, this phenomenon has been observed with the DME for cadmium in 1 M hydrochloric acid solution. However, the summit current obtained with the PMDCE in the presence of dissolved oxygen is increased more than in the absence of such oxygen. This is considered to be a special feature of this electrode, but it has not yet been explained.

Summary

A. C. polarography with the PMDCE has been investigated, using cadmium in 1 M hydrochloric acid.

A satisfactory proportionality between the summit current and the concentration is obtained in the range from 1×10^{-4} to 2×10^{-6} M, and the summit current obtained with the PMDCE (in the presence of dissolved oxygen at the stirring rate of 600 r. p. m.) for the cadmium depolarizer is about thirty times as large as the corresponding diffusion current obtained with the DME.

The a. c. polarogram obtained with the PMDCE shows a gradual decrease in the summit current as the stirring increases; this decrease is considered to be due to the quasi-irreversibility at the electrode reaction because of the increase in the rate of mass transfer caused by the convection. The relation between the summit current and the stirring rate is exponential in the range from 600 to 1200 r. p. m.

The authors wish to express their thanks to the Ministry of Education, which defrayed a part of the expense of this study.

Faculty of Education
Shizuoka University
Ooiwa, Shizuoka

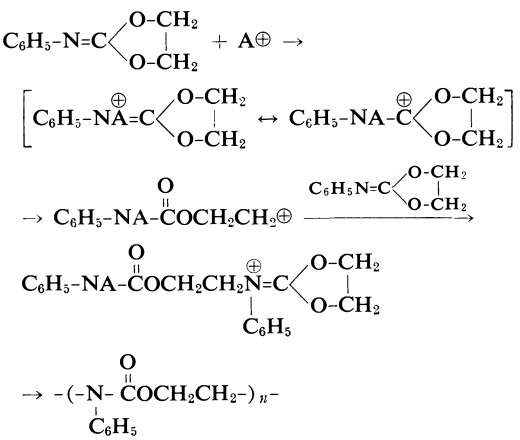
4) J. Jordan, *Anal. Chem.*, 27, 1708 (1955).
5) I. M. Kolthoff and J. Jordan, *J. Am. Chem. Soc.*, 75, 4869 (1953).
6) P. Delahay, "New Instrumental Methods in Electrochemistry," Interscience Publishers, New York (1953), pp. 217–249.

The Synthesis and 1, 4-Addition Type Ring-opening Polymerization of N-Substituted Cyclic Iminocarbonates

By Tamotsu FUJISAWA, Yorikazu TAMURA and Teruaki MUKAIYAMA

(Received December 11, 1963)

It has been shown in a previous paper that ethylene *N*-phenyl iminocabonate affords poly-(ethylene *N*-phenylcarbamate) by ring-opening polymerization when treated with cationic catalysts.[1]

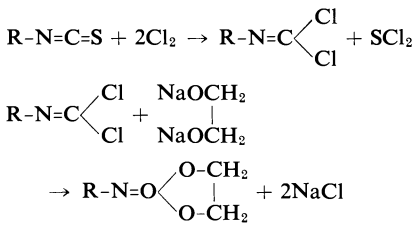


In the initiation step of the polymerization of ethylene *N*-phenyl iminocarbonate, a cationic catalyst adds to the imino group of the iminocarbonate to form a reactive addition compound. The addition compound in turn decomposes, with oxygen-carbon bond fission, to generate a new open-chained carbonium ion by the shift of an electron pair. The chain propagates by the rapid addition of the carbonium ion to a new monomer, a step which may be repeated many times.

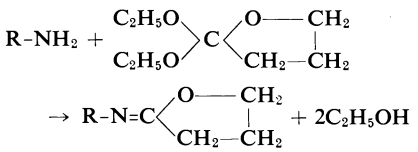
As is shown above, the polymerization proceeds by 1, 4-addition; therefore, it can be termed a "1, 4-addition type ring-opening polymerization." This involves the ring-opening polymerizations of such imino compounds as 2-iminotetrahydrofurans[2] and 2-imino-1, 3-oxazolizines,[3] 4-methylene-1, 3-dioxalane,[4] β-pinene,[5,6] diketene[7-9] and 1, 4, 6-trioxaspiro-[4, 4] nonane.[10]

In the present work, the syntheses of various *N*-substituted iminocarbonates and their ring-opening polymerization have been studied.

N-Alkyl and *N*-aryl ethylene iminocarbonates were prepared from the corresponding imidophosgenes and sodium ethylene glycolate according to a procedure similar to that used for ethylene *N*-phenyl iminocarbonate.[11] Alkyl and aryl imidophosgenes were prepared by passing chlorine into a chloroform or carbon tetrachloride solution of the corresponding alkyl and aryl isothiocyanates under cooling. The solvents, yields, physical properties and analysis for these imidophosgenes and iminocarbonates are listed in Tables I and II.



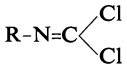
By a procedure similar to that used in the preparation of *N*-substituted iminotetrahydrofurans described in a previous paper,[2] the



preparation of *N*-substituted cyclic iminocarbonates from 2, 2-diethoxy-1, 3-dioxolane[12] and various primary amines was attempted. In contrast to the case of 2-iminotetrahydrofurans, the reaction of 2, 2-diethoxy-1, 3-di-

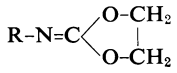
1) T. Mukaiyama, T. Fujisawa, H. Nohira and T. Hyugaji, *J. Org. Chem.*, **27**, 3337 (1962).
2) T. Mukaiyama and K. Sato, This Bulletin, **36**, 99 (1963).
3) H. Nohira, Y. Nishikawa and T. Mukaiyama, ibid., **37**, 797 (1964).
4) M. Goodman and A. Abe, Am. Chem. Soc. Meeting, New York (1963), polymer preprints, Vol. 4, No. 2, p. 557.
5) W. J. Roberts and A. R. Day, *J. Am. Chem. Soc.*, **72**, 1226 (1950).
6) C. S. Marvel, J. R. Hanley, Jr., and D. T. Longone, *J. Polymer Sci.*, **40**, 551 (1959).
7) J. Furukawa, T. Saegusa and N. Mise, *Makromol. Chem.*, **39**, 243 (1960).
8) R. Oda, S. Munemiya and M. Okano, ibid., **43**, 149 (1961).
9) J. Furukawa, T. Saegusa and N. Mise, *J. Chem. Soc. Japan, Ind. Chem. Sec.* (*Kogyo Kagaku Zasshi*), **65**, 254 (1962).
10) K. Bodenbenner, *Ann.*, **623**, 183 (1959).
11) T. Mukaiyama, T. Fujisawa and T. Hyugaji, This Bulletin, **35**, 687 (1962).
12) This compound was prepared from ethylene carbonate, triethyl oxonium fluoroborate and sodium ethoxide by modified procedure for the preparation of carbon tetraethoxide by Meerwein et al., *Chem. Ber.*, **89**, 2060 (1956); yield 18%; b. p. 124~127°C. Found: C, 51.58; H, 8.86. Calcd. for $C_7H_{14}O_4$: C, 51.84; H, 8.70%.

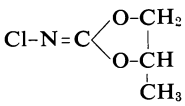
TABLE I. THE SYNTHESIS OF ALKYL AND ARYL IMIDOPHOSGENES



R	Solvent	Yield %	B. p. (m. p.) °C/mmHg		Analysis C, %	H, %	N, %
	CCl_4	95	100/30	Found	47.02	6.24	7.74
				Calcd.	47.02	6.16	7.77
n-C_6H_{13}-	CCl_4	52	94～96/24	Found	46.87	7.24	7.91
				Calcd.	46.17	7.20	7.69
p-Cl-C_6H_4-	CCl_4	71	80～82/1	Found	40.13	2.11	6.94
				Calcd.	40.24	1.91	6.71
p-NO_2-C_6H_4-	$CHCl_3$	68	120～130/8 (60～63)				

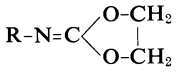
TABLE II. THE SYNTHESIS OF ETHYLENE *N*-SUBSTITUTED IMINOCARBONATES



R	Yield %	M. p. (b. p.) °C (°C/mmHg)	Recrystallization solvent		Analysis C, %	H, %	N, %
	48	(110～113/0.3)		Found	62.56	9.02	8.09
				Calcd.	63.88	8.94	8.28
n-C_6H_{13}-	50	(94～96/0.18)		Found	62.70	9.94	8.05
				Calcd.	63.13	10.00	8.18
p-Cl-C_6H_4-	54	88～89	Ether	Found	54.67	4.05	7.09
				Calcd.	54.72	4.33	7.33
p-NO_2-C_6H_4-	15	121～123	Ether	Found	51.92	3.87	13.46
				Calcd.	51.11	3.65	14.38
Cl-	12	33～35	Ether	Found	29.47	3.14	11.76
				Calcd.	29.66	3.32	11.52
Br-	34	62～64*	Ether	Found	21.88	2.44	8.33
				Calcd.	21.71	2.42	8.43
	37	85～88/0.25		Found	35.76	4.74	9.94
				Calcd.	35.44	4.46	10.33

* Decomposition point.

TABLE III. 1,4-ADDITION TYPE RING OPENING POLYMERIZATION OF ETHYLENE *N*-SUBSTITUTED IMINOCARBONATES

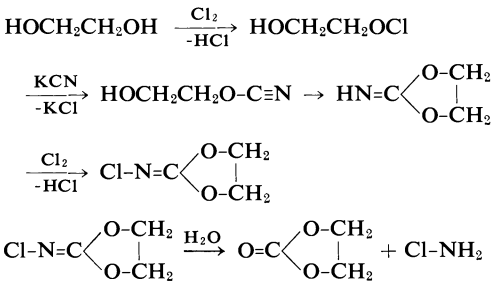


R	Catalyst	Reaction Time hr.	Reaction Temp.	*N*-Substituted poly(ethylene carbamate) Yield %	M. p. (decomp. p.) °C	$[\eta]^{30°*}_{CHCl_3}$	Reprecipitation solvent
	$BF_3O(C_2H_5)_2$	96	Room	14	178～183	0.11	Chloroform-acetone
	H_2SO_4 (96%)	14	Room	32	185～190	0.20	Chloroform-acetone
n-C_6H_{13}-	$BF_3O(C_2H_5)_2$	70	Room	100	Oily	0.05	
p-Cl-C_6H_4-	$BF_3O(C_2H_5)_2$	Instant	100°C	56	135～142	0.24	Chloroform-petroleum ether
p-NO_2-C_6H_4-	$BF_3O(C_2H_5)_2$	27	Room	100	230～240	—	
Cl-	$BF_3O(C_2H_5)_2$	240	Room	98	(60)	0.14	Chloroform-petroleum ether

* $[\eta]^{30°}_{CHCl_3}$ = intrinsic viscosity measured in chloroform at 30°C.

oxolane with primary amines, such as aniline and cyclohexylamine, did not give the corresponding iminocarbonates, even when they were heated at 130°C for 10 hr. in the presence of an acidic catalyst and most of the starting materials were recovered.

Next, *N*-halogeno cyclic iminocarbonates were prepared by the reactions of potassium cyanide, various glycohols and such halogenes, as chlorins and bromine in an alkaline solution. Their yields were comparatively low since they are rapidly hydrolyzed to yield ethylene carbonate when the reaction media become acidic.

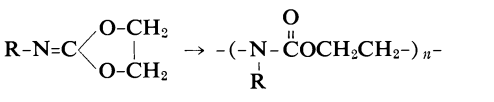


It is to be noted that ethylene *N*-bromo iminocarbonate was unstable enough to decompose readily in the air and that it darkened within 8 hr., even when stored in an ethereal solution.

The *N*-halogeno cyclic iminocarbonates thus obtained were less reactive toward acidic substances than ethylene *N*-phenyl iminocarbonate,[11,13] and they did not react with benzoic acid when refluxed in benzene for 2 hr. and the starting materials were recovered quantitatively.

On the other hand, attempts to prepare unsaturated ethylene iminocarbonate by means of ester exchange between diethyl iminocarbonate and glycol, or by means of reductions of *N*-halogeno cyclic iminocarbonates with arsenious trioxide or with fluorene, failed.

When the ring-opening polymerization of *N*-substituted cyclic iminocarbonates was tried in the presence of such cationic catalysts as boron trifluoride etherate or sulfuric acid, the corresponding poly(ethylene *N*-substituted carbamates) were obtained, as Table III shows.



Compared with ethylene *N*-phenyl iminocarbonate, the polymerization of these cyclic iminocarbonates, except for ethylene *N*-*p*-chlorophenyl iminocarbonate, took a long time and their intrinsic viscosities in chloroform were low.

Polyurethane obtained from ethylene *N*-chloro iminocarbonate was comparatively unstable and was gradually decomposed above 60°C, with the evolution of chlorine.

These results show that various poly(ethylene *N*-substituted carbamates) can be produced by the 1, 4-addition-type ring-opening polymerization of cyclic iminocarbonates. On the other hand, the polyurethane can not be successfully produced from oxazolidone, 5-membered cyclic urethane, since it yields exclusively polyethyleneimine, with the evolution of carbon dioxide.

The ease of the 1, 4-addition type ring-opening polymerization of these cyclic iminocarbonates may be interpreted in the following way: since the cyclic iminocarbonates are an enol isomer of cyclic urethane, which seems to be more unstable than the corresponding keto-form structure, it is reasonable to consider that these compounds are readily converted into the polymers with a keto-form structure by the ring-opening polymerization.

Experimental

Alkyl and Aryl Isothiocyanates. — Cyclohexyl isothiocyanate was prepared from cyclohexyl amine, carbon disulfide and mercuric chloride following the procedure of Skita.[14] *n*-Hexyl isothiocyanate was prepared from *n*-hexyl amine, carbon disulfide and ethyl chlorocarbonate by a method analogous to that used for the preparation of methyl isothiocyanate by Moore;[15] yield, 46%, b. p. 80~82°C/3 mmHg. *p*-Chlorophenyl and *p*-nitrophenyl isothiocyanates were prepared from corresponing anilines and thiophosgene according to the methods of Dyson[16] and Dyer.[17]

The Preparation of Cyclohexyl Imidophosgene. —A solution of 40 g. of cyclohexyl isothiocyanate in an equal volume of carbon tetrachloride was saturated with dry chlorine until the reaction mixture became dark red. Since an evolution of heat was noticed during the reaction, the reaction mixture was cooled in ice-water. After the solvent and sulfur dichloride had been removed by distillation, cyclohexyl imidophosgene was fractionated; yield, 48.0 g. (95%); b. p. 100°C/30 mmHg.

In a similar way, *n*-hexyl, *p*-chlorophenyl and *p*-nitrophenyl imidophosgenes were prepared from the corresponding isothiocyanates and chlorine as is shown in Table I.

The Preparation of Ethylene *N*-Cyclohexyl Iminocarbonate.—Into 5.4 g. (0.05 mol.) of sodium ethylene glycolate suspended in 30 ml. of dry benzene was added dropwise a solution of 9.0 g. (0.05 mol.) of cyclohexyl imidophosgene in 20 ml. of dry benzene with vigorous stirring. Then the

13) T. Mukaiyama, Y. Tamura and T. Fujisawa, This Bulletin, 37, 628 (1964).

14) A. Skita and H. Rolfes, *Ber.*, 53, 1242 (1920).

15) M. L. Moore and F. S. Crossley, "Organic Syntheses," Coll. Vol. 3, 599 (1955).

16) G. M. Dyson, ibid., Coll. Vol. 1, 165 (1948).

17) E. Dyer and T. B. Johnson, *J. Am. Chem. Soc.*, 54, 777 (1932).

reaction mixture was refluxed on a water bath for 2 hr. while being continuously stirred. It was then poured into water and extracted with benzene. After washing with water, the benzene solution was dried with calcium chloride. The benzene was then removed completely in vacuo and ethylene *N*-cyclohexyl iminocarbonate was distilled; yield, 4.0 g. (48%); b. p. 110~113°C/0.3 mmHg. The infrared absorption bands are 1700(s), 1410(ms), 1370(ms), 1250~1100(ms) broad, 1030(s) and 760(ms) cm^{-1}.

In a similar manner, ethylene *N*-*n*-hexyl, *N*-*p*-chlorophenyl and *N*-*p*-nitrophenyl iminocarbonates were prepared from the corresponding imidophosgenes and sodium ethylene glycolate as listed in Table II.

The Preparation of Ethylene *N*-Chloro Iminocarbonate.[18]—Into a solution of 16.0 g. (0.4 mol.) of sodium hydroxide, 13.0 g. (0.2 mol.) of potassium cyanide and 12.4 g. (0.2 mol.) of ethylene glycol in 80 ml. of water, was passed chlorine with vigorous stirring under cooling by ice-water until red litmus paper no longer changed to blue. When the aqueous solution, became neutral, ethylene *N*-chloro iminocarbonate floated on the surface of the solution. The iminocarbonate was filtered and was recrystallized from ether; yield, 2.9 g. (12%); m. p. 33~35°C. The infrared absorption bands are at 1650(s), 1400(ms), 1230(s), 1060(s) and 700(ms) cm^{-1}.

Similarly, propylene *N*-chloro iminocarbonate was prepared following the above method by using propylene glycol in place of ethylene glycol. Ethylene *N*-bromo iminocarbonate was also prepared by using bromine, of which about 50 g. was required, instead of chlorine as in the above experiment. The yields, physical properties and analysis for these iminocarbonates are also indicated in Table II.

The Polymerization of Ethylene *N*-Cyclohexyl Iminocarbonate.—Into 1.0 g. of ethylene *N*-cyclohexyl iminocarbonate was added a catalytic amount of boron trifluoride etherate; the mixture was then allowed to stand at room temperature for 14 hr. Then poly(ethylene *N*-cyclohexylcarbamate) was reprecipitated from chloroform-acetone. Yield, 0.14 g. (14%); m. p. 178~183°C. Its infrared absorption bands are at 1680(s), 1420(ms), 1230(ms), 1150(ms) and 760(ms) cm^{-1}.

Found: C, 63.23; H, 9.06; N, 7.96. Calcd. for $(C_9H_{15}O_2N)_n$: C, 63.88; H, 8.94; N, 8.28%.

The polymerizations of other *N*-substituted cyclic iminocarbonates were carried out in a similar method under the reaction conditions indicated in Table III in the presence of a small amounts of catalyst (7~10 mg.). The catalysts, yields, physical properties, intrinsic viscosities and solvents of reprecipitation for the polyurethane obtained are also shown in the same table.

18) The preparation of this compound has aleady been published; H. E. Simnous, U. S. Pat. 2972620; *Chem. Abstr.*, 55, 14481 (1961).

Summary

As one of a series of studies of 1, 4-addition type ring-opening polymerizations, the synthesis and ring-opening polymerization of *N*-substituted cyclic iminocarbonates have been studied.

N-Alkyl and *N*-aryl cyclic iminocarbonates have been prepared by the reaction of sodium ethylene glycorate with the corresponding imidophosgenes. *N*-Halogeno cyclic iminocarbonates have been prepared from glycols, potassium cyanide and halogenes.

The ring-opening polymerization of the *N*-substituted cyclic iminocarbonates, which are considered to be cyclic enol derivatives of urethanes, in the presence of cationic catalysts gives the corresponding poly(ethylene *N*-substituted carbamates).

The authors wish to express their hearty thanks to Miss Toshiko Aoyagi for her microanalyses.

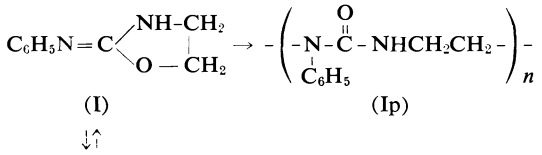
Laboratory of Organic Chemistry
Tokyo Institute of Technology
Meguro-ku, Tokyo

The Preparation of Poly(ethylene N,N'-Disubstituted Ureas) by the 1,4-Addition Type Ring-opening Polymerization of 2-Imino-1,3-oxazolidines

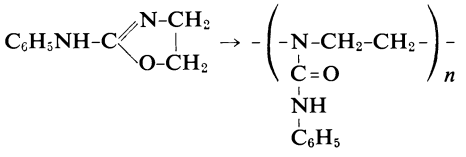
By Hiroyuki NOHIRA, Yoshihiro NISHIKAWA and Teruaki MUKAIYAMA

(Received December 12, 1963)

A new type of ring-opening polymerization of ethylene iminocarbonates, cyclic ketene acetals and 2-iminotetrahydrofurans, to give polyurethans, polyesters and polyamides respectively, has been reported in preceding papers.[1,2] It was shown there that the polymerization of 2-phenylimino-1,3-oxazolidine (I) gives a polymer with urea linkage; however, both the melting temperature and the intrinsic viscosity of the resulting polymer are low. Moreover, a troublesome problem remained concerning the structure of the polymer, since there are two possible pathways for the polymerization to yield poly(ethylene *N*-phenyl urea) (Ip) and the polyethylene imine-type polymer (Ip'), which have been attributed to the existence of two tautomeric forms, 2-phenylimino-1,3-oxazolidine (I) and 2-anilino-2-oxazoline (I'), respectively. In this connection, in the present investigation, the polymerizations of 2-imino-3-substituted-1,3-oxazolidines, which have no labile hydrogen atom at the 3-position, have been studied in order to establish the ring-openig polymerization which yields polyureas of the type Ip.



(I) (Ip)



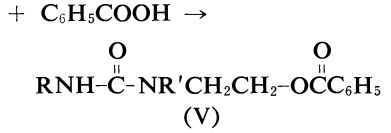
(I') (Ip')

Several methods for the preparation of *N*, *N'*-disubstituted-2-imino-1,3-oxazolidines (III) have been reported: from β-hydroxyethyl thioureas by the action of mercuric oxide,[3] from guanidinoethanols by refluxing in xylene,[4] or from β-chloroethylureas by the action of potassium hydroxide.[5] Although the last route seems to be the most convenient, the yields of the desired compounds are low, and the corresponding cyclic ureas IV have resulted as main products.

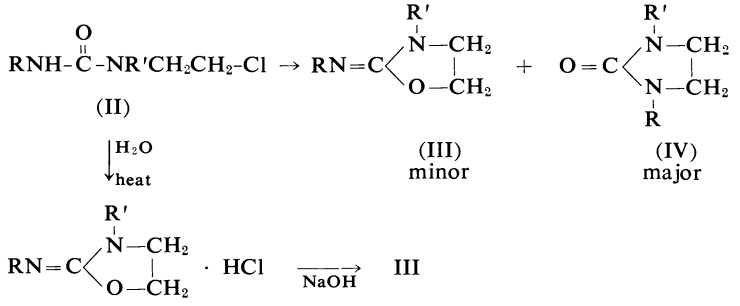
It has now been found that II gives the cyclic pseudo ureas III in good yields when treated with hot water and neutralized with sodium hydroxide.

On the other hand, the cyclic pseudo ureas with an unsubstituted imino group (III, R = H) were prepared from ethanolamines and cyanogen bromide through the hydrobromides.[6]

When III was heated with benzoic acid in benzene, ring-opening adducts V were obtained in fairly good yields.



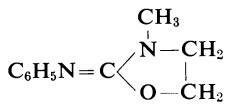
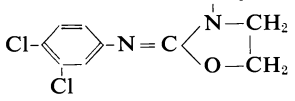
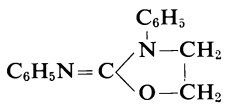
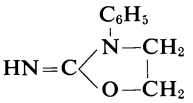
(V)



(II) (III) minor (IV) major

1) T. Mukaiyama, T. Fujisawa, H. Nohira and T. Hyugaji, *J. Org. Chem.*, **27**, 3337 (1962).
2) T. Mukaiyama and K. Sato, This Bulletin, **36**, 99 (1963).
3) F. B. Dains, R. Q. Brewster, J. S. Blair and W. C. Thompson, *J. Am. Chem. Soc.*, **44**, 2637 (1922).
4) B. Adcock, A. Lawson and D. H. Miles, *J. Chem. Soc.*, **1961**, 5120.
5) R. W. Luckenbaugh, U. S. Pat. 2902356 (1959).
6) J. T. Thurston, U. S. Pat. 2479525 (1949).

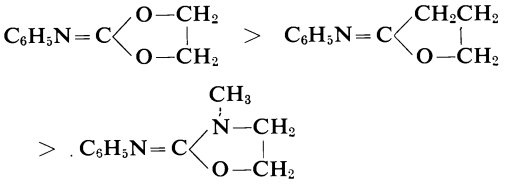
TABLE I. BULK POLYMERIZATION OF 2-IMINO 1, 3-OXAZOLIDINES (III)

Monomer	Polymerization conditions: Catalyst	%	Temp. °C	Time hr.	Properties of polymers: Yield %	P. M. T. °C	$[\eta]^{30°}_{\text{chloroform}}$
	BF_3[E]	1.0	120	4	90(a)	187～190	0.14
	BF_3[O]	1.0	140	3	95(b)	190～193	0.26
	BE_3[O]	1.0	160	2	95(b)	184～187	0.20
					63(a)	184～187	0.33
	BF_3[E]	0.3	85	36	90(b)	125～140	0.06
	$AlCl_3$	0.3	85	36	20(b)	125～140	—
	$TiCl_4$	0.3	85	36	20(b)	105～140	—
	BF_3[E]	1.1	140	1	85(c)	345～350	0.50 (*m*-cresol)
	BF_3[O]	1.1	160	0.33	100(c)	350～353	0.33 (*m*-cresol)
	BF_3[O]	0.2	160	1	60(c)	348～355	0.55 (*m*-cresol)
	BF_3[E]	1.0	140	4	50(d)	130～160	0.10
	H_2SO_4	1.0	140	4	40(d)	120～140	0.05
	BF_3[O]	1.0	160	3	80(d)	100～130	0.03

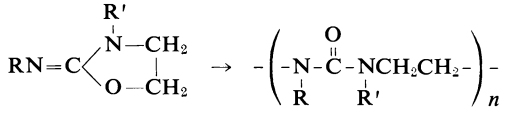
P. M. T., Polymer melting temperature; BF_3[E], Boron trifluoride etherate; BF_3[O], Boron trifluoride 2-imino-3-phenyl-1,3-oxazolidine complex (VI); (a)—(d): reprecipitating media (a), chlroform-acetone; (b), chloroform-petroleum ether; (c), *m*-cresol-acetone; (d), chloroform-ether

This reaction is similar to those of ethylene iminocarbonates or 2-iminotetrahydrofurans with acids reported in the previous papers,[1,2] and it suggests the possibility of a 1, 4-addition type ring-opening polymerization of the imino-oxazolidines.

Successful ring-opening polymerizations of the iminooxazolidines in question were carried out when these oxazolidines were heated in the presence of a cationic catalyst such as boron trifluoride etherate at a temperature between 85 and 160°C. Higher temperatures were necessary for this polymerization than for the polymerization of the ethylene iminocarbonates (25～100°C) and the 2-iminotetrahydrofurans (60～100°C). This result agrees with that of a kinetic study[7] of the 1, 4-addition type ring-opening reaction of three typical cyclic imino-compounds with carboxylic acids, where the order of the reactivities was shown to be as follows:



The structure of the resulting polymers was confirmed to be of the polyethylene-urea-type (IIIp) by means of infrared spectroscopy. That is, the monomers show an absorption in the range 1670～1680 cm^{-1} due to the exo-imino group of the five-membered ring, while all polymers absorb at the region about 1650 cm^{-1}, the same region as that where non-cyclic substituted ureas absorb.

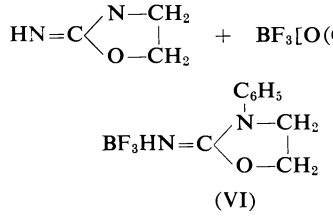


(III) (IIIp)

The polymerization conditions and properties of the resulting polymers are listed in Table I.

2-Phenylimino-3-phenyl-1, 3-oxazolidine (III, R, R' = C_6H_5) gave a hard, tough polymer with a fairly high polymer-melting temperature of 350°C. It was soluble in *m*-cresol, but insoluble in acetone, chloroform, methylene dichloride and dimethylsulfoxide. These properties may be attributable to the high density and to the symmetrical arrangement of phenyl groups along the ethylene urea linkages. The unsubstituted imino oxazolidine (III, R = H, R' = C_6H_5–) gave a polymer with a low polymer melting temperature and a low viscosity in low yields. In addition, the oxazolidine was found to give a stable complex with boron trifluoride when it was mixed with boron trifluoride etherate in a dilute ether solution:

7) T. Mukaiyama, Y. Tamura and T. Fujisawa, This Bulletin, 37, 628 (1964).



(VI)

The difficulty of the polymerization of the oxazolidine may be connected with the stability of the complex VI as this complex can be weighed in small quantities, an attempt was made to use this as a catalyst in the polymerization of the other disubstituted imino oxazolidines. It was found that the complex VI was as effective as boron trifluoride etherate in these polymerizations.

2-Imino-3-methyl-1, 3-oxazolidine (III, R=H, R'=CH_3) did not give any solid polymers, even when it was heated at 120°C for 5 hr.

Experimental

1-(2-Chloroethyl)-3-phenyl-1-methyl Urea (II, R=C_6H_5, R'=CH_3) and 1-(2-Chloroethyl)-3-(3, 4-dichlorophenyl)-1-methyl Urea (II, R=3, 4-$Cl_2C_6H_3$, R'=CH_3).—These compounds were prepared from the corresponding hydroxyethyl ureas and thionyl chloride according to the methods described in the patent literature.[5]

By an analogous method, 1-(2-chloroethyl)-1, 3-diphenyl urea (II, R, R'=C_6H_5) was obtained from 1-(2-hydroxyethyl)-1, 3-diphenyl urea (which had been prepared from phenyl isocyanate and *N*-phenyl ethanolamine in dioxane as a viscous liquid) and thionyl chloride in a 65% yield. It was recrystallized from ligroin (70 parts) and benzene (30 parts). M. p. 71°C.

Found; C, 65.43, H, 5.47; N, 10.43. Calcd. for $C_{15}H_{15}ClN_2O$: C, 65.57, H, 5.50; N, 10.19.

2-Phenylimino 3-Methyl 1, 3-Oxazolidine (III, R=C_6H_5, R=CH_3).—Eleven grams of 1-(2-chloroethyl)-3-phenyl-1-methyl urea was heated with 50 ml. of water with vigorous stirring in a boiling water bath for 30 min. After cooling, the solution was neutralized with aqueous sodium hydroxide. The precipitate was recrystiallized from ligroin. Yield, 7.2 g. (80%); m. p. 74.5~75.5°C (lit.[4] m. p. 82°C). The infrared spectrum (KBr) showed strong absorptions at 1678 cm^{-1} (N=C) and 1039 cm^{-1} (O−C).

Found: C, 68.16, H, 6.86; N, 15.90. Calcd. for $C_{10}H_{12}N_2O$: C, 68.01, H, 7.04; N, 16.10%.

2-(3, 4-Dichlorophenylimino)-3-methyl-1, 3-oxazolidine (III, R=3, 4-$Cl_2C_6H_3$, R'=CH_3) was prepared in the same way. Yield, 80%; m. p. 64~65°C (lit.[5] m. p. 45~47°C). The infrared spectrum (KBr) showed strong absorptions at 1673 cm^{-1} (N=C) and 1035 cm^{-1} (O−C).

Found: N, 11.58. Calcd. for $C_{10}H_{10}Cl_2N_2O$; N, 11.43%.

2-Phenylimino-3-phenyl-1, 3-oxazolidine (III, R, R'=C_6H_5).—This compound was also prepared by a similar method except for the use of a larger amount of water: Ten grams of 1-(2-hydroxyethyl-1, 3-diphenyl urea was heated with 500 ml. of water for one hour. It was then recrystallized from ligroin. Yield, 5.6 g. (65%); m. p. 124°C. A strong absorption due to the imino group appeared at 1679 cm^{-1} (KBr) in the infrared spectrum. This material was identical in all respects with a sample prepared from 1-(2-hydroxyethyl)-1, 3-diphenyl thiourea and mercuric oxide[3].

2-Imino-3-phenyl-1, 3-oxazolidine (III, R=H, R'=C_6H_5) and 2-Imino-3-methyl-1, 3-oxazolidine (III, R=H, R'=CH_3).—These compounds were prepared by the method of Thurston[6] except for the use of cyanogen bromide instead of cyanogen chloride.

2-Imino-3-phenyl-1, 3-oxazolidine: Yield, 46%; m. p. 99~100°C, after recrystallization from ligroin (lit.[6] m. p. 99~100°C).

2-Imino-3-methyl-1, 3-oxazolidine: Yield, 50%; b. p. 56~57°C 3 mmHg. Found: C, 47.80, H, 8.29; N, 26.74. Calcd. for $C_4H_8N_2O$: C, 47.98, H, 8.05; N, 27.98%.

Ring-opening Adducts of the Imino Oxazolidines with Benzoic Acid. (V)—A mixture of 2-phenylimino-3-methyl-1, 3-oxazolididine (1.0 g.) and benzoic acid (0.85 g.) in 5 ml. of dry benzene was refluxed for 2 hr. The solvent was removed under reduced pressure, and the residual 1-(2-benzoyloxyethyl)-3-phenyl-1-methyl urea (V, R=C_6H_5, R'=CH_3) was washed with aqueous sodium carbonate. It was then recrystallized from ligroin and benzene; yield, 1.1 g. (65%); m. p. 116~117°C. The infrared spectrum (KBr) showed strong absortions at 1720 cm^{-1} (C=O of ester linkage) and at 1646 cm^{-1} (C=O of urea linkage).

Found: C, 67.42, H, 6.09; N, 9.67. Calcd. for $C_{17}H_{18}N_2O_3$: C, 68.44, H, 6.08; N, 9.39%.

Similarly, 1-(2-benzoyloxyethyl)-3-(3, 4-dichlorophenylimino)-1-methyl urea (V, R=3, 4-$Cl_2C_6H_3$-, R'=CH_3) was obtained from 2-(3, 4-dichlorophenylimino)-3-methyl-1, 3-oxazoline and benzoic acid in a 60% yield (m. p. 103~104°C) after recrystallization from ligoin and benzene. The infrared spectrum (KBr) showed strong absorptions at 1720 cm^{-1} (C=O of ester linkage) and at 1650 cm^{-1} (C=O of urea linkage).

Found: C, 55.86, H, 4.47; N, 7.80, Calcd. for $C_{17}H_{16}Cl_2N_2O_3$: C, 55.60, H, 4.36; N, 7.83%.

The Boron Trifluoride Complex of 2-Imino-3-phenyl-1, 3-oxazolidine (VI).—To a 2% solution of 2-imino-3-phenyl-1, 3-oxazolidine in dry ether cooled in an ice water bath was added, an equivalent amount of boron triflurorido etherate. The resulting precipitate was filtered and washed with dry ether. The yield was almost quantitative. It is very sensitive to moisture and easily deliquesces. It melts at the range 97~105°C.

Found: N, 11.70. Calcd. for $C_9H_{10}N_2OBF_3$: N, 12.17%.

Polymerizations of the above mentioned imino oxazolidines were carried out in bulk polymerizations. The catalysts, polymerizing temperature and time, reprecipitating media, yields, melting temperature and intrinsic viscosities are shown in Table I. The infrared spectra (KBr) of poly(ethylene *N*-phenyl-*N'*-methylurea), poly[ethylene

N-(3, 4-dichlorophenyl) *N'*-methylurea] and poly-(ethylene *N*, *N'*-diphenylurea) showed strong absorptions at 1648 cm^{-1}, 1647 cm^{-1} and 1659 cm^{-1} respectively. These are attributable to the non-cyclic disubstituted urea linkages.

Summary

Various 2-imino-1, 3-oxazolidines have been prepared from β-chloroethylureas or from ethanolamines and cyanogen bromide.

N, *N'*-Disubstituted 2-imino-1, 3-oxazolidines give poly(ethylene *N*, *N'*-disubstituted ureas) by 1, 4-addition type ring-opening polymerization in the presence of a cationic catalyst such as boron trifluoride etherate. On the other hand, 2-unsubstituted imino-1, 3-oxazolidines polymerize with difficulty and give polymers with low melting temperatures.

The authors wish to express their hearty thanks to Miss Toshiko Aoyagi for her microanalyses.

Laboratory of Organic Chemistry
Tokyo Institute of Technology
Meguro-ku, Tokyo

The Determination of Water by Gas Chromatography

By Seishi YAJIMA, Koreyuki SHIBA, Muneo HANDA and Yoshihisa TAKAHASHI

(Received December 17, 1963)

In the determination of water, the introduction of a sample directly into a gas chromatograph has been reported by many workers, who have used a wide variety of column packings.[1-5] However, the retention time of water was very long and the peak of water in gas chromatograms was very broad, both of which features interfered with the analysis of the other gases in the sample. In analysing gas samples containing water, Desty et al.[6] decomposed the water to hydrogen, using calcium hydride, before introducing it into gas chromatography they thus obtained satisfactory results for the gases other than water vapor in the sample.

Recently, Arnett[7] ascertaind the amount of heavy water in light water by decomposing the heavy water to DH and by analysing the DH using a charcoal column. Green[8] has reported results obtained by decomposing water to hydrogen, using an iron powder bed heated electrically to heat.

However, detailed experimental conditions have not been examined for the adsorption of water on calcium hydride, for the complete decomposition of water by calcium hydride, for the limitation of detection, for the reaction between calcium hydride and other gases, or for the reproducibility of the experiments.

The present authors used a lithium aluminum hydride, which is widely used in organic chemistry, to reduce water to hydrogen, and developed a method for determining the amount of water by gas chromatography. By this method they could determine water in amounts as small as 0.1 μg. in 10 ml. of a gas sample with a high degree of accuracy. The reaction between lithium aluminum hydride and water follows this chemical equation:[9]

$$LiAlH_4 + 4H_2O = LiOH + Al(OH)_3 + 4H_2$$

To determine such small amounts of water, the following experiments were carried out. By using water of crystallization in hydrated copper sulfate as a standard, it was first confirmed that lithium aluminum hydride could decompose water completely to hydrogen at room temperature. Second, the reactions between lithium aluminum hydride and oxygen, nitrogen, carbon dioxide, carbon monoxide, methane and C_2–C_4 hydrocarbons were studied. Third, the adsorption of water vapor on the lithium hydride surface was studied. Fourth, in order to the limitations of the detection of

1) P. W. Darby and C. Kemball, *Trans. Faraday Soc.*, **55**, 833 (1959).
2) K. G. Woolmington, *J. Appl. Chem.*, **11**, 114 (1961).
3) C. E. Benett, S. D. Nogare and L. W. Sabranski, "Treatise on Analytical Chemistry," Part I, Vol. 3, Interscience Publishers, New York and London (1961), p. 1703.
4) L. Brealey, S. A. Elvidge and K. A. Proctor, *Analyst*, **84**, 221 (1959).
5) D. A. Elvidge, and K. A. Proctor, ibid., **84**, 461 (1959).
6) D. H. Desty, T. J. Warhan and B. H. F. Whyman, "Vapor Phase Chromatography," Butterworths Scientific Publications, London (1957), p. 346.
7) E. M. Arnett, M. Strem, N. Hepfinger, J. Lipowits and D. McGuire, *Science*, **131**, 1680 (1961).
8) G. W. Green, *Nature*, **180**, 295 (1957).
9) A. E. Finhort, A. C. Bond, Jr., and H. I. Schlesinger, *J. Am. Chem. Soc.*, **69**, 1199 (1947).

water, a molecular sieve-5A column and completely-purified argon carrier gas were used for determining the hydrogen; thereby 10 p.p.m. of hydrogen could be determined in 10 ml. of a gas sample. Last, by applying the above method, the gas content of uranium dioxide was studied; satisfactory results were obtained. One example of the results is reported on in this paper.

Experimental

Apparatus.— A flow diagram of the experimental apparatus is shown in Fig. 1. The apparatus consists of an electric furnace, a U-tube packed with lithium aluminum hydride powder, and an automatic Toepler pump. The sample was heated by the electric furnace, the temperature of which was controlled by an automatic temperature regulator.

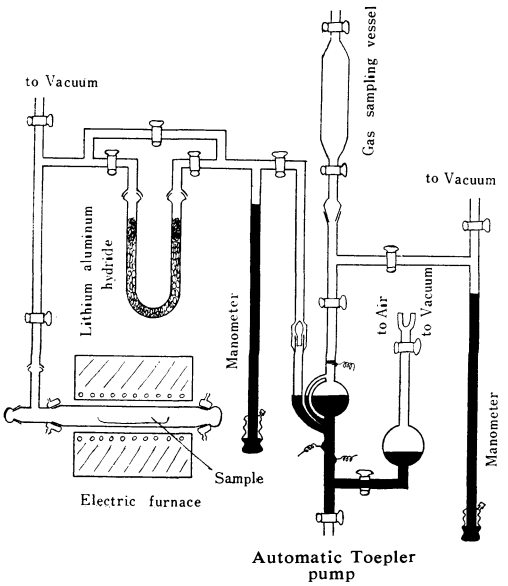


Fig. 1. Apparatus.

The automatic Toepler pump took one minute for one cycle, and its effective volume was about 100 ml., that is, if the pump was operated at S. T. P., it could draw out 100 ml. of gas per minute. The pump could bring the apparatus up to a pressure of 10^{-2} mmHg.

To Pack Lithium Aluminum Hydride into the U-Tube and to Degas the Impurity Gases Adsorbed on It.—The lithium aluminum hydride commercially available is a white powder with particle sizes of less than one micron and with various impurity gases adsorbed on its surfaces.

When lithium aluminum hydride is used as it is sold, these impurity gases are released slowly during the experiment and make the accuracy of the analysis poor. To remove these impurity gases, lithium aluminum hydride was heated for two hours at 100°C in a vacuum. The release rate of the impurity gases was reduced to 0.001 μl. per minute for the degassed lithium aluminum hydride; this release rate was negligible within the range of experimental error. To increase the passage of sample gases through the U-tube, lithium aluminum hydride was mixed with glass wool, which was then packed into the U-tube.

The amount of lithium aluminum hydride packed in the U-tube was about 0.5 g. The U-tube used was 1 cm. in diameter and 20 cm. long.

Procedure.—The sample was placed in the center of an electric furnace, and the whole apparatus was evacuated by a rotary pump to less than 10^{-3} mmHg. Then the automatic Toepler pump was operated, and the temperature in the electric furnace was raised to a given temperature.

The water vapor and the other gases released from the sample were passed through the U-tube packed with lithium aluminum hydride, where the water vapor was decomposed to hydrogen; the hydrogen was collected in the gas-sampling vessel by the automatic Toepler pump, along with other gases. The collected gases were then analysed by means of a gas chromatograph.

Gas Analysis.—A GC-IA type Shimazu gas chromatograph was used in all the experiments. Sample of gas were introduced by an attached apparatus, which is used to make the calibration curve. This apparatus is shown in Fig. 2; it is so designed that the current of the carrier gas is not interrupted during the sampling. The gas-sampling vessel containing the gas sample was attached to this calibration apparatus. Then the gas sample was transferred into a gas pipet by replacing it with mercury in the gas-sampling vessel, and a definite volume of gas was transferred from the pipet to vessel A (cf. Fig. 2).

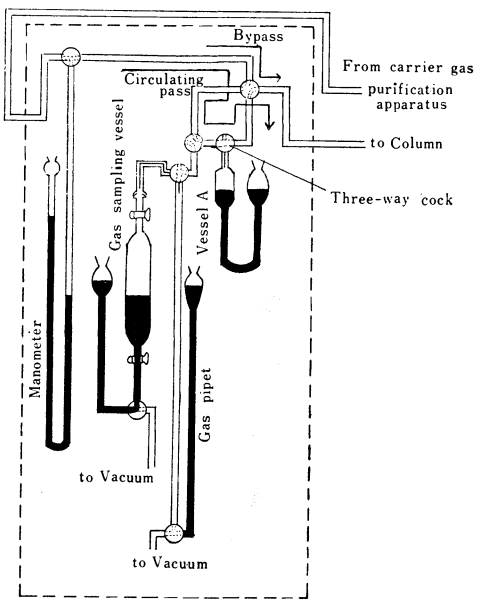


Fig. 2. Apparatus for making calibration curve.

The flow of the carrier gas was changed from the bypass to the circulating path in which the gas sample in vessel A was pushed by mercury; the sample gas was then sent to the gas chromato-

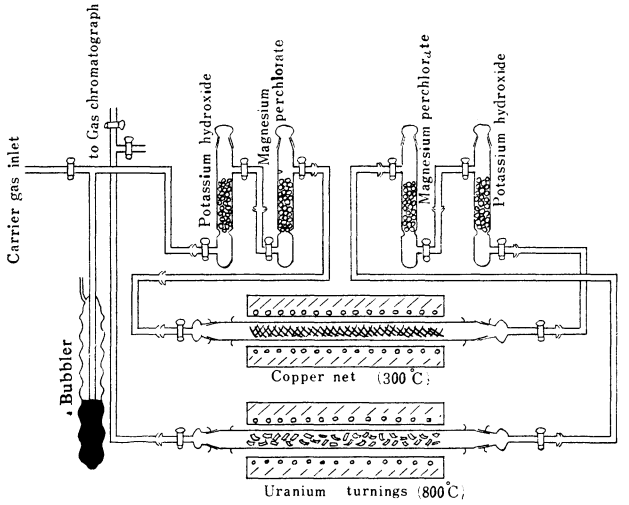


Fig. 3. Carrier gas purification apparatus.

TABLE I. DETERMINATION OF WATER OF CRYSTALLIZATION IN HYDRATED COPPER SULFATE

Weight of $CuSO_4 \cdot 5H_2O$ g.	Volume of H_2 released from $CuSO_4 \cdot 5H_2O$ (Experimental value) ml.	Weight of water in $CuSO_4 \cdot 5H_2O$ (Experimental value) g.	Weight of water in $CuSO_4 \cdot 5H_2O$ (Calculated value) g.	The ratio of the third and fourth columns
0.0358	15.85	0.0127	0.0129	1.0157
0.0779	34.17	0.0274	0.0273	0.9963
0.0883	39.87	0.0320	0.0318	0.9937
0.1503	68.47	0.0550	0.0542	0.9854
				1 ± 0.0022*

* Standard deviation

graph, along with the carrier gas. The determination was carried out with a ball-disc-type automatic integrator fixed on the SAP-type recorder. A molecular sieve-5A column was used for the separation of the components (0.6 cm. in diameter and 75 cm. long). The flow rate of the carrier gas was 40 ml. per minute. For the determination of hydrogen, argon gas was used as the carrier, while for oxygen, nitrogen, methane and carbon monoxide, helium gas was used. Both the carrier gases were completely purified by the gas purification apparatus shown in Fig. 3. A constant flow rate of the carrier gas was obtained by maintaining a constant pressure at the inlet of the chromatograph by using the mercury bubbler set in the gas purification apparatus. The sensitivity of the recorder was increased to 30 μV. per full scale by using an electronic galvanometer, model AD-6, made by the Toa Dempa Kogyo Co.

Results and Discussion

The Determination of the Water of Crystallization in Hydrated Copper Sulfate.—To confirm the complete decomposition of water to hydrogen by lithium aluminum hydride at room temperature, hydrated copper sulfate was used as standard material and the water of crystallization in it was determined. The copper sulfate weighed was heated in the furnace at 250°C, and the water vapor released was passed through the U-tube with lithium aluminum hydride powder packing, in which the vapor was decomposed to hydrogen. The hydrogen was then drawn into and collected in the gas sampling vessel by the automatic Toepler pump, and analysed by the gas chromatograph. The results obtained are shown in Table I.

As the table shows, the water completely decomposed to hydrogen by lithium aluminum hydride under the experimental conditions.

The Reaction of Lithium Aluminum Hydride with Gases Other than Water Vapor.—It was confirmed that lithium aluminum hydride quantitatively reduced water to hydrogen at room temperature. Then the reactions between lithium aluminum hydride and other gases were examined. The results of the reaction between lithium aluminum hydride and oxygen are shown in Fig. 4, where the small circles indicate the oxygen calibration points which were obtained by passing it through the U-tube packed with lithium aluminum hydride, and the small triangles show the calibration points which were obtained by not passing it through it. The points obtained for both cases

TABLE II. DETERMINATION OF WATER IN STANDARD SAMPLE

Volume of standard sample introduced to gas chromatograph ml.	Volume of water in standard sample (Experimental value) ml.	Concentration of water in standard sample (Experimental value) %	Concentration of water in standard sample (Calculated value) %	The ratio of the third and fourth columns
7.90	0.018	0.228	0.230	0.9913
7.33	0.017	0.232	0.230	1.0097
5.45	0.001	0.020	0.019	1.0536
				1±0.0311*

* Standard deviation

TABLE III. VOLUME AND COMPOSITION OF GASES EVOLVED BY 50 g. OF URANIUM DIOXIDE

Temp. °C	Heated time hr.	Volume ml.	Gas constituents, %				
			H_2O	O_2	N_2	CH_4	CO
300	6.0	13.1	94.3	0.0	3.0	2.8	0.0
300	18.0	2.7	100.0	0.0	0.0	0.0	0.0
600	6.0	3.7	39.8	4.5	42.7	13.0	0.0
600	18.0	3.4	0.0	0.0	100.0	0.0	0.0
1000	6.0	15.9	0.0	0.0	100.0	0.0	0.0
1000	18.0	6.7	0.0	0.0	100.0	0.0	0.0
Total	72.0	45.5					

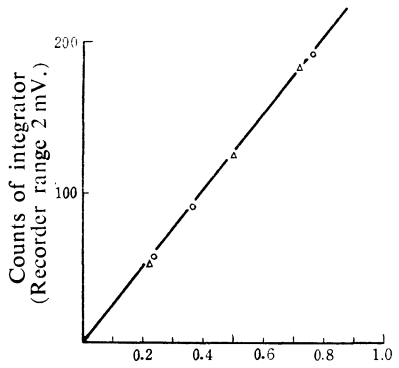


Fig. 4. Calibration curve of oxygen.

Carrier gas; Helium
Flow rate; 70 ml./min.
Column; Molecular sieve-5A, 1.5 m.

lie on the same line.

From the results, it is clear that the reaction between lithium aluminum hydride and oxygen does not occur. Following the same procedure, the reactions between lithium aluminum hydride and nitrogen, carbon monoxide, carbon dioxide methane and C_2-C_4 hydrocarbons were examined; no reactions could be detected.

The Adsorption of Water on the Surface of Lithium Aluminum Hydride.—As lithium aluminum hydride is a fine powder, the adsorption of water vapor on its surface must be checked under the experimental conditions.

Standard samples of water with water vapor contents of 0.230 and 0.019% were prepared. The water was decomposed to hydrogen and analysed by the gas chromatograph. The results obtained are shown in Table II. This table shows that the adsorption of water on the surface of lithium aluminum hydride is negligible within the range of experimental error under the present experimental conditions.

The Gas Content of Uranium Dioxide.*—Because of its good heat resistance, good chemical stability, etc., uranium dioxide is widely used as a nuclear fuel. However, uranium dioxide adsorbs various kinds of impurity gases on its surfaces. These gases are released gradually during the reactor operation, which has various harmful effects on the reactor operation, such as reacting with the zirconium used to protect to graphite moderator from the sodium coolant, leading to the deterioration of the physical properties of the zirconium.[10,11]

The analytical method stated above was used to determine the gas content of uranium dioxide, and satisfactory results were obtained. An example of the results is shown in Table III.

The sample of uranium dioxide which was used for the experiments had been stored in a laboratory, sealed in a polyethylene bottle, while the uranium dioxide was purchased from the Yokogawa Kagaku Co., Ltd.

In Table III, the first column shows the

* The gas content of many samples of uranium dioxide was ascertained. The results will be reported in the Journal of the Atomic Energy Society of Japan.

10) S. Siegel, R. L. Carter, F. E. Bowman and B. R. Hayward, "Proceedings of the International Conference on the Peaceful Uses of Atomic Energy," 9 (1956), p. 829.

11) H. J. Anderson and R. J. Anicetti, "Specification for High Density Uranium Dioxide (Nuclear Grade)," HW-74204, July (1962).

degassing temperature; the second, the degassing time; the third, the volume of gas released equivalent to that at S. T. P., and the fourth and other columns, the results of the analysis of the released gases. About 50 g. of uranium dioxide powder was used for this experiment.

The Limitation of the Determination of Water.—Concentrations of hydrogen as low as about 10 p. p.m. could be determined by the present gas chromatographical method. When 10-ml. gas samples are used, the limitation of the determination of water is as follows. In the decomposition of water by lithium aluminum hydride, one mole of hydrogen is obtained from one mole of water. That is, 10 p. p. m. of water in 10-ml. sample gases (0.1 μl. of water) is the limitation of the determination for water. Converting this value to weight, it follows that about 0.1 μg. is the limitation for water.

Division of Nuclear Engineering
Reactor Fuel Laboratory
Japan Atomic Energy Research Institute
Tokai, Ibaraki

An Automatic Recording Analyzer for the Determination of Dissolved Oxygen in Boiler Feed Water[*1]

By Kazuo TANNO

(Received December 28, 1963)

In thermal power plants, the dissolved-oxygen content of feed water for boilers is rigidly controlled in order to prevent the corrosion of the boiler and other equipment. The allowable dissolved-oxygen content is less than a few parts per billion.

The dissolved-oxygen content of the feed water in these plants is usually determined by means of an analyzer with thermal conductivity cells.[1,2),*2] However, when hydrazin is used for reducing the dissolved-oxygen content, the results of oxygen determination by the above type of analyzer are erroneous. This is because nitrogen is formed during the treatment of the feed water with hydrazin, and the thermal conductivity of nitrogen is nearly the same as that of oxygen. Therefore, a new type of oxygen analyzer is required for the determination of dissolved oxygen in hydrazin-treated feed water. The design of such an analyzer was undertaken at this laboratory; it is described in this paper. The underlying principle is to determine the dissolved oxygen automatically by Winkler's method.[3,4)]

Although, while the present work was being conducted, Ridley et al.[5)] published a paper describing the design of an instrument for dissolved-oxygen determination by the same method, their instrument appears to be useful only when the dissolved-oxygen content is of the order of some parts per million. On the other hand, the instrument described in this paper is designed for determination in the range of oxygen concentration up to 50 parts per billion.

Outline of the Method and the Reagents Used

Method.—Briefly, the method involves two main steps: (1) the fixation of dissolved oxygen, and (2) amperometric titration. The dissolved oxygen is fixed by adding the following reagents to the sample water in the order named: an alkaline iodide solution (made alkaline with potassium hydroxide), a manganous sulfate solution, and a sulfuric acid solution. The reactions taking place in this step are the formation of manganous hydroxide (Eq. 1), the oxidation of manganous hydroxide to manganic hydroxide by dissolved oxygen (Eq. 2), and the liberation of iodine (Eq. 3).

$$MnSO_4 + 2KOH = Mn(OH)_2 + K_2SO_4 \quad (1)$$

$$2Mn(OH)_2 + 1/2O_2 + H_2O = 2Mn(OH)_3 \quad (2)$$

$$2Mn(OH)_3 + 2KI + 3H_2SO_4 = 2MnSO_4 + I_2 + K_2SO_4 + 6H_2O \quad (3)$$

*1 Presented at the Autumn Meeting of the Chemical Society of Japan, Tokyo, November, 1962.

1) D. M. Considine, "Process Instruments and Controls Handbook," McGraw Hill, New York (1957), pp. 6–184.

2) H. W. Holy, *Trans. Soc. Instr. Tech.*, **12**, 145 (1960).

3) ASTM Standards, Designation D888-49T (1949).

4) Japanese Industrial Standard, B8224 (1961).

*2 Although a variety of dissolved-oxygen analyzers have been developed in these several years, this type of analyzer has been most widely used.

5) J. E. Ridley, D. B. L. Elliott and A. B. Oaten, *Analyst*, **85**, 508 (1960).

As may be seen from Eq. 3, the iodine liberated is equivalent to the dissolved oxygen. The iodine is, therefore, amperometrically back-titrated with a standard solution of potassium iodate after the addition of an excessive thiosulfate solution.

A blank determination is also carried out in order to make a correction for the effect of the interfering substances both in the sample water and in the reagents. In this case, the reagents for oxygen fixation are added to the sample water in the following order: an alkaline iodide solution, a sulfuric acid solution, and a manganous sulfate solution. The titration is then performed in the same way as has been described above.

The dissolved-oxygen content is calculated from the difference between the quantities of titrant used in the sample and blank titrations by the following equation:

$$X = \frac{8\times10^6}{V}\{m(K'-K)-D\} \qquad (4)$$

Where X = the dissolved-oxygen concentration in parts per billion (p. p. b.)
V = the volume of sample water taken for analysis, ml.
m = the concentration of the potassium iodate solution, N
K = the volume of the potassium iodate solution used in the sample titration, ml.
K' = the volume of the potassium iodate solution used in the blank titration, ml., and
D = the correction for the dissolved oxygen in the reagents.

In the present instrument, 550 ml. of sample water is analyzed by the use of the reagents described below; the quantities of reagents used for oxygen fixation are: 3 ml. of the alkaline iodide solution, 2 ml. of the manganous sulfate solution, and 3 ml. of the sulfuric acid solution. Therefore, Eq. 4 reduces to:

$$X = 72.7\{(K'-K)-0.13\} \qquad (5)^{*3}$$

This is a working formula for use with the present instrument. Although the concentrations and quantities of the reagents employed for oxygen fixation in the present method are different from those specified in the standard method, the present method gives the same results as the standard method.*4

Reagents.—The reagents used in the present instrument are as follows: Alkaline iodide solution (solution A): The concentrations of potassium hydroxide, potassium iodide, and iodine in the solution are: potassium hydroxide 8.3 N, potassium iodide 10%, and iodine 0.003 N.

Manganous sulfate solution (solution B): 32.5% solution.

Sulfuric acid solution (solution C): 18 N solution.

Standard potassium iodate solution: 0.005 N solution.

Thiosulfate solution: Approximately 0.005 N solution.

Automatic Recording Analyzer

A diagram of the automatic recording analyzer is shown in Fig. 1. This instrument was so designed as to perform automatically most of the operations involved in manual analysis, such as sampling, the addition of reagents, titration, recording, and cleansing. In order that such operations might be carried out in a systematic way, a time-cycle-control system was employed. The operations described below are automatically performed in the order of description.

Sequence of Operations.*5—*Cleansing and Sampling.*—The valves,*6 V14, V12, V10, V13, and V11, are opened, and the water to be analyzed is passed through the two fixation vessels, K and L, for a fixed period of time in order to cleanse them. Thereafter, the valves are closed. Thus, the fixation vessels are filled with the sample water.

Fixation.—The fixation of dissolved oxygen in the fixation vessel, K, is carried out first. Solutions A, B, and C in the reservoirs are simultaneously fed to the respective reagent pipets, F, G, and H; then, after the pipets are filled with the reagents, the stirrer*7 in the fixation vessel, K, is started. The reagents in the pipets are then injected into the fixation vessel in the following order: solution A, solution B, and solution C. When these solutions are forced into the fixation vessel, the surplus liquid in the vessel is drained from the top of vessel. After the injection of solution C is completed, the stirrer is stopped.

The blank operation in the fixation vessel, L, is carried out in the same way except that

*3 The value of D has been determined on the following ground. The concentrations of alkaline iodide and sulfuric acid solutions employed in the present method are, respectively, 2/3 the concentrations specified in the standard method; however, the quantities of these solutions used for dissolved-oxygen fixation are 1.5 times as large as the quantities specified in the standard method. The correction term, D, in Eq. 4 was calculated according to the equation of Adams et al.[6] and White et al.[7]

*4 For purposes of comparison, the results of analysis by the two methods are summarized in Appendix Table I.

*5 Wherever necessary, the literal symbols used to designate the parts of instrument in Fig. 1 are used in the description under this head.

*6 All the valves used in this instrument are of the electromagnetic type and systematically operated.

*7 This and two others (in vessels, L and M) are magnetic stirrers.

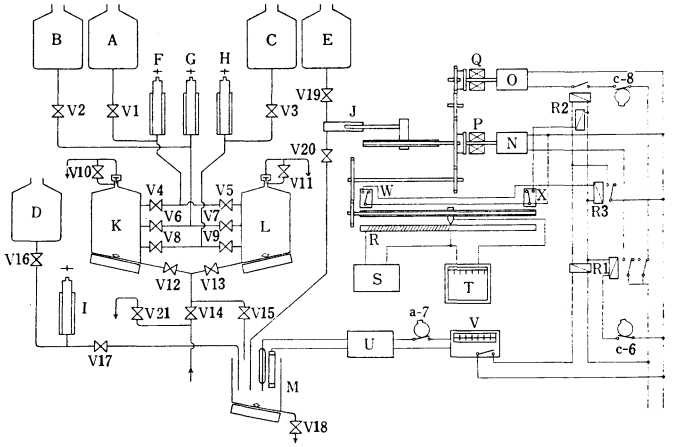


Fig. 1. Diagramatic representation of automatic recording analyzer.

A Reservoir for solution A
B Reservoir for solution B
C Reservoir for solution C
D Reservoir for sodium thiosulfate solution
E Reservoir for potassium iodate solution
F Reagent pipet for solution A
G Reagent pipet for solution B
H Reagent pipet for solution C
I Reagent pipet for sodium thiosulfate solution
J Titration pipet
K Sample fixation vessel
L Blank fixation vessel
M Titration vessel
N Titration motor
O Back-drive motor
P Titration clutch
Q Back-drive clutch
R Potentiometer
S Constant voltage source
T Recorder
U Amplifier
V Indicating controller
W Safety switch
X Slide-range=setting switch
R1, R2, R3 Relays
V1, V2,··· V21 Valves
a-7 Cam switch in controller a
c-6, c-8 Cam switches in controller c

the reagents in the pipets are injected into the fixation vessel in the order: solution A, solution C, and solution B.

Titration and Recording.—As soon as the fixation in the fixation vessel, K (sample), is completed, all the solution in this vessel is transferred to the titration vessel, M. (Here, the V10 valve, besides V12 and V15, is opened.) At the same time, the reagent pipet, I, is filled with the thiosulfate solution from the reservoir, D. The thiosulfate solution is then delivered to the titration vessel, and the stirrer in this vessel started. Next, the titration motor, N is started in order to deliver the standard potassium iodate solution (in pipet, J) to the titration vessel. (The titration pipet is filled with the titrant as soon as the previous titration is completed.)

In the course of titration, a small residual current flows between the platinum and calomel electrodes in the titration vessel until the end point is reached. After this point is reached, the diffusion current, the magnitude of which is proportional to the quantity of iodine liberated from the excess iodate added, flows between the electrodes. The diffusion current is amplified by the amplifier, U. As soon as the diffusion current attains the predetermined value, the switch in the indicating controller, V, closes, stopping the titration motor. During the titration, on the other hand, the contactor of the potentiometer, R, is driven by the screw connected by gears and a clutch to the titration motor.

After the titration is completed, the titration pipet, J, is refilled with the titrant, and the potentiometer contactor is brought back to the original position. The titrated solution in the vessel is drained, and the vessel washed with the fresh sample water delivered via the V14 and V15 valves. The vessel is then emptied and made ready for the next titration.

After the sample titration, the blank titration is carried out in the same way.

As has been indicated, all the above operations are systematically carried out as a result of the adoption of a time-cycle-control system. This system consists of four controllers, designated as a, b, c, and d. Controller b operates those parts of the instrument which are concerned with the fixation operation. Controller c operates the parts concerned with the titration operation. Controller d operates the indicating lamps. These controllers are, in turn, operated by controller a, which also carries out the operations not performed by the other controllers.

The series of operations described above (the operations in sample analysis together with the operations in blank analysis) is

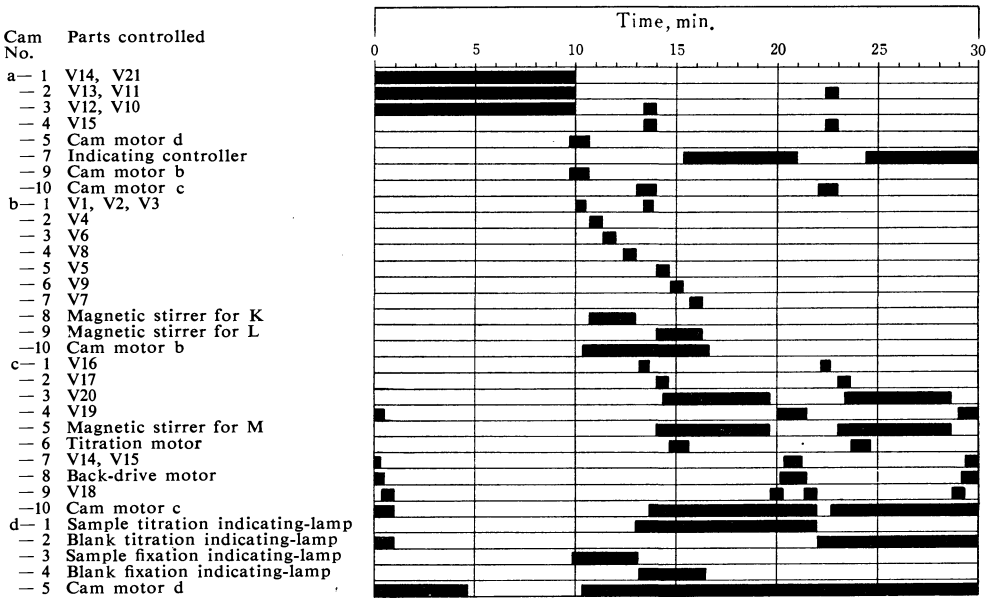


Fig. 2. Time table.
V1, V2, ····· , V21 : Valves indicated in Fig. 1. K : Fixation vessel K.
L : Fixation vessel L. M : Titration vessel M.

completed in 30 min. The time table for this series of operations is given in Fig. 2.

Apparatus and Some Particular Parts.—*Reagent Pipet.*—As is shown in Fig. 3, the pipet is a modified hypodermic syringe fitted with a branched capillary tube. One of the branches is an entry tube, and the other, an exit tube. When the entry valve is opened, the piston is raised by the hydrostatic head up to the movable stop, which is placed in position by a fine adjustment. When the entry valve is closed and the exit valve opened, the reagent in the pipet is discharged by the hydrostatic head and the weight of the piston. Table I shows that the precision in operation of the pipet is very high and is not affected by the movement of the plugs in the entry and exit valves.

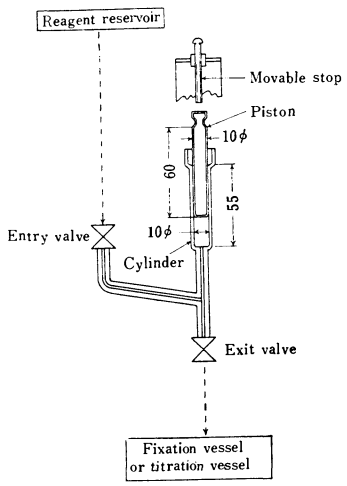


Fig. 3. Reagent pipet.

TABLE I. PRECISION IN OPERATION OF REAGENT PIPET

Pipet	Quantity of reagent transferred, g.*	
	Mean of 10 determinations	Standard deviation
With electromagnetic valves	2.1541	0.0024
With ordinary glass cocks†	1.9857	0.0030

* The reagent is the sodium thiosulfate solution.
† The valves attached to the pipet in the analyzer were replaced by ordinary glass cocks, and the cocks were manually operated.

Fixation Vessel.—In the fixation operation it is necessary that the sample water should not come in contact with air and that the reagents should be mixed thoroughly with the sample in order that complete reactions may be effected. It is also necessary that the quantity of solution remaining in the vessel after the transfer to the titration vessel should be as small as possible. These requirements were met by employing a vessel of the type shown in Fig. 4. The full capacity of the vessel used is 550 ml. The mercury-sealed

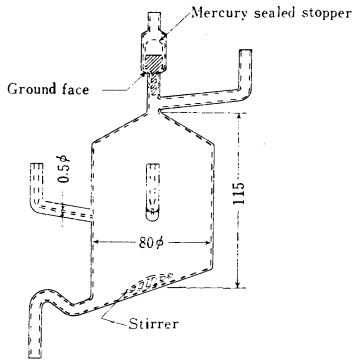


Fig. 4. Fixation vessel.

stopper can readily be raised by the liquid in the vessel when an excess of liquid is introduced. Through the capillary tube (0.5 mm. in inside diameter) attached to the side of vessel, the reagents are introduced into the vessel. The U-bent part of the tube attached to the bottom corner prevents manganese precipitate from entering the valve at the end of the tube.

Electromagnetic Valve.—The construction of the valve and the circuit diagram are shown in Fig. 5. The upper coil is used to open the valve, while the lower coil used to close the valve. The current for the coils is transmitted through a cam-switch-operated relay.

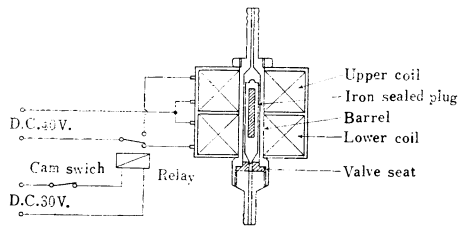


Fig. 5. Electromagnetic valve.

Titration Unit.—The titration pipet is made up of a cylinder and a narrow rod serving as a piston. The piston is 6 mm. in diameter. The pipet delivers the reagent at a rate of 0.42 ml./min., and it can discharge 2 ml. of reagent in the one-stroke operation of piston. The piston is connected by a gear mechanism and clutch either to the titration motor or to the back-drive motor. The clutches (P and Q in Fig. 1) are of the electromagnetic type; when the magnets are energized, the clutches are disengaged. During titration, the back-drive clutch, Q, is disengaged, and the connection between the piston and the back-drive motor (O in Fig. 1) is cut off. In the back drive of piston, the titration clutch, P, is disengaged to cut off the connection between the piston and the titration motor (N in Fig. 1).

The potentiometer has a slide wire 15 cm. long, and the range of movement of the contactor is adjusted by the position of the slide-range-setting switch (X in Fig. 1).

Titration Vessel and Electrodes.—The titration vessel has a capacity of 600 ml.; capillary tubes for delivering sodium thiosulfate and potassium iodate solutions are inserted in the vessel. The platinum electrode is a spiral made by winding a platinum wire 0.5 mm. in diameter and 50 mm. long.*8 The calomel electrode is one commonly used in pH measurement. These electrodes are connected by a 15 kΩ resistor*9 in the amplifier.

Indicating Controller.—The controller is a Hitachi indicating controller. The internal resistance is 100 Ω, and the reading range is 0~1000 μ.

Recorder.—A Hitachi TVK-B recorder is used. The full scale reading is 30 mV.

Performance Tests and Discussion

The instrument was tested by analyzing the water deaerated with or without the addition of hydrazin.

The deaeration was carried out in the following way by employing the apparatus shown diagrammatically in Fig. 6. Pure water was charged to both the boiler and the deaerator, and the boiler was heated. The steam from the boiler was blown into the water in the deaerator, and the water in the deaerator was, in turn, pumped into the boiler. The dissolved air was expelled with steam through

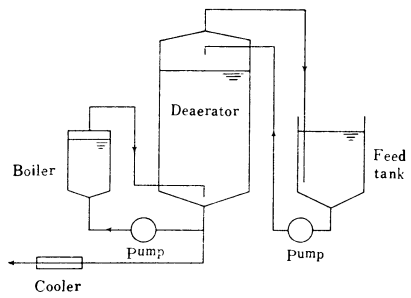


Fig. 6. Deaeration apparatus.

*8 The platinum electrode, after its preparation, is immersed in Mohr's salt solution. If this treatment has been made, the residual current, which flows before the end point is reached, can be not only minimized but also stabilized.

*9 The value of the resistor was determined experimentally. In the experiment, seven resistors (1, 5, 15, 50, 200 and 500 kΩ and 100 MΩ) were tried, and the reproducibility and the slope of titration curve were examined. From the results, a 15 kΩ resistor is considered appropriate for use in the present instrument. The data obtained in the experiment are given in Appendix Table II.

the submerged pipe in the feed tank. This procedure is based on the fact that, above 100°C., the concentration of oxygen in the vapor phase is far greater than the concentration in the liquid phase.[8] In two of the trials made, acidic hydrazin was added to pure water before deaeration by the above procedure.

After the dissolved-oxygen content of water in the deaerator had been reduced, the water was delivered to the analyzer through the cooler, and the analyzer was set in operation. The test was continued for several hours with no interruption in the operation of the deaerator.

A typical chart from the instrument, showing the results of analysis, is presented in Fig. 7. The full scale of the chart corresponds to 0.934 ml. of the titrant used. The oxygen contents calculated from such recorded data are summarized in Tables II and III, together with the results of determination by manual analysis. The data in Table III were obtained in the tests carried out by using the water deaerated with the addition of hydrazin. The hydrazin concentration decreased gradually during the run of test. However, according to Harshman and Woodmard,[9] the reaction between hydrazin and oxygen proceeds very slowly at low pH and low hydrazin concentrations, and it appeared that the conditions prevailing in the deaerator during the test were not such as to favor the reaction. It is, therefore, considered that the oxygen concentration actually remained constant, or nealry so, during the run of test. Hydrazin may have undergone thermal degradation.

The results of oxygen determination by the analyzer agree approximately with the results

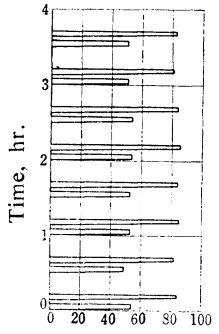


Fig. 7. Typical chart showing the results of analysis.

Table II. Analysis of the water deaerated without the addition of hydrazin

Run no.		Dissolved oxygen, p. p. b. Mean of n determinations	Standard deviation
1	Automatic analysis	12(n=5)	2.0
	Manual analysis	13(n=3)	1.2
2	Automatic analysis	11(n=8)	0.9
	Manual analysis	9(n=4)	1.2
3	Automatic analysis	11(n=8)	0.9
	Manual analysis	9(n=4)	1.5

Table III. Analysis of the water deaerated with the addition of hydrazin

Run no.		Dissolved oxygen, p.p.b. Mean of n determinations	Standard deviation
4*	Automatic analysis	1.6(n=9)	1.7
	Manual analysis	1.2(n=4)	2.4
5†	Automatic analysis	1.6(n=8)	1.3
	Manual analysis	1.0(n=2)	—

* pH : 4.0~4.1 ; hydrazin, p. p. b. : 7~12
† pH : 5.2~5.8 ; hydrazin, p. p. b. : 4~10

obtained by manual analysis. The precision of determination by the analyzer is not greater than 2 p. p. b., and the reproducibility is better than that of manual analysis.

Table IV shows the results of the test of the titration unit. In the test, a definite quantity

Table IV. Precision of automatic titration

	Titrant added, ml. Mean of 10 determinations	Standard deviation
Example 1	0.438	0.008
Example 2	0.637	0.006

of a sodium thiosulfate solution was automatically introduced into the titration vessel and titrated with the standard potassium iodate solution, the quantity of titrant added being recorded on the recorder chart. As may be seen from the table, the standard deviation is quite small. Since 0.006 ml. of the potassium iodate solution used corresponds to an oxygen concentration of 0.4 p. p. b., the difference between the error of the integral analytical operation performed by the analyzer and the error of the operation performed by the titration unit appears to be attributable mainly to the fixation operation. The titration unit may also be used for some other types of analysis.

As has been mentioned, the above tests were carried out in the laboratory by empolying a special apparatus for producing the deaerated water. Besides these tests, similar tests were also performed in a thermal power

6) R. C. Adams, R. E. Barnett and D. E. Keller, Jr., *Proceedings, Am. Soc. Testing Mats.*, **43**, 1252 (1943).
7) A. H. White, C. H. Leland and D. W. Button, *Proceedings, Am. Soc. Testing Mats.*, **36** part II, 707 (1936).
8) M. Abe, E. Okumura, K. Tanno and N. Kawashima, *Hitachi Hyoron*, **45**, 561 (1963).
9) R. C. Harshman and E. R. Woodmard, *Trans. Am. Soc. Mech. Eng.*, **77**, 869 (1955).

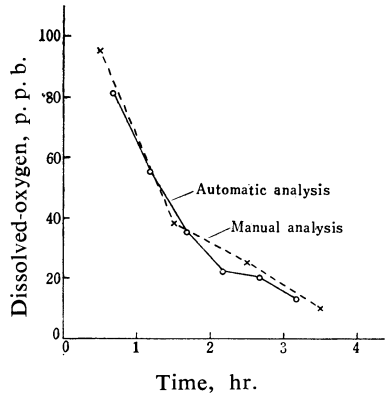


Fig. 8. Results of test in a power plant (During the start-up period)

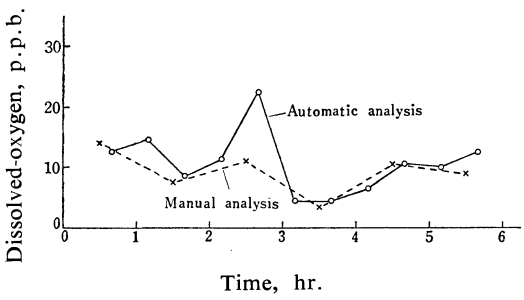


Fig. 9. Results of test in a power plant (During the start-up period)

plant. The analyzer was set in operation at the start-up of the power plant, and in each run, a manual analysis was made at intervals for purposes of comparison. The potassium iodate and thiosulfate solutions used for the analysis in the start-up stage of the boiler operation were 0.01 N solutions, because, during the start-up period, the dissolved-oxygen content was greater than that to be determined by the use of the reagents specified in this paper. The results obtained during the start-up period are shown in Fig. 8, while the results obtained after this period are shown in Fig. 9. In spite of the facts that it was impossible to take the samples simultaneously for both automatic and manual analyses and that the dissolved-oxygen content was apt to fluctuate, a relatively good agreement is again observed between the automatic and manual analyses.

Besides dissolved oxygen and hydrazin, traces of ammonia, iron, copper and silica are contained in feed water. The concentration of ammonia is controlled to around 0.1 part per million[8] as to keep the pH value of feed water within the limits shown in Appendix Table III, and the amounts of other components are usually kept below the limits in the table. Iron and copper exist in ionic state in part, but their possible disturbing influence on the determination of dissolved oxygen is removed by the blank operation as mentioned above.

Summary

An automatic recording analyzer for the determination of dissolved oxygen (in concentrations up to 50 p. p. b.) in boiler feed water by Winkler's method has been described. The instrument is so designed as to perform automatically most of the operations involved in manual analysis, such as sampling, the addition of reagents, titration, recording, and cleansing. The series of required operations (all of the operations in both sample and blank analyses) is completed in 30 min. and is automatically repeated. A more important feature of the instrument is that hydrazin-treated feed water, as well as feed water not treated with hydrazin, can be analyzed with accuracy. The oxygen content, however, cannot be read directly on the recorder chart and must be calculated from the recorded quantities of the titrant used. The precision of oxygen determination is within 2 p. p. b. The reproducibility is better than that of manual analysis.

The author wishes to express his thanks to Professor Mutsuaki Shinagawa of Osaka University, Dr. Isao Makino of Naka Works, Hitachi, Ltd., and Dr. Takeshi Nakatogawa, Dr. Natsuki Kawashima, and Dr. Kaoru Sakai of Hitachi Research Laboratory, Hitachi, Ltd., for their advice and encouragement in this work.

Hitachi Research Laboratory
Hitachi, Ltd.
Hitachi-shi, Ibaraki

APPENDIX TABLE I. DISSOLVED-OXYGEN DETERMINATION WITH THE REAGENTS PREPARED ACCORDING TO DIFFERENT SPECIFICATIONS

Run no.	Dissolved-oxygen content*, p. p. b., determined with: Reagents prepared according to the standard specifications	Reagents prepared according to the present specifications
1	7	—
	—	6
	7	—
	—	9
2	5	—
	—	5
	6	—
	—	4
	4	—
	—	2
	1	—
	—	2
	2	—

* The data are arranged in the order of increasing time in the run.

Appendix Table II. Data for the selection of the resistor for coupling the platinum and calomel electrodes

Resistance Ω	Maximum difference in three determinations (Expressed in ml. of titrant)		Voltage increase per unit volume of titrant, E' (mV./0.1 ml.)	E'/E	Response†
	At equivalence point	At predetermined voltage, E (mV.)*			
1 k	0.03	0.06(0.9)	0.44	0.5	F
5 k	0.01	0.03(6)	2.4	0.4	F
15 k	0.01	0.01(15)	6.6	0.4	F
50 k	0.02	0.02(50)	22	0.4	F
200 k	0.01	0.03(160)	76	0.5	RS
500 k		0.02(200)	155	0.8	S
100M		0.02(300)	55	0.2	VS

* The voltage is such that the titrant volume reading at this voltage exceeds the reading at the equivalence point by a small fixed amount.

† F: fast, RS: rather slow, S: slow, VS: very slow

Appendix Table III. Examples of feed water limits

	Natural circulation boiler with operating pressure (kg./cm²)			Monotube boiler
	100	130	180	
pH	8.6~8.9	8.6~8.9	8.6~8.9	8.6~8.9
Dissolved oxygen, p. p. b.	7	7	7	7
Total iron, p. p. b.	20	20	10	10
Total copper, p. p. b.	20	10	5	5
Silica, p. p. b.	—	—	—	20

*Semiconducting Properties of Organic Polyiodides**

By Shigekazu KUSABAYASHI, Hiroshi MIKAWA, Shichio KAWAI, Madoka UCHIDA and Ryôiti KIRIYAMA

(Received January 6, 1964)

A new class of organic salts, formed from the radical anion of tetracyanoquinodimethane (abbreviated as TCNQ, or simply as T) and various cations has been reported,[1] and the electrical resistivties of these compounds have also been reported.[2] Quinolinium TCNQ anion radical salt (M^+T^-), for example, has a resistivity of $10^4\Omega$ cm., whereas quinolinium TCNQ anion radical complex salt (M^+T^-T), which contains one molecule of neutral TCNQ in addition to M^+T^-, has such a low resistivity as $10^{-2}\Omega$ cm.

The mechanism of the electrical conduction of M^+T^-T salt is presumed to be essentially the successive electron transfer between T^- and T, resulting in a delocalization of the electrons through the crystal. The M^+ cation seems to be of subordinate importance in the conduction mechanism, acting merely to keep the entity electrically neutral. In other words, the electrical conduction of M^+T^-T salt is primarily the conduction through the charge transfer complex T_2^-, with T^- acting as a donor and T acting as an acceptor. In this sense, M^+T^-T may also be written as $M^+T_2^-$.

Organic polyiodides, $M^+I_x^-$, are a class of compound analogous to TCNQ anion radical complex salts. The only difference between TCNQ complex salt and the polyiodide, except for their different crystal structures, is that the

* Presented at the 16th Annual Meeting of the Chemical Society of Japan, Tokyo, April, 1963.

1) D. S. Acker, R. J. Harder, W. R. Hertler, W. Mahler, L. R. Melby, R. E. Benson and W. E. Mochel, *J. Am. Chem. Soc.*, **82**, 6408 (1960).

2) R. G. Kepler, P. E. Bierstedt and R. E. Merrifield, *Phys. Rev. Letters*, **5**, 503 (1960).

former is an anion radical salt containing π-electron system and the latter is an ionic salt of a highly-polarized polyatomic ion. The crystal structures of these four organic polyiodides have been analysed: tetraphenylarsonium triiode,[3] tetramethylammonium pentaiodide,[4] tetraethylammonium heptaiodide[5] and tetramethylammonium enneaiodide[6]. The structure of tetramethylammonium pentaiodide, for example, consists of layers of iodine atoms, with V-shaped pentaiodide ions arranged so as to form a nearly square net of iodine. The iodine-iodine distances within an ion are 2.81 and 3.17 Å, whereas the shortest distance between the iodine atoms belonging to the nearest neighboring ions is 3.63 Å; however, the net to net distance is 4.3 Å. The nets are so arranged as to leave large holes for the tetramethylammonium cations.

As for the crystalline polyiodides stated above, it is generally observed that the iodine-iodine distances within each ion are longer than the I–I distance of the I_2 molecule in crystalline iodine (2.68 Å),[7] and that they are considerably smaller than the sum of the normal ionic radius of the I^- ion, 2.16 Å[8], and the covalent radius of iodine, 1.34 Å. These facts show that, as Hach and Rundle have suggested[4], polyiodide ions result from the interaction of a negative iodide ion with a highly-polarizable iodine molecule, the interaction leading to a partial charge transfer through the resonance of the covalent bond. Furthermore, the interpretation of the structure of polyiodide by the molecular orbital method has confirmed the possibility of the delocalization of the outer p-electron.[4,9]

Although quite a large number of organic semiconductors have already been investigated, not so many ionic compounds have been investigated except for some ionic dyes. The present paper will, therefore, deal with the electrical properties of organic polyiodides.

Experimental

Material.—*Monoiodides.*— Tetramethylammonium iodide, trimethylphenylammonium iodide, 1-methyl-2-picolinium iodide and 1-methylquinolinium iodide were prepared by the method of Vogel[10] by the action of methyl iodide on the parent tertiary amines. These were recrystallized three times from water or alcohol. The melting points agreed with those reported in the literature.

Polyiodides.—The following polyiodides were prepared from iodine and monoiodides and were recrystallized twice from alcohol or an iodine-alcohol solution. Single crystals of several polyiodides were grown from a solution over a several-weeks period. *Tetramethylammonium Polyiodides* were prepared by the method of Buckles, Yuk and Popov.[11] The melting points found (and those reported in the literature) are as follows. Triiodide, 116.5~117.5°C (117.0~117.2°C); pentaiodide, 129~130°C (129~130°C). *Trimethylphenylammonium Polyiodides* were prepared by the method of Geuther.[12] Triiodide, 117.0~117.5°C (115°C); pentaiodide, 83.3~83.6°C (82°C); heptaiodide, 63.5~64.0°C (65°C). *1-Methyl-2-picolinium Polyiodides* were prepared by the method of Murrill.[13] Triiodide, 135.5~136.0°C (134°C); pentaiodide, 61.5~62.5°C (60°C); heptaiodide, 57.5~59.0°C (57°C). *1-Methylquinolinium Polyiodides* were prepared by the method of Trowbridge.[14] Triiodide, 109.1~109.3°C (108.6~109.6°C[15]); pentaiodide, 70.5~71.5°C (70°C).

Measurements.—Measurements were mainly carried out on a compressed disk of crystalline powder. Since it is inert to iodine or iodides, graphite was used as the electrode material. The electrode assembly is shown in Fig. 1. Two disk electrodes, 0.4~0.5 mm. thick and 8 mm. in diameter, were prepared first by pressing graphite powder with a 5t/cm² apparatus. Crystalline powder was then

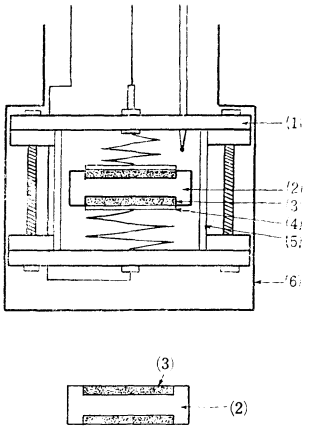


Fig. 1. Electrode assembly.

(1) Teflon (2) Specimen (3) Graphite electrode (4) Platinum plate (5) Glass tube (6) Shield box

3) R. C. L. Mooney Slater, *Acta Cryst.*, **12**, 187 (1959).
4) R. J. Hach and R. E. Rundle, *J. Am. Chem. Soc.*, **73**, 4321 (1951); J. Broekema, E. E. Havinga and E. H. Wiebenga, *Acta Cryst.*, **10**, 596 (1957).
5) E. E. Havinga and E. H. Wiebenga, *Proc. Roy. Ac. Amsterdam*, B, **58**, 412 (1955); E. E. Havinga and E. H. Wiebenga, *Acta Cryst.*, **11**, 733 (1958).
6) W. J. James, R. J. Hach, D. French and R. E. Rundle. *Acta Cryst.*, 8, 814 (1955).
7) A. I. Kitaĭgorodskiĭ, T. L. Khotsyanova and Yu. T. Struchkov, *Zhur. Fiz. Khim.*, **27**, 780 (1953) from *Chem. Abstr.*, **49**, 2145 (1955).
8) L. C. Pauing, "The Nature of the Chemical Bond," 3rd ed., Cornell University Press, Ithaca, New York (1960), p. 518.
9) E. E. Havinga and E. H. Wiebenga, *Rec. Trav. Chem.*, **78**, 724 (1959); G. C. Pimentel, *J. Chem. Phys.*, **19**, 446 (1951).
10) A. I. Vogel, "A Text-book of Practical Organic Chemistry," Longmans, Green and Co., London (1951), p. 631.
11) R. E. Buckles, J. P. Yuk and A. I. Popov, *J. Am. Chem. Soc.*, **74**, 4379 (1952).
12) A. Geuther, *Ann.*, **240**. 66 (1887).
13) P. Murrill, *J. Am. Chem. Soc.*, **21**, 828 (1899).
14) P. F. Trowbridge, ibid., **21**, 66 (1899).
15) C. Schall, *Z. Elektrochem.*, **14**, 397 (1908).

packed between these two graphite electrodes in a mold with a diameter of 13 mm. and pressed at 2.7 t/cm^2 in a vacuum. The thickness of the specimen-between-electrodes thus obtained was about 0.5 mm. Platinum plates with lead wires were attached to the graphite electrodes. In the case of a single crystal, both ends of the crystal rod were wrapped with graphite powder and held with platinum plates. A copper-constantan thermocouple was placed near one of the platinum plates. The whole was closed in a Teflon container of a 3 cc. capacity. The electrode assembly was entirely shielded and placed in a glass vessel.

The resistance was measured by the d. c. method with a Toa Denpa Model PM 18 microvolt-ammeter for the specimens with a high resistivity. A National Model PV 910 A vacuum-tube voltmeter was used for the specimens with a lower resistivity. The applied voltage was less than 70 V./cm. The temperature range of the measurements was from room temperature to about 10~20°C below the melting point.

As graphite had to be used as the electrode material, it was impossible to apply a guard ring electrode. The surface leakage current is, however, negligible, because ε values, the band-gap energy of electrical conduction, do not change, even after the heating and cooling cycles which accompany the slight color change of the material surface, bulk conduction evidently being predominant.

Results and Discussion

In tetramethylammonium pentaiodide, for example, a linear relationship was observed between current and applied voltage as long as the voltage was kept below about 2000 V./cm.

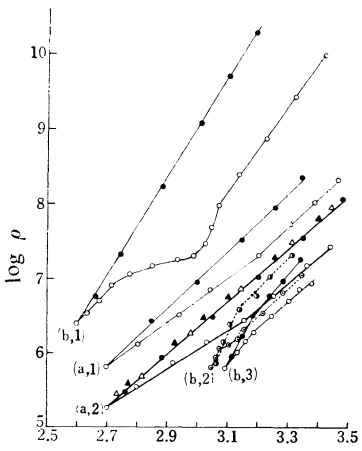


Fig. 2. Temperature dependence of the electrical resistivity of organic polyiodides.

(a) Tetramethylammonium polyiodides
(b) 1-Methyl-2-picolinium polyiodides
(1) Triiodide (2) Pentaiodide (3) Heptaiodide
○ or ⊙ first heating, ● or ◑ first cooling, △ second heating, ▲ second cooling

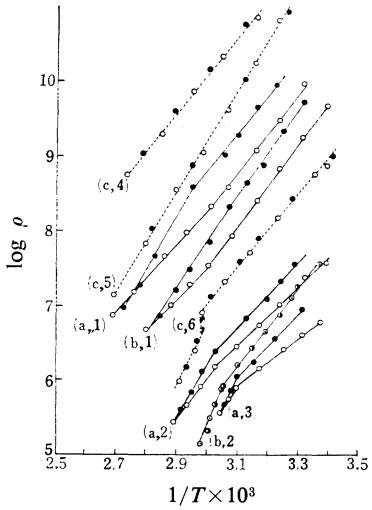


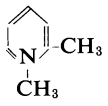
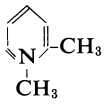
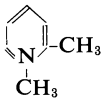
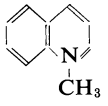
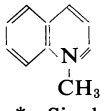
Fig. 3. Temperature dependence of the electrical resistivity of organic polyiodides.

(a) Trimethylphenylammonium polyiodides
(b) 1-Methylquinolinium polyiodides
(c) Single crystal of trimethylphenylammonium polyiodides (Values of log ρ are arbitrary.)
(1) Triiodide (2) Pentaiodide (3) Heptaiodide
(4) Parallel to the cleavage plane of triiodide
(5) Normal to the cleavage plane of triiodide
(6) Parallel to the cleavage plane of pentaiodide
○ or ⊙ heating, ● or ◑ cooling

The relationship between the logarithm of resistivity and the reciprocal of temperature is shown for various compounds in Figs. 2 and 3. Generally speaking, the plots obtained for the heating cycle do not agree with those for the cooling cycle. For the reasons to be discussed below, the values of the resistivities and the slopes observed at relatively low temperature for the heating cycle seem to be correct. The specific resistivities at 20°C (ρ_{20}) and the band-gap energy (ε) as calculated from the low temperature slope by the equation $\rho = \rho_0 \exp(\varepsilon/2kT)$ are tabulated in Table I. The values of the specific resistivity and the band-gap energy for several organic polyiodides range between 10^7~10^{10} Ωcm. and 1.3~2.6 eV. respectively.

On the Shape of log ρ versus $1/T$ Curves.— Curve (a, 2) of Fig. 2. shows the log ρ versus $1/T$ curve for tetramethylammonium pentaiodide, where the heating and cooling cycles are repeated successively twice. During the first course of the heating cycle, a distinct break was observed. Moreover, different ρ values were observed in the heating and cooling cycles. However, the plots of the second heating and cooling cycles were found on the same line and coincided with the plots in the first cooling cycle. Besides, no change in ε

TABLE I. ELECTRICAL PROPERTIES OF ORGANIC POLYIODIDES

Substance	ρ_{20} Ω cm.	ε, eV. Heating cycle Low temp.	Heating cycle High temp.	Cooling cycle Low temp.	Cooling cycle High temp.	Temp. range
$(CH_3)_4N\ I_3$	1.2×10^{8}	1.58	1.17	1.64		16— 97
$(CH_3)_4N\ I_5$	2.1×10^{7}	1.36	1.00	1.37		16— 97
$(CH_3)_3C_6H_5N\ I_3$	2.7×10^{10}	2.09	1.89	2.04	3.10	29—100
$(CH_3)_3C_6H_5N\ I_3$	*	2.65		2.65		36—100
$(CH_3)_3C_6H_5N\ I_3$	**	2.00		2.00		41— 91
$(CH_3)_3C_6H_5N\ I_5$	5.2×10^{7}	1.63	2.15	1.73	3.30	24— 71
$(CH_3)_3C_6H_5N\ I_5$	**	2.03	3.43	2.03	3.43	26— 71
$(CH_3)_3C_6H_5N\ I_7$	8.2×10^{6}	1.29	2.96	2.12	3.68	25— 56
	I_3 9.6×10^{9}	2.25	1.81	2.68		20—104
	I_5 2.2×10^{7}	1.65	4.97	1.73	5.22	26— 55
	I_7 1.2×10^{7}	1.39	1.98	2.19	3.48	24— 50
	I_3 7.0×10^{9}	2.08	1.74	2.14	2.66	21— 85
	I_5 7.2×10^{7}	1.96	4.33	1.96	4.33	25— 63

* Single crystal: normal to the cleavage plane.
** Single crystal: parallel to the cleavage plane along the growth axis.

values was observed throughout all the cycles except just after the break in the first heating cycle.

One possible explanation for the break and the difference in ρ values is the annealing of the strain originally existing in the virgin specimen, i. e. that caused by some unstable grain contact which existed first; the thermal annealing gradually removed such unstable contact in the temperature region higher than a certain temperature. In the case of single crystals, the reproducibility was observed in the $\log\rho$ versus $1/T$ plots, as is shown in Fig. 3, as can be well understood from the assumption that no unstable contact exists in a single crystal.

After the measurement, the surface of the specimen showed some color change, evidently because some iodine was lost from the surface of the material. No color change was observed in the inner part of the specimen, however, and the X-ray powder pattern also remained quite unchanged. As the contact surface between the material and the electrode graphite is deep in the specimen, as Fig. 1 show, it may safely be assumed that the values obtained, especially at relatively low temperatures, are correct.

The general features of the shape of the $\log\rho$ versus $1/T$ plots just explained above using tetramethylammonium pentaiodide as an example are about the same as those observed in other pentaiodides as well as those in the several triiodides investigated, as Figs. 2 and 3 show. The values of ρ and ε calculated at a relatively low temperature seem to be correct for these compounds also.

For heptaiodides the slopes of the plots for the heating and cooling cycles do not agree, as is shown in Figs. 2 and 3. As heptaiodide is the most unstable compound among the polyiodides investigated, the difference in the slopes of the plots for the heating and cooling cycles seems to be due to the slight irreversible decomposition of the compound. Here again the values calculated at low temperatures will be the correct ones.

Although the possible annealing of the strain

which originally existed in the specimen was suggested as the cause of the rather complex feature of the $\log \rho$ versus $1/T$ plots observed with almost every polyiodides, the effects of, say, impurities, lattice defects and a phase transition during the measurements should not be left out of consideration.

Single Crystal.—For the trimethylphenylammonium triiodide single crystal, a considerable anisotropy was observed in ε values between the normal direction and that parallel to the cleavage plane along the growth axis. Although in some organic semiconductors a considerable anisotropy is reported in conductivity, ε values remain isotropic without exception.[2,16] This is natural because the energy gap should remain isotropic in so far as an energy-band scheme is applicable to the conduction in different directions. Hence, it is possible that band-scheme conduction and hopping conduction are taking place in different directions, in the hopping conduction some excess activation energy for hopping being required in addition to the energy of carrier formation.

It is interesting to note that the ε value of a specimen tablet made of powdered trimethylphenylammonium triiodide at a low temperature is about the same as the value of the single crystal measured parallel to the cleavage plane along the growth axis. The absolute value of the specific resistivity can not be estimated at present with a single crystal, because the estimation of the electrode area is not possible. Thereby, it is impossible to ascertain the anisotropy in specific resistivity. To find this, a large single crystal is now being grown.

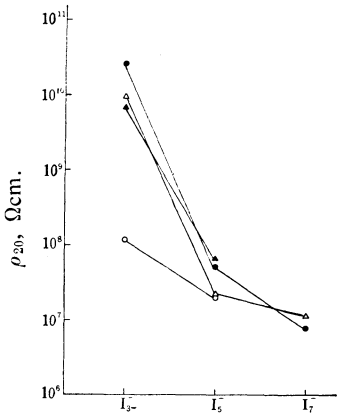


Fig. 4. Resistivities of organic polyiodides.
○ Tetramethylammonium
● Trimethylphenylammonium
△ 1-Methyl-2-picolinium
▲ 1-Methylquinolinium

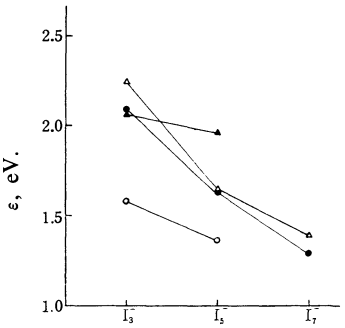


Fig. 5. Band-gap energies of organic polyiodides.
○ Tetramethylammonium
● Trimethylphenylammonium
△ 1-Methyl-2-picolinium
▲ 1-Methylquinolinium

Electrical Properties and Crystal Structure.—Figures 4 and 5 show how the values of ρ_{20} and ε change with the number of iodine atoms in polyiodide anions. It is indicated clearly that both values decrease with an increase in the number of iodine atoms, the influence of cations being of subordinate importance. That iodine has an important effect upon the conduction of polyiodides is understandable in the light of the crystal structure of the polyiodides. With regard to enneaiodide, the details will be discussed in a forthcoming paper.

As has been stated previously, the crystal structures of tetraphenylarsonium triiodide, tetramethylammonium pentaiodide, tetraethylammonium heptaiodide and tertamethylammonium enneaiodide are known. Although it is sure that the structure of many other polyiodides will deform according to the difference in the nature of the cations, it is certain that the structure will remain essentially similar to the known structures.

The structure of the molecular crystal of iodine itself is also known. In its layer structure, the I–I bond length and the I_2–I_2 intermolecular distance in the layer are 2.68 and 3.56 Å respectively.[7] The values of the electrical resistivity at room temperature are 2×10^{11} and $6\times10^{7}\,\Omega$ cm. for both the normal direction and the direction parallel to the cleavage plane,[17] while the ε value is 1.24~1.30 eV.[18]

As is evident from Table II, the shortest

16) H. Mette and H. Pick, *Z. Physik.*, **134**, 566 (1953); P. L. Kronick and M. M. Labes, *J. Chem. Phys.*, **35**, 2016 (1961); G. H. Heilmeier, G. Warfield, S. E. Harrison and J. Assour, Abstracts of Organic Crystal Symposium. Ottawa, October, 1962., p. 133; H. Kokado, K. Hasegawa and W. G. Schneider, ibid., p. 186; Y. Maruyama, H. Inokuchi and Y. Harada, This Bulletin, **36**, 1193 (1963).

17) R. Bersohn, *J. Chem. Phys.*, **36**, 3445 (1962).

18) T. S. Moss "Photoconductivity in the Elements," Butterworths, London (1952), p. 240.

TABLE II. SHORTEST DISTANCE BETWEEN NEIGHBORING POLYIODIDE ANIONS IN ORGANIC POLYIODIDE CRYSTALS OF KNOWN STRUCTURE

Polyiodide		Shortest distance Å
Anion	Cation	
Triiodide	tetraphenylarsonium	5.29[3] ($I_3^- - I_3^-$)
Triiodide	(caesium)	4.03* ($I_3^- - I_3^-$)
Pentaiodide	tetramethylammonium	3.63[4] ($I_5^- - I_5^-$)
Heptaiodide	tetraethylammonium	3.47[7] ($I_3^- - I_2$)**
(Iodine)		3.56[7] ($I_2 - I_2$)

* Value reported for CsI_3 (H. A. Tasman and K. H. Boswijk, *Acta Cryst.*, 8, 59 (1955).). $I_3^- - I_3^-$ distances of organic polyiodides investigated for electrical properties in the present report may come, because of the bulkiness of the cation, between 4~5Å.

** I_7^- anion in crystal is better understood as being composed of I_3^- and I_2.

distances between neighboring polyiodide anions in crystsal decrease with an increase in the number of iodine atoms of polyiodide anions. In so far as the electrical conduction is effected through the overlap of molecular orbitals of polyiodide anions, it is quite understandable that the ρ_{20} and ε values of these compounds decrease with an increase in the number of iodine atoms in polyiodide anions.

Although, as has been discussed above, the iodine framework may be of primary importance in the electrical conduction in the crystal, it is possible that the cation has some influence on the conduction, although it should be remembered that the iodine framework itself is being deformed by the differences in the size and shape of the cations. It is possible, for example, that some cation with conjugated double bonds may form a charge transfer complex with the polyiodide anion.

Thermoelectric Power.—To ascertain the sign of the majority carriers, a preliminary examination of the thermoelectric power was made. The flow of the current was clearly observed in pentaiodides, heptaiodides and tetramethylammonium enneaiodide. The direction of the current indicated that the positive hole contributed more to the current than the electron. In other polyiodides the results were not so clear as in the compounds stated above; the positive hole seems, however, to be the main carrier there also. It has been reported that, in the space-charge-limited photocurrent in iodine, the hole conduction was predominant over the electron conduction.[19]

Details of the measurement of thermoelectric power will be reported on in a forthcoming paper.

Optical Properties. — The optical absorption spectra of quaternary ammonium polyiodides in various solvents have been reported.[11,20]

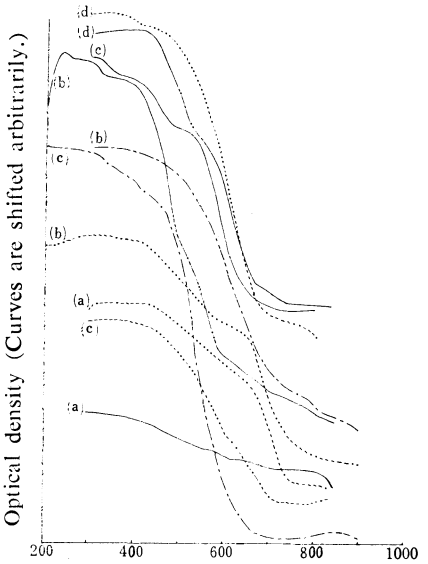


Fig. 6. Absorption spectra of organic polyiodides.
—— Triiodides
- - - Pentaiodides
-·-· Heptaiodides
(a) Tetramethylammonium
(b) Trimethylphenylammonium
(c) 1-Methyl-2-picolinium
(d) 1-Methylquinolinium

As in connection with the electrical properties of a solid, we are interested in the absorption spectra of solid; they were measured and are shown in Fig. 6. Polyiodides were melted between two glass or quartz plates and then cooled slowly, and the absorption was measured with the usual spectrophotometer. The absorption curves are rather diffuse, and the band-gap energies, as calculated from the temperature dependence of the electrical resistivity, do not agree with the absorption maxima, being grouped rather near the very beginning of the first absorption.

Preliminarily it is observed that all the

19) A. Many, M. Simhony, S. Z. Weisz and J. Levinson, *J. Phys. Chem. Solids*, 22, 285 (1961).
20) C. K. Tinkler, *J. Chem. Soc.*, 1908, 1611; F. L. Gilbert, R. R. Goldstein and T. M. Lowry, ibid., 1931, 1092; R. E. Buckles and J. F. Mills, *J. Am. Chem. Soc.*, 76, 6021 (1954).

polyiodides investigated show a photoconductivity response. Details will be published later.

Summary

1) The electrical conductivities of ten organic polyiodides have been measured: tetramethylammonium triiodide, tetramethylammonium pentaiodide, trimethylphenylammonium triiodide, trimethylphenylammonium pentaiodide, trimethylphenylammonium heptaiodide, 1-methyl-2-picolinium triiodide, 1-methyl-2-picolinium pentaiodide, 1-methyl-2-picolinium heptaiodide, 1-methylquinolinium triiodide and 1-methylquinolinium pentaiodide. At the room temperature specific resistivities are $10^{7}\sim10^{10}\Omega$ cm. and the band-gap energies, as calculated from $\rho=\rho_0 \exp(\varepsilon/2kT)$, are 1.3~2.6 eV.

2) Both ε and ρ_{20} decrease with an increase in the number of iodine atoms in the polyiodide anion, not so much difference in these values being observed with different kinds of cations. The iodine framework in the crystal structure is of primary importance in determining the electrical conductivity.

3) For the trimethylphenylammonium triiodide single crystal, an anisotropy of ε values was observed between the normal direction and the direction parallel to the cleavage plane along the growth axis.

4) Preliminary thermoelectric power measurements show that the majority carrier is the hole.

5) The solid absorption spectra of polyiodides have been measured. The band-gap energy, ε, does not agree with the absorption maximum, being rather near the very beginning of the first absorption.

6) All the polyiodides investigated show a photoconductivity response.

The authors wish to express their thanks to Miss Seiko Oka for her help in the measurement of the absorption spectra.

Institute of Scientific and Industrial Research
Osaka University
Sakai-shi, Osaka

Colloid Chemical Studies of Starching Materials. VI. Viscometric Studies of the Interaction between Polyvinyl Alcohol and Sodium Dodecyl Sulfate

By Masayuki NAKAGAKI* and Yukiko NINOMIYA

(Received January 6, 1964)

In a previous paper[1] of this series,[2] the intrinsic viscosity of polyvinyl alcohol in a sodium laurate solution was studied, and it was concluded that the effect of sodium laurate may be classified into three types, depending on the detergent concentration. Similar studies made in a sodium dodecyl sulfate (SDS) solution will be reported on here.

Experimental

Materials.—Two samples of polyvinyl alcohol, the same as in a previous paper, were used. They are Gohsenol NM-14 (the degree of polymerization is about 1400; the degree of saponification is 99.3%) and Gohsenol GM-14 (the degree of polymerization is about 1400; the degree of saponification is 87.6%), provided by the Nippon Gosei Kagaku Kogyo K. K. To dissolve the polymer, a weighed sample was added to cold distilled water and heated to 90°C within 15 min.; heating was continued at the same temperature for a further 30 min. As the detergent, sodium dodecyl sulfate, provided by the Nihon Yushi K. K., was recrystallized twice from distilled *n*-butanol and dried in vacuum at room temperature.

Apparatus.—The dilution viscometer used was the same as was described in the a previous paper. All measurements were made in a thermostat at 40°C. A series of viscometric measurements was undertaken in solutions of varying polymer concentrations but of a constant detergent concentration, and the viscosity values were expressed relative to that of the detergent solution, in order to obtain the intrinsic viscosity and related quantities of the polymer at that detergent concentration.

Results and Discussion

The Viscosity of the SDS Solution.—The viscosity of the aqueous SDS solution, used as

* Present address: Faculty of Pharmaceutical Sciences, Kyoto University, Sakyo-ku, Kyoto.

1) M. Nakagaki and H. Nishibayashi, This Bulletin, 31, 477 (1958).

2) V of this series: M. Nakagaki and T. Nishii, ibid., 37, 60 (1964).

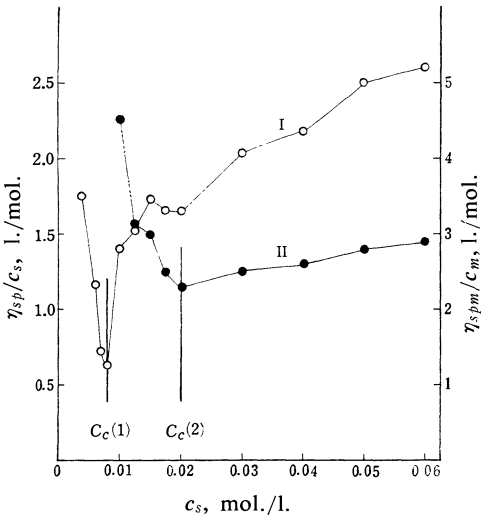


Fig. 1. Reduced viscosity of the SDS solution. Curve I: η_{sp}/c_s, Curve II: η_{spm}/c_m (on the right side ordinate)

the "solvent" in further experiments, was measured; the results are shown in Fig. 1. The relation between the reduced viscosity, η_{sp}/c_s, and the SDS concentration, c_s (mol./l.), as shown by curve I in Fig. 1, reaches a minimum at the SDS concentration of 0.008 mol./l. The minimum point is believed[3] to correspond to the critical micelle concentration, c_c, and agrees well with the values already reported by many authors.[4]

Therefore, the reduced viscosity for the micelle, η_{spm}/c_m, is shown by curve II in Fig. 1, where

$$\eta_{spm}/c_m=(\eta_s/\eta_c-1)/(c_s-c_c) \qquad (1)$$

Here η_s is the relative viscosity of SDS solution (relative to distilled water), and η_c is the relative viscosity at $c_c=0.008$ mol./l. A minimum point is found at 0.02 mol./l. This is believed to correspond to the "second" critical micelle concentration.[3,5] Thus, the following results were obtained:

$$\left.\begin{aligned} c_c(\mathrm{I})&=0.008 \text{ mol./l.} \\ c_c(\mathrm{II})&=0.02 \text{ mol./l.} \end{aligned}\right\} \qquad (2)$$

A Method to Obtain Intrinsic Viscosity.—In order to obtain the intrinsic viscosity, $[\eta]$, the extrapolation to zero of the polymer concentration, c_p (g./100 ml.), was usually made on the basis either of Huggins' equation:

$$f_1=\eta_{sp}/c_p=[\eta]+k_1[\eta]^2c_p \qquad (3)$$

or Staudinger's equation:

$$f_2=\ln \eta_r/c_p=[\eta]-k_2[\eta]^2c_p \qquad (4)$$

It has already been pointed out by Heller[6] that the simultaneous use of f_1 and f_2, together with the mathematical consequence:

$$k_1+k_2=0.5 \qquad (5)$$

can appreciably reduce the arbitrariness in the extrapolation. This method has been used in one of our previous papers.[1]

The new method used in the present paper (in addition to the one described above), is based on the fact that the difference, Δf, between f_1 and f_2 should be proportional to the polymer concentration at a sufficiently low concentration range. The following equation, as readily derived from Eqs. 3, 4 and 5, can be used to estimate the value of $[\eta]$:

$$\Delta f=f_1-f_2=0.5[\eta]^2c_p \qquad (6)$$

An example for NM-14 in a 0.03 mol./l. SDS solution is shown in Fig. 2. As may be seen

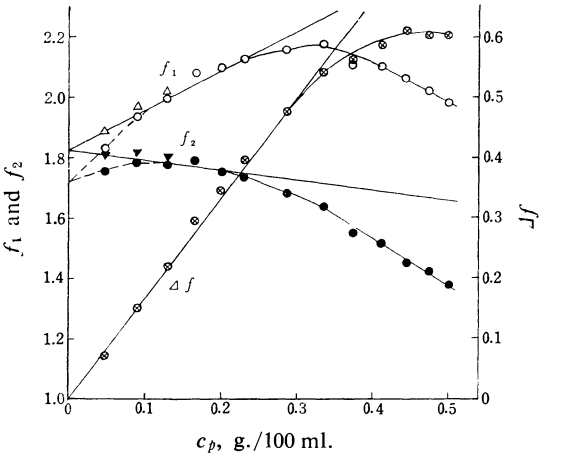


Fig. 2. An example of c_p dependencies of f_1, f_2 and Δf for NM-14 in 0.03 mol./l. SDS solution.
Corrected values for f_1(△) and f_2(▼)

in Fig. 2, a linearity between Δf and c_p holds, and the tangent will give the value of $[\eta]$ according to Eq. 6. Figures similar to Fig. 2 were drawn for all the instances in this paper, and the values of $[\eta]$, k_1 and k_2 were determined to satisfy Eqs. 3, 4, 5 and 6 at the range of small c_p values.

Anomalies at Low Polymer Concentrations.—It is often found in experiments of this kind that the experimentally-obtained values show a kind of anomalous deviation from the linearity to be expected on the basis of Eqs. 3 or 4 at low polymer concentrations. This anomaly is, of course, partly due to the

3) N. Sata and K. Tyuzyo, ibid., 26, 177 (1953).
4) R. Goto and T. Sugano, "Surface Chemistry," (Vol. 7 in the "Zikken Kagaku Koza" series), Maruzen, Tokyo (1963), p. 167. The value of c_c varies between 0.003 and 0.010 mol./l.
5) K. Hess, W. Philippoff and H. Kiessig, *Kolloid-Z.*, 88, 40 (1939).
6) W. Heller, *J. Colloid Sci.*, 9, 547 (1954).

experimental error unavoidable because of the low value of the polymer concentration, but, more often, a systematic deviation from the linearity is observed. One of the expected reasons for this is the effect of the electric charge given to the polymer molecules by the combination of detergent anions, a charge which results in a positive deviation from the linearity; that is, the greater the experimental f-values, the smaller the polymer concentration, as has already been discussed in the previous paper.[1] Another reason should, however, be considered to explain the negative deviation from the linearity shown, for example, in Fig. 2 by broken curves.

The f_1 and f_2 values in the present paper have been calculated by using the viscosity values relative to the viscosity, η_s, of the "solvent," that is, the detergent solution not containing any polymer. If a part of the detergent is combined with the polymer, however, the actual value of the viscosity of the "solvent," η_s^0, should be the value at a concentration a little smaller than the analytical detergent concentration. Then, the values of f_1 and f_2 should be recalculated to f_1^0 and f_2^0. The results will probably show the linearity anticipated by Eqs. 3 and 4. The relations between f_1, f_2, f_1^0 and f_2^0 are given by the following:

$$\left.\begin{aligned} f_1 &= (\eta_s^0/\eta_s)f_1^0 - (1-\eta_s^0/\eta_s)/c_p \\ f_1^0 &= (\eta/\eta_s^0 - 1)/c_p \end{aligned}\right\} \quad (7)$$

and

$$\left.\begin{aligned} f_2 &= f_2^0 - [\ln(\eta_s/\eta_s^0)]/c_p \\ f_2^0 &= [\ln(\eta/\eta_s^0)]/c_p \end{aligned}\right\} \quad (8)$$

where η is the relative viscosity of a solution containing a polymer as well as a detergent. If the amount of detergent combined with the polymer is so small that η_s^0/η_s is very close to unity, $\ln(\eta_s/\eta_s^0)$ can be expanded in a power series of $(1-\eta_s^0/\eta_s)$ and the terms of the second and higher powers can be neglected. Then, Eq. 8 can be appoximated as:

$$f_2 = f_2^0 - (1-\eta_s^0/\eta_s)/c_p \quad (8a)$$

Equations 7 and 8a can explain how a negative deviation is observed when c_p is so small that the value is comparable to $(1-\eta_s^0/\eta_s)$, if $\eta_s^0 < \eta_s$ because of the deficiency of free detergent molecules as a result of the combination with the polymer. Equations 7 and 8a indicate, too, that Δf will not show any serious deviation from the linearity at the low polymer concentration because of the cancellation of the $(1-\eta_s^0/\eta_s)/c_p$ term in both equations (cf. Fig. 2).

$$\Delta f = f_1 - f_2 = (\eta_s^0/\eta_s)f_1^0 - f_2^0 \quad (9)$$

In the example shown in Fig. 2, $\eta_s = 1.060$ was used. If the value $\eta_s^0 = 1.057$ is adopted and if the values of f_1^0 and f_2^0 are calculated, the corrected values (△ and ▼) are on the straight lines, as expected.

The Intrinsic Viscosity of PVA in an SDS Solution.—For the solutions of polyvinyl alcohol NM-14 and GM-14 in an SDS solution, the intrinsic viscosity, $[\eta]$, and the constants, k_1 and k_2, of Eqs. 3 and 4 are as shown in Figs. 3, 4 and 5 respectively, taking the SDS concentration on the abscissa. According to Eqs. 7 and 8a, the corrected intrinsic viscosity, $[\eta_0]$, should be:

$$(\eta_s/\eta_s^0)\,[\eta_1] \geqq [\eta_0] \fallingdotseq [\eta_2] \quad (10)$$

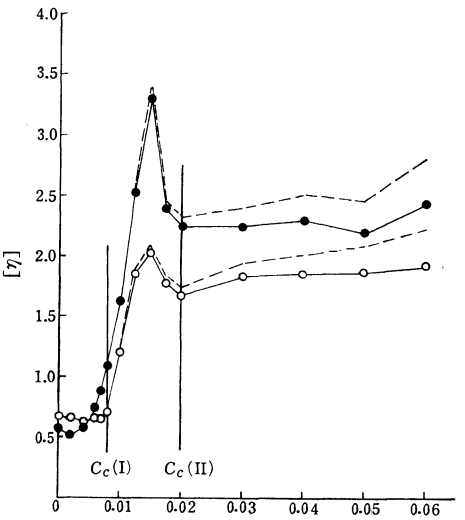


Fig. 3. Intrinsic viscosity of NM-14 (○) and GM-14 (●) in the SDS solution.

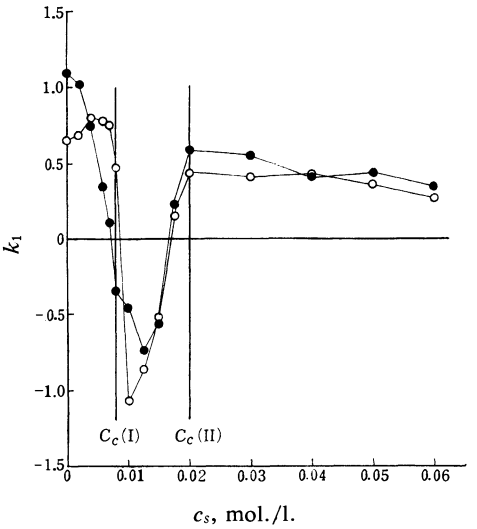


Fig. 4. Huggins' constant k_1 of NM-14 (○) and GM-14 (●) in the SDS solution.

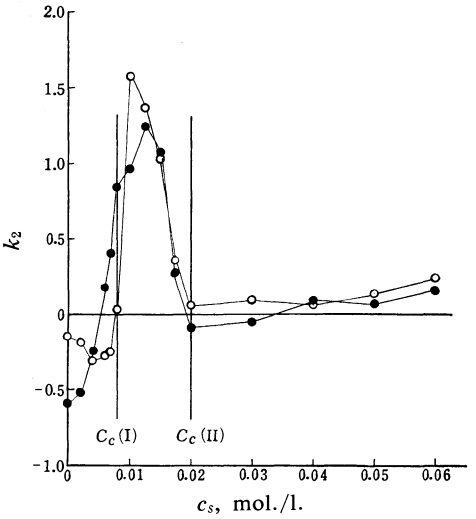


Fig. 5. Staudinger's constant k_2 of MN-14 (○) and GM-14 (●) in the SDS solution.

where $[\eta_1]$ and $[\eta_2]$ are the values of f_1 and f_2 respectively as extrapolated from the concentration range $c_p \gg (1-\eta_s^0/\eta_s)$ to the infinite dilution $c_p \to 0$. Since the correct value of η_s^0 should be larger than that of pure water, or $\eta_s > \eta_s^0 > 1$, the possible upper limit of $[\eta_0]$ is $\eta_s[\eta]$. The unrealizable upper limit, at which all the detergent is assumed to be combined with the polymer and nothing is left free in the solution, is shown in Fig. 3 by broken lines. The actual $[\eta_0]$ is expected to be much closer to $[\eta]$ than to $\eta_s[\eta]$; e. g., in the case of NM-14 in a 0.03 mol./l. SDS solution (cf. Fig. 2), $[\eta]=1.820$ and $\eta_s[\eta]=1.931$, while the value corresponding to the corrected values (△ and ▼) in Fig. 2 is $[\eta_0]=1.825$. Therefore, the errors, which might be caused by the decrease in the viscosity of the medium because of the combination of SDS with the polymer molecules, neither change the essential features of Fig. 3 nor affect the following discussion.

Figures 3, 4 and 5 show that the entire range of detergent concentration, c_s, is divided into three ranges by the first, c_c(I), and the second, c_c(II), critical micelle concentrations of the detergent. These three ranges for SDS exactly correspond to the three ranges described for sodium laurate in a previous paper,[1] although it was not noticed in that paper that the boundary concentration between the second and the third range is equal to the second critical micelle concentration.

The viscometric behavior of the polymer in these three ranges is as follows: (I) In SDS solutions at concentrations lower than c_c(I), $[\eta]$ is small, k_1 is positive and k_2 is negative. In this region, the effect of the detergent seems to be negligible, and the polymer behaves as if it were in water. (2) In SDS solutions of concentrations between c_c(I) and c_c(II), $[\eta]$ becomes large, k_1 becomes negative, and k_2 becomes large. The negative value of k_1, or a rapid increase in η_{sp}/c_p with a decreasing polymer concentration, is usually observed in aqueous solutions of polyelectrolytes. Polyvinyl alcohol molecules are, therefore, presumed to be combined with the SDS anions and to behave like polyelectrolytes. The maximum of $[\eta]$ is explained by the circumstances that the electric repulsion responsible for the expansion of the polymer molecules is partially shielded by the ion atmosphere of the counter ions (sodium ions) with the increase in the detergent concentration. (3) In SDS solutions at concentrations higher than c_c(II), $[\eta]$ is still large, although the value is a little smaller than the value at the maximum point. The value of k_1 is about 0.5, while the value of k_2 is nearly equal to zero. In this range, the viscometric behavior characteristic of the polyelectrolyte was not observed, probably because the electric charges of detergent anions combined with the polymer were almost completely shielded by the counter ions at this high detergent concentration. The high value of the intrinsic viscosity, indicating the high affinity to the medium or the extended configuration of the polymer molecules, may be due, as was already pointed out in the previous paper,[1] to the hydrophilic property of the polymer strengthened by the combination of detergent anions, to the intramolecular repulsion between electric charges resulting from the combination of detergent anions, to the expansion of the polymer molecules in order to secure the space necessary for the combined detergent molecules, or to the decrease in the flexibility of the polymer molecules because of the combination of detergent molecules.

The second critical micelle concentration, c_c(II), is said to be the concentration above which the I-band of X-ray diffraction is observed. It is presumed that this means that the solution is saturated with the usual micelle and that the excess of the detergent forms a large lamellar micelle or a kind of crystallite at concentrations higher than c_c(II). In this range of detergent concentrations, on the other hand, the variations in $[\eta]$, k_1, and k_2 with the concentration, c_s, is not large. This is probably due to the saturation of the solution with the usual micelle.

A Comparison between SDS and SL.—The shape of the curve, $[\eta]$ vs. c_s, for the SDS solution is very similar to that for the sodium laurate (SL) solution reported on in the previous paper,[1] except that the concentration ranges of the detergents used are different.

The difference is obviously due to the difference in the critical micelle concentration, c_c(I), the values being 0.025 N for SL and 0.008 N for SDS. Therefore, it is supposed that all the experimental plots would come onto one curve if the scales of the ordinate and abscissa were changed properly, and that the reduced abscissa would be c_s/c_c. As for the ordinate, it is noticeable that the value of $[\eta]$ shows a tendency to approach a limiting value $[\eta_\infty]$ when c_s becomes large. The values of $[\eta_\infty]$ are assumed to be as cited in Table I, and the reduced curve is drawn as in Fig. 6, in which the data for SL reported in the previous paper are plotted, as well as the data for SDS.

From Table I, it may be seen that the $[\eta_\infty]$ value for GM-14 is about 1.28 times larger than that for NM-14 in either detergent solution, and that $[\eta_\infty]$ in SDS is about 1.08 times larger than in SL for either polymer. In other words, GM, with an imperfectly-saponified polymer, expands more readily when subjected to a combination of detergents than NM, with a completely saponified polymer, and SDS, with a higher lipophilicity can expand the polymers more than SL, with a lower lipophilicity. This would suggest that the polymer-detergent interaction is due to the contact of the hydrophobic parts of the molecules, if it is presupposed that the greater expansion of the polymer is caused by the larger amount of detergent combined.

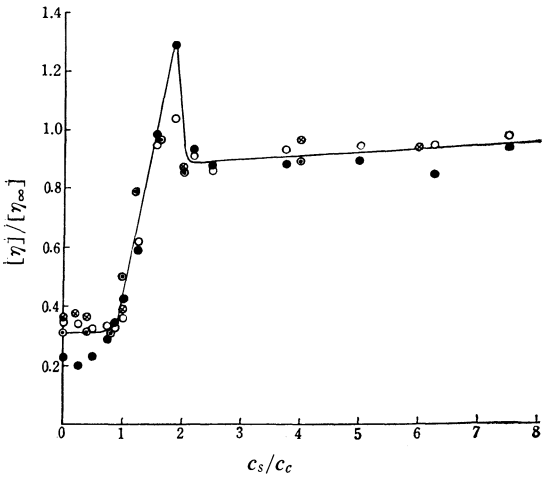


Fig. 6. Reduced curve of intrinsic viscosity vs. detergent concentration.
NM(○) and GM(●) in SDS, and NM(⊗) and GM(⊙) in SL

TABLE I. ASSUMED VALUES OF $[\eta_\infty]$

	NM	GM	GM/NM	Aver.
SDS	1.95	2.56	1.31	1.28±0.03
SL	1.86	2.32	1.25	
SDS/SL	1.05	1.10		1.08±0.03

Summary

The intrinsic viscosity and related constants have been measured for polyvinyl alcohol NM-14 and GM-14 in a sodium dodecyl sulfate solution. At a detergent concentration lower than the first critical micelle concentration (0.008 N), the viscometric property of the polymer is close to that in distilled water. At an intermediate detergent concentration between the first and the second critical micelle concentration (0.02 N), the viscometric property of the polymer is like that of polyelectrolyte, probably because of the electric charges given by detergent anions combined with the polymer. At a detergent concentration higher than the second critical micelle concentration, the intrinsic viscosity of the polymer is high and the polymer combined with the detergent is more extended than in distilled water. The interaction between the polymer and the detergent is very likely due to the contact of hydrophobic parts of the molecules.

The authors wish to thank the Nippon Gosei Kagaku Kogyo K. K. and the Nihon Yushi K. K. for their support of this project.

Faculty of Living Science
Osaka City University
Nishi-ku, Osaka

Electron Spin Resonance Study of Substituted Nitrobenzene Negative Ions Produced by Electroreduction

By Taitiro FUJINAGA, Yasuo DEGUCHI and Kisaburo UMEMOTO

(Received December 14, 1963)

A number of organic anion radicals, obtained by chemical reduction with metals, have been studied by means of electron spin resonance (ESR). Since the formation of free radicals can be expected in the course of electrochemical reductions, it seemed to us that the radical formation could be conveniently detected by ESR measurements.

Austen et al.[1] electrolyzed certain organic compounds, such as anthracene anthraquinone and benzophenone, and observed the ESR spectra of the free radicals in a frozen state in a dimethylformamide (DMF) solution. This was the first time that the electrolytic formation of organic free radicals was proved directly. However, since the ESR measurements were performed in the frozen solid state, the hyperfine structure (hfs) was lost in the broadened absorption-line width, and no detailed information about the electronic structure could be obtained. A similar method was used by Geske and Maki,[2] who carried out the electrolysis in the cavity and recorded the ESR spectrum of the nitrobenzene anion radical in an acetonitrile solution at room temperature. These authors[3,4] also used this "in situ" method for their study of the ESR of many para-substituted nitrobenzene anion radicals, with interesting results.

Ever since, the electrolytic technique has been employed by many authors[5-8] as a convenient method for the preparation of free radicals for ESR measurements.

Recently some investigators have used ESR measurements for the elucidation of electrode processes by studying the radicals formed during electrolysis;[9,10] Rieger et al.,[11] for instance, elucidated the reduction mechanism of many aliphatic and aromatic nitrile compounds by studying the ESR spectra obtained at different electrode potentials.

The present communication will deal with the investigation of the hfs in the ESR spectra of a series of substituted nitrobenzene anion radicals, obtained by electrochemical reduction. The mechanism of the electrolytic reduction of some halonitrobenzenes will also be studied.

Experimental

Nitrobenzene, a series of ortho-, para- and meta-substituted nitrobenzene derivatives, in the form of their chloro, bromo, iodo, methyl, methoxyl, amino, hydroxyl, cyano and aldehyde compound, as well as anthraquinone and naphthoquinone, were used. Most of the reagents were of an extra pure grade and were supplied by the Maruwaka Chemicals Co., Osaka; an they were used without further purification. Acetonitrile of an extra pure grade was used as a solvent in all ESR measurements unless otherwise mentioned. It was first dried with phosphorous pentoxide and then with anhydrous carbonate.

All solutions were approximately 1 mM and contained 0.1 M tetra-*n*-propylammonium perchlorate as the supporting electrolyte. The electrolytic cell was similar to that used by Geske and Maki.[2] Purified nitrogen gas was used for the de-oxygenation of the solutions; the electrolysis was carried out at a constant potential, the value of which was chosen in accordance with the results of polarographic measurements.

The ESR spectra of chloro, bromo and iodonitrobenzene were observed in both acetonitrile and a DMF solution. The DMF was dried with anhydrous potassium carbonate, and the fraction distilling at 152~153°C was used. The ESR spectrometer was an X-band instrument, manufactured by the Japan Electron Optics Co., Model JES-3B-type; it employs a rectangular reflection cavity, 100 kc./sec. field modulation, and a JES electromagnet with 300 mm.ϕ pole pieces. For all field measurements, the spectrum of the peroxylamine disulfonate anion radical, which shows three lines with a 13.0 gauss separation, due to nitrogen splitting, was referred to as the standard.

Results and Discussion

ESR Spectra.—*Nitrobenzene.*—The spectrum of the nitrobenzene anion is shown in Fig. 1;

1) D. E. G. Austen, P. H. Given, D. J. E. Ingram and M. E. Peover, *Nature*, **182**, 1784 (1958).
2) D. H. Geske and A. H. Maki, *J. Am. Chem. Soc.*, **82**, 2671 (1960).
3) A. H. Maki and D. H. Geske, *J. Chem. Phys.*, **33**, 825 (1960).
4) A. H. Maki and D. H. Geske, *J. Am. Chem. Soc.*, **83**, 1852 (1961).
5) P. H. Rieger and G. K. Fraenkel, *J. Chem. Phys.*, **37**, 2795 (1962); **39**, 609 (1963).
6) J. Gendell, J. H. Freed and G. K. Fraenkel, ibid., **37**, 2832 (1962).
7) P. H. Rieger and G. K. Fraenkel, ibid., **37**, 2811 (1962).
8) I. Bernal, P. H. Rieger and G. K. Fraenkel, ibid., **37**, 1489 (1962).
9) P. Ludwig and R. N. Adams, *Anal. Chem.*, **34**, 917 (1962).
10) H. Lee and R. N. Adams, ibid., **34**, 1587 (1962).
11) P. H. Rieger, I. Bernal, W. H. Reinmuth and G. K. Fraenkel, *J. Am. Chem. Soc.*, **85**, 683 (1963).

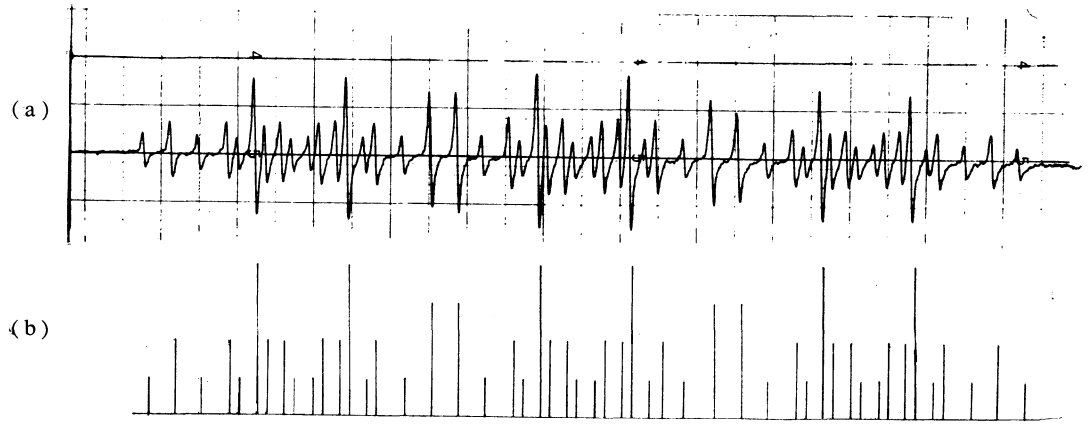


Fig. 1. (a) The ESR spectrum of nitrobenzene anion radical.
(b) Spectrum calculated based upon the coupling constants shown in the Table I.

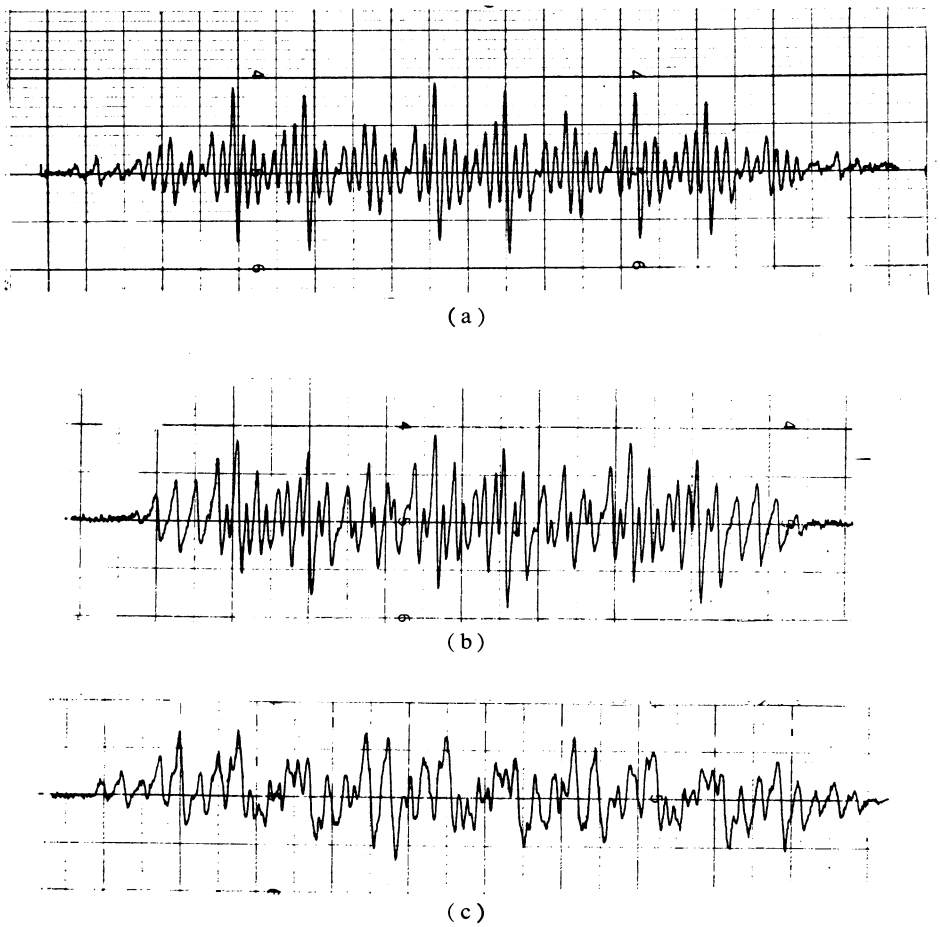
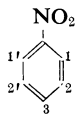
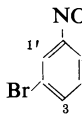
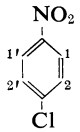
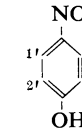
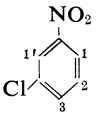
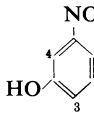
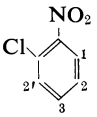
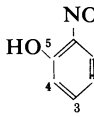
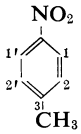
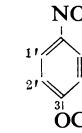
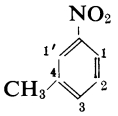
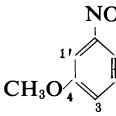
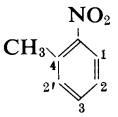
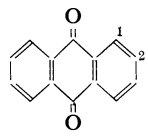
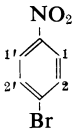
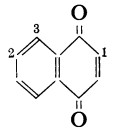


Fig. 2. ESR spectra of (a) *p*- (b) *m*- (c) *o*-nitrotoluene anion radicals.

TABLE I. ESR HYPERFINE COUPLING CONSTANTS

	a_N = 10.62	a_{H_1} = 3.30	a_{H_2} = 1.03		a_N = 9.78	a_{H_1} = 3.36	a_{H_2} = 1.02
	a_{H_3} = 3.82				a_{H_3} = 4.22		
	a_N = 9.70	a_{H_1} = 3.42	a_{H_2} = 1.12		a_N = 13.8	a_{H_1} = 3.14	a_{H_2} = 0.72
	a_N = 9.60	a_{H_1} = 3.20	a_{H_2} = 0.93		a_N = 12.3	a_{H_1} = 2.76	a_{H_2} = 0.92
	a_{H_3} = 4.07				a_{H_3} = 2.98	a_{H_4} = 3.33	
	a_N = 9.95	a_{H_1} = 3.30	a_{H_2} = 1.13		a_N = 12.5	a_{H_1} = 3.59	a_{H_2} = 0.61
	a_{H_3} = 3.92				a_{H_3} = 3.59	a_{H_4} = 1.01	a_{H_5} = 0.46
	a_N = 11.0	a_{H_1} = 3.31	a_{H_2} = 1.14		a_N = 11.5	a_{H_1} = 3.33	a_{H_2} = 1.06
	a_{H_3} = 3.90				a_{H_3} = 0.31		
	a_N = 10.7	a_{H_1} = 3.39	a_{H_2} = 1.09		a_N = 10.3	a_{H_1} = 3.30	a_{H_2} = 1.04
	a_{H_3} = 3.84	a_{H_4} = 1.09			a_{H_3} = 3.80	$a_{H_4} \ll 0.1$	
	a_N = 11.3	a_{H_1} = 3.32	a_{H_2} = 1.04		a_{H_1} = 0.95	a_{H_2} = 0.31	
	a_{H_3} = 3.74	a_{H_4} = 3.32					
	a_N = 9.80	a_{H_1} = 3.36	a_{H_2} = 1.13		a_{H_1} = 3.30	a_{H_2} = 0.60	a_{H_3} = 0.30

it is very similar to that obserbed by Geske and Maki[2] though there is a slight difference in the hyperfine coupling constants. This difference might be due to the presence of traces of water in the solvent used, in accordance with the results we reported previously when dealing with the solvent effect on the width of the line due to nitrogen coupling in the cases of diphenyl nitric oxide[12] and di-*p*-anisyl nitric oxide.[13] It was shown there that the nitrogen-coupling constant obtained in an aqueous solution was larger than that obtained in acetonitrile. Piette et al.[14] also examined the dependence of the nitrogen coupling constant of nitro compounds on the water content of the solvent and showed that the presence of small quantities of water considerably increases the magnitudes of the constant.

Nitrotoluene.—The ESR spectra of electrolytically reduced *o*-, *m*- and *p*-nitrotoluenes are shown in Figs. 2a, 2b and 2c. The coupling constants given in Table I are in good agreement with the observed spectra. The coupling constants were assigned to each proton by referring to the results of Hückel's molecular orbital (MO) method of calculation. It was found that all three methyl protons had the same coupling constant; this shows that there is a hyperconjugative interaction between the methyl group rotating at high speed and the ring π system. In the case of *o*-nitrotoluene, one would expect that the molecule will have an unequal spin distribution in the ring system because of the molecular asymmetry; however, the two protons in the meta position to the nitro group showed the same coupling constant.

12) Y. Deguchi, This Bulletin, **35**, 260 (1962).
13) K. Umemoto, Y. Deguchi and H. Takagi, ibid., **36**, 560 (1963).
14) L. H. Piette, P. Ludwig and R. N. Adams, *J. Am. Chem. Soc.*, **84**, 4212 (1962).

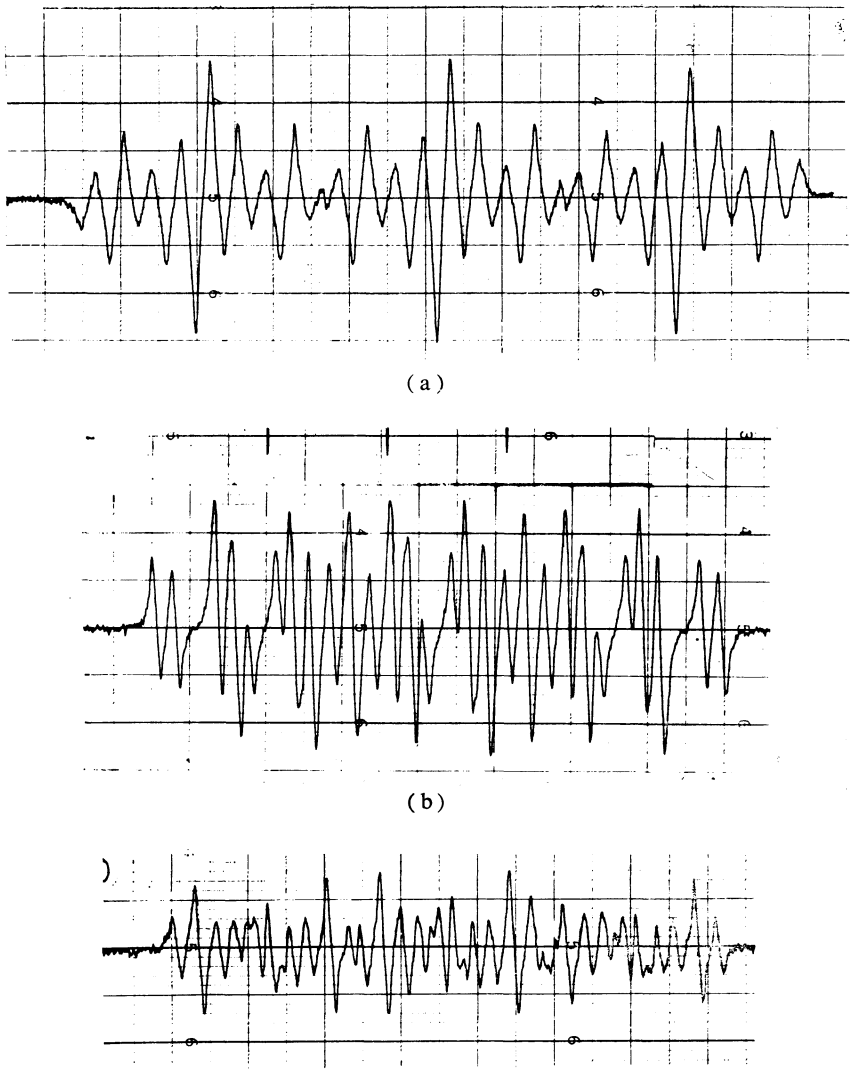


Fig. 3. ESR spectra of (a) *p*- (b) *m*- (c) *o*-nitrochlorobenzene anion radicals.

In the case of *m*-nitrotoluene, the two ortho protons were found to be equivalent. Hence, the spin distribution in the molecule seems to be little affected by the substitution of a ring proton with a methyl group. The nitrogen-coupling constats are a little larger than that of the nitrobenzene anion, showing that the methyl group has an electron-repelling effect. The fact that the ortho and para isomers have a larger nitrogen-splitting constant than the meta compound explains why the electron-repelling effect of the methyl group is directed towards the ortho and para positions.

Chloronitrobenzene.—The ESR spectra of the reduced ortho, meta and para isomers are shown in Figs. 3a, 3b and 3c. Once again the coupling constants shown in Table I agree well with the observed spectra. It was not possible to obtain an hfs spectrum of chlorine. Wertz and Vivo,[15] who studied the ESR spectra of chloro compounds in an aqueous solution, were also unable to observe the hfs of the chlorine because of the small nuclear magnetic moment of this atom. As in the case of nitrotoluene, the two meta protons of the ortho isomer and two ortho protons of the meta isomer have the same coupling constant. Hence, the chloro-substitution seems to affect the spin distribution of the molecule very little. The nitrogen-coupling constants were somewhat smaller than that of the nitrobenzene anion because of the electron-attracting effect of the chlorine

15) J. E. Wertz and J. L. Vivo, *J. Chem. Phys.*, 23, 2441 (1955).

TABLE II. ^{14}N COUPLING CONSTANTS OF SUBSTITUTED NITROBENZENE

	-OH	$-NH_2$	$-OCH_3$	$-CH_3$	-Br	-Cl	-CN	-CHO	$-NO_2$*
para	13.8	12.2	11.5	11.0	9.80	9.70	7.05	5.91	1.74
meta	12.3	—	10.3	10.7	9.78	9.60	9.09	6.60	4.68
ortho	12.7	12.3	11.4	11.3	—	9.95	7.70	7.55	3.22

* Data from Ref. 3.

atom. The nitrogen-coupling constants of the ortho isomers of nitrotoluene and nitrochlorobenzene are little larger than those of the corresponding meta and para isomers, indicating a small steric effect. It has been pointed out by Geske and Ragel[16] that the a_N value in an aromatic anion radical approaches that of the aliphatic counterpart when the nitro-group is twisted out of the plane of the benzene ring by steric effects of bulky substituents.

Bromonitrobenzene.—The ESR spectra of the reduced para and meta isomers were very similar to those of the corresponding chloronitrobenzene compounds. However, the ortho isomer showed the same ESR spectrum as the nitrobenzene anion radical, indicating that the elimination of the bromine atom occurs prior to the formation of the free radical.

Iodonitrobenzene.—The electrolytic reduction products of ortho, meta and para isomers all showed the same ESR spectrum as the nitrobenzene anion radical. This once again indicates that the iodine is eliminated prior to the reduction of the nitro group.

Other Substituted Nitrobenzenes.—The coupling constants of other substituted nitrobenzene anion radicals are also listed in Table I. The different nitrogen-coupling constants are given in Table II; the substituents are arranged according to their increasing electron-attracting effect. Electron-attracting substituents generally reduce the nitrogen-coupling constant, whereas the electron-repelling substituents increase it. In both cases, the electron effect is more pronounced in the case of ortho and para than in the case of meta substitution. *o*-Nitrobenzaldehyde gave an abnormally large nitrogen-splitting constant, and the usual order observed with electron-attracting groups, viz. para<ortho<meta, does not hold; this seems to indicate a strong ortho effect of the aldehyde group.

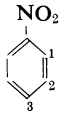
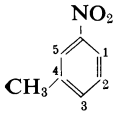
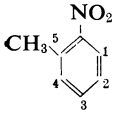
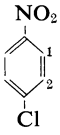
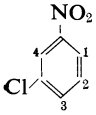
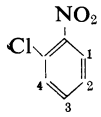
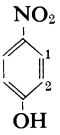
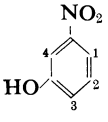
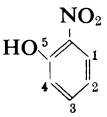
As regards nitrophenol, the authors have discussed the effect of hydrogen bonding in a previous publication.[17]

Hückel's Molecular Orbital Calculations.—Using the coupling constants shown in Table I, the spin density distribution could be calculated from the following relation: $a_i^H = Q_{CH}{}^H \rho_i^\pi$, where $Q_{CH}{}^H = 28$ gauss[18] and, for the methyl group, $a_{CH_3}{}^H = Q_{CCH_3}{}^H \rho^\pi$, where $Q_{CCH_3}{}^H = 30$ gauss.[19] By Hückel's MO method, the spin density in the molecules could also be calculated. The results are listed in Table III, where the parameters employed in this calculation are also listed. The calculated spin density in the ortho and para positions relative to the nitro group is in fairly good agreement with the experimental values; by contrast the calculated meta position is not in agreement with the experimental results. Rieger and Fraenkel[5] calculated the spin density distribution for some nitrile and nitro compounds by both Hückel's MO method and McLachlan's procedure, which employs the concept of approximate configuration interaction; these authors also found that Hückel's MO method generally gave good results for ortho- and para- but not for meta-substitution, while McLachlan's approximation method generally gave very good agreement with the experimental results.

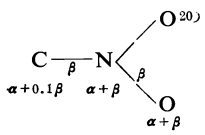
Electrochemical Process.—*Nitrobenzene.*—The nitrobenzene anion radical was generated by electrolysis at −1.3 V. vs. SCE (saturated calomel electrode), that is, at a potential slightly more negative than that of the first wave in the polarogram. The radical was stable for about 30 min. It is known that at the potential of the second wave the mono negative ion is further reduced to the di-negative radical, which is generally rapidly protonated by the reaction with the solvent. Therefore, no ESR spectrum would be expected a priori. However, an ESR spectrum was observed in the potential range of the second wave, although the intensity was reduced to some extent. This shows that the process corresponding to the second wave is slower than the radical formation. When phenol was added as a proton donor to the 1 mM nitrobenzene DMF solution, the radical formation at −1.3 V. vs. SCE was not affected until the concentration of the added phenol reached about 2 mM; at higher potentials, the stability of the radical decreased. Upon the further addition of phenol, the rate of the radical formation at the potential of the first wave

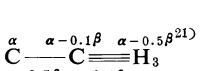
16) D. H. Geske and L. Ragle, *J. Am. Chem. Soc.*, **83**, 3532 (1961).
17) T. Fujinaga, Y. Deguchi and K. Umemoto, This Bulletin, **36**, 1539 (1963).
18) H. S. Jarrett, *J. Chem. Phys.*, **25**, 1289 (1956).
19) D. J. E. Ingram, "Free Radicals as Studied by Electron Spin Resonance," Butterworths Scientific Publications, London (1958), p. 116.

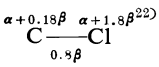
TABLE III. CALCULATED AND EXPERIMENTAL SPIN DENSITY

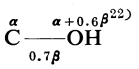
	Position	Spin density: experimental	Spin density: calculated
	1	0.120	0.0942
	2	0.038	0.0023
	3	0.136	0.1030
	1	0.118	0.09356
	2	0.041	0.00202
	3	0.130	0.10190
	1	0.121	0.09397
	2	0.039	0.00226
	3	0.137	0.10280
	4	0.039	0.00224
	5	0.121	0.09447
	1	0.1194	0.09401
	2	0.0372	0.00202
	3	0.1335	0.10238
	4	0.0372	0.00252
	5	0.1194	0.09305
	1	0.1220	0.09351
	2	0.0400	0.00085
	1	0.1145	0.09243
	2	0.0332	0.00231
	3	0.1450	0.10129
	4	0.1145	0.09633
	1	0.1180	0.09674
	2	0.0404	0.00083
	3	0.1400	0.10232
	4	0.0404	0.00484
	1	0.1122	0.09091
	2	0.0257	0.00063
	1	0.0985	0.08719
	2	0.0329	0.00248
	3	0.1063	0.09614
	4	0.1189	0.10279
	1	0.1282	0.10520
	2	0.0218	0.00067
	3	0.1282	0.09956
	4	0.0360	0.01777
	5	0.0164	0.04044

Parameters used in this calculation are as follows.



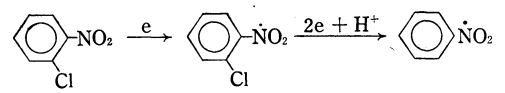






decreased as well, indicating rapid protonation and, hence, a decreased life time of the free radical.

Chloronitrobenzene.—The reducttion products of the three isomers of chloronitrobenzene, prepared by electrolysis at −1.3 V. vs. SCE in an acetonitrile solution, showed an ESR spectrum. In DMF the para and meta isomers gave their characteristic spectra. When the applied potential was changed from −1.2 V. to −2.0 V. vs. SCE the generated radical species showed little change, although the intensity of the spectrum decreased at potentials lower than −1.8 V. vs. SCE. When the ortho isomer was electrolyzed at −1.3 V. vs. SCE in a 1 mM DMF solution, its ESR spectrum could be observed soon after the electrolysis began, but after about fifteen minutes the spectrum showed the beginning formation of the nitrobenzene radical, which after 45 min. was the major component present. When the applied voltage was changed to −1.5 V. vs. SCE the ESR spectrum became identical with that of the nitrobenzene anion radical, indicating a dehalogenation reaction according to:



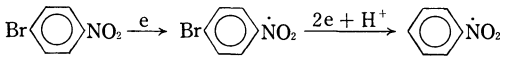
The ease of dehalogenation in the case of the ortho isomer might be due to steric reasons. When phenol was added in about an equimolar quantity, the dehalogenation was impeded, and when a quantity about three times greater was added, no dehalogenation was observed at potentials above −1.7 V. vs. SCE; no radical formation could be detected at lower potentials because of enhanced protonation.

Bromonitrobenzene.—The reduction products of the para and meta isomers gave their characteristic ESR spectra when prepared by electrolysis at −1.3 V. vs. SCE in an acetonitrile solution, whereas the ortho derivative, under the same conditions, showed the ESR spectrum of the nitrobenzene anion, indicating dehalogenation in the DMF solution.

In the DMF solution the meta isomer did not show any sign of dehalogenation in the potential range from −1.1 V. to −2.0 V. vs. SCE, whereas the ortho isomer was completely dehalogenated. The reduction product of the para isomer showed its own characteristic spectrum when prepared by electrolysis at −1.0 V. vs. SCE in a 1 mM solution; at −1.3 V. vs. SCE the beginning formation of the

20) J. I. F. Alonso., *Compt. rend.*, **233**, 403 (1951).
21) C. A. Coulson and U. A. Crawford, *J. Chem. Soc.*, **1953**, 2052.
22) H. H. Jaffé, *J. Chem. Phys.*, **20**, 279 (1952).

nitrobenzene anion radical could be observed, while as the electrolysis proceeded, the formation of increasing quantities of nitrobenzene anion could be seen. At −1.6 V. vs. SCE a clear spectrum of the nitrobenzene anion alone could be observed. When the concentration of the para isomer was raised to 5 mM, the spectrum of the reduced para isomer alone was observed in the potential region from −1.0 V. to −1.4 V. vs. SCE, whereas at lower potentials dehalogenation became evident. These results suggets the following electrode process:



Indonitrobenzene.—All three isomers showed the formation of the nitrobenzene anion radical, even in a 5 mM solution at −1.2 V. vs. SCE both in acetonitrile and in the DMF solution. Hence, complete dehalogenation occurred in all cases. The reaction can be represented by:



The experiments show that the ease with which the halonitrobenzenes are dehalogenated during the electrolytic reduction follows the order:

$$p, m\text{-Cl}, \quad m\text{-Br} < o\text{-Cl} < p\text{-Br} < o\text{-Br}, \quad p, m, o\text{-I}$$

This series seems to indicate that the ease of dehalogenation depends on steric considerations.

Details of the polarographic studies of the halonitrobenzenes will be reported later.[23]

The authors wish to acknowledge the helpful suggestions of Visiting Professor B. Breyer of the University of Sydney.

Chemistry Institute
Faculty of Science
Kyoto University
Sakyo-ku, Kyoto

23) T. Fujinaga and T. Arai, *J. Chem. Soc. Japan, Pure Chem. Sec.* (*Nippon Kagaku Zasshi*), in press.

*Emission and Absorption of the Sodium D-Line behind a Shock Wave in Argon, Nitrogen- and Carbon Monoxide-Argon Mixtures Containing a Trace of Sodium Vapor**

By Soji TSUCHIYA

(Received December 25, 1963)

Large translational energies are given to gaseous atoms or molecules in the duration of several collisions in a shock wave. These thermal energies are transferred by atomic or molecular collisions to other degrees of freedom, such as electronic states, vibration, rotation and chemical conversion or ionization. Therefore, the shock wave technique is a powerful tool for studying the process of energy transfer and high-speed chemical reactions.

This paper will be concerned with the temperature measurement of the shock-heated gas by the simultaneous measurement of the emission and absorption of the sodium D-resonance line ; it aims at the verification of the relation of the excitation and quenching of sodium atoms to the measured temperatures. Gaydon and Hurle have studied the same problems and have concluded that the temperature observed by the sodium D-line reversal method agrees with the vibrational temperature of shock-heated diatomic molecules.[1] Also, they found that the reversal temperature of argon gas behind a shock wave was lower than the calculated value; they explained the observed discrepancy as being due to the existence of a radiative non-equilibrium state. The present report will give a more quantitative elucidation of those problems proposed by Gaydon and Hurle, and will attempt to clarify the physical back-ground of the sodium D-line reversal method.

Sobolev and his collaborators have, using a

* Presented at the Symposium on Photochemistry, Sendai, Oct., 1963.

1) A. G. Gaydon and I. R. Hurle, Eighth International Symposium on Combustion, William Wilkins Pub., N. Y. (1962), p. 309 and cited references.

spectral line of barium ion, observed the reversal temperature in shock-heated argon and have obtained a value of 4×10^{-17} cm^2 as an effective quenching cross-section of an argon atom.[2] Only a little is known about the quenching or exciting atomic collisions of electronic states. The shock wave technique provides an experimental method which can inform us how the excitation of electronic states of atoms occurs by slow thermal atomic or molecular collisions. Preceding shock wave works on this problem have been undertaken from the viewpoint that the excitation of the electronic states of atoms depends on collisions with electrons rather than on collisions with atoms or molecules in the shock wave.[3,4]

Experimental

The shock tube used here is constructed with steel pipe sections 10 cm. in inner diameter; the inner walls are plated with hard chromium. Some of these sections are connected to form a driver section and a low pressure section; the lengths of these sections are 160 cm. and 480 cm. respectively. The low pressure section is pumped out to pressure below 10^{-4} mmHg by an oil diffusion pump, and the leak rate of the tube is about 3 μHg/hr. Lumirror film (polyethylene terephthalate) is used as bursting diaphragms, which are ruptured spontaneously by the accumulating pressure of the driver gas of hydrogen. There are two windows 410 cm. downstream from the diaphragm position in order to make the spectroscopic measurement. Four platinum-resistance gauges are positioned at intervals 30 cm. upstream from the window. The time interval of the two signal pulses from two platinum-resistance gauges, 60 cm. apart from each other, is measured by a 1 Mc. counter, and the shock velocity is determined. One of the other gauges is used to trigger the synchroscope which records the spectroscopic data.

The real shock velocity is not constant along the entire passage through the shock tube. Simultaneous measurements of shock velocity at two positions along the tube are performed using the four platinum-resistance gauges and the synchroscope. The results show that the uncertainty of shock velocity obtained here is less than 0.5%; this corresponds to the temperature fluctuation of about 30°K in the present experimental conditions.

The sample gases are argon, nitrogen and carbon monoxide, with nominal purities of 99.99, 99.96 and 99.5% respectively. These gases are used without further purification. Gaseous mixtures which contain nitrogen or carbon monoxide of less than 1% are made by successive dilution, and the concentrations are measured by the manometric method. Complete mixing is obtained by allowing at least 2 days for diffusion. A very small amount of sodium vapor is introduced into the test gas as follows: the sample gas is fed into the shock tube through a glass tube in which a piece of sodium metal is heated to 250~350°C. By this method, roughly controlled quantities of sodium vapor, which perhaps forms colloidal dust before the passage of the shock wave, can be mixed with the shock-heated gas. The intensity of the sodium D-line is independent of the time between the shock experiment and the introduction of the sample gas, and the time required for colloidal sodium to vaporize is very short.

The emission and absorption of the sodium D-line is observed by a two-channel monochromator. This monochromator has already been described in detail in another paper.[5] The monochromator is of the Littrow type, with two glass prisms whose apex angle is 60°. The calculated spectral slit width is 8.9 cm^{-1} at 5890 Å when the entrance and exit slit width is 0.1 mm. The doublet lines of the sodium D-line can be resolved by the monochromator, and the experiment is performed using one of the doublet lines corresponding to the $^2P_{3/2}-{}^2S_{1/2}$ transition. The accuracy of the measured temperature has been discussed in the preceding paper; the maximum error is considered to be about $\pm$50°K at 2500°K.

The Temperature Measurement of Shock-heated Gas

The gas temperature is calculated from the measured data of the emission and absorption of a resonance spectral line. In order to discuss the physical limitation of this method, the nature of the radiation from a gaseous distributed emitter should first be considered.

A gaseous atom is here assumed to have only two levels, upper and lower. When the atoms are included within an opaque enclosure, the following equilibrium is attained:

$$N_1[A_{1\to2}+B_{1\to2}\rho(\omega_{12}, T)] - N_2B_{2\to1}\rho(\omega_{12}, T)=0 \quad (1)$$

where N_1, N_2 are populations of atoms on the upper and lower levels respectively, where $A_{1\to2}$, $B_{1\to2}$, $B_{2\to1}$ are Einstein's coefficients for spontaneous emission, induced emission and absorption respectively, and where $\rho(\omega_{12}, T)$ is a radiation density at the wave number of ω_{12}, which corresponds to the energy difference between upper and lower levels. The intensity of radiation in the wave number interval $(\omega, \omega+d\omega)$ can be defined as the amount of radiant energy falling on the unit solid angle in the unit time; it is formulated as:

$$B^\circ(\omega, T)d\omega=\frac{1}{4\pi}c\rho(\omega, T)d\omega$$

2) N. N. Sobolev et al., "Proc. of Fifth International Conference on Ionization Phenomena in Gases," Ed. by H. Maecker, North-Holland Pub. Co., Amsterdam (1962), p. 2122 and cited references.

3) T. Wilkerson, *Univ. Michigan, Technical Note*, AFOSR 1151 (1961).

4) S. H. Bauer, J. H. Kiefer and B. E. Loader, *Can. J. Chem.*, **39**, 1113 (1961).

5) S. Tsuchiya, *J. Chem. Soc. Japan, Pure Chem. Sec. (Nippon Kagaku Zasshi)*, **84**, 300 (1963).

where $\boldsymbol{c}$ is the light velocity. $(1/2)B^\circ(\omega, T)\mathrm{d}\omega$ equals the radiant energy emitted from the black body into the unit solid angle in the unit time in the wave number interval $(\omega, \omega+\mathrm{d}\omega)$. The absorption coefficient per unit optical length is formulated by the equation:

$$k(\omega_{12}) = \boldsymbol{h}\omega_{12}(N_2B_{2\to1} - N_1B_{1\to2}) = \frac{\boldsymbol{h}\omega_{12}}{\rho(\omega_{12}, T)}N_1A_{1\to2} \quad (2)$$

Equation 1 does not hold in the case of a gaseous body which is not contained in an opaque enclosure. In this case, the radiation density, $\rho'(\omega_{12}, T)$ is different from $\rho(\omega_{12}, T)$ in Eq. 1, and it is approximated as constant within the gaseous body. The intensity of radiation from the gaseous body concerned can be defined by the use of $\rho'(\omega_{12}, T)$ as follows:

$$B(\omega_{12}, T)\mathrm{d}\omega = \frac{1}{4\pi}\boldsymbol{c}\rho'(\omega_{12}, T)\mathrm{d}\omega$$

The radiation intensity depends on the optical thickness of the gaseous body; this circumstance may be described in the following manner. When the radiation flux passes through the optical length $\mathrm{d}X$, the radiation intensity takes a value of $B(\omega_{12}, T)+\mathrm{d}B(\omega_{12}, T)$. The radiation quanta emitted in the unit time and volume are $\{N_1[A_{1\to2}+B_{1\to2}\rho'(\omega_{12}, T)] - N_2B_{2\to1}\cdot\rho'(\omega_{12}T)\}$. Therefore, the increase in radiation intensity, $\mathrm{d}B(\omega_{12}, T)$, can be formulated as:

$$\mathrm{d}B(\omega_{12},T) = \frac{\boldsymbol{hc}\omega_{12}}{4\pi}\{N_1[A_{1\to2}+B_{1\to2}\rho'(\omega_{12}, T)] - N_2B_{2\to1}\rho'(\omega_{12}, T)\}\mathrm{d}X \quad (3)$$

which is simplified by the introduction of $k(\omega_{12})$ in Eq. 2 as follows:

$$\mathrm{d}B(\omega_{12}, T) = k(\omega_{12})\frac{\boldsymbol{c}}{4\pi}[\rho(\omega_{12}, T) - \rho'(\omega_{12}, T)]\mathrm{d}X = k(\omega_{12})[B^\circ(\omega_{12}, T) - B(\omega_{12}, T)]\mathrm{d}X$$

Therefore, by integrating the above equation, the spectral intensity:

$$B(\omega_{12}, T) = B^\circ(\omega_{12}, T)\{1-\exp[-k(\omega_{12})X]\} \quad (4)$$

is derived.

It is important to notice that the equilibrium condition is admitted into Eq. 4 inexplicitly by introducing the absorption coefficient $k(\omega_{12})$, which is defined in condition 1 of the radiation equilibrium. This means that the Boltzmann distribution between the upper and lower levels is maintained;

$$N_1/N_2 = (g_1/g_2)\exp(-\boldsymbol{hc}\omega_{12}/\boldsymbol{k}T) \quad (5)$$

where g_1 and g_2 are the statistical weights of the upper and lower levels respectively. In Eq. 4, the factor $\{1-\exp[-k(\omega)X]\}$ is a spectral emissivity, and an emission from any body may be represented by such an emissivity and the radiation density of "hohlraum radiation." The emissivity is the function of the concentration of atoms or molecules emitting a spectral line and of the optical length of the gaseous system. The assumption that the emission from the gaseous body is the thermal radiation originates from the acknowledgement of equilibrium relation 5 in the gas.

It is convenient to define the effective emissivity, E_ω, since the emission from the gaseous body is measured by the monochromator, which has a finite spectral resolving power. If $g(\omega', \omega)$ is a spectral slit function when the monochromator is set at a certain wave number, ω, an effective emissivity is:

$$E_\omega = \int g(\omega', \omega)\{1-\exp[-k(\omega')X]\}\mathrm{d}\omega'/\overline{\Delta\omega} \quad (6)$$

and,

$$\overline{\Delta\omega} = \int g(\omega', \omega)\mathrm{d}\omega'$$

where $\overline{\Delta\omega}$ is a spectral slit width expressed in wave numbers.

The observed intensity of the sodium D-line from the high-temperature gas containing sodium atoms is;

$$I_d = \int g(\omega', \omega_d)B^\circ(\omega', T_g) \times\{1-\exp[-k(\omega')X]\}\mathrm{d}\omega'\cdot\Delta\Omega\cdot\Delta s = E_dB^\circ(\omega_d, T_g)\overline{\Delta\omega}\cdot\Delta\Omega\cdot\Delta s \quad (7)$$

where ω_d is the wave number of the sodium D-line, T_g is the temperature of a gas, E_d is the effective emissivity of the sodium D-line, and $\Delta\Omega$ and Δs are the solid angle of a light-flux incident on the monochromator and the area of the slit respectively. Also, the intensity of the light beam from the standard light source, whose spectral radiancy is the same as the black body of the temperature, T_0, is represented as a sum of emission and absorption terms that is,

$$I_l = [E_dB^\circ(\omega_d, T_g) + (1-E_d)B^\circ(\omega_d, T_0)]\overline{\Delta\omega}\cdot\Delta\Omega\cdot\Delta s \quad (8)$$

The light beam from the standard light source without an absorption by the gaseous body has an intensity of

$$I_0 = B^\circ(\omega_d, T_0)\overline{\Delta\omega}\cdot\Delta\Omega\cdot\Delta s \quad (9)$$

The following relation can be derived from Eqs. 7, 8 and 9:

$$\frac{I_l-I_0}{I_d} = 1 - \frac{B^\circ(\omega_d, T_0)}{B^\circ(\omega_d, T_g)} \quad (10)$$

If Wien's radiation formula is applied to Eq. 10, the relation between the temperatures of gas and the light source is shown by the equation:

$$\frac{1}{T_g}=\frac{1}{T_0}+\frac{k}{hc\omega_d}\ln\left(1-\frac{I_l-I_0}{I_d}\right) \qquad (11)$$

Thus, the temperature of the gas can be obtained by the measurement of I_l and I_d; this temperature is the same as the so-called reversal temperature. The physical meaning of the temperature is given by Eq. 5;[6] that is,

$$\frac{[\mathrm{Na}(^2\mathrm{P})]}{[\mathrm{Na}(^2\mathrm{S})]}=\frac{g_{^2\mathrm{P}}}{g_{^2\mathrm{S}}}\exp\left(-\frac{hc\omega_d}{kT_g}\right) \qquad (12)$$

It is necessary to remember that the temperature observed in the simultaneous measurement of emission and absorption is not always the gaseous temperature; it is defined as the population temperature in the upper and lower levels concerned. This population temperature, of course, agrees with the thermodynamic temperature when the whole system is in thermal equilibrium.

In order to clarify the assumption that the sodium D-line in the shock-heated gas containing a trace of sodium vapor is thermal radiation, the relative intensities of the sodium D-line were measured in the cases of various shock velocities.

The effective emissivity of the sodium D-line may be obtained by the relation;

$$E_d=\frac{I_d}{I_0}\left(1-\frac{I_l-I_0}{I_d}\right) \qquad (13)$$

Further, the following relation can be derived from Eqs. 9, 11 and 13;

$$\ln\frac{I_d}{E_d}=-\frac{hc\omega_d}{kT_g}+\text{const.} \qquad (14)$$

If the complete equilibrium between sodium atoms and shock-heated gas is maintained (see below), the temperature, T_2, calculated from the shock velocity equals the temperature, T_g, obtained by the present method. Therefore, the observed emission intensity is expected to be illustrated by the temperature T_2.

The graphic plot of I_d/E_d vs. $1/T_2$ are shown in Fig. 1. The data used are the mean values of the intensities in the steady region behind the shock fronts. (As to the profiles of emission, a more detailed description will be given in the next section). It may be seen in Fig. 1 that the experimental points accord with the theoretical linear slope. It is reasonable that the emission of the sodium D-line in the present experiments arises from a thermal mechanism but not from the other sources, e.g., a chemical luminescence.

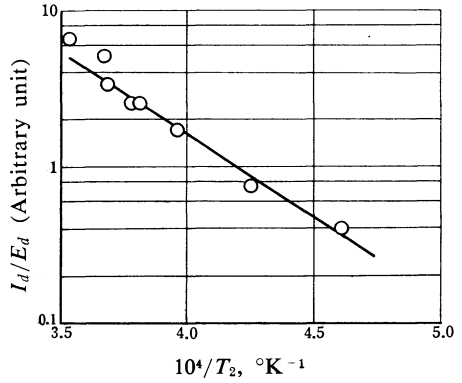


Fig. 1. Relation of sodium D-line emission intensity to reciprocal of the temperature T_2 calculated from shock velocity. The experimental points are the data from shock-heated 1% N_2-99% Ar mixture. The solid line shows the theoretical slope, $-hc\omega_d/k$.

Results

Figure 2 shows the emission and the emission-plus-absorption profiles of the sodium D-line in argon gas behind the shock wave; the temperatures calculated from these two curves are also given. The intensity of the emission rises very fast in less than 10 μsec. (lab. time) after the passage of the shock front, and it is almost constant in the high temperature region between the shock front and the intermixing zone. It is found that the emission becomes more intense near the intermixing zone; this may be attributable to the diffusional mixing of the driver hydrogen and argon gas. These phenomena are also found in the case of argon gas containing less than 0.1% of nitrogen or carbon monoxide. To avoid the confusion

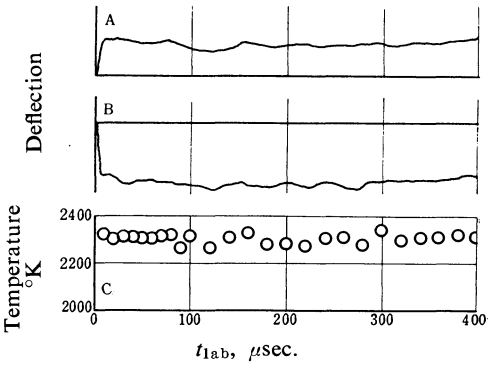


Fig. 2. Emission (A), emission-plus-absorption (B), and temperature (C) profiles behind the shock wave in pure argon gas.
Run No. 012, $v_s=1.724$ mm./μsec., $T_2^{calc}=2921$°K, $p_2^{calc}=1017$ mmHg, $T_0=2583$°K.

6) A. G. Gaydon and H. G. Wolfhard, "Flames," Chapman and Hall, London (1960) p. 234.

which arises from the intermixing of argon and hydrogen, the present observations and discussion are limited to the region of about 300 μsec. after the passage of the shock front.

The observed profile of emission behind the shock front confirms that the vaporization of the colloidal sodium introduced into the argon gas occurs in less than 30 μsec. (gas time), and that the concentration of sodium vapor is almost constant throughout the shock-heated gas. In the later section, the concentration of sodium atoms is calculated to be $10^{12}\sim10^{13}$ atoms/cc. The observed temperature profile is the same as the emission intensity, about 600°K lower than the theoretical temperature calculated from the shock velocity. Gaydon and Hurle have observed that the reversal temperature in the shock-heated argon is 100~200°K lower than the calculated value.[1] Their observed temperature is much higher than the present results; this discrepancy may be attributed to the existence of impurities in their argon gas or to a less efficient vacuum in their shock tube.

An example of the experimental results in the case of nitrogen-argon mixtures is shown in Fig. 3. The emission of the sodium D-line

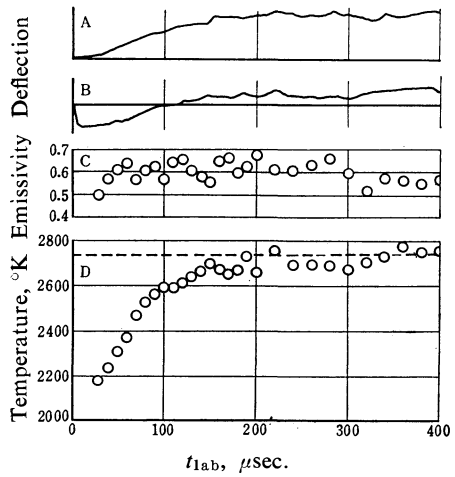


Fig. 3. Profiles of emission (A), emission-plus-absorption, (B), effective emissivity (C), and temperature (D) behind the shock wave in 1% N_2-99% Ar mixture. The dotted line in (D) shows the temperature T_2 calculated from shock velocity. Run No. 1101, v_s=1.662 mm./μsec., T_2^{calc}=2714°K, p_2^{calc}=766mmHg, T_0=2583°K.

rises gradually after the shock front and reaches a steady value of intensity which is much larger than that observed in the case of pure argon gas shocked to the same shock velocity. The rise of the emission intensity just behind the shock front seems to indicate an induction time or a relaxation process. The observed emissivity profile shows that the concentration of sodium vapor is almost constant behind the shock front, even if the emission intensity is low compared with the steady state. In the profile of emission-plus-absorption in Fig. 3, a remarkable intensity decrease is observed just behind the shock front. This decrease is due to low excitation temperature behind the shock front. However, the observed temperature in the steady region agrees well with the theoretical temperature. The difference between these results and those in pure argon can be attributed to the existence of a small amount of nitrogen gas in the mixture.

The time required to reach the steady value of the emission intensity is independent of the concentration of nitrogen in the range of 1~0.1%, and it becomes shorter as the temperature or pressure is raised. On the contrary, the mean temperature in the steady region far from the shock front drops in the shock-heated argon containing less nitrogen. This circumstance is shown in Fig. 4. These findings confirm that, rather than argon atoms, nitrogen molecules in the mixture, even if their concentration is very small, play an important role in the excitation of sodium atoms.

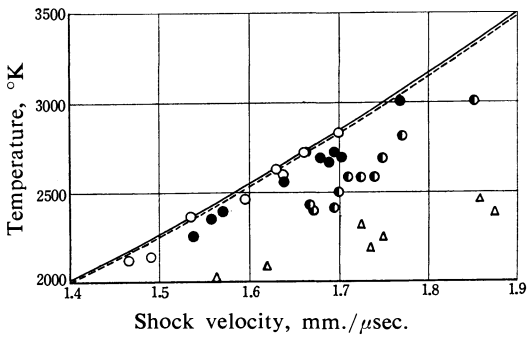


Fig. 4. Temperature obtained from the simultaneous measurement of emission and emission-plus-absorption in the steady regions far from shock front in the case of N_2-Ar mixtures.
——: Calculated temperature for pure argon
----: Calculated temperature for 1% N_2-99% Ar mixture
○: 1.03% N_2 ●: 0.09% N_2
◐: 0.04% N_2 in argon △: pure argon

The same observations have been made in the carbon monoxide-argon mixture behind the shock wave. The only difference between the experimental results of the carbon monoxide- and nitrogen-argon mixtures is that the emission of the sodium D-line in the carbon monoxide-argon mixture behind the shock front rises a little faster than in the case of the nitrogen-argon mixture. Figure 5 shows

one of the experimental observations in the case of the carbon monoxide-argon mixture.

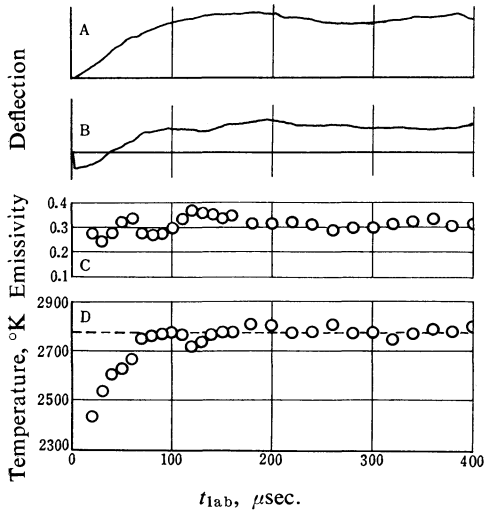


Fig. 5. Profiles of emission (A), emission-pulse-absorption (B), effective emissivity (C), and temperature (D) behind the shock wave in 0.5% CO-99.5% Ar mixture. The dotted line in (D) shows the temperature calculated from shock velocity. Run No. 2203, $v_s=1.675$ mm./μsec., $T_2^{calc}=2774$°K, $p_2^{calc}=1010$ mmHg, $T_0=2583$°K.

The Excitation and Quenching of Sodium Atoms

It has been described that the temperature observed by the present method determines the populations of the ^2P and ^2S states of sodium atom, provided that the populations are distributed by Boltzmann's law. The experimental findings that the measured temperatures are about 600°K lower than the theoretical temperatures calculated from shock velocity in the shock-heated argon and agree with the theoretical temperatures in the nitrogen-argon mixtures, are to be explained by the aforementioned nature of the measured temperature. That is, sodium atoms in the pure argon gas do not attain a thermal equilibrium with argon atoms since the effective cross-section of collisions between sodium and argon atoms is very small. The existence of nitrogen molecules, which have a large cross section in collision with a sodium atom, can excite sodium atoms to ^2P states, thus resulting in the thermal equilibrium of the whole system. These conclusions will be more quantitatively treated in the latter part of this section.

The populations of sodium atoms in the ^2P and ^2S states are supposed to be determined by the following reaction scheme:

$$\begin{aligned} \mathrm{Na}(^2S) + \mathrm{M}^* &\rightarrow \mathrm{Na}(^2P) + \mathrm{M} \\ \mathrm{Na}(^2P) + \mathrm{M} &\rightarrow \mathrm{Na}(^2S) + \mathrm{M}^* \\ \mathrm{Na}(^2P) &\rightarrow \mathrm{Na}(^2S) + \boldsymbol{h}c\omega_d \end{aligned} \qquad (15)$$

where M may be either an atom, a molecule and an electron, and M* is an M which possesses enough energy to excite a sodium atom to the ^2P state. The ionization via the ^2P state of sodium is disregarded in the above scheme. The ionization from the excited electronic state occurs by means of the collisions with electrons, whose content is expected to be too small to make effective collisions with excited atoms (see the latter part of this paper).

As a mean of determining the populations of the ^2P and ^2S states, however, the scheme is not a perfect one. The light quanta emitted spontaneously from ^2P sodium atoms are re-absorbed by the neighboring atoms, re-emitted, and so on. This phenomenon is characteristic of the resonance spectral line, and is called the "radiation imprisonment."

Radiation Imprisonment. — The theoretical treatment of the imprisonment of resonance radiation has been made by Bieberman[7] and Holstein.[8] Their method of analysis may be applied to the present problem. Let $N_1(\boldsymbol{r})$ and $N_2(\boldsymbol{r})$ represent the concentration of sodium atoms in the ^2P and ^2S states respectively at a position, $\boldsymbol{r}$, within the gaseous body. If the reactions 15 represent the mechanism of the excitation or quenching of sodium atoms, $N_1(\boldsymbol{r})$ obeys the following integro-differential equation:

$$\frac{\partial N_1(\boldsymbol{r})}{\partial t} = Z_E N_2(\boldsymbol{r}) - Z_Q N_1(\boldsymbol{r}) - \gamma N_1(\boldsymbol{r}) + \gamma \int N_1(\boldsymbol{r}') G(\boldsymbol{r}', \boldsymbol{r}) \mathrm{d}\boldsymbol{r}' \qquad (16)$$

where Z_E, Z_Q are collision frequencies per unit time of the excitation and quenching respectively, where γ is the reciprocal of the radiative life time, and where the last term expresses the imprisonment of the resonance radiation. $G(\boldsymbol{r}', \boldsymbol{r})$ represents the probability that a light quantum emitted from the $\boldsymbol{r}'$ position in the gaseous body is re-absorbed in the volume element, $\mathrm{d}\boldsymbol{r}$, at the $\boldsymbol{r}$ position, and the integration in Eq. 16 is accomplished over the whole volume of the gaseous body.

Since the present problem concerns the steady state behind the shock wave, $\partial N_1(\boldsymbol{r})/\partial t=0$. Two extreme cases are expected to occur in Eq. 16.

(i) In the case of Z_E, $Z_Q \gg \gamma$, the third and fourth terms in Eq. 16 can be disregarded, and

7) L. M. Bieberman, *J. Exptl. Theoret. Phys.* (*U. S. S. R.*), **17**, 416 (1946).
8) T. Holstein, *Phys. Rev.*, **72**, 1212 (1947); **83**, 1159 (1951).

the following relation is derived;

$$(N_1/N_2)^{equil}=Z_E/Z_Q$$
$$=(g_1/g_2)\exp(-\boldsymbol{hc}\omega_{12}/\boldsymbol{k}T) \quad (17)$$

The exciting or quenching collisions are predominant over the transitions due to the spontaneous emission; therefore, the thermal equilibrium between the atoms emitting the resonance line and the surrounding gaseous particles is maintained.

(ii) In the case of $G(\boldsymbol{r}', \boldsymbol{r})=0$, i.e., when the concentration of atoms is too low to reabsorb the light quanta emitted, Eq. 16 may be arranged to the relation:

$$(N_1/N_2)=Z_E/(Z_Q+\gamma) \quad (18)$$

This formula is an analogous form of the Stern-Volmer equation which is frequently used in the photochemical experiment of the quenching.

For the analysis of the present results, it is convenient to introduce the parameter $y(\boldsymbol{r})$:

$$y(\boldsymbol{r})=\frac{N_1(\boldsymbol{r})}{N_2(\boldsymbol{r})}\Big/\frac{Z_E}{Z_Q} \quad (19)$$

which represents a degree of non-equilibrium between the atoms emitting the resonance line and the gaseous particles; i.e., a value of y is 1 in the complete thermal equilibrium and less than 1 in the radiative non-equilibrium state, where the insufficient energy transfer from the gaseous particles to the atoms results in the lean populations in the upper electronic state.

The mean value of the parameter y, is obtained in the present experiment in the following manner. The physical meaning of the observed temperature, T_g, has already been described by Eq. 12. When the complete equilibrium between sodium atoms and gaseous particles is maintained behind the shock wave, T_g equals T_2 calculated from the shock velocity; i.e.,

$$\left\{\frac{[\mathrm{Na}(^2\mathrm{P})]}{[\mathrm{Na}(^2\mathrm{S})]}\right\}_{equil}=(g^2\mathrm{P}/g^2\mathrm{S})\exp(-\boldsymbol{hc}\omega_d/\boldsymbol{k}T_2)$$
$$=Z_E/Z_Q$$

Therefore, the experimental value of the parameter y is expressed as:

$$y=\frac{[\mathrm{Na}(^2\mathrm{P})]}{[\mathrm{Na}(^2\mathrm{S})]}\Big/\left\{\frac{[\mathrm{Na}(^2\mathrm{P})]}{[\mathrm{Na}(^2\mathrm{S})]}\right\}_{equil}$$
$$=\exp\left[-(\boldsymbol{hc}\omega_d/\boldsymbol{k})\left(\frac{1}{T_g}-\frac{1}{T_2}\right)\right] \quad (20)$$

The introduction of $y(\boldsymbol{r})$ into Eq. 16 gives the equation:

$$1-\left(1+\frac{\gamma}{Z_Q}\right)y(\boldsymbol{r})+\frac{\gamma}{Z_Q}\int y(\boldsymbol{r}')G(\boldsymbol{r}', \boldsymbol{r})\mathrm{d}\boldsymbol{r}'=0 \quad (21)$$

where $N_2(\boldsymbol{r})$ is approximated as equal to N of the total concentration of the emitting atoms. The dependence of $y(\boldsymbol{r})$ upon the position, $\boldsymbol{r}$, in the gaseous body is disregarded in Eq. 21. Therefore, y may be formulated as:

$$y=1\Big/\left[1+\frac{\gamma}{Z_Q}<1-\int G(\boldsymbol{r}, \boldsymbol{r}')\mathrm{d}\boldsymbol{r}'>_{Av}\right] \quad (22)$$

where the symmetric property of the function G, i.e., $G(\boldsymbol{r}', \boldsymbol{r})=G(\boldsymbol{r}, \boldsymbol{r}')$ is used. $\left[1-\int G(\boldsymbol{r}, \boldsymbol{r}')\mathrm{d}\boldsymbol{r}'\right]$ is described as the probability that the light quanta emitted at the $\boldsymbol{r}$ position escape from the enclosure of the gas. Though this probability is dependent on the coordinate $\boldsymbol{r}$, mean probability is adopted here:

$$<1-\int G(\boldsymbol{r}, \boldsymbol{r}')\mathrm{d}\boldsymbol{r}'>_{Av}$$
$$=\int\left[1-\int G(\boldsymbol{r}, \boldsymbol{r}')\mathrm{d}\boldsymbol{r}'\right]\mathrm{d}\boldsymbol{r}\Big/\int\mathrm{d}\boldsymbol{r}$$

By the use of the escaping probability of the resonance light quanta, the effective radiative life time may be defined;

$$\tau_{eff}=\tau/<1-\int G(\boldsymbol{r}, \boldsymbol{r}')\mathrm{d}\boldsymbol{r}'>_{Av} \quad (23)$$

τ_{eff} depends on the absorption coefficient of the gas and the geometrical shape of the gaseous body. y is represented from Eq. 22 as;

$$y=1\Big/\left(1+\frac{\gamma_{eff}}{Z_Q}\right) \quad (24)$$

where

$$\gamma_{eff}=1/\tau_{eff}$$

The assumption that $y(\boldsymbol{r})$ does not depend on the $\boldsymbol{r}$ coordinate contradicts the expectation that the concentration of the emitting atoms in the upper state at the border of the gaseous body is less than in the center part, because the light quanta emitted from the atoms at the border have a great possibility of escaping from the gaseous body. However, in the case of the dense concentration of the atoms, this treatment is satisfactory for the present purpose. The situations may be explained by the following consideration. The light quanta emitted from the atoms can travel only a very short distance because of the great possibility of capture by the neighboring atoms, and at the border of the gaseous body, there is only a thin layer of atoms which have lower value of y than the atoms in the center part have. In addition to this, the experimental value of y obtained from the measured temperature is a mean value, since it is assumed that the radiation density, $\rho'(\omega_{12}, T)$, is constant over the gaseous body in Eq. 3. Walsh confirmed the suitability of the approximation by more

detailed calculations.[9]

The Derivation of the Escaping Probability. —The quantity $G(\boldsymbol{r}', \boldsymbol{r})$ is formulated in terms of the distance, $x=|\boldsymbol{r}'-\boldsymbol{r}|$, and the absorption coefficient of the gas. Holstein shows

$$G(|\boldsymbol{r}'-\boldsymbol{r}|)=\frac{1}{4\pi x^2}\frac{\partial T(x)}{\partial x} \tag{25}$$

where $T(x)$ is the probability that the radiation quantum travels the distance x without absorption; this can be explained by the equation:

$$T(x)=\int_{-\infty}^{+\infty}\varepsilon(\omega)e^{-k(\omega)x}\mathrm{d}\omega \tag{26}$$

The factor $\varepsilon(\omega)$ in Eq. 26 is the distribution function which represents the wave number profile of the emitted line; it is assumed to be proportional to $k(\omega)$. Holstein has given the approximate formula for $T(x)$ as follows:

$$T(x)=1/k_0x(\pi \ln k_0x)^{1/2},$$

for the Doppler line shape (27)

$$T(x)=1/(\pi k_cx)^{1/2},$$ for the

collision-broadened line shape (28)

where k_0 and k_c are the peak absorption coefficients in the Doppler and collision-broadened lines respectively.

In order to calculate the numerical value of the escaping probability, it is necessary to know the geometry of the gaseous body emitting the resonance line. Under present experimental conditions, sodium vapor in the shock-heated gas is enclosed in a cylinder whose diameter and height are the radius of the shock tube and the distance between the shock front and the contact discontinuity respectively. Here, the solution in the enclosure of an infinite slab with the thickness L is applied to the present problem. Though the infinite cylinder is expected to be a better approximation to the real geometry than the infinite slab, Holstein has shown that the escaping probability is nearly equal in these two cases. The above approximation is also based on the the same conditions which are introduced into the definition of the mean escaping probability; in other words, the light quanta emitted from atoms travels only a small distance before absorption.

According to Holstein's calculation, the escaping factor in the case of an infinite slab is as follows:

for a Doppler-broadened spectral line,

$$<1-\int G(\boldsymbol{r}, \boldsymbol{r}')\mathrm{d}\boldsymbol{r}'>_{Av}=\frac{1}{k_0L}\left(\frac{1}{\pi}\ln\frac{k_0L}{2}\right)^{1/2} \tag{29}$$

9) P. J. Walsh, *Phys. Rev.*, **107**, 338 (1957).

for a collision- or dispersion-broadened spectral line,

$$<1-\int G(\boldsymbol{r}, \boldsymbol{r}')\mathrm{d}\boldsymbol{r}'>_{Av}=\frac{4}{3(\pi k_cL)^{1/2}} \tag{30}$$

The Determination of the Absorption Coefficient. — The absorption coefficient may be derived from the effective emissivity obtained from the experiment. The spectral shape of the sodium D-line is considered to be a combined form of the Doppler and the collision broadening in the present shock wave experiment. The absorption coefficient has already been given as a function of parameter a, which is defined as $a=(\ln 2)^{1/2}(\Delta\omega_N+\Delta\omega_c)/\Delta\omega_D$, where $\Delta\omega_N$, $\Delta\omega_c$, $\Delta\omega_D$ are the half-widths of the natural and collision and Doppler-broadened lines respectively.[10] The total absorption of the spectral line is given by the integration:

$$A=\int_{-\infty}^{+\infty}\{1-\exp[-k(|\omega-\omega_0|)L]\}\mathrm{d}\omega \tag{31}$$

where ω_0 is the wave number at the center of the spectral line. The value of A has been calculated numerically in the case of various values of a and is given by the "curves of growth". Since the spectral slit width, $\overline{\Delta\omega}$, is much wider than the half-width of a pure Doppler- or collision-broadened line (e.g., in the present case, $\overline{\Delta\omega}=8.9\,\mathrm{cm}^{-1}$ against $\Delta\omega_D$ or $\Delta\omega_c=0.1\sim0.15\,\mathrm{cm}^{-1}$), the total absorption can be obtained from the observed effective emissivity by the relation:

$$E_d=\int g(\omega,\omega_d)\{1-\exp[-k(\omega)L]\}\mathrm{d}\omega\Big/\int g(\omega,\omega_d)\mathrm{d}\omega\fallingdotseq A_d/\overline{\Delta\omega} \tag{32}$$

For the numerical evaluation of k_0 by the use of the curves of growth*, the collision half-width, $\Delta\omega_c$, is necessary. This is given by the classical collision-damping theory[11]:

$$\Delta\omega_c=\sigma^2\bar{v}N'/c$$

where N' is the concentration of perturbing atoms or molecules, $\bar{v}$, the gas kinetic mean velocity, and σ^2, the optical cross-section of collisions with perturbing particles. Hinnov measured the total absorption of the sodium D_2-line in the acetylene-air flame and obtained

10) S. S. Penner, "Quantitative Molecular Spectroscopy and Gas Emissivities," Addison-Wesley Pub. Co., Mass. (1959), p. 38.

* The relation $k_c=k_0/\sqrt{\pi}\ a$ can be derived, since in any shape of the spectral line, $\int k(|\omega-\omega_0|)\mathrm{d}\omega=(\pi e^2/mc^2)Nf$, where e and m are the electron's charge and mass respectively, and f is the f-number of the concerned spectral line. In the latter part of this paper, the absorption coefficient, k_0, will be used as a measure of optical thickness instead of k_c, because the total absorption is given in terms of k_0L in the curves of growth.

11) S. Chen and M. Takeo, *Rev. Mod. Phys.*, **29**, 20 (1957).

TABLE I. CALCULATED QUENCHING CROSS SECTION OF NITROGEN AND CARBON MONOXIDE FROM SHOCK WAVE DATA

Test gas	N_2 0.05%-Ar 99.95%					CO 0.03%-Ar 99.97%				
Run No.	1802	1803	1805	1809	1811	2401	2403	2404	2406	2408
T_1 (°K)	303	303	303	303	303	302	302	302	302	302
v_s (mm./μsec.)	1.657	1.649	1.700	1.690	1.675	1.648	1.657	1.675	1.680	1.680
T_2^{calc} (°K)	2737	2713	2868	2837	2792	2709	2736	2791	2806	2806
p_2^{calc} (mmHg)	839	834	886	943	894	881	865	880	879	876
T_g^{steady} (°K)	2430	2395	2330	2440	2590	2405	2530	2450	2325	2270
E_d	0.44	0.35	0.115	0.18	0.95	0.41	1.0	0.44	0.14	0.14
y^{steady}	0.32	0.31	0.14	0.25	0.51	0.32	0.48	0.29	0.17	0.13
k_0L	460	280	40	62	1770	360	2040	300	43	38
Z_Q ($\times 10^6$ sec^{-1})	1.40	1.46	1.43	2.35	1.39	1.43	1.65	1.36	1.68	1.33
σ^2_{eff} ($\times 10^{-15}$ cm^2)	1.4	1.5	1.4	2.1	1.3	2.1	2.5	2.1	2.5	2.0
σ^2_{eff}*	14 Å^2 for nitrogen					28 Å^2 for carbon monoxide				

* Effective cross section from Norrish and Smith's data.

value of σ^2 as 64Å^2 for nitrogen-sodium collisions.[12a] Margenau and Watson observed the absorption profile of the sodium D_1- and D_2-lines in the atmosphere of nitrogen and argon[12b] and found that the half-width of the absorption line in argon at high pressure was larger than that in nitrogen. However, half-widths at less than 1 atm. are almost the same in both cases, as is shown in Fig. 4 of their paper. The difference between half-widths in argon and nitrogen at high pressure may be considered to be due to the fact that the degrees of assymmetrical broadening and the shift of the spectral line are different in argon and in nitrogen. The value of σ^2 obtained by Hinnov is used in the present case, since the present experimental conditions, i. e., high temperature and about 1 atm., resemble Hinnov's case and the sodium D-line is expected to be broadened equally by nitrogen- and argon-sodium collisions.

Effective Collision Cross-section.—The aforementioned procedures make it possible to calculate the numerical value of the quenching collision frequency, Z_Q, by the use of an experimental y value. Table I shows the experimental results of the temperature measurement in the cases of shock-heated nitrogen- and carbon monoxide-argon mixtures, and it also gives the calculated values of k_0L and Z_Q. The value of k_0L is obtained from the curves of growth using the total absorption estimated from the observed emissivity. Z_Q is calculated by Eq. 24, where the value of γ_{eff} is obtained from Eq. 30. Here the value of 1.6×10^{-8} sec. is adopted as the radiative lifetime of the $Na^2P_{3/2}-{}^2S_{1/2}$ transition.[13] In the above calculation, the spectral line, which has a shape combining the Doppler and the collision brandening, is considered to be a pure collision-broadened line, and k_0L is converted to k_cL using the relation $k_cL=k_0L/\sqrt{\pi}a$. This approximation is reasonable taking into account the fact that the spectral shape of the sodium D-line is close to the collision-broadened line in the present experimental conditions.

The calculated Z_Q's have an order of 10^6 sec^{-1} in the cases of both the 0.05% nitrogen and 0.03% carbon monoxide mixtures. This Z_Q should be interpreted from the viewpoint that some particles in the shock-heated heated nitrogen- or carbon monoxide-argon mixture have large efficiencies in exciting or quenching collisions with sodium atoms. The effective collision cross-section, σ^2_{eff}, is defined by the equation;

$$Z_Q=\sigma^2_{eff}\left[8\pi RT\left(\frac{1}{M_{Na}}+\frac{1}{M_q}\right)\right]^{1/2}N_q \quad (33)$$

where M_{Na} and M_q are the atomic or molecular weights of sodium and the quencher respectively, and N_q is the number of quenchers per unit volume.

In order to explain the obtained value of Z_Q in nitrogen- and carbon monoxide-argon mixtures, it is assumed that the collisional excitation and quenching of sodium atoms are performed by nitrogen or carbon monoxide molecules involved in the shock-heated mixtures. The values of σ^2_{eff} for nitrogen or carbon monoxide in collisions with sodium atoms can be calculated on the above assumption; they are shown in Table I. These values agree well with the experimental values given by Norrish and Smith,[14] even though many approximations are made in the process of the

12a) E. Hinnov, *J. Opt. Soc. Am.*, **47**, 151 (1957).
12b) H. Margenau and W. W. Watson, *Phys. Rev.*, **44**, 92 (1933).
13) A. C. G. Mitchell and M. W. Zemansky, "Resonance Radiation and Excited Atoms," Cambridge University Press, London (1934), p. 146.
14) R. G. W. Norrish and W. MacF. Smith, *Proc. Roy. Soc.* (*London*), **176A**, 295 (1945).

calculation. However, the value of σ^2_{eff} obtained here has only one significant figure, i. e., σ^2_{eff} (for N_2) $=(1.4\pm0.5)\times10^{-15}$ cm^2, because of the uncertainty in the estimation of the absorption coefficient and because of the approximation used in the analysis of the radiation imprisonment. The agreement of σ^2_{eff} with Norrish and Smith's value leads to the conclusion that molecular collisions with sodium atoms are dominant in quenching Na(^{2}P), that is, in exciting Na(^{2}S) in the nitrogen- and carbon monoxide-argon mixtures even if the concentration of nitrogen or carbon monoxide is less than 0.1%. The present values of σ^2_{eff} are obtained in the gas with a high temperature of about 2800°K. On the other hand, the experiment of Norrish and Smith was performed at room temperature. The agreement of the present values with their experimental values shows that the activation energy of the quenching process is zero. Mori has calculated quantum-mechanically the potential surface of the sodium-nitrogen system; the calculated potentials have no activation energy.[15]

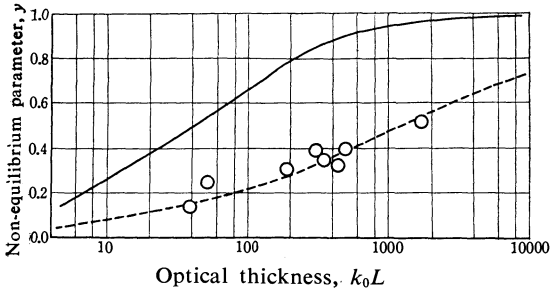


Fig. 6. Relation of non-equilibrium parameter y to optical thickness k_0L. The calculation is carried out in the case of $Z_Q=1.53\times10^6$ sec^{-1} which corresponds to the quenching collision frequency of nitrogen in 0.05%N_2-99.95%Ar mixture at 900 mmHg and 2800°K. In this case, $y=0.0239$ at $k_0L\to0$. Solid and dotted lines shows values of y calculated in the case of Doppler- and collision-broadened spectral lines, respectively. Experimental points are adopted from Table I.

The graphical representation of the theoretical y value vs. the optical thickness, k_0L, is shown in Fig. 6. The theoretical curves are calculated by Eq. 24 in the case of $Z_Q=1.53\times10^6$ sec^{-1}. This value of Z_Q is the collision frequency of quenching by nitrogen molecules in a 0.05% nitrogen - 99.95% argon mixture, which is shocked to the temperature of 2800°K and the pressure of 900 mmHg. Experimental results are also given in Fig. 6, although the experimental shock conditions are not precisely the same as the conditions used in the calculation. The experimental points lie on the curve of y calculated in the case of the collision-broadened line shape.

It is seen in Fig. 6 that the values of y increases as the optical thickness, k_0L, becomes larger. This is due to the radiation imprisonment. If all the light quanta emitted spontaneously from sodium atoms escape from the gaseous enclosure, i. e., if $\tau_{eff}=\tau$ and $k_0L=0$, expected value of y is 0.0239 as calculated from Eq. 25. Gaydon and Wolfhard have explained the radiative non-equilibrium state between sodium atoms and a high temperature medium by the use of τ rather than of τ_{eff}.[16] However, the populations of the ^{2}P state of sodium atoms are much closer to the values of the thermal equilibrium state than those without the imprisonment of resonance radiation.

Vibrational-Electronic Energy Exchange

In this section, the rise of the emission behind the shock wave will be discussed. The results show that a lab. time of 50~100 μsec. after the passage of the shock front is required for the emission intensity to attain a steady value in the nitrogen- or the carbon monoxide-argon mixture. On the contrary, the emission rises in less than 10 μsec. (lab. time) in the shock-heated argon.

Gaydon has described that the excitation of sodium atoms occurs by collision with vibrationally-excited molecules, because the quenching cross-sections of the fluorescence are large when the quenchers are molecules and extremely small when they are inert monoatomic gases.[17] He obtained the vibrational relaxation time on the assumption that the reversal temperature equals the vibrational temperature of diatomic gases.[1] Karl and Polanyi investigated the infrared emission of carbon monoxide, which quenched electronically-excited mercury, and found that the electronic energy of the mercury atom was transferred to the vibrational freedom of carbon monoxide by collisions of second kind.[18] Their findings can be applied to the present problem.

The mechanism of the collisional excitation of the sodium atom may be represented by the following scheme:

$$N_2(v=0) + Ar \rightleftarrows N_2(v=1) + Ar \rightleftarrows N_2(v=2) + Ar \rightleftarrows \quad (34)$$

15) Y. Mori, This Bulletin, 35, 1591 (1962).

16) A. G. Gaydon and H. G. Wolfhard, *Proc. Phys. Soc. (London)*, 65, 19 (1952).

17) A. G. Gaydon, "Energy Transfer in Hot Gases," Natl. Bur. Standards, Circular 523, Washington (1954), p. 1.

18) G. Karl and J. C. Polanyi, *J. Chem. Phys.*, 38, 271 (1963).

$$Na(^2S) + N_2(v \geq v^*) \rightleftarrows Na(^2P) + N_2(v < v^*) \quad (35)$$

The successive excitation or de-excitation of vibrational states of carbon monoxide has been recently experimentally ascertained.[19] This has been predicted by Landau-Teller's classical theory of vibrational relaxation, and Eq. 34 reflects this mechanism. Equation 35 represents how the excitation of sodium atoms occurs in collisions with nitrogen of a high vibrational state ($v^* \geq 8$).

First, it will be shown that the process of Eq. 35 is much faster than that of Eq. 34. Equation 16 represents the concentration of $Na(^2P)$ and is formulated by the use of γ_{eff} as follows:

$$dN_1/dt = Z_E N_2 - (Z_Q + \gamma_{eff}) N_1 \quad (16')$$

where the exciting collision frequency, Z_E, is a function of a concentration of vibrationally-excited nitrogen molecules. If Eq. 34 keeps complete equilibrium, that is, if nitrogen molecules are in equilibrium with argon atoms at any moment after the passage of the shock front, Z_E is constant throughout the high temperature region behind the shock front, and the rate of the process of Eq. 35 is represented by Ep. 16'. On the assumption that $N_2 \fallingdotseq N$, Eq. 16' may be integrated to give the relation:

$$N_1 = N_1^{steady}\{1 - \exp[-(Z_Q + \gamma_{eff})t]\} \quad (36)$$
$$N_1^{steady} = NZ_E/(Z_Q + \gamma_{eff})$$

where the integration is carried with the initial condition, $N_1 = 0$ at $t = 0$, and N_1^{steady} is a value of N_1 at the steady region far from the shock front.

Since the emission intensity of the sodium D-line is proportional to the concentration of excited sodium atoms, the profiles of the emission intensity behind the shock front is expressed by Eq. 36. In the case of a 1% nitrogen-99% argon mixture, the time required for N_1 to reach 90% of N_1^{steady} is estimated by Eq. 36; this corresponds to the rise time of the emission intensity behind the shock front. Under the present experimental conditions, $\gamma_{eff} \fallingdotseq 10^6\ sec^{-1}$ and $Z_Q \fallingdotseq 10^7\ sec^{-1}$. The corresponding rise time of the emission intensity is calculated to have an order of 10^{-7} sec., which is much shorter than the rise time observed in the experiment. The discrepancy between this argument and the experimental findings is due to the assumption that Eq. 34 keeps complete equilibrium. Therefore, it can be concluded that the process of Eq. 34 rather than that of Eq. 35 is the rate-determining step of the excitation of sodium atoms; i. e., the distribution of sodium atoms in the ^2S and ^2P states are always in equilibrium with nitrogen molecules in the various vibrational states.

Montroll and Shuler have calculated the relaxational process of harmonic oscillators which are involved in a heat bath with a constant temperature.[20] Their calculations are based on the Landau-Teller-type relaxation, and the solution is applicable to the present problem. Their calculations show that when the temperature of a heat bath is suddenly raised, as in the shock wave, the initial Boltzmann distribution of harmonic oscillators goes to the final distribution, maintaining the Boltzmann distribution at any moment of the relaxation process. Therefore, the vibrational temperature, $T(t)$, of oscillators can be defined as a function of the time, t, after the sudden increase in the temperature of the heat bath. At a large value of t, Montroll and Shuler gave the equation;

$$\Theta - \theta \fallingdotseq e^{-t/\tau}\left[\frac{(1-e^{-\theta})}{(1-e^{-\theta_0})}(1-e^{\theta-\theta_0})\right] - O(e^{-2t/\tau}) \quad (37)$$

In this equation, τ is the vibrational relaxation time of $v=1 \rightarrow v=0$; $O(e^{-2t/\tau})$ is a function of terms higher than $e^{-2t/\tau}$, and $\Theta = \boldsymbol{hc}\omega_{vib}/\boldsymbol{kT}(t)$, $\theta_0 = \boldsymbol{hc}\omega_{vib}/\boldsymbol{kT}(0)$, $\theta = \boldsymbol{hc}\omega_{vib}/\boldsymbol{kT}(\infty)$, where $T(0)$ and $T(\infty)$ are the initial and final temperatures of the system of oscillators, and ω_{vib} is the fundamental vibration frequency of the oscillator. Equation 37 can be arranged to give the relation;

$$\ln\left[\frac{1}{T(t)} - \frac{1}{T(\infty)}\right] \fallingdotseq -\frac{t}{\tau} + \text{const.} \quad (38)$$

As a results of the preceding consideration of the energy transfer between sodium atoms and nitrogen molecules, the observed excitation temperature of the sodium D-line may be concluded to correspond to $T(t)$ of the vibrational temperature of nitrogen. The emission intensity of the sodium D-line is described by Eq. 4, and if the concentration of sodium is constant behind the shock wave, the ratio of the intensities at any time, t, and at the steady state of $t=\infty$ is represented by;

$$\frac{I(t)}{I(\infty)} = \exp\left\{-\frac{\boldsymbol{hc}\omega_d}{\boldsymbol{k}}\left[\frac{1}{T(t)} - \frac{1}{T(\infty)}\right]\right\}$$

therefore,

$$\ln\left[\ln\frac{I(\infty)}{I(t)}\right] \fallingdotseq -\frac{t}{\tau} + \text{const.} \quad (39)$$

Figure 7 shows the experimental determination of τ from the measured temperature and the emission intensity profiles behind the shock wave in the case of the 1% nitrogen-99%

19) W. J. Hooker and R. C. Millikan, ibid., 38, 214 (1963).

20) E. W. Montroll and K. E. Shuler, ibid., 26, 454 (1957).

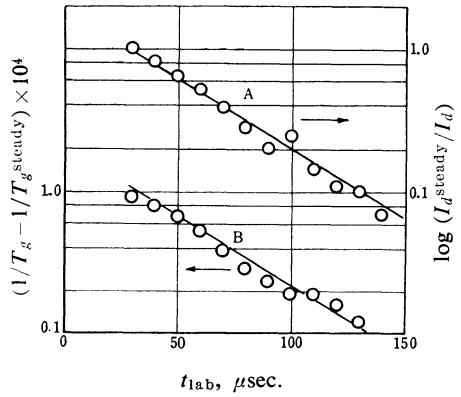


Fig. 7. Determination of vibrational relaxation time from the measured emission intensity(A) and temperature (B) profiles behind shock wave in 1%N_2-99%Ar mixture. Both linear slopes give the same relaxation time. Run No. 1101.

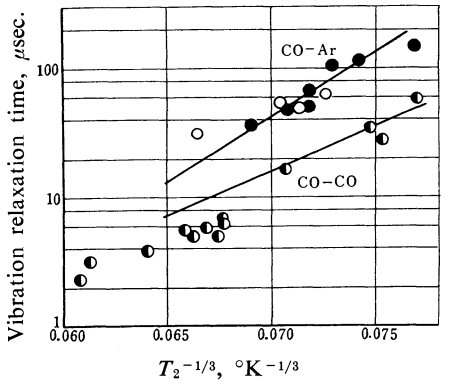


Fig. 9. Vibrational relaxation time in CO-Ar collisions.

○ : 1.16% CO in argon
● : 0.12% CO in argon
◐ : Matthew's data[23]
——: Hooker and Millikan's data

argon mixture. Two methods, i. e., Eqs. 38 and 39, of obtaining the vibrational relaxation time give the same value. In Figs. 8 and 9, the obtained vibrational relaxation times at 1 atm. are given. Since the measurements are made in 1% and 0.1% nitrogen or carbon monoxide in argon, the contribution of nitrogen-nitrogen or carbon monoxide-carbon monoxide collisions to the relaxation time is negligible. The results of the relaxation time measured by the present method in pure nitrogen behind the shock wave agree with the extrapolated value of

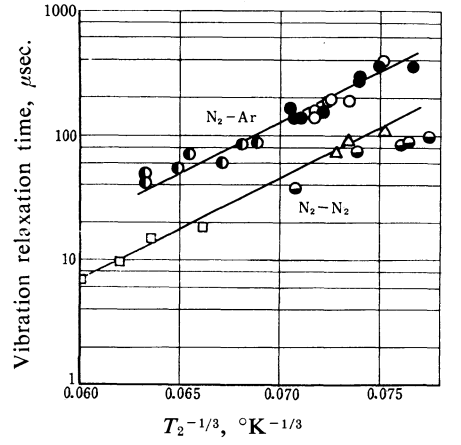


Fig. 8. Obtained vibrational relaxation time at 1 atm. in N_2-Ar and N_2-N_2 collisions.

○: 1.0% N_2 in argon, data obtained from temperature profile
◐: 1.0% N_2, from emission profile
●: 0.09% N_2, from temperature profile
△: data obtained from temperature profile in shocked nitrogen
□: Blackman's data[21]
◒: Gaydon and Hurle's data

Blackman's data,[21] as has already been pointed out by Gaydon.[1] On the other hand, the relaxation times in the 1% nitrogen-99% argon mixture are about three times longer than in the pure nitrogen. This is consistent with Camac and Vaughan's measurement in an oxygen-argon mixture,[22] and Hooker and Millikan's data on a carbon monoxide-argon mixture.[19] The plots of the relaxation time vs. $T^{-1/3}$ give the relation;

$$\log_{10}\tau_{N_2-Ar} = 85T^{-1/3} - 9.8$$

$$\log_{10}\tau_{N_2-N_2} = 81T^{-1/3} - 10$$

where τ is described in sec. The results obtained in carbon monoxide-argon mixtures are the same as Hooker and Millikan's data:

$$\log_{10}\tau_{CO-Ar} = 101T^{-1/3} - 11.45$$

$$\log_{10}\tau_{CO-CO} = 69.3T^{-1/3} - 9.64$$

It is reasonable to expect a longer vibrational relaxation time in nitrogen-argon collisions than in nitrogen-nitrogen collisions, since only a translational-vibrational energy exchange, and novibrational-vibrational one, occurs in nitrogen-argon collisions.

The Excitation of the Sodium Atom in Argon behind the Shock Wave

In order to discuss the mechanism of the excitation of sodium atoms in the shock-heated argon, the method of analysis already described will be applied to the experimental results. Table II shows that the quenching collision frequency, Z_Q, derived from the measured tem-

21) V. Blackman, *J. Fluid Mech.*, **1**, 61 (1956).
22) M. Camac and A. Vaughan, *J. Chem. Phys.*, **34**, 448 (1961).
23) D. L. Matthews, ibid., **34**, 639 (1961).

TABLE II. CALCULATED QUENCHING COLLISION FREQUENCIES OF ARGON ATOMS WITH SODIUM ATOM FROM SHOCK WAVE DATA

Run No.	012	022	025	036	040	053	057	058
T_1 (°K)	282	282	282	296	297	297	297	297
v_s (mm./μsec.)	1.724	1.749	1.734	1.929	1.874	1.618	1.562	1.522
T_2^{calc} (°K)	2921	3000	2953	3609	3422	2616	2456	2342
p_2^{calc} (mmHg)	1017	852	773	556	242	1031	1053	1074
T_g^{steady} (°K)	2320	2250	2170	2390	2385	2085	2020	1925
E_d	0.73	0.61	0.48	0.28	0.078	0.71	0.66	0.53
y^{steady}	0.11	0.064	0.050	0.032	0.045	0.093	0.12	0.10
k_0L	580	810	470	140	51	930	800	510
N_{Na} ($\times 10^{13}$ atoms/cc.)	3.8	5.3	3.1	0.92	0.33	6.1	5.2	3.3
Z_Q ($\times 10^5$ sec^{-1})	3.1	1.3	1.2	1.1	1.8	2.2	1.6	3.4
σ^2_{eff} ($\times 10^{-19}$ cm^2)	1.3	0.69	0.73	1.1	3.6	0.93	0.55	1.3

perature has an order of 10^5 sec^{-1}. By the use of this value, it can be determined what sort of particles in the shock-heated argon performs the excitation and de-excitation by collisions with sodium atoms.

First, the collisions between sodium and argon atoms will be discussed. The effective cross sections can be calculated from the obtained Z_Q's; the values are shown to be about $10^{-19}\sim10^{-20}$ cm^2 in Table II. Laidler has discussed the physical quenching of an excited sodium atom by considering the potential surface between a sodium atom and a quencher;[24] he has concluded that the inert atoms would be poor quenchers, since the potential curves of the $Na^+ + M^-$ (M=inert atom) system do not cross the curves of the Na(^{2}P) + M and Na(^{2}S) + M systems. A very small effective cross-section obtained from the present data reflects these circumstances. Gaydon has proposed the possibility of quenching by an inert atom;[25] though both Na(^{2}S) + Ar and Na(^{2}P) + Ar have potential curves of a repulsive type, the Na(^{2}P) + Ar system is less repulsive than Na(^{2}S) + Ar, and the intersection of the two potential curves occurrs at a high energy point, as Fig. 10 shows. The same discussions were cited by Herzberg.[26] In this mechanism, an activation energy is necessary for quenching.

The present data may be interpreted by the above scheme. It is reasonable that the crossing point of the two potential curves, Na(^{2}P) + Ar and Na(^{2}S) + Ar, lies at an atomic distance of about 10^{-8} cm. Therefore, the collision cross-section is expected to have an order of 10^{-16} cm^2; the $10^{-3}\sim10^{-4}$ factor might come from the necessity of the activation energy for

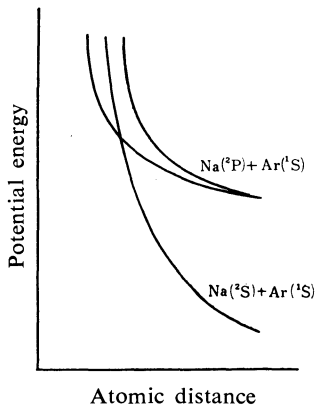


Fig. 10. Potential curves explaining the excitation of sodium atom by collision with argon atom. Two states $^2\Sigma$, $^2\Pi$ are considered in the system Na(^{2}P) + Ar(^{1}S).

quenching, i. e., the energy difference between the crossing point of two potential curves and the energy level of Na(^{2}P) + Ar at a large atomic distance. This activation energy may be expected to be 40~60 kcal. from the results of the present experiment. If the above explanation correctly accounts for the excitation of the sodium atom by collisions with argon atoms, the effective cross-section is strongly dependent on the temperature of the shock wave. The temperature dependency is not certain in the present experiments. Moreover, the constant cross-section is not obtained from the experiments carried out at the various pressures behind the shock wave. These negative facts appear to deny the possibility of the excitation of a sodium atom by collisions with argon atoms.

The collisional excitation of the sodium atom by other particles in argon gas behind the shock wave should also be examined. When the concentration of sodium atoms in the shock-heated argon is calculated from the obtained value of k_0, it is shown to be

24) K. J. Laidler, ibid., 10, 34 (1942).
25) A. G. Gaydon and I. R. Hurle, "The Shock Tube in High Temperature Chemical Physics," Chapman and Hall London (1963), p. 230.
26) G. Herzberg, "Molecular Spectra and Molecular Structure I. Spectra of Diatomic Molecules," D. Van Nostrand Co., N. Y. (1950), p. 463.

$10^{12}\sim10^{13}$ atoms/cc. (cf. Table II). The collisions between sodium atoms cannot take a dominant role in the shock wave unless the effective cross section for a sodium atom is extraordinarily large. There is no possibility of the excitation by Na_2 molecules, which exist in a small concentration because of the low dissociation energy. The other possibility is collision with the nitrogen or oxygen which is involved in argon gas as an impurity. The Z_Q of $10^5\,sec^{-1}$ at 1000 mmHg and 3000°K requires the contamination of about 0.003% nitrogen in argon. The argon gas used in the present experiment contains nitrogen, oxygen, hydrogen and water vapor as follows: $N_2<0.007\%$, $O_2<0.001\%$, $H_2<0.001\%$, $H_2O<0.001\%$. Therefore, the excitation of sodium atoms by these impurities must be taken into consideration; the observed Z_Q can be explained by this scheme. However, there is a phenomenon which contradicts the reality of the excitation by the impurity whose main component is nitrogen; i. e., the rise time of the emission intensity just behind the shock front is very short compared with that in the case of the 1% nitrogen-99% argon mixture. The following explanation of this fact is possible. The proportion of oxygen, hydrogen or other impurities to the amount of nitrogen is much larger than that of the 1% nitrogen - 99% argon mixture. The vibrational relaxation times of oxygen, hydrogen and water vapor are much shorter than that of nitrogen. This is the probable reason why the emission of the sodium D-line rises rapidly behind the shock front. In order to gain a more rigid conclusion, however, it is necessary to perform the experiment using highly pure argon and a highly-evacuated shock tube.

Bauer, Kiefer and Loader have measured the temperature dependency of the emission rise of the chromium line in the 10% nitrogen-90% argon mixture behind the shock wave[4] and have concluded that chromium atoms are excited predominantly by collisions with electrons. Since the large cross-section for the excitation of sodium atoms is expected in collisions with electrons, electrons which are produced by the ionization of sodium atoms can make the quenching collisions of $Z_Q \fallingdotseq 10^5\,sec^{-1}$ if the equilibrium ionization is attained. However, the ionization is known to occur after some delay in the inert gas behind the shock wave. Haught has observed the delayed luminosity in the shock wave of a cesium-argon mixture[27] and has described that the ionization by atom-atom collisions is less effective by a factor of 10^{-3} than electron-atom collisions, and that atom-atom collisions occur only just behind the shock front in argon. In the shocked gas higher than 3500°K, the delayed rise of the emission is observed 100$\sim$300 μsec. (lab. time) later behind the passage of the shock front; this is perhaps attributable to the ionization of sodium atoms. A detailed investigation of this phenomenon will be discussed in another place. Therefore, the emission of the sodium D-line in the shock-heated argon is not due to the ionization of sodium atoms.

The above arguments lead to the conclusions that the excitation of sodium atoms in the shock-heated argon does not occur by sodium-argon collisions in the 2500$\sim$3500°K temperature range, and that molecular impurities such as nitrogen, oxygen and hydrogen, rather than electrons play a dominant role as to the excitation of sodium atoms. This conclusion is compatible with the fact that the translational-electronic energy exchange in nitrogen-sodium collisions cannot occur in the case of a shock-heated nitrogen-argon mixture.

Conclusion

The so-called reversal temperature can be obtained by simultaneous measurements of the emission and of the absorption of the sodium D-line. The physical meaning of the temperature is such that the obtained temperature determines the distribution of populations in the ^2P and ^2S states of the sodium atom according to the Boltzmann distribution. The measured temperatures in argon containing a trace of sodium vapor are about 600°K lower than the values calculated from the shock velocity. However, in the shock-heated 1% nitrogen-99% argon mixture, the measured temperatures agree with the calculated ones, and a complete equilibrium between sodium atoms and the gaseous particles is attained.

These results can be explained by the fact that the effective cross-section for the excitation of the sodium atom in collisions with argon atoms is too small to maintain the thermal equilibrium. The collision frequencies of the second kind can be obtained with the correction of radiation imprisonment, and the calculations show that sodium-nitrogen collisions rather than sodium-argon collisions play a dominant role in the shock wave of a temperature between 2000$\sim$3000°K, even if the concentration of nitrogen is 0.05%. Quite the same conclusions are obtained in the case of a carbon monoxide-argon mixture. The present shock wave experiment may provide a method for obtaining the effective cross-section of collison for quenching an excited atom.

Concerning the feature of the emission rise

27) A. F. Haught, *Phys. Fluid*, 5, 1337 (1962).

in the nitrogen-argon mixture just behind the shock front, the observed temperature follows the vibrational temperature of nitrogen defined by Montroll and Shuler; that is, the electronic excitation occurs in collisions with vibrationally-activated nitrogen molecules. The vibrational relaxation time in nitrogen-argon collisions has a value about three times greater than the value in nitrogen-nitrogen collisions in the temperature range of 2000~3000°K.

The effective quenching cross-section of $Na(^2P)$ for the argon atom has been calculated to be 10^{-19}~10^{-20} cm^2 at 2500~3500°K from the measured temperatures in the shock-heated argon. However, collisions with other impurities, e. g., nitrogen, electrons etc., must be taken into consideration. It has been concluded that molecular impurities, such as nitrogen or oxygen, rather than argon atoms or electrons make exciting collisions with sodium atoms in the shock-heated argon.

The author wishes to express his sincere thanks to Professor Kenji Kuratani for his kind advice and encouragement throughout this work. His thanks are also expressed to Mr. Takuji Sakai for his help in the experimental work.

Aeronautical Research Institute
The University of Tokyo
Meguro-ku, Tokyo

*Photoconductivity of Polyacenaphthylene and Its Nitrated Derivatives**

By Akira INAMI, Kazuhisa MORIMOTO and Yoshiki HAYASHI

(Received January 10, 1964)

During the last decade a renewed interest in the photoconductive properties of organic compounds has been shown, and many studies of the photoconductivities of polynuclear molecules and of miscellaneous dyes have been reported.

Recently a few photoconductive polymers have been discovered, such as poly-*N*-vinyl carbazole,[1-4] irradiated polyvinylidene chloride,[5] the thermal conversion product of polyacrylonitrile,[6] polyvinylchloride-leuco base complexes[7] and a polymer containing a triphenylpyrazoline group which has been reported on in a previous paper of ours.[8]

The semiconductivity of charge-transfer complexes of polyacenaphthylene with Lewis acids in the dark was studied by Slough.[9] The present authors, in studying the photoconductive behavior of polyacenaphthylene, have detected that the photoconduction of this polymer is small initially but that it increases with adequate nitration of the polymer.

Experimental

Polymerization of Acenaphthylene.[10]—Ten grams of acenaphthylene was dissolved in 10 ml. of ethyl benzene and emulsified with 100 ml. of a sodium stearate solution.** As an initiator, 0.4 g. of potassium persulfate was added to the emulsion, and then the mixture was agitated in a closed container for 10 hr. at 45°C. The resultant polymer was coagulated from the solution by dropping it slowly into dilute hydrochloric acid. The coagulated polymer was then filtered off, dissolved in benzene, and precipitated into methyl alcohol. Yield, 74%. $[\eta]=0.53$ (at 25°C in benzene).

Nitration of Polyacenaphthylene. — The polyacenaphthylene thus obtained was dissolved in a mixture of benzene (or monochlorobenzene) and glacial acetic acid (or acetic anhydride); then the mixture was stirred and concentrated nitric acid (s. g. 1.40) was slowly added. After the addition of nitric acid, the mixture was stirred at a constant temperature and then poured into methyl alcohol. The pale yellow polymer was twice reprecipitated from a monochlorobenzene solution by pouring it into methyl alcohol and then dried at room temperature. The molar per cent of sub-

* Presented at the 12th Annual Meeting of the Society of Polymer Science of Japan, Tokyo, May, 1963.

1) J. Weigl, Internationales Kolloquim über wissenschaftliche Photographie, Zürich, Sept., 1961.

2) C. Claus, *Photo. Sci. Eng.*, **7**, 5 (1963).

3) H. Mikawa et al., Symposium of the Society of Electrophotography of Japan, Tokyo, June, 1963.

4) Y. Hayashi and A. Inami, 12th Annual Meeting of the Society of Polymer Science of Japan, Tokyo, May, 1963.

5) G. Oster, G. Oster and M. Kryszewski, *J. Polymer Sci.*, **57**, 937 (1962).

6) K. Daito and Y. Oshina, 11th Annual Meeting of the Society of Polymer Science of Japan, Nagoya, May, 1962.

7) H. Greig, *R. C. A. Rev.*, **23**, 413 (1962).

8) K. Morimoto, Y. Hayashi and A. Inami, This Bulletin, **36**, 1651 (1963).

9) W. Slough, *Trans. Faraday Soc.*, **58**, 2360 (1962).

10) U. S. Pat. 2563524 (1951).

** This emulsion consisted of 600 ml. of water, 14 g. of stearic acid, and 6 g. of potassium hydroxide.

Table I. Nitration of polyacenaphthylene

No.	Polymer/HNO_3 mole ratio	Solvent ml.		Temp. °C	Time hr.	$-NO_2$ group mol. %
2	1/1	Benzene	60	70	2	7.9
		Acetic acid	10			
3	1/1	Acetic acid	10	75	6	16.4
4	1/1	Benzene	60	70	2	28.7
		Acetic acid	30			
5	1/1.2	Chlorobenzene	60	70	2	40.6
		Acetic anhydride	20			

stituted nitro groups were calculated from the nitrogen contents by the Dumas' microanalysis. Table I shows the reaction conditions and results. The degrees of nitration varied from 7.9 to 40.6 molar per cent, according to the condition of the reaction. The photoconductive properties of these nitrated polyacenaphthylenes were studied.

Photoconductivity of Polymers. — The photoconductivity was investigated by using the same sandwich-type cell as was used in another paper.[8] The preparation of the cell was carried out by the following technique; a 10% polymer solution of monochlorobenzene was placed uniformly flat onto a NESA conductive glass plate used as a transparent electrode, and then the solvent was thoroughly evaporated. After the solvent had been evaporated, the specimen film was 10 μ thick. The second electrode was formed thereafter by the vacuum-evaporation coating of aluminum onto the surface of the specimen film.

The sandwich-type cell thus obtained was then placed in a closed glass chamber, which was kept in a vacuo of 10^{-3} mmHg. The applied field of the specimen was 1600 V./cm., taken from a 1.6 V. drybattery source, and the current measurement was carried out with the aid of a vibration-reed electronic micro-micro ammeter (Takeda Riken, type TR-85) and an electronic X-T recorder (Toa-Dempa, type EPR-2). The light source used for measuring the photocurrent of the cell was a 100 W. tungsten lamp.

From the fact that the V-I plots in the dark passed through the point of origin, it may be seen that the dark currents of specimens obeyed Ohm's law and that the contacts between the specimen films and the aluminum layer, or the NESA conductive surface, were perfect.

Relative Surface Potential.—The resistances in the dark were so high and both rise and decay responses were so slow that the ordinary methods of the mere detection of the photocurrents described above were not enough to determine their photoconductive behaviors. In order to reexamine them, the authors introduced a method of comparing the relative surface potential in the light with that in the dark, a method which had been applied in the determination of the photosensitivity of electrophotographic conductive layers. A typical difference between the sandwich-type cell method and the relative-surface-potential method is that the internal field of the specimen in the latter (ca. 10^6 V./cm.) is much higher than in the former (ca. 10^3 V./cm.).

As has been stated in detail in another paper,[4] a thin specimen film 3 μ thick was formed on an aluminum plate. The top surface of a plate was sensitized in the dark to a potential of 200~300 V. (V_d) by negative corona-charging. Actinic light produces electron-hole pairs, which, under the influence of the electric field, are separated; the hole moves to the surface to neutralize a negative charge, and the negative electron is accelerated to the conductive aluminum base, where it neutralizes the induced positive charge. Therefore, the surface potential decreased with the illuminated time to V_l. The relative-surface-potential was defined as a ratio of potential V_l to V_d, and so the time in which V_l/V_d is reduced to one-half represents the half-decay time $(V_l/V_d)_{1/2}$, which serves as an index of photoconductivity. The experimental results obtained when the surface was illuminated with an incandescent light at 1000 luxes are shown in Table II.

Results

Photocurrents under Illumination with an Incandescent Lamp.—*Polyacenaphthylene.* — When a powerful incandescent light (10^5 luxes) is applied to the negative electrode of the cell, a photocurrent increases slowly, attaining a peak after 200 sec. Then the current tends to decay slowly; when the light is switched off, it decays to the initial value, as Fig. 1 shows.

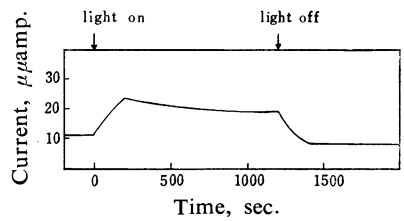


Fig. 1. Rise of the photocurrent under illumination and its decay, polyacenaphthylene.

Nitrated Polyacenaphthylenes. — The time-responses of the photocurrents of the nitrated polyacenaphthylenes are shown in Fig. 2. No photocurrent is observed in the case of Experiment No. 5. The time-responses are very slow; that is, even after 1400 sec. the photocurrents increase gradually. This is the same

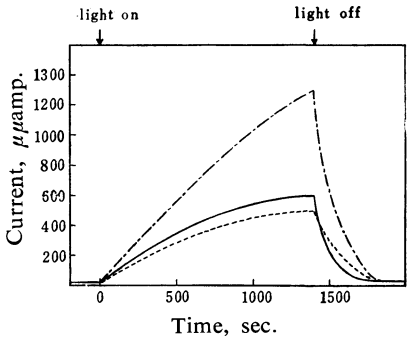


Fig. 2. Rise of the photocurrent under illumination and its decay, nitrated polyacenaphthylenes.
7.9% nitration (dotted line)
16.4% nitration (solid line)
28.7% nitration (broken line)

phenomenon as was observed in crystal violet by Vartanian,[11] and so it can be seen that something in nitrated polymers seems to act as electron-traps.

When a powerful incandescent light (10^4 to 10^5 luxes) is applied to the cell, the photocurrents increase, as is shown in Fig. 3.

The photoconductive natures of these polymers are listed in Table II. In the case of the sandwich-cell method, the sample of 16.4 molar per cent nitration is the most photoconductive, while in the relative-surface-potential method, the sample of 28.7 molar per cent nitration is the most photoconductive. This difference may be due to the different measuring methods. In any case it is clear that the photoconductivity of polyacenaphthylene increases upon the nitration of the polymer.

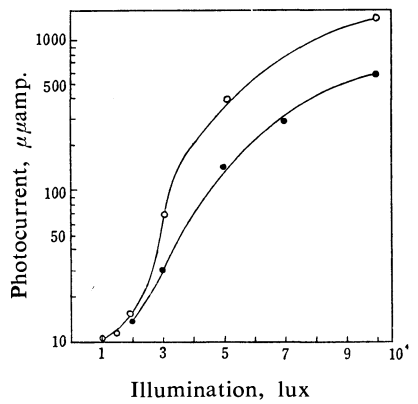


Fig. 3. Photoconductivity curve.
16.4% nitration (○)
28.7% nitration (●)

TABLE II. PHOTOCONDUCTIVE INDEXES OF POLYACENAPHTHYLENE AND NITRATED

No.	$-NO_2$ group mol. %	I_d μμamp.	I_l μμamp.	I_l/I_d	$(V_l/V_d)_{1/2}$ sec.
1	0	11	24	2	100
2	7.9	15	500	33	46
3	16.4	18	1300	72	14
4	28.7	18	600	33	4.5
5	40.6	37	37	1	74

Discussion

The number of the conjugated double bonds or mobile π electrons of polyacenaphthylene are equal to those of polyvinylnaphthalene, which our experiment establishes as having no photoconductivity. The photoconductivity of polyacenaphthylene, therefore, can not be explained by the mere existence of the mobile π electrons. It may be considered that the conductivity of this polymer depends on the stereoregularity. Between the electron clouds of the acenaphthene groups, which lie one against the other, there are, by virtue of a slight overlapping, interaction forces which cause a slight splitting of the electron orbitals of the groups and, consequently, the formation of narrow energy bands.

The fact that the nitration brings more photoconductivity may be interpreted with a charge-transfer mechanism. The nitrated acenaphthene group may be an electron-donor. When these groups are put in order, as has been discussed above, a charge-transfer complex may be formed between an acenaphthene group and a nitrated acenaphthene group.

Summary

The photoconductive properties of polyacenaphthylene and nitrated polyacenaphthylene have been studied using both the sandwich-cell method and the relative-surface-potential method. The polyacenaphthylene shows little photoconductivity, while the nitrated polymer obtained by the partial nitration of polyacenaphthylene shows considerable photoconductivity. The photocurrent depends on the degree of nitration.

The authors are grateful to Dr. Shunkichi Kisaka, Manager of this Laboratory, for his helpful advice, and to Mr. Yosihisa Ogasawara and Mr. Makoto Kuroda for their co-operation in this work.

Research Laboratory, Wireless Division
Matsushita Electric Industrial Co., Ltd.
Kadoma, Osaka

11) A. Terenin, *Proceed. Chem. Soc.*, **1961**, 321.

The Condensation of Thujopsene with Formaldehyde

By Shoji WATANABE and Kyoichi SUGA

(Received January 11, 1964)

In a previous paper,[1] the thermal condensation of thujopsene with formaldehyde was reported. The reaction of thujopsene with formaldehyde in an acetic acid solution is the subject of this paper.

In this study thujopsene (I) was added to a slurry of paraformaldehyde in glacial acetic acid at 50~60°C. The crude products were isolated by fractional distillation and liquid chromatography. A dioxane II was isolated as the major product. The minor product was an unsaturated alcohol III.

The analytical results ($C_{17}H_{28}O_2$) and the molecular weight of the major product indicated that the product was an adduct of two moles of formaldehyde to I. The infrared absorption spectrum showed characteristic absorption bands of an ethearic group (dioxane type) at 1045 cm^{-1} and 1175 cm^{-1}. It gave no positive reaction with a potassium permanganate solution and bromine water for a double bond; it was not suggested that II had a double bond.

The nuclear magnetic resonance spectrum of II is shown in Fig. 1. The four strong signals, at 8.90, 8.96, 9.45 and 8.52 τ., correspond to the four methyl groups. The quartet signal at 5.30 is presumably due to protons on the ethearic ring (AB type, $-O-CH_2-O-$). The multiplet signal at 6.0~6.7 τ is due to the ABX-type spectrum caused by two non-

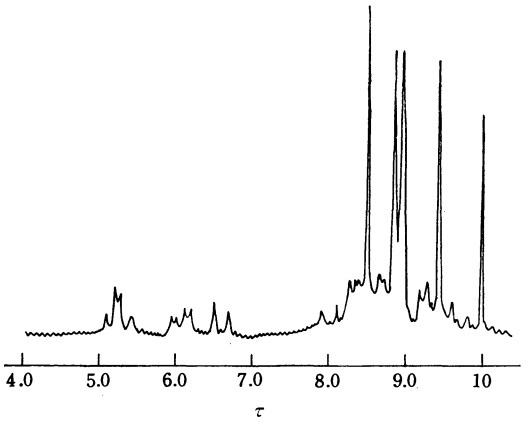
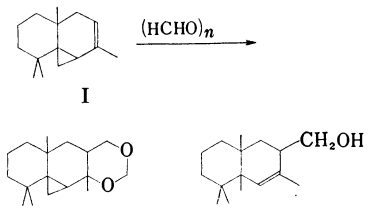


Fig. 1. The nuclear magnetic resonance spectrum of II.



I II III

equivalent protons of $-\overset{|}{C}H-CH_2-O-$.[2] The infrared spectrum exhibits the absorptions at 1000 cm^{-1} and 3050 cm^{-1} which have been reported to be characteristic of the cyclopropane ring.[3,4] The nuclear magnetic resonance spectrum shows the signal of the methylene group of the cyclopropane ring at 9.3 τ. The substance gave a pale yellow color reaction with tetranitromethane, which also indicated the presence of a cyclopropane ring.[5,6] The hydration of II gave an oily product, and the infrared absorption spectrum of this product did not indicate the absorption of the cyclopropane ring at 1000 cm^{-1} and 3050 cm^{-1}. These results indicated that the structure was 1, 3, 5, 6, 7, 8, 9, 9_a-octahydro-4_a, 5, 5, 8_a-tetramethyl-10,10_a-methano-2,4-dioxaanthracene (II).

The structure of the minor product included III. It was demonstrated as follows: the infrared absorption spectrum and gas chromatogram of the substance agreed with those of the authentic III which was prepared from the thermal condensation of I with formaldehyde.

Experimental

The Reaction of Thujopsene with Formaldehyde. —To a mixture of 60 g. of paraformaldehyde, 500 g. of glacial acetic acid and 60 g. of isopropyl ether, 300 g. of thujopsene was added at 60~70°C while the mixture was being vigorously agitated. After the completion of the addition, the mixture

1) S. Watanabe and K. Suga, *J. Chem. Soc. Japan, Pure Chem. Sec.* (*Nippon Kagaku Zasshi*), **84**, 993 (1963).

2) L. M. Jackman, "Application of NMR Spectroscopy in Organic Chemistry," Pergamon Press, London (1959), p. 90.

3) L. J. Bellamy. "The Infrared Spectra of Complex Molecules," "Methuen & Co., London (1958), pp. 17, 29.

4) G. Büchi, M. Schach v. Wittenau and D. M. White, *J. Am. Chem. Soc.*, **81**, 1968 (1959).

5) T. Norin, *Acta Chemica Scandinavica*, **15**, 1676–1694 (1961).

6) A. Zurcher, O. Jeger and L. Ruzicka, *Helv. Chim. Acta*, **37**, 2145 (1954).

was heated at 60°C while being stirred for an additional 7 hr. The reaction mixture was then dissolved in ether, and the resultant solution was washed with water. The distillation of this solution gave the following fraction: 317 g., b. p. 100~185°C/3 mmHg. The redistillation of this product (250 g.) gave 73 g. of thujopsene (b. p. 102°C/3 mmHg) and the residue (136 g.). The residue was dissolved in acetone, and 44 g. of white polymer was removed to give 92 g. of the clear oil. The liquid chromatography of this oil (15 g.) with silica gel (100 g.) gave 3 g. of viscous II from the elution of benzene; b. p. 154°C/6 mmHg, n_D^{14} 1.5189. It did not give the positive reaction with potassium permanganate and bromine solution for a double bond. It was not hydrogenated over a nickel catalyst under high pressure (40 kg./cm^2) and at a high temperature (120°C). II gave a pale yellow color reaction with tetranitromethane.

Found: C, 77.27; H, 10.43. Calcd. for $C_{17}H_{28}O_2$: C, 77.22; H, 10.67%.

III was given from the elution of methanol. Its nature was confirmed comparing its infrared absorption spectrum and gas chromatogram with those of an authentic sample.

From the elution of benzene and methanol, an ethearic compound was obtained; its structure has not yet, however, been determined.

The Hydration of II.—A mixture of 1 g. of II and 100 cc. of 10% sulfuric acid was agitated at 10~15°C for 10 hr. It was then extracted with ether. When the etheric solution was treated as usual, a small amount of a viscous oil was given. The infrared absorption spectrum did not show the absorptions of the cyclopropane ring at 1000 cm^{-1} and 3050 cm^{-1}.

The authors are indebted to the Takasago Perfumary Co., Ltd., for providing materials, and Dr. Sho Ito of Tohoku University and Dr. Atsuaki Arai of the Kobayashi Institute of Physical Research for the nuclear magnetic resonance spectra.

Department of Applied Chemistry
Faculty of Technology
Chiba University
Matsudo Chiba

Asymmetric Hydrogenation with Modified Raney Nickel. III. Studies of the Modified Hydrogenation Catalyst. IV

By Susumu TATSUMI, Masami IMAIDA, Yoshio FUKUDA
Yoshiharu IZUMI and Shiro AKABORI

(Received January 13, 1964)

The asymmetric hydrogenation of methyl acetoacetate to methyl 3-hydroxybutyrate has been achieved by the use of a R-Ni* catalyst modified with optically active 2-amino or 2-hydroxycarboxylic acids, and it has been found that the asymmetric activity of the catalyst is much influenced by the pH and by the temperature of the modifying solution.[1,2]

In the present investigation, optically-active 2-hydroxycarboxylic acids prepared from L-valine, L-leucine, L-isoleucine and L-phenylalanine were tested as modifying reagents and compared with the parent amino acids.

The modifying effects of diacetyl-D-tartaric acid and monobenzoyl-D-tartaric acid were also tested to study the mode of asymmetric modification.

Materials

Modifying Reagents. — The L-2-hydroxycarboxylic acids used in this report were prepared from L-2-aminocarboxylic acids by the following common reaction:

$$\mathrm{R\text{-}\overset{*}{C}H\text{-}COOH} \xrightarrow{HNO_2} \mathrm{R\text{-}\overset{*}{C}H\text{-}COOH}$$
$$\quad\;\; \mathrm{NH_2} \qquad\qquad\qquad\quad \mathrm{OH}$$

The absolute configurations of amino acids are believed to be maintained during this reaction, and the 2-hydroxycarboxylic acids obtained must have the same configurations as the parent amino acids.

Thus, L-2-hydroxyisovaleric, L-2-hydroxyisocaproic, L-2-hydroxy-3-methylvaleric and L-2-hydroxy-3-phenylpropionic acids were prepared as described by Winitz.[3] *O,O'*-Diacetyl-D-tartaric acid and *O*-monobenzoyl-D-tartaric acid were prepared according to the directions

* Abbreviation: R-Ni, Raney Nickel.

1) Y. Izumi, M. Imaida, H. Fukawa and S. Akabori, This Bulletin, **36**, 21 (1963).

2) Y. Izumi, M. Imaida, H. Fukawa and S. Akabori, ibid., **36**, 155 (1963).

3) M. Winitz, L. Bloch-Frankenthal, N. Izumiya, S. M. Birnbaum, C. G. Baker and J. P. Greenstein, *J. Am. Chem. Soc.*, **78**, 2423 (1956).

TABLE I. MELTING POINT AND OPTICAL ROTATION OF L-2-HYDROXYCARBOXYLIC ACID AND *O*-ACYLATED D-TARTARIC ACID

Hydroxycarboxylic acid	M. p., °C	$[\alpha]_D^{20}$	Lit. value M. p., °C	Lit. value $[\alpha]_D^{20}$
L-2-Hydroxyisovaleric	71	−1.0°[a]	—	−1.0°[3]
L-2-Hydroxyisocaproic	81～83	−12.6[a]	80～82[6]	−13.3[3]
L-2-Hydroxy-3-methylvaleric	49～50	+4.0[a]	47～49[7]	+3.9[3]
L-2-Hydroxy-3-phenylpropionic	126	−20.4[a]	124～126[8]	−20.0[3]
O-Acylated-D-tartaric acid				
O, *O*'-Diacetyl-D-tartaric	117	−23.6[b]	118[4]	−24.57[4]
O-Monobenzoyl-D-tartaric	205～206	−4.6[c]	202～203[5]	−4.4[5]

a) One to four per cent aq. solution
b) Ten per cent acetone solution
c) Six per cent ethanol solution

of Austin[4] and Langenbeck[5] respectively.

The melting points and the optical rotations $[\alpha]_D^{20}$ of the L-2-hydroxycarboxylic acids, *O*, *O*'-diacetyl-D-tartaric acid and *O*-monobenzoyl-D-tartaric acid, used in the present work are shown in Table I.

Results and Discussion

The Effect of the pH of the Modifying Solution.—Measurements were made of the asymmetric activities of the catalyst modified at 0°C with solutions of L-2-hydroxyisovaleric acid, L-2-hydroxyisocaproic acid, L-2-hydroxy-3-methylvaleric acid and L-2-hydroxy-3-phenylpropionic acid, the pH of which had been adjusted to specified values; the results are shown in Table II.

TABLE II. EFFECT OF pH OF MODIFYING SOLUTION (AT 0°C)

Modifying reagent	pH of modifying solution	$[\alpha]_D^{20}$ of methyl 3-hydroxybutyrate
L-2-Hydroxyisovaleric acid	2.9	+1.05°
	5.0	+1.09
	10.5	−0.08
L-2-Hydroxyisocaproic acid	2.9	+1.26
	4.0	+0.71
	5.0	+0.82
	6.4	+0.76
	10.5	+0.07
L-2-Hydroxy-3-methylvaleric acid	2.9	+1.48
	5.0	+1.14
	7.4	−0.06
	10.5	−0.08
L-2-Hydroxy-3-phenylpropionic acid	2.9	+0.70
	4.0	+0.62
	5.0	+0.75
	5.8	+0.13
	7.0	+0.19
	10.5	0

The neutralization curve of L-2-hydroxy-3-phenylpropionic acid, and the asymmetric activities of the catalysts modified at 0°C with solutions of L-2-hydroxy-3-phenylpropionic acid, are shown in Fig. 1.

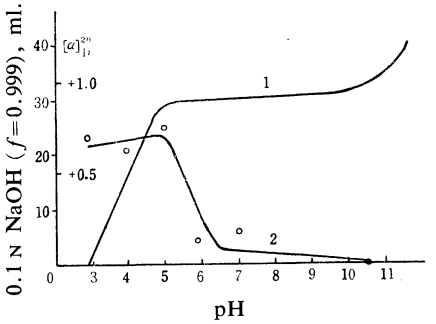


Fig. 1. Effect of pH of L-2-hydroxy-3-phenylpropionic acid solution.
Curve 1, titration curve
Curve 2, asymmetric activity of modified catalyst

With other L-2-hydroxycarboxylic acids, figures similar to those in Fig. 1 are obtained.

Greater asymmetric activities were observed when R-Ni catalysts were treated at pH values below the pH jump of the titration curves of the hydroxycarboxylic acids, as the figure and Table II show. Table II shows that the catalysts modified with L-2-hydroxycarboxylic acids at pH 2.9～10.5, at 0°C, produced dextrorotatory methyl 3-hydroxybutyrate, except for those modified with L-2-hydroxyisovaleric acid at pH 10.5 and with L-2-hydroxy-3-methylvaleric acid above pH 7.4.

The results described above show that L-2-hydroxycarboxylic acids have an asymmetric

4) P. C. Austin and J. R. Park, *J. Chem. Soc.*, **127**, 1933 (1925).
5) W. Langenbeck and O. Herbst, *Chem. Ber.*, **86**, 1524 (1953).
6) C. G. Baker and A. Meister, *J. Am. Chem. Soc.*, **73**, 1336 (1951).
7) O. Lutz and B. Jirgensons, *Ber.*, **65**, 784 (1932).
8) H. A. Dakin and H. W. Dudley, *J. Biol. Chem.*, **18**, 29 (1914).

effect upon the R-Ni catalyst the reverse of that of the corresponding 2-aminocarboxylic acids. The same relationship has been observed between L-aspartic acid and L-malic acid, as was reported in a previous paper[2].

The difference between 2-amino and 2-hydroxycarboxylic acid can be explained by the difference in the coordination form at the active metallic center of these two series of compounds. Probably the former is tetrahedral and the latter planar, so that stereochemically-different active centers are produced.

The Effect of the Modifying Temperature.—The effect of the temperature of the modifying solution was studied at pH values of 2.9 and 5.0, at 0°C and 70°C. The results are shown in Table III. The catalytic activity of the R-Ni catalyst modified at 100°C was too low to permit any hydrogenation experiments.

Under the conditions shown in Table III, dextrorotatory methyl 3-hydroxybutyrate was formed predominantly on the hydrogenation of methyl acetoacetate.

The catalysts modified at pH 2.9 always showed an increase in their asymmetric activities with an elevation of the modifying temperature. On the other hand, the asymmetric activities of the catalysts modified at pH 5.0 were not always increased by an elevation of the modifying temperature.

TABLE III. EFFECT OF TEMPERATURE OF MODIFYING SOLUTION

Modifying reagent	Modifying conditions pH	Temp., °C	$[\alpha]_D^{20}$ of methyl 3-hydroxybutyrate
L-2-Hydroxyisovaleric acid	2.9	0	+1.05°
	2.9	40	+1.45
	2.9	70	+1.48
	5.0	0	+1.09
	5.0	40	+1.17
	5.0	70	+1.31
L-2-Hydroxyisocaproic acid	2.9	0	+1.26
	2.9	40	+1.27
	2.9	70	+1.54
	5.0	0	+0.82
	5.0	40	+1.12
	5.0	70	+1.01
L-2-Hydroxy-3-methyl-valeric acid	2.9	0	+1.48
	2.9	40	+2.18
	2.9	70	+2.60
	5.0	0	+1.14
	5.0	40	+1.62
	5.0	70	+1.71
L-2-Hydroxy-3-phenyl-propionic acid	2.9	0	+0.70
	2.9	40	+1.03
	2.9	70	+1.08
	5.0	0	+0.75
	5.0	40	+0.86
	5.0	70	+0.47

Modification with *O*-Acylated D-Tatraric Acid.—Catalysts modified with *O*,*O'*-diacetyl-D-tartaric acid and *O*-monobenzoyl-D-tartaric acid were tested for their asymmetric activities in order to study the role of the hydroxy group in the modification of the catalyst.

The effect of the modifying temperature was studied at pH 5.1~5.2, since the catalyst modified at this pH with tartaric acid showed the greatest asymmetric activity, as was reported in a previous paper.[2] The results are shown in Table IV.

TABLE IV. MODIFICATION WITH *O*-ACYLATED D-TARTARIC ACID AND D-TARTARIC ACID SOLUTION

Modifying reagent	Modifying condition pH	Temp. °C	$[\alpha]_D^{20}$ of methyl 3-hydroxybutyrate
Diacetyl-D-tartaric acid	5.1	0	−0.66°
	5.1	50	−0.41
	5.1	100	−0.18
Monobenzoyl-D-tartaric acid	5.2	0	−2.15
	5.1	50	−2.64
	5.2	100	−2.29
D-Tartaric acid[2]	5.1	0	−5.30
	5.2	40	−5.25
	5.2	70	−7.23
	5.2	100	−8.37

The above results show that *O*,*O'*-diacetyl-D-tartaric acid and *O*-monobenzoyl-D-tartaric acid have smaller asymmetric effects upon the R-Ni catalyst than D-tartaric acid.

It is clearly conceivable that the hydroxy group has a certain important role in the asymmetric modification of the R-Ni catalyst, but no reasonable explanation of the effect of acylation on the mode of asymmetric catalytic activity seems possible at present.

Experimental

The Preparation of the R-Ni Catalyst.—The R-Ni catalyst used in the present work was prepared as described in a previous paper.[1]

The Modification of the Catalyst.—The modification of the catalyst was carried out as described in a previous paper.[1] One hundred milliliters of 1% aqueous solutions of each hydroxycarboxylic acid, the pH of which had been adjusted to a specified value with a N sodium hydroxide solution, were added to the newly-prepared R-Ni catalyst; these mixtures were then allowed to stand, with occasional shakings, at a constant temperature for 1.5 hr. After the modifying solution had been removed by decantation, the catalyst was washed with water and then with methanol, and then it was separated by centrifugation.

The Hydrogenation of Methyl Acetoacetate.—Newly-distilled methyl acetoacetate (17.0 g.) was hydrogenated in the presence of the modified R-Ni catalyst prepared from 1.5 g. of alloy. The reaction was run at 60°C under an initial hydrogen pressure of 80~90 kg./cm^2 in a shaking autoclave. The catalyst was filtered off, and the filtrate was distilled under reduced pressure. The main fraction was collected at 61~62°C/12 mmHg.

The Asymmetric Activity of the Catalyst.—The asymmetric activity of the catalyst was measured as described in a previous paper.[1]

Summary

1) The asymmetric activities of R-Ni catalysts modified with L-2-hydroxyisovaleric acid, L-2-hydroxyisocaproic acid, L-2-hydroxy-3-methylvaleric acid and L-2-hydroxy-3-phenylpropionic acid have been compared with those of catalysts modified with the corresponding L-amino acids, which had the same stereochemical configurations.

2) On modification with L-2-hydroxycarboxylic acids, the greatest asymmetric activities are obtained when the catalysts are treated at pH values below the pH jump of the titration curves of the acids.

3) Catalysts modified with L-2-hydroxycarboxylic acids have asymmetric activities the reverse of those modified with L-amino acids with the same configurations.

4) The modifying effects of *O*, *O'*-diacetyl-D-tartaric acid and *O*-monobenzoyl-D-tartaric acid upon the R-Ni catalyst are entirely different from that of D-tartaric acid.

Division of Organic Chemistry
Institute for Protein Research
Osaka University
Kita-ku, Osaka

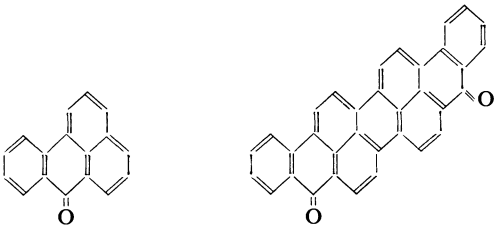
The Paramagnetism of "Violanthrone-B"

By Hideo AKAMATU, Tsuneo MAEKAWA, Yôichi IIDA and Minoru KINOSHITA

(Received January 18, 1964)

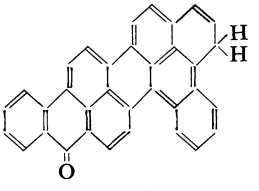
Violanthrone (II), a purplish-blue vat dye, is prepared from benzanthrone (I) by alkali fusion in the presence of phenol or sodium acetate. In this process, a dark violet compound is obtained as a by-product. Maki[1] has found that this compound is barely vattable at 65~70°C and slightly soluble in chlorobenzene, while violanthrone is insoluble; he has named this compound "violanthrone-B," as distinguished from the violanthrone which he called "violanthrone-A." He assumed formula III for this compound. However, its formula has not been definitely proven, and an alternative formula (IV) has been suggested by Aoki.[2] According to these proposed formulae, violanthrone-B consists of nine condensed rings with one carbonyl group, and one of its peripheral carbon atoms is attached by two hydrogen atoms, so that it possesses a tetrahedral type of bonding.

In a preliminary experiment, we have found that violanthrone-B is paramagnetic and shows a strong ESR absorption.[3] However, a question remains concerning its spin concentration, which has not been established. The purpose of the present investigation is to verify the paramagnetic nature of this compound. If it is a paramagnetic compound, the semiconductive properties of this compound will be of interest in comparison with those of other condensed polycyclic aromatic compounds.

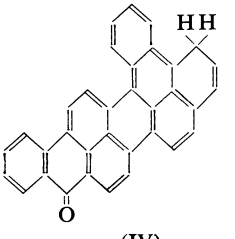


(I)

(II)



(III)



(IV)

1) T. Maki, *J. Soc. Chem. Ind., Japan* (*Kōgyō Kwagaku Zasshi*), **35**, 1441 (1932); **38**, 1390 (1935).
2) J. Aoki, This Bulletin, **34**, 1817, 1820 (1961).
3) H. Akamatu, S. Mrozowski and D. C. Wobschall, Proceedings of the 3rd. Conference on Carbon, Pergamon Press, New York (1959), p. 135.

Material

Violanthrone-B was supplied by Mr. J. Aoki, who prepared it from benzanthrone following the procedure described in Maki's paper[1] with a little modification for the condition of alkali fusion.[2] For the purpose of purification, the sublimation method is not applicable to this compound, for it is not stable enough when heated. It was boiled in glacial acetic acid for 2 hr. and then washed with ethanol. Further purification was made by chromatography. The *o*-dichlorobenzene solution of violanthrone-B was passed through the adsorption column of sodium carbonate anhydride. When the adsorbed layer was washed with the same solvent, it developed into two zones. The zone which traveled faster contained impure components and showed a greenish fluorescence under ultraviolet light. All the procedure was carried out in the dark. The separated solution was concentrated by distillation under reduced pressure, after which violanthrone-B was precipitated by adding ethanol. The absorption spectrum of the violanthrone-B is illustrated in Fig. 1.

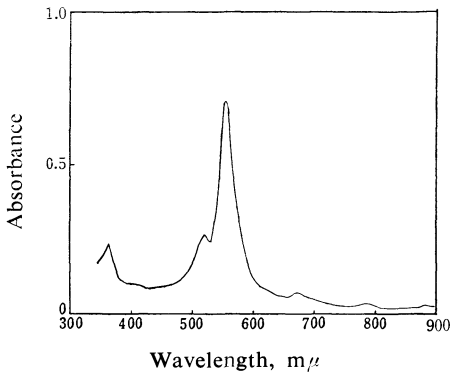


Fig. 1. The absorption spectrum of violanthrone-B in a trichlorobenzene solution.

Magnetic Susceptibility

The magnetic susceptibility of violanthrone-B and its variation with the temperature were measured by the Faraday method. All the measurements were performed under the reduced pressure of 10^{-2}mmHg.

The specific susceptibility was $+0.470\times10^{-6}$ at 259°K and increased with a lowering of the temperature. When the Curie-Weiss law is applied, the susceptibility, χ, can be described by:

$$\chi=\chi_{dia}+\frac{C}{T-\theta} \qquad (1)$$

where the first term, χ_{dia}, is the diamagnetic part of the susceptibility; the second term, the paramagnetic part; T, the absolute temperature, C, the Curie constant, and θ, the Curie point. The diamagnetic susceptibility of violanthrone-B is not known. A large value may be anticipated for a condensed polycyclic aromatic compound because of the contribution of anisotropic diamagnetism. This is ascribed to the non-localized orbitals of π-electrons and depends on the shape and the size of condensed aromatic molecules.[4] It can be said that the skeleton of the violanthrone-B molecule (III or IV) is not much different from that of the violanthrone molecule (II). Violanthrone is diamagnetic, and its molar susceptibility is -247.4×10^{-6}.[5] From this value, corrected by Pascal's rule for the difference in composition, an approximate value for the diamagnetic susceptibility of violanthrone-B was assumed as:

-252.1×10^{-6} for molar susceptibility,

or

-0.572×10^{-6} for specific susceptibility.

Using this value for χ_{dia}, a good linear relationship was obtained when $1/(\chi-\chi_{dia})$ was plotted against T. This is shown in Fig. 2. Hence, the following values were estimated for C and θ:

$$C=0.306\times10^{-3} \text{ emu°K/g.}$$
$$\theta=-45°\text{K}$$

The paramagnetism of violanthrone-B may be associated with the presence of unpaired electrons. As will be discussed in a later section, we assume that some of the violanthrone-B is in the state of a free radical. Therefore, the Curie constant may be given by:

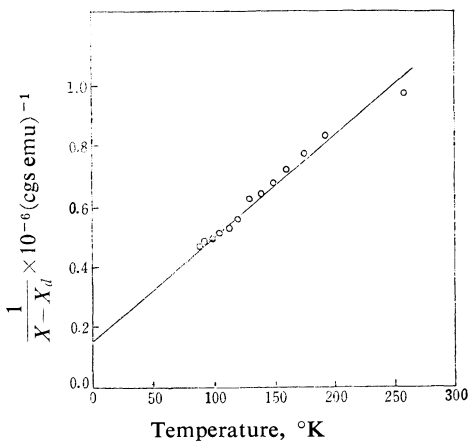


Fig. 2. The temperature dependence for the specific susceptibility of violanthrone-B.

4) H. Akamatu and Y. Matsunaga, This Bulletin, 26, 364 (1953).

5) This value is more plausible than published.[4]

$$C=\frac{Ng^2S(S+1)\beta^2}{3k} \qquad (2)$$

where k is the Boltzmann constant; β, the Bohr magneton; S, the electron spin; $g=2.00$, and N, the number of molecules, each of them possessing an unpaired electron. This gives $N=2.15\times10^{23}$ per mole. This value indicates that about 36 per cent of the molecules possess unpaired electrons.

ESR Absorption

The experiments of ESR absorption were performed at a frequency of 9400 Mc. sec^{-1} in association with a Hitachi MPS-1 spectrometer. The violanthrone-B power showed a strong absorption in a vacuum and in air. Its g-value was 2.0041 ± 0.0005, which was determined in comparison with ultramarine ($g=2.0279$). The line width at the half-intensity maximum, $\Delta H_{1/2}$, was 2.32 gauss in a vacuum. It was broadened to 3.88 gauss in air by the oxygen effect.

The spin concentration at room temperature was determined by a comparison of the integrated ESR absorption with that of a standard sample. A sample of α,α-diphenyl-β-picrylhydrazyl (DPPH) was employed as the standard sample. For this purpose, the spin concentration of the DPPH had to be known. This was determined from the magnetic susceptibility and its variation with the temperature. The Curie point of DPPH has been reported as $\theta=-17°K$.[6] Using this value, when the observed susceptibility was plotted against $1/(T-\theta)$, a good linear relationship was found in the temperature range of 80~260°K. Hence, the Curie constant for the DPPH was estimated as $C=0.857\times10^{-3}$ emu°K/g., and the diamagnetic susceptibility as $\chi_{dia}=-0.533\times10^{-6}$ emu/g. (or -210×10^{-6} emu/mol.). Equation 2 can be applied to its Curie constant. This gives the spin concentration $N=5.42\times10^{23}$ per mole. Thus, our sample of DPPH contained free radicals of 90.3 per cent of all the moles.[7]

In practice, a subsidiary standard sample was used. This was a sample of "crude" violanthrone,[8] the spin concentration of which was determined in comparison with the standard DPPH.

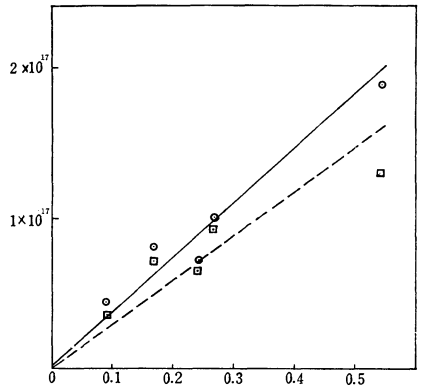


Fig. 3. The number of unpaired electrons in violanthrone-B.
⊙—— in vacuo, ⊡- - - in air

The number of spins of violanthrone-B was measured in air and in a vacuum for the same specimen. The results are shown in Fig. 3. The spin concentration was estimated as 4.9×10^{20} per g. in air and 5.9×10^{20} per g. in vacuum. When we assume that a spin center is a molecule which possesses an unpaired electron, the number of such molecules will be 35.7 per cent of the total molecules in air, and 42.7 per cent of those in a vacuum. A slightly larger value was thus observed in a vacuum than in air. However, the difference is so small as to be within the range of experimental error; thus one can say that the air has essentially no effect on the spin concentration. On the average, the molecules of 39 per cent of the total molecules possess unpaired electrons.

In some cases, the spin population of a solid material increases when the material is ground. In such a case, one can assume a spin center which is ascribed to a trapped electron at a crystal defect. This was not the case with violanthrone-B. For violanthrone-B, when it was ground in an agate-mortar to a fine powder, the line width increased to 5.3 gauss in air, but no appreciable change in the spin concentration has been found.

Furthermore, the ESR-absorption of the violanthrone-B was observed in a dilute solution in trichlorobenzene (0.1 mg. per 1.). Although the hyperfine structure could not be resolved, the absorption line spread into a broad one, the over-all width of which was about 30 gauss.

6) J. Turkevich and P. Selwood, *J. Am. Chem. Soc.*, 63, 1077 (1941); W. Duffy, Jr., *J. Chem. Phys.*, 36, 490 (1962).

7) The purity of the DPPH was determined on the basis of its paramagnetism. Alternatively, spectroscopy can be used for the same purpose. For a chloroform solution of the same sample, the absorbance at absorption maximum (532.5 mμ) gave the extinction coefficient $\varepsilon=30.9\,g^{-1}l.\,cm^{-1}$ for DPPH, after correction had been made for the free radical content as determined from its magnetic susceptibility. The value of $32.3\,g^{-1}l.\,cm^{-1}$ for chemically-pure DPPH has been reported by J. A. Lyons and W. F. Watson [*J. Poly. Sci.*, 18, 141 (1955).].

8) The ESR absorption of violanthrone was reported by Y. Yokozawa and I. Tatsuzaki [*J. Chem. Phys.*, 22, 2087 (1954)]. It has been found, however, that the spin concentration of this substance decreased progressively when it was purified repeatedly. Therefore, a large part of the unpaired spins in "crude" violanthrone seem due to the presence of an impurity. The most probable impurity is violanthrone-B.

After the solution had been kept in a cool, dark place for a month, no appreciable change in the signal intensity was found. This indicates that the absorption is due to a fairly stable free radical.

Physico-Chemical Properties

Violanthrone-B is not stable in solution when it is kept in the light. Its *o*-dichlorobenzene solution gradually lost its deep violet color when it was illuminated with ultraviolet light from a mercury lamp. It was also found that the spectroscopic concentration of violanthrone-B decreased rapidly. In this process, a black substance precipitated, and a benzene-soluble product was obtained. Neither part of the products showed any appreciable ESR absorption.

It is well known that, in a polymerization reaction, a stable free radical, for instance DPPH, can terminate the chain propagation. The effect of violanthrone-B on the thermal polymerization of stylene at 80~100°C was examined in comparison with that of DPPH. The rate of polymerization was measured qualitatively by the increase of viscosity. It was remarkably supressed when stylene contained violanthrone-B or DPPH in a concentration of one milligram per 100 cc. The color of both solutions was deep violet at the beginning, but it changed to orange for the violanthrone-B solution and to colorless for the DPPH solution as the polymerization reaction proceeded. It was concluded that violanthrone-B inhibited the thermal polymerization of stylene even more strongly than did DPPH.

Semiconductivity

The electrical resistivity of violanthrone-B and its variation when temperature ranges from 10 to 160°C were examined with the DC method. The measurements were performed with the sample powder under a compression of 80 kg. per cm^2 between brass electrodes in a quartz cylinder. A good linear relationship was obtained when the logarithm of the resistivity was plotted against the reciprocal of the absolute temperature. Hence, the resistivity (ρ) was described by:

$$\rho = \rho_0 \exp(E/\boldsymbol{k}T) \qquad (3)$$

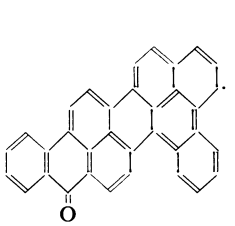
where E, the activation energy for conduction, was 0.34 ± 0.01 eV. and ρ_0 was 8.5 ohm. cm; the resistivity at room temperature was $\rho_{15°} = 6.9 \times 10^6$ ohm. cm. These data should be compared with those for violanthrone: $E = 0.39_5$ eV., $\rho_0 = 1.6 \times 10^4$ ohm. cm. and $\rho_{15°} = 1.1 \times 10^{11}$ ohm. cm.

Discussion

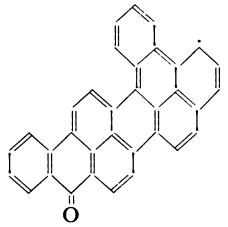
Polycyclic aromatics give often a signal of ESR absorption. The origin of spin centers is not known. Usually these signals are weak and are considered to be due to impurities which could be produced incidentally in synthetic processes. In such cases, the signal decreases as the sample is purified repeatedly. However, this was not the case with violanthrone-B. The crude sample of violanthrone-B gave an absorption with a broad line width. When it was purified by chromatography, the line width became narrower and the integrated intensity increased.

There are many reasons to believe that the observed paramagnetism for violanthrone-B is of a free radical. The g-value observed, 2.0041, is similar to those of many organic free radicals. The absorption line width is as narrow as 2.32 gauss, as is characteristic of crystalline-stable free radicals. The same can be said for the relatively high negative Curie point of $-45°K$.[6] The ESR absorption is observable in a dilute solution; this implies that a spin center exists on a molecule. Furthermore, the physico-chemical behavior also suggests the free radical nature of violanthrone-B.

If the observed paramagnetism is a property of violanthrone-B, instead of the structure III or IV, $C_{34}H_{18}O$, the structure V or VI, $C_{34}H_{17}O$, can be assumed as the most plausible one to explain its free radical nature. The tetrahedral bonding in the former structures is replaced by a trigonal bonding in the latter structures, in which the unpaired electron will be delocalized and in which it will be stabilized by some delocalization energy.



(V)



(VI)

Assuming the free radical $C_{34}H_{17}O$, its concentration was estimated from the spin concentration which was observed to be 39 per cent of all the moles. This value coincides with the result of magnetic susceptibility measurements. Hence, although not all the molecules are free radicals, two out of five molecules are. Thus, violanthrone-B might be a mixture of $C_{34}H_{18}O$ and $C_{34}H_{17}O$.

It is uncertain that these two species are in

a chemical equilibrium:

$$C_{34}H_{18}O = C_{34}H_{17}O + \frac{1}{2}H_2$$

However, the free radical may be produced by such a dissociation process. Thus, violanthrone-B behaves as if it were a free radical.

There remain a few points to be discussed. There is no direct proof for the proposed structure, V or VI. Hoping to derive information from the infrared absorption spectrum, we examined it by the KBr-disk technique. The stretching vibration of C=O of violanthrone-B is of particular interest in comparison with that of violanthrone. For violanthrone the absorption peak due to the C=O stretching was observed at 1642 cm^{-1}, while for the violanthrone-B two peaks were observed, at 1619 cm^{-1} and 1643 cm^{-1}, in the same region of frequency. The latter peak coincides with that of violanthrone and may be ascribed to the C=O stretching of $C_{34}H_{18}O$. The peak at 1619 cm^{-1}, which fairly shifts to the low-wave number side, might be due to the C=O stretching of $C_{34}H_{17}O$; this implies somewhat of a reduction of the bond order, which can result from the contribution of the structure of $\geqslant C-\dot{O}$ because of the delocalization of the unpaired electron.

Usually the sharp line width of ESR absorption is ascribed to the narrowing that occurs when electrons are exchanged between the orbitals of different molecules. The line width of violanthrone-B was as narrow as 2.32 gauss, which is comparable with that of DPPH, 2.4 gauss.[9] In this case, however, not all the molecules are free radicals; only two out of five molecules have unpaired spins, and they still showed the effect of exchange interaction.

The semiconductive property of violanthrone-B may be interestingly compared with that of violanthrone, as the molecules of these two compounds have nearly the same shape and size, even though the former has a free radical character. Eley[10] has proposed a potential box model to describe the semiconductive properties of organic solids. This model, assuming the tunnel effect for electron transfer between molecules, indicated that a solid free radical would behave as a semiconductor, with a very small or zero energy gap ($\varepsilon = 2E$). The small value of the activation energy of DPPH (0.13 eV.) was interpreted by means of this model. This theory can not be strictly applied to violanthrone-B, as it contains free radicals only partially. Nevertheless, it is noteworthy that no apprecible difference in the activation energy between violanthrone-B and violanthrone could be found. On the other hand, the electrical conductivity of violanthrone-B is improved more than 10^4 times at room temperature as compared with that of violanthrone. The higher conductivity of violanthrone-B may be ascribed to its free radical character. However, the mechanism for the contribution of unpaired electrons to the conduction still remains in question.

9) H. Inokuchi and M. Kinoshita, This Bulletin, 33, 1627 (1960).

10) D. D. Eley and G. D. Parfitt, *Trans. Faraday Soc.*, 51, 1529 (1955); D. D. Eley and M. R. Willis, Symposium on Electrical Conductivity in Organic Solids, Wiley, New York (1960).

Summary

The paramagnetic nature of "violanthrone-B" has been studied. The spin concentration in this substance has been determined by the ESR absorption, which is consistent with the value estimated from the magnetic susceptibility and its variation with the temperature. It has been concluded that the molecules of violanthrone-B, in the amount of about 40 per cent of all the molecules, are in a free radical state. It has been suggested, according to the proposed structure of violanthrone-B, that the free radical might result from detaching a hydrogen atom from a peripheral carbon of the tetrahedral type of bonding, which changes thereafter to the trigonal type of bonding.

The authors wish to express their thanks to Mr. Junji Aoki, who prepared the sample of violanthrone-B, and to Dr. Chizuko Tanaka, who examined the infrared absorption spectra of violanthrone and violanthrone-B.

Department of Chemistry
Faculty of Science
The University of Tokyo
Hongo, Tokyo

*The Synthesis of Deuterated Polypropylenes**

By Shunsuke MURAHASHI, Shun'ichi NOZAKURA and Katsutoshi YASUFUKU

(Received January 18, 1964)

The deuteration of polymers is a useful method for the structural study of high polymers. In previous papers,[1] the authors reported the infrared spectroscopic study of deuterated polystyrenes and were led to the conclusion that some of infrared crystalline sensitive bands observed in isotactic polystyrene originate from the helical structure of the polymer.

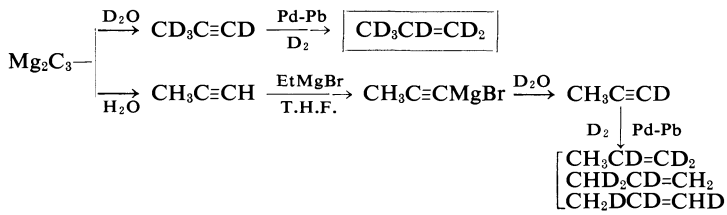
The structure of isotactic polypropylene is being investigated extensively by many authors using infrared spectra of deuterated polymers. Propylene-*cis*-1-d_1, -*trans*-1-d_1,[2] -1, 1-d_2, -2-d_1,[3,4] -3, 3, 3-d_3,[4] and -3-d_1,[5] have hitherto been prepared, and the infrared spectra of their polymers have been discussed.

In the present paper, for the purpose of an infrared spectroscopic study of isotactic polypropylene, the authors carried out the preparation and polymerization of propylene-1, 1, 2-d_3 and -d_6. A recent note by Liang and Lytton[6] on polypropylene-d_6 prompted the present authors to report on the syntheses of the two polymers and on interesting information obtained from the copolymerization of the monomers. A more detailed study of infrared spectra of the polymers will be published elsewhere.

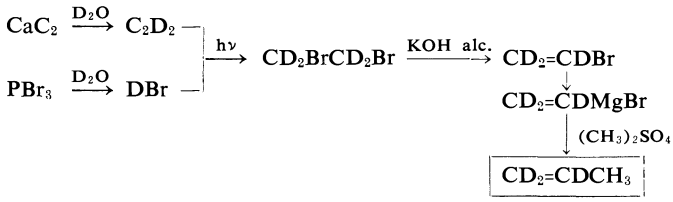
Results and Discussion

Propylene-d_6 was prepared by the half-reduction of deuterated propyne, which had been obtained from the hydrolysis of magnesium carbide (method 1) with deuterium oxide. Method 1 was proved unsuitable for the preparation of propylene-1, 1, 2-d_3. It was, however, successfully prepared by the reaction of deuterated vinyl magnesium bromide (method 2). Methods 3 and 4 were also tried. However, method 3 gave a very low overall yield in preliminary runs, while method 4 gave an impure propyl alcohol which was found rather difficult to purify and so was felt unsuitable for the synthesis of the pure end product.

Propylene-d_6.—Magnesium carbide is the only carbide which gives C_3-acetylenic hydrocarbon on hydrolysis.[7] The preparation of propyne-d_4 from magnesium carbide was reported by Leitch.[8] Using the method of Novak,[7] magnesium carbide was prepared by the reaction of



Method 1



Method 2

* Paper XI in a series on "Stereoregular Polymers." For the preceding paper, see This Bulletin, **35**, 1686 (1962).

1) H. Tadokoro, T. Kitazawa, S. Nozakura and S. Murahashi, *Chem. High Polymer (Kobunshi Kagaku)*, **17**, 231 (1961); This Bulletin, **34**, 381 (1961).

2) G. Natta, *SPE Journal*, **15**, 373 (1959).

3) M. Peraldo and M. Farina, *Chim. e ind.*, **42**, 1349 (1960).

4) C. Y. Liang and M. R. Lytton, *J. Polymer Sci.*, **44**, 549 (1960); **54**, 523 (1961).

5) H. Tadokoro, T. Kitazawa, S. Nozakura and S. Murahashi, This Bulletin, **34**, 1209 (1961).

6) C. Y. Liang and M. R. Lytton, *J. Polymer Sci.*, **61**, S45 (1962).

7) J. Novak, *Z. physik. Chem.*, **73**, 513 (1910).

8) L. C. Leitch and R. Renaud, *Can. J. Chem.*, **30**, 79 (1952).

$$CD_3CDO \xrightarrow[HCl]{EtOH} CD_3CDClOEt \xrightarrow{Br_2} CD_2BrCDBr\text{-}O\text{-}Et$$

$$CD_2BrCDBr\text{-}O\text{-}Et \xrightarrow{CH_3MgBr} CD_2BrCD(CH_3)\text{-}O\text{-}Et$$

$$CD_2BrCD(CH_3)\text{-}O\text{-}Et \xrightarrow{Zn} CD_2{=}CDCH_3$$

Method 3

$$CD_2\text{-}CD_2 \xrightarrow{CH_3MgBr} CH_3CD_2CD_2OH \rightarrow CH_3CD{=}CD_2$$

(O)

Method 4

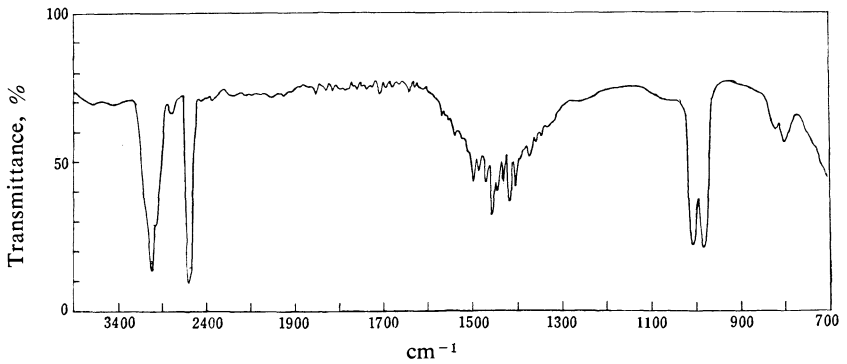


Fig. 1. IR spectrum of propyne-1-d_1.

magnesium metal and *n*-pentane at 680±20°C. Hydrolysis of the carbide with deuterium oxide gave crude propyne-d_4, which contained allene (11.2%) and acetylene (0.4%) as by-products. Acetylene was removed from the crude product by repeated distillation. The propyne, which still contained allene, was used in subsequent hydrogenation without further purification. The degree of the deuteration of propyne was estimated by mass spectrographic analysis to be 88.5%. The product was then deuterated over a Lindlar catalyst to propylene-d_6, which was found to contain a considerable amount of propane-d_8 (15.7%) and the unreacted propyne-d_4 (6.0%) the latter being removed as mercuric salt. The propylene, which still contained propane, was used for the polymerization without further purification, since the existence of propane does not impair the succeeding polymerization or the resulting polymer. The degree of the deuteration of propane-d_8 was found to be 78.7% by mass spectrography, and so that of propylene-d_6 could be estimated to be around 82%.

Method 1 was found to be unsuitable for the synthesis of propylene-1, 1, 2-d_3. Propyne-1-d_1, which was obtained by the hydrolysis of propynyl magnesium bromide with deuterium oxide, was found to be highly deuterated, showing no ≡C–H stretching band at 3300 cm^{-1} and a strong ≡C–D stretching absorption at 2550 cm^{-1} in the infrared spectrum (Fig. 1). After the half-reduction with deuterium, however, the product showed a weak absorption at 3060 cm^{-1}, indicating the presence of $=CH_2$ and/or =CHD. Furthermore, a polymer obtained from this product showed a $-CH_2-$ stretching absorption at 2836 cm^{-1}, the inten-

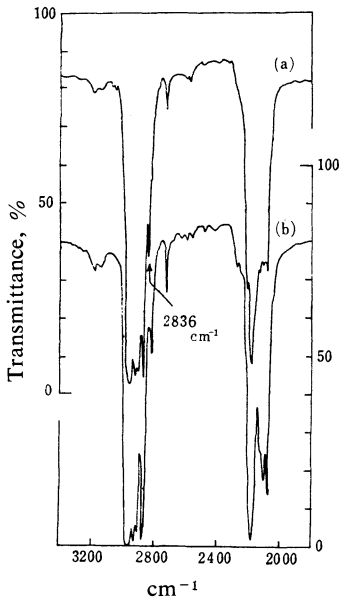


Fig. 2. IR spectra of isotactic polypropylene-1,1,2-d_3, (a) prepared by method 1 and (b) by method 2.

sity of which suggests the existence of more than 15% $-CH_2-$ units in total methylene units (Fig. 2). This unexpectedly high $=CH_2$ group content suggests that there is an equilibrium between propyne and allene on the surface of the Lindlar catalyst. The equilibrium concentration of allene at 100°C is known to be about 14%,[9] and allene is known to be more rapidly hydrogenated than propyne.[10] The observed values of more than 15% $-CH_2-$ in the polymer mentioned above indicates the existence of more than 30% allene in the mixture with propyne. Therefore, allene should have been supplied continuously by the isomerization of propyne during hydrogenation.

Propylene-1, 1, 2-d_3.—Propylene-1, 1, 2-d_3 was successfully prepared by method 2 starting from calcium carbide. The yield of the dedeuterobromination product of deutero-dibromoethane was found to be rather low (30%) compared with the yield of more than 70% in the case of the dehydrobromination of dibromoethane. The yield in the former case could not be improved by various modifications of reaction conditions. This may be explained as follows: The reaction can be considered competitive between an elimination and a substitution reaction. It is known that the substitution reaction is usually accelerated by the deuteration of the substrate ($k_D/k_H = \sim 1.1$),[11] while the elimination reaction is retarded ($k_D/k_H = 1/4 \sim 1/6$).[12] The observed isotope effect in the yield of vinyl bromide, therefore, may be the result of the composite effect of two competing reactions.

The reaction of deuterated vinyl magnesium bromide with dimethyl sulfate gave propylene-1, 1, 2-d_3 in a good yield. The impurity was found by gas chromatography to consist of very small amounts of ethane and butadiene. Since butadiene was expected to be objectionable in the preparation of the pure polymer, it was removed by repeated distillation. The degree of the deuteration of the propylene-1, 1, 2-d_3 thus prepared was estimated to be fairly high from the fact that its infrared absorption spectrum did not show any of the characteristic absorptions which are ascribed to the other partially-deuterated propylenes[13] (Fig. 3). A notable difference of between the infrared spectrum and those of the other deuteropropylenes is found in the position of the stretching mode of the C=C double bond. Propylene-1, 1, 2-d_3 shows the absorption at 1604 cm^{-1}, while propylene, propylene-2-d_1, -1, 1-d_2, and -d_6 show it at 1651, 1613, 1612 and 1587 cm^{-1} respectively.[14]

Polymerization.—The deuterated propylenes obtained above were polymerized to isotactic polymers with a Ziegler-Natta catalyst. The results are shown in Table I, while infrared spectra of the polymers are presented in Fig. 4.

The Infrared Characteristics of Copolymer.—An interesting fact was observed in the infrared spectrum of the copolymer of propylene-

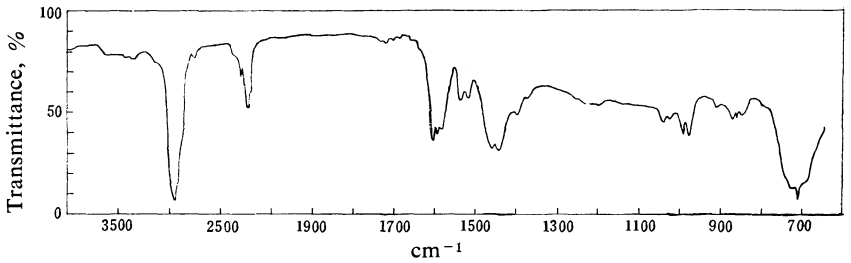


Fig. 3. IR spectrum of propylene-1,1,2-d_3.

TABLE I. POLYMERIZATION OF PROPYLENES WITH $TiCl_3$-$AlEt_3$ CATALYST IN HEPTANE AT 60°C

Monomer	g.	Catalyst		Polymn. time hr.	Polymer yield g.	Heptane insoluble part	
		Ti/monomer	Ti/Al			% in total polymer*	M. p. °C
$CD_3CD=CD_2$	ca. 2.3	0.04	1.0	67	1.7	80.9	166
$CH_3CD=CD_2$	ca. 1.3	0.02	0.9	46	1.2	56.0	167

* Extracted with boiling heptane for 10 hr.

9) J. F. Cordes and H. Gunzler, *Chem. Ber.*, **92**, 1055 (1959).
10) G. C. Bond and J. Sheridan, *Trans. Faraday Soc.*, **48**, 651 (1952).
11) S. I. Miller, *J. Phys. Chem.*, **66**, 978 (1962).
12) K. B. Wiberg, *Chem. Revs.*, **55**, 713 (1955).
13) M. Farina and M. Peraldo, *Gazz. chim. ital.*, **90**, 973 (1960).
14) G. Zerbi, M. Peraldo and E. Mantica, International Symposium on Molecular Structure and Spectroscopy, Tokyo, Papers of Abstract, C213-1, 1962.

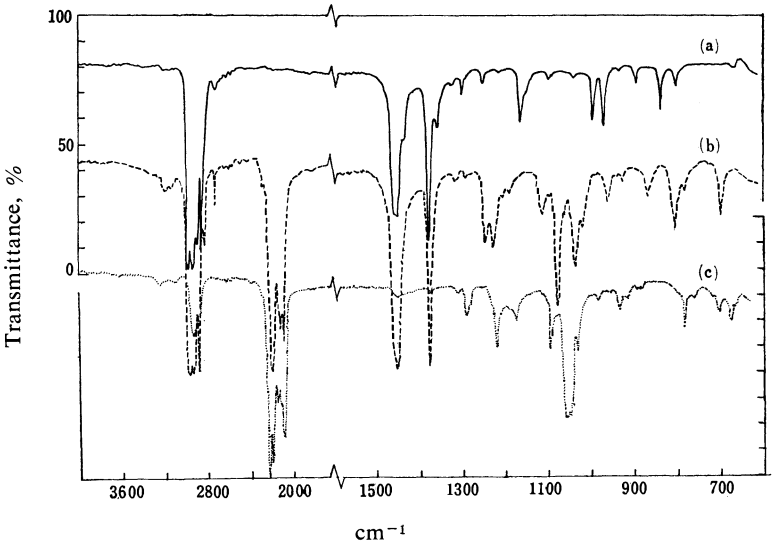


Fig. 4. IR spectra of isotactic polypropylene (a), propylene-1,1,2-d_3 (b), and polypropylene-d_6 (c).

1,1,2-d_3 and propylene. The isotactic copolymer is compared with an artificial mixture of the isotactic homopolymers of these two monomers in Fig. 5. An X-ray examination of the copolymer specimen showed the same order of crystallinity as those of the homopolymers. However, the infrared spectrum of the copolymer is quite dfferent from that of the artificial mixture. The crystalline sensitive bands (shown by arrows in Fig. 5) of polypropylene exist in the spectrum of the artificial mixture, but they do not exist or diminish in that of the copolymer. This suggests that the occurrence of crystalline-sensitive bands in isotactic polypropylene is not due to intermolecular interaction but to intramolecular interaction, as in the case of isotactic polystyrene.[1] If the crystalline-sensitive bands were originated from intermolecular interaction, they would disappear, or at least diminish, in the case of the artificial mixture too. The fact also suggests a random distribution of the deuterated monomer units along a polymer chain, resulting in the complete disturbance of the original intrachain interaction.

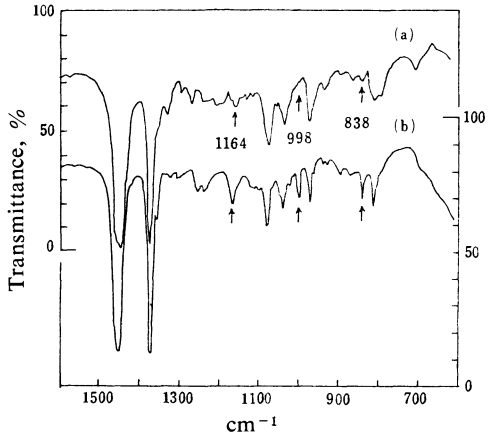


Fig. 5. IR spectra of isotactic propylene-propylene-1,1,2-d_3 copolymer (a), and an artificial mixture of the two homopolymers having the same composition (b). Arrows show the crystalline sensitive bands of the isotactic polypropylene.

Experimental

Mg_2C_3.—Magnesium carbide was prepared by the method of Novak.[7] The vapor of pentane (100 cc.) with a stream of hydrogen was brought into contact with magnesium powder (20 g.) at 680±20°C for 6 hr., yielding 27 g. of the dark gray carbide covered with black carbon powder. On hydrolysis the carbide (20 g.) evolved a gas which was condensed by a dry ice-acetone trap to 14 ml. (−78°C) of liquid products. The gas was found by gas chromatography (1m. silica gel column, 100°C) to be composed of 89.2% propyne, 10.4% allene and 0.4% acetylene.

Propyne-1, 3, 3, 3, d_4.—In a 100 ml. three-necked flask equipped with a stirrer, a condenser and a dropping funnel, magnesium carbide (20 g.) was placed suspended in 50 ml. of dry dioxane. The top of the condenser was connected to a trap kept at about −20°C and then to a collecting trap cooled in dry ice-acetone. Deuterium oxide (26 g., 99.65% purity) was added drop by drop to magnesium carbide at room temperature, yielding 12 ml. (−78°C) of a liquid product. The product was found by gas chromatography to contain 88.4% deuterated propyne, 11.2% deuterated allene and 0.4% deuterated acetylene. In order to remove acetylene, the product was evaporated at about −25°C and condensed at −78°C. Evaporation and

condensation was repeated several times until no acetylene was detected by gas chromatography. The degree of deuteration of the C_3D_4 mixture was found to be 88.5% by mass spectrography.

Propyne-1-d_1.—A mixture of propyne and allene was obtained by the hydrolysis of magnesium carbide with water, and it was freed from acetylene in a manner similar to that mentioned above. The mixture was passed through a solution of ethyl magnesium bromide in tetrahydrofuran, and the unreacted component, allene, was swept by a stream of dry nitrogen while the solution was being refluxed. The tetrahydrofuran solution of propynyl magnesium bromide thus obtained was hydrolyzed by a solution of deuterium oxide (15 g.) in tetrahydrofuran, yielding 14 ml. (−78°C) of propyne-1-d_1. A trace of impurity, ethane-1-d_1, was removed by repeated distillation. The infrared spectrum of the product showed no absorptoin at 3300 cm^{-1}.

Propylene-d_6.—The Lindlar catalyst was prepared as follows. Palladium chloride was dissolved in dilute hydrochloric acid and then absorbed on pumice[10] (Pd/pumice=1/100) by evaporating the solvent. The supported palladium chloride (10 g.) was reduced in a stream of hydrogen at 300°C, and then the cooled catalyst was poisoned by treating it with an aqueous solution of 0.34 g. $Pb(OAc)_4 \cdot 3H_2O$. Propyne-1, 3, 3, 3-d_4 (12 ml. of a liquid at −78°C) was reduced in the stream of deuterium at a flow ratio of $CD_3C{\equiv}CD/D_2=1.2$ at 60～90°C over 8 g. of the Lindlar catalyst. The catalyst had been pretreated by deuterium three times at 70°C in vacuo before use. The product was 6 ml. (at −78°C) of a liquid, which was found to be composed of 15.7% deuterated propane, 78.7% propylene and 6.0% unreacted propyne. The crude product was freed from propyne by treatment with a mixed solution of mercuric iodide (0.4 g.), potassium iodide (0.5 g.), potassium hydroxide (0.3 g.) and water (3 ml.) in a pressure-glass bottle at room temperature. The final product was found to be composed of 14.7% propane-d_8 and 85.3% propylene-d_6. The degree of the deuteration of propane-d_8 was found to be 78.7% by mass spectrography. That of propylene-d_6 could not be measured directly from a mass spectrum, but it may be estimated at 82% if we assume that the same order of impurity was introduced at each step of the reduction.

Dibromoethane-d_4.—Acetylene-d_2, deuterium bromide and dibromoethane-d_4 were prepared by the method of Leitch.[15] The yield of acetylene-d_2 was 75% and that of deuterium bromide was 94% based on deuterium oxide. Dibromoethane-d_4 was obtained by photochemical addition reaction in a vacuum system. The crude product was washed with a dilute aqueous solution of potassium carbonate, dried with sodium sulfate, and distilled; b. p. 128～129°C. The yield was 93% from acetylene.

Vinyl-bromide-d_3.—In a 500 ml. three-necked flask equipped with a stirrer, a Dimroth condenser cooled at 20°C and a dropping funnel, a mixture of 120 ml. of water, 200 ml. of ethanol and 20 g. of potassium hydroxide was placed. Dibromoethane-d_4 (80 g.) was stirred into the mixture at 50°C. Vinyl-bromide-d_3 gas was evolved gradually for 2 hr. and was then condensed in a cold trap. The crude product was dried over calcium chloride overnight and then distilled through a Vigreux column, yielding 14.1 g. of the product (31%) (b.p. 17.3°C).

Propylene-1, 1, 2-d_3.—In a 200 ml. two-necked flask equipped with a magnetic stirrer, a dropping funnel, and a reflux condenser with a gas outlet tube, a dioxane solution of vinyl magnesium bromide-d_3 was prepared under nitrogen from magnesium (2.92 g.) vinyl-bromide-d_3 (12.9 g.), and tetrahydrofuran (50 ml.). The content of the flask was degassed twice and covered with nitrogen. The outlet tube was connected with a trap kept at −20°C and then with a trap cooled at −78°C. Then, 15.2 g. of dimethyl sulfate dissolved in 10 ml. of tetrahydrofuran was vigorously stirred in at room temperature over a one-hour period and heating was continued for an additional two hours. The evolved gaseous product was condensed in the second trap. The yield was 70% (6 ml. at −78°C). The product was found to contain small amounts of ethane and butadiene, which were removed by repeated distillation.

Polymerization.—Polymerizations were carried out in glass pressure tubes. The monomer was charged in vacuo into the tube in which Ziegler-Natta catalyst had previously been prepared, and it was polymerized with occasional shaking at 60°C. The polymerization was quenched by the addition of a methanol-concentrated hydrochloric acid mixture. The precipitated polymer was washed with methanol and dried in vacuo. The atactic part of the polymer was removed by extraction with boiling heptane for 10 hr.

Copolymerization.—Propylene-1, 1, 2-d_3 (0.526 g.) and propylene (0.415 g.) were charged and weighed successively. The mixture of the monomers was transferred by vacuum technique to the polymerization tube containing the catalyst and polymerized for 5.3 hr.

Artificial Mixture.—A mixture of isotactic polypropylene-1, 1, 2-d_3 and isotactic polypropylene was dissolved in toluene at 130°C and precipitated by pouring the hot solution into methanol.

Summary

The synthesis of propylene-d_6 and propylene-1, 1, 2-d_3 has been attempted for the purpose of an infrared spectroscopic study of the isotactic polymers.

Propylene-d_6 has been synthesized by the half-deuteration of the propyne-d_4 which had been obtained by the hydrolysis of magnesium carbide with deuterium oxide, and propylene-1, 1, 2-d_3 has been synthesized by the reaction of deuterovinyl magnesium bromide and dimethyl sulfate. In the half-reduction of propyne-d_1 with a Lindlar catalyst, it was found that an equilibrium between propyne-1-d_1 and allene-1-d_1 exists on the catalyst.

The polymerization of these monomers was carried out with a Ziegler-Natta catalyst, and

15) L. C. Leitch and A. T. Morse, *Can. J. Chem.*, **30**, 924 (1952).

isotactic polymers were obtained. In the copolymerization of propylene and propylene-1,1,2-d_3 with a Ziegler-Natta catalyst, it was observed that some of the infrared crystalline sensitive bands of isotactic polypropylene, 1164, 998 and 838 cm^{-1}, do not exist (or at least diminish) in the copolymer but do exist in artificial mixtures of the homopolymers. This fact evidently suggests that these infrared bands are due to an intrachain interaction in the crystalline part of the polymer.

Department of Polymer Science
Faculty of Science
Osaka University
Nakanoshima, Osaka (S. M. & S. N.)

Institute of Physical & Chemical Research
Bunkyo-ku, Tokyo (K. Y.)

The Synthesis of S-Guaiazulene from Hinokitiol

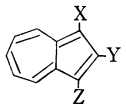
By Yoshio KITAHARA and Tadahiro KATO

(Received January 30, 1964)

In recent years, a marvelous method of synthesizing azulenes have been developed by Nozoe and his co-workers.[1,2] This method is based on the reaction of tropolone methyl ether (1: X=OCH_3) or 2-halotropones (1: X=Cl, Br) with malononitrile or ethyl cyanoacetate in the presence of sodium methoxide, and it is particularly useful for the synthesis of azulenes (2) having substituents (X, Y and Z) at their 1-, 2- and 3-positions.



(1)

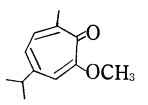


(2)

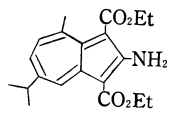
Thus, a number of azulene derivatives of this type were obtained and examined for their properties. Azulene itself (2: X, Y and Z=H) was successfully derived, by the same authors, from 1,3-dicarboethoxy-2-aminoazulene (2: X and Z=CO_2Et, Y=NH_2), which might be recorded as one of the important azulene syntheses.

The syntheses of natural azulenes from tropolones by the above method have, however, so far been unsuccessful.

It was reported,[3] for instance, that in the reaction of 2-methoxy-4-isopropyl-7-methyltropone (3) and cyano ethyl acetate under similar conditions, the formation of an azulene nucleus (4) was impossible because of the steric interference of the methyl group at the 7 position.



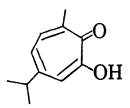
(3)



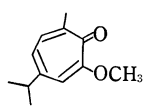
(4)

We tried to synthesize *S*-guaiazulene from hinokitiol although this compound had already been synthesized by Plattner and his coworkers.[4]

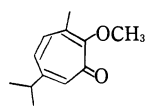
3-Methyl-6-isopropyltropolone (I)[5] gives its methyl ether almost quantitatively by reaction with diazomethane. This methyl ether is assumed to be a mixture of IIa and IIb, which are possible isomers to each other.



(I)

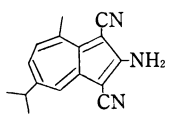


(IIa)

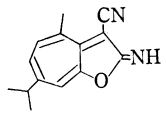


(IIb)

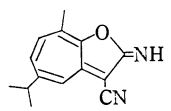
1,3-Dicyano-2-aminoazulene derivative III was obtained in a 48% yield by the addition of malononitrile directly to the mixture of IIa and IIb in the presence of sodium methoxide. In this reaction a small amount of a compound (m. p. 140°C) corresponding to IVa or IVb was isolated.



(III)



(IVa)



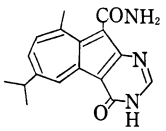
(IVb)

It is known that cyano groups at the 1 and

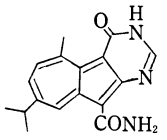
1) T. Nozoe, S. Matsumura, Y. Murase and S. Seto, *Chem. & Ind.*, **1955**, 1257.
2) T. Nozoe, S. Seto, S. Matsumura and Y. Murase, This Bulletin, 35, 1179 (1962).
3) T. Asano, Ph. D. Thesis, Tohoku University (1959).
4) Pl. A. Plattner, A. Furst, L. Marti and H. Schmid, *Helv. Chim. Acta.*, 32, 2137 (1949).
5) See Experimental Section.

3 positions of the azulene nucleus are generally very stable and resist hydrolysis in acids and alkalis.[6-8] However, when III was heated in a mixture of concentrated sulfuric acid and formic acid, it gave a red crystalline compound, the infrared spectrum of which indicates the absence of a cyano group and which has multiple bands in the 3100~3400 cm^{-1} region which are more complicated than those of III. This suggests the presence of a carbamoyl group.

This compound is deduced to have the structure Va from the results of micro analysis and from its behavior with relation to bases (it does not dissolve in a sodium bicarbonate solution although it does dissolve in a 2 N solution of sodium hydroxide, and the original substance is recovered on acidification).



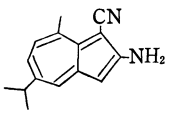
(Va)



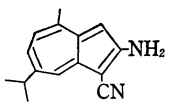
(Vb)

An attribution of the structure Vb to this compound is also possible, but, as will be mentioned later, the cyano group at the 1 position is more apt to be hydrolyzed than the other one. Therefore, Va rather than Vb seems to be more probable for this compound.

When III was heated in concentrated sulfuric acid for a considerable period, it blackened, evolving sulfur dioxide gas, and did not afford any clear product. However, when III was heated in 100% phosphoric acid[9] at 100°C, it gradually generated bubbles to yield a red crystalline compound in a 65% yield. Its infrared spectrum has a band of one cyano group (2150 cm^{-1}); its micro analysis data fits either VIa or VIb.



(VIa)



(VIb)

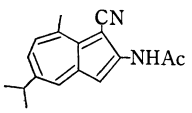
This hydrolysis is considered to proceed through the phosphoric acid ester formed with phosphoric acid and the cyano group. The formation of phosphoric acid ester from the cyano group at the 3-position might be difficult because of the steric interference of the methyl group at the peri position; accordingly, hydrolysis of the cyano group will also become difficult. Therefore, the obtained product is deduced to have the structure VIa. This deduction was finally proved to be true by the synthesis of *S*-guaiazulene from this compound.

We next tried to introduce a formyl group to the 1 position of VIa. It was already known[10] that the 1- and 3-positions of azulenes are easily formylated by the application of the Vilsmeier-Haack reaction.[11]

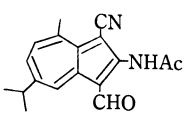
After the acetylation of the amino group at the 2-position of VIa, the acetylamino compound VII was treated with phosphorous oxychloride-dimethylformamide. Two compounds were produced, m. p. 176°C, and m. p. 232°C (decomp.), in a ratio of almost 3 : 1.

The infrared spectrum of the compound (m. p. 176°C) indicates the presence of a formyl group (2850 and 1626 cm^{-1}), and an acetyl group (1708 cm^{-1}), and the results of its micro analysis are satisfactory for 1-cyano-2-acetylamino-3-formylazulene (VIII). The alkaline hydrolysis of VIII gave X, the formyl group of which reacts easily with hydrazine to give XI.

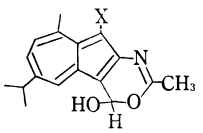
The red crystalline compound (m. p. 232°C (decomp.)) has the same composition ($C_{18}H_{18}NO_2$) as that of VIII; therefore, it is assumed to be an isomer of VIII. However, its infrared absorption spectrum has the broad band of a hydroxyl group (3450 cm^{-1}) and the band of neither an acetyl group nor of a formyl group. From this infrared spectural date it may be concluded that the compound (m. p. 232°C (decomp.)) would have the structure IX. IX was easily hydrolyzed, when heated with 100% phosphoric acid, producing a red oil (XII):



(VII)



(VIII)



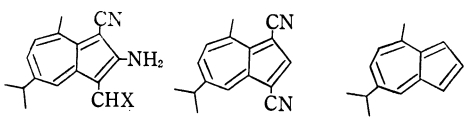
(IX) X=CN
(XII) X=H

In this way, it became clear that the cyano groups at both the 1 and 3 positions, the

6) T. Nozoe, T. Sato, S. Matsumura, T. Asano and H. Akino, Presented at the 9th Annual Meeting of the Chemical Society of Japan, Kyoto, April, 1956.
7) T. Asano, Presented at the 12th Annual Meeting of the Chemical Society of Japan, Kyoto, April, 1959.
8) W. Treibs, J. Hiebsch, and H. J. Neupert, *Chem. Ber.*, **92**, 606 (1959).
9) R. B. Wagner and H. D. Zook, "Synthetic Organic Chemistry," John Wiley & Sons, Inc., New York (1953), p. 412.
10) K. Hafner, *Angew. Chem.*, **69**, 533 (1957); W. Treibs, *Chem. Ber.*, **92**, 141 (1959); K. Hafner and C. Bernhard, *Ann.*, **625**, 108 (1959).
11) A. Vilsmeir and A. Haach, *Chem. Ber.*, **60**, 119 (1927).

hydrolysis of which has hitherto been regarded as being difficult, could be hydrolyzed using 100% phosphoric acid. Since the yield of IX from VII was so low that it seemed difficult to obtain the last objective *S*-guaiazulene from IX, the preparation of 1, 3-dicyano-4-methyl-7-isopropylazulene (XIII) by the deamination of III, followed by its transformation into 4-methyl-7-isopropylazulene (XIV) was planned.

The diazotization of III is difficult by the usual manner. However, when a concentrated sulfuric acid solution of sodium nitrite was added to a solution of III in concentrated sulfuric acid and formic acid under ice cooling, III was easily diazotized, affording a bright violet solution, which was reductively decomposed, using hypophosphorous acid-copper powder, to give a crystalline compound in a 53% yield. The band of the amino group in the infrared spectrum of this compound disappears, and the ultraviolet absorption spectrum is very similar to that of 1, 3-dicyanoazulene.[12] When heated with phosphoric acid, XIII gave, under an evolution of gas, a small amount of blue oil and a green oil as the main products. The infrared spectrum of the green oil clearly indicates the presence of a hydroxyl group, which suggests that the hydration to the nucleus takes place. XIII can be hydrolyzed neither by sulfuric acid-formic acid nor by alkaline reagents, such as potassium hydroxide and sodium ethoxide, to recover the starting substance XIII. Therefore, the introduction of a methyl group to the 1-position of VIa was tried next.

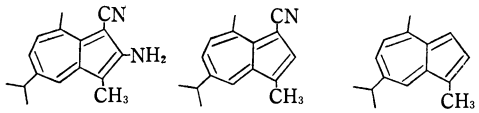


(X) X=O (XI) X=N·NH$_2$ (XIII) (XIV)

As has been mentioned before, the Vilsmeier reaction of VII produces a mixture of VIII and XI in a low yield; therefore, the above reaction was applied to VIa.

Since it was anticipated[13] that the formyl group at the 1-position of X would be very active in an acidic medium and would form an intermolecular Schiff's base with the amino group at the 2-position, X was directly subjected to Huang-Minlon reduction[14] without isolation and purification. As a result, a red crystalline compound was obtained in a 34% yield calculated from VIa. Its infrared spectrum has a band assigned to the cyano group at 2200 cm^{-1} and several bands at 3220, 3330 and 3450 cm^{-1} assigned to the amino group. The results of its micro analysis also fits the structure XV.

The diazonium salt of XV was reductively decomposed by ethanol, giving, in a 41% yield, a blue compound (m. p. 69~70°C) which is soluble in most organic solvents. The results of its micro analysis are satisfactory for XVI. The melting point, type of crystals, characteristic infrared absorption spectrum, and visible absorption curves of XVI[15] all coincide perfectly with those of 3-cyano-1, 4-dimethyl-7-isopropylazulene, which has already been prepared from *S*-guaiazulene by Stafford et al.[16]



(XV) (XVI) (XVII)

The phosphoric acid hydrolysis of XVI gave a blue oil in a 80% yield.[17] The oil was characterized by means of its trinitrobenzene complex (m. p. 147~148°C) and its picrate (m. p. 116~117°C), which were undepressed upon admixture with authentic samples[18] prepared from natural *S*-guaiazulene XVII. The infrared spectra of this oil and of natural *S*-guaiazulene are entirely identical.

Experimental

3-Methyl-6-isopropyltropolone (I).—To a mixture of hinokitiol (4-isopropyltropolone) (50 g.) and formaline (50 ml.), morpholine (50 ml.) was added. The generation of heat was observed. After being kept at room temperature for 1 hr., the mixture was heated at 60°C for 30 min. and then kept in a refrigerator overnight. 3-Morpholinomethyl-6-isopropyltropolone (m. p. 50°C) was obtained in a more than 90% yield.

The Reduction of 3-Morpholinomethyl-6-isopropyltropolone.—To a palladium chloride solution (30 ml.) prepared by Vogel's method[19] Norit (3 g.) was added; then hydrogen was absorbed to this mixture. When a sodium salt aqueous solution of 3-morpholinomethyl-6-isopropyltropolone (40 g.) was added to the palladium-carbon mixture and catalytically reduced at room temperature, a total of 4.2 l. of hydrogen was absorbed. With the progress of the reduction, sodium salt of the reduction product, 3-methyl-6-isopropyltropolone (I), was deposited.

12) W. Treibs, ibid., **92**, 606 (1959).
13) K. Hafner and C. Bernhard, *Angew. Chem.*, **69**, 533 (1957); E. C. Kirby and D. H. Reid, *J. Chem. Soc.*, **1960**, 494.
14) K. Hafner and C. Bernhard, *Ann.*, **625**, 108 (1959).
15) D. H. Reid, W. H. Stafford and W. I. Stafford, *J. Chem. Soc.*, **1958**, 1118; W. Treibs, *Chem. Ber.*, **92**, 606 (1959).
16) See Ref. 15.
17) As a trinitrobenzene complex.
18) Pl. A. Plattner, *Helv. Chim. Acta*, **25**, 581 (1942); **32**, 284, 2137 (1949).
19) A. I. Vogel, "A Text-book of Practical Organic Chemistry," Longmans, Green and Co., New York (1951), p. 996.

The first 1 molar equivalent of hydrogen was rapidly absorbed, but the absorption of the second 1 molar equivalent of hydrogen was rather slow; a total of 2 molar equivalents of hydrogen were absorped. In methanol or acidic methanol solutions, however, hydrogen absorption did not stop even after 2 molar equivalents of hydrogen had been absorbed, so the reduction of the tropolone nucleus must have been taken place.

After the hydrogen absorption had ceased, 2 N sodium hydroxide (50 ml.) and water (200 ml.) were added to the reduction mixture, and then the crystals and palladium-carbon were filtered and dissolved in 2 N sulfuric acid. The solution was extracted with chloroform, and palladium-carbon was filtered off. On the other hand, the alkaline filtrate was acidified with 6 N sulfuric acid and extracted with chloroform. The extracts were combined with the former chloroform extracts, washed with water twice, and dried over magnesium sulfate. When the chloroform was removed and the remaining residue distilled under reduced pressure, 3-methyl-6-isopropyltropolone (I) (25.2 g.) was obtained as a yellow oil in a 91.5% yield.

The Tosylation of I. — *p*-Toluenesulfonyl chloride (4.6 g.) was added to a solution of 3-methyl-6-isopropyltropolone (3.65 g.) dissloved in absolute pyridine (10 ml.). After the mixture had been kept overnight and the pyridine removed under reduced pressure, colorless crystals were obtained on the addition of water. The recrystallization of these crystals from benzene-cyclohexane (1 : 1) gave colorless needles (m. p. 86~87°C) (3.7 g.).

Found: C, 65.08; H, 5.95. Calcd. for $C_{18}H_{20}O_4S$: C, 65.05; H, 6.07%.

The Methyl Ether of I.—To I (25.2 g.) dissolved in ether (100 ml.) an excess of a diazomethane ether solution was added, and the mixture was kept at room temperature overnight. This reaction proceeded extremely slowly. After the ether had been removed and the residue had been distilled, the methyl ether, IIa and IIb, 26.8 g. was obtained in a 98% yield.

The Reaction of 2-Methoxy-4-isopropyl-7-methyltropone (IIa and IIb) with Malononitrile.—To a sodium methoxide solution prepared from absolute methanol (5 ml.) and sodium metal (100 mg.), malononitrile (360 mg.), and IIa and IIb, (400 mg.) were added successively; the mixture was kept at room temperature overnight. Then it was heated under reflux for 2.5 hr., and the resultant red solution was diluted with ethyl acetate and washed with a saturated sodium chloride aqueous solution three times and then dried over magnesium sulfate. After the removal of the solvent, there remained a red oil, which was then dissolved in benzene and chromatographed on alumina. From the benzene eluate, IVa or IVb (m. p. 140~141°C) was obtained in the form of yellow scales.

Found: C, 74.36; H, 6.63; N, 12.19. Calcd. for $C_{14}H_{14}N_2O$: C, 74.31; H, 6.26; N, 12.38%.

UV λ_{max}^{MeOH} mμ (log ε): 242 (4.29), 295 (4.65).

From benzene-ethyl acetate (5 : 1), an eluate, III (250 mg., 48% yield) was obtained as orange prisms from ethanol. M. p. 184~185°C.

Found: C, 77.05; H, 6.19; N, 17.02. Calcd. for $C_{16}H_{15}N_3$: C, 77.08; H, 6.06; N, 16.86%.

UV λ_{max}^{MeOH} mμ (log ε): 235 (4.57), 315 (4.68), 325 (4.75), 390~400 (sh.).

The Hydrolysis of III. — *With Sulfuric Acid-Formic Acid.*—A mixture of III (350 mg.), 80% formic acid (2 ml.) and concentrated sulfuric acid (2 ml.) was heated at 85~95°C at 1 hr. The addition of water then afforded a red solution. A red crystalline substance (350 mg.) (m.p.>270°C) was obtained by neutralization (pH 4~5) with 2 N sodium hydroxide. Recrystallization from dimethylformamide gave Va (m.p.>270°C) in the form of red scales. The compound did not dissolve in a saturated sodium bicarbonate solution, but it did dissolve in 2 N sodium hydroxide.

Found: C, 69.29; H, 5.77; N, 14.23. Calcd. for $C_{17}H_{17}N_3O_2$: C, 69.13; H, 5.80; N, 14.23%.

UV λ_{max}^{MeOH} mμ (log ε): 315 (4.61), 362 (3.84), 380 (3.85), IR 3370, 3270, 3170, 3070, 1655, 1605, 1585, 1510 cm^{-1}.

With 100% Phosphoric Acid. — 100% phosphoric acid (5 ml.) prepared by the addition of an excess quantity of phosphoric acid anhydride to 85% phosphoric acid was added to III (720 mg.), and the mixture was heated at 100°C for 3.5 hr. After water had been added to the reaction mixture, it was neutralized with sodium bicarbonate and extracted with ethyl acetate. The combined ethyl acetate extract was washed with water and dried, and the solvent was removed, giving a red crystalline compound (420 mg.). Recrystallization from ethanol gave VIa (m. p. 157~158°C) as red prisms in a 65% yield.

Found: C, 80.39; H, 7.42; N, 12.79. Calcd. for $C_{15}H_{15}N_2$: C, 80.32; H, 7.19; N, 12.49%.

UV λ_{max}^{MeOH} mμ (log ε): 228 (4.30), 305 (4.76), 315 (4.82), 355 (3.91), IR 3400, 3300, 3200, 2150, 1640, 1540 cm^{-1}.

With 100% Phosphoric Acid at 120°C—A mixture of III and 100% phosphoric acid (3 ml.) was heated at 120°C for 5 hr., water was added, and the mixture was neutralized with sodium bicarbonate and extracted with benzene. The benzene extract was washed with water, dried, concentrated and chromatographed on alumina. The benzene eluate afforded a red oil. After this oil had been heated with acetic anhydride under reflux for 1 hr., the removal of the acetic anhydride gave a red crystalline compound. Recrystallization from dimethylformamide afforded blackish violet prisms (m. p. 250°C.)

Found: C, 88.48 (88.66); H, 8.13 (7.86); N, 3.85 (3.70). Calcd. for $C_{28}H_{31}N$: C, 88.14; H, 8.19; N, 3.67%.

The Acetylation of VIa.—A mixture of VIa (300 mg.) and acetic anhydride (4 ml.) was heated under reflux for 30 min.; the solvent was removed under reduced pressure, and then water was added. The filtered crystals were recrystallized from benzene (m. p. 182~184°C) VII as long red needles.

Found: C, 77.04; H, 6.88; N, 10.68. Calcd. for $C_{17}H_{18}N_2O$: C, 76.66; H, 6.81; N, 10.52%.

UV λ_{max}^{MeOH} mμ (log ε): 240 (4.30), 307 (4.75), 317 (4.85), 355 (3.90), 370 (3.93).

The Vilsmeier Reaction of VII.—To VII (260 mg.) dissolved in dimethylformamide (10 ml.) phosphorus oxychloride (300 mg.) was added and the mixture was heated at 90°C for 1 hr. The reaction mixture was poured into water (100 ml.) yielding a crystalline compound IX. The filtrate was neutralized with 2 N sodium hydroxide and extracted with ethyl acetate. From the ethyl acetate extract, VIII was obtained. The recrystallization of VIII from ethanol gave orange prisms (130 mg.) (m. p. 175~176°C).

Found: C, 73.88; H, 6.07; N, 9.85. Calcd. for $C_{18}H_{18}N_2O_2$: C, 73.45; H, 6.16; N, 9.52%.

UV λ_{max}^{MeOH} mμ (log ε): 232 (4.34), 252 (4.41), 287 (4.40), 322 (4.61).

The recrystallization of IX from dimethylformamide afforded red needles (50 mg.) (m. p. 232~233°C (decomp.).

Found: C, 73.48; H, 5.53; N, 9.71. Calcd. for $C_{18}H_{18}N_2O_2$: C, 73.45; H, 6.16; N, 9.52%.

UV λ_{max}^{MeOH} mμ (log ε): 240 (4.46), 320 (4.66), 335 (4.70), 370 (3.83), 390 (4.02), 415 (4.17).

The Hydrolysis of IX with 100% Phosphoric Acid.—A mixture of IX (150 mg.) and 100% phosphoric acid (7 ml.) was heated at 120~130°C for 5 hr., then it was diluted with water, neutralized with 2 N sodium hydoxide, and extracted with benzene. After the combined extract had been washed with water and dried, the removal of the solvent gave a reddish violet oil (XII). Picrate: m. p. >250°C, green needles.

Found: C, 55.74; H, 3.91; N, 11.34. Calcd. for $C_{23}H_{22}N_4O_9$: C, 55.42; H, 4.45; N, 11.24%.

The Hydrolysis of VIII. — To VIII (130 mg.) dissolved in methanol was added 2 N sodium hydroxide under reflux. After the methanol had been removed by heating on a water bath, a yellow crystalline compound was obtained on the addition of water. Recrystallization from methanol gave crange scales (X) (90 mg., m.p. 168~169°C).

Found: C, 76.03; H, 6.55; N, 11.32. Calcd. for $C_{16}H_{16}N_2O$: C, 76.16; H, 6.39; N, 11.10%.

UV λ_{max}^{MeOH} mμ (log ε): 230 (4.30), 252 (4.43). 282 (4.48), 335 (4.74).

The Condensation of X with Hydrazine.—An ethanol solution of XI and an excess quantity of hydrazine was heated for 10 min., and then water was added. After being kept overnight, a reddish crystalline product was obtained. Recrystallization from ethanol afforded XI as reddish brown needles (m. p. 158~160°C (decomp.)).

Found: C, 71.73; H, 6.79; N, 21.03. Calcd. for $C_{16}H_{18}N_4$: C, 72.15; H, 6.81; N, 21.04%.

UV λ_{max}^{MeOH} mμ (log ε): 260 (4.41), 300 (4.45), 310 (4.45), 350 (4.76) 400 (sh.).

The Deamination of III. — III (1 g.) was dissolved in a mixture of 86% formic acid (50 ml.) and concentrated sulfuric acid (10 ml.). To this solution sodium nitrite (400 mg.) in concentrated sulfuric acid (20 ml.) was added. The solution turned a bright reddish violet. After the addition of the sodium nitrite solution, the mixture was allowed to stand for 30 min., then a small amount of copper powder and 38% hypophosphorous acid (8 g.) were added. When the resultant mixture was kept in a refrigerator overnight, the solution turned red. After the solution had been stirred at room temperature for 5 hr. to complete the reaction, water was added. The reaction mixture was neutralized with 2 N sodium hydroxide and extracted with benzene. The combined benzene extract was concentrated to a proper volume and chromatographed on alumina. From benzene eluate, a red crystalline compound (500 mg.) was obtained. Recrystallization from ethanol gave XIII (53% yield) as red needles (m. p. 145~146°C).

Found: C, 82.11; H, 5.96; N, 11.80. Calcd. for $C_{16}H_{14}N_2$: C, 82.02; H, 6.02; N, 11.96%.

UV λ_{max}^{MeOH} mμ (log ε): 237 (4.71), 300 (4.55), 340 (3.89), 368 (4.02).

Attempts to Hydrolyze XIII. — a) XIII was dissolved in 100% phosphoric acid (1 ml.) and heated at 95~100°C for 2 hr., but no gas evolution was noticed. After being heated at 120~130°C for 2.5 hr., water was added. The reaction mixture was neutralized with 2 N sodium hydroxide and extracted with ethyl acetate. After the ethyl acetate had been removed, the residual oil was dissolved in benzene and chromatographed on alumina. From benzene eluate a blue oil was obtained. The infrared spectrum of this oil indicates the absence of a cyano group and this oil afforded its picrate of green needles, but its identity was not confirmed because of its small quantity. The ethyl acetate eluate gave a green oil, the infrared spectrum of which indicates the presence of a hydroxyl group (3400 cm^{-1}) and the absence of a cyano group. This oil gave a picrate, but its identity was not confirmed because of its small quantity.

b) XIII was dissolved in 10% sodium ethoxide-ethanol and heated at 95°C for 1 hr. The solvent was almost all removed. Water was then added to the residue, and it was extracted with ethyl acetate. From the ethyl acetate solution, the starting material was recovered.

c) A mixture of XIII, formic acid and concentrated sulfuric acid was heated for 1 hr. on a water bath. Only the starting substance was recovered.

The Synthesis of 1-Cyano-2-amino-*S*-guaiazulene (XV). — To VIa (550 mg.) dissolved in dimethylformamide (10 ml.), phosphorus oxychloride (1 g.) was added, and the mixture was kept overnight. Then the mixture was added to a heated ethanolic 2 N sodium hydroxide solution, ethanol (10 ml.) and hydrazine (2 ml.) were added, and the resultant mixture was heated for 30 min. on a water bath. After the addition of an ethylene glycol solution (5 ml.) of potassium hydroxide, which had been prepared by dissolving potassium hydroxide (5.6 g.) in ethylene glycol (25 ml.), the mixture was heated at 190~200°C with reflux for 1.5 hr. Then it was diluted with water and extracted with ethyl acetate, and the combined ethyl acetate extract was washed with water and dried. After the ethyl acetate had been removed, it was chromatographed on alumina. From the benzene-ethyl acetate (1 : 1) eluate, a red crystalline substance was obtained. Recrystallization from methanol afforded red scales (m. p. 120~121°C).

Found: C, 80.20; H, 7.63; N, 11.53. Calcd, for $C_{16}H_{18}N_2$: C, 80.63; H, 7.61; N, 11.76%.

UV λ_{max}^{MeOH} mμ (log ε): 230 (4.25), 310 (4.78), 320 (4.82), 355 (3.95), 395~400 (sh.), 420~430 (sh.).

The Deamination of XV. — XV (230 mg.) was dissolved into a mixture of ethanol (10 ml.) and concentrated sulfuric acid (0.4 ml.). Isoamyl nitrite (130 mg.) was added to the mixture under ice cooling, and it was stirred for 30 min. Then the mixture was added to boiling ethanol (10 ml.) and heated for 30 min. After neutralization with 2 N sodium hydroxide, the mixture was extracted with benzene. The benzene extract was washed with water and dried, and the benzene was removed. When the resulting residue was dissolved in cyclohexane - ether (4 : 1) and chromatographed on alumina, a crystalline compound (90 mg.) (m. p. 64~67°C) was obtained. Purification by sublimation gave XVI of bluish violet needles (m. p. 68.5~69.5°C).

Found: C, 86.12; H, 7.99; N, 5.97. Calcd. for $C_{16}H_{17}N$: C, 86.05; H, 7.76; N, 6.27%.

UV λ_{max}^{MeOH} mμ (log ε): 245 (4.44), 298 (4.58), 312 (4.47), 380 (3.98), 558 (2.75).

IR 2190, 1554, 1539, 1526, 1417, 1330, 1295 (doublet), 1208, 1160, 1123, 1097, 1055, 1020, 995, 953, 915 cm^{-1}.

The Hydrolysis of XVI. — A mixture of XVI (90 mg.) and 100% phosphoric acid (1 ml.) was heated at 98~99°C°. It first became a clear solution, but then a compound, which might be carbamoyl-*S*-guaiazulene, was separated out. After this temperature had been maintained for an additional 4 hr., water was added. The resultant solution was neutralized with sodium bicarbonate and extracted with petroleum ether. The combined extract was washed with water and dried, and the solvent was removed. When the residual oil was chromatographed on alumina using petroleum ether, a blue oil was obtained. This oil was dissolved in ethanol (2 ml.), of which 0.5 ml. was used for the preparation of its picrate. The picrate (m. p. 116~118°C) was obtained as blackish green needles. Similarly, from the ethanol solution (0.5 ml.), 1, 3, 5-trinitrobenzene complex (30 mg.) was obtained as green crystals. Recrystallization from ethanol afforded green needles (m. p. 147~148°C). They were both identical with the authentic sample obtained from *S*-guaiazulene as determined by mixed melting point determination.

The authors gratefully acknowledge financial help from the Sankyo Co., Ltd., to cover part of the expenses of the present work. They are also indebted to Miss Yoko Endo and Miss Yukiko Endo of this Institute for their elemental analyses.

The Chemical Research Institute of Non-Aqueous Solutions
Tohoku University
Katahira-cho, Sendai

*A Novel Method of Acetylation Using Acetoxypyridines**

By Yoshio UENO, Takao TAKAYA and Eiji IMOTO

(Received November 9, 1963)

Pyridoxine, cytosine, thymine, guanine and adenine, which play important roles in biological systems, have an azine or a diazine ring and also one or more hydroxyl and/or amino substituents. Though it had been known that the hydroxyl and the amino groups of these compounds are important in constructing the double spiral structure of nucleic acids by means of hydrogen bonds, the chemical meaning of these groups had not yet been known. A hydroxyl group and an amino group attached to such a heteroaromatic ring as an azine or a diazine have interesting properties. For example, 2- or 4-hydroxypyridine tends to from 2- or 4-pyridone. It may, therefore, be assumed that acyloxy derivatives of pyridine and pyrimidine behave as acylating reagents. Moreover, if so, it is expected that the hydroxyl and the amino groups of the basic components in nucleic acids will play their chemical role of offering an electrophilic reaction intermediate if they act chemically.

In this paper the satisfactory acetylation of alcohols, phenols, amines and acid compounds with 2- and 3-acetoxypyridines is reported.

Experimental

2-Acetoxypyridine.—This compound was prepared by the Tschitschibabin method[1] from acetyl chloride and the sodium salt of 2-hydroxypyridine,[2] which had been prepared from 2-aminopyridine. B. p. 110~112°C/10 mmHg.

3-Acetoxypyridine.—This compound was prepared from acetic anhydride and 3-hydroxypyridine by

* This article was presented at the 16th Annual Meeting of the Chemical Society of Japan, Tokyo, April, 1963.

1) A. E. Tschitschibabin and P. G. Szolow, *Ber.*, **58**, 2650 (1925).

2) R. Adams and V. V. Jones, *J. Am. Chem. Soc.*, **69**, 1803 (1947).

the Fischer method,[3] b. p. 92°C/9 mmHg.

The Acetylation of Butyl Alcohol. — *The Preperation of Butyl Acetate.*—Butyl alcohol (3.96 g.) and 3-acetoxypyridine (8.23 g.) were placed in a flask equipped with a condenser and a calcium chloride tube; the mixture was refluxed for 7 hr., then cooled, acidified with dilute hydrochloric acid and extracted with ether. The ethereal extract was washed with an aqueous solution of sodium bicarbonate and then with water, and dried with anhydrous sodium sulfate. After the ether had been distilled off, the residue was combined with 10 ml. of dry xylene and fractionated under atmospheric pressure to give 5.78 g. of butyl acetate. Yield, 93%. When butyl alcohol (6.07 g.) was acetylated with 2-acetoxypyridine (10.47 g.) in tetrahydrofuran (5 ml.) at 25°C for 3 hr. and when the reaction mixture was then treated in a way similar to that described above, the same yield (92%) of butyl acetate was obtained.

The Acetylation of Amines and Phenols. — *General Method.*—In a 50 ml. flask equipped with a condenser and a calcium chloride tube, an amine or a phenol was acetylated with acetoxypyridine under various conditions. The details of reaction conditions are summarized in Table I. After the solvent had been distilled under reduced pressure at room temperature, the residue was washed with 1 N hydrochloric acid or a 1 N sodium hydroxide solution according to the case and then washed with water several times. The acetyl derivative obtained was recrystallized from an adequate solvent. The product was identified with an authentic sample. In case the product was a liquid, such as acetobutylamide or acetodiethylamide, the aqueous hydrochloric acid solution was extracted with ether and the ethereal solution was dried over anhydrous sodium sulfate. After the ether had been distilled off, the residue was fractionated in a vacuum. In the case of urea, the residue was washed with absolute alcohol and the monoacetyl derivative was obtained.

3-Benzoxypyridine.—In a flask equipped with a condenser and a calcium chloride tube, benzoic acid (6.11 g.) and 3-acetoxypyridine (7.11 g.) were placed in 5 ml. of dry xylene, and the mixture was refluxed for 1 hr. After the acetic acid produced had been distilled off, ether was added to the residue. The ethereal solution was washed with an aqueous dilute solution of sodium carbonate and then with water. After drying over anhydrous sodium sulfate, the ether was distilled off and the residue was fractionated under reduced pressure. The fraction boiling at 168~171°C/12 mmHg was collected, m. p. 49~50°C. The yield of 3-benzoxypyridine was 85% on the basis of the 3-acetoxypyridine.

The Friedel-Crafts-type Acetylation of Anisole. —In a round-bottomed three-necked flask equipped with a condenser, a calcium chloride tube, a dropping funnel, a thermometer, and a sealed stirrer there were placed anisole (13.5 g.) and 3-acetoxypyridine (13.7 g.) in 50 ml. of dry carbon disulfide. Aluminum chloride (37 g.) was added to the stirred solution over a period of 15 min., with occasional cooling with water. The solution was then stirred under gentle reflux for 2 hr. After the carbon disulfide had been distilled under reduced pressure, the residue was poured onto ice containing hydrochloric acid. The decomposed mixture was extracted with ether, and the combined ether extracts were washed with water, with a 10% aqueous solution of sodium hydroxide and again water. After drying over sodium sulfate, the ether was distilled and the residue was fractionated under reduced pressure. The yield of acetylanisole was 76% on the basis of 3-acetoxypyridine. Acetyl derivatives of benzene and toluene were obtained in similar manners; the results are shown in Table II.

3) O. Fisher and E. Renouf, *Ber.*, **17**, 1896 (1889).

Results

The remarkable differences in the reactivity of 2- and 3-acetoxypyridine are shown in Tables I and II. In general, the yields of

Table I. Acetylation of Amines, Alcohols and Phenols

Sample	Acetylating reagent*	Solvent**	Temp. °C	Yield %
Butylamine	3	None	Reflux	70
Diethylamine	3	None	Reflux	91
Urea	3	Xylene	Reflux	80
Aniline	2	THF	25	77
Aniline	3	THF	25	78
o-Toluidine	2	THF	Reflux	81
o-Toluidine	2	THF	25	73
o-Toluidine	3	Xylene	Reflux	46
o-Toluidine	3	THF	Reflux	0
p-Toluidine	2	THF	Reflux	95
p-Toluidine	2	THF	25	88
p-Toluidine	3	THF	Reflux	93
p-Toluidine	3	THF	30	70
p-Nitroaniline	2	THF	Reflux	95
p-Nitroaniline	2	THF	25	82
p-Nitroaniline	3	Xylene	Reflux	0
β-Naphthylamine	2	THF	Reflux	96
β-Naphthylamine	2	THE	25	89
β-Naphthylamine	3	Xylene	Reflux	66
β-Naphthylamine	3	THF	Reflux	0
Diphenylamine	2	Xylene	Reflux	95
Diphenylamine	2	THF	Reflux	0
Diphenylamine	3	Xylene	Reflux	0
Benzanilide	2	Xylene	Reflux	0
Butanol	2	THF	25	92
Butanol	3	None	Reflux	93
α-Naphthol	2	THF	Reflux	45
α-Naphthol	2	THF	25	0
β-Naphthol	2	THF	Reflux	68
β-Naphthol	2	THF	25	37
β-Naphthol	3	Xylene	Reflux	33
β-Naphthol	3	THF	Reflux	0

* 2: 2-Acetoxypyridine
3: 3-Acetoxypyridine
** THF: Tetrahydrofuran

TABLE II. FREIDEL-CRAFTS TYPE ACETYLATION OF BENZENE, TOLUENE, AND ANISOLE

Sample	Acetylating reagent*	Yield %
Benzene	2	32
Benzene	3	0.7
Toluene	2	50
Toluene	3	25
Anisole	2	81
Anisole	3	76

* 2 : 2-Acetoxypyridine
3 : 3-Acetoxypyridine

acetylated compounds with 2-acetoxypyridine were higher than those with 3-acetoxypyridine. *o*-Toluidine and *p*-nitroaniline did not react with 3-acetoxypyridine under reflux in xylene, but they did reacted with 2-acetoxypyridine to give the corresponding acetyl compounds without catalyzers under mild conditions. For example, *o*-acetotoluide was obtained in a 81% yield in refluxing tetrahydrofuran and in a 73% yield at 25°C in the same solvent. The acetyl derivatives of *p*-nitroaniline, β-naphthylamine, diphenylamine and β-naphthol were obtained in good yields with 2-acetoxypyridine under mild conditions. In the Friedel-Crafts-type acetylation, it was found that the main acetyl-substituted products of aromatic compounds were *p*-derivatives and that *o*-derivatives were very small in quantity. As may be seen from Table III, interesting results were obtained. The boron trifluoride etherate was found to be a good catalyzer for this acetylation. On the other hand, because cupric sulfate and cupric acetate were sparingly soluble in dry organic solvents, they were unsuitable as catalyzers. For example, *p*-nitroaniline was acetylated with 3-acetoxypyridine in chloroform containing boron trifluoride etherate, but it was not acetylated with either cupric sulfate or cupric acetate. The solvent effect was not clear in these experiments. The interexchange reaction between benzanilide and 2-acetoxypyridine did not proceed in refluxing xylene or tetrahydrofuran containing boron trifluoride etherate as a catalyzer. The effect of the temperature and the catalyzer on the reactivity of aniline was investigated with 3-acetoxypyridine. As is shown in Table IV, the yield was little changed above 25°C, but at 10°C it decreased to the extent of 40% of the yield.

TABLE III. THE EFFECT OF CATALYZER IN ACETYLTION OF *p*-NITROANILINE WITH 3-ACETOXYPYRIDINE

Catalyzer	Solvent*	Temp. °C	Yield %
None	THF	Reflux	0
$CuSO_4$	THF	Reflux	0
$Cu(AcO)_2$	THF	Reflux	0
BF_3	THF	Reflux	70
None	$CHCl_3$	Reflux	0
$CuSO_4$	$CHCl_3$	Reflux	0
$CuSO_4$	$(Me)_2SO$	66	0
BF_3	$CHCl_3$	Reflux	72

* THF : Tetrahydrofuran

TABLE IV. THE EFFECT OF TEMPERATURE AND CATALYZER IN ACETYLATION OF ANILINE WITH 3-ACETOXYPYRIDINE

Solvent*	Catalyzer	Temp. °C	Yield %
Xylene	None	Reflux	87
Benzene	None	Reflux	91
THF	None	35	81
THF	None	25	78
THF	None	10	36
THF	CH_3I	25	83
THF	BF_3	25	76
THF	$Cu(AcO)_2$	25	72

* THF : Tetrahydrofuran

This study has not established the best experimental conditions, nor has it found the specific property in reactivity.

Department of Applied Chemistry
College of Engineering
The University of Osaka Prefecture
Sakai, Osaka

Ultrasonic Studies of the Hydration of Various Compounds in an Ethanol-Water Mixed Solvent. I. Hydration of Inorganic Compounds

By Tatsuya YASUNAGA, Yasutomo HIRATA, Yoshihiko KAWANO and Masaji MIURA

(Received December 9, 1963)

The problem of the hydration of electrolytes in an aqueous solution has been studied in our laboratory for the past few years. One of the present authors[1] determined the amount of hydration by measuring the ultrasonic velocity and density on the basis of the assumption that the hydrated water molecules are incompressible because of the strong electrostatic interaction between the ion and the surrounding water. A theoretical study on this problem has also been reported by Yasunaga,[2] who assumed that the strength of interaction between the ion and the surrounding water molecules depends only on the distance between them for the ions of identical charge, and that the lower limit of the strength of interaction is that of a hydrogen bond in ice.

In general, the definitions of hydration in the various methods hitherto reported are somewhat arbitrary, and the discordance among the data of hydration numbers found in the literature suggests the need of further research. The hydration numbers obtained by various methods are compared in Table III.

It has been known that the velocity of sound in an ethanol-water mixture[3] shows unusual behavior withre spect to its concentration dependence as do such other physical properties as viscosity, volume contraction, heat capacity, heat of mixing, and sound absorption. According to Parshad,[4] a maximum in the plot of the velocity of sound against the concentration is shifted to the lower concentration side by the addition of electrolytes.

In the present study, an attempt is made to determine the degree of the hydration of electrolytes by using this phenomenon, assuming that the shift of the peak is caused only by the decrease in the amount of free water in the solution.

Theoretical

As has been mentioned above, the plot of the velocity of sound against the concentration of ethanol in water exhibits a peak, the maximum of which is shifted toward the lower concentration side by the addition of an electrolyte. Now it is assumed that this shift is caused only by the hydration, and that there is no interaction between the electrolyte dissolved and the ethanol. Therefore, the amount of hydration can be estimated from the relationship:

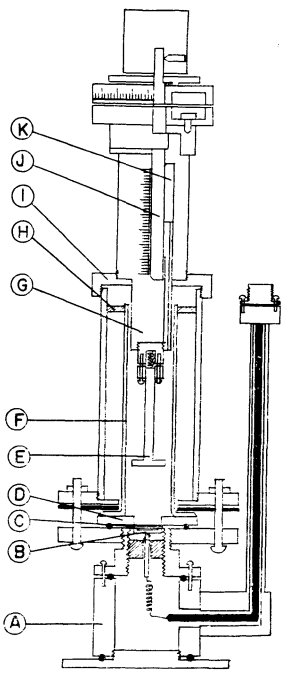


Fig. 1. Ultrasonic interferometer.

A	Base	B	Crystal supporter
C	Crystal	D	Terex glass plate
E	Reflector	F	Cell
G	Reflector shaft	H	Neoprene
I	Cell cap	J	Leading screw
K	Threaded bushing		

1) T. Yasunaga, *J. Chem. Soc. Japan, Pure Chem. Sec.* (*Nippon Kagaku Zassi*), **72**, 87, 89 (1951); T. Sasaki, T. Yasunaga and H. Fujiwara, ibid., **73**, 181 (1952).
2) T. Yasunaga, *J. Sci. Hiroshima Univ., Ser. A*, **23**, 133 (1959).
3) P. Vigoureux, "Ultrasonics," John Wiley & Sons Inc., New York (1951), p. 116.
4) R. Parshad, *J. Acoust. Soc. Am.*, **21**, 175 (1949).

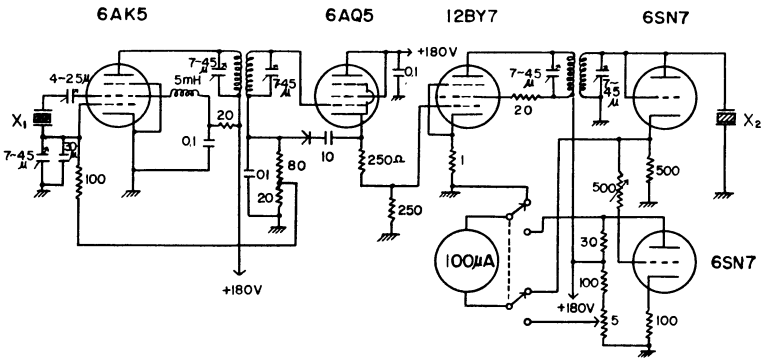


Fig. 2. Electronic circuits for the interferometer.

Resistances in kiloohm unless marked Ω; capacitances in microfarads unless marked μ (micromicrofarad)

TABLE I. SOME RECENT VALUES OF THE VELOCITY OF SOUND IN WATER AT 25°C

Author	Method	Frequency Mc./sec.	Velocity m./sec.
Hubbard and Loomis[5] (1928)	Interferometer	0.5	1498.1
Seifen[6] (1938)	Optical	5	1497.15
Schreuer[7] (1939)	Optical	6~12	1497.2
Gucker and Haag[8] (1953)	Interferometer	4	1497.0
Owen and Simons[9] (1957)	Interferometer	2.5~10	1496.7
Ours (1963)	Interferometer	5	1496.8

TABLE II. SOLUBILITIES OF SOME INORGANIC COMPOUNDS IN ETHANOL[10]

Salt	Solubility
NaCl	0.065 g./100 g. ethanol (25°C)
KCl	0.022 g./100 g. ethanol (25°C)
K_2CO_3	0.095 g./100 g. solution of 90.65% ethanol (23~26°C)
$BaCl_2$	0.014 g./100 g. ethanol 97% (15°C)

$$\frac{W_{alc.0}}{W_{w.0}} = \frac{W_{alc}}{W_w - W_x} = a \qquad (1)$$

where W_{alc}, W_w and W_x are the amounts of ethanol, total water and hydrated water at the peak point respectively, and the subscript 0 refers to the values at infinite dilution with respect to the electrolyte. This equation is derived on the basis of a working hypothesis that the position of the maximum is determined only by the ratio of the amounts of ethanol and free water.

Experimental

Apparatus.—The velocity of sound was measured with an ultrasonic interferometer. A partially-exploded diagram of the interferometer-cell is show in Fig. 1. A vertical glass tube 15 cm. long and 3.8 cm. in diameter is sealed with a glass plate of 4.213 mm. thick, without grease at the bottom, below which is placed a gold plated x-cut quartz crystal with a resonance frequency of 5 Mc.

The reflector is made of a plane glass plate, which moves vertically without and rotation, and its position is determined within an accuracy of 0.002 mm. with a micrometer with a travelling range of 5 cm.

The electronic circuits are given in Fig. 2. The temperature change of the frequency was minimized by keeping the quartz crystal of the main oscillator in a thermostat. The frequency of the oscillator was measured in each experimental run with the standard frequency of the JJY station. The drift of frequency was less than 10 c./day.

The velocity of sound in water as measured with the present apparatus is given in Table I, together with the data found in the literature. The present result is in good agreement with those results, especially with those of Owen and Simons, and with those of Gucker and Haag, who used interferometers of a similar type.

Materials.—Sodium chloride, potassium chloride, potassium carbonate, and barium chloride were used

5) J. C. Hubbard and A. L. Loomis, *Phil. Mag.*, **5**, 1177 (1928).
6) N. Seifen, *Z. Physik*, **108**, 681 (1938).
7) E. Schreuer, *Akust. Z.*, **4**, 215 (1939).
8) F. T. Gucker and R. M. Haag, *J. Acoust. Soc. Am.*, **25**, 470 (1953).
9) B. B. Owen and H. L. Simons, *J. Phys. Chem.*, **61**, 479 (1957).
10) A. Seidell, "Solubilities of Inorganic and Metal Organic Compounds," D. Van Nostrand Company, Inc., New York (1940).

as the electralytes. The mutual interaction between the ion and ethanol for these electrolytes is negligible, as is seen from their solubilities in ethanol as shown in Table II. Guaranteed pure reagents were used without further purification. Ethanol was purified by the usual method to a purity of 99.86%.

Results

The velocities of sound in the solutions of sodium chloride, potassium chloride, potassium carbonate and barium chloride in the mixture of ethanol and water are shown in Figs. 3—6. The concentration of ethanol at the maximum velocity of sound decreased with the increase in the concentration of electrolytes, as has

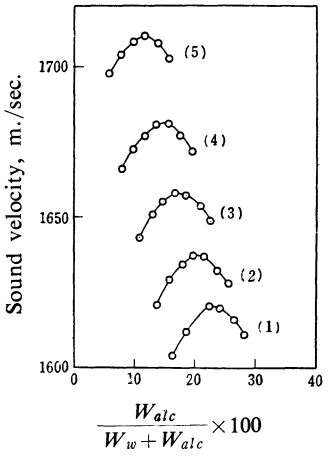


Fig. 3. Sound velocity in ethanol-water solutions of sodium chloride.
The concentration of sodium chloride in M;
(1) 0 (2) 0.689 (3) 1.478
(4) 2.227 (5) 3.063

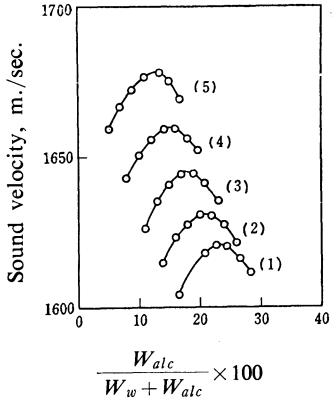


Fig. 4. Sound velocity in ethanol-water solutions of potassium chloride.
The concentration of potassium chloride in M;
(1) 0 (2) 0.692 (3) 1.417
(4) 2.215 (5) 3.021

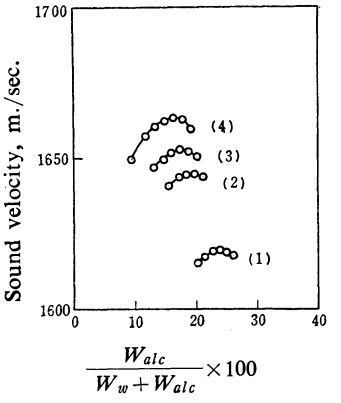


Fig. 5. Sound velocity in ethanol-water solutions of potassium carbonate.
The concentration of potassium carbonate in M;
(1) 0 (2) 0.505 (3) 0.640 (4) 0.789

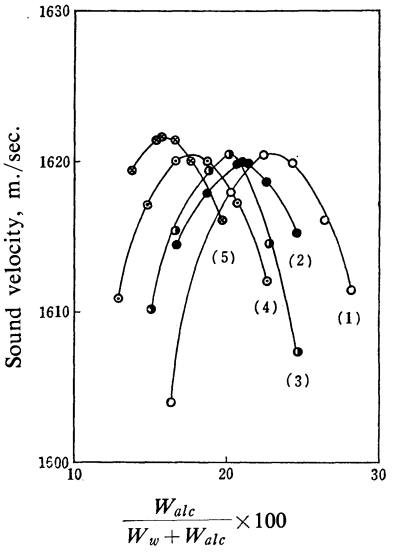


Fig. 6. Sound velocity in ethanol-water solutions of barium chloride.
The concentration of barium chloride in M;
(1) 0 (2) 0.282 (3) 0.375
(4) 0.657 (5) 0.886

been reported by Parshad.[4] The concentration of ethanol at the maximum velocity of sound is plotted against that of the electrolyte in Fig. 7. The degrees of hydration at various concentrations of the electrolytes calculated from these data by using Eq. 1 are shown in Fig. 8. The degree of hydration of sodium chloride and potassium chloride decreased slightly with the increase in the concentration, while that of potassium carbonate and that of barium chloride were constant over the range of concentration studied. The values for the degree of hydration at infinite dilution, as obtained from Fig. 8 by extrapolation, are

TABLE III. COMPARISON OF THE HYDRATION NUMBER

Author	Method	Hydration number			
		NaCl	KCl	K_2CO_3	$BaCl_2$
Ulich[11]	Ionic entropy	7	6		14
Haggis[12]	Dielectric	6±1	5±1		
Yasunaga[1]	Compressibility	6.7	5.2	21.7	14.8
Azzam[13]	Theoretical	7.4	5.8		
Yasunaga[2]	Theoretical	2.31	1.99		
Present work	Sound velocity	8.5	7.1	24.4	14.8

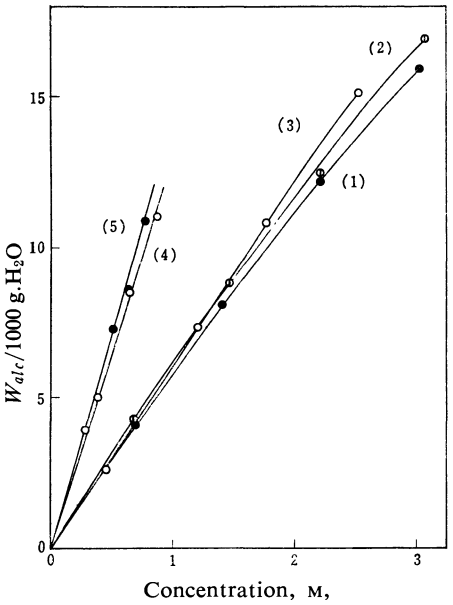


Fig. 7. Relation between the concentration of solute and that of ethanol at the maximum in the velocity of sound.
(1) KCl (2) NaCl (3) NaCl+KCl
(4) $BaCl_2$ (5) K_2CO_3

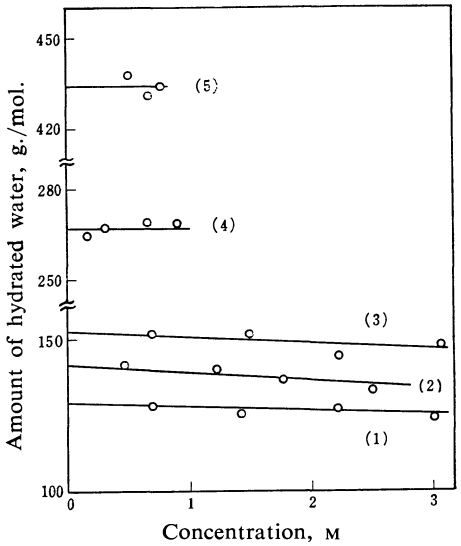


Fig. 8. Amount of hydration.
(1) KCl (2) NaCl+KCl (3) NaCl
(4) $BaCl_2$ (5) K_2CO_3

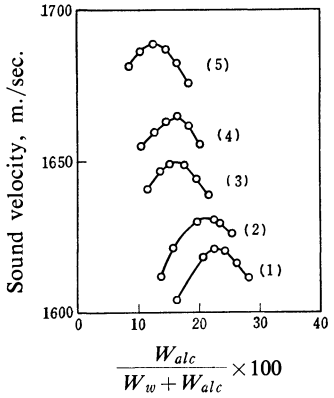


Fig. 9. Sound velocity in ethanol-water solution of sodium chloride and potassium chloride.
The concentration of each of sodium chloride and potassium chloride in M;
(1) 0 (2) 0.464 (3) 1.224
(4) 1.777 (5) 2.523

shown in Table III, where the data found in the literature are appended. As may be seen in Table III, the present result is slightly higher than the other data.

The results obtained for the mixtures of sodium chloride and potassium chloride are shown in Figs. 7, 8 and 9. As may be seen in the figures, the degree of hydration in the mixture of two electrolytes is just the arithmetic sum of those of the individual ions.

Discussion

The significant points in the present results are as follows. 1) The degree of hydration is independent of the concentration. The slight deviation from constancy for the concentrated solutions of sodium and potassium chloride can be ascribed to the ion association. 2) The degree of hydration of a mixture of two electrolytes is additive. 3) The amounts of hydration are in good agreement with those

11) H. Ulich, *Z. physik. Chem.*, **168**, 141 (1934).
12) G. H. Haggis, J. B. Hasted and T. J. Buchanan, *J. Chem. Phys.*, **20**, 1452 (1952).
13) A. M. Azzam, *Z. Elektrochem.*, **58**, 889 (1954).

obtained by various methods. These facts confirm, at least empirically, the validity of our assumption that the position of the maximum of sound velocity is determined by the relative concentration of free water.

The extension of the research with different types of compounds is in progress; this will shed light on the problems of hydration and of the solution properties of a three-component system.

Department of Chemistry
Faculty of Science
Hiroshima University
Hiroshima

Preparation of Some Bis(fluorodimethylsilyl)alkanes

By Makoto KUMADA, Kiyomi NAKA and Yoshihiro YAMAMOTO

(Received January 31, 1964)

Sommer and his co-workers[1] observed that certain organosilicon structures undergo the selective cleavage of one methyl group from each trimethylsilyl grouping, Me_3Si, as methane, when treated with concentrated sulfuric acid. It has also been well established that the demethylation reaction takes place smoothly, even in heterogeneous systems. For example, Sommer and Ansul[2] found that 1,4-bis(trimethylsilyl)butane can be converted into 2,7-dimethyl-2,7-difluoro-2,7-disilaoctane by sulfuric acid cleavage, followed by hydrolysis and then by treatment with boron trifluoride etherate.

$$n\mathrm{Me_3Si(CH_2)_4SiMe_3} \xrightarrow[2)\ H_2O]{1)\ H_2SO_4} \left[-\mathrm{Si(Me)_2(CH_2)_4Si(Me)_2-O-}\right]_n + 2n\mathrm{CH_4}$$

$$\mathrm{FMe_2Si(CH_2)_4SiMe_2F} \xleftarrow{BF_3\cdot Et_2O} \left[-\mathrm{Si(Me)_2(CH_2)_4Si(Me)_2-O-}\right]_n$$

Kumada and his co-workers[3] observed that hexamethyldisilane behaves towards concentrated sulfuric acid in a manner similar to that of the above silahydrocarbon except that the demethylation reaction in this case proceeds in two distinct steps. Thus, chloro(or fluoro)-pentamethyldisilane or 1,2-dichloro(or 1,2-difluoro)tetramethyldisilane can be obtained selectively if the reaction mixture is treated with ammonium chloride (or fluoride) when, respectively, one or two equivalents of methane have been evolved.

$$\mathrm{Me_3SiSiMe_3} \xrightarrow[2)\ NH_4X]{1)\ H_2SO_4} \begin{cases} \mathrm{Me_3SiSiMe_2X} + \mathrm{CH_4} \\ \mathrm{XMe_2SiSiMe_2X} + 2\mathrm{CH_4} \end{cases}$$

In the present study we have established that the demethylation by sulfuric acid, followed by fluorination by the same method as above, can successfully be used for the method generally applicable to the preparation of bis(fluorodimethylsilyl)alkanes (Eq. 1), important intermediates for the preparation of hybrid paraffin-siloxanes.

$$\mathrm{Me_3SiRSiMe_3} \xrightarrow[2)\ NH_4F\cdot HF]{1)\ H_2SO_4} \mathrm{FMe_2SiRSiMe_2F} + 2\mathrm{CH_4} \qquad (1)$$

The starting compounds selected for the present study were eight bis(trimethylsilyl)-alkanes and one chlorine-substituted compound: bis(trimethylsilyl)methane (I), 1,1-bis(trimethylsilyl)ethane (II), 1,2-bis(trimethylsilyl)ethane (III), 1,3-bis(trimethylsilyl)propane (IV), 2,2-bis(trimethylsilyl)propane (V), 1,4-bis(trimethylsilyl)butane (VI), 1,5-bis(trimethylsilyl)pentane (VII), 1,6-bis(trimethylsilyl)hexane (VIII) and bis(trimethylsilyl)-chloromethane (IX). The respective normal products, bis(fluorodimethylsilyl)alkanes, are as follows: bis(fluorodimethylsilyl)methane (X), 1,1-bis(fluorodimethylsilyl)ethane (XI), 1,2-bis(fluorodimethylsilyl)ethane (XII), 1,3-bis(fluorodimethylsilyl)propane (XIII), 2,2-bis(fluorodimethylsilyl)propane (XIV), 1,4-bis(fluorodimethylsilyl)butane (XV), 1,5-bis(fluorodimethylsilyl)pentane (XVI), 1,6-bis(fluorodimethylsilyl)hexane (XVII) and bis(fluorodimethylsilyl)chloromethane (XVIII). The reaction conditions employed for the demethylation and the yields of fluorinated products are listed in Table I; the physical properties, together with analytical data for $FMe_2SiRSiMe_2F$, are shown in Table II.

1) a) L. H. Sommer, N. S. Marans, G. M. Goldberg, J. Rockett and R. P. Pioch, *J. Am. Chem. Soc.*, 73, 882 (1951); b) L. H. Sommer, R. P. Pioch, N. S. Marans, G. M. Goldberg, J. Rockett and J. Kerlin, ibid., 75, 2392 (1953).

2) L. H. Sommer and G. R. Ansul, ibid., 77, 2482 (1955).

3) M. Kumada, M. Yamaguchi, Y. Yamamoto, J. Nakajima and K. Shiina, *J. Org. Chem.*, 21, 1264 (1956).

TABLE I. CLEAVAGE OF SOME SILAHYDROCARBONS $Me_3SiRSiMe_3$ BY SULFURIC ACID, FOLLOWED BY FLUORINATION

Compound			H_2SO_4	Temp.	Gas evolved[a]	$NH_4F \cdot HF$	Yield of product, g. (%)		
No.	R	g. (mol.)	g.	°C	%	g.	Me_3SiF	$FMe_2SiRSiMe_2F$	$HRSiMe_2F$
I	CH_2	30 (0.19)	130	30	65	17	5.5(32)	14.5(46)	5.5(32)[b]
II	CHMe	21.5(0.12)	89	30	75	12	5 (44)	10 (45)	6 (46)[c]
III	$(CH_2)_2$	18 (0.10)	80	30	80	11	2.5(26)	10.5(58)	2.6(25)[d]
IV	$(CH_2)_3$	19 (0.10)	70	43	80	11	1 (11)	13 (67)	1 (10)[e]
V	CMe_2	21 (0.11)	80	30	100	10	0	20 (92)	0
VI	$(CH_2)_4$	40 (0.19)	180	40~45	94	30	2 (8)	28 (72.5)	3 (12)[f]
VII	$(CH_2)_5$	24 (0.11)	80	60~63	95	11	0.8(8)	19 (77)	1.5(9)[g]
VIII	$(CH_2)_6$	30 (0.10)	80	62~65	95	10	0.8(9)	19 (79)	2 (12)[h]
IX	CHCl	18 (0.09)	80	38	95	12	Trace	16 (86)	Trace

a) Not analyzed.
b) In addition, 1.5 g. of a liquid, b. p. 26°C was caught in a trap cooled at −78°C. It is believed to be tetramethylsilane, b. p. 26~27°C [A. Bygden, *Z. physik. Chem.*, **90**, 243 (1915)].
c) B. p. 51°C, n_D^{20} 1.3543, d_4^{20} 0.7972 (Found: F, 17.73. Calcd. for $C_4H_{11}FSi$: F, 17.89%). B. p. 51°C, n_D^{15} 1.3570 are reported by C. Eaborn, *J. Chem. Soc.*, **1949**, 2755; **1952**, 2846.
d) B. p. 51°C, n_D^{20} 1.3540, d_4^{20} 0.7958 (Found: F, 17.73. Calcd. for $C_4H_{11}FSi$: F, 17.89%).
e) B. p. 77~78°C, n_D^{20} 1.3660.
f) B. p. 103°C, n_D^{20} 1.3810, d_4^{20} 0.8119 (Found: F, 14.20. Calcd. for $C_6H_{15}FSi$: F, 14.15).
g) B. p. 36°C/26 mmHg, n_D^{20} 1.3900, d_4^{20} 0.8212 (Found: F, 12.75. Calcd. for $C_7H_{17}FSi$: F, 12.81 %).
h) B. p. 44°C/14 mmHg, n_D^{20} 1.3980, d_4^{20} 0.8222 (Found: F, 11.76. Calcd. for $C_8H_{19}FSi$: F, 11.71%).

TABLE II. PHYSICAL PROPERTIES AND ANALYTICAL DATA FOR $FMe_2SiRSiMe_2F$

Compound		B. p.	n_D^{20}	d_4^{20}	F, %	
No.	R	°C/mmHg			Calcd.	Found
X[a]	CH_2	115	1.3810	0.9203	22.57	22.50
XI	CHMe	114.5	1.3934	0.9377	20.84	20.68
XII	$(CH_2)_2$	136~137	1.3870	0.9193	20.84	20.58
XIII[b]	$(CH_2)_3$	156	1.3926	0.9137	19.38	19.0
XIV	CMe_2	149	1.4055	0.9410	19.38	19.13
XV[c]	$(CH_2)_4$	176	1.7990	0.9664	18.06	18.2
XVI	$(CH_2)_5$	93/26	1.4050	0.9113	16.93	16.89
XVII	$(CH_2)_6$	95/14	1.4087	0.9037	15.93	15.90
XVIII	CHCl	53/21	1.4105	1.0700	18.74	18.55

a) B. p. 114~116°C, n_D^{20} 1.3780, d_4^{20} 0.920 are reported by B. A. Bluestein, *J. Am. Chem. Soc.*, **70**, 3068 (1948).
b) Reported values:[6] b. p. 160.5°C, n_D^{20} 1.3945, d_4^{20} 0.9124.
c) Reported value:[1] b. p. 176°C.

The mixture of a silahydrocarbon and sulfuric acid was stirred vigorously in a vessel connected to a gas-collecting apparatus. The reaction system was heterogeneous initially, but it became homogeneous as the reaction went on. In the $Me_3Si(CH_2)_xSiMe_3$ series of compounds, it was necessary to increase the reaction temperature along with an increase in the value of x in order to cause the demethylation to occur at a reasonable rate. At the temperatures indicated in Table I the reaction appeared to be completed within a few hours.

In agreement with the observation by Sommer and Ansul[2] of the cleavage of 1,4-bis(trimethylsilyl)butane (VI) by sulfuric acid, some percentage of the reaction gave a cleavage between silicon and the R grouping, while Si-Me cleavage was the main reaction in most cases. Less than a theoretical amount of methane (2 mol. of methane per mole of $Me_3SiRSiMe_3$) was evolved; accordingly, the fractional distillation of fluorinated products gave trimethylfluorosilane and alkyldimethylfluorosilanes, $HRMe_2SiF$, in some and nearly equal yields in most cases. With compound I, however, a small amount of a liquid believed to be tetramethylsilane was also detected.

Apart from the detailed reaction mechanism, undoubtedly these products were formed through the two different courses indicated by

Eqs. 2a-2b and 3a-3b:

$$Me_3SiRSiMe_3 \xrightarrow{H_2SO_4} Me_3Si(HSO_4) + HRSiMe_3 \quad (2a)$$

$$HRSiMe_3 \xrightarrow{H_2SO_4} HRSiMe_2(HSO_4) + CH_4 \quad (2b)$$

$$MeSiRSiMe_3 \xrightarrow{H_2SO_4} Me_3SiRSiMe_2(HSO_4) + CH_4 \quad (3a)$$

$$Me_3SiRSiMe_2(HSO_4) \xrightarrow{H_2SO_4} Me_3Si(HSO_4) + HRSiMe_2(HSO_4) \quad (3b)$$

Apparently tetramethylsilane is a product in reaction 2a; this volatile (b. p. 27°C) and paraffin-like compound leaves the reaction system without being attacked by concentrated sulfuric acid. Compounds of the $HRSiMe_2F$ type are probably produced through both courses, 2a-2b and 3a-3b.

Since the results in Table I are over-all ones from complicated reactions, heterogeneous and homogeneous, we cannot discuss the mechanism of silicon-carbon cleavage in detail. However, the following listing by relative ease of Si-R cleavage may be established on the basis of the yields of products:

$$CH_2,\ CHMe > (CH_2)_2 > (CH_2)_3 > (CH_2)_4,$$
$$(CH_2)_5,\ (CH_2)_6 > CHCl > CMe_2$$

These results seem to be fairly well explained in terms of electronic and steric effects of substituents on the methylene carbon to be attacked by the acid.

In order to learn more about the reaction path, further investigation into the homogeneous reaction using compounds such as $Me_3SiRSiMe_2OEt$ is being undertaken.

Experimental

Materials.—All the compounds used (I—IX) are known and prepared by known methods with the exception of compounds III and VIII, the preparation of which is described below. In the following list, the references given after the compounds are to the source or method of preparation: I,[4] b. p. 132~134°C, n_D^{20} 1.4172; II,[5] b. p. 160~161°C, n_D^{20} 1.4331; IV,[6] b. p. 170°C, n_D^{20} 1.4224; V,[7] b. p. 178°C, n_D^{20} 1.4459; VI,[2] b. p. 191°C, n_D^{20} 1.4272; VII,[5] b. p. 88°C/12 mmHg, n_D^{20} 1.4310; IX,[5] b. p. 71°C/21 mmHg, n_D^{20} 1.4491.

1,2-Bis(trimethylsilyl)ethane (III).—To a Grignard solution prepared from 40 g. (0.33 mol.) of Me_3SiCH_2Cl and 7.8 g. (0.33 g. atom) of magnesium turnings in ether, 7 g. of anhydrous cobaltous chloride was added in several portions. To the resulting black solution 40 g. of Me_3SiCH_2Cl was added, and the reaction mixture was kept under reflux for 40 hr. After hydrolysis, an organic layer was separated, dried and fractionally distilled to give 21 g. of unchanged Me_3SiCH_2Cl and 14.3 g. (a 34% yield on the basis of the Me_3SiCH_2Cl unrecovered) of 1,2-bis(trimethylsilyl)ethane; b. p. 149~150°C, n_D^{20} 1.4202, d_4^{20} 0.7506 (reported:[9] b. p. 152°C, n_D^{20} 1.4204, d_4^{20} 0.7536).

1,6-Bis(trimethylsilyl)hexane (VIII).—This compound was prepared by the following sequence of reaction:

$$CH_2=CHCH_2CH_2CH=CH_2 + 2MeSiHCl_2 \rightarrow Cl_2MeSi(CH_2)_6SiMeCl_2$$
XIX
$$XIX + 2MeMgBr \rightarrow VIII$$

In a 100-ml. three-necked flask fitted with a thermometer, a dropping funnel and an efficient reflux condenser, there was placed 25 g. (0.35 mol.) of diallyl and 0.5 ml. of a 0.1 M $H_2PtCl_6 \cdot 6H_2O$ solution in isopropyl alcohol.[10] The exit of the apparatus was sealed with mercury so that the reaction might be carried out at temperatures higher than the boiling points of the starting materials. To the mixture 76 g. (0.66 mol.) of methyldichlorosilane was added drop by drop under reflux conditions. The reaction temperature gradually increased to 140~150°C over a period of 13 hr. Fractional distillation gave two products: 5-hexenylmethyldichlorosilane (b. p. 91°C/26 mmHg; 26 g., in a 41% yield based on the diallyl used (Found: Cl, 35.96. Calcd. for $C_7H_{14}Cl_2Si$: Cl, 36.20%)) and 1,6-bis(dichloromethylsilyl)hexane (XIX) (b. p. 155~156°C/13 mmHg; 42 g., yield 44% (Found: Cl, 44.91. Calcd. for $C_8H_{18}Cl_4Si_2$: Cl, 45.46%)).

To a Grignard solution containing about 1 mol. of methylmagnesium bromide 68 g. (0.22 mol.) of compound XIX was added over a 2/3-hr. period. The reaction mixture was allowed to stand overnight, refluxed for 1 hr. and then hydrolyzed with dilute hydrochloric acid. After a work-up in the usual way, the product was fractionally distilled to give 33 g. (66% yield) of 1,6-bis(trimethylsilyl)hexane; b. p. 101°C/7 mmHg, n_D^{25} 1.4322, d_4^{25} 0.773 (reported:[8] b. p. 109.5°C/16 mmHg, n_D^{25} 1.4298, d_4^{25} 0.772).

The Demethylation, Followed by Fluorination, of Silahydrocarbons.—The technique followed in detail that used in the demethylation, followed by the fluorination, of hexamethyldisilane.[3] The organic products were fractionally distilled through a small Stedman column rated at about 20 theoretical plates to give, in most cases, trimethylfluorosilane (b. p. 16°C), alkyldimethylfluorosilanes and bis(fluorodimethylsilyl)alkanes (see Tables I and II).

Summary

It has been established that the demethylation of bis(trimethylsilyl)alkanes of the

4) M. Kumada and M. Yamaguchi, *J. Chem. Soc. Japan, Ind. Chem. Sec.* (*Kogyo Kagaku Zasshi*), **57**, 175 (1954).
5) M. Kumada and M. Ishikawa, *J. Organometallic Chem.*, **1**, 411 (1964).
6) M. Kumada and A. Habuchi, *J. Inst. Polytech. Osaka City Univ., Ser. C*, **3**, 65 (1952).
7) M. Kumada, K. Naka and M. Ishikawa, *J. Organometallic Chem.*, in press.
8) R. West and E. G. Rochow, *J. Org. Chem.*, **18**, 303 (1953).
9) D. C. Noller and H. W. Post, *J. Am. Chem. Soc.*, **74**, 1361 (1952).
10) J. L. Speier, J. A. Webster and G. H. Barnes, *J. Am. Chem. Soc.*, **79**, 974 (1957).

general formula $Me_3SiRSiMe_3$ by concentrated sulfuric acid, followed by fluorination with ammonium hydrogenfluoride, can successfully be used for the method generally applicable to the preparation of bis(fluorodimethylsilyl)-alkanes, $FMe_2SiRSiMe_2F$. Although Si-Me cleavage was the main reaction in most cases, some part of the reaction gave a cleavage between silicon and the R grouping. The ease of the cleavage of R from silicon was found to decrease in the following order :

CH_2, $CHMe > (CH_2)_2 > (CH_2)_3 > (CH_2)_4$, $(CH_2)_5$, $(CH_2)_6 > CHCl > CMe_2$

We are indebted to the Tokyo Shibaura Electric Co., Ltd., for its support of this work.

Department of Synthetic Chemistry
Faculty of Engineering
Kyoto University
Sakyo-ku, Kyoto

*Studies of Polybutene. I. Determination of the End-groups and the Molecular Weight by the Infrared Method**

By Kazuyoshi IIMURA, Ryūichi ENDŌ and Masatami TAKEDA

(Received February 1, 1964)

A practical method for the determination of the molecular weight of commercial liquid polybutenes of a low molecular weight has been developed by an infrared technique. Moreover, the types of unsaturated terminal groups of the polymer chain have been ascertained. However, the application of this method to polymers of a higher molecular weight would be difficult, because of the undetectably weak relative-intensity of the band assignable to the end-group.

Experimental

Materials.—The samples of the commercial polybutenes used in this investigation are Indopol from Amoco, Oronite from California Chemicals, and Polyvis from Cosden. Benzene was washed with sulfuric acid and water, and distilled after drying over calcium chloride. The treated benzene was purified by fractional distillation over sodium wire before use.

Technique.—The molecular weight of the samples was determined by a cryoscopic method, using benzene as the solvent, and also by an iodine-value method[1] reported on in a preceding paper. The infrared absorption was measured by a Hitachi EPI-2 infrared spectrometer with an NaCl optical system. A group-type analysis was applied in the determination of the content of the end group and of the molecular weight. In this case, the absorption coefficient of the band characteristic of the type of structure must usually be determined. In the present work, however, this procedure was eliminated by applying the data of the absorption coefficients, reported by McMurry and Thornton,[2] of the bands caused by the structural types in question; the proportionality of the absorption coefficient can be held between the data reported by McMurry and our measurements.

Results and Discussion

The Molecular Weight of the Polybutenes.—Table I gives the molecular weight obtained by the iodine-value method on the assumption that each polymer molecule contains only one unsaturated double bond at the end, and those obtained from the cryoscopic method. As may be seen in the table, there is a close agreement in molecular weight between the two methods. This fact justifies the assumption indicated above when the molecular weight is determined by the iodine-value method.

TABLE I. THE MOLECULAR WEIGHT OF POLYBUTENES

Sample	Cryoscopic method	Iodine-value method
Polyvis 3	650	660
Polyvis 5	710	690
Polyvis 10	900	870
Polyvis 30	1300	1150
Indopol L-10	310	310
Indopol H-35	630	640
Indopol H-50	700	660
Indopol H-100	780	840
Indopol H-300	1090	1100
Oronite 24	680	830
Oronite 32	1240	1030

* Presented at the 12th Annual Meeting of the Society of Polymer Science, Japan, Tokyo, May, 1963.

1) R. Endo, K. Iimura and M. Takada, to be pubeished in this Bulletin as Part II.

2) H. I. McMurry and V. Thornton, *Anal. Chem.*, **24**, 318 (1952).

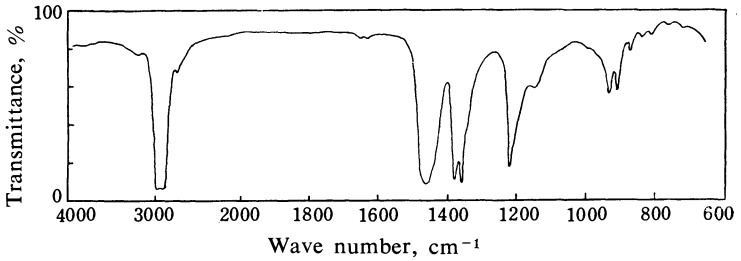


Fig. 1-a. Infrared spectrum of Polyvis 10.

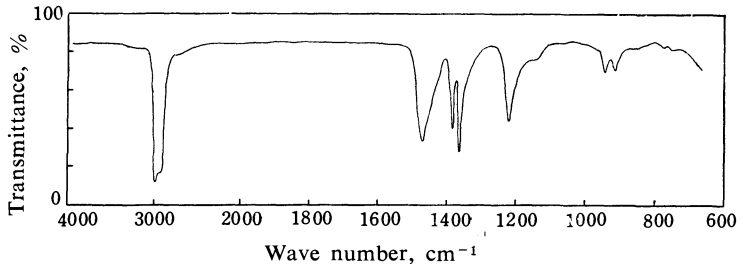


Fig. 1-b. Infrared spectrum of polyisobutylene (Vistanex LM-MH).

The Structures of the Polybutenes. — The infrared spectra of eleven samples are all identical to that of polyisobutylene except in the double-bond stretching and the out-of-plane =CH deformation regions. For example, the infrared spectra of Polyvis 10 and polyisobutylene (Vistanex LM-MH from the Esso Standard, $\bar{M}_w$: 10000~11700) are shown in Fig. 1. The absorption caused by the unsaturated double bonds is observed in all samples. The two weak absorption bands at 1660 and at 1640 cm^{-1} can be assigned to the C=C stretching vibrations. The disappearance of the bands at 892 and at 830 cm^{-1} on the iodation of the samples (cf. Fig. 2) suggests that these bands arise from the CH out-of-plane bending vibration at the C=C bond. The bands at 1660 and 830 cm^{-1} are assigned to the vibration of the tri-substituted ethylenic double bond, while those at 1640 and 892 cm^{-1} have been assigned to the vibration of the vinylidene-type double bond by Dainton and Sutherland[3] and by other investigators.[4-6]

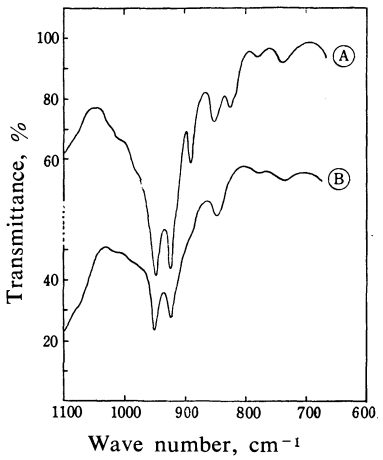


Fig. 2. Infrared spectra of Polyvis 10 before and after treating with I_2; A: original, B: treated with I_2.

From this finding, together with that obtained in the first section, it would seem that the commercial polybutenes are low molecular weight polyisobutylene, and that they are mixtures of two types of polymer chains consisting of one vinylidene-type end-group per one polymer molecule and one tri-substituted ethylenic end-group per another polymer molecule.

The Quantitative Determination of the End-groups.—In the infrared study of low molecular weight polyisobutylene, Dainton and Sutherland[3] and Flett and Plesch[6] have suggested that the termination of the polymer occurs mainly in the vinylidene-type unsaturation. In the sample used in this investigation, however, a considerable amount of the tri-substituted ethylenic end-group exists in the polymer chain, together with the vinylidene-type end-group.

The measurement of the absorption intensities of the bands at 892 and 830 cm^{-1}, which

3) F. S. Dainton and G. B. B. M. Sutherland, *J. Polymer Sci.*, **4**, 37 (1949).
4) W. S. Richardson, ibid., **10**, 353 (1954).
5) W. S. Gallaway and M. J. Murray, *J. Am. Chem. Soc.*, **70**, 2584 (1948).
6) M. St. C. Flett and P. H. Plesch, *J. Chem. Soc.*, **1952**, 3355.

are assigned to the CH out-of-plane vibration of the vinylidene-type end-group and that of the tri-substituted ethylenic end-group respectively, gives the concentration of the end-groups. The absorption coefficients of the bands at 892 and 830 cm^{-1} have been determined as 14×10^4 mol./ml./cm. and 4.0×10^4 mol./ml./cm. respectively by McMurry and Thornton.[2] Using these values, it is possible to obtain the content of the end-groups from the measured intensity ratio of the bands.

If the intensities of the bands at 830 and 892 cm^{-1} are proportional to the concentrations of the respective end-groups, the following relation can be proved:

$$C_{830}/C_{892} = (k_{892}/k_{830}) \times (D_{830}/D_{892}) = (14/4.0) \times (D_{830}/D_{892}) \quad (1)$$

where C is the molar concentration of the end-group, k is the absorption coefficient, and D is the optical density of the band at the wave numbers shown by the subscript. The ratio of the contents of the tri-substituted ethylenic end-group to that of the vinylidene-type end-group is given by C_{830}/C_{892}. The contents calculated from C_{830}/C_{892} are listed in Table II.

TABLE II. END-GROUP CONTENT

Sample	D_{830}/D_{892}	C_{830}/C_{892}	V	T
Polyvis 3	0.431	1.51	0.40	0.60
Polyvis 5	0.427	1.49	0.40	0.60
Polyvis 10	0.461	1.61	0.38	0.62
Polyvis 30	0.437	1.53	0.40	0.60
Indopol L-10	0.306	1.07	0.48	0.52
Indopol H-35	0.436	1.53	0.40	0.60
Indopol H-50	0.490	1.72	0.37	0.63
Iodopol H-100	0.623	2.18	0.31	0.69
Indopcl H-300	0.402	1.41	0.41	0.59
Oronite 24	0.573	2.01	0.33	0.67
Oronite 32	0.520	1.82	0.35	0.65

Note: V provides a vinylidene-type end-group. T provides a tri-substituted ethylenic end-group.

Unlike the results obtained by Dainton and Sutherland[3] and by Flett and Plesch[6] on their samples, the tri-substituted ethylenic end-group is predominant in our samples.

The Determination of the Degree of Polymerization by the Infrared Method.—The band at 855 cm^{-1} is caused by the $R\text{–}CH_2\text{–}C(CH_3)_2\text{–}CH_2\text{–}R$ group in the polyisobutylene chain, and its absorption coefficient is estimated as 0.2×10^4 mol./ml./cm.[2] As has been described in the second section, if we assume that these samples are mixtures of two kinds of polyisobutylene chains, one with the tri-substituted ethylenic end-group and the other with the vinylidene end-group, the contribution from the dimethyl branching of these two chains to the intensity of the band at 855 cm^{-1} must be considered. That is, the number-average degree of polymerization, $\bar{P}_n$, of the samples can be calculated from the following formulas:

$$\bar{P}_n = \{(V\times D_{855}\times k_{892})/(D_{892}\times k_{855})\}+1 \quad (2)$$

or

$$\bar{P}_n = \{(T\times D_{855}\times k_{830})/(D_{830}\times k_{855})\}+1 \quad (3)$$

where V is the content of the vinylidene-type end-group and T is that of the tri-substituted ethylenic end-group. The degree of polymerization, therefore, can be obtained from the content of the end-group by applying Eq. 2 or 3.

Table III gives the degree of polymerization obtained by the above method and those obtained from the cryoscopic and iodine-value methods. There is considerable agreement between the results obtained by the three methods. These experimental results demonstrate that the infrared technique can be used as a practical and rapid method for the determination of the types and numbers of the end-group in the commercial polybutenes and the molecular weight of polymers.

TABLE III. DEGREE OF POLYMERIZATION OBTAINED BY INFRARED AND OTHER METHODS

Sample	Infrared		Cryo-scopic	Iodine-value
Polyvis 3	10.9[a]	10.8[b]	11.6[c]	11.8[c]
Polyvis 5	12.9	13.0	12.7	12.3
Polyvis10	15.0	15.1	16.0	15.5
Polyvis30	20.0	19.5	23.2	20.5
Indopol L-10	9.0	9.0	5.5	5.5
Indopol H-35	13.5	13.3	11.1	11.4
Indopol H-50	15.3	15.2	12.5	11.8
Indopol H-100	14.9	15.7	13.9	15.0
Indopol H-300	20.0	20.4	19.4	19.6
Oronite 24	16.3	16.4	12.1	14.8
Oronite 32	20.3	20.7	22.1	18.4

Note: a) From the content of the vinylidene-type end-group.
b) From the content of the tri-substituted ethylenic end-group.
c) Obtained by dividing the respective molecular weight by 56.1, the monomeric molecular whight.

The authors are indebted to Mr. Kazuo Saotome for his assistance.

Tokyo College of Science
Department of Chemistry
Faculty of Science
Shinjuku-ku, Tokyo

A Cobalt(III) Complex with Trimethylenediaminetetraacetate

By Nobuyuki TANAKA and Hiroshi OGINO

(Received February 3, 1964)

The preparation and the properties of the cobalt(III) complexes with ethylenediaminetetraacetate (edta) have been extensively investigated. The cobalt(III) complexes with propylenediaminetetraacetate (pdta) and *trans*-1, 2-cyclohexanediaminetetraacetate (cydta) have also been reported on.[1,2] In these complexes, the chelate rings around the central cobalt(III) ions are all five-membered.

This paper will present the synthesis of a cobalt(III) complex with trimethylenediaminetetraacetate (trdta, $(^{-}OOCH_2C)_2N(CH_2)_3N(CH_2COO^{-})_2$) in which a six-membered chelate ring involving two nitrogen atoms is formed. The infrared, visible and ultraviolet absorption spectra of the complex, as well as those of edta-, pdta- and cydta-cobalt(III) complexes, are also presented and discussed.

Experimental

Preparation.—H_4pdta,[1] H_4hdta[3] (hexamethylenediaminetetraacetic acid, $(HOOCH_2C)_2N(CH_2)_6N(CH_2COOH)_2$), Na[Coedta]·$4H_2O$,[4] K[Copdta]·$H_2O$[1] and K[Cocydta]·$3H_2O$[2] were preparaed in essentially the same way as has been reported in the literature. The H_4edta and H_4cydta used were purchased from Dojindo & Co., Ltd.

Trimethylenediaminetetraacetic acid: Twenty-eight grams of monochloroacetic acid in 25 ml. of water was cooled in an ice-bath and then 16.5 g. of potassium hydroxide dissolved in 30 ml. of water was added drop by drop with stirring, followed by the addition of 5 g. of trimethylenediamine. The resulting solution was heated for 1 hr. After cooling, the pH of the solution was adjusted to 2.3 with concentrated hydrochloric acid. The solution was filtered and evaporated on a water-bath to a volume of 40 ml. Then, the deposited potassium chloride was removed and the solution kept in a refrigerator until white powder appeared. This powder was collected and washed with water, alcohol and ether. The filtrate was concentrated on a water-bath, and the same procedure was repeated to recover the compound from the solution; yield, 6 g. The compound was recrystallized from aqueous alcohol and dried at 110°C.

Found: C, 43.24; H, 6.06; N, 9.23. Calcd. for $C_{11}H_{18}N_2O_8$: C, 43.14; H, 5.92; N, 9.15%.

Schwarzenbach and Ackermann[5] reported that H_4trdta did not precipitate upon the acidification of the condensation-mixture of monochloroacetic acid, sodium hydroxide and trimethylenediamine. In this study, however, H_4trdta was successfully crystallized by the careful adjustment of the pH of the condensation-mixture (pH 2.3).

K[Cotrdta]·$2H_2O$: 6.1 g. of H_4trdta, 12 g. of potassium acetate and 5.0 g. of cobalt(II) acetate tetrahydrate were dissolved into 100 ml. of water, to which 2 g. of active charcoal and 4 ml. of 30% hydrogen peroxide were then added. Air was passed through the mixture for 50 hr. at room temperature. Then the solution was filtered and the filtrate evaporated to 25 ml. on a water-bath. During the evaporation the solution was bubbled with a current of air. After the solution had been cooled to 0°C, the reddish violet crystals deposited were collected and washed with alcohol and ether. The compound was recrystallized from water by the addition of alcohol and dried over a silica gel desiccator.

Found: C, 30.27; H, 3.93; N, 6.26; H_2O, 8.13. Calcd. for K[Co($C_{11}H_{14}N_2O_8$)]·$2H_2O$: C, 30.28; H, 4.16; N, 6.42; H_2O, 8.26%.

Apparatus.—The crystalline water of the complexes was determined by a Shimadzu RT-2 recording thermobalance. The infrared spectra were measured with a Hitachi EPI-2G recording infrared spectrophotometer by the potassium bromide disk method. The visible and ultraviolet spectra were obtained by using a Hitachi EPU-2 spectrophotometer at room temperature.

Results and Discussion

Infrared Absorption Spectra.—The carboxyl stretching bands of H_4edta and the related compounds are shown in Fig. 1. In Table I are summarized the frequencies of the absorption bands of these compounds. The values obtained for H_4edta and H_4pdta almost agree with those reported in the literature.[6,7] It has been known that the ionized COO^{-} stretching band occurs at 1610~1550 cm^{-1} and the unionized COOH stretching band at 1725~1700 cm^{-1}.[8] The compounds investigated in

1) F. P. Dwyer and F. L. Garvan, *J. Am. Chem. Soc.*, **81**, 2955 (1959).
2) F. P. Dwyer and F. L. Garvan, ibid., **83**, 2610 (1961).
3) A. Müller and T. Bersin, *Helv. Chim. Acta*, **38**, 1708 (1955).
4) S. Kirschner, *Inorg. Syntheses*, **5**, 186 (1957).
5) G. Schwarzenbach and H. Ackermann, *Helv. Chim. Acta*, **31**, 1029 (1948).
6) D. T. Sawyer and P. J. Paulsen, *J. Am. Chem. Soc.*, **80**, 1597 (1958).
7) K. Nakamoto, Y. Morimoto and A. E. Martell, ibid., **85**, 309 (1963).
8) L. J. Bellamy, "The Infrared Spectra of Complex Molecules," John Wiley and Sons, Inc., New York, N. Y. (1954).

TABLE I. INFRARED ABSORPTION OF H_4trdta AND THE RELATED COMPOUNDS (cm^{-1})

Compound	COOH	COO^-
H_4trdta	1724, 1656	—
H_4edta	1704, 1634	—
H_4cydta	1751, 1730, 1706, 1656	1587
H_4pdta	1704, 1626	—
H_4hdta	1709(sh), 1686	—

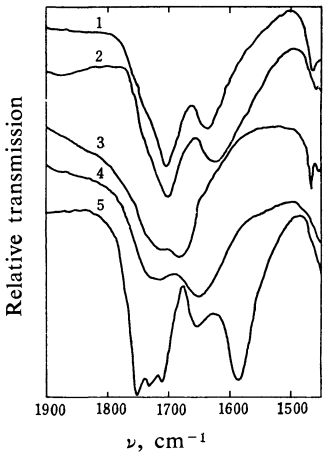


Fig. 1. Infrared absorption spectra of H_4edta (1), H_4pdta (2), H_4hdta (3), H_4trdta (4) and H_4cydta (5).

this study show similar absorption spectra, except that H_4cydta gives an additional strong and sharp absorption band at 1587 cm^{-1}, a band which can be assigned as ionized COO^-. This may be the evidence for the fact that H_4cydta forms a so-called "zwitter ion" in the solid state.

The coordinated $COO^-\cdots M$ stretching bands of the cobalt(III)-trdta and the related complexes are listed in Table II. The values obtained for the cobalt(III)-edta and the cobalt(III)-pdta complexes agree with that reported by Busch and Bailar[9] and those by Gillard[10] and Swaminathan and Busch[11] respectively. Busch et al. found that the cobalt(III)-edta complex gave a single and strong carboxylate band at higher frequencies than those of the free COO^- band, and they considered this to be the indication of the covalent character of the metal-carboxylate bond.[9,12] The results given in Table II indicate that the character of the metal-carboxylate bond in the cobalt(III) complexes with trdta, pdta and cydta closely resembles that in the cobalt(III)-edta complex. Although the carboxylate band of K[Cotrdta]·$2H_2O$ split into two absorption peaks at 1661 cm^{-1} and 1639 cm^{-1} (Fig. 2), both peaks are considered to be associated with the coordinated carboxyl groups. This strongly suggests that a quadrivalent trdta anion in the cobalt(III) complex is hexadentate.

TABLE II. INFRARED ABSORPTION OF Co(III)-trdta AND THE RELATED COMPLEXES (cm^{-1})

Compound	$COO^-\cdots M$
K[Cotrdta]·$2H_2O$	1661(sh), 1639
Na[Coedta]·$4H_2O$	1639
K[Cocydta]·$3H_2O$	1645
K[Copdta]·H_2O	1653

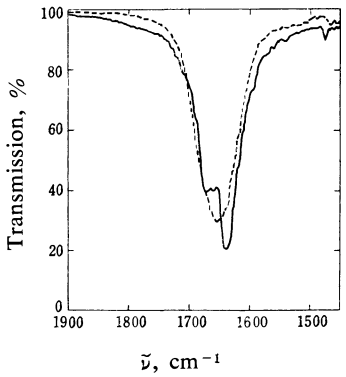


Fig. 2. Infrared absorption spectra of K[Copdta]·H_2O (dotted line) and K[Cotrdta]·$2H_2O$ (full line).

Visible and Ultraviolet Absorption Spectra.— The characteristic numerical data of the visible and ultraviolet spectra for the cobalt(III) complexes with trdta and the related complexes are presented in Table III, from which it can be seen that the absorption spectra of Na[Coedta]·$4H_2O$, K[Copdta]·H_2O and K[Cocydta]·$3H_2O$ are essentially identical, while those of K[Cotrdta]·$2H_2O$ are somewhat different. The intensities of the first and the second absorption bands of K[Cotrdta]·$2H_2O$ are smaller than, and the wavelength of the first band of K[Cotrdta]·$2H_2O$ is longer than, those of the other three complexes. Furthermore, as may be seen in Fig. 3, the broadening of the first band is observed with K[Cotrdta]·$2H_2O$. Yamatera predicted from the molecular orbital calculations that the first band of a complex of the $[CoA_4B_2]$ type splits into two components.[13] The broadening of the first band of K[Cotrdta]·$2H_2O$ seems to support Yamatera's prediction. Although the broadening or splitting of the first band was not

9) D. H. Busch and J. C. Bailar, Jr., *J. Am. Chem. Soc.*, **75**, 4574 (1953).
10) R. D. Gillard, Nature, **188**, 487 (1960).
11) K. Swaminathan and D. H. Busch, *J. Inorg. Nucl. Chem.*, **20**, 159 (1961).
12) M. L. Morris and D. H. Busch, *J. Am. Chem. Soc.*, **78**, 5178 (1956).
13) H. Yamatera, This Bulletin, **31**, 95 (1958).

TABLE III. VISIBLE AND ULTRAVIOLET ABSORPTION MAXIMA (10^{13} sec^{-1}) AND log ε FOR Co(III) COMPLEXES WITH trdta AND THE RELATED COMPLEXES

Compound	B band		I band		II band		Specific band	
	max.	log ε	max.	log ε	max.	log ε	max.	log ε
K[Cotrdta]·$2H_2O$	ca. 43	ca. 0.3	54.3	2.12	79.1	2.05	133	4.40
Na[Coedta]·$4H_2O$[14]	ca. 43	ca. 0.4	55.9	2.51	78.1	2.36	133	4.33
K[Cocydta]·$3H_2O$	ca. 43	ca. 0.5	55.8	2.50	78.6	2.34	134	4.43
K[Copdta]·H_2O	ca. 43	ca. 0.5	56.1	2.50	78.8	2.34	133	4.34

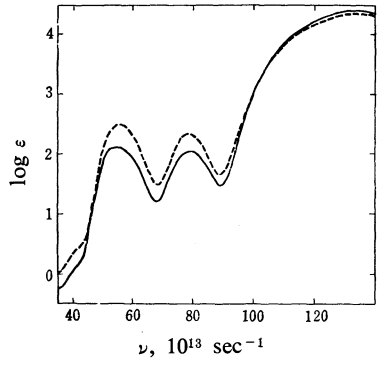


Fig. 3. Visible and ultraviolet absorption spectra of K[Cotrdta]·$2H_2O$ (full line) and K[Copdta]·H_2O(dotted line).

observed with the Na[Coedta]·$4H_2O$, K[Copdta]·H_2O and K[Cocydta]·$3H_2O$, Hidaka et al.[14] concluded from their analysis of the optical rotatory dispersion curve that the first absorption band of [Coedta]$^-$ may have two component absorptions.

14) J. Hidaka, Y. Shimura and R. Tsuchida, ibid., 33, 847 (1960).

Summary

The synthesis of a new cobalt(III) complex, K[Cotrdta]·$2H_2O$ (trdta, $(^-OOCH_2C)_2N(CH_2)_3N(CH_2COO^-)_2$), has been carried out. The infrared, visible and ultraviolet absorption spectra indicate that a quadrivalent trdta anion in this complex is hexadentate. The infrared, visible and ultraviolet absorption spectra of the cobalt(III) complexes with ethylenediaminetetraacetate, propylenediaminetetraacetate and *trans*-1,2-cyclohexanediaminetetraacetate have also been observed and discussed.

Department of Chemistry
Faculty of Science
Tohoku University
Katahira-cho, Sendai

Kinetic Energies of Fragment Ions from n-Butane Resulting from Electron Impact

By Miyako INOUE and Akibumi DANNO

(Received February 10, 1964)

Fragment ions from polyatomic molecules produced by electron impact sometimes possess considerable kinetic energy, the so-called initial energy, which may amount to several electron volts. In early studies the initial energy of ions was measured to determine the ionization potential of ions from their appearance potential. Recently, however, the kinetic energy has come to be of importance in itself, because it provides valuable information on the molecular structure and on the primary processes of the radiation chemistry.

The kinetic energy of fragment ions from *n*-butane produced by electron impact has been studied by many workers. Using the retarding potential method, Fox and Hipple[1] reported that fragment ions of a small mass and those formed by complex dissociation processes always had a high kinetic energy. Taubert[2] carried out a systematic measurement of the kinetic energy of fragment ions from some paraffins and mono-olefines; varying the repeller voltage, he showed that more abundant fragment ions normally have lower kinetic

1) R. E. Fox and J. A. Hipple, *Rev. Sci. Instr.*, **19**, 462 (1948).
2) R. Taubert, "Advances in Mass Spectrometry," p. 486 (1959).

energies. Mohler et al.[3] observed some ions of a high kinetic energy from polyatomic molecules, and they proposed that these ions are produced from the decomposition of doubly-charged molecule-ions. On the other hand, Washburn and Berry[4] attempted to estimate the initial energies of various ions from *n*-butane, using a discrimination method.

Conventional mass spectrometers exhibit a phenomenon called "discrimination," in which ions having initial energies tend to fail to pass through the slit system of the ion-source and the analyzer tube because of the effect of the velocity components perpendicular to the principal motion through the system. On the basis of his experiments, Berry[5] pointed out that the initial velocity distribution could be obtained from the discrimination data and that it was possible to utilize the discrimination effect to determine the average value of initial kinetic energies; he studied theroretically and experimentally the effects of discrimination using the slit system of a mass spectrometer.

The purposes of the present work are two: (a) To investigate the influence of the initial kinetic energy of ions on the relative intensity of the mass spectrum. We studied the difference between the discrimination for ions produced from rare gases in which the initial energy was in equilibrium with the thermal energy, and that for some fragment ions produced from *n*-butane, ions which were believed to have a certain amount of initial energy. (b) On the basis of the information gained about the discrimination effect of the ions with some kinetic energy, the amount of kinetic energy for fragment ions is estimated and the mechanisms of dissociation processes from doubly-charged molecule-ions are considered.

Experimental

A model 21-103-C C.E.C. mass spectrometer was used in the present research. The temperature of the ion-source was kept at 250°C as determined by a thermocouple. The energy of the ionizing electrons was 70 V. and the current was 9.5 μamp. in all experiments. In the instrument, the ions formed in the electron beam are forced through the first slit by a weak repeller voltage and are accelerated in the region between the first and second slits by a high voltage. Between the second slit and the collector slit, the ions travel at a constant speed, but they are caused to move in a circular path by the uniform magnetic field. The mass analyzer tube which is immersed in the magnetic field is a 180° type.

As the instrument is the electric-field scanning type, the ion-accelerating voltage varies in inverse proportion to the mass-chage ratio, *m/e*, of the ions. To determine the discrimination curve, the relative intensity of various ions was measured by scanning accelerating voltage at several magnetic fields.

The samples used in this experiment were standard samples for mass spectrometric analysis and were 99.9% pure.

Experimental Results

The Effect of the Initial Energy on the Relative Intensities of the Mass Spectrum.—The discrimination efficiency is defined as the ratio of the number of ions of a given mass passing through the collector slit in a unit of time to the number of ions initially produced by electron impact. Since the discrimination efficiency depends on the initial energy of ions, on the accelerating voltage, on the repeller voltage, and on the geometry of the

TABLE I. RELATIVE ABUNDANCE FOR FRAGMENT IONS FROM *n*-BUTANE AT TWO DIFFERENT MAGNETIC FIELDS

Electron impact voltage was 70 V.

Ion	*m/e*	Low magnetic field mag. curr. =255 mamp.	High magnetic field mag. curr. =300 mamp.
C_2^+	24	0.07	0.10±0.002
C_2H^+	25	0.78±0.01	0.93±0.004
$C_2H_2^+$	26	9.19±0.04	10.12±0.01
$C_2H_3^+$	27	45.76±0.01	47.60±0.07
$C_2H_4^+$	28	35.27±0.15	36.13±0.20
$C_2H_5^+$	29	45.32±0.01	45.52±0.06
$C_2H_6^+$	30	1.06±0.003	1.06±0.004
C_3^+	36	0.14±0.004	0.15±0.003
C_3H^+	37	1.72±0.004	1.92±0.003
$C_3H_2^+$	38	3.06±0.003	3.35±0·01
$C_3H_3^+$	39	18.13±0.10	19.44±0.02
$C_3H_4^+$	40	2.67±0.01	2.87±0.002
$C_3H_5^+$	41	33.22±0.04	33.65±0.02
$C_3H_6^+$	42	13.03±0.03	13.08±0.01
$C_3H_7^+$	43	100.	100.
$C_3H_8^+$	44	3.44±0.02	3.49±0.005
C_4^+	48	1.00±0.003	0.12±0.003
C_4H^+	49	0.63±0.001	0.69±0.003
$C_4H_2^+$	50	1.97±0.002	2.11±0.003
$C_4H_3^+$	51	1.48±0.001	1.56±0.002
$C_4H_4^+$	52	0.35±0.003	0.36±0.004
$C_4H_5^+$	53	0.97±0.001	1.01±0.001
$C_4H_6^+$	54	0.24±0.001	0.24±0.001
$C_4H_7^+$	55	1.11±0.003	1.13±0.001
$C_4H_8^+$	56	0.87±0.004	0.89±0.01
$C_4H_9^+$	57	2.54±0.012	2.60±0.004
$C_4H_{10}^+$	58	11.64±0.008	11.78±0.03
$C_4H_{10}^+$ (i)	59	0.51±0.007	0.52±0.002

3) F. L. Mohler, V. H. Dibeler and R. M. Reese, *J. Chem. Phys.*, **22**, 394 (1954).
4) H. W. Washburn and C. E. Berry, *Phys. Rev.*, **70**, 559 (1946).
5) C. E. Berry, ibid., **78**, 597 (1960).

slit system, it is possible to find information on the initial energy of ions from the experimental relation between the discrimination efficiency and the accelerating voltage.

TABLE II. RELATIVE ABUNDANCE FOR THE KRYPTON ISOTOPE IONS AT TWO DIFFERENT MAGNETIC FIELDS

Ion m/e	Low magnetic field mag. curr. =240 mamp.	High magnetic field mag. curr. =316 mamp.	Sensitivity ratio H_{316}/H_{240}
78	0.635±0.01	0.645±0.002	1.051
80	4.07 ±0.01	4.03 ±0.01	1.059
82	20.43 ±0.005	20.36 ±0.004	1.061
83	20.25 ±0.01	20.23 ±0.003	1.064
84	100.	100.	1.064
86	30.35 ±0.00	30.38 ±0.09	1.066

At the normal repeller voltage and at the fixed geometry of the slit system, the measured relative abundance for ions with an initial energy was measured as a function of the ion-accelerating voltage. Table I shows the relative abundance of fragment ions from *n*-butane at two different magnetic fields. The second column of the table shows the relative intensity for fragment ions preduced at a lower magnetic field (the magnetic current was 255 mamp), while the third column shows those at a higher magnetic field (the magnetic current was 300 mamp). The relative intensities for most of the fragment ions, such as the ions of $m/e=$ 58, 42 and 29, are nearly independent of the magnetic field strength and are all about the same, varying only within a few per cent. On the other hand, the relative intensities for

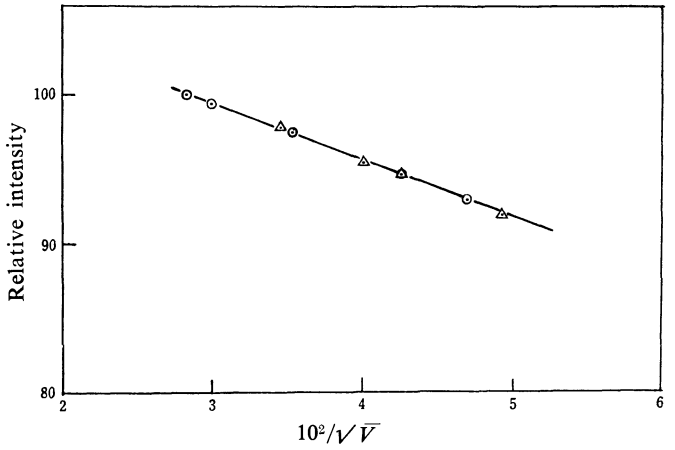


Fig. 1. Discrimination curve for $^{40}Ar^+$ and $^{80}Kr^+$.
⊙ Argon-40 △ Krypton-80

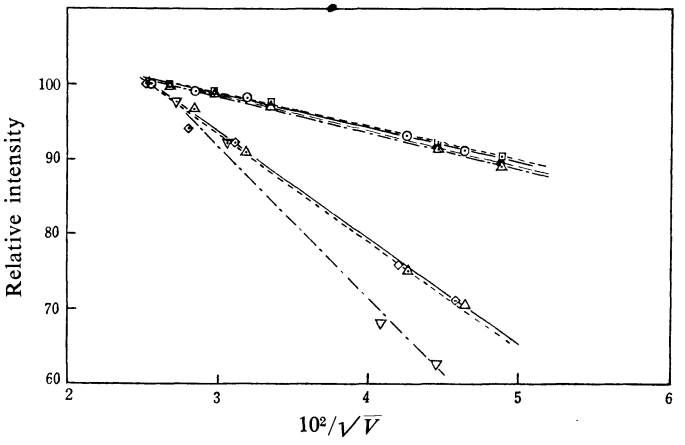


Fig. 2. Discrimination curves for argon, carbon dioxide, propane and some fragment ions from *n*-butane.

—⊙— Argon-40
--△-- Carbon dioxde-44
---▣--- Propane-44
--O-- *n*-Bu-43
—△— *n*-Bu-40
---◇--- *n*-Bu-39
---▽--- *n*-Bu-37

certain ions, such as the ions of m/e =39, 40 and 26, are considerably dependent on the field strength. For instance, the change in relative intensity at the two different magnetic field strengths is about 7% for m/e=39 and about 10% for m/e=26.

Table II shows the relative intensities for krypton isotopes at two different magnetic field strengths. The relative intensities for each isotope ion at the different field strengths are nearly equal, but they have a small dependence on the field strength; that is, the relative intensity of isotopes gradually increases at a high magnetic field as the mass-charge ratio of the ions increases.

Figure 1 shows the relation between the relative intensity of the isotopes of krypton and argon and the accelerating voltage. In this experiment, the accelerating voltage was determined by using the relation between the accelerating voltage and the magnetic field strength, which was adjusted by means of the magnetic current. Although there is a great difference between the mass of argon (m=40) and krypton (m=80), the relative intensities of both ions lie on the same discrimination curve, since the ions for argon and krypton are produced with no initial energy but have only thermal energy which is determined by the temperature of the ions-source, From this finding, it may be concluded that the ions which have only thermal energy but whose mass-charge ratios are different receive the same discrimination effect.

In this instrument, since ions are analyzed by the electric-field scanning, the ions are accelerated by the voltage obtained from the following eqation:

$$V_1/V_2=(B_1/B_2)^2 \qquad (1)$$

where V is the accelerating voltage, B is the magnetic field strength, and the subscripts represent two different magnetic fields. Since the accelerating voltage decreases with an increase in the mass-charge ratio of ions, the discrimination efficiency for ions with the same mass increases with an increase in the magnetic field strength, as is shown in Fig. 1. This is a reason why the sensitivity ratios for krypton isotopes measured at different magnetic fields increase with an increase in the mass of ions, as is shown in Table II.

The relative intensities for fragment ions from n-butane were measured at different magnetic fields. Figure 2 shows the discrimination curves for several ions of n-butane. In this figure, the discrimination curves for argon, carbon dioxide and propane ions which were produced with no initial energy are also shown. The relative intensity of the most abundant ion (m/e=43) from n-butane lies on the same discrimination curve as argon, carbon dioxide and propane ions. On the other hand, the curves for the fragment ions, such as ions of m/e=37, 39 and 40, are seen to be extremely steep compared with the former curves. It is reasonable to conclude that these ions are produced with certain amounts of initial energy from the dissociation processes. Furthermore, from the slope of the curves it may be seen that the initial energy for the ion of m/e=37 is greater than those of ions of m/e=39 and 40.

From the effect of discrimination, it may be concluded that the relative intensity of fragment ions with initial kinetic energies greater than the thermal energy is markedly dependent on the conditions of measurement, such as the accelerating voltage or the magnetic field strength.

The Kinetic Energy of the Fragment Ions from n-Butane.—Since the discrimination efficiency for ions with an initial energy markedly depends on the accelerating voltage and on the geometry of the slit system, there is a possibility of utilizing the discrimination effect to determine the average value of initial energies. Berry[5] pointed out that the collection efficiency, N, namely, the ratio of the number of ions of a given mass-charge ratio passing through the collector slit in a unit of time to the number of ions passing the second slit is given by the following equation:

$$N=\frac{1}{2}\left[(1+k)-\frac{L}{w}\sqrt{\frac{V_0}{V}}\right] \qquad (2)$$

where k, w and L are constants determined by the geometry of the slit system, V is the accelerating voltage, and V_0 is the initial energy of the ions. When the initial energy of ions is not so large as the thermal energy, the discrimination effect at the second slit is not so appreciable that the above equation can be applied. On the basis of the results of Figs. 1 and 2, Eq. 2, seems to give a good approximation for the collection efficiency of these ions, because the discrimination effect for ions with the same kinetic energy is not dependent on the mass of ions, as is shown in Figs. 1 and 2, and because the discrimination curves for fragment ions linearly decrease with an increasing $1/\sqrt{V}$, as is shown in Fig. 2.

On the basis of Eq. 2, the kinetic energy for a given ion can be estimated as in Fig. 3. Line (a) in the figure shows a discrimination curve for the A^+ ion with the known kinetic energy of V_{oa}. The dotted lines on both sides of the line are extrapolations of the observed points to $V\rightarrow\infty$, or to the relative intensity, $\rightarrow$0. The line (b) shows a discrimination curve

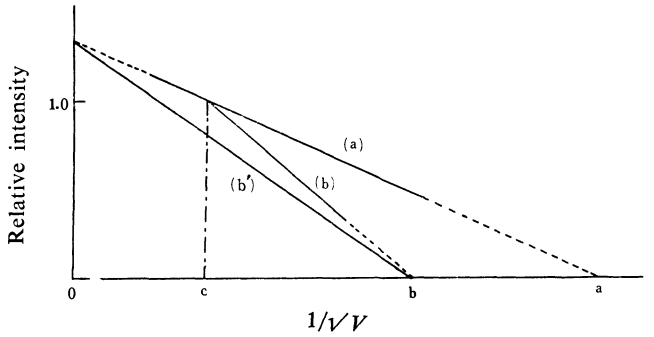


Fig. 3. Calculation of the kinetic energy for ions having initial energy by a graphical method.

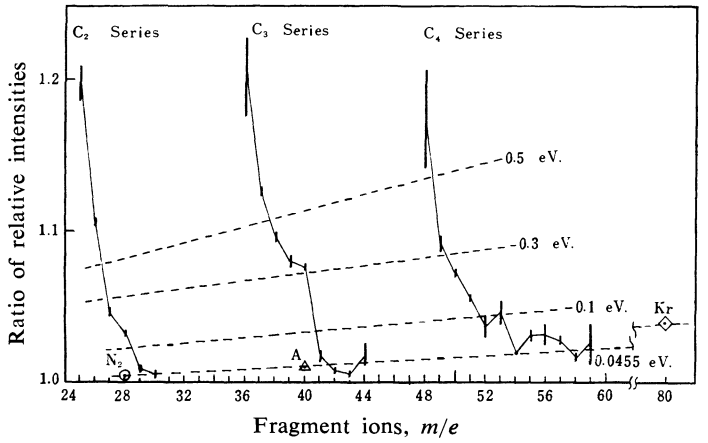


Fig. 4. Ratio of relative intensities at two different magnetic fields and kinetic energies for fragment ions from *n*-butane. Low magnetic field strength was 2386 G and the high field strength was 2807 G.

for the B^+ ion with the unknown kinetic energy of V_{ob}, and the relative intensity for B^+ is normalized at a point C, which is usually the highest voltage obtained. To compare the kinetic energies for the A^+ and B^+ ions, line (b) must be transferred to line (b'), which is normalized at $1/\sqrt{V}=0$. Line (b') is easily obtained as shown in Fig. 3. Let the slopes of lines (a) and (b') be t_a and $t_{b'}$; then the kinetic energy of the B^+ line is given by the following equation:

$$V_{ob}=(t_{b'}/t_a)^2 V_{oa} \qquad (3)$$

Since the kinetic energy of the argon ion of $m/e=40$ is in equilibrium at the wall of the ion-source and is estimated to be 0.0455 eV. at 250°C, the kinetic energy for the fragment ion of $m/e=40$ is estimated to be about 0.31 eV. from the results of Fig. 2 and from the relation of Eq. 3.

The ratio of the relative intensities for a given ion at two different magnetic fields, or at two difierent accelerating voltages of V_1 and V_2, provides information about the initial energy of the ion. Figure 4 shows the ratio of relative intensities for fragment ions from *n*-butane obtained by successive operations (to eliminate an error arising from the pressure drop). In this figure, the dotted lines show the iso-energy curve obtained by the above method for ions with difierent initial energies. The curves for ions of N_2^+, Ar^+ and Kr^+ were obtained with this instrument. The other curves for 0.3 and 0.5 eV. were calculated from Eq. 3, assuming that the kinetic energies for N_2^+, Ar^+ and Kr^+ were thermal energy. From the results of Fig. 4, some information about the initial energy for fragment ions from *n*-butane is obtained: (1) All ions produced from *n*-butane by the scission of CH_3 or C_2H_5 have lower kinetic energies, energies which are comparable with the thermal energy. (2) The ions which are represented by the following formulas have high kinetic energies;

$$C_nH_m^+, \quad n=2,3,4 \quad m=0,1,\ldots,n+1 \qquad (4)$$

In general, the kinetic energy of these ions increases with a decrease in the number of hydrogen atoms; that is, as the number of scissions of the C–H bond increases, the initial

TABLE III. INITIAL ENERGIES AND RELATIVE ABUNDANCES FOR FRAGMENT IONS FROM *n*-BUTANE PRODUCED BY ELECTRON IMPACT

	Parent ion	Fragment ion			
		Thermal energy		Kinetic energy	
	1	2	3	4	5
C_4-Series	$C_4H_{10}^+$ (11.6)	(2.5) $C_4H_9^+$	(1.1) $C_4H_7^+$	[0.1] (1.0) $C_4H_5^+$	[0.15] (1.5) $C_4H_3^+$
		(0.9) $C_4H_8^+$	(0.2) $C_4H_6^+$	[0.08] (0.3) $C_4H_4^+$	[0.25] (2.0) $C_4H_2^+$
C_3-Series	$C_4H_{10}^+$ or $(C_4H_{10})^{2+}$	(3.4) $C_3H_8^+$	(13) $C_3H_6^+$	[0.31] (2.6) $C_3H_4^+$	[0.45] (3.6) $C_3H_2^+$
		(100) $C_3H_7^+$	(33) $C_3H_5^+$	[0.35] (18) $C_3H_3^+$	[0.55] (1.7) C_3H^+
C_2-Series	$C_3H_{10}^+$ or $(C_4H_{10})^{2+}$		(1.0) $C_2H_6^+$	[0.15] (35) $C_2H_4^+$	[0.7] (9.1) $C_2H_2^+$
			(45) $C_2H_5^+$	[0.25] (46) $C_2H_3^+$	[2.0] (0.9) C_2H^+

[ ]: Kinetic energy ( ): Relative abundance

energy for the ions rapidly increases.

Discussion

Fragment ions from *n*-butane produced by electron impact are divided into C_2, C_3 and C_4 series depending on the number of carbon atoms in the ions. The $C_4H_{10}^+$ ion is the parent ion, but its relative intensity is small compared with that of the $C_3H_7^+$ ion, which is the most abundant. This result indicates that the $C_4H_{10}^+$ ion is so unstable that the ion decomposes further into a number of fragment ions as soon as it is formed.

The initial energies obtained in the present experiment for various fragment ions are summarized in Table III. The fragment ions in the second and third columns of the table have only thermal energy. On the other hand, the ions in the fourth and fifth columns have initial kinetic energies larger than the thermal energy. With regard to the relative abundances, in the C_3 series, the intensities of the $C_3H_7^+$ and $C_3H_5^+$ ions are larger than those of the $C_3H_6^+$ and $C_3H_4^+$ ions, and in the C_4 series the intensities of the $C_4H_9^+$ and $C_4H_7^+$ ions are larger than those of the $C_4H_8^+$ and $C_4H_6^+$ ions. In general it is found that the relative intensities of ions with odd numbers of hydrogen atoms are larger than those with even numbers of such atoms. Therefore, it is reasonable to conclude that the fragment ions in a series are formed by splitting hydrogen molecules successively.[6]

However, in the C_2 series the above relation does not hold, because the relative intensity of the $C_2H_4^+$ ions is quite large; it is, in fact, of nearly the same order as that of the $C_2H_5^+$ and $C_2H_3^+$ ions. Moreover, with regard to the initial energies, the $C_2H_5^+$ ion has only thermal energy, while the $C_2H_4^+$ and $C_2H_3^+$ ions have certain amounts of initial energy. Therefore, it is not always true that the less abundant ions have higher initial energies, as Taubert[2] proposed.

It was pointed out by Berry[5] and Mohler et al.[3] that the CH_3^+ ion from *n*-butane produced by electron impact possessed an initial energy of several electron volts. Mohler et al. proposed the mechanism leading to the high initial energy of the CH_3^+ ion. The ion with a high kinetic energy comes from the dissociation of the doubly-charged molecule-ion, because the Coulomb repulsion of these two charges can dissociate the molecule and most of this Coulomb energy will appear as kinetic energy of the fragment ions. The maximum kinetic energy of the CH_3^+ ion was measured as 1.6 eV. by Berry and as 2.2 eV. by Mohler et al. If the high energy of the CH_3^+ ion is produced by the dissociation of doubly charged molecules, the remaining fragment ions will also possess a high kinetic energy.

On the basis of the above assumption, the process for producing the kinetic energies for the $C_3H_3^+$ and $C_3H_4^+$ ions may be explained as follows:

$$(C_4H_{10})^{2+} \rightarrow CH_3^+ + 2H_2 + C_3H_3^+$$
$$\rightarrow CH_4^+ + H_2 + C_3H_4^+$$

When the kinetic energy for the CH_3^+ ion is selected as 1.6 eV., the kinetic energy for the $C_3H_3^+$ ion formed by the above dissociation

6) F. H. Field and J. L. Franklin, "Electron Impact Phenomena," Academic Press Inc., New York (1957), p. 88.

process is calculated as 0.61 eV. On the other hand, the kinetic energy for the $C_3H_4^+$ ion is estimated as 0.64 eV., provided that the kinetic energy of the CH_4^+ ion is of the same magnitude as that of the CH_3^+ ion.

In the case of the C_2 series, the processes for producing the kinetic energies for the $C_2H_3^+$ and $C_2H_4^+$ ions may also be explained by the same assumption:

$$(C_4H_{10})^{+2} \rightarrow C_2H_3^+ + 2H_2 + C_2H_3^+$$
$$\rightarrow C_2H_4^+ + H_2 + C_2H_4^+$$

The kinetic energies for the $C_2H_3^+$ and $C_2H_4^+$ ions are measured as about 0.25 eV. and 0.15 eV. respectively.

In the present experiment, however, the initial energy distribution for ions could not be obtained, although the average energy for mixtures of thermal and high energy ions was obtained. The discrimination effect is larger for high energy ions than for low energy ions. Therefore, the observed values of 0.35 eV. for the $C_3H_3^+$ ion and of 0.31 eV. for the $C_3H_4^+$ ion may turn out to be somewhat smaller than the actual kinetic energy. Using a deflection method, Berry obtained the maximum value of the initial energy for the $C_3H_3^+$ ion as 1.2 eV.[5]; its average value is calculated to be about 0.3 eV. Therefore, the present results are in good agreement with his result. Moreover, these results indicate that a considerable portion of the $C_3H_3^+$ ions is produced by the dissociation of doubly-charged molecule-ions.

Summary

The discrimination effect on the fragment ions from *n*-butane produced by electron impact has been investigated using a conventional mass spectrometer. From the effect of discrimination, it has been concluded that the relative intensity of fragment ions with initial energies larger than their thermal energy is markedly dependent on the conditions of measurement. On the basis of the information gained about the effect of discrimination on ions, the amount of the kinetic energy for fragment ions from *n*-butane has been estimated. From the results of our experiments, it is reasonable to consider that considerable portions of $C_3H_3^+$, $C_3H_4^+$, $C_2H_4^+$ and $C_2H_3^+$ ions are produced with high kinetic energies from the dissociation of the doubly-charged molecule-ion, according as the high kinetic enegy of the CH_3^+ ion is produced.

The authors wish to express their sincere thanks to Dr. Tsutomu Watanabe and Mr. Masamitsu Washino for their valuable discussions, and also to Mr. Hitoshi Hashimoto for assisting in the experimental work described in this paper.

Japan Atomic Energy Research Institute
Tokai-mura, Ibaraki-ken

NOTES

Terpenoids. VII. The Isolation of Sandaracopimarinol from the Wood Oil of "Sugi"[*1]

By Shizuo NAGAHAMA[*2]

(Received September 19, 1963)

A recent investigation by Kondo, Imamura and Suda[1] showed the presence of isopimaric acid, sugiol, xanthoperol, ferruginol, β-sitosterol and a new diterpene alcohol, phyllocradanol, in the heartwood extractive of Sugi (*Cryptomeria japonica* D. Don.).

An acetone extract of the sawdust of Sugi wood gave an oil which afforded sandaracopimarinol[2] together with some of the compounds cited above. This is the first time sandaracopimarinol has been found in a natural source. Since sandaracopimaric acid[3] has already been found in the exudates of Sugi, the existence of sandaracopimarinol in the wood is of interest in view of a biogenetic pathway.

A diterpene hydrocarbon with a conjugated diene system was also isolated.

Experimental

The Isolation of an Oily Mixture.—Sawdust of Sugi (12 kg.) collected at a saw-mill on Mt. Seburi, near Fukuoka City, was extracted with hot acetone for 20 hr. The acetone was evaporated off, and the remaining oil was stirred into a tenfold volume of petroleum ether. The petroleum ether solution was then successively washed with a saturated aqueous sodium hydrogen carbonate, 5% sodium hydroxide, and water. After evaporation of the solvent from the solution, the volatile oil (6.35 g.) was removed by steam distillation. The residue was extracted with petroleum ether, which was evaporated off after drying over sodium sulfate, yielding a neutral material (36 g.). This substance was divided by simple distillation into three parts: fraction a, b. p. 110~117°C/4 mmHg (5.5 g.); fraction b, b. p. 177~185°C/4 mmHg (5.5 g.); and fraction c, residue (about 25 g.).

The Separation of Fraction b.—The fraction was chromatographed on an alumina column (100 g.). Petroleum ether eluted an oily diterpene hydrocarbon (1.88 g.) which gave a single peak on gas chromatograph.[*3]

Found: C, 88.04; H, 11.94. Calcd. for $C_{20}H_{32}$: C, 88.16; H, 11.84%.

n_D^{25} 1.5272, λ_{max} 241.5 mμ, ε 12300. ν_{max} 1628, 886 cm^{-1}.

A mixture of petroleum ether and ether (1 : 1) eluted a carbonyl compound (0.06 g.), and ether containing 1% methanol eluted an alcohol fraction (total: 3.40 g.), from which phyllocradanol (0.6 g., m. p. 187.5~188.5°C, recrystallized from methanol) and sandaracopimarinol were isolated (see below).

The Separation of the Residue c.—The residue was chromatographed on another alumina column (190 g.). The results are shown in Table I.

TABLE I

Fr.	Solvent	Volume cc.	Yield g.
1	Petroleum ether	100	0.67
2	Petroleum ether	250	0.22
3	Petroleum ether+Ether (1%)	50	0.12
4	Ether	50	3.35
5	Ether	50	2.25
6	Ether	450	3.47
7	Ether+Methanol (1%)	300	0.82
8	Ether+Methanol (1%)	100	0.90
9	Ether+Methanol (5%)	150	3.59
10	Methanol	300	1.87

Fraction 1 was the same diterpene hydrocarbon that was obtained from fraction b. The presence of an ester was recognized in fractions 2 to 5. Ferruginol was separated from fraction 4 by further chromatography and was identified by infrared spectrum measurement.

[*1] Contribution No. 50 from the Department of Organic Synthesis, Faculty of Engineering, Kyushu University.

[*2] Present address: Central Research Laboratories, Teijin Limited, Hino, Tokyo.

1) T. Kondo, H. Imamura and M. Suda, *Bull. Agr. Chem. Soc.*, **23**, 233 (1959); ibid., **24**, 65 (1960).

2) V. Galik, J. Kuthan and F. Petrů, *Chem. & Ind.*, **1960**, 722. Added in proof: The identity was later confirmed by direct comparion with authentic sample. The author thanks Professor F. Petrů for the identification.

3) S. Keimatsu, T. Ishiguro and G. Fukui, *J. Pharm. Japan* (*Yakugaku Zassi*), **57**, 69 (1937); J. W. Apsimon, B. Green and W. B. Whalley, *J. Chem. Soc.*, **1961**, 752; V. P. Arya, C. Enzell and H. Erdtman, *Acta Chem. Scand.*, **15**, 682 (1961); A. Tahara, O. Hoshino and N. Ikekawa, *Chem. Pharm. Bull.*, **10**, 995 (1962).

[*3] The author is indebted to Professor Yoshio Kitahara and Dr. Akira Yoshikoshi for the gas chromatography and elementary analysis of this hydrocarbon.

Fractions 6 to 9 contained mainly sandaracopimarinol and phyllocradanol. A crude sandaracopimarinol fraction (970 mg.) obtained from fraction 9 was treated with excess acetic anhydride and was left overnight.*4 A petroleum ether extract gave the residue (1.05 g.), which was chromatographed on an alumina column. Petroleum ether eluted the acetate of sandaracopimarinol (495 mg.), and ether eluted phyllocradanol (286 mg.). The saponification of the acetate with ethanolic potassium hydroxide afforded crude sandaracopimarinol (m. p. 40~62°C). 3, 5-Dinitrobenzoate, m. p. 150.5~151.5°C (from a petroleum ether - benzene mixture). Pure sandaracopimarinol, m. p. 63~65°C, $[\alpha]_D$ −11° (*c* 2.34, chloroform), was obtained by the saponification of the 3, 5-dinitrobenzoate.

A crystalline ketone (m. p. 85°C, 0.03g.) was obtained from fraction 6. Fraction 10 solidified on standing and recrystallization from methanol afforded β-sitosterol (m. p. 136~137°C, 435 mg.).

The Oxidation of Sandaracopimarinol.—The alcohol (530 mg.) in acetone (100 cc.) was oxidized with a Jones reagent[4] (about 3 cc.) in 30 min. The mixture was poured into water and extracted with ether. The crude acid (84 mg.) separated in the usual manner was recrystallized from acetone and was purified by silica gel chromatography to afford sandaracopimaric acid (m. p. 171~175°C (from acetone)). No depression was observed by mixed melting point test with an authentic sample. The infrared spectra of the two samples were superimposable.

*4 On the acetylation of the distilled diterpene alcohol fraction, most of the phyllocradanol was precipitated from the acetic anhydride solution.

4) A. Bowers, T. G. Halsall and E. R. H. Jones, *J. Chem. Soc.*, **1953**, 2555.

The author wishes to express his gratitude to Professor Ernest Wenkert, Indiana University, U. S. A., for the authentic sandaracopimaric acid and to Professor Tamio Kondo of this University for the other authentic samples. Thanks are also due to Professor Emeritus Saburo Akiyoshi for his interest and encouragement, to Assistant Professor Masashi Sumimoto of this University for his valuable discussions, and to Dr. Tamaki Kubota for material.

Department of Organic Synthesis
Faculty of Engineering
Kyushu University
Hakozaki, Fukuoka

The Selective Nuclear Hydrogenation of Benzyl-type Alcohols. On the Effect of the Solvent

By Yoshiyuki ICHINOHE and Hirotoshi ITŌ

(Received December 16, 1963)

It has been well known that the aromatic nuclear catalytic hydrogenation of benzyl-type oxygen compounds is accompanied by the hydrogenolysis of carbon-oxygen linkage.[1] In recent years, studies concerning the selective nuclear hydrogenation have been described by many investigators. Especially, Nishimura[2] reported that the catalytic hydrogenation of benzyl alcohol (I) by means of Adams' platinum oxide catalyst gave cyclohexylcarbinol (II) in a high yield of 88% at ordinary temperature and pressure in ethanol containing a trace of glacial acetic acid. However, no report on the effect of the solvent has been made.

In order to prepare 1,4-dihydroxymethylcyclohexane (III), an important intermediate of synthetic fiber,[3] we studied the selective nuclear hydrogenation of *p*-xylylene glycol (IV), which had not yet been described. Since IV has two carbon-oxygen linkages susceptible to hydrogenolysis, the hydrogenation of IV to III seemed to be more difficult than that of I to II.

We now wish to report that we have been able to synthesize compound III in an almost quantitative yield at ordinary temperature and high hydrogen pressure in *t*-butanol containing a trace of glacial acetic acid by the use of Adams' platinum oxide catalyst.

It has been found that alcohols used as solvents strongly influence the selectivity of the nuclear hydrogenation of benzyl-type alcohols. The selectivity increases in the following order of the solvent alcohols: prim-<sec-<tert-alcohol. This effect of solvents may be caused by some affinity between the solvent and the catalyst. Supposing that there exist active centers of nuclear hydrogenation and of hydrogenolysis on the surface of the

1) W. H. Hartung and R. Simonoff, "Organic Reactions," 7, 263 (1953).
2) S. Nishimura, This Bulletin, 32, 1155 (1959).
3) E. V. Martin, *Textile Research Journal*, 32, 619 (1962).

TABLE I. CATALYTIC HYDROGENATION OF *p*-XYLYLENE GLYCOL AND BENZYL ALCOHOL

No.	Compound g.	Solvent ml.	Organic acids added ml.	Catalyst g.	Temp. °C	H_2 press. kg./cm²	Time min.	H_2 up-take %	Conversion* %	Selectivity* %
1	*p*-Xylylene glycol 7.0	EtOH 70	AcOH 1.15	PtO_2 0.35	28	20～10	75	80.7	100	63.8
2	*p*-Xylylene glycol 7.0	EtOH 70	AcOH 1.15	PtO_2 0.35	28	20～10	20	28.7	30.0	62.3
3	*p*-Xylylene glycol 7.0	EtOH 70	AcOH 1.15	PtO_2 0.35	25	96～90	90	29.0**	30.0	81.0
4	*p*-Xylylene glycol 7.0	EtOH 70	AcOH 1.15	PtO_2 0.35	50	20～10	50	79.0	100	51.0
5	*p*-Xylylene glycol 7.0	EtOH 70	AcOH 1.15	(7:3) 0.35 Pt-Pt	27	20～10	45	20.8**	24.8	
6	*p*-Xylylcne glycol 7.0	*iso*-PrOH 70	AcOH 1.15	PtO_2 0.35	25	20～10	120	80.0	100	70.5
7	*p*-Xylylene glycol 7.0	Dioxane 70	AcOH 1.15	PtO_2 0.35	24	20～10	135	41.7**	44.9	75.0
8	*p*-Xylylene glycol 7.0	*t*-BuOH 70	AcOH 1.15	PtO_2 0.35	25	20～10	120	98.0	100	89.5
9	*p*-Xylylene glycol 7.0	*t*-BuOH 70	AcOH 1.15	PtO_2 0.35	29	95～70	75	91.9	100	97.9
10	*p*-Xylylene glycol 7.0	*t*-BuOH 70	AcOH 1.15	(10:1) 0.35 Pt-Rh	29	20～10	120	28.8	22.6	
11	*p*-Xylylene glycol 7.0	*t*-BuOH 70	AcCH 1.15	(10:1) 0.35 Pt-Pd	27	20～10	120	27.6**	32.8	70.0
12	*p*-Xylylene glycol 7.0	*t*-BuOH 70	$EtCO_2H$ 1.35	PtO_2 0.35	26	20～10	120	ca. 12.0**	ca. 10.0	ca. 90.0
13	*p*-Xylylene glycol 7.0	*t*-BuOH 70	MeCH(OH) CO_2H 1.57	PtO_2 0.35	27	20～10	180	88.6	100	50.5
14	Benzyl alcohol 7.0	MeOH 70	AcOH 1.15	PtO_2 0.35	22	20～10	90	18.5**	10.7	42.0
16	Benzyl alcohol 7.0	EtOH 70	AcOH 1.15	PtO_2 0.35	27	20～10	210	45.0**	45.5	69.0
16	Benzyl alcohol 7.0	*n*-BuOH 70	AcOH 1.15	PtO_2 0.35	25	20～10	210	48.5**	43.0	71.0
17	Benzyl alcohol 7.0	*s*-BuOH 70	AcOH 1.15	PtO_2 0.35	22	20～10	90	30.3**	21.5	74.0
18	Benyzl alcohol 7.0	*t*-BuOH 70	AcOH 1.15	PtO_2 0.35	26	20～10	270	101.0	100	98.5
19	Benzyl alcohol 7.0	*t*-AmOH 70	AcOH 1.15	PtO_2 0.35	25	20～10	210	99.3	100	97.0

TABTE II. CATALYTIC HYDROGENATION OF *p*-XYLYLENE GLYCOL DIACETATE

Compound g.	Solvent ml.	Catalyst g.	Temp. °C	H_2 press. kg./cm²	Time min.	H_2 up-take %	Conversion %*	Selectivity %*
7.0	EtOH 70	PtO_2 0.35	25	20～10	45	107	100	0
7.0	EtOH 70	PtO_2 0.35	25	80～70	30	106	100	0
7.0	EtOH 70	(7 : 3) Rh-Pt 0.35	25	20～10	20	105	100	0
7.0	EtOH 70	(7 : 3) Rh-Pt 0.35	25	80～70	4	121	100	Trace
7.0	*t*-BuOH 70	PtO_2 0.35	25	20～10	20	103	100	Trace

* Analytical value by gas chromatogram. (The ratio of cis- to trans-form of III obtained in the experiment No. 1 was about 7 to 3.)

** Hydrogen up-take became extremely slow and almost stopped at these points.

catalyst, the larger the electron density of the oxygen atom of an alcohol the stronger may be the poisoning with the alcohol which occurs on the active centers of hydrogenolysis, which are supposed to be of an electrophilic character. Therefore, the nuclear hydrogenation is considered to occur selectively.

The experimental data on the hydrogenation of I and IV are shown in Table I. Hydrogenations were carried out in a magnetic, mechanically-stirred autoclave (600 r.p.m.) made of SUS-32 stainless steel.

Runs No. 1 and No. 2, the conversion rates of which were 30 and 100% respectively, show no difference in selectivity, so it seems that subreactions are concurrent.

In tests using various alcohols as solvents, the initial rate of hydrogen absorption in the hydrogenation of IV decreased in the following order; prim->sec->tert-alcohol (cf. Fig. 1).

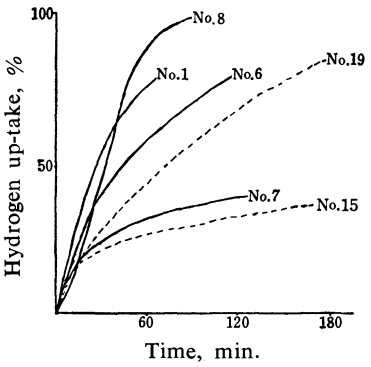


Fig. 1. Effect of solvent on the rate of hydrogen absorption.
Full lines; hydrogenation of IV
Broken lines; hydrogenation of IV

However, the absorption rates of primary and secondary alcohols show a tendency to decrease after the hydrogen absorption goes over 30~40% of the theoretical amount. On the contrary, no such tendency was observed in *t*-butanol. The selectivity of the nuclear hydrogenation diminished in the order: tert->sec->prim-alcohol. Dioxane seemed to make the selectivity higher than primary alcohol, but hydrogen absorption was very slow at the initial stage, and it soon stopped entirely. In the case of I, where the reaction was slower than in the case of IV, the solvent effect was similar to that in the case of IV, and II was obtained in a quantitative yield by the use of *t*-alcohols as the solvent.

The effects of hydrogen pressure on the hydrogenation of IV were studied in about 15 kg./cm^2 and 90 kg./cm^2. The selectivity was higher at the higher pressure, when either ethanol or *t*-butanol was used as the solvent.

In *t*-butanol, the initial rate of hydrogen up-take at the higher pressure was about twice as great as that at the lower pressure, while in ethanol, under the increased hydrogen pressure, the hydrogen up-take was slower and stopped when less than 30% of the theoretical amount.

In the hydrogenation of IV with platinum-rhodium catalysts of the Adams type, the reaction proceeded slowly, both in ethanol and in *t*-butanol, and it stopped halfway (Nos. 5 and 10)*. An analogous result was obtained with the use of a platinum-palladium catalyst of the Adams type (No. 11). On adding 30% of II to I at the starting of a repeated test of No. 14, no hydrogen absorption occurred. When the influence of added organic acids was investigated in *t*-butanol, acetic acid was bound to be the most effective. When a weaker acid was added, the rate of hydrogen absorption was extremely slow; when a stronger acid was added it was fast, but the selectivity was lower (Nos. 8, 12 and 13). Thus, it is necessary to add a proper organic acid in order to accelerate the hydrogenation without inviting hydrogenolysis.

The hydrogenation of IV with palladium, palladium-carbon or nickel on a kieselguhr catalyst gave no III; with Raney nickel (W-2), it gave just a trace of III.

p-Xylylene glycol diacetate (V) more easily underwent hydrogenolysis than IV, and its aromatic nucleus was scarcely be hydrogenated without inviting an extensive hydrogenolysis, as Table II shows.

The authors wish to express their deep thanks to Dr. Nobuto Ohta, Chief of the Department of Organic Synthetic Chemistry, Government Chemical Industrial Research Institute, Tokyo, for many helpful discussions and suggestions during this work.

Tokyo Research Laboratory
Mitsubishi Rayon Company, Ltd.
Chuo-ku, Tokyo

* S. Nishimura (Rh, Pt(3:1))[4] and J. H. Stocker (Rh)[5] have observed similar phenomenon in the hydrogenation of benzyl alcohol.

4) S. Nishimura, This Bulletin, **34**, 32 (1961).
5) J. H. Stocker, *J. Org. Chem.*, **27**, 2288 (1962).

The Assignment of the Methyl Proton Signals in the NMR Spectrum of Hibaene[*1]

By Yoshio KITAHARA and Akira YOSHIKOSHI

(Received December 26, 1963)

Hibaene, a diterpene isolated from the essential oil in the leaves of *Thujopsis dolabrata* Sieb. et Zucc., has been shown[1] to have structure I.

In order to assign the methyl proton signals in the NMR spectrum of hibaene, the chemical shifts have been compared with those of dihydrohibaene (II), isophyllocladene (III), and phyllocladane (IV).

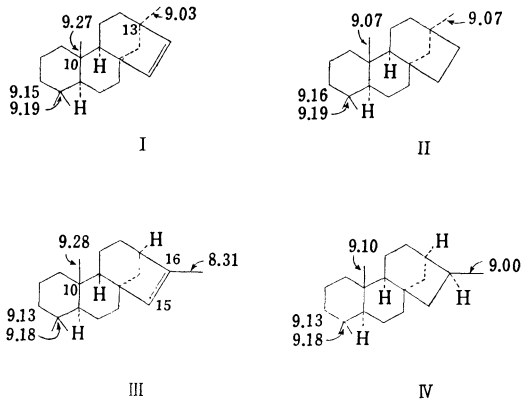


Fig. 1. Chemical shifts of methyl protons.

Hibaene shows four methyl proton signals;[*2] on the other hand, in dihydrohibaene[1] (II), the positions of some of the methyl group signals are displaced in comparison with those of hibaene. This is considered to be due to some of the methyl groups in hibaene being influenced by the anisotropy effect of the double bond. Such effects have been observed, for example, in Δ^7-steroids.[2]

The signals at τ, 8.31 (J=2 c. p. s.) of isophyllocladene[3] (III) and at τ, 9.00 (J=6 c. p. s.) of phyllocladane[4] (IV) appear as doublets; they are, therefore, to be assigned to the C_{16}-methyl group, which is coupled with the C_{15}-proton in III and with the C_{16}-proton in IV. Because there is no change in the chemical shifts of the peaks at τ, 9.13 and 9.18 of III compared to the corresponding peaks of IV, it is deduced that these signals are due to the *gem*-dimethyl group. The remaining methyl signal at τ, 9.28 in III corresponds, therefore, to the C_{10}-angular methyl group; the corresponding signal in IV appears at a lower field (τ, 9.10). The C_{10}-angular methyl group in III is recognized to be shielded by the anisotropy of the double bond.

By applying the results of the above assignments to the spectra of I and II, the methyl proton signals were assigned as follows: (a) the signals at τ, 9.15 and 9.19 of I and at τ, 9.16 and 9.19 of II originate from their respective *gem*-dimethyl groups; (b) the signal at τ, 9.07 of II is due to the C_{10}-angular methyl-group; this is shielded in the the case of I and appears at a high field (τ, 9.27); (c) consequently, the signal at τ, 9.07 of II is assigned to the C_{13}-methyl group in II; this signal appears at a low field (τ, 9.03) in the case of I because of deshielding.

The results of these assignments are depicted in Fig. 1. The C_{10}-angular methyl and the C_{13}-methyl group in I are subject to bond anisotropy effects of the opposite sign, a finding which is in agreement with what would be expected from an inspection of the molecular models.

We wish to thank Dr. Shizuo Nagahama of Kyushu University for the donation of isophyllocladene, and the Shionogi Research Laboratories, Shionogi and Co. for the measurement of the NMR spectra.

The Chemical Research Institute of Non-Aqueous Solutions
Tohoku University
Katahira-cho, Sendai

*1 Reported at the 16th Annual Meeting of the Chemical Society of Japan, March, 1963.

1) Y. Kitahara and A. Yoshikoshi, to be published.

*2 Measurements were made on a Varian A60 NMR spectrometer using CCl_4 solutions.

2) J. N. Shoolery and M. T. Rogers, *J. Am. Chem. Soc.*, **80**, 5121 (1958).

3) P. K. Grant and R. Hodges, *Tetrahedron*, **8**, 261 (1960).

4) L. H. Briggs, B. F. Cain, R. C. Cambie and B. R. Davis, *J. Chem. Soc.*, **1962**, 1840.

*The Synthesis of 3α-Chloro-5, 6α-epoxy-5α-cholestane**

By Michio SHIOTA and Taeko TOYOTA**

(Received December 28, 1963)

One of the present authors (M. S.) and his co-workers have previously reported on a study of the formation and the reactions of 3α-chloro-5, 6β-epoxy-5β-cholestane.[1] This paper will describe a study of the synthesis of an isomeric epoxide, 3α-chloro-5, 6α-epoxy-5α-cholestane.

6β-Chloro-5α-cholestane-3β, 5-diol[2] (I) was chlorinated with phosphorus oxychloride and pyridine.[3] The elementary analysis and infrared spectrum of the product II showed that one of the hydroxyl groups in I was replaced by chlorine. The chlorohydrine II was not acetylated with acetic anhydride and pyridine at room temperature, and it differed from 3β, 6β-dichloro-5α-cholestan-5-ol derived from 3β-chloro-5, 6α-epoxy-5α-cholestane.[4] From these observations it was concluded that the chlorohydrin II is 3α, 6β-dichloro-5α-cholestan-5-ol. The configuration at C_3 was further confirmed by a study of the reactions of the epoxide derived from II.

The chlorohydrin was treated with alkali to afford 3α-chloro-5, 6α-epoxy-5α-cholestane (III). The epoxide was converted into II with hydrochloric acid, and the reaction of III with boron trifluoride-ether complex[5] gave 6-ketone. Whereas 3α-chloro-5, 6β-epoxy-5β-cholestane failed to be reduced with lithium aluminum hydride at the boiling point of ether,[1] the epoxide III was reduced with the reagent to give 3α-chloro-5α-cholestan-5-ol.[3] Hydrolytic cleavage was also effected to give 3α-chloro-5α-cholestane-5, 6β-diol. These reactions confirmed that the epoxide is 3α-chloro-5, 6α-epoxy-5α-cholestane.

Experimental***

3α, 6β-Dichloro-5α-cholestan-5-ol (II). — To a stirred solution of 1 g. of 6β-chloro-5α-cholestane-3β, 5-diol in 25 ml. of pyridine, 10 ml. of freshly distilled phosphorus oxychloride was added over a period of 30 min. at room temperature. Stirring was continued for another hour at room temperature, and then the product was isolated according to the procedure of Shoppee.[3] A pale yellow, oily residue was dissolved in 50 ml. of *n*-hexane, and the solution was stirred with 2 g. of silica gel for 30 min. at room temperature. The removal of the solvent from the filtered solution afforded a colorless crystalline residue. Recrystallization from acetone gave 180 mg. of 3α, 6β-dichloro-5α-cholestan-5-ol (m. p. 118~119.5°C) $[\alpha]_D$ 0° (*c* 2.23, $CHCl_3$).

Found: C, 70.86; H, 10.04. Calcd. for $C_{27}H_{46}Cl_2O$: C, 70.87; H, 10.13%.

The acetylation of the chlorohydrin with acetic anhydride and pyridine at room temperature was attempted, but the starting material was recovered unchanged. 3β, 6β-Dichloro-5α-cholestan-5-ol (m. p. 149~150°C) derived from 3β-chloro-5, 6α-epoxy-5α-cholestane was different from II.

3α-Chloro-5, 6α-epoxy-5α-cholestane (III). — A mixture of 130 mg. of II, 9 ml. of ethanol and 0.4 ml. of 15% aqueous sodium hydroxide was heated under reflux for 30 min. The solvent was then removed under reduced pressure, and the product was isolated with ether in the usual way. Two recrystallizations from methanol gave 72 mg. of the colorless crystalline product, which sintered at 158°C and melted at 160~162°C. Filtration through alumina, followed by recrystallization from methanol, did not raise the melting point. $[\alpha]_D$ −37.7° (*c* 3.18, $CHCl_3$). It gave no yellow color with tetranitromethane and showed no hydroxyl infrared absorption. Infrared absorptions at 1261, 1036 and 875 cm^{-1} (KBr disk) seemed to indicate the 5,6-epoxy group.

Found: C, 76.95; H, 10.29. Calcd. for $C_{27}H_{45}ClO$: C, 77.01; H, 10.77%.

The Reduction of the Epoxide III with Lithium Aluminum Hydride.—The epoxide was reduced with lithium aluminum hydride at the boiling point of ether in the usual way to give 3α-chloro-5α-cholestan-5-ol in an almost quantitative yield (m. p. 118~120°C (lit.,[3] m. p. 118~119°C)).

The Reaction with Boron Trifluoride-Ether Complex. — Freshly-distilled boron trifluoride-ether complex (4 drops) was added to a solution of 50 mg. of III in 5 ml. of dry benzene. After the mixture had been allowed to stand at room temperature for 20 min., it was treated with aqueous sodium bicarbonate and washed with water. The removal of the solvent from the dried solution gave a brown oily residue (52 mg.), which showed hydroxyl and ketonic infrared absorptions. The attempted crystallization of the oil from various

* Presented at the 14th Annual Meeting of the Chemical Society of Japan, Tokyo, April, 1961.

** Present address: Yawata Chemical Engineering Co., Ltd., Ginza-higashi, Chuo-ku, Tokyo.

1) M. Shiota, T. Ogihara and Y. Watanabe, This Bulletin, **34**, 40 (1961).

2) D. H. R. Barton and E. Miller, *J. Am. Chem. Soc.*, **72**, 370 (1950).

3) Cf. A. J. Fudge, C. W. Shoppee and G. H. R. Summers, *J. Chem. Soc.*, **1954**, 958.

4) C. W. Shoppee, R. J. Bridgwater, D. N. Jones and G. H. R. Summers, ibid., **1956**, 2492.

5) H. B. Henbest and T. I. Wrigley, *J. Chem. Soc.*, **1967**, 4596, 4765.

*** All melting points are uncorrected

solvents was not successful. The oily material was heated with 3 drops of concentrated hydrochloric acid in 10 ml. of ethanol to give a semicrystalline product, from which 3α-chloro-5α-cholestan-6-one was isolated in about a 50% yield by recrystallization from acetone. From this result, it was inferred that the oily product contained 3α-chloro-5β-cholestan-6-one,[4] a rearrangement product of the epoxide III, which was isomerized to 5α-6-one by treating it with hydrochloric acid.

The Hydrolytic Cleavage of the Epoxide III. — A mixture of 60 mg. of III, 4 ml. of acetone and 0.1 ml. of a 5% phosphomolybdic acid solution (in acetone) was kept at 28~30°C for 2.5 hr.[6] The solution was then treated with ammonia solution to remove phosphomolybdic acid, and the product was isolated with ether. An oily residue (60 mg.) was crystallized from methanol to give a crystalline product (30 mg.). Recrystallization from methanol gave 3α-chloro-5α-cholestane-5, 6β-diol in needles (20 mg.) (m. p. 130~134°C). The acetylation of the diol afforded an acetate (m. p. 129~130°C). The acetate was identified by comparing it with the acetate derived from 6β-acetoxy-5α-cholestane-3β, 5-diol.

6β-Acetoxy-3α-chloro-5α-cholestan-5-ol from 6β-Acetoxy-5α-cholestane-3β, 5-diol. — 6β-Acetoxy-5α-cholestane-3β, 5-diol[7] (1 g.) was chlorinated with 10 ml. of freshly-distilled phosphorus oxychloride in 25 ml. of pyridine as described above. An oily product was crystallized from methanol to give 650 mg. of a crude crystalline product (m. p. ca. 118°C). Two recrystallizations from acetone-methanol gave 350 mg. of 6β-acetoxy-3α-chloro-5α-cholestan-5-ol (m. p. 129~131°C). $[\alpha]_D$ −34.9°C (*c* 1.65, $CHCl_3$).

Found: C, 72.41; H, 10.17. Calcd. for $C_{29}H_{49}ClO_3$: C, 72.39; H, 10.27%.

The acetate was identical with the acetate derived from the hydrolytic cleavage product of 3α-chloro-5, 6α-epoxy-5α-cholestane (mixed melting point test and infrared spectrum).

The authors wish to express their thanks to the Ministry of Education for its grant-in-aid for fundamental scientific research.

Chemical Laboratory
Ochanomizu University
Bunkyo-ku, Tokyo

6) Procedure according to M. Sawai, presented at the 10th Annual Meeting of the Chemical Society of Japan, Tokyo, April, 1957.

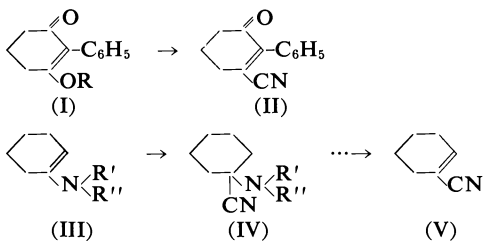
7) B. Ellis and V. A. Petrow, *J. Chem. Soc.*, 1939, 1078.

The Reaction of Enamines with Acetonecyanohydrin

By Yujiro NOMURA, Takiko SHIMURA and Yoshito TAKEUCHI

(Received December 29, 1963)

Betts and Davey[1] reported that the alkoxy group in the enol ethers (I) of 2-phenylcyclohexane-1, 3-dione was replaced by a cyano group by a reaction with acetonecyanohydrin, yielding 2-phenyl-3-cyano-2-cyclohexen-1-one (II). In connection with the resemblance of the properties of enol ethers and enamines, the reaction of the enamines (III) of cycloalkanone with acetonecyanohydrin has been investigated and found to yield aminonitrile (IV).



(I) (II)

(III) (IV) (V)

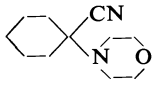
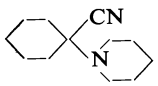
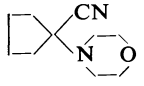
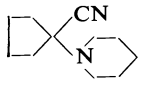
No further reaction to cyanocycloalkene (V) could be observed, even when IV was treated with thionyl chloride in pyridine.[2] Thus, the reaction of 1-morpholino-1-cyclohexene, 1-piperidino-1-cyclohexene, 1-morpholino-1-cyclopentene and 1-piperidino-1-cyclopentene with acetonecyanohydrin in chloroform in the presence of triethylamine gave 1-cyano-1-morpholinocyclohexane (VI) (m.p. 44～45°C), 1-cyano-1-piperidinocyclohexane (VII) (m. p. 67～68°C), 1-cyano-1-morpholinocyclopentane (VIII) (m. p. 53～54°C), and 1-cyano-1-piperidinocyclopentane (IX) (b. p. 88°C/3 mmHg) respectively. Of these aminonitriles, VIII and IX are new substances.

The identity of these products was confirmed by a comparison with authentic samples prepared by the condensation of cycloalkanone-cyanohydrin with morpholine or piperidine. The infrared spectra of these aminonitriles (VI—IX) in a carbon tetrachloride solution had an absorption at 2225～2230 cm^{-1}, indicating the presence of a cyano group.

1) B. E. Betts and W. Davey, *J. Chem. Soc.*, **1961**, 3333.

2) H. O. House, V. Paragamian, R. S. Ro and D. J. Wluka, *J. Am. Chem. Soc.*, **82**, 1461 (1960).

TABLE I. AMINONITRILES PRODUCED BY THE REACTION OF ENAMINE WITH ACETONECYANOHYDRIN

Aminonitrile	No.	Yield %	B. p. °C/mmHg	M. p. °C	IR cm^{-1}	N % Calcd.	N % Found
	VI	74 (almost quanti.)	127~133/4[a]	44~45[a] (45)	2230 1122 (2230) (1120)	14.42	14.31
	VII	57 (47)	(120~121/3)	67~68[b] (67~68)	2230	14.57	14.80
	VIII	55 (almost quanti.)	98~99/2.5	53~54 (52~53)	2225 1117	15.54	15.61
	IX	48 (50)	88/3 (104/4)	n_D^{19} 1.4908 ($n_D^{20.8}$ 1.4901)	2225	15.71	15.70

a) The reported[3] boiling point of VI is 120°C/1 mmHg, and the melting point is 35°C. It was prepared by the catalytic reduction (Pd-charcoal) of 1-cyano-1-morpholino-2-iodocyclohexanein methanol in the presence of triethylamine.

b) The reported[4] melting point of VII is 59°C. It was prepared from piperidine hydrochloride, sodium cyanide and cyclohexanone in an aqueous ethanol solution.

Experimental

All temperatures are uncorrected. The infrared spectra were determined with a Nihon Bunko Model Koken DS 301 spectrophotometer.

The Reaction of Enamines with Acetonecyanohydrin.—To a solution of enamine (0.1 mol.) and triethylamine (0.1 mol.) in 100 ml. of chloroform, one molar equivalent of acetonecyanohydrin was added. After the exothermic reaction had subsided, the mixture was heated under reflux for two hours. The solution was then cooled and poured into 300 ml. of water which had been neutralized with 6 N hydrochloric acid (Congo red). The layers were separated, and the aqueous layer was extracted with three 50 ml. portions of ether. The combined chloroform layer and ether extracts were washed with dilute hydrochloric acid and then with water. After the solution had been dried over anhydrous magnesium sulfate and the solvent had been removed, the crude aminonitrile appeared; this was purified by distillation at reduced pressure or by recrystallization from ethanol.

The aminonitriles obtained by this procedure are listed in Table I along with the results obtained by the condensation of cycloalkanonecyanohydrin with morpholine or piperidine (in parentheses).

Department of Chemistry
College of General Education
The University of Tokyo
Meguro-ku, Tokyo

3) E. Fusco, G. Bianchetti and S. Rossi., *Gazz. Chim. Ital.*, **91**, 825 (1961).

4) A. Kötz and P. Merkel *J. prakt. Chem.*, [2], **111**, 74 (1926); G. Le Ny and Z. Welvart, *Compt. rend.*, **245**, 434 (1957); Parke, Davis & Co., Brit. Pat. 851782 (1960) [cf. *Chem. Abstr.*, **55**, 10477 (1961)].

The Reaction of Phthalic Anhydride with Cyanoacetic Acid

By Toshio HAYASHI

(Received January 18, 1964)

Yale reported that the reaction of phthalic anhydride with malonic acid, in the presence of pyridine, gave *o*-acetophenonecarboxylic acid in a good yield.[1] The present author has attempted a similiar reaction using cyanoacetic acid in place of malonic acid, expecting to obtain *o*-carboxy-*α*-cyanoacetophenone (I). However, the reaction of phthalic anhydride with cyanoacetic acid in pyridine, in addition to unaltered phthalic anhydride and a small quantity of phthalic acid, yielded a new, bright yellow compound (II) (m. p. 221~222°C, $C_{12}H_6ON_2$).

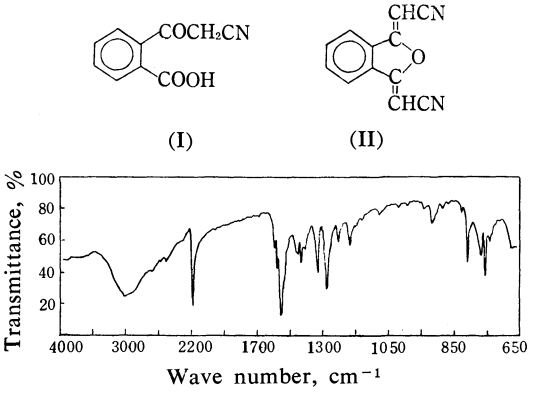


Fig. 1. Infrared spectrum of II in KBr disk.

The infrared spectrum of II (Fig. 1) unexpectedly lacks an absorption band in the C=O stretching region; on the other hand, it does show a sharp and strong band at 2208 cm^{-1} indicating the presence of a conjugated cyano group, and a strong absorption at 1576 cm^{-1}, which is regarded as the C=C stretching frequency which is shifted to the lower wave number region by conjugation with the benzene nucleus and with the cyano group. The enhanced intensity of this band is possibly due to the substitution of a hydrogen atom by an oxygen atom on one of the carbon atoms constituting the double bond. It also shows the out-of-plane deformation band of hydrogen atom of the tri-substituted double bond at 821 cm^{-1} and that of hydrogen atoms of the ortho-di-substituted benzene ring at 768 cm^{-1}. Biscyanomethylenephthalan (II) is the most probable structure to explain all the facts mentioned above. All attempts to hydrolyze II according to the usual method failed giving further evidence that the cyano groups are conjugated with double bonds.

Experimental

Biscyanomethylenephthalan (II).—A finely-powdered mixture of 26.5 g. (0.18 mol.) of phthalic anhydride and 18.0 g. (0.21 mol.) of cyanoacetic acid was heated with 20 ml. of pyridine on a water bath for 1.5 hr. Carbon dioxide was evolved throughout the heating. The clear red solution, on dilution with 200 ml. of water, results in the separation of a colorless solid (m. p. 124~126°C). When this was filtered and dried, it was identified as unaltered phthalic anhydride by a mixed melting point determination with an authentic sample. After the filtrate had been treated with 20 ml. of concentrated hydrochloic acid and allowed to stand for three days at room temperature, the precipitates which formed were filtered and identified as phthalic acid. To the filtrate 20 ml. of concentrated hydrochloric acid was again added and the mixture allowed to stand for additional three days. Clusters of yellow plates appeared on the sides of the flask. These were filtered off; weight 2.3 g. One crystallization of this sample from aqueous ethanol gave bright yellow plates (m. p. 221~222°C).

Found: C, 74.09; H, 2.88; N, 14.03. Calcd. for $C_{12}H_6ON_2$: C, 74.22; H, 3.11; N, 14.03%.

The Institute of Physical and Chemical Research
Bunkyo-ku, Tokyo

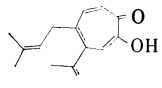
1) H. L. Yale, *J. Am. Chem. Soc.*, **69**, 1547 (1947).

The Synthesis of Procerin

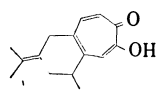
By Yoshio KITAHARA and Tadahiro KATO

(Received January 23, 1964)

In the course of his investigation of the tropolone constituents of *Juniperus procera Hochst*, Buneberg found a propolone, $C_{15}H_{18}O_2$, of a new sesquiterpene type to which he gave the name of procerin. From the chemical and physical experimental facts, the same author proposed structure I for it.[1] However, the synthesis of procerin has not yet been published.



(I)



(II)

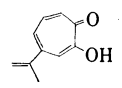
Nootkatin (II)[2,3] which has structure similar to that of procerin, has already been synthesized by Kitahara and Funamizu[4] by applying the Claisen rearrangement reaction. We have expected that procerin may be synthesized by the application of the above method to β-dolabrin (III).

The reaction of the silver complex salt of dolabrin and γ,γ-dimethyl allyl bromide in ether afforded the corresponding allyl ether (IV) of III in a 60% yield. IV was anticipated to be a mixture of two isomers, i. e., IVa and IVb, although several efforts to separate them were all unsuccessful.

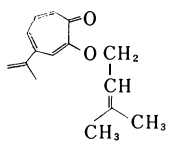
After a mixture of IVa and IVb had been heated in xylene to perform the Claisen rearrangement, the tropolone part was placed in an alkaline solution; this was extracted with ether after an acidification. From the sodium bicarbonate-soluble fraction of the ether solution, III was recovered in a 6.5% yield, while the sodium carbonate-soluble part of it gave a white crystalline compound V (m. p. 68~69°C), whose infrared spectrum is entirely the same as that of natural procerin. Furthermore, the results of the microanalysis of V and its copper complex (m. p. 199~200°C) are satisfactory for procerin and for its copper complex respectively.

We have not isolated the compound VI, which might be formed by the rearrangement which occurs at the ortho position.

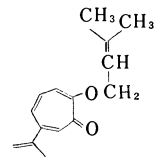
Since the synthesis of III had already been carried out, the total synthesis of procerin has now accomplished.



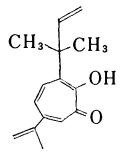
(III)



(IVa)



(IVb)



(VI)

Experimental

Silver Salt of Dolabrin (III). — Dolabrin (III) (1.62 g.) was dissolved into water (300 ml.), and the solution was neutralized with 2 N sodium hydroxide, using phenolphthalein as an indicator. To the solution was added silver nitrate (1.8 g.) in an aqueous solution (50 ml.). The separated yellow precipitate (2.5 g., 97%) were filtered off and dried at 100°C at reduced pressure for 2 hr., using phosphoric acid anhydride.

γ,γ-Dimethyl Allyl Ether IV of III.—(A) well-dried silver complex (2.5 g.) was suspended in absolute ether (30 ml.), and into this suspension γ,γ-dimethyl allyl bromide (1.5 g.) was stirred at room temperature. After being stirred for 1 hr., it was heated under reflux for 2 hr., the separated silver bromide was filtered off, and the ether was removed. Distillation of the resultant residue under reduced pressure afforded a yellow oil (IVa and IVb) (1.27 g., 60%), which has a slight color reaction to a ferric chloride solution.

The Claisen Rearrangement Reaction of γ,γ-Dimethyl Allyl Ether (IV). — A solution of IV (1.27 g.) in xylene (3 ml.) was refluxed for 3 hr. under a nitrogen atmosphere; then the solution was diluted with ether (20 ml.) and extracted with 0.1 N aqueous sodium hydroxide. The sodium hydroxide solution was acidified with sulfuric acid and extracted with ether. The combined ether

1) J. Buneberg, *Acta Chem. Scand.*, **15**, 645 (1961).
2) B. Carlssin, H. Erdtman, A. Frank and W. E. Harvey, ibid., **6**, 690 (1952).
3) W. E. Harvey, *Chem. & Ind.*, **1952**, 1267.
4) Y. Kitahara and M. Funamizu, This Bulletin, **31**, 782 (1958).

solution was extracted three times with a saturated sodium bicarbonate aqueous solution, which was then separated from the ether solution (E_1). The combined sodium bicarbonate solution was washed with ether once, and the ether washing was combined with E_1. The sodium bicarbonate solution was acidified and extracted with ether. The ether extract gave a white crystalline compound (60 mg.) (m. p. 50~53°C), which was identified as dolabrin by mixed melting point determination. E_1 was extracted with a saturated sodium carbonate aqueous solution, which was then separated from the ether solution (E_2). The sodium carbonate solution was washed with ether once, and the ether washing was combined with E_2. The separated sodium carbonate solution was acidified and extracted with ether. The ether solution gave a white crystalline compound (70 mg., 5.5%) (m. p. 68~69°C).

Found: C, 78.72; H, 8.16. Calcd. for $C_{15}H_{18}O_2$: C, 78.23; H, 7.88%.

Copper complex: m. p. 198~200°C, green needles (from ethanol).

Found: C, 69.39; H, 6.56. Calcd. for $C_{15}H_{17}O_2 \cdot Cu_{1/2}$: C, 69.01; H, 6.56%.

E_2 was washed with water and dried. The removal of the solvent gave a yellow oil.

The authors are indebted to Miss Yoko Endo and Miss Yukiko Endo of this Institute for their elemental analyses. The authors are also grateful to the Sankyo Co., Ltd., for its financial support of the present research.

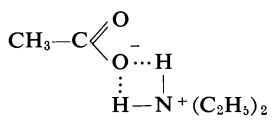
The Chemical Research Institute of Non-Aqueous Solutions
Tohoku University
Katahira-cho, Sendai

The Instability of Carbon Tetrachloride as a Solvent in the Study of Acid-Base Reactions

By Tai-ichi SHIBUYA* and Yasumasa I'HAYA

(Received January 28, 1964)

Barrow and Yerger[1] studied the acid-base reactions between acetic acid and diethylamine in carbon tetrachloride and chloroform, which are usually recognized as non-dissociating solvents, and reported that an interesting ion-pair with the structure:



(I)

is formed in carbon tetrachloride, but not in chloroform. This conclusion mainly followed from the fact that a new infrared absorption band appears just midway between the monomer and dimer carbonyl-stretching vibration bands of acetic acid in the carbon tetrachloride solution.

We reinvestigated the same system and also the benzoic acid-diethylamine reaction. We observed the same intermediate band as Barrow and Yerger reported, but we also found a new feature, that its intensity increases continuously as time passes. This is schematically shown in Fig. 1. It was also found that a crystalline substance gradually precipitates in the cell and that the solution becomes first yellow and then blue after the solution is taken out of the cell. This was seen over a wide range of concentrations of acids and diethylamine. It can be concluded that the crystalline substance is diethylamine hydrochloride from the fact that its infrared absorption spectrum and melting point agree very well with those of pure diethylamine hydrochloride. This compares favorably with the report of Collins.[2]

We also noticed that diethylamine in the carbon tetrachloride solution itself always shows a weak absorption band at 1741 cm^{-1}, the intensity of band increasing very much in about half an hour and a crystalline substance precipitating in the ordinary cell with a spacer of lead-amalgam. The crystalline substance in this case also was confirmed to be diethylamine hydrochloride. We have, therefore, concluded that the 1741 cm^{-1} band should *not* be assigned to the carbonyl group of the ion-pair (I). Since diethylamine hydrochloride does not show any infrared absorption in the carbonyl-stretching frequency region, the 1741 cm^{-1} band has to be ascribed to another substance, one which is supposed to be produced

* Present address: Department of Physics, University of the Pacific, Stockton, Calif.

1) G. M. Barrow and E. A. Yerger, *J. Am. Chem. Soc.*, **76**, 5211 (1954); E. A. Yerger and G. M. Barrow, ibid., **77**, 4474 (1955).

2) R. F. Collins, *Chem. & Ind.*, **1957**, 704.

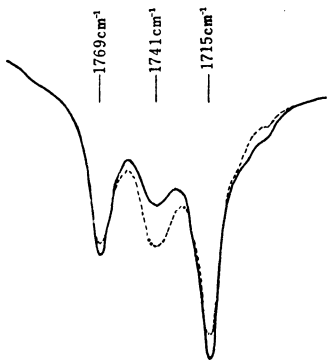


Fig. 1. Non-reproducibility of the infrared absorption curve for the system of 0.001 M acetic acid — 0.001 M diethylamine in the carbon tetrachloride solution. The time interval between first run (solid curve) and second run (dotted curve) is about 2 min. 1769 cm^{-1} band: free carbonyl stretching; 1715 cm^{-1} band: bound carbonyl stretching.

through organic reactions involving a process producing hydrogen chloride. As Ard and Fontaine reported,[3] the mixed solution of diethylamine and carbon tetrachloride, when used as an infrared solvent, tends to become opaque in an ordinary cell with a lead-amalgam spacer, but it is kept transparent for a while in a cell with a polyethylene spacer. We confirmed that this unknown organic reaction is promoted by the existence of a lead-amalgam—the solution rapidly becomes yellow, and soon a sticky, dark brown liquid floats on the surface of the solution, while the amount of the crystalline substance produced increases. We found that carbon tetrachloride acts on triethylamine in the same way as on diethylamine. The previous results obtained for acid-base reactions in carbon tetrachloride by infrared spectroscopy[1] seem, therefore, to be quite disputable, even qualitatively.

3) J. S. Ard and T. D. Fontaine, *Anal. Chem.*, 23, 133 (1951).

One of the authors especially (T. S.) wishes to thank Professor Keizo Suzuki, Dr. R. F. Collins and Mr. Noboru Suzuki for their helpful discussions.

Department of Chemistry
Tokyo University of Education
Otsuka, Tokyo (T. S.)

Laboratory of Physical Chemistry
The University of Electro-Communications
Chofu-shi, Tokyo (Y. I.)

SHORT COMMUNICATIONS

The Appearance of Free Radicals during Grignard Reactions

By Kazuhiro MARUYAMA*

(Received February 14, 1964)

Although ionic mechanisms are generally assumed for most Grignard reactions, I have been able to observe free radicals during the course of the addition of Grignard reagents to certain ketones by ESR techniques. Such aromatic ketones as benzophenone, 4-chlorobenzophenone, 4-aminobenzophenone, 4-methoxybenzophenone, 4, 4'-dimethoxybenzophenone, acetophenone and *p*-bromoacetophenone produce free radicals in their reactions with C_2H_5MgI, C_6H_5MgBr and p-$CH_3C_6H_4MgBr$ in tetrahydrofuran (THF).[1] Some aliphatic ketones (such as pentamethylacetone and hexamethylacetone) and benzonitrile also produce free radicals in the reaction.

The ESR measurements were carried out as follows: The carbonyl compounds and the Grignard reagent (each at about 10^{-3} mol.) were mixed at a dry-ice-acetone temperature in the absence of air and moisture. The sapmle was then inserted into a cavity which had previously been cooled with a stream of boiling liquid nitrogen, and the ESR spectrum was measured.

* Present address: Department of Chemistry, Faculty of Science, Kyoto University, Kyoto.

1) The Grignard reagents were prepared from reagent grade magnesium turnings for a Grignard reagent and the corresponding halides.

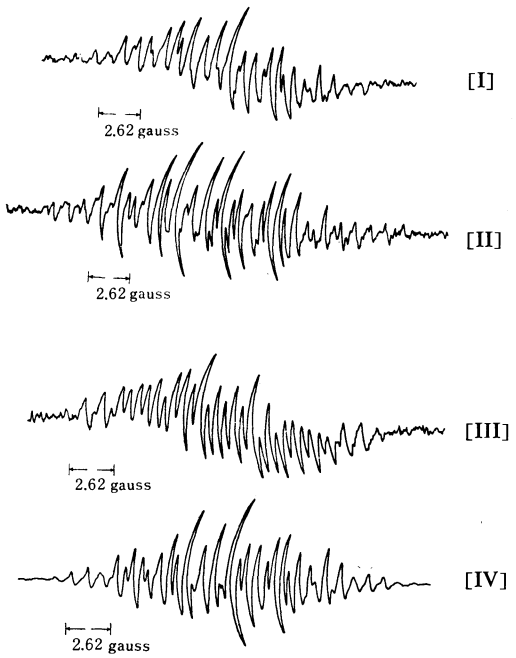


Fig. 1. The ESR spectra obtained during the course of some Grignard reaction.
[I] Benzophenone/phenylmagnesium bromide reacting system at −25°C
[II] Benzophenone/*p*-tolylmagnesium bromide reacting system at −25°C
[III] *p*-Chlorobenzophenone/phenylmagnesium bromide reacting system at −20°C.
[IV] Benzophenone-magnesium ketyl at −20°C

Benzophenone and 4-chlorobenzophenone give well-resolved hyperfine spectra during the course of the reactions with the Grignard reagents mentioned (Fig. 1). The other compounds give a single line. Although it is clear that the free radical in each Grignard reaction is not the ketyl which is obtained through the reduction of the corresponding carbonyl compound with Mg/Hg, a comparison of their ESR spectra and visible absorption spectra indicate that they are quite similar.

Table I. Absorption maximum in the visible absorption spectra of carbonyl/Grignard reacting systems and of the corresponding ketyls

Carbonyl compound	Carbonyl/Grignard system in THF	Ketyl in THF
Benzophenone	555 mμ	615 mμ
4-Chlorobenzophenone	570 mμ	623 mμ

It was also found that the amount of the free radical which is produced in the course of the Grignard reaction depends on the concentration of the Grignard reagent (Table II).

Although the mechanism of the free radical formation can not be clarified by only the ESR technique, the facts described above seem to suggest that the free radical is of the ketyl type and that it is produced through the reduction of ketone by a species such as $(MgX)_2(RMgX)_n$ or $(MgR)_2(RMgX)_n$ which might exist in the Grignard reagent.[2)]

The scope of the formation and the problem of the structure of such free radical species are now under study.

Table II. Concentration of free radicals produced in the course of reaction between $C_6H_5COC_6H_5$ and C_6H_5MgBr

Benzophenone*2 (B) mol.	Phenylmagnesium*1 bromide (G) mol.	Mol. ratio (B/G)	Maximum concn. of*2 free radicals (%)
1.8×10^{-3}	1.9×10^{-3}	1	3.4
4.5×10^{-4}	11.3×10^{-4}	1/ 3	3.7
3.8×10^{-5}	7.5×10^{-4}	1/20	24.0

*1 Dissolved in 10 ml. of THF.
*2 Calculated value based on the amount of benzophenone.

2) There is no conclusive information about the components of Grignard reagents. The existence of an equilibrium such as $2RMgX \rightleftarrows RMgR\ MgX_2 \rightleftarrows RMgR + MgX_2$ is generally believed in, but this is not enough to explain the complex behavior of Grignard reagents. See H. Gilman "Organic Chemistry," Vol. 1, John Wiley & Sons, New York (1949), p. 489; A. D. Vreugdenhill and C. Blomberg, *Rec. trav. chim.*, **28**, 453 (1963); N. M. Bikales and E. I. Becker, *Can. J. Chem.*, **41**, 1329 (1963); K. Maruyama, a paper which will soon appear in this Bulletin; A. F. Scott "Survey of Progress in Chemistry," Vol. 1, Academic Press, New York (1963), p. 300, etc.

Department of Chemistry
Washington University
St. Louis 30, Mo., U. S. A.

The Polarographic Behavior of Hydroxylycoctonine

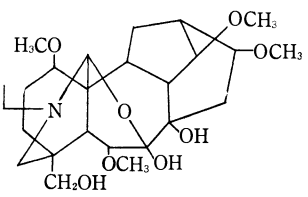
By Shozo YAMADA

(Received February 19, 1964)

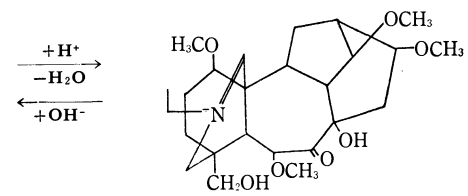
Hydroxylycoctonine[1,2] exhibited well-defined polarographic waves in an acidic medium. As is shown in Table I and in Fig. 1, the first wave was observed in the pH range of 2~8 and the second in the pH range of 5~8; the heights of both waves became smaller as the pH became greater, and the waves entirely disappeared at pH values greater than 8.

TABLE I. HALF-WAVE POTENTIAL AND WAVE HEIGHT OF HYDROXYLYCOCTONINE IN BRITTON-ROBINSON BUFFER SOLUTION
1.2 mmol./l; $m^{2/3}t^{1/6}=1.26\ mg^{2/3}\ sec^{-1/2}$

pH	$E_{1/2}$, −V. vs. SCE		i_d, μamp.	
	I	II	I	II
1.9	0.73		3.648	
3.9	0.75		3.648	
4.3	0.755		3.498	
4.85	0.76		3.318	
5.45	0.765		2.712	
5.9	0.77	1.725	1.464	3.0
6.9	0.775	1.725	0.240	1.56
7.75	unmeasurable			



I



II

A slope of 10 mV. per unit change of pH in the $E_{1/2}$~pH curve, a slope of 80 mV. in the log (i/i_d-i)~E curve at pH 1.9, and an $E_{1/4}-E_{3/4}$ value of 100 mV. at pH 1.9 were obtained, these values confirming the irreversibility of

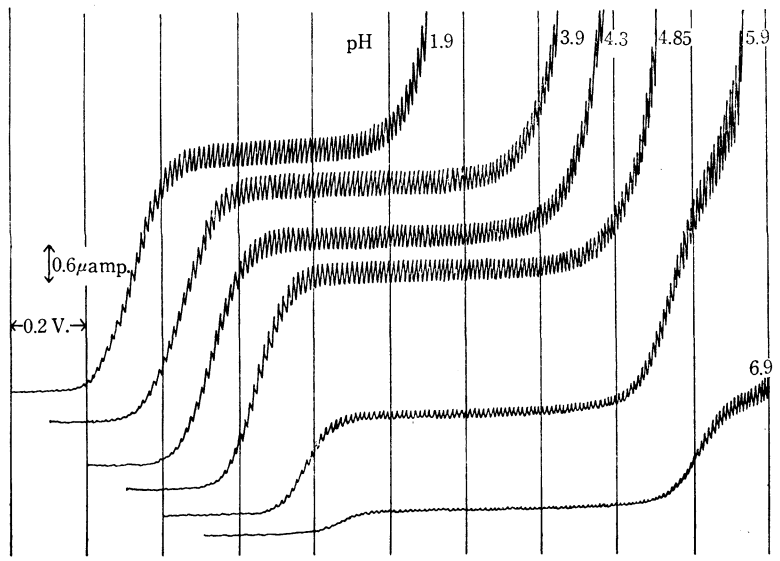


Fig. 1. Polarograms of hydroxylycoctonine in buffers at various pH values. (Curves start from −0.4 V.)

1) H. Suginome and K. Ohno, *J. Fac. Sci., Hokkaido Univ., Ser. III, Chem.*, 4, 36 (1950).

2) O. E. Edwards and L. Marion, *Can. J. Chem.*, 30, 627 (1952).

the electrode process. The irreversibility was observed also in the a.c. polarography of hydroxylycoctonine.

Applying Ilkovic equation with the D value estimated from the molecular weight, $n=2.0$ was obtained.

From the $i_d \sim$pH curve the apparent pK_a of hydroxylycoctonine was assumed to be 5.8; this value was concordant with the reported pK_a (5.8) in a 50% methanol solution.[3]

The limiting current of the wave was confirmed to be diffusion-controlled from the relationship between the height of the mercury column and the limiting current height; it was linearly proportional to the concentration between 0 and 0.27 mmol./l. at pH 1.9.

This polarographic behavior of hydroxylycoctonine can be readily interpreted from the defined structures[3,4] of hydroxylycoctonine (I) and its anhydronium salt (II). Therefore, it is considered that the first wave of the polarogram is due to the $>C=N^+<$ bond and the second to the ketone group in II,* which is formed in an acidic medium.

Similar behavior was observed also in the polarography of acetylanhydrolycoctonine** and of anhydrolycoctonine.***

Further details of the experiment will be published shortly.

Osaka City Institute of Hygiene
Kita-ku, Osaka

3) O. E. Edwards, M. Los and L. Marjon, ibid., **37**, 1996 (1959).

4) Z. Valenta, *Chem. & Ind.*, **1959**, 633; Z. Valenta and I. G. Wright, *Tetrahedron*, **9**, 284 (1960).

* The same immonium structure as that in hydroxylycoctonine has been reported in the case of diacetyldelcosine (T. Amiya and T. Shima. *J. Org. Chem.*, **26**, 2616 (1961)).

** Suginome's monoacetyl derivative, m. p. 132~133°C;[1] $C_{27}H_{41}O_7N$, $[\alpha]_D^{31}+11°$, ν_{max}^{Nujol} 1730, 1224 (ester), 1721 cm^{-1} (C=O).

*** Alkali hydrolysis product of acetylanhydrolycoctonine; $C_{25}H_{39}O_6N$, m. p. 158~160°C, $[\alpha]_D^{28}+21°$, ν_{max}^{Nujol} 3497 (OH), 1721 cm^{-1}(C=O).

Eine π-Dien-Eisentricarbonyl-Komplexverbindung als ein öllöslicher Hydrierungskatalysator

von Ikuei OGATA und Akira MISONO

(Eingegangen am 26. Februar, 1964)

Das π-C_{18}-Dien-carbonsäure-ester-eisentricarbonyl, welches immer bei der Hydrierung des als Fettsäurezusammensetzung Diensäure enthaltenden Öles mit Eisenpentacarbonyl entsteht und bisher für ein Nebenprodukt oder für einen Zwischenkörper im Hydrierungsvorgang gehalten wurde,[1] erwies sich, dass es als ein aktiver Katalysator mit grösserer Aktivität als Eisenpentacarbonyl selbst auf die Hydrierung der CC-Doppelbindung von ungesättigten Fettsäureestern wirkt und sich selbst dabei allmählich—in der Monoen-Körper-Hydrierung ziemlich schneller—zersetzt.

Jeder Versuch wurde mit der einem 0.4～0.8 Gew. % metallischen Eisen entsprechenden Komplexverbindung, welche durch die in der letzten Arbeit[2] berichtete Methode hergestellt wurde, in einem kleinen Edelstahlautoklaven durchgeführt. Das Reaktionsprodukt wurde zur Entfärbung in Äther mit Salzsäure (1 : 1) geschüttelt, und seine Fettsäurezusammensetzung wurde als Methylester durch Gaschromatographie gemessen. Einige Versuchsergebnisse sind in der folgenden Tabelle zusammengestellt.

Bei geeigneten Reaktionsbedingungen verlief die Hydrierung ziemlich selektiv und die Umwandlung von Dien-Körpern, besonders von Konjugierter, in Monoen war bevorzugt. Dabei trat im Vergleich zu Arbeiten mit Festkatalysator verhältnissmässig geringfügige Transisomerisierung ein. Als Eigentümlichkeit des homogenen Katalysators waren die Selektivität und die Geschwindigkeit bei der Hydrierungsreaktion davon unabhängig, ob die Probe als Methylester order als Glycerid zu der Reaktion verwendet wurde. Freie Fettsäuren dagegen, die unter den Versuchsbedingungen kein Komplex bilden, wurden nicht reduziert und verhalten sich wie ein Katalysatorgift, wie es bereits bei der Hydrierung mit Eisenpentacarbonyl bemerkt wurde. Andererseits wurde aber reines Methyloleat hydriert,[3]

1) A. Misono, I. Ogata und F. Funami, *J. Japan Oil Chemists' Soc.* (*Yukagaku*), **13**, 21 (1964).

2) I. Ogata und A. Misono, Diese Bulletin, **84**, 439 (1964).

3) I. Ogata, unveröffentlicht.

TABELLE I. VERSUCHSERGEBNISSE*1

Ausgangsstoff	DHCO-Me*2		Baumwollsaat-Öl	Baumwollsaat-Methylester	Leinöl	Walöl	Methyloleat
Autoklavenfüllung, g							
Öl od. Ester	2.34	2.50	2.39	2.28	27.55	34.43	2.47
Komplex	0.15	0.11	0.08	0.07	1.42*3	1.74	0.13
Wasserstoffdruck, kg/cm² bei 20°C							
Anfang	29.8	35.0	30.0	30.0	100	29.2	30.0
End	23.8	30.1	27.1	27.2	86	10.8	26.1
Temperature, °C	190	180	190	190	190	190	190
Reaktionszeit, Min*4	120	195	90	90	95	170	125
Absorbiertes							
Wasserstoff, cm³	175	146	90	87	1060	1205	110
Analyse der Produkte							
Fettsäureaufbau, %							
C_{16}	1.7	1.7 (2.9)	22.7	24.5 (25.0)	6.5 (4.6)		7.4 (7.6)
C_{18}	15.8	8.1 (1.6)	6.3	5.9 (2.0)	8.0 (6.4)	*5	63.5 (2.1)
$C_{18}F_1$	78.5	77.4 (7.3)	65.0	63.3 (18.0)	37.2 (21.6)		29.1 (84.1)
$C_{18}F_2$ (nonkonj.)	4.0	12.8 (57.7)	6.0	6.3 (55.0)	20.3 (15.2)		0.0 (6.2)
$C_{18}F_2$ (konj.)	0.0	0.0 (30.5)	—	—	—		—
$C_{18}F_3$	—	—	—	—	28.0 (52.2)		—
Jod-Z. (Wijs)	—	—	—	—	134 (178)	78 (120)	—
trans-Isomer (Gew.%)	35	40 (>50)*6	28	28 (Spur)	17 (Spur)	24 (Spur)	—
Smp. (°C)*7	18	8 (<0)	33	8 (—)	7 (<0)	23 (13)	39 (<0)

*1 Die Zahl in Klammen gibt die Zahl des Ausgangsöles.
*2 Methylestergemisch von Fettsäuren des dehydrierten Rizinusöl.
*3 Reinheit 60%.
*4 Bis die Wasserstoffaufnahmgeschwindigkeit abnimmt.
*5 Identisch mit Ausgangsstoff. Nur die länger kettigen, hochungesättigten wurden reduziert,
*6 Der cis-trans-Konjugierte wurde nicht berechnet.
*7 Durch JOCS Official Method Cc 4—25 gemessen,

obgleich unter den gleichen Umständen auch keine Komplexbildung beobachtet wurde. Das System, welches das im gesättigten Fettsäureester und unter Wasserstoffatmosphäre durch thermische Zersetzung von Eisencarbonylen erzeugte kolloidale Eisen enthält, zeigte keine katalytische Aktivität für die Hydrierung.

Zur Aufklärung dieses Ergebnisses können wir vermuten, dass die Bildung von π-Dieneisentricarbonyl-Komplex keine notwendige Voraussetzung für die weitere Hydrierungsreaktion ist, sondern dass der Komplex in ein Eisencarbonylradikal wie $Fe(CO)_3$ dissoziiert, das auch aus Eisenpentacarbonyl in beschränkten Zuständen erzeugt werden könne und alsbald ins unbekannte aktive Eisencarbonylwasserstoffradikal wie $HFe(CO)_3$[4] übergehen und die Hydrierung verursachen werde. Der Reaktionsmechanismus mit freien Säure ist noch nicht klar.

Technische Fakultät
Institut für Technische Chemie
Universität Tokio
Hongo, Tokio

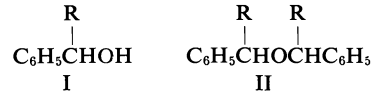
4) T. A. Mannuel, *J. Org. Chem.*, **27**, 3941 (1962).

The Intermolecular Dehydration Reaction of Benzhydrols in Dimethyl Sulfoxide

By Takeo SATO, Akihiko TAKATSU and Kazuo HATA

(Received February 29, 1964)

It has been shown[1] that the treatment of α-(bromomesityl)-benzyl alcohol (Ib) with polyphosphoric acid gives α-(bromomesityl)-benzyl ether (IIb). This mild reaction, which takes place when the mixture is warmed on a water bath for 15 minutes, constitutes the first example of the intermolecular dehydration of alcohol by means of polyphosphoric acid.



I II

a, R=phenyl
b, R=bromomesityl

The current interest in dimethyl sulfoxide as an efficient dehydrating agent, which gives olefins from aliphatic tertiary alcohols or secondary and tertiary benzylic alcohols[2] and substituted tetrahydrofurans from 1, 4-glycols,[3] has lead the present authors to reinvestigate the ether formation reaction of compound Ib in dimethyl sulfoxide.[4] The same reaction was also applied to benzhydrol (Ia) and 9-hydroxyfluorene.

Benzhydrol (0.010 mol.) was heated in dimethyl sulfoxide[5] (0.20 mol.) at 165~170°C for 8 hours under an atmosphere of nitrogen. The dilution of the reaction mixture with water, followed by the filtration and recrystallization of the crystalline product, afforded a 87.5% yield of bis(diphenylmethyl) ether (IIa) (m. p. 108~109°C; ν_{max}^{KBr} 1050, 737 and 698 cm^{-1}). The shorter reaction period employed apparently lowered the yield to 62.5% (4 hr.), whereas the longer heating did not affect the yield since 80% of IIa was obtained after 24 hr. α-(Bromomesityl)-benzyl alcohol (Ib) in the form of colorless prisms (m. p. 65~67°C) (Found: C, 62.77; H, 5.51. Calcd. for $C_{16}H_{17}OBr$: C, 62.96; H, 5.61%) was obtained in a 95% yield by the reduction of benzoylbromomesitylene[6] with a lithium aluminum hydride slurry in ether. It formed an acetate as colorless prisms (m. p. 99~100°C) (Found: C, 62.07; H, 5.21. Calcd. for $C_{18}H_{19}O_2Br$: C, 62.26; H, 5.51%). The treatment of Ib in dimethyl sulfoxide at 165~170°C for 16 hours, followed by the isolation procedure

1) M. Ōki and T. Sato, unpublished work, done in connection with their study of the sterically-hindered polyphenylethylenes. Cf. M. Ōki, This Bulletin, **26**, 161 (1953).

2) V. J. Traynelis, W. L. Hergenrother, J. R. Livingston and J. A. Valicenti, *J. Org. Chem.*, **27**, 2377 (1962).

3) B. T. Gillis and P. E. Beck, ibid., **28**, 1388 (1963).

4) After the completion of the present study, two reports along this line appeared: V. J. Traynelis, W. L. Hergenrother, H. T. Hanson and J. A. Valicenti, *J. Org. Chem.*, **29**, 123 (1964); V. J. Traynelis and W. L. Hergenrother, *J. Am. Chem. Soc.*, **86**, 298 (1964).

5) Dimethyl sulfoxide was dried over potassium hydroxide and fractionally distilled through a Vigreux column under a current of nitrogen; b. p. 84~84.5°C/18 mmHg, n_D^{20} 1.4791.

6) J. F. Hyde and R. Adams, *J. Am. Chem. Soc.*, **50**, 2503 (1928).

described above, afforded 20% of the crude ether as colorless prisms (m. p. 156~158°C), the same compound as the product of dehydration reaction by polyphosphoric acid.[1] By a combination of fractional crystallization and chromatography on alumina it gave α-(bromomesityl)-benzyl ether (IIb) (m. p. 176~177°C) (Found: C, 64.51; H, 5.51. Calcd. for $C_{32}H_{32}OBr_2$: C, 64.86; H, 5.44%), together with a low melting compound (m. p. 152~154°C), probably the structural isomer.

As a related compound, 9-hydroxyfluorene was heated in dimethyl sulfoxide for 24 hours at 165~170°C. It, however, gave 9-fluorenone as a major product (56%), with only a 14% yield of 9-fluorenyl ether. Benzyl alcohol has also been found to give an oxidation product on prolonged heating (20 hr.) in dimethyl sulfoxide at the same temperature; benzaldehyde was obtained in a 15.7% yield, characterized as 2,4-dinitrophenylhydrazone, about 60% of the starting alcohol being recovered by distillation.

Department of Chemistry
Faculty of Science
Tokyo Metropolitan University
Setagaya-ku, Tokyo

The Trans-Configuration in Dimethyltin and Dimethyllead Bis(acetylacetonates)

By Yoshikane KAWASAKI, Toshio TANAKA and Rokuro OKAWARA

(Received March 4, 1964)

Recently, a series of diorganotin bis(8-hydroxyquinolinates) and diorganotin (2,2'-bipyridyl)dichlorides have been characterized by the authors[1] and others[2]; all of these compounds seem to have a chelate structure containing a hexa-coordinated tin atom. It is not clear, however, whether they have a cis- or a trans-configuration with regard to the methyl groups. It seemed that it would be interesting to identify one of the isomers which is of either a cis- or a trans-configuration among similar compounds with a hexa-coordinated tin atom.

We have, therefore, prepared dimethyltin and dimethyllead bis(acetylacetonates). Dimethyltin bis(acetylacetonate). M. p. 177～178°C. Found: C, 41.03; H, 5.83; Sn, 34.25. Calcd. for $C_{12}H_{20}O_4Sn$: C, 41.54; H, 5.81; Sn, 34.21%. Dimethyllead bis(acetylacetonate). M. p. 163～163.5°C. Found: C, 33.10; H, 4.58; Pb, 47.53. Calcd. for $C_{12}H_{20}O_4Pb$: C, 33.10; H, 4.60; Pb, 47.58%.

The infrared spectra of these compounds were measured as mulls in Nujol and in hexachlorobutadiene, using a Hitachi EPI-2G grating infrared spectrophotometer for 2～25 μ and a Leitz infrared spectrophotometer equipped with CsBr optics for 15～33 μ. Furthermore, the Raman spectrum of dimethyltin bis(acetylacetonate) was measured in the solid state, using a Nippon Yūki-gōsei Raman spectrograph. The absorption bands and the Raman lines in the 300～600 cm^{-1} region of these spectra are shown in Table I, together with the assignment of the M–C and M–O stretching vibrations. The assignment of the remaining bands will be discussed elsewhere.

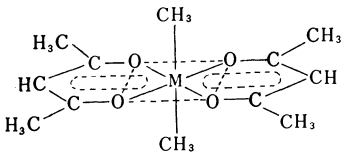
The most interesting characteristic of the infrared spectrum of dimethyltin bis(acetylacetonate) is that the only strong antisymmetric stretching vibration of the Sn–C bond was observed at 556 cm^{-1}, while the symmetric one disappeared. On the other hand, the latter was observed at 508 cm^{-1} in the Raman spectrum, as Table I shows. In the infrared

TABLE I. INFRARED AND RAMAN SPECTRA OF DIMETHYLTIN AND DIMETHYLLEAD BIS(ACETYLACETONATES) IN THE REGION OF 300～600 cm^{-1}

$(CH_3)_2Sn(acac)_2$		$(CH_3)_2 \cdot Pb(acac)_2$	
IR	Raman	IR	
576 s	568 w	553 w	
556 s	—	541 s	M–C antisym. str.
—	508 s	—	M–C sym. str.
421 sh	—	—	
406 s	417 m	391 s	M–O str.

1) T. Tanaka, M, Komura, Y. Kawasaki and R. Okawara, *J. Organometal. Chem.*, in press.
2) D. Blake, G. E. Coates and J. M. Tate, *J. Chem. Soc.*, **1961**, 756; D. L. Alleston and A. G. Davies, ibid., **1962**, 2050.

spectrum of dimethyllead bis(acetylacetonate), similarly, the only antisymmetric stretching vibration of the Pb–C bond was found at 541 cm^{-1}. Considering the selection rules of the infrared and the Raman spectra, two methyl groups in these compounds will be in the trans-position with the central tin or lead atom. The absorption bands due to the ligand of the tin or lead chelate are similar to those of copper acetylacetonate,[3] in which four Cu–O bonds are considered to be equivalent. The four Sn–O or Pb–O bonds in these acetylacetonates seem, therefore, to be nearly equivalent. From these facts, the most probable structure of dimethyltin and dimethyllead bis(acetylacetonates) is considered to be:



Trans-dimethylmetal bis(acetylacetonates)
M=Sn, Pb

3) K. Nakamoto and A. E.Martell, *J. Chem. Phys.*, 32, 588 (1960); K. Nakamoto, P. J. McCarthy and A. E. Martell, *J. Am. Chem. Soc.*, 83, 1272 (1961); M. Mikami, I. Nakagawa and T. Shimanouchi, The 17th Annual Meeting of Japan Chem. Soc., 31X-21 (1964).

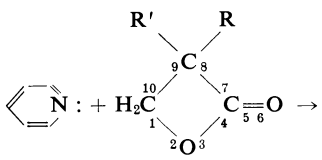
Department of Applied Chemistry
Osaka University
Miyakojima, Osaka

A Molecular Orbital Interpretation of the Ring-opening Polymerization

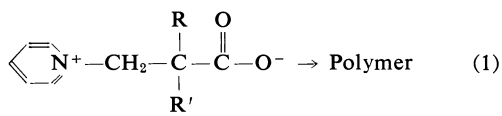
By Kenichi FUKUI, Hiroshi KATO, Teijiro YONEZAWA and Seizo OKAMURA

(Received March 9, 1964)

One of the most interesting problems in ring-opening polymerization is that of the fission of a particular bond in a definite catalyst. No quantum mechanical interpretation of the results, however, has yet been proposed. In this short communication, it will be shown that the reactivity indices for σ electron systems, that is, the delocalizability (D_r) and the frontier electron density (f_r) proposed in our previous paper,[1] are useful in explaining the experimental results of ring-opening polymerizations of β-propiolactone derivatives by Watanabe, Hayashi and Okamura.[2] It will be pointed out that, in β-propiolactone derivatives (I), the bond fission takes place at the β C–O bond with a basic catalyst such as pyridine:



(I)



(1)

The rate of the polymerization in these derivatives is found to decrease as follows:

α,α-bischloromethyl β-propiolactone >
α-ethyl, α-chloromethyl β-propiolactone >
α-methyl, α-chloromethyl β-propiolactone >
β-propiolactone > α,α-dimethyl
β-propiolactone

With an acid catalyst such as BF_3OEt_2, the order of the reaction rate is reversed; hence, it may be supposed that the magnitude of the σ electron density at the β-carbon atom may be correlated with the experimental results presented above.

We have tentatively treated these compounds by the C–C skeleton method[3] for the sake of simplicity. The values of the parameters used may be summarized as follows:

Coulomb integrals:

$$C(sp^3)=\alpha,\ C(sp^2)=\alpha+0.1\beta,$$
$$\text{and } O(\text{etheric})=O(\text{ketonic})=\alpha+0.3\beta.$$

Resonance integrals:

$$C(sp^3)\text{–}C(sp^3)=\beta,\ C(sp^3)\text{–}C(sp^2)=\beta,$$
$$C(sp^3)\text{–}O(\text{etheric})=0.6\beta,$$
$$C(sp^2)\text{–}O(\text{etheric})=0.7\beta,$$
$$C(sp^2)\text{–}O(\text{ketonic})=1.2\beta,$$

1) K. Fukui, H. Kato and T. Yonezawa, This Bulletin, **34**, 443, 1111 (1961).
2) H. Watanabe, K. Hayashi and S. Okamura, *Summary of the 12th Symposium on High Polymers*, Nagoya, (1963), p. 221.
3) H. Yoshizumi, *Trans. Faraday Soc.*, **53**, 125 (1957): K. Fukui, H. Kato and T. Yonezawa, This Bulletin, **33**, 1197 (1960).

$C(sp^3)-C(sp^3)=0.34\beta$,
$C(sp^2)-C(sp^2)=0.40\beta$,
$O-O=0.30\beta$,
} between two hybridized orbitals of the same atom.

In order to characterize the electronic effect of the substituent group at the α-carbon atom in β-propiolactone, two symbols are employed. M denotes an electron-repelling group, and X, an electron-attracting group. We make use of one parameter to represent their electronic effect. The value of the Coulomb integral of M is taken tentatively to be -0.2 (for ethyl)* and to be 0 (for the methyl group), and that of X, to be $+0.2$ and $+0.4$ for the chloromethyl group. The values of the resonance integral for C–M and C–X are taken to be β.

Since it is evident from our frontier electron concept that the frontier orbital of pyridine for an electron acceptor is the highest-occupied lone-pair orbital of nitrogen, we can assume a weak interaction between the nitrogen lone-pair electrons in pyridine and the σ orbital in β-propiolactone derivative molecules at the transition state. Hence, $D_r^{(N)}$ and $f_r^{(N)}$ are employed as the reactivity indices. In Fig. 1, the calculated values of $f_r^{(N)}$ with respect to several lactones are listed. The position of

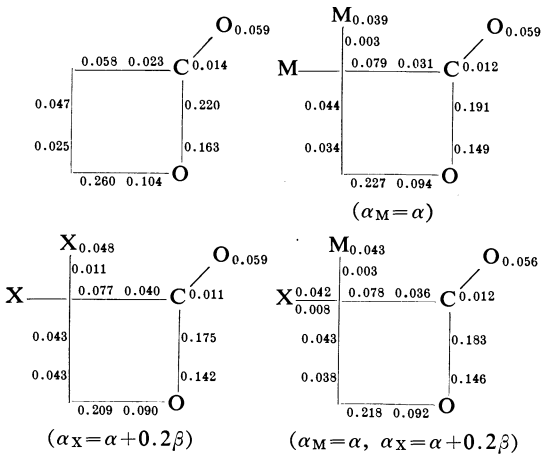


Fig. 1. Values of $f_r^{(N)}$ of some β-propiolactone derivatives.

* Altough this value may be too large, it is adopted just for the convenience of calculation.

Table I. Calculated values of $D_r^{(N)}$ at σ orbital (1) in various β-propiolactone derivatives

$X^{a)}=+0.4$, $X=+0.4$	1.570
$X=+0.2$, $X=+0.2$	1.538
$M=0$, $X=+0.2$	1.536
$M=0$, $X=+0.2$	1.522
$M=-0.2$, $X=+0.4$	1.519
M none, X none	1.510
$M=0$, $M=0$	1.510
$M=-0.2$, $M=-0.2$	1.489

a) X and M denote the values of the Coulomb integral of X and M respectively.

the largest $f_r^{(N)}$ is common with respect to all of these compounds and is the orbital 1 (cf. Eq. (1). This finding is compatible with the experimental evidence.[2] The calculated $D_r^{(N)}$'s of σ orbitals at the β-C atom in the C–O bond are shown in Table I. In view of this finding the more repulsive the substituent group is, the lower is the reactivity of the compound. In the case of the electron-attracting substituent, the more attracting the substituent group is, the higher is the reactivity. This theoretical results is approximately consistent with the experiment which is indicated in Reaction (1).

Accordingly, it may be seen that $D_r^{(N)}$ and $f_r^{(N)}$ are appropriate indices for discussing the reactivity of ring-opening polymerization.

For the case of acidic catalysts, the electrophilic reactivity indices, $D_r^{(E)}$ and $f_r^{(E)}$, can be used. These results will be published in the near future.

The calculation has been carried out on a KDC-I digital computer at Kyoto University.

Faculty of Engineering
Kyoto University
Sakyo-ku, Kyoto

The Solubility and Anion Exchange Behavior of Heavy Lanthanide Elements in a Potassium Carbonate Solution

By Tomitsugu TAKETATSU

(Received March 13, 1964)

In a previous paper,[1] the present author reported that several lanthanide elements dissolved in a potassium carbonate solution were adsorbed on an anion exchange resin and that both the amount dissolved and that adsorbed increase with the increase in atomic number. However, it was impossible to distinctly detect the order of these amounts dissolved and adsorbed, as well as the position of yttrium among those of lanthanide elements, because of the lack of data for heavy lanthanide elements.

This study treats the behavior of tripositive lanthanide elements other than cerium and promethium. Since the solubilities of lanthanum and praseodymium are small and since the convenient concentration for an anion exchange measurement can not be obtained, both these elements are eliminated from the measurement. From the results obtained, it was observed that there was a distinct difference between the heavy lanthanide elements (Er, Tm, Yb, Lu and Y) and the other light elements. The standard solutions were prepared by dissolving the pure oxides (purity more than 99.8~99.9%) in dilute hydrochloric acid. The quantities of these lanthanide elements and the volumes of the potassium carbonate solutions used in this experiment were identical, i. e., ca. 2×10^{-4} mol. and 5 ml. for the measurement of the solubility (S), and ca. 2×10^{-5} mol. and 20 ml. for that of the distribution coefficient (K_d, cc./g.) respectively. The anion exchange resin used was 1 g. of Dowex 1, X-8, in the carbonate form, of the size of 50~100 mesh.

Figure 1 shows that, when the amount dissolved is more than about 3×10^{-5} mol./ml., the solubility increases with the increase in atomic number, and that, on the other hand, when the amount is less than that, the slope of the curve $\log S$ vs. $\log CO_3^{2-}$ in the heavy lanthanide elements obviously differs from that in other light elements. It may be thought that the order of the solubility varies with the concentration of potassium carbonate. Figure 2 shows the logarithmic plot of the K_d values of four representative lanthanide elements against various concentrations of potassium carbonate. All the curves of $\log K_d$ vs. $\log CO_3^{2-}$ obtained in this experiment give a linearity,

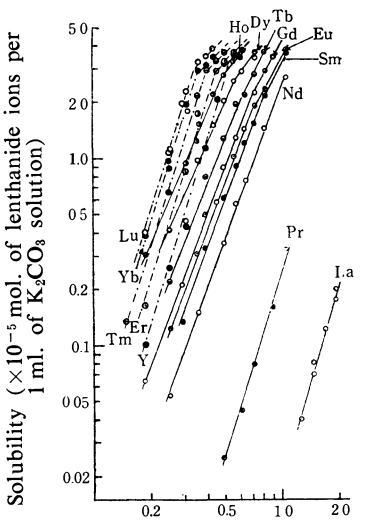


Fig. 1. Relation between the solubility of lanthanide elements and the concentration of potassium carbonate at 20°C.

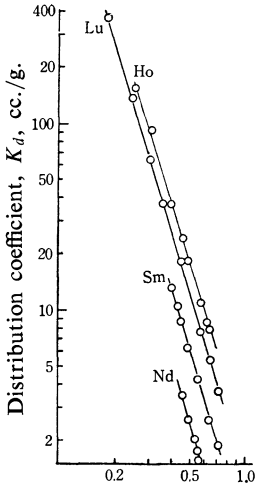


Fig. 2. Distribution coefficient of lanthanide ions between Dowex 1 and potassium carbonate solution at about 20°C.

1) T. Taketatsu, This Bulletin, 35, 1573 (1962).

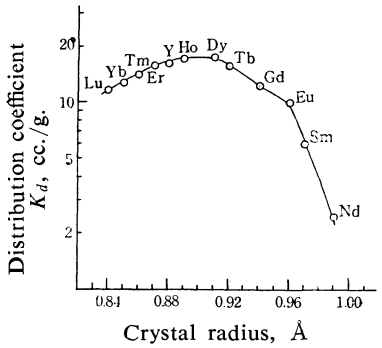


Fig. 3. Relation between the K_d value in a 0.5 M potassium carbonate solution and the crystal radius of tripostive lanthanide ions at about 20°C.

and the lines are parallel to one another, with a negative slope. The relation between the K_d values in a 0.5 M potassium carbonate solution and the crystal radii of tripositive lanthanide ions given by Zachariasen[2] is shown in Fig. 3. These K_d values increase with the increase in atomic number from neodymium to dysprosium or holmium; on the other hand, the values decrease with the increase from erbium to lutetium. The position of yttrium is found to be between erbium and holmium. It is interesting to consider that the maximum K_d value corresponds with the maximum magnetic susceptibility of the lanthanide element.

The details of the experimental procedure will be presented and the findings discussed elsewhere.

General Education Department
Kyushu University
Otsubo-machi, Fukuoka

2) W. H. Zachariasen, *Phys. Rev.*, **73**, 1104 (1948).

Some Stable Sigma-bonded Alkyl Derivatives of Nickel

By Hiroshi YAMAZAKI and Nobue HAGIHARA

(Received March 23, 1964)

In recent years a variety of compounds has been reported in which an aryl or ethynyl group is attached to nickel[1-3] by means of a sigma-bond. However, alkyl derivatives have not been isolated because of their instability, though evidence has been obtained about their formation in solution.[1,4] We now wish to report the preparation of stable sigma-bonded alkyl derivatives of nickel.

The treatment of a solution of methyl magnesium iodide in ether with a solution of triphenylphosphine-π-cyclopentadienyl nickel chloride[5] (decomp. p. 138~139°C. Found: C, 65.53; H, 4.82%.) in benzene under cooling, followed by hydrolysis with aqueous ammonium chloride, chromatography on alumina, and recrystallization from hexane resulted in the formation of dark green crystals of triphenylphosphine-π-cyclopentadienylmethylnickel, (π-C_5H_5)Ni(PPh_3)CH_3 (Yield, 67%; m. p. 115~118°C (decomp.). Magnetic measurement: diamagnetic, $\chi_{mol} = -149 \times 10^{-6}$. PMR: 2.56$\tau$ (C_6H_5); 4.94 τ (C_5H_5); 10.82 τ (CH_3), doublet (J=6 c. p. s.). Found: C, 71.64; H, 5.99; mol. wt. (cryoscopic in benzene), 387. Calcd. for $C_{24}H_{23}PNi$: C, 71.86; H, 5.78%; mol. wt., 401.).

The crystals are stable enough to handle in the air. They are soluble in most organic solvents, although poorly soluble in alcohols; they decompose immediately in carbon tetrachloride. The green solution in benzene is fairly stable under nitrogen, but unstable in the air.

Triphenylphosphine-π-cyclopentadienylethylnickel, (π-C_5H_5)Ni(PPh_3)C_2H_5, was also obtained by a similar procedure (green crystals; yield, 61%; decomp. p. 90~100°C (without melting). PMR: 2.56 τ (C_6H_5); 4.94 τ (C_5H_5); 9.46 τ (C_2H_5), unresolved broad peak. Found: C, 72.64; H, 6.15. Calcd. for $C_{25}H_{25}PNi$: C, 72.33; H, 6.07%). The crystals can be handled in the air, but their solution is less stable than that of the methyl derivative.

More stable phenyl, ethynyl and phenylethynyl derivatives were also prepared by the

1) J. Chatt and B. L. Shaw, *J. Chem. Soc.*, **1960**, 1726.
2) M. Tsutsui and H. Zeiss, *J. Am. Chem. Soc.*, **82**, 6255 (1960).
3) R. Nast, *Angew. Chem.*, **72**, 26 (1960).
4) M. Tsutsui and H. Zeiss, *J. Am. Chem. Soc.*, **81**, 6090 (1959).
5) U. S. Pat. 3054815 (1962); *Chem. Abstr.*, **58**, 1494 (1963).

reaction of triphenylphosphine-π-cyclopentadienyl nickel chloride and the corresponding Grignard reagents.

(π-C_5H_5)Ni(PPh_3)Ph: dark green crystals. Yield, 77%. M. p. 137~139°C (decomp.). Found: C, 75.03; H, 5.53. Calcd. for $C_{29}H_{25}PNi$: C, 75.20; H, 5.44%.

(π-C_5H_5)Ni(PPh_3)C≡CH: dark green crystals. Yield, 75%. M. p. 111.5~112.5°C (decomp.). Found: C, 72.96; H, 5.30. Calcd. for $C_{25}H_{21}PNi$: C, 73.03; H, 5.15%. IR (Nujol): 3300 (≡C–H stretching), 1970 cm^{-1} (C≡C stretching).

(π-C_5H_5)Ni(PPh_3)C≡CPh: green crystals. Yield, 65%. M. p. 135°C (decomp.). Found: C, 76.71; H, 5.26. Calcd. for $C_{31}H_{25}PNi$: C, 76.42; H, 5.17%. IR (Nujol): 2160 cm^{-1} (C≡C stretching).

Studies of these compounds are now in progress.

The Institute of Scientific and Industrial Research
Osaka University
Sakai, Osaka

The Fractionation of Polypropylene by Extraction with Boiling Hydrocarbons with Increasing Boiling Points

By Akio Nakajima and Hiroshi Fujiwara

(Received July 16, 1963)

The fractionation of polypropylene is generally carried out either by the fractional solution method in a column or by the fractional extraction method in a Soxhlet-type apparatus. As to the column method, two techniques are known: the gradient elution fractionation is achieved at a given temperature by making use of solvents with gradually increasing solvent power, or the increasing temperature fractionation is performed with a given solvent at increasing temperatures. According to the findings on column techniques by Wijga and others,[1] the gradient elution method at a temperature (150°C) sufficiently near the melting point of the polymer separates fractions only according to molecular weight, whereas the increasing temperature method fractionates the polymer mainly according to tacticity. On the other hand, in the fractional extraction in a vapor-jacketed Soxhlet apparatus with boiling solvents with increasing boiling points, separation is considered to be conducted mainly by tacticity. However, in the reports[2-4] published so far, the solvents used for a series of fractional extractions of polypropylene have been comparatively few in number and, moreover, detailed information on the solubilities of polypropylene in these solvents has not been reported.

One of the present authors[5] previously fractionated polyethylene and its thermally degradated product by extraction with boiling hydrocarbons with increasing boiling points in a range from 45°C to 95°C, and pointed out that both the degree of crystallinity (density and melting point) and the molecular weight of the fractionated fraction increase with an increase in the boiling point of the hydrocarbons. Accordingly, this method of fractionation may be regarded as promising for polypropylene also.

In this study, 17 hydrocarbon fractions, mainly based on normal paraffins, with different boiling temperatures in the range from 35°C to 135°C, were used for the fractional extraction of polypropylene in a Soxhlet-type apparatus. With this method, successive fractionations are carried out with hydrocarbons, with different carbon numbers and with different solubilities, at different extraction temperatures corresponding to their boiling temperatures. Thus, fractionation, in this case, is conducted by two parameters. We will discuss the characteristic features of this method in comparison with other methods of fractionation and will also investigate the correlation between the solubility parameters of the solvents at their extraction temperatures and those of polymer fractions extracted at these temperatures, working with experimental findings on molecular weight, degree of crystallinity, tacticity, melting point, and extraction temperature.

Experimental

Material.—The polypropylene used was Moplen AS. Moplen AS pellets were dissolved in a low-boiling-range fraction of kerosene at 140~145°C and precipitated in powder form by cooling the solution to room temperature; then the solvent was evaporated in vacuo at 60°C. The powdered polypropylene thus obtained was used for the fractionation experiments.

Solvents for Extraction.—Purified petroleum ether, petroleum benzine and high-boiling-range ligroin were fractionated by fractional distillation to obtain hydrocarbon fractions with a sharp boiling range. 17 hydrocarbon fractions covering boiling temperatures of 35~130°C were prepared. The boiling temperature range of each hydrocarbon fraction is shown in the second column of Table I. Gas chromatographic examinations of these fractions disclosed that the main components in the fractions were normal paraffin hydrocarbons with carbon number from 5 to 8.

Fractionation Apparatus.—The fractional extraction was carried out in a vapor-jacketed Soxhlet-type apparatus, as is shown in Fig. 1, consisting of a extraction cell equipped with a G-1 glass filter, condensers and a solvent container. The outside of the apparatus was covered with asbestos to keep the temperature constant. With this apparatus, the extraction temperature (see Table I) were kept constant within ±0.3°C.

1) P. W. O. Wijga, J. van Schooten and J. Boerma, *Makromol. Chem.*, **36**, 115 (1960).
2) G. Natta, *J. Polymer Sci.*, **34**, 531 (1959).
3) S. Newman, ibid., **47**, 111 (1960).
4) C. A. Russell, *J. Appl. Polymer Sci.*, **4**, 219 (1960).
5) A. Nakajima, *Chem. High Polymers, Japan* (*Kobunshi Kagaku*), **7**, 64 (1950).

TABLE I. RESULTS OF FRACTIONATION EXPERIMENTS

No.	Solvent b. p., °C	Extr. °C	Main comp.	Extr. g.	$[\eta]$	$\bar{P}$	d^{30}	D_{995}/D_{974}	T_m, °C
1	35~ 38	36.0	Pentane	0.413	0.400	672	0.851	0	none
2	50~ 55	50.0		0.521	0.390	652	0.862	0	none
3	60~ 65	60.5		0.463	0.435	765	0.876	0.327	101
4	65~ 70	65.0		0.282	0.360	590	0.875	0.537	118
5	70~ 75	71.0	Hexane	0.274	0.275	421	0.884	0.653	120
6	75~ 80	75.5		0.651	0.345	645	0.891	0.752	128
7	85~ 90	89.0		0.502	0.382	635	0.891	0.758	138
8	90~ 95	92.5		0.209	0.410	694			
9	95~100	99.5	Heptane	0.360	0.485	856	0.897	0.794	139
10	102~104	102.5		2.730	1.150	2517	0.911	0.926	159.5
11	106~108	106.0		0.340	1.634	3905	0.912	0.929	163.0
12	110~112	111.0		3.149	2.520	6712	0.912	0.955	163.0
13	114~116	115.0		1.418	3.60	10478	0.912	0.962	172.0
14	118~120	119.0		0.105	4.86	15254	0.912		
15	122~124	123.5		2.883	4.60	13444	0.913	0.970	178.0
16	124~126	126.0	Octane	1.079	6.50	21317	0.911	0.979	178.0
17	126~130	128.5		0.282	7.38	25541	0.913	0.968	178.5

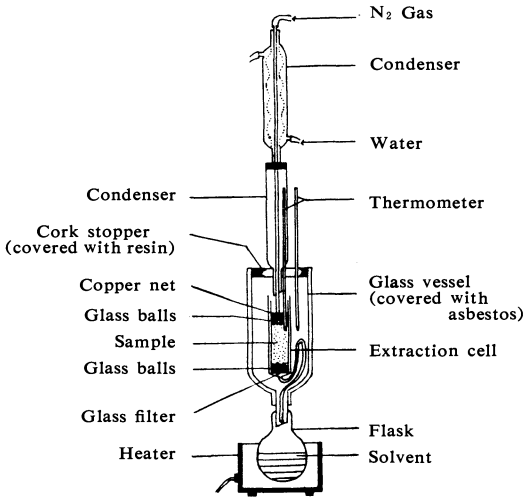


Fig. 1. Extraction apparatus.

Fractionation.—Fifteen grams of a sample was placed in the extraction cell. The extraction of each fraction was performed in 10 hr. by circulating the solvent under flushing (100 cc./min.) nitrogen. The amount of solvent placed in the flask was 400 ~500 ml., and the time needed for one cycle of solvent circulation through the cell was about 10 min. In cases of extractions at above 100°C, 2, 6-di-*t*-butyl-*p*-cresol was added (0.5% of the amount of solvent) to prevent the thermal decomposition of the polymer. The polymer fractions extracted below 100°C were recovered by evaporating the solvent, while those extracted above 100°C were collected in acetone to remove the stabilizer, filtered, and dried in a vacuum oven. The amount of fractions extracted is given in the fifth column of Table I.

Molecular Weight Determination. — The molecular weights, M, of the fractions were estimated by determining the limiting viscosity numbers in decalin, including a small amount of 2, 6-di-*t*-butyl-*p*-cresol, at 135°C, with the equation:[6]

$$[\eta] = 1.10 \times 10^{-4} M^{0.8} \quad (1)$$

where the limiting viscosity number, $[\eta]$, is given in dl./g. units. The viscosity measurements were carried out in a nitrogen atmosphere.

Density Measurement.—Samples were molded in film form under the same conditions and were thoroughly annealed at temperatures suited to the fractions. Density measurements were then carried out by the flotation method in a water-methanol system at 30°C. The degree of crystallization at 30°C, X_c, was estimated by means of Eq 4.

Infrared Spectra. — Samples were dissolved in ligroin with a high boiling point and then cast in films, ca. 20 μ thick, by evaporating the solvent. Infrared absorption spectra were obtained for these films by using a Shimadzu spectrometer (Type AR-275-2S). The ratio of optical densities at 995 cm^{-1} and 974 cm^{-1}, D_{995}/D_{974}, was used to estimate the isotacticity X_i of the samples according to the method of Luongo.[7]

Melting Point Measurement.—The melting points of the samples were determined by visual observations on sufficiently-annealed samples sealed in capillary tubes by raising the temperature at a rate of about 1°C/hr.

Results and Discussion

Fractionation. — Table I shows the boiling temperatures of the solvents, the extraction temperatures, the main components of the solvents, the amounts of the polymer fractions extracted, the limiting viscosity numbers, the degrees of polymerization (P), the densities

6) J. B. Kinsinger and R. E. Hughes, *J. Phys. Chem.*, **63**, 2002 (1959).
7) J. P. Luongo, *J. Appl. Polymer Sci.*, **3**, 302 (1960).

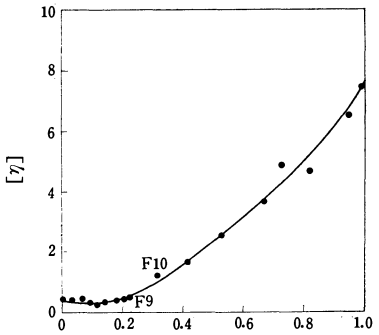


Fig. 2. Integral weight fraction plotted against the intrinsic viscosity.

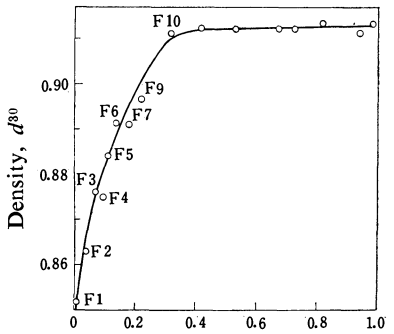


Fig. 3. Integral weight fraction plotted against the density of the fractions.

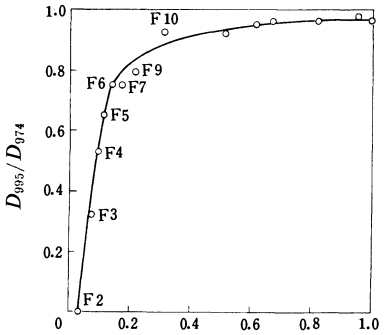


Fig. 4. Integral weight fraction plotted against D_{995}/D_{974}.

(d^{30}), the optical density ratios, and the melting points of the fractions.

In Figs. 2, and 4, the integral weight fraction is plotted against the limiting viscosity number, the density, and the optical density ratio of the fractions respectively. A characteristic feature of the curve shown in Fig. 2 is that the limiting viscosity number of the fractions is almost constant up to about a 0.2 integral weight fraction. This means that the fractionation in the low molecular weight range did not occur according to the molecular weight of the polymer. On the other hand, the curve shown in Fig. 3 or 4 means that the fractionation in the low molecular weight range (F1–F9) was rather determined by the crystallinity or tacticity of the fractions, but that the fractions above F10 were fractionated according to molecular weight and have almost the same crystallinity or tacticity. The integral weight fraction at above 0.3 is abruptly increased with an increase in the density or in the optical density ratio. This behavior is similar in the low molecular weight range to the results obtained for increasing temperature fractionation by the column technique and in the high molecular weight range to those obtained by the gradient elution method. Compared with the increasing temperature method, the maintenance of a constant temperature in the method used here was much easier. Between the melting points of the fractions and the extraction temperatures, a linear relationship was obtained, as is shown in Fig. 5. Presumably, the extraction was carried out at or near the critical solution temperatures of the corresponding polymer fractions. To confirm this,

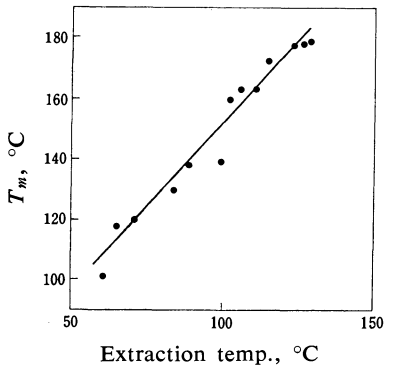


Fig. 5. Melting points of the fractions plotted against the extraction temperature.

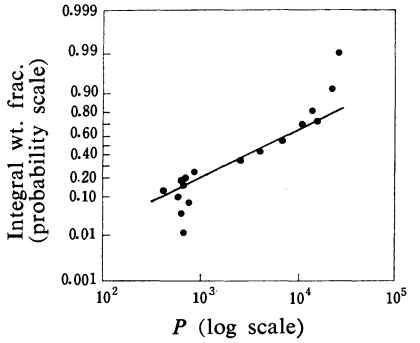


Fig. 6. Integral weight fraction plotted on logarithmic paper. P denotes the degree of polymerization.

some experiments were undertaken. In Fig. 6, the integral weight fraction is plotted against the degree of polymerization on logarithmic probability paper after Wesslau.[8] A straight line was obtained from about a 0.1 to a 0.8 integral weight fraction. Taking into account the fact that the fractionation up to a 0.3 integral weight fraction is carried out according to the degree of crystallinity, it may be concluded that the molecular weight distribution of the sample is given approximately by a log-normal molecular weight distribution except in a sufficiently high molecular weight range. From the slope of the straight line, the ratio of the weight average to the number average degree of polymerization, P_w/P_n, is obtained by using the expression:

$$P_w/P_n = \exp \sigma^2 \qquad (2)$$

were σ is the standard deviation of the Gaussian distribution of the weight fractions against the logarithm of the molecular weight of the fractions; it is determined by the equation: $\sigma = [\sqrt{2\pi}P(\mathrm{d}I/\mathrm{d}P)_{P=P_0}]^{-1}$, in which I denotes the integral weight fraction and P_0 is the degree of polymerization at $I=0.5$. The value of P_w/P_n obtained was 13, which falls in the range of $P_w/P_n=12\sim35$ found[1] for some commercial polypropylene samples.

The Characterization of the Fractions.—Before discussing the solubility of polypropylene, we should refer to the stereoregularity and crystallinity of the fractions. Luongo,[7] after taking into account the fact that the degree of crystallinity of samples with the same tacticity is scarcely affected by the method of sample preparation, obtained a relationship between the tacticity of polypropylene and the D_{974}/D_{995} value from data obtained for a series of mixtures composed of a 100% isotactic and a 100% atactic sample. In this study, the isotacticity, X_i, was obtained from D_{974}/D_{995} using Luongo's method.

On the other hand, the crystallinity, X_c, was calculated from the density of the fractions at 30°C by using the relation:

$$\frac{1}{d} = X_c\frac{1}{d_c} + (1-X_c)\frac{1}{d_a} \qquad (3)$$

in which d_c and d_a are the densities of crystalline and amorphous polypropylene respectively. With $d_c=0.936$, which was obtained by Natta et al.[9] from X-ray data, and with $d_a=0.850$, also obtained by Natta et al.,[10] Eq. 3 becomes:

$$X_c = 11.68 - (9.966/d) \qquad (4)$$

The linear relationship shown in Fig. 7 was obtained between X_i and X_c, from which it is known that the intermediate fractions are different in their tacticities. The extrapolated value of X_c to $X_i=1$ is about 0.8. Since X_i indicates the fraction of maximum crystallizable component, the result means that about 80% of a crystallizable component is really crystallized.

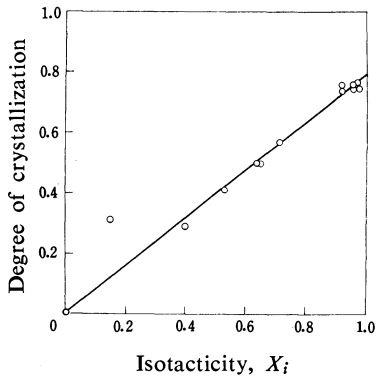


Fig. 7. Relation between the degree of crystallization and the isotacticity of the fractions.

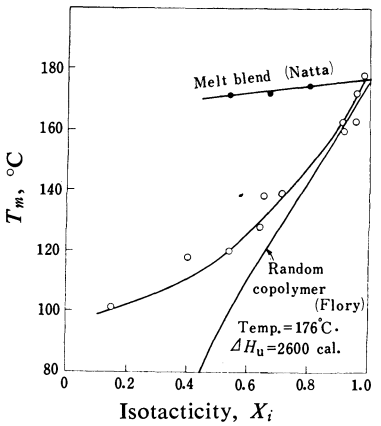


Fig. 8. Melting point-isotacticity relation.

Figure 8 shows the relation between the melting points of the fractions and their isotacticities, together with the results obtained on melt blends of amorphous and crystalline polymers by Natta.[11] Obviously, the melting points of our fractions are much lower than those of melt blends of the same isotacticity. This may mean that our intermediate fractions are composed of copolymers which are built up of components of *d*- and *l*-configurations. Now, we shall apply Flory's[12] equation, proposed for a random copolymer composed of

8) H. Wesslau, *Makromol. Chem.*, **20**, 111 (1956).
9) G. Natta, P. Corradini and M. Cesari, *Lincei-Rend. Sc. fis. mat. e nat.*, **22**, 11 (1957).
10) G. Natta, F. Danusso and G. Moraglio, *Angew. Chem.*, **69**, 686 (1957).
11) G. Natta, *J. Polymer Sci.*, **34**, 531 (1959).
12) P. J. Flory, *J. Chem. Phys.*, **17**, 223 (1949).

crystalline and amorphous components, to the polypropylene fractions. For the present case, the melting point depression should be a function of X_t, instead of the mole fraction of crystalline component in the case of the random copolymer. Thus, we have:

$$\frac{1}{T_m}-\frac{1}{T_m{}^0}=-\frac{R}{\Delta H_u}\ln X_t \qquad (5)$$

in which T_m and $T_m{}^0$ donote the melting point of the fractions and that of $X_t=1$ respectively, and in which ΔH_u indicates the heat of the melting of the polymer.

The curve, T_m against X_t, calculated with $T_m{}^0=176$°C and $\Delta H_u=2600$ cal./mol., a value obtained by Danusso,[13] is given also in Fig. 8. A comparison between the observed and calculated curves shows that the two coincide at higher values of X_t, but at lower values of X_t the observed melting points are higher than the calculated ones for a random copolymer. Such results may suggest that these fractions are composed of stereoblock copolymers (as designated by Natta), which are built up, in a somewhat different fashion in the low X_t range from usual random copolymers, of sequences of *d*- and *l*-configurations of various lengths. In other words, the distribution of such stereoregular-sequence length may differ from that of crystalline-sequence length in random copolymers.

The Fractionation Mechanism in Connection with Solubility Parameters of Solvents.—The solvents used for extraction and the polymer are both aliphatic hydrocarbons, so the solvent-polymer interaction may be approximated by the geometrical mean of the solvent-solvent interaction and the polymer-polymer interaction. Thus, we may discuss the mechanism of the extraction fractionation in connection with the solubility parameter of the solvent, δ_s, and of the polymer, δ_p. Since the partial molar heat of dilution, $\Delta\bar{H}_1$, for the polymer solution is related[14] to the heat parameter, κ_1, by the equation:

$$\kappa_1=\frac{\Delta\bar{H}_1}{RTv_2{}^2} \qquad (6)$$

where v_2 denotes the volume fraction of the polymer in solution, the equation given by Hildebrand;[15]

$$\Delta\bar{H}_1=V_1(\delta_s-\delta_p)^2v_2{}^2 \qquad (7)$$

is rewritten in the form:

$$\frac{\kappa_1}{V_1}=(\delta_s-\delta_p)^2/RT \qquad (8)$$

in which V_1 represents the molar volume of the solvent, and in which the solubility parameter of solvent, δ_s, is calculated by the equation:[16]

$$\delta_s=\frac{\Delta H_v-RT}{V_1} \qquad (9)$$

where ΔH_v is the heat of the vaporization of the solvent at temperature T. Our extraction fractionation was carried out at the boiling points of hydrocarbons with different boiling points. Now we shall estimate the solubility parameters of solvents at their boiling points. It is possible to estimate the heat of vaporization from the boiling point, provided the liquid is nonpolar, by the aid of the "Hildebrand rule." Between the heats of vaporization at the normal boiling point, $\Delta H_{v,b}$ (cal./mol.), and the normal boiling points, T_b (°K), the following relation was found by Scott:[17]

$$\Delta H_{v,b}=17.0\,T_b+0.009\,T_b{}^2 \qquad (10)$$

Thus, we can estimate δ_s at the boiling point of the solvent, the temperature regarded as the extraction temperature, with Eqs. 9 and 10 if the molal volume of the liquid at the boiling point is known.

In Table II, the boiling point, T_b, the molar volume, V_1, of the liquid at T_b, and the solubility parameter of the solvent at T_b are listed. The numerical values of V_1 for the solvents used here were obtained in the following way. At first, the values of V_1 at the boiling points of *n*-pentane, *n*-hexane, *n*-heptane and *n*-octane were calculated using the equation proposed by Sakurada and one of the present authors:[18]

$$V_1=1.143+0.00089\,t+\frac{1}{(0.50-0.00110\,t)n} \qquad (11)$$

where n is the number of carbon atoms in normal paraffin and t is the temperature in °C. Plotting these V_1-values against the boiling temperatures of the corresponding paraffins, we obtained the V_1 values of the solvents used here by interpolation. The δ_s values of normal paraffins at their boiling points are plotted against their boiling points in Fig. 9 (the broken line less sloped). In Fig. 9 also the δ_s values of normal paraffins at temperatures up to their boiling points are plotted against the temperatures (the broken lines more sloped). Our extractional fractionation is carried out along the former broken line; on the other hand, the increasing temperature

13) F. Danusso, G. Moraglio and E. Flores, *Lincei-Rend. Sc. fis. mat. e nat.*, **25**, 520 (1958).
14) P. J. Flory, "Principles of Polymer Chemistry," Cornell University Press, Ithaca, N. Y. (1953), p. 523.
15) J. H. Hildebrand and R. L. Scott, "The Solubility of Nonelectrolytes," 3rd. ed., Reinhold Pub. Corp., N. Y. (1950), p. 180.
16) Ibid., p. 424.
17) Ibid., p. 427.
18) I. Sakurada and A. Nakajima, *Chem. High Polymers, Japan (Kobunshi Kagaku)*, **3**, 95 (1946).

method, using a given solvent and the column technique, is performed along a curve as shown by the latter broken lines. In both cases, δ_s decreases with an increase in the temperature; however, the slopes of the curves are different.

TABLE II. SOLUBILITY PARAMETERS OF SOLVENTS AT BOILING POINTS

No.	T_b, °C	V_1 at T_b	δ_s at T_b
1	36.0	118	6.90
2	50.0	128	6.80
3	60.5	135	6.78
4	65.0	138	6.74
5	71.0	142	6.70
6	75.5	146	6.67
7	89.0	156	6.60
8	92.5	159	6.58
9	99.5	164	6.54
10	102.5	166	6.52
11	106.0	170	6.50
12	111.0	174	6.47
13	115.0	177	6.44
14	119.0	180	6.42
15	123.5	184	6.40
16	126.0	186	6.39_5
17	128.5	188	6.39

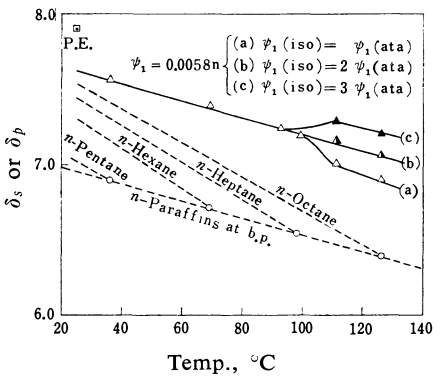


Fig. 9. Cohesive energy density of solvent, δ_s (broken line), and of polymer, δ_p (solid line), as a function of temperature.

Now we would like to speculate about the solubility parameter of the polymer, δ_p. We assume that extraction is carried out at the critical solution temperature, T_c, of the extracted polymer fraction with regard to the hydrocarbon used for extraction. According to Flory,[14] the heat parameter, κ_1, is related to the entropy parameter, ψ_1, and the free energy parameter, χ_1, by $\chi_1 = 0.5 + \kappa_1 - \psi_1$, and the value of χ_1 at the critical temperature is expressed by the equation:

$$\chi_{1,c} = \frac{(1+x^{1/2})^2}{2x} \tag{12}$$

Accordingly, by combining these equations with Eq. 8, we obtain:

$$(\delta_s - \delta_p)^2_{T=T_c} = \frac{RT_c}{V_1}\left[\frac{1}{2x} + \frac{1}{x^{1/2}} + \psi_1\right] \tag{13}$$

where x means the ratio of the molar volume of the polymer to that of the solvent. As the entropy parameter, ψ_1, is independent of the temperature, if ψ_1 is known for the corresponding solvent-polymer system, then we can calculate the δ_p at $T=T_c$ from Eq. 13.

So far we do not have any information about the ψ_1 of polypropylene in aliphatic hydrocarbons. However, the results obtained by Fox[19] for the ψ_1 of polyisobutylene-aliphatic hydrocarbon systems may serve as a reference. The relationship obtained between ψ_1 and the number of carbon atoms in aliphatic hydrocarbons, n, is

$$\psi_1 = 0.0058\, n \tag{14}$$

The δ_p values, calculated from Eq. 13 by the use of the ψ_1 values obtained by assuming Eq. 14 for polypropylene, are plotted against the temperature as curve a in Fig. 9. The curve shows that δ_p is abruptly changed at the fraction (F10) extracted near 100°C. This change in δ_p may be due to the change in T_c arising from the marked effect in tacticity. As is obvious from Fig. 3, the densities of the fractions above F10 are quite high and are almost all the same. Previously we pointed out, on the basis of experiments on polymethyl methacrylate in several solvents,[20] that the ψ_1 of the isotactic polymer is always larger than that of the atactic polymer. If we apply this fact for polypropylene and assume $\psi_1(\text{iso}) = 2\psi_1(\text{atac})$ and $\psi_1(\text{iso}) = 3\psi_1(\text{atac})$, then we obtain curves b and c in Fig. 9. In these estimations, we regarded the fractions extracted at above 100°C as isotactic and used the ψ_1(iso) value, and the fractions extracted at below 100°C as atactic and used the ψ_1(atac) value, the value calculated by Eq. 14. In the case of curve b, δ_p was nearly linearly decreased with the temperature, but in the case of c, the δ_p of the fractions above F10 were located higher than those given by curve b. If we extrapolate the linear portion of these curves for higher fractions, then we have, at a given temperature, $\delta_p(\text{iso}) \gtrless \delta_p(\text{atac})$ according to the condition of a, b, and c. In the present polymer-solvent system, the case c means that the energy interaction between the crystalline segment and the solvent is larger than that between the amorphous segment and the solvent. Such a case is the same as the model

19) T. G. Fox, *Polymer*, 3, 111 (1962).
20) I. Sakurada, A. Nakajima, O. Yoshizaki and K. Nakamae, *Koll-Z.*, **186**, 41 (1962).

introduced by Oyama[21] for a crystalline polymer solution. Thus, the condition as given in c seems most probable so far as Eq. 14 is concerned.

So far as Eq. 14 is concerned, the δ_p value of polypropylene at 25°C is estimated as 7.6. This value may be compared to $\delta_p=7.9$ for polyethylene[21] and $\delta_p=8.05$ for polyisobutylene.[22] Taking into account the value obtained here for polypropylene at 25°C, the solubility parameter, δ_s, of *n*-octane or *n*-nonane at 25°C is very close to that of polypropylene at that temperature.

Department of Polymer Chemistry
Kyoto University
Sakyo-ku, Kyoto

21) T. Oyama, *Chem. High Polymers, Japan* (*Kobunshi Kagaku*), **18**, 420, 426 (1961).

22) M. Magat, *J. Chim. Phys.*, **46**, 344 (1949); H. A. Stuart, "Das Makromolekül in Lösungen," Springer-Verlag, Berlin (1953), p. 204.

Some Novel Reactions of 1, 1-Diphenyl-3, 3-dibromoprop-1-ene

By Fumio TODA and Hisaya TANI

(Received November 27, 1963)

In previous papers,[1] the synthesis of 1,1-diphenyl-3,3-dibromoprop-1-ene (I) from 1,1-diphenylprop-2-yn-1-ol and phosphorus tribromide in acetic acid has been reported.

During the course of the studies of the reactions of the *gem*-dibromide (I), some novel reactions were found. The present paper deals with these reactions and will discuss the reaction mechanism.

The treatment of the *gem*-dibromide (I) with sodium ethoxide in ethanol resulted in *trans*-1,1-diphenyl-1-ethoxy-3-bromoprop-2-ene (IIIa) in a 33% yield. The structure of the compound IIIa was determined by infrared and ultraviolet spectral determination. The ultraviolet spectrum of IIIa is almost identical with that of benzene, indicating the absence of conjugation between benzene nuclei and the double bond. The infrared spectrum of IIIa shows the presence of a non-conjugated trans double bond, an ethoxy group and ether linkage (Fig. 2).

As is shown in the Scheme, this reaction may be attributable to the S_N2' mechanism. At the transition state, the less hindered intermediate (II) most reasonably produces the trans-compound (IIIa).

Although the crystals of IIIa were fairly stable for several days in the absence of air, IIIa was converted into an oily material in about one hour in the presence of air. Some parts of the oil gradually solidified, and the solid was identified as the *gem*-dibromide (I) by mixed melting point determination with an authentic specimen. The unsolidified oil was determined to be 3,3-diphenylprop-3-en-1-al (IV) by infrared spectroscopy. It may be most reasonable to consider the mechanism of this reaction to be the disproportionation of IIIa. The aldehyde IV was also obtained by the hydrolysis of I.[1]

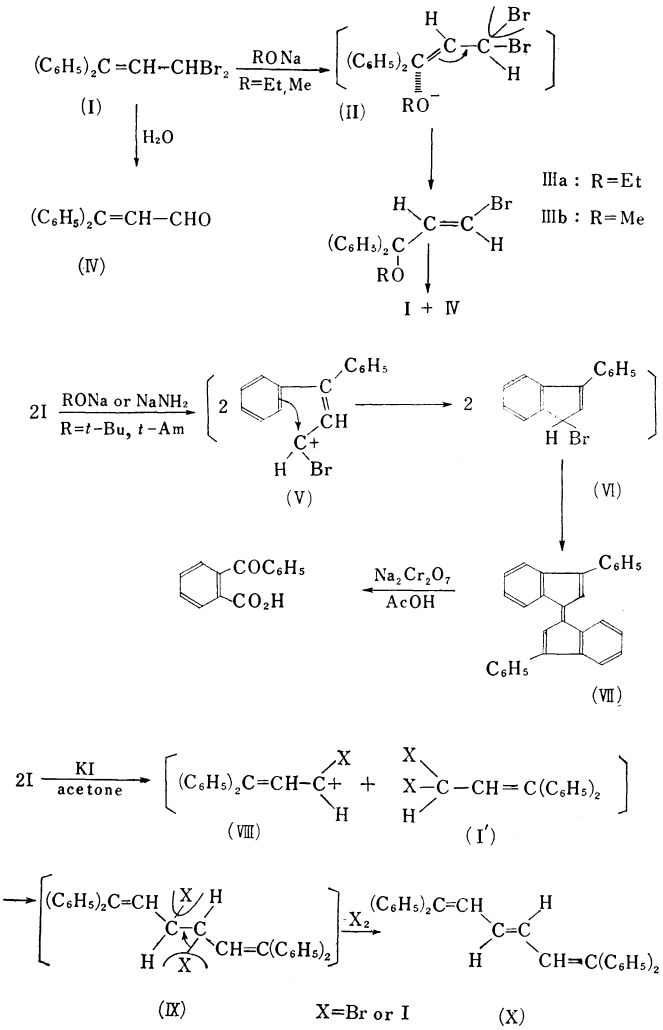
A lower homologue of IIIa, IIIb, obtained by the similar treatment of I with sodium methoxide in methanol, behaved in the same way as IIIa. The less hindered methoxy compound IIIb was less stable than IIIa.

In contrast with the reactions with sodium methoxide or sodium ethoxide, the reaction of I with sodium amide in liquid ammonia resulted in the formation of 3,3'-diphenyl-bis-(1-indenylidene) (VII) in a 50% yield. The compound VII was also obtained, by the treatment of I with sodium *t*-butoxide or sodium *t*-amyloxide, in a 40% yield in both cases. The electronic spectrum (Fig. 1) of the bis(1-indenylidene) (VII) is typical of fulvene derivatives and is similar to that of 3,3'-dibromo-bis(1-indenylidene).[2] The oxidation of VII with potassium bichromate in acetic acid gave *o*-benzoylbenzoic acid. Satisfactory analysis and consistent infrared (Fig. 2) and NMR spectra were also obtained for the compound VII.

As is shown in the Scheme, the formation of VII can be interpreted as the result of the ionic dimerization of the cyclic compound VI produced by the intramolecular cyclization of

1) H. Tani and F. Toda, *Chem. & Ind.*, **1963**, 1083; This Bullein, **37**, 470 (1964).

2) F. Straus, R. Kuhnel and R. Haensel, *Ber. dtsch. Chem. Ges.*, **66**, 1847 (1933).



the cationic intermediate V initially formed from I.

The heating of the *gem*-dibromide (I) with potassium iodide in acetone for two hours led to *trans*-1, 1, 6, 6-tetraphenylhexa-1, 3, 5-triene (X) in a 74% yield. The ultraviolet (Fig. 1) and infrared (Fig. 2) spectra of X are identical with that recorded by Kuhn and Fischer[3] for X prepared by the partial hydrogenation of 1, 1, 6, 6-tetraphenylhexapentaene. The triene melted at 204°C with or without the addition of an authentic sample, kindly supplied by Professor Richard Kuhn.

On the basis of the experimental finding that the *trans*-triene was obtained exclusively, the following mechanism may be put forward. As is shown in the Scheme, an S_N2 attack of a cationic intermediate VIII on a *gem*-dihalide (I') leads to a dihalogeno compound IX, in which two halogens are located in meso-form fashion, and the intermediate IX finally gives *trans*-triene (X) by the trans-elimination of halogens.

During the reaction of I with potassium iodide, an ionic salt containing an iodide anion formulated as $[C_{30}H_{24}\cdot H_2O]^+I^-$ was isolated as purple black needles; m. p. 155°C. The salt was easily converted into the triene (X) by treatment with ethanol. The structure of this salt is being investigated.

Experimental*

1, 1-Diphenyl-1-ethoxy-3-bromoprop-2-ene (IIIa). —I (1.0 g.) was dissolved in 30 ml. of a 1% solution of sodium ethoxide in ethanol. The mixture was refluxed for 30 min., thus causing sodium bromide

3) R. Kuhn and H. Fischer, *Chem. Ber.*, 93, 2285 (1960).

* All melting points are uncorrected. Molecular weights were determined in a benzene solution using a Mechrolab Vapor Pressure Osmometer, model 301 A.

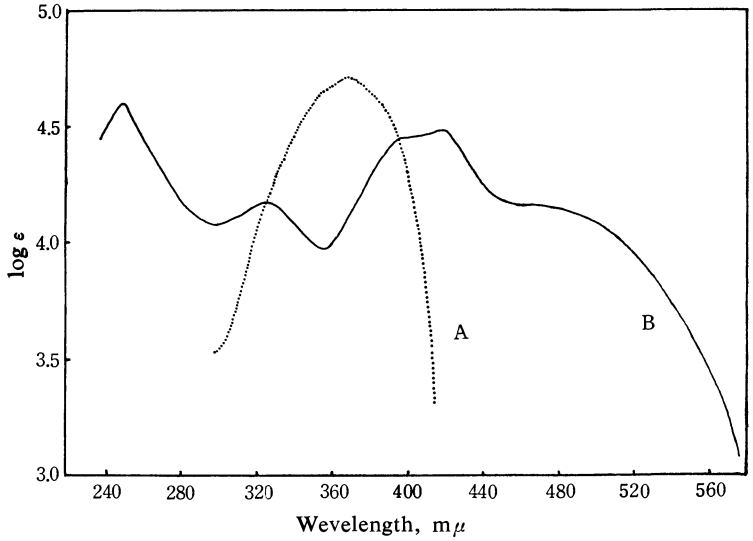


Fig. 1. Electronic absorption spectra.

A *trans*-1,1,6,6-Tetraphenylhexa-1,3,5-triene (X)
B 3,3'-Diphenyl-bis(1-indenylidene) (VII), in dioxane

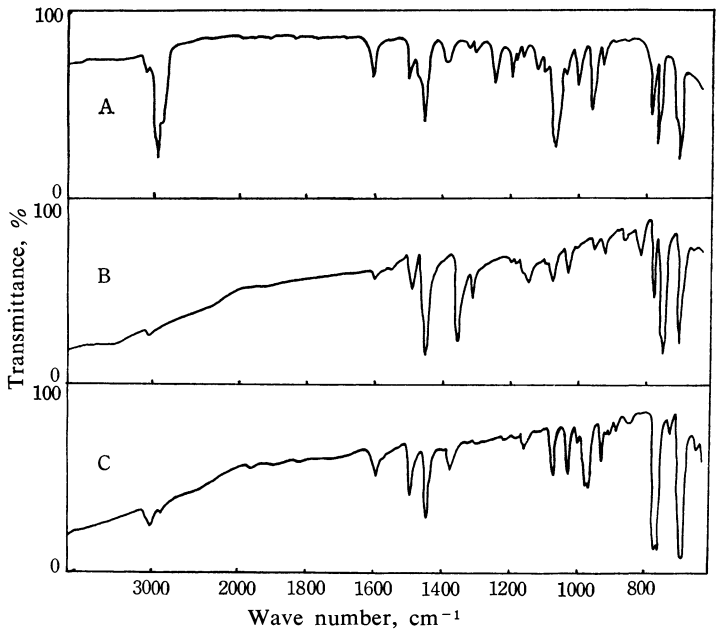


Fig. 2. Infrared absorption spectra.

A *trans*-1,1-Diphenyl-1-ethoxy-3-bromoprop-2-ene (IIIa)
B 3,3'-Diphenyl-bis(1-indenylidene) (VII)
C. *trans*-1,1,6,6-Tetraphenylhexa-1,3,5-triene (X)
A: Nujol mull; B, C: KBr disk

to be deposited. The reaction mixture was poured into water, and the oily material was extracted with ether. The ether layer was washed with water and dried over sodium sulfate. The oily substance obtained by the evaporation of the ether gradually solidified. Recrystallization of the solid from aqueous ethanol yielded IIIa as colorless needles (0.3 g. (33%), m. p. 60°C). IR: KBr disk, 2980 (ethoxy), 1620 (double bond), 1060 (ether) and 952 cm^{-1} (trans). UV: $\lambda_{max}^{Dioxane}$, 253 (470) and 259 mμ (ε, 530).

Found: C, 64.28; H, 5.30; Br, 25.96. Calcd. for $C_{17}H_{17}BrO$: C, 64.35; H, 5.36; Br, 25.24%.

When treated with 2,4-dinitrophenylhydrazine,

IIIa gave directly 2,4-dinitrophenylhydrazone of 3,3-diphenylprop-3-en-1-al quantitatively (m. p. 200 °C (lit.[4] 196°C)).

On being kept standing for an hour, IIIa was degraded into an oily material, some of which was converted into rhombic plates. The crystals melted at 75~78°C and were identified as the *gem*-dibromide (I) by mixed melting point determination.

1,1-Diphenyl-1-methoxy-3-bromoprop-2-ene (IIIb).—By the same treatment employed for the preparation of IIIa, IIIb was obtained from I and sodium methoxide as colorless needles (30%); m. p. 58°C. IR: KBr disk, 1615 (double bond), 1075 (ether) and 970 cm^{-1} (trans).

Found: C, 63.21; H, 5.01. Calcd. for $C_{16}H_{15}BrO$: C, 63.70; H, 5.01%.

IIIb behaved similarly to IIIa but was less stable.

3,3'-Diphenyl-bis(1-indenylidene) (VII), Sodium Amide Method.—To a stirred suspension of sodium amide (3.9 g., 0.1 mol.) in liquid ammonia (100 ml.), a solution of I (8.5 g., 0.024 mol.) in tetrahydrofuran (20 ml.) was added drop by drop over a period of 10 min. After the stirring had then been continued for a further hour, the reaction mixture was decomposed with ammonium chloride (7.0 g.). The solid which remained after the evaporation of the ammonia was extracted with benzene (200 ml.). The benzene solution was washed with water and dried over sodium sulfate. The recrystallization from ethyl acetate of the crude crystals obtained by the evaporation of the solvent from the benzene solution afforded VII as purple red needles (2.3 g. (50%); m. p. 208°C). UV: $\lambda_{max}^{Dioxane}$, 249 (39400), 325 (14800), 400 (27800), 418 (30700) and 500 mμ (shoulder) (ε, 12000).

Found: C, 94.31; H, 5.35. Mol. wt., 380. Calcd. for $C_{30}H_{20}$: C, 94.70; H, 5.30%. Mol. wt., 380.

3,3'-Diphenyl-bis(1-indenylidene) (VII), Sodium *t*-Butoxide Method.—The *gem*-dibromide (I) (0.5 g.) was added to 30 ml. of a 5% solution of sodium *t*-butoxide in *t*-butyl alcohol. The mixture was heated at 90°C. for 10 min. After the reaction mixture had been decomposed by the addition of water, the crude solid which remained was collected by filtration and washed with water and methanol. Two successive recrystallizations of this dried solid from ethyl acetate yielded VII as purple red needles (0.1 g. (40%); m. p. 208°C); these did not show any depression of melting point when mixed with the authentic sample obtained above.

The same treatment of I with sodium *t*-amyloxide in *t*-amyl alcohol also gave VII in a 40% yield.

The Potassium Bichromate Oxidation of VII.—A mixture of VII (0.2 g.), potassium bichromate (1.0 g.) and acetic acid (20 ml.) was heated at 90°C for 30 min. and then refluxed for a further hour. After cooling, the reaction mixture was poured into dilute hydrochloric acid. The crude crystals which separated were collected by filtration and dissolved in ether. The ether solution was extracted with aqueous sodium bicarbonate. Crystals obtained from the acidified alkaline layer were recrystallized from petroleum ether (b. p. 60~70°C) to give *o*-benzoylbenzoic acid as colorless needles (0.1 g. (43%); m. p. 127°C (lit.[5] 127°C)). The substance showed no depression of its melting point on admixture with an authentic specimen.

***trans*-1,1,6,6-Tetraphenylhexa-1,3,5-triene (XI).**—A mixture of I (0.50 g.), finely powdered potassium iodide (0.75 g.) and acetone (20 ml.) was heated under reflux for 2 hr. After the acetone had been removed, the residue was decomposed with water and extracted with ether. The ether layer was washed with aqueous sodium thiosulfate and water, and dried over sodium sulfate. The crude crystals obtained by the evaporation of the solvent were suspended in ethanol and heated for 10 min. The yellow solid collected by filtration was recrystallized from ethyl acetate to yield XI as bright yellow needles (0.2 g. (74%); m. p. 204°C). A mixed melting point determination with an authentic sample, kindly supplied by Professor Richard Kuhn, showed no depression. IR: KBr disk, 977, 968 cm^{-1} (trans) UV: $\lambda_{max}^{Dioxane}$, 355 (shoulder) (42100), 370 (51200) and 390 mμ (shoulder) (ε, 37100).

Found: C, 93.34; H, 6.35. Calcd. for $C_{30}H_{24}$: C, 93.71; H, 6.29%.

The authors wish to express their thanks to Professor Richard Kuhn for supplying a sample of *trans*-1,1,6,6-tetraphenylhexa-1,3,5-triene. They are also indebted to Professor Yasuhide Yukawa and Professor Shigeru Oae for their valuable discussions.

Department of Polymer Science
Faculty of Science
Osaka University
Nakanoshima. Osaka

4) H. Lorenz and R. Wizinger, *Helv. Chim. Acta*, **28**, 600 (1945).

5) T. C. McMullen, *J. Am. Chem. Soc.*, **44**, 2055 (1922).

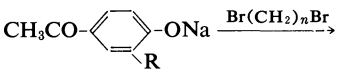
Oligomers and Polymers Containing Triple Bonds. III. Derivatives of α,ω-Bis(4-ethynylphenoxy)alkane[1]

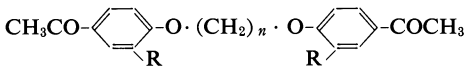
By Hisaya TANI, Ken MURAYAMA and Fumio TODA

(Received December 7, 1963)

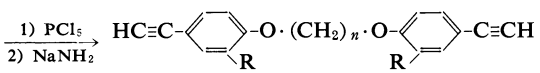
In previous papers[2,3] the oxidative polymerization of conjugated diethynyl compounds to produce conjugated linear polymers containing triple bonds has been reported.

The present paper deals with the oxidative polymerization of non-conjugated diethynyl compounds, α,ω-bis(4-ethynylphenoxy)alkanes (II: R=H) and α,ω-bis(4-ethynyl-2-methylphenoxy)alkanes (II: R=CH_3). In connection with the polymerization, the relation among the kinds of catalysts, the degree of polymerization and the crystallinity of polymers and that between the degree of polymerization and the length of the polymethylenic chain of the monomeric compound (*n*) have been studied.

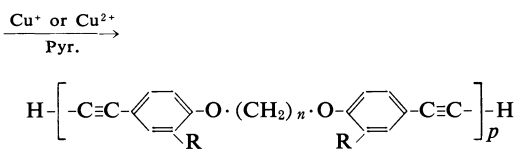




(I)



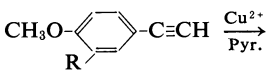
(II)



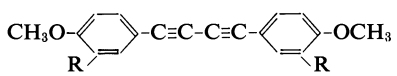
(III)

R=H: n=1, 2, 3, 4, 5, 6 and 10

R=CH_3: n=1, 2, 3, 4, 5 and 6



(IV)



(V) R=H, CH_3

The influence of a methyl group substituted at the benzene ring on the degree of polymerization and on the crystallinity has also been investigated.

Following the method employed for the preparation of α,ω-di(2-ethynylphenoxy)alkane,[4] sodium 4-acetylphenoxide or sodium 4-acetyl-2-methylphenoxide was treated with α,ω-dibromoalkanes in boiling dimethylformamide to produce the diketones (I: R=H or R=CH_3), usually in moderate yields. These diketones were then converted to the chlorinated compounds with phosphorus pentachloride, followed by dehydrochlorination with sodium amide in liquid ammonia to give the diethynyl compounds (II).

The oxidative polymerization of the diethynyl monomers (II) using cupric or cuprous salt in pyridine afforded the corresponding polymers, which were insoluble in common organic solvents. Under some conditions, however, some linear oligomers were produced; for example, when the polymerization of a monomer (II: R=CH_3, n=6) was carried out using cupric salt in pyridine-methanol, the linear dimer (III: R=CH_3, n=6) was obtained as colorless crystals. Although the polymers were stable at temperatures below 150°C, when heated above 200°C in a air bath they turned brown and finally black.

The infrared spectra of most of the polymers show the ethynyl absorption band at ca. 3300 cm^{-1} (Fig. 1); this provides evidence for the linear structure of the polymers. Another confirmatory piece of evidence for the structure involving diphenyldiacetylene and diphenoxyalkane linkages was obtained by comparing the infrared spectra of the polymers with those of standard compounds involving the monomers II, the linear dimer (II: R=CH_3, n=6, p=2), 4,4'-dimethoxydiphenyldiacetylene (V: R=H) and 4,4'-dimethoxy-3,3'-dimethyldiphenyldiacetylene (V: R=CH_3).

The degree of polymerization of the polymer (III) was estimated by comparing the intensity of the ethynyl absorption maximum with that of the corresponding monomer (II),[1,2] as represented by the example shown in Fig. 1.

Although some polymers (III: R=CH_3, n=1, 3, 5) do not show any ethynyl band at ca.

1) Preliminary report: *Chem. & Ind.*, **1962**, 1980.
2) H. Tani, F. Toda and K. Matsumiya, This Bulletin, **36**, 391 (1963).
3) H. Tani, S. Tanaka and F. Toda, ibid., **36**, 1268 (1963).
4) F. Toda and M. Nakagawa, ibid., **34**, 862 (1961).

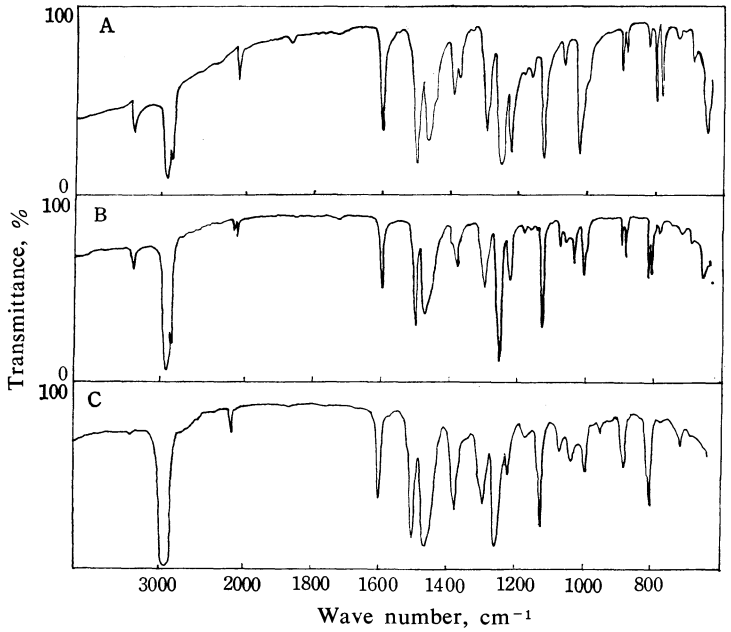


Fig. 1. Infrared spectra (Nujol mull).

A: α,ω-Bis(4-ethynyl-2-methylphenoxy)hexane (II: R=CH_3, n=6)
B: Linear dimer of II R=CH_3, n=6 (III: R=CH_3, n=6, p=2)
C: Polymer (III: R=CH_3, n=6, p=36)

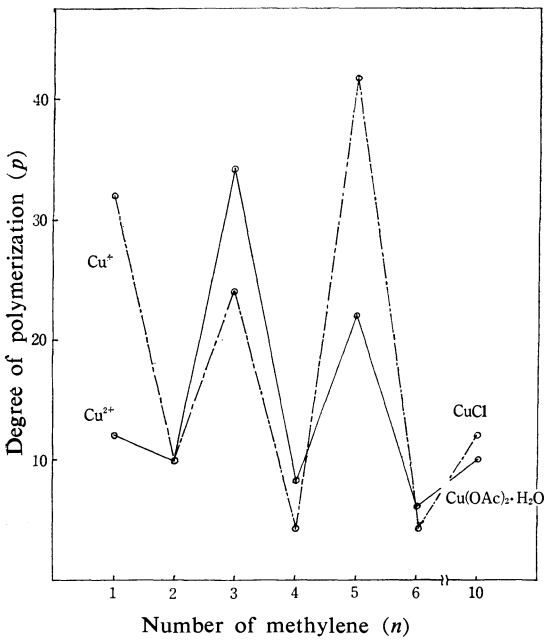


Fig. 2. Relation between the degree of polymerization (p) and the number of methylene (n) in the oxidative polymerization of II: R=H.

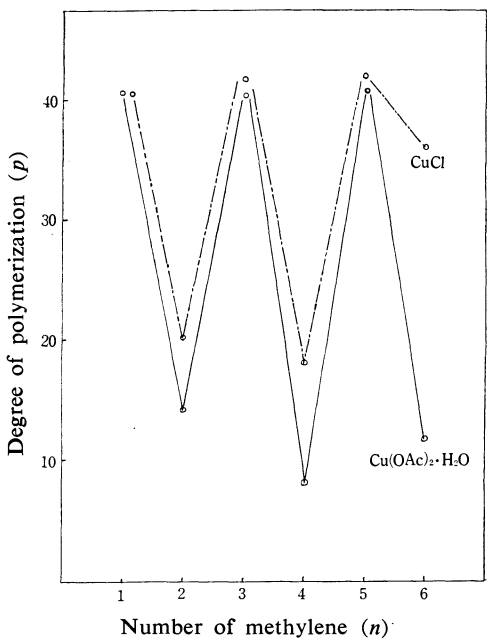


Fig. 3. Relation between the degree of polymerization (p) and the number of methylene (n) in the oxidative polymerization of II: R=CH_3.

TABLE I. OXIDATIVE POLYMERIZATION OF α,ω-BIS(4-ETHYNYLPHENOXY)ALKANE (II: R=H)

II: R=H		Catalyst			Reaction		Atmosphere	Degree of polymerization
n	mg.	CuCl mg.	$Cu(OAc)_2 \cdot H_2O$ mg.	Pyridine ml.	Temp. °C	Time min.		p
1	200		800	15	55	70	Air	12
	300	300		50	55	70	Air	32
2	50		500	10	60	150	Air	10
	50	50		10	50	75	O_2	10
3	300		2800	25	60	95	Air	34
	200	200		15	45	80	O_2	24
4	70		300	15	55	70	Air	8
	70	50		15	60	120	O_2	4
5	100		400	10	55	100	Air	22
	100	100		10	55	100	Air	42
6	100		400	20	50	110	Air	6
	100	100		20	55	120	O_2	4
10	100		400	20	55	100	Air	10
	100	100		20	55	100	Air	12

TABLE II. OXIDATIVE POLYMERIZATION OF α,ω-BIS(4-ETHYNYL-2-METHYLPHENOXY)ALKANE (II: R=CH_3)

All reactions were carried out at 55°C under atmosphere of air.

II: R=CH_3		Catalyst			Reaction time	Degree of polymerization
n	mg.	CuCl mg.	$Cu(OAc)_2 \cdot H_2O$ mg.	Pyridine ml.	min.	p
1	100		400	15	60	>36
	100	100		15	60	>36
2	60		240	10	90	14
	60	60		10	90	20
3	100		400	10	100	>36
	100	100		10	100	>36
4	100		400	10	100	8
	100	100		10	100	18
5	40		160	6	100	>36
	40	40		10	100	>36
6	100		400	10	100	12
	100	100		10	100	36

3300 cm^{-1}, their degrees of polymerization are assumed to be higher than 36, since the monomer (II: R=H, n=1, 3 and 5) with an odd number of n yielded higher polymers than those obtained from the monomers (II: R=H, n=2, 4, 6 and 10) showing even mumbers of n, as is shown in Figs. 2 and 3 as well as in Tables I and II, moreover, the polymer (III: R=CH_3, n=4) was estimated to have 36 degree of polymerization according to the spectral estimation cited above.

The high crystallinity of the polymers (III) shown by the X-ray diagrams and the fact that the larger the degree of polymerization, the higher is the crystallinity of the polymer, indicate that the polymers are substantially linear and are arranged in a regular manner.

The degree of polymerization (p) is scarcely affected by the kind of catalyst or by the length of the methylenic chain of the monomer (n), but it is strikingly influenced by whether n is odd or even (see Figs. 2 and 3, Tables I and II).

Experimental*

α,ω-Bis(4-acetylphenoxy)alkanes (I: R=H, n=1, 2, 3, 4, 5, 6 and 10).—Sodium 4-acetylphenoxide prepared from 4-acetylphenol (15.8 g., 0.12 mol.) and a nearly equivalent amount of sodium ethoxide in ethanol, was dried under reduced pressure, mixed with dibromomethane (11.5 g., 0.066 mol.), a small amount of potassium iodide and dimethylformamide (27 ml.), and then heated under reflux for 3 hr. The cooled reaction mixture was poured into ice-water, and the solid which deposited was collected by filtration, washed with water and then recrystallized from ethanol to afford I, R=H, n=1, (15.2 g., 89%) in the form of colorless needles (m. p.

* Melting points are not corrected.

104～105°C). IR: Nujol mull, 1680 (CO), 1275 (=C-O-) and 820 cm^{-1} (*p*-disubstituted benzene).

Found: C, 71.95; H, 5.64. Calcd. for $C_{17}H_{16}O_4$: C, 71.82; H, 5.67%.

A similar treatment of sodium 4-hydroxyacetophenone with α,ω-dibromoalkanes (n=2,3,4,5,6 and 10) yielded the following ketones:

I: R=H, n=2, colorless needles (14%), m. p. 165 °C.

Found: C, 72.40; H, 6.03. Calcd. for $C_{18}H_{18}O_4$: C, 72.46; H, 6.08%.

I: R=H, n=3, colorless needles (21%), m. p. 126 °C.

Found: C, 72.96; H, 6.44. Calcd. for $C_{19}H_{20}O_4$: C, 73.06; H, 6.45%.

I: R=H, n=4, colorless leaflets (60%), m. p. 145.5 ～146.5°C.

Found: C, 73.44; H, 6.79. Calcd. for $C_{20}H_{22}O_4$: C, 73.60; H, 6.79%.

I: R=H n=5, colorless leaflets (62%), m. p. 89～90°C.

Found: 74.06; H, 7.16. Calcd. for $C_{21}H_{24}O_4$: C, 74.09; H, 7.11%.

I: R=H, n=6, colorless leaflets (57%), m. p. 123 ～124.5°C.

Found: C, 74.21; H, 7.93. Calcd. for $C_{22}H_{26}O_4$: C, 74.55; H, 7.39%.

I: R=H, n=10, colorless leaflets (67%), m. p. 105 °C.

Found: C, 75.95; H, 8.35. Calcd. for $C_{26}H_{34}O_4$: C, 76.06; H, 8.34%.

α,ω-Bis (4-ethynylphenoxy) alkanes (II: R=H, n=1,2,3,4,5,6 and 10).—A mixture of I: R=H, n=1 (14.2 g., 0.05 mol.), phosphorus pentachloride (27 g., 0.13 mol.) and phosphorus oxychloride (20 ml.) was heated at 70°C for 2 hr. The crude chloride which remained after the removal of the solvent under reduced pressure was dissolved in dry ether (100 ml.), and the solution was added to sodium (10 g., 0.43 g. atom) amide in liquid ammonia (500 ml.). After the ammonia had been evaporated, the residue was decomposed with water and extracted with ether. The ethereal solution was washed with water, dried over magnesium sulfate, and evaporated. The crude crystals thus obtained were recrystallized from ethanol to give II, R=H, n=1, (7.4 g., 60%); m. p. 85.5～86°C. IR: Nujol mull, 3295 (-C≡CH), 2095(-C≡C-), 1220 (=C-O-) and 813, 833 cm^{-1} (*p*-disubstituted benzene).

Found: C, 82.19; H, 4.88. Calcd. for $C_{17}H_{12}O_2$: C, 82.24; H, 4.87%.

Further purification of the compound for oxidative polymerization was carried out by means of column chromatography on alumina from carbon tetrachloride.

By the same method as that employed for II, R=H, n=1, the following diethynyl compounds were prepared:

II: R=H, n=2, colorless needles (37%), m. p. 170.5 °C.

Found: C, 82.80; H, 5.54. Calcd. for $C_{18}H_{14}O_2$: C, 82.42; H, 5.38%.

II: R=H, n=3, colorless needles (36%), m. p. 124 ～124.5°C.

Found: C, 82.35; H, 5.83. Calcd. for $C_{19}H_{16}O_2$: C, 82.58; H, 5.84%.

II: R=H, n=4, colorless needles (47%), m. p. 118.5 ～119°C.

Found: C, 82.26; H, 6.42. Calcd. for $C_{20}H_{18}O_2$: C, 82.73; H, 6.25%.

II: R=H, n=5, colorless needles (70%), m. p. 97～98.5°C.

Found: C, 82.68; H, 6.59. Calcd. for $C_{21}H_{20}O_2$: C, 82.86; H, 6.62%.

II: R=H, n=6, colorless leaflets (32%), m. p. 111～111.5°C.

Found: C, 82.18; H, 7.10. Calcd. for $C_{22}H_{22}O_2$: C, 82.98; H, 6.96%.

II: R=H, n=10, colorless leaflets (56%), m. p. 110 ～111.5°C.

Found: C, 82.34; H, 7.98. Calcd. for $C_{26}H_{30}O_2$: C, 83.38; H, 8.07%.

α,ω-Bis(4-acetyl-2-methylphenoxy)alkanes (I: R=CH_3, n=1,2,3,4,5 and 6).—In the same manner as that described in the preparation of II, R=H, n=1, 2-methyl-4-acetylphenol (30 g., 0.2 mol.) was first converted to its sodium derivative and then treated with dibromomethane (17.4 g., 0.1 mol.) and a small amount of potassium iodide in dimethylformamide (100 ml.) to afford I, R=CH_3, n=1. Recrystallization from ethanol gave colorless needles (10.3 g., 33%), m. p. 132.5～133.5°C. IR: Nujol mull, 1680 (CO), 1275 (=C-O-) and 815 cm^{-1} (1,2,4-trisubstituted benzene).

Found: C, 73.12; H, 6.44. Calcd. for $C_{19}H_{20}O_4$: C, 73.06; H, 6.45%.

A similar treatment of sodium 2-methyl-4-acetylphenoxide with α,ω-dibromoalkanes yielded the following ketones:

I: R=CH_3, n=2, colorless needles (25%), m. p. 167～167.5°C.

Found: C, 73.34; H, 6.77. Calcd. for $C_{20}H_{22}O_4$: C, 73.60; H, 6.79%.

I: R=CH_3, n=3, colorless leaflets (52%), m. p. 108.5～109.5°C.

Found: C, 73.98; H, 7.13. Calcd. for $C_{21}H_{24}O_4$: C, 74.09; H, 7.11%.

I: R=CH_3, n=4, colorless leaflets (64%), m. p. 114.5～115.5°C.

Found: C, 74.45; H, 7.34. Calcd. for $C_{22}H_{26}O_4$: C, 74.55; H, 7.39%.

I: R=CH_3, n=5, colorless leaflets (52%), m. p. 81.5～82.5°C.

Found: C, 74.98; H, 7.58. Calcd. for $C_{23}H_{28}O_4$: C, 74.97; H, 7.66%.

I: R=CH_3, n=6, colorless leaflets (76%), m. p. 87～88°C.

Found: C, 75.21; H, 7.90. Calcd. for $C_{24}H_{30}O_4$: C, 75.36; H, 7.91%.

α,ω-Bis(4-ethynl-2-methylphenoxy)alkanes (II: R=CH_3, n=1,2,3,4,5 and 6).—I, R=CH_3, n=1 (7.8 g., 0.025 mol.) was chlorinated with phosphorus pentachloride (11.5 g., 0.055 mol.) in phosphorus oxychloride (20 ml.) at 60°C for 2 hr., and the crude product was treated in the manner shown in the preparation of II, R=H, n=1, to yield II, R=CH_3, n=1, which was then recrystallized to give colorless needles (3 g., 44%), m. p. 138.5～139 °C. IR: Nujol mull, 3260 (-C≡CH), 2100 (-C≡C-), 890 (isolated H) and 815 cm^{-1} (1,2,4,-trisubstituted benzene).

Found: C, 82.63; H, 5.80. Calcd. for $C_{19}H_{16}O_2$: C, 82.58; H, 5.84%. Further purification was carried out by column chromatography on alumina from carbon tetrachloride.

Using the method employed for I, R=CH_3, n=1, the following diethynyl compounds were prepared:

II: R=CH_3, n=2, colorless needles (20%), m. p. 166~167°C.

Found: C, 82.73; H, 6.25. Calcd. for $C_{20}H_{18}O_2$: C, 82.73; H, 6.25%.

II: R=CH_3, n=3, colorless plates (46%), m. p. 67.5~69°C.

Found: C, 82.68; H, 6.63. Calcd. for $C_{21}H_{20}O_2$: C, 82.86; H, 6.62%.

II: R=CH_3, n=4, colorless needles (38%), m. p. 103~104°C.

Found: C, 82.70; H, 6.97. Calcd. for $C_{22}H_{22}O_2$: C, 82.98; H, 6.96%.

II: R=CH_3, n=5, colorless needles (34%), m. p. 87~88°C.

Found: C, 82.69; H, 7.24. Calcd. for $C_{23}H_{24}O_2$: C, 83.10; H, 7.28%.

II, R=CH_3 n=6, colorless leaflets (71%), m. p. 91.5~93°C.

Found: C, 83.10; H, 7.61. Calcd. for $C_{24}H_{26}O_2$: C, 83.20; H, 7.56%.

3-Methyl-4-methoxyphenylacetylene (IV: R=CH_3).—A mixture of 3-methyl-4-methoxyacetophenone[5] (8.8 g., 0.053 mol.), chloroform (25 ml.), and phosphorus pentachloride (15.5 g., 0.074 mol.) was heated at 60°C for 2 hr. After the chloroform had been removed under reduced pressure, the crude product was suspended in dry tetrahydrofuran (100 ml.), and the suspension was stirred drop by drop to sodium (6 g., 0.265 g. atom) amide into liquid ammonia (300 ml.). The stirring was continued for a further 1.5 hr. After the ammonia had evaporated, the residue was decomposed with water and extracted with ether. The ethereal layer was washed with water and dried over sodium sulfate. The removal of the solvent afforded IV, R=CH_3 (3.5 g., 44%) as an oily material which partly solidified when kept standing at room temperature. The recrystallization of the solid from ethanol yielded the pure substance in the form of colorless plates; m. p. 75~77°C. IR: Nujol mull, 3295 (-C≡CH), 2095 (-C≡C-), 2850 (-OCH_3) and 898, 820 cm^{-1} (1,2,4-trisubstituted benzene).

Found: C, 82.41; H, 6.82. Calcd. for $C_{10}H_{10}O$: C, 82.16; H, 6.90%.

3,3'-Dimethyl-4,4'-dimethoxydiphenyldiacetylene (V: R=CH_3).—A mixture of IV, R=CH_3, as the crude oil (1.8 g.), cupric acetate monohydrate (1.8 g.) and pyridine (20 ml.) was stirred at 55°C for 2 hr. The solvent was removed in vacuo and the residue was decomposed with water and extracted with ether. The ethereal layer was washed with water, dried over sodium sulfate and evaporated. On recrystallization of the residue from acetone V, R=CH_3, was obtained in a very high yield in the form of colorless needles (m. p. 163~165°C). IR: Nujol mull, 2140 (-C≡C-) and 890, 810 cm^{-1} (1,2,4-trisubstituted benzene). UV: $\lambda_{max}^{Ethanol}$, 262 (56700), 268 (58000), 281 (41000), 300 (37400), 319 (45000) and 342 mμ (ε, 36900).

Found: C, 82.51; H, 6.18. Calcd. for $C_{20}H_{18}O_2$: C, 82.73; H, 6.25%.

4-Methoxyphenylacetylene (IV: R=H) and 4,4'-Dimethoxydiphenyldiacetylene (V: R=H).—4-Methoxyacetophenone[6] (3 g., 0.02 mol.) was treated with phosphorus pentachloride (5 g., 0.024 mol.) and then with sodium amide (0.086 mol.) in liquid ammonia to yield IV, R=H, as an oil which was used for the following coupling reaction without further purification, though it was still somewhat inhomogeneous. IR: liquid, 3300 (-C≡CH), 2850 (-OCH_3), 2140 (-C≡C-) and 835 cm^{-1} (p-disubstituted benzene). In the same manner as that employed for IV, R=CH_3, IV, R=H, was coupled giving quantitatively diacetylene V, R=H, in the form of colorless needles (m. p. 143.5°C). IR: Nujol mull, 2130 (-C≡C-) and 843, 822 cm^{-1} (p-disubstituted benzene). UV: $\lambda_{max}^{Ethanol}$, 267 (27700), 281 (28700), 299 (34000), 317(44000) and 341 mμ (ε, 36700).

Found: C, 82.10; H, 5.37. Calcd. for $C_{18}H_{14}O_2$: C, 82.42; H, 5.38%.

The General Procedure for the Oxidative Polymerization of II.—A mixture or II, pyridine and cupric acetate monohydrate or cuprous chloride was stirred under the conditions summarized in Tables I and II. The precipitate formed was collected by filtration, washed successively with dilute hydrochloric acid, water and methanol, and then dried in vacuo.

The Linear Dimer of 1,6-Bis(4-ethynyl-3-methylphenoxy)hexane (II: R=CH_3, n=6).—When the oxidative coupling of II, R=CH_3, n=6, was carried out in methanol-pyridine (30:1) with cupric acetate monohydrate, a small amount of the linear dimer (III: R=CH_3, n=6, p=2) was produced. along with a large amount of an insoluble polymer, Colorless leaflets, m. p. 114~116°C. IR: Nujol mull, 3305 (-C≡CH), 2130, 2090 (-C≡C-) and 885, 815, 805 cm^{-1} (1,2,4-trisubstituted benzene). UV: $\lambda_{max}^{Ethanol}$, 269 (32200), 282 (34300), 298 (40400), 318 (40400) and 340 mμ (ε, 39800).

Found: C, 83.24; H, 7.29. Mol. wt., 699 (camphor). Calcd. for $C_{48}H_{50}O_4$: C, 83.44; H, 7.30%. Mol. wt., 695.

Department of Polymer Science
Faculty of Science
Osaka University
Nakanoshima, Osaka

5) C. A. Dalal, K. V. Bokil and K. S. Nargund, *J. Univ. Bombay 8*, pt. 3, 190 (1939).

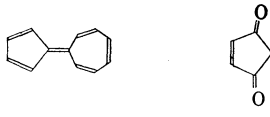
6) L. Gattermann, R. Ehrhardt and H. Maisch, *Ber.*, 23, 120 (1890).

The Synthesis and Reaction of Sesquifulvalene-1, 4-quinone[1]

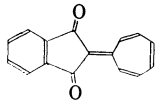
By Yoshio KITAHARA, Ichiro MURATA and Takashi ASANO*

(Received December 20, 1963)

One of the non-alternant hydrocarbons, sesquifulvalene (I), has been synthesized recently by Prinzbach and Rosswog[2] and found to be less stable than was expected from the molecular orbital theory.[3-6] On the other hand, Roberts[7] has pointed out that such



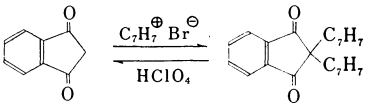
(I) (II)



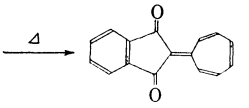
(III)

unsaturated cyclic hydrocarbons would be expected to form stable quinone derivatives. In this paper we will report on the synthesis and the chemical properties of the following five-membered ring quinone derivatives of sesquifulvalene; sesquifulvalene-1, 4-quinone (II) and 2, 3-benzosesquifulvalene-1, 4-quinone (III).

The reaction of indane-1, 3-dione (IV)[8] with 2 mol. equiv. of tropylium bromide (V) in an aqueous solution afforded 2, 2-ditropylindane-1, 3-dione (VI)[9] in a good yield. The two tropyl groups in compound VI were easily cleaved,[10] by the action of perchloric acid, to yield IV and tropylium perchlorate. The thermal decomposition[11] of VI gave 2, 3-benzosesquifulvalene-1, 4-quinone (III) as red needles.



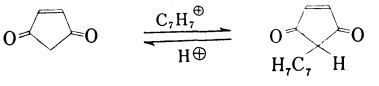
(IV) (VI)



(III)

When cyclopentene-3, 5-dione[12] was allowed to react with 2 mol. equiv. of V, 4, 4-ditropylcyclopentene-3, 5-dione (VIII) was obtained in a very low yield; however, by adjusting the reaction mixture to pH 7 with sodium hydrogen carbonate, VIII could be obtained in an almost quantitative yield.

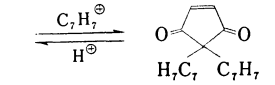
When an attempt was made to obtain sesquifulvalene-1, 4-quinone (II) by the thermal decomposition of VIII, the only product isolated was a reddish-brown resinous substance. This reaction will be discussed later. On the other hand, it is to be expected that II would be produced by the dehydrogenation of 4-tropylcyclopentene-3, 5-dione (IX). The preparation of this compound IX from VII was attempted, but even when 1 mol. equiv. of V was used, no monotropyl compound IX could be detected. The following equilibrium is supposed to be involved in the tropylation of cyclopentene-3, 5-dione (VII):



(VII) (IX)

↓

II



(VIII)

* Present address: Santoku Chemical Co., Sendai.

1) Preliminary communication: Y. Kitahara, I. Murata and T. Asano, This Bulletin, **34**, 589 (1961).

2) H. Prinzbach and W. Rosswog, *Angew. Chem.*, **73**, 543 (1961).

3) J. F. Tinker, *J. Chem. Phys.*, **19**, 981 (1951).

4) B. Pullman, A. Pullman, E. D. Bergmann, H. Berthod, E. Fisher, Y. Hirshberg, D. Lavie and M. Mayot, *Bull. soc. chim. France*, **1952**, 73.

5) R. D. Brown, *Trans. Faraday Soc.*, **45**, 296 (1949); **46**, 146 (1950).

6) B. Pullman and A. Pullman, "Les Theories Electroniques de la Chimie Organique," Masson et Cie., Paris (1952).

7) J. D. Roberts, *Record of Chem. Progr.*, **17**, 107 (1956).

8) L. F. Fieser, "Experiments in Organic Chemistry," D. C. Heath and Co., Boston (1957), p. 127.

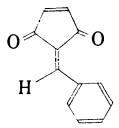
9) N. W. Jordan and I. W. Elliot, *J. Org. Chem.*, **27**, 1455 (1962).

10) K. Conrow, *J. Am. Chem. Soc.*, **81**, 5461 (1959).

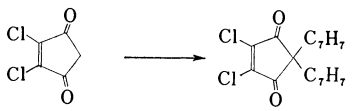
11) Cf. T. Nozoe, T. Mukai, K. Osaka and N. Shishido, This Bulletin, **34**, 1384 (1961).

12) C. H. DePuy and E. F. Zaweski, *J. Am. Chem. Soc.*, **81**, 4920 (1959).

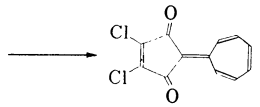
This means that, if 1 mol. equiv. of acid were to be used in the reaction, even though VIII were formed, the action of the protons would be expected to cause cleavage in VIII and thus to shift the equilibrium towards the monotropyl compound IX. In fact, when the tropylation was carried out in the presence of a 1 mol. equiv. of hydrogen bromide, an oily substance resulted, and on dehydrogenation with chloranil in xylene, the oil gave II as red plates (m. p. 180~181°C). The possibility that the rearrangement to a benzene derivative might take part in the reaction was excluded by the finding reported below. The expected rearrangement product of II is 4-benzylidene-cyclopentene-3, 5-dione (structure shown below). This compound has already been synthesized by DePuy as pale yellow needles (m.p. 146~146.5°C[13]) and is obviously different from the product (II) (m. p. 180~181°C), obtained above.



The thermal decomposition of 1, 2-dichloro-4, 4-ditropylcyclopentene-3, 5-dione (XI), which was derived from 1, 2-dichlorocyclopentene-3, 5-dione (X),[14] gave 2, 3-dichlorosesquifulvalene-1, 4-quinone (XII) in a good yield.



(X) (XI)



(XII)

All the sesquifulvalene quinone derivatives synthesized as above are red to reddish-orange crystals with high melting points; they are quite stable to air, heat and light.

It is noteworthy that the double bond at the 2, 3-position of the parent compound II is comparatively reactive. Thus, it reacted with bromine in chloroform to give a dibromide XIII as an adduct, and with cyclopentadiene in benzene, even at room temperature, a Diels-Alder reaction occurred to yield an adduct XIV; furthermore, by the action of diazomethane it afforded a pyrazoline derivative XV.

The highly unsaturated nature of the unsubstituted 2, 3-double bond in II accounts for the fact that, in the case of the 2, 3-benzo and 2, 3-dichloro derivatives where the 2, 3-position is substituted, the thermal decomposition of the ditropyl compounds, VI and XI, give III and XII respectively in good yields. Under the same conditions, however, only resinous products were obtained from VIII. This can be understood because, in the latter case, addition would occur between sesquifulvalene-1, 4-quinone and cycloheptatriene,[15] both of which would be formed during the thermal decomposition of VIII.

The ultraviolet absorption maxima[16] and the carbonyl-stretching frequencies[17] of the sesquifulvalene-1, 4-quinones and their 2, 3-adducts are shown in Tables I and II.

Table I. Ultraviolet absorption maxima: mμ (log ε)

II	III	XII
222 (4.35)	247 (4.43)	230 (4.20)
253 (4.16)	257 (4.40)	255 (4.36)
420 (4.37)	452 (4.57)	422 (4.42)
$\Delta\lambda$ 0	+32	+2
XIII	**XIV**	**XV**
225 (4.30)	227 (4.27)	225 (4.33)
267 (4.21)	264 (4.15)	266 (4.23)
452 (4.43)	450 (4.42)	451 (4.42)
+32	+30	+31

Table II. C=O Stretching frequencies: cm^{-1}; KBr-disk

II	III	XII	XIII	XIV	XV
1643	1645	1660	1627	1620	1618
$\Delta\nu$ 0	+2	+17	−16	−23	−25

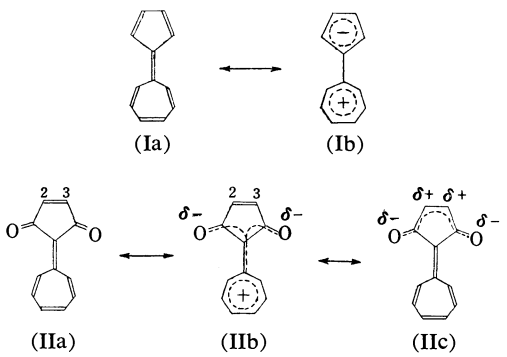
With reference to the 2, 3-adducts, XIII, XIV and XV it is significant that their ultraviolet absorption maxima at the longest wavelength show a bathochromic shift of about 30 mμ, and that their carbonyl-stretching frequencies, in the infrared spectra, are decreased by about 20 cm^{-1} compared with those of the 2, 3-unsaturated compounds, II and XII.

It appears to be rather strange that, despite the decrease of conjugation due to the 2, 3-positions being saturated in the adducts, the absorption maxima are shifted towards longer

13) C. H. DePuy and P. R. Wells, ibid., 82, 2909 (1960).
14) B. T. McBee, C. W. Roberts and K. Dinbergs, ibid., 78, 489 (1956).
15) The product from the thermal decompostion of VIII; it had the characteristic odor of cycloheptatriene, although none of this compound was actually isolated.
16) The ultraviolet spectra were recorded on a Hitachi photoelectric spectrometer model EPU-2 and are for methanol solutions.
17) The infrared spectra were measured on a Perkin-Elmer model 21 spectrometer and are for KBr-disks.

wavelengths. This apparent discrepancy could be explained as follows.

In sesquifulvalene (I), there appears to be quite a large contribution by the ionic structure Ib, a dipolar species possessing a positive seven-membered ring and a negative five-membered ring; for this reason a large dipole moment is expected.[4]



A contribution by the ionic structure may also naturally be expected in II. However, in this case the negative charge is not delocalized over the whole five-membered ring, as is the case in the species Ib; rather, it is probably localized on the two more electronegative oxygen atoms and a charge distribution as depicted in IIb is obtained. The charge transfer between the seven-membered ring and the two oxygen atoms seems to be rather strongly inhibited by the charge transfer IIc which occurs between the double bond at the 2, 3-position and the oxygen atoms. Naturally, the conditions for the transfer of the charge from the seven-membered ring become more favorable when the 2, 3-double bond is removed by the addition of bromine, cyclopentadiene, or diazomethane. The shifts in the ultraviolet and infrared spectra are thus understandable. This speculation is also supported by dipole moment measurements.[18]

Experimental

2, 2-Ditropylindane-1, 3-dione (VI).—Tropylium bromide (3.4 g., 0.02 mol.) in water (50 ml.) was stirred in, drop by drop over a period of 10 min., into a solution of indane-1, 3-dione (1.46 g., 0.01 mol.) in acetonitrile (25 ml.) at room temperature; stirring was then continued for a further 5 hr. The crystalline deposit was filtered off (3.15 g., 97.2%, m. p. 164~166°C) and recrystallized from ethanol to afford colorless prisms of VI (m. p. 167.5~168°C).

IR ν_{max}^{KBr} : 3015, 1728, 1699, 1590, 765 cm^{-1}. UV λ_{max}^{MeOH} $m\mu$ (log ε) : 227 (4.69), 252 (4.31).

Found: C, 84.29; H, 5.41. Calcd. for $C_{23}H_{18}O_2$: C, 84.64; H, 5.56%.

The Reaction of 2, 2-Ditropylindane-1, 3-dione with Perchloric Acid.—To a stirred solution of 2, 2-ditropylindane-1, 3-dione (0.65 g., 0.002 mol.) in 5 ml. of glacial acetic acid 60% perchloric acid (0.4 ml., 0.004 mol.) was added at room temperature; crystals were deposited almost immediately. After the mixture had been allowed to stand for 3 hr., the crystals of tropylium perchlorate (0.68 g., 89.4%) were filtered off. Its infrared absorption spectrum coincided with that of authentic tropylium perchlorate.

The filtrate was then diluted with water (300 ml.) and extracted with ether. The ether layer was washed with water, dried, and evaporated to yield crystals (0.25 g., 85.6%; m. p. 124~127°C), which showed no depression on a mixed melting point test with indane-1, 3-dione.

2, 3-Benzosesquifulvalene-1, 4-quinone (III).—2, 2-Ditropylindane-1, 3-dione (1.0 g., 0.00307 mol.), in a test tube fitted with a side arm which was connected via a dry-ice trap to a vacuum pump, was heated, under reduced pressure, in an oil bath at 175°C for 30 min. During this time an oil was observed to distil into the trap. After distillation of the oil had ceased, the pressure was kept at 2 mmHg for a further 10 min. The oil in the trap was then refluxed with maleic anhydride in xylene for 4 hr. The recrystallization of the crystalline product from carbon tetrachloride gave colorless rods (m.p. 98~100°C). No depression in the melting point was observed when a mixed melting point test was carried with the maleic anhydride adduct of cycloheptatriene.

The residue which remained in the test tube after the above thermal decomposition was a red solid (0.70 g., 97.5%; m. p. 194~200°C) which, after four recrystallizations from benzene, afforded red needles of III (m. p. 244~245°C).

UV λ_{max}^{MeOH} $m\mu$ (log ε) : 247 (4.43), 257 (4.40), 452 (4.57). IR ν_{max}^{KBr} : 1645, 1628, 1590, 760 cm^{-1}.

Found: C, 81.71; H, 4.13. Calcd. for $C_{16}H_{10}O_2$: C, 82.04; H, 4.30%.

4, 4-Ditropylcyclopentene-3, 5-dione (VIII).—(a) Tropylium bromide (1.71 g., 0.01 mol.) in water (30 ml.) was stirred drop by drop during 10 min. into a solution of cyclopentene-3, 5-dione (0.96 g., 0.01 mol.) in water (20 ml.). After the reaction mixture had been allowed to stand for 3 hr. at room temperature, the resulting precipitate was taken up in ether. The ether layer was washed with water, dried over magnesium sulfate, and then evaporated. The residue, dissolved in benzene, was chromatographed on an alumina column (1× 10 cm.). From the combined yellow benzene eluates 0.55 g. of crystals was obtained (m. p. 118~121°C). Recrystallization from cyclohexane gave yellow prisms (m. p. 121~122°C).

UV λ_{max}^{MeOH} $m\mu$ (log ε) : 225 (4.17), 250 (3.90). IR ν_{max}^{KBr} : 3015, 1735, 1696, 740 cm^{-1}.

Found: C, 82.45; H, 5.84. Calcd. for $C_{19}H_{16}O_2$: C, 82.58; H, 5.84%.

(b) Tropylium bromide (3.42 g., 0.02 mol.) in 75% ethanol (15 ml.) was added, in one lot, to a

18) S. Katagiri, I. Murata, Y. Kitahara and H. Azumi, to be published.

stirred solution of cyclopentene-3,5-dione (0.96 g., 0.01 mol.) in ethanol (20 ml.) at room temperature. After being stirred for 10 min., the solution was adjusted to pH 6.5~7.0 with saturated aqueous sodium hydrogen carbonate. The precipitated crystals of 4,4-ditropylcyclopentene-3,5-dione (2.58 g., 93.5%; m. p. 118~120°C) were then filtered off.

Sesquifulvalene-1, 4-quinone (II).—To a stirred solution of cyclopentene-3,5-dione (1.92 g., 0.02 mol.) in water (40 ml.) 3.2 g. of 48% hydrobromic acid was added; then to this mixture, a solution of tropylium bromide (3.42 g., 0.02 mol.) in water (50 ml.) was stirred in drop by drop over a period of 30 min. The yellow oil which separated was extracted into ether, and the ether solution was washed with water, dried over magnesium sulfate, and then evaporated. The residual oil (3.7 g.), without further purification, was dissolved in xylene (40 ml.). Chloranil (4.8 g.) was added to the solution, and the solution was refluxed for 3 hr. and then allowed to stand overnight. The precipitated tetrachlorohydroquinone was filtered off, and the filtrate was concentrated under reduced pressure. The benzene-soluble fraction of the residue was chromatographed on an alumina column (2×15 cm.). The red benzene eluate yielded red crystals (0.37 g., 10% yield based on tropylium bromide; m. p. 172~175°C). Recrystallization from benzene afforded red plates of II (m. p. 180~181°C).

UV λ_{max}^{MeOH} mμ (log ε): 222 (4.35), 253 (4.16), 420 (4.37). IR ν_{max}^{KBr}: 3060, 1643, 1515, 1262, 849 cm^{-1}.

Found: C, 78.41; H, 4.26. Calcd. for $C_{12}H_8O_2$: C, 78.25; H, 4.38%.

1, 2-Dichloro-4, 4-ditropylcyclopentene-3, 5-dione (XI).—Tropylium bromide (12.1 g., 0.0708 mol.) in acetonitrile (150 ml.) was stirred drop by drop into a solution of 1,2-dichlorocyclopentene-3,5-dione (5.5 g., 0.033 mol.) in acetonitrile (50 ml.) at room temperature. Pyridine (5 ml.) was then added, and stirring was continued for a further 30 min. The yellow crystals (11.2 g., 97.3%) which precipitated on the addition of water (500 ml.) had a m. p. of 98~100°C; recrystallization from methanol afforded yellow plates of XI (m. p. 103~104°C).

IR ν_{max}^{KBr}: 3020, 1757, 1712, 1584, 1200 cm^{-1}.

Found: C, 66.21; H, 4.20. Calcd. for $C_{19}H_{14}O_2Cl_2$: C, 66.11; H, 4.09%.

2, 3-Dichlorosesquifulvalene-1, 4-quinone (XII).—1,2-Dichloro-4,4-ditropylcyclopentene-3,5-dione (1.72 g., 0.005 mol.) was pyrolysed in a test tube with a side arm at 150°C under reduced pressure. During the reaction, the material in the tube melted, then began to bubble, and finally resolidified after about 10 min. Methanol was added to the residue, and the red crystals (1.1 g., 86.9%; m. p. 250°C (decomp.)) which were obtained in filtering the suspension were recrystallized from benzene to give reddish-orange scales of XII (m. p. 263°C (decomp.)).

UV λ_{max}^{MeOH} mμ (log ε): 230 (4.20), 255 (4.36), 422 (4.42). IR ν_{max}^{KBr}: 1660, 1615 cm^{-1}.

Found: C, 57.07; H, 2.59. Calcd. for $C_{12}H_6O_2Cl_2$: C, 56.95; H, 2.39%.

The Reaction of Sesquifulvalene-1, 4-quinone (II) with Bromine.—Bromine (0.08 g.) in chloroform (1 ml.) was added to a stirred solution of sesquifulvalene-1,4-quinone (0.09 g.) in chloroform (4 ml.) with ice-cooling. The crystalline orange precipitate (0.12 g; m. p. 80~95°C) which was produced was then filtered off and recrystallized from ethanol to yield golden-yellow scales of XIII (m. p. 148°C (decomp.)).

UV λ_{max}^{MeOH} mμ (log ε): 225 (4.30), 267 (4.21), 452 (4.43). IR ν_{max}^{KBr}: 1627 cm^{-1}.

Found: C, 42.51; H, 2.42. Calcd. for $C_{12}H_8O_2Br_2$: C, 41.89; H, 2.34%.

The Reaction of Sesquifulvalene-1, 4-quinone (II) with Diazomethane.—Ethereal diazomethane was stirred into an ice-cold solution of sesquifulvalene-1,4-quinone (0.09 g.) in a mixture of benzene (4 ml.) and ether (50 ml.). Orange crystals began to be formed within a few minutes; the mixture was then allowed to stand for 30 min., after which time the crystals (0.08 g.; m. p. 290°C) were filtered off and recrystallized three times from ethanol to afford orange needles of XV (m. p. 290°C).

UV λ_{max}^{MeOH} mμ (log ε): 225 (4.33), 266 (4.23), 451 (4.42). IR ν_{max}^{KBr}: 1618 cm^{-1}.

Found: C, 68.67; H, 4.33; N, 12.08. Calcd. for $C_{13}H_{10}O_2N_2$: C, 69.01; H, 4.46; N, 12.38%.

The Reaction of Sesquifulvalene-1, 4-quinone (II) and Cyclopentadiene.—A solution of sesquifulvalene-1,4-quinone (0.09 g.) and freshly-distilled cyclopentadiene (0.07 g.) in benzene (6 ml.) was set aside for 24 hr. in a tightly-stoppered flask at room temperature. The residue remaining after the removal of the benzene was treated with light petroleum, and the insoluble residue (m. p. 182~183°C) was recrystallized from benzene; red prisms of XIV (m. p. 188~189°C) were obtained.

UV λ_{max}^{MeOH} mμ (log ε): 235 (3.82), 289 (3.83), 450 (4.43). IR ν_{max}^{KBr}: 1620 cm^{-1}.

Found: C, 81.51; H, 5.25. Calcd. for $C_{17}H_{14}O_2$: C, 81.58; H, 5.64%.

The authors are indebted to Miss Yoko Endo and Miss Yukiko Endo of this Institute for their elementary analyses. They are also grateful to the Sankyo Co., Ltd., for its financial support in the present research.

The Chemical Research Institute of Non-Aqueous Solutions
Tohoku University
Katahira-cho, Sendai

Radiolysis of Solid Glycine

By Gisuke MESHITSUKA, Kotaro SHINDO, Atsuko MINEGISHI, Hiroshi SUGURO and Yoshiharu SHINOZAKI

(Received January 8, 1964)

The mechanism of radiation-induced reactions in a glycine aqueous solution has been extensively studied in many laboratories.[1,2] The radiolysis of solid glycine, however, has not been investigated thoroughly; although some of the radicals produced have been examined from the ESR spectra of irradiated solid glycine,[3,4] there has been insufficient interpretation of the spectra.

In the present work, products are measured after dissolving irradiated solid glycine in water, and mechanisms for the primary reaction of solid glycine radiolysis and for the secondary reaction, giving final products, are proposed with reference to the results of ESR studies.

Experimental

Materials. — Glycine (Yuki Gosei Kogyo Co., Special grade) was purified by recrystallization from water at least four times. Sodium chromotropate (Merck, Reagent) and *p*-dimethylaminobenzaldehyde (Daiichi Kagaku Yakuhin Co., Special grade) were used without further purification as reagents for the analysis of the products.

Irradiation.—Glycine powder (100~200 mesh) in glass vessels was evacuated for 8 hr. at 110°C in vacuo ($<10^{-4}$ mmHg) and then sealed. A 3000-curie cobalt source was used for γ-ray irradiation. The dose range employed was 0.5×10^{20} eV. g^{-1} to 2.7×10^{21} eV. g^{-1} at dose rates of $9.5\times10^{18}\sim4.1\times10^{19}$ eV. $g^{-1}\,hr^{-1}$. Dosage was determined by the Fricke-dosimeter technique with a $G(Fe^{3+})$ value of 15.6.

Analysis. — Hydrogen collected by conventional techniques directly from the irradiated solid samples was analyzed with a gas chromatograph (Shimadzu, GC-1A) and a mass spectrometer (Hitachi, RMU-5B).

All the other products, volatile bases, organic acids, formaldehyde etc. were analyzed from the solutions after dissolving the irradiated samples in water in and out of the presence of oxygen.

Nitrogen-containing Products.—The total amount of the volatile bases (NH_3, CH_3NH_2) was measured by two different methods, the Kjeldahl method and separation with an anion-exchange resin. In the latter case, Dowex 1 resin (OH form, 100~200 mesh, 8% crosslinked) was used. Aqueous solutions of the irradiated glycine were poured onto the top of the column (40 cm. high by 2 cm. in diameter), and the effluents were collected in the excess of sulfuric acid and back-titrated with sodium hydroxide, using phenolphthalein as an indicator. The results of the two methods agreed well. In some runs, a radiofrequency titration method was also applied.

Methylamine was identified and measured by an infrared absorption spectrum of methylamine hydrochloride obtained by evaporating the effluents after neutralization with hydrochloric acid. Methylamine was measured also from extinction at 540 mμ induced by the reaction with lactose.[5] The amount of ammonia was obtained by substracting the amount of methylamine from that of the total volatile base.

The amount of hydrazine tested colorimetrically with *p*-dimethylbenzaldehyde[6] was negligibly small. Amino acids were not detected by the use of an amino acid analyzer or by paper chromatography.

Acids and Formaldehyde.—Organic acids were separated from glycine and other products with cation exchange resin Dowex 50 (H form, 50~100 mesh, 8% crosslinked). Aqueous solutions of the irradiated glycine were poured onto the column (40 cm. high, 2 cm. in diameter), and the effluents were titrated with sodium hydroxide, using cresol red as an indicator, under an atmosphere of nitrogen. In some runs, the effluents were degassed by conventional techniques to remove the carbon dioxide and then titrated in order to measure the real amount of organic acids. The amount of carbon dioxide was obtained from the decrease in the total of acid produced by the degassing. The components of the organic acid were identified as glyoxilic acid and acetic acid from the infrared absorption spectra of the sodium salts obtained by freeze-drying after titration.

Glyoxilic acid was measured by techniques modified from the method used for the analysis of formaldehyde by MacFadyen.[7] The irradiated glycine (0.01~0.05 g.) was dissolved in 0.5 ml. of water and 5 ml. of 2 N hydrochloric acid; 0.05 ml. of sodium chromotropate (0.1 g. ml^{-1}) and 5 ml. of concentrated sulfuric acid were then added, and

1) C. R. Maxwell, D. C. Peterson and N. E. Sharpless, *Radiation Research*, **1**, 530 (1954); C. R. Maxwell, D. C. Peterson and W. C. White, ibid., **2**, 431 (1955).
2) B. M. Weeks and W. M. Garrison, ibid., **9**, 291 (1958).
3) D. K. Ghosh and D. H. Whiffen, *Mol. Phys.*, **2**, 285 (1959); D. K. Ghosh and D. H. Whiffen, *J. Chem. Soc.*, **1960**, 1869.
4) R. F. Weiner and W. S. Koski, *J. Am. Chem. Soc.*, **85**, 873 (1963).
5) A. A. Ormsby and S. Johnson, *J. Biol. Chem.*, **187**, 711 (1950).
6) "Bunseki Kagaku Binran," Maruzen, Tokyo (1961), pp. 463–464.
7) D. A. MacFadyen, *J. Biol. Chem.*, **158**, 107 (1945).

the mixture was boiled for 30 min., cooled, and diluted to 10 ml. with water. From the absorption spectra of the solution, glyoxilic acid was measured by the extinction at 440 mμ.

The amount of acetic acid was obtained by subtracting the amount of glyoxilic acid from the total of organic acid. A small amount of formaldehyde was measured by the same method as glyoxilic acid from the extinction at 568 mμ.

Results and Discussion

Yields.—Figures 1 and 2 show the relations between the amounts of the products and the irradiation doses. All products except H_2 increase linearly with the dose. Hydrogen shows a plateau from a relatively low dose. Figure 1 shows that oxygen dissolved in water,

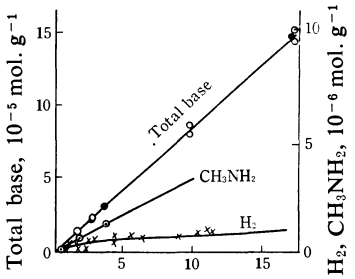


Fig. 1. The yields of basic products and H_2 from glycine irradiated by ^{60}Co γ-rays. Total base was obtained by dissolving the sample in oxygen containing water (○) or degassed water (●).

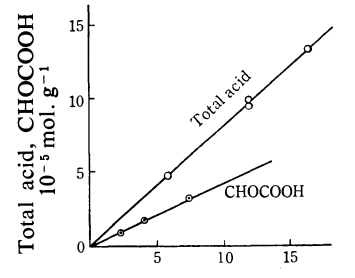


Fig. 2. The yields of acidic products from glycine irradiated by ^{60}Co γ-rays.

TABLE I. YIELDS OF PRODUCTS

Product	G
H_2	~0.2
NH_3	4.8
CH_3NH_2	0.2
$CHOCO_2H$	2.5
CH_3CO_2H	2.3
CO_2	~0.2
HCHO	trace (~0.0_3)

which is used to dissolve the irradiated samples, does not remarkably affect the yields of the total base. The yields of the products obtained from the slopes of Figs. 1 and 2 are listed in Table I. The initial yield of H_2 was estimated to be approximately 0.2 from the initial slope of the curve.

Mechanism. — From the studies of ESR spectra of the irradiated solid glycine, some evidence concerning radicals in irradiated solid glycine was obtained.[8] The results were interpreted by assuming that the free radicals primarily produced are NH_2 and $CH_2CO_2^-$, with a trace of $\overset{+}{N}H_3CHCO_2^-$, and that NH_2 and $CH_2CO_2^-$ slowly decrease to produce $\overset{+}{N}H_3CHCO_2^-$ and an unknown radical (presumably $\overset{+}{N}H_2CH_2CO_2^-$).

Irradiated glycine was dissolved in water, immediately after irradiation or after having been kept at room temperature for a long time. In the latter case, the radicals originally produced should have completely changed. Nevertheless, the chemical analysis of the final products of the two cases gave the same results.

The CH_3NH_2 obtained ($G=0.2$) appears to be due to a direct molecular dissociation of the glycine molecule, as was proposed by Garrison[2] in the radiolysis of aqueous solutions.

From these results, the following mechanism of the radiolysis of solid glycine may be proposed:

$$\overset{+}{N}H_3CH_2CO_2^- \rightsquigarrow H^+ + NH_2 + CH_2CO_2^- \quad (1)$$

$$\overset{+}{N}H_3CH_2CO_2^- \rightsquigarrow CH_3NH_2 + CO_2 \quad (2)$$

$$\overset{+}{N}H_3CH_2CO_2^- \rightsquigarrow \overset{+}{N}H_3CHCO_2^- + H \quad (3)$$

$$H + \overset{+}{N}H_3CH_2CO_2^- \longrightarrow H_2 + \overset{+}{N}H_3CHCO_2^- \quad (4)$$

With an increasing dose, radicals are accumulated (the estimated value is, for instance, 10^{-5} mol. g^{-1} at a dose of 1×10^{20} eV. g^{-1}) and scavenge H atom to give a plateau of the H_2 yield.

$$H + R \longrightarrow RH \quad (5)$$

The primary process 1 seems to be not so simple; it may contain dissociative electron-capture mechanism to give the same resultant radicals. The results of the investigation of this point will be published elsewhere.

When the irradiated glycine is dissolved in

8) G. Meshitsuka, Y. Shinozaki and K. Shindo. *Annual Report, Tokyo Metropolitan Isotope Center*, 2, 181 (1963).

water, particular radicals, NH_2 and $CH_2CO_2^-$, abstract H from the glycine molecule to produce ammonia, acetic acid and $\overset{+}{N}H_3CHCO_2^-$:

$$NH_2 + \overset{+}{N}H_3CH_2CO_2^- \longrightarrow NH_3 + \overset{+}{N}H_3CHCO_2^- \quad (6)$$

$$CH_2CO_2^- + \overset{+}{N}H_3CH_2CO_2^- \longrightarrow CH_3CO_2^- + \overset{+}{N}H_3CHCO_2^- \quad (7)$$

Hydrogen abstraction may occur at the amino group to form $\overset{+}{N}H_2CH_2CO_2^-$, but it is probable that the radical changes to a more stable radical, $\overset{+}{N}H_3CHCO_2^-$, by the H atom migration:

$$\overset{+}{N}H_2CH_2CO_2^- \longrightarrow \overset{+}{N}H_3CHCO_2^- \quad (8)$$

Glycine radicals give NH_3, $CHOCO_2H$, HCHO and CO_2 by the following reactions, as proposed in the radiolysis of aqueous solutions:[2]

$$2\overset{+}{N}H_3CHCO_2^- \longrightarrow \overset{+}{N}H_2CHCO_2^- + \overset{+}{N}H_3CH_2CO_2^- \quad (9)$$

$$\overset{+}{N}H_2CHCO_2^- + H_2O \longrightarrow NH_3 + CHOCO_2H \quad (10)$$

$$\longrightarrow NH_3 + HCHO + CO_2 \quad (11)$$

Reaction 9′ has been proposed by Garrison[2] in the radiolysis of oxygen-containing aqueous solutions:

$$\overset{+}{N}H_3CHCO_2^- + O_2 \longrightarrow \overset{+}{N}H_2CHCO_2^- + HO_2 \quad (9')$$

However, oxygen in water does not have any remarkable effect on the yields of the total base. It seems, therefore, that $\overset{+}{N}H_3CHCO_2^-$ reacts mainly in the disproportionation reaction 9 instead of in reaction 9′, even in the presence of dissolved oxygen. If the scavenging reaction 5 holds, $G(CH_3CO_2H)$ should be a little higher than $G(CHOCO_2H)$. On the contrary, however, the results show $G(CHO\cdot CO_2H)$ to be a little higher than $G(CH_3CO_2H)$, indicating that reaction 9′ also occurs to a small extent.

According to the mechanism, the following relationships may be expected:

$$G(\text{total acid}) = G(\text{total base})$$

$$G(NH_3) = G(CHOCO_2H) + G(CH_3CO_2H)$$

$$G(CO_2) = G(CH_3NH_2) + G(HCHO)$$

As Table I shows, the experimental results satisfy these relationships well. The yields of the primary processes are estimated as follows:

$$G(1) = G(CH_3CO_2H) = 2.3$$

$$G(2) = G(CH_3NH_2) = 0.2$$

and $G(3) = G(H_2) \sim 0.2$

Summary

Solid glycine has been radiolyzed by ^{60}Co γ-rays in vacuo at room temperature, and all the products except H_2 have been measured after dissolving the irradiated samples in water. The hydrogen has been collected and measured directly from the irradiated solid samples. All products except H_2 increase linearly with the dose, while H_2 shows a plateau from a relatively low dose. The yields of products are as follows: $G(H_2) \sim 0.2$, $G(NH_3) = 4.8$, $G(CH_3NH_2) = 0.2$, $G(CHOCO_2H) = 2.5$, $G(CH_3CO_2H) = 2.3$, $G(CO_2) \sim 0.2$, and $G(HCHO) \sim 0.03$. The mechanisms of the primary process and the reactions to give final products have been proposed with reference to the results of the ESR studies.

Tokyo Metropolitan Isotope Center
Setagaya-ku, Tokyo

A Study of the Sorption of Metal Ions by Cotton Cloth

By Reiko KOGA, Yoshiharu SHINOZAKI, Gisuke MESHITSUKA and Toshizo TITANI

(Received January 8, 1964)

The interactions of cellulose with metal ions in aqueous solutions have long been known. For example, cellulose can react with metal ions in such strong alkaline media as Schweizer's solution. In connection with the structure and the nature of cellulose, mechanisms for the sorptions of metal ions by cellulose have been discussed by various workers.[1-5] Some of them ascribe the sorption phenomena to an acidic action of hydroxyl groups and a complex formation,[4] and some, to an ion-exchange reaction of the carboxyl groups which exist in cellulose.[3,5]

The present paper will study, by means of the tracer technique, the sorption phenomena of metal ions by cotton cloth in the aqueous media. In the neutral and the acidic region, the exchange mechanism by the carboxyl grou s has again been confirmed. Since it has been another object of this work to obtain information on the decontamination of metal ions from cotton cloth, the relative affinities of metal ions, i. e., Cu^{2+}, Co^{2+}, Zn^{2+}, Ca^{2+}, Sr^{2+}, Cs^{+}, K^{+} and Na^{+}, to cotton cloth have also been determined.

Experimental

Materials.—The cotton print cloth (Nitto Boseki K. K.) was purified by extracting it with hot ethanol and boiling for 2.5 hr. in a 1% sodium hydroxide solution. The residual sodium hydroxide was removed from the cotton by washing it with distilled water; it was then acidified with dilute acetic acid, again neutralized with dilute aqeous ammonia, and finally washed with deionized distilled water. The cotton thus obtained was dried and stored. The Cu-value was found to be 0.048.

Commercial metal salts (reagent grade) were used without further purification. The water employed was treated with ion exchange resin and distilled. Radioisotopes, ^{45}Ca, ^{60}Co and ^{137}Cs, were diluted to the proper activity level for use.

Procedures. — *The Determination of Uptake.* — Weighed samples of cotton cloth, about 4.5 cm^2 in apparent area (ca. 0.05 g.), were immersed into 20 ml. of a metal salt solution of a known concentration containing the radioisotope as a tracer and shaken for 2 hr. at a desired constant temperature (usually 25°C) in most cases. Then the cotton sample was taken out of the solution, pressed between two sheets of filter paper, and reweighed to determine the amount of the moisture retained in the sample. The activity of the air-dried sample was measured by a Geiger-Mueller counter or a scintillation counter, while the total number of metal ions taken up by the sample was calculated by means of the calibration curve which had been obtained in the preliminary experiment for the sample soaked with a known number of the metal ions. The real amount of sorbed metal ions was obtained by correcting for the moisture retained in the sample. In this correction it was assumed that the concentration of the metal ion in the retained moisture was the same as that in the bulk solution.

The Determination of Rates of Sorption. — The rates of the sorption of Co^{2+} were determined at 2, 4.7, 25 and 38°C by measuring the uptake at appropriate intervals by a method similar to that mentioned above until equilibrium was achieved.

pH Adjustment.—In the studies of the pH dependence, hydrogen ion concentrations were changed by adding hydrochloric acid to solutions while keeping the amount of metal hydroxide constant.

The Determination of Relative Affinities. — The maximum uptakes of Co^{2+} from mixed solutions of Co^{2+} and any one of the following ions, Cu^{2+}, Zn^{2+}, Ca^{2+}, Cs^{+}, K^{+} and Na^{+}, were determined. The initial concentrations of the two ions in the mixed solutions were the same (10^{-3} M). An affinity series was determined from the order of the maximum uptake of Co^{2+}. A similar experiment was undertaken for mixed solutions of Ca^{2+} and any one of the following ions, Cu^{2+}, Co^{2+}, Zn^{2+}, Cs^{+}, K^{+} and Na^{+}.

Results and Discussion

pH Dependence. — The equilibrium uptakes of Co^{2+}, Ca^{2+} and Cs^{+} by cotton cloth exhibit a marked dependence upon the hydrogen ion concentration of the media, as is shown, for instance, for Ca^{2+} in Fig. 1. The uptake becomes perceptible around pH 3 and increases rapidly with the increasing pH, with an intermediate approximate plateau in the neutral region. This suggests two mechanisms for the

1) G. F. Davidson and T. P. Nevell, *Shirley Inst. Mem.*, **21**, 46 (1947).
2) H. F. Church, *J. Soc. Chem. Ind. (London)*, **66**, 221 (1947).
3) R. J. Demint and J. C. Arthur, Jr., *Textile Research J.*, **29**, 276 (1959).
4) D. S. Belford, A. Myers and R. D. Preston, *Biochim. Biophs. Acta*, **34**, 47 (1959).
5) R. I. C. Michie, *Nature*, **190**, 803 (1961).

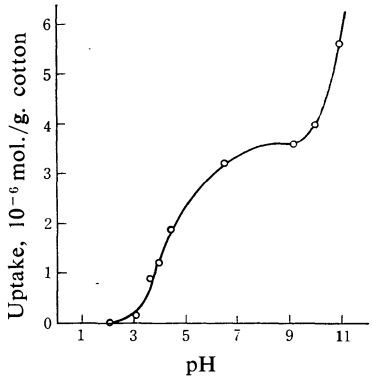


Fig. 1. pH dependence of Ca^{2+} uptake on cotton cloth.
$[Ca^{2+}]=1.1\times10^{-3}$ M, 25°C

sorption, one effective in the acidic and neutral regions, and the other only in the strongly alkaline region. The former is a cation exchange mechanism of the carboxyl groups, in accordance with Michie's[5] observation that the uptake of copper is proportional to the carboxyl content and with Demint and Arthur's[3] study of the exchanging properties of γ-ray irradiated cotton.

The latter mechanism is an acidic action of the hydroxyl groups in cellulose. Complex formations of this groups have long been known in strongly alkaline media, such as Schweizer's solution. In the strongly alkaline region, however, cotton shows a swelling which may increase the active sites. This renders the interpretation difficult. Therefore, the following experiments are restricted to the sorption in the acidic and neutral regions.

The Rate of Sorption. — The rates of the sorption of Co^{2+} were measured at various temperatures and at various concentrations of Co^{2+} at pH ca. 4.7. As is shown in Fig. 2, the uptakes increase with time approaching the equilibrium values.

According to the mechanism of cation exchange between the hydrogen ion of the caboxyl groups, H^+, and the metal ions, M^+, the following rate expression may be expected

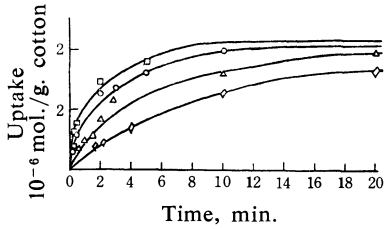


Fig. 2a. Uptake of Co^{2+} at various temperatures.
($[Co^{2+}]=1\times10^{-4}$ M)
2°C (◇), 4.7°C(△), 25°C (○), 38°C (□)

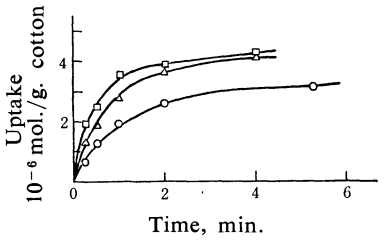


Fig. 2b. Uptake of Co^{2+} at various concentrations. (25°C)
4×10^{-4} M (□), 2×10^{-4} M (△), 1×10^{-4} M (○)

to hold as a first approximation;

$$dx/dt=k_1(a-x)[M^+]-k_2x[H^+] \qquad (1)$$

where x is the uptake at time t, a is the total number of sites available for ion exchange, and k_1 and k_2 are rate constants. Equation 1 was derived by assuming a hypothetical homogeneous solution. Further, it can be assumed that $[H^+]$ and $[M^+]$, practically speaking, do not change during the sorption under our experimental conditions. Thus, from Eq. 1, a linear relationship for $\ln(1-x/x_e)$ vs. t plots follows, where x_e is the equilibrium uptake. The experimental results under the various conditions are illustrated in Fig. 3. The deviation from linearity in Fig. 3 indicates that the simplified model mentioned above is not accurate. The actual process is a heterogeneous one. Possibly, delayed transporting phenomena of the metal ions from the surface into the inner sorption site of the cotton are responsible for the non-linearity obtained.

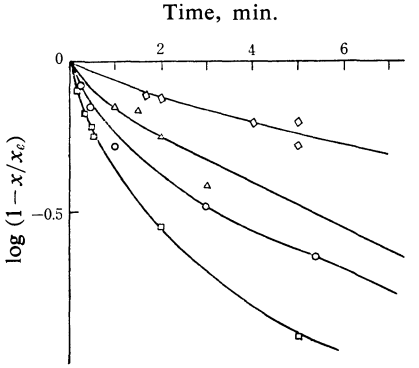


Fig. 3. $\log(1-x/x_e)$ vs. t plots.
2°C (◇), 4.7°C (△), 25°C (○), 38°C (□)

However, as the limiting case of Eq. 1, the following relation may be applied for an initial stage of the sorption;

$$(dx/dt)_0=k_1a[M^+] \qquad (2)$$

where $(dx/dt)_0$ means the initial velocity. $(dx/dt)_0$ can be obtained from the 'initial

slopes of curves in Fig. 2. Equation 2 is satisfied as illustrated in Fig. 4, as far as the change of $[M^+]$ is concerned in the sorption of Co^{2+}. k_1 can be calculated from the slope of the straight line in Fig. 4, using the maximum uptake, a, obtained in the equilibrium experiments.

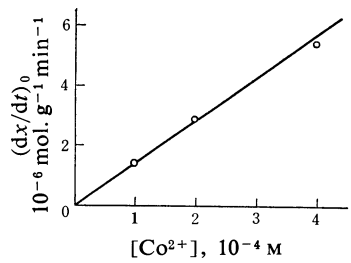


Fig. 4. Initial rates of Co^{2+} uptake at various concentrations (25°C).

An activation energy for the sorption of Co^{2+} was calculated from k_1 values at various temperatures (Fig. 5) to be 7.6 kcal./mol. It is interesting to note that this value is of the same order as the activation energies of the diffusion of metal ions in aqueous solutions.[6,7]

The facts may indicate that the diffusion of Co^{2+} to the cotton surface is the rate-determining step in the early stage of the sorption of the ion.

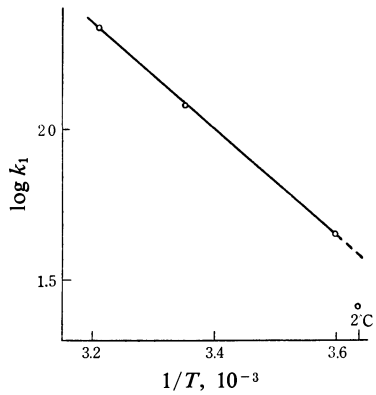


Fig. 5. Temperature dependence of initial rate constants of uptake of Co^{2+}.

The Concentration Dependence of the Uptake. —The equilibrium uptakes at various concentrations of Co^{2+} are expressed as a Langmuir-type sorption isotherm (Fig. 6).

Assuming a cation exchange mechanism,

$$RH + M^+ \rightleftharpoons RM + H^+$$

a Langmuir-type isotherm (Eq. 5) is derived as follows:

$$\frac{(RM)\,[H^+]}{(RH)\,[M^+]} = K_H^M \tag{3}$$

$$(RH) + (RM) = a \tag{4}$$

$$a = \frac{(RM)\,[H^+]}{K_H^M\,[M^+]} + (RM)$$

$$\frac{[M^+]}{(RM)} = \frac{[H^+]}{aK_H^M} + \frac{[M^+]}{a} \tag{5}$$

where (RH) and (RM) are the total number of sites per gram of cotton occupied by H^+ and M^+ respectively, and $[H^+]$ and $[M^+]$ are the concentrations of H^+ and M^+ respectively in the solution.

The total amount of available sites a mol. per gram of cotton can be obtained as the maximum uptake experimentally. The value, 4.2×10^{-6} mol./g. cotton, calculated for a from Fig. 6 is about 10^{-3} times the number of hydroxyl groups in cellulose. These results seem to indicate that some special group, possibly a carboxyl group, is responsible for the sorption phenomena in the acidic region.

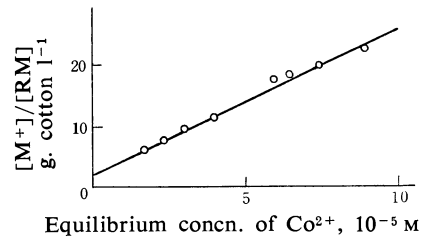


Fig. 6. Langmuir absorption isotherm of Co^{2+} (25°C).

The Heat of Sorption. — The heat of the sorption of Co^{2+} was determined to be ca. -2 kcal./mol. from the variation of uptake with temperature. Because of the small effect of the temperature on the uptake, it was difficult to ascertain the heat of sorption accurately. The low value of the heat of sorption may be an evidence for the exchange mechanism of the sorption.

The Affinities of Various Metal Ions.—When two kinds of metal ions, M_1^+ and M_2^+, coexist in the sorption system, the following exchange equilibria are to be expected;

$$RH + M_1^+ \rightleftharpoons RM_1 + H^+$$

$$RH + M_2^+ \rightleftharpoons RM_2 + H^+$$

$$RM_1 + M_2^+ \rightleftharpoons RM_2 + M_1^+$$

The relative affinity of these metal ions to the cotton can be given as;

$$K_{M_1}^{M_2} = \frac{K_H^{M_2}}{K_H^{M_1}} = \frac{\dfrac{(RM_2)\,[H^+]}{(RH)\,[M_2^+]}}{\dfrac{(RM_1)\,[H^+]}{(RH)\,[M_1^+]}} = \frac{(RM_2)\,[M_1^+]}{(RM_1)\,[M_2^+]} \tag{6}$$

6) J. H. Wang, *J. Phys. Chem.*, **58**, 686 (1952).
7) F. Fukuoka, *J. Chem. Soc. Japan, Ind. Chem. Sec.* (*Kogyo Kagaku Zassi*), **56**, 51 (1953).

where $K_{M_1}^{M_2}$ denotes the relative affinity of M_2^+ with respect to M_1^+. The uptake of the metal ions of 10^{-3} M on a RH ion exchanger was found to be almost equal the maximum uptake, a. Therefore, in this case the following relation holds.

$$a=(RM_1)+(RM_2) \tag{7}$$

Therefore, Eq. 6 can be written;

$$K_{M_1}^{M_2}=\frac{(a-(RM_1))\,[M_1^+]}{(RM_1)\,[M_2^+]} \tag{8}$$

Using ^{45}Ca or ^{60}Co as a tracer, K_{Ca}^{M} or K_{Co}^{M} were determined experimentally using Eq. 8, and then K_H^M was calculated using the value of K_H^{Ca} (=0.26) obtained from the studies of pH dependence. The results are given in Table I. This order nearly parallels that of the stabilities of metal complexes[8] and that of the catalytic activities of metal ions in the oxygen exchange reaction between lactose and water.[9]

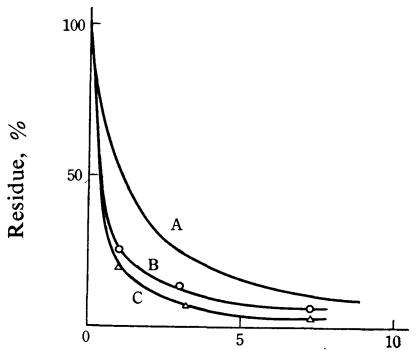


Fig. 7. Decontamination efficiency of Cu^{2+}.
Decontamination of Co
Decontamination of Ca
Solid lines show calculated values.
A, decontamination by the same ion $K_M^M=1$
B, decontamination by the same ion $K_{Co}^{Cu}=3.6$
C, decontamination by the same ion $K_{Ca}^{Cu}=5.3$

8) M. Yasuda, K. Yamasaki and H. Ohtaki, This Bulletin, 33, 1067 (1960).
9) T. Titani and K. Goto, *Catalysis* (*Shokubai*), 3, 123 (1948).

TABLE I. RELATIVE AFFINITIES

Ion	Cu^{2+}	Zn^{2+}	Co^{2+}	Ca^{2+}	Sr^{2+}	Cs^+	K^+	Na^+
K_H^M	1.4	0.54	0.36	0.26	0.11	0.03	0.03	~0

The Decontamination of Radioactive Metal Ions from Cotton.—It can be expected that metal ions sorbed by cotton cloth may be effectively replaced by an ion which has a much stronger affinity to cotton. This was ascertained by the following experiments. Cotton cloth which had been contaminated by ions, ^{60}Co or ^{45}Ca, was immersed in a solution of Cu^{2+}. After the solution had been shaken for 2 hr., the residual contamination was measured. As Fig. 7 shows, of ^{60}Co or ^{45}Ca can be decontaminated very efficiently by using a Cu^{2+} solution. The solid lines show the theoretical values calculated by using these relative affinities; A: $K_M^M=1$, B: $K_{Co}^{Cu}=3.6$, and C: $K_{Ca}^{Cu}=5.3$. Thus, the order of relative affinities in Table I turns out to be useful as a guide for the decontamination problems.

Summary

The uptakes of the metal ions, Co^{2+}, Ca^{2+} and Cs^+, by cotton cloth have been determined by using the tracer technique. In the acidic and the neutral media, the isotherms were the Langmuir type, and the cation exchange mechanism of the special groups (probably the carboxyl group) has been confirmed. The heat and the activation energy for the sorption of Co^{2+} were -2 kcal./mol. and 7.6 kcal./mol. respectively (at pH ca. 4.7). In the alkaline media, the cotton cloth showed marked uptakes. The order of the affinity of various metal ions to cotton cloth was also determined as follows:

$$Cu^{2+}>Zn^{2+}>Co^{2+}>Ca^{2+}>Sr^{2+}>Cs^+, K^+>Na^+$$

The order is useful for the purpose of decontamination.

Tokyo Metropolitan Isotope Center
Setagaya-ku, Tokyo

Studies of the Organic Reactions of Metal Carbonyl. IV. The Acceleration Effect of the Addition of Organic Compounds on the Reaction of Olefin Oxide with Cobalt Hydrocarbonyl and on the Hydroformylation of Olefin Oxide

By Yoshinobu TAKEGAMI, Chikao YOKOKAWA and Yoshihisa WATANABE

(Received January 16, 1964)

It has been demonstrated elsewhere[1,2] that olefin oxides react with cobalt hydrocarbonyl and carbon monoxide to form β-hydroxyacylcobalt carbonyls which can be converted to the corresponding esters of β-hydroxycarboxylic acid by cleavage with iodine and alcohol. On the other hand, the present authors have recently reported[3] that propylene oxide undergoes hydroformylation to form β-hydroxy-*n*-butyraldehyde as the major product.

The authors have found that the alcohol used in the cleavage reaction has an acceleration effect on the reaction of olefin oxide with cobalt hydrocarbonyl. The present investigation has aimed at examining in detail the effect of the addition of various organic compounds on these types of reaction. The results described in this paper indicate that some organic compounds, such as alcohol, ketone, ether and ester, accelerate remarkably the reaction of olefin oxide with cobalt hydrocarbonyl. A similar effect has been also observed in the hydroformylation of olefin oxide.

Experimental

Reaction Procedures.—The reactions of olefin oxide with cobalt hydrocarbonyl were carried out in the way described in a previous paper[2] using 50 ml. of a 0.09 M cobalt hydrocarbonyl solution in toluene. Various amounts of organic compounds were added at the beginning or during the reaction.

The hydroformylation of olefin oxide was investigated, in the manner which has been described previously,[3] in the presence of ethyl alcohol using dicobalt octacarbonyl as a catalyst.

Analytical Procedures.—The reaction products were analyzed by gas chromatography and by means of infrared spectra which had been taken on a Shimadzu model IR-27 infracord spectrophotometer. The details were given in previous papers.[2,3] The hydroformylation product of ethylene oxide was isolated as 2,4-dinitrophenylhydrazone and recrystallized from chloroform.

Meterials.—Ethylene oxide, propylene oxide, styrene oxide, epichlorohydrin and the other organic compounds employed in this study were commercial products, all of which were proved to be sufficiently pure by gas chromatography.

Results and Discussion

The Reactions of Propylene Oxide with Cobalt Hydrocarbonyl in the Presence of Various Organic Compounds.—All reactions were carried out at the mole ratio*1 of 1.6, at which the reaction without additives proceeds very slowly.[2] The results of the reactions in the presence of ethyl alcohol are summarized in Table I and in Figs. 1, 2 and 3. In Fig. 1 the amounts of carbon monoxide absorbed at 0°C are plotted against the reaction time. These gas absorption curves indicate a remarkable increase of the reaction rate upon the addition of a relatively small amount of ethyl alcohol. Without the additive (curve A),

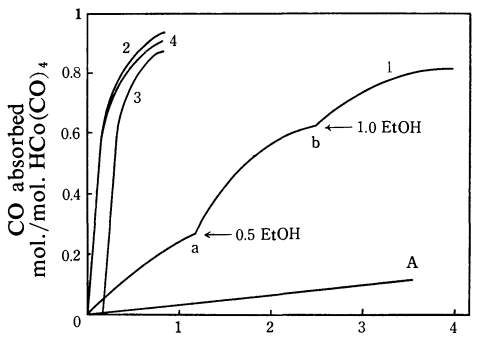


Fig. 1. CO absorption vs. time plots for the reactions of propylene oxide in the presence of ethyl alcohol at 0°C.
A: without ethyl alcohol
Numbers (1—4) correspond with Exp. No. in Table I.
a and b: At these points, 0.5 and 1.0 mol. of ethyl alcohol were added, respectively.

1) R. F. Heck, *J. Am. Chem. Soc.*, **85**, 1460 (1963).
2) Y. Takegami, C. Yokokawa, Y. Watanabe and H. Masada, This Bulletin, **37**, 672 (1964).
3) C. Yokokawa, Y. Watanabe and Y. Takegami, ibid., **37**, 677 (1964).

*1 Mole of propylene oxide per mole of cobalt hydrocarbonyl used.

TABLE I. THE REACTION OF PROPYLENE OXIDE WITH COBALT HYDROCARBONYL IN THE PRESENCE OF ETHYL ALCOHOL

Exp. No.	Reaction condition*1		EtOH added (mol./mol.-$HCo(CO)_4$)	CO absorbed (mol./mol.-$HCo(CO)_4$)	Product	
	Temp. °C	Time min.			Ester*2 (mol./mol.-$HCo(CO)_4$)	Aldehyde*3 (mol./mol.-$HCo(CO)_4$)
1	0	250	0.5+1.5*4	0.80	0.34	—
2	0	50	2.0	0.93	0.49	—
3	0	50	3.0	0.88	0.47	—
4	0	80	4.0	0.87	0.40	0.05
5	−30	155	2.0	0.93	0.55	—
6	−30	170	2.0	0.82	0.53	—
7	−30	110	3.0	0.72	0.52	—
8	−45	220	1.0	0.88	0.66	—
9	−45	230	2.0+2.0*4	0.89	0.64	0.05
10	−45	90	2.0	0.62	0.48	—
11	−55	330	2.0	0.82	0.63	—
12*5	0	100	2.0	0.90	0.24	—
13*5	−45	265	2.0+2.0*4	0.94	0.59	—

*1 Under one atmosphere of carbon monoxide and 1.6 mol. ratio of propylene oxide The speed of stirring was 900 r. p. m.
*2 Ethyl β-hydroxy-*n*-butyrate
*3 β-Hydroxy-*n*-butyraldehyde
*4 Added during the reaction
*5 In *n*-heptane solvent

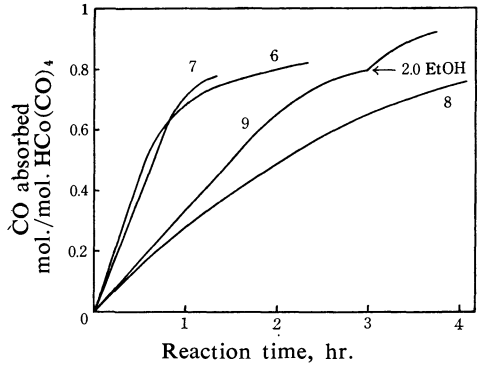


Fig. 2. CO absorption vs. time plots for the reactions of propylene oxide in the presence of ethyl alcohol at −30 and −45°C.

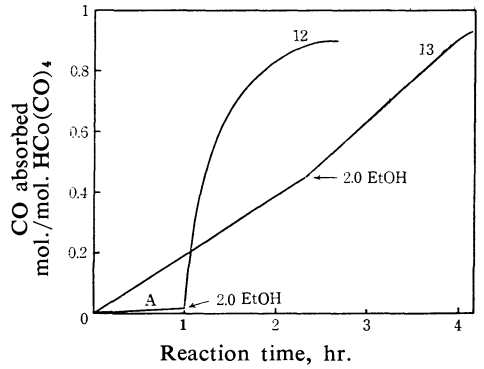


Fig. 3. CO absorption vs. time plots for the reactions of propylene oxide in *n*-heptane.
A: without ethyl alcohol

only 0.1 mol.*2 of the gas was absorbed in three hours. When 0.5 mol.*3 of the alcohol was added (Exp. 1 and curve 1), 0.3 mol. of the gas was absorbed in 70 min. Additional amounts of the alcohol (0.5 and 1.0 mol.) also promoted the gas absorption. By the addition of 2.0 mol. of the alcohol (Exp. 2) in the beginning, the rate of the gas absorption was about one hundred and twenty times larger than that of the standard run. The increase in the rate of the gas absorption with the increase in the amount of the alcohol added seemed to cease, however, at the amount of 2.0 mol. since the rates of Exps. 3 and 4 (3.0 and 4.0 of the alcohol were added respectively) were comparable to that of Exp. 2. No gas absorption was observed in the systems of cobalt hydrocarbonyl and ethyl alcohol or of propylene oxide and ethyl alcohol.

The main product in these reactions was ethyl β-hydroxy-*n*-butyrate.*4 In addition to this ester and a small amount of β-hydroxy-*n*-butyraldehyde, there was no indication of the presence of other product in the gas chromatogram. The total yield of the ester and aldehyde, based on the amount of gas absorbed, is about 50% almost the same as that of the reactions without the alcohol.[2]

The acceleration effect of the alcohol was also observed at −30 and −45°C, as Fig. 2

*2,*3 Mole per mole of cobalt hydrocarbonyl used.
*4 This compound can be obtained from the corresponding acylcobalt carbonyl by cleavage with iodine and ethyl alcohol.[2]

TABLE II. THE REACTION OF PROPYLENE OXIDE WITH COBALT HYDROCARBONYL IN THE PRESENCE OF VARIOUS KINDS OF ORGANIC COMPOUND

Exp. No.	Reaction*1 time min.	Compound added Name	(mol./mol.-$HCo(CO)_4$)	CO absorbed (mol./mol.-$HCo(CO)_4$))	Relative absorption rate*2	Product Ester*3 (mol./mol.-$HCo(CO)_4$)
A	180	None	—	0.10	1	—
14	90	Ethyl alcohol	2.0	0.93	120	0.45
15	210	Ethylene chlorohydrin	2.0	0.81	10	—
16	35	*n*-Butyl alcohol	3.0	0.87	120	0.48*4
17	40	*t*-Butyl alcohol	3.0	0.53	120	0.32
18	180	Acetone	3.0	0.70	25	0.33
19	240	Chloroacetone	3.0	0.73	9	—
20	270	Acetylacetone	3.0	0.81	14	0.40
21	150	Acetophenone	2.0	0.49	12	0.29
22	265	Ethyl ether	2.0+2.0+2.0	0.71	6	0.43
23	180	Tetrahydrofuran	3.0	0.71	30	—
24	270	Acetal	3.0	0.86	17	0.42
25	210	Benzaldehyde	3.0	0.64	9	—
26	210	Ethyl acetate	3.0	0.86	12	0.42
27	180	Acetonitrile	3.0	0.61	12	0.43
28	50	Nitromethane	3.0	0.06	1～2	—
29	60	Phenol	2.0	0	—	—

*1 Other reaction conditions : under one atmosphere of carbon monoxide, at 0°C and at 1.6 mol. ratio of propylene oxide

*2 The relative value of the absorption rate at the early stage of the reaction to the rate of Exp. A

*3 Ethyl β-hydroxy-*n*-butyrate

*4 Ethyl β-hydroxy-*n*-butyrate 0.40 and *n*-butyl β-hydroxy-*n*-butyrate 0.08

shows although the rate of the gas absorption decreased with a decrease in the reaction temperature. The yield of the ester increased at low temperatures; the total yields of the ester and aldehyde, based upon the amount of the gas absorbed, are about 70 or 80% at −30 and at −45 or −55°C respectively. The low yield of the ester at the relatively high reaction temperature seems to be partly due to the thermal instability of alkyl- and/or acyl-cobalt carbonyl.

From Fig. 3, it is evident that ethyl alcohol also has an acceleration effect in *n*-heptane. However, the effect seems to be about half of that for the reactions in toluene.

The effects of several organic compounds other than ethyl alcohol on this reaction at 0°C were examined; the results are summarized in Table II, in which the value of the gas absorption rate at the early stage of the reaction relative to the absorption rate in Exp. A is shown as a measure of the acceleration effect of the individual compound.

The results shown in Table II indicate that various kinds of organic compounds also have this effect, though their effects are considerably influenced by their structures. *n*- and *t*-butyl alcohols have an effects comparable to that of ethyl alcohol, but the effect of ethylene chlorohydrin is about one-twelfth that of ethyl alcohol. The compounds with functional groups other than an aliphatic hydroxy group, such as acetone, tetrahydrofuran, acetal, benzaldehyde, ethyl acetate and acetonitrile, also show the effect, but it is much smaller than that of ethyl alcohol. These facts seem to suggest that the compounds which have the effect are not limited to the above-mentioned compounds but may also include their homologues, i. e., alcohols, ketones, ethers, esters of carboxylic acids and nitriles.

The acceleration effect seems to be due to the basicity of these compounds. This consideration is supported by the following facts: phenol has no effect, and ethylene chlorohydrin, chloroacetone and acetylacetone have a smaller effect, than ethyl alcohol and acetone respectively. The chlorine atom and the acetyl group are considered to decrease the basicity of hydroxy and carbonyl groups with their nagative inductive effect.

The main product was ethyl β-hydroxy-*n*-butyrate in all of these cases. Even the reactions which were carried out in the presence of *n*- or *t*-butyl alcohol gave this ethyl ester*5 as a main product. This fact indicates that

*5 Ethyl alcohol was used in the cleavage reaction with iodine.

TABLE III. THE REACTION OF STYRENE OXIDE WITH COBALT HYDROCARBONYL IN THE PRESENCE OF ETHYL (OR PROPYL) ALCOHOL

Exp. No.	Reaction condition*1			Alcohol added (mol./mol.-$HCo(CO)_4$)	CO absorbed (mol./mol.-$HCo(CO)_4$)	Product*2		
	Time min.	Mole ratio*3				Ester (mol./mol.-$HCo(CO)_4$)	α	β
30	30	1.4	None	—	0	—	—	—
31	170	1.4	EtOH	2.0	0.72	—	—	—
32	120	1.2	EtOH	3.0	0.77	0.2	0.06	trace
33	160	1.2	PrOH	3.0	0.82	0.2	0.06	trace

*1 Other conditions: under one atmosphere of carbon monoxide and at −45°C
*2 Ester: α-phenyl-β-hydroxy- or β-phenyl-β-hydroxypropionate
α: α-phenylethyl alcohol β: β-phenylethyl alcohol
*3 Mole of styrene oxide per mole of cobalt hydrocarbonyl used

TABLE IV. THE REACTION OF EPICHLOROHYDRIN WITH COBALT HYDROCARBONYL IN THE PRESENCE OF ETHYL ALCOHOL

Exp. No.	Reaction condition*1		EtOH added (mol./mol.-$HCo(CO)_4$)	CO absorbed (mol./mol.-$HCo(CO)_4$)	Relative absorption rate*2	Product Ester*3 (mol./mol.-$HCo(CO)_4$)
	Time min.	Mole ratio				
34	225	1.5+1.5+1.5+1.5	3.0	0.82	—	0.55
35	60	14.5	0	0.10	—	—
36	180	14.5	1.0	0.61	1	0.4
37	150	14.5	2.0	0.86	2	0.6
38	85	14.5	8.0	0.93	10	0.6
39	100	5.8	8.0	0.81	4	0.55
40	70	5.8	12.0	0.97	6.5	0.6
41	160	2.9	8.0	0.82	2	0.55

*1 Other conditions: under one atmosphere of carbon monoxide and at 0°C
*2 The relative value of the gas absorption rate at the early stage of the reaction to the rate of Exp. 36
*3 Ethyl γ-chloro-β-hydroxy-*n*-butyrate

the alcoholysis of β-hydroxy-*n*-butyrylcobalt carbonyl did not occur in the course of the reaction. Thus, all of the additives appear to be acting as kinds of catalysts.

The Reactions of Styrene Oxide and Epichlorohydrin with Cobalt Hydrocarbonyl in the Presence of Ethyl Alcohol. — Styrene oxide was submitted to the reaction at −45°C; the results are summarized in Table III.

No gas absorption was observed in the reaction without ethyl alcohol under the conditions of Exp. 30, but a rapid gas absorption was observed in the presence of ethyl or propyl alcohol (Exp. 31—33), probably the carbonylation reaction was promoted by the addition of the alcohols. An ester-like compound was obtained as a main product after the cleavage of the reaction mixture with iodine and alcohol.*6 This ester may reasonably be considered to be β-phenyl-β-hydroxypropionate or α-phenyl-β-hydroxypropionate. As the minor by-products, α- and β-phenylethyl alcohols, which are the major products of the reaction without the alcohol at 0°C and at a relatively small mole ratio (1∼2),[2] were identified. These facts seem to support the supposition that the alcohol added accelerates the carbonylation reaction selectively. The low yield of the corbonylation product may be attributed to the instability of the corresponding acylcobalt carbonyl complex.

The results with epichlorohydrin are summarized in Table IV and in Fig. 4. The reactivity of epichlorohydrin is about several tenths that of propylene oxide;[2] at a relatively small mole ratio of epichlorohydrin (5∼6) no gas absorption was observed. Although the acceleration effect of the addition of alcohol has also been observed for the reaction of epichlorohydrin, the magnitude of this effect is smaller than those for propylene oxide and styrene oxide. The effect of the addition of ethyl alcohol was scarcely observed at a 1.5 mole ratio of epichlorohydin, even when 3 mol. of the alcohol, which is a sufficient amount in the reactions of propylene

*6 The infrared spectrum of the products in toluene had a band at 1730 cm^{-1} corresponding to a carbonyl group. The retention time of the product (ester) in gas chromatography increased as the molecular weight of the alcohol used in the cleavage increased. The retention time of the ethyl ester was longer than that of ethyl hydrocinnamate.

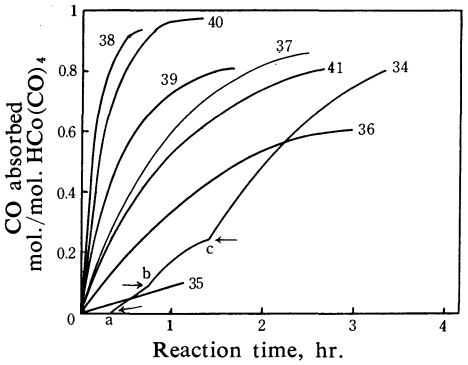


Fig. 4. CO absorption vs. time plots for the reactions of epichlorohydrin in the presence of ethyl alcohol.
a, b, and c: At these points, 1.5 mol. of epichlorohydrin per mole of $HCo(CO)_4$ was added.

oxide and styrene oxide, was added, but when additional amounts of epichlorohydrin were added successively, the acceleration of the gas absorption was clearly observed (Exp. 34 and and curve 34). At a 14.5 mol. ratio of epichlorohydrin at which a very slow gas absorption was observed without the alcohol (Exp. 35), a faster gas absorption evidently occurred when a larger amount of alcohol was added (Exp. 36—38).

The values of the gas absorption rate relative to the rate of Exp. 36 at an early stage of the reactions are shown in Table IV. At 14.5 and 5.8 mol. ratios, the rate increased proportionally with the increased amount of alcohol (Exp. 36—40). On the other hand, the rate increased with the increased amount of epichlorohydrin when the amount of the alcohol was fixed at 8.0 mol. (Exp. 38, 39 and 41). Thus, the rate of the gas absorption may be represented by the following equation:

$$\text{rate} = k\,[\text{epichlorohydrin}]\,[\text{ethyl alcohol}]$$

The main product of these reactions has been proved to be ethyl γ-chloro-β-hydroxy-*n*-butyrate from the considerations described previously.[2] Thus, this carbonylation reaction is also promoted by the addition of alcohol.

In the reactions of propylene oxide or styrene oxide, however, the relationship given by the above equation was not observed. This observation may be interpreted in terms of the fact that propylene oxide and styrene oxide are much more reactive, in other words, the same relationship may exist under well-controlled reaction conditions, such as a lower reaction temperature and a smaller concentration.

In the light of the above equation, ethyl alcohol seems to form some complex with epichlorohydrin and/or cobalt hydrocarbonyl as the first step of the reaction; this complex is considered to be more reactive than epichlorohydrin and/or cobalt hydrocarbonyl.

The Hydroformylation of Ethylene Oxide in the Presence of Ethyl Alcohol.—The effect of the addition of ethyl alcohol on the hydroformylation of ethylene oxide has been examined.

Although ethylene oxide seems to undergo hydroformylation at 80~90°C, even without ethyl alcohol,[3] only a little acrolein is obtained; some side reactions, such as isomerization, dehydration and polymerization may decrease the yield of the hydroformylation product considerably. By the addition of the alcohol (0.5~1.0 mol./mol.-ethylene oxide), however, the side reactions seemed to be considerably decreased, and then the hydroformylation product (β-hydroxypropionaldehyde*[7]) was obtained, though its yield was not good (at 80°C, about 15% of the amount of ethylene oxide used).

Summary

It has been observed that organic compounds with various kinds of functional groups have an accelerating effect on the reaction of olefin oxide with cobalt hydrocarbonyl and on the hydroformylation of olefin oxide.

1) The addition of a relatively small amount of ethyl alcohol promotes the carbonylation of propylene oxide with cobalt hydrocarbonyl until it is about 120 times faster than that of the standard run, carried out without alcohol. The amount of the alcohol necessary for this effect is about 2.0 mol./mol. $HCo(CO)_4$. As the reaction products, only compounds with a β-hydroxy-*n*-butyryl structure (ester and aldehyde) have been obtained.

2) The compounds other than ethyl alcohol, such as *n*- and *t*-butyl alcohol, ethylene chlorohydrin, acetone, tetrahydrofuran, ether, acetal, benzaldehyde, ethyl acetate and acetonitrile, also have the same effect on this reaction. Among these compounds, ethyl and butyl alcohols have the largest effect. On the other hand, phenol has no effect. The accelerating effect is considered to be due to the basicity of these compounds.

3) The reactions of styrene oxide and epichlorohydrin with cobalt hydrocarbonyl are also promoted by the addition of ethyl alcohol.

*[7] Identified by gas chromatography. 2,4-Dinitrophenylhydrazone. Found: C, 45.7; H, 3.39; N, 24.8. Cald. for $C_9H_8O_4N_4$: C, 45.8; H, 3.38; N, 23.7%. M. p. 164~166°C. A mixed melting point with the hydrazone of authentic acrolein gave no depression. β-Hydroxypropionaldehyde is dehydrated to give acrolein in the formation of the hydrazone.

A relatively small amount of the alcohol accelerates selectively, the carbonylation of styrene oxide which is comparatively readily hydrogenated with cobalt hydrocarbonyl.[2] For epichlorohydrin, the following relationship was observed to exist at an early stage of the reaction: rate of the gas absorption $=k$ [epichlorohydrin] [ethyl alcohol].

4) The hydroformylation of ethylene oxide seems to be selectively promoted by the addition of ethyl alcohol, which gives β-hydroxypropionaldehyde, in a low yield.

Department of Fuel Chemistry
Faculty of Engineering
Kyoto University
Sakyo-ku, Kyoto

Crystal Structure of Salicylamide

By Yoshio SASADA, Tsunehiro TAKANO and Masao KAKUDO

(Received January 20, 1964)

The polymorphism observed in the crystals of most amides may be expected to correspond to the varied types of molecular arrangement connected by hydrogen bonds with each other.[1] Such variations in molecular linkage are due to the fact that the amide group is a bivalent donor and a bivalent acceptor of hydrogen bonding at the same time.

If a group attached to an amide group is a donor or an acceptor of hydrogen bonding, more different types of molecular association can be presumed, and this compound might show more crystallographic modifications. In fact, one of the authors has observed that pyrazinamide has four modifications and has determined, from the structure determination, that each modification has a characteristic molecular linkage by hydrogen bonds.[1-3]

The determination of the molecular arrangement in amide crystals will be of some interest in determining the relationship between the delicate balance of intermolecular interactions and the molecular geometry. As a part of a series of studies of the amide crystals,[1-4] this account will deal with the crystal structure of salicylamide obtained from X-ray analysis.

Experimental and Crystal Data

Crystals were obtained from an alcohol-water solution as colorless laths elongated along the b-axis. Twins were found frequently, and X-ray photographs showed that this twinning occurs with a common ba plane.

The crystal and physical data found are as follows:

Salicylamide: $C_7H_7NO_2$, m. p. 139°C
Monoclinic: $a=12.92\pm0.04$, $b=4.98\pm0.02$, $c=21.04\pm0.05$ Å, $\beta=91.8\pm0.4°$
Absent spectra: (hkl) when $h+k+l$ is odd, $(h0l)$ when h and l are odd, $(0kl)$ when $k+l$ is odd, $(hk0)$ when $h+k$ is odd, and $(0k0)$ when k is odd.
Space group: I $2_1/a-C_{2h}^6$
Eight molecules per unit cell
Volume of the unit cell: 1353.0 Å^3
Density (by floatation): 1.34_9 g. cm^{-3}
Density (calculated): 1.34_5 g. cm^{-3}
Linear absorption coefficient for Cu$K\alpha$ radiation: $\mu=9.73$ cm^{-1}
Total number of electrons per unit cell: $F(000)=576$

Using Cu$K\alpha$ radiation with a nickel filter, complete sets of relative intensities for $(h0l)$, $(h1l)$ and $(h2l)$ were obtained by the Weissenberg procedure. The specimen used was 0.04×0.02 cm. at right angles to the axis of rotation. Precession photographs were also taken using Cu$K\alpha$ radiation for the $(0kl)$ and $(hk0)$ zones. Intensities were estimated by visual comparison with a calibrated scale prepared using the same crystal. The multiple-film technique was applied to correlate strong and weak reflections, ranging in relative intensity from 5400 to 1. The maximum $2\sin\theta$ observed was 1.95. Within this range, 133 reflections were measured out of the 172 possible $(h0l)$.

Corrections for Lorentz and polarization factors were applied in the usual way, while that for absorption was neglected. The observed structure factors were first set onto an absolute scale by Wilson's method,[5] and the scale factor was further improved during the later stage of the refinement.

1) C. Tamura, H. Kuwano and Y. Sasada, *Acta Cryst.*, **14**, 693 (1961).
2) Y. Takaki, Y. Sasada and T. Watanabe, ibid., **13**, 693 (1960).
3) Y. Takaki et al., to be published.
4) S. Orii, T. Nakamura, Y. Takaki, Y. Sasada and M. Kakudo, This Bulletin, **36**, 788 (1963).
5) A. J. C. Wilson, *Nature*, **150**, 152 (1942).

TABLE I. ATOMIC COORDINATES AND TEMPERATURE FACTORS

Atom	x/a	y/b	z/c	B_{11}	B_{33}	B_{13}
C_1	0.0799	0.177	0.3720	0.00440	0.00180	−0.00003
C_2	0.1861	0.230	0.3601	0.00405	0.00153	0.00015
C_3	0.2600	0.067	0.3934	0.00450	0.00188	0.00020
C_4	0.2284	−0.124	0.4360	0.00533	0.00190	0.00000
C_5	0.1254	−0.174	0.4468	0.00568	0.00200	0.00035
C_6	0.0524	−0.020	0.4150	0.00533	0.00213	0.00040
C_7	0.2120	0.452	0.3134	0.00358	0.00138	0.00033
N_8	0.3099	0.480	0.3005	0.00360	0.00150	0.00065
O_9	0.1424	0.580	0.2870	0.00375	0.00175	0.00020
O_{10}	0.0050	0.326	0.3418	0.00405	0.00223	0.00015

Structure Determination

Structure Projected on the (010) Plane.—It seemed reasonable to set up a planar molecular model of salicylamide on the basis of the information already obtained on some related crystal structures. The problem in the first step was to determine the arrangement of these hypothetical molecules in the unit cell. From the unit cell dimensions and the disposition of symmetry elements required by the space group, the molecule could not be inclined steeply with respect to the (010) plane but would lie approximately in the region with the dimensions of $a/4 \times c/4$. There are four possible arrangements of the symmetry elements, as Fig. 1 shows, and the hydroxyl and amide groups can be arbitrarily taken to point downward in this drawing. It was expected from the normal van der Waals radii and hydrogen bond distances that the atoms would be located only outside the circles centered on the symmetry elements shown in Fig. 1. The initial coordinates of the atoms in the molecule were chosen in the rather limited allowable region so as to give large calculated values for some strong reflections, such as (202). By the systematic use of the structure factor maps for reflections with a larger spacing than 2 Å, the coordinates were adjusted so that a fairly good agreement between observed and calculated structure factors was obtained. Ordinary Fourier syntheses followed. After four cycles of Fourier refinement, the (F_o-F_c) synthesis technique was applied twice in succession. Four hydrogen atoms were first placed on the molecular plane at a distance of 1.0 Å from the carbon atoms, and the hydrogen atoms of the hydroxyl and amino groups were located at positions which could reasonably be expected from the second difference map. At this stage, the discrepancy index, $R=\sum||F_o|-|F_c||/\sum|F_o|$, was 0.16. After that, the anisotropy in the thermal motion of each atom was taken into account in terms of $\exp\{-(h^2B_{11}+hlB_{13}+l^2B_{33})\}$. The anisotropic temperature factors were derived and refined from four successive (F_o-F_c) syntheses by the method of Takaki and Sakata.[6] The effect of secondary extinction was also allowed for. The discrepancy index thereby decreased to 0.087. The final atomic coordinates and the temperature factors of carbon, nitrogen and oxygen atoms are listed in Table I, while the observed and calculated structure factors are shown in Fig. 2. In the refinement stage, all calculations of the structure factors and Fourier syntheses were made on an automatic digital computer, NEAC 2203, using programs devised by Yoriko Ogawa of this laboratory. The final electron density distribution projected on the (010) plane is shown in Fig. 3.

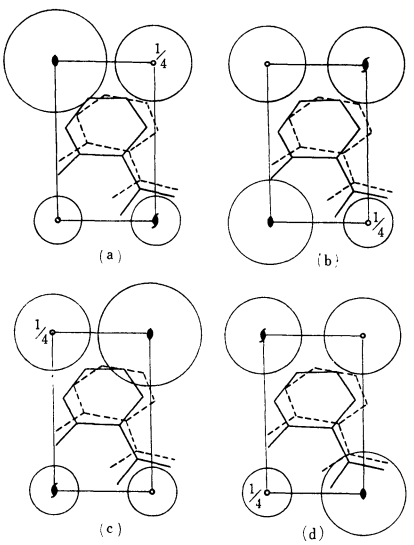


Fig. 1. Arrangement of symmetry elements and trial structure (solid line). Final projected structure is shown by broken lines. Correct arrangement of symmetry elements is (b).

Determination of the y-Parameters.—As no

6) Y. Takaki and Y. Sakata, *Memoirs of the Osaka University of Liberal Arts and Education*, **9**, 98 (1960).

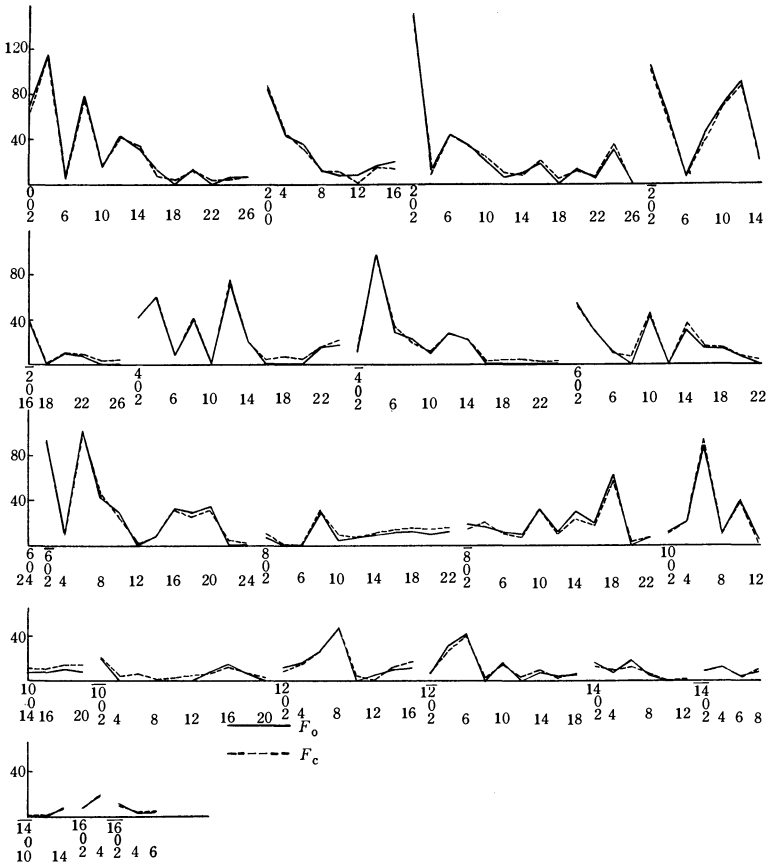


Fig. 2. Observed and calculated structure factors, $F(h0l)$.

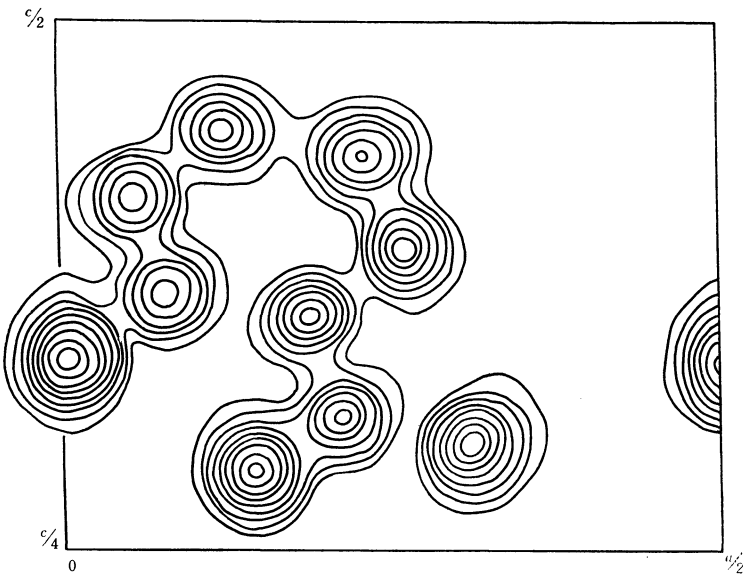


Fig. 3. The final electron density projection on (010). Contours at intervals of 1 e. Å^{-2}, with the lowest solid contour of 2 e. Å^{-2}.

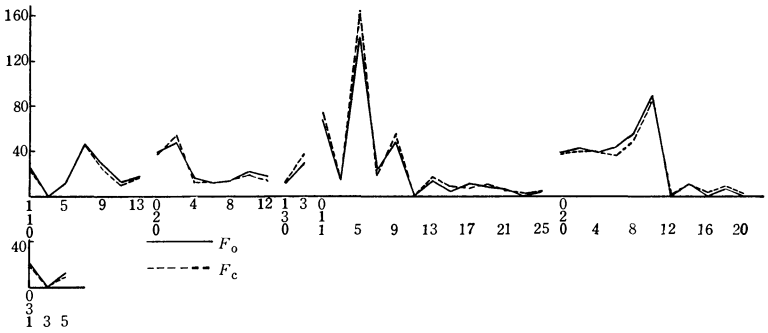


Fig. 4. Observed and calculated structure factors, $F(hk0)$ and $F(0kl)$.

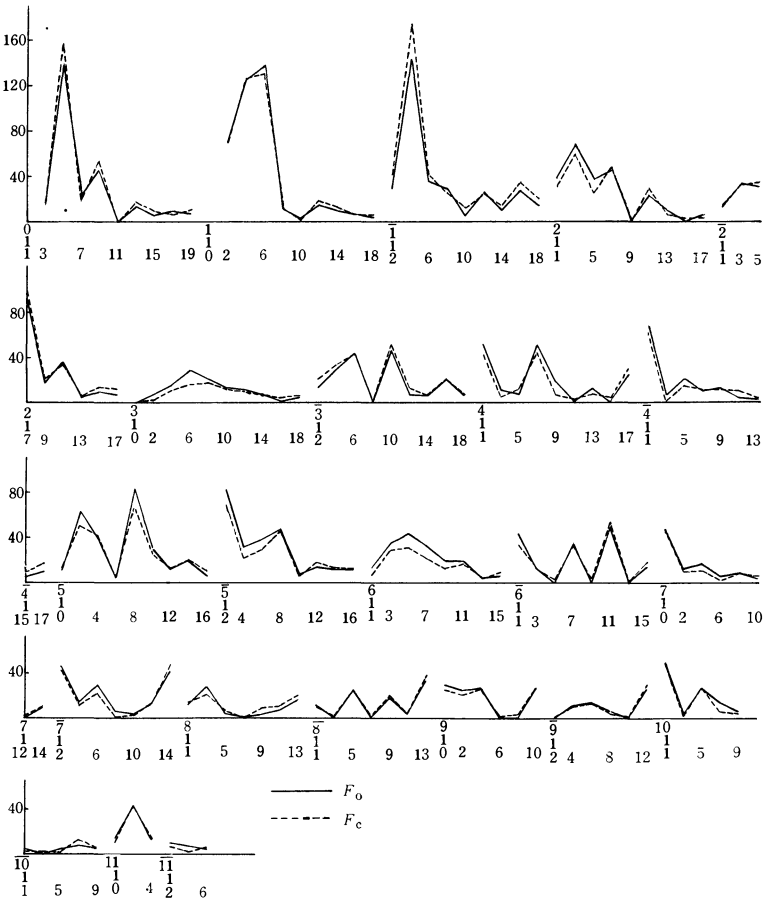


Fig. 5. Observed and calculated structure factors, $F(h1l)$.

complete intensity set for $(0kl)$, $(hk0)$ or (hkl) was taken and a serious overlapping of atoms was expected in the projections along the a and c axes, we attempted to refine the y-coordinates by the full-matrix least-squares technique for $(hk0)$ and $(0kl)$ intensity data, with fixed x and z coordinates obtained from the (010) projection. The structure projected on the (010) plane suggested that the relative arrangement of the symmetry elements in Fig. 1(c) is impossible because of too close van der Waals contacts around C_4. Arrangements (a) and (d) also seemed to be less probable. As the inclination of the molecular plane with respect to the (010) plane could be estimated, it was not difficult to choose approximate y-coordinates for the atoms referred to the arrangement (b) of the symmetry elements,

thus explaining some characteristic structure factors using the structure factor maps. The program of the full-matrix least-squares refinement was written in MALT language[7] and executed on an electronic computer NEAC 2206. After a few cycles of refinement, the discrepancy index decreased from 0.47 to 0.22. As the molecule suffered considerable deformation, however, the y-coordinates so obtained were adjusted to recover a reasonable molecular shape and were then again refined by the least-squares program. When this process was repeated several times, the discrepancy index reached 0.120. The overall isotropic temperature factor was 3.27.

The unsatisfactory convergence at the earlier stages of refinement may be due to the shortage of the intensity data and to the less accuracy of some of the structure factors. We had the feeling that in such a case a technique similar to that used in the analysis of 2-amino azulene[8] would be adequate, although we did not actually apply one.

Observed and calculated structure factors for (*hk*0) and (0*kl*) are shown in Fig. 4. To confirm the above-mentioned results further, we have calculated the structure factors for (*h*1*l*). The agreement between observed and calculated structure factors for (*h*1*l*) was fairly good, as Fig. 5 shows; the discrepancy index was 0.184.

Description of the Structure and Discussion

Molecular Structure.—Bond lengths and bond angles in salicylamide are shown in Fig. 6.

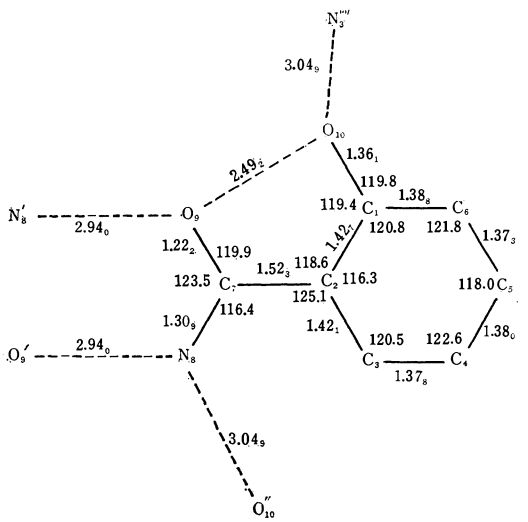


Fig. 6. Bond lengths (Å) and bond angles (°).

Although small fluctuations among the C–C bond lengths in the benzene ring are observed and the slight elongation of C_1–C_2 is probably of some significance, no detailed discussion will be given because of low degree of accuracy of the y-coordinates. The average C–C bond length in the benzene ring is 1.39_5 Å, and the average bond angle C–C–C is 120.0°, in good agreement with the standard value. The bond length, C_1–O_{10}, is 1.36_1 Å, which is nearly the same as the values observed in salicylic acid,[9] 1.36_1 Å, and in *p*-amino salicylic acid,[10] 1.37 Å. The dimensions of amide group found in the present compound are close to those found in the related compounds: for example, C–N= 1.31_2 Å and C–O=1.24_6 Å in α-pyrazinamide.[2]

The final (F_o-F_c) synthesis projected on the (010) plane is shown in Fig. 7; this was obtained using the structure factors calculated without the contributions from hydrogen. Electron density peaks corresponding to hydrogen atoms are easily recognized, although their heights and coordinates are not so accurate. The hydrogen atom attached to O_{10} lies near the line joining O_9 and O_{10}. The position of this hydrogen atom and the interatomic distance between O_9 and O_{10}, 2.49 Å, clearly show that an intramolecular hydrogen bond is formed between these atoms, as has been observed in salicylic acid[9] and *p*-amino salicylic acid[10] also.

The plane of the benzene ring (including C_7 and O_{10}) can be represented by the equation:

$$y=-0.0526\,x'-1.1098\,z'+9.6211$$

where x', y and z' are referred to the orthogonal axes a, b and c*, so that $x'=x+z\cos\beta^*$ and $z'=z\sin\beta^*$; the values of the coefficients were determined by means of the least-squares method. The perpendicular displacements of atoms from the mean plane, shown in Table

TABLE II. PERPENDICULAR DISPLACEMENTS OF ATOMS FROM THE MEAM PLANE OF THE BENZENE RING

Atom	Displacement Å
C_1	0.010
C_2	0.003
C_3	0.013
C_4	−0.012
C_5	0.001
C_6	−0.003
C_7	−0.009
N_8	0.085
O_9	−0.012
O_{10}	−0.002

7) Y. Yasui, to be published.
8) Y. Takaki, Y. Sasada and I. Nitta, *J. Phys. Soc. Japan*, **14**, 771 (1959).
9) W. Cochran, *Acta Cryst.*, **6**, 260 (1953).
10) F. Bertinotti, G. Giacomello and A. M. Liquori, ibid., **7**, 808 (1954).

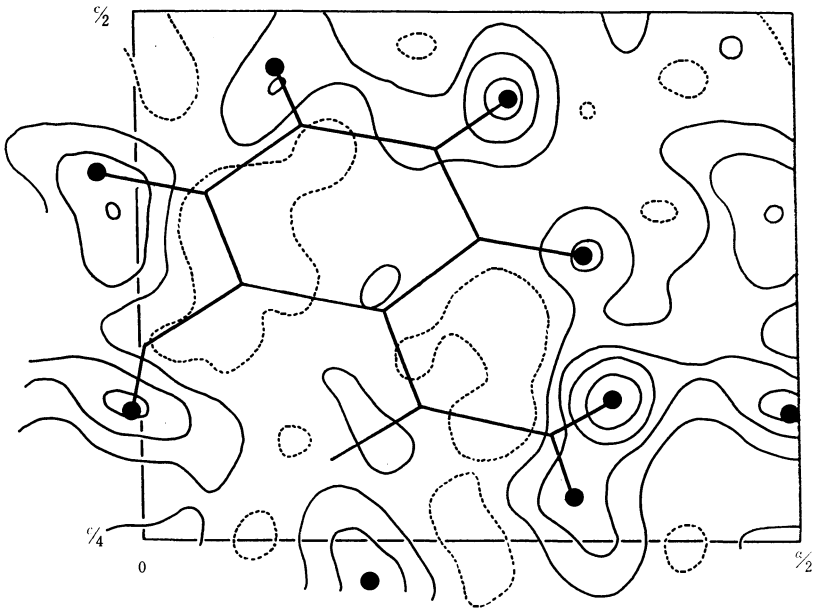


Fig. 7. The final (F_o-F_c) projection on (010).
Contours at intervals of 0.2 e. Å^{-2}, zero contour being broken.

II, vary from 0.001 to 0.013 Å, the mean value being 0.007 Å. On the other hand, oxygen and nitrogen atoms in the amide group considerably deviate from the mean plane, and the angle between planes of amide and benzene ring is about 3°. In many related amide crystals,[3,4,11,12] it is observed that the amide group twists around the connecting C–C bond and that the planes of amide and ring make an angle of about 25°. This twist has been interpreted as the effect of steric hindrance between hydrogen atom in the amino group and that in the ortho position of the ring. In the present compound, however, it may be suggested that this kind of steric hindrance is balanced with the effects of the intramolecular hydrogen bond on another side of the amide group, together with other intermolecular forces, and that the whole molecule remains approximately planar. In this connection, it is of some interest that the C_2–C_7 distance in this molecule is longer than those in similar amide compounds.[3,4,11,12]

Crystal Structure.—The crystal structure of salicylamide is shown in Fig. 8, in which the hydrogen bond is represented by bold broken lines. The molecules are connected by two NH–O hydrogen bonds, the first set, 2.94 Å in length, forming a dimer across the center of symmetry, and the second set, 3.05 Å in length, joining such dimers into an endless chain extended along the a axis. As the latter set is located across the two-fold axis, the

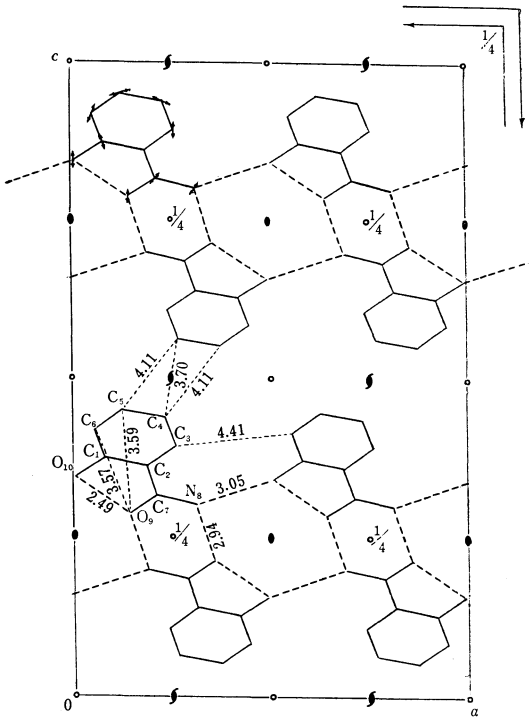


Fig. 8. Arrangement of molecules in the (010) projection with intermolecular distances (Å). Arrows show the direction of the maximum thermal oscillation of atoms.

11) W. B. Wright and G. S. D. King, *Acta Cryst.*, **7**, 283 (1954).
12) B. R. Penfold and J. C. B. White, ibid., **12**, 130 (1959).

inclination of component dimers in a chain changes alternately. In α-pyrazinamide,[2] the atom in the ortho position is a donor of the hydrogen bond which connects the pyrazinamide dimers with each other. It might be said that in this sense the molecular linkage in α-pyrazinamide is similar to that found in the present crystal, although there are some differences between them.

McCrone and Hinch[13] have reported another modification obtained from melt. It is supposed that the molecular association in this modification might be of a type similar to that in β- or δ-pyrazinamide.[3]

The directions of the maximum thermal motions of atoms are illustrated by arrows in Fig. 8; they ase derived from the anisotropic temperature factors in Table I. The length of the arrow is proportional to the mean-square displacement of the atom by the thermal motion in this direction. By inspection it seems probable that the molecule is making an angular oscillation around the mass center of a single molecule, suggesting that the NH–O hydrogen bonds forming the dimer are not very strong, a similar situation having also been observed in the crystal of α-pyrazinamide.[2]

This molecular arrangements can reasonably explain the existence of the cleavage parallel to the ba plane and also the twinned crystals frequently obtained, in which the twinning plane is the ba.

The authors wish to express their thanks to Miss Yoriko Ogawa for her assistance in the experiments and for her computations using the electronic computer.

Institute for Protein Research
Osaka University
Kita-ku, Osaka

13) W. C. McCrone and R. J. Hinch, *Analyt. Chem.*, **25**, 1277 (1953).

Pyrolysis of Fluorinated Organic Compounds. I. The Pyrolysis of 1, 2-Dibromo-1-chloro-1, 2, 2-trifluoroethane and Some Related Halogenated Ethane Derivatives

By J. D. PARK, R. W. LAMB[1] and J. R. LACHER

(Received January 17, 1964)

It is known that chemical bonds may be broken homolytically by heat to produce free radicals which may further react to produce other compounds. This study involves the homolytic scission of the least thermally stable bonds in CF_2Br–$CFClBr$ and related compounds. A temperature was selected for the pyrolysis which probably caused primarily carbon bromine bonds to be broken in the initiation steps of the reaction. The products were isolated and used as evidence to postulate reaction paths involving intermediate free radicals.

Results and Discussion

It was shown that pyrolysis of CF_2Br–$CFClBr$ (I) produced two major products, CF_2Cl–$CFClBr$ (II) and CF_2Br–$CFBr_2$ (III) in addition to starting material. The following reactions can be used to explain the products.

$$\mathrm{I} \xrightarrow{\text{heat}} \begin{cases} \rightarrow \dot{C}F_2\text{-}CFClBr + \dot{B}r \\ \rightarrow CF_2Br\text{-}\dot{C}FCl + \dot{B}r \end{cases} \quad \text{(initiation)} \quad (1)$$

$$\dot{C}F_2\text{-}CFClBr + \mathrm{I} \rightarrow CF_2Br\text{-}\dot{C}FBr + \mathrm{II} \quad (2)$$

$$CFBr\text{-}\dot{C}FCl + \mathrm{I} \rightarrow CF_2Br\text{-}CFCl_2\ (\mathrm{IV}) + CF_2Br\text{-}\dot{C}FBr \quad (3)$$

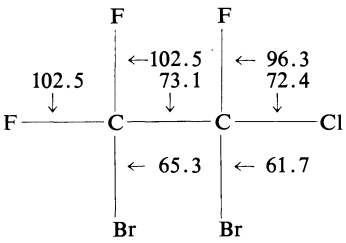
$$CF_2Br\text{-}\dot{C}FBr + \mathrm{I} \rightarrow CF_2Br\text{-}\dot{C}FCl \text{ or } \dot{C}F_2\text{-}CFClBr + \mathrm{III} \quad (4)$$

(propagation)

The bond dissociation energies (kcal./mol.) were calculated for the starting material I, according to the equation developed by Errede.[2]

1) Frank J. Seiler Research Laboratory, Office of Aerospace Research, United States Air Force Academy, Colorado. This paper represesnts part of a thesis submitted by R. W. Lamb to the Graduate School, University of Colorado, in partial fulfillment of the requirements of the Ph. D. degree, June, 1961.

2) L. A. Errede, *J. Phys. Chem.*, **64**, 1031 (1960).



Assuming that the ease of breaking a bond in the initiation step is a function of the bond dissociation energy, it is postulated that the initiation step in the pyrolysis of I involves primarily the rupture of carbon-bromine bonds as is shown in reaction 1.

A small amount of CF_2Cl-$CFBr_2$ (VI) was also shown to be present in the product which indicates the presence of the free radical, $\dot{C}F_2$-$CFBr_2$ or CF_2Cl-$\dot{C}FBr$, during the course of the reaction. Both of these free radicals could originate from the further reaction of the products obtained in reactions 2 and 3.

There was no IV · isolated in the product, therefore, the rate of reaction 3 must be slow compared to 2 and 4.

When a mixture of I and bromine was pyrolyzed, the same products were obtained in the same proportions as was obtained when elemental bromine was not used in the reaction. However, the yield was drastically reduced when I was pyrolyzed in the presence of nitric oxide as would be expected for a reaction involving free radicals.

When II was pyrolyzed, CF_2Cl-$CFCl_2$ (V), I and VI were the only products isolated. These products can be accounted for using the following reactions.

$$\text{II heat} \rightarrow CF_2Cl\text{-}\dot{C}FCl + \dot{B}r \quad \text{(initiation)} \quad (5)$$

$$\text{II} + CF_2Cl\text{-}\dot{C}FCl \rightarrow \text{V} + \dot{C}F_2\text{-}CFClBr \quad \text{or } CF_2Cl\text{-}\dot{C}FBr \quad (6)$$

$$\text{II} + \dot{C}F_2\text{-}CFClBr \rightarrow \text{I} + CF_2Cl\text{-}\dot{C}FCl \quad (7)$$

$$\text{II} + CF_2Cl\text{-}\dot{C}FBr \rightarrow \text{VI} + CF_2Cl\text{-}\dot{C}FCl \quad (8)$$

(6), (7), (8): (propagation)

Pyrolysis of an equimolar mixture of III and V produced I, II and VI as the major products. Four different free radical intermediates are possible from the pyrolysis of III and V. The combination of these intermediates with a bromine or chlorine atom should lead to the formation of the products as follows :

$$\dot{C}F_2\text{-}CFCl_2 \xrightarrow{\text{Abstract Br}} \text{IV} \quad (9)$$

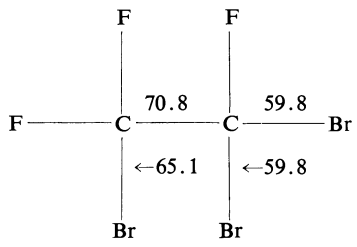
$$CF_2Cl\text{-}\dot{C}FCl \xrightarrow{\text{Abstract Br}} \text{II} \quad (10)$$

$$\dot{C}F_2\text{-}CFBr_2 \xrightarrow{\text{Abstract Cl}} \text{VI} \quad (11)$$

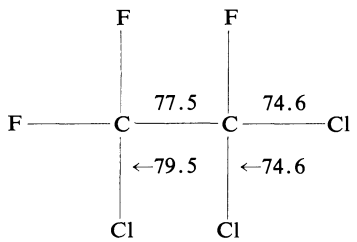
$$CF_2Br\text{-}\dot{C}FBr \xrightarrow{\text{Abstract Cl}} \text{I} \quad (12)$$

The products which were isolated furnish evidence for reactions 10, 11 and 12. Since IV could not be isolated from the pyrolysis, it appears that either appreciable amounts of $\dot{C}F_2$-$CFCl_2$ are not present during the reaction or reaction 9 is slow compared to 10, 11, and 12. It is presumed that the carbon-chlorine bond in the chlorodifluoromethyl moiety of V is not appreciably broken under the conditions of the reaction. This particular bond is known to be relatively strong because of the strong negative inductive effect of the two fluorine substituents.[3]

Using the equation developed by Errede,[2] a quantitative comparison of the strengths of the bonds in III and V can be made. The following model illustrates some calculated bond dissociation energies in kcal./mol.



III



V

It is presumed from the above calculated bond dissociation energies that the initiation step involves primarily the breaking of carbon-bromine bonds in III. Furthermore, the rate of production of CF_2Br-$\dot{C}FBr$ should exceed that of $\dot{C}F_2$-$CFBr_2$ because of the difference in the bond dissociation energies of the carbon-bromine bonds in III. Production of free radicals from V probably occurs during the propagation steps by the reaction of V with either $\dot{C}F_2$-$CFBr_2$ or CF_2Br-$\dot{C}FBr$. The high boiling liquid obtained from the pyrolysis of CF_2Br-$CFBr_2$ in the presence of nitric oxide was probably formed from the coupling of

3) R. K. Steunenberg and G. H. Cady, *J. Am. Chem. Soc.*, **74**, 4165 (1952).

free radicals, such as $CF_2Br-\dot{C}FBr$ or $\dot{C}F_2-CFBr_2$.

An infrared spectrum of the slightly blue product showed no absorption peak at 6.25 μ, where the nitroso should absorb. The nitroso blue color is very intense; therefore, the presence of a small amount of nitroso compound could be enough to give a slight coloration to the product, but not enough to show up on a gas chromatogram, or in an infrared spectrum. This small amount of nitroso compound is to be expected. Nitric oxide is a known free radical scavenger; therefore, it would be expected to react with the free radicals formed in the following manner:

$$CF_2Br-\dot{C}FBr + NO \rightarrow CF_2Br-\underset{\displaystyle NO}{\underset{|}{CFBr}} \quad (1)$$

$$\dot{C}F_2CFBr_2 + NO \rightarrow \underset{\displaystyle NO}{\underset{|}{CF_2}}-CFBr_2 \quad (2)$$

These reactions represent termination steps; therefore, the products should be present only in small amounts. No attempt was made to isolate and identify the high boiling compound, which was a minor product, when $CF_2Br-CFBr_2$ was pyrolyzed in the presence of nitric oxide.

Experimental

General Procedures.—All pyrolysis runs were made using the same general procedures. When the reactants were liquids, as was the case in all but one reaction, they were added from a 50 ml. burette into a pyrolysis tube enclosed in an electric furnace. In the one reaction involving a gaseous reactant and a liquid reactant, the same apparatus was used except that the gas was introduced into the line leading to the pyrolysis tube via a T-connection just below the burette.

The tube used for pyrolysis was a platinum-lined nickel tube with an outside inconel jacket about 24 inches long and 3/4 inches in diameter. A section of the tube about 12 inches long was enclosed in the furnace. In order to make a distinct boundary for the region of pyrolysis, tap water was circulated through copper coils wrapped around the tube at the ends of the furnace. The volume of the section of tube used for pyrolysis was required in order to calculate the contact time. The temperature of the reaction was measured with a chromel-alumel thermocouple, which was inserted into the furnace along with the pyrolysis tube. The contact time was calculated by dividing the volume of the pyrolysis tube by the rate of flow of the reactants through the tube.

Gas chromatography was used to determine the composition of mixtures of liquids. All percentages are given in weight percents.

1, 2-Dibromo-1-chloro-1, 2, 2-trifluoroethane.—1,2-Dibromo-1-chloro-1, 2, 2-trifluoroethane was prepared by bubbling chlorotrifluoroethylene through liquid bromine in the presence of actinic light. In a typical reaction, 290 g. (2.50 mol.) of olefin was added to 375 g. (2.34 mol.) of bromine over a four hour period. The distilled product obtained was 637 g. (92% conversion), b. p. 86.5°C/630 mmHg (lit.[4] 92~92.5°C/760 mmHg). Gas chromatography showed this material to be pure.

Pyrolysis of 1, 2-Dibromo-1-chloro-1,2,2-trifluoroethane.—*A) at 500°C.*—Exactly 155 g. (0.56 mol.) of $CF_2Br-CFClBr$ was pyrolyzed at 500°C at a contact time of about 26~27 sec. The reactant was added at a uniform rate over a total time of four hours. All of the products (150 g.) were collected in a trap maintained at room temperature. Fractionation through a Todd column yielded the following three main fractions: a) $CF_2Br-CFClBr$ (I), b. p. 86~87°C/630 mmHg (84%); b) $CF_2Cl-CFClBr$ (II), b. p. 63°C/630 mmHg (5.5%) and c) $CF_2Br-CFBr_2$ (III), b. p. 108°C/630 mmHg (7.9%).

II was shown to be $CF_2Cl-CFClBr$ by comparison of its infrared spectrum with that of an authentic sample obtained from the addition of chlorine to trifluorobromoethylene. Similarly, compound III was compared with an authentic sample obtained form the bromination of trifluorobromoethylene.

B) At 600°C.—Although a trap maintained at −80°C was in the exit line, nearly all the products were collected in the trap kept at room temperature. In a typical reaction, 382 g. of $CF_2Br-CFClBr$ was pyrolyzed over a 3.5 hr. period to yield 367 g. of product. The product was washed with 5% sodium bisulfite solution to remove some bromine, washed with water, and dried over magnesium sulfate. The product was filtered and fractionated through a 50 cm. Todd column. The following materials were isolated and identified: a) mixture A consisting of $CF_2Br-CFClBr$ and $CF_2Cl-CFBr_2$, b. p. 86~87°C/630 mmHg: n_D^{25} 1.4254 (33%); b) $CF_2Cl-CFClBr$ (14%) and c) $CF_2Br-CFBr_2$ (19%).

The yields of the various components were calculated from a chromatogram of the mixture of undistilled products. The isomers, $CF_2Br-CFClBr$ and $CF_2Cl-CFBr_2$ gave only one peak on the chromatogram; therefore, they were treated as one compound in calculating yields.

The infrared spectrum of the mixture was compared with the spectrum of $CF_2Br-CFClBr$ prepared by adding bromine to chlorotrifluoroethylene. The spectrum of the mixture contained all of the absorption peaks of $CF_2Br-CFClBr$ plus two additional peaks at 9.75 μ and 13.27 μ. This evidence indicated that mixture A consisted of the two positional isomers, $CF_2Br-CFClBr$ and $CF_2Cl-CFBr_2$. In order to verify this supposition, and to determine the relative amounts of each isomer, A was treated with zinc and the resulting gaseous olefins brominated. The two isomers reacted by the following paths giving two products, which were easily separated by fractionation:

4) R. N. Haszeldine, *J. Chem. Soc.*, 1952. 3423.

$$\left.\begin{matrix} CF_2Br\text{-}CFClBr \\ \\ CF_2Cl\text{-}CFBr_2 \end{matrix}\right\} \xrightarrow{\text{Zn in ethanol}} \left\{\begin{matrix} CF_2{=}CFCl \\ + \\ CF_2{=}CFBr \end{matrix}\right\}$$

$$\xrightarrow[\text{light}]{Br_2} \left\{\begin{matrix} CF_2Br\text{-}CFClBr \text{ b. p. } 86°C/630 \text{ mmHg} \\ + \\ CF_2Br\text{-}CFBr_2 \text{ b. p. } 107°C/630 \text{ mmHg} \end{matrix}\right.$$

The amount of each component was determined from a vapor phase chromatogram of the product. The product was found to be 73 mol. percent CF_2Br-$CFClBr$ and 27 mol. percent CF_2Br-$CFBr_2$.

Pyrolysis of a Mixture of 1, 2-Dibromo-1-chloro-1, 2, 2-trifluoroethane and Bromine at 600°C.—A mixture consisting of 535 g. (1.93 mol.) of CF_2Br-$CFClBr$ and 309 g. (1.93 mol.) of bromine was pyrolyzed at 600°C at a contact time of about 10 sec. The pyrolysis reaction was run over a period of fourteen hours and fifty minutes. The product was collected in a trap maintained at room temperature. It was then washed with a solution of 5% sodium bisulfide to remove the excess bromine, washed with water and dried over magnesium sulfate. The composition of the product was calculated from a gas chromatogram of the undistilled material. The individual peaks corresponding to each component of the products were identified by their retention times. The following products were obtained: a) mixture A consisting of CF_2Br-$CFClBr$ and CF_2Cl-$CFBr_2$ (32%); b) CF_2Cl-$CFClBr$ (13.6%) and c) CF_2Br-$CFBr_2$ (24%).

The reaction was repeated with a mixture consisting of 200 g. (0.72 mol.) of CF_2Br-$CFClBr$ and 109 g. (0.69 mol.) of bromine using a longer contact time (21.1 sec.). Apparently, there was very little change in the distribution of the pyrolyzates from that obtained above. The distribution was 27%, 13.6% and 19% for mixture A, CF_2Cl-$CFClBr$ and CF_2Br-$CFBr_2$, respectively.

Pyrolysis of a Mixture of 1, 1, 2-Tribromo-1, 2, 2-trifluoroethane and Nitric Oxide at 600°C.—Approximately 40 g. of CF_2Br-$CFBr_2$ was pyrolyzed in the presence of nitric oxide at 600°C over a 1.5 hr. period. The apparatus described under "General Procedures" was used, except that the nitric oxide was added at the rate of approximately 100 ml. per second. The product was all collected in the trap maintained at room temperature. It was washed with water, dried over magnesium sulfate, and filtered. The product was slightly blue, indicating a possible trace of a nitroso compound; however, the infrared spectrum of the product showed no absorption at the wavelengths, where the nitroso group should absorb. Calculations based on a gas chromatogram of the product indicate that it is approximately 92% starting material and 8.0% high boiling compound. The high boiling compound is probably a product of coupling of free radicals produced in the pyrolysis.

Pyrolysis of 1-Bromo-1, 2-dichloro-1, 2, 2-trifluoroethane at 600°C.—About 110 g. of CF_2Cl-$CFClBr$ was pyrolyzed at 600°C at a contact time of about 11 sec. over a period of one hour and thirty-five minutes. All of the product (102 g.) were collected in the trap, maintained at room temperature. It was washed with a solution of 5% sodium bisulfite to remove some bromine, washed with water and dried over magnesium sulfate. The product was fractionated through a Todd column. The pure products were obtained for identification from the distillation, but the yields were calculated from a chromatogram of the original mixture of products. The following products were identified. The yields given were based on the amount of starting material: a) CF_2Cl-$CFCl_2$ (10%); b) CF_2Cl-$CFClBr$ (43%), and c) mixture A consisting of CF_2Cl-$CFBr_2$ and CF_2Br-$CFClBr$ (9.5%).

Pyrolysis of a Mixture of 1, 1, 2-Tribromo-1, 2, 2-trifluoroethane and 1, 1, 2-Trichloro-1, 2, 2-trifluoroethane at 600°C.—A mixture consisting of 56 g. (0.17 mol.) of CF_2Br-$CFBr_2$ and 32 g. (0.17 mol.) of CF_2Cl-$CFCl_2$ was pyrolyzed at 600°C at a contact time of about 14 sec. The pyrolysis was run over a 1.5 hr. period. All of the product (49 g.) were collected in the trap kept at room temperature. It was washed with a solution of 5% sodium bisulfite to remove some bromine, washed with water, and dried over magnesium sulfate. The product was fractionated through a Todd column. The pure products were obtained for identification from the distillation; however, the yields were calculated from a chromatogram of the original mixture of products. The following products were isolated and identified from the reaction. The calculated yields were based on the total amount of material obtained from the pyrolysis: a) CF_2Cl-$CFCl_2$ (37.4%); b) CF_2Cl-$CFClBr$ (7.6%); c) mixture A consisting of CF_2Br-$CFClBr$ and CF_2Cl-$CFBr_2$ (14.5%) and d) CF_2Br-$CFBr_2$ (40.5%).

Dehalogenation of a Mixture of 1, 2-Dibromo-1-chloro-1, 2, 2-trifluoroethane and 1, 1-Dibromo-2-chloro-1, 2, 2-trifluoroethane.—About 166 g. (0.6 mol.) of a mixture of CF_2Cl-$CFBr_2$ and CF_2Br-$CFClBr$ was treated with zinc in ethanol to yield a mixture of $CF_2{=}CFBr$ and $CF_2{=}CFCl$. The reaction was carried out in a three-neck flask equipped with a stirrer, addition funnel, and a condenser. The halocarbons were added dropwise to a stirred suspension of powdered zinc in ethanol via an addition funnel. The exit line from the top of the condenser was collected to a dry-ice acetone trap, in which the olefins were collected. The olefins were used as a mixture in the next reaction, in which they were brominated.

Bromination of a Mixture of 1-Bromo-1, 2, 2-trifluoroethylene and 1-Chloro-1, 2, 2-trifluoroethylene.—Approximately 30 g. of a mixture, consisting of a mixture of $CF_2{=}CFCl$ and $CF_2{=}CFBr$, was passed from a trap through a glass frit into a glass flask approximately 6 cm. × 50 cm. The glass flask, which contained the bromine, was irradiated with light from a tungsten lamp to catalyze the reaction. The glass flask was equipped with a water-cooled condenser. The exit line was connected to a bubbler, which was connected to a dry-ice acetone-cooled trap to recover some unreacted olefin. The crude product was washed with a 10% sodium bisulfite solution to remove the excess bromine, washed with water, and dried over magnesium sulfate. Gas chromatography showed that the product (72 g.) consisted of a mixture of 78%

CF_2Br-CFClBr and 22% CF_2Br-$CFBr_2$.

Pyrolysis of CF_2Br-$CFBr_2$ in the Presence of Nitric Oxide.—A sample of CF_2Br-$CFBr_2$ was pyrolyzed at 350°C in the presence of nitric oxide. At this temperature, 93% of the starting material was recovered and the absence of blue color was noted. This indicated no nitroso compounds, such as CF_2NO-$CFBr_2$ and CF_2Br-CFBrNO, were formed.

When the pyrolysis was run at 600°C a great deal of decomposition took place. After washing the product with water and drying, it retained a blue color, indicating that some nitroso compounds could be in the product. However, a gas chromatogram of the product showed it to consist of 92% of CF_2Br-$CFBr_2$ and 8% of an unidentified high boiling liquid.

Summary

The synthesis of various halogenated ethane derivatives was performed by the pyrolysis of CF_2Br-CFClBr and other similar compound. The reactions were carried out in a platinum-lined tube at temperatures ranging from 350°C to 600°C alone and in the presence of nitric oxide or bromine. Various products were isolated and identified. A mechanism is postulated for the reaction.

We wish to take this opportunity to thank the Minnesota Mining and Manufacturing Co., St. Paul, Minnesota for partial support of this work through a grant-in-aid.

Department of Chemistry
University of Colorado
Boulder, Colorado
U. S. A.

*Studies of Polybutene. II. On the Molecular Weight Distribution and the Solution Properties**

By Ryūichi ENDŌ, Kazuyoshi IIMURA and Masatami TAKEDA

(Received February 1, 1964)

Various commercial polybutenes have been obtained from several sources. Infrared study makes it seem that the polybutene is almost identical with a low-molecular-weight polyisobutylene.[1] Far fewer studies of the solution properties of the polymers with molecular weights ranging from 1000 to 10000 were carried out than on the usual high polymers, although recently the vapor pressure osmometer has become available for these low-molecular-weight polymers. Previous investigation of the polybutene has only dealt with its rheological property,[2] not with its solution property because of its extremely low molecular weight.

The present investigation has been undertaken to study the molecular weight and the molecular weight distribution of polybutene. Furthermore, according to the theory of Stockmayer and Fixman,[3] the unperturbed dimension of the polybutene fractions has been calculated from the relationship between the intrinsic viscosity and the molecular weight, and compared with the data reported by Fox and Flory[4] on low-molecular-weight polyisobutylene.

Experimental

Samples.—All the polybutenes employed were commercial products: Indopol of Amoco, Oronite of California Chemicals, and Polyvis of Cosden. All these samples except Indopol L-10 appeared as transparant viscous liquids.

The solvent and non-solvent were purified in the usual ways.[5]

Fractionation. — Fractional extraction has been applied with benzene as a solvent and methanol as a non-solvent. The fractionation was carried out using benzene-methanol mixtures, initially with a mixture rich in the non-solvent and finally with a mixture rich in the solvent, at room temperature. Then, the lowest-molecular-weight fraction was extracted from the sample. All the sample were divided into about eight or nine fractions.

Viscosity Measurement.—Samples were dissolved into benzene at room temperatures. The viscosities were measured with dilution in an Ubbelohde-type

* Presented at the 12th Annual Meeting of the Society of Polymer Science, of Japan, Tokyo, May, 1963.

1) K. Iimura, R. Endō and M. Takeda, This Bulletin, 37, 874 (1964).

2) H. Leaderman, R. G. Smith and R. W. Jones, *J. Polymer Sci.*, 14, 47 (1954).

3) W. H. Stockmayer and M. Fixman, *J. Polymer Sci.*, Part C, No. 1, 137 (1963).

4) T. G. Fox and P. J. Flory, *J. Phys. and Colloid Chem.*, 53, 197 (1949).

5) J. A. Riddick and E. E. Toops, Jr., "Organic Solvents," Interscience Publishers, N. Y. (1955).

viscometer at 30°C. The temperature of the double water bath, in which the viscometer was mounted vertically by using a specially-designed clamp, was maintained constant within ±0.005°C. Intrinsic viscosities were treated by the Huggins relation, and the data were calculated by the least-square method.

Molecular Weight Measurement.—The molecular weight of unfractionated samples was determined by the cryoscopic method in benzene. The molecular chain of polybutene is known to be a linear chain with one double bond at the end of the chain.[6]

Therefore, it is possible to determine the molecular weight of the same samples by the end-group analysis. The number of double bonds was determined using a modified Hübler method[7] in the following manner: about 1 g. of a sample was dissolved into 20 ml. of chloroform in a 500 ml. Erlenmeyer flask and added to a definite volume of an iodine solution ($I_2+Hg_2Cl_2$ in alcohol). The flask was then shaken frequently by hand. The reaction to the double bond with iodine was carried out in a dark oven at 30°C; the reaction mixture was kept there for 48 hr. (e. g., see Fig. 3). The molecular weight was calculated from the following equation (1);

$$\overline{M}_n = 1/[I_2] \quad (1)$$

The observed values agreed closely with that determined by the cryoscopic method. Since the amount of each fraction was limited, the molecular weight was determined mainly by the end-group analysis method.

Results and Discussion

Fractionation and Intrinsic Viscosity.—The solubility in a benzene-methanol mixed solvent was determined for Indopol L-10 as the lower, the Indopol H-35 as the medium, and for Indopol H-300 as the higher molecular weight sample respectively. The results are shown in Fig. 1. Figure 1 shows that the fractionation can be carried out with the mixed solvents by varying the volume fraction of benzene. Because these polymers have lower molecular weights, it seems likely that the fractionation is effected only by the difference in the dissolution energy of polymer molecules in mixed solvents and not by the entropy effect as in the usual high polymers. According to Brönsted's law of partition,[8] there exists a relation:

$$N_1/N_2 = \exp(-ME/RT) \quad (2)$$

where N_1 is the concentration of polymers in the solution phase, N_2 is the concentration of polymers in the gel phase, M is the molecular weight of dissolved polymers, and E is the dissolution energy of a monomer unit of polybutene. If the dissolution energy of some mixed solvent is a constant, the value of N_1/N_2 becomes smaller for the larger M. Generally, the value of N_1/N_2 increases with an increase in the dissolution energy or with the larger volume fraction of benzene in the mixed solvent. If the fractionation follows Eq. 2, a linear relation may be obtained between $\ln N_1/N_2$ and the dissolution energy, E, of mixed solvents.

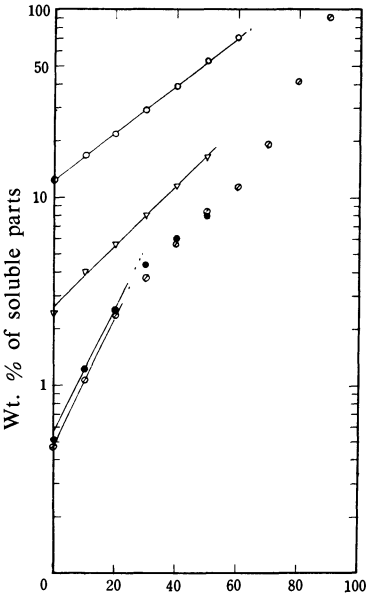


Fig. 1. Relation between the volume fraction of benzene in benzene-methanol mixed solvent and the weight fraction of soluble part.
○ L-10, ▽ H35, ⊘ H300, ● 32

For Indopol L-10, which is of the lowest molecular weight, a linear relation was obtained, but not for Indopol H-35 and Indopol H-300. A more general theory[9] it necessary for treating these samples. The fractions obtained from each sample are given in Table I(a)—(f). The reduced viscosities are plotted against the concentration for Indopol H-300 and Polyvis 3 in Fig. 2(a)—(b). It may be seen from Fig. 2 that the Huggins' relation holds for these samples up to higher concentrations, but for higher-molecular-weight polymers, the non-linear relation[10] appears in the range of higher concentrations. The intrinsic viscosities of unfractionated samples are shown in Table II.

6) C. E. Schildknecht, "Vinyl and Related Polymers," John Wiley & Sons, Inc., New York (1959), p. 560.
7) J. Arima, "Analytical Methods of Organic Compounds" (in Japanese), Iwanami, Tokyo, p. 190.
8) Brönsted, *Z. phys. Chem.*, Bodenstein Festband 257 (1931).
9) P. J. Flory, "Principles of Polymer Chemistry," Cornell Univ. Press, Ithaca, N. Y. (1953).
10) M. Nakamuta, *J. Chem. Soc. Japan, Pure Chem. Sec.* (*Nippon Kagaku Zassi*), 77, 702, 705, 858, 861 (1956).

Table I. Intrinsic viscosities and molecular weights of the fractions of polybutenes

(a) Indopol L-10

Fraction No.	Weight	Weight-fraction	$[\eta]$	$\bar{M}_{end}$	$\bar{M}_v$
F-1	1.173_5	12.4_4	0.011_3	240	230
F-2	1.521_7	16.1_3	0.011_5	270	230
F-3	2.303_3	24.4_1	0.012_6	350	260
F-4	2.004_4	21.2_4	0.013_5	350	290
F-5	0.974_1	10.3_2	0.018_0	(330)	430
F-6	0.293_8	3.1_1	0.023_6	390	630
F-7	0.214_9	2.2_8	0.033_5	600	1040
F-8	0.949_8	10.0_7	0.065_3	—	2580

(b) Indopol H-35

Fraction No.	Weight	Weight-fraction	$[\eta]$	$\bar{M}_{end}$	$\bar{M}_v$
F-1	1.899_4	19.0_8	0.015_8	380	360
F-2	1.575_5	15.8_3	0.018_3	370	440
F-3	1.331_4	13.3_7	0.023_4	480	620
F-4	1.194_7	12.0_0	0.026_4	830	740
F-5	0.992_8	9.9_7	0.037_3	1460	1190
F-6	0.800_0	8.0_4	0.044_2	—	1500
F-7	0.670_4	6.7_3	0.051_8	(5560)	1870
F-8	1.490_9	14.9_8	0.076_1	—	3190

(c) Indopol H-300

Fraction No.	Weight	Weight-fraction	$[\eta]$	$\bar{M}_{end}$	$\bar{M}_v$
F-1	0.676_7	6.6_7	0.019_1	460	470
F-2	1.553_1	15.3_1	0.024_0	600	650
F-3	2.022_9	19.9_4	0.032_8	990	970
F-4	1.980_7	19.5_2	0.040_7	1400	1340
F-5	1.219_1	12.0_2	0.047_3	2070	1650
F-6	1.107_8	10.9_2	0.061_2	3800	2360
F-7	0.745_0	7.3_4	0.076_7	4330	3220
F-8	0.390_1	3.8_5	0.084_2	—	3670
F-9	0.449_2	4.4_3	0.125_4	—	6370

(d) Polyvis 3

Fraction No.	Weight	Weight-fraction	$[\eta]$	$\bar{M}_{end}$	$\bar{M}_v$
F-1	1.906_8	19.2_8	0.016_8	360	390
F-2	1.797_3	18.1_7	0.019_6	420	490
F-3	1.635_8	16.5_4	0.025_0	510	680
F-4	1.441_8	14.5_8	0.029_3	730	850
F-5	1.115_6	11.2_8	0.036_8	1630	1170
F-6	0.864_3	8.7_4	0.046_5	—	1610
F-7	0.643_8	6.5_1	0.053_5	—	1960
F-8	0.484_7	4.9_0	0.070_7	—	2880

(e) Polyvis 30

Fraction No.	Weight	Weight-fraction	$[\eta]$	$\bar{M}_{end}$	$\bar{M}_v$
F-1	0.647_9	6.3_6	0.014_8	420	330
F-2	1.237_0	12.2_5	0.023_6	710	630
F-3	1.614_0	15.8_5	0.031_8	860	950
F-4	1.766_0	17.3_5	0.040_0	1360	1310
F-5	1.370_0	13.4_6	0.046_9	2250	1630
F-6	1.462_8	14.3_7	0.058_9	2920	2240
F-7	1.266_3	12.4_4	0.073_6	3800	3040
F-8	0.513_6	5.0_5	0.086_6	—	3810
F-9	0.302_4	2.9_7	0.115_1	—	5650

(f) Oronite 32

Fraction No.	Weight	Weight-fraction	$[\eta]$	$\bar{M}_{end}$	$\bar{M}_v$
F-1	0.685_1	6.8_3	0.017_4	430	410
F-2	1.344_9	13.4_1	0.023_4	710	620
F-3	1.725_3	17.2_0	0.031_6	890	940
F-4	1.952_6	19.4_0	0.040_5	1310	1330
F-5	1.390_6	13.8_6	0.047_4	2280	1660
F-6	1.178_7	11.7_5	0.061_5	2870	2370
F-7	0.897_6	8.9_5	0.072_7	3520	2990
F 8	0.494_4	4.9_3	0.090_3	4980	4040
F-9	0.363_0	3.6_2	0.125_9		6400

Molecular Weight.—The molecular weight of unfractionated samples was determined by means of the cryoscopic method and are listed as $\bar{M}_{cry}$ in Table II. Figure 3 shows the plots of the iodine concentration against the reaction time. Therefore, the molecular weights with an end-group titration $\bar{M}_{end}$ were determined after 48 hr.; they are shown in Table I(a)—(f), and Table II. The agreement of $\bar{M}_{end}$ and $\bar{M}_{cry}$ is fair. Therefore, it has been proved that the molecular chain of polybutene has only one double bond in each chain.

Therefore, the molecular weight determination of fractions has been carried out mainly by end-group analysis, because it requires a smaller amount of sample than does the cryoscopic method.

Table II. Viscosities and molecular weights of unfractionated samples

Sample	$[\eta]$	$\bar{M}_{end}$	$\bar{M}_{cry}$
Indopol L-10	0.019_6	310	310
Indopol H-35	0.034_6	640	630
Indopol H-300	0.051_6	1100	1090
Polyvis 3	0.030_2	660	650
Polyvis 30	0.061_9	1150	1300
Oronite 32	0.052_6	1030	1240

The Relationship between Intrinsic Viscosity and Molecular Weight.—The intrinsic viscosity of fractions is plotted against the molecular weight in Fig. 4. The Mark-Houwink equation was determined by the least squares method to be:

$$[\eta] = 2.24 \times 10^{-4} \bar{M}_n^{0.72_2} \quad (3)$$

On the other hand, Fox and Flory[4] obtained for polyisobutylene with molecular weights from 1000 to 1300000:

$$[\eta] = 6.1 \times 10^{-4} \bar{M}^{0.56} \quad (4)$$

For comparison, a dotted line expressing Flory's equation (4) is also drawn in Fig. 4. The value of the exponent in Eq. 3 is larger than that in Flory's equation (4). Since it is known that the system of polyisobutylene

TABLE III. MOLECULAR WEIGHTS OF POLYBUTENES

Sample	$\bar{M}_{end}$[a]	$\bar{M}_{cry}$[b]	$\bar{M}_w$[c]	$\bar{M}_n$[c]	$\bar{M}_w/\bar{M}_n$	$\mu_2\times10^{-4}$
Indopol L-10	310	310	280	260	1.08	0.54
Indopol H-35	640	630	1260	750	1.008	38.25
Indopol H-300	1100	1010	1590	1040	1.53	57.32
Polyvis 3	660	650	990	650	1.52	21.97
Polyvis 30	1150	1300	1780	940	1.89	78.64
Oronite 32	1030	1240	1680	990	1.70	68.61

a) Determined by the end-group analysis.
b) Determined by the cryoscopic method.
c) Calculated from the molecular weight distribution.

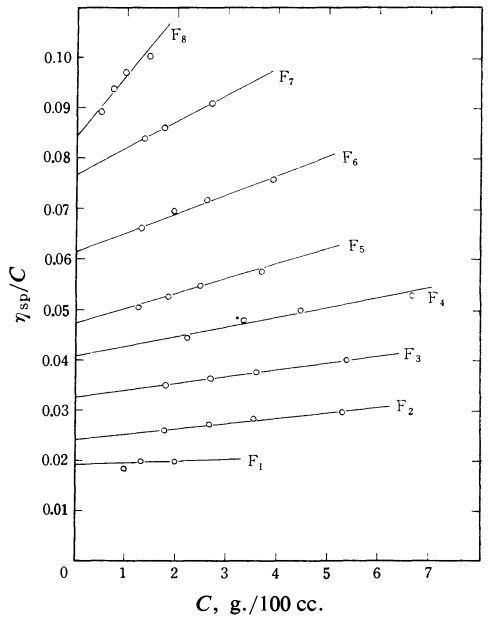


Fig. 2(a). Relation between the reduced viscosity and the concentration of Indopol H-300, at 30°C.

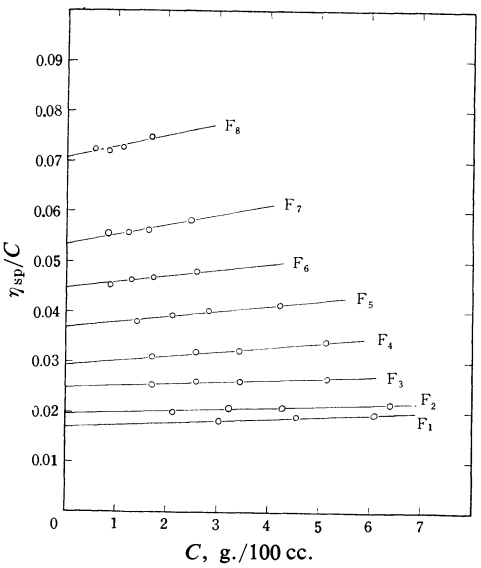


Fig. 2(b). Relation between the reduced viscosity and the concentration of Polyvis 3, at 30°C.

in benzene has the theta temperature at 25°C,[11] the obtained α for polybutene seems to be large. In polymerization, the branching of the polymer chain may occur mainly at the molecule with a higher molecular weight. Because the polyisobutylene has a higher molecular weight than polybutene, it seems that the branching exists in the molecular chain. Since polybutene seems to consist of linear chain molecules with molecular weights ranging from 240 to 7000, the value of the α of polybutene is thought to become larger than that of polyisobutylene.

Recently, Stockmayer and Fixman[3] have demonstrated a means to estimate the unperturbed dimension factor K from the intrinsic viscosity $[\eta]$ by means of the following equation:

$$[\eta] = KM^{1/2}\alpha_\eta^3 \tag{5}$$

$$[\eta] = KM^{1/2} + 0.51\Phi_0 BM \tag{6}$$

$$K = \Phi_0 A^3 \tag{7}$$

$$A^2 = \langle\bar{L}^2\rangle_0/M \tag{8}$$

where Φ_0 is the universal viscosity constant for chain polymers in theta solvents, B is the polymer-solvent interaction parameter, α_η is the viscosity expansion factor,[12] and $\langle\bar{L}^2\rangle_0$ is the mean square unperturbed end-to-end distance. Equation 6 gives the unperturbed molecular dimension, A^2, from the measured value of K without using the theta solvent. If the plots of $[\eta]M^{-1/2}$ against $M^{1/2}$ are extrapolated to zero molecular weight, we have the value of K. Experimental results are shown in Fig. 5. The value of K obtained

11) T. G. Fox and P. J. Flory, *J. Am. Chem. Soc.*, 73, 1909 (1951).

12) M. Kurata and W. H. Stockmayer, *Progress Polymer Phys. Japan*, 5, 23 (1962).

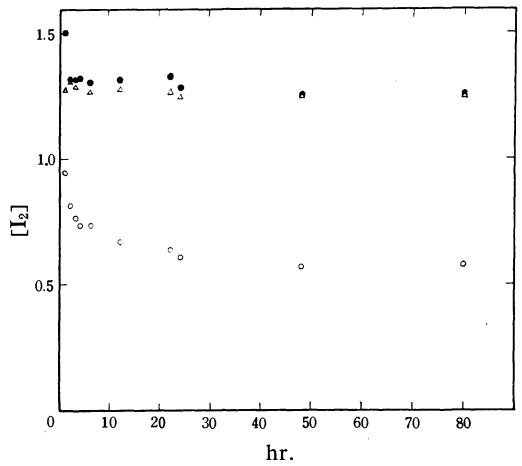


Fig. 3. Change of iodine value with time. The open circle and triangle are the Indopol L-10 and Polyvis 30 respectively. The closed circle is blank test.

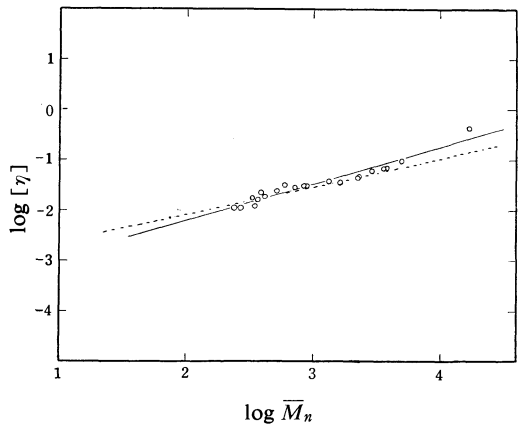


Fig. 4. Relation between the intrinsic viscosity and the molecular weight. Dotted line shows Flory's result.

in the theta solvent is given[9] as 10.6×10^{-4}, as is shown on the ordinate axis by an arrow in Fig. 5. Although the experimental points are scattered widely, the value of K obtained from the present work shows a tendency to be smaller than 10.6×10^{-4}. This effect seems to arise from the end-effect of the molecular chain of polybutene because of its smaller molecular weight.[13]

Molecular Weight Distribution. — The end-group analysis is less reliable for the determination of the molecular weight of higher fractions. The molecular weight of all fractions was re-calculated by using Eq. 3 and is shown as $\overline{M}_v$ in Table I (a)—(f).

Integral distribution curves are expressed as

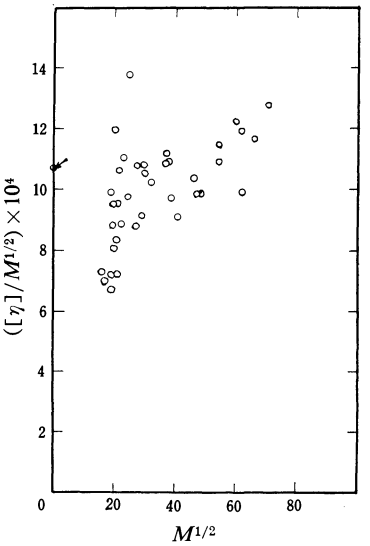


Fig. 5. Relation between $[\eta]M^{-1/2}$ and $M^{1/2}$. The arrow shows the value of K obtained in θ-solvent.

plots of the cumulative weight fraction against the molecular weight. The cumulative weight fraction corresponding to the molecular weight, M_i, of the i-th fraction, designated as W_i, is expressed by the following equation;

$$W_i = w_i/2 + \sum_{j=1}^{i-1} w_j \qquad (9)$$

where w_i and w_j are the weight fractions of the i-th and j-th fractions respectively. The integral distribution curves are then converted into the differential distribution curves (cf. Fig. 6 (a)—(f)). The number-average molecular weight $\overline{M}_n$, the weight-average molecular weight $\overline{M}_w$, the $\overline{M}_w/\overline{M}_n$ ratio and a variance, μ_2, were also calculated[14] for these distributions; they are shown in Table III. The calculated values of the number-average molecular weight, with the exception of Indopol L-10, are essentially identical with the observed values. The values of $\overline{M}_w/\overline{M}_n$, also with the exception of Indopol L-10, are equal to those of high polymers in general. Therefore, it is found that such a low-molecular-weight polymer keeps the inhomogeneity of molecular weight.

We have tried to fit Schulz's molecular weight distribution function[15] to our experimental results. This function is:

$$f(M) = M \ln^2 aa^M \qquad (10)$$

where M is the molecular weight and a is the probability of propagation for the active

13) M. Kurata and W. H. Stockmayer, *Fortschr. Hochpolym.-Forsch.*, 3, 196 (1963).

14) R. Endō *Chem. High Polymers Japan* (*Kōbunshi Kagaku*), **18**, 214 (1961).

15) G. V. Schulz, *Z. phys. Chem.*, **B30**, 379 (1935).

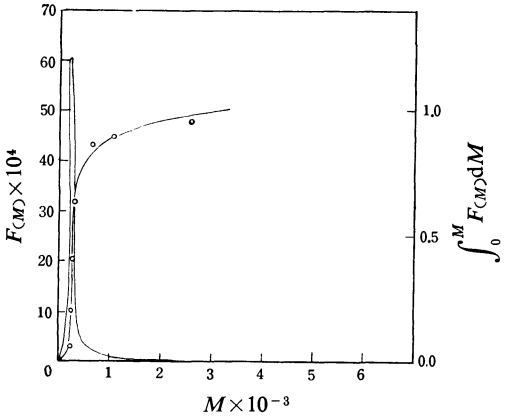


Fig. 6(a). Molecular weight distribution curve of Indopol L-10.

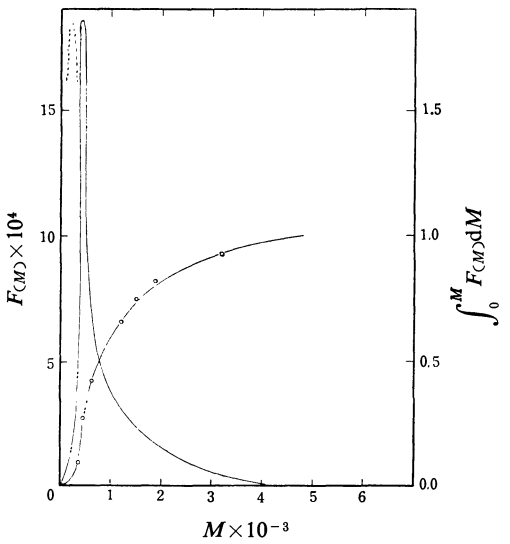


Fig. 6(b). Molecular weight distribution curve of Indopol H-35. Dotted curve was calculated from Schulz's function.

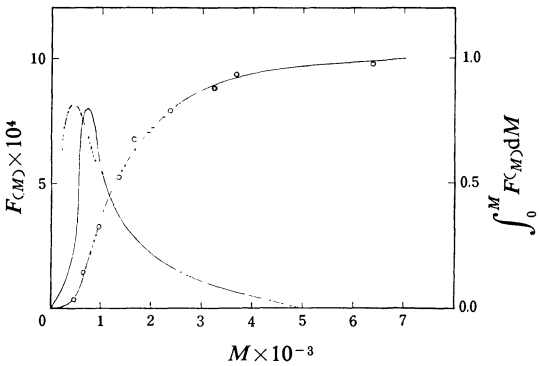


Fig. 6(c). Molecular weight distribution curve of Indopol H-300. Dotted curve was calculated from Schulz's function.

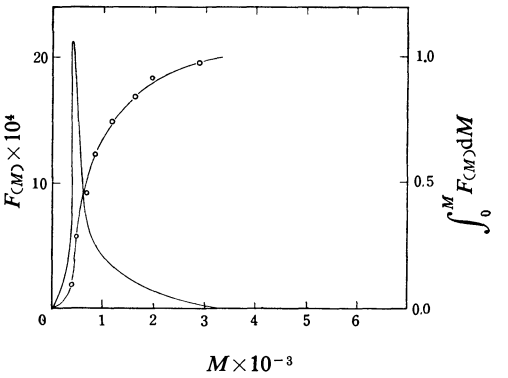


Fig. 6(d). Molecular weight distribution curve of Polyvis 3.

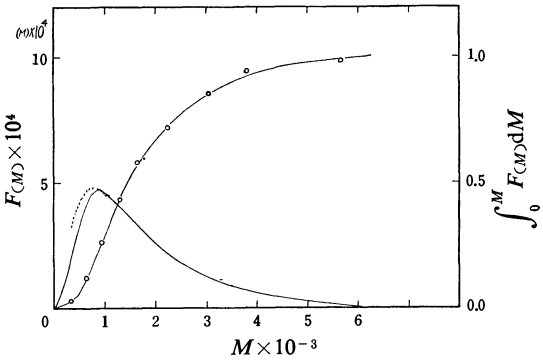


Fig. 6(e). Molecular weight distribution curve of Polyvis 30. Dotted curve was calculated from Schulz's function.

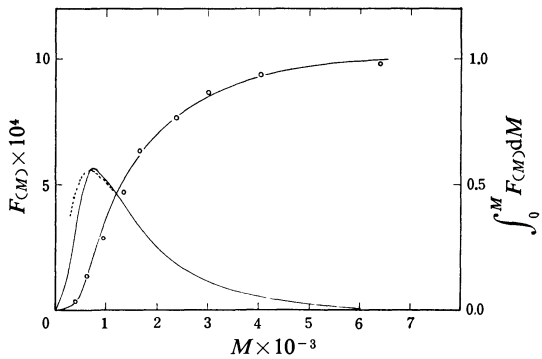


Fig. 6(f). Molecular weight distribution curve of Oronite 32. Dotted curve was calculated from Schulz's function.

Table IV. The values of a and χ

Sample	a	χ*	Ref.
Indopol H-35	(0.9950)	(0.0050)	This work
Indopol H-300	(0.9978)	(0.0022)	This work
Polyvis 30	0.9987	0.0013	This work
Oronite 32	0.9985	0.0015	This work
Polyisobutylene	0.9982	0.0018	17

* $1-\chi=a$ where $\chi \ll 1$.

molecule in polymerization. The parameters a in Eq. 10 were calculated from the observed distribution function; they are listed in Table IV. For comparison, theoretical curves expressing Eq. 10 are also given as dotted lines in Figs. 6(b), 6(c), 6(e) and 6(f). Some difference between the theoretical and the observed curves may be seen in Fig. 6(b). The theoretical curves are not drawn in Figs. 6(a) and 6(d) because the observed curves are not in good agreement with the theoretical ones. These disagreements are thought to be caused by their smaller molecular weights. Though the Indopol H-300 shown in Fig. 6(c) is of a higher molecular weight than the other three samples, the agreement between the observed curve and the theoretical one for it is not very good. In general, it is felt that the observed curves for the samples of Indopol series do not agree with the theoretical curves. On the other hand, the curves for the other samples shown in Figs. 6(e) and 6(f) are in close agreement with theoretical ones.

The ratio of the probability of termination to the probability of propagation, χ, is then calculated from the value of a; it is also shown in Table IV. For comparison, the value of a for polyisobutylene[16] is also listed in Table IV. Because the material gas of polybutene consists of mixed olefin with carbon numbers from two to six, it seems difficult to compare the mechanism of its polymerization directly with that of polyisobutylene. However, as the values of a are nearly equal to that of polyisobutylene, it may suggest that the polymerization mechanism of polybutene is similar to that of polyisobutylene.

The authors are indebted to Miss Kazumi Nakamura for her assistance.

Tokyo College of Science
Department of Chemistry
Faculty of Science
Kagurazaka, Shinjuku-ku
Tokyo

16) M. Imoto, "*Chemistry of Synthetic High Polymers*" (in Japanese), Sōgensha, Tokyo (1950), p. 84.

The Synthesis of Lactones from ω-Chlorocarboxylic Acids

By Kazuo SAOTOME

(Received February 8, 1964)

Various intermediates for polymers have been prepared by Russian authors[1] from ω-chlorocarboxylic acids, which are the basic derivatives from the tetrachloroalkanes obtained by the telomerization of ethylene with carbon tetrachloride. However, the hydrolysis of these ω-chlorocarboxylic acid has been little studied.

In the present work, the author will report on the kinetics of the hydrolysis of δ-chlorovaleric and ω-chloroheptanoic acids in an aqueous solution. Joyce et al.[2] derived δ-valerolactone from δ-chlorovaleric acid by heating it with sodium hydroxide in methanol. δ-Chlorovaleric acid is easily hydrolyzed in an aqueous alkaline solution to δ-hydroxyvaleric acid, which is then immediately converted to δ-valerolactone by neutralizing the solution. When an aqueous solution of sodium δ-chlorovalerate is heated, the oily layer of δ-valerolactone appears. On the other hand, the hydrolysis product from sodium ω-chloroheptanoate in an aqueous solution remains ω-hydroxyheptanoic acid. Its polyester is produced by removing water from the solution.

The dimeric lactone of ω-hydroxyheptanoic acid was obtained by the thermal decomposition of the polyester according to the method of Spangel and Carothers.[3] The monomeric

1) R. Kh. Freidlina and Sh. A. Karapetyan, "Telomerization and New Synthetic Materials," Pergamon Press (1961).

2) R. M. Joyce, W. E. Hanford and J. Harmon, *J. Am. Chem. Soc.*, **70**, 2529 (1948).

3) E. W. Spangel and W. H. Carothers, ibid., **57**, 929 (1935).

Table I. The thermal decomposition of the polyester-NaCl mixture
$Cl(CH_2)_6COOH$, 82.5 g. Catalyst, 1.0 g.

Catalyst	Temp. (bath) °C	Distillate g.	Frac. I g.	Frac. II g.	Residue g.	Crystals g.
——	310～330	49.5	14.0	28.5	6.5	12.5
$MgCl_2 \cdot 6aq.$	300～310	55.0	19.5	28.0	7.0	23.5
$SnCl_2 \cdot 2aq.$	310～320	53.0	18.0	27.5	7.0	22.0
$FeCl_2 \cdot 4aq.$	310～320	53.5	18.5	27.5	7.5	23.0
$CoCl_2 \cdot 6aq.$	320～330	50.0	17.5	25.0	7.0	15.5
$MnCl_2 \cdot 4aq.$	300～310	51.0	19.5	26.0	3.0	19.0
Mg powder	290～300	40.0	19.0	16.5	3.5	9.0
MgO	300～310	44.0	25.0	11.0	6.5	7.0
$MgCO_3$	300～310	45.5	24.0	14.0	4.0	7.5
$PbCl_2$	310～320	36.0	16.0	16.5	3.0	12.0
$ZnCl_2$	310～320	55.0	26.0	24.0	4.5	19.0

lactone was also isolated from the lower-boiling by-products. Stoll and Rouve[4] early obtained the dimeric lactone by treating ω-hydroxyheptanoic acid in a large amount of benzene (the dilution method).

Practical methods for the preparation of δ-valerolactone from δ-chlorovaleric acid were investigated on the basis of the kinetic studies.

Experimental

The Hydrolysis of ω-Chlorocarboxylic Acids.—Sample solutions were prepared by neutralizing δ-chlorovaleric and ω-chloroheptanoic acids with a dilute aqueous solution of sodium hydroxide, using phenolphthalein as an indicator, while stirring and cooling the solutions with ice-water. The fresh solution was diluted to a given concentration and immediately subjected to the reaction in a thermostat. In the case of ω-chloroheptanoic acid, the reaction was carried out in a sealed ampoule. As the reaction proceeded, a portion of the solution was taken up and titrated with a standard solution of silver nitrate.

The Preparation of δ-Valerolactone.—1) A mixture of δ-chlorovaleric acid (136.5 g.) and an equivalent aqueous sodium hydroxide was heated while evaporating water with an aspirator. After the removal of the water, the residue was distilled under reduced pressure to afford δ-valerolactone; yield 92.0 g. (92%). Repeated distillation gave an analytically pure sample of δ-valerolactone; b. p. 75～76°C/3 mmHg, n_D^{25} 1.4555, d_4^{20} 1.0988 (lit. b. p. 88°C/4 mmHg, n_D^{20} 1.4600, 1.4503, d_4^{20} 1.0794, 1.094). The above sample was easily polymerized in the presence of acid catalysts. Its infrared spectrum shows, at 1725 cm^{-1}, a strong absorption band attributable to C=O stretching in lactone. 2) An aqueous solution (400 ml.) of sodium δ-chlorovalerate (1.0 mol.) was refluxed for 2 hr. After it had been cooled, the reaction mixture was extracted three times with benzene. The extract was distilled under reduced pressure to give δ-valerolactone; yield 92.5 g. (92.5%).

4) M. Stoll and A. Rouve, *Helv. Chim. Acta*, **18**, 1087 (1935).

The Thermal Decomposition of a Polyester-Sodium Chloride Mixture.—A solid mixture of the polyester and sodium chloride was prepared by evaporating water from the aqueous solution of sodium ω-chloroheptanoate. The mixture was decomposed by heating it with a niter-bath above 300°C under reduced pressure (1 mmHg) in the presence of various catalysts. By the repeated distillation of the decomposition product, two fractions were obtained: fraction I, b. p. 45～70°C/1 mmHg; fraction II, b. p. 115～130°C/1 mmHg. White crystals were precipitated by cooling the methanol solution of the fraction II with dry ice-methanol. Recrystallization from methanol afforded the dimeric lactone of ω-hydroxyheptanoic acid; m. p. 46°C (lit.[4] m. p. 41°C).

Found: C, 65.77; H, 9.37. Calcd. for $C_{14}H_{24}O_4$: C, 65.59; H, 9.44%.

This 16-membered dimeric lactone has a fairly strong musk odor. Its infrared spectrum indicates the characteristic absorption band at 1725 cm^{-1} due to the lactonic carbonyl. From these results, the crystalline product was proved to be the dimeric lactone of ω-hydroxyheptanoic acid.

The fractional distillation of fraction I afforded a liquid; b. p. 96～98°C/10 mmHg, n_D^{20} 1.4520. This was treated with potassium permanganate in an aqueous alkaline solution. The manganese dioxide produced was filtered out. From the ether extract of the filtrate, a crystalline product identified with pimelic acid (m. p. 103～104°C) was obtained.

The infrared spectrum of this fraction is similar to that of the dimeric lactone and shows the characteristic band at 1720 cm^{-1} due to the lactonic carbonyl. The above sample, after being allowed to stand for a few days, was converted into a polymer which was identified analytically with the polyester from ω-hydroxyheptanoic acid. These results indicate this fraction to be the monomeric lactone of ω-hydroxyheptanoic acid. Details of the reaction are shown in Table I.

The Thermal Decomposition of the Polyester.—A mixture of ω-chloroheptanoic acid (329 g.), potassium acetate (300 g.) and glacial acetic acid (400 ml.) was refluxed for 16 hr. The reaction mixture was then diluted with water and extracted with benzene. After being washed several times with water, the ether extract was distilled

Table II. The thermal decomposition of the polyester
Polyester, 64 g. Catalyst, 1.0 g.

Catalyst	Temp.(bath) °C	Distillate g.	Frac. I g.	Frac. II g.	Residue g.	Crystals g.
$MgCl_2 \cdot 6aq.$	300~310	38.5	10.0	22.0	6.0	12.5
$SnCl_2 \cdot 2aq.$	310~320	24.5	9.5	12.0	3.0	7.0
MgO	300~310	35.0	20.5	9.5	4.0	4.5

Table III. Rate constants (min^{-1}) in the hydrolysis of δ-chlorovaleric acid
A=1.0 mol./l.

Time	Temp., 50°C		Temp., 55°C		Temp., 60°C		Temp., 65°C	
min	conv. %	$k \cdot 10^2$	conv. %	$k \cdot 10^2$	conv. %	$k \cdot 10^2$	conv. %	$k \cdot 10^2$
10	—	—	—	—	24.3	2.87	34.1	4.30
15	13.6	0.99	—	—	—	—	52.6	4.96
20	18.5	1.02	30.8	1.84	49.0	3.37	62.0	4.83
25	—	—	—	—	—	—	67.6	4.51
30	27.8	1.09	42.6	1.85	62.7	3.29	74.9	4.61
40	36.0	1.12	53.3	1.90	70.2	3.03	—	—
50	42.9	1.12	61.2	1.89	75.6	2.84	—	—
60	49.0	1.12	66.2	1.80	—	—	—	—
70	54.9	1.14	—	—	—	—	—	—
(average)*		(1.12)		(1.86)		(3.06)		(4.67)

* In calculating the average values we neglected those in the initial stage of the reaction.

Table IV. Rate constants (min^{-1}) in the hydrolysis of ω-chloroheptanoic acid
A=1.0 mol./l.

Time	Temp., 90°C		Temp., 95°C		Temp., 100°C		Temp., 105°C	
min.	conv. %	$k \cdot 10^2$	conv. %	$k \cdot 10^2$	conv. %	$k \cdot 10^2$	conv. %	$k \cdot 10^2$
30	12.5	0.441	—	—	23.3	0.888	31.7	1.20
60	21.0	0.393	28.9	0.568	34.1	0.698	47.1	1.06
90	28.2	0.369	37.2	0.518	43.0	0.623	57.7	0.954
120	33.0	0.337	44.3	0.490	52.1	0.614	64.5	0.863
150	37.4	0.312	49.3	0.457	—	—	70.6	0.817
180	41.7	0.300	53.7	0.428	—	—	—	—
(average)		(0.359)		(0.490)		(0.706)		(0.979)

under reduced pressure to give ω-acetoxyheptanoic acid (b. p. 147~150°C/1 mmHg, n_D^{20} 1.4430). The product (335 g.) was saponified with a small excess of sodium hydroxide in an aqueous methanol solution. The solution was acidified with hydrochloric acid and extracted with ether. The polyester of ω-hydroxyheptanoic acid was prepared by evaporating ether from the extract and by heating the residue a further 3 hr. under reduced pressure (about 3 mmHg). The polyester was decomposed as in the previous experiments. The results are given in Table II.

Results and Discussion

The Hydrolysis of ω-Chlorocarboxylic Acids. —The rate of hydrolysis was expressed by the following first-order equation:

$$dx/dt = k(A-x)$$

where A represents the initial concentration of the reactant, and x denotes the concentration of sodium chloride produced. The results are summarized in Tables III and IV.

In Table III, the rate constants at each temperature are calculated with a good constancy except for those at the beginning of the reaction. In the case of ω-chloroheptanoic acid, however, the rate constants tend to decrease as the reaction proceeds. Since the reaction product is in an equilibrium between δ-hydroxyvaleric acid and δ-valerolactone, a large change in pH valne, which is considered to affect the reaction rate, is prevented in the course of the reaction. On the other hand, the reaction solution of ω-chloroheptanoic acid becomes weakly acidic as the reaction proceeds.

The decrease in pH during the reaction, at any rate, is rather small, for the reaction system is a buffer solution. Therefore, the average values were employed for the calculation of rate constants.

The relation between the temperature and

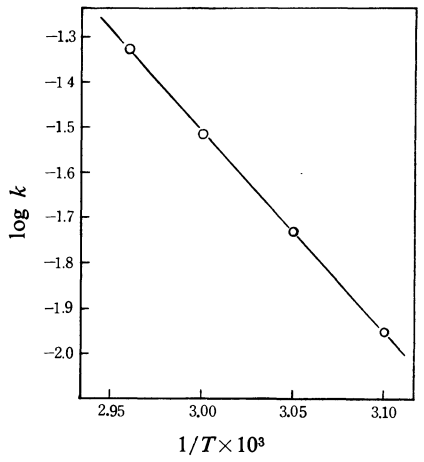


Fig. 1. Arrhenius plot for the hydrolysis of δ-chlorovaleric acid.
E=19900 cal./mol.

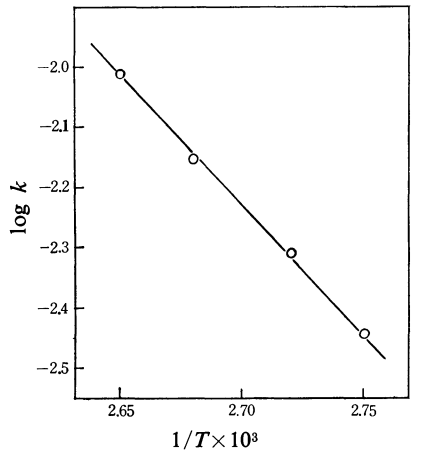


Fig. 2. Arrhenius plot for the hydrolysis of ω-chloroheptanoic acid.
E=19700 cal./mol.

the rate constants is plotted in Figs. 1 and 2.

The energies and entropies of the activation in these reactions are calculated as: E=19900 cal./mol., $\Delta S^{\neq}=-14$ e.u. (δ-chlorovaleric acid); and E=19700 cal./mol., $\Delta S^{\neq}=-24$ e. u. (ω-chloroheptanoic acid). The rate equations are expressed as follows:

for δ-chlorovaleric acid:

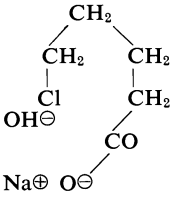
$$dx/dt=3.5\cdot10^{11}\cdot e^{-19900/RT}(A-x)$$
$$(\text{mol. } l^{-1}\text{min}^{-1})$$

for ω-chloroheptanoic acid:

$$dx/dt=2.6\cdot10^{9}\cdot e^{-19700/RT}(A-x)$$
$$(\text{mol. } l^{-1}\text{min}^{-1})$$

While an equal value is obtained for the activation energies in these two reactions, a large difference is obterved between the activation entropies.

These facts suggest that the chlorine atom in δ-chlorovaleric acid is far more accessible to hydroxyl ions than that in ω-chloroheptanoic acid. The chlorine atom at the δ-position is considered to be located close to the ion-pair (−COO⊖ Na⊕), which accelerates the hydrolysis as below:



The large difference between the activation entropies in these reactions may be realized by the above explanation.

Summary

1) The kinetics of the hydrolysis of δ-chlorovaleric and of ω-chloroheptanoic acids in an aqueous solution of their sodium salts has been studied. The reason for the difference between the activation entropies has been discussed.

2) The methods for the preparation of δ-valerolactone from δ-chlorovaleric acid have been established.

3) By the thermal decomposition of the polyester from ω-hydroxyheptanoic acid, the dimeric lactone of the acid has been prepared, and the formation of the monomeric lactone has also been ascertained.

Technical Research Laboratory
Asahi Chemical Industry Co., Ltd.
Itabashi-ku, Tokyo

The Bromination of Aromatic Compounds with a Mixture of Peroxyacetic Acid and Bromine in Acetic Acid

By Yoshiro OGATA, Yoshiaki FURUYA and Kenji OKANO

(Received February 8, 1964)

It is well known that the bromination of aromatic compounds with molecular bromine is catalyzed by some electrophilic reagents such as ferric bromide and that, without these catalysts, the bromination of benzene is very slow. In the course of our study of some reactions using peroxycarboxylic acid, we discovered that peroxyacetic acid could accelerate the bromination of benzene. Although the yield of bromobenzene was not high (56%), the probable mechanism and attacking species of this reaction is of interest since the reaction mixture constitutes a homogeneous system suitable for a kinetic study. Thus far there have seemed to be two mechanisms for the bromination of aromatics; i. e., one is the rate-determining abstraction of bromide ions from the π-complex between an aromatic molecule and a bromine molecule, followed by the rapid elimination of the proton to give brominated aromatics;[1] the other is an attack of the bromonium ions formed from bromine and the electrophilic reagent on aromatics.[2] The present paper summarizes our data on the mechanism of bromination by a mixture of peroxyacetic acid and bromine in acetic acid. The data suggest a mechanism which involves the intermediary formation of acetyl hypobromite, CH_3COOBr. The mechanism was studied kinetically and, in addition, by the spectrophotometric detection of acetyl hypobromite.

Experimental

Materials.—Peroxyacetic acid was prepared by the reaction of acetic anhydride with hydrogen peroxide[3] and was stored as an acetic acid solution. Acetyl peroxide was prepared by dropping water into a suspension of sodium peroxide in an ethereal solution of acetic anhydride;[4] the ether was evaporated after the addition of acetic acid to prepare an acetic acid solution of acetyl peroxide for safe storage. Aqueous hypobromous acid was prepared by the addition of aqueous bromine to a suspension of an excess of mercuric oxide in water.[5] Acetyl hypobromite[7] was prepared by mixing an acetic acid solution of bromine and a suspension of silver acetate in acetic acid.

The Preparation of Bromobenzene.—An acetic acid solution of peroxyacetic acid was added slowly to a solution containing acetic acid, bromine and benzene. Aqueous sodium hydroxide was added to the resulting solution to remove unreacted bromine; the benzene layer was washed with water, dried and then distilled, yielding bromobenzene (b. p. 156~157°C). The trace of α-benzene hexabromide which was identified in the product is probably formed by the photochemical reaction. The results, including those of the other brominations, are shown in Table I. The yields were calculated on the basis of the original bromine.

Reaction Products Criterion.—Bromobenzene (b. p. 156~157°C) was identified by gas chromatography in comparison with an authentic sample. *p*-Chlorobromobenzene and *p*-dibromobenzene were identified by mixed melting point determinations with authentic samples; m. p. and mixture m. p., 66°C and 84°C, respectively. α-Benzene hexabromide was identified by a mixed m. p. determination (m. p. and mixture m. p. 214°C), together with a comparison of its infrared spectrum with that of an authentic sample prepared by the photochemical bromination of benzene.

A Typical Procedure for the Rate Measurements.—An acetic acid solution containing known amounts of benzene, peroxyacetic acid and sulfuric acid was brought to the constant temperature of 60°C. A known amount of an acetic acid solution of bromine was then added to the solution to start the reaction. Aliquots (each 5 ml.) were pipetted out at regular intervals and poured into ice-cooled aqueous 0.04 M phenol (50 ml.) to remove the bromine. After a few minutes, 5% aqueous potassium iodide (5 ml.) was added. The iodine liberated by peroxyacetic acid was titrated with 0.005 N aqueous sodium thiosulfate.

It was preliminarily confirmed that no appreciable reaction occurred between phenol and peroxyacetic acid under these conditions. The concentration of peroxyacetic acid was corrected by a blank test which estimated the extent of the decomposition of peroxyacetic acid alone (3~4% at 60°C for 100 min.).

1) R. M. Keefer and L. J. Andrews, *J. Am. Chem. Soc.*, **78**, 255, 4549 (1956).
2) P. B. D. de la Mare and J. T. Harvey., *J. Chem. Soc.*, **1956**, 36; **1957**, 131; **1957** 923.
3) M. W. C. Smit, *Rec. trav. chim.*, **49**, 674 (1930).
4) J. R. Slagle and H. J. Shine, *J. Org. Chem.*, **24**, 107 (1959).
5) M. Christen and Hch. Zollinger, *Helv. Chim. Acta*, **45**, 2057 (1962).

Results and Discussion

Synthetic Experiments.—The results on the synthetic bromination of benzene are shown in Table I. The data show that the addition of a small quantity of sulfuric acid increases the yield of bromobenzene, and that the reaction is an electrophilic substitution. The formation of a small amount of α-benzene hexabromide suggests a radical attack in part; its formation is not due to the presence of diacetyl peroxide,[6] because no hexabromide was formed upon the addition of acetyl peroxide to the corresponding benzene solution of bromine.

TABLE I. BROMINATION OF SUBSTITUTED BENZENES

Molar ratio, $C_6H_5X : Br_2 : CH_3CO_3H = 1.28 : 0.11 : 0.27$
Reaction temp., 80~85°C
Reaction time, 2.5~4 hr.

Substituted group of C_6H_5X	Product	Yield, %
H	C_6H_5Br	31.1
	α-Benzene hexabromide	a small amount
$H(H_2SO_4)$[a]	C_6H_5Br	56.0
H[b]	C_6H_5Br	18.5
Cl	p-Cl-C_6H_4-Br	5.0
Br	p-Br-C_6H_4-Br	7.6
NO_2	—	0.0
CN	—	0.0

Molar ratio are as follows:
a) $C_6H_6 : Br_2 : CH_3CO_3H : H_2SO_4 : CH_3CO_2H = 1.0 : 0.1 : 0.14 : 0.135 : 0.5$
b) $C_6H_6 : Br_2 : CH_3CO_3H : CH_3CO_2H = 1.0 : 0.1 : 0.14 : 1.0$

Kinetics.—The rate data are shown in Table II. The table indicates that the rate is expressed as

$$-d[CH_3CO_3H]/dt = k_2[CH_3CO_3H][Br_2] \quad (1)$$

where k_2 is independent of the concentration of benzene and also independent of the acidity of the solution. Hence, the rate-determining step is the reaction of bromine and peroxyacetic acid to form reactive species which can react rapidly with benzene. It is known that bromine reacts with some oxidizing agents, e. g., mercuric oxide, to give bromine monoxide Br_2O, which may be formed in this reaction, but it should react rapidly with acetic acid or water to form acetyl hypobromite or hypobromous acid as follows:

$$CH_3CO_3H + Br_2 \overset{\text{slow}}{\rightleftarrows} CH_3CO_2H + Br_2O \quad (2)$$

$$Br_2O + H_2O \overset{\text{fast}}{\rightleftarrows} 2HOBr \quad (3)$$

$$CH_3CO_2H + HOBr \overset{\text{fast}}{\rightleftarrows} CH_3CO_2Br + H_2O \quad (4)$$

or

$$2CH_3CO_2H + Br_2O \rightleftarrows 2CH_3CO_2Br + H_2O \quad (5)$$

The rate-determining formation of bromine monoxide, followed by the rapid attack of acetyl hypobromite on benzene, was supported by the determination of the rate of the bromination of benzene with authentic acetyl hypobromite; i. e., the second-order rate constant was 3.20×10^{-2} M^{-1} sec^{-1} at 60°C, which was ca. 20 times as high as the rate constant of bromination with a mixture of bromine and peroxyacetic acid.

A Discussion of Active Attacking Species.—The ultraviolet spectrum of bromine showed a maximum at 266 mμ both in water (Fig. 1, curve 4) and in anhydrous acetic acid (curve 2), but neither an aqueous hypobromous acid solution (curve 5) nor an acetic acid solution of acetyl hypobromite (curve 3) showed a maximum at a wavelength longer than 250 mμ. The apparent maxima at ca. 243 mμ (curves 3 and 6 in Fig. 1) were found to be caused by the high absorption and, hence, too wide a slit width, which prevented scanning of the spectrophotometer, because the maxima shifted by changing the thickness of the layer for measurements and the maximum disappeared in a pure ethereal solution of acetyl hypobromite (curve 7). Hence, the maximum at 324 mμ for acetyl hypobromite reported by by Anber and Dostrovsky[7] is doubtful.

The molar extinction coefficient at 250 mμ for acetyl hypobromite is higher than that of hypobromous acid (curves 3 and 6 in Fig. 1); the extinction for acetyl hypobromite is comparatively stable, but that for hypobromous acid is decreased rapidly by the decomposition of the acid.

The addition of peroxyacetic acid to an acetic acid solution of bromine gave rise to an increase in extinction corresponding to that of acetyl hypobromite, the extinction being increased as the reaction proceeded.

The addition of water to an acetic acid solution of acetyl hypobromite results in a decrease in the extinction at 250 mμ (Figs. 1 and 2) and also in the appearance of a maximum at 266 mμ (bromine). These phenomena indicate the hydrolysis of acetyl hypobromite

6) Y. Ogata, Y. Furuya, J. Maekawa and K. Okano, *J. Am. Chem. Soc.*, **85**, 961 (1963).

7) M. Anber and J. Dostrovsky, *J. Chem. Soc.*, **1954**, 1105; Cf. P. B. D. de la Mare, I. C. Hilton and C. A. Vernon, ibid., **1960**, 4039.

TABLE II. THE RATE DATA FOR THE CONSUMPTION OF PEROXYACETIC ACID WITH A MIXTURE OF BROMINE AND PEROXYACETIC ACID AT 60°C

Catalyst: Sulfuric acid

$[CH_3CO_3H]$ M	$[Br_2]$ M	$[C_6H_6]$ M	$[H_2SO_4]$ M	H_0[a)]	$k_2\times10^3$ $M^{-1}\,sec^{-1}$
0.0113	0.0118	0.05	0	—	1.55
0.0241	0.0114	0.05	0	—	1.66
0.0091	0.0056	—	0.036	−1.13	1.60
0.0188	0.0056	0.05	0.036	−1.13	1.64
0.0093	0.0056	0.05	0.036	−1.13	1.66
0.0123	0.0056	0.05	0.063	−1.39	1.64
0.0115	0.0056	0.05	0.117	−1.68	1.44
0.0114	0.0056	—	0.117	−1.68	1.43

a) N. F. Hall and W. F. Spengeman, *J. Am. Chem. Soc.*, **62**, 2487 (1940).

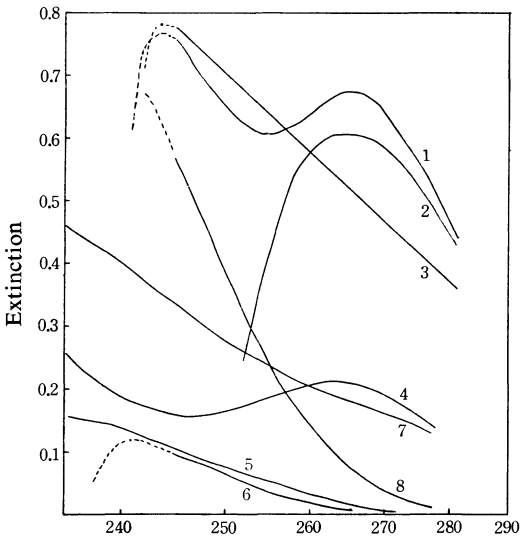


Fig. 1. Ultraviolet spectra of probable attacking species in the bromination of aromatic compounds.[a,b)]

(1) An acetic acid solution of 5.04×10^{-3} M bromine containing 0.18% water
(2) An anhydrous acetic acid solution of 2.00×10^{-2} M bromine
(3) An acetic acid solution of 8.43×10^{-3} M acetyl hypobromite
(4) An aqueous solution of 4.82×10^{-3} M bromine
(5) An aqueous solution of 1.36×10^{-3} M hypobromous acid
(6) An aqueous acetic acid solution of 1.36×10^{-3} M hypobromous acid
(7) An ethereal solution of 3.6×10^{-4} M acetyl hypobromite
(8) An aqueous (0.18% water) acetic acid solution of a mixture of 6.23×10^{-2} M bromine and a slight excess of peroxyacetic acid

a) The thickness of layer: 2 mm. for 1—6, 10 mm. for 7 and 1 mm. for 8
b) All experiments were done by using corresponding solution as reference.

to hypobromous acid, followed by its rapid decomposition to give bromine. Moreover, the presence of a small percentage of water in an acetic acid solution of bromine gave the extinction corresponding to acetyl hypobromite (compare curves 1 and 2 in Fig. 1). Therefore, the following equilibria are probable:

$$Br_2O + H_2O \rightleftarrows 2HOBr$$

$$CH_3CO_2H + HOBr \rightleftarrows CH_3CO_2Br + H_2O$$

It is well known that bromine monoxide, Br_2O, or hypobromous acid readily decomposes to evolve oxygen and bromine; this must be the main cause of the poor yield of bromobenzene in the present reaction.

$$4HOBr \rightleftarrows O_2 + 2H_2O + 2Br_2$$

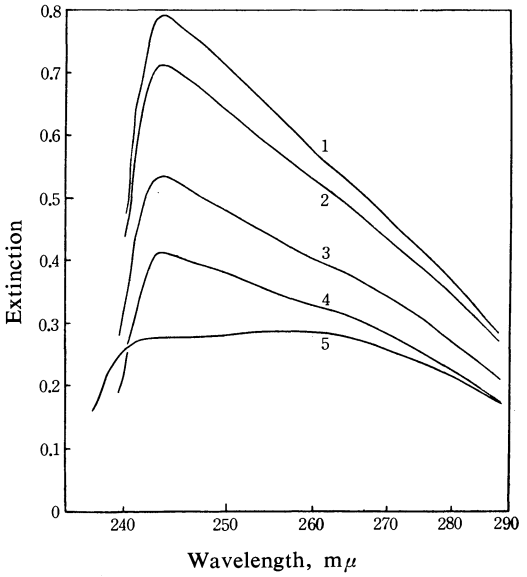
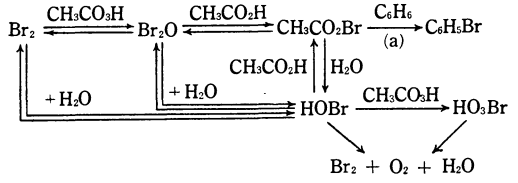


Fig. 2. Effect of the water content on the decomposition of 8.43×10^{-3} M acetyl hypobromite in acetic acid at 20°C.

Contents of water (%), (1) 0.18%; (2) 1.18; (3) 5.18; (4) 10.18; (5) 50.18

It was confirmed by gas chromatography (column, molecular sieve, 13X, 80~100 mesh, column temp., 32.5°C; carrier gas, helium 30 ml. min^{-1}) that a mixture of peroxyacetic acid and bromine in acetic acid evolved oxygen. Simultaneously, the mixture liberated bromine which could be titrated with 0.01 N sodium thiosulfate. In this reaction using both reactants in 0.04 M, the titer of peroxyacetic acid decreased to ca. 1/2 after 8 hr. at 50°C, while that of bromine held constant.

Over-all Mechanism. — These findings suggest the following mechanism for the over-all reaction:



A comparison of the electrophilicity of hypobromous acid with that of acetyl hypobromite strongly suggests that acetyl hypobromite, which has the electron-attracting carbonyl group, should be more powerful and a more probable agent for the electrophilic attack on the benzene ring.

The formation of acetyl hypobromite is slower than its reaction with benzene and is little influenced by the acidity of the solution. However, the addition of sulfuric acid to the reaction mixture appreciably increased the yield of bromobenzene (Table I), which implies that the bromination of benzene (step a) is done by protonated acetyl hypobromite.

Summary

Bromobenzene is obtained in a 56% yield when an acetic acid solution of peroxyacetic acid is slowly added to an acetic acid solution of bromine, benzene and a catalytic amount of sulfuric acid. The rate of the consumption of peroxyacetic acid has been expressed as $v=k_2[CH_3CO_3H][Br_2]$, where k_2 is independent of the concentration of benzene and of the acidity of solution. However, the rate of the formation of bromobenzene is accelerated by sulfuric acid and a more effective use of the attacking species is possible. A mechanism has been suggested which involves the rate-determining formation of bromine monoxide or acetyl hypobromite, followed by its rapid attack on benzene. The rate is slower with benzene substituted with electron-attracting groups. Some evidence for the formation of acetyl hypobromite has been obtained by ultraviolet spectrophotometry.

Department of Applied Chemistry
Faculty of Engineering
Nagoya University
Chikusa-ku, Nagoya

Long-range Proton Spin-Spin Interactions in Ketones. II. The Substitution Effect*

By Kensuke TAKAHASHI

(Received February 11, 1964)

A previous communication[1] has reported that multiplet structures have been observed in the spectra of the methyl group adjacent to the carbonyl group in ethyl methyl ketone and isopropyl methyl ketone. A similar multiplet structure was observed also in the $^{13}CH_3$ satellites of acetone by Holmes and Kivelson.[2] The aim of the present article is to get more extensive data to aid in understanding the mechanism of the long-range proton spin-spin interactions through the carbonyl groups in these ketones. In this paper we should like to present our experimental results and to discuss the substitution effect on such a long-range coupling in some substituted acetones. Some studies related to this problem have been

* Presented at the Symposium on Molecular Structure of the Chemical Society of Japan, Sendai, October, 1963. This is part II in the series (see Ref. 1 and Ref. 14 for parts I and III).

1) K. Takahashi, This Bulletin, **35**, 1046 (1962).

2) J. R. Holmes and D. Kivelson, *J. Am. Chem. Soc.*, **83**, 2959 (1961).

TABLE I. PMR DATA FOR THE SUBSTITUTED ACETONE IN A 5 MOL. % CARBON TETRACHLORIDE SOLUTION, AT 60 Mc. p. s.

No.	Compound	Coupling c. p. s.	Chemical shift, p. p. m.*1		
			CH_3CO	CH_2XCO	CHX_2CO
1	CH_3COCH_3	0.57±0.03*2	2.09	—	—
2	$CH_3COCH_2CH_3$	0.48±0.05*2	2.05_5	2.38	—
3	$CH_3COCH(CH_3)_2$	0.45±0.05*2	2.06	—	2.40
4	$CH_3COC(CH_3)_3$		2.05	—	—
5	$CH_3COCH_2CH_2COCH_3$	~0.2	2.12_5	2.59	—
6	$CH_3COCH_2COCH_3$	0.45±0.05	2.16_5	3.46	—
7	$CH_3COCH_2COOC_2H_5$	0.42±0.03	2.20	3.29_5	—
8	$CH_3COCH_2SC_6H_5$	0.42±0.03	2.18_5	3.51_5	—
9	CH_3COCH_2Br	0.37±0.03	2.34	3.76	—
10	$CH_3COCHBr_2$	0.40±0.03	2.54_5	—	5.69_5
11	$CH_2BrCOCH_2Br$		—	4.09_5	—
12	CH_3COCH_2Cl	0.22±0.05	2.28	3.93_5	—
13	$CH_3COCHCl_2$	0.30±0.03	2.42_5	—	5.68_5
14	$CH_3COCH(OH)CH_3$	<0.2	2.15	—	4.12
15	$CH_3COCH=C(CH_3)_2$	*3	2.07	—	—
16	$CH_3COCH=CH_2$	<0.2	2.20_5	—	—
17	$CH_3COCH=CHC_6H_5$	<0.2	2.27_5	—	—

*1 Referred to TMS.
*2 The value in the pure liquid.
*3 Not clear because of overlapping.

reported recently by Sasaki,[3] Wittstruck[4] and van Meurs.[5] In 2, 3-dihalopropenes, the solvent-dependence of the long-range coupling constants and rotational isomerism have been reported by Whipple.[6]

Experimental

The wiggle beat method[7] for measuring these small couplings was used in addition to the steady-state method used in the previous report.[1] The compounds examined were commercially-available products except for dibromoacetone, chloroacetone and phenylmercapto-2-propanone. Dibromoacetone was measured in the mixture with monobromoacetone and other small amounts of by-products which had been prepared by the bromination of acetone. Measurements were carried out with 5 mol.% solutions in carbon tetrachloride, which had been degassed and which contained small amounts of tetramethylsilane (TMS) as an internal reference. Spectra were obtained at a temperature of 22.8± 0.5°C, and at a frequency of 60 Mc.p.s. on a Varian 4300B spectrometer. The sweep rate of the magnetic field for chemical shift measurements was calibrated by measuring the displacement between the two peaks for a benzene-cyclohexane mixture (1 : 1 by volume). The value for this displacement in the present work is taken to be 5.746 p.p.m.[8]

Results and Discussion

The results of the measured coupling constants are shown in Table I, along with the values previously reported in measurements for the pure liquid state. In this table <0.2 shows no evidence of coupling; ~0.2 does show some evidence of coupling, but it is too small to resolve. For convenience, the chemical shifts are also given in the same table in p. p. m. with reference to TMS. In the case where the signal is split by the indirect spin-spin interaction, the chemical shift given in Table I is that for the center of the multiplet structure. The magnitude of the long-range coupling in question, as shown in Table I, seems to decrease as the electronegativity of the substituent, such as methyl, bromine or chlorine, increases; that is, the more the electronegativity of the substituent, the less the coupling constant seems to become. In the case of acetoin (No. 14 in Table I), the hydroxy-substituted compound of ethyl

3) Y. Sasaki, paper presented at the 1st Symposium on High-resolution NMR of the Chemical Society of Japan, Tokyo, November, 1961; Y. Sasaki, Y. Kondo and G. Miyajima, paper presented at the 3rd Symposium on NMR of the Chemical Society of Japan, Osaka, November, 1963.
4) T. A. Wittstruck, private communication; T. A. Wittstruck, S. K. Malhotra, H. T. Ringold and A. D. Cross, *J. Am. Chem., Soc.*, **85**, 3038 (1963).
5) N. van Meurs, *Spectrochim. Acta*, **19**, 1695 (1963).
6) E. B. Whipple, *J. Chem. Phys.*, **35**, 1039 (1961).
7) J. J. Turner, *Mol. Phys.*, **3**, 417 (1960).
8) The author wishes to express his thanks to Dr. M. Matsuoka (the Institute for Solid State Physics, the University of Tokyo) for measuring this displacement by the usual side-band technique; it is 232.50±0.25 c.p.s. at 40.462 Mc.p.s. and 24.0±0.1°C.

methyl ketone, there is no evidence of the coupling in question via the carbonyl group. This shows quite a decrease in the coupling as compared with that of ethyl methyl ketone. On the other hand, the sulfur compound of No. 8 holds a coupling of about 0.4 c. p. s. Consequently, it can be assumed that the introduction of an electronegative substituent, such as a halogen or hydroxyl group, causes the decrease in the coupling constant under consideration.

However, a further examination of the compounds listed under No. 16 in Table I shows no clear evidence of coupling. In these ketones, the first atom in the substituent is carbon, so that it may, from the consideration described just before, be expected to have a coupling of about 0.4 c. p. s. Similar is the case of 2, 5-hexanedione, No. 5 in Table I. Moreover, in the cases of the disubstituted acetones, isopropyl methyl ketone shows some decrease in coupling constant as compared with ethyl methyl ketone, but dichloro- and dibromoacetone show some increase as compared with chloro- and bromoacetone respectively.

For the sake of a plausible explanation of these results, first of all, it will be supposed that the internal rotation about the carbon-carbon bond in $CO-CHX_2$ may be more hindered than that in $CO-CH_2X$. The consideration of this kind of rotational hindrance brings the discussion to a consideration of the angular dependence of the long-range couplings in these ketones. Karplus[9] presented an approximate formula of the long-range coupling in some unsaturated hydrocarbons as follows:

$$A_{HH'}(\pi) = 2.1 \times 10^{-15} \sum (a_H \cdot a_{H'} / \Delta\pi)$$

where $\Delta\pi$ is the average singlet-triplet excitation energy in eV., and a_H is the hyperfine constant for a π-electron radical fragment in c. p. s. in ESR spectra. Holmes and Kivelson[2] have also shown an expression similar to the coupling observed in acetone, assuming the $CH_3-\dot{C}-\dot{O}$ triplet. The hyperfine constant a_H in radicals of the $CH_3-\dot{C}$ type has been found, both experimentally[10] and theoretically[11], to be positive and of the form:

$$a_H = A_0 + A_1 \cos^2\varphi$$

where φ is the dihedral angle between the H–C–$\dot{C}$ plane and the axis of the unpaired π-electron. The ESR data show us that A_0 is negligible as compared with A_1, so that it may be assumed to be $a_H \propto \cos^2\varphi$. This comes to $a_H = 0$ at $\varphi = 90°$. The absence of the coupling in the compounds of Nos. 16 and 17 prompts us to regard this assumption as reasonable. In these ketones, Nos. 16 and 17, if the conjugation between C=O and C=C bonds is supposed, φ will be nearly 90° and a_H will be approximately zero in ageement with the experimental results.

To predict the long-range coupling in ketones, depending upon the dihedral angle assumed above, it is necessary to average $a_H(\varphi)$ for all possible conformations, weighted with respect to the potential barrier hindering internal rotation. If such a barrier is significantly greater than RT, it is sufficient only to sum up the couplings for the conformation of some considerable rotational isomers. In each ketone, the NMR spectrum of the methylene or the methyl protons shows no differently-oriented conformations, only a single peak as a mean in the measurement at room temperature.

Now we will consider two extreme cases; the one is free rotation, and the other is a fixed conformation about the CO–CH bond as an axis. In each case, the factor $(\cos^2\varphi)$ of the long-range coupling in question, depending on the dihedral angle stated above, is shown in Table

Table II. $\cos^2\varphi$

No. of protons	3	2	1
Free rotation	1/2	1/2	1/2
Fixed conformation ($\varphi = 0 \sim 2\pi$)	1/2	1/4~3/4	0~1

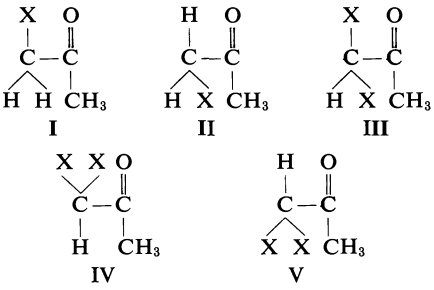
II. In the case of the protons in CH_2 or CH_3, we took the average between the factors of two or three protons respectively. If we want to include some substituted acetones, the combination of two proton groups must be considered, as is shown in Table III. If any other constants remain approximately constant, the factor depending on the dihedral angle must play a significant role in the coupling. The variation of this factor appears rather large in the cases concerned with a smaller number of protons, such as the methine-methine system. The magnitude of the coupling observed in acetone is about 0.5 c. p. s., and if the methyl group in acetone is assumed to rotate freely around the CO–CH axis, the factor must be taken to be 1/4. Therefore, under these conditions, a coupling of about 2 c. p. s. may be observed in some cases. Further studies of some other ketones, such as cyclic ketones with limited conformations, would be of interest.

9) M. Karplus, *J. Chem. Phys.*, **33**, 1842 (1962).
10) C. Heller and H. M. McConnell, ibid., **32**, 1535 (1960); D. Pooley and D. H. Whiffen, *Mol. Phys.*, **4**, 81 (1961).
11) A. D. McLachlan, ibid., **1**, 233 (1958); W. Derbyshire, ibid., **5**, 225 (1962).

TABLE III. $\cos^2\varphi$

No. of protons	Combination of rotation				Range of variation
	Free-Free	Free-Fix	Fix-Free	Fix-Fix	
3-3	1/4	1/4	1/4	1/4	1/4
3-2	1/4	1/8～3/8	1/4	1/8～3/8	1/8～3/8
3-1	1/4	0～1/2	1/4	0～1/2	0～1/2
2-2	1/4	1/8～3/8	1/8～3/8	1/16～9/16	1/16～9/16
2-1	1/4	0～1/2	1/8～3/8	0～3/4	0～3/4
1-1	1/4	0～1/2	0～1/2	0～1	0～1

In chloroacetone, Mizushima[12] and Bellamy[13] suggested two rotational isomers, I and II, on the basis of their infrared and dipole moment studies. The carbonyl-stretching frequencies of this compound were observed at 1752 and 1726 cm^{-1} in a carbon tetrachloride solution,[13] corresponding to the two rotational isomers, the cis-form (I) and the trans-form (II) with respect to the Cl-atom and the CO group respectively. The former is more polar than the latter, so that a very marked change in the relative intensities of these bands was observed on passing from the solution in carbon tetrachloride to that in acetonitrile.[13] Similar is the case with dichloroacetone, as is shown in III, IV and V. In theses cases, the hyprefine constants,



which are considered to depend upon the dihedral angle, φ, in question, are as follows:

$$\bar{a}\,(\mathrm{Cl}) \fallingdotseq P_{\mathrm{I}}a(30°) + P_{\mathrm{II}}[a(30°) + a(90°)]/2$$
$$\fallingdotseq (1+P_{\mathrm{I}})\ a(30°)/2$$
$$\bar{a}'(\mathrm{Cl_2}) \fallingdotseq P_{\mathrm{III}}a'(30°) + (P_{\mathrm{IV}}+P_{\mathrm{V}})a'(90°)$$
$$\fallingdotseq a'(30°)$$

where P_i is the population of the i isomer (i. e., $P_{\mathrm{I}}+P_{\mathrm{II}}=1$ for chloroacetone and $P_{\mathrm{III}} \fallingdotseq 1$ for dichloroacetone; P_{IV} and P_{V} are supposed to be negligible in view of the band intensities of the carbonyl-stretching frequencies). From the consideration of electronegativity described before, it is rather difficult to explain the decrease in the coupling in chloroacetone as compared with dichloroacetone. However, it is possible to explain the experimental results if we consider the contribution of some rotational isomers. Even in the case of $a(30°) > a'(30°)$, $\bar{a}(\mathrm{Cl})$ depends upon the population of P_{I} in a very limited sense; therefore, $\bar{a}(\mathrm{Cl}) < \bar{a}'(\mathrm{Cl_2})$ is possible under some conditions.

Now we do not know enough to come to a final conclusion, but it must be noted about the long-range coupling in some substituted acetones, CH_3COCH_2X or CH_3COCHX_2, that (1) the more electronegative X is, the less the constant becomes, and that (2) this coupling is dependent upon the dihedral angle between the C–H bond and the π-orbital of carbon atom in the carbonyl group. From this standpoint, it is of interest of investigate the solvent or temperature effects of these coupling constants. Only a few compounds have been examined briefly in pure liquid and in a carbon tetrachloride solution.[14] The coupling constants in chloroacetone and bromoacetone seem to decrease upon dilution with carbon tetrachloride. This supports the assumptions of the dependence of the coupling constant on the dihedral angle and of the presence of the rotational isomers in these haloketones. These points are now under investigation.

The author wishes to express his gratitude to Professors Genjiro Hazato and Tsuneo Ikenoue for their continuous encouragement and valuable discussion, and to Mr. Akio Hanabuchi for his help in measuring the spectra.

The Chemical Research Institute of Non-Aqueous Solutions
Tohoku University
Katahira-cho, Sendai

12) S. Mizushima, T. Shimanouchi, T. Miyazawa, I. Ichishima, K. Kuratani, I. Nakagawa and N. Shido, *J. Chem. Phys.*, **21**, 815 (1953).
13) L. J. Bellamy and R. L. Williams, *J. Chem. Soc.*, **1957**, 4394.
14) K. Takahashi, This Bulletin, **37**, 291 (1964).

Syntheses and Ultraviolet Spectra of Aromatic Azo Compounds. III. Methoxyazobenzene Derivatives

By Yujiro NOMURA, Hiroyuki ANZAI, Ryokichi TARAO and Kengo SHIOMI

(Received February 20, 1964)

In continuing our studies[1,2] of the synthesis of aromatic azo compounds by the reaction of diazonium salt with a Grignard compound, we wish in this paper to report on the synthesis of methoxyazobenzene derivatives.

Although several azobenzenes which have a methoxyl group at the ortho- or para-position with respect to the azo group are known, many other methoxyazobenzene derivatives have not hitherto been prepared.

Nine tolylazoanisoles (I—IX), six dimethoxyazobenzenes (X—XV), and six bromophenylazoanisoles (XVI—XXI) have been synthesized by the reactions of the zinc chloride double salts of diazonium chlorides with Grignard compounds following the procedure described in previous papers.[1,2] These azo compounds are listed in Table I, in which new compounds are asterisked. Although the yields of the azo compounds by this method were not always satisfactory, many of these azo compounds are also difficult to prepare by the method known hitherto.

The electronic absorption maxima of methoxyazobenzene derivatives are shown in Table II. It can be seen that the wavelengths of the *K*-bands of *m*-methoxyazobenzenes are shorter than those of the corresponding *o*- or *p*-isomers.

Experimental

2-(*o*-Tolylazo)anisole (I).—Following the procedure of a previous paper,[2] *o*-anisidine was diazotized and precipitated as the zinc chloride double salt by adding solid zinc chloride to the diazotized solution.

The suspension of 21.5 g. (0.09 mol.) of the dry powdered double salt in ether was vigorously stirred, and the ethereal solution of *o*-tolylmagnesium bromide prepared from 12 g. (0.07 mol.) of *o*-bromotoluene and the excess of magnesium was added slowly to it at the rate necessary to maintain reflux. After the mixture had been stirred for an additional 60 min. at room temperature, the deep red ether solution was separated by filtration with suction from the solid, which was then washed several times with ether. The ether filtrate and washings were combined and washed with dilute hydrochloric acid and then with water, dried over anhydrous sodium sulfate, and evaporated. The remaining crude azo compound (5.2 g.) was recrystallized twice from ethanol and then from petroleum ether (b. p. 40~60°C) to give orange crystals; m. p. 73.5~75°C; yield, 2.8 g. (18% theoretical based on *o*-bromotoluene).

2-(*p*-Tolylazo)anisole (III).—The brown red oil (2.6 g.) was obtained by the reaction of the zinc chloride double salt of *o*-methoxybenzenediazonium chloride (23.4 g., 0.098 mol.) with *p*-tolylmagnesium bromide (prepared from 0.07 mol. of *p*-bromotoluene). The oil was dissolved in petroleum ether (b. p. 40~60°C) and passed through a 40 cm. alumina column. The same solvent was employed as the eluent. Colorless crystals (0.1 g.) were isolated from the early fractions, which were identified as 4, 4'-dimethoxybiphenyl by melting point and mixed melting point determinations with an authentic sample. Deep red crystals (1.7 g., 11%) were obtained from the red elute; m. p. 56~57°C.

3-(*m*-Tolylazo)anisole (V).—The deep red oil (9.3 g.) was obtained by the reaction of the zinc chloride double salt of *m*-methoxybenzenediazonium chloride (23.9 g., 0.1 mol.) with *m*-tolylmagnesium bromide (prepared from 0.09 mol. of *m*-bromotoluene). The crude oil was extracted by petroleum ether (b. p. 40~60°C). The petroleum ether solution was evaporated and the remaining oil was distilled in vacuo to yield 4.1 g. (20%) of the azo compound (b. p. 168°C/6 mmHg), which could not be induced to crystallize.

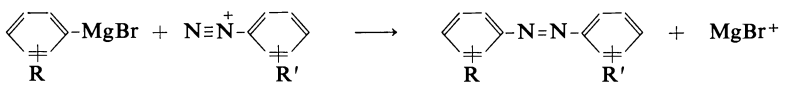
Summary

1) Nine tolylazoanisoles, six dimethoxyazobenzenes, and six bromophenylazoanisoles have been synthesized by the reactions of Grignard reagents with zinc chloride double salts of diazonium compounds; thirteen of them are new compounds.

2) The ultraviolet and visible absorption spectra of the methoxyazobenzene derivatives have been measured, and some regularities of the absorption maxima have been observed in them.

1) Y. Nomura, This Bulletin, **34**, 1648 (1961).
2) Y. Nomura and H. Anzai, ibid., **35**, 111 (1962).
3) R. C. Farmer and A. Hantzsch. *Ber.*, **32**, 3097 (1899).
4) H. Wieland, ibid., **48**, 1107 (1915).
5) B. M. Bogoslovskii, *J. Gen. Chem.*, **16**, 193 (1946); cf. *Chem. Abstr.*, **41**, 104*i* (1947).
6) Th. Rotarski, *Ber.*, **41**, 865 (1908).
7) K. Kinoshita, This Bulletin, **32**, 777 (1959).
8) Si-Jung Yeh and H. H. Jaffé, *J. Am. Chem. Soc.*, **81**, 3274 (1959).
9) G. M. Badger and R. G. Buttery, *J. Chem. Soc.*, **1954**, 2243.

TABLE I. METHOXYAZOBENZENES PREPARED BY THE REACTION:



No.	R	R′	[M. p.], (B. p.)[a]	Yield, %[b]	Color	Found: N, %[c]
I*	2-CH_3	2′-CH_3O	[73.5～75°C]	18	Orange	12.34
II*	3-CH_3	2′-CH_3O	(176°C/6 mmHg)	11	Deep red	12.37
III*	4-CH_3	2′-CH_3O	[56～57°C]	11	Orange	12.14
IV*	2-CH_3	3′-CH_3O	(160～165°C/7 mmHg)	29	Deep red	12.18
V*	3-CH_3	3′-CH_3O	(168°C/6 mmHg)	20	Deep red	12.44
VI*	4-CH_3	3′-CH_3O	[78～79°C]	14	Orange yellow	12.43
VII	2-CH_3	4′-CH_3O	(173°C/6 mmHg) [58～59°C][d]	8.9	Deep red	12.15
VIII*	3-CH_3	4′-CH_3O	(171°C/6 mmHg) [56～57°C]	4.0	Orange	12.16
IX	4-CH_3	4′-CH_3O	[109～110°C][e]	13	Orange yellow	12.18
X	2-CH_3O	2′-CH_3O	[143～144°C][f]	1.4	Orange	11.16
XI*	3-CH_3O	2′-CH_3O	167°C/6 mmHg]	11.3	Deep red	11.50
XII*	4-CH_3O	2′-CH_3O	(165～172°C/ 6.5 mmHg) [41～42°C]	7.3	Deep red	11.62
XIII	3-CH_3O	3′-CH_3O	[77～77.3°C][g]	7.6	Orange yellow	11.79
XIV*	3-CH_3O	4′-CH_3O	[41～42°C]	34	Orange yellow	11.39
XV	4-CH_3O	4′-CH_3O	[145～155°C][h]	6.9	Yellow	11.26
XVI*	2-CH_3O	3′-Br	[65～65.5°C]	8.8	Orange	9.50
XVII*	3-Br	3′-CH_3O	[86～87°C]	17.1	Yellow	9.76
XVIII	4-CH_3O	3′-Br	[59～60°C][i]	10.3	Orange red	9.60
XIX	2-CH_3O	4′-Br	[81.5～82.5°C][i]	2.0	Orange	9.45
XX*	3-CH_3O	4′-Br	[88.5～89.5°C]	0.9	Orange	9.58
XXI	4-CH_3O	4′-Br	[146～146.5°C][k]	14	Yellow	9.54

* New compound

a) M. p. and b. p. are uncorrected.

b) Based on the bromo compound used to prepared the Grignard reagent.

c) Calcd. % of N for tolylazoanisole $C_{14}H_{14}N_2O$ (I—IX) : 12.38.
Calcd. % of N for dimethoxyazobenzene $C_{14}H_{14}N_2O_2$ (X—XV) : 11.56.
Calcd. % of N for bromophenylazoanisole $C_{13}H_{11}BrN_2O$ (XVI—XXI) : 9.62.

d) The reported[3] m. p. of VII is 59°C; it was prepared by the condensation of *o*-nitrosotoluene with *p*-anisidine.

e) The reported[4] m. p. of IX is 110～111°C; it was prepared by the condensation of *p*-nitrosotoluene with *p*-anisidine.

f) The reported[5] m. p. of X is 153～153.5°C; it was prepared by the decomposition of *o*-methoxybenzenediazonium chloride in the presence of cuprous chloride.

g) The reported[6] m. p. of XIII is 76～77°C; it was synthesized by the reduction of *m*-azoxyanisole, which was prepared from *m*-nitroanisole.

h) The reported[7] m. p. of XV is 162～163°C; it was prepared by the air oxidation of *p*-anisidine in pyridine containing cuprous chloride.

i) The repored[8] m. p. of XVIII is 62～63°C; it was synthesized by the methylation of 4-(*m*-bromophenylazo)phenol, which was prepared by the coupling of *m*-bromobenzenediazonium chloride with phenol.

j) The reported[9] m. p. of XIX is 83°C; it was synthesized by heating the mixture of *o*-nitroanisole and *p*-bromoaniline with powdered sodium hydroxide.

k) The reported[8] m. p. of XXI is 148～149°C; it was prepared by the methylation of 4-(*p*-bromophenylazo)phenol.

TABLE II. ELECTRONIC ABSORPTION MAXIMA OF METHOXYAZOBENZENES IN ETHANOL

			K-band			
	λ, mμ	ε	λ, mμ	ε	λ, mμ	ε
I	238.5	8815	316.0	7382	435.0	1127
			352.0	7382		
II	236.3	9102	311.0	7837	435.0	1077
			353.0*	6920		
III	239.3	9852	320.0	9124	433.0	1355
			340.0*	8816		
			356.0	8559		
IV	237.0	10470	323.5	12360	440.0	773.7
V	236.0	11310	318.0	14390	435.5	782.4
VI	237.0	12180	325.6	16370	437.5	966.1
VII	239.0	11340	347.0	15470	402.5	1271
VIII	237.8	12650	344.6	20370	437.0	2009
IX	239.0	12120	346.0	21330	435.0	1428
X	243.5	8870	310.0	5059	445.0*	1537
			371.0	5497		
XI	241.5	9641	313.0	7370	430.0*	1151
			357.0	7126		
XII	242.0	11910	363.5	16600	435.0*	1943
XIII	242.9	11350	316.0	12530	436.0	881.2
XIV	243.0	13480	349.0	20260	434.0	1251
XV	241.0	12980	354.0	18370	430.0*	2160
	245.0*	12850				
XVI	238.0*	10230	315.0	9920	435.0*	1042
			363.0	8782		
XVII	237.7	11930	316.0	14660	436.0	794.7
XVIII	241.5	12780	350.0	18790	437.0	1277
XIX	239.0	9540	316.0	9700		
			364.0	8780		
XX	237.0	12200	323.0	17700	432.0	1180
XXI	241.0	6018	351.0	9511	438.0	1509
	245.5	5982				

* Wavelength of shoulder.

Department of Chemistry
College of General Education
The University of Tokyo
Meguro-ku, Tokyo

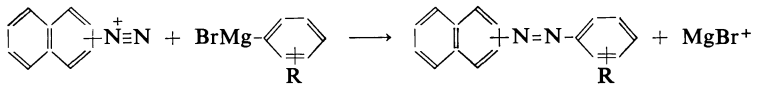
Syntheses and Ultraviolet Spectra of Aromatic Azo Compounds. IV. Naphthylazobenzene Derivatives

By Yujiro NOMURA and Hiroyuki ANZAI

(Received March 5, 1964)

In the previous papers[1-3] of this series it was shown that many azobenzene derivatives could be prepared conveniently by the reactions of the zinc chloride double salts of

TABLE I. NAPHTHYLAZOBENZENES PREPARED BY THE REACTION:



No.	Naphthyl	R	M. p., °C[a]	Yield, %[b]	Color	Found: N, %[c]
I	α-	H	66.5~67.5[d]	22	Red	12.00
II	β-	H	81.5~82.5[e]	11	Orange	11.76
III	α-	*o*-CH_3	67~68[f]	7	Red	11.00
IV*	β-	*o*-CH_3	70~71	12	Orange	11.24
V	α-	*m*-CH_3	42~43[g]	23	Red	11.13
VI*	β-	*m*-CH_3	98~99.5	6	Orange yellow	11.03
VII*	α-	*p*-CH_3	81~82	20	Red	11.17
VIII*	β-	*p*-CH_3	126~127	7	Orange yellow	11.20
IX*	α-	*o*-CH_3O	102~103	12	Red	10.92
X	β-	*o*-CH_3O	93~94.5[h]	11	Orange	10.88
XI*	α-	*m*-CH_3O	55~56	12	Orange red	10.92
XII*	β-	*m*-CH_3O	67~68	6.4	Orange yellow	10.40
XIII*	α-	*p*-CH_3O	73~74.5	9	Orange red	10.42
XIV*	β-	*p*-CH_3O	102~103	11	Orange	10.40
XV*	α-	*o*-Br	103~104	3.5	Orange red	9.11
XVI*	β-	*o*-Br	92.5~93	12	Orange yellow	9.08
XVII*	α-	*m*-Br	84~85	4.2	Red	8.95
XVIII*	β-	*m*-Br	117~118	12	Orange yellow	9.26
XIX*	α-	*p*-Br	132~133	11.4	Orange red	9.23
XX*	β-	*p*-Br	142.5~143	13	Orange red	8.85

* New compound

a) All temperatures in Tables I—III are uncorrected.

b) Based on the bromo compound used to prepare the Grignard reagent.

c) Calcd. % of N for naphthylazobenzene $C_{16}H_{12}N_2$ (I, II) : 12.06.
Calcd. % of N for naphthylazotoluene $C_{17}H_{14}N_2$ (III—VIII) : 11.29.
Calcd. % of N for naphthylazoanisole $C_{17}H_{14}N_2O$ (IX—XIV) : 10.68.
Calcd. % of N for naphthylazobromobenzene $C_{16}H_{11}BrN_2$ (XV—XX) : 9.00.

d) The reported m. p. of I is 63.5°C[4] or 70°C[5]. It was prepared by the deamination of 4-phenylazo-1-naphthylamine.

e) The reported[5] m. p. of II is 84°C. It was prepared by condensing nitrobenzene with β-naphthylamine in the presence of sodium hydroxide at 180°C.

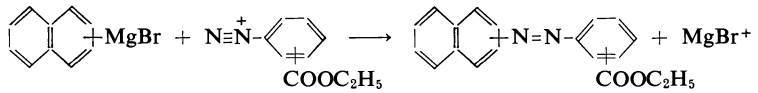
f) The reported[4] m. p. of III is 52°C. It was synthesized by the deamination of 4-(*o*-tolylazo)-1-naphthylamine, which had been prepared by the coupling of *o*-toluenediazonium chloride with α-naphthylamine.

g) The reported[6] m. p. of V is 43~44°C. It was prepared by the reaction of *N*-sulfinyl-α-naphthylamine with *m*-tolylhydroxylamine.

h) The reported[7] m. p. of X is 92.5°C. It was prepared by condensing *o*-nitroanisole with β-naphthylamine in the presence of sodium hydroxide at 170~180°C.

1) Part III: Y. Nomura, H. Anzai, R. Tarao and K. Shiomi, This Bulletin, **37**, 967 (1964).
2) Y. Nomura, ibid., **34**, 1648 (1961).
3) Y. Nomura and H. Anzai, ibid., **35**, 111 (1962).
4) R. Nietzki and R. Zehntner, *Ber.*, **26**, 143 (1893).
5) G. M. Badger and G. E. Lewis, *J. Chem. Soc.*, **1953**, 2151.
6) A. Michaelis and K. Petou, *Ber.*, **31**, 995 (1898).
7) G. M. Badger and R. G. Buttery, *J. Chem. Soc.*, **1954**, 2243.
8) G. Kalischer, R. Müller and F. Frister, *Friedl.*, **15**, 716 (1925).

TABLE II. ETHYL NAPHTHYLAZOBENZOATES PREPARED BY THE REACTION:



No.	Naphthyl	$COOC_2H_5$	[M. p.], (B. p.), °C	Yield, %[a]	Color	Found: N, %[b]
XXI*	α-	*o*-	(170/11 mmHg)	trace	Deep red	—[c]
XXII*	β-	*o*-	oil[d]	1	Deep red	8.69
XXIII*	α-	*m*-	[101~102]	25	Orange	9.40
XXIV*	β-	*m*-	[88~89]	1	Orange	8.96
XXV*	α-	*p*-	[88.5~89]	4	Orange	9.43
XXVI*	β-	*p*-	[112.5~113.5]	trace	Orange	9.22

* New compound

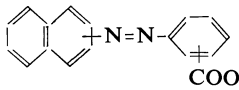
a) Based on the α- or β-bromonaphthalene used to prepare the Grignard reagent.

b) Calcd. % of N for ethyl naphthylazobenzoate $C_{19}H_{16}N_2O_2$: 9.21.

c) The yield was poor, and analytically pure sample could not be obtained after distillation in vacuo. However, its structure was confirmed by hydrolyzing it to the free acid (XXVII of Table III).

d) Purified by column (alumina) chromatography.

TABLE III. NAPHTHYLAZOBENZOIC ACIDS



No.	Naphthyl	COOH	M. p., °C	Color	Found: N, %[a]
XXVII*	α-	*o*-	141~142	Orange red	10.21
XXVIII*	β-	*o*-	146~146.5	Orange yellow	10.01
XXIX	α-	*m*-	207 and >320[b]	Orange	9.97
XXX*	β-	*m*-	220~221	Orange yellow	10.02
XXXI*	α-	*p*-	234~234.5	Orange	10.02
XXXII*	β-	*p*-	220	Orange yellow	9.91

* New compound

a) Calcd. % of N for naphthylazobenzoic acid $C_{17}H_{12}N_2O_2$: 10.14.

b) XXIX melted at 207°C and solidified above its melting point to needles, which did not melt even at 320°C. The reported[8] m. p. of XXIX is 207°C. It was prepared by the deamination of *m*-(4-amino-1-naphthylazo)benzoic acid, which had been obtained by coupling *m*-carboxybenzenediazonium chloride with α-naphthylamine.

TABLE IV. ELECTRONIC ABSORPTION MAXIMA OF NAPHTHYLAZOBENZENES IN ETHANOL

					K-Band			
No.	λ, mμ	ε	λ, mμ	ε	λ, mμ	ε	λ, mμ	ε
I	217.4	52300	270.0	12630	371.7	14390		
II	230.0*	23940	260.0*	10250	328.5	23970		
			264.2	13540				
			277.0	14420				
			287.5	14570				
III	214.7*	25840	256.9	5966	374.7	8199		
IV	229.1	21990	263.5	12280	332.4	23060	443.3	1028
			277.6	12060				
			288.5	12320				
V			264.9	9938	371.5	12680		
			272.9*	9690				
			294.7	8101				
VI	230.0*	22880	265.9	12840	330.0	22370	440.0*	1228
			277.6	13090				
			288.2	13350				
VII	215.3	40580	262.9	9220	373.5	12780		
			309.4	8498				
VIII	234.7	22020	262.3	12600	335.0	25510	450.0*	1295
			278.8	12440				
			290.0	12720				

TABLE IV (Continued)

No.	λ, mμ	ε	λ, mμ	ε	K-Band λ, mμ	K-Band ε	λ, mμ	ε
IX			270.0*	8773	385.0	12730		
			293.2	6120				
X			263.2	12470	325.9	15820		
			278.5	11680	367.6	17140		
			289.4	11710				
XI			253.1*	12550	374.1	13620		
			292.4	7440				
XII			266.0*	13410	325.6	20430	460.0*	1018
			276.9	12980				
			287.4	12930				
XIII			250.0*	9540	378.6	11480	490.0*	590
			290.0*	3302				
XIV	242.4	22310	282.4	9582	345.9*	25780		
			294.1	9714	357.0	26400		
XV	245.9*	11990	268.2	9901	382.9	11820		
			276.5	9581				
			295.0*	7275				
XVI	251.8	14870	267.7*	13210	332.7	22760		
			278.3	12400				
			287.9	12040				
XVII			272.9*	9716	378.2	10680		
			276.5	9850				
			285.9*	7746				
XVIII	235.9*	24410	266.0	15250	330.9	26430		
			276.3	15940				
			286.5	15610				
XIX	216.5	44690	267.6	10760	379.1	15440		
			275.4	10810				
			302.0	10270				
XX	231.5	22040	265.9	12350	335.4	28110		
			278.2	12950				
			288.8	13270				
XXII	236.5	18400	287.3	12000	325.9	19000		
XXIII			275.3	9960	378.2	9020		
XXIV	238.2	24000	274.7	15900	330.0	22100		
	247.1	23000	287.1	14700				
	255.3	23500						
XXV	236.5	10400	276.5	15100	387.1	12500		
XXVI			268.2	15400	334.7	25200		
			277.7	15500				
			288.2	15100				
XXVII	238.7	12300	288.8	8030	372.4	11300		
XXVIII	237.6	18400	260.0	14200	330.0	19900		
			276.5	12500				
			288.8	12200				
XXIX	237.3	17600	293.5	7900	371.8	10600		
XXX	252.4	20900	275.9	12900	328.8	20200		
			288.2	12700				
XXXI	238.8	11900	263.8	11000	378.8	11800		
			300.0	8750				
XXXII			267.1	10200	337.1	22100		
			279.4	10400				
			290.9	10800				

* Wavelength of shoulder.

diazonium chlorides with Grignard reagents. We would now like to report, in extension of this investigation, on the synthesis of naphthylazobenzenes and their derivatives by the same reaction.

α- and β-Naphthylazobenzene (I, II) and their eighteen derivatives (III—XX) carrying a substituent such as methyl, methoxyl, or bromine on a benzene ring have been prepared by the reactions of the zinc chloride double salt of α- or β-naphthalenediazonium chloride with substituted phenylmagnesium bromides. They are summarized in Table I, in which new compounds are asterisked.

Six ethyl naphthylazobenzoates (XXI—XXVI) have been obtained by the reactions of the zinc chloride double salt of ethoxycarbonylbenzenediazonium chloride with α- or β-naphthylmagnesium bromide. They are all new compounds and are listed in Table II. By the hydrolysis of ethyl naphthylazobenzoates, the corresponding free acids (XXVII—XXXII) were prepared; they are listed in Table III.

The electronic absorption spectra of these naphthylazobenzenes were measured in ethanol solutions; their maxima are listed in Table IV.

The K-band of the α-naphthylazobenzene derivatives shifts towards a wavelength longer by about 45 mμ than that of the corresponding β-isomers, in spite of the β-naphthyl dyes having a considerably greater intensity. A similar difference of spectra between α- and β-naphthylazobenzene was pointed out and discussed theoretically by Robin and Simpson.[9]

Experimental

The Preparation of Naphthylazobenzenes.—α- and β-Naphthylazobenzene (I, II) and their derivatives (III—XXVI) were prepared by the method used in a previous paper.[1] They have been summarized in Tables I and II.

***m*-(α-Naphthylazo)benzoic Acid (XXIX).**—One gram of ethyl *m*-(α-naphthylazo)benzoate was dissolved in 10 ml. of ethanol containing 0.2 g. of sodium hydroxide. The solution was refluxed on a water bath for an hour, diluted with 50 ml. of water, and acidified with dilute hydrochloric acid to precipitate *m*-(α-naphthylazo)benzoic acid, which was then recrystallized from ethanol. The yield (0.9 g.) was almost that theoretically expected.

Other naphthylazobenzoic acids were also prepared by the hydrolysis of the corresponding ethyl esters. They have been summarized in Table III.

The Measurement of Spectra. — The absorption spectra were obtained in 95% ethanol as a solvent on a Cary Model 14 M self-recording spectrophotometer with 1 cm. quartz cells.

Summary

1) α- and β-Naphthylazobenzene and their twenty-four derivatives with a substituent on a benzene ring have been synthesized by the reactions of Grignard reagents with zinc chloride double salts of diazonium salts. Twenty-one of them are new compounds.

2) Six naphthylazobenzoic acids have been prepared by the hydrolysis of the corresponding ethyl esters; five of them are new compounds.

3) The ultraviolet and visible absorption spectra of these naphthylazobenzene derivatives have been measured.

Department of Chemistry
College of General Education
The University of Tokyo
Meguro-ku, Tokyo

9) M. B. Robin and W. T. Simpson, *J. Chem. Phys.*, **36**, 585 (1962).

The Infrared Absorption Spectra of $(NH_2CONH-)_2$, $NH_2CONHNH_2$, $(NH_2CSNH-)_2$ and $NH_2CSNHNH_2$

By Mitsuo MASHIMA

(Received February 21, 1964)

The infrared absorption spectra of hydrazides containing the -CONHNHCO-[1] or $-CONHNH_2$[2] group have been investigated and the frequencies characteristic of those groups obtained by the present author. On the other hand, Suzuki[3,4] has discussed the frequency of the stretching vibration of the C=S bond adjacent to the C-N bond in thioamides in connection with the results of infrared measurements and normal vibration calculations. He has concluded that the band of thioformamide[3] at 843 cm^{-1} is associated with an almost pure C=S stretching vibration.

For the present study, the infrared spectra of hydrazine-*N*, *N'*-bis-carbonic acid amide, semicarbazide, hydrazine-*N*, *N'*-bis-thiocarbonic acid amide, thiosemicarbazide, acetyl-semicarbazide, formyl- and acetyl-thiosemicarbazide and the *N*-deuterated derivatives of these compounds were examined in the rock salt region. For the sake of comparison, semicarbazide hydrochloride and its *N*-deuterated derivative were examined spectroscopically. The frequencies obtained were tentatively assigned to the fundamental vibrational modes by comparing the spectra with those of related compounds.

Experimental

Hydrazine-*N*,*N'*-bis-carbonic Acid Amide (HCA): $(NH_2CONH-)_2$.—This compound was obtained by heating a mixture of urea (2 mol.) and hydrazine hydrate (1 mol.) in a sealed tube,[5] and it was purified by recrystallization from water (m. p. 267°C).

Semicarbazide (SC): $NH_2CONHNH_2$.—This compound was synthesized by heating the 1 : 1 (in mole) mixture of urea and hydrazine hydrate in a sealed tube,[6] and it was purified by recrystallization from ethanol (m. p. 96°C). Semicarbazide hydrochloride was prepared with hydrochloric acid and semicarbazide, and it was purified by recrystallization from water (m. p. 174°C). This hydrochloride was examined analytically.

Found: Cl, 30.4%. Calcd. for $NH_2CONHNH_2 \cdot HCl$: Cl, 31.8%.

Acetyl-semicarbazide (ASC): $CH_3CONHNH \cdot CONH_2$.—This compound was synthesized with acetic anhydride and semicarbazide,[7] and it was purified by recrystallization from ethanol (m. p. 165°C).

Hydrazine-*N*, *N'*-bis-thiocarbonic Acid Amide (HTCA): $(NH_2CSNH-)_2$.—This compound was synthesized with hydrazine sulfate and ammonium rhodanide[8] and was purified by recrystallization from water (m. p. 215°C).

Thiosememicarbazide (TSC): $NH_2CSNHNH_2$.—This compound was synthesized by the method presented by Freund and Imagat[9] and was purified by recrystallization from water (m. p. 180°C).

Formyl-thiosemicarbazide (FTSC): $HCONHNH \cdot CSNH_2$.—This compound was synthesized with thiosemicarbazide and formic acid[10] and was purified by recrystallization from water (m. p. 175°C).

Acetyl-thiosemicarbazide (ATSC): $CH_3CONH \cdot NHCSNH_2$.—This compound was synthesized with thiosemicarbazide and acetic anhydride[11] and was purified by recrystallization from water (m. p. 164°C).

The *N*-deuterated derivatives examined were prepared in a sealed tube in the presence of heavy water (99.8%). The excess of heavy water was evaporated in a vacuum.

The spectra of all of the compounds in the solid state were studied with KBr disks. A double-beam Hitachi infrared spectrophotometer, Type EPI-2, was used in the rock salt region.

Results and Discussion

The infrared spectra obtained are shown in Figs. 1 to 3.

The ν(C=O)*1 Frequency.—SC and HCA are considered to show a strong band which is mainly associated with the ν(C=O) vibration because, for urea[12] and oxamide[13], corresponding band has been found at 1686 and 1656 cm^{-1} respectively. In ASC, FTSC and ATSC,

1) M. Mashima, This Bulletin, **35**, 332, 338, 423 (1962).
2) M. Mashima, ibid., **35**, 1882, 2020 (1962); **36**, 210 (1963).
3) I. Suzuki, ibid., **35**, 1286 (1962).
4) I. Suzuki, ibid., **35**, 1449 (1962).
5) T. Curtius, *Ber.*, **26**, 405 (1893).
6) T. Curtius and K. Heidenreich, ibid., **27**, 56 (1894).
7) O. Widman and A. Cleve, ibid., **31**, 381 (1898).
8) M. Freund and S. Wischewiansky, ibid. **26**, 2877 (1893).
9) M. Freund and H. Imagat, ibid., **28**, 948 (1895).
10) M. Freund and C. Meinecke, ibid., **29**, 2513 (1896).
11) M. Freund and C. Meinecke, ibid., **29**, 1515 (1896).
*1 In this paper the following notations are used: ν: bond stretching, β: bending, δ: deformation, r: rocking, w: wagging, t: twisting, π: out-of-plane deformation, τ: tortional, a: asymmetric and s: symmetric.
12) A. Yamaguchi, *J. Chem. Soc. Japan, Pure Chem. Sec.* (*Nippon Kagaku Zassi*), **78**, 1467 (1957).
13) T. A. Soctt, Jr., and E. L. Wagner, *J. Chem. Phys.*, **30**, 465 (1959); see also T. Miyazawa, *J. Chem. Soc. Japan, Pure Chem. Sec.* (*Nippon Kagaku Zassi*), **75**, 86 (1954).

TABLE I. THE ν(C=O) AND AMIDE I BANDS IN cm^{-1}

$NH_2CONHNH_2$	1661	$ND_2CONDND_2$	1640
$NH_2CONHNH_3^+$	1687	$ND_2CONDND_3^+$	1642
$(NH_2CONH-)_2$	1687	$(ND_2COND-)_2$	1625
$CH_3CONHNHCONH_2$	1668	$CH_3CONDNDCOND_2$	1663
$HCONHNHCSNH_2$	1690	$HCONDNDCSND_2$	1684, 1661
$CH_3CONHNHCSNH_2$	1706	$CH_3CONDNDCSND_2$	1670

TABLE II. THE ν(C=S) FREQUENCY IN cm^{-1}

	$HCSNH_2$[a]	$(NH_2CSNH-)_2$	$NH_2CSNHNH_2$	$HCONHNHCSNH_2$	$CH_3CONHNHCSNH_2$
ν(C=S)	830	831	803	858	837
	$HCSND_2$[a]	$(ND_2CSND-)_2$	$ND_2CSNDND_2$	$HCONDNDCSND_2$	$CH_3CONDNDCSND_2$
ν(C=S)	996	901	928	908	910
$r(ND_2)$	752	735	700	726	743

a) See Ref. 3.

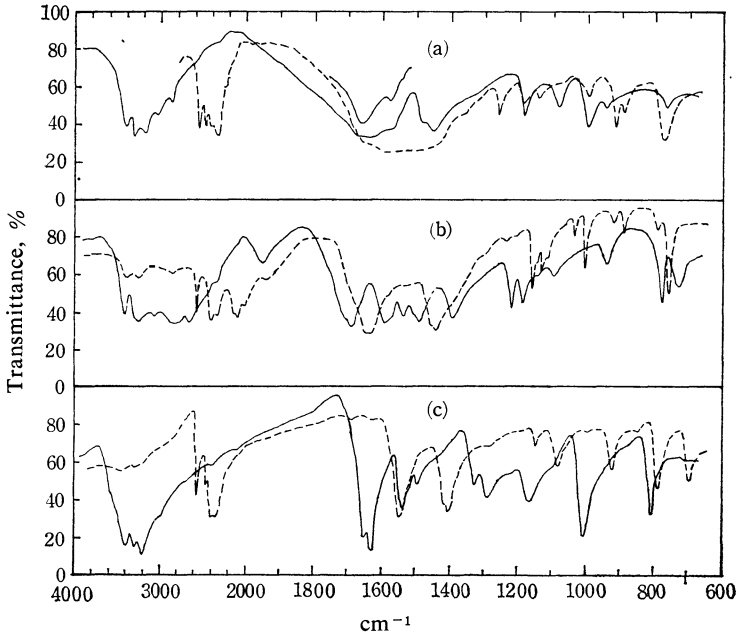


Fig. 1. Infrared spectra of SC (a), SC·HCl (b), and TSC (c) (solid lines) and their *N*-deuterated derivatives (broken lines) in the solid state.

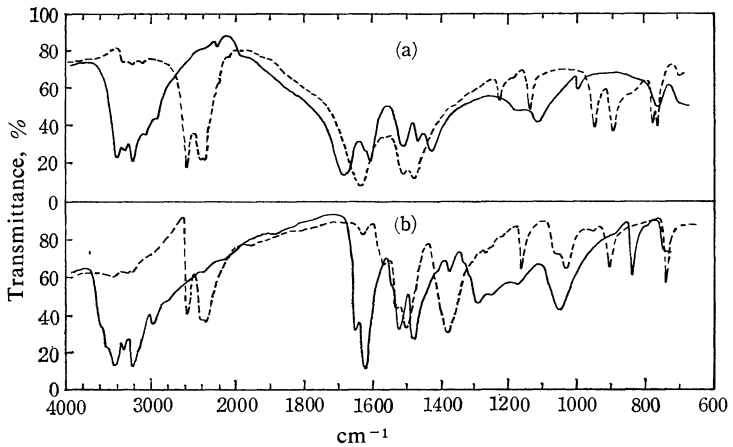


Fig. 2. Infrared spectra of HCA (a) and HTCA (b) (solid lines) and their *N*-deuterated derivatives (broken lines) in the solid state.

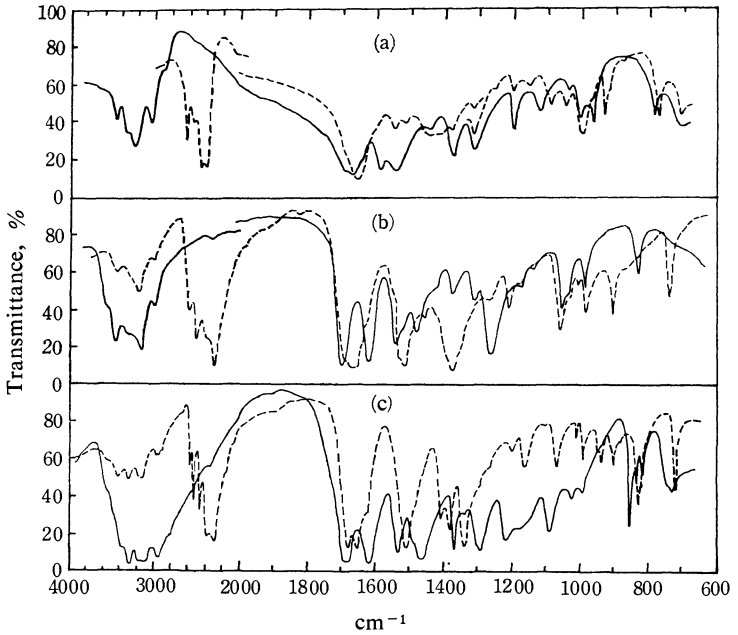


Fig. 3. Infrared spectra of ASC (a), ATSC (b), and FTSC (c) (solid lines) and their *N*-deuterated derivatives (broken lines) in the solid state.

the amide I band characteristic of monosubstituted amides is expected to appear. In fact, these bands are very easily identified in the spectra of those compounds. The ν(C=O) and amide I band are summarized in Table I.

The ν(C=S) Frequency.—This frequency has been found in the 1400~1150 cm^{-1} range in thioureas. This wide range has been ascribed to varying degrees of coupling with other vibrations.[14] Recently, Suzuki concluded that, judging from the normal vibration calculations, the ν(C=S) vibration in simple thioamides may couple with other vibrations; the band of thioformamide[3] at 830 cm^{-1} is associated with an almost pure ν(C=S) vibration, while the band of thioacetamide[4] at 718 cm^{-1} is due to a hybridized vibration mainly composed of the ν(C=S) motion. The spectra of HTCA, TSC, and ATSC are comparatively simple in the region 900~700 cm^{-1}, and they have only a moderately strong band near 830 cm^{-1}: 831 cm^{-1} of HTCA, 803 cm^{-1} of TSC, and 837 cm^{-1} of ATSC. In place of this band, their *N*-deuterated derivatives have two bands, near 910 and 730 cm^{-1}. It is of interest that the 830 $^{-1}$ band of thioformamide disappears on *N*-deuteration and that, in place of it, two bands appear, at 996 and 752 cm;[1-3] the latter two bands have been assigned to vibrations composed of the ν(C=S) and $r(ND_2)$ vibrations. The bands corresponding to these two bands may very easily be identified with the bands at 901 and 735 cm^{-1} for HTCA-d_6 and 910 and 743 cm^{-1} for ATSC-d_4, because they have only those two bands in this region. On the other hand, TSC-d_5 has three moderately strong bands, at 928, 792 and 700 cm^{-1}; of these, the first and last bands are considered to correspond to the two bands mentioned above. In this region the spectrum of FTSC is rather complicated, and it is comparatively hard to find the corresponding bands, but the band at 858 cm^{-1} may be taken as the ν(C=S) band because, on *N*-deuteration, it is displaced by new bands at 908*2 and 726 cm^{-1}.

The ν(C=S) frequencies in thioformamide and the compounds examined here are summarized in Table II, which also contains the bands associated with the hybridized vibrations, mainly composed of the ν(C=S) and $r(ND_2)$ vibrations. As may be seen in Table II, the ν(C=S) frequency in this class of compounds falls in the range of 860~800 cm^{-1}, which is rather lower than that of 1400~1150 cm^{-1} in thioureas and that in other classes of compounds containing the C=S bond.[14]

The $\beta(NH_2)$*1 Frequency.—For TSC and HTCA this frequency will be easily found because no band, except for one associated with the $\beta(NH_2)$ vibration, is considered to

14) L. J. Bellamy, "The Infrased Spectra of Complex Molecules," Methuen & Company, London (1958), p. 356.

*2 FTSC shows several bands in the region where the band mentioned in the text is considered to appear. By comparing the value of this frequency with those of HTCA, TSC, and ATSC, this frequency was used for the band considered just now.

appear in the region from 1650 to 1600 cm^{-1}. In fact, these compounds have a strong band at 1626 and 1617 cm^{-1} respectively. Since they disappear on *N*-deuteration, we can safely take them as $\beta(NH_2)$ frequencies. The $\beta(ND_2)$ frequency is easily found at 1150 cm^{-1} for TSC-d_6 and 1158 cm^{-1} for HTCA-d_6.

The bands at 1624 cm^{-1} for FTSC and 1633 cm^{-1} for ATSC may also be safely taken as $\beta(NH_2)$ bands. This assignment is supported by the spectroscopic observations for these compounds in the acetonitrile solution. In changes of state, the 1624 cm^{-1} band of FTSC shifts to 1618 cm^{-1} and the 1633 cm^{-1} band of ATSC, to 1613 cm^{-1}. These frequency shifts are, in direction and value, in accordance with those obtained for the $\beta(NH_2)$ bands of thioformamide[3] and thioacetamide.[4] HCA has a band at 1604 cm^{-1} which is accompanied with a shoulder band at 1622 cm^{-1}. They disappear on *N*-deuteration. Accordingly, they are taken as $\beta(NH_2)$ frequencies. In the remaining compounds, SC and ASC, the location of the $\beta(NH_2)$ band is very difficult to ascertain. As has been indicated above, TSC-d_5 and HTCA-d_6 have the $\beta(ND_2)$ band at ca. 1150 $^{-1}$. The corresponding band has been obtained at 1118 $^{-1}$ for $HCOND_2$,[15] 1145 cm^{-1} for $HCSND_2$,[3] 1189 cm^{-1} for CH_3COND_2,[16] and 1160 cm^{-1} for CH_3CSND_2[4]. Therefore, the $\beta(ND_2)$ band of the remaining five compounds is expected to appear near at 1150 cm^{-1}. It has been obtained as summarized in Table III.

Bands in the Region from 1590 to 1340 cm^{-1}. —In ASC, ATSC and FTSC, the amide II band is considered to appear in this region. Recently, Suzuki obtained amide II-like bands for *N*-methylthioamides: 1550 cm^{-1} of $HCSNH\cdot CH_3$ and 1564 cm^{-1} of $CH_3CSNHCH_3$.[17] On the other hand, the ν(C–N) vibration of the $CO(S)NH_2$ group is considered to give rise to a band in this region because the ν(C–N) frequency has been found at 1464 cm^{-1} for urea[12] and 1470 cm^{-1} for thiourea.[18]

In this region the observed frequencies of ASC, ATSC and FTSC are collected in Table IV(a). ASC has two strong bands at 1587 and 1542 cm^{-1}, one of which may be taken as the amide II band and the other as the ν(C–N) band. On *N*-deuteration, the amide II band usually moves to lower frequencies and the so-called amide II′ band occurs; e.g., $CH_3\cdot CONHCH_3$[19] shows the 1567 (amide II) and 1475 (amide II′) cm^{-1} bands. ASC-d_4 shows a relatively weak band at 1552 cm^{-1} and two strong bands at 1445 and 1410 cm^{-1}. The amide II′ band of $CH_3CONHCH_3$ has been ascribed to the ν(C–N) vibration interacting with other vibrational modes.[19] In ASC-d_4, it is considered that the ν(C–N) vibration interacts with at least the $\delta_a(CH_3)$ vibration, and two strong bands are shown as has been indicated above. The bands at 1443 and 1372 cm^{-1} of ASC may be safely assigned to the $\delta_a(CH_3)$ and $\delta_s(CH_3)$ vibrations respectively, because the values of frequency lie in the normal ranges for those vibrations of the C–CH_3 group. The band of ASC-d_4 at 1380 cm^{-1} may safely be ascribed to the $\delta_s(CH_3)$ vibration.

Since the bands at 1545 cm^{-1} for ATSC and 1540 cm^{-1} for FTSC correspond in fuequency to the amide II band of *N*-methylthioamides,[17] these bands may be taken as amide II bands. Two strong bands, at 1513 and 1437 cm^{-1}, of $HCSNDCH_3$[17] have been ascribed to the hybridized vibrations composed of the ν(C–N) and $\delta_a(CH_3)$ vibrations, while in $CH_3CSND\cdot CH_3$[17] the coupling occurs among the ν(C–N), $\delta_a(CH_3)_N$ and $\delta_a(CH_3)_C$ vibrations and three bands have been observed at 1515, 1483 and 1442 cm^{-1}. ATSC-d_4 and FTSC-d_4 also have strong bands at 1517 and 1515 cm^{-1} respectively; their frequency-values are in good accordance with those of the bands at 1513 cm^{-1} for $HCSNDCH_3$ and 1515 cm^{-1} for $CH_3CSNDCH_3$. Therefore, they seem to be bands characteristic of the –CSND– group (amide II′). The band of ATSC at 1485 cm^{-1} is displaced by a strong band at 1380 cm^{-1} on *N*-deuteration. The former may be associated with the amide II band; the latter is suitable in frequency to the $\delta_s(CH_3)$ vibration, but it appears more strongly than that vibration. Probably, the 1380 cm^{-1} band will be the $\delta_s(CH_3)$ band overlapped with the amide II′ band come from the CH_3COND– group. The band of FTSC at 1472 cm^{-1} moves to 1346 cm^{-1} on *N*-deuteration; they may be taken as the amide II and II′ bands respectively. In ATSC two bands at 1430 and 1379 cm^{-1} are easily associated with the $\delta_a(CH_3)$ and $\delta_s(CH_3)$ vibrations respectively. The band at 1374 cm^{-1} of FTSC corresponds to the band at 1384 cm^{-1} of FTSC-d_4, and these may safely be assigned to the δ(C–H) vibration.

In this region HCA shows three bands at 1505, 1465, and 1426 cm^{-1} which are displaced by two strong bands at 1506, 1473 cm^{-1} and a weak band at 1221 cm^{-1} on *N*-deuteration. For SC, the corresponding bands are found at 1577, 1484 and 1452 cm^{-1}. In the spectrum of SC-d_5, the location of the bands corresponding

15) I. Suzuki, This Bulletin, **33**, 1359 (1960).
16) I. Suzuki, ibid., **35**, 1279 (1962).
17) I. Suzuki, ibid., **35**, 1456 (1962).
18) A. Yamaguchi, R. B. Penland, S. Mizushima, T. J. Lange, C. Curran and J. V. Quagliano, *J. Am. Chem. Soc.*, **80**, 527 (1958).
19) T. Miyazawa, T. Shimanouchi and S. Mizushima, *J. Chem. Phys.*, **29**, 611 (1958).

Table III. The $\beta(NH_2)$ and $\beta(ND_2)$ frequencies in cm^{-1}

	$(NH_2CSNH-)_2$	$NH_2CSNHNH_2$	$CH_3CONHNHCSNH_2$	$HCONHNHCSNH_2$	$(NH_2CONH-)_2$	$NH_2CONHNH_2$	$CH_3CONHNHCONH_2$
$\beta(NH_2)$	1642 1617	1648 1626	1633	1624	1622 1604	—a)	—a)
	$(ND_2CSND-)_2$	$ND_2CSNDND_2$	$CH_3CONDNDCSND_2$	$HCONDNDCSND_2$	$(ND_2COND-)_2$	$ND_2CONDND_2$	$CH_3CONDNDCOND_2$
$\beta(ND_2)$	1158	1150	1142	1168	1130	1190 1142	1152

a) The corresponding bands were not located with certainty.

Table IV. The observed frequencies in the region from 1590 to 1340 cm^{-1}

(a) ABC, ATSC, and FTSC

	$CH_3CONHNHCONH_2$	$CH_3CONDNDCOND_2$	$CH_3CONHNHCSNH_2$	$CH_3CONDNDCSND_2$	$HCONHNHCSNH_2$	$HCONDNDCSND_2$
Amide II (II') and ν(C-N)	1587(s) 1542(s)	1552(m) 1445(s)	1545(m) 1527(sh) 1485(m)	1532(sh) 1517(s)	1540(s) 1493(sh) 1472(s)	1515(s) 1413(m) 1346(s)
$\delta_a(CH_3)$	1443(w)	1410(s)	1430(w)	1458(w)		
$\delta_s(CH_3)$	1372(m)	1380(m)	1379(w)	1380(s)		
δ(CH)					1374(m)	1384(m)

(b) HCA, SC, HTCA, and TSC

	$(NH_2CONH-)_2$	$(ND_2COND-)_2$	$NH_2CONHNH_2$	$ND_2CONDND_2$	$(NH_2CSNH-)_2$	$(ND_2CSND-)_2$	$NH_2CSNHNH_2$	$ND_2CSNDND_2$
Amide II (II') and ν(C-N)	1505(s) 1465(m) 1426(s)	1506(s) 1473(s)	1577(s) 1484(m) 1452(s)	—a) —a)	1517(s) 1473(s) 1368(w)	1523(w) 1493(s) 1374(s)	1536(m) 1491(m) 1391(vw)	1550(s) 1418(sh) 1407(s)
		1221(w)		1259(w)				

a) It is difficult to locate the corresponding band.

Table V (a). The observed frequencies of HCA, SC, HTCA and TSC in the region from 1340 to 700 cm^{-1}

	$(NH_2CONH-)_2$	$(ND_2COND-)_2$	$NH_2CONHNH_2$	$ND_2CONDND_2$	$(NH_2CSNH-)_2$	$(ND_2CSND-)_2$	$NH_2CSNHNH_2$	$ND_2CSNDND_2$
Amide III					1287(m)		1322(m) 1287(m)	
$\delta(NH_2)$[a]			1182(m)					
$r(NH_2)$	1110(m)		1080(m)		1049(m)		1164(m)	
Amide III'						1028(m)		1086(m)
$\delta(NH_2)$[a]			996(m)				1001(s)	
δ(O=C-N)	996(w)		946(w)					
$\delta(ND_2)$[a]				997(w)				
$r(ND_2)+\delta$(O=C-N)		943(m) 883(m)		917(m) 891(m)				
$\delta(ND_2)$[a]				834(vw)				792(w)
π(O=C-N_2)	759(w)	771(m) 758(m)	767(w)	772(m)				

a) It is of the hydrazine residue.

Table V (b). The observed frequencies of ASC, ATSC and FTSC in the region from 1340 to 700 cm^{-1}

	$CH_3CONHNHCONH_2$	$CH_3CONDNDCOND_2$	$CH_3CONHNHCSNH_2$	$CH_3CONDNDCSND_2$	$HCONHNHCSNH_2$	$HCONDNDCSND_2$
Skeletal	1313(m)	1315(m)	1318(m)	1213(m)		
Amide III	1197(m)		1265(s)		1298(s) 1223(m)	
Skeletal	1121(w)	1089(w)	1180(w)	1185(w)	1093(m)	1074(m)
$r(CH_3)$ and $\nu(C-C)$	1037(w) 1002(m) 996(m)	1043(w) 998(m) 931(w)	1058(m) 1045(m) 990(m)	1058(m) 1034(w) 992 983 (m)		
$\pi(C-H)$					1029(w) 1001(w)	1019(w)
Amide III′						997(w) 946(w)
Skeletal					840 823 (w)	837 827 (m)
$\pi(O=C-N_2)$	783(m)	774(m)				
Skeletal	700(m)	706(m)				

Table VI (a). The observed frequencies of HCA and HTCA in the region from 3000 to 2000 cm^{-1}

	$(NH_2CONH-)_2$	$(ND_2COND-)_2$	$(NH_2CSNH-)_2$	$(ND_2CSND-)_2$
$\nu_a(NH_2)$	3360(s) 3280(s)		3380(s) 3280(m)	
$\nu_s(NH_2)$ and $\nu(NH)$	3190(s, b) 3040(w) 2920(w)		3170(s) 3100(sh) 2940(m)	
$\nu_a(ND_2)$		2560(s)		2540(s)
$\nu_s(ND_2)$ and $\nu(ND)$		2390 2340 (s)		2400 2320 (s)
	2210(w)	2180(w)		

Table VI (b). The observed frequencies of SC and TSC in the region from 3000 to 2000 cm^{-1}

	$NH_2CONHNH_2$	$ND_2CONDND_2$	$NH_2CONHNH_3^+$	$ND_2CONDND_3^+$	$NH_2CSNHNH_2$	$ND_2CSNDND_2$
$\nu_a(NH_2)$	3410(s)		3410(s)		3370(s)	
$\nu(NH_2)$	3310(s)				3270(s)	
$\nu_s(NH_2)$ and $\nu(NH)$	3200(s) 3060(w) 2890(w)		3220(s) 3050(m)		3190(s) 2980(m)	
$\nu_a(NH_3^+)$			2850(s)			
$\nu_s(NH_3^+)$			2640(s)			
$\nu_a(ND_2)$		2850(m)		2570(m)		2560(m)
$\nu(ND_2)$		2470(m)				2470(m)
$\nu_s(ND_2)$ and $\nu(ND)$		2410 2330(s)		2390 2320(s)		2400 2330(s)
$\nu_a(ND_3^+)$				2150(sh) 2090(s)		
$\nu_s(ND_3^+)$				2020(m)		

Table VI (c). The observed frequencies of ASC, ATSC and FTSC in the region from 3000 to 2000 cm^{-1}

	$CH_3CONHNHCONH_2$	$CH_3CONDNDCOND_2$	$CH_3CONHNHCSNH_2$	$CH_3CONDNDCSND_2$	$HCONHNHCSNH_2$	$HCONDNDCSND_2$
$\nu_a(NH_2)$	3440(m)		3440(s)		3390(w) 3295(s)	
$\nu(NH)$	3310(m)		3310(m)		3155(s)	
$\nu_s(NH_2)$ and $\nu(NH)$	3230(s) 3040(m) 2900(vw)		3170(s) 3000(m)		2970(s) 2830(w)	
$\nu_s(ND_2)$		2620(m)		2590(w)		2590(w)
$\nu(ND)$		2530(w)		2500(m)		2550(m) 2470(m)
$\nu_s(ND_2)$ and $\nu(ND)$		2440 2400(s)		2390 2310(s)		2390 2310(s)
			2340(vw)		2350(vw)	

to the 1506 and 1473 cm^{-1} bands of HCA-d_6 is very difficult to determine because of the presence of strong back-ground absorptions, while the band corresponding to the 1221 cm^{-1} band is easily found at 1259 cm^{-1}. HTCA and TSC show absorptions a little different from those of HCA and SC: HTCA has only two strong bands at 1517 and 1473 cm^{-1} which are displaced by strong bands at 1493 and 1374 cm^{-1} on *N*-deuteration; TSC has also two moderately strong bands at 1536 and 1491 cm^{-1} and TSC-d_5, at 1550 and 1407 cm^{-1}. A detailed assignment is difficult from the present observations only, but these bands may be taken as the amide II and ν(C–N) bands.

The Bands in the Region from 1340 to 700 cm^{-1}.—The observed frequencies of HCA, SC, HTCA, and TSC are collected in Table V(a). The band of HCA at 759 cm^{-1} is displaced by a band with two peaks at 771 and 758 cm^{-1} on *N*-deuteration. SC has a band at 767 cm^{-1} which moves to 772 cm^{-1} on *N*-deuteration; ASC has also a corresponding band at 783 cm^{-1} and ASC-d_4, one at 774 cm^{-1}, as is indicated in Table V (b). A band of urea[12] at 776 cm^{-1}, which moves to 785 cm^{-1} on *N*-deuteration, has been assigned to the $\pi(OCN_2)$*1 vibration. Therefore, the band near 770 cm^{-1} is considered to be one characteristic of these compounds and has been assigned to the $\pi(OCN_2)$ vibration.

HCA has, further, a moderately strong band at 1110 cm^{-1} and a weak band at 996 cm^{-1}; they are considered to be due to fundamental vibrational modes because they are displaced by two moderately strong bands, at 943 and 888 cm^{-1}, on *N*-deuteration. Urea[12] shows a band at 1150 cm^{-1} which has been assigned to the $r(NH_2)$ vibration of the A_1 and B_1 species: urea-d_4[12] has the $r(ND_2)$ bands at 1001 cm^{-1} (A_1) and 887 cm^{-1} (B_1). For oxamide,[13] the $r(NH_2)$ frequency has been obtained at 1103 cm^{-1} and the $r(ND_2)$ frequency at 927 cm^{-1}. The 1110 cm^{-1} band of HCA is determined to come from a vibration mainly due to the $r(NH_2)$ vibration by comparing the value of the frequency with those of the corresponding frequencies in urea and oxamide. In consequence, the 943 and 883 cm^{-1} bands of HCA-d_6 are considered to arise from the $r(ND_2)$ vibration strongly interacting with another vibration. Assuming the symmetry of C_{2h} for a molecule of HCA,*3 of a total of thirty-six (3N-6) normal vibrations, eighteen are infrared active; six of these are of species A_u, and twelve of species B_u. Seven of them will give rise to bands outside the region examined here. They may be deformation N–N–C and N–C–N vibrations (species B_u) or torsional N–C and N–N vibrations, wagging and twisting NH_2 vibrations and out-of-plane N–H deformation vibrations (species A_u); the τ(N–N–)*1 frequency of NH_2NH_2 is 377 cm^{-1},[20] the τ(C–N) frequency of $HCONHCH_3$[21] is 353 cm^{-1}, the δ(N–N–C) frequency of CH_3NHNH_2 is 433 cm^{-1},[22] and the δ(N–C–N) frequency of $NH_2 \cdot CONH_2$ is 556 cm^{-1}.[12] The π(N–H), $w(NH_2)$ and $t(NH_2)$*1 frequencies are considered to be found in this region,*4 but in the spectrum of HCA no band corresponding to them is observed. In consequence, eleven frequencies will be found for HCA in the region examined here. Of these only one has not yet been accounted for, the δ(O=C–N) frequency. Therefore, the 996 cm^{-1} band of HCA is considered to be due to that vibration, while the 943 and 888 cm^{-1} bands of HCA-d_6 may be ascribed to the hybridized vibrations composed of $r(ND_2)$ and δ(O=C–N) vibrations. The above assignment is supported by the fact that, for HTCA, no band corresponding to them is observed.

SC has four bands, not yet accounted for, at 1182, 1080, 996 and 946 cm^{-1}. In order to explain these bands, the spectrum of SC was compared with that of SC·HCl. Of the four, only the third band has no band corresponding in frequency to it in the spectrum of SC·HCl, and it moves to 834 cm^{-1} on *N*-deuteration. Therefore, it may be ascribed to a $\delta(NH_2)$ vibration of the hydrazine residue*5 contained in SC. The second and fourth bands are considered to correspond to the 1110 and 996 cm^{-1} bands of HCA, and they may be taken as the $r(NH_2)$ and δ(O=C–N) bands respectively. Since they are displaced by two bands at 917 and 891 cm^{-1} on *N*-deuteration, we can apply the same explanation to

*3 Since the infrared spectrum of diformylhydrazine has been reasonably explained with a model of the transplanar configuration of the -CONHNHCO- group (T. Miyazawa, T. Shimanouchi and S. Mizushima, *J. Chem. Phys.*, **24**, 408 (1956); T. Miyazawa, *J. Chem. Soc. Japan, Pure Chem. Sec.* (*Nippon Kagaku Zassi*), **76**, 341 (1955)), that group contained in HCA may be assumed to have a similar structure. On the other hand, the spectrum of urea has been interpreted by means of a model of the planar structure of a molecule (see Ref. 12) and part of the $-NHCONH_2$ of a molecule of HCA is considered to have a planar configuration. In that case, HCA has the symmetry of C_{2h}.

20) A. Yamaguchi, I. Ichishima, T. Shimanouchi and S. Mizushima, *J. Chem. Phys.*, **31**, 843 (1959).

21) I. Suzuki, This Bulletin, **35**, 540 (1962).

22) D. W. E. Axford, G. J. Janz and K. E. Russel, *J. Chem. Phys.*, **19**, 704 (1951).

*4 The π(N–H) frequencncy has been obtained at 720 cm^{-1} for *N*-methylformamide (see Ref. 21): the $w(NH_2)$ and $t(NH_2)$ frequencies have been found at 792 and 678 cm^{-1} for oxamide (see Ref. 13) and at 719 and 500 cm^{-1} for urea (see Ref. 12).

*5 In SC·HCl, HCl is considered to attach itself to the hydrazine residue because the NH_2 group of this residue is considered to be more basic in nature than that group of $-CONH_2$.

the latter two bands as was applied to the 943 and 888 cm^{-1} bands of HCA-d_6. The first band also has a partner band at 1180 cm^{-1} in the spectrum of SC·HCl and moves to 997 cm^{-1} on *N*-deuteration; it may be ascribed to a $\delta(NH_2)$ vibration of the hydrazine residue. This assignment will be considered further later in this paper.

HTCA has a moderately strong band at 1049 cm^{-1} which is disappears on *N*-deuteration; its frequency-value is suitable for it to be assigned to the $r(NH_2)$ vibration. The $r(ND_2)$ frequency of HTCA-d_6 has been considered previously (see Table II). The band at 1287 cm^{-1} of this compound shifts to 1028 cm^{-1} on *N*-deuteration and corresponds in frequency to the amide III band of HCSNH·CH_3[17] at 1297 cm^{-1}. Therefore, we can take it as the amide III band characteristic of the –CSNH– group.

TSC has four bands, at 1332, 1287, 1164 and 1001 cm^{-1}, all of which are displaced on *N*-deuteration. In this compound an $r(NH_2)$ vibration in the $-CSNH_2$ plane*6 and NH_2 deformation vibrations of the hydrazine residue will give rise to bands in the region just considered. Of the above four, the 1164 and 1001 cm^{-1} bands seem to be suitable in frequency for the $r(NH_2)$ and the NH_2 deformation vibrations respectively. In TSC-d_5 the 928 and 700 cm^{-1} bands have been assigned to the hybridized vibrations composed of the $r(ND_2)$ and ν(C=S) vibrations (see Table II). TSC-d_5 has a further band at 792 cm^{-1} which may be assigned to the ND_2 deformation vibration of the hydrazine residue. One of the 1322 and 1287 cm^{-1} bands of TSC is considered to correspond to the band at 1086 cm^{-1} of TSC-d_5 and may be taken as the amide III band.

The observed frequencies of ASC, FTSC and ATSC in this region are collected in Table V (b), except for the ν(C=S) frequency accounted for already. All of these compounds are considered to show the amide III band characteristic of the –CONH– group; ASC and ATSC show the bands due to the $r(CH_3)$ and ν(C–C) vibrations, and FTSC, the band due to the π(C–H) vibration. The bands at 1298 cm^{-1} of FTSC and 1265 cm^{-1} of ATSC may safely be taken as amide III bands because they disappear on *N*-deuteration, and their frequency-values are considered to be suitable for amide III bands. In ASC a band at 1197 cm^{-1} disappears on *N*-deuteration; we can take this as the amide III band. In the region where the $r(CH_3)$ and ν(C–C) vibrations will give rise to bands, three bands are found, at 1037, 1002 and 996 cm^{-1} for ASC and at 1058, 1045 and 990 cm^{-1} for ATSC. They may be ascribed to the $r(CH_3)$ and ν(C–C) vibrations or to the hybridized vibrations composed of those and the $r(NH_2)$, skeletal stretching vibrations. In ASC the above three bands are displaced by bands at 1043, 998 (relatively broad) and 931 cm^{-1}; those of ATSC are displaced by two bands, at 1058 and 1034 cm^{-1}, and a band with two peaks at 992 and 983 cm^{-1}. The 998 cm^{-1} band of ASC-d_4 and the doublet band of ATSC-d_4 may be regarded as the amide III′ band overlapping with a band arising from one of the hybridized vibrations indicated above. Now, ASC has three bands not yet accounted for, at 1313, 1121 and 700 cm^{-1}; the first and last bands are scarcely changed in frequency on *N*-deuteration, and, accordingly, they may be considered to come from skeletal stretching vibrations; the second shifts to 1089 cm^{-1}, but this is also due to a skeletal vibration. ATSC has two bands at 1318 and 1180 cm^{-1}; the latter is hardly changed on *N*-deuteration, while the former shifts to 1213 cm^{-1}. A detailed assignment of the two bands is not easy, but they are considered to come from skeletal vibrations. In the spectrum of FTSC, bands at 1093, 840 and 823 cm^{-1} are hardly changed on *N*-deuteration. Therefore, they may be ascribed to skeletal vibrations. In this compound the π(C–H) and $r(NH_2)$ vibrations will give rise to bands in this region. They may be associated with the relatively weak bands at 1029 and 1001 cm^{-1}. In FTSC-d_4 the band at 1019 cm^{-1} may be assigned to the π(C–H) vibration. A moderately strong band at 1223 cm^{-1} may be taken as the amide III band because it disappears on *N*-deuteration. In FTSC-d_4 the bands at 997 and 946 cm^{-1} are suitable in frequency for the amide III′ bands characteristic of the –COND– and –CSND– groups. The band at 733 cm^{-1} also disappears on *N*-deuteration and may be associated with the wagging or twisting NH_2 vibration.

The $\nu(NH_2)$ and ν(NH) Frequencies.—The frequencies observed above 2000 cm^{-1} and a tentative assignment of them are given in Tables VI (a), (b) and (c). As may be seen from Table VI (a), HCA and HTCA have two strong bands, near 3370 and 3190 cm^{-1}. They correspond in frequency to the $\nu_a(NH_2)$ band of 3335 cm^{-1} and the $\nu_s(NH_2)$ band of 3145 cm^{-1} for thioformamide[3] respectively. For formamide[15] the $\nu_a(NH_2)$ frequency has been found at 3330 cm^{-1} and the $\nu_s(NH_2)$ frequency, at 3190 cm^{-1}. Therefore, the bands near 3370 and 3190 cm^{-1} may safely be assigned to the $\nu_a(NH_2)$ and $\nu_s(NH)_2$ vibrations respectively.

*6 It may be assumed that this group is planar because the infrared spectrum of $HCSNH_2$ has been reasonably explained with a planar model of the molecule (see Ref. 3).

Table VII. The observed frequencies of SC·HCl in the region from 1600 to 700 cm^{-1}

	$NH_2CONHNH_3^+$	$ND_2CONDND_3^+$
$\delta_a(NH_3^+)$	1586(s)	
$\delta_s(NH_3^+)$	1529(m)	
Skeletal	1486(s)	1459(s)
		1441(s)
	1387(s)	1391(sh)
$r(NH_3^+)$	1215(m)	
	1180(m)	
$\delta_a(ND_3^+)$		1160(m)
		1146(vw)
$\delta_s(ND_3)^+$		1130(m)
		1112(vw)
$r(NH_2)$	1088(w)	
$r(ND_3^+)$		1036(w)
		1005(m)
δ(O=C-N)	933(w)	
$r(ND_2)$, δ(O=C-N)		918(w)
		892(w)
$\pi(O=CN_2)$	768(m)	761(m)
$w(NH_2)$ or $t(NH_2)$	717(m)	

As has been mentioned already, it is assumed that a molecule of HCA has the point symmetry C_{2h}, so that only the ν(NH) vibration is infrared-active. The hydrazides[1] containing the -CONHNHCO- group show a band about 3200 cm^{-1} which has been associated with the ν(NH) vibration. On *N*-deuteration, the 3360 cm^{-1} band of HCA moves to 2565 cm^{-1}, while the 3190 cm^{-1} band is displaced by a doublet band with two peaks at 2390 and 2340 cm^{-1}. Therefore, it seems possible that the 3190 cm^{-1} band is the $\nu_s(NH_2)$ band overlapping with the ν(NH) band. Such a doublet band, which has two peaks at 2400 and 2320 cm^{-1}, is also found for HTCA-d_6.

SC and TSC are considered to show rather complicated absorption bands associated with the $\nu(NH_2)$ and ν(NH) vibrations because of the less symmetrical structure of their molecules. In fact, SC shows three strong bands at 3410, 3310 and 3200 cm^{-1} and TSC, at 3370, 3270 and 3190 cm^{-1} (see Table VI(b)). On *N*-deuteration, the SC 3410 cm^{-1} band of SC moves to 2580 cm^{-1}, and the 3370 cm^{-1} band of TSC, to 2560 cm^{-1}. SC·HCl also has a band at 3410 cm^{-1} which is displaced by a band at 2570 cm^{-1} on *N*-deuteration. Therefore, the band about 3400 cm^{-1} may be assigned to the $\nu_a(NH_2)$ vibration of the $-CONH_2$ group. On the other hand, no band corresponding to the band near 3300 cm^{-1} is observed in SC·HCl; therefore, this band may be associated with the $\nu(NH_2)$ vibration of the $-NHNH_2$ group. This assignment is supported by the fact that the hydrazides[2] contaning the $-CONHNH_2$ group show a band ca. 3300 cm^{-1}. The 3200 cm^{-1} band of SC is displaced by a doublet band with two peaks at 2410 and 2330 cm^{-1} on *N*-deuteration. This band corresponds in frequency to, and behaves on *N*-deuteration like, the 3190 cm^{-1} band of HCA; therefore, it may be the $\nu_s(NH_2)$ band of the $-CONH_2$ group overlapping with the ν(NH) band. TSC also has the corresponding band at 3190 cm^{-1} which is displaced by a doublet band, 2400 and 2330 cm^{-1}, on *N*-deuteration. The band of SC·HCl at 3220 cm^{-1} may be similarly explained because it is displaced by a doublet band, 2390 and 2320 cm^{-1}, on *N*-deuteration. SC·HCl further shows two strong bands at 2850 and 2640 cm^{-1} which are displaced by two bands at 2090 and 2020 cm^{-1} on *N*-deuteration; therefore, they may be associated with the NH_3^+ stretching vibrations.

ASC shows strong or moderately strong bands at 3440, 3310 and 3230 cm^{-1}; ATSC has corresponding bands at 3440, 3310, 3170 cm^{-1}. Of these three, the former two move to about 2600 and 2500 cm^{-1} on *N*-deuteration, while the third band corresponds in frequency to, and behaves on *N*-deuteration like, the bands about 3200 cm^{-1} of the compounds in Tables VI(a) and (b). Therefore, the band about 3200 cm^{-1} of ASC and ATSC may also be taken as the $\nu_s(NH_2)$ band overlapping with the ν(NH) band. On the other hand, the 3440 and 3310 cm^{-1} bands are considered to arise from the $\nu_s(NH_2)$ and ν(NH) vibrations respectively. For FTSC the corresponding bands are found at 3295, 3155 and 2970 cm^{-1}.

The Bands of SC·HCl.—The observed frequencies of this compounds have partly been accounted for in previous sections. Let us now consider the frequencies charateristic of the NH_3^+ structure. A number of investigations have been made of the infrared spectra of amino acids and their hydrochlorides. These compounds usually show two characteristic

bands in the 1600～1500 cm^{-1} region which are associated with the NH_3^+ deformation vibrations; many amino acids have a further band near 1300 cm^{-1} and their hydrochlorides, a band near 2000 cm^{-1}.[23] Mizushima and Nakagawa[24] have obtained the 1650～1560 cm^{-1} range for the $\delta_a(NH_3)$ frequency, the 1350～1150 cm^{-1} range for the $\delta_s(NH_3)$ frequency, and the 950～650 cm^{-1} range for the $r(NH_3)$ frequency in ammine complex salts. On the other hand, the corresponding frequencies of the NH_3^+ structure have been found at 1613, 1504, 1133 and 1109 cm^{-1} for glycine[25] and 1620, 1515 and 1497, and 1185 and 1112 cm^{-1} for *C*-deuterated glycine.[26]

The observed frequencies of SC·HCl in the region from 1600 to 700 cm^{-1} and their assignments are summarized in Table VII. In the range for the $\delta_a(NH_3)$ frequency indicated above, SC·HCl has only a strong band at 1586 cm^{-1}; this disappears on *N*-deuteration and so may be associated with the $\delta(_aNH_3^+)$ frequency. The band at 1529 cm^{-1} also disappears on *N*-deuteration and corresponds in frequency to the $\delta_s(NH_3^+)$ band of glycine. Therefore, it may be ascribed to the $\delta_s(NH_3^+)$ vibration. This hydrochloride shows two bands at 1215 and 1180 cm^{-1} in place of the 1182 cm^{-1} band of SC, and on *N*-deuteration those two bands shift to 1036 and 1005 cm^{-1} respectively. Their frequency-values are a little high, but they may be taken as $r(NH_3^+)$ frequencies. This assignment is consistent with the fact that these two bands appear in place of the 1882 cm^{-1} band of SC which has been ascribed to a $\delta(NH_2)$ vibration of the hydrazine residue. In SC·HCl-d_6 the two bands at 1160 and 1130 cm^{-1} are considered to arise from the $\delta_a(ND_3^+)$ and $\delta_s(ND_3^+)$ vibrations respectively.

Since three bands, at 1088, 933, and 768 cm^{-1} of SC·HCl and 918, 892 and 761 cm^{-1} of SC·HCl-d_6, have their partner bands in the spectra of SC and SC-d_5 respectively, these bands may be explained in the same way as those partner bands have been. It is especially interesting to see that the 1088 and 933 cm^{-1} bands of SC·HCl are displaced by two bands at 918 and 892 cm^{-1} on *N*-deuteration. In consequence, this observation supports the assignment presented already (see Table V(a)); i. e., the 1080 and 946 cm^{-1} bands of SC are associated with the $r(NH_2)$ and δ(O=C–N) vibrations of the $-CONH_2$ group, and the 917 and 891 cm^{-1} bands of SC-d_5, with the hybridized vibrations composed of the $r(ND_2)$ and δ(O=C–N) vibrations. The two bands at 1486 and 1387 cm^{-1} are displaced by bands at 1459 and 1441 cm^{-1} on *N*-deuteration, and these may be ascribed to skeletal stretching vibrations. A moderately strong band at 717 cm^{-1} disappears on *N*-deuteration and may be associated with a $w(NH_2)$ or $r(NH_2)$ vibration.

The weak band of SC·HCl at 1926 cm^{-1} seems to be one characteristic of the NH_3^+ structure, but it may be ascribed to a combination or overtone band because it is scarcely changed in frequency on *N*-deuteration.

Conclusions

(1) For HTCA, TSC, ATSC, and FTSC a ν(C=S) frequency has been obtained in the 860～800 cm^{-1} range which is rather lower than that obtained in other classes of compounds containing the C=S bond. In *N*-deuterated species, the ν(C=S) vibration interacts with the $r(ND_2)$ vibration and two bands which may be regarded as characteristic of the $-CSND_2$ group appear. In consequence, the conclusion obtained for thioamides[15,16] has been confirmed by the present observations.

(2) The spectra of HCA and SC are rather more like that of urea than those of hydrazides containing a –CONHNHCO– or –CONH·NH_2 group; the observed frequencies have tentatively been explained by comparing the spectra with the spectrum of urea.

(3) In ASC, ATSC, and FTSC the amide I, II, and III bands characteristic of the –CONH– group have without ambiguity been located. HTCA, TSC, ATSC, and FTSC show amide II- and III-like bands; these two bands are regarded as characteristic of the –CSNH– group, as previously been found for monosubstituted thioamides.[17]

(4) For SC·HCl the frequencies characteristic of the NH_3^+ structure have without much difficulty been obtained. By comparing the spectrum of SC·HCl with that of SC, the $r(NH_2)$ and δ(O=C–N) frequencies of the $-CONH_2$ group and two frequencies due to hybridized vibrations composed of the $r(ND_2)$ and δ(O=C=N) vibrations have been obtained.

The author is grateful to Professor Yoshiya Kanda of Kyushu University for the use of the spectrophotometer. He is also indebted to the Ministry of Education for its financial support.

Department of Literature and Science
Saga University
Saga

23) See Ref. 14, pp. 234-244.
24) S. Mizushima and I. Nakagawa, *J. Chem. Soc. Japan, Pure Chem. Sec.* (*Nippon Kagaku Zasshi*), **80**, 124 (1959).
25) M. Tsuboi, T. Onishi, I. Nakagawa, T. Shimanouchi and S. Mizushima, *Spectrochim. Acta*, **12**, 253 (1958).
26) K. Nakamura, *J. Chem. Soc. Japan, Pure Chem. Sec.* (*Nippon Kagaku Zasshi*), **80**, 118 (1959).

The Electronic Structure of the α-Amino Acids of Proteins. II. Dissociation Constants

By Teijiro YONEZAWA,* Giuseppe DEL RE** and Bernard PULLMAN

(Received February 21, 1964)

In a previous paper[1] we obtained a satisfactory correlation between the charge distribution in the α-amino acids, as determined by a semi-empirical procedure derived from the molecular orbital method,[2] and the proton chemical shifts of these compounds. In the present paper we will report some approximate results concerning the dissociation constants of the same compounds.

The simplest α-amino acids dissociate according to the schemes:

$$RNH_3{}^+COOH \rightleftharpoons RNH_3{}^+COO^- + H^+ \quad (I)$$

and

$$RNH_3{}^+COO^- \rightleftharpoons RNH^2COO^- + H^+ \quad (II)$$

The pK's corresponding to these two dissociation processes are conventionally denoted as pK_1 and pK_2. Only these processes will be discussed in the present paper.

The Method

Simple electrostatic models[3] have already led to the conclusion that the dissociation constant of an acidic group is affected by the electrostatic effect of the neighbouring groups. We have assumed, therefore, that the energy variation involved in the dissociation process is given by two essential contributions: a) the change in the sum of the bond energies of the amino acid molecule in passing from the non-dissociated form to the dissociated form; and b) the change in the electrostatic energy of the proton because, in the final dissociated state, it is no longer subject to the attractions or repulsion of the other atoms of the molecule.

Several theoretical chemists have attempted to interpret dissociation constants on the basis of more or less refined calculations. They have, however, studied conjugated compounds almost exclusively and based their considerations on calculations for the π systems of such molecules. Therefore, their procedures cannot be directly applied to our problem. However, some of their considerations have, of course, a general significance. Thus, the basicity of conjugated molecules has been related to the chang in π energy during the dissociation[4] and to the value of the π charge of the protonated heteroatom[5]. The use of a combined index taking into account both the change in π energy and the change in the energy due to an additional electrostatic interaction has also been proposed[6] and shown to be particularly successful. Finally, it has been observed that taking the solvation into account leads to useful improvements.[7]

Only a classical electrostatic theory has been proposed,[3] as far as we know, in connection with saturated compounds.

We have adopted a point of view similar to that of Ref. 6. Already in Ref. 2, the method proposed in that paper was used for a semi-qualitative discussion of dissociation constants. In particular, the total σ-electron energy of a given molecule was calculated by adding the σ energies of the various bonds, according to the formulas;

$$E = \sum_{\substack{\text{bonds} \\ \mu\nu}} E_{\mu\nu} \quad (1)$$

where*

$$E_{\mu\nu} = 2\alpha + \{(\delta_\mu + \delta_\nu) + 2\varepsilon_{\mu\nu}\sqrt{1+Q^2{}_{\mu\nu}}\}\beta \quad (2)$$

and

$$Q_{\mu\nu} = \frac{\delta_\mu - \delta_\nu}{2\varepsilon_{\mu\nu}} \quad (3)$$

(The parameters α and β are the usual standard Coulomb and bond integrals; δ_μ and δ_ν are defined by the condition that $\alpha+\delta_\mu\beta$ and $\alpha+\delta_\nu\beta$ are the Coulomb integrals of the μ-th and ν-th atom respectively; $\varepsilon_{\mu\nu}\beta$ is the bond

* On leave from Faculty of Engineering, Kyoto University, Kyoto, Japan.

** Universita di Napoli, Istituto di Fisica Teorica, Naples, Italy.

1) G. Del Re, B. Pullman and T. Yonezawa, *Biochem. Biophys. Acta*, **75**, 153 (1963).

2) G. Del Re, *J. Chem. Soc.*, **1958**, 4031.

3) N. Bjerrum, *Z. physik. Chem.*, **106**, 219 (1923); J. G. Kirkwood and F. H. Westheimer, *J. Chem. Phys.*, **6**, 506, 513 (1938); F. H. Westheimer and M. W. Shookhoff, *J. Am. Chem. Soc.*, **61**, 555 (1939).

4) H. C. Longuet-Higgins, *J. Chem. Phys.*, 18, 275 (1950).

5) B. Pullman and A. Pullamn, "Les Théories Electroniques de la Chimie Organique," Masson, Paris (1952).

6) T. Nakajima and A. Pullman, *J. chim. phys.*, **1958**, 793: B. Pullman and T. Nakajima, *Bull. soc. chim. France*, **1959**, 590.

7) O. Chalvet, R. Daudel and F. Peradejordi, *J. chim. phys.*, **1962**, 709.

* In Ref. 2 the factor 2 before $\varepsilon_{\mu\nu}$ had been ommitted in the formula for $E_{\mu\nu}$

integral of the $\mu\nu$ bond.)

If formula 1 is applied to a series of protonated molecules and to the corresponding free bases, one gets energy differences which can be expected to a first approximation to be linearly related to the pK's of the corresponding dissociation equilibria (of course, the changes in the solvation and nuclear repulsion energies are assumed to be constant).

These considerations have been taken as a starting point of the present paper. The ΔE's, however, have been calculated according to the refined formula:

$$\Delta E = E_\sigma(\text{final}) - E_\sigma(\text{initial}) - \sum_\mu \frac{Q_H Q_\mu e^2}{R_{H\mu}} \qquad (4)$$

Here E_σ(initial) denotes the energy of the protonated compound, and E_σ(final), that of the base. The third term corresponds to the electrostatic interaction between the proton and the other atoms in the protonated compound. Q_H is the net charge (in e units) of the proton; $Q\mu$, the net charge of μ-th atom, and $R_{H\mu}$, their mutual distance. The calculation of $R_{H\mu}$ was carried out using a formula proposed by Eyring,[8] and by Kirkwood and Westheimer.[9] This formula gives the root-mean square distance between the hydrogen and the atom located at the end of the n-th bond, assuming free rotation around the bonds. Let $\eta_{m\ m+1}$ be the cosine of the supplement of the angle between the m-th and $m+1$-th bond and l_k, the length of the k-th bond; then,

$$\overline{R_n}^2 = \sum_{k=1}^{n} l_k^2 + 2\sum_{k=1}^{n}\sum_{s=1}^{k-1} l_k l_s \prod_{m=s}^{k-1} \eta_{m\ m+1} \qquad (5)$$

A few remarks are important in connection with Eq. 4:

1) The net charge, Q_μ, of the μ-th atom must be calculated by adding the charge, $Q_\mu{}^\sigma$, due to the σ electrons to $Q_\mu{}^\pi$, the net charge due to the π electrons, if present:

$$Q_\mu = Q_\mu{}^\sigma + Q_\mu{}^\pi \qquad (6)$$

The net charges, $Q_\mu{}^\pi$, calculated for our compounds by the ordinary Hückel method are shown in Fig. 1.

2) ΔE should be given by the difference between the total energy of the final and initial molecules in Eqs. I and II the total energy of a molecule being:

$$E_\pi + E_\sigma + \sum_{\mu>\nu} \frac{Q_\mu Q_\nu e^2}{R_{\mu\nu}} \qquad (7)$$

(E_π and E_σ denote the total π and σ energies, and the third term denotes the core repulsion energy in the molecule). Equation 4 represents this ΔE only if the variation of the total π-electron energy is assumed to be constant, and only if one may reasonably assume that the variation of the third term can be written as:

$$\Delta\sum_{\mu>\nu} \frac{Q_\mu Q_\nu e^2}{R_{\mu\nu}} = C - \sum_\mu \frac{Q_H Q_\mu e^2}{R_{H\mu}} \qquad (8)$$

where C is a constant.

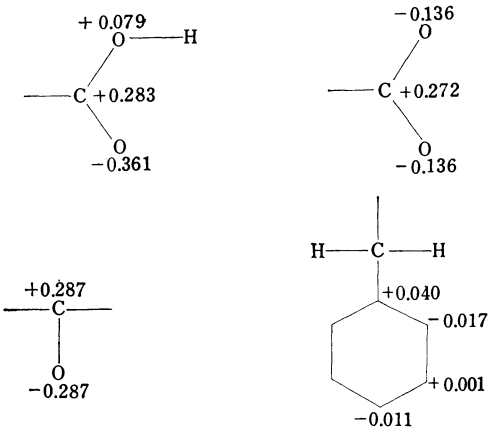


Fig. 1 The net charge of π-electrons in the conjugated parts of the amionacids.

3) The last term in Eq. 4 corresponds to the dielectric constant of the solvent being equal to 1. Different values have been adopted in classical theory,[3] but no serious modification could arise if we introduced the same kind of correction, as the change in the dielectric constant has always been taken to be small.

4) The contribution of the solvation energy is not taken into account.

5) The hyperconjugation effects, which may take place in certain amino acids, are ignored throughout all the calculations.

Results and Discussion

The results of the calculation are listed in Tables I and II, together with the experimental values of pK_1 and pK_2 for the various compounds. In the second columns of these tables, the variations of the total σ energies in the course of reactions I and II are given in units of $-\beta$. In the fourth columns the calculated values of the ΔE's (Eq. 4) are listed in units of eV.'s. The calculation of the ΔE's has required the determination of a value for $-\beta$. We have chosen 5.2 electron volts, a value not unreasonable for this type of property judging from other investigations of saturated compounds[10] and corresponding to a least-square

8) H. Eyring, *Phys. Rev.*, **39**, 746 (1932).
9) J. Kirkwood and F. H. Westheimer, *J. Chem. Phys.*, **6**, 506 (1938).
10) K. Fukui, H. Kato, T. Yonezawa, K. Morokuma, A. Imamura and C. Nagata, This Bulletin, **35**, 38 (1962).

TABLE I. THE DISSOCIATION CONSTANT pK_1' AND CALCULATED RESULTS

Compound	ΔE_σ (in units of $-\beta$)	$\sum_\mu \frac{Q_H Q_\mu}{R_{H\mu}} e^2$ (in units of eV.)	$\Delta E_\sigma - \sum_\mu \frac{Q_H Q_\mu}{R_{H\mu}} e^2$ (in units of eV.)	Apparent dissociation constants pK_1'*
Glycine	1.852	−0.037	9.527	2.34
Alanine	1.821	−0.014	9.483	2.34
Valine	1.815	−0.031	9.469	2.32
Serine	1.815	−0.010	9.448	2.21
Proline	1.803	−0.062	9.437	1.99
β-Alanine	1.818	−0.235	9.689	3.60
Leucine	1.815	−0.094	9.548	2.36
Methionine	1.821	−0.024	9.493	2.28
Aspartic acid	1.821	+0.057	9.412	1.88
Asparagine	1.815	+0.017	9.421	2.02
Phenylalanine	1.811	−0.032	9.449	1.83

* These values are quoted from Tables 4-11 of J. P. Greenstein and M. Winitz, "Chemistry of the Aminoacids," Vol. 1, John Wiley and Sons (1961).

TABLE II. THE DISSOCIATION CONSTANT pK_2' AND CALCULATED RESULTS

Compound	ΔE_σ (in units of $-\beta$)	$\sum_\mu \frac{Q_H Q_\mu}{R_{H\mu}} e^2$ (in units of eV.)	$\Delta E_\sigma - \sum_\mu \frac{Q_H Q_\mu}{R_{H\mu}} e^2$ (in units of eV.)	Apparent dissociation constants pK_2'*
Glycine	3.367	+0.799	16.709	9.60
Alanine	3.363	+0.794	16.694	9.69
Valine	3.357	+0.782	16.674	9.62
Serine	3.367	+0.791	16.717	9.15
Methionine	3.363	+0.891	16.597	9.21
Proline	3.603	+0.871	17.784	10.60
β-Alanine	3.387	+0.877	16.735	10.19
Asparagine	3.363	+0.850	16.638	8.80
Leucine	3.371	+0.811	16.718	9.60
Phenylalanine	3.366	+0.789	16.714	9.13

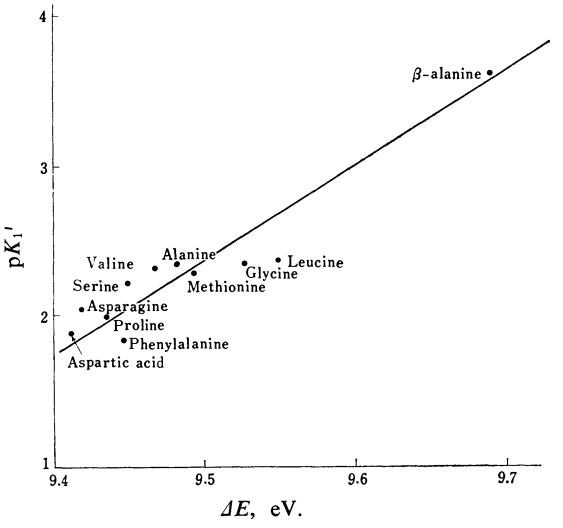


Fig. 2 The dissociation constant pK_1' vs. $\Delta E\left(\Delta E_\sigma - \sum_\mu \frac{Q_H Q_\mu}{R_{H\mu}} e^2\right)$

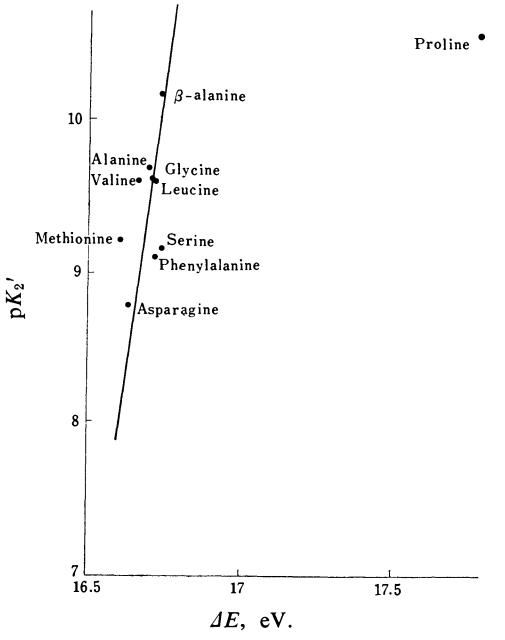


Fig. 3 The dissociation constant pK_2' vs. ΔE.

TABLE III. STATIC REPULSION ENERGY

Dipolar ion	Free rotation $-\sum_{\mu}\frac{Q_{\mu}Q_{H}}{R_{H\mu}}e^2$	Hindered rotation $-\sum_{\mu}\frac{Q_{H}Q_{\mu}}{R_{H\mu}}e^2$	Hinderd rotation $\Delta\sum_{\nu>\mu}\frac{Q_{H}Q_{\mu}}{R_{H\mu}}e^2$	$+C$
Glycine	−0.799	−0.247	−2.006	−1.759
Alanine	−0.794	−0.363	−2.105	−1.742

fitting of the ΔE vs. pK_1 plot by a straight line.

As regards the relationship between the ΔE's and the pK_1's, Table I and Fig. 2 show that it corresponds to a straight line as far as could be expected with such drastic simplifications as have been introduced. In Table I, a remarkable contribution of the repulsion term is observed, for instance, in the case of β-alanine. This confirms that one cannot ignore the contributions of the third term of Eq. 4.

In the case of the pK_2's, the agreement between the experimental and theoretical results is less satisfactory (Table II and Fig. 3). For proline, which has the largest pK_2 value, we do obtain the largest calculated value of ΔE: this value, however, deviates to a large extent from the rough linear relationship observed for the other pK_2's.

It may be useful to consider the influence of some possible refinements in the calculations on these results. Thus, e. g., the present treatment introduces two kinds of approximations in connection with interatomic distances. First of all, the interatomic distances are calculated by means of Eq. 5, assuming that there is free rotation around the bonds; second, the repulsion term is assumed to consist only of those repulsions or attractions which take place between the hydrogen atom which is involved in the dissociation and the other atoms of the initial molecule, to the exclusion of the changes in other repulsion energies (Eq. 8).

As to the first approximation, one may note that, especially in reaction I, the Lewis acid from which the proton dissociates probably has a special steric conformation, so that the free rotation around the various bonds is hindered to some exten. In order to evaluate the changes brought about in the repulsion energy by the assumption of a fixed configuration, let us assign to the dipolar ion of reaction II the configuration shown in Fig. 4. The

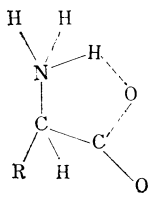


Fig. 4 Assumed conformation in $RNH_3^+COO^-$.

static repulsion terms, $\sum_{\mu}\frac{Q_{H}Q_{\mu}e^2}{R_{H\mu}}$, for this conformation of the glycine and alanine dipolar ions are given in Table III.

To check the validity of our second assumption, we have also evaluated the variation in the core repulsion energy, $\sum_{\mu>\nu}\frac{Q_{\mu}Q_{\nu}e^2}{R_{\mu\nu}}$, for the same molecules in a similar conformation of the anions, i. e., with a hydrogen bond between the $-COO^-$ group and the NH_2 group. Its values are also given in Table III, together with the values of $\sum_{\mu}\frac{Q_{H}Q_{\mu}e^2}{R_{\mu H}}$ corresponding to the freely rotating structure. Table III shows that the values of C (Eq. 8) become −1.759 and −1.742 for glycine and alanine respectively, they are thus approximately the same. These results strongly suggest that the above assumptions do not cause serious errors in connection with dissociation constants, therefore, e. g., the disagreement we have found between calculated and experimental values of the pK_2's may very probably be explained in a different way.

Another dubious point concerns the contribution of the solvation energy to ΔE, since this contribution is not taken into account in our calculation. No suitable method for estimating the extent of this contribution is available; therefore, we can only estimate it roughly with the help of the Hush-Blackledge and Daudel formula:[7,11]

$$E_s \simeq -\sum_{\mu} Q_{\mu}^2 \qquad (9)$$

where the solvation energy, E_s, is considered to be proportional to the sum of the squares of the net charges in the molecule. Formula 9 leads to nearly the same values of ΔE_s for all the aminoacids, so that no important improvement of the results can be expected for this correction.

Conclusion

The results reported in the present note seem to make possible another encouraging stop forward in the difficult process of correlating, by means of semi-empirical quantum

11) N. S. Hush and J. Blackledge, *J. Chem. Phys.*, 23, 514 (1955).

theoretical methods, the properties of α-amino acids. The particularly severe difficulties connected with the treatment of dissociation constants make the deviations from a linear relationship quite expected; therefore, it is gratifying that the overall correlation, especially of the pK_1's, is quite satisfactory.

Improvements should probably be looked for through refinements concerning the solvation effects and possibly through the inclusion of long-range exchange effects.

This work was sponsored by the Convention N° 61-FR-134 of the Délégation Générale à la Recherche Scientifique et Technique of France, and Grant CY-3073 of the United States Public Health Service.

Université de Paris
Institut de Biologie Physico-Chimique
13, rue Pierre Curie, Paris 5e, France

The Polarographic Behavior of Mercuric Diethyldithiocarbamate in a Ternary Solvent Mixture

By Taitiro FUJINAGA and Kazuo YAMASHITA

(Received February 21, 1964)

Sodium-diethyldithiocarbamate has long been used as one of the most useful analytical reagents in methods involving solvent extraction for the separation and concentration of the trace constituents of a sample.

As is well known, the method of solvent extraction has been widely applied to the analysis of trace elements, particularly in colorimetric determinations. However, in order to apply the extraction method to electrochemical analyses, either the sample solution has to be evaporated and the residue redissolved in water or, alternatively, the solution must be reextracted with water after a suitable adjustment of the physico-chemical conditions.

The present authors, in a previous paper,[1] proposed a third method, in which a ternary mixture is used as a solvent for the polarographic analysis after extraction; they applied the method to the determination of traces of lead in sodium chloride of analytical grade. In this procedure, the chloroform layer, into which the lead chelate of diethyldithiocarbamate had been extracted, was mixed directly with a solution consisting of ethylene glycol monomethyl ether (methyl-cellosolve), and aqueous hydrochloric acid as the supporting electrolyte. Even though chloroform is insoluble in water, the addition of methyl-cellosolve makes it possible to obtain a homogeneous solution. It was found that this homogeneous ternary mixture had a dielectric constant high enough to ensure the electrolytic dissociation of dissolved salts. The ohmic drop in this solution was about the same as that in a purely aqueous solution. Hence, it was possible to carry out the polarographic analysis directly, without any further treatment.

In the present work, the polarographic reduction of mercuric-diethyldithiocarbamate has been investigated in a ternary solvent mixture consisting of chloroform, methyl-cellosolve and water, in the presence of 0.5 M perchloric acid as a supporting electrolyte. In this solution, $Hg(DDTC)_2$ usually gives two d. c. cathodic waves, though a small anodic step appears at a more positive potential when the temperature is lowered below 15°C. The first cathodic step (step A in Fig. 1, curve 1) was found to be proportional to the bulk concentration of $Hg(DDTC)_2$ over the concentration range of 0.1 mM to 0.4 mM; it is probably due to the reduction of unadsorbed $Hg(DDTC)_2$. The height of the second step (step B in Fig. 1, curve 1), on the other hand, was almost constant and independent of the concentration of $Hg(DDTC)_2$ and, hence, seems due to the reduction of $Hg(DDTC)_2$ adsorbed onto the surface of the dropping electrode. Step B, therefore, represents a so-called anomalous polarographic step.[2] In the present case, the oxidised form of the depolarizer, $Hg(DDTC)_2$, is adsorbed strongly onto the electrode surface and, consequently, a post-step B appears at a more negative potential than the normal step A. Though many

1) T. Fujinaga, H. Brodowsky, T. Nagai and K. Yamashita, *Review of Polarography (Japan)*, 11, 217 (1963).

examples of anomalous waves[2-6] have been found for the adsorption of the reduced form which produces a prewave, examples of the present case have rarely been reported.

Experimental

The reagents and the apparatus used were the same as those reported on in the previous paper.[1] Throughout the experiments, two dropping mercury electrodes with the following characteristics were used: Electrode A: $m=0.73$ mg./sec., $t=3.75$ sec., and $h=65$ cm., and Electrode B: $m=0.64$ mg./sec., $t=4.63$ sec., and $h=65$ cm. in an air-free ternary solvent mixture at open circuit. The polarographic measurements were carried out in the absence of air; the potential values quoted refer to the saturated calomel electrode, which was connected to the electrolyte solution through an agar bridge (5% agar, 7.5% sodium perchlorate).

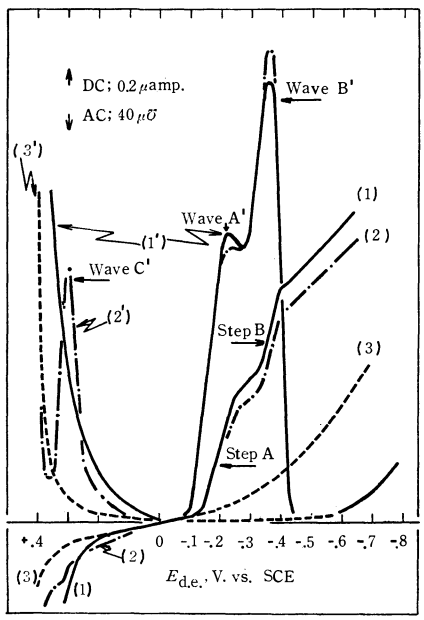


Fig. 1.

(1) D. C. polarogram of 3×10^{-4} M mercuric-diethyldithiocarbamate $Hg(DDTC)_2$ and 0.5 M perchloric acid in the ternary solvent mixture at 25°C.
(1') A. C. polarogram of the same solution as in (1).
(2) D. C. polarogram of the same solution as in (1) at 10°C.
(2') A. C. polarogram of the same solution as in (1) at 10°C.
(3) D. C. polarogram of 0.5 M perchloric acid in the ternary mixture at 25°C
(3') A. C. polarogram of the same solution as in (3).

Results

It is well known that $Hg(DDTC)_2$ can be extracted completely into chloroform from an aqueous solution over a wide pH range.[7,8] The solution of $Hg(DDTC)_2$ in the ternary solvent mixture was prepared as follows: 1 ml. of an aqueous solution of 0.4% sodium diethyldithiocarbamate was added to 2 ml. of water which contained from 1 mM to 10 mM mercuric ions. To this solution 5 ml. of chloroform were added. After this mixture had been shaken for five minutes, 11 ml. of methyl-cellosolve and 1 ml. of concentrated perchloric acid were added and the solution was shaken until a clear solution was obtained. The proportion of water, methyl-cellosolve and chloroform in the final solution was 4 : 11 : 5 by volume.

D. C. Polarography.—With a solution of less than 0.1 mM $Hg(DDTC)_2$, only a single step is observed around −0.4 V. vs. SCE. When the concentration of $Hg(DDTC)_2$ is raised above 0.1 mM, however, two steps appear, one at −0.2 and the other at −0.4 V., as is shown by curve 1, Fig. 1.

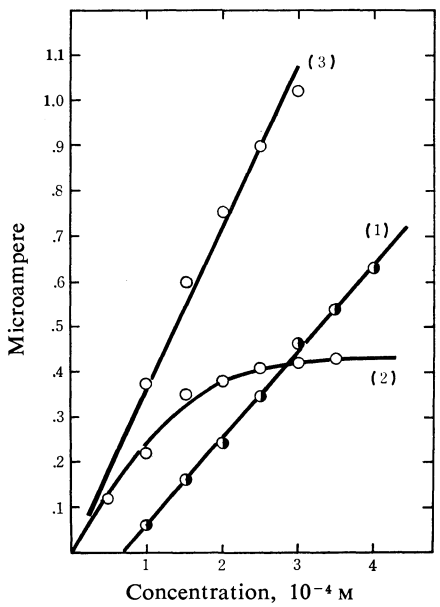


Fig. 2. Calibration curves of D. C. steps (1) A, (2) B and (3) the total step height in 0.5 M perchloric acid, and in ternary solvent mixture, $h=65$ cm.; $m=0.64$ mg./sec.; $t=4.63$ sec.; T, 25°C.

2) R. Brdicka, *Collection Czechoslov. Chem. Communs.*, **12**, 522 (1947).
3) O. H. Müller, *Trans. Electrochem. Soc.*, **87**, 441 (1941).
4) R. C. Kage and H. I. Stonehill, *J. Chem. Soc.*, **1942**, 3244.
5) Y. Asahi, *Review of Polarography*, **8**, 1 (1960).
6) B. Breyer and T. Biegler, *Collection Czechoslov. Chem. Communs.*, **25**, 3348 (1960).
7) H. Bode, *Z. anal. Chem.*, **142**, 414; **143**, 182 (1954).
8) Y. Hamamoto and M. Kotakemori, *J. Agr. Chem. Soc. Japan*, **34**, 885 (1960).

TABLE I. EFFECT OF THE HEIGHT OF THE MERCURY COLUMN ABOVE THE CAPILLARY TIP, h_{Hg}, ON THE CURRENTS OF STEPS B AND TOTAL FOR 0.3 mM SOLUTION OF $Hg(DDTC)_2$ IN 0.5 M PERCHLORIC ACID IN THE TERNARY MIXTURE

h_{Hg} cm.	m, mg./sec.	t, sec. at −0.4 V.	$\bar{i}$(mm.) $\bar{i}_B$	$\bar{i}$(mm.) $\bar{i}_T$	$h_{corr.}$ cm.	$\bar{i}_B/h_{corr.}$	$\bar{i}_T/h^{1/2}_{corr.}$
60.2	0.667	4.52	35.5	72.0	58	0.61_2	9.4_6
65.2	0.717	4.12	38.0	75.5	63	0.60_3	9.5_1
70.2	0.771	3.88	41.5	79.0	68	0.61_0	9.5_8
75.2	0.823	3.57	45.0	83.0	73	0.61_6	9.7_1
80.2	0.874	3.32	48.0	86.0	78	0.61_5	9.7_3
85.2	0.928	3.10	52.5	90.0	83	0.63_2	9.8_7

Figure 2 illustrates the dependence of the heights of step A (1), step B (2) and of the total step height (3) on the concentration of $Hg(DDTC)_2$. The limiting currents of step A, step B and of the total step height were measured at −0.25 and at −0.40 V., respectively. The height of step B increases with the concentration of $Hg(DDTC)_2$ in a fashion corresponding to a Langmuir adsorption isotherm; it shows a limiting value when the concentration of $Hg(DDTC)_2$ reaches a value of 0.3 mM. The height of step A increases linearly with the concentration of $Hg(DDTC)_2$, but the step does not appear at concentrations of $Hg(DDTC)_2$ below 0.1 mM because of its adsorption onto the electrode surface which produces step B. The total wave height (curve 3) also increases approximately linearly with the concentration of $Hg(DDTC)_2$.

The electrocapillary curves obtained are shown in Fig. 3. In the presence of $Hg(DDTC)_2$, a marked decrease of the drop time is observed between +0.4 and −0.4 V. (curve 3). At more negative potentials than −0.4 V., the drop time in the presence of $Hg(DDTC)_2$ is equal to that in its absence (curve 2). This indicates that the substance is adsorbed between +0.4 and −0.4 V. and is desorbed from the electrode surface at about −0.4 V. The potential at which $Hg(DDTC)_2$ is desorbed corresponds to that at which step B appears.

The relationship between the heights of steps A and B and the concentration of $Hg(DDTC)_2$ also confirms the supposition that step B is due to the reduction of the adsorbed form of $Hg(DDTC)_2$, whilst step A is due to the reduction of the unadsorbed form. This assumption is also confirmed by experimental results to be reported on below.

The temperature coefficients of the heights of steps A and B and of their sum were +1.63%, +1.28% and +1.46% respectively in the 15~30°C range (Fig. 4).

The effect of the height of the mercury reservoir was also studied. The results are shown in Table I. The height of step B was

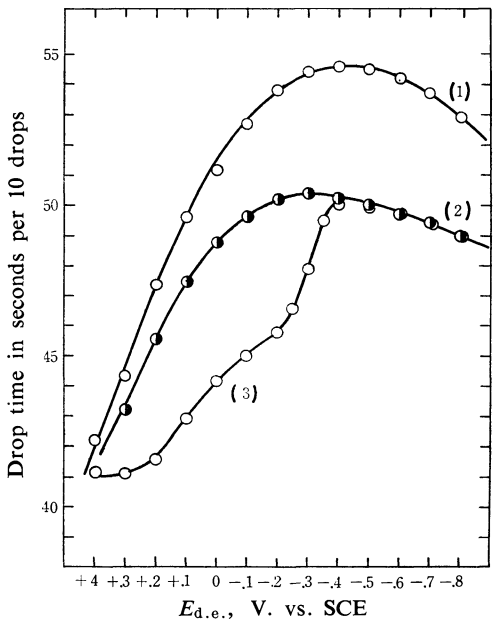


Fig. 3. Electrocapillary curves of (1) 0.5 M perchloric acid in water, (2) 0.5 M perchloric acid in ternary solvent mixtures and (3) 3×10^{-4} M concentration of $Hg(DDTC)_2$, h= 65 cm.; m=0.73 mg./sec.; t=3.75 sec.; T, 25°C.

approximately linearly proportional to h, whilst the total step height was approximately proportional to $h^{1/2}$. This agrees well with the assumption that step B is anomalous. The fact that surfactants, such as polyacrylamide (PAM 75) or gelatine, had little effect on the polarograms shows that $Hg(DDTC)_2$ is more strongly adsorbed than these surfactants.

A. C. Polarography.—A. C. polarograms obtained with a solution of 0.3 mM $Hg(DDTC)_2$ in the ternary solvent mixture are shown in Fig. 1. At 25°C, two a. c. waves were observed (curve 1', A' and B') at potentials corresponding to the two d. c. steps.

Below 15°C, however, a new a. c. wave (wave C') was observed at about +0.3 V., a

wave which corresponds to the small anodic wave in the d.c. polarogram (Fig. 1). The height of wave A′ increased linearly with the concentration of $Hg(DDTC)_2$ at concentrations below 0.5 mM (Fig. 5, curve 1). The calibration curves of waves B′ and C′ have the shape of a Langmuir adsorption isotherm (Fig. 5, curve 2, and Fig. 6). Hence, these two waves seem to be connected with the adsorption and desorption of $Hg(DDTC)_2$.

The effects of temperature are shown in Figs. 7 and 8. The height of wave A′ increases with the increasing temperature (Fig. 7, curve 1); the height of wave B′, however, decreases with the increasing temperature. This behavior shows that the a.c. current of wave B′ has both a tensammetric and a faradaic component

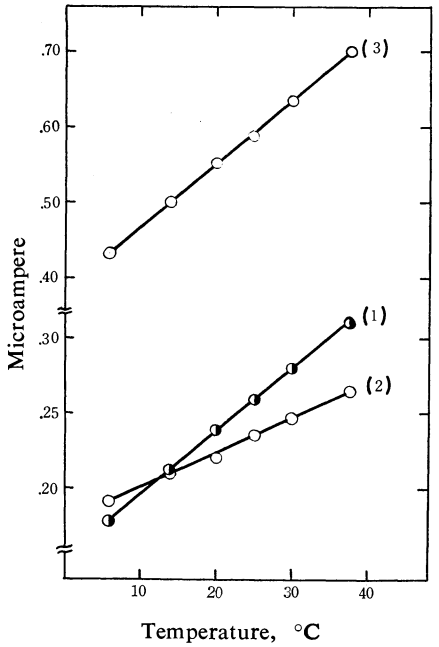


Fig. 4. Effect of temperature on heights of steps (1) A, (2) and (3) total step height in 0.5 M perchloric acid in the ternary solvent mixture, h=65 cm.; m=0.73 mg./sec.; t=3.75 sec.; T, 25°C.

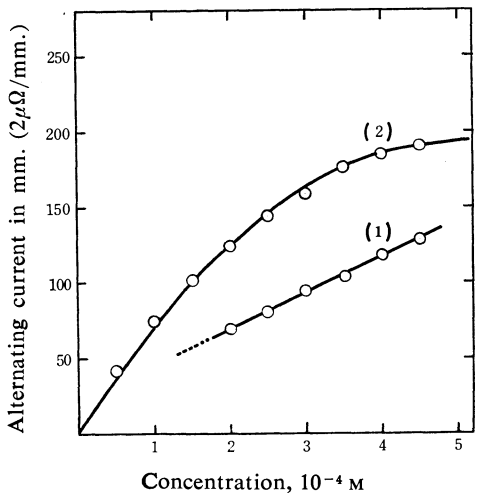


Fig. 5. Calibration curves of waves (1) A′ and (2) B′ of $Hg(DDTC)_2$ in 0.5 M perchloric acid in the ternary solvent mixture, h=65 m.; m=0.64mg./sec.; t=4.63 sec. at open circuit; T, 25°C; A.C. 15 mV. r.m.s.

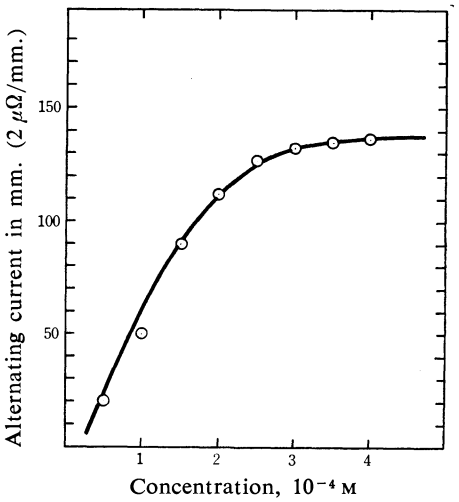


Fig. 6. Calibration curves of tensammetric wave (wave C′) of $Hg(DDTC)_2$ in 0.5 M perchloric acid in the ternary solvent mixture, h=65 cm., m=0.64 mg./sec., t=4.63 sec., at zero applied potential, T, 10°C; A.C. 15 mV. r.m.s.

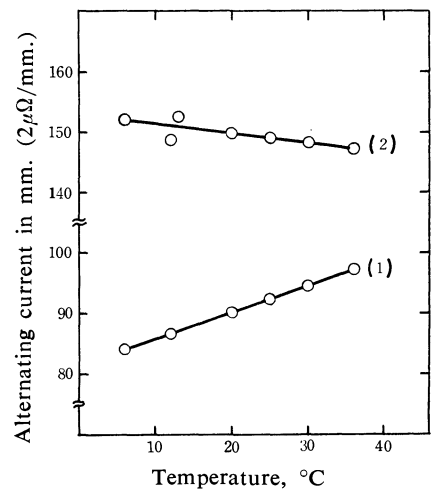


Fig. 7. Effect of temperature on the heights of A.C. waves (1) A′ and (2) B′; h=65 cm.; m=0.64 mg./sec.; t=4.63 sec.; T, 25°C; A.C. 15 mV. r.m.s.

("rearrangement current"[9]). The results obtained by the a. c. polarographic method are also in good agreement with the assumption that waves B and B′ are anomalous, that is, that they are due to the fact that the strongly adsorbed $Hg(DDTC)_2$ is reduced and desorbed from the electrode surface.

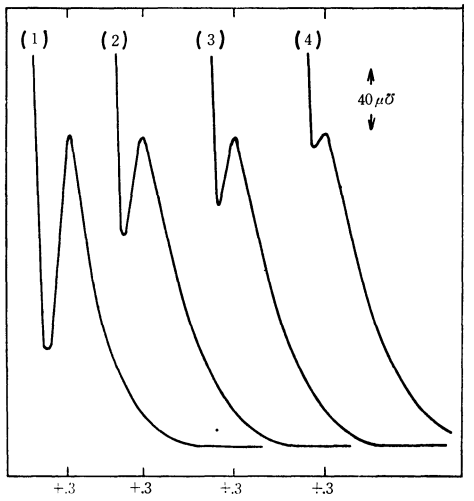


Fig. 8. Effect of temperature on the appearance of the tensammetric wave (wave C′) in 0.5 M perchloric acid in the ternary solvent mixture; h=65 cm; m=0.64 mg./sec.; t=4.63 sec.; A. C. 15 mV. r. m. s. (1) 10°C, (2) 13°C, (3) 14°C, (4) 15°C.

Discussion

The appearance of wave C′ in the a. c. polarogram in the absence of a d. c. polarographic step indicates that this a. c. wave is tensammetric in nature. The adsorption of $Hg(DDTC)_2$ onto the dropping mercury electrode, therefore, begins at this potential.

When the concentration of $Hg(DDTC)_2$ is small (below about 0.1 mM), all the molecules which diffuse to the electrode surface are adosorbed to be reduced at the B potential corresponding to step in d. c. polarography. If the concentration of $Hg(DDTC)_2$ becomes larger than that sufficient for the electrode surface to be completely covered with adsorbed molecules, unadsorbed molecules reach the electrode surface and are reduced, forming wave A. In d. c. polarography, wave B is called an anomalous polarographic wave. As has been pointed out already, the current of the a. c. wave B′ is a rearrangement current, that is, it contains both a faradaic and a tensammetric component; this is in good agreement with the postulate that it is due to the reduction of adsorbed $Hg(DDTC)_2$. Incidentally, we believe that this is one of the first instances where the existence of the theoretically-predicted rearrangement current has been proved experimentally.

If we assume that the reduction of $Hg(DDTC)_2$ proceeds according to:

$$Hg(DDTC)_2 + 2e = Hg + 2(DDTC)^- \qquad (1)$$

we would expect that the $(DDTC)^-$ anion so formed would give rise to an oxidation step. However, it has been reported by Bode[7] and by Gregg[10] that the $(DDTC)^-$ anion is decomposed immediately in a strongly acidic solution, such as 0.5 M perchloric acid, according to:

$$(C_2H_5)_2N\text{-}C\langle^{S^-}_{S} + H^+ = (C_2H_5)_2NH + CS_2$$

In fact, we did not observe an oxidation step of $DDTC^-$ ions in 0.5 M perchloric acid, though we did see one in a basic solution.

If the concentration of $Hg(DDTC)_2$ in the solution is large enough, the electrode surface is completely covered with a mono-layer of $Hg(DDTC)_2$ and the excess of $Hg(DDTC)_2$ produces step A.

The average current ($\bar{i}$) at the potential of wave A can be expressed as:

$$\bar{i} = \bar{i}_I - \bar{i}_B \qquad (2)$$

where $\bar{i}_I$ is the theoretical current, that is, that calculated from the Ilkovič equation under the assumption that $Hg(DDTC)_2$ is unadsorbed. $\bar{i}_I$ is defined by:

$$\bar{i}_I = 2Km^{2/3}t^{1/6}(C_0^* - C_0^0) \qquad (3)$$

where C_0^* is the concentration of $Hg(DDTC)_2$ in the bulk of the solution and C_0^0, that at the electrode surface, while $\bar{i}_B$ is the current corresponding to step B, i. e., the current due to the reduction of adsorbed $Hg(DDTC)_2$. $\bar{i}_B$ is practically independent of the concentration of $Hg(DDTC)_2$ and can be expressed by the following equation:

$$\bar{i}_B = 2Fz\Delta q \qquad (4)$$

where F: Faraday constant, z: maximum number of moles adsorbed per unit area, and Δq: the mean increase of the surface area per time unit ($\Delta q = 0.85\, m^{2/3}t^{-1/3}$).

From Eqs. 2 and 3, we obtain:

$$\bar{i} = 2Km^{2/3}t^{1/6}(C_0^* - C_0^0) - \bar{i}_B$$

$$C_0^0 = C_0^* - (\bar{i} + \bar{i}_B)/2Km^{2/3}t^{1/6} \qquad (5)$$

9) B. Breyer and H. H. Bauer, "Alternating Current Polarography and Tensammetry," Interscience Publishers, New York (1963), pp. 74, 268.

10) E. C. Gregg and W. P. Tyler, *J. Am. Chem. Soc.* 72, 4561 (1950).

Since, as has already been explained, $(DDTC)^-$ ions cannot exist in an acid solution, we can write:

$$\bar{i}=K'm^{2/3}t^{1/6}C_R{}^0$$

where $C_R{}^0$ is the surface concentration of $(DDTC)^-$.

Therefore,

$$C_R{}^0=\bar{i}/K'm^{2/3}t^{1/6} \quad (6)$$

Assuming that the redox reaction 1 occurs reversibly, the potential at any point of wave A is given by the Nernst equation:

$$E_{d.e.}=E_0-0.0295\log(C^\circ{}_{DDTC^-})^2/C^\circ{}_{Hg(DDTC)_2} \quad (7)$$

Solving Eqs. 5, 6 and 7, we obtain

$$E_{d.e.}=E_0'-0.0295\log(\bar{i}^2/(2C_0{}^*Km^{2/3}t^{1/6}-\bar{i}-\bar{i}_B))$$

where E_0' is equal to $E_0-0.0295\log(K/K'm^{2/3}t^{1/6})$ and is almost constant at a constant $m^{2/3}t^{1/6}$. $2C_0{}^*Km^{2/3}t^{1/6}$ is equal to the total limiting current and is given by the sum of $\bar{i}_B$ and $\bar{i}_A$ (average limiting current of step A).

Hence, we can write:

$$E_{d.e.}=E_0'-0.0295\log\bar{i}^2/(\bar{i}_A-\bar{i}) \quad (8)$$

Thus a plot of $E_{d.e.}$ vs. $\log\bar{i}^2/(\bar{i}_A-\bar{i})$ of wave A should have a slope of 29.5 mV. The experimental results agreed well with this prediction, as Fig. 9 shows; log-plots were found to have a slope between 28 and 31 mV. This fact suggests that the reduction of $Hg(DDTC)_2$ is a reversible, two-electron process.

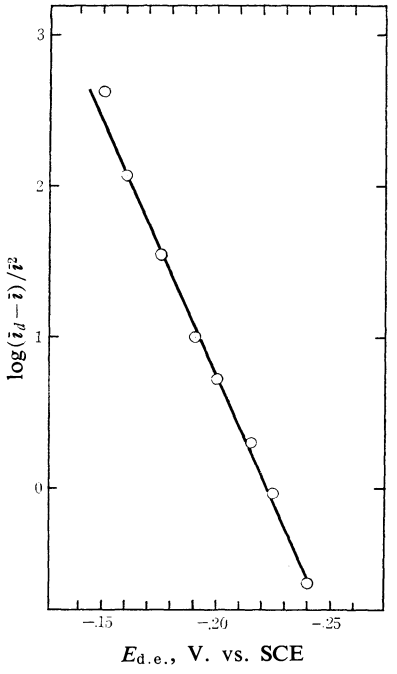


Fig. 9. Relationship between $\log(\bar{i}^2/\bar{i}_A-\bar{i})$ and $E_{d.e.}$ of the D. C. step A T, 25°C.

Relationship 4 makes it possible to evaluate directly the maximum number of molecules per unit area of the electrode surface. At a concentration of 0.3 mM of $Hg(DDTC)_2$, the number of moles of $Hg(DDTC)_2$ adsorbed per unit area of the electrode surface was calculated as:*

$$Z_1=5.7\times10^{-10}\ \text{mol./cm}^2$$

Similary, at a concentration of 0.1 mM, when wave A begins to appear:

$$Z_2=2.3\times10^{-10}\ \text{mol./cm}^2$$

From the value of Z_1, the area which one molecule of $Hg(DDTC)_2$ occupies is 30 Å^2/molecule, assuming that the adsorbed molecules form a monolayer. If we consider that $Hg(DDTC)_2$ is adsorbed vertically upon the electrode surface, this value seems reasonable, considering the area calculated from the crystal data reported by Simonsen and Wah Ho.[11] From the Z_2 value, the occupied area is found to be 75 Å^2/molecule; this value is in fairly good agreement with the value calculated by assuming that the chelate is adsorbed horizontally onto the electrode. We think that the difference between Z_1 and Z_2 might be due to a different orientation of the adsorbed chelate molecule at the electrode surface. However, it is also possible that the adsorbed film may be a multi- and not a monolayer.

The behavior of the $Hg(DDTC)_2$ dimethylformamide solution will be reported on in a subsequent paper.

The authors wish to acknowledge the helpful suggestions of Visiting Professor Bruno Breyer, formerly of the University of Sydney.

Chemistry Institute
Faculty of Science
University of Kyoto
Sakyo-ku, Kyoto

11) S. H. Simonsen and u. J. Wah Ho, *Acta Cryt.* **6**, 430 (1953).

* For the calculation, the following data were used:

$\bar{i}_B=(\bar{i}_{total})_{corr.}-\bar{i}_A$,

$(\bar{i}_{total})_{corr.}=(\bar{i}_{total})_{obs.}(t_A/t_B)^{1/6}$

where t_A=4.66 sec., $\bar{i}_A$=0.475 microampere at −0.29., t_B=4.97 sec., and $(\bar{i}_{total})_{obs.}$=0.905 microampere at −0.40 V.

Determination of Lead and Thallium(I) in Presence of Each Other by Amperometric Titrations

By D. S. JAIN and J. N. GAUR

(Received November 30, 1963)

Thallium in presence of lead has been determined by Winn[1] in urine by digesting a sample of urine with a mixture of sulphuric, perchloric and nitric acids. Thallium was oxidised to the trivalent state with bromine water and then extracted with a chloroform solution of dithiozone, while lead under these conditions, remained in the water phase. The chloroform extract was used for the polarographic estimation of thallium.

In supporting electrolytes which do not complex lead ions, the thallium and lead waves coincide. The half-wave potentials of lead and thallous ion in 1 M potassium nitrate has been found to be -0.38 V.[2] and -0.46V.[3] respectively against SCE at 25°C and thus their polarographic determination in presence of each other presents some difficulty, but by employing sodium or potassium hydroxide supporting electrolyte the half-wave potential of lead shifts to -0.76 V.[4] Thallium can thus easily be determined in presence of lead. In the present communication a method will be described by which lead and thallium (ous) can be determined in presence of each other amperometrically without oxidizing thallous to thallic ion.

Apparatus and Experimental

Heyrovsky LP55 polarograph was used. The dropping mercury electrode had the following characteristics: $m=2.12$ mg./sec., $t=3.6$ sec. (at -1.0 V. vs. SCE in 0.1 M potassium nitrate solution).

All measurements were done at 20°C, purified hydrogen was used for the removal of dissolved oxygen.

All reagents employed were of A. R. grade. Purity of the samples was checked by standard methods.

Determination of Lead in Presence of Thallium Ion.—The principles involved in the method are as follows: (i) Tl^+ does not form a complex with potassium ferrocyanide[5] in concentrations below 0.1 M, but lead does at all concentration; and (ii) when a potential of -0.4 V. vs. SCE is applied to a solution containing both lead and thallium ion, it is the thallous ion which can be reduced.

Solutions of different strength containing Pb^{2+} and Tl^+ were prepared in 1 M potassium nitrate. One thousandth percent solution of triton×100 was used as maxima suppressor in the final solution. The mixture was titrated with a standard potassium ferrocyanide solution at an applied voltage of -0.4 V. vs. SCE. Hydrogen was passed after every addition. Titrations were performed both by the direct and reverse methods. The results are recorded in Tables I and II.

Determination of Thallium in Presence of Lead.—(i) In alkaline solution (pH 11.5) of

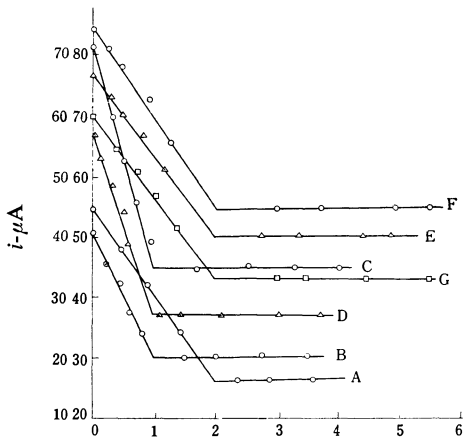


Fig. 1. Direct titration of Pb^{2+} in presence of Tl^+ with 0.1 M $K_4Fe(CN)_6$.

Curve A: 1 ml. of 0.2 M Pb^{2+} + 0.2 ml. of 0.1 M Tl^+.
B: 0.5 ml. of 0.2 M Pb^{2+} + 0.2 ml. of 0.1 M Tl^+.
C: 0.5 ml. of 0.2 M Pb^{2+} + 1 ml. of 0.1 M Tl^+.
D: 0.5 ml. of 0.2 M Pb^{2+} + 0.4 ml. of 0.1 M Tl^+.
E: 1.0 ml. of 0.2 M Pb^{2+} + 2 ml. of 0.1 M Tl^+.
F: 1.0 ml. of 0.2 M Pb^{2+} + 5 ml. of 0.1 M Tl^+.
G: 1.0 ml. of 0.2 M Pb^{2+} + 10 ml. of 0.1 M Tl^+.

1) G. S. Winn, F. L. Godfrey and K. W. Nelson, *Arch. Ind. Hyg. Occupational Med.*, **6**, 14 (1952).
2) H. M. Hershenson, M. E. Smith and D. N. Hume, *J. Am. Chem. Soc.*, **75**, 507 (1953).
3) L. Meites, ibid., **73**, 4155 (1951).
4) J. Heyrovsky and D. Ilkovic, *Collection Czechoslov. Chem. Communs.*, **7**, 198 (1935).
5) J. N. Gaur, H. C. Gaur and A. K. Bhattacharya, *J. Indian Chem. Soc.*, **35**, 144 (1958).

TABLE I. DIRECT TITRATION OF Pb IN PRESENCE OF THALLIUM

Sample No.	Composition of mixture (10 ml.) in 1 M KNO_3	Volume of sol. taken in cell ml.	Volume of 0.1 M $K_4Fe(CN)_6$ used ml.	Amount of Pb^{2+} found g.	Amount of Pb^{2+} actually present (calcd.) g.
A	5 ml. of 0.2 M Pb^{2+} 1 ml. of 0.1 M Tl^+	20	2.0	0.04144	0.04144
B	2.5 ml. of 0.2 M Pb^{2+} 1 ml. of 0.1 M Tl^+	10	1.0	0.02072	0.02072
C	2.5 ml. of 0.2 M Pb^{2+} 5 ml. of 0.1 M Tl^+	10	1.0	0.02072	0.02072
D	2.5 ml. of 0.2 M Pb^{2+} 2 ml. of 0.1 M Tl^+	10	1.0	0.02072	0.02072
E	5 ml. of 0.2 M Pb^{2+} 10 ml. of 0.1 M Tl^+	20	2.0	0.04144	0.04144
F	5 ml. of 0.2 M Pb^{2+} 25 ml. of 0.1 M Tl^+	20	2.0	0.04144	0.04144
G	5 ml. of 0.2 M Pb^{2+} 50 ml. of 0.1 M Tl^+	20	2.0	0.04144	0.04144

TABLE II. REVERSE TITRATION OF Pb^{2+} IN PRESENCE OF Tl^+

Sample No.	Composition of mixture (100 ml.) in 1 M KNO_3	Strength and volume of $K_4Fe(CN)_6$ in the cell	Volume of mixture used ml.	Amount of Pb^{2+} found g.	Amount of Pb^{2+} present (calcd.) g.
1	50 ml. of 0.2 M Pb^{2+} 5 ml. of 0.2 M Tl^+	40 ml. of 5 mM	2.0	0.04144	0.04144
2	50 ml. of 0.2 M Pb^{2+} 10 ml. of 0.2 M Tl^+	40 ml. of 5 mM	2.0	0.04144	0.04144
3	20 ml. of 0.2 M Pb^{2+} 20 ml. of 0.2 M Tl^+	40 ml. of 2 mM	2.00	0.01666	0.01666

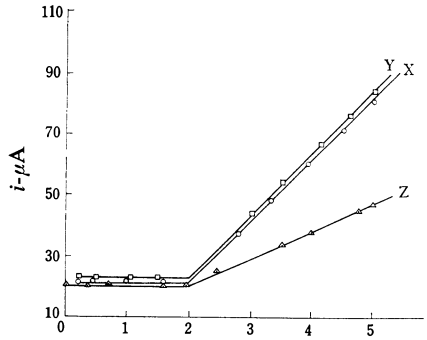


Fig. 2. Reverse titration of Pb^{2+} in presence of Tl^+ with $K_4Fe(CN)_6$.
Curve X: 0.1 M Pb^{2+} + 0.01 M Tl^+ added to 40 ml. of 5 mM $K_4Fe(CN)_6$.
Y: 0.1 M Pb^{2+} + 0.02 M Tl^+ added to 40 ml. of 5 mM $K_4Fe(CN)_6$.
Z: 0.04 M Pb^{2+} + 0.04 M Tl^+ added to 40 ml. of 2 mM $K_4Fe(CN)_6$.

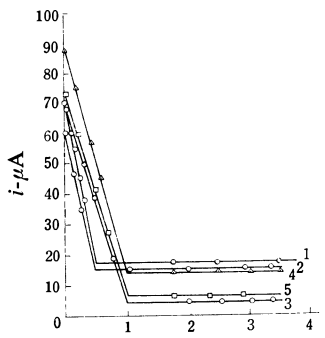


Fig. 3. Direct titration of Tl^+ in presence of Pb^{2+} with K_2CrO_4.
Curve 1: 0.25 ml. of 0.2 M Tl^+ + 0.25 ml. of 0.2 M Pb^{2+} titrated with 0.05 M K_2CrO_4.
2: 0.5 ml. of 0.2 M Tl^+ + 0.5 ml. of 0.2 M Pb^{2+} titrated with 0.1 M K_2CrO_4.
3: 5.0 ml. of 0.2 M Tl^+ + 5.0 ml. of 0.2 M Pb^{2+} titrated with 0.5 M K_2CrO_4.
4: 1.0 ml. of 0.2 M Tl^+ + 1.0 ml. of 0.2 M Pb^{2+} titrated with 0.5 M K_2CrO_4.

thallium and lead, only thallium is precipitated as thallous chromate and lead remains in solution as sodium plumbate. (ii) As a potential of −0.5 V. vs. SCE is applied, only thallium is reduced in the alkaline medium. After adjusting the pH of the solution of 11.5 by adding sodium hydroxide the mixture was titrated with a standard solution of potassium chromate. Titrations were done by the direct as well as reverse methods. The results are recorded in Tables III and IV.

TABLE III. DIRECT TITRATION OF Tl^+ IN PRESENCE OF Pb^{2+}

Sample No.	Composition of the mixture (50 ml.) in NaOH (pH=11.5)	Volume of mixture in the cell ml.	Strength and volume of K_2CrO_4 used	Amount of Tl^+ found g.	Amount of Tl^+ present (calcd.) g.
1	1.25 ml. of 0.2 M Tl^+ 1.25 ml. of 0.2 M Pb^{2+}	10	0.5 ml. of 0.05 M	0.01022	0.01022
2	2.5 ml. of 0.2 M Tl^+ 2.5 ml. of 0.2 M Pb^{2+}	10	0.5 ml. of 0.1 M	0.02044	0.02044
3	12.5 ml. of 0.2 M Tl^+ 12.5 ml. of 0.2 M Pb^{2+}	20	1.0 ml. of 0.5 M	0.20439	0.20439
4	2.5 ml. of 0.2 M Tl^+ 2.5 ml. of 0.2 M Pb^{2+}	20	1.0 ml. of 0.1 M	0.40878	0.40878
5	12.5 ml. of 0.2 M Tl^+ 25.0 ml. of 0.2 M Pb^{2+}	20	1.0 ml. of 0.5 M	0.20439	0.20439

TABLE IV. REVERSE TITRATION OF Tl^+ IN PRESENCE OF Pb^{2+}

Sample No.	Composition of the mixture (50 ml.) in NaOH (pH=11.5)	Strength and volume of K_2CrO_4 in cell	Volume of mixture used ml.	Amount of Tl^+ found g.	Amount of Tl^+ present (calcd.) g.
1	1.25 ml. of 0.2 M Tl^+ 1.25 ml. of 0.2 M Pb^{2+}	10 ml. of 1.0 mM	4.0	0.00409	0.00409
2	2.5 ml. of 0.2 M Tl^+ 2.5 ml. of 0.2 M Pb^{2+}	10 ml. of 0.5 mM	1.0	0.00204	0.00204
3	12.5 ml. of 0.2 M Tl^+ 12.5 ml. of 0.2 M Pb^{2+}	10 ml. of 1.0 mM	4.0	0.04087	0.04087
4	2.5 ml. of 0.2 M Tl^+ 25.00 ml. of 0.2 M Pb^{2+}	20 ml. of 1.0 mM	2.0	0.00409	0.00409
5	12.5 ml. of 0.2 M Tl^+ 25.0 ml. of 0.2 M Pb^{2+}	10 ml. of 1.0 mM	4.0	0.04087	0.04087

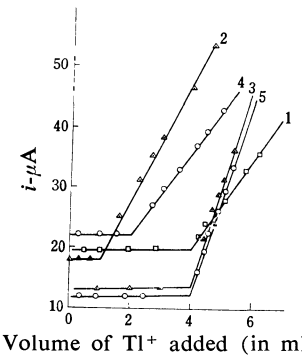


Fig. 4. Reverse titration of Tl^+ in presence of Pb^{2+} with K_2CrO_4.
Curve 1: 0.005 M Tl^++0.005 M Pb^{2+} titrated with 10 ml. of 1.0 mM of K_2CrO_4.
2: 0.01 M Tl^++0.01 M Pb^{2+} titrated with 10 ml. of 0.5 mM of K_2CrO_4.
3: 0.05 M Tl^++0.05 M Pb^{2+} titrated with 10 ml. of 1.0 mM of K_2CrO_4.
4: 0.01 M Tl^++0.1 M Pb^{2+} titrated with 20 ml. of 1.0 mM of K_2CrO_4.
5: 0.05 M Tl^++0.1 M Pb^{2+} titrated with 10 ml. of 1.0 mM of K_2CrO_4.

Discussion

It has been found that the results obtained by the direct and reverse titrations of thallium by potassium ferrocyanide suggest an excellent method of determining lead in presence of thallium in small concentrations (0.01 M Pb^{2+} in 0.05 M Tl^+). The concentration of the thallium ion should not go beyond 0.1 M, since it reacts with potassium ferrocyanide. At pH 11.5 it has been possible to determine thallous ion in presence of lead by titration with potassium chromate. Under these conditions lead does not interfere. It is possible to determine accurately as small as 0.005 M Tl^+ in 0.1 M of Pb^{2+}.

Summary

A method has been described in which thallium(I) can be determined in presence of lead and vice versa. Thallium is determined amperometrically in presence of lead at pH 11.5 and is titrated with potassium chromate, while lead is determined in presence of thallium by titrating with potassium ferrocyanide. It is possible to determine small amounts of lead in large quantities of thallium and vice versa.

Department of Chemistry
University of Rajasthan
Jaipur, India

*The Inhibitive Behavior of the Fluoride Ion and the Destruction of Its Protective Film in the Corrosion of Magnesium in Neutral Solutions**

By Goro WADA and Seihei MAEKAWA

(Received December 25, 1963)

Fluoride ions accelerate the corrosion rate of aluminum in a manner quite similar to that of other halide ions.[1] Iron is corroded in a dilute solution of potassium fluoride as well as in a solution of potassium chloride, but its corrosion is suppressed in a solution of potassium fluoride more concentrated than 0.8 N.[2,3] The inhibitive action of chromate ions on the corrosion of zinc is considerably strengthened by the addition of fluoride ions.[4,5] Now, in the case of magnesium, the fluoride ion has been known to be a good inhibitor and to exhibit a somewhat different behavior from that of such other ionic inhibitors as the chromate, bichromate and nitrate ions.[6] In this paper, a mechanism for the formation of protective films by the fluoride ions and their destruction by corrosive ions will be presented on the basis of electrochemical kinetics.

Experimental

Materials. — The magnesium metal used was obtained from the E. Merck Chemical Company, Darmstadt, Germany, in the form of a ribbon 3.18 mm. in average width, 0.26 mm. in average thickness, and 99.93% pure. The impurities, as found by spectrographic analysis,[7] are shown in Table I.

TABLE I. IMPURITIES IN MAGNESIUM (%)

Fe	Mn	Cu	Al	Si	Ca	Zn
0.017	0.014	0.005_1	0.002_0	0.003_5	0.0003_7	<0.01
Sn	Sr	Ni	Cr	V	Ti	Pb
<0.005	<0.005	<0.001	<0.001	<0.005	+	−

After a magnesium specimen was cut in an appropriate length, the connection to the leading wire was sealed completely by paraffin so as not to come in contact with the corroding reagent. The effective surface area of magnesium acting as an electrode was determined by a micrometer microscope, considering its surface to be flat enough, or its roughness factor to be unity, and disregarding the edge effect in the course of reaction. The magnesium was cleaned by acetone just before the measurements.

Polarization Characteristics of Magnesium in Various Solutions. — The stationary potentials of magnesium at various external current densities in several corrosion media are shown in Fig. 1. The anodic polarization curves in corrosive media, such as the aqueous solutions of potassium chloride and potassium bromide, are almost horizontal, while those in solutions containing inhibitive reagents, such as potassium nitrate, potassium chromate and potassium fluoride, are displaced towards nobler potentials and have steeper slopes; especially in the case of potassium fluoride, the curve is quite vertical and the anodic current is markedly retarded.

On the other hand, all the cathodic polarization curves are very similar to one another.

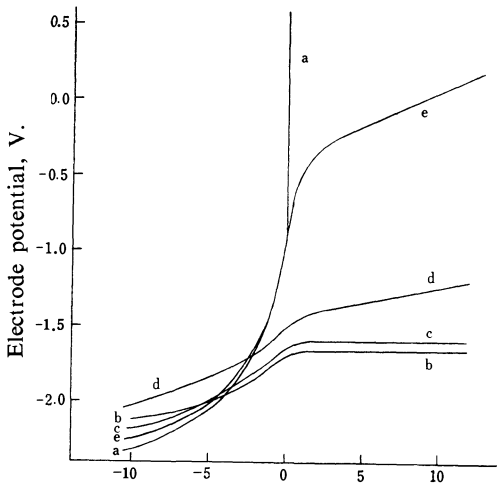


Fig. 1. Polarization characteristic curves of magnesium in 0.1 N aqueous solutions of various electrolytes at 20°C.
(a) KF (d) KNO_3
(b) KCl (e) K_2CrO_4
(c) KBr

* Corrosion Reaction of Magnesium. Part XIV. The previous report appeared in *J. Chem. Soc. Japan, Pure Chem. Sec.* (*Nippon Kagaku Zassi*), **79**, 1461 (1958).

1) M. Izuyama and Y. Hayakawa. *J. Electrochem. Soc. Japan*, **29**, 873 (1961).
2) A. W. Chapman, *J. Chem. Soc.*, **1930**, 1546.
3) U. R. Evans, "The Corrosion and Oxidation of Metals, Scientific Principles and Practical Applications," Edward Arnold Publishers, London (1960), p. 176.
4) U. R. Evans, ibid., p. 185.
5) C. V. King, E. Goldschmidt and N. Mayer, *J. Electochem. Soc.*, **99**, 423 (1952); C. V. King and E. Hilmer, ibid., **101**, 79, (1954); C. V. King and E. Rau, ibid., **103**, 331 (1956).
6) G. Wada, *J. Chem. Soc. Japan, Pure Chem. Sec.* (*Nippon Kagaku Zassi*), **75**, 279 (1954).
7) N. Oda, S. Tuno and M. Idohara, *J. Electrochem. Soc. Japan*, **30**, 350, E-111 (1962).

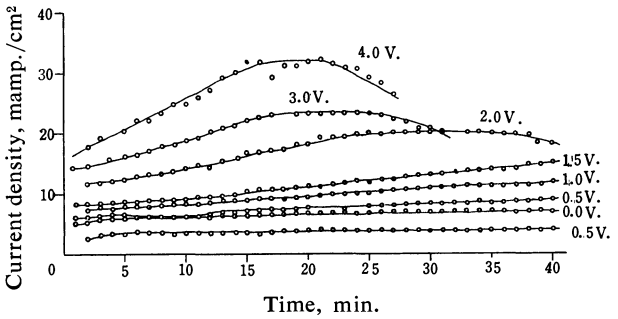


Fig. 2. Variations of anodic current densities with time at various potentials in a 0.001 N KCl solution at 20°C.

The Formation of Fluoride Films.—The inhibitive action of the fluoride ion on the corrosion of magnesium has been attributed to the formation of fine protective films composed of insoluble magnesium fluoride on the magnesium surface. Concerning this, the following facts were found in this experiment: a) 4.9 μg./cm^2 of the fluoride ion was deposited on the surface when magnesium was anodically polarized at 2 V. in a 0.1 N solution of potassium fluoride for 15 min., using a 0.1 N calomel electrode as the reference; b) 69.0 μg./cm^2 of the fluoride ion was also deposited when the magnesium was left alone in the same solution for 40 days. Provided that these amounts of deposited fluoride ions form homogeneous films of magnesium fluoride over the surface, their thicknesses would be about 280 Å in the case of a) and about 4000 Å in the case of b). In the experiment, the determination of small quantities of fluoride ion was carried out by the method of spectrophotometric titration using sodium alizarin monosulfonate.[8]

The quantity of electricity accumulated in the film during the 15 min. period was calculated to be about 0.03 coul./cm^2 from the observed current density-time relation,[9] while the theoretical quantity of electricity necessary to form the film in the case of a) is equal to about 0.025 coul./cm^2. Therefore, the current efficiency is nearly equal to unity for the formation of the magnesium fluoride film. Moreover, the result in the case of b) indicates that the magnesium fluoride film still continues to grow spontaneously by the diffusion of charged particles through the film, even in the natural, or externally unpolarized, state.[10]

The Destruction of Magnesium Fluoride Films by Corroding Reagents.—Figures 2 and 3 show the time variations in the potentiostatic external current densities observed at various electrode potentials

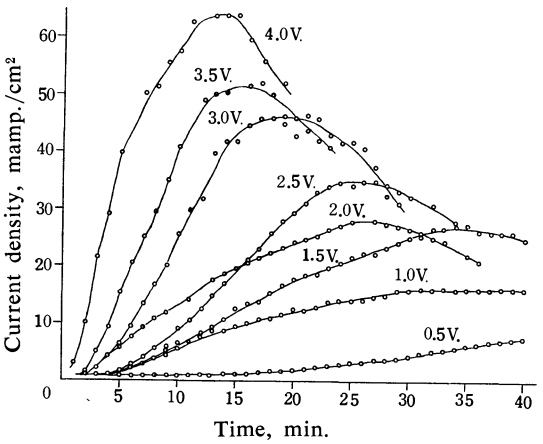


Fig. 3. Variations of anodic current densities with time at various potentials in a 0.001 N KCl+0.1 N KF solution at 20°C.

in the corrosive solutions, where magnesium had previously been covered with a magnesium fluoride film by treating it in a 0.1 N potassium fluoride solution under the same conditions as in the case of a) mentioned above.

In any case, the current density increases with time at the first stage, reaches a maximum, and then gradually begins to decrease. At the stage of increase, the destruction or the stripping of the magnesium fluoride film mainly occurs; at the stage of decrease, on the other hand, perhaps the surface is covered by the products of corrosion, the hydroxide of magnesium.

When fluoride ions coexist with chloride ions in the solution, the current density is rather larger than when the chloride ion alone is present. The fluoride ion itself must have the power to promote corrosion like other halide ions if magnesium fluoride were not insoluble.

Discussion

The Mechanism of Film Rupture.—As the fine film of magnesium fluoride covering the surface is quickly destroyed and stripped off by the attack of corrosive ions, the bare area of

8) W. P. Pickhardt, *Anal. Chem.*, 34, 863 (1962).

9) The electric current was quite large at the instant when magnesium was brought into contact with a 0.1 N potassium fluoride solution and afterwards reduced abruptly to an extremely low value.

10) Since the densities of magnesium fluoride and metallic magnesium are 3.17 and 1.74 g./cm^3, the atomic densities with respect to magnesium are 5.0×10^{-2} and 7.2×10^{-2} g.-atom/cm^3 respectively. Accordingly, there occurs as much as a 44% expansion in the volume of magnesium with the transformation from the metallic state into a magnesium fluoride film.

the surface, without the film, expands and, accordingly, the apparent current density increases. However, since the products of the corrosion, such as magnesium hydroxide soon begin to interfere with the contact of the bare area with the corroding reagent, the apparent current density begins to decrease after reaching its maximum. Now, if the fractions of three kinds of surface areas, namely the bare and those covered with magnesium hydroxide and magnesium fluoride, are denoted by s_1, s_2 and s_3 respectively, and if the true current densities at a certain potential, E, on the respective areas are denoted by i_1, i_2 and i_3, the following relations can be established, where I represents the averaged current density over the total surface:

$$s_1+s_2+s_3=1 \tag{1}$$

$$\frac{ds_1}{dt}+\frac{ds_2}{dt}+\frac{ds_3}{dt}=0 \tag{2}$$

$$I=s_1i_1+s_2i_2+s_3i_3 \tag{3}$$

$$\left(\frac{\partial I}{\partial t}\right)_E=i_1\left(\frac{\partial s_1}{\partial t}\right)_E+i_2\left(\frac{\partial s_2}{\partial t}\right)_E+i_3\left(\frac{\partial S_3}{\partial t}\right)_E \tag{4}$$

Judging from the nature of the surface, $i_1 \gg i_2$, and $i_3 \approx 0$. Therefore, Eq. 4 may be written as:

$$\left(\frac{\partial I}{\partial t}\right)_E=-i_1\left(\frac{\partial s_3}{\partial t}\right)_E-(i_1-i_2)\left(\frac{\partial s_2}{\partial t}\right)_E \tag{5}$$

In the cases as shown in Figs. 2 and 3, $s_1=s_2=0$ and $s_3=1$ at the beginning of the reaction, but s_1 has fluctuating values between zero and unity in the midst of the reaction and afterwards converges again to zero. Consequently, the slopes of the nearly straight lines appearing before and after the peaks in Figs. 2 and 3 are approximately expressed by Eqs. 6 and 7 respectively, and the condition corresponding to the maximum point is expressed by Eq. 8.

$$\left(\frac{\partial I}{\partial t}\right)_E \simeq -i_1\left(\frac{\partial s_3}{\partial t}\right)_E \quad \text{Initial stage} \tag{6}$$

$$\left(\frac{\partial I}{\partial t}\right)_E \simeq -(i_1-i_2)\left(\frac{\partial s_2}{\partial t}\right)_E \quad \text{Final stage} \tag{7}$$

$$-\left(\frac{\partial s_3}{\partial t}\right)_E \simeq \left(\frac{\partial s_2}{\partial t}\right)_E \quad \text{Maximum point} \tag{8}$$

The intrinsic anodic polarization characteristic curves for the respective kinds of areas are schematically shown in Fig. 4, where i_1 is, of course, by far the largest among the three throughout the whole range of the potential. The Tafel relation holds on the bare area as long as the potential is low, but i_1 gradually fails and reaches a saturation value which is controlled by the diffusion at the higher potentials.[11] The electrode potential on the mixed surface of the areas with different natures is denoted by E in Fig. 4, as "a compromise potential."[13]

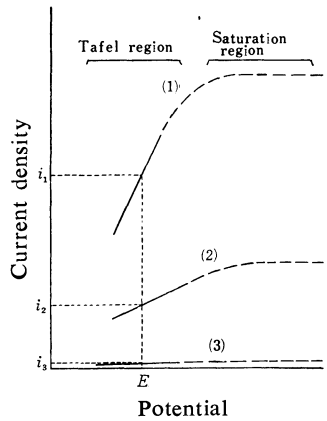


Fig. 4. Schematic diagram for the anodic polarization characteristic curves of different surface areas.
(1) Bare
(2) Covered with $Mg(OH)_2$
(3) Covered with MgF_2

Now, when the logarithms of the slopes of the initial and the final stages, $\log(\partial I/\partial t)_E$, in Figs. 2 and 3 are polotted against the potential, straight lines are obtained, as Fig. 5 shows. Therefore, recognizing that the potentials are high enough for i_1, i_2 and i_3 to be already saturated and hardly to vary with the potential, as can be seen in Fig. 4, the following relations can be derived:

$$R_F=\frac{A_F}{i_1}\exp\frac{\alpha_F FE}{RT} \tag{9}$$

$$R_O=\frac{A_O}{i_1-i_2}\exp\frac{\alpha_O FE}{RT} \tag{10}$$

where $R_F \equiv -(\partial s_3/\partial t)_E$, i.e., the rate of the destruction of the magnesium fluoride film; $R_O \equiv (\partial s_2/\partial t)_E$, i.e., the rate of the fomation of the magnesium hydroxide film; A_F and A_O are the characteristic constants; α_F and α_O are the transfer coefficients,[14] and F is the Faraday constant. Table II shows the transfer coefficients calculated from Fig. 5.

11) The anodic polarization curve of magnesium in a potassium chloride solution as shown in Fig. 1 is nearly horizontal. This was obtained by the steady-state method. If determination were performed on a fresh surface of magnesium by the rapid method, the curve should have a somewhat steeper slope in quite the same way as in the case of aluminum.[12]

12) G. Okamoto, T. Morozumi and F. Arai, *J. Electrochem. Soc. Japan*, 27, 437 (1559).

13) U. R. Evans, Ref. 3, p. 893.

14) M. Maeda, "Denkyoku no Kagaku (Chemistry of Electrodes)," Gihodo Series 12, Tokyo (1961), p. 102.

TABLE II. TRANSFER COEFFICIENTS OF THE POTENTIAL CURVES ALONG THE REACTION COORDINATES IN THE REACTIONS OF THE MgF_2-FILM DESTRUCTION, α_F, AND OF THE $Mg(OH)_2$-FILM FOMATION, α_O

Solution	α_F	α_O
0.001 N KCl	2.8×10^{-2}	0.41×10^{-2}
0.001 N KCl×0.1 N KF	2.3×10^{-2}	2.1×10^{-2}

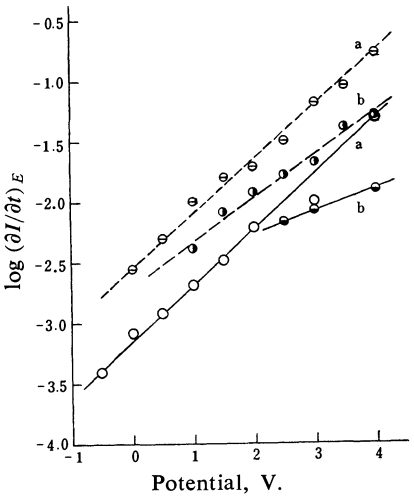


Fig. 5. Variations of $\log(\partial I/\partial t)_E$ of (a) the initial and (b) the final stages with the potential of magnesium.
—— 0.001 N KCl solution
---- 0.001 N KCl+0.1 N KF solution

In the reaction of the magnesium fluoride-film destruction, α_F's have values similar to each other irrespective of the presence of fluoride ions in the solutions, while in the magnesium hydroxide-film formation, the α_O's in the different solutions are quite different from each other. In the former reaction, a step which the existing ions do not seriously influence would be rate-determining, although it is not clear whether the reaction proceeds through a mechanical stripping-off of the film or through a chemical oxidation of fluoride ions. The films of magnesium hydroxide formed by the latter reaction, on the contrary, would all be different because of the adsorption of different ions.

The Activation Energy of the Destruction Reaction of the Magnesium Fluoride-film and That of the Cathode Reaction on the Same Surface.—The apparent activation energy of the reaction of the magnesium fluoride-film destruction at 0.5 V. in a 0.001 N KCl+0.1 N KF solution in the temperature range between 15 and 40°C was found to be nearly 19 kcal./mol. by plotting the logarithms of $(\partial I/\partial t)_E$ at the initial stage against the reciprocals of the temperature. This value is only one-fourth of the electron affinity of fluorine, 3.94 eV.[15] and seems to be too low if the destruction reaction involves a real electrochemical oxidation of fluoride ions. Therefore, it is probable that the destruction of the film is forced to occur through a mechanical stripping caused by the invasion of the corrosive reagent between the film and the metal. On the other hand, the apparent activation energies of the cathode reaction on the surface covered with magnesium fluoride, which had been formed beforehand in a 0.1 N potassium fluoride solution at 2.0 V. for 15 min., could be obtained from the temperature variations of the cathodic current density at −2.1V.; they are 3.0 kcal./mol. in a solution of 0.1 N potassium fluoride and 3.3 kcal./mol. in one KF 0.001 N KCl+0.1 N KF respectively.

As it could be ascertained that neither the reduction of Mg^{2+} ions nor the deposition of magnesium occurred at all through the magnesium fluoride film in the cathode reaction, it may be said, taking the very low values of both apparent activation energies into account, that the electric conduction through the film is not ionic but electronic. However, when the metal is polarized anodically, electricity is conducted through the magnesium fluoride-film neither by electrons nor by ions, in spite of the fact that the magnesium fluoride-film can grow by means of the diffusion of certain ions through the film, as has been mentioned. Thus the rectifying phenomenon by the magnesium fluoride-film can be recognized when the solution contains no other anions but fluoride ions.

Summary

Fluoride ions exhibit an anomalous inhibitive ability against the corrosion of magnesium; this may be attributed to the formation of a fine film of insoluble magnesium fluoride. This film conducts the cathodic current fairly well, but it conducts the anodic current not at all, as far as it is not destroyed. The cathode reaction through the magnesium fluoride film has a low apparent activation energy because of its electronic conduction, while, when magnesium is anodically polarized, the film is no longer electron-conductive and still permits to a lesser extent the diffusion of any other charged particles; consequently, this is a kind of rectifier in a solution containing potassium fluoride alone.

If a solution contains chloride ions in addition to fluoride ions, the matter is quite

15) "Kagaku Benran," Ed. by Chem. Soc. Japan, Maruzen, Tokyo (1952), p. 635.

different and fluoride ions rather promote the corrosion, like other halide ions. When magnesium, the surface of which has previously been covered with magnesium fluoride is anodically polarized in a solution containing only chloride ions or containing fluoride ions as well as chloride ions, the film soon begins to be destroyed at the initial stage, the bare area of high conductivity appears, and then the surface is gradually again covered with the bulky products, magnesium hydroxide, at the later stage. The destruction of the magnesium fluoride film may occur through a mechanical process regardless of the presence of fluoride ions.

The authors wish to thank Mr. Jujiro Nishijo, who helped in this investigation, and Dr. Nakaaki Oda of the Nippon Soda Co. Ltd. for his help in the special analysis of the magnesium sample.

Department of Chemistry
Faculty of Science
Kobe University
Rokko-dai, Kobe

Studies of Thio Acids. I. The Synthesis of Thiostearic Acid[*1]

By Yoshio HIRABAYASHI, Masateru MIZUTA and Tetsuro MAZUME[*2]

(Received December 26, 1963)

Many studies have been made of lower aliphatic thio acids, such as thioacetic acid and simple aromatic thio acids, and the knowledge recognized hitherto of the properties of thio acids has been mainly based on the properties of thioacetic acid or on those of thiobenzoic acid.[1,2] On the other hand, the studies of higher aliphatic thio acids have been very scanty, except for some short reports of the synthesis[3],[*3] of thiomyristic acid and thiopalmitic acid, and their properties have scarcely been studied at all.[4]

The authors made a series of studies for the purpose of obtaining extensive knowledge of higher aliphatic thio acids and examining the general properties of thio acids.

In this first paper of the present series, the synthesis of thiostearic acid from stearoyl chloride and sodium hydrogen sulfide will be described.

Stearoyl chloride prepared from stearic acid and thionyl chloride was added drop by drop into the ethanol solution of sodium hydrogen sulfide with heating. By the fractional crystallization of the crude product (Table I), thiostearic acid was obtained in the form of colorless crystals (m. p. 39.8~40.3°C), together with small amounts of distearoyl disulfide (m. p. 81.8~82.3°C), stearic acid, and ethyl stearate.

The separation of thiostearic acid from these by-products was achieved by fractional crystallization from petroleum ether or hexane; it was difficult to achieve by fractional distillation under reduced pressure or by fractional crystallization from other solvents.

The quantities of by-products depend upon the condition of the reaction. The yield of thiostearic acid was higher when the liquid temperature at dropping was higher, the time of dropping was shorter, the stirring was more vigorous, and the molar ratio of sodium hydrogen sulfide to chloride was larger. For example, the yields of thiostearic acid at the reaction temperatures of 40°C and 65°C were 25.2% and 53.3%[*4] respectively, other conditions being the same. The formation of ethyl

*1 Most of this study was presented at the 9th Annual Meeting of the Chemical Society of Japan, Kyoto, April, 1956.

*2 Present Address: Shimogamo-Kishimotocho, Sakyo-ku, Kyoto.

1) H. Gilman, "Organic Chemistry, An Advanced Treatise," Vol. I, John Wiley and Sons, Inc., New York (1949), p. 929.

2) D. S. Tarbell and D. P. Harrish, *Chem, Revs.*, **49**, 1 (1951).

3) V. Auger and M. Billy, *Compt. rend.*, **136**, 555 (1903).

*3 After the authors presented this study at the 9th Annual Meeting of the Chemical Society of Japan (1956), a report on thiostearic acid was found (F. J. Ritter, *Rubber Stickting, Delft, Commun.*, **No. 324**, 100 (1956); *Chem. Abstr.*, 50, 16168 (1956)). The synthetic method in the report corresponds well with the authors' method in this paper, but the melting point of the thiostearic acid obtained was reported to be 29~51°C, indicating the presence of an impurity.

4) K. S. Markley, "Fatty Acids," Intersience Publishers, Inc., New York (1947), p. 520.

*4 The yields were calculated for pure thiostearic acid separated from the crude product by recrystallization. If the sulfur contents (iodine method) in the crude product were attributed solely to thiostearic acid, the quantities of thiostearic acid in the crude product should be 72.2% and 90.9% respectively.

stearate made the separation of thiostearic acid difficult in fractional crystallization and gave a lower yield of thiostearic acid.

Distearoyl disulfide was obtained from the fraction with the higher melting point. Ethyl stearate was isolated from the mother liquor of the recrystallization of thiostearic acid by applying a method similar to the lead salt-alcohol method for the separation of solid fatty acids from liquid ones.

It is assumed that thiostearic acid and ethyl stearate were produced according to Eqs. 1—4 below and that distearoyl disulfide was produced as follows: in the preparation of a sodium hydrogen sulfide-ethanol solution, some sodium disulfide was produced, and then this reacted with stearoyl chloride to produce distearoyl disulfide.

$$RCOCl + C_2H_5OH \longrightarrow RCOOC_2H_5 + HCl \quad (1)$$

$$\left.\begin{array}{l} RCOCl + NaSH \longrightarrow RCOSH + NaCl \\ RCOSH + NaSH \rightleftarrows RCOSNa + H_2S \\ RCOSNa + RCOCl \longrightarrow RCOSOCR + NaCl \end{array}\right\} \quad (2)$$

$$\left.\begin{array}{l} 2\,NaSH \rightleftarrows Na_2S + H_2S \\ 2\,RCOCl + Na_2S \longrightarrow RCOSOCR + 2NaCl \end{array}\right\} \quad (3)$$

$$RCOSOCR + C_2H_5OH \longrightarrow RCOOC_2H_5 + RCOSH \quad (4)$$

$R = C_{17}H_{35}-$

The ultraviolet absorption spectrum of the obtained thiostearic acid in a cyclohexane solution is shown in Fig. 1, in which $\lambda_{max} = 221$ mμ and $\varepsilon_{max} = 1800$. An inflection is indicated at 260~280 mμ in the 0.1% solution,*5 but it is not observed in the 0.01% solution. In the infrared absorption spectra measured by the Nujol-mull method and by the potassium bromide-disk method (Fig. 2), an absorption band for the S–H group evidently appears at 2548 cm^{-1} as well as an absorption band for the C=O group at 1662 cm^{-1}, indicating that the synthesized thiostearic acid assumes the thiolic acid form; this is in accordance with the view of Sheppard[5] and Crouch[6] that thioacetic acid has the thiolic acid form.

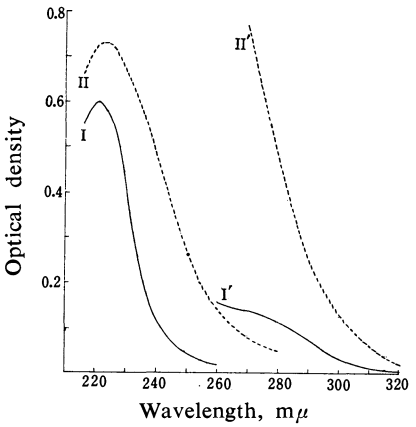


Fig 1. Ultraviolet absorption spectra of thiostearic acid (I, I') and distearoyl disulfide (II, II') in cyclohexane.
I, II, 0.01; I', II', 0.1% solution

Experimental

The Synthesis of Stearoyl Chloride.—Stearic acid (a product of the Nippon Yushi Co.) was recrystallized several times from methanol (neutralization value, 197.3; m. p. 70.0~70.5°C). When stearoyl chloride was synthesized by Ralston's process[7] from freshly-distilled thionyl chloride (85 g.) and stearic acid (105 g.), 100 g. of the fraction with the b. p. of 180~183°C/2.5 mmHg was retained.

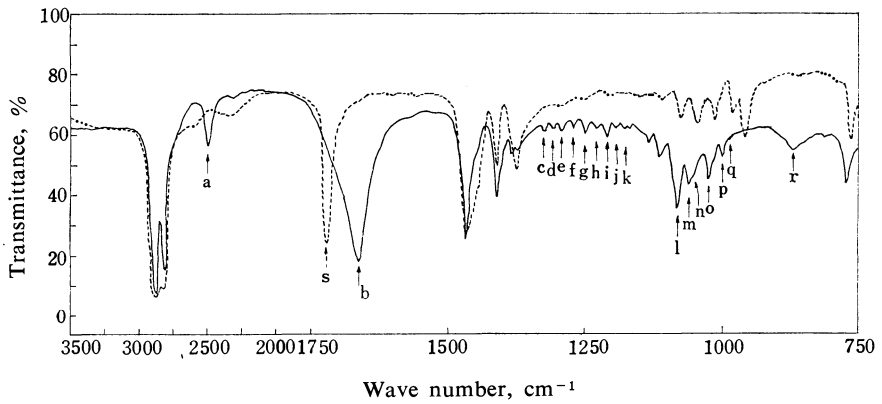


Fig. 2. Infrared absorption spectra of thiostearic acid (T) (——) in potassium bromide disk and distearoyl disulfide (J) (- - -) in Nujol mull.

*5 Ultraviolet absorption spectrum will be discussed later.

5) N. Sheppared, *Trans. Faraday Soc.*, 45, 693 (1949).

6) W. W. Crouch, *J. Am. Chem. Soc.*, 74, 2926 (1952).

7) A. W. Ralston and W. M. Selby, ibid., 61, 1019 (1939).

The Preparation of a Sodium Hydrogen Sulfide-Ethanol Solution. — Metallic sodium (10 g.) was dissolved in 150 ml. of absolute ethanol (previously distilled with the addition of metallic sodium), and then purified and dried hydrogen sulfide[8] was rapidly introduced into the solution until an excess of hydrogen sulfide was produced. The solution was colored a light yellow and was somewhat turbid.

The Synthesis of Thiostearic Acid.—Stearoyl chloride (31 g.) was vigorously stirred, drop by drop, into the above sodium hydrogen sulfide-ethanol solution at 40°C in 10 min. Then the mixture was refluxed on a water bath for 1 hr., followed by the separation of ethanol under a vacuum to obtain a white jelly residue. The residue was dissolved in 3 l. of water, acidified with dilute hydrochloric acid, and extracted with ether, and the ether layer was washed with water. An insoluble white matter suspended between the ether and the water was filtered off: 0.4 g. (A'). The ether layer was dried over anhydrous sodium sulfate, and the ether was expelled to obtain 27 g. of a crude product (light yellow colored; m. p. 32~34 °C; neutralization value 138.3; and sulfur content 7.7% (by the iodine method)). The crude product (23.0 g.) was recrystallized from hexane. The yields and melting points of several crystallization fractions are shown in Table I. These fractions were identified as follows:

TABLE I. YIELDS AND MELTING POINTS OF FRACTIONS OBTAINED BY RECRYSTALLIZATION OF CRUDE PRODUCT (23.0 g.)

Fraction	Yield, g.	M. p., °C
A	0.3	81.8~82.3
B	0.1	
C	1.1	69.5~70.0
D	1.6	51 ~55
E	5.8	39.8~40.3
F	4.5	31 ~35
G	8.4	30 ~31

(A): Obtained by the recrystallization of A' from benzene; colorless crystals.

Found: S, 0 (iodine method), 10.70 (Kitamura's method[9]). Calcd. for $C_{36}H_{70}O_2S_2$: S, 10.60%

This product did not show any depression in melting point when mixed with authentic distearoyl disulfide. Furthermore, the ultraviolet and infrared spectra of the two products were quite identical.

(C): Neutralization value 197.2. No depression in melting point was observed by mixing it with stearic acid.

(E): Colorless. Found: neutralization value 185.9; C, 72.03; H, 12.16; S, 10.57 (iodine method), 10.60 (Kitamura's method), 10.61 (Carius method). Calcd. for $C_{18}H_{36}OS$: neutralization value 186.7; C, 71.94; H, 12.07; S, 10.67%.

This fraction was thus identified as thiostearic acid $C_{17}H_{35}COSH$.

G): The neutralization value of 88.7, the sulfur content of 5.00% (iodine method) or 5.20% (Kitamura's method), and the melting point did not vary when recrystallization was repeated from hexane. A solution of this product (6 g.) in ethanol (20 ml.) was neutralized with a 0.1 N potassium hydroxide-ethanol solution. A soluton of lead acetate (0.4 g.) in ethanol (20 ml.) was added to the above solution, and the mixture settled for 3 hr. at room temperature. The solution was filtered, and then the filtrate was decomposed with dilute hydrochloric acid and extracted with ether; ethyl stearate (0.3 g.) was obtained: m. p. 33~34°C, saponification value 184.4. The precipitate was decomposed with dilute hydrochloric acid and extracted with ether to obtain a mixture of thiostearic acid and a small amount of stearic acid: m. p. 37.5~39°C, neutralization value 175.1, sulfur content (iodine method) 9.5%.

The Synthesis of Distearoyl Disulfide.—An iodine solution (0.1N) was added drop by drop into a mixture of thiostearic acid (3 g.) and ethanol (100 ml.) until coloring was observed; the reaction mixture was diluted by water, and the product (3 g.) was recrystallized from benzene to give 2.8 g. of the crystals with a m. p. of 81.8~82.3°C.

Found: C, 72.22; H, 11.83; S, 0 (iodine method), 10.70% (Kitamura's method). Calcd. for $C_{36}H_{70}O_2S_2$: C, 72.18; H, 11.78; S. 10.69%.

Infrared Absorption Spectra.—The infrared absorption spectra of thiostearic acid (T) and distearoyl disulfide (J) are shown in Fig. 2. A Hilger H-800 infrared spectrophotometer was used for measuring.

In T, the S-H stretching band is evidently indicated at 2548 cm^{-1} (a). The C=O stretching bands are indicated at 1662 (b) in T and at 1713 cm^{-1}(s) in J. In the spectrum of T measured by the potassium bromide disk method, absorption bands corresponding to the progression bands reported by Jones[10] appear at 1327(c), 1307(d), 1288(e), 1268(f), 1248(i), 1228(h), 1208(i), 1188(j) and 1172 cm^{-1} (k), but they are not evident in the spectrum measured by the Nujol mull method. Absorption bands appear at 1081(l), 1060(m), 1045(n), 1025(o), 996(p), and 977 cm^{-1} (q) in T, but their assignments are not evident. A low-intensity absorption band is indicated at 868 cm^{-1} (r) in T; this is probably due to the S-H group.

Ultraviolet Absorption Spectra. — They were measured by using a Shimadzu Quartz spectrophotometer, model QB-50, and silica cells (1 cm.).

Department of Industrial Chemistry
Faculty of Engineering
Gifu University
Kagamigahara-shi, Gifu

8) G. Brauer, "Handbuch der Präparativen Anorganischen Chemie," Verdinand Enke, Stuttgart (1954), p. 270.

9) R. Kitamura, *J. Pharm. Soc. Japan* (*Yakugaku Zasshi*), **57**, 31 (1937).

10) R. N. Jones, A. F. Mckay and R. G. Sinclair, *J. Am. Chem. Soc.*, **74**, 2575 (1952).

An Analysis of the NMR Spectra of the $ABKLX_3Y_3$ System

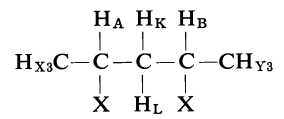
By Yuzuru FUJIWARA and Shizuo FUJIWARA

(Received December 27, 1963)

2, 4-Disubstituted pentane is often used as a model compound for vinyl-type polymers in investigating their physical and chemical properties. In the field of NMR, the analysis of the spectra of model compounds is of value in obtaining information concerning polymers. As disubstituted pentane has a much lower molecular weight than a polymer, the molecular motions are sufficient to give well-resolved spectra which permit unambiguous analysis. 2, 4-Disubstituted pentane has ten protons interacting with each other and belongs to the $ABKLX_3Y_3$ system. Analysis of the NMR spectra of this compound is simple in theory. However, the large number of included protons complicates the treatment. General formulas for NMR analysis are given for spin systems of three or less. For spin systems of four or more, the analysis is possible only in special cases or by numerical calculation. For the present analysis, the calculation was made by reducing the entire system to two six-spin systems and one four-spin system. The six-spin systems of the ABB'CC'D type[1] and the A_mBX_n type[2] were previously analysed, but the calculation of $AKLX_3$ type given below has not been previously reported.

The Analysis of $ABKLX_3Y_3$

2, 4-Disubstituted pentane has the following structure;



Suffixes have been assigned to protons. Though these ten protons interact with each other, the spin-spin coupling constants between methylene protons and methyl protons are likely to be negligibly small compared with the others and with the chemical shifts (as is the usual case), and it is not always necessary to consider all the protons in the calculation at the same time. This makes it possible to reduce the system to several simple subgroups. The specra of methyl protons are quite simple because they interact with only one methine proton, either H_A or H_B, and are of the AX_3 or BX_3 type. Methylene protons interact with two methine protons. Since they are not necessarily they are analyzed as the KL part in the ABKL system. Methine protons give the most complicated spectra to be analyzed since they are coupled with two methylene protons and three methyl protons. Therefore, this system is expressed as $AKLX_3$ or $BKLY_3$; the transitions concerned merely with A or B are taken into account. The calculation procedure was the usual one; the results are shown in Tables I to IV. The present calculation is confined to the case where the spin-spin coupling constants between methine and methylene protons are small compared with the corresponding chemical shift. Therefore, the large off diagonal terms are $H_{3,4}$, $H_{8,9}$, $H_{12,13}$, $H_{16,17}$, $H_{20,22}$ $H_{24,25}$, $H_{28,29}$, $H_{31,32}$, $H_{35,36}$, $H_{37,38}$, $H_{41,42}$, $H_{44,45}$, $H_{48,49}$, $H_{51,52}$, $H_{55,56}$ and $H_{59,60}$. The diagonalization of the energy matrix is effected by solving sixteen 2×2 determinants. The absence of a spin-spin coupling between methyl and methylene protons simplifies the spectrum, since it makes the parameters R_a, R_c, S_a, and S_c all equal, and R_b, R_d, S_b, S_d all equal.

Discussion

The spectrum of the KL part has an asymmetric form; the effect of the sings of the coupling constants and chemical shifts will now be discussed in relation to this spectrum. The change in sign of the geminal coupling constants between two methylene protons leads to the same spectrum because the resonance frequency and the intensity of the lines reverse themselves at the same time, so that the resultant spectrum remains identical. If the sign of the vicinal coupling constant between methine and methylene protons is reversed, the parameters C and the resonance position interchange between 1 and 4, and between 2 and 3, and no change in the resultant spectrum occurs, although the line assignment becomes different. These considerations enable one to conclude that the spectrum of the KL

1) S. Fujiwara and H. Shimizu, *J. Chem. Phys.*, **32**, 1636 (1962).
2) P. L. Corio, *J. Mol. Spectr.*, **8**, 193 (1962).

TABLE I. BASIC PRODUCT FUNCTIONS AND DIAGONAL MATRIX ELEMENTS FOR $AKLX_3$

n	ϕ_n	F_z	Sym-metry	H_{nn}									
				ν_A	ν_K	ν_L	ν_X	J_{AK}	J_{AL}	J_{AX}	J_{KL}	J_{KX}	J_{LX}
				2	2	2	2	4	4	4	4	4	4
1	$\alpha\alpha\alpha\alpha\alpha\alpha$	3	a_3	+	+	+	+3	+	+	+3	+	+3	+3
2	$\beta\alpha\alpha\alpha\alpha\alpha$	2	a_2	−	+	+	+3	−	−	−3	+	+3	+3
3	$\alpha\beta\alpha\alpha\alpha\alpha$	2	a_2	+	−	+	+3	−	+	+3	−	−3	+3
4	$\alpha\alpha\beta\alpha\alpha\alpha$	2	a_2	+	+	−	+3	+	−	+3	−	+3	−3
5	$\alpha\alpha\alpha(\beta\alpha\alpha+\alpha\beta\alpha+\alpha\alpha\beta)/\sqrt{3}$	2	a_2	+	+	+	+	+	+	+	+	+	+
6	$\alpha\alpha\alpha(\beta\alpha\alpha+\alpha\beta\alpha-2\alpha\alpha\beta)/\sqrt{6}$	2	e_2	+	+	+	+	+	+	+	+	+	+
7	$\alpha\alpha\alpha(\beta\alpha\alpha-\alpha\beta\alpha)/\sqrt{2}$	2	e_2	+	+	+	+	+	+	+	+	+	+
8	$\beta\beta\alpha\alpha\alpha\alpha$	1	a_1	−	−	+	+3	+	−	−3	−	−3	+3
9	$\beta\alpha\beta\alpha\alpha\alpha$	1	a_1	−	+	−	+3	−	+	−3	−	+3	−3
10	$\alpha\beta\beta\alpha\alpha\alpha$	1	a_1	+	−	−	+3	−	−	+3	+	−3	−3
11	$\beta\alpha\alpha(\beta\alpha\alpha+\alpha\beta\beta+\alpha\alpha\beta)/\sqrt{3}$	1	a_1	−	+	+	+	−	−	−	+	+	+
12	$\alpha\beta\alpha(\beta\alpha\alpha+\alpha\beta\beta+\alpha\alpha\beta)/\sqrt{3}$	1	a_1	+	−	+	+	−	+	+	−	−	+
13	$\alpha\alpha\beta(\beta\alpha\alpha+\alpha\beta\beta+\alpha\alpha\beta)/\sqrt{3}$	1	a_1	+	+	−	+	+	−	+	−	+	−
14	$\alpha\alpha\alpha(\beta\beta\alpha+\beta\alpha\beta+\alpha\beta\beta)/\sqrt{3}$	1	a_1	+	+	+	−	+	+	−	+	−	−
15	$\beta\alpha\alpha(\beta\alpha\alpha+\alpha\beta\alpha-2\alpha\alpha\beta)/\sqrt{6}$	1	e_1	−	+	+	+	−	−	−	+	+	+
16	$\alpha\beta\alpha(\beta\alpha\alpha+\alpha\beta\alpha-2\alpha\alpha\beta)/\sqrt{6}$	1	e_1	+	−	+	+	−	+	+	−	−	+
17	$\alpha\alpha\beta(\beta\alpha\alpha+\alpha\beta\alpha-2\alpha\alpha\beta)/\sqrt{6}$	1	e_1	+	+	−	+	+	−	+	−	+	−
18	$\alpha\alpha\alpha(\beta\beta\alpha+\beta\alpha\beta-2\alpha\beta\beta)/\sqrt{6}$	1	e_1	+	+	+	−	+	+	−	+	−	−
19	$\beta\alpha\alpha(\beta\alpha\alpha-\alpha\beta\alpha)/\sqrt{2}$	1	e_1	−	+	+	+	−	−	−	+	+	+
20	$\alpha\beta\alpha(\beta\alpha\alpha-\alpha\beta\alpha)/\sqrt{2}$	1	e_1	+	−	+	+	−	+	+	−	−	+
21	$\alpha\alpha\beta(\beta\alpha\alpha-\alpha\beta\alpha)/\sqrt{2}$	1	e_1	+	+	−	+	+	−	+	−	+	−
22	$\alpha\alpha\alpha(\beta\beta\alpha-\beta\alpha\beta)/\sqrt{2}$	1	e_1	+	+	+	−	+	+	−	+	−	−
23	$\beta\beta\beta\alpha\alpha\alpha$	0	a_0	−	−	−	+3	+	+	−3	+	−3	−3
24	$\beta\beta\alpha(\beta\alpha\alpha+\alpha\beta\alpha+\alpha\alpha\beta)/\sqrt{3}$	0	a_0	−	−	+	+	+	−	−	−	−	+
25	$\beta\alpha\beta(\beta\alpha\alpha+\alpha\beta\alpha+\alpha\alpha\beta)/\sqrt{3}$	0	a_0	−	+	−	+	−	+	−	−	+	−
26	$\alpha\beta\beta(\beta\alpha\alpha+\alpha\beta\alpha+\alpha\alpha\beta)/\sqrt{3}$	0	a_0	+	−	−	+	−	−	+	+	−	−
27	$\beta\alpha\alpha(\beta\beta\alpha+\beta\alpha\beta+\alpha\beta\beta)/\sqrt{3}$	0	a_0	−	+	+	−	−	−	+	+	−	−
28	$\alpha\beta\alpha(\beta\beta\alpha+\beta\alpha\beta+\alpha\beta\beta)/\sqrt{3}$	0	a_0	+	−	+	−	−	+	−	−	+	−
29	$\alpha\alpha\beta(\beta\beta\alpha+\beta\alpha\beta+\alpha\beta\beta)/\sqrt{3}$	0	a_0	+	+	−	−	+	−	−	−	−	+
30	$\alpha\alpha\alpha\beta\beta\beta$	0	a_0	+	+	+	−3	+	+	−3	+	−3	−3
31	$\beta\beta\alpha(\beta\alpha\alpha+\alpha\beta\alpha-2\alpha\alpha\beta)/\sqrt{6}$	0	e_0	−	−	+	+	+	−	−	−	−	+
32	$\beta\alpha\beta(\beta\alpha\alpha+\alpha\beta\alpha-2\alpha\alpha\beta)/\sqrt{6}$	0	e_0	−	+	−	+	−	+	−	−	+	−
33	$\alpha\beta\beta(\beta\alpha\alpha+\alpha\beta\alpha-2\alpha\alpha\beta)/\sqrt{6}$	0	e_0	+	−	−	+	−	−	+	+	−	−
34	$\beta\alpha\alpha(\beta\beta\alpha+\beta\alpha\beta-2\alpha\beta\beta)/\sqrt{6}$	0	e_0	−	+	+	−	−	−	+	+	−	−
35	$\alpha\beta\alpha(\beta\beta\alpha+\beta\alpha\beta-2\alpha\beta\beta)/\sqrt{6}$	0	e_0	+	−	+	−	−	+	−	−	+	−
36	$\alpha\alpha\beta(\beta\beta\alpha+\beta\alpha\beta-2\alpha\beta\beta)/\sqrt{6}$	0	e_0	+	+	−	−	+	−	−	−	−	+
37	$\beta\beta\alpha(\beta\alpha\alpha-\alpha\beta\alpha)/\sqrt{2}$	0	e_0	−	−	+	+	+	−	−	−	−	+
38	$\beta\alpha\beta(\beta\alpha\alpha-\alpha\beta\alpha)/\sqrt{2}$	0	e_0	−	+	−	+	−	+	−	−	+	−
39	$\alpha\beta\beta(\beta\alpha\alpha-\alpha\beta\alpha)/\sqrt{2}$	0	e_0	+	−	−	+	−	−	+	+	−	−
40	$\beta\alpha\alpha(\beta\beta\alpha-\beta\alpha\beta)/\sqrt{2}$	0	e_0	−	+	+	−	−	−	+	+	−	−
41	$\alpha\beta\alpha(\beta\beta\alpha-\beta\alpha\beta)/\sqrt{2}$	0	e_0	+	−	+	−	−	+	−	−	+	−
42	$\alpha\alpha\beta(\beta\beta\alpha-\beta\alpha\beta)/\sqrt{2}$	0	e_0	+	+	−	−	+	−	−	−	−	+
43	$\beta\beta\beta(\beta\alpha\alpha+\alpha\beta\alpha+\alpha\alpha\beta)/\sqrt{3}$	−1	a_{-1}	−	−	−	+	+	+	−	+	−	−
44	$\beta\beta\alpha(\beta\beta\alpha+\beta\alpha\beta+\alpha\beta\beta)/\sqrt{3}$	−1	a_{-1}	−	−	+	−	+	−	+	−	+	−
45	$\beta\alpha\beta(\beta\beta\alpha+\beta\alpha\beta+\alpha\beta\beta)/\sqrt{3}$	−1	a_{-1}	−	+	−	−	−	+	+	−	−	+
46	$\alpha\beta\beta(\beta\beta\alpha+\beta\alpha\beta+\alpha\beta\beta)/\sqrt{3}$	−1	a_{-1}	+	−	−	−	−	−	−	+	+	+
47	$\beta\alpha\alpha\beta\beta\beta$	−1	a_{-1}	−	+	+	−3	−	−	+3	+	−3	−3
48	$\alpha\beta\alpha\beta\beta\beta$	−1	a_{-1}	+	−	+	−3	−	+	−3	−	+3	−3
49	$\alpha\alpha\beta\beta\beta\beta$	−1	a_{-1}	+	+	−	−3	+	−	−3	−	−3	+3
50	$\beta\beta\beta(\beta\alpha\alpha+\alpha\beta\alpha-2\alpha\alpha\beta)/\sqrt{6}$	−1	e_{-1}	−	−	−	+	+	+	−	+	−	−
51	$\beta\beta\alpha(\beta\beta\alpha+\beta\alpha\beta-2\alpha\beta\beta)/\sqrt{6}$	−1	e_{-1}	−	−	+	−	+	−	+	−	+	−
52	$\beta\alpha\beta(\beta\beta\alpha+\beta\alpha\beta-2\alpha\beta\beta)/\sqrt{6}$	−1	e_{-1}	−	+	−	−	−	+	+	−	−	+
53	$\alpha\beta\beta(\beta\beta\alpha+\beta\alpha\beta-2\alpha\beta\beta)/\sqrt{6}$	−1	e_{-1}	+	−	−	−	−	−	−	+	+	+

TABLE I (contnd.)

n	ϕ_n	F_z	Sym-metry	H_{nn}									
				ν_A	ν_K	ν_L	ν_X	J_{AK}	J_{AL}	J_{AX}	J_{KL}	J_{KX}	J_{LX}
				2	2	2	2	4	4	4	4	4	4
54	$\beta\beta\beta(\beta\alpha\alpha-\alpha\beta\alpha)/\sqrt{2}$	−1	e_{-1}	−	−	−	+	+	+	−	+	−	−
55	$\beta\beta\alpha(\beta\beta\alpha-\beta\alpha\beta)/\sqrt{2}$	−1	e_{-1}	−	−	+	−	+	−	+	−	+	−
56	$\beta\alpha\beta(\beta\beta\alpha-\beta\alpha\beta)/\sqrt{2}$	−1	e_{-1}	−	+	−	−	−	+	+	−	−	+
57	$\alpha\beta\beta(\beta\beta\alpha-\beta\alpha\beta)/\sqrt{2}$	−1	e_{-1}	+	−	−	−	−	−	−	+	+	+
58	$\beta\beta\beta(\beta\beta\alpha+\beta\alpha\beta+\alpha\beta\beta)/\sqrt{3}$	−2	a_{-2}	−	−	−	−	+	+	+	+	+	+
59	$\beta\beta\alpha\beta\beta\beta$	−2	a_{-2}	−	−	+	−3	+	−	+3	−	+3	−3
60	$\beta\alpha\beta\beta\beta\beta$	−2	a_{-2}	−	+	−	−3	−	+	−3	−	−3	+3
61	$\alpha\beta\beta\beta\beta\beta$	−2	a_{-2}	+	−	−	−3	−	−	−3	+	+3	+3
62	$\beta\beta\beta(\beta\beta\alpha+\beta\alpha\beta-2\alpha\beta\beta)/\sqrt{3}$	−2	e_{-2}	−	−	−	−	+	+	+	+	+	+
63	$\beta\beta\beta(\beta\beta\alpha-\beta\alpha\beta)/\sqrt{2}$	−2	e_{-2}	−	−	−	−	+	+	+	+	+	+
64	$\beta\beta\beta\beta\beta\beta$	−3	e_{-3}	−	−	−	−3	+	+	+3	+	+3	+3

TABLE II. TRANSITIONS OF A PART IN AKLX$_3$

Transition	Frequency	Relative intensity
1−2	$\nu_A+1/2(J_{AK}+J_{AL}+3J_{AX})$	1
5−11, 6−15, 7−19	$\nu_A+1/2(J_{AK}+J_{AL}+J_{AX})$	3
14−27, 18−34, 22−40	$\nu_A+1/2(J_{AK}+J_{AL}-J_{AX})$	3
30−47	$\nu_A+1/2(J_{AK}+J_{AL}-3J_{AX})$	1
10−23	$\nu_A+1/2(-J_{AK}-J_{AL}+3J_{AX})$	1
26−43, 33−50, 39−54	$\nu_A+1/2(-J_{AK}-J_{AL}+J_{AX})$	3
46−58, 53−62, 57−63	$\nu_A+1/2(-J_{AK}-J_{AL}-J_{AX})$	3
61−64	$\nu_A+1/2(-J_{AK}-J_{AL}-3J_{AX})$	1
3′−8′	$\nu_A+3/2J_{AX}+R_a-R_b$	$\cos^2(\theta R_a-\theta R_b)$
12′−24′, 16′−31′, 20′−37′	$\nu_A+1/2J_{AX}+S_a-S_b$	$3\cos^2(\theta S_a-\theta S_b)$
28′−44′, 35′−51′, 41′−55′	$\nu_A-1/2J_{AX}+S_c-S_d$	$3\cos^2(\theta S_c-\theta S_d)$
48′−59′	$\nu_A-3/2J_{AX}+R_c-R_d$	$\cos^2(\theta R_c-\theta R_d)$
4′−8′	$\nu_A+3/2J_{AX}-R_a-R_b$	$\sin^2(\theta R_a-\theta R_b)$
12′−24′, 17′−31′, 21′−37′	$\nu_A+1/2J_{AX}-S_a-S_b$	$3\sin^2(\theta S_a-\theta S_b)$
29′−44′, 36′−51′, 42′−55′	$\nu_A-1/2J_{AX}-S_c-S_d$	$3\sin^2(\theta S_c-\theta S_d)$
49′−59′	$\nu_A-3/2J_{AX}-R_c-R_d$	$\sin^2(\theta R_c-\theta R_d)$
3′−9′	$\nu_A+3/2J_{AX}+R_a+R_b$	$\sin^2(\theta R_a-\theta R_b)$
12′−25′, 16′−32′, 20′−38′	$\nu_A+1/2J_{AX}+S_a+S_b$	$3\sin^2(\theta S_a-\theta S_b)$
28′−45′, 35′−52′, 41′−56′	$\nu_A-1/2J_{AX}+S_c+S_d$	$3\sin^2(\theta S_c-\theta S_d)$
48′−60′	$\nu_A-3/2J_{AX}+R_c+R_d$	$\sin^2(\theta R_c-\theta R_d)$
4′−9′	$\nu_A+3/2J_{AX}-R_a+R_b$	$\cos^2(\theta R_a-\theta R_d)$
13′−25′, 17′−32′, 21′−38′	$\nu_A+1/2J_{AX}-S_a+S_b$	$3\cos^2(\theta S_a-\theta S_b)$
29′−45′, 36′−52′, 42′−56′	$\nu_A-1/2J_{AX}-S_c+S_d$	$3\cos^2(\theta S_c-\theta S_d)$
49′−60′	$\nu_A-3/2J_{AX}-R_c+R_d$	$\cos^2(\theta R_c-\theta R_d)$

where

$R_a=1/2[(\nu_L-\nu_K-1/2J_{AK}+1/2J_{AL}-3/2J_{KX}+3/2J_{LX})^2+J^2_{KL}]^{1/2}$ $\quad \theta R_a=1/2\sin^{-1}J_{AB}/2R_a$

$R_b=1/2[(\nu_L-\nu_K+1/2J_{AK}-1/2J_{AL}-3/2J_{KX}+3/2J_{LX})^2+J^2_{KL}]^{1/2}$ $\quad \theta R_b=1/2\sin^{-1}J_{AB}/2R_b$

$R_c=1/2[(\nu_L-\nu_K-1/2J_{AK}+1/2J_{AL}+3/2J_{KX}-3/2J_{LX})^2+J^2_{KL}]^{1/2}$ $\quad \theta R_c=1/2\sin^{-1}J_{AB}/2R_c$

$R_d=1/2[(\nu_L-\nu_K+1/2J_{AK}-1/2J_{AL}+3/2J_{KX}-3/2J_{LX})^2+J^2_{KL}]^{1/2}$ $\quad \theta R_d=1/2\sin^{-1}J_{AB}/2R_d$

$S_a=1/2[(\nu_L-\nu_K-1/2J_{AK}+1/2J_{AL}-1/2J_{KX}+1/2J_{LK})^2+J^2_{KL}]^{1/2}$ $\quad \theta S_a=1/2\sin^{-1}J_{AB}/2S_a$

$S_b=1/2[(\nu_L-\nu_K+1/2J_{AK}-1/2J_{AL}-1/2J_{KX}+1/2J_{LK})^2+J^2_{KL}]^{1/2}$ $\quad \theta S_b=1/2\sin^{-1}J_{AB}/2S_b$

$S_c=1/2[(\nu_L-\nu_K-1/2J_{AK}+1/2J_{AL}+1/2J_{KX}-1/2J_{LK})^2+J^2_{KL}]^{1/2}$ $\quad \theta S_c=1/2\sin^{-1}J_{AB}/2S_c$

$S_d=1/2[(\nu_L-\nu_K+1/2J_{AK}-1/2J_{AL}+1/2J_{KX}-1/2J_{LK})^2+J^2_{KL}]^{1/2}$ $\quad \theta S_d=1/2\sin^{-1}J_{AB}/2S_d$

TABLE III. BASIC PRODUCT FUNCTIONS FOR ABKL SYSTEM

No.	ϕ_n K	L	A	B	F_z	H_{nn} ν_K 2	ν_L 2	ν_A 2	ν_B 2	J_{KL} 4	J_{AK} 4	J_{BK} 4	J_{AL} 4	J_{BL} 4	J_{AB} 4
1	α	α	α	α	2	+	+	+	+	+	+	+	+	+	+
2	β	α	α	α	1	−	+	+	+	−	−	−	+	+	+
3	α	β	α	α	1	+	−	+	+	−	+	+	−	−	+
4	α	α	β	α	1	+	+	−	+	+	−	+	−	+	−
5	α	α	α	β	1	+	+	+	−	+	+	−	+	−	−
6	β	β	α	α	0	−	−	+	+	+	−	−	−	−	+
7	β	α	β	α	0	−	+	−	+	−	+	−	−	+	−
8	α	β	β	α	0	+	−	−	+	−	−	+	+	−	−
9	β	α	α	β	0	−	+	+	−	−	−	+	+	−	−
10	α	β	α	β	0	+	−	+	−	−	+	−	−	+	−
11	α	α	β	β	0	+	+	−	−	+	−	−	−	−	+
12	β	β	β	α	−1	−	−	−	+	+	+	−	+	−	−
13	β	β	α	β	−1	−	−	+	−	+	−	+	−	+	−
14	β	α	β	β	−1	−	+	−	−	−	+	+	−	−	+
15	α	β	β	β	−1	+	−	−	−	−	−	−	+	+	+
16	β	β	β	β	−2	−	−	−	−	+	+	+	+	+	+

TABLE IV. FREQUENCIES AND INTENSITIES OF KL SPECTRUM FOR ABKL SYSTEM

Transition	Frequency relative to $(\nu_K+\nu_L)/2$ J_{AK} 4	J_{AL} 4	J_{BK} 4	J_{BL} 4	J_{KL} 2	Relative intensity	
1 − 2	+	+	+	+	+	$-C_1$	$1+\sin 2\theta_1$
1 − 3′	+	+	+	+	+	$+C_1$	$1-\sin 2\theta_1$
2′− 6	+	+	+	+	−	$+C_1$	$1+\sin 2\theta_1$
3′− 6	+	+	+	+	−	$-C_1$	$1-\sin 2\theta_1$
4 − 7′	−	−	+	+	+	$-C_2$	$1+\sin 2\theta_2$
4 − 8′	−	−	+	+	+	$+C_2$	$1-\sin 2\theta_2$
7′−12	−	−	+	+	−	$+C_2$	$1+\sin 2\theta_2$
8′−12	−	−	+	+	−	$-C_2$	$1-\sin 2\theta_2$
5 − 9′	+	+	−	−	+	$-C_3$	$1+\sin 2\theta_3$
5 −10′	+	+	−	−	+	$+C_3$	$1-\sin 2\theta_3$
9′−12	−	−	+	+	−	$+C_3$	$1+\sin 2\theta_3$
10′−12	−	−	+	+	−	$-C_3$	$1-\sin 2\theta_3$
11 −14′	−	−	−	−	+	$-C_4$	$1+\sin 2\theta_4$
11 −15′	−	−	−	−	+	$+C_4$	$1-\sin 2\theta_4$
14′−16	−	−	−	−	−	$+C_4$	$1+\sin 2\theta_4$
15′−16	−	−	−	−	−	$-C_4$	$1-\sin 2\theta_4$

$C_1=1/2[(\nu_{LK}-1/2J_{AK}-1/2J_{BK}+1/2J_{AL}+1/2J_{BL})^2+J^2_{KL}]^{1/2}$ $\theta_1=1/2\sin^{-1}J_{KL}/2C_1$

$C_2=1/2[(\nu_{LK}+1/2J_{AK}-1/2J_{BK}-1/2J_{AL}+1/2J_{BL})^2+J^2_{KL}]^{1/2}$ $\theta_2=1/2\sin^{-1}J_{KL}/2C_2$

$C_3=1/2[(\nu_{LK}-1/2J_{AK}+1/2J_{BK}+1/2J_{AL}-1/2J_{BL})^2+J^2_{KL}]^{1/2}$ $\theta_3=1/2\sin^{-1}J_{KL}/2C_4$

$C_4=1/2[(\nu_{LK}+1/2J_{AK}+1/2J_{BK}-1/2J_{AL}-1/2J_{BL})^2+J^2_{KL}]^{1/2}$ $\theta_4=1/2\sin^{-1}J_{KL}/2C_4$

part does not contribute to the determination of the sign of the coupling constants through an approximation of this kind.

The sign of the chemical shift between K and L in a methylene group is determined when the relative magnitude of two vicinal coupling constants between methine and methylene protons are determined; i. e., the relative magnitude of the coupling constants decides the sign of the chemical shift. The change of the sign of the chemical shift results in an interchange of parameters between C_1 and C_4 and between C_2 and C_3, but the relative resonance positions are not altered, therefore the asymmetric spectrum is reversed against the field direction.

Another point of interest is that the present approximation makes the calculation fairly simple, though the application is limited to cases where the coupling constants between methine

and methylene protons are not very large compared with chemical shift. The perturbation method can be used in cases where the coupling constants are not very small but are still considerably smaller than the chemical shift. If the coupling constants are larger, a secular equation which includes determinants higher than 2×2 must be solved.

The present treatment may be applied to pentanes substituted by electronegative atoms or groups, such as halogens and OH, but it is not suitable for those groups which do not affect the electron density or the magnetic state surrounding methine hydrogen.

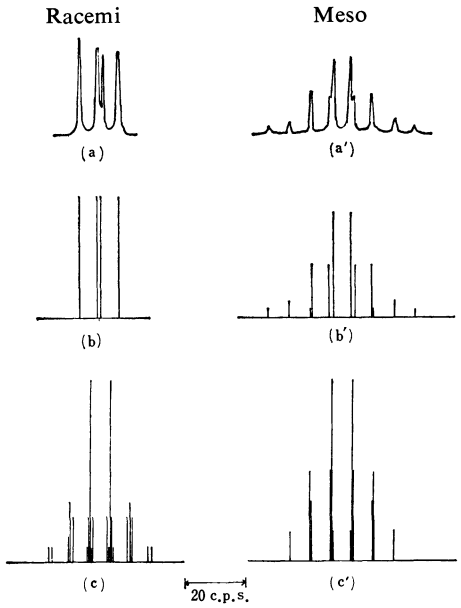


Fig. 1. NMR Spectra of 2,4-dichloropentane.
(a) and (a') : methylene spectra observed at 60 Mc.[3]
(b) and (b') : calculated methylene spectra
(c) and (c') : calculated methine spectra.

Example

The NMR spectra of 2,4-dichloropentane were analysed using the spin-decoupling technique[3]. This compound has two isomers (racemic and meso) and shows two corresponding spectra. The spectra of methylene protons and the results of analysis are shown in Fig. 1 and Table V respectively, where chemical shifts between methylene protons are estimated from the decoupled pattern with the assumption that the spin coupling constants between methylene protons are the same for both isomers.

The calculated spectra with the values in Table V are compared with the observed ones in Fig. 1.

Table V. Chemical shifts and coupling constants of 2,4,-dichloropentane

	Chemical shift ν_{LK}, c.p.s.	Coupling constant c.p.s.		
		CH_3-CH	CH_2	CH_2-CH
Racemi	0	6.7	14.5	5.8 7.1
Meso	15.6	6.7	14.5	7.0

The agreement of the methylene spectra is quite satisfactory. L=K for racemic compound and K≠L for meso one. The calculated spectrum of the methine proton in the racemic compound is more complicated than the simple sextet which appears for the meso compound. This is also in good agreement with the experimental results reported.[3] Another example of K≠L will be given in a succeeding paper.[4]

Added in Proof: Calculated spectrum of Fig. 1b was constructed from the values in Table V. Same spectrum can be obtained by using another set of parameters, $\nu_{LK}=0$, $J_{AK}=J_{BL}=10.8$ and $J_{AL}=J_{BK}=2.2$. In the latter case, Fig. 1c, should be replaced with a figure of different shape, that is also a complex sextet. The set seems to be a more plausible one.

Department of Chemistry
Faculty of Science
The University of Tokyo
Hongo, Tokyo

3) S. Sato, R. Chujo and E. Nagai, Proceedings of 3rd Simposium on NMR, Osaka, (1963) p. 51.
4) Y. Fujiwara and S. Fujiwara, This Bulletin., 37, 8450 (1964).

The NMR Spectra of the Acetal of 2, 4-Pentanediol

By Yuzuru FUJIWARA and Shizuo FUJIWARA

(Received December 27, 1963)

2, 4-Pentanediol is a model compound of polyvinylalcohol (PVA), with the lowest molecular weight among this series and with optical isomers corresponding to the stereoregularity of the polymer. It has been shown, through a comparison of the reaction rate of the meso type of 2, 4-pentanediol (which corresponds to isotactic PVA) with that of the racemic type (which corresponds to syndiotactic PVA), that the rate of acetal formation from PVA and acetaldehyde depends upon the stereospecificity. The rate of the formation of the racemic acetal is about 20 times that of the meso type.[1] The reaction rate of PVA is of the same order as that of pentanediol, according to its tacticity. In determining the difference in reaction rates, two kinds of acetal were separated by gas chromatography and identified by NMR. The identification of these compounds was straightforward. A process for calculating the energy levels and transition probabilities of the $ABKLX_3Y_3$ system has been developed.[2] This process made it possible to accomplish the complete analysis of the NMR spectra of the compounds. Through this analysis, spin-spin coupling constants and chemical shifts are obtained, as well as information concerning the structures and conformations of the acetals.

Experimental

Acetal was formed by adding *p*-toluene sulfonic acid to a solution of 2,4-pentanediol and acetaldehyde at 60°C. After the water had been eliminated, the product was distilled. The acetal was allowed to pass through a gas chromatographic column 4 mm. in diameter and 2 m. long which was maintained at 100°C, using hydrogen as a carrier gas. This column was filled with Shimadzu DOP-A. The two species of acetal were completely separated. The first fraction was designated f_1, and the second one, f_2. The NMR spectra were measured at 60 Mc./sec. and 40 Mc./sec. at room temperature. The positions of spectral lines and coupling constants were determined by the usual side-band method.

1) K. Fujiiwara, S. Matsumoto and Y. Fujiwara, Abstracts of the 12th Symposium on Polymer Chemistry, Tokyo (1963) p. 114.
2) Y. Fujiwara and S. Fujiwara, This Bulletin, 37, 1005 (1964).

Results and Discussion

The NMR spectra of f_1 and f_2 are shown in Fig. 1, and all lines have been assigned as shown, with consideration given to the position and the shape. f_1 has two doublets of methyl protons, one being about twice the size of the other, while f_2 has three doublets with almost equal intensity. Two different structures of acetal are formed in accordance with the structures of pentanediol (Fig. 2). Structure I comes from the meso type, and structure II, from the racemic type. Structure I has two methyl groups in equatorial positions at 4 and 6 carbons and one at 2 carbon. Structure II has one equatorial methyl group at 6, one axial methyl group at 4 and one at 2; i. e., the three methyl groups are not equivalent. This suggests that f_1 has structure I and f_2 has structure II. This identification is confirmed through the analysis of protons other than methyl groups.

The spectra of methine and methylene protons were analyzed by the method previously described;[2] the results are shown in Table I.

TABLE I. COUPLING CONSTANTS AND CHEMICAL SHIFTS FOR $ABKLX_3Y_3$ SYSTEM

	(A=B X=Y)		(A≒B X≒Y)	
	60 Mc.	40 Mc.	60 Mc.	40 Mc.
$\lvert J_{AK} \rvert$	10.73	10.73	11.26	11.26
$\lvert J_{AL} \rvert$	2.62	2.62	3.06	3.06
$\lvert J_{AX} \rvert$	6.20	6.20	6.14	6.14
$\lvert J_{KL} \rvert$	13.06	13.06	12.70	12.70
ν_{LK}	21.32	14.21	−25.94	−17.29
ν_{BA}	0	0	16.22	10.81
$\lvert J_{BK} \rvert$	10.73	10.73	7.02	7.02
$\lvert J_{BL} \rvert$	2.62	2.62	0.58	0.58
$\lvert J_{BX} \rvert$	6.20	6.20	6.80	6.80

in c.p.s.

The coupling constants and chemical shifts obtained were confirmed by comparison with the observed and calculated spectra at 60 and 40 Mc./sec. as shown in Figs. 3 to 6. Though some combination lines are missing because of their low intensity, the agreement is quite satisfactory. It is shown that, as expected, A is equivalent to B and X to Y for

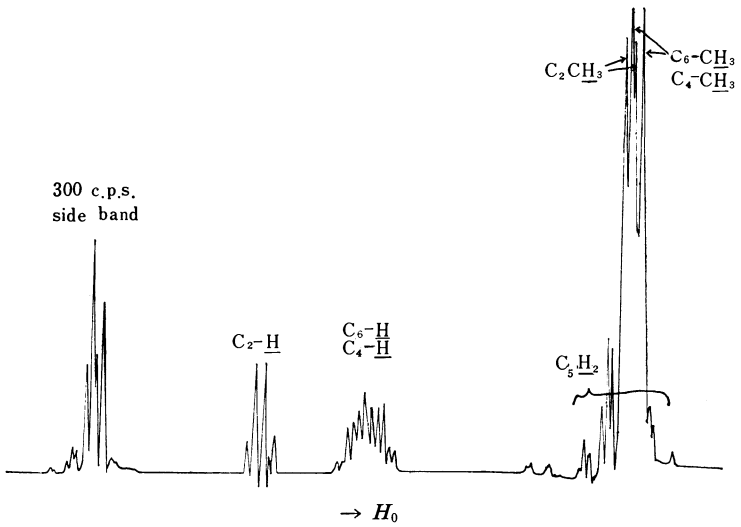


Fig. 1. a) NMR spectra of f_1 at 60 Mc./sec.

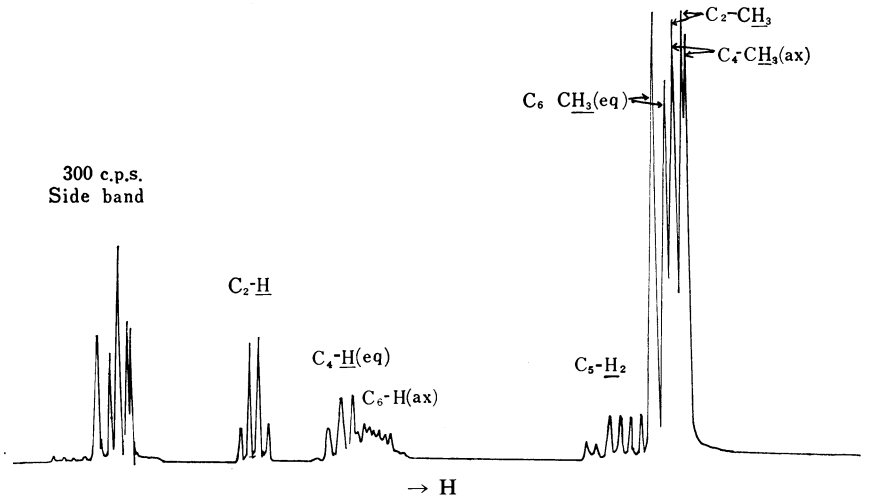


Fig. 1. b) NMR spectrum of f_2 at 60 Mc./sec.

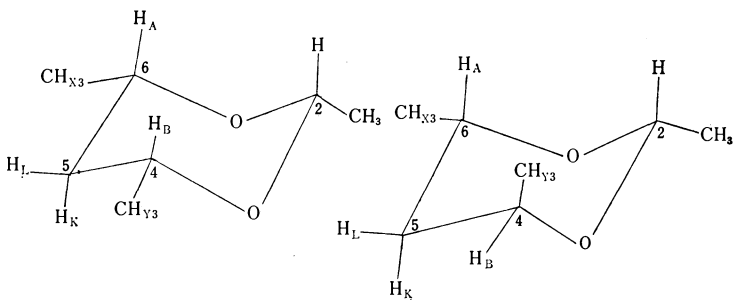


Fig. 2. Structures of acetals of 2,4-pentanediol.

f_1, but that A is not equivalent to B and X not to Y for f_2. It is noted that $J_{BK} \neq J_{BL}$ for f_2. Contrary to this finding, the structure suggests that $J_{BK}=J_{BL}$, because both couplings are vicinal ones in the gauche position. The discrepancy may result from strain in the structure caused by an outward slanting of the axial methyl. ν_{LK} is expected to be smaller for structure II than for structure I. However, experimental results show that the ν_{LK} for f_2 has a larger absolute value than f_1 and that the sign is negative. J_{AK} is quite large compared with J_{AL}, and it is not unlikely that both A and K are axial protons. Therefore the negative value of ν_{LK} means that the axial proton at 5 carbon appears at a lower field

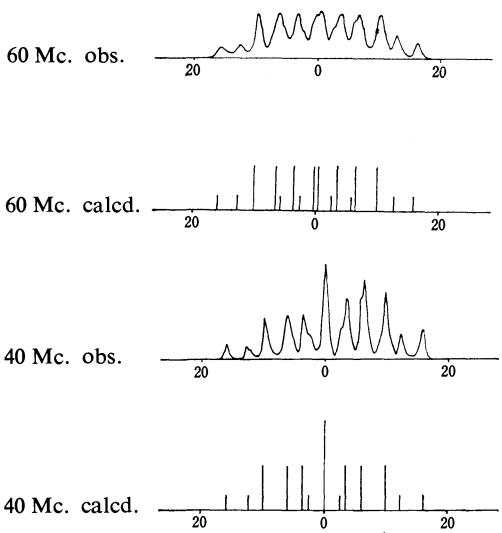


Fig. 3. NMR spectra of A in $AKLX_3$.

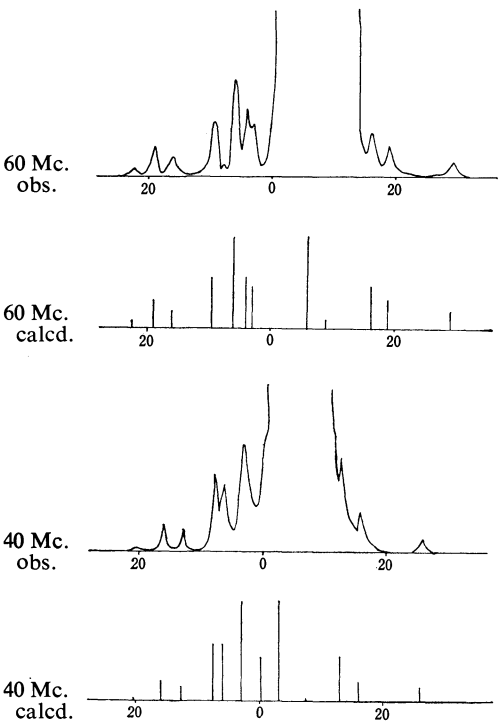


Fig. 4. NMR spectra of KL in A_2KL system.

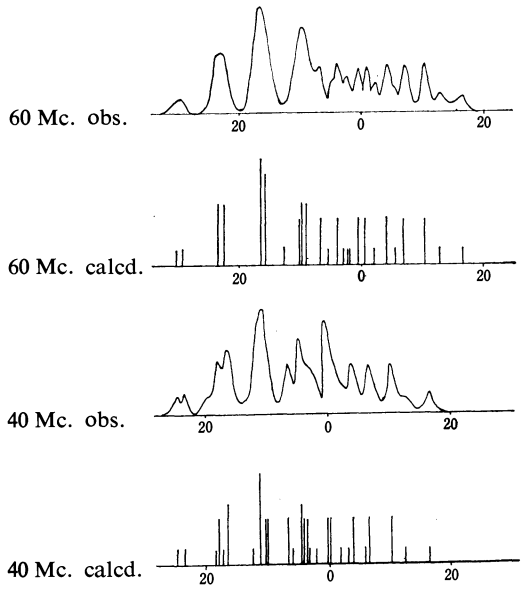


Fig. 5. NMR spectra of AB in $ABKLX_3Y_3$.

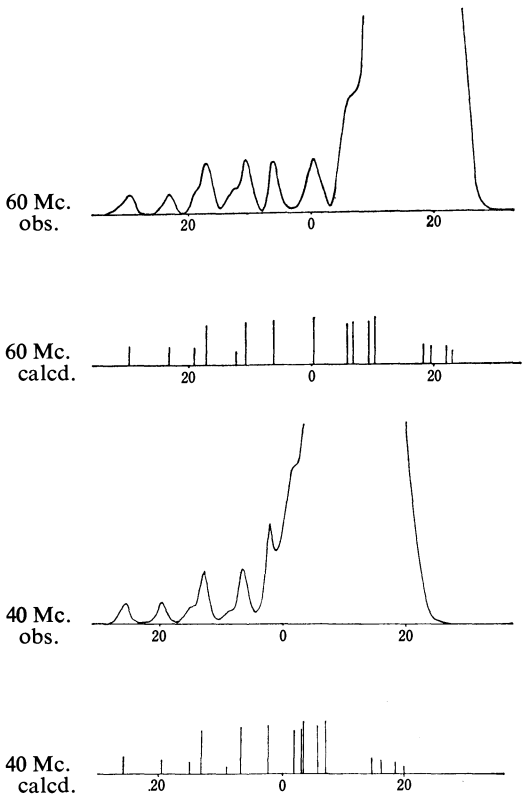


Fig. 6. NMR spectra of KL in $ABKLX_3Y_3$.

than the equatorial one. This may be attributed partly to the structural strain mentioned above, and partly to the difference in magnetic anisotropy between oxygen and carbon. There is a slight possibility of missassignment of the spectrum due to one spectrum of this system being partly hidden by the large methyl signal, leading to such an apparent anomaly.

The methyl group at 2 is supposed to be equatorial, since if two kinds of methyl groups are positioned at 2 carbon, the methine proton at 2 must give two quartets; this is contradictory to the experimental findings.

A possible exchange between two chair forms is excluded by the fact of a large difference in the chemical shifts and coupling contants of the methylene protons, K and L; any such exchange would make the two protons nearly equivalent. This has been confirmed also by the temperature effects on the spectra. 1, 3-Dioxane undergoes ring inversion at temperatures higher than $-80°C$.[4] For 4, 4-dimethyl-1, 3-dioxane the incipient temperature is about $-50°C$.[4] 2, 4-Pentanediol-acetal (2, 4, 6-trimethyl-1, 3-dioxane) is supposed to have a higher incipient temperature because of high structural hindrance. The temperature change from $-77°C$ to $+150°C$ does not effect any change in the spectra of 2, 4, 6-trimethyl-1, 3-dioxane except for slight changes in the chemical shift. The same reasons may be given to explain the exclusion of the boat form of f_2.

As f_1, it can be said that only one stable form exists; this seems to be a chair form with all methyl groups in quatorial positions. This conclusion is consistent with energy considerations and with the structure of paraacetaldehyde.[3]

The authors wish to thank Messrs. Osamu Yamamoto of the Government Chemical Industrial Research Istitute, Shoichi Hayashi of The Institute of Physical and Chemical Research, and Naohiro Hayakawa of the Japan Atomic Energy Research Institute for their aid in obtaining the NMR spectra. They also wish to thanks Dr. Kiyoshi Fujii of the Kurashiki Rayon Co., Ltd., for preparing the samples.

Department of Chemistry
Faculty of Science
The University of Tokyo
Hongo, Tokyo

3) P. Diehl and R. Freeman, *Mol. Phys.*, **4**, 39 (1961).
4) H. Frieblin, S. Kabuss, W. Maier and A. Lüttringhaus, *Tetrahedron Letters* (1962), 683.

A Study of the Reaction between Nitrosobenzene and the Grignard Reagent

By Kazuhiro MARUYAMA*

(Received January 25, 1964)

Although the ionic mechanism has generally been assumed for most Grignard reactions, it has been shown, as will be described below, that free radicals can be observed during the course of the reaction between nitrosobenzene and a Grignard reagent by the electron-spin resonance (ESR) technique. The reaction between nitrosobenzene and phenylmagnesium bromide was the subject of an extensive investigation by Wieland and his co-workers about fifty years ago,[1] and this reaction has been established as the usual synthetic method of diphenylhydroxylamine.

The present investigation is concerned mainly with reactions between nitrosobenzene and phenylmagnesium bromide, between *p*-nitrosotoluene and phenylmagnesium bromide and between nitrosobenzene and *p*-tolylmagnesium bromide. The free radical species produced during the reactions were determined from the hyperfine structures of their ESR spectra. The equilibrium among the reaction products will be discussed below.

Experimental

ESR Measurements.—An ESR spectrometer with an X-band and a 100 Kc. modulation was used in this work. The ESR measurement of the reaction

* Present address: Department of Chemistry, Faculty of Science, Kyoto University, Kyoto.

1) H. Wieland and S. Gambarjan, *Ber.*, **36**, 1499 (1906); H. Wieland and A. Roseeu, ibid., **45**, 494 (1912); H. Wieland and M. Offenbächer, ibid., **47**, 2111 (1914); H. Wieland and K. Roth, ibid., **53**, 210 (1920); H. Wieland and F. Kögl, ibid., **55**, 1798 (1922).

between nitrosobenzene and a Grignard reagent was carried out as follows: prior to the sealing of part A of the reaction vessel, the ether used as a solvent was evaporated as completely as possible under a high vacuum (about 10^{-6} mmHg), and this part was connected with part B of the vessel (see Fig. 1). Thereafter, part B of the vessel which contained nitrosobenzene was evacuated under a high vacuum, a known amount of tetrahydrofuran was distilled into this vessel, and the vessel was sealed off from the vacuum line. Nitrosobenzene and a Grignard reagent which had been separated from each other by a break seal were mixed at the dry ice - acetone temperature in the absence of air and moisture. The reacting mixture was then inserted into the cavity, which had previously been cooled to the desired temperature with a stream of boiling liquid nitrogen. The reaction temperature in the cavity was controlled by regulating the boiling rate of liquid nitrogen. The reaction vessel is shown in Fig. 1.

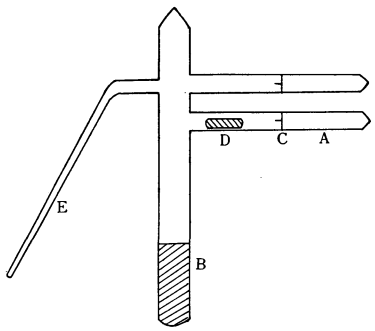


Fig. 1. Reaction vessel.
A : Grignard reagent
B : Nitrosobenzene in THF
C : Break seal
D : Hammer
E : Inserted into the cavity

Materials.—*Nitrosobenzene.*—Commercial Fulka special-grade reagent was twice recrystallized from ethanol. This sample did not show any ESR signal in tetrahydrofuran. M. p. 68°C.

p-Nitrosotoluene.—This was prepared by the oxidation of *p*-tolylhydroxylamine with an aqueous ferric chloride solution.[2] This sample did not show any ESR signal in tetrahydrofuran. M. p. 48.5°C.

Phenylmagnesium Bromide.—Phenylmagnesium bromide was prepared from bromobenzene and magnesium turnings of reagent grade suitable for the Grignard reagent in ether. This reagent was stored in a sealed bottle, and the upper transparent solution was used for the reaction. The concentration of this reagent was determined by the acid titration method.[3] This Grignard reagent did not show any ESR signal in tetrahydrofuran.

p-Tolylmagnesium Bromide.—*p*-Tolylmagnesium bromide was prepared from *p*-bromotoluene and reagent-grade magnesium turnings for the Grignard reagent in ether. The succeeding treatment was the same as in the case of phenylmagnesium bromide. This reagent did not show any ESR signal in tetrahydrofuran.

Methylmagnesium Iodide and Ethylmagnesium Bromide.—Methylmagnesium iodide and ethylmagnesium bromide were prepared according to the method used for the above two reagents.

2) E. Bamberger, ibid., 28, 247 (1895).
3) H. Gilman, E. A. Zoeller and J. B. Dickey, *J. Am. Chem. Soc.*, 51, 1576 (1929).

Results and Discussion

The Identification of Free Radicals.—The reaction between phenylmagnesium bromide and nitrosobenzene was carried out as follows: after the two reacting components (the mole ratio of the Grignard reagent to nitrosobenzene is 1/1～5/1) had been mixed in a dry ice - acetone bath, the color of the mixture suddenly became brown, and at the same time strong ESR signals, which indicate the existence of free radical species, could be observed. This free radical was identified as diphenylnitric oxide by a comparison of the hyperfine structure of its ESR spectrum with that of pure diphenylnitric oxide, which was prepared by the oxidation of diphenylhydroxylamine with silver oxide[1] (see Fig. 2 and Eq. 1).

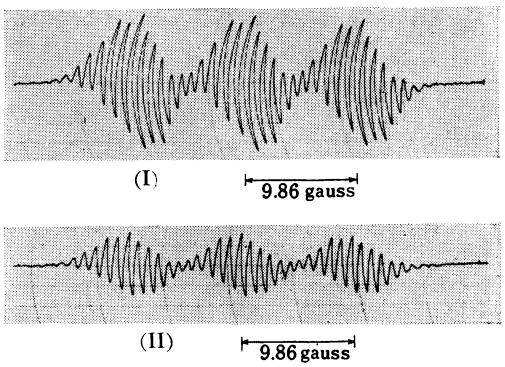


Fig. 2. A comparison of ESR spectra of the free radical produced with that of pure diphenylnitric oxide.
(I) ESR spectrum of the reaction mixture resulting from the reaction between nitrosobenzene and phenylmagnesium bromide.
(II) ESR spectrum of pure diphenylnitric oxide.

$$C_6H_5NO + C_6H_5MgBr \longrightarrow C_6H_5-\underset{\displaystyle O}{\underset{|}{N}}-C_6H_5 \quad (1)$$

The reaction between phenylmagnesium bromide and *p*-nitrosotoluene was carried out in just the same way as that between phenylmagnesium bromide and nitrosobenzene. A large amount of a free radical was also observed

in this reaction. This free radical was identified as *p*-methyldiphenylnitric oxide by a comparison of its hyperfine structure with a known sample.[1]

The reaction between *p*-tolylmagnesium bromide and nitrosobenzene was also examined, and the features of the reaction were quite the same as that of the above two. The ESR signals of the free radical produced were just the same as those of the free radical obtained in the reaction between phenylmagnesium bromide and *p*-nitrosotoluene (see Fig. 3 and Eq. 2).

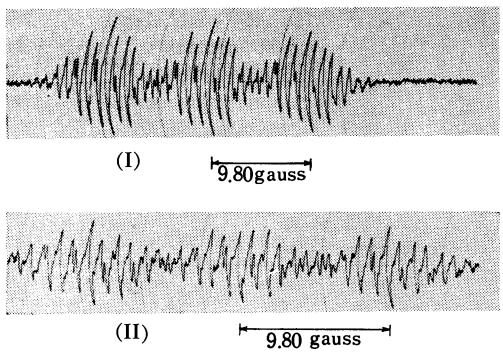


Fig. 3. A comparison of the ESR spectra.
(I) ESR spectrum of the reaction mixture resulting from the reaction between nitrosobenzene and *p*-tolylmagnesium bromide.
(II) ESR spectrum of the reaction mixture resulting from the reaction between *p*-nitrosotoluene and phenylmagnesium bromide.

$$\begin{matrix} C_6H_5NO+ \\ p\text{-}CH_3C_6H_4MgBr \end{matrix} \longrightarrow p\text{-}CH_3C_6H_4\text{—}N(\cdot)\text{—}C_6H_5 \quad (O) \longleftarrow \begin{matrix} p\text{-}CH_3C_6H_4NO+ \\ C_6H_5MgBr \end{matrix} \qquad (2)$$

The above three reactions indicate that the production of free radical species is due solely to the reaction between nitrosobenzene and the Grignard reagent and not to any other cause, such as the decomposition of nitrosobenzene.

The reaction between nitrosobenzene and methylmagnesium iodide and the reaction between nitrosobenzene and ethylmagnesium bromide were also examined. A large amount of free radicals could be observed in these reactions by the ESR technique. The free radical species, however, could not be identified because of the complication of their hyperfine structures (see Fig. 4).

The Equilibrium between the Free Radicals Produced and the Grignard Reagent.—In several

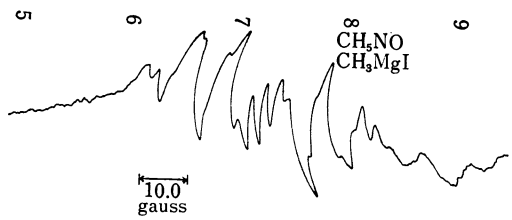


Fig. 4. The ESR spectra of free radicals produced by reaction between nitrosobenzene and methylmagnesium bromide.

preliminary reactions, it was found that the total amount of free radicals in the reaction mixture is considerably influenced by the mole ratio of the two reacting components. The quantitative determination of the free radicals in the reaction mixture was performed by the overmodulated modulation technique of ESR[4] (sweep range, about 200 gauss; modulation amplitude, 11.2 gauss; crystal current, 60 mamp.). A solution of diphenylpicrylhydrazyl in tetrahydrofuran whose concentration was known was used as the standard sample. The results obtained are shown in Table I.

The change in the concentration of free radicals on the successive addition of nitrosobenzene to the solution with a constant amount of the Grignard reagent (phenylmagnesium bromide) was examined by the successive breaking of break seals; thereby the reaction mixture and a known amount of nitrosobenzene in a vacuum tube (in this case, the Grignard reagent dissolved in 10 ml. of tetrahydrofuran is in part B of the reaction vessel and nitrosobenzene is in part A of the vessel) were separated. The results are shown in Table II.

Although the above two series of reactions suggest the existence of an equilibrium in the reaction mixture, the analysis of the reaction product was carried out when nitrosobenzene was mixed with a large excess of phenylmagnesium bromide in order to ascertain whether or not the disappearance of the free radicals is caused by a further reaction, such as a formation of diphenylamine. Thus, two vessels, containing phenylmagnesium bromide dissolved in tetrahydrofuran and nitrosobenzene dissolved in tetrahydrofuran respectively, were degassed and connected with each other by using a break seal; then they were cooled to $-80°C$ and mixed by breaking the seal. The whole reaction vessel was kept at this temperature for thirty minutes after mixing. A rather large amount of a white crystalline precipitate was formed. Then the reaction

4) J. S. Hyde and H. W. Brown, *J. Chem. Phys.*, 37, 368 (1962); K. Halbach, *Phys. Rev.*, 119, 1230 (1960).

TABLE I. YIELDS OF FREE RADICALS IN THE REACTION MIXTURE OF C_6H_5MgBr AND C_6H_5NO

	C_6H_5NO* mol.	C_6H_5MgBr* mol.	Mol. ratio C_6H_5NO/C_6H_5MgBr	Yields of radicals based on C_6H_5NO used, %
i	7.5×10^{-4}	7.5×10^{-4}	1	76.6
ii	2.5×10^{-4}	7.5×10^{-4}	1/3	36.4
iii	1.5×10^{-4}	7.5×10^{-4}	1/5	13.5
iv	7.5×10^{-5}	7.5×10^{-4}	1/10	0

* These two reagents react in 10 ml. of tetrahydrofuran.

TABLE II. CHANGES IN THE CONCENTRATION OF FREE RADICALS ON SUCCESSIVE ADDITIONS OF C_6H_5NO TO A CONSTANT AMOUNT OF C_6H_5MgBr

	Components of the reaction mixture	Yieds of free radicals based on the total C_6H_5NO, %
Solution 1	C_6H_5MgBr*: 7.5×10^{-4} mol. + C_6H_5NO: 7.5×10^{-5} mol.	0
Solution 2	Solution 1 + C_5H_5NO: 7.5×10^{-5} mol.	12.8
Solution 3	Solution 2 + C_6H_5NO: 7.5×10^{-5} mol.	37.0

* This was dissolved in 10 ml. of tetrahydrofuran.

TABLE III. ANALYSIS OF THE REACTION PRODUCT OF C_6H_5NO WITH C_6H_5MgBr

	C_6H_5NO (I)	C_5H_5MgBr (II)	Mol. ratio I/II	Yield of DPHA based upon C_6H_5NO mg. (%)
1	45×10^{-4} mol. in 20 ml. THF	450×10^{-4} mol. in 20 ml. THF	1/10	810 (93)
2	45×10^{-4} mol. in 20 ml. THF	450×10^{-4} mol. in 20 ml. THF	1/10	845 (98)

DPHA : Diphenylhydroxylamine

mixture was allowed to stand until its temperature reached 0°C. The reaction mixture was hydrolyzed by a usual method under a stream of nitrogen. After the evaporation of tetrahydrofuran, an almost colorless crystalline mass was obtained. This was nearly pure diphenylhydroxylamine. Recrystallization of this sample from ligroin gave pure diphenylhydroxylamine (m. p. 59~60°C) (see Table III). The results of this reaction indicate unambiguously that the disappearance of free radicals which occurs when a large excess of phenylmagnesium bromide to nitrosobenzene is used is not brought about by a further reaction.

Furthermore, the dependency of the concentration of free radicals in the reaction mixture on the temperature was examined by the ESR technique. The results are shown in Fig. 5. The plots in Fig. 5 were completely reproducible at each temperature.

Reaction Mechanism.—It was described above that free radical species could not be observed

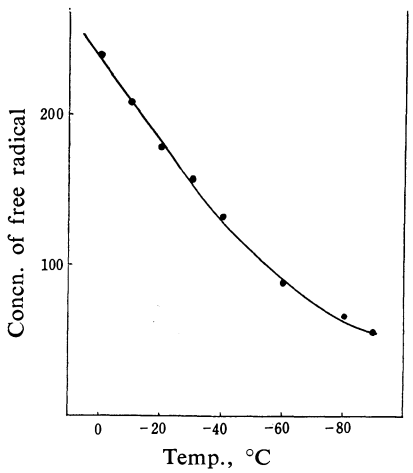


Fig. 5. Change in free radical concentration with temperature.
Sample : reaction mixture between 2.5×10^{-4} mol. of nitrosobenzene and 7.5×10^{-4} mol. of phenylmagnesium bromide.

in the reaction mixture at the equilibrium state in which the mole ratio of the reacting components (C_6H_5NO/C_6H_5MgBr) was 1/10. However, even in this reaction mixture, free radicals could be detected shortly after the mixing of the reacting components (2~3 min. at −50°C) by ESR and until its equilibrium was attained. This fact excludes the possibility (of Eq. 3) that a Grignard-type complex is formed at first through an ionic mechanism, and that then this complex dissociates into free radicals:

$$C_6H_5NO+C_6H_5MgBr \longrightarrow C_6H_5-\underset{\underset{O-MgBr}{|}}{N}-C_6H_5 \rightleftarrows C_6H_5-\underset{\underset{O\cdot}{|}}{N}-C_6H_5+\cdot MgBr \quad (3)$$

From the discussion so far, it seems reasonable to conclude that the reaction between nitrosobenzene and a Grignard reagent proceeds through the free radical mechanism and that the following equilibrium exist between the free radicals formed and the mixture of Grignard reagents:

$$C_6H_5NO+(C_6H_5MgBr)_n \longrightarrow \begin{matrix} C_6H_5 \\ C_6H_5 \end{matrix}\!\!>\!N-O\cdot+\cdot MgBr(C_6H_5MgBr)_{n-1} \underset{\uparrow}{\downarrow} \left(\begin{matrix} C_6H_5 \\ C_6H_5 \end{matrix}\!\!>\!N-OMgBr\right)(C_6H_5MgBr)_{n-1} \quad (4)$$

Although the Grignard reagent is one of the most familiar reagents to organic chemists, its structure is still the subject of great controversy.[5] It has been accepted, in general, that the reagent is an equilibrium mixture, that is:

$$2\ RMgX \rightleftarrows RMgR+MgX_2 \quad (5)$$

However, a simple mixture of one mole of RMgR and one mole of MgX_2 is less reactive than the reagent prepare from Mg and RX.[6] On the other hand, it was confirmed that a large excess of the Grignard reagent ($C_6H_5\cdot MgBr$) can combine with pure diphenylnitric oxide to result in the disappearance of this free radical (see Fig. 6).

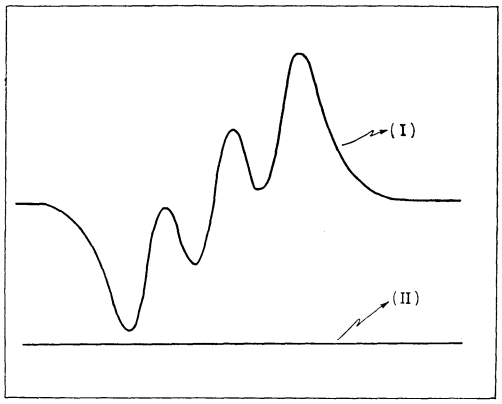


Fig. 6. Reaction of diphenylnitric oxide with phenylmagnesium bromide, ESR spectra of solutions.
(I) 1.25×10^{-4} mol. solution of diphenylnitric oxide in 10 ml. THF.
(II) After addition of 7.5×10^{-4} mol. of phenylmagnesium bromide to solution I.

These facts seem to suggest that the Grignard reagent contains some sort of $(MgBr)_2\cdot(RMgBr)_n$-type complex.[7] Therefore, the existence of an equilibrium between diphenylnitric oxide and an excess of the Grignard reagent seems not surprising.

The author wishes to express his sincere gratitude to Professor S. I. Weissman for his fruitful suggestions, discussions, and encouragement. This work was done with the financial support of the National Science Foundation of the U. S. A.

Department of Chemistry
Washington University
St. Louis 30, Missouri, U. S. A.

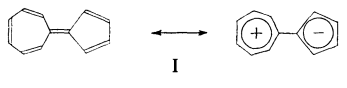
5) N. M. Bikales and E. I. Becker, *Can. J. Chem.*, **41**, 1329 (1963); A. D. Vreugdenhill and C. Blomberg, *Rec. trav. chim.*, **28**, 453 (1963).
6) H. Gilman, "Organic Chemistry," Vol. I, John Wiley and Sons, New York (1949), p. 489.
7) The Grignard reagent can produce ketyl-like free radicals from the ketones, which can be easily reduced to the corresponding metal ketyls. This investigation will be reported on later.

The Fragmentation Reaction of 4-(7-Tropyl)pyrazoles by Bromination[1]

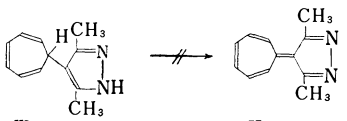
By Toshio MUKAI and Haruki TSURUTA

(Received on February 24, 1964)

Because of its peculiar ring system, a synthesis of sesquifulvalene (I) has been attempted by many chemists. Recently Prinzbach and Rosswog[2] and Kitahara and Funamizu[3] reported the synthesis of I, but they failed in the isolation of I in a pure state, it being very unstable. In an attempt to synthesize a nitrogen analog (II) of sesquifulvalene by the dehydrogenation of 3, 5-dimethyl-4-(7-tropyl)-pyrazole (III), the present authors found that, instead of the expected product resulting, fragmentation had occurred during the bromination-dehydrobromination of III, yielding tropyrium ino and pyrazole derivatives. This report will describe details of the results obtained.



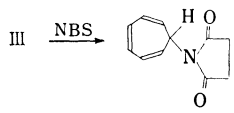
I



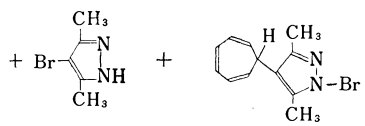
III II

3, 5-Dimethyl-4-(7-tropyl)pyrazole (III) was obtained quantitatively from the reaction of tropylacetylacetone[4,5] with hydrazine. The acetylation of III gave a monoacetate. The dehydrogenation of III by heating it with chloranil in xylene afforded a dark green resinous material. The treatment of III with alkaline hydorgen peroxide[6] resulted in the recovery of III. Refluxing III with selenium dioxide in dioxane afforded a viscous oil which could not be purified.

The reaction of III with *N*-bromosuccinimide in *t*-butanol containing water and pyridine[7] yielded three kinds of products besides succinimide: colorless crystals (IV) $C_{11}H_{11}O_2N$ (m. p. 144~146°C); colorless crystals (V) $C_5H_7N_2Br$ (m. p. 122°C), and an oil (VI) $C_{12}H_{13}N_2Br$ (b. p. 150~160°C/3 mmHg). On the basis of their elementary analyses and their ultraviolet and infrared spectra (see Experimental section), IV and V were confirmed to be *N*-(7-tropyl)succinimde[8] and 4-bromo-3, 5-dimethylpyrazole[9] respectively. From its elementary analysis and the fact that it has no absorption due to the NH stretching vibration, but still has the tropyl group, (see Experimental section) VI was assumed to be 1-bromo-3, 5-dimethyl-4-tropylpyrazole. Further evidence for the structure of VI was provided by its NMR spectrum,[10] which has the multiplicities, chemical shifts (τ value), relative areas and interpretations of the signals produced in carbon tetrachloride shown below: two singlets, at 8.12 and 8.03 τ, relative area 3 and 3, two methyl groups in the pyrazole ring; a triplet, at 6.58, 1, C_7-proton of the tropyl group; three multiplets, centered at 5.02, 4.59 and 4.08, 2, 2 and 2, the protons of the $C_{1,6}$, $C_{2,5}$ and $C_{3,4}$ of the tropyl group. VI did not yield the expected sesquifulvalene derivative (II) on attempted dehydrogenation with collidine at 100°C or when refluxed with sodium acetate in ethanol; it was recovered unchanged.



IV



V VI

1) Presented at the General Meeting of the Tohoku district of the Chemical Society of Japan, Yonezawa, October, 1961,

2) H. Prinzbach and W. Rosswog, *Angew. Chem.*, **73**, 543 (1961).

3) Presented at the 15th Annual Meeting of the Chemical Society of Japan, Kyoto, April, 1962.

4) K. Conrow, *J. Am. Chem. Soc.*, **81**, 5461 (1959).

5) M. E. Volpin, I. S. Arkem and D. N. Kursanov, *Izvest. Akad. Nauk S. S. S. R., Otdel Khim. Nauk.*, **1957**, 1501.

6) G. T. Newbola and F. S. Spring, *J. Chem. Soc.*, **1947**, 373; K. Alder and H. Niklas, *Ann.*, **585**, 81 (1954).

7) T. Nozoe, T. Mukai, K. Osaka and N. Shishido, This Bulletin, **34**, 1384 (1961).

8) H. L. Dryden, Jr., and B. E. Burgert, *J. Am. Chem. Soc.*, **77**, 5633 (1955).

9) G. T. Morgan and I. Ackermann, *J. Chem. Soc.*, **1956**, 2026.

10) All NMR spectra were measured in the Laboratory of professor Hazato of the Chemical Resesarch Institute of Non-aqueous Solutions, Tohoku University.

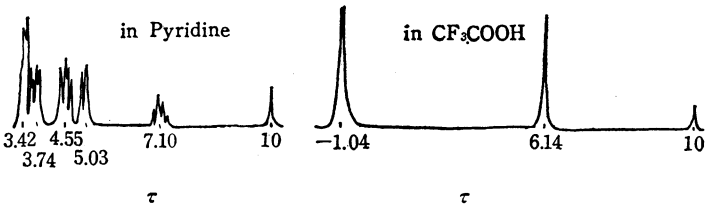


Fig. 1. NMR spectra of tropylmalononitrile (60 Mc.).

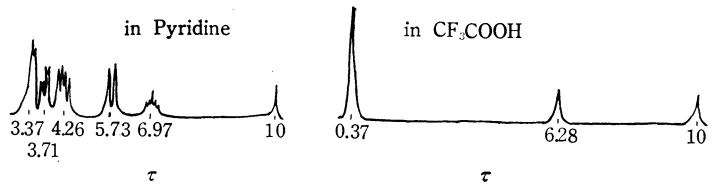


Fig. 2. NMR spectra of tropylmalonic acid (60 Mc.).

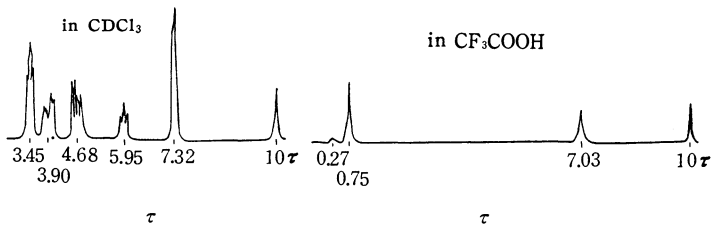


Fig. 3. NMR spectra of tropylsuccinimide (IV) (60 Mc.).

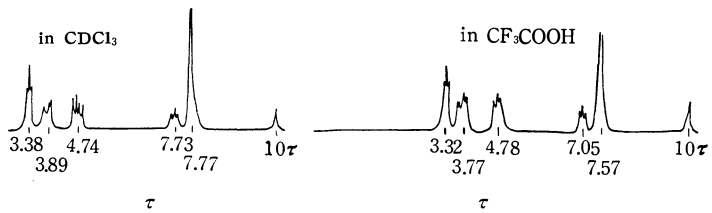
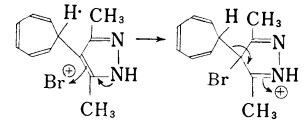
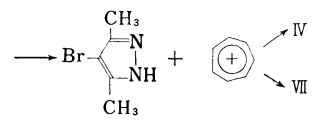


Fig. 4. NMR spectra of 3,5-dimethyl-4-(7-tropyl)pyrazole (III) (60Mc.). Tetramethylsilane was used as an internal reference in all spectra.

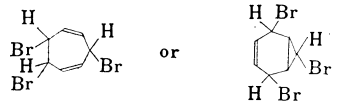
When III was heated with *N*-bromosuccinimide in carbon tetrachloride in the presence of benzoyl peroxide, the same products, IV, V, VI and succinimide, were obtained as when a polar solvent was used, as above. The bromination of III, when carried out by the addition of bromine in a chloroform solution, yielded V, benzaldehyde and yellow plates (VII) $C_7H_7Br_3$ (m. p. 115°C(decomp.)), which has no maximum in the ultraviolet spectrum. When VII was heated in ethanol or water, it yielded benzaldehyde. These facts indicate that VII was probably identical with the compound obtained by Dewar and Petit[11] by the bromination of tropylium ions; the identity of the two compounds was confirmed by a comparison of their infrared spectra and by a mixed melting point determination. The fragmentation of III can be explained by the

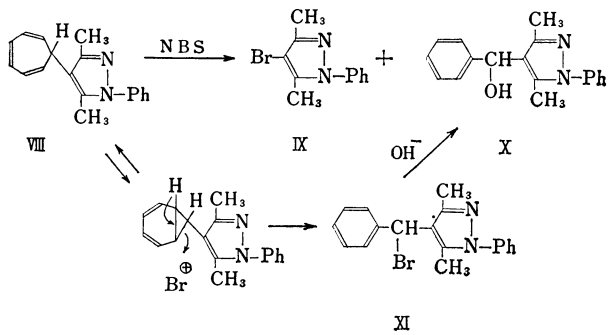




V

11) M. J. S. Dewar and R. Petit, *J. Chem. Soc.*, **1956**, 2026. They proposed the following structure for VII:





following mechanism (p. 1019), which is initiated by the attack of a bromonium ion; the driving force would be the formation of the stable tropylium ion.

It has already been reported by Conrow[3] that the fragmentation of the tropyl derivatives, in general, results from the action of an acid or of electrophilic reagents. For example, tropylmalononitrile, tropylmalonic acid and IV are readily cleaved into tropylium ions and the corresponding components. This situation can be clearly seen from a comparison of the NMR spectra of the above three compounds measured in chloroform or pyridine and that measured in trifluoroacetic acid (Figs. 1, 2 and 3). 3, 5-Dimethyl-4-(7-tropyl)pyrazole (III), however, was recovered unchanged after treatment with acetic acid containing perchloric acid, and the NMR spectrum of III in trifluoroacetic acid showed that the fragmentation of III dose not occur, but that a salt is formed, being clear from the shift to a lower field of signals due to the protons of the methyl groups at the pyrazole and due to the C_7-proton of the tropyl group (Fig. 4).

The hydrobromide salt of III was obtained as colorless crystals (m. p. 195°C (decomp.)) when hydrogen bromide gas was passed through a benzene solution of III.

In order to compare it with the bromination of III, 3, 5-dimethyl-1-phenyl-4-(7-tropyl)pyrazole (VIII) was brominated with *N*-bromosuccinimide or bromine under the same condition as were used above. VIII or the bisphenylhydrazone of tropylacetylacetone was obtained by the reaction of tropylacetylacetone with phenylhydrazine, depending on the reaction conditions. The bromination of VIII in chloroform with bromine also afforded the fragmentation products, tropylium ions and 4-bromo-3, 5-dimethyl-1-phenylpyrazole[12] .(IX) as an oil (b. p. 175~180°C/2 mmHg), as well as a considerable amount of an unidentified viscous oil. The reaction of VIII with *N*-bromosuccinimide in *t*-butanol containing pyridine and water resulted in the formation of IX and colorless crystals (X), $C_{18}H_{18}ON_2$ (m. p. 102~106°C). The infrared spectrum of X shows the presence of the hydroxyl group at 3230 and 1020 cm^{-1}. The NMR spectrum of X in carbon tetrachloride reveals no signal characteristic of the tropyl group, but the following multiplicities, chemical shifts (τ value), relative areas and assignments of the signals: a singlet, at 8.13, 6, the methyl groups of the pyrazole ring; a singlet, at 5.14, 1, the hydroxyl-proton; singlet, at 4.56, 1, the benzylic proton; diffused singlet, at 2.96, about 10, protons of the benzene rings. From these data, X was assumed to be 3, 5-dimethyl-4-(α-hydroxybenzyl)-1-pheylpyrazole. Compound XI may be an intermediate in the formation of X from VIII, but it must be examined further.

From this series of experiments, it became clear that the 1-phenyl derivative (VIII) also suffered from fragmentation when brominated with *N*-bromosuccinimide or bromine.

However, the yield of tropylium ions and IX from VIII was rather lower than in the case of III. This may be attributed to the effect of the 1-phenyl group. The treatment of VIII with perchloric acid in acetic acid or with hydrogen bromide in benzene resulted in the recovery of VIII without the formation of the corresponding salt.

Experimental[13,14]

3, 5-Dimethyl-4-(7-tropyl)pyrazole (III). — To a solution of 3.12 g. (16.4 mmol.) of 7-tropylacetylacetone dissolved in 48 ml. of ethanol, 2.1 ml. (32.8 mmol.) of 80% hydrazine hydrate was added; the reaction mixture was then refluxed on a water bath for 2 hr. After the ethanol had been removed, the solution was diluted with water and extracted with ether. The ether-extract was washed with water, dried over magnesium sulfate, and evaporated to

12) L. Balbiano, *Ber.*, 23, 1452 (1890).

13) All melting points are uncorrected.

14) The microanalyses were carried out by Miss Ayako Iwanaga and Miss Mutsuko Suzuki in this Laboratory.

yield 3 g. of III, which on recrystallization from ethanol afforded colorless prisms (m. p. 144～146°C). IR in Nujol: 3195, 3135, 3086, 1575, 1442, 1389, 1311, 1279, 1149, 1042, 1006, 847, 765, 749, and 705 cm^{-1}. λ_{max}^{MeOH} mμ (log ε): 260 (3.55).

Found: C, 77.20; H, 7.21; N, 14.80. Calcd. for $C_{12}H_{14}N_2$: C, 77.38; H, 7.58; N, 15.04%.

A solution of 200 mg. of III dissolved in 0.5 ml. of acetic anhydride was heated on a boiling water bath for 30 min. and evaporated under reduced pressure to give 240 mg. of an acetylated compound of III (m. p. 36～41°C.) Recrystallization from ethanol afforded colorless needles (m. p. 36～41°C) IR in KBr disk: 1720, 1598, 1424, 1382, 1370, 1336, 856, 750, and 710 cm^{-1}.

Found: C, 73.50; H, 6.88; N, 12.00. Calcd. for $C_{14}H_{16}ON_2$: C, 73.65; H, 7.06; N, 12.27%.

The Reaction of 3, 5-Dimethyl-4-(7-tropyl)pyrazole (III) with *N*-Bromosuccinimide. — *a) In a Polar Solvent.*—To a solution of 800 mg. (4.3 mmol.) of III dissolved in 20 ml. of *t*-butanol, 8 ml. of pyridine and 3 ml. of water, 900 mg. (5.0 mmol.) of *N*-bromosuccinimide was added. The mixture was then allowed to stand for 48 hr. at room temperature and extracted with chloroform after being diluted with water. The chloroform-extract was washed with water, dried over magnsium sulfate, and evaporated up to an oil containing some crystals. After being diluted with a small amount of ethanol or benzene, 180 mg. of crystals (m. p. 142～145°C) were filtered out, on recrystallization from ethanol or ethyl acetate these afforded colorless plates (IV) (m. p. 144～146°C.) IR in Nujol: 1779, 1695, 1408, 763, 748, 708, and 678 cm^{-1}. λ_{max}^{MeOH} mμ (log ε): 258 (4.13).

Found: C, 70.55; H, 5.58; N, 7.41. Calcd. for $C_{11}H_{11}O_2N$: C, 69.82; H, 5.86; N, 7.40%.

IV was found to be identical with authentic *N*-(7-tropyl)-succinmide[8] (m. p. 146°C) by mixed melting point determination and by a comparison of their infrared spectra.

After the solvent had been evaporated, the filtrate of the crude IV was dissolved in petroleum ether-benzene and chromatographed through a column containing 30 g. of alumina. The evaporation of the elute with the same solvent gave 270 mg. of a yellow oil (VI) (b. p. 150～160°C/3 mmHg) IR in oily state: 3030, 2925, 1548, 1471, 1422, 1345, 1266, 1065, 743, and 706 cm^{-1}. λ_{max}^{MeOH} mμ (log ε): 230 (3.86) 265 (3.52).

Found: C, 54.38: H, 4.62; N, 9.70. Calcd. for $C_{12}H_{13}N_2Br$: C, 54.34; H, 4.90; N, 10.26%,

The subsequent elute with benzene-ether (49 : 1) gave 40 mg. of IV (m. p. 139～142°C) while the elute with ether-ethanol (60 : 1) afforded 390 mg. of crystals, (m. p. 116～119°C) which on recrystallization from ethanol-water gave colorless crystals (V) (m. p. 122°C), IR in Nujol: 3225, 3123, 1586, 1431, 1310, 1098, 1042, 1000, 830, and 768 cm^{-1}. λ_{max}^{MeOH} mμ (log ε): 226 (4.04).

Found: C, 34.28; H, 4.00; N, 16.02. Calcd. for $C_5H_7N_2Br$: C, 34.68; H, 4.07; N, 15.51%.

V was confirmed to be identical with authentic 4-bromo-3, 5-dimethylpyrazole,[9] (m. p. 122°C) by mixed melting point determination.

b) In a Nonpolar Solvent.—A solution of 800 mg. (4.3 mmol.) of III, 740 mg. (4.2 mmol.) of *N*-bromosuccinimide and 50 mg. of benzoyl peroxide dissolved in 16 ml. of carbon tetrachloride was refluxed in a nitrogen atmosphere for 3 hr. After the succinimide which separated had been filtered off, the filtrate was concentrated by distillation at reduced pressure to give a mixture of an oil and crystals. Filtration afforded 180 mg. of IV (m. p. 140～144°C) and an oily part. The latter was chromatographed using 30 g. of alumina by the same way as in a). Thus, 380 mg. of VI, (as an oil) and 200 mg. of V (m. p. 110～118°C) were obtained.

The Reaction of 3, 5-Dimethyl-4-(7-tropyl)pyrazole (III) with Bromine.—Into a solution of 500 mg. 2.7 mmol.) of III in 2 ml. of chloroform, a solution of 860 mg. (5.4 mmol.) of bromine in 0.6 ml. of chloroform was stirred while the solution was being cooled by ice. The mixture was stirred for 20 min. The crystals which formed during the reaction were filtered off to give 210 mg. of yellow crystals, (m. p. 104～106°C) which on recrystallization from ethanol afforded crystals (VII) (m. p. 115°C (decomp.)). IR in Nujol: 3050, 3005, 1586, 1274, 1218, 976, and 866 cm^{-1}.

Found: C, 25.77; H, 2.10. Calcd. for $C_7H_7Br_3$: C, 25.37; H, 2.11%.

VIII was identified with the compound (m. p. 115°C (decomp.)) which was obtained by the bromination of tropylium ions[11] by a comparison of their infrared spectra. The ethanolic filtrate of VII, upon being treated with 1.2 ml. of an ethanol solution containing 240 mg. of 2, 4-dinitrophenylhydrazine, afforded 80 mg. of 2, 4-dinitrophenylhydrazone of benzaldehyde (m. p. 220°C). The chloroform-mother liquor was poured into water and shaken. The separated chloroform layer was washed with water and dried over magnesium sulfate. The evaporation of the chloroform afforded 460 mg. of an oil, which was then dissolved in benzene and chromatographed through a column containing 22 g. of alumina. The evaporation of thebenzene-elute gave 20 mg. of an oil, which then afforded 2, 4-dinitrophenylhydrazone of benzaldehyde. The elute with ether gave 90 mg. of 4-bromo-3, 5-dimethylpyrazole (V) (m. p. 121°C). The elute with ether-ethanol (15 : 1) gave 270 mg. of colorless crystals (m. p. about 175°C) (Found: C, 56.51; H, 5.19; N, 15.17%), which were difficult to recrystallize from the usual solvents. IR in Nujol: three peaks about 3145, 1585, 1542, 1492, 731, and 695 cm^{-1}.

The Stability of 3, 5-Dimethyl-4-(7-tropyl)pyrazole (III) towards Acids.—a) Hydrogen bromide gas was passed into a solution of 200 mg. (1.1 mmol.) of III dissolved in 6 ml. of benzene, giving colorless crystals. Filtration gave 145 mg. of colorless crystals (m. p. 193°C (decomp.)) which, on recrystallization from a mixture of ethanol and ethyl acetate, gave crystals (m. p. 195°C (decomp.)).

Found: C, 54.23; H, 5.63; N, 10.40. Calcd. for $C_{12}H_{15}N_2Br$: C, 53.93; H, 5.66; N, 10.48%.

After standing the filtrate afforded 80 mg. of crystals (m. p. 132～155°C). The hydrobromide salt was added to an aqueous solution of sodium bicarbonate and extracted with ether. The ether-extract was washed with water, dried over sodium

sulfate, and evaporated to give III (m. p. 139~142°C) quantitatively.

b) To a solution of 200 mg. of III in 7 ml. of acetic acid, 0.3 ml. of 60% perchloric acid was added. Since no tropylium perchlorate precipitated when the mixture had been stood for 30 min., one further ml. of 60% pechloric acid was added to the solution. After being diluted with water and neutralized with a 2N sodium hydroxide solution the solution was extracted with ether. The ether-extract was washed with water, dried over sodium sulfate, and evaporated, giving 180 mg. of III (m. p. 145°C).

The Preparation of 3, 5-Dimethyl-1-phenyl-4-(7-tropyl)pyrazol (VIII) and Bisphenylhydrazone of 7-Tropylacetylacetone.—a) To a solution of 2 g. (10.7 mmol.) of 7-tropylacetylacetone in 25 ml. of ethanol, 1.5 ml. (13.8 mmol.) of phenylhdrazine was added. The reaction mixture was refluxed on a water bath for 1 hr. and then diluted with a large amount of water and extracted with ether. The ether-extract was washed with water and dried over magnesium sulfate, and the ether was evaporated to give 2.5 g. of an oil containing crystals. The filtration afforded 680 mg. of colorless crystals (m. p. 122~125°C) as the first crop and 240 mg. of crystals (m. p. 123~125°C) as the second crop. The residual part was dissolved in benzene-petroleum ether and chromatographed through a column containing 60 g. of alumina. The evaporation of the elute with the same solvent gave 390 mg. of a brownish yellow oil. 1.1 g. of crystals (m. p. 116~125°C) was obtained from the elute with benzene. The crystals obtained here were combined and recrystallized from ethanol, giving colorless prisms (VIII) (m. p. 126~127.5°C). IR in Nujol: 1577, 1565, 1505, 1450, 1427, 1386, 1364, 1137, 1070, 1015, 914, 856, 804, 800, 767, 752, 713, 702, and 683 cm^{-1}. λ_{max}^{MeOH} $m\mu$ (log ε) : 245 (4.01).

Found: C, 81.97; H, 6.73; N, 10.68. Calcd. for $C_{18}H_{18}N_2$: C, 82.40; H, 6.92; N, 10.68%.

b) A solution of 0.5 g. (2.7 mmol.) of 7-tropylacetylacetone and 0.9 g. (8.1 mmol.) of phenylhydrazine in 10ml. of ethanol was refluxed on a water bath for 20 min. and then allowed to stand in a refrigerator overnight. The crystals which precipitated were collected and recrystallized from ethanol to yield 200 mg. of bisphenylhydrazone of 7-tropylacetylacetone as colorless needles (m. p. 165~167°C). IR in Nujol: 3448, 1603, 1504, 755, 745, 725, and 695 cm^{-1}.

Found: C, 77.94; H, 6.77; N. 14.84. Calcd. for $C_{24}H_{26}N_4$: C, 77.80; H, 7.07; N, 15.12%.

The Bromination of 3, 5-Dimethyl-1-phenyl-4-(7-tropyl)pyrazole (VIII).—To a well-stirred solution of 600 mg. (2.3 mmol.) of VIII in 2 ml. of chloroform, a solution of 400 mg. (2.5 mmol.) of bromine in 1.5 ml. of chloroform was added drop by drop while the solution was being cooled by ice. The reaction mixture was then stirred for 30 min., diluted with a large amount of chloroform, and washed with water. The addition of acetylacetone to the water-washing afforded 30 mg. of 7-tropylacetylacetone (m. p. 123°C), indicating the presence of tropylium ions.[4] The chloroform-layer was dried over sodium sulfate and evaporated, yielding 670 mg. of a brownish yellow oil. This oil was dissolved in petroleum ether - benzene (1 : 1) and chromatographed through a column containing 20 g. of alumina. The evaporation of the elute with the same solvent afforded 230 mg. of an oil, which on distillation under reduced pressure gave two fractions, b. p. 175~180°C/2 mmHg (IX) and b. p. 215~220°C/2 mmHg (Found: C, 74.83; H, 6.92; N, 8.82%), in a ratio of 2 : 1. IX has the following data: IR in an oily state: 1595, 1546, 1504, 1465, 1412, 1377, 1362, 1080, 1041, 1022, 739, 793, 696, and 682 cm^{-1}.

Found: C, 54.11; H, 4.47; N, 10.19. Calcd. for $C_{11}H_{11}N_2Br$: C, 53.59; H, 4.38; N, 11.11%.

The infrared spectrum of IX was superposed on that of an authentic sample of 4-bromo-3, 5-dimethyl-1-phenylpyrazole.[12] The elutes with ether and ethanol afforded 220 mg. of a viscous oil which was not further studied.

The Reaction of 3, 5-Dimethyl-1-phenyl-4-(7-tropyl)pyrazole (VIII) with *N*-Bromosuccinimide.—To a solution of 800 mg. (3.0 mmol). of VIII in 20 ml. of *t*-butanol containing 7 ml. of pyridine and 2 ml. of water, 650 mg. (3.7 mmol.) of *N*-bromosuccinimide was added, and the resulting mixture was allowed to stand at room temperature for 48 hr. The solution was then diluted with water and extracted with chloroform. After being washed with water and dried over magnesium sulfate, the chloroform-extract was evaporated at reduced pressure to give 465 mg. of a viscous oil. The oil was dissolved in petroleum ether - benzene and chromatographed through a column containing 14 g. of alumina. The evaporation of the elute with the same solvent afforded 90 mg. of a yellow oil (b. p. 165~175°C/2 mmHg) which was found to be identical with IX by a comparison of their infrared spectra. The elute with benzene-ether (1 : 1) and ether gave 125 mg. of a viscous oil, which crystallized after standing for a long period of time. These crystals were difficult to recrystallize from usual organic solvents, but on digestion with ethyl acetate they gave colorless crystals (X) (m. p. 102~106°C). IR in Nujol: 3230, 1595, 1562, 1507, 1487, 1427, 1331, 1283, 1256, 1165, 1144, 1022, 810, 790, 769, 729, and 702 cm^{-1}. λ_{max}^{MeOH} $m\mu$ (log ε) : 251 (4.07).

Found: C, 77.37; H, 6.22; N, 10.17. Calcd. for $C_{18}H_{15}ON_2$: C, 77.67; H, 6.52; N, 10.07%.

The Stability of 3, 5-Dimethyl-1-phenyl-4-(7-tropyl)pyrazole (VIII) towards Acids.—a) A solution of 100 mg. of VIII in 2 ml. of benzene was saturated with hydrogen bromide gas and allowed to stand at room temperature for 2 hr., during which no crystal formed. After the solution had been washed with water and dried over magnesium sulfate, the removal of the benzene regenerated 65 mg. of VIII, (m. p. 126~128°C).

b) To a solution of 50 mg. of VIII in 1.5 ml. of acetic acid, 0.1 ml. of 60% perchloric acid was added; no crystal formed during a 5-min. period. Then 0.1 ml. of 60% perchloric acid was added to the solution and the solution was allowed to stand at room temperature for 20 min. After being diluted with a large amount of water, the solution was extracted with ether. The ether-extract was

washed with water, dired over magnesium sulfate, and evaporated to give 35 mg. of VIII (m. p. 122~125°C).

The authors wish to take this opportunity to express their deep gratitude to Professor Tetsuo Nozoe for his kind guidance throughout the course of this work. They also wish to thank Professor Genjiro Hazato and his colleages of the Chemical Institute of Non-aqueous Solutions, Tohoku University, for their measurement of the NMR spectrum and the Sankyo Co. for the donation of research funds which covered a part of the expenses of this work.

Department of Chemistry
Faculty of Science
Tohoku University
Katahira-cho, Sendai

Studies on the Chemical Decomposition of Simple Sugars. XV. The Synthesis of 1-O-Benzoyl-3,4; 5,6-di-O-isopropylidene-L-xylo-2-hexulose

By Hiroyuki MIZOIRI, Akira SERA and Ryozo GOTO

(Received February 24, 1964)

Syntheses of keto-hexuloses have been made by many investigators since 1941. For instance, some synthetic procedures working through the condensation of acetylated aldonyl chlorides with diazomethane[1] and the oxidation of substituted hexitols with chromium trioxide[2,3] have been reported. However, the synthesis of diisopropylidene-keto-L-sorbose has not been reported. In accordance with the research program in our laboratory studying the decomposition mechanism of simple sugars, 1-*O*-benzoyl-3,4; 5,6-di-*O*-isopropylidene-L-*xylo*-2-hexulose, i. e., 1-*O*-benzoyl-3,4; 5,6-di-*O*-isopropylidene-keto-L-sorbose, has been synthesized. As the starting compound 1,2-*O*-isopropylidene-D-sorbitol was used.

The benzoylation of 1,2-*O*-isopropylidene-D-sorbitol[4] (I) with an equimolar amount of benzoyl chloride in anhydrous pyridine gave 1,2-*O*-isopropylidene-6-*O*-benzoyl-D-sorbitol (II). When II was treated with acetone in the presence of anhydrous copper sulfate, diacetone-monobenzoyl-D-sorbitol (III) was obtained. After the debenzoylation of III, one mole of di-*O*-isopropylidene-D-sorbitol obtained consumed one mole of sodium periodate. Therefore, III was confirmed to be 1,2; 3,4-di-*O*-isopropylidene-6-*O*-benzoyl-D-sorbitol, and the presence of 1,2; 4,5-di-*O*-isopropylidene isomer was excluded.

Compound II has three adjacent hydroxyl groups, attached to the carbons 3, 4 and 5. The adjacent hydroxyl groups attached to C_4 and C_5 have an erythro-, and those attached to C_3 and C_4 have a threo-configuration. In order to condense with acetone to form a five-membered ring, the two hydroxyl groups must have an eclipsed conformation. In such circumstances, the twist around the C_4–C_5 bond axis causes a large steric repulsion between the bulky groups (R_2 and $R_1 + C_3$ in Fig. 1), while that around the C_3–C_4 bond axis makes the steric repulsion (Fig. 2) so small that the condensation with acetone may take place and 1,2; 3,4-di-*O*-isopropylidene-6-*O*-benzoyl-D-sorbitol is produced exclusively.

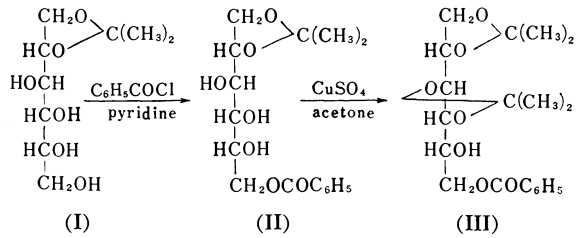
The oxidation of 1,2; 3,4-di-*O*-isopropylidene-6-*O*-benzoyl-D-sorbitol (III) with chromium trioxide gave 1-*O*-benzoyl-3,4; 5,6-di-*O*-isopropylidene-keto-L-sorbose (IV) in a 49% yield. The deacetonation of ketose (IV) was effected by using the ion-exchange resin, Amberlite IR-120 (H-form). The crystalline 1-*O*-benzoyl-L-sorbose (V) obtained was debenzoylated by transesterification with methanol in the presence of sodium methoxide to give crystalline L-sorbose (VI).

Further investigations related to those described in this communication are in progress.

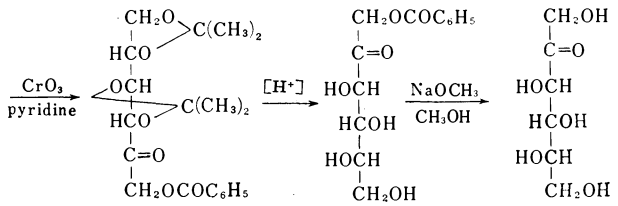
Experimental

1,2-*O*-Isopropylidene-6-*O*-benzoyl-D- sorbitol (II).—To an ice-cooled solution of 1,2-*O*-isopropylidene-D-sorbitol (18 g.) in 130 ml. of anhydrous pyridine, benzoyl chloride (12 ml.) was added with vigorous stirring drop by drop. After standing overnight at

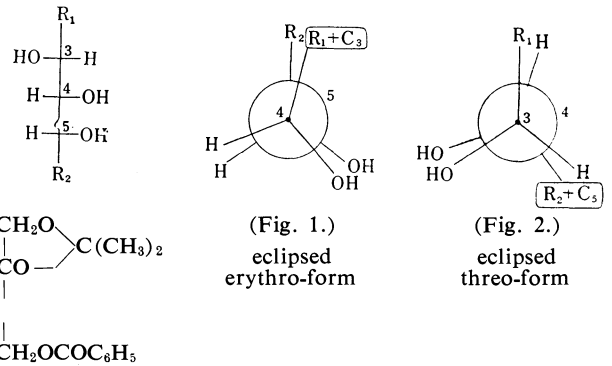
1) W. Pigman, "The Carbohydrates," Academic Press, New York (1957), p. 111.
2) W. R. Sullivan, *J. Am. Chem. Soc.*, **67**, 837 (1945).
3) J. M. Sugihara and G. U. Yuen, ibid., **79**, 5780 (1957); G. U. Yuen and J. M. Sugihara, *J. Org. Chem.*, **26**, 1598 (1961).
4) L. Anderson, B. C. Pressmann and H. A. Lardy, *J. Am. Chem. Soc.*, **72**, 2404 (1950).



(I) (II) (III)



(IV) (V) (VI)



(Fig. 1.) eclipsed erythro-form

(Fig. 2.) eclipsed threo-form

room temperature, the solution was concentrated under reduced pressure. The resulting sirup was poured into 300 ml. of ice and water, and the crystalline precipitate was filtered and recrystallized from isopropyl ether containing a small amount of ethanol. 1,2-*O*-Isopropylidene-6-*O*-benzoyl-D-sorbitol(II) (m. p. 120.0~124.6°C) was obtained. After several recrystallizations, the compound had a m. p. of 124.7~125.1°C (13.5 g.), $[\alpha]_D^{25}$ +3° (*c* 1, pyridine).

Found: C, 58.91; H, 6.88; C_6H_5CO, 34.14, 33.17. Calcd. for $C_{16}H_{22}O_7$: C, 58.86; H, 6.74; C_6H_5CO, 32.21%.

Infrared spectrum: ν_{OH}, 3540, 3450; $\nu_{C=O}$, 1709; $\nu_{C=C}$, 1604, 1589 cm^{-1}.

Moles of periodate consumed/one mole of II: 2.08 (15 min.), 2.09 (20 min.), 2.09 (30 min.) and 2.13 (45 min.). Moles of formic acid produced/one mole of II: 1.05 (17 min.), 1.12 (1 hr.), 1.16 (2 hr.) and 1.24 (4 hr.).

1,2; 3,4-Di-*O*-isopropylidene-6-*O*-benzoyl-D-sorbitol (III).—To a solution of 1,2-*O*-isopropylidene-6-*O*-benzoyl-D-sorbitol (II) (2 g.) in 70 ml. of anhydrous acetone, 5 g. of anhydrous copper sulfate was added, and the mixture was gently refluxed for 30 hr. After the inorganic salt had been filtered off, the filtrate was concentrated under reduced pressure to a sirup, which crystallized slowly when 10 ml. of isopropyl ether was added. The crude material (1.3 g.) had a m. p. of 66.7~67.1°C. After several recrystallizations from isopropyl ether, 1,2; 3,4-di-*O*-isopropylidene-6-*O*-benzoyl-D-sorbitol (III) showed a m. p. of 68.2~68.5°C, $[\alpha]_D^{25}$ +19.3° (*c* 1.03, pyridine).

Found: C, 62.19; H, 7.14. Calcd. for $C_{19}H_{26}O_7$: C, 62.28; H, 7.15%.

Infrared spectrum: ν_{OH}, 3550; $\nu_{C=O}$, 1713 cm^{-1}.

After the benzoyl residue of III had been removed, the product was oxidized with sodium periodate in aqueous dioxane. Moles of periodate consumed/one mole of 1,2; 3,4-di-*O*-isopropylidene-D-sorbitol; 1.18 (10 min.), 1.21 (20 min.), 1.25 (40 min.) and 1.28 (50 min.).

When copper sulfate was replaced with zinc chloride in the above procedure, 1,2-*O*-isopropylidene-6-*O*-benzoyl-D-sorbitol was recovered unchanged (90%).

1-*O*-Benzoyl-3,4; 5,6-di-*O*-isopropylidene-L-*xylo*-2-hexulose (IV). — Chromium trioxide (9 g.) was added to anhydrous pyridine while being agitated mechanically. To this mixture, 1,2; 3,4-di-*O*-isopropylidene-6-*O*-benzoyl-D-sorbitol (III) (7 g.) was added quickly, and the mixture was kept at 60°C for 7 hr. while being continuously stirred. The mixture was then poured into 300 ml. of ice and water and extracted with ether (200 ml.×7). The ethereal solution was washed successively with dilute hydrochloric acid, aqueous sodium hydrogen carbonate, and water, and then dried over anhydrous

magnesium sulfate. The removal of the solvent gave white crystalline needles (3.4 g.; m. p. 69~70°C). After several recrystallizations from aqueous ethanol, 1-*O*-benzoyl-3,4; 5,6-di-*O*-isopropylidene-L-*xylo*-2-hexulose (IV), (m. p. 75.0°~75.4°C) was obtained. $[\alpha]_D^{25}$ −38.4° (*c* 1, pyridine).

Found: C, 62.70; H, 6.86. Calcd. for $C_{19}H_{24}O_7$: C, 62.62; H, 6.64%. Infrared spectrum: $\nu_{C=O}$, 1742, 1724; $\nu_{C=C}$, 1604, 1588 cm^{-1}. No absorption peak was observed near 3550 cm^{-1}, where the parent compound had an absorption peak.

1-*O*-Benzoyl-L-sorbose (V).—Amberlite IR-120 (H-form) (7 g.) was added to a solution of 1-*O*-benzoyl-3,4; 5,6-di-*O*-isopropylidene-L-*xylo*-2-hexulose (IV) (3 g.) in 100 ml. of acetone and water (3 : 1 by volume). The mixture was kept at 40°C for 30 hr. After the resin had been removed by filtration, the filtrate was concentrated under reduced pressure. A crude material (2.2 g.) was obtained (m. p. 122~125°C). After several recrystallizations from isopropyl ether containing a small amount of ethanol, 1-*O*-benzoyl-L-sorbose (V) showed a m. p. of 132.5~133.0°C. $[\alpha]_D^9$ −2.1° (*c* 5, methanol). (Reported[2] m. p. 133.5°C, $[\alpha]_D^{26}$ −3.4° in methanol (*c* 5)).

Found: C, 54.66; H, 5.74. Calcd. for $C_{13}H_{16}O_7$: C, 54.93; H, 5.67%.

Infrared spectrum: ν_{OH}, 3540, 3350 (broad); $\nu_{C=O}$, 1709, 1697; $\nu_{C=C}$, 1610, 1595 cm^{-1}.

L-Sorbose (VI).—1-*O*-Benzoyl-L-sorbose (V) (1.7 g.) was dissolved in 25 ml. of anhydrous methanol, and the solution was cooled with an ice-bath. Into the cold solution, 6 ml. of 0.1 N sodium methoxide in anhydrous methanol was added. After 2 hr., the cooling bath was removed and the solution allowed to stand overnight at room temperature. The solvent was then distilled off under reduced pressure to a sirup, which crystallized spontaneously (900 mg.; m. p. 158~161°C). After several recrystallizations from aqueous ethanol, L-sorbose showed a m. p. of 164~165°C; it was undepressed when the substance was admixed with an authentic specimen of L-sorbose. $[\alpha]_D^9$ −42.9° (*c* 2.4, water).

Found: C, 40.14; H, 6.83. Calcd. for $C_6H_{12}O_6$: C, 40.00; H, 6.71%.

Insitute of Chemistry
Faculty of Science
Kyoto University
Sakyo-ku, Kyoto

Studies on the Disproportionation Reaction of Methylnaphthalene

By Etsuro ECHIGOYA, Tōru WATANABE and Kiyoshi MORIKAWA

(Received February 25, 1964)

The disproportionation reaction of toluene and xylene over a silica-alumina catalyst has been studied by several investigators,[1-3] but that of methylnaphthalene (M. N.)[1] has been scarcely studied at all.

This work has been done in order to clarify the promoter action of chromium oxide on the silica-alumina catalyst[4] and also to obtain a kinetic equation for the disproportionation reaction of methylnaphthalene over the catalyst.

Experimental

The reaction was studied by means of the flow method under various pressures. As the reactor for this reaction, a quartz tube (I. D. 2.5 cm.) and a stainless steel tube (I. D. 2.9 cm.), both containing 30 cc. of the catalyst, were used under

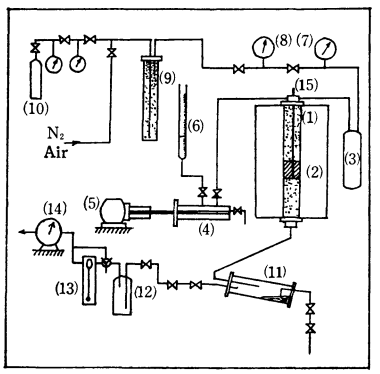


Fig. 1. Flow sheet of the disproportionation reaction of methylnaphthalene.

(1) stainless steel reactor
(2) electric furnace
(3) pressure storage
(4) liquid feed pump
(5) motor
(6) mess cylinder
(7) pressure gauge
(8) pressure gauge
(9) drier (silica gel)
(10) hydrogen cylinder
(11) gas-liquid pa-se rator
(12) dry ice - methanol trap
(13) orifice meter
(14) gas meter
(15) thermocouple

1) R. C. Hansford, C. G. Myers and A. Sachanen, *Ind. Eng. Chem.*, 37, 617 (1945).
2) P. M. Pitts, Jr., J. E. Connor, Jr., and L. N. Leum, ibid., 47, 770 (1955).
3) K. Tarama, S. Teranishi, K. Hattori and M. Shimobayashi, on the 15th Annual Meeting of the Chemical Soceity of Japan.
4) T. Matsuda, T. Takahashi, T. Kakuzen and H. Chiyajima, *J. of the Fuel Soc. Japan*, 41, 593 (1962).

atmospheric pressure and 3~6 atms. respectively. The flow sheet of this reaction under pressure is shown in Fig. 1. Methylnaphthalene was diluted with hydrogen which was free from oxygen and was introduced into the reactor.

The reaction products from the reactor were caught by methanol - dry ice cold traps and were analyzed by means of the gas chromatographic method.

Raw Material.—The methylnaphthalene employed in these experiments was provided by Mitsui Chemical Industries and was an equiliburium mixture of α and β isomers. (The sulfur content was about 1 wt.%).

Catalysts. — *Nalcat.* — The fine powders (over 100 mesh) of the commercial nalcat silica-alumina cracking catalyst (aluminum oxid content, 12~13 wt.%) were pelletized to a 4 mm. in diameter.

Chromium Oxide - added Nalcat. — Nalcat powders were immersed in a chromic sulfate solution (1 wt.%), and a small amount of dextrin (5 wt.%) was used as a binder in pelletizing.

Chromia - Alumina Gel Mixed Catalyst. — Aqueous gels of alumina and chromia, both prepared by precipitation from nitrate solutions (3 N) with aqueous ammonia, were kneaded well and dried in granules. The Chromium oxide content of this catalyst was 15 wt.%.

Results and Discussion

Reactions under Atmospheric Pressue. — The Effect of Reaction Temperature on the Disproportionation of Methylnaphthalene. — The reaction over the nalcat catalyst was carried out under the following conditions: SV, 600 hr^{-1}; mole ratio of hydrogen to methylnaphthalene, 4.5. The amounts of liquid

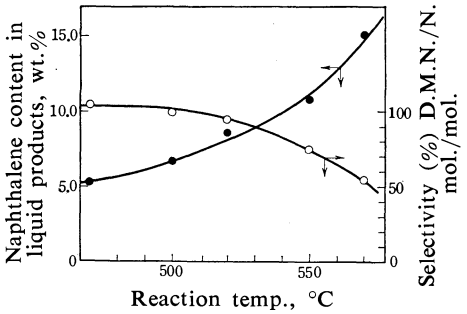


Fig. 2. Activity of SiO_2-Al_2O_3 catalyst for the disproportionation reaction of M. N.
S.V.=600 (hr^{-1}), H_2/M.N.=4.5 (mol. ratio)

products (%) recovered varied a little from experiment to experiment. Figure 2 shows that at lower temperatures, 450~520°C, the yield of naphthalene was quite small (about 7%), but that the selectivity of this reaction was excellent (about 100%); on the other hand, at higher temperatures, 550~570°C, the yield increased up to 15%, but the corresponding selectivity decreased to about 55% because of the increased demethylation reaction.

The Effect of the Chromium Oxide added to the Silicon Oxide - Aluminum Oxide Catalysts on the Disproportionation Reaction. — When several kinds of silica-alumia catalysts were tested, the nalcat was found to give the best result and, therefore, the promoter effect of chromium oxide for this catalyst was examined with nalcat. Figure 3 shows that, as the amount of chromium oxide increased, the yield of naphthalene varied through a maximum, while the selectivity varied through a minimum, in the temperature range of 520~560°C.

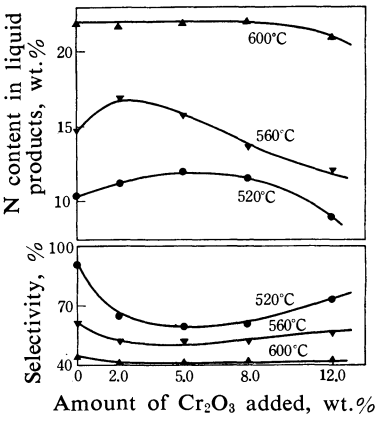


Fig. 3. Effect of addition of Cr_2O_3 on the activity of SiO_2-Al_2O_3 catalysts for the disproportionation reaction of M. N.

The activity of the chromia-alumina catalyst was quite low at 520°C under the same reaction conditions, and the yield of methylnaphthalene was only 4 wt.% even at 560°C. Naphthalene obtained over this catalyst was produced by demethylation, not by disproportionation reaction.

The Structure of Chromium Oxide - added Catalyst.—The nalcat catalyst showed diffuse X-ray patterns, indicating its amorphous structure, while the chromium oxide - added catalyst (5 wt.%) gave markedly sharp diffraction patterns of chromium oxide crystals.

The chromium oxide crystal content was estimated from this pattern to be 3.5 wt.%, amounting to 70% of the chromium oxide added.

The residual 30% of chromium oxide might be in an amorphous state, but its chemical state is not clear.

The mean magnitude of the crystallite of the chromium oxide - added catalyst was calculated by the Scherrer method to be D_{110}=400 Å. This crystal might be free from carriers, since this value was almost the same as those found

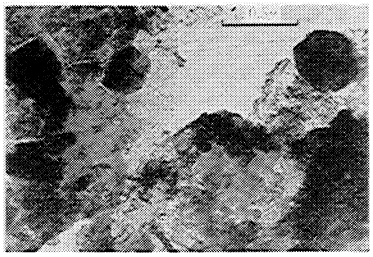


Fig. 4. Electron Micrograph (taken by Mr. A. Kitahara of T. I. T.)
Sample: Cr_2O_3 (5 wt%) on nalcat.

in literature for pure chromium oxide crystals.

Figure 4 shows the electro-micrograph of chromium oxide (5 wt.%)-added nalcat, which was examined by a one-step powder replica method, depositing carbon vapor. This picture shows that many fine crystals (30~80Å), besides a few large hexagonal single crystals (2000~5000Å), exist in very fine nalcat particles.

On the basis of the above results, it may be concluded that most of the added chromium oxide (about 70%) did not chemically combine with silica-alumina and did not widely disperse on the surface, but rather developed into large crystals. The residual chromium oxide (about 30% which was not observed as crystals in the electro-micrographic picture would be in a very finely-dispersed state and exert a promoter action on this reaction, thus explaining the results of Fig. 3 satisfactorily.

Experiments under Pressure. — The experiments under pressure were carried out to study the kinetics of the disproportionation reaction of methylnaphthalene over the chromium oxide (5 wt.%) - added silica-alumina catalyst.

The change in catalytic activity with reaction time was tested under the following conditions: reaction temperature, 470°C; reaction pressure, 17 atm.; mole ratio of H_2 to methylnaphthalene, 10, and contact time, 11 sec. The selectivity for this reaction was almost 100%, but the conversion decreased as the reaction proceeded.

It was further found that there was little difference between the activity of the nalcat with and without chromium oxide. The former, however, was used for this kinetic study under pressure, with carbon deposit being avoided as much as possible.

A Kinetic Analysis of this Catalytic Reaction Accompanied by Activity Degradation. — The rate of the reaction in the flow system may commonly be obtained from the relationship between the conversion and the time factor (W/F). The catalytic activity, however, decreased gradually as the reaction proceeded. Therefore, the degradation curves as shown in Fig. 5 were prepared; they indicate the change in catalytic activities with the reaction time at the constant value of W/F and at each reaction temperature. The initial activities of the catalyst at each W/F can be obtained by extrapolating each curve to the zero reaction time point.

The following reaction conditions were used: the catalyst, 30 cc. (19.2 g.); reaction temperature, 470~430°C; mole ratio H_2 to M. N., 10.0; feed rate of M.N., 12 g./hr.~40 g./hr. (W/F 60~250 hr. g. cat./mol. M. N.), and reaction pressure range, 3.0~15.0 atm. The reaction products were collected four times every two hours and were analyzed. The conversion of the disproportionation reaction was assumed to be twice that of the dimethylnaphthalene (D. M. N.) (mol.%) found. The side reaction of destruction, which may be connected with the carbon deposition, occured

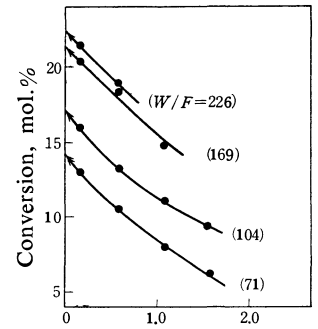


Fig. 5. Chart to read the initial activities of catalysts from the degradation curves.

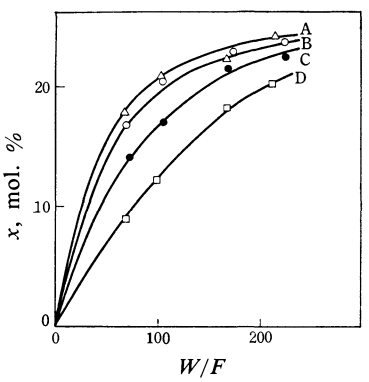


Fig. 6. Relationship between x and W/F under the definite pressures.
H_2/M.N. (mol. ratio), 10.0 Temp., 470°C
π; Total pressure (atm.)
A π=16.0 atm. C π=6.0
B π=11.0 D π=3.0

to some extent. Figure 6 shows the experimental results, that is, the relationship between the conversion, x, and the time factor, W/F, under several different pressures.

Analysis of the Experimental Results Obtained. — According to the concept of the Langumuir-Hinshelwood mechanism, three rate-controlling steps: (1) adsorption, (2) surface reaction and (3) desorption, may be considered for this surface reaction.

The initial reaction rates r_0 obtained from Fig. 6 were plotted against the corresponding total pressures, π, as Fig. 7-I shows. The shape of the curve in this figure indicates that step 2, the surface reaction, may be the real rate-controlling step for this reaction.

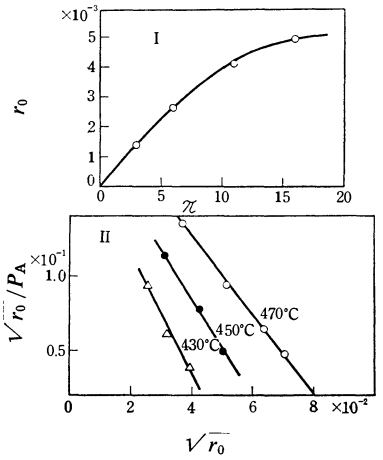


Fig. 7. I: Initial rate vs. total pressure.
II: $\sqrt{r_0}/P_A$ vs. $\sqrt{r_0}$.

Thus, the rate equation (r) and the initial rate equation (r_0) for this reaction may be expressed as follows:

$$r=\frac{k(K_A^2P_A^2-(1/K)K_RK_SP_RP_S)}{(1+K_AP_A+K_AP_A+K_SP_S+K_IP_I)} \quad (1)$$

$$r_0=\frac{kK_A^2P_A^2}{(1+K_AP_A+K_IP_I)^2} \quad (2)$$

Assuming that K_IP_I would be negligibly small in comparison with K_AP_A,

$$\sqrt{r_0}/P_A=a-\sqrt{r_0}+\sqrt{c} \quad (3)$$

where a is K_a and c is $k\,K_a^2$.

The plots of $\sqrt{r_0}/P_a$ vs. $\sqrt{r_0}$ gave straight lines, as Fig. 7-II shows; from this figure a and c can be estimated, while the rate equation at 470°C is given by the following equation.

$$r=\frac{0.0523(1-x)^2-0.414x^2}{(11.0/\pi+2.55(1-x)+7.71x)^2} \quad (4)$$

The full lines in Fig. 8, which were calculated using Eq. 4, agree with the experimental data satisfactorily. Figure 9 shows the temperature dependency of k and K_A, from which the activation energy of this reaction and the heat of adsorption of methylnaphthalene can be estimated to be 32.4 kcal./mol. and 12.6 kcal./mol. respectively.

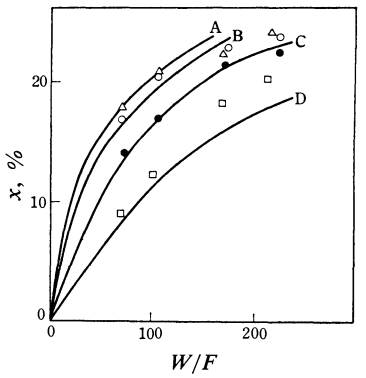


Fig. 8. Test of Eq. 4 with experiments. Full lines indicate the calculated ones after Eq. 4, and all the points indicate the estimated initial activities from the observed conversion-time curves (cf. Fig. 4).
A $\pi=16.0$ atm. C $\pi=6.0$
B $\pi=11.0$ D $\pi=3.0$
React. temp. 470°C

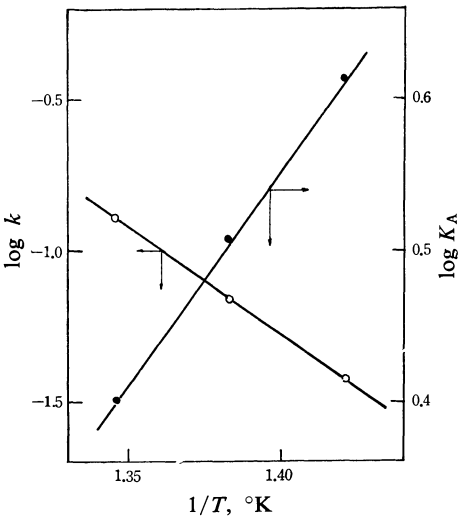


Fig. 6. Temperature dependency of k and K_A.

Summary

The effect of the addition of chromium oxide on the activity of silicon oxide - aluminum oxide for the disproportionation reaction of methylnaphthalene has been studied.

1) As the amount of chromium oxide added increased the yield of naphthalene increased, but the selectivity for this reaction decreased

in the low temperature range of 450～520°C. The 5 wt.%, chromium oxide added catalyst gave the best results.

2) It has been concluded, from the observation of X-ray and electromicrograph of the chromium oxide-added nalcat catalyst, that most of the chromium oxide added developed into large hexagonal crystals which had little activity and that the residue (about 30%), which is supposedly dispersed very finely, is probably responsible for the promotion of the catalytic activity.

3) It has been concluded from the analyses of the experimental data obtained that this disproportionation reaction can be expressed by the kinetic equation based on the surface reaction which is rate-controlling.

Nomenclature

r: reaction rate (mol. M. N./hr. g. cat.)
k: rate constant of surface reaction
K: equilibrium constant
K_A: adsorption equilibrium constant of methylnaphthalene
K_R: adsorption equilibrium constant of naphthalene
K_S: adsorption equilibrium constant of demethylnaphthalene
K_I: adsorption equilibrium constant of hydrogen
P_a: partial pressure of methylnaphthalene (atm.)
P_R: partial pressure of naphthalene (atm.)
P_S: partial pressure of demethylnaphthalene (atm.)
P_I: partial pressure of hydrogen (atm.)
x: conversion of disproportionation reaction (mol.%)
μ: total pressure (atm.)

The authors wish to thank the Mitsui Chemical Co. and the Maruzen Petroleum Co. for providing samples and the Nippon Petroleum Co. for its analyses of the sulfur content of the samples.

They would also like to express their appreciation to Dr. T. Shirasaki for his help in the X-ray and electro-micrograph observation.

Research Laboratory of Resources Utilization
Tokyo Institute of Technology
Meguro-ku, Tokyo (E. E. & K. M.)

Kawasaki Kasei Kogyo Co., Ltd.
Kawasaki (T. W.)

Terpenoids. VIII. Sesquiterpenoids from the Wood Oil of "Sugi" (Cryptomeria japonica D. Don.)[*1,*2]

By Shizuo NAGAHAMA[*3]

(Received February 26, 1964)

The main components of the oil of Sugi wood have been shown to be sesquiterpenoids.[1-5] Among these, however, a cadinene has been the only component unsatisfactory characterized, except for the recent work by Sumimoto and his co-workers[6] on the isolation and characterization of cryptomeridiol (selinan-4α, 11-diol).

The results of experiments on two samples of Sugi-wood oil, kindly supplied by Professor Tamio Kondo, are described in this paper.

Oil I, obtained by steam-distillation, was analyzed by distillation, followed by chromatography; the complete results are given in Table I. Sesquiterpene alcohols are distributed over all fractions, and two alcohols are obtained

*1 Contribution No. 64 from the Department of Organic Synthesis, Faculty of Engineering, Kyushu Univesity. Part VII, This Bulletin, **37**, 886 (1964).

*2 Partly presented before the 6th Symposium on Perfumery, Terpene and Essential Oil Chemistry held at Shinshu University, Ina, August, 1962, and the 7th Symposium on the same subjects held at Kochi University, Kochi, October, 1963.

*3 Present address: Central Reserch Institute, Teijin Ltd., Hino, Tokyo.

1) C. Kimoto, *Tokyo Imp. Univ. Agr.*, **4**, 403 (1902); *Chem. Zent.*, **1902**, II, 382.

2) H. Kimura, a) *J. Pharm. Soc. Japan* (*Yakugaku Zasshi*), No. 284, 905 (1905); b) *Ber. Deutsch. Pharm. Ges.*, **19**, 369 (1909); *Chem. Zent.*, **1910**, I, 275.

3) K. Keimatsu, *J. Chem. Soc. Japan* (*Tokyo Kagaku Kaishi*), **26**, 315 (1905); *J. Pharm. Soc. Japan* (*Yakugaku Zasshi*), No. 277, 189 (1905).

4) M. Yano, *J. Soc. Chem. Ind. Japan* (*Kogyo Kagaku Zasshi*), **16**, 443 (1913).

5) K. Hoshino, ibid., **22**, 969 (1919).

6) M. Sumimoto, H. Ito, H. Hirai and K. Wada, *Chem. & Ind.*, **1963**, 780; M. Sumimoto, ibid., **1963**, 1356.

in the crystalline form. The one, $C_{15}H_{26}O$, (m. p. 140~141°C), was identified as pilgerol (=δ-cadinol) by a direct comparison with the sample provided by Professor Erdtman.*4 It seems quite probable that the "isocryptomeriol" (m. p. 135~136°C) described by Kimura[2b] is identical with this alcohol. Another alcohol (m. p. 63~74°C) was still impure, but its infrared spectrum was almost identical with that of β-eudesmol.[7],*5 Furthermore, a new monocyclic ketone, named cryptomerion, $C_{15}H_{22}O$, was isolated from fraction 7.

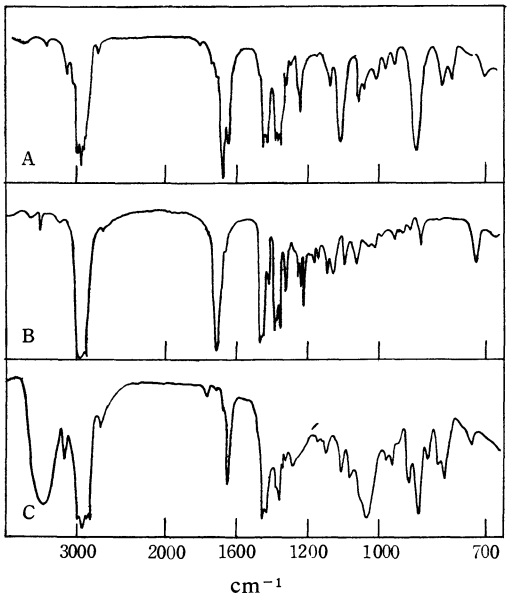


Fig. 1. Infrared spectra of cryptomerion (A); hexahydrocryptomerion (B); and unsaturated alcohol (C).

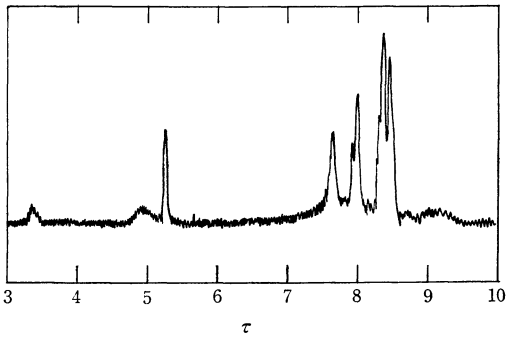
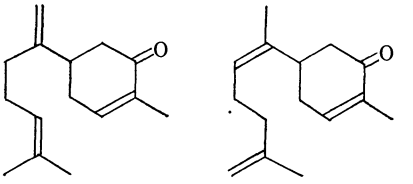


Fig. 2. NMR spectrum of cryptomerion (CCl_4 solution 10%).

Cryptomerion possesses an α,β-unsaturated ketone group (λ_{max} 236, 304 mμ and ν_{max} 1685 cm^{-1}; Fig. 1A). The infrared spectrum of the corresponding unsaturated alcohol (Fig. 1C) obtained by reduction of cryptomerion with lithium aluminum hydride clearly shows the presence of a terminal methylene group (ν_{max} 3130, 1650 and 888 cm^{-1}). The NMR spectrum*6 of cryptomerion (Fig. 2) indicates the presence of the following groups; one hydrogen and one methyl group on the conjugated ketone system (τ value 3.38 and 8.00), one hydrogen on a trisubstituted double bond (4.98), one terminal methylene group (5.25), one methylene group adjacent to the carbonyl group (7.66), and two methyl groups on one (or two) double bond(s) (8.37 and 8.46). The catalytic reduction of cryptomerion gave a hexahydroderivative (Fig. 1B), which was reduced to the corresponding hydrocarbon by the Huang-Minlon method. The infrared spectrum of this hydrocarbon is identical with that of hexahydrobisabolene.[8],*7 When the groups detected by the NMR spectrum are arranged on the bisabolane skeleton, the possible structures are limited to two, namely, I and II. Structure I is preferred for cryptomerion from the biogenetic point of view.[9]



(I) (II)

Oil II, obtained by methanol extraction, was used for the analysis of sesquiterpene hydrocarbons. The fraction corresponding to fractions 1 to 4 of oil I was distilled by a spinning-band column (the results are shown in Table II) with each fraction subjected to the chromatographic separation. Fractions 10 to 13 show two main peaks in the gas chromatography. They were separated pure by chromatography and identified as δ-cadinene[10] and

7) F. J. McQuillin and J. D. Parrack, *J. Chem. Soc.*, **1956**, 2973.

*4 The author thanks Professor H. Erdtman for his kindness in providing him with the authentic sample.

*5 The presence of eudesmol (=cryptomeradol) in the root oil of Sugi was reported by H. Wienhaus and H. Scholz, *Ber. Schimmel Jubiläum Ausgabe*, 267 (1929); *Chem. Zent.*, **1930**, I, 137. cf. L. Ruzicka, D. R. Koolhaas and A. H. Wind, *Helv. Chem. Acta*, **14**, 1178 (1931); Y. Sugii and T. Sengoku *J. Pharm. Soc. Japan* (*Yakugaku Zasshi*), **51**, 196 (1931).

*6 The NMR spectrum was measured with Varian A 60. The author is indebted to Dr. T. Matsuo and Mr. Y. Nakayama for the measurement and instructive discussions.

*7 The author thanks Professor V. Herout for the donation of the reprints.

*8 The author is indebted to Dr. Y. Hirose of the University of Tokyo for the identification of infrared spectrum of copaene.

8) J. Pliva, V. Herout and F. Šorm, *Chem. Listy*, **45**, 117 (1951).

9) J. B. Hendrickson, *Tetrahedron*, **7**, 82 (1959).

10) J. Pliva, V. Herout, B. Schneider and F. Šorm, *Coll. Czecko. Chem. Communs.*, **18**, 500 (1953).

TABLE I.

Fraction	B. p. °C/7 mmHg	n_D^{21}	Yield g.	Yield %	Results of chromatography, % Sesquiterpene Hydrocarbon	Sesquiterpene Ether	Sesquiterpene Alcohol	Sesquiterpene Ketone	Diterpene Hydrocarbon
1	105~110	1.5060	1.5	6.3	5.2	0.5	0.2		
2	110~115	1.5075	3.5	14.5	10.9	0.9	1.8		
3	115~120	1.5075	1.5	6.3	2.9		3.1		
4	120~125	1.5055	1.1	4.6	0.7		3.9		
5	125~130	1.5055	2.9	12.1	1.2		10.9		
6	130~140	1.5112	2.0	8.4			8.4		
7	140~155	1.5152	1.6	6.7			5.0	1.2	0.4
	Hold up		1.0	4.2			1.2	0.1	1.2
	Residue		7.5	31.1					4.1
	Total		22.6	94.2	20.9	1.4	34.5	1.3	5.7

calamenene.[10] From fraction 13 and from the pot residue a small amount of pure calacorene[10] was separated. Fractions 1 to 3 are complex mixtures of hydrocarbons; at least seven peaks were observed in gas chromatography, besides δ-cadiene and calamenene, and a small amount of copaene*6 was separated from fractions 1 and 2.

Experimental

The Analysis of Oil I.—The oil obtained by steam distillation was brown and viscous n_D^{22} 1.5130, d_{22} 0.982. The neutral fraction (24 g.) was distilled with a concentric column 26 cm. high, and each fraction was chromatographed on an alumina or silica gel column. The results are tabulated in Table I.

Sesquiterpene Alcohols.—Fraction 6 (2.0 g.) was chromatographed on an alumina column (25 g.). A mixture of alcohols (oil) was eluted by a mixture of petroleum ether and ether. The next fraction was solidified (m. p. about 60°C) (300 mg.); the melting point was raised to 63~74°C after repeated crystallization from petroleum ether. 3, 5-Dinitrobenzoate, m. p. 125~136°C. This alcohol was considered to be impure β-eudesmol. The fractions eluted by ether gave another crystalline alcohol (257 mg.), which was recrystallized from petroleum ether and sublimed under reduced pressure. M. p. and mixed m. p. with authentic pilgerol, 140~141°C; $[\alpha]_D$ −100° (*c* 0.48, chloroform). The infrared spectra of the two alcohols are superimposable. Crued pilgerol was also obtained from fractions 4 (21 mg.), 5 (420 mg.) and 7 (42 mg.).

The Presence of Ethers.—Fraction 2 (3.33 g.) was chromatographed on a silica gel column (65 g.). After the elution of hydrocarbon (2.51 g.) with petroleum ether, a fraction (705 mg.) was eluted with ether. This fraction, on further chromatography on an alumina column (15 g.), afforded fractions of n_D^{24} 1.4745~1.4725 (total, 200 mg.). The infrared spectra of these fractions showed strong bands at 1135~1070 cm^{-1}.

Cryptomerion.—Fraction 7 (1.5 g.) was chromatographed on an alumina column (20 g.), Petroleum ether eluted an oily diterpene hydrocarbon (102 mg.) and a ketone (243 mg.) successively. The same ketone was obtained from a commercial (root ?) oil. The ketone (cryptomerion) showed n_D^{26} 1.5050, d_{26} 0.954, MR 68.19. Calcd. for $C_{15}H_{22}OF_3$, 67.90, $[\alpha]_D$ −38° (*c* 1.45, chloroform), λ_{max} 236 and 304 mμ (ε 9600 and 110, ethanol). Infrared spectrum, Fig. 1A. 2, 4-Dinitrophenylhydrazone m. p. 168~171°C.

Hexahydroketone. — n_D^{26} 1.4597, d_{26} 0.884, $[\alpha]_D$ +17° (*c* 0.92, chloroform) (infrared spectrum, Fig. 1B) was obtained by catalytic hydrogenation with Willstätter's platina black in ethanol. 2, 4-Dinitrophenylhydrazone, m. p. 74~77.5°C.

Found: C, 62.29; H, 8.08; N, 13.69. Calcd. for $C_{21}H_{32}O_4N_4$: C, 62.35; H, 7.97; N, 13.85%.

The Huang Minlon reduction of the hexahydroketone (208 mg.) gave a saturated hydrocarbon (123 mg., purified through an alumina column). Its infrared spectrum was identical with that of hexahydrobisabolene.[8] The lithium aluminum hydride reduction of cryptomerion gave an oily unsaturated alcohol (infrared spectrum, Fig. 1C). 3, 5-Dinitrobenzoate, m. p. 65.5~67°C (from petroleum ether).

Found: C, 63.33; H, 6.25; N, 6.68. Calcd. for $C_{22}H_{26}O_6N_2$: C, 63.75; H, 6.32; N, 6.76%.

The Separation of Sesquiterpene Hydrocarbons from Oil II.—The fractions (b. p. 105~115°C/10 mmHg (31.5 g.) and 115~140°C/10 mmHg (24 g.)) of oil II (which was obtained by methanol extraction) were distilled by a spinning-band column (Tokyo Kagaku Seiki Model SB 815); the fractions boiling below 131°C/11 mmHg were combined and distilled twice on sodium metal and finally by the same spinning-band column. The results of the final distillation is shown in Table II.

The Isolation and Identification of Individual Hydrocarbons.—The purity of the fractions was determined by gas chromatography.

Apparatus.—Shimadzu gas chromatograph, Type GC-2A. Column PEG 6000 on Shimalite; 2 m. Temp., 180°C. Carrier gas, H_2. The infrared spectra were compared with those published by F. Šorm,

TABLE II.

Fraction	B. p. °C/11 mmHg	cc.	n_D^{23}
1	108~114	1.20	1.4930
2	114~115.5	1.40	1.4945
3	115.5~117	1.18	1.4995
4	117~119	1.68	1.5040
5	119~120	1.20	1.5055
6	120~121	1.06	1.5056
7	121	2.30	1.5060
8	121	2.00	1.5069
9	121	1.64	1.5080
10	121	2.65	1.5080
11	121	1.65	1.5084
12	121	1.86	1.5097
13	121	1.30	1.5107

V. Herout and their colleagues in Collection Checkoslovak Chem. Communs.*[7]

Copaene.—Fraction 1 was chromatographed on an alumina column (100 g.), and the first fraction (412 mg.) was rechromatographed twice to yield copaene (70 mg. n_D^{26} 1.4813).

δ-Cadinene.—Fractions 8—13 were chromatographed on a hundred-fold of alumina. The first fraction yielded δ-cadinene, n_D^{28} 1.5072, d_4^{28} 0.9133, $[\alpha]_D$ +27.8° (*c* 4.1 1, chloroform). Dihydrochloride, m. p. 118°C, $[\alpha]_D$ −36.1° (*c* 3.39, chloroform).

Calamenene.—The tail fractions of the chromatography of fractions 5—13 yielded calamenene, which was then purified by further chromatography. n_D^{28} 1.5155, d_4^{28} 0.9276, $[\alpha]_D$ −67.0° (*c* 2.40, chloroform).

Calacorene.—On chromatography the pot residue yielded a middle fraction calacorene of high purity (88 mg.) n_D^{23} 1.5405.

The author wishes to express his gratitude to Professor Tamio Kondo, of the Faculty of Agriculture of this University, for supplying the materials and to Professor Emeritus Saburo Akiyoshi, who took a special interest in this work, for his encouragement. He wishes also to thank Miss Reiko Tomita and Miss Katsumi Mera for their infrared and ultraviolet measurements.

Department of Organic Synthesis
Faculty of Engineering
Kyushu University
Hakozaki, Fukuoka

The Radiation Annealing of Phosphorus-32 with Cobalt-60 Gamma-rays for Several Neutron-irradiated Inorganic Phosphorus Compounds

By Kichizo TANAKA

(Received February 7, 1964)

The distribution of chemical species formed by neutron capture in several oxy-acids has been shown to depend on thermal and radiation effects during neutron irradiation in a nuclear reactor.

Boyd, Cobble and Wexler[1] pointed out that the chemical yield of bromine-82 as bromide was considerably influenced by the time of neutron irradiation in a reactor when the bromine-82 of a high specific activity was produced by the Szilard-Chalmers effect in potassium bromate. They showed that the shorter the irradiation time in a reactor, the higher the chemical yield of bromine-82 of a high specific activity. Cobble and Boyd[2] also indicated that the retention as bromate was increased by re-irradiation with cobalt-60 gamma-rays for neutron-irradiated potassium bromate. Maddock and Müller[3] observed that the retention increased in neutron-irradiated calcium bromate when it was re-irradiated with 1.8 MeV. electrons. Green, Harbottle and Maddock[4] noticed that the distribution of chemical species containing chromium-51 formed by the neutron irradiation of potassium chromate in a reactor was changed by re-irradiation with gamma-rays. Claridge and Maddock[5] reported that the retention increased for potassium dihydrogen phosphate and ammonium

1) G. E. Boyd, J. W. Cobble and S. Wexler, *J. Am. Chem. Soc.*, **74**, 237 (1952).
2) J. W. Cobble and G. E. Boyd, ibid., **74**, 1282 (1952).
3) A. G. Maddock and H. Müller, *Thans. Faraday Soc.*, **56**, 509 (1960).
4) J. H. Green, G. Harbottle and A. G. Maddock, ibid., **49**, 1413 (1953).
5) R. F. C. Claridge and A. G. Maddock, "Chemical Effects of the Nuclear Transformations," Vol I, IAEM, Prague (1961), p. 475.

hydrogen phosphate when they were irradiated with 1.8 MeV. electrons or an ultraviolet light. However, their results are somewhat ambiguous, as has been pointed out by Wazer,[6] because they used the precipitation method in separating the chemical species.

In their recent paper, Baba, Tanaka and Yoshihara[7] reported that the retention increased in several neutron-irradiated phosphates when they were thermally treated; in their experiment, the chemical species were separated by one-dimensional paper-partition chromatography. They observed that all phosphorus-32 species other than parent species decreased when heated for over 10^4 min. in the temperature range of 85~200°C. The rate of the decrease in the polyphosphate was larger than that of the reduced species. The fractional amount of the reduced species was extremely small[8] at long irradiations or at irradiations at a high power operation in nuclear reactors. This fact can not be explained by the process expected from the thermal annealing experiments. In the preparation of phosphorus-32 of a high specific activity by the Szilard-Chalmers effect,[9] the decrease in the recovery might be attributed to the radiation annealing effect. In the present paper, radiation annealing with cobalt-60 gamma-rays was studied for several neutron-irradiated inorganic phosphorus compounds, mainly in dehydrated forms.

Experimental

Target Materials.—Series of sodium orthophosphates and potassium orthophosphates, sodium orthophosphates, sodium orthophosphite, sodium hypophosphite and sodium pyrophosphate were used in anhydrous forms. Hydrated salts were dehydrated by heating and then drying them in vacuo over phosphorus pentoxide overnight. The anhydrous salts thus prepared were assayed for purity by the radioactivation method and by flame photometry, as has been previously reported[7].

Neutron Irradiation.—The salts were sealed in a polyethylene tube and subjected to neutron irradiation in hole No. 12 (a vertical hole; the nominal neutron flux was 0.48×10^{12} n/cm^2-sec.) for 15 hr. and in hole No. 16 (a pneumatic tube, the nominal neutron flux was 0.64×10^{12} n/cm^2-sec.) for 2 hr. in JRR-1 (a waterboiler type, operated at 40 kW.). Immediately after irradiation, the samples were cooled with dry ice to avoid any change in the distribution of the chemical species containing phosphorus-32 during storage.

Gamma-ray Irradiation.—Neutron-irradiated samples were again sealed in a polyethylene tube or in a glass ampoule and exposed to high intensity gamma-rays from a cobalt-60 source of 0.7×10^4 curies in a thermally-controlled vessel at temperatures from −196°C to 100°C. The irradiated samples were then stored in a vessel cooled with dry ice.

Chemical Separation.—The chemical species containing phosphorus-32 were separated by one-dimensional paper-partition chromatography by the same procedure as before.[7] The decomposition of the sample by gamma irradiation was measured by colorimetric analysis of the products separated from the parent species by the anion exchange method.[10,11]

Counting Procedure.—After it had been developed and dried, the paper was cut into pieces 1 cm. wide and the radioactivity was measured by a thin end-window-type GM counter at a constant geometry. Counting was made at least ten days after the termination of neutron irradiation in order to avoid errors from the radioactivity of sodium-24 or potassium-42.

Thermal Annealing.—Neutron-irradiated sodium orthophosphates were subjected to thermal annealing at an elevated temperature, as has been previously reported,[7] and the effect of neutron irradiation conditions on thermal annealing behaviors was tested for the phosphorus-32 species. The distribution of chemical species containing phosphorus-32 obtained from irradiation for 2 hr. in a pneumatic tube was considerably different from that of 15 hr. irradiation in the vertical hole of the JRR-1. In both cases, however, all the chemical species other than parent species decreased, only the parent species increased with the salts were heated, and the polyphosphate was more predominantly annealed than the reduced species. It was concluded that the thermal-annealing behavior does not depend on the neutron irradiation conditions. All samples were stored in two vessels: one portion was stored at 30°C, and the other at a lower temperature obtained by cooling with dry ice. During the storage for 16 days, no change was observed in the distribution of chemical species containing phosphorus-32.

Results and Discussion

The Decomposition of the samples by Gamma-ray Irradiation.—When the phosphate salts are irradiated by gamma-rays, the decomposition of the sample may be expected as a result of radiation effects. Pyrophosphate was detected in the gamma-irradiated orthophosphates. Except for the case of dipotassium hydrogen phosphate, the amounts of pyrophosphate formed by gamma irradiation were so small that the amounts detected were near the detection limit (approximately 5 μg. per gram of the sample),

6) J. R. Van Wazer, "Phosphorus and its Compounds," Vol. I, Interscience Publishers, Inc., New York (1957), p. 441.
7) H. Baba K. Yoshihara, H. Amano, K. Tanaka and N. Shibata, This Bulletin, **34**, 590 (1961); H. Baba, K. Tanaka and K. Yoshihara, ibid., **36**, 928 (1963).
8) K. Tanaka, to be published.
9) K. Tanaka, to be published.
10) H. J. Weiser, Jr., *J. Am. Oil Chemists' Soc.*, **34**, 124 (1957).
11) N. Shibata K. Yoshihara, K. Tanaka, H. Baba and K. Kurosawa, Fifth Conference of Radioisotopes in Japan, B/P-C 10 (1963).

TABLE I. ESTIMATED G VALUES FOR PYROPHOSPHATE FORMATION OF SEVERAL ORTHOPHOSPHATES

Target material	G Values	
	20°C	50°C
NaH_2PO_4	0.17	−0.16
Na_2HPO_4	0.11	0.15
Na_3PO_4	0.075	0.08
KH_2PO_4	0.05	0.02
K_2HPO_4	<1.4	<1.5

even at the total dose of 1×10^7 r. The estimated G values of pyrophosphate formation are tabulated in Table I. Pyrophosphate was also formed when orthophosphates containing hydrogen in the molecule were heated above 150°C. Because pyrophosphate formation in the orthophosphate salts was prominent as a result of thermal reaction at an elevated temperature, the effects of gamma-rays on the formation of pyrophosphate could not be detected in this case. The formation curves obtained by irradiation at temperatures of 150~200°C for sodium dihydrogen phosphate and disodium hydrogen phosphate were exactly the same as those obtained by the thermal reaction, within the range of experimental error. The formation of no polyphosphates other than pyrophosphate was observed by the anion exchange separation for all samples. The evolution of gaseous products was not studied; this evolution may be disregarded considering the results obtained by Sellers and his co-workers.[12]

The Change by Gamma Irradiation of the Chemical Species Containing Phosphorus-32.— The distribution of chemical species containing phosphorus-32 in neutron-irradiated phosphates varies with the irradiation conditions in the reactor. All the salts were irradiated in the same capsule to compare the annealing effects of irradiation for the different salts.

The radiation annealing of species containing phosphorus-32 in several orthophosphate salts (irradiated for 2 hr., in a pneumatic tube of the JRR-1 and re-irradiated with cobalt-60 gamma-rays at −50°C) results in an increase in retention and in a decrease in the reduced species. The behavior of the polyphosphates in irradiation varies considerably among the different orthophosphates studied. The results are shown in Figs. 1—3, where the fraction of each species is plotted against the radiation dose. The retention as orthophosphate increases rapidly in the low dose region and gradually in the higher dose region. This is more prominent in the case of sodium dihydrogen phosphate. The polyphosphate in di-

12) P. A. Sellers, T. R. Sato and H. H. Strain, *J. Inorg. Nucl. Chem.*, 5, 31 (1957).

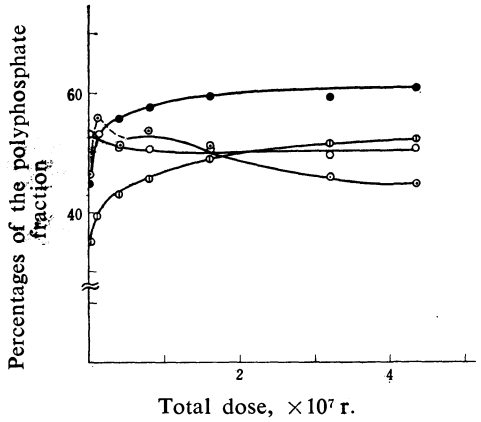


Fig. 1. Gamma ray annealing of ^{32}P in the polyphosphate fraction.

—○— NaH_2PO_4 —●— Na_2HPO_4
—◑— Na_3PO_4 —⊙— KH_2PO_4

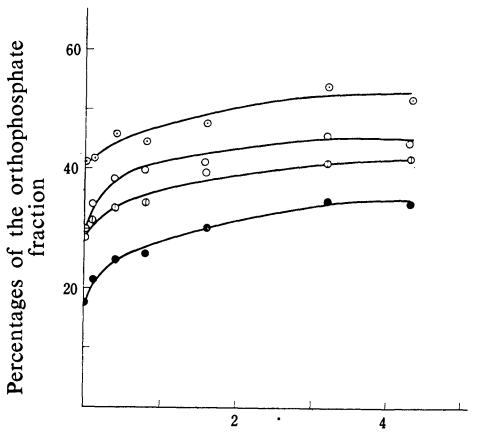


Fig. 2. Gamma ray annealing of ^{32}P in the orthophosphate fraction.

—○— NaH_2PO_4 —●— Na_2HPO_4
—◑— Na_3PO_4 —⊙— KH_2PO_4

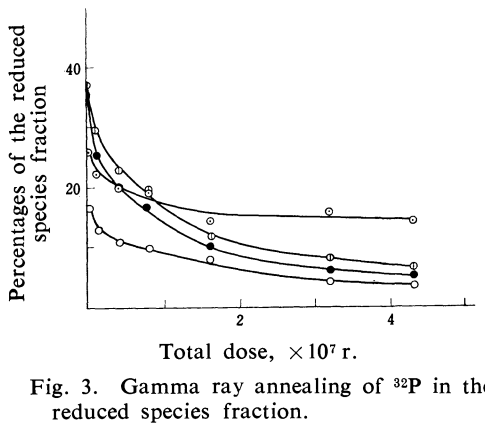


Fig. 3. Gamma ray annealing of ^{32}P in the reduced species fraction.

—○— NaH_2PO_4 —●— Na_2HPO_4
—◑— Na_3PO_4 —⊙— KH_2PO_4

sodium hydrogen phosphate and in trisodium phosphate shows a fast rise in the initial low-dose region and gradually approaches a plateau, whereas the polyphosphate in sodium dihydrogen phosphate initially increases and then decreases. However, the reduced species clearly decreases in all of the orthophosphate salts studied. These changes in fractions are summarized in Fig. 4 for disodium hydrogen phosphate. In the figure, experimental results are given by the solid line, while the dotted lines show the estimated values obtained by the analysis of the curves, assuming the plateau values for each corresponding curve.

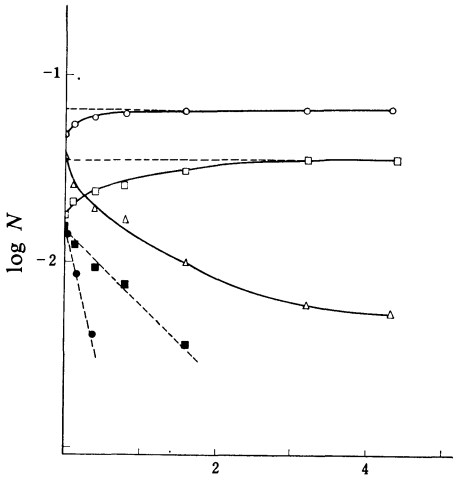


Fig. 4. Gamma ray annealing of the chemical species containing ^{32}P in disodium hydrogen phosphate.

—○— the polyphosphate fraction
—□— the orthophosphate fraction
—△— the reduced species fraction
--■-- estimated increase of the orthophosphate fraction
--●-- estimated increase of the polyphosphate fraction

The estimated values for the increase in the polyphosphates and those for the orthophosphate are linear on a semilog plot. This suggests that the reactions in the increase in the polyphosphates and orthophosphate follow the first order kinetics, in which the sum of these increases in two fractions corresponds to the decrease in the reduced species. The number of species in the sample is proportional to their percentages in the sample. The ordinates show the logarithmic number of species on an arbitrary scale. By an analysis of these curves, two main processes of the radiation annealing of species containing phosphorus-32 are indicated: (I) the reduced species to the polyphosphate, and (II) the reduced species to the orthophosphate. The reduced species is converted to the phosphorus(V) state by oxidation with a potassium permanganate solution, whereas the polyphosphate is not changed. The polyphosphate is converted to the orthophosphate by hydrolysis with a mineral acid such as hydrochloric or sulfuric acid. The polyphosphate thus contains phosphorus(V). The radiation-induced oxidation process is a predominant reaction in the radiation annealing of orthophosphate salts. This finding is in good agreement with the recent results of Claridge and Maddock[13] which have indicated that phosphorus(III) is oxidized to phosphorus(V) by irradiation with an ultraviolet light or by 1.8 MeV. electrons in several neutron-irradiated phosphates.

The radiation-annealing curves obtained by 15 hr. irradiation in a reactor (with a vertical hole of the JRR-1) seemed to be similar to those by shorter irradiations, except that the polyphosphate fraction is slightly lower in the former. Besides the two main processes stated, other processes were observed; the third process III, the polyphosphate to the orthophosphate, is indicated by the results listed in Table II. The decrease in the polyphosphate at longer irradiations in a reactor suggests that the polyphosphate curve. in Fig. 4 shows a pseudoplateau attained by the rate equilibrium between the two processes, " the reduced species to the polyphosphate " and " the polyphosphate to the orthophosphate." The polyphosphate fractions in the other orthophosphate salts studied show the same behavior as that in disodium hydrogen phosphate.

Annealing behaviors were also studied for neutron-irradiated sodium orthophosphite and sodium hypophosphite. Little change was observed in the distribution of chemical species containing phosphorus-32 in gamma irradiation in the dose range from 1.0×10^6 to 1.5×10^7 r. for these two salts. The hypophosphite fraction in sodium orthophosphite and the orthophosphite fraction in sodium hypophosphite salts were found to be unchanged.

The Effect of the Dose Rate.—The dose-rate dependence of the annealing behavior was studied in the dose range of 3.7×10^4 to 2.1×10^6 r./hr. at the total dose and at the temperature used above. The results obtained are shown in Table II. Only slight differences are observed among the different dose rates.

The Rate Constants in Gamma-ray Annealing.—Assuming that the radiation annealing of chemical species containing phosphorus-32

13) R. F. C. Claridge and A. G. Maddock, *Trans. Faraday Soc.*, 59, 935 (1963).
14) R. R. Williams, *J. Phys. Colloid Chem.*, 52, 603 (1948).

TABLE II. TYPICAL EXAMPLE OF LONGER IRRADIATION IN A REACTOR AND DOSE RATE DEPENDENCIES OF THE CHEMICAL DISTRIBUTION OF ^{32}P

Target materials	Neutron irradiation in a JRR-1 reactor n/cm² sec.	^{60}Co gamma ray irradiation: Dose rate r./hr.	^{60}Co gamma ray irradiation: Total dose r.	Percentages of each fraction of species (^{32}P): Ortho-phosphate	Poly-phosphate	Reduced species
Na_2HPO_4	2 hr. at 5.0×10^{11}	0	0	17.3	45.4	33.8
	2 hr. at 5.0×10^{11}	3.7×10^{4}	1.5×10^{7}	22.0	60.4	17.6
	2 hr. at 5.0×10^{11}	1.7×10^{5}	1.5×10^{7}	19.1	62.9	18.0
	2 hr. at 5.0×10^{11}	2.1×10^{6}	1.5×10^{7}	22.6	56.4	20.9
Na_2HPO_4	15 hr. at 1.9×10^{11}	0	0	40.4	52.5	7.0
	15 hr. at 1.9×10^{11}	1.2×10^{5}	4.8×10^{6}	42.7	52.2	5.2
	15 hr. at 1.9×10^{11}	1.2×10^{5}	1.5×10^{7}	45.8	49.6	4.8
	15 hr. at 1.9×10^{11}	2.2×10^{5}	1.5×10^{7}	45.5	49.8	4.7
	15 hr. at 1.9×10^{11}	4.7×10^{5}	1.5×10^{7}	47.3	49.1	3.4
	15 hr. at 1.9×10^{11}	2.2×10^{5}	5.2×10^{7}	53.2	43.9	3.3
NaH_2PO_4	2 hr. at 5.0×10^{11}	0	0	31.4	45.3	23.4
	2 hr. at 5.0×10^{11}	3.7×10^{4}	1.5×10^{7}	33.9	60.0	6.1
	2 hr. at 5.0×10^{11}	1.7×10^{5}	1.5×10^{7}	35.4	60.1	4.5
	2 hr. at 5.0×10^{11}	2.1×10^{6}	1.5×10^{7}	37.5	55.9	6.6
KH_2PO_4	2 hr. at 5.0×10^{11}	0	0	36.6	52.9	10.4
	2 hr. at 5.0×10^{11}	3.7×10^{4}	1.5×10^{7}	39.1	58.3	2.6
	2 hr. at 5.0×10^{11}	1.7×10^{5}	1.5×10^{7}	39.6	58.6	1.7
	2 hr. at 5.0×10^{11}	2.1×10^{6}	1.5×10^{7}	38.0	58.7	3.3

TABLE III. RATE CONSTANTS FOR THE CHANGES OF CHEMICAL SPECIES CONTAINING ^{32}P BY GAMMA IRRADIATION

Target material	Rate constants, hr^{-1}, 1.7×10^{5} r./hr.: Irradiated at −50°C, k_1*	Irradiated at −50°C, k_2**	Irradiated at 20°C, k_1	Irradiated at 20°C, k_2	Irradiated at 20°C, k_3***
NaH_2PO_4	uncertain	9×10^{-2}	1×10^{0}	3×10^{-1}	1.8×10^{-3}
Na_2HPO_4	4.7×10^{-2}	2.5×10^{-2}	6×10^{-1}	4.5×10^{-2}	1.5×10^{-3}
Na_3PO_4	2.7×10^{-2}	2.7×10^{-2}	3×10^{-1}	4.5×10^{-2}	9×10^{-4}
KH_2PO_4	uncertain	1.2×10^{-2}	—	4×10^{-2}	8×10^{-4}
K_2HPO_4	—	—	6.5×10^{-2}	4×10^{-2}	5×10^{-4}
$K_3P_4O_4$	—	—	4.5×10^{-2}	4.5×10^{-2}	—

* k_1, a rate constant corresponding to the increase of the polyphosphate fraction
** k_2, a rate constant corresponding to the increase of the orthophosphate fraction
*** k_3, a rate constant corresponding to the decrease of the polyphosphate fraction

follows the kinetics which contains several processes of the first order,[14] the rate constants for these processes can be defined. Since the rate is proportional to the number of species containing phosphorus-32, the formula, $dN_i/dt=k_iN_i$, expresses the process, where k_i is the rate constant for the change in the number of species and N_i is the number of species which contribute to the i-th process. The rate constant can be obtained at a fixed dose rate. The annealing curves were obtained for the several orthophosphate salts, and an analysis was made in order to estimate the rate constant from the numbers of the increases of the polyphosphates and orthophosphate, as Fig. 4 shows. In the case of polyphosphate, a correction was made for the contribution of the third process, which resulted in the slow decrease in the polyphosphate. The results obtained for the rate constants at given temperatures are shown in Table III. In the table, k_1 is the rate constant for the reduced species to the polyphosphate (process I) and k_2 is the rate constant for the reduced species to the orthophosphate (process II). In these estimates, samples were irradiated for 2 hr. in a pneumatic tube of the JRR-1. In order to estimate k_3, the rate constant for the polyphosphate to the orthophosphate (process III), samples were irradiated for 15 hr. in the vertical hole. In gamma irradiation at −50°C, only a slight change induced by this process is observed, even at the highest dose of 5×10^{7} r. The rate constants obtained for sodium or potassium orthophosphates are of the order of 10^{-4} hr^{-1} (−50°C, 1.7×10^{5} r./hr.). The rate constants obtained at 20°C are listed in Table III.

Similar experiments were made to estimate the rate constants for sodium pyrophosphate. The decrease in the reduced species uniquely

follows the first-order kinetics, and the rate constant is $1.7\times10^{-3}\,hr^{-1}$ ($-50°C$, 1.7×10^{5} r./hr.). This value is one order smaller than those for the orthophosphate salts.

The Effect of Temperature During Gamma Irradiation.—The temperature dependence of gamma-ray annealing is studied for all the salts mentioned. The decrease in the reduced species in sodium or potassium orthophosphates and in sodium pyrophosphate is clearly affected by the temperature during gamma irradiation. In Fig. 5, the decrease in the reduced species in sodium and potassium orthophosphate salts is plotted as a function of the total dose at 20°C. In the salts containing hydrogen atoms, the decrease in the reduced species is divided into two parts: the initial rapid decrease corresponding to processes I and II, and the slow decrease which is predominant in trisodium and tripotassium phosphates, as Fig. 5 shows. The former process is the same as that observed at $-50°C$. The decrease in the reduced species corresponds to the sum of the increases of the polyphosphate and orthophosphate. However, the latter slow process, which is not clearly observed at $-50°C$, is probably a different

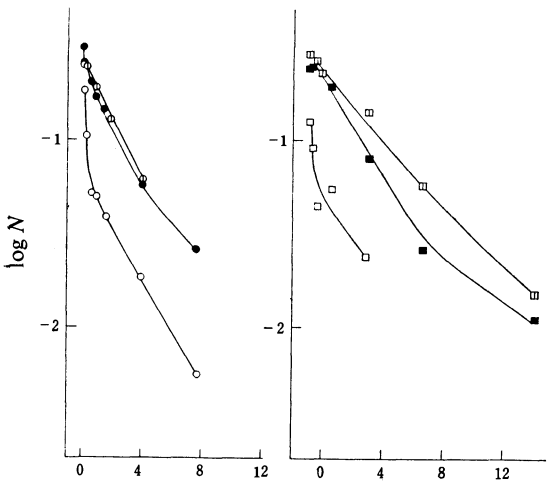


Fig. 5. Gamma ray annealing of ^{32}P species of the reduced species fraction for several orthophosphate salts.

—○— NaH_2PO_4 —□— KH_2PO_4
—●— Na_2HPO_4 —■— K_2HPO_4
—◑— Na_3PO_4 —◫— K_3PO_4

process from those mentioned above; it probably corresponds to the slow increase in the orthophosphate.

The changes in the reduced species in disodium hydrogen phosphate at several different temperatures are shown in Fig. 6. In a series of the sodium orthophosphate salts and in a

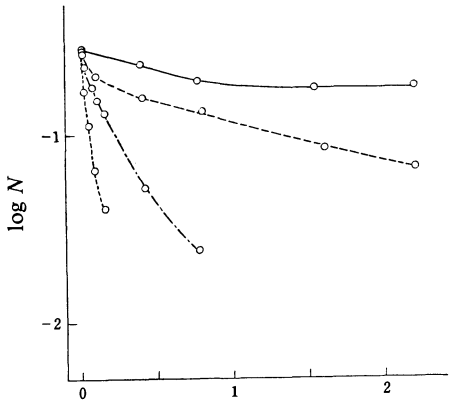


Fig. 6. Gamma ray annealing as functions of temperature during gamma ray irradiation—the decrease of ^{32}P for the reduced species fraction in disodium hydrogen phosphate.

—○— at $-196°C$ —--○--- at 20°C
--○-- at $-50°C$ ----○---- at 100°C

series of the potassium orthophosphate salts studied, the reduced species considerably decreased, even irradiation at $-196°C$. If the log k is plotted against $1/T$, the curve is quite different from the linear shape, where T is the absolute temperature. The log k decreases as the temperature is lowered to approximately $-20°C$, then it nearly approaches a constant at $-196°C$. The reaction induced by gamma irradiation at a low temperature seemed to involve another process. The process is apparently different from the higher temperature process above $-20°C$.

Comparisons of Gamma-ray Annealing with the Chemical Form of the Samples.—From the comparison of the decreases in the reduced species by the gamma irradiation for the series of the orthophosphate salts, it is clear that the higher the hydrogen content in the sample, the greater the decrease in the reduced species.

Disodium hydrogen phosphate dodecahydrate was also studied. The change in the distribution of chemical species containing phosphorus-32 are similar to those in the anhydrous salt. The rate of decrease in the reduced species in sodium pyrophosphate is also affected by the temperature during gamma irradiation, whereas in sodium orthophophite and sodium hypophosphite, no change in chemical species by gamma irradiation is observed, even in irradiation at 20°C.

The rate-constant values obtained can not be compared in detail with the other observations in oxy-acid salts because the experimental conditions are different. However, the rate of the change of retention in orthophosphate salts is at least approximately 10^2 times greater than

those in the other salts; namely, for bromine-82 in potassium bromate,[2] and chromium-51 in potassium chromate.[15]

From the results of the present experiment, it is to be expected that the neutron irradiation for relatively long periods of time or at high operating power will give the reduced species of low fractions in sodium or potassium orthophosphate salts.[8]

Summary

Radiation annealings with cobalt-60 gamma-rays have been investigated for several neutron-irradiated inorganic phosphorus compounds. The group separation technique by one-dimensional paper-partition chromatography was adopted to separate chemical species containing phosphorus-32. The reduced species in the sodium and potassium orthophosphate salts and in the sodium pyrophosphate salt decreased upon gamma irradiation, and an increase in the retention was observed. However, the polyphosphate increased initially in the several orthophosphate salts.

Three processes has been observed, the rate constants for these processes have been estimated, and two other processes have been suggested. The main process is the oxidation of the reduced species to phosphorus(V) species.

Radiation annealing have been studied for phosphates as a functions of the dose rate, the total dose of irradiation, and the temperature during gamma irradiation, it has been found that annealings are dependent upon the total dose and the temperature during irradiation and are independent of the dose rate. In orthophosphates and pyrophosphate, chemical species other than the parent species are easily annealed by gamma irradiation, whereas no detectable annealing has been observed in sodium orthophosphite or sodium hypophosphite.

In series of sodium and potassium orthophosphates, annealing was affected by the hydrogen content of the salts.

The author wishes to express his appreciation to Dr. Kenjiro Kimura, Director of this Institute, to Dr. Nagao Shibata, and to Professor Shizuo Fujiwara of the University of Tokyo for their interest and encouragement. The author also wishes to express his thanks to Professor Nobufusa Saito of the University of Tokyo, to Dr. Kenji Yoshihara, and to Mr. Hiroshi Baba for their discussions.

Radioisotope Production Laboratory
Japan Atomic Energy Research Institute
Tokai-mura Ibaraki-ken

15) G. Harbottle, *J. Chem. Phys.*, **22**, 1083 (1954).

Spectrophotometric Studies of the Metallic Chelates of 2-Picolylamine. I. The Electronic Absorption Spectra of Some Nickel, Copper(II) and Cobalt(III) Chelates

By Shunji UTSUNO and Kôzô SONE

(Received March 2, 1964)

2-Picolylamine (2-aminomethylpyridine; abbreviation: "pic") is a chelating agent which is structurally intermediate between ethylenediamine ("en") and 2,2'-bipyridine ("bip"). Recently Sutton[1] found that 2-picolylamine forms a large number of chelates with various metals, and that their properties in many respects resemble those of ethylene diamine chelates.[2] His data on the absorption spectra of these chelates were of special interest to us, since they reflect a number of important features of their electronic structures; this interest inspired us to carry out a series of more detailed spectrophotometric studies of these and related chelates, the first results of which shall be reported in this paper.

Experimental

Reagents.—The 2-picolylamine used in this work was the product of the Aldrich Chemical Co. (Milwaukee, Wisc., U. S. A.). In the preparation of the chelates, it was used without further purification; in the spectral study of the systems contain-

1) G. J. Sutton, *Australian J. Chem.*, **13**, 74, 222, 473 (1960); **14**, 37, 545, 550 (1961); **15**, 232, 563 (1962).

2) The stabilities of some of these chelates were studied also by D. E. Goldberg and W. C. Fernelius (*J. Phys. Chem.*, **63**, 1246 (1959)) and T. J. Lane, C. S. C. and J. W. Thompson (*J. Am. Chem. Soc.*, **82**, 4179 (1960)).

ing the free ligand, it was purified by vacuum distillation (b. p. 89°C/15 mmHg). All the other reagents used were "Extra Pure" chemicals, most of which were the products of the Wako Pure Chemicals Co. (Osaka, Japan).

Apparatus. — The visible, ultraviolet and near infrared spectra of the aqueous solutions of the chelates were measured with a Shimadzu QR-50 quartz spectrophotometer, using silica cells of 10 mm. and 1 mm. light paths.

The Preparation of the Chelates.—These chelates —[Co pic$_3$](ClO$_4$)$_3$, [Co pic$_2$(NO$_2$)$_2$]NO$_3$·1/2H$_2$O, Ni·pic$_2$Cl$_2$, [Ni pic$_3$]Cl$_2$·2H$_2$O and Cu pic$_2$Cl$_2$– were prepared according to the methods of Sutton.[1] When all these chelates were analyzed with respect to their metals, satisfactory agreement between experimental and theoretical values was obtained in every case. In addition, the following chelates (a)—(d) were prepared for the present study:

(a) Ni pic Cl$_2$·H$_2$O. — NiCl$_2$·6H$_2$O (2.4 g.; 10^{-2} mol.) was dissolved in 3 ml. of water by heating, and 2-picolylamine (1.1 g.; 10^{-2} mol.) was added. When the blue mixture was concentrated by heating, green crystals were formed; after cooling, they were washed with 95% ethanol and then with absolute ethanol and ether. (Yield, 2.12 g.; 83%) (Found: Ni, 22.68; C, 28.33; H, 4.04; N, 11.21. Calcd. for $C_6H_{10}N_2Cl_2ONi$: Ni, 22.95; C, 28.17; H, 3.94; N, 10.95%).

(b) Ni pic SO$_4$·2H$_2$O.—NiSO$_4$·6H$_2$O (2.6 g.; 10^{-2} mol.) was dissolved in 5 ml. of water by heating, and 2-picolylamine (1.1 g.; 10^{-2} mol.) was added. The mixture was left standing for a week or more in a dessicator or in the open air, and the greenish blue crystals which formed were filtered, washed repeatedly with ethanol and then with ether, and dried at room temperature in the open air. The obtained crystals contained about 3 molec. of water of crystallization; when they were heated at 150°C for several hours, a part of the water was lost, leaving the pale blue dihydrate. (Yield, 2.58 g.; 86%). (Found: Ni, 19.28; C, 22.84; H, 4.12; N, 9.42. Calcd. for $C_6H_{12}N_2SO_6Ni$: Ni, 19.64; C, 23.10; H, 4.04; N, 9.37%).

(c) Cu pic Cl$_2$.—CuCl$_2$·2H$_2$O (1.7 g.; 10^{-2} mol.) and 2-picolylamine (1.1 g.; 10^{-2} mol.) were dissolved separately in 90% ethanol (10 ml. each). When the two solutions were mixed, a green precipitate was formed at once; this became blue when the mixture was heated for some time. After the completion of this color change, the precipitate was filtered and washed with ethanol and ether. The pale blue crystalline powder which was obtained was recrystallized by dissolving it in 10 ml. of water by heating and then adding the same volume of ethanol. (Yield, 2.16 g.; 90%). (Found: Cu, 25.92; C, 29.32; H, 3.23; N, 11.72. Calcd. for $C_6H_8N_2Cl_2Cu$: Cu, 26.19; C, 29.71; H, 3.32; N, 11.55%).

(d) Cu pic SO$_4$·2H$_2$O.—CuSO$_4$·5H$_2$O (2.5 g.; 10^{-2} mol.) was dissolved in 5 ml. of water, and 2-picolylamine (1.1 g.; 10^{-2} mol.) was added. The mixture was left standing overnight in a refrigerator, and the blue crystals which separated out were washed with ethanol and ether, dried at room temperature in the open air, and recrystallized from water. (Yield, 2.37 g.; 79%). (Found: Cu, 21.13; C, 26.71; H, 3.14; N, 10.44. Calcd.:[3] Cu, 20.91; C, 26.92; H, 3.01; N, 10.46%).

Results and Discussion

The Formation of Some Nickel and Copper Chelates. — Sutton[1] prepared a number of nickel chelates of 2-picolylamine with metal: ligand ratios of 1:2 and 1:3, and copper chelates with the ratio of 1:2. On the other hand, it is well known that both ethylenediamine and 2,2'-bipyridine can form 1:1, 1:2 and 1:3 chelates with these metals, either in an aqueous solution or in the state of crystalline complexes; therefore, it is to be expected that 2-picolylamine can also form 1:1 chelate with nickel and copper, and a 1:3 chelate with copper, at least in aqueous solutions, and probably in the state of crystalline complexes, too. In fact, Fernelius et al.[2] found that such 1:1 complexes of considerable stability are formed in solution, and now we have found the crystals of the Ni pic Cl$_2$·H$_2$O, Ni pic SO$_4$·2H$_2$O, Cu pic Cl$_2$ and Cu pic SO$_4$·2H$_2$O chelates can be easily obtained from the solutions of their components. The nickel chelates are greenish blue (sulfate) or green (chloride), and they give blue solutions in water, while the copper chelates are blue, both in the solid state and in aqueous solutions.

The common coordination numbers of Ni^{2+} and Cu^{2+} are 6 and 4 respectively, and the tendencies of organic amines, water, Cl^- and SO_4^{2-} to form coordinate bonds with these ions generally decrease in the order: amines $>H_2O>$ anions. Therefore, the most probable coordination formulas of the copper chelates are [Cu pic Cl$_2$] and [Cu pic (OH$_2$)$_2$]SO$_4$ respectively, while the coordination of both water and anions must be assumed to explain the compositions of the nickel chelates. In aqueous solutions, however, the coordinated anions seem to be displaced by water, forming the chelate ions $[Cu\ pic\ (OH_2)_2]^{2+}$ and $[Ni\ pic(OH_2)_4]^{2+}$; this is proved by the fact that the solutions of all these chelates show the immediate reactions of their anions, by the fact that the absorption spectra of these solutions are practically independent of their anions (i. e., the curves of Ni pic Cl$_2$·H$_2$O and Cu pic Cl$_2$ are nearly identical with those of Ni pic SO$_4$·2H$_2$O and Cu pic SO$_4$·2H$_2$O respectively), and, further, by the fact that these spectra are quite insensitive to the addition of their anions in a considerable excess.

3) While the value for Cu refers to the dihydrate ($C_6H_{12}N_2SO_6Cu$), those for C, H and N refer to the anhydrous state, since this chelate loses all of its water in the course of vacuum dessication prior to the organic analysis (5 mmHg, 80°C, 2 hr.).

TABLE I. LIGAND FIELD BANDS OF ETHYLENEDIAMINE, 2-PICOLYLAMINE AND 2,2'-BIPYRIDINE CHELATES

Chelate	λ_{max} (log ε_{max})			Literature
$[Ni\ en\ (OH_2)_4]^{2+}$	973 (0.68)	618 (0.54)	370 (0.76)	6a
$[Ni\ pic\ (OH_2)_4]^{2+}$	960 (0.62)	610 (0.50)	367 (0.81)	*
$[Ni\ bip\ (OH_2)_4]^{2+}$	942 (0.62)	595 (0.42)	(( ))	6a
$[Ni\ en_2\ (OH_2)_2]^{2+}$	940 (0.81)	571 (0.71)	357 (0.87)	6a
$[Ni\ pic_2\ (OH_2)_2]^{2+}$	910 (0.91)	556 (0.73)	(( ))	*
$[Ni\ bip_2\ (OH_2)_2]^{2+}$	929 (0.97)	560 (0.87)	(( ))	6a
$[Ni\ en_3]^{2+}$	898 (0.85)	547 (0.81)	345 (0.90)	6a, 6c
$[Ni\ pic_3]^{2+}$	860 (0.96)	536 (1.03)	(( ))	*
$[Ni\ bip_3]^{2+}$	789 (0.84)	519 (1.08)	(( ))	6a, 6b
$[Cu\ en\ (OH_2)_2]^{2+}$		662 (1.51)		6a
$[Cu\ pic\ (OH_2)_2]^{2+}$		685 (1.51)		*
$[Cu\ bip\ (OH_2)_2]^{2+}$ a)		699 (1.48)		6a
$[Cu\ en_2]^{2+}$		556 (1.85)		6a
$[Cu\ pic_2]^{2+}$		580 (1.82)		*
$[Cu\ bip_2]^{2+}$		750 (1.99)		6a
$[Co\ en_3]^{3+}$	467 (1.93)	338 (1.90)		6c
$[Co\ pic_3]^{3+}$	464 (2.11)~335 (~2.2, sh.)			*
$[Co\ bip_3]^{3+}$ a)	448 (1.83)	(( ))		6d
cis-$[Co\ en_2\ (NO_2)_2]^{+}$	435 (2.10)	(( ))		12
trans-$[Co\ en_2\ (NO_2)_2]^{+}$	429 (2.20)	(( ))		12
$[Co\ pic_2\ (NO_2)_2]^{+}$	440 (2.46)	(( ))		*

(( )): The band hidden by the strong ultraviolet absorption of the ligand.
sh: Shoulder.
*: Data of the present study.
a) According to Ito (Ref. 6a), these chelates should be formulated as $[Cu\ bip\ (OH_2)_4]^{2+}$ and $[Cu\ bip_2\ (OH_2)_2]^{2+}$, respectively.

TABLE II. STRONG ULTRAVIOLET BANDS OF 2-PICOLYLAMINE CHELATES

Chelate	λ_{max} (log ε_{max})	Chelate	λ_{max} (log ε_{max})	
(2-Picolylamine)	260 (3.48)	$[Co\ pic_3]^{3+}$	~260 (3.95, sh.)	
$[Ni\ pic\ (OH_2)_4]^{2+}$	260 (3.46)	$[Co\ pic_2\ (NO_2)_2]^{+}$	338 (3.70)	252 (4.34)
$[Ni\ pic_2\ (OH_2)_2]^{2+}$	260 (3.74)	*cis*-$[Co\ en_2\ (NO_2)_2]^{+}$	323 (3.68) a)	
$[Ni\ pic_3]^{2+}$	260 (3.98)	*trans*-$[Co\ en_2\ (NO_2)_2]^{+}$	339 (3.44) a)	249 (4.37) a)
$[Cu\ pic\ (OH_2)_2]^{2+}$	247 (3.59)			
$[Cu\ pic_2]^{2+}$	247 (3.92)			

a) Data of Kuroya and Tsuchida (Ref. 12a.). Later data of Basolo (Ref. 12b) in MeOH-H_2O agree reasonably well with these authors', but add one more band at 240 mμ (log ε_{max} 4.22) for *cis*-$[Co\ en_2\ (NO_2)_2]^{+}$.

We also tried to prove our second expectation, i.e., the formation of the chelate ion. $[Cu\ pic_3]^{2+}$, and we found rather convincing evidence for its existence in solution. Figure 1 shows three representative curve taken from our data on the absoprtion spectra of aqueous solutions containing $[Cu\ pic_2]^{2+}$ and free 2-picolylamine; it can be seen that, with the increase in free ligand concentration, the absorption band of $[Cu\ pic_2]^{2+}$ at 580 mμ is gradually intensified and shifted toward a longer wavelength, until, in a 8.46 M solution of 2-picolylamine (the highest concentration tried), the λ_{max} and ε_{max} values become 612 mμ and 109 respectively. A comparison of these data with the spectra of the $[Cu\ en_2]^{2+}$-ethylenediamine system studied by Bjerrum and Nielsen[4] reveals the general resemblance of these two systems, and an approximate analysis of the data by their method indicates that the chelate ions $[Cu\ pic_3]^{2+}$ are progressively formed in these solutions. The third stability constant (k_3) of this chelate was estimated to be 2~3, which is somewhat larger than the k_3 value (~0.1) of $[Cu\ en]^{2+}$ reported by Bjerrum and Nielsen, but much

4) J. Bjerrum and E. J. Nielsen, *Acta Chem. Scand.*, 2, 297 (1948).

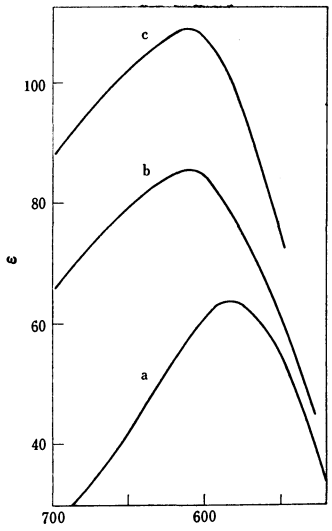


Fig. 1. The effect of excess 2-picolylamine on the spectrum of $[Cu\ pic_2]^{2+}$.

a: $[Cu\ pic_2]^{2+}$ $(6.82\times10^{-3}$ M)
b: $[Cu\ pic_2]^{2+}$ $(5.09\times10^{-3}$ M) + 2-picolylamine $(7.901\times10^{-1}$ M) + HNO_3 $(6.87\times10^{-2}$ M)
c: $[Cu\ pic_2]^{2+}$ $(5.09\times10^{-3}$ M) + 2-picolylamine (8.465 M). Temp.: 25°C
μ: 1 M KNO_3; cell thickness: 10 mm.

smaller than the value of $[Cu\ bip_3]^{2+}$ (~2000) reported by Irving and Mellor.[5] This fact, and the fact that the λ_{max} and ε_{max} values of $[Cu\ pic_3]$ given above are quite near to the values of $[Cu\ en_3]^{2+}$ reported by Bjerrum and Nielsen, are new examples of the close resemblance between 2-picolylamine and ethylenediamine chelates, a resemblance which has already been pointed out by Sutton[1] and which will be discussed further in the next section.

The Electronic Absorption Spectra of the Chelates.—The visible, ultraviolet and near infrared spectra of the chelates prepared are summarized in Figs. 2—4 and in Tables I and II. Table I shows the λ_{max} and $\log \varepsilon_{max}$ values of the relatively weak absorption bands appearing between 350 and 1000 mμ, bands which are undoubtedly due to the ligand-field splittings of the metal 3d orbitals; this table also presents the data of the corresponding ethylenediamine and 2,2'-bipyridine chelates taken from the literature.[6] The results already mentioned in the preceding section, and the remark of Sutton[1] that Ni pic_2 Cl_2 and Cu pic_2 Cl_2 are converted into $[Ni\ pic_2\ (OH_2)_2]^{2+}$ and $[Cu\ pic_2]^{2+}$

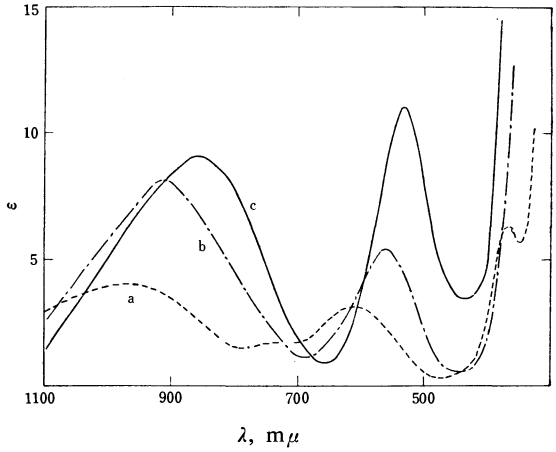


Fig. 2. Absorption spectra of nickel chelates.
a: $[Ni\ pic(OH_2)_4]^{2+}$
b: $[Ni\ pic_2(OH_2)_2]^{2+}$
c: $[Ni\ pic_3]^{2+}$
Concn.: $10^{-1}\sim5\times10^{-2}$ M; temp: 13°C; cell thickness: 10 mm.

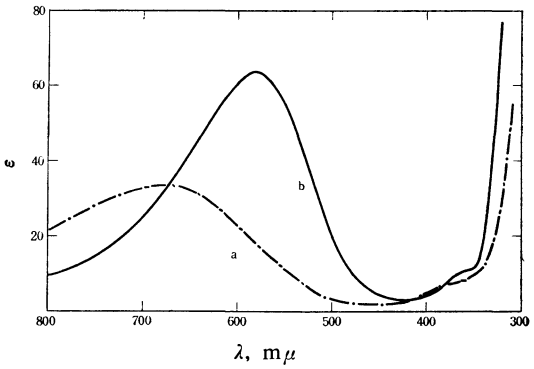


Fig. 3. Absorption spectra of copper chelates.
a: $[Cu\ pic(OH_2)_2]^{2+}$ b: $[Cu\ pic_2]^{2+}$
Concn.: $10^{-2}\sim7\times10^{-3}$ M; temp.: 18°C; cell thickness: 10 mm.

in their aqueous solutions, were taken into account in the preparation of this table.

It can be seen from this table and from the corresponding curves in Figs. 2—4 that, in general, the spectrum of a 2-picolylamine chelate is intermediate between those of the ethylenediamine and 2,2'-bipyridine chelates of the corresponding structure. This is what one can expect from the structure of 2-picolylamine; however, it can be seen further that, in most cases, the spectral similarity to the ethylenediamine chelates is more apparent than that to the 2,2'-bipyridine chelates. This fact is in conformity with the remark of Sutton mentioned above; two groups of chelates can be distinguished in this respect: (i) those in which the λ_{max} values decrease in the order: ethylenediamine ≳ 2-picolylamine > 2,2'-bipyridine and (ii) those in which they increase in

5) H. Irving and D. H. Mellor, *J. Chem. Soc.*, **1962**, 5222.
6) a) H. Ito, *J. Chem. Soc. Japan, Pure Chem. Sec.* (*Nippon Kagaku Zassi*), **77**, 1383 (1956); b) K. Sone and M. Kato, *Naturwiss.*, **45**. 10 (1958); c) C. K. Jørgensen, *Acta Chem. Scand.*, **8**, 1497 (1954); d) B. Martin and G. M. Waind, *J. Chem. Soc.*, **1958**, 4284.

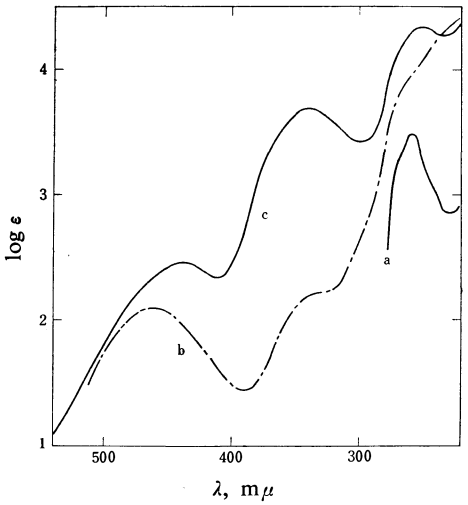


Fig. 4. Absorption spectra of cobalt chelates.
a: 2-picolylamine
b: $[Co\ pic_3]^{3+}$
c: $[Co\ pic_2(NO_2)_2]^{+}$
Concn.: $2\times10^{-3}\sim10^{-4}$ M; temp.: 18~24°C; cell thickness: 10 mm. and 1 mm.

the order: ethylenediamine ≲2-picolylamine< 2, 2'-bipyridine.

The chelates $[Ni\ R\ (OH_2)_4]^{2+}$, $[Ni\ R_3]^{2+}$, and $[Co\ R_3]^{3+}$ belong to the first group. According to the concept of the spectrochemical series,[7] this type of spectral change means that the strength of the effective ligand field increases in the order; ethylenediamine ≲ 2-picolylamine < 2, 2'-bipyridine. In fact, this is a very conceivable order, because it is generally accepted that, in the 2, 2'-bipyridine chlates, there is a special stabilization of the resonance system of the bipyridine molecule because of the chelate formation, presumably through the formation of metal-ligand π-bonds and the introduction of some "aromaticity" into the chelate ring. On the other hand, such effects are absent in ethylenediamine chelates, and, in the case of 2-picolylamine chelates, it is apparent that they are, at most, much smaller than in 2, 2'-bipyridine chelates, since there is only one pyridine ring and no conjugation between the ring and the $-CH_2NH_2$ chain in their ligand. Therefore, we can expect that the most effective binding of the metal ions, or, in other words, the operation of the strongest ligand field, is realized in 2, 2'-bipyridine chelates, and that the corresponding effects decrease in ethylenediamine and 2-picolylamine chelates in just the observed order.

$[Cu\ R_2]^{2+}$ and $[Cu\ R\ (OH_2)_2]^{2+}$ belong to the second group. Here the chief factor governing the spectra seems to be a different one, i. e., the steric effect. It has formerly been pointed out by Ito[8] that the spectro-chemical series in its simple form is not obeyed by many of the copper(II) complexes; according to him, their λ_{max} values are strongly influenced by their actual coordination number. A similar opinion was expressed by Jørgensen, who further argued that it is possible to study the shape of a copper(II) complex from the magnitude of the σ_{Cu}/σ_{Ni} ratio for it, i. e., the ratio between the wave number of its absorption band and that of the first band of the corresponding nickel complex. According to him, the complex is highly tetragonal if this ratio is 1.6~1.8, and if it is smaller than this, the tetragonality is accordingly lower; for example, $[Cu\ en_2]^{2+}$ (the 1.73 ratio) belongs to the former group, while $[Cu\ bip_2]^{2+}$ (the 1.1 ratio) belongs to the latter, most probably because of the steric repulsion caused by the 6, 6'-H atoms of bipyridine molecules, a repulsion which deforms the chelate strongly from the planar structure favored by copper(II).[5]

Now the λ_{max} value of $[Cu\ pic_2]^{2+}$ is much closer to that of $[Cu\ en_2]^{2+}$ than to that of $[Cu\ bip_2]^{2+}$, and the value of σ_{Cu}/σ_{Ni} is 1.56. These data indicate that this chelate is nearly tetragonal in shape, and that the repulsion between the ligands is quite small. This indication is again a very reasonable one, since it can be expected that this chelate exists chiefly in the trans-planar form in solution, and the model of this form is practically free from the repulsion of this kind.

In the chelates $[Cu\ R\ (OH_2)_2]^{2+}$, the steric repulsion of this kind should be completely absent. The differences among the λ_{max} values of the three chelates of ethylenediamine, 2-picolylamine and 2, 2'-bipyridine are, accordingly, quite small, but they are still in the same order as those of $[Cu\ R_2]^{2+}$. This may be due to the existence of some kind of steric effect even in this case, although we cannot be very certain about its nature.[9,10]

In the chelates, $[Ni\ R_2\ (OH_2)_2]^{2+}$ the spectral order is rather irregular (ethylenediamine>

7) Cf. C. K. Jørgensen, "Absorption Spectra and Chemical Binding in Complexes," Pergamon Press, London (1962), Chapter 7.

8) H. Ito, Ref. 6a.

9) It is interesting to compare the spectral data in Table I with the values of the stability constants of these chelates reported by Irving and Mellor (Ref. 5) and by Goldberg and Fernelius (Ref. 2). Although the data of these two sets of authors are not strictly comparable with each other, it can be seen that there exists a certain degree of parallelism between the spectral and stability data; for example, the order of stabilities for the chelates $[Ni\ R_3]^{2+}$ is; ethylenediamine<2-picolylamine≪2, 2'-bipyridine, while that for $[Cu\ R_2]^{2+}$ is: ethylenediamine> 2-picolylamine≫2, 2'-bipyridine.

10) The existence of some steric effect in $[Cu\ bip(OH_2)_2]^{2+}$ and $[Cu\ phen(OH_2)_2]^{2+}$ was also pointed out by Irving and Mellor (Ref. 5).

2, 2'-bipyridine > 2-picolylamine). If R is a symmetrical ligand (ethylenediamine or bipyridine), this type of chelate can exist in either a cis or in a trans form; if R is unsymmetrical (2-picolylamine), two cis and two trans forms are possible. However, as in the case of the copper chelates, the formation of the trans chelate will be hindered in the case of $[Ni \cdot bip_2(OH_2)_2]^{2+}$, and the cis form will be formed predominantly in solution; on the other hand, in the case of ethylenediamine and 2-picolylamine chelates, the trans forms will be more stable because of their higher symmetries, and, therefore, they will be formed predominantly in solution. This difference may be, at least in part, the reason for the irregular order observed here.[11]

Apart from the bands shown in Table I, the chelates studied also have a band or bands in the ultraviolet region which are much stronger than those in Table I (cf. Table II). 2-Picolylamine itself shows a strong band at 260 mμ while the nickel chelates also show a band at this wavelength. In the case of the copper chelates, this band is considerably broadened, and the apparent maximum is shifted to 247 mμ. $[Co\ pic_3]^{3+}$ also shows a shoulder at abuot 260 mμ. $[Co\ pic_2(NO)_2]^{+}$ shows two strong bands at 338 and 252 mμ, the latter of which is still much stronger than the band of 2-picolylamine. A comparison of the absorption curve of this chelate with those of the two isomers of $[Co\ en_2(NO_2)_2]^{+}$ indicates that these bands are not due to the absorption of coordinated picolylamine, and that they should, rather, be ascribed to the absorption of coordinated NO_2^- ions, which probably occupy trans positions with regard to each other.[12] Thus, these spectral data support the original view of Sutton[1] that this chelate has the trans structure, although the corresponding cis isomer could not be obtained by him, and our several trials in this direction all ended in failure.

11) However, the spectrum of $[Ni\ bip_2(OH_2)_2]^{2+}$ cited in Table I is that in its alcoholic solution, and, therefore, it is also possible that this irregularity is due to some effect of this solvent on the structure or electronic state of chelate. All the other data in this table refer to the spectra of aqueous solutions.

Summary

1) In addition to the nickel chelates (1 : 2 and 1 : 3) and copper chelates (1 : 2) already described by Sutton, it has been found that 2-picolylamine also forms 1 : 1 chelates (chlorides and sulfates) with these metals, which can be obtained in the state of crystals, and the chelate ions $[Cu\ pic_3]^{2+}$ of low stability, in solution.

2) A comparison of the electronic absorption spectra of all these chelates and two cobalt(III) chelates of 2-picolylamine with those of the chelates of ethylenediamine and 2, 2'-bipyridine has indicated that, in general, the spectrum of a 2-picolylamine chelate is intermediate between the spectra of the corresponding chelates of the latter two ligands; however, the similarity to the ethylenediamine chelate is more apparent in most cases.

3) Certain structural features of the 2-picolylamine chelates have been discussed on the basis of these spectral data.

Chemical Laboratory
Aichi Gakugei University
Higashi-ku, Nagoya (S. U.)

Chemical Laboratory
Department of General Education
Nagoya University
Chikusa-ku, Nagoya (K. S.)

12) a) H. Kuroya and R. Tsuchida, This Bulletin, 15, 427 (1940); b) F. Basolo, *J. Am. Chem. Soc.*, 72, 4393 (1950).

Bis(succinimidato)copper(II) Complexes with Pyridine, Picolines and Lutidines

By Seiko MIKI and Shoichiro YAMADA

(Received March 3, 1964)

Succinimidate, which is derived when succinimide (Fig. 1) loses a proton, forms a number of copper (II) complexes with different amines bound together. In a previous communication,[1] a series of red bis(succinimidato)-bis(alkylamine)copper(II) complexes were examined, and the factors favoring the formation of these red copper(II) complexes discussed. In order to confirm and extend the conclusions previously derived, it was thought to be interesting to examine complexes of a similar type with other amines. The present paper deals with bis(succinimidato)copper(II) complexes combining pyridine, picolines and lutidines.

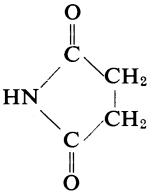


Fig. 1. Succinimide.

Experimental

Materials. — *Pyridine Complexes.* — [Cu(*sucim*)$_2$-(*py*)(OH$_2$)] was prepared in violet, cubic crystals according to the method of Tschugaeff,[2] where *sucim* and *py* denote a succinimidate ion and a pyridine molecule respectively. The crystals were stable in the atmosphere and were recrystallized from ethanol containing a few drops of pyridine.

Found: C, 43.9; H, 4.60; N, 11.6. Calcd. for $C_{13}H_{15}N_3O_5Cu$: C, 43.8; H, 4.24; N, 11.8%.

[Cu(*sucim*)$_2$(*py*)$_2$] was prepared, by a method similar to that used for [Cu(*sucim*)$_2$(*py*)(OH$_2$)], from 10 g. (0.1 mol.) of succinimide, 3 g. (0.05 g. atom) of copper powder, and 12 g. (0.15 mol.) of pyridine, with ethanol as a solvent. Since this compound was rather unstable in the atmosphere, the product was filtered in the dry air and stored in a tightly-closed bottle or in a desiccator containing sodium hydroxide. The crystals were recrystallized from an ethanol-pyridine mixture. The brown-red crystals, which were not quite free from the mother liquor, turned violet on exposure to the air, a co-ordinated pyridine molecule being replaced by a water molecule in the atmosphere. The compound was comparatively stable in the atmosphere when completely free from the mother liquor.

Found: C, 51.7; H, 4.50; N, 13.4. Calcd. for $C_{18}H_{18}N_4O_4Cu$: C, 51.7; H, 4.34; N, 13.4%.

Picoline Complexes. — [Cu(*sucim*)$_2$(*α-pic*)(OH$_2$)·CH$_3$OH] was prepared from 3 g. (0.05 g. atom) of copper powder, 10 g. (0.1 mol.) of succinimide and 10 g. (0.1 mol.) of α-picoline by a procedure similar to that used for [Cu(*sucim*)$_2$(*py*)$_2$], except that 50 ml. of methanol was used as a solvent. The notation '*pic*' denotes picoline. The product was filtered in the dry air and dried over phosphorus pentoxide in a vacuum desiccator. Recrystallization was carried out from methanol containing a suitable amount of the amine. Since these crystals turned from blue to green in the atmosphere, the compound was stored in a desiccator over sodium hydroxide.

Found: C, 45.0; H, 5.45; N, 10.0. Calcd. for $C_{15}H_{21}N_3O_6Cu$: C, 44.7; H, 5.25; N, 10.4%.

[Cu(*sucim*)$_2$(*α-pic*)$_2$] was obtained from [Cu-(*sucim*)$_2$(*α-pic*)(OH$_2$)·CH$_3$OH]. An excess of [Cu·(*sucim*)$_2$(*α-pic*)(OH$_2$)·CH$_3$OH] was added to methylene dichloride containing a small amount of α-picoline, and the solution was stirred for two hours; the blue crystals of the starting complex changed to red microcrystals. The product was filtered in the dry air and dried over phosphorus pentoxide in a vacuum desiccator. Recrystallization of the compound was carried out from ethanol containing an excess of α-picoline. The brown-red color of these crystals soon turned green in the atmosphere. The compound, however, was comparatively stable in the air when completely free from the mother liquor.

Found: C, 53.9; H, 4.99; N, 12.8. Calcd. for $C_{20}H_{22}N_4O_4Cu$: C, 53.9; H, 4.97; N, 12.6%.

[Cu(*sucim*)$_2$(*β-pic*)$_2$·2H$_2$O] was prepared by a method similar to the oxidation method of Tschugaeff, except that the filtration of the product was carried out in the dry air. The product consisted of deep-blue, needle-like crystals, which were hygroscopic. The crystal changed its color from deep-blue to red when stored for half a day over phosphorus pentoxide in a vacuum desiccator. The red compound is most probably [Cu(*sucim*)$_2$-(*β-pic*)$_2$], which is considered to be formed by the removal of two co-ordinated water molecules from [Cu(*sucim*)$_2$(*β-pic*)$_2$·2H$_2$O].

Found: C, 49.9; H, 5.29; N, 11.3. Calcd. for $C_{20}H_{26}N_4O_6Cu$: C, 49.8; H, 5.44; N, 11.6%.

Red crystals of [Cu(*sucim*)$_2$(*β-pic*)$_2$] were obtained from a methylene dichloride solution of [Cu-(*sucim*)$_2$(*β-pic*)$_2$·2H$_2$O]. When the solution was evaporated over phosphorus pentoxide in a vacuum desiccator, red crystals separated out. Since these

1) S. Yamada and S. Miki, This Bulletin, **36**, 680 (1963).
2) L. Tschugaeff, *Ber.*, **38**, 2900 (1905).

red crystals turned blue immediately on exposure to the air, it was quite difficult to analyze the complex and to examine its properties. However, a comparison with other complexes of a [Cu(*sucim*)$_2$-(*pic*)$_2$]-type shows that the red product is most probably [Cu(*sucim*)$_2$(β-*pic*)$_2$].

[Cu(*sucim*)$_2$(γ-*pic*)$_2$·H_2O] was easily prepared by a method similar to the oxidation method of Tschugaeff. The complex was obtained as violet-blue, cubic crystals which were stable in the atmosphere.

Found: C, 51.8; H, 5.22; N, 12.2. Calcd. for $C_{20}H_{24}N_4O_5Cu$: C, 51.8; H, 5.21; N, 12.1%.

[Cu(*sucim*)$_2$(γ-*pic*)(OH$_2$)] was prepared by a procedure similar to that used for [Cu(*sucim*)$_2$(α-*pic*)$_2$], except that [Cu(*sucim*)$_2$(γ-*pic*)$_2$·H_2O] was used in place of [Cu(*sucim*)$_2$(α-*pic*)(OH$_2$)·CH_3OH]. The compound was obtained as violet microcrystals. The compound was comparatively stable in the atmosphere when completely free from the solvent or mother liquor.

Found: C, 44.4; H, 4.61; N, 11.8. Calcd. for $C_{14}H_{17}N_3O_5Cu$: C, 45.3; H, 4.62; N, 11.3%.

[Cu(*sucim*)$_2$(γ-*pic*)$_2$] was obtained in brown-red, plate-like crystals by a method similar to that used for [Cu(*sucium*)$_2$(*py*)$_2$], except that 14 g. (0.15 mol.) of γ-picoline was used in place of 12 g. of pyridine. On exposure to the atmosphere, the crystals changed into blue crystals of [Cu(*sucim*)$_2$(γ-*pic*)$_2$·H_2O].

Found: C, 53.5; H, 4.88; N, 12.8. Calcd. for $C_{20}H_{22}N_4O_4Cu$: C, 53.9; H, 4.97; N, 12.6%.

Cu(*sucim*)$_2$(γ-*pic*)(OH$_2$)$_n$·CH_3OH was obtained as deep-blue crystals by the same method as that used for [Cu(*sucim*)$_2$(α-*pic*)(OH$_2$)·CH_3OH]. When exposed to the air, or when stored over phosphorus pentoxide in a vacuum desiccator, the product underwent decomposition. Accurate elemental analyses, therefore, were difficult, but the analyses agreed with the above formula, with n having a value between one and two.

Lutidine Complexes. — [Cu(*sucim*)$_2$(2,4-*lut*)$_2$]·0.5-H_2O, in which the notation '*lut*' denotes lutidine, was obtained as red crystals by a method similar to that used for [Cu(*sucim*)$_2$(*py*)$_2$], except that 15 g. (0.15 mol.) of 2,4-lutidine was used in place of 12 g. of pyridine. On exposure to the air, the crystals gradually decomposed, finally forming a sky-blue powder.

Found: C, 53.8; H, 5.48; N, 12.3. Calcd. for $C_{22}H_{27}N_4O_{4.5}Cu$: C, 54.7; H, 5.64; N, 11.6%.

[Cu(*sucim*)$_2$(3,5-*lut*)$_2$·H_2O] was obtained, by a method similar to the oxidation method of Tschugaeff, from 5 g. (0.05 mol.) of succinimide, 1.5 g. (0.025 g. atom) of copper powder, and 5.5 g. (0.05 mol.) of 3,5-lutidine. This complex formed blue plate-like microcrystals which were stable in the air.

Found: C, 53.2; H, 5.88; N, 11.5. Calcd. for $C_{22}H_{28}N_4O_5Cu$: C, 53.7; H, 5.74; N, 11.4%.

Red crystals of [Cu(*sucim*)$_2$(3,5-*lut*)$_2$] were obtained by the same method as that used for [Cu-(*sucim*)$_2$(β-*pic*)$_2$], except that [Cu(*sucim*)$_2$(3,5-lut)$_2$·H_2O] was used in place of [Cu(*sucim*)$_2$(β-*pic*)$_2$2H_2O]. On exposure to the atmosphere, the compound readily absorbed water to form [Cu(*sucim*)$_2$(3,5-*lut*)$_2$$H_2O$].

Cu(*sucim*)$_2$(OH$_2$)$_2$ was obtained as a sky-blue powder by a procedure similar to that used for Cu(*sucim*)$_2$(*py*)(OH$_2$), using 10 g. (0.1 mol.) of succinimide, 3 g. (0.05 g. atom) of copper powder and 11 g. (0.1 mol.) of 2,6-lutidine.

Found: C, 33.1; H, 4.19; N, 9.73. Calcd. for $C_8H_{12}N_2O_6Cu$: C, 32.5; H, 4.09; N, 9.47%.

All the compounds prepared in the present work, with the exception of Cu(*sucim*)$_2$(OH$_2$)$_2$, were soluble in chloroform, methylene dichloride, ethanol, methanol and pyridine, forming a greenish-blue or a dark-blue solution.

Pyridine, α-picoline and 2,6-lutidine, used as solvents for spectral measurements, were purified by distillation after having been dried over potassium hydroxide for several weeks.[3] The chloroform, which was purchased from Wako Co., was of extra-pure reagent grade, containing less than 0.05% water.

Measurements.—Quantitative dichroism measurements of the crystals were carried out at room temperature by Tsuchida and Kobayashi's microscopic method,[4] using polarized light in the visible and ultraviolet regions. The symbol α represents the absorption coefficient per mm. of a crystal. No correction was made for reflection on the surface of the crystal.

The absorption spectra of the compounds in organic solvents were determined at room temperature with a Beckman DU spectrophotometer.

Reflection spectra were determined with a Hitachi EPU 2A spectrophotometer. The symbols in the text are those conventionally used.

Results and Discussion

The Configuration of Bis(succinimidato)copper(II) Complexes with Pyridine.—As has been discussed in a previous paper,[1] a succinimidate ion is combined with a copper(II)-ion through its nitrogen atom when this behaves as a unidentate (Fig. 1).

The electronic absorption spectra of bis(succinimidato)copper(II) complexes with pyridine are shown in Fig. 2. The absorption bands between 50 and 70×10^{13} sec^{-1} observed with [Cu(*sucim*)$_2$(*py*)$_2$] in the crystalline state are regarded as "ligand field bands" which are due to the *d-d* transitions.[1] The main band maximum (about 62×10^{13} sec^{-1}) lies in a frequency region much higher than that of the cupric complexes of an ordinary kind. In the same way as in the previous paper,[1] the high frequency of the ligand field band maximum shows that [Cu(*sncim*)$_2$(*py*)$_2$] has a square-planar configuration of the [Cu(N)$_4$]-type, with the fifth and the sixth co-ordination sites left vacant.

The crystal structure analysis of the complex

3) D. J. Royer, *J. Inorg. Nucl. Chem.*, **11**, 151 (1959).
4) R. Tsuchida and M. Kobayashi, "The Colour and the Structure of Metallic Compounds" (Kinzokukagōbutsu no Iro to Kōzō), Zōshindo, Osaka (1944), p. 180.

TABLE I. ABSORPTION MAXIMA OF BIS(SUCCINIMIDATO)COPPER(II) COMPLEXES WITH PYRIDINE, PICOLINES AND LUTIDINES IN SOLID STATE

Complex	ν_{max} (half width)		Type
Cu(*sucim*)$_2$(*py*)$_2$	62*	52*	I Cu(N)$_4$ Red
Cu(*sucim*)$_2$(*α-pic*)$_2$	63.6 (15.1)	50.4 (11)	
Cu(*sucim*)$_2$(*β-pic*)$_2$	unstable		
Cu(*sucim*)$_2$(*γ-pic*)$_2$	unstable		
Cu(*sucim*)$_2$(2,4-*lut*)$_2$·0.5H$_2$O	61.8 (14.8)	50.0 (11)	
Cu(*sucim*)$_2$(3,5-*lut*)$_2$	unstable		
Cu(*sucim*)$_2$(*py*)(OH$_2$)	58.2*	53*	II Cu(N)$_3$O Violet
Cu(*sucim*)$_2$(*γ-pic*)(OH$_2$)	55.2 (14.4)	47 (sh)	
Cu(*sucim*)$_2$(*α-pic*)(OH$_2$)·CH$_3$OH	unstable		IV Cu(N)$_3$O$_n$ Deep-blue
Cu(*sucim*)$_2$(*γ-pic*)(OH$_2$)$_2$·CH$_3$OH	unstable		
Cu(*sucim*)$_2$(*β-pic*)$_2$·2H$_2$O	50.8 (12.4)	44 (sh)	III Cu(N)$_4$O$_n$ Deep-blue
Cu(*sucim*)$_2$(*γ-pic*)$_2$·H$_2$O	52.0 (14.5)	44 (sh)	
Cu(*sucim*)$_2$(3,5-*lut*)$_2$·H$_2$O	51.2 (14.1)	44 (sh)	
Cu(*sucim*)$_2$(OH$_2$)$_2$	45.0 (13.8)		Sky-blue

ν and half width : 10^{13} sec^{-1}, * : in crystalline state, sh : shoulder

TABLE II. ABSORPTION MAXIMA OF BIS(SUCCINIMIDATO)COPPER(II) COMPLEXES WITH PYRIDINE, PICOLINES AND LUTIDINES IN CHLOROFORM SOLUTION

Complex	ν_{max}	log ε	h. w.	Type
Cu(*sucim*)$_2$(*py*)$_2$	44	1.63	16.8	I
Cu(*sucim*)$_2$(*α-pic*)$_2$	44	1.61	18.5	
Cu(*sucim*)$_2$(*β-pic*)$_2$		unstable		
Cu(*sucim*)$_2$(*γ-pic*)$_2$	44	1.57	16.7	
Cu(*sucim*)$_2$(2,4-*lut*)$_2$·0.5H$_2$O	44	1.64	17.1	
Cu(*sucim*)$_2$(3,5-*lut*)$_2$		unstable		
Cu(*sucim*)$_2$(*py*)(OH$_2$)	44	1.63	17.6	II
Cu(*sucim*)$_2$(*γ-pic*)(OH$_2$)	45	1.60	17.1	
Cu(*sucim*)$_2$(*α-pic*)(OH$_2$)·CH$_3$OH	45	1.63	21.0	IV
Cu(*sucim*)$_2$(*γ-pic*)(OH$_2$)$_2$·CH$_3$OH		unstable		
Cu(*sucim*)$_2$(*β-pic*)$_2$·2H$_2$O	44	1.60	17.2	III
Cu(*sucim*)$_2$(*γ-pic*)$_2$·H$_2$O	45	1.64	16.4	
Cu(*sucim*)$_2$(3,5-*lut*)$_2$·H$_2$O	44	1.62	17.0	
Cu(*sucim*)$_2$(OH$_2$)$_2$*	45	1.68	17.4	

* Alcohol solution, ν : 10^{13} sec^{-1}, h. w. : half width in 10^{13} sec^{-1}

is not yet available, and usually the planes of the complexes in the crystal are not exactly parallel to each other. However, it may readily be found that the A- and B-absorption in Fig. 2 represent the main features of the xy- and the z-absorption respectively of the square-planar complex, since previous studies have shown that, for ligand field absorption band, the xy-absorption has a larger oscillator strength than the z-absorption.[5]

The violet complex, [Cu(*sucim*)$_2$(*py*)(OH$_2$)], in the crystalline state shows a peak at about 58.2×10^{13} sec^{-1} which is remarkably dichroic and which is regarded as a ligand field band due to the cupric ion. The frequency at the band maximum is regarded as quite high for a cupric complex of the [Cu(N)$_3$O]-type. Thus, [Cu(NH$_3$)$_4$]$^{2+}$ and [Cu *en*$_2$]$^{2+}$ in water show absorption maxima at 49.2 and 54.6×10^{13} sec^{-1} respectively. It is concluded that [Cu(*sucim*)$_2$(*py*)(OH$_2$)] has a square-planar configuration of the [Cu(N)$_3$O]-type, with the fifth and the sixth sites left vacant.

The Configuration of Bis(succinimidato)copper(II) Complexes with Picolines and Lutidines. —The electronic absorption spectra of bis(succinimidato)copper(II) complexes with picolines and lutidines in the solid state were determined. An inspection of the data given in Table I indicates that there are three main types of succinimidato-copper(II) complexes with the amines, which are red, violet and deep-blue respectively. The difference in color between these types is so apparent that

5) S. Yamada and R. Tsuchida, *Ann. Reports Faculty of Sci., Osaka Univ.*, **4**, 79 (1956); This Bulletin, **29**, 289, 694 (1957).

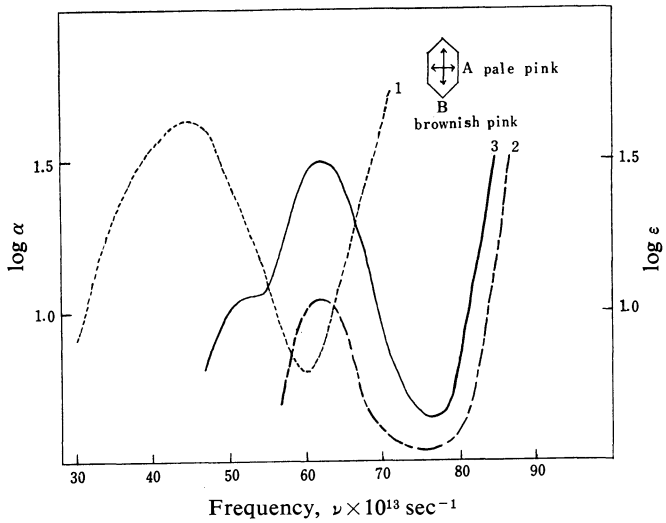


Fig. 2. Electronic absorption spectra of Cu(*sucim*)$_2$(*py*)$_2$ in the crystalline state and in chloroform.

1, soln.; 2, A-absorption in crystalline state; 3, B-absorption

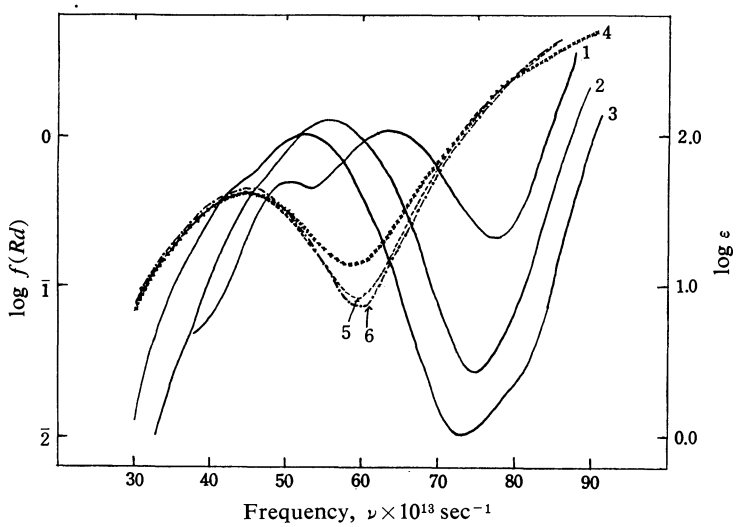


Fig. 3. Electronic absorption spectra of bis(succinimidato)copper(II) complexes in the solid state and in chloroform.

Cu(*sucim*)$_2$(*α-pic*)$_2$ (1, solid; 4, soln.), Cu(*sucim*)$_2$(*γ-pic*)(OH$_2$) (2, solid; 5, soln.) and Cu(*sucim*)$_2$(*γ-pic*)$_2$·H$_2$O (3, solid; 6, soln.). The solid spectra were determined by the reflection method.

in most cases it is possible to assign a compound to one of these types with little ambiguity (Table I). Besides these, there is a green type for *α*-picoline.

A typical spectrum of the red crystals is shown in Fig. 3. From the data in Table I, it is found that the red crystals show the main peak of the ligand field band at about 61.5×10^{13} sec^{-1} or at higher frequencies. The red crystals, which are denoted as type I, consist of square-planar complexes of the [Cu(*sucim*)$_2$(amine)$_2$]-type, since the frequency of the main peak of the ligand field band is exceedingly high.

The deep-blue or indigo crystals of type III show the peak of ligand field bands at about 50×10^{13} sec^{-1}, a frequency which corresponds to a much lower frequency than the peak for the red, square-planar complexes of the [Cu(N)$_4$]-type. Thus, deep-blue crystals of [Cu(*sucim*)$_2$(*β-pic*)$_2$·2H$_2$O] and [Cu(*sucim*)$_2$(*γ-pic*)$_2$·H$_2$O] show their ligand field bands at

about 50.8 and 52.0×10^{13} sec^{-1}, respectively (Table I). These frequencies are much lower than those of the square-planar complexes of the $[Cu(N)_4]$-type, and are very close to the values for the complexes, which have already been established to consist of a $[Cu(N)_4(O)_n]$-type, n being either one or two.[1,6] It may be concluded that, in the crystals of $[Cu(sucim)_2(\beta\text{-}pic)_2\cdot2H_2O]$ and $[Cu(sucim)_2(\gamma\text{-}pic)_2\cdot H_2O]$, one or two molecules of water occupy additional co-ordination sites above and below the $[Cu(N)_4]$-plane to form a quinque-co-ordinate, tetragonal-pyramidal or a sexa-co-ordinate, pseudo-octahedral complex of the $[Cu(N)_4(OH_2)_n]$-type.

The complexes classified as type IV may be interpreted in a similar way. It is most likely that in these complexes the methanol molecule is combined with the copper(II) ion, $[Cu(N)_3(O)_n]$ being thereby formed, where n is either two or three.

Of the compounds of type II, the pyridine compound, $[Cu(sucim)_2[(py)(OH_2)]$, has been discussed above. The violet compounds of type II reported in the present paper show the peak of the ligand field bands at about 55 to 59×10^{13} sec^{-1}, a frequency which is slightly lower than the frequency for the red crystals but remarkably higher than the frequency for the complexes of the $[Cu(N)_4(OH_2)_n]$-type. It is, therefore, presumed that the violet crystals of type II consist of square-planar complexes of the $[Cu(sucim)_2(amine)(OH_2)]$-type, in which the fifth and the sixth co-ordination sites around the copper(II) ion are left vacant.

In the case of α-picoline, a green type is also obtained when the red crystals of $[Cu(sucim)_2(\alpha\text{-}pic)_2]$ are left to stand in the atmosphere. The green type of the α-picoline complex shows a peak corresponding to the ligand field band at about 51.5×10 sec^{-1}; the band is, however, quite broad. It is most likely that the compound is polynuclear, with hydroxyl groups serving as bridges, judging from its properties. The detailed structure of the compound is not established in the present study. A similar procedure for the preparation of the red compound using 2,6-lutidine instead of the other lutidines or picolines gives none of the three types; instead, a pale-blue compound with an empirical formula of $Cu(sucim)_2(OH_2)_2$ was obtained. The pale-blue complex of $Cu(sucim)_2(OH_2)_2$ shows a ligand field band at about 45×10^{13} sec^{-1} which is comparatively symmetrical. Although the precise structure of the compound has not yet been completely clarified, the low frequency of the band maximum indicates that the compound consists of a sexa-co-ordinate complex of the $[Cu(N)_2(O)_4]$-type, with oxygen atoms of water molecules possibly serving as bridges.

It should be noted that the quadri-co-ordinate copper(II) complexes of type I show ligand field bands which are less symmetrical, with a shoulder on the lower frequency side of the main band. This fact may be understood mainly in terms of the symmetry of the complexes, since the tetragonal nature of the ligand field is regarded as more pronounced in the complexes of type I than in those of type II as well as of type III.

General Consideration.—It is to be noted that the red crystals of the $Cu(sucim)_2(pic)_2$ formula were isolated with all of the α-, β- and γ-picolines. The red crystals of all the compounds obtained are quite unstable, taking up molecules of water in the atmosphere to turn green in the case of the α-picoline and deep-blue in the case of the β- or γ-picoline complexes.

The red complexes of β- and γ-picoline readily take the fifth and the sixth ligands, while the corresponding complex of α-picoline does not. Moreover, the isolation of the blue crystals of the $[Cu(sucim)_2(amine)_2(OH_2)_n]$-type is possible only with β- and γ-picolines, not with α-picoline. These facts may be understood mainly in terms of the steric factor.

The behavior of the lutidine-complexes of the $[Cu(sucim)_2(lut)_2]$-type may be interpreted in the same way as that of the corresponding complexes of picolines. Thus, the red 2,4-lutidine-complex in the atmosphere does not combine with a water molecule at the fifth or the sixth co-ordination sites; instead, the bond between the copper(II) ion and lutidine is readily broken, the original square-planar complex being changed into sky-blue $Cu(sucim)_2(OH_2)_2$. On the other hand, the red complex, $[Cu(sucim)_2(3,5\text{-}lut)_2]$, takes up one water molecule at the fifth site. The isolation of the blue crystals of the $[Cu(sucim)_2(lut)_2(OH_2)_n]$-type is found to be possible with those lutidines with no substituent on the α-carbon atom. This behavior is quite similar to that of the corresponding picoline-complexes of copper(II).

It should also be noted that the red pyridine-complex, $[Cu(sucim)_2(py)_2]$, has a much weaker tendency to combine additional ligands at the fifth and sixth co-ordination sites than do the complexes of the picolines and lutidines. Moreover, the square-planar, violet complex of $[Cu(sucim)_2(py)(OH_2)]$ is formed when the red $[Cu(sucim)_2(py)_2]$ is left in the air, but the corresponding violet complex is not formed with the picoline- or lutidine-complexes under the same conditions. Instead, the deep-blue complex of $[Cu(sucim)_2(pic)_2(OH_2)_n]$ or $[Cu(sucim)_2(lut)_2(OH_2)_n]$ is formed when the red

6) S. Miki and S. Yamada, to be submitted shortly.

complex of the $[Cu(sucim)_2L_2]$-type is left in the atmosphere. The corresponding deep-blue complex was not isolated with pyridine. It seems certain that bis(succinimidato)copper(II) complexes of pyridine have a stronger tendency to keep the fifth and sixth co-ordination sites vacant. This difference between the pyridine complexes and the complexes of picolines may be ascribed to the nature of the copper(II)-ligand bond, since the steric factor alone can not explain these differences. A definite explanation of this is not given in the present paper, but it may be ascribed to the difference in the π-bonding contribution, if it is assumed, on the basis of the concepts presented previously, that the π-bonding is important in stabilizing the square-planar configuration with the fifth and the sixth sites left vacant.[1)]

The Configuration of Bis(succinimidato)copper(II) Complexes in Non-donor Solvents.—The electronic absorption spectra of red diaminebis(succinimidato)copper(II) complexes were examined in chloroform (Table II and Fig. 3). An enormous bathochromic shift of the ligand field band (about $18\times10^{13}\,sec^{-1}$) is observed on going from the solid to the solution. It is considered that the molecular configuration in the solid state is not present in the solution. Since Beer's law is obeyed, and since the solution is unchanged in several days, there is a very slight possibility of the decomposition of the complex. Moreover, the shift is much larger than that which would be expected if the solvent molecules were co-ordinated to the copper(II) ion, since the bonding of the solvent molecule with the copper(II) ion would be very weak. In the same way as has been discussed previously,[1)] it is considered that the molecule of $[Cu(sucim_2)(amine)_2]$ in the solution is distorted from the square-planar configuration.

The violet and deep-blue complexes of types II and III also show ligand field bands at about 44 and $45\times10^{13}\,sec^{-1}$. The observed bathochromic shift on going from the solid to the solution is quite remarkable for the shift expected if the co-odination of chloroform molecules to the cupric ion takes place. It is considered that the field produced by ligands surrounding the copper(II) ion is distorted from the tetragonal symmetry to a considerable extent.

The bathochromic shift on going from the solid to the solution in the case of type III is considerably smaller than that in the case of types I and II, although the shift in the former case is still so great that some configurational change is to be assumed. A detailed discussion of them will be deferred until more materials become available.

The absorption spectra of these complexes in methylene dichloride are quite similar to those in chloroform. The molecular configuration of these complexes, therefore, is considered to be similar in all these solvents.

The absorption spectra of the compounds of type I in ethanol are similar to the spectra of the compounds in chloroform. Therefore, the same conclusion as that above is obtained. On the contrary, the absorption spectra of the complexes of types II and III in ethanol are more complicated, and the discussion of them will be deferred until more materials become available.

The Configuration of Bis(succinimidato)copper(II) Complexes in Pyridine, Picolines and Lutidines.—In donor solvents such as pyridine, the situation may be different from that in non-donor solvents. The red bis(pyridine)bis(succinimidato)copper(II) in pyridine shows a ligand field band at about $47\sim48\times10^{13}\,sec^{-1}$, a frequency which is much higher than that (about $44\times10^{13}\,sec^{-1}$) of the same compound in non-donor solvents. It may thus be inferred that the pyridine molecules are probably bound with the copper(II) ion to complete its sexa-co-ordination, the tetragonal symmetry of the ligand field being kept.

On the contrary, the red complexes of type I in 2,6-lutidine show a ligand field band at about $58\times10^{13}\,sec^{-1}$, a frequency which is much higher than those of the same compounds in pyridine as well as in other non-donor solvents (Fig. 4). It is most certain, from the steric ground, that the molecules of 2,6-lutidine are not bound with the copper(II) ion in the same sense as the molecules of pyridine are bound. The high frequency of the band maximum of the complex in 2,6-lutidine (Fig. 4) is taken as indication that the symmetry of the ligand field around the copper(II) ion is tetragonal,

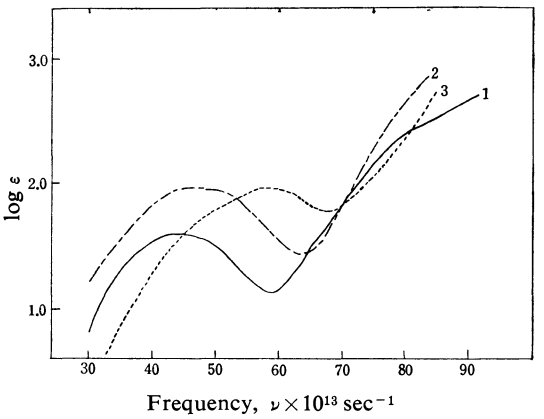


Fig. 4. UV-spectra of $Cu(sucim)_2(\alpha\text{-}pic)_2$ in organic solvents.

1, Chloroform; 2, Pyridine; 3, 2,6-Lutidine

and that the slight bathochromic shift of the band maximum relative to the band maximum of the crystal may be due to a feeble effect of the 2,6-lutidine molecules on the copper(II) ion. It is likely that the 2,6-lutidine molecules point toward the copper(II) ion at a farther distance in such a way that the ligand field around the copper(II) ion keeps the tetragonal symmetry.

Summary

Bis(succinimidato)copper(II) complexes with pyridine and its derivatives have been prepared, the derivatives involving α-, β- and γ-picoline, 2,4-lutidine and 3,5-lutidine. Depending upon the reaction conditions the following types of complexes have been obtained: (1) red complexes of [Cu(*sucim*)$_2$(amine)$_2$], (2) violet complexes of [Cu(*sucim*)$_2$(amine)(OH$_2$)], and (3) indigo or dark-blue complexes of [Cu(*sucim*)$_2$-(amine)$_2$(OH$_2$)$_n$]. When 2,6-lutidine is employed, however, none of the three types is obtained; rather, a blue compound with the formula of Cu(*sucim*)$_2$(OH$_2$)$_2$ is isolated.

The configuration of the three types of complexes has been examined, mainly on the basis of the electronic absorption spectra. The complexes of types 1 and 2 consist of quadri-coordinate complexes with a square-planar configuration. The compounds of type 3 consist of quinque- or sexa-co-ordinate complexes.

The configuration of these complexes of the three types in non-donor solvents has also been discussed.

The authors are grateful to Mrs. Miyoko Kōsaka for her experimental assistance and to the Ministry of Education for financial support.

Department of Chemistry
Faculty of Science
Osaka Univesity
Nakanoshima, Osaka

The Beckmann Rearrangement of Alkyl Methyl Ketoximes

By Masato KAWAKAMI and Yasuhide YUKAWA

(Received March 19, 1964)

The mechanism of the Beckmann rearrangement has been discussed by several authors with attention to the intermediate, the stereospecificity, and the kinetics. Kuhara and his co-workers established the kinetics of the rearrangement of benzophenone oxime acetate[1]. Pearson et al. studied the effect of substituents on the rate of substituted acetophenone oximes[2] and symmetrical dialkyl ketoximes in sulfuric acid.[3] Ogata and Okano measured the rate of cyclohexanone oxime in oleum.[4] For the reaction in sulfuric acid, it has been known that the rate-determining step involves the breaking of the nitrogen-oxygen bond. The actual migration may rapidly proceed after the fission (the iminonium ion mechanism) or simultaneously with the fission (the concerted mechanism). At first sight, the stereospecificity of the reaction would support the concerted mechanism, since the group trans to the nitrogen-oxygen bond migrates preferentially. However, one can assume the formation of an ion pair between the iminonium ion and the hydroxyl ion, followed by rapid migration; therefore, the iminonium ion mechanism does not conflict with the stereospecificity of the reaction. Pearson reported that the polar effect of the aryl group in aryl methyl ketoximes influenced the rate of the reaction. A good linearity was found between the rates and Hammett's sigma values corrected for the additional electrophilic resonance effect using Yukawa-Tsuno's equation.[5] The effect can be explained satisfactorily either by the concerted mechanism or the iminonium ion mechanism. The direct participation of the aryl group in the former or the polar assistance through the C=N bond to the breaking of the N–O bond in the latter fits the equation as well.

The rates of the rearrangement of the several

1) M. Kuhara, M. Matsumiya and N. Matsunami, *Memoirs Coll. Sci. Kyoto*, **1**, 105 (1916).
2) D. E. Pearson, J. E. Boxter and J. C. Martin, *J. Org. Chem.*, **17**, 1511 (1952): D. B. Pearson and J. D. Burton, ibid., **19**, 957 (1954).
3) P. T. Scott, D. E. Pearson and L. J. Bircher, ibid., **19**, 1815 (1954).
4) Y. Ogata and M. Okano, *J. Am. Chem. Soc.*, **77**, 4643 (1955).
5) Y. Tsuno, T. Ibata and Y. Yukawa, This Bulletin, **32**, 960 (1959).

alkyl methyl ketoximes were measured and the influence of the steric bulkiness of the migrating group were studied in this paper.

Experimental

Ketoximes.—The ketoximes used were prepared by the usual procedure from the corresponding ketones and were purified by recrystallization from petroleum ether or by distillation under reduced pressure.

n-Amyl methyl ketoxime	b. p. 107~107.5°C/21 mmHg
Cyclopentyl methyl ketoxime	b. p. 114~116°C/20 mmHg
2-Methylcyclopentyl methyl ketoxime	b. p. 120.5~121°C/20 mmHg
Cyclohexyl methyl ketoxime	m. p. 60°C
Cycloheptyl methyl ketoxime	m. p. 53~54°C b. p. 145°C/23 mmHg

Rearrangement Products.—After one milliliter of sulfuric acid had been added to 0.5 g. of ketoxime contained in a 30 ml. Erlenmeyer flask, the flask was held in the thermostat at 80°C for 10~15 hr. Ten milliliters of water was then added to the flask and the reaction mixture refluxed for 5~7 hr. to hydrolyze the acetamides produced. The solution was made strongly basic by adding a concentrated aqueous solution of potassium hydroxide, and the amine was extracted with 10 ml. of ether three times. After the removal of the solvent, it was derived to *N*-alkyl-*N'*-phenylurea by the reaction with phenyl isocyanate or to *N*-alkylbenzamide by Schotten-Baumann reaction. The melting points of these derivatives were not depressed by admixture with respective authentic samples prepared by the usual procedure.

N-*n*-Amyl-*N'*-phenylurea (from *n*-amyl methyl ketoxime), m. p. 237~238°C

N-Cyclopentyl-*N'*-phenylurea (from cyclopentyl ketoxime), m. p. 205°C

N-(2-Methylcyclopentyl)-benzamide (from 2-methylcyclopentyl methyl ketoxime), m. p. 116°C

N-Cyclohexyl-*N'*-phenylurea (from cyclohexylmethyl ketoxime), m. p. 182~182.5°C

N-Cycloheptyl-*N'*-phenylurea (from cycloheptyl methyl ketoxime), m. p. 182.5~183°C

Spectra of the 2,4-Dinitrophenylhydrazones in the Visible and Ultraviolet Region.—The absorption spectra of the 2,4-dinitrophenylhydrazones of alkyl methyl ketones in carbon tetrachloride were measured with a Hitachi photo-spectrometer. The spectra were essentially identical. The absorption curve in the case of *n*-amyl methyl ketone is shown in Fig. 1. The absorbance at 410 mμ was chosen for quantitative analysis. The correlation of the optical density with the concentration of the 2,3-dinitrophenylhydrazone of *n*-amyl methyl ketone is shown in Fig. 2.

Analysis of Ketoximes.—Pearson's method for the analysis of acetophenone oxime was modified as follows. A stock solution of ketoxime in 10% sulfuric acid was prepared. An aliquot of the solution was added from a burrett to each 100 ml. glass-stoppered flask with the flasks being weighed

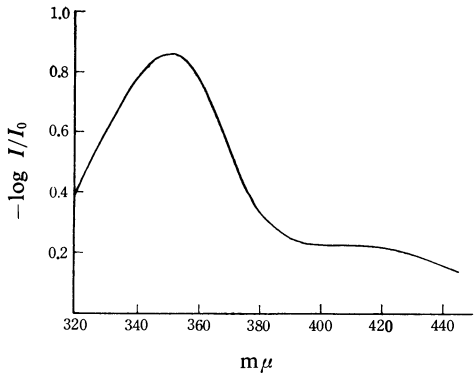


Fig. 1. The absorption curve of 2,4-dinitrophenylhydrazone of *n*-amyl methyl ketone.

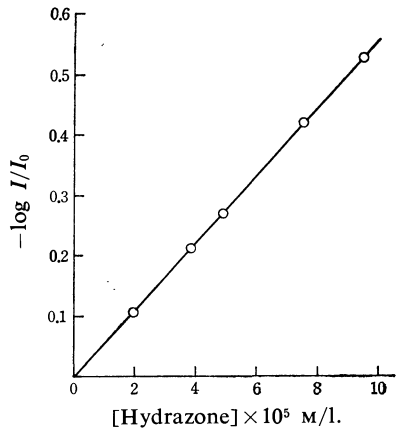


Fig. 2. Correlation of the optical density at 410 mμ to the concentration of 2,4-dinitrophenylhydrazone of *n*-amyl methyl ketone.

accurately before and after the addition. Twenty-five milliliters of 4% sulfuric acid and 0.300 g. of 2,4-dinitrophenylhydrazine were added to each flask. The flask was then sealed with a glass stopper and placed in a bath at 50°C for about 18 hr. After the flask had cooled, 25 ml. of carbon tetrachloride was added. The flask was then thoroughly shaken and allowed to stand for 18 hr. at room temperature. The carbon tetrachloride layer was transferred to a 100 ml. measuring flask using a separatory funnel fitted with a cotton filter. Another 5 ml. of carbon tetrachloride were added to wash the funnel and cotton filter and were combined with the filtrate. The combined solution was then diluted to 100 ml. with carbon tetrachloride. The optical density of this solution was determined at 410 mμ using a photo-spectrometer. A typical run is shown in Fig. 3.

Rate Determination.—About 500 mg. of ketoxime was weighed accurately and then dissolved in 20 ml. of sulfuric acid which had been weighed exactly in a glass-stoppered flask. The flask was sealed and immersed in a thermostatted bath (49.70~49.95°C±0.01°C). At approximately equal time intervals, from zero time to a half-life, each 2 ml. portion of the solution was pipetted out and the

TABLA I.

Ketoxime	$k\times10^3$, min^{-1}	Taft's σ	Temp., °C
Acetone*	0.025	0.00	50.0
Diethyl ketone*	1.33	—	50.0
Diisopropyl ketone*	84.8	—	50.0
n-Amyl methyl ketone	1.07±0.06	−0.162	49.95±0.01
Cyclopentyl methyl ketone	2.32±0.04	−0.20	49.82±0.01
2-Methylcyclopentyl methyl ketone	3.55±0.13	—	49.70±0.01
Cyclohexyl methyl ketone	26.4 ±0.5	−0.15	49.70±0.01
Cycloheptyl methyl ketone	26.0 ±0.4	—	49.75±0.01
Acetophenone*	1.107	—	50.0

Taft's σ : R. W. Taft, Jr., *J. Am. Chem. Soc.*, **75**, 4231 (1953).
* Calculated from D. E. Pearson's data (Refs. 2 and 3).

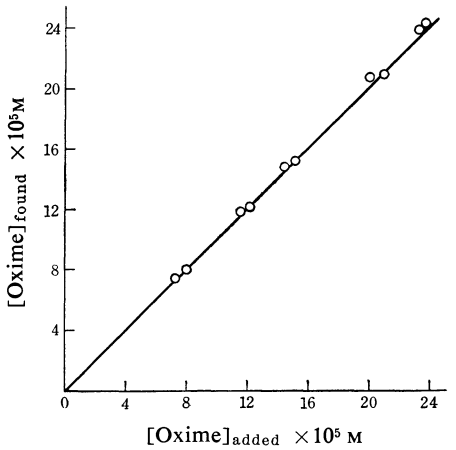


Fig. 3. Analysis of *n*-amyl methyl ketoxime.

quantity of unchanged keoxime was determined.

The rate is first order to ketoxime, the rate constant was calculated by the following equation.

$k=\ln(a/(a-x))\ (1/t)$

k: rate constant
t: time in minutes
a: concentration of initial ketoxime
x: concentration of reacted ketoxime at time t

The results are shown in Table I.

Results and Discussion

The first order rate-constants are given in Table I. The sequence of the rates was found to be: cycloheptyl≈cyclohexyl>2-methylcyclopentyl>cyclopentyl>*n*-amyl. As the steric bulkiness of the alkyl group in oximes is far greater than that of methyl, oximes have a methyl-syn configuration. It has been known that the group trans to the hydroxyl group in oxime migrates preferentially in sulfuric acid.*

Actually, the migration of the bulkier group was ascertained from the derivatives of the main products in the reaction, and the measured rates are those for the migration of alkyl groups.

The effect of the alkyl group upon the rates of reaction cannot be explained on the basis of the polar effect only, and there is no corre lation between the relative rates and Taft's sigma star values. The results can be elucidated only by the steric effect of the migrating group. The bulkiness of the *n*-amyl group would be smaller than that of cyclopentyl. Those of cycloheptyl and cyclohexyl would be the greatest, as these two groups have a non-planar ring.

If we consider the steric compression between the migrating alkyl group and the non-migrating methyl group, the sequence can be understood. When steric compression decreases in the transition state, the greater the steric compression in the initial state, the faster the reaction rate. The compression decreases during the reaction by means of: 1) the expansion of the angle between the migrating group and the non-migrating group, and 2) the increase of the length of the bond between the migrating group and the carbonyl carbon.

Our results can be explained by considering that the decrease of the steric compression might happen at the rate-determining step. On the basis of Pearson's data,[3] the ratios of k(diethyl ketone)/k(acetone) and k(diisopropyl ketone)/k(acetone) are 53 and 3400 respectively. The striking value in diisopropyl ketone may be also explained because the steric compression between two isopropyl groups is very much greater than that between two methyl groups or two ethyl groups. Pearson reported that the rate of *o*-methylacetophenone was much faster than that of acetophenone and explained the phenomenon as follows: The resonance interaction between phenyl group and the *d*-oximinoethyl group is diminished by the steric effect of the ortho substituent;

* This does not always hold in other media. (cf. S. Kim and Y. Yukawa, Unpublished.)

therefore, the ring system is geometrically more susceptible to participating with the nitrogen atom. Yukawa and Tsukamoto suggested the presence of the resonance inhibition due to the steric compression between the *o*-tolyl group and the methyl group of the oxime in its ultra-violet absorption spectra and also noticed the effect of the resonance inhibition in the aryl-carbonyl bond on the relative stability of *o*-substituted benzophenone oxime isomers.[6]

These suggestions agree with the above explanation of our results. The decrease in the steric compression seems to contribute to the rate. This implies that the migrating group participates in the cleavage of the N–O bond in the rate-determining step in sulfuric acid. The iminonium ion mechanism can not offer any explanation, but the concerted mechanism is supported. The carbon-14 kinetic isotope effect in a Beckmann rearrangement undertaken to confirm the mechanism will be reported in a succeeding paper.

The Institute of Scientific and Industrial Research
Osaka Universiy
Sakai, Osaka

6) Y. Yukawa and A. Tsukamoto, Abstracts of 8th Annual Meeting, Chemical Society of Japan, 1955, p. 67.

*Sesquiterpenes from Dictyopteris divaricata. I**

By Toshi IRIE, Koji YAMAMOTO and Tadashi MASAMUNE

(Received March 23, 1964)

In 1951, Takaoka and Ando[1] isolated a sesquiterpene alcohol from *Dictyopteris divaricata*, Okamura, and they suggested that it was a new type of cadinol. Recently acquired knowledge about the constitution and stereochemistry of sesquiterpenes[2] has prompted us to re-examine the sesquiterpenes of the brown alga.

The methanol extracts of the air-dried seaweed, *Dictyopteris divaricata*[3] (92 kg.), were concentrated to a small volume in vacuo, and the residual light brown oil was then distilled with steam. The ether extracts of the distillate were washed with 5% aqueous potassium hydroxide and then by 1 N hydrochloric acid.

The neutral essential oil (790 g.)[4] thus obtained was subjected to fractional distillation in vacuo; each fraction was chromatographed on alumina or silica gel, the homogeneity was tested by gas chromatography and thin-layer chromatography, and six components were isolated in a pure state.

Four sesquiterpenes among them were identified as (−)-copaene,[5] (−)-γ_1-cadinene,[6] cadalene and (−)-δ-cadinol[7] by a comparison of their infrared absorption spectra and other physical constants with those the corresponding sesquiterpenes given by Šorm.[8] The alcohol was also shown to be identical with that isolated by Takaoka and Ando.[1]

A new hydrocarbon (b. p. 97°C/5 mmHg, $[\alpha]_D^{23}$ +12.8°) showed an infrared spectrum which was superimposable on that of (−)-β-elemene.[8] The NMR spectrum showed the presence of one quaternary methyl (τ=9.07, s), two methyls attached to the double bond (τ=8.38, ss), one vinyl group (τ=4.45, q; 5.35, d; 5.43, d) and four olefinic protons (τ=5.45~5.65). These data have shown that the hydrocarbon is the optical antipode of (−)-β-elemene. This was further confirmed by a comparison of the retention time on gas chromatography with that of authentic (−)-β-elemene.[9]

The further investigation of another sesquiterpene, a newly isolated secondary alcohol, $C_{15}H_{24}O$, $[\alpha]_D^{23.5}$ −13.6°, is now in progress; details will be presented elsewhere.

* "Terpenoids from Marine Plants," Part I.

1) M. Takaoka and Y. Ando *J. Chem. Soc. Japan, Pure Chem. Sec.* (*Nippon kagaku Zassi*), **72**, 999 (1951).

2) Cf. P. de Mayo, "Mono- and Sesquiterpenoids", Interscience Publ., New York (1959); F. Šorm, "Fortschritte der Chemie Organischer Naturstoffe," XIX, Wien-Springer-Verlag (1961) p. 1; T. G. Halsall and D. W. Theobald, *Quart. Rev.*, **16**, 101 (1962).

3) Collected at Oshoro Bay, Hokkaido.

4) The gas chromatogaphic analysis showed that it consisted of at least thirteen components.

5) G. Büchi and S. H. Feairheller, *Proc. Chem. Soc.*, **1963**, 214; V. K. Kapadia, B. A. Nagasampagi, V. G. Naik and S. Dev, *Tetrahedron Letters*, **1963**, 1933.

6) V. Herout and V. Sykora, *Tetrahedron*, **4**, 246 (1958).

7) W. G. Dauben, B. Weinstein, P. Lim and A. B. Anderson, ibid., **15**, 217 (1961).

8) J. Pliva, M. Herac, V. Herout and F. Šorm, "Die Terpene. Sammlung der Spektren und physikalischen Konstanten," Teil I, Akademie-Verlag, Berlin (1960).

TABLE I. THE FRACTIONAL DISTILLATION OF THE NEUTRAL ESSENTIAL OIL (774 g.)

Fraction	B. p., °C/mmHg	Yield, g.	Principal component*
D-1	65~85/9	0.15	
2	100~105/9	1.47	
3	109~129/9	21.00	crude (−)-copaene
4	89.5~91/5	18.51	two components
5	96~98/5	75.90	crude (+)-β-elemene
6	102~104/5	12.86	two or three components
7	104.5~108/5	26.53	three components
8	108.5~110/5	73.45	two or three components
9	105~109/4.5	42.86	two or three components containing γ_1-cadinene
10	109~110/4.5	33.55	
11	110.5~114/4.5	13.53	
12	114.5/4.5	90.05	two components
13	101~104/4	80.00	five or six components
14	105~106.5/4	27.53	five or six components
15	106.5/4	4.93	
16	residue	ca. 80	

* Checked by gas chromatography on PEG-4000

Experimental

The melting points are uncorrected. Fractional distillation was carried out with a high-efficiency concentric-tube Kyowa fractionator. The gas chromatographic analyses were carried out with a Hitachi gas chromatograph KGL-2 at 200°C, using PEG-4000 and helium gas. The ultraviolet and infrared spectra were measured using a Hitachi ESP-2 spectrophotometer and a Nippon Bunko 401-G spectrophotometer respectively. The NMR measurements were performed with a Nippon Denshi 60 Mc. spectrophotometer, and carbon tetrachloride and tetramethylsilane were used as the solvent and the internal standard respectively.

The Extraction and Fractionation of the Essential Oil.—The air-dried seaweed, *Dictyopteris divaricata*, Okamura (92 kg.), was extracted with methanol at room temperature for two weeks, after which the methanol extracts were concentrated in vacuo. The light brown residual oil then distilled with steam, and the distillate was extracted with ether. After the solvent had been removed from the ethereal extracts, 890 g. of a light yellow essential oil was obtained (yield, 0.97%).

The crude essential oil was dissolved in ether, and the ethereal solution was washed with 5% aqueous potassium hydroxide and then by 1 N hydrochloric acid. The neutral fraction thus obtained amounted to 790 g. (0.86%). Gas chromatography showed that this fraction consisted of at least thirteen components. The neutral fraction was then fractionated in a nitrogen stream under diminished pressure using a high-efficiency (theoretical plates about 80) fractional column. The results are shown in Table I.

(−)-Copaene.—Fraction D-3 was subjected to redistillation in vacuo, and a fraction boiling at 87~87.5°C/3 mmHg was then chromatographed on silica gel. (−)-Copaene, $C_{15}H_{24}$ ($n_D^{21.5}$ 1.4922, $[\alpha]_D^{23}$ −26.1°, IR (liquid film): 3040, 1642, 1320, 1177, 1166, 1156, 1045, 1032, 1010, 930, 879, 824, 777, 740 cm^{-1}) was obtained from the fraction eluted with petroleum ether.

The NMR spectrum showed peaks at 5.20 (1H, singlet), 8.28 (3H, doublet, J=2.4 c.p.s.), 9.02 (3H, singlet), and 9.08 τ (6H, doublet, J=6.6 c.p.s.).

(+)-β-Elemene.—Fraction D-5 was redistilled in vacuo, and a fraction boiling at 97°C/5 mmHg (yield 66.2%) was collected. This was chromatographed on silica gel. A pure hydrocarbon n_D^{22} 1.4920, $[\alpha]_D^{23}$ +12.8°, was obtained.

Found: C, 87.87; H, 11.69. Calcd. for $C_{15}H_{24}$: C, 88.16; H, 11.84%.

The infrared spectrum (liquid film) (3080, 1640, 1003, 907, 885 cm^{-1}) was superimposable on that of (−)-β-elemene.[8] The NMR spectrum showed peaks at 4.45 (1H, quartet, J=9.5, 17.5 c.p.s.), 5.35 (1H, doublet, J=9.5 c.p.s.), 5.43 (1H, doublet, J=17.5 c.p.s.), 5.45~5.65 (4H), 8.38 (6H, singlet), and 9.07 τ (3H, singlet). When the comparison of this hydrocarbon and authentic (−)-β-elemene was carried out by Šorm[9] using gas chromatography, the same retention time was observed.

(−)-γ_1-Cadinene.—Fractions D-9, 10, and 11 were combined and redistilled in vacuo, and a fraction boiling at 108.5~109°C/5 mmHg was identified as (−)-γ_1-cadinene ($[\alpha]_D^{25}$ −19.6°, IR (liquid film): 3070, 1642, 886, 833, 812 cm^{-1}).

Cadalene.—Fraction D-15 was chromatographed on neutral alumina, and the first petroleum ether eluate yielded cadalene, $C_{15}H_{18}$, (picrate, m. p. 111~113°C. UV: λ_{max}^{EtOH} 231 (4.67), 290 (3.72), 325 mμ (log ε 2.75); IR (liquid film): 3070, 1625, 1603, 1517, 828, 806, 777 cm^{-1}; NMR: 2.23 (2H, multiplet), 2.75 (1H, doublet, J=2 c.p.s.), 2.92 (2H, singlet), 6.38 (1H, multiplet), 7.42 (3H, singlet), 7.50 (3H, singlet), 8.64 (3H, doublet, J=5.7 c.p.s.) and 8.66 τ (3H, doublet, J=5.7 c.p.s.).

(−)-δ-Cadinol.—The D-16 residue was distilled in vacuo; the results are shown in Table II.

9) F. Šorm, private communication.

TABLE II. VACUUM DISTILLATION OF THE RESIDUE D-16 (10 ml.)

Fraction	B. p., °C/mmHg	Yield, ml.
D-16-1	123.5~128/3	1.60
2	128~131/3	1.00
3	131.5~132.5/3	0.54
4	130.5/2.5	0.51
5	130.5~133/2.5	0.53
6	139~146.5/1.5	0.52
7	149.5~170/1.5	0.58

Fraction D-16-3, boiling at 131.5~132.5°C/3 mmHg, (417 mg.) was chromatographed on neutral alumina, and from the benzene-ether (3 : 2) eluate, colorless crystals (m. p. 110~130°C) were isolated (71 mg.) ; these were repeatedly recrystallized from methanol to have an m. p. of 137.5~138.5°C and $[\alpha]_D^{27}$ −108°.

Found : C, 81.22 ; H, 11.75. Calcd. for $C_{15}H_{26}O$: C, 81.02 ; H, 11.79%.

The infrared spectra in chloroform, 3590, 1133, 1117, 1101, 947, 873 cm^{-1}, and in Nujol, 3305, 1108, 871 cm^{-1}, were identical with those of (−)-δ-cadinol. NMR : 4.64 (1H, doublet), 8.37 (3H, singlet), 8.77 (3H, singlet), 9.11 (3H, doublet, J=5.5 c.p.s.) and 9.21 τ (3H, doublet, J=5.5 c.p.s.). The cadinol isolated by Takaoka and Ando[1] was found to be identical with this (−)-δ-cadinol on the basis of a mixed melting point determination and the infrared spectra.[10]

A Sesquiterpene Alcohol.—The D-16 residue (25 g.) was chromatographed on neutral alumina, and from the benzene-ether (4 : 1) eluate, a sesquiterpene alcohol (1.73 g.) was obtained, $[\alpha]_D^{23.5}$ −13.6°C.

Found : C, 81.87 ; H, 10.91. Calcd. for $C_{15}H_{24}O$: C, 81.76 ; H, 10.98%.

IR (liquid film) : 3360, 1033, 1015 (OH), 3080, 1643 885 cm^{-1} (>C=CH_2) ; NMR : 4.77 (1H, multiplet), 5.36 (2H, broad singlet), 6.65 (1H, multiplet), 8.27 (3H, singlet), 8.42 (3H, singlet) and 9.29 τ (3H, doublet). The structure elucidation of this alcohol is in progress.

The authors wish to express their thanks to Dr. Yoshiaki Ando, the Institute of Health, Hokkaido, for his helpful suggestions and for providing them with a sample of cadinol, and to Professor F. Šorm, the Czeckoslovak Academy of Science, for his kind advice. They are also indebted to Mr. Shigezo Shimokawa for his NMR measurements and to Miss Akiko Maeda for her microanalyses.

Department of Chemistry
Faculty of Science
Hokkaido University
Sapporo

10) Cf. Footnote 6 and B. Weinstein, *Experientia*, in press.

The Ultraviolet Absorption Spectra of Nitramide and Ethyl Nitrate

By Koji KAYA, Keiji KUWATA and Saburo NAGAKURA

(Received March 24, 1964)

The electronic absorption spectra of various molecules which contain both electron donating and accepting groups have been studied by several workers from both experimental and theoretical points of view.[1-9] Consequently, it has been found that these molecules exhibit absorption bands characteristic of the interaction between electron donor and acceptor. The absorption bands of this kind have been called intramolecular charge-transfer bands from an analogy with Mulliken's nomenclature[10] for the intermolecular case.

In the present paper, the study of the intramolecular charge-transfer band was extended to nitramide and ethyl nitrate, in which the nitro group as an electron acceptor and the amino or ethoxyl group as an electron donor are connected directly with each other. Our principal purposes are to discover intramolecular charge-transfer bands for these two systems, and to obtain quantitative knowledge about the interaction between the nitro group and the amino or ethoxyl group by combining the experimental data of the absorption spectra

1) S. Nagakura and J. Tanaka, *J. Chem. Phys.*, **22** 236 (1954); S. Nagakura, ibid., **23** 1441 (1955); J. Tanaka, S. Nagakura and M. Kobayashi, ibid., **24**, 311 (1956).
2) J. Tanaka, This Bulletin, **36**, 833 (1963).
3) S. Nagakura, *Mol. Phys.*, **3**, 105 (1960); S. Nagakura, K. Kaya and H. Tsubomura, *J. Mol. Spectroscopy*, **13**, 1 (1964).
4) H. Hosoya, J. Tanaka and S. Nagakura, This Bulletin, **33**, 850 (1960)
5) S. Nagakura, *Pure and Applied Chem.*, **7**, 79 (1963).
6) H. C. Longuet-Higgins and J. N. Murrell, *Proc. Phys. Soc.*, **A68**, 601 (1955).
7) J. N. Murrell, ibid., **A68**, 969 (1955).
8) J. N. Murrell, *Tetrahedron*, **19**, Suppl. 2, 277 (1963).
9) J. E. Bloor, *Canad. J. Chem.*, **39**, 2256 (1961)
10) R. S. Mulliken, *J. Phys. Chem.*, **56**, 801 (1952).

with the theoretical results based on the molecular orbital calculations.

Experimental

Materials.—Ethyl nitrate was synthesized from ethanol and nitric acid.[11] It was purified by distillation and stored in a desiccator at low temperature.

Nitramide was synthesized by the decomposition of nitrourethane and was purified by recrystallization from petroleum ether.[12] It was stored in a desiccator with potassium hydroxide under reduced pressure and at low temperature.

Measurement.—The ultraviolet absorption measurements down to 1900 Å were made with a Cary recording spectrophotometer, model 14 M, quartz cells 0.1 and 1 cm. long being used.

A vacuum ultraviolet spectrophotometer constructed in our laboratory[13] was used for the measurements in the vacuum ultraviolet region. In this case, a quartz cell 0.01 cm. thick was used for the measurements of solutions, and gas cells 0.7 cm. and 3 cm. long and equipped with lithium fluoride windows were used for the measurements in the gaseous state.

The absorption spectra of nitramide and ethyl nitrate was measured in various solvents. We succeeded in measuring the absorption spectrum in the gaseous state for ethyl nitrate, but we could not do so for nitramide because of its explosive character at high temperatures. The observed absorption spectra are shown in Figs. 1 and 2. The peak wavelengths, molar extinction coefficients and oscillator strengths are tabulated in Table I.

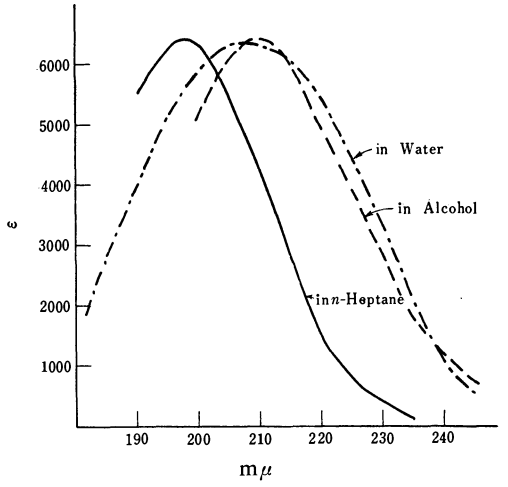


Fig. 1. The ultraviolet absorption spectra of nitramide.

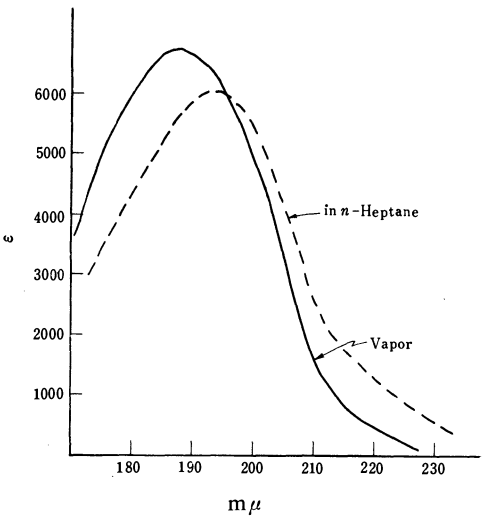


Fig. 2. The ultraviolet absorption spectra of ethyl nitrate.

TABLE I. THE OBSERVED PEAK WAVELENGTHS AND MOLAR EXTINCTION COEFFICIENTS FOR NITRAMIDE AND ETHYL NITRATE

Sample	Solvent	λ_{max}(mμ)	ε_{max}
Nitramide	Water	207~208	6300
	Alcohol	209	6400
	n-Heptane	198	—
Ethyl nitrate	*n*-Heptane	193	5800
	Gas	190	6800

Theoretical

The π-electron energy levels and the wave functions of nitramide and ethyl nitrate were calculated by taking into account the configurational interaction among several electron configurations. That is to say, each of the two molecules was separated into the two components, the electron donor (NH_2 or C_2H_5O) and the electron acceptor (NO_2). The interaction between them was considered by means of the configurational interaction among π-electron configurations which have been constructed by putting the six π-electrons into the appropriate orbitals of the components. The electron configurations actually taken up in the present calculation are shown in Fig. 3. In addition to the ground configuration, G, a charge-transfer configuration, CT, which is caused by an electron transfer from the electron donor toward the electron acceptor, three locally excited configurations, LE_1, LE_2, LE_3, and one doubly excited configuration, D, were considered. A characteristic point in the present calculation is that we took the locally excited configuration LE_3, corresponding to the transition within the electron donating group,

11) L. Gattermann and H. Wieland, "Laboratory Method of Organic Chemistry," MacMillan and Co., Ltd., London (1952), p. 148.
12) C. A. Marlies, V. K. La Mer and J. Greenspan, "Inorg. Synth," Vol. 1, McGrow-Hill Book Co. Inc., New York (1939), p. 68.
13) H. Tsubomura, K. Kimura, K. Kaya, J. Tanaka and S. Nagakura, This Bulletin, 37, 818 (1964).

and the D configuration corresponding to a two electron excitation.

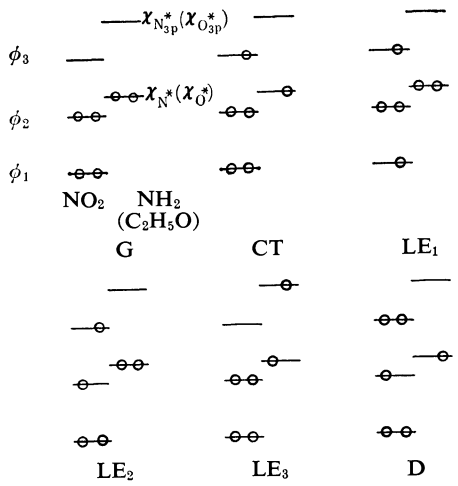


Fig. 3. The electron configurations of nitramide and ethyl nitrate.

The geometrical structure of nitramide was studied by Beevers and Trotman-Dickenson[14] with the X-ray crystal analysis technique and by Tyler[15] with the microwave spectrum analysis technique. The bond lengths and bond angles determined by the latter, which are shown in Fig. 4, were used in the present calculations. There has been no investigation of the structure of ethyl nitrate, so we assumed the structure of ethyl nitrate from the electron diffraction data of methyl nitrate by Pauling and Brockway[16] and from the X-ray crystal analysis data of pentaerythritol tetranitrate by Booth and Llewellyn.[17] The bond lengths and bond angles of ethyl nitrate used in the present calculation are also shown in Fig. 4.

The above-mentioned structure of ethyl

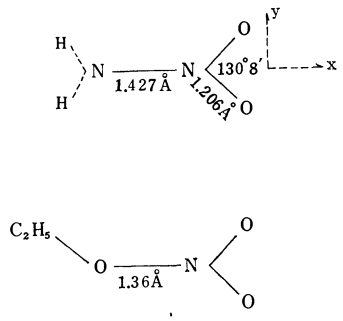


Fig. 4. The geometrical structures of nitramide and ethyl nitrate.

nitrate shows that the lone-pair electron orbital on the oxygen atom of the ethoxyl group is pure 2p. The situation is the same for planar nitramide. According to the study by Tyler, however, the two hydrogen atoms of the amino group of gaseous nitramide are out of the $N-NO_2$ plane by 51°47′. In this case, the lone-pair electron orbital of the nitrogen atom on the amino group can be represented by the hybridization of 2p and 2s orbitals.

In the present study, we first calculated the π-electron structures for the planar ethyl nitrate and nitramide molecules, and then we considered the effect of the distortion from the planarity for nitramide.

The energy of the ground configuration was taken as the standard. The energy of the charge-transfer configuration (H_{CT}) was calculated by the following equation:

$$H_{CT}=I_D-A_{NO2}+E(D^+-A^-) \qquad (1)$$

Here, I_D is the ionization potential of the electron donating group (NH_2 or C_2H_5O); it was determined to be 10.25 and 10.44 eV. for the amino and ethoxyl groups respectively, from the ionization potentials of ammonia and ethanol obtained by Watanabe.[18] A_{NO2} is the electron affinity of the electron accepting group (NO_2); it was assumed to be +0.40 eV, the value taken for a series of nitro compounds.[19,20] $E(D^+-A^-)$ is the electrostatic interaction energy between the electron donor and the acceptor after electron migration and can be represented by the following equations:

$$\left.\begin{aligned} &E(NH_2^+-NO_2^-)=0.4912(N^*N^* \mid NN) \\ &\quad -1.4912\ (N^*N^* \mid OO) \text{ for nitramide} \\ &E(C_2H_5O^+-NO_2^-)=0.4912(O^*O^* \mid NN) \\ &\quad -1.4912\ (O^*O^* \mid OO) \text{ for ethyl nitrate} \end{aligned}\right\} \qquad (2)$$

where $(\mu\mu \mid \nu\nu)$ indicates the two center Colomb repulsion integral between the $2p\pi$ atomic orbitals on the μ and ν atoms, and where N* is the nitrogen atom of the NH_2 group, O* is the oxygen atom of the C_2H_5O group, and N and O indicate the nitrogen and oxygen atoms of the NO_2 group respectively.

Two center Coulomb repulsion integrals were evaluated by Pariser and Parr's method.[21] The evaluation of these integrals needed valence state ionization potentials and electron affinities, so they were taken from the tables of Pritchard and Skinner[22] and of Moore[23].

14) C. A. Beevers and A. F. Trotman-Dickenson, *Acta Cryst.*, **10**, 34 (1957).
15) J. K. Tyler, *J. Mol. Spectr.*, **11**, 39 (1963).
16) L. Pauling and L. O. Brockway, *J. Am. Chem. Soc.*, **59**, 13 (1937).
17) N. D. Booth and F. J. Llewellyn, *J. Chem. Soc.*, **1947**, 837.
18) K. Watanabe, *J. Chem. Phys.*, **22**, 1564 (1954).
19) S. Nagakura, *Mol. Phys.*, **3**, 152 (1960).
20) S. Nagakura, M. Kojima and Y. Maruyama, *J. Mol. Spectroscopy*, in press.
21) R. Pariser and R. G. Parr, *J. Chem. Phys.*, **21**, 466, 767 (1953).
22) H. O. Pritchard and H. A. Skinner, *Chem. Revs.*, **55**, 745 (1955).
23) C. E. Moore, "Atomic Energy Levels" Vol. I, National Bureau of Standards (1949).

TABLE II. THE ENERGIES AND WAVE FUNCTIONS OF THE CONFIGURATIONS

Energy	Wave function[a]
$H_G=0$ eV.	$\varphi_G=(1\bar{1}2\bar{2}N^*\bar{N}^*)$
$H_{CT}=4.96$ eV. (NH_2NO_2) 5.13 eV. ($EtONO_2$)	$\varphi_{CT}=1/\sqrt{2}\{(1\bar{1}2\bar{2}N^*\bar{3})+(1\bar{1}2\bar{2}3\bar{N}^*)\}$
$H_{LE_1}=6.26$ eV.	$\varphi_{LE_1}=1/\sqrt{2}\{(1\bar{1}2\bar{3}\bar{N}^*N^*)+(1\bar{1}32N^*\bar{N}^*)\}$
$H_{LE_2}=11.15$ eV.	$\varphi_{LE_2}=1/\sqrt{2}\{(1\bar{3}2\bar{2}N^*\bar{N}^*)+(3\bar{1}2\bar{2}N^*\bar{N}^*)\}$
$H_{LE_3}=8.18$ eV. (NH_2NO_2) 10.99 eV. ($EtONO_2$)	$\varphi_{LE_3}=1/\sqrt{2}\{(1\bar{1}2\bar{2}N^*\bar{N}^*_{3p})+(1\bar{1}22N^*_{3p}N^*)\}$
$H_D=9.43$ eV.	$\varphi_D=1/\sqrt{2}\{(1\bar{1}233\bar{N}^*)+(1\bar{1}3\bar{2}N^*\bar{3})\}$

a) The exact formula for $(1\bar{1}2\bar{2}N^*\bar{N}^*)$ as an example is as follows;
$(\bar{1}12\bar{2}N^*N^*)=1/\sqrt{6!}\sum(-1)^p p\begin{Bmatrix}\phi_1(1)\phi_1(2)\phi_2(3)\phi_2(4)\chi_N^*(5)\phi_N^*(6)\\ \alpha(1)\beta(2)\alpha(3)\beta(4)\alpha(5)\beta(6)\end{Bmatrix}$ [b,c]

b) ϕ_1, ϕ_2 and ϕ_3 are the SCF molecular orbitals of the nitro group calculated by Tanaka *(J. Chem. Soc. Japan, Pure Chem. Sec. (Nippon Kagaku Zasshi)*, **78**, 1643(1957)) and are represented as below;
$\phi_1=0.7133\,\chi_N+0.7009/\sqrt{2}\,(\chi_O+\chi_{O'})$
$\phi_2=1/\sqrt{2}\,(\chi_O-\chi_{O'})$
$\phi_3=0.7009\,\chi_N-0.7133/\sqrt{2}\,(\chi_O+\chi_{O'})$
Here, χ_N and χ_O ($\chi_{O'}$,) indicate the $2p\pi$ atomic orbitals of the nitrogen and the two oxygen atoms of the nitro group.

c) χ_N^* and $\chi_N^*{}_{3p}$ are the $2p\pi$ and the $3p\pi$ atomic orbitals of the nitrogen atom of the amino group in the case of nitramide. In the case of ethyl nitrate, N^* and $N^*{}_{3p}$ must be changed into χ_O^* and $\chi_O^*{}_{3p}$ which represent the $2p\pi$ and the $3p\pi$ atomic orbitals of the oxygen atom of the ethoxyl group.

TABLE III. THE OFF-DIAGONAL ELEMENTS USED IN THE PRESENT CALCULATION

$H_{G\cdot CT}=0.9912\ \beta_{NN}^*(\beta_{NO}^*)$ $\quad H_{CT\cdot LE_1}=-0.7133\ \beta_{NN}^*(\beta_{NO}^*)$
$H_{CT\cdot LE_3}=0.7009\ \beta_{NN}^*{}_{3p}\ (\beta_{NO}^*{}_{3p})$ $\quad H_{LE_2\cdot D}=0.7133\ \beta_{NN}^*(\beta_{NO}^*)$
$H_{G\cdot LE_1}=H_{G\cdot LE_3}=H_{CT\cdot LE_2}=H_{LE_1\cdot LE_3}=0$

$\beta_{NN}^*=\int\chi_N H_{core}\chi_N^*d\tau=-2.14$ eV. $\quad \beta_{NO}^*=\int\chi_N H_{core}\chi_O^*d\tau=-2.18$ eV.

$\beta_{NN}^*{}_{3p}=\int\chi_N H_{core}\chi_N^*{}_{3p}d\tau=-2.52$ eV. $\quad \beta_{NO}^*{}_{3p}=\int\chi_N H_{core}\chi_O^*{}_{3p}d\tau=-2.49$ eV.

As has been mentioned above, we considered three locally excited configurations, LE_1, LE_2, LE_3. Among these, LE_1 and LE_2 are caused by local excitation within the nitro group. The energy of the LE_2 configuration, H_{LE2}, is lower than that of the LE_1 configuration. H_{LE2} was taken to be 6.26 eV. from the position of the observed $\pi\rightarrow\pi^*$ transition band of nitromethane.[19] Concerning the energy of the locally excited configuration LE_1, the corresponding value has never been observed; therefore, it was calculated by the following equation:

$$H_{LE1}=-2\sqrt{2}\,\beta_{NO}+K_{13} \qquad (3)$$

where β_{NO} is the core resonance integral between the $2p\pi$ atomic orbitals of the nitrogen and oxygen atoms of the nitro group and K_{13} represents the exchange repulsion integral between the lowest (ϕ_1) and the highest (ϕ_3) π molecular orbitals of the nitro group, the actual forms of which are shown in Table II. The value of β_{NO} was calculated by the following approximate equation:[24]

$$\beta_{\mu\nu}=\frac{(I_\mu+I_\nu)S_{\mu\nu}\beta_{CC}}{2(I_C S_{CC})} \qquad (4)$$

Here, I_μ I_ν and I_C are the ionization potentials of the μ atom, the ν atom and the carbon atom of benzene respectively. $S_{\mu\nu}$ and S_{C-C} are the overlap integrals between $2p\pi$ atomic orbitals of the μ and ν atoms[25] and between the $2p\pi$ atomic orbitals of the neighboring carbon atoms of benzene respectively. By the use of the above equation, β_{NO} was evaluated to be -3.25 eV. The K_{13} value was resolved into two center Coulomb integrals and found to be 1.96 eV. Therefore, the value of H_{LE} was determined to be 11.15 eV.

The energy of the LE_3 configuration corresponding to the $2p\rightarrow3p$ transition within the

24) R. S. Mulliken, *J. Phys. Chem.*, **56**, 295 (1952).
25) R. S. Mulliken, C. A. Rieke, D. Orloff and H. Orloff *J. Chem. Phys.*, **17**, 210 (1949).

TABLE IV. THE WAVE FUNCTIONS FINALLY OBTAINED WITH NITRAMIDE AND ETHYL NITRATE

Nitramide (planar)

Energy, eV.	Wave function
$W_0=-0.85$	$\phi_0=0.9244\,\varphi_G+0.3714\,\varphi_{CT}-0.0472\,\varphi_{LE_1}+0.0725\,\varphi_{LE_3}$
$W_1=4.67$	$\phi_1=-0.3684\,\varphi_G+0.8128\,\varphi_{CT}-0.1912\,\varphi_{LE_2}+0.4088\varphi_{LE_3}$
$W_2=5.65$	$\phi_2=0.9280\,\varphi_{LE2}+0.3726\,\varphi_D$
$W_3=8.88$	$\phi_3=0.0851\,\varphi_G-0.3571\,\varphi_{CT}+0.2398\,\varphi_{LE_1}+0.8988\,\varphi_{LE_3}$
$W_4=10.04$	$\phi_4=-0.3726\,\varphi_{LE_2}+0.9280\,\varphi_D$
$W_5=11.59$	$\phi_5=-0.0497\,\varphi_G+0.2720\,\varphi_{CT}+0.9506\,\varphi_{LE_1}-0.1409\,\varphi_{LE_3}$

Nitramide (non-planar)

Energy, eV.	Wave function
$W_0=-0.63$	$\phi_0=0.9433\,\varphi_G+0.3250\,\varphi_{CT}-0.0364\,\varphi_{LE_1}+0.0564\,\varphi_{LE_3}$
$W_1=4.83$	$\phi_1=-0.3125\,\varphi_G+0.8462\,\varphi_{CT}-0.1769\,\varphi_{LE_1}+0.3864\,\varphi_{LE_3}$
$W_2=5.80$	$\phi_2=0.9546\,\varphi_{LE_2}+0.2979\,\varphi_D$
$W_3=8.76$	$\phi_3=0.0732\,\varphi_G-0.3492\,\varphi_{CT}+0.1933\,\varphi_{LE_1}+0.9140\,\varphi_{LE_3}$
$W_4=9.96$	$\phi_4=-0.2979\,\varphi_{LE_2}+0.9546\,\varphi_D$
$W_5=11.48$	$\phi_5=-0.0380\,\varphi_G+0.2375\,\varphi_{CT}+0.9644\,\varphi_{LE_1}-0.1102\,\varphi_{LE_3}$

Ethyl nitrate

Energy, eV.	Wave function
$W_0=-0.85$	$\phi_0=0.9287\,\varphi_G+0.3639\,\varphi_{CT}-0.0472\,\varphi_{LE_1}+0.0537\,\varphi_{LE_3}$
$W_1=5.12$	$\phi_1=-0.3656\,\varphi_G+0.8661\,\varphi_{CT}-0.2233\,\varphi_{LE_1}+0.2576\,\varphi_{LE_3}$
$W_2=5.64$	$\phi_2=0.9273\,\varphi_{LE_2}+0.3744\,\varphi_D$
$W_3=10.04$	$\phi_3=-0.3744\,\varphi_{LE_2}+0.9273\,\varphi_D$
$W_4=11.07$	$\phi_4=0.0067\,\varphi_G-0.0343\,\varphi_{CT}+0.6900\,\varphi_{LE_1}+0.7229\,\varphi_{LE_3}$
$W_5=11.92$	$\phi_5=-0.0618\,\varphi_G+0.3410\,\varphi_{CT}+0.6869\,\varphi_{LE_1}-0.6388\,\varphi_{LE_3}$

TABLE V. THE OBSERVED AND CALCULATED TRANSITION ENERGIES AND OSCILLATOR STRENGTHS

	Transition	Transition energy, eV.			Oscillator strength	
		Obs.		Cald.	Obs.	Cald.
Nitramide	W_0-W_1	5.94	6.26	5.52	0.233	0.11
	W_0-W_2			6.50		0.61
Ethyl nitrate	W_0-W_1	6.43	6.52	5.97	0.233	0.15
	W_0-W_2			6.49		0.59

electron-donating group was determined to be 8.18 eV. and 10.99 eV. for the NH_2 and C_2H_5O groups, respectively. The former value was obtained by adding the energy difference between the 3s and 3p orbitals[23] to the observed Rydberg transition energy of ammonia.[26] The latter value was assumed to be equal to the difference between the 2p and 3p orbitals of the oxygen atom taken form Moore's table.[23] The energy of the doubly excited configuration D was evaluated by the following equation:

$$H_D=H_{LE_1}+I_D-A_{NO_2}{}^*+E^*(D^+-A^-)$$
$$=9.430\,\text{eV. for } NH_2NO_2$$
$$=9.426\,\text{eV. for } EtONO_2 \qquad (5)$$

Here $A_{NO_2}{}^*$ is the electron affinity for bringing an additional electron into the ϕ_3 orbital of the nitro group in the locally excited state LE_2; it was assumed to be 1.03 eV.[27] $E^*(D^+-A^-)$ is the electrostatic interaction energy between the electon donating and accepting groups in the D configuration and was evaluated by the use of the above-mentioned two center Coulomb integrals of the $(\mu\mu\,|\,\nu\nu)$ type. The energies and the wave functions of the configurations used in the present calculations are tabulated in Table II.

The off-diagonal matrix elements of the total electronic Hamiltonian which represent the magnitudes of the interaction between different configurations were evaluated according to the formulations by Pople[28] and by Longuet-Higgins and Murrell.[6] They are given in Table III in terms of the core resonance integrals $\beta_{NO}{}^*$, $\beta_{NN}{}^*$, $\beta_{NO_3p}{}^*$ and $\beta_{NN3p}{}^*$. The definitions and values of these

26) A. B. F. Duncan, *Phys. Rev.*, **50**, 700 (1936).

27) According to the exact calculations, the energy difference between A^*_{NO2} and A_{NO2} can be written as follows:

$$A^*_{NO2}-A_{NO2}=J_{23}+K_{23}-J_{33}=+0.63\,\text{eV}. \qquad (6)$$

Here, J_{ij} and K_{ij} represent, respectively, the Coulomb and exchange repulsion integrals between the ϕi and ϕj molecular orbitals of the nitro group.

28) J. A. Pople, *Trans. Faraday Soc.*, **49**, 1375 (1953).

core resonance integrals evaluated by Eq. 4 are also shown in Table III.

Using these diagonal and off-diagonal matrix elements, we set up the secular equations of the fourth and second orders for the symmetric and antisymmetric configurations respectively. Solving these equations by an electronic computer, a Facom 202 in our Institute, we obtained the π-electron energy levels and the wave functions for planar nitramide and ethyl nitrate. The energy levels and wave functions are shown in Figs. 5 and 6 and in Table IV. From these results, the transition

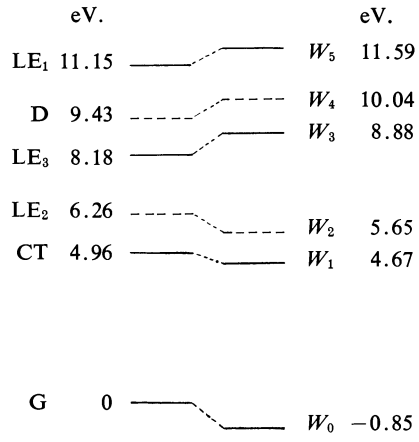


Fig. 5. The π-electron energy levels of nitramide.

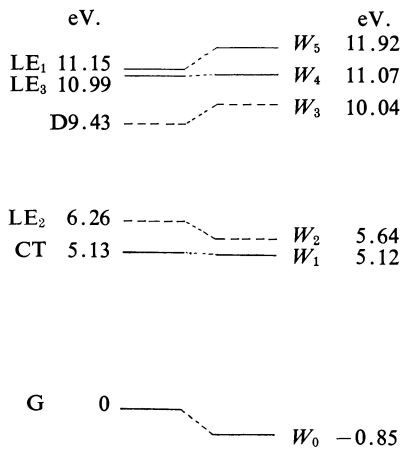


Fig. 6. The π-electron energy levels of ethyl nitrate.

energies and oscillator strengths were calculated for the longest two $\pi \rightarrow \pi^*$ transition bands of nitramide and of ethyl nitrate. The results are shown in Table V, together with the observed results.

As may be seen in the paper by Tyler,[15] there is some doubt concerning the planar structure of nitramide. Therefore, it seems to be necessary to consider the effect of the distortion from planarity on the absorption spectrum of nitramide.

From one 2s and three 2p atomic orbitals of the nitrogen atom of the amino group, four hybridized orbitals, which are independent and orthonormal from each other, are constructed; two of them are directed towards the two hydrogen atoms of the amino group, and the third one, towards the nitrogen atom of the nitro group. The last one constitutes the lone pair electron orbital of the amino group. If we take the coordinate of the molecule as shown in Fig. 4, the geometrical structure of nitramide determined by Tyler leads to the conclusion that the principal axis of the lone pair orbital is on the xz plane and makes an angle of 14°35′ from the z axis.

Since this angle is rather small and therefore, the lone pair electron orbital has an overwhelmingly large contribution from the π-electron orbital,[29] the effect of distortion from the planarity of the molecule on the calculated energy levels and wave functions may be thought to be small. This is shown to be true by the actual calculations. The theoretical result calculated by considering the changes of the core resonance integral β_{NN}^* and of the two center Coulomb integrals due to the distortion from the planarity is very similar to that for the planar molecule, as is seen in Table IV. Therefore, we will hereafter consider only the case of planar nitramide.

Results and Discussion

As is easily seen in Figs. 1 and 2, both nitramide and ethyl nitrate show rather broad bands near 200 mμ. The peak wave lengths and the molar extinction coefficients obtained by us are summarized in Table I. The ultraviolet spectrum of nitramide was first measured by Jones.[30] According to his results, nitramide has its absorption maximum at 225 mμ in an aqueous solution. This result is obviously different from our result, which shows the absorption maximum near 200 mμ. Our sample was identified by the aid of the infrared absorption measurements and of the elementary analysis of nitrogen. Therefore, Jones' finding on the ultraviolet absorption spectrum of nitramide may conceivably be erroneous.

According to the theoretical results shown

29) The lone pair orbital of the amino group ϕ_N^* can be written as follows:

$$\phi_N^* = 0.4448\ \chi_{2s} + 0.8668\ \chi_{2pz} + 0.2255\ \chi_{2px}$$

where χ_{2s}, χ_{2qz} and χ_{2px} represent the 2s, $2p_z$ and $2p_x$ atomic orbital wave functions on the nitrogen atom of the amino group.

30) R. Jones, *Canad. J. Reaserch*, **B27**, 828 (1949).

in Table V, the first $\pi \rightarrow \pi^*$ band corresponding to the $W_0 \rightarrow W_1$ transition should appear at 225 and 208 mμ for nitramide and ethyl nitrate respectively, with the oscillator strength value of 0.14 and 0.15. As will be mentioned below, however, another strong band corresponding to the $W_0 \rightarrow W_2$ transition may be expected to appear near 200 mμ for either of these two molecules. Therefore, it seems reasonable to consider that the $W_0 \rightarrow W_1$ transition band may be covered by the $W_0 \rightarrow W_2$ transition band. This expectation seems to be supported by the broadness of the observed bands. As may easily be seen by comparing the wave function of the first excited state with that of the ground state, the first $\pi \rightarrow \pi^*$ band may be regarded as an intramolecular charge-transfer band caused by interaction between the electron donating group (NH_2 or OC_2H_5) and the electron accepting group (NO_2).

The present calculation shows that near 200 mμ there should exist the $W_0 \rightarrow W_2$ transition bands, which have the character of local excitation within the nitro group. Their calculated oscillator strengths are 0.61 and 0.59 for nitramide and ethyl nitrate respectively. Therefore, the observed broad bands of nitramide and ethyl nitrate can be interpreted as the superposition of the two bands corresponding to the $W_0 \rightarrow W_1$ and $W_0 \rightarrow W_2$ transitions. Of course, the $W_0 \rightarrow W_2$ transition band makes the main contribution to the observed band, since the calculated oscillator strength value of this band is about five times larger than that of the $W_0 \rightarrow W_1$ transition band.

By looking at the findings on the energy value, W_0, of the ground state given in Table IV, it may be seen that the ground state is lower by 0.85 eV. = 19.5 kcal./mol. for both nitramide and ethyl nitrate than the unperturbed ground configuration. These stabilization energies, which are mainly brought about by interaction between the ground and charge-transfer configurations, may be regarded as corresponding to the vertical resonance energy due to the resonance hybrid between the following two structures for each molecule:

$$H_2N\text{–}NO_2 \leftrightarrow H_2N^+\text{=}NO_2^-$$

$$H_5C_2O\text{–}NO_2 \leftrightarrow H_5C_2O^+\text{=}NO_2^-$$

The Institute for Solid State Physics
The University of Tokyo
Azabu, Tokyo (K. Kaya and S. N.)

Department of Chemistry
Faculty of Science
Osaka University
Nakanoshima, Osaka (K. Kuwata)

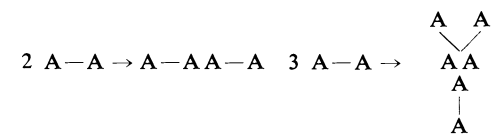
A Theory of Gel Formation with a Multifunctional Interunit Junction

By Tokio YAMABE and Kenichi FUKUI

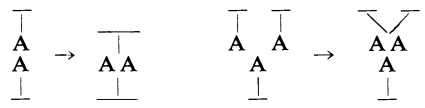
(Received March 10, 1964)

The ways in which high polymer substances are formed from monomeric units or by the crosslinking of polymer chains may be classified according to the number of functional groups involved in the formation of an interunit junction. Each case may be referred to as polymerization by a bi-, a ter-, a quadri-, a ···, or a multifunctional interunit junction. A schematic representation follows:

Polymerization:



Crosslinking:



bifunctional interunit junction

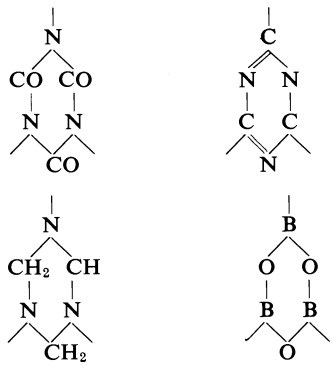
terfunctional interunit junction

In the polymerization by a bifunctional interunit junction, the theory of molecular size distribution and gel formation has been studied by Flory,[1] Stockmayer[2] and many other

1) P. J. Flory, "Principles of Polymer Chemisty," Cornell University Press, Ithaca, New York (1953), Chaps. 8 and 9.

2) W. H. Stockmayer, *J. Chem. Phys.*, **11**, 45 (1943); **12**, 125 (1944).

researchers.[3] The theory of gel formation with a terfunctional interunit junction has been developed by the present authors[4] for the case in which any monomer possesses equivalent f functional groups. Recently such a type of polycondensation by a terfunctional interunit junction has come to our attention as we attempted to prepare thermosetting resins. For example:



where the interunit junctions are the isocyanuric ring, the *s*-trizine ring, the hexahydro-*s*-triazine ring, and the boroxin ring respectively. These interunit junctions are applicable to the crosslinking of polymer chains, as was realized in the crosslinking of polyacrylonitrile[5] or of polyacrylhydroxanic acid.[6] In the present paper, the theory is extended to a more general case than those previously considered, namely, the case of the formation of a multifunctional interunit junction (say, j functional: $j=2, 3, 4, \cdots$) not only in the polycondensations of a monomer with f equivalent functional groups ($f \geqq 2$), but also in the cross linking of a system of chains with an arbitrary initial size distribution. Of course, the $j=2$ case is equivalent to that of the bifunctional interunit junction, while $j=3$ is equivalent to that of a terfunctional interunit junction. Here the methods developed by Stockmayer are employed to derive the distribution of molecular sizes up to the gel point, and as was done in his papers, we also neglect the formation of macrorings, namely, rings which contain two or more endocyclic interunit junctions, for the first approximation.

f-Functional Monomer

In this part, each monomer possesses f equivalent functional groups, and those monomers are combined as polymer by a j-functional interunit junction, where j is the number of functional groups composing an interunit junction. If ν is the number of interunit junctions in an n-mer, and if the symbol ${}_jM_\nu^{(f)}$, is used for the number of n-mers ($n=(j-1)\nu+1$), the total number of units, N, and the total number of molecules, M, can be expressed as follows:

$$\sum_{\nu \geqq 0}((j-1)\nu+1)\,{}_jM_\nu^{(f)}=N \tag{1}$$

$$\sum_{\nu \geqq 0}{}_jM_\nu^{(f)}=M \tag{2}$$

Therefore, the most probable molecular size distribution may be written as:

$${}_jM_\nu^{(f)}=A\frac{{}_jW_\nu^{(f)}}{N!}B^n \tag{3}$$

where ${}_jW_\nu^{(f)}$ is the number of different ways in which a polymeric molecules can be formed from n monomeric units (therefore, with ν interunit junctions) and is equal to:

$${}_jW_\nu^{(f)}=\frac{f^{(j-1)\nu+1}((f-1)(j-1)\nu+f-1)!\,((j-1)\nu)!}{\nu!\,((fi-f-j)\nu+f)!\,\{(j-1)!\}^\nu} \tag{4}$$

A and B are Lagrangian multipliers to be determined from Eqs. 1 and 2. Those summations can easily be evaluated by introducing Eq. 3 into Eqs. 1 and 2; the results are:

$$N=\frac{AB}{(1-\alpha)^f} \tag{5}$$

$$M=B\left(1-\frac{j-1}{j}f\alpha\right) \tag{6}$$

where

$$\frac{(fB)^{j-1}}{(j-1)!}=\alpha(1-\alpha)^{(f-1)(j-1)-1} \tag{7}$$

The molecular size distribution may then be rewritten:

$${}_jM_\nu^{(f)}=f\cdot N\times\frac{((f-1)(j-1)\nu+f-1)!\,((j-1)\nu)!}{\nu!\,((j-1)\nu+1)!\,((f-1)\nu-\nu+f)!}\times\alpha^\nu(1-\alpha)^{(f-1)(j-1)\nu-\nu+f} \tag{8}$$

The fraction of reacted functional groups is obtained from Eqs. 5 and 6:

$$p=\frac{\sum_{\nu \geqq 0}j\nu\,{}_jM_\nu^{(f)}}{fN}=\frac{j(N-M)}{(j-1)N}=\alpha \tag{9}$$

which means that α is equal to the fraction of reacted functional groups. The number and weight-average molecular size can easily be calculated from Eq. 6 and by direct summation:

3) M. Gordon *J. Chem. Phys.*, **22**, 610 (1954); F. E. Harris, ibid., **23**, 1518 (1955); L. C. Case, *J. Polymer Soc.*, **26**, 333 (1957).
4) K. Fukui and T. Yamabe, *J. Polymer Sci.*, **45**, 305 (1960).
5) K. Takemoto, *Chemistry (Kagaku)*, **17**, 124 (1962).
6) W. Kern and R. C. Schulz, *Angew. Chem.*, **69**, 153 (1957).

$$\langle W\rangle_{\mathrm{av.}}=\frac{\sum_{\nu\geqq 0}(j-1)\nu+1)^2{}_jM_\nu^{(f)}}{\sum_{\nu\geqq 0}((j-1)\nu+1){}_jM_\nu^{(f)}}$$

$$=\frac{1+(j-1)\alpha}{1-(f-1)(j-1)\alpha} \tag{10}$$

$$\langle N\rangle_{\mathrm{av.}}=\frac{\sum_{\nu\geqq 0}((j-1)\nu+1){}_jM_\nu^{(f)}}{\sum_{\nu\geqq 0}{}_jM_\nu^{(f)}}$$

$$=\frac{N}{M}=\frac{1}{1-(j-1)f\alpha/j} \tag{11}$$

Therefore, the gel point is characterized by the following equation:

$$\alpha_{\mathrm{gel}}=\frac{1}{(f-1)(j-1)} \tag{12}$$

For the special case of $j=2$, Eqs. 10 and 11 become:

$$\langle n\rangle_{\mathrm{av.}}=\frac{1}{1-f\alpha/2},\qquad \langle w\rangle_{\mathrm{av.}}=\frac{1+\alpha}{1-(f-1)\alpha}$$

which agree with Stockmayer's results,[2] For yet another case, $j=3$, these equations are:

$$\langle n\rangle_{\mathrm{av.}}=\frac{1}{1-2f\alpha/3},\quad \langle w\rangle_{\mathrm{av.}}=\frac{1+2\alpha}{1-2(f-1)\alpha}$$

which are in accord with our previous results.[4]

The Crosslinking of Polymer Chains

In this section, the theory of the crosslinking of polymer chains by a j function interunit junction will be treated. For the sake of simplicity, the treatment is restricted to cases in which all units in the chains carry a functional group, all of which are assumed to be equivalent and of the same reactivity. Let the system contain N_1 monomeric chains, N_2 dimeric chains,$\cdots$, N_s s-meric chains,$\cdots$, etc. The number-average size of the chain that initially exist is thus:

$$\lambda_n=\frac{\sum_s sN_s}{\sum_s N_s}=\frac{1}{\sum_s W_s/s} \tag{13}$$

and the weight-average size is:

$$\lambda_w=\frac{\sum_s s^2N_s}{\sum_s sN_s}=\sum_s sW_s \tag{14}$$

where W_s, the weight fraction of s-meric chains, is given by:

$$W_s=\frac{sN_s}{\sum_s sN_s} \tag{15}$$

and where, therefore,

$$\sum_s W_s=1 \tag{16}$$

The description of any crosslinked molecules requires the specification of the number of chains of each size which it coniains. We denote by n_1, n_2, n_3,$\cdots$, n_s, etc., these numbers of chains and represent any particular set of these numbers by the symbol $\{n_s\}$. The symbole $m\{n_s\}$ will be used for the number of molecules described by a particular set $\{n_s\}$ (which is joined with ν j-functional interunit juctions). The most probable molecular size distribution is, therefore, written as:

$$m\{n_s\}=A\cdot{}_jW_\nu\{n_s\}\prod_s \xi_s n_s/n_s! \tag{17}$$

where A and ξ_s are Lagrangian multipliers which must be so chosen that

$$N_t=\sum_{\mathrm{all}\{n_s\}} n_t m\{n_s\} \tag{18}$$

$$M=\sum_{\mathrm{all}\{n_s\}} m\{n_s\} \tag{19}$$

and ${}_jW_\nu\{n_s\}$ is the number of different ways in which a molecule described by $\{n_s\}$ can be constructed from its constituent chains by ν interunit junctions. The use of the Stockmayer method for calculating this number gives the result:

$${}_fW_\nu\{n_s\}=\frac{(\sum_s(s-1)n_s)!((j-1)\nu)!}{(\sum_s(s-1)n_s-(\nu-1))!\,\nu!\,((j-1)!)^\nu}\prod_s s^{n_s} \tag{20}$$

where

$$\sum_s n_s=(j-1)\nu+1 \tag{21}$$

Using Eq. 20, Eq. 17 may be rewritten as folloms:

$$m\{n_s\}=(\sum_s sN_s)\frac{(\sum_s(s-1)n_s)!((j-1)\nu)!}{\nu!(\sum_s(s-1)n_s-(\nu-1))!}\times\alpha^\nu(1-\alpha)^{\sum_s(s-1)n_s-(\nu-1)}\times\prod_s\frac{W_s^{n_s}}{n_s!} \tag{22}$$

where

$$s\xi_s=\{(j-1)!\,\alpha(1-\alpha)^{-j}\}^{1/(j-1)}W_s(1-\alpha)^s$$

$$A=(\sum_s sN_s)\{(j-1)!\,\alpha(1-\alpha)^{-j}\}^{-1/(j-1)}$$

which satisfies the conditions of Eqs. 18 and 19, as is shown in the Appendix. After the evaluation of the necessary sums, the number- and weight-average molecular sizes are obtained as follows:

$$\bar{P}_n=\frac{\sum_s(\sum sn_s)m\{n_s\}}{\sum m\{n_s\}}=\frac{1}{1-(j-1)\alpha\lambda_n/j} \tag{23}$$

$$\bar{P}_w=\frac{\sum_s(\sum sn_s)^2m\{n_s\}}{\sum_s(\sum sn_s)m\{n_s\}}=\frac{1+(j-1)\alpha\lambda_w}{1-(j-1)(\lambda_w-1)\alpha} \tag{24}$$

Therefore, the gel-point is given by

$$\alpha_{gel}=\frac{1}{(j-1)(\lambda_w-1)} \tag{25}$$

Of course, for the special case of $j=2$, these results are consistent with those of Stockmayers.

In the above formulations, the size distribution of the chains which initially exist is arbitrary, but the distribution of almost all the synthesized polymer chains is the most probable distribution. In this case, the molecular size distribution and the average sizes in the course of cross linking are found to be as follows. It is well known that the most probable molecular size distribution of chain polymers is given by $W_s=s\rho^{s-1}(1-\rho)^2$, where s is the number of units in a chain, and ρ is the probability that the reactive group in the unit has reacted. Let $m_{p,\nu}$ be the number of crosslinked polymeric molecules composed of p units and jointed with functional interunit junctions. This $m_{p,\nu}$ can be expressed:

$$m_{p,\nu}=\sum m\{n_s\} \tag{26}$$

where the summation should cover all possible sets, $\{n_r\}$, with the conditions:

$$\sum_s n_s=(j-1)\nu+1,\quad \sum_s sn_s=p \tag{27}$$

Equation 26 easily be evaluated, with the result that

$$m_{p,\nu}=\frac{((j-1)\nu)!\,(p+(j-1)\nu)!}{\nu!((j-1)\nu+1)!\,(p-j\nu)!\,(2(j-1)\nu+1)!}\times\alpha^\nu(1-\alpha)^{p-j\nu}\rho^{-(j-1)\nu-1}(1-\rho)^{2(j-1)\nu+2} \tag{28}$$

Form Eqs. 23 and 24, the number- and weight-average size are found to be;

$$\bar{P}_n=\frac{1}{1-\rho-(j-1)\alpha/j} \tag{29}$$

$$\bar{P}_w=\frac{(1+\rho)(1+(j-1)\alpha)}{1-\rho-2(j-1)\alpha\rho} \tag{30}$$

$$\alpha_{gel}=\frac{1-\rho}{2(j-1)\rho} \tag{31}$$

since $\lambda_n=1/(1-\rho)$, and $\lambda_w=(1+\rho)/(1-\rho)$ for the case of chains with the most probable distribution. When $j=2$, the result is consistent with that of Ohiwa derived by the kinetical method.[7]

7) M. Ohiwa, *J. Chem. Soc. Japan, Pure Chem. Sec. (Nippon Kagaku Zassi)*, **75**, 1244 (1954).

Department of Fuel Chemistry
Faculty of Engineering
Kyoto University
Sakyo-ku, Kyoto

Appendix

We wish to show that the distribution law:

$$m\{n_s\}=\{\sum_s sN_s\}\frac{(\sum_s(s-1)n_s!\,((j-1)\nu)!}{(\sum_s(s-1)n_s-(\nu-1))!\,\nu!}\times\alpha^\nu(1-\alpha)^{\sum_s(s-1)n_s-(\nu-1)}\prod_s\frac{W_s^{n_s}}{n_s!}$$

satisfies the conditions:

$$N_t=\sum n_t m\{n_s\} \tag{A-1}$$

$$M=\sum m\{n_s\} \tag{A-1}$$

Putting $\nu_t=n_t-1$ and $\nu_s=n_s(s\neq t)$, and expanding the power of $(1-\alpha)$ in Eq. A-1, we have;

$$\sum n_t m\{n_s\}=(\sum_s sN_s)W_t\sum_{q=0}\frac{(-\alpha)^q}{q!}\sum_{\nu=0}^{q}\binom{q}{\nu}(-1)^\nu\times\sum\frac{(\sum_s(s-1)\nu_s+(t-1))!\,(\sum_s\nu_s)!}{(\sum_s(s-1)\nu_s+(t-1)-(q-1))}\times\prod_s\frac{W_s^{\nu_s}}{\nu_s!} \tag{A-3}$$

where $\sum_s\nu_s=(j-1)\nu$

Consider now the function:

$$\mathscr{H}(x)=(1-(\sum_s W_s x^{s-1})^{j-1})^q x^{t-1}$$

$$=\sum_{\nu=0}^{q}\binom{p}{\nu}(-1)^\nu\sum(\sum_s\nu_s)!\prod_s\frac{W_s^{\nu_s}}{\nu_s!}\times x^{\sum_s(s-1)\nu_s+t-1}$$

where q is an integer greater than one.

Repeated differentiations give:

$$\left[\left(\frac{d}{dx}\right)^{q-1}\mathscr{H}(x)\right]_{x=1}=\sum_{\nu=0}^{q}\binom{p}{\nu}(-1)^\nu\times\sum\frac{(\sum_s(s-1)\nu_s+t-1)!\,(\sum_s\nu_s)!}{(\sum_s(s-1)\nu_s+t-1-(q-1))!}\prod_s\frac{W_s^{\nu_s}}{\nu_s!}$$

which is recognized as the sum required in Eq. A-3. However, since this derivative necessarily contains the $(1-(\sum_s W_s)^{j-1})$ factor, its value is zero, and the sum of Eq. A-3 is reduced to the term of $q=0$. Evaluating these, we obtain

$$\sum n_s m\{n_s\}=\frac{W_t}{t}(\sum_s sN_s)=N_t$$

Since the procedure for the summation of Eq. 18 resembles that used above, it may be omitted.

The Intramolecular Force Field and Normal Vibrations of Isotactic Polypropylene and Deuterated Derivatives[*1]

By Tatsuo MIYAZAWA and Yoshiko IDEGUCHI

(Received February 24, 1964)

The infrared active normal vibrations of isotactic polypropylene (IPP), poly(propylene-2-d_1) (IPP-CD), poly(propylene-1, 1-d_2) (IPP-CD_2) and poly(propylene-3, 3, 3-d_3) (IPP-CD_3) in the 1500~650 cm^{-1} region have been treated in previous studies.[1,2] The high-frequency CH stretching modes of the CH, CH_2, and CH_3 groups have been separated and the internal rotation modes have not been taken into account since the internal rotation potential terms do not contribute much to the frequencies above 650 cm^{-1}. Thus, the "effective" potential constants have been calculated, by the method of least squares,[3] from the observed frequencies. In the present study, a complete normal coordinate treatment of isotactic polypropylene and deuterated derivatives was made, one in which the CH stretching modes and the internal-rotation modes about the CH–CH_2 and CH–CH_3 bonds were all taken into account.

Normal Coordinate Treatment

Internal Coordinates.—A general method for the treatment of the molecular vibrations of helical polymers has been described.[1] The internal coordinate (or the local symmetry coordinate) vectors, $R_{1,n}$~$R_{18,n}$, of the nth repeating unit of isotactic polypropylene have been given in Eqs. 1—6 of Ref. 2. In addition, the C–H stretching coordinates and the internal rotation coordinaten shown below were used in the present study:

$$R_{19,n}(\text{CH stretch.}) = \Delta r(1,n;\ 5,n) \tag{1}$$

$$\begin{bmatrix} R_{20,n}(\text{CH}_3 \text{ sym. stretch.}) \\ R_{21,n}(\text{CH}_3 \text{ asym. stretch.}) \\ R_{22,n}(\text{CH}_3 \text{ asym. stretch.}) \end{bmatrix} = \begin{bmatrix} 1/3^{1/2} & 1/3^{1/2} & 1/3^{1/2} \\ 1/6^{1/2} & 1/6^{1/2} & -2/6^{1/2} \\ 1/2^{1/2} & -1/2^{1/2}, & 0 \end{bmatrix} r(\text{CH}_3)_n \tag{2}$$

$$\begin{bmatrix} R_{23,n}(\text{CH}_2 \text{ sym. stretch.}) \\ R_{24,n}(\text{CH}_2 \text{ asym. stretch.}) \end{bmatrix} = \begin{bmatrix} 1/2^{1/2} & 1/2^{1/2} \\ 1/2^{1/2} & -1/2^{1/2} \end{bmatrix} r(\text{CH}_2)_n \tag{3}$$

where the elements of the vector $r(CH_3)$ in Eq. 2 are $\Delta r(3,n;\ 7,n)$, $\Delta r(3,n;\ 8,n)$, and $\Delta r(3,n;\ 9,n)$; the elements of the vector r-$(CH_2)_n$ in Eq. 3 are $\Delta r(2,n;\ 4,n)$ and $\Delta r(2,n;\ 6,n)$; and Δr's are the stretching coordinates for which the numbering of carbon and hydrogen atoms has been shown in Fig. 1 of Ref. 2.

The internal-rotation coordinates[4] for the nth unit are;

$$\begin{aligned} R_{25,n}(\text{CH–CH}_3 \text{ bond}) &= \Delta t(1,n;\ 3,n) \\ &= [\Delta\tau(2,n-1;\ 1,n;\ 3,n;\ 7,n) \\ &\quad + \Delta\tau(2,n-1;\ 1,n;\ 3,n;\ 8,n) \\ &\quad + \Delta\tau(2,n-1;\ 1,n;\ 3,n;\ 9,n) \\ &\quad + \Delta\tau(2,n;\ 1,n;\ 3,n;\ 7,n) \\ &\quad + \Delta\tau(2,n;\ 1,n;\ 3,n;\ 8,n) \\ &\quad + \Delta\tau(2,n;\ 1,n;\ 3,n;\ 9,n) \\ &\quad + \Delta\tau(5,n;\ 1,n;\ 3,n;\ 7,n) \\ &\quad + \Delta\tau(5,n;\ 1,n;\ 3,n;\ 8,n) \\ &\quad + \Delta\tau(5,n;\ 1,n;\ 3,n;\ 9,n)]/9 \end{aligned} \tag{4}$$

$$\begin{aligned} R_{26,n}(\text{axial CH–CH}_2 \text{ bond}) &= \Delta t(1,n;\ 2,n) \\ &= [\Delta\tau(2,n-1;\ 1,n;\ 2,n;\ 4,n) \\ &\quad + \Delta\tau(2,n-1;\ 1,n;\ 2,n;\ 6,n) \\ &\quad + \Delta\tau(2,n-1;\ 1,n;\ 2,n;\ 1,n+1) \\ &\quad + \Delta\tau(3,n;\ 1,n;\ 2,n;\ 4,n) \\ &\quad + \Delta\tau(3,n;\ 1,n;\ 2,n;\ 6,n) \\ &\quad + \Delta\tau(3,n;\ 1,n;\ 2,n;\ 1,n+1) \\ &\quad + \Delta\tau(5,n;\ 1,n;\ 2,n;\ 4,n) \\ &\quad + \Delta\tau(5,n;\ 1,n;\ 2,n;\ 6,n) \\ &\quad + \Delta\tau(5,n;\ 1,n;\ 2,n;\ 1,n+1)]/9 \end{aligned} \tag{5}$$

$$\begin{aligned} R_{27,n}(\text{equatorial CH–CH}_2 \text{ bond}) &= \Delta t(2,n;\ 1,\ n+1) \\ &= [\Delta\tau(1,n;\ 2,n;\ 1,n+1;\ 2,n+1) \\ &\quad + \Delta\tau(1,n;\ 2,n;\ 1,n+1;\ 3,n+1) \\ &\quad + \Delta\tau(1,n;\ 2,n;\ 1,n+1;\ 5,n+1) \\ &\quad + \Delta\tau(4,n;\ 2,n;\ 1,n+1;\ 2,n+1) \end{aligned}$$

*1 This is Part VI of *Molecular Vibrations and Structures of High Polymers*. The present study was, in part, published at the Confernce on Vibrational Spectra of High Polymers, Milan, July, 1963.

1) T. Miyazawa, Y. Ideguchi and K. Fukushima, *J. Chem. Phys.*, **38**, 2709 (1963).

2) T. Miyazawa and Y. Ideguchi, This Bulletin, **36**, 1125 (1963).

3) D. E. Mann, T. Shimanouchi, J. H. Meal and L. Fano, *J. Chem. Phys.*, **27**, 43 (1957).

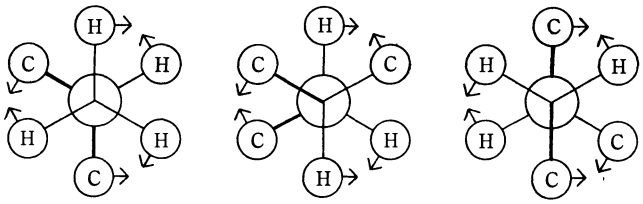


Fig. 1 The internal-rotation modes about the C-methyl bond (t_{C-CH_3}), about the axial C-C bond (t_{CC}^{ax}), and about the equatorial C-C bond (t_{CC}^{eq}) of isotactic polypropylene chain (the right-handed helix). Main chain C-C bonds are drawn with heavy lines.

$$+\Delta\tau(4,n;\ 2,n;\ 1,n+1;\ 3,n+1)$$
$$+\Delta\tau(4,n;\ 2,n;\ 1,n+1;\ 5,n+1)$$
$$+\Delta\tau(6,n;\ 2,n;\ 1,n+1;\ 2,n+1)$$
$$+\Delta\tau(6,n;\ 2,n;\ 1,n+1;\ 3,n+1)$$
$$+\Delta\tau(6,n;\ 2,n;\ 1,n+1;\ 5,n+1)]/9 \qquad (6)$$

where $\Delta\tau$'s are the torsional coordinates. These internal-rotation coordinates are schematically shown in Fig. 1. The elements of the inverse kinetic energy matrix associated with the internal-rotation modes were calculated by the use of the general formulas.[4]

Potential Function.—In deriving the potential energy matrix, the modified Urey-Bradley field was supplemented with these internal-rotation potential term.[4,5]

$$V(\text{internal-rotation}) = \frac{1}{2}\sum_n \{Y(\text{CH–CH}_2)\,[\Delta t(1,n;\ 2,n)]^2 + Y(\text{CH–CH}_2)\,[\Delta t(2,n;\ 1,n+1)]^2 + Y(\text{CH–CH}_3)\,[\Delta t(1,n;\ 3,n)]^2\} \qquad (7)$$

The potential constants of isotactic polypropylene used in the present study are listed in Table I. Common potential constants, K(C–C) and Y(C–C), were used for the axial and equatorial CH–CH$_2$ bonds, since the arrangements of the carbon and hydrogen atoms adjacent to these C–C bonds are the same. The repulsion constants, F(H–C–H) and F(C–C–H), were transferred from the ethane molecule as treated by Takahashi and Shimanouchi.[6] The initial set of the remaining potential constants (except for the CH stretching constant) were transferred from the previous study[2] and were then adjusted by the method of least squares[3] with reference to the fundamental frequencies of IPP, IPP-CD, IPP-CD$_2$, and IPP-CD$_3$ as observed by Peraldo and Farina[7] in the region above 650 cm^{-1} and to the far infrared frequencies of IPP in the region below 650 cm^{-1}.[1,8] The adjustments of the potential constants were repeated until

Table I. Modified Urey-Bradley potential constants*1 (and standard error*2) of isotactic polypropylene

K(C-H)	4.255±0.003	CH_3 group
	3.980±0.005	CH_2 group
	4.030±0.003	CH group
K(C-C)	2.240±0.108	CH–CH_2 bond
	2.270±0.110	CH–CH_3 bond
Y(C-C)	0.176±0.042	CH–CH_2 bond
	0.080±0.002	CH–CH_3 bond
H(H-C-H)	0.366±0.002	CH_3 group
	0.353±0.004	CH_2 group
H(H-C-C)	0.231±0.011	CH_3 group
	0.218±0.006	CH_2 group
	0.235±0.016	CH group
H(C-C-C)	0.350±0.100	C–CH_2–C angle
	0.390±0.035	C–CH–C angle
F(H-C-H)	0.200*3	
F(H-C-C)	0.480*3	
F(C-C-C)	0.280±0.065	
κ	−0.028±0.008	CH_3 group
	0.002±0.012	CH_2 group
	−0.130±0.055	CH group
T	0.118±0.007	H-C-C-H (trans)
G	−0.038±0.007	H-C-C-H (gauche)
p(C-H)	−0.115±0.005	CH_3 group
	−0.115±0.015	CH_2 group
l(C-C-H)	0.000±0.005	C–CH_2–C

*1 K, stretching (mdyn./Å); Y, internal rotation (mdyn.Å); H, bending (mdyn./Å;) F, repulsion (mdyn./Å); T, trans-coupling (mdyn.Å); G, gauche-coupling (mdyn.Å); κ, intramolecular tension (mdyn.Å), l, angle-interaction (mdyn. Å), and p, stretching-interaction (mdyn./Å).
*2 Ref. 10.
*3 Transferred from ethane (Ref. 6).

4) T. Miyazawa and K. Fukushima, 16th Annual Meeting of the Chemical Society of Japan, Tokyo, April, 1963.
5) T. Shimanouchi, *Pure Appl. Chem.*, **7**, 131 (1963).
6) H. Takahashi and T. Shimanouchi, Symposium on Molecular Structure, Sendai, October (1963).
7) M. Peraldo and M. Farina, *Chim. Ind. (Milan)*, **42**, 1349 (1960).
8) T. Miyazawa, K. Fukushima and Y. Ideguchi, *J. Polymer Sci.* **B1**, 385 (1963).

finally, for each constant, the calculated correction was reduced to a point where it was negligible compared with the standard error. In the adjustment of the potential constant, the element of the Jacobian matrices were calculated by the equation reported previously.[9] The standard errors were calculated according to the method derived by Ogawa and Miyazawa.[10]

Potential Constants. — The final set of the potential constants and their standard errors are listed in Table I. The C–H stretching constants, K(C–H), of the CH_2 and CH groups are calculated to be slightly smaller than for the CH_3 group, where the repulsion constants, F(H–C–H) and F(C–C–H), have been transferred from ethane. The stretching-interaction constants, p(C–H), for the CH_3 and CH_2 groups were taken independently, but they have finally been calculated to be the same. Therefore, a common stretching-interaction parameter may be used for the CH_3 and CH_2 groups.

The stretching constants, K(C–C), for the CH–CH_2 and CH–CH_3 bonds were also taken independently, but these two constants finally coincided within the standard errors. Therefore, these two constants may well be reduced to a common parameter $[(2.240+2.270)/2 = 2.255]$.

The bending constants of the H–C–H angle of the CH_3 and CH_2 groups are nearly the same, but the difference is greater than their standard errors. The bending constants for the C–C–H angles of the CH_3, CH_2, and CH groups all lie in the range between 0.235 and 0.215 mdyn./Å.

The values of the intramolecular tension [κ] and angle-interaction term [l(C–C–H)]*2 for the CH_2 group are almost negligible compared with the corresponding standard errors; accordingly, these parameters may well be neglected, at least in the treatment of polypropylene. It may be recalled that the corresponding contants for malonitrile, $CH_2(CN)_2$, are also negligible.[5]

The trans and gauche coupling constants of IPP agree closely with those of ethane ($T=0.107$ and $G=-0.024$) and of polyethylene ($T=0.100$ and $G=-0.033$).[5]

The internal-rotation constants, Y(C–C), may be used for estimating the barrier height of the internal-rotation potential, which is assumed to be threefold and sinusoidal. Thus, the potential barrier for the CH–CH_2 bond of the main chain and for the CH–CH_3 bond are estimated to be 5.7±1.4 and 2.9±0.1 kcal./mol. (approximately corrected for anharmonicity[4]) respectively.

The diagonal elements of the potential energy matrix associated with genuine vibrational modes may be obtained satisfactorily from the observed frequencies, although the off diagonal elements are not necessarily so.[5] Accordingly, the final values of the diagonal elements associated with "local" symmetry coordinates of isotactic polypropylene are listed in Table II.

Table II. The diagonal elements*1 of the potential energy matrix of isotactic polypropylene

CH_3 sym. stretch. (R_{20})	4.798
asym. stretch. (R_{21}, R_{22})	4.726
CH_2 sym. stretch. (R_{23})	4.614
antisym. stretch. (R_{24})	4.566
CH stretch. (R_{19})	4.756
CH–CH_2 stretch. (R_{12}, R_{18})	3.854
CH–CH_3 stretch. (R_6)	4.067
CH_3 sym. deform. (R_9)	0.584
asym. deform. (R_7, R_8)	0.519
rock. (R_{10}, R_{11})	0.686
CH_2 bend. (R_{14})	0.547
wag. (R_{15})	0.677
twist. (R_{16})	0.675
rock. (R_{17})	0.677
CH bend. (R_1, R_2)	0.657
C–CH_2–C bend. (R_{13})	1.021
C–CH$\langle$C sym. deform. (R_3)	0.810
C asym. deform. (R_4, R_5)	1.145
CH–CH_2 internal rotation (R_{26}, R_{27})	0.176
CH–CH_3 internal rotation (R_{25})	0.080

*1 The elements associated with the stretching modes are given in unit of mdyn./Å and the elements associated with the bending and internal rotation coordinates are given in unit of mdyn.Å.

The A and E($2\pi/3$) frequencies of IPP, IPP-CD, IPP-CD_2, and IPP-CD_3 were calculated with the final set of potential constants and are listed in Tables III—IX, together with the observed frequencies. The calculated and observed frequencies are also compared in Figs. 2 and 3. For the region above 650 cm^{-1}, the r.m.s. frequency deviations are: IPP: 0.9%; IPP-CD: 0.9%; IPP-CD_2: 0.8%; and IPP-CD_3: 1.0%; while the overall r.m.s. deviation was 0.9%. Since the calculated frequencies agreed so closely with the observed frequencies, the potential energy distributions were also calculated as aids in assigning the infrared bands. The distributions, $(PED)_{ii}$,

9) T. Miyazawa, *J. Chem. Soc. Japan, Pure Chem. Sec.* (*Nippon Kagaku Zassi*), **76**, 1132 (1955).

10) T. Ogawa and T. Miyazawa, *Spectrochim. Acta*, **20**, 557 (1964).

*2 The parameter, l(C-C-H), is correlated somewhat with the internal-rotation constant for the CH-CH_2 bond. In our previous treatment, the internal-rotation potential terms were neglected and the value of l(C-C-H) was adjusted to 0.014 mdyn./Å.[2]

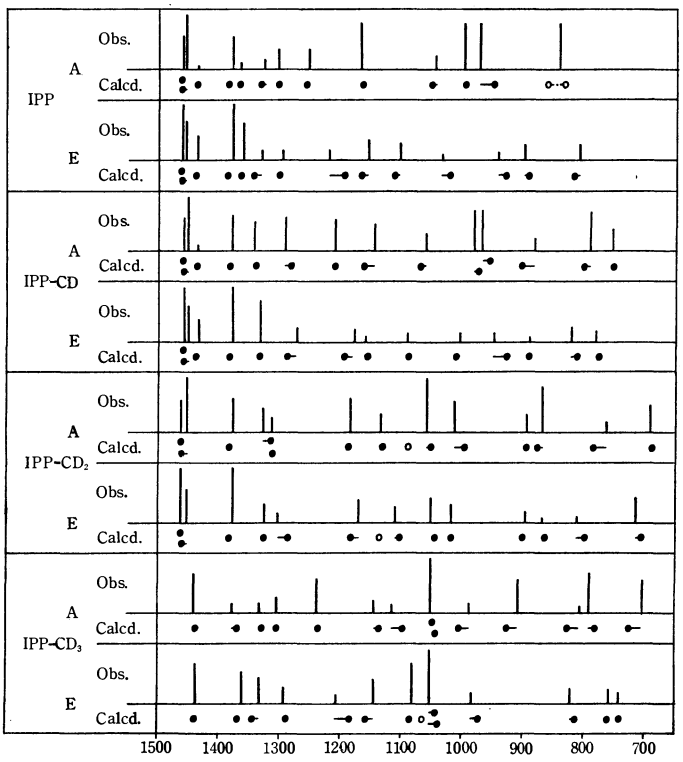


Fig. 2 Observed frequencies (cm^{-1}) and relative intensities (Ref. 7) and calculated frequencies of isotactic polypropylene [IPP], poly(propylene-2-d) [IPP-CD], poly(propylene-1, 1-d_2) [IPP-CD_2], and poly(propylene-3, 3, 3-d_3) [IPP-CD_3].

TABLE III. THE C-H AND C-D STRETCHING FREQUENCIES OF ISOTACTIC POLYPROPYLENE [IPP], POLY(PROPYLENE-2-d) [IPP-CD], POLY(PROPYLENE-1, 1-d_2) [IPP-CD_2], POLY(PROPYLENE-3, 3, 3-d_3) [IPP-CD_3]

IPP	IPP-CD	IPP-CD_2	IPP-CD_3	ν_{calcd}	Assignment
2959(vs, ∥)	2959(vs, ∥)	2961(vs, ∥)		2962(A) 2962(E)	CH_3 asym. stretch. (antisym. with respect to the H-C-CH_3 plane)
2950(vs, ⊥)	2950(vs, ⊥)	2949(vs, ⊥)		2962(E) 2962(A)	CH_3 asym. stretch. (sym. with respect to the H-C-CH_3 plane)
2921(vs, ⊥)		2922(s, ⊥)	2918(vs, ⊥)	2923～2927(E) 2924～2926(A)	CH stretch.
2879(s, ⊥)	2882(sh, ⊥)		2885(m, ⊥)	2903～2906(E) 2906(A)	CH_2 antisym. stretch.
	2868(w, ∥)	2874(m, ∥)		2873～2874(A)	CH_3 sym. stretch.
2868(s, ⊥)	2867(m, ⊥)	2868(s, ⊥)		2873～2874(E)	
2838(m)	2837(s)		2837(s)	2848～2849(E) 2845～2848(A)	CH_2 sym. stretch.
			2215(vs, ∥)	2196(A) 2196(E)	CD_3 asym. stretch. (antisym. with respect to the H-C-CD_3 plane)
			2204(s, ⊥)	2196(E) 2196(A)	CD_3 asym. stretch. (sym. with respect to the H-C-CD_3 plane)
		2171(s, ⊥)		2153(E) 2154(A)	CD_2 antisym. stretch.
		2169(w, ∥)			
	2162(m, ⊥)			2141(E) 2142(A)	CD stretch.
	2154(w, ∥)				
		2092(m, ⊥)		2065(E) 2062(A)	CD_2 sym. stretch.
		2085(m, ∥)			
			2067(m, ⊥)	2058(E) 2058(A)	CD_3 sym. stretch.
			2066(m, ∥)		

TABLE IV. THE OBSERVED AND CALCULATED FREQUENCIES (IN cm^{-1}) AND POTENTIAL ENERGY DISTRIBUTIONS (IN %) OF ISOTACTIC POLYPROPYLENE IN THE REGION 1500~600 cm^{-1}

ν_{obs}*1	ν_{calcd}	Potential energy distributions*2
1460(s, ⊥)	1463(ν_7^E)	CH_3 δ_a(ax : 10, eq : 70)
	1462(ν_7^A)	CH_3 δ_a(ax : 30, eq : 50)
1454(m, ∥)	1461(ν_8^A)	CH_3 δ_a(ax : 50, eq : 30)
	1461(ν_8^E)	CH_3 δ_a(ax : 75, eq : 10)
1435(m, ⊥)	1439(ν_9^E)	CH_2 bend. (100)
	1436(ν_9^A)	CH_2 bend. (100)
1378(m, ∥)	1385(ν_{10}^A)	CH_3 δ_s(90)
1377(s, ⊥)	1386(ν_{10}^E)	CH_3 δ_s(85)
1365(vw, ∥)	1367(ν_{11}^A)	CH_2 wag. (40), CH bend.^{ax} (30), CH_3 δ_s(15)
1360(m, ⊥)	1365(ν_{11}^E)	CH bend.^{eq} (30), CH_2 twist. (20), CH_2 wag. (15), CH_3 δ_s (15)
1330(w, ⊥)	1344(ν_{12}^E)	CH_2 wag. (35), CH bend.^{ax} (35)
1326(vw, ∥)	1332(ν_{12}^A)	CH bend.^{eq} (60)
1304(m, ∥)	1304(ν_{13}^A)	CH_2 wag. (50), CH_2 twist. (25), CH bend.^{ax} (15)
1296(w, ⊥)	1301(ν_{13}^E)	CH_2 wag. (40), CH bend. (ax : 20, eq : 20)
1254(m, ∥)	1264(ν_{14}^A)	CH_2 twist. (35), CH bend. (ax : 20, eq : 10)
1220(w, ⊥)	1195(ν_{14}^E)	CH_2 twist. (25), CH bend. (15), r_{CC}^{eq}(20)
1168(s, ∥)	1165(ν_{15}^A)	r_{CC}^{ax} (40), CH_3 rock.^{ax} (25)
1155(m, ⊥)	1166(ν_{15}^E)	r_{CM} (20). CH bend. (15)
1103(m, ⊥)	1112(ν_{16}^E)	CH_3 rock. (ax : 20, eq : 10), r_{CC}^{ax} (25)
1045(m, ∥)	1051(ν_{16}^A)	r_{CM} (35), r_{CC}^{eq} (30)
1034(vw, ⊥)	1021(ν_{17}^E)	r_{CM} (30), CH_2 twist. (15), CH bend. (15), CH_3 rock.^{eq} (15)
998(s, ∥)	996(ν_{17}^A)	CH_3 rock.^{eq} (35), r_{CM} (35), CH bend. (15), CH_2 twist. (15)
973(s, ∥)	950(ν_{18}^A)	CH_3 rock.^{ax} (50), r_{CC}^{ax} (20), r_{CC}^{eq} (20)
941(w, ⊥)	930(ν_{18}^E)	CH_3 rock. (ax : 35, eq : 10), r_{CC}^{ax} (35)
899(m, ⊥)	892(ν_{19}^E)	CH_3 rock.^{eq} (35), CH_2 rock. (20), CH bend.^{eq} (15)
842(s, ∥)	862(ν_{19}^A)	CH_3 rock. (ax : 10, eq : 25), r_{CC}^{eq} (30)
	833(ν_{20}^A)	CH_2 rock. (75), CH bend.^{ax} (15)
809(m, ⊥)	818(ν_{20}^E)	CH_2 rock. (35), r_{CM} (25), r_{CC}^{eq} (20)

*1 s, strong; m, medium; w, weak; vw, very weak; ∥, parallel band; and ⊥, perpendicular band (observed by Peraldo and Farina[7]).

*2 CH_3 δ_s and δ_a, the symmetric and asymmetric deformation modes, respectively, of the methyl group; r_{CM}, C-methyl stretching; r_{CC}^{ax} and r_{CC}^{eq}, axial and equatorial C-C stretching modes, respectively.

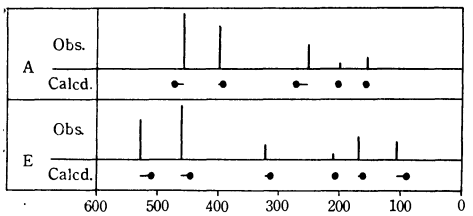


Fig. 3 Observed frequencies (cm^{-1}) and relative intensities (Refs. 1 and 8) and calculated frequencies of isotactic polypropylene (A : parallel band, E : perpendicular band) in the region below 600 cm^{-1}.

are shown in Tables IV–IX, which list only the terms greater than 15%.

The calculated frequencies of IPP below 650 cm^{-1} did not agree with the observed frequencies as closely as did the calculated higher frequencies. The potential constants, H(C–C–C), F(C–C–C), κ(CH), and Y(C–C) [CH–CH_2 bond], are primarily associated with these low frequency vibrations, accordingly, their standard errors are calulated to be relatively large. The correction terms for the Urey-Bradley force field are undoubtedly necessary for more refined treatments of the low frequency vibrations, but they have not been established as yet. The r. m. s. frequency deviation for the vibrations of IPP below 650 cm^{-1} is 3.7% except for the ν_{26}^E vibration at 106 cm^{-1}. This lowest frequency vibration is possibly considerably affected by the intermolecular force field.

C–H and C–D Stretching Vibrations

The infrared spectra of IPP and deuterated derivatives in the 3000~2000 cm^{-1} region have been measured by Peraldo and Farina,[7] by Liang et al.[11] and by McDonald and Ward.[12] Their assignments, as well as the

11) C. Y. Liang, M. R. Lytton and C. J. Boone, *J. Polymer Sci.*, **47**, 139 (1960).
12) M. P. McDonald and I. M. Ward, *Polymer (London)*, **2**, 341 (1961).

TABLE V. THE CALCULATED AND OBSERVED FREQUENCIES (IN cm^{-1}) AND POTENTIAL ENERGY DISTRIBUTIONS (IN %) OF ISOTACTIC POLY(PROPYLENE-2-d) IN THE REGION 1500~600 cm^{-1}

ν_{obs}*1	ν_{calcd}	Potential energy distributions*2
1459(s, ⊥)	1459(ν_7^E)	CH_3 δ_a (ax : 25, eq : 65)
	1459(ν_7^A)	CH_3 δ_a (ax : 20, eq : 65)
1451(s, ∥)	1460(ν_8^A)	CH_3 δ_a (ax : 65, eq : 20)
	1460(ν_8^E)	CH_3 δ_a (ax : 65, eq : 25)
1435(m, ⊥)	1438(ν_9^E)	CH_2 bend. (100)
	1436(ν_9^A)	CH_2 bend. (100)
1379(m, ∥)	1382(ν_{10}^A)	CH_3 δ_s (100)
1378(s, ⊥)	1383(ν_{10}^E)	CH_3 δ_s (100)
1342(m, ∥)	1340(ν_{11}^A)	CH_2 wag. (85)
1334(m, ⊥)	1333(ν_{11}^E)	CH_2 wag. (85)
1291(m, ∥)	1282(ν_{12}^A)	CH_2 twist. (75)
1273(w, ⊥)	1289(ν_{12}^E)	CH_2 twist. (55)
1210(m, ∥)	1210(ν_{13}^A)	r_{CC}^{ax} (25), r_{CC}^{eq} (25), CH_3 rock. (15), CD bend. (ax : 15, eq : 10)
1179(w, ⊥)	1195(ν_{13}^E)	r_{CM} (20), r_{CC}^{eq} (15), CD bend. (15), CH_3 rock. (15)
1160(vw, ⊥)	1156(ν_{14}^E)	r_{CC}^{ax} (25), CH_3 rock.^{ax} (25)
1145(m, ∥)	1162(ν_{14}^A)	CH_3 rock. (ax : 15, eq : 15), CD bend.^{eq} (15)
1091(w, ⊥)	1089(ν_{15}^E)	CH_3 rock.^{eq} (30), r_{CM} (15)
1060(w, ∥)	1070(ν_{15}^A)	CH_3 rock.^{eq} (25), CH_2 rock. (20)
1005(w, ⊥)	1010(ν_{16}^E)	CH_3 rock. (ax : 15, eq :10), CH_2 rock. (20), CD bend. (15)
981(s, ∥)	974(ν_{16}^A)	r_{CM} (40), CH_3 rock.^{ax} (25), CD bend.^{ax} (15)
969(s, ∥)	955(ν_{17}^A)	CH_3 rock. (ax : 25, eq : 15), r_{CC}^{ax} (20), r_{CM} (15)
949(w, ⊥)	927(ν_{17}^E)	r_{CC}^{ax} (40), CH_3 rock. (ax : 30, eq : 10), r_{CC}^{eq} (15)
890(vw, ⊥)	891(ν_{18}^E)	CD bend. (ax : 40, eq 10), r_{CM} (20)
881(w, ∥)	903(ν_{18}^A)	r_{CC}^{eq} (55), CD bend.^{eq} (15)
821(m, ⊥)	812(ν_{19}^E)	CD bend. (ax : 10, eq : 30), r_{CM} (20), CH_3 rock.^{eq} (15)
790(s, ∥)	801(ν_{19}^A)	CD bend.^{eq} (50), CH_3 rock. (ax : 10, eq : 20)
781(w, ⊥)	776(ν_{20}^E)	CD bend. (ax : 25, eq : 30), CH_2 rock. (35)
754(m, ∥)	752(ν_{20}^A)	CH_2 rock. (50), CD bend.^{ax} (50)

*1,*2 See *1,*2 of Table IV.

observed spectra, were critically reviewed in the present study with reference to the calculated frequencies and their possible shifts due to the anharmonicity. It was expected that the observed C–H stretching frequency would be slightly lower than the calculated C–H stretching frequency, while the observed C–D stretching frequency would be slightly higher than the calculated frequency in the final stage of the calculation based on the method of least squares.

The observed frequencies, intensities, and dichroism of IPP and deuterated derivatives,[7] the calculated frequencies, and the vibrational assignments are shown in Table III. When the potential energy distribution was calculated for each vibration, the potential energy was found to be localized in the single mode as listed in Table III.

The band at about 2870 cm^{-1} has been assigned by Liang et al.[11] to the CH_3 symmetric stretching vibration.*3 The parallel component (A) is weaker than the perpendicular component (E), in accordance with the expected intensity ratio of $I_A/I_E=0.4$.[13] The bands due to the CH_3 asymmetric stretching mode[7,11-13] are split into two components of nearly the same intensity; the parallel component at about 2960 cm^{-1} is assigned to the mode which is antisymmetric with respect to the H–C–CH_3 plane [denoted as $\nu_a(CH_3)_0$[13]]. The dichroism of this component has been estimated to be $I_E/I_A=0.1$. The perpendicular component at about 2950 cm^{-1} is assigned to the mode which is symmetric with respect to the H–C–CH_3 plane [denoted as $\nu_a(CH)_i$[13]]. The dichroism of this component has been estimated to be $I_A/I_E=0.8$. The stretching vibrations of the CD_3 groups are observed at 2215 cm^{-1} (∥) and 2204 cm^{-1} (⊥) [asymmetric] and at 2066~2067 cm^{-1} [symmetric].

The nondichroic band at 2838 cm^{-1} has been assigned to the CH_2 symmetric stretching mode.[7,11-13] The perpendicular band at about 2880 cm^{-1} is assigned, in the present study, to the CH_2 antisymmetric stretching vibration.*4

*3 Krimm assigned this band to an overtone,[13] whereas McDonald and Ward[12] assigned the two bands at 2925 and at 2868 cm^{-1} to the CH_3 symmetric stretching modes.

13) S. Krimm, *Fortschr. Hochpolymer.-Forsch.*, **2**, 51 (1960).

*4 This band has been assigned to the CH_3 symmetric stretching mode (E) [13] or to an overtone.[11,12]

TABLE VI. THE OBSERVED AND CALCULATED FREQUENCIES (IN cm^{-1}) AND POTENTIAL ENERGY DISTRIBUTIONS (IN %) OF ISOTACTIC POLY(PROPYLENE-1, 1-d_2) IN THE REGION 1500~600 cm^{-1}

ν_{obs}*1	ν_{calcd}	Potential energy distributions*2
1461(s, ⊥)	1462(ν_7^E)	CH_3 δ_a (ax : 20, eq : 60)
	1462(ν_7^A)	CH_3 δ_a (ax : 20, eq : 60)
1452(s, ∥)	1461(ν_8^A)	CH_3 δ_a (ax : 65, eq : 20)
	1460(ν_8^E)	CH_3 δ_a (ax : 65, eq : 20)
1377(s, ⊥)	1383(ν_9^E)	CH_3 δ_s (100)
	1383(ν_9^A)	CH_3 δ_s (100)
1327(m, ∥)	1315(ν_{10}^A)	CH bend. (ax : 10, eq : 65)
1325(m, ⊥)	1326(ν_{10}^E)	CH bend. (ax : 15, eq : 55)
1313(w, ∥)	1312(ν_{11}^A)	CH bend. (ax : 65, eq : 10)
1303(w, ⊥)	1286(ν_{11}^E)	CH bend. (ax : 65, eq : 15)
1184(s, ∥)	1187(ν_{12}^A)	r_{CC}^{ax} (45), CD_2 wag. (20)
1170(m, ⊥)	1183(ν_{12}^E)	r_{CC}^{eq} (35)
	1136(ν_{13}^E)	r_{CC}^{ax} (30), CD_2 wag. (20), r_{CM} (15), CH_3 rock. (15)
1134(m, ∥)	1131(ν_{13}^A)	CH_3 rock.^{eq} (15), CD_2 twist. (15), r_{CM} (15)
1110(m, ⊥)	1102(ν_{14}^E)	CH_3 rock.^{eq} (25), CD_2 wag. (15)
	1088(ν_{14}^A)	r_{CM} (20), r_{CC}^{eq} (20), CH_3 rock.^{ax} (20)
1058(s, ∥)	1052(ν_{15}^A)	CD_2 bend. (60), CH_3 rock.^{eq} (15)
1051(m, ⊥)	1045(ν_{15}^E)	CD_2 bend. (75)
1018(m, ⊥)	1018(ν_{16}^E)	CD_2 wag. (40), CH_3 rock.^{ax} (25), r_{CM} (20)
1013(s, ∥)	996(ν_{16}^A)	r_{CM} (30), CD_2 wag. (20), r_{CC}^{eq} (20), CH_3 rock.^{ax} (20)
896(w, ⊥)	901(ν_{17}^E)	CH_3 rock. (ax : 10, eq : 25), r_{CC}^{ax} (20)
894(m, ∥)	895(ν_{17}^A)	CH_3 rock.^{eq} (25), CD_2 wag. (20), CD_2 twist. (25)
868(s, ∥)	877(ν_{18}^A)	CH_3 rock. (ax : 30, eq : 20), CH bend. (15), r_{CC}^{ax} (15)
868(w, ⊥)	865(ν_{18}^E)	CH_3 rock. (ax : 20, eq : 15), r_{CC}^{ax} (20), CD_2 twist. (20)
811(w, ⊥)	799(ν_{19}^E)	CD_2 twist. (55)
764(w, ∥)	785(ν_{19}^A)	CD_2 twist. (40), r_{CC}^{eq} (20), r_{CM} (15)
715(m, ⊥)	705(ν_{20}^E)	CD_2 rock. (50), r_{CM} (15)
691(m, ∥)	689(ν_{20}^A)	CD_2 rock. (80)

*1,*2 See *1,*2 of Table IV.

The corresponding bands of the CD_2 group are observed at about 2170 cm^{-1} (antisymmetric stretching), while the bands due to the CD_2 symmetric stretching mode[7] appear to be split into the parallel component at 2085 cm^{-1} and the perpendicular component at 2092 cm^{-1}. The stretching vibrations of the CHD group of poly(propylene-1-d_1) are observed at 2870 cm^{-1} (CH stretching) and at about 2135 cm^{-1} (CD stretching).[7,14]

The strong perpendicular bands at about 2920 cm^{-1} are assigned to the stretching vibration of tertiary CH group in the present study.*5 The perpendicular component has been expected to be stronger than the parallel component ($I_A/I_E=0.8$).[13] The band due to the CD stretching vibration[7] appears to be split into the weak parallel component at 2154 cm^{-1} and the strong perpendicular component at 2162 cm^{-1}.

*5 This band has been assigned to the CH_2 antisymmetric stretching mode.[11-13] Instead, the bands near 2800 cm^{-1} have been assigned to the CH stretching modes.[12,13]

14) T. Miyazawa and Y. Ideguchi, to be published.

Infrared Bands in the 1500~650 cm^{-1} Region

In our previos study, the potential energy distributions for the vibrations lying in the 1500~650 cm^{-1} region have been approximately calculated and the vibrational assignments of the infrared bands discussed in detail.[2] In the present study, the potential energy distributions (PED) were refined by a complete normal coordinate treatment (Table IV–VII). However, the potential energy distributions did not change essentially, except as noted below: (1) The potential energy of the vibrations of IPP at 1377~1379 cm^{-1} are associated almost exclusively with the CH_3 symmetric deformation mode, although in the previous treatment a slight coupling with the C–H bending modes was deduced. (2) As for the C–H and C–D bending modes, and the degenerate deformation and rocking modes of the CH_3 and CD_3 groups, the fractions of the potential energy associated with the axial and equatorial components have changed more or less for several vibrations. Except for these changes, the detailed analyses of the infrared bands reported previously are still valid. Therefore,

TABLE VII. THE OBSERVED AND CALCULATED FREQUENCIES (IN cm^{-1}) AND POTENTIAL ENERGY DISTRIBUTIONS (IN %) OF ISOTACTIC POLY(PROPYLENE-3, 3, 3-d_3) IN THE REGION 1500～600 cm^{-1}

ν_{obs}*1	ν_{calcd}	Potential energy distributions*2
1440(m, ∥)	1437(ν_7^A)	CH_2 bend. (100)
1438(m, ⊥)	1439(ν_7^E)	CH_2 bend. (100)
1379(w, ∥)	1369(ν_8^A)	CH_2 wag. (45), CH bend.^{ax} (35)
1361(m, ⊥)	1367(ν_8^E)	CH bend.^{eq} (35), CH_2 wag. (20), CH_2 twist. (25)
1334(w, ∥)	1329(ν_9^A)	CH bend.^{eq} (60), CH_2 twist. (15)
1333(m, ⊥)	1343(ν_9^E)	CH_2 wag. (40), CH bend.^{ax} (35)
1305(m, ∥)	1305(ν_{10}^A)	CH_2 wag. (50), CH_2 twist. (25), CH bend.^{ax} (20)
1293(m, ⊥)	1288(ν_{10}^E)	CH bend. (ax : 30, eq : 25), CH_2 wag. (35)
1239(m, ∥)	1236(ν_{11}^A)	CH bend. (ax : 25, eq : 25), CH_2 twist. (35)
1206(w, ⊥)	1183(ν_{11}^E)	CH_2 twist. (25), CH bend. (ax : 15, eq : 10), r_{CC}^{eq} (20)
1145(m, ⊥)	1156(ν_{12}^E)	r_{CM} (30), CH bend. (20)
1145(w, ∥)	1136(ν_{12}^A)	r_{CC}^{ax} (55)
1115(w, ∥)	1097(ν_{13}^A)	CD_3 δ_s (70), r_{CM} (45)
1081(m, ⊥)	1085(ν_{13}^E)	CD_3 δ_s (35), r_{CC}^{ax} (25), r_{CC}^{eq} (15)
	1064(ν_{14}^E)	CD_3 δ_s (35), CD_3 δ_a^{ax} (15), r_{CC}^{ax} (20)
1054(s, ⊥)	1043(ν_{15}^E) 1048(ν_{14}^A)	CD_3 δ_a (ax : 15, eq : 80) CD_3 δ_a (ax : 15, eq : 65)
1051(s, ∥)	1043(ν_{15}^A) 1038(ν_{16}^E)	CD_3 δ_a (ax : 75, eq : 15) CD_3 δ_a (ax : 60, eq : 10)
989(w, ∥)	1005(ν_{16}^A)	r_{CC}^{eq} (40), CD_3 δ_s (20)
984(w, ⊥)	971(ν_{17}^E)	CH_2 rock. (15), r_{CM} (15), CD_3 δ_s (15)
909(m, ∥)	926(ν_{17}^A)	r_{CM} (25)
821(m, ⊥)	814(ν_{18}^E)	CH_2 rock. (30), r_{CM} (15)
807(vw, ∥)	827(ν_{18}^A)	CH_2 rock. (70), CH bend. (15)
791(s, ∥)	781(ν_{19}^A)	CD_3 rock. (ax : 40, eq : 35)
759(m, ⊥)	760(ν_{19}^E)	CD_3 rock. (ax : 50, eq : 20)
743(w, ⊥)	741(ν_{20}^E)	CD_3 rock. (ax : 15, eq : 50)
703(m, ∥)	725(ν_{20}^A)	CD_3 rock. (ax : 40, eq : 35)

*1,*2 See *1,*2 of Table IV.

TABLE VIII. THE FREQUENCIES (IN cm^{-1}) OF THE FAR INFRARED BANDS AND THE POTENTIAL ENERGY DISTRIBUTIONS (%) OF ISOTACTIC POLYPROPYLENE

ν_{obs}*1	ν_{calcd}*2	Potential energy distributions*3
528(⊥)	ν_{21}^E 509	δ^a (40), δ (25)
460(⊥)	ν_{22}^E 445	δ^s (65)
456(∥)	ν_{21}^A 473	δ^a (75)
398(∥)	ν_{22}^A 392	δ^s (35), δ^a (40)
321(⊥)	ν_{23}^E 314	δ^a (60)
251(∥)	ν_{23}^A 272	δ^s (40), δ^a (20)
210(⊥)	ν_{24}^E 207	t_{C-CH_3} (95)
200(∥)	ν_{24}^A 203	t_{C-CH_3} (85)
169(⊥)	ν_{25}^E 162	δ^a (40), δ (30), t_{CC}^{ax} (15)
155(∥)	ν_{25}^A 157	δ (40), t_{CC}^{eq} (35)
106	ν_{26}^E 90	t_{CC}^{ax} (70)

*1 Observed frequencies (Refs. 1 and 8); ∥ : parallel band; and ⊥ : perpendicular band.
*2 Calculated frequencies.
*3 δ^s and δ^a : the symmetric and asymmetric deformation modes of the C-CH-C group; δ : C-CH_2-C (with C below CH); bending; t_{CC}^{eq}, t_{CC}^{ax} and t_{C-CH_3} : the internal rotation modes about the equatorial and axial C-C bonds and the C-methyl bond, respectively.

TABLE IX. FREQUENCIES (ν_c IN cm^{-1}) AND POTENTIAL ENERGY DISTRIBUTIONS (PED IN %)*1 CALCULATED FOR THE LOW FREQUENCY VIBRATIONS

$[-CH_2-CD(CH_3)-]_p$

A species		E species	
ν_c	PED	ν_c	PED
467	δ^a (75)	497	δ^a (35), δ (25)
387	δ^s (35), δ^a (40)	438	δ^s (65)
269	δ^s (40), δ^a (20)	310	δ^a (60)
202	t_{C-CH_3} (85)	207	t_{C-CH_3} (95)
154	t_{CC}^{eq} (35), δ (35)	160	δ^a (40), δ (30), t_{CC}^{ax} (15)
		89	t_{CC}^{ax} (75)

$[-CD_2-CH(CH_3)-]_p$

A species		E species	
ν_c	PED	ν_c	PED
446	δ^a (70)	483	δ^a (40), δ (30)
367	δ^s (40), δ^a (30)	394	δ^s (60), CD_2 rock. (15)
249	δ^s (30), δ^a (25), t_{C-CH_3} (15)	297	δ^a (60)
202	t_{C-CH_3} (80)	207	t_{C-CH_3} (95)
153	t_{CC}^{eq} (35), δ (35)	155	δ^a (40), δ (30), t_{CC}^{ax} (15)
		88	t_{CC}^{ax} (70)

$[-CH_2-CH(CD_3)-]_p$

A species		E species	
ν_c	PED	ν_c	PED
441	δ^a (65)	484	δ^a (30), δ (25)
362	δ^s (30), δ^a (45)	420	δ^s (60)
260	δ^s (40), δ^a (20), t_{CC}^{eq} (15)	291	δ^a (60)
154	t_{C-CD_3} (50), δ (20)	157	t_{C-CD_3} (45), δ^a (25), δ (15)
137	t_{C-CD_3} (40), t_{CC}^{eq} (25), δ (20)	138	t_{C-CD_3} (55), δ^a (20), δ (15)
		82	t_{CC}^{ax} (75)

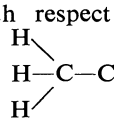
*1 See *3 of Table VIII.

the nature of the infrared bands of IPP, IPP-CD, IPP-CD_2 and IPP-CD_3 will be briefly described.

$[-CH_2CH(CH_3)-]_p$.—The perpendicular band at 1460 cm^{-1} and the parallel band at 1454 cm^{-1} are assigned to the CH_3 asymmetric deformation vibrations, while the bands at 1377~1378 cm^{-1} are assigned to the CH_3 symmetric deformation vibrations. The bands of IPP, IPP-CD, and IPP-CD_3 at 1435~1440 cm^{-1} are assigned to the CH_2 bending vibrations. The abnormal dichroic behavior of the bands of IPP and IPP-CD may possibly be due to the slight coupling of the CH_2 and CH_3 deformation modes.[2)]

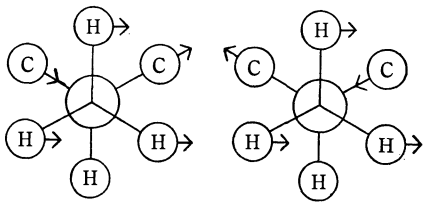
In the 1370~1200 cm^{-1} region, the observed bands are due to the hybridized vibrations of the CH_2 wagging and twisting modes and the axial and equatorial CH bending modes.*6 The interactions among these modes are primarily due to the trans- and gauche-coupling terms in the vibrational potential function. These vibrational couplings depend upon the internal-rotation about the main-chain CH–CH_2 bonds. The remarkable spectral change upon the fusion of the isotactic sample may be understood in relation to the coupling of the CH_2 and CH modes across the CH–CH_2 bonds.

The infrared bands of IPP in the 1200~800 cm^{-1} region arise from the hybridized vibrations of the axial and equatorial C–C stretching modes, the C–methyl stretching modes, the axial and equatorial CH_3 rocking modes, and the CH_2 rocking modes. The strong parallel bands at 1168, 998, and 973 cm^{-1} are primarily due to the C–C stretching and CH_3 rocking modes. The parallel bands at 973 cm^{-1} and 1168 cm^{-1} arise from the coupled vibrations of the antisymmetric stretching mode of the axial and equatorial C–C bonds and of the methyl rocking modes, which is nearly antisymmetric with respect to the H–C–CH_3 plane. For the



group, the atomic displacements of the vibrations at 973 cm^{-1} and 1168 cm^{-1} are schematically

*6 The intrinsic frequencies of the CH_2 wagging and twisting modes are located at 1330~1340 cm^{-1} and 1270~1290 cm^{-1} respectively, while the intrinsic C-H bending frequency is located at 1305~1325 cm^{-1}.



(a) (b)

Fig. 4 Atomic displacements of the vibrations of $H-\overset{H}{\underset{H}{C}}-\overset{H}{\underset{C}{C}}-H$ group at 950 cm^{-1} (a) and at 1150 cm^{-1} (b).

shown in Figs. 4a and 4b respectively. The band at 998 cm^{-1} arises from the C–methyl stretching mode and the methyl rocking mode in the H–C–CH_3 plane. The parallel band at 842 cm^{-1} is due either to the ν_{19}^A vibration or to the ν_{20}^A vibration. The ν_{19}^A vibration is associated with the methyl rocking mode (in the H–C–CH_3 plane) as coupled with the nearly symmetric stretching mode of the axial and equatorial C–C bonds and the C–methyl bonds.

[–CH_2–$CD(CH)_3$–]$_p$—Since the intrinsic C–D bending frequency is much lower than 1250 cm^{-1}, the CH_2 wagging and twisting modes of this molecule are not coupled with the C–D bending modes. The bands at 1342 cm^{-1} (∥) and 1334 cm^{-1} (⊥) are due to the CH_2 wagging modes, while the bands at 1291 cm^{-1} (∥) and 1273 cm^{-1} (⊥) are due to the CH_2 twisting modes. The infared bands of IPP–CD in the 1250～750 cm^{-1} region arise from the coupled vibrations of the C–D bending modes, the CH_3 and CH_2 rocking modes, and the C–C stretching modes. The intrinsic frequencies of all these modes may be located in the 1100～800 cm^{-1} region. It is remarkable to note that the contributions of the C–D bending modes are greater than 15% for many vibrations in the 1250～750 cm^{-1} region.

[–CD_2–$CH(CH_3)$–]$_p$.—For this molecule, the intrinsic CD_2 wagging and twisting frequencies are shifted lower than 1200^{-1}, and, consequently, the CH bending modes are not coupled with the CD_2 bending modes. The bands at 1327 cm^{-1}, 1325 cm^{-1}, 1313 cm^{-1}, and 1303 cm^{-1} arise almost exclusively from the C–H bending modes.

The bands primarily due to the CD_2 bending modes are observed at 1058 cm^{-1} (∥) and 1051 cm^{-1} (⊥), while the band due to the CD_2 rocking modes are observed at 764 cm^{-1} (∥) and 811 cm^{-1} (⊥).

The CD_2 wagging and twisting modes are strongly coupled with the methyl rocking modes and the C–C stretching modes and give rise to the infrared bands in the 1200～800 cm^{-1} region.

[–CH_2–$CH(CD_3)$–]$_p$.—The strong bands of IPP–CD_3 at 1051 cm^{-1} (∥) and at 1054 cm^{-1} (⊥) are due to the CD_3 asymmetric deformation modes. The CD_3 symmetric deformation modes are strongly coupled with the axial and equatorial C–C stretching modes and give rise to bands in the 1100～1000 cm^{-1} region. The parallel bands at 791 and 703 cm^{-1} and the perpendicular bands at 759 and 743 cm^{-1} arise from the CD_3 rocking modes.

Far Infrared Vibrations of Isotactic Polypropylene

The far infrared spectra of the uniaxially oriented films of isotactic polypropylene have been measured in the 600～300 cm^{-1} region[1] and in the 400～80 cm^{-1} region[8] (the dichroism has been measured in the region above 100 cm^{-1}). (A preliminary normal coordinate treatment had previously been made as an aid in the vibrational assignments.[8]) The potential energy distributions of the far infrared vibrations of isotactic polypropylene were recalculated in the present study and are listed in Table VIII.

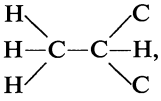
These low frequency vibrations are associated with the C–C–C bending modes of the $C-CH_2-C$ and $C-CH\langle^{C}_{C}$ groups and with the internal-rotation modes about the C–methyl bond and the equatorial and axial C–C bonds. The weak bands at 200 cm^{-1} (∥) and 210 cm^{-1} (⊥) arise from the internal-rotation modes of the CH_3 group about the C–methyl bond. The low frequency modes of isotactic polypropylene are not localized in a repeating unit. Therefore, these modes give rise to well-defined bands only for highly-ordered helical conformations in the crystalline region.[8]

The far infrared spectra of the deuterated derivatives of isotactic polypropylene have not been published. However, the frequencies and potential energy distributions calculated for deuterated derivatives are shown in Table IX.

Liquid Spectra of Isotactic Polypropylene

Well-defined infrared bands observed in the liquid spectra of isotactic polypropylene and deuterated derivatives have been discussed before with reference to the potential energy distributions calculated for the helical structure. Moreover, the liquid bands arising from the CH_3 symmetric and asymmetric deformation modes, the CH_2 bending wagging, and twisting modes and the CH bending modes,

and the CD_3 rocking modes have already been analyzed.[2]

For isotactic polypropylene, two strong bands are observed at 971 and 1151 cm^{-1} in the liquid state; these are naturally considered to arise from the C–C stretching modes and the methyl rocking modes. An empirical analysis has been made before in view of the "intrinsic" methyl rocking frequency.[2] In the present study, the normal vibrations of the model system,  , were treated. The elements of the potential energy matrix were transferred from the corresponding elements of isotactic polypropylene. In the 1200~800 cm^{-1} region, three A' vibrations (symmetric with respect to the H–C–CH_3 plane) were calculated at 864, 1015 and 1062 cm^{-1}, whereas two A'' vibrations (antisymmetric with respect to the H–C–CH_3 plane) were calculated at 948 cm^{-1} (ν_a) and 1134 cm^{-1} (ν_b). The atomic displacements of the ν_a and ν_b vibrations are schematically shown in Fig. 4. The calculated vibration at 948 cm^{-1} appears to correspond to the liquid frequency of 971 cm^{-1}, and its potential energy is associated 60% with the rocking mode and 40% with the C–C stretching modes. On the other hand, the calculated vibration at 1134 cm^{-1} corresponds to the liquid frequency of 1151 cm^{-1}, and its potential energy is associated 50% with the C–C stretching mode and 20% with the methyl rocking mode. If either one of these vibrations is excited in phase throughout the main chain, as is shown in Fig. 5, the vibrations of adjacent units will

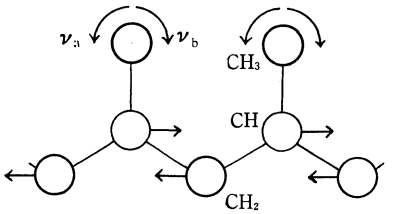


Fig. 5. In-phase vibrations of the ν_a or ν_b mode.

tend to displace the common CH_2 group in nearly the same direction (at least not in the opposite direction), and only minor vibrational interactions may be expected among CH–CH_3 groups. Such a vibrational mode may not be very sensitive to changes in the internal-rotation arrangements, and accordingly, well-defined strong absorption peaks may be expected, even in the liquid state. In support of these considerations, the in-phase ν_a and ν_b vibrations give rise to the strong bands at 973 cm^{-1} and 1168 cm^{-1} for isotactic polypropylene (in the crystalline region) and to the strong bands at 1153 cm^{-1} and 974 cm^{-1} for syndiotactic polypropylene (in the crystalline region).[15]

The strong parallel band of isotactic polypropylene at 998 cm^{-1} disappears on melting. As Table IV shows, this band is due to the hybridized vibration of the methyl rocking mode, the C–methyl stretching mode, and the CH_2 twisting mode. The coupling with the CH_2 twisting mode depends upon the internal-rotation about the main-chain CH–CH_2 bonds. This vibration, therefore, is very much affected by the rearrangements of the main-chain conformations and does not give rise to a well-defined band in the liquid state.

Summary

The infrared active normal vibrations of isotactic polypropylene and its deuterated derivatives in the crystalline state have been treated. The modified Urey-Bradley-Shimanouchi force field has been used for the calculations. A total of 23 potential constants have been adjusted by the method of least squares with reference to a total of 166 frequencies observed by Peraldo and Farina. The standard errors of the potential constants have also been calculated. The r. m. s. deviation of the calculated frequencies from the observed ones is as small as 0.9%. The potential energy distributions have also been calculated for the discussion of the nature of the observed infrared bands. Vibrational assignments of the liquid bands of isotactic polypropylene have also been made.

The authors wish to thank Professor Takehiko Shimanouchi and his group at the University of Tokyo for their stimulating discussions and Mr. Hiroatsu Matsuura of Osaka University for his assistance in the preparation of all the figures.

Institute for Protein Research
Osaka University
Kita-ku, Osaka

15) T. Miyazawa and Y. Ideguchi, presented at the 17th Annual Meeting of the Chemical Society of Japan, Tokyo, April, 1964; T. Miyazawa, *J. Polymer Sci.*, to be published.

NOTES

The Separation of Lanthanons by Paper Precipitation Chromatography with 8-Quinolinol. II. The Separation and Detection of Lanthanum, Cerium, Praseodymium and Uranium

By Hideo NAGAI

(Received May 17, 1963)

It was shown in the preceding paper[1] that the use of an aqueous *n*-butyric acid solution saturated with isobutanol (as a developer) made it possible to obtain rare earth ions on oxine-impregnated filter paper in the form of separated circular bands of precipitates.

In the present study, a modified developer composed of a *n*-butyric acid solution and a water-miscible organic solvent has been applied to the separation of ions from mixtures containing lanthanum, cerium(III), praseodymium and uranyl ions. It has been found that the separation is much improved by the use of the new developer when a small amount of uranyl ions is added to the sample solution.

Experimental

The apparatus, the method of development and the preparation of the sample were essentially the same as have been reported previously,[1] but some changes were made:

1) The distance between the liquid surface of the developer and the oxine-impregnated filter paper was 3.5~4.0 mm. when a container 6 cm. in diameter was used. The width of the strip at the center of the filter paper disk was 3.5~4.0 mm., larger than that of the strip used in the previous study.[1]

2) Oxine (1.000±0.003 g.) in 80 ml. of ethanol was used to impregnate 100 sheets of filter paper (Toyo Filter Paper No. 5B, 9 cm. in diameter). In order to obtain reproducible results, it is essential to keep the oxine content in the filter paper disk as constant as possible.

3) A *n*-butyric acid solution (1~3%) could be used as the developer when a small quantity of uranyl nitrate (ca. 1 mg./ml. as uranium) was added to the sample solution, although the results were not satisfactory because of the low dissolution. *n*-Butyric acid solutions containing various organic solvents were examined and found to be much more useful for the separation of ions.

4) A 2.5% solution of *n*-butyric acid was used as one of the components of the developer. This concentration of the acid is higher than that used in the previous study.[1]

5) After development, the chromatograms were exposed ammonia vapor in order to insure the precipitation of the oxinates. The color of the cerium band thereupon changed from yellow to violet, but most of the cerium which had been coprecipitated together with the other rare earth elements (contaminants of the other rare earth bands) remained unchanged. The distribution of cerium was determined in detail by spraying about a 3 N aqueous solution of potassium chromate.

Development.—Table I shows the results obtained with mixtures in water of organic solvents and 2.5% *n*-butyric acid in various proportions (20± 1°C).

There is almost no change in the chromatogram when only a small quantity of the organic solvent (shown by ±) is added. Then the development is gradually improved as the quantity of organic

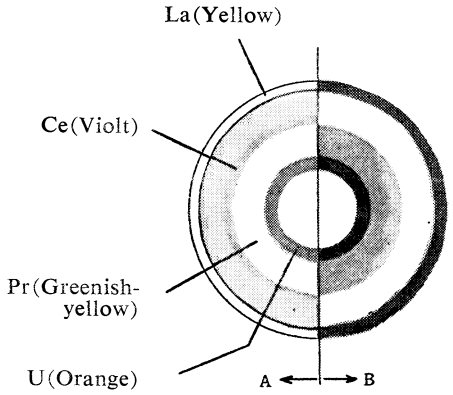


Fig. 1. Chromatogram and its radioautogram.
A. Chromatogram of uranyl and three rare earth element ions.
B. Radioautogram: chromatogram was irradiated with thermal neutrons (ca. 1×10^{11} n/cm²/sec., 5 hr.) and attached to the photographic plate from 90 till 170 hr. after irradiation.

1) H. Nagai, This Bulletin, 33, 715 (1960).

TABLE I.* RESULTS OF DEVELOPMENT WITH VARIOUS SOLVENTS

Volume ratio of the 2.5% *n*-butyric acid solution	300	200	100	60	30	10	5	2	1	1	1
Volume ratio of the organic solvent	1	1	1	1	1	1	1	1	1	2	3
Dioxane				±	+	++	++	M	S		
n-Propanol		±	+	+	++	++	M	M	S		
Isopropanol		±	+	++	+++	++	M	M	S		
Ethanol	±	+	++	+	+	+	+	+	M	M	S
Methanol			±	+	+	++	++	+	M	S	

* This table is explained below.

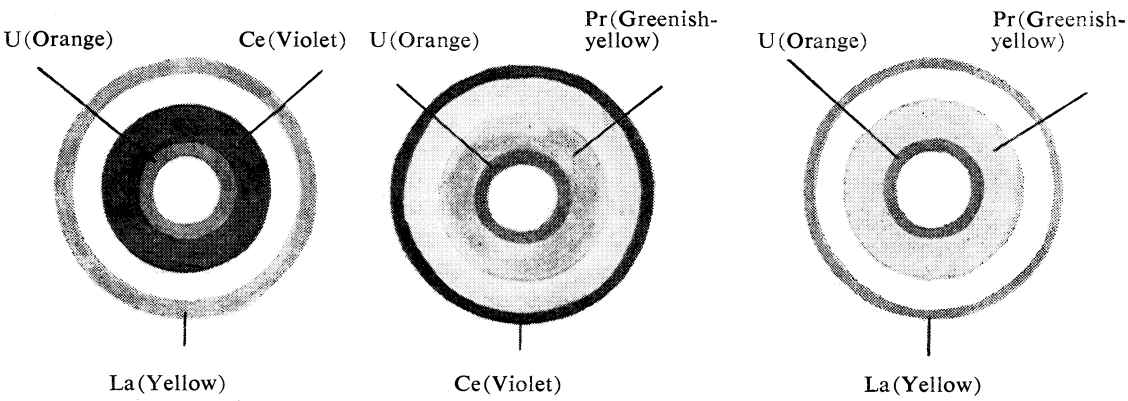


Fig. 2. Chromatograms of ternary mixtures.

solvent is increased (the degree of improvement is indicated by +, ++, and +++). When the mixing ratio of organic solvent is increased beyond this region, some of the bands begin to dissolve before the completion of the development; the chromatogram obtained is an intermediate one between the precipitation- and soluble-type chromatograms. This region is indicated as M. When the mixing ratio of the organic solvent is increased further, the chromatogram finally comes to be a true soluble type (indicated as S). In the present study, the author does not deal with these regions, M and S.

When a sample solution containing uranyl, praseodymium, cerium and lanthanum ions was developed in precipitation chromatography with a suitable developer, the bands of the components were formed in the order described above counting from the center to the periphery (Fig. 1). Table I shows that a 30 : 1 mixture of 2.5% *n*-butyric acid and isopropanol is the best developer. In this case, however, a considerable amount of the lanthanum ions was retained in the praseodymium and cerium bands. This defect was reduced by adding dioxane to the developer. The best result, in this experiment, was obtained with a developer composed of 2.5% butyric acid, isopropanol and dioxane in a volume ratio of 50 : 4 : 1. It is important to stop the development immediately after the formation of the bands of all the components; thus, in order to obtain satisfactory results, the development is stopped when the uranyl band formed begins to dissolve slightly. The results of the development were as follows.

When all of the four cations were present, the only band which could be obtained in an almost pure state was the uranyl band (the innermost). The lanthanum band (the outermost) was slightly contaminated by cerium. The praseodymium and the cerium bands, between the two bands mentioned above, however, almost entirely overlapped one another, and a considerable quantity of lanthanum was contained in these bands, although the characteristic color of each band could still be observed (praseodymium, a greenish yellow, and cerium, violet).

Better results were obtained with samples containing three kinds of ions, two kinds of rare earth ions and the uranyl ion. The uranyl ion was separated in an almost pure state in all cases, and the separation of praseodymium and cerium, which had been almost impossible before, was possible, though the separation was not satisfactory. Concerning the separation of lanthanum and cerium the lanthanum band was found to be almost pure; the cerium band, however, was contaminated by a considerable quantity of lanthanum. The separation of lanthanum and praseodymium was most satisfactory in these experiments; the amount of lanthanum in the other band was much less than that in the case of the separation of cerium and lanthanum. Figure 2 shows these chromatograms.

Discussion

Optimum Mixing Ratio. — When chromatograms were obtained with a series of organic solvents, with various mixing ratios the area of a band was the largest at the optimum

mixing ratio. It might be that the rate of precipitation was the slowest in this solution, as in the case of the other precipitation reactions.

The Estimation of the Separation of Ions.— In order to estimate the degree of the separations, the following methods were employed; observation under day- and ultraviolet-light, a radioautogram, and spraying with a potassium chromate solution. A radioautogram is a very convenient way to find out the distribution of the components (Fig. 1), but several months are necessary to determine the distribution of cerium. The potassium chromate spray can, however, give almost the same results as the long exposure-radioautography does.

The author wishes to express his appreciation to the Ministry of Education for having made available part of the Scientific Research Fund of the Ministry of Education for this study.

Department of Chemistry
Faculty of Science
Kumamoto University
Kurokami-machi, Kumamoto

The Synthesis of L-*Theanine*

By Toshiyuki FURUYAMA, Takeshi YAMASHITA and Saburo SENOH

(Received February 15, 1964)

In the course of investigations of flavor substances in Japanese green tea, Sakato discovered L-glutamic acid γ-ethyl amide in the water extract and named theanine.[1] The synthesis of this substance has since been reported by several authors.[2-8] Sakato et al.,[3] for instance, synthesized it from *N*-carbobenzoxy-L-glutamic acid γ-ethyl ester, and Hashizume[4] and Tsuchiya et al.,[8] from pyrrolidonecarboxylic acid.

The synthesis described here is based on the reaction between amino groups of amino acids and carbon disulfide in the presence of alkali, giving dithiocarbamates and protecting the amino group.[9] The procedure is as follows: In the solution of 10 ml. of ethanol and 2 ml. of carbon disulfide, 4 g. of γ-methyl L-glutamate was dispersed. To the mixture, 50 ml. of anhydrous ethylamine*1 was added under cooling with ice-water. The solution was left to stand for ten days at room temperature in a sealed flask. The excess ethylamine, carbon disulfide and ethanol were then distilled off in vacuo. The residual oily material was suspended in 25 ml. of 5 N acetic acid and heated for 30 min. at 60°C under reduced pressure. The carbon disulfide which had protected the amino group of the product was split off by this procedure. The residual solution was concentrated to some extent, and ethanol added. L-Theanine crystallized out in a yield of 1 g. Recrystallization from water-ethanol afforded L-theanine (m.p. 215°C with decomp.) and $[\alpha]_D^{18}$ +8.7° (*c* 1.743, water).*2

Found: C, 48.11; H, 8.06; N, 16.01. Calcd. for $C_7H_{14}O_3N_2$: C, 48.26; H, 8.10; N, 16.08%.

The favorable protection of the amino group with carbon disulfide gave L-theanine without any racemization. Boissonnas previously synthesized optically-pure L-glutamine by protecting the amino group by carbon disulfide.[10] When his scheme was used, scarcely any formation of pyrrolidonecarboxylic acid occured. The present reaction appears to proceed in a manner analogous to Boissonnas' scheme.

Technical Research Laboratory
Asahi Chemical Industry Co., Ltd.
Itabashi-ku, Tokyo

1) Y. Sakato, *J. Agr. Chem. Soc. Japan* (*Nippon Nogei Kagaku Kaishi*), **23**, 262 (1949).
2) N. Lichtenstein, *J. Am. Chem. Soc.*, **64**, 1021 (1942).
3) Y. Sakato, T. Hashizume and Y. Kishimoto, *J. Agr. Chem. Soc. Japan* (*Nippon Nogei Kagaku Kaishi*), **23**, 269 (1949).
4) T. Hashizume, ibid., **25**, 25 (1951).
5) Y. Tsuchiya, Japanese Pat. Pub. No. 27-3417 (1952).
6) J. Edelson, C. G. Skinner and W. Shive, *J. Med. Pharm. Chem.*, **1**, 165 (1959).
7) G. B. Kline, U.S. Pat. 2873294 (1959).
8) Y. Tsuchiya, Y. Yamada and M. Sakurai. Japanese Pat. Pub. No. 37-11661 (1962).
9) M. Siegfried and O. Wiedenkanpt, *Z. physiol. Chem.*, **70**, 152 (1910).

*1 This specimen of ethylamine was prepared by the distillation of a commercial 70% aqueous solution in the presence of sodium hydroxide pellets. If 70% ethylamine is used, the main product will be pyrrolidonecarboxylic acid instead of theanine.

*2 A Rudolph photo-electric polarimeter, model 200, was used.

10) R. Boissonnas, German Pat. 1080113 (1960).

A New Method of Synthesizing Tetrabenzo[a, cd, j, lm]perylene and Dibenzo[cd, lm]perylene

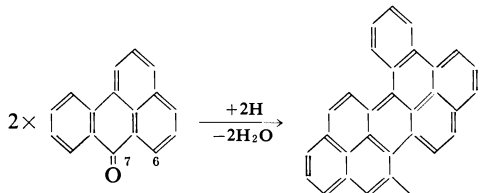
By Junji AOKI

(Received February 2, 1964)

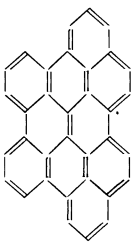
When the 6- and 7-positions of one benzanthrone (I) molecule couple with the 7- and 6-positions of another one, tetrabenzo[a, cd, j, lm]perylene (II) is formed. Similarly, by a coupling related to the carbonyl groups of two moles of benzonaphthenone (IV), dibenzo[cd, lm]perylene (V) is formed. Although the syntheses of these two hydrocarbons have already been carried out by Clar,[1,2] the procedures were quite different. Tetrabenzoperylene (II) was prepared by the condensation of two moles of benzanthrone in a benzene solution through the action of zinc dust and anhydrous aluminum chloride, while dibenzoperylene (V) was synthesized by the zinc dust fusion of benzonaphenone.

However, the present author has succeeded in the synthesis of both of them by the one following method.

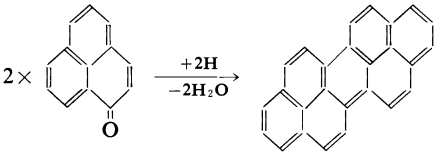
A mixture of ketone (1 part), copper powder (1 part), zinc chloride (5 parts) and sodium chloride (1 part) is kept at 220~230°C for 30~60 min. Then the mixture is treated with diluted hydrochloric acid, and the insoluble part collected. After the extraction of this material with chlorobenzene or *o*-dichlorobenzene, the crude product is purified by recrystallization or chromatography.



I II



III



IV V

This method is not only easy to perform, but it gives rather a good yield. The author, therefore, recommends it as a general method for the condensation of such a substance.

Experimental

Tetrabenzo[a, cd, j, lm]perylene (II) and Dibenzo[hi, uv]bisanthene (III).—A mixture of benzanthrone (5.0 g.), copper powder (5.0 g.), zinc chloride (25 g.) and sodium chloride (5 g.) was kept at 220°C for 30 min. As the reaction proceeded, the reaction mixture became thicker and its color changed from red to black. Then the mixture was treated with warm water containing a small amount of hydrochloric acid, and the insoluble part was collected, washed and dried. Yield, 11.1 g. This product was refluxed with 100 g. of chlorobenzene for 2 hr., and the insoluble material and copper powder were removed by hot filtration. When the filtrate was concentrated, 3.95 g. of a brown crystalline powder was obtained (insoluble part, 6.65 g.). A solution of 1 g. of this product in 30 cc. of chlorobenzene was passed through a column of alumina and eluted with chlorobenzene. The first passing yellow band was separated and concentrated, giving long, fine, yellow needles (0.2 g.) which melted at 331°C (uncor.). This product was soluble in an organic solvent with a lemon yellow color and a strong grey blue fluorescence, while in a concentrated sulfuric acid solution it is blue. The absorption spectrum in benzene was identical with that of II reported by Clar.[2]

Found: C, 95.94; H, 4.34. Calcd. for $C_{34}H_{18}$· (II): C, 95.75; H, 4.25%.

On the other hand, 2.0 g. of above product (3.95 g.) was refluxed with 50 g. of benzene, and, after hot filtration, the insoluble part was sublimated in a high vaccum (10^{-3}~10^{-4} mmHg). The orange sublimed material was collected and recrystallized from *o*-dichlorobenzene and then chlorobenzene, giving orange crystals (m. p. 305~307°C). This substance is soluble in xylene with a greenish

1) E. Clar, D. R. P. 621861.
2) E. Clar, *Chem. Ber.*, **76**, 458 (1943).

yellow color and a green yellow fluorescence, while in a concentrated sulfuric acid it is blue. Found: C, 95.95; H, 3.92. Calcd. for $C_{34}H_{16}$(III): C, 96.20; H, 3.80%. This by-product is considered to be the III reported by Clar.[2]

Dibenzo[cd, lm]perylene (V). — A mixture of 2.0 g. of benzonaphthenone (IV), 2.0 g. of copper powder, 10 g. of zinc chloride and 2 g. of sodium chloride was kept at 220~230°C for 40 min. Then the mixture was treated with diluted hydrochloric acid, and the insoluble part was collected, washed and dried. Yield, 5.0 g. This material was refluxed with alcohol (30 ml.) for 2 hr. After the solution had cooled the insoluble part was filtered off and refluxed with xylene (50 g.) for 2 hr. The insoluble substance was then removed by hot filtration, and the filtrate was concentrated, giving 1.1 g. of a brown solid. This crude product was twice recrystallized from *o*-dichlorobenzene, giving 0.6 g. of gold yellow leaflets (m. p. 373~374°C). The sample, purified by means of chromatography on alumina with chlorobenzene, melted at 375~376°C (uncor.), and the absorption spectrum in alcohol was identical with that of V reported by Clar.[2] Found: C, 95.42; H, 4.53. Calcd. for $C_{26}H_{14}$(V): C, 95.68; H, 4.32%.

Department of Chemistry
Faculty of Science
Toho University
Narashino, Chiba

Infrared-Active Lattice Vibrations in a Few Fluorite-type Crystals

By Minoru TERADA and Masamichi TSUBOI

(Received February 24, 1964)

In an attempt to obtain information about the crystalline force field, we have observed the infrared absorptions of three metal oxides with fluorite-type lattices, namely, uranium dioxide (UO_2), thorium dioxide (ThO_2), and cerium dioxide (CeO_2).

The sample of UO_2 was prepared by the Mitsubishi Metal Mining Company, that of ThO_2 was prepared by the Linsay Chemical Company (U.S.A.), and that of CeO_2 was prepared by Dr. Hiroshi Takahashi (the University of Tokyo), who kindly placed it at our disposal. The fact that all three of these samples fluorite-type crystal structures[1] was ascertained by an X-ray diffraction method.* The infrared absorption measurement was carried out by the use of a far-infrared spectrophotometer constructed by Professor H. Yoshinaga and his collaborators.[2] Each of the samples were mounted on the spectrophotometer in the form of a dispersion in a polyethylene film[3] (mostly with 200 mg. of oxide per 1.5 g. of polyethylene and 0.2 mm. thick).

The results of our infrared absorption measurement are shown graphically in Fig. 1. As may be seen in the figure, each of these oxides shows only one strong absorption band in the spectral region 4000~200 cm^{-1}. This is just what was expected from the crystal structure of these oxides. In a previous paper,[4] it has been shown that the fluorite (CaF_2)-type lattice (space group O_h^5) has only one infrared-active (F_{1u}) lattice vibration, and that its frequency ν (cm^{-1}) is given approximately by

$$4\pi^2c^2\nu^2=(4/3)K(\mu_F+2\mu_{Ca}) \qquad (1)$$

In this equation, c is the velocity of light, K, the stretching force constant of the Ca-F bond, and μ_F and μ_{Ca}, the reciprocal masses of the F and Ca atoms respectively. Table I gives the observed frequencies ν of the oxides in question and the metal-oxygen bond stretching force constants K as calculated by Eq. 1. In the third column of Table I, the metal-oxygen bond distances,[1] r, are also given.

As may be seen in Table I, the metal-oxygen bond is strongest in UO_2, next strongest in

1) V. M. Goldschmidt and L. Thomassen, *Videnskaps-selsk. Skr.*, 5, 12 (1923).

* In an X-ray diffraction examination kindly made by Dr. Y. Iitaka (the University of Tokyo), the sample of CeO_2 used gave sharp reflections: at d=0.81569, 0.82518, 0.85549, and 0.91454 Å (the calibration has been made by the use of silicon powder). These reflections are indexed as (622), (533), (620), and (531) respectively, with a fluorite-type cell and with a=5.411 Å. The exact cell dimension has been obtained, by an extrapolation at $2\theta=180°$ (2θ being the angle of diffraction), as a=5.4108 Å. On the basis of the results of the examination and by referring, for example, to "Standard X-ray Diffraction Powder Patterns" (United States Departmet of Commerce, National Bureau of Standards), the sample used may be considered to be practically pure CeO_2 for the present purposes.

2) H. Yoshinaga, S. Hujita, S. Minami, A. Mitsuishi, R. A. Oetjen and Y. Yamada, *J. Opt. Soc. Am.*, 28, 315 (1958).

3) H. Yoshinaga and R. A. Oetjen, ibid., 45, 1085 (1955).

4) T. Shimanouchi, M. Tsuboi and T. Miyazawa, *J. Chem. Phys.*, 35, 1597 (1961).

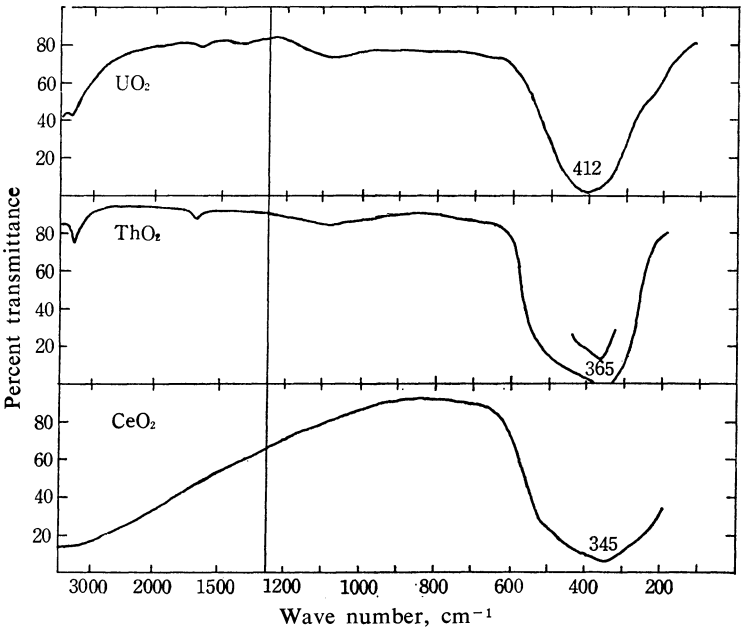


Fig. 1. Infrared absorptions of uranium dioxide, thorium dioxide, and cerium dioxide crystals, all of which have the fluorite type structures.

TABLE I

	Frequency ν cm^{-1}	Force constant, K mdyn./Å	Bond length, r Å
UO_2	412	1.057	2.36
ThO_2	365	0.827	2.42
CeO_2	345	0.685	2.34

ThO_2, and weakest in CeO_2. (However, the metal-oxygen bond length is shortest in CeO_2.) It is noticeable that the metal-oxygen bond stretching force constants in the oxides in question are much greater than the Ca-F bond stretching force constant (0.31 mdyn./Å) in fluorite crystal[4] or the Na-Cl bond stretching force constant (0.11 mdyn./Å) in sodium chloride crystal,[4] where the Ca-F or the Na-Cl bond is considered to be ionic. On the other hand, the metal-oxygen bond stretching force constants in question are much smaller than the C-C, C-Si, or U-O bond stretching force constants (2.8, 2.0, or 1.7 mdyn/Å respectively) in diamond,[4] silicon carbide,[5]** or α-uranium trioxide[6] crystals respectively; where the C-C, C-Si, or U-O bond is considered to be rather covalent.

We wish to express our sincere thanks to Professor H. Yoshinaga and Dr. A. Mitsuishi for their kindness in allowing us to use the far-infrared spectrometer of Osaka University.

Mitsubishi Atomic Power Industries, Inc.
Research and Engineering Laboratory
Amagasaki, Hyogo (M. Terada)

Faculty of Pharmaceutical Sciences
The University of Tokyo
Hongo, Tokyo (M. T.)

5) M. Tsuboi, ibid., **40**, 1326 (1964).

** For hexagonal silicon carbide, the stretching force constant of the C-Si bond (1.890 Å in length) along the c axis is slightly lower than that of the C-Si bond (1.886 Å in length), which makes a nearly tetrahedral angle with the c axis. The difference, however, was found to be less than 0.1 mdyn./Å. It was also found that the force constant of the latter C-Si bond is practically equal to the force constant of the C-Si bond (1.886 Å in length) in cubic silicon carbide.

6) M. Tsuboi, M. Terada and T. Shimanouchi, *J. Chem. Phys.*, **36**, 1301 (1962).

The Preparation of Bis(2-acetamido-6-acetylthio-O-acetyl-glucopyranosyl)sulfides

By Tadao Ishii and Teiichiro Ito

(Received March 6, 1964)

In 1959 M. Černý and J. Pacák[1] reported that 2, 3, 4, 6-tetra-*O*-acetyl-1-thio-β-D-glucopyranose condensed with alkyl halides, giving alkylthioglucopyranosides. The present work describes the application of this procedure to 2-acetamido-3, 4-di-*O*-acetyl-6-*S*-acetyl-2, 6-dideoxy-1, 6-dithio-β-D-glucopyranose (I)[2,3] for the preparation of bis (2-acetamido-6-acetylthio-*O*-acetyl-glucopyranosyl) sulfides.

The treatment of compound I with ethylene dibromide in acetone containing potassium carbonate afforded bis-(2, 2'-diacetamido-3, 4, 3', 4'-tetra-*O*-acetyl-2, 6, 2', 6'-tetra-deoxy-6, 6'-di-*S*-acetyl-6, 6'-dithio-β, β'-D-glucopyranosyl) ethylene disulfide (II) in an 80% yield. It showed $[\alpha]_D^{22}$ −23° in chloroform. Bis(2, 3, 4, 6, 2', 3', 4', 6'-octa-*O*-acetyl-β, β'-D-glucopyranosyl) ethylene disulfide was reported[1] to have $[\alpha]_D$ −38.5° in chloroform.

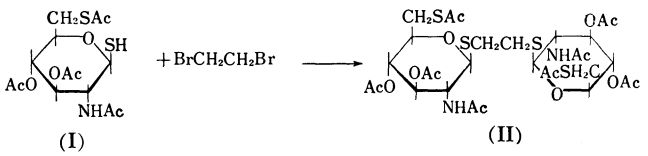
By a similar procedure, bis(2, 2'-di-acetamido-3, 4, 3', 4'-tetra-*O*-acetyl-2, 6, 2' 6'-tetra-deoxy-6, 6'-di-*S*-acetyl-6,6'-dithio-β, β'-D-glucopyranosyl) pentamethylene disulfide (III) was prepared from compound I and pentamethylene dibromide.

When compound I was treated with 2-acetamido-3, 4-di-*O*-acetyl-2, 6-dideoxy-6-*S*-acetyl-6-thio-D-glucopyranosyl chloride[3] (V) in acetone containing potassium hydroxide, bis (2, 2'-diacetamido-3, 4, 3', 4'-tetra-*O*-acetyl-2, 6, 2', 6'-tetra-deoxy-6, 6'-di-*S*-acetyl-6, 6'-dithio-β, β'-D-glucopyranosyl) sulfide (IV) was formed. The β, β' configuration has been suggested for compound IV on the basis of a comparison of rotation ($[\alpha]_D^{21}$ −16° in chloroform) with that of bis (2, 2', 3, 3', 4, 4', 6, 6'-octa-*O*-acetyl-β, β'-D-glucopyranosyl) sulfide ($[\alpha]_D^{18}$ −38° in chloroform).[4]

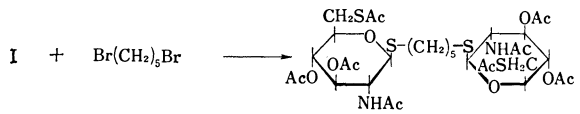
Experimental

Melting points are uncorrected.

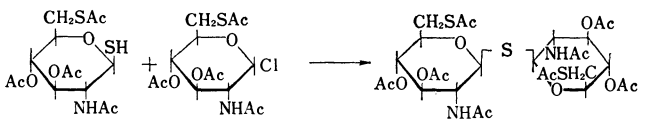
Bis(2, 2'-di-acetamido-3, 4, 3', 4'-tetra-*O*-acetyl-2, 6, 2', 6'-tetradeoxy-6, 6'-di-*S*-acetyl-6, 6'-dithio-β,β'-D-glucopyranosyl) Ethylene Disulfide (II).—Into a solution of 2-acetamido-3, 4-di-*O*-acetyl-6-*S*-acetyl-2, 6-di-deoxy-1, 6-dithio-β-D-glucopyranose (I) (1 g.) and ethylene dibromide (0.25 g.) in dry acetone (7.5 ml.), a solution of potassium carbonate (0.35 g.) in a small amount of water was added. After the solution had been stirred for 30 min. at room temperature, the solution was poured on ice water. The precipitates were filtered, washed with water



(I) (II)



(III)



(V) (IV)

1) M. Černý and J. Pacak, *Collection Czechoslov. Chem. Communs.*, **24**, 2566 (1959).
2) T. Ito, *Agr. Biol. Chem.*, **26**, 831 (1962).
3) T. Ito and T. Ishii, *Agr. Biol. Chem.*, **27**, 423 (1963).
4) M. Akagi, S. Tejima, M. Haga and M. Sakata, *Chem. Pharm. Bull.*, **11**, 1081 (1962).

and ether, and recrystallized from ethyl alcohol to give 0.83 g. (80%) of colorless crystals; m. p. 257 ~258°C, $[\alpha]_D^{22}$ −23° (*c* 0.5, chloroform).

Found: C, 45.52; H, 5.57; N, 3.72; S, 16.42. Calcd. for $C_{30}H_{44}N_2O_{14}S_4$: C, 45.90; H, 5.65; N, 3.57; S, 16.34.%

Bis(2, 2'-di-acetamido-3, 4, 3', 4'-tetra-*O*-acetyl-2, 6, 2', 6'-tetradeoxy-6, 6'-di-*S*-acetyl-6, 6'-dithio-β,β'-D-glucopyranosyl) Pentamethylene Disulfide (III).—This material was prepared in a manner analogous to that used for II above. Yield, 78, m. p. 227~228°C, $[\alpha]_D^{25}$ −6° (*c* 0.1, chloroform).

Found: C, 47.41; H, 6.06; N, 3.21; S, 16.10. Calcd. for $C_{33}H_{50}N_2O_{14}S_4$: C, 47.93; H, 6.09; N, 3.39; S, 15.51%.

Bis(2, 2'-di-acetamido-3, 4, 3', 4'-tetra-*O*-acetyl-2, 6, 2', 6'-tetradeoxy-6, 6'-di-*S*-cetyl-6, 6'-dithio-β, β'-D-glucopyranosyl) Sulfide (IV).—To a solution of 2-acetamido-3, 4-di-*O*-acetyl-2, 6-dideoxy-6-*S*-acetyl-6-thio-D-glucopyranosyl chloride (V) (0.64 g.) in acetone (10 ml.), a solution of compound I (0.63 g.) in 1% ethanolic potassium hydroxide (10 ml.) was added. After 24 hr. at room temperature, the inorganic precipitate was filtered out.

This filtrate was then evaporated to 12 ml., diluted with chloroform and poured into cold water. The chloroform layer was separated and then dried and evaporated in vacuo to give the crystalline product, which was washed with dry ether. The yield was 0.93 g. (78%). M. p. 281~282°C. $[\alpha]_D^{21}$ −16° (*c* 0.5, chloroform).

Found: C, 46.42; H, 5.43; N, 3.74; S, 13.49. Calcd. for $C_{28}H_{40}N_2O_{14}S_3$: C, 46.40; H, 5.56; N, 3.86; S, 13.27%.

The authors are grateful to Dr. Hiroshi Ogawa of this laboratory for his kind advice and encouragement and also to Miss Keiko Hibino for her elemental analysis.

Research Laboratories
Meiji Seika Kaisha, Ltd.
Kohoku-ku, Yokohama

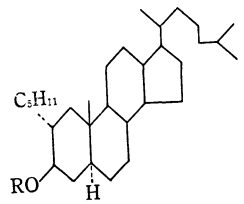
SHORT COMMUNICATIONS

The Structure of "α-Cholestanol"

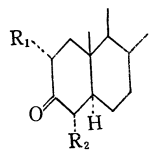
By Nobukatsu KATSUI, Yumiko YASUNARI, Isamu SUZUKI, Tadashi MASAMUNE and Toshi IRIE

(Received March 17, 1964)

"α-Cholestanol" obtained[1,2] by the treatment of cholesterol with sodium and isoamyl alcohol, has been presumed to be isoamylated dihydrocholesterol,[3,4] but it has received no generally accepted structural assignment. We will now describe findings which show Diels and Abderhalden's "α-cholestanol" ($C_{32}H_{58}O$, m. p. 124~127°C, sintering at 120°C, $[\alpha]_D$ −15° ($CHCl_3$)) to be 2α-isoamylcholestan-3β-ol (I).

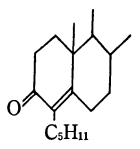


I: R=H
IV: R=Ac

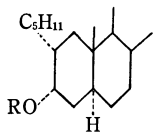


II: R_1=Isoamyl, R_2=H
VII: R_1=H, R_2=Isoamyl

1) C. Neuberg, *Salkowski Festschrift*, 279 (1904).
2) O. Diels and E. Abderhalden, *Ber.*, **39**, 884 (1906).



VI



III: R=H
V: R=Ac

The secondary alcoholic function of I has been well characterized[2,3,5] by the formation of a benzoate and by oxidation to a ketone (II) named "α-cholestanone" ($C_{32}H_{56}O$, m. p. 118~120°C, $[\alpha]_D$+23° ($CHCl_3$), $[\alpha]_D$+22°C (MeOH), ν_{max} 1702 cm^{-1} ($CHCl_3$)). The absence of a double bond has now been confirmed by the following results; (i) Neither I

3) A. Windaus and C. Uibrig, ibid., **46**, 2487 (1913).
4) H. Sobota, "The Chemistry of the Steroids," The Williams and Wilkins Co., Baltimore (1938), p. 210; L. F. Fieser and M. Fieser, "Steroids," Reinhold Publishing Corporation, New York, (1959), p. 29.
5) O. Diels and K. Linn, *Ber.*, **41**, 544 (1908); O. Diels and E. Stamm, ibid., **45**, 2228 (1912).

nor II had any peak due to an olefinic proton in the NMR spectra (ii) the ketone II was stable to acid or base and showed no absorption due to α,β-unsaturated ketone in the infrared and ultraviolet spectra.

The reduction of II with lithium aluminum hydride in ether gave rise to I (80%), along with an isomeric alcohol III (16%) ($C_{32}H_{58}O$; m.p. 95~96°C), which had a larger R_f value than the former I on thin layer chromatography. The acetylation of I with acetic anhydride and pyridine at room temperature yielded an acetate (IV) ($C_{34}H_{60}O_2$, m.p. 67~68°C, $[\alpha]_D$ −32° ($CHCl_3$), ν_{max} 1245 cm^{-1} (CS_2) (type A),[6] τ_{CDCl_3} 5.60 (half-width 23 c.p.s.)). The same treatment of III afforded an isomeric acetate (V) ($C_{34}H_{60}O_2$, m.p. 97~98°C, ν_{max} 1241 and 1234 cm^{-1} (CS_2) (type B)[6], τ_{CDCl_3} 5.14 (half-width 6 c.p.s)). All these results indicate[6,7] that the alcohol I has an equatorial hydroxyl group and that its isomer III has an axial one.

The lower carbonyl-stretching frequency of II, compared with those of the usual 3-keto steroids, suggests[8,9] that II is a C-2 or C-4 alkylated steroid, and the rotatory dispersion curve showed a positive Cotton effect, implying that the ketone was a derivative of 5α-cholestane. By following Atwater's procedure,[10] Δ^4-cholesten-3-one was isoamylated, using isoamyl iodide and potassium in boiling *t*-butyl alcohol; we thus isolated 4-isoamyl-Δ^4-cholesten-3-one (VI) (m.p. 66~67°C, $[\alpha]_D$+92° ($CHCl_3$), λ_{max} 251 mμ (ε 15400, ethanol), ν_{max} 1670 and 1605 cm^{-1} (Nujol)). The NMR spectrum of VI showed no signal due to the olefinic proton. Thus, all the spectral behavior indicated that an extra alkyl group was introduced at the C-4 position, as had been expected. The Birch reduction of VI under the conditions employed for the reduction[6] of 4-methyl-Δ^4-cholesten-3-one afforded the corresponding dihydro compound, $C_{32}H_{56}O$ (m.p. 68~69°C, $[\alpha]_D$+26° ($CHCl_3$), ν_{max} 1702 cm^{-1}), which had a positive Cotton effect. In view of the analogous reduction products of 4-methyl-[8] or 4-ethyl-Δ^4-cholesten-3-one,[11] the dihydro compound may be assigned the 4α-isoamylcholestanone structure (VII). The physical constants and the infrared spectrum of VII were different from those of II.

The isoamylation at the 2-position of cholesten-3-one was then attempted by a procedure[8] similar to that used for monomethylation, treating it with isoamyl iodide and potassium in boiling *t*-butyl alcohol for 10 min. The resulting crude product was successfully separated in a few components by chromatography on alumina. The material (16%), which was eluted with petroleum ether - benzene (24 : 1 and 4 : 1), had an m.p. of 118~120°C and was found to be identical with "α-cholestanone" (II). Since the direct alkylation of cholestanone should afford 2α-alkyl derivative,[8] the ketone II can be identified as 2α-isoamylcholestan-3-one. In agreement with this structure, there is no appreciable solvent effect[8] in the specific rotation of II, as has been mentioned above. Therefore, "α-cholestanol" is 2α-isoamylcholestan-3β-ol.

Department of Chemistry
Faculty of Science
Hokkaido University
Sapporo

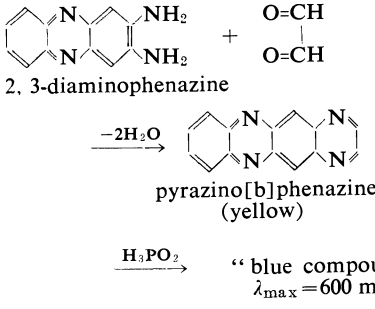
6) R. N. Jones, P. Humphries, F. Herling and K. Dobriner, *J. Am. Chem. Soc.*, **73**, 3215 (1951).
7) C. W. Shoppee and G. M. Summer, *J. Chem. Soc.*, **1950**, 687; V. Cerny, J. Joska and L. Labler, *Collection Czechoslov. Chem. Communs.*, **26**, 1658 (1961); O. R. Vail and D. M. S. Wheeler, *J. Org. Chem.*, **27**, 3863 (1962).
8) Y. Mazur and F. Sondheimer, *J. Am. Chem. Soc.*, **80**, 5220 (1958).
9) C. Cherrer, *Compt. rend.*, **225**, 1063 (1947).
10) N. W. Atwater, *J. Am. Chem. Soc.*, **79**, 5315 (1957).
11) B. R. Brown, P. W. Trown and J. M. Woodhouse, *J. Chem. Soc.*, **1961**, 2478.

The Determination of Submicrogram Quantities of Selenium by Means of a New Catalytic Reaction

By Motoharu TANAKA, Takuji KAWASHIMA and Harunaga MIWA*

(Received March 28, 1964)

The following reaction has been proposed for the determination of glyoxal:[1,2]



It was found that the reaction is catalyzed by selenium(IV). The effect of selenium(IV) on the rate of formation of the " blue compound " is demonstrated in Fig. 1. The absorption maximum of the resulting " blue compound " is found at 600 mμ.[1,2]

The procedure given by Ullmann and Mauthner[3] was followed, with a slight modification in the preparation of 2, 3-diaminophenazine. The product does not melt below 360°C, in accordance with the findings of Dechary et al.[1]

2, 3-Diaminophenazine hydrochloride (12.5 mg.) is dissolved in 250 ml. of 0.1 M hydrochloric acid. If some crystals separate out, it is necessary to warm the solution before use.

To 5 ml. of sample solution containing 0.1～0.2 μg. of selenium, 1 ml. of the 2, 3-diaminophenazine solution, one drop of 40% glyoxal and 1 ml. of 50% hypophosphorous acid are added. The acidity is adjusted to a pH value of about 0.65 with 1 M hydrochloric acid, and the whole diluted to 10 ml. The solution is then kept at 60°±1°C in a thermostat for 12 min. Then it is cooled quickly with tap-water and the extinction read at 600 mμ, using a similarly-treated reagent blank as a reference. The extinction should be read within 30 min., preferably within 10 min.

A typical calibration curve is shown in Fig. 2.

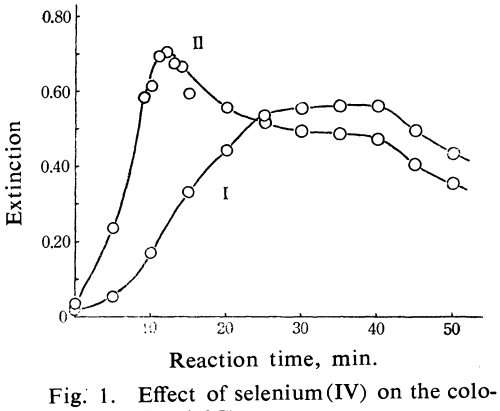


Fig. 1. Effect of selenium(IV) on the coloration (at 60°C).
Curve I: Reaction in the absence of selenium;
Curve II: Reaction in the presence of 0.5 μg. of selenium in 10 ml.

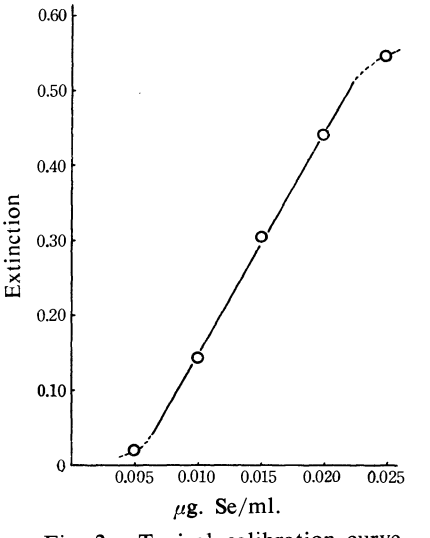


Fig. 2. Typical calibration curve.
Condition: Heating for 12 minutes at 60°±1°C; pH 0.65; effective light path of 16 mm.

The molar extinction coefficient is calculated from the difference in extinctions for 0.01 μg. and 0.02 μg. Se/ml. on the molar basis of

* Present address: Iwakuni Plant, Mitsui Petrochemical Industries, Ltd., Iwakuni, Yamaguchi.

1) J. M. Dechary, E. Kun and H. C. Pitot, *Anal. Chem.*, **26**, 449 (1954).
2) E. Sawicki, T. R. Hauser and R. Wilson, ibid., **34**, 505 (1962).
3) F. Ullmann and F. Mauthner, *Ber.*, **35**, 4302 (1902).

selenium : $\varepsilon_{600m\mu}=1.46\times10^6$. By an appropriate modification of such conditions as the reaction time, the reaction temperature and the pH, it is possible to extend the range of concentration for the determination and/or to double the sensitivity.

The following elements do not interfere with the determination of 0.1 μg. selenium, at least up to the specified quantities: Mg(1 mg.), Ca(10 mg.), Ba(4 mg.), Ni(10 mg.), Co(10 mg.), Mn(II) (1 mg.), Zn(150 μg.), Al(40 μg.), Mo(VI) (60 μg.), Fe(III) (10 μg.), and V(V) (5 μg.). Cu(II), V(V) (>10 μg.), Te(IV), As(III) and As(V) interfere, giving rise to a similar coloration. The addition of EDTA is effective in suppressing the interference of copper (II).

Details will be published elsewhere.

Laboratory of Analytical Chemistry
Faculty of Science
Nagoya University
Chikusa-ku, Nagoya

On the Anomalous Gas Evolution in the Electrooxidation of Absolute Methanol

By Kazuo SASAKI, Chisato HAMAGUCHI and Shigeo NAGAURA

(Received April 9, 1964)

The mechanism of the electrooxidation of methanol has recently become the subject of great interest in connection with the present development of liquid fuel cells. Although this problem has thus been quite familiar to us, however, the mechanisms so far proposed can not be accepted with full agreement.

Here, we would like to report an interesting finding concerning the electrooxidation of a non-aqueous methanolic solution of inorganic salts. In this experiment, the methanol used had been dehydrated by single distillation in the presence of metallic magnesium. About 0.1 mol./1. each of sodium methylate, sodium hydroxide and sodium perchlorate were used as supporting electrolytes. The current densities were 2 to 5 mamp./cm^2 for the most part, but 10 to 20 mamp./cm^2 in some cases; these values of current density will be referred to as lower and higher current densities below. The solution was deaerated by nitrogen before the electrolysis.

The anodic product of the electrooxidation of absolute methanol is formaldehyde, in the case of an aqueous solution, on the other hand, methanol is oxidized to carbon dioxide via formic acid. Usually the gas evolution from the anode could hardly be observed except when a higher current density was applied; however, a minor amount of gas was found to be accumulated at the bottom of the sintered glass disk used to separate the cathode chamber and so prevent the mixing of the cathode gas. Through careful examination we have found an anomalous phenomenon, that is, the formation of the anode gas at the lower surface of the glass filter and not at the anode itself. This was quite reproducible.

We first suspected this to be a misconception caused by some errors. However, even when the anode was shielded from the cathode chamber by triplicated glass filters, the gas is still formed at the nearest glass filter surface. The shape of the electrolytic cell or the relative spacing of two electrodes and the separater in the electrolytic cell did not appreciably affect the anomaly. The effects of the kind of electrolyte, sodium methylate, sodium hydroxide and sodium perchlorate were also examined, but there was no appreciable effect.

Furthermore, the following facts were ascertained. When the abnormal gas formation once occurred, it continued during the electrolysis. The gas formation ceased upon the discontinuance of the current, but it resumed at the resumption of the current, provided that the time of the discontinuance of the current did not exceed two or three minutes. When the period of current discontinuance lasted more than five to ten minutes, the gas formation is not restored by the electrolysis. Thus, the gas formation disappeared when the electrodes had been kept in the solution for a prolonged time without passing a current through. However, even in such a case, we could see the anomaly when the anode was dried in air. This clearly indicates that the gas formation is a phenomenon induced by the anodic reaction and not by other reasons. Perhaps the existence of a catalytic amount

of oxygen is required for this gas formation. The above experiments were made with platinized platinum anode. Although the anomaly was also found for the smooth platinum anode, it was occasional and the reproducibility was poor.

The relative composition of the gases evolved from the anode surface (at the higher current density) and of the separater was determined by a mass spectrometer; it is given in Table I.

TABLE I

	Methanol	Formaldehyde	CO
Gas evolved from the anode surface	0.84	0.06	0.19
Gas accumulated at the separater	0.79	0.21	0.00

Beside solvent methanol, formaldehyde was the only component of the gas, while carbon monoxide was the main component of the gas evolved from the anode surface.

At the end of the electrolysis for the gas collection, the concentration of formaldehyde could never exceed 10^{-3} in its mole ratio to methanol: this proportion could not cause such a high concentration of formaldehyde as was observed in the evolved gas.

On the basis of the facts described, we propose the following sequence of reactions:

At the anode

$$MeOH \rightarrow MeO + H^+ + e \quad (1)$$

Detachment and diffusion

$$MeO(ads) \rightarrow MeO\ (bulk) \quad (2)$$

Disproportionation

$$2MeO \rightarrow MeOH + HCHO \quad (3)$$

We have some evidence that the radicals formed by electrooxidation are methoxyl (CH_3O) and not hydroxymethylene radicals (CH_2OH),[1] although it seems that the real process of methoxyl radical formation is not so simple as to be expressed by Eq. 1. The methoxyl radical is comparatively stable,[2] and the following decomposition is heavily endothermic ($q = -20$ to 35 kcal.[3]).

$$MeO \rightarrow HCHO + H$$

Therefore, it is not surprising that an appreciable number of the radicals formed by Eq. 1 do not undergo further oxidation upon the electrode surface but detach from the electrode and diffuse into the bulk solution. If the association of two radicals occurs, large exothermic disproportionation ($q = +85$ kcal. for Eq. 3) would occur readily, presumably at the glass filter surface.

Faculty of Engineering
Osaka City University
Kita-ku, Osaka

1) K. Sasaki, K. Uneyama, C. Hamaguchi and S. Nagaura, 17th Annual Meeting of the Chemical Society of Japan, Tokyo (1964).
2) P. Gray and A. Williams, *Chem. Revs.*, **59**, 239 (1959).
3) N. Semenov, "Some Problems in the Chemical Kinetics and Reactivity" (Translated into Japanese), Iwanami, Tokyo (1963), p. 95.

A Kinetic Structure of Ammonia Synthesis

By Kenzi TAMARU

(Received April 28, 1964)

The adsorption measurements during surface catalysis[1] have been extended to the study of the reactivity of chemisorbed species on the catalyst surface as a function of the pressures and coverages of such species as reactants, products and intermediates.[2] Accordingly, the mechanism of the overall reaction can be elucidated by studying each step in the overall reaction.

The ammonia synthesis on a doubly promoted iron catalyst has been treated by the new approach, and the chemisorption of nitrogen and its desorption, the reaction between the chemisorbed nitrogen and hydrogen to form ammonia have been separately studied under the reaction conditions.[2-4] The rates of the three steps ($\vec{V}_1$, $\overleftarrow{V}_1$ and $\vec{V}_2$, respectively) are expressed in the following manner according to the experimental results:

$$\vec{V}_1 = AP_{N_2} \exp(-\gamma x) \quad (1)$$

$$\overleftarrow{V}_1 = B \exp(\beta x) \quad (2)$$

1) K. Tamaru, This Bulletin, **31**, 666 (1958).
2) K. Tamaru, *Catalyst* (*Shokubai*), **4**, 30 (1962).
3) K. Tamaru, *Trans. Faraday Soc.*, **59**, 979 (1963).
4) K. Tamaru, This Bulletin, **37**, 771 (1964).

$$\vec{V}_2 = CP_{H_2} \exp(\alpha x) \quad (3)$$

where x is the amount of nitrogen chemisorbed A, B, C, α, β, γ, are constants, and P_N and P_H are the pressures of nitrogen and hydrogen respectively.

If we postulate that the backward reaction of the latter step ($\overleftarrow{V}_2$) is first order as to ammonia, as has been reported in the case of a tungsten catalyst, $\overleftarrow{V}_2$ should conform to the following equation from the equilibrium conditions:

$$\overleftarrow{V}_2 = D(P_{NH3}/\sqrt{P_{H_2}})\exp(-\delta x) \quad (4)$$

where $B/A = C^2/(D^2K_p)$, $\alpha+\beta = 2(\gamma+\delta)$, and K_p is the equilibrium constant of the reaction, $N_2+3H_2=2NH_3$.

The $\overleftarrow{V}_1/\vec{V}_2$ ratio can be taken as a criterion to identify the rate-determining step of the overall reaction; if it is much larger than unity, the latter step is rate-determining, while if it is much smaller than unity, the former step is.

$$\overleftarrow{V}_1/\vec{V}_2 = (B/C)\exp[(\beta-\gamma)x]/P_{H_2} \quad (5)$$

The experimental results revealed that β is approximately equal to γ and that the activation energy for $\overleftarrow{V}_1$, which is the sum of that for $\vec{V}_1$ and the heat of adsorption of nitrogen, is markedly larger than that for $\vec{V}_2$. Accordingly, at a higher temperature and a lower pressure of hydrogen, the latter step is likely to be rate-determining.

If the steady-state approximation is applied, the kinetic expression of the overall reaction can be derived in the following way:

$$\vec{V}_1+\overleftarrow{V}_2 = \overleftarrow{V}_1+\vec{V}_2$$

$$AP_{N_2}\exp(-\alpha x)+D(P_{NH_3}/\sqrt{P_{H_2}})\exp(-\delta x) = B\exp(\beta x)+CP_{H_2}\exp(\gamma x)$$

$$\exp[(\alpha+\beta)x/2] = \frac{1}{2(B+CP_{H_2})}\left[D\frac{P_{NH_3}}{\sqrt{p_{H_2}}}+\sqrt{D^2\frac{P^2_{NH_3}}{p_{H_2}}+4AP_{N_2}(B+CP_{H_2})}\right] \quad (6)$$

$$\text{Overall rate } (V_0) = \vec{V}_1-\overleftarrow{V}_1 = AP_{N_2}\exp(-\alpha x)-B\exp(\beta x) \quad (7)$$

Equation 6 gives the nitrogen coverage under given reaction conditions, while Eq. 7 gives the overall reaction rate at the nitrogen coverage.

If the former step is rate-determining, the Temkin-Pyzhev treatment[5] is exactly applicable as follows:

$$V_0 = A^{\frac{\beta}{\alpha+\beta}}(K_pB)^{\frac{\alpha}{\alpha+\beta}}P_{N_2}(P^3_{H_2}/P^2_{NH})^{\frac{\alpha}{\alpha+\beta}} - (A/K_p)^{\frac{\beta}{\alpha+\beta}}B^{\frac{\alpha}{\alpha+\beta}}(P^2_{NH3}/P^3_{H_2})^{\frac{\beta}{\alpha+\beta}} \quad (8)$$

From the experimental results, $\alpha/(\alpha+\beta)=0.6$ was obtained, which conforms to the value hitherto obtained kinetically.

If the synthesis reaction proceeds in the presence of a negligible amount of ammonia, V_0 can be expressed as follows, putting P_{NH_3} as zero in Eqs. 6 and 7:

$$V_0 = AP_{N_2}[(AP_{N_2}/(B+CP_{H_2})]^{\frac{-\alpha}{\alpha+\beta}} - B[AP_{N_2}/(B+CP_{H_2})]^{\frac{\beta}{\alpha+\beta}} \quad (9)$$

The orders of the forward reaction as to nitrogen and hydrogen are, accordingly, $\beta/(\alpha+\beta)$ and $\alpha/(\alpha+\beta)$ respectively, provided $CP_{H_2} \gg B$. It is of great interest to note that Temkin et al.[6] recently reported that the ammonia synthesis in the presence of a negligible amount of ammonia is half-order as to both nitrogen and hydrogen. On the basis of this fact, they suggested that the hydrogenation step of the chemisorbed nitrogen participates in the rate-determining step of the overall reaction. Equation 9 reasonably agrees with the observed kinetics, which seemingly supports the validity of the general kinetic treatment of the overall reaction on the basis of the kinetics of each component step of the overall reaction.

Department of Chemistry
Faculty of Science
The University of Tokyo
Hongo, Tokyo

5) M. I. Temkin and V. Pyzhev, *Acta Physicochim.*, **12**, 327 (1940).

6) M. I. Temikin, N. M. Morozov and E. N. Shapatina, *Kinetics and Catalysis* (*U. S. S. R*), **4**, 260, 565 (1963).

Electron Paramagnetic Resonance Spectra of Phosphate Glasses Irradiated with Gamma-rays

By Yasuo NAKAI

(Received April 30, 1964)

The electron spin resonance (ESR) of irradiated glasses has been reported on several times in the past five years,[1] since the paramagnetic centers have been expected to contain localized electrons and holes.

ESR study of the defect centers in irradiated glasses containing phosphorus was first reported on by Karapetyan and Yudin.[2] They observed an ESR spectrum consisting of two lines at $g=2.0038$. This two-line structure was attributed to hyperfine interaction with a P nucleus. In the present investigation, it was found that there are three distinct types of defect centers in irradiated phosphate glasses.

Phosphate glass samples with the composition of (RPO_3) [R=Li, Na, Ca, Ba,], where R/P=1, were irradiated at room temperature with Co^{60} gamma-rays ($5\sim6\times10^6$r.). The derivative curve was obtained with a Varian 4501 ESR spectrometer at room temperature, employing a modulation frequency of 100 kc./sec.

The irradiated lithium phosphate glasses ($LiPO_3$) exhibit the ESR spectra of two strong lines (P_1 and P_2) and of the other two weak absorption lines (Fig. 1). One of the weak

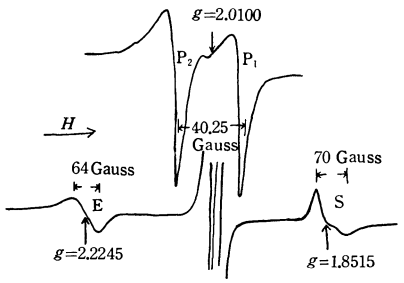


Fig. 1. The ESR spectrum obtained for a γ-ray irradiated (5×10^6 r.) lithium phosphate glass ($LiPO_3$).

absorption lines appear to display a broad derivative peak on the low magnetic field side ($g=2.2245$), and the other, a broad asymmetric derivative peak on the high magnetic field side ($g=1.8575$). The former is denoted by E, and the latter, by S.

The intensity of the two-line structure can easily be reduced by heating at 100°C. The fading speed by the thermal treatment is dependent on the kinds of alkali or alkaline earth modifiers. The derivative peaks denoted by P_1 and P_2 are spaced with a spacing of 40.25 gauss, and the g value at the center of these two peaks is observed to be $g=2.0100$. This two-line structure has the same response to both the thermal annealing and the optical bleach, and it is independent of the type of alkali or alkaline earth modifiers.

The observed g value of the two-line structure is larger than that of the free electron. This suggests that the paramagnetic center is a hole trapped on a singly bonded oxygen. The hyperfine structure arises from the overlap of the hole orbital on a phosphorus atom with a spin of 1/2. The principal values of g in the axial field are given by $g_{\parallel}=2.0243$ and $g_{\perp}=2.0100$.

The process of this creation can perhaps be interpreted as follows. An electron in the π-orbital of oxygen associated with the P=O link is thrown out because of the action of γ-rays. Thus, migrating through the valence zone, the formed hole goes to the nucleus of a four coordinate phosphorus ion.

Karapetyan and Yudin have interpreted the magnetic centers of phosphate glasses as arising from electron capture in the (PO_4) groups, not as oxygen vacancies in the vicinity of the alkali or alkaline earth ions. In this present work, however, we found that the shapes of the other weak resonance lines (E and S) were dependent on the kinds of alkali or alkaline earth ions. The resonance spectra in irradiated phosphate glasses containing a calcium or barium modifier appear as is shown in Fig. 2. In the case of a sodium or potassium modifier, the spectra disappear on both the low and the high magnetic field sides. The sample of (KPO_3), however, is not in the state of glass but is a highly polymerized crystal.

In phosphate glasses modified with such ions

1) R. A. Weeks, *J. Appl. Phys.*, 27, 1376 (1956); Y. Nakai, *J. Chem. Soc. Japan, Pure Chem. Sec.* (*Nippon Kagaku Zasshi*), 82, 1629 (1961); S. Lee and P. J. Bray, *Phys. Chem. Glasses*, 3, 37 (1962); S. Lee and P. J. Bray, *J. Chem. Phys.*, 39, 2863 (1963).

2) G. O. Karapetyan and D. M. Yudin, *Fiz. Tverd. Tela*, 4, 2647 (1962).

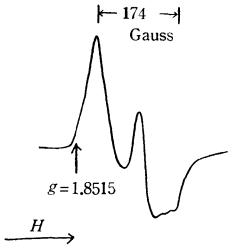


Fig. 2. The ESR spectrum (S band) obtained for a γ-ray irradiated ($\sim 10^5$ r.) calcium phosphate glass ($CaPO_3$).

as calcium, barium or lithium, that can coordinate with the tetrahedral oxygen atom in the glass network, the two weak resonance lines seem to appear just as well as with a low dosage of γ-rays irradiation.

The g value of the E band is far larger than that of the free electron, and yet it depends upon the kinds of alkaline earth ions. Consequently, it is possible that it has something to do with new valence zone of alkali ions coordinated with the oxygen atom in the glass network.

The intensity of the S band is hardly reduced at all by heat treatment at 200°C for 5 hr. This suggests that the S band may arise from electrons trapped at oxygen vacancies in the vicinity of the alkali ions, as has been assumed previously.[3)]

Central Research Laboratory
Tokyo Shibaura Electric Co., Ltd.
Kawasaki-shi, Kanagawa

3) R. A. Weeks, *J. Appl. Phys.*, **27**, 1376 (1956).

The Electrometric Titration of Thorium with Tellurite

By V. K. SHARMA and J. N. GAUR

(Received August 27, 1963)

Berzelius prepared tellurites of thorium, zirconium, berylium, aluminium, yttrium, etc. by mixing a solution of each of their salts with a sodium tellurite solution.[1] We ourselves have previously used tellurite for the estimation of zirconium by electrometric methods.[2] Results of similar investigations with thorium have been reported in the present communication.

Experimental

Solutions from thorium nitrate (99.0% pure) and potassium tellurite (97.0% pure) were prepared and standardized by gravimetric methods.

Conductometric Measurements.—Solutions prepared from conductivity water were used for the purpose of conductometric titrations.

When thorium nitrate solutions are taken into the cell, two breaks, at ratios of approximately 1 : 1 and 1 : 2, are obtained, whereas reverse titrations show only one break, at the 1 : 2 ratio. Results of direct as well as reverse titrations have been incorporated in Table I, while typical curves are shown in Fig. 1.

TABLE I

S. No.	Volume and strength of $Th(NO_3)_4$ soln.	Volume and strength of K_2TeO_3 soln.	Ratio Th : Te
	Direct titration		
1	20 ml., 0.0025 M	2.0 ml., 0.05 M	1 : 2
2	20 ml., 0.0020 M	1.6 ml., 0.05 M	1 : 2
3	20 ml., 0.00125 M	1.0 ml., 0.05 M	1 : 2
	Reverse titration		
4	2.0 ml., 0.05 M	20 ml., 0.01 M	1 : 2
5	1.6 ml., 0.05 M	20 ml., 0.008 M	1 : 2
6	1.0 ml., 0.05 M	20 ml., 0.005 M	1 : 2

Potentiometric Titration. — pH measurements were made with a battery-operated Cambridge pH meter. Direct and reverse titrations show a sharp break at the 1 : 2 (Th : Te) ratio. Results have been summarized in Table II, while typical curves are given in Fig. 2.

Direct Volumetric Titrations.—pH titrations show

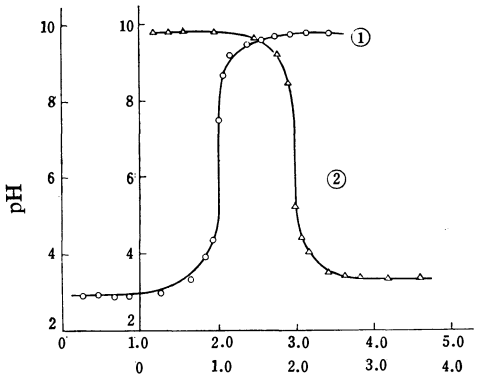


Fig. 2. Titration of (1) 10 ml., 005 M $Th(NO_3)_4$ with 0.05 M K_2TeO_3 and (2) 10 ml., 0.02 M K_2TeO_3 with 0.05 M $Th(NO_3)_4$.

TABLE II

S. No.	Volume and strength of $Th(NO_3)_4$ soln.	Volume and strength of K_2TeO_3 soln.	Ratio Th : Te
	Direct tirtration		
1	10 ml., 0.005 M	2.0 ml., 0.05 M	1 : 2
2	10 ml., 0.004 M	1.6 ml., 0.05 M	1 : 2
3	10 ml., 0.0025 M	1.0 ml., 0.05 M	1 : 2
	Reverse titration		
4	2.0 ml., 0.05 M	10 ml., 0.02 M	1 : 2
5	1.6 ml., 0.05 M	10 ml., 0.016 M	1 : 2
6	1.0 ml., 0.05 M	10 ml., 0.01 M	1 : 2

that there is a sharp change in pH from the acidic side to the alkaline side at the end point. Thus, the possibility of using phenolphthalein for the visual detection of the end point can not be ruled out. In was actually found that phenolphthalein gave reliable results, even in dilute solutions of thorium nitrate, and that hence potassium tellurite could be used for the direct volumetric estimation of the thorium nitrate solution. Results are summarized in Table III.

TABLE III

S. No.	Volume and strength of $Th(NO_3)_4$ soln.	Volume and strength of K_2TeO_3 soln.	Ratio Th : Te
1	10 ml., 0.005 M	2.0 ml., 0.05 M	1 : 2
2	10 ml., 0.004 M	1.6 ml., 0.05 M	1 : 2
3	10 ml., 0.0025 M	1.0 ml., 0.05 M	1 : 2

1) J. J. Berzelius, "Jahrez," 1833; *Pogg. Ann.*, **28**, 396 (1833). Handlinger 1833, 277; *Pogg. Ann.*, **32**, 1-577 (1834); *Ann. Chem. Physics* (*2*), **58**, 225 (1835).

2) V. K. Sharma and J. N. Gaur, *J. Electroanal. Chem.*, **5**, 375 (1963).

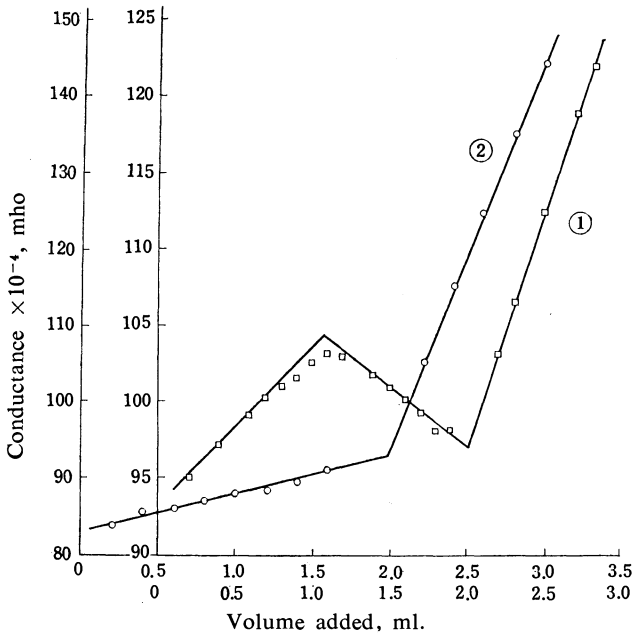


Fig. 1. Titration of (1) 20 ml. 0.0025 M $Th(NO_3)_4$ with 0.05 M K_2TeO_3 and (2) 20 ml. 0.01 M K_2TeO_3 with 0.05 M $Th(NO_3)_4$.

Discussion

Conductometric and potentiometric titrations show a sharp break at 1:2 (Th:Te) ratio; hence, thorium can be estimated using potassium tellurite by conductometric and potentiometric methods. A direct estimation of thorium can also be effected using phenolphthalein as an indicator, as is evident from the results of Table III. All these titrations show the formation of normal thorium tellurite.

Summary

Potentiometric and conductometric titrations of thorium nitrate solutions with tellurite show a sharp break at the 1:2 (Th:Te) ratio. Direct volumetric titrations using phenolphthalein as an indictator also show the 1:2 ratio, indicating the formation of normal tellurite. The estimation of thorium by potentiometric, conductometric and direct volumetric titrations using potassium tellurite has been suggested.

Department of Chemistry
University of Rajasthan
Jaipur, India

ESR Studies of the Negative Ions of Biphenyl Derivatives. II. Electron Spin Resonance Hyperfine Spectra of 3-Methyl Biphenyl, m, m'-Bitolyl, 2-Methyl Biphenyl, and o, o'-Bitolyl Mononegative Ions

By Kazuhiko Ishizu*

(Received September 13, 1963)

In a previous paper,[1] the author reported the results of an ESR study of 4-methyl biphenyl and *p, p'*-bitolyl mononegative ions; this study has also provided us with some information on methyl proton splitting which will be referred to later in this paper.

In this article, work on the ESR spectra of 3-methyl biphenyl, *m, m'*-bitolyl, 2-methyl biphenyl, and *o, o'*-bitolyl mononegative ions will be presented in order to clarify further the effect of methyl substitution at various positions on the biphenyl ring in terms of hyperconjugation and the steric effect.

Experimental

The radical anions were produced with potassium metal in dimethoxyethane (DME) and also in tetrahydrofuran (THF). The experimental procedures were described in the preceding paper.

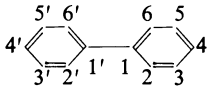
Results

The resolution of the observed hyperfine lines in the ESR spectra for each specimen was found to be better in DME than in THF, except for 3-methyl biphenyl; thus, the spectra observed in DME will be discussed.

With reference to the theoretically-calculated spin density given in Table II, the hyperfine structures of the observed spectra were interpreted adequately by assuming that the magnitude of the methyl splittings and of the ring-proton splittings were almost equal to those at the same positions on biphenyl, in which the splitting ratios at the para-, ortho-, and meta-positions were approximately 8 : 4 : 1.

The proton hyperfine splittings at the meta- and the ortho-positions were derived from an analysis of the terminal and the next-inner groups of the spectrum, while those at the para-positions were derived through the trial and error method by observing the intense splittings around the center of the spectrum.

The general structure of a biphenyl ring is:



In the following sections, ΔH_n and ΔH_n (CH_3) represent the hyperfine coupling constants* of, respectively, the ring protons and of the methyl protons attached to the ring carbon C_n, where n denotes a position on the biphenyl ring.

3-Methyl Biphenyl.—The observed spectrum measured in DME at room temperature is shown in Fig. 1(a). Although he made careful observations in range from room temperature to −60°C, the author could not observe any good resolved patterns of ESR hyperfine lines; thus, it was difficult to determine the coupling constants precisely. The integral intensity of each hyperfine line, however, seems to be in good agreement with the theoretical intensity, as is shown in Fig. 1 (b).

The overall width, the number of the groups in which hyperfine lines flocked, and the location of strong intensity lines in the spectrum were all similar to the conditions in biphenyl. Thus, one may assume that the para (ΔH_4 and $\Delta H_{4'}$)-, or the ortho (ΔH_2, $\Delta H_{2'}$, ΔH_6 and $\Delta H_{6'}$)- ring proton splittings are about 5.4 gauss and 2.7 gauss respectively, not far from those of biphenyl. The ring-proton splitting ($\Delta H_{3'}$, $\Delta H_{5'}$ and ΔH_5) and the methyl proton splittings ($\Delta H_3(CH_3)$) at the meta-positions were all about 0.43 gauss.

The methyl splitting was identified from the integration of the septet lines in the terminal groups.

The proton hyperfine splittings thus determined are:

$$\Delta H_4 \simeq \Delta H_{4'} = 5.4 \text{ gauss}$$

$$\Delta H_2 \simeq \Delta H_{2'} \simeq \Delta H_6 \simeq \Delta H_{6'} = 2.7 \text{ gauss}$$

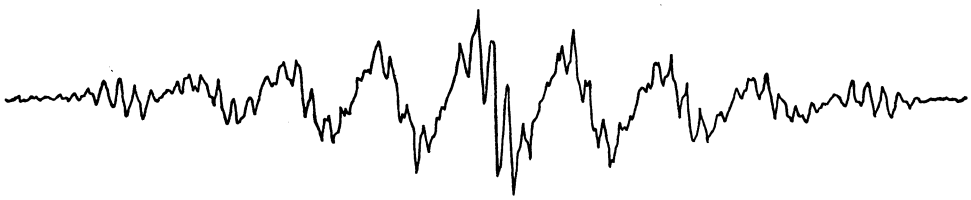
$$\Delta H_3(CH_3) = \Delta H_{3'} = \Delta H_5 = \Delta H_{5'} = 0.43 \text{ gauss}$$

***m, m'*-Bitolyl.**—The observed spectrum measured at −15°C is shown in Fig. 2(a). The overall width and the grouping of every hyperfine line in the spectrum can be easily

* On leave from the Department of Chemistry, Faculty of Literature and Science, Yamaguchi University, as a research fellow at Kyoto University (1963-1964); leave sponsored by the Japan Society for the promotion of science.

1) K. Ishizu, This Bulletin, **36**, 938 (1963).

* The hyperfine coupling constant is a synonym of the splitting coefficient which was used in the previous report.



10 gauss

Fig. 1 (a)

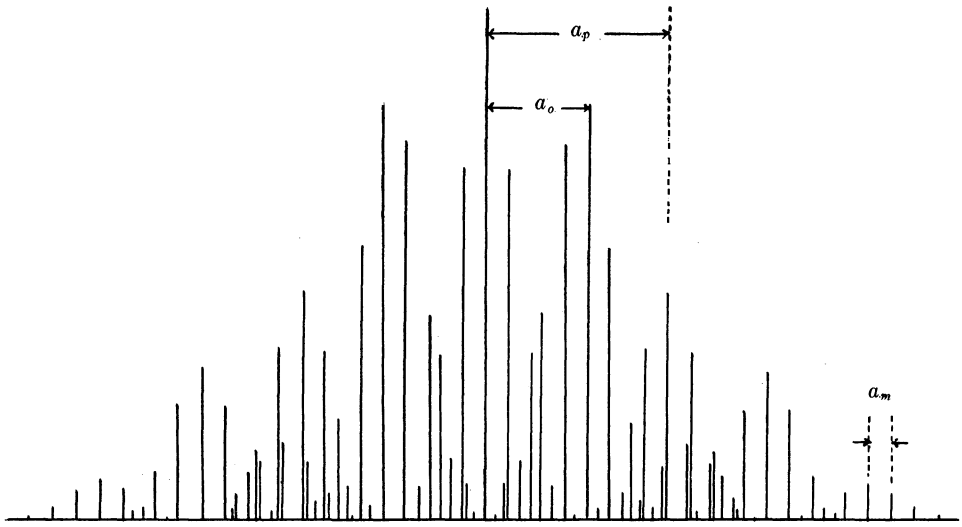


Fig. 1 (b)

Fig. 1. 3-Methyl biphenyl.

(a) : ESR spectrum
(b) : Intensity diagram constructed based upon theoretically calculated spin densities assuming that the splitting parameter of the methyl proton was equal to that of the ring proton. Each of a_p, a_o and a_m is the theoretical proton splitting at the para-, the ortho-, and the meta-position.

compared with those of biphenyl. The observed spectrum consists of three triplets originating from a pair of para (5.15 gauss)-, and two pairs of ortho (2.82, 2.33 gauss)-, ring protons. Each line then splits further into a triplet septet caused by a pair of the metaring protons and the six methyl protons.

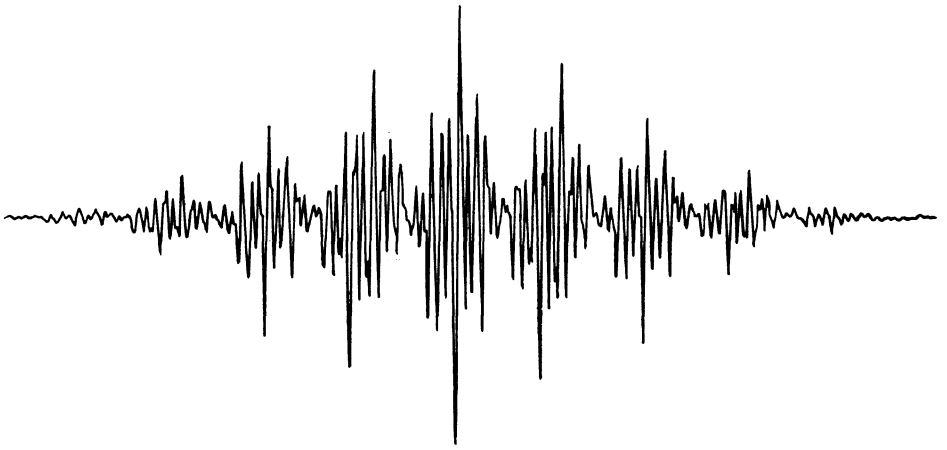
With reference to Hückel's MO calculation, in which $\rho_6 > \rho_2$*, the ΔH's of each proton thus determined are as follows:

$\Delta H_4 = 5.15$, $\Delta H_6 = 2.82$, $\Delta H_2 = 2.33$, $\Delta H_3(CH_3) = 0.49$, $\Delta H_5 = 0.27$ gauss.

The relative intensities of the hyperfine lines estimated on the basis of these ΔH's are shown in Fig. 2(b).

2-Methyl Biphenyl.—The spectrum measured at room temperature is shown in Fig. 3(a). As is illustrated in Fig. 3(b), the terminal group of the spectrum consists of six lines, whose relative intensity ratios are 1 : 1 : 2 : 2 : 1 : 1, and the line spacing is alternatively 0.42 and 0.23 gauss. One would expect the hyperfine structures of these six lines to appear as a triplet due to a pair of equivalent ring-proton splittings (0.65 gauss), followed by a doublet due to a pair of equivalent ring-proton splittings (0.42 gauss) at the meta-positions. Thus, it may reasonably be expected that any coupling constant of the remaining meta-proton will be too small to split the hyperfine lines. One may assume that an equivalent pair exists for the meta-ring protons in the non-substituted phenyl group, taking the theoretical prediction of spin density into account. Thus, the ring proton splittings at each meta-position are determined to be:

* ρ_n: a theoretically-calculated spin density on the ring carbon atom, C_n, of the biphenyl ring.



10 gauss

Fig. 2 (a)

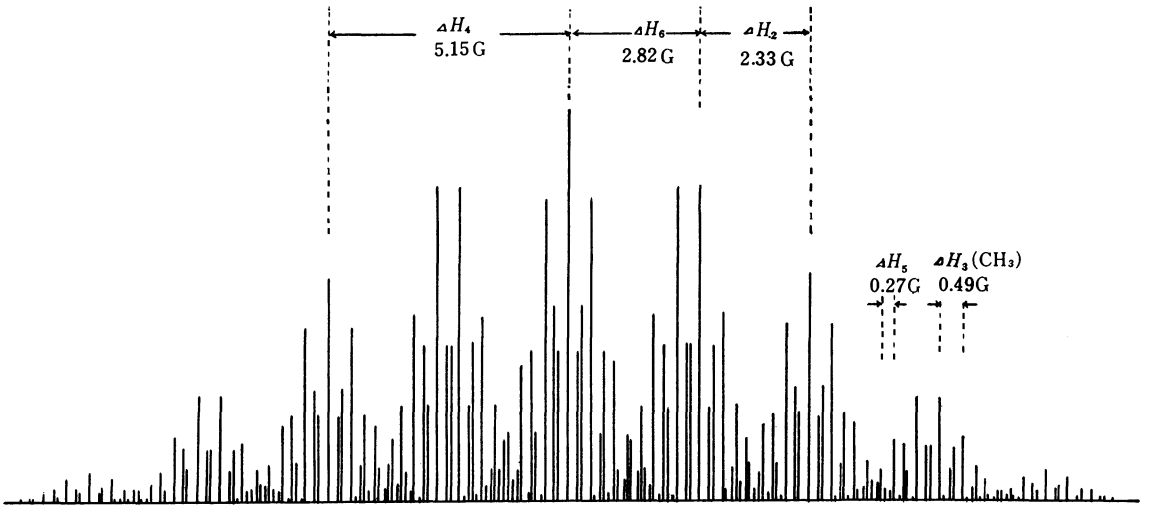


Fig. 2 (b)

Fig. 2. *m*, *m'*-Bitolyl.

(a) : ESR spectrum

(b) : Calculated spectrum based on experimentally determined proton coupling constants

$\Delta H_{3'}=\Delta H_{5'}=0.65$, $\Delta H_5=0.42$, and

$\Delta H_3<0.03$* gauss.

The analysis of the wing groups in the spectum shows that the ring and the methyl protons at the ortho-positions will give two kinds of splittings, a triplet (2.88 gauss) and a quintet (2.41 gauss), respectively.

Taking the theoretical spin density at the ortho-positions into account, a triplet is assigned to the ortho-ring proton splittings in the non-substituted phenyl group, and a quintet, to an ortho-ring proton and the three methyl proton splittings in the substituted phenyl group; that is, $\Delta H_{2'}=\Delta H_{6'}=2.88$ and $\Delta H_2(CH_3)=\Delta H_6=2.41$ gauss. Finally, the para-(ΔH_4, $\Delta H_{4'}$) proton splitting was found to be 5.25 gauss by the trial and error method. The relative intensities of the hyperfine lines are shown in Fig. 3 (c).

The $\Delta H_{5'}$ thus determined are:

$\Delta H_4=\Delta H_{4'}=5.25$, $\Delta H_{2'}=\Delta H_{6'}=2.88$,

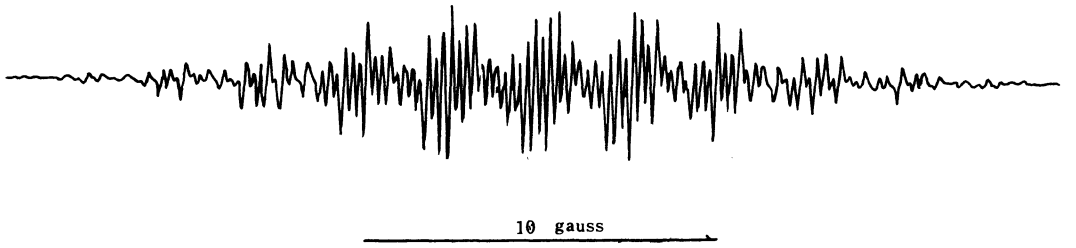
$\Delta H_2(CH_3)=\Delta H_6=2.41$,

$\Delta H_{3'}=\Delta H_{5'}=0.65$, $\Delta H_5=0.42$, and

$\Delta H_3<0.03$ gauss.

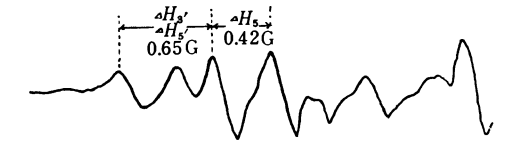
***o, o'*-Bitolyl.**—The spectrum measured at -15°C is shown in Fig. 4(a). The relative intensity ratios of the seven hyperfine lines in

* The ultimate resolvable width of the spectrometer.



10 gauss

Fig. 3 (a)



2 gauss

Fig.3 (b)

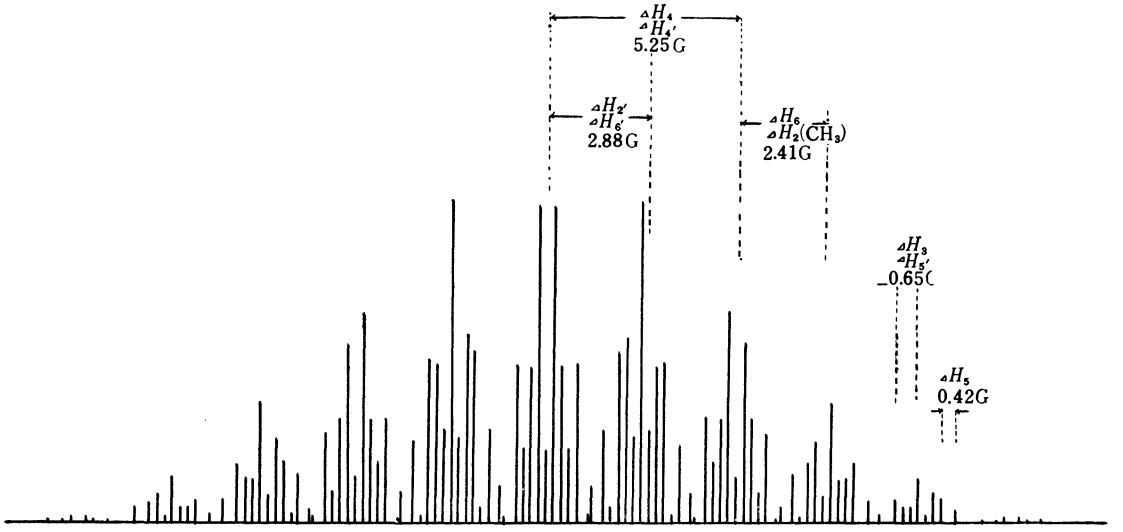


Fig. 3 (c)

Fig. 3. 2-Methyl biphenyl.
(a) : ESR spectrum (b) : An end group of spectrum (c) : Calculated spectrum based on experimentally determined proton coupling constants

all three groups at the wing of the spectrum illustrated in Fig. 4(b), are equal to 1 : 2 : 3 : 4 : 3 : 2 : 1. The ring proton and the methyl proton splittings at the ortho-positions are all equal; that is, $AH_2(CH_3) = AH_6$. Furthermore, the proton splitting ratio at the meta-position is equal to 2 : 1. The AH's thus determined are as follows:

$AH_4 = 5.12$, $AH_2(CH_3) = AH_6 = 2.20$,

$AH_5 = 0.56$, and $AH_3 = 0.28$ gauss.

The spectrum which has been constructed on the basis of the observed coupling constants is shown in Fig. 4(c). Table I gives the overall width, the g-values, and the observed coupling constants of both ring protons and methyl protons in mononegative ions of biphenyl and its derivatives.

Discussion

The Ring Proton Splitting.—The theoretical spin density on both ring carbons and methyl protons were derived by means of Hückel's MO calculation, assuming that each aromatic ring would be on a plane and estimating the resonance integral between neighboring ring carbon atoms (β_{C-C}) and the Coulomb integral

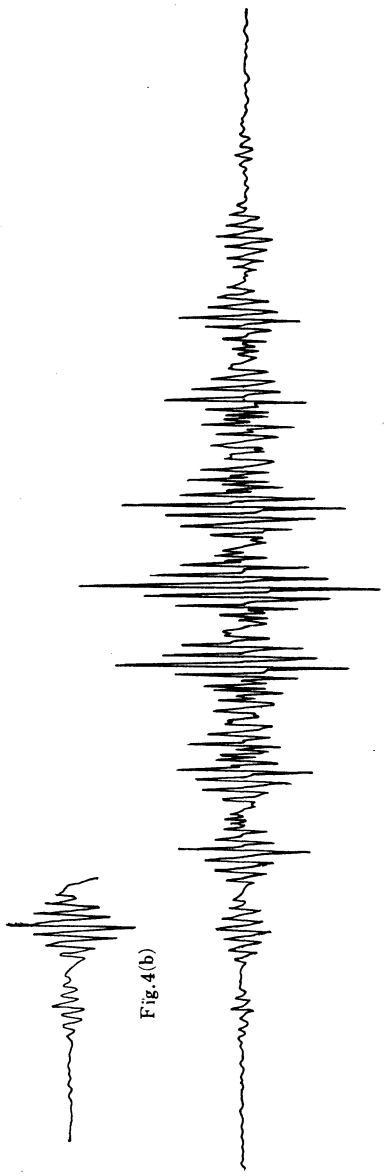


Fig. 4(b)

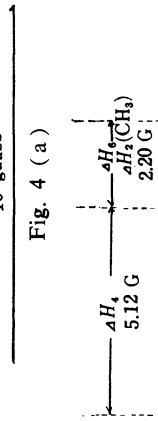


Fig. 4 (a)

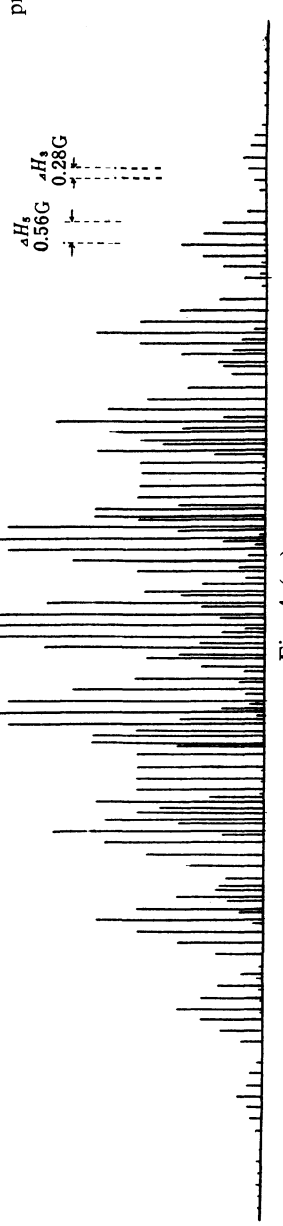


Fig. 4 (c)

Fig. 4. *o, o'*-Bitolyl.
(a) : ESR spectrum
(b) : Three groups in a wing of spectrum
(c) : Calculated spectrum based on experimentally determined proton coupling constants

TABLE I. OVERALL WIDTHS, g-VALUES AND OBSERVED PROTON COUPLING CONSTANTS OF BIPHENYL AND METHYL DERIVATIVE MONONEGATIVE IONS

	g	Overall	ΔH_s									
			2	2'	3	3'	4	4'	5	5'	6	6'
Biphenyl	2.0025	23.5	2.66	2.66	0.41	0.41	5.31	5.31	0.41	0.41	2.66	2.66
4-Methyl	2.0024	33.6	2.85	2.51	0.64	0.32	†5.43	5.43	0.64	0.32	2.85	2.51
p, p'-Bitolyl	2.0025	46.7	2.66	2.66	0.51	0.51	†5.63	†5.63	0.51	0.51	2.66	2.66
3-Methyl-	2.0025	23.7	2.7	2.7	†0.43	0.43	5.4	5.4	0.43	0.43	2.7	2.7
m, m'-Bitolyl	2.0024	23.8	2.33	2.33	†0.49	†0.49	5.15	5.15	0.27	0.27	2.82	2.82
2-Methyl-	2.0027	27.5	†2.41	2.88	<0.03	0.65	5.25	5.25	0.42	0.65	2.41	2.88
o, o'-Bitolyl	2.0025	29.5	†2.20	†2.20	0.28	0.28	5.12	5.12	0.56	0.56	2.20	2.20

†: Methyl proton splitting, Overall ΔH_s: (gauss)

TABLE II. THEORETICAL SPIN DENSITY OF BIPHENYL AND METHYL DERIVATIVE MONONEGATIVE IONS

	ρ												
	1	2	3	4	5	6	1'	2'	3'	4'	5'	6'	CH_3
Biphenyl	0.123	0.090	0.020	0.158	0.020	0.090	0.123	0.090	0.020	0.158	0.020	0.090	—
4-Methyl-	0.123	0.088	0.020	0.157	0.020	0.088	0.120	0.088	0.019	0.155	0.019	0.088	0.0125
p, p'-Bitolyl	0.120	0.087	0.020	0.154	0.020	0.087	0.120	0.087	0.020	0.154	0.020	0.087	0.0125
3-Methyl-	0.122	0.088	0.020	0.159	0.019	0.090	0.123	0.089	0.020	0.158	0.020	0.089	0.0016
m, m'-Bitolyl	0.123	0.088	0.020	0.158	0.019	0.090	0.123	0.088	0.020	0.158	0.019	0.090	0.0016
2-Methyl-	0.123	0.091	0.018	0.157	0.021	0.087	0.122	0.089	0.019	0.157	0.019	0.089	0.0074
o, o'-Bitolyl	0.122	0.090	0.018	0.155	0.020	0·086	0.122	0.090	0.018	0.155	0.020	0.086	0.0074

of a ring carbon atoms (α_C) to be the same as those of benzene (β, α).

Coulson-Crawford's[2] parameters were employed here for the calculation of the methyl fraction ($-C_1-C_2\equiv H_3$); that is, $\beta_{C_1-C}=0.7\ \beta$, $\alpha_{C_2}=\alpha-0.1\ \beta$, $\beta_{C=H_3}=2.5\ \beta$, and $\alpha_{H_3}=\alpha-0.5\ \beta$. The overlap integrals were disregarded for the above cases. For the ring proton splitting, Jarret's[3] calculation agreed well with the observed values, deviating by only about 15%, indicating that the ring-proton splitting parameter is 28 gauss.

However, with regard to the observed proton splitting given in Table I, some distinct spin distribution can be recognized in the case of both ortho-derivatives compared with those of the other meta- or para-derivatives. In the case of 2-methyl biphenyl, there is a certain difference in spin distribution at the ortho- and the meta-positions between a substituted and a non-substituted phenyl group; this difference may be due to a steric effect caused by the methyl group. In the case of o, o'-bitolyl, the magnitude of the proton splitting at the ortho-positions was much reduced, whereas that at the para-position was not.

Comparing the ring-proton splitting ratios $\Delta H_4/\Delta H_6$ of o, o'-bitolyl negative ions with those at the para- and the ortho-positions of other derivatives (e.g., $\Delta H_4/\Delta H_6$ or $\Delta H_4/\Delta H_2$), the largest value was obtained in the case of o, o'-bitolyl (2.35), although those of the others are all within the 1.80~2.17 range; moreover, the theoretical values are all equal to 1.76, including that of o, o'-bitolyl.

Recently McLachlan[4] has suggested that a reduction of the ring-proton splitting will take place selectively at the ortho- and at the meta-positions, so that $\Delta H_4/\Delta H_6$ will increase when both phenyl rings are assumed to be twisted in the biphenyl negative ion. Thus, a large $\Delta H_4/\Delta H_6$ value in the o, o'-bitolyl negative ion will probably indicate the presence of steric hindrance, as will be described in the following section.

The Methyl Proton Spitting.—In an ESR investigation of methylated, aromatic free radicals, hyperconjugation has been studied from two distinct theoretical points of view. One is the molecular orbital theory, in which the π-π coupling between the methyl group and the odd-ring orbital is considered to play an important role. Several workers' investigations have applied the method to the study of methyl substituted semiquinones[5] and methyl anthracene[6], using Coulson and Crawford's parameters. The other is the valence bond theory; McLachlan[7] calculated the hyperfine

2) C. A. Coulson and V. A. Crawford, *J. Chem. Soc.*, **1953**, 2052.
3) H. S. Jarret, *J. Chem. Phys.*, **25**, 1066 (1956).
4) A. D. McLachlan, *Mol. Phys.*, **3**, 244, (1960).
5) R. Bersohn, *J. Chem. Phys.*, **24**, 1066 (1956).
6) J. R. Bolton, A. Carrington and A. D. McLachlan, *Mol. Phys.*, **5**, 31 (1962).
7) A. D. McLachlan, ibid., **1**, 233 (1958).

splitting produced by protons of a methyl group in a π-electron radical such as Würster's blue, invoking the spin exchange polarization between the odd electron and the methyl group.

Taking these theoretical studies of hyperconjugation into consideration, the methyl proton splitting in each methylated biphenyl may be calculated in the following way.

The spin density (a_M) on the methyl protons is calculated on the basis of Hückel's MO method, utilizing Coulson-Crawford's parameters; then the theoretical methyl proton splittings (a_M) are calculated by making use of the following relation 1. The results are shown in Table III (A).

$$a_M = \rho_H \times 502 \text{ gauss} \quad (1)$$

where the splitting of a bare proton was estimated to be 502 gauss.

Furthermore, by referring to McLachlan's suggestion, the theoretical methyl splittings (a_M) were calculated on the basis of Hückel's spin density (ρ_C) on the corresponding ring carbon atoms of the biphenyl negative ion, using the following relation 2;

$$a_M = Q_M \rho_C \quad (2)$$

where Q_M is the methyl proton splitting parameter (which had been found to be 25~28 gauss after McLachlan)

Here, Q_M is estimated to be 28 gauss, since the magnitudes of the observed methyl splittings are all close to those of the ring proton at the relevant positions on the biphenyl ring. The results are shown in Table III (B).

TABLE III. THE ODD π ELECTRON ENERGY LEVELS AND THE EXPERIMENTAL AND THEORETICAL METHYL SPLITTINGS OF METHYLATED BIPHENYL MONO-NEGATIVE IONS

	Energy ($\times\beta$)	Methyl splitting (gauss)		
		(A)	(B)	(C)
Biphenyl	−0.704	—	—	—
4-Methyl-	−0.702	6.27	4.42	5.42
p, p-Bitolyl	−0.699	6.27	4.42	5.63
3-Methyl-	−0.704	0.80	0.56	0.43
m, m'-Bitolyl	−0.704	0.80	0.56	0.49
2-Methyl-	−0.703	3.71	2.52	2.41
o, o'-Bitolyl	−0.702	3.71	2.52	2.20

(A) Theoretical methyl splitting predicted by the Hückel's MO method by using the Coulson-Crawford parameters.
(B) Theoretical methyl splitting calculated from the relation $a_M = Q_M \rho_C$.
(C) Experimentally determined methyl splitting.

The molecular orbital calculations (A) agree well with the observed (C) and the calculated values in the case of the para-derivatives, while McLachlan's predictions (B) give satisfactory results in the case of the meta-derivatives.

As for the energy level of the odd π orbital shown in Table III, which was calculated in the course of the molecular orbital treatment (A), it is recongnized that the most effective perturbation of the energy level occurs in the case of the para-substitution, whereas there is no change in energy level in the case of the meta-derivatives compared with that of a biphenyl negative ion.

In the process of the interaction between the unpaired electron and the methyl group in these negative ions, when the π-π interaction is dominant, it may be assumed that the delocalization of the unpaired electron will perturb the energy level of the odd π orbital; thus, the magnitude of the methyl splitting will vary according to the perturbed energy level of the odd π orbital. Therefore, the theoretical methyl splitting calculated by the molecular orbital method A would be close to the observed values in this case.

However, when spin polarization is an important process, the perturbation of the energy level is assumed to be small. Thus, it may reasonably be expected that the hyperfine interaction of the methyl proton will be solely proportional to the spin density on the relevant ring carbon atoms of the unsubstituted negative ion; hence, McLachlan's prediction B would be more reliable than A.

From these arguments for the theoretical calculation, one may assume that the π-π interaction between the methyl group and a ring π orbital is likely to be the main process of hyperconjugation in the case of the para-derivatives. On the other hand, spin polarization would be dominant in the case of the meta-derivatives.

In the case of the ortho-derivative, one may suppose that the steric effect may change the methyl splitting as well as the ortho-ring proton splitting. In the case of 2-methyl biphenyl, the theoretical value obtained by the relation 2 is in good agreement with those observed. However, in the case of *o, o'*-bitolyl, the magnitude of the observed methyl splitting is appreciably less than that of the 2-methyl biphenyl negative ion or the theoretical value. It will be established in the following section that the reduction of the methyl splitting originates in steric hindrance in the case of the *o, o'*-bitolyl negative ion.

The Effect of Steric Hindrance.—In order to confirm the steric effect on both the ring

proton and the methyl proton splitting, the spin density was calculated with the modification that the resonance integral of C_1–C_1 bond was estimated to be $\beta \cos\theta$, where θ is a twisting angle between both phenyl rings. The dependence of the spin density of the ring carbon atoms and that of the methyl splitting on the twisting angle θ are shown in Figs. 5 and 6 respectively.

In Fig. 6(a), the methyl splitting is presented by the relation 1 on the basis of the spin densities on the methyl protons which were calculated for twisted models of the o,o'-bitolyl negative ion. In Fig. 6(b), the methyl splitting is calculated by utilizing the relation 2 described in the last section on the basis of the theoretical spin density of a twisted biphenyl negative ion.

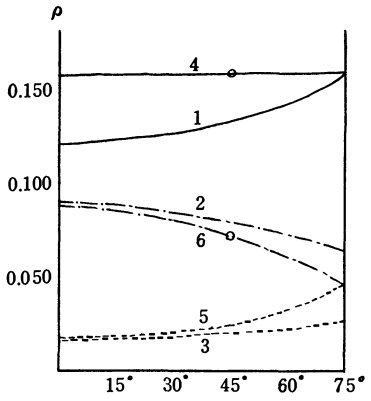


Fig. 5. Dependence of theoretical spin density of ring carbon atoms on twisting angle θ between the phenyl rings in o,o'-bitolyl negative ion, where the numbers represent the positions on the biphenyl ring.

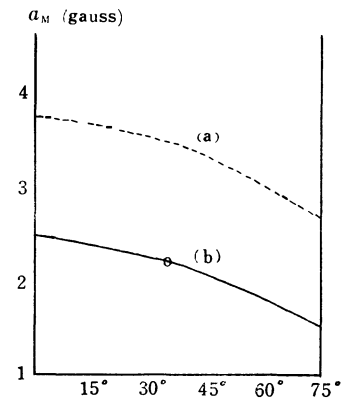


Fig. 6. Dependence of theoretical methyl splitting on twisting angles θ between the phenyl rings in o,o'-bitolyl negative ion.
(a) is plotted with the theoretical methyl splitting predicted by the Hückel's MO method using the Coulson-Crawford's parameter, applied for the twisted model of o,o'-bitolyl negative ion.
(b) is plotted with the theoretical methyl splitting obtained from the relation $a_M = Q_M \rho_C$, where the spin density on the ring carbon atom (ρ_C) are calculated for twisted biphenyl negative ion, and the methyl splitting parameter Q_M is estimated to be 28 gauss.

As is illustrated in Fig. 5, the spin density on the ring carbon atoms at the para (ρ_4)-position was enhanced gradually with an increment of θ, while conversely, those of the ortho (ρ_2, ρ_6)-positions were reduced.

This is a possible reason why the observed ring-proton splitting ratio, $\Delta H_4/\Delta H_6$, becomes larger in the o,o'-bitolyl negative ion than in other derivatives.

One will see that the theoretical spin density ratio, ρ_4/ρ_6, approaches the observed proton splitting ratio around $\theta = 45°$. Furthermore, it will be found that the magnitude of theoretical methyl splitting decreases with the increment of θ, as is shown in Fig. 6; hence, the theoretical value becomes equal to the observed values around $\theta = 30°$ in Fig. 6(b). In Fig. 6(a), the theoretical value is considerably larger than the observed values because of overstimated parameters in the methyl fraction.

When the results of both the ring proton splitting and the methyl proton splitting discussed in twisted models of the o,o'-bitolyl negative ion were put together, Hückel's calculation led to the conclusion that the two phenyl rings are twisted about 30°~45° from each other.

It has been well known on the basis of the investigation of the electronic spectra,[8] that the phenyl rings are twisted out about 70° in the neutral molecule of o,o'-bitolyl. When these twisting angles in the negative ion are compared with those in the neutral molecule, one may conclude that there is a greater tendency toward coplanarity between the two phenyl rings in the negative ion than in the neutral molecule of o,o'-bitolyl.

Recent ESR studies of such other ortho-derivatives as o-terphenyl,[9] o,o'-dinitro-biphenyl[10] have also suggested that this conclusion is justified.

Summary

The electron spin resonance of 3-methyl-biphenyl, 2-methyl-biphenyl, m,m-bitolyl, and o,o'-bitolyl has been observed. The overall

8) H. Suzuki, This Bulletin, 32, 135 (1959).
9) H. Nishiguchi, Y. Nakai, K. Nakamura, Y. Deguchi and H. Takaki, *Rev. Phys., Chem. Japan.*, 32, 57 (1962).
10) K. Kawamura, Y. Nakai, Y. Deguchi and H. Takaki, Private communication.

width and ring-proton coupling constants of the mononegative ions of each methylated biphenyl have been interpreted by utilizing the calculated spin density derived by Hückel's MO treatment. It has been found that the splitting parameters of the ring proton and the methyl proton were both about 28 gauss.

Hyperconjugation has been effected through the π-π interaction in the case of the para-derivatives, while spin polarization is important in the case of the meta-derivatives. In the case of the ortho-derivatives, the magnitude of the methyl splitting decreased with steric hindrance, which either brought about a fair amount of unbalanced spin density on biphenyl carbon atoms, or markedly reduced the magnitude of the ortho-proton splitting.

From Hückel's calculation, one may conclude that both of the phenyl rings are twisted about $30°\sim45°$ in the *o,o'*bitolyl negative ion, in which the twisting angle is much smaller than that in the neutral molecule.

The author wishes to thank Professors Hideo Takaki and Ryozo Goto for making the ESR spectrometer available for this study. He is also much obliged to Dr. Yasuo Deguchi for his helpful discussions and encouragement through the course of this work. The author wishes to express his gratitude to Professor Kenichi Fukui and to Dr. Keiji Morokuma for their computations of molecular orbitals. He is also indebted to Mr. Isao Yokomichi for the synthesis of the samples.

Deparment of Chemistry
Faculty of Science
Kyoto University
Sakyo-ku, Kyoto

The Colorimetric Determination of Minute Amounts of Iodide and Iodate in Sea Water by Means of Their Catalytic Effects

By Norinobu YONEHARA

(Received November 6, 1963)

It is known that iodine in sea water exists in the form of both iodide and iodate. Sugawara and Terada[1] determined the iodide and total iodine contents in sea water, but the method they proposed requires a considerable amount of sample and a time-consuming procedure. Barkley and Thompson[2] determined the iodate and total iodine contents in a relatively small amount of sample by using an amperometric or spectrophotometric method. The amperometric method was, however, accompanied by a somewhat complicated procedure, while the spectrophotometric method was applicable only to the determination of total iodine. The present author and others have reported in a preceding paper[3] a colorimetric method for the determination of ultramicro amounts of iodine in the form of both iodide and iodate by utilizing their catalytic effect on the color-fading of ferric thoicyanate. By this method, the iodate and total iodine contents in river and rain waters can be determined. However, as for sea water, this method is suitable for determining only the total iodine, but not the iodate iodine, because the separation of iodide from iodate is not performed quantitatively in the presence of the large amount of chloride contained in sea water. In the present work, therefore, the quantitative separation of iodide from iodate in sea water is attempted by means of the oxidation of iodide with an appropriate oxidizing agent. Because it improves the concentration of the reagents concerned and the conditions of the reaction, this catalytic method appears to be more sensitive and accurate than the method previously proposed, at least sensitive and accurate enough to determine the iodate and total iodine contents in sea water.

1) K. Sugawara and K. Terada, *J. Earth Sci., Nagoya Univ.*, **5**, 81 (1957).
2) R. A. Barkley and J. G. Thompson, *Anal. Chem.*, **32**, 154 (1960).
3) I. Iwasaki, S. Utsumi and N. Yonehara, *J. Chem. Soc. Japan, Pure Chem. Sec.* (*Nippon Kagaku Zasshi*), **85**, 36 (1964).

Experimental

Apparatus.—A Hirama photoelectric-colorimeter with a 460 filter (with maximum transmission at 460 mμ) and 10 mm. cells was used to measure the absorbance.

The reaction was carried out at 60.00±0.05°C using a water bath with a Taiyo Thermo Unit.

Reagents. — All the chemicals used were of guaranteed reagent quality.

Ferric Ammonium Sulfate - Nitric Acid Solution.— Six grams of ferric ammonium sulfate dissolved in 100 ml. of a 7.0 N nitric acid solution was stored in a brown glass bottle.

Potassium Thiocyanate Solution (0.01 M).—A potassium thiocyanate solution (0.1 M), standardized by Volhard's method, was diluted to a 0.01 M solution and stored in a brown glass bottle.

Sodium Nitrite Solution (0.014 M). — Sodium nitrite, 0.483 g. dissolved in redistilled water, was diluted to 500 ml. in a volumetric flask, and stored in a brown glass bottle.

Sodium Chloride Solution (20 g. of Chloride per l.). —Sodium chloride (32.970 g.) was dissolved in redistilled water and diluted to exactly 1 l.

Standard Iodide Solution. — A potassium iodide solution (0.1 M) was standardized by Volhard's method;[4] the working solution was then prepared by diluting this solution adequately.

Standard Iodate Solution. — Potassium iodate 0.843 g. was dissolved in redistilled water and diluted to exactly 500 ml. The working solution was prepared by successive dilutions.

Procedures and Calibration Curves. — The chlorinity of sea water was determined, and then it was diluted with redistilled water, to give a chlorinity of 2%.

Procedure (1) (for the Determination of Total Iodine).—Ten milliliters of the diluted sample is taken into a glass tube. One milliliter of a 0.014 M sodium nitrite solution and 1.0 ml. of a 0.01 M potassium thiocyanate solution are added and thoroughly mixed. The glass tube is then placed in the water bath at 60.0±0.1°C for about 10 min. The reaction is initiated by adding 2.0 ml. of a nitric acid solution of ferric ammonium sulfate (at the same temperature), mixing them thoroughly, and replacing the glass tube in the water bath.

After 20 min. ±5 sec. after the addition of the ferric ammonium sulfate solution, the absorbance of the solution is measured at the wavelength of 460 mμ, using redistilled water as a reference. It is recommended that the solution in the glass tube be removed from the water bath and poured into the cell 20 sec. before the scheduled time.

The calibration curve I shown in Fig. 1 was obtained by procedure 1 by using standard iodide and iodate solutions of known concentrations and containing chloride of the concentration of 2000 p. p. m. As can be seen in Fig. 1, in the cases of iodide and iodate, the absorbance is identical for the corresponding concentrations.

Procedure (2) (for the Determination of Iodate in the Presence of Iodide).—To 10.0 ml. of the diluted sample taken in a separatory funnel, 1.0 ml. of a 0.014 M sodium nitrite solution is added and thoroughly mixed, followed by the addition of 2.0 ml. of a nitric acid solution of ferric ammonium sulfate, mixing, and the further addition of 5 ml. of carbon tetrachloride. The separatory funnel is shaken for about 10 sec. and the layers allowed to separate. The aqueous layer is then transferred to the glass tube; a small amount of carbon tetrachoride does not disturb the subsequent procedure. The glass tube containing the aqueous layer thus obtained is placed in the water bath at 60.0±0.1°C for about 10 min. Then the reaction is initiated by adding 1.0 ml. of a 0.01 M potassium thiocyanate solution (at the same temperature); the solution is mixed thoroughly, and the glass tube with the solution is replaced in the water bath. At 20.0 min. after mixing, the absorbance of the solution is measured in the same way as in procedure 1.

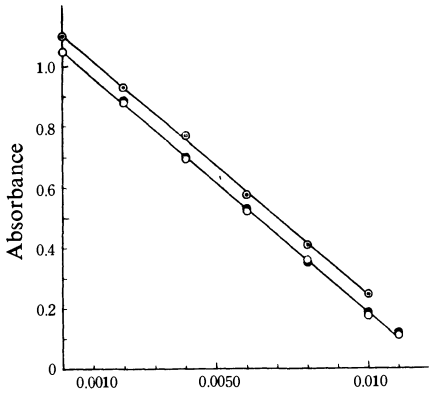


Fig. 1. Calibration curves.
In the presence of 2000 p. p. m. chloride
-○- I^- and -●- IO_3^- (I)
-⊙- IO_3^- (II)

The calibration curve II shown in Fig. 1 was obtained by procedure 2 by using standard iodate solutions of known concentrations and containing chloride of the concentration of 2000 p. p. m.

A difference between calibration curves I and II in Fig. 1 is probably caused by a loss (about 0.2 ml.) of solution during the extraction of procedure 2.

The catalytic reaction should be carried out in a dark place, thus avoiding an acceleration of the fading by sun light.[5]

Results and Discussion

The Effect of the Reaction Time.—Ten milliliters of a 0.010 p. p. m. iodide solution in the presence of 2000 p. p. m. chloride, 1.0 ml. of a 0.014 M sodium nitrite solution, 1.0 ml. of a 0.01 M potassium thiocyanate solution, and 2.0 ml. of a nitric acid solution of ferric ammonium sulfate were mixed and kept at 60°C. Reaction rate curve I shown in Fig. 2 was obtained by measuring the absorbances of this solution at various reaction times. Curves II and III in Fig. 2 were obtained by using a 0.005 p. p. m. iodide solution and redistilled water. It may be seen in Fig. 2 that the reaction rate increases with the amount of iodide and that differences in absorbances

4) F. P. Treadwell and W. T. Hall, "Analytical Chemistry," Vol. II, John Wiley & Sons, Inc., New York (1935), p. 657.

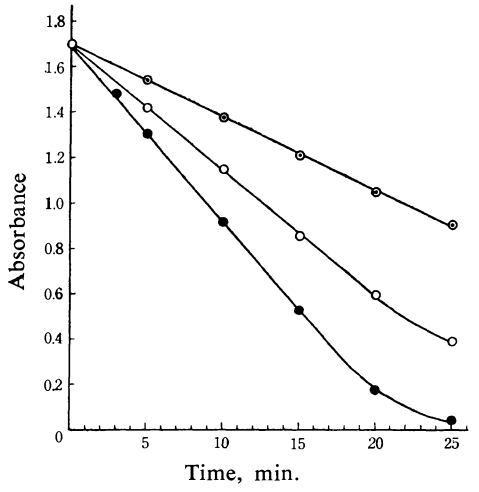


Fig. 2. Reaction rate curves.
60°C, in the presence of 2000 p. p. m. chloride
-●- 0.010 p. p. m. I^- (I)
-○- 0.005 p. p. m. I^- (II)
-⊙- Redistilled water (III)

among the three curves increase with the reaction time. These results indicate that the sensitivity of the method increases with the reaction time. The solution with 0.010 p. p. m. iodide becomes almost colorless after 25 min. A reaction time of 20 min. is adequate because of the high sensitivity.

The Effect of Chloride.—In the absence of chloride, iodate showed a different catalytic effect on the reaction rate than did iodide.[5] However, it has been reported by Dubravčić[6] that iodate showed the same catalytic effect as iodide in the presence of a large amount of chloride in the ceric-arsenous acid method. The same effect was also found in this color-fading method. In the present work, the effects of chloride have also been examined, therefore.

Three curves, I, II and III, shown in Fig. 3 were obtained by procedure 1 by using both iodide and iodate solutions containing various amounts of chloride. In the presence of more than 1000 p. p. m. chloride, iodide solutions show the same absorbance as that of iodate solutions in the same concentrations. The presence of 2000 p. p. m. chloride is adequate to determine the amount of total iodine. Sea water diluted ten times, containing chloride of about 2000 p. p. m., is, consequently, suitable for determination by this method. Satisfactory results obtained by using mixtures of iodides and iodates of different concentration

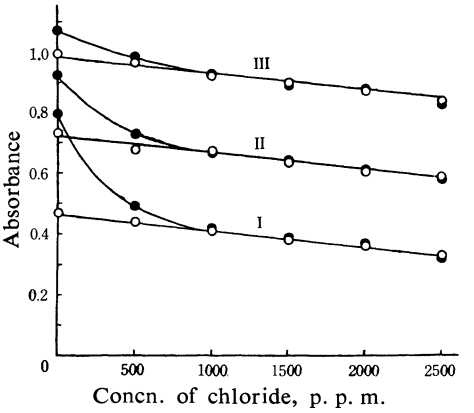


Fig. 3. Effect of concentrations of chloride.
60°C, 20 min.
-○- I^-, -●- IO_3^-
(I) 0.008 p. p. m. iodine
(II) 0.005 p. p. m. iodine
(III) 0.002 p. p. m. iodine

TABLE I. CHECK OF DETERMINATION OF TOTAL IODINE IN THE MIXTURE
(in the presence of 2000 p. p. m. chloride)

Concn. of I^- p. p. m.	Concn. of IO_3^- (as iodine) p. p. m.	Concn. of total iodine p. p. m.	Absorbance	
0.0020	0	0.0020	0.87_9	0.87_9
0.0010	0.0010		0.87_7	0.85_9
0	0.0020		0.87_9	0.88_0
0.0060	0	0.0060	0.53_5	0.53_3
0.0050	0.0010		0.53_9	0.53_9
0.0030	0.0030		0.54_9	0.54_0
0.0020	0.0040		0.52_0	0.52_8
0	0.0060		0.53_8	0.52_6
0.0080	0	0.0080	0.37_3	0.35_5
0.0060	0.0020		0.35_4	0.37_0
0.0040	0.0040		0.35_8	0.37_5
0.0010	0.0070		0.36_5	0.35_3
0	0.0080		0.35_4	0.36_4

ratios are listed in Table I.

The Concentration of Reagents. — A suitable concentration of a sodium nitrite solution was first sought. As iodide and iodate react with each other in an acidic solution, iodide must be oxidized to free iodine and then removed before the iodide-iodate reaction takes place. In the previous paper[3] a nitric acid solution of ferric ammonium sulfate was used for oxidation, but in the presence of a large amount of chloride, the separation of iodide from iodate was not quantitative. Both a sodium nitrite solution and a nitric acid solution of ferric ammonium sulfate are used for the oxidation of iodide. These reagents are not only the oxidizing agents, but also the reagents in the catalytic fading reaction. As an

5) S. Utsumi, M. Shiota, N. Yonehara and I. Iwasaki, *J. Chem. Soc. Japan, Pure Chem. Sec.* (*Nippon Kagaku Zasshi*), **58**, 32 (1964).
6) M. Dubravčić, *Analyst*, **80**, 149 (1955).

oxidizing agent, 1 ml. of a 0.014 M nitrite solution was necessary for the quantitative separation of iodide from iodate.

After a satisfactory concentration of a nitrite solution was determined, the concentration of the thiocyanate solution was adjusted to provide a suitable calibration curve covering the range from 0.001 to 0.01 p. p. m. of iodine.

The Removal of Iodide. — An attempt was made to remove the iodide of various concentrations in solutions by procedure 2. The results listed in Table II show that satisfactory removals of iodide were carried out by this procedure. Absorbances by using iodide solutions are identical with that of the redistilled water within the range of experimental error.

The results listed in Table III were obtained by precedure 2 in the presence of various amounts of both iodide and iodate. As can be seen in Table III, the iodate remains quantitatively in the aqueous layer, while the iodide is completely removed. In the experiments described above, the extraction in procedure 2 was carried out within 15 min.

TABLE II. REMOVAL OF IODIDE

Concn. of I^- p. p. m.	Absorbance	
Blank	1.09_2	1.08_6
0.002	1.08_6	1.08_1
0.004	1.08_6	1.08_1
0.006	1.08_6	1.07_5
0.008	1.07_1	1.06_8
0.010	1.07_6	1.06_6

TABLE III. REMOVAL OF IODIDE IN THE PRESENCE OF IODATE

Concn. of IO_3^- (as iodine) p. p. m.	Concn. of I^- p. p. m.	Absorbance	
0.0010	0	1.00_9	1.00_0
	0.0020	1.00_4	0.99_1
	0.0050	1.00_0	1.00_0
	0.0090	1.00_4	0.99_1
0.0020	0	0.92_8	0.91_4
	0.0010	0.92_8	0.93_1
	0.0040	0.93_1	0.91_7
	0.0080	0.93_1	0.90_0
0.0040	0	0.76_0	0.77_0
	0.0010	0.76_2	0.78_7
	0.0030	0.77_0	0.76_0
	0.0060	0.78_2	0.79_0
0.0060	0	0.57_2	0.57_5
	0.0020	0.57_7	0.58_2
	0.0040	0.58_5	0.56_9
0.0080	0	0.40_9	0.40_0
	0.0010	0.40_0	0.38_6
	0.0020	0.41_1	0.38_8

TABLE IV. EFFECT OF DIVERSE IONS

Ion	Added as	Concn. p. p. m.	Absorbance: Reagent blank	Absorbance: 0.005 p. p. m. I^-	Absorbance: 0.005 p. p. m. IO_3^- (as iodine)
None		0	1.05_1	0.62_0	0.62_5
K^+	KNO_3	100	1.04_6	0.62_0	0.63_8
Mg^{2+}	$Mg(NO_3)_2 \cdot 6H_2O$	200	1.04_6	0.61_6	0.63_3
Ca^{2+}	$Ca(NO_3)_2 \cdot 4H_2O$	100	1.04_6	0.60_2	0.62_2
Sr^{2+}	$SrSO_4$	10	1.01_7	0.60_4	0.62_0
Br^-	KBr	50	1.04_6	0.61_4	0.62_2
SO_4^{2-}	K_2SO_4	300	1.04_6	0.58_8	0.60_0
HCO_3^-	$NaHCO_3$	100	1.05_6	0.64_6	0.65_4
Borate ion	H_3BO_3	10	1.04_6	0.61_7	0.62_2
Silicate ion	(as SiO_2)	100	1.03_7	0.61_2	0.62_0
F^-	NaF	10	1.04_2	0.61_4	0.62_2
NO_3^-	$NaNO_3$	6200	1.00_9	0.55_1	0.56_5
		1000	1.04_6	0.62_0	0.62_5
PO_4^{3-}	$NaH_2PO_4 \cdot H_2O$	100	1.04_6	0.58_8	0.61_4
BrO_3^-	$KBrO_3$	1	1.04_1	0.59_9	0.62_0
CrO_4^{2-}	K_2CrO_4	10	1.00_0	0.58_3	0.58_3
$S_2O_3^{2-}$	$Na_2S_2O_3 \cdot 5H_2O$	10	0.99_5	0.58_8	0.60_0
ClO_3^-	$KClO_3$	1	1.04_1	0.61_6	0.63_6
Hg^{2+}	$HgSO_4$	0.1	1.05_1	0.78_5	0.79_8
		0.01	1.04_6	0.62_9	0.65_0
Ag^+	Ag_2SO_4	1	1.04_6	0.70_3	0.71_9
		0.1	1.05_0	0.62_0	0.62_0

TABLE V. DETERMINATIONS OF PREPARED MIXTURE SOLUTIONS

Added			Found					
Total iodine p. p. m.	IO_3^- (as iodine) p. p. m.	I^- p. p. m.	Concn. of total iodine p. p. m.	error	Concn. of IO_3^- (as iodine) p. p. m.	error	Concn. of I^- p. p. m.	error
0.0020	0.0010	0.0010	0.002_2	+0.0002	0.001_1	+0.0001	0.001_1	+0.0001
			0.002_2	+0.0002	0.001_0	0	0.001_2	+0.0002
	0	0.0020	0.002_2	+0.0002	0.000_1	+0.0001	0.002_1	+0.0001
			0.001_9	−0.0001	0.000_0	0	0.001_9	−0.0001
0.0040	0.0010	0.0030	0.004_2	+0.0002	0.001_1	+0.0001	0.003_1	+0.0001
			0.004_1	+0.0001	0.001_0	0	0.003_1	+0.0001
	0.0020	0.0020	0.004_0	0	0.001_9	−0.0001	0.002_1	+0.0001
			0.004_3	+0.0003	0.002_0	0	0.002_3	+0.0003
	0.0040	0	0.004_0	0	0.003_9	−0.0001	0.000_1	+0.0001
			0.004_0	0	0.003_7	−0.0003	0.000_3	+0.0003
0.0060	0.0010	0.0050	0.006_0	0	0.001_0	0	0.005_0	0
			0.006_2	+0.0002	0.001_1	+0.0001	0.005_1	+0.0001
	0.0030	0.0030	0.005_9	−0.0001	0.002_7	−0.0003	0.003_2	+0.0002
			0.006_0	0	0.002_7	−0.0003	0.003_3	+0.0003
	0.0050	0.0010	0.006_0	0	0.004_9	−0.0001	0.001_1	+0.0001
			0.006_1	+0.0001	0.004_8	−0.0002	0.001_3	+0.0003
	0	0.0060	0.006_0	0	0.000_2	+0.0002	0.005_8	−0.0002
			0.006_1	+0.0001	0.000_1	+0.0001	0.006_0	0
0.0090	0.0010	0.0080	0.008_9	−0.0001	0.001_1	+0.0001	0.007_8	−0.0002
			0.008_9	−0.0001	0.001_1	+0.0001	0.007_8	−0.0002
	0.0020	0.0070	0.008_9	−0.0001	0.001_9	−0.0001	0.007_0	0
			0.009_0	0	0.001_9	−0.0001	0.007_1	+0.0001
	0.0040	0.0050	0.008_9	−0.0001	0.004_0	0	0.004_9	−0.0001
			0.008_9	−0.0001	0.003_7	−0.0003	0.005_2	+0.0002
	0.0060	0.0030	0.009_0	0	0.006_1	+0.0001	0.002_9	−0.0001
			0.008_9	−0.0001	0.005_7	−0.0003	0.003_2	+0.0002
	0.0080	0.0010	0.008_9	−0.0001	0.007_8	−0.0002	0.001_1	+0.0001
			0.009_0	0	0.007_8	−0.0002	0.001_2	+0.0002
	0.0090	0	0.008_8	−0.0002	0.008_8	−0.0002	0.000_0	0
			0.008_9	−0.0001	0.008_9	−0.0001	0.000_0	0

after the addition of the oxidizing agent. However, when this period was prolonged over 40 min., the results did not have a tolerable reproducibility.

The Effect of Diverse Ions.—To make clear the effect of diverse ions on this method, some experiments were made in the presence of 0.005 p. p. m. of both iodide and iodate ions, and in their absence. The experimental results are given in Table IV. Nitrate does not interfere at 1000 p. p. m., but it gives a slightly low absorbance at 6200 p. p. m. (about 0.1 M). Sulfate does not significantly interfere at 300 p. p. m. Oxidizing or reducing agents interfere at relatively low concentrations. Mercury and silver interfere remarkably. Most sea waters do not contain these substances in concentrations which cause serious interference. Most ions commonly occuring in sea water do not interfere.

The Results of Determination.—The determinations of the total iodine and iodate-iodine were made by using mixed solutions containing known amounts of iodide and iodate and 2000 p. p. m. of chloride. The results listed in Table V indicate the maximum error of ± 0.0003 μg. per l. Iodide-iodine is calculated by the difference between the total-iodine and the iodate-iodine.

The total iodine and iodate-iodine contents in several sea waters were determined by using sea water diluted about ten and twenty times with the addition of known amounts of chloride to give the concentration of 2000 p. p. m. of chloride. The results listed in Table VI are calculated to original concentrations, and the comparison of the two results mentioned above shows good agreement. The method was also checked by adding known amounts of both iodide and iodate to sea water to show the good recovery of both iodide and iodate (Table VII).

According to these results, it may be concluded that the present method is quite satisfactory for the determination of iodide and iodate contents in sea water.

TABLE VI. DETERMINATIONS OF IODIDE AND IODATE CONTENTS IN SEA WATERS

Sea water		Concn. of total iodine p. p. m.	Concn. of IO_3^- (as iodine) p. p. m.	Concn. of I^- p. p. m.	Chlorinity ‰
Artificial sea water*1	Diluted ten times	0.07_1 0.07_0	0.02_1 0.02_0		18.68
	Average	0.07_1	0.02_1	0.05_0	
Standard sea water	Diluted ten times	0.05_6 0.05_5	0.03_5 0.03_4		19.37
	Average	0.05_6	0.03_5	0.02_1	
Sea water*2 No. 1	Diluted ten times	0.05_2 0.05_4	0.03_4 0.03_4		
	Diluted twenty times	0.05_4 0.05_5	0.03_4 0.03_6		18.80
	Average	0.05_4	0.03_5	0.01_9	
Sea water*3 No. 2	Diluted ten times	0.05_3 0.05_1	0.04_5 0.04_2		
	Diluted twenty times	0.05_2 0.05_2	0.04_4 0.04_4		19.37
	Average	0.05_2	0.04_4	0.00_8	
Sea water*4 No. 3	Diluted ten times	0.03_4 0.03_3	0.01_6 0.01_5		
	Diluted twenty times	0.03_6 0.03_4	0.01_6 0.01_4		18.61
	Average	0.03_4	0.01_5	0.01_9	

*1 Artificial sea water[7] contains 0.050 p. p. m. iodide-iodine and 0.020 p. p. m. iodate-iodine.
*2 The sample was taken 200 m. apart from the east coast of Satsuma-Iwo-jima, Kagoshima, August, 1962.
*3 The sample was taken 10 km. apart from the north coast of O-sima, Tokyo, March, 1962.
*4 The sample was taken on the coast of Mito, Ibaraki, August, 1962.

TABLE VII. DETERMINATIONS OF IODIDE AND IODATE CONTENTS IN SEA WATERS CONTAINING KNOWN ADDED IODIDE AND IODATE

Sample		Concn. of total iodine p. p. m.	Concn. of IO_3^- (as iodine) p. p. m.	Concn. of I^- p. p. m.
No. 1	Originally present	0.05_4	0.03_5	0.01_9
	Added	0.030	0.015	0.015
	Total	0.08_4	0.05_0	0.03_4
	Found*	0.08_4	0.05_1	0.03_3
	Recovered	0.03_0	0.01_6	0.01_4
No. 2	Originally present	0.05_2	0.04_4	0.00_8
	Added	0.030	0.015	0.015
	Total	0.08_2	0.05_9	0.02_3
	Found*	0.08_2	0.05_8	0.02_4
	Recovered	0.03_0	0.01_4	0.01_6
No. 3	Originally present	0.03_4	0.01_5	0.01_9
	Added	0.030	0.015	0.015
	Total	0.06_4	0.03_0	0.03_4
	Found*	0.06_2	0.02_9	0.03_3
	Recovered	0.02_8	0.01_4	0.01_4

* Average of two determinations.

7) J. Lyman and R. H. Fleming, *J. Marine Research*, 3, 134 (1940).

Summary

In the presence of 2000 p. p. m. chloride, iodide and iodate show the same catalytic effect on the color-fading reaction of a solution of ferric thiocyanate. The total iodine content in sea water may be determined by estimating the absorbance of a sample diluted about ten times.

The iodide in the sample is first oxidized to free iodine by a sodium nitrite solution and a nitric acid solution of ferric ammonium sulfate. The resulting free iodine is removed by extraction with carbon tetrachloride. The iodate which remains quantitatively in the aqueous layer is determined by a similar procedure. The difference between the total iodine and the iodate-iodine gives the iodide-iodine.

By this method, the iodate and total iodine contents in sea water can be determined rapidly and accurately. It takes only about 2 ml. of sea water to determine both the total iodine and the iodate-iodine.

The author wishes to express his thanks to Professor Iwaji Iwasaki of the Tokyo Institute of Technology for advice and encouragement given in the course of the work. Thanks

are also due to Dr. Satori Utsumi of the Nihon University for his valuable advice. He is also much obliged to the members of the Laboratory of Analytical Chemistry and Geochemistry, Tokyo Institute of Technology, for their fruitful discussions.

Laboratory of Analytical Chemistry
and Geochemistry
Tokyo Institute of Technology
Meguro-ku, Tokyo

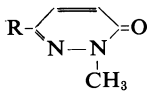
*The Tautomerism and Methylation of 3, 6-Disubstituted Pyridazines**

By Makoto FUJISAKA, Yoshio UENO, Hiroyuki SHINOHARA and Eiji IMOTO

(Received December 10, 1963)

The tautomerism of heteroaromatic compounds containing two different potentially tautomeric groups has not been widely studied. A recent investigation of 4-amino-6-hydroxypyrimidine and its related compounds reported by Brown and Harper[1] represents the only published case in which a 6-hydroxyl group exists predominantly in the keto form. This paper will deal with the tautomerism of 3, 6-disubstituted pyridazines which contain two different potentially tautomeric groups, such as OH, SH and NH_2. Furthermore, the attempted methylation of 3,6-disubstituted pyridazines will be discussed in connection with their tautomeric forms.

TABLE I. IONIZATION CONSTANTS OF SUBSTITUTED PYRIDAZINES, IN WATER AT 20°C

Compound R	Compound R′	Acidic pK_a	Basic pK_a
SH	OH	3.32	−1.39
SCH_3	OH	10.11*	(−)
SH	OCH_3	6.95*	−2.36
SCH_3	OCH_3	—	1.84
Cl	NH_2	—	3.85
SH	NH_2	9.05*	−0.14
SCH_3	NH_2	—	5.61
Cl	$NHCH_3$	—	4.01
SH	$NHCH_3$	9.46*	−0.04
SCH_3	$NHCH_3$	—	5.94
Cl		—	3.51
SH		9.31	−0.06
SCH_3		—	5.13
			
R			
OH		5.46*	−1.32
SCH_3		—	(−)

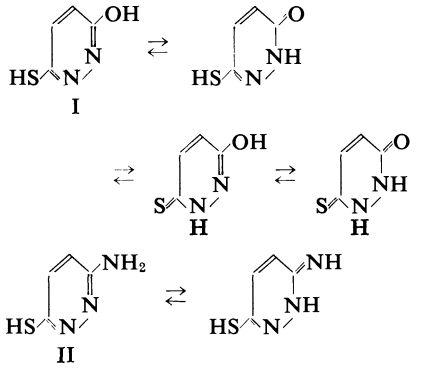
* These values were obtained by potentiometric titration and the values without asterisk were measured by means of spectrophotometric method. (−) means that spectrophotometric method did not allow to give pK_a value.

* Part of the data given in this article were presented at the 16th Annual Meeting of the Chemical Society of Japan, Tokyo, April, 1963.

Results and Discussion

The compounds studied in this work are listed in Table I, together with their ionization constants in aqueous solutions. These compounds were prepared by the method shown in Fig. 1, and their pK_a values were determined by potentiometric titration or the spectrophotometric method.[2]

Preferred Tautomeric Forms. — The conceivable tautomeric forms for 3-hydroxy-6-mercaptopyridazine (I)[3] and 3-amino-6-mercaptopyridazine (II)[4] in aqueous solutions may be written as follows:



I

II

1) D. J. Brown and J. S. Harper, *J. Chem. Soc.*, **1961**, 1298.

2) L. A. Flexser, L. P. Hammett and A. Dingwall, *J. Am. Chem. Soc.*, **57**, 2103 (1935).

3) J. Druey, Kd. Meier and K. Eichenberger, *Helv. Chim. Acta*, **37**, 121 (1954).

4) H. G. Morren, Belg. Pat. 579291 (1959).

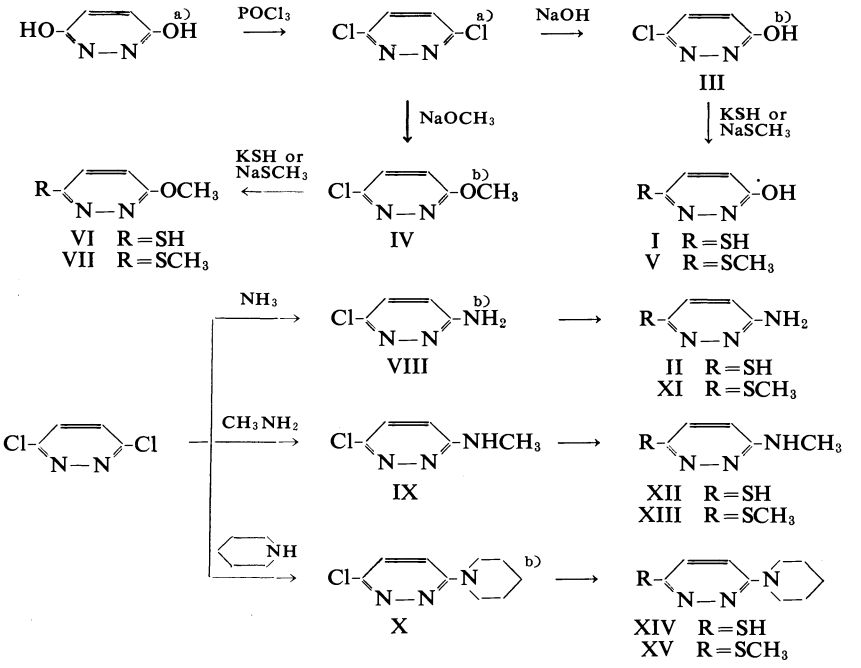
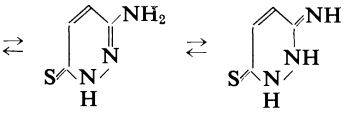


Fig. 1. The synthesis of the compounds.

a) R. H. Mizzoni and P. E. Spoerri, *J. Am. Chem. Soc.*, **73**, 1873 (1951).

b) J. Druey, Kd. Meier and K. Eichenberger, *Helv. Chim. Acta*, **37**, 121 (1954).



These compounds are also capable of existing in three forms, i. e., the neutral, anionic and cationic forms, depending on the pH values of the solutions. In the pH regions above the acidic values and below the basic values of their pK_a's, these compounds would be largely in the anionic and cationic forms respectively. In the pH range between the acidic and basic values of their pK_a's, these compounds would predominantly be in neutral forms and exhibit the tautomeric equilibria shown above.

In order to assign the preferred tautomer of 3-hydroxy-6-mercaptopyridazine (I) in an aqueous solution, the ultraviolet spectrum of the neutral species of I measured at pH 3.02 was compared with that of 3-mercapto-6-methoxypyridazine (VI) in which the tautomerism of the hydroxyl group of I had been inhibited. The spectra of the two compounds closely resemble each other in shape, as is shown in Fig. 2. Thus, it is highly probable that the lactim form predominates over the lactam form in the tautomerism of I. Furthermore, since the spectrum of I is markedly different from that of 3-methoxy-6-methylthiopyridazine (VII), the proportion of the thiolactam form of I should be very large. However,

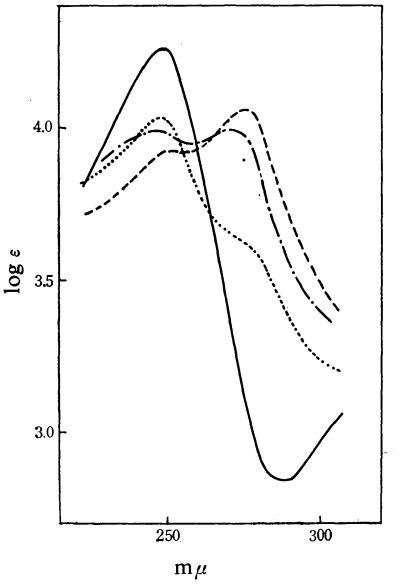


Fig. 2. Ultraviolet absorption spectra of neutral species in the aqueous solution;

---- 3-hydroxy-6-mercaptopyridazine (I) (pH 3.02),

- - - - 6-mercapto-3-methoxypyridazine (VI) (pH 2.87),

—— 3-hydroxy-6-methylthiopyridazine (V) (pH 6.28) and

------ 3-methoxy-6-methylthiopyridazine (VIII) (pH 5.38).

the spectrum of the neutral species of 3-hydroxy-6-methylthiopyridazine (V) differs from that of the compound VII. This seems to mean that V exists predominantly in the lactam form.

For assigning the preferred tautomers of 3-amino-6-mercaptopyridazine (II), 3-mercapto-6-methylaminopyridazine (XII) and 3-mercapto-6-piperidinopyridazine (XIV) in aqueous solutions, the tautomerism between amino and imino forms for II and XII was first examined. The ultraviolet absorption spectra of 3-amino-6-chloropyridazine (VIII) and 3-chloro-6-methylaminopyridazine (IX) were measured and compared with that of 3-chloro-6-piperidinopyridazine (X), in which the tautomeric hydrogen atom is lacking. The spectra of VIII, IX and X closely resemble one another in shape, as may be seen in Fig. 3.

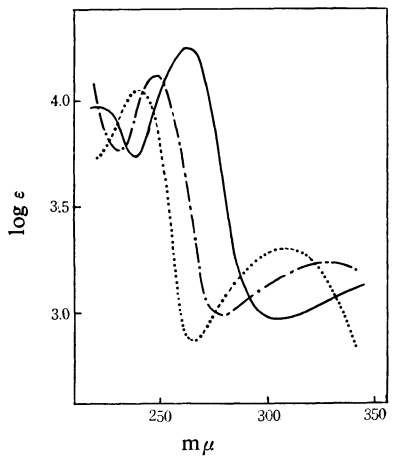


Fig. 3. Ultraviolet absorption spectra of neutral species in the aqueous solution;
------ 3-amino-6-chloropyridazine (VIII) (0.1N NaOH),
—·— 6-chloro-3-methylaminopyridazine (IX) (0.1N NaOH) and
—— 6-chloro-3-piperidinopyridazine (X) (0.1N NaOH).

Therefore, the amino group of II and the methylamino group of XII may exist predominantly in the amino and methylamino forms respectively. The marked differences which appeared in the spectra of the neutral species of the three pairs, II and XI, XII and XIII, and XIV and XV, (cf. Fig. 4), provide strong evidence that II, XII and XIV exist predominantly in the thiolactam forms rather than in thiol forms in aqueous solutions.

The Infrared Spectra of Substituted Pyridazines. — The infrared spectra of substituted pyridazines were measured in the solid states to verify the above conclusions. The results

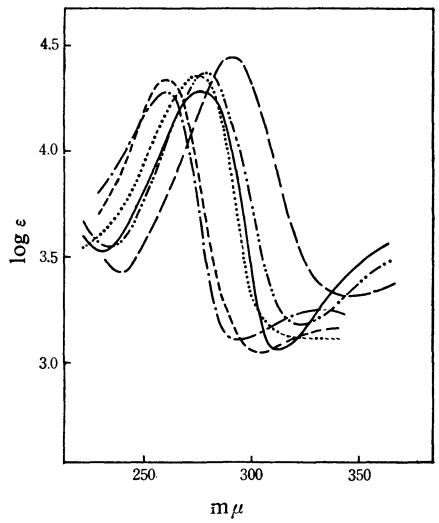


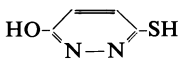
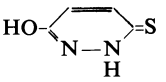
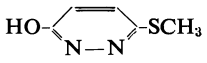
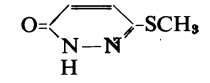
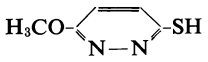
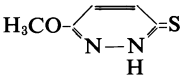
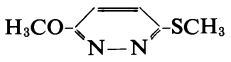
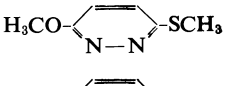
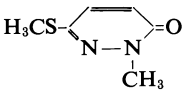
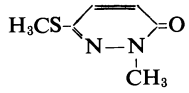
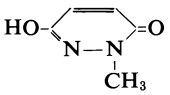
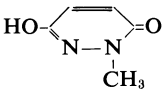
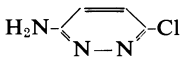
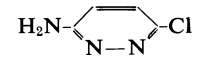
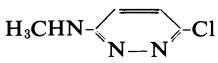
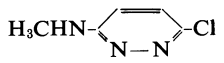
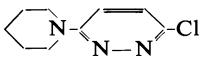
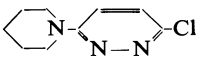
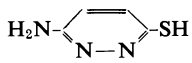
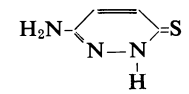
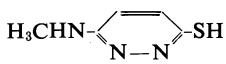
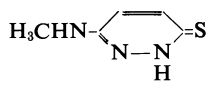
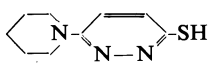
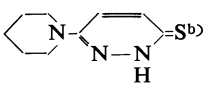
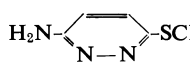
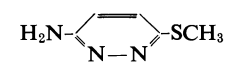
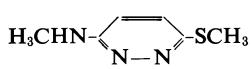
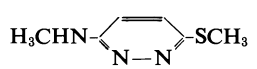
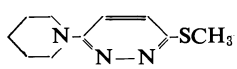
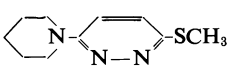
Fig. 4. Ultraviolet absorption spectra of neutral species in the aqueous solution;
—— 3-amino-6-mercaptopyridazine (II) (pH 5.38),
---- 3-amino-6-methylthiopyridazine (XI) (pH 6.28),
-·-·- 3-methylamino-6-mercaptopyridazine (XII) (pH 5.38),
- - - - 3-methylamino-6-methylthiopyridazine (XIII) (pH 6.28),
—— 6-mercapto-3-piperidinopyridazine (XIV) (pH 6.33) and
------ 6-methylthio-3-piperidinopyridazine (XV) (0.1N NaOH).

are summarized in Table II. As Table II illustrates, the structures of pyridazine derivatives in the solid states may be presumed to be identical with those of the neutral species suggested above in aqueous solutions.

The Ultraviolet Absorption Spectra of I and II in Various Solvents. — Since tautomerism is known to be affected by the nature of the solvents, the ultraviolet absorption spectra of I and II were measured in various solvents with different dielectric constants. Figure 5 shows that the absorption maxima shift toward the longer wavelength region with the decrease in dielectric constants for the solvents used.

Methylation of Compounds I and II. — The methylation of I and II with methyl iodide or dimethyl sulfate was studied. The results are listed in Table III. The thiol groups of I and II were found to be methylated more readily than the amino or the hydroxy groups under any conditions examined. However, when the methylation of I was carried out with dimethyl sulfate under the conditions described in Table III, a compound with an m.p. of 27~29°C, (XVI), was obtained as the major product. The results of the elementary analysis of XVI were in agreement with the calculated values

TABLE II. INFRARED SPECTRA OF SUBSTITUTED PYRIDAZINES

Compound	$\nu_{C=N}$ or $\nu_{C=C}$ cm^{-1}	$\nu_{C=O}$ cm^{-1}	ν_{N-H} cm^{-1}	$\nu_{C=S}$[a] cm^{-1}	Assumed structure
	1529 s	—	—	1086 s	
	1591 s	1713 s	—	—	
	1567 s	—	—	1080m	
	1597 s	—	—	—	
	1619 s 1575 s	1661 s 1644 s	—	—	
	1600 s	1671 s	—	—	
	1656 s 1608 s	—	3435 s 3231 s	—	
	1617 s	—	3264 s	—	
	1587 s	—	—	—	
	1653 s 1631m 1576 s	—	3585 s 3518 s 3400m sh 3288m	1126 s	
	1627m	—	3241m 3110m	1143 s	
	1612w	—	3160m 3100m	?	
	1641 s 1619 s	—	3312m 3140m	—	
	1621 s	—	3353m 3245m	—	
	1593 s	—	—	—	

Estimated band intensities are given as strong (s), medium (m) and weak (w), and a shoulder band is shown as (sh). a) E. Spinner, *J. Chem. Soc.*, **1960**, 1237. b) The structure of this compound was not certain because $\nu_{C=S}$ could not be found for this compound.

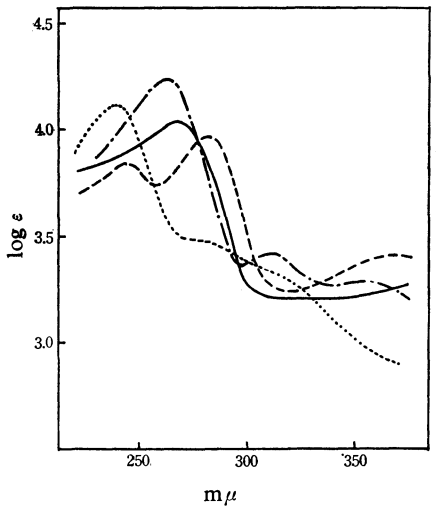


Fig. 5-a. Ultraviolet absorption spectra of 3-hydroxy-6-mercaptopyridazine; ---- in ethanol, —— in ethanol-water 1 : 1, —·— in water and ------ in 40% sulfuric acid.

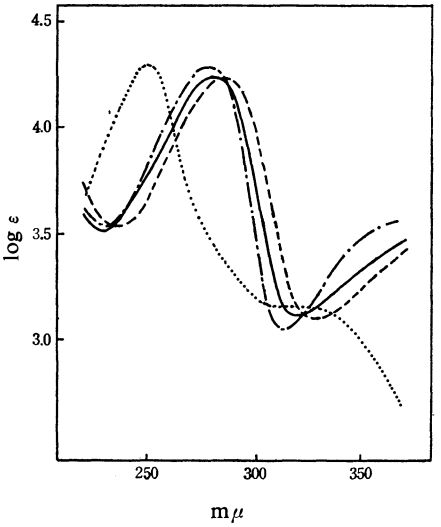


Fig. 5-b. Ultraviolet absorption spectra of 3-amino-6-mercaptopyridazine; ---- in ethanol, —— in ethanol-water 1 : 1, —·— in water and ------ in 20% sulfuric acid.

for the dimethylated compound of I. The spectrum of the neutral species of XVI closely resembles that of the neutral species of 3-hydroxy-6-methylthiopyridazine (V), the preferred tautomeric form of which was proposed in a previous section of this paper to be the lactam form (see Fig. 6).

The infrared spectrum of XVI shows a very strong absorption band at 1682 cm^{-1} due to carbonyl stretching vibration. On the basis of these results, the most reasonable structure assigned for XVI seems to be 2-methyl-6-methylthio-2, 3-dihydropyridaz-3-one.

Table III. Methylation of I and II

Compound	Methylating agent	Solvent	Added base	Reaction Temp. °C	Reaction Time hr.	Product	Yield %
I	CH_3I[a]	CH_3OH	$NaOCH_3$	70	1	V	78
I	CH_3I[b]	CH_3OH	$NaOCH_3$	120	2	V	72
I	CH_3I[a]	CH_3OH - H_2O	$NaHCO_3$	75	1	V	63
I	$(CH_3)_2SO_4$[a]	—	—	100	1	V	72
						XVI	8
I	$(CH_3)_2SO_4$[b]	—	—	140	3	XVI	80
II	CH_3I[a]	CH_3OH	$NaOCH_3$	reflux	1	XI	63
II	CH_3I[b]	CH_3OH	$NaOCH_3$	75	1	XI	72
II	CH_3I[a]	CH_3OH - H_2O	$NaHCO_3$	reflux	1	XI	81

a) The molar ratio of methylating agent to I or II was 1.
b) The molar ratio of methylating agent to I or II was 2.

Table IV. 3-Substituted 6-mercaptopyridazines

3-Substituent	Reaction condition Temp., °C	Time, hr.	Yield %	M. p. °C	Analysis N% Calcd.	Found
$-OCH_3$	135~145	6	57	191~193	19.70	19.34
$-NHCH_3$	80~ 90	3	52	234~237 (decomp.)	29.77	29.87
	170~180	9	76	147~149	21.52	21.07

Recrystallization were carried out with the following solvents; $-OCH_3$: aqueous ethanol, $-NHCH_3$: water,  : water.

TABLE V. 3-SUBSTITUTED 6-METHYLTHIOPYRIDAZINES

3-Substituent	Reaction condition Temp., °C	Time, hr.	Yield %	M. p. °C	Analysis N% Calcd.	Found
-OH	140~160	6	60	132~133	19.70	20.28
$-OCH_3$	140~160	6	65	85~ 87	17.94	18.21
$-NH_2$	120~130	9	70	116~117	29.77	30.27
$-NHCH_3$	130~140	8	83	83~ 84	27.08	27.12
-N⟨ ⟩	170~180	9	60	77~ 79	20.08	20.04

Recrystallizations were carried out with the following solvents; -OH and $-OCH_3$: water, $-NH_2$: benzene, $-NHCH_3$: ligroin, -N⟨ ⟩: cyclohexane.

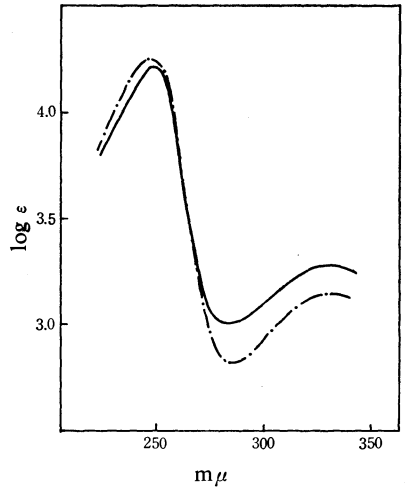


Fig. 6. Ultraviolet absorption spectra of neutral species in the aqueous solution;
—— 2-methyl-6-methylthio-2, 3-dihydropyridaz-3-one (XVI) (0.1 M H_2SO_4),
---- 3-hydroxy-6-methylthiopyridazine (V) (0.1M H_2SO_4).

Experimental

The Measurement of pK_a's Values.—pK_a values for the compounds which were soluble in water were measured by potentiometric titration, and those for the compounds which were sparingly soluble in water, by the spectrophotometric method.

The Measurement of the Ultraviolet Spectra.—The ultraviolet spectra were measured with a Hitachi EPS-2 spectrophotometer. The measurements were made in buffered, acidic or alkaline solutions and the pH value of each solution was adjusted so that more than 99% of the compound might exist in the form of neutral, cationic or anionic species in the solution, as expected from the pK_a values for the compound.

The Measurement of Infrared Spectra. — The infrared spectra were recorded with a Hitachi EPI-2 spectrophotometer by means of the potassium bromide disk technique.

Materials.—The compounds, I,[3] II,[4] 3-amino-6-chloropyridazine,[3] 3-chloro-6-hydroxypyridazine[3] and 3-chloro-6-methoxypridazine,[3] were synthesized by the known methods and purified until their physical constants gave values identical with those given in the literature.

3-Chloro-6-methylaminopyridazine (IX).—A mixture of 3.5 g. of 3,6-dichloropyridazine[5] and an aqueous solution containing 1 g. of methylamine was heated in a sealed tube at 120~130°C for 9 hr. After it had cooled, the resultant solid was collected by filtration. Recrystallization from water gave 2.3 g. of colorless needles of IX, m. p. 198~199°C. Found: N, 29.28. Calcd. for $C_5H_6ClN_3$: N, 29.27%.

A General Method for the Preparation of 3-Substituted 6-Mercaptopyridazine from 3-Substituted 6-Chloropyridazine. — A mixture of 3-substituted 6-chloropyridazine and 2 N ethanolic potassium hydrogen sulfide was heated in a sealed tube. After it had cooled, the reaction mixture was filtered to remove potassium chloride, and then the filtrate was evaporated to dryness under reduced pressure. The residue was recrystallized from a suitable solvent to obtain the product, as is shown in Table IV.

A General Method for the Preparation of 3-Substituted 6-Methylthiopyridazine from 3-Substituted 6-Chloropyridazine.—A mixture of 3-substituted 6-chloropyridazine and a 40% aqueous solution of sodium thiomethylate was heated in a sealed tube. The reaction mixture was then evaporated to dryness under reduced pressure, and the residue was recrystallized from a suitable solvent to obtain the product, as is shown in Table V.

The Methylation of I with Methyl Iodide.—a) To a solution of sodium methoxide which had been prepared from 0.3 g. of sodium and 20 ml. of methanol, 1.3 g. of 3-hydroxy-6-mercaptopyridazine (I) and 1.5 g. of methyl iodide were added. The mixture was heated in a sealed tube at 70°C for 1 hr. and then cooled and filtered to remove sodium iodide. The filtrate was evaporated to dryness, and the residue was dissolved in water and then acidified to precipitate the product. Recrystallization from water gave 1.1 g. of colorless crystals (m. p. 131.5 ~133°C, undepressed on admixture with an authentic sample of 2-hydroxy-6-methylthiopyridazine (V)). The reaction products were always the same although the molar ratios of I to methyl iodide changed from one to two.

b) When sodium hydrogen carbonate was used instead of sodium methoxide, only V was obtained, in a 63% yield.

The Methylation of I with Dimethyl Sulfate.—A mixture of 1 g. of I and 1 g. of dimethyl

5) R. H. Mizzoni and P. E. Spoerri, *J. Am. Chem. Soc.*, 73, 1873 (1951).

sulfate was heated on a steam bath for 1 hr. After the reaction mixture had been made alkaline by the addition of an aqueous solution of sodium carbonate, the solid which precipitated was collected by filtration. Recrystallization from water gave 0.8 g. of colorless crystals of V, m. p. 130~132°C. When the alkaline solution was extracted with ether, the ether extract gave 0.1 g. of colorless crystals, (m.p. 27~29°C) after evaporation.

The Methylation of II with Methyl Iodide.—a) The methylation was carried out in a sealed tube at 70°C for 1 hr. by a procedure similar to that used in the methylation of I. The product, 3-amino-6-methylthiopyridazine (XI), recrystallized from benzene, melted at 116~117°C and was not depressed on admixture with an authentic sample.

b) When sodium hydrogen carbonate was used instead of sodium methoxide, the reaction product was also only XI, in an 81% yield.

Department of Applied Chemistry
Faculty of Engineering
University of Osaka Prefecture
Sakai, Osaka

The Thermal Isomerization and Nuclear Magnetic Resonance Spectra of Tropyltropolones

By Takahiro TEZUKA

(Received December 13, 1963)

Nozoe et al.[1] have obtained five different tropyltropolones by the reaction of tropylium ions with tropolone. Of those tropyltropolones, structures for isomeric 5-tropyltropolone (II) and 3-tropyltropolone (III) have been suggested on the basis of ultraviolet spectral data.[1]

In order to obtain a more definite basis for the assigned structures, the present author has compared the nuclear magnetic resonance (NMR) spectra of several tropilidene derivatives and found the assigned structure to be correct. This paper will deal with these results, as well as with the thermal isomerization of tropyltropolones.

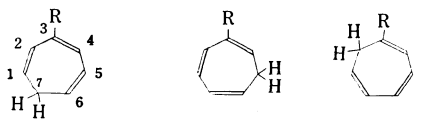
In the 40 Mc. NMR spectra of 5-tropyltropolone (I), a triplet (J=4.0 c.p.s.), a quartet, a multiplet and a triplet (J=1 c.p.s.) appear at 7.34, 4.82, 3.87 and 3.44 τ respectively. The proton ratio of these absorptions is 1 : 2 : 2 : 2 (Fig. 1). In the NMR spectra of the other 7-substituted tropilidenes (III, IV, V, VI, VII, VIII and XI), the same coupling patterns concerning the absorption of the tropyl group appear at approximately the same position and with the same proton ratio as those of 5-tropyltropolone, as is indicated in Table I. Therefore, the author has classified the proton absorptions of the tropyl group of those derivatives into four groups: A, B, C and D.*

A is a triplet (J=4~6 c.p.s.) at 6.5~7.8 τ (the position of which is especially affected by the substituent group at C_7), B is a quartet at 4.5~4.8 τ, C is a multiplet at 3.6~3.9 τ, and D is a triplet (J=2~3 c.p.s.) at 3.3~3.5 τ.

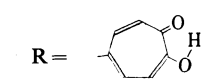
Proton assignments of tro ilidene have been made by Burton et al.[2] and by Isobe[3]. A comparison of these results shows that the absorptions A, B, C and D should be assigned to the protons at C_7, C_1+C_6, C_2+C_5 and C_3+C_4 respectively.

Taking this assignment into account, we will compare the NMR spectra of isomeric 5-tropyltropolone (II) with I to derive a reasonable structure for II.

Three possible formulae can be written for the isomeric 5-tropyltropolone structure (IIa, IIb and IIc):



IIa IIb IIc



The triplet at 7.71 τ in the NMR spectrum of II rules out the formula IIc. The formula

1) T. Nozoe, T. Mukai and T. Tezuka, This Bulletin, **36**, 1470 (1963).

* The 60 Mc. NMR spectra of phenyltropilidene (VII), taken with a Varian Associate HR-60 spectrometer, reveals that the basic coupling pattern is just the same as that of 40 Mc. The only difference is that the former has the fine structure of the each peak, A, B, C and D, due to the long-range coupling. The author wishes to thank Dr. Roy King for his measurement of the NMR spectra and his discussions.

2) R. Burton, L. Pratt and G. Willikinson, *J. Chem. Soc.*, **1961**, 594.

3) T. Isobe, presented at the 12th Annual Meeting of the Chemical Society of Japan, Kyoto, April, 1959.

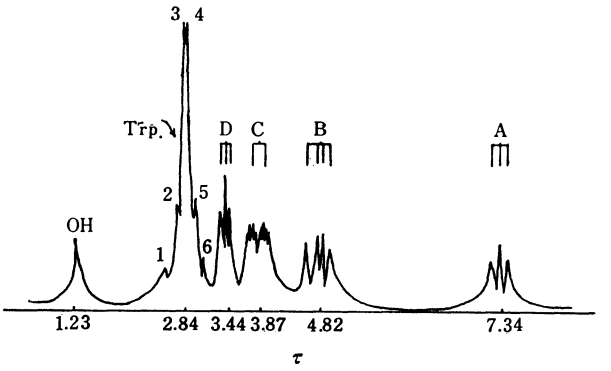


Fig. 1. NMR spectrum of compound I at 40 Mc.

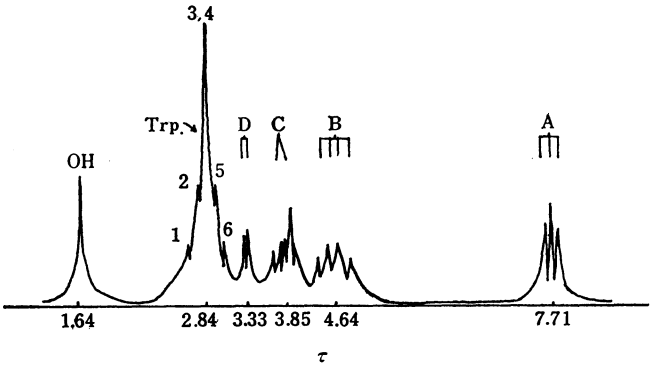


Fig. 2. NMR spectrum of compound II at 40 Mc.

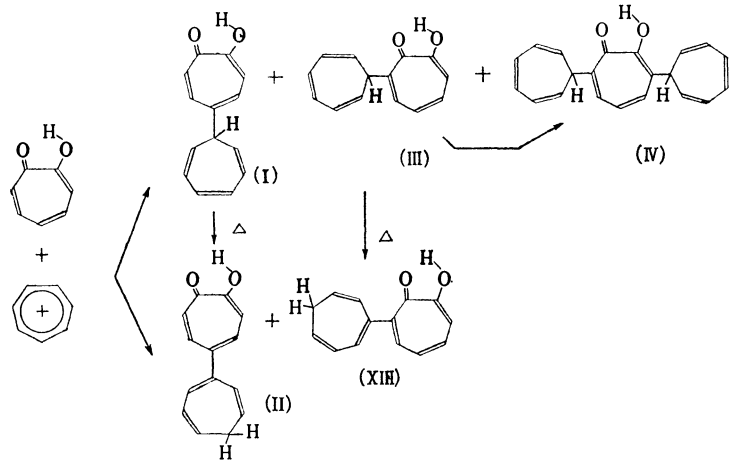
IIb may also be ruled out for the following reasons.

In the NMR spectra of I and II, the most significant difference is observed in the absorptions C and D. In the NMR spectrum of II (Fig. 2) a doublet (J=4.4 c.p.s.) and a multiplet appear at 3.33 τ (corresponding to the D absorption) and at 3.85 τ (C) respectively, while in the NMR spectrum of I a triplet and a multiplet apprear at 3.44 τ (D) and at 3.87 τ (C) respectively. The proton ratio of the absorption D to the absorption C of II is 1 : 2, while that of I is 2 : 2. These results are most reasonably explained by assuming the formula IIa thus ruling out IIb. A proton of C_4 in IIa appears at 3.33 τ, giving rise to a doublet, and the protons of C_2+C_5 at 3.84 τ, giving the multiplet. Therefore, the formula IIa is concluded to be correct for the structure of II; this is quite consistent with Nozoe's result.[1]

Nozoe et al.[1] have also mentioned that the isomeric 5- and 3-tropyltropolones, II and XIII, were obtained when the raection mixture of tropylium ions and tropolone was distilled at 180°C while the other tropyltropolones, I, III and IV, were obtained when the separation was carried out with the reaction mixture by recrystallization. This evidence seems to suggest that the isomeric tropyltropolones II and XIII come from either I, III, or IV by thermal isomerization when distilled. This assumption is justified as follows. The distillation of 5-tropyltropolone (I) at 180°C gives an oil (b. p. 173°C/3 mmHg) which soon crystallizes to afford the isomeric 5-tropyltropolone (II) (m. p. 98°C) in a good yield. Because only a small amount of 3-tropyltropolone (III) is available, the thermal isomerization reaction has not been carried out with III. The same treatment of 3, 7-ditropyltropolone (IV), however, gives neither the isomeric 3, 7-ditropyltropolone nor 3- and 5-tropyltropolones, XIII and II. Therefore, it may be concluded on the basis of the evidence given by Nozoe et al.[1] and by the present author that the isomeric 3-tropyltropolone (XIII) comes from III by thermal isomerization. 3, 7-Ditropyltropolone (IV) is derived from 3-troplytropolone (III) by the reaction of one mole equivalent of tropylium ions.

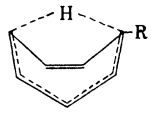
The above relationship between tropyltropolones can be given as:

The isomer IIa was the only product obtained by the isomerization of I. The reason for this is that the most stable isomer with regard to the length of the conjugated system



and the steric conditions is IIa. While IIc has the longest conjugation system between three double bonds of the tropyl group and the tropolone molecule, the methylene group of C_7 prevents the coplanality of the tropyl group with the tropolone molecule, thus inhibiting the resonance stabilization, and making IIc less stable than IIa. In IIb, there is no such steric hindrance, but the conjugated system is shorter; thus IIb is less stable than IIa.

For the mechanism of the migration of hydrogen in the thermal isomerization of 7-d-tropilidene, Ter Borg et al.[4] have proposed the 1, 5-transannular migration of hydrogen, as is pictured in XIV. It is also probable that the 1, 5-transannular migration of hydrogen is involved in our case, as is indicated in XV.[5] The conjugation of the tropolone molecule in the transition state decreases the activation energy for this migration, facilitating the isomerization.



XIV: R=D XV: R=Tropolone

The auther wishes now to discuss the NMR spectra of the tropilidene derivatives listed in Table I.

The most striking fact to be pointed out is the difference in the chemical shift of the methine and methylene protons (absorption A) of those derivatives. Looking at the chemical shift of methine protons of the compounds I, VII and VIII, we find that these protons appears at a lower field by 0.4~0.5 p.p.m. than the methylene protons of tropilidene (XII). On the other hand, the methylene protons of the tropyl derivatives, II, IX and 3-phenyltropilidene,[11] which are the isomer of I, VIII and VII respectively, appear at approximately the same position as tropilidene (XII). Obviously, the cause of this low field shift of the methine protons should be attributed to the effect of the phenyl or tropolone molecule substituted at the C_7 of tropilidene. However, it is rather surprising that the low field shift is not so large as would be expected from the usual substituent effect of the phenyl group.[6]

α-Protons are usually affected by the phenyl group to show a low field shift of approximately 1.5 p.p.m. when the phenyl group is substituted for hydrogen on an alkane.[6] Thus the methylene protons of *n*-propane appear at 8.75 τ, while the methine proton of isopropylbenzene appears at 7.10 τ.[6]

The reason for this small shift seems to be that the double bonds of the tropyl group have some shielding effect upon the methine proton.[7,8] Although the theory and the magnitude of the shielding effect of the tropyl group are not clear, we can understand such a tendency of the tropyl group when we look at the NMR spectrum of ditropyl (XI). The shift of the methine protons of XI are slightly higher than that of the methylene protons of tropilidene, suggesting that the double bonds of the tropyl group have the effect of increasing the effective shielding of the methine proton at C_7.[7,8]

The fact that the methine proton of 5-tropyltropolone (I) shifts to a low field by the

4) Ter Borg, H. Kloosteaziel and N. van Meurs, *Proc. Chem. Soc.*, **1962**, 359.

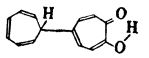
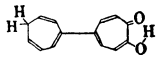
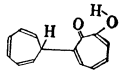
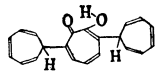
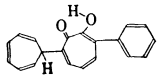
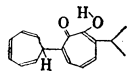
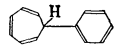
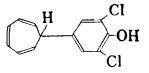
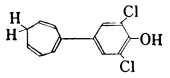
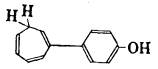
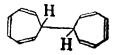
5) The author has found that the compound VIII is also converted to IX upon heating at 200°C. T. Tezuka, unpublished work.

6) L. M. Jackman, "Application of NMR Spectroscopy in Organic Chemistry," Pergamon Press, London (1959), pp. 58-60.

7) The author is deeply indebted to Professor Orville L. Chapman for discussing the shielding effect of the double bonds of the tropyl group.

8) O. L. Chapman, T. Tezuka and R. King, to be published.

TABLE I. THE PROTON CHEMICAL SHIFT OE THE TROPYL GROUP IN THE SUBSTITUTED TROPILIDENES

No.	Compound	Group A (τ)	B	C	D	Ref.
I		7.34 (J=4.0)	4.82	3.87	3.44	1 (J=c.p.s.)
II		7.71 (J=6.0)	4.64	(3.85)	(3.33)	1
III		6.50 (J=5.7)	4.76	3.88	3.52	1
IV		6.48 (J=5.1)	4.64	3.76	3.40	1
V		6.37 (J=4.8)	4.82	3.87	3.63	10
VI		6.58	4.72	3.80	3.46	10
VII		7.30 (J=5.0)	4.78	3.80	3.34	11,12
VIII		7.41	4.57	3.85	3.33	5
IX		7.67	4.50	3.62	3.28	5
X		7.75 (J=6.7)	4.64	—	—	14
XI		8.10 (J=3.0)	4.82	3.88	3.42	13
XII		7.84 (J=6.2)	4.81	3.94	3.54	2,3

same degree as in phenyl tropilidene (VII) indicates that the tropolone molecule also has the effect of deshielding the methin protons by the same degree as benzene. Probably, the six-π-electron circulation in the tropolone molecule occurs when it is placed in a magnetic field as in the benzene molecule.

One more point of interest is that the different coupling patterns of the tropolone ring protons are observed with different tropyltropolones. The ring protons of 5-tropyltropolones (I and II) are expected to show A_2B_2-type coupling, while 3,7-ditropyltropolone (IV) show AB_2-type coupling. Actually, the symmetrical A_2B_2-type coupling[9] are observed at 2.84 τ in the NMR spectra of I and II, as is indicated in Figs. 1 and 2. In the case of I, six lines can be recognized.

An unsymmetrical coupling pattern of the

9) L. M. Jackman, "Application of NMR Spectroscopy in Organic Chemistry," Pergamon Press, London (1959), pp. 91-95.

* A figure of the NMR spectra of this compound is indicated in Ref. 10.

10) T. Nozoe and T. Tezuka, This Bulletin, in press.

11) T. Nozoe, T. Mukai, T. Tezuka and K. Osaka, *J. Chem. Soc. Japan, Pure Chem. Sec.* (*Nippon Kagaku Zasshi*), **84**, 662 (1963).

12) H. Horino obtained phenyltropilidene (VII) as colorless crystal (m. p. 32°C) and kindly provided a sample; to him the authors thanks are due.

13) Professor Toshio Mukai kindly gave the sample of ditropyl (XI) (m. p. 61°C); the author wishes to thank him.

14) K. Kitahara, Doctoral Thesis, Tohoku Univ. (1963).

tropolone ring proton of compound IV[1],* is oberved which is very similar to the theoretical pattern of the AB_2 system.[9] Almost the same coupling is observed for the ring protons of compound VI.[10],*

The methine proton lines of the tropyl group of compounds III, IV, V and VI, in which the tropyl groups are present at the ortho-position of tropolone, appear at an even lower field than those of compounds I, VII and VIII. The chemical shifts of those protons are lower by 1.3 p.p.m. than the methylene protons of tropilidene. The methine protons of III, IV, V and VI will be greatly deshielded by both the ring current and the oxygen functions of of tropolone. However, the details of these effects are too complicated to discuss here; further studies are necessary.

Experimental

Isomeric 5-Tropyltropolone (II) from I. — I (500 mg.) was heated at 180~200°C for 20 min. and then distilled to give an oil, b. p. 170°C/4 mmHg, which soon crystallized to afford 500 mg. of crystals, m. p. 80~85°C. Recrystallization from the mixed solvent of ethanol and benzene gave yellow needles, m. p. 98°C (II), identified by a mixed melting point determination and by a comparison of the infrared spectra with those of an authentic sample.[1]

3, 7-Ditropyltropolone (IV) from III.—A mixture of 250 mg. of III and 117 mg. of ditropylether[14] in 2.5 ml. of absolute ethanol was heated under reflux for 3 hr. The evaporation of the solvent gave 360 mg. of crystals, m. p. 90~100°C, which afforded yellow needles, m. p. 135°C (IV), on recrystallization from ethanol. The crystals obtained were confirmed to be identical with 3,7-ditropyltropolone[1] by mixed melting point determination and by a comparison of infrared spectra.

NMR Spectra Measurement.—The NMR spectra of the tropyl derivatives (I—X) were measured with a Varian Associates V 4200 B spectrometer (40 Mc.) in carbon tetrachloride solutions, using cyclohexane as an inner reference.* The NMR spectrum of IX was measured with a 60 Mc. Hitachi NMR spectrometer in a carbon tetrachloride solution, using tetramethyl silane as an inner reference.

The author wishes to express his gratitude to Professor Tetsuo Nozoe for his guidance throughout this study. The author also wishes to express many thanks to Professors Toshio Mukai, Kahei Takase, Taro Isobe, Dr. Takashi Toda and Mr. Kenichi Abe for their helpful discussions and assistance.

Department of Chemistry
Faculty of Science
Tohoku University
Katahira-cho, Sendai

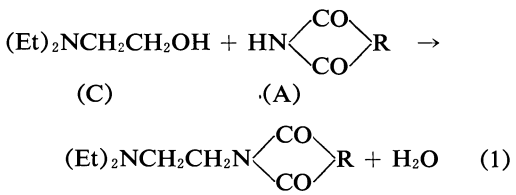
* For the NMR measurement, the author wishes to thank Mr. Kensuke Takahashi, Dr. Masaki Iwaizumi and Mr. Makoto Hanabuchi.

*The Reaction of 2-(Diethylamino)ethanol with Imides**

By Tsuyoshi OGATA

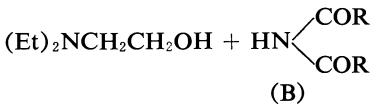
(Received December 27, 1963)

In the previous paper of this series,[1] it was reported that the imides of dibasic acids (A) were condensed with 2-(diethylamino)ethanol (C) with the elimination of water, while the imides of monobasic acids (B) were converted into the corresponding amides and the esters of the aminoalcohol (C) in good yields.



$$(Et)_2NCH_2CH_2OH + HN\begin{matrix}CO\\CO\end{matrix}R \rightarrow (Et)_2NCH_2CH_2N\begin{matrix}CO\\CO\end{matrix}R + H_2O \quad (1)$$

(C) (A)



$$(Et)_2NCH_2CH_2OH + HN\begin{matrix}COR\\COR\end{matrix} \rightarrow (Et)_2NCH_2CH_2O\cdot COR + RCONH_2 \quad (2)$$

(B)

The present investigation has been undertaken to clarify the cause of the different in reactivity on the aminoalcohol (C) between the imides of dibasic acids (A) and those of monobasic acids (B).

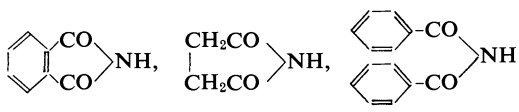
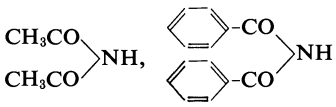
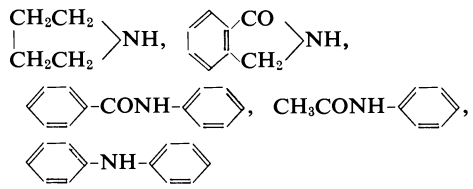
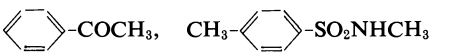
Experimental Results and Discussion

The Reaction of 2-(Diethylamino)ethanol (C) with Imides or Their Analogues.[1]—The rerults summarized in Table I show that: 1) The presence of two carbonyl groups attached to

* Presented at the Symposium on Organic Reaction Mechanisms, Fukuoka, October, 1963. This is the third paper of the series, "Studies of the Reaction of 2-(Diethylamino)ethanol with Imides."

1) R. Goto and T. Ogata, *J. Chem. Soc. Japan, Pure Chem. Sec.* (*Nippon Kagaku Zasshi*), **84**, 653 (1963).

TABLE I. RELATIVE REACTIVITIES OF IMIDES AND THEIR ANALOGUES ON THE AMINOALCOHOL (C)

No.	Imides or their analogues	Type of reaction	Note
(I)		Eq. 1	The aminoalcohol (C) does not react below 180°C. Usual alcohols and amino-*t*-alcohol do not react with imides (A).
(II)		Eq. 2	Usual alcohols react with imides (B).
(III)		No reaction	
(IV)		No reaction	

an imino group is essential to both reactions, 1 and 2.

2) The imides of dibasic acids (cyclic imides)** (A) are condensed with the aminoalcohol (C) with the elimination of water.

3) The imides of monobasic acids (straight-chain imides)** (B) are converted into the corresponding amides and the esters of the aminoalcohol (C).

4) Usual alcohols do not react with the imides of dibasic acids (A). Therefore, a diethylamino group in the aminoalcohol (C) is necessary for reaction 1.

5) The imides of monobasic acids (B) react with alcohols in the same manner as with the aminoalcohol (C). Thus, an attack of the alcohol or the aminoalcohol (C) on acyl groups seems to be easier than that on an imino group of imide (B).

Reaction of 2-(Diethylamino)ethanol (C) with Unsymmetrical Imides of Monobasic Acids (B).[2] —In these experiments the reactivities of the two acyl groups in imide were compared. The experimental data are shown in Table II.

The data in Table II lead to the following conclusions:

1) In the cases of I, II, IV, and V, unsymmetrical imides predominantly yield the esters of the stronger acids. In the cases of VI and VII, however, unsymmetrical imides yield the esters of the weaker acids exclusively. Therefore, it seems that the steric influence predominates over the acidity of the acyl group.

2) I and II, where the parent acids are of approximately the same strength, gave the esters in a different molar ratios. These results may be explained by the greater steric hindrance of the isobutyryl group over that of the propionyl group.

3) In the case of III, the ester of the weaker acid forms predominantly.

As Fig. 1 shows, the resonance in the benzoyl group would disperse the postive charge of the carbonyl carbon atom into a benzene ring, making the benzoyl group less susceptible to a nucleophilic attack than the acetyl group, which would be polarized by the inductive effect of the methyl group.[3]

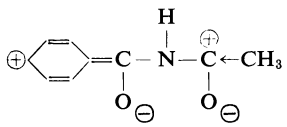


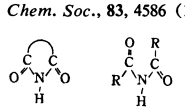
Fig. 1.

Reaction Mechanism

1) In discussing the reaction mechanism, it is first necessary to consider the role of a diethylamino group in 2-(diethylamino)ethanol (C).

Recently, Komori and his co-workers[4]

** From the measurement of the dipole moments of imides, only a cis-cis conformation (a) is possible in cyclic imides (A), while a cis-trans conformation (b) is likely in straight-chain imides (B). W. D. Kumler and C. M. Lee, *J. Am. Chem. Soc.*, **83**, 4586 (1961); **84**, 571 (1962).



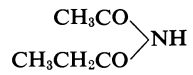
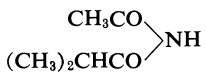
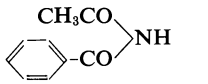
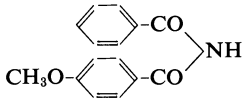
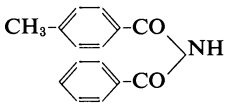
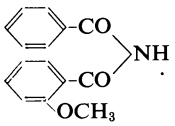
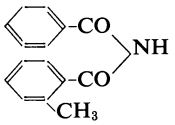
(a) (b)

2) R. Goto and T. Ogata, *J. Chem. Soc. Japan, Pure Chem. Sec.* (*Nippon Kagaku Zasshi*), **84**, 849 (1963).

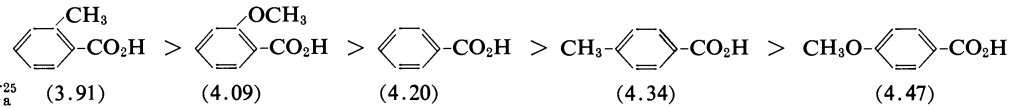
3) P. S. Baily and Y.-G. Chang, *J. Org. Chem.*, **27**, 1193 (1962).

4) S. Komori, M. Ochiai and Y. Ōki, *J. Chem. Soc. Japan, Ind. Chem. Sec.* (*Kogyo Kagaku Zasshi*), **64**, 1588 (1961); **65**, 1830 (1962).

TABLE II. RELATIVE REACTIVITIES OF UNSYMMETRICAL IMIDES OF MONOBASIC ACIDS ON THE AMINOALCOHOL (C)

No.	Unsymmetrical imides*	Esters formed**	Molar ratio of esters fromed
(I)		$RO\cdot COCH_3$: $RO\cdot COCH_2CH_3$	1 : 0.93
(II)		$RO\cdot COCH_3$: $RO\cdot COCH(CH_3)_2$	1 : 0.51
(III)		$RO\cdot COCH_3$: $RO\cdot CO$-C$_6$H$_4$	1 : 0.51
(IV)		$RO\cdot CO$-C$_6$H$_4$: $RO\cdot CO$-C$_6$H$_4$-OCH_3	1 : 0.25
(V)		$RO\cdot CO$-C$_6$H$_4$: $RO\cdot CO$-C$_6$H$_4$-CH_3	1 : 0.29
(VI)		$RO\cdot CO$-C$_6$H$_4$: $RO\cdot CO$-C$_6$H$_4$-OCH_3	1 : 0.08
(VII)		$RO\cdot CO$-C$_6$H$_4$: $RO\cdot CO$-C$_6$H$_4$-CH_3	only $RO\cdot CO$-C$_6$H$_5$

* The order of acidities (pK_a^{25}) of monobasic acids, of which unsymmetrical imides are constituted, is as follows.



pK_a^{25}	(3.91)	(4.09)	(4.20)	(4.34)	(4.47)

$> CH_3CO_2H > (CH_3)_2CHCO_2H > CH_3CH_2CO_2H$
(4.76) (4.85) (4.88)

"Series of Comprehensive Organic Chemistry (Dai Yuki-kagaku)," Additional Vol. 2, Asakura Publishing Co., Tokyo (1963), p. 638.

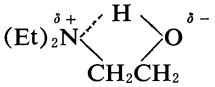
** $R = (Et)_2NCH_2CH_2-$

reported that, in the preparation of polyhydroxyethylene alkyl ether from alcohol and ethylene oxide in the presence of tertiary amine serving as a catalyst, the reaction rate increased in proportion to the basicity of the amine and considerably decreased as *N*-substituents of the amine became bulky. In this reaction, therefore, it seems that a hydroxyl group in alcohol is activated by tertiary amine, as is shown in Eq. 3.

$$ROH + R'_3N \rightarrow R-\overset{\delta-}{O}-H\cdots\overset{\delta+}{N}R'_3 \qquad (3)$$

Douheret and Pariaud[5] suggested the presence of an intramolecular hydrogen bond in dialkylaminoethanol on the basis of their measurement of its infrared sepctrum in carbon tetrachloride. Therefore, a hydroxyl group in 2-(diethylamino)ethanol seems to be activated by a diethylamino group, as is shown in Eq. 4.

$$(Et)_2NCH_2CH_2OH \rightleftharpoons$$



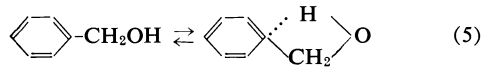
(4)

Furthermore, in the reaction of benzyl alcohol on dibenzamide, benzamide and benzyl benzoate were produced in good yields.[1] In the case of lauryl alcohol, however, in spite of a longer reaction time, benzamide

5) G. Douheret and J. C. Pariaud, *J. Chim. Phys.*, **59**, 1021 (1962).

and lauryl benzoate were produced in lower yields than in benzyl alcohol.

Ōki and Iwamura[6] concluded that in benzyl alcohol there is an interaction between an aromatic nucleus and a hydroxyl group, as is shown in Eq. 5. Therefore, it seems that a hydroxyl group is activated by an aromatic nucleus and that, toward dibenzamide, benzyl alcohol is more reactive than lauryl alcohol.



(5)

2) Lamberton and Standage[7] investigated the alkaline and acid hydrolysis of some *N*-acylbenzamides ($x\,C_6H_4CONRCOR'$) and found that in the alkaline medium the ortho-substituent x almost completely prevented the attack of hydroxyl ions on the nearer carbonyl group, while meta- and para-substituent did not have such a steric effect. Thus, *N*-acyl ortho-substituted benzamides gave ortho-substituted benzamide ($x\,C_6H_4CONHR$) and acid (R'COOH) upon alkaline hydrolysis, while meta- and para-substituted benzamides gave the stronger acid preferentially.

In the acid hydrolysis, on the other hand, the ortho-substituent showed no sign of the steric effect. In meta- and para-substituted benzamides, the weaker acid was liberated preferentially.

From these facts, it may be generally concluded that in the alkaline hydrolysis, the S_N2-type mechanism is operative, as is shown in Fig. 2-A, while in the acid hydrolysis, the results are explicable by the formation of acylium ions, as is shown in Fig. 2-B.

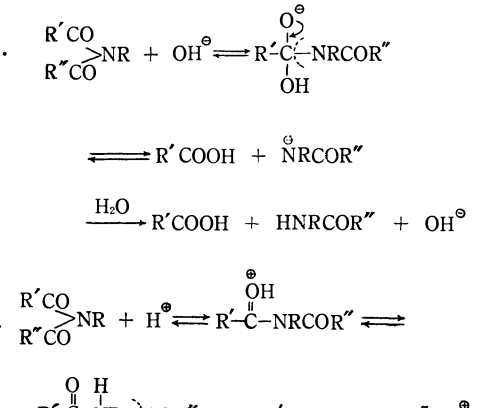
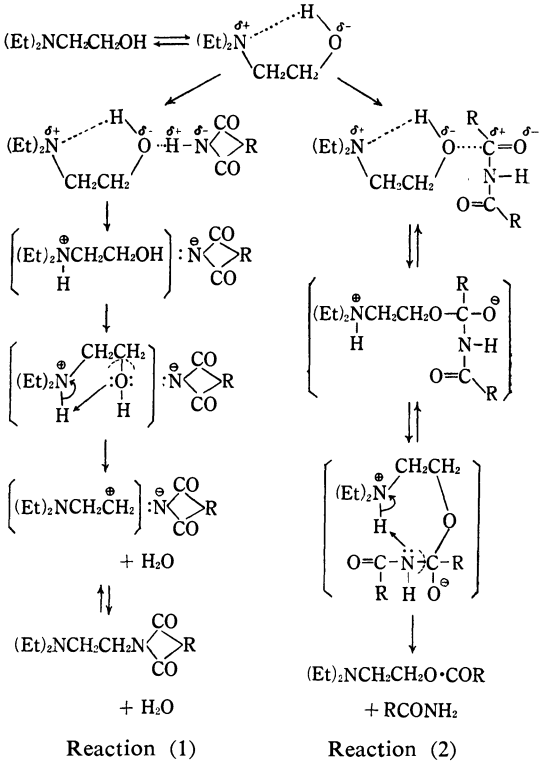


Fig. 2.

Tedder[8] summarized the reactions of unsymmetrical carboxylic anhydrides on amines or ethanol and showed that these reactions proceeded in the same fashion as the alkaline hydrolysis of diacylamines mentioned above. Furthermore, he showed that Friedel-Crafts acylation by unsymmetrical carboxylic anhydrides in the presence of aluminum chloride proceeded in the same fashion as the acid hydrolysis of diacylamine, and that the ketones derived from the weaker acids were produced preferentially.

On the basis of these data, reasonable conclusions may be deduced as follows:

i) In the case of the imides of monbasic acids (B), a nucleophilic attack of the aminoalcohol (C) will occur preferentially at the more positive carbonyl group and, when the position is sterically hindered, at another, less hindered carbonyl group.



Reaction (1) Reaction (2)

Fig. 3. Reaction mechanism of 2-(diethylamino)ethanol with imides

ii) In the case of the imides of dibasic acids (A), it seems that, on account of the steric hindrance of the carbonyl group of the imide, a nucleophilic attack of the aminoalcohol (C) is almost completely prevented and that an attack of the aminoalcohol (C) will

6) M. Ōki and H. Iwamura, This Bulletin, **32**, 955 (1959).
7) A. H. Lamberton and A. E. Standage, *J. Chem. Soc.*, **1960**, 2957.
8) J. M. Tedder, *Chem. Revs.*, **55**, 805 (1955).

occur at the imino group.

These conclusions are schematically summarized in Fig. 3.

The author wishes to express his deep gratitude to Professor Ryozo Goto of Kyoto University, for his discussion and encouragement throughout the course of this work.

Department of Chemistry
Faculty of Science
Kyoto University
Sakyo-ku, Kyoto

*The Absorption Spectra of Thiourea and Potassium Iodide on Nickel Metal**

By Wataru SUËTAKA

(Received January 6, 1964)

Organic or inorganic compounds are extensively used for corrosion inhibitors. Many interesting studies on the mechanism of corrosion inhibition have been reported; the chemical adsorption of organic compounds or inorganic ions on metal surfaces is considered to be the most important process.[1] The great majority of works, however, have been gravimetric or electrochemical. Because these data do not directly furnish information about the interaction between inhibitor molecules or ions and metal surfaces, there has been much speculation on this point. Absorption sorption spectroscopy has proven to be one of the most powerful tools for studying intermolecular interaction. Absorption spectra of organic compounds adsorbed on silica or alumina have been studied by several investigators, and many interesting results have been published.[2] Inorganic surface complex formation on different adsorbents has also been revealed by diffuse reflection spectra.[3]

Thiourea and the iodine ion are effective corrosion inhibitors. They have a very strong absorption band near 230 mμ, a band which facilitates the measurement of the spectrum of adsorbed species. Thiourea has the most simple structure in the homologue, and the potassium ion has no absorption band near 230 mμ. For these reasons thiourea and potassium iodide were chosen to investigate the mechanism of corrosion inhibition. In the present paper the absorption spectra of thiourea adsorbed on nickel surfaces and the diffuse reflection spectra of its solid complexes with some divalent metal salts will be reported on. The absorption spectra of the iodine ion on nickel surfaces in aqueous solutions will also be described.

Experimental

Absorption spectra were observed by means of a Hitachi EPU-2A photoelectric spectrophotometer. A diffuse reflectance attachment of the R-3 type was employed for the measurement of the diffuse reflection spectra of solid thiourea complexes. The spectral slit widths of the absorption and diffuse reflection spectra were 2 and 5 mμ respectively.

The reflection cells shown in Fig. 1 were used for measuring the absorption spectra of thiourea

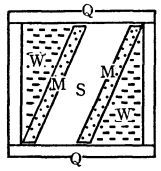


Fig. 1. Reflection cell.

M: Nickel plate
S: Solution
Q: Quartz window
W: Paraffin wax for fixing the nickel plate

or the iodine ion adsorved on nickel. A light beam was reflexed twice at the nickel surfaces in the cell. Nickel of a 99.9% purity was used for the adsorbent and reflection mirror, since its ion in an aqueous solution has no remarkable absorption band in the observed region of the spectra and does not interfere with the measurement of the spectra of the inhibitors. The surfaces of nickel were polished with the 0/4 emery paper and with buff. The polished plates were then cleaned successively in dilute hydrochloric acid and pure water. The

* Presented at the 16th Annual Meeting of the Chemical Society of Japan, Tokyo, April, 1963.

1) N. Hackerman and A. C. Mackrides, *Ind. Eng. Chem.*, **46**, 523 (1954).

2) A. N. Terenin, *Zhur. Fiz. Khim.*, **14**, 1111 (1940); M. Okuda and T. Tachibana, This Bulletin, **33**, 863 (1960).

3) G. Kortüm, *Trans. Faraday Soc.*, **58**, 1625 (1962).

TABLE I. EFFECT OF NICKEL SALT ON THE ABSORPTION BAND OF THIOUREA

Concn. of thiourea mol./l.	Salt: Compd.	Salt: Concn. mol./l.	Solvent	λ_{max}, mμ	A_{max}
6.0×10^{-5}	None	—	0.1 N H_2SO_4	236	0.785
	$NiSO_4$	1.0		234	0.762
5.0×10^{-5}	None	—	Water	236	0.608
	$NiSO_4$	0.030		236	0.619

Spectral slit width: 2 mμ
A: Absorbance

energies of light which had passed through a reflection cell filled with a solution and of light which had passed through the same cell filld with pure water were measured over the 215~320 mμ region. The ratio of the energies gave an absorption curve. The lengths of the light path in the reflection cells were estimated from the intensity of a weak absorption band at 260 mμ of acetone of known concentrations. The concentrations of acetone were sufficiently high to avoid any significant change in the intensity of the band by adsorption.

Complexes of thiourea with cadmium, zinc and nickel chlorides were prepared by the method reported by Nardelli et al.[4] Fine particles of the complexes, the diameters of which were less than 40 μ, were collected for the diffuse reflectance measurement. No diluent was used so as to avoid any eventual change in the spectrum by adsorption on a diluent. Magnesium oxide was used as the reference standard.

Corrosion inhibitors are used in an acid solution. The surfaces of nickel are generally covered with an oxide layer which dissolves in acid. The absorption spectra were, therefore, observed in acid solutions for the most part.

Thiourea, acetone, potassium iodide, nickel chloride and sulfate, cadmium chloride, zinc chloride, hydrochloric acid and sulfuric acid of guaranteed grades were used in the experiments. Water was purified by distillation and ion exchange. Immediately after the purification, the specific electric conductivity of water was less than 2×10^{-7} mho/cm.

Results and Discussion

Thiourea. — The Absorption spectra of a thiourea solution as measured with a reflection cell and an absorption cell are shown in Fig. 2. In this figure a considerable intensity decrease in a band at 236 mμ in the reflection spectrum can be clearly seen. It is considered that nickel or nickel oxide on the surfaces of metal plates is dissolved in the dilute acid solution used in the experiment, though the dissolved quantity might be very small, and that the nickel ion in the solution can form complexes with thiourea. The absorption band of thiourea may change in its position and intensity upon complex formation. The hypothesis that the observed intensity decrease arose from the complex formation in the solution might be postulated. The absorption spectra of thiorurea in acid or in water with or without nickel salt were also observed (Table I). The change in the intensity of the absorption band upon the addition of salt is very small and can be considered to be within the limit of experimental error. A slight blue shift of band was observed only for a solution containing salt in a high concentration. The hypothesis can, therefore, be ruled out from the results of the experiments mentioned above.

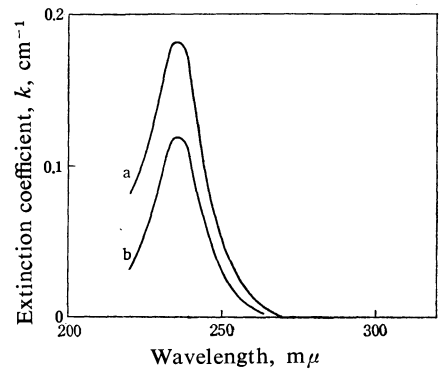


Fig. 2. Absorption spectra of thiourea.
a : Transmission measurement
b : Reflection measurement
Solvent : 0.001 N HCl

An intensity decrease in the absorption band upon adsorption has been reported by some investigators.[5] At first sight, the intensity decrease observed in the present work may be considered to be one example of this phenomenon. The observed reduction in intensity, however, seems to be too large to be regarded as the result of an intensity change upon adsorption, since the number of thiourea molecules in the solution is probably larger than that on nickel surfaces and since the

4) M. Nardelli, L. Cavalca and A. Braibanti, *Gazz. chim. ital.*, **86**, 867, 1037 (1956).

5) M. Robin and K. N. Trueblood, *J. Am. Chem. Soc.*, **79**, 5138 (1957); H. Kobayashi, *J. Chem. Soc. Japan, Pure Chem. Sec.* (*Nippon Kagaku Zasshi*), **80**, 1399 (1959); K. Fueki, K. Hirota and H. Otouma, Paper presented at the 15th Annual Meeting of the Chemical Society of Japan, Tokyo, April, 1962.

contribution to the intensity of the absorption band from the molecules in solution should be larger than that from the molecules on nickel surfaces. Furthermore, the intensity decrease upon adsorption is generally accompanied by a change in band shape, and the bands of adsorbed molecules are diffuse.[5] The absorption band observed with the reflection cell has the same shape as that observed with the absorption cell, as Fig. 2 shows. It is difficult, therefore, to deduce that the observed intensity decrease was caused by the reduced intensity of the absorption band of adsorbed molecules.

The structure of thiourea and of a number of its complexes with divalent metal salts was studied with infrared absorption spectra and X-ray diffraction techniques. These studies have shown that sulfur-to-metal bonds are formed in these complexes.[6] The interatomic distance between sulfur and its nearest neighbors in the crystals was determined by the X-ray diffraction method. A value of 2.45 Å was calculated for the distance between sulfur and the cadmium atom in a thiourea-cadmium chloride complex,[7] and the distance of 3.45 Å was reported for the intermolecular contact between sulfur and the amino group in a thiourea crystal.[8] The observed interatomic distance between sulfur and cadmium is almost equal to the sum of the covalent radii, 2.52 Å.[9] The interatomic distance between sulfur and hydrogen in a thiourea crystal can be estimated to be larger than 2.45 Å, because the length of the N–H bond is about 1.0 Å. The sum of the covalent radii of sulfur and hydrogen is 1.34 Å,[9] which is considerably shorter than the estimated distance. The intermolecular perturbation to the thiocarbonyl group can, therefore, be deduced to be larger in the complex than in thiourea.

The diffuse reflection spectra of thiourea and its complexes with cadmium, zinc and nickel chlorides in the form of fine powder were observed. The obtained results are shown in Fig. 3, except for the spectrum of the thiourea-nickel chloride complex, in which an absorption band at a longer wavelength due to thiourea was difficult to isolate because of overlapping with a strong absorption band of nickel. A diffuse reflection spectrum of cadmium chloride is also shown in this figure for the sake of comparison. The bands near 250 mμ of complex crystals are considered to correspond to a band at 273 mμ of thiourea. This blue shift of the band is probably caused by the perturbation of electronic states through the sulfur atom. In this connection, a blue shift of the band at 236 mμ of thiourea in solution upon adsorption on nickel surfaces can be expected, because in acid solutions protons attach to amino groups and the sulfur atom may play an important role upon adsorption.[10]

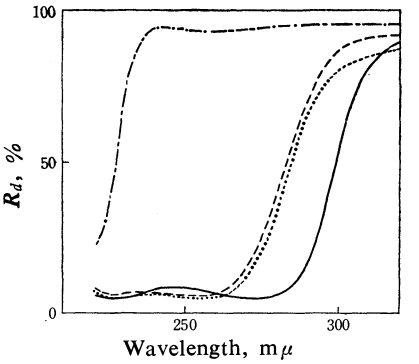


Fig. 3. Diffuse reflection spectra of thiourea and its complexes.

——— Thiourea
——— Thiourea-$CdCl_2$ complex
····· Thiourea-$ZnCl_2$ complex
—·—· $CdCl_2$
Particle size; $d \leqq 40\ \mu$

The concentration of adsorbed thiourea was estimated on the assumption that the absorption band of adsorbed molecules shifted to the unobserved region of shorter wavelengths (Table II). A roughness factor of 2 was assumed in the calculation, since the surfaces were polished mechanically. On the other hand, nickel plates were dipped in solutions of thiourea for several minutes. After the plates had been withdrawn, the solutions were subjected to the measurement of the absorption spectrum. The results obtained are shown in Table III. The reproducibility of the experiment is rather poor, but a remarkable intensity decrease is clearly seen. The reduction in intensity can be considered to be caused by the removal of thiourea adsorbed on nickel from the solution. The values of the concentration of adsorbed molecules on dipped nickel surfaces calculated with the assumption of the same roughness factor, values which are shown in Table III, are in fairly good agreement with the values shown in Table II. The agreement of the

6) M. Nardelli, *Gazz. chim. Ital.*, **89**, 1616 (1959); M. Brufani, D. Duranti, G. Giacomello and L. Zambonelli, ibid., **91**, 287 (1961); A. Yamaguchi, R. B. Penland, S. Mizushima, J. T. Lane, C. Curran and J. V. Quagliano, *J. Am. Chem. Soc.*, **80**, 527 (1958).

7) L. Cavalca, M. Nardelli and A Braibanti, *Gazz. chim. Ital.*, **87**, 137 (1957).

8) R. W. G. Wycoff and R. B. Corey, *Z. Krist.*, **81**, 386 (1932).

9) L. Pauling, "Nature of the Chemical Bond," Cornell University Press, Ithaca (1940), p. 179.

10) W. Suëtaka and S. Shimodaira, *Sci. Rept. Res. Inst., Tohoku Univ., Ser. A*, **15**, 313 (1963).

TABLE II. TRANSMISSION AND REFLECTION MEASUREMENT OF ABSORPTION SPECTRUM OF THIOUREA

Concn. of thiourea mol./l.	Method	k_{max} cm^{-1}	Vol. of soln. cc.	App. surface area cm^2	Concn. of adsorbed molecules mol./cm^2
1.4×10^{-5}	Trans.	0.180	—	—	—
	Ref.	0.108	1.0	7.8	3.6×10^{-10}
		0.116	1.2	7.4	4.0×10^{-10}
1.4×10^{-5}	Trans.	0.174	—	—	—
	Ref.	0.106	1.2	7.4	4.4×10^{-10}
6.1×10^{-5}	Trans.	0.796	—	—	—
	Ref.	0.699	1.2	7.4	4.9×10^{-10}

Spectral slit width: 2 mμ
Solvent: 1/1000 N HCl
k: Extinction coefficient

TABLE III. CONCENTRATION OF THIOUREA ADSORBED ON NICKEL PLATES

Concn. of thiourea mol./l.	A_{max}	Vol. of soln. cc.	App. surface area cm^2	Concn. of adsorbed molecules mol./cm^2
1.7×10^{-5}	a*: 0.201	—	—	—
	b**: 0.144	3.0	15	4.4×10^{-10}
1.4×10^{-5}	a: 0.174	—	—	—
	b: 0.126	3.0	22	2.7×10^{-10}
6.1×10^{-5}	a: 0.796	—	—	—
	b: 0.689	3.0	24	4.2×10^{-10}

* a: Before dipping the nickel plates
** b: After withdrawal of plates
Solvent: 1/1000 N HCl

TABLE IV. TRANSMISSION AND REFLECTION MEASUREMENT OF ABSORPTION SPECTRUM OF POTASSIUM IODIDE

Solvent	Concn. of KI mol./l.	Method	λ_{max} mμ	k_{max} cm^{-1}
H_2O	1.2×10^{-5}	Trans.	226	0.147
		Ref.	226	0.142
H_2O	2.4×10^{-5}	Trans.	226	0.328
		Ref.	226	0.329
0.002 N HCl	2.4×10^{-5}	Trans.	226	0.358
		Ref.	227	0.301
0.001 N H_2SO_4	2.4×10^{-5}	Trans.	226	0.353
		Ref.	227	0.291
0.002 N H_2SO_4	2.2×10^{-5}	Trans.	226	0.303
		Ref.	227	0.250

Spectral slit width: 2 mμ

calculated concentrations can be considered to support the hypothesis that the intensity decrease observed in the reflection spectra arose from the large blue shift of the absorption band upon adsorption.

The decomposition of thiourea on nickel surfaces should be taken into account. It is believed, however, to be of small importance, because, as can be seen from Table II, the concentration of thiourea on nickel surfaces did not vary with the change of concentration in the solution. A more conclusive result would be obtained from research into the absorption spectrum of adsorbed thiourea in the shorter wavelengths, which could not be measured in the present work.

Potassium Iodide.—The results of the absorption spectrum measurement of potassium iodide obtained with the reflection cells are collected in Table IV. In this table, the results of normal absorption measurement are also shown. While a remarkable intensity reduction of the

charge transfer band of the iodine ion at 226 mμ in reflection measurements was observed for acid solutions, no important change was seen for solutions in pure water. Nickel plates could be attacked by the acid solution used to a slight extent, and the resulting nickel ions in the solution might cause an intensity decrease of the absorption band. The absorption spectrum of potassium iodide in a dilute (1×10^{-3} N) sulfuric acid aqueous solution containing nickel sulfate in the concentration of 7×10^{-4} mol./l. was observed in the 200~320 mμ region. The addition of the nickel salt caused only a negligible reduction in the intensity of the band at 226 mμ. These facts suggest that, while a strong interaction can be expected between the iodine ion and the nickel surface in acid solutions, the interaction should be very small in pure water. A new absorption band was observed at 310 mμ in the reflection measurement of acid solutions (Fig. 4). The nickel ion in an acid aqueous solution, the concentration of which is as high as 1.0 mol./l., does not show an absorption band at the same wavelength. This band may arise from nickel atoms on the metal surfaces or from a surface complex formed on the nickel plates, but it is premature to advance a discussion of this point.

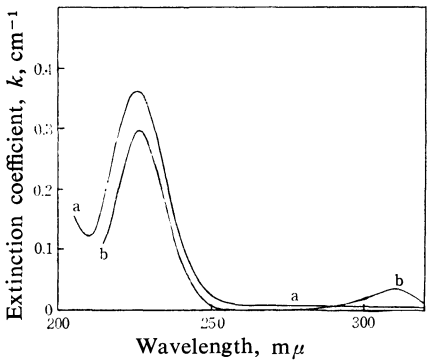


Fig. 4. Absorption spectra of potassium iodide.

a : Transmission measurement
b : Reflection measurement
Solvent : 0.001 N H_2SO_4

Summary

The absorption spectra of thiourea molecules adsorbed on nickel surfaces in acid aqueous solutions have been observed by means of reflection cells. A new band did not appear in the observed region, but the intensity of the absorption band at 236 mμ decreased remarkably. The absorption spectra of potassium iodide have also been observed with reflection cells. For acidic solutions an absorption band at 226 mμ decreased in intensity and a new band appeared at 310 mμ, while for the solutions in pure water no change in the spectrum has been observed. The observed results have been discussed and a hypothesis of surface complex formation presented.

The author wishes to express his deep thanks to Professor Saburo Shimodaira for his valuable discussion. Thanks are due to Mr. Takuya Sato for his assistance in the experiment.

Department of the Chemistry of Metal Surfaces
Research Institute for Iron, Steel and Other Metals
Tohoku University
Katahira-cho, Sendai

The Low Temperature NMR Spectrum of Triethylaluminum

By Osamu YAMAMOTO

(Received January 23, 1964)

In a previous paper,[1)] the author reported on the NMR spectra of triethylaluminum and diethylaluminum monohalides at room temperature and pointed out an anomaly in the δ value of triethylaluminum: in general, the δ value (the internal chemical shift betweeen methyl and methylene protons in the ethyl group) for metal ethyl compounds increases when one of the ethyl groups is replaced by a halogen atom. In contrast with this, the δ value for triethylaluminum (-0.72 p. p. m. for a pure liquid sample) is larger than that for diethylaluminum chloride (-0.81 p. p. m. for pure liquid). In the previous paper it was suggested that this anomaly may be attributed to the rapid exchange of the

1) O. Yamamoto, This Bulletin, **36**, 1463 (1963).

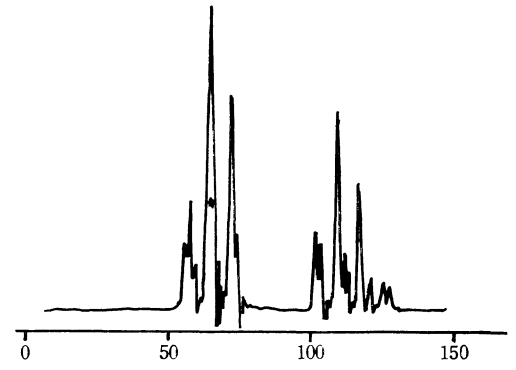
ethyl groups between bridge and terminal positions in the triethylaluminum dimer, so that a weighted mean of two kinds of ethyl spectra is observed as the spectrum of triethylaluminum at room temperature. If this suggestion is valid and if the rapid exchange becomes slower as the temperature is lowered, the NMR spectrum of triethylaluminum at a sufficiently low temperature will show two separate ethyl signals, due to the terminal and bridge groups respectively. To confirm this, the low temperature spectra of triethylaluminum have been studied in this work.

Experimental

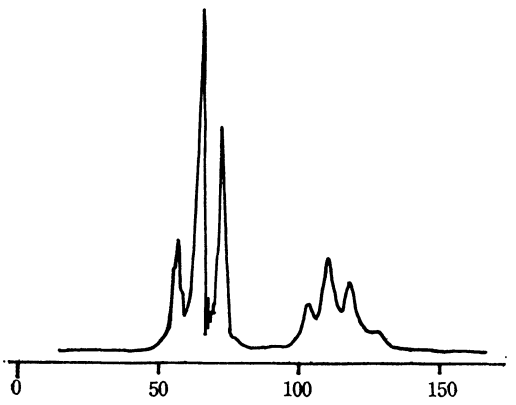
The measurement of the NMR spectea and the preparation of the samples were made in the manner previously reported,[1] except that a Varian-temperature variable cell at 60 Mc. was employed for the low temperature measurements and toluene was used as the solvent. The temperature in the cell was calibrated by the usual technique.

Results and Disussion

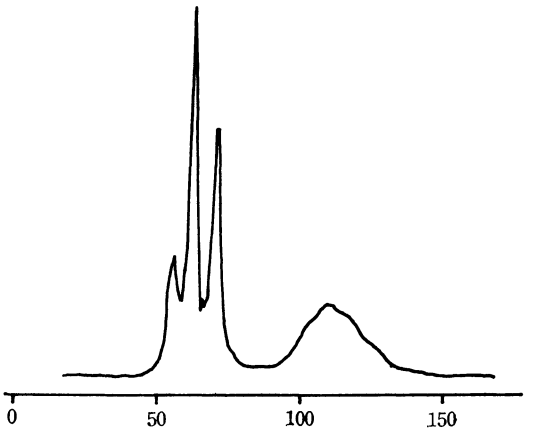
The NMR spectra of triethylaluminum in toluene (a 31.3 mol.% solution) obtained at various temperatures are shown in Fig. 1.



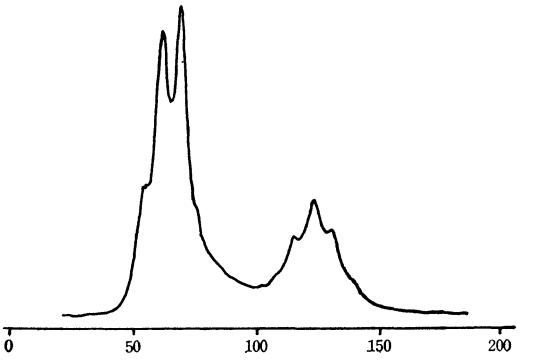
(a) 29.5°C



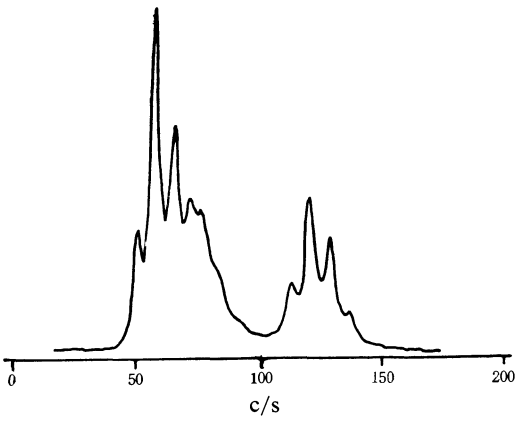
(b) −29°C



(c) −40°C



(d) −61°C



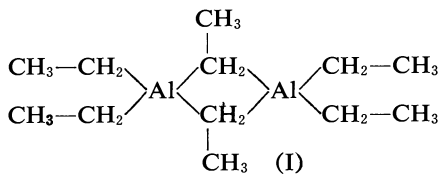
(e) −80°C

Fig. 1(a—e). The NMR traces of triethylaluminum in toluene (31.3 mol.% solution) at various temperatures (chemical shifts are referred to the methyl signal of solvent toluene). The intensity scale was changed arbitrarily from one to the others.

When other samples with different concentrations were also measured, they were found to give similar spectra, with only slight differences in the chemical shift due to the dilution effect. As is shown in the figures, the signals of an A_3B_2 pattern, which are quite sharp at room temperature, broaden as the temperature decreases, especially for methylene signals (the higher-field side ones). At $-40°C$, the methylene signals are almost collapsed. As the temperature decreases further, the signals become slightly sharper; at the same time, a group of new signals appears on the higher-field side of the methyl signals. At $-80°C$, the temperature which seems to be the lowest limit for the apparatus used, the spectrum of triethylaluminum consits of three groups: a triplet with the strongest intensity at the lowest field, a quartet at the highest field, and a group of new signals in the middle portion. The quartet signal is found to be at a higher field than the methylene quartet at room temperature, while the triplet is at only a slightly lower field than the methyl signals at room temprature.

Muller and Pritchard[2] and Growenewege and others[3] observed two singlet signals for trimethylaluminum at $-75°C$, but only one singlet signal at room temperature. The two singlet signals were separated by about 1 p. p. m. from one another and were positioned at either side of the original signal found at room temperature. They concluded from their NMR studies that, in a dimeric structure for trimethylaluminum with a bridged form[4] similar to the I shown below, the rapid exchange of the methyl group occurs between bridge and terminal positions at room temperatune. Judging from a consideration of the intensity of the $-75°C$ spectrum, the higher-field side singlet was due to terminal methyl groups, and the lower-side one, to bridge methyl groups, in the dimer.

In a similar way, if the following methylene-bridged structure I is assumed for triethylaluminum, an assignmet of the signals will be obtained rather straightforwardly:



(I)

In model I, the bridge-forming group is the methylene group. By analogy with the methyl compound, the signals of the protons in the bridge-forming group at a sufficiently low temperature will appear at a lower field when the group is in the bridge position, and at a higher field when it is in the terminal position, than the averaged signals at room temperature. On the other hand, the signals of the protons which do not directly take part in the bridge formation are expected to show only a small change in their resonance position through the exchange process. In the spectrum obtained at $-80°C$, the methylene signals show a considerable shift (about 12 c. p. s. to a higher field) from the position at room temperature, while the methyl signals show only a small shift (about 6 c. p. s. to a lower field). Thus, the methylene-bridge model I seems to be reasonable for the structure of triethylaluminum.

Since the bridge methylene signals are at a lower field than for the terminal methylene, the higher field quartet of triethylaluminum at $-80°C$ must be responsible for the terminal methylene, and, correspondingly, the triplet at a lower field, for the terminal methyl, and the middle portion, for the bridge ethyl group. It is considered that a group of signals with a complex appearance in the middle portion results from the fact that the δ value in the bridge ethyl group becomes comparable to the coupling constant (presumably about 8 c. p. s.) between the methyl and methylene protons.

To confirm this assignment, the intensity ratio between the highest side quartet and the remainder of the signals was measured and found to be 0.39, while the expected value for the formula I is 0.37. This agreement between the observed and the expected values is very good.

Thus, as in the case of trimethylaluminum, triethylaluminum gives a single ethyl spectrum at room temperature because of a rapid exchange between the terminal and the bridge ethyl groups, and a compound spectrum of two kinds of ethyl groups at a sufficiently low temperature because of the decreased exchange rate.[5] In contrast with the methyl compound, however, the bridge-forming group in triethylaluminum is the methylene group.

This seems to be the first positive experimental evidence that triethylaluminum forms a dimer bridged *through the methylene group*, although formula I has been used for the triethylaluminum dimer in the literature.[6]

2) N. Muller and D. E. Pritchard, *J. Am. Chem. Soc.*, **82**, 248 (1960).

3) M. P. Growenewege, J. Smidt and H. de Vries, ibid., **82**, 4425 (1960).

4) P. H. Lewis and R. E. Rundle, *J. Chem. Phys.*, **21**, 986 (1953).

5) Unfortunately the rate and the activation energy for the exchange process can not be found because of the complex nature of the spectrum.

6) For example, see H. Zeiss, "Organometallic Chemistry," Reinhold Publishing Corportaion, New York (1960), p. 207.

The σ values for the terminal and bridge ethyl groups are calculated from the $-80°C$ spectrum to be -1.11 p. p. m. and about -0.2 p. p. m. respectively. Since the monohalogen derivatives of triethylaluminum are halogen-bridged dimer,[7] the ethyl groups are always at the terminal position. Thus, in comparing the δ values of triethylaluminum and diethylaluminum monohalides, the value for the terminal group should be used. Since the δ value of diethylaluminum monochloride in benzene (at almost the same concentration of aluminum compound as that in the present work) is about -0.85 p.p. m.,[1] triethylaluminum has a smaller δ value in its terminal ethyl group than do diethylaluminum monohalides. Therefore, the general trend for the δ values of metal ethyl compounds stated at the beginning of this paper still holds for the case of aluminum compounds, and the origin of the anomaly mentioned in the previous paper is elucidated satisfactorily.

Government Chemical Industrial Research Institute, Tokyo
Shibuya-ku, Tokyo

7) O. Yamamoto, This Bulletin, 35, 619 (1962), and the references cited therein.

Electron Spin Resonance of Peroxy Radicals in Gamma-irradiated Polytetrafluoroethylene

By Hazime TANAKA, Akira MATSUMOTO and Nobuhisa GOTO

(Received January 25, 1964)

Quite a few ESR investigations have been carried out on polytetrafluoroethylene (PTFE) irradiated by gamma- or X-rays.[1-8] When irradiation and measurements have been made in the absence of oxygen, the ESR spectra of PTFE specimens have been found to consist mainly of double quintets, arising from the fluoroalkyl radical, $-CF_2\dot{C}FCF_2-$, produced by the removal of a fluorine atom from the polymer chain. Some measurements of the oriented samples have also been made; they have given information concerning the relation between the polymer structure and the ESR spectra.[7]

The double-quintets signal disappeared, giving an asymmetrical spectrum, when PTFE specimens irradiated in vacuo were aged in air.[3] The kinetics of this reaction was analyzed under the assumptions: $\dot{R}+O_2 \rightleftarrows R\dot{O}_2$, and $[\dot{R}]+[R\dot{O}_2]=[\dot{R}]_0$, where $\dot{R}$ and $R\dot{O}_2$ represent fluoroalkyl radical and its peroxy radical respectively and $[\dot{R}]_0$ was the initial concentration.[9] On the other hand, it has been reported[8] that the ESR spectra of peroxy radicals can be separated into two components. One of them is associated with the peroxy radical derived from the aforesaid fluoroalkyl radical, while the other is ascribed to the peroxy radical originating in the chain scission-type radical.

This paper intends to pretent an examination of the transition process from the spectrum observed in vacuo to the spectrum which is obtained in a specimen aged in air, considering two sorts of peroxy radicals, and also an examination of the stability of these peroxy radicals under heat treatment. The nature of the peroxy radicals will be discussed in the light of data on the orientation dependence of their ESR spectra and the crystalline arrangement of PTFE.

Experimental

All the ESR spectra were measured at a frequency of 24000 Mc./sec. with a superheterodyne-type spectrometer,[10] which displays the first derivative

1) W. B. Ard, H. Shield and W. Gordy, *J. Chem. Phys.*, **23**, 1727 (1955).
2) H. N. Rexrord and W. Gordy, ibid., **30**, 399 (1959).
3) Yu. D. Tsvetkov, N. N. Boubnov, M. A. Makulskii, Yu. S. Lazurkin and V. V. Voevodskii, *Doklady Akad. Nauk, SSSR*, **122**, 1053 (1958).
4) N. Tamura, *J. Phys. Soc. Japan*, **15**, 943 (1960).
5) Ya. S. Lebedev, Yu. D. Tsvetkov, and V. V. Voevodskii, *Optics and Spectroscopy*, **8**, 426 (1960).
6) N. Tamura, *J. Chem. Phys.*, **37**, 479 (1962).
7) D. W. Ovenall, ibid., **38**, 2448 (1963).
8) T. Matsugashita and K. Shinohara, ibid., **35**, 1652 (1961).
9) Yu. C. Tsvetkov, Ya. S. Lebedev and V. V. Voevodskii, *Vyskomol. Soedinenie*, **1**, 1519 (1959); ibid.. **1**, 1634 (1959).
10) This spectrometer was designed and constructed by the Applied Electric Laboratory Co. It consists of an automatic frequency-control unit, two 24V10 klystrons, a klystron power supply, a sweep generator an electromagnet, a magnet power supply, and a field scanning unit.

of the resonance curve. Some spectra were recorded as absorption figures with an integrator. For the determination of the correct line width, proton resonance signals at 36.5 Mc./sec. with 100 kc./sec. side bands were recorded. Small quantities of 1,1-diphenyl-2-picrylhydrazyl (DPPH) were employed as a standard for the g-factor and intensity of spectra.

The specimens of PTFE films and powder were supplied by the Daikin Kogyo Co., Ltd. The film, 0.2 mm. thick, had a density of 2.17, and the degree of crystallinity was estimated to be about 55%.[11] In preparing oriented samples, the film was stretched further by using a screw-jacket elongation apparatus up to 200%. All samples were placed in quartz tubes 3 mm. in o. d. In the case of irradiation in vacuo, the samples were sealed off after evacuation with an oil diffusion pump for 24 hr. The irradiation was carried out with Co-60 gamma rays, the intensity of which was about 10^5 rad./hr. the total dose reached up to about 10^7 rad.

Results and Discussion

The ESR Spectrum of Peroxy Radicals in Powder.—The dominating feature of the ESR spectrum in the powder sample irradiated and measured in vacuo is the double quintets. This spectrum shows a slight asymmetry, as a result of the g-anisotropy. This appears more clearly in the present K-band measurement than in the reported X-band spectra.[1-4]

Upon exposure of the sample to oxygen, the double quintets disappear rapidly and new resonance lines build up. This new spectrum gives an appearance of the superposition of two components, one symmetric and the other asymmetric, as may be seen in Fig. 1. Matsugashita and Shinohara obtained the symmetrical signal and the asymmetrical signal, which disappear upon the re-evacuation of the oxygenated sample, at 250°C and 150°C respectively.[8] In the present case, no treatment is required to resolve them. The intensity of the symmetrical component, I_s, is obtained under the assumption that the line shape is Lorentzian. By subtracting I_s from the total intensity, the intensity of the asymmetrical component, I_a, is obtained. If the sample is irradiated in the presence of air, the intensity ratio of the symmetrical component, I_s/I_a, increases by a factor of two.

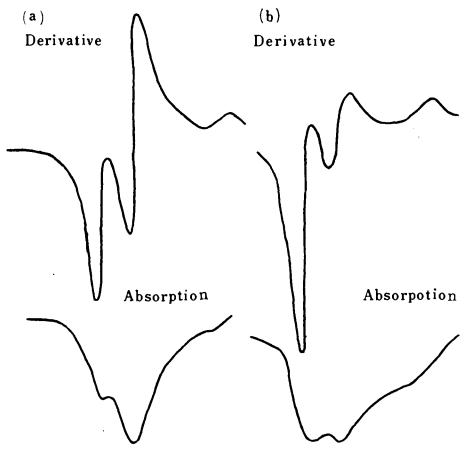


Fig. 1. ESR spectra of peroxy radicals in PTFE powders, (a) irradiated and observed in air, (b) irradiated in vacuo and observed in air.

The Transition Process.—In order to examine the transition process from the spectrum in vacuo to that of oxygenated sample, a small quantity of oxygen is introduced, with a velocity of 10^{-3} cc./min. (reduced to 1 atm.), into a sample tube containing about 30 mg. of PTFE powder irradiated in vacuo. The variation of the spectrum with time is shown in Fig. 2. A decrease in the double quintets

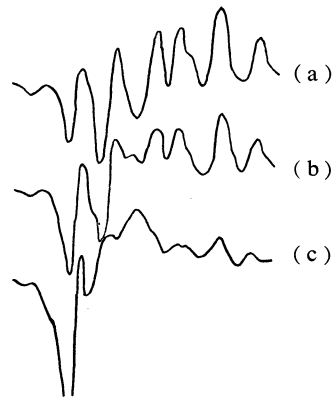


Fig. 2. Changes in shape of ESR spectrum in PTFE powder, upon exposure of oxygen.
(a) Before admission of oxygen
(b) Some 5 min. after admission of oxygen
(c) Some 15 min. after admission of oxygen

accompanies the increase in the asymmetrical component. The intensity of each component in the double quintets, I_{dq}, is expressed by:

$$I_{dq} = I^{\circ}_{dq} \exp(-\lambda t) \qquad (1)$$

where I°_{dq} is the initial intensity of each component of the double quintets, t is the time in minutes, and λ is a constant (0.035/min. in the present case). The intensity of the asymmetrical component in the oxygenated spectrum, I_p, is given by:

$$I_p = I_p^{\infty}\{1-\exp(-\lambda t)\} \qquad (2)$$

where I_p^{∞} is the intensity of the asymmetrical component after equilibrium, and λ is the same constant in Eq. 1. The initial intensity

11) P. E. Thomas, J. F. Lontl, C. A. Sperati and J. L. McPherson, *SPE Journal*, June, 89 (1956).

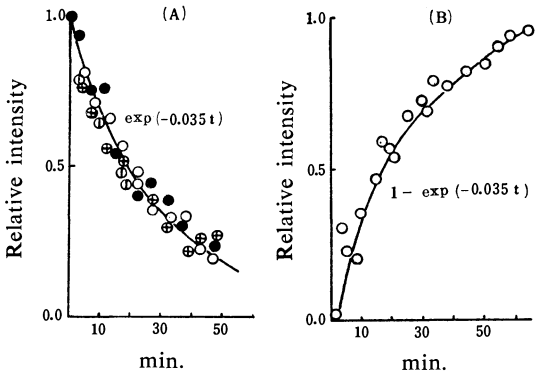


Fig. 3. Intensity variation of ESR spectrum in irradiated PTFE powder, as a function of time after exposure of air, (A) relative intensity of each component of double quintets, (B) relative intensity of an asymmetrical signal of peroxy radicals.

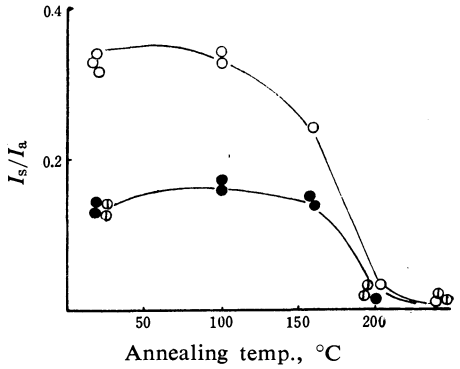


Fig. 4. Effect of anneal temperature on the intensity ratio of a symmetrical component to an asymmetrical one, I_s/I_a, in ESR spectrum of PTFE peroxy radicals.

	Irrad.	Anneal.
○	in air	in air
●	in vac.	in air
⦶	in vac.	in vac.

of the double quintets agrees with the final intensity of the asymmetrical component.

These results accord with those of Tsvetkov, Lebedev and Voevodskii,[9] though the present experiment was carried out with samples smaller in size and at lower oxygen pressures. The experiment shows only that the fluoroalkyl radical is converted into the peroxy radical, $-CF_2CF(O\dot{O})CF_2-$ which gives the asymmetrical component of the ESR spectrum in air, but it does not bring out information about the symmetrical component.

The Thermal Stability of Peroxy Radicals.—The intensity ratio of the symmetrical component to the asymmetrical component changes upon heat treatment. In the experiment, three groups of PTFE powder were used: (1) irradiated and heated in air, (2) irradiated and heated in vacuo before aging in air, and (3) irradiated in vacuo and heated in air. The change in I_s/I_a when it is heated for 30 min. at various temperatures is shown in Fig. 4. It is evident that the radical which gives the symmetrical component is unstable at temperatures above 150°C; the I_s/I_a ratio decreases rapidly at an annealing temperature of 150°C, though the I_a intensity does not change greatly until 250°C.

It has bee reported[12] that one of the peaks of the mechanical loss tangent of crystalline PTFE exists near 130°C in the dynamical measurement at 1 c./sec. This shows the presence of a configurational transition of the material in this temperature region.[13] The decomposition of the radical species which give a symmetrical spectrum must be related to this transition. From the symmetrical profile, this "heat sensitive radical" must be trapped in the region where the motional freedom of the polymer, for example, vibrational or rotational motion, is large and local order does not exist. The "heat sensitive radical" does not seem to come from the fluoroalkyl radical which gives the double quintets signal, but from radicals of a different type, for example, the type with "carbon-carbon bond" breakage. The scission of the main chain destroys the local order and gives much more motional freedom. The situation holds even after aging in air, so that the peroxy radical derived from the scission-type radical shows a symmetrical spectrum. As the temperature rises beyond 130°C, the chain motion increases and the radicals trapped at the ends of the chains disappear as a result of recombination and decomposition. This estimate accords substantially with that of Matsugashita and Shinohara.

The asymmetrical spectrum, on the contrary, holds even above about 250°C. It must originate from the fluoroalkyl radical trapped in PTFE crystallite.

The Anisotropy of the *g* Factor in an Oriented Sample.—Further investigation of the asymmetric component has been undertarken from the point of view of the angular dependence of its *g* factor. The ESR spectrum of peroxy radicals in oriented films can be resolved into two singlets when the axis of the molecular chain is along the orientation axis. One has a stronger intensity than the other.

The resonance field position of the strong signal changes as a function of the angle between the orientation axis and the external magnetic field; the *g* factor shows a maximum

12) K. H. Illers and E. Jenckel, *Kolloid-Z.*, **160**, 97 (1958).
13) Y. Wada, *J. Phys. Soc. Japan*, **16**, 1226 (1961).

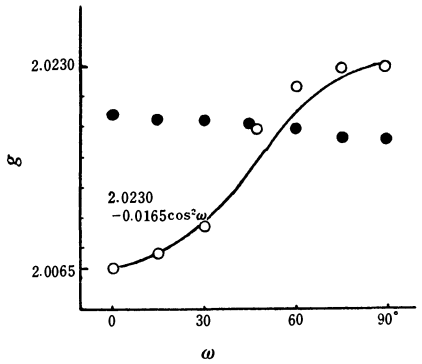


Fig. 5. Variation of g factor of ESR in oriented PTFE films irradiated and observed in air, as a function of the orientation of the sample in the magnetic field.
○ Stronger signal
● Weaker signal

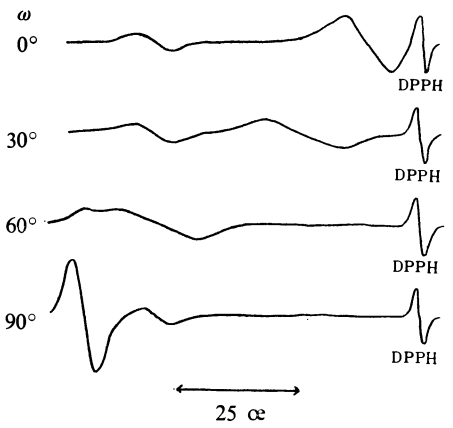


Fig. 5a. Change of the ESR spectrum with the angle, ω, between the orientation of PTFE films and the magnetic field.

value of 2.0230 when the magnetic field is perpendicular to the orientation axis, and it reaches a minimum value of 2.0065 when the magnetic field is parallel to the orientation axis, as may be seen in Fig. 5. The weak signal hardly changes its field position throughout the angle variation. Its g factor, 2.018, agrees with the value obtained from the symmetrical component in the powder spectrum. It becomes evident that the weak signal gives nearly the same profile in both oriented films and powder, while the strong signal appears asymmetric in powder because of its g anisotropy.

The Origin of the g Anisotropy—One can consider the origin of the g anisotropy in the oriented sample to be as follows. The fluoroalkyl radical to which the oxygen molecule is attached forms the peroxy radical, $-CF_2CF(OO)CF_2-$. To the first approximation it is assumed that the local order of original PTFE does not change markedly during the desertion of the fluorine atom and the insertion of the oxygen molecule. The crystal structure of PTFE is pseudo-hexagonal at room temperature,[14] and its C–C chain has a torsion whose period is 6.5 carbon atoms along the crystal c axis (see Fig. 6). Now, we suppose

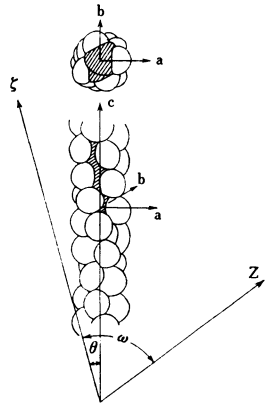


Fig. 6. The crystal structure of polytetrafluoroethylene.
▨ C atom ○ F atom

that the oxygen molecule in the defect of the fluorine atom forms a C–O–O bond perpendicular to the crystal c axis. The unpaired electron localized on the oxygen atom has an axially symmetrical distribution around the C–O–O axis. We choose three Cartesian coordinates, (x, y, z), (ξ, η, ζ), and (x', y', z'), connected with each other by the Eulerian angles shown in Fig. 7, where the system x', y', z' is connected with the system (ξ, η, ζ) by three angles, θ, φ and ψ, and where ω is an angle between the ζ axis and the z axis. In these systems we assume that the crystal c

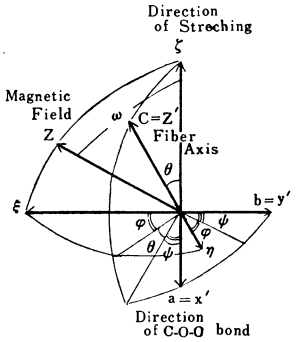


Fig. 7. The relation among three Cartesian coordinate systems, xyz, $\xi\eta\zeta$, and $x'y'z'$.

14) I. Nitta, "X-sen Kessyogaku," Maruzen, Tokyo (1961).

axis of PTFE is along the z′ axis, and that the x′ axis is approximately in the direction of the C–O–O bond, which is the symmetrical axis of the unpaired electron density. The ζ axis is taken as in the direction of the orientation axis, while the z axis is in the direction of the external magnetic field. Then, the rotation of the ζ axis in the z−x plane about the y axis is expressed only by the angle ω.

If the principal values of the g tensor are g_1, g_2, and g_3, the g factor can be written as follows:

$$g^2=g_1^2\alpha^2+g_2^2\beta^2+g_3^2\gamma^2 \tag{3}$$

where α, β, and γ are the direction cosines of the external magnetic field with respect to the principal axis system. We can assume that g_1 is the g factor along the x′ axis, and that g_2 $(=g_3)$ is perpendicular to it. The direction cosines in Eq. 3 may be calculated easily using the above assumption. The defects of the fluorine atom are distributed at random about the crystal c axis, so that the angles φ and ψ have no definite values. Therefore, we must caluculate the average values of α^2, β^2, γ^2 with respect to the equally-probable distribution of φ and ψ.

$$\langle\alpha^2\rangle,\langle\beta^2\rangle=\frac{1}{4}\{(1+\cos^2\theta)+(1-3\cos^2\theta)\cos^2\omega\}$$

$$\langle\gamma^2\rangle=\frac{1}{2}\{(1-\cos^2\theta)-(1-3\cos^2\theta)\cos^2\omega\} \tag{4}$$

Then,

$$g^2=\frac{1}{4}[\{(g_1^2+3g_2^2)+(g_1^2-g_2^2)\cos^2\theta\}+\{(g_1^2-g_2^2)+3(g_2^2-g_1^2)\cos^2\theta\}\cos^2\omega] \tag{5}$$

For the purpose of comparing the calculated results with the experimental data, it is convenient to introduce the new parameters $g_\parallel$ and $g_\perp$; $g_\parallel$ is the component of g along the crystal c axis, while $g_\perp$ is perpendicular to it: $g_{11}=g_2$, $g_\perp=\sqrt{(g_1^2+g_2^2)/2}$.

$$g^2=\frac{1}{2}[\{(g_\perp^2+g_\parallel^2)+(g_\perp^2-g_\parallel^2)\cos^2\theta\}+\{(g_\perp^3-g_\parallel^2)+3(g_\parallel^2-g_\perp^2)\cos^2\theta\}\cos^2\omega] \tag{6}$$

Equation 6 shows the axial symmetry of g around the orientation axis. If $\theta=0$, Eq. 6 becomes

$$g^2=g_\perp^2+(g_\parallel^2-g_\perp^2)\cos^2\omega \tag{7}$$

and as a simple approximation; $g\fallingdotseq g_\perp-\Delta g\cos^2\omega$, where $\Delta g=g_\perp-g_\parallel\langle\langle g_\perp, g_\parallel$.

The results shown in Fig. 5 show this axially symmetrical property of the g factor. The deviation of the experimental data from the curve, $g=2.0230-0.0165\cos^2\omega$, suggests the presence of distribution in θ. The values of g_1 and g_2 are estimated as 2.037 and 2.0065 respectively.

If the local order of PTFE does not exist, the average values of $\langle\alpha^2\rangle$, $\langle\beta^2\rangle$, and $\langle\gamma^2\rangle$ in Eq. 4 become 1/3, and the value of the g factor is 2.017, which is in good agreement with the value obtained from the symmetrical component of the ESR spectrum in air.

The spectrum of the powder sample, taken off the symmetrical component, must be composed of the sum of randomly-oriented radicals. It shows a fairly good agreement with the curve obtained from the calculations under the assumptions[15,16] of axial symmetry, a Lorentzian line shape and the random orientation of the crystallites, as Fig. 8 shows.

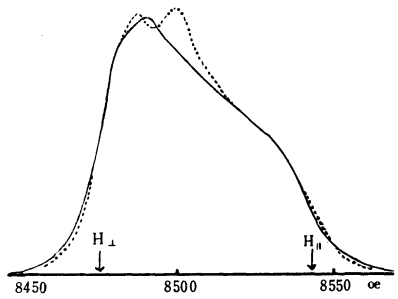


Fig. 8. ESR absorption curve of peroxy radicals in irradiated PTFE powder. Calculated curve obtained from the observed values in oriented sample; $g_\parallel=2.0065$, $g_\perp=2.0230$, and $b=10$ oe. (b: half width at half power.)
—— Calculated ------ Experimental

Summary

In the oriented sample of irradiated PTFE, the ESR spectrum of peroxy radicals consists of two singlets. One of them has an angular dependent g factor: $g=2.0230-0.0165\cos^2\omega$, where ω is an angle between the orientation of the PTFE crystal and the direction of the magnetic field applied. This spectrum shows an asymmetrical profile in a powder sample. It has been interpreted in the light of the crystalline arrangement of PTFE. Additional peroxy radical, which gives an angle-independent ESR signal, is unstable at temperatures above 150°C.

The authors wish to express their hearty thanks to Professor Hidetaro Abe of the

15) A. K. Chirkov and A. A. Kokin, *J. Exptl. Theoret. Phys. SSSR*, **39**, 1381 (1961).
16) J. A. Ibers and J. D. Swalen, *Phys. Rev.*, **127**, 1941 (1962).

Institute for Solid State Physics, the University of Tokyo, for his helpful discussions. The aid of Mr. Jiro Nishimura in some calculations is also greatly appreciated.

The Central Research Laboratory
Showa Denko K. K.
Ohta-ku, Tokyo

Sorboses. V. The Reactions of the Tosyloxy Groups of 2,3-O-Isopropylidene-α-L-sorbofuranoses in Liquid Ammonia[1]

By Kanji TOKUYAMA

(Received January 28, 1964)

The results presented in the preceding paper demonstrated that liquid ammonia is an excellent solvent for the nucleophilic displacement reaction of *O*-tosylsorbofuranoses.[1] In this paper we will report on some further examples of the nucleophilic displacement of *O*-tosyl derivatives of 2,3-*O*-isopropylidene-α-L-sorbofuranose (I) in liquid ammonia.

Reactions with Liquid Ammonia

The treatment of 1-*O*-tosyl-2,3 : 4,6-di-*O*-isopropylidene-α-L-sorbofuranose (II)[2] with liquid ammonia resulted in the formation of the secondary amine, di(1-deoxy-2,3 : 4,6-di-*O*-isopropylidene-α-L-sorbofuranose-1-)-amine (III), but not of the primary amine, 1-deoxy-1-amino-2,3 : 4,6-di-*O*-isopropylidene-α-L-sorbofuranose (IV) ; this latter was, however, obtained in the presence of sodium amide. On the other hand, as has been reported in a previous paper,[3] the treatment of 1,6-di-*O*-tosyl-2,3-*O*-isopropylidene-α-L-sorbofuranose (V)[4] and 6-*O*-tosyl-2,3-*O*-isopropylidene-α-L-sorbofuranose (VI) with liquid ammonia, even in the absence of sodium amide, gave the primary amines, namely 1,6-dideoxy-1,6-diamino- (VII) and 6-deoxy-6-amino-2,3-*O*-isopropylidene-α-L-sorbofuranose (VIII) respectively. These facts suggest that the reactivities of the tosyloxy groups of sorbofuranoses are influenced by free hydroxyl groups.

Potassium Cyanide in Liquid Ammonia

The treatment of II with potassium cyanide in ethanol did not give any derivatives with a nitrile group, only 2,3 : 4,6-di-*O*-isopropylidene-α-L-sorbofuranose (IX).[5] Similarly, 6-*O*-tosyl-1,4-anhydro-2,3-*O*-isopropylidene-α-L-sorbofuranose (X)[3] was obtained by the treatment of V with potassium cyanide in ethanol. Ammonium cyanide also did not give the nitrile derivatives. As these unexpected results

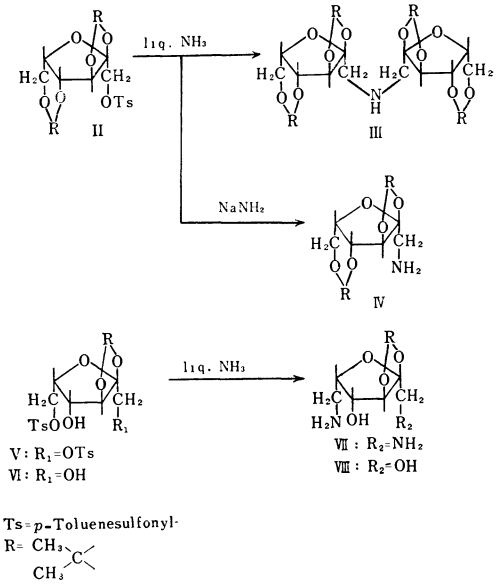


Chart 1.

seemed to be due to the fact that potassium cyanide is insoluble in organic solvents, containing dissolved tosylsorboses, we searched for suitable solvents with better solubilities for both sugars and potassium cyanide; we found liquid ammonia to be suitable for the above purpose.

The heating of II with potassium cyanide in liquid ammonia gave a sirup, the infrared

1) Part IV of this series: K. Tokuyama and M. Kiyokawa, *J. Org. Chem.*, **29**, 1475 (1946).
2) W. Sullivan, *J. Am. Chem. Soc.*, **67**, 837 (1945).
3) K. Tokuyama, M. Kiyokawa and N. Hōki, This Bulletin, **36**, 1392 (1963).
4) H. Ohle, *Ber.*, **71**, 562 (1938).
5) T. Reichstein, *Helv. Chim. Acta*, **17**, 311 (1934).

spectrum of which showed the bands of an amide at 1620 and 1690 cm^{-1}, but no bands of a nitrile group. Therefore, the structure of the sirup was determined to be 1-deoxy-1-carbamoyl-2, 3 : 4, 6-di-*O*-isopropylidene-α-L-sorbofuranose (XI). The cyanation of II to 1-deoxy-1-cyano-2, 3 : 4, 6-di-*O*-isopropylidene-α-L-sorbofuranose (XII), followed by hydrolysis or by ammonolysis, seemed to give XI or 1-deoxy-1-amidino-2, 3 : 4, 6-di-*O*-isopropylidene-α-L-sorbofuranose (XIII), which was then hydrolyzed to XI.

When the above-described reaction was carried out under strictly anhydrous conditions, another kind of alkaline sirup was obtained; this was easily converted into XI by the evolution of ammonia gas. The purification of the sirup was unsuccessful because of its instability for humidity, but the treatment of it with diethyl malonate in the presence of sodium gave a sirup, the ultraviolet spectrum of which showed an absorption maximum at 250 and 280 mμ in an alkaline medium, suggesting that it is a pyrimidine derivative. Therefore, the structure of the former sirup was determined as XIII and that of the latter sirup, as 2-(1'-deoxy-2', 3': 4', 6'-di-*O*-isopropylidene-α-L-sorbofuranose-1')-4, 6-dihydroxypyrimidine (XIV). The infrared spectrum of XIII exhibited bands, at 1713 and 1668 cm^{-1}, which should be ascribed to an amidino group. As these two bands were shifted to wave numbers higher and lower respectively than those of a guanidine,[6] XIII

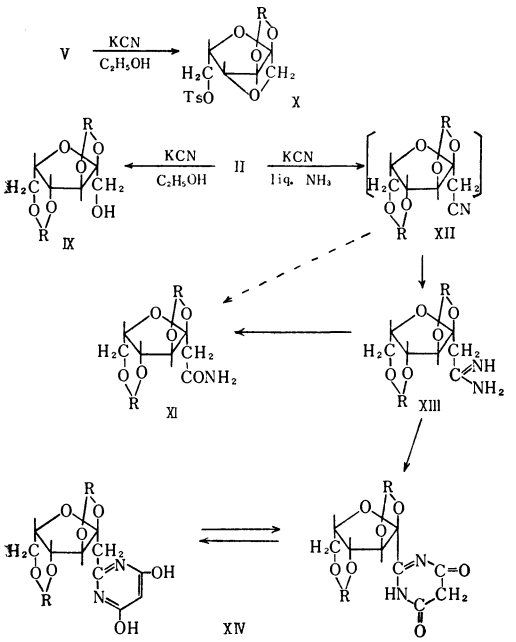


Chart 2.

6) J. Fabian, M. Legraud and P. Poirier, *Bull. soc. chim. France*, **85**, 1461, 1499 (1956).

was supposed to be a dimer. This fact was also supported by the weak absorption bands of the amino group at 3000 and 3200 cm^{-1}. On the basis of above-described facts, it is clear that II was converted into XI via XIII, which was derived from the probable intermediate, XII. On the other hand, when II was treated with potassium cyanide in liquid ammonia containing a small amount of water, only IV was obtained. This means that the equilibrium between potassium cyanide and liquid ammonia shown in Eq. 1[7] shifted to the right side because of the decomposition of ammonium cyanide by water:

$$KCN + NH_3 \rightleftharpoons NH_4CN + KNH_2 \qquad (1)$$

Potassium Thiocyanate in Liquid Ammonia

No displacement reaction of the tosyloxy group of sorbofuranose by thiocyanate was observed in either liquid ammonia or ethanol. Since the treatment of II with potassium thiocyanate in liquid ammonia gave IV, potassium thiocyanate was considered to react like sodium amide.

Sodium Hydroxide in Liquid Ammonia

Sodium hydroxide in liquid ammonia has received renewed attention in recent years because its reactivities are similar to those of sodium amide in liquid ammonia; e.g., it reacts with diethyl malonate to give the sodium salt or accelerates the amination reaction.[8] The treatment of II with a large excess of sodium hydroxide in liquid ammonia at room temperature or on heating on a boiling water-bath gave IX, but not IV. This appears to be the first reported example of hydroxylation with sodium hydroxide in liquid ammonia. Although only an equimolecular sodium hydroxide to a tosylsorbose would be required for this purpose, no displacement was observed under these conditions. This means that the reaction occurred on the surface of sodium hydroxide, which is insoluble in liquid ammonia. The treatment of V with sodium hydroxide gave 1, 4-anhydro-2, 3-*O*-isopropylidene-α-L-sorbofuranose (XV)[9] in liquid ammonia. Similarly, I and XV were obtained from VI and 1-*O*-tosyl-2, 3-*O*-isopropylidene-α-L-sorbofuranose (XVI)[1] respectively. These reactions were observed with potassium hydroxide, but not with lithium hydroxide.

7) S. Takizawa, *Bull. Chem. Research Inst. Non-aqueous Solutions, Tohoku Univ.*, **1**, 93 (1951).

8) R. Asami and K. Shimo, *Sci. Repts. Research Insts., Tohoku Univ.*, **9A**, 341 (1957); *Chem. Abstr.*, **52**, 36677 (1958); K. Shimo and S. Wakamatsu, *J. Org. Chem.*, **24**, 19 (1959).

9) The formation of X by the tosylation of XV clearly established the structure of XV.

Sodium Hydrosulfide in Liquid Ammonia

As has been described above, the tosyloxy group was displaced by a hydroxide group with sodium hydroxide in liquid ammonia to give a hydroxyl compound. Therefore, similar displacement reactions by sodium hydrosulfide in liquid ammonia were investigated. Although the solubility of hydrosulfide in liquid ammonia is much higher than that of sodium hydroxide,[10] no displacement of the tosyloxy group by a mercapto group was observed at room temperature. The treatment of II, VI, XVI and V with sodium hydrosulfide in liquid ammonia at room temperature recovered the starting materials without any aminated compounds. However, the heating of II on a boiling water-bath with a sodium hydrosulfide-liquid ammonia solution gave the product when the tosyloxy group is replaced by a mercapto group, 2, 3 : 4, 6-di-*O*-isopropylidene-1-thio-α-L-sorbofuranose (XVII).[1]

Similarly, the heating of V with sodium hydrosulfide gave 1, 4-anhydro-2, 3-*O*-isopropylidene-6-thio-α-L-sorbofuranose (XVIII),[11] which

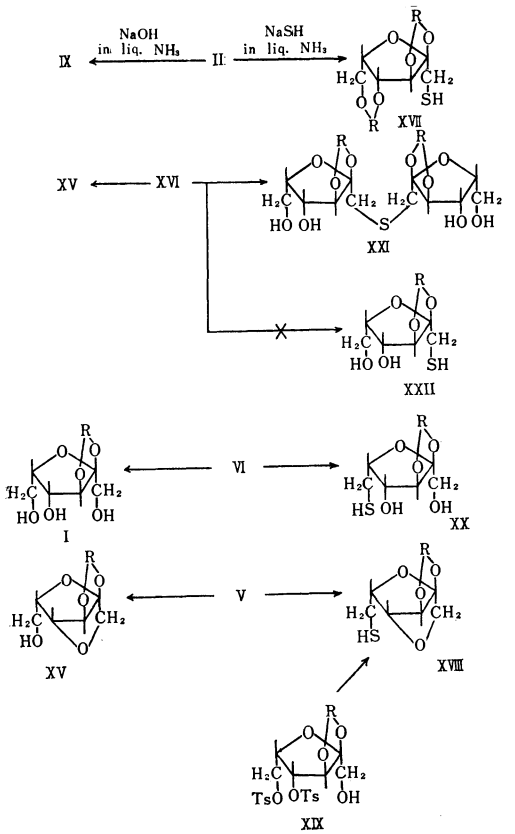


Chart 3

was also obtained from 4, 6-di-*O*-tosyl-2, 3-*O*-isopropylidene-α-L-sorbofuranose (XIX)[3] by the same reaction. Furthermore, 2, 3-*O*-isopropylidene-6-thio-α-L-sorborfuranose (XX)[1] was obtained from VI, and di-(1-deoxy-2, 3-*O*-isopropylidene-α-L-sorbofuranose-1-)-sulfide (XXI), from XVI. In the last case, 2, 3-*O*-isopropylidene-1-thio-α-L-sorbofuranose (XXII)[1] was not formed.

From the standpoint of the introduction of a mercapto group into a sugar, the above-described method, composed of only one step, considered to be much more convenient for use in the preparation of thiosugars than others reported hitherto.

Experimental

The Reactions of 1-*O*-Tosyl-2, 3 : 4, 6-di-*O*-isopropylidene-α-L-sorbofuranose (II) with Liquid Ammonia.—i) A solution of II (5 g.) in liquid ammonia (8 ml.) was heated on a boiling water-bath for 60 hr. After the liquid ammonia had been removed, the residue was extracted with chloroform; the extract was then washed with water, dried, and evaporated to give a dark brown sirup (3 g.). A solution of the sirup (3 g.) and *p*-nitrobenzoyl chloride (2 g.) in dry pyridine (10 ml.) was stirred at room temperature for 3 hr. The reaction mixture was poured into a saturated aqueous solution of sodium carbonate under cooling and extracted with chloroform. The chloroform extract was washed with water and evaporated in vacuo. Recrystallization of the residue from ethanol gave *p*-nitrobenzoate of III (1.7 g.); m. p. 252°C (decomp.).

Found: C, 57.28; H, 6.67; N, 4.30. Calcd. for $C_{31}H_{42}N_2O_{13}$ (650): C, 57.31; H, 6.47; N, 4.31%.

ii) A solution of II (2 g.) in liquid ammnoia containing sodium amide (prepared from sodium (0.2 g.) in liquid ammonia (10 ml.)) was heated on a boiling water-bath for 20 hr. The reaction mixture was neutralized with ammonium chloride. After the ammonia had been removed, the residue was extracted with chloroform, and the extract was washed with water and evaporated. Recrystallization of the residue from *n*-hexane gave IV (0.6 g.); m. p. 71.5°C, $[\alpha]_D^{23}$ −3.7 (*c* 1.035, chloroform).

Found: C, 55.82; H, 8.14; N, 5.20. Calcd. for $C_{12}H_{21}NO_5$ (259): C, 56.03; H, 8.24; N, 5.44%.

The Reactions of 1-*O*-Tosyl-2, 3 : 4, 6-di-*O*-isopropylidene-α-L-sorbofuranose (II) with Potassium Cyanide.—i) A solution of II (1 g.) and dry potassium cyanide (3 g.) in liquid ammonia (10 ml.) (dried with sodium) was heated on a boiling water-bath for 45 hr. After the ammonia had been removed, the residue was extracted with dry ether, and the ether extract was dried with sodium sulfate and evaporated in vacuo to obtain a sirup, XIII (0.3 g.), which could not be purified. a) After the sirup had been heated with a trace of water at 80°C for 1 hr., the residue was purified by silica-gel chromatography with benzene. A pale yellow sirup, XI, was obtained. The yield was 0.1 g., $[\alpha]_D^{22}$ −4.8 (*c* 1.011, chloroform).

10) S. Takizawa and Y. Abe, paper presented at the 16th Annual Meeting of the Chmical Society of Japan, Tokyo, April, 1963.

11) As the mild hydrolysis of XVIII gave XX, the structure of XVIII was confirmed.

Found: C, 54.20; H, 6.83; N, 4.75. Calcd. for $C_{13}H_{21}NO_6$ (287): C, 54.36; H, 7.13; N, 4.31%.
b) A solution of XIII (0.3 g.,), sodium (0.15 g.) and diethyl malonate (0.6 g.) in absolute ethanol (10 ml.) was warmed at 60°C for 8 hr. After the ethanol had been removed, water (15 ml.) was added to the residue and the insoluble sirup was removed by decantation. When the aqueous solution was made weakly acidic with acetic acid, a brown sirup was precipitated. This was dissolved in a 1 N sodium carbonate solution and reprecipitated with acetic acid. After this procedure had been repeated several times, XIV was obtained as a brown sirup (8 mg.), which was very hygroscopic.
Found: N, 7.80. Calcd. for $C_{16}H_{22}N_2O_7$ (354): N, 7.91%.

ii) A solution of II (1 g.), potassium cyanide (2 g.) and one drop of water in liquid ammonia (10 ml.) was heated on a boiling water-bath for 45 hr. After the ammonia had been removed, the residue was extracted with chloroform, and the extract was washed with water and then evaporated. Recrystallization from *n*-hexane gave IV (0.4 g.); m. p. 71.5°C.

iii) A mixture of II (1 g.) and potassium cyanide (2 g.) in ethanol (10 ml.) was simultaneously boiled and stirred for 20 hr. and then poured into water and extracted with chloroform, from which IX (0.5 g.) was obtained m. p. 78°C. X (0.5 g.) from V (1 g.) was obtained by the same procedure; m. p. 115°C.

The Reaction of 1-*O*-Tosyl-2, 3 : 4, 6-di-*O*-isopropylidene-α-L-sorbofuranose (II) with Potassium Thiocyanate in Liquid Ammonia.—A solution of II (1 g.) and potassium thiocyanate (1 g.) in liquid ammonia (8 ml.) was heated on a boiling water-bath for 40 hr. or kept at room temperature for two weeks. After the ammonia had been removed, the residue was extracted with chloroform, from which IV (0.5 g.) was obtained.

The Reactions with Sodium Hydroxide in Liquid Ammonia. — *1-O-Tosyl-2, 3 : 4, 6-di-O-isopropylidene-α-L-sorbofuranose (II).*—A mixture of II (3 g.) and powdered sodium hydroxide (2 g.) in liquid ammonia (12 ml.) was kept at room temperature for 10 days or heated on a boiling water-bath for 40 hr. The ammonia was allowed to evaporate, the residue was extracted with acetone, and the solution was dried and evaporated. Recrystallization from *n*-hexane gave IX (1.4 g.); m. p. 78°C.

1, 6-Di-O-tosyl-2, 3-O-isopropylidene-α-L-sorbofuranose (V).—A mixture of V (1 g.) and sodium hydroxide (1 g.) in liquid ammonia (10 ml.) was kept at room temperature and occasionally shaken for two weeks. After the ammonia had been removed, the residue was diluted with water and extracted with chloroform, which was evaporated to give a sirup. Recrystallization of the sirup from *n*-hexane gave colorless needles (XV) (0.4 g.); m. p. 92°C, $[\alpha]_D^{24.5}$ −34.5 (*c* 1.051, chloroform).

Found: C, 53.47; H, 6.90. Calcd. for $C_9H_{14}O_5$ (202): C, 53.41; H, 7.01%.

A solution of the crystals (0.4 g.) and *p*-nitrobenzoyl chloride (0.8 g.) in dry pyridine (2 ml.) was stirred at room temperature for 5 hr. The raction mixture was then poured into a saturated solution of sodium hydroxide and extracted with chloroform, from which *p*-nitrobenzoate of XV was obtained (0.6 g.). M. p. 5°C (decomp.) (recrystallized from ethanol).

Found: C, 54.58; H, 4.71; N, 4.01. Calcd. for $C_{16}H_{17}NO_8$ (351): C, 54.70; H, 4.80; N, 3.99%.

6-O-Tosyl-2, 3-O-isopropylidene-α-L-sorbofuranose (VI).—A reaction mixture of VI (1 g.) and powdered sodium hydroxide (1 g.) in liquid ammonia (12 ml.) was worked up by the procedure used for the reaction of II. The yield of I was 0.5 g. (recrystallized from ethyl acetate).

1-O-Tosyl-2, 3-O-isopropylidene-α-L-sorbofuranose (XVI).—A reaction mixture of XVI (1 g.) and sodium hydroxide (1 g.) in liquid ammonia (12 ml.) was worked up by the procedure used for the reaction of V. The yield of *p*-nitrobenzoate of XV was 0.5 g.; m. p. 85°C (decomp.).

The Reactions with Sodium Hydrosulfide in Liquid Ammonia. — *1-O-Tosyl-2, 3 : 4, 6-di-O-isopropylidene-α-L-sorbofuranose (II).*—A solution of II (1 g.) and sodium hydrosulfide (1 g.) in liquid ammonia (10 ml.) was heated on a boiling water-bath for 50 hr. After the ammonia had been removed, the residue was diluted with water and then extracted with chloroform. This was washed with water, dried, and evaporated. Recrystallization from *n*-hexane and ethyl acetate gave XVII (0.2 g.); m. p. 136°C.

1, 6-Di-O-tosyl-2, 3-O-isopropylidene-α-L-sorbofuranose (V).—A mixture of V (2 g.) and sodium hydrosulfide (2 g.) in liquid ammonia (10 ml.) was heated on a boiling water-bath for 44 hr. After the ammonia had been removed, the residue was diluted with water and extracted with chloroform; the extract was then washed with water, dried, and evaporated to obtain a sirup. The sirup was chromatographed on silica gel: first fraction (benzene) 100 ml.; second fraction (benzene : ether, 9 : 1, v/v), 100 ml., and third fraction (benzene : ether, 7 : 3, v/v), 1 l. From the third fraction, XVIII (600 mg.) was obtained as a sirup; $[\alpha]_D^{27}$ +19.2 (*c* 1.184, chloroform).

Found: C, 49.14; H, 6.69; S, 14.56. Calcd. for $C_9H_{14}O_4S$ (218): C, 49.34; H, 6.42; S, 14.79%.

The Reaction of 4, 6-Di-O-tosyl-2, 3-O-isopropylidene-α-L-sorbofuranose (XIX) with Sodium Hydrosulfide in Liquid Ammonia was the same as that of XV with sodium hydrosulfide in liquid ammonia.

6-O-Tosyl-2, 3-O-isopropylidene-α-L-sorbofuranose (VI).—A solution of VI (2.5 g.) and sodium hydrosulfide (2.5 g.) in liquid ammonia (25 ml.) was heated on a boiling water-bath for 40 hr. After the ammonia had been removed, the residue was diluted with water and extracted with chloroform; the extract was then washed with water, dried, and evaporated. The recrystallization of the residue from ethyl acetate and *n*-hexane gave XX (0.6 g.); m. p. 160°C.

1-O-Tosyl-2, 3-O-isopropylidene-α-L-sorbofuranose (XVI).—A solution of XVI (2.5 g.) and sodium hydrosulfide (2.5 g.) in liquid ammonia (25 ml.) was heated on a boiling water-bath for 40 hr. XXI was obtained by the above-described procedure. Yield, 0.5 g.; m. p. 108°C. $[\alpha]_D^{25.5}$ +32.7 (*c* 0.954, chloro-

form).

Found: C, 49.21; H, 6.91; S, 7.29. Calcd. for $C_{18}H_{30}O_{10}S$ (438): C, 49.40; H, 6.85; S, 7.19%.

The Tosylation of 1, 4-Anhydro-2, 3-*O*-isopropylidene-α-L-sorbofuranose (XV).—A solution of XV (0.5 g.) and tosyl chloride (1.0 g.) in dry pyridine (3 ml.) was stirred at room temperature for 6 hr. The reaction mixture was then poured into a saturated solution of sodium carbonate and extracted with chloroform; from the extract X (0.9 g.) was obtained. M. p. 115°C.

The Hydrolysis of 1, 4-Anhydro-2, 3-*O*-isopropylidene-6-thio-α-L-sorbofuranose (XVIII).—A solution of XVIII (0.5 g.) in 80% methanol (20 ml.) containing sodium hydroxide (0.1 g.) was boiled for 2 hr. under a nitrogen stream. After cooling, the solution was diluted with water, extracted with chloroform, washed with water, and dried. The removal of the chloroform gave XX (0.2 g.); m. p. 160°C.

The author wishes to express his grattiude to Dr. Ken'ichi Takeda, Director of the labratory, and to Dr. Kaname Hamamoto, Assistant Director of this laboratory, for their encouragement. He is also indebted to Dr. Yoshiki Matsui of this laboratory for his valuable discussions of the infrared spectra.

Shionogi Research Laboratory
Shionogi & Co., Ltd.
Fukushima-ku, Osaka

The Stability of Fused Rings in Metal Chelates. II. Copper(II) Complexes of Schiff Bases Derived from Pyruvic Acid and Amino Acids or Diamines[1]

By Akitsugu NAKAHARA, Haruyo YAMAMOTO and Hironobu MATSUMOTO

(Received February 1, 1964)

It has long been observed that an increase in the number of rings within a particular chelate structure results in the greater stability of the chelate. For example, when Calvin and Bailes[2] studied polarographically the relationship between structure and stability for the salicylaldimine copper(II) chelates, they concluded that the effect of tying together the coordinating groups to form additional rings is most essential in stabilizing the chelate. The same trend was also pointed out by Schwarzenbach[3] for a number of zinc complexes from a comparison of their formation constants. No attempt has, however, yet been made to investigate systematically how the structural factors of individual rings in a metal polydentate influence the stability of the whole fused-ring system.

The present paper is a report on a more or less quantitative survey to determine the influence of an alteration of the size of individual rings upon the stability of the fused-ring system in copper(II)-Schiff base chelates. Spectroscopic and polarographic methods were applied to determine the relative stability of those chelates. Glycine, β-alanine, ethylenediamine and trimethylenediamine were selected as amino compounds to form Schiff bases with carbonyl compounds, such as pyruvic acid, acetylacetone and salicylaldehyde. Consequently, we have succeeded in isolating four new copper(II) complexes derived from pyruvic acid. The preparation and properties of these new chelates will also be described in this paper.

Experimental

The Preparation of Copper(II) Chelates.—*Copper(II) Chelate of the Schiff Base Derived from Pyruvic Acid and Glycine, A.*—To a solution of 12.5 g. of glycine in 50 ml. of aqueous ethanol (two to one by volume mixture) was added 14.3 g. of pyruvic acid. The resulting mixture was stirred and heated at about 40°C. To this was added 33.3 g. of copper(II) acetate monohydrate. The reaction mixture was kept at 40°C for about two more hours while being constantly stirred. A dark blue solution was gradually obtained, accompanied by a precipitation of pale blue microscopic crystals. The precipitate was filtered by suction and recrystallized from a small amount of water.

The final pure product appears as thin, pale blue plates which begin to decompose at 192°C. The compound is soluble in water and is slightly soluble in ethanol, but it is insoluble in acetone

1) Part I of this series: A. Nakahara, H. Yamamoto and H. Matsumoto, *Sci. Rep., College of Gen. Ed., Osaka Univ.*, **12**, 11 (1963).
2) M. Calvin and R. H. Bailes, *J. Am. Chem. Soc.*, **68**, 949 (1946).
3) G. Schwarzenbach, *Chimia (Buenos Aires)*, **3**, 1 (1949).

or chloroform.

Found: C, 23.13; H, 4.23; N, 5.57; H_2O, 20.50. Calcd. for dihydrate of A, $[Cu(pyv=gly)(H_2O)]\cdot 2H_2O$: C, 23.00; H, 4.21; N, 5.36; H_2O, 20.65%.

Copper(II) Chelate of a Schiff Base Derived from Pyruvic Acid and β-Alanine, B.—To a solution of 6.5 g. of β-alanine in 50 ml. of water 6.4 g. of pyruvic acid was added. The mixture was stirred and heated at about 45°C. To this was added copper(II) hydroxide or oxide freshly precipitated from an aqueous solution containing 20 g. of copper(II) sulfate pentahydrate. The resulting mixture was kept at 45°C for about five hours while being constantly stirred. The color of the solution gradually changed from dark green to bluish geen. The solution was then filtered to remove unreacted copper(II) hydroxide and was allowed to stand at 0°C. Beautiful blue monoclinic crystals were obtained after 24 hr. The compound was found to decompose at 210°C. The compound is soluble in water and ethanol, but it is insoluble in acetone or chloroform.

Found: C, 26.15; H, 4.64; N, 5.11; H_2O, 19.43. Calcd. for dihydrate of B, $[Cu(pyv=\beta\text{-ala})(H_2O)]\cdot 2H_2O$: C, 26.20; H, 4.73; N, 5.09; H_2O, 19.65%.

Copper(II) Chelate of the Schiff Base Derived from Pyruvic Acid and Ethylenediamine, C.—To a solution of 7.5 g. of ethylenediamine in 100 ml. of methanol in an ice-bath, 22 g. of pyruvic acid was gradually added. After the completion of a vigorous reaction, the resulting mixture was stirred and heated at about 50°C. Hereupon an yellowish orange precipitate resulting from the formation of the Schiff base was obtained. The precipitate was filtered by suction and dissolved in 100 ml. of water without further purification. To this was added cupric oxide freshly precipitated from an aqueous solution containing 35 g. of copper(II) sulfate pentahydrate. The resulting mixture was kept at 50°C for two hours while being constantly stirred. The reaction mixture was filtered while it was warm. A large amount of acetone was then added to the filtrate. Hereupon, a dark green, crystalline solid was deposited. To purify the chelate, the above procedure of adding a large amount of acetone to the concentrated aqueous solution of the chelate was repeated several times. Since the compound which had not completely dried readily became sticky on being exposed to air, in order to accomplish complete dehydration it was necessary to dry the compound in vacuo for three days.

The compound appears green and was found to decompose at 184°C. The compound is soluble in water but insoluble in common organic solvents.

Found: C, 37.92; H, 4.26; N, 10.42. Calcd. for C, $[Cu(pyv=en=pyv)]$: C, 36.71; H, 3.82; N, 10.71%.

Copper(II) Chelate of the Schiff Base Derived from Pyruvic Acid and Trimethylenediamine, D.—To a solution of 8.8 g. of trimethylenediamine in 10 ml. of water 22 g. of pyruvic acid was added. The solution changed to yellowish orange on account of the formation of the Schiff base. To this was added copper(II) hydroxide or oxide freshly precipitated from an aqueous solution containing 32 g. of copper(II) sulfate pentahydrate. The resulting mixture was kept at 45°C for three hours while being constantly stirred and was then filtered. When the solution was allowed to stand at 0°C, blue crystals were deposited. These were recrystallized from water to give beautiful needles which decompose at 208°C. The compound is soluble in water and pyridine, but insoluble in ethanol, acetone and chloroform.

Found: C, 36.54; H, 4.75; N, 9.61. Calcd. for monohydrate of D, $[Cu(pyv=trim=pyv)]\cdot H_2O$: C, 36.85; H, 4.77; N, 9.54%.

Copper(II) Chelates of Schiff Bases Derived from Acetylacetone and Diamines, E and F. — These two chelates were prepared according to the directions of McCarthy et al.[4] The compound E in the crystalline state appears purple right after the recrystallization from methanol, but when it comes in contact with water vapor, when allowed to stand in the atmosphere, it gradually changes green. This is probably because of an additional coordination of the water molecule around copper(II), as has been demonstrated for the copper(II) chelates of salicylaldehyde-Schiff bases.[5,6]

On the other hand, the compound F only appears green in spite of having no crystal water. The compound E was found decompose at 144°C, while F decomposed at 97°C. Both the two compounds are readily soluble in common organic solvents but only slightly soluble in water.

Copper(II) Chelates of Schiff Bases Derived from Salicylaldehyde and Diamines, G and H. — These two chelates were prepared by the method of Pfeiffer et al.[7] from a mixture of 1 : 2 : 1 copper(II) : salicylaldehyde : ethylene- or trimethylenediamine. No decomposition was observed, at least below 260°C, for these two compounds. The chelate G is green in the crystalline state, purple in a chloroform solution and bluish green in a pyridine solution. It is insoluble in water, ethanol and acetone. On the other hand, the chelate H is purple in the crystalline state and green in chloroform and pyridine solutions. The color of these chelates is apparently closely related to the additional coordination of solvent molecules around copper(II) as well as to their original chelate structure. This point, however, awaits further investigation.

Spectroscopic Measurements. — The visible and ultraviolet absorption spectra of the chelates were determined with a Shimadzu spectrophotometer Type QB-50 at room temperature. The solvent used here was water in all cases, and the concentrations of the solutions varied from 10^{-3} to 10^{-5} M.

Polarographic Measurements. — Measurements were made with a Yanagimoto recording polarograph model PA-102. An "H" cell was used, the reference electrode being a saturated calomel electrode and the whole cell being thermostated at 25±0.5°C.

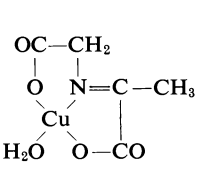
Pure distilled mercury was used throughout. C. p. chemicals were used in all cases. Tank nitrogen was bubbled without any further purification

4) P. J. McCarthy, R. J. Hovey, K. Ueno and A. E. Martell, *J. Am. Chem. Soc.*, **77**, 5820 (1955).
5) F. J. Llewellyn and T. N. Waters, *J. Chem. Soc.*, **1960**, 2639.
6) T. Tanaka, This Bulletin, **29**, 93 (1956).
7) P. Pfeiffer, E. Breith, E. Lübbe and T. Tsumaki, *Ann.*, **503**, 85 (1933).

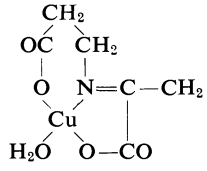
through the samples to remove dissolved oxygen. The concentration of the copper(II) chelates varied from 10^{-4} to 10^{-3} M. The supporting electrolyte used was 0.1 M potassium nitrate in all cases. As for the maximum suppressor, methyl red was employed in all cases. A point was plotted for each individual drop on the rising part of the curve, and at least six values were used along the mid-portion of the curve. The plot of log $i/(i_d-i)$ against the voltage invariably resulted in a straight line with an allowable scatter of points and a slope of either nearly 0.06 or 0.03. The half-wave potential was taken as that value of the voltage for which the log term was zero.

Results and Discussion

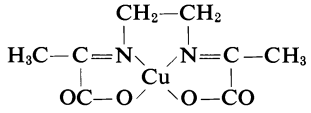
As was described in the preceding section, pyruvic acid condenses in the presence of copper(II) with glycine, β-alanine, ethylenediamine and trimethylenediamine, giving rise to the respective copper(II)-Schiff base chelate. It seems quite reasonable to assign the following structures, A → D, to the four copper(II) chelates on the basis of the analytical data and the quadri-coordinating character of copper(II) complexes.



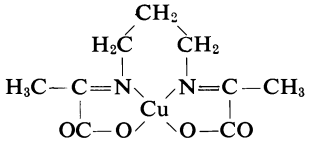
(A)
[Cu(pyv=gly)(OH$_2$)]



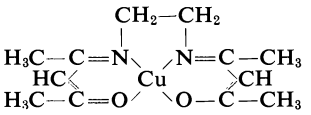
(B)
[Cu(pyv=β-ala)(OH$_2$)]



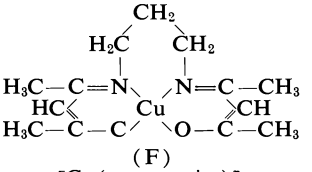
(C)
[Cu(pyv$_2$=en)]



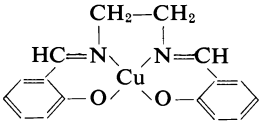
(D)
[Cu(pyv$_2$=trim)]



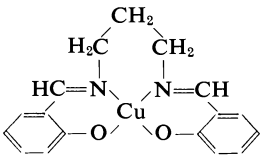
(E)
[Cu(acac$_2$=en)]



(F)
[Cu(acac$_2$=trim)]



(G)
[Cu(salal$_2$=en)]



(H)
[Cu(salal$_2$=trim)]

The difference in structure between A and B, or between C and D, is only the number of methylene groups in the same part of the organic residues. The four atoms bound to copper(II) are exactly the same in each pair. In other words, the skeletal structure of A consists of two adjacent five-membered rings, 5-5,* while that of B is five- and six-membered rings, 5-6.* In the same way, the skeletal structures of C and D are expressed as 5-5-5 and 5-6-5 respectively.

From a comparison of the properties of the respective aqueous solution, A is considered to be less stable than B. For instance, A is more difficult to recrystallize from water than B because it is accompanied by a decomposition to some extent in an aqueous solution. A slight difference is observed also in a comparison of their decomposing temperatures, as is shown in Table I.

Since the decomposing temperature of A is distinctly lower than that of B, the same relationship in relative stability, A<B, is supported here again. This situation seems to be characteristic of this type of fused-ring system, since it has been known that glycine generally forms a more stable chelate ring than β-alanine.[8-10] The same characteristic is observed also in a comparison of the other pair, C and D. Trimethylenediamine seems to be more favorable than ethylenediamine to forming stable interlocked rings around copper(II) between two pyruvate residues, unlike when they are respectively coordinated to a metal to form a single ring.[11,12] The difference in stability is observed to be much greater in

* Hereafter the notation "5-5" will be adopted for this type of fused rings. In the same manner, the fused rings in B, C and D will be expressed as 6-5, 5-5-5 and 5-6-5 respectively.

8) A. Nakahara, This Bulletin, **29**, 925 (1956).
9) C. B. Monk, *Trans. Faraday Soc.*, **47**, 285 (1951).
10) R. M. Keefer, *J. Am. Chem. Soc.*, **68**, 2329 (1946).
11) P. Pfeiffer and E. Lübbe, *J. Prakt. Chem.*, [2], **136**, 321 (1933).
12) M. Calvin and A. E. Martell, "Chemistry of the Metal Chelate Compounds," Prentice-Hall, Inc., New York (1952), p. 522.

this particular case, C<D. While D is readily recrystallized from hot water to give typical beautiful crystals, C is not satisfactorily recrystallized from any solvent, as has been described in the preceding section. The same order in stability is confirmed from a comparison of their decomposing temperature, as is shown in Table I.

The influence of the ethylene- and trimethylene-diamine chelate rings upon the stability of the respective fused-ring system, however, is reversed in the case of the acetylacetone- or salicylaldehyde-Schiff base complex, as is clear from Table I, E>F, G>H. The evidence for this is not obtainable from the same preliminary tests as employed above, but it is given by spectroscopic and polarographic data, as will be discussed in the later part of this paper. At any rate, ethylenediamine is considered to have an advantage over trimethylenediamine in forming fused rings around copper(II) with two acetylacetone or salicylaldehyde residues. This is probably a very important example to demonstrate the influence of the alteration of the size of individual rings upon the stability of the whole fused-ring system in metal polydentates. That is to say, a five-membered ring stabilizes the fused-ring system more than a six-membered ring does when either is respectively located between two six-membered rings, while the same five-membered ring stabilizes the fused-ring system less than the six-membered ring does when either is located between two five-membered rings, (5-5-5<5-6-5, 6-5-6>6-6-6).

Hence, it may be concluded that the stability of a fused-ring can not be predicted from the simple summation of the stabilty of the individual rings contained in the fused-ring system. It is considered that this is because no stress on any individual ring in metal polydentate chelates is deposited in the same ring; rather, it spreads to some extent over the whole fused-ring system, being sometimes strengthened and at other times weakened or even completely cancelled by another stress on another ring in the system.

After all, the stability of metal polydentate chelates increases with the decreasing stress over the whole fused-ring system.

For example, ethylenediamine, which is located between two pyruvate rings as a bridge in a polydentate ligand, does not weaken the stress on the adjacent copper-pyruvate rings, probably because of its too short chain, but trimethylenediamine is supposed to be long enough to weaken the stress in such a case. The above consideration can easily be supported by a simple test making use of the Stuart model. On the other hand, if the adjacent metal chelate rings are six-membered rings, such as metal-acetylacetone or -salicylaldehyde, it is not necessary to assume a significant stress on those metal-chelate rings. Hence, trimethylenediamine, which is located between two those six-membered rings, would preferably be unfavorable to forming a stable structure because of its too long chain. Ethylenediamine may fit in such a situation contrary to the above case. The greater stability of the β-alanine-pyruvate complex, B, compared with the glycine-pyruvate complex, A, is explainable from the same point of view.

Spectroscopic Studies.—It is also of interest to compare the relationship between the structure and the light absorption for those copper(II) chelates. The color of A is pale bule, while that of B is a little more intense blue. The chelate C appears green, while D appears blue. This is a great difference compared with their difference in structure.

The visible and ultraviolet absorption spectra

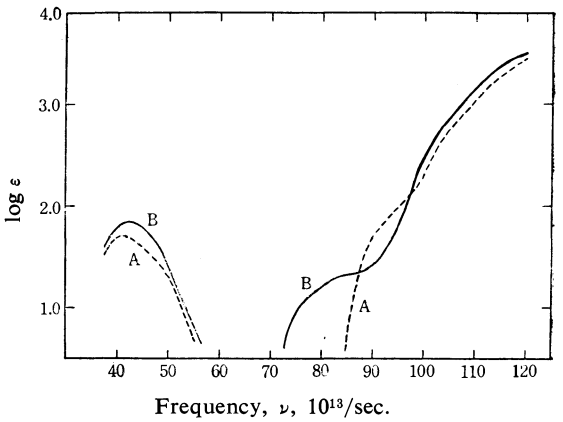


Fig. 1. Absorption spectra of copper(II)-chelates, A [Cu(pyv=gly)(OH_2)], and B [Cu(pyv=β-ala)(OH_2)].

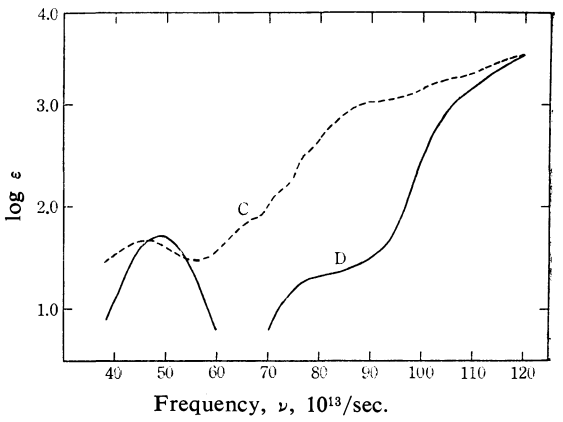


Fig. 2. Absorption spectra of copper(II)-chelates, C [Cu(pyv=en=pyv)], and D [Cu(pyv=trim=pyv)].

TABLE I. PROPERTIES OF COPPER(II)-SCHIFF BASE COMPLEXES

	Schiff base (ligand)	Skeletal structure of fused rings	Color and melting (or decomposing) point	Absorption maximum (ν_{max} in 10^{13}/sec. and log ε_{max}) in the visible region	Half-wave potential $E_{1/2}$ vs. SCE at 25°C
(A)	Pyruvic acid and glycine	5-5	Pale blue (cryst.) Pale blue (aq. soln.) 192~206°C (decomp.)	ν, 41.4 log ε, 1.70	$E_{1/2}^{(1)}$, −0.11 V.}two-step $E_{1/2}^{(2)}$, −0.37 V.}reduction
(B)	Pyruvic acid and β-alanine	6-5	Blue (cryst.) Blue (aq. soln.) 210~213°C (decomp.)	ν, 42.3 log ε, 1.85	$E_{1/2}^{(1)}$, −0.22 V.}two-step $E_{1/2}^{(2)}$, −0.35 V.}reduction
(C)	2:1 Pyruvic acid: Ethylenediamine	5-5-5	Green (cryst.) Green (aq. soln.) 184°C (decomp.)	ν, 46.1 log ε, 1.68	$E_{1/2}$, −0.29 V., irrev.
(D)	2:1 Pyruvic acid: Trimethylenediamine	5-6-5	Blue (cryst.) Blue (aq. soln.) 208°C (decomp.)	ν, 48.8 log ε, 1.72	$E_{1/2}$, −0.51 V., one-step reduction
(E)	2:1 Acetylacetone: Ethylenediamine	6-5-6	Green (hydrate cryst.) Violet (non-hydrate cryst.) Violet (solution) 144°C (m. p.)	ν, 55.6 log ε, 2.13	$E_{1/2}$, −1.12 V., irrev.
(F)	2:1 Acetylacetone: Trimethylenediamine	6-6-6	Green (cryst.) Green (aq. soln.) 97°C (m. p.)	ν, 50.8 log ε, 2.05	$E_{1/2}$, −0.79 V., irrev.
(G)	2:1 Salicylaldehyde: Ethylenediamine	6-5-6	Green (cryst.) Violet (in chloroform) Bluishgreen (in pyridine)	ν, 53.1 log ε, 2.55 (in $CHCl_3$)	$E_{1/2}$, −0.94 V., irrev. (0.1 M KNO_3 / 50% H_2O-pyridine)
(H)	2:1 Salicylaldehyde: Trimethylenediamine	6-6-6	Violet (cryst.) Green (in chloroform) Green (in pyridine)	ν, 49.6 log ε, 2.37 (in $CHCl_3$)	$E_{1/2}$, −0.66 V., irrev.

of those four chelates in an aqueous solution are shown in Fig. 1 (A and B), and in Fig. 2 (C and D), while their numerical data are shown in Table I.

It is expected that the greater the stress through the fused-ring system, the greater the weakening of the ligand field around copper(II). Moreover, the weakening of the ligand field is supposed to be reflected in the degree of bathochromic shifting of the absorption band.

Therefore, the ligand-field absorption band in each spectrum may be considered to be a measure of the stability of those chelates. From this point of view, a more or less quantitative survey may be made on the basis of spectroscopic studies to decide the influence of the alteration of the size of individual rings upon the stability of the whole fused-ring system in copper(II) chelates. The stability order, (A) 5-5<(B) 5-6; (C) 5-5-5<(D) 5-6-5, is confirmed here again by the results of the spectroscopic investigation. As to the acetylacetene-Schiff base chelates, the same stability order as mentioned above, (E) 6-5-6>(F) 6-6-6, is reaffirmed in the same way.

Polarographic Studies. — A comparison of half-wave potentials for the same type of complexes under the same conditions may be an important approach to ascertaining the relative stability of the complexes against the reduction at the dropping mercury electrode. Of course, the more negative the value of the half-wave potential, the greater the stability of the complex. The numerical data are summarized in Table I.

It is necessary to consider at least two electrode reactions for the cases of the comparatively unstable chelates, such as A, B, C and D: (1) the direct reduction of the copper(II) chelate; and (2) the reduction of unchelated Cu^{2+}, which is produced by the dissociation of the copper(II) chelate. This is because each polarogram more or less contains a reduction wave which coincides with that of the simple cupric ion as well as with that of the copper(II) chelate concerned. Since, however, the redution wave of simple cupric ion* mostly appears considerably away from that of the chelated copper(II), there was no interference with the determination of the half-wave potentials.

* The half-wave potential of the simple cupric ion for the reduction of Cu^{2+} to Cu^0 was determined to be +0.05 V. vs. SCE at 30°C in a 0.1 M potassium nitrate solution containing 0.01% gelatine.

On the other hand, it is unnecessary to take the decomposition of complexes into account for the cases of fairly stable chelates such as E and F, since the dissociation is slow compared to the direct reduction of the chelate at the electrode. The absorption spectra of those very stable chelate solutions also showed no indications of dissociation occurring.

The half-wave potential presented by Calvin and Bailes.[2] for the copper(II) chelate of salicylaldehyde-ethylenediamine, G, is −0.75 V., showing a considerable discrepancy with the present value, −0.94 V. (cf. Table I). This is understandable when we remember the difference in the conditions applied in the respective measurements. In the present work, the measurements for G and H were made with a 0.1 M potassium nitrate solution of a 50% (by volume) mixture of pyridine and water, using methyl red as the maximum suppressor. Calvin and Bailes used hydrochloric acid instead of potassium nitrate, and used no maximum suppressor. At any rate, it is not significant to discuss the cases of G and H quantitatively since they are certainly not reversible waves. At the same time, it is not necessary to know the precise values of the half-wave potentials in all cases either, since our present purpose is a qualitative comparison of the effects of changes in structure upon the nature of the chelate. However, all the polarograms other than those of G and H are supposed to be at least good enough for a semi-quantitative discussion.

The order in stability established by the polarographic studies shows a precise coincidence with that obtained from preliminary tests or spectroscopic studies previously described: (A) 5-5 < (B) 6-5; (C) 5-5-5 < (D) 5-6-5; (E) 6-5-6 > (F) 6-6-6; (G) 6-5-6 > (H) 6-6-6.

Summary

The preparation and some properties of four new copper(II) chelates of Schiff bases produced from pyruvic acid and amino acids or diamines have been reported.

The relative stability of these compounds as well as of other rather popular copper(II) chelates has been discussed on the basis of spectroscopic and polarographic investigations.

It has been demonstrated that any stress on any individual ring in metal polydentate chelates does not generally tend to be deposited in the same ring, but rather spreads to some extent over the whole fused-ring system, sometimes strengthened and at other times weakened or even completely cancelled by another stress on another ring in the system. Therefore, the stability of fused rings should not be discussed on the basis of a simple summation of the stability of individual rings contained in the fused-ring system. It has been concluded that the stability of metal polydentate chelates increases with a decrease in stress over the whole fused-ring system.

A part of the expenses for this work was defrayed by a grant from the Ministry of Education, to which the authors' thanks are due.

Institute of Chemistry
College of General Education
Osaka University
Toyonaka, Osaka

The Thermal and Radiation Oxidation of Benzene to Phenol in Aqueous Solutions Containing Metal Ions at Elevated Temperatures. V. The Thermal Oxidation of Phenol and Maleic Acid

By Kazuo SHIMADA, Nobutake SUZUKI, Nobue ITATANI and Hiroshi HOTTA*

(Received February 3, 1964)

The thermal oxidation of phenol in aqueous solutions was studied under the same conditions as for that of benzene to phenol in order to understand the benzene oxidation reported on in previous papers,[1] for the phenol produced might be also oxidized successively to other compounds. The oxidation of maleic acid was also studied with reference to this subject.

Experimental

Oxidation Procedure. — 5.35×10^{-2} M of phenol was dissolved in neutral and 0.1 N sulfuric acid solutions, to which ferrous, ferric and cupric sulfates were then added by 0.01 M as metal ions. These solutions were oxidized for 30 min. at 100~200°C under an oxygen pressure of 30 atmospheres (at room temperature) by means of that procedure mentioned in Part II.[2] For reference, the same experiment was also carried out without any metal ions. This initial concentration of phenol is about 2~3 times as great as the largest amount of phenol produced in the previous oxidation of benzene.[2]

Analytical.—After a thermal oxidation, the aqueous solutions were quantitatively analyzed directly by gas chromatography using a polyethylene-glycol (PEG 6000) column at the several temperatures (cf. Table I), depending upon the products to be

TABLE I. TEMPERATURE OF PEG COLUMN, °C

Carbon dioxide	70
Acetaldehyde	70
Acetone	70
Formaldehyde	100
Acetic acid	130
Formic acid	130
Phenol	180

analyzed. The order of the substance described in Table I is that of their retention time. Some of their peaks were assigned by other methods (to be mentioned later) as well as by the retention time. Some products were also identified by thin-layer chromatography.

The concentration of iron species in the solution after the reaction was determined by the same methods as in Part II.[2]

* From whom reprints should be requested.

1) N. Suzuki and H. Hotta, This Bulletin, 37, 244 (1964).

2) H. Hotta, A. Terakawa, K. Shimada and N. Suzuki, ibid., 36, 721 (1963).

Results

The results in all the figures except Figs. 2, 3 and 9 are shown by circle (⊙ and ●), triangle (△ and ▲) and square (▣ and ■) marks for ferrous, ferric and cupric sulfates respectively. The open marks and solid lines are for the neutral solutions, while the solid marks and dotted lines are for the 0.1 N sulfuric acid solutions. The results without any metal ion are shown by crosses (×) for the aqueous solution and by circle crosses (⊗) for the 0.1 N sulfuric acid solution.

Phenol and Metal Ions after Reaction.—The amounts of phenol after reaction are shown in Fig. 1. The results can be interpreted in the terms used for the effect of metal ions on the benzene oxidation in previous papers.[1,2] The decomposition of phenol is suppressed in the acidic solutions, in which the concentration of ions is lowered. The effect of cupric sulfate can be understood by the fact that the concentration is high even at elevated temperatures,

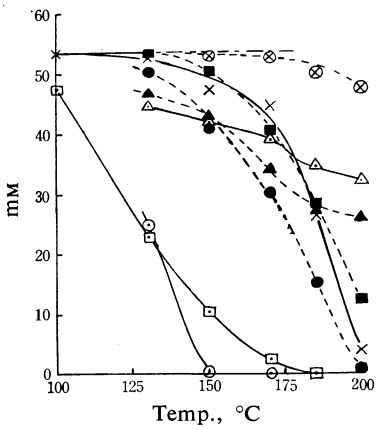


Fig. 1. Amounts of phenol after reaction in the solutions of ferrous (⊙ and ●,) ferric (△ and ▲) and cupric (▣ and ■) sulfates, and without any metal ion (× and ⊗). The results of the aqueous solutions are represented by open marks and crosses (×), and those of the 0.1 N sulfuric acid solutions by solid marks and circle crosses (⊗).

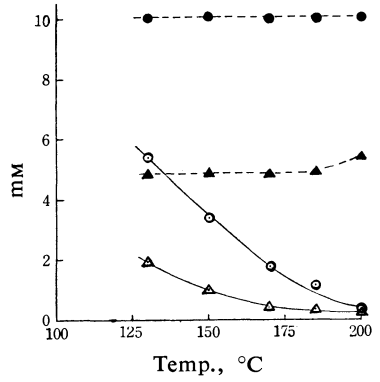


Fig. 2. Concentrations of iron species (⊙ and ●) and ferrous species (△ and ▲) after reaction in the ferrous sulfate solutions. Open marks are for the neutral solution, and solid marks for the 0.1 N sulfuric acid one.

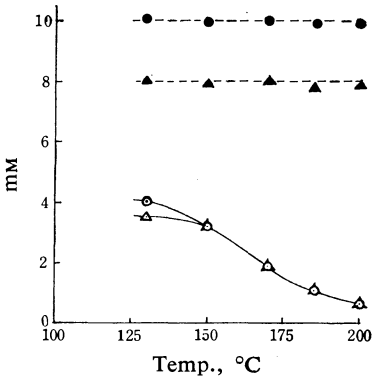


Fig. 3. Concentrations of iron and ferrous species after reaction in the ferric sulfate solutions. Marks are the same as in Fig. 2.

unlike iron salts.[1]

The total concentrations of iron species (⊙ and ●) and the contents of ferrous species (△ and ▲) dissolved in the solutions of ferrous and ferric sulfates after reaction are shown in Figs. 2 and 3 respectively. The open marks are for the neutral solutions, while the solid marks for the 0.1 N sulfuric acid solutions.

Acetic and Formic Acids.—The amounts of acetic acid produced are shown in Fig. 4. Acetic acid was identified by the mass-spectrum of the fraction obtained by gas chromatography, the chemical shift of its unclear magnetic resonance spectrum, and the behavior for extraction procedure, as well as by the retention time of the gas chromatography. It was also confirmed by the presence of acetaldehyde among the products, as will be mentioned below.

There was a peak other than that of acetic acid for the gas chromatography of the samples oxidized at 200°C. This is supposed to be of

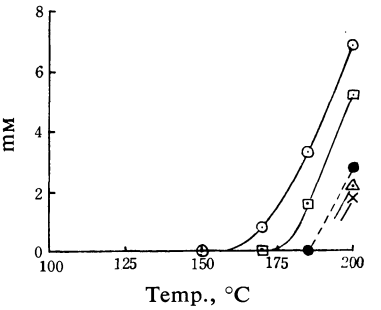


Fig. 4. Amounts of acetic acid produced in the various solutions. Marks are the same as in Fig. 1.

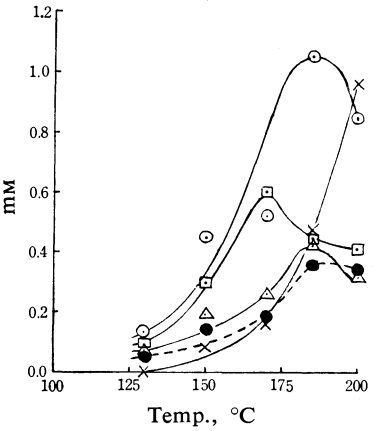


Fig. 5. Amounts of acetaldehyde produced in the various solutions. Marks are the same as in Fig. 1.

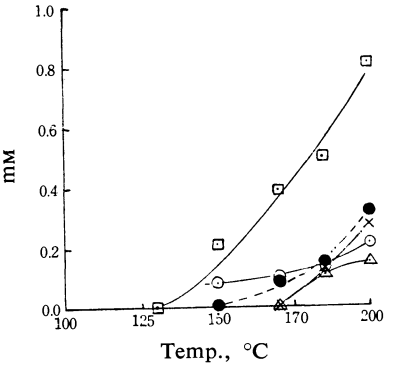


Fig. 6. Amounts of formaldehyde produced in the various solutions. Marks are the same as in Fig. 1.

formic acid judging from the retention time and the behavior of the extraction procedure, especially, the fact that the peak disappears when extracted by ether.

Aldehydes and Acetone. — The amounts of acetaldehyde and formaldehyde are shown in Figs. 5 and 6 respectively. The amounts of acetone produced are also shown in Fig. 7.

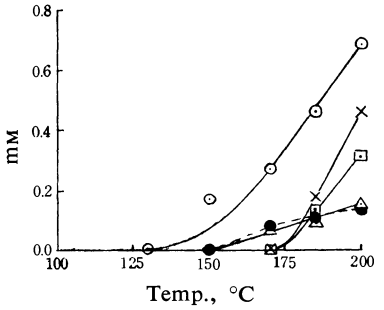


Fig. 7. Amounts of acetone produced in the various solutions. Marks are the same as in Fig. 1.

The carbonyl compounds were identified as their 2,4-dinitrophenyl hydrazone according to Johnson and Scholes.[3] They gave two absorption peaks at 360 and 560 mμ in the ethanolic alkaline solution dissolved after having been extracted into carbon tetrachloride. The former peak is usually given by monoaldehydes, and the latter by glyoxal and *p*-quinone. The uncorrected melting points of the hydrazones, given from the sample oxidized at 200°C in the aqueous solution of cupric sulfate, were 138~141°C and 160°C for the fraction dissolved in methanol, and 270~280°C for the insoluble fraction respectively. The melting points of the related hydrazones in the literature[4] are listed in Table II.

Table II. Melting point of 2,4-dinitrophenyl hydrazone derivatives, °C

Acetone	126
Acetaldehyde	147, 168
Formaldehyde	166
p-Quinone	267~268
Glyoxal	328

The reduction of ferric ions to ferrous ions, as seen in Figs. 2 and 3, is due not only to their reactions with aldehydes, but also to those with hydroperoxides in the chain oxidation process, as has been pointed out in our previous papers;[1] that is,

$$ROOH + M^{2+} = ROO + H^{+} + M^{+}$$

Carbon Dioxide.—The concentrations of carbon dioxide dissolved in the aqueous phase at the first day after reaction are shown in Fig. 8. They have been estimated approximately according to Seidell's textbook.[5]

Thin-layer Chromatography.—Some products

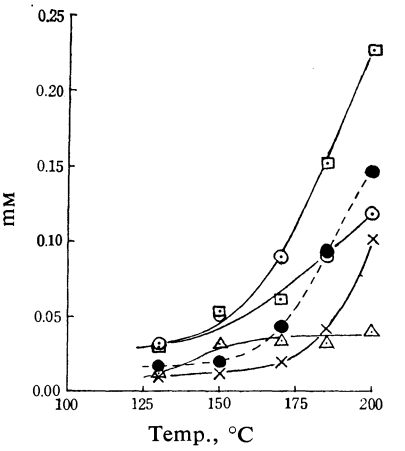


Fig. 8. Concentrations of carbon dioxide dissolved in the aqueous solutions at the first day after reaction. Marks are the same as in Fig. 1.

were detected by thin-layer chromatography using silica gel as an adsorbent on a glass plate[6] as follows (the detailed results will be described elsewhere).

When the sample, oxidized at 130°C in the aqueous solution of ferrous sulfate, was developed on the plate with a solvent composed of benzene 75+ethyl formate 24+formic acid 1, there were three spots of low R_f-values and two spots of high R_f-values. The former spots, colored by bromocresol green, were identified as oxalic, maleic and fumaric acids, and the latter spots, colored by a 5% iodine solution of ethanol, as *o*- and *p*-dihydroxybenzenes, from their R_f-values. The sample, oxidized at 200°C, gave only the spot of oxalic acid, suggesting that all the above products except oxalic acid decomposed at the higher temperature. *o*- and *p*-Dihydroxybenzenes have been reported to be found in the aqueous oxidation of phenol by Fenton's reagent or by X-rays at room temperature.[7]

Discussion

When the production of the decomposition products is compared with the consumption of phenol in Fig. 1, the amounts of the decomposition products are found to increase at higher temperatures, at which almost a part of phenol is consumed, suggesting that there are some fairly stable intermediates. This is shown clearly by the results concerning the aqueous solution of ferrous sulfate.

Since maleic and fumaric acids are detected by thin-layer chromatography, the oxidation

3) G. R. A. Johnson and G. Scholes, *Analyst*, **79**, 217 (1954).
4) "Beilsteins Handbuch der Organische Chemie," XVI Zweittes Ergz., Springer-Verlag, Berlin (1951).
5) A. Seidell, "Solubilities of Inorganic and Metal-organic Compounds," Vol. 1, D. Van Nostrand Co., New York (1953).
6) E. Stahle, *Pharmazie*, **11**, 633 (1956); *Chemker Ztg.*, **82**, 323 (1958).
7) G. Stein and J. Weiss, *J. Chem. Soc.*, **1951**, 3265.

of these acids (4.33×10^{-2} M) in the aqueous solution of ferrous sulfate by means of the same procedure as was used for phenol was examined by gas chromatography and by the absorptiometry of 2,4-dinitrophenylhydrazone derivatives. The results, shown in Fig. 9, indicate that maleic acid gave acetic acid, acetaldehyde and formaldehyde. However, since fumaric acid is very stable, it did not give these products except for a trace amount of acetaldehyde. Therefore, it is likely that maleic acid is the stable precursor of these products in the oxidation of phenol. This is also supported by the fact that the amounts of acetic acid and aldehydes increase with the rise in temperature, while maleic and fumaric acids decrease at higher temperature, as is seen in thin-layer chromatography. Acetone was not given by these acids.

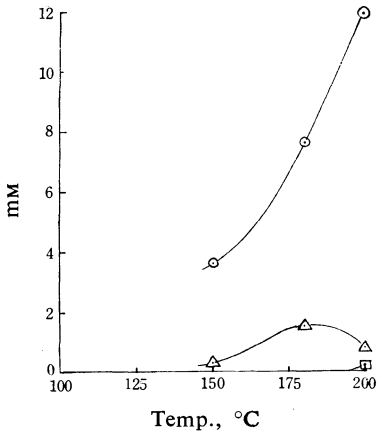


Fig. 9. Amounts of products from maleic acid (4.33×10^{-2} M) in the aqueous solution of ferrous sulfate; acetic acid (⊙), acetaldehyde (△) and formaldehyde (▣).

According to Bernatek et al.,[8-10] the ozonolysis of phenols, i.e., phenol, catechol, resorcinol and quinol, gives carbon dioxide, formic acid, oxalic acid and glyoxal, while that of *p*-benzoquinone gives formic acid, mesooxalic dialdehyde, glyoxylic acid, oxalic acid, maleic acid and carbon dioxide. However, they did not detect acetic acid and acetone.

Summary

The products of the oxidation of phenol in the aqueous solution (100~200°C) were analyzed by gas chromatography and by thin-layer chromatography. The amounts of the decomposition products, acetic acid, formic acid, acetaldehyde, formaldehyde, acetone and carbon dioxide, increase with a rise in temperature. On the other hand, maleic acid, fumaric acid and dihydroxybenzene decrease with a rise in temperature. Since the oxidation of maleic acid gives acetaldehyde, formaldehyde, and acetic acid, these products are considered to be produced through maleic acid from phenol. However, acetone is not given from maleic acid, but from phenol.

Japan Atomic Energy Research Institute
Tokai, Ibaraki

8) E. Bernatek and K. A. Sraumsgård, *Acta Chem. Scand.*, **13**, 178 (1959).
9) E. Bernatek and C. Frengen, ibid., **15**, 471 (1961).
10) E. Bernatek, J. Møkleland and K. Valen, ibid., **15**, 1454 (1961).

The Thermal and Radiation Oxidation of Benzene to Phenol in Aqueous Solutions Containing Metal Ions at Elevated Temperatures. VI. The By-products of Benzene Oxidation

By Hiroshi HOTTA, Nobutake SUZUKI, Nobue ITATANI and Kazuo SHIMADA

(Received February 3, 1964)

The oxidation of benzene catalyzed by metal ions has been discussed in previous papers,[1-3] in which the phenol yield has been shown to increase very little with the rise in temperature above 170°C. The present paper will analyze the by-products and compare them with those of phenol oxidation, which were reported on in Part V.[4]

Unpurified benzene was oxidized thermally in aqueous solutions of 0.01 M ferrous and cupric sulfates, while purified benzene was oxidized with gamma-ray irradiation in these solutions, both procedures being the same as in previous papers.[1,3] The products were then analyzed by means of gas chromatography as in Part V.[4] The amounts produced are shown in Fig. 1 for the ferrous solution and in Fig. 2 for the cupric solution, with open marks

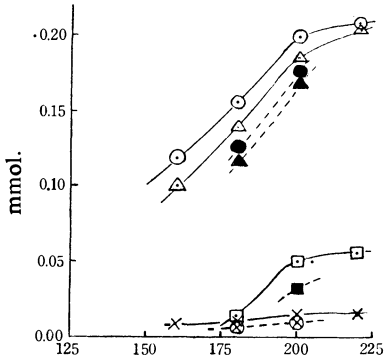


Fig. 1. Amounts of products produced in the aqueous solution of ferrous sulfate for the thermal oxidation of unpurified benzene (open marks and ×) and the radiation oxidation of purified benzene (solid marks and ⊗) : phenol by optical absorption, ⊙ and ● ; phenol by gas chromatography, △ and ▲ ; acetic acid by GC, ▣ and ■ ; and acetaldehyde by GC, × and ⊗.

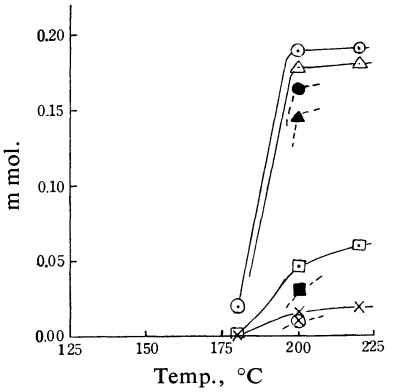


Fig. 2. Amounts of products produced in the aqueous solution of cupric sulfate ; marks are the same as in Fig. 1.

representing unpurified benzene and solid marks, purified benzene respectively. In the figures, the amounts of phenol dissolved in the aqueous phase, as analyzed by gas chromatography, are shown by triangles (△ and ▲). They are somewhat smaller than the amounts analyzed by optical absorption after ether extraction as in Parts II[1] and IV[3] and shown by circles (⊙ and ●). The amounts of acetic acid produced, shown by squares (▣ and ■), increased with the rise in temperature, even at 220°C, at which point the amount of phenol did not increase so much. The amounts of acetaldehyde produced, shown by crosses (×) for unpurified benzene and by circle-crosses (⊗) for purified benzene, did not increase at temperatures higher than 200°C, as in the case of phenol. The other products which had been found in the decomposition of phenol in Part V[4] were also detected in the present study. Formaldehyde and acetone were found to be in the greatest quantity by about 1.5×10^{-6} mole at 200°C.

When these results are compared with those in Part V, it may be concluded that the phenol produced is violently decomposed to acetic acid through acetaldehyde at high temperatures. That is, the saturation of the phenol yield at elevated temperatures is neither due to the self-inhibition effect of phenols on the oxidation

1) H. Hotta, A. Terakawa, K. Shimada and N. Suzuki, This Bulletin, 36, 721 (1963).
2) H. Hotta, N. Suzuki and A. Terakawa, ibid., 36, 1255 (1963).
3) N. Suzuki and H. Hotta, ibid., 37, 224 (1964).
4) K. Shimada, N. Suzuki, N. Itatani and H. Hotta, ibid.. 37, 1143 (1964).

reactions,[5,6] nor to some termination and competing reactions with the chain-carrying radicals.[1] No biphenyl was detected for any of the ether extracts from the aqueous and benzene phases or in the inorganic precipitates after the reaction; gas chromatography with a PEG column at 180°C was the method employed.

Dihydroxybenzene, which was detected by thin-layer chromatography in Part V,[4] was found, by optical absorption for the thermal oxidation of benzene, in the ferrous sulfate solution by Terakawa et al.[7]

The presence of aldehydes among the oxidation products suggests that the reduction of ferric ions to ferrous ions, as seen in Part II,[1] is partly due to their reactions with aldehydes, not only to those with hydroperoxides, as has been discussed previously.[3]

The temperature dependences of the phenol yield in Figs. 1 and 2 are somewhat different from those in previous papers.[1,3] The present yields are somewhat smaller than those in the previous ones at the corresponding temperature, and they increase even at the temperature where there was saturation previously.[1,3] This is due to the difference of impurities in benzene, as has been discussed in Part IV.[3] In fact, the present unpurified benzene is rather pure, as may be seen by comparing Table I (the result of gas chromatography using a TCP-column at 70°C) with Table I of Part IV.[3]

Table I. Impurities in unpurified benzene, M

Carbon disulfide	2.7×10^{-4}
n-Hexane	1.7×10^{-4}
Cyclohexane	trace
Cyclohexene	trace
Thiophene	$<6\times10^{-4}$
Toluene	1.8×10^{-3}
Xylene	0

As may be seen in Figs. 1 and 2, phenol is produced from the purified benzene, which gave no appreciable peak of impurities in gas chromatography, unlike as in Part IV.[3] Therefore, the idea that the oxidation is initiated by benzene itself, as was assumed in Part II,[1] cannot be discarded, even if the impurities promote the oxidation process.

Japan Atomic Energy Research Institute
Tokai, Ibaraki

5) K. U. Ingold, *Chem. Revs.*, **61**, 563 (1961).
6) M. A. Proskurnin and Y. M. Kolotyrkin, *Proc. 2nd U. N. Conf., Geneva*, **29**, 52 (1961).
7) A. Terakawa, Y. Hosaka, M. Nitto and T. Hirayama, *J. Chem. Soc. Japan, Ind. Chem. Sec.* (*Kogyo Kagaku Zasshi*), **66**, 1328 (1963).

The Reaction Rate in Binary Mixed Solvents

By Yasuhiko KONDO* and Niichiro TOKURA*

(Received February 3, 1964)

The rate-determining factors in the reactions in a solution are considered to be (1) the type of reaction, (2) the nature of the chemical species of the reaction, and (3) the nature of the solvent used for the reaction, in addition to (4) such ordinarily-accepted factors as the reaction temperature, the concentration of the solutes and the viscosity of the solution. Studies of these factors up to the present time seem to have been concentrated on (2) and (4). The dependence of the reaction rate on the kind of the solvent, generally referred to as "the solvent effect," includes quite complicated problems, such as "the selectivity of the solvent,"[1] the details of which have not yet been solved.

Various attempts have been made to specify the type of effect exerted by solvents on the reaction rate. For example, several reports have been published on the participation of the solvent[2] and on the effects of the dielectric constants,[3] the *Y*-values[4] or the *Z*-values[5] of the solvents. However, all these researches relate only to a few special reactions. The

* Present Address : Department of Applied Chemistry, Faculty of Engineering, Osaka University, Higashinoda, Miyakojima-ku, Osaka.

1) J. B. Hyne, *J. Am. Chem. Soc.*, **82**, 5129 (1960), J. B. Hyne, R. Wills and R. E. Wonka, ibid., **84**, 2944 (1962); J. B. Hyne and R. Wills, ibid., **85**, 3650 (1960).
2) H. E. Zaugg, ibid., **83**, 837 (1961).
3) A. A. Frost and R. G. Pearson, "Kinetics and Mechanism," John Wiley & Sons, New York (1953), p. 133.
4) E. Grunwald and S. Winstein, *J. Am. Chem. Soc.*, **70**, 2700 (1951).
5) E. M. Kosower, ibidi, **80**, 3253 (1958).

determination of the reaction rate can hardly be made for each quantity since each solvent has different selectivities during the course of the reaction.

When two solvents with different selectivities are chosen and mixed, the selectivity is expected to vary with the composition; therefore, the examination of the reaction rate in such mixtures must be profitable for the study of the dependence of the reaction rate on the nature of the solvent. To discuss the reaction rate in a mixed solvent system, the most important problem is whether there exists a general relation between the rate and the composition, a relation which would enable us to construct an empirical formula. Therefore, first an attempt was made to obtain a formula which would generalize the reaction.

The meanings of the parameters which appear in the experimentally-deduced formula will also be discussed.

The Method and the Results

When the relation between the rate constant and the composition of the solvent is discussed, the first problem to be solved is the choice of the measures with which the rate constant, k, and the composition, n, of the solvent are to be expressed. Log k was adopted for the purpose of discussing the reaction rate from the view point of the free energy of activation. Molar fraction was adopted for the expression of the composition of the solvent for the convenience of the discussion of the reaction rate, the rate equation of which is

$$k=\kappa(\boldsymbol{k}T/h)e^{-\Delta F^{\neq}/RT}$$

This equation is based on the absolute rate theory; in it, k is the rate constant, κ is the transmission coefficient, $\boldsymbol{k}$ is the Boltzmann constant, and $\Delta F^{\neq}$ is the free energy of activation.

If there is no selectivity, the plot of log k vs. the composition of the mixed solvent, x, should be linear. Howerer, the relation, as Fig. 1 shows, generally curves upward or downward. This indicates that the rate constant, $\boldsymbol{k}$, in the mixed solvent system would consist of two components, one of which depending on a linear correlation of log k vs. x (the linear plot in Fig. 1) and the other corresponding to the deviation from ideality.

Further treatment enables us to clarify the situation. When the deviation of log k from the linear correlation, $\Delta \log k$, taken on the abscissa, the curve shown in Fig. 2 is obtained. The general features of Fig. 2 indicate the following points. (In the figures, the pure solvent which gives the larger rate constant, A, is placed on the right end of the abscissa.

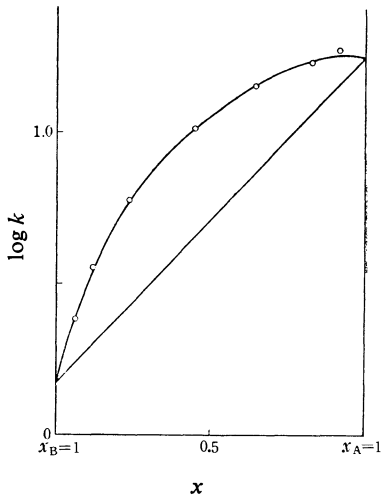


Fig. 1. Correlation between log k vs. the composition of the solvent mixture x.
The Menschutkin reaction in acetone (x_A)-benzene (x_B) mixture, between triethylamine and ethyl iodide.[11] Temp. 40°C

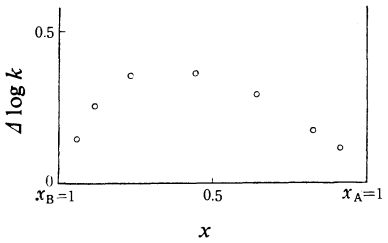


Fig. 2. A relationship between $\Delta \log k$ vs. x.
The Menschutkin reaction between triethylamine and ethyl iodide.[11]
x_A: Acetone, x_B: Benzene, Temp. 40°C

1) $\Delta \log k$ is always positive; i.e., $\Delta \log k>0$.

2) The maximum of $\Delta \log k$ lies at a molar composition smaller than $x_A=0.5$, where x_A is the molar composition of the solvent A.

Over twenty reactions in various solvent systems were examined to find if the above rules hold true (Table I). These reactions were the most elementary reactions involving (1) the chlorination of aromatic hydrocarbons, (2) the acylation of aromatic bases, and (3) the Menschutkin reactions, the details of which will be described in the following part of this paper.

An empirical equation is derived as follows:

(1) The part of the relation showing the linearity where the additivity rule is rate controlling is:

$$\log k_1=x_A \log k_A+x_B \log k_B \qquad (1)$$

where x_A and x_B are the molar compositions of the components A and B, and k_A and k_B are the rate constants of the same reaction in

the pure solvents A and B ($k_A > k_B$), respectively.

(2) The part representing the deviation from linearity may be expressed in correspondence with the theory of non-electrolyte solutions as follows:

$$\Delta \log k = x_A x_B \{a + b(x_A - x_B) + c(x_A - x_B)^2 + d(x_A - x_B)^3\} \quad (2)$$

Thus, the resultant rate formula must be:

$$\log k \text{ (mixture)} = (1) + (2) = \log k_1 + \Delta \log k = x_A \log k_A + x_B \log k_B + x_A x_B \{a + b(x_A - x_B) + c(x_A - x_B)^2 + d(x_A - x_B)^3\} \quad (4)$$

In view of the significance of the mixed solution, this equation may reasonably be accepted for the purpose of studying the reaction rate in a mixed solution.

The appicabilty of expression 4 depends on the third terms in the equation, where *a*, *b*, *c* and *d* are the parameters indicating the deviation from ideality or the long and short range interactions of the solvents. For the estimation of these parameters, the following method was adopted. The empirically-found $\Delta \log k$'s were plotted against the molar composition of the solvents. A curve passing through these plots was then drawn. From this curve the values of $\Delta \log k$'s at some selected points ($x_A = 0.15$, 0.35, 0.65 and 0.85 molar fractions) were obtained and substituted into Eq. 4. A number of the simultaneous equations thus obtained were solved to obtain the values of the respective parameters, *a*, *b*, *c* and *d*.

The curves calculated by the *a*, *b*, *c* and *d* parameters and the experimental plots of $\Delta \log k$ vs. x_A are compared in Figs. 3 and 4. As is indicated in Table I. The experimental results can be expressed with a good accuracy for various reactions by the appropriate choice of parameters.

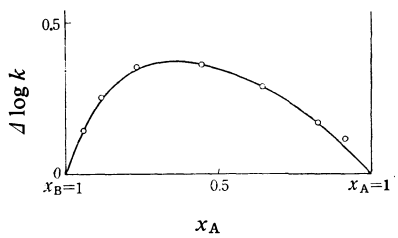


Fig. 3. Plots of $\Delta \log k$ vs. x_A.
The Menschutkin reaction between triethylamine and ethyl iodide.[11]
x_A: Acetone, x_B: Benzene
a, 1.39, *b*, −0.570, *c*, 0.696, *d*, −0.346
○ obtained, —— calcd.

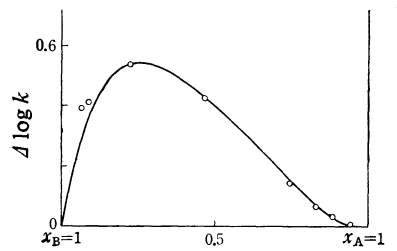


Fig. 4. Plots of $\Delta \log k$ vs. x_A.
Benzoylation of *m*-nitroaniline.[7]
x_A: Nitrobenzene, x_B: Benzene
a, 1.60, *b*, −1.70, *c*, 1.02, *d*, −1.51,
Temp., 25°C
○ obtained, —— calcd.

Discussion

The Theoretical Derivation of Expression 4.— When the solvent effect of a reaction in a solution is discussed, it is necessary to take the effect of solvation into consideration. Taking the state in a vacuum as the standard, the relationship of the free energies with the reaction process is considered. In Fig. 5 the free energies of activation in a vacuum and in a solution are compared.

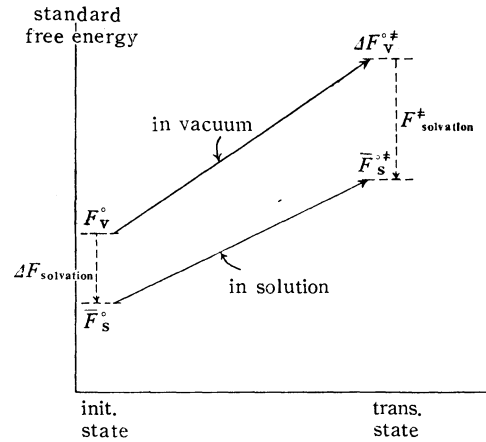


Fig. 5

The free energies of activation are indicated as:
Free energy of activation in a vacuum:

$$\Delta F_v^{\circ\ddagger} = \Delta F_v^{\circ\ddagger} - F_v^{\circ}$$

Free energy of activation in a solution:

$$\Delta \bar{F}_s^{\circ\ddagger} = \Delta \bar{F}_s^{\circ\ddagger} - \bar{F}_s^{\circ}$$

$$\bar{F}_s^{\circ} = F_v^{\circ} + \Delta F_{solvation}$$

and

$$\bar{F}_s^{\circ\ddagger} = F_v^{\circ\ddagger} + \Delta F^{\ddagger}_{solvation}$$

where F_v°, $F_v^{\circ\ddagger}$, $\bar{F}_s^{\circ}$ and $\bar{F}_s^{\circ\ddagger}$ are the free energies of the initial and the transition states in

Table I. Results of calculation of the parameters, a, b, c and d in Eq. 4

No.	Reaction	Solvent system	Reactants	Temp. of reaction, C°	Parameter				Ref.
					a	b	c	d	
1	Chlorination	CH_3CN-nitromethane	Toluene+Cl_2	25	−0.3	—	—	—	6)
2			2-Chloronaphthalene+Cl_2	25	0	0	0	0	6)
3	Acylation	Benzene-nitrobenzene	*i*-Butyryl Cl+*m*-Nitroaniline	25	1.28	−1.42	−0.0917	−1.25	7)
4			Benzoyl Cl+*m*-Nitroaniline	25	1.60	−1.70	1.02	−1.51	7)
5			Benzoyl Cl+*m*-Chloroaniline	25	1.16	−0.853	0.424	−1.10	7)
6		Benzene-phenylcyanide	Benzoyl Cl+*m*-Nitroaniline	25	3.12	−1.70	1.52	−1.41	7)
7	The Menschutkin reaction	Benzene-nitrobenzene	Triethylamine+MeI	100	1.94	−0.610	0.740	−1.370	8)
8			Triethylamine+*i*-PrI	100	2.20	−1.73	0.485	0.454	8)
9			Pyridine+MeI	100	2.10	−1.06	0.290	0.420	9)
10			Pyridine+*i*-PrI	100	1.96	−1.07	0.936	−0.710	8)
11		*i*-Pr-ether-nitrobenzene	Pyridine+MeI*	100	1.460	1.925	0.863	−6.833	9)
12		Benzene-EtOH	Pyridine+MeI	100	0.84	−0.80	0.963	−0.10	9)
13		Acetone-nitrobenzene	Pyridine+MeI	100	0.80	0	0	0	9)
14		Diphenylether-propylenecarbonate	4-Picoline+*n*-BuBr	100	1.56	−1.20	0.92	−0.055	10)
15		Benzene-acetone	Triethylamine+EtI**	100	1.070	−0.138	0.639	−0.426	11)
16			Pyridine-MeI	100	1.400	−0.510	0.686	−0.420	9)
17		Benzene-nitrobenzene	Triethylamine+MeI	40	1.80	−1.10	1.03	−0.764	8)
18			Pyridine+Benzyl Br	45	2.00	−0.948	0.868	−1.27	12)
19			Triethylamine+Benzyl Br	45	1.60	−0.980	1.370	−1.330	12)
20		Benzene-EtOH	Pyridine+Benzyl Br	45	1.780	−1.53	1.340	−0.870	12)
21			Triethylamine+Benzyl Br	45	1.740	−1.260	1.200	−0.614	12)
22		Dioxane-acetone	Triethylamine+EtI	40	1.14	−0.489	0.349	−0.318	11)

* The reaction was too complex to be expressed with four parameters.
** The results are not clear because the numbers of the data are scarce.

a vacuum and in a solution respectively, and where $\Delta F_v^{\circ\ddagger}$ and $\Delta \overline{F}_s^{\circ\ddagger}$ are the free energies of activation in a vacuum and in a solution respectively.

Therefore,

$$\Delta \overline{F}_s^{\circ\ddagger} = \Delta F_v^{\circ\ddagger} + (\Delta F_{\text{solvation}}^{\ddagger} - \Delta F_{\text{solvation}}) \quad (5)$$

The reason why the solvent effect appears in the reaction in a solution must be due mostly to the difference in $(\Delta F_{\text{solvation}}^{\ddagger} - \Delta F_{\text{solvation}})$ for various solvents. What is most important in the discussion of the solvent effect is $\overline{F}_s^{\circ}$ and $\overline{F}_s^{\circ\ddagger}$, namely, the standard free energies of the initial and the transition states in the solution.

The free energies of the standard state of a solute in solvents 1 and 2 are expressed by $\overline{F}_1^{\circ}$ and $\overline{F}_2^{\circ}$, and the free energy of the solute in the standard state in a mixture of 1 and 2, by $\overline{F}_{12}^{\circ}$; x_1 and x_2 are the molar fractions of solvents 1 and 2 in the mixture. The next relation is assumed to hold when the free energy of the solute in the mixed solvent affected by component 1 is $F_{1x_1x_2}^{\circ}$:

$$\begin{aligned}\overline{F}_{1x_1x_2}^{\circ} = \overline{F}_1^{\circ} &+ \boldsymbol{RT}\cdot a_{12}x_2^2 + \boldsymbol{RT}b_1x_2^2(x_1-x_2) \\ &+ \boldsymbol{RT}\cdot c_{12}\cdot x_2^2(x_1-x_2)^2 \\ &+ \boldsymbol{RT}\cdot d_{12}\cdot x_2^2(x_1-x_2)^3 \end{aligned} \quad (6)$$

Similarly, the free energy of the solute affected by component 2, $\overline{F}_{2x_1x_2}^{\circ}$, is as follows:

$$\begin{aligned}\overline{F}_{2x_1x_2}^{\circ} = \overline{F}_2^{\circ} &+ \boldsymbol{RT}\cdot x_1^2\{a_{21} + b_{21}\cdot(x_2-x_1) \\ &+ c_{21}\cdot(x_2-x_1)^2 + d_{21}(x_2-x_1)^2\} \end{aligned} \quad (7)$$

and in a 1—2 system:

$a_{12}=a_{21}$, $b_{12}=-b_{21}$, $c_{12}=c_{21}$ and $d_{12}=-d_{21}$

When n_1 mole of the solute in solvent 1 is mixed with n_2 mole of the solute in solvent 2, the total free energy of the solute in the solvent is $(n_1+n_2)\overline{F}_{12}^{\circ}$; therefore,

$$\begin{aligned}(n_1+n_2)\overline{F}_{12}^{\circ} &= n_1\overline{F}_1^{\circ} + n_1\boldsymbol{RT}x_2^2\{a_{12} \\ &+ b_{12}(x_1-x_2) + c_{12}(x_1-x_2)^2 + d_{12}(x_1-x_2)^3\} \\ &+ n_2\boldsymbol{RT}x_2^2\{a_{21} + b_{21}(x_2-x_1) + c_{21}(x_1-x_1)^2 \\ &+ d_{21}(x_2-x_1)^3\} = n_1\overline{F}_1^{\circ} + n_2\overline{F}_2^{\circ} + (n_1\boldsymbol{RT}x_2^2 \\ &+ n_2\boldsymbol{RT}x_1^2)\{a_{12} + b_{12}(x_1-x_2)^2 + c_{12}(x_1-x_2)^2 \\ &+ d_{12}(x_1-x_2)^3\} \end{aligned} \quad (8)$$

Since $n_1/(n_1+n_2)=x_1$ and $n_2/(n_1+n_2)=x_2$

$$\begin{aligned}\overline{F}_{12}^{\circ} = x_1\overline{F}_1^{\circ} + x_2\overline{F}_2^{\circ} &+ \boldsymbol{RT}x_1x_2\{a_{12} + b_{12}(x_1-x_2) \\ &c_{12}(x_1-x_2)^2 + d_{12}(x_1-x_2)^3\} \end{aligned} \quad (9)$$

A similar relation holds for $\overline{F}_{12}^{\circ\ddagger}$. Therefore, the free energy of the activation in the mixture is:

$$\begin{aligned}\Delta \overline{F}_{12}^{\circ\ddagger} = \overline{F}_{12}^{\circ\ddagger} - \overline{F}_{12}^{\circ} &= x_1\Delta\overline{F}_1^{\circ\ddagger} + x_2\Delta\overline{F}_2^{\circ\ddagger} \\ &+ \boldsymbol{RT}x_1x_2\{a'_{12} + b'_{12}(x_1-x_2) \\ &+ c'_{12}(x_1-x_2)^2 + d'_{12}(x_1-x_2)^3\} \end{aligned} \quad (10)$$

where a'_{12}, b'_{12}, c'_{12} and d'_{12} are the arithmetic sums of the initial and the transition states respectively.

According to the absolute reaction rate theory cited above,

$$\boldsymbol{RT}\ln k = \text{const} - \Delta F^{\ddagger}$$

Consequently, it is clear that the following relation holds so long as Eqs. 6 and 7 are valid;

$$\begin{aligned}\log k_{12} = x_1\log k_1 + x_2\log k_2 + x_1x_2 \\ \times\{a + b(x_1-x_2) + c(x_1-x_2)^2 + d(x_1-x_2)^3\} \end{aligned} \quad (11)$$

In the above discussion, the free energies of standard state in pure solvents are $\overline{F}_1^{\circ}$ and $\overline{F}_2^{\circ}$. When two solvents are mixed together, the free energy of the mixture is sufficiently expressed by $(x_1\overline{F}_1^{\circ} + x_2\overline{F}_2^{\circ})$ if the change is ideal. Actually, however, various interactions occur; therefore, a series of terms must be added as corrections. The parameters of the solution, then enable us to determine the interaction in the real mixtures.

A Discussion of the Calculated Parameter: The Nature of *a*.—The important factors which determine the rate constant of the reaction are; (1) the type of reaction (or the charge type), (2) the nature and the structure of the reaction species, and (3) the nature of the solvent used, as has been mentioned above. The four parameters in Eq. 11, *a*, *b*, *c* and *d*, are the quantities that relate to the rate constant. Therefore, it is quite reasonable to suppose that *a*, *b*, *c* and *d* are affected by the three factors described above as is the rate constant.

It is sure from the nature of the proposed formula 11 that *a* is the most important parameter of the four. The value of *a* may easily be calculated, since it is $\log k/x_1x_2$ at an equimolar mixture of solvents 1 and 2. When the mixed solution consists of equal or nearly equal molar amounts of the components (1 and 2), Eq. 11 reduces to:

$$\log k_{12} = x_1\log k_1 + x_2\log k_2 + x_1x_2a \quad (12)$$

Moreover, in discussing the deviation from

6) R. H. Keefer and L. J. Andrews, *J. Am. Chem. Soc.*, **84**, 3635 (1962).
7) H. S. Venkataraman and C. N. Hinshelwood, *J. Chem. Soc.*, **1960**, 4986.
8) H. C. Rains and C. N. Hinshelwood, ibid., **1939**, 1379.
9) R. A. Fairclough and C. N. Hinshelwood ibid., **1937**, 1573.
10) M. Watanabe and R. M. Fuoss, *J. Am. Chem. Soc.*, **78**, 527 (1956).
11) E. Tomila and P. Kauranen, *Acta Chem. Scand.*, **8**, 1152 (1954).
12) G. Michin, R. Ginsburg and Ch. Moissejewa, *J. Chim. de l'Ukraine, L. Wissenschaft Teil*, **136**; *Chem. Zentralb.*, **1926**, II, 2376.

ideality, the parameter a is convenient for the mixed solution, while the ideal mixture exhibits the following relation;

$$\log k_{12} = x_1 \log k_1 + x_2 \log k_2 \quad (13)$$

The three kinds of reaction shown in Table I will now be considered. Although the magnitude of a can not be determined from the type of reaction only, it keeps an almost constant value even when the reactants vary over a wide range as long as the solvent system is the same during reactions of the same type (for example, Nos. 1 and 2, Nos. 3, 4 and 5, Nos. 7, 8, 9 and 10, Nos. 15 and 16, Nos. 17, 18 and 19, and Nos. 20 and 21 in Table I). However, it changes greatly if the solvent system is different, even when both the reaction and the reactants are the same (for example, Nos. 4 and 6, and Nos. 9, 11, 12, 13 and 16 in Table I). From the characteristics of a's described above, it can be concluded that a is sensitive to the type of reaction and the solvent system, but that it is not affected by the nature of the reactant as long as the solvent system and the type of reaction are the same.

The Theoretical Derivation of The Additivity of the Parameter a.—The following formulae will hold when a two-component system changes ideally for three kinds of solvent, the components being 1, 2 and 3 respectively:

$$\Delta\overline{F}_{12}^{\circ\ddagger} = x_1\Delta\overline{F}_1^{\circ\ddagger} + x_2\Delta\overline{F}_2^{\circ\ddagger} \qquad x_1+x_2=1 \quad (14)$$

$$\Delta\overline{F}_{23}^{\circ\ddagger} = x_2\Delta\overline{F}_2^{\circ\ddagger} + x_3\Delta\overline{F}_3^{\circ\ddagger} \qquad x_2+x_3=1 \quad (15)$$

$$\Delta\overline{F}_{13}^{\circ\ddagger} = x_1\Delta\overline{F}_1^{\circ\ddagger} + x_3\Delta\overline{F}_3^{\circ\ddagger} \qquad x_1+x_3=1 \quad (16)$$

Let us now discuss the relation among $\Delta\overline{F}_{12}^{\circ\ddagger}$, $\Delta\overline{F}_{23}^{\circ\ddagger}$ and $\Delta\overline{F}_{13}^{\circ\ddagger}$. When a 1—2 solvent system and a 2—3 solvent system are mixed,

$$\Delta\overline{F}_{12}^{\circ\ddagger} + \Delta\overline{F}_{23}^{\circ\ddagger} = x_1\Delta\overline{F}_1^{\circ\ddagger} + x'_2\Delta\overline{F}_2^{\circ\ddagger} + x'_2\Delta\overline{F}_2^{\circ\ddagger} + x'_3\Delta\overline{F}_3^{\circ\ddagger} \quad (17)$$

where (x_1 and x_2) are the molar fractions in the 1—2 system and (x'_2 and x'_3) are those in the 2—3 solvent system, (x_1 and x_2) being independent of (x'_2 and x'_3). If the condition $x_1+x'_3=1$ is satisfied, the sum for each independent system comes to show the behavior of the 1—3 system. Thus, the activation free energy of the 1—3 system can be calculated from the sum of the 1—2 and 2—3 mixed component systems:

$$\Delta\overline{F}_{12}^{\circ\ddagger} + \Delta\overline{F}_{23}^{\circ\ddagger} = x_1\Delta\overline{F}_1^{\circ\ddagger} + (1-x_1)\Delta\overline{F}_1^{\circ\ddagger} + (1-x_3')\Delta\overline{F}_2^{\circ\ddagger} + x_3'\Delta\overline{F}_3^{\circ\ddagger} \quad (17')$$

Since $x_1+x_3'=1$,

$$\Delta\overline{F}_{12}^{\circ} + \Delta\overline{F}_{23}^{\circ\ddagger} = \Delta\overline{F}_2^{\circ\ddagger} + x_1\Delta\overline{F}_1^{\circ\ddagger} + x_2'\Delta\overline{F}_3^{\circ\ddagger} \quad (18)$$

If ($x_1+x_3'=1$) is rewritten as ($x_1+x_3=1$),

$$\Delta\overline{F}_{12}^{\circ\ddagger} + \Delta\overline{F}_{23}^{\circ\ddagger} = \Delta\overline{F}_2^{\circ\ddagger} + \Delta\overline{F}_{12}^{\circ\ddagger} \quad (19)$$

The above consideration may be continued further and applied to the system which has the term a the deviation from an ideal system:

$$\Delta\overline{F}_{12}^{\circ\ddagger} = x_1\Delta\overline{F}_1^{\circ\ddagger} + x_2\Delta\overline{F}_2^{\circ\ddagger} + \boldsymbol{RT}x_1x_2a_{12}, \qquad x_1+x_2=1 \quad (20)$$

$$\Delta\overline{F}_{23}^{\circ\ddagger} = x_2\Delta\overline{F}_2^{\circ\ddagger} + x_3\Delta\overline{F}_3^{\circ\ddagger} + \boldsymbol{RT}x_2x_3a_{23}, \qquad x_2+x_3=1 \quad (21)$$

$$\Delta\overline{F}_{13}^{\circ\ddagger} = x_1\Delta\overline{F}_1^{\circ\ddagger} + x_3\Delta\overline{F}_3^{\circ\ddagger} + \boldsymbol{RT}x_1x_3a_{13}, \qquad x_1+x_3=1 \quad (22)$$

As before, when $x_1+x_3=1$,

$$\begin{aligned}\Delta\overline{F}_{12}^{\circ} + \Delta\overline{F}_{23}^{\circ} &= x_1\Delta\overline{F}_1^{\circ\ddagger} + (1-x_1)\Delta\overline{F}_2^{\circ\ddagger} \\ &\quad + \boldsymbol{RT}x_1(1-x_1)a_{12} + x_3\Delta\overline{F}_\infty^{\circ\ddagger} \\ &\quad + (1-x_3)\Delta\overline{F}_2^{\circ\ddagger} \boldsymbol{RT}x_3(1-x_3)a_{23} \\ &= \Delta\overline{F}_2^{\circ\ddagger} + x_1\Delta\overline{F}_1^{\circ\ddagger} + x_3\Delta\overline{F}_3^{\circ\ddagger} \\ &\quad + \boldsymbol{RT}x_1x_3(a_{12}+a_{23}) \end{aligned} \quad (23)$$

If the relation of Eq. 19 holds as in the ideal change, the relation

$$a_{12} + a_{22} = a_{13} \quad (24)$$

must also hold.

The Additivity of the Parameter a in the Menschutkin Reaction.—Relation 24, obtained above, may be applied to the case of the Menschutkin reaction.

When benzene, acetone and nitrobenzene are taken as the solvent components 1, 2 and 3 respectively, the relation among them is described in Table II and in Fig. 6. While $a_{12}+a_{23}=2.03$ from the sum of the average values of a_{12} and a_{23} as listed in Table II, the average value of a_{13} experimentally obtained

TABLE II. THE PARAMETER a'S IN THE MENSCHUTKIN REACTION AT 100°C, IN BENZENE (1), ACETONE (2) AND NITROBENZENE (3) SYSTEMS

Benzene-acetone a_{12}		Acetone-nitrobenzene a_{23}		Benzene-nitrobenzene a_{13}	
Triethylamine+EtI	1.07[11]	Pyridine+MeI	0.80[9]	Triethylamine+MeI	1.94[8]
Pyridine+MeI	1.40[9]			Triethylamine+*i*-PropI	2.20[8]
				Pyridine+MeI	2.10[9]
				Pyridine+*i*-PropI	1.96[8]
Average	1.28			Average	2.05

is 2.05. Therefore, it was found that the additivity rule 24 holds among these three a's if the deviation from ideal is taken into account up to the first term, as in Eq. 12.

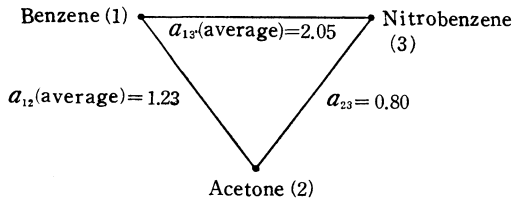


Fig. 6.

Summary

The reaction rate in binary mixed solvents have been discussed and following facts confirmed:

1) A linear relation does not hold between $\log k$ and the molar fraction of the components in most cases.

2) The deviation from linearity is usually positive, and the maximum deviation is found at $x_A \leq 0.5$, x_A is the molar fraction of a component in which the rate is faster than in another component.

3) The experimental results may be expressed with good accuracy by the formula:

$$\log k = x_A \log k_A + x_B \log k_B + x_A x_B a + b(x_A - x_B) + c(x_A - x_B)^2 + d(x_A - x_B)^3$$

4) The parameter a depends upon the type of reaction and the solvent system, but it does not depend on the nature of the reactants.

5) The additivity of has been proved theoretically and confirmed a for the Menschutkin reaction in various solvent mixtures.

The authors wish to thank Professor Yasukatsu Tamai of Tohoku University and Professor Kiyoharu Ishida of Shizuoka University for their helpful discussions of this work.

The Chemical Research Institute of Non-Aqueous Solutions
Tohoku University
Katahira-cho, Sendai

The Preparation and the Co-ordination Chemistry of Cobalt Complexes with Schiff Bases Derived from Salicylaldehyde and Alkyl Amines

By Hiroaki NISHIKAWA and Shoichiro YAMADA

(Received February 5, 1964)

The cobalt complexes of Schiff bases involve many problems of fundamental importance in the co-ordination chemistry of cobalt. As a step to the elucidation of these problems, the present authors previously characterized and discussed the electronic absorption spectra of the Schiff-base complexes of cobalt(II), which necessarily have a square-planar configuration because of their steric condition.[1] It is now appropriate and possible to make a similar study of these cobalt complexes which are not necessarily required to take a square-planar configuration by the steric reason alone. The present paper deals with the preparation and the stereochemistry of cobalt(II) and cobalt-(III) complexes of *N*-alkyl-salicylideneimines (Fig. 1).

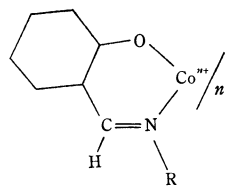


Fig. 1. Cobalt-complexes of *N*-alkyl-salicylideneiminate.

Experimental

Materials. — Bis(*N*-α-branched alkyl-salicylideneiminato) (cobalt(II) complexes were prepared in the atmosphere by the following two methods. 1)[2] A mixture of calculated amounts of cobalt(II) acetate tetrahydrate, salicylaldehyde, and an α-branched-alkyl amine was heated in ethanol. To this solution a 4 N solution of sodium carbonate (about 75% of the calculated amount) was added to neutralize the acetic acid which was expected to be liberated

1) H. Nishikawa and S. Yamada, This Bulletin, **37**, 8 (1964).

2) H. Nishikawa, S. Yamada and R. Tsuchida, *Z. Naturforsch.*, **17b**, 78 (1962).

in the reaction. When the solution was cooled or evaporated, the red crystals of the compound were obtained in a good yield. 2) Bis(salicylaldehyde)-cobalt(II) dihydrate, $Co(sal)_2 \cdot 2H_2O$,* and a slight excess of an α-branched alkyl amine were heated in methanol or ethanol for about ten minutes. When the solution was evaporated, red crystals were obtained in a good yield.

Bis(*N*-isopropyl- and bis(*N*-*s*-butyl-salicylideneiminato)cobalt(II) were reported previously.[2]

Bis(*N*-*t*-butyl-salicylideneiminato)cobalt(II) was obtained in the form of prismatic red crystals. Recrystallization was carried out from ethanol. The crystals are quite soluble in common organic solvents.

Found: C, 64.41; H, 7.03; N, 6.73. Calcd. for $C_{22}H_{28}N_2O_2Co$: C, 64.2; H, 6.86; N, 6.81%.

The compound has also been reported by Sacconi et al.[3]

Bis(*N*-1-ethylpropyl-salicylideneiminato)cobalt(II) was obtained in red, needle-like crystals. Recrystallization was carried out from *n*-hexane. It is very soluble in common organic solvents.

Found: C, 65.4; H, 7.41; N, 6.46. Calcd. for $C_{24}H_{32}N_2O_2Co$: C, 65.6; H, 7.34; N, 6.37%.

In general, the above-described compounds of cobalt(II) are stable, and they are not oxidized either in solution or in the crystalline state in the atmosphere.

Tris(*N*-*n*-alkyl-salicylideneiminato)cobalt(III) complexes were prepared by a method previously reported.[2] There was a mistake in the original direction; a 4 N sodium carbonate ought to be employed instead of a 0.3 N solution.

All these cobalt(III) complexes, which are obtained as dark-green crystals, are very stable to the air both in the crystalline state and in solution.

Tris(*N*-methyl-,[4] tris(*N*-ethyl-,[5] tris(*N*-*n*-propyl-[2] and tris(*N*-*n*-butyl-salicylideneiminato)cobalt(III)[2] were reported earlier.

Bis(*N*-*n*-alkyl-salicylideneiminato)cobalt(II) complexes are readily oxidized by the atmospheric oxygen. For the preparation of these complexes, it is necessary to carry out the procedures in an oxygen free atmosphere. Recently Sacconi et al.[6] reported the preparation of bis(*N*-*n*-butyl- and bis(*N*-*n*-amyl-salicylideneiminato)cobalt(II). The present authors have succeeded in preparing these complexes by the following novel method, which is also applicable to the synthesis of bis(*N*-*n*-alkyl-salicylideneiminato)-cobalt(II) in general: A methanolic solution of bis(salicylaldehyde)cobalt(II) dihydrate, $Co(sal)_2 \cdot 2H_2O$, and a trace of formaldehyde was boiled in a flask. When the space in the flask was filled with the methanol vapor, a slight excess of the amine was added quickly; then the flask was closed with a stopper in order to prevent the air from coming in. The closed flask was heated under stirring at the boiling temperature of the solvent for a reaction period of from 10 to 40 min.; then the solution was left to cool. The crystals which separated out were filtered quickly in the air and dried in vacuo.

For the preparation of bis(*N*-methyl-salicylideneiminato)cobalt(II), 3.0 g. of bis(salicylaldehyde)-cobalt(II) dihydrate and 2.5 ml. of a 30% aqueous solution of methyl amine were used, with 60 ml. of methanol, as a solvent, containing 2 ml. of a 37% formaldehyde solution. Following the general method described above, the reaction was continued for 10 min. at about 60°C. After the closed flask was left at room temperature for a day, brown crystals separated out.

Found: C, 58.7; H, 4.98; N, 8.58. Calcd. for $C_{16}H_{16}N_2O_2Co$: C, 58.7; H, 4.92; N, 8.56%.

Bis(*N*-ethyl-salicylideneiminato)cobalt(II) was prepared from 3.0 g. of bis(salicylaldehyde)cobalt(II) dihydrate and 1.4 g. of a 70% aqueous solution of ethyl amine. The solvent used was methanol (60 ml.) containing 26 ml. of water and 2 ml. of a 37% aqueous solution of formaldehyde. The general method was followed, the reaction being continued for 30 min. at 60°C. After the reaction was over, the cooled flask was left at room temperature for a day; well developed red plate-like crystals then separated out.

Found: C, 60.9; H, 5.67; N, 7.80. Calcd. for $C_{18}H_{20}N_2O_2Co$: C, 60.9; H, 5.67; N, 7.89%.

Bis(*N*-*n*-propyl-salicylideneiminato)cobalt(II) was prepared and red crystals by a method similar to that used in the case of bis(*N*-ethyl-salicylideneiminato)cobalt(II).

Found: C, 62.9; H, 6.41; N, 7.08. Calcd. for $C_{20}H_{24}N_2O_2Co$: C, 62.7; H, 6.31; N, 7.31%.

Bis(*N*-*n*-butyl-salicylideneiminato)cobalt(II) was prepared in red crystals from 3.0 g. of bis(salicyl-aldehyde)cobalt(II) dihydrate and 2.5 g. of *n*-butyl amine. The solvent employed was methanol (80 ml.) containing 2 ml. of a 37% aqueous solution of formaldehyde. The same general method was followed, the reaction being continued for about 10 min. at 60°C.

Found: C, 64.3; H, 6.78; N, 6.83. Calcd. for $C_{22}H_{28}N_2O_2Co$: C, 64.2; H, 6.85; N, 6.81%.

This complex has also been prepared by Sacconi et al.[6] by a more complicated method.

Bis(*N*-benzyl-salicylideneiminato)cobalt(II) was prepared from 3.5 g. of bis(salicylaldehyde)cobalt-(II) dihydrate and 3.5 g. of benzyl amine, with 60 ml. of methanol as a solvent. The same general method was followed, the reaction being continued for about 20 min. at 60°C. After the flask, in which crystals of the compound had already started to separate out, was left to cool, well-developed red crystals were collected. This compound had been prepared previously by Endo[4] using another method.

Found: C, 70.0; H, 5.02; N, 5.77. Calcd. for $C_{23}H_{24}N_2O_2Co$: C, 70.2; H, 5.05; N, 5.84%.

Comparison shows that this compound, which gradually undergoes oxidation in organic solvents in the atmosphere, is less stable to oxidation than the *N*-α-branched alkyl-derivatives, but more stable than the corresponding *N*-*n*-alkyl-derivatives.

* The notation "sal" represents an anion formed when a proton is liberated from a molecule of salicylaldehyde.

3) L. Sacconi, P. Paoletti and M. Ciampolini, *J. Am. Chem. Soc.*, **85**, 411 (1963).
4) J. Endo, *J. Chem. Soc. Japan (Nippon Kwagaku Kwaisi)*, **65**, 428 (1944).
5) B. O. West, *J. Chem. Soc.*, **1952**, 3115.
6) L. Sacconi, M. Ciampolini, F. Maggio and F. P. Cavasino, *J. Am. Chem. Soc.*, **84**, 3246 (1962).

Measurements.—The electronic absorption spectra of the complexes in solution were determined with a Beckman DU spectrophotometer. The solvents used were chloroform, benzene, ethanol and pyridine. It was confirmed that Beer's law was obeyed in the concentration range of the present work, which varied between 10^{-2} and 10^{-5} molar.

Results and Discussion

Cobalt(II) Complexes of Schiff Bases Derived from Salicylaldehyde and α-Branched Alkyl Amines.—Examination with a Stewart model shows that the steric condition due to the *t*-butyl groups prevents bis(*N*-*t*-butylsalicylideneiminato)cobalt(II) from taking a planar configuration.[7] The absorption spectrum of this compound in benzene, which is shown in Fig. 2, is essentially similar to the spectrum of the compound in such other organic solvents as methanol, ethanol and pyridine; therefore, no remarkable solvent effect on the structure of the molecules is present in the case of this compound. The absorption bands due mainly to the ligand groups come into the region of quite low frequencies, being superposed on a part of the ligand-field bands. It is generally possible, however, to see the main features of the ligand-field bands of these cobalt complexes. The ligand-field bands are quite different from those of the related cobalt(II) complexes with a square-planar configuration.[1] The spectum of bis(*N*-*t*-butylsalicylideneiminato)cobalt(II) also bears an apparent resemblance to the spectrum of such tetrahedral cobalt(II) complexes as tetrahalogeno-cobalt(II) ions. As with the spectra of tetrahalogeno-cobalt(II) complexes with a tetrahedral configuration, the absorption band of bis(*N*-*t*-butylsalicylideneiminato)cobalt(II) with the main peak at about 24.6×10^{13} sec^{-1} is assigned to the spin-allowed transition, $^4A_2\rightarrow{}^4T_1(F)$. The next band, at 54 to 60×10^{13} sec^{-1}, is similarly assigned to the transition $^4A_2\rightarrow{}^4T_1(P)$. In the corresponding *s*-butyl, isopropyl or 1-ethylpropyl complexes, the steric hindrance to the square-planar configuration is more or less serious enough to prevent the square-planar configuration, but this is not so complete as in the case of the *t*-butyl derivative. The absorption spectra of these complexes in non-donor solvents, however, are quite similar to the spectrum of the *t*-butyl-complex with ligand-field bands in the visible and near-infrared regions characteristic of the tetrahedral cobalt(II) complexes (Fig. 2). It may be concluded that bis(*N*-isopropyl-, bis(*N*-*s*-butyl- and bis(*N*-1-ethylpropyl-salicylideneiminato)cobalt(II) are distorted significantly from the square-planar configuration. The assignment of the ligand-field bands of these tetrahedral complexes is made in a way similar to that used for the *t*-butyl complex.

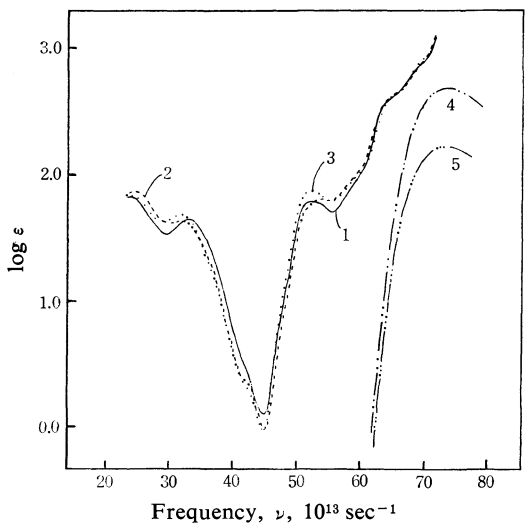


Fig. 2. Electronic absorption spectra of Co(O·C_6H_4·CH : NR)$_2$ in benzene and HO·C_6H_4·CH : NR′ in chloroform.
1, R=Isopropyl (——)
2, R=*t*-Butyl (----)
3, R=1-Ethylpropyl (·····)
4, R′=*t*-Butyl (—·—)
5, R′=isopropyl (—·····—)

It is significant that bis(*N*-α-branched alkyl-salicylideneiminato)cobalt(II) complexes show quite similar spectra, with absorption bands at nearly identical frequencies, when the substituent represents *t*-butyl, isopropyl, *s*-butyl, 1-ethylpropyl and cyclohexyl groups. Since the extent of the steric hindrance to the square-planar configuration of the cobalt(II)-complex is expected to be different for these substituents, the above observation suggests that the distortion from the square-planar configuration occurs to a nearly equal extent among all the above cobalt(II) complexes with α-branched alkyls as substituents. Judging from the considerable distortion from the square-plane in the case of the *t*-butyl-derivative, it is concluded that the tetrahedral configuration is most likely for these cobalt(II) complexes.

Cobalt-Complexes of Schiff Bases Derived from Salicylaldehyde and *n*-Alkyl Amines.—In the preceding part of this paper, it has been concluded that the configuration around the cobalt(II) ion in bis(*N*-α-branched alkyl-salicylideneiminato)cobalt(II) complexes is tetrahedral. It seemed interesting, therefore, to examine whether the configuration around the cobalt(II) ion is tetrahedral or square-planar in bis(*N*-*n*-alkyl-salicylideneiminato)cobalt(II)

7) S. Yamada and H. Nishikawa, This Bulletin, **36**, 755 (1963).

complexes, in which there is no serious steric hindrance to either the tetrahedral or the square-planar configuration.

The *N*-*n*-alkyl-substituted complexes of cobalt(II) are so readily oxidized that these complexes can not be prepared by the conventional procedures in the atmosphere which have proved applicable to the preparation of the *N*-α-branched alkyl-complexes. Diehl and Chao[8] reported the preparation of bis(*N*-*n*-alkyl-salicylideneiminato)cobalt(II) with methyl, ethyl, *n*-propyl, *n*-butyl and *n*-amyl groups as the substituent. These compounds, however, were not obtained in the form of crystals, but only as a solid mass. Sacconi et al.[6] recently reported the *n*-butyl- and *n*-amyl-derivatives of this series, but their method is not quite suitable for the preparation of the methyl-, ethyl- and *n*-propyl-derivatives, which are particularly susceptible to oxidation.

The present authors succeeded in synthesizing cobalt(II) complexes of the Schiff bases, with methyl, ethyl, *n*-propyl and *n*-butyl as the substituent, by means of a new method which proved applicable to the synthesis of the corresponding compounds with higher alkyls. The electronic spectra may be used diagnostically in examining the configuration of the cobalt(II) complexes of this type, since the spectrum of the square-planar cobalt(II) complex is quite different from that of the tetrahedral cobalt(II) complex.[1,2,7] Bis(*N*-*n*-alkyl-salicylideneiminato)cobalt(II) complexes all show absorption spectra similar to each other and to the spectra of bis(*N*-α-branched alkyl-salicylideneiminato)cobalt(II) complexes (cf. Fig. 3). It may be concluded that these bis(*N*-*n*-alkyl-salicylideneiminato)cobalt(II) complexes have a tetrahedral configuration.[9] In the spectra of bis(*N*-*n*-alkyl-salicylideneiminato)cobalt(II), an absorption band with the main peak at about 25×10^{13} sec^{-1} is assigned to a transition $^4A_2\rightarrow{}^4T_1(F)$.

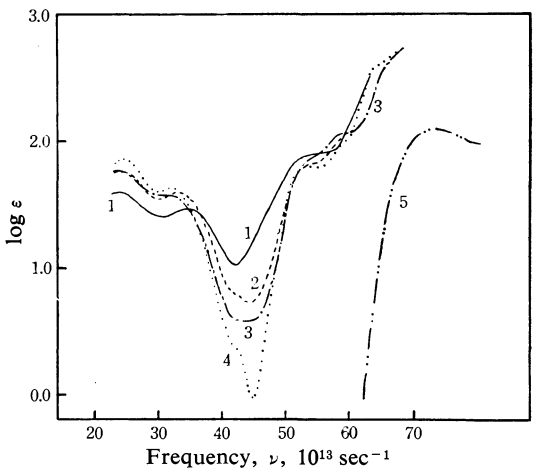


Fig. 3. Electronic absorption spectra of Co·(O·C_6H_4·CH : NR)$_2$ and HO·C_6H_4·CH : NR'·
1, R=Methyl, in methylene dichloride (——)
2, R=Ethyl, in ethanol (----)
3, R=Benzyl, in ethanol (—·—)
4, R=*t*-Butyl, in benzene (·····)
5, R'=Methyl, in chloroform (—···—)

The absorption maxima of the ligand-field bands of the *n*-alkyl-substituted cobalt(II) complexes are nearly identical with those of the *t*-butyl-derivative, which is regarded as remarkably distorted from the square-planar configuration on the steric ground alone. In the corresponding complexes of copper(II) and nickel(II), a gradual shift of the ligand-field band toward a lower frequency was observed in the following order, depending upon the extent of the distortion from the square-plane: *n*-alkyl, isopropyl, *t*-butyl.[7] It may, therefore, be concluded that the distortion from the square-planar configuration in bis(*N*-*n*-alkyl-salicylideneiminato)cobalt(II) complexes is as great as in the corresponding *t*-butyl derivative. It is thus clear that the configuration of the bis(*N*-alkyl-salicylideneiminato)cobalt(II) complexes, in general, is tetrahedral, whether or not there is steric hindrance to the square-planar configuration. The configuration around the cobalt(II) ion in bis(*N*-*n*-butyl-salicylidene iminato)cobalt(II) has been reported to be tetrahedral from magnetic measurements and X-ray powder photographs.[6,10]

Comparison readily reveals that the tetrahedral configuration is much more stabilized in the cobalt(II) complex than in the nickel(II) and the copper(II) complex[7] when complexes with identical ligands are compared. This is in agreement with what has been predicted on the basis of the crystal-field theory,[11] which demands much more crystal-field stabilization energy for the cobalt(II) ion with a d^7 configuration than for the nickel(II) and copper(II) ions. The color of bis(*N*-methyl-salicylideneiminato)cobalt(II) in the solid state is different from that of the other bis(*N*-alkyl-salicylideneiminato)cobalt(II) in the solid state,

8) H. Diehl and T. S. Chao, *Iowa State Coll. J. Sc.*, **22**, 126 (1947).

9) It was formerly stated that bis(*N*-methyl-salicylideneiminato)cobalt(II) was square-planar (H. Nishikawa, S. Yamada and R. Tsuchida, *Z. anorg. u. allg. Chem.*, **316**, 278 (1962)). In the light of the present work, this statement is not correct, although the configuration of the corresponding cobalt(II) complexes of ethyl, propyl and higher alkyls was correctly concluded in that paper to be distorted from the square-planar configuration.

10) E. Frasson and C. Panatoni, *Z. Krist.*, **116**, 154 (1961).

11) See, for example, L. E. Orgel, "An Introduction to Transition-metal Chemistry," Methuen and Co., London (1961).

although both of them consist of tetrahedral molecules in non-donor solvents. The examination of the methyl-substituted complex in the solid state is now in progress; it will be reported later, together with other materials.

The electronic absorption spectra of bis(*N*-*n*-alkyl-salicylideneiminato)cobalt(II) complexes in pyridine have been examined; some of them are shown in Fig. 4. The spectra of

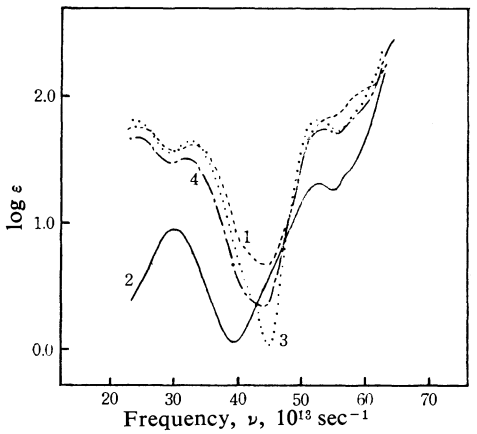


Fig. 4. Electronic absorption spectra of Co·(O·C$_6$H$_4$·CH : NR)$_2$.
1, R=*n*-Butyl, in ethanol (----)
2, R=*n*-Butyl, in pyridine (——)
3, R=*s*-Butyl, in ethanol (·····)
4, R=*s*-Butyl, in pyridine (—·—)

these *n*-alkyl-derivatives in pyridine, which are quite different from the spectra of the same compounds in non-donor solvents, may be interpreted as those of the sexa-co-ordinate cobalt(II) complexes. It may, therefore, be concluded that bis(*N*-*n*-alkyl-salicylideneiminato)cobalt(II) complexes in pyridine combine with two additional pyridine molecules to form sexa-co-ordinate complexes of cobalt(II). In agreement with this seems to be a fact that the recrystallization from pyridine of these cobalt(II) complexes yields crystals of the compounds with two molecules of pyridine per formula, molecules which are most probably bound with the cobalt(II) ion.

The absorption band at about 30×10^{13} sec^{-1} is assigned to the $^4T_{1g} \rightarrow {}^4T_{2g}$ transition, and the absorption band at about 53.6×10^{13} sec^{-1}, to the $^4T_{1g}(F) \rightarrow {}^4T_{1g}(P)$ transition, on the basis of the notation of the O_h field symmetry.

On the contrary, the *N*-α-branched alkyl complexes keep their tetrahedral configuration in pyridine, since their spectra in pyridine are closely similar to their spectra in non-donor solvents (Fig. 4) and since they give no pyridine adducts on recrystallization from pyridine. This behavior is considered to be due partly to the steric condition originating from the branched alkyl groups, which prevent a pyridine molecule from combining with the cobalt(II) ion to a greater or lesser extent. This behavior also shows that the tetrahedral configuration is more favored for cobalt(II) than for nickel(II), since bis(*N*-isopropyl-salicylideneiminato)nickel(II) in pyridine, for example, is sexa-co-ordinate with the solvent molecules combined.[12] It is worth noting that this is exactly the case with the cyclohexyl-derivative. Bis(*N*-cyclohexyl-salicylideneiminato)cobalt(II) in pyridine does not keep a tetrahedral configuration, but probably forms a quinque-co-ordinate complex of cobalt(II), with a molecule of pyridine as one of the ligands.[13]

Tris(*N*-*n*-alkyl-salicylideneiminato)cobalt(III). —The electronic spectra of tris(*N*-*n*-alkyl-salicylideneiminato)cobalt(III) complexes, which are very stable in the atmosphere, are quite similar to each other. Only some of them are, therefore, shown in Fig. 5. The spectra

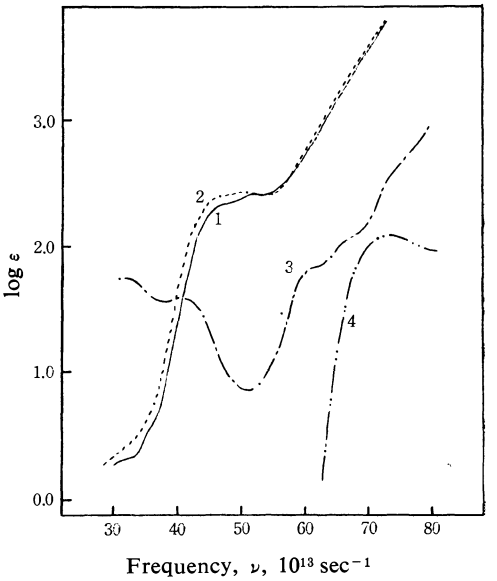


Fig. 5. Electronic absorption spectra of:
1, Co(O·C$_6$H$_4$·CH : N·CH$_3$)$_3$, in benzene (——);
2, Co(O·C$_6$H$_4$·CH : N·*n*-C$_3$H$_7$)$_3$, in benzene (----);
3, Co(O·C$_6$H$_4$·CH : N·*n*-C$_3$H$_7$)$_2$, in ethanol (—·—);
4, HO·C$_6$H$_4$·CH : N·CH$_3$, in chloroform (—··—).

12) S. Yamada and H. Nishikawa, unpublished.
13) The pyridine solution of the cyclohexyl-substituted complex obeys Beer's law; therefore, an equilibrium between the original complex and the pyridine adduct seems to be non-existent. Upon recrystallization from pyridine, this cobalt(II)-complex yields an adduct with one molecule of pyridine. The details will be presented later elsewhere.

of these complexes, which are quite different from the spectra of the cobalt(II)-complexes with the corresponding Schiff bases show, a ligand-field band at about $50\times10^{13}\,sec^{-1}$, a band which is assigned to the $^1A_{1g}\rightarrow{}^1T_{1g}$ transition in the notation of the O_h field symmetry. Judging from the maximum frequency of this band, the Schiff bases of this type stand a little higher than water and acetylacetonate, but much lower than ammonia in the spectrochemical series.

Bis(*N*-α-branched alkyl-salicylideneiminato)-cobalt(II) is stable in solution as well as in the solid state. An ordinary procedure of refluxing cobalt(II) acetate, salicylaldehyde and one of the α-branched alkyl amines in the atmosphere yields the cobalt(II)-complex, but no cobalt(III)-complex. So far, all attempts with α-branched alkyls as a substituent, even those using oxidizing agents, to prepare tris-(*N*-alkyl-salicylideneiminato)cobalt(II) have been unsuccessful. This is probably due to the steric condition. This also shows the relatively high stability of the tetrahedral configuration for bis(*N*-α-branched alkyl-salicylideneiminato)cobalt(II).

The Relative Stability of Tetrahedral Cobalt(II) Complexes.—The tetrahedral bis(*N*-*n*-alkyl-salicylideneiminato)cobalt(II) complexes are much more easily oxidized to give tris(*N*-*n*-alkyl-salicylideneiminato)cobalt(III) than the corresponding *N*-aryl-substituted cobalt(II)-complexes. Thus, by refluxing cobalt acetate, salicylaldehyde and one of the *n*-alkyl amines in the atmosphere, the cobalt(III) complexes of the Schiff bases are obtained in the form of dark green crystals, while a similar procedure using aromatic amines instead of the *n*-alkyl amines yields red crystals of the cobalt(II) complexes of the corresponding Schiff bases. Moreover, when heated on a water-bath, tris-(*N*-aryl-salicylideneiminato)cobalt(III)-complexes in solution convert themselves into the cobalt(II)-complexes, while tris(*N*-*n*-alkyl-salicylideneiminato)cobalt(III)-complexes do not.

This difference between *n*-alkyl and aromatic amines may be due partly to the steric factor, which destabilizes the octahedral tris(*N*-aryl-salicylideneiminato)cobalt(III)-complexes. This fact also seems to show that the *N*-*n*-alkyl-salicylideneiminate yields a stronger ligand field than the *N*-aryl-salicylideneiminate ion, since it is known that the higher stability of the sexa-co-ordinate cobalt(III)-complex is attained with ligands producing a stronger ligand field.

The stability of the quadri-co-ordinate cobalt(II)-complex to oxidation by atmospheric oxygen seems to be correlated with the strength of the field produced by the ligands. Inspection shows that, in the spectrochemical series, water as ligand lies on the border above which the cobalt(III)-complex is more stable than the cobalt(II)-complex in the atmosphere. Thus the hexaquo-cobalt(III)-complex is known although it readily changes into the hexaquo-cobalt(II)-complex. On the other hand, the acetylacetonate ion, which is just above water in the series, forms a stable cobalt(III)-complex, but its cobalt(II)-complex is readily oxidized to yield the cobalt(III)-complex in the atmosphere, unless sexa-co-ordinate diaquo-bis(acetylacetonato)cobalt(II) is formed. Since *N*-alkyl- or *N*-aryl-salicylideneiminate ions lie slightly above water and acetylacetonate in the spectrochemical series, the observed stability of *N*-substituted salicylideneiminato-cobalt-complexes is found to be understandable in terms of the strength of the ligand field. Inspection also reveals that those ligands, such as halide and isothiocyanate, which stand below acetylacetonate in the spectrochemical series form tetrahedral cobalt(II)-complexes which are stable in the atmosphere, unless sexa-co-ordinate complexes are formed.

Bis(*N*-benzyl-salicylideneiminato)cobalt(II).—Bis(*N*-benzyl-salicylideneiminato)cobalt(II) in non-donor solvents shows an absorption spectrum quite similar to the spectra of the other cobalt(II)-complexes which have been concluded to be tetrahedral (Fig. 3). It may similarly be concluded that the *N*-benzyl-substituted complex of cobalt(II) has a tetrahedral co-ordination.

The compound is comparatively stable to oxidation in the atmosphere. The stability of the complex to oxidation seems to lie between that of the *N*-*n*-alkyl and *N*-α-branched alkyl derivatives, as may be inferred from the following properties of these complexes: 1) The *N*-benzyl-substituted cobalt(II) is considerably stable in the atmosphere, while the *N*-*n*-alkyl-derivatives of cobalt(II) are very susceptible to the atmospheric oxygen and are likely to give the cobalt(III)-complexes. When left in the air for a long time, however, the *N*-benzyl-derivative of cobalt(II) undergoes oxidation to the cobalt(III) state. 2) In the typical procedure using cobalt(II) acetate, salicylaldehyde and benzyl amine in the atmosphere, bis(*N*-benzyl-salicylideneiminato)cobalt-(II) is formed as red crystals; on prolonged heating these crystals are changed into dark green crystals of tris(*N*-benzyl-salicylideneiminato)cobalt(III).

This behavior may be regarded as showing that the field of *N*-benzyl-salicylideneiminate to the metal ion is weaker than that of the *N*-alkyl-substituted one but stronger than that of the *N*-aryl-substituted one.

Summary

A novel method has been described for preparing bis(*N*-*n*-alkyl-salicylideneiminato)cobalt(II), where *n*-alkyl represents methyl, ethyl, *n*-propyl, *n*-butyl and higher alkyls. Bis(*N*-α-branched alkyl-salicylideneiminato)cobalt(II)-complexes have been prepared by a simpler method, where α-branched alkyl denotes isopropyl, 1-ethylpropyl, *s*-butyl, *t*-butyl and cyclohexyl. The benzyl derivative has also been prepared. Tris(*N*-*n*-alkyl-salicylideneiminato)cobalt(III) complexes have been prepared.

On the basis of electronic absorption spectra, it has been concluded that bis(*N*-alkyl-salicylideneiminato)cobalt(II)-complexes have a tetrahedral configuration, whether the alkyl used as a substituent represents an *n*-alkyl or an α-branched alkyl.

The relative stability and the configuration of cobalt(II)-complexes have been discussed.

The present authors are grateful to the late Professor Ryutaro Tsuchida for his interest in this work, and to Professor Yoshiharu Izumi and Dr. Kensaku Morihara of the Protein Research Institute for advice about the syntheses of some of the ligands. Special thanks are also due to Professors Tokuichi Tsumaki and Juitsu Endo for their painstaking and pioneering work in this field of co-ordination chemistry. This work was supported in part by the Ministry of Education.

Department of Chemistry
Faculty of Science
Osaka University
Nakanoshima, Osaka

*Thermogravimetric Analysis of Polyoxymethylene**

By Shoichi IGARASHI,** Itaru MITA and Hirotaro KAMBE

(Received February 11, 1964)

Several studies[1,2] of the thermal decomposition of polyoxymethylene in the bulk state have been made; in them the weight loss of the polymer has been measured during its degradation at a constant temperature in the 100~350°C range. Recently, Dudina and his co-workers[3-7] have also extensively studied the thermal and thermo-oxidative degradation of polyoxymethylene. However, there has been little attempt to make a thermogravimetric analysis (TGA) of polyoxymethylene. In this technique the temperature of the polymer is elevated at a constant rate until the sample decomposes completely; then the general character of the thermal degradation process and the thermal stability of the polymeric materials can be determined.

The data presented in this paper are based largely on the thermogravimetric analysis of polyoxymethylene, acetylated polyoxymethylene and commercial Delrin resin, both in air and in nitrogen. The derivative thermogravimetric analysis (DTGA) curves of the three samples show two peaks in each case. In order to clarify the above observations, the effect of the concentration of oxygen on the DTGA curve was also investigated. From the TGA in a vacuum, some knowledge of the volatility of pyrolysates and their thermal decomposition character in a very low concentration of oxygen has been obtained.

It has been found that the first stage is due to the chain depolymerization as well as to the oxidative decomposition and that the second stage is to be attributed to the random degradation of a stable fragment formed during first-stage decomposition. Moreover, an increase of carbonyls in the polyoxymethylene as a result of the degradation has been confirmed by the infrared absorption method.

Experimental

Materials.—The polyoxymethylene ($[\eta]=1.6$ g./

* Presented in part at the 15th Annual Meeting of the Chemical Society of Japan, Kyoto, April, 1962.

** Central Research Laboratories, Toyo Rayon Company, Ltd., Sonoyama, Otsu, Shiga.

1) C. E. Schweitzer, R. N. MacDonald and J. O. Punderson, *J. Appl. Polymer Sci.*, **1**, 158 (1959).
2) W. Kern and H. Cherdron, *Makromol. Chem.*, **40**, 101 (1960).
3) L. A. Dudina and N. S. Enikolopyan, *Vysokomolek. Soed.*, **5**, 861 (1963).
4) L. A. Dudina and N. S. Enikolopyan, ibid., **5**, 986 (1963).
5) L. A. Dudina and N. S. Enikolopyan, ibid., **5**, 1135 (1963).
6) L. A. Dudina, L. V. Karmilova and N. S. Enikolopyan, ibid., **5**, 1160 (1963).
7) L. A. Dudina, L. A. Agayants, L. V. Karmilova and N. S. Enikolopyan, ibid., **5**, 1245 (1963).

100 ml. in *p*-chlorophenol at 60°C) used in this work was supplied by the Toyo Rayon Co., Ltd. It was free from additives. The acetylation of polyoxymethylene was carried out using acetic anhydride and sodium acetate at 139°C.[1] Commercial Delrin 5000X was also used without further purification.

Apparatus. — The automatic recording thermobalance[8] used in this work consists of a tungsten spring balance and a linear variable differential transformer to detect the elongation of the spring. The temperature of the furnace regulated by a program controller.

Procedure. — A weighed quantity of polymer (eigher 100 mg. or 10 mg.) was placed in a glass crucible with a diameter of 12 mm. and a depth of 10 mm. The weight loss of the polymer was recorded against the time using the automatic recording thermobalance while the sample was heated at the rate of about 1°C/min. or, in some cases, at 0.5°C/min., from room temperature to about 350°C in various concentrations of oxygen. The DTGA curves were obtained by the graphical differentiation of the weight loss versus the temperature curves.

The isothermal decomposition of polyoxymethylene was conducted in nitrogen at temperatures ranging from 200 to 240°C and in air at 177~225°C.

The infrared spectra were recorded with a Shimadzu IR-2A spectrophotometer. The sample, decomposed partially during the thermogravimetric measurements, was used after having been rapidly cooled to room temperature. The infrared analysis was carried out by using potassium bromide pellets.

Results

Thermogravimetric Analysis in Nitrogen and in Air.—The TGA curves of polyoxymethylene, acetylated polyoxymethylene and Delrin using a sample of 100 mg. in nitrogen are shown in Fig. 1. All of these polymers show two peaks in each DTGA curve. Polyoxymethylene alone shows a large peak at 200°C, whereas the others exhibit no large weight loss in this temperature. The temperature at which the sample decomposes completely becomes higher in the order of polyoxymethylene, acetylated polyoxymethylene and Delrin.

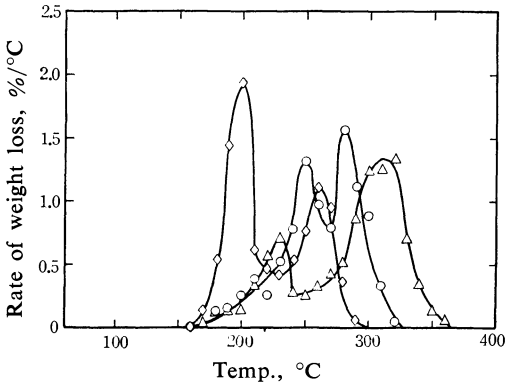


Fig. 1. Thermogravimetric analysis curves for polyoxymethylene (POM), acetylated polyoxymethylene (POMAc) and Delrin in nitrogen atmosphere.
◇ POM, ○ POMAc, △ Delrin 5000X

The DTGA curves of these polymers using a sample of 100 mg. in air are shown in Fig. 2. In each curve of these polymers, two peaks were observed, as in nitrogen. However, both polyoxymethylene and acetylated polyoxymethylene showed a large weight loss over the range from 150 to 200°C. In the case of oxidative decomposition, the completely decomposing temperature is the highest for Delrin and the lowest for polyoxymethylene.

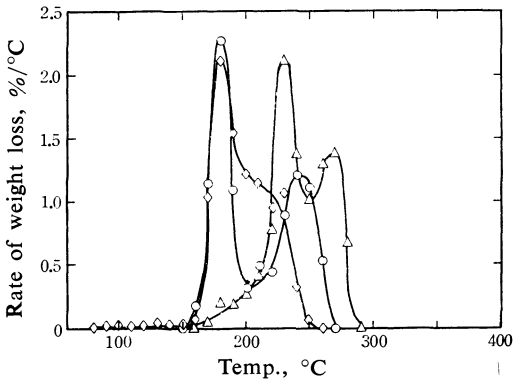


Fig. 2. Thermogravimetric analysis curves for polyoxymethylene (POM), acetylated polyoxymethylene (POMAc) and Delrin in air.
◇ POM, ○ POMAc, △ Delrin 5000X

Isothermal Decomposition of Polyoxymethylene in Nitrogen and in Air.—The thermal decomposition of polyoxymethylene was isothermally studied at temperatures in the 200~240°C range. The plot of the logarithm of the weight loss of the sample against the time in nitrogen is shown in Fig. 3. A deviation of the reaction rate from the first-order law was observed. The decomposition seems to occur in two stages.

The plot of the logarithm of the weight loss of the sample against the time at various temperatures in air is shown in Fig. 4. In this case, no simple straight line was observed; accordingly, the oxidative decomposition is more complex than the thermal decomposition in a nitrogen atmospher (cf. Fig. 3).

Effect of the Concentration of Atmospheric Oxygen on Thermal Decomposition. — As has been mentioned above, the thermal decomposition of polyoxymethylene is significantly affected by the concentration of oxygen.

8) H. Kambe and S. Igarashi, *Rept. Aeronaut. Res. Inst., Univ. Tokyo*, **28**, 145 (1963).

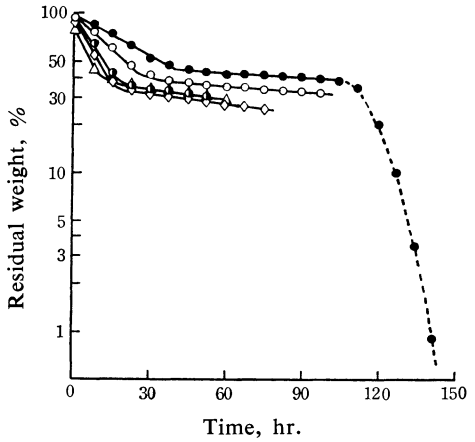


Fig. 3. Thermal decomposition of polyoxymethylene in nitrogen at various temperatures.
Broken line; at 300°C
● 200°C, ○ 210°C, ◑ 220°C
◇ 230°C, △ 240°C

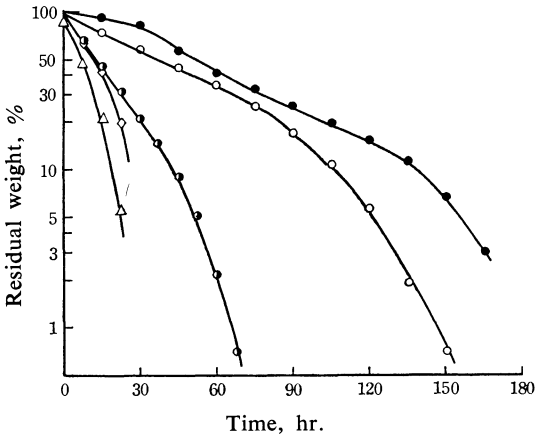


Fig. 4. Thermal decomposition of polyoxymethylene in air at various temperatures.
● 177°C, ○ 185°C, ◑ 200°C
◇ 215°C, △ 225°C

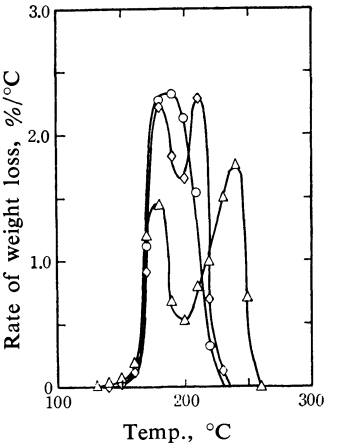


Fig. 5. Thermal decomposition of polyoxymethylene in various concentrations of oxygen.
(△) 0.24 mol. %; (◇) 5.6 mol. %;
(○) 21.0 mol. %

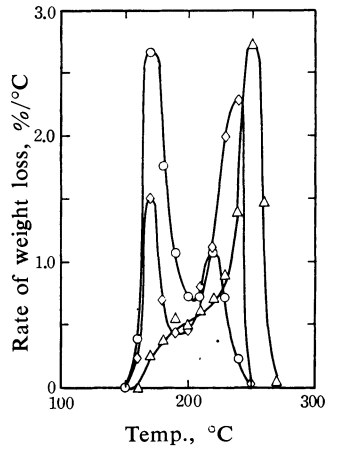


Fig. 6. Thermal decomposition of acetylated polyoxymethylene in various concentrations of oxygen.
(△) 0.24 mol. %; (◇) 5.6 mol. %;
(○) 21.0 mol. %

Therefore, TGA measurements were performed in various concentrations of oxygen. The typical curves for the decomposition of polyoxymethylene shown in Fig. 5 indicate a significant difference between the DTGA curves. The weight loss at the first stage, from 150 to about 200°C, increases with the concentration of oxygen. The weight of the sample used in these measurements was about 10 mg. From Figs. 2 and 5, the weight loss at the first stage for experiments using a sample of 10 mg. may be seen to have been greater than for measurements using a sample of 100 mg. in air (i.e., 21.0 mol. % of oxygen). This will be discussed furthere below.

The DTGA curves for the decomposition of acetylated polyoxymethylene are shown in Fig. 6. The weight loss at the first stage, from 150 to about 200°C, increases with the concentration of oxygen. The weight losses at the first stage in the decomposition for polyoxymethylene and its acetylated sample calculated from Figs. 5 and 6 are plotted against the concentration of oxygen in mole per cent in Fig. 7. The weight loss of the first peak for both samples increases clearly with the concentration of oxygen, and the weight loss for polyoxymethylene is greater than that for acetylated polyoxymethylene.

The effects of the concentration of oxygen on the thermal decomposition of polyoxymethylene and acetylated polyoxymethylene are listed in Table I.

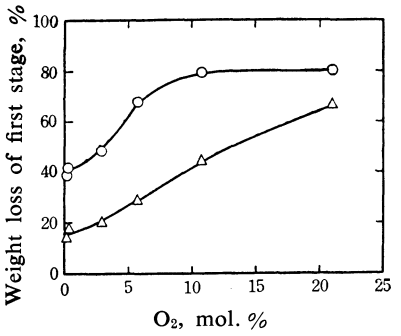


Fig. 7. Effect of the concentration of oxygen on the first stage of thermal decomposition of polyoxymethylene (POM) and acetylated polyoxymethylene (POMAc).
(○) POM, (△) POMAc

TABLE I. EFFECT OF THE CONCENTRATION OF OXYGEN ON THE FIRST STAGE OF THERMAL DECOMPOSITION

Oxygen in the atmosphere	Polyoxymethylene		Acetylated polymer	
	Wt. loss at the 1st stage	Temp. range	Wt. loss at the 1st stage	Temp. range
mol. %	%	°C	%	°C
21.0[a]	80.8	130~200	66.6	150~200
10.8	79.5	130~200	44.7	150~190
5.6	67.8	130~200	28.8	150~190
2.9	47.9	130~200	20.1	150~200
0.24[b]	41.9	130~200	17.5	150~200

a) In air.
b) In nitrogen.

Thermogravimetric Analysis in a Vacuum.—We consider that the effect of oxygen on the decomposition of polyoxymethylene can be eliminated by carrying out the thermogravimetric measurements in a vacuum. The DTGA curves of polyoxymethylene and acetylated polyoxymethylene in a vacuum are shown in Fig. 8. Polyoxymethylene shows a sharp peak at about 180°C and a second peak over the range from 200 to 330°C. For polyoxymethylene, there is no significant difference between the curve obtained at 1°C/min. and that at 0.5°C/min.

Acetylated polyoxymethylene shows two peaks in the DTGA curves; the former is in the region from 150 to 200°C, and the latter, from 200 to 340°C. Moreover, the first peak is smaller than the second one.

The TGA results obtained in the several atmospheres are summarized in Table II.

Infrared Analysis of Partially-Degraded Polyoxymethylene.—Infrared analysis was carried out for polyoxymethylene heated from room temperature to a desired maximum temperature. A great change in the infrared spectra

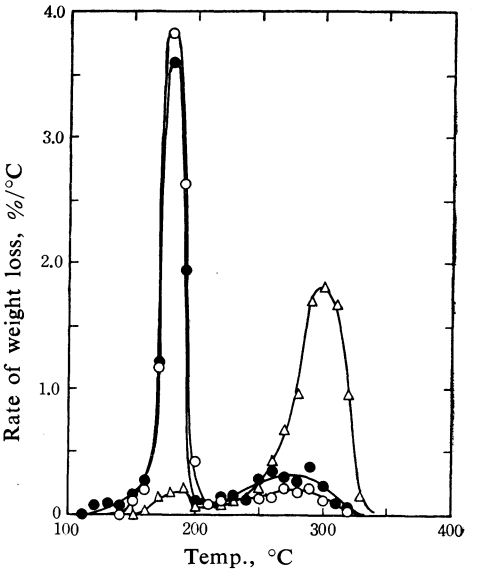


Fig. 8. Thermogravimetric analysis curves for polyoxymethylene (POM) and acetylated polyoxymethylene (POMAc) in a vacuum at different heating rates.
○ POM 1°C/min., ● POM 0.5°C/min.
△ POMAc 1°C/min.

TABLE II. THERMOGRAVIMETRIC ANALYSIS OF POLYOXYMETHYLENE AND ACETYLATED POLYOXYMETHYLENE

	Wt. loss at the 1st stage %	Wt. loss at the 2nd stage %	Temp. range °C	Energy of activation[a] kcal./mol.	Residue %
Polyoxymethylene					
In air[b]	80.8		130~200	40	0
		19.2	200~230		
In N_2[c]	41.9		130~200	45	0
		58.1	200~260	43	
In vacuum	84.7		140~210	57	0
		15.1	210~320	18	
Acetylated polyoxymethylene					
In air[b]	66.6		150~200		6
		27.4	200~250		
In N_2[c]	17.5		150~200	28	3
		79.5	200~280	37	
In vacuum	6.9		150~210		4
		89.1	210~340	31	

a) Values estimated from the DTGA curves by assuming that the reaction is of the first order.
b) 21.0 mol. % of oxygen, sample weight used is 10 mg.
c) 0.24 mol. % of oxygen, sample weight used is 10 mg.

because of carbonyl groups is observed at the absorption of the 1740 cm^{-} band. The ratio

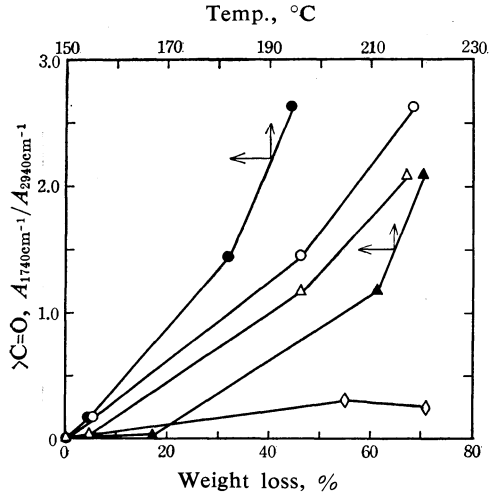


Fig. 9. The increase of carbonyls in polyoxymethylene with the decomposition in the different atmospheres.
○ in air, △ in N_2, ◇ in vacuum

TABLE III. INFRARED ANALYSIS OF DEGRADED POLYOXYMETHYLENE

Atmosphere	Wt. loss	Relative absorbance $A_{1740cm^{-1}}/A_{2940cm^{-1}}$	Maximum temp.
	%		°C
Air	0	0	
	5	0.17	154
	46	1.45	182
	68	2.63	194
Nitrogen	4	0.04	167
	46	1.18	211
	67	2.09	220
Vacuum	55	0.308	230[a]
	71	0.260	250[a]

a) Isothermal decomposition.

of the absorbance at the 1740 cm^{-1} band to that at the 2940 cm^{-1} band is plotted against the weight loss and also against the maximum heated temperature in air and in nitrogen in Fig. 9. The results obtained by infrared analysis are listed in Table III.

Discussion

Thermal Decomposition Character.—Dainton, Ivin and Walmsley,[9] Schweitzer and MacDonald,[1] and Kern and Cherdron,[2] found that the thermal degradation of polyoxymethylene is of the chain-depolymerization type, involving the successive release of formaldehyde from a hydroxyl end group, and that the oxidative degradation may occur at random along the chain. Recent investigation[3] has revealed that the isothermal decomposition of polyoxymethylene occurs in two stages.

As is shown in the DTGA curves in Figs. 1 and 2, polyoxymethylene, acetylated polyoxymethylene and Delrin undergo thermal and oxidative degradation in two stages. The results in Fig. 1 clearly show that the polyoxymethylene with an acetyl end group is thermally more stable than the original polymer with a hydroxyl end group; the weight loss of the former in the 200°C region is smaller than that of the latter. Although polyoxymethylene is stabilized by the acetylation of the hydroxyl end group, the stabilization of the chain ends has a minor effect on the oxidative decomposition, as may be seen in Fig. 2. This means that, in air, the chain scission due to oxidation occurs at random points along the chain. Since the decomposition of polyoxymethylene in the 200°C region occurs also in nitrogen, it may be deduced that its oxidative decomposition in this stage occurs as a combination of random degradation and chain depolymerization. Delrin shows a good thermal stability at temperatures in the above-mentioned region. This may be attributed to the effects of a stabilization of the end group and of an antioxidant added to the polymer upon decomposition.

The two steps of degradation observed by TGA are confirmed by the isothermal decomposition, as is shown in Fig. 3. Each peak in the DTGA curve may correspond to two straight lines in the isothermal decomposition, which is a reaction of the first order. The isothermal decomposition character of polyoxymethylene in air illustrated in Fig. 4 is similar to that reported by Kern.[2]

The effect of the concentration of oxygen on the DTGA curve is shown in Figs. 5 and 6 for polyoxymethylene and acetylated polyoxymethylene, respectively. The weight losses of the first stage in the 200°C region increases with the concentration of oxygen, as Fig. 7 shows. This indicates that the oxidative decomposition occurs more easily as the concentration of oxygen increases. Acetylated polyoxymethylene undergoes the oxidative decomposition entirely, but polyoxymethylene decomposes preferentially at the chain ends in addition to the decomposition which occurs as a result of the random attack of oxygen. This may be a reason why the weight loss of polyoxymethylene is larger than that of acetylated polyoxymethylene.

The thermogravimetric measurements were conducted in a vacuum at 10^{-2} mmHg. The results in Fig. 8 reveal clearly that the

9) F. S. Dainton, K. J. Ivin and D. A. G. Walmsley, *Trans. Faraday Soc.*, 55, 61 (1959).

degradation occurs in two stages in such a low concentration of oxygen. The fraction of the weight loss in the first stage of polyoxymethylene is larger than that obtained in nitrogen at atmospheric pressure (see Table II). The rate of the vaporization of the degradation products from polyoxymethylene will depend on the pressure of the atmosphere. There is no significant difference between the curves obtained at different heating rates, as Fig. 8 shows. Accordingly, it is interesting that the thermal decomposition polyoxymethylene did not all occur in one stage. It is deduced that the second stage of weight loss corresponds to the decomposition of the stable fragments formed during the first stage of degradation. The scission of the main chain of the acetylated polyoxymethylene molecule occurs mainly over the range from 200 to 340°C. The small peak below 200°C is probably to be attributed to the thermal decomposition of an unacetylated polyoxymethylene.

The Mechanism of Decomposition. — The results in Fig. 9 and in Table III show that the carbonyl groups are formed during the decomposition of polyoxymethylene in each atmosphere and that its amount increases with the degree of degradation. The carbonyls are formed even in a vacuum. Since the oxygen remaining in a vacuum had no influence on the DTGA curve, it may be supposed that this formation is due to the interchange of the ether linkage into the carbonyl group (see step II below).

The following mechanism for the thermal decomposition of polyoxymethylene in the absence of oxygen is proposed:

$$\mathrm{HO\text{-}CH_2\text{-}O\text{-}CH_2\text{-}O\text{-}CH_2\text{-}O\text{-}CH_2\text{-}O\text{-}}\sim$$

$$\rightarrow \mathrm{HO\cdot} + \mathrm{\cdot CH_2\text{-}O\text{-}CH_2\text{-}O\text{-}CH_2\text{-}O\text{-}CH_2\text{-}O\text{-}}\sim \quad \text{(I)}$$

monomer, etc.

$$\sim\mathrm{CH_2\text{-}O\text{-}CH_2\text{-}O\text{-}CH_2\text{-}O\text{-}CH_2\text{-}O\text{-}}\sim$$

$$\rightarrow \sim\mathrm{CH_2\text{-}O\text{-}CH_2\text{-}O\text{-}CH_2\text{-}O\text{-}CH\text{-}O\text{-}}\sim + \mathrm{\cdot H}$$

$$\rightarrow \sim\mathrm{CH_2\text{-}O\text{-}CH_2\text{-}O\text{-}CH_2}$$

$$+\mathrm{O{=}CH\text{-}O\text{-}CH_2\text{-}O\text{-}}\sim \quad \text{(II)}$$

In the light of the above mechanism, it may be deduced that a stable fragment with carbonyl groups at the chain ends decomposes in the second stage in the DTGA curve of polyoxymethylene in a vacuum.

In the presence of oxygen, the following scheme is well known:

$$\sim\mathrm{CH_2\text{-}O\text{-}CH_2\text{-}O\text{-}CH_2\text{-}O\text{-}CH_2\text{-}O\text{-}}\sim + \mathrm{O_2}$$

$$\rightarrow \sim\mathrm{CH_2\text{-}O\text{-}CH_2\text{-}O\text{-}CH_2\text{-}O\text{-}CH(OOH)\text{-}O\text{-}}\sim$$

$$\rightarrow \sim\mathrm{CH_2\text{-}O\text{-}CH_2\text{-}O\text{-}CH_2\text{-}O\text{-}CH(O\cdot)\text{-}O\text{-}}\sim$$

$$+\mathrm{\cdot OH}$$

$$\rightarrow \sim\mathrm{CH_2\text{-}O\text{-}CH_2\text{-}O\text{-}CH_2\text{-}O\text{-}C(=O)H}$$

$$+\mathrm{\cdot O\text{-}CH_2\text{-}O\text{-}CH_2\text{-}}\sim$$

The fact that the quantity of carbonyl groups formed in the decomposition in air is larger than that in nitrogen, as has been mentioned already, reflects the above mechanism for the oxidative degradation of polyoxymethylene.

Effect of Sample Size on the Thermogravimetric Analysis Curve.—It may be seen from Figs. 5 and 6 that the temperature of the second stage is altered to a lower temperature with an increase in the concentration of oxygen. Moreover, it should be noticed that the feature of the DTGA curve is dependent on the weight of the sample used for measuring. For instance, by comparing the curve for polyoxymethylene using a sample of 100 mg. in air (see Fig. 2) with that for polyoxymethylene using sample of 10 mg. in air (i. e., 21.0 mol. % of oxygen in Fig. 5), it is confirmed that the DTGA curve for the oxidative decomposition is greatly affected by the weight of the sample used. A similar effect for the oxidative decomposition of polyethylene has been reported in a previous paper.[10]

Summary

The character of the thermal decomposition of polyoxymethylene, acetylated polyoxymethylene and Delrin in air and in nitrogen has been studied by thermogravimetric analysis. Two peaks have been observed in each atmosphere in the derivative thermogravimetric analysis curves for these samples.

It has been confirmed that the feature of doublet peaks is related to the concentration of oxygen during the decomposition and, thus, that the first stage is due to the chain depolymerization as well as to the oxidative decomposition, and that the second stage is to be attributed to the random degradation of a stable fragment formed during the first stage decomposition.

An increase of carbonyl groups in the polymer molecule with the degradation was confirmed by infrared spectroscopy.

Department of Materials
Aeronautical Research Institute
The University of Tokyo
Komaba, Meguro-ku, Tokyo

10) S. Igarashi and H. Kambe, This Bulletin, 37, 176 (1964).

The Base-catalyzed Condensation of Nitrophenylpyruvates. I. α-Oxo-β-(o-nitrophenyl)-γ-(o-nitrobenzyl)-γ-ethoxycarbonyl-γ-butyrolactone

By Takeo SAKAN, Masahiko KATO, Toshio MIWA and Nobuo NAKAMURA

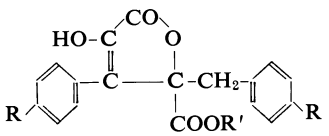
(Received February 11, 1964)

In connection with our synthetic study of the amino acid metabolism, we wished to prepare a quantity of ethyl *o*-nitrophenylpyruvate. The ester had been studied extensively by Wislicenus and Thoma,[1] who prepared it by the condensation of *o*-nitrotoluene with ethyl oxalate in the presence of potassium ethoxide in dry ether.

We attempted, however, to prepare the ester more economically by modifying the DiCarlo method[2] for the acid. *o*-Nitrotoluene was condensed with ethyl oxalate in the presence of sodium ethoxide in boiling ethanol. The reaction mixture was saturated with hydrogen chloride. From a benzene solution of the reaction product, the keto ester was isolated as a bisulfite adduct. When the adduct was decomposed with mineral acid, a crystalline substance, $C_{20}H_{26}O_9N_2$, insoluble in benzene was obtained. This compound usually appeared as needles decomposing at 180°C; however, it was occasionally obtained as rhombi decomposing at 183.5°C. Most of the reactions were carried out with the former.

A comparison of the composition of this compound with that of ethyl *o*-nitrophenylpyruvate indicated that the compound had been formed by the condensation of two moles of the pyruvate with a loss of one mole of ethanol. The enolate anion from the starting ester might attack another mole of the ester, either at the ester carbonyl or at the keto carbonyl, to form a triketo ester I or a ketolactone ester II respectively.

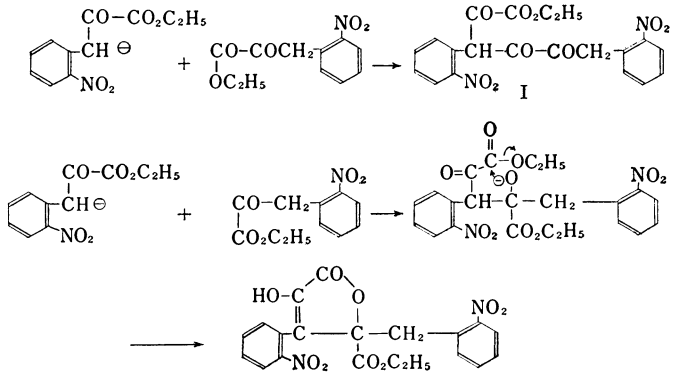
Hemmerlé[3] has found the self-condensation products of phenylpyruvic esters to be α-oxo-β-phenyl-γ-benzyl-γ-alkoxycarbonyl-γ-butyrolactone (III, R=H). Cagniant[4] obtained analogous compounds III (R=NO_2 and CH_3O, R'=H) from *p*-nitro- and *p*-methoxyphenylpyruvic acids.



III

Similarly, the compound obtained here also may probably be expressed by the structure II. This will be established by the following chemical evidence.

The compound II is weakly acidic and soluble in aqueous alkali. The acetylation of II with acetic anhydride gave a monoacetate IV, and treatment with diazomethane yielded



II

1) W. Wislicenus and E. Thoma, *Ann.*, **436**, 42 (1924).
2) F. T. DiCarlo, *J. Am. Chem. Soc.*, **66**, 1420 (1944).
3) R. Hemmerlé, *Ann. chim.*, [9] **7**, 226 (1917).
4) Mme. P. Cagniant, ibid., **7**, 442, 457, 470 (1952).

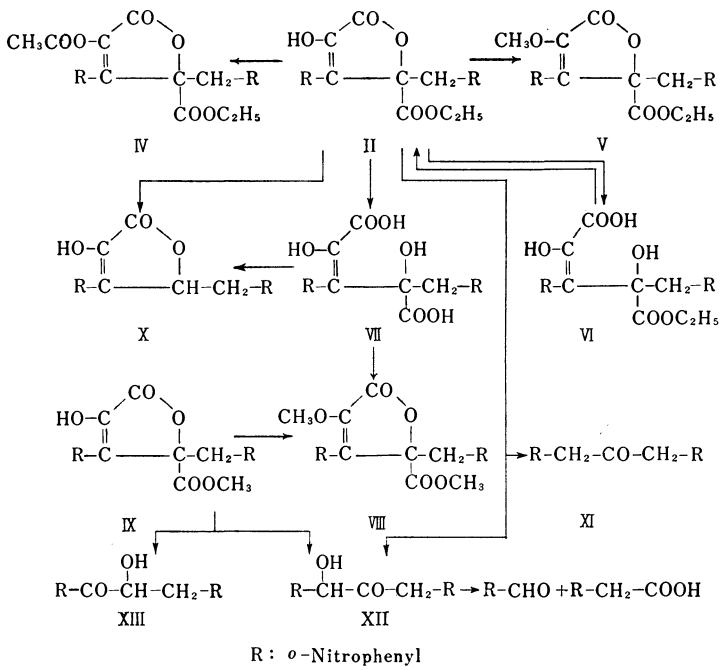


Chart 1.

a monomethyl ether V. They were no longer acidic.

The hydrolysis of II with aqueous sodium hydroxide at room temperature for one and a half hours gave a pale green acid, VI, melting at ca. 95°C.[5] The methylation of the acid VI with diazomethane gave the methyl ether V, while esterification with ethanolic hydrogen chloride formed the original ester II.

In contrast to the above hydrolysis, the hydrolysis of II with aqueous sodium hydroxide at room temperature for 22 hr. gave an acid, VII, decomposing at 144.5~145°C. This acid, on treatment with diazomethane, was changed to a methyl ether VIII (m. p. 169.5~170.5°C), whose composition, $C_{20}H_{16}O_9N_2$, was less by CH_2 than that of the ethyl ester V. The methyl ether VIII was identified with the enol methyl ether of the methyl ester IX which was prepared by the condensation of *o*-nitrotoluene with methyl oxalate under the same conditions as used for the ethyl ester II.

The attempted esterification of the acid VII with ethanolic hydrogen chloride gave a lactone X (m. p. 191~191.5°C), the structure of which was determined on the basis of its composition, $C_{17}H_{14}O_7N_2$, and its infrared spectrum (see Experimental). This compound was still weakly acidic, as was to be expected from its structure, and gave a methyl ether with diazomethane. The hydrolysis of II with a mixture of hydrochloric and acetic acids gave the same compound X; however, the hydrolysis was very hard.

The oxidation of II or IX with alkaline hydrogen peroxide gave various results, as did the alkaline hydrolysis.[5] Three neutral products were isolated. One of them, a ketone XI, $C_{15}H_{12}O_5N_2$, was identified with the 1,3-bis(*o*-nitrophenyl)-2-propanone prepared by the nitration of dibenzyl ketone. The positions of the nitro groups in the synthetic sample were confirmed by permanganate oxidation to *o*-nitrobenzoic acid. The second product, XII ($C_{15}H_{12}O_6N_2$; m. p. 142~143°C), gave a positive Fehling reaction indicative of a ketol function. This compound was assumed to possess the structure XII from the fact that the Treibs oxidation of this compound yielded *o*-nitrobenzaldehyde and *o*-nitrophenylacetic acid. The third product, XIII (m. p. 95°C), was isomeric with the ketol XII and was tentatively assigned the structure of 1,3-bis(*o*-nitrophenyl)-2-propanol-1-one from its infrared spectrum (see Experimental); however, it gave a negative Fehling reaction.

Jarrousse[6] has noted that the α-ketol analogous to XIII obtained by the decarboxylation of an acid that had been obtained by the permanganate oxidation of di-(phenylpyruvic acid) is isomerized readily to the α-ketol corresponding to XII. The fact that no such

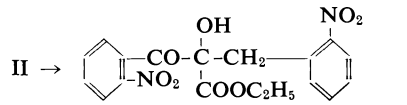
5) The product was erratic, varying in response to slight differences in the reaction conditions, and so was hard to purify.

6) J. Jarrousse, *Ann. chim.*, **9**, 157 (1938).

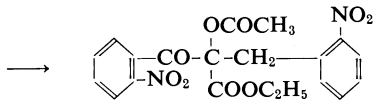
isomerization was observed with the compound XIII made the postulated structure doubtful.

The above transformations of the compound II are summerized in Chart 1.

The permanganate oxidation of II in acetone gave a hydroxy ester XIV (m. p. 131.5~132°C), together with *o*-nitrobenzoic and oxalic acids. This compound gave a negative ferric chloride reaction; its structure was postulated from the composition, $C_{18}H_{18}O_8N_2$, and its infrared spectrum (see Experimental). The acetylation of XIV with acetic anhydride gave an acetate, XV. The acetate was so stable that it was sublimed without decomposition on attempted pyrolysis under reduced pressure.[7]



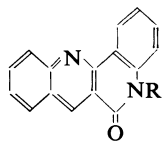
XIV



XV

The hydrolysis of XIV with hydrochloric acid gave *o*-nitrophenylacetic acid in a 69% yield. The mechanism of the unexpected formation of this acid has not been clarified.

The hydrogenation of XIV in the presence of palladium-on-carbon gave yellow crystals melting at 354°C. This compound exhibited an ultraviolet spectrum completely identical with that of 5-methylquino[4, 3-b]quinoline-6(5*H*)-one[8] (XVII) and was assigned the structure of the quinoquinolone XVI.



XVI: R=H
XVII: R=CH_3

Experimental[9]

α-Oxo-β-(*o*-nitrophenyl)-γ(*o*-nitrobenzyl)-γ-ethoxycarbonyl-γ-butyrolactone (II).—Into a sodium ethoxide solution prepared from 23 g. of sodium and 270 cc. of ethanol was added a mixture of 137 g. of *o*-nitrotoluene and 146 g. of diethyl oxalate in one portion with stirring at room temperature. The resulting deep-red mixture was heated while continuously being stirred at 125°C for half an hour. After cooling, the mixture was acidified by bubbling dry hydrogen chloride. The precipitated sodium chloride was filtered off, and the filtrate was concentrated. The residue as a benzene solution was treated with aqueous sodium bisulfite (360 g. in 600 cc. of water) to form a quantity of precipitates. The precipitates were filtered, washed with benzene, and decomposed by treatment with diluted sulfuric acid (90 cc. in 350 cc. of water) and 250 cc. of benzene at 50~60°C for one hour. The insoluble material was then filtered from the cooled mixture (43.8 g.). The benzene layer of the filtrate was diluted with ether and then extracted with 10% aqueous sodium carbonate. The acidification of the extract gave an additional 6.4 g. of the precipitates, which were combined with the above-mentioned insoluble material (total 50.2 g., 23%) and twice recrystallized from ethanol to yield pure ester II as a powder, decomposing at 182~182.5°C. ν_{max} 3330 (OH), 1773, 1698 (C=O or C=C), 1529, 1348, 1335 cm^{-1} (NO_2). (Found: C, 56.07; H, 3.74; N, 6.45. Calcd. for $C_{20}H_{16}O_9N_2$: C, 56.08; H, 3.77; N, 6.54%.) Allowing the mother liquor of recrystallization to evaporate gave a mixture of needles and rhombi; these two forms of crystals were separated by hand. Since the needles (Found: C, 56.21; H, 3.94%), decomposing at 183.5°C, showed the same infrared spectrum as the ester in powder, the ester in powder was assumed to be mainly composed of this form. The rhombi decomposed at 183.5°C (Found: C, 56.18; H, 4.01%). ν_{max} 3330 (OH), 1748 (C=O), 1695 (C=C), 1522, 1355 cm^{-1} (NO_2).

Monoacetate IV.—Heating 0.5 g. of II with acetic anhydride for five hours at 100°C gave 0.5 g. of IV, which, after recrystallization from acetic acid, melted at 170.5~171°C (Found: C, 56.49; H, 3.95; N, 5.97. Calcd. for $C_{22}H_{18}O_{10}N_2$: C, 56.17; H, 3.86; N, 5.96%).

Monomethyl Ether V.—A solution of 1 g. of II in aqueous potassium hydroxide (0.39 g. in 8 cc. of water) was treated with 0.9 g. of dimethyl sulfate to give a yellow oil which solidified in a short time. Extraction with benzene, followed by washing with aqueous sodium carbonate and the evaporation of the solvent, gave yellow plates, which, after three recrystallizations from benzene, melted at 140.5~141.5°C (Found: C, 57.12; H, 4.09; N, 6.53; mol. wt. (Rast): 406. Calcd. for $C_{21}H_{18}O_9N_2$: C, 57.01; H, 4.10; N, 6.33%; mol. wt. 442).

The methylation of 1 g. of II in methanol with diazomethane gave 0.9 g. of the methyl ether V melting at 137~138.5°C. Recrystallization from benzene gave 0.73 g. of a pure material which melted at 137.5~138.5°C. Mixed melting point determination with the above methyl ether did not show any depression.[10]

The Alkaline Hydrolysis of II.—*Carboxylic Acid VI.*—A solution of II (2 g.) in 23 cc. of N aqueous sodium hydroxide was allowed to stand

7) Steric circumstances might hinder the formation of a six-membered-ring transition state favorable for pyrolysis.

8) J. T. Braunholtz and F. G. Mann, *J. Chem. Soc.*, **1955**, 381.

9) All melting points are uncorrected. The infrared spectra were measured in Nujol mull and are expressed in ν_{max} cm^{-1}. The authors are much indebted to Mr. Jun'ichi Gōda and his associates for their elementary analyses and to Mrs. Michino Butsugan and Miss Hiromi Tokuda for their infrared spectral measurements.

10) The discrepancy between the melting points is due to the use of different thermometers.

for half an hour at room temperature. Acidification with N hydrochloric acid precipitated a pale-green acid, which, after recrystallization from acetic acid-ligroin, decomposed at 95°C, solidified at 100°C, and then decomposed at 159~165°C again. ν_{max} 3300 (OH), 1786, 1695 (C=O).

Carboxylic Acid VII.—Allowing a solution of II in 20 cc. of 2 N sodium hydroxide to stand for 22 hr. at room temperature gave an acid VII, which, after three recrystallizations from acetic acid-ligroin, decomposed at 152.5°C. (Found : C, 52.64; H, 3.04; N, 6.80. Calcd. for $C_{18}H_{14}O_{10}N_2$: C, 51.68; H, 3.37; N, 6.70%).

The Attempted Esterification of the Acid VI with Ethanolic Hydrogen Chloride.—Into a solution of 200 mg. of acid VI in 5 cc. of dry ethanol hydrogen chloride was bubbled for half an hour, and then the mixture was refluxed for 40 min. After the removal of the solvent, the residue was dissolved in ether, washed with aqueous sodium bicarbonate and water successively, and dried. The distillation of the ether left a colorless powder, decomposing at 182~183°C, in a quantitative yield. It was identified with II by admixture test and infrared comparison.

The Methylation of the Acid VI with Diazomethane.—The methylation of VI with methanolic diazomethane afforded a neutral compound melting at 146.5~147°C, which was identified with the methyl ether V by mixed melting determination and infrared comparison.

The Attempted Esterification of the Acid VII with Ethanolic Hydrogen Chloride. — *α-Oxo-β-(o-nitrophenyl)-γ-(o-nitrobenzyl)-γ-butyrolactone (X).* — A suspension of 0.14 g. of VII in 4 cc. of dry ethanol was refluxed for 30 min. while hydrogen chloride was being introduced. Rubbing the neutral fraction with benzene-ethanol gave 88 mg. of crystals, which, after recrystallization from ethanol, melted at 187~189°C. ν_{max} 3300 (OH), 1745 (C=O), 1695 cm^{-1} (C=C).

Found : C, 57.59; H, 3.36; N, 7.64. Calcd. for $C_{17}H_{12}O_7N_2$: C, 57.31; H, 3.40; N, 7.86%.

α-Oxo-β-(o-nitrophenyl)-γ-(o-nitrobenzyl)-γ-methoxycarbonyl-γ-butyrolactone (IX). — Into a sodium methoxide solution prepared from 11.5 g. of sodium and 94 cc. of methanol, 59 g. of dimethyl oxalate and then 68.5 g. of *o*-nitrotoluene were added. The mixture was refluxed vigorously for 20 min. and acidified by the introduction of dry hydrogen chloride. After the removal of salt by filtration and that of the solvent by evaporation, the residue was treated with ice and benzene to separate a yellow, insoluble material. The benzene layer, after filtration, was extracted with three portions of 10% aqueous sodium carbonate, and the extract was acidified with 2 N hydrochloric acid to give reddish brown precipitates, which were combined with the above-obtained, insoluble material and recrystallized from ethanol to yield colorless crystals decomposing at 185~186°C. (Found : C, 55.31; H, 3.62; N, 7.03. Calcd. for $C_{19}H_{14}O_9N_2$: C, 55.07; H, 3.38; N, 6.76%.)

α-Methoxy-β-(o-nitrophenyl)-γ-(o-nitrobenzyl)-γ-methoxycarbonyl-$\Delta^{\alpha,\beta}$-butenolide (VIII).—*The Methylation of the Acid VII with Diazomethane.*—The methylation of VII with diazomethane in methanol gave a methyl ether melting at 169.5~170.5°C. (Found : C, 56.29; H, 4.03; N, 6.83. Calcd. for $C_{20}H_{16}O_9N_2$: C, 56.08; H, 3.77; N, 6.54%.) This methyl ether was identified with the methyl ether VIII synthesized below by the admixture test and by an infrared spectral comparison.

The Methylation of Compound IX.—The methylation of IX with methanolic diazomethane gave a methyl ether which, after recrystallization from benzene, melted at 167°C.

The Oxidation of Compound II or IX with Alkaline Hydrogen Peroxide.—*The Formation of 1, 3-Bis(o-nitrophenyl)-2-propanone.*—A solution of 2 g. of II in 20 cc. of N sodium hydroxide was treated with 40 cc. of 30% hydrogen peroxide. An exothermic reaction occurred. The mixture was allowed to stand overnight, and was then acidified and extracted with ether. The ether extract, after being washed with aqueous sodium bicarbonate, gave yellow crystals, which, after recrystallization from ethanol, melted at 136~137°C. This material was identified with the specimen synthesized below by the admixture test and by a comparison of the infrared spectra.

The Formation of Compound XII.—A solution of 1 g. of II in 5 cc. of N sodium hydroxide was left to stand with 20 cc. of 30% hydrogen peroxide for two days. Within one hour the mixture became cloudy. After extraction with ether, an additional amount of N sodium hydroxide was added to the aqueous layer to cause an exothermic reaction. The mixture was then allowed to stand overnight and extracted with ether. The combined ether extracts were shaken with aqueous sodium bicarbonate. The aqueous layer was acidified with hydrochloric acid and extracted with ether again. The extract, after the removal of the solvent, left a yellow oil, which solidified and was repeatedly recrystallized from ethanol to give the ketol XII, melting at 142~143°C. This compound reduced the Fehling solution. ν_{max} 3480 (OH), 1727 cm^{-1} (C=O). (Found : C, 57.44; H, 3.93; N, 8.64. Calcd. for $C_{15}H_{12}O_6N_2$: C, 56.96; H, 3.82; N, 8.86%.)

The Formation of Compound XIII.—A solution of 3 g. of compound IX in 60 cc. of N sodium hydroxide was allowed to stand for 50 min. and then treated with 2 cc. of 30% hydrogen peroxide. The mixture was left overnight and then acidified to give 2.39 g. of precipitates decomposing at 151~159°C. The precipitates were dissolved in 12 cc. of N sodium hydroxide and treated with 48 cc. of hydrogen peroxide. After the mixture had been left to stand overnight, it was acidified to give precipitates, which afforded 0.81 g. of an acid fraction and 0.98 g. of neutral fraction. The acid fraction was treated with hot benzene. The benzene-soluble acid (0.21 g.) melted at 131~134°C and was identified with *o*-nitrophenylacetic acid. The benzene-insoluble fraction was methylated with diazomethane to give a compound melting at 166°C, which was identified with the methyl ether VIII. The neutral fraction was recrystallized from benzene to give 0.25 g. of a compound melting at 138~141°C, which was found to be identical with the compound XII obtained above. From the mother

liquor of the recrystallization compound XIII (m. p. 95°C) was obtained. This compound did not reduce the Fehling solution. ν_{max} 3380 (OH), 1705 cm^{-1} (C=O).

Found: C, 57.34; H, 3.93; N, 8.34. Calcd. for $C_{15}H_{12}O_6N_2$: C, 56.96; H, 3.82; N, 8.86%.

1, 3-Bis(*o*-nitrophenyl)-2-propanone.—Into 4 g. of fuming nitric acid (d=1.53) was added a mixture of 2 g. of dibenzyl ketone and 4 g. of acetic anhydride at −3∼−5°C with stirring. After 40 min. the mixture was poured onto ice, and the resulting oil was extracted with benzene. The benzene extract was washed successively with aqueous sodium bicarbonate and water, followed by drying and chromatography on active alumina. The first fraction eluted with benzene yielded colorless plates (450 mg.), which, after recrystallization from ethanol, melted at 141∼141.5°C. (Found: C, 60.23; H, 4.06; N, 9.31. Calcd. for $C_{15}H_{12}O_5N_2$: C, 60.00; H, 4.00; N, 9.33%.) This compound, on oxidation with potassium permanganate in aqueous alkali, produced *o*-nitrobenzoic acid (m. p. 147°C).

The Treibs Oxidation of Compound XII.—Into a warm solution of XII in 2 cc. each of methanol and ethanol was added one drop of a vanadium pentoxide solution, prepared from 100 mg. of vanadium pentoxide and 5 cc. of 30% hydrogen peroxide, and then 0.8 cc. of 30% hydrogen peroxide in three portions; white precipitates were thus produced. After the addition of a sufficient amount of acetone to make a clear solution, the solution was left to stand for three days. The solvent was distilled off and the residue, after the addition of water, was extracted with benzene-ether. The acid fraction gave an acid melting at 137.5∼138°C, which was identified with *o*-nitrophenylacetic acid by mixed melting point determination. The neutral fraction was converted to a 2, 4-dinitrophenylhydrazone decomposing at 235∼250°C, which was identified with that of *o*-nitrobenzaldehyde, decomposing at 250°C, by infrared comparison.

The Permanganate Oxidation of Compound II.—Into a solution of 2.57 g. of II in 400 cc. of acetone 2.53 g. of potassium permanganate was added in one portion, and then the mixture was stirred for 7 hr. at room temperature. The acetone solution, after the filtration of manganese dioxide and the distillation of the solvent, gave 1.66 g. of a residue, which, after recrystallization from benzene-ligroin, melted at 131.5∼132°C. ν_{max} 3485 (OH), 1730 (shoulder), 1712 cm^{-1} (C=O). (Found: C, 55.87; H, 4.30; N, 7.21. Calcd. for $C_{15}H_{16}O_8N_2$: C, 55.67; H, 4.15; N, 7.21%.)

Acetate XV.—A mixture of 0.5 g. of XIV and 5 cc. of acetic anhydride was heated for one hour in the presence of one drop of concentrated sulfuric acid to give a crude acetate in a quantitative yield. Two recrystallizations from ethanol provided the pure acetate melting at 129°C. ν_{max} 1745, 1705 cm^{-1} (C=O) (Found: C, 56.33; H, 4.38; N, 6.70; mol. wt. (Rast), 423. Calcd. for $C_{20}H_{18}O_9N_2$: C, 55.81; H, 4.22; N, 6.51%; mol. wt., 430).

The Hydrolysis of XIV.—A mixture of 400 mg. of XIV, 100 cc. of 2 N hydrochloric acid and 30 cc. of acetic acid was boiled under reflux for 18 hr. The acid fraction gave 100 mg. of *o*-nitrophenylacetic acid (m. p. 136.5°C). The neutral fraction gave 88 mg. of the recovered XIV.

The Hydrogenation of XIV.—A solution of 200 mg. of XIV in 40 cc. of acetic acid was hydrogenated in the presence of 40 mg. of palladium-on-carbon under ordinary pressure. Six molar equivalents of hydrogen were absorbed in 5 hr., 20 min. After the catalyst had been removed, the solvent was distilled under reduced pressure to give 170 mg. of a yellow powder, which, after recrystallization from acetic acid, decomposed at 354°C. The analytical sample was purified by sublimation at 270°C/10 mmHg. ν_{max} 3175 (NH), 1667cm^{-1} (C=O). λ_{max}^{EtOH} mμ (log ε): 227 (4.54), 233 (4.52), 274 (4.82), 290 (4.36), 362 (3.66). (Found: C, 77.68; H, 4.33; N, 12.34. Calcd. for $C_{16}H_{10}ON_2$: C, 78.03; H, 4.09; N, 11.38%.)

Faculty of Science
Osaka City University
Sumiyoshi-ku, Osaka

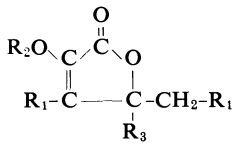
The Base-catalyzed Condensation of Nitrophenylpyruvates. II. The Absorption Spectra of α-Oxo-β-aryl(or alkyl)-γ-aryl-methyl(or alkyl)-γ-ethoxycarbonyl-γ-butyrolactones

By Takeo SAKAN, Masahiko KATO and Toshio MIWA

(Received February 11, 1964)

In the preceding paper,[1] the base-catalyzed condensation of ethyl *o*-nitrophenylpyruvate (in situ) was reported to give a dimeric condensate, the structure of which was confirmed by chemical means to be α-oxo-β-(*o*-nitrophenyl)-γ-(*o*-nitrobenzyl)-γ-ethoxycarbonyl-γ-butyrolactone (I). However, the infrared spectra of this compound and its derivatives do not agree, in some respects, with their structures. In order to make a correct interpretation of the spectra, those compounds in which the two *o*-nitrophenyl groups in compound I had been substituted with two methyl or two phenyl groups were prepared and their absorption spectra were comparatively examined. Table I lists the compounds used in this study and the references for their preparation.[2,3]

TABLE I. LIST OF COMPOUNDS



Compd. No.	R_1	R_2	R_3	Ref.
I	*o*-$NO_2C_6H_4$	H	CO_2Et	1
II	Me	H	CO_2Et	2
III	Me	Me	CO_2Et	*
IV	Me	Ac	CO_2Et	2
V	Me	H	H	2
VI	Me	Ac	H	2
VIII	*o*-$NO_2C_6H_4$	Me	CO_2Et	1
IX	*o*-$NO_2C_6H_4$	Ac	CO_2Et	1
X	*o*-$NO_2C_6H_4$	H	H	1
XI	Ph	H	CO_2Et	3
XII	Ph	Me	CO_2Et	3
XIII	Ph	Ac	CO_2Et	*
XIV	Ph	H	H	3

* New compounds.

1) T. Sakan, M. Kato, T. Miwa and N. Nakamura, This Bulletin, **37**, 1161 (1964).
2) J. Monnin, *Helv. Chim. Acta*, **40**, 1983 (1957).
3) R. Hemmerlé, *Compt. rend.*, **162**, 758 (1915); *Ann. chim.*, [9] **7**, 226 (1917).

Infrared Absorption Spectra

The spectral data[4] are listed in Table II. The ester $\nu_{C=O}$ of compounds II, III, and IV appeared in the normal position for esters[5] (1740~1742 cm^{-1}), and there is no such effect of an α-alkoxyl group on carbonyl as that observed by Jones and his co-workers[6] in ketones and by Singh[7] in a lactone. This is probably due to the presence of a double bond in the α, β-position of the lactone. On the other hand, the absorption spectra of II and V, and of IV and VI[8] showed that the $\nu_{C=O}$ due to lactone had shifted by 8~15 cm^{-1} to a higher wave number region in II and IV, apparently due to the presence of an ethoxycarbonyl group. The $\nu_{C=O}$ and ν_{OH} of lactone carbonyl and enol in II and V are split in two, even in a dilute solution; this is considered to show that these compounds are present as a mixture of enols with and without hydrogen bonding,[9] because the intramolecular hydrogen bond of VII-type is a labile five-membered ring.[10] A dicarbonyl type is possible but, since compounds of this type exist completely in the enol type[11] in an aqueous solution (dielectric constant of the solvent: 81[12])[13] and since a

4) Infrared absorption spectra were measured with a Hitachi model EPI-2 infrared spectrophotometer. We are indebted to Miss Hiromi Tokuda for the measurements.
5) L. J. Bellamy, "The Infrared Spectra of Complex Molecules," Methuen & Co., London; John Wiley & Sons, New York (1954), p. 152.
6) R. N. Jones, V. Z. Williams, M. J. Whalen and K. Dobriner, *J. Am. Chem. Soc.*, **70**, 2030 (1948).
7) G. Singh, ibid., **78**, 6109 (1956).
8) In IV and VI, the $\nu_{C=O}$'s of lactone and acetate completely overlap to form one peak.
9) The absorptions on the lower wave number side in these peaks are those due to the intramolecular hydrogen bonding.
10) W. Klyne, "Progress in Stereochemistry," Vol. I, Butterworths Publications, London (1954), p. 224.
11) G. S. Hammond, in M. S. Newman, "Steric Effects in Organic Chemisty," John Wiley & Sons, New York (1956), p. 449.
12) A. E. Remick, "Electronic Interpretation of Organic Chemistry," John Wiley & Sons, New York (1949), p. 256.
13) In general, keto-enol tautomers are more likely to exist in the keto form in an aqueous solution than in other solvents. See A. E. Gillam and E. S. Stern, "An Introduction to Electronic Absorption Spectroscopy in Organic Chemistry," Edward Arnold Ltd., London (1954), p. 227.

TABLE II. INFRARED ABSORPTION SPECTRA*

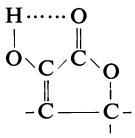
Compd. No.	ν_{max} cm^{-1}					
I	3550^{s}	3350^{bw}	1785^{vs}	1739^{s}	1528	1352
II	3580	3395^{b}	1785^{vs}	1768^{sh}		
			1742^{s}			
III			1783^{vs}	1740^{s}		
			1690^{ms}			
IV			1798^{s}	1739		
			1703^{vw}			
V	3570^{m}	3365	1770	1753		
			1728	1717^{sh}		
VI			1790	1705		
VIII			1787^{vs}	1738^{s}	1528	1350
IX			1798^{vs}	1739^{s}	1528	1355
X	3500		1764^{s}		1526	1350
XI	3540	3340^{b}	1778^{s}	1747^{s}		
XII			1778^{vs}	1748^{s}		
XIII			1800^{vs}	1750		
XIV	3550	3325^{b}	1770^{s}	1748^{sh,w}		

* Spectra of compounds with R_1=Me and Ph were measured in CCl_4 solution, and those of compounds with R_1=*o*-$NO_2C_6H_4$ were taken in $CHCl_3$ solution.

TABLE III. ULTRAVIOLET ABSORPTION SPECTRA

Compd. No.	λ_{max}^{EtOH} mμ	(log ε)
I	248	(4.28)
II	242	(3.92)
III	235	(3.91)
IV	212	(4.04)
V	234.5	(3.95)
VI	213.5	(4.09)
VIII	244	(4.02)
IX	266	(3.79)
X	253	(4.28)
XI	288	(4.28)
XII	283	(4.28)
XIII	276	(4.14)
XIV	288	(4.30)

ν_{OH} of a very strong intensity appears in their infrared absorption spectra in carbon tetrachloride (dielectric constant of the solvent: 2.24[12]), it is apparent that they are mainly present in the enol type in these solution.[14] When the hydroxyl is methylated (III), ν_{OH} disappears and the lactone $\nu_{C=O}$ alone remains, at 1783 cm^{-1}. When this is derived to an acetate, IV, there is no change in the $\nu_{C=O}$ of ethoxycarbonyl, but the lactone $\nu_{C=O}$ shifts further to a higher wave number region as a result of the interaction of the lactone with the newly-introduced acetate group.



VII

In the compounds with a phenyl ring, XI and XII, the $\nu_{C=O}$ due to lactone is shifted by 5~7 cm^{-1} to a lower wave number side than that of the corresponding compounds with a

TABLE IV. ULTRAVIOLET ABSORPTION SPECTRA OF $R-\underset{R_1}{\overset{|}{C}}=\underset{R_2}{\overset{|}{C}}-COR_3$

			K-Band λ_{max} mμ (log ε)				$\Delta\lambda_{max}$ mμ
			R=Me		R=Ph		
R_1	R_2	R_3					
H	H	OH	204	(4.07)*1	273	(4.32)*1	69
OH	H	Me	ca. 270	(4.08)*1	ca. 310	(4.18)*1	ca. 40
H	Me	OH	216	(3.98)*2	259~263	(4.22)*3	ca. 45

*1 A. E. Gillam and E. S. Stern, "An Introduction to Electronic Absorption Spectroscopy in Organic Chemistry," Edward Arnold Ltd., London (1954).
*2 W. E. Parham, W. N. Moulton and A. Zuckerbraun, *J. Org. Chem.*, **21**, 72 (1956).
*3 A. Mangini and F. Montanari, *Gazz. chim. ital.*, **88**, 1081 (1958).

14) As will be stated later, these compounds are present almost in an enolized form even in ethanol, and completely their ultraviolet absorption spectra can be interpreted on the same structural basis.

TABLE V. ANALYTICAL VALUES AND PHYSICAL CONSTANTS OF α-OXO-β-METHYL-γ-ETHYLBUTYROLACTONES

Compd. No.	C, % Found	C, % Calcd.	H, % Found	H, % Calcd.	B. p., °C mmHg. Found	B. p., °C mmHg. Lit.*1	n_D °C Found	n_D °C Lit.*1
II	56.40	56.07	7.06	6.59	86 (0.04)	112～115 (0.1)	1.4779 (25)	1.4785 (20)
III	57.69	57.88	7.09	7.07	70～74 (0.02)	—	1.4652 (22)	—
IV	56.30	56.24	6.54	6.29	100～104 (0.02)	100～102 (0.01)	1.4630 (22)	1.4636 (21)
V	57.51	57.34*2	7.51	7.22*2	90～94 (0.2)	78～79 (0.05)	1.4868 (22)	—
VI	58.41	58.69	6.72	6.57	110～141*3 (0.01)	90～92 (0.05)	1.4685 (16)	1.4660 (23)

*1 Ref. 2.

*2 +1/4 H_2O. Due to hygroscopicity.

*3 Bath temperature due to small amount available.

TABLE VI. MELTING POINTS OF α-OXO-β-PHENYL-γ-BENZYLBUTYROLACTONES

Compd. No.	M. p. °C	Lit. m. p. °C
XI	141～141.3	140[8]
XII	80.0～80.5	80[8]
XIII*	93～94	—
XIV	171.2～172.2	171[8]

* Found: C, 69.76; H, 5.48. Calcd.: C, 69.46; H, 5.30%.

methyl group (II and III) as a result of conjugation with the phenyl ring,[15] while the ester $\nu_{C=O}$ is shifted by 9～10 cm^{-1} to a higher wave number region, now being present at 1747～1750 cm^{-1}. The reason for the latter shift is still not clear.[16] The splitting of the ν_{OH} of compounds XI and XIV in two, without the splitting of the carbonyl $\nu_{C=O}$, is probably due to hydrogen bonding with the π-electron of the phenyl ring.[17]

In the infrared absorption spectra of I and X with an enol structure, there are only one $\nu_{C=O}$ due to lactone carbonyl and one ν_{OH} in the higher wave number region, and practically no evidence of an intramolecular hydrogen bonding. In the methyl ether compound VIII and the acetate IX, absorptions in the $\nu_{C=O}$ region are similar to that of the corresponding III and IV with a methyl group in place of the phenyl. This indicates that the *o*-nitrophenyl ring is not conjugated with the lactone ring.

15) In CH_3=$CHCO_2CH_3$ (*trans*) and C_6H_5CH=$CHCO_2C_2H_5$ (*trans*), the difference is −11 cm^{-1}, not greatly different from the above shift. See J. L. H. Allan, G. D. Menkins and M. C. Whiting, *J. Chem. Soc.*, **1955**, 1874.

16) The change in absorption wave numbers may be due to interaction with π-electrons of the phenyl ring.

17) There is no splitting of the $\nu_{C=O}$ and a close proximity of the hydroxyl and phenyl ring is possible. Such an example has been observed in the β-phenylethyl alcohol derivatives. See G. Büchi, L. Crombie, P. J. Godin, J. S. Kaltenbornn, K. S. Siddalingiah and D. A. Whiting, *J. Chem. Soc.*, **1961**, 2843.

Ultraviolet Absorption Spectra

The results[18] are shown in Table III. As has already been stated, α-oxo-γ-butyrolactone is completely enolized in an aqueous solution and is expected to be present chiefly in the enolized form in the ethanol solution (dielectric constant of the solvent: 25.7[12]) in which its ultraviolet absorption spectrum was measured. Actually, the absorptions of the enols, II and XI, are shifted by 7 and 5 mμ respectively to a longer wavelength region than those of the methyl ethers, III and XII,[19] without any change in their intensity; this is evidence for the above assumption.[20]

Compared to the spectrum of II, that of the acetate IV shows a hypsochromic shift of 31 mμ; this is in good agreement with the generally accepted value of 34 mμ.[21] The absorption maximum of V seems to have shifted slightly to a shorter wavelength side; the reason for this is not clear.

In general, α, β-unsaturated carbonyl compounds with a phenyl group in the β-position show the so-called K-band in a region of wavelengths longer by 40～65 mμ than those with a methyl group in the same position, as is illustrated in Table IV. Consequently, in compounds with a phenyl group such as R_1, the absorptions of XI and XII show a bathochromic shift of 46～48 mμ compared to the corresponding methyl compounds, II and III,

18) The ultraviolet apsorption spectra were measured with a Hitachi model EPS-2 recording spectrophotometer.

19) P. Grossmann, *Z. physik. Chem.*, **109**, 327 (1924). The difference between the enol form of ethyl acetoacetate (245 mμ) and ethyl β-ethoxycrotonate (232 mμ) is 13 mμ.

20) H. Schinz and M. Hinder (*Helv. Chim. Acta*, **30**, 1349 (1947)) have reported that α-oxobutyrolactones have an absorption maximum at 232 mμ (log ε 4.1); but the direct bonding of a methyl group with the chromophore group should cause a shift of about 10 mμ to the longer wavelength region and 242 mμ in II seems to be a normal value.

21) K. Hirayama, "Zikken Kagaku Kōza," I/1, Maruzen, Tokyo (1957), p. 104.

indicating that the phenyl group is in conjugation with the enol in the α-oxobutyrolactone ring. The presence of the absorption of the acetate XIII on a longer wavelength side than is to be expected is inexplicable.[22] The absorption maximum of XIV is in a normal position and is not different from that of XI.

In compounds with an *o*-nitrophenyl group, absorptions in the enol I and the enol methyl ether VIII are in a shorter wavelength region than those of the corresponding compounds with a phenyl group. In these cases, the introduction of an *o*-nitrophenyl group probably prevents the conjugation of the phenyl group with the α,β-unsaturated lactone ring and the *o*-nitrotoluene-type absorption (λ_{max} 260 mμ) of a weak intensity overlaps the absorption of II or III to show the absorption in a somewhat longer wavelength region. In the deethoxycarbonylated compound X this steric hindrance is diminished slightly and a weak conjugation appears,[25] which probably results in the presence of absorption in a longer wavelength region and with an increased intensity. Since there is no absorption absorption around 235 mμ in the acetate IX the of the *o*-nitrotoluene system alone must have appeared in a weak intensity.

Conclusion

To summarize the above results, we may say that all compounds in which R_1 is methyl show absorptions in the position to be expected for an enol and its ether and ester. Compounds in which R_1 is phenyl have the lactone ring and phenyl ring in the same plane and a complete conjugation is established. The compounds in which R_1 is an *o*-nitrophenyl group, however, do not have the *o*-nitrophenyl ring and lactone ring in the same plane; they are present as separate and individual chromophores. However, a slight conjugation phenomenon is observed in X in which the ethoxycarbonyl group has been liberated.

Experimental

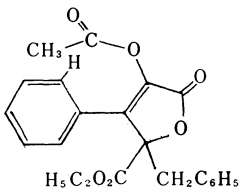
The α-oxo-β-methyl-γ-ethyl-γ-butyrolactones (II, IV, V, and VI) were synthesized according to the procedure reported by Monnin.[2] Compound III, a new compound, was prepared by the addition of an ether solution of diazomethane to a solution of II in methanol-ether (1 : 1 v/v); after the mixture had stood overnight, it was distilled. These were all oily substances and were confirmed through elemental analysis and a comparison of their physical constants (Table V).

The α-oxo-β-phenyl-γ-benzylbutyrolactone derivatives (XI, XII, XIV) were synthesized according to the method of Hemmerlé.[3] Compound XII was obtained by heating XI with acetic anhydride on a water bath for one hour. The melting points of these compounds are compared in Table VI.

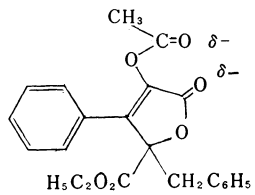
The synthesis of α-oxo-β-(*o*-nitrophenyl)-γ-(*o*-nitrobenzyl)-butyrolactone derivatives (I, VIII, IX, X) has been reported in a previous paper.[1]

Faculty of Science
Osaka City University
Sumiyoshiku, Osaka

22) It appears that conformation i is impossible because of steric interference, and that conformation ii, with two oxygen atoms in close proximity, will result. Consequetly, the unshared electron pair of ether oxygen in the ester takes part in the conjugation system; this probably causes the shift of the absorption to a longer wavelength region. Such a consideration has been used by Jones and his co-workers,[23] and by others[24] in explaining infrared absorption spectra.



(i)



(ii)

In comparing the infrared absorption spectra of IV and XIII, the $\nu_{C=O}$ of XIII is found to be shifted to a little higher wave number side by the same cause.

23) R. N. Jones, P. Humphries, F. Herling and K. Dobriner, *J. Am. Chem. Soc.*, 74, 2820 (1952).

24) L. J. Bellamy and R. L. Williams, *J. Chem. Soc.*, 1957, 861.

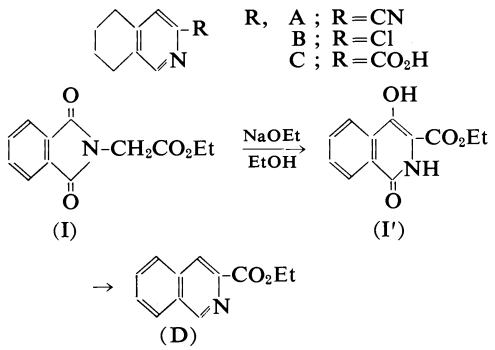
25) The conjugation phenomenon is manifested as the function of $\cos^2\theta$, where θ is the angle formed by the two rings. E. A. Braude and F. C. Nachod, "Determination of Organic Structures by Physical Methods," Academic Press, New York (1955), p. 174.

Beiträge zur Umlagerung der Cyclischen Imidoester

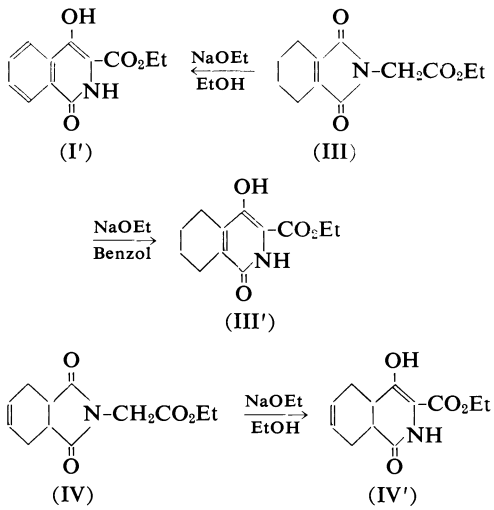
Von Tsuneyuki NAGASE

(Eingegangen am 12. Februar, 1964)

Im Laufe eines synthetischen Versuches im hiesigen Laboratorium brauchten wir 5, 6, 7, 8-Tetrahydroisochinolin-Derivate, die an der C_3-Stellung eine Nitril- order Carbalkoxyl-Gruppe tragen. Über 3-Cyano-5, 6, 7, 8-tetrahydroisochinolin (A), von dem Sempervirin abgeleitet wurde, hat schon Swan[1] geschrieben, es wurde aber über seine Darstellung nichts berichtet. Die Einwirkung von Kaliumcyanid auf 3-Chlor-5, 6, 7, 8-tetrahydroisochinolin (B) ergab kein (A) sondern 3-Carboxy-5, 6, 7, 8-tetrahydroisochinolin (C) mit nur ca. 20%iger Ausbeute.[2] Andererseits wurde nun gezeigt, dass 3-Carbäthoxyisochinolin (D) aus α-Phthalimidoessigsäureäthylester (I) durch Umlagerung nach Gabriel und Colmann[3] mittels Natriumäthylates über 3-Carbäthoxy-4-hydroxyisocarbostyril (I') ableitbar ist.[4]



Diese Umlagerung, die nicht nur beim (I) sondern auch bei verschiedenen aromatischen *o*-Dicarboximidoderivaten, wie α-Phthalimidoketonen,[5] Chinolyl-[6] oder Cinchomeronylimidoessigsäureäthylester,[7] mit Erfolg festgestellt wurde, verlief beim α-Δ^1-Tetrahydrophthalimidoessigäthylester (III) leider nicht glatt. Beim Erhitzen von III mit Natriumäthylat in abs. Äthanol wurde kein 3-Carbäthoxy-4-hydroxy-5, 6, 7, 8-tetrahydroisocarbostyril (III'), sondern I', das Dehydrierungsprodukt von III', mit einer Ausbeute von nur 5～6% der Theorie erhalten und erst beim Erhitzen mit demselben Katalysator in Benzol wurde, III' mit ebenso geringer Ausbeute isolient. α-Δ^4-Tetrahydrophthalimidoessigsäureäthylester (IV) ergab dagegen beim Erhitzen mit demselben Katalysator in abs. Äthanol 3-Carbäthoxy-4-hydroxy-5, 8, 9, 10-tetrahydroisocarbostyril (IV') mit einer Ausbeute von 63% der Theorie.

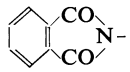
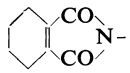
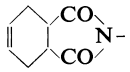
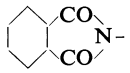
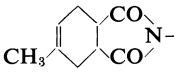
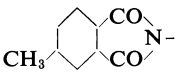
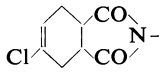
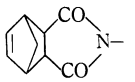
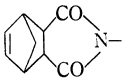
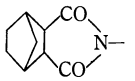
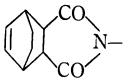
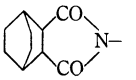


Um dieses merkwürdig verschiedene Verhalten beider Ester bei der Umlagerung, das vermutlich von sterischem und polarem Effekt beeinflusst wird, näher zu untersuchen, wurde nun die Reaktion auch bei einigen nicht aromatischen Cyclischen *o*-Dicarboximidoessigester, deren Eigenschaften in Tabelle I gezeigt werden, weiter probiert. Die Tabelle II stellt die Eigenschaften der normalen Umlagerungsprodukte samt ihren Ausbeuten dar. Die Verbindungen, bei denen keine Umlagerung stattfand, spalteten ihren Imidoring und ergaben die entsprechenden Carbonamidosäuren, deren Eigenschaften samt ihren Ausbeuten in der Tabelle III gezeigt wurden.

Diese Ergebnisse zeigen, dass die Umlagerung nicht nur bei den aromatischen und alicyclischen *o*-Dicarboximidoderivaten, sondern auch selbst beim Succinimidoessigsäureäthylester (II) erfolgt. Sehr merkwürdig ist die Tatsache,

1) G. A. Swan, *J. Chem. Soc.*, **1950**, 1534.
2) R. M. Anderson, G. R. Clemo und G. A. Swan, ebenda, **1954**, 2579.
3) S. Gabriel und J. Colmann, *Ber.*, **33**, 980 (1900); **35**, 2421 (1902).
4) T. Nagase: Auf der 16. Jahrestagung der Japanische Chemische Gesellschaft vorgetragen (1963).
5) S. Gabriel und J. Colmann, *Ber.*, **33**, 2630 (1900).
6) E. Ochiai, K. Miyaki und S. Sato, ebenda, **70**, 2018 (1937).
7) E. Ochiai und I. Arai, *J. Pharm. Soc. Japan*, **59**, 458 (1939).

TABELLE I.

No.	R-CH_2CO_2Et	Schmp. °C (Siedp./mmHg)	Ausbeute %	Formel	Analyse Ber./Gef. C	H	N	Cl
I*[1]		105	93	$C_{12}H_{13}O_4N$	61.80 61.77	4.75 4.76	6.01 6.00	
II		62～63	85	$C_8H_{11}O_4N$	51.88 51.79	5.99 5.97	7.56 7.48	
III		45～47	80	$C_{12}H_{13}O_4N$	60.75 60.96	6.37 6.24	5.90 6.34	
IV		81～82	Quant.	$C_{12}H_{15}O_4N$	60.75 60.96	6.37 6.31	5.90 6.17	
V*[2]		(141～142/1)	Quant.	$C_{12}H_{17}O_4N$	60.24 60.16	7.16 7.09	5.83 5.53	
VI		(139～140/1)	90	$C_{13}H_{17}O_4N$	62.14 61.81	6.82 6.84	5.57 5.57	
VII*[3]		(150～151/1)	Quant.	$C_{13}H_{19}O_4N$	61.64 61.68	7.56 7.51	5.53 5.68	
VIII		69～70	Quant.	$C_{12}H_{14}O_4NCl$	53.04 53.03	5.19 5.08	5.19 5.02	13.04 13.02
IX*[4]	 *cis-endo*	(151～152/1)	86	$C_{13}H_{15}O_4N$	62.64 62.97	6.07 6.25	5.62 5.78	
X	 *cis-exo*	77～78	80	$C_{13}H_{15}O_4N$	62.64 62.94	6.07 5.95	5.62 5.56	
XI*[5]	 *cis-endo*	(161～162/1)	Quant.	$C_{13}H_{17}O_4N$	62.14 62.21	6.82 6.76	5.57 5.45	
XII	 *cis-endo*	81～82	Quant.	$C_{14}H_{17}O_4N$	63.86 64.00	6.51 6.50	5.32 5.27	
XIII*[6]	 *cis-*	55～56	Quant.	$C_{14}H_{19}O_4N$	63.38 63.19	7.22 6.83	5.28 5.26	

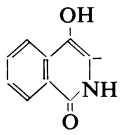
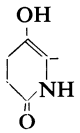
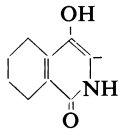
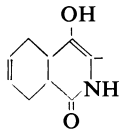
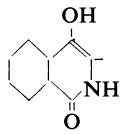
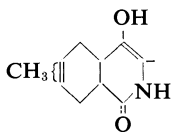
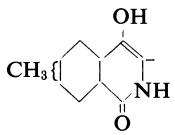
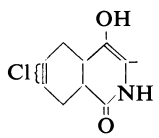
*1 3)
*2 Hergestellt aus IV durch katalytische Reduktion.
*3 Hergestellt aus VI durch katalytische Reduktion.
*4 M. Furdik und V. Sutoris, *Chem. zvesti*, **17**, 31 (1963).
*5 Hergestellt aus IX durch katalytische Reduktion.
*6 Hergestellt aus XII durch katalytische Reduktion.

dass die Umlagerung beim α-4-Methyl-Δ^4-tetrahydrophthalimidoessigsäureäthylester (V) nur mit einer Ausbeute von 8～10% der Theorie erfolgt, während sie beim entsprechenden Chlorderivat (VIII) oder beim gesättigten α-4-Methylhexahydrophthalimidoessigsäureäthylester (VII) mit mehr als 60%iger Ausbeute stattfand.[8] Ferner ergaben die bicyclischen *o*-Dicarboximidoessigester, deren gebrückte carbocyclische Ringe im Vergleich zum VII ziemlich gespannt sind, kein Umlagerungsprodukt, sondern die entsprechende Carbonamidosäure unter Abspaltung ihres Imidoringes.

Für den Verlauf dieser Base-katalysierten

8) Die Stellung der Substituenten in den Umlagerungsprodukten wurde noch nicht festgestellt.

TABELLE II.

No.	R-CO_2Et*1	Schmp. °C	Ausbeute*2 %	Formel	Analyse Ber./Gef. C	H	N	Cl
I′		194	80	$C_{12}H_{11}O_4N$	61.80 61.54	4.75 4.54	6.01 5.97	
II		151～152	35	$C_8H_{11}O_4N$	51.88 51.71	5.99 5.86	7.56 7.71	
III′		222	5～6	$C_{12}H_{15}O_4N$	60.75 60.50	6.37 6.18	5.90 5.83	
IV′		148～150	65	$C_{12}H_{15}O_4N$	60.75 60.80	6.37 6.27	5.90 5.81	
V′		155～157	60	$C_{12}H_{17}O_4N$	60.24 60.29	7.16 6.88	5.85 5.83	
VI′		168～169	8～10	$C_{13}H_{17}O_4N$	62.14 62.21	6.82 6.69	5.57 5.26	
VII′		154～155	60	$C_{13}H_{19}O_4N$	61.64 61.15	7.56 7.32	5.53 5.53	
VIII′		193～195	62	$C_{12}H_{14}O_4NCl$	53.04 52.77	5.19 5.08	5.19 4.98	13.04 13.16

*1 Alle Verbindungen zeigen eine tief blaue Färbung mit Eisenchlorid-Lösung.
*2 Aus Äthanol umkristallisiert.

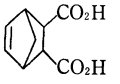
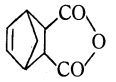
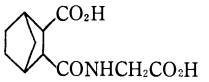
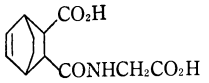
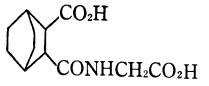
Umlagerung sind die nachfolgenden Mechanismen denkbar.

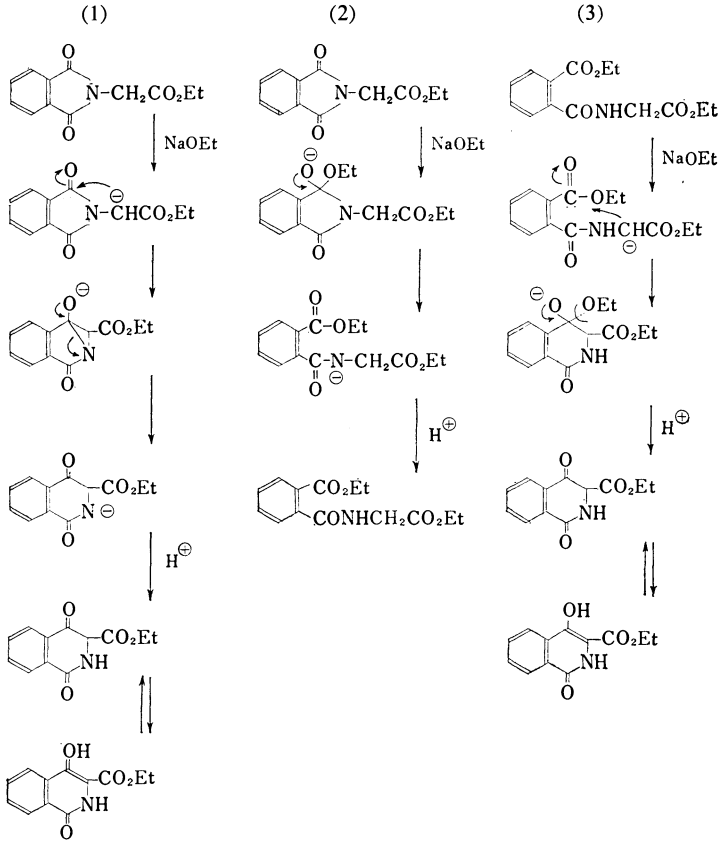
Der Mechanismus 2 wurde durch Misserfolg der Umlagerung beim *N*-Benzylphthalimid gestützt,[9] bei welchem die Reaktion, wegen der Schwierigkeit der Bildung des für den Reaktionsverlauf nach 3 nötigen Carbanions, mit der Stufe des Phthalamidoesters gehindert ist.

Die Konformation des *N*-Carbäthoxymethyl-bicyclo[2, 2, 1]hepten-(5)-2, 3-dicarboximides (IX) bzw. des entsprechenden *N*-Carbäthoxymethyl-bicyclo[2, 2, 2]octen-(5)-2, 3-dicarboximides (XII), das durch Diels-Alder-Reaktion von Cyclopentadien bzw. Cyclohexadien mit Maleinsäureanhydrid hergestellt wurde, ist sicher cis-endo-Form und der mit dem ebenen Imidoring kondensierte Cyclohexenring ist boot-förmig. Das π-Orbital der cyclischen Doppelbindung an der Stellung 5 und die Imidoring-Ebene sind fast parallel und liegen ziemlich nahe beieinander, sodass ein elektrostatischer Feldeffekt zwischen ihnen denkbar ist. Die elektrophile Aktivität der beiden Carbonyl-Kohlenstoffe im Imidoring wird vermutlich durch Feldeffekt der Doppelbindung in der Masse neutralisiert, sodass keine Umlagerung, sondern nur die Ringspaltung stattfindet. Dieses Ergebnis, sowie die Tatsache, dass XII, dessen Ringspannung im Vergleich zum

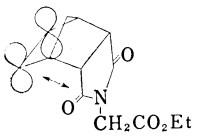
9) R. C. Elderfield, "Heterocyclic Compounds," Vol. 4, John Wiley and Sons, New York (1952), S. 378.

TABELLE III.

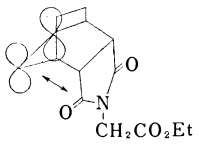
No.	Produkt	Schmp. °C	Ausbeute %	Formel	Analyse Ber./Gef. C	H	N
IX′	 *cis-endo*	147～148	75	$C_9H_{10}O_4$	59.33 58.87	5.47 5.65	
X′	 *cis-exo*	138～140	70	$C_9H_8O_3$	65.78 65.30	4.91 5.12	
XI′	 *cis-endo*	167	78	$C_{11}H_{15}O_5N$	54.76 54.67	6.27 6.33	5.81 5.73
XII′	 *cis-endo*	135～136	85	$C_{12}H_{17}O_5N$	56.91 57.13	5.97 5.69	5.53 5.59
XIII′	 *cis-*	178～179	80	$C_{12}H_{17}O_5N$	56.40 56.55	6.71 6.61	5.49 5.26



IX geringer ist, ebenfalls nur das Ringspaltungsprodukt ergibt, scheint mit dem Mechanismus nach dem Sinn von 3 schwer vereinbar zu sein. Ein derartiger Feldeffekt wurde auch bei der elektrophilen Addition von 2, 4-Dinitrobenzolsulfenylchlorid auf *cis-endo-* und *cis-exo*-Bicyclo [2, 2, 1] hepten-(5)-2, 3-dicarbonsäureanhydrid[10] oder bei der Epoxydierung des 7-Diphenylmethylen-*N*-methyl-bicyclo [2, 2, 1] hepten-(5)-2, 3-dicarboximides[11] bemerkt, bei welchem die ungesättigte Eigenschaft der Kerndoppelbindung durch Feldeffekt des Anhydridringes oder Imidoringes vermindert ist.

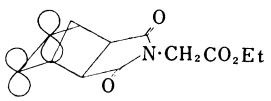


(IX)



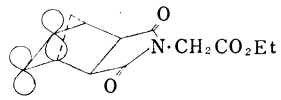
(XII)

Mit dieser Erklärung allein ist jedoch die Spaltung des Imidoringes beim *cis-exo*-Carbäthoxymethyl - bicyclo [2, 2, 1] hepten - (5)-2, 3-dicarboximid (X) schwer verständlich, bei welchem das π-Orbital und der Imidoring fast senkrecht zueinander liegen. Zu bemerken ist dabei, dass die Distanz zwischen der Ringebene und der Brückenmethylen-Gruppe im Vergleich zu IX weit kleiner geworden ist.[12] Hierbei scheint irgendein anderer Einfluss einzugereifen.



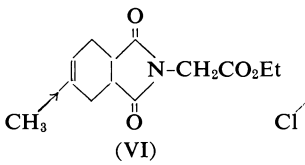
(X)

Bei der Verbindung, die ausgenommen diese Brückenmethylen-Gruppe eine ähnliche Konformation besitzt, sollte diesser Effekt noch deutlicher erscheinen. So findet beim α-Δ^4-Tetrahydrophthalimidoessigsäureäthylester (IV), welcher aus *cis*-Δ^4-Tetrahydrophthalsäureanhydrid abgeleitet wurde und dementsprechend eine cis-Form darstellt, die Umlagerung ziemlich glatt statt. Beim *cis*-Δ^4-Tetrahydrophthalsäureanhydrid ist nach Buckels[13] die von den zwei möglichen boot-förmigen Konformationen stabiler, in der der Anhydridring *quasiäquatorial* liegt. Diese Vermutung wurde durch das Ergebnis der Epoxydierung, sowie durch das Ergebnis von Imid unterstützt.[14] Die Konformation von IV entspricht daher derjenigen der Verbindung, die aus X nur durch Ausfallen der Methylenbrücke entstanden ist. Sein Imidoring ist von dem π-Orbital der Doppelbindung an der Stellung 4 weiter entfernt und liegt beinahe senkrecht dazu und ist daher von dem letzteren weniger beeinflusst, sodass die Umlagerung ziemlich glatt stattfindet.

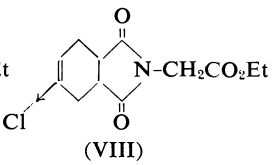


(IV)

Beim 4-Methyl-Δ^4-derivat (VI) wird der induktive Effekt der Methylgruppe die Elektronendichte der Doppelbindung vergrössern, so dass die Umlagerung in der Masse gestört wird, während beim 4-Chlor-Δ^4-derivat (VIII), wegen des umgekehrten induktiven Effekts des Chloratoms, die Umlagerung ebenso glatt erfolgt, wie beim X sowie bei den gesättigten Derivaten (V und VII). Bei der entsprechenden Δ^1-Verbindung (III) wird die Imidocarbonylgruppe wegen der Konjugierung mit der Doppelbindung etwas deaktiviert und ferner wird die Spannung des halbsessel-förmigen Cyclohexenrings im Vergleich zur Δ^4-Verbindung grösser, so dass die Neigung zur Aromatisierung vor der Umlagerung beobachtet wird.



(VI)



(VIII)

Experimentelles

Die Säureanhydride, die in diesem Versuch verwendet wurden, sind nach den bekannten Methoden hergestellt, und zeigen die folgenden Schmelzpunkte.

	Schmp. °C
Δ^1-Tetrahydrophthalsäureanhydrid[15]	74
cis-Δ^4-Tetrahydrophthalsäureanhydrid[16]	103～104
cis-4-Methyl-Δ^4-tetrahydrophthalsäureanhydrid[17]	63～64
cis-4-Chlor-Δ^4-tetrahydrophthalsäureanhydrid[18,19]	57～58

10) H. Kwart und L. J. Miller, *J. Am. Chem. Soc.*, **83**, 4552 (1961).
11) G. I. Poos und J. D. Rosenau, *J. Org. Chem.*, **28**, 665 (1963).
12) Die gaschromatographische Tatsache, dass die Retention-Zeit der cis-exo-Form (X) im Vergleich zur cis-endo-Form (IX) kleiner ist, die auf einen sterisch dichteren Zustand hinzudeuten scheint, stimmt mit dieser Vermutung überein.
13) R. E. Buckels, *Chem. Revs.*, **57**, 643 (1957).
14) A. P. Gray, D. E. Heitmeier und H. Kraus, *J. Am. Chem. Soc.*, **90**, 91 (1962).
15) W. Hückel und U. Lampert, *Ber.*, **67**, 1812 (1934).
16) O. Diels und K. Alder, *Ann.*, **460**, 98 (1928); *Ber.*, **62**, 2087 (1929).
17) E. H. Farmer und F. L. Warren, *J. Chem. Soc.*, **1931**, 3221.
18) W. H. Carothers, I. Williams, A. M. Collins und J. E. Kirby, *J. Am. Chem. Soc.*, **53**, 4203 (1931).

cis-endo-Bicyclo[2, 2, 1]hepten-(5)-2, 3-dicarbonsäureanhydrid[20,21]	164
cis-exo-Bicyclo[2, 2, 1]hepten-(5)-2, 3-dicarbonsäureanhydrid[22]	143
cis-endo-Bicyclo[2, 2, 2]octen-(5)-2, 3-dicarbonsäureanhydrid[23]	144～145

Die Imide wurden aus Säureanhydriden nach der Methoden von Ficken und Linstead[24] durch 30～40 minutiges Erhitzen mit Harnstoff auf 150～160°C hergestellt und aus Alkohol umkristallisiert.

	Schmp. °C
Δ^1-Tetrahydrophthalimid[24]	169～170
cis-Δ^4-Tetrahydrophthalimid[25]	136～137
cis-4-Methyl-Δ^4-tetrahydrophthalimid	97
$C_9H_{11}O_2N$: Ber., C, 65.44 ; H, 6.71 ; N, 8.48. Gef., C, 65.53 ; H, 6.54 ; N, 8.52%.	
cis-4-Chlor-Δ^4-tetrahydrophthalimid	101～102
$C_8H_8O_2NCl$: Ber., C, 51.77 ; H, 4.29 ; N, 7.54 ; Cl, 19.10. Gef., C, 51.90 ; H, 4.61 ; N, 7.60 ; Cl, 18.98%.	
cis-endo-Bicyclo[2, 2, 1]hepten-(5)-2, 3-dicarboximid[26]	187 (aus Alkohol-Äther)
cis-exo-Bicyclo[2, 2, 1]hepten-(5)-2, 3-dicarboximid	160～161
$C_9H_9O_2N$: Ber., C, 66.24 ; H, 5.56 : N, 8.58. Gef., C, 66.20 ; H, 5.38 ; N, 8.75%.	
cis-endo-Bicyclo[2, 2, 2]octen-(5)-2, 3-dicarboximid[27]	204～205 (aus Benzol-Ligroin)

Imidoessigester. — Ein Mol Imid wurde durch Einwirkung von 1 Mol Kaliumäthylat in abs. Alkohol-Lösung in das Kaliumsalz übergeführt und nach dem Abdestillieren des Lösungmittels 1 Mol Monochloressigsäureäthylester zugegeben und im Ölbad auf 150～155°C 2 Stunden lang erhitzt. Nach dem Erkalten wurde das Reaktionsgemisch mit kaltem Wasser behandelt und dann mit Chloroform geschüttelt. Die Chloroform-Lösung wurde nach dem Trocknen über Natriumsulfat eingeengt und der Rückstand durch Umkristallisieren aus Äthanol oder durch Destillieren unter vermindertem Druck gereinigt.

Umlagerung der Imidoessigester. — *Umlagerung des cis-Δ^4-Tetrahydrophthalimidoessigsäureäthylester (IV).*—Zu einer Lösung von 2.1 g Natrium in 40 ccm abs. Äthanol wurden 7.11 g IV zugegeben und auf dem Wasserbad unter Rückfluss 1 Stunde lang erhitzt. Nach dem Erkalten wurde das Lösungsmittel unter vermindertem Druck abdestilliert, der Rückstand nach Zusatz einer geringen Menge Wasser mit 10%iger Salzsäure angesäuert. Die hierbei ausgeschiedenen Kristalle wurden abgesaugt und aus Äthanol umkristallisiert. 4.62 g (65%) farblose Nadeln von Schmp. 148～150°C (IV'). IR ν (KBr) : 1670 cm.$^{-1}$ UV λ_{max}^{EtOH} 294, 232 mμ. Färbte sich purpur mit Eisenchlorid-Lösung.

Einwirkung von Natriumäthylat auf N-Carbäthoxymethyl - bicyclo [2, 2, 2] octen - (5) - 2, 3 - dicarboximid (XII).—Zu einer Lösung von 0.07 g Natrium in 5 ccm abs. Äthanol wurden 0.26 g. XII zugegeben und auf dem Wasserbad 30 Min lang unter Rückfluss erhitzt. Bei analoger Aufarbeitung wie bei IV und beim Umkristallisieren des Produktes aus Äthanol-Wasser wurden 0.225 g Nadeln von Schmp. 136～137°C (XII') erhalten.

Die Umlagerungsreaktion der anderen Ester wurde wie bei IV durchgeführt.

Dehydrogenierung vom Umlagerungsprodukt (IV'). —0.1 g IV' wurde mit 0.05 g 10% iger Pd-Kohle innig gemischt und auf dem Ölbad 30 Min lang auf 170°C erhitzt. Nach dem Erkalten wurde das Reaktionsgemisch mit Äthanol extrahiert und die vom Katalysator abfiltrierte Lösung eingeengt. Die hierbei ausgeschiedenen Kristalle ergaben beim Umkristallisieren aus Äthanol 0.08 g Nadeln von Schmp. 193～194°C. Eine Mischprobe mit 3-Carbäthoxy-4-hydroxy-isocarbostyril (I') zeigte keine Schmelzpunkterniedrigung. Die IR-und UV-Spektren beider Präparate stimmten auch völlig überein.

Ich bin Herrn Professor Eiji Ochiai von diesem Institut für die Anregung zu dieser Arbeit und das ihr entgegengebrachte Interesse, und Herrn Dr. H. Tanida von der Shionogi A. G. für seine freundliche Diskussion dieser Abhandlung zu grossem Dank verpflichtet. Alle Analysen dieser Abhandlung wurden von der mikroanalytischen Abteilung dieses Institutes durchgeführt, wofür ich sehr dankbar bin.

des Instituts für Physikalische und Chemische Forschungen
Komagome, Bunkyo-ku, Tokyo

19) Das Chloropren zur Herstellung dieser Verbindung verdanke ich Herrn Dr. S. Fujiiye von der Denki-Kagaku Industrie A. G.
20) O. Diels und K. Alder, *Ann.*, **460**, 98 (1928).
21) O. Diels und K. Alder, ebenda., **460**, 115 (1928).
22) D. Graig, *J. Am. Chem. Soc.*, **73**, 4889 (1951).
23) Das Präparat verdanke ich Herrn Dr. M. Fujimoto von der Shionogi A. G.
24) G. E. Ficken und R. P. Linstead, *J. Chem. Soc.*, **1952**, 4850.
25) H. R. Snyder and G. I. Poos, *J. Am. Chem. Soc.*, **72**, 4104 (1950) ; J. E. Grill und J. Munro, *J. Chem. Soc.*, **1952**, 4631.
26) S. C. Harvey, *J. Am. Chem. Soc.*, **71**, 1121 (1949).
27) M. Fujimoto und K. Okabe, *Chem. Pharm. Bull.*, **10**, 717 (1962).

The Thermal Decomposition of Zinc Oxide

By Tatsuya IMOTO, Yoshio HARANO and Yasuhide NISHI

(Received February 19, 1964)

In previous papers on the reduction of zinc oxide by hydrogen,[1-3] it has been suggested that the reduction is not a surface reaction, but a successive reaction consisting of the following two processes: the decomposition of zinc oxide into zinc vapor and oxygen, and the subsequent reaction of oxygen with hydrogen. Further, the former is a rate-determining step in the presence of a small amount of zinc oxide and the latter an excessive amount of it respectively.

The present work was carried out in order to obtain information of the decomposition process in the reduction and to discuss further the reduction mechanism.

As for the thermal decomposition of zinc oxide, it has been known that zinc oxide decomposes into zinc vapor and oxygen rather than subliming as zinc oxide vapor.[4,5] When Moore and Williams[6] investigated the decomposition rate in a stream of oxygen, nitrogen and zinc vapor by measuring the weight loss, they found that the rate is fastest in zinc vapor. No quantitative studies of the decomposition, however, have yet been carried out.

Experimental

The decomposition rate was determined by using a thermobalance and a McLeod gauge. The zinc oxide used in this work was the same commercial superior product supplied by the Sakai Chemicals Co., Ltd., as was used in the previous work.

Since zinc oxide is a structure-sensitive compound and since its surface state is affected by a slight variation in the pretreatment, it was necessary to fix the standard pretreating conditions as follows: after evacuating below 10^{-5} mmHg for one hour at 190°C, the reaction tube was heated to the standard temperature (740°C) within half an hour, and then the reaction system was kept at 740°C for half an hour. During the heating process, the evacuation was stopped. The pressure of the oxygen evolved in this interval was estimated to be one in the initial decomposition equilibrium. Then the system was reevacuated below 10^{-5} mmHg and the decomposition was started. In this work, 200 min. was taken as a standard decomposition time.

Results and Discussion

The relation between the initial amount (w_0) and the decomposed amount of zinc oxide after 200 min., at 740 and 780°C (Δw), is shown in Fig. 1. In Fig. 1 it can be seen that, when

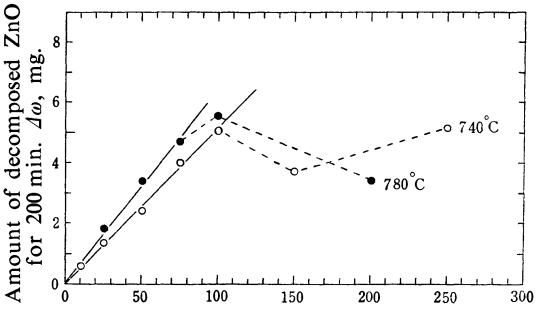


Fig. 1. The relationship between initial and decomposed amount of zinc oxide.

the amount of zinc oxide is less than 100 mg. at 740°C, the ratio ($\Delta w/w_0$) is nearly constant. On the other hand, when there is more than 100 mg. of zinc oxide, the relation deviates from linearity and the ratio is occasionally observed to be smaller than the former one. The deviation from linearity seems to take place because of the decrease in the effective surface of zinc oxide by its aggregation rather than because of the decrease in the surface of the zinc oxide lying in the lower part of the basket. Since the aggregation increases with a rise in the temperature, the deviation tends to appear in a smaller region of zinc oxide. Moreover, when pre-sintered and then crushed zinc oxide is used, the linearity appears over a wider range.

The decomposition ratios ($\Delta w/w_0$) at 740°C are plotted against the time for various initial amounts (w_0: 25, 50, 75 and 100 mg.) in Fig. 2. This figure shows that the relations between the ratio and the time are represented by an identical curve, regardless of the amount

1) T. Imoto, Y. Harano and Y. Nishi, *J. Chem. Soc. Japan Pure Chem. Sec.* (*Nippon Kagaku Zasshi*), **84**, 115 (1963).
2) T. Imoto, Y. Harano, Y. Nishi and S. Masuda, ibid., **85**, 106 (1964).
3) T. Imoto, Y. Harano, Y. Nishi and S. Masuda, This Bulletin, **37**, 441 (1964).
4) E. A. Secco, *Can. J. Chem.*, **38**, 596 (1960).
5) L. Brewer and D. F. Mastick, *J. Chem. Phys.*, **19**, 834 (1951).
6) W. J. Moore and E. L. Williams, *J. Phys. Chem.*, **63**, 1516 (1959).

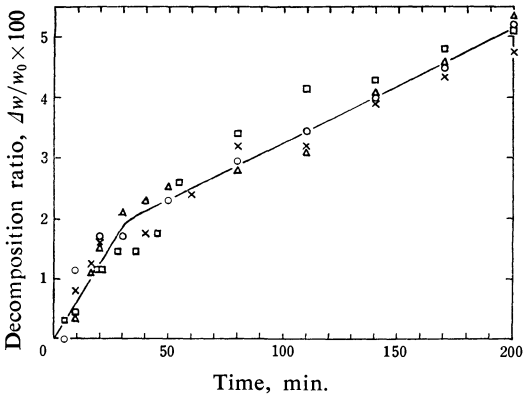


Fig. 2. The relationship between decomposition ratio and decomposition time.

w_0, mg. w_0, mg. w_0, mg. w_0, mg.
○ 25 × 50 △ 75 □ 100

of zinc oxide, and that in the early stages, the decomposition proceeds rapidly, but after it has proceeded for about half an hour, it proceeds at a nearly constant rate which is slower than that in the earlier part. Since the curve in Fig. 2 is nearly straight under these experimental conditions, the decomposition rate seems to be proportional to the surface area of zinc oxide.

Gray[7] investigated the sintering of zinc oxide and reported that the surface area of zinc oxide rapidly decreases in the initial half hour, but that it scarcely varies thereafter. In this work, zinc oxide was kept at a decomposition temperature for half an hour before the reaction. It is, however, still doubtful whether or not the faster decomposition stage is caused by the incompleteness of the sintering. Therefore, the following experiment was undertaken with zinc oxide which had been presintered for about two hours at the decomposition temperature in order to sinter it completely; the results obtained are shown in Fig. 3-b. From Fig. 3, it was found that the b decomposition curve has the same profile and the same slope as does the a standard curve which is identical with that in Fig. 2, and that zinc oxide also decomposes rapidly for the initial half hour. Consequently, the initial rapid decomposition seems not to be due to the variation in the surface area during the reaction.

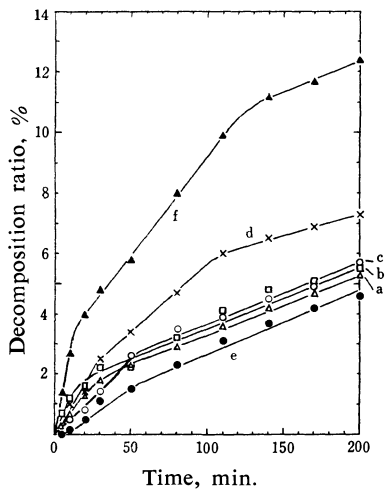


Fig. 3. Decomposition profiles of zinc oxide pretreated at various conditions (at 740°C).

△ a Standard (30 min.)
□ b Standard (200 min.)
○ c Presintered normal
× d Presintered Zn rich
● e O_2 treatment
▲ f H_2 treatment

The effect of the surface state on the decomposition rate is also shown in Fig. 3. Curves c and d show the results obtained with zinc oxide pretreated in vacuo. After sintering, the samples were exposed to air at a sintering temperature of 800°C, in case c, or cooled down to room temperature in vacuo and then exposed to admitted air, in case d. Sample c is fluffy and white, whereas sample d is coarse and gray. Such phenomena were also reported by Gray,[7] who found the surface pretreated as in sample d to be rich in zinc. Curve c is the same as the standard one (curve a), whereas curve d is different and has a longer stage of initial rapid reaction. Curves e and f show the results obtained with the sample pretreated in an atmosphere of oxygen (80 mmHg) or hydrogen (40 mmHg) respectively. In case e, the initial rapid decomposition does not appear, while in case f the reaction proceeds much faster than in the others.

The initial decomposition equilibrium pressures of oxygen in the standard experiments at 740°C are shown in Table I. In Table I,

TABLE I. INITIAL DECOMPOSITION PRESSURE OF OXYGEN (mmHg)

Sample mg.	Pretreatment period at 740°C	
	0.5 hr.	2.0 hr.
100	1.30×10^{-1}	1.15×10^{-1}
75	0.92×10^{-1}	1.45×10^{-1}
50	1.07×10^{-1}	1.42×10^{-1}
		1.30×10^{-1}
25	0.61×10^{-1}	0.99×10^{-1}
10	0.67×10^{-1}	

the pressure slightly fluctuates, there is, however, no difference between the samples kept at the decomposition temperature for half an hour and that kept for two hours. Assuming

7) T. J. Gray, *J. Am. Cer. Soc.*, 37, 534 (1954).

that an amount of zinc corresponding stoichiometrically to oxygen is also evolved during the pretreatment, the weight loss of zinc oxide may be calculated to be 0.07 to 0.16 mg., since the volume of the reaction vessel is 358 cc. and the volume ratio of the vessel outside and inside of the electric furnance is 1.47. If only oxygen is evolved, the weight loss would be 0.014 to 0.032 mg. From the facts that the weight loss during the above standard pretreatment was unmeasurable (less than 0.03 mg.) at 740°C and that no deposition of zinc metal on the cooler part of the reaction vessel was observed, one may say that oxygen is evolved without any accompanying evolution of zinc vapor. Therefore, the surface of the zinc oxide will be rich in zinc. Since the equilibrium decomposition pressures of oxygen in both the a and b cases were identical (cf. Table I), their surface states may also be considered to be the same. Therefore, the a and b decomposition curves (in Fig. 3) may be almost identical. On the other hand, when zinc oxide is pretreated in an atmosphere of oxygen at a higher pressure than the equilibrium pressure, no evolution of oxygen takes place, and hence, no initial rapid decomposition is observed.

As a result, it may be suggested that the fewer oxygen atoms relative to zinc atoms are involved on the surface of zinc oxide, the faster the initial reaction proceeds and the longer its rapid stage becomes. Consequently, the rate of the decomposition of zinc oxide treated by hydrogen will be very fast, since the surface has a marked deficiency of oxygen. Oxygen on the surface of the zinc oxide pretreated in vacuo will be quite scarce. On the other hand, when zinc oxide pretreated in vacuo is exposed to air at a high temperature, relatively many zinc atoms on its surface will be reoxydized and the surface will return to the original state.

Further, when the surface affected by the pretreatments has disappeared as decomposition proceeds, each sample will decompose at the same rate, regardless of the various pretreatments. Figure 3 also indicates the above suggestion.

As has been mentioned above, the pretreatment causes the surface state of zinc oxide to deviate from its stoichiometry and accelerates its initial decomposition rate. Now let us cmpare the extent of the deviation from stoichiometry with the amount of decomposition acceleration. Extraporating the linear parts of the a and b curves in Fig. 3, an intersection with the ordinate of 1.5%, is obtained. That is, the evolution of oxygen in a and b accelerates the decomposition by 1.5%. The amounts of zinc oxide which result in the non-stoichiometric state upon the evolution of oxygen, are calculated to be 0.08 to 0.02% of the initial zinc oxide, 25 to 100 mg. (assuming the non-stoichiometric substance to be zinc), and 0.16 to 0.04% (assuming, Zn_2O*1) ; hence these values are too small to explain the value of 1.5%.

Consequently, the accelerated decomposition will be caused not only by the non-stoichiometric substance, but also by the lattice defect

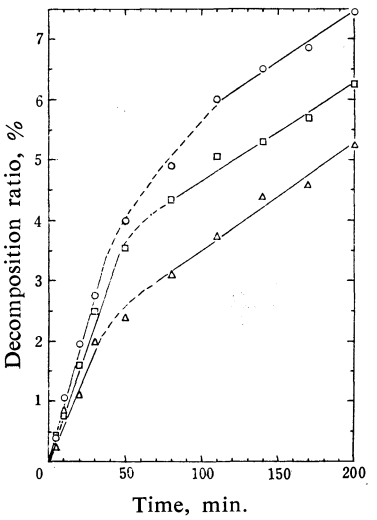


Fig. 4. The relationship between reaction rate and temperature (standard sample).
○ 820°C □ 780°C △ 740°C

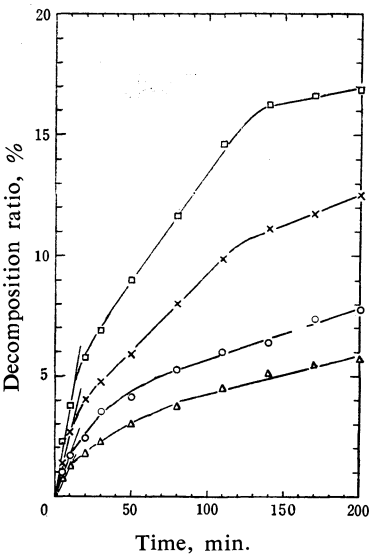


Fig. 5. The relationship between reaction rate and temperature (hydrogen pretreated sample).
□ 780°C × 740°C ○ 700°C △ 660°C

*1 Some investigators have suggested that, on the surface of zinc oxide in the state of oxygen deficiency, zinc suboxide, e.g., Zn_2O, is formed.[4,6]

TABLE II. INITIAL DECOMPOSITION RATE OF PRETREATED ZINC OXIDE BY H_2 (ca. 40 mmHg) AND IN VACUO ($\times 10^2\,min^{-1}$)

Temp. °C	Conditions of pretreatment	
	H_2 ca. 40 mmHg	in vacuo
820		0.094
780	0.411	0.083
740	0.274	0.066
700	0.198	
660	0.143	

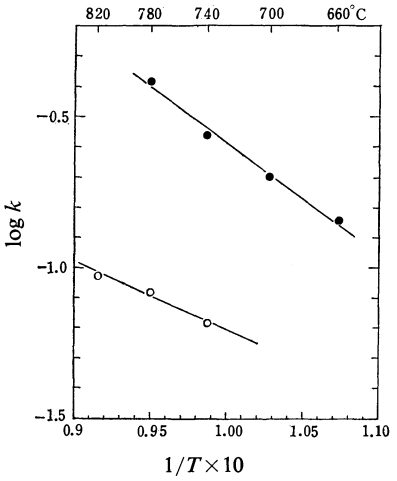


Fig. 6. Arrhenius relationships.
○ Standard ● H_2 treated

resulting from the lack of oxygen.

The results at various temperatures obtained with zinc oxide pretreated under standard conditions and by hydrogen are shown in Figs. 4 and 5. From Figs. 4 and 5, the initial reaction rates,*2 which are thought to be dependent upon the pretreatments, shown in Table II are obtained. Figure 6 shows the Arrhenius plots, from which the activation energies have been found to be 9.7 and 16.6 kcal./mol. The latter value, 16.6 kcal./mol., is in good agreement with the 17.0 kcal./mol. value obtained in the previous studies[2] of the rate of the reduction of zinc oxide by hydrogen controlled by the decomposition process of zinc oxide.

Considerations Upon the Rate of Oxygen Evolution.—After the decomposition had proceeded into the linear stage, as is shown in Fig. 2, the evacuation from the reaction system was stopped and the amount of oxygen which had accumulated in the system was measured. Figure 7 shows the typical curves of the accumulating rate of oxygen. Assuming that the rate of the oxygen evolution is proportional to the

*2 The slopes of the lines in the initial reaction stage in Figs. 4 and 5 represent the initial reaction rate.

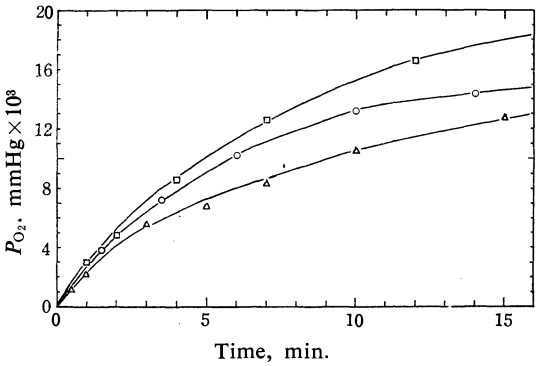


Fig. 7. Typical curves of accumulating rate of oxygen.
△ 100 mg. $P_e=13.8\times10^{-3}$ mmHg
□ 30 mg. $P_e=19.1\times10^{-3}$ mmHg
○ 10 mg. $P_e=16.1\times10^{-3}$ mmHg

pressure difference of oxygen between that at the decomposition equilibrium, P_e, and that at time t, P_{O_2}, the rate equation may be given by Eq. 1:

$$\frac{dP_{O_2}}{dt}=k_0(P_e-P_{O_2}) \qquad (1)$$

Integrating Eq. 1,

$$-\log\frac{P_e-P_{O_2}}{P_e}=k_0't \qquad (2)$$

In Fig. 8, the $\log(P_e-P_{O_2})/P_e$ obtained from Fig. 7 is plotted against the time. Figure 8 shows that every datum gives good straight lines and that Eqs. 1 and 2, based on the above assumption, are satisfied.

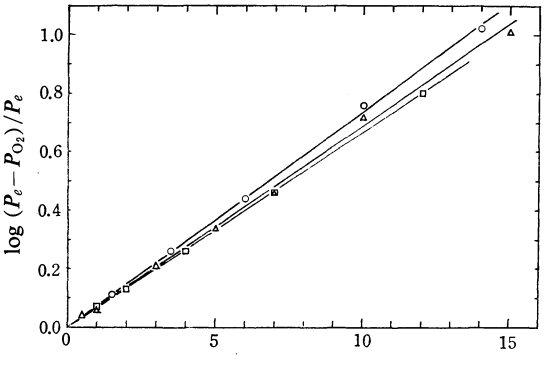


Fig. 8. $-\log(P_e-P_{O_2})/P_e$ vs. t.
△ 100 mg. □ 30 mg. ○ 10 mg.

The amount of zinc oxide is plotted against k_0' in Fig. 9, where the k_0' value is independent of the initial amounts of the zinc oxide, provided that zinc oxide is present in a larger amount. Consequently, in this region, the diffusion process of oxygen from the surface of

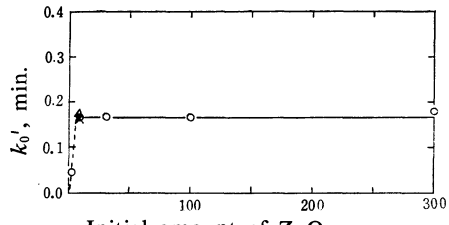


Fig. 9. The relationship between k_0' and the amount of zinc oxide.
○ 700°C × 740°C △ 780°C

zinc oxide into the ambient gas is considered to be the rate-controlling step in the overall decomposition. On the contrary, at smaller amounts of zinc oxide, the decomposition rate is found to be proportional to the amount of zinc oxide; hence, the rate of the overall reaction is controlled by the decomposition process.

From the initial decomposition rate (3.2×10^{-3} mmHg/min.) at $t=0$, $w_0=10$ mg. in Fig. 7, the rate of the weight loss is calculated to be 0.033 mg./hr. if only oxygen is evolved, and 0.17 mg./hr. if both oxygen and zinc are stoichiometrically evolved. When the above values are compared with the experimental value, 0.12 mg./hr., obtained from the slope in Fig. 2 (where w_0 is assumed to be 10 mg.), it may be concluded that the evolution of oxygen is predominant over the vaporization of zinc and that zinc oxide grows richer in zinc as the decomposition proceeds.

A Comparison of the Rate Constants of the Decomposition with the Reduction by Hydrogen. —As has been mentioned above the activation energy of the decomposition of zinc oxide is found to be in good agreement with that of the reduction by hydrogen controlled by the decomposition process. In this section, in order to discuss further the relations between these two reactions, their rate constants will be compared. The following two results, obtained at nearly the same temperature, are chosen for the comparison: at 738°C, $k_2'=0.158$ cmHg$^{1/3}\cdot$min^{-1}, sample 40 mg., from Ref. 2., and at 740°C, $k=0.00274$ min^{-1}, from Table II in this paper. The rate constant, k_2', of the reduction of zinc oxide was obtained according to Eq. 3, which had been deduced from the assumption that the reduction rate is proportional to the surface area of zinc oxide:

$$(P_0-P_\infty)^{1/3}-(P-P_\infty)^{1/3}=k_2'(t-t_0) \qquad (3)$$

where

$$k_2'=k_1\left(\frac{\pi n}{3a}\right)^{1/3}\left(\frac{2}{\rho}\right)^{2/3} \qquad (4)$$

$$a=\frac{(P-P_\infty)}{w} \qquad (5)$$

where k_1 is the reduction rate per unit surface area in a unit of time, g./cc. min., n is the number of zinc oxide particles, w and ρ are the mass and density of zinc oxide respectively, and P_0 and P_∞ are the hydrogen pressures when the reduction starts to obey Eq. 3 and the zinc oxide is completely used up respectively (shown in Fig. 10). In this work, the characteristic value, a, defined by Eq. 5 equals 0.00947 g./(cmHg of hydrogen) at 738°C.

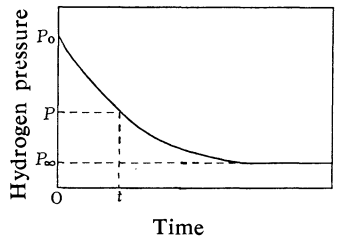


Fig. 10. The typical curve of the reduction of zinc oxide by hydrogen, which proceeds according to Eq. 3.

Since the amounts of zinc oxide is 40 mg. and since its specific surface area is 10 m^2/g.,*3 n is calculated to be 1.2×10^{13}. Therefore, from Eqs. 4 and 5, k_1 is given by Eq. 6:

$$k_1=k_2'\left(\frac{3a}{n\pi}\right)^{1/3}\left(\frac{\rho}{2}\right)^{2/3}$$
$$=2.85\times10^{-6}\ \text{g./cm}^2\cdot\text{min.} \qquad (6)$$

On the other hand, in this decomposition of the pellet-type zinc oxide, the decomposed amounts in 200 min. at 780°C, Δw, were 0.6 and 0.8 mg. for the samples with the surface areas of 4.41 and 4.39 cm^2 respectively, and, hence, 0.7 mg. for 4.40 cm^2 on the average. From Fig. 1, the decomposed amount, Δw, of 0.7 mg. will be found to correspond to the initial amount w_0 (10 mg.) of zinc oxide powder. Therefore, the effective specific surface area for the decomposition of zinc oxide powder is 4.40 cm^2/10 mg.$=$440 cm^2/g.*3 Consequently, the decomposition rate per unit of surface area in this work is 0.00274 min^{-1}/440 (cm^2/g.) $=6.23\times10^{-6}$ g./cm$^2\cdot$min. Considering the experimental errors and the requirement of some assumptions for the comparison, the above value, 2.85×10^{-6} g./cm$^2\cdot$min., may be regarded to be in good agreement with the experimental value, 6.23×10^{-6} g./cm$^2\cdot$min.

A Discussion of the Reverse Reaction. —During the course of the investigation of the

*3 There is the marked difference in the specific surface area of zinc oxide between the two samples, the one used in the decomposition, and the other in the reduction. This may be caused by the difference in particle diameter. The former contains about 30 wt.% which is larger than 250μ in particle diameter whereas in the latter only 0.03% are larger than 44 μ.[1] The electron-microscope study also shows the above fact.

TABLE III. THE WEIGHT LOSS OF ZINC OXIDE AND PRESSURE CHANGE OF HYDROGEN DURING HYDROGEN PRETREATMENT

Run No.	Temp. °C	Initial hydrogen pressure mmHg	Weight loss during hydrogen pretreatment mg.	Hydrogen pressure	
				Corresponding to weight loss of ZnO mmHg	After pretreatment mmHg
69	740	32.3	142.0	76.6	>16.8
70	740	33.1	140.1	75.6	>16.8
71	740	32.3	76.00	41.0	>16.8
73	700	33.1	67.46	36.4	28.2
74	700	30.7	60.75	32.8	28.9
79	660	32.3	24.70	13.3	>17.0
80	660	31.5	30.90	16.7	>17.0
85	780	29.1	121.2	65.5	16.3
87	780	29.9	71.39	35.8	23.8
88	780	29.1	59.66	32.2	25.8

reduction of zinc oxide by hydrogen,[1-3] a deposit consisting of zinc oxide and zinc metal was observed on the cooler part of the reaction vessel. The following three reasons for zinc oxide film may be suggested.

1) The sublimed zinc oxide condenses on the cooler part of the vessel before it is reduced by hydrogen.

2) Zinc oxide decomposes into zinc vapor and oxygen, and then the reverse reaction takes place to produce the zinc oxide.

3) Zinc oxide is produced by the reaction of zinc vapor and gaseous water.

In this study of the decomposition, the zinc oxide film was not produced on the cooler part of the reduction tube. Therefore, reasons 1 and 2 above have been found to be invalid. Reason 3 was also supported by the additional observation that hydrogen, which is produced by the reaction*4 of water and zinc, will contribute to the reduction of zinc oxide again. Table III shows the weight loss by the pretreatment of zinc oxide placed in the basket, the initial hydrogen pressure for the pretreatment, and the hydrogen pressure cooresponding to the weight loss (each value being converted at 0°C). In all the runs (except No. 79 and 80 in Table III), the hydrogen pressure corresponding to the weight loss caused by the reduction of hydrogen*6 is found to be higher than the initial hydrogen pressure. Consequently, the hydrogen reproduced by reason 3 is suggested to reduce further the zinc oxide placed in the basket.

Department of Applied Chemistry
Faculty of Engineering
Osaka City University
Sumiyoshi-ku, Osaka

*4 Since the equilibrium constant K of the reaction: $ZnO(s)+H_2 \rightleftarrows Zn(g)+H_2O(g)$ is very small*5, the vapor pressure of wate is very low. Consequently, the reduction rate can be followed by measuring the pressure in the system as reported in Ref. 1.

*5 $K=1.1\times10^{-3}$, $P_{H_2O}=0.85$ mmHg at 1 atm. H_2, 723°C
$K=2.4\times10^{-3}$, $P_{H_2O}=1.85$ mmHg at 1 atm. H_2, 823°C
from G. B. Taylor and H. W. Starkweather, *J. Am. Chem. Soc.*, 52, 2314 (1930).

*6 In this case, the decomposed amount of zinc oxide is much less than the amount of zinc oxide reduced by hydrogen.

*The Redox Reaction of 1-Ethoxy-n-heptyl Hydroperoxide**

By Shinji MURAI, Noboru SONODA and Shigeru TSUTSUMI

(Received February 27, 1964)

In our previous study of the redox reaction of an ether-hydroperoxide,[1] we reported that hexane-1, 6-diol diformate and γ-butyrolactone are produced by the redox reaction of tetrahydrofuran hydroperoxide (a heterocyclic ether hydroperoxide) with ferrous sulfate, and that, in the case of the reaction with cuprous and cupric chlorides, 3-formoxypropyl chloride and γ-butyrolactone are produced. We then suggested that these products might be formed by carbon-carbon bond fission and carbon-hydrogen bond fission at the α-position of the 2-tetrahydrofuranoxy radical generated as an intermediate. The corresponding carbon-oxygen bond fission might lead to the formation of *a carbonyl product*, 4-hydroxybutanal, which was obtained in a trace amount. Now it has become desirable to investigate the redox reaction of the hydroperoxide of a linear ether; therefore, the redox decomposition of 1-ethoxy-*n*-heptyl hydroperoxide (I) has been carried out in order to clarify the nature of these reactions.

Results and Discussion

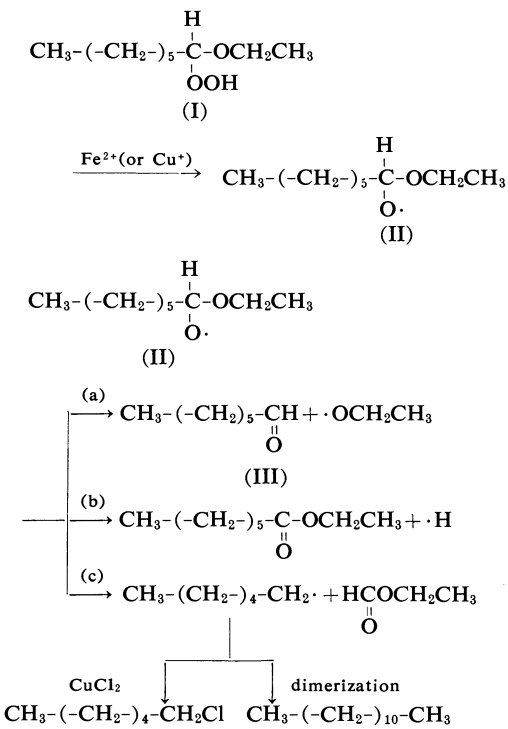
Analytically pure 1-ethoxy-*n*-heptyl hydroperoxide (I) was prepared by the ozonolysis of octene-1 in ethanol. The decomposition reaction of the hydroperoxide (I) was carried out using some metal ions such as ferrous or cuprous ions. When the hydroperoxide I was decomposed in the presence of ferrous sulfate at 7~9°C, ethyl formate, *n*-heptanal, ethyl heptanoate and *n*-dodecane were obtained; they might be formed through the fragmentation of the 1-ethoxy-*n*-heptoxy radical (II) produced by the reductive cleavage of the hydroperoxide I with ferrous ions. In the presence of cupric and cuprous chlorides, the decomposition of I gave ethyl formate, *n*-hexyl chloride, *n*-heptanal and ethyl heptanoate, whereas the formation of *n*-dodecane was not observed because of the chlorination of the *n*-hexyl radical with the cupric chloride used as an alkyl radical scavenger. The *n*-heptanal (III) obtained in both reactions is *the carbonyl product* corresponding to the product which might be given by the carbon-oxygen bond fission of the radical II. However, the mechanism of the carbonyl-product formation is more complicated, as will be discussed later. The results are summarized in Table I.

TABLE I. DECOMPOSITION PRODUCTS OF 1-ETHOXY-*n*-HEPTYL HYDROPEROXIDE

	Decomposition with $FeSO_4$ Yield, %	Decomposition with $CuCl$-$CuCl_2$ Yield, %
Ethyl formate	30[a]	22
n-Hexyl chloride	—	20
n-Heptanal	38	26
Ethyl heptanoate	27	26
n-Dodecane	18	0

a) see Experimental section.

In these reactions, the initial step may be the reductive cleavage of the hydroperoxide I to yield the radical II, which would then react according to the following scheme:

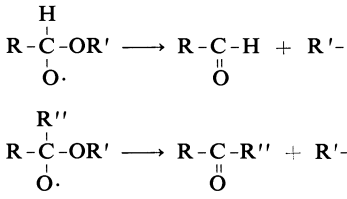


* Presented at the 16th Annual Meeting of the Chemical Society of Japan, Tokyo, April, 1963.

1) S. Murai, N. Sonoda and S. Tsutsumi, This Bulletin, 36, 527 (1963).

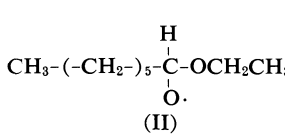
In these reactions, path a comprises the homolytic cleavage of the carbon-oxygen bond, while paths b and c also comprise the fission of the carbon-hydrogen bond and of the carbon-carbon bond of the radical II respectively. The *n*-hexyl radical produced in path c would dimerize to produce *n*-dodecane and also would give *n*-hexyl chloride in the presence of cupric chloride used as an alkyl radical scavenger.

Little attention has been paid to the formation of carbonyl products, aldehydes or ketones in the redox decomposition of the ether-hydroperoxides.

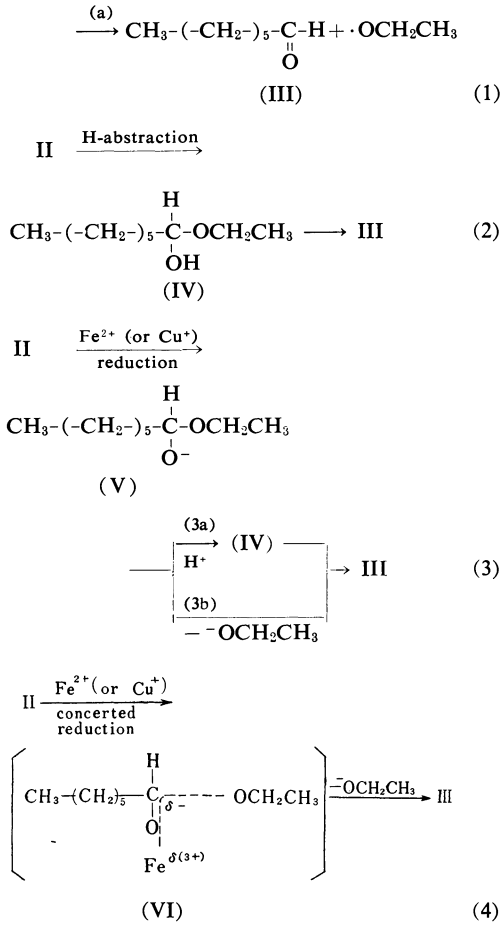


In some cases the hydroperoxides were prepared from carbonyl compounds or ethers and were subjected to reaction without isolation; thus, it was more difficult to clarify the formation of carbonyl products in the redox reaction, and in other cases no effort was made to detect them.[2] Sharp and Patrick reported the formation of aldehydes in a small amount in the ferrous ion-catalyzed decomposition of ether-hydroperoxides.[3] However, the hydroperoxides were not reacted in isolation and were reacted at a rather high temperature, which would induce thermal decomposition. Milas et al. suggested[4] the possible formation of 2-hydroxytetrahydropyran[5] in the ferrous ion-catalyzed decomposition of 2-hydroperoxytetrahydropyran, but the formation of this compound was not reported in a recent investigation of this same system.[6]

In contrast with these results, a rather large amount of a carbonyl compound, *n*-heptanal, was obtained in the present experiment. Some possible reaction pathways for the formation of *n*-heptanal (III) are:



(II)



(III) (1)

(IV) (2)

(V) (3)

(VI) (4)

It may be assumed that the pathway shown by Eq. 4 is the most plausible from the following consideration; since the transition state for the homolytic cleavage of an alkoxy radical involves the stretching of the breaking bond, the free energy of the activation for the cleavage would be expected to be raised as the stability of the leaving radical is decreased. Therefore, the homolytic cleavage of the carbon-oxygen bond, Eq. 1, would be unable to compete with the carbon-carbon bond cleavage (step c) or the carbon-hydrogen bond cleavage (step b) because of the relative instability of the leaving ethoxy radical. Furthermore, as to Eq. 2, there may exist a few hydrogen donors for H-abstraction except the hydroperoxide itself and its decomposition products, which may be insufficient in amount to serve efficiently. Equation 3 shows the reduction of the alkoxy radical II to the corresponding anion V, followed by the protonation 3a or by the leaving of the ethoxide ion 3b. Such a reduction of an alkoxy radical with reducing metal ions has been reported by Kochi.[7]

2) For example, a) J. K. Kochi and F. F. Rust, *J. Am. Chem. Soc.*, **84**, 3946 (1962); b) R. V. Digman and D. F. Anderson, *J. Org. Chem.*, **28**, 239 (1963).

3) D. B. Sharp and T. M. Patrick, Jr., *J. Org. Chem.*, **26**, 1389 (1961).

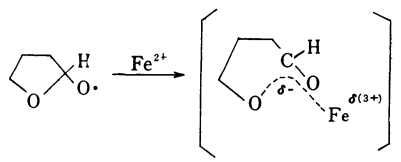
4) N. A. Milas, R. L. Peeler, Jr., and O. L. Mageli, *J. Am. Chem. Soc.*, **76**, 2322 (1954).

5) This compound is in equilibrium with 5-hydroxypentanal and corresponds to the carbonyl product.

6) E. A. Youngman, F. F. Rust, G. M. Coppinger and H. E. De La Mare, *J. Org. Chem.*, **28**, 144 (1963).

7) J. K. Kochi, *J. Am. Chem. Soc.*, **84**, 1193 (1962).

Equation 3, however, cannot explain the different results that, in the present reaction of the hydroperoxide of the linear ether, a carbonyl product was obtained in a better yield than in the case of the cyclic ether system reported on previously.[1] This result may be explained most reasonably in terms of the concerted reduction, Eq. 4, in which the partial breaking of the carbon-oxygen bond might be more sterically favorable in the transition state VI than in a cyclic ether system VIII.



(VIII)

⟶ 4-Hydroxybutanol

Because of the reasons described above, it seems reasonable to assume that *n*-heptanal is produced by the reduction of radical II with ferrous or cuprous ions, followed concertedly by the leaving of the ethoxide ion, which may be a suitable leaving anion.

There assumptions are also supported by the fact that cyclohexanone was generated as a carbonyl product in the redox reaction of 1-ethoxycyclohexyl hydroperoxide under the same conditions as is described above.[8]

Experimental

1-Ethoxy-*n*-heptyl Hydroperoxide (I). — Eighteen grams of 1-octene was dissolved in 350 ml. of ethanol, and a stream of ozone containing oxygen was passed at −70°C until the completion of the reaction was indicated by the liberation of iodine in an aqueous solution of potassium iodide at the gas outlet. The solvent and the cleavaged fragment were removed under reduced pressure at room temperature, and then further removed in vacuo (0.5 mmHg) at room temperature for three hours. The residual colorless oil (26 g.) showed infrared absorptions at 3400 cm^{-1} (-OH) and 1100 cm^{-1} (C-O-C) and reacted positively to a lead tetraacetate test. The amount of active oxygen was determined by iodometry to be 9.27% (Calcd. for $C_9H_{20}O_3$: 9.08%). Molecular weight (in benzene) 180 (Calcd. for $C_9H_{20}O_3$: 176.3%).

The Reaction of 1-Ethoxy-*n*-heptyl Hydroperoxide (I) with Ferrous Sulfate.—Into a solution of 15.0 g. of ferrous sulfate heptahydrate in 70 ml. of water 8.0 g. of the hydroperoxide I was vigorously stirred, drop by drop, over a period of 20 min. at 7~9°C. The stirring was then continued for a further three hours at a room temperature. From the reaction mixture a low boiling material was distilled out directly, at room temperature and at 10 mmHg, in to a trap cooled at −70°C.

After the removal of water from this trap by a separatory funnel, 1.1 g. of ethyl formate was obtained. By gas chromatographic analysis this fraction was shown to contain a small amount of *n*-hexane and hexene-1, but no effort was made to make a quantitative determination of these compounds.

The reaction mixture, after the removal of the low boiling material, was extracted with five 100 ml. portions of ether. The ether extract was dried over anhydrous magnesium sulfate. The evaporation of the ether gave 6.0 g. of products which were estimated by gas chromatography to contain 2.2 g. of *n*-heptanal, 2.3 g. of ethyl heptanoate and 1.5 g. of *n*-dodecane; column, Silicon DC-550 and PEG 6000; column temperature, 130°C; carrier gas, H_2. The 2, 4-dinitrophenylhydrazone of *n*-heptanal was prepared by treating the above-mentioned reaction mixture with a hydrochloric acid solution of 2, 4-dinitrophenylhydrazine; its melting point and mixed melting point with an authentic sample were each 108~109°C.

The Reaction of 1-Ethoxy-*n*-heptyl Hydroperoxide (I) with Cuprous Chloride and Cupric Chloride.—Into a suspension of 5.0 g. of cuprous chloride and 8.8 g. of cupric chloride dihydrate in 100 ml. of water 8.0 g. of the hydroperoxide I was vigorously stirred, drop by drop, over a period of 30 min. at 5~7°C. The stirring was then continued for a further three hours. The reaction mixture was treated in the manner mentioned above. From the low boiling product, 0.7 g. of ethyl formate, and from the ether extract, 1.0 g. of *n*-hexyl chloride, 1.5 g. of *n*-heptanal and 2.1 g. of ethyl heptanoate were obtained, although no formation of *n*-dodecane was observed by gas chromatographic analysis.

Summary

1) The reaction of 1-ethoxy-*n*-heptyl hydroperoxide with ferrous sulfate has given ethyl formate, *n*-heptanal, ethyl heptanoate and *n*-dodecane, while the reaction with a mixture of cuprous and cupric chlorides has given ethyl formate, *n*-hexyl chloride, *n*-heptanal and ethyl heptanoate.

2) The formation of *n*-heptanal in both reactions has been attributed to the reduction of the 1-ethoxy-*n*-heptanoxy radical with ferrous or cuprous ions to the corresponding anion, followed concertedly by the leaving of the ethoxide ion.

3) The probable reaction pathway, especially the difference between the natures of the heterocyclic ether syetem and the linear ether system, has been discussed.

8) S. Murai, N. Sonoda and S. Tsutsumi, unpublished work: Analytically pure 1-ethoxycyclohexyl hydroperoxide was prepared by the ozonolysis of methylenecyclohexane in ethanol; b. p. 50~58°C (ca. 10^{-2} mmHg); n_D^{20}, 1.4602.

The authors wish to thank Dr. Yoshinobu Odaira for his helpful suggestions and encouragement.

Department of Chemical Technology
Faculty of Engineering
Osaka University
Miyakojima-ku, Osaka

Studies of the Organic Reaction of Metal Carbonyl. V. The Reaction of Cobalt Hydrocarbonyl with Olefin—The Effects of the Reaction Conditions and of the Structure of Olefin

By Yoshinobu TAKEGAMI, Chikao YOKOKAWA, Yoshihisa WATANABE, Hiromitsu MASADA and Yasukazu OKUDA

(Received February 27, 1964)

In connection with the oxo reaction, several studies[1-4] of the reaction of cobalt hydrocarbonyl with olefin have been published. It have been established[3,4] that 1-olefin gives two isomeric acylcobalt carbonyls and aldehydes in this reaction. Heck and Breslow[3] have suggested that the direction of the addition of cobalt hydrocarbonyl to some olefins, such as methyl acrylate and isobutylene, at 0°C is essentially the reverse of that of hydroformylation reaction at 120°C. It has thus seemed of considerable interest to study the reaction in greater detail. Previous work[5] in this laboratory has shown that some alkyl- and acylcobalt carbonyls isomerize readily. It is, accordingly, considered that the distribution of two isomeric acylcobalt carbonyls is affected by the isomerization as well as by the direction of the addition.

In the present paper, this type of reaction has been investigated by examing the effect of the reaction conditions and the structure of olefin, mainly on the nature of the reaction and on the distribution of the products.

Experimental

The Reaction Procedures.—The reactions under one atmosphere of carbon monoxide or nitrogen were carried out in the way described in previous papers,[5,6] using 50 ml. of a 0.09 M cobalt hydrocarbonyl solution in toluene. The reactions under two atmospheres of carbon monoxide were carried out using a 200 ml. glass autoclave.

The Analytical Procedures.—The solution of crude products was treated with iodine and alcohol as described previously,[5,6] and the excess of iodine was reduced with crystalline sodium thiosulfate. After concentration, the analyses of the reaction products were carried out by gas chromatography and by means of the infrared spectra, which were measured on a Shimadzu model IR-27 spectrophotometer.

The Materials.—Ethyl acrylate, styrene, *n*-butyl vinyl ether and pentene-1 were commercial products, all of which had been proved to be sufficiently pure by gas chromatography.

Results and Discussion

The Reaction of Ethyl Acrylate.—The results of the reaction of ethyl acrylate, which were carried out under one atmosphere of carbon monoxide or nitrogen at various temperatures, are summarized in Table I and Fig. 1.

The gas absorption curves in Fig. 1 indicate that the amount of gas absorbed increased with a decrease in the reaction temperature, though the rate of the gas absorption decreased; for instance, at −15°C, 0.6 mol.*1 of the gas was absorbed in 4 hr.; then the gas absorption ceased, but at 25°C about 0.4 mol. of the gas was absorbed in half an hour.

The reaction temperature had a significant effect on the distribution of the products; at

1) I. Wender, H. W. Sternberg and M. Orchin, *J. Am. Chem. Soc.*, **75**, 3041 (1953); P. Pino, R. Ercoli and F. Calderazzo, *Chim. e Ind. (Milan)*, **37**, 783 (1955); L. Kirch and M. Orchin, *J. Am. Chem. Soc.*, **80**, 4428 (1958); **81**, 3597 (1959).

2) R. F. Heck and D. S. Breslow, *Chem. & Ind.*, **1961**, 467.

3) R. F. Heck and D. S. Breslow, *J. Am. Chem. Soc.*, **83**, 4023 (1961).

4) G. L. Karapinka and M. Orchin, *J. Org. Chem.*, **26**, 4187 (1961).

5) Y. Takegami, C. Yokokawa, Y. Watanabe and Y. Okuda, This Bulletin, **37**, 181 (1964).

6) Y. Takegami, C. Yokokawa, Y. Watanabe and H. Masada, ibid., **37**, 662 (1964).

*1 Mole of the gas absorbed per mole of cobalt hydrocarbonyl used.

TABLE I. THE REACTION OF ETHYL ACRYLATE WITH COBALT HYDROCARBONYL

Exp. No.	Reaction conditions*1			CO Absorbed (mol./mol. $HCo(CO)_4$)	Product	
	Atmosphere	Temp. °C	Time min.		Esters*2 (mol./mol. $HCo(CO)_4$)	Distribution of esters $B/(B+S)$*2 $\times 10^2$
1	CO	25	120	0.39	0.31	3
2	CO	0	180	0.47	0.78	97
3	CO	0	180	0.51	0.72	97
4	CO	−10	210	0.55	0.72	97
5	CO	−15	250	0.59	0.57	97
6	CO	−20	240	0.32	0.28	97
7	N_2	0	120	—	0.21	30
8	N_2	−10	180	—	0.18	40
9	N_2-CO*3	0	20～120	0.09	0.21	33

*1 Other condition: 10 mol. of ethyl acrylate per mol. of cobalt hydrocarbonyl used. Under one atmosphere of carbon monoxide or nitrogen.
*2 B: a ester with the branched structure, diethyl methylmalonate.
S: a ester with the straight structure, diethyl succinate.
*3 At first under nitrogen atmosphere and then under carbon monoxide.

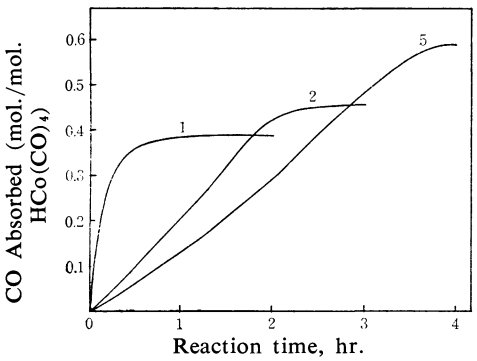


Fig. 1. CO Absorption vs. time plots for the reaction of ethyl acrylate at various temperatures.
Number corresponds with Exp. No. in Table I.
Curve 1; at 25°C, curve 2; at 0°C and curve 5; at −15°C.

25°C, diethyl succinate*2 was the major product, and only a trace of diethyl methylmalonate*3 was also identified (Exp. 1). On the other hand, at 0～−20°C, diethyl methylmalonate was the major product, and only a small amount of diethyl succinate was formed (Exp. 2—6). These facts, it would seem, can be interpreted by the following assumption; at a relatively low temperature, some effect of the ester group (-COOEt) on the adjacent carbon atom is more important, and then α-carbon atom is selectively carbonylated to form the acylcobalt carbonyl with the branched structure. However, at 25°C the steric effect is more important, and then a more stable acylcobalt carbonyl with a straight chain structure is formed.

At 0 and −10°C, the quantity of diethyl methylmalonate formed was more than that expected from the amount of the gas absorbed. It would seem that this fact can be explained by the following equilibrium:

$$\begin{array}{l} \text{C–C–COOEt} \\ \quad\vert \\ \text{COCo(CO)}_3 \end{array} + \text{CO} \rightleftarrows \begin{array}{l} \text{C–C–COOEt} \\ \quad\vert \\ \text{COCo(CO)}_4 \end{array}$$

At nitrogen atmosphere also had a significant effect on the distribution of the products, as was demonstrated by Exps. 7 and 8; even at 0 and −10°C, diethyl succinate was the major product, and a relatively large amount of diethyl methylmalonate was also formed, though the yield of the esters was not good. Under a nitrogen atmosphere, however, the color of the reaction solution changed much more readily than under carbon monoxide from yellow to brown; it took less than five minutes, even at −10°C. The reaction was carried out in two stages at 0°C, at first under a nitrogen atmosphere for 20 min. and then under a carbon monoxide. At the second stages, only 0.09 mol. of the gas was absorbed, and the yield of the esters was comparable to that under nitrogen (cf. Exps. 7 and 9). This fact seemed to indicate that under nitrogen, side reactions other than the formation of the acylcobalt carbonyl occurred rapidly to consume a large part of cobalt hydrocarbonyl used. Such a effect of a nitrogen atmosphere has been also observed in the reaction of olefin oxide with cobalt hydrocarbonyl.[6]

Heck and Breslow[3] have suggested that a nitrogen atmosphere promotes the carbonylation of olefin and that the inhibitory effect of a carbon monoxide atmosphere may be explained by the following equilibrium:

*2,*3 Believed to have been derived from the corresponding acylcobalt carbonyls by cleavage with iodine and ethyl alcohol. Identified by gas chromatography and infrared spectrum using authentic samples.

TABLE II. THE REACTION OF ETHYL ACRYLATE—EFFECT OF CO PRESSURE

Exp. No.	Reaction conditions*1			CO Absorbed (mol./mol. $HCo(CO)_4$)	Product	
	Atmosphere	Temp. °C	Time min.		Esters*2 (mol./mol. $HCo(CO)_4$)	Distribution of esters $B/(B+S)\times10^2$
10	CO*3	0	240	0.71	0.73	97
11	CO*3	0	240	0.76	0.67	97
12	CO*3	25	240	0.76	0.32	12
13	CO*4	0	240	0.41	0.45	97

*1 10 mol. of ethyl acrylate per mol. of cobalt hydrocarbonyl used.
*2 Diethyl methylmalonate and diethyl succinate.
*3 Under two atmosphere of carbon monoxide.
*4 Under one atmosphere of carbon monoxide.

TABLE IIIa. THE REACTION OF PENTENE-1 WITH COBALT HYDROCARBONYL

Exp. No.	Reaction conditions*1			CO Absorbed (mol./mol. $HCo(CO)_4$)	Product	
	Atmosphere	Temp. °C	Time min.		Esters*2 (mol./mol. $HCo(CO)_4$)	Distribution of esters $B/(B+S)$*2$\times10^2$
14	CO	25	120	0.26	0.1	
15	CO	15	180	0.70	0.45	25
16	CO	0	420	0.54	0.35	25
17	CO	−10	960	0.44	0.33	30
18	N_2	0	5	—	0.03	—
19	N_2	0	30	—	0.03	—
20	N_2	0	180	—	0.03	—
21	N_2	0	780	—	0.03	—
22	N_2-CO*3	0	5～300	0.07	0.06	—
23	N_2-CO	0	30～180	～0	0.05	—

TABLE IIIb. THE REACTION OF METHYL IODIDE WITH POTASSIUM COBALT CARBONYL

24	CO	0	200	1.00	—	—
25	N_2-CO	0	5～200	1.00	—	—
26	N_2-CO	0	30～200	0.96	—	—
27	N_2-CO	0	60～280	0.70	—	—

*1 10 mol. of pentene-1 per mol. of cobalt hydrocarbonyl used.
5 mol. of methyl iodide per mol. of potassium cobalt carbonyl used.
*2 B: ethyl α-methyl-*n*-valerate.
S: ethyl *n*-caproate.
*3 At first under nitrogen and then under carbon monoxide.

$$HCo(CO)_4 \rightleftarrows HCo(CO)_3+CO$$

that is, cobalt hydrotricarbonyl is more reactive.

In regard to this assumption, the reactions were carried out under two atmospheres of carbon monoxide to examine the effect of the pressure of carbon monoxide on the reaction. The resuluts are summarized in Table II. Under these conditions, the reaction seemed to occur relatively more smoothly because a larger amount of the gas was absorbed than under one atmosphere of carbon monoxide (cf. Exp. 11 and 13*4), suggesting that higher pressures of carbon monoxide are more advantageous fos this reaction, the formation of the acylcobalt carbonyls. This observation is not interpreted by Heck and Breslow's assumption. The reaction temperature, under these conditions, had almost the same effect on the distribution of the products as under one atmosphere of carbon monoxide.

In order to examine the effect of the atmosphere in greater detail, pentene-1 and methyl iodide were submitted to reactions with cobalt hydrocarbonyl and potassium cobalt tetracarbonyl respectively. The results are summarized in Table III.

Pentene-1 is evidently less reactive than ethyl acrylate (cf. Fig. 4). In this case, the reaction temperature (25～10°C) had no effect on the distribution of the products; ethyl *n*-caproate was the major product, and ethyl α-methylvalerate was the minor (Exps. 14—17). Under a nitrogen atmosphere at 0°C, only 0.03 mol

*4 Carried out under one atmosphere of carbon monoxide using the same glass autoclave.

TABLE IV. THE REACTION OF ETHYL ACRYLATE—EFFECT OF THE CHANGE OF THE REACTION TEMPERATURE IN STAGES ON THE DISTRIBUTION OF PRODUCTS

Exp. No.	Reaction conditions*1			CO Absorbed (mol./mol. $HCo(CO)_4$)	Product	
	Atmosphere	Temp. °C	Time min.		Esters*2 (mol./mol. $HCo(CO)_4$)	Distribution of esters B/(B+S) $\times 10^2$
28*3	CO	25~10	120~150	0.34	0.29	3
29	CO	−10~25	220~60	0.58+0.42*4	0.65	3
30	CO	−10~25	120~60 ~120	0.43+0.43	0.29	5
31	CO	−10~25	180~60	0.48+0.52	0.58	3
32	CO	−10~15	190~160	0.53−0.16 +0.35	0.39	35
33*5	CO	0~25	180~120	0.55	0.70	40
34	CO	25	10	0.40	0.30	23
35	CO	0	300	0.50	0.57	90
36	CO	0	900	0.46	0.44	55
37	N_2	0	10	—	0.22	76
38	N_2	0	240	—	0.15	14

*1 10 mol. ethyl acrylate/mol. $HCo(CO)_4$.
*2 Diethyl methylmalonate and diethyl succinate.
*3 At first at 25°C for 120 min. and then at −10°C for 150 min.
*4 Absorbed at 25°C (at the second stage).
*5 Under two atmospheres of carbon monoxide.

of the ester, mainly ethyl α-methylvalerate, was identified independently of the reaction time from 5 min. to 13 hr. (Exps. 18—21); C_6-aldehyde seemed not to be formed its 2,4-dinitrophenylhydrazone was not obtained.

The reaction was carried out in two stages, as has been mentioned above: at the second stage under carbon monoxide, a small amount of the gas was absorbed (Exps. 22 and 23), and the amount of gas evolved by the treatment with an excess of iodine after the reaction was comparable to that calculated for the cobalt hydrocarbonyl used. However, the reaction of methyl iodide with potassium cobalt tetracarbonyl was not affected evidently by the pre-treatment with a nitrogen atmosphere (Exps. 25—27). Therefore, in the reaction of pentene-1 under nitrogen, a large part of the cobalt hydrocarbonyl used seemed to be consumed in less than 5 min. by side reaction other than the carbonylation. It may, accordingly, be concluded that a carbon monoxide atmosphere is advantageous for the carbonylation of olefin.

The Isomerization of Acylcobalt Carbonyl.— As has been described above, the reaction temperature and atmosphere have a significant effect on the distribution of the products from ethyl acrylate. In regard to this fact, several reactions were carried out in two or three stages by changing the reaction temperature (from 25°C to −10°C or from −10°C to 25°C, etc.) and by changing the reaction atmosphere in the course of an individual run.

By the change of the reaction temperature from 25°C to −10°C, the distribution of the products was not affected, as in Exps. 28 and 1. However, by the change from −10°C to 25°C or 15°C, the distribution was remarkably affected (cf. Exp. 4); at the first stage, at −10°C, about 0.6 mol. of the gas was absorbed in about 200 min. and the gas absorption ceased, but at the second stage, at 25°C, about 0.4 mol. more of the gas was absorbed in about 60 min. (curve 29 in Fig. 2) and then diethyl succinate was obtained as the major product (Exp. 29). This fact indicates that the acyl-cobalt carbonyl (or/and the alkyl-) with the branched structure isomerized to that with the

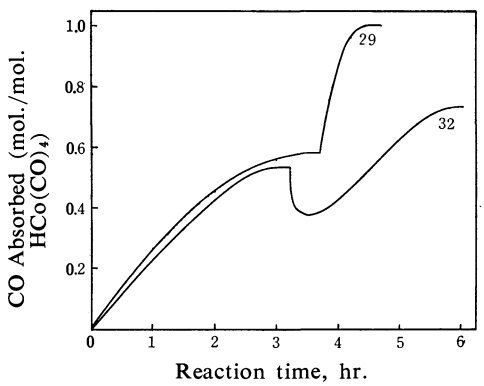
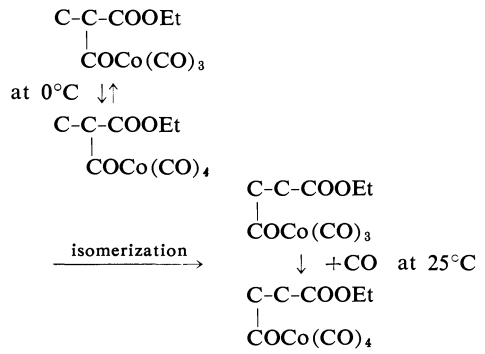


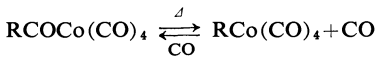
Fig. 2. CO Absorption vs. time plots for the reaction of ethyl acrylate——Effect of the change of the reaction temperature in stages.
Curve number: Exp. No.
Curve 29; at first at −10°C and then at 25°C.
Curve 32; at first at −10°C and then at 15°C.

straight one in this treatment; this may be represented as follows:

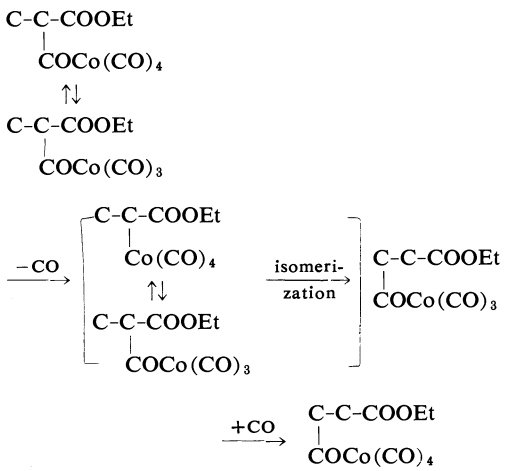


that is, the gas absorption at the second stage seemed to be due to the acylcobalt tricarbonyl with the straight-chain structure formed by the isomerization. The reverse isomerization, from the acylcobalt carbonyl with the straight-chain structure to that with the branched one, occurs only with difficulty, it seems.

When the reaction temperature at the second stage was set at 15°C, the gas evolution occurred first, followed by the gas absorption (curve 32 in Fig. 2). In this case diethyl succinate predominated in the product, but a relatively large amount of diethyl methylmalonate was also formed (Exp. 32); at 15°C, the isomerization also occurred, but more slowly than at 25°C. The gas evolution seemed to be due to the following change, as has been reported previously:[5]



Thus, it seems that the overall reaction scheme may be represented as follows:



that is, the carbon monoxide-lacking state, such as in the alkylcobalt tetracarbonyl and the acylcobalt tricarbonyl, seemed to undergo isomerization.

Even at 25°C, when the reaction was carried out only for 10 min., the proportion of diethyl methylmalonate formed was larger than that formed in the reaction which was carried out for 2 hr. (Exps. 34 and 1), suggesting that, at 25°C, the acylcobalt carbonyl with the branched structure is formed at first and that it then isomerizes rapidly to that with the straight structure. Thus, at an elevated temperature this type of isomerization is considered to occur more easily. The distribution of the products obtained in the oxo condition seems to be considerably affected by the isomerization as well as by the direction of the addition of cobalt hydrocarbonyl to a C=C bond.

Under two atmospheres of carbon monoxide, the same isomerization occurred with the change in the reaction temperature from 0°C to 25°C, but more slowly than under one atmosphere of carbon monoxide (cf. Exps. 33 and 29). The fact that a relatively high pressure of carbon monoxide is unfavorable for the isomerization seemed to support the above mechanism.

Even at 0°C under one atmosphere of carbon monoxide, this isomerization occurred very slowly; after 15 hr. the amount of diethyl succinate was almost comparable to that of diethyl methylmalonate (Exp. 36). On the other hand, under nitrogen this isomerization occurred more rapidly than under carbon monoxide; at 0°C, when the reaction was carried out for only 10 min., mainly diethyl methylmalonate was formed (Exp. 37), but after 2 or 4 hr. diethyl succinate predominated (Exps. 38 and 7). Thus, a nitrogen atmosphere promotes the isomerization.

By the change of the reaction atmosphere in such stages, as from carbon monoxide to nitrogen, the distribution of the products was also affected (Table V). When the reaction was carried out in two stages at 0°C, at the second stage under nitrogen about 0.2 mol. of a gas was evolved in about 20 min., and then the gas absorption followed slowly, as is shown in Fig. 3 (curve 40). The amount of the isomerized product, diethyl succinate, increased with an increase in the reaction time under nitrogen (Exps. 39—41); a nitrogen atmosphere promoted the isomerization. This observation seemed to be interpreted well by the mechanism of the isomerization.

As has been described above (Exp. 9), pretreatment for 20 min. with a nitrogen atmosphere remarkably reduced the amound of the gas adsorbed at the second stage under carbon monoxide. However, when the reaction was carried out at first under carbon monoxide for

TABLE V. THE REACTION OF ETHYL ACRYLATE—EFFECT OF THE CHANGE OF REACTION ATMOSPHERE IN STAGES ON THE DISTRIBUTION OF PRODUCTS

Exp. No.	Reaction conditions*1		CO Absorbed (mol./mol. $HCo(CO)_4$)	Product	
	Atmosphere	Time min.		Esters*2 (mol./mol. $HCo(CO)_4$)	Distribution of esters $B/(B+S)\times10^2$
39*3	$CO-N_2$	120～60	0.44－0.20	0.59	82
40	$CO-N_2$	120～180	0.54－0.22＋0.20*4	0.31	52
41	$CO-N_2$	120～300	0.45－0.20＋0.20	0.34	25
42*5	$CO-N_2-CO$	120～60～120	0.47－0.25＋0.30	0.4	75
43	$CO-N_2-CO$	15～30～120	0.14－0.07＋0.36	0.32	70
44	$CO-N_2-CO$	15～120～60	0.14－0.05＋0.18	0.13	30
45	$CO-N_2-CO$	30～30～135	0.26－0.07＋0.34	0.38	80
46	$CO-N_2-CO$	30～120～80	0.26－0.07＋0.23	0.27	25

*1 Other conditions: at 0°C 10 mol. of ethyl acrylate/mol. $HCo(CO)_4$.
*2 Diethyl methylmalonate and diethyl succinate.
*3 At first under carbon monoxide for 120 min. and then under nitrogen for 60 min. At the second stage 0.20 mol. of the gas was evolved.
*4 Absorbed at the second stage.
*5 Carried out in three stages: at the third stage 0.30 mol. of the gas was absorbed.

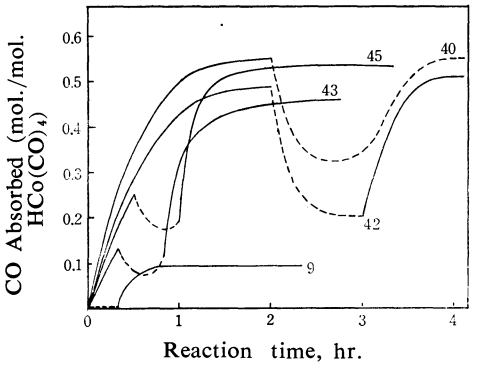


Fig. 3. CO Absorption vs. time plots for the reaction of ethyl acrylate——Effect of the change of the reaction atmosphere in stages.
Curve number: Exp. No.
(------) under a nitrogen atmosphere and
(——) under a carbon monoxide.

only 15 or 30 min.,*5 a nitrogen atmosphere for 30 min.*6 (or 120 min.) at the second stage did not prevent the gas absorption at the third stage under carbon monoxide (Exps. 43—46); in these runs the overall amount of gas absorbed was almost comparable to that absorbed when the reaction which was carried out under carbon monoxide (cf. Exp. 2). This fact seemed to support the consideration that, under nitrogen at the first stage, the cobalt hydrocarbonyl used is rapidly consumed by some side reaction other than the carbonylation. In these case the proportion of the isomerized product, diethyl succinate, also increased with an increase in the reaction time under nitrogen.

The Reaction of *n*-Butyl Vinyl Ether and Styrene.—With relation to ethyl acrylate, the effects of the reaction conditions on the reactions of *n*-butyl vinyl ether and styrene have been also investigated; the results are summarized in Tables VI and VII. These olefins are much more reactive than ethyl acrylate and pentene-1 (cf. Fig. 4);*7 with *n*-butyl vinyl ether, even at −30°C, 0.96 mol. of the gas was absorbed in one hour. In these cases, the reaction temperature and the atmosphere had a similar effect on the distribution of the products and on the isomerization, as in the reaction of ethyl acrylate; under carbon mono-

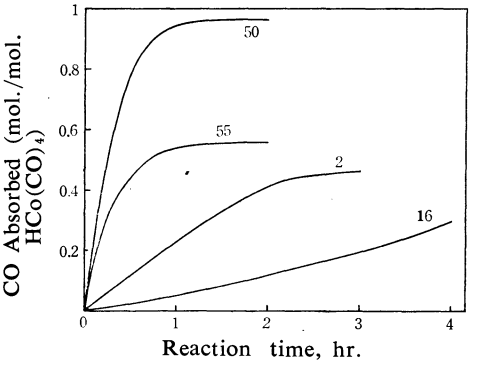


Fig. 4. CO Absorption vs. time plots for the reaction of several kinds of olefin.
Curve number: Exp. No.
Curve 50; *n*-butyl vinyl ether at −30°C, curve 55; styrene at 0°C, curve 2; ethyl acrylate at 0°C and curve 16; pentene-1 at 0°C.

*5 The reaction was not finished; only 0.14 and 0.26 mol. of the gas were absorbed.
*6 A relatively samll amount of the gas was evolved.
*7 Styrene was relatively readily hydrogenated to give some ethyl benzene.

TABLE VI. THE REACTION OF *n*-BUTYL VINYL ETHER WITH COBALT HYDROCARBONYL

Exp. No.	Reaction conditions*1			CO Absorbed (mol./mol. $HCo(CO)_4$)	Product	
	Atmosphere	Temp. °C	Time min.		Esters*2 (mol./mol. $HCo(CO)_4$)	Distribution of esters B/(B+S)*2×10²
47	CO	25	120	0.36	0.25	3
48	CO	0	120	0.70	0.36	75
49	CO	−20	120	1.00	0.60	97
50	CO	−30	120	0.96	0.63	97
51	N_2	0	120	—	0.28	13
52	CO	−20∼25	120∼120	0.99−0.32	0.29	20

*1 2 mol. *n*-butyl vinyl ether/mol. $HCo(CO)_4$.
*2 B: an ester with the branched structure, ethyl α-*n*-butoxypropionate.
S: an ester with the straight structure, ethyl β-*n*-butoxypropionate.

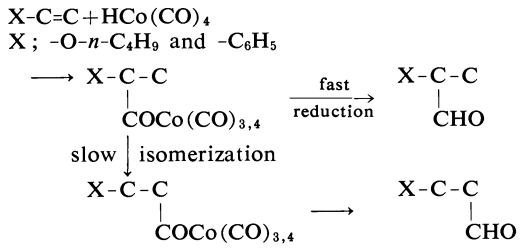
TABLE VII. THE REACTION OF STYRENE WITH COBALT HYDROCARBONYL

Exp. No.	Reaction conditions*1			CO Absorbed (mol./mol. $HCo(CO)_4$)	Product		
	Atmosphere	Temp. °C	Time min.		Ethylbenzene (mol./mol.	Esters*2 $HCo(CO)_4$)	Distribution of esters B/(B+S)*2×10²
53	CO	25	120	0.43	0.2	0.25	30
54	CO	20	180	0.43	0.2	0.25	40
55	CO	0	120	0.56	0.2	0.38	96
56	CO	−10	300	0.51	0.2	0.38	97
57	CO	−20	340	0.52	0.2	0.35	97
58	N_2	0	120	—	0.2	0.25	55
59	CO	0∼25	120∼200	0.48	0.2	0.25	40
60	CO	−10∼20	240∼90	0.51	0.2	0.31	70

*1 10 mol. styrene/mol. $HCo(CO)_4$.
*2 B: ethyl α-phenylpropionate.
S: ethyl hydrocinnamate.

xide at a relatively low temperature (0∼−30°C), esters with a branched structure, ethyl α-*n*-butoxypropionate*8 and ethyl α-phenylpropionate,*9 predominated (Exps. 48—50 and 55—57), but at 25°C, esters with a straight-chain structure, ethyl β-*n*-butoxypropionate*10 and ethyl hydrocinnamate,*11 were mainly obtained (Exps. 47 and 53). Under nitrogen, even at 0°C, the esters with the straight-chain structure predominated (Exps. 51 and 58). Moreover, the isomerization of the acylcobalt carbonyls with the branched structure to those with the straight-chain structure occurred with the change in the reaction temperature from −20°C or 0°C to 25°C (Exps. 52 and 59). However, the isomerization of α-phenylpropionylcobat carbonyl seemed to occur more slowly than in the cases of ethyl acrylate and *n*-butyl vinyl ether (cf. Exps. 29, 52 and 59). Thus, the *n*-butoxy and phenyl groups have an effect essentially similar to that of the ester group of ethyl acrylate on this type of reaction.

At an elevated temperature (in the oxo condition), the formation as the main products of branched aldehydes, methylphenylacetaldehyde and α-butoxypropionaldehyde, from styrene and *n*-butyl vinyl ether[7] respectively, may be explained by the following reaction scheme:



*8 Identified by gas chromatography and by means of its infrared spectrum, which had a band at 1760 cm^{-1} corresponding to a carbonyl grop with α-electronegative substituents.
*9 Infrared spectrum, 1720 cm^{-1}.
*10 Infrared spectrum, 1735 cm^{-1}. Further evidence; the retention time of the products (esters) increased as the molecular weight of the alcohol used for the cleavage reaction increased.
*11 Identified by using authentic ethyl hydrocinnamate.

7) H. Adkins and G. Krsek, *J. Am. Chem. Soc.*, 70, 383 (1948); 71, 3051 (1949).

that is, the methylphenylacetyl and α-butoxypropionylcobalt carbonyls formed at the first step undergo reduction more rapidly than isomerization to give the corresponding aldehydes. On the other hand, in the case of ethyl acrylate, the isomerization of the branched acylcobalt carbonyl seems to occur more rapidly than the reduction; therefore, an aldehyde with a straight-chain structure, ethyl γ-oxobutyrate, is mainly formed.

Summary

It has been observed that the reaction of 1-olefin with cobalt hydrocarbonyl is remarkably affected by the reaction conditions and by the structure of olefin.

Some functional groups, such as the ester, *n*-butoxy and phenyl groups, adjacent to a C=C bond increase the reactivity of the C=C bond; the order of the reactivity is *n*-butyl vinyl ether, 10^3>styrene, 20>ethyl acrylate, 5>pentene-1. (The numbers indicate the relative reactivities, which have been roughly calculated from the gas absorption curve.)

At a relatively low temperature (below 0°C), the α-carbon atom of the C=C bond of all these olefins except pentene-1 is selectively carbonylated; the reaction scheme may be considered to be as follows; suggesting that cobalt hydrocarbonyl is acting as an acid:

$$C{=}C{-}X \xrightarrow{H^+} C{-}\overset{+}{C}{-}X \xrightarrow{[Co(CO)_4]^-} C{-}C{-}C \quad (Co(CO)_4 \text{ on the second C})$$

$$\xrightarrow{CO} C{-}C{-}X \quad (COCo(CO)_{3,4} \text{ on the second C})$$

X: -COOEt, -O-*n*-C_4H_9 and -C_6H_5

However, these acylcobalt carbonyls with the branched structure isomerize to those with the straight one:

$$C{-}C{-}X \quad (COCo(CO)_{3,4}) \xrightarrow{\text{isomerization}} C{-}C{-}X \quad (COCo(CO)_{3,4})$$

A relatively high temperature (25°C) and a nitrogen atmosphere promote this isomerization considerably. The reverse isomerization seems to occur only with difficulty. On the other hand, these olefins mainly give the β-carbon carbonylated product at 25°C, the formation of which seems to result from the two successive reactions, the carbonylation of the α-carbon atom and the isomerization of the corresponding acylcobalt carbonyl. However, the distribution of the products from pentene-1 is not affected by the reaction temperature.

A relatively high pressure of carbon monoxide is advantageous for this reaction. Under a nitrogen atmosphere, some reaction other than the carbonylation seems to occur very rapidly, consuming a large part of the cobalt hydrocarbonyl used; a nitrogen atmosphere has an inhibitory effect on the carbonylation.

Department of Fuel Chemistry
Faculty of Engineering
Kyoto University
Sakyo-ku, Kyoto

The Preparation of 2,5-Thiophenedicarboxaldehyde

By Tyo Sone

(Received March 7, 1964)

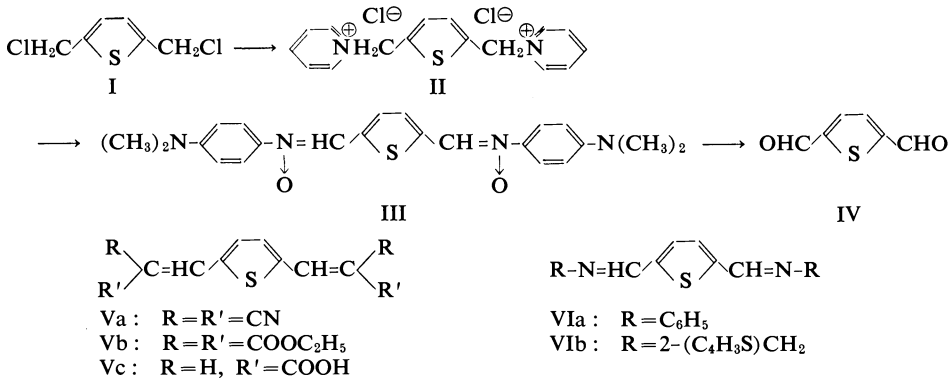
Although thiophenedicarboxaldehydes are of interest as synthetic intermediates, only two of them have appeared in the literature; Steinkopf and Köhler prepared 3,4-dichloro- and 3,4-dibromo-2,5-thiophenedicarboxaldehydes by hydrolyses of the corresponding 3,4-dihalogeno-2,5-bis-(dihalogenomethyl)thiophenes.[1]

The present paper will describe the preparation of 2,5-thiophenedicarboxaldehyde (IV) from 2,5-bis(chloromethyl)thiophene (I). In general, the procedures used for the preparation of benzene derivatives can not always be applied to the thiophene analogues, and such is also the case in the preparation of IV. In connection with an investigation of the reactions of methoxymethylthiophenes, the present author previously attempted to synthesize IV by treating 2,5-bis(methoxymethyl)thiophene with bromine in carbon tetrachloride, but instead of the expected dialdehyde a small amount of another material containing bromine was obtained.[2] The method was virtually identical with that described by Markees for preparing terephthaldehyde from *p*-bis(methoxymethyl)-benzene.[3] The cupric nitrate oxidation of I

1) W. Steinkopf and W. Köhler, *Ann.*, **532**, 250 (1937).

2) Y. Matsuki and T. Sone, *J. Chem. Soc. Japan, Ind. Chem. Sec.* (*Kogyo Kagaku Zasst*), **62**, 1559 (1959).

3) D. G. Markees, *J. Org. Chem.*, **23**, 1490 (1958).

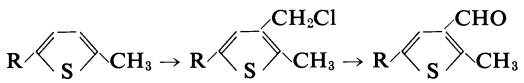


or the application of the Sommelet procedure to I was also unsuccessful.

The dialdehyde was easily available by means of Kröhnke's method.[4] The reaction of I with pyridine afforded 1,1'-(2,5-thiophenediyldimethylene)bis[pyridinium chloride] (II) almost quantitatively. The reaction of II with *p*-nitroso-*N*,*N*-dimethylaniline gave α,α'-(2,5-thiophenediyl)bis[*N*-(*p*-dimethylaminophenyl)-nitrone] (III), which was converted into IV by hydrolysis with hydrochloric acid (overall yield, 60%.) The application of the Sommelet procedure to a mixture of 4- and 5-chloromethyl-2-thiophenecarboxaldehydes[5] afforded only a small amount of the dialdehyde.

The dialdehyde IV is highly reactive and reacts with various active methylene compounds and amines to give the corresponding condensation products (V) and the Schiff bases (VI) respectively.

2-Methyl-5-thiophenecarboxaldehyde (VII) was easily chloromethylated by the usual chloromethylation procedure to give 2-methyl-3-chloromethyl-5-thiophenecarboxaldehyde (VIII), which was then converted into 2-methyl-3,5-thiophenedicarboxaldehyde (IX) by the Sommelet procedure. Similarly, the chloromethylation of 2-methyl-5-acetylthiophene (X), followed by oxidation, gave 2-methyl-5-acetyl-3-thiophenecarboxaldehyde (XII). 2-Methyl-3,5-thiophenedicarboxylic acid (XIII), which is difficult to obtain by the usual manner, was prepared from IX by silver oxide oxidation.



VII: R=CHO VIII: R=CHO IX: R=CHO
X: R=$COCH_3$ XI: R=$COCH_3$ XII: R=$COCH_3$

Experimental[6]

1,1'-(2,5-Thiophenediyldimethylene)bis[pyridinium chloride] (II).—When a mixture of 2,5-bis(chloromethyl)thiophene[7] (I, 4.5 g.), pyridine (5.2 g.), and absolute ethanol (5 ml.) was warmed on a water bath, colorless precipitate separated within a few minutes. After the mixture had been warmed for a further 30 min., the precipitate was collected and washed with ether, by which process II was obtained in a nearly quantitative yield. Recrystallization from ethanol afforded colorless hygroscopic crystals (m. p. above 280°C).

Found: N, 7.60. Calcd. for $C_{16}H_{16}Cl_2N_2S$: N, 8.25%.

α,α'-(2,5-Thiophenediyl)bis[*N*-(*p*-dimethylaminophenyl)-nitrone] (III).—Into a mixture of II (9.2 g.), *p*-nitroso-*N*,*N*-dimethylaniline (7.5 g.), and ethanol (150 ml.), a solution of sodium hydroxide (2 g.) in water (50 ml.) was stirred while the mixture was being ice-cooled. After being stirred for 1 hr. under ice cooling and then at room temperature for a further 2 hr., the mixture was diluted with water (100 ml.) and allowed to stand overnight. The brownish red precipitate which deposited was collected and recrystallized from ethanol; m. p. 254~255°C (decomp.). Yield, 8.0 g. (72%).

Found: C, 64.63; H, 5.49; N, 13.36. Calcd. for $C_{22}H_{24}O_2N_4S$: C, 64.68; H, 5.92; N, 13.71%.

2,5-Thiophenedicarboxaldehyde (IV).—III (8.2 g.) was added to ice-cooled 2 N hydrochloric acid (160 ml.), and the resultant brownish red solution was stirred for 30 min. while being cooled with ice, during which time a pale yellow precipitate was formed. The mixture was allowed to stand overnight at room temperature. The precipitate was collected and washed well with cold water to give 2 g. of the crude aldehyde (m. p. 115~116°C). The filtrate was extracted with ether, and the ether was evaporated to give an additional 0.3 g. of the product (m. p. 109~114°C). The total yield was 82.5%. Recrystallization from petroleum ether gave pale yellow leaflets (m. p. 115~116°C).

Found: C, 51.53; H, 2.88. Calcd. for $C_6H_4O_2S$: C, 51.41; H, 2.87%.

4) S. J. Angyal, "Organic Reactions," Vol. 8, Ed. by R. Adams, John Wiley & Sons, Inc., New York (1954), p. 203.

5) T. Sone, unpublished work.

6) All melting points are uncorrected. The ultraviolet spectra were measured with a Hitachi EPU-2-A-type spectrophotometer, while the infrared spectra were measured with a Hitachi EPI-2A spectrophotometer. Microanalyses were carried out by Misses Yoko Endo and Yukiko Endo of this Institute, to whom the author is indebted.

7) J. M. Griffing and L. F. Salisbury, *J. Am. Chem. Soc.*, **70**, 3416 (1948).

UV λ_{max}^{MeOH} mμ (log ε): 290 (4.23), 269 (4.15; shoulder), IR (KBr disk): ν_{CO} 1664 cm^{-1}.

2,5-Bis(2,2-dicyanovinyl)thiophene (Va). — A mixture of IV (140 mg.), malononitrile (150 mg.), and absolute ethanol (2 ml.) was allowed to stand for a few minutes while occasionally being stirred; by this method yellow crystals precipitated (190 mg.; m. p. 265~266°C (decomp.)). Recrystallization from a mixture of acetone and methanol afforded fine yellow needles (m. p. 265~266°C (decomp.)).

Found: C, 60.29; H, 1.32; N, 23.47. Calcd. for $C_{12}H_4N_4S$: C, 61.00; H, 1.70; N, 23.71%.

2,5-Bis(2,2-diethoxycarbonylvinyl)thiophene (Vb). —A mixture of IV (140 mg.), ethyl malonate (400 mg.), piperidine (2 drops), and absolute ethanol (2 ml.) was allowed to stand overnight. The mixture was then treated with 2 N hydrochloric acid, and the precipitate thereby formed was collected by filtration and washed with dilute ethanol (200 mg.; m. p. 65~68°C). Recrystallization from petroleum ether afforded pale yellow leaflets (m. p. 68~69°C).

Found: C, 57.06; H, 5.65. Calcd. for $C_{20}H_{24}O_8 \cdot S$: C, 56.59; H, 5.69%.

2,5-Bis(2-carboxyvinyl)thiophene (Vc).—A mixture of IV (350 mg.), malonic acid (550 mg.), piperidine (3 drops), and pyridine (3 ml.) was heated on a water bath for 3 hr. and then, after 5 min. refluxing, acidified with hydrochloric acid. The precipitate thereby formed was collected (490 mg.; m. p. above 300°C). Recrystallization from ethanol yielded a brownish yellow powder.

Found: C, 53.19; H, 3.89. Calcd. for $C_{10}H_8O_4S$: C, 53.56; H, 3.59%.

2,5-Bis[(phenylimino)methyl]thiophene (VIa). —After a mixture of IV (140 mg.), aniline (200 mg.), and ethanol (2 ml.) had been allowed to stand at room temperature, a yellow precipitate began to separate (270 mg.; m. p. 201~202°C). Recrystallization from a mixture of ethanol and benzene afforded pale yellow leaflets (m. p. 202~203°C).

Found: C, 74.79; H, 4.67; N, 9.41. Calcd. for $C_{18}H_{14}N_2S$: C, 74.45; H, 4.85; N, 9.64%.

2,5-Bis[(2-thenylimino)methyl]thiophene (VIb). —A mixture of IV (140 mg.), 2-thenylamine (240 mg.), and ethanol (5 ml.) was allowed to stand at room temperature; a precipitate formed within 10 min. (230 mg.; m. p. 133~137°C). Recrystallization from ethanol afforded coloress leaflets (m. p. 146~147°C).

Found: C, 58.19; H, 3.93; N, 8.03. Calcd. for $C_{16}H_{14}N_2S_3$: C, 58.14; H, 4.26; N, 8.47%.

The Chloromethylation of 2-Methyl-5-thiophenecarboxaldehyde (VII).—Into a mixture of VII (12.6 g.), trioxane (5.0 g.), zinc chloride (5.0 g.), and carbon tetrachloride (50 ml.), a stream of dry hydrogen chloride was stirred over a 30 min. period. Then the mixture was gradually warmed to 50°C and stirred for 1 hr. at the same temperature, while a stream of hydrogen chloride continued to pass through. The resultant solution was diluted with water, and then the layers were separated. The organic layer was washed well with water, a dilute sodium carbonate solution, and again with water, and then dried. After the carbon tetrachloride had been removed, the residue was fractionated in vaccuo, yielding 13.8 g. (79%) of crude 2-methyl-3-chloromethyl-5-thiophenecarboxaldehyde (VIII) (b. p. 105~110°C/2.5~3 mmHg; m. p. 49~51°C), which was recrystallized from a mixture of ether and petroleum ether to give colorless needles (m. p. 50~51°C).

Found: C, 48.07; H, 4.09. Calcd. for C_7H_7ClOS: C, 48.13; H, 4.03%.

UV λ_{max}^{MeOH} mμ (log ε): 222 (3.95), 264 (4.03), 299 (4.00). IR (KBr disk): ν_{CO} 1659 cm^{-1}.

2-Methyl-3,5-thiophenedicarboxaldehyde (IX).— A mixture of VIII (7.0 g.), hexamethylenetetramine (5.6 g.), and chloroform (20 ml.) was heated on a water bath for 30 min. and then cooled, after which the resulted salt was filtered off. The salt was dissolved in a mixture of water (30 ml.) and acetic acid (30 ml.) and boiled for 30 min. The solution was cooled and extracted with chloroform. The extract was dried, and the chloroform was evaporated to give 3.5 g. the crude aldehyde (m. p. 102~104°C, 57%). Recrystallization from boiling water afforded colorless needles (m. p. 106~107°C).

Found: C, 54.56; H, 4.14. Calcd. for $C_7H_6O_2S$: C, 54.52; H, 3.92%.

UV λ_{max}^{MeOH} mμ (log ε): 246 (4.49), 290 (3.99). IR (KBr disk): ν_{CO} 1690, 1665 cm^{-1}.

The Chloromethylation of 2-Methyl-5-acetylthiophene (X).—Paraformaldehyde (4.5 g.), X (14.0 g.), zinc chloride (5 g.), and carbon tetrachloride (50 ml.) were used; the procedure was the same as described previously for VII. Crude 2-methyl-3-chloromethyl-5-acetylthiophene (XI, 14.0 g. (74%) b. p. 130~135°C/3~3.5 mmHg; m. p. 69.5~71.5°C) was recrystallized from petroleum ether to yield colorless leaflets (m. p. 72~73°C).

Found: C, 50.70; H, 5.07. Calcd. for C_8H_9ClOS: C, 50.92; H, 4.80%.

UV λ_{max}^{MeOH} mμ (log ε): 223 (4.00), 264 (4.03), 297 (4.02). IR (KBr disk): ν_{CO} 1654 cm^{-1}.

2-Methyl-5-acetyl-3-thiophenecarboxaldehyde (XII).—This aldehyde (m. p. 110~111°C, 330 mg.) was obtained from XI (2.0 g.), hexamethylenetetramine (1.8 g.), and chloroform (8 ml.) by the method used with IX. Recrystallization from ligroin gave colorless needles, but it did not alter the melting point.

Found: C, 57.26; H, 4.92. Calcd. for $C_8H_8O_2S$: C, 57.12; H, 4.80%.

VU λ_{max}^{MeOH} mμ (log ε): 246 (4.65), 283 (4.10). IR (KBr disk): ν_{CO} 1659, 1680 cm^{-1}.

2-Methyl-3,5-thiophenedicarboxylic Acid (XIII). —Into a mixture of silver oxide (0.4 g.) and an aqueous sodium hydroxide solution (10%, 8 ml.), 0.2 g. of IX was swirled. After the reaction mixture had been allowed to stand overnight, the black silver was filtered off. The filtrate was acidified with hydrochloric acid, and the precipitate which separated thereby was collected (180 mg., m. p. 258~260°C (decomp.)). Sublimation under reduced pressure raised the melting point to 275~276°C (decomp.) (lit.[8] m. p. above 250°C (decomp.)).

Found: C, 44.99; H, 3.55. Calcd. for $C_7H_6O_4S$: C, 45.16; H, 3.24%.

UV λ_{max}^{MeOH} mμ (log ε): 222 (4.36), 259 (3.92). IR (KBr disk): ν_{CO} 1680 cm^{-1}.

8) M. Janda, *Collection Czechoslov. Commun.*, **26**, 1889 (1961).

Summary

The application of Kröhnke's method to 2, 5-bis(chloromethyl)thiophene has afforded 2, 5-thiophenedicarboxaldehyde, from which some condensation products with amines and active methylene compounds have then been derived. 2-Methyl-5-acetyl-3-thiophenecarboxaldehyde and 2-methyl-3, 5-thiophenedicarboxaldehyde have also been prepared, from 2-methyl-3-chloromethyl-5-acetylthiophene and 2-methyl-3-chloromethyl-5-thiophenecarboxaldehyde respectively, by the Sommelet procedure.

The author wishes to express his deep gratitude to Professor Yasuo Matsuki for his unfailing guidance throughout the course of this work.

The Chemical Research Institute
of Non-Aqueous Solutions
Tohoku University
Katahira-cho, Sendai

A Geochemical Study of Selenium in Volcanic Exhalation and Sulfur Deposits

By Tetsuro SUZUOKI

(Received February 21, 1964)

Several investigations have previously been made concerning the abundance and behavior of selenium in various terrestrial materials. Recently, Anderson[1] summarized the geochemical work on this chemical element. Many studies reveal that selenium is usually enriched in pneumatolytic and high temperatured hydrothermal sulfide rather than in sulfide ores of low temperatured hydrothermal or sedimentary origin.[2,3] It has also been reported that most of the selenium in sedimentary sulfide or rock is not accumulated in pyrite but in independent minerals such as ferroselite.[4] As to the native sulfur, it is known that selenium is usually concentrated in sulfur deposits of volcanic origin. The variation of selenium content in Kilauean sulfur deposits was regarded as being due to a partial sublimation of selenium during deposition.[1,5] It is also said that the low selenium content in the sulfur which is produced in Mexico, West Indies, and Iceland may represent a selenium-poor, residual fraction of sulfur.

It was found by the continuous observation of the chemical constituents of the condensed water from an exhalation collected at a fumarole of the Showashinzan volcano on Hokkaido Island, Japan (42°30'N, 140°53'E), that the behavior or sulfur in volcanic gases was different from that of the other constituents.[6] According to Matsuo and Mizutani, the sulfur content showed less variation with time than do those of such other constituents as halogen and boron.

This study was undertaken to investigate the content and distribution of selenium in volcanic matter from fumarolic gases and associated sulfur sublimates at the Nasudake (36°07'N, 139°57'E) and Kuju (33°07'N, 131°13'E) volcanoes, Japan.

Sampling Sites and Samples

Nasudake volcano is situated at 36°07'N 139°57'E on Honshu, Japan. The activity of the volcano is moderate at present, but a large amount of volcanic gases is emitted from fumaroles near the top of the dome. As is shown in Fig. 1, these fumaroles are divided into three groups, NA, NB, and NC and ND, according to their locations, which are roughly in the order of decreasing gas temperature, ranging from 420 to 120°C.*

Kuju volcano is situated at 33°07'N 131°13'E in the north-eastern part of Kyushu Island, Japan. The active, high-temperatured fumaroles are gathered in the area KA near the top of volcano. These fumaroles also are divided into three groups according to their locations

1) M. S. Anderson, H. W. Lakin, K. C. Beeson, F. F. Smith and E. Thacker, Agriculture Handbook No. 200, U. S. Department of Agriculture, 3 (1961).
2) A. B. Edwards and G. C. Calos, *Australian Inst. Min. Metallurgy Proc.*, No. 172, 31 (1954).
3) R. G. Coleman and M. Delevaux, *Economic Geology*, **54**, 499 (1957).
4) E. Z. Bur'yanova, *Geochemistry* (English translation), No. 7, 669 (1961).
5) H. G. Byers, K. T. Williams and H. W. Lakin, *Ind. & Eng. Chem.*, **28**, 821 (1936).
6) S. Matsuo and Y. Mizutani, *Bull. Volcanol. Soc. Japan, 2nd Ser.*, **3**, 119 (1959).

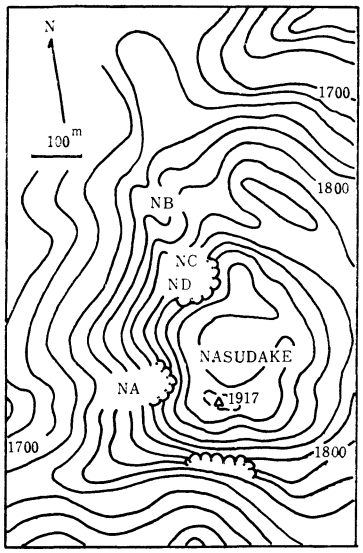


Fig. 1. Distribution of fumaroles at Nasudake.

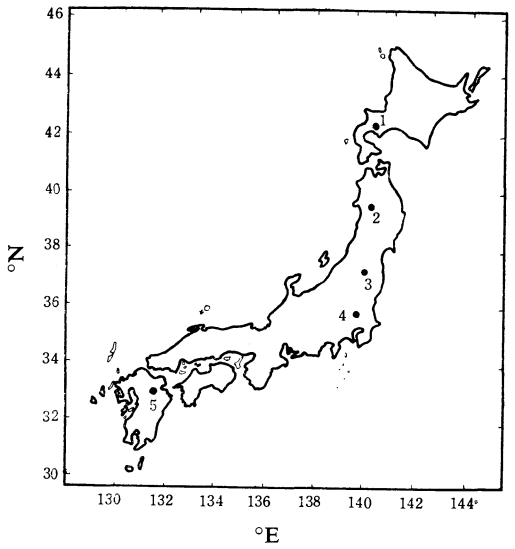


Fig. 2. Location of volcanoes where samples were collected.
1 Showashinzan 2 Tamagawa
3 Issaikyo 4 Nasudake
5 Kuju

KA, KB and KC, of which the temperature ranges from about 120 to 300°C.*

Sulfur is economically mined in both volcanoes. It is, however, usually difficult to collect gas sample directly from the natural outlet of a fumarole. Because, in order to collect a sulfur deposit efficiently, the gases emitted from the fumaroles are introduced into tunnels, as is shown schematically in Fig. 3. Therefore, most of samples were collected from leaks and from the outlets of tunnels.

Two kinds of sulfur deposits were collected, one obtained at leaks and the other, at the outlets of tunnels. The former (deposit I) is a sublimation deposit from gases, while the latter (deposit II) is the solidified sulfur from the out-flow of the liquid.

At Nasudake, three samples of condensed water and sulfur deposits from the NB area were collected from three different leaks of the same tunnel. At Kuju, two kinds of sulfur deposits, as has been mentioned above, were collected from the outlet of each tunnel.

The Method of Sampling and Analysis

Sampling Method.—Fumarolic gases are introduced into an ice-cooled water trap as is shown in Fig. 4. Water and other condensable substances are trapped in a cold trap containing sodium hydroxide. Selenium, sulfur and chlorine in condensed water are analyzed in laboratory.

Analytical Method. — 1) *Sulfur* is determined by the gravimetric method as barium sulfate after oxidation.

2) *Chlorine* is determined by the colorimetric method with mercuric thiocyanate and iron alum.[7]

3) *Selenium* is determined by the colorimetric

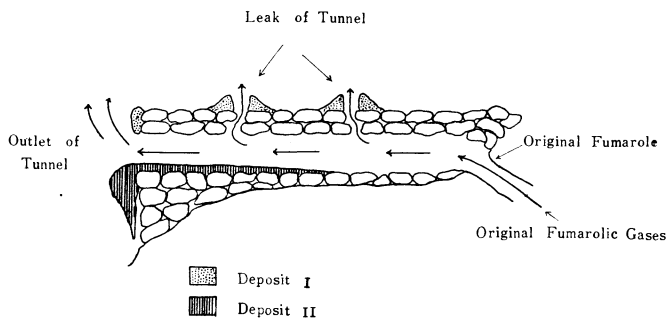


Fig. 3. Schematic diagram of artificial tunnel, which is made of piled stones.

* There are fumaroles at Nasudake and Kuju, the gas temperature of which may be 500°C or higher. It is, however, diffcult to get a gas sample directly from those fumaroles.

7) S. Utsumi, *J. Chem. Soc. Japan, Pure Chem. Sec.* (*Nippon Kagaku Zasshi*), **81**, 401 (1960).

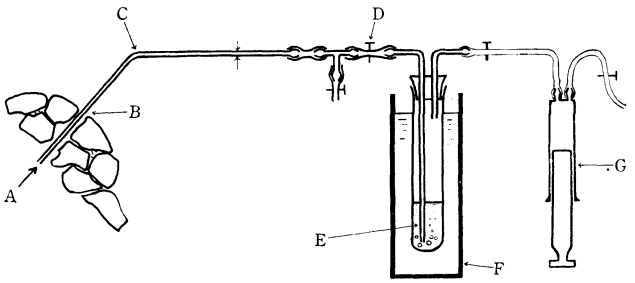


Fig. 4. Apparatus for collection of volcanic gases.

A Volcanic gases B Outlet of fumarole C Quartz tubing D Stop cock
E Condensed water F Cold trap G Injector

method using 3,3'-diaminobenzidine.[8,9] As 3,3'-diaminobenzidine reacts only with quadrivalent selenium, it is necessary to convert all the selenium to a quadrivalent state. Selenium of various ionic forms is first oxidized with hydrogen peroxide to a sexivalent state, and then reduced, by using hydrochloric acid, to a quadrivalent state. Generally the oxidation proceeds smoothly, while the reduction is strongly affected by the concentration of hydrogen chloride and by the time of heating. As is shown in Figs. 5 and 6, a time for heating of longer than 90 min. and a concentration higher than 4 M for hydrochloric acid are required for complete reduction. The concentration of hydrochloric acid must be adjusted during the heating, because selenium forms volatile compound such as Se_2Cl_2 and $SeO_2 \cdot HCl$ when the concentration of acid rises. Sulfate ion interferes with the coloration when its concentration exceeds 16 g.-SO_4/l. in the final solution (ca. 50 ml.) for solvent extraction.[10] In addition, the S/Se ratio (by weight) should be kept below 5.6×10^4 in the final solution. The excess amount of sulfate is removed as barium sulfate after reducing the selenate to selenite in order to avoid the coprecipitation of selenium.

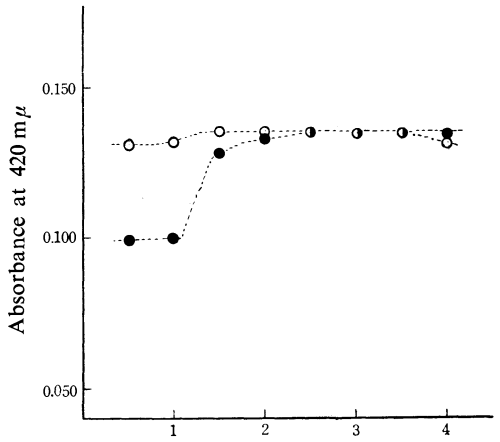


Fig. 5. Time of heating and reduction of selenium(VI) to selenium(IV).
●: 4 M HCl solution ○: 8 M HCl solution

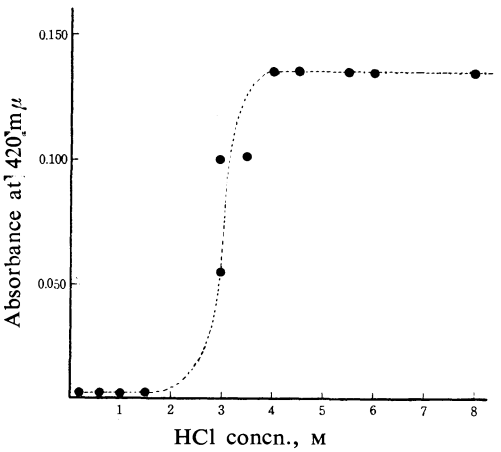


Fig. 6. HCl concentration and reduction of selenium(VI) to selenium(IV).

The Procedure of Sample Preparation for the Solvent Extraction of Selenium.—Native sulfur is pulverized and ground about finer than 100 mesh. One tenth to 0.3 g. of ground sulfur and 2 g. of sodium hydroxide are put into a test tube and heated on a water bath. Hydrogen peroxide is added to the tube until free sulfur disappears. An aliquot of this solution or condensed water is then transferred into a 100 or 200 ml. beaker with a few grams of sodium hydroxide. A small amount of hydrogen peroxide (30%) is added to the solution to assure complete oxidation. The solution is heated on a water bath to approximate dryness. After the residue is neutralized with a (1 : 1) hydrochloric acid solution, the volume of the solution is doubled with concentrated hydrochloric acid. The solution is then heated on a water bath for 180 min., after which the solution is neutralized again with dilute ammonium hydroxide (1 : 1). To remove the excess sulfur, a 20% barium chloride solution is added to the solution after it has been heated with hydrochloric acid. The barium sulfate precipitate is removed by centrifuge, and the filtrate is neutralized with ammonium hydroxide. After the solution is evaporated to a volume less than about 50 ml.

8) J. Hoste and J. Gillis, *Anal. Chim. Acta*, **12**, 158 (1955).
9) K. L. Cheng, *Anal. Chem.*, **28**, 1738 (1956).
10) T. Danzuka and K. Ueno, ibid., **30**, 1370 (1958).

on a water bath, the selenium content is determined by the colorimetric method using 3,3'-diaminobenzidine.

TABLE I. SELENIUM, SULFUR AND CHLORINE CONTENTS, AND S/Se RATIO IN THE CONDENSED WATER FROM EXHALATION OF NASUDAKE FUMAROLES

Locality No.	Temp. °C	S p.p.m.	Se p.p.m.	S/Se 10^4	Cl p.p.m.
NA-2d	421	4390	0.23	1.9	
NA-2c	410	6270	0.25	1.8	554
NA-3a	386	4730	0.25	1.9	
NA-3b	380.5	4790	0.22	2.2	
NA-3c	291	6300	0.18	3.5	
NA-2a	261	4430	0.22	2.0	8340
NA-3d	252	5690	0.08	7.1	
NA-2e	241	7150	0.13	5.5	
NA-2f	236	6800	0.08	8.5	
NA-3e	226	5350	0.15	3.6	
NB-2	195	23300	0.12	19	960
NB-1	181	25400	0.09	28	1000
NB-3	118	14700	0.01	150	1300
NC-1	120	5590	0.01	560	390
ND-1	118	9490	0.01	950	5000

TABLE II. SELENIUM CONTENT AND S/Se RATIO IN SULFUR DEPOSITS OF NASUDAKE AND KUJU

Locality No.	Temp. °C	Se p.p.m.	S/Se 10^3	Type*
(Nasudake)				
NA-2a	261	368	2.72	I
NA-3	120	291	3.34	II
NB-2	195	124	8.05	I
NB-1	181	175	5.98	I
NB-3	118	49	21.6	I
NB-4	119	404	2.54	II
NC-1	120	20	50	II
ND-1	118	20	50	II
(Kuju)				
KA-a	297.5	213	3.20	I
		741	1.35	II
KA-b	118.5	15.5	64.5	I
		22.3	44.8	II
KA-c	228.5	201	4.97	I
		369	2.71	II
KA-d	278.5	335	2.99	I
		555	1.80	II
KA-d'	285.0	578	1.73	II
KA-f	126.5	77.8	12.9	I
		490	2.09	II
KB-1	205.0	36.9	27.1	I
		98.1	10.1	II
KB-2	128.0	14.8	67.6	I
		15.2	65.9	II
KC-1	133.0	17.4	57.6	I
		49.7	20.1	II
KC-2	155.0	18.3	54.6	I
		89.8	11.1	II

* Type I and II represent respectively deposit I and II which are described in page 1201.

Results

In Tables I and II, the selenium, sulfur, and chlorine contents in condensed water and two types of sulfur are given. The amount of selenium and sulfur in the tables represent the total amounts, regardless of their chemical forms.

A) The following results were obtained for condensed water and the sulfur deposits of the Nasudake volcano:

Condensed Water.—The sulfur content ranges from 4390 to 25400 p.p.m. In the NB area it was several times higher than in other areas. The NB area is thus characterized by a higher total concentration of sulfur. The chlorine content and selenium content range from 390 to 8340 p.p.m. and 0.01 to 0.35 p.p.m. respectively. The variation in the selenium content is greater than those of sulfur and chlorine.

Sulfur Deposits. — The selenium content in deposits I and II ranges from 49 to 368 p.p.m. and 20 to 404 p.p.m. respectively.

TABLE III. SELENIUM IN VOLCANIC SULFUR

Location	Se p.p.m.	Reference
Colorado, U.S.A.	8350	Byers[11]
Kilauea, Hawaii	1400	Byers et al.[5]
	2200	
	1600	Lakin et al.[1]
	1600	
	900	
	4	
Mexico	0.6	Williams et al.[12]
	0.5	
	10	
	0	
West Indies	5	Byers et al.[13]
Alaska	1200	Zies[14]
Iceland	18.9	Friend et al.[15]
Showashinzan, Japan (42°31'N, 140°53'E)	129	Suzuoki
	92.9	
Tamagawa, Japan (39°56'N, 140°44'E)	89.9	
	45.3	
Issaikyo, Japan (37°45'N, 140°15'E)	214	
Nasudake, Japan (36°07'N, 131°13'E)	20	
	404	
Kuju, Japan (33°07'N, 131°13'E)	15.5	
	741	

11) H. G. Byers, *U. S. Department of Agriculture Tech. Bull.*, **482**, 47 (1935).
12) K. T. Williams, H. G. Byers and H. W. Lakin, ibid., **702**, 59 (1940).
13) H. G. Byers, J. T. Miller, K. T. Williams and H. W. Lakin, ibid., **601**, 74 (1938).
14) E. G. Zies, *Natl, Geog. Soc. Contrib. Papers, Katomai Ser.*, **1**, No. 4, 79 (1929).
15) J. N. Friend and J. P. Allchin, *Mineralogist Mag.*, **26**, 9 (1941).

B) The following results were obtained regarding the sulfur deposits of the Kuju volcano:

Sulfur Deposits. — The selenium content in deposits I annd II ranges from 14.8 to 355 p.p.m. and 15.2 to 741 p.p.m. respectively.

Selenium is richer in deposit II than in deposit I. The selenium content in the sulfur deposits of Kuju is a little higher than that of Nasudake. It may be said that volcanic gases and sulfur from the two volcanoes contain various amounts of seleninum according to the location of the fumaroles. A comparison of the selenium contents in various volcanic sulfurs is given in Table III. It should be noted that the selenium content in sulfur from Mt. Kilauea, Hawaii, is about ten times higher than that of several volcanoes, the selenium contents of which have been determined by the present author.

C) The Continuous Observation of Fumarolic Gas at Nasudake.—A continuous observation over a short period was made in order to study the time variation of the sulfur and selenium contents in volcanic gases from a certain fumarole at the Nasudake volcano. The sulfur and selenium contents of seven samples which were collected from a fumarole (NA-3a) at intervals of 40 min. were determined (cf. Table IV). As Table IV shows, the time variation of the sulfur content in condensed water is small, whereas a considerable variation, ranging from 0.20 to 0.31 p.p.m., was found in the selenium content.

TABLE IV. THE TIME VARIATION OF SELENIUM AND SULFUR CONTENT IN THE CONDENSED WATER FROM NA-3a FUMAROLE OF NASUDAKE (30 AUGUST 1962)

Sample	Time hr. min.	S p.p.m.	Se p.p.m.	S/Se $\times 10^4$
1	9 40	4500	0.22	2.04
2	10 20	4490	0.29	1.55
3	11 00	4530	0.27	1.68
4	11 40	4440	0.31	1.43
5	12 20	4410	0.20	2.21
6	13 00	4430	0.21	2.11
7	13 40	4440	0.23	1.93

Discussion

As it is known that selenium forms certain volatile compounds with chlorine, the relationship between selenium and chlorine was studied. The results showed that there is no correlation between the two elements in condensed water. This suggests that selenium is not exclusively transferred by fumarolic gases in the form of a compound with chlorine. It was also found that selenium and sulfur in condensed water have no correlation with each other.

The relation between the temperature of gases at the outlet of the fumarole and the selenium content in condensed water and sulfur deposits was also considered. As is shown in Fig. 7, the higher the temperature, the higher the selenium concentration. A sharp correlation between the S/Se ratio (by weight) and the outlet temperature was also observed, as may be seen in Figs. 8, 9 and 10. The

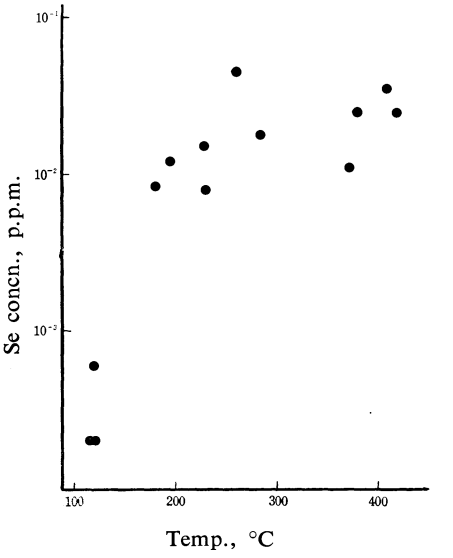


Fig. 7. Relationship between gas temperature and selenium content in condensed water.

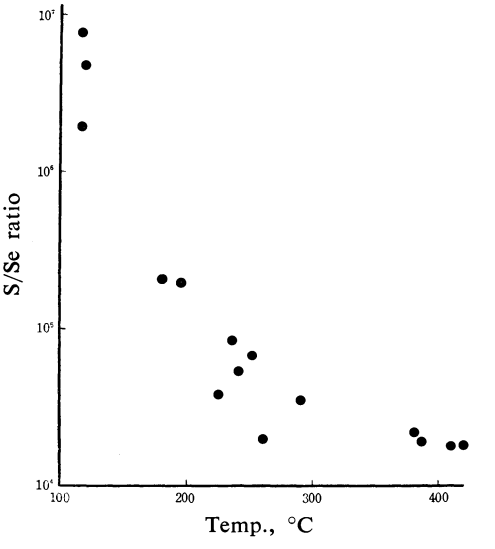


Fig. 8. Relationship between S/Se ratio and gas temperature in condensed water from Nasudake.

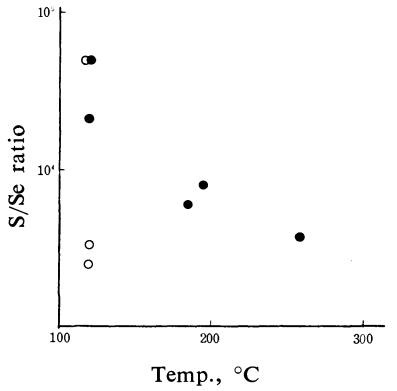


Fig. 9. Relationship between S/Se ratio and gas temperature in sulfur deposit from Nasudake.

●: Deposit-I ○: Deposit-II

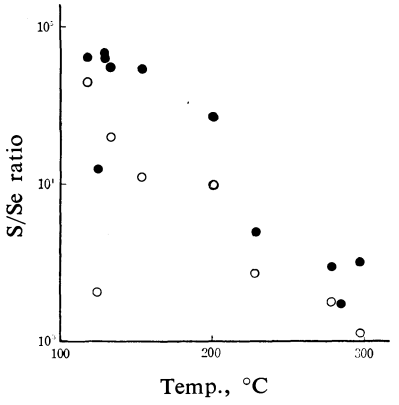


Fig. 10. Relationship between S/Se ratio and gas temperature in sulfur deposit from Kuju.

●: Deposit-I ○: Deposit-II

S/Se ratio in both condensed water and sulfur deposits has an inverse correlation with the gas temperature. This fact implies that the fractionation between selenium and surfur depends on the temperature of the fumarolic gases. The values of the $r=\{$(S/Se) condensed water/(S/Se) volcanic sulfur$\}$ ratio for condensed water and sulfur deposits from the same outlet of fumaroles are listed in Table V. These values which extend from 7.5 to an extremely high number, may be said to reflect the degree of the fractionation of selenium and sulfur between volcanic gases and sulfur deposits. In addition, this factor is controlled by other factors related to the mechanism of the transportation of chemical elements in volcanic gases. The relationship between the ratio r and the outlet temperature is given in Fig. 11, which shows the temperature dependency of the ratio r.

TABLE V. VALUE OF (S/Se) CONDENSED WATER/(S/Se) VOLCANIC SULFUR RATIO (r)

Locality, No.	Temp., °C	r
Na-2a	261	7.3
NB-2	195	23.6
NB-1	181	50.0
NB-3	118	93.0

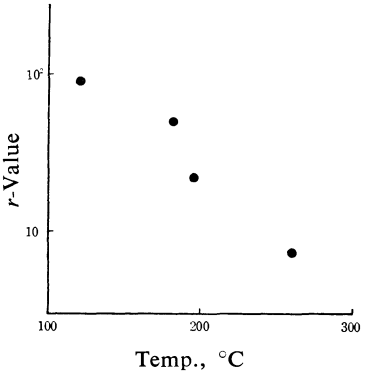


Fig. 11. Relationship between gas temperature and (S/Se) condensed water/(S/Se) volcanic sufur ($=r$).

The same correlation of the selenium content with the temperature was also observed in deposit I, as is shown in Figs. 9 and 10. On contrary, some of deposit II is high in selenium content and low in S/Se ratio, unlike deposit I. The variation of the S/Se ratio in deposit II independently of the outlet temperature may be explained as follows. From field observation, it is known that deposit II is formed through the movement of separated sulfur in a liquid form toward the outlet of tunnel and that then the sulfur is deposited at the outlet of the tunnel. Judging from the outlet temperature of the tunnel, most of the sulfur and selenium would be completely trapped inside the tunnel during the effusion processes. From the above considerations, the lack of relationship between the temperature and the selenium content (and the S/Se ratio) in deposit II might be due to the difference in the mode of deposition rather than to that in temperature between the two types of deposits. In addition, the S/Se ratio in deposit II might depend mainly on the temperature at the original outlet on the fumaroles. Accordingly, the S/Se ratio in deposit II will be taken to serve to estimate the physical and chemical conditions at original outlet such as the S/Se ratio, the temperature, and the structure of the tunnel. From the observed data, it was found that the same separation process due to temperature gradient as in the tunnel occurs also inside the natural conduit of volcanic gases, and that the source gas at some fumarole areas (NC and ND) has

an essentially lower selenium concentration than that in other areas.

The NA area is regarded as the most active area in Nasudake, as has been mentioned before. If fumarolic gages in this field have the same origin, it may be said that the S/Se ratio in the original volcanic gases of Nasudake is close to that found in NA fumarolic gases of the highest temperature (1.8×10^4).

Conclusion

On the basis of our observations, it may be concluded that the temperature at the fumarole outlet is one of the main factors controlling selenium concentration in volcanic gases and sulfur deposits. In the case of sulfur deposits collected at the outlet of tunnels, deposit II, the temperature of the source gases and the structure of the tunnel seem to play an important role in governing the selenium content. The variation in selenium content in the volcanic sulfur suggests the fractional distillation of selenium and sulfur through either natural or artificial conduits of volcanic exhalation. On the basis of findings that the S/Se ratio in sulfur deposits and gases increases with the decrease in the temperature at the sampling sites, it may also be concluded that the S/Se ratio gives an indication of the condition which governs the effussion process of volcanic gases.

There remain, however, a number of problems to be solved concerning selenium in volcanic matter, such as the mechanism of the fractionation of selenium and sulfur, and the reason for the variation in selenium content with respect to each fumarole and its general area.

Summary

Regarding selenium in volcanic materials collected at fumaroles of the Nasudake (36° 07'N, 139°57'E) and the Kuju (33°07'N, 131° 13'E) volcanoes, Japan, the following results have been obtained.

1) The selenium content in condensed water has no relation to that of sulfur and chlorine. The selenium content in certain sulfur deposits is strongly affected by the mode of occurrence, such as sublimation and solidification, as well as by the outlet temperature of the fumarole. The ratio of selenium to sulfur in both condensed water and sulfur deposit is related with gas temperature at the outlet of fumarole. The higher the gas temperature, the lower the degree of fractionation between selenium and sulfur.

2) The S/Se ratio in the original volcanic gases at Nasudake is close to 1.8×10^4, found in fumarolic gases with the highest temperature. The S/Se ratio in sulfur deposit is at least one-seventh that in condensed water.

3) Continuous observation over a short period (3 hr.) showed that the selenium content in condensed water varies considerably with time, while the sulfur content remains constant.

This study was made under the guidance of Professor Shinya Oana, Institute of Earth Sciences, Faculty of Science, Nagoya University, to whom the present author wishes to express his hearty thanks. Thanks are also due to Dr. Yoshihiko Mizutani and Mr. Tsutomu Sugiura for their help in the collection of samples.

The author wishes also to thank Professor Yasuo Miyake and Dr. Sadao Matsuo, Department of Chemistry, Faculty of Science, Tokyo Kyoiku University, who gave him valuable advice on many points.

Department of Chemistry
Faculty of Science
Tokyo Kyoiku University
Otsuka, Tokyo

*The Catalytic Hydrogenolysis of 5,6β-Epoxy-5β-cholestan-3β-ol**

By Shigeo NISHIMURA, Michio SHIOTA and Aiko MIZUNO

(Received March 11, 1964)

In the catalytic hydrogenolysis of 5,6β-epoxy-5β-cholestan-3β-ol and related 5β,6β-epoxy-compounds, there often occurs a rather extensive over-hydrogenolysis beyond the mere reductive cleavage of the oxide ring. Chuman[1] obtained 5α-cholestane in the catalytic hydrogenolysis of 5,6β-epoxy-5β-cholestan-3β-ol (I) with platinum oxide in acetic acid. 3β-Acetoxy-5,6β-epoxy-5β-cholestane (II) has also been reported to give 5α-cholestane and 3β-acetoxy-5α-cholestane, along with 3β-acetoxy-5α-cholestan-6β-ol, under similar conditions.[1,2] Such an over-hydrogenolysis has also been found to take place in the catalytic hydrogenolysis of 5,6β-epoxy-5β-cholestan-3α-ol[3] and 3α-chloro-5,6β-epoxy-5β-cholestane.[4] From the observations that the reduction of the epoxide II with lithium aluminum hydride afforded about 20% of 5β-cholestane-3β,5-diol along with 60% of 5α-cholestane-3β,6β-diol, and that the yield of the 3β,5β-diol nearly amounted to the sum of 5α-cholestane and 3β-acetoxy-5α-cholestane obtained in the catalytic hydrogenolysis, it has been suggested that 3β-acetoxy-5β-ol was also produced in the catalytic hydrogenolysis, but further reduced to give 5α-cholestane and 3β-acetoxy-5α-cholestane.[5] There is no evidence for the assumption, however, and it seems not probable that the catalytic hydrogenolysis or the dehydration, followed by the hydrogenation, of the 5β-hydroxy compound would be involved in the reaction, because the 5β-hydroxyl group is not activated by any unsaturated groups and the condition of the reaction is not so drastic.

This paper will present the results of the reinvestigation of the catalytic hydrogenolysis of 5,6β-epoxy-5β-cholestan-3β-ol with platinum, (7:3) rhodium-platinum and palladium oxides as catalysts. 5β-Cholestane-3β,5-diol[6] was also subjected to hydrogenolysis with platinum oxide in order to observe the behavior of the tertiary hydroxyl group under the conditions.

Table I summarizes the products formed in the catalytic hydrogenolysis of the epoxide I in acetic acid at room temperature and under the atmospheric pressure of hydrogen. The elimination of oxygen groups increases with respect to the catalysts in the following order: (7:3) rhodium-platinum, platinum, palladium. In every case 5β-compounds, which had not been isolated previously, were also produced, though in smaller yields than the corresponding 5α-compounds. Palladous oxide, which caused the most extensive over-hydrogenolysis, gave no diols and only a trace of 5α-cholestan-3β-ol-6-one. The catalyst also gave a considerable amount of 5α-cholestan-3-one, along with 5α-cholestan-3β-ol. These carbonyl compounds were not found in the products obtained with platinum and (7:3) rhodium-platinum catalysts. Platinum oxide and (7:3) rhodium-platinum oxide gave 3,6-diols in 36% and 74% yields respectively, the 5α-diol being formed more predominantly than the 5β-diol. Thus, the compounds carrying no oxygen at C_6 were produced mostly on palladous oxide, while in only a 25% yield on (7:3) rhodium-platinum oxide.

If these compounds were formed via 5β-cholestane-3β,5-diol, the hydrogenolysis of the oxide ring of the epoxide I should have occurred almost exclusively at C_6 on the palladium catalyst, while mostly at C_5 on the (7:3) rhodium-platinum catalyst. It may be rather unreasonable to assume that there exists such a great difference in selectivity between the catalysts in the mere hydrogenolysis of the oxide ring in acetic acid at room temperature.*1 Further evidences against

* Presented in part at the 16th Annual Meeting of the Chemical Society of Japan, Tokyo, April, 1963.

1) M. Chuman, *J. Chem. Soc. Japan (Nippon Kwagaku Zassi)*, **64**, 1486 (1943).

2) Pl. A. Plattner, Th. Petrzilka and W. Lang, *Helv. Chim. Acta*, **27**, 513 (1944).

3) Y. Urushibara and K. Mori, This Bulletin, **31**, 1068 (1958).

4) M. Shiota, T. Ogihara and Y. Watanabe, ibid., **34**, 40 (1961).

5) Pl. A. Plattner, H. Heusser and M. F. Feurer, *Helv. Chim. Acta*, **32**, 587 (1949). L. F. Fieser and M. Fieser, "Steroids," Reinhold Publishing Corporation, New York (1959), p. 199.

6) Pl. A. Plattner, H. Heusser and A. B. Kulkarni, *Helv. Chim. Acta*, **31**, 1885 (1948).

1* The catalytic hydrogenolysis of 1,2-epoxy-1-methylcyclohexane in acetic acid at room temperature gave 7% of 1-methylcyclchexanol and 93% of 2-methylcyclohexanol with platinum oxide, 8% of 1-methylcyclohexanol and 92% of 2-methylcyclohexanol with (7:3) rhodium-platinum oxide, and 8.5% of 1-methylcyclohexanol, 53.5% of 2-methylcyclohexanol and 38% of 2-methylcyclohexanone with palladous oxide. Thus, the ratio of 1-methylcyclohexanol to 2-methylcyclohexanol or to 2-methylcyclohexanol plus 2-methylcyclohexanone differs only slightly between the three catalysts (unpublished results by the present authors).

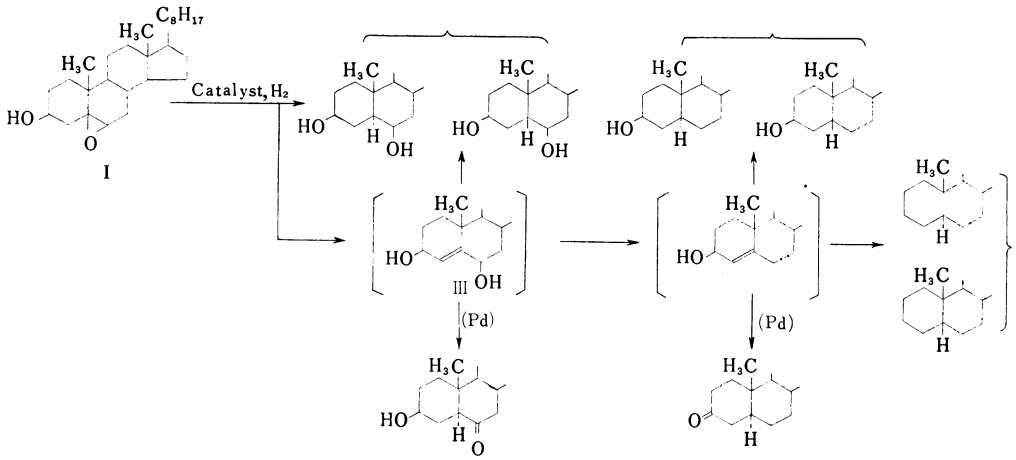


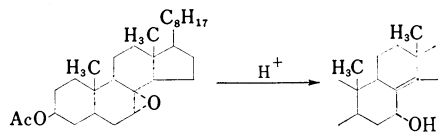
Fig. 1. The catalytic reduction of 5, 6β-epoxy-5β-cholestan-3β-ol.

TABLE I. PERCENTAGE PRODUCTS OF CATALYTIC REDUCTION OF 5,6β-EPOXY-5β-CHOLESTAN-3β-OL (I) AND OF CHOLEST-4-ENE-3β,6β-DIOL (III)[a]

Product	Compound I Catalyst			Compound III Catalyst	
	Pt	(7 : 3)Rh-Pt	Pd	Pt	(7 : 3)Rh-Pt
5β-Cholestane	3	trace	14	5	trace
5α-Cholestane	28	3	32	43	2
5β-Cholestan-3β-ol	11	6	7	13	4
5α-Cholestan-3β-ol	23	16	27	28	9
5α-Cholestan-3-one	—	—	20	—	—
5β-Cholestane-3β,6β-diol	6	26	—	5	46
5α-Cholestane-3β,6β-diol	30	48	—	6	39
5α-Cholestan-3β-ol-6-one	—	—	trace	—	—

a) All the reductions were carried out in acetic acid at room temperature and atmospheric pressure of hydrogen.

the assumption are the facts that 5β-cholestane-3β, 5-diol does not absorb any hydrogen in the presence of platinum oxide in acetic acid, and that the starting diol was recovered unchanged.[7] From these results, it is very probable that the over-hydrogenolyzed products would be formed via a different reaction path from that via the 3β, 5β-diol. These results will be best explained if we assume that the epoxide I is partly isomerized to cholest-4-ene-3β, 6β-diol (III) during the catalytic hydrogenolysis, and that this is further hydrogenated to give hydrocarbons, cholestanols (or cholestanone) and cholestanediols as illustrated in Fig. 1. The isomerization of an epoxide to an allylic alcohol has been described, for example, by Fieser and Goto,[8] who have shown that 7α, 8α-epoxy-5α-cholestan-3β-ol acetate is isomerized to the allylic alcohol V upon



IV V

standing briefly in chloroform shaken with 10% sulfuric acid. The hydrogenolysis of the epoxide I not accompanied with the isomerization may occur simultaneously, since the hydrogenolysis of the epoxide I gives a greater yield of 5α-cholestane-3β, 6β-diol than the hydrogenation of cholest-4-ene-3β, 6β-diol (see Table I). The attack of hydrogen from the β-face will be more hindered in the hydrogenolysis of the oxide ring at C_5 than in the hydrogenation of the 4, 5-double bond of the cholestenediol. The formation of carbonyl

7) The difficult hydrogenolysis of the tertiary hydroxyl group of a saturated compund in acetic acid at room temperature was also confirmed in the hydrogenation of *cis*- and *trans*-1-methyl-4-*t*-butylcyclohexanol, using platinum oxide as the catalyst.

8) L. F. Fieser and T. Goto, *J. Am. Chem. Soc.*, **82**, 1693 (1960).

compounds on a palladium catalyst may also be explained without difficulty by means of the schema shown in Fig. 1. Cholest-4-ene-3β, 6β-diol formed from the epoxide I is partly isomerized to 5α-cholestan-3β-ol-6-one*2 and mostly hydrogenolyzed to give cholest-4-en-3β-ol, which affords 5α-cholestan-3-one, along with hydrocarbons and cholestanols. Such an isomerization is supposed to occur to some extent also on (7 : 3) rhodium-platinum oxide, which would hydrogenate the resulting ketone to the corresponding alcohol. However, platinum oxide will give rise to this isomerization to a much less extent, as is expected from the fact that the isomerization of allyl alcohol to propionaldehyde during the hydrogenation in ethanol at room temperature occurs to the extent of about 30% on palladous oxide and about 20% on (7 : 3) rhodium-platinum oxide, while there is practically no isomerization on platinum oxide.[9]

Experimental

Catalysts.—The catalysts were prepared by the fusion of their chlorides with sodium nitrate according to the procedures described in the literature.[10-12]

Hydrogenation.—The hydrogenation was carried out at an ordinary temperature and pressure, using acetic acid as the solvent. The substrate was added after the metal oxide had been pre-reduced to black with hydrogen in the solvent.

5, 6β-Epoxy-5β-cholestan-3β-ol. — This compound (200 mg.) was hydrogenated with 50 mg. of the catalyst in 30 ml. of acetic acid. The hydrogenation was completed in 30 min. with platinum oxide (1.7 mol./mol. of hydrogen being absorbed), in 50 min. with (7 : 3) rhodium-platinum oxide (1.2 mol./mol. of hydrogen being absorbed), and in 1 hr. 20 min. with palladous oxide (1.8 mol./mol. of hydrogen being absorbed).

Cholest-4-ene-3β, 6β-diol. — When this compound (70 mg.) was hydrogenated with 30 mg. of platinum oxide in 15 ml. of acetic acid, 2.3 mol./mol. of hydrogen was absorbed in 20 min. The hydrogenation with (7 : 3) rhodium-platinum oxide in acetic acid has already been described in a previous paper by one of the present authors (S. N.) and Mori.[13]

5β-Cholestane-3β, 5-diol.—This compound (30 mg.) was subjected to hydrogenolysis with 15 mg. of platinum oxide in 15 ml. of acetic acid for about 1 hr., but no hydrogen was absorbed. Though the melting point of the recovered material was somewhat lower than that of the starting 3,5-diol, the following analytical values show that the recovered material did not lose any hydroxyl group :

Found : C, 80.19 ; H, 11.91. Calcd. for $C_{27}H_{48}O_2$: C, 80.14 ; H, 11.96%.

Analysis of the Products.—The reaction mixture was neutralized with aqueous sodium hydroxide and extracted with ether, and the residue after the evaporation of the ether was analyzed by gas-liquid partition chromatography with a GC-1B of Shimadzu Seisakusho, Ltd. (hydrogen-flame ionization-detector type) and a column of 1% SE-30 silicone on Chromosorb W (60~80 mesh).

The authors wish to thank Dr. Nobuo Ikekawa for his gas chromatographic analysis and for his discussion of the results, and Mrs. Misako Nohira for her collaboration in this work.

A part of the expense has been defrayed by a grant given by the Ministry of Education, to which the authors' thanks are due.

The Institute of Physical and Chemical Research
Bunkyo-ku, Tokyo (S. N.)

Chemical Laboratory
Ochanomizu University
Bunkyo-ku, Tokyo (M. S. & A. M.)

*2 It may also be possible that 5α-cholestan-3β-ol-6-one was formed directly from the epoxide I, but the fact that a much larger amount of 5α-cholestan-3-one was formed, along with the 6-one, seems to suggest that the more probable course of the occurrence of 3β-ol-6-one would be the one via III.

9) S. Nishimura, unpublished. Cf. T. Fukuda, *J. Chem. Soc. Japan, Pure Chem. Sec.* (*Nippon Kagaku Zasshi*), **83**, 1119 (1962).
10) R. Adams, V. Voorhees and R. L. Shriner, "Organic Syntheses," Coll. Vol. I, 2nd Ed., 463 (1941).
11) R. L. Shriner and R. Adams, *J. Am. Chem. Soc.*, **46**, 1683 (1924).
12) S. Nishimura, This Bulletin, **34**, 1544 (1961).
13) S. Nishimura and K. Mori, ibid., **36**, 318 (1963).

The Metal Chelates of p-(3-Formyl-4-hydroxyphenylazo)benzene Sulfonic Acid and Its Derivatives

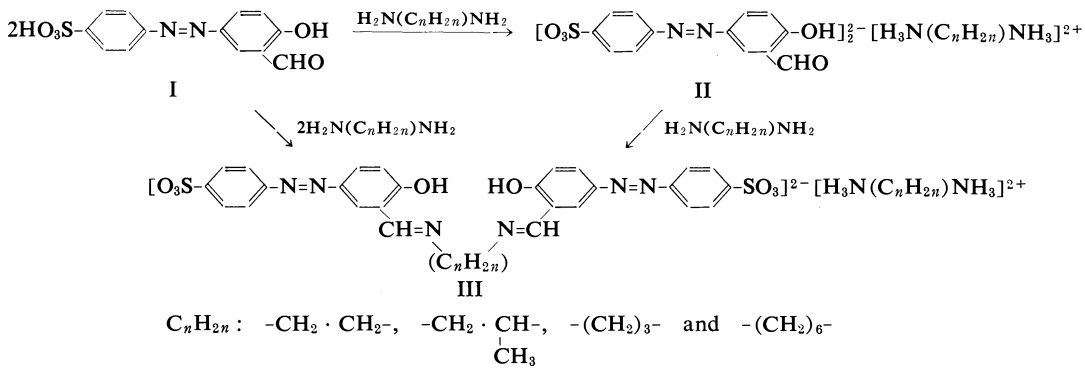
By Mitsunori TANAKA

(Received March 14, 1964)

Several syntheses of *p*-aminosalicylaldehyde have been attempted in the hope that the physiological activity of *p*-aminosalicylic acid in the treatment of tuberculosis would be improved by changing the lipophobic carboxyl group into a lipophillic aldehyde group. These attempts, however, have resulted in the formation of a resinous product of a high molecular weight because of the spontaneous condensation of the amino group of one molecule with the aldehyde group of the other. Derivatives of *p*-aminosalicylaldehyde in which the amino group is protected by an acyl group, thus preventing condensation or polymerisation, have been synthesized.

The present work is a preliminary study to approach the synthesis of *p*-aminosalicylaldehyde derivatives retaining a free amino group formed by the reductive cleavage of azo linkage in an azo compound derived from salicylaldehyde. As the aromatic amino component to be used for the diazotization and for the subsequent coupling to salicylaldehyde sulfanilic acid was adopted, since it was expected both to enhance the solubility of the resultant azo compound and to ease in the isolation of the *p*-aminosalicylaldehyde derivative from the amino component formed on reduction. We tried to suppress the chemical activity of the aldehyde group by coordinating the oxygen atom of the aldehyde group with a metal atom and by allowing the aldehyde group to react with a diamine. In this way, the reaction products of *p*-(3-formyl-4-hydroxyphenylazo)-benzene sulfonic acid or 5-(*p*-sulfophenylazo)-salicylaldehyde (I) with several alkylenediamines and their metal chelates were synthesized.

A number of complex salts of hydroxyazo-compounds whose azo group participates in the complex formation are known[1], but there



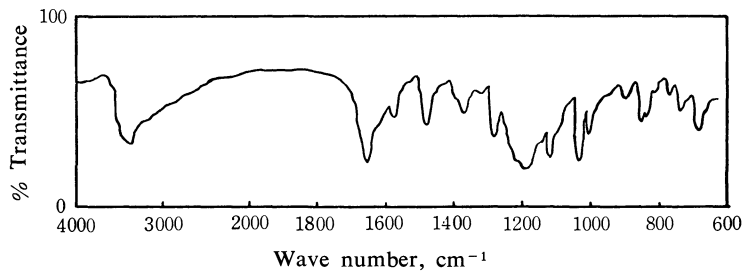


Fig. 1. Infrared spectrum of the *p*-(3-formyl-4-hydroxyphenylazo)benzene sulfonic acid.

1) For instance, A. H. Knight, *J. Soc. Dyecs Colourists*, **66**, 34 (1950); N. M. Mackenzie, H. E. Millson and B. L. West, *Ind. Eng. Chem.*, **44**, 1017 (1952); H. Pfitzner, *Angew. Chem.*, **62**, 242 (1950).

are a few instances[2] in which the nitrogen atoms of the azo-groups do not coordinate with central metal ions. The metal chelates in the present paper belong to the latter group.

The starting material, *p*-(3-formyl-4-hydroxyphenylazo) benzene sulfonic acid (I), was prepared by a modified Tummely[3] method; the barium salt of the sulfonic acid was used in place of sodium salt for the isolation of the free acid with a satisfactory purity and in a better yielde.

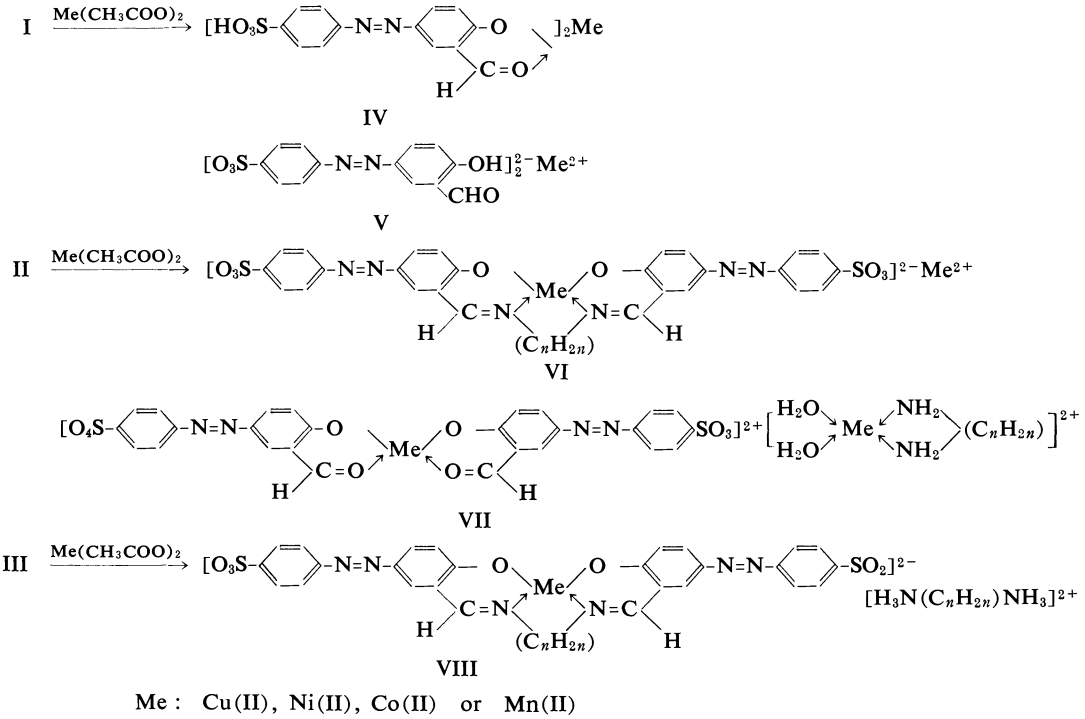
When two moles of the sulfonic acid (I) was treated with one mole of alkylene diamine, alkylene diammonium salts (II) of sulfonic acid invariably formed; those were confirmed by their infrared spectra. No formation of Schiff's base between aldehyde and diamines could be observed. As the alkylene diamine components, ethylene diamine, propylene diamine, trimethylene diamine and hexamethylene diamine were used. Figures 1 and 2 show the infrared spectra of the sulfonic acid and its ethylene diammonium salt respectively. The band in the 3200~3000 cm^{-1} region in Fig. 2 indicates the presence of a $-NH_3^+$ vibration.

On the the other hand, when the sulfonic acid was mixed with each of the above alkylene diamines in a molar ratio of 1 : 1, the Schiff's base represented by formula III was formed. Of course, the base could also be obtained from alkylene diammonium salt (II) by the action of 0.5 mol. of alkylene diamine. The infrared spectrum of one of the bases is given in Fig. 3. The band at 1625 cm^{-1} can be assigned to the -CH=N- vibration, which has already been discussed by Murase.[4]

The metal compounds of the sulfonic acid could be obtained easily when the latter was treated with metal acetates in an aqueous ethanolic medium. These metal compounds cannot be considered to be ionic metal sulfonates (V) on the basis of their infrared spectra (Fig. 4); they must be genuine chelate compounds as represented by formula IV.

It is generally accepted that, in the case of such a sulfonic acid, the formation of simple metal salts does not cause any appreciable change in their infrared spectra.

However, when the curves in Fig. 4 are compared with the curve of the original sulfonic acid (Fig. 1), a considerable change is observed. For instance, the carbonyl band of the free acid at 1650 cm^{-1} shifts towards the 1600 cm^{-1} region in the copper compound (Fig. 4, curve Cu), indicating the presence of a strong chelation; the magnitude of the shift is comparable to that between salicylaldehyde and its copper chelate.[5] The nickel, cobalt or



Me : Cu(II), Ni(II), Co(II) or Mn(II)

2) H. Ohta, K. Nawata, C. Soejima and T. Tsumaki, *Memoirs of the Faculty of Science, Kyushu University, Series C, Chemistry*, Vol. 5, No. 1. 1. (1962).
3) E. Tummely, *Ann.*, **251**, 180.
4) I. Murase, This Bulletin, **32**, 828 (1959).
5) L. J. Bellamy and R. F. Branch, *J. Chem. Soc.*, **1954**, 4491.

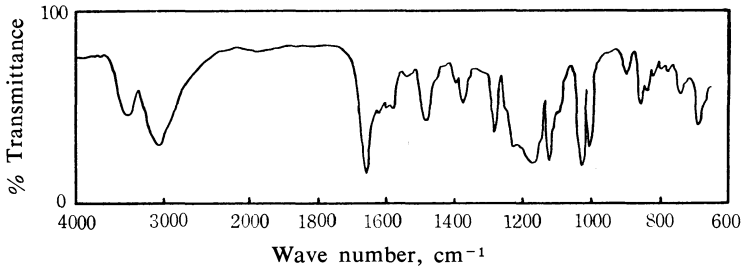


Fig. 2. Infrared spectrum of the ethylene diammonium *p*-(3-formyl-4-hydroxyphenylazo)-benzene sulfonate.

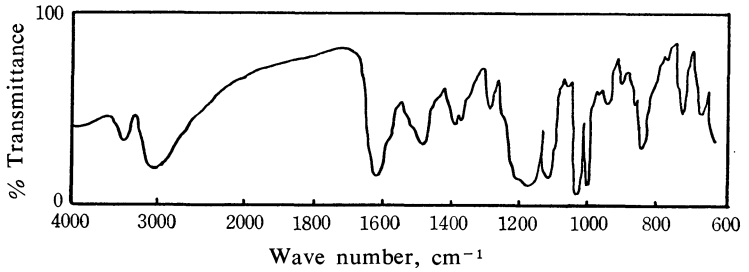


Fig. 3. Infrared spectrum of the ethylene diammonium salt of *N*, *N'*-bis[5-(*p*-sulfophenylazo)salicylidene]ethylene diamine.

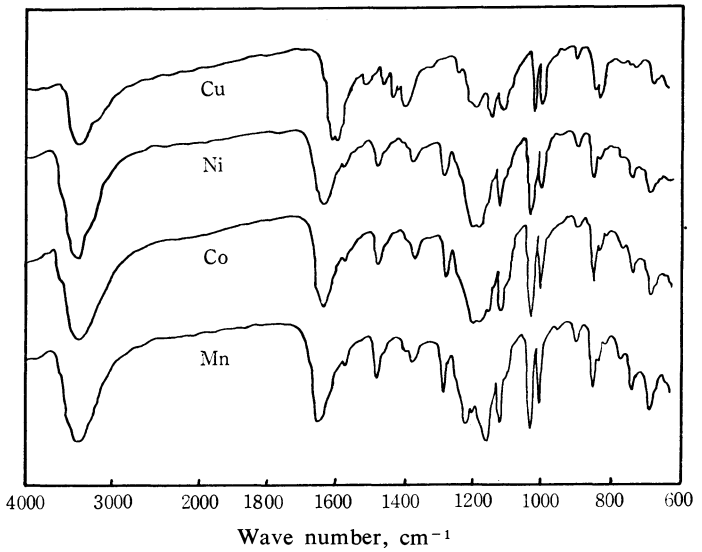


Fig. 4. Infrared spectra of the bis[5-(*p*-sulfophenylazo)salicylaldehyde]metal chelates.

manganese compound also shows a definite shift, though its magnitude is not as large.

The chelate compounds corresponding to formula VI were obtained when one mole of the alkylene diammonium salts (II) was mixed with 2 mol. of metal acetates. Figs. 5a and 5b give the infrared spectra of the copper and the nickel compounds (formula VI); the presence of the -CH=N- vibration band at 1600 cm^{-1} excludes formula VII for the nickel compound, for formula VII would require the chelated carbonyl absorption to be present at a greater wave number (ordinarily at 1640 cm^{-1}), as can be seen, for example, in the case of bis(salicylaldehyde)-nickel[5] or the nickel chelate of the sulfonic acid mentioned above (Fig. 4, curve Ni). Moreover, the band in the 3200~3000 cm^{-1} region of the $-NH_3^+$ vibration in Fig. 2 apparently has disappeared in the infrared spectra shown in Figs. 5a and 5b. Therefore, it can be concluded that, during the reaction, alkylene diamine is replaced by

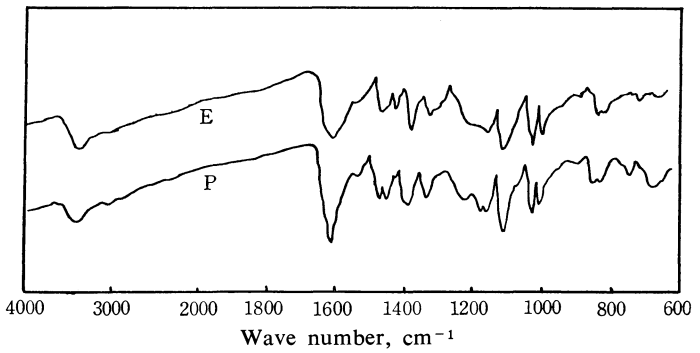


Fig. 5a. Infrared spectra of the copper(II) salt of *N*, *N*-bis[5-(*p*-sulfophenylazo)salicylidene]-alkylene diamine-copper(II).
E: Ethylene diamine, P: Propylene diamine.

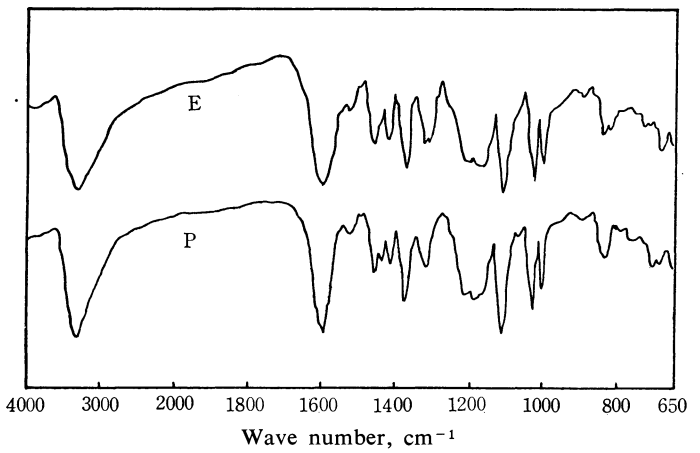


Fig. 5b. Infrared spectra of the nickel(II) salt of *N*, *N'*-bis[5-(*p*-sulfophenylazo)salicylidene]-alkylene diamine-nickel(II).
E: Ethylene diamine, P: Propylene diamine.

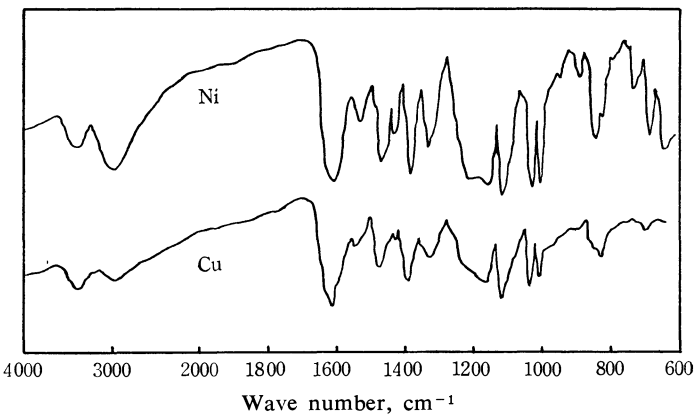


Fig. 6. Infrared spectra of the alkylene diammonium salt of *N*, *N'*-bis[5-(*p*-sulfophenylazo)-salicylidene]alkylene diamine-metal chelate.
Ni: Ethylene diamine, Cu: Trimethylene diamine

a bivalent metal ion and that the diamine molecule enters into condensation with the aldehyde group to form a Schiff's base. In the case of the copper or cobalt compound, the data indicate the same conclusion.

By the reaction of metal acetates with the alkylene diammonium salts of *N, N'*-bis[5-(*p*-sulfophenylazo)salicylaldehyde] alkylene diamine (III) or by the reaction of the metal acetates with the sulfonic acid (I) and alkylene diamines, the chelates represented by formula VIII were obtained; they are supported by the analytical data and infrared spectra (Fig. 6).

Experimental

The Infrared Spectra.—Those in Figs. 1, 2, 3, 4, 5a and 6 were measured with an Hitachi I. R. spectrophotometer, model EPI-2, and that in Fig. 5b, with an Hitachi I. R. spectrophotometer, model EPI-S2.

Chelating Agent. — *p-(3-Formyl-4-hydroxyphenylazo)benzene Sulfonic Acid (I).*—The sodium salt of the sulfonic acid was prepared by Tummely's method.[3] For the isolation of free sulfonic acid, the sodium salt was dissolved in water, and then, by the addition of an aqueous barium chloride solution, it was converted into barium salt, which was obtained as a yellowish brown precipitate. It was then decomposed with a theoretical amount of dilute sulfuric acid in an aqueous solution. The barium sulfate was removed, and the filtrate was concentrated in a vacuum desiccator. The sulfonic acid crystallized out as red or yellowish red prisms.

Alkylene Diammonium p-(3-Formyl-4-hydroxyphenylazo)benzene Sulfonate (II).—As the diamine components, ethylene diamine, propylene diamine, trimethylene diamine and hexamethylene diamine were used. One thousandth mol. of alkylene diamine was added slowly to a warm aqueous or ethanolic solution of 0.002 mol. of sulfonic acid (I). The sulfonate, which immediately separated out, was filtered and recrystallized from hot water, forming yellow needles or prisms. The analytical data are given in Table I.

TABLE I. ALKYLENE DIAMMONIUM *p*-(3-FORMYL-4-HYDROXYPHENYLAZO)BENZENE SULFONATE (Formula II).

Alkylene diamine component	Appearance	Analysis (%) Found C	H	N	Calcd. for II C	H	N
Ethylene diamine[a]	Yellow needles	49.20	4.35	11.93	49.33	4.29	12.33
Propylene diamine[b]	Yellow needles	48.21	4.71	11.51	48.19	4.74	11.63
Trimethylene diamine[c]	Yellow needles	49.14	4.60	11.34	49.43	4.58	11.93
Hexamethylene diamine[d]	Yellow needles	52.39	5.11	11.17	52.09	5.05	11.39

Percentage were calculated according to the Formulae a) $C_{28}H_{28}O_{10}N_6S_2 \cdot 0.5H_2O$, b) $C_{29}H_{30}O_{10}N_6S_2 \cdot 2H_2O$, c) $C_{29}H_{30}O_{10}N_6S_2 \cdot H_2O$ and d) $C_{32}H_{36}O_{10}N_6S_2 \cdot 0.5H_2O$.

TABLE II. ALKYLENE DIAMMONIUM SALT OF *N, N'*-BIS[5-(*p*-SULFOPHENYLAZO)-SALICYLIDENE]-ALKYLENEDIAMINE (Formula III).

Alkylene diamine component	Appearance	Analysis (%) Found C	H	N	Calcd. for III C	H	N
Ethylene diamine[a]	Orange yellow needles	51.53	4.77	15.88	51.71	4.63	16.08
Propylene diamine[b]	Yellowish orange crystalline powder	52.34	4.97	15.06	52.38	5.08	15.27
Trimethylene diamine[c]	Yellowish orange needles	52.28	5.05	15.18	52.38	5.08	15.27
Hexamethylene diamine[d]	Orange crystalline powder	55.98	5.97	13.49	55.80	6.04	13.70

Percentage were calculated according to the Formulae a) $C_{30}H_{32}O_8N_8S_2$, b) $C_{32}H_{36}O_8N_8S_2 \cdot 0.5H_2O$, c) $C_{32}H_{36}O_8N_8S_2 \cdot 0.5H_2O$ and d) $C_{38}H_{48}O_8N_8S_2 \cdot 0.5H_2O$.

TABLE III. BIS[5-(*p*-SULFOPHENYLAZO)SALICYLALDEHYDE]METAL CHELATE (Formula IV).

Metal	Appearance	Analysis (%) Found C	H	N	Me	Calcd. for IV C	H	N	Me
Cu[a]	Yellowish green needles	37.94	4.43	6.77	7.38	37.75	4.26	6.77	7.68
Ni[b]	Yellow needles	38.58	4.27	6.65	7.26	38.82	4.14	6.97	7.30
Co[c]	Yellow needles	40.23	4.16	7.23	7.48	40.16	3.89	7.21	7.58
Mn[d]	Yellow needles	38.94	4.24	6.94	7.02	39.01	4.15	7.00	6.86

Percentages were calculated according to the Formulae a) $C_{26}H_{18}O_{10}N_4S_2Cu \cdot 8.5H_2O$, b) $C_{26}H_{18}O_{10}N_4S_2Ni \cdot 7.5H_2O$, c) $C_{26}H_{18}O_{10}N_4S_2Co \cdot 6H_2O$ and d) $C_{26}H_{18}O_{10}N_4S_2Mn \cdot 7.5H_2O$.

TABLE IV. METAL SALT OF *N*, *N'*-BIS[5-(*p*-SULFOPHENYLAZO)SALICYLIDENE]ALKYLENE DIAMINE METAL CHELATE (Formula VI).

Alkylene diamine component	Metal	Appearance	Analysis (%) Found C	H	N	Me	Calcd. for VI C	H	N	Me
Ethylene diamine	Cu hydrate[a]	Green powder	38.73	3.87	9.92	14.47	38.75	3.72	9.68	14.64
	Cu pyridinate[b]	Dark green needles	51.93	4.43	12.42	10.80	51.84	3.99	12.59	11.43
	Ni hydrate[c]	Orange red needles	39.34	3.84	9.62	13.73	39.19	3.76	9.79	13.68
	Ni pyridinate[d]	Orange red needles	48.29	4.56	11.73	9.77	48.34	4.56	11.75	9.85
Propylene diamine	Cu pyridinate[e]	Green needles	49.41	4.61	11.80	11.08	49.12	4.54	11.69	10.61
	Ni hydrate[f]	Orange red needles	39.22	3.84	9.54	13.39	39.13	4.08	9.44	13.19
	Ni pyridinate[g]	Reddish orange needles	53.47	4.67	12.58	9.04	53.33	4.70	12.65	8.84
Trimethylene diamine	Cu pyridinate[h]	Dark green prisms	50.25	4.72	11.65	10.82	50.25	4.39	11.96	10.85
	Ni hydrate[i]	Reddish orange crystals	39.91	4.08	9.53	13.81	39.94	3.93	9.64	13.46
	Ni pyridinate[j]	Red needles	49.47	4.67	11.49	9.93	49.52	4.58	11.78	9.88
Hexamethylene diamine	Cu pyridinate[k]	Dark green powder	49.65	5.00	11.18	10.41	49.63	4.97	11.13	10.10

Percentages were calculated according to the Formulae a) $C_{28}H_{20}O_8N_6S_2Cu_2 \cdot 6H_2O$, b) $C_{28}H_{20}O_8N_6S_2Cu_2 \cdot 4C_5H_5N \cdot 2H_2O$, c) $C_{28}H_{20}O_8N_6S_2Ni_2 \cdot 6H_2O$, d) $C_{28}H_{20}O_8N_6S_2Ni_2 \cdot 4C_5H_5N \cdot 7H_2O$, e) $C_{29}H_{22}O_8N_6S_2Cu_2 \cdot 4C_5H_5N \cdot 6H_2O$, f) $C_{29}H_{22}O_8N_6S_2Ni_2 \cdot 7H_2O$, g) $C_{29}H_{22}O_8N_6S_2Ni_2 \cdot 6C_5H_5N \cdot 5H_2O$, h) $C_{29}H_{22}O_8N_6S_2Cu_2 \cdot 4C_5H_5N \cdot 4.5H_2O$, i) $C_{29}H_{22}O_8N_6S_2Ni_2 \cdot 6H_2O$ j) $C_{29}H_{22}O_8S_2N_6S_2Ni_2 \cdot 4C_5H_5N \cdot 6H_2O$ and k) $C_{32}H_{29}O_8N_6S_2Cu_2 \cdot 4C_5H_5N \cdot 7H_2O$.

TABLE V. ALKYLENE DIAMINE SALT OF *N*, *N'*-BIS[5-(*p*-SULFOPHENYLAZO)SALICYLIDENE]ALKYLENE DIAMINEMETAL CHELATE (Formula VIII)

Alkylene diamine component	Metal	Appearance	Analysis (%) Found C	H	N	Me	Calcd. for VIII C	H	N	Me
Ethylene diamine	Cu[a]	Green needles	45.45	4.45	14.58	8.22	45.36	4.31	14.11	8.00
	Ni[b]	Orange red needles	46.82	4.21	14.28	7.74	46.71	4.18	14.52	7.61
Propylene diamine	Cu[c]	Green needles	45.06	5.05	12.66	7.67	44.78	4.93	13.05	7.40
	Ni[d]	Red needles	44.18	5.02	13.08	6.83	44.10	5.08	12.86	6.74
Trimethylene diamine	Cu[e]	Green needles	44.73	5.05	13.08	7.65	44.78	4.93	13.05	7.40
	Ni[f]	Orange red prisms	43.53	5.54	12.83	6.65	43.21	5.21	12.60	6.60
Hexamethylene diamine	Cu[g]	Green crystalline powder	46.97	5.97	11.85	6.65	47.07	5.93	11.56	6.55

Percentages were calculated according to the Formulae a) $C_{30}H_{30}O_8N_8S_2Cu \cdot 2H_2O$, b) $C_{30}H_{30}O_8N_8S_2Ni \cdot H_2O$, c) $C_{32}H_{34}O_8N_8S_2Cu \cdot 4H_2O$, d) $C_{32}H_{34}O_8N_8S_2Ni \cdot 5H_2O$, e) $C_{32}H_{34}O_8N_8S_2Cu \cdot 4H_2O$, f) $C_{32}H_{34}O_8N_8S_2Ni \cdot 6H_2O$ and g) $C_{38}H_{46}O_8N_8S_2Cu \cdot 5.5H_2O$.

In the case of the copper chelate of the propylene diamine analogue, it was prepared by mixing the sulfonic acid (I), propylene diamine and copper acetate in an aqueous solution.

Alkylene Diammonium Salt of N, N'-Bis[5-(p-sulfophenylazo)salicylidene]alkylene Diamine (III).—To a warm solution of 0.002 mol. of the sulfonic acid (I) in 100 ml. of water, a solution of 0.002 mol. of alkylene diamine in 10 ml. of water was added. The yellow precipitate thus obtained was recrystallized from a large quantity of water, a pyridine-water mixture, or an ethanol-water mixture. The salts are listed in Table II.

Metal Chelate. — *Bis-[5-(p-sulfophenylazo)salicylaldehyde]metal Chelate (IV).*—The copper, the nickel, the cobalt and the manganese chelates were synthesized by adding a solution of 0.0005 mol. of metal acetate in 10 ml. of water to a solution of 0.001 mol. of the sulfonic acid (I) in 50 ml. water. The mixture was heated on a water-bath for a short time and then left to cool. The precipitate was collected and recrystallized from water. The results are listed in Table III.

The Metal Salt of N, N'-Bis[5-(p-sulfophenylazo)-salicylidene]alkylene Diamine-metal Chelate (VI).—Four alkylene diammonium sulfonates of Table I were used as the ligand components, and copper and nickel acetate as the metal components. The chelates thus obtained are listed in Table IV. A solution of 0.001 mol. of copper acetate or nickel acetate in 10 ml. of water was added to a warm solution of 0.0005 mol. of the alkylene diammonium salt (III) in 200 ml. of water (50 ml. of a pyridine-water mixture was used for the preparation of copper chelates). The mixture was filtered when necessary, boiled for a short time, and concentrated on a water-bath until the precipitation of the chelate was completed. The chelates thus obtained were recrystallized from a pyridine-water mixture or from an ethanol-water mixture. All of the nickel chelates were obtained in the form of hydrates or pyridinates. They are listed in Table IV.

Alkylene Diammonium Salt of N, N'-Bis[5-(p-sulfophenylazo) - salicylidene]alkylene Diamine-metal Chelate (VIII).—These salts are listed in Table V. A solution of 0.0005 mol. of metal acetate in 20 ml. of water was added to a solution of 0.0005 mol. of the salt (III) in 100 ml. of a hot pyridine-water mixture (in the case of the ethylene diamine analogue, 800 ml. of hot water was used). The mixture was heated for a short time and concentrated on a water-bath to an adequate volume. The precipitate was then collected and recrystallized from an ethanol-water mixture or a pyridine-water mixture.

The author wishes to express his thanks to President Dr. Tokuichi Tsumaki of the Kyushu Institute of Technology and to Professor Dr. Tamotsu Yoshida and Dr. Masaru Yamaguchi of Kyushu University for their exceedingly kind direction of this work. The author also wishes to thank Professor Dr. Yoshiya Kanda of Kyushu University for his measurement of the infrared spectra and Mr. Michio Shido and his group for their elementary analysis.

The Faculty of Liberal Arts & Education,
Kagawa University
Saiwaicho, Kagawa

Vibrational Spectra of Tetracyanoethylene

By Tohru TAKENAKA and Soichi HAYASHI

(Received March 17, 1964)

Since tetracyanoethylene (TCNE) was synthesized for the first time by Cairns et al.,[1] much attention has been directed to the π-complexes formed by TCNE with aromatic compounds. However, previous work on the vibrational spectra and assignments of this molecule has been very limited. The infrared spectrum of TCNE was first reported by Looney and Downing,[2] who also gave the C≡N and C=C stretching frequencies in the infrared and Raman spectra. When we were almost finished with the present work, Long and George[3] published a paper in which the infrared and Raman spectra of the powdered solid were treated, together with the infrared spectrum of solution, and tentative assignments were given on the basis of spectra correlations.

On the other hand, in the normal coordinate treatments of molecules with π-electron systems, it was found necessary to supplement the basic Urey-Bradley force field (UBFF)[4,5] with additional cross terms, for example, "resonance-interaction terms" between the C—C stretching coordinates in benzene,[6-8] and

1) T. L. Cairns, R. A. Carboni, D. D. Coffman, V. A. Engelhardt, R. E. Heckert, E. L. Little, E. G. McGeer, B. C. Mckusick, W. J. Middleton, R. M. Scribner, C. W. Theobald and H. E. Winberg, *J. Am. Chem. Soc.*, **80**, 2775 (1958).

2) C. E. Looney and J. R. Downing, ibid., **80**, 2840 (1958).

3) D. A. Long and W. O. George, *Spectrochim. Acta*, **19**, 1717 (1963).

4) H. C. Urey and C. A. Bradley, *Phys. Rev.*, **38**, 1969 (1931).

5) T. Simanouchi, *J. Chem. Phys.*, **17**, 245, 734, 848 (1949).

6) S. Califano and B. Crawford, Jr., *Spectrochim. Acta*, **16**, 889 (1960).

7) J. R. Scherer and J. Overend, ibid., **17**, 719 (1961).

8) W. D. Jones, *J. Mol. Spectrosc.*, **10**, 131 (1963).

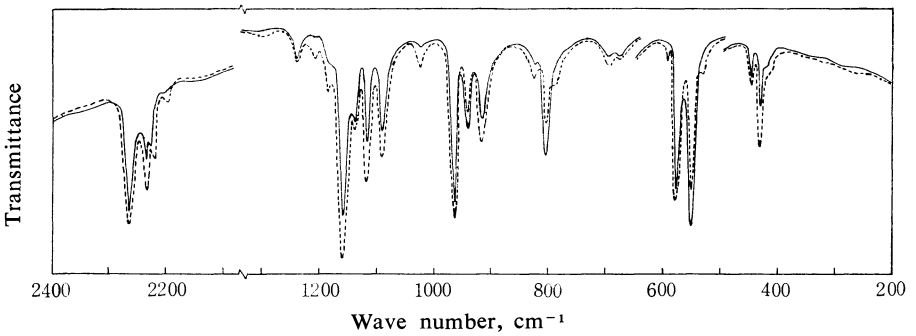


Fig. 1. Infrared spectrum of highly-oriented crystal of tetracyanoethylene.
—— Electric vector perpendicular to direction of crystal growth
---- Electric vector parallel to direction of crystal growth

" trans-interaction terms " between trans-hydrogen bending coordinates[9] or " bond-flexibility terms "[9,10] in ethylene and its derivatives. Thus, one might not expect the basic UBFF to be a satisfactory description of the potential function for TCNE, for in this case it is well recognized that resonance plays an important structural role.

In the present work, we have studied the polarized infrared spectrum of a highly-oriented crystal of TCNE and the Raman spectrum of a sample consisting of several lumps of the crystals. The infrared spectra of the powdered solid, solution, and vapor were also measured for comparison. In order to make vibrational assignments and to determine the force constants for this molecule, the normal coordinate treatments for the in-plane vibrations were carried out by using the basic UBFF and also a slight modification of it.

Experimental and Observed Spectra

A sample of TCNE kindly supplied by Dr. Kenichi Kudo was twice sublimed at 130~140°C/1~2 mmHg. The colorless, crystalline solid thus obtained melts at 199~200°C in a sealed capillary tube, the melting point being in good agreement with the literature values.[1,11]

Infrared Spectra. — The infrared absorption spectra in the region 4000~480 cm^{-1} were obtained by using a Perkin-Elmer model 21 spectrophotometer equipped with a lithium fluoride or sodium chloride prism, and by a Nippon Bunko model DS-301 (double monochromator) spectrophotometer equipped with two potassium bromide prisms. For measurements in the far-infrared region, 500~200 cm^{-1}, a Parkin-Elmer model 221 spectrophotometer equipped with a cesium bromide prism and a Nippon Bunko model DS-402G grating spectrophotometer were used.

Solid. — The highly-oriented, tabular crystals of TCNE were carefully prepared by the gradual heating of the purified solid up to about 140°C with a slight temperature gradient and at a pressure of 1~2 mmHg. The maximum size of these crystals was ca. 6×3 mm.; polarization microscopic examination was used to choose the best oriented crystal to be placed in the spectrophotometer beam. By X-ray diffraction studies, it was found that the solid TCNE prepared in the present work has the same crystal form as that (monoclinic crystals of the space group $P2_1/n$—C_{2h}^5) obtained by Bokoe and Trueblood[12] by recrystallization from a mixture of carbon tetrachloride and ethyl acetate, and that the crystals grew elongated along the b axis with the tabular ($\bar{1}01$) face.

Infrared polarization measurements for the crystal were made with silver chloride transmission polarizers, except in the far-infrared region, where transmission polarizers made of polyethylene sheets were used. The observed absorption spectra are shown in Fig. 1. The solid and broken lines represent the absorption curves obtained with polarized radiation, with the electric vector perpendicular to and parallel to the direction of crystal growth respectively. From Fig. 1, it may be seen that the absorption bands can be classified by their dichroic properties into three groups: (1) a group of bands which exhibit a high parallel dichroism ($\parallel$ band), (2) a group of bands which show nearly the same absorption intensities for both the parallel and perpendicular polarized radiations with a slight predominance of absorption intensity for the former · ($\parallel \perp$ band), and (3) a group of bands which exhibit perpendicular dichroism ($\perp$ band). The observed bands, their relative intensities, and their dichroic properties are listed in Table I. The infrared spectrum of the powdered solid was also recorded by the use of the potassium bromide disk and Nujol mull; this procedure showed the same frequencies and relative intensities as those in the spectrum of the crystal.

Solution. — The infrared spectra of TCNE were

9) J. R. Scherer and J. Overend, *J. Chem. Phys.*, **33**, 1681 (1960).
10) T. Shimanouchi, ibid., **26**, 594 (1957).
11) "Organic Syntheses," Vol. 39, 64 (1959).
12) D. A. Bekoe and K. N. Trueblood, *Z. Kristallogr.*, **113**, 1 (1960).

also measured for the saturated solution in dichloromethane or dibromomethane by using various fixed-thickness cells (0.2~1.0 mm.). The solution spectrum over the region 4000~200 cm^{-1} could be obtained by using either of these solvents, thus avoiding the strong interference due to solvent absorptions. Because of the limited solubilities of TCNE in these solvents, however, only the absorption bands which correspond to the relatively intense bands in the solid spectrum were observed. The observed bands and their relative intensities are given in Table I.

TABLE I. OBSERVED FREQUENCIES (cm^{-1}) OF TETRACYANOETHYLENE*1

Infrared				Raman
Crystal		Solution*2	Vapor*3	Crystal
				2313 vw
2262 m	∥ ⊥	2255 m	2248 s	
		2249 vw		
				2250 s
				2237 s
2230 m	∥	2222 m	2217 m	
2221 vw	⊥			
2216 vw	∥			
				2195 vw
2194 vw	∥			
				1573 s
				1537 w
				1284 m
1233 w	∥ ⊥			
1206 vw	∥			
1181 vw	∥			
1155 s	∥	1153 s	1153 s	
1138 vw	∥ ⊥			
1115 m	∥	1109 m	1111 m	
1086 m	∥	1079 m	1070 m	
1021 w	∥			
959 s	∥ ⊥	956 s	953 m	
935 m	⊥	927*w		
916 m	∥	905*m	902 m	
825 w	∥		822 w	
804 m	⊥		785 m	
797 sh	∥			
696 w	∥			
675 w	∥ ⊥			
				679 m
				592 vw
586 vw	∥			
579 s	∥ ⊥	575 m		
555 s	⊥	553 s		
537 vw	∥			
				536 vw
				508 vw
444 w	∥ ⊥			
429 m	∥			
ca. 420 sh				
				370 vw
				360 vw
				251 w

*1 s: strong, m: medium, w: weak, vw: very weak, sh: shoulder.

*2 Measured with a saturated solution in CH_2Cl_2 except for bands marked with * which are measured with a saturated solution in CH_2Br_2.

*3 Measured only in the LiF and NaCl prism regions.

Vapor.—The vapor spectrum in the region 4000~650 cm^{-1} was obtained by using a 10 cm. cell kept at ca. 200°C[13] by electric heaters. From Looney and Downing's data[2] the vapor pressure of TCNE was estimated to be more than 150 mmHg at this temperature. The spectrum obtained gave broad bands instead of fine structures due to the rotation of the molecule. The observed bands and their relative intensities are given in Table I, together with similar data for the corresponding bands of solid and solution. The correspondence of the bands among vapor, solution, and solid is fairly good as far as the comparison can be made indicating intermolecular forces in the solid phase are so weak that the intense bands of solid TCNE are correlated with the fundamental vibrational modes of the vapor molecules.

Raman Spectrum.—The Raman spectrum of solid TCNE was recorded photoelectrically by using a Cary model 81 spectrometer and photographically by using a Yuki Gosei model RL-II spectrometer. Several lumps of crystals prepared in the same way as those for the infrared polarization measurement were used as samples. The observed frequencies and their relative intensities are summarized in Table I. Attempts to determine the depolarization ratios by using the polarized incident-light technique were unsuccessful.

The Symmetry of Molecule and Selection Rule

According to X-ray analysis by Bekoe and Trueblood,[12] a TCNE molecule in crystal should have the site symmetry of C_i; in fact, slight difference is found between two C-C bond lengths of one wing of the molecule, and also between two bond angles formed by the two C-C bonds and the C=C bond (the C-C bond lengths: 1.454±0.007 Å and 1.443±0.006 Å; the C-C=C bond angles: 120.2° and 122.4°). However, it is reasonable to assume that the vibrational spectra of the crystal can virtually be treated under the molecular point group V_h for the following reasons: (1) The difference between the two C-C bond lengths, as well as that between the two C-C=C bond angles, is very small, as has been described above, and the planarity of the molecule is fairly

13) Since it was shown[11] that TCNE slowly evolves hydrogen cyanide when exposed to moist air even at room temperature, the gas cell was evacuated before heating, but weak bands due to hydrogen cyanide were still observed at ca. 3320 and 712 cm^{-1}.

TABLE II. SYMMETRY COORDINATES* FOR TETRACYANOETHYLENE

Species	Symmetry coordinate	Mode
A_g	$S_1=\Delta R$	C=C stretching
	$S_2=1/2(\Delta r_2+\Delta r_3+\Delta r_4+\Delta r_5)$	C-C stretching
	$S_3=1/2(\Delta l_6+\Delta l_7+\Delta l_8+\Delta l_9)$	C≡N stretching
	$S_4=1/\sqrt{3}\{(\Delta\alpha_0+\Delta\alpha_1)-1/2(\Delta\beta_2+\Delta\beta_3+\Delta\beta_4+\Delta\beta_5)\}$	C-C-C bending
	$S_5=1/2(\Delta\theta_6+\Delta\theta_7+\Delta\theta_8+\Delta\theta_9)$	C-C≡N bending
B_{1g}	$S_6=1/2(\Delta r_2-\Delta r_3+\Delta r_4-\Delta r_5)$	C-C stretching
	$S_7=1/2(\Delta l_6-\Delta l_7+\Delta l_8-\Delta l_9)$	C≡N stretching
	$S_8=1/2(\Delta\beta_2-\Delta\beta_3+\Delta\beta_4-\Delta\beta_5)$	C-C-C rocking
	$S_9=1/2(\Delta\theta_6-\Delta\theta_7+\Delta\theta_8-\Delta\theta_9)$	C-C≡N bending
B_{2u}	$S_{10}=1/2(\Delta r_2-\Delta r_3-\Delta r_4+\Delta r_5)$	C-C stretching
	$S_{11}=1/2(\Delta l_6-\Delta l_7-\Delta l_8+\Delta l_9)$	C≡N stretching
	$S_{12}=1/2(\Delta\beta_2-\Delta\beta_3-\Delta\beta_4+\Delta\beta_5)$	C-C-C rocking
	$S_{13}=1/2(\Delta\theta_6-\Delta\theta_7-\Delta\theta_8+\Delta\theta_9)$	C-C≡N bending
B_{3u}	$S_{14}=1/2(\Delta r_2+\Delta r_3-\Delta r_4-\Delta r_5)$	C-C stretching
	$S_{15}=1/2(\Delta l_6+\Delta l_7-\Delta l_8-\Delta l_9)$	C≡N stretching
	$S_{16}=1/\sqrt{3}\{(\Delta\alpha_0-\Delta\alpha_1)-1/2(\Delta\beta_2+\Delta\beta_3-\Delta\beta_4-\Delta\beta_5)\}$	C-C-C bending
	$S_{17}=1/2(\Delta\theta_6+\Delta\theta_7-\Delta\theta_8-\Delta\theta_9)$	C-C≡N bending

* Redundant coordinates are excluded.

good.[12] (2) The correspondence of the infrared bands among vapor, solution, and solid is fairly good. (3) The infrared bands of the crystal are classified into three groups according to their dichroic properties. Thus, the normal vibrations of TCNE divide into symmetry species as follows:

$$\Gamma = 5A_g(R) + 4B_{1g}(R) + 4B_{2u}(IR) + 4B_{3u}(IR) + 2A_u(\text{inactive}) + 2B_{1u}(IR) + 2B_{2g}(R) + B_{3g}(R)$$

where the first four are the in-plane vibrations, and the rest are the out-of-plane vibrations.

Normal Coordinate Treatment for In-plane Vibrations

The *GF* matrix method developed by Wilson[14] was used. A representative of each type of internal coordinate is shown in Fig. 2, while the symmetry coordinates are shown in Table II. The equilibrium bond lengths adopted are those determined from X-ray analysis by Bekoe and Trueblood:[12] $R_0=1.317$ Å, $r_0=1.449$ Å,[15] and $l_0=1.15$ Å. For the bond angles, $\alpha_0=\beta_0=120°$ and $\theta_0=180°$ were assumed for the sake of simplicity. In order to solve the secular equation, the symmetrization of the *GF* matrix was made according to the usual method.[16-18]

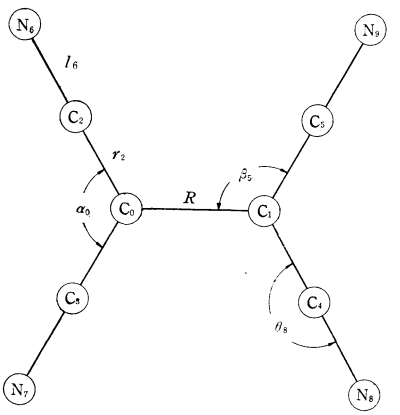


Fig. 2. Internal coordinates for tetracyanoethylene.

The numerical calculations were carried out by using the KDC-1 electronic digital computer constructed in the Faculty of Engineering of Kyoto University.

The basic UBFF[4,5] was used at first as the potential function for TCNE. Then, three bond-stretching (K(C=C), K(C-C), and K(C≡N)), three angle-bending (H(C-C-C), H(C-C=C), and H(C-C≡N)), and four non-bonded repulsion force constants (F(C-C-C), F(C-C=C), F(C-C≡N), and C) were necessary. The constants, C, represents the repulsion between two

14) E. B. Wilson, Jr., *J. Chem. Phys.*, **7**, 1047 (1939); **9**, 76 (1941).
15) The average of the individual bond lengths (see above).
16) T. Miyazawa, *J. Chem. Phys.*, **29**, 246 (1958).
17) T. Shimanouchi, "Jikken-Kagaku Koza," 3, Maruzen, Tokyo (1957), Chap. 5.
18) W. J. Taylor, *J. Chem. Phys.*, **18**, 1301 (1950).

carbon atoms in the cis-position.[9,19,20] Since Urey-Bradley force constants transferable to conjugated nitriles have not been reported, for the first calculation the force constants were assumed to have the values found for alkylnitriles,[21,22] tetrahalogenoethylenes,[20] and methyl-substituted ethylenes.[23] Repetitions of the calculation with several sets of force constants were then carried out by the trial-and-error method by the use of the Jacobian matrix.[24] The final set of force constants thus obtained is shown in Column I of Table III, and the frequencies calculated with these constants are compared in Column I of Table IV with the observed values. The agreement is satisfactory except in the case of the frequency 679 cm^{-1} (ν_3) of the A_g species.

In order to obtain a better agreement for this frequency, the basic UBFF was modified by introducing new cross terms between the C–C and C=C bonds to take the presumed resonance interaction into account. The modified potential function is written as:

$$2V_{\text{mod. UBFF}} = 2V_{\text{UBFF}} + 2\rho\sum_{i=2}^{5}(\Delta R)(\Delta r_i)$$

The new cross terms appear only on the A_g factor of the $\boldsymbol{F}$ matrix. Hence, by putting $\rho = 0.75$ mdyn./Å, $K(C{=}C) = 7.79$ mdyn./Å, and other constants equal to those of Set I, considerable improvements were made for the frequencies of the A_g species without any altration of the frequencies for other species. The

TABLE III. FORCE CONSTANTS* FOR TETRACYANOETHYLENE (mdyn./Å)

	I UBFF	II Mod. UBFF
K(C=C)	6.31	7.79
K(C-C)	4.80	4.80
K(C≡N)	16.84	16.84
H(C-C-C)	0.05	0.05
H(C-C=C)	0.16	0.16
H(C-C≡N)	0.13	0.13
F(C-C-C)	1.11	1.11
F(C-C=C)	1.04	1.04
F(C-C≡N)	0.08	0.08
C	0.11	0.11
ρ	—	0.75

* $F' = -0.1F$, $C' = -0.1C$

TABLE IV. COMPARISON BETWEEN OBSERVED AND CALCULATED FREQUENCIES (cm^{-1}) FOR IN-PLANE FUNDAMENTAL VIBRATIONS OF TETRACYANOETHYLENE

Species	No.	Obs. freq. Raman	Obs. freq. Infrared	I Calcd. freq.	I Dev.* %	II Calcd. freq.	II Dev.* %
A_g	ν_1	2250		2250	0.0	2246	−0.2
	ν_2	1573		1573	0.0	1573	0.0
	ν_3	679	Inact.	647	−4.7	659	−2.9
	ν_4	536		525	−2.1	530	−1.1
	ν_5	—		122	—	122	—
B_{1g}	ν_6	2237		2232	−0.2	2232	−0.2
	ν_7	1284	Inact.	1304	+1.5	1304	+1.5
	ν_8	508		503	−1.0	503	−1.0
	ν_9	251		251	0.0	251	0.0
B_{2u}	ν_{10}		2230	2239	+0.4	2239	+0.4
	ν_{11}	Inact.	1155	1152	−0.3	1152	−0.3
	ν_{12}		429	433	+0.9	433	+0.9
	ν_{13}		—	111	—	111	—
B_{3u}	ν_{14}		2262	2257	−0.2	2257	−0.2
	ν_{15}	Inact.	959	980	+2.2	980	+2.2
	ν_{16}		579	591	+2.1	591	+2.1
	ν_{17}		—	157	—	157	—

* $100 \times (\nu_{\text{calcd}} - \nu_{\text{obs}})/\nu_{\text{obs}}$

19) D. E. Mann, T. Shimanouchi, J. H. Meal and L. Fano, *J. Chem. Phys.*, **27**, 43 (1957).
20) D. E. Mann, L. Fano, J. H. Meal and T. Shimanouchi, ibid., **27**, 51 (1957).
21) I. Nakagawa and T. Shimanouchi, *Spectrochim. Acta*, **18**, 513 (1962).
22) T. Fujiyama, I. Nakagawa and T. Shimanouchi, Symposium on Structural Chemistry, Tokyo, October, 1961.
23) S. Mizushima and T. Shimanouchi, "Sekigaisen-kyushu to Raman Koka," Kyoritsu, Tokyo (1958).
24) T. Miyazawa, *J. Chem. Soc. Japan, Pure Chem. Sec.* (*Nippon Kagaku Zassi*), **76**, 1132 (1955).

TABLE V. POTENTIAL ENERGY DISTRIBUTIONS (%) FOR IN-PLANE FUNDAMENTAL VIBRATIONS OF TETRACYANOETHYLENE

	A_g				
	ν_1 2246 cm^{-1}	ν_2 1573 cm^{-1}	ν_3 659 cm^{-1}	ν_4 530 cm^{-1}	ν_5 122 cm^{-1}
S_1	0.0	78.0	0.0	1.2*	0.4*
S_2	13.4*	13.2*	83.5	5.1*	0.9
S_3	86.6	0.0*	13.1	0.4*	0.0
S_4	0.0*	8.1	2.4	63.2	32.8*
S_5	0.0*	0.7	1.0	30.0	65.8
	B_{1g}				
	ν_6 2232 cm^{-1}	ν_7 1304 cm^{-1}	ν_8 503 cm^{-1}	ν_9 251 cm^{-1}	
S_6	15.5*	52.0*	26.3	1.7	
S_7	84.0	7.6*	4.8	0.6	
S_8	0.5	39.7	49.3	13.2	
S_9	0.0*	0.6*	19.7*	84.5	
	B_{2u}				
	ν_{10} 2239 cm^{-1}	ν_{11} 1152 cm^{-1}	ν_{12} 433 cm^{-1}	ν_{13} 111 cm^{-1}	
S_{10}	16.3	83.0	0.0	1.5*	
S_{11}	83.6*	14.4	0.2*	0.0	
S_{12}	0.0*	2.2*	50.6*	46.2	
S_{13}	0.0	0.4	49.1	52.3	
	B_{3u}				
	ν_{14} 2257 cm^{-1}	ν_{15} 980 cm^{-1}	ν_{16} 591 cm^{-1}	ν_{17} 157 cm^{-1}	
S_{14}	15.8*	62.8*	16.9*	0.0	
S_{15}	84.1	10.1*	4.1*	0.0	
S_{16}	0.0	23.8	57.3*	23.2	
S_{17}	0.0	3.3	21.6*	76.7*	

* The sign of the corresponding element of $\boldsymbol{L}$ matrix is negative.

results are shown in Column II of Table III and Table IV. The additional introduction of cross terms between the C–C and C≡N bonds improved the situation little. Table V shows the potential energy distribution (for Set II) among the symmetry coordinates calculated from the expression:[25]

$$P_{tj}=L_{tj}^2F_{tt}/\sum_i L_{tj}^2F_{tt}$$

where L_{tj} denotes the element of the $\boldsymbol{L}$ matrix whose columns are the characteristic vectors of the $\boldsymbol{GF}$ matrix.

Vibrational Assignments

In-plane Fundamental Vibrations. — In view of the fact that, in the polarized infrared spectrum of the TCNE crystal, the two medium-strength bands observed at 2262 and 2230 cm^{-1} (due to the C≡N stretching modes) exhibit a ∥ ⊥ and a ∥ dichroism respectively, it is evident that one of the two species, B_{2u} and B_{3u}, should have one of these dichroic properties, and the remaining one, the other.

On the other hand, comparisons of the four C–X stretching frequencies on each tetrahalogenoethylene ($X_2C=CX_2$) belonging to the point group V_h always result in the sequence $\nu(B_{1g})>\nu(B_{2u})>\nu(B_{3u})>\nu(A_g)$,[20] as is shown in Table VI. Therefore, it is reasonable to

TABLE VI. C–X STRETCHING FREQUENCIES (cm^{-1}) OF $X_2C=CX_2$ MOLECULES (POINT GROUP V_h)

Species	X=F*	Cl*	Br*	CN Present work
A_g	778	447	265	679
B_{1g}	1340	1000	880	1284
B_{2u}	1337	908	766	1155
B_{3u}	1186	777	635	959

* Ref. 20.

assume that the four C–C stretching modes of TCNE should be arranged in the same sequence of frequencies. Thus, the two strong infrared bands at 1155(∥) and 959 cm^{-1}(∥ ⊥) are associated with the B_{2u} and B_{3u} C–C stretching modes respectively, while the two medium-strength Raman lines at 1284 and 679 cm^{-1} are associated with the corresponding B_{1g} and A_g modes respectively (Table VI). These assignments are confirmed by the present normal coordinate analysis. In each species, the potential energy of this vibration is predominantly associated with the C–C stretching mode, its magnitude depending upon the species. These assignments are different from those given by Long and George,[3] who attributed the two infrared bands at 1155 and 959 cm^{-1} to the B_{3u} and B_{2u} C–C stretching modes respectively, and the two Raman lines at 1250[26] and 1280 cm^{-1} to the corresponding B_{1g} and A_g modes respectively.

The assignments of the C–C stretching modes reveal that the infrared acitive species B_{2u} and B_{3u} should have a ∥ and a ∥ ⊥ dichroism respectively. Hence, the ∥ ⊥ band at 2262 cm^{-1} is assigned to the B_{3u} C≡N stretching mode, and the ∥ band at 2230 cm^{-1}, to the corresponding B_{2u} mode. Since the two strong Raman lines at 2250 and 2237 cm^{-1} (due to the C≡N stretching modes) have almost the same intensity, it is difficult to assign these lines to the respective species experimentally. Therefore, with the aid of the normal coordinate

25) Y. Morino and K. Kuchitsu, *J. Chem. Phys.*, **20**, 1809 (1952).

26) We could not find this Raman line in our spectrum even in careful measurements (see Table I).

TABLE VIII. ASSIGNMENTS OF OBSERVED BANDS (LINES) DUE TO OVERTONE AND COMBINATION VIBRATIONS OF TETRACYANOETHYLENE

	Freq. cm^{-1}	Intensity	Dichroism	Assignment
Raman line	2313	vw		$1155(B_{2u})\times 2=2310(A_g)$
	2195	vw		$1233(B_{3u})+959(B_{3u})=2192(A_g)$
	1537	w		$1284(B_{1g})+251(B_{1g})=1535(A_g)$; $959(B_{3u})+579(B_{3u})=1538(A_g)$
Infrared band	1115	m	∥	$679(A_g)+429(B_{2u})=1108(B_{2u})$
	1086	m	∥	$579(B_{3u})+508(B_{1g})=1087(B_{2u})$
	1021	w	∥	$916(B_{2u})+122^*(A_g)=1038(B_{2u})$; $1155(B_{2u})-122^*(A_g)=1033(B_{2u})$
	935	m	⊥	$579(B_{3u})+360(B_{2g})=939(B_{1u})$
	916	m	∥	$555(B_{1u})+370(B_{3g})=925(B_{2u})$
	825	w	∥	$579(B_{3u})+251(B_{1g})=830(B_{2u})$
	804	m	⊥	$444(B_{3u})+360(B_{2g})=804(B_{1u})$
	696	w	∥	$444(B_{3u})+251(B_{1g})=695(B_{2u})$; $959(B_{3u})-251(B_{1g})=708(B_{2u})$
	675	w	∥ ⊥	$429(B_{2u})+251(B_{1g})=680(B_{3u})$
	444	w	∥ ⊥	$579(B_{3u})-122^*(A_g)=457(B_{3u})$

* Calculated value for ν_5 (see Table IV).

analysis, we attributed the former to the A_g mode and the latter to the B_{1g} mode.

The strongest Raman line, at 1573 cm^{-1}, is undoubtedly to be assigned C=C stretching mode (A_g). In fact, the potential energy of this vibration is primarily associated with the C=C stretching mode (78%), although the contributions of the C–C stretching (13%) and C–C–C bending modes (8%) are appreciable.

A strong infrared band at 579 cm^{-1} and a medium-strength one at 429 cm^{-1} exhibit ∥ ⊥ and ∥ dichroisms and are assigned to the B_{3u} and B_{2u} vibrations respectively. As Table V shows, the band at 579 cm^{-1} (calculated as 591 cm^{-1}) is due to the hybridized mode of the C–C–C bending (57%), C–C≡N bending (22%), and C–C stretching modes (17%). The band at 429 cm^{-1} (calculated as 433 cm^{-1}) is also due to the hybridized mode of the C–C–C rocking (51%)[27] and C–C≡N bending mode (49%). In the region 600∼500 cm^{-1} of the Raman spectrum, three very weak lines are observed at 592, 536 and 508 cm^{-1}. Of these Raman lines, the most intense one, at 536 cm^{-1} (calculated as 530 cm^{-1}), is attributed to the A_g mode involving the C–C–C bending (63%)[28] and C–C≡C bending modes (30%). The line at 508 cm^{-1} (calculated as 503 cm^{-1}) is attributed to the B_{1g} mode involving the C–C–C rocking (49%), C–C≡N bending (20%), and C–C stretching modes (26%). The assignment of the remaining line, at 592 cm^{-1}, will be discussed later.

A weak Raman line at 251 cm^{-1} is assigned to the lowest B_{1g} vibration. The potential energy of this vibration is associated with the C–C≡N bending (85%) and C–C–C rocking modes (13%). The Raman line assigned to the lowest A_g vibration (calculated as 122 cm^{-1}) and two infrared bands assigned to the lowest B_{2u} and B_{3u} vibrations (calculated as 111 and 157 cm^{-1} respectively) could not be observed, because their frequencies are lower than the 200 cm^{-1} limit of the present work. In each species, the potential energy of this vibration of associated predominantly with the C–C≡N bending mode but also partly with the C–C–C bending (or rocking) mode, the distribution of the energy between these two modes depending upon the species.

Out-of-plane Fundamental Vibrations.—Since the B_{2u} and B_{3u} species have been shown to have ∥ and ∥ ⊥ dichroisms, respectively it is apparent that the out-of-plane vibrations of the B_{1u} species give rise to ⊥ bands in the infrared spectrum. For this reason, and also because of its reasonable frequency, the strong infrared band at 555 cm^{-1} (⊥) is assigned to the B_{1u} C–C–C wagging mode. By using a frequency correlation with this mode, the very weak Raman line at 592 cm^{-1} is assigned to

27) Long and George gave a 715 cm^{-1} (medium-strength) infrared band in Table 6 of their paper,[3] and assigned it to the B_{2u} C–C–C rocking mode. This band, however, could be identified neither in their own spectrogram (Fig. 3 of Ref. 3) nor in that obtained by Looney and Downing (Fig. 1 of Ref. 2). No band was observed at this frequency in our spectrum either (see Fig. 1 and Table I).

28) Long and George[3] assigned the Raman line at 678 cm^{-1} to the A_g C–C–C bending mode. In the present work, however, this line (679 cm^{-1}) was attributed to the A_g C–C stretching mode as mentioned above.

the corresponding B_{2g} mode.

In the region 400~300 cm^{-1} of the Raman spectrum, a pair of very weak lines are observed at 370 and 360 cm^{-1}. Each of these lines may be associated with one of the B_{2g} and B_{3g} C–C≡N (out-of-plane) bending modes, because these correlate well with the corresponding modes of malononitrile, which have been observed at 371 and 337 cm^{-1}.[22] Here, the line at 370 cm^{-1} is tentatively assigned to the B_{3g} mode, and the line at 360 cm^{-1}, to the B_{2g} mode, in consideration of the assignments for combination vibrations mentioned below. No infrared ⊥ band to be assigned to the B_{1u} C–C≡N (out-of-plane) bending mode was observed in the region higher than 200 cm^{-1}. The results obtained for the out-of-plane fundamental vibrations are summarized in Table VII.

TABLE VII. ASSIGNMENTS OF OBSERVED BANDS (LINES) DUE TO OUT-OF-PLANE FUNDAMENTAL VIBRATIONS OF TETRACYANOETHYLENE

	Freq. cm^{-1}	Intensity	Assignment
Infrared band	555 (⊥)	s	C-C-C wagging (B_{1u})
	—		C-C≡N bending (B_{1u})
Raman line	592	vw	C-C-C wagging (B_{2g})
	360	vw	C-C≡N bending (B_{2g})
	370	vw	C-C≡N bending (B_{3g})

Overtone and Combination Vibrations.—Besides the bands (lines) assigned to the fundamental vibrations, there remain three weak Raman lines and a number of infrared bands, including five medium-strength ones, which are attributable to the overtone or combination vibrations. According to the selection rule, these Raman lines and infrared bands were assigned as is shown in Table VIII. It may be noticed that all the Raman lines are exclusively associated with the A_g mode. Since the A_u frequencies have not yet been established, the overtones and combinations involving the A_u vibrations were not considered. Nevertheless, for each of the observed frequencies, one or two possible assignments were found, and the agreement between the calculated and observed values is satisfactory, as Table VIII shows.

Summary

The polarized infrared spectrum of a highly-oriented crystal of TCNE have been measured, tegether with the Raman spectrum of a sample consisting of several lumps of the crystals. The infrared spectra of the powedered solid, solution, and vapor have also been observed for comparison. Under the assumption of the V_h symmetry, the normal vibrations of TCNE have been calculated for the in-plane modes by the use of the ***GF*** matrix method. The basic UBFF, as well as the modified one containing cross terms between the C=C and C–C bonds, has been used as the potential function for this molecule. The frequencies calculated with the modified UBFF agree well with the observed values. The potential energy distributions have also been calculated, and the nature of the in-plane fundamental vibrations has been elucidated. The tentative assignments have been made to the out-of-plane fundamental vibrations and to the overtone and combination vibrations.

The authors wish to express their gratitude to Professor Rempei Gotoh for his continuing interest and encouragement during the course of this work. Thanks are also due to Dr. Katsunosuke Machida of Kyoto University for his helpful discussions, to Dr. Kenichi Kudo of Sumitomo Atomic Energy Industries, Ltd., for supplying the TCNE, to Dr. Tatsuo Miyazawa of Osaka University for giving the chance to use the Perkin-Elmer model 221 spectrophotometer, and to Dr. Yoshiki Matsui of Shionogi and Co., Ltd., and Miss Michiko Matsushima of the Government Chemical Industrial Research Institute of Tokyo for measuring the Raman spectra of TCNE.

Institute for Chemical Research
Kyoto University
Takatsuki

Calculation of the State Energies of Benzaldehyde. I. Semi-Empirical Molecular Orbital Method

By Kōzō INUZUKA and Toshio YOKOTA

(Received March 9, 1964)

Experimental and theoretical studies of the electronic structures of organic molecules have been made by many authors. In particular, the benzene molecule, a representative aromatic compound, has been investigated thoroughly. Studies now extend to the electronic structures of the derivatives of benzene. Benzaldehyde is an example of these derivatives. The ultraviolet absorption measurement of benzaldehyde at longer wavelengths (n-π transition) has been carried out by Imanishi et. al.[1] The theoretical assignment of the absorption bands at shorter wavelengths (π-π transition) has been made by Tanaka.[2] Recently, the phosphorescence and the S–T absorption spectra of benzaldehyde were measured by Kanda.[3]

For benzaldehyde there are experimental data concerning the singlet and triplet states, which can be compared with the results of the theoretical calculation. In spite of these experimental studies, however, there are few theoretical considerations of its electronic structure.

The semi-empirical molecular orbital method proposed by Pariser and Parr[4] succeeded in the calculation of the π, π state energies and was extended to that of the n, π state energies by Anno et al.[5,6] In this article, the calculation of the state energies of benzaldehyde will be carried out by the use of the semi-empirical molecular orbital method.

Calculation Procedure

Conventional Hückel Type LCAO MO's.—In the calculation of electronic state energies of benzaldehyde, we adopted the molecular structure model shown in Fig. 1. In actual benzaldehyde, which belongs to the C_s-symmetry group, all electronic transitions are allowed. Therefore, if we take account of the C_s symmetry we must solve an 8th-order seqular equation. Calculations then become more complex and tedious. In the present calculations we assume a simplified model with the C_{2v} symmetry for the structure of the benzaldehyde molecule and use Hückel type MO's.

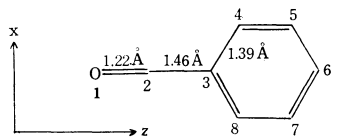


Fig. 1. The C_{2v} model* of benzaldehyde
* The bond distances were estimated from the calculated bond order and the experimental data for carbonyl compounds.

The Coulomb integral, α_1, of the oxygen atom and the resonance integral, β_{12}, between the carbon atom, 2, and the oxygen atom, 1, are expressed as:

$$\alpha_1 = \alpha + \delta_1 \cdot \beta$$

$$\beta_{12} = \rho_{12} \cdot \beta$$

where α is the Coulomb integral of the carbon atom and β is the resonance integral over the neighboring carbon atoms in benzene. The resonance integral, β_{23}, between the benzene ring and the carbonyl group is given by the usual approximation:

$$\beta_{23} = (S_{23}/S)\beta$$

where S_{23} is the overlap integral between the carbon atoms 2 and 3, and S the overlap integral of the neighboring carbon atoms in benzene. In the present calculations, the numerical values of the parameters δ_1 and ρ_{12} and the S_{23}/S ratio are chosen as follows:

$$\delta_1 = 1.5, \qquad \rho_{12} = \sqrt{2}, \qquad S_{23}/S = 0.894$$

The results of the calculations for Hückel MO's and their energies are listed in Table I, where χ_i is the $2p\pi$AO of the ith-atom.

In addition to the above MO's, the benzaldehyde molecule has a nonbonding orbital which can be represented approximately as follows:

$$\varphi_n = \chi_n$$

where χ_n is the $2p\pi$ AO of the oxygen atom. Its nodal plane is perpendicular to the molecular plane and contains the CO axis. Therefore, the symmetry of χ_n is b_1.

State Energies without Configuration Interaction.—In order to calculate the state energies of benzaldehyde by the methods proposed by Pariser and Parr[4] and by Anno et al[5,6] we need the values of the core integrals and the electronic repulsion integrals. The problem of obtaining these values

1) S. Imanishi, K. Semba, M. Ito and T. Anno, This Bulletin, 25, 150 (1952).
2) J. Tanaka, *J. Chem. Soc. Japan, Pure Chem. Sec.* (*Nippon Kagaku Zassi*), 79, 1114 (1958).
3) Y. Kanda, Private Communication.
4) R. Pariser and R. G. Parr, *J. Chem. Phys.*, 21, 466, 767 (1953).
5) T. Anno, I. Matubara and A. Sadō, This Bulletin, 30, 168 (1957).
6) T. Anno, I. Matubara and A. Sadō, *J. Chem. Phys.*, 26, 967 (1957).

is reduced to the calculation of Coulomb repulsion integrals over atomic orbitals, Coulomb integrals, α_p, and resonance integrals, β_{pq}. The values of Coulomb repulsion integrals are evaluated by the use of the equation derived by Roothaan and by Anno et al.[5] in the case of $r>2.80$ Å and $r\leqq 2.80$ Å respectively. The value of the resonance integral β_{CC} over carbon and oxygen atoms is calculated by

TABLE I. HÜCKEL MO'S AND THEIR ENERGIES OF BENZALDEHYDE

MO*	Sym	χ_1	χ_2	χ_3	$(\chi_4\pm\chi_8)$	$(\chi_5\pm\chi_7)$	χ_6	Energy, e_i
φ_1	b_2	0.73575	0.52737	0.31893	0.16511	0.09610	0.07647	−2.51368
φ_2	b_2	0.36631	0.11745	−0.32283	−0.36782	−0.39567	−0.40510	−1.95344
φ_3	b_2	0.28326	−0.09035	−0.55409	−0.25020	0.29165	0.55611	−1.04889
φ_4	a_2				0.50000	0.50000		−1.00000
φ_5	b_2	0.40548	−0.58446	−0.28942	0.33917	0.10679	−0.39667	0.53844
φ_6	a_2				0.50000	−0.50000		1.00000
φ_7	b_2	0.25937	−0.52573	0.39329	−0.03371	−0.34722	0.50819	1.36650
φ_8	b_2	0.11211	−0.28625	0.49861	−0.39834	0.34231	−0.32431	2.11106

* The ith-MO φ_i is $\sum_p C_{pi}\,\chi_p$, where C_{pi}'s are listed under the corresponding χ_p. The signs + and − refer to MO's of symmetry b_2 and a_2 respectively.

TABLE II. TRANSITION ENERGIES OF THE n-π AND π-π TRANSITIONS OF BENZALDEHYDE WITHOUT CONFIGURATION INTERACTION (E in eV.)

	Orbital Jump	Calculated	Observed		Jump	Calculated	Observed
$^3A_2$:	n-5	3.955	3.22[a]	$^1A_2$:	n-5	4.235	3.34[a,b]
	n-7	7.374			n-7	7.488	
	n-8	10.289			n-8	10.311	
$^3B_2$:	n-6	7.905		$^1B_2$:	n-6	7.905	
$^3A_1$:	4−6	4.192		$^1A_1$:	4−6	6.261	6.36[c,d]
	3−5	4.688			3−5	6.229	5.32[e]
	3−7	6.342			3−7	7.599	
	1−5	6.376			1−5	8.022	
	2−5	7.674			2−5	8.569	
	3−8	8.035			3−8	8.913	
$^3B_1$:	4−5	5.172		$^1B_1$:	4−5	6.054	4.50[e]
	4−7	6.783			4−7	7.514	
	3−6	6.861			3−6	8.047	
	2−6	7.754			2−6	8.624	
	4−8	7.988			4−8	8.817	
	1−6	9.929			1−6	10.049	

a) Ref. 3, b) Ref. 1, c) Ref. 9, d) Ref. 10, e) Ref. 2,

TABLE III. WAVE FUNCTIONS* FOR THE GROUND AND LOWER EXCITED STATES OF BENZALDEHYDE

$^1A_1$: $\phi_1 = 0.9900V_0-0.0758V_3^5+0.0039V_4^6-0.1008V_3^7+0.0079V_1^5+0.0285V_2^5-0.0545V_3^8$

$\phi_2 = 0.0136V_0+0.7102V_3^5-0.5794V_4^6-0.3870V_3^7+0.0042V_1^5-0.0455V_2^5-0.0888V_3^8$

$\phi_3 = 0.0432V_0+0.5777V_3^5+0.7449V_4^6-0.0058V_3^7-0.2196V_1^5-0.2250V_2^5-0.1030V_3^8$

$^3A_1$: $\phi_1 = -0.5140T_3^5+0.7607T_4^6-0.3711T_3^7-0.0297T_1^5-0.1132T_2^5-0.0756T_3^8$

$\phi_2 = 0.8533T_3^5+0.4640T_4^6-0.2252T_3^7-0.0483T_1^5+0.0290T_2^5-0.0517T_3^8$

$^1B_1$: $\phi_1 = 0.8314V_4^5-0.4298V_4^7+0.3380V_2^5+0.0452V_2^6-0.0835V_4^8+0.0285V_1^6$

$^3B_1$: $\phi_1 = 0.8653T_4^5-0.4725T_4^7-0.0767T_3^6+0.0582T_2^6-0.1343T_4^8-0.0257T_1^6$

$^1A_2$: $\phi_1 = 0.9025V_n^5+0.4103V_n^7+0.1307V_n^8$

$^3A_2$: $\phi_1 = 0.8962T_n^5+0.4216T_n^7+0.1382T_n^8$

* V_0 represents the ground configurational wave function. V_i^j and T_i^j represent singlet and triplet excited configurational wave functions respectively, in which an electron has been raised from ψ_i to ψ_j. The subscript n represents nonbonding orbital.

TABLE IV. COMPARISON OF EXPERIMENT AND HÜCKEL MO CALCULATION WITH INTERACTION OF SINGLY-EXCITED CONFIGURATIONS

State	Calculated		Experimental	
	E, eV.	f	E, eV.	f
$^1A_1$	0	0	0	0
$^1B_1$	5.333	0.091	4.50[a]	0.026[a]
$^1A_1$	5.567	0.057	5.32[a]	0.29[a]
$^1A_1$	6.658	0.832	6.36[b,c]	0.45[b,c]
$^3A_1$	3.930			
$^3B_1$	4.318			
$^3A_1$	4.472			
$^1A_2$	3.614	0	3.34[d,e]	0.55×10^{-3} [d]
$^3A_2$	3.124		3.22[d]	1.8×10^{-7} [d]

a) Ref. 2, b) Ref. 9, c) Ref. 10, d) Ref. 3, e) Ref. 1

the use of Kon's formula,[8] while the value of β_{CC} over carbon atoms is obtained by Pariser and Parr's formula.[4] The Coulomb penetration integrals, which are needed to evaluate the Coulomb integrals, α_p, are estimated approximately by taking account of the integrals over only the nearest neighboring atoms. The π electronic states belong to the irreducible representations, A_1 and B_1, of the symmetry group C_{2v}. Electronic transitions from the ground state, A_1, to the excited A_1 and B_1 states will have a transitions moment directed along the z axis and the x axis respectively. In the n-π excitation, there are two symmetry types, A_2 and B_2, since the symmetry of the n orbital is b_1. Type A_2 is forbidden, but type B_2 is allowed. The transition moment is perpendicular to the molecular plane; that is, it is parallel to the y axis. This conclusion comes from the assumption of C_{2v} symmetry. In actual benzaldehyde, which has a C_s symmetry, the n-π transition of the A_2 type will also be allowed. In Table II we show all the energies of the n-π and π-π transitions within the range of about 10 eV. These energies are in poor agreement with the experimental values.

State Energies with Configuration Interaction.— Configuration mixing with respect to the π-π transition leads to an 11th-order seqular equation for the $^1A_1$ singlet state, a 10th-order equation for the $^3A_1$ triplet state, and two 6th-order equations for the $^1B_1$ and $^3B_1$ states respectively. As configurations of remarkably higher energies have a negligible effect on lower-lying states, we need consider only the configurations listed in Table II. In the present calculations of the π-π transition, we solve a 7th-order seqular equation for the $^1A_1$ state and a 6th-order equation for the $^3A_1$ state. In the case of n-π transition, configuration mixing leads to two 3rd-order seqular equations, for $^1A_2$ and $^3A_2$ respectivly. The solution of these seqular equations leads to a set of state energies and wave functions. These results are listed in Tables III and IV. The ground state energy is lowered by 0.168 eV.

From a comparison with Tables II and IV, it may be seen that the effect of the configuration interaction for the states separated by a small energy is large and that it is important for complex molecules.

Discussion

Benzaldehyde has four absorption bands in the region from 400 to 190 mμ. An absorption band on the longer wavelength side of this region was measured by Imanishi et al.[1] They assigned this band to an n-π transition and observed that the 0-0 band of the n-π transition is at 26,929 cm^{-1}. The energy, 3.614 eV. in Table IV, which is the $^1A_1$-$^1A_2$ transition energy, may correspond to the above n-π transition. In the present calculations, this transition is forbidden because of the assumption of the C_{2v} symmetry, but it is allowed in the actual molecule, with a symmetry C_s. The observed oscillator strength of this transition is 0.55×10^{-3}.[3]

Three absorption bands are observed in the region from 300 to 190 mμ. These are assigned to π-π transitions. The band at 285 mμ (4.50 eV.) is the weakest of them; it may correspond to the energy 5.333 ev. in Table IV, although the calculated value is larger than the observed value. Therefore, this band at 285 mμ is assigned to the $^1A_1$-$^1B_1$ transition. The next stronger band is at 233 mμ (5.32 eV.)[2]; this may be correlated with the energy 5.567 eV. in Table IV and is assigned to the $^1A_1$-$^1A_1$ transition. The strongest band is at 195 mμ (6.36 eV.);[9,10] it may be assigned to the $^1A_1$-$^1A_1$ transition (6.658 eV.). In the above assignments, the theoretically-calculated values of the oscillator strengths of these π, π bands are in poor agreement with the results of the experiments.

According to the experiment of Kanda,[3] the

7) C. C. J. Roothaan, *J. Chem. Phys.*, **19**, 116 (1951).
8) H. Kon, This Bulletin, **28**, 275 (1955).
9) W. C. Price and A. D. Walsh, *Proc. Roy. Soc.*, **A191**, 22 (1947).
10) H. B. Klevens and J. R. Platt, Technical Report, Laboratory of Molecular Structure and Spectra," (1953-1954).

S–T absoption spectrum appears at 25,195 cm^{-1} (3.22 eV.), and its oscillator strength is 1.8×10^{-1}. In Table IV this may be related to the energy 3.124 eV. of the n, π triplet state. Therefore, the above band may be assigned to $^1A_1$–$^3A_2$ transition.

The exsistence of π, π triplet states has not yet been confirmed experimentally, but in the present calculations three lower-lying π, π triplet states are obtained. The energies of these triplet states are about 4 ev; they are also listed in Table IV. These values seem reasonable judging from an average S–T separation for the π-π transition.[11]

The charge densities for the ground and two excited states are shown in Fig. 2. In the ground state, the charge density of the meta position is higher than those of the ortho- and para-positions. This is consistent with the tendency toward a meta orientation of the carbonyl group for electrophylic reagents. Similarly, from Fig. 2 it may be seen that the $^1B_1$ state has a tendency toward a para orientation and that the 1st $^1A_1$ excited state has a tendency toward meta and ortho orientations. Tanaka[2] pointed out that the transition from the ground state to the 1st $^1A_1$ excited state is attended with the migration of electrons from the benzene ring to the carbonyl group, and he assigned it to the charge transfer band. A similar phenomenon is seen in Fig. 2. The charge density on the carbonyl group becomes larger in the 1st $^1A_1$ excited state than in the ground state. This is in agreement with Tanaka's assignment. The calculation of charge density is very sensitive to the wave function used. Therefore, it is better to calculate it by the use of SCF MO's under a C_s symmetry than by the use of Hückel MO's assuming a C_{2v} symmetry. The results of such improved calculations[12] will be reported in the near future.

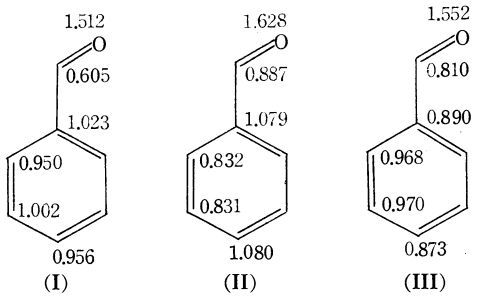


Fig. 2. π Electron densities of benzaldehyde
(I) in the ground state;
(II) in the 1st excited $^1B_1$ state;
(III) in the 1st excited $^1A_1$ state.

Summary

The electronic structure and the nature of the electronic transitions in the benzaldehyde molecule have been elucidated by the use of a semi-empirical MO method assuming a C_{2v} symmetry. The results of the calculations conform to the observed values for the singlet and triplet states in spite of the use of a crude approximation. In benzaldehyde, it has been found that the n, π triplet state is the lowest. The charge transfer band may be explained by means of our calculations.

The authors wish to express their thanks to Mr. Masuo Suzuki and Dr. Toshinori Munakata for their kind assistance in carrying out the digital computations. They also wish to express their gratitude to Professor Yoshiya Kanda of Kyushu University, who had the kindness to send them his experimental data. The present study was partially financed by the Scientific Research Fund of the Ministry of Education.

Department of Applied Science
Tokyo Electrical Engineering College
Kanda, Chiyoda-ku, Tokyo

11) C. Reid, *J. Chem. Phys.*, **21**, 1906 (1953).

12) K. Inuzuka and T. Yokota, to be published.

NOTES

Studies of the Mucilage of the Root of "Tororo-aoi" (Abelmoschus manihot, MEDIC). IV.[1] *An Aldotriouronic Acid Isolated from the Mucilage*

By Saburo INOKAWA, Ryozo GOTO, Toshiro BAN, Takane UCHIDA and Kiyoaki WAKAIZUMI

(Received March 2, 1964)

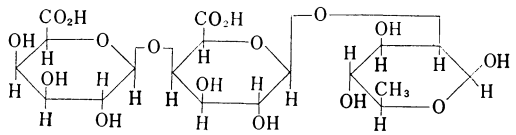
There have been many studies[2] of the mucilage of "Tororo-aoi" (*Abelmoschus manihot*, MEDIC), and the purified mucilage has been found to be composed of rhamnose and galacturonic acid, but the chemical structure of the mucilage has not yet been clarified in detail.

Oshibuchi[3] has suggested the presence of an aldotriouronic acid (rhamno-di-galacturonic acid) in the hydrolysate of the mucilage. In the present paper, the chemical structure of this aldotriouronic acid will be determined.

Hydrolysis of the mucilage with 4 percent sulfuric acid, followed by the precipitation of the neutralized hydrolysate with ethanol, gave a mixture of barium salts, from which an aldotriouronic acid was isolated as white crystals $[\alpha]_D^{13}$ +74° (*c* 1, water) by de-ionizing the mixture with ion-exchange resins and using cellulose column chromatography. The aldotriouronic acid was found to be composed of rhamnose and galacturonic acid by hydrolysis and paper chromatography. The equivalent weight of the aldotriouronic acid, as determined by titration with alkali, was 260, which shows that the aldotriouronic acid consists of rhamnose and galacturonic acid in a mole ratio of 1 : 2.

The aldotriouronic acid was converted into a neutral trisaccharide by the reduction of the methyl ester of the methyl glycoside with sodium borohydride. The methylation of the trisaccharide gave a derivative which, on acid hydrolysis, gave 2, 3, 4, 6-tetra-*O*-methylgalactose, 2, 3, 6-tri-*O*-methylgalactose, and 3, 4-di-*O*-methylrhamnose.

The structure of the aldotriouronic acid is, therefore, determined to be *O*-α-D-galacturonosyl-(1→4)-*O*-α-D-galacturonosyl-(1→2)-*O*-L-rhamnose, the anomeric configuration of which is supposed from the optical rotation:



Experimental

Paper-partition chromatography was carried out with the upper layer of butanol - acetic acid - water (4 : 1 : 5). Paper ionophoresis was carried out in a 0.2 M borate buffer at pH 10. R_{gal} and R_G (or M_G) values are proportional to the rates of the migration of galactose and 2, 3, 4, 6-tetra-*O*-methylglucose respectively. The *R* values observed were compared with those of authentic samples.

The Preparation of Purified Mucilage.—After the roots of "Tororo-aoi" had been ground and soaked in distilled water for 2 days at 0°C, the mucilage was filtered through a cotton cloth. The crude mucilage was then homogenized with a mixer, filtered through a cellite-bed, and precipitated with ethanol-ether (8 : 2), and the precipitate was redissolved in water, re-precipitated with ethanol, washed with absolute ethanol and dry ether, and dried in vacuum.

The Partial Hydrolysis of Purified Mucilage with Dilute Sulfuric Acid.—Dry purified mucilage (10 g.) was heated in 4 percent sulfuric acid 100°C for 11 hr. The filtered solution was neutralized with barium carbonate and then filtered, and the filtrate was concentrated under reduced pressure to a light syrup (100 ml.), which was then stirred into ethanol (400 ml.). The precipitate was washed thoroughly with 80 percent ethanol, absolute ethanol, and dry ether, and dried in a vacuum. The precipitate was redissolved in water (100 ml.) and the solution was poured into ethanol (400 ml.), washed, and dried similarly to give a white powder

1) Part III: S. Inokawa. This Bulletin, **34**, 29 (1961).
2) See S. Inokawa and R. Goto, *Wood Research* (Japan), No. 17, 50 (1956); S. Inokawa, This Bulletin, **33**, 1473 (1960).
3) T. Oshibuchi and H. Kusunose, *J. Agr. Chem. Soc. Jaapan* (*Nippon Nogei-Kagaku Kaishi*), **31**, 481 (1957).

(4.1 g.). On a paper chromatogram after having been de-ionized with IR-120 resin, the product gave two spots, namely, galactose and R_{gal} 0.32.

The Isolation of Aldotriouronic Acid. — The white powder (2 g.) described above was de-ionized with IR-120 resin, and a portion corresponding to R_{gal} 0.32 was separated on a cellulose column (5× 40 cm.) with butanol - acetic acid - water (12 : 3 : 5) to give white crystals (0.40 g.), $[\alpha]_D^{13}$ +74° (*c* 1, water). On titration with a 0.005 N sodium hydroxide solution, the equivalent weight of the material was 260 (calc. for rhamno-di-galacturonic acid; 258). The crystals were then completely hydrolysed with 2 N sulfuric acid in a sealed tube at 100°C for 24 hr. The neutralized solution, de-ionized with IR-120 resin, gave rhamnose and galacturonic acid on a paper chromatogram.

The Identification of the Aldotriouronic Acid. —The aldotriouronic acid (300 mg.) was refluxed with 1.8 percent methanolic hydrogen chloride (50 ml.) for 7 hr., neutralized with silver carbonate, and filtered. The filtrate was evaporated to dryness, the residue dissolved in water (6 ml.), and the solution added slowly to a solution of sodium borohydride (200 mg.) in water (3 ml.). After 2 hr., the excess borohydride was destroyed by adding dilute acetic acid, and the solution was de-ionized with IR-120 and IR-45 resins and evaporated under reduced pressure to dryness to give white prisms (120 mg.), $[\alpha]_D^{13}$ +2° (*c* 1, water). The crystals were completely hydrolysed, and the neutralized solution gave only rhamnose and galactose on a paper chromatogram.

The crystals were methylated three times with methyl sulfate and sodium hydroxide, and, after the extraction of the acidified mixture with chloroform, the product was further methylated three times with methyl iodide and silver oxide to give a pale yellow oil (100 mg.).

The oil was hydrolysed with N sulfuric acid (10 ml.) at 100°C for 18 hr. in a sealed tube. The hydrolysate was neutralized with barium carbonate and extracted with chloroform. The chloroform solution was evaporated to give a syrup (30 mg.) which gave an intensive spot (R_G 0.89) and a faint spot (R_G 0.74) on a paper chromatogram. The aqueous residual solution was de-ionized with IR-120 resin and evaporated to give a syrup (10 mg.) which gave an intensive spot (R_G 0.74), a faint spot (R_G 0.89), and a very faint spot (R_G 0.58) on a paper chromatogram. The spots at R_G 0.74 and 0.58 corresponded to 2,3,6-tri-*O*-methylgalactose and 4-*O*-methylrhamnose respectively. The spot at R_G 0.89, by paper ionophoresis,[4] was separated into two spots, $M_G \fallingdotseq 0$ and M_G 0.39, which corresponded to 2,3,4,6-tetra-*O*-methylgalactose and 3,4-di-*O*-methylrhamnose, respectively.

This work was partially supported by a grant from the Hattori Hokokai, to which the authors' thanks are due.

Department of Chemistry
Faculty of Science
Kyoto University
Sakyo-ku, Kyoto

4) A. B. Foster, *J. Chem. Soc.*, **1953**, 982.

Thermal Effects on the Lattices of η- and γ-Aluminum Oxide

By Hiroaki YANAGIDA and Goro YAMAGUCHI

(Received April 13, 1964)

In a previous paper,[1] the present authors found that the lattice dimensions and the tetragonal axial ratio of γ-aluminum oxide vary with hydrothermal and heat treatments and proposed that η-aluminum oxide may be an end-member of the γ-aluminum oxide series with little tetragonal deformation. In the present paper, the lattice dimensions of η- and γ-aluminum oxide will be measured with a high temperature X-ray diffraction apparatus at various temperatures and after various heat treatments in order to discuss further the relation between η- and γ-aluminum oxide.

The γ-aluminum oxide examined had a tetragonal axial ratio of 1.0357 and was obtained from a hydrothermal treatment, at 500°C under 50 atm. for 20 hr., of γ-aluminum oxide which had been formed from the dehydration

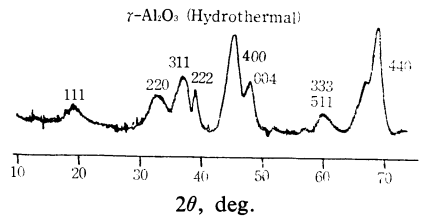


Fig. 1 The X-ray diffraction diagram of γ-Al_2O_3(hydrothermal), Cu$K\alpha$ ray.

1) G. Yamaguchi and H. Yanagida, This Bulletin, 35, 1896 (1962).

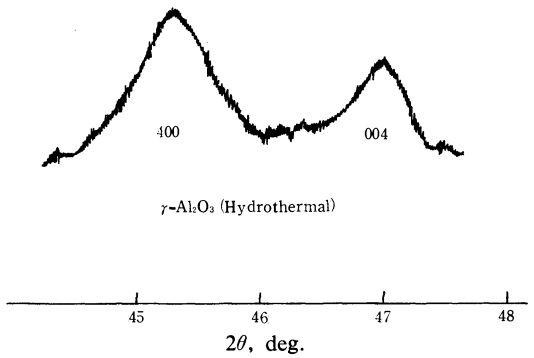


Fig. 2. The slow-scanning X-ray diffraction pattern of γ-Al_2O_3 about the (400) peak in the spinel indices; Cu$K\alpha$, 35kV., 12 amp. 1°1° 0.2 mm. slit system; rate meter 8; time constant 4 sec.; scanning speed 1°/4 min. Geigerflex.

of well-crystallized boehmite AlOOH in air at 700°C. The X-ray diffraction diagram is shown in Fig. 1, while the slow-scanning pattern about the (400) peak in the spinel indices is in Fig. 2. This specimen contained 7.5% water at 150°C. Another γ-aluminum oxide with the axial ratio of 1.0183 was also examined; it contained 3.5% water at 150°C.

The η-aluminum oxide with little tetragonal deformation was obtained from the dehydration, at 700°C in air, of bayerite $Al(OH)_3$ which had been formed by the neutralization of an aqueous solution of aluminum chloride by ammonia. The (400) peak of this specimen is hardly split at all. This had 3.8% water at 150°C.

Table I. The lattice dimensions of γ-Al_2O_3 measured with a high temperature X-ray diffraction apparatus Cu$K\alpha$, 35 kV., 15 mamp.; 1°1° 0.02 mm. slit system; rate meter 8; time constant 4 sec.; scanning speed 1°/4 min.; Geigerflex

No. of Heating procedure	d(400 and 040)* Å	d(004)* Å	Tetragonal** Axial ratio
1 Room temperature	2.0015	1.9325	1.0357
2 130°C	2.0043	1.9321	1.0374
3 270°C	2.0089	1.9340	1.0387
4 Room temperature	2.0005	1.9314	1.0358
5 400°C	2.0055	1.9331	1.0375
6 Room temperature	1.9984	1.9300	1.0354
7 600°C	1.9914	1.9300	1.0318
8 Room temperature	1.9856	1.9182	1.0351
9 800°C	1.9918	1.9298	1.0321
10 Room temperature	1.9799	1.9167	1.0330
11 900°C	1.9934	1.9329	1.0313
12 Room temperature	1.9799	1.9163	1.0332

* The d-values are ±0.0008Å

** The axial ratios ±0.0006

Table II. The lattice dimensions of η-Al_2O_3 measured with a high temperature X-ray diffraction apparatus

Cu$K\alpha$, 35 kV., 15 mamp.; 1°1° 0.2 mm. slit system; rate meter 8; time constant 4 sec.; scanning speed 1°/2 min; Geigerflex

No. of Heating procedure	d(400, 040 and 004)* Å
1 Room temperature	1.9799
2 130°C	1.9819
3 270°C	1.9831
4 Room temperature	1.9815
5 400°C	1.9840
6 Room temperature	1.9815
7 600°C	1.9873
8 800°C	1.9918
9 Room temperature	1.9799

* The d-values are ±0.0012Å

The curves plotting the heating temperatures versus the lattice dimensions of η-aluminum oxide and γ-aluminum oxide are shown in Tables I and II and in Figs. 3 and 4. The curve for η-alumnum oxide is reversible whereas that for γ-aluminium oxide is not reversible. The lattice dimensions of γ-aluminum oxide decrease, and, at the same time, the degree of tetragonal deformation is lowered through the heat treatments numbered 5—9 in Table I and in Fig. 3. The axial ratios decreased 1.0357 to 1.0332 and 1.0183 to 1.0158. Curves plotting the heating temperatures versus the amount of water in or on the aluminas are shown in Fig. 5, in which the axial ratios of the starting γ-aluminum

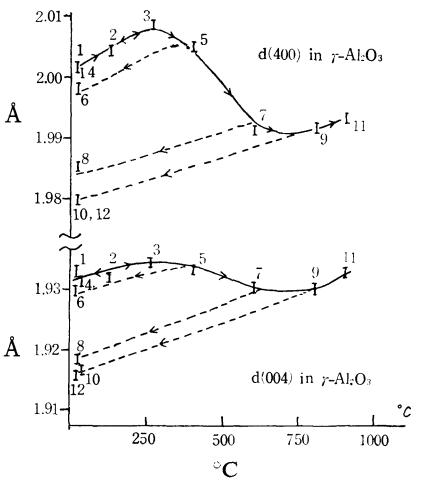


Fig. 3. The lattice dimension of γ-Al_2O_3 measured with a high temperature X-ray diffraction apparatus; Cu$K\alpha$, 35kV., 15 amp.; 1°1° 0.2 mm. slit system; rate meter 8; time constant 4 sec.; scanning speed 1°/4 min. Geigerflex.

oxide are also indicated. We can see the loss of water from the aluminas take place through the heat treatments. The changes in the lattice dimensions and the tetragonal axial ratio are accompanied by the loss of water from the γ-aluminum oxide, while the loss of water from the η-aluminum oxide does not cause those changes.

These results lead us to consider that a certain type of water should be present in the lattice of γ-aluminum oxide with considerable tetragonal deformation, especially in such a hydrothermal substance,[1] but the water of this type is not there in the lattice of η-aluminum oxide as an end-member of the γ-aluminum oxide series with little tetragonal deformation. Unfortunately, we cannot discuss the type of water and the relation between the amount of this water and the axial ratio in the present work. We will try to clarify the relation in a later paper.

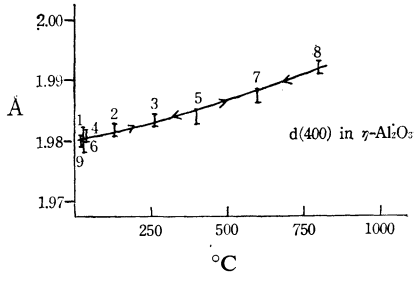


Fig. 4. The lattice dimension of η-Al_2O_3 measured with a high temperature X-ray diffraction apparatus ; Cu$K\alpha$, 35kV., 15 amp. ; 1°1° 0.2 mm. slit system ; rate meter 8 ; time constant 4 sec. ; scanning speed 1°/2 min. ; Geigerflex.

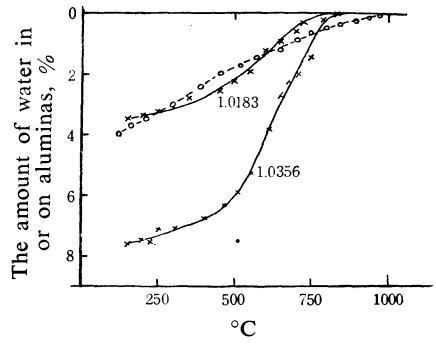


Fig. 5. The relation between the temperatures and the amount of water in or on η-Al_2O_3 (-○-) and γ-Al_2O_3 (-×-).

Department of Industrial Chemistry
Faculty of Engineering
The University of Tokyo
Hongo, Tokyo

SHORT COMMUNICATIONS

A New Reagent for the p-Nitrophenylation of Carboxylic Acids

By Shumpei SAKAKIBARA and Noriyoshi INUKAI*

(Received May 2, 1964)

The *p*-nitrophenylester of acylamino acid is well known to be a convenient intermediate in peptide synthesis. Bodanszky[1] originally prepared this compound by heating a mixture of *p*-nitrophenol and carbobenzoxy amino acid chloride or mixed anhydride. Since then, Schwyzer et al.[2] have developed two new reagents, di-*p*-nitrophenyl sulfite and tri-*p*-nitrophenyl phosphite, for the *p*-nitrophenylation of carbobenzoxy amino acid. Later, Bodanszky and du Vigneaud[3] prepared the same *p*-nitrophenylesters by using dicyclohexylcarbodiimide as a coupling reagent.

In the present study, it was found that *p*-nitrophenyl trifluoroacetate (I) was a useful reagent for the same purpose. A solution of trifluoroacetic anhydride (62 g., 0.3 mol.) and *p*-nitrophenol (28 g., 0.2 mol.) in dry benzene

* Present address: Yamanouchi Pharmaceutical Co. Ltd., Azusawa-cho, Itabashi-ku, Tokyo.

1) M. Bodanszky, *Nature*, **175**, 685 (1955).

2) R. Schwyzer, B. Iselin and P. Sieber, *Helv. Chim. Acta*, **40**, 373 (1957).

3) M. Bodanszky and V. du Vigneaud, *J. Am. Chem. Soc.*, **81**, 5688, 6072 (1959).

TABLE I. FORMATION OF *p*-NITROPHENYLESTERS BY ESTER-EXCHANGE REACTIONS WITH CARBOXYLIC ACIDS

Carboxylic acid	Reagent	Yield %	Melting point, °C		$[\alpha]_D$, *c* 2 in DMF (temp., °C)	
			Found	Cited	Found	Cited
CH_3COOH	$CF_3COOPNP$	80	78～80	79～80[a]		
C_6H_5COOH	$CF_3COOPNP$	90.5	143	142.5[b]		
Z-Gly-OH	$CF_3COOPNP$	93	126～127.5	127.5～128.5[c]		
Z-L-Pro-OH	$CF_3COOPNP$	83.5	94～95.5	94～96[d]	−70.0(22)	−68(20)[d]
Z-L-Phe-OH	$CF_3COOPNP$	85.5	125～126	126～126.5[e]	−24.7(22)	−24.7(25)[e]
Z-L-Glu(NH_2)-OH	$CF_3COOPNP$	63.5	151～153	155～156[d]	−24.0(21.5)	−24(20)[d]
Z-Gly-Gly-OH	$CF_3COOPNP$[f]	89	160～162[g]			
Z-L-Phe-OH	$CH_2ClCOOPNP$[h]	37	124～126	126～126.5[e]	−24.7(20)	−24.7(25)[e]
Z-L-Pro-OH	$CCl_3COOPNP$[h]	57	94～96	94～96[d]	−70.0(22)	−68(20)[d]

a) A. Kaufmann, *Ber.*, **42**, 3482 (1909). b) Beilstein Vol. 9, p. 119. c) M. Bodanszky and V. du Vigneaud, Biochemical preparation Vol. 9, p. 110. d) M. Bodanszky and V. du Vigneaud, *J. Am. Chem. Soc.*, **81**, 5688 (1959). e) M. Bodanszky and V. du Vigneaud, ibid., **81**, 6072 (1959). f) The reaction was carried out for two hours at room temperature. g) Found: C, 55.88; H, 4.36; N, 10.61. Calcd. for $C_{18}H_{17}N_3O_7$: C, 55.81; H, 4.42; N, 10.85%. h) The reaction was carried out by refluxing the pyridine solution for about 10 min.

(Z: Carbobenzoxy; PNP: *p*-nitrophenyl; DMF: dimethyl formamide)

(60 ml.) was refluxed for about 5 hr., and then the solution was concentrated to dryness; the yield of crystalline product I was quantitative (m. p. 37～39°C). This product was used without further purification in the following reactions. A part of the product was subjected to sublimation in vacuo for analysis; m. p. 36～38°. Found: C, 41.11; H, 1.89. Calcd. for $C_8H_4O_4NF_3$: C, 40.86; H, 1.71%. A solution of a carboxylic acid such as carbobenzoxy amino acid (0.005 mol.) in dry pyridine (1.5～3 ml.) was treated with I (0.005 mol.) at room temperature. After about 10 min., water (20 ml.) was added to the reaction mixture to precipitate the resulting *p*-nitrophenylester of the carboxylic acid as crystals. The product was collected by filtration and then recrystallized from a suitable solvent system. The yields and physical constants of the reaction products are listed in Table I. In contrast with this, it was confirmed that the mono-, di- or trichloroacetic acid *p*-nitrophenylester was only reactive with carbobenzoxy amino acids in boiling pyridine, and gave poor yields of the desired products, together with colored by-products.

In carbobenzoxy peptides, however, the ester-exchange reaction of I was slower than that in carbobenzoxy amino acids. In these cases, the heating of the reaction mixture or the prolongation of the reaction time at room temperature was necessary in order to complete the reaction, and the racemization of the *C*-terminal amino acid residues might occur to some extent during the reaction. The advantages of the new method over the Schwyzer method[2] are as follows: 1) Since the reaction occurred within 10 min. at room temperature (with acylamino acids), such undesirable side-reactions as racemization were few. 2) The only co-product of the reaction was trifluoroacetic acid, which can easily be removed from the reaction mixture. Therefore, the product could easily be purified.

Peptide Center
Institute for Protein Research
Osaka University
Kita-ku, Osaka

A Polarographic Study of the Tetracyanomono(ethylenediamine)-cobaltate(III) Complex

By Nobufumi MAKI and Kuwako OKAWA*

(Received May 7, 1964)

Previously, the $[Co^{III}(CN)_4(SO_3)_2]^{5-}$ ion (probably the trans-form) was found to be reduced in one step to the cobaltate(I) complex in a sulfite medium at the dropping mercury electrode (DME).[1]

In the present report, the tetracyanomono(ethylenediamine)cobaltate(III) complex, K-$[Co^{III}(CN)_4\ en]\cdot H_2O$ (cis-form)[2], will be found to be reduced irreversibly to the metal through the cobaltate(I) complex in a 0.5 M sodium sulfate solution containing 2 M ethylenediamine.

More specifically, the $[Co^{III}(CN)_4\ en]^-$ ion gave rise to well-defined two-step waves at the DME. The ratio of the height of the first wave to that of the second was roughly 2 : 1. The first wave, corresponding to an acceptance of two electrons, represents the reduction from the cobalt(III) to the cobalt(I) state, while the second, corresponding to a gain of one electron, represents the reduction to the metal.

The limiting current of both waves was proportional to the concentration of the complex in the range between 10^{-2} and 10^{-4} F and was diffusion-controlled.

In the absence of excess ethylenediamine, the wave of apparently one step, corresponding to a three-electron reduction, was obtained.

Figure 1 shows the d.c. polarograms for this complex in the presence or in the absence of excess ethylenediamine. For the sake of comparison, the wave of the two electron-reduction of the dicyanobis(dimethylglyoximato)cobaltate(III) complex, whose resulting cobaltate(I) complex was ascertained by isolation in vacuo[3] is also shown. It can be seen that the wave-height is roughly proportional to the electron-number of the reduction process.

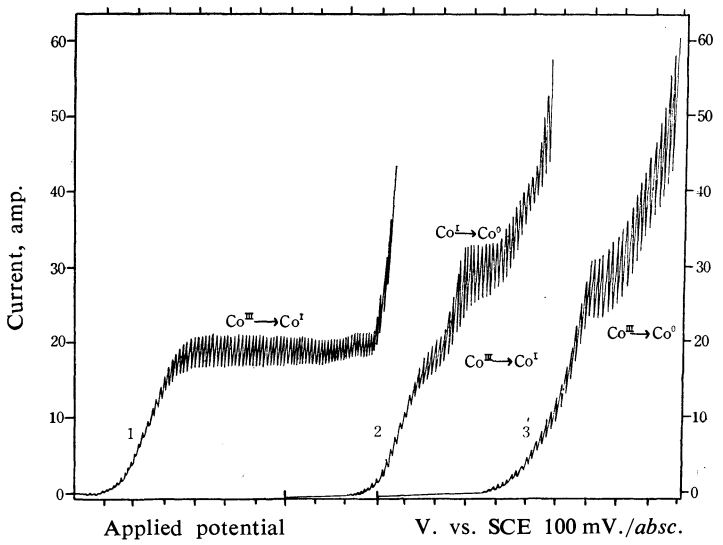


Fig. 1. D. C. polarograms of cyano-cobaltate(III) complexes obtained at the concentration of $5\cdot10^{-3}$F/1(25°C).

1) $K[Co^{III}(CN)_2\ dg_2]\cdot 3/2\ H_2O$ in 0.5 F Na_2SO_4 aq. soln. Recorded from −0.90 V. vs. SCE. $E_{1/2}=-1.10_5$ V. vs. SCE.

2) $Na[Co^{III}(CN)_4\ en]\cdot 3.5\ H_2O$, in 0.5 F Na_2SO_4 + 2 M en + 0.0078% Triton X 100. Recorded from −1.00 volt vs. SCE.

3) $Na[Co^{III}(CN)_4\ en]\cdot 3.5\ H_2O$, in 0.5 F Na_2SO_4 aq. soln. Recorded from −0.50 V. vs. SCE.

* Present address: Department of Chemistry, Osaka University, Kita-ku, Osaka.

1) N. Maki and R. Tsuchida, This Bulletin, **34**, 891 (1961).

2) J. Fujita and K. Okawa, unpublished.

3) N. Maki, *Nature*, **188**, 227 (1960).

TABLE I. HALF-WAVE POTENTIALS OF THE CYANO-COBALT(III) COMPLEXES (25°C)

Compund	$E_{1/2}$ of 1st wave Co(III) → Co(I)	$E_{1/2}$ of 2nd wave Co(I) → Co(0)	Supporting electrolyte
$Na[Co(CN)_4\ en]\cdot 3.5\ H_2O$	-1.36_4	-1.51	0.5 F Na_2SO_4+2 M en 0.0078% Triton X 100*
$Na_5[Co(CN)_4(SO_3)_2]$	-1.36	No reduction	0.5 F Na_2SO_3
$K_4[Co(CN)_5SO_3]\cdot 2\ H_2O$	-1.53_5	No reduction	1 F KCl

* Triton X 100=Alkyl-aryl-polyether alcohol (Rohm & Haas Inc.)
Voltage unit : volt vs. SCE. Concentration of the complex : $5\cdot 10^{-3}$ F/l

These overall processes of the electrode reaction are considered to be most plausible:

$$[Co^{III}(CN)_4\ en]^- \xrightarrow{e} [Co^{II}(CN)_4\ en]^{2-} \xrightarrow[(A)]{e} [Co^{I}(CN)_4\ en]^{3-}$$

$$[Co^{II}(CN)_4(OH_2)_2]^{2-},\ \text{etc.} \xleftarrow{(B)} [Co^{II}(CN)_4\ en]^{2-}$$

$$[Co^{I}(CN)_4\ en]^{3-} \xrightarrow{e} [Co^{0}(CN)_4]^{4-} \xrightarrow{2e} \text{Co(metal)}$$

(aquated species)

The reaction takes place in two ways. When the aquation of the cobalt(II) ion is prevented, the reaction proceeds mainly along path A rather than along path B. Otherwise, the aquated cobalt(II) ions would all be reduced to the metal directly, not through the cobalt(I) state.

Therefore, the resulting cobalt(I) complex was presumed to have the hexacoordinate formula, $[Co^{I}(CN)_4\ en]^{3-}$, in solution, judging from the properties of the other tetracyano complexes.[1,4]

This is the first time that the type of polarographic reduction Co(III)→Co(I)→Co(0) has been observed for the cobalt(III) complexes.

Radiation Center of Osaka Prefecture
Sakai, Osaka

4) G. W. Watt and R. J. Thompson, *J. Inorg. Nucl. Chem.*, **9**. 311 (1959).

Electrical Conductivity of α, α'-Diphenyl-β-picrylhydrazyl under High Pressure

By Hiroo INOKUCHI, Ichimin SHIROTANI and Shigeru MINOMURA

(Received May 26, 1964)

Recently, several examinations of the effect of pressure on such molecular crystals as polycyclic aromatic compounds, have been reported.[1,2,3] As a function of the intermolecular distance, in this article we will present the effect of pressure on the electrical conductivity of the organic free radical, α, α'-diphenyl-β-picrylhydrazyl (DPPH), and also on that of some polycyclic aromatic compounds.

The electrical resistance cell employed consisted of a cylinder and two opposed pistons of Carboloy, with truncated cone ends and press-fitted in hard-steel outer jackets. The specimen (1.2 mm. in diameter and 0.08 mm. thick), encased in a pellet of pyrophyllite, was compressed between the flat centre sections of the pistons.[4] The piston was electrically insulated from the press with mica. Because of the fairly low insulation of the high pressure cell itself, $10^7\ \Omega$, it was not possible to measure the resistivity of the specimen above $10^7\ \Omega$ cm. An appropriate apparatus for the measurement of a high resistance, up to $10^{11}\sim10^{12}\ \Omega$, with a boron nitride pellet is now being prepared.

The abrupt change in the electrical resistance of bismuth or lead at a phase-transition point was used to calibrate the pressure applied to the cell. The transition of bismuth occurs at 2.5×10^4 kg./cm^2 and 8.8×10^4 kg./cm^2, and that of lead, at 1.61×10^5 kg./cm^2.

1) H. Inokuchi, This Bulletin, **28**, 570 (1955).
2) R. S. Bradley, J. D. Grace and D. C. Munro, *Trans. Faraday Soc.*, **58**, 776 (1962).
3) G. A. Samara and H. G. Drickamer, *J. Chem. Phy.*, **37**, 474 (1962).
4) A. S. Balchan and H. G. Drickamer, *Rev. Sci. Inst.*, **32**, 308 (1961).

A sharp drop in the electrical resistance of the purified free radical[5] was found at a lower pressure range, 10^4 kg./cm^2, as is illustrated in Fig. 1. The atmospheric resistivity of DPPH was found to be $10^{13}\,\Omega$cm. at room temperature.[5]

The behaviour was reproducible, and no chemical change could be found under high compressiron. Under the high pressure, the molecules are brought closer together, and this leads to a larger molecular orbital overlap between neighbouring molecules. A quantitative treatment with a band theory for this increments of the overlapping of molecular orbitals will be reported elsewhere.[6]

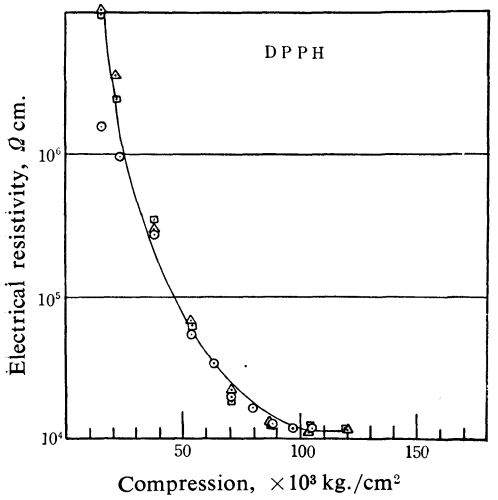


Fig. 1. The resistivity change of DPPH under high pressure.
Different marks, △ ▣ ⊙, are shown different specimens of the free radical.

No chemical reactions among the free radical molecules were found under the compression of 10^5 kg./cm^2. A further compression, however, may induce a solid phase reaction in the D. P. P. H. crystal. A similar result for several organic semiconductors, violanthrone, pentacene and quaterrylene, was obtained as illustrated in Table I.

Table I. The semiconductivity ($\rho=\rho_0\cdot\exp(\Delta\varepsilon/2kT)$) of polycyclic aromatic compounds under a high pressure

Compound	At atmospheric pressure		at 1.6×10^5 kg./cm^2	
	$\rho_{15°C}$**	$\Delta\varepsilon$**	$\rho_{15°C}$**	$\Delta\varepsilon$**
Quaterrylene	1.2×10^8	0.60	6×10^3	0.16
Violanthrone	2.3×10^{10}	0.78	7×10^2	0.18
Pentacene*	10^{14}	1.5	6×10^3	0.14

* A decomposition of the compound under a high pressure may occur.
** $\rho=\Omega$ cm. and $\Delta\varepsilon=$eV.

The Institute for Solid State Physics
The University of Tokyo
Azabu, Tokyo

5) H. Inokuchi, Y. Harada and Y. Maruyama, This Bulletin, 35, 1559 (1962).

6) Y. Harada, Y. Maruyama, I. Shirotani and H. Inokuchi, This Bulletin, in press

The Formation of Three Isomeric Mononitro Derivatives in the Nitration of 2-Thenyl Chloride

By Tyo SONE and Yasuo MATSUKI

(Received June 3, 1964)

It is commonly assumed that the electrophilic substitution of thiophene derivatives with an *o*-, *p*-directing group in the 2-position occurs almost exclusively at the 5-position because of the overlapping of the directive effects of the nuclear sulfur atom and the substituent; it occurs at the 3-position to only a minor extent. Recently, it has been suggested by the NMR technique that, besides the 5-substituted isomers, considerable amounts of the 3-substituted ones are formed in the nitrations of 2-methylthiophene,[1] 2-thenyl chloride (I)[2] and 2-thenyl acetate.[3] However, no report on the formation of 4-substituted isomer has been made. A further study of the product obtained from the nitration of I has revealed the formation of, in addition to

1) R. A. Hoffman and S. Gronowitz, *Arkiv Kemi*, 16, 563 (1960).
2) T. Sone and Y. Matsuki, *J. Chem. Soc. Japan, Pure Chem. Sec.* (*Nippon Kagaku Zasshi*), **83**, 496 (1962).
3) T. Sone, K. Takahashi and Y. Matsuki, This Bulletin, 35, 1420 (1962).

the 3- and 5-substituted isomers, the 4-substituted isomer, which would not be expected from the assumption mentioned above.

Figure 1 shows the NMR spectrum of the product at 60 Mc. (b. p. 105~109°C/2 mmHg)[2] in the nitration of I by the nitric acid - acetic anhydride procedure. The assignment of the peaks to each of the isomers is based on the ring-coupling constants[1] and on the couplings[4,5] between the methylene protons and the ring protons. A set of four strong peaks, consisting of two triplets and a doublet (J= 4.1$_5$ c. p. s. and J_{CH_2}=0.8 c. p. s.), is typical for the ring protons of 5-substituted 2-thenyl derivatives[4,5] and can be assigned to 5-nitro-2-thenyl chloridet (II), the main product. The

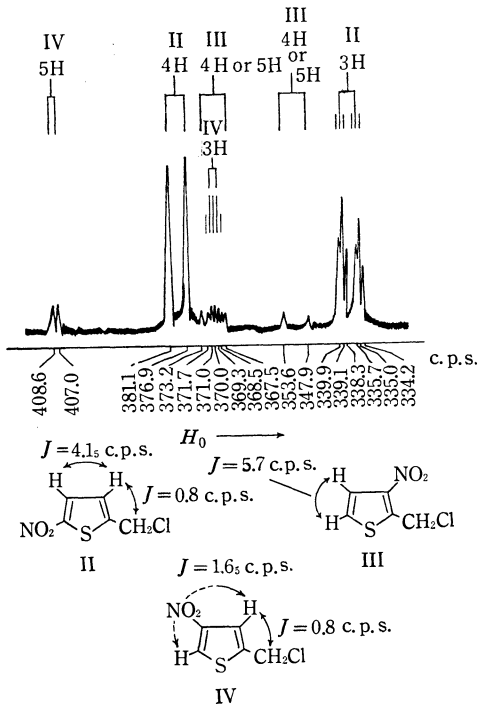


Fig. 1. NMR spectrum of the ring protons of a mixture of 5-nitro-2-thenyl chloride (II), 3-nitro-2-thenyl chloride (III) and 4-nitro-2-thenyl chloride (IV) in carbon tetrachloride at 60 Mc.

4) K. Takahashi, T. Sone, Y. Matsuki and G. Hazato, This Bulletin, 36, 108 (1963).

5) Data obtained from the NMR spectra of some thenyl chlorides will be published later.

remainder may be explained as follows. The doublet (J=5.7 c. p. s.) centered about 350 c. p. s., with reference to cyclohexane, is clearly due to one[6] of the two ring protons of 3-nitro-2-thenyl chloride (III), while the doublet (J=1.6 c. p. s.) on the lowest field side is due to the proton at the 5-position of 4-nitro-2-thenyl chloride (IV).[7] Among the seven peaks in the 367.5 c. p. s.~373.2 c. p. s. region, the two peaks at the two outermost sides are due to one[6] of the two ring protons of III, while the other five peaks are related to the proton at the 3-position of IV; the overlapping of two triplets, which is caused by the coupling of the proton at the 3-position with both that at the 5-position and with the neighboring methylene protons, forms five peaks with an estimated intensity of 1 : 2 : 2 : 2 : 1, and the observed coupling constants (J_{35}=1.7 c. p. s. and J_{2CH_2-3}=0.8 c. p. s.) are in accord with the expected ones. The signals correspond well with those of authentic IV (b. p. 105~107°C/2 mmHg, n_D^{20} 1.6065, d_4^{20} 1.4825. Found: C, 33.89; H, 2.02; N, 7.52. Calcd. for $C_5H_4ClNO_2S$: C, 33.81; H, 2.27; N, 7.88%) prepared by the chloromethylation of 3-nitrothiophene, although attempts to isolate IV, itself or as a derivative, from the nitration product were unsuccessful.

The NMR spectrum of the product in the nitration of 2-thenyl acetate also suggests the formation of the 4-nitro derivative as a by-product.[8]

The authors wish to thank Mr. Kensuke Takahashi for his NMR spectral measurements and for his many helpful suggestions on the spectra.

The Chemical Research Institute of Non-Aqueous Solutions
Tohoku University
Katahira-cho, Sendai

6) At present, it is not possible to determine which of the doublets should be assigned to the proton at the 5-position or to that at the 4-position.

7) The agreement of the spacing both at 40 Mc. and at 60 Mc. assures the assignment of this doublet to one of the two ring protons of the 4-substituted isomer coupling with the other proton.

8) 4-Nitro isomer: J_{35}=1.5 c.p.s. and J_{2CH_2-3}=0.6 c.p.s. In a preceeding paper,[3] two peaks on the lowest field side in the NMR spectrum (40 Mc.) were ascribed to the dinitro isomer.

Electron Spin Resonance Studies of Deuterated Borate Glasses Irradiated with Gamma Rays at Liquid Nitrogen Temperature

By Yasuo NAKAI

(Received June 4, 1964)

The present investigation was undertaken with the expectation that paramagnetic absorption measurements would yield information regarding the hydrogen atoms produced in the radiolysis of B–O–H–O–B or H_2O in borate glass.

For the purpose of examining the effect of water or B–O–H–O–B in glass, borate glass, B_2O_3, was deuterated. The deuterated B_2O_3 glass used was made from the melting of D_3BO_3 prepared by the hydrolysis of trimethyl borate with D_2O.

The infrared spectrum of the deuterated B_2O_3 glass is shown in Fig. 1. The components of the hydrogen and deuterium atoms in the glass seem to be H : D = 1 : 1.

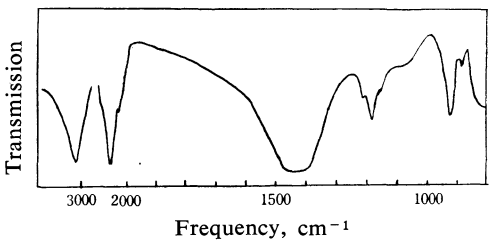


Fig. 1. The IR spectrum of deuterated borate glass.

The sample was irradiated at liquid nitrogen temperature with Co^{60} gamma rays (1×10^6 r). Derivative curves were obtained with a Varian 4501 ESR spectrometer at liquid nitrogen temperature employing a modulation frequency of 100 kc./sec.

The first derivative curve of the spectrum is shown in Fig. 2. The derivative peaks denoted by P_2, P_3, P_4 and P_5, and P_b (Bray's symbol) were found to be the same as have been reported previously.[1] The observed spectrum at 77°K appears to display other new derivative peaks. The additional peaks will be denoted by H_1 and H_2 for the outer pair, and D_1, D_2 and D_3 for the inner lines.

The paramagnetic resonance spectra of a free atomic hydrogen (S = 1/2, I = 1/2) would be expected to consist of a doublet with a

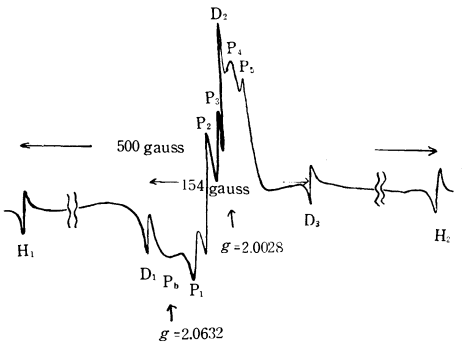


Fig. 2. The ESR spectrum obtained from γ-ray irradiated (1×10^6 r) deuterated borate glass.

separation of 506 gauss, while those of a free atomic deuterium (S = 1/2, I = 1) would consist of a triplet with a separation of 156 gauss between outer components.[2]

Therefore, H and D resonances seem to arise from the hydrogen atom center, H^0 of interstitial vacancy produced by the radiolysis of B–O–H–O–B or H_2O in glass. The derivative peaks denoted by D_1, D_2 and D_3 cannot be observed in nondeutrated samples.

At room temperature, hydrogen atoms may diffuse to form hydrogen molecules or BOH. Thus, no paramagnetic resonance absorption due to H^0 and D^0 centers can be observed.

Central Research Laboratory
Tokyo Shibaura Electric Co., Ltd.
Kawasaki-shi, Kanagawa

1) Y. Nakai *J. Chem. Soc. Japan, Pure Chem. Sec.* (*Nippon Kagaku Zasshi*), **82**, 1629 (1961); S. Lee and P. J. Bray, *J. Chem. Phys.*, **39**, 2863 (1963).

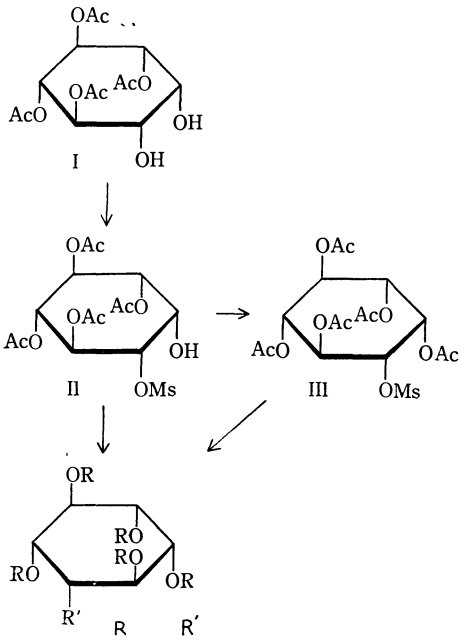
2) P. Kusch, *Phys. Rev.*, **100**, 1188 (1955).

Aminocyclitols. IV. The New Synthesis of Inosamine

By Tetsuo SUAMI and Seiichiro OGAWA

(Received June 4, 1964)

In a previous paper[1] of this series, the displacement of the mesylate group of the 2-amino-1, 3-cyclohexanediol derivative with an azide ion has been described. The replacement of the mesylate group of *myo*-inositol by an azide ion will be studied and the synthesis of inosamine will be described in the present communication.



IV Ac N_3
V Ac NHAc
VI H NHAc
VII H $NH_3^+Cl^-$

The starting material for the synthesis is a known (±)-1, 4, 5, 6-tetra-*O*-acetyl-*myo*-inositol (I).[2] By treating I with one mole of methanesulfonyl chloride in pyridine, (±)-1, 4, 5, 6-tetra-*O*-acetyl-3-*O*-mesyl-*myo*-inositol (II), m. p. 207~208°C, is obtained in 72% yield. II is further acetylated with acetic anhydride and pyridine to give (±)-3-*O*-mesyl-*myo*-inositol pentaacetate (III), m. p. 159~161°C, in 88% yield. It is found that III is different in melting point and in infrared spectra from 2-*O*-mesyl-*myo*-inositol pentaacetate, m. p. 190~192°C which is prepared from 1, 3, 4, 5, 6-penta-*O*-acetyl-*myo*-inositol[3] by the ordinary procedure of mesylation. Since tosyl chloride attacks an equatorial hydroxyl group rather than an axial one in the *myo*-inositol derivative,[4] the attacking of mesyl chloride might take place in a similar manner; therefore, the assignment of the attaching point of the mesylate group to C-3 (or C-1) in II seems to be reasonable. This is further confirmed by the NMR spectrum of III, which reveals a sharp signal at 7.00 τ, as is expected from the protons of an equatorial mesylate group.[5]

When II is then treated with sodium azide in boiling aqueous 2-methoxyethanol for 15 hr., an oily product is obtained. As it has been partially deacetylated during the reaction with sodium azide, this product is acetylated with acetic anhydride and pyridine to yield IV, which shows the characteristic infrared absorption of an azide group at 2115 cm^{-1}. IV is reduced with hydrogen in the presence of Raney nickel. The reduction product shows the infrared absorption of an amide group at 1645 and 1570 cm^{-1}; accordingly, a migration of the acyl group from O to N must have occurred[6] during the course of the reduction. Further treatment with acetic anhydride and pyridine gave hexaacetyl-inosamine (V), m. p. 205~205.5°C in 43% yield from II.

V is also obtained from III by the procedure mentioned above.

The selective deacetylation of V with ammonia in methanol yields *N*-acetyl-inosamine (VI), m. p. 224~225°C. The hydrolysis of VI with 6 N hydrochloric acid gives inosamine hydrochloride (VII), which shows a single spot of R_f 0.18 in ascending paper chromatography in an ethyl acetate - pyridine - acetic

1) T. Suami and S. Ogawa, This Bulletin, 37, 733 (1964).
2) S. J. Angyal, P. T. Gilham and C. G. Macdonald, *J. Chem. Soc.*, 1957, 1417.
3) E. L. May, *J. Org. Chem.*, 17, 286 (1952).
4) S. J. Angyal and L. Anderson, "Advances in Carbohydrate Chemistry," Vol. XIV, Academic Press, New York (1959), p. 167.
5) The NMR spectra of an axial and an equatorial mesylate groups in cyclohexanetriol were presented at the 17th Annual Meeting of the Chemical Society of Japan, Tokyo, April 1964.
6) G. Fordor and J. Kiss, *J. Am. Chem. Soc.*, 72, 3495 (1950); L. Anderson and H. A. Lardy, ibid., 72, 3141 (1950).

acid - water (5 : 5 : 3 : 1) system[7] at 20°C (R_f of D-glucosamine hydrochloride : 0.25).

Not enough examples of the reactions of the sulfoxylate group with sodium azide have been accumulated to predict the stereochemistry of the reaction product, but there are three possible configurations for V: hexaacetyl-*myo*-inosamine-(1),[8] *rac*-inosamine-(2),[9] and *muco*-inosamine-(1).[10] The melting point of V and the R_f value of VII are different from those of the former two. Therefore, hexaacetyl-*muco*-inosamine-(1) seems to be the most probable structure for V.

Department of Applied Chemistry
Faculty of Engineering
Keio University
Koganei-shi, Tokyo

7) F. G. Fischer and H. Dorfel, *Hoppe-Seyler's Z. physiol. Chem.*, **301**, 224 (1955).
8) F. W. Lichtenthaler, *Chem. Ber.*, **94**, 3071 (1961).
9) M. Nakajima, N. Kurihara and A. Hasegawa, ibid., **95**, 141 (1962).
10) M. Nakajima, A. Hasegawa and N. Kurihara, ibid., **95**, 2708 (1962).

Sensitized Luminescence of Tb^{3+}

By Hideo MIZUNO and Mutsuo MASUDA

(Received June 8, 1964)

Recently rare earth-activated phosphors have been studied in order to develop new laser materials. It is well known that rare earth-activated phosphors show line absorption spectra and line emission spectra, and that the intensities of these spectra are weak because the absorption and emission are due to $f-f$ forbidden transitions. Some experiments have been made to sensitize the luminescence of rare earth ions.[1] The authors have found that the emission of Tb^{3+} could be sensitized by heavy metals, such as Cu^+ and Tl^+.

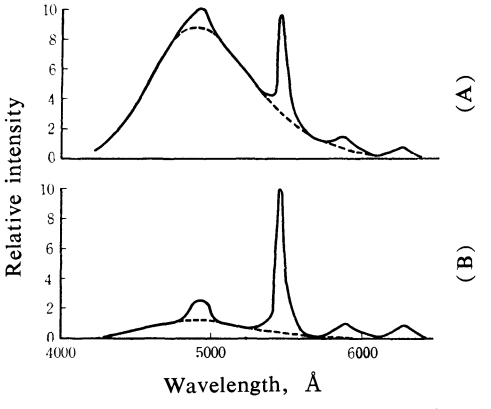


Fig. 1. Emission spectra of Cu and Tb activated phosphors.
(A) $Sr_{2.5}Mg_{0.3}(PO_4)_2$: 0.024 Cu, 0.01 Tb
(B) $Sr_{2.5}Mg_{0.3}(PO_4)_2$: 0.024 Cu, 0.1 Tb

Phosphors of the composition $Sr_{2.5}Mg_{0.3}(PO_4)_2$ activated with Tb^{3+} or the combination of Tb^{3+} with a heavy metal were fired in N_2 or mixed gas (10% H_2+90% N_2) for two hours at 1200°C. The emission spectra were measured at room temperature with a Kipp and Zonen double monochromator. The phosphors activated with Cu^+ and Tb^{3+} show the broad emission spectrum of Cu^+ with a maximum at 4900Å and the line emission spectrum of Tb^{3+} with peaks at 4900, 5460, 5880 and 6250Å, as is shown in Fig. 1. With an increasing Tb^{3+} content, the intensity of the Cu^+ emission decreases while that of the Tb^{3+} emission increases. The phosphor activated only with Tb^{3+} shows a weak emission under 3650Å radiation, but no emission under 2537Å radiation.

When Tb^{3+} coexists with Cu^+ in the host crystal, a strong emission of Tb^{3+} appears under 2537Å radiation. The excitation spectra were measured at room temperature by a Xe-lamp. The excitation spectrum for the Tb^{3+} emission of the phosphors was measured for the 5460Å line in the Tb^{3+} emission spectrum, which was separated from the Cu^+ emission by filters. As is shown in Fig. 2, the excitation spectrum for the Cu^+ activated phosphor is a broad band with a maximum at 3000Å, while the one for the Tb^{3+} activated phosphor is a line spectrum with a complicated structure and with a peak near 3700Å. The excitation spectrum for the Tb^{3+} emission in

1) W. W. Holloway, Jr., M. Kestigian and R. Newman, *Phys. Rev. Letters*, **11**, 458 (1963).

the phosphors activated with Cu^+ and Tb^{3+} shows the broad band corresponding to the excitation spectrum of Cu^+-activated phosphors. From these results it may be concluded that the Tb^{3+} emission is sensitized by Cu^+. It is reasonable to consider that the energy absorbed by Cu^+ is transferred to the $^5D_4$ level of Tb^{3+} by resonance transfer, and that the four lines of the Tb^{3+} emission spectrum with peaks at 4900, 5460, 5880 and 6250Å correspond to the transitions from $^5D_4$ to $^7F_6$, $^7F_5$, $^7F_4$ and $^7F_3$ of the Tb^{3+} energy levels respectively.[2]

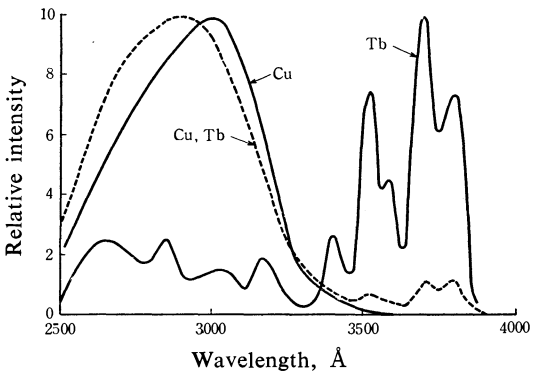


Fig. 2. Excitation spectra of $Sr_{2.5}Mg_{0.3}(PO_4)_2$: 0.1 Tb and $Sr_{2.5}Mg_{0.3}(PO_4)_2$: 0.024 Cu, 0.1 Tb.
Tb : Excitation spectrum for the Tb activated phosphor
Cu : Excitation spectrum for the Cu activated phosphor
Cu, Tb : Excitation spectrum for the Tb emission in the phosphors activated with Cu and Tb

Following the same procedure, it was found that the Tb^{3+} emission is sensitized by Tl^+ in the phosphors activated with Tl^+ and Tb^{3+}. Under 2537Å radiation the phosphors activated with Tl^+ and Tb^{3+} show the broad spectrum of Tl^+ with two maxima at 3400 and 3900Å, as well as the line spectrum of Tb^{3+}, which includes four new peaks at 3840, 4150, 4380 and 4570Å, in addition to the four peaks already described above. Therefore, it is reasonable to consider that, under 2537Å radiation, in the phosphors activated with Tl^+ and Tb^{3+} the energy absorbed by Tl^+ is transferred to the $^5D_3$ level of Tb^{3+} by resonance transfer, and that the former four peaks correspond to the transitions from the $^5D_3$ level, while the latter ones correspond to the transitions from the $^5D_4$ level, to which the energy is transferred from the $^5D_3$ level by radiationless transition.

In the present investigation it has been found that the Tb^{3+} emission is sensitized by such heavy metal ions as Cu^+ and Tl^+, and that Tb^{3+} is excited to the $^5D_4$ level by the sensitizer with an emission peak at about 4900Å, while Tb^{3+} is excited to the $^5D_3$ level by the sensitizer with an emission peak at about 3400～3800Å. In the line spectrum of Tb^{3+}, the 5460Å line is strongest. This emission corresponds to the transition from a $^5D_4$ to a $^7F_5$ level, which is located 2000 cm^{-1} above the ground state $^7F_6$. Consequently, it may be considered that these materials can be used as laser materials by creating a negative temperature state between the $^7F_5$ and $^5D_4$ levels.

Matsushita Electronics Corporation
Takatsuki, Osaka

2) G. H. Dieke, *J. Opt. Soc. Am.*, **51**, 820 (1961).

Effects of Basic Substances on the Rate and Equilibrium of the Tautomeric Reaction between Anthrone and Anthranol

By Hiroaki BABA and Takeshi TAKEMURA

(Received June 8, 1964)

The rate and equilibrium of the keto-enol tautomeric reaction in solution between anthrone and anthranol are known to be strongly dependent upon the solvent employed.[1] In hydrocarbons the reaction is so slow that it requires several days to reach the equilibrium, starting from one of the tautomeric pair. This makes it practically impossible to determine the equilibrium constant, K, in such inert solvents. We have recently observed spectroscopically, however, that the tautomeric reaction in hydrocarbon solvents is markedly affected both in rate and in equilibrium by the presence of basic substances.

The absorption spectrum of anthrone in benzene is shown in Fig. 1, together with the spectrum of the equilibrium mixture of anthrone and anthranol. The equilibrium was established by the addition of a small amount of triethylamine to the benzene solution, the concentration of the amine being only 10^{-4} mol./l. Triethylamine of this low concentration sufficiently accelerates the keto-enol transformation, the rate being increased by a factor of 10^3, but it exerts almost no influence on the equilibrium itself. Consequently, from an analysis of the absorption spectra, the equilibrium constant could be determined to be $K=0.0025$ at 20°C in benzene. In the same way we obtained $K=0.0021$ at 20°C in isooctane. Furthermore, the temperature dependence of the K values led to the following ΔH values: $\Delta H=2.6$ kcal./mol. in benzene and $\Delta H=3.3$ kcal./mol. in isooctane. Both the K and ΔH values indicate that the keto form is more stable than the enol form in hydrocarbons. The present experimental data will be useful in dealing with the problem of keto-enol tautomerism in general.[2,3]

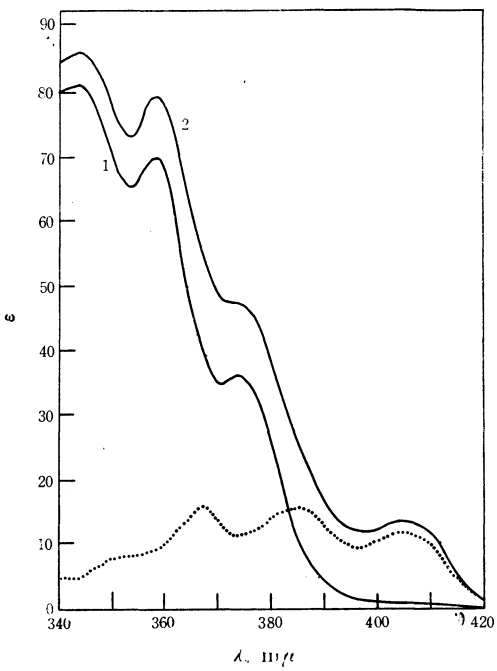


Fig. 1. Absorption spectra of anthrone and the equilibrium mixture of anthrone and anthranol in benzene at 20°C. Solid curve 1, anthrone; solid curve 2, the equilibrium mixture; dotted curve, difference of absorptions 2 and 1, corresponding to the absorption due to anthranol.

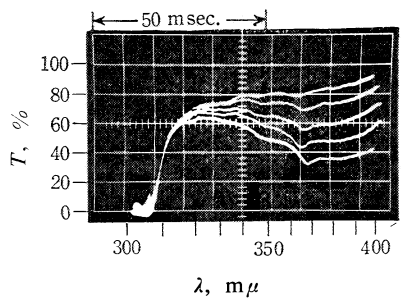


Fig. 2. Spectrophotometric tracing of the base-catalyzed transformation reaction from anthrone to anthranol. The spectra from top to bottom are at 1.5, 4.5, 10, 20, and 120 sec., respectively, after mixing of isooctane solution of anthrone and the same solution of triethylamine. The concentrations of anthrone and triethylamine at the beginning of the reaction are, respectively, 6.1×10^{-4} and 0.9 mol./l. The cell length is 11 mm. and the temperature is 24°C.

1) Y. Bansho and K. Nukada, This Bulletin, **33**, 579 (1960); K. Nukada and Y. Bansho, ibid., **26**, 454 (1953).

2) B. Pullman and A. Pullman, "Quantum Biochemistry," Interscience, New York (1963), pp. 121-123.

3) A. Streitwieser, "Molecular Orbital Theory for Organic Chemists," John Wiley and Sons, New York (1961), pp. 248-255.

The equilibrium between anthrone and anthranol is affected by the amine with higher concentrations. It is noticeably displaced to the side of the enol form with an increasing concentration of added amine. Thus, for the amine concentration of 1 mol./l., the enol form amounts to about 10 per cent of the keto form. This phenomenon can be satisfactorily interpreted as due to the formation of a hydrogen bond between the enol form and the amine. When the concentration of triethylamine is of the order of 10^{-1} to 1 mol./l., the tautomeric equilibrium is reached in isooctane within one or two minutes. The keto-enol reaction was traced by the use of a rapid-scan spectrophotometer[4] constructed recently in our laboratory; this spectrophotometer can display transmission curves on a cathode-ray tube for the wavelength region from 220 to 650 mμ, with a scanning time of 0.3 sec. The results are given in Fig. 2, from which it can be seen that the reaction is of the first order.

Several other basic compounds have also been investigated. Pyridine has essentially the same effect as in the case of triethylamine on both the reaction rate and the equilibrium. Dioxane produces no appreciable change in the reaction rate, but it has a definite effect on the keto-enol equilibrium. Details of the work will be published later.

Research Institute of Applied Electricity
Hokkaido University
Sapporo

4) H. Baba and Y. Shindo, *Bull. Res. Inst. Appl. Elec., Hokkaido Univ.*, 15, 107 (1963).

On a New Type of Cyclododecatriene - Silver Nitrate Complex

By Shunsuke KURIBAYASHI, Noritake YASUOKA, Toshiko MITSUI, Hiroshi TAKAHASHI and Muneaki YAMAGUCHI

(Received June 19, 1964)

In the course of X-ray work on the cyclododecatriene - silver nitrate complex, we have found a new type of complex.

Zakharkin and Korneva reported[1] that *trans, trans, cis*-cyclododecatriene-1, 5, 9 (abbreviated *t, t, c*-CDT) forms a complex with silver nitrate and gave it the formula $(C_{12}H_{18})AgNO_3$ (m. p. 166~167°C). This complex crystallizes as a platelet. In the course of a structure analysis by X-ray diffraction, we found a few needle-like crystals among them. These needles gave X-ray diffraction patterns different from those of platelets. We cite below the former (needles) as the β-type and the latter (platelets) as the α-type. The β-type crystal melts at 149°C and was found by elementary analyses to be of the formula $(C_{12}H_{18})_2AgNO_3$. (Found: C, 58.37, 58.67; H, 7.33, 7.27; Calcd. C, 58.30; H, 7.34%.) Crystallographic data of both complexes are shown in Table I.

The infrared absorption spectra of *t, t, c*-CDT and of both complexes are shown in Fig. 1. The absorption maximum at 970 cm^{-1}, which is assigned to an out-of-plane bending of the CH bond related to the trans C=C bond, is shifted to 990 cm^{-1} in the case of the α-type.

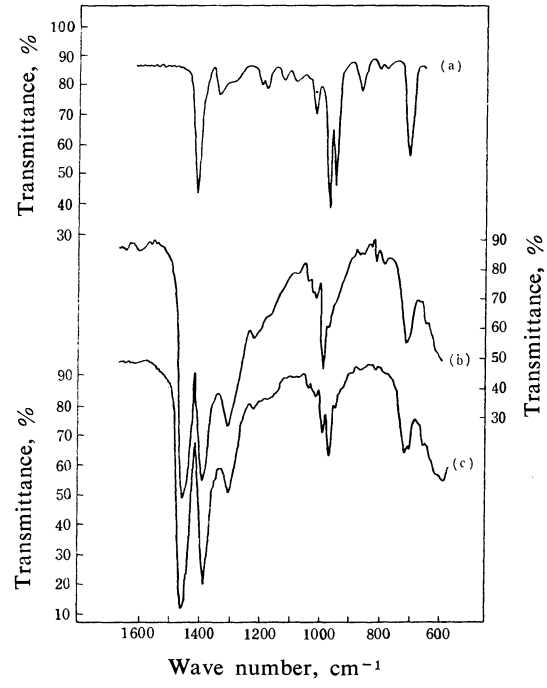


Fig. 1. Infrared spectra of
(a) *trans, trans, cis*-Cyclododecatriene,
(b) α-Type complex in Nujol and
(c) β-Type complex in Nujol.

1) L. I. Zakharkin and V. V. Korneva, *Doklady Akad. Nauk. S.S.S.R.*, 132, 1078 (1960).

TABLE I. CRYSTALLOGRAPHIC DATA OF *trans, trans, cis*-CYCLODODECATRIENE-SILVER NITRATE

	Crystal system	a (A)	b (A)	c (A)	Probable space groups from missing reflections
α-Type	Orthorhombic	15.72	17.62	9.66	$Cmc2_1$, $Cmcm$, $C2cm$
β-Type	Orthorhombic	5.35	15.34	29.80	$Pbcn$

On the other hand, in the case of β-type crystals, the absorption band at 970 cm^{-1} still remains, and that at 990 cm^{-1} is also observed. The absorption at 720 cm^{-1}, assigned to an out-of-plane bending of the CH bond related to the cis C=C bond, remains unchanged in both cases.

These facts suggest that both of the two trans C=C bonds of the α-type coordinate to the Ag^+ ion, but that only one of them does in the case of the β-type and that the cis C=C bond remains free in both cases.

Preliminary X-ray work supports these conclusions. Details of the results of our X-ray crystal structure analysis will be reported in the near future.

Government Industrial Research Institute, Osaka
Oyodo-ku, Osaka

The Far Infrared Spectra of Trimethylaluminum

By Teiichiro OGAWA, Kozo HIROTA and Kunio FUKUSHIMA

(Received June 23, 1964)

The peculiar structure and the high reactivity of trimethylaluminum has provided a very interesting subject for chemists. The vibrational spectra of this molecule have been measured by several authors. Hoffmann,[1] for instance, has published his extensive investigation of the infrared and Raman spectra in the region above 400 cm^{-1}. The infrared measurement was extended to the region from 400 to 120 cm^{-1} by the present authors.[2] Recently Gray,[3] and Onishi and Shimanouchi[4] have described the infrared spectra in the region above 280 cm^{-1}.

As to the assignments of the spectra, however, Hoffmann and Gray gave contradictory views; therefore, in order to settle the problem, observation in the far infrared region has had to be carried out. In the present communication, the far infrared spectra of

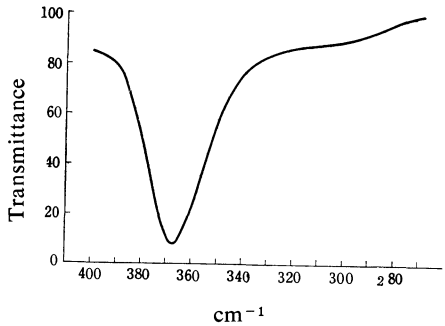


Fig. 1. The far infrared spectra of trimethylaluminum in the 400 to 270 cm^{-1} region. A band lies at 367 cm^{-1}.

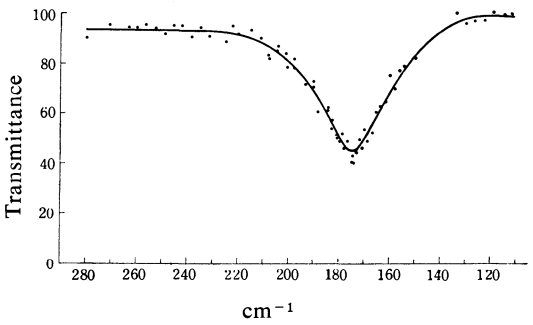


Fig. 2. The far infrared spectra of trimethylaluminum in the 280 to 110 cm^{-1} region. A band lies at 175 cm^{-1}.

1) E. G. Hoffmann, *Z. Elektrochem.*, **64**, 616 (1960).
2) T. Ogawa, K. Hirota, T. Imanaka, K. Fukushima and T. Miyazawa, International Symposium on Molecular Structure and Spectroscopy, A309, Tokyo, September, 1962.
3) A. P. Gray, *Can. J. Chem.*, **41**, 1511 (1963).
4) T. Onishi and T. Shimanouchi, *Spectrochim. Acta*, **20**, 325 (1964).

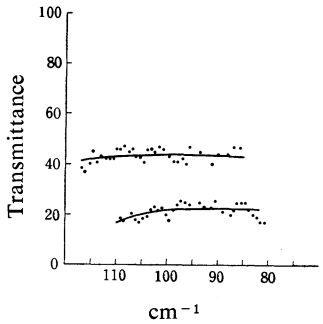


Fig. 3. The far infrared spectra of trimethylaluminum in the 120 to 85 cm^{-1} and 110 to 80 cm^{-1} region. Any band is not observed.

trimethylaluminum will be reported.

Commercial trimethylaluminum (Ethyl Corporation, New York) was purified by vacuum distillation and then transferred into a liquid cell made of two polyethylene films 0.5 mm. thick. This cell was then kept by itself in a vacuum of about 10^{-2} mmHg for several days. The infrared spectra in the 700~270 cm^{-1} region were measured by a Perkin-Elmer Model 221 spectrophotometer with CsBr optics, and the spectra in the 500~65 cm^{-1} region, by a Perkin-Elmer Model 201C far infrared spectrometer. The spectra in the region above 400 cm^{-1} were also measured by a Nippon Bunko Model DS402G spectrometer and found to be similar to those described in the literature.[1,3]

The observed spectra are shown in Figs. 1, 2 and 3. The thickness of the sample is not the same in all measurements but greater in the longer-wavelength region. Two absorption bands were found at 367 cm^{-1} and 175 cm^{-1} in the observed far infrared region.

Department of Chemistry
Faculty of Science
Osaka University
Nakanoshima, Osaka
(T. O. & K. H)

Institute for Protein Research
Osaka University
Kita-ku, Osaka
(K. F.)

The Acyl-Exchange Reactions of N-Acyl Lactams with Amines. A Novel Synthesis of N-Substituted Amides

By Hisaya TANI, Nobuki OGUNI and Takeo ARAKI

(Received October 23, 1963)

The *N*-acylated lactam has two carbonyl groups in each molecule, so two types of nucleophilic reaction are possible. If an amine attacks the ring carbonyl, a ring-opening reaction may be expected to occur, while if it attacks the acyl carbonyl, an acyl-exchange reaction will occur.

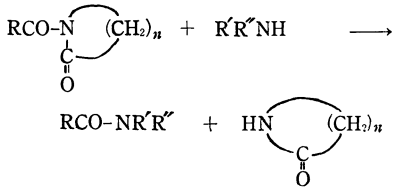
The hydrolysis of the acyl lactam has been investigated,[1] but its aminolysis has not yet been reported. Of various amides, on the other hand, acylimidazole has been successfully used as an acylating reagent in the synthesis of peptides, and it is thought to be an active amide.[2,3]

The present paper is concerned with the aminolysis of some acyl lactams, i. e., the *N*-acetyl or *N*-benzoyl derivatives of 2-pyrrolidone, 2-piperidone and ε-caprolactam. The reactions were studied by means of product isolation techniques; it was found that *N*-acyl lactams generally exchange their *N*-acyl groups readily with a hydrogen atom of the amines, thus producing corresponding amides in good yields. The results obtained indicate that *N*-acyl lactams can be considered as a kind of active amides.

Results and Discussion

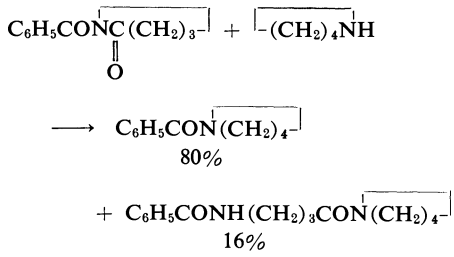
The general procedure for the aminolysis of *N*-acyl lactams was as follows: a tetrahydrofuran solution of an *N*-acyl lactam and an amine (aniline, benzylamine, *n*-butylamine, diethylamine, pyrrolidine or piperidine) was sealed in a glass tube and kept standing for a predetermined length of time in a bath. The temperature of the bath was about 50°C in the case of *N*-benzoyl lactams and about 90°C in the case of *N*-acetyl lactams, varying with the reactivity of the series of lactams.

All of the acetyl lactams used readily reacted with amines and gave corresponding amides in good yields. *N*-Benzoyl lactam also reacted with amines and gave satisfactory results. These results are summarized in Tables II and III.



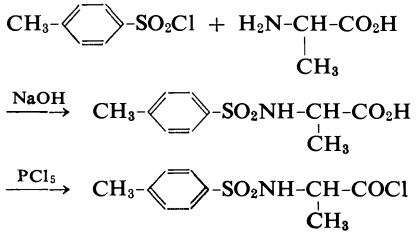
The chemical behavior of the acyl lactams described above indicates that these compounds are good acylating reagents and may be regarded as active amides.

It is noteworthy that small amounts (ca. 20%) of ring opened products were obtained by the reaction of *N*-benzoyl-2-pyrrolidine with such secondary amines as diethylamine, pyrrolidine and piperidine. In the other cases studied, however, no ring-opened product was obtained.

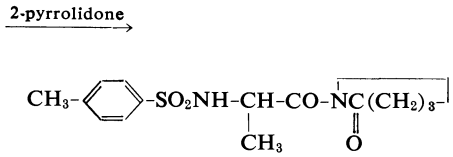


On the other hand, the results of alkaline hydrolysis by potassium hydroxide (Table IV) indicate that the ring-opened products were always obtained, along with lactams, regardless of the number of carbon atoms in the lactam rings. The reason why secondary amines attack the carbon atom of the ring carbonyl of *N*-benzoyl-2-pyrrolidone in an exceptional manner is an interesting but as yet unclarified problem.

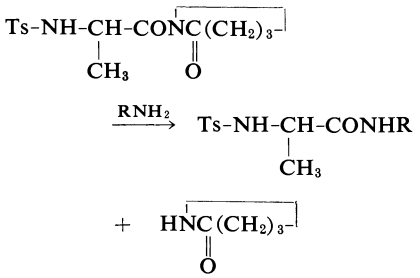
Applications: The novel acyl-exchange reaction presented above was applied to peptide synthesis. *N*-Tosyl-DL-alanyl-2-pyrrolidone was synthesized by the following route.



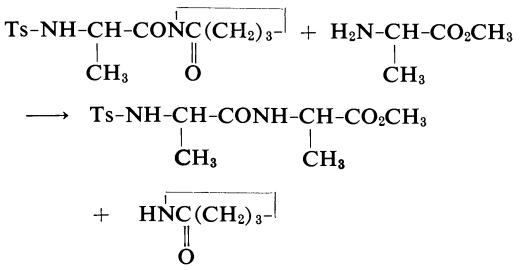
1) A. R. Battersby and J. C. Robinson, *J. Chem. Soc.*, 1956, 2076.
2) G. W. Anderson and R. Paul, *J. Am. Chem. Soc.*, **80**, 4423 (1958).
3) R. Paul and G. W. Anderson, ibid., **82**, 4596 (1960).



Tosyl-DL-alanyl-2-pyrrolidone was converted almost quantitatively to tosyl-DL-alanine *N*-benzylamide by reaction with benzylamine, or to tosyl-DL-alanine *N*-(*n*-butyl)amide by reaction with *n*-butylamine. The results are listed in Table V.



The extension of this reaction to dipeptide synthesis seemed to be interesting. In fact, when the alanine methyl ester was allowed to react with *N*-(tosyl-DL-alanyl)-2-pyrrolidone, the normal acyl-exchange reaction occurred and gave a dipeptide in a good yield:



Experimental

Materials.—*N*-Acetyl lactams were prepared by the acylation of corresponding lactams with acetyl or benzoyl chloride in benzene containing triethylamine. Crude *N*-acyl lactams were purified by fractional distillation or repeated recrystallization. The *N*-acyl lactams used are listed in Table I.

Solvent.—Tetrahydrofuran (THF) was purified by the usual method.

The Reaction of *N*-Acyl Lactams with Amines.—*General Procedure.—i) Reaction*: An *N*-acyl lactam 0.01~0.04 mol. (1 part) and 0.02~0.08 mol. of an amine were dissolved in THF (10~70 ml.). The mixture was then heated in a sealed tube for 16~48 hr. at temperatures ranging from 50 to 90°C.

ii) Methods of Fractionation: The solvent and the unreacted amine were removed under reduced pressure. When the residue solidified, it was purified by recrystallization from suitable solvents (procedure A). When the residue was oily, it was purified by distillation under reduced pressure (procedure B). When the oily residue could not be distilled, two methods were used. One was to dissolve the residue in ethyl acetate and to wash the solution first with 0.5 N hydrochloric acid and second with water, and then to dry it with anhydrous sodium sulfate (procedure C); the other was column chromatography on activated alumina (procedure D). The results are tabulated in Tables II and III, together with the experimental conditions and the methods of purification.

The Hydrolysis of *N*-Benzoyl Lactams.—*General Procedure.*—An *N*-benzoyl lactam (1.9 g.) was dissolved in 20 ml. of dioxane containing 20 ml. of 0.5 N potassium hydroxide and an excess of water (10 ml.). After the mixture had been allowed to stand for half an hour at 14°C, the solution was concentrated in vacuo to one-third of its volume. After the concentrate had been extracted twice with 10 ml. of ethyl acetate, the water layer was acidified (pH 3) with 3 N hydrochloric acid and extracted five times with petroleum benzine (150 ml.). By evaporating the petroleum extract, benzoic acid (m. p. 120~121°C) was obtained. The water layer of the extraction was re-extracted with ethyl acetate. After the ethyl acetate had been removed, the corresponding *N*-benzoyl-*ω*-amino acid was obtained; this was then recrystallized from ethyl acetate. The corresponding *N*-benzoyl-*ω*-amino acids were thus obtained. The results are listed in Table IV.

Tosyl-DL-alanine.—Into a solution of DL-alanine (0.7 mol.) dissolved in 330 ml. of 2 N sodium hydroxide and 400 ml. of water, tosyl chloride

TABLE I. *N*-ACYL LACTAMS PREPARED

Lactam	M. p. °C	B. p. °C/mmHg	n_D	Analysis % C	H	N
	N-Acetyl lactams					
N-Acetyl-2-pyrrolidone	—	90~91/4	1.4843[a]	57.01	7.22	10.86
N-Acetyl-2-piperidone	—	109/9	1.4890[b]	59.56	7.85	9.81
N-Acetyl-ε-caprolactam	—	97~99/5		62.12	8.52	8.79
	N-Benzoyl lactams					
N-Benzoyl-2-pyrrolidone	92~93	—	—	68.53	5.91	7.47
N-Benzoyl-2-piperidone	110~111	—	—	70.64	6.45	6.78
N-Benzoyl-ε-caprolactam	74~ 75	—	—	71.91	6.93	6.29

a) At 8.3°C b) At 25°C

Table II. Reactions of *N*-acetyl lactams with amines

Amine	Methods of fractionation[a]	Product	Uncorrected M. p. °C	Uncorrected B. p. °C/mmHg	Yield %	Analysis % C	Analysis % H	Analysis % N	Identification[e]	Presence of the ring-opened product	Reaction temp. °C
		N-Acetyl-2-pyrrolidone[b]									
Aniline[c]	A	Acetanilide[d]	112~114	—	69	70.59	6.62	10.30	IR, Mixing	None	90
Benzylamine[f]	A	*N*-Benzylacetamide[g]	60~ 61	—	87	72.56	7.36	9.35	IR, Mixing	None	70
		N-Acetyl-2-piperidone[h]									
Aniline	A	Acetanilide[d]	113~115	—	65	71.15	6.65	10.18	IR, Mixing	None	90
Benzylamine	B	*N*-Benzylacetamide[g]	60~ 61	139~140/5	76	72.38	7.47	9.30	IR, Mixing	None	90
n-Butylamine	D[i]	*N*-(*n*-Butyl)acetamide	—	116/7	91	61.06	11.40	11.98	IR	None	90
Diethylamine	B	*N*, *N*-Diethylacetamide	—	58~60/5.5	72	61.99	11.31	10.93	IR	None	90
Pyrrolidine	B	*N*-Acetylpyrrolidine	—	85~88/6.5	92	62.39	9.69	12.27	IR	None	90
Piperidine	D[i]	*N*-Acetylpiperidine	—	89/5	91	65.52	10.30	10.90	IR	None	90
		N-Acetyl-ε-caprolactam[j]									
Aniline	A	Acetanilide[k]	113	—	74	70.86	6.43	10.38	IR, Mixing	None	90
Benzylamine	A	*N*-Benzylacetamide[k]	59.8	—	66	72.17	7.56	9.39	IR, Mixing	None	90
n-Butylamine	D[i]	*N*-(*n*-Butyl)acetamide	—	116~117/7	75	62.27	11.29	12.01	IR	None	90
Diethylamine	B	*N*, *N*-Diethylacetamide	—	56.5~61.5/5	97	63.24	11.46	12.15	IR	None	90
Pyrrolidine	B	*N*-Acetylpyrrolidine	—	82~86/9	93	64.47	9.73	12.39	IR	None	90
Piperidine	B	*N*-Acetylpiperidine	—	65~70/2	78	66.09	10.23	10.28	IR	None	90

a) See text. b) 0.01 mol. of lactam and 0.02 mol. of amine were used. Reaction was continued for overnight. c) Solvent 10 ml. was used. d) Recrystallized from hot water. e) "IR" denotes that infrared spectrum of sample was identical with that of authentic one which was prepared through other route. "Mixing" denotes that the melting point did not show any of depression by mixing with the authentic sample. f) Solvent 20 ml. was used. g) Recrystallized from ether. h) 0.04 mol. of lactam and 0.08 mol. of amine were used. Solvent 70 ml. Reaction was continued for 36~40 hr. i) Elute of ethyl acetate was collected. Chromatographic column had a dimension of 22.5 mm.×102 mm. j) 0.04 mol. of lactam and 0.08 mol. of amine were used. Solvent 70 ml. Reaction time was 20 hr. k) Recrystallized from the mixture of ethyl acetate and *n*-hexane (1 : 1 v/v).

TABLE III. REACTIONS OF *N*-BENZOYL LACTAMS WITH AMINES

Amine	Methods of fraction-ation[a]	Product	M. p. °C	B. p. °C/mmHg	Yield %	Analysis % C	H	N	Identification[b]	Presence of the ring-opened products	Reaction temp. °C
		N-Benzoyl-2-pyrrolidone[c]									
Aniline	A	*N*-Phenylbenzamide[d]	160～161	—	86	78.70	5.63	6.94	IR, Mixing	None	50
Benzylamine	A	*N*-Benzylbenzamide[e]	105～105.5	—	96	79.89	6.28	6.68	IR, Mixing	None	28
n-Butylamine	A	*N*-(*n*-Butyl)benzamide[d]	40～41	—	89	74.86	8.56	7.73	IR, Mixing	None	50
Pyrrolidine	B	*N*-Benzoylpyrrolidine	—	153～154/7	80	74.90	7.60	7.72	IR	$C_6H_5CONH(CH_2)_3\overline{CON(CH_2)_4}$ is ring-opened one	50
	A	$C_6H_5CONH(CH_2)_3\overline{CON(CH_2)_4}$[f]	170～171	—	16	69.09	7.71	10.86	IR[g]		
Piperidine	B	*N*-Benzoylpiperidine	—	145～147/4	63	76.48	8.04	7.66	IR	$C_6H_5CONH(CH_2)_3\overline{CON(CH_2)_5}$ is ring-opened one	50
	A	$C_6H_5CONH(CH_2)_3\overline{CON(CH_2)_5}$[e]	86～87	—	22	69.77	7.96	10.26	IR[g]		
Diethylamine	B	*N*, *N*-Diethylbenzamide	—	115～118/4	63	74.40	8.53	7.57	IR	Some but unidentified[h]	50
		N-Benzoyl-2-piperidone[c]									
Aniline	A	*N*-Phenylbenzamide[e]	162	—	Quant.	78.91	6.27	7.04	IR, Mixing	None	50
Benzylamine	A	*N*-Benzylbenzamide[i]	106	—	Quant.	79.69	6.19	6.47	IR, Mixing	None	50
n-Butylamine	C	*N*-(*n*-Butyl)benzamide[d]	40～41	—	91	72.96	8.54	7.33	IR, Mixing	None	50
Pyrrolidine	B	*N*-Benzoylpyrrolidine	—	135/2	91	74.24	7.55	8.03	IR	None	50
Piperidine	B	*N*-Benzoylpiperidine	—	134～134.5/2	Quant.	73.14	8.17	7.52	IR	None	50
Diethylamine	B+C	*N*, *N*-Diethylbenzamide	—	115～120/4	62	74.40	8.53	7.57	IR	None	50
N-Methylaniline	No reaction occured										50
		N-Benzoyl-ε-caprolactam[c]									
Aniline	A	*N*-Phenylbenzamide[f]	160.5～162	—	90	78.79	5.54	6.92	IR, Mixing	None	50
Benzylamine	A	*N*-Benzylbenzamide[j]	102～103	—	95	79.73	6.21	6.55	IR, Mixing	None	50
n-Butylamine	C	*N*-(*n*-Butyl)benzamide[d]	40～41	—	90	73.77	8.48	7.59	IR, Mixing	None	50
Diethylamine	B+C	*N*, *N*-Diethylbenzamide	—	104/2	76	74.56	8.47	7.80	IR	Trace, if present[k]	50
Piperidine	B	*N*-Benzoylpiperidine	—	121～123/1	95	75.97	8.23	7.61	IR	None	50
N-Methylaniline	No reaction occured										50

a) See text. b) See foot-note e) of Table II. c) 0.01 mol. of lactam and 0.02 mol. of amine were used. Solvent 20 ml. Reaction was continued for overnight. d) Recrystallized from ethanol. e) Recrystallized from ethyl acetate. f) Recrystallized from methanol. g) Infrared-absorption bands were seen at 1623 cm^{-1} and 1546 cm^{-1}. h) Infrared spectrum seemed to contain some ring-opened products. i) Recrystallized from petroleum benzine. j) Recrystallized from 60% methanol. k) Very small amounts of amorphus precipitate was obtained.

TABLE IV. ALKALINE HYDROLYSIS OF *N*-BENZOYL LACTAMS

Lactam	Benzoic acid %	Ring-opened product	M. p. °C	%
N-Benzoyl-2-pyrrolidone	82	$C_6H_5CONH(CH_2)_3CO_2H$[a]	81～82	13.5
N-Benzoyl-2-piperidone	33	$C_6H_5CONH(CH_2)_4CO_2H$[b]	106～107	50
N-Benzoyl-ε-caprolactam	67	$C_6H_5CONH(CH_2)_5CO_2H$[a]	76～77	30

a) Recrystallized from ethyl acetate. b) Recrystallized from chloroform.

TABLE V. REACTIONS OF *N*-(TOSYL-DL-ALANYL)-2-PYRROLIDONE WITH AMINES

	Methods of fractionation[a]	Product	M. p. °C	Yield %	Analysis % C H N	Identification
Benzylamine[b]	A	*N*-(Tosyl-DL-alanyl)-benzylamide[c]	133～134	98	Found 61.53 6.12 8.24 Calcd. 61.42 6.06 8.43	IR (Presence of amide I, II and absence of ring carbonyl)
n-Butylamine[d]	A	*N*-(Tosyl-DL-alanyl)-*n*-butylamide[e]	104～105	92	Found 56.14 7.44 9.47 Calcd. 56.37 7.38 9.40	IR
DL-Alanine methyl ester[f]	A	Tosyl-DL-alanyl-DL-alanine methyl ester[g]	95～97	89	Found 51.72 6.19 8.55 Calcd. 51.29 6.10 8.53	IR

a) See text of the reactions of *N*-acyl lactam with amines. b) *N*-(Tosyl-DL-alanyl)-2-pyrrolidone 0.003 mol. and amine 0.01 mol. were used with 20 ml. of THF. Reaction was continued for overnight at 60°C c) Recrystallized from ethyl acetate. d) *N*-(Tosyl-DL-alanyl)-2-pyrrolidone 0.005 mol. and amine 0.03 mol. were used with 20 ml. of THF, at 60°C for overnight. e) Recrystallized from ether. f) *N*-(Tosyl-DL-alanyl)-2-pyrrolidone 0.003 mol. and DL-alanine methyl ester 0.006 mol. in 10 ml. of THF were used, at 60°C for overnight. g) Recrystallized from the mixture of acetone and petroleum ether.

(1 mol.) was stirred; the stirring was then continued for 5 hr. at room temperature. After the reaction had been completed, the reaction mixture was extracted with benzene in an adjusted basic media (pH 9). The residue was acidified to pH 3 by adding 3 N hydrochloric acid. A crystalline material precipitated. It was recrystallized from ethyl acetate, m. p. 136～137°C. Yield, 72.5%.

Tosyl-DL-ananyl-2-pyrrolidone.—Eighteen grams of phosphorus(V) chloride were added to the solution of 19.2 g. of tosyl-DL-alanine in 280 ml. of ether, and the mixture stirred for half an hour. After the removal of the ether, colorless needles were obtained. They were then dissolved in 240 ml. of THF, and the solution was cooled to 0°C. Fifty milliliters of THF solution containing 2-pyrrolidone (16 ml.) and triethylamine (8.8 g.) was then added drop by drop to the tosylalanyl chloride solution. The precipitate was separated off, and the THF was removed. The residue was dissolved in 100 ml. of ethyl acetate. The solution was washed with a 5% solution of potassium bicarbonate, a 5% solution of hydrochloric acid, and then with water, and dried with sodium sulfate. After the ethyl acetate had been removed, a crystalline material was obtained. It was recrystallized from ethyl acetate, m. p. 133～134°C. Yield, 76%.

Found: C, 54.05; H, 5.78; N, 8.95. Calcd. for $C_{14}H_{18}O_4N_2S$: C, 54.18; H, 5.58; N, 9.03%.

The Reaction of *N*-(Tosyl-DL-alanyl)-2-pyrrolidone with Amines.—The procedure was the same as that in the reaction of *N*-acyl lactams with amines. The results are listed in Table V.

Summary

N-Acetyl and *N*-benzoyl lactams consisting of a five-to-seven-membered ring were found to be good acylation reagents. Several amines were acylated with these reagents to give the corresponding amides in good yields.

When *N*-benzoyl-2-pyrrolidone was used, ring-opened by-products were obtained by the reaction with a secondary amine, such as pyrrolidine and piperidine.

Tosylalanyl-2-pyrrolidone reacted with primary amines to produce the corresponding tosylalanine amides. The alanine methyl ester reacted as a primary amine with tosylalanyl-2-pyrrolidone to afford a dipeptide.

The authors are indebted in some parts of their experiments to Mr. Sigeru Tanaka, Mr. Hiroshi Kagawa and Mr. Hajime Yasuda; grateful acknowledgment is hereby made to these persons.

Department of Polymer Science
Faculty of Science
Osaka University
Nakanoshima, Osaka

Studies in the Equilibrium Dyeing of Cotton with Direct Dyes: The Determination of the Activity and Affinity of Direct Dyes for Cellulose

By E. H. DARUWALLA and G. G. KULKARNI

(Received December 7, 1963)

The three main theories which have been put forth to explain the effect of dye and salt concentration and temperature on the equilibrium dyeing of cellulosic fibres with direct dyes are those suggested by Hanson, Neale and Stringfellow,[1] by Willis, Warwicker, Standing and Urquhart,[2] and by Peters and Vickerstaff.[3] Peters and Vickerstaff are of the opinion that the driving force during dyeing can be best represented by the Gibbs free energy changes involved; they obtained a quantitative measure of the tendency of dye to pass from the aqueous phase to the fibre phase, which they termed as "affinity." These workers in the development of the treatment were faced with the great difficulty of expressing the activity of dye in the fibre phase, as no precise information was available regarding the saturation values of cellulose with regard to direct dyes. They were, therefore, compelled to introduce a term for the volume of cellulosic fibres, the values of which were deduced arbitrarily from the results of the adsorption of Chrysophenine G by cellulosic fibres, which gave linear plots of unit slope when the logarithm of ionic products in fibre and in the solution at equilibrium were plotted. Recently, Daruwalla and D'Silva[4] developed a new thermodynamic approach in which the activity of dye in cellulosic fibre substances is expressed in terms of the fraction of total sites occupied at a particular stage of dyeing. On the basis of this thermodynamic approach, they obtained consistent values of affinity for three direct dyes under different experimental conditions.

The present work was undertaken with a view of seeing whether the thermodynamic treatment of Daruwalla and D'Silva could be applied to other direct dyes, dyes with different chemical structures and aggregation tendencies. Attempts have also been made to test the validity of this treatment in explaining the behaviour of Chlorazol Sky Blue FF and Chrysophenine G during dyeing from a mixed dyebath.

Experimental Procedure

Materials.—The cellulosic fibre substance used was 20^s yarn made from Indian cotton and from which, by suitable treatments, impurities other than cellulose in the fibre substance were removed. Pure samples of Congo Red (C. I. Direct Red 28), Benzopurpurine 4B (C. I. Direct Red 2), Benzopurpurine 10B (C. I. Direct Red 7), Chloramine Purple 10BC (C. I. Direct Red 61), Chlorazol Corinth GW (C. I. Direct Red 10), Benzocorinth B (C. I. Direct Violet 21), Diazol Violet R (C. I. Direct Violet 43), Chlorazol Blue B (C. I. Direct Blue 6), Chlorazol Blue G (C. I. Direct Blue 10), Durazol Blue 2R (C. I. Direct Blue 71) and Chlorazol Orange RN (C. I. Direct Orange 8) were obtained from commercial dyes by purification, using the technique recommended by Robinson and Mills,[5] the purity of the samples was determined from an analysis of the elements present. All the other chemicals used were of Analar quality.

The Determination of the Heat of Dyeing.—The determination of the heat of dyeing was carried out by a technique similar to that described by Gilbert,[6] in which a fibre containing a constant amount of a dye is brought to equilibrium at different temperatures with solutions containing different amounts of dye. The details of the determination are the same as those mentioned by Daruwalla and D'Silva.[4]

The Determination of the Fibre Degradation of NaOCl-treated Dyed Cotton.—A definite weight of dyed or undyed cotton was treated with a 50 ml. sodium hypochlorite solution (3 g./l. available chlorine) buffered to pH 7 at 30°C for 3 min. The oxidised sample was washed thoroughly, antichlored, washed, and dried; the fluidity of the solution containing oxidised sample dissolved in a cuprammonium hydroxide solution was then determined according to A. S. T. M. Standards specifications.[7]

For the determination of the values of $[D_\phi]$, the amount of dye in the fibre phase (g. ions/kg.) and $[D_\sigma]$, the amount of dye in the solution (g. ions/l.) in equilibrium at different temperatures, the desorption technique for attaining equilibrium was used. This method of approach for obtaining the values of $[D_\phi]$ and the corresponding values of $[D_\sigma]$ at different temperatures was preferred to the

1) J. Hanson, S. M. Neale and W. A. Stringfellow, *Trans. Faraday Soc.*, **31**, 1718 (1935).
2) H. F. Willis, J. O. Warwicker, H. A. Standing and A. R. Urquhart, ibid., **41**, 506 (1945).
3) R. H. Peters and T. Vickerstaff, *Proc. Roy. Soc.*, **A192**, 292 (1948).
4) E. H. Daruwalla and A. P. D'Silva, *Textile Research J.*, **33**, 40 (1963).
5) C. Robinson and H. A. T. Mills, *Proc. Roy. Soc.*, **A131**, 576 (1931).
6) G. A. Gilbert, ibid., **A183**, 167 (1944).
7) Apparent Fluidity of Dispersions of Cellulose Fibres, D-539-53, A. S. T. M. Standards, Part 10, 233 (1958).

normal method of obtaining these values from adsorption experiments because, in the latter case, longer times are required for the establishment of equilibrium, with a risk of the decomposition of dyes and changes in the structure of the cellulosic fibres. It was found that the affinity values calculated from the appropriate values of $[D_\phi]$ and $[D_s]$ obtained from desorption experiments were close to those recorded in the literature where the adsorption technique for attaining equilibrium conditions between the dye in the fibre substance and the dye in the bath was employed.

Results and Discussion

For the direct dyes studied, the results of the present investigation indicate that, except for the initial low concentration of adsorbed dye, the values of the heat of dyeing remain constant over a fairly wide range of dye concentration in the fibre, and that, beyond a critical dye concentration, the values tend to decrease continuously as the amount of adsorbed dye in the fibre is increased (Figs. 1–3). The critical dye concentration beyond which the values decrease is peculiar to each dye studied (Table I). In view of the fact that the cellulose-water system is not homogeneous, the sorption affinity of dye will not be identical over all the surface with which dye may come in contact, with the result that the values of the heat of dyeing associated with different portions of cotton will be different. The values of the heat of dyeing generally indicate overall changes in the heat content of the system, but to some extent these values may also be considered to indicate the energy of the association of a particular dye with cellulose. The fact that constant values of the heat of dyeing over a sufficiently wide range of adsorbed dye are obtained in the present study goes to show that, within this range, the dye

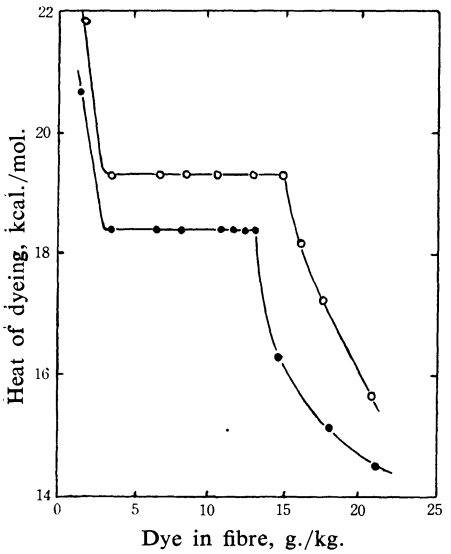


Fig. 1. Heats of dyeing of Benzopurpurine 10B and Benzopurpurine 4B on cotton.
—○— Benzopurpurine 10B
—●— Benzopurpurine 4B

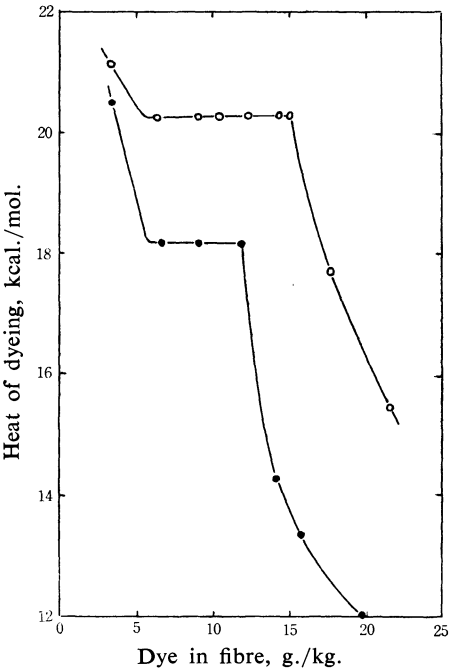


Fig. 2. Heats of dyeing of Chloramine Purple 10BC and Chlorazol Orange RN on cotton.
—○— Chloramine Purple 10BC
—●— Chlorazol Orange RN

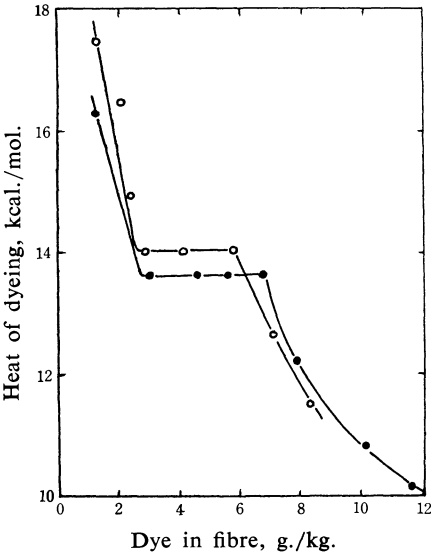
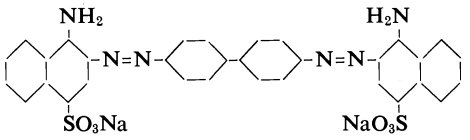
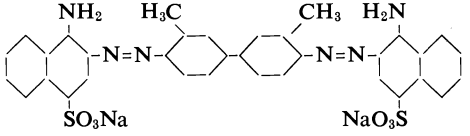
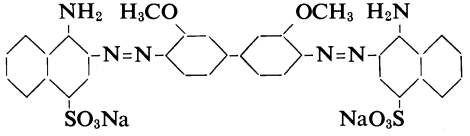
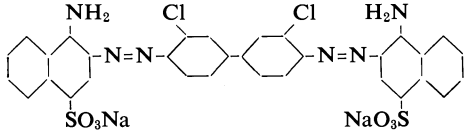
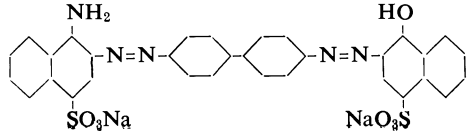
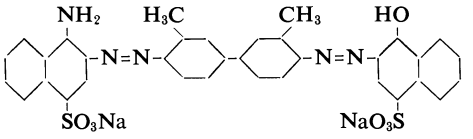
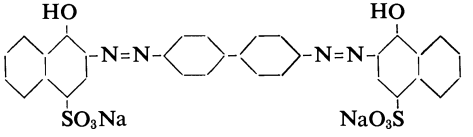
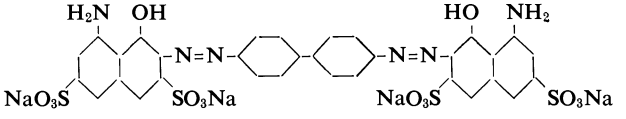
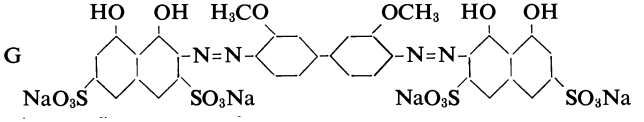
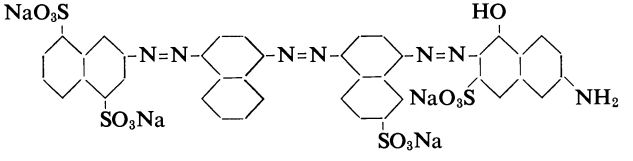
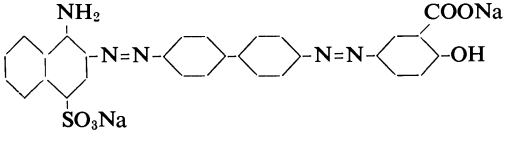


Fig. 3. Heats of dyeing of Chlorazol Blue G and Chlorazol Blue B on cotton.
—○— Chlorazol Blue G
—●— Chlorazol Blue B

TABLE I. HEATS OF DYEING, SATURATION VALUES, AVERAGE AFFINITY VALUES AT DIFFERENT TEMPERATURES AND ENTROPY OF DYEING OF DIRECT DYES ON COTTON

No.	Dye	Structure	$-\Delta H^\circ$ kcal./mol. (from desorption measurements)	Saturation value mM/kg. dry fibre		$-\Delta G^\circ$, kcal./mol. 60°C	70°C	80°C	90°C	$-\Delta H^\circ$ kcal./mol. (from affinity values)	ΔS° cal./°C/mol.
1	Congo Red		20.24	18.67	B	9.73	9.44	9.13	8.85	19	31
					C	7.22	6.85	6.47	6.11	20	39
2	Benzopurpurine 4B		18.40	17.96	B	9.55	9.28	9.05	8.79	18	27
					C	7.32	6.98	6.69	6.36	18	33
3	Benzopurpurine 10B		19.32	19.85	B	9.28	8.97	8.74	8.40	19	30
					C	7.16	6.78	6.49	6.09	19	37
4	Chloramine Purple 10BC		20.24	19.61	B	9.98	9.71	9.44	9.17	19	31
					C	7.85	7.52	7.18	6.84	19	37
5	Chlorazol Corinth GW		16.10	—	C	7.18	6.92	6.66	6.40	16	27

6	Benzocorinth B		16.10	—	C	7.10	6.81	6.55	6.28	16	27
7	Diazol Violet R		6.0	—	C	—	—	—	7.80	—	—
8	Chlorazol Blue B		14.03	7.24	B	7.96	7.79	7.60	7.44	14	18
					C	5.01	4.75	4.47	4.22	14	27
9	Chlorazol Blue G		14.03	5.78	B	8.14	7.96	7.79	7.61	14	18
					C	4.89	4.61	4.35	4.07	14	27
10	Durazol Blue 2R		21.62	—	C	6.85	6.40	5.95	5.50	22	44
11	Chlorazol Orange RN		18.17	19.64	B	8.56	8.34	8.11	7.90	17	29
					C	6.39	6.10	5.81	5.54	17	35

Mechanism B: Dye anions adsorbed on specific sites and sodium ions diffusely adsorbed.
Mechanism C: Dye anions and sodium ions diffusely adsorbed,

is likely to form a monomolecular layer in the substrate. With further absorption of dye, multimolecular layers are likely to be formed; moreover, because the energy released in sorbate-sorbate interaction is generally lower than that released in the sorbate-solvent interaction, the values of the heat of dyeing show a tendency to decrease as soon as multimolecular layer formation commences. The critical concentration beyond which the values of the heat of dyeing tend to decrease may, therefore, be taken as a stage of the completion of the formation of a monolayer of a particular dye in a cellulosic fibre substance. Although it is not possible to indicate very conclusively whether or not, up to the stage of constancy in the values of the heat of dyeing, a monomolecular layer of the dye is formed in the substrate, indirect evidence in support of this concept is available from the results of the density measurements of dyed cellulose[4] and from the results of the oxidation of cellulose containing different amounts of dye with a sodium hypochlorite solution. As did Daruwalla and D'Silva, the present authors found that, in the case of cotton containing increasing amounts of dye (Chloramine Purple 10BC, Chlorazol Orange RN and Chlorazol Blue B), catalytic oxidation is very rapid, but that beyond a critical dye concentration in the fibre, the extent of oxidation does not change appreciably (Fig. 4). This critical dye concentration is analogous to the stage beyond which the values of the heat of dyeing tend to decrease. Thus, because of the formation of a monolayer of dye in cellulose, the dye which is in close proximity to cellulose is more effective in increasing cellulose oxidation than when additional dye going into the fibre gets adsorbed on the monolayer of the dye present in the substrate. Furthermore, as will be discussed later, when these critical concentrations of dyes are considered to be saturation values and when the activity of dye in the fibre and the subsequent affinity values are calculated on the basis of a mechanism of the adsorption of dye anions on specific sites, plots correlating the activity of dye in the fibre with that in solution at equilibrium are linear with slopes close to unity and affinity values are fairly consistent over a wide range of dye concentration in the bath at different dyebath temperatures. Direct evidence is also available from the results of the present study regarding the saturation value of a direct dye for cotton when the reciprocals of the dye in the fibre to that in solution are plotted at different temperatures of dyeing (Fig. 5). These curves are linear, indicating a Langmuir type of adsorption, and the intercept on the $1/[D_\phi]$ axis corresponds to a figure very close to that obtained for monolayer formation from the experiments of the heat of dyeing measurements (Table II).

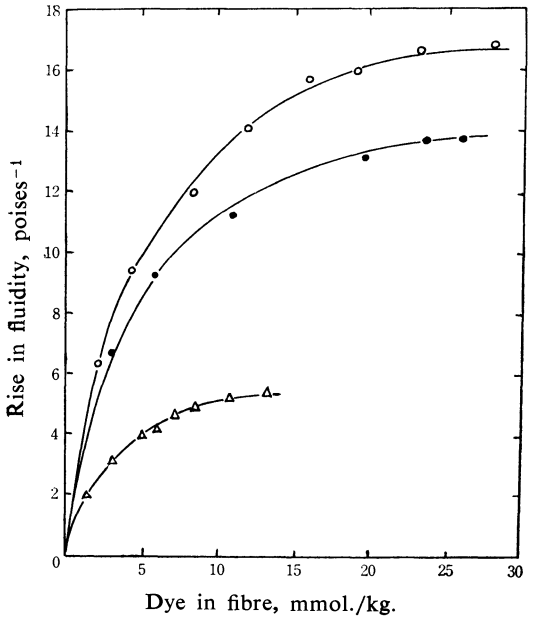


Fig. 4. Relation between rise in fluidity of cotton after oxidation and amount of dye in cotton.
—○— Chloramine Purple 10BC
—●— Chlorazol Orange RN
—△— Chlorazol Blue B

TABLE II. COMPARISON BETWEEN THE SATURATION VALUES OBTAINED FROM HEATS-OF-DYEING MEASUREMENTS AND THOSE OBTAINED FROM ADSORPTION MEASUREMENTS

Dye	Saturation values obtained from heats of dyeing, mmol./kg. dry fibre	Saturation values obtained from adsorption, mmol./kg. dry fibre
Congo Red	18.67	17.86
Benzopurpurine 4B	17.96	20.83
Chloramine Purple 10BC	19.61	18.52
Chlorazol Blue B	7.24	8.30
Chlorazol Blue G	5.78	6.17

The amounts of dye required for the formation of a monolayer as obtained from the heat of dyeing measurements vary between 6 and 19 mol./kg. of cotton for the different dyes studied. When a comparison is made between the saturation values of different dyes studied, it appears that there is not much difference between dyes of similar structure (namely dye nos. 1–4), but when large sulphonic acid groups are introduced in the dye molecule, as

TABLE III. SLOPES OF PLOTS OF LOG ACTIVITY OF DYE IN FIBRE AND IN DYEBATH

Dye	Temp. °C	Mechanism A	Mechanism B	Mechanism C
Congo Red	60	2.66	1.20	0.69
	70	2.73	1.20	0.69
	80	2.70	1.18	0.70
	90	2.78	1.21	0.70
Benzopurpurine 4B	60	2.66	1.16	0.94
	70	2.66	1.11	0.86
	80	2.56	1.08	0.84
	90	2.71	1.10	0.89
Benzopurpurine 10B	60	1.89	0.91	0.71
	70	1.88	0.91	0.70
	80	1.80	0.91	0.67
	90	1.73	0.93	0.70
Chloramine Purple 10BC	60	2.83	1.23	0.95
	70	2.63	1.16	0.90
	80	2.58	1.17	0.89
	90	2.50	1.13	0.86
Chlorazol Blue B	60	—	1.60	1.20
	70	—	1.53	1.20
	80	—	1.58	1.21
	90	—	1.55	1.20
Chlorazol Blue G	60	—	1.58	1.03
	70	—	1.50	1.03
	80	—	1.43	0.96
	90	—	1.37	1.07
Chlorazol Orange RN	60	—	2.28	1.78
	70	—	2.22	1.67
	80	—	2.06	1.50
	90	—	1.91	1.45

Mechanism A : Dye anions and sodium ions adsorbed on specific sites.
Mechaaism B : Dye anions absorbed on specific sites and sodium ions diffusely adsorbed.
Mechanism C : Dye anions and sodium ions diffusely adsorbed.

in the case of Chlorazol Blue B and Chlorazol Blue G, the saturation values drop appreciably (Table I).

With most of the dyes studied, at a low dye concentration the values of the heat of dyeing are always higher than the normal values, indicating that there exist a limited number of sites in cotton for which dye has high affinity and that, when dye is adsorbed on these highly-active sites, dyeing on the less active and more plentiful sites takes place. These observations are in agreement with those of Gnehm and Kaufler,[8] and Jackson and Turner,[9] who found that the last traces of direct cotton dyes could not be removed by repeated washing or by extraction with an aqueous solution of pyridine, and with those of Mann and Marrinan,[10] who observed that, during the rehydrogenation of deuterated groups in cellulose, a few of these groups were very resistant to rehydrogenation. Very recently, Daruwalla and Shet,[11] who studied the kinetics of the rate of the removal of primary adsorbed water in different cellulosic fibres, observed that the rate of removal during the last stages was extremely low compared with the rate of the removal of primary adsorbed water. No correlation was observed between the nitrogen content of the fibre substance or free-COOH groups in the fibre and the amount of dye in the fibre substance where high values of the heat of dyeing are obtained. It appears that the high energy of association between

8) Von R. Gnehm and F. Kaufler, vide T. Vickerstaff, "The Physical Chemistry of Dyeing," Oliver and Boyd, London (1954), p. 233.
9) J. H. E. Jackson and H. A. Turner, *J. Soc. Dyers Colourists*, **68**, 345 (1952).
10) J. Mann and H. J. Marrinan, *Trans. Faraday Soc.*, **52**, 481 (1956).
11) E. H. Daruwalla and R. T. Shet, *J. Polymer Sci.*, **A2**, 943 (1964).

TABLE IV. ABSORPTION OF BENZOPURPURINE 4B ON COTTON (5 g./l. NaCl)

Temp. °C	$[D_\phi]$ 10^{-3}	$[Na_\phi]$ 10^{-3}	$[D_\sigma]$ 10^{-3}	$[Na_\sigma]$ 10^{-3}	θ	$-\Delta G°$, kcal./mol. Mechanism B	$-\Delta G°$, kcal./mol. Mechanism C
70	4.37	30.38	0.0006	85.47	0.243	9.15	7.05
	5.50	31.72	0.0009	85.47	0.306	9.17	7.00
	6.17	32.54	0.0011	85.47	0.344	9.19	6.99
	6.92	33.47	0.0014	85.47	0.385	9.21	6.97
	7.77	34.55	0.0017	85.47	0.433	9.26	6.96
	8.72	35.80	0.0020	85.47	0.485	9.33	6.96
80	4.37	30.38	0.0013	85.47	0.243	8.92	6.76
	6.17	32.54	0.0023	85.47	0.344	8.95	6.69
	6.92	33.47	0.0028	85.47	0.385	8.99	6.68
	7.77	34.55	0.0034	85.47	0.433	9.03	6.67
	8.71	35.80	0.0041	85.47	0.485	9.10	6.67
	9.78	37.22	0.0050	85.48	0.545	9.18	6.66
90	4.37	30.38	0.0028	85.47	0.243	8.63	6.41
	6.17	32.54	0.0048	85.47	0.344	8.68	6.35
	6.92	33.47	0.0058	85.48	0.385	8.72	6.35
	7.77	34.55	0.0069	85.48	0.433	8.78	6.34
	8.72	35.80	0.0083	85.48	0.485	8.84	6.34
	9.78	37.22	0.0101	85.49	0.545	8.93	6.34

Mechanism B: Dye anions adsorbed on specific sites and sodium ions diffusely adsorbed.
Mechanism C: Dye anions and sodium ions diffusely adsorbed.

TABLE V. ADSORPTION OF BENZOPURPURINE 10B ON COTTON (5 g./l. NaCl)

Temp. °C	$[D_\phi]$ 10^{-3}	$[Na_\phi]$ 10^{-3}	$[D_\sigma]$ 10^{-3}	$[Na_\sigma]$ 10^{-3}	θ	$-\Delta G°$, kcal./mol. Mechanism B	$-\Delta G°$, kcal./mol. Mechanism C
60	5.27	31.44	0.0004	85.47	0.265	9.30	7.31
	5.91	32.31	0.0005	85.47	0.298	9.27	7.24
	6.63	33.11	0.0007	85.47	0.334	9.25	7.19
	7.44	34.14	0.0009	85.47	0.375	9.22	7.12
	8.35	35.30	0.0012	85.47	0.421	9.23	7.08
	10.51	38.21	0.0020	85.47	0.529	9.28	7.03
70	5.27	31.44	0.0009	85.47	0.265	9.01	6.96
	5.91	32.21	0.0012	85.47	0.298	8.97	6.88
	6.63	33.11	0.0016	85.47	0.334	8.93	6.81
	8.35	35.30	0.0027	85.47	0.421	8.93	6.71
	9.36	36.68	0.0036	85.47	0.472	8.93	6.65
	10.51	38.21	0.0047	85.47	0.529	8.96	6.60
80	5.27	31.44	0.0019	85.47	0.265	8.79	6.68
	5.91	32.21	0.0025	85.47	0.298	8.75	6.61
	6.63	33.11	0.0032	85.47	0.334	8.71	6.53
	8.35	35.30	0.0055	85.48	0.421	8.69	6.41
	10.51	38.21	0.0098	85.48	0.529	8.70	6.28
	11.26	39.26	0.0115	85.49	0.567	8.73	6.25
90	5.27	31.44	0.0043	85.47	0.265	8.45	6.27
	6.63	33.11	0.0073	85.48	0.334	8.38	6.13
	7.44	34.14	0.0096	85.48	0.375	8.35	6.06
	9.36	36.68	0.0163	85.50	0.472	8.36	5.95
	10.51	38.21	0.0210	85.51	0.529	8.40	5.91
	11.26	39.26	0.0252	85.52	0.567	8.42	5.86

Mechanism B: Dye anions adsorbed on specific sites and sodium ions diffusely adsorbed.
Mechanism C: Dye anions and sodium ions diffusely adsorbed.

TABLE VI. ADSORPTION OF CHLORAMINE PURPLE 10BC ON COTTON (5 g./l. NaCl)

Temp. °C	$[D_\phi]$ 10^{-3}	$[Na_\phi]$ 10^{-3}	$[D_\sigma]$ 10^{-3}	$[Na_\sigma]$ 10^{-3}	θ	$-\Delta G°$, kcal./mol. Mechanism B	Mechanism C
70	4.13	30.11	0.0003	85.47	0.211	9.60	7.59
	5.20	31.37	0.0004	85.47	0.265	9.61	7.55
	5.84	32.15	0.0005	85.47	0.298	9.62	7.52
	6.55	33.01	0.0006	85.47	0.334	9.64	7.51
	7.35	34.02	0.0007	85.47	0.375	9.68	7.50
	8.25	35.18	0.0008	85.47	0.421	9.71	7.49
80	4.13	30.11	0.0006	85.47	0.211	9.34	7.27
	5.84	32.15	0.0011	85.47	0.298	9.35	7.19
	6.55	33.01	0.0013	85.47	0.334	9.36	7.17
	7.35	34.02	0.0015	85.47	0.375	9.40	7.16
	8.25	35.18	0.0019	85.47	0.421	9.44	7.15
	9.25	36.52	0.0023	85.47	0.472	9.50	7.15
90	4.13	30.11	0.0012	85.47	0.211	9.09	6.95
	5.20	31.37	0.0018	85.47	0.265	9.08	6.90
	5.84	32.15	0.0022	85.47	0.298	9.08	6.87
	6.55	33.01	0.0027	85.47	0.334	9.09	6.84
	7.35	34.02	0.0032	85.47	0.375	9.12	6.82
	8.25	35.18	0.0040	85.47	0.421	9.16	6.81

Mechanism B: Dye anions absorbed on specific sites and sodium ions diffusely adsorbed.
Mechanism C: Dye anions and sodium ions diffusely adsorbed.

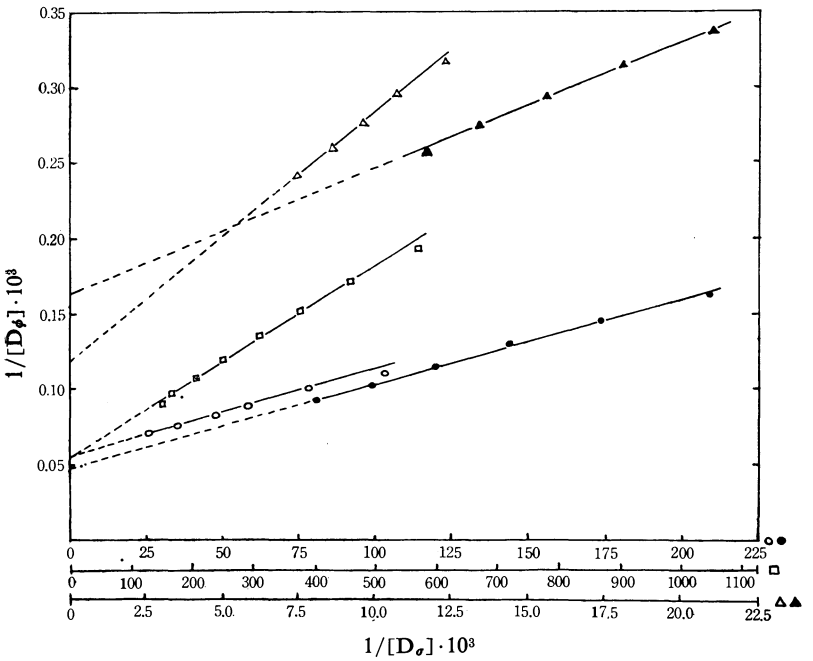


Fig. 5. Plots of $1/[D_\phi]$ and $1/[D_\sigma]$ at 90°C on cotton.
—△— Chlorazol Blue B —▲— Chloramine Blue G
—□— Chloramine Purple 10BC —○— Congo Red
—●— Benzopurpurine 4B

TABLE VII. ADSORPTION OF DYE MIXTURES BY CELLOPHANE SHEET (2 g./l. NaCl)

Temp. °C	F_ϕ g. ions/ kg. $\times 10^{-3}$	F_σ g. ions/ l. $\times 10^{-6}$	F'_σ g. ions/ l. $\times 10^{-6}$	F_c g. ions/ l. $\times 10^{-6}$	G_ϕ g. ions/ kg. $\times 10^{-3}$	G_σ g. ions/ l. $\times 10^{-6}$	G'_σ g. ions/ l. $\times 10^{-6}$	G_c g. ions/ l. $\times 10^{-6}$	G_σ/F_σ	G_c/F_c
70	3.40	9.78	3.29	6.49	0.40	8.90	2.36	6.54	0.91	1.0
	2.87	9.91	2.0	7.90	0.51	10.91	2.90	8.0	1.10	1.0
	1.56	9.75	0.52	9.23	1.32	19.95	9.08	10.87	2.05	1.18
	0.72	9.92	0.14	9.78	2.34	39.61	19.1	20.51	3.99	2.09
	0.44	9.92	0.08	9.84	3.18	59.77	30.0	29.77	6.02	3.03
	0.29	10.01	0.04	9.97	3.92	79.75	42.0	37.75	7.97	3.78
90	1.87	9.74	6.20	3.5	0.10	4.98	1.5	3.5	0.51	1.0
	1.72	9.77	5.25	4.52	0.18	7.48	2.9	4.6	0.77	1.0
	1.63	9.64	4.7	4.9	0.30	10.02	4.9	5.1	1.04	1.04
	0.71	10.01	1.2	8.8	1.02	39.83	18.9	20.9	3.98	2.37
	0.51	9.94	0.77	9.17	1.53	59.63	30.9	28.6	6.00	3.13
	0.37	9.90	0.51	9.4	1.94	79.60	42.12	37.5	8.04	3.99

dye and fibre at low concentrations may be due both to adsorption on sites of high activity and to steric factors which prevent the dye molecules trapped in the network of cellulose from passing from the fibre phase to the solution phase.

When the affinities of direct cotton dyes for cellulose are to be determined, the main parameters required are the activity of dye in the fibre and in the dyebath. Affinity can be represented by the equation:

$$-\Delta G^\circ = RT \ln a_\phi - RT \ln a_\sigma \qquad (1)$$

where R is the gas constant; T, the absolute temperature of dyeing; a_ϕ, the activity of dye in fibre, and a_σ, the activity of dye in an aqueous solution. If the dye is assumed to be completely ionised in a solution and if the activity coefficient is considered to be unity, the activity of the dye in solution can be represented by the product of the ionic concentration of the dye anions and sodium ions in the solution, and

$$-\Delta G^\circ = RT \ln a_\phi - RT \ln [D_\sigma] [Na_\sigma]^z \qquad (2)$$

where $[D_\sigma]$ and $[Na_\sigma]$ are the ionic concentrations of dye anions and sodium ions in the solution at equilibrium (g. ions/l.) and z is the valency of the dye. For assigning a value to the activity of dye in the cellulose phase, a choice of a suitable function to represent the activity will depend on the mechanism of dyeing which is postulated. If the dye is assumed to be completely ionised in the substrate, the activity of dye in the fibre will vary depending on which of the following three thermodynamic mechanisms is operative during the dyeing:

A. Both the dye anions and sodium ions are adsorbed on specific sites in the fibre in a monomolecular layer and are not subjected to interference, either electrical or otherwise, from the adjacent adsorbed anions.

B. Only the dye anions are adsorbed on specific sites, while the sodium ions are diffusely adsorbed.

C. Both the dye anions and sodium ions are attracted to the fibre-solvent interphase and there is a possibility of formation of a multimolecular layer. Vickerstaff[12] has considered these three thermodynamic approaches for expressing the activity of dye in the fibre phase and has developed appropriate equations for the calculation of activity in the fibre and of affinity values for each of these mechanisms.

Until now only mechanism C could be considered and tested because in the other two mechanisms it was essential to know the exact amount of dye required to form a monolayer in the fibre substance. Peters and Vickerstaff[3] adopted the mechanism of diffused adsorption for both dye anions and gegenions; this mechanism necessitated the use of the volume term V, which represents the volume of the surface of the fibre substance which takes part in the dyeing. The validity of this term has, however, been questioned by Preston, Mhatre and Narasimhan,[13] by Nishida[14] and by Horiki[15]. It was, therefore, thought desirable to test the alternative approach of expressing the activity of a direct dye in a fibre substance as the fraction of the total sites occupied at a specific stage of equilibrium dyebath adsorption. From the knowledge of the saturation value of a direct dye for cotton obtained with

12) T. Vickerstaff, "The Physical Chemistry of Dyeing," Oliver and Boyd, London (1954), pp. 106-111.
13) J. M. Preston, S. H. Mhatre and K. I. Narasimhan, *J. Soc. Dyers Colourists*, **65**, 17 (1949).
14) K. Nishida, *J. Soc. Textile Cellulose Ind. Japan*, **7**, 539 (1951).
15) Y. Horiki, This Bulletin, **33**, 974 (1960).

precision from the determination of the heat of dyeing at different concentrations of adsorbed dye in the fibre, the two mechanisms, A and B, could be investigated. When mechanism A is applied to the results of the present study, it is found that it is not valid, the slopes of the plots correlating $(z+1)\log\theta_D/(1-\theta_D)$, where θ_D is the fraction of total sites occupied by dye anions, with $\log[D_\sigma][Na_\sigma]^z$ are far from unity (Table III), and the calculated affinity values are not at all consistent. This is because the dyebath contains both dye and electrolyte; therefore, the total number of sodium ions present in the fibre would not only be equal to those required for maintaining electrical neutrality but would also be equal to the sum of sodium ions surrounding dye anions in an equivalent number and to those arising from the electrolyte present in the fibre phase in equilibrium with the solution phase, according to the Donnan membrane equilibrium.

When mechanism B is considered in connection with the results of the present sudy, under different temperatures and conditions of dye concentration in the bath, plots correlating $\log\theta_D/(1-\theta_D)\cdot[Na_\phi]^z/V^z$ with $\log[D_\sigma][Na_\sigma]^z$ are linear, except for Chlorazol Blue B, Chlorazol Blue G and Chlorazol Orange RN, with slopes close to unity (Figs. 6–8 and Table III), and the affinity values are consistent (Tables IV–VI). $[Na_\phi]$ is the ionic concentration of dye anions in the fibre phase (g. ions/kg.); it can be determined by means of the Donnan equilibrium between sodium ions and chloride ions in the fibre and in the external solution according to the equation derived by Peters and Vickerstaff.[3] V is the surface volume in l./kg. dry fibre, which is taken to be 0.3 l./kg. for cotton. In the case of Congo Red, Benzopurpurine 4B and Benzopurpurin 10B, the plots correlating the activity of dye in the fibre to that in the solution are closer to unity, and the affinity values agree more closely with one another when mechanism B is considered than is the case when the treatment of Marshall and

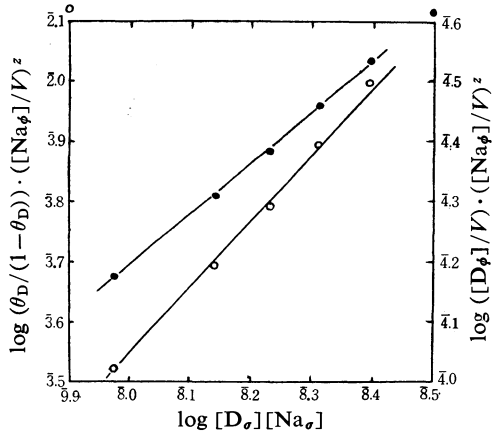


Fig. 6. Plots of log activity of dye in fibre and in bath for Benzopurpurine 4B on cotton at 80°C (5 g./l. NaCl).
—○— Dye ions adsorbed on specific sites and sodium ions diffusely adsorbed
—●— Dye ions and sodium ions diffusely adsorbed

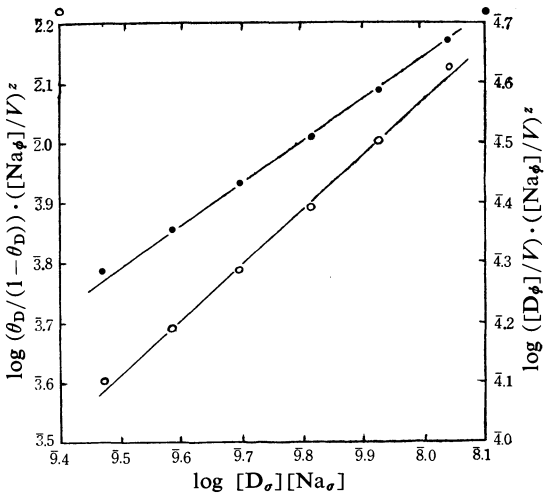


Fig. 7. Plots of log activity of dye in fibre and in bath for Benzopurpurine 10B on cotton at 60°C (5 g./l. NaCl).
—○— Dye ions adsorbed on specific sites and sodium ions diffusely adsorbed
—●— Dye ions and sodium ions diffusely adsorbed

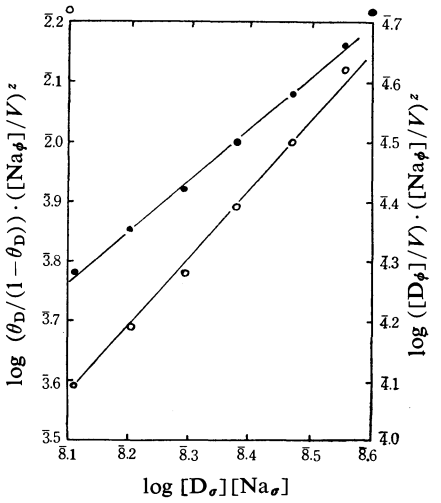


Fig. 8. Plots of log activity of dye in fibre and in bath for Chloramine Purple 10BC on cotton at 90°C (5 g./l. NaCl).
—○— Dye ions adsorbed on specific sites and sodium ions diffusely adsorbed
—●— Dye ions and sodium ions diffusely adsorbed

Peters[16] is considered (mechanism C). The affinity values obtained from the results of dyeing equilibria at different temperatures and the values of the heat dyeing determined from the slopes of the linear plots correlating $\Delta G^\circ/T$ with $1/T$ are given in Table I. It can be seen that the values of the heat of dyeing obtained are close to those obtained from the desorption experiments mentioned earlier, where the method of determining the heat of dyeing does not involve the expression of the activity of the dye in the fibre phase.

The following are the main points which serve to show that the mechanism based on the adsorption of dye anions on specific sites and sodium ions being diffusely adsorbed is more probable for dyeing equilibria with direct dyes on cellulose than that developed by earlier workers based on diffused adsorption for both the ions.

(1) The saturation values which are used to calculate the total number of sites available for dye adsorption in order to determine the activity of the dye in the cellulose substrate are actually obtained from experimental data rather than arbitrarily accepting the volume term, V, to fit the experimental results with the postulated theory.

(2) Plots correlating the logarithm of the activity of the dye in the fibre to that in the solution are linear, with slopes approaching unity.

(3) The calculated values of the affinity of a dye are consistent with one another under different conditions of dye concentrations in the bath at each of the dyebath temperatures studied.

(4) Plots correlating $\Delta G^\circ/T$ against $1/T$ are linear, and the values of the heats of dyeing obtained from the slopes of these curves are very close to those obtained from desorption experiments where the treatment used does not involve the expression of the activity of the dye in the fibre.

The Adsorption of the Dye Mixture.—Boulton, Delph, Fothergill and Morton,[17] Neale and Stringfellow[18] and Derbyshire and Peters[19] have shown that, with binary mixtures of Chrysophenine G and Chlorazol Sky Blue FF, the equilibrium adsorption of either of the two dyes was reduced when the other dye was present in the dyebath. The main factors which are likely to influence the adsorption of direct dyes from mixtures are competition between different dye anions for available sites in the fibre substance, the effect of each dye in contributing to the surface charge of the cellulose and sodium ion concentrations in the fibre, and interaction between dyes in the solution. As the fibre at a low concentration of adsorbed dye is very far from being saturated, however, competition for available sites is not likely to have much effect. According to Neale and Stringfellow,[18] the effect of each dye on the charge on the fibre surface and on the sodium ion concentration in the fibre is inadequate to explain the reduced adsorption from the mixed dyebath. Thus, the main contribution to the reduction in the dye uptake from a mixed dyebath appears to arise from the interaction of dyes in the solution.

Horiki[15] could explain satisfactorily in a quantitative way the adsorption of Chrysophenine G and Chlorazol Sky Blue FF from a mixed dyebath at 90°C by a cellophane sheet, assuming the formation of 1 : 1 complex and adopting the thermodynamic treatment of Marshall and Peters[16] for equilibrium dyeing. At higher concentrations of Chrysophenine G in the dyebath, however, he could not explain the adsorption behaviour on the basis of the 1 : 1 complex.

In the present study, in order to explain the behaviour of Chrysophenine G and Chlorazol Sky Blue FF when applied from a mixed dyebath, the data given by Horiki[15] have been considered and the saturation values and affinity values for these two dyes in cellophane have been determined by the desorption experiments mentioned before. Assuming that the thermodynamic treatment mentioned before is valid in the case of mixtures also, the effective dyebath concentration of each dye which would effect a specific equilibrium adsorption on cellophane can be calculated from the equation:

$$-\Delta G^\circ = RT \ln \theta_D/(1-\theta_D) \cdot [Na_\phi]^z/V^z - RT \ln [D'_\sigma] [Na_\sigma]^z \quad (3)$$

where $[D'_\sigma]$ is the effective dyebath concentration of a particular dye (g. ions/l.), when the affinity values of the dyes at a particular temperature and the saturation values of cellophane for these dyes are known. From the knowledge of the effective dyebath concentration of each dye under different concentrations of combinations and at different temperatures, the amount of each dye in the mixture which is ineffective in dyeing can be obtained and the types of complexes of these two dyes likely to be formed under different conditions can be predicted. These results for the dyeing temperatures of 70 and 90°C have been

16) W. J. Marshall and R. H. Peters, *J. Soc. Dyers Colourists*, **63**, 446 (1947).
17) J. Boulton, A. E. Delph, F. Fothergill and T. H. Morton, *J. Textile Inst.*, **24**, P113 (1933).
18) S. M. Neale and W. A. Stringfellow, *J. Soc. Dyers Colourists*, **59**, 241 (1943).
19) A. N. Derbyshire and R. H. Peters, ibid., **72**, 268 (1956).

recorded in Table VII, where F_ϕ and G_ϕ represent the concentrations of Chlorazol Sky Blue FF and Chrysophenine G in cellophane at equilibrium (g. ions/kg.), F_σ and G_σ are the equilibrium dyebath concentrations of Chlorazol Sky Blue FF and Chrysophenine G in a mixture dyebath (g. ions/l.), F'_σ and G'_σ are the effective dyebath concentrations of Chlorazol Sky Blue FF and Chrysophenine G (g. ions/l.) as calculated from Eq. 3 and F_c and G_c are the dyebath concentrations of Chlorazol Sky Blue FF and Chrysophenine G ineffective in adsorption because of the interaction of dyes in the mixture (g. ions/l.) (they correspond to $(F_\sigma - F'_\sigma)$ and $(G_\sigma - G'_\sigma)$ respectively). The affinity values of Chlorazol Sky Blue FF for cellophane at 70 and 90°C have been calculated as 8.9 and 7.9 kcal./mol. respectively; the corresponding figures for Chrysophenine G are 6.0 and 5.6 kcal./mol. The saturation values of Chlorazol Sky Blue FF and Chrysophenine G for cellophane as obtained from the measurements of the heats of dyeing are 0.01512 g. ions/kg. dry cellophane and 0.02647 g. ions/kg. dry cellophane respectively. V, the volume term of the cellulose phase in cellophane, is considered to be 0.45 l./kg., a figure also used by Marshall and Peters[16] for the calculation of affinity values.

It can be seen from the results of Table VII that the experimental data for the adsorption of these dyes from a mixed dyebath at 70 and 90°C can be explained on the basis of the formation of a 1 : 1 complex between these two dyes up to the stage where the ratio of the amount of Chlorazol Sky Blue FF to that of Chrysophenine G is less than 1 : 2, but at higher concentrations of Chrysophenine G, complexes other than 1 : 1 (namely, 1 : 2, 1 : 3 and 1 : 4) appear to be formed in the dyebath. The types of complexes formed for the same ratio of Chlorazol Sky Blue FF to Chrysophenine G as starting dyebath concentrations appear to be the same at both 70 and 90°C. These results are in agreement with those recorded by Derbyshire and Peters,[19] who, from calorimetric measurements of the magnitude of the heats of interaction between Chrysophenine G and Chlorazol Sky Blue FF, have indicated the possibility of the formation of a considerable proportion of complexes richer in Chrysophenine G in the presence of an excess of this dye in an aqueous solution. These workers have also shown that the adsorption spectrum of a mixture of these two dyes in an aqueous solution is not the same as the sum of the spectra of its constituents and that, even at 90°C, the formation of a 1 : 1 complex takes place in the aqueous solution to an appreciable extent. In agreement with the deductions obtained in the present study from the equilibrium adsorption measurements of these two dyes from a mixed dyebath and the subsequent calculation of the effective dyebath concentration, these workers showed that, when an excess of Chrysophenine G was present in the dyebath, for a constant proportion of Chlorazol Sky Blue FF, the absorption maxima of Chlorazol Sky Blue FF shifted to longer wavelengths, this shows that the formation of higher complexes does take place to a certain extent under these dyebath conditions.

In conclusion, from the results of the present study it may be noted that the thermodynamic treatment developed by Daruwalla and D'Silva[4] is valid for a number of direct cotton dyes with different chemical constitutions and different aggregation behaviours. The affinity values obtained with the present treatment with all the dyes studied are higher than those obtained by adopting the treatment of Marshall and Peters.[16] It is rather difficult, however, to state which of these two sets of values may be considered to represent the true values. Nevertheless, it appears that the values obtained by adopting the thermodynamic treatment developed in the present study, values which are based on experimentally-determined value for the activity of dye in the fibre as calculated from the fraction of the total sites occupied, are likely to be more representative. Futhermore, the thermodynamic treatment used in the present study also explains in a semiquantitative way the equilibrium adsorption behaviour on cellulose of Chrysophenine G and Chlorazol Sky Blue FF when they are applied from mixed dyebaths.

Department of Chemical Technology
University of Bombay
Matunga, Bombay, India

*The Synthesis of Methylacetylene by the Pyrolysis of Propylene. I. The Effect of Pyrolysis Conditions on Product Yields**

By Yasumasa SAKAKIBARA

(Received February 5, 1964)

Methylacetylene would be a valuable material in the field of synthetic chemistry. For example, it is known that methylacetylene is carbonylated with carbon monoxide to give methacrylate,[1] just as acetylene gives acrylate. Although various methods have been reported for the synthesis of methylacetylene, however, there is no economically attractive one. The present author was interested in obtaining methylacetylene by the pyrolysis of light hydrocarbons, especially by the direct dehydrogenation of propylene.

Rice et al.[2] were the first to report the synthesis of methylacetylene and allene, both being isomeric and equilibrated thermo-catalytically,[3] by the pyrolysis of isobutylene. In many investigations[4-14] of the pyrolysis of propylene, methylacetylene has not been detected in the products, while Szwarc[15] alone has found allene as a main product. He pyrolyzed propylene at temperatures ranging from 680 to 870°C and at pressures from 2 to 15 mmHg; there was a low conversion of 0.01 to 2 per cent. Recently, in the course of this study, it has been announced (U. S. Pat.[16]) that allene and methylacetylene were produced by contacting propylene with a metal filament heated over 900°C, at low pressure and with a short contact time. The purpose of the present investigation is to determine suitable conditions for the production of methylacetylene and allene by the pyrolysis of propylene and to obtain data on the distribution of the pyrolysis products.

Experimental

Materials.—Propylene was prepared by the vapor phase dehydration of isopropyl alcohol, using activated clay as a catalyst. After it had been washed with about a 15% solution of sodium hydroxide, it was stored in a 25 l. water-gas holder. Gas chromatographic analysis showed that the purity was better than 99.0 mol. % and that the principal impurities were hydrogen, methane, ethylene, and propane. Cylinder nitrogen of 99.9 mol.% purity was used as a reference gas, a known amount (about one-fourth of the propylene volume) being added to the propylene. The change in the volume (rate of expansion) of the reactant gas upon pyrolysis was calculated from the change in the concentration (mol.%) of the nitrogen.

Apparatus and Procedure. — The apparatus is shown in Fig. 1. The reactant gas, consisting of about 80 vol.% propylene and 20 vol.% nitrogen, was introduced into a silica (or porcelain) reaction tube from the gas holder through a water bubbler, a drying tower containing calcium chloride, and a needle valve. The gas pressure in the gas holder was always kept at atmospheric pressure by allowing water to run into it. To carry out experiments over a wide temperature range, various silica reaction tubes, from 2.9 to 11.0 mm. in inside diameter, and two different types of electric furnaces, one 30 cm. long (furnace I) and the other 10 cm. long (furnace II), were employed. Furnace II, having been constructed from a spiral "Siliconit" heating element,* was used mainly for heating to 1100°C and above. The reaction tube was suspended in the center of another silica tube, which extended through the furnace. The exhausted gas from the reaction tube was rapidly cooled with running water at the exit of the tube; it then passed through a trap immersed in ice-water to remove any liquid products and then through a 300-ml. glass gas-sampling flask, which was attached to a

* Presented at the 14th Annual Meeting of the Chemical Society of Japan, Tokyo, April, 1961.

1) J. W. Copenhaver and M. H. Bigelow, "Acetylene and Carbon Monoxide Chemistry," Reinhold Publishing Corp., New York (1949), p. 299.
2) F. O. Rice and W. S. Haynes, *J. Am. Chem. Soc.*, **70**, 964 (1948); F. O. Rice and L. A. Wall, ibid., **72**, 3967 (1950).
3) J. F. Cordes and H. Günzler, *Chem. Ber.*, **92**, 1055 (1959); *Z. Naturforsch.*, **15b**, 682 (1960); German Pat. 1093350 (1960).
4) E. F. Frey and D. F. Smith, *Ind. Eng. Chem.*, **20**, 948 (1928).
5) R. H. Wheeler and W. L. Wood, *J. Chem. Soc.*, **1930**, 1819.
6) C. D. Hurd and R. N. Meinert, *J. Am. Chem. Soc.*, **52**, 4978 (1930).
7) V. Schneider and P. K. Frolich, *Ind. Eng. Chem.*, **23**, 1405 (1931).
8) C. D. Hurd and L. K. Eilers, ibid., **26**, 776 (1934).
9) H. Tropsch, C. I. Parrish and G. Egloff, ibid., **28**, 581 (1936).
10) V. G. Moor, N. V. Strigaleva and A. V. Frost, *J. Gen. Chem. U. S. S. R.*, **7**, 860 (1937); *Chem. Abstr.*, **31**, 5662 (1937).
11) H. D. Burnham and R. N. Pease, *J. Am. Chem. Soc.*, **64**, 1404 (1942).
12) K. U. Ingold and F. J. Stubbs, *J. Chem. Soc.*, **1951**, 1749.
13) R. E. Kinney and D. J. Crowley, *Ind. Eng. Chem.*, **46**, 258 (1954).
14) K. J. Laidler and B. W. Wojciechowski, *Proc. Roy. Soc.*, **A259**, 257 (1960).
15) M. Szwarc, *J. Chem. Phys.*, **17**, 284 (1949).
16) M. J. Hogsed, U. S. Pat. 2925451 (1960).

* Manufactured by the Siliconit Kōnetsu Kōgyo Co., Ltd.

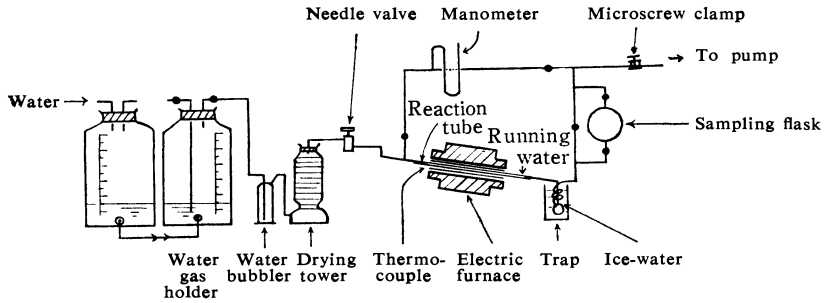


Fig. 1. Apparatus for pyrolysis.

bypass. The gas leaving the flask passed through a microscrew clamp and was continuously pumped out by an oil pump. The reactant-gas feed and the pressure, measured at the entrance of the reaction tube and at the exit of the sampling flask, were regulated to the desired grades by means of the needle valve before the reaction tube and the microscrew clamp.

The temperature was measured by a Pt-Pt·Rh thermocouple tied to the external wall of the reaction tube. The total volume of the reaction tube was measured, and a section, 20 cm. long in furnace I and 7 cm. long in furnace II, was assumed to be heated to the recorded temperature. The volume of the reaction zone, calculated on the basis of the above assumption, was used in the calculation of the contact time by means of the formula:

$$\text{Contact time (sec.)} = V_R/F$$

where V_R = the volume of the reaction zone (ml.)
F = the flow rate of the reactant gas corrected to the temperature and pressure of the reaction zone (ml./sec.)

The pyrolysis was performed under conditions varying over the following wide range: temperature, 800~1400°C; contact time, 4.4×10^{-4}~2.3 sec.; pressure, 50~200 mmHg (partial pressure of propylene, about 40~160 mmHg).

Analysis.—All hydrocarbon products through C_4 were analyzed, using mainly an 11.0-wt.% β,β'-oxydipropionitrile on silica gel column (1.0 or 2.4 m.) at 60°C and a 30-wt.% dioctyl phthalate column (2.4 m.) at room temperature and with hydrogen as the carrier gas. Although the β,β'-oxydipropionitrile-modified silica gel column was found by the present author to give a good separation of air and most of hydrocarbons through C_4 at temperatures below 70°C, the dioctyl phthalate column appeared to be more suitable for the rapid analysis of small quantities of methylacetylene and allene in the pyrolyzed gas. In practice, the latter column was used for the analysis of allene, methylacetylene, the isobutene-1-butene pair, and the 2-butenes-butadiene pair. For the sake of convenience, the overlapped peaks of isobutene-1-butene and 2-butenes-butadiene were adopted as those of 1-butene and butadiene respectively, because in most cases, the amounts of isobutene and 2-butenes formed were negligible (particularly of the former) or, at most, slight. For the quantitative analysis, relative gas volume response factors which had been measured for a series of hydrocarbons for hydrogen were used. The factors (per unit chromatographic peak area, propylene=1.00) used for methylacetylene and allene were 1.07 and 1.10 respectively. Hydrogen was analyzed using the above β,β'-oxydipropionitrile-modified silica gel column and using nitrogen as the carrier gas. In a gas-sampling procedure for gas chromatography, the gas sample of reduced pressure in the sampling flask was introduced into one to five milliliters glass sample tubes using a vacuum system.

In several cases, acetylenic hydrogen of methylacetylene and acetylene was determined chemically by a concentrated silver nitrate solution.[17] The results were in full accord with those of gas chromatography.

Results and Discussion

The conversion of propylene (per cent of propylene pyrolyzed) and the yield of each product (moles per 100 mol. of propylene pyrolyzed) to be given below were obtained by the formulas:

$$\text{Conversion} = \{(a-b\cdot f)/a\}\times 100$$

$$\text{Yield} = \{p\cdot f/(a-b\cdot f)\}\times 100$$

where a, the volume percentage of propylene in the reactant gas; b, the volume percentage of propylene in the pyrolyzed gas; f, the rate of the expansion of the reactant gas by pyrolysis; the ratio of the volume percentage of nitrogen before to that after pyrolysis; and p, the volume percentage of the product.

In the composition of the pyrolyzed gas, the volume percentage was calculated on the basis of gases from hydrogen through C_4 hydrocarbons, though C_5 and higher hydrocarbons were present to a slight degree. Such treatment is possible without distorting the conversion and yield, because they are determined only on the basis of the ratio of each component to nitrogen. Furthermore, since methylacetylene and allene are equilibrated rapidly over catalysts,[3] the total yield was used to evaluate conditions for the synthesis of methylacetylene. In order to examine the hydrogen and carbon balance,

17) L. Barnes, Jr. and L. J. Molinini, *Anal. Chem.*, **27**, 1025 (1955).

TABLE I. PYROLYSIS OF PROPYLENE AT VARIOUS TEMPERATURES

	Pressure, 100 mmHg								
Run No.	17*	97*	95*	22	92*	31	36	70	73
Temp., °C	800	800	900	1000	1000	1100	1200	1300	1400
Contact time, 10^{-3} sec.	1100	1100	92	9.4	11	2.5	1.4	0.83	0.46
Nitrogen content in reactant gas, vol. %	19.9	20.6	20.2	22.4	20.0	20.2	20.2	20.0	20.0
Composition of pyrolyzed gas, vol. %									
Nitrogen	19.2	19.9	19.4	21.6	19.1	19.4	19.3	19.0	19.2
Hydrogen	1.3	1.3	1.4	1.2	1.8	1.6	2.0	1.9	1.8
Methane	4.0	4.0	3.9	3.1	4.2	3.4	3.3	3.6	2.7
Ethylene	3.9	3.9	3.7	2.8	3.9	3.0	3.1	3.4	2.5
Acetylene	0.3	0.3	0.5	0.4	0.7	0.5	0.6	0.8	0.7
Propylene	69.5	68.5	68.0	67.9	66.2	68.7	68.3	67.4	70.1
Allene	0.4	0.5	1.2	1.3	1.9	1.6	1.8	1.9	1.5
Methylacetylene	0.4	0.4	0.9	0.8	1.3	1.0	1.1	1.3	1.0
1-Butene	0.3	0.5	0.5	0.5	0.5	0.5	0.4	0.4	0.3
Butadiene	0.7	0.7	0.5	0.4	0.4	0.3	0.3	0.3	0.2
Rate of expansion	1.039	1.034	1.041	1.039	1.049	1.042	1.047	1.051	1.040
Conversion, %	9.9	10.7	11.2	9.1	13.1	10.3	10.4	11.4	8.8
Yield, mol./100 mol. of propylene pyrolyzed									
Hydrogen	17.1	15.6	16.4	18.0	17.8	20.0	24.9	22.3	26.3
Methane	52.8	48.5	45.4	46.0	42.1	43.3	41.2	41.5	40.5
Ethylene	51.3	48.0	43.9	40.7	38.8	38.1	39.2	39.8	37.4
Acetylene	3.3	3.6	5.6	6.3	6.5	6.5	7.4	8.7	10.7
Allene	5.8	6.0	14.0	18.3	19.4	20.5	22.2	21.9	21.7
Methylacetylene	4.7	4.7	10.9	11.6	12.8	12.3	13.5	14.8	15.0
1-Butene	4.6	5.6	5.5	7.0	5.1	6.1	5.0	5.1	4.6
Butadiene	8.6	8.4	5.7	5.7	4.0	3.3	3.3	3.1	2.8
Total yield of methylacetylene and allene	10.5	10.7	24.9	29.9	32.2	32.8	35.7	36.7	36.7
Percentage of hydrogen and carbon accounted for in gaseous products through C_4 hydrocarbons									
Hydrogen	97.9	93.7	96.5	100.9	94.3	96.4	98.1	98.9	97.7
Carbon	82.1	79.9	88.0	93.5	88.6	89.5	91.6	93.8	92.1

* Furnace I was used.

the percentages of hydrogen and carbon accounted for in gaseous products through C_4 hydrocarbons were calculated from their yields.

Concerning pyrolysis products, no ethane was detected in any experiment, except in those at 200 mmHg pressure, in which a trace of ethane was found. Propane was disregarded, because the reactant gas was contaminated with a small amount (0.4%) of propane and its amount decreased with increasing conversion until it showed only a trace at conversion levels above about 20%. Also, the total of butadiene and 2-butenes, the latter being much smaller than the former, was given as butadiene, as was described in the analytical procedure section.

The Effect of Temperature on Product Yields. —The results obtained in the conversion range from 8 to 14% are shown in Table I and Fig. 2. The yields of both methylacetylene (M-C_3H_4) and allene (A-C_3H_4) increased with an increase in the temperature in the range investigated, from 800 to 1400°C; the total yield [(M+A)-C_3H_4] ranged from 10 mol. at 800°C up to 37 mol. at 1300°C. Although the total yield increased rapidly in the lower part of the temperature range, it was almost constant (36 to 37 mol.) at high temperatures, ranging from 1200 to 1400°C. Thus, a high temperature of 1200 to 1300°C was found to be suitable for the synthesis.

The main products through C_4 hydrocarbons, except for methylacetylene and allene, were methane, ethylene, hydrogen, acetylene, 1-butene, and butadiene. The approximate decreasing order of yield is as just listed. The yields of methane and ethylene, formed in the ratio of about 1 to 1, decreased with an increase in the temperature from about 50 mol. to 40 mol. Contrarily, the yields of hydrogen and acetylene increased regularly with an increase in the temperature, reaching 26 mol. and

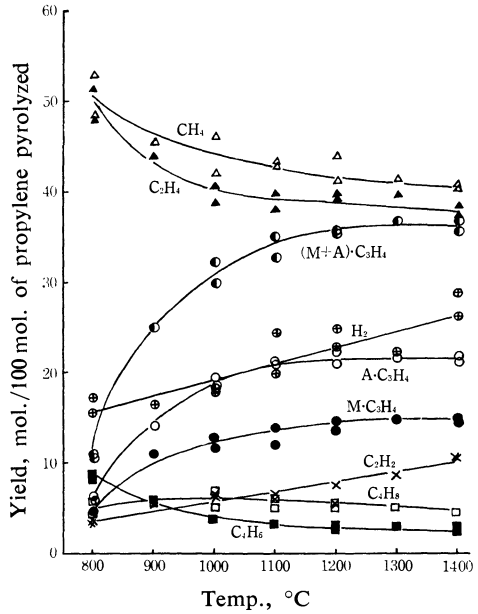


Fig. 2. Effect of temperature on product yields. Conversion, 9 to 14%

10 mol. respectively at 1400°C. The amount of 1-butene was nearly constant at about 5 mol., while that of butadiene fell from 8 mol. at 800°C to 3 mol. at 1400°C.

Some amounts of higher hydrocarbons (C_5 and higher) and coke appeared to be formed. In Table I, the deficiencies of the hydrogen and carbon accounted for in the gaseous products (in hydrogen and in hydrocarbons through C_4) must be explained in terms of the formation of higher hydrocarbons, and of them and coke respectively, when these deficiencies are not due to experimental error. Thus, the

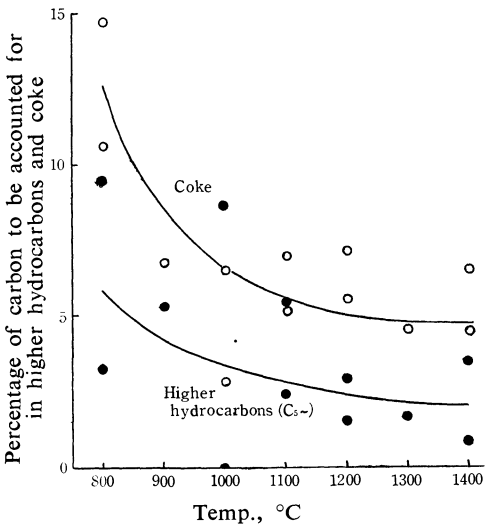


Fig. 3. Estimated amounts of higher hydrocarbons and coke.

percentage of carbon to be accounted for in the higher hydrocarbons and coke (Fig. 3) was derived from the deficiencies of the hydrogen and carbon, on the assumption of an average ratio of carbon to hydrogen of 3:4 in the higher hydrocarbons (probably olefins, cycloolefins, aromatics etc.[14]) formed. On the whole, the estimated amounts (in percentages of carbon) of both higher hydrocarbons and coke, though a part of their values are scattered, fall at a considerable rate with an increase in the temperature.

The Effect of Contact Time (Conversion) on Yields. — The results of the pyrolysis at 100 mmHg pressure and 1200°C, which was a suitable temperature for the synthesis, are shown in Table II (Run No. 36—52) and Fig. 4. The

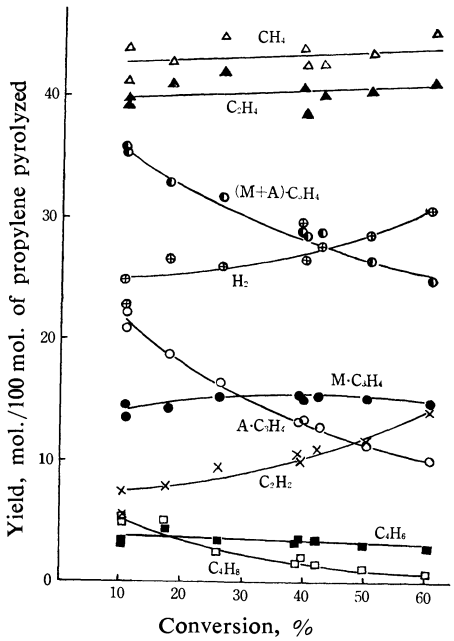


Fig. 4. Effect of contact time (conversion) on product yields. Temp., 1200°C

total yield of methylacetylene and allene decreased with the increasing conversion, ranging from 36 mol. at 10% conversion down to 25 mol. at 60% conversion. In this connection, the yield of allene fell at a considerable rate as the conversion was increased, while that of methylacetylene was fairly constant at 13 to 15 mol. over the wide conversion range studied. Thus, taking account of an equilibrium relation between methylacetylene and allene, it seems probable that methylacetylene is not a primary but a secondary product of the isomerization of allene. On the other hand, the yields (in moles per 100 mol. of entering propylene) of methylacetylene and allene increased with the increasing conversion, being 9 mol.

Table II. Pyrolysis of propylene at various contact times and pressures*

	Temp., 1200°C														
Run No.	87	88	89	81	36	40	47	38	51	52	80	83	82	84	90
Press., mmHg	50	50	50	50	100	100	100	100	100	100	200	200	200	200	200
Contact time, 10^{-3} sec.	1.1	1.7	2.2	2.9	1.4	1.8	2.4	2.7	3.5	4.5	2.6	3.0	3.4	4.4	4.8
Nitrogen content in reactant gas, vol. %	19.8	19.8	19.8	20.0	20.2	19.4	21.0	19.9	21.1	21.1	20.1	20.1	20.1	20.0	19.8
Composition of pyrolyzed gas, vol. %															
Nitrogen	19.0	17.9	17.4	16.1	19.3	17.9	18.7	16.8	17.3	16.4	19.3	18.9	18.5	17.4	17.2
Hydrogen	1.4	4.1	5.4	9.1	2.0	3.4	4.7	7.8	9.3	11.4	1.5	2.5	3.6	6.2	7.6
Methane	2.7	6.9	8.8	13.7	3.3	5.5	8.2	11.6	14.2	16.8	2.9	4.6	6.7	10.2	11.9
Ethylene	2.7	6.8	8.4	12.7	3.1	5.3	7.7	10.8	13.2	15.3	2.8	4.4	6.4	9.7	10.9
Acetylene	0.5	1.5	2.3	4.3	0.6	1.0	1.7	2.8	3.8	5.2	0.6	0.9	1.3	2.1	2.7
Propylene	70.2	55.0	48.5	32.2	68.3	61.4	52.0	41.3	32.2	24.3	70.3	64.7	58.2	47.5	42.9
Allene	1.8	3.7	4.1	4.5	1.8	2.4	3.0	3.5	3.7	3.8	1.3	1.6	2.0	2.5	2.8
Methylacetylene	0.9	2.9	3.7	5.8	1.1	1.9	2.8	4.1	4.9	5.5	0.9	1.5	2.1	2.9	2.6
1-Butene	0.5	0.5	0.6	0.5	0.4	0.6	0.5	0.4	0.4	0.2	0.3	0.4	0.5	0.6	0.5
Butadiene	0.2	0.6	0.8	1.2	0.3	0.6	0.6	0.8	1.0	1.1	0.2	0.5	0.6	0.8	0.9
Rate of expansion	1.040	1.106	1.138	1.242	1.047	1.085	1.124	1.182	1.220	1.288	1.042	1.063	1.089	1.150	1.149
Conversion, %	9.0	24.1	31.2	50.0	10.4	17.4	26.0	39.0	50.2	60.4	8.4	14.0	20.7	31.8	44.2
Yield, mol./100 mol. of propylene pyrolyzed															
Hydrogen	21.0	23.7	24.5	28.2	24.9	26.6	26.0	29.6	28.6	30.8	23.4	23.5	23.9	28.3	28.3
Methane	39.6	39.8	40.2	42.5	41.2	42.9	45.0	44.1	43.7	45.4	44.5	43.5	44.4	46.4	44.3
Ethylene	39.1	39.0	38.2	39.5	39.2	41.1	42.2	40.9	40.6	41.3	43.0	42.1	42.5	44.0	40.5
Acetylene	6.9	8.8	10.6	13.2	7.4	7.9	9.5	10.6	11.7	14.1	9.0	8.6	8.5	9.7	10.0
Allene	26.1	21.1	18.7	14.0	22.2	18.7	16.6	13.3	11.4	10.2	20.1	15.6	13.3	11.2	10.4
Methylacetylene	13.5	16.6	17.0	18.0	13.5	14.3	15.3	15.5	15.2	14.9	14.3	13.9	13.9	13.2	9.6
1-Butene	6.7	3.0	2.6	1.4	5.0	5.0	2.5	1.6	1.1	0.7	5.0	4.0	3.2	2.5	1.7
Butadiene	3.0	3.4	3.5	3.6	3.3	4.3	3.3	3.2	3.1	2.9	3.9	4.5	4.2	3.5	3.5
Total yield of methylacetylene and allene	39.6	37.7	35.7	32.0	35.7	33.0	31.9	28.8	26.6	25.1	34.4	29.4	27.2	24.4	20.0
Percentage of hydrogen and carbon accounted for in gaseous products through C_4 hydrocarbons															
Hydrogen	100.1	95.9	94.7	95.3	98.1	100.5	97.9	94.6	91.9	93.3	102.6	97.6	95.3	96.0	88.4
Carbon	96.4	91.4	89.8	88.0	91.6	92.3	89.1	84.2	81.6	82.0	95.8	89.8	85.9	83.7	75.4

* Furnace II was used.

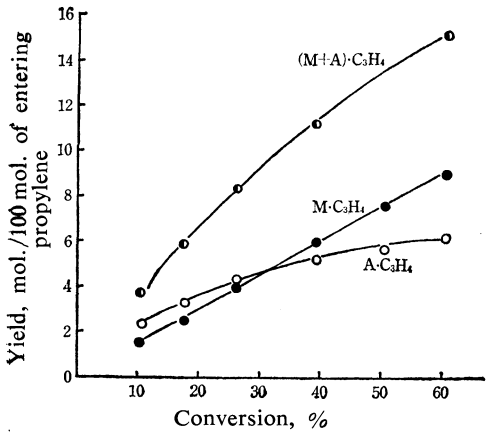


Fig. 5. Variation of yields (in moles per 100 mol. of entering propylene) of methylacetylene and allene with conversion. Temp., 1200°C

and 6 mol. respectively (total 15 mol.) at the highest conversion, 60% (Fig. 5).

The yields of both methane (42~44 mol.) and ethylene (39~41 mol.) hardly varied over the conversion range investigated. The yields of hydrogen and acetylene, however, increased fairly rapidly with the increasing conversion, being 31 mol. and 14 mol. at 60% conversion respectively. In the conversion range, butadiene, formed probably by the secondary decomposition of 1-butene, was obtained in a constant yield of about 3 mol., while the yield of 1-butene decreased with the increasing conversion from 5 mol. to 1 mol. The percentage of hydrogen and carbon accounted for in the gaseous products decreased with an increase in the contact time (conversion). Admittedly, the decrease of hydrogen means that the formation of higher hydrocarbons becomes striking. Furthermore, in view of the results that the yield of methylacetylene-allene, because it is unstable as compared with propylene, decreased fairly rapidly with the increasing contact time, it may be supposed that they react easily with propylene or various radicals, e.g., allyl, to form higher hydrocarbons.

The variations in the yields of methylacetylene and allene, and in the total yield with conversion at 1100°C and 1300°C, in addition to that at 1200°C, are shown in Fig. 6. In the cases of 1100°C and 1300°C, the variation in their yields with conversion was almost the same as that at 1200°C, except that it was somewhat lower at 1100°C.

The Effect of Pressure on Yields.—In addition to the experiments made at 100 mmHg pressure (partial pressure of propylene, about 80 mmHg), a number of experiments were carried out at 50 and 200 mmHg pressure (partial pressure of propylene, about 40 and 160 mmHg respectively). The results are shown in Table II. Also, Fig. 7 shows the effect of pressure on the yields of methylacetylene and allene, as well as the total yields. When yields at fixed conversions are compared, the total yields and also each yields are found to increase with a decrease in the pressure. The differences in the total yields between different pressures were larger at higher conversions. The highest

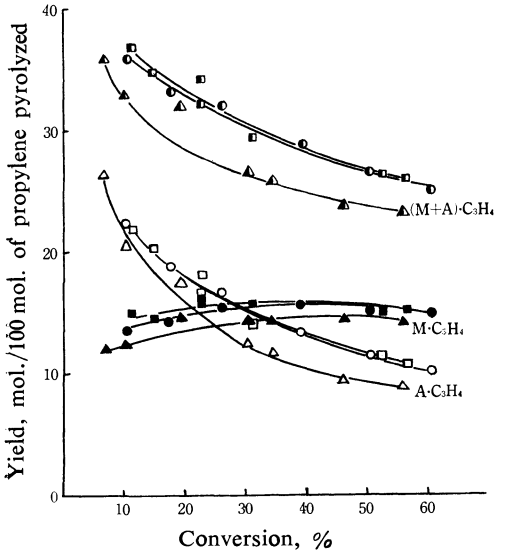


Fig. 6. Variation of yields of methylacetylene and allene with conversion at various temperatures.
Triangles, 1100°C; Circles, 1200°C; Squares, 1300°C

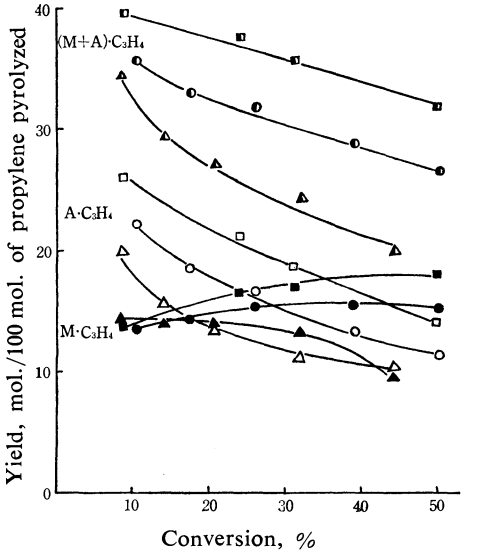


Fig. 7. Effect of pressure on yields of methylacetylene and allene.
Triangles, 200 mmHg; Circles, 100 mmHg; Squares, 50 mmHg.

total yield of 40 mol. was obtained when the pressure (50 mmHg) and the conversion (9.0%) were the lowest studied. It is noticeable that, with 100 mmHg pressure, the yield of methylacetylene is fairly constant over the conversion range, while with 50 mmHg pressure the yield increases with the increasing conversion.

The yields of other gaseous products varied slightly with pressure over the range investigated. Namely, with a decrease in the pressure the yields of methane and ethylene decreased slowly, while reversely, that of acetylene increased. On the other hand, the yields of 1-butene and butadiene almost did not vary at all with the pressure. The percentage of hydrogen and carbon accounted for in the gaseous products increased with the decrease in the pressure from 88% and 75% at 200 mmHg pressure (44% conversion) to 95% and 88% at 50 mmHg pressuse (50% conversion) respectively. On the basis of the above variation in the distribution of pyrolysis products with pressure, it is assumed that the formation of higher hydrocarbons by the additions to propylene of propylene, allene, and methylacetylene (as molecules or radicals derived from them) is diminished as the pyrolysis pressure is decreased, and that, consequently, the yield of methylacetylene-allene is increased.

Summary

Propylene has been pyrolyzed in a flow system over a wide range of conditions (temperature, 800~1400°C; contact time, 4.4×10^{-4} ~2.3 sec.; pressure, 40~160 mmHg) to find suitable conditions for producing methylacetylene (and allene) and for obtaining data concerning the distribution of pyrolysis products. Under proper conditions, the pyrolysis occurred without any appreciable production of tarry and carbonaceous materials. High temperatures (1200~1300°C), short contact times (millisecond order; conversions below 30%), and low pressures (below 100 mmHg) were found to required for the good production of methylacetylene-allene. A methylacetylene-allene yield of 38 mol. per 100 mol. of propylene pyrolyzed was realized at 1200°C, 50 mmHg pressure (partial pressure of propylene, 40 mmHg), and 24% conversion (contact time, 1.7 msec.). The other gaseous products were found to be methane, ethylene, hydrogen, acetylene, 1-butene and butadiene, in decreasing order.

The author wishes to express his thanks to Professor Sango Kunichika of Kyoto University for his helpful advice and kind encouragement throughout this work.

Institute for Chemical Research
Kyoto University
Daigaku-cho, Takatsuki

The Synthesis of Methylacetylene by the Pyrolysis of Propylene. II. The Mechanism of the Pyrolysis[*1]

By Yasumasa SAKAKIBARA

(Received March 23, 1964)

Previously,[1] when the present author investigated the pyrolysis of propylene with the object of finding suitable conditions for the production of methylacetylene-allene,[*2] he found that high temperatures (1200~1300°C), low pressures (below 100 mmHg), and short contact times (conversion below 30%) were required for good results. In this paper the mechanism for the pyrolysis will be reported on.

The distribution of the products of the pyrolysis varies considerably with pyrolysis conditions, and on the basis of observed results several mechanisms have been suggested in recent years. Ingold and Stubbs,[2] investigating the pyrolysis at temperatures from 570 to 650°C and at pressures from 50 to 500 mmHg, proposed a series of molecular

*1 Presented at the 15th Annual meeting of the Chemical Society of Japan, Kyoto, Apil, 1962.

1) Y. Sakakibara, This Bulletin, 37, 1262 (1964).

*2 Both materials are isomeric and are equilibrated over catalysts at 250 to 300°C.

2) K. U. Ingold and F. J. Stubbs, *J. Chem. Soc.*, 1951, 1749.

rearrangement reactions. At higher temperatures, however, it is quite possible that a radical mechanism may predominate. Szwarc,[3] who used higher temperatures (680~870°C), lower pressures (2~15 mmHg), and very low conversions (0.01~2%), found that allene, methane, ethylene, and hydrogen were the main products; he suggested a free-radical chain mechanism for the primary decomposition reaction. Another radical mechanism was proposed by Laidler and Wojciechowski,[4] who reinvestigated the pyrolysis under conditions similar to those used by Ingold and Stubbs and found a considerable amount of higher hydrocarbons but did not detect any allene. The mechanism was partly different from the Szwarc mechanism; namely, a step in the Szwarc method, $CH_2=CH-CH_2\cdot \rightarrow CH_2=C=CH_2 + H$, was replaced by the reaction, $CH_2=CH-CH_3 + CH_2=CH-CH_2\cdot \rightarrow$ higher hydrocarbons + H.

In the present investigation, an effort was made to clarify the mechanism for the pyrolysis at higher temperatures (800~1400°C). Special attention was given to the development of mechanisms for the formation of allene and methylacetylene and for their subsequent decomposition, mechanisms by which we can account for the experimental results. In order to obtain information about secondary reactions involving allene, the pyrolysis of allene itself also was investigated under conditions similar to those of propylene.

Experimental

The Pyrolysis of Propylene. — A large number of experimental results have already been described.[1] The present additional experiments were carried out similarly.

The Pyrolysis of Allene. — The experimental methods were the same as those for propylene.

Allene was prepared by the debromination of 2,3-dibromopropene with zinc.[5] The crude allene was passed through two wash bottles, containing a 10% sodium hydroxide solution and a 3 M silver nitrate solution, and a cooled trap at −20°C, and was then condensed in an ethanol-dry ice trap. It was distilled roughly and stored over a saturated sodium chloride solution in a 25 l. gas holder. Gas chromatographic analysis showed that the purity was about 93 mol. %, the remainder being almost all propylene.

Results and Discussion

The Pyrolysis Products of Propylene. — The primary gaseous products were determined by extrapolating the products to zero conversion (the zero conversion method). With low conversion data obtained at 1100°C and 80 mmHg pressure, the extrapolation was easily treated (Fig. 1). From the figure it may be concluded that hydrogen, methane, ethylene, allene, and 1-butene are the primary products, and that methylacetylene, acetylene, and butadiene are the secondary products. Of the primary products, allene and 1-butene, which are less stable to heat than the original material, would undergo considerable subsequent decomposition, even at low conversion levels, to produce such secondary products as methylacetylene and butadiene respectively.

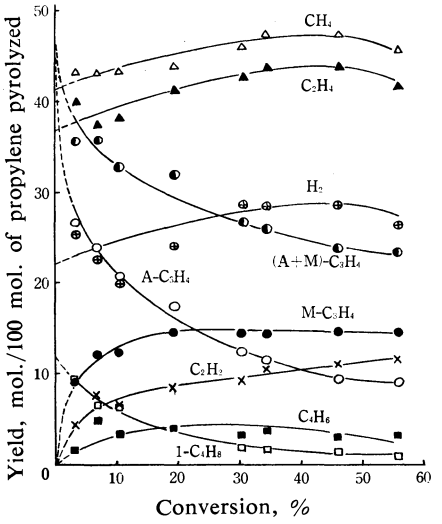


Fig. 1. Extrapolation of gaseous products from propylene to zero conversion (1100°C): A-C_3H_4, allene; M-C_3H_4, methylacetylene.

The formation of acetylene appears to be due to the decomposition of methylacetylene rather than to that of ethylene and methane, particularly at low conversion levels, in view of the results of the pyrolysis of allene described below. The effects of temperature (800~1400°C) and pressure (40~160 mmHg) on the product yield are shown in Tables I and II respectively.

Some higher hydrocarbons (C_5 and higher) and carbonaceous matter appeared to be formed, though they were not identified. Their amounts formed under the present conditions had previously been[1] estimated on the basis of the deficiencies of the percentage of hydrogen and carbon accounted for in the gaseous products (Table I). Laidler and Wojciechowski[4] obtained such liquid products as benzene, cyclopentadiene, cyclohexadiene, etc.

The Pyrolysis of Allene.—The data of the

3) M. Szwarc, *J. Chem. Phys.*, 17, 284 (1949).
4) K. J. Laidler and B. W. Wojciechowski, *Proc. Roy. Soc.*, A259, 257 (1960).
5) A. T. Blomquist and J. A. Verdol, *J. Am. Chem. Soc.*, 78, 109 (1956).

TABLE I. EFFECT OF TEMPERATURE ON YIELD OF PRODUCTS FROM PROPYLENE PYROLYSIS
Composition of reactant gas, propylene 80%+nitrogen 20%; pressure, 100 mmHg

Run No.	97	95	92	31	36	70	73
Temp., °C	800	900	1000	1100	1200	1300	1400
Contact time, 10^{-3} sec.	1100	92	11	2.5	1.4	0.83	0.46
Conversion, %	10.7	11.2	13.1	10.3	10.4	11.4	8.8
Yield, mol./100 mol. of propylene pyrolyzed							
Hydrogen	15.6	16.4	17.8	20.0	24.9	22.3	26.3
Methane	48.5	45.4	42.1	43.3	41.2	41.5	40.5
Ethylene	48.5	43.9	38.8	38.1	39.2	39.8	37.4
Acetylene	3.6	5.6	6.5	6.5	7.4	8.7	10.7
Allene	6.0	14.0	19.4	20.5	22.2	21.9	21.7
Methylacetylene	4.7	10.9	12.8	12.3	13.5	14.8	15.0
1-Butene	5.6	5.5	5.1	6.1	5.0	5.1	4.6
Butadiene	8.4	5.7	4.0	3.3	3.3	3.1	2.8
Total yield of allene and methylacetylene	10.7	24.9	32.2	32.8	35.7	36.7	36.7
Percentage of hydrogen and carbon accounted for in gaseous products through C_4 hydrocarbons							
Hydrogen	93.7	96.5	94.3	96.4	98.1	98.9	97.7
Carbon	79.9	88.0	88.6	89.5	91.6	93.8	92.1

TABLE II. EFFECT OF PRESSURE ON YIELD OF PRODUCTS FROM PROPYLENE PYROLYSIS
Composition of reactant gas, propylene 80%+nitrogen 20%; temp., 1200°C

Run No.	87	89	36	38	80	84
Press., mmHg	50	50	100	100	200	200
Contact time, 10^{-3} sec.	1.1	2.2	1.4	2.7	2.6	4.4
Conversion, %	9.0	31.2	10.4	39.0	8.4	31.8
Yield, mol./100 mol. of propylene pyrolyzed						
Hydrogen	21.0	24.5	24.9	29.6	23.4	28.3
Methane	39.6	40.2	41.2	44.1	44.5	46.4
Ethylene	39.1	38.2	39.2	40.9	43.0	44.0
Acetylene	6.9	10.6	7.4	10.6	9.0	9.7
Allene	26.1	18.7	22.2	13.3	20.1	11.2
Methylacetylene	13.5	17.0	13.5	15.5	14.3	13.2
1-Butene	6.7	2.6	5.0	1.6	5.0	2.5
Butadiene	3.0	3.5	3.3	3.2	3.9	3.5
Total yield of allene and methylacetylene	39.6	35.7	35.7	28.8	34.4	24.4
Percentage of hydrogen and carbon accounted for in gaseous products through C_4 hydrocarbons						
Hydrogen	100.1	94.7	98.1	94.6	102.6	96.0
Carbon	96.4	89.8	91.6	84.2	95.8	83.7

pyrolysis of allene,*3 particularly at high temperatures and low pressures, were necessary for clarifying the mechanisms for the secondary reactions involving allene, in the pyrolysis of propylene. The results of the pyrolysis at temperatures of 800 to 1200°C and at a pressure of about 80 mmHg are shown in Table III. Allene was much less stable than propylene, as is shown by the relative stability of propylene and allene (Table V). At high temperatures, the isomerization to methylacetylene occurred predominantly, though lower temperatures favor polymerization rather than isomerization or decomposition (see footnote *3). Methylacetylene was a main gaseous product; much smaller amounts of hydrogen, methane, ethylene, and acetylene were found, together with a trace of C_4 hydrocarbons. At 800°C, the isomerization of allene

*3 Although a few investigations have been reported, none of them was applied to the conditions under which the pyrolysis of propylene was studied by the present author. Cf. R. N. Meinert and C. D. Hurd, *J. Am. Chem. Soc.*, 52, 4540 (1930); A. T. Blomquist and J. A. Verdol, ibid., 78, 109 (1956).

TABLE III. PYROLYSIS OF ALLENE AT VARIOUS TEMPERATURES*

Pressure, 100 mmHg

Run No.	7	5	8	9	2	13	14	10	11	17	16	19	18
Temp., °C	800	800	800	800	800	1000	1000	1000	1000	1200	1200	1200	1200
Contact time, 10^{-3} sec.	88	120	200	320	930	3.3	4.4	8.0	16	0.40	0.53	0.81	1.3
Composition of reactant gas, vol. %													
Nitrogen	19.5	20.9	19.6	19.6	19.9	19.9	19.1	19.7	19.7	20.5	20.5	20.5	20.5
Allene	74.0	74.3	73.9	73.9	75.5	73.5	74.4	73.8	73.8	74.0	74.0	74.0	74.0
Propylene	6.5	4.8	6.5	6.5	4.6	6.6	6.5	6.5	6.5	5.5	5.5	5.5	5.5
Composition of pyrolyzed gas, vol. %													
Nitrogen	20.1	23.2	22.5	22.9	23.4	20.2	19.6	20.4	21.1	20.6	20.8	20.8	20.5
Hydrogen	0.4	1.6	4.8	6.3	13.1	0.2	0.7	1.8	4.9	0.3	1.1	3.7	6.3
Methane	0.3	1.7	6.4	9.1	20.4	0.2	0.6	2.0	6.6	0.2	0.8	3.8	6.6
Ethylene	1.0	2.4	4.5	5.5	8.0	0.4	0.7	1.5	2.8	0.4	0.6	1.3	2.0
Acetylene	0.1	0.7	2.6	3.9	8.1	0.1	0.3	1.3	4.7	0.1	0.6	3.6	6.9
Propylene	7.2	6.0	7.6	7.6	3.4	6.9	7.1	6.5	5.7	5.5	5.4	4.6	3.7
Allene	61.7	45.0	21.3	14.4	2.6	64.5	54.6	33.7	15.7	63.3	47.7	24.1	16.0
Methylacetylene	6.9	14.4	20.9	20.3	7.1	7.3	15.7	28.1	30.0	9.3	22.2	35.3	31.1
1-Butene (+Isobutene)	0.0	0.2	0.4	0.4	0.1	0.0	0.0	0.1	0.0	0.0	0.0	0.0	0.0
Butadiene (+2-Butene)	0.0	0.0	0.3	0.3	0.4	0.0	0.0	0.1	0.4	0.0	0.0	0.3	0.6
Volume ratio of methylacetylene/allene	0.11	0.32	0.98	1.41	2.73	0.11	0.29	0.84	1.91	0.15	0.47	1.47	1.94
Rate of expansion	0.970	0.903	0.871	0.856	0.851	0.984	0.975	0.970	0.935	0.996	0.989	0.985	1.002
Conversion, %	19.1	45.4	75.0	83.4	97.1	13.7	28.4	55.9	80.2	14.5	36.4	68.0	78.2
Yield, mol./100 mol. of allene pyrolyzed													
Hydrogen	2.6	4.3	7.5	8.8	15.2	2.0	3.0	4.3	7.7	2.7	4.1	7.3	10.9
Methane	2.2	4.5	10.1	12.7	23.7	1.9	2.6	4.8	10.4	1.9	3.1	7.5	11.4
Ethylene	7.2	6.4	7.1	7.6	9.3	3.5	3.3	3.5	4.5	3.3	2.4	2.6	3.4
Acetylene	1.0	1.9	4.1	5.4	9.4	0.6	1.5	3.0	7.5	1.0	2.3	7.0	11.9
Propylene**	3.2	1.8	0.2	0.0	(−2.3)	2.0	1.9	(−0.5)	(−2.0)	0.0	(−0.7)	(−2.0)	(−3.1)
Methylacetylene	47.1	38.4	32.9	28.2	8.3	71.5	72.4	66.2	47.3	86.6	81.6	69.0	53.8
1-Butene (+Isobutene)	0.0	0.5	0.6	0.6	0.1	0.0	0.0	0.3	0.1	0.0	0.0	0.0	0.0
Butadiene (+2-Butene)	0.0	0.0	0.4	0.4	0.4	0.0	0.0	0.2	0.6	0.0	0.0	0.5	1.0
Percentage of hydrogen and carbon accounted for in gaseous products through C_4 hydrocarbons													
Hydrogen	63.1	56.1	58.0	57.4	52.6	81.2	83.4	78.5	68.9	93.7	89.5	84.5	78.0
Carbon	56.5	47.9	45.3	42.4	28.6	76.9	78.4	72.5	58.6	90.1	85.3	77.0	67.1

* Furnace I was used for Run Nos. 2—9 and furnace II for the others (See Ref. 1).

** The values were calculated in taking account of the amount of propylene contained in the reactant gas. The minus values shown in parentheses mean that propylene was pyrolyzed in the ratio of these values to 100 mol. of allene pyrolyzed.

to methylacetylene was incomplete. Judging from the low percentages of hydrogen and carbon accounted for in the gaseous products, considerable amounts of polymerized products appeared to be formed. On the other hand, at 1200°C and low conversion levels, other reactions than isomerization were considerably suppressed and the isomerization was performed efficiently. With increasing contact time (conversion), the yields of methylacetylene decreased rapidly. The methylacetylene/allene ratio, however, slowly approached the value of a theoretically calculated equilibrium constant for the allene $\rightleftarrows$ methylacetylene isomerization as was to be expected from the equilibrium relation (Table IV).

TABLE IV. EQUILIBRIUM CONSTANT FOR THE ISOMERIZATION OF ALLENE*
(CH_2=C=CH_2 $\rightleftarrows$ CH_3-C≡CH)

Temp., °K	800	1000	1200	1400	1500
$K_p=\frac{[CH_3\text{-}C\equiv CH]}{[CH_2=C=CH_2]}$	4.53	3.75	3.15	2.94	2.77

* The values were calculated on the basis of the $\Delta G°/T$ given in "Landolt-Börnstein Zahlenwerte und Funktionen" (6 Aufl. II Bd. 4 Teil, 453 (1961)); see also J. F. Cordes and H. Günzler, *Chem. Ber.*, **92**, 1055 (1959).

The main gaseous products other than methylacetylene, though they were found in much smaller quantities than those of methylacetylene, varied remarkably with the temperature and the rate of conversion. Figures 2 and 3 show the distribution of main gaseous products, exclusive of methylacetylene, and the methylacetylene/allene ratio at 800 and 1200°C. The conversion and yield described in these figures were those calculated by regarding both allene and its isomerization product, methylacetylene, as unreacted allene. The results of the zero conversion method suggest that ethylene is the primary product (Figs. 2 and 3).

This is supported also by the fact that, at both 800 and 1200°C, the yield of ethylene decreased with the increase in the methylacetylene/allene ratio which resulted from the isomerization of allene. Furthermore, it is reasonable that the decrease was rapid in the case of 1200°C, at which temperature the ratio increased rapidly with the increasing conversion. Hydrogen also appears to be a primary product. On the other hand, methane and acetylene are the secondary products, as determined by the zero conversion method. In the case of 1200°C, it should be noted that the yields of methane and acetylene were about the same, and that they increased rapidly with the increase in the methylacetylene/allene ratio. From these facts, it may be concluded that methane and acetylene are the decomposition products of methylacetylene, which is itself the isomerization product of allene.

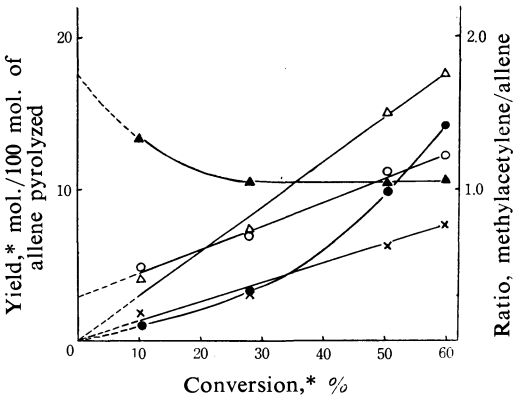


Fig. 2. Yields of main gaseous products (exclusive of methylacetylene) from allene pyrolysis at 800°C: ○, hydrogen; △, methane; ×, acetylene; ▲, ethylene; ●, methylacetylene/allene ratio.
* These values were calculated by regarding both allene and its isomerization product, methylacetylene, as unreacted allene.

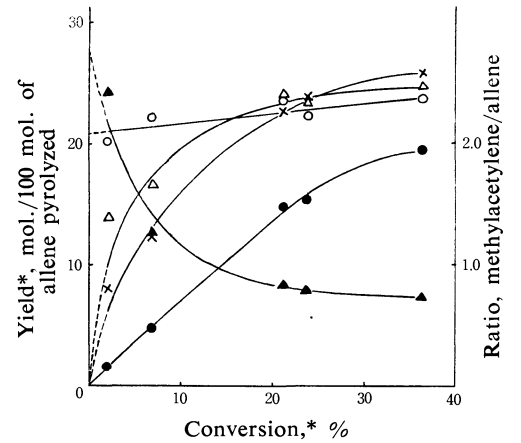


Fig. 3. Yields of main gaseous products (exclusive of methylacetylene) from allene pyrolysis at 1200°C: ○, hydrogen; △, methane; ×, acetylene; ▲, ethylene; ●, methylacetylene/allene ratio.
* See footnote* to Fig. 2.

Mechanism.—On the basis of the experimental results, a mechanism for the pyrolysis of propylene may be proposed. This mechanism may be developed by observing the following restrictions. Even at low conversions, secondary reactions involving such unstable products as allene and methylacetylene are considered to be important and are thus included. However, secondary reactions involving stable

TABLE V. RELATIVE STABILITY OF PROPYLENE AND ALLENE

Temp., °C	800	1000	1200	1200
Conversion, %	20	20	20	40
Contact time,* sec.				
Propylene	2.1	1.3×10^{-2}	1.9×10^{-3}	3.0×10^{-3}
Allene**	8.9×10^{-2}	3.7×10^{-3}	4.4×10^{-4}	5.5×10^{-4}
	(0.10)	(8.2×10^{-3})	(8.1×10^{-4})	(1.5×10^{-3})
Ratio of contact time, propylene/allene	24	3.5	4.3	5.5
	(21)	(1.6)	(2.4)	(2.0)

* Contact times for fixed conversions were obtained from the curves of the contact time vs. the conversion.

** The values shown in parentheses are those of cases in which conversion was calculated by regarding both allene and its isomerization product, methylacetylene, as unreacted allene.

pyrolysis products are disregarded. The order of the decreasing stability of methane and light olefins is as follows: methane>ethylene >propylene>2-butene> 1-butene > isobutene.[6] Judging from the relative stability of propylene and allene, it may be said that allene is much less stable than propylene, especially at the lower temperatures investigated (Table V).

Although higher hydrocarbons (C_5 and higher) formed in the pyrolysis would readily undergo subsequent decomposition, these reactions are disregarded.

With the above restrictions in mind, the following mechanism was developed:

Primary reactions

$$CH_2{=}CH{-}CH_3 \rightarrow CH_2{=}CH{-}CH_2\cdot + H \quad (1)$$

$$CH_2{=}CH{-}CH_3 + H \rightarrow CH_2{=}CH{-}CH_2\cdot + H_2 \quad (2)$$

$$CH_2{=}CH{-}CH_3 + H \rightarrow CH_3{-}CH_2{-}CH_2{}^*\cdot \quad (3)$$

$$CH_3{-}CH_2{-}CH_2{}^*\cdot \rightarrow C_2H_4 + CH_3\cdot \quad (4)$$

$$CH_2{=}CH{-}CH_3 + CH_3\cdot \rightarrow CH_2{=}CH{-}CH_2\cdot + CH_4 \quad (5)$$

$$CH_2{=}CH{-}CH_3 + CH_2{=}CH{-}CH_2\cdot \rightarrow \text{higher hydrocarbons(HHC)(A)} + H(CH_3\cdot) \quad (6)$$

$$CH_2{=}CH{-}CH_2\cdot \rightarrow CH_2{=}C{=}CH_2 + H \quad (7)$$

$$CH_2{=}CH{-}CH_2\cdot + H \rightarrow CH_2{=}CH{-}CH_3 \quad (8)$$

$$CH_2{=}CH{-}CH_2\cdot + CH_3\cdot \rightarrow CH_2{=}CH{-}CH_2{-}CH_3 \quad (9)$$

Secondary reactions involving allene and methylacetylene

$$CH_2{=}C{=}CH_2 \rightleftarrows \begin{matrix} CH_2{=}C{=}CH\cdot \\ \updownarrow \\ \cdot CH_2{-}C{\equiv}CH \end{matrix} + H \rightleftarrows CH_3{-}C{\equiv}CH \quad (10)$$

$$CH_2{=}C{=}CH_2 + CH_2{=}CH{-}CH_2\cdot \rightarrow \text{HHC(B)} + H \quad (11)$$

$$CH_2{=}C{=}CH\cdot \leftrightarrow \cdot CH_2{-}C{\equiv}CH$$

$$+ CH_2{=}CH{-}CH_3 \rightarrow \text{HHC(C)} + H \quad (12)$$

$$CH{\equiv}C{-}CH_3 + CH_2{=}CH{-}CH_2\cdot \rightarrow \text{HHC(D)} + H \quad (13)$$

$$CH{\equiv}C{-}CH_3 + H \rightarrow C_2H_2 + CH_3\cdot \quad (14)$$

involving 1-butene

$$CH_2{=}CH{-}CH_2{-}CH_3 \xrightarrow{\text{(or by radicals R)}} CH_2{=}CH{-}\dot{C}H{-}CH_3 + H(RH) \quad (15)$$

$$CH_2{=}CH{-}\dot{C}H{-}CH_3 \rightarrow CH_2{=}CH{-}CH{=}CH_2 + H \quad (16)$$

(The asterisks indicate a hot radical which decomposes easily into C_2H_4 and $CH_3\cdot$.)

The known frequency factors and activation energies for the elementary reactions 1 to 9 are shown in Table VI. Those shown in parentheses are less certain values assumed by Laidler and Wojciechowski,[4] and by Amano and Uchiyama.[7]

In this mechanism, part of the primary decomposition reaction (reacitons 1–9) is a

TABLE VI. KINETIC PARAMETERS (AT 1000°K) FOR ELEMENTARY REACTIONS*

Reaction	Frequency factor sec^{-1} or l./mol. sec.	Activation energy kcal./mol.
(1)	(10^{15})	79
(2)	$10^{10.1}$	1.5
(3)	$10^{10.5}$	1.5
(4)	$10^{13.4}$	30.4
(5)	$10^{7.8}$	7.7
(6)	(10^{6})	(15)
(7)	$(10^{13.6})$	(70)
(8)	(10^{9})	(0)
(9)	(10^{8})	(0)

* For the source of these values, see Ref. 7.

6) a) H. Tropsch, C. I. Parrish and G. Egloff, *Ind. Eng. Chem.*, **28**, 581 (1936); b) H. Tropsch and G. Egloff, ibid., **27**, 1063 (1935).

7) A. Amano and M. Uchiyama, *J. Phys. Chem.*, **67**, 1242 (1963).

chain process. Reaction 1 is the chain initiation, reactions 2-6, 2-7, 3-4-5-6, and 3-4-5-7 are four chain propagation processes, and, finally, reactions 8 and 9 are the chain termination. Reactions 10 to 16 are the main secondary reactions, chiefly involving allene and methylacetylene.

The compatibility of the proposed mechanism with the observed experimental data can now be examined.

Products and Processes of Formation.—All the primary gaseous products, hydrogen, ethylene, methane, allene, and 1-butene, are formed by reactions 2, 4, 5, 7, and 9 respectively. Reaction 6, proposed by Laidler and Wojciechowski[4] for the formation of higher hydrocarbons, is also included in this mechanism, because considerable amounts of higher hydrocarbons appeared to be formed at the lower part of the temperature range investigated. In reaction 6, instead of hydrogen atoms, the splitting of methyl radicals would also be possible in view of the fact that C_5 olefins, such as cyclopentene,[8] cyclopentadiene,[4] and pentadiene,[9] were formed in the early stage of the pyrolysis of propylene or in that of the reaction of allyl radicals with propylene. Reaction 9 is included as a termination reaction in addition to reaction 8, though Szwarc,[3] and Laidler and Wojciechowski[4] adopted only reaction 8. This is a result of the fact that 1-butene was obtained as the primary product and the observation by Dominey and Danby[9] that the formation of butyl radicals by the addition of methyl radicals to propylene occurred only at temperatures below 400°C. In addition, it has been shown, most recently by Amano and Uchiyama,[7] that in the reaction $CH_3\cdot + C_3H_6 \rightarrow$ butyl, the equilibrium ratio of [methyl]/[butyl] is 10^3 at 1000°K by calculation from thermodynamic data; therefore, the reverse reaction is faster.

Of secondary reactions, those involving allene and methylacetylene may be presumed to be predominant in view of the relative stability of propylene and allene (Table V). Allene isomerizes to methylacetylene according to reaction 10, and the allene/methylacetylene ratio approaches the equilibrium constant. It has been shown by Collin and Lossing[10] that the loss of a H atom from allene results in the formation of a C_3H_3 radical which has a propagyl rather than an allenyl configuration and that the $CH{\equiv}C{-}CH_2\cdot$ and $\cdot CH{=}C{=}CH_2$ forms are probably resonance hybrids. Furthermore, they have presented the bond dissociation energies of 82.8 kcal./mol. for $CH{\equiv}C{-}CH_2{-}H$ and 81.2 kcal./mol. for $CH_2{=}C{=}CH{-}H$. The formation of higher hydrocarbons from allene and methylacetylene, which would clearly be responsible for the loss of allene—methylacetylene, may be ascribed to the reactions with allyl radicals (reactions 11 and 13) as in the case of propylene and to the reaction of propagyl radicals, produced from allene and methylacetylene, with propylene (reaction 12). Acetylene is probably produced by the reaction of methylacetylene with hydrogen atoms (reaction 14), in view of the experimental data of the pyrolysis of allene (Fig. 2 and 3). Considering the relative stability of ethylene and propylene,[6a] another process for the production of acetylene, the dehydrogenation of ethylene, appears to be less important in the early stage of the pyrolysis of propylene. Butadiene is probably produced by the dehydrogenation of 1-(and 2-)butene (reactions 15 and 16).

The Rates of the Formation of Products and Yields.—According to this mechanism, whenever an ethylene molecule is produced by reaction 4 a methyl radical is formed; this radical may give rise to a methane molecule by reaction 5 or, in a lesser degree, a 1-butene molecule by reaction 9. Therefore, the ethylene/(methane+1-butene) ratio must be 1:1. The experimental data seem to confirm this 1:1 ratio, considering that some amounts of methane are produced also from the methyl radicals formed by reaction 6 and by secondary reaction 14 (Fig. 1 and Table I).

The hydrogen/ethylene ratio should be independent of the pressure of propylene, since reactions 2 and 3, the latter followed by reaction 4 leading to the formation of ethylene, are the same reaction of propylene with hydrogen atoms. This is consistent with the experimental data (Table II). On the other hand, since the activation energies for both reaction processes are small (both 1.5 kcal./mol.), the hydrogen/ethylene ratio should be nearly independent of the temperature. The experimental data seem to confirm this requirement, and the experimental ratios are in fairly good agreement with the values (about 0.4) calculated from kinetic parameters (Table I).

Inspections were also made of allene and methylacetylene, whose production is an important object of this series of investigations. According to this mechanism, allyl radicals, which give allene by the elimination of a hydrogen atom, are produced by reactions 2

8) W. A. Bryce and D. J. Ruzicka, *Can. J. Chem.*, **38**, 835 (1960).
9) D. A. Dominey and C. J. Danby, *J. Chem. Soc.*, **1962**, 4656.
10) J. Collin and F. P. Lossing, *Can. J. Chem.*, **35**, 778 (1957).

and 5, together with reaction 1. The allyl radicals disappear in any one of four reaction processes, 6, 7, 8, and 9. Of these processes, the last two, which are the chain-terminating reactions, are disregarded if the chain is long. In fact, however, it appears to be very short in view of the amount of 1-butene and the chain length estimated by Szwarc.[3]

First, the rates of the formation of higher hydrocarbons by reaction 6 (v_6) and of allene by reaction 7 (v_7) will be compared. Table VII shows the v_6/v_7 ratio, at various temperatures and at a 80 mmHg pressure, as calculated on the basis of the kinetic parameters shown in Table VI. From the calculated values, it follows that at 900°C the rate of reaction 7 is more rapid than that of reaction 6 and that reaction 6 may be practically disregarded above 1000°C.

TABLE VII. RATIO OF THE RATES OF REACTIONS 6 AND 7

$$\frac{v_6}{v_7}=\frac{k_6}{k_7}[C_3H_6]=10^{-7.6}e^{\frac{55000}{RT}}\times\frac{1.28}{T}$$

Temp., °C	800	900	1000	1100
v_6/v_7	5.0	0.40	0.062	0.013

Next, assuming that the chain reaction is terminated only by reaction 9, it can be shown via the steady-state approximation method, that the yield (in moles per 100 mol. of propylene pyrolyzed) of allene is calculated by the following equation:

$$\text{Yield of allene}=\frac{L(1+C_1)}{(L+1)(2+C_1)(1+C_2)+LC_2(1+C_1)}\times 100$$

where L=chain length
C_1=ratio of rates of reactions 2 and 3, v_2/v_3
C_2=ratio of rates of reactions 6 and 7, v_6/v_7

Figure 4 compares the experimental yields of allene-methylacetylene (in 9~13% conversion) and the calculated yields of allene at various temperatures. The calculated values are those obtained by assuming that $L=5$, $C_1=0.50$, and $C_2=$ the values shown in Table VII. The results of the calculation (calculated yields I) show that the temperature has a remarkable effect on the yield of allene, as was observed in the experiments (Table I), and that high temperatures are suitable for the production of allene. Furthermore, considering that the values of kinetic parameters for elementary reactions 6 and 7 are uncertain and that allene undergoes secondary reactions readily, the experimental yields are in fair agreement with the calculated ones. The experimental yields however, can reasonably be accounted for on the basis of the yields of allene calculated by assuming $E_7-E_6=50$ kcal./mol., which is lower by 5 kcal./mol. than the value estimated by Laidler-Wojciechowski.[4] The second calculated yields (calculated yields II) are shown in Fig. 4 to be comparable with the experimental

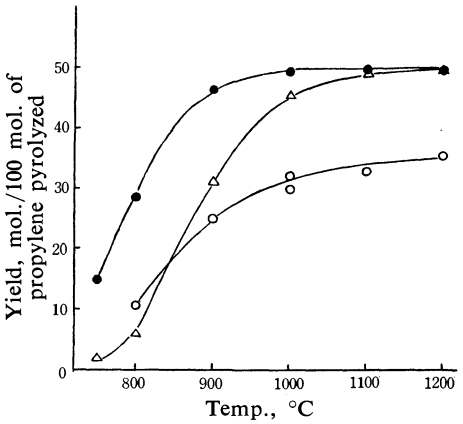


Fig. 4. A comparison of the experimental yields of allene-methylacetylene and the calculated yields of allene: ○, experimental yields; △, calculated yields I; ●, calculated yields II.

yields of allene-methylacetylene. The experimental values are considerably lower than the calculated ones. This may be supposed to be due to the loss of allene-methylacetylene by secondary reactions, probably by reactions 10 to 14, which proceed considerably even at low conversion levels. Furthermore, judging from the fact that the stability of allene-methylacetylene approaches that of propylene fairly rapidly with the increase in the temperature (Table V), it may be concluded that the degree of the loss by secondary reactions decreases with the increasing temperature and that, therefore, at high temperatures, for example, at 1100°C, allene-methylacetylene is obtained in yields comparatively close to the calculated yields.

The rapid decrease in the yield of allene-methylacetylene with the increase in conversion may be supposed to be due to the loss of allene, methylacetylene, and propylene, probably by various secondary reactions involving reactions 10 to 14. The variation in the methylacetylene/allene ratio with conversion can be accounted for by the equilibrium relation between the two. Namely, the experimental ratio (1.6 at 56% conversion) approached the calculated equilibrium constant (3.0 at 1100°C) with the increasing conversion (Fig. 1).

The decrease in the pressure of propylene

suppresses secondary reactions 11 to 14, by which means allene, methylacetylene, and propylene are lost; moreover, reaction 6 leads to the formation of higher hydrocarbons. Therefore, it may be expected that low pressures give better yields of allene-methylacetylene. The experimental data seem to confirm this (Table II).

Summary

A study has been made of the mechanism of the pyrolysis of propylene at high temperatures (800~1400°C). Of the gaseous products, hydrogen, methane, ethylene, allene, and 1-butene, obtained in the yields of 25, 43, 40, 27, and 9 mol. per 100 mol. of propylene pyrolyzed (3% conversion) respectively, have been found to be the primary products, while methylacetylene, acetylene, and butadiene, obtained in the yields of 9, 4, and 2 mol. respectively, have been found to be the secondary products. In view of the results of the pyrolysis of allene itself, even at a low conversion of 3%, allene appears to undergo considerable secondary reactions, such as isomerization to methylacetylene, addition to propylene and allyl radicals, and decomposition, for example, to acetylene and methane via methylacetylene. On the basis of the observed results, free-radical mechanisms have been proposed for the primary reactions and main secondary reactions. The mechanism for the primary decomposition reaction is a chain process in which the chain is initiated by the reaction $C_3H_6 \rightarrow C_3H_5\cdot$ (allyl radical) + H, and is, via the chain-propagating step, terminated by two types of reactions, $C_3H_5\cdot + H \rightarrow C_3H_6$ and $C_3H_5\cdot + CH_3\cdot \rightarrow 1\text{-}C_4H_8$. The formation of allene-methylacetylene has been satisfactorily explained by considering secondary reactions.

The author wishes to express his thanks to Professor Sango Kunichika of Kyoto University for his helpful advice and kind encouragement throughout this work.

Institute for Chemical Research
Kyoto University
Daigaku-cho, Takatsuki

The Separation of Potassium by Solvent Extraction

By Tadashi IWACHIDO and Kyoji TÔEI

(Received February 12, 1964)

Very few investigations of the solvent extraction of potassium have been made because potassium is highly ionic and so it is difficult to extract it by an ordinary solvent immiscible with water. This paper will describe the extraction of the potassium ion in an aqueous solution by nitrobenzene. The potassium ion is extracted in the form of potassium dipicrylaminate (DPA-K) and is stripped from the nitrobenzene layer by shaking it with a hydrochloric acid solution. The potassium ion is then determined gravimetrically with sodium tetraphenylborate (TPB-Na).

Experimental and Discussion

Reagents.—A dipicrylaminate aqueous solution, 0.1 M, was made by dissolving Hexyl Natrium (Mitsubishi Kasei Co., Ltd.) in water, while a 0.05 M dipicrylaminate nitrobenzene solution was prepared by dissolving Hexyl Natrium in nitrobenzene. The potassium chloride and the other reagents were of the analytical grade.

Organic Solvent. — To find out a suitable solvent, one immiscible with water and one which extracts potassium dipicrylaminate from an aqueous solution, the following solvents were tested: nitrobenzene, cyclohexanone, butylacetate and *o*-nitrotoluene. Among these solvents, nitrobenzene was best in extractability, and so it was used in all the extraction procedures.

Extraction. — As is shown in Fig. 1, two procedures were used in this experiment:

Procedure 1: The extraction by nitrobenzene from a solution containing deposited crystals of DPA-K formed by adding the reagent aqueous solution.

Procedure 2: The extraction from a solution containing potassium by adding the reagent nirobenzene solution which is almost saturated

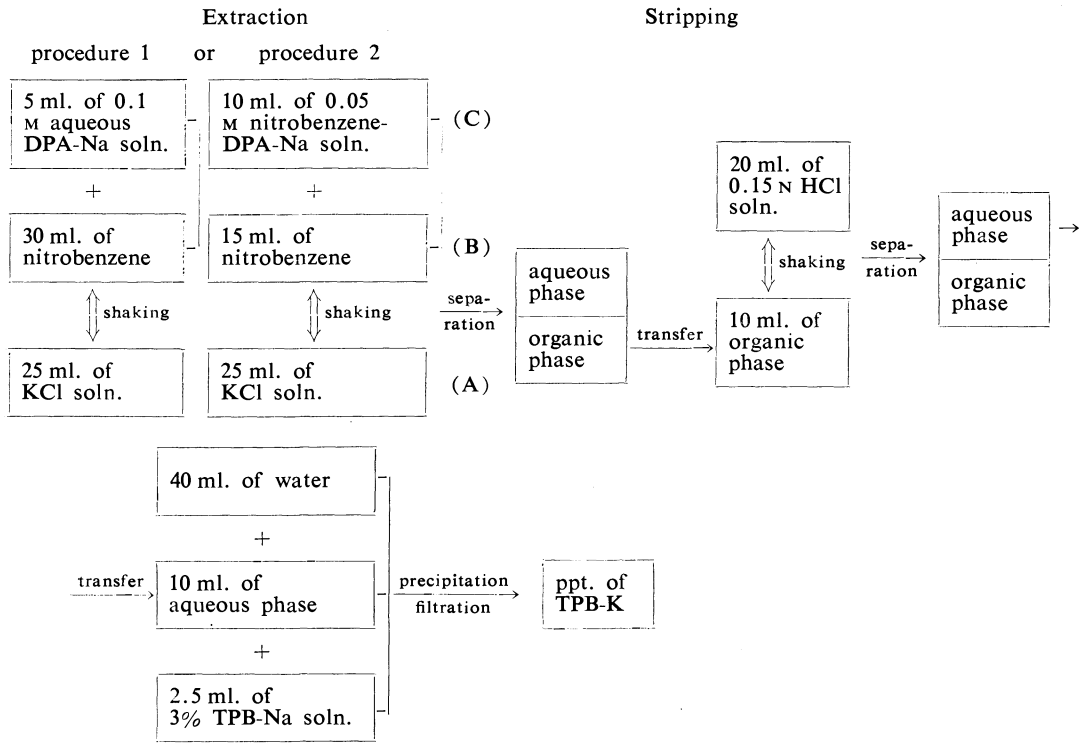


Fig. 1. Scheme of standard procedure.

with DPA-Na (0.05 M).

The molarity of the reagent was kept twice that of potassium throughout this experiment; the concentration of potassium chloride was also kept constant at 0.01023 M, corresponding to the potassium concentration of sea water.

Twenty-five milliliters of an aqueous potassium chloride solution were pipetted into a 100-ml. separatory funnel. In procedure 1, adequate amounts of the reagent aqueous solution and nitrobenzene were added to the potassium solution, or in procedure 2, the reagent nitrobenzene solution and nitrobenzene were added to the solution. After having been shaken for one or two minutes, this solution was allowed to stand overnight in order to separate it completely into two layers. The nitrobenzene solution was drained into a 100-ml. beaker.

Stripping Procedure.—Ten milliliters of the organic phase containing potassium dipicrylaminate was again pipetted into a 100-ml. separatory funnel, and then 20 ml. of 0.15 N hydrochloric acid were added. The two solutions were mixed well by shaking them until the color of the organic phase turned from orange-red to yellow. After the mixture had been allowed to stand for 2 hr., 10 ml. of the colorless aqueous solution was transferred into a 100-ml. beaker.

The Determination of the Potassium.[1]—The aqueous solution was diluted to 50 ml. with water, and then a 3 per cent solution of sodium tetraphenylborate (Kalibor, Dojindo & Co., Ltd.) was added drop by drop, with a gentle swirling. After the solution had cooled for 20 to 30 min. in a refrigerator, the precipitate was filtered through a No. 4 or 5 porosity glass filter, washed well with distilled water, and dried at 125°C for 1 hr. This was cooled in a desiccator and weighed. The precipitate was dissolved in acetone in Soxhlet's apparatus. The amount of potassium was calculated from the loss of weight. All the procedures are shown schematically in Fig. 1.

After 25 ml. of a potassium chloride solution (0.01023 M) had been shaken with the same volume of nitrobenzene, the amount of potassium was determined gravimetrically by means of the above method. The weight of TPB-K was always 0.8 mg. smaller than the calculated value. This negative error is due to the very small amount of TPB-K in a dilute solution (ca. 40 mg./50 ml.).[2]

Extractability. — The extractability, E, was calculated from the following equation, taking the above correction into consideration:

1) K. Tamaoku, *J. Japanese Chem.* (*Kagaku-no-Ryoiki*), 17, 39 (1963).
2) K. Sporek and A. F. Williams, *Analyst*, 80, 347 (1955).

$$E=D/(D+V_a/V_o)$$

where D is the distribution ratio, and V_o and V_a are the volumes of the organic and the aqueous layers respectively.

The Effect of the Volume Ratio, V_o/V_a.—Procedures 1 and 2 were compared in extractability under various volume ratios (Fig. 2).

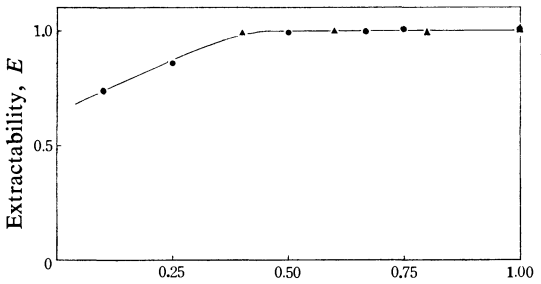


Fig. 2. Dependence of the volume ratios of organic to aqueous phase on extractability.
Sample: 0.01023 M KCl soln.
Procedure:
procedure 1 ($V_o/V_a=1.00$, (A)=25.0 ml.; $V_o/V_a=0.75\sim0.25$, (A)=50.0 ml.): ●
procedure 2 ($V_o/V_a=1.00\sim0.60$, (A)=25.0 ml.; $V_o/V_a=0.40$, (A)=50.0 ml.): ▲

Figure 2 shows that there is no appreciable difference between the two procedures; moreover, in the range of $V_o/V_a>0.5$, the extraction is almost perfect. In the range of $V_o/V_a<0.5$, however, somewhat lower values were obtained.

The Effect of pH. — Sodium in sodium dipicrylaminate will be displaced by hydrogen rather than by potassium in an acidic solution, so the experiment was carried out in a neutral or alkaline solution. The desired basicity was obtained by adding a small amount of a sodium hydroxide solution; the concentration of potassium was kept constant at 0.01023 M. The extractability decreased with the increase in pH, as is shown in Fig. 3. From the results, it must be concluded that the extraction is best in a neutral solution.

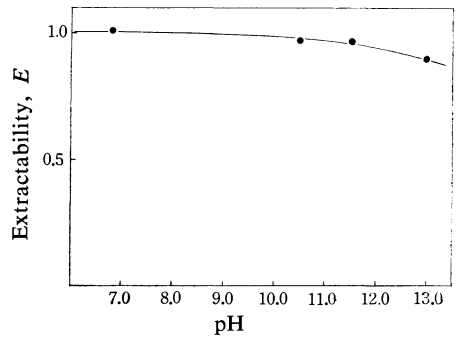


Fig. 3. Effect of pH.
Sample: 0.01023 M KCl soln. (+NaOH)
Procedure: standard procedure 1

The Effect Sodium Ions.—When an aqueous solution containing only potassium chloride was extracted by the reagent nitrobenzene solution, no turbidity was found in the organic phase, but in the presence of both sodium and potassium ions in a solution, the organic phase was turbid, even after standing overnight. In order to eliminate this turbidity, the solution was filtered through a dry filter paper or centrifuged at 2000 r. p. m. for 10 min. These two methods were compared in extractability by varying the time of standing in the stripping procedure. In these experiments, it was found that the extractability does not depend upon the stripping time; moreover, no significant difference between these two procedures was observed.

From Table I and Fig. 4, it is clear that the extractability decreases with the increase in the ratio of sodium to potassium ions, and that, thus, the co-existence of sodium hydroxide should similarly decrease the extractability (Fig. 3). The turbidity in the organic phase increases with the quantity of sodium ions.

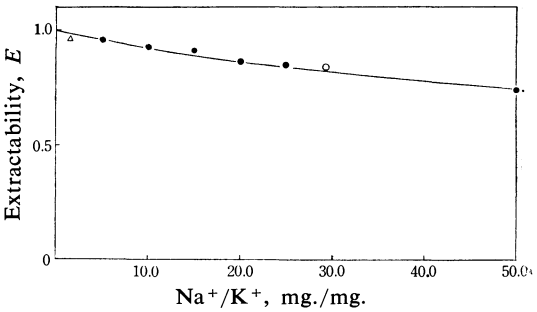


Fig. 4. Effect of sodium ion.
Sample: {Mixture of KCl and NaCl: ●; Bittern: △; Sea water: ○}
Procedure: procedure 2

For rapidity and convenience of experimentation, procedure 2 and the method of the elimination of turbidity by filtration were adopted for the following experiments.

The Separation of Potassium from Sea Water and Bittern by Solvent Extraction.—The extractabilities obtained with bittern (Table II) and sea water are shown in Table III. In Fig. 4, these values are plotted with open symbols against the ratio of sodium to potassium ions.

From Table III it may be concluded that, among all the ions which disturb the extraction, sodium ion has the most undesirable effect, but the co-existence of even a large

TABLE I. EFFECT OF SODIUM ION

A* Na+K soln. ml.	B ml.	C ml.	Na^+/K^+ mg./mg.	TPB-K found mg.	TPB-K** corr. mg.	E
25.0	15.0	10.0	5.0	16.7	17.5	0.955
25.0	15.0	10.0	10.0	16.1	17.0	0.925
25.0	15.0	10.0	15.0	15.8	16.6	0.907
25.0	15.0	10.0	20.0	14.9	15.7	0.857
25.0	15.0	10.0	25.0	14.5	14.7	0.845
25.0	15.0	10.0	50.0	12.6	13.5	0.734

* The concentration of potassium was kept constant at 0.01023 M.
** The calculated value of TPB-K is 18.32 mg.

TABLE II. COMPOSITION OF BITTERN* (g./l.)

Be[1]	Temp.** °C	pH	$MgSO_4$	$MgBr_2$	$MgCl_2$ g./l.	KCl	NaCl
32.0	13.6	7.28	72.32	3.79	209.55	41.34	74.98

* By courtesy of Mr. M. Komatsu (Kinkai Engyo Co., Ltd.).
** For extraction, supernatant solution at this temperature was used.

TABLE III. EXTRACTION OF POTASSIUM FROM SEA WATER AND BITTERN*

	Sample soln. ml.	B ml.	C ml.	V_o/V_a ml./ml.	Na^+/K^+ mg./mg.	TPB-K found mg.	TPB-K corr. mg.	E
Sea water**	25.0	15.0	10.0	1.0	29.3	13.5	14.3	0.841
Bittern	2.0	0	40.0	20.0	1.36	49.0	49.9	0.960

* The direct determination of potassium gave the results of 34.05 mg./10 ml. for sea water and 19.96 mg./10 ml. for bittern (diluted ten times with water).
** Tamashima Shi, Okayama Prefecture.

amount of magnesium ions has a negligible effect on the extractability.

In conclusion, by solvent extraction using sodium dipicrylaminate and nitrobenzene, the quantitative separation of potassium was not attained when sodium ions were also present. When sodium ions are absent, however, potassium can be quantitatively separated from the other ions.

The authors are very grateful to the Society of Salt Science, Japan, for its financial support, and also to Dr. Syozo Sato (Mitsubishi Kasei Co., Ltd.) for his generous gifts of Hexyl Natrium.

Department of Chemistry
Faculty of Science
Okayama University
Tsushima, Okayama

Chlorination by Sulfuryl Chloride. III.[1] *The Reactivities of the C–H Bond to Sulfuryl Chloride*

By Mannosuke ARAI

(Received March 16, 1964)

In a previous paper,[2] the author established that the action of sulfuryl chloride, in the presence of peroxide, on aromatic aldehydes with various nuclear substituents other than hydroxyl, resulted in the replacement of aldehydic hydrogen by chlorine, giving the corresponding acid chlorides.

$$ArC\overset{H}{\underset{O}{\diagdown}} + SO_2Cl_2 \xrightarrow[Bz_2O_2]{} ArC\overset{Cl}{\underset{O}{\diagdown}} + HCl + SO_2$$

Aliphatic hydrocarbons and the side chain of aralkyl hydrocarbons have also been established by Kharasch and Brown[3] to undergo a similar chlorination reaction. In order to establish the reactivity of various types of C–H bonding in relation to that of aldehydic hydrogen, the competitive chlorination of benzaldehyde and aralkyl and alicyclic hydrocarbons has now been carried out using sulfuryl chloride. The results are presented in this paper.

Experimental

Materials and Reagents.—Toluene, cyclohexane, cumene and *t*-butyl benzene (all reagent grade) were purified in advance by fractional distillation, and the purified materials were redistilled before use.

Benzaldehyde (reagent grade) was purified by vacuum distillation under a nitrogen atmosphere; freshly-distilled middle-cut was used for the experiment.

Sulfuryl chloride (first grade) was fractionally distilled, stored in a bottle wrapped with aluminum foil, and kept in a desiccator.

General Procedure for Chlorination.—The materials to be chlorinated competitively were placed in a 100 ml. round-bottomed flask equipped with a stirrer, a dropping funnel, and a reflux condenser, to which a calcium chloride tube was attached. After the air in the system had been replaced by dry nitrogen, benzoyl peroxide (0.1% of the weight of the sulfuryl chloride used) was added to the flask and the system was heated to 80±1°C. When sulfuryl chloride was gradually added through the dropping funnel, the evolution of gas was observed after some induction period. Heating was continued until the gas evolution ceased. After cooling, the hydrogen chloride formed was driven off by passing nitrogen through.

Analytical Procedures.—The reaction mixture obtained by the method descrived above was weighed. Any loss of weight during the reaction was distributed to each starting material according to the relative ratio of the vapor pressure.

The total chlorine content was determined by Rauscher's method[4] the reaction mixture (2 ml.) was heated with sodium in xylene for 2 hr. under reflux. *n*-Butanol was used to accelerate the reaction in place of amyl alcohol, which has been reported to contain halogens as impurities.[5] The sodium chloride obtained was determined by Mohr's method, using silver nitrate.

In order to determine the amount of benzoyl chloride produced, the reaction mixture (2 ml.) was decomposed by 80% ethanol at room temperature for 3 hr., thus forming hydrochloric acid, which was then titrated with sodium hydroxide potentiometrically. This method was established by experimentation using known amounts of benzoyl chloride and benzyl chloride in a mixture of toluene and benzaldehyde. It is also known that 2-chloro-2-phenylpropane, the chlorination product of the α-position of cumene, is decomposed quantitatively by 80% ethanol.[6]

Results and Discussion

The relative reactivity of toluene to benzaldehyde was first determined by means of competitive chlorination, using ca. 1/10 mol. of sulfuryl chloride. Under these conditions, the formation of dichlorocompounds can be ignored. The results are shown in Table I.

The relative reactivity is determined by the following scheme, using benzaldehyde as a standard:

$$RH + \cdot SO_2Cl \xrightarrow{k} R\cdot + HCl + SO_2$$

$$BzH + \cdot SO_2Cl \xrightarrow{k'} Bz\cdot + HCl + SO_2$$

$$\frac{k}{k'} = \frac{\log([RH]_{Int}/[RH]_{fin})}{\log([BzH]_{Int}/[BzH]_{fin})}$$

1) Part II: M. Arai, This Bulletin, 35, 1271 (1962).
2) M. Arai, *J. Chem. Soc. Japan, Pure Chem. Sec.* (*Nippon Kagaku Zasshi*), 81, 1450 (1960).
3) M. S. Kharasch and H. C. Brown, *J. Am. Chem. Soc.*, 61, 2142 (1939).
4) W. H. Rauscher, *Ind. Eng. Chem., Anal. Ed.*, 9, 296 (1937).
5) C. Walling and B. Miller, *J. Am. Chem. Soc.*, 79, 4181 (1957).
6) G. A. Russell and H. C. Brown, ibid., 77, 4578 (1955).

TABLE I. COMPETITIVE CHLORINATION OF BENZALDEHYDE AND TOLUENE AT 80°C[a]

Reactant	mol.	mol.
Benzaldehyde	0.280	0.171
Toluene	0.253	0.326
Sulfuryl chloride	0.040	0.034
Product		
Total chlorides	0.0398	0.0338
Benzoyl chloride	0.0308	0.0211
Benzyl chloride[b]	0.0090	0.0127
Benzaldehyde[c]	0.249	0.150
Toluene[c]	0.244	0.313
Reactivity of toluene	0.305	0.310
Mean	0.31	

a) In the presence of benzoyl peroxide
b) Total chlorides minus benzoyl chloride
c) Initial quantity minus the amount substituted and the amount vaporized

where $[\ ]_{int}$ and $[\ ]_{fin}$ denote the initial and the final concentration respectively.

Table I shows the reactivity of toluene to be 0.31 that of benzaldehyde.

Similar experimentation on and calculations of cyclohexane and benzaldehyde lead to the results listed in Table II, which shows the reactivity of cyclohexane to be 3.64 times that of benzaldehyde.

TABLE II. COMPETITIVE CHLORINATION OF BENZALDEHYDE AND CYCLOHEXANE AT 80°C[a]

Reactant	mol.	mol.
Benzaldehyde	0.248	0.339
Cyclohexane	0.261	0.245
Sulfuryl chloride	0.043	0.042
Product		
Total chlorides	0.0416	0.0421
Benzoyl chloride	0.0091	0.0123
Chlorocyclohexane[b]	0.0325	0.0298
Benzaldehyde[c]	0.239	0.327
Cyclohexane[c]	0.228	0.215
Reactivity of cyclohexane	3.65	3.62
Mean	3.64	

a) In the presence of benzoyl peroxide
b) Total chlorides minus chlorocyclohexane
c) Initial quantity minus the amount substituted and the amount vaporized

From the relative reactivity (0.31) of toluene to benzaldehyde, the value of 11.8 was derived as that of cyclohexane vs. toluene. The value thus derived indirectly is somewhat smaller than the value (13.1) obtained by Russell and Brown through the competitive chlorination of cyclohexane and toluene at 80°C directly.[6]

Next, the relative reactivity of cumene vs. benzaldehyde was examined. Since cumene has two kinds of hydrogen—a tertiary hydrogen at the α-position and six primary hydrogens at the β-position—all of which can be subjected to abstraction, it is of interest to determine each of the isomers formed and to see the relative reactivity of these two different hydrogens. Cumene was reacted at 80°C with ca. 1/10 mol. of sulfuryl chloride and benzoyl peroxide; the total amounts of chlorides and α-chloride (2-chloro-2-phenylpropane) in the product were determined separately, the amount of β-chloride (1-chloro-2-phenylpropane) being obtained as the difference between these two figures. The ratio of the isomers in the product is summarized in Table III.

TABLE III. ISOMER DISTRIBUTION OF CUMENE BY CHLORINATION AT 80°C[a]

Reactant	mol.	mol.
Cumene	0.334	0.496
Sulfuryl chloride	0.034	0.062
Product		
Total chlorides	0.0334	0.0622
α-Chloride	0.0270	0.0544
β-Chloride[b]	0.0044	0.0078
α-Chloride/β-Chloride	6.59	7.00
Mean	6.80	

a) In the presence of benzoyl peroxide
b) Total chlorides minus α-chloride

The ratio, 6.80, of α-chloride to β-chloride gives 40.8 per hydrogen at both positions. This value is rather close to the figure obtained by Kharasch[3] in 1939 from a similar reaction

TABLE IV. COMPETITIVE CHLORINATION OF BENZALDEHYDE AND CUMENE AT 80°C[a]

Reactant	mol.	mol.
Benzaldehyde	0.182	0.154
Cumene	0.275	0.378
Sulfuryl chloride	0.039	0.039
Product		
Total chlorides	0.0380	0.0392
(HCl)[b]	0.0346	0.0354
Cumene-β-chloride[c]	0.0034	0.0038
Cumene-α-chloride[d]	0.0231	0.0258
Benzoyl chloride[e]	0.0115	0.0096
Benzaldehyde[f]	0.170	0.144
Cumene[f]	0.248	0.348
Reactivity of cumene	1.51	1.23
Mean	1.37	

a) In the presence of benzoyl peroxide
b) The amount of HCl by hydrolysed with 80% EtOH, —— cumene-α-chloride and benzoyl chloride
c) Total chlorides minus (HCl)
d) 6.80 times β-chloride
e) (HCl) minus α-chloride
f) Initial quantity minus the amount substituted and the amount vaporized

in benzene, but it is different from the value, 2.13, derived from the photochlorination using chlorine.[7]

The competitive chlorination of benzaldehyde and cumene was realized, after a consideration of the isomer distribution. The ratio of the reactivity of cumene to that of benzaldehyde is shown to be 1.37 (Table IV); that is, the ratio is 4.43 to toluene. Our direct comparison of the reactivities of cumene and toluene is summarized in Table V.

Table V shows that the cumene vs. toluene ratio is 4.33, which is in good agreement with the value obtained indirectly in Table IV.

TABLE V. COMPETITIVE CHLORINATION OF TOLUENE AND CUMENE AT 80°C[a]

Reactant	mol.
Toluene	0.221
Cumene	0.230
Sulfuryl chloride	0.037
Product	
Total chlorides	0.0373
Cumene-α-chloride	0.0265
Cumene-β-chloride[b]	0.0039
Benzyl chloride[c]	0.0069
Toluene[d]	0.214
Cumene[d]	0.200
Reactivity of cumene	4.33

a) In the presence of benzoyl peroxide
b) (1/6.80) α-Chloride
c) Total chlorides minus cumene α- and β-chlorides.
d) Initial quantity minus the amount substituted and the amount vaporized

TABLE VI. COMPETITIVE CHLORINATION OF BENZALDEHYDE AND *t*-BUTYLBENZENE AT 80°C[a]

Reactant	mol.
Benzaldehyde	0.164
t-Butylbenzene	0.255
Sulfuryl chloride	0.041
Product	
Total chlorides	0.0406
Benzoyl chloride	0.0289
Neophyl chloride[b]	0.0117
Benzaldehyde[c]	0.135
t-Butylbenzene[c]	0.243
Reactivity of *t*-butylbenzene	0.25

a) In the presence of benzoyl peroxide
b) Total chloride minus benzoyl chloride
c) Initial quantity minus the amount substituted and the amount vaporized

7) G. A. Russell and H. C. Brown, ibid., 77, 4031 (1955).

The results of a similar reaction of benzaldehyde and *t*-butyl benzene are summarized in Table VI, which shows that the reactivity of the latter is 25% that of the former. The relative value of *t*-butyl benzene to toluene is found from this value to be 0.80, which is again in good agreement with Russell's value,[6] 0.81, derived from the direct competitive reaction.

The results obtained above are summarized in Table VII and in Fig. 1.

TABLE VII. RELATIVE REACTIVITY ON A MOLECULAR AND BOND BASIS

	Molecule[a] A	Molecule[a] B	C-H Bond[b]
Benzaldehyde	1.00	3.23	9.7
Toluene	0.31	1.00	1.00
Cumene	1.37	4.42 (4.23)[c]	
t-Hydrogen			11.6
prim-Hydrogen			0.28
t-Butylbenzene	0.25	0.80 (0.81)[c]	0.27
Cyclohexane	3.64	11.8 (13.2)[c]	2.9

a) Reactivity per molecule
b) Reactivity per C-H bond
c) The numerical values in parentheses are based upon the competitive reaction with toluene

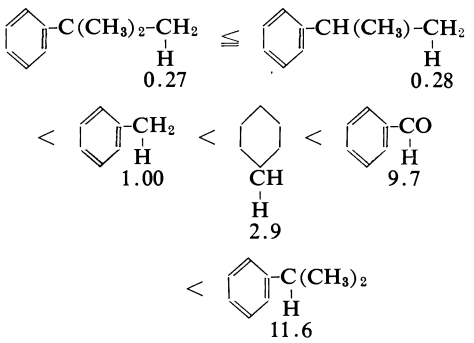


Fig. 1

The results of the chlorination by sulfuryl chloride are listed in Table VIII; those obtained by other halogenation reagents are shown for the sake of comparison.

The reaction with sulfuryl chloride is similar to the photochlorination using chlorine, but it has a higher selectivity. The hydrogen abstraction from the C-H bond in toluene would be expected to be accelerated by the formation of a stable benzyl radical in comparison with the case of cyclohexane, where no such acceleration can be expected. However, the reverse has been found to be the case

TABLE VIII. COMPARISON OF RADICAL HALOGENATION AGENTS

	SO_2Cl_2	Cl_2[3]	Br_2[a]	C_4H_9OCl[b]
Toluene	1.0	1.0	1.0	1.0
Cumene				
(*tert.*)	11.6	4.0	>1	6.84
(*prim.*)	0.28	0.31	v. small	0.26
t-Butylbenzene	0.27	0.22	v. small	0.105
Cyclohexane	2.9	2.8	0.004	1.5

a) P. C. Anson, P. S. Fredericks and J. M. Tedder, *J. Chem. Soc.*, **1959**, 918.
b) C. Walling and B. B. Jacknow, *J. Am. Chem., Soc.*, **82**, 6108 (1960).

in the present study. This phenomenon can be rationalized, following Russell's explanation in his photochlorination, in terms of the inductive effect of the phenyl group in toluene. The aldehydic hydrogen in benzaldehyde has, as is shown in Table VII, a higher relative reactivity. This may be explained, together with the case of the tertiary hydrogen in cumene, by the greater stability of the radical formed in its transition state and by the weaker polar effect. However, more extensive studies are necessary before any definite conclusion can be drawn on this point.

The ratio of isomer formation in the chlorination of cumene (*tert/prim*) is 6.80, as has been described, which is far different from the ratio, 3.13, in photochlorination. This difference is of interest and is meaningful in connection with the reaction mechanism of the chlorination by sulfuryl chloride. Two mechanisms have hitherto been proposed for the radical chlorination by the reagent. One is that the chlorosulfonyl radical produced by the initiator decomposes to form the chlorine atom, which is the actual reacting species (equilibrium 1 and reaction 2).

$$SO_2Cl\cdot \rightleftarrows SO_2+Cl\cdot \quad (1)$$

$$RH+Cl\cdot \rightarrow R\cdot+HCl \quad (2)$$

$$RH+SO_2Cl\cdot \rightarrow R\cdot+SO_2+HCl \quad (3)$$

$$R\cdot+SO_2Cl_2 \rightarrow RCl+SO_2Cl\cdot \quad (4)$$

The other, alternative mechanism is that the chlorosulfonyl radical itself is responsible for the hydrogen abstraction (reaction 3). The latter mechanism has been established in the peroxide-catalyzed reaction of sulfuryl chloride with olefins.[8,9] Therefore, the different isomer distributions in the products obtained from cumene by photochlorination and by sulfuryl chloride chlorination is assumed to be based upon the difference between the actions of the chlorine atom and the chlorosulfonyl radical.

Russell[10] has concluded that, as a result of the solvent effect in the radical chlorination reaction, sulfuryl chloride reacts as does chlorosulfonyl radical in the presence of aliphatic solvents, while in aromatic solvents solvated chlorine atoms are the reacting species, as in the case in photochlorination. Since the isomer ratio in the chlorination products of cumene is supported experimentally by Kharasch,[3] an active hydrogen such as tertiary hydrogen in cumene is assumed to be abstracted by the chlorosulfonyl radical, which has greater selectivity than the chlorine atom, even in the aromatic solvent, contrary to Russell's explanation.

The author wishes to express his gratitude to Professor Mamoru Yamaguchi of Tohoku University for his constant guidance in the course of this work.

Kawauchi College
Tohoku University
Kawauchi, Sendai

8) M. S. Kharasch and A. F. Zavist, ibid., **73**, 964 (1951).
9) A. Y. Yakubovich and Y. M. Zinovev, *J. Gen. Chem. (U. S. S. R.)*, **17**, 2028 (1947); *Chem. Abstr.*, **43**, 1248 (1949).
10) G. A. Russell, *J. Am. Chem. Soc.*, **80**, 5002 (1958).

Isomerization of cis-Azobenzene in the Solid Phase

By Morizo TSUDA and Kenji KURATANI

(Received March 18, 1964)

Various solid phase reactions have been studied by many authors, but there have been few studies concernd with the simplest case, that is, with

$$A(solid) \rightarrow B(solid)$$

reaction. The isomerization and phase transformation belong to this case; the thermal isomerization of crystalline *cis*-azobenzene to *trans*-azobenzene will be considered as an example. The isomerization rate of *cis*-azobenzene in several solvents or in the liquid phase has been studied by Hartley[1] and Le Févre,[2] and it has been concluded that the thermal isomerization rate in these cases is expressed as a first order reaction. Along with the thermal change, the photo-isomerization in the various solvents has been studied by Zimmerman[3] and Birnbaum[4], and the results have been explained well by the reversible zeroth order reaction scheme. However, there has been no information about the solid phase, and, therefore, it appears that it would be valuable to learn of the effect of the crystalline lattice on the isomerization procsses.

Experimental

Materials.—*cis*-Azobenzene was prepared from the commercial reagent of G. R. grade, according to Hartley's method.[1]

trans-Azobenzene was recrystallized from an alcohol solution after having been boiled for several hours in a dark room. The melting points of cis- and trans-isomers, measured by the capillary method, were 69.0~71.5°C, and 66.0~68.0°C respectively.

Apparatus and Procedure.—The infrared absorption spectra of these crystals were measured by the KBr disk method in the range of 600~4000 cm^{-1}, using a Perkin-Elmer Model 112 spectrometer equipped with a NaCl prism. KBr disks were prepared under the pressure of 10 ton/cm^2 in vacuo, and were 12 mm. in diameter. The concentration of azobenzene in the disk was 0.7 mg./300 mg. KBr. In order to observe continuously the spectral intensity change of the disk at a constant temperature, a thermostat-cell was made and placed in front of the entrance slit of the spectrometer. A KBr disk was located at the center of the cell, and the radiation from the globar was transmitted through it. The medium circulating through the thermostat was liquid paraffin, while the temperature fluctuation of the thermostat-cell was ±0.2°C throughout the long run at nearly the middle point of the disk.

A calibration curve for the determination of the fractional isomerization, α, was prepared according to the following procedure; it is shown in Fig. 1.

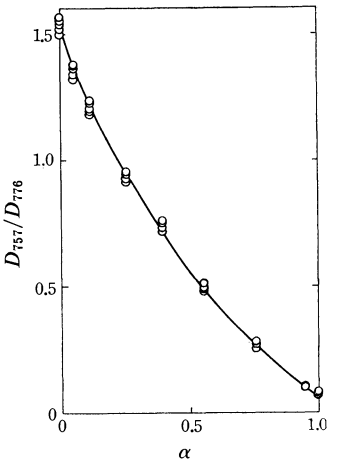


Fig. 1. Calibration curve for fractional isomerization.

Several lots of KBr disks having different mixing ratios of cis- and trans-isomers were prepared from the mechanical mixtures of isomers. Then the ratio of the optical density of the sharp band at 757 cm^{-1} to the that of 776 cm^{-1} was measured with these disks,* and was plotted against the isomeric mixing ratio, which was supposed to be equivalent to the fractional isomerization. In order to examine the reliability of the experimental process, the thermal isomerization rate of a 3 wt.% *cis*-azobenzene solution in cyclohexane at 50°C was measured according to a similar calibration curve. The reaction rate in solution was of the first order, as had been expected, and the rate constant at 50°C was 2.7×10^{-3} sec^{-1}. This value agrees well with the findings of Le Févre and Northcott.[2]

Poor reproducibility was found when the isomerization rate was measured with disks made from different lots of a KBr-azobenzene mixture, mean-

1) G. S. Hartley, *J. Chem. Soc.*, **1938**, 633.
2) R. J. W. Le Févre and J. Northcott, ibid., **1953**, 867.
3) G. Zimmerman, Lue-yung Chow and Nu-jin Paik, *J. Am. Chem. Soc.*, **80**, 3528 (1958).
4) P. P. Birnbaum and D. W. G. Style, *Trans. Faraday Soc.*, **50**, 1192 (1954).

* These absorption bands are assigned to the out-of-plane vibration of benzene rings. The 757 cm^{-1} band is characteristic of the cis-isomer, while the 776 cm^{-1} band is attributable to both trans- and cis-isomers.

ing that the isomerization rate is affected a little by the degree of the crystal grinding, since the azobenzene crystal used for preparing disks was always of the same lot. However, the grinding condition was rather difficult to control. In order to overcome this difficulty, the following procedure was adopted: several disks were prepared at one time from the same lot of the KBr-azobenzene mixture, and the isomerization rates at different temperatures were then measured spectroscopically with these disks. The quantitative discussion of the experimental results was limited to the data obtained from the disks of the same lot.

Results

Appropriate Expression for Kinetics. — The thermal isomerization rates were measured at 36, 50 and 58°C. The change with time in the fractional isomerization α is shown as sigmoid curves in Fig. 2. This figure shows that three

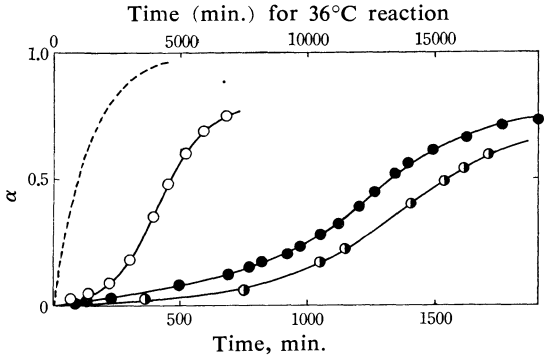


Fig. 2. Thermal isomerization of crystalline *cis*-azobenzene.
○ : 58.3±0.2°C
◑ : 50.2±0.2°C
● : 36.3±0.2°C (time scale ×10)
--- : isomerization rate in liquid phase calculated from Hartley's data

stages in the isomerization process can be distinguished, the induction, acceleration and decay periods. In the present case, the induction period is relatively short, and our interest is concentrated on the acceleration period. Jacobs and Tompkins have written an excellent review of the kinetics equations of solid reactions and have deduced some theoretical expressions.[5] To know which of these equations is the most suitable for the present case, experimental results have been plotted according to these equations. Most of them, such as:

$$\log \alpha = k_3 t + c$$

$$\log(1-\alpha) = kt + c$$

$$1-(1-\alpha)^{1/2} = kt$$

$$1-(1-\alpha)^{1/3} = kt$$

$$\alpha = 1/2(k_2 t/a)^3 - 3/16(k_2 t/\alpha)^2$$

do not adequately represent the characteristics of experimental results.

However, the acceleration period in Fig. 2 can be represented by the following two equations. In the range of $\alpha = 0 \sim 0.6$, the Prout-Tompkins law,

$$\log[\alpha/(1-\alpha)] = k_3 t + \text{const.} \quad (1)$$

is a good approximation, while in the little narrower range of $\alpha = 0.03 \sim 0.5$, the power law,

$$\log \alpha = n \log t + \text{const.} \quad (2)$$

appears to be also applicable.

Figure 3 shows the relation between $\log[\alpha/(1-\alpha)]$ and the reaction time, and Fig. 4 shows the relation between $\log \alpha$ and $\log t$. However, the value of n in Eq. 2, which was estimated by the method of the least square, varied at random with the reaction temperature (i.e., it was 2.35 at 58°C, 3.00 at 50°C and 2.20 at 36°C), and no significant correlation

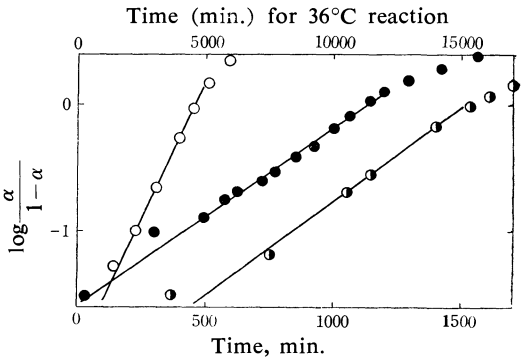


Fig. 3. Relationship between $\log[\alpha/(1-\alpha)]$ and reaction time.
○ : 58.3±0.2°C
◑ : 50.2±0.2°C
● : 36.3±0.2°C (time scale ×10)

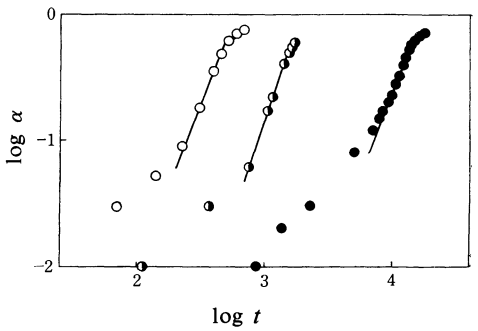


Fig. 4. Relationship between $\log \alpha$ and $\log t$.
○ : 58.3±0.2°C
◑ : 50.2±0.2°C
● : 36.3±0.2°C

5) P. W. M. Jacobs and F. C. Tompkins, "Classification and Theory of Solid Reaction," in "Chemistry of the Solid State," Ed. by W. E. Garner, Butterworths Sci. Pub., London (1955), p. 184.

between n and reaction temperature could be found. This suggests that the power law is not applicable for the present reaction kinetics.

The Effect of the Pre-irradiation. — Prout-Tompkins' equation 1 is derived according to the assumptions that the nucleus formation is completed at a comparatively early stage of the reaction, that the nucleus branches into chains as the reaction proceeds, and that these chain branchings of reaction sites cause an increase in the chemical reaction rate. The termination of the branching by the interaction between growing nuclei should also be considered. The relation between the probabilities of chain branching, k_3, and of termination, k_4, is assumed to be $k_4=k_3(\alpha/\alpha_i)$, where α_i is the fractional isomerization at the points of inflection, which is approximated as 0.5. These circumstances are confirmed by the following pre-irradiation effect.

Pre-irradiation with a mercury lamp shortens the apparent induction period, and the Prout-Tompkins plots with the *cis*-azobenzene disks pre-irradiated for 0.5, 5, and 10 min. are parallel to that obtained with the non-irradiated pure *cis*-azobenzene disk. These plots are shown in Figs. 5a and 5b. This result can be explained if the influence of the irradiation is concerned only with the increase in the number of potential nucleus-forming sites or with that of the nuclei themselves. In the present case, the latter may occur, since the initial values of α_0 observed with the pre-irradiated disks are nearly 0.02 to 0.04. Therefore, the increase in the initial number of nuclei formed by the pre-irradiation makes the branching and termination steps predominant at the early stage of the thermal treatment, and the induction period is reduced significantly. Moreover, the irradiation does not affect the branching and termination rate constants; therefore, the slopes of Prout-Tompkins' plots are independent of the irradiation, as may actually be observed in Figs. 5a and 5b. The lateral shift of these plots is due to the difference in the initial value of α_0 or in the initial number of nuclei produced by the pre-irradiation.

The Effect of Grinding.—As has been previously described, the reaction rates observed with the disks from the different lots are not the same. This discrepancy is due to the difference in the degree of crystal grinding among the different lots of the KBr-azobenzene mixture. Two series of data are illustrated in Fig. 6. One series of data is obtained with disks made from one lot of the mixture, while the other series is observed with disks of the other lot. The reaction rates of the disks with different histories are not the same, even at the same temperature, and the reaction rate constants are also different. However, the activation energies in the rate constant, k_3, are nevertheless similar in these two series. This finding is not unreasonable considering the relation between the grinding action and the increase in the points of crystal defects. In fact, the same effect of grinding was revealed in the thermal decomposition of potassium and silver permanganates.[6,7]

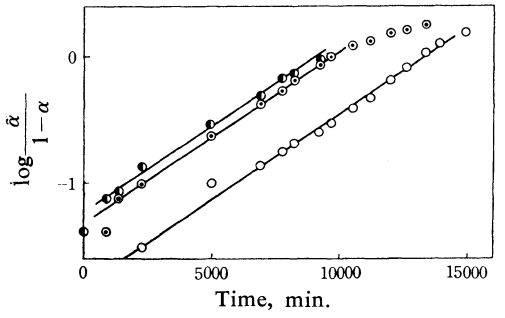


Fig. 5a. Effect of Hg-lamp pre-irradiation on cis→trans thermal isomerization at 36.3°C of crystalline azobenzene. Pre-irradiation times are ○ : 0, ⊙ : 5, ◑ : 10 min.

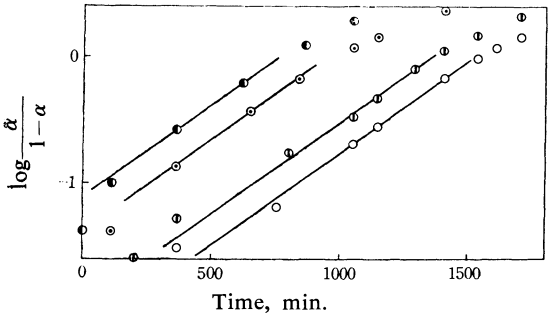


Fig. 5b. Effect of Hg-lamp pre-irradiation on cis→trans thermal isomerization of crystalline azobenzene at 50.2°C. Pre-irradiation times are ○ : 0, ◐ : 0.5, ⊙ : 5, ◐ : 10 min.

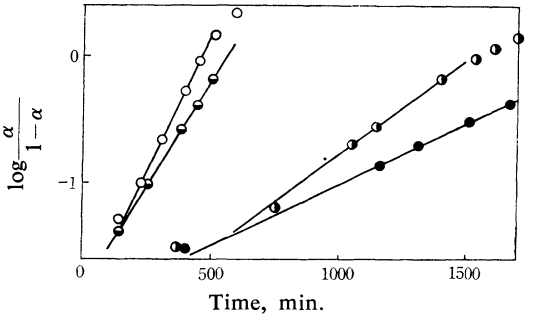


Fig. 6. Dependency of k_3 on KBr-mixture lots; lot A, ○ : 58.2, ◑ : 50.2°C, lot B, ◒ : 58.3, ● : 49.9°C.

6) E. G. Prout, *J. Inorg. Chem.*, **7**, 368 (1958).
7) E. G. Prout and M. J. Sole, ibid., **9**, 232 (1959).

Photo-isomerization. — The photo-isomerization of azobenzene in the solid state by prolonged irradiation with a mercury lamp (Toshiba SHL-100 UV) was observed at 12°C. The results are shown in Fig. 7; in contrast

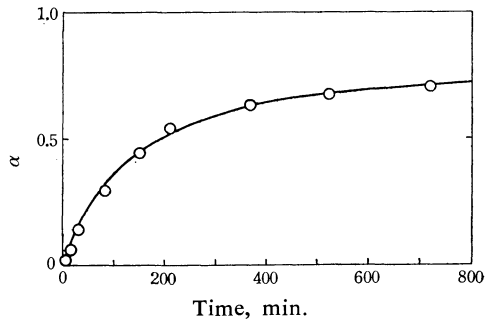


Fig. 7. Photo-isomerization of crystalline *cis*-azobenzene.

to the thermal process, there is no induction period. A similar contrast between the photo and thermal processes in the solid phase was observed in the case of the decomposition of barium azide.[8] The photo-decomposition of barium azide is more complicated than in the present case. That is, it proceeds linearly after some duration of the deceleration period, and there is also no induction period before the onset of the decomposition. However, the thermal decomposition of barium azide starts after the induction period, and the length of this induction period is effectively reduced by pre-irradiation with ultraviolet light.

Another striking characteristic of the solid-phase photo-process is that the photo-isomerization from trans to cis isomer does not occur in the solid-phase, as it does in the liquid-phase, (The photo-isomerization process in various solutions is utilized in preparing cis-azobenzene.) Pre-treatment, such as X-ray or γ-ray irradiation, in which an increase in the number of nucleus-forming sites can be expected, does not alter this characteristic. This behavior may be explained by assuming the stabilization of *trans*-azobenzene molecules by the crystalline lattice field.

Discussion

In the present study, it is important to establish the non-existence of the liquid phase, since partial melting often occurs in the course of the thermal reaction, especially in the case of organic compounds. The crystal of single isomeric azobenzene does not melt at temperatures lower than 68°C. However, mixing with the other isomer lowers its melting point to 41°C, i. e., to the eutectic point.[1] If the isomerization proceeds at temperatures lower than the eutectic point, the isomerization can be recognized as a perfect solid-state reaction. However, no reliable kinetics data could be obtained in the temperature range lower than 30°C, since the reaction rate became too slow. In order to avoid this difficulty, the reaction rates were measured at temperatures higher and lower than the eutectic point, i. e., in the range of 36~58°C; it was found that the kinetics at any temperature in this range could be treated with the same reaction mechanism, i, e., with Prout-Tompkins' law.

From the reaction kinetics obtained with the pure *cis*-azobenzene at the temperatures of 36, 50 and 58°C, the values of k_3 were estimated by the least-square method, and their logarithmic values were plotted against the reciprocal of the reaction temperature. This plot gives a straight line, as is shown in Fig. 8. This finding certifies that, even at the tem-

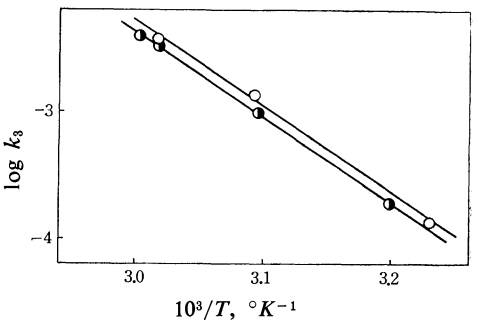


Fig. 8. Relationship between log k_3 and reaction temperature; ○ : lot A, ◑ : lot B. (cf. Fig. 6).

perature of 58°C, no partial melting occurred throughout the isomerization process. This conclusion is supported by the considerations that, if the liquid phase existed in the course of the thermal isomerization at temperatures highe than the eutectic point, the values of log k_3 at 50 and 58°C would not lie on a single straight line with the value at 36°C, and that the activation energy in the temperature range lower than the eutectic point would be larger than that in the higher temperature range.

This is confirmed further by another series of thermal isomerization studies, i. e., at the temperatures of 64, 58, 50 and 38°C. The relationship between $\log[\alpha/(1-\alpha)]$ and the reaction time at the temperatures of 58 and 50°C is shown in Fig. 6, while the Arrhenius plot of k_3 is given in Fig. 8, together with the results of the first series.

Following the Prout-Tompkins' reaction scheme, the activation energy of k_3 is found

8) J. G. N. Thomas and F. C. Tompkins, *Proc. Roy. Soc.*, **A209**, 550 (1951); **A210**, 111 (1951).

to be 31.3±0.3 kcal./mol. This value is reasonable, because Hartley has shown that the activation energy of the cis→trans isomerization of liquid-phase azobenzene is 23 kcal./mol. Because of the strain energy which exists on the interface of *cis*- and *trans*-azobenzene lattice, the activation energy in the solid-phase reaction must be larger than the one in the liquid-phase isomerization.

Summary

The thermal and photo-isomerizations of crystalline *cis*-azobenzene have been studied by infrared spectrophotometry in the temperature range of 36~58°C, It has been found that the thermal isomerization follows Prout-Tompkins' law, and the values of k_3 at 36, 50 and 58°C have been estimated. The Arrhenius plot of K_3 is linear, and the activation energy of k_3 is 31.3±0.3 kcal./mol. Pre-irradiation with a mercury lamp shortens the induction period, but it does not change the value of k_3. On the other hand, the value of k_3 is affected by the degree of grinding of azobenzene crystals. In this case, the activation energy is not altered by crystal grinding.

The photo-isomerization at 12°C, in contrast to the case of thermal isomerization, has no induction period. However, the trans→cis photo-isomerization does not occur even if the crystal is treated by X-ray or by γ-ray pre-irradiation.

The authors wish to thank Mr. Soji Tsuchiya for his helpful discussions throughout this work and Mr. Takuji Sakai for his assistance in preparing the apparatus.

Aeronautical Research Institute
The University of Tokyo
Meguro-ku, Tokyo

3-Phenoxytropolone and 2-Phenoxytropone

By Kahei TAKASE

(Received March 19, 1964)

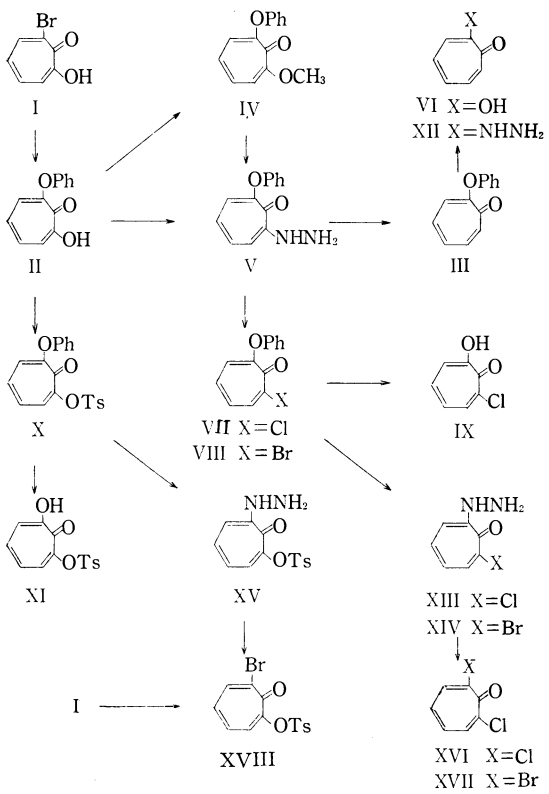
It has been reported[1] that the reaction of 3-bromotropolone (I) and sodium phenoxide affords 3-phenoxytropolone (II) and that its phenoxyl group is not hydrolyzed by heating it with concentrated hydrochloric acid, as in diphenyl ether. In order to make clear the behavior of the phenoxyl group attached to the tropone or tropolone ring, in comparison with diphenyl ether, 2-phenoxytropone (III) and its derivatives were prepared from II and the reactivities of the phenoxyl group in the phenoxytropones toward some nucleophilic reagents, especially dilute alkali and hydrazine, were examined.

The heating of 3-bromotropolone (I) with 2~3 molar equivalents of sodium phenoxide in phenol, in the presence of a catalytical amount of copper acetate, gave 3-phenoxytropolone (II) in a good yield while in the absence of copper acetate the yield of II was low. The reaction did not proceed at all when only one molar equivalent of sodium phenoxide was used. The tropolonic nature of II was shown from the facts that II was soluble in aqueous alkali hydroxide solution, turned red in chloroform with a ferric chloride solution, and formed a pale green copper chelate. The prolonged heating of II which acid or alkali did not produce any change.

The methylation of II with diazomethane gave a crystalline methyl ether (IV), together with an oily substance. When IV was treated with hydrazine, it gave a hydrazinotropone derivative (V), in which the methoxyl was replaced by hydrazine. The oxidative decomposition of V by heating it with copper sulfate in acetic acid afforded phenoxytropone (III), which was easily hydrolyzed by heating it with dilute alkali to give tropolone (VI) and phenol. This result shows that III is 2-phenoxytropone and that IV and V are 7-methoxy- and 7-hydrazino-2-phenoxytropone respectively; consequently, it was concluded that the phenoxyl group of II was located in the 3-position of the tropolone ring. From this evidence, it was clear that the reaction of I and sodium phenoxide under these conditions was not accompanied by an abnormal substitution reaction such as was observed in the case of alkali hydroxide.[1]

1) Y. Kitahara, *Sci. Repts., Tohoku Univ.*, I, **39**, 265 (1956).

The oxidative decomposition of V by heating it with copper sulfate in concentrated hydrochloric acid or hydrobromic acid afforded 7-chloro- (VII) or 7-bromo-2-phenoxytropone (VIII), respectively. When VII or VIII was heated with dilute alkali, the phenoxyl group was easily hydrolyzed to give 3-chloro-[2,3] (IX) or 3-bromotropolone (I) respectively. The treatment of II with *p*-toluenesulfonyl chloride afforded a *p*-toluenesulfonate (X), in a quantitative yield; this gave a hydrolyzed product (XI) when heated with dilute alkali. From its reddish coloration with a ferric chloride solution and its ultraviolet absorption spectrum, which was similar to those of tropolones, XI was assumed to be 3-(*p*-tolylsulfonyloxy)tropolone; consequently, X was assumed to be 7-(*p*-tolylsulfonyloxy)-2-phenoxytropone.



The phenoxyl group in II remains unchanged upon treatment with acid or alkali; this behavior is similar to that of diphenyl ether. On the contrary, as has been mentioned above, the reactivities of the phenoxyl groups in 2-phenoxytropones (III, VII, VIII and X) differ greatly from that in II, and they are easily hydrolyzed with alkali. In order to make clear the different behavior of the phenoxyl group in 2-phenoxytropones and 3-phenoxytropolone, the reaction with hydrazine was examined. 2-Phenoxytropone (III) easily reacted with hydrazine to form 2-hydrazinotropone (XII). The phenoxyl group of VII, VIII and X were also replaced by hydrazine to give 7-chloro- (XIII), 7-bromo- (XIV)[4] and 7-(*p*-tolylsulfonyloxy)-2-hydrazinotropone (XV) respectively. The structure of XIII was confirmed through the formation of the known 2, 7-dichloro- (XVI) and 2-bromo-7-chlorotropone (XVII)[3] by oxidative decomposition with copper sulfate in concentrated hydrochloric or hydrobromic acid. The structure of XV, which afforded an acetate and an isopropylidene derivative, was also comfirmed by its derivation, when heated with copper sulfate in concentrated hydrobromic acid, to 2-bromo-7-(*p*-tolylsulfonyloxy)tropone (XVIII), which was also obtained by the tosylation of I.

From the foregoing experiments, it was found that the phenoxyl group of 2-phenoxytropones, rather than the halogen or the *p*-tolylsulfonyloxyl group, was replaced easily by hydrazine, as in the case of alkaline hydrolysis. This bavarior is rather interesting when compared with the behavior of 7-methoxy-2-phenoxytropone (IV) toward hydrazine, in which not the phenoxyl but methoxyl group is replaced. From these findings, the substituents at the 2- (or 7) position of the tropone ring may be arranged in the order of ease (methoxyl, phenoxyl, *p*-tolylsulfonyloxyl and halogen), with which they are replaced by a nucleophile.

When II was heated with hydrazine in ethanol, not the phenoxyl but the hydroxyl group was replaced to give V. This is interesting since tropolones in general do not react with ketonic reagents, and only specific tropolone derivatives, such as, 5-nitroso- and 5-arylazotropolones,[5] which can exist in the tautomeric diketone form, are known to react with ketonic reagents. It is also known that 3-carboxy- and 3-cyanotoropolone react with hydrazine to form 2-hydrazinotropones; this is considered to be due to the electron-attracting nature of the carboxyl or cyano group.[6] 3-Phenoxytropolone (II) cannot take the diketone structure; consequently, the replacement of the hydroxyl group by hydrazine must be due to the electron attraction of the phenoxyl

2) T. Nozoe, S. Seto, S. Ito, M. Sato and T. Katono, *Sci. Repts., Tohoku Univ.*, I, 37, 191 (1953).
3) S. Seto, ibid., I, 37, 275, 377 (1953).
4) T. Nozoe, S. Seto, H. Takeda, S. Morosawa and K. Matsumoto, *Proc. Japan Acad.*, 28, 192 (1952); *Sci. Repts., Tohoku Univ.*, I, 36, 126 (1952).
5) T. Nozoe, M. Sato and K. Matsui, ibid., I, 37, 407 (1953); S. Ito, ibid., 42, 236 (1958); 43, 216 (1959); T. Nozoe, S. Ito, S. Suzuki and K. Hiraga, *Proc. Japan Acad.*, 32, 344 (1956).
6) T. Nozoe, Y. Kitahara, K. Takase and I. Murata, This Bulletin, 37, 1292 (1964).

group, which renders the tropolone ring more liable to the attack of nucleophilic reagents.

Experimental[7]

3-Phenoxytropolone (II).—A mixture of 3-bromotropolone (I) (20.1 g.), sodium phenoxide (35 g.) and copper acetate (0.2 g.) in phenol (80 ml.) was heated at 135~140°C for 5 hr. The reaction mixture was then dissolved in a mixture of benzene (100 ml.) and water (100 ml.), acidified with 6 N sulfuric acid, and extracted with benzene. After being dried over sodium sulfate, the solvent was evaporated and the phenol was distilled off under reduced pressure. The residue was recrystallized from methanol to give II (18.3 g.) as colorless prisms, m. p. 106~107°C; reported 105~105.5°C.[1]

Copper Chelate.—M. p. 320°C; pale green crystals.

Found: C, 64.23; H, 3.89. Calcd. for $(C_{13}H_9O_3)_2Cu$: C, 63.73; H, 3.07%.

In this reaction, when copper acetate was not used, 30% of I was recovered and II was formed in a 49% yield after heating for 20 hr.

7-Methoxy-2-phenoxytropone (IV).—Into a cooled suspension of II (1.07 g.) in ether (15 ml.), an ethereal solution of diazomethane (10 ml.) was stirred. After the mixture had been allowed to stand overnight, the crystals which had formed were collected by filtration to give IV (0.41 g.), m. p. 92~95°C. Recrystallization from a mixture of benzene-petroleum ether gave colorless needles, m. p. 95°C.

λ_{max}^{MeOH} mμ (log ε); 242 (4.44), 325 (4.00), 353 (3.99).

Found: C, 73.55; H, 5.58. Calcd. for $C_{14}H_{12}O_3$: C, 73.67; H, 5.30%.

From the mother liquor, an oily substance was obtained. This oil failed to form a picrate and blackened with hydrazine.

7-Hydrazino-2-phenoxytropone (V).—*a) From IV.*—A mixture of IV (200 mg.) and 80% hydrazine hydrate (0.2 ml.) in ethanol (0.2 ml.) was warmed at 80°C for a few minutes to give V (140 mg.), m. p. 198°C (decomp.). Recrystallization from ethanol gave yellow prisms, m. p. 199°C (decomp.).

λ_{max}^{MeOH} mμ (log ε); 250 (4.32), 340 (4.12), 412 (4.04).

Found: C, 68.50; H, 5.17; N, 12.53. Calcd. for $C_{13}H_{12}O_2N_2$: C, 68.41; H, 5.30; N, 12.27%.

Acetate.—M. p. 189~190°C, pale yellow prisms (from methanol).

λ_{max}^{MeOH} mμ (log ε); 252 (4.31), 335 (4.12), 395 (3.99).

Found: C, 66.92; H, 4.77; N, 10.15. Calcd. for $C_{15}H_{14}O_3N_2$: C, 66.65; H, 5.22; N, 10.37%.

Isopropylidene Derivative.—M. p. 156~157°C, yellowish orange prisms (from acetone).

λ_{max}^{MeOH} mμ (log ε); 267 (4.36), 357 (4.33), 418 (4.20).

Found: C, 71.50; H, 5.82; N, 10.48. Calcd. for $C_{16}H_{16}O_2N_2$: C, 71.62; H, 6.01; N, 10.44%.

b) From II.—A mixture of II (1.00 g.) and a 50% ethanolic solution of hydrazine (1.5 ml.) was refluxed for 5 hr. to give V (0.77 g.) as yellow scales, m. p. 197°C. When the reaction period was short, the hydrazine salt of II was obtained as yellow needles m. p. 148°C (decomp.).

Found: C, 63.09; H, 5.65; N, 11.17. Calcd. for $C_{13}H_{14}O_3N_2$: C, 63.40; H, 5.73; N, 11.38%.

2-Phenoxytropone (III).—To a hot solution of V (500 mg.) in a mixture of glacial acetic acid (7.5 ml.) and water (3.5 ml.), a hot solution of copper sulfate (1.2 g.) in water (3 ml.) was added in one lot. After being heated for 5 min., the mixture was cooled, diluted with water (30 ml.), and extracted with chloroform. The solvent was then evaporated and the residue passed through a short alumina column, as with the benzene solution. The eluted substance was distilled under reduced pressure at 150°C to give III (320 mg.) as a colorless oil, which solidified on being allowed to stand, forming colorless crystals, m. p. 43~45°C.

λ_{max}^{MeOH} mμ (log ε); 228 (4.41), 322 (3.98).

Found: C, 79.19; H, 5.17. Calcd. for $C_{13}H_{10}O_2$: C, 78.77; H, 5.09%.

The Hydrolysis of III.—A mixture of III (100 mg.), ethanol (2 ml.) and a 2 N potassium hydroxide solution (2 ml.) was refluxed for 5 hr. and then acidified with 6 N hydrochloric acid and extracted with benzene. The benzene extract was shaken with 2 N sodium carbonate solution, and the aqueous layer was acidified and extracted with benzene. The evaporation of the solvent from the extract left crystals (60 mg.), m. p. 45~49°C; these crystals and its picrate, m. p. 81~83°C, shown no depression of melting point on admixture with tropolone (VI), m. p. 50°C, and its picrate, m. p. 83°C respectively.

7-Chloro-2-phenoxytropone (VII).—To a heated suspension of V (500 mg.) in concentrated hydrochloric acid (10 ml.), a hot solution of copper sulfate (3 g.) in water (7 ml.) was added in one lot. After it had been heated for 5 min., the mixture was cooled, diluted with water, and extracted with benzene. The benzene extract was passed through a short alumina column to give VII (480 mg.), m. p. 137~140°C. Recrystallization from cyclohexane afforded colorless prisms, m. p. 141~142°C.

λ_{max}^{MeOH} mμ (log ε); 242 (4.44), 328 (3.99), 355 (3.91).

Found: C, 67.33; H, 4.13. Calcd. for $C_{13}H_9O_2Cl$: C, 67.11; H, 3.90%.

7-Bromo-2-phenoxytropone (VIII).—When heated suspension of V (500 mg.) in concentrated hydrobromic acid (10 ml.) was treated with an aqueous copper sulfate solution as in the above experiment, VIII (320 mg.), m. p. 139~142°C, was obtained. Recrystallization from cyclohexane afforded colorless prisms, m. p. 142~143°C.

λ_{max}^{MeOH} mμ (log ε); 252 (4.33), 330 (3.98), 355 (3.91).

Found: C, 56.61; H, 3.37. Calcd. fo $C_{13}H_9O_2Br$: C, 56.34; H, 3.27%

3-Chlorotropolone (IX): The Hydrolysis of VII.—When VII (200 mg.) was treated with a 2 N potassium hydroxide solution, as in the experiment concerning the hydrolysis of III, it afforded crystals

7) All melting poins are uncorrected.

(80 mg.), m. p. 98~103°C, Sublimation at reduced pressure and recrystallization from ethanol gave colorless prisms, m. p. 103~104°C, this melting point was undepressed on admixture with an authentic specimen.[3]

λ_{max}^{MeOH} mμ (log ε); 248 (4.51), 324 (3.89), 379 (3.76), 398 (3.38).

3-Bromotropolone (I): The hydrolysis of VIII. —The treatment VIII (100 mg.) as in above experiment afforded I (40 mg.), m. p. 106~107°C.

7-(*p*-Tolylsulfonyloxy)-2-phenoxytropone (X).—Into a cooled solution of II (630 mg.) in pyridine (1.5 ml.), *p*-toluenesulfonyl chloride (600 mg.) was stirred; the mixture was then stirred for an additional hour and allowed to stand overnight. Water (20 ml.) was added, and the crystals (1.05 g.), m. p. 119~123°C, thereby obtained were recrystallized from methanol to give X (980 mg.), m. p. 114~116°C. Further recrystallization from methanol gave colorless prisms, m. p. 127~128°C.

λ_{max}^{MeOH} mμ (log ε); 228 (4.52), 325 (3.95), 350 (3.90).

Found: C, 64.96; H, 4.54. Calcd. for $C_{20}H_{15}O_5S$: C, 65.22; H, 4.26%.

3-(*p*-Tolylsulfonyloxy)tropolone (XI).—A mixture of X (370 mg.), ethanol (1 ml.) and a 2 N potassium hydroxide solution (1 ml.) was heated for 10 min. and then acidified. The crystals (240 mg.), m. p. 83~115°C, so obtained were recrystallized twice from benzene to give XI (70 mg.) as colorless needles, m. p. 169~170°C.

λ_{max}^{MeOH} mμ (log ε); 232 (4.43), 328 (3.85), 375 (3.76), 400 (3.54).

Found: C, 57.68; H, 4.10. Calcd. for $C_{14}H_{12}O_5S$: C, 57.54; H, 4.14%.

2-Hydrazinotropone (XII): The Reaction of III with Hydrazine. — A mixture of III (100 mg.), ethanol (0.5 ml.) and 80% hydrazine hydrate (0.05 ml.) was heated for 2 min., diluted with water, and extracted with chloroform. The chloroform extract was washed with a 2 N sodium hydroxide solution and evaporated to dryness, leaving crystals (60 mg.), m. p. 90~93°C, which were then recrystallized from benzene to give XII as yellow needles, m. p. 92~93°C.

λ_{max}^{MeOH} mμ (log ε); 247 (4.37), 238 (4.09), 406 (4.05).

7-Chloro-2-hydrazinotropone (XIII).—To a suspension of VII (230 mg.) in ethanol (1 ml.), 80% hydrazine hydrate (0.06 ml.) was added, and the mixture was heated for 2 min., affording XIII (160 mg.) as yellow needles, m. p. 165°C (decomp.), after recrystallization from ethanol.

λ_{max}^{MeOH} mμ (log ε); 255 (4.35), 342 (4.07), 416 (4.05).

Found: C, 49.43; H, 4.28; N, 16.32. Calcd. for $C_7H_7ON_2Cl$: C, 49.28; H, 4.14; N, 16.42%.

Acetate.—M. p. 205°C (decomp.), yellow needles (from ethanol).

λ_{max}^{MeOH} mμ (log ε); 255 (4.40), 338 (4.08), 404 (4.07).

Found: C, 50.89; H, 4.39; N, 13.02. Calcd. for $C_9H_9O_2N_2Cl$: C, 50.83; H, 4.27; N, 13.18%.

7-Bromo-2-hydrazinotropone (XIV). — To a suspension of VIII (140 mg.) in ethanol (0.5 ml.), 80% hydrazine hydrate (0.03 ml.) was added, and the mixture was heated for 1 min. to give XIV (100 mg.), m. p. 150°C. Recrystallization from ethanol afforded yellow needles, m. p. 156°C (decomp.).

λ_{max}^{MeOH} mμ (log ε); 253 (4.26), 345 (4.03), 418 (4.07).

Found: C, 38.99; H, 3.17; N, 12.84. Calcd. for $C_7H_7ON_2Br$: C, 39.10; H, 3.28; N, 13.02%.

Acetate. — M. p. 196°C (decomp.), pale yellow, silky needles (from ethanol).

λ_{max}^{MeOH} mμ (log ε); 258 (4.35), 3.40 (4.04), 406 (4.07).

Found: C, 41.42; H, 3.47; N, 10.58. Calcd. for $C_9H_9O_2N_2Br$: C, 42.04; H, 3.53; N, 10.90%.

Isopropylidene Derivative.—M. p. 101~103°C, pale orange prisms (from ethanol).

λ_{max}^{MeOH} mμ (log ε); 272 (4.38), 358 (4.23), 428 (4.31).

Found: C, 47.44; H, 4.39; N, 10.83. Calcd. for $C_{10}H_{11}ON_2Br$: C, 47.08; H, 4.35; N, 10.98%.

Neither the acetate nor the isopropylidene derivative of XIV showed any depression of the melting point on admixture with the respective derivative prepared from authentic 7-bromo-2-hydrazinotropone.[4]

7-(*p*-Tolylsulfonyloxy)-2-hydrazinotropone (XV). —To a suspension of X (630 mg.) in ethanol (4 ml.), 80% hydrazine hydrate (0.4 ml.) was added, and the mixture was heated for 2 min. to give XV (520 mg.) as yellow microneedles, m. p. 204°C.

λ_{max}^{MeOH} mμ (log ε); 230 (4.37), 250 (4.31), 340 (4.05), 412 (4.10).

Found: C, 55.44; H, 4.35; N, 9.30. Calcd. for $C_{14}H_{14}O_4N_2S$: C, 54.89; H, 4.61; N, 9.15%.

Acetate.—M. p. 187~188°C (decomp.), pale yellow prisms (from ethanol).

λ_{max}^{MeOH} mμ (log ε); 230 (4.38), 335 (4.00), 402 (4.09).

Found: C, 55.52; H, 4.86; N, 8.29. Calcd. for $C_{16}H_{16}O_5N_2S$: C, 55.16; H, 4.63; N, 8.04%.

Isopropylidene Derivative. — M. p. 165~166°C, yellow prisms (from ethanol).

λ_{max}^{MeOH} mμ (log ε); 227 (4.37), 267 (4.34), 353 (4.19), 422 (4.29).

Found: C, 58.94; H, 5.23; N, 8.09. Calcd. for $C_{17}H_{18}O_4N_2S$: C, 58.90; H, 4.93; N, 8.19%.

2,7-Dichlorotropone (XVI).—To a hot solution of XIII (100 mg.) in concentrated hydrochloric acid (2 ml.), a 25% aqueous copper sulfate solution (2 ml.) was added; the mixture was then heated for 2 min. Water was added and the crystals thereby obtained were collected and sublimed at reduced pressure to give XVI (90 mg.), m. p. 127~129°C. Recrystallization from benzene-cyclohexane afforded colorless needles, m. p. 130~131°C.

λ_{max}^{MeOH} mμ (log ε); 248 (4.46), 328 (3.92).

Found: C, 48.29; H, 2.53. Calcd. for $C_7H_4OCl_2$: C, 48.04; H, 2.30%.

2-Bromo-7-chlorotropone (XVII). — When a suspension of XIII (100 mg.) in concentrated hydrobromic acid (2 ml.) was treated with a copper sulfate solution as in the foregoing experiment, XVII

(100 mg.), m. p. 148~150°C, was obtained. Recrystallization from benzene-cyclohexane afforded pale yellow plates, m. p. 150~151°C.

λ_{max}^{MeOH} mμ (log ε) ; 220 (4.04), 253 (4.29), 337 (3.87).

Found : C, 38.65 ; H, 2.05. Calcd. for $C_7H_4OBr\cdot Cl$: C, 38.73 ; H, 1.79%.

2-Bromo-7-(*p*-tolylsulfonyloxy)tropone (XVIII). — *a) From XV.* — To a hot solution of XV (460 mg.) in concentrated hydrobromic acid (10 ml.), a 30% aqueous copper sulfate solution (10 ml.) was added ; the mixture was then heated for 1 min. The reaction mixture was diluted with water and extracted with chloroform. When the residue obtained after the evaporation of the solvent was passed through a short alumina column, as with the benzene solution, XVIII (250 mg.), m. p. 114~116°C, was obtained. Recrystallization from methanol afforded colorless needles, m. p. 117~118°C.

λ_{max}^{MeOH} mμ (log ε) ; 227 (4.35), 248 (4.27), 325 (3.87).

Found : C, 47.30 ; H, 3.03. Calcd. for $C_{14}H_{11}\cdot O_4SBr$: C, 47.33 ; H, 3.12%.

b) From 3-Bromotropolone (I). — Into a cooled solution of I (200 mg.) in pyridine (1 ml.), *p*-toluenesulfonyl chloride (200 mg.) was stirred. The mixture was then stirred for 3 hr., diluted with water (20 ml.), and allowed to stand, thus giving XVIII (150 mg.), m. p. 113~115°C. Recrystallization from methanol afforded colorless needles, m. p. 117~118°C.

The author wishes to express his deep gratitude to Professor Tetsuo Nozoe for his kind guidance and to Professor Yoshio Kitahara for for his valuable suggestions. Thanks are also due to Miss. Kuni Kato and Miss. Ayako Iwanaga for their elemental analyses.

Department of Chemistry
Faculty of Science
Tokyo University
Katahira-cho, Sendai

The Reaction of 3-Carboxy- and 3-Cyanotropolone with Hydrazine

By Tetsuo NOZOE, Yoshio KITAHARA, Kahei TAKASE and Ichiro MURATA

(Received on March 19, 1964)

It has been known that tropolones generally do not react with the ketonic reagents, with a few exceptions, such as nitro-,[1] nitroso-[2,3] and arylazotropolone[3]. In our previous studies, however, it has been found that 3-carboxytropolone reacts with *o*-phenylenediamine to form cyclohepta[b]quinoxaline (benzo[b]tropazine).[4] The present authors have now carried out some studies of 3-carboxy- and 3-cyanotropolone and found that these tropolones react easily with hydrazine to give hydrazinotropone derivatives. Furthermore, 2-cyano- and 2-carboxytropone have been derived from 3-cyanotropolone by utilizing this reaction.

When 3-carboxytropolone (I) was heated with hydrazine in ethanol, 2-hydrazinotropone (II)[5] was obtained. Since tropolone itself does not react with hydrazine under these conditions, it is clear that the formation of II from I is not due to the reaction of hydrazine on tropolone, which would be formed by the decarboxylation of I, but to the decarboxylation of 2-carboxy-7-hydrazinotropone (III) (or its isomer; 3-carboxy-2-hydrazinotropone) formed as an intermediate.

3,5-Dibromo-7-carboxytropolone (IV)[6] also reacted with hydrazine, but no decarboxylation occurred in this case; 3,5-dibromo-7-carboxy-2-hydrazinotropone (V) (or its isomer, 5,7-dibromo-3-carboxy-2-hydrazinotropone) was obtained. The structure of V was confirmed from its analytical value, the similarity of its ultraviolet spectrum to that of II, and the formation of IV by its hydrolysis with 75% sulfuric acid.

In the reaction of 3-cyanotropolone (VI) and hydrazine in ethanol, the hydrazine salt of VI was first formed; this was changed by heating to afford a hydrazinotropone derivative (VII). The ultraviolet spectrum of VII is similar to that of II. The hydrolysis of VII with concentrated hydrochloric acid afforded

1) T. Nozoe, *Science of Drugs*, 3, 191 (1949); *Sci. Repts. Tohoku Univ.*, I, **34**, 225 (1950); T. Nozoe, Y. Kitahara, K. Doi and T. Arai, *Bull. Chem. Research Inst. Non-Aqueous Solns., Tohoku Univ.*, **7**, 13 (1957).

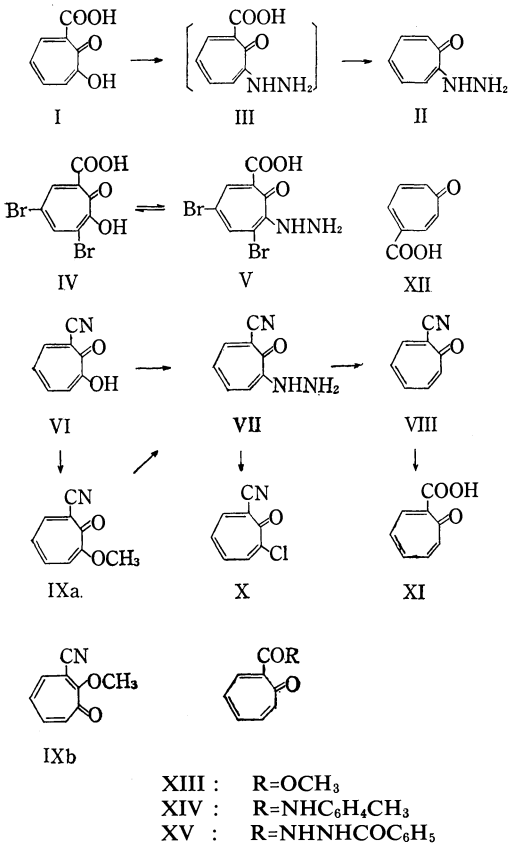
2) T. Nozoe, M. Sato and K. Matsui, *Sci. Repts. Tohoku Univ.*, I, **37**, 407 (1953); S. Ito, ibid., **42**, 236 (1958); **43**, 216 (1959).

3) T. Nozoe, S. Ito, S. Suzuki and K. Hiraga, *Proc. Japan Acad.*, **32**, 344 (1956).

4) T. Nozoe, Y. Kitahara, K. Takase and M. Sasaki, ibid., **32**, 349 (1956).

5) T. Nozoe, S. Seto, H. Takeda, S. Morosawa and K. Matsumoto, ibid., **28**, 192 (1952); *Sci. Repts. Tohoku Univ.*, I, **36**, 126 (1952).

6) Y. Kitahara, ibid., I, **40**, 74 (1956).



XIII : R=OCH_3
XIV : R=$NHC_6H_4CH_3$
XV : R=$NHNHCOC_6H_5$

VI, and the oxidative decomposition of VII in acetic acid with cupric sulfate afforded 2-cyanotropone (VIII).[7] This evidence suggests that VII is 7-cyano-2-hydrazinotropone. The methylation of VI with diazomethane afforded two methyl ethers, 2-cyano-7-methoxytropone (IXa) and 3-cyano-2-methoxytropone (IXb); one of these, IXa, gave VII when treated with hydrazine, thus establishing the structures of these methyl ethers. When VII was oxidatively decomposed in concentrated hydrochloric acid with cupric sulfate, 2-chloro-7-cyanotropone (X) was obtained.

The above-mentioned results show that the tropolonic hydroxyl group of I and VI is substituted with hydrazine to the hydrazino group. This is, presumably, due to the electron-withdrawing nature of the carboxyl or cyano group, by which the tropolone nucleus is more liable to the attack of hydrazine than is usual tropolone.

The hydrolysis of 2-cyanotropone (VIII) by heating it in 75% sulfuric acid gave 2-carboxytropone (XI) in a good yield. The isomeric 4-carboxytropone (XII) has only been synthesized by Johnson et al.;[8] therefore, the XI obtained here is of interest as one of the fundamental troponoids. Its ultraviolet absorption spectrum in methanol (maxima at 231 and 316 mμ; log ε, 4.25 and 3.85 respectively) is similar to those of the usual tropones, and its pK_a value, 3.73,[9] is smaller than those of acetic acid or benzoic acid. The bromination of XI afforded an oily substance which gave 2, 7-dibromotropone[10] when heated. Methylation with diazomethane gave an oily methyl ester (XIII), while treatment with thionyl chloride afforded an unstable acid chloride. *p*-Toluidide (XIV) and benzoylhydrazide derivative (XV) of the acid XI were derived through this methyl ester or acid chloride.

Experimental[11]

The Reaction of 3-Carboxytropolone (I) with Hydrazine.—A mixture of I (330 mg.) and 80% hydrazine hydrate (300 mg.) in ethanol (10 ml.) was refluxed for 5 hr. The solvent was then evaporated, and the residue sublimed under reduced pressure. The sublimate (130 mg.) was recrystallized from benzene to give yellow needles (110 mg.); m. p. 92~93°C, which was undepressed on admixture with 2-hydrazinotropone (II).[5] λ_{max}^{MeOH} mμ (log ε); 246 (4.37), 338 (4.09), 406 (4.05).

3, 5-Dibromo-7-carboxy-2-hydrazinotropone (V).—A mixture of 3, 5-dibromo-7-carboxytropolone (IV) (160 mg.) and 80% hydrazine hydrate (50 mg.) in ethanol (20 ml.) was refluxed for 24 hr. The removal of the solvent and recrystallization from ethanol afforded V (150 mg.) as yellow needles, m. p. 216°C (decomp.)

λ_{max}^{MeOH} mμ (log ε); 268 (4.37), 352 (4.05), 431 (3.96).

Found: N, 8.29. Calcd. for $C_8H_6O_3N_2Br_2$: N, 8.55%.

The hydrolysis of V by heating it with 75% sulfuric acid afforded IV in a good yield.

2-Cyano-7-hydrazinotropone (VII).—*From 3-Cyanotropolone (VI).*—To a hot solution of VI (600 mg.) in ethanol (20 ml.), 80% hydrazine hydrate (800 mg.) was added; hydrazine salt of VI was then crystallized out as yellow needles, m. p. 166~168°C (Found: N, 23.27. Calcd. for $C_8H_9O_2N_3$: N, 23.45%). This mixture was refluxed for 3 hr., and the crystals thereby obtained were recrystallized from ethanol to give VII (550 mg.) as orange needles, m. p. 205°C (decomp.).

λ_{max}^{MeOH} mμ (log ε); 214 (4.22), 252 (4.14), 268 (4.08), 355 (3.87), 438 (4.24). Found: C, 59.52; H, 4.71; N, 26.13. Calcd. for $C_8H_7ON_3$: C, 59.62; H, 4.38; N, 26.08%.

7) T. Nozoe, S. Seto and S. Matsumura, *Proc. Japan Acad.*, **28**, 483 (1952).

8) J. R. Bartels-Keith, A. W. Johnson and A. Langemann, *J. Chem. Soc.*, **1952**, 4461.

9) N. Tanaka, I. T. Oiwa, T. Kurosawa and T. Nozoe, This Bulletin, **32**, 92 (1959).

10) T. Nozoe, S. Seto and S. Matsumura, *Proc. Japan Acad.*, **28**, 483 (1952); T. Nozoe, T. Mukai, K. Takase and T. Nagase, ibid., **28**, 477 (1952); S. Seto, *Sci. Repts. Tohoku Univ.*, I, **37**, 275 (1953).

11) All melting points are uncorrected.

From 2-Cyano-7-methoxytropone (IXa). — To a suspension of IXa (150 mg.) in methanol (10 ml.), 80% hydrazine hydrate (100 mg.) was added; when the mixture was then allowed to stand for 2 hr. at room temperature, it gave VII (110 mg.) as orange needles, m. p. 205°C (decomp.).

The heating of VII in concentrated hydrochloric acid for 3 hr. gave VI.

The Acetate of VII; m. p. 260°C, yellow needles (from ethanol).

λ_{max}^{MeOH} mμ (log ε); 215 (4.12), 247 (4.22), 273 (4.12), 345 (3.87), 430 (4.27).

Found: C, 59.32; H, 4.73; N, 20.69. Calcd. for $C_{10}H_9O_2N_3$: C, 59.10; H, 4.46; N, 20.68%.

2-Cyanotropone (VIII).—To a hot solution of VII (200 mg.), in a mixture of glacial acetic acid (6 ml.) and water (6 ml.) a 10% cupric sulfate solution (12 ml.) was added in one lot. After it has been heated for 15 min., the mixture was diluted with water and extracted with chloroform. The solvent was removed, the residue was sublimed under reduced pressure at 130°C, and the sublimate (60 mg.), m. p. 132~137°C, was recrystallized from benzene to give VIII as yellow needles, m. p. 136~137°C (decomp.), which was identified by mixed melting point and by a comparison of its infrared spectrum with that of an authentic specimen.[7] λ_{max}^{MeOH} mμ (log ε); 238 (4.32), 305 (3.71), 320 (3.73), 340 (3.70).

2-Cyano-7-methoxytropone (IXa) and 3-Cyano-2-methoxytropone (IXb).—Into a suspension of VI (2.0 g.) in methanol (40 ml.), an ethereal solution of diazomethane was added under cooling; the mixture was then allowed to stand overnight. The crystals which separated out were collected by filtration and recrystallized from water to give IXa (530 mg.) as pale yellow needles, m. p. 173.5~174.5°C.

λ_{max}^{MeOH} mμ (log ε); 250 (4.31), 311 (3.68), 327 (3.73).

Found: C, 66.54; H, 4.45. Calcd. for $C_9H_7O_2N$: C, 67.07; H, 4.38%.

The crystalline material (1.53 g.) obtained by the removal of the solvent from the mother liquor was dissolved in benzene and chromatographed on an aluminum column. From the first effluent, IXb was obtained as pale yellow scales, m. p. 141~142°C, after recrystallization from methanol.

λ_{max}^{MeOH} mμ (log ε); 234 (4.23), 331 (3.82).

Found: C, 66.89; H, 4.69. Calcd. for $C_9H_7O_2N$: C, 67.07; H, 4.38%.

7-Chloro-2-cyanotropone (X).—To a mixture of VII (500 mg.) and concentrated hydrochloric acid (6 ml.), a 30% cupric sulfate solution (6 ml.) was added in one lot, the mixture was then heated for 5 min. The crystals which were precipitated were collected and sublimed under reduced pressure to give X (410 mg.), m. p. 155~158°C, which was recrystallized from ethanol to afford yellow needles, m. p. 162~162.5°C.

Found: C, 58.13; H, 2.86; N, 8.79. Calcd. for C_8H_4ONCl: C, 58.02; H, 2.43; N, 8.46%.

2-Carboxytropone (XI).—A mixture of VIII (220 mg.) and 75% sulfuric acid (2 ml.) was heated for 1 hr. at 120~125°C and then poured into ice-water and extracted with chloroform. The solvent was removed, and the residue was recrystallized from benzene to give XI (200 mg.) as cream-colored needles, m. p. 149°C (decomp.).

Found: C, 63.78; H, 4.19. Calcd. for $C_8H_6O_3$: C, 64.00; H, 4.03%.

The Bromination of XI.—To a solution of XI (50 mg.) in glacial acetic acid (2 ml.) bromine (160 mg.) was added; the mixture was then stirred for 1 hr. The addition of water and extraction with chloroform gave an oily substance. This oil was heated in glacial acetic acid for 1 hr., and then the mixture was diluted with water, affording crystals. Recrystallization from benzene afforded 2, 7-dibromotoropone as pale orange plates (m. p. 169~170°C), identified by admixture with an authentic specimen.[10]

Methoxycarbonyltropne (XIII).—To a solution of XI (100 mg.) in methanol (1 ml.), an ethereal solution of diazomethane was added under cooling. The removal of the solvent gave an oily XIII. λ_{max}^{MeOH} mμ (log ε); 228 (4.18), 305 (3.77).

A mixture of XIII *p*-toluidine and methanol was heated for 1 hr. The removal of the solvent and recrystallization from benzene gave a *p*-toluidide derivative (XIV) as colorless plates, m. p. 152~153°C.

Found: N, 5.70. Calcd. for $C_{15}H_{13}O_2N$; N, 5.85%.

The Reaction of XI with Thionyl Chloride.—A mixture of XI (100 mg.) and thionyl chloride (100 mg.) in dry benzene (2 ml.) was refluxed for 3 hr.; the removal of the solvent then gave acid chloride, m. p. 155~156°. To a solution of this acid chloride in benzene (2 ml.), a solution of benzoylhydrazide (200 mg.) in benzene (5 ml.) was added, and the new mixture was refluxed for 30 min. The crystals thereby obtained were recrystallized from methanol to give a benzoylhydrazide derivative (XV) (200 mg.) as yellow prisms, m. p. 191~192°C.

Found: N, 10.78. Calcd. for $C_{15}H_{12}O_3N_2$: N, 10.44%. λ_{max}^{MeOH} mμ (log ε); 235 (4.44), 305 (3.86).

The expenses of the present series of experiments were defrayed by a grant-in-aid for Scientific Research from the Ministry of Education, to which the authors' thanks are due.

Department of Chemistry
Faculty of Science
Tohoku University
Katahira-cho, Sendai

The Synthesis and Some Reactions of Polyphenoxytropolones

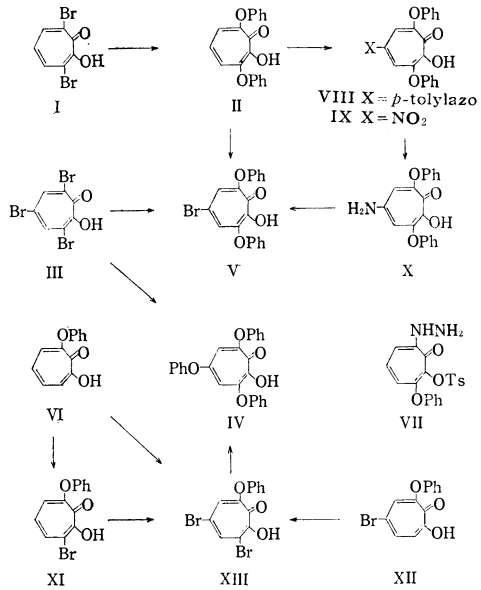
By Kahei TAKASE

(Received March 24, 1964)

In a previous paper,[1] it was described how the bromine of 3-bromotropolone was easily replaced with a phenoxyl group by heating it with sodium phenoxide, affording 3-phenoxytropolone. This reaction has now been extended to polybromotropolones, such as 3, 7-dibromotropolone and 3, 5, 7-tribromotropolone, in order to obtain polyphenoxytropolones, which are expected to be interesting from the point of view of synthetical studies in troponoid chemistry. In this paper, the synthesis of polyphenoxytropolones and some of their reactions will be reported.

The heating of 3,7-dibromotropolone (I) with an excess of sodium phenoxide in phenol, in the presence of a catalytic amount of copper acetate, gave 3, 7-diphenoxytropolone (II), in which both bromine atoms were replaced with a phenoxyl group. However, even with one or two molar equivalents of sodium phenoxide, no monosubstituted product was obtained. Similarly, when heated with an excess of phenoxide, 3, 5, 7-tribromotropolone (III) afforded 3, 5, 7-triphenoxytropolone (IV), while heated with three molar equivalents of phenoxide, a diphenoxy compound (V) was obtained. By analogy with the formation of 3-phenoxytropolone from 3-bromotropolone,[1] the phenoxyl groups of II and IV are assumed to be located at the 3 : 7 and positions 3 : 5 : 7 respectively. The structure of V was established as 5-bromo-3, 7-diphenoxytropolone from the fact that the bromination of II also afforded V.

These polyphenoxytropolones, like the common tropolones, are soluble in alkali, are colored red in chloroform with a ferric chloride solution, and give methyl ethers with diazomethane and tosylates with *p*-toluenesulfonyl chloride. When heated with hydrazine, II did not give any hydrazinotropone derivative as 3-phenoxytropolone (VI) did,[1] but only hydrazine salt. By heating in acid, the tosylate of II was hydrolyzed to reproduce II, but it gave a resinous substance in alkali. When the tosylate of II was heated with hydrazine, one of the phenoxyl groups was replaced with hydrazine to give a hydrazino derivative (VII). From the similarity of its ultraviolet absorption curve to that of 2-hydrazinotropone, VII may be assumed to be 7-hydrazino-3-phenoxy-2-(*p*-tolylsulfonyloxy)tropone. The methyl ether of II, however, afforded only a resinous product with hydrazine.



The azo-coupling of II with *p*-tolyldiazonium chloride gave a *p*-tolylazo compound VIII in a good yield. The treatment of II with sodium nitrite in acetic acid did not give any nitroso compound, but it did give a nitro compound IX. The catalytic reduction of both VIII and IX gave the same amino compound, X, which then afforded 5-bromo-3, 7-diphenoxytropolone (V) by Sandmeyer reaction. This evidence indicates that VIII, IX and X are 5-(*p*-tolylazo)-, 5-nitro- and 5-amino-3, 7-diphenoxytropolone respectively.

The bromination of 3-phenoxytropolone (VI) in methanol afforded a monobromo derivative (XI), which is different from the 5-bromo-3-phenoxytropolone (XII)[2] obtained from 5-amino-3-phenoxytropolone. On the other hand, the bromination of VI in acetic acid, in the presence of sodium acetate, afforded a dibromo compound XIII, which was also obtained by the bromination of both XI and XII in acetic acid. The treatment of XIII with

1) K. Takase, This Bulletin, 37, 1288 (1964).

2) K. Takase, ibid., 37, 1298 (1964).

sodium phenoxide gave 3, 5, 7-triphenoxytropolone (IV). From this evidence, XI and XIII may be considered to be 7-bromo-3-phenoxytropolone and 5, 7-dibromo-3-phenoxytropolone respectively.

The above-mentioned results show that bromine atoms of bromotropolones are easily replaced by phenoxide and that the chemical natures of polyphenoxytropolones thereby obtained are similar to those of common tropolones. That is, they are acidic, show positive in ferric chloride tests, give ethers or esters, and are capable of the electrophilic substitution reaction at the 3-, 5- and 7-positions. It is interesting that a nitro compound IX was produced in place of a nitroso compound by the action of nitrous acid. This unexpected result is considered to result from the action of nitrogen dioxide, or its equivalent, formed in the reaction medium.

Experimental[3]

3, 7-Diphenoxytropolone (II). — A mixture of 3, 7-dibromotropolone (I) (2.00 g.), dried sodium phenoxide (4.00 g.), copper acetate (50 mg.) and phenol (8 ml.) was heated at 135～140°C for 5 hr. The reaction mixture was then dissolved in a mixture of benzene and water, acidified with 6 N hydrochloric acid, and extracted with benzene. All the benzene extracts were combined, the benzene and phenol were distilled under reduced pressure, and the residue was recrystallized from methanol, affording II (1.95 g.) as colorless prisms, m. p. 138～139°C.

λ_{max}^{MeOH} mμ (log ε) ; 255 (4.39), 332 (3.95), 375 (3.79), 405 (3.64).

Found : C, 74.46 ; H, 4.49. Calcd. for $C_{19}H_{14}O_4$; C, 74.45 ; H, 4.60%.

Hydrazine Salt : M. p. 173°C (decomp.), yellow needles (from ethanol).

Found : C, 67.81 ; H, 4.87 ; N, 7.90. Calcd. for $C_{19}H_{18}O_4N_2$: C, 67.44 ; H, 5.36 ; N, 8.28%.

Methyl Ether : M. p. 78～79°C, colorless prisms (from benzene - petroleum ether).

λ_{max}^{MeOH} mμ (log ε) ; 225 (4.39), 325～345 (3.92).

Found : C, 74.90 ; H, 5.00. Calcd. for $C_{20}H_{16}O_4$: C, 74.99 ; H, 5.03%.

Tosylate : M. p. 118～119°C, colorless microcrystals (from methanol).

λ_{max}^{MeOH} mμ (log ε) ; 228 (4.47), 335 (3.91).

Found : C, 67.89 ; H, 4.37. Calcd. for $C_{26}H_{20}O_6S$: C, 67.82 ; H, 4.38%.

3, 5, 7-Triphenoxytropolone (IV).—*a) From 3,5,7-Tribromotropolone (III).*—A mixture of III (1.44 g.), dried sodium phenoxide (2.3 g.), copper acetate (10 mg.) and phenol (4 g.) was heated at 135～140°C for 5 hr. The reaction mixture was then treated as described in the above experiment to give IV (1.20 g.), m. p. 155～156°C. Recrystallization from benzene-methanol afforded pale yellow microprisms, m. p. 162～163°C.

λ_{max}^{MeOH} mμ (log ε) ; 262 (4.49), 337 (4.05), 390 (3.91).

Found : C, 75.14 ; H, 4.47. Calcd. for $C_{25}H_{18}O_5$: C, 75.37 ; H, 4.55%.

Methyl Ether : M. p. 96～97°C, pale yellow prisms (from methanol).

λ_{max}^{MeOH} mμ (log ε) ; 260 (4.48), 347 (4.08).

Found : C, 75.59 ; H, 4.86. Calcd. for $C_{26}H_{20}O_5$: C, 75.71 ; H, 4.89%.

Tosylate : M. p. 146～148°C, colorless needles (from methanol).

λ_{max}^{MeOH} mμ (log ε) ; 230 (4.52), 257 (4.42), 342 (4.33).

Found : C, 69.39 ; H, 4.28. Calcd. for $C_{32}H_{24}O_7S$: C, 69.56 ; H, 4.38%.

b) From 5, 7-Dibromo-3-phenoxytropolone (XIII). When a mixture of XIII (370 mg.), dried sodium phenoxide (350 mg.), copper acetate (10 mg.) and phenol (1 g.) was treated as described in a), IV (310 mg.) was obtained as pale yellow microprisms, m. p. 162～163°C.

5-Bromo-3,7-diphenoxytropolone (V).—*a) From 3, 5, 7-Tribromotropolone (III).*—A mixture of III (720 mg.), dried sodium phenoxide (720 mg.), copper acetate (10 mg.) and phenol (2 g.) was heated at 135～140°C for 5 hr. The reaction mixture was treated as described in the above experiment, and V (370 mg.), m. p. 138～139°C was obtained. Recrystallization from methanol afforded pale yellow prisms, m. p. 140～141°C.

λ_{max}^{MeOH} mμ (log ε) ; 258 (4.40), 350 (4.06), 425 (3.81).

Found : C, 59.22 ; H, 3.45. Calcd. for $C_{19}H_{13}O_4Br$: C, 59.24 ; H, 3.40%.

b) The Bromination of 3, 7-Diphenoxytropolone (II).—To a suspension of II (30 mg.) and sodium acetate (140 mg.) in glacial acetic acid, a solution of bromine (160 mg.) in the same solvent (0.5 ml.) was added ; the mixture was then stirred under cooling for 4 hr. The reaction mixture was diluted with water and extracted with chloroform. After the solvent had been removed from the extract, the residual oil was solidified by the addition of methanol, affording V (220 mg.) as pale yellow prisms, m. p. 140～141°C.

c) The Sandmeyer Reaction of 5-Amino-3, 7-diphenoxytropolone (X).—A solution of X (110 mg.) in dioxane (1 ml.) containing 6 N sulfuric acid (0.3 ml.) was diazotized by the addition of a solution of sodium nitrite (30 mg.) in water (0.3 ml.) at 0～5°C over a 40 min. period. This diazotized mixture was then stirred into a solution of cuprous bromide (200 mg.) in concentrated hydrobromic acid (2 ml.) at room temperature. After being stirred for a further 2 hr., the mixture was diluted with water, and the copper chelate thereby formed was collected and dried. Into a suspension of this copper chelate in chloroform, hydrogen sulfide gas was passed, and the copper sulfide thereby formed was filtered off. The removal of the solvent from the filtrate and the recrystallization of the residue from methanol gave V (80 mg.) as pale yellow prisms, m. p. 140～141°C.

7-Hydrazino-3-phenoxy - 2 -(*p* - tolylsulfonyloxy)-tropone (VII).—A mixture of the tosylate of II

3) All melting points are uncorrected.

(100 mg.), 80% hydrazine hydrate (0.2 ml.) and ethanol (2 ml.) was heated for 1 min., affording VII (80 mg.) as yellow micro-needles, m. p. 194°C (decomp.).

λ_{max}^{MeOH} mμ (log ε); 228 (4.34), 260 (4.41), 343 (3.95), 404 (4.13).

Found: C, 60.32; H, 4.60; N, 6.81%. Calcd. for $C_{20}H_{18}O_5N_2S$: C, 60.30; H, 4.55; N, 7.03%.

5-(*p*-Tolylazo)-3, 7-diphenoxytropolone (VIII).—A *p*-tolyldiazonium chloride solution prepared from *p*-toluidine (110 mg.), 6 N hydrochloric acid (0.5 ml.) and sodium nitrite (80 mg.) was stirred into a solution of II (300 mg.) in pyridine (4 ml.). After it had stirred for 2 hr., water was added, and the crystals thereby formed were collected and washed with methanol to give VIII (400 mg.), m. p. 194~197°C. Recrystallization from ethyl acetate afforded orange silky needles, m. p. 200~201°C.

λ_{max}^{MeOH} mμ (log ε); 307 (4.22), 414 (4.36), 462 (4.30).

Found: C, 73.37; H, 4.49; N, 6.92. Calcd. for $C_{26}H_{20}O_4N_2$: C, 73.57; H, 4.75; N, 6.60%.

5-Nitro-3, 7-diphenoxytropolone (IX).—Into a cooling suspension of II (200 mg.) in glacial acetic acid (3 ml.), a solution of sodium nitrite (150 mg.) in water (0.5 ml.) was stirred. After it had been stirred for a further 3 hr., the mixture was diluted with water, giving yellow crystals (120 mg), m. p. 172°C (decomp.). Recrystallization from methanol gave IX (80 mg.) as yellow silky needles, (m. p. 188°C (decomp.).

λ_{max}^{MeOH} mμ (log ε); 220 (4.38), 404 (4.23).

Found: C, 64.77, 64.91; H, 3.52, 3.90; N, 3.64. Calcd. for $C_{19}H_{13}O_6N$: C, 64.96; H, 3.73; N, 3.99%.

5-Amino-3, 7-diphenoxytropolone (X).—*a) The Hydrogenolysis of VIII.*—A suspension of VIII (200 mg.) in methanol (5 ml.) was shaken with hydrogen in the presence of platinum oxide (5 mg.); 27 ml. of hydrogen gas was absorbed in a period of 1.5 hr. The catalyst was then filtered off, and the filtrate was concentrated to a small volume to give X (110 mg.), m. p. 235~239°C. Recrystallization from methanol afforded yellow plates, m. p. 240~241°C.

λ_{max}^{MeOH} mμ (log ε); 258 (4.45), 353 (4.15), 410 (3.94).

Found: C, 70.82; H, 4.63; N, 4.41. Calcd. for $C_{19}H_{15}O_4N$: C, 71.02; H, 4.71; N, 4.36%.

N-Acetate: M. p. 216~217°C, pale yellow micro-needles (from ethanol.)

λ_{max}^{MeOH} mμ (log ε); 465 (4.42), 348 (4.11).

Found: C, 68.68; H, 4.39; N, 3.91. Calcd. for $C_{21}H_{17}O_5N$: C, 69.41; H, 4.72; N, 3.86%.

b) The Hydrogenolysis of IX.—A suspension of IX (90 mg.) in methanol (3 ml.) was skaken with hydrogen in the presence of platinum oxide (5 mg.); 23 ml. of hydrogen gas was absorbed in a period of 1 hr. After the removal of the catalyst and the solvent, the residue was recrystallized from methanol, affording X (60 mg.) as yellow plates, m. p. 240~241°C.

7-Bromo-3-phenoxytropolone (XI).—Into a cooling suspension of 3-phenoxytropolone (VI) (640 mg.) in methanol (10 ml.), a solution of bromine (530 mg.) in methanol (1 ml.) was stirred. After the mixture had been stirred for 1 hr., the removal of the solvent gave an oily material, which was chromatographed through a column of silica gel as a solution in benzene. From the second effluent, the evaporation of the solvent gave crystals (220 mg.), m. p. 91~94°C, which were then recrystallized from cyclohexane, affording XI as pale yellow needles, m. p. 98~99°C.

λ_{max}^{MeOH} mμ (log ε); 260 (4.45), 335 (3.96), 415 (3.89).

Found: C, 53.32; H, 3.23. Calcd. for $C_{13}H_9O_3Br$: C, 53.26; H, 3.10%.

5, 7-Dibromo-3-phenoxytropolone (XIII).—*a) The Bromination of 3-Phenoxytropolone (VI).*—To a suspension of VI (210 mg.) and sodium acetate (240 mg.) in glacial acetic acid (1 ml.), bromine (320 mg.) was added. After the mixture had been stirred for 2 hr., water was added and the crystals thereby formed were collected to give XIII (340 mg.), m. p. 136~138°C. Recrystallization from methanol afforded pale yellow needles, m. p. 140~141°C.

λ_{max}^{MeOH} mμ (log ε); 262 (4.50), 350 (4.14), 435 (3.97).

Found: C, 42.17; H, 2.29. Calcd. for $C_{13}H_8O_3Br_2$: C, 41.99; H, 2.17%.

b) The Bromination of 7-Bromo-3-phenoxytropolone (XI).—To a suspension of XI (30 mg.) and sodium acetate (10 mg.) in glacial acetic acid (0.5 ml.), bromine (20 mg.) was added. After it had been stirred for 2 hr., the mixture was treated as described in a) and XIII (30 mg.) was obtained as pale yellow needles, m. p. 140~141°C.

c) The Bromination of 5-Bromo-3-phenoxytropolone (XII).—When XII (60 mg.) was brominated as in a), XIII (40 mg.) was obtained, m. p. 140~141°C.

The author wishes to take this opportunity to express his sincere gratitude to Professor Tetsuo Nozoe for his kind guidance throughout the course of this work, and to Professor Shuichi Seto and Professor Yoshio Kitahara for much helpful advice. Thanks are also due to Miss Kuni Kato and Miss Ayako Iwanaga for their elementary analyses.

Department of Chemistry
Faculty of Science
Tohoku University
Katahira-cho, Sendai

The Synthesis of 4-Substituted Tropolones from 3-Phenoxytropolone

By Kahei TAKASE

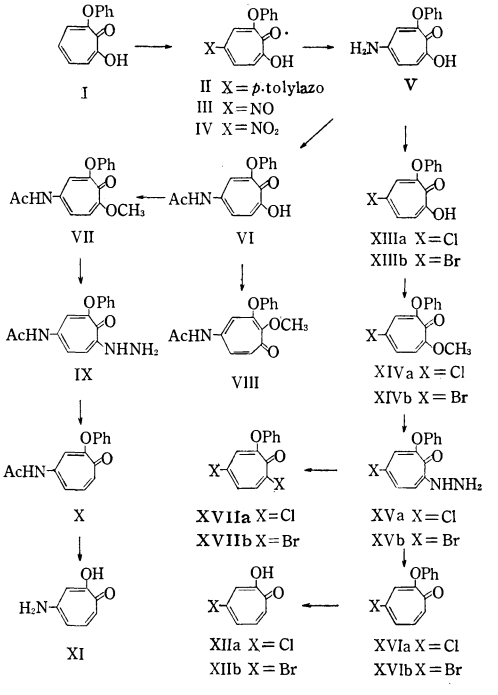
(Received March 24, 1964)

In a previous paper,[1] it was described how 2-phenoxytropone has been synthesized from 3-phenoxytropolone through a hydrazinotropone derivative. This reaction has now been extended to 5-substituted 3-phenoxytropolones in order to synthesize some 4-substituted tropolones, such as 4-amino-, 4-chloro- and 4-bromotropolone, which are fundamental compounds in troponoid and are interesting in their chemical natures.

The azo-coupling of 3-phenoxytropolone (I)[1] with *p*-tolyldiazonium chloride afforded a *p*-tolylazo compound (II). On the other hand, the nitrosation of I with sodium nitrite in acetic acid afforded a nitroso compound (III), and the nitration of I with fuming nitric acid afforded a nitro compound (IV). By catalytic reduction all of these compounds (II, III and IV) gave the same amino compound (V.) From the general tendency in the electrophilic substitution of tropolones, which suggests that azo and nitroso groups are located at the 5-position of the tropolone ring,[2] II and III are assumed to be 5-(*p*-tolylazo)- and 5-nitroso-3-phenoxytropolone respectively; consequently, IV and V are 5-nitro- and 5-amino-3-phenoxytropolone respectively.

The acetylation of V gave a monoacetate (VI), which is assumed to be 5-acetamido-3-phenoxytropolone from its acidic nature, its positive color reaction with ferric chloride, and its infrared spectrum, which shows an absorption at 1683 cm^{-1} (C=O of amide). The methylation of VI with diazomethane afforded two methyl ethers (VII and VIII.) When heated with hydrazine, one of these methyl ethers, VII, gave a hydrazinotropone derivative (IX,) in which the methoxyl group was replaced with hydrazine. The oxidative decomposition of IX with copper sulfate in acetic acid afforded a dehydrazinated compound (X,) which is assumed to be 4-acetamido-2-phenoxytropone from its infrared spectrum, which shows absorptions at 1704 cm^{-1} (C=O of amide) and 827 cm^{-1}.[3] The alkaline hydrolysis of X afforded an amino compound, which was identical with the 4-aminotropolone (XI) obtained from 4-acetyltropolone by a Schmidt reaction[4] or from 3-iodotropolone by an abnormal substitution reaction in liquid ammonia.[4] On the basis of these results, it is established that IX and X are 4-acetamido-7-hydrazino-2-phenoxytropone and 4-acetamido-2-phenoxytropone respectively, and that, consequently, methyl ether VII and VIII are 4-acetamido-7-methoxy-2-phenoxytropone and 5-acetamido-2-methoxy-3-phenoxytropone respectively.

4-Chlorotropolone (XIIa) and 4-bromotropolone (XIIb) were synthesized from 5-amino-3-phenoxytropolone (V) as described in the following sequence. By a Sandmeyer reaction, V was converted to 5-chloro-3-phenoxytropolone (XIIIa) and 5-bromo-3-phenoxytropolone (XIIIb), which in turn gave crystalline methyl ethers, 4-chloro-7-methoxy-2-phenoxytropone (XIVa) and 4-bromo-7-methoxy-2-phenoxytropone (XIVb) with diazomethane respectively. The heating of methyl ethers, (XIVa and XIVb) with hydrazine afforded



1) K. Takase, This Bulletin, 37, 1288 (1964).
2) T. Nozoe, *Fortsh. Chem. org. Naturstoffe*, 13, 273 (1956).
3) 2,4-Disubstituted tropones show the characteristic absorption in the 810~840 cm^{-1} range (T. Nozoe, K. Takase and M. Yasunami, to be published).
4) K. Doi, This Bulletin, 34, 497, 501 (1961).

4-chloro-7-hydrazino-2-phenoxytropolone (XVa) and 4-bromo-7-hydrazino-2-phenoxytropone (XVb) respectively, in both of which the methoxyl group was replaced with hydrazine. The oxidative decomposition of hydrazino compounds, (XVa and XVb,) with copper sulfate in acetic acid afforded 4-chloro-2-phenoxytropone (XVIa) and 4-bromo-2-phenoxytropone (XVIb), the alkaline hydrolysis of which gave the known 4-chlorotropolone (XIIa)[6] and 4-bromotropolone (XIIb)[5,6] respectively. By the oxidative decomposition of hydrazino compounds, (XVa and XVb,) with copper sulfate in concentrated hydrochloric acid or hydrobromic acid, 4, 7-dichloro-2-phenoxytropone (XVIIa) and 4, 7-dibromo-2-phenoxytropone (XVIIb) were obtained. The above-mentioned results confirm that 4-substituted tropolones were synthesized from 3-phenoxytropolone.

Experimental[7]

5-(*p*-Tolylazo)-3-phenoxytropolone (II).—Into a solution of 3-phenoxytropolone (I) (420 mg.) in a N potassium hydroxide solution (10 ml.), *p*-tolyldiazonium chloride solution prepared from *p*-toluidine (240 mg.) was stirred. The mixture was then stirred for a further 2 hr. and acidified with 6 N hydrochloric acid. The crystals (640 mg.) m. p. 141~143°C, so obtained were recrystallized from benzene, affording II (520 mg.) as red needles, m. p. 156~157°C.

λ_{max}^{MeOH} mμ (log ε) ; 232 (4.32), 300 (4.11), 402 (4.38).

Found: C, 72.43; H, 5.10; N, 8.52. Calcd. for $C_{20}H_{16}O_3N_2$: C, 72.28; H, 4.85; N, 8.43%.

5-Nitroso-3-phenoxytropolone (III).—To a stirred solution of I (4.28 g.) in glacial acetic acid (28 ml.), a solution of sodium nitrite (4.0 g.) in water (8 ml.) was added over a 1 hr. period at 0~5°C. The mixture was stirred for a further hour, and then allowed to stand overnight in an ice-box. The crystals thereby obtained were collected by filtration and washed with water, affording III (3.57 g.), m. p. 198°C (decomp.). Recrystallization from a large amount of ethanol afforded yellowish orange rhombo prisms, m. p. 202°C (decomp.).

λ_{max}^{MeOH} mμ (log ε) ; 250 (3.93), 298 (4.05), 460 (3.50).

Found: C, 64.07; H, 3.68; N, 5.64. Calcd. for $C_{13}H_9O_4N$: C. 64.20; H, 3.73; N, 5.76%.

5-Nitro-3-phenoxytropolone (IV).—To a solution of I (210 mg.) in glacial acetic acid (2 ml.), fuming nitric acid (0.05 ml.) was added under cooling, and the mixture was then stirred for 1 hr. The addition of water to the mixture gave IV (70 mg.) as yellow crystals, m. p. 139~142°C, which were recrystallized from methanol, affording yellow needles, m. p. 143~144°C.

λ_{max}^{MeOH} mμ (log ε) ; 245 (4.25), 390 (4.17), 432 (4.25).

Found: C, 60.03; H, 3.60; N, 5.54. Calcd. for $C_{13}H_9O_5N$: C, 60.23; H, 3.50; N, 5.40%.

5-Amino-3-phenoxytropolone (V).—*a) From 5-(p-Tolylazo)-3-phenoxytropolone (II).*—A suspension of II (150 mg.) in methanol (10 ml.) was shaken with hydrogen in the presence of 5% palladium on carbon (20 mg.) ; 23 ml. of hydrogen (23°C, 760 mmHg) was absorbed during 5 hr. The catalyst was then removed and the solvent evaporated, affording a mixture of crystals and an oily substance. Benzene was added to this mixture, and soluble part was decanted off. The residue was recrystallized from methanol to give V (70 mg.) as yellow needles, m. p. 90~94°C, which showed the same melting point upon further recrystallization from the same solvent.

λ_{max}^{MeOH} mμ (log ε) ; 235 (4.38), 358 (4.24).

Found: C, 65.03, 64.88; H, 5.52, 5.34; N, 5.57, 5.54. Calcd. for $C_{13}H_{11}O_3N \cdot CH_3OH$: C, 64.36; H, 5.79; N, 5.36%.

b) From 5-Nitroso-3-phenoxytropolone (III).—When a suspension of III (2.43 g.) in methanol (40 ml.) was hydrogenated in the presence of 5% palladium on carbon (200 mg.), 490 ml. of hydrogen (20°C, 760 mmHg) was absorbed during 1 hr. The catalyst was then filtered off and the filtrate concentrated to give V (1.91 g.) as yellow needles, m. p. 92~94°C.

The hydrogenolysis of III in the presence of platinum oxide also gave V.

c) From 5-Nitro-3-phenoxytropolone (IV).—When a solution of IV (60 mg.) in methanol (5 ml.) was hydrogenated in the presence of platinum oxide, V (30 mg.) was obtained as yellow needles, m. p. 90~93°C, after the treatment described in b).

5-Acetamido-3-phenoxytropolone (VI).—When a mixture of V (1.86 g.) and acetic anhydride (3.7 ml.) was heated for 5 min. and then cooled, it afforded VI (1.55 g.) as yellow needles, m. p. 190~191°C.

λ_{max}^{MeOH} mμ (log ε) ; 242 (4.38), 348 (4.18).

Found: C, 66.76; H, 4.94; N, 5.10. Calcd. for $C_{15}H_{13}O_4N$: C, 66.41; H, 4.83; N, 5.16%.

4-Acetamido-7-methoxy-2-phenoxytropone (VII) and 5-Acetamido-2-methoxy-3-phenoxytropone (VIII).—To a stirred suspension of VI (1.35 g.) in a mixture of ether (2.5 ml.) and ethyl acetate (5 ml.), an ethereal solution of diazomethane (10 ml.) was added under cooling with ice-water. After the mixture had been stirred for a further 6 hr., the crystals (940 mg.), m. p. 191~194°C, so obtained were collected by filtration and recrystallized from methanol, affording VII (540 mg.) as pale yellow prisms, m. p. 216~218°C.

λ_{max}^{MeOH} mμ (log ε) ; 245 (4.34), 343 (4.15), 368 (4.12).

Found: C, 67.31; H, 5.68; N, 4.80. Calcd. for $C_{16}H_{15}O_4N$: C, 67.36; H, 5.30; N, 4.91%.

All the filtrates were combined, the solvent was removed, and the residue was dissolved in ethyl acetate and chromatographed through and alumina column. The first effluent gave crystals (470 mg.), m. p. 120~124°C, which were then recrystallized

5) K. Doi, ibid., **34**, 504 (1961).
6) T. Sato, *J. Chem. Soc. Japan, Pure Chem. Sec.* (*Npipon Kagaku Zasshi*), **80**, 1171 (1959).
7) All melting points are uncorrected.

from ethyl acetate, affording VIII as yellow scaels, m. p. 126~127°C.

λ_{max}^{MeOH} mμ (log ε); 245 (4.35), 340 (4.18).

Found: C, 67.48; H, 5.27; N, 4.86. Calcd. for $C_{16}H_{15}O_4N$: C, 67.36; H, 5.30; N, 4.91%.

From the second effluent, VII (250 mg.) was obtained, m. p. 214~216°C after recrystallization from methanol.

4-Acetamido-7-hydrazino-2-phenoxytropone (IX).—A mixture of VII (540 mg.), ethanol (1.5 ml.) and 80% hydrazine hydrate (0.2 ml.) was warmed for 2 min. and then cooled to give IX (460 mg.) as yellow needles, m. p. 210°C (decomp.).

λ_{max}^{MeOH} mμ (log ε); 258 (4.37), 360 (4.27), 428 (3.99).

Found: C, 63.13; H, 5.13; N, 15.10. Calcd. for $C_{15}H_{15}O_3N_3$: C, 63.15; H, 5.30; N, 14.73%.

Acetate: M. p. 247°C (decomp.), pale yellow needles (from ethanol).

λ_{max}^{MeOH} mμ (log ε); 252 (4.39), 355 (4.29), 410 (4.01).

Found: C, 62.17; H, 5,01; N, 12.59. Calcd. for $C_{17}H_{17}O_4N_3$: C, 62.37; H, 5.24; N, 12.84%.

4-Acetamido-2-phenoxytropone (X).—A solution of IX (200 mg.) in a mixture of glacial acetic acid (3 ml.) and water (1 ml.) was heated at about 100°C; to this, a 30% copper sulfate solution (1.2 ml.) was added in one lot and heating was continued for 2 min. The reaction mixture was then diluted with water (15 ml.) and extracted with chloroform, and the chloroform solution was passed through a short alumina column. The evaporation of the solvent from the effluent left crystals (130 mg.), m. p. 168~171°C, which were recrystallized from a mixture of chloroform and ethyl acetate to give X as colorless needles, m. p. 174~175°C.

λ_{max}^{MeOH} mμ (log ε); 268 (4.25), 358 (4.05).

Found: C, 70.16; H, 5.45; N, 5.47. Calcd. for $C_{15}H_{13}O_3N$: C, 70.58; H, 5.13; N, 5.49%.

4-Aminotropolone (XI).—A mixture of X (120 mg.) in ethanol (2 ml.) and a 2 N potassium hydroxide solution (1 ml.) was heated under reflux for 2 hr. and then neutralized to pH 7 with 2 N hydrochloric acid and extracted with chloroform. After the evaporation of the solvent, the residue was sublimed in vacuo and recrystallized from methanol to give XI (40 mg.) as colorless needles, m. p. 187~188°C, which showed no depression of melting point on admixture with an authentic specimen.[4]

N-Acetate: M. p. 167°C; pale brown prisms (from ethanol).

λ_{max}^{MeOH} mμ (log ε); 267 (4.56), 335 (3.75), 365 (3.85).

Found: C, 60.51; H, 5.00; N, 7.74. Calcd. for $C_9H_9O_3N$: C, 60.33; H, 5.06; N, 7.82%.

5-Chloro-3-phenoxytropolone (XIIIa).—To a stirred mixture of V (920 mg.) in 50% aqueous dioxane (10 ml.) containing concentrated sulfuric acid (0.6 ml.), a solution of sodium nitrite (360 mg.) in water (1 ml.) was added over a 30 min. period at 0~5°C. After being stirred for an additional hour, the mixture was stirred into a solution of cuprous chloride (1.4 g.) in concentrated hydrochloric acid (7.5 ml.); stirring was then continued for one hour. Water was added, and the copper chelate thereby obtained was collected by filtration and dried. Into a suspension of this copper chelate in chloroform, hydrogen sulfide gas was passed, and the copper sulfide thereby formed was filtered off. The evaporation of the solvent from the filtrate gave XIIIa (710 mg.), m. p. 100~103°C, which was recrystallized from methanol, affording pale yellow prisms, m. p. 106~107°C.

λ_{max}^{MeOH} mμ (log ε); 248 (3.40), 342 (4.09), 385 (3.77), 416 (3.68).

Found: C, 62.95; H, 3.96. Calcd. for $C_{13}H_9O_3Cl$: C, 62.79; H, 3.65%.

5-Bromo-3-phenoxytropolone (XIIIb).—A diazotized solution of III (920 mg.), as in the above experiment, was treated with a solution of cuprous bromide (1.4 g.) in concentrated hydrobromic acid (7.5 ml.). The copper chelate so obtained was treated with hydrogen sulfide gas to give XIIIb (870 mg.), m. p. 93~96°C. Recrystallization from methanol afforded pale yellow needles, m. p. 100~101°C).

λ_{max}^{MeOH} mμ (log ε); 250 (4.42), 342 (4.17), 390 (3.75), 416 (3.79).

Found: C, 53.34, H, 2.09. Calcd. for $C_{13}H_9O_3Br$: C, 53.26; H, 3.10%.

4-Chloro-7-methoxy-2-phenoxytropone (XIVa).—To a stirred suspension of XIIIa (950 mg.) in ether (8 ml.), an ethereal solution of diazomethane (6.5 ml.) was added while it was being cooled with ice-water; then the mixture was stirred for 3 hr. and allowed to stand overnight. The crystals so obtained were collected by filtration and recrystallized from ethanol, affording XIVa (430 mg.) as pale yellow needles, m. p. 133~134°C.

λ_{max}^{MeOH} mμ (log ε); 248 (4.37), 330 (4.05), 362 (3.91).

Found: C, 63.96; H, 3.99. Calcd. for $C_{14}H_{11}O_3Cl$: C, 64.01; H, 4.23%.

The removal of the solvent from the filtrate gave an oily substance, which was then dissolved in benzene and chromatographed through an alumina column. The first effluent gave an oily substance (300 mg.), while the second effluent gave XIVa (100 mg.).

4-Bromo-7-methoxy-2-phenoxytropone (XIVb).—The same treatment of XIIIb (1.03 g.) with diazomethane as in the above experiment and recrystallization from ethanol afforded XIVb (470 mg.) as pale yellow needles, m. p. 155~156°C.

λ_{max}^{MeOH} mμ (log ε); 428 (4.42), 330 (4.05), 360 (3.94).

Found: C, 54.92; H, 3.09. Calcd. for $C_{14}H_{11}O_3Br$: C, 54.74; H, 3.61%.

The filtrate was chromatographed as in the above experiment, giving an oily substance (300 mg.) and XIVb (70 mg.).

4-Chloro-7-hydrazino-2-phenoxytropone (XVa).—When mixture of XIVa (400 mg.) in ethanol (2 ml.) and 80% hydrazine hydrate (0.2 ml.) was warmed for 2 min., XVa was obtained as yellow needles, m. p. 205°C (decomp.).

λ_{max}^{MeOH} mμ (log ε) ; 256 (4.22), 352 (4.14), 430 (3.92).

Found : C, 59.64 ; H, 3.98 ; N, 10.48. Calcd. for $C_{13}H_{11}O_2N_2Cl$: C, 59.43 ; H, 4.23 ; N, 10.68%.

Acetate : M. p. 155～157°C ; pale yellow needles (from methanol).

λ_{max}^{MeOH} mμ (log ε) ; 255 (4.32), 348 (4.12), 398 (3.94), 414 (3.96).

Found : C, 59.09 ; H, 4.13 ; N, 9.01. Calcd. for $C_{15}H_{13}O_3N_2Cl$: C, 59.12 ; H, 4.33 ; N, 9.19%.

4-Bromo-7-hydrazino-2-phenoxytropone (XVb).—The treatment of XIVb (400 mg.) with hydrazine, as in the above experiment, afforded XVb (340 mg.) as yellow needles, m. p. 199°C (decomp.).

λ_{max}^{MeOH} mμ (log ε) ; 258 (4.19), 355 (4.09), 430 (3.80).

Found : C, 50.69 ; H, 3.74 ; N, 8.90. Calcd. for $C_{13}H_{11}O_2N_2Br$: C, 50.83 ; H, 3.61 ; N, 9.12%.

Acetate : M. p. 185～186°C, yellow needles (from ethanol).

λ_{max}^{MeOH} mμ (log ε) ; 255 (4.33), 348 (4.22), 395 (3.93), 412 (3.95).

Found : C, 51.74 ; H, 3.65 ; N, 7.79. Calcd. for $C_{15}H_{13}O_3N_2Br$: C, 51.59 ; H, 3.75 ; N, 8.02%.

4-Chloro-2-phenoxytropone (XVIa).—A solution of XVa (180 mg.) in a mixture of glacial acetic acid (2 ml.) and water (1 ml.) was heated at about 100°C ; to this, a 30% copper sulfate solution (1.5 ml.) was added in one lot and heating was continued for 15 min. The mixture was then diluted with water and extracted with chloroform, and the chloroform solution was passed through a short alumina column. The removal of the solvent from the effluent left crystals (110 mg.), m. p. 80～83°C, which were recrystallized from a mixture of benzene and cyclohexane to give XVIa as colorless prisms, m. p. 85～86°C.

λ_{max}^{MeOH} mμ (log ε) ; 238 (4.37), 332 (3.95).

Found : C, 66.52 ; H, 3.61. Calcd. for $C_{13}H_9O_2Cl$: C, 67.11 ; H, 3.90%.

4-Bromo-2-phenoxytropone (XVIb). — The same treatment of XVb (210 mg.) with a copper sulfate solution, as in the above experiment, and recrystallization from a mixture of benzene and cyclohexane afforded XVIb (100 mg.) as colorless prisms, m. p. 94～95°C.

λ_{max}^{MeOH} mμ (log ε) ; 242 (4.37), 332 (4.00).

Found : C, 56.40 ; H, 3.23. Calcd. for $C_{13}H_9O_2Br$: C, 56.34 ; H, 3.27%.

4-Chlorotropolone (XIIa).—A solution of XVIa (70 mg.) in a mixture of ethanol (1 ml.) and a 2 N potassium hydroxide solution (1 ml.) was heated under reflux for 2 hr. and then acidified with 6 N hydrochloric acid and extracted with benzene. The benzene layer was shaken with a 2 N potassium carbonate solution, and the carbonate layer was acidified and extracted with chloroform. The removal of the solvent from the extract and the sublimation of the residue in vaccuo afforded colorless crystals, m. p. 68～71°C. Recrystallization from ethanol gave XIIa, m. p. 79～80°C, as colorless needles, which showed no depression of melting point on admixture with an authentic specimen.[6]

4-Bromotropolone (XIIb). — The hydrolysis of XVIb (70 mg.), as in the above experiment, afforded colorless crystals (40 mg.), m. p. 80～83°C. Recrystallization from ethanol gave XIIb, m. p. 87～88°C, as colorless needles, which showed no depression of melting point on admixture with an authentic specimen.[5,6]

4, 7-Dichloro-2-phenoxytropone (XVIIa).—A suspension of XVa (100 mg.) in concentrated hydrochloric acid (2 ml.) was heated at about 100°C ; to this, a 20% copper sulfate solution (2 ml.) was added in one lot, and heating was continued for 2 min. The mixture was then diluted with water and extracted with chloroform. The solvent was evaporated, and the residue was passed through a short almina column in a benzene solution to give XVIIa (70 mg.), m. p. 112～115°C. Recrystallization from methanol afforded colorless needles, m. p. 115～116°C.

λ_{max}^{MeOH} mμ (log ε) ; 248 (4.42) ; 340 (3.99).

Found : C, 58.19 ; H, 3.08. Calcd. for $C_{13}H_8O_2Cl_2$: C, 58.45 ; H, 3.02%.

4, 7-Dibromo-2-phenoxytropone (XVIIb). — The treatment of XVb (100 mg.) in concentrated hydrobromic acid with a copper sulfate solution, as in the above experiment, afforded XVIIb (50 mg.), m. p. 112～114°C. Recrystallization from methanol afforded pale yellow needles, m. p. 117～119°C.

λ_{max}^{MeOH} mμ (log ε) ; 262 (4.33), 345 (3.99).

Found : C, 43.68 ; H, 2.75. Calcd. for $C_{13}H_8O_2Br_2$: C, 43.54 ; H, 2.26%.

The author wishes to take this opportunity to express his sincere gratitude to Professor Tetsuo Nozoe for his kind guidance throughout the course of this work, and to Professor Shuichi Seto and Professor Yoshio Kitahara for much helpful advice.

Department of Chemistry
Faculty of Science
Tohoku University
Katahira-cho, Sendai

*Spectroscopic Studies of the Complex Produced by Trimethylaluminum and Diphenylamine**

By Makoto KAWAI, Teiichiro OGAWA and Kozo HIROTA

(Received March 19, 1964)

In order to make clear the polymerization mechanism of lower olefins and epoxides by the use of a Ziegler-type catalyst, it is most important to know the chemical and physical nature of the catalyst. In our previous work, the structure of trialkylaluminum was studied by infrared spectroscopy.[1] The present papar will report on the structure of the complex obtained by the reaction of trimethylaluminum and diphenylamine. Since trimethylaluminum is the lowest member of the trialkylaluminum series, this compound has been well investigated in spite of its low reactivity toward lower olefins. Until recently only a few compounds of $R_2Al\text{–}NR'_2$ type have been reported.

Formerly Brown and Davidson studied a trimethylaluminum and dimethylamine complex.[2] Then Fetter and Bartocha reported on the reaction of trimethylaluminum with various methyl hydrazines.[3] Hoffmann and Tornau described the compound $(Et_2Al\text{-}NC_9H_8)_2$[4] and Murahashi et al. investigated the polymerization of methyl methacrylate by an $EtAl\text{-}N(C_6H_5)$ catalyst.[5] In the publication mentioned above, it was concluded that most of the compounds a covalent aluminum-nitrogen bond was formed by a general reaction scheme:

$$AlR_3 + R'_2NH \rightarrow R_3Al : NHR'_2$$
$$\rightarrow R_2Al\text{–}NR'_2 + HR$$

The compound of the $R_2Al\text{–}NR'_2$ type has been suggested as associating to form a dimer through nitrogen bridges.[2,3] As the complex was sensitive both to air and to moisture, the reaction and subsequent manipulation were carried out under a high vacuum.

Experimental

Materials. — Trimethylaluminum (Ethyl Corp.) was transferred to several break-sealed ampoules in a dry nitrogen atmosphere and then distilled into storage ampoules under a high vacuum. Diphenylamine was recrystallized from alcohol, and was dried and degassed in vacuo before use. Cyclohexane (optical grade) was dried with calcium hydride and evaporated sodium film and then distilled in vacuo into break-sealed storage ampoules.

Reaction. — The reaction was carried out in a conventional high-vacuum system. Trimethylaluminum was transferred to a cold reactor (−196°C) containing diphenylamine. By warming the reactor toward room temperature, some gas was gradually evolved indicating the commencement of the reaction. After the mixture had been heated to the melting point of the product so as to complete the reaction, the excess trimethylaluminum and evolved gas were pumped out. The product was solid at room temperature and liquid at an elevated temperature. Cyclohexane was distilled into the reactor so as to dissolve the product. Then the solution was led into an NMR tube and a break-sealed capsule (for ultraviolet absorption measurements) previously attached to the reactor. Both NMR tube and break-sealed capsule were sealed and removed from the vacuum line.

Apparatus and Measurements.—The evolved gas was analyzed by a Hitachi Model RMU-5B mass-spectrometer installed at the Institute for Protein Reserch of Osaka University. Measurements of the ultraviolet spectra were made with a Hitachi Model EPS-2 spectrometer using 1-cm. quartz cells at room temperature. Samples were prepared under a high vacuum in a U-tube attached to the ampoule (Fig. 1). At first, the break-sealed capsule was broken, the cyclohexane in the ampoule was then transferred to the capsule, and the solution was introduced into the cell. The sample was diluted by distilling cyclohexane into the cell. The proton resonance spectra were obtained with a Varian Model A-60 high-resolution NMR spectrometer at 60 Mc. The sweep rate was about 1 p.p.m./min. For the measurement of the temperature dependence of the rate of methyl group exchange in the system of trimethylaluminum and the complex, the standard equipment of the spectrometer was used. The solvent was used as an internal reference (8.56 p.p.m. in τ value).

* Paper read at the Symposium on Molecular Structure (held by the Chemical Society of Japan), Sendai, October, 1963.

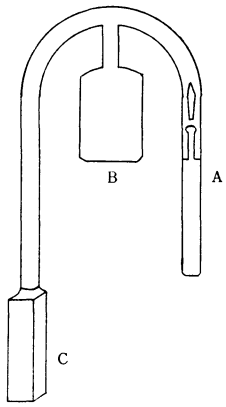
1) K. Hirota, K. Kuwata and T. Imanaka, *J. Chem. Soc. Japan, Pure Chem. Sec.* (*Nippon Kagaku Zasshi*), **83**, 1302 (1962); T. Ogawa, K. Hirota, T. Imanaka, K. Fukushima and T. Miyazawa, International Symposium on Molecular Structure and Spectroscopy, A309, Tokyo, September, 1962.

2) N. Davidson and H. C. Brown, *J. Am. Chem. Soc.*, **64**, 316 (1942).

3) N. R. Fetter and B. Bartocha, *Can. J. Chem.*, **39**, 2001 (1961).

4) E. G. Hoffmann and W. Tornau, *Z. anal. Chem.*, **186**, 231 (1962).

5) S. Murahashi, H. Yuki, T. Niki and K. Hatada, The 11th Annual Meeting of the High Polymer Society of Jappan, Nagoya, May, 1962; S. Murahashi, H. Yuki and T. Obugata, The Symposium on High Polymers and Rubber, Nagoya, November, 1963.



Fi. 1. U-tube for ultraviolet absorption measurement.

A: Break-sealed capsule
B: Ampoule
C: Cell

Results and Discussion

The ultraviolet spectra of diphenylamine, diphenylammonium ion and the complex are shown in Fig. 2. The long wavelength bands of diphenylammonium ion and the complex show the vibrational structure characteristic of weakly-perturbed benzene rings. The spectrum of the complex resembles the spectra of polyphenyl compounds, which have no lone electron pair at the central atom directly bonded to phenyl radicals (for example $(C_6H_5)_3PO$).[6] The long wavelength band of the complex (274 mμ) is located between the corresponding bands of the diphenylammonium ion (255 mμ) and of diphenylamine (285 mμ). Hence, it may be concluded that the several phenyl rings in the complex are not appreciably conjugated with one another and that, therefore,

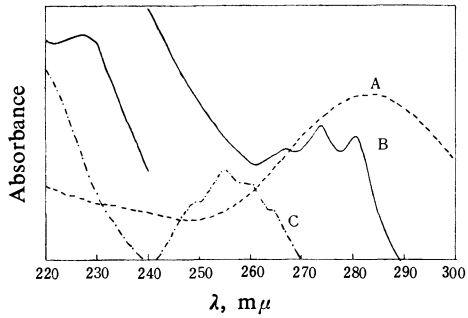


Fig. 2. Ultraviolet absorption spectra.

A: Diphenylamine in cyclohexane
B: The complex in cyclohexane
C: Diphenylammonium ion in water

the nitrogen atom in the complex will take approximately a hybride sp^3 orbital.

The proton magnetic resonance spectrum of the complex (Fig. 3) shows two groups of peaks, with chemical shifts (in τ value) of 2.90 p.p.m. and 10.58 p.p.m. The unresolved low field peaks represent all the protons of the phenyl rings. This group of peaks occurs at a lower field position than that of diphenylamine (3.20 p.p.m.). Groenewege et al. have reported a value of 10.67 p. p. m. for the outer methyls in trimethylaluminum dimer and 9.53 p. p. m. for the bridge methyls.[7] Hoffmann has described a shift of 10.54 p. p. m. of the outer methyls in a dimethylaluminum tertiary-butoxyl dimer.[8] Compounds of the $(Me_2AlX)_2$ type (with X=OR, NR_2,$\cdots$) form bridges only across X. However, their spectra do not yield the outer-methyl signal position of the trimethylaluminium, because the inductive and co-ordinative influences of the X substituents separately alter the effective electronegativity of the molecule residue.

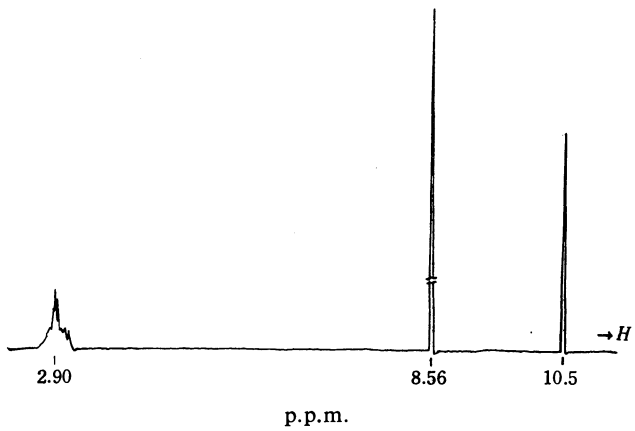


Fig. 3. NMR spectrum of the complex in cyclohexane.

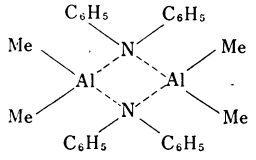
6) H. H. Jaffe, *J. Chem. Phys.*, 22, 1430 (1954).
7) M. P. Groenwege, J. Smidt and H. de Vries, *J. Am. Chem. Soc.*, 82, 4425 (1960).
8) E. G. Hoffmann, *Trans. Faraday Soc.*, 58, 642 (1962).

Me_2Al〈. Negative polarizing substituents which asociate through a lone electron pair (X=OR, NR_2) show the sum of both influences. Thus, the sharp high field peak was assigned to methyl protons in the complex. The intensity ratios of both peaks were found to be approximately 5 : 3 by integration. This suggests that the ratio of phenyl groups to methyl groups in the complex is 1 : 1. The gas evolved in the course of the reaction was found to be methane.

From these observations of the complex, as well as from the results of previous works, the reaction of trimethylaluminum with diphenylamine may be expressed by Eq. I.

$$Al_2Me_6 + 2(C_6H_5)_2NH \rightarrow [(C_6H_5)_2NAlMe_2]_2 + 2CH_4 \quad (I)$$

The structure of the complex may be a dimer through nitrogen bridges, which are perpendicular to the plane of four methyl groups.



(II)

The dimer shown in formula II may be called a aluminum diphenylamide complex. In order to confirm this structure of the complex, the NMR spectra of the mixtures of the complex and trimethylaluminum at various ratios were measured in cyclohexane. Figure 4 shows methyl group signals of mixtures at room temperature. The molar ratios of the complex to trimethylaluminum are about 1 : 1 and 1 : 3.2.

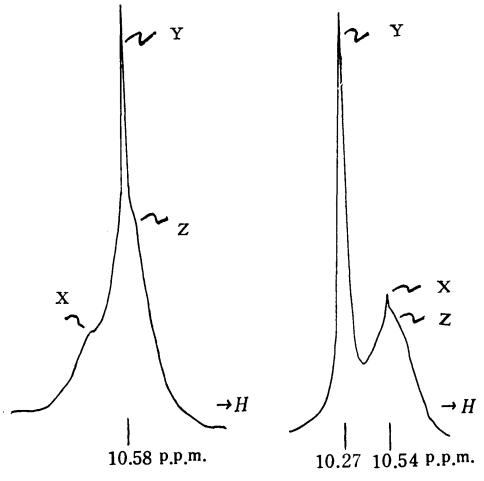


Fig. 4. NMR spectra of mixtures at the molar ratio of (a) 1 : 1 and (b) 1 : 3.2 (the complex : trimethylaluminum) at room temperature.

In the molar ratio 1 : 1, there is no sharp methyl group signal of trimethylaluminum at 10.29 p.p.m., but a sharp methyl group signal (X) and broadened signals are superposed. The position of the former signal coincides with that of the complex. In the mixture, (1 : 3.2) there are two broad and one sharp signals of the methyl group, as is shown in Fig. 4(b). A broad signal with a chemical shift of 10.27 p.p.m. (Y) and a sharp signal (X) with one of 10.54 p.p.m. are assigned to trimethylaluminum and the complex respectively. The broadened signals in those systems show that some exchange takes place in the system.

Each sample was measured at various temperatures to make clear the mechanism of this exchange. The temperature dependences of the NMR spectra of the mixture of the complex and trimethylaluminum in the molar ratios of 1 : 1 and 1 : 3.2 are shown in Fig. 5 and Fig. 6 respectively. The figures illustrate the broadening and coalescence of NMR peaks when they pass through the transition region between slow and fast exchange.

All the results and assignments are summarized in Table I. In the mixture, (1 : 3.2) two broadened signals (Y and Z) at room temperature move together as the temperature rises and coalescence into a single peak (T) at about 50°C. The sharp signal (X) decreases

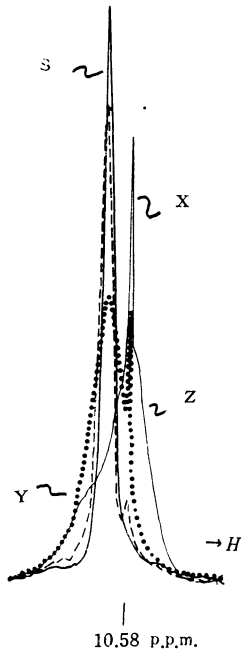


Fig. 5. The temperature dependence of the NMR spectrum of the mixture 1 : 1; (the complex : trimethylaluminum).

—— room temperature ····· 50°C
--- 70°C ——— 90°C

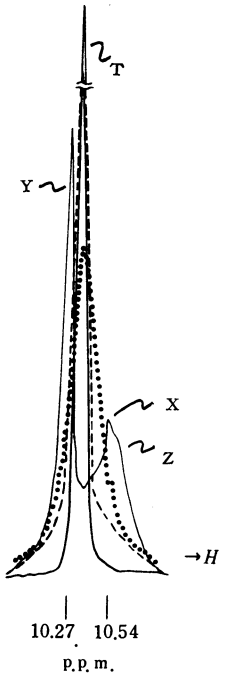


Fig. 6. The temperature dependence of the NMR spectrum of the mixture 1 : 3.2; (the complex : trimethylaluminum).

—— room temperature ····· 50°C
--- 70°C ——— 90°C

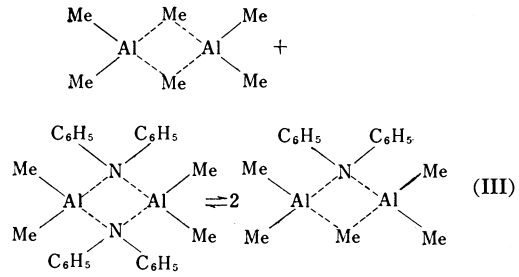
TABLE I. CHEMICAL SHIFTS OF METHYL GROUPS (p.p.m.)

Signal*	Assignment	Obs. Room temp.	Obs. 90°C	Calcd. 90°C
X	Dimer complex	10.58	—	—
Y	Trimethylaluminum, B_2	10.29	—	—
Z	Outer methyls of mixed dimer, AB	~10.58	—	—
S	Mixed dimer,** AB	—	10.40	—
T	Mixture, 1 : 3.2	—	10.34	10.34

* See Fig. 4, Fig. 5 and Fig. 6.
** An averaged position for all protons of AB.

its intensity as the temperature is elevated and finally disappears at about 70°C. At 90°C, the spectrum becomes sharp and narrow. Figure 5 shows the same behavior of methyl group signals in mixture (1 : 1). These results reveal behavior of methyl group signals in the mixture (1 : 1). These results reveal the presence of three chemical species in the system.

The dimer structure of the complex suggested above permits us to interpret the three species and also these exchange phenomena by assuming the following reaction:



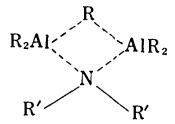
i.e. $B_2 + A_2 \rightleftharpoons 2AB$

where A stands for $AlMe_2N(C_6H_5)$ and B, for $AlMe_3$. The broad signal (Z) is assigned to the outer methyl groups of the mixed dimer AB. The existence of the three species could not be explained by a monomer structure. There are five different sites which can be occupied by the methyl groups. In the previous study of trimethylaluminum by proton resonance, it was concluded that the exchange between B_2 and B_2 (including intramolecular exchange) was fast at room temperature.[8] At room temperature, the NMR spectrum of Fig. 5 shows a sharp methyl group signal at 10.58 p.p.m. (X) corresponding to A_2 and broadened methyl group signals, which originate from a slow exchange between AB and B_2 and between AB and AB. At 50°C the rate of this exchange is probably fast enough for the two broadened peaks to coalescence into a single peak (S), as is shown in Fig. 6. A sharp methyl group signal (X) corresponding to A_2 decreases with the increasing temperature and disappears at 90°C. This shows that reaction III proceeds toward the right side with the increasing temperature. At 90°C, therefore, AB is the predominant species in the system and shows a sharp signal (S), which indicates a fast exchange between AB and AB. This observation shows that the rate of the three exchanges between B_2 and B_2, between AB and AB, and between AB and A_2 are in the observable region of proton resonance.

Using the value, 10.40 p.p.m. of AB and 10.29 p.p.m of B_2, the τ-value of the mixture (1 : 3.2) at 90°C was calculated** shown in Table I. The agreement of the observed and the calculated τ-values for the mixture (1 : 3.2) at 90°C supports the present assignment of proton magnetic resonance spectra.

Ziegler et al. reported that the mixtures of dialkylaluminum amide $(R_2AlNR'_2)_2$ and trialkyl aluminum do not polymerize ethylene, and that a mixed dimer of the type

** This τ-value was the weighted average of the τ-values of B_2 and AB, assuming that reaction III proceeded completely towards the right side at 90°C.



(IV)

is not produced in the system.[9]

The results of the present NMR study clearly show the existence of the mixed dimer (IV) in the present case. A similar system was reported to polymerize methyl methacrylate.[5] Aliphatic amines and aromatic amine might be different in activity in forming a complex.

Summary

The reactive complex produced by the reaction of trimethylaluminum with diphenylamine has been studied by the ultraviolet absorption and proton magnetic resonance methods. The ultraviolet absorption of the complex has shown two bands, at 228 mμ and 274 mμ, in cyclohexane. Proton magnetic resonance spectrum of the complex has been shown to consist of two groups of peaks, with an intensity ratio of approximately 5 : 3 and with chemical shifts of 2.90 p.p.m. and 10.58 p.p.m. These shifts have been assigned to phenyl protons and methyl protons respectively. In the mixture of trimethylaluminum and the complex, an exchange of methyl groups occurs. The structure of the complex has been concluded to be dimeric through two nitrogen bridges, as is shown in formula II.

The authors wish to express their thanks to Professor Heimei Yuki (Faculty of Engineering Science, Osaka University) for his helpful discussions in the course of this study.

Department of Chemistry
Faculty of Science
Osaka University
Nakanoshima, Osaka

9) K. Ziegler and W. R. Kroll, *Ann.*, **629**, 167 (1960).

*Infrared Spectra of Adsorbed Formic Acid**

By Teiichiro OGAWA, Kosaku KISHI and Kozo HIROTA

(Received May 4, 1964)

In order to investigate the mechanism[1] of the catalytic decomposition of formic acid, the infrared spectra of adsorbed formic acid have been already studied by Hirota, Kuwata and Nakai,[2] and by others[3]. Hirota et al. found new bands at 1590 cm^{-1} and 1360 cm^{-1} for the silica-supported zinc catalyst[2] and assigned these bands to the chemisorbed formate anion.

The adsorbent hitherto investigated have, however, been confined to the metal oxides and supported metals, and their spectral region has usually been in the range from 2000 cm^{-1} to 1250 cm^{-1}.[2] In order to clarify the reaction mechanism, a spectroscopic study of the adsorbed state on pure metals and an extension of the wavelength region have to be carried out. In the present report, a new cell for infrared measurement is devised and adsorbed states on evaporated metal films are investigated in the four ranges from 4000 cm^{-1} to 400 cm^{-1}.

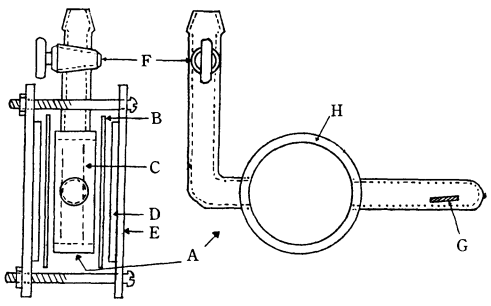


Fig. 1. Diagram of the cell.
A, hard glass cell; B, polyethylene window; C, polyethylene substratum; D, rubber sheet; E, brass holder; F, stopcock; G, zinc metal; H, ground glass

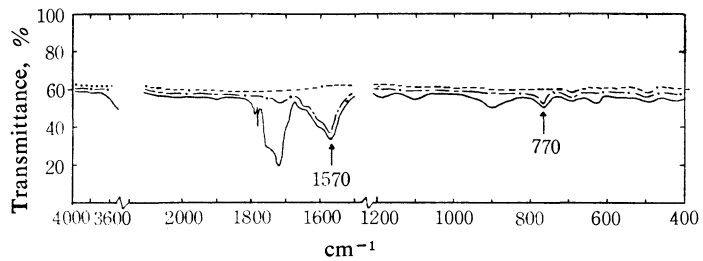
* Presented at the Symposium on Molecular Structure, Sendai, September, 1963.

1) Cf. "Advances in Catalysis and Related Subjects," Vol. 14, Academic Press, New York (1963), p. 35.

2) K. Hirota, K. Kuwata and Y. Nakai, This Bulletin, **31**, 861 (1958); K. Hirota, K. Kuwata and S. Asai, *J. Chem. Soc. Japan, Pure Chem. Sec. (Nippon Kagaku Zasshi)*, **80**, 701 (1959); K. Hirota, T. Otaki and S. Asai, *Z. physik. Chem. N. F.*, **21**, 438 (1959).

3) J. Fabrenfort and H. F. Hazebroek, ibid., **20**, 105 (1959); T. K. A. Clarke and A. D. E. Pullin, *Trans. Faraday Soc.*, **56**, 534 (1960).

4) Landolt-Börnstein, Table I, 2, p. 237 (1957); Cf. K. Ito and H. J. Bernstein, *Can. J. Chem.*, **34**, 170 (1956).



Fig, 2. Spectra of formic acid on evaporated zinc film at room temperature. Two bands of adsorbed state are indicated by arrows.
—— at 30 mmHg of HCOOH.
---- after an hour's evacuation.
---- background spectrum of zinc film.

TABLE I. THE INFRARED SPECTRA OF FORMATE ANION AND ADSORBED SPECIES

	ν_1	ν_2	ν_3	ν_4	ν_5	ν_6
Adsorbed formate; present study			770	1570		
Adsorbed formate; by Hirota et al.[2]		1360		1590	1360	
Zinc formate; present study	2900?	1355	767	1580	1380	1075?
Formate ion in solution[6]	2803	1351	760	1585	1383	1069
Assignment	ν(CH)	ν(CO)	δ(OCO)	ν(CO)	δ(CH)	δ(CH)

Experimental

The cell was made of hard glass, on which windows of polyethylene films 0.5 mm. thick were stuck with a small amount of glyptal resin, as is shown in Fig. 1. Similar films 0.1 mm. thick were set in the cell as substrata for the evaporated metal film. The cell was then degassed and kept under about 10^{-2} mmHg for several days. The use of polyethylene as optical windows made it possible to measure the 4000 cm^{-1}~3100 cm^{-1}, 2500 cm^{-1}~1500 cm^{-1}, 1250 cm^{-1}~750 cm^{-1} and below 700 cm^{-1} regions. Zinc metal could easily be evaporated on the thin polyethylene films by heating it externally with a gas-burner.

The spectra were recorded with a Nippon Bunko Model DS402G spectrometer. Polyethylene films and a wire netting were inserted in the reference beam during the measurement. Formic acid was dried by anhydrous cupric sulfate.

Results and Discussion

The spectrum of the evaporated zinc film was measured first, and then formic acid was introduced into the cell at about 30 mmHg. The two spectra are shown in Fig. 2 by a dotted and a solid line respectively. Successive evacuation and spectral measurements were carried out; one of such spectra is shown in the figure by a dot-dash line.

The observed bands are summarized in Table I. The bands which disappeared after ten minutes' evacuation were assigned to formic acid in the vapor state. The two band which remained after an hour's evacuation were considered to arise from the chemisorbed species and were assigned to the adsorbed formate anion on the basis of a comparison of them with the spectra of the zinc formate and the formate anion in solution.

The effects of polyethylene or glyptal resin on the adsorbed state were checked; no band of the formate anion or others was observed without the metal film after ten minutes' of pumping. The saturated hydrocarbon as polyethylene is chemically inactive and is considered to have less influence on the adsorbed states than does a silica or alkali halides crystal. The present method, therefore, not only makes it possible to find a new band at 770 cm^{-1}, but also reveals the less unperturbed adsorbed states.

Summary

The infrared spectra of adsorbed formic acid on zinc have been measured. Two bands have been found at 1570 cm^{-1} and 770 cm^{-1} and assigned to the adsorbed formate anion.

Department of Chemistry
Faculty of Science
Osaka University
Nakanoshima, Osaka

High-kinetic Energy Fragment Ions from Organic Compounds under Electron Impact. IV. Methanol

By Toshikazu TSUCHIYA

(Received March 24, 1964)

It has long been known[1,2] that fragment ions formed from polyatomic molecules under electron impact often have excess kinetic energy,* and studies of KE fragment ions from hydrocarbons have been reported.[1-7] Hustrulid et al.[1] suggested that these ions with a high kinetic energy result from the dissociation of doubly-charged ions formed by electron impact. Mohler et al.[3] computed the repulsive energies of ions fromed from various compounds on this assumption.

In the present ariticle, some findings on the KE fragment ions from methanol will be reported, and a mechanism of the production of the KE ions will be suggested according to the proposal made by Hustrulid and Mohler.

Measurement

Methanol was a special-grade reagent obtained from the Nippon Rikagaku Shiyaku Co. and was purified by distillation. It was found to be mass-spectroscopically pure. The procedure for the measurement of KE ions has previously been reported.[6]

The results of measurement are given in Table I. Column two gives the kinetic energy, E, of the KE ions CH_2^+, CH_3^+ and OH^+, while columns three and four give the intensity of the KE ion, I_k, and that of TE ion, I_t, respectively in arbitrary units. The last column gives the lowest electron energy, A, at which the KE ions could be detected. In each instance, the given result is the mean value of four measurements. The reproducibility of E values was ± 0.2 eV. The + mark in the I_k column indicates the presence of a weak peak.

Table I. Ions of high kinetic energy in the mass spectrum of methanol

m/e	E, eV.	I_k	I_t	A, eV.
14		+		
15	2.7	0.7	74.3	37
17	1.9	1.3	2.0	36

E, kinetic energy
I_k, intensity of the high kinetic-energy peak,
I_t, intensity of the thermal energy peak,
A, minimum electron energy at which the kinetic-energy peak was observed.
+ indicates the presence of a weak peak.

Discussion

KE peaks appear at m/e 14, 15 and 17, which indicate CH_2^+, CH_3^+ and OH^+ ions respectively. The kinetic energy of the CH_2^+ ion could not be measured, as its intensity was too small. CH_3^+ and OH^+ KE ions may be produced individually or simultaneously from methanol by one or more of the following reactions:

$$CH_3OH \rightarrow CH_3OH^+ \rightarrow \begin{cases} CH_3^+ + OH & 19.2 \quad (1) \\ CH_3^+ + O + H & 23.6 \quad (2) \\ OH^+ + CH_3 & 21.0 \quad (3) \\ OH^+ + CH_2 + H & 24.5 \quad (4) \\ OH^+ + CH + 2H & 28.8 \quad (5) \\ OH^+ + C + 3H & 31.2 \quad (6) \end{cases}$$

$$CH_3OH \rightarrow CH_3OH^{2+} \rightarrow CH_3^+ + OH^+ \qquad 31.5 \quad (7)$$

The figures after each formula indicate the energy of formation in eV. computed from the measured kinetic energy in Table I and from other appropriate data,[8] assuming the conservation of the momentum of fragments.

Since the intensities of KE ions were rather weak over a fairly wide range of electron energies, the precise values of the appearance potentials could not be estimated. A comparison of the tangent of the ionization efficiency curves of the ions with that of neon indicates that the appearance potentials of the KE ions are somewhat lower than the minimum electron energy given in Table I. Hence, in the following discussions, we will confine our

1) A. Hustrulid, P. Kusch and J. T. Tate, *Phys. Rev.*, **54**, 1037 (1938).
2) J. A. Hipple, R. E. Fox and E. U. Condon, ibid., **69**, 347 (1946).
* For convenience, ions with excess kinetic energies will hereafter be described as KE ions, and ions with thermal energies corresponding to the temperature of the ion-source, as TE ions. The peak height of the KE and TE ions will be indicated by I_k and I_t respectively.
3) F. L. Mohler, V. H. Dibeler and R. M. Reese, *J. Chem. Phys.*, **22**, 394 (1954).
4) H. E. Stanton, *J. Chem. Phys.*, **30**, 1116 (1959).
5) T. Tsuchiya, *J. Chem. Phys.*, **36**, 568 (1962).
6) T. Tsuchiya, This Bulletin, **35**, 1221 (1962).
7) T. Tsuchiya, ibid., **36**, 1290 (1963).
8) F. H. Field and J. L. Franklin, "Electron Impact Phenomena," Academic Press, New York (1957); M. B. Wallenstein, Thesis, Univ. of Utah (1951).

investigation to these reactions that require energies larger than about 30 eV. Thus, reactions 1—4 were discarded, assuming the produced fragments are not in excited states.

The peak height of the OH^+ KE ion is larger than that of the CH_3^+ KE ion, as may be seen from Table I. As both ions are focused at about the same ion acceleration voltage, their "sensitivities" are considered to be approximately equal.[9] Under the present experimental conditions, the number of ions produced in the ion source is considered to be proportional to the area of the recorded ion peak rather than to the height of the peak, and it is expected that the higher the initial kinetic energy of the ions, the larger the recorded ion peak width.[10] Even taking such circumstances and the amount of kinetic energies of the OH^+ ion and the CH_3^+ ion in Table I into consideration, the number of CH_3^+ ions of high energy is considered to be smaller than that of the OH^+ ion. Since, by reaction 7, CH_3^+ and OH^+ are expected to be produced in the same amount, reactions 5 and 6, which should produce the OH^+ KE ion only, must be considered. In the investigation described above, the possibility of a simultaneous production of CH_2^+ and OH^+ KE ions was disregarded, as the intensity of CH_2^+ was very small.

The CH_3^+ KE ion is expected to be produced only by reaction 7, which involves the disruption of a doubly-charged ion proposed by Hustrulid[1] and Mohler[3]. On this base, the two ions produced simultaneously are expected to have the same momentum. From the measured kinetic energies given Table I, the momenta of CH_3^+ and OH^+ are computed to be proportional to 9.2 and 8.0 respectively. Even taking into account the experimental errors, these two values are not expected to coincide with each other. The discrepancy may be explained as follows. Hitherto we have assumed that the two fragments produced in reaction 7 have only translational energies. However, the circumstances are quite different if we suppose that the OH^+ KE ion can carry away energy in some other form, such as rotational energy, because of the particular molecular structure of the mother substance.

Lyman,[11] in a study of the band spectrum of the hydroxyl radical produced by a discharge through water vapor, pointed out that a part of the OH radical exhibits "abnormal rotation." Many authors have studied the abnormal rotation of the hydroxyl radical,[12-15] and similar phenomena have been reported in a study of water vapor bombarded by electrons.[14,15] This phenomenon has been explained as follows. A water molecule has the equilibrium form of an isosceles triangle at the ground state, two hydrogen atoms bonding with an oxygen atom at about 105°. When a water molecule is excited to an unstable excited state by vacuum discharge or electron bombardment, however, one of the two hydrogen atoms will fly off in a direction normal to the line joining the initial position and the oxygen atom, leaving the other to rotate about the oxygen atom. The amount of the abnormal rotational energy is reported to be about 0.4 eV.[14] in this event. A similar abnormal rotation of OH is also observed in the case of ethanol.[13]

More recently Chupka,[16] in a study of appearance potentials, has pointed out that appreciable excess rotational energy may be present where the dissociation into fragments with excess kinetic energy occurs in a direction not along the line connecting the centers of the mass of the two fragments.

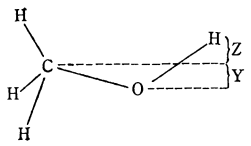


Fig. 1. Molecular structure of methanol.

C-H	1.096±0.010Å
C-O	1.427±0.007Å
O-H	0.956±0.015Å
y	0.083±0.005Å
z	0.802Å
∠HCH	109.03±0.75°
∠COH	108.9±2°

P. Venkateswarlu and W. Gordy, *J. Chem. Phys.*, **23**, 1200 (1955).

The molecular structure of methanol is shown in Fig. 1,[17] the C–O–H angle is about 108°. If it is assumed that, according to the mechanism proposed by Hustrulid and Mohler, at first two electrons are removed from the methanol molecule, leaving a positive charge on the CH_3 and OH groups, and that then the doubly-charged molecular ion dissociates into CH_3^+ and OH^+ KE ions by means of the Coulomb repulsion, a part of the Coulomb

9) C. Berry, *Phys. Rev.*, **78**, 597 (1950).
10) C. A. McDowell and J. W. Warren, *Discussions Faraday Soc.*, **10**, 53 (1951).
11) T. Lyman, *Phys. Rev.*, **53**, 379 (1938).
12) R. J. Dwyer and O. Oldenberg, *J. Chem. Phys.*, **12**, 35 (1944).
13) K. Niira, *Busseironkenkyu*, **11**, 1 (1948) (in Japanese).
14) K. Niira, *J. Phys. Soc. Japan*, **4**, 230 (1949).
15) C. Hayakawa, *Proc. Phys. Math. Soc. Japan*, **26**, 78 (1944).
16) W. A. Chupka, *J. Chem. Phys.*, **30**, 191 (1959).
17) J. D. Swalen, ibid., **23**, 1739 (1955); P. Venkateswarlu and W. Gordy, ibid., **23** 1200 (1955).

energy may be considered to be transferred to the rotational energy of the fragment ions. Because of the structure of the parent ion, OH^+ rather than CH_3^+ is expected to obtain rotational energy in the main. If OH^+ is assumed to carry away energy by rotational motion, we may judiciously elucidate the phenomenon that the momenta of the two fragment ions in reaction 7 differ greatly, the OH^+ ion having the smaller momentum.

The difference between the sum of the measured kinetic energies of the two fragments and the total energy computed from the kinetic energy of the CH_3^+ ion is 0.5 eV. If it is assumed that the CH_3^+ ion has only a translational energy, and that vibrational motion of OH^+ is only slightly excited, a value of 0.5 eV. may be assigned to the rotational energy of the OH^+ ion. This value is considered to be compatible in order of magnitude with the value reported for the abnormal rotational energy of the OH molecule from water,[14] taking the accuracy of the present experiment into account. According to Mohler et al., the distance between two charges in the present case is estimated to 2.8 Å. However, since nothing is known about the actual distance between the charges in CH_3OH^{2+}, the postulate given above cannot be corroborated from this point of view, although the assumed distance would not be unacceptable. If the CH_3^+ ion has additional excitation energy, a smaller distance may be assumed.[3]

Summary

Fragment ions with high kinetic energies have been produced from methanol by electron impact, as in the cases of many hydrocarbons. Assuming that a fragment has a rotational energy of the order of 0.5 eV. most of the high-energy ions from methanol can be ascribed to a doubly-charged molecule ion that dissociates into two singly-charged fragments.

The author wishes to express his thanks to Mr. Mikitake Nakayama for his assistance in purifying the sample and to Mr. Ryuzo Shiota for his kind discussions and survey of the manuscript.

Government Chemical Industrial Research Institute, Tokyo
Shibuya-ku, Tokyo

An Application and Modification of the Freeze-out Technique by Quiram and Biller for the Determination of Pollutants in the Atmosphere by Mass Spectrometry

By Hiroko HOSHINO, Nobuhide WASADA and Toshikazu TSUCHIYA

(Received March 24, 1964)

Many works[1-5] have reported on concentrating air pollutants in a cold trap in order to analyze the concentrates by mass spectrometry. It has long been known that water can be passed through an ordinary in-seal trap at the temperature of liquid air,[6] even though its vapor pressure is almost 10^{-26} mmHg at these temperatures. Extremely small frozen particles are formed at these low temperatures, and these fine crystals are carried into the gas stream through the trap. Contaminants contained in air, other than water, may also pass more or less through a trap in a similar manner. To collect from air sufficient pollutants for subsequent analysis, Shepherd et al.[1] and Quiram and Biller[5] used a cold trap of glass wool or one of silica gel. To compensate the passover of the pollutants, Shepherd et al. took a large amount of the air sample. Quiram's method, on the other hand, requires only 3 l. NTP of air. In his method, by handling glass stop cocks manually, a part of the air sample was introduced into the trap and was then left in contact with the glass wool for about 30 sec. in order to improve the condensation efficiency of the pollutants; then the air sample in the trap was evacuated off.

1) M. Shepherd, S. M. Rock, R. Howard and J. Stormes, *Anal. Chem.*, **25**, 1431 (1951).
2) P. P. Mader, M. W. Heddon, R. T. Lofberg and R. H. Koehler, ibid., **24**, 1899 (1952).
3) E. R. Quiram, S. J. Metro and J. B. Lewis, ibid., **26**, 352 (1954).
4) K. Suzuki, S. Araki and S. Hirano, *J. Chem. Soc. Japan, Ind. Chem. Sec.* (*Kogyo Kagaku Zasshi*), **61**, 26 (1958).
5) E. R. Quiram and W. F. Biller, *Anal. Chem.*, **30**, 1166 (1958).
6) M. Shepherd and A. Martin, *J. Res. Natl. Bur. Standards*, **2**, 1145 (1929).

This procedure was repeated about 50 times until the air in the 3 l. sample bottle was exhausted. By this method they improved the collection efficiency and could collect sufficient hydrocarbons contained in the atmosphere above 10 p.p.m. for subsequent analysis with a mass spectrometer. Though excellent in its capacity of collection, the method of Shepherd et al. is somewhat unhandy to apply in field work, while in that of Quiram and Biller it is very troublesome to handle the stopcocks.

We have employed the method of Quiram and Biller, investigating its usefulness for several pollutants, notably for a trace of mercury vapor in air. Since the results proved to be satisfactory, as will be described below, we have slightly improved the freeze-out technique by automatically circulating the air sample through a glass-wool trap instead of handling the stopcocks manually. Synthetic air samples were analyzed by this procedure, and the results checked.

Experimental

The assembly of the sample-collecting apparatus is shown schematically in Fig. 1. The apparatus is essentially the same as that employed by Quiram and Biller, but it was modified by the addition of

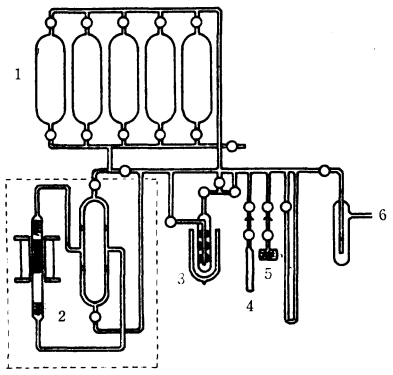


Fig. 1. Sample collecting manifold.

1 Sample bottles
2 Circulation pump
3 Glass-wool trap
4 Contaminant concentration thimble
5 Drying agent
6 To vacuum pump

a magnetic circulating pump, which is shown in Fig. 1, encircled with a dotted line. The volume of the gas-collecting bottle was about 3 l. Five gas-collecting bottles were assembled in order to prepare synthetic blended samples by a dilution technique using these bottles successively. Blends of appropriate concentrations in the bottles were diluted with air, and could be used immediately to get a calibration curve.

The magnetic circulation pump was equipped with only one solenoid. The principal features of the pump have been reported by Livingston.[7] The 2000-turn coil driving the piston was of enamel wire, 1.5 mm. in diameter. The solenoid was activated by an electronic timer obtained from the Sakashita Factory. When adjusted to an optimum stroke, the pump circulated air at atmospheric pressure at the rate of 3 l./min. with a power consumption of about 50 W. When necessary, the pump can be shunted out from the gas sample manifold by stop cocks. Under these conditions, the method of Quiram and Biller was tested.

The procedure of manual operation for the freezing out of the contaminants from the air sample was the same as that reported by Quiram and Biller. In the mercury analysis, a mercury manometer in the gas-handling manifold of the mass spectrometer was demounted in order to eliminate the mercury background.

In the circulation method, the air sample was repeatedly circulated from a sample bottle through a cold trap for an appropriate period. The other operations were the same as in Quiram and Biller's method. Carbon dioxide was not removed from the collected contaminants in the present experiment, however. Rather, the amount of carbon dioxide in the room air itself was determined beforehand using argon as the internal standard, and in the subsequent analysis of the various components in the collected pollutants, carbon dioxide, collected simultaneously, was used as the internal standard, since one of the main components of the substance frozen-out from the air itself of the room was carbon dioxide, and the same air was introduced into the sample bottle containing an appropriate amount of blended materials in order to prepare the air sample.

In order to determine the appropriate circulating time, the carbon dioxide in the room air was collected under various circulating times, ranging from 5 to 60 min. The amount of carbon dioxide collected was then determined, using argon as the internal standard. Table I shows the result. Since a 10-min. circulation was found to be sufficient to attain a maximum, an almost constant collection efficiency in the case of carbon dioxide, all the samples were circulated for 10 min. in the following determinations.

The gases used to prepare the samples were standard gases obtained from the Takachiho Chemicals Co. Anhydrous magnesium perchlorate, the

Table I. Circulation time versus freezed-out amount of carbon dioxide from room air

Circulation time min.	Argon added as internal standard mmHg×ml.	(CO_2/Ar) ratio determined by mass spectra	Carbon dioxide collected* mmHg×ml.
5	55.77	16.08	896.8
10	57.53	16.59	954.0
20	54.02	17.59	932.8
30	63.57	15.20	966.7
60	59.67	18.01	994.5

* Corrected for volume of sample bottle.

7) R. Livingston, *J. Phys. Chem.*, 33, 956 (1929).

drying agent, was a guaranteed reagent obtained from the Toyama Kagaku Co. A Consolidated Electrodynamics Corp. mass spectrometer, type 21-103C, was used.

Results and Discussion

Mercury Determination. — Table II shows the mean deviation of the determination of the mercury vapor in the air by Quiram and Biller's method. The samples were prepared as follows. An evacuated 3 l. sample bottle containing a drop of mercury was immersed in water, which was kept at a constant temperature. The atmosphere in the bottle was found to come to an equilibrium with liquid mercury in about an hour. After 3 hr. of immersion, the mercury drop was removed from the bottle containing the mercury vapor corresponding to the temperature of the water; then, by opening a cock, the bottle was filled with room air. The pressure of mercury in the sample bottle was estimated from the Table recording vapor pressure versus temperature.[8] The samples in Table II and Table III were obtained by successively diluting the air prepared by the procedure. The data in Table III indicate the known content of mercury and the ratio of the mercury found to the known content. The rather low value of the ratio is probably due to poor collection efficiency, since little memory effect was observed in the mass spectrometer. For analysis we used a working curve. Figure 2 indicates such a working curve. A synthetic air sample containing 1.7×10^{-2} p.p.m. of mercury vapor was analyzed by the method. The result was 2.0×10^{-2} p.p.m., which is 20% over the blended value. As much mercury vapor contained in atmosphere as the maximum allowable tolerance, i.e., about 1/100 p.p.m., may be determined by this method, with a mean deviation of about 20% (Table II), whereas, according to our experiment, with hydrocarbons contained in the air, the detection limit of the present technique was 1 p.p.m.*

TABLE II

Concn. of mercury in air p.p.m.	Peak height of *m/e* 202 of concd. material arbitrary unit	Deviation	Standard deviation
1.4	43.1	5.0	
1.4	33.1	5.0	
1.4	38.0	0.1	
1.4	38.1	0.0	
mean	38.1	2.6	3.6

Electron current, 9 μamp. Sample is air in equilibrium with mercury at 18.5±0.3°C.

Concn. of mercury in air p.p.m.	Peak height of *m/e* 202 of conced. material arbitrary unit	Deviation	Standard deviation
0.015	1.4	0.0	
0.015	1.2	0.2	
0.015	1.7	0.3	
mean	1.4	0.2	0.2

Electron current, 30 μamp.

Volume of air sample, ca. 3 l. Electron voltage, 70 eV.

All freezed-out mercury was introduced into the reservoir of MS.

TABLE III. MERCURY CONTENT AND COLLECTION EFFICIENCY

Dilution ratio	1*	1/2	1/4	1/8	1/32	1/96
Collection efficiency, %	84	63	50	35	28	15

* 1.03 μHg of mercury is contained. Other samples were prepared from the same one by successive dilution.

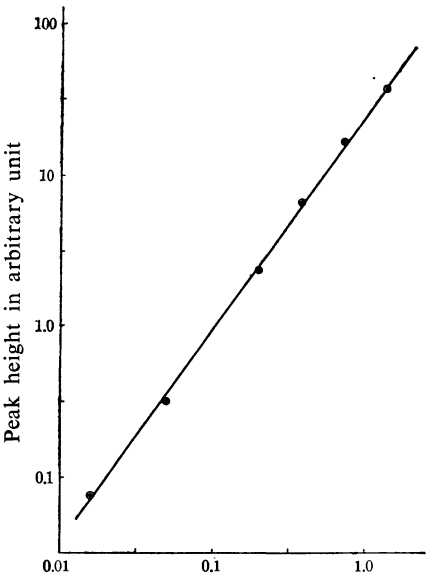


Fig. 2. Working curve of mercury in air.

Circulation Method.—Air samples containing about 10 p.p.m. to 100 p.p.m. each of acetylene, ethane, propylene, *n*-butane and freon-12 were blended for analysis. Table IV shows the results of a run. In analysis we used a working curve, since a part of the blended pollutant

8) International Critical Tables, Vol. III, McGraw-Hill, New York (1928).

* Quiram determined pollutants below 10 p.p.m. by another freeze-out technique.

TABLE IV. ANALYSIS OF SYNTHETIC BLEND

Component	Pressure in gas reservoir of MS μHg	Content*	
		Collected	Synthesized
Acetylene	0.16	7.83	8.44
Ethane	0.19	8.99	7.98
Propylene	0.18	9.25	10.19
n-Butane	0.19	9.44	10.71
Freon-12	0.19	9.74	11.02
Carbon dioxide	26.57		
Total	27.48**		

Pressure of carbon dioxide (internal standard) in air determined beforehand was 0.4471 mmHg.
Electron current: 9 μamp., ionizing voltage: 70 eV.
* (mmHg·ml.) in 3 l. of air.
** Measured with micromanometer, introduced pressure was 25.02 μ.

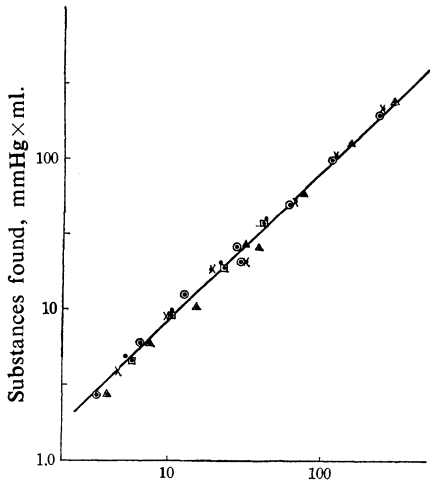


Fig. 3. Found amount versus synthetic values of various substances in air (1 atm.).
⊙ C_2H_2 △ C_2H_6 • C_3H_6
× C_4H_{10} ▣ F 12

is not recovered. Figure 3 shows the relation between the amount of blended compounds and the amount collected. As may be seen in the figure, the working curves of various compounds coincide remarkably in this range of concentration. This is not surprising, however, as these pollutants are physically, rather than chemically, adsorbed on glass-wool. When samples of the same composition were analyzed several times, the reproducibility of the analysis was found to be about ±10%. Blended samples of various compositions were analyzed, but no interference effect among components was observed.

In the range of 10~100 p.p.m., about 90% of each of the pollutants was recovered. With the object of seeing the whereabouts of the uncollected pollutants, the remaining air of the once-freezed-out sample containing *n*-butane was treated afresh. By this treatment, about 10% of the original amount of *n*-butane was collected. From this result it seems that the uncollected portion of the pollutants is not lost in the process, but remains in the gas phase.

The compounds in the lowest concentration blend tested, which contained about 10 p.p.m. of each of the compounds, gave peak heights of 20~80 divisions of the recorder chart of mass spectrometer, according to their sensitivities. Since a difference of one division has significance under favorable circumstances, a one- or two-fold decrease in concentration, depending on the compounds, may be tolerated in analyzing a sample of air of this size. The time necessary for the sample manipulation, including mass spectrometric recording, is about 3 hr. per sample.

The merit of the present procedure is that it requires only mechanical operations, no mental concentration. The method has, however, a few limitations. One of these concerns the fact that some contaminants which are often encountered, such as carbon monoxide, methane and hydrogen, cannot be collected by this technique. Those substances which dissolve or attack vacuum grease, such as benzene or boronfluoride, also do not give reliable results when one uses ordinary greased stopcocks. For a similar reason, a drying agent may also limit the usefulness of the method.

Summary

Quiram and Biller's freeze-out method, originally devised to determine hydrocarbons contained in air above 10 p.p.m. and using a mass spectrometer, was tried on a trace (down to 1/100 p.p.m.) of mercury vapor in atmosphere; it was proved to give satisfactory results. The freeze-out procedure was then slightly modified. To collect the pollutants, the air sample was circulated automatically for ten minutes through the freezing-out trap instead of repeatedly handling the stopcocks. By this procedure, a blended air sample containing various pollutants above 10 p.p.m. have been analyzed. The precision is about ±10%.

The authors would like to express their thanks to Dr. Shun Araki for his advice and to Mr. Ryuzo Shiota for his valuable discussions and survey of the manuscript.

Government Chemical Industrial Research Institute, Tokyo
Shibuya-ku, Tokyo

The Spectrophotometric Determination of a Small Amount of l-Ascorbic Acid with the Iron(III)-1, 10-Phenanthroline Reagent

By Isao ONISHI and Tadashi HARA

(Received March 24, 1964)

Though several methods[1-4] have been reported for the spectrophotometric determination of ascorbic acid on the basis of the oxidation-reduction reaction between *l*-ascorbic acid and the coloring agents, they seem to be either complicated or unreliable because the absorptivity of the colored solution varies with time. The purpose of the present study is to establish a simple and accurate spectrophotometric method, which is indispensable for the investigation of the catalytic effects of metal complexes on the autoxidation of *l*-ascorbic acid.

It is well known that the iron(II) - 1, 10-phenanthroline complex shows an intense red color and is more stable than the corresponding ferric complex over a wide pH range. On the other hand, the ferric complex has been found by the authors to be quantitatively reduced to the ferrous complex by *l*-ascorbic acid. Use is made of these facts for the present purpose. Because of the instability of the colored solution, no report has been presented for the determination of *l*-ascorbic acid using the ferric complex as a coloring agent. The instability of the colored solution seems to be caused by the photo-reduction of the ferric complex, because the iron(III) - 1,10-phenanthroline solution gradually shows a red color in visible light.[5]

The photo-reduction of the ferric complex, however, has been avoided by adding a chelating agent such as ethylenediaminetetraacetic acid (EDTA) to mask excessive ferric iron after the color development. The method has been further applied to the measurement of the catalytic activities of metal complexes for the autoxidation of *l*-ascorbic acid.

Experimental

Apparatus.—Absorbance mearurements were made with a Shimadzu spectrophotometer, Model QR-50, using 1 cm. glass cells.

Reagents. — *l-Ascorbic Acid Solution.* — For the determination, 0.2 g. of l-ascorbic acid manufactured by Merck & Co. is dissolved in water, and the solution is diluted to 100 ml. A 10 ml. portion is pipetted out and diluted to 500 ml. For the catalytic reaction, 0.2 g. of *l*-ascorbic acid is directly dissolved in 500 ml. of water. These solutions are freshly prepared for every use.

1,10-Phenanthroline Solution.—Prepared by dissolving 1.4401 g. of 1,10-phenanthroline hydrochloride in water, and by diluting this to 1000 ml. with water.

Ferric Iron Solution. — Prepared by dissolving 0.9858 g. of ferric ammonium sulfate in 1000 ml. of water.

EDTA Solution.—Prepared by dissolving 9.2555 g. di-sodium salt of EDTA in water, and by diluting it to 500 ml.

Metal Salt Solutions.—Prepared as 10^{-4}M solutions.

Buffer Solution.—Prepared by mixing each of 1 M acetic acid and sodium acetate solution at a moderate ratio.

Water.—Prepared by redistilling ordinary distilled water with an all-glass-jointed Pyrex glass apparatus, and by saturating it with purified air.

Procedure. — Take 5.0 ml. each of iron(III) and buffer solutions in a 50 ml. measuring flask, add a sample solution containing *l*-ascorbic acid, and, then 5.0 ml. of the 1,10-phenanthroline solution. Add 1.0 ml. of the EDTA solution after 1 min., dilute to the mark with water, and measure the absorbance of the colored solution at 514 mμ against a reagent blank solution within an hour.

Results and Discussion

Absorption Spectra.—The absorption spectra of the blank, iron(II)- and iron(III)-complexes are shown in Fig. 1. The maximum absorbances for both A and B in Fig. 1 are observed at 514 mμ, where the blank shows a slight absorption. The shapes of the absorption spectra are quite similar for A and B, and the λ_{max} gives a good agreement with the values reported in the literature.

The Effect of pH. — The absorbance of the mixture of 5.0 ml. each of iron(III) and 1, 10-phenanthroline solutions and of 10 ml. of a *l*-ascorbic acid solution was measured at various pH values. The results obtained are shown in Fig. 2. The absorbances of the colored solutions are almost the same at pH 3.6~5.8.

1) J. A. Owen, B. Iggo and D. B. Horn, *Nature*, **174**, 701 (1954).
2) M. Schmall, C. W. Pifer, E. G. Wollish et al., *Anal. Chem.*, **26**, 1521 (1954).
3) H. Fukuba, J. Yamazaki and N. Inagaki, *Vitamin (Japan)*, **9**, 312 (1955).
4) C. G. King, *Ind. Eng. Chem.*, **13**, 225 (1942).
5) Cf. C. C. Tsen, *Anal. Chem.*, **33**, 849 (1961).

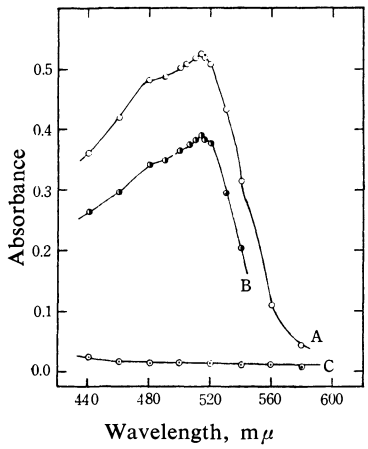


Fig. 1. Absorption spectra.

A: Fe(III) + (ascorbic acid) + 1,10-phenanthroline)
B: Fe(II) + (1,10-phenanthroline)
C: Fe(III) + (1,10-phenanthroline)

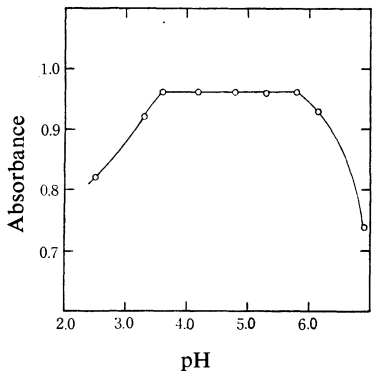


Fig. 2. Relationship between pH and absorbance of the colored solution.

The Stability of the Colored Solution.—The relations between the absorbance and the time after the color development are shown in Fig. 3. It is apparent from Fig. 3 that the absorbance of the colored solution increases with time in the absence of a chelating agent, while it is almost constant in the presence of a moderate amount of EDTA or phosphoric acid. The increase in the absorption mentioned above seems to be due to the photo-reduction of the ferric complex, because the mixed solution of iron(III) and 1,10-phenanthroline easily turns red under sunlight, and the stable coloration seems to be based on the masking of the excessive iron(III) with EDTA or phosphoric acid. The coloration is stable for at least an hour in the presence of a chelating agent.

Calibration Curve. — Solutions containing various amounts of *l*-ascorbic acid were treated by the preceding procedure; the results are plotted in Fig. 4. As can be seen from Fig. 4,

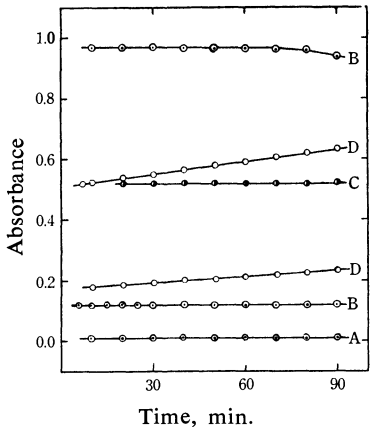


Fig. 3. Stability of the colored solution.

A: Fe(III) + (1,10-phenanthroline) + (1 ml. of 0.05 M EDTA)
B: Fe(III) + (1,10-phenanthroline) + (different amount of *l*-ascorbic acid) + (1 ml. of 0.05 M EDTA)
C: Fe(III) + (1,10-phenanthroline) + (*l*-ascorbic acid) + (1 ml. of 0.15 M H_3PO_4)
D: Fe(III) + (1,10-phenanthroline) + (*l*-ascorbic acid)

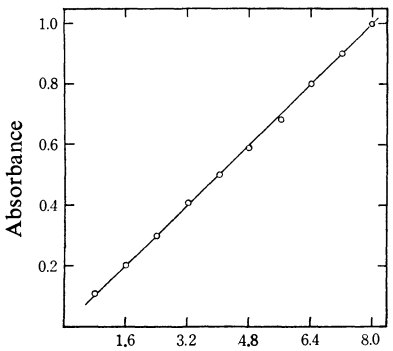


Fig. 4. Calibration curve for *l*-ascorbic acid at 514 mμ.

up to 8.0 p.p.m. *l*-ascorbic acid obeys Beer's law.

Diverse Ions.—The method is interfered with not only strong oxidizing or reducing agents, but also by small amounts of cations. The effects of metal ions on the catalytic oxidation of *l*-ascorbic acid were measured by the following procedure: Take a definite amount of metal ions in a test-tube fitted with a glass-stopper, adjust the pH to 4.3 with the acetate buffers, and dilute to 90 ml. with water. Take an aliquot volume of an *l*-ascorbic acid solution in another test-tube. Stopper both tubes and place them in a thermostat held at 25±0.1°C for about two hours. Pipette out 10 ml. of the *l*-ascorbic acid solution, add it to the other

test-tube, mix, and let it stand in the thermostat. Pipette a 10 ml. portion out of the solution as soon as possible, and estimate the amount of *l*-ascorbic acid in it by the preceding method, where the time is regarded as zero. The residual amounts of *l*-ascorbic acid in the mixed solution are determined by the same treatment after a definite interval.

The values of $\log C_0/C$ are plotted against the time, "t," and the rate constant, "k," is calculated from the equation, $k=(2.303/t)\times\log C_0/C$. The results obtained are shown in Table I and in Fig. 5. The catalytic effects of various metal ions are compared by the k values, the order of which is as follows:

$$\text{Cu(II)} \gg \text{Fe(II)} > \text{Cd} > \text{Zn} > \text{Al} > \text{Fe(III)}$$

Among these, copper(II) is the most active, followed by iron(II), iron(III), cadmium, zinc and aluminum. The other metal ions, such as silver(I), cobalt(II), mercury(II), magnesium, manganese(II), nickel(II), lead(II), palladium and chromium(III), do not show any remarkable activity. Since the linear relationships as shown in Fig. 5 are obtained between $\log C_0/C$ and t with regard to the active ions, the oxidation is consider to proceed as of the first order with respect to the ascorbic acid. The reaction rate of *l*-ascorbic acid against various pH values in the presence of a definite amount of copper(II) is shown in Fig. 6. Judging from the reaction mechanism reported in the literature,[6,7] the following conditions seem to be at least necessary for the catalytic oxidation of *l*-ascorbic acid with metal ions: (1) the coordination of *l*-ascorbic acid to the metal ions, and (2) the valency change of the metal ion by the coordination. Since the complex formation proceeds witd the pH increase, the results shown in Fig. 6 are understandable.

According to Mellor and Maley,[8] the stability of bivalent metal complexes is ordered as follows:

TABLE I. OXIDATION RATE OF *l*-ASCORBIC ACID IN THE PRESENCE OF VARIOUS KINDS OF METAL IONS
(25 ± 0.1°C, pH=4.3, metal ion: 5×10^{-6} M/l.)

Metal ion	Salt	Rate constant k, $\times10^3$ min^{-1}
—	—	3.14
Ag	$AgNO_3$	3.14
Cd	$Cd(NO_3)_2$	6.90
Co	$Co(CH_3COO)_2$	3.03
Cu	$CuSO_4$	33.7
Fe	$FeSO_4(NH_4)_2SO_4$	7.32
Hg	$Hg(NO_3)_2$	2.68
Mg	$MgCl_2$	2.74
Mn	$MnCl_2$	2.49
Ni	$NiCl_2$	4.22
Pb	$Pb(CH_3COO)_2$	4.23
Pd	$PdCl_2$	3.86
Zn	$ZnCl_2$	6.30
Al	$Al_2(SO_4)_3$	6.12
Cr	$Cr(NO_3)_3$	4.72
Fe	$Fe_2(SO_4)_3(NH_4)_2SO_4$	5.48

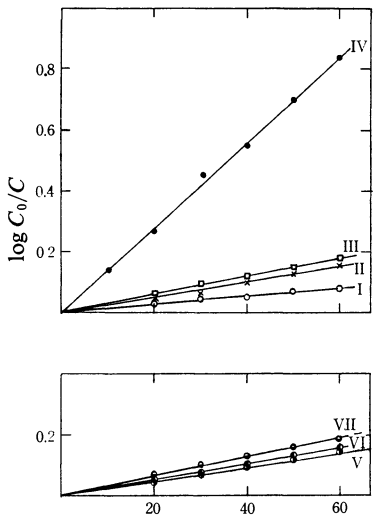


Fig. 5. Relationship between "t" and $\log C_0/C$.
I: blank, II: Zn, III: Cd, IV: Cu, V: Fe(III), VI: Al, VII: Fe(II)

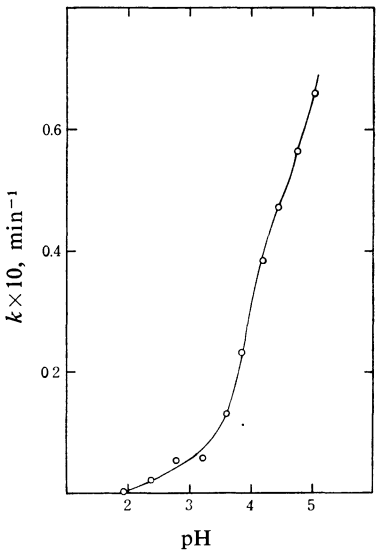


Fig. 6. Relationship between pH and "k" for the oxidation of *l*-ascorbic acid in the presence of a definite amount of Cu^{2+}, at 25°C.

6) A. Weissberger, J. E. LuValle and D. S. Thomas, Jr., *J. Am. Chem. Soc.*, **65**, 1934 (1943).
7) A. Weissberger and J. E. LuValle, ibid., **66**, 700 (1944).
8) D. P. Mellor and L. Maley, *Nature*, **159**, 370 (1947); **161**, 436 (1948).

$$Pd > Cu > Ni > Pb > Co > Zn > Cd > Fe > Mn > Mg$$

In view of this stability series and the reversibility of the valency change, the order of the catalytic activity is also understandable, except for iron(III). The inactivity of iron(III) seems to be closely related to the hydrolysis at pH 4.3. The inactivity of palladium is considered to be based on the irreversibility of its valency, since palladium(II) is easily reduced to palladium(0).

Summary

A simple and accurate spectrophotometric method with the iron(III) - 1, 10-phenanthroline reagent has been established for the determination of a small amount of *l*-ascorbic acid; it has been applied to the measurement of the catalytic effects of metal ions on the autoxidation of *l*-ascorbic acid.

The authors wish to express their heartly thanks to Miss Mikiko Kobata and Miss Masako Onishi for their skillful technical assistance.

Department of Chemistry
Faculty of Engineering
Doshisha University
Kamikyo-ku, Kyoto

The Catalytic Effects of Copper Complexes on the Oxidation of l-Ascorbic Acid

By Isao ONISHI and Tadashi HARA

(Received March 24, 1964)

In the preceding paper,[1] the catalytic effects of metal ions on the oxidation of *l*-ascorbic acid were examined, and copper(II) was found to be the most active among them. The present study has been carried out in order to determine the relationship between the catalytic acitivity of various kinds of copper(II) complexes and the stability of the complexes. Though the discussions have often been made qualitatively with regard to the relationship between the catalytic activity of metal complexes and their stability, no quantitative relationship has been reported. The catalytic activity of copper(II) decreases more or less in the presence of the chelating agent, which forms a stable complex with copper(II). Since the decrease in the catalytic activity changes depending on the kinds of chelating agents and on the mole ratios of copper to the chelating agents, the stability constants of copper complexes can be calculated by measuring the rate constant with the solutions of the same composition as the copper(II) complexes. The results obtained by this method will be compared with those obtained by the polarographic method, etc. As for the relationship between k and the stability constant, K_s, k will be found to be inversely proportional to the $\log(1+K_s\cdot[Y]^n)$, in which [Y] means the concentration of the dissociated chelating agent.

1) I. Onishi and T. Hara, This Bulletin, 37, 1314 (1964).

Experimental

Apparatus and Reagents.—The same apparatus and reagents were used as in the preceding paper except for the following. For the measurement of the polarogram, a Yanagimoto polarograph, Model PR-2, was used. Each chelating agent was prepared as $n\times10^{-4}$ M solution by taking the mole ratio, n, of the chelating agent to copper into consideration.

Procedure.—Take a definite amount of metal ions or an additional chelating agent in a test-tube fitted with a glass-stopper, adjust the pH to either 4.3 or 6.0 with an acetate buffer, and dilute to 90 ml. with water. Take an aliquot volume of an *l*-ascorbic acid solution in another test-tube. Stopper the test-tubes, place in the thermostat held at 25±0.1°C, and treat in a manner similar to that described in the preceding paper.

Results and Discussion

The Relation between the Amount of Copper(II) and *k*.—The rate constant, k, for the oxidation of *l*-ascorbic acid was measured in

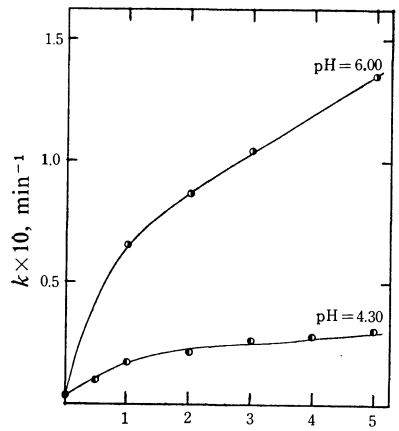


Fig. 1. Relations between the amount of Cu^{2+} and k.

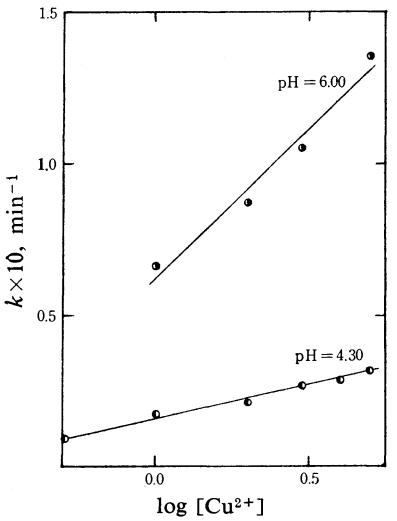


Fig. 2. Relations between log $[Cu^{2+}]$ and k.

the presence of various amounts of copper(II) and with an accuracy of within 5%. The results obtained are shown in Fig. 1. By taking the logarithm of the copper concentration in Fig. 1, Fig. 2 is obtained. As can be seen from Fig. 2, there are two straight lines, and the relations between the amount of copper(II) and k are generally given by Eq. 1;

$$k=a\log[Cu^{2+}]+b \qquad (1)$$

Since a and b are constant under the limited conditions and since their numerical values may easily be estimated from Fig. 2, Eq. 1 is replaced by Eq. 2 or 3 respectively:

$$\text{at pH}=4.3 \quad k_{4.3}=0.023\log[Cu^{2+}]+0.0155 \qquad (2)$$

$$\text{at pH}=6.0 \quad k_{6.0}=0.100\log[Cu^{2+}]+0.064 \qquad (3)$$

By measuring the value of $k_{4.3}$ or $k_{6.0}$ and by substituting them into Eq. 2 or 3, log $[Cu^{2+}]$ is easily found.

The Effects of Chelating Agents on k.—The rate constant for the oxidation of *l*-ascorbic acid was measured in the presence of various kinds of chelating agents, which were added to copper(II) in the same ratios as with copper complexes. The results obtained are shown in Table I. It is apparent from Table I that the values of k vary with the chelating agents, but no definite relation exists between the stability constant and k. The relation between k and the mole ratio of EDTA to copper(II) is

Table I. The rate constants in the presence of various kinds of chelating agents ($[Cu^{2+}]$: 5×10^{-6} M/l., 25±0.1°C)

Chelating agent	mole ratio	$k\times10$, min^{-1} pH=4.30	$k\times10$, min^{-1} pH=6.00
—*	—	0.031	0.031
Cu alone	—	0.313	1.360
Citric acid	1	0.302	1.270
NTA**	1	0.131	0.134
EDTA***	1	0.077	0.403
1, 10-Phenanthroline	2	0.200	0.524
Oxine	2	0.228	0.400
α, α'-Dipyridyl	2	0.054	0.420
Oxalic acid	2	0.259	1.350
Glycine	2	0.298	1.320
Ethylenediamine	2	0.292	1.370

* Blank
** Nitrilotriacetic acid
*** Ethylenediaminetetraacetic acid

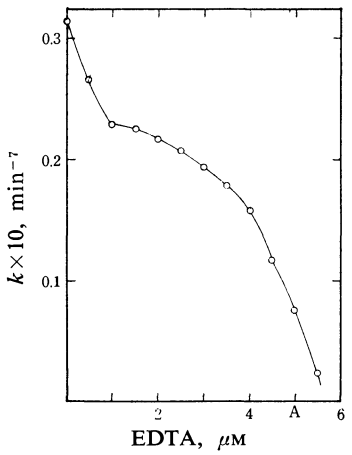


Fig. 3. Relation between k and the mole ratio of EDTA to Cu^{2+}.
Cu^{2+}: 5 μM, A: equivalence point

shown in Fig. 3. As can be seen from Fig. 3, the value of k decreases with an increase in the mole ratio of EDTA to copper(II). Therefore, the catalytic activity of the copper-EDTA system is considered to be due to the free copper ion alone. This was later confirmed by the agreement between the experimental and the theoretical results.

The Estimation of the Stability Constant.—The stability constants of copper(II) complexes are calculated on the basis of the assumption that the catalytic activity of copper(II) complexes are due to the free copper ions which have been liberated from the copper(II) complexes at equilibrium.

If Cu is made to react with n mol. of dissociated chelating agents, Y, to form CuY_n, the formation reaction is expressed by Eq. 4. (Here, the charges on the ions are omitted for the sake of simplicity.)

$$Cu + nY \rightleftarrows CuY_n \tag{4}$$

$$K = [CuY_n] / [Cu]\,[Y]^n \tag{5}$$

If the initial concentration of Cu, $[Cu]_0$, is known,

$$[CuY_n] = [Cu]_0 - [Cu] \tag{6}$$

Similarly, Eq. 7 is derived:

$$[Y]_t = [Y]_0 - n[CuY_n] = n[Cu] \tag{7}$$

where $[Y]_0$: initial concentration of chelating agent,

$[Y]_t$: total concentration of unbound chelating agent at equilibrium.

$[Y]$ is calculated from $[Y]_t$ by the following process. The dissociation of the chelating agent, H_mY, is given by Eq. 8:

$$\begin{aligned} &H_mY \rightleftarrows H^+ + H_{m-1}Y \\ &\qquad K_{d_1} = [H^+]\,[H_{m-1}Y] / [H_mY] \\ &H_{m-1}Y \rightleftarrows H^+ + H_{m-2}Y \\ &\qquad K_{d_2} = [H^+]\,[H_{m-2}Y] / [H_{m-1}Y] \\ &\qquad \cdots\cdots\cdots\cdots \\ &H_2Y \rightleftarrows H^+ + HY \\ &\qquad K_{d_{m-1}} = [H^+]\,[HY] / [H_2Y] \\ &HY \rightleftarrows H^+ + Y \quad K_{d_m} = [H^+]\,[Y] / [HY] \end{aligned} \tag{8}$$

$[Y]_t$ is also given by Eq. 9:

$$[Y]_t = [H_mY] + [H_{m-1}Y] + \cdots\cdots + [HY] + [Y] \tag{9}$$

The terms, $[H_mY] \sim [HY]$ in Eq. 9 are given by rewriting Eq. 8;

$$\begin{aligned} &[HY] = [H^+]\,[Y] / K_{d_m} \\ &[H_2Y] = [H^+]^2\,[Y] / K_{d_m} \cdot K_{d_{m-1}} \\ &[H_mY] = [H^+]^m\,[Y] / K_{d_m} \cdot K_{d_{m-1}} \cdots \\ &\qquad \cdot K_{d_2} \cdot K_{d_1} \end{aligned} \tag{10}$$

By substituting Eq. 10 into Eq. 9, Eqs. 11 and 12 are obtained:

$$[Y]_t = \frac{[H^+]^m\,[Y]}{K_{d_1} \cdot K_{d_2} \cdot \cdots \cdot K_{d_m}} + \frac{[H^+]^{m-1}\,[Y]}{K_{d_2} \cdot K_{d_1} \cdot \cdots \cdot K_{d_m}} + \cdots \frac{[H^+]\,[Y]}{K_{d_m}} + [Y] \tag{11}$$

$$[Y] = [Y]_t / \left(\frac{[H^+]^m}{K_{d_1} \cdots K_{d_m}} + \cdots + \frac{[H^+]}{K_{d_m}} + 1 \right) \tag{12}$$

If k is measured in the presence of a copper-complex, $\log [Cu]$ is found by Eq. 2 or 3, followed by the calculation of $[CuY_n]$ and $[Y]_t$ by Eqs. 6 and 7. $[Y]$ is also calculated by Eq. 12, and the stability constant is finally calculated by Eq. 5. The results obtained by this method are shown in Table II, along with those obtained by the polarographic method, etc. The results agree well with those obtained by other methods.

Table II. The stability constants of copper complexes calculated from k (pH=4.3, 25±0.1°C, ionic strength=0.2)

Chelating agent	lok k_s from rate constant	lok k_s from polarographic method*	lok k_s from literature
EDTA	15.2	15.1	18.80[2]
NTA	12.1	13.8	12.96[3]
1, 10-Phenanthroline	12.9	—	12.45[4]
α, α'-Dipyridyl	14.1	12.3	—
Oxine	25.4	—	26.22[5]
Oxalic acid	10.4	—	10.3[6]

* Calculated from the shifts of half-wave potentials.

Correlation among k, K_s and Y.—Figure 4 is obtained by plotting k against $\log (1 + K_s \cdot [Y]^n)$. As can be seen from Fig. 4, k is inversely proportional to $\log (1 + K_s [Y]^n)$. This relationship may also be derived theoretically. Eq. 5 is expressed by Eq. 13:

$$K_s = ([Cu]_0 - [Cu]) / [Cu]\,[Y]^n \tag{13}$$

By rewriting Eq. 13,

$$[Cu] = [Cu]_0 / (1 + K_s [Y]^n) \tag{14}$$

By taking a logarithm and combining it with Eq. 1,

$$k = a \log [Cu]_0 - a \log (1 + K_s [Y]^n) + b \tag{15}$$

2) G. Schwarzenbach et al., *Helv. Chim. Acta*, **37**, 937 (1954).
3) G. Schwarzenbach et al., ibid., **38**, 1144 (1955).
4) F. P. Dwyer and R. Nyholm, *J. Proc. Roy. Soc., New South Wales*, **80**, 28 (1946).
5) W. D. Johnston and H. Freiser, *J. Am. Chem. Soc.*, **74**, 5239 (1952).
6) L. Meites, ibid., **72**, 184 (1950).

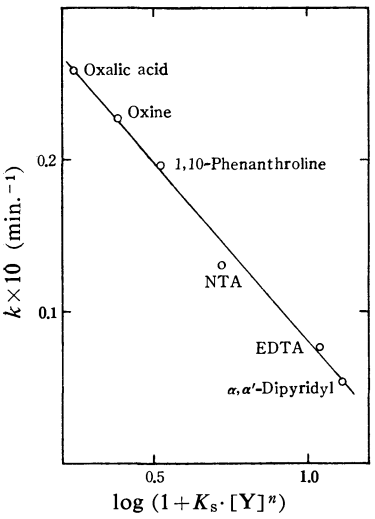


Fig. 4. Relation between k and $\log(1+K_S[Y]^n)$ (pH=4.3, ionic strength=0.2, 25±0.1°C)

Since the first term on the right-hand side is thought to be a constant, Eq. 16 is glven:

$$k = -a \log(1+K_s[Y]^n) + b' \qquad (16)$$

According to Fig. 4, the value of k for a given copper-complex at a definite pH can be estimated by the use of the values for K_S and Y. It is expected that Eq. 16 generally holds for the various kinds of reactions which proceed as of the first order.

Summary

The stability constants of various kinds of copper complexes have been estimated on the basis of the decrease in the catalytic activity of copper(II) in the presence of chelating agents. The rate constant, k, has been found to be inversely proportional to $\log(1+K_s[Y]^n)$.

The authors wish to express their hearty thanks to Mr. Shozo Fukui and Miss Keiko Yamamoto for their skillful technical assistance.

Department of Chemistry
Faculty of Engineering
Doshisha University
Kamikyo-ku, Kyoto

*The Effect of the Type of Radiation on the Radiation-Induced Addition of Acetaldehyde to Cyclohexene**

By Akira SHINGYOUCHI, Motoyoshi HATADA and Kozo HIROTA

(Received February 21, 1964)

An earlier report[1] studied the gamma-ray-induced addition of acetaldehyde to cyclohexene; cyclohexyl ketone was the main product. The products were different from those when ultraviolet irradiation was carried out.[2] Since such a discrepancy might be caused by the difference in irradiation sources, the effect of the type of radiation will be investigated in the present report by comparing the results obtained by use of gamma-rays,[1] ultraviolet light, and electron beams.

* Chain-Telomerization Induced by Radiation. VII. Presented at the Annual Meeting of the Chemical Society of Japan, April, 1963.

1) M. Hatada, J. Takezaki and K. Hirota, This Bulletin, 37, 1661 (1964).

2) P. de Mayo, I, B. Stothers and W. Templeton, *Can. J. Chem.*, 39, 488 (1961).

Experimental

Materials.—Acetaldehyde was prepared by the method which has previously been described in the present series of studies. Commercial cyclohexene was used after distillation. Commercial DPPH was used without any further purification.

Irradiation Procedures.—For electron-beam irradiations, spot electron beams (1.5 MeV., 50 μamp) from a Van de Graaff accelerator were used. Figure 1 shows the apparatus for the irradiation. The sample (40 ml.) was irradiated in a vessel equipped with a magnetic stirrer, A, and an aluminum window, B, through which the electron beams penetrated into the vessel. During the irradiation, the sample was cooled with an ice water bath.

The dose rate was estimated to be 0.77×10^{20} eV./sec. by the use of a cerric-cerrous dosimeter in

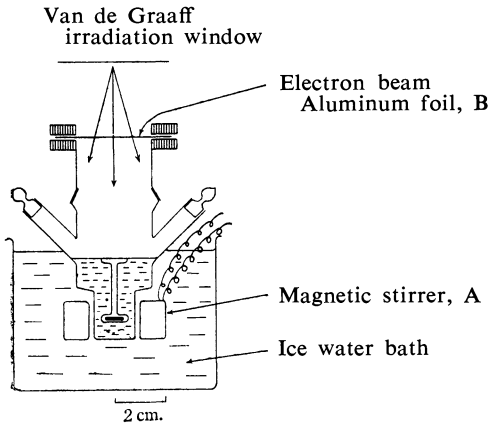


Fig. 1. Apparatus for electron beam irradiation.

the vessel used for the irradiation of the mixture. Details of the dosimetry will be described elsewhere.[3]

For the irradiation with an ultraviolet light, a high-pressure mercury lamp (Toshiba H400 P type) was used as the irradiation source. The sample (8 ml.) was degassed and distilled into a quartz tube under vacuum. Having been sealed off, the tubes were then subjected to the irradiation at 17°C for 5 hr.

Analysis. — After irradiation, the samples were subjected to gas chromatographic analyses, the conditions of which were as follows:

Column, P. E. G. 6000; column length, 3.0 m; carrier gas, He; flow rate, 60 ml./min.; column temperature, 180°C; apparatus; Shimadzu GCIB.

For the identification of the peaks which appeared in the gas chromatograms, a mass spectrometer (Hitachi RMU-5) and an infrared spectrometer (Shimadzu AR275) were used.

Results and Discussion

Identification of the Irradiation Products.— Typical gas chromatograms of the irradiated samples with γ rays,* electron beams, and ultraviolet are shown in Figs. 2a, 2b, and 2c respectively. The peaks which appeared in the gas chromatograms are designated as P^i_γ, P^i_e and P^i_{UV} respectively, where the subscripts denote the type of radiations while the superscripts, $i=1, 2, 3,\ldots\ldots$ denote the order in which the peaks appeared in the gas chromatograms.

By a comparison of the retention times of the peaks obtained by different irradiation sources, some of the products may be assumed to be the same. They may be grouped in parentheses as follows:

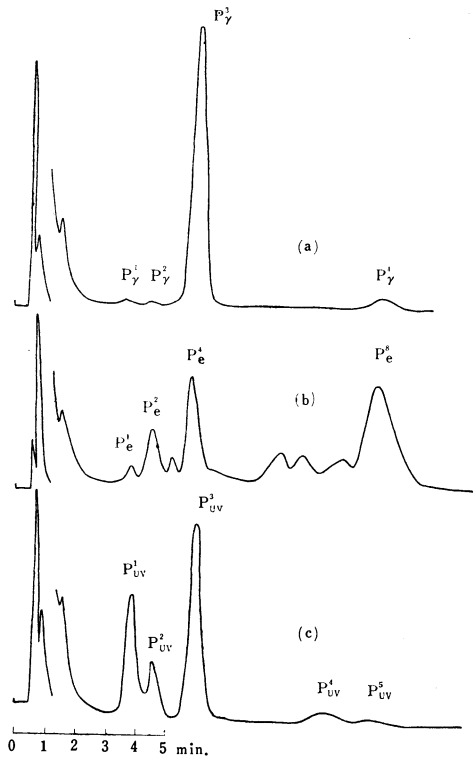
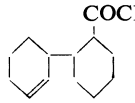


Fig. 2. Gas chromatograms of irradiated mixtures.
a) with γ-rays, b) with electron beams from the Van de Graaff accelerator, and c) with ultraviolet light from the high pressure mercury lamp.
Column: Polyethylene glycole 6000, 3.0 m.
Column temp.: 180°C
Carrier gas: He 60 cc./min.

$$A(P^1_\gamma, P^1_e, P^1_{UV}),\ B(P^2_\gamma, P^2_e, P^2_c),$$
$$C(P^3_\gamma, P^4_e, P^3_{UV}),\ D(P^4_\gamma, P^8_e, P^5_{UV})$$

The mass spectra and the infrared spectra of these fractions, A, C and D, are shown in Figs. 3a, 3b and 3c respectively, but the spectra of the fraction B were difficult to obtain because of its small yield as well as because of lack of a standard samples. The fraction A, which gives the same mass spectrum, infrared spectrum and retention time in the gas chromatogram as acetoin, $CH_3\overset{O}{\overset{\|}{C}}-\overset{OH}{\overset{|}{\underset{H}{\underset{|}{C}}}}-CH_3$, is identified as this compound. The fraction C is assigned to be methyl cyclohexyl ketone (McHK) from the mass and infrared spectra shown in Fig. 3b. The D fraction is estimated to be 1-acetyl-2(3-cyclohexenyl)-cyclohexane,



in the mass spectrum and from

3) Y. Nakai et al., Annual Meeting of the Physical Society of Japan, 1963.

* Almost all the data on γ-ray irradiations in this report are reproduced from a former report[1] for the sake of comparison.

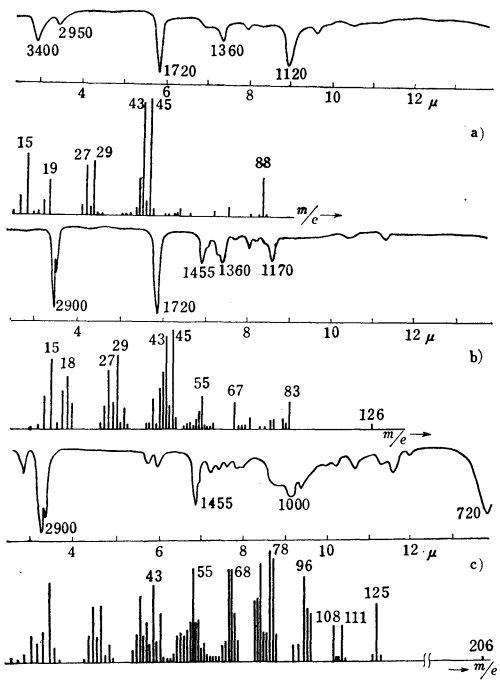
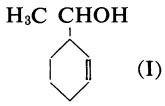


Fig. 3. Mass spectra and infrared spectra of fractions corresponding to the peaks appeared in the gas chromatogramms:
a) P^1_γ, P^1_e, P^1_{UV}, b) P^3_γ, P^4_e, P^3_{UV} and
c) P^4_γ, P^8_e

the absorptions of ν_{CH_2,CH_3} (2900~2950 cm^{-1}) and ν_{CO} (1720 cm^{-1}) in the infrared spectrum in Fig. 3c.* Although the identification of this product is not so definite as the former two, it will be supported by the experimental results below.



(I)

In the present experiment, 1-cyclohex-2'-enylethan-1-ol(I) was not found as has been reported by Mayo[2], even when ultraviolet was used as the irradiation source. Since the separating factor of the column used in this experiment is not as large as that of Mayo's, there may be some ambiguity concerning the separation of (I) from McHK. However, this ambiguity is reduced to some extent by the fact that the absorption of ν_{OH} is not found in the infrared spectrum of this fraction. At any rate further experiments using higher resolution colums will be needed to elucidate this problem.

* The absorption band at ν_{OH}~3300 cm^{-1} appeared in the IR spectrum of the fraction C. This band seems to be attributed to a trace of water condensed in the fraction collector from the atmosphere, and it seems to become significant when the fraction is difficult to collect effectively because of its lower vapor pressure.

The Effect of the Irradiation Time on the Yields. — The amounts of the products are plotted against the irradiation time in Figs. 4-1 and 4-2, practically giving a linear increase of the amount of the products. However in the region of higher doses, the rates of formation decrease because of the decomposition of the products as a result of irradiation.

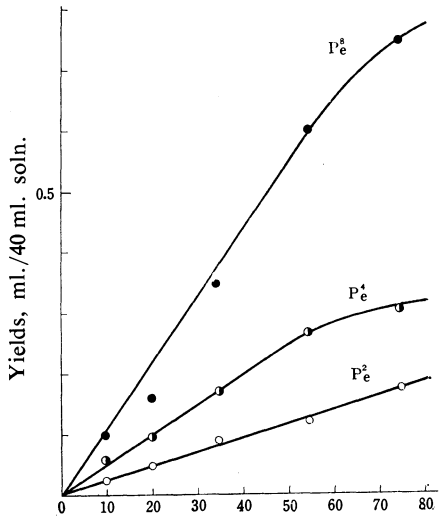


Fig. 4-1. The yields of products vs. irradiation time (electron beam irradiation).
Cyclohexene: 35 ml., Acetaldehyde: 5 ml.
Irradiation temp.: 0°C
Electron accelerating voltage: 1.5 MeV.
Electron beam current: .50 μA.

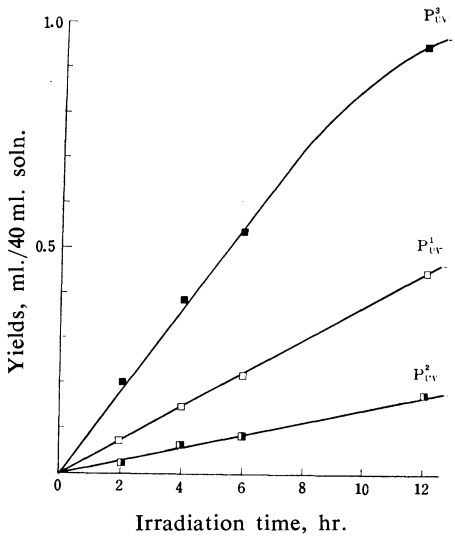


Fig. 4-2. The yields of products vs. irradiation time (ultra-violet light irradiation).
Cyclohexene: 2 ml., Acetaldehyde: 6 ml.
Irradiation temp.: 17°C

The Effect of the Compositions of the Feed on the Yields.—The results are shown in Fig. 5, where the yields of the products are plotted against the volume percent of cyclohexene. For the methyl cyclohexylketone formation, the concentration of that cyclohexene in the feed which gives a maximum yield of McHK seems to depend on the type of radiation. It reaches its highest value at 40% in the electron

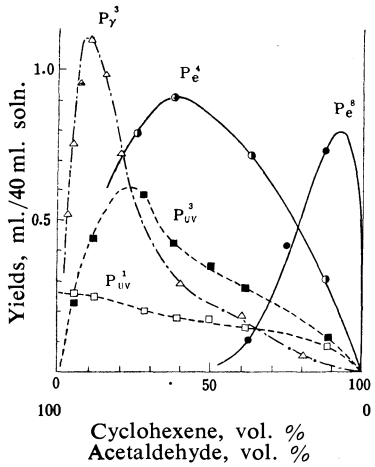


Fig. 5. The yields of products vs. cyclohexene in the feed.

irradiation, at 25% in ultraviolet irradiation, and at 10% in the γ-ray irradiation.

Acetoin was produced most favorably in pure acetaldehyde. The yield of 1-acetyl-2-(3-cyclohexenyl)cyclohexane reaches a maximum in the cyclohexene-rich mixture (ca. 90%). These relations between the yields and the cyclohexene fraction in the feed seem to be reasonable judging from the structure of the product molecules.

The Temperature Dependencies on the Yields.—The yield of McHK increases with the rise in irradiation temperature in the case of ultraviolet irradiation, as Fig. 6 shows. The Arrhenius plot for the McHK formation gives an overall activation energy of 3.5 kcal./mol., which is approximately equal to that obtained in the γ-ray irradiation. This coincidence indicates that the mechanism of the McHK formation is the same in both systems.

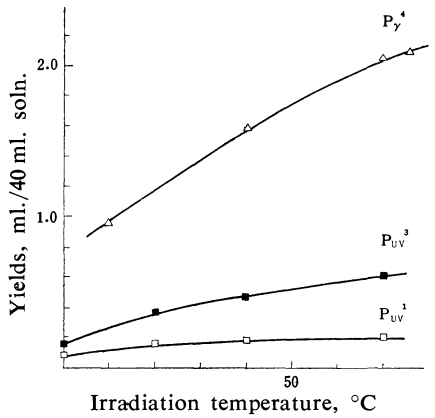


Fig. 6. The yields of products vs. irradiation temperature.

The Effect of the Dose Rate on the Yields.—The effects of the dose rate of the electron beams on the formation of McHK and 1-acetyl-2-(3-cyclohexenyl)cyclohexane are shown in Fig. 7. The yield of McHK is proportional to 1/2 power of the beam current, while that of 1-acetyl-2-(3-cyclohexenyl)cyclohexane is proportional to 1. The reason for this will be discussed below.

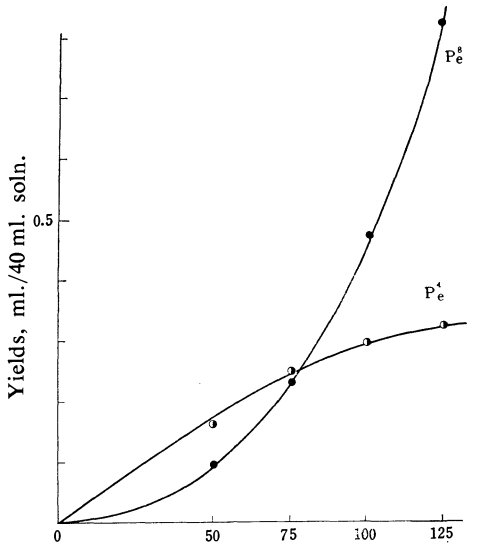
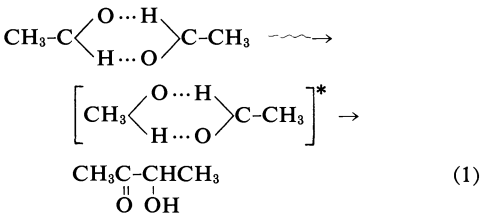


Fig. 7. The yields of products vs. electron beam current.
Cyclohexene: 30 ml., Acetaldehyde: 10 ml.
Irradiation time: 20 min.
Irradiation temp.: 0°C
Accelerating voltage: 1.5 MeV.

The Effect of Additives.—When ultraviolet was used as the irradiation source, the peaks P^1_{UV} and P^2_{UV} in the gas chromatogram were not affected by the addition of DPPH, but P^3_{UV} decreased markedly. However, when the electron beams were used as the irradiation source, the peaks P^1_e, P^2_e and P^3_e were not changed, while P^4_e and P^8_e decreased markedly upon the addition of DPPH.

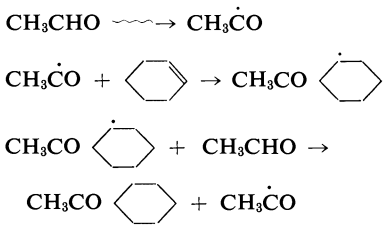
The Reaction Mechanism of Acetoin Formation.—Acetoin was formed by ultraviolet and electron beam irradiations in the acetaldehyde-rich mixture, but it was formed in only a small quantity by the γ-ray irradiation. As

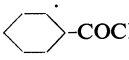
has been mentioned above, the formation of acetoin was not inhibited by the addition of DPPH. These facts indicate that acetoin was formed via a bimolecular process 1 which involves the excitation of the acetaldehyde dimer thus, forming a chelate ring. This reaction does not proceed via a chain mechanism, so it plays only a minor role in the case of the γ-ray irradiation, where the dose rate is significantly lower than in the other.



$$CH_3C(=O)CH(OH)CH_3 \quad (1)$$

Methyl Cyclohexylketone.—McHK was formed by γ-ray, electron beam and ultraviolet irradiations. Its formation was inhibited by the addition of DPPH, and its rate of formation depends on the 1/2 power of the dose rate. On the basis of these results, McHK formation may be attributed to the following radical chain process, as was suggested in a previous report:[1]



Fraction C (1-Acetyl-1-(3-cyclohexenyl)-cyclohexane).—This productwas formed only when a cyclohexene-rich mixture was irradiated with electron beams. The formation of this compound was inhibited by the addition of DPPH, and its rate of formation depends on the first power of the dose rate. Consequently, this fraction was formed by a recombination reaction of the two radicals, probably  * and  .

The fact that this product is formed in only a small amount in the two types of radiation other than that of electron beams may stem from the situation that the radicals which react to form this fraction are not produced effectively in the case of ultraviolet irradiation because cyclohexene does not absorb the ultraviolet light of this wavelength region, and that the concentrations of these radicals are small in the case of γ-ray irradiation because of its low dose rate.

Summary

Several kinds of products have been found to be formed from mixtures of cyclohexene and acetaldehyde by the irradiation of γ-rays, electron beams, and ultraviolet. Both the yields and the kind of product seem to depend on the type of radiation because of their dose rate and bond-dissociating power.

The present authors wish to express their thanks to Dr. Yohta Nakai for his operation of the Van de Graaff apparatus.

Japanese Association for Radiation Research on Polymers
Osaka Laboratories
Neyagawa-shi, Osaka
(A. S., M. H., & K. H.)

Department of Chemistry
Faculty of Science
Osaka University
Kita-ku, Osaka (K. H.)

* It has been reported that the cyclohoxenyl radical may be produced by irradiating cyclohexene at −198°C with electron beams from the Van de Graaff apparatus. Cf. S. Ohnishi and I. Nitta, *J. Chem. Phys.*, **39**, 2848 (1963).

Studies on Organic Catalytic Reactions. II. The Hydration of Nitriles to Amides with Nickel Catalysts

By Ken-ichi WATANABE

(Received March 23, 1964)

In a preliminary note,[1] it was reported that nitriles are hydrated to the corresponding amides by the catalytic action of nickel. It is notably important that the hydration of nitriles is effected in water without any acid, alkali or hydrogen peroxide and that it is generally stopped at the amide stage. This paper will describe and discuss the results of further investigation of the hydration of nitriles.

In general, aromatic nitriles are hydrated to the corresponding amides, the yields of amides range from 30 to 90 per cent of the nitriles used except in special cases. The reaction of aliphatic nitriles is somewhat complicated and is different from that of aromatic ones: the yield of the amides is comparatively lower than that from aromatic nitriles, and the hydration reaction is accompanied by side reactions forming some acidic compounds. The catalysts used are Urushibara nickel (U-Ni),[2] Raney nickel, "stabilized nickel"[3] and related substances. The general procedure for the hydration is completed by refluxing a nitrile for five to ten hours in water with a suitable amount of a nickel catalyst. During the reaction, a small quantity of ammonia is generated; this can be detected with litmus. After the reaction, the catalyst is filtered off, and the solution is evaporated to a solid mass which consists of a crude amide.

In a few cases, a very small quantity of the corresponding acid is obtained by hydrolysis. However, benzamide itself is hardly ever hydrolyzed to benzoic acid, even when it is refluxed for a long time with a newly-prepared nickel catalyst. Amines are obtained in some cases because of the hydrogenation of the nitrile with hydrogen adsorped on the nickel catalyst. The yield of amines increases largely when a solvent other than water, especially ethanol, is used. In some cases, the formation of a metal complex is observed by a presumable side reaction between the nitrile and the catalyst. In general, the hydration to an amide is predominant over the other side reactions mentioned above if the condition of the reactions is suitable: the features of this metal-catalyzed hydration are peculiar and are unlike those of acid- or base-catalyzed hydration.

The Effect of the Nature and the Position of the Substituents in Substituted Benzonitriles.— The results of experiments on the hydration of various nitriles with U-Ni-B in water are given in Table I. As is shown in the table, the hydration of substituted benzonitriles is governed largely by the nature and the position of the substituent in the benzene nucleus. It is rather remarkable that amides can not be obtained from *p*-hydroxybenzonitrile (Exp. 6), ethyl *o*- and *p*-cyanobenzoates (Exp. 13 and 14) or *p*-cyanobenzaldehyde (Exp. 16). On the other hand, a complex-formation between the nitrile (or intermediate) and the catalyst metal is observed with *p*-hydroxybenzonitrile (Exp. 6), *p*-nitrobenzonitrile (Exp. 7), *o*- and *p*-aminobenzonitriles (Exp. 9 and 10), mesitonitrile (Exp. 11), ethyl *o*- and *p*-cyanobenzoates (Exp. 13 and 14) and *p*-cyanobenzaldehyde (Exp. 16). The yield of the complexes varies with the kind of nitrile.

It has been found that there are two types of complexes, one containing zinc and the other containing nickel. Zinc complexes are obtained from *p*-cyanobenzoic acid, ethyl *o*- and *p*-cyanobenzoates and *p*-hydroxybenzonitrile. Nickel complexes are obtained from *p*-nitrobenzonitrile, *o*- and *p*-aminobenzonitriles and *p*-cyanobenzaldehyde. The former is easily decomposed to the corresponding carboxylic acids with acid or aqueous alkaliliberating ammonia. On the other hand, the latter is very stable to acid, alkali and oxidizing agents. As a whole, electron-releasing substituents retard the hydration reaction and electron-attracting substituents effect the formation of metal complexes. 3-Cyanopyridine gives rise to a very high yield of the amide, the nitrogen in the pyridine nucleus having an important electron-attracting effect on the cyano group.

A remarkable ortho effect is observed in this hydration reaction, which has been similarly recognized in the case of acid or alkaline hydration. The yield of amides is

1) K. Watanabe, This Bulletin, **32**, 1280 (1959).
2) Y. Urushibara and S. Nishimura, ibid., **27**, 480 (1954); **28**, 446 (1955).
3) T. Yamanaka and Y. Takagi, *J. Sci. Res. Inst.*, **51**, 168 (1957); **52**, 143, 224 (1958).

TABLE I. THE HYDRATION OF NITRILES TO AMIDES WITH U-Ni-B IN WATER
(4 g. of U-Ni-B was used in each run)

Exp. No.	Nitriles	Water (solvent) g.	Water (solvent) cc.	Reaction time hr.	Yield[1] of amides %	Recovered nitrile %	Other products
1	Benzonitrile	5	80	8	78	–	
2	*o*-Tolunitrile	5.5	80	12	49	–	Unidentified oil
3	*p*-Tolunitrile	7	100	8	63	–	
4	*o*-Methoxybenzonitrile	10	100	10	33	32	Phenolic substance, amine
5	*p*-Methoxybenzonitrile	10	100	10	65	+	Amine
6	*p*-Hydroxybenzonitrile	4.5	100	5	—	–	Metal complex (3.5 g.), tarry matter
7	*o*-Nitrobenzonitrile	5	150	10	54	–	*o*-Aminobenzamide (43%), tarry matter
8	*p*-Nitrobenzonitrile	5	200	10	50	–	*p*-Aminobenzonitrile, metal complex (2 g.)
9	*o*-Aminobenzonitrile	5	100	5	ca. 45	20	Metal complex (0.5 g.) (purple)
10	*p*-Aminobenzonitrile	5	100	5	65	+	Metal complex (0.9%.) (yellow)
11	Mesitonitrile	7	100	10	?	The most part	Metal complex (0.6 g.), amine
12	Benzyl cyanide	10	150	10	52	30	Amine
13	Ethyl *p*-cyanobenzoate	5	150	8	—	>40	Metal complex (2 g.)
14[2]	Ethyl *p*-cyanobenzoate	5	150	10	—	+	Metal complex (2 g.), unidentified oil
15	*p*-Cyanobenzoic acid	5	100	12	—	–	Metal complex
16	*p*-Cyanobenzaldehyde	5	150	8	—	–	Metal complex (5 g.)
17	α-Naphthonitrile	7	100	8	19	35.7	Amine
18	Acetonitrile	7	100	5	47	–	Acids
19[3]	Enanthonitrile	3.6	50	5	38	+	
20	Adiponitrile	10	100	10	14	–	Unidentified oil, acidic substance
21	3-Cyanopyridine	7	100	10	89	–	

1) Yield of amides was calculated from the weight of amides obtained.
2) It was almost the same with a reaction on *p*-cyanobenzoic acid.
3) Two grams of the catalyst was used.

more or less diminished with ortho-substituted benzonitriles, such as *o*-tolunitrile (Exp. 2), *o*-methoxybenzonitrile (Exp. 4), *o*-nitrobenzonitrile (Exp. 7), *o*-aminobenzonitrile (Exp. 9), mesitonitrile (Exp. 11), ethyl *o*-cyanobenzoate (Exp. 13) and α-naphthonitrile (Exp. 17), the largest effect being observed with mesitonitrile. The reaction velocity becomes slower, and often a considerable quantity of the starting materials is recovered unchanged. In some cases, unfavorable side reactions are alternated.

The Effect of the Nature of the Catalyst.— When *o*-nitrobenzonitrile was hydrogenated with a nickel catalyst in either the liquid[4] or the vapor phase, it was reported that a considerable quantity of *o*-aminobenzamide was formed by the hydration of the nitrile group.[5] It has been presumed that the hydrogenating activity of the nickel catalyst is largely depressed by poisoning with the amino group produced by the reduction of the nitro group,[6] and that the nitrile group is hydrated with water produced by the hydrogenolysis of the nitoro group or originally present in the solvent. The present investigation shows that such is the case, since the ability of nickel catalysts to effect the hydration of nitrile group has been proved. Ordinary nickel catalysts for

4) H. Rupe, *Helv. Chim. Acta*, **8**, 832 (1925).

5) K. Watanabe, *J. Chem. Soc. Japan, Pure Chem. Sec.* (*Nippon Kagaku Zassi*), **76**, 398 (1955); *Chem. Abstr.*, **51**, 17815 (1957).

6) K. Watanabe, *J. Chem. Soc. Japan, Pure Chem. Sec.* (*Nippon Kagaku Zassi*), **77**, 225 (1956); *Chem. Abstr.*, **51**, 17816 (1957).

hydrogenation are generally available for the hydration of nitriles.

In this connection, precipitated nickel, precipitated copper, nickel oxide, cupric oxide and Urushibara copper (U-Cu) were also tested with relation to the hydration of benzonitrile. The results of representative experiments are shown in Table II. The highest yield of benzamide was given with U-Ni-B, followed by those with U-Ni-A, Raney nickel and stabilized

Table II. The hydration of benzonitrile to benzamide with various catalysts

Exp. No.	Catalysts	g.	Weight of benzonitrile g.	Solvent	cc.	Reaction time hr.	Yield of benzamide %	Recovered benzonitrile g.	Other products
1*	U-Ni-B	4	5	Water	80	8	78	–	
2	U-Ni-A	3	5	Ethanol	60	8	5	1.6	Amine
3	U-Ni-A	3	3	Water	80	8	71.5	–	
4	U-Ni-BA	4	5	Ethanol	80	9	5	1.7	Amine
5	U-Ni-BA	4	5	Water	80	9	34.5	1.4	Amine
6	U-Cu-A	4	5	Ethanol	60	8	+	0.8	Amine
7	U-Cu-A	4	5	Water	100	8	24	–	
8	U-Cu-B	4	5	Ethanol	60	8	7	–	Amine, unidentified oil and crystals
9	ppt. Ni (Zn)	4	10	Ethanol	100	13	–	–	Complex of amine and nickel (6.8 g.), amine-HCl (3 g.), unidentified oil
10	ppt. Ni (Zn)	4	10	Water	150	10	–	–	Complex of amine and zinc, unidentified crystals
11	ppt. Cu (Zn)	4	5	Ethanol	80	8	7	–	Amine-HCl (1.7 g.), unidentified oil
12	Reduced Ni	4	5	Water	80	16	10.7	>0.8	
13	Raney Ni (W-4)	4	10	Ethanol	100	8	+	>5	
14	Raney Ni (W-4)	4	10	Water	100	8	65	–	
15	Stabilized Ni	10	2	Water	50	6	70	–	
16	NiO+CuO	5	5	Ethanol	80	10	5	2.5	

* Same as Exp. I, Table I
U-Ni-B in ethanol: see Table III

Table III. The hydration of benzonitrile to benzamide in various solvents
(Catalyst: U-Ni-B)

Exp. No.	Weight of benzonitrile g.	Weight of catalyst g.	Solvent	cc.	Reaction time hr.	Yield of benzamide %	Recovered benzonitrile g.	Other products
1	5	2	Water	80	9	57	+	
2	5	4	Water	80	11	73	–	
3	5	4	Water	80	8	78	–	
4	15	8	Water	150	10	74	–	
5	5	4	Ethanol	60	9	11	–	Amine-HCl (4 g.), tarry matter
6	5	8	Ethanol	100	2.5	19	0.6	Amine-HCl (2 g.), tarry matter
7	10	8	Ethanol	100	8	19	1	Amine-HCl (3.6 g.), tarry matter
8	10	4	Methanol	100	10	12	ca. 4	Amine
9	5	4	1-Butanol	80	4	7	–	Amine-HCl (3.4 g.), unidentified oil
10	10	8	Dioxane	100	12	34	+	Amine-HCl (1.5 g.), unidentified crystal; m. p. 220°C

* Sample as Exp. I, Table I

nickel. The other substances mentioned above gave poor results as catalysts for the hydration, and they sometimes caused unexpected side reactions.

It should be noted that the procedure for the preparation of U-Ni may be simpler for the hydration than for hydrogenation. Common city water serves well enough for preparing the catalyst, and it does not matter if the catalyst is exposed to air during the preparation. To prepare Raney nickel (W-4) for the hydration, caution is unnecessary with regard to the temperature, air and water. The stabilized nickel and the reduced nickel catalysts are less active than the U-Ni's and Raney nickel. It was found that the precipitated nickel or copper is of no use at all for the hydration of nitriles to amides, a large amount of complexes of corresponding amines and zinc being formed.

The results of the experiments indicate that the hydrating activity of the nickel catalysts depends on the size of the crystallites of the catalysts. It is known that the approximate sizes of the crystallites of U-Ni-A, U-Ni-B, U-Ni-BA, U-Cu and reduced nickel are 40 Å 40 Å, 120 Å, 260 Å and 350 Å respectively. The yields of benzamide obtained with these catalysts follows the above-mentioned order. If too small a quantity of a catalyst is used, or if the reaction time is insufficient for the hydration, the nitrile is sometimes recovered unchanged in a considerable quantity. Gas chromatographic research shows that about 90 per cent of benzonitrile is changed after five hours with a U-Ni-B catalyst. When the catalyst is not so active, a large quantity is necessary for a satisfactory hydration, as is shown by Exp. 15 and 16 in Table II.

In the previous experiments, any specific behavior of thiophene or pyridine as a promoter of the catalyst was examined, and it was shown shat a small quantity of thiophene or pyridine exhibited no promoter action in an ethanolic solution but, rather, had an unfavorable effect. In the present investigation, however, some different information was put forward on this subject. It is noteworthy in Table I that nitriles of basic character, such as 3-cyanopyridine and *p*-aminobenzonitrile, give good yields of amides, whereas those of an acidic character, such as *p*-hydroxybenzonitrile and *p*-cyanobenzoic acid, give no hydration products. The aliphatic nitriles, some of which are hydrolyzed to acids during the reaction, also give unfavorable results, as in the normal hydration. From these results, it may be inferred that the hydration of nitriles is due to the catalytic action of the basic contact sites (active center) of the nickel catalysts.

It is assumed that a nickel catalyst acts in two different ways, exhibiting acidic and basic functions. It has been suggested that the catalytic hydrogenation of nitriles and nitro groups is due to the acidic contact sites of the catalyst,[7] as is the reductive dehydroxymethylation of primary alcohols.[8] On the other hand, the catalytic hydrogenation of carbonyl groups[9] and the dehydroxylation of alcohols are attributed to basic sites.[8] In the hydration of nitriles, acidic substances or acidic parts of the nitrile molecules may cover the basic sites of the catalyst, resulting in the depression of the hydration reaction. Ammonia, generated by the hydrogenolysis of nitriles during the reaction, and basic parts of the nitrile molecules may cover the acidic sites of the catalyst and accentuate the catalytic activity of the basic sites to realize a favorable hydration. According to the studies of the reaction mechanism of the hydrolysis of nitriles with acid or alkali, the hydration has been assumed to be initiated at the carbon atom of a nitrile group, endowed with a carbonium character. In the catalytic hydration of nitriles, the reaction may be similarly initiated at the carbon atom attached to the basic sites of the catalyst. Our preliminary test for the effects of pyridine and thiophene on the hydration of benzyl cyanide proved that the former increases the yield of the amide, while the latter decreases it. This will be discussed in a subsequent report of this series.

The Effect of Solvents:—Methanol, ethanol, 1-butanol, dioxane and water were examined for as possible solvents for the catalytic hydration of benzonitrile. Water was proved to be the most excellent of all. When any other solvent than water is used, the nitrile group is hydrogenated more or less by hydrogen adsorped on the catalyst; sometimes undesirable side reactions are caused. The reactions in water generally give good yields of amides. The results of the experiments are listed in Table III, while the results of the hydration in water and ethanol are compared in Table II. It is noteworthy that water suppresses the catalytic activity for hydrogenation and emphasizes the catalytic activity for hydration.

Experimental

The Preparation of Catalysts for the Hydration of Nitriles.—*U-Ni-A.*—To 40 g. of commercial zinc

7) K. Watanabe, *J. Chem. Soc. Japan, Pure, Chem. Sec.* (*Nippon Kagaku Zassi*), **78**, 1478 (1958); *Chem. Abstr.*, **54**, 1370 (1960).
8) H. Pines, M. Shamaienger and W. S. Postal, *J. Am. Chem. Soc.*, **77**, 5099 (1955).
9) D. R. Levering, F. L. Morritz and E. Lieber, ibid., **72**, 1190 (1950).

dust in a 1000 ml. Erlenmeyer flask, a small quantity of was added, and the mixture was heated to boil. In another vessel, 40 ml. of a nickel chloride solution containing 16 g. of $NiCl_2 \cdot 6H_2O$ was heated to 60°C and then added to the zinc dust with vigorous shaking. A violent exchange reaction took place, depositing nickel on the surface of the zinc. When the generation of hydrogen had ceased, about 640 ml. of 13% acetic acid, prepared from 83 ml. of CH_3COOH and 560 ml. of water and heated to about 70°C in advance, was added gradually while the mixture was shaken well, lest the contents should overflow as a results of the vigorous generation of hydrogen. The whole was occasionally shaken for about twenty minutes, until the liquid turned slightly green; then the mixture was diluted with cold water. The acid solution was decanted off, and the residue was washed with water several times by decantation until the washing became neutral to litmus. The catalyst thus prepared was used directly for the reaction in water. For use in other solvents, it was collected by filtration and pressed between filter paper before adding it to the solvents. The catalyst thus obtained contains about 3 g. of nickel.

U-Ni-B.—For the preparation of U-Ni-B, 640 g. of a sodium hydroxide solution (70 g. of sodium hydroxide and 570 ml. of water) were used to digest the precipitated nickel. The procedure was the same as for U-Ni-A in other respects. The finished catalyst was repeatedly washed with water until the washing became neutral to phenolphthalein paper. The U-Ni-B thus obtained contains 4 g. of nickel and is more voluminous than U-Ni-A.

U-Ni-BA.—To 20 g. of aluminum grains of 40~80 mesh in a 1000 ml. Erlenmeyer flask, a small quantity of hot water was added, and then 40 ml. of a hot nickel chloride solution containing 16 g. of $NiCl_2 \cdot 6H_2O$ was added. The whole was occasionally shaken until the reaction mixture became slushy. The exchange reaction was controlled by either cooling with cold water or heating with hot water. The precipitate was washed with cold water by decantation, and 500 g. of a 20% sodium hydroxide solution (100 g. of sodium hydroxide and 400 ml. of water), heated to about 60°C in advance, was gradually added. Because of the vigorous exothermic reaction, the contents were shaken well. The aluminum dissolved completely in a short time. The solution was decanted off, and the residue was washed three or four times with cold water by decantation until the washings became neutral to phenolphthalein. The catalyst thus obtained contains about 4 g. of nickel.

U-Cu.—U-Cu was prepared by almost the same procedure as that used for U-Ni, cupric chloride being used instead of nickel chloride. The precipitated copper could not be digested well with aqueous alkali, but it was digested well with aqueous acetic acid.

Precipitate Nickel (or Copper).—The precipitated nickel (or copper), prepared from nickel (or copper) chloride and zinc dust, was used directly after being washed with only water. The catalyst is very voluminous and contains much more adsorbed hydrogen.

Stabilized Nickel.—This is a kind of reduced nickel supported on kieselguhr and stabilized by treatment with carbon dioxed. The KSY-6 FC type (Nikko Shokai, Tokyo) was used for the hydration of benzonitrile.

The Hydration of Nitriles.—The procedure for the hydration of benzonitrile to benzamide with U-Ni-B (Exp. I, Table I) is shown as an example. The nickel catalyst (containing 4 g. of nickel) in 80 ml. of water was placed in a 200 ml. round flask, and 5 g. of benzonitrile was added. The flask was fitted with an Allihn condenser. The mixture was refluxed vigorously for about eight hours until the oil drops of benzonitrile on the water disappeared. The catalyst was separated by filtration while hot and washed with hot water and ethanol. The filtrate, admixed with the washings, was evaporated on a water bath. Benzamide was obtained in white crystals. The yield was 4.5 g. (78%). The crude amide, although it was fairly pure, was recrystallized from hot water with a small quantity of active charcoal. M. p. 127~128°C. It was identified by hydrolyzing to benzoic acid with alkali.

The author wishes to express his hearty thanks to Professor Kazuo Hata for his kind advice.

Department of Chemistry
Faculty of Science
Tokyo Metropolitan University
Setagaya-ku Tokyo

The Mechanism of the Thermal Decomposition of Hexamminecobalt(III) Chloride

By Nobuyuki TANAKA and Michio NANJO

(Received March 28, 1964)

The thermal decomposition of hexamminecobalt(III) complexes has been extensively studied by several researchers,[1-6] and the stoichiometric relation,

$$6[Co(MH_3)_6]Cl_3(s) \rightarrow 6CoCl_2(s) + N_2(g) + 6NH_4Cl(s) + 28NH_3(g)$$

has been proposed for the complete decomposition.[6] Its mechanism, however, is not fully understood. In the course of a reinvestigation of the thermal decomposition of metal complexes in this laboratory, some preliminary results suggested that the decomposition of cobalt(III) complexes was often initiated by the electron transfer from either a ligand atom or an outer-sphere ion to the central cobalt(III) atom, forming a less stable cobalt(II) complex. These results have been confirmed by polarographic and infrared spectroscopic measurements of the thermal decomposition product of hexamminecobalt(III) chloride, as well as by the measurement of the infrared spectra of the complex at elevated temperatures. The results will be briefly presented in this paper. A similar conclusion has been obtained by Wendlandt and Smith[7] from the thermomagnetic measurement of cobalt(III) ammine complexes.

Experimental

Hexamminecobalt(III),[8] hexamminecobalt(II)[9] and hexamminechromium(III)[10] chlorides were prepared by the methods given in the literature cited; they were identified by the measurement of their infrared absorption spectra.

The thermogravimetric curves were recorded with an automatic-recording thermobalance, Shimadzu Thermano Balance Type RT-2, in a nitrogen atmosphere. A 400-mg. sample was used in each measurement unless otherwise stated. The furnace heating rate was approximately linear with the time at about 3°C per min. The particle sizes of the samples ranged between 100 and 200 mesh.

Polarograms were recorded with a Yanagimoto PR-2 Polarorecorder equipped with an automatic potential scanner. The samples which had been taken out of the furnace were dissolved in supporting electrolyte solutions containing 1 M ammonium chloride, 1 M ammonium hydroxide and 0.005% gelatin. The dropping mercury electrode used had an m value of 2.06 mg./sec. and a drop time, t_d, of 3.72 sec., when measured at −0.80 V. vs. SCE in the same supporting electrolyte solution.

A Hitachi EPI-2G double-beam instrument with a KBr foreprism and gratings was used for the measurement of the infrared absorption spectra. The KBr disk method was employed unless otherwise stated.

Results and Discussion

The thermogravimetric curves of hexamminecobalt(III), hexamminecobalt(II) and hexamminechromium(III) chlorides are reproduced

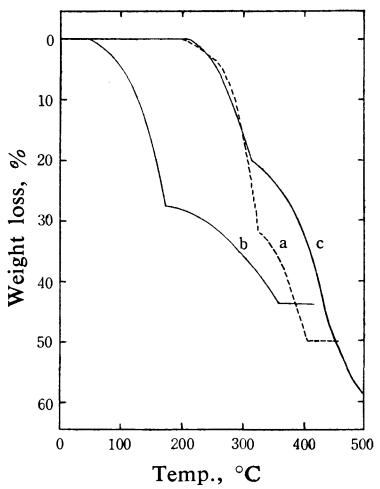


Fig. 1. Thermogravimetric curves of (a) $[Co(NH_3)_6]Cl_3$, (b) $[Co(NH_3)_6]Cl_2$ and (c) $[Cr(NH_3)_6]Cl_3$ obtained in nitrogen atmosphere.

1) W. Biltz, *Z. anorg. Chem.*, **83**, 177 (1913).
2) G. L. Clark, A, J. Quick and W. D. Harkins, *J. Am. Chem. Soc.*, **42**, 2496 (1920).
3) L. Kekedy, A. Szurkos, P. Krobl and E. Kekedy, *Acad. Rep. populare Romine, Filiala Cluj, Studii certetări chim.*, **9**, 79 (1958); *Chem. Abstr.*, **53**, 18721 (1959).
4) L. Kekedy, A. Szurkos, E. Kekedy and P. Krobl, ibid., 9, 91 (1958); *Chem. Abstr.*, **53**, 18721 (1959).
5) M. Mori and R. Tsuchiya, This Bulletin, **32**, 467 (1959).
6) W. W. Wendlandt. *J. Inorg. Nucl. Chem.*, **25**, 545 (1963).
7) W. W. Wendlandt and J. P. Smith, *J. Inorg. Nucl. Chem.*, **25**, 1267 (1963).
8) J. Bjerrum and J. P. McReynolds, "Inorganic Syntheses," Vol. II, Ed. by W. C. Fernelius, McGraw-Hill, New York (1946), p. 216.
9) W. Biltz and Fetkenheuer, *Z. anorg. Chem.*, **89**, 130 (1914).
10) M. Mori, *J. Chem. Soc. Japan, Pure Chem. Sec. (Nippon Kagaku Zassi)* **74**, 253 (1953).

in Fig. 1. The decomposition of hexamminecobalt(III) chloride begins at 205°C, whereas that of hexamminecobalt(II) chloride begins at 50°C.

Polarograms of heated samples of hexamminecobalt(III) chloride are given in Fig. 2, where, for convenience of comparison, the current is represented with a value for one millimolar

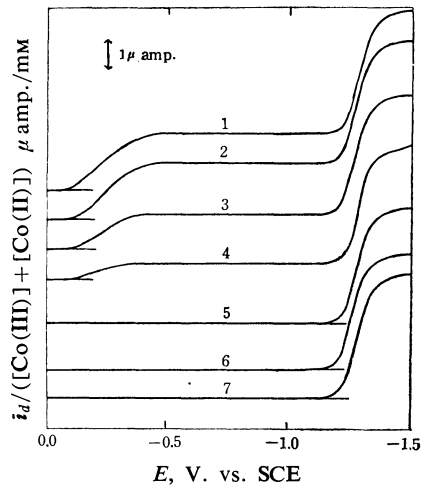


Fig. 2. Polarograms of the $[Co(NH_3)_6]Cl_3$ subjected to the thermal treatment, being recorded in 1 M NH_4Cl - 1 M NH_4OH containing 0.005% gelatin: The numbers represent the sample numbers given in Table I. Polarograms are corrected for the residual currents and the current is represented with the value for one millimolar of the total concentration of Co(III) and Co(II).

of the total concentration of cobalt(III) and cobalt(II). The temperatures at which the samples were taken out of the furnace are given in Table I. On curves 1 to 4, the first wave starts around −0.1 V. vs. SCE, which corresponds to the reduction of cobalt(III) to cobalt(II). The change in the limiting current with various heights of the mercury reservoir shows that the limiting current is diffusion-controlled. The second wave can be attributed to the reduction of cobalt(II) to cobalt(0). The height of the first wave decreased with an increase in the temperature at which the samples were treated. This indicates that the amount of cobalt(III) in the sample is less when treated at a higher temperature. Curve 5, which was obtained with the sample taken out of the furnace at 305°C, shows that the cobalt(III) was completely reduced to cobalt(II). Percentages of the decrease in weight and cobalt(III) content are given in Table I.

Table I. Loss in weight and Co(III) content in the $[Co(NH_3)_6]Cl_3$ subjected to the thermal treatment

Sample no.	Temp.* °C	Loss in weight, %	Loss in Co(III) content, %
1	Not treated	—	—
2	170	0	0
3	285	11.9	35
4	295	22.8	76
5	305	30.7	100
6	340	37.6	100
7	475	48.6	100

* Temperatures at which the samples were taken out of the furnace.

Infrared spectra of hexamminecobalt(III) chloride treated at various temperatures are given in Fig. 3. The absorption band due to the NH_3 symmetric deformation vibrations at 1320 cm^{-1} and that due to the NH_3

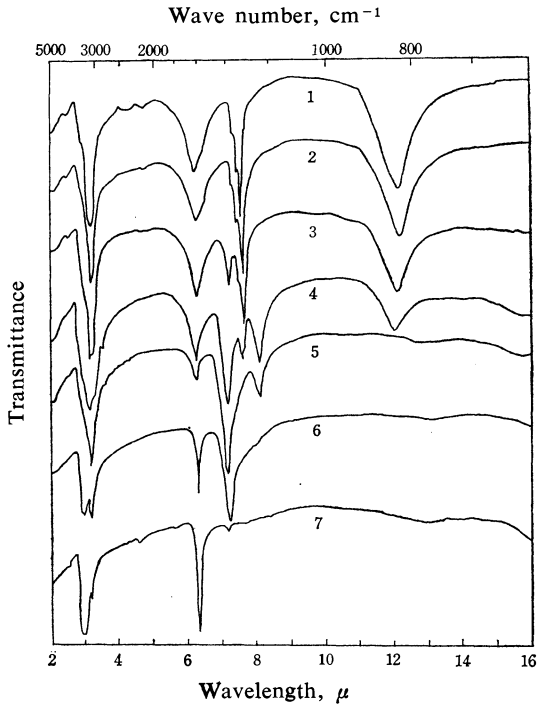


Fig. 3. Infrared absorption spectra of the $[Co(NH_3)_6]Cl_3$ subjected to the thermal treatment: The numbers represent the sample numbers given in Table I. Transmittance scale displaced arbitrarily.

rocking vibrations at 830 cm^{-1} decrease in intensity as temperature increases until they disappear at 340°C. A new absorption band appears at 1400 cm^{-1}; this is assigned to the ν_4 vibration of NH_4^+ ions. In samples 6 and 7, the NH_3 degenerate deformation band at 1608 cm^{-1} overlaps with a sharp ν_4 band of free ammonia molecules. These changes in the infrared absorption spectra may indicate a decrease in cobalt(III) content as well as

the formation of ammonium ions and free ammonia molecules. These experimental results indicate that, at higher temperatures, cobalt(III) in a hexammine complex is reduced to cobalt(II) to form a less stable cobalt(II) ammine complex, which then immediately dissociates ammonia molecules and undergoes decomposition, as may be seen from the thermogravimetric curve of hexamminecobalt(II) chloride in Fig. 1. Mori and Tsuchiya[6] have proposed that the thermal decomposition of hexamminecobalt(III) chloride proceeds according to the reaction,

$$[Co(NH_3)_6]Cl_3(s) \rightarrow [CoCl(NH_3)_5]Cl_2(s) + NH_3(g)$$

However, they also found the formation of ammonium chloride at temperatures higher than 170°C. This result seems to indicate that the decomposition reaction is not so simple as they proposed.

In this connection, the infrared absorption spectra of hexamminecobalt(III) chloride which were recorded at elevated temperatures by means of the potassium chloride disks should be noted (Fig. 4). The NH_4^+ band at 1400 cm^{-1}

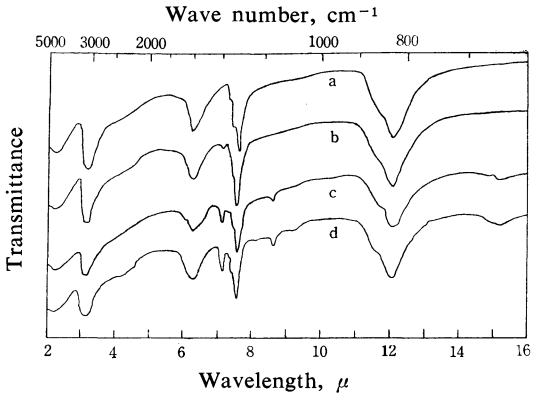


Fig. 4. Infrared absorption spectra of the $[Co(NH_3)_6]Cl_3$ in KCl disks at (a) room temperature, (b) 200°C, (c) 260°C and (d) after cooling of (c). Transmittance scale displaced arbitrarily.

appears on the spectra obtained at 200°C and higher. At temperatures higher than 260°C, two new absorption bands are observed, at 1160 cm^{-1} and 655 cm^{-1}; these are considered to be due to the NH_3 symmetric deformation vibration and the NH_3 rocking vibration of cobalt(II) ammine complexes respectively. Cobalt(III) in the hexammine complex is reduced to cobalt(II) by accepting an electron from either a ligand molecule or an outer-sphere ion to form a cobalt(II) ammine complex. Since the complex is kept in the potassium chloride disk, it retains its structure without dissociating all of the ammonia molecules and gives the absorption bands characteristic of the cobalt(II) ammine complex.

It has been known that the Co–N bond in cobalt(III) ammine complexes is stronger than the Cr–N bond in chromium(III) ammine complexes.[11] This seems to contradict the result obtained from the thermogravimetric measurement, that hexamminecobalt(III) chloride does not decompose more easily than hexamminechromium(III) chloride (see Fig. 1). This contradiction may be explained by considering that the decomposition of hexamminecobalt(III) chloride is initiated by the electron transfer from either a ligand or an outer-sphere ion and that the decompositions of these two complexes, consequently, proceed according to entirely different mechanisms.

Summary

The thermal decomposition of hexamminecobalt(III) chloride has been investigated by thermogravimetric, polarographic and infrared spectroscopic method. The results indicate that the reaction is initiated by the electron transfer from either a ligand molecule or an outer-sphere ion to the central cobalt atom, forming a less stable cobalt(II) complex, which immediately dissociates ammonia molecules and undergoes decomposition.

The measurements of infrared absorption spectra were carried out by Mr. Mitsuo Shoji. The authors wish to thank the Ministry of Education for the financial support granted for this research.

Department of Chemistry
Faculty of Science
Tohoku University
Katahira-cho, Sendai

11) M. Kobayashi and J. Fujita, *J. Chem. Phys.*, **23**, 1354 (1955).

The Solvent Extraction and Spectrophotometric Determination of Uranium using Benzoyltrifluoroacetone as the Chelating Reagent

By Tsunenobu SHIGEMATSU, Masayuki TABUSHI and Masakazu MATSUI

(Received April 9, 1964)

It has been generally known that β-diketones are useful chelating reagents in analytical chemistry, chelate chemistry and radiochemistry. Fluorinated β-diketones such as TTA are especially useful in the solvent extraction of metals, because a fluoromethyl group increases the acidity of the enol form.[1]

As do many other metals, uranium reacts with β-diketones to form extractable chelates, which are widely utilized for the separation of the metal. The present authors have studied the chelates of uranium with acetylacetone (AA),[2] dibenzoylmethane (DBM)[3] and trifluoroacetylacetone (TFA),[4] and have developed methods for the extraction separation and the photometric determination of uranium using these β-diketones.

An extraction using benzoyltrifluoroacetone (BTFA), a fluorinated β-diketone, might have some advantages: Quantitative extraction can be expected at a lower pH range from the lower pK_D value of the reagent;[5] high extractability can be anticipated from its low solubility in water, and the extraction may be facilitated by the shielding effect of the phenyl group against hydration to the central metal.

From this view-point, the authors have investigated the solvent extraction of uranium as a BTFA chelate and will propose a procedure for the separation and the spectrophotometric determination of the element.

Experimental

Apparatus. — Spectrophotometric measurements were made with a Shimadzu automatic recording spectrophotometer, model UV-50, and a Hitachi photoelectric spectrophotometer, model EPU-2A, using 1 cm. transmission cells. Radioactivity countings were performed with a Kobe Kogyo NaI(Tl) (4.45 cm.×5.08 cm.) well-type scintillation counter, model PS-300, connected to a transistorized scaler, model SA-230, and a Metro automatic decatron scaler, model D-5, using a Philips halogen-quenched G-M tube 1905. A Hitachi-Horiba glass electrode pH meter, model P, was used for the pH measurements.

The Standard Solution of Uranium, 100 μg./ml. — A stock solution was prepared by dissolving $UO_2(NO_3)_2 \cdot 6H_2O$ with water; the concentration was determined gravimetrically as U_3O_8. The stock solution was diluted to make the standard solution.

The Benzoyltrifluoroacetone Solution, 1 M. — 4.3232 g. of BTFA was dissolved and diluted to 20.0 ml. with acetone.

The EDTA-Ca Solution. 0.2 M.

Acetic acid. 1 M.

Boric acid. 1 M.

The Lutetium-177, Zirconium-Niobium-95 and Fission Products Solution. — The radioisotopes were obtained from ORNL. Lutetium and zirconium-niobium were converted to sulfate by fuming them with sulfuric acid. These sulfates and fission products solution were diluted to give a 1~5 μc./ml. solution.

Organic Solvents. — Chloroform was purified by washing it with a diluted sodium hydroxide solution, water, diluted hydrochloric acid, and three portions of water, followed by distillation. Butyl acetate was washed with water and distilled. Reagent-grade benzene was used without further purification. All the other reagents used were reagent-grade materials.

Results and Discussion

Absorption Spectra. — The absorption spectra of the uranium BTFA chelate were obtained by the following procedure. To the solution containing 100 μg. of uranium, the pH of which adjusted to 5~6, 0.1 ml. of a 1 M BTFA acetone solution was added. The solution was then diluted to 10 ml. and shaken with 10.0 ml. of benzene, chloroform or butyl acetate. The organic layer was separated, and the absorption was measured against the reagent blank.

Figure 1 shows the absorption curve of the uranium chelate in butyl acetate. The absorption curve exhibits a maximum at 380 mμ; that is almost the same as in the case of benzene or chloroform. For practical purposes, however, it seems suitable to make the measurements at a longer wavelength such as 385

1) G. H. Morisson and H. Freiser, "Solvent Extraction in Analytical Chemistry," John Wiley & Sons, New York (1957), p. 159.

2) M. Tabushi, *Bull. Inst Chem. Res., Kyoto Univ.*, **37**, 237 (1959).

3) T. Shigematsu and M. Tabushi, *J. Chem. Soc. Japan, Pure Chem. Sec. (Nippon Kagaku Zasshi)*, **81**, 265 (1960); T. Shigematsu, M. Tabushi and T. Tarumoto, *Bull. Inst. Chem. Res., Kyoto Univ.*, **40**, 388 (1962).

4) T. Shigemtsu, M. Tabushi and M. Matsui, presented at the 16th Annual Meeting of the Chemical Society of Japan, Tokyo, April, 1963.

5) L. G. van Uitert, W. C. Fernelius and E. Douglas, *J. Phys. Chem.*, **75**, 457 (1953).

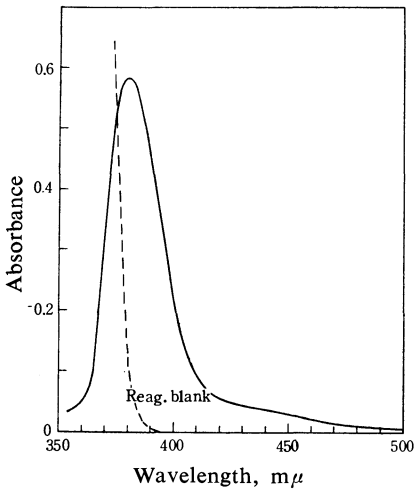


Fig. 1. Absorption spectrum of uranium BTFA chelate.
Solvent: butyl acetate U: 10.0 p.p.m
BTFA: 1×10^{-2} M

mμ, because of the quite high absorption of the reagent blank found around and below 380 mμ. Measurements were therefore performed at 385 mμ and 400 mμ in the following experiments.

The Effect of pH. — The effect of the pH value on absorbance and, consequently, on the extraction of uranium was studied by extracting 100 μg. of uranium with 10.0 ml. of an organic solvent from 10 ml. of an aqueous solution, which had a variable pH value and which contained 0.1 ml. of 1 M BTFA and sodium chloride or acetic acid at and below pH 7, or boric acid above pH 7 in the final concentration of 0.1 M. The influence of EDTA was also studied by using a solution containing 0.02 M EDTA-Ca and 0.1 M acetic acid.

The absorption of the reagent blank extracted from an acidic or neutral solution is independent of the pH value, but it is affected by the pH when the extraction is made from an alkaline solution. In the latter case absorbances of the reagent blank in benzene or chloroform media decreased, while that in a butyl acetate medium increased, with an increase in the pH value. Accordingly, the effect of pH in an alkaline solution was examined by measuring absorbances at 400 mμ but not at 385 mμ.

The results are shown in Figs. 2, 3 and 4.

These figures reveal that butyl acetate is convenient as an extracting solvent for the uranium BTFA chelate, because the absorbance is kept constant over a wider pH range and the acetate buffer hardly affects the extraction, as may be seen in Fig. 4. The phenomenon that butyl acetate is superior in the extraction of the uranium β-diketone chelate has previously been recognized in the acetylacetone and dibenzoylmethane systems.

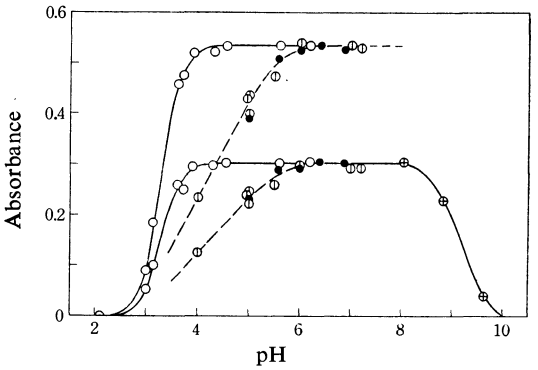


Fig. 2. Effect of pH.
Solvent: benzene U: 10.0 p. p. m.
BTFA: 1×10^{-2} M
Aqueous solution:
-○- 0.1 M NaCl, -⊖- 0.1 M acetate,
-⊕- 0.1 M borate, -●- 0.02 M EDTA-Ca and 0.1 M acetate

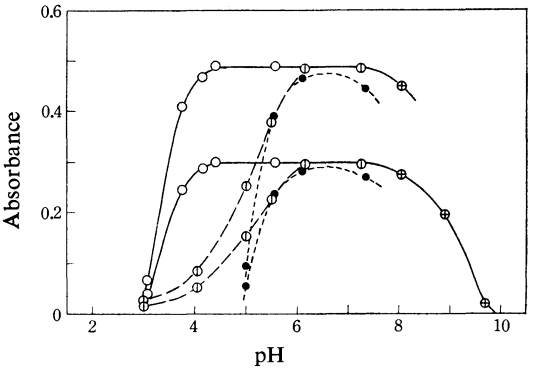


Fig. 3. Effect of pH.
Solvent: chloroform
Others are same to in Fig. 2.

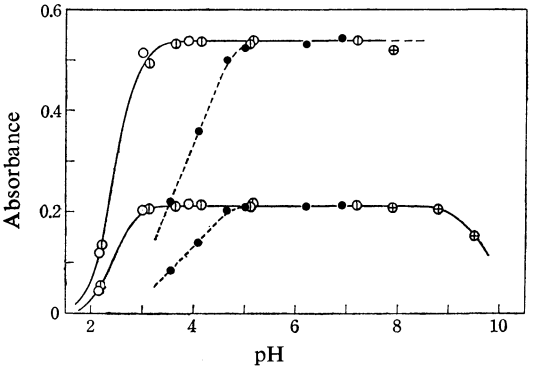


Fig. 4. Effect of pH.
Solvent: butyl acetate. Others are same to in Fig. 2.

Analytical Procedure and Calibration Curve. —From the above experimental results, a procedure for the spectrophotometric determination of uranium was designed as follows.

To a sample solution containing 5~150 μg. of uranium, add 1 ml. of a 1 M acetic acid and 0.2 M EDTA-Ca solution. Dilute the solution to about 10 ml., adjust the pH to 5.5~6.0, and add 0.1 ml. of a 1 M BTFA acetone solution. After it has been left standing for 10~15 min., extract the uranium chelate with 10.0 ml. of butyl acetate and then measure the absorbance at 385 mμ or 400 mμ against the reagent blank.

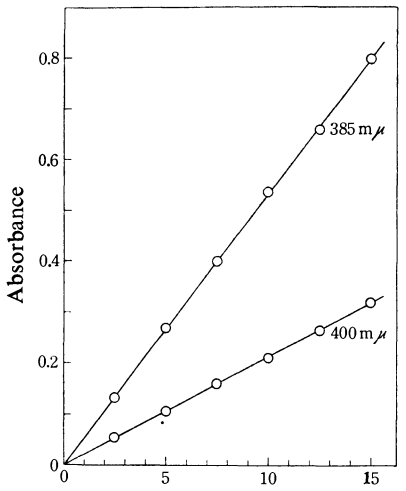


Fig. 5. Calibration curve.
Solvent: butyl acetate BTFA: 1×10^{-2} M
pH: 5.5~6.0

TABLE I. INFLUENCE OF DIVERSE IONS
(U present: 100 μg.)

Ion present	mg.	U found (μg.) 385 mμ	400 mμ	Remark
Ag^{+}	10			oxide ppt.
Al^{3+}	10			hydroxide ppt.
	2	99.4	100.0	
Bi^{3+}	10	101.3	100.9	
Cd^{2+}	10	100.7	100.5	
Co^{2+}	10	108.1	106.6	
Cu^{2+}	10			ppt. by adding BTFA
	2	102.3	104.3	
Cr^{3+}	1			hydroxide ppt.
Cr^{6+}	1	98.0	99.1	
Mn^{2+}	2	103.0	104.3	
Fe^{3+}	1			hydroxide ppt.
	0.2	107.0	121.3	
Ni^{2+}	10	101.1	101.4	
Mo^{6+}	10	99.6	101.4	
Pb^{2+}	10	100.0	100.5	
Sn^{4+}	1			hydroxide ppt.
Ti^{4+}	1			hydroxide ppt.
Th^{4+}	1	100.9	99.5	
W^{6+}	2	59.2	60.7	
V^{5+}	5	26.8	26.5	
	1	99.6	100.9	
Zn^{2+}	10	100.0	100.0	

Diverse Ions. — To investigate the influence of several metal ions, the measurements were made on a solution containing a proper amount of foreign cations with 100 μg. of uranium. The results are presented in Table I.

Silver, chromium(III), iron(III), tin(IV), titanium and large amounts of aluminum interfere because of the formation of hydroxide; a few milligrams of copper precipitate when the chelating reagent is added and a milligram or more of tungsten and vanadium-(V) gives a negative error.

The Extraction Recovery of Uranium. — Extractability was estimated by determining uranium remaining in the aqueous layer by means of the DBM method.

Uranium was extracted as the BTFA chelate by the above procedure, and the aqueous layer was washed with 10 ml. of butyl acetate. The pH value of the solution was adjusted to 6.5, and 0.5 ml. of a 5% DBM acetone solution was added. The uranium DBM chelate was extracted with 10.0 ml. of butyl acetate, and the absorbance was measured at 410 mμ or 420 mμ against the reagent blank.

The extraction recovery of the uranium BTFA chelate was found to be more than 99.9 per cent.

The Separation from Lutetium-177, Zirconium-Niobium-95 and Fission Products.—Extractions were carried out on a solution containing

TABLE II. DECONTAMINATION FACTORS OF LUTETIUM-177, ZIRCONIUM-NIOBIUM-95 AND FISSION PRODUCTS

Nuclide	Decontamination factor (1)*	(2)*
Lutetium-177	1.2×10^{3}	2.5×10^{3}
Zirconium-niobium-95	4.0×10^{3}	6.3×10^{3}
Fission products (gross γ)	1.7×10^{2}	2.4×10^{2}
Fission products (gross β)	1.1×10^{2}	1.6×10^{2}

*(1) Radioactivities were measured on organic and aqueous solution obtained by the described procedure.
(2) Measurements were made after organic layers were washed with 10 ml. of aqueous solution, which had the composition similar to the extraction condition.

TABLE III. COMPARISON OF FOUR β-DIKETONE METHODS

β-Diketone	pK_D*	Concn.** (M)	pH***	Molar extinction coef. and wavelength
Trifluoroacetylacetone	8.7	2×10^{-2}	4～7.5	4690 at 358 mμ
Benzoyltrifluoroacetone	9.2	1×10^{-2}	3.5～8.5	14000 at 385 mμ
Acetylacetone	12.7	5×10^{-2}	6～7.5	2640 at 365 mμ
Dibenzoylmethane	13.7_5	1×10^{-2}	5～9	20300 at 400 mμ

* The pK_D values were obtained in 74.5 vol. per cent dioxane (Ref. 5).
** Concentration in organic layer after distribution.
*** In the absence of EDTA-Ca.

100 μg. of uranium and 1～5 μc. of lutetium-177, zirconium-niobium-95 or mixed fission products. One milliliter of the counting samples pipetted out from the solvent and from each of the aqueous layers, and γ- and β-activities were measured with a well-type NaI(Tl) scintillation counter and a G-M counter respectively.

The decontamination factors summarized in Table II indicate that the extraction procedure recommended for the determination of uranium can be successfully applied to the separation of uranium from rare earth elements, zirconium and mixed fission products.

In Table III, the method proposed in this paper is compared with the methods using AA, TFA, and DBM as the reagents.

The order of the minimum pH value for the complete extraction do not agree with that of the pK_D value; AA and DBM, and TFA and BTFA, are reversed. This may be due to the difference in solubility in water and to the shielding effect of the phenyl group.

As is shown in Table III, the uranium BTFA chelate can be extracted at the lowest pH value and from the widest pH range among the chelates of these four β-diketones. Therefore, the BTFA method is most suitable for the extraction of uranium, although it is less sensitive than the DBM method with regard to the spectrophotometric method.

The authors wish to thank the Ministry of Education for the financial support granted for this research.

Institute for Chemical Research
Kyoto University
Sakyo-ku, Kyoto

The Vacuum Ultraviolet Absorption Spectra of Aniline and Some of Its N-Derivatives

By Katsumi KIMURA,* Hiroshi TSUBOMURA* and Saburo NAGAKURA

(Received April 10, 1964)

Concerning the effect of substituent groups upon the electronic spectrum of benzene, a number of theoretical and experimental studies have already been carried out.[1-17] This effect may be discussed from two different viewpoints: one of them is the wavelength shift and the intensity change of the bands pertinent to the benzene molecule, and the other is the appearance of an additional new band caused by the charge-transfer interaction between the

* Present address: Department of Chemistry, Faculty of Engineering Science, Osaka University, Toyonaka, Osaka.

1) K. F. Herzfeld, *Chem. Revs.*, **41**, 233 (1949).
2) F. A. Matsen, *J. Am. Chem. Soc.*, **72**, 5243 (1950).
3) S. Nagakura and H. Baba, ibid., **74**, 5693 (1952).
4) I. Fischer, *Ark. Fys.*, **5**, 377 (1952); I. Fischer-Hjalmars, ibid., **21**, 123 (1962).
5) L. Goodman and H. Shull, *J. Chem. Phys.*, **27**, 1388 (1957).
6) K. Nishimoto and R. Fujishiro, This Bulletin, **31**, 1036 (1958).
7) Y. I'Haya, *J. Am. Chem. Soc.*, **81**, 6120, 6127 (1959).
8) H. Baba, This Bulletin, **34**, 76 (1961).
9) N. Mataga, ibid., **36**, 1607 (1963).
10) S. Nagakura and J. Tanaka, *J. Chem. Phys.*, **22**, 236 (1954); S. Nagakura, ibid., **23**, 1441 (1955).
11) J. Tanaka, This Bulletin, **36**, 833 (1963).
12) H. C. Longuet-Higgins and J. N. Murrell, *Proc. Phys. Soc.*, **A68**, 601 (1955); J. N. Murrell, ibid., **A68**, 969 (1955).
13) S. Nagakura, *Pure and Applied Chem.*, **7**, 79 (1963); S. Nagakura, M. Kojima and Y. Maruyama, *J. Mol. Spectroscopy*, **13**, 174(1964).
14) J. N. Murrell, *Tetrahedron*, **19**, Suppl. **2**, 277 (1963).
15) T. E. Peacock, *Mol. Phys.*, **3**, 453 (1960).
16) J. E. Bloor and F. Peradejordi, *Theoret. Chim. Acta*, **1**, 83 (1962); J. E. Bloor, *Canad. J. Chem.*, **39**, 2256 (1961).
17) H. Labhart and G. Wagnière, *Helv. Chim. Acta*, **46**, 1314 (1963).

substituent groups and the benzene ring. The latter band is called an intramolecular charge-transfer or electron-transfer band. Since 1954, the latter phenomenon has been studied by one of the present authors and Tanaka, by Longuet-Higgins and Murrell and by others;[11-15] the intramolecular charge-transfer band has been observed with such substituted benzenes as nitrobenzene, benzoic acid, and *p*-nitroaniline.

Concerning aniline, Nagakura and Tanaka[10] first pointed out the possibility of an intramolecular charge-transfer band for the 235 mμ band. Murrell[12] studied this problem theoretically in detail and assigned the 235 mμ band to an intramolecular charge-transfer band whose transition is accompanied by an electron transfer from the amino group to the benzene ring. In addition, several authors have made quantum mechanical considerations of this problem by various kinds of approximate methods.

Their results are not always consistent with each other in the interpretation of the 235 mμ band of aniline. For instance, some authors interpret this band as the shifted band of the 200 mμ band of benzene. In order to determine which of the two interpretations is correct and, moreover, in order to obtain accurate knowledge about the π-electron structure of aniline, the experimental data of vacunm ultraviolet absorption spectra corresponding to higher-energy transitions are undoubtedly important. In spite of this, only a few experiments of absorption spectra in the vacuum ultraviolet have hitherto been carried out with aniline and its derivatives, although Klevens and Platt have measured absorption spectra for aniline, *N*-methylaniline and *N*, *N*-dimethylaniline in heptane solutions in the 1700~2300 Å region.[18]

Under these circumstances, we undertook to extend absorption measurements down to 1500 Å for aniline and some members of its *N*-derivatives in the vapor phase, using a recording vacuum ultraviolet spectrophotometer. In doing so, we succeeded in finding some new absorption bands in the vacuum ultraviolet region and in confirming the appearance of the intramolecular charge-transfer band. Furthermore, we could obtain more reliable knowledge than before about the π-electron structures of aniline and its derivatives by combining the present experimental results with theoretical considerations.

18) H. B. Klevens and J. R. Platt, *J. Am. Chem. Soc.*, 71, 1714 (1949); Technical Report of the Laboratory of Molecular Structure and Spectra, Department of Physics, University of Chicago (1954-1955).

Experimental

Absorption measurements for aniline and its *N*-derivatives were carried out in the vapor phase at room temperature. A recording vacuum ultraviolet spectrophotometer constructed in our laboratory was used for the measurements in the region from 1500 to 2200 Å, the apparatus using a Bausch and Lomb concave grating with a radius of 995.4 mm. The details of this apparatus have been published elsewhere.[19] Gas cells with paths 10 and 30 mm. long and with lithium fluoride windows were used.

The compounds studied were aniline, *N*-methylaniline, *N*-ethylaniline, *N*, *N*-dimethylaniline, *N*, *N*-diethylaniline, and *N*-*n*-butylaniline. The commercial materials of these compounds were fractionally distilled in a vacuum glass line, and the vapor of the purified samples was transferred through it into the gas cell for absorption measurements. The vapor pressure was measured with an accuracy of ±0.02 mmHg by using a mercury manometer with a travelling microscope attached. Spectra were carefully measured for different vapor pressures under the same optical conditions. Absorption measurements in the quartz region over 1900 Å were also carried out with a Cary spectrophotometer Model 14 M, a gas cell 10 cm. long being used. A comparison between the absorption spectra taken with the two apparatus in the overlap region of wavelength gave us an opportunity to check the accuracy of the intensity measurements made by means of our vacuum ultraviolet spectrophotometer.

The vapor phase spectum of benzene was also taken in the region over 1500 Å; it gives reference data for interpreting the electronic spectra of the anilines reported here. The *N*-*n*-butylaniline spectrum was measured only in the region over 2000 Å, because its vapor pressure at room temperature is too low to measure a vacuum ultraviolet spectrum with the gas cells employed in the vacuum apparatus.

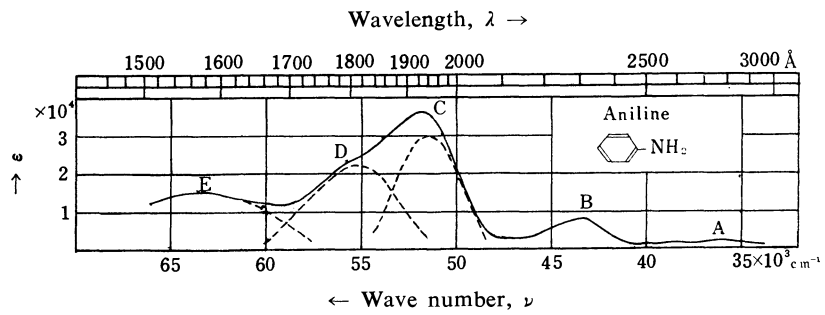
Experimental Results

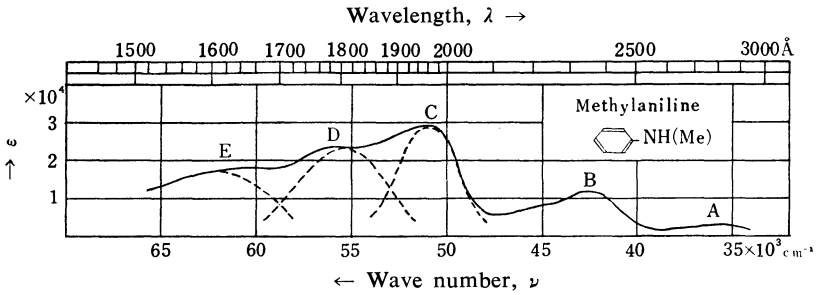
Our measurement for benzene indicated that the wavelengths of the three absorption peaks in the vapor phase are: 1776 Å (6.98 eV.) for the $^1A_{1g} \rightarrow {}^1E_{1u}$ transition, 2008 Å (6.17 eV.) for the $^1A_{1g} \rightarrow {}^1B_{1u}$ transition, and 2534 Å (4.89 eV.) for the $^1A_{1g} \rightarrow {}^1B_{2u}$ transition,[20] with oscillator strengths of 1.035, 0.126, and 0.01 respectively.

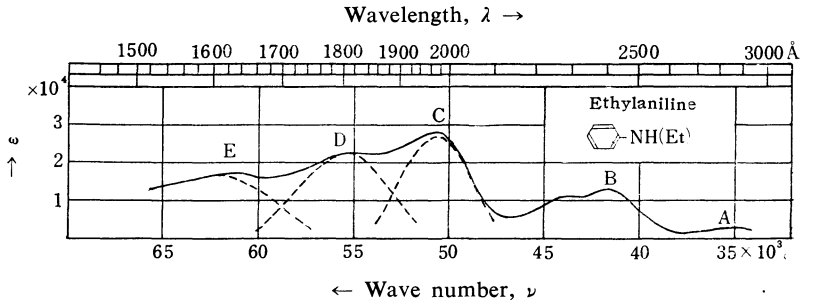
The absorption spectra of the anilines observed in the present work are shown in Fig. 1. The spectra show five characteristic bands near

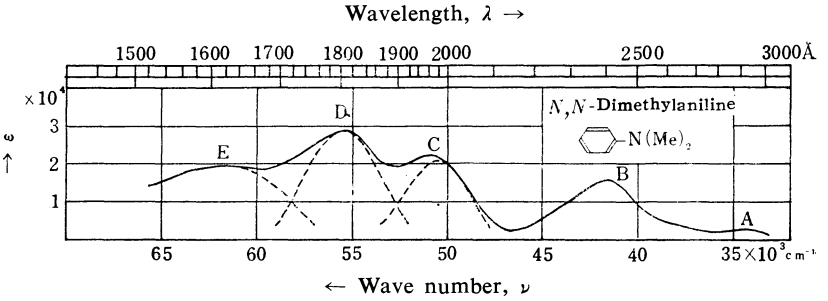
19) H. Tsubomura, K. Kimura, K. Kaya, J. Tanaka and S. Nagakura, This Bulletin, 37, 417 (1964).

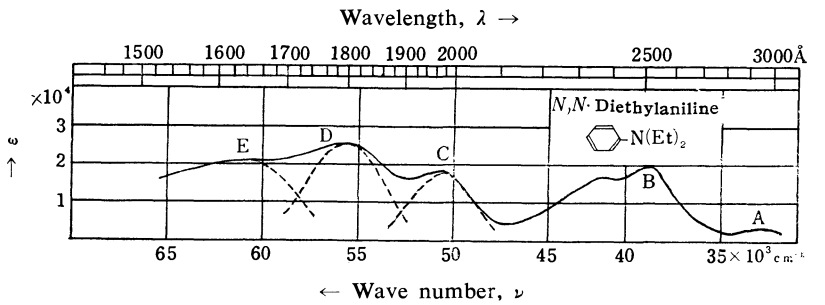
20) The $A_{1g} \rightarrow B_{1u}$ and $A_{1g} \rightarrow B_{2u}$ absorptions are accompanied with vibrational structures. The above-mentioned peak wavelength values for these absorptions were taken from the position of the strongest maximum for each absorption. Klevens and Platt[18] determined the $A_{1g} \rightarrow E_{1u}$, $A_{1g} \rightarrow B_{1u}$ and $A_{1g} \rightarrow B_{2u}$ transition energies to be 6.74, 6.14, and 4.89 eV. respectively by measuring the benzene spectrum in a heptane solution.


Wavelength, λ →
1500 1600 1700 1800 1900 2000 2500 3000 Å
×10⁴
ε →
3
2
1
C
D
E
B
A
Aniline
NH₂
65 60 55 50 45 40 35×10³ cm⁻¹
← Wave number, ν


Wavelength, λ →
1500 1600 1700 1800 1900 2000 2500 3000Å
×10⁴
ε →
3
2
1
C
D
E
B
A
Methylaniline
NH(Me)
65 60 55 50 45 40 35×10³ cm⁻¹
← Wave number, ν


Wavelength, λ →
1500 1600 1700 1800 1900 2000 2500 3000 Å
×10⁴
ε →
3
2
1
C
D
E
B
A
Ethylaniline
NH(Et)
65 60 55 50 45 40 35×10³
← Wave number, ν


Wavelength, λ →
1500 1600 1700 1800 1900 2000 2500 3000Å
×10⁴
ε →
3
2
1
D
E
C
B
A
N,N-Dimethylaniline
N(Me)₂
65 60 55 50 45 40 35×10³ cm⁻¹
← Wave number, ν


Wavelength, λ →
1500 1600 1700 1800 1900 2000 2500 3000Å
×10⁴
ε →
3
2
1
E
D
C
B
A
N,N-Diethylaniline
N(Et)₂
65 60 55 50 45 40 35×10³ cm⁻¹
← Wave number, ν

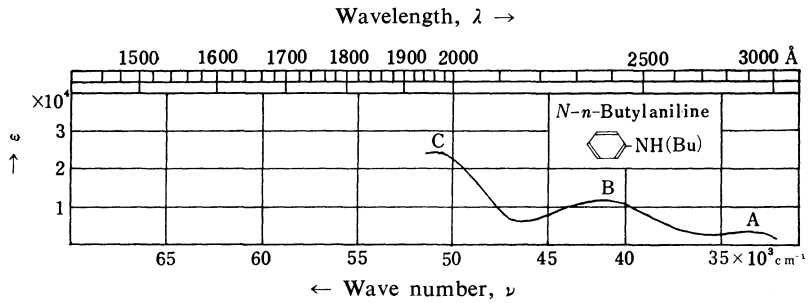


Fig. 1. Ultraviolet absorption spectra of aniline, *N*-methylaniline, *N*-ethylaniline, *N*, *N*-dimethylaniline, *N*, *N*-diethylaniline, and *N*-*n*-butylaniline. The A and B bands of aniline have vibrational structures which are neglected in this figure.

2850, 2350, 1950, 1800, and 1600 Å; they are designated as A, B, C, D and E respectively. Among these bands, the C and D bands are superposed to a considerable extent. The resolution of these two bands is made under the assumption that the curves of these bands are approximately of the Gaussian type and that the C bands and the D bands have the same half-widths.

The experimental oscillator strengths, f, were computed from the integral areas under the curves by the following equation:

$$f=4.32\times10^{-9}\int\varepsilon d\nu \qquad (1)$$

where ε is the molar extinction coefficient and ν is the frequency in cm^{-1}. Table I summarizes the experimental results concerning the peak wavelengths, the molar extinction coefficients, the transition energies, and the oscillator strengths for the anilines.

It may be seen from Fig. 1 and Table I that the spectral feature changes in the following order:[21]

$$\text{Ph-NH}_2,\ \text{Ph-NH(Me)},\ \text{Ph-NH(Et)},$$
$$\text{Ph-N(Me)}_2,\ \text{Ph-N(Et)}_2 \qquad (2)$$

The A and B bands show red shifts and increasing f values in the above order, from aniline to *N*, *N*-diethylaniline. On the other hand, the C and D bands, roughly speaking, shift to a small extent to longer wavelengths with appreciably decreasing f values and the differences in the absorption intensity between the C and D bands decrease going from aniline to *N*, *N*-diethylaniline. It should also be noticed that the E bands are commonly broad for all the compounds under consideration. This may conceivably show that the E bands are composed of two closely overlapping bands. The above interpretation is supported by the present theoretical consideration, details of which will be described below.

21) Ph-NH(*n*-Bu) is located at next to Ph-NH(Et) so far as its spectral data in the quartz region is concerned.

Theoretical

The present method of calculating the π-electron structures of the anilines is essentially based on that presented by Longuet-Higgins and Murrell,[12] in particular, on that of the calculation of aniline by Murrell,[12] in which the interaction between the two fragments of the benzene ring and the amino group is taken into account by configurational interaction among the ground, charge-transfer and locally excited configurations.

Although no detailed structural data of the anilines, even of the aniline molecule itself, have yet been reported, we assumed in the present theoretical treatment that the molecules are coplanar and belong to the symmetry group C_{2v}. In actual calculations, we took seven electron configurations; that is to say, besides the ground configuration, two charge-transfer configurations and four locally-excited configurations. The wave functions and energies for the locally excited configurations corresponding to the $A_{1g}\rightarrow B_{2u}$, $A_{1g}\rightarrow B_{1u}$, $A_{1g}\rightarrow E_{1u}$ excitations of benzene are as follows:

Wave function	Energy, eV.	
$\psi_{B_{1u}}=2^{-1/2}\{(\phi_3^{-1}\phi_5)-(\phi_2^{-1}\phi_4)\}$	4.89	
$\psi_{B_{1u}}=2^{-1/2}\{(\phi_3^{-1}\phi_4)+(\phi_2^{-1}\phi_5)\}$	6.17	
$\psi_{E_{1u}}=2^{-1/2}\{(\phi_3^{-1}\phi_5)+(\phi_2^{-1}\phi_4)\}$	6.98	
$\psi_{E_{1u}'}=2^{-1/2}\{(\phi_3^{-1}\phi_5)-(\phi_2^{-1}\phi_5)\}$	6.98	(3)

where the ϕ_i's are the molecular orbitals of benzene expressed in terms of the six carbon $2p\pi$ atomic orbitals.[22] The energy values given

22) The six molecular orbitals of benzene are:
$\phi_1=6^{-1/2}(\chi_1+\chi_2+\chi_3+\chi_4+\chi_5+\chi_6)$
$\phi_2=12^{-1/2}(2\chi_1+\chi_2-\chi_3-2\chi_4-\chi_5+\chi_6)$
$\phi_3=2^{-1}(\chi_2+\chi_3-\chi_5-\chi_6)$
$\phi_4=2^{-1}(\chi_2-\chi_3+\chi_5-\chi_6)$
$\phi_5=12^{-1/2}(-2\chi_1+\chi_2+\chi_3-2\chi_4+\chi_5+\chi_6)$
$\phi_6=6^{-1/2}(\chi_1-\chi_2+\chi_3-\chi_4+\chi_5-\chi_6)$.

TABLE I. EXPERIMENTAL AND THEORETICAL RESULTS FOR ANILINE AND ITS *N*-DERIVATIVES
(Energies are given in eV.)

Aniline

	Absorption band		Transition energy		f		Transition
	λ, Å	ε	Obs.	Theoret.	Obs.	Theoret.	
A	2817	1500	4.40	4.72	0.028	0.021	$W_0 \rightarrow W_1$
B	2299	8000	5.39	5.42	0.140	0.174	$W_0 \rightarrow W_2$
C	1938	29800	6.40	6.42	0.510	0.416	$W_0 \rightarrow W_3$
D	1800	23000	6.88	6.86	0.570	0.505	$W_0 \rightarrow W_4$
E	1575	15000	7.87	8.04 8.05	(0.68)	0.745 0.416	$W_0 \rightarrow W_5$ $W_0 \rightarrow W_6$

N-Methylaniline

	Absorption band		Transition energy		f		Transition
	λ, Å	ε	Obs.	Theoret.	Obs.	Theoret.	
A	2833	2200	4.37	4.66	0.031	0.024	$W_0 \rightarrow W_1$
B	2380	12000	5.20	5.28	0.190	0.179	$W_0 \rightarrow W_2$
C	1960	28000	6.31	6.32	0.478	0.330	$W_0 \rightarrow W_3$
D	1800	22500	6.88	6.85	0.556	0.440	$W_0 \rightarrow W_4$
E	1587	16000	7.80	7.95 7.97	(0.71)	0.826 0.472	$W_0 \rightarrow W_5$ $W_0 \rightarrow W_6$

N-Ethylaniline

	Absorption band		Transition energy		f		Transition
	λ, Å	ε	Obs.	Theoret.	Obs.	Theoret.	
A	2857	2300	4.34	4.63	0.048	0.025	$W_0 \rightarrow W_1$
B	2398	13000	5.17	5.22	0.230	0.181	$W_0 \rightarrow W_2$
C	1972	27000	6.28	6.28	0.450	0.304	$W_0 \rightarrow W_3$
D	1800	22200	6.88	6.85	0.530	0.426	$W_0 \rightarrow W_4$
E	1600	16000	7.75	7.92 7.95	(0.77)	0.850 0.475	$W_0 \rightarrow W_5$ $W_0 \rightarrow W_6$

N, *N*-Dimethylaniline

	Absorption band		Transition energy		f		Transition
	λ, Å	ε	Obs.	Theoret.	Obs.	Theoret.	
A	2882	2300	4.30	4.61	0.044	0.026	$W_0 \rightarrow W_1$
B	2404	16000	5.15	5.17	0.256	0.182	$W_0 \rightarrow W_2$
C	1980	21000	6.25	6.25	0.350	0.279	$W_0 \rightarrow W_3$
D	1800	28500	6.88	6.85	0.575	0.409	$W_0 \rightarrow W_4$
E	1613	19000	7.68	7.90 7.93	(0.81)	0.875 0.497	$W_0 \rightarrow W_5$ $W_0 \rightarrow W_6$

N, *N*-Diethylaniline

	Absorption band		Transition energy		f		Transition
	λ, Å	ε	Obs.	Theoret.	Obs.	Theoret.	
A	2941	4000	4.21	4.55	0.051	0.027	$W_0 \rightarrow W_1$
B	2480	17000	5.00	5.06	0.280	0.186	$W_0 \rightarrow W_2$
C	1980	18200	6.25	6.18	0.318	0.233	$W_0 \rightarrow W_3$
D	1800	25200	6.88	6.84	0.535	0.377	$W_0 \rightarrow W_4$
E	1626	21000	7.62	7.86 7.89	(0.88)	0.920 0.525	$W_0 \rightarrow W_5$ $W_0 \rightarrow W_6$

N-*n*-Butylaniline

	Absorption band		Transition energy		f		Transition
	λ, Å	ε	Obs.	Theoret.	Obs.	Theoret.	
A	2865	4000	4.32	4.63	0.050	0.025	$W_0 \rightarrow W_1$
B	2398	13000	5.17	5.22	0.250	0.181	$W_0 \rightarrow W_2$
C	1975	25000	6.27	6.28	—	0.304	$W_0 \rightarrow W_3$

here are taken from the electronic absorption spectrum data of benzene measured by the present authors. Taking an elelctron from the nonbonding π-orbital of the amino group (θ), and putting it into the lowest vacant orbitals of benzene (ϕ_4 and ϕ_5), we could obtain the two charge-transfer configurations, which might be represented by[23];

$$\psi_{CTa}=(\theta^{-1}\phi_5) \text{ and } \phi_{CTb}=(\theta^{-1}\phi_4) \quad (4)$$

the corresponding energies being

$$E_{CTa}=I-A-Q_1 \text{ and } E_{CTb}=I-A-Q_2 \quad (5)$$

Here I is the ionization potential of the substituent, A the electron affinity of benzene, Q_1 and Q_2 the electrostatic energies given by;

$$Q_1=1/3\{(C_1C_1/NN)+1/2(C_2C_2/NN)+1/2(C_3C_3/NN)+(C_4C_4/NN)\}$$
$$Q_2=1/2\{(C_2C_2/NN)+(C_3C_3/NN)\} \quad (6)$$

The two-center integrals (CC/NN) were calculated by the use of a quadratic equation with the atomic distance r_{CN}:

$$(CC/NN)=0.1922r_{CN}^2-2.502r_{CN}+10.83 \quad (7)$$

which was derived in the way suggested by Pariser and Parr.[24]** Concerning atomic distances, it was assumed that the C–C distances are the same in benzene (i. e., $r_{CC}=1.397$ Å[25]), and that the distance of the C–N bond is equal to that in 2, 5-dichloroaniline determined recently by an X-ray crystal analysis technique (i. e., $r_{CN}=1.407$[26]). From this geometry, Q_1 and Q_2 were calculated to be 5.44 and 5.00 eV.

Off-diagonal matrix elements of the total electron Hamiltonian were evaluated by the method of Longuet-Higgins and Murell[12] and also by that of Pople[27] as follows:

$$H_{G.CTa}=-\frac{2}{\sqrt{6}}(\beta-\beta')$$
$$H_{CTa.B_{1u}}=-\frac{1}{\sqrt{6}}(\beta+\beta')$$
$$H_{CTa.E_{1u}}=\frac{1}{\sqrt{6}}(\beta+\beta')$$
$$H_{CTb.B_{2u}}=\frac{1}{\sqrt{6}}(\beta+\beta')$$
$$H_{CTb.E_{1u}'}=-\frac{1}{\sqrt{6}}(\beta+\beta') \quad (8)$$

where β is the resonance integral between two atomic orbitals belonging to the nitrogen and adjacent carbon atoms, and β' is that belonging to the nitrogen and ortho-position carbon atoms. The ratio of β' to β was assumed to be equal to that of the corresponding overlap integrals, $\beta'=\beta(S'/S)=0.116\beta$, where S and S' are the overlap integrals corresponding to β and β'. The inclusion of β' is one of the characteristics of the present calculation. This seems to be necessary in order to improve the coincidence between the observed and theoretical transition energies. This point will be discussed later in some detail.

In the present calculations, β and β' were assumed to be parameters common to all the compounds under consideration, and the $(I-A)$ values were regarded as pertinent to the individual molecules. We determined these parameters in such a way that the calculated transition energies fit as well as possible to the experimental values of the anilines reported here by a trial-and-error method. The secular equations were solved by the aid of a Facom 202 electronic computer for various sets of parameters; the β value ranges from -1.4 to -2.6 eV., with an interval of 0.2 eV., and the $(I-A)$ values, from 9.5 to 12.5 eV, with an interval of 0.1 eV. From the systematic comparison, it was found that the best values for β and β' are -1.94 and -0.25 eV. respectively.

The transition energies ΔW evaluated by the use of the above β and β' values are plotted against the $(I-A)$ values in Fig. 2, from which it may be found that the best $(I-A)$ values in eV units are: 11.34 for aniline, 11.04 for *N*-methylaniline, 10.94 for *N*-ethylaniline, 10.84 for *N*, *N*-dimethylaniline, and 10.64 for *N*, *N*-diethylaniline. Table II gives the energy levels and wave functions calculated with the best values for β, β' and $(I-A)$. Furthermore, the relation between the electron configurations used in the present calculation and the energy levels finally obtained is shown in Fig. 3, *N*, *N*-dimethylaniline being taken as an example.

The oscillator strengths were calculated by the use of the following equation:

$$f_{ih}=1.085\times10^{11}\nu_{ih}D_{ih}^2 \quad (9)$$

Where ν_{ih} and D_{ih} are, respectively, the transition energy (in cm^{-1}) and the transition moment (in cm.) for the $i\rightarrow h$ transition. In calculating theoretical oscillator strengths, we took the three following integrals into account:

** In the derivation of Eq. 7, data for the valence state ionization potentials and electron affinities for carbon and nitrogen were taken from the table recently given by G. Pilcher and H. A. Skinner (*J. Inorg. Nucl. Chem.*, **24**, 937 (1962)).

23) One is symmetric and the other is antisymmetric with regard to the symmetry plane vertical to the molecular plane; they are denoted with the letters "a" and "b" respectively,

24) R. Pariser and R. G. Parr, *J. Chem. Phys.*, **21**, 767 (1953).

25) K. Kimura and M. Kubo, ibid., **32**, 1776 (1960).

26) T. Sakurai, M. Sundaralingam and G. A. Jefferey, *Acta Cryst.*, **16**, 354 (1963).

27) J. A. Pople, *Proc. Phys. Soc.*, **A68**, 81 (1955).

$$\int \psi_{E_{1u}} \boldsymbol{r} \psi_{CT_a} \, d\nu \approx (Sl/\sqrt{6})\boldsymbol{j}$$
$$\int \psi_{B_{1u}} \boldsymbol{r} \psi_{CT_b} \, d\nu \approx (Sl/\sqrt{6})\boldsymbol{j} \qquad (10)$$
$$\int \psi_{G} \boldsymbol{r} \psi_{CT_b} \, d\nu \approx (-2Sl/\sqrt{6})\boldsymbol{j}$$

which have usually been disregarded in such calculations. Here, $\boldsymbol{j}$ is a unit vector along the molecular axis, and l is the destance between the center of the benzene ring and that of the C–N bond. The final results on the transition energies and oscillator strengths are included in Table I where they are compared with the experimental results.

TABLE II. CALCULATED ENERGY LEVELS AND WAVE FUNCTIONS OF ANILINE AND ITS *N*-DERIVATIVES

Aniline

Energy, eV.	Wave function
$W_6 = 7.73$	$\psi_6 = -0.344\psi_{B_{1u}} + 0.715\psi_{E_{1u}} - 0.107\psi_G - 0.599\psi_{CT_a}$
$W_5 = 7.72$	$\psi_5 = -0.198\psi_{B_{2u}} + 0.757\psi_{E_{1u}'} + 0.622\psi_{CT_b}$
$W_4 = 6.54$	$\psi_4 = 0.729\psi_{B_{1u}} + 0.612\psi_{E_{1u}} + 0.063\psi_G + 0.300\psi_{CT_a}$
$W_3 = 6.10$	$\psi_3 = -0.463\psi_{B_{2u}} - 0.632\psi_{E_{1u}'} + 0.622\psi_{CT_b}$
$W_2 = 5.10$	$\psi_2 = -0.591\psi_{B_{1u}} + 0.337\psi_{E_{1u}} + 0.192\psi_G + 0.707\psi_{CT_a}$
$W_1 = 4.40$	$\psi_1 = 0.864\psi_{B_{2u}} - 0.165\psi_{E_{1u}'} + 0.475\psi_{CT_b}$
$W_0 = -0.32$	$\psi_0 = 0.031\psi_{B_{1u}} - 0.028\psi_{E_{1u}} + 0.974\psi_G - 0.225\psi_{CT_a}$

N-Methylaniline

Energy, eV.	Wave function
$W_6 = 7.63$	$\psi_6 = -0.338\psi_{B_{1u}} + 0.756\psi_{E_{1u}} - 0.100\psi_G - 0.551\psi_{CT_a}$
$W_5 = 7.61$	$\psi_5 = -0.187\psi_{B_{2u}} + 0.803\psi_{E_{2u}'} + 0.565\psi_{CT_b}$
$W_4 = 6.51$	$\psi_4 = 0.768\psi_{B_{1u}} + 0.565\psi_{E_{1u}} + 0.062\psi_G + 0.294\psi_{CT_a}$
$W_3 = 5.98$	$\psi_3 = -0.524\psi_{B_{2u}} - 0.568\psi_{E_{2u}'} + 0.634\psi_{CT_b}$
$W_2 = 4.94$	$\psi_2 = -0.543\psi_{B_{1u}} + 0.327\psi_{E_{1u}} + 0.208\psi_G + 0.745\psi_{CT_a}$
$W_1 = 4.32$	$\psi_1 = 0.831\psi_{B_{2u}} - 0.178\psi_{E_{1u}'} + 0.527\psi_{CT_b}$
$W_0 = -0.32$	$\psi_0 = 0.032\psi_{B_{1u}} - 0.029\psi_{E_{1u}} + 0.971\psi_G - 0.235\psi_{CT_a}$

N-Ethylaniline and *N*-*n*-butylaniline

Energy, eV.	Wave function
$W_6 = 7.60$	$\psi_6 = -0.335\psi_{B_{1u}} + 0.769\psi_{E_{1u}} - 0.097\psi_G - 0.535\psi_{CT_a}$
$W_5 = 7.58$	$\psi_5 = -0.183\psi_{B_{2u}} + 0.817\psi_{E_{1u}'} + 0.547\psi_{CT_b}$
$W_4 = 6.50$	$\psi_4 = 0.780\psi_{B_{1u}} + 0.550\psi_{E_{1u}} + 0.062\psi_G + 0.291\psi_{CT_a}$
$W_3 = 5.94$	$\psi_3 = -0.545\psi_{B_{2u}} - 0.547\psi_{E_{1u}'} + 0.635\psi_{CT_b}$
$W_2 = 4.88$	$\psi_2 = -0.527\psi_{B_{1u}} + 0.324\psi_{E_{1u}} + 0.214\psi_G + 0.756\psi_{CT_a}$
$W_1 = 4.29$	$\psi_1 = 0.818\psi_{B_{2u}} - 0.182\psi_{E_{1u}'} + 0.545\psi_{CT_b}$
$W_0 = -0.34$	$\psi_0 = 0.033\psi_{B_{1u}} - 0.029\psi_{E_{1u}} + 0.970\psi_G - 0.239\psi_{CT_a}$

N, *N*-Dimethylaniline

Energy, eV.	Wave function
$W_6 = 7.58$	$\psi_6 = -0.332\psi_{B_{1u}} + 0.782\psi_{E_{1u}} - 0.095\psi_G - 0.519\psi_{CT_a}$
$W_5 = 7.55$	$\psi_5 = -0.178\psi_{B_{2u}} + 0.830\psi_{E_{1u}'} + 0.529\psi_{CT_b}$
$W_4 = 6.50$	$\psi_4 = 0.792\psi_{B_{1u}} + 0.535\psi_{E_{1u}} + 0.061\psi_G + 0.288\psi_{CT_a}$
$W_3 = 5.90$	$\psi_3 = -0.566\psi_{B_{2u}} - 0.526\psi_{E_{1u}'} + 0.635\psi_{CT_b}$
$W_2 = 4.82$	$\psi_2 = -0.511\psi_{B_{1u}} + 0.319\psi_{E_{1u}} + 0.220\psi_G + 0.767\psi_{CT_a}$
$W_1 = 4.26$	$\psi_1 = 0.805\psi_{B_{2u}} - 0.186\psi_{E_{1u}'} + 0.564\psi_{CT_b}$
$W_0 = -0.35$	$\psi_0 = 0.033\psi_{B_{1u}} - 0.030\psi_{E_{1u}} + 0.969\psi_G - 0.243\psi_{CT_a}$

N, *N*-Diethylaniline

Energy, eV.	Wave function
$W_6 = 7.53$	$\psi_6 = -0.324\psi_{B_{1u}} + 0.805\psi_{E_{1u}} - 0.090\psi_G - 0.489\psi_{CT_a}$
$W_5 = 7.50$	$\psi_4 = -0.170\psi_{B_{2u}} + 0.853\psi_{E_{1u}'} + 0.494\psi_{CT_b}$
$W_4 = 6.48$	$\psi_4 = 0.814\psi_{B_{1u}} + 0.505\psi_{E_{1u}} + 0.060\psi_G + 0.281\psi_{CT_a}$
$W_3 = 5.82$	$\psi_3 = -0.609\psi_{B_{2u}} - 0.484\psi_{E_{1u}'} + 0.628\psi_{CT_b}$
$W_2 = 4.70$	$\psi_2 = -0.481\psi_{B_{1u}} + 0.310\psi_{E_{1u}} + 0.231\psi_G + 0.787\psi_{CT_a}$
$W_1 = 4.10$	$\psi_1 = 0.775\psi_{B_{2u}} - 0.194\psi_{E_{1u}'} + 0.601\psi_{CT_b}$
$W_0 = -0.36$	$\psi_0 = 0.035\psi_{B_{1u}} - 0.031\psi_{E_{1u}} + 0.967\psi_G - 0.251\psi_{CT_a}$

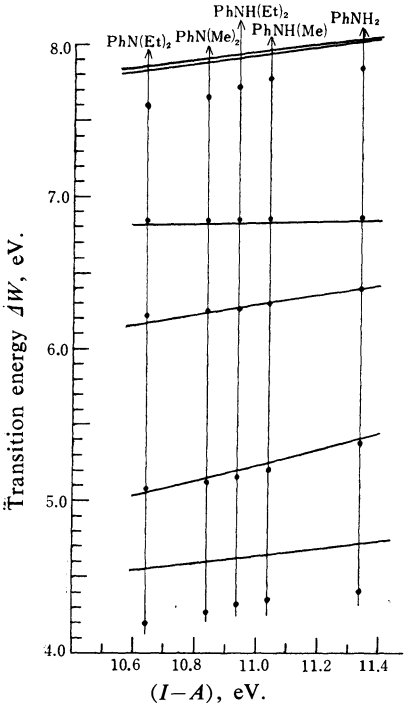


Fig. 2. The calculated best curves of the transition energy ΔW plotted against $(I-A)$ values. The circles show the experimental transition energies obtained from the absorption spectra.

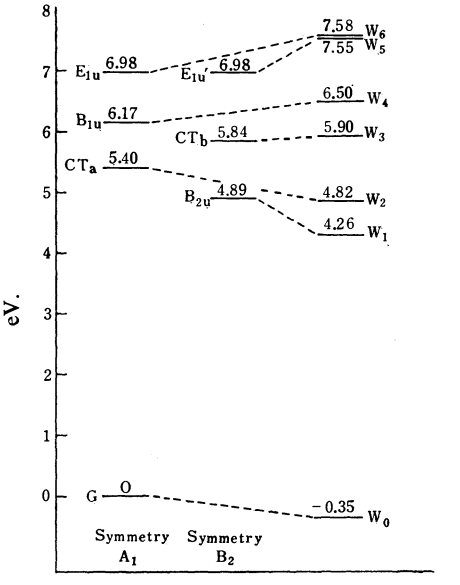


Fig. 3. Energy levels of *N*, *N*-dimethylaniline. The energy levels before and after the configuration interactions are shown, and the correlations are denoted with the broken lines.

TABLE III. COMPARISON OF THE PRESENT RESULTS OF ANILINE WITH THOSE BY OTHER AUTHORS (Transition energies, $E-E_0$, are given in eV.)

Symmetry of the excited state	Present work: Obs. (gas) $(E-E_0)$	Present work: Obs. (gas) f	Present work: Theoret. $(E-E_0)$	Present work: Theoret. f
B_2	4.40	0.028	4.72	0.021
A_1	5.39	0.144	5.42	0.174
B_2	6.40	0.510	6.42	0.416
A_1	6.88	0.570	6.86	0.505
B_2	7.87	(0.68)	8.04	0.745
A_1			8.05	0.416

Klevens and Platt[18] Obs. (heptane solution) $(E-E_0)$	Klevens and Platt[18] Obs. (heptane solution) $\log\varepsilon_{max}$	Mataga[9] Theoret. $(E-E_0)$	Mataga[9] Theoret. f
4.32	3.1	4.5324	0.05
5.31	3.9	5.4652	0.31
6.32	4.3	6.5656	0.84
7.06	4.5	6.7248	1.04

Fischer-Hjalmars[4] Theoret. $(E-E_0)$	Fischer-Hjalmars[4] Theoret. f	Bloor and Peradejordi[16] Theoret. $(E-E_0)$	Bloor and Peradejordi[16] Theoret. f
4.699	0.015	4.24	0.09
5.581	0.19	5.29	0.44
6.503	0.55	6.57	
6.668	0.68	6.61	
7.496	0.61		
7.396	0.41		

Baba[8] Theoret. $(E-E_0)$	Baba[8] Theoret. f	Peacock[15] Theoret. $(E-E_0)$	Murrell[12] Theoret. $(E-E_0)$
4.28	0.091	4.3	4.91
5.38	0.289	4.3	5.16
6.53	0.773	6.1	6.34
6.59	1.051	7.6	6.67
		8.3	7.58
		10.1	7.39

Discussion

As may be seen in Table I, we obtained an excellent agreement in the transition energies and oscillator strength values between the theoretical and the experimental results. It is interesting that the changes in the absorption spectra of the compounds can be well interpreted in terms of the change in the $(I-A)$ values or the energies of the charge-transfer configurations on the assumption that β and β' are constant for the series of compounds under consideration. The resuls on aniline obtained by other authors are compared with the present results in Table III. The results by Fischer-Hjalmars and by Murrell are similar to ours, although their results are somewhat different from ours in that the calculated transition energies for the three higher frequency transitions are considerably smaller than the observed values.

The most important point of our experimental results is that the five absorption bands were found in the wavelength region of 160 mμ to 300 mμ. On the basis of the absorption intensity and the shape of absorption curve, these bands can safely be assigned to the $\pi \rightarrow \pi^*$ transition bands. This means that some additional bands appear in the absorption spectra of the anilines, in addition to the shifted bands of the 180, 200 and 260 mμ bands of benzene. According to our interpretation, the additional bands are intramolecular charge-transfer bands caused by the interaction between the electron donor (NH_2, NHMe, etc.) and the electron acceptor (the benzene ring). The additional bands of this kind could not observed with phenol and toluene, as will be mentioned in a following paper. In other words, the absorption bands of these two compounds can be interpreted as the shifted bands of benzene. In this point the absorption spectra of the anilines exhibit a striking contrast to those of phenol and toluene. At any rate, it may be said that theoretical treatment[1-3,8] in which the substituent effect is considered to be only a weak perturbation to the energy levels of benzene itself, can not be applied to the anilines.

The transitions to the lowest excited states (W_1) which give rise to the A bands correspond mainly to the transition to the B_{2u} state of benzene. The contributions from the charge-transfer configuration in the W_1 state are 22% for aniline, 36% for *N*, *N*-diethylaniline, and so on. There is no doubt that the B bands appearing around 240 mμ, which are called intramolecular charge-transfer bands, are to be assigned to the transitions to the W_2 states to which the charge-transfer configurations are mainly contributed; for instance, their contributions are, respectively, 50% and 62% for aniline and *N*, *N*-diethylaniline.

According to the present experimental results, going from aniline to *N*, *N*-diethylaniline, the C and D bands show very small red shifts and the oscillator strengths of the C bands decrease appreciably. These phenomena can be well explaind by the present theoretical study. The decrease in the intensity of the C band may be due to the decreasing contributions of the E_{1u} locally excited configuration, going from aniline to *N*, *N*-diethylaniline.

The shortest wavelength band for each compound is most likely to be attributed to two transitions, $W_0 \rightarrow W_5$ and $W_0 \rightarrow W_6$, whose transition energies are almost equal to each other. This seems to be a reason for the broadness of the band. As is shown in Table II, the calculated results show that, going from aniline to *N*, *N*-diethylaniline, the fifth and the sixth bands both shift toward the longer wavelengths and, at the same time, their f values increase, with increasing contributions from the E_{1u} locally excited configuration of benzene. These features derived by the theoretical calculations agree well with those of the observed E bands.

As can be seen in Table II, the contributions of the charge-transfer configurations to the ground states are 5% for aniline, 6% for *N*, *N*-diethylaniline, and so on, while the calculated stabilization energies due to conjugation are 7.37 kcal./mol. for aniline, 8.29 kcal./mol. for *N*, *N*-diethylaniline, and so on. The conjugation energy of aniline coincides well with the extra resonance energy estimated empirically (6 kcal./mol.)[28]. This seems to establish that the present theoretical results on the conjugation effect in the ground states are reasonable.

As may be easily seen from Fig. 2, the present calculations indicate that the $(I-A)$ values decrease in the order of aniline > *N*-methylaniline > *N*-ethylaniline > dimethylaniline > *N*, *N*-diethylaniline. The changes in the $(I-A)$ values should be attributed to those in the ionization potentials of the substituents. In Fig. 4, the $(I-A)$ values of aniline, *N*-methylaniline and *N*, *N*-dimethylaniline are compared with the ionization potentials of ammonia and amines. It may be said that the differences in the $(I-A)$ values obtained for the anilines reflect a general tendency in th effect of methyl and ethyl substituents upon the ionization potential of ammonia.

Taking the value of I as equal to the ionization potential of ammonia, 10.25 eV., we can

28) L. Pauling, "The Nature of the Chemical Bond," Cornell University Press, Ithaca (1960), p. 208.

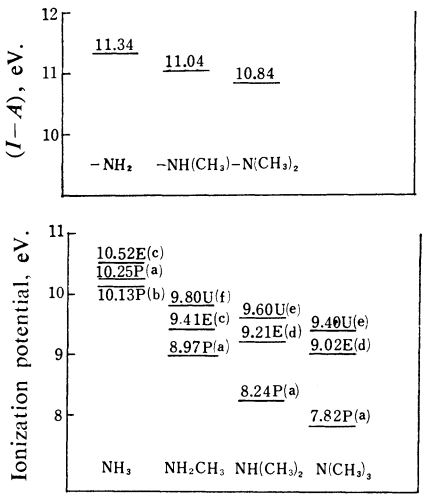


Fig. 4. The upper diagram shows the $(I-A)$ values for aniline, *N*-methylaniline, and *N*, *N*-dimethylaniline. The lower one shows the ionization potentials of ammonia and amines; NH_3, $NH_2(CH_3)$, $NH(CH_3)_2$, and $M(CH_3)_3$. (a) K. Watanabe, *J. Chem. Phys.*, **22**, 1564 (1954); **26**, 542 (1957). (b) E. C. Y. Inn, *Phys. Rev.*, **91**, 1154, 1194 (1953). (c) J. D. Morrison and A. J. C. Nicholson, *J. Chem. Phys.*, **20**, 1021 (1952). (d) I. Ohmura, K. Higasi and H. Baba, This Bulletin, **29**, 504 (1956). (e) T. M. Sugden, A. D. Walsh and W. C. Price, *Nature*, **148**, 372 (1941). (f) W. C. Price, *Chem. Revs.*, **41**, 257 (1947).
E: Electron impact P: Photo-ionization
U: Ultraviolet

estimate the electron affinity of benzene to be $A=-1.00$ eV. from the $(I-A)$ value of 11.25 eV. obtained for aniline. We have a few theoretical data on the electron affinity of benzene available for comparison with the present data; one is the -1.63 eV. given by Hedges and Matsen,[29] and the other, the -0.54 eV. given by Pople and Hush.[30] From the comparison of these values, it may be said that the present electron affinity value of benzene seems to be reasonable. Similar attempts to estimate the electron affinity of benzene from the $(I-A)$ values obtained for the aniline derivatives have been unsuccessful because of the large fluctuations among the experimental ionization potential data for amines (see Fig. 4.)

The present values of $\beta(CN)=-1.94$ eV. may be compared with the other data used in the theoretical calculations of aniline by several other authors. Murrell[12] has used $\beta(CN)=-1.60$ eV., and Fischer-Hjalmars[4] has used $\beta(CN)=-1.452$ eV. in her calculation using the Pariser-Parr-Pople method, while Bloor and Peradejordi's value[16] was $\beta(CN)=-2.74$ eV.

In the present calculations, it should be emphasized that taking β' (the resonance integral for the N···C(ortho) atom pair) into account leads to considerably better results than when it is disregarded. As can be seen from Eq. 8, β' $(=0.116\beta)$ makes the off-diagonal term, $H_{G.CTa}$, smaller by about 12%, while it makes all the other terms in Eq. 8 greater by about 12%. This effect brings about a lower transition energy value for the longest wavelength band; consequently, a good agreement between the theoretical and experimental results was obtained.

Furhermore, we checked the effect of the other electron configurations with higher energies upon the transition energies,[31] although we could well reproduce the observed spectra of the anilines by the above-mentioned calculation, taking the seven electron configurations into account. The results show that the effect is not important.

Extra peaks appearing at about 230 mμ for *N*-methylaniline, *N*-ethylaniline, and *N*-butylaniline, and at about 250 mμ for *N*, *N*-diethylaniline may be attributed to the $n \rightarrow \sigma^*$ transitions, since the ultraviolet absorption measurements with saturated amines have indicated that a relatively weak absorption band due to an $n \rightarrow \sigma^*$ transition appears around 200 mμ; for instance, for trimethylamine it appears at 212 mμ.[19]

Summary

The vacuum ultraviolet absorption spectra of anilne, *N*-methylaniline, *N*-ethylaniline, *N*, *N*-dimethylaniline, *N*, *N*-diethylaniline and *N*-*n*-butylaniline have been measured in the vapor phase by a recording vacuum ultraviolet spectrophotometer, with which the absorption measurements have been extended down to

29) R. M. Hedges and F. A. Matsen, *J. Chem. Phys.*, **28**, 950 (1958).
30) J. A. Pople and N. S. Hush, *Trans. Faraday Soc.*, **51**, 600 (1955).

31) We checked how the other electron configurations with higher energies affect the calculated results. In order to check this point, we tried to calculate by including several additional higher energy configurations of the following types:
$(\phi_2^{-1}\phi_6)$, $(\phi_3^{-1}\phi_6)$, $(\theta^{-1}\phi_6)$, $(\theta^{-1}w)$, $(\phi_2^{-1}w)$ and $(\phi_3^{-1}w)$ which correpond to transitions to the highest vacant orbital of benzene (ϕ_6) and to the $3p\pi$ atomic orbatal of nitrogen (w). Assuming roughly that all the diagonal elements of the new configurations are 9.0 eV., and that the resonance integral between the nitrogen $3p\pi$ orbital and the adjacent carbon $2p\pi$ orbital is -2.0 eV., we obtaind transition energies by solving 5th- and 8th-order secular equations built up with the thirteen configurations. The resulting transition energies (in eV.) for seven original configurations were found to be 4.97 (4.72) for the $W_0 \rightarrow W_1$ transition, 5.53 (5.42) for the $W_0 \rightarrow W_2$, 6.65 (6.42) for the $W_0 \rightarrow W_3$, 7.04 (6.86) for the $W_0 \rightarrow W_4$, 7.81 (8.04) for the $W_0 \rightarrow W_5$, and 8.18 (8.05) for the $W_0 \rightarrow W_6$; the values in parentheses indicate the corresponding energies listed in Table I.

1500 Å. Some new bands have been found in the vacuum ultraviolet region, and in total five $\pi \rightarrow \pi^*$ transtion bands with molar extinction coefficients larger than 1500 have been observed commonly for the anilines. In order to clarify the nature of these bands, a theoretical treatment has been made by considering the configuration interaction among the ground, locally excited and charge-transfer configurations. An excellent agreement has been obtained between the experimental and the calculated results. It has been concluded that the anilines studied here exhibit intramolecular charge-transfer bands characteristic of the electron transfer interaction between the substituents and the benzene ring.

The Institute for Solid State Physics
The University of Tokyo
Azabu, Tokyo

The Szilard-Chalmers Reaction of Several Neutron-Irradiated Inorganic Phosphorus Compounds

By Kichizo TANAKA

(Received Appril 11, 1964)

In 1948, Williams[1] reported that, in the Szilard-Chalmers process, the longer the irradiation time in a reactor, the higher was the retention of the parent form for potassium ferrocyanide and antimony pentafluoride. This high retention for long irradiations was postulated as resulting from radiation annealing, particularly with gamma-rays.

In a series of studies by the author on the Szilard-Chalmers effects on several inorganic phosphorus compounds, such post-irradiation processes as thermal annealing[2] and gamma-ray annealing[3] were reported in the distribution of chemical species containing phosphorus-32 for several neutron-irradiated phosphates. In an experiment[4] concerned with the preparation of phosphorus-32 of a high specific activity by means of the (n, γ) reaction of phosphates, the recovery and enrichment factors were affected by the irradiation conditions.

In the present paper, studies will be made of the neutron irradiation of several phosphates under various irradiation conditions in order to find the optimum conditions of irradiation for the preparation of phosphorus-32 of a high specific activity. For the group separation of the chemical species of phosphorus-32, the results obtained by paper partition chromatography[5] will be compared with those obtained by the ion-exchange method and with those obtained by paper electrophoresis.[6-9] The effects of radiation in a reactor on the distribution of chemical species containing phosphorus-32 will also be discussed.

Experimental

Target Materials.—Guaranteed reagents were used without further purification. Hydrated salts were dehydrated, dried, and analyzed as previously reported.[2]

Neutron Irradiation.—Samples sealed in a polyethylene tube were irradiated in the holes of JRR-1 (operated at 40 kW.) or of JRR-2 (operated at 5 MW.). Thin gold foils were used as thermal neutron flux monitors, and thin aluminum foils and small nickel pellets, as fast neutron flux monitors. These monitors were irradiated by being placed in a capsule holding the target material. When irradiated in a glory hole of JRR-1 and in a vertical hole of JRR-2, the samples were sealed in a quartz tube which was then placed in an aluminum container. The samples were irradiated at ambient reactor temperatures.

Separation Procedure.—After irradiation, the samples were stored in a vessel cooled with dry ice. Each sample was then dissolved in water so that the concentration was made 0.1 M. The solution was submitted to one-dimenssional paper partition chromatography. Two different systems were used for the separation; one used *n*-butanol saturated with 2 N nitric acid as the developing agent, and the other, a mixture of 1 N ammonia, dioxane and *n*-butanol (1 : 1 : 1, volume ratio). The

1) R. R. Williams, *J. Phys. Colloid Chem.*, **52**, 603 (1948).
2) H. Baba, K. Tanaka and K. Yoshihara, This Bulletin, **36**, 928 (1963).
3) K. Tanaka, ibid., **37**, 1032 (1964).
4) K. Tanaka, to be published.
5) K. Yoshihara and T. Yokoshima, This Bulletin, **34**, 123 (1961).
6) P. A. Sellers, T. R. Sato and H. H. Strain, *J. Inorg. Nucl. Chem.*, **5**, 31 (1957).
7) T. R. Sato, P. A. Sellers and H. H. Strain, ibid., **11**, 84 (1959).
8) T. R. Sato, *Anal. Chem.*, **31**, 841 (1959).
9) H. Michl, *J. Chrom.*, **1**, 93 (1958).

TABLE I. THE DISTRIBUTION OF CHEMICAL SPECIES CONTAINING PHOSPHORUS-32 FOR DISODIUM HYDROGEN PHOSPHATE: COMPARISON OF THREE SEPARATION METHODS

By paper partition chromatography	%	By paper electrophoresis	%	By ion exchange method	%
Polyphosphates	46.1	Polyphosphates	45.0	Fraction absorbed with an aqueous chlorides solution	62.2
		Isohypophosphate and hypophosphate	18.4		
Orthophosphate	22.0	Orthophosphate	23.1	Fraction eluted with an aqueous chlorides solution	37.8
		Orthophosphite	9.9		
Reduced species (P(I)	32.0 2.9)	Hypophosphite	3.6		

procedure was the same as has previously been described.[2] The ion exchange method used to prepare phosphorus-32 of a high specific activity was also the same as in a previous paper.[4] When the sample solution in an equimolar mixture of 0.025 M potassium chloride and 0.025 M hydrochloric acid was passed through the column, orthophosphate, orthophosphite, and hypophosphite ions were eluted with an equimolar mixed solution of 0.025 M potassium chloride and 0.025 M hydrochloric acid, and the absorbed phosphorus-32 was completely eluted with 8 M hydrochloric acid. The distribution of the chemical species containing phosphorus-32 formed in phosphates by neutron irradiation was very complex; therefore, the distribution of the phosphorus oxy-acid species obtained by the two methods were compared with that obtained by paper electrophoresis. Recently, the usefulness of high voltage electrophoresis for the separation of a complex phosphate mixture has been recognized; in such an electrophoresis voltage gradients up to 80 V./cm. were attained. Lindner and Harbottle[10] applied this method to finding the distribution of the chemical species containing phosphorus-32 in neutron irradiated phosphates. In the present experiment, the sample was dissolved in 0.1 M lactic acid, and a 0.1 M lactic acid solution was used as the electrolyte. The voltage gradient was 80 V./cm. During development, the filter paper (Whatman 3 MM) was clamped between two glass plates, the upper plate being cooled with ice. The separation took about one hour.

Counting Procedure.—After separation, the filter paper was dried and cut into pieces 1 cm. wide. These pieces were placed on the bottom of a glass planchet (2.5 cm. in diameter) and counted with a gas-flow GM counter, an automatic sample changer made by the Tracer-Lab Inc. also being used. Each piece was counted at least ten days after neutron irradiation to avoid error arising from contamination by sodium-24 or potassium-42. The total count was 2^{10} counts for each piece. The sample in a solution was evaporated in a glass planchet (2.5 cm. in diameter) and counted with a thin end-window-type gas flow GM counter. The gamma-ray spectra were measured with a 256-channel scintillation spectrometer equipped with a NaI crystal (7.4 cm.×7.4 cm.).

The Chemical Analysis of Phosphorus.—Trace amounts of phosphorus were determined by colorimetry, as has been reported by Gaitanis.[11] For macroamounts, gravimetric determination was used after precipitating the phosphorus with ammonium molybdate.

Results and Discussion

The distribution of the chemical species containing phosphorus-32 was studied using the three different separation methods described above, and the distributions were compared with each other. Each sample was irradiated for 2 hr. in a pneumatic tube of JRR-1 (the nominal neutron flux, 0.64×10^{12} n./cm^2-sec). The results obtained for disodium hydrogen phosphate are shown in Table I. In all three separations the storage time was also the same. In the paper partition chromatography, three fractions, the polyphosphates, the orthophosphate and the reduced species, were separated. The polyphosphates and the reduced species consisted of mixed phosphorus oxy-acid species, as has previously been reported.[2] From the analysis of the R_f values, tripolyphosphate and pyrophosphate were observed in the chromatographic histogram for the polyphosphates. Hypophosphite was observed by separation with a mixture of 1 N ammonia, dioxane and *n*-butanol. As may be seen in the table, the percentages of phosphorus-32 in the polyphosphates and in the orthophosphate are the same as those obtained by the paper electrophoresis. On the other hand, the percentage of the reduced species is much larger than the sum of the orthophosphite and hypophospphite given by the paper electrophoresis. This difference corresponds exactly to the percentages of the isohypophosphate and hypophosphate in the paper electrophoresis.

In the ion exchange separation, the activities of the fractions which are absorbed on the anion exchange resin from the aqueous chloride

10) L. Lindner and G. Harbottle, "Proceedings of Chemical Effects of the Nuclear Transformations," Vol. I, IAEA, Prague (1961), p. 485.

11) M. J. Gaitanis, "Master Analytical Manual," Section 1-12 TID-7015 (1957).

solutions are higher than those of the polyphosphates obtained by the other separations. In the case of the ion exchange separation, the elutions were made successively with a potassium chloride solution, as has been reported by Weiser.[12] Appoximately one-half of the total activity of the absorbed fraction is found in pyrophosphate and tripolyphosphate; the remaining half is not identified. The percentages of the sum of the polyphosphates, isohypophosphate and hypophosphate in the paper electrophoresis were approximately equal to those absorbed on the anion exchange resin. For the neutron-irradiated orthophosphate salts treated with anion exchange resin, the eluted solution with 8 M hydrochloric acid was evaporated to near dryness by heating the solution and submitting it to one-dimenssional paper partition chromatography. Phosphorus-32 was observed in the orthophosphate and reduced species. Because orthophosphite and hypophosphite ions were eluted with an aqueous chloride solution, this provided other evidence that the reduced polyphosphate species were formed by the Szilard-Chalmers process of orthophosphate salts. These species were absorbed on the resin from the aqueous chloride solutions.

Several orthophosphate salts, sodium orthophosphite and sodium hypophosphite were irradiated in a pneumatic tube of JRR-1. The distribution of the chemical species containing phosphorus-32 which was obtained by paper partition chromatography is plotted in Fig. 1—3 as a function of the neutron irradiation time. For the orthophosphate salts, the shorter the irradiation time, the higher was the percentage of the reduced species, but the lower were those of the polyphosphates and orthophosphate. The fraction of orthophosphate is considerably reduced by irradiating it for shorter periods of time. However, the distribution of the phosphorus oxy-acid species contaianing phosphorus-32 was apparently independent of the irradiation time for sodium orthophosphite and sodium hypophosphite, although the fraction of hypophosphite in sodium orthophosphite slightly decreases when the sample is irradiated for longer periods of time.

The samples were irradiated at various locations in the reactor of JRR-1. The results obtained from these irradiations are shown in Table II. The thermal neutron fluxes measured with a thin gold foil by a calibrated ionization chamber are shown in the third column in Table II. The fast neutron fluxes in the fourth column were obtained from the induced activity of magnesium-27 by the $^{27}Al(n, p)^{27}Mg$ reaction, assuming that the cross section was 3.1 millibarns.[13] The energy distribution of the fast neutrons at any location in a reactor was assumed to be the same as that of the

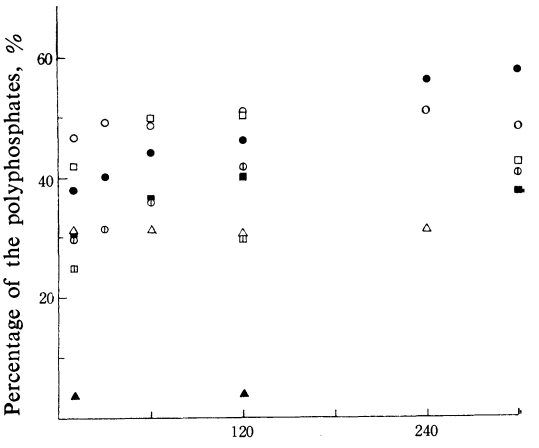


Fig. 1. The polyphosphates as a function of irradiation time.
○ Sodium dihydrogen phosphate
● Disodium hydrogen phosphate
◐ Trisodium phosphate
□ Potassium dihydrogen phosphate
■ Dipotassium hydrogen phosphate
◫ Tripotassium phosphate
△ Sodium orthophosphite
▲ Sodium hypophosphite

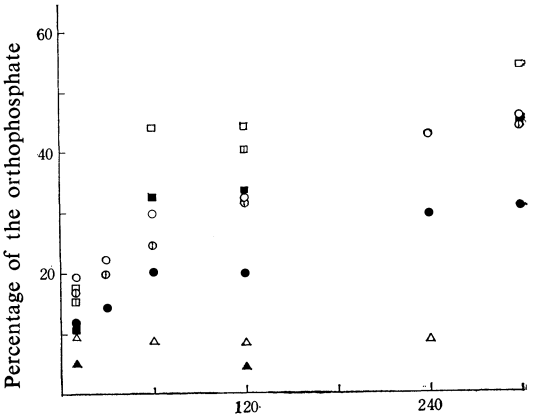


Fig. 2. The orthophosphate as a function of irradiation time.
○ Sodium dihydrogen phosphate
● Disodium hydrogen phosphate
◐ Trisodium phosphate
□ Potassium dihydrogen phosphate
■ Dipotassium hydrogen phosphate
◫ Tripotassium phosphate
△ Sodium orthophosphite
▲ Sodium hypophosphite

12) H. J. Weiser, Jr., *J. Am. Oil Chemists Soc.*, **34**, 124 (1957).

13) J. C. Roy and J. J. Hawton, CRC-1003 (1960).

TABLE II. THE DISTRIBUTION OF CHEMICAL SPECIES CONTAINING PHOSPHORUS-32 ON IRRADIATION AT VARIOUS LOCATIONS IN JRR-1

Neutron irradiation Hole	Time	Thermal neutron n./cm²-sec.	Fast neutron n./cm²-sec.	Gamma ray r./hr.	Polyphosphates %	Orthophosphate %	Reduced species %
			NaH_2PO_4				
No. 1	10 min.	1.2×10^{12}	1.2×10^{12}	1.3×10^{7}	59.6	31.4	9.0
No. 2	10 min.	4.2×10^{11}	3×10^{10}	2×10^{6}	48.9	23.3	27.9
No. 3	10 min.	3.9×10^{11}	7.7×10^{10}	1×10^{6}	48.4	21.4	30.3
No. 12	10 min.	3.5×10^{11}	10^{9}	4.5×10^{5}	39.2	24.1	36.7
No. 1	5 hr.	1.2×10^{12}	1.2×10^{12}	1.3×10^{7}	36.9	63.1	0.0
			Na_2HPO_4				
No. 1	10 min.	1.2×10^{12}	1.2×10^{12}	1.3×10^{7}	64.5	16.2	19.3
No. 2	10 min.	4.2×10^{11}	3×10^{10}	2×10^{6}	32.7	15.9	51.4
No. 3	10 min.	3.9×10^{11}	7.7×10^{10}	1×10^{6}	33.4	16.1	50.5
No. 12	10 min.	3.5×10^{11}	10^{9}	4.5×10^{5}	38.4	14.9	46.7
No. 1	5 hr.	1.2×10^{12}	1.2×10^{12}	1.3×10^{7}	53.9	45.9	0.2
			KH_2PO_4				
No. 1	10 min.	1.2×10^{12}	1.2×10^{12}	1.3×10^{7}	51.5	36.0	12.4
No. 12	10 min.	3.5×10^{11}	10^{9}	4.5×10^{5}	32.1	25.7	42.2
No. 1	5 hr.	1.2×10^{12}	1.2×10^{12}	1.3×10^{7}	19.4	80.3	0.3

TABLE III. THE DISTRIBUTION OF CHEMICAL SPECIES CONTAINING PHOSPHORUS-32 OBTAINED BY IRRADIATION IN A PNEUMATIC TUBE OF JRR-1* AND OF JRR-2** for 20 min.

Target material	Polyphosphates, %		Orthophosphate, %		Reduced species, %	
	JRR-1	JRR-2	JRR-1	JRR-2	JRR-1	JRR-2
NaH_2PO_4	47.2	51.4	20.8	46.4	31.8	2.2
Na_2HPO_4	39.0	56.4	14.5	32.7	46.5	11.4
KH_2PO_4	45.8	41.6	26.0	56.4	28.0	1.9
K_2HPO_4	32.0	43.0	14.3	46.7	53.6	10.3
K_3PO_4	25.7	38.2	19.2	43.2	55.0	18.6

* Thermal neutron flux, 5.0×10^{11} n./cm²-sec.
Fast neutron flux, 6.0×10^{10} n./cm²-sec.
** Thermal neutron flux, 3.0×10^{13} n./cm²-sec.
Fast neutron flux, 1.0×10^{12} n./cm²-sec.
Gamma flux, $\sim1\times10^{8}$ r./hr. (JAERI Memo, No. 1098 (1963))

fission neutrons.[14,15] The fast neutron fluxes obtained by this reaction were checked by those from other reactions, $^{27}Al(n,\alpha)^{24}Na$ and $^{58}Ni(n,p)^{58}Co$.

At the central position in the glory hole of JRR-1 at 40 kW. operation, the fast neutron flux obtained by this method agreed with other observations,[16] $1.2\sim1.5\times10^{12}$ n./cm²-sec. For the gamma-ray intensity in the reactor, the data shown by Nakadoi et al.[17] were used. When irradiated for the same period of time, the distribution of the chemical species containing phosphorus-32 was strongly dependent on the location where they were irradiated. For sodium dihydrogen phosphate, the reduced species obtained by irradiation in the glory hole considerably differed from those of the other locations. The reduced species in two different salts were compared. The percentages of the reduced species in the sodium dihydrogen phosphate salt and in the disodium hydrogen phosphate salt were approximately the same when irradiated in the vertical hole No. 12; however, the percentage of the reduced species in the disodium hydrogen phosphate salt was approximately twice that in the sodium dihydrogen phosphate salt when irradiated in the glory hole.

The orthophosphate salts were irradiated in a pneumatic tube of JRR-2 (operated at 5 MW). The distributions obtained by the chromatographic separation were compared with those of JRR-1 as shown in Table III. Low proportions of the reduced species were observed when they were irradiated at a high operating

14) T. O. Passell and R. L. Heath, *Nucl. Science and Engineering*, **10**, 309 (1961).
15) B. E. Watt, *Phys. Rev.*, **57**, 1037 (1952).
16) H. Ezure et al., private communication.
17) S. Nakadoi et al., private communication.

TABLE IV. ENRICHMENT OF PHOSPHORUS-32 BY ION EXCHANGE SEPARATION USING JRR-2

Target material	Neutron irradiation		Thermal neutron flux (n./cm²-sec.)	Recovery %	Enrichment factor
	Hole	Time			
KH_2PO_4	Pneumatic tube	20 min.	9.4×10^{12}	55.2	1.7×10^{4}
KH_2PO_4	Vertical hole	50 hr.	6.2×10^{12}	14.0	8.0×10^{3}
NaH_2PO_4	Vertical hole	72 hr.*	2.5×10^{13}	30.1	0.95
Na_2HPO_4	Vertical hole	72 hr.	2.5×10^{13}	66.9	1.3

* Ambient reactor temperature at 170°C.

TABLE V. THE APPARENT RATE CONSTANTS FOR THE VARIATION OF THE ORTHOPHOSPHATE AND FOR THOSE OF THE REDUCED SPECIES

Irradiation conditions			Apparent rate constants, hr^{-1}				Ratio of the apparent rate constants between two salts $k_{(NaH_2PO_4)}/k_{(Na_2HPO_4)}$	
			Orthophosphate		Reduced species			
Reactor	Hole	Time	NaH_2PO_4*	Na_2HPO_4*	NaH_2PO_4	Na_2HPO_4	Orthophosphate	Reduced species
JRR-1	No. 1	10 min.	9.0	15	36	18	0.6	2.0
JRR-1	No. 2	10 min.	3.5	4.0	9.0	1.7	0.9	5.2
JRR-1	No. 3	10 min.	2.5	4.1	7.7	1.8	0.6	4.3
JRR-1	No. 12	10 min.	3.8	3.2	4.8	2.8	1.2	1.7
JRR-1	No. 16	10 min.	1.4	1.4	5.9	2.0	1.0	3
JRR-2	pneumatic tube	20 min.	14	9.3	73	14	1.5	5.2

* Sample salts tested.

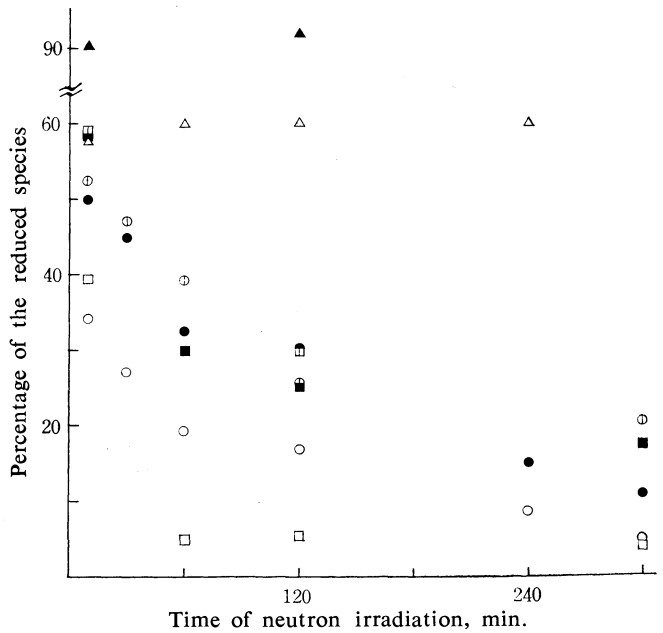


Fig. 3. The reduced species as a function of irradiation time.

○ Sodium dihydrogen phosphate
◐ Trisodium phosphate
■ Dipotassium hydrogen phosphate
△ Sodium orthophosphite
● Disodium hydrogen phosphate
□ Potassium dihydrogen phosphate
⊞ Tripotassium phosphate
▲ Sodium hypophosphite

power. This is due to the greater dose exposures in the reactor. Some of the orthophosphate salts were irradiated in a vertical hole of JRR-2 and subjected to ion exchange separation. Decreases in the recovery were observed for longer periods of irradiations, as Table IV shows. When the salts were neutron-irradiated for 72 hr. at ambient reactor temperatures up to 170°C in a vertical hole of JRR-2 for sodium dihydrogen phosphate and disodium hydrogen phosphate, the enrichment factor decreased to approximately unity. This can be explained by the thermal pyrolysis of the orthophosphate salts. The ambient reactor temperature was measured with a very thin (0.3 mmϕ) alumelchromel thermo-couple placed adjacent to the sample. The low fractions of the polyphosphates in Table IV are the results for irradiations at high ambient reactor temperatures. They can be attributed to the effects not only of radiation annealing but also of thermal annealing.

When the irradiation time was extrapolated to zero, the retention as orthophosphate approached approximately 8 to 15% for the orthophosphate salts studied. Although this retention was obtained for irradiation at ambient reactor temperatures of JRR-1, much difference was not seen between the retention estimated by the extrapolation of the irradiation time to zero and those obtained by irradiation cooled with liquid nitrogen for 2 hr.[18]. This suggests that the distribution of the chemical species containing phosphorus-32 at an irradiation time of zero, which is called the initial distribution, is independent of such post-irradiation effects as thermal and radiation annealing.[3]

As the chemical species were annealed by gamma irradiation, an attempt was made to analyze the variation of the distribution of the chemical species with the neutron irradiation time[1] in a reactor. On irradiation in JRR-1, the effect of radiation annealing would be the greatest cause of the variation of the distribution, because ambient reactor temperatures were not so high[19] that the thermal annealing was prominent for the variation of the distribution. Roughly speaking, if the rate of the annealing of the chemical species containing phosphorus-32 is proportional to the numbers of the chemical species present, the apparent rate constant is dependent on the intensity of radiation in a reactor; then

$$N_t = N_0 \frac{\lambda}{\lambda+k}\left[\frac{1-\exp\{-(\lambda+k)t\}}{1-\exp(-\lambda t)}\right]$$

where k is the apparent rate constant for the variation of the distribution, λ is the decay constant of phosphorus-32, and N_0 and N_t are the numbers of the chemical species at irradiation time zero and at irradiation time t respectively. For this analysis, the initial distribution was assumed to be independent of the post-irradiation effects. For the initial distribution, N_0, the extrapolated values at irradiation time zero for the reduced species were used. However, those for the polyphosphates and orthophosphate were estimated in a different way because these fractions increased with the increase of neutron irradiation time, and the sum of the increase of these two fractions corresponded to the decrease of the reduced species. At an infinitely long irradiation time, N_t approached a constant value; namely, $N_{t=\infty} = \lambda/(\lambda+k)$. If $k \gg \lambda$ were attained as expected from the results of the radiation-annealing experiment, this value might be assumed to be zero at a long irradiation time. The difference between the numbers of the polyphosphates obtained by a 5 hr.-neutron irradiation of JRR-1 and those of the fraction at irradiation time zero was assumed to be the initial distribution of the annealable species in the increase of the polyphosphates. The remaining fraction of the reduced species was then assigned to be the initial distribution of those in the increase of the orthophosphate.

The estimation of the apparent rate constants is based on the best fit of each experimental value, N_t at irradiation time t. The apparent rate constants are shown in Fig. 1, where the neutron irradiation time is shown on the absissa. The apparent rate constants thus

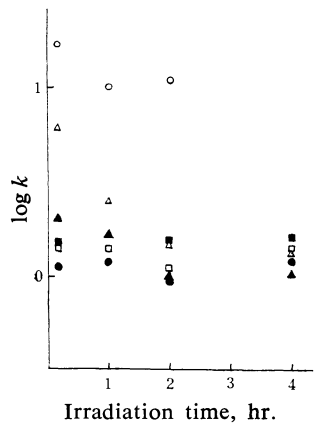


Fig. 4. The apparent rate constants.
Polyphosphate
○ NaH_2PO_4 ● Na_2HPO_4
Orthophosphate
□ NaH_2PO_4 ■ Na_2HPO_4
Reduced species
△ NaH_2PO_4 ▲ Na_2HPO_4

18) R. F. C. Claridge and A. G. Maddock, *Trans. Faraday Soc.*, 59, 935 (1963).
19) K. Tomabechi, private communication.

obtained for the variation of the reduced species vary with the neutron irradiation time; the shorter the irradiation time, the higher the apparent annealing rate. However, this is to be expected from the finding that the radiation annealing takes place by means of mixed processes for the reduced species, as was shown in a previous paper.[3] In the increase of the orthophosphate, however, the apparent rate constants seemed to be independent of the neutron irradiation time. The results shown in Table II and Table III were also analyzed for sodium dihydrogen phosphate and disodium hydrogen phosphate. The ratio between the apparent rate constants for the two salts is compared with different locations on irradiation. This is shown in Table V. The apparent rate constants change roughly with the pile factor, and the ratio of these constants for the two salts seemed to fluctuate independent of the irradiation conditions. The effects of fast neutrons in a reactor were probably suggested by the ratio of these rate constants among the salts in which the hydrogen content was a variable, because the effective dose was attributed to the hydrogen atoms in the salts. The does rates were estimated from the results of fast neutron fluxes obtained above. For this estimation, it was assumed that the energy distribution was the same as that of fission neutrons, and that all the energies of the scattered atoms were absorbed into the sample. It was approximately one-fourth of the gamma ray dose intensity for dihydrogen phosphate and one-twentieth of that for monohydrogen phosphate at the maximum (No. 1 hole of JRR-1). However, the ratio was not increased. Fast neutrons were probably less effective for the annealing process during irradiation in a reactor.

Summary

The distribution of the chemical species containing phosphorus-32 formed by the (n, γ) reaction has been studied for several phosphates as functions of the irradiation conditions in a reactor. The variation in the distribution has been discussed in connection with the radiation annealing process during irradiation, and a comparison of the distribution of the chemical species containing phosphorus-32 by three separation methods has been made.

By means of the analysis of the variation curves of the distribution of the chemical species containing phosphorus-32, the apparent rate constants have been estimated. It has been suggested that the variations in the distribution may be approximately expressed by radiation annealing processes, and that they are affected by pile factors.

The author wishes to express his appreciation to Professor Shizuo Fujiwara for his guidance and encouragement, and to Dr. Kenjiro Kimura for his valuable advice. His thanks are also due to Dr. Nagao Shibata and to Dr. Kenji Yoshihara for their discussions and valuable suggestions.

Radioisotope Reduction Laboratory
Japan Atomic Energy Reserch Institute
Tokai-mura, Ibaraki-ken

Radiolysis of n-Butane in the Gas, Liquid and Solid Phases

By Tetsuo MIYAZAKI, Shigeyoshi ARAI, Shoji SHIDA and Shiro SUNOHARA

(Received April 11, 1964)

Many investigations have been made of the radiolysis of alkanes in order to elucidate the radiolysis mechanism. Although the phase seems to influence the mechanism of the radiolysis, experimental studies of its effect have been few. A comparison of the gas phase with the liquid phase was made by Dewhurst[1] for the radiolysis of *n*-hexane. He reported that the vapor-phase radiolysis showed a much higher proportions of products which must ultimately result from C–C bond cleavage, while the liquid-phase radiolysis showed a higher proportion of product, which must result from C–H bond cleavage. Hamashima et al.[2] compared the radiolysis of neopentane in the gas and the liquid phases.

1) H. A. Dewhurst, *J. Am. Chem. Soc.*, **83**, 1050 (1961).

2) M. Hamashima, M. P. Reddy and M. Burton, *J. Phys. Chem.*, **62**, 246 (1958).

The present authors have studied the phase effect on the radiolysis of *n*-butane; it is the simplest hydrocarbon which contains two types of C–C bond and is easily liquefied. They found a clear difference between the C–C bond scissions in the gas and the condensed phases.

Experimental

Materials.—A commercial pure-grade *n*-butane, stated to be of 99.7% purity, was used without further purification. The gas chromatographic analysis of this material showed 0.036% isobutane and 0.130% isopentane, but no unsaturated impurities were detected.

Irradiation.—The radiolysis in the gas phase was carried out in a glass cylinder 1 liter in volume. The cell used for the liquid and solid radiolyses was a heavy-walled glass tube 1.5 cm. in diameter and 13 cm. long. The samples were irradiated with 1.5 MeV. electrons from a Van de Graaff accelerator with γ-rays from cobalt-60 of 200 c. and 16000 c. The gas samples were irradiated with electrons at room temperature. The hydrogen yield ($G(H_2)=1.3$) from irradiated ethylene at 100 mmHg was used as the measure of the gas dosimetry.[3] The liquid samples were irradiated with γ-rays and electrons at room temperature. The dose rate of γ-rays was 1.5×10^{19} eV./g. hr. and 3.1×10^{19} eV./g hr. Doses were determined by a Fricke dosimeter, taking $G(Fe^{+3})=15.5$. The solid radiolysis was carried out at −196°C.

Product Analysis. — After irradiation, non-condensable gas (a mixture of hydrogen and methane) at −196°C was transferred to a gas burette by a Toepler pump and then analyzed using a copper oxide furnace. Condensable gas was vaporized into a gas holder, an aliquot of which was subjected to gas chromatography. The columns used were of dimethyl sulfolane at room temperature for C_2–C_5 hydrocarbons, of silica gel at 40°C for ethane and ethylene, and of dinonyl phthalate at 80°C for C_6–C_8 hydrocarbons. For runs with iodine added, alkyl iodide products were analyzed by gas chromatography with a dinonyl phthalate column at 80°C.

Results and Discussion

***G*-Value.** — The amounts of the major irradiation products of liquid *n*-butane are plotted against the energy absorbed in Fig. 1 and Fig. 2.

The initial yield was calculated from the initial slopes of these curves, since the amount of olefin did not increase linearly with the energy absorbed.

The radiolytic yields obtained in the gaseous, liquid and solid phases are listed in Table I.

The *G*-values obtained for gaseous and liquid *n*-butane are in good agreement with those reported in the previous works.[4-7]

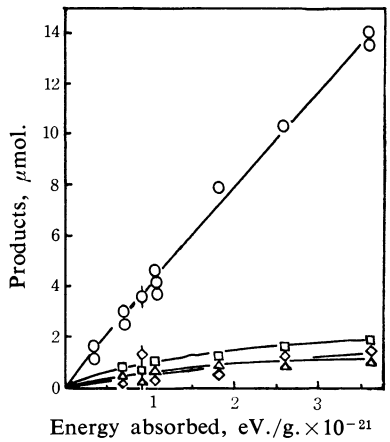


Fig. 1. Product formation in the liquid phase radiolysis as a function of the energy absorbed. Ordinates represent the yield from 1000 μmol. *n*-butane. The hydrogen yield in the electron bombardment was assumed to be equal to that in the γ-rays radiolysis.

	γ-Rays	Electrons
H_2	○	○
C_4H_8-1	□	□
trans C_4H_8-2	◇	◇
cis C_4H_8-2	△	△

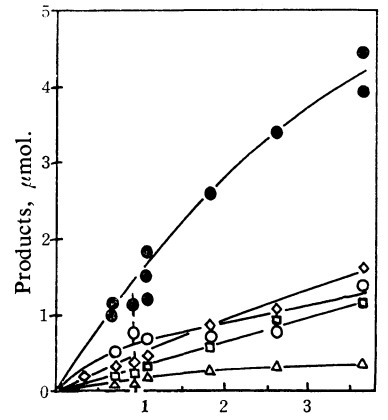


Fig. 2. Product formation in the liquid phase radiolysis as a function of the energy absorbed. Ordinates represent the yield from 1000 μmol. *n*-butane.

	γ-Rays	Electrons
CH_4	◇	△
C_3H_8	□	□
C_3H_6	△	△
C_2H_6	●	●
C_2H_4	○	○

3) M. C. Sauer and L. M. Dorfman, ibid., **66**, 322 (1960).
4) S. C. Lind and D. C. Bardwell, *J. Am. Chem. Soc.*, **48**, 2235 (1926).
5) A. Kuppermann and M. Burton, *Radiation Research*, **10**, 636 (1959).
6) R. P. Borkowski and P. J. Ausloos, *J. Chem. Phys.*, **39**, 818 (1963).
7) C. D. Wagner, *J. Phys. Chem.*, **67**, 1793 (1963).

TABLE I. G VALUES OF THE RADIOLYSIS OF n-BUTANE

Product	Gas[a] (room temp.)	Liquid[b] (room temp.)	Solid[c] (−196°C)
H_2	5.06	4.73	2.84
CH_4	0.96	0.50	0.21
C_2H_6	1.89	1.29	0.69
C_2H_4	0.59	0.58	0.23
C_3H_8	2.12	0.29	0.13
C_3H_6	0.18	0.16	0.03
C_4H_8-1	0.23	0.88	0.74
trans-C_4H_8-2	0.64	0.50	0.43
cis-C_4H_8-2	0.18	0.48	0.10
C_5	0.32	0.18	—
C_6	0.38	0.38	—
C_7	0.09	0.05	—
C_{8A}	0.26	0.38	0.20

a) Results are the averages at the pressure of 50 and 100 mmHg. The total dose is 2.5×10^{21} eV./g.
b) The yields of hydrogen and lower hydrocarbons (C_1-C_4) were determined by extrapolation to zero dose. The yields of C_5-C_8 hydrocarbons represent the mean values of two runs at the total dose 3.7×10^{21} eV./g.
c) The mean values of three individual irradiations, that is, two runs at 3.7×10^{21} eV./g. and one run at 2.6×10^{21} eV./g.

Formation of C_2 and C_3 Products.—n-Butane has two types of C–C bonds, and the major products from these C–C bond scissions are C_1, C_2 and C_3 hydrocarbons. It is noted in Table I that the $G(C_2)$ of the liquid phase is approximately the same as that of the gas phase, while for $G(C_3)$ this is not the case.

Since the irradiation with 1.5 MeV. electrons and γ-rays gave the same yield (Fig. 1 and Fig. 2), the different $G(C_3)$ values cannot be ascribed to the different dose rate and, therefore, must be due to the different radiolysis mechanisms in the two phases.

Table II compares the radiolyses in the gas, liquid and solid phases, the vacuum ultraviolet photolysis (1470A and 1236A),[8,9] the mass spectral fragmentation[10] and the appearance potentials of ions from n-butane.[11]

The C_2/C_3 ratios in the radiolyses of liquid and solid butane are 4.2 and 5.7 respectively. These values are similar to the value of the photolysis, where only the cracking of neutral excited butane takes part, but not to that of mass spectral fragmentation. Since the parent ion in the mass spectral fragmentation is highly excited, the fragmentation of low excited ions which may take part in the condensed-phase radiolysis would be different from that in the mass spectroscopy. As may be seen in Table II, the appearance potential of $C_3H_7^+$ is lower than that of $C_2H_5^+$ and, accordingly, the low-excited ion produces C_3 products mainly; the C_2/C_3 in the fragmentation of the low excited ion should be less than 1.43. Therefore, the values of C_2/C_3 in the liquid and solid radiolyses cannot be explained, even by the fragmentation of such a low-excited butane ion.

On the contrary, the C_2/C_3 in the radiolysis of n-butane in the gas phase is analogous to that of mass spectral fragmentation, but not so that of the photolysis.

Bond Dissociation Energy.—In the radiolysis of liquid hydrocarbons, it has been shown that weaker bonds are preferentially broken.[12,13]

Since the difference between the gas and liquid radiolyses of n-butane obviously cannot be explained by the bond strength of the neutral molecule alone, the bond strength of the butane ion is also considered here.

The bond dissociation energies of n-butane and the butane ion are given below.

TABLE II. COMPARISON OF RADIOLYSIS OF n-BUTANE WITH OTHER CRACKING PROCESSES

	Solid	Liquid	Gas	Photolysis (1470A, 1236A)	Mass spectrum[b]	A. P. of ions from n-butane
C_2/C_3[a]	5.7	4.2	1.1	3-4	1.4	$C_4H_{10}^+$ 10.4 eV.
						$C_3H_6^+$ 11.0 eV.
						$C_3H_7^+$ 11.2 eV.
						$C_2H_4^+$ 11.6 eV.
						$C_2H_5^+$ 12.1 eV.

a) C_2 represents the sum of the yields of ethane and ethylene. C_3 represents the sum of the yields of propane and propylene.
b) The complementarity between ion and radical is assumed to hold in the mass spectral fragmentation.

8) M. C. Sauer and L. M. Dorfman, *J. Chem. Phys.*, **35**, 497 (1961).
9) H. Okabe and D. A. Becker, ibid., **39**, 2549 (1963).
10) American Petroleum Institute Research Project No. 44, Mass Spectral Data.
11) M. B. Loffel and R. A. Lad, *J. Chem. Phys.*, **16** 420 (1948).
12) H. Yamazaki and S. Shida, ibid., **32**, 950 (1960).
13) K. Fueki and K. Hirota, *J. Chem. Soc. Japan, Pure Chem. Sec.* (*Nippon Kagaku Zasshi*), **81**, 209 (1960).

	n-Butane molecule	ΔH (kcal./mol.)
$CH_3CH_2CH_2CH_3$	$\rightarrow CH_3 + C_3H_7$	84.0
	$\searrow 2\ C_2H_5$	81.0
	Butane ion	
$CH_3CH_2CH_2CH_3^+$	$\rightarrow CH_3 + C_3H_7^+$	3.5
	$\searrow C_2H_5 + C_2H_5^+$	30.2

The bond dissociation energies of the butane ion have been derived by assuming the heats of formation of C_4H_{10}, $C_3H_7^+$, $C_2H_5^+$, CH_3 and C_2H_5 to be 219, 190, 224, 32.4 and 25.2 kcal./mol. respectively.[14] In the butane molecule, the second bond is weaker than the first bond, while in the butane ion the first bond is much weaker than the second bond. Therefore, one may expect that C_2 products are more readily formed than C_3 products from the fragmentation of the butane molecule, while C_3 products become the major product from that of the butane ion.

Radical Detection by the Scavenger Method. —*n*-Butane saturated with iodine was irradiated with γ-rays in the gaseous and liquid phases. The yields of alkyl iodide, which represent the yields of the radical, and the decrement of each product upon the addition of DPPH are shown in Table III.

TABLE III. *G* VALUES OF RADICALS IN THE RADIOLYSIS OF *n*-BUTANE AND IODINE (or DPPH) MIXTURE[a]

	Gas[b] (I_2)	Liquid[c] (I_2)		Liquid[d] (DPPH)
CH_3I	1.54	0.29	ΔCH_4	0.22
C_2H_5I	0.69	0.59	ΔC_2	0.83
iso-C_3H_7I	0.33	0.15	ΔC_3	0.16
n-C_3H_7I	—	0.06		

a) Results are the averages of two or more runs at the total dose 3.7×10^{21} eV./g. The dose rate is 8×10^{18} eV./g. hr.
b) The pressure of *n*-butane is 200 mmHg and that of I_2 is 0.3 mmHg.
c) The concentration of I_2 is 0.025 mol./l.
d) The concentration of DPPH is about 0.001 mol./l. ΔCH_4, ΔC_2 and ΔC_3 represent the difference between the initial yield and the molecular yield of methane, C_2-products and C_3-products respectively. This difference can be thought to represent the yield of radical.

The present data on liquid butane are not similar to the reported values.[15] The disagreement seems to be due to the different analytical techniques. McCauley et al. separated the alkyl iodides by fractional distillation, but in the present study iodides were analyzed by gas chromatography.

The yield of the propyl radical is only one-fifth of that of the methyl radical in the gas phase, while in the liquid phase the amounts of methyl and propyl radicals are approximately equal. From this result, it seems that in the liquid phase the homolytic dissociation of the butane molecule into two radicals occurs, while in the gas phase this mode of dissociation is of minor importance. From the mass spectral study, the scission of the first C–C bond of the butane ion is known to produce the propyl ion and the methyl radical, but not the propyl radical or the methyl ion. Since the yield of the methyl radical is extremely high as compared with that of the propyl radical in the gas phase radiolysis, the dissociation of the butane ion seems to occur in the gas phase.

Conclusion

From these discussions it seems that the fragmentation of butane ion is important in the gas phase radiolysis, but that in the condensed phases that of the butane molecule is important. The main reactions are as follows:

Solid and liquid radiolyses

$$n\text{-}C_4H_{10} \sim\sim\rightarrow n\text{-}C_4H_{10}' \rightarrow C_3H_7 + CH_3$$
$$\searrow 2\ C_2H_5$$
$$C_3H_7 + n\text{-}C_4H_{10} \xrightarrow[\text{solid, liquid}]{} C_3H_8 + C_4H_9$$
$$C_3H_7 + R \xrightarrow[\text{liquid}]{} C_3H_6, \text{ Products}$$

Gas radiolysis

$$n\text{-}C_4H_{10} \sim\sim\rightarrow C_4H_{10}^+ \rightarrow C_3H_7^+ + CH_3$$
$$\searrow C_2H_5^+ + C_2H_5$$
$$C_3H_7^+ + n\text{-}C_4H_{10} \longrightarrow C_3H_8 + C_4H_9^+$$
$$C_4H_9^+ + e \longrightarrow C_4H_8, \text{ Products}$$

N. B. C_4H_{10}' represents a neutral precursor of fragmentation.
R represents some radicals.

We wish to express our appreciation to Dr. Shin Sato for his very valuable suggestions and to Mr. Kiyoshi Furukawa and Mr. Tomoyoshi Kudo for their fruitful discussions. We appreciate also the help of the Japan Atomic Energy Institute in performing the irradiation.

Laboratory of Physical Chemistry
Tokyo Institute of Technology
Meguro-ku, Tokyo (T. M., S. A. & S. Sh.)

Tokyo Laboratories
Japanese Association for Radiation Research on Polymers
Bunkyo-ku, Tokyo (S. Su.)

14) F. H. Field and J. L. Franklin, "Electron Impact Phenomena," Academic Press, New York (1957).
15) C. E. McCauley and R. H. Schuler, *J. Am. Chem. Soc.*, **79**, 4008 (1957).

A Method of Synthesizing Pure Violanthrene

By Junji Aoki

(Received April 28, 1964)

Zinc dust fusion is a convenient and excellent method for obtaining aromatic hydrocarbons from their quinones.[1] The preparation of violanthrene (III) from violanthrone (II) is a mere application of the above method, but little attention has been paid to the purity of violanthrone. This quinone as usually supplied is one of the condensation products obtained by the alkali fusion of benzanthrone (I). It is, therefore, unavoidable that by-products[2] are mixed in it as impurities. Among these by-products, violanthrone B and all the other substances except isoviolanthrone (IV) can be removed by means of the differences in their solubility and vattability, but the removal of isoviolanthrone is very difficult since isoviolanthrone is as vattable at 55~60°C and as difficult to dissolve in organic solvent as is violanthrone. Although the proportion of isoviolanthrone decreases as the temperature of alkali fusion is raised,[3] it has been found by the author that, even in a sample prepared under proper conditions, 6~7 per cent of the sample is isoviolanthrone.[4]

When the zinc dust fusion was applied to such a sample, isoviolanthrone was also reduced to isoviolanthrene (V). In consequence, a mixture of violanthrene and isoviolanthrene was obtained as the reduction product; the separation of these two hydrocarbons was also very difficult. It may, therefore, be asserted that, in seeking to obtain pure violanthrene, such material must not be used.

The reliable sample of pure violanthrene which had been prepared by the present author from pure violanthrone synthesized by Scholl's mothod[5] (Scheme 1) gave the absorption spectrum shown in Fig. 1. It has one high peak at 496 mμ, and the peak at 365 mμ is lower than that at 385 mμ. On the other hand, the absorption spectrum of isoviolanthrene has two high peaks, at 363 and 521 mμ (Fig. 1).

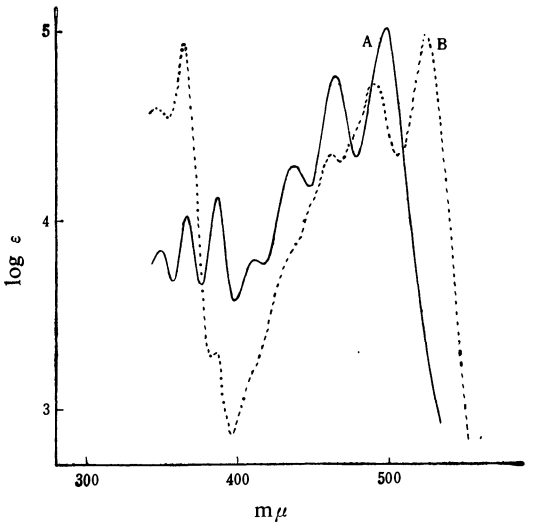


Fig. 1. Absorption spectra of violanthrene (A) and isoviolanthrene (B) (in 1,2,4-trichlorobenzene).

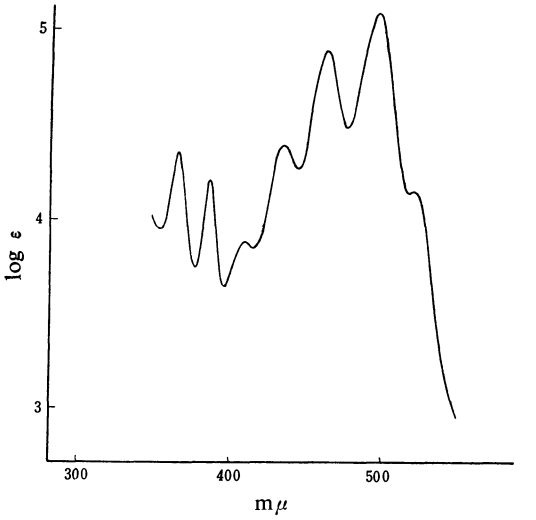
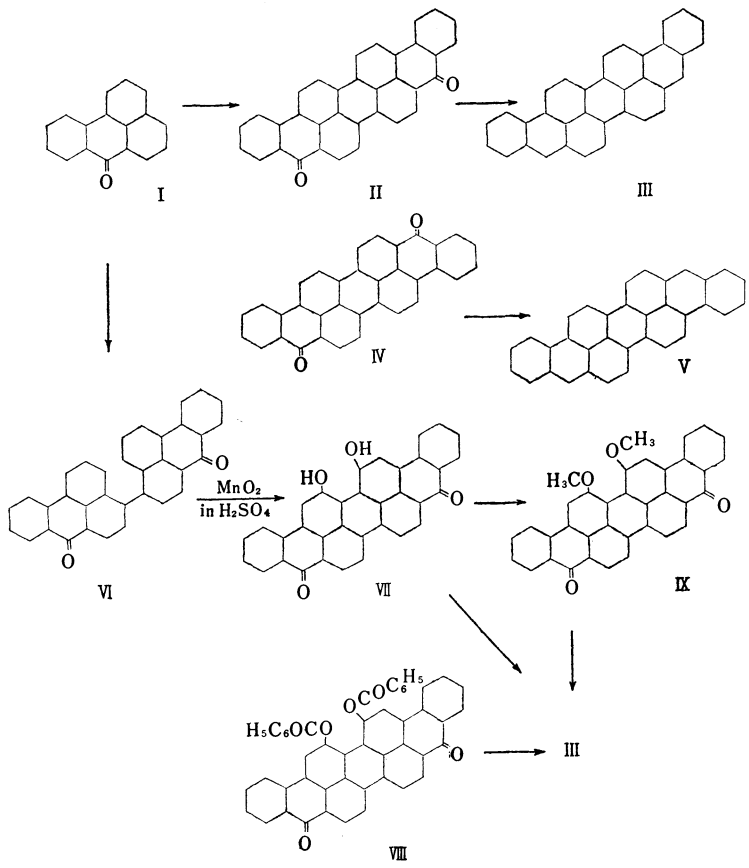


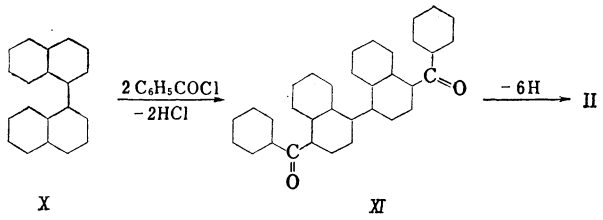
Fig. 2. Absorption spectrum of violanthrene contained isoviolanthrene (in 1,2,4-trichlorobenzene).

However, the absorption spectrum of the reduction product obtained from violanthrone containing isoviolanthrone was very characteristic, as is shown in Fig. 2. As a result of the

1) E. Clar, *Ber.*, **72**, 1645 (1939).
2) Isoviolanthrone, violanthrone B, 4,4'-dibenzanthronyl (VI), etc.
3) This relation was reported by Lüttringhaus and Neresheimer (*Ann.*, **473**, 259 (1921)), in which paper it was also stated that isoviolanthrone was not produced under the proper conditions (220~230°C).
4) J. Aoki, Y. Usui, and S. Fujisawa, Presented at the 16th Annual Meeting of the Chemical Society of Japan, Tokyo, April, 1963.
5) R. Scholl and Chr. Seer, *Ann.*, **394**, 171 (1912).



Scheme 1



presence of isoviolanthrene, it has a low peak at nearly 520 mμ, and the peak at nearly 365 mμ is unexpectedly higher than that at nearly 385 mμ. These facts confirm that violanthrone, the material needed to obtain pure violanthrene, must be supplied by means of Scholl's method, not by alkali fusion.

However, Scholl's method, which was devised for the determination of the structure of violanthrone, is not an adequate synthetic method, since it consists of many steps and contains processes difficult to perform.

The present author has found, however, that the zinc dust fusion of 16, 17-dihydroxyviolanthrone (VII),[6] its dibenzoate (VIII) and a dimethyl ether (IX) gives pure violanthrene. Since the dimethyl ether, 16,17-dimethoxyviolanthrone, is a component of "Indanthrene Brilliant Green FFB" and since 16, 17-dihydroxyviolanthrone is its intermediate product, these substances can be readily supplied.

Consequently, the above facts indicate an advantageous method of synthesizing pure violanthrene; the author especially recommends the use of the dibenzoate of 16, 17-dihydroxyviolanthrone, since this substance can be readily purified by recrystallization.

6) This substance should be prepared from 4, 4'-dibenzanthronyl (VI), as will be described below. Although it is obtained by the oxidation of violanthrone, the purity of the raw material is again questionable.

7) C. S. Schoepfle, *J. Am. Chem. Soc.*, **45**, 1569 (1924).

8) T. Maki and M. Maezawa, This Bulletin, **28**, 77 (1955).

In addition, judging from the facts that these materials are applied to obtain the pure sample of violanthrene, it may be considered that these substances contain little or no isomer of the isoviolanthrone type, because the cyclization of 4,4'-dibenzanthronyl is carried out by the action of manganese dioxide in a concentrated sulfuric acid, not by alkali fusion.

Experimental

Violanthrone (II) (Scholl's Method). — This material was synthesized in the steps shown in Scheme 1. Dinaphthyl (1,1') (X) was prepared from α-bromonaphthalene by the method described in Ref. 7. From this product, violanthrone was synthesized following Scholl's method.[5] The crude product was refluxed with 100 parts of chlorobenzene for 2 hr., and the soluble impurities were removed by hot filtration. Further purification was carried out by the vatting method. Thus pure violanthrone was obtained.

Yield: 0.6 g. of II from 1.0 g. of XI, 1.6 g. of XI from 2.5 g. of X, and 3.2 g. of X from 50 g. of α-bromonaphthalene.

16,17-Dihydroxyviolanthrone (VII). — The synthesis was carried out by the method described in Ref. 8.

Dibenzoate (VIII).—A mixture of 2.0 g. of VII, 2.0 g. of pyridine and 200 g. of *o*-dichlorobenzene was refluxed for 30 min. Then, 4.5 g. benzoyl chloride was added, and boiling was continued for 30 min. After standing overnight, the reaction mixture was filtered to remove the unchanged substance as the insoluble material (0.9 g.). The filtrate was slightly warmed and 100 ml. of alcohol added, giving fine black needles with a certain green brightness. Yield: 1.5 g.; m. p. higher than 400°C. This product, 16,17-dibenzoate, is soluble in an organic solvent; the solution shows a purple color with a strong red fluorescence. In addition, as a result of the examination of the above method, it was found that pyridine was indispensable for this reaction and that more of it was necessary than the mole ratio of benzoyl chloride,

Found: C, 82.58; H, 3.53. Calcd. for $C_{48}H_{24}O_6$ (VIII): C, 82.75; H, 3.47%.

16,17-Dimethoxyviolanthrone. — "Indanthrene Brilliant Green FFB" (Mitsui Chemical Industries Ltd.) was refluxed with 50 parts of 96, 60 and 20 % alcohol successively; the insoluble part was then collected, washed with water, and dried. This material, after the water-soluble substances had been removed, was finely powdered, refluxed with 100 parts of chlorobenzene for 2 hr. and the insoluble part used as the sample.

Zinc Dust Fusion (Violanthrene).—Violanthrone or its derivative was treated as in Ref. 9.

The sample of Fig. 2 was prepared from impure violanthrone (violanthrone 92.7, isoviolanthrone 7.3 %[10]); by comparing the absorption spectra, the amount of isoviolanthrene in this reduction product was estimated at about 10 per cent.

The author wishes to thank Mrs. Yasuko Usui for her assistance during the dibenzoate experiment.

Department of Chemistry
Faculty of Science
Toho University
Narashino, Chiba

9) J. Aoki, This Bulletin, 34, 1818, 1821 (1961).
10) This value was obtained from the absorption spectra in concentrated sulfuric acid. The details will be dealt with in a later report.

The Spectrophotometric Determination of Trace Amounts of Arsenate and Arsenite in Natural Waters with Special Reference to Phosphate Determination

By Ken SUGAWARA and Satoru KANAMORI

(Received April 6, 1964)

The current methods for the determination of arsenic,[1-5] in which molybdoarsenate or its reduction product, "*molybdenum blue*", is determined spectrophotometrically, are only applicable to microgram quantities of the element and are inconvenient for usual natural waters, the arsenic content of which is from several tenths to several micrograms per liter. It is a time-consuming and laborious work to concentrate the necessary liters of a sample. Furthermore, when the available amount of the sample is limited or the sample is extremely

1) N. W. Rakestraw and F. B. Lutz, *Biol. Bull.*, **65** 397 (1933).
2) S. Gorgy, N. W. Rakestraw and D. L. Fox, *J. Mar. Research*, **7**, 22 (1948).
3) M. Ishibashi, T. Shigematsu, Y. Nakagawa and Y. Ishibashi, *Bull. Chem. Research, Kyoto Univ.*, **24**, 68 (1951).
4) K. Sugawara and S. Kanamori, This Bulletin, **29**, 670 (1956).
5) W. Dozanska and H. Czarnodolowa, *Roczniki Panstwowego Zakladu Hig.*, **10**, 217 (1959).

diluted, the methods are useless.

The present authors have previously reported a spectrophotometric method for determining submicrogram quantities of orthophosphate in natural waters.[6] The principle was to isolate molybdophosphate by solvent extraction, to liberate molybdate by decomposition from the extracted molybdophosphate in which the molybdenum is coordinated to phosphate in the ratio of 1 : 12, and finally to determine the liberated molybdenum spectrophotometrically.

In the present work the authors have extended this principle so that it is possible to separately determine 0.01~1.00 μg. of phosphate-P, 0.02~2.00 μg. of arsenate-As, and 0.02~2.00 μg. of arsenite-As from a sample smaller than 250 ml.

The method consists of the following five steps: 1) Phosphate and arsenate are extracted as molybdophosphate and molybdoarsenate successively with the proper solvents. 2) The arsenite in the remaining solution is oxidized into arsenate. Then the arsenate is extracted according to step 1. 3) The three fractions, phosphate, arsenate and arsenite, are washed. 4) The respective heteropolymolibdate are stripped and subjected to decomposition, with the liberation of free molybdate. 5) The liberated molybdate is spectrophotometrically determined as thiocyanate for the respective fractions.

Experimental

Apparatus. — The absorbance is measured by the use of a Beckman spectrophotometer, type DU, with 10 mm. cells of Pyrex glass.

All glass vessels must be free from any contamination of arsenic. Especially, it is recommended that the 500 ml. separatory funnel for the extraction of molybdoarsenate be washed with hot mineral acid for several days.

Reagents. — All reagents should be of the analyzed reagent grade, and water distilled with copper still must be used.

Ascorbic Acid: a 0.05% aqueous solution.

Hydrochloric Acid: concentrated. One milliliter of methanol is added per liter of the acid to reduce the trace of chlorine.

n-Butanol, Chloroform and Acetone: distilled.

Solvent A: *n*-butanol and chloroform are mixed in a 4 : 6 proportion by volume.

Solvent B: *n*-butanol, chloroform and acetone are mixed in a 3 : 7 : 3 proportion by volume.

Ammonium Molybdate: a 10% aqueous solution.

Washing Solution A: 60 ml. of *n*-butanol and 40 ml. of concentrated nitric acid are dissolved to 1 l. with distilled water.

Washing Solution B: 60 ml. of *n*-butanol, 140 ml. of acetone, and 10 ml. of concentrated nitric acid are dissolved to 1 l. with distilled water.

Potassium Iodate: a saturated aqueous solution.

Sodium Hydroxide: a 1 N aqueous solution.

Ferrous Ammonium Sulfate: 1 g. of the hexahydrate is dissolved in 100 ml. of 0.2 N sulfuric acid.

Potassium Thiocyanate: a 10% aqueous solution.

Stannous Chloride: 10 g. of the dihydrate is dissolved in 100 ml. of 1 N hydrochloric acid.

Phosphate Standard Solution. — A stock solution containing 1 mg. of phosphate-P per ml. is prepared by dissolving 0.439 g. of potassium dihydrogen phosphate to 100 ml. with distilled water. The addition of a few drops of chloroform keeps the solution from a mold growth. The working standard solutions are prepared by properly diluting the stock solution.

Arsenite Standard Solution. — A stock solution containing 1 mg. of arsenite-As per ml. is prepared as follows, 0.132 g. of arsenic trioxide is dissolved in 10 ml. of a 1 N sodium hydroxide solution, slightly acidified with diluted hydrochloric acid and made up to 100 ml. This stock solution is properly diluted for the preparation of working standard solutions.

Arsenate Standard Solution. — One milliliter of an arsenite stock standard solution is evaporated up with 20 ml. of concentrated nitric acid and 1 ml. of concentrated hydrochloric acid on a water bath, and then the residue is dissolved in hot water and properly diluted.

Procedure. — *The Separation of Phosphate, Arsenate and Arsenite.* — Into a 500 ml. separatory funnel, 250 ml. of a sample water, 0.3 ml. of an ascorbic acid solution, 4 ml. of hydrochloric acid, 15 ml. of *n*-butanol, and 10 ml. of solvent A are taken; the funnel is then shaken for 3 min. to saturate the aqueous phase with solvent A. The addition of the ascorbic acid protects the arsenite from any possible oxidation, leaving the coexisting phosphate and arsenate untouched. The organic layer is replaced by a new 5 ml. of solvent A. After 2.5 ml. of the ammonium molybdate solution is added, the funnel is immediately shaken for 3 min. The extract is transferred to a 100 ml. separatory funnel. The extraction is repeated with another 5 ml. of solvent A. For the determination of phosphate, these two extracts of the phosphate-fraction are combined in a 100 ml. separatory funnel.

The remaining aqueous phase is again subjected to extraction by two or more 5 ml.-portions of the solvent A to remove the last trace of phosphate. Then 7.5 ml. of the ammonium molybdate solution and 35 ml. of acetone are added to the funnel and the arsenate is extracted by shaking the mixture for 3 min. with two 5 ml.-portions of solvent B. For the determination of arsenate, these two extracts of the arsenate fraction are combined in a 100 ml. separatory funnel.

The remaining aqueous phase is extracted with two or more 5 ml.-portions of solvent B to ensure the complete separation of the arsenate. Then 5 drops of a saturated potassium iodate solution are added to oxidize the arsenite to arsenate. The arsenate thus formed is extracted according to the step for the separation of arsenate described above,

6) K. Sugawara and S. Kanamori, This Bulletin, **34**, 258 (1961).

and the extracts of the arsenite fraction are combined in a 100 ml. separatory funnel.

*The Determination of Phosphate**. — The phosphate fraction separated above is shaken for 3 min. with 50 ml. of washing solution A to wash out any uncombined molybdate and any contaminative heteropolymolybdate other than molybdophosphate. The remaining organic layer is then transferred to a 50 ml. separatory funnel. After the addition of 10 ml. of the 1 N sodium hydroxide solution the funnel is shaken for 1 min. to strip the molybdophosphate completely from the oily phase, and then the organic layer is drawn off. Next, 3 ml. of concentrated hydrochloric acid, 1 ml. of the ferrous ammonium sulfate solution, 3 ml. of the potassium thiocyanate solution and 3 ml. of the stannous chloride solution are successively added. The molybdenum thiocyanate with an amber color is extracted with two small portions of solvent A. The extract is made up to 5 ml. in order to subject it to spectrophotometry at 475 mμ. Here, to protect the ferrous iron from oxidation, the addition of a few small crystals of stannous chloride to the joint extract is recommended.

The Determination of Arsenate. — The arsenate fraction is shaken with two 50 ml.-portions of washing solution B for 3 min. Through the washing process, only molybdoarsenate remains in the organic phase; the other molybdenum compounds contaminating the molybdoarsenate are washed out.

The organic layer is transferred to a 50 ml. separatory funnel in order to subject it to the stripping of molybdoarsenate with an alkali solution and to the final step of spectrophotometry, as has been described in the determination of phosphate.

The Determination of Arsenite. — The extract of the arsenite fraction is processed as described in the determination of arsenate.

Discussion

The Separation of Phosphate, Arsenate and Arsenite.—*The Extraction of Molybdophosphate.* —Figures 1 and 2 show the relation of the percent extraction of phosphate, arsenate, germanate and silicate as respective heteropolymolybdates to the acidity in hydrochloric acid and to the concentration of ammonium molybdate in the sample solution before extraction. When the concentration of ammonium molybdate is fixed at 0.08%, the extraction of molybdophosphate is practically complete at the acidity of higher more than 0.19 N and when the acidity is fixed at 0.19 N, it is complete at the concentration of ammonium molybdate of higher more than 0.08%. More-

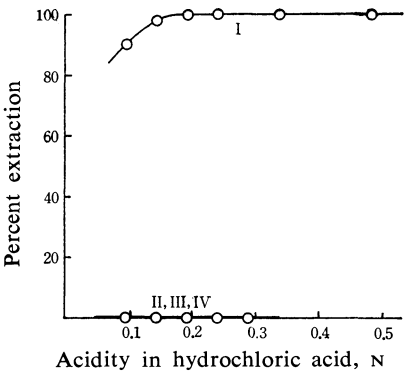


Fig. 1. Percent extraction of phosphate, arsenate, germanate and silicate and the acidity of aqueous phase before extraction.
I: Phosphate II: Arsenate
III: Germanate IV: Silicate
The concentration of ammonium molybdate: 0.08%

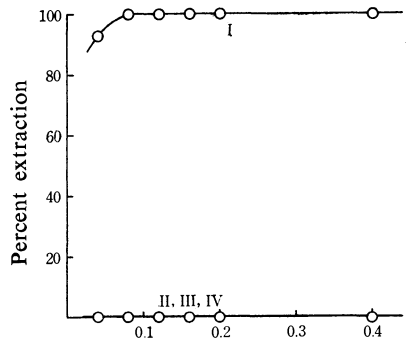


Fig. 2. Percent extraction of phosphate, arsenate, germanate and silicate and concentration of ammonium molybdate before extraction.
I: Phosphate II: Arsenate
III: Germanate IV: Silicate
The acidity in hydrochloric acid: 0.19 N

over the extraction of the other ions is less than 0.3% in the whole range examined and shows a tendency to increase with the acidity and the concentration of molybdate. Accordingly, the acidity of 0.19 N and the concentration of ammonium molybdate of 0.1% are chosen as the optimum conditions for the extraction of phosphate, under which conditions the other ions are extracted in percentages of less than 0.01%.

The Extraction of Molybdoarsenate.—Figures 3 and 4 show the relation of the percent extraction of arsenate, germanate and silicate as respective heteropolymolybdates to the acidity in hydrochloric acid and to the concentration of ammonium molybdate. When the concentration of ammonium molybdate is fixed

* When more than 2 μg. of phosphate-P is treated with, 2 ml. of the stannous chloride solution and 10 ml. of chloroform are added to the extract, which is then swirled to reduce the extracted molybdophosphate to the "molybdenum blue" completely. Then, 10 ml. of 1 N hydrochloric acid is added and the funnel is shaken for 1 min. to back-extract the "*molybdenum blue*" into the aqueous phase, which is subjected to spectrophotometry at 740 mμ.

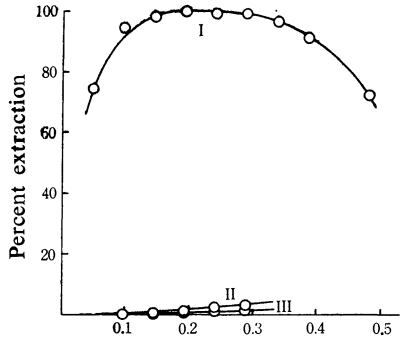


Fig. 3. Percent extraction of arsenate, germanate and silicate and acidity of aqueous phase before extraction.
I: Arsenate II: Germanate III: Silicate
The concentration of ammonium molybdate: 0.1%

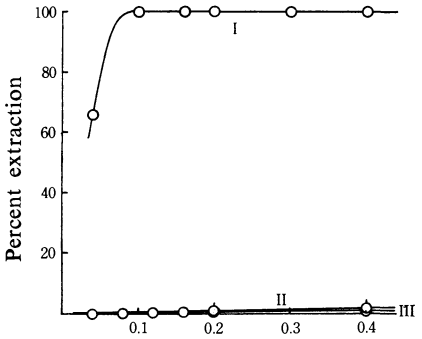


Fig. 4. Percent extraction of arsenate, germanate and silicate and concentration of ammonium molybdate in aqueous phase before extraction.
I: Arsenate II: Germanate III: Silicate
The acidity in hydrochloric acid: 0.19 N

at 0.1%, the extraction of arsenate is complete in the acidity range from 0.19 N to 0.24 N, and when the acidity is fixed at 0.19 N, it is complete at the concentration of ammonium molybdate of higher more than 0.1%. Moreover, the extraction of the other ions increases with the acidity and the concentration of molybdate up to 4 per cent. However, as will be shown later, a large amount of silicate interefers with the extraction of arsenate, because a considerable amount of molybdate is consumed by the silicate. Therefore, the acidity of 0.19 N and the concentration of ammonium molybdate of 0.4% are chosen as an appropriate conditions under which germanate and silicate are extracted in percentages as small as 1.5% and 0.5% respectively.

The Washing of the Extracts.—*The Washing of the Phosphate Fraction.*—Figure 5 shows the

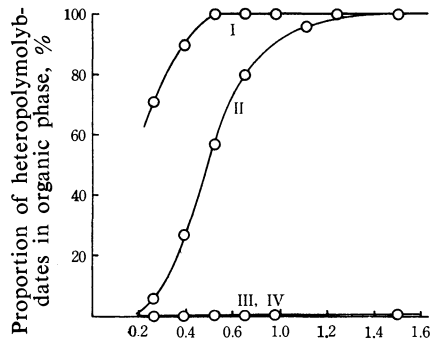


Fig. 5. Distribution of heteropolymolybdates of phosphate, arsenate, germanate and silicate and acidity of aqueous phase.
I: Molybdophosphate
II: Molybdoarsenate
III: Molybdogermanate
IV: Molybdosilicate

distribution of four heteropolymolybdates between 10 ml. of solvent A and 50 ml. of the 6% *n*-butanol aqueous solution at various acidities in nitric acid. The molybdophosphate remains completely in the organic phase at an acidity of higher more than 0.52 N, while almost all of the molybdogermanate and molybdosilicate is in the aqueous phase, and the proportion of molybdoarsenate in the organic phase increases with the increase in acidity. When the phosphate fraction of the extracts is washed with washing solution A (0.52 N in acidity), 57% of molybdoarsenate and less than 0.5% of the other heteropolymolybdates remain in the organic phase.

The Washing of the Arsenate Fraction. — The distribution of molybdoarsenate, molybdogermanate and molybdosilicate between 10 ml.

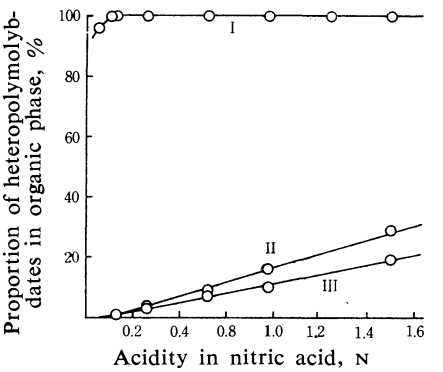


Fig. 6. Distribution of heteropolymolybdates of arsenate, germanate and silicate and acidity of aqueous phase.
I: Molybdoarsenate
II: Molybdogermanate
III: Molybdosilicate

TABLE I. THE DETERMINATION OF PHOSPHATE, ARSENATE AND ARSENITE IN THE PRESENCE OF GERMANATE AND SILICATE*

Added					Found		
Phosphate -P μg.	Arsenate -As μg.	Arsenite -As μg.	Germanate -Ge μg.	Silicate -Si μg.	Phosphate -P μg.	Arsenate -As μg.	Arsenite -As μg.
0.50	10	10	0	0	0.51		
0.50	0	0	100	0	0.50		
0.50	0	0	0	1000	0.51		
100	0.50	0.50	0	0		0.50	0.49
0	0.50	0.50	100	0		0.51	0.49
0	0.50	0.50	0	200		0.50	0.50
0	0.50	0.50	0	1000		0.06	0.05
0	0.50	0.50	0	1000		0.51**	0.50**

* The experiment was carried out with 50 ml. of the aqueous phase.
** The extraction of molybdoarsenate was carried out at the ammonium molybdate concentration of 1.2%.

TABLE II. APPLICATION OF THE PRESENT METHOD TO NATURAL WATERS

Sample	Sample taken ml.	Added Phosphate -P μg.	Added Arsenate -As μg.	Added Arsenite -As μg.	Found Phosphate -P μg.	Found Arsenate -As μg.	Found Arsenite -As μg.
Ground water from a well on the campus of Nagoya University	250	0	0	0	11.3	0.08	0.03
	250	3.0	0.05	0.05	14.2	0.14	0.07
Sea water from the north-western Pacific Ocean (33°12'N; 139°53'E)	250	0	0	0	13.6	0.25	0.13
	250	2.0	0.50	0.50	15.8	0.76	0.63

of solvent B and 50 ml. of a washing solution containing 6% *n*-butanol and 14% acetone at various acidities in nitric acid is shown in Fig. 6. The molybdoarsenate remains completely in the organic phase at an acidity of higher more than 0.10 N, and a small proportion of the other ions remains in the organic phase, although this proportion increases with the acidity. At the acidity of 0.13 N in washing solution B, less than 1% of molybdogermanate and molybdosilicate remain in the organic phase. Usual natural waters contain several milligrams of dissolved silica per liter, and, therefore, duplicated washing is needed to get exact results for arsenate determination.

Standard Curve. — The standard curves for phosphate-P and arsenate-As are shown in Fig. 7.

The molecular extinction coefficients were measured as 15.5×10^3 for molybdenum thiocyanate and as 185×10^3 and 184×10^3 for phosphate- and arsenate-equivalents respectively. Therefore, the P/Mo and As/Mo ratios in the extracted chemical species are 12.0 and 11.9 respectively; this shows that both extracted molybdophosphate and molybdoarsenate are 12-acid.

As is shown in Fig. 7, the sensitivity of the present method is high enough to be applicable to natural waters with no need to concentrate samples previously.

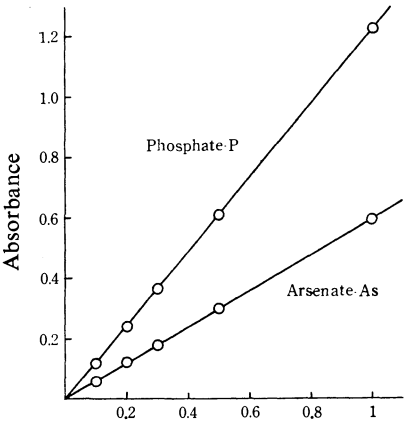


Fig. 7. Standard curves.

Interference

The detailed discussion of the successive isolation of phosphate, arsenate and arsenite

in the previous section suggests an applicability of the present method to the analysis of trace amounts of these ions in the presence of considerable amounts of germanate and silicate. This is also proved to be satisfactory by the results listed in Table I. Thus, 200 μg./l. each of arsenate-As and arsenite-As, 2 mg./l. of germanate-Ge, and 20 mg./l. of silicate-Si do not interfere with the determination of phosphate. One hundred micrograms of phosphate-P, 2 mg./l. of germanate-Ge, and 4 mg./l. of silicate-Si do not interfere with the determination of arsenate or arsenite, but 20 mg./l. of silicate-Si shows a marked negative interference; this is avoided by the extraction of molybdoarsenate at an increased concentration of ammonium molybdate (1.2%).

Large amounts of titanium(IV), vanadium(V) and tungsten(VI) interfere, but they are tolerated up to the concentrations of 20 μg./l., 20 μg./l. and 200 μg./l. respectively.

Sodium, potassium, calcium, magnesium, chloride, sulfate and nitrate cause no interference up to the concentrations found in sea water.

When a sample contains some oxidizing agent, there is danger that a part of the arsenite will be converted to arsenate during the process of analysis. The addition of a small amount of ascorbic acid will protect the arsenite from this oxidation.

Examples of the application of the present method to natural waters are listed in Table II.

The authors wish to thank Dr. Motoharu Tanaka for his many helpful discussions and suggestions during this work.

Chemical Institute
and Water Research Laboratory
Faculty of Science
Nagoya University
Chikusa-ku, Nagoya

On the Study of the Copper Chelates of Ephedrine and Related Compounds. II. The Crystal Structure of the Bis-l-ephedrine Copper(II) Chelate Benzene Clathlate

By Yoshiharu AMANO, Kenji OSAKI* and Tokunosuké WATANABÉ**

(Received April 23, 1964)

As is well known, when a copper(II) salt is added to an aqueous solution of *l*-ephedrine in the presence of alkali hydroxide, the color of the solution changes to blue-violet. If the mixture is extracted with *n*-hexane or benzene, a reddish-violet solution is obtained; from it well-defined crystals can be obtained. In a previous paper,[1] it was concluded that the crystal consisted of bis-*l*-ephedrine copper(II) chelate (abbreviated as ephedrine copper chelate in the following), and that the copper atom had a square-planar coordination.

Ephedrine copper chelate exhibits peculiar properties. It reacts at room temperature with carbon tetrachloride of other halogenated hydrocarbons, yielding chloride ions and the oxidation products of ephedrine.[2] It dissolves easily in non-polar solvents such as *n*-hexane in spite of having hydrophillic groups in its molecule.

In order to clarify the above-mentioned peculiar properties of the ephedrine copper chelate, a crystal structure analysis of this compound was conducted; the experimental results obtained and a discussion based on the structure will be presented below.

Experimental

Efforts were made to prepare single crystals of the ephedrine copper chelate, crystals suitable for X-ray crystal structure analysis. From a benzene solution, hexagonal plates or prisms a deep violet in color were obtained. These crystals have a cleavage plane parallel to the hexagonal basal plane. The examination, by means of ultraviolet absorption, of the volatile components of the solution obtained by dissolving these crystals in *n*-hexane showed the presence of a benzene molecule in the crystal. The results of the elemental analysis also suggest that the crystal contained two benzene

* Present address: Faculty of Pharmaceutical Sciences, Kyoto University, Kyoto.
** Present address: College of General Education, Osaka University, Toyonaka, Osaka.

1) T. Uno and Y. Amano, *Yakugaku Zasshi*, **82**, 1176 (1962).
2) Y. Amano and T. Uno, to be published.

TABLE I. ELEMENTAL ANALYSIS

	C, %	H, %	N, %	Cu, %
Found	65.11	7.232	6.287	14.34
Calcd.(1)	61.28	7.200	7.146	16.21
Calcd.(2)	64.91	7.256	6.310	14.31

(1) $(C_{10}H_{14}ON)_2 \cdot Cu$
(2) $(C_{10}H_{14}ON)_2 \cdot Cu \cdot 2/3C_6H_6$

molecules per three chelate molecules. The results of the elemental analysis are shown in Table I.

The unit cell dimensions were determined by precession photographs. These photographs show that the Laue symmetry of the crystal is $\bar{3}$m. There remain two possible space groups, P312 and P321, on the basis of the extinction rules and the Laue symmetry. In these two space groups, the mirror planes of the reciprocal lattice have different orientations with respect to the crystal axes. From the examination of the symmetry of the reciprocal lattice, it was found that .there are mirror planes parallel to the a*c* planes. Therefore, it was concluded that the space group is P321-D_3^2 and that the a-axis is a two-fold axis. The density as calculated from the composition, $(C_{10}H_{14}ON)_2 \cdot Cu \cdot 2/3C_6H_6$, as was suggested by the elemental analysis, agreed with the observed value.

The specimens for the intensity measurements were cut out along the a- and c-axes from hexagonal plates or prisms. The sets of intensities were obtained from equi-inclination Weissenberg photographs using both multiple-films and varying exposures, with copper $K\alpha$ radiation filtered through nickel foil. The zeroth to third layers about the a-axis and the zeroth layer about the c-axis were recorded.

The intensities were estimated by visual comparison with a calibrated intensity scale prepared with the same specimen and reduced to the same scale.

Corrections for Lorentz and polarization factors were applied in the usual way, but none were made for absorptions since μr is 0.37 for the a-axis specimen and 0.47 for the c-axis specimen. The preliminary scale factor and temperature factors were determined by Wilson's method and were further improved during the later stages of the refinements. The crystallographic data are shown in Table II.

TABLE II. CRYSTALLOGRAPHIC DATA

$a = 11.89$ Å $\quad c = 15.32$ Å
Laue symmetry : $\bar{3}$m
Space group : P321-D_3^2
Three formula units per unit cell
Volume of unit cell : 1875.7 Å^3
Linear absorption coefficient for Cu$K\alpha$ rapiation : 14.78 cm^{-1}
Density
observed : 1.20 g./cm^3
calculated : 1.18 g./cm^3

TABLE III. COMPARISON OF STATISTICALLY DISTRIBUTED BENZENE MOLECULE AND FOUR SETS OF FIXED BENZENE MOLECULE

	Coordinates			Corresponding R value
	x	y	z	%
1	Statistically distributed			16.3
2	0.3333	0.5482	0.3650	16.3
	0.2149	0.5482	0.3650	
3	0.2967	0.5343	0.3650	15.9
	0.2011	0.5699	0.3650	
4	0.2636	0.5302	0.3650	16.5
	0.1968	0.5985	0.3650	
5	0.2365	0.5343	0.3650	16.2
	0.2011	0.6305	0.3650	

TABLE IV. THE FINAL ATOMIC COORDINATES AND THE THERMAL PARAMETERS

Atom	Coordinates			Thermal parameter
	x	y	z	
Cu	0.0000	0.1977	0.0000	7.3
O	−0.1084	0.1260	0.0980	6.7
N	0.1446	0.2910	0.0906	6.2
C(1)	−0.2444	0.1517	0.2403	7.3
C(2)	−0.3169	0.1552	0.3141	8.2
C(3)	−0.2766	0.1541	0.4025	10.1
C(4)	−0.1637	0.1497	0.4096	10.3
C(5)	−0.0855	0.1552	0.3368	8.2
C(6)	−0.1184	0.1504	0.2501	7.9
C(7)	−0.0355	0.1498	0.1761	6.5
C(8)	0.0782	0.2982	0.1707	8.1
C(9)	0.0337	0.3986	0.1593	8.0
C(10)	0.2561	0.4170	0.0633	7.8
C(B1)	0.3333	0.5482	0.3655	9.6
C(B2)	0.2967	0.5343	0.3655	9.6
C(B3)	0.2636	0.5302	0.3655	9.6
C(B4)	0.2365	0.5343	0.3655	9.6
C(B5)	0.2149	0.5482	0.3660	9.3
C(B6)	0.2011	0.5699	0.3660	9.3
C(B7)	0.1968	0.5985	0.3660	9.3
C(B8)	0.2011	0.6305	0.3660	9.3

The Determination of the Structure

The number of atoms in the unit cell gives the following information. The copper atoms must lie on the two-fold symmetry axis, so that the chelate molecule has the two-fold rotational symmetry. The center of the solvated benzene molecule lies on the three-fold axis.

Because the a-axis is shorter than the c-axis, we first attempted to proceed with a projection corresponding to the ($h0l$) reflections and to use the other layer-line spectra to confirm the structure. The sharpened Patterson synthesis using the ($h0l$) reflections showed that the copper atom was located at a position with $x=0$, $y=0.1935$, and $z=0$. This conclusion agreed with the results of the vector analysis.

A trial model was set up from this Patterson map using the vector convergence diagram method and also on the basis of the molecular packing. The solvated benzene molecules were disregarded at this stage.

On the basis of this trial model, the values of the $F(h0l)$ were calculated. From a comparison of these with the observed structure amplitudes, it was possible to deduce the signs of about one-third of all the $F(h0l)$ reflections obtained. Using these signs, the first Fourier synthesis was calculated. In this projection, there appeared, in addition to the expected peaks of the atoms of the copper chelate, an extended hill-like cluster almost perpendicular to the z-axis and symmetrically situated with respect to the three-fold axis. It was suggested that this hill-like cluster be the projected structure of the solvated benzene molecule. This was thought admissible because the space which the benzene molecule is to occupy corresponds to quite a large hole between the copper chelates. It was further suggested that the six carbon atoms of the benzene molecule are statistically distributed along the ring which has a radius of 1.39Å. Therefore, the effect of the benzene molecule was added in the following computations of the structure factor, where each carbon atom was assumed to lie at four equally-spaced positions with a weight of 1/4.

After several successive Fourier and difference Fourier refinements, the R values for 259 $F(h0l)$ and 49 $F(hk0)$ reflections became 26.5% and 18.8% respectively.

The Refinement of the Structure

The positional and thermal parameters were refined by the three-dimensional least-squares method using the $(h0l)$, $(h1l)$, $(h2l)$ and $(h3l)$ structure factors. The positional and isotropic individual thermal parameters were refined by disregarding the off-diagonal terms other than the x, y-interaction terms, to minimize the value of $\sum w||F_o|^2-|F_c|^2|^2$. The weights applied to the terms were:

TABLE V

h	k	l	$\|F_o\|$	F_c	h	k	l	$\|F_o\|$	F_c	h	k	l	$\|F_o\|$	F_c
0	0	2	4.77	−12.78	1	0	−3	34.87	32.73	2	0	−7	28.71	36.31
		3	74.97	82.79			−4	39.29	40.97			−8	7.53	−6.11
		4	62.25	−67.84			−5	10.84	−11.99			−9	11.80	−18.63
		5	50.11	58.71			−6	33.37	37.50			−10	12.88	−18.52
		6	17.90	19.72			−7	18.50	25.38			−11	20.13	−6.32
		7	4.77	4.72			−8	0.00	3.47			−12	12.94	−9.83
		8	29.72	30.92			−9	25.79	31.44	3	0	0	81.71	−84.56
		9	15.27	15.93			−10	5.08	3.67			1	9.74	8.64
		10	21.07	22.31			−11	14.44	16.32			2	1.80	6.62
		11	29.96	32.04			−12	18.59	22.46			3	11.24	−15.69
		12	34.70	41.05			−13	3.44	−3.62			4	27.29	25.70
		13	12.54	17.27	2	0	0	119.84	−113.35			5	8.63	6.85
		14	0.00	−1.93			1	51.79	55.98			6	12.57	15.77
		15	0.00	−2.19			2	98.67	−94.17			7	8.02	8.95
		16	0.00	2.92			3	34.52	−36.30			8	16.38	−16.55
		17	6.37	4.42			4	11.40	−5.70			9	10.28	−14.33
1	0	1	92.99	88.76			5	3.47	−3.52			10	9.82	−12.56
		2	16.90	16.48			6	22.61	28.43			11	6.94	−9.75
		3	45.75	−43.55			7	23.67	−21.09			−1	40.54	−41.80
		4	10.40	12.80			8	10.50	−11.99			−2	28.38	−29.00
		5	38.09	37.37			9	5.58	3.55			−3	47.93	−47.97
		6	11.68	−8.72			10	3.66	5.63			−4	22.17	−23.45
		7	14.16	16.90			11	6.73	−6.85			−5	0.00	6.45
		8	17.36	17.89			12	5.78	−8.58			−6	15.99	19.63
		9	10.91	10.64			13	7.33	2.91			−7	0.00	6.97
		10	26.84	33.88			−1	78.20	−87.20			−8	0.00	5.22
		11	7.78	18.65			−2	68.01	79.66			−9	9.64	−11.39
		12	14.05	13.06			−3	12.06	−12.34			−10	10.72	−8.84
		13	8.42	9.74			−4	15.74	20.31			−11	5.65	−2.80
		−1	88.87	85.50			−5	8.84	−8.52			−12	12.94	−12.58
		−2	35.13	34.46			−6	14.08	11.20	4	0	0	12.45	−10.64

TABLE V (continued)

h k	l	$\|F_o\|$	F_c	h k	l	$\|F_o\|$	F_c	h k	l	$\|F_o\|$	F_c
4 0	1	30.20	26.80	6 0	1	10.67	−12.88	8 0	−8	4.25	−1.86
	2	35.37	32.21		2	3.34	2.73	9 0	0	3.47	0.21
	3	45.83	46.67		3	11.93	11.49		1	6.00	4.05
	4	44.12	45.45		4	19.73	16.02		2	0.00	2.56
	5	16.27	15.30		5	19.26	18.90		3	0.00	−0.52
	6	35.13	33.59		6	16.20	16.49		4	0.00	−5.94
	7	15.67	14.17		7	19.82	18.23		5	0.00	1.40
	8	4.59	−2.70		8	8.38	4.33		6	7.33	4.93
	9	0.00	−0.28		9	10.18	6.03		7	0.00	1.27
	10	0.00	−1.00		10	12.06	10.74		8	7.47	6.48
	11	10.63	8.17		11	8.17	5.50		9	7.85	5.71
	12	3.44	4.32		−1	33.83	33.78		−1	4.89	3.76
	13	3.47	4.93		−2	29.52	27.74		−2	10.67	10.04
	14	8.34	7.08		−3	27.19	19.32		−3	11.51	11.55
	−1	2.05	−6.67		−4	5.24	10.85		−4	5.50	9.87
	−2	17.36	13.88		−5	10.67	10.67		−5	0.00	−0.31
	−3	8.70	13.00		−6	7.50	11.36		−6	0.00	0.62
	−4	7.82	6.90		−7	8.42	11.54		−7	2.41	3.02
	−5	38.81	38.86		−8	4.03	1.08	10 0	0	8.76	1.92
	−6	27.49	31.64		−9	0.00	4.68		1	11.41	7.54
	−7	9.64	13.18		−10	7.33	8.40		2	10.28	8.96
	−8	19.45	23.96		−11	3.47	2.11		3	5.90	2.47
	−9	10.55	13.33		−12	7.67	5.93		4	8.93	5.59
	−10	8.24	10.15		−13	7.75	7.25		5	9.96	6.38
5 0	0	32.80	31.61		−14	4.89	3.19		6	7.96	5.82
	1	10.28	2.53	7 0	0	16.45	19.32		7	6.29	5.58
	2	53.92	55.73		1	5.21	1.57		8	4.25	3.80
	3	30.15	27.39		2	0.00	−4.69		9	2.80	2.84
	4	38.09	32.15		3	0.00	−5.80		10	2.60	1.73
	5	55.25	54.04		4	6.29	−6.00		−1	10.01	3.93
	6	44.27	36.07		5	8.51	−5.94		−2	9.08	3.94
	7	27.40	25.27		6	13.40	−16.67		−3	7.62	6.76
	8	17.19	17.24		−1	0.00	0.87		−4	5.33	4.96
	9	9.69	5.13		−2	0.00	4.00		−5	5.26	4.02
	10	8.56	1.52		−3	0.00	4.40		−6	9.47	5.63
	11	11.51	9.28		−4	0.00	−4.40		−7	7.72	3.80
	12	6.52	6.19		−5	8.51	−6.61		−8	4.25	3.15
	13	0.00	3.79		−6	19.23	−18.64		−9	2.80	2.28
	14	6.62	6.53		−7	10.92	−8.42		−10	4.49	2.98
	15	5.31	5.23		−8	4.21	−2.26		−11	3.98	2.44
	16	4.28	4.08	8 0	0	0.00	3.51	11 0	0	0.00	−0.66
	−1	65.56	69.61		1	8.38	12.20		1	0.00	0.71
	−2	10.90	10.13		2	0.00	−7.37		2	7.96	6.36
	−3	24.23	25.07		3	0.00	−3.74		3	8.71	6.44
	−4	33.91	36.41		4	9.84	−7.46		4	7.35	4.48
	−5	35.60	37.59		5	15.27	−15.58		−1	0.00	0.87
	−6	34.00	35.42		6	8.80	−8.32		−2	0.00	−1.14
	−7	18.91	20.17		7	0.00	−0.51		−3	0.00	−0.56
	−8	17.89	19.03		8	8.17	5.61		−4	0.00	1.04
	−9	11.44	9.45		−1	10.63	−5.80		−5	5.50	2.75
	−10	9.50	8.71		−2	7.01	−1.46		−6	4.84	3.67
	−11	8.46	7.46		−3	4.72	−5.24		−7	4.21	3.01
	−12	9.19	5.89		−4	0.00	3.54		−8	4.28	2.62
	−13	11.39	9.54		−5	4.18	−3.02		−9	3.47	2.03
	−14	6.17	5.54		−6	13.57	−11.54				
6 0	0	15.40	18.18		−7	9.84	−8.96				

TABLE V (continued)

h k	*l*	$\|F_o\|$	$\|F_c\|$	A_c	B_c
0 1	2	29.45	34.46	34.46	0.00
	3	35.55	32.73	32.73	0.00
	4	40.38	40.97	40.97	0.00
	5	10.18	11.99	−11.99	0.00
	6	35.02	37.50	37.50	0.00
	7	20.02	25.38	25.38	0.00
	8	0.00	3.47	3.47	0.00
	9	22.58	31.44	31.44	0.00
	10	9.74	3.67	3.67	0.00
	11	10.38	16.32	16.32	0.00
	−2	13.34	16.48	16.48	0.00
	−3	40.60	43.55	−43.55	0.00
	−4	7.20	12.80	12.80	0.00
	−5	35.82	37.37	37.37	0.00
	−6	9.71	8.72	−8.72	0.00
	−7	13.64	16.90	16.90	0.00
	−8	15.96	17.89	17.89	0.00
	−9	0.00	10.64	10.64	0.00
	−10	32.33	33.88	33.88	0.00
	−11	16.42	18.65	18.65	0.00
1 1	0	71.53	61.74	−41.37	45.15
	1	67.23	67.09	−37.12	55.87
	2	4.59	7.46	2.54	7.01
	3	38.69	36.46	30.81	−19.49
	4	7.66	11.86	−10.57	5.38
	5	28.65	30.42	2.92	30.28
	6	45.04	52.04	12.89	50.42
	7	21.80	27.81	−12.46	25.01
2 1	0	92.15	93.63	−30.60	88.49
	1	17.83	24.70	−22.64	9.87
	2	41.49	41.88	−14.54	39.27
	3	51.24	50.35	−8.10	49.70
	4	45.25	45.52	−9.07	44.61
	5	44.24	43.21	−6.30	42.74
	6	49.64	48.13	−28.18	39.02
	7	27.23	27.98	−18.65	20.86
	8	0.00	16.48	−15.80	4.70
	9	21.23	20.99	−12.12	17.14
	10	22.66	14.49	−9.28	11.13
	11	17.02	22.16	−18.53	12.16
	12	11.23	15.83	−5.83	14.71
	−1	93.90	96.34	−57.19	77.52
	−2	24.58	23.52	−22.29	7.49
	−3	36.75	33.35	−10.50	31.65
	−4	13.71	16.61	−5.91	15.52
	−5	25.70	27.07	−13.50	23.46
	−6	42.49	41.54	−27.24	31.36
	−7	13.73	21.43	−7.51	20.08
	−8	19.32	22.30	−12.17	18.69
	−9	20.38	23.15	−18.32	14.16
	−10	17.55	21.76	−12.51	17.80
	−11	16.15	17.89	−12.64	12.65
3 1	0	78.35	72.69	−8.75	72.16
	1	32.75	32.07	7.99	31.06
	2	18.58	22.80	22.76	−1.38
	3	23.79	22.54	7.26	21.34
3 1	4	30.84	33.73	−0.83	33.72
	5	25.54	24.34	−11.12	21.66
	6	20.93	18.90	−15.21	11.21
	7	14.64	13.94	1.41	13.87
	8	9.36	2.05	−1.88	0.81
	−1	41.56	43.02	−34.70	25.42
	−2	38.01	37.66	−27.97	25.20
	−3	17.51	18.06	−0.29	18.06
	−4	7.26	11.05	−9.42	−5.79
	−5	20.01	21.83	3.33	21.57
	−6	14.41	18.89	3.89	18.48
	−7	0.00	15.17	−10.32	11.11
	−8	13.23	12.51	4.15	11.80
4 1	0	26.41	21.45	20.17	7.30
	1	35.82	35.93	28.25	22.20
	2	30.67	31.74	28.10	−14.77
	3	24.71	23.00	20.38	−10.66
	4	12.98	17.62	17.61	0.59
	5	11.29	9.37	7.83	5.14
	6	17.41	17.62	16.22	−6.88
	7	12.57	17.68	15.76	−8.01
	−1	30.91	27.10	21.08	−17.03
	−2	16.20	22.73	7.85	21.33
	−3	23.45	22.72	21.47	7.41
	−4	28.45	35.36	35.15	3.81
	−5	19.55	17.07	15.96	6.05
	−6	21.57	17.13	16.02	−6.06
	−7	13.44	17.01	15.39	7.24
5 1	0	32.58	32.70	6.62	−32.02
	1	0.00	12.26	10.46	6.40
	2	0.00	6.55	2.80	5.92
	3	8.34	12.07	10.30	−6.28
	4	19.53	16.49	16.48	−0.57
	5	22.91	21.05	21.03	−0.79
	6	20.35	22.49	22.35	2.56
	7	14.50	17.81	17.78	1.10
	8	10.70	15.54	15.54	−0.26
	−1	35.11	26.11	20.56	−16.10
	−2	36.02	30.58	29.45	8.20
	−3	15.94	10.59	10.13	3.09
	−4	20.36	20.17	18.41	8.23
	−5	23.58	26.60	26.57	1.22
	−6	16.52	17.22	17.16	−1.43
6 1	0	0.00	4.57	−1.99	−4.11
	1	0.00	9.02	−1.73	8.85
	2	14.52	20.21	−6.82	19.02
	3	9.85	13.69	−9.54	9.81
	−1	0.00	4.76	1.01	4.65
	−2	19.36	11.33	9.20	6.62
7 1	0	15.94	6.29	−0.16	6.29
	1	0.00	4.70	0.60	4.67
	2	10.64	14.56	−0.11	14.56
	3	20.85	14.56	−4.74	13.77
	4	15.44	15.33	−5.25	14.40
	−1	24.58	21.99	−8.23	20.40
	−2	23.79	21.73	−16.33	14.33

TABLE V (continued)

h k	l	$\|F_o\|$	$\|F_c\|$	A_c	B_c	h k	l	$\|F_o\|$	$\|F_c\|$	A_c	B_c
7 1	−3	18.65	11.30	−9.09	6.70	3 2	0	49.68	45.88	44.31	−11.91
−1 2	3	37.26	36.46	30.81	19.49		1	24.57	20.78	18.40	9.66
	4	10.45	11.86	−10.57	−5.38		2	15.09	17.26	−15.74	7.07
	5	29.60	30.42	−2.92	−30.28		3	9.05	6.81	−5.38	−4.16
	6	45.12	52.04	12.89	−50.42		4	42.26	44.38	−44.37	−1.28
	7	24.28	27.81	−12.16	−25.01		5	40.20	36.21	−36.17	−1.78
0 2	2	77.10	79.66	79.66	0.00		6	17.37	18.35	−11.01	14.68
	3	15.38	12.34	−12.34	0.00		7	17.29	15.47	−14.45	5.52
	4	17.42	20.31	20.31	0.00		−1	9.83	13.39	−13.05	−3.00
	5	6.35	8.52	−8.52	0.00		−2	10.06	9.52	−6.77	−6.69
	6	9.89	11.20	11.20	0.00		−3	0.00	10.58	−7.68	−7.28
	7	31.32	36.31	36.31	0.00		−4	23.34	20.49	−20.25	−3.16
	8	0.00	6.11	−6.11	0.00		−5	22.47	18.88	−18.58	3.34
	9	0.00	18.63	−18.63	0.00		−6	26.06	27.24	−23.16	14.34
	10	22.05	18.52	−18.52	0.00	4 2	0	24.52	21.06	12.56	−16.91
	−2	89.19	94.17	−94.17	0.00		1	0.00	12.44	−8.09	−9.45
	−3	31.95	36.30	−36.30	0.00		2	0.00	8.96	−5.88	6.76
	−4	11.30	5.70	−5.70	0.00		3	0.00	4.28	0.10	−4.28
	−5	0.00	3.51	−3.52	0.00		4	15.66	15.26	−14.28	−5.36
	−6	23.72	28.43	28.43	0.00		5	14.42	14.65	0.95	−14.62
	−7	25.57	21.09	−21.09	0.00		−1	32.40	25.68	8.60	−24.19
1 2	0	91.28	93.63	−30.60	88.49		−2	31.09	26.59	−0.62	−26.58
	1	101.12	96.34	−57.19	77.52		−3	22.17	18.14	11.62	−13.93
	2	28.82	23.52	−22.29	7.49		−4	12.28	12.32	4.61	−11.42
	3	37.64	33.35	−10.50	31.65		−5	16.42	15.29	−14.56	−4.67
	4	16.96	16.61	−5.91	15.52		−6	22.81	19.47	−6.00	−18.52
	5	28.43	27.07	−13.50	23.46		−7	19.30	20.01	−9.79	−17.45
	6	43.17	41.54	−27.24	31.36	5 2	0	15.71	15.87	−15.74	−2.01
	7	17.60	21.43	−7.51	20.08		1	0.00	8.68	−1.87	8.48
	8	24.68	22.30	−12.17	18.69		2	18.44	21.74	−20.39	7.53
	9	26.23	23.15	−18.32	14.16		3	18.21	15.78	−15.20	4.27
	10	24.77	21.76	−12.51	17.80		−1	0.00	15.43	−8.55	−12.84
	11	21.51	17.89	−12.64	12.65	6 2	0	21.50	18.19	−12.83	12.88
	−1	21.62	24.70	−22.64	9.87		1	20.33	13.14	−4.46	12.36
	−2	44.23	41.88	−14.54	39.27		2	19.86	17.84	−4.81	17.18
	−3	54.27	50.35	−8.10	49.70		3	23.25	16.68	−12.95	10.52
	−4	50.70	45.52	−9.07	44.61		−1	25.92	16.12	−11.00	11.77
	−5	45.16	43.21	−6.30	42.74		−2	26.14	20.31	−17.49	10.33
	−6	52.35	48.13	−28.18	39.02		−3	23.25	17.85	−9.98	14.80
	−7	25.55	27.98	−18.65	20.86		−4	27.01	23.02	−9.08	21.16
	−8	12.34	16.46	−15.80	4.70		−5	20.29	14.30	−5.82	13.06
	−9	20.57	20.99	−12.12	17.14	7 2	0	25.92	16.17	−13.89	8.28
	−10	14.30	14.49	−9.28	11.13		1	15.64	11.80	−9.47	7.03
	−11	22.17	22.16	−18.53	12.16		2	13.62	5.51	−2.92	4.68
2 2	0	25.32	23.21	10.35	20.77		−1	22.12	14.99	−10.31	10.87
	1	45.90	46.60	−9.24	45.67		−2	21.55	15.47	−11.62	10.21
	2	41.26	38.32	−11.71	36.48		−3	20.99	15.22	−11.18	10.32
	3	42.58	34.56	−27.51	20.92	−1 3	2	23.19	23.52	−22.29	−7.49
	4	38.88	38.04	−17.63	33.71		3	37.62	33.35	−10.50	−31.65
	5	49.47	43.87	−26.13	35.24		4	18.88	16.61	−5.91	−15.52
	6	62.56	62.59	−54.78	30.27		5	29.53	27.07	−13.50	−23.46
	7	22.86	24.81	−18.43	16.60		6	45.66	41.54	−27.24	−31.36
	8	20.33	21.33	−5.81	20.52		7	21.68	21.43	−7.51	−20.08
	9	20.25	17.10	−3.81	16.67		8	24.62	22.30	−12.17	−18.69
	10	17.35	12.47	−3.74	11.90		9	28.13	23.15	−18.32	−14.16
	11	15.56	17.70	−4.80	17.04		10	23.88	21.76	−12.51	−17.80

TABLE V (continued)

h k	*l*	$\|F_o\|$	$\|F_c\|$	A_c	B_c
−1 3	11	17.99	17.89	−12.65	−12.65
	12	11.68	13.49	−9.69	−9.39
	−2	37.20	41.88	−14.54	−39.27
	−3	49.59	50.35	−8.10	−49.70
	−4	47.73	45.52	−9.07	−44.61
	−5	46.07	43.21	−6.30	−42.74
	−6	52.93	48.13	−28.18	−39.02
	−7	30.00	27.98	−18.65	−20.86
	−8	9.78	16.48	−15.80	−4.70
	−9	19.89	20.99	−12.12	−17.14
	−10	16.22	14.49	−9.28	−11.13
	−11	18.67	22.16	−18.53	−12.16
	−12	10.44	15.83	−5.83	−14.71
0 3	0	80.12	84.56	−84.56	0.00
	1	43.58	41.80	−41.80	0.00
	2	31.92	29.00	−29.00	0.00
	3	54.44	47.97	−47.97	0.00
	4	25.69	23.45	−23.45	0.00
	5	5.43	6.45	6.45	0.00
	6	19.52	19.63	19.63	0.00
	−1	9.85	8.64	8.64	0.00
	−2	5.02	6.62	6.62	0.00
	−3	14.13	15.69	−15.69	0.00
	−4	31.47	25.70	25.70	0.00
	−5	6.26	6.85	6.85	0.00
	−6	11.44	15.77	15.77	0.00
	−7	7.55	8.95	8.95	0.00
	−8	13.60	16.55	−16.55	0.00
1 3	0	79.88	72.69	−8.75	72.16
	1	47.11	43.02	−34.70	25.42
	2	42.00	37.65	−27.97	25.20
	3	22.02	18.06	−0.29	18.06
	4	7.02	11.05	−9.42	−5.79
	5	26.10	21.83	3.33	21.57
	6	16.85	18.89	3.89	18.48
	7	7.43	15.17	−10.32	11.11
	8	8.57	12.51	4.15	11.80
	−1	36.01	32.01	7.99	31.06
	−2	23.10	22.80	22.76	−1.38
	−3	28.87	22.54	7.26	21.34
	−4	37.44	33.73	−0.83	33.72
	−5	30.01	24.34	−11.12	21.66
	−6	23.83	18.90	−15.21	11.21
	−7	15.13	13.94	1.41	13.87
	−8	11.81	2.05	−1.88	0.81
2 3	0	41.83	45.88	44.31	−11.91
2 3	1	10.24	13.39	−13.05	−3.00
	2	0.00	9.52	−6.77	−6.69
	3	14.49	10.58	−7.68	−7.28
	4	23.35	20.49	−20.25	−3.16
	5	21.87	18.88	−18.58	3.34
	6	25.83	27.24	−23.16	14.34
	−1	26.21	20.78	18.40	9.66
	−2	12.76	17.26	−15.74	7.07
	−3	6.65	6.81	−5.38	−4.16
	−4	46.71	44.38	−44.37	−1.28
	−5	41.94	36.21	−36.17	−1.78
	−6	21.83	18.35	−11.01	14.68
	−7	10.86	15.47	−14.46	5.52
3 3	0	7.54	13.73	2.28	−13.54
	1	28.36	24.71	5.22	−24.15
	2	31.41	29.05	−10.61	−27.04
	3	28.80	27.85	−17.50	−21.66
	4	34.74	29.17	−16.13	−24.30
	5	39.13	35.63	−30.28	−18.78
	6	30.29	26.86	−24.16	−11.72
	7	22.52	18.66	−14.31	−11.97
	8	13.81	16.01	−5.14	−15.16
4 3	0	26.08	22.29	−18.91	−11.78
	1	27.16	21.74	−19.19	−10.20
	2	32.24	26.95	−14.99	−22.39
	3	26.25	20.92	−8.76	−19.00
	4	17.01	13.84	−9.88	−9.69
	5	22.64	20.08	−7.50	−18.63
	6	19.55	17.33	−5.19	−16.53
	7	11.52	11.58	−9.86	−6.06
	−1	25.58	20.40	−6.46	−19.35
	−2	29.72	25.50	−6.00	−24.78
	−3	33.54	28.09	−8.39	−26.81
	−4	27.78	23.51	−8.42	−21.95
	−5	19.74	18.44	−15.10	−10.58
	−6	20.12	18.15	−10.59	−14.74
	−7	19.66	20.91	−6.79	−19.77
5 3	0	9.15	4.98	−4.88	−0.96
	1	0.00	2.37	−2.18	−0.93
	−1	0.00	13.44	−13.01	−3.39
	−4	12.80	9.95	−8.96	4.34
	−5	0.00	3.94	−0.20	−3.94
	−6	10.19	5.47	3.03	−4.55
6 3	0	0.00	5.54	−1.48	5.34
	1	0.00	7.17	−2.83	6.59
	−1	11.29	10.78	−7.41	7.84

$w = 0.25$ for $|F_o| \leq 5$

$w = |F_o|/20$ for $5 \leq |F_o| \leq 20$

$w = 1.0$ for $20 \leq |F_o| \leq 30$

$w = 30/|F_o|$ for $30 \leq |F_o|$

After each cycle of the refinements, the positional and thermal parameters of the atoms of the copper chelate were improved. Those of the carbon atoms of the benzene molecule, however, showed unreasonable shifts. Therefore, no shifts were applied to the parameters of the benzene molecule. After several cycles of least-squares, the R value was reduced to 16.3% for all the reflections used, including the non-observed reflections.

At this stage, we tried to see if any model of the structure with the benzene molecule at

a definite orientation would improve the structure factors. The structure factors were calculated by using the parameters obtained for the atoms of the copper chelate, and by adding the contribution of the benzene molecule in either of the four sets of coordinates listed in Table III. No significant differences were found in the R values among the four sets of the carbon atoms and the statistical model described earlier. However, the R value increased to 23.1% if we disregarded the contributions of the benzene molecule. The final set of positional and thermal parameters corresponding to the statistical model is listed in Table IV. The observed and calculated structure factors are reproduced in Table V.

A Description and Discussion of the Structure

The intermolecular bond lengths and angles of the copper chelate molecule as calculated on the basis of the above atomic parameters are shown in Fig. 1. Although the accuracy of the results is not still adequate to enable us to discuss the bond lengths and angles quantitatively, the overall stereochemical relation of the atoms in the copper chelate molecule and the mutual disposition of the copper chelates are clear.

Molecular Structure. — In a previously reported paper,[1] it was concluded that the hydrogen atom of the alcoholic hydroxyl group of the ephedrine molecule was replaced by the copper ion in the chelate formation, and also that the chelate ring was built by a four-coordinated square-planar configuration. The results of the X-ray crystal structure analysis not only confirmed the above prediction, but also led to useful information about the structure, as will be described below.

The copper atom lies on the two-fold rotational axis and is surrounded by two oxygen and two nitrogen atoms in a square configuration. These four atoms are almost coplanar with the copper atom, and there are no atoms

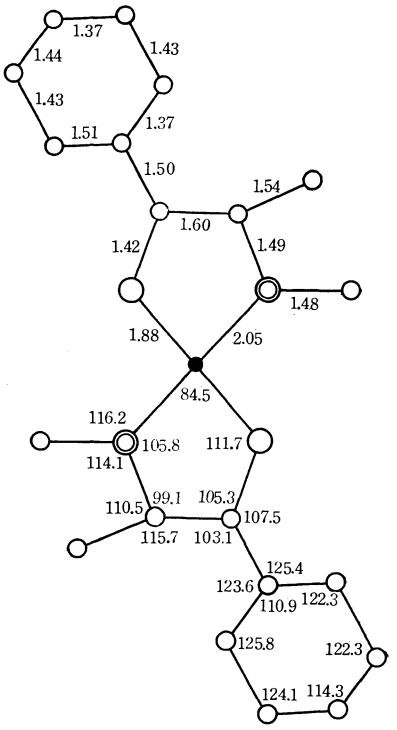


Fig. 1. Interatomic bond lengths and angles.

between the copper atoms in the adjacent unit cells in the direction perpendicular to the plane of the square. As is well known, however, the majority of cupric compounds, have distorted octahedral configurations, in agreement with the conclusions of the theory of Orgel[3] based on the Jahn-Teller effect.[4] In the ephedrine copper chelate, therefore, its configuration can be regarded as a limiting case of the usual distorted octahedral configuration with two ligands completely removed. This configuration of the copper chelate coordinated through the alcoholic hydroxyl group of the ephedrine molecule, without using two available orbitals, would be related to the peculiar property of the ephedrine copper chelate, namely, its reactivity with the halogenated hydrocarbons,[2] and also

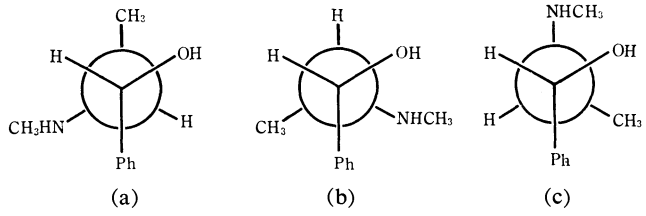


Fig. 2. Conformations of ephedrine molecule.

3) L. E. Orgel, *J. Chem. Soc.*, **1952**, 4756.

4) L. E. Orgel and J. D. Dunitz, *Nature, Lond.*, **179**, 462 (1957).

to its light absorption associated with copper-(II), which has its maximum at 518 mμ.

With respect to the ephedrine molecule, there are three possible conformations (cf. Figs. 2 (a), (b) and (c)). Conformation (a) has been proposed for the free ephedrine molecule by Close.[5] For the ephedrine molecule of the copper chelate, however, there remain two possible conformations, (b) and (c), bacause the nitrogen and oxygen atoms must be close together to form a chelate with the copper atom. The conformation of the ephedrine molecule of the copper chelate as found by present investigation is concluded to be the conformation (c), which is the same as that reported for ephedrine hydrochloride.[6]

Intermolecular Relation of the Chelate.— Although the positions of the hydrogen atoms were not determined, the existence of the hydrogen bonds can be inferred from the observed interatomic distances and from the possible distribution of the hydrogen atoms. In this crystal, three chelate molecules related by the three-fold symmetry form a trimer structure by means of six hydrogen bonds, as is shown in Fig. 3. In this trimer structure, the normals of the three square planes formed by the copper, oxygen and nitrogen atoms point to the three-fold symmetry axis. The distance between the two copper atoms in the trimer molecule is 4.07Å, which is the shortest copper-copper atom distance in this crystal. There will be no direct coupling between these copper atoms. The main force forming the trimer structure would be the six intermolecular hydrogen bonds of the NH···O type.

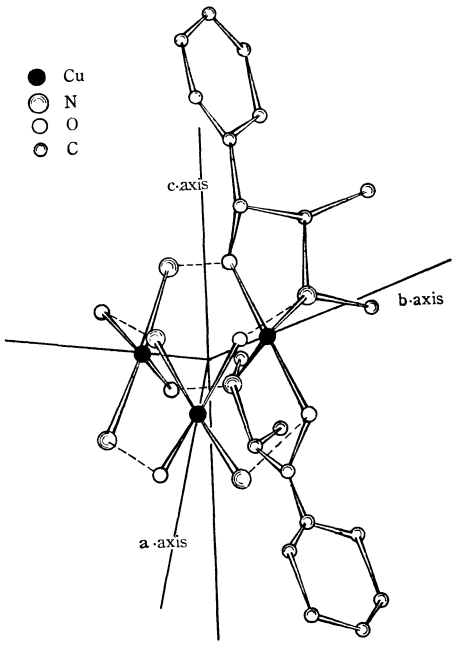


Fig. 3. Trimer structure of chelate molecule.

An infrared absorption spectrum of the crystal had already shown the presence of a hydrogen-bonded N–H stretching band, the type of molecular association which existed in the crystal had not yet been determined. This problem can now be interpreted, without any doubt, on the basis of the trimer structure of the chelate molecule described above. The observed absorption frequeny, 3130 cm^{-1}, in the infrared absorption spectrum agrees well with the value

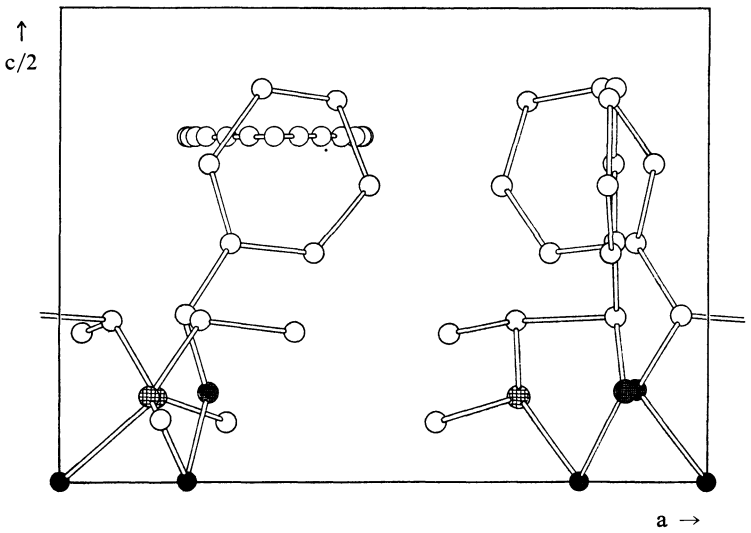


Fig. 4. Projection along b-axis.

5) W. J. Close, *J. Org. Chem.*, **15**, 1131 (1950).

6) D. C. Phillips, *Acta Cryst.*, **7**, 159 (1954).

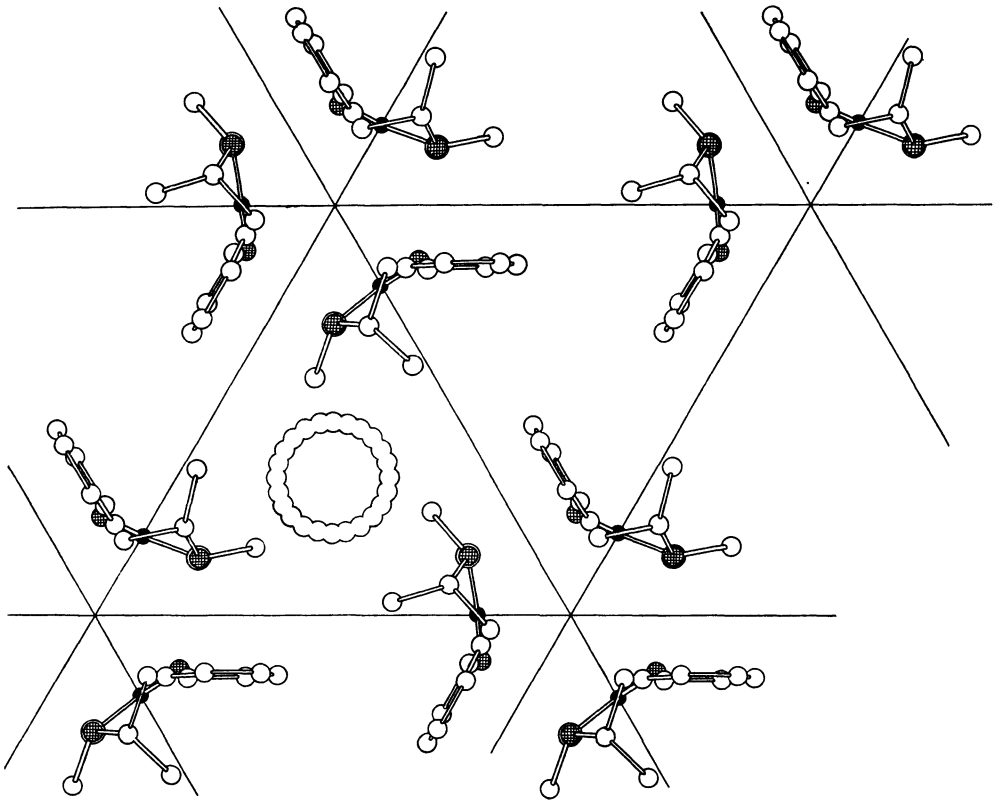


Fig. 5. Bounded projection $B(x, y;\ z=0 \rightarrow z=1/2)$.

obtained from the intermolecular N(H)–O bond length (2.87Å), using the table given by Nakamoto et al.[7]

The ephedrine copper chelate is easily soluble in non-polar solvents, such as *n*-hexane or benzene. This indicates that the ephedrine copper chelate still retains its trimer structure in these solvents, because it is hardly acceptable that the monomer chelate molecule with hydrophillic groups would dissolve in non-polar solvents. In fact, the absorption spectrum of the crystal is almost identical with the spectrum of its *n*-hexane or benzene solution in the visible region.

Molecular Packing.—The arrangement of the trimer chelate molecules in this crystal structure leaves two large cavities in the unit cell; the benzene molecules are enclosed in these cavities (Fig. 4 and Fig. 5). This crystal can, therefore, be considered to be a sort of clathlate compound. Namely, the trimer chelate is the host, and the benzene the guest molecule. It may be suggested that these benzene molecules are also responsible for holding together the trimer chelate molecules by virtue of the van der Waals attraction forces. It is highly probable that they rotate or are distributed statistically about the symmetry axis.

Throughout this study, the calculation of the structure factor, the Fourier summation and the least-squares method were carried out on the NEAC 2203 and the NEAC 2206 at the Computation Center of Osaka University, using partial modifications of programs originaly written by one of the authors (K. O.).

Faculty of Pharmaceutical Sciences
Kyoto University
Sakyo-ku, Kyoto (Y. A.)

Depertment of Physics
Faculty of Science
Osaka University
Nakanoshima, Osaka
(K. O. & T. W.)

7) K. Nakamoto, M. Margoshes and R. E. Rundle, *J. Am. Chem. Soc.*, 77, 6480 (1955).

Studies of Crystal Hydrates. VII.[1] *The Dielectric Properties of Capillary Water in Single Crystals of* DL-$[Co(en)_3]Cl_3 \cdot nH_2O$*

By Hideaki CHIHARA, Setsuo OKAWA** and Syûzo SEKI

(Received May 1, 1964)

The molecules of water of crystallization in DL-$[Co(en)_3]Cl_3$ hydrate are packed in linear, four-lane array in cylindrical channels which extend in the direction of the crystallographic c axis of this hexagonal crystal.[2] The partial dehydration of the hydrate crystal does not produce any substantial change in its X-ray diffraction patterns; this suggests a zeolitic nature of the dehydration. The thermodynamic properties of the dehydration[3] are also consistent with the structural studies and, further, suggest that the water is in a state similar to capillary-condensed water, such as is found in zeolite minerals. Water molecules in zeolites are usually so mobile that they are detected by means of high-resolution nuclear magnetic resonance at room temperatures.[4] However, the structural studies of zeolites have not been successful in locating the water molecules in the crystal lattice, and even had this been done, the arrangement of water molecules would still be quite complex.

The water molecules in DL-$[Co(en)_3]Cl_3 \cdot nH_2O$, where n runs from 0 to 4, were located by the X-ray diffraction technique; a brief account of the structure and the arrangement of the water molecules has already been given in a previous paper.[3] An investigation into the extent to which these molecules are mobile in the crystalline channels was considered to be of interest; it was also thought that the dielectric absorption study would give us some clue to the mode of motion of the water molecules. A preliminary experiment on the dielectric absorption[3] has shown that a relaxation absorption occurs below room temperature in the radio frequency region; this merits more detailed systematic study.

Experimental

Material. — The powdered DL-$[Co(en)_3]Cl_3$ used was from the same source as has been described previously.[3] Single crystals were grown by slowly cooling the nearly-saturated solution from 40°C. at the rate of about 1°C/day. Hexagonal prism crystals about 1'' long and 3/4'' across were readily obtained; these were shaped with Emery powder and kerosene into disks about 1 mm. thick. Kerosene was washed with benzene, and the crystals were finally polished with a drop of water. The crystals were then stored over powdered DL-$[Co(en)_3]Cl_3 \cdot 3.6H_2O$ for at least a month prior to the measurements in order to secure a uniform water content throughout. In obtaining disks with (0001) faces, drops of water had to be used instead of Emery powder and kerosene because the crystal was readily cleaved parallel to the c axis.

Apparatus and Equipment. — Measurements of the dielectric constant and loss between 40 c./s. and 5 Mc./s. were made with a mutual-inductance bridge of the Cole type[5] (Ando Elec. Co., Model TR-1B), which works between 30 c./s. and 5 Mc./s. Oscillators were of the low-distortion type, General Radio 1301A and Ando Elec. GET-2. A Q-meter of the Yokogawa Elec. Works, Model QM-101, was used to determine rough estimates at higher frequencies in order to check the consistency.

The measuring electrodes were designed so as to chill the specimen close to 90°K and to secure good electrical contacts between the electrodes and the specimen at all temperatures by making allowance for the thermal expansion and contraction of the crystal. Several pieces of measuring apparatus of slightly different designs were constructed; the one which is illustrated in Fig. 1 is typical of them. Here, A is a bakelite base for an electron tube (type Z), C is the glass stem with six Ni lead wires fused in, D are mica-disk spacers, E is a brass electrode (high-impedance side) 5 mm. in diameter and 1 mm. thick, and H is the other electrode (low-impedance side) with a spring of music wire, G, underneath, one end of which is soft-soldered to the electrode, H, and the other end of which is soldered to the supporting brass plate, F. The lead wires J are brass rods 2 mm. thick and are connected to Ni wires at the upper ends with soft solder. The temperature of the crystal was measured with a copper-constantan thermocouple junction, I, which was attached to the lower electrode, H (electrically insulated).

* Read before the XVIIIth International Congress of Pure and Applied Chemistry, Montréal, Québec, Canada, August, 1961. Abstract of Paper A2-37.

** Present address: The Asahi Shimbun, Kawaramachi, Kyoto.

1) Part VI: This Bulletin, 32, 908 (1959).

2) K. Nakatsu, Y. Saito and H. Kuroya, ibid., 29, 428 (1956).

3) H. Chihara and K. Nakatsu, ibid., 32, 903 (1959).

4) R. Kiriyama, H. Kiriyama and T. Wada, 12th Annual Meeting of the Chemical Society of Japan, Kyoto, April, 1959. Abstract of Paper No. 4048.

5) R. H. Cole and P. M. Gross, Jr., *Rev. Sci. Instr.*, 20, 252 (1949).

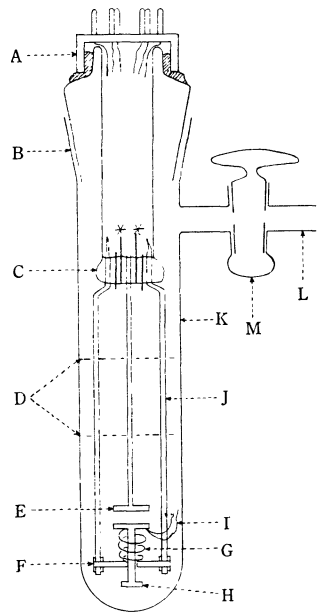


Fig. 1. Sample cell and electrodes for dielectric measurements.

The glass jacket, K, had a side tubing, L, which permitted control of the ambient pressure. The whole jacket was cemented to the six-legged base, A, with an Epoxy resin above the ground-glass joint, B. The apparatus was inserted in a Dewar vessel below the level of L and further placed in a shielded enclosure. To minimize the external disturbances, two of the fused lead wires (* marks in Fig. 1) and one of the thermocouple lead wires were electrically grounded.

Such construction of the apparatus, particularly the use of the base, A, proved to make the calibration procedure easy if a needle-and-mercury switch was employed to reduce the variation of the stray capacitance when the measuring cell was switched on and off.

Determination of the Cell Constants.—As there are no guard electrodes in the apparatus, the edge corrections had to be estimated experimentally. This was done in conjunction with the determination of the stray capacity by referring to the dielectric constant (5.30) of the (001) face of sodium chloride. The apparent total capacity of the cell was determined with single crystals of sodium chloride (aluminum foils of $1\times1\,cm^2$ on either side) of different thicknesses (between 0.99 and 1.37 mm.) inserted between the measuring electrodes. The apparent capacity, plotted against the reciprocal of the crystal thickness, gave a good straight line; the slope gave the cell constant, including the edge corrections, and the intercept gave the stray capacity. This was further checked favorably with a single crystal of potassium chloride ($\varepsilon'_{100}=4.41$).

Procedure and Determination of the Water Content of the Crystal in situ. — The specimen crystals were sandwiched, for the measurements, between aluminum foils $1\times1\,cm^2$ which were glued on the crystal with a very thin film of silicone grease. The thickness of the crystal was measured to within 0.01 mm. and was found to be uniform all over within these limits. The initial water content of the crystal was determined gravimetrically. The practical limit of the hydration of DL-$[Co(en)_3]Cl_3\cdot nH_2O$ is $n=3.6$ at room temperature, as may be seen from the sorption-desorption isotherm.[3] Crystals of a smaller degree of hydration were prepared in the dielectric apparatus. The side tubing (L in Fig. 1) was connected to a vacuum line through a trap with an appendix glass tube with narrow walls. The specimen having been placed, the glass jacket, K, was chilled with liquid nitrogen and evacuated. After the crystal had been warmed to room temperature, some water of crystallization was distilled into the trap cooled with liquid nitrogen for a variable length of time. The distilled water was then recollected in the appendix tube, which was then fused off and weighed. The same procedure was repeated in situ after dielectric measurements had

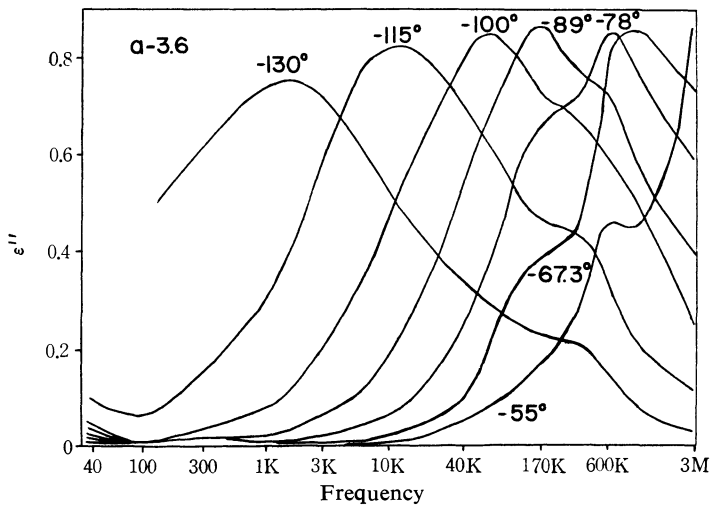


Fig. 2. Dielectric loss of specimen a-3.6.

been made at particular water contents, the final weight of the crystal being used to monitor the accuracy of the amounts of the water distilled between the successive series of dielectric measurements. Usually the total weight of the trapped water and the weight loss of the crystal agreed to within several parts per cent. Where the rate of dehydration is high (for a large n value) it was necessary to cool the crystal during the distillation. For crystals with (0001) flat faces, the distillation was slower than for those with $(10\bar{1}0)$ faces. After a certain amount of dehydration, the stopcock, M, was closed and the crystal was allowed to regain its transparency (quick dehydration often made the surface of the crystal opaque). It took about a week for a new equilibrium to be achieved. Dielectric measurements were made in most cases with a rising temperature at about 1 deg./min. from -170°C at a prefixed frequency. In one case, at -78°C, the apparatus was immersed in a dry ice-petroleum benzine mixture and the frequency was scanned from 40 c./s. to 3 Mc./s. in order to compare it with the other measurements.

Experimental Results and Discussion

The experimental results were converted to plots of ε' or ε'' as a function of the frequency at several selected temperatures; some of them are shown in Figs. 2 through 5, where a-3.6, for example, denotes that the external electric field was perpendicular to the $(10\bar{1}0)$ or a plane (i.e., perpendicular to the axis of the channel) and that the water content of the crystal was 3.6 mol. per formula unit of the salt.

The anomalous dispersion and absorption were found to depend on the water content of the crystal and are apparently associated with some motion of the water molecules in the channels. The wavelengths and the temperatures where the absorption is seen are low for the water of crystallization. This suggests considerable mobility in the water molecules. Thus, the frequency of the maximum absorption, when extrapolated to room temperature, comes very close to the critical frequency for liquid water.[3)]

There are two absorptions in the frequency range examined; one is larger than the other and is markedly displaced to higher frequencies at higher temperatures. The smaller peak (300 to 600 kc.) does not seem to move with the change in temperature, although it seems to change with the water content. This temperature-independent absorption is rather difficult to interpret.* Therefore, we will here consider only the temperature-dependent part of the dielectric absorption.

The anisotropy of the absorption is rather small. The only difference is in the additional large dielectric loss, which increases towards lower frequencies when the electric field is

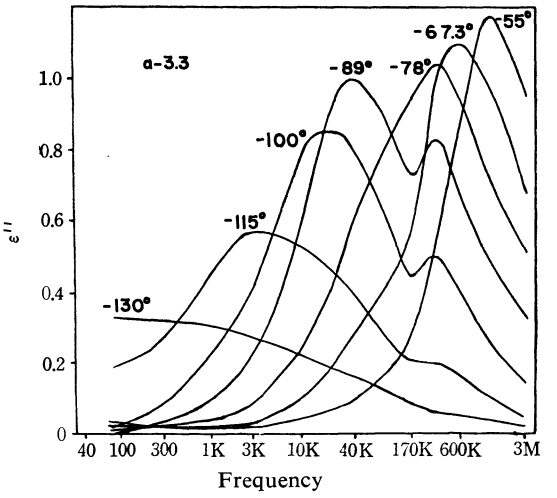


Fig. 3. Dielectric loss of specimen a-3.3.

parallel to the crystallographic c axis (see Fig. 5 for the results with c-3.6). This additional loss is most probably due to d.c. conductivity; it is also seen in a-2.7 and to a much smaller extent in a-3.6. The appearance of d.c. conductivity in the "a" specimens indicates that the crystal starts to fissure as the water of crystallization is successively removed. The d.c. conductivity would thus be due to the grain-boundary diffusion of water in the "a" specimens. The "c" specimens, on the other hand, shows a large d.c. conductivity, even with a good crystal; this may be reasonably accounted for by the ionic conduction due to proton jumps through the hydrogen bond between α and β sites in cooperation with the rotation of water molecules at both types of sites.

The shape of the absorption curve changes with the temperature, as Fig. 3 shows. It generally becomes sharper at higher temperatures; this tendency is more pronounced as the water content is decreased.

The main dielectric loss peak is the relaxation absorption due to the hindered rotation of the water molecules. The relaxation is

* On the basis of the crystal structure described previously,[3)] two possibilities which would give rise to the almost temperature-independent absorption were considered. One is the rotational isomerism between the two gauche configurations of ethylenediamine units that coordinate a Co^{3+} ion. However, such isomerism has to take place in synchronism at least among the three ethylenediamine molecules belonging to the same Co^{3+} ion. The other possibility is the rotation of the water molecules at the α sites about the axis of the hydrogen bond, O-H·····Cl^-. Because the other hydrogen atom of this water is only very weakly engaged in the O-H·····O hydrogen bond to a water molecule at a β site, such axial rotation would require a very small activation energy, which in turn might cause the absorption to be almost independent of the temperature. While this seems to be a plausible explanation, the frequencies at which the absorption is observed are too low for such a mechanism.

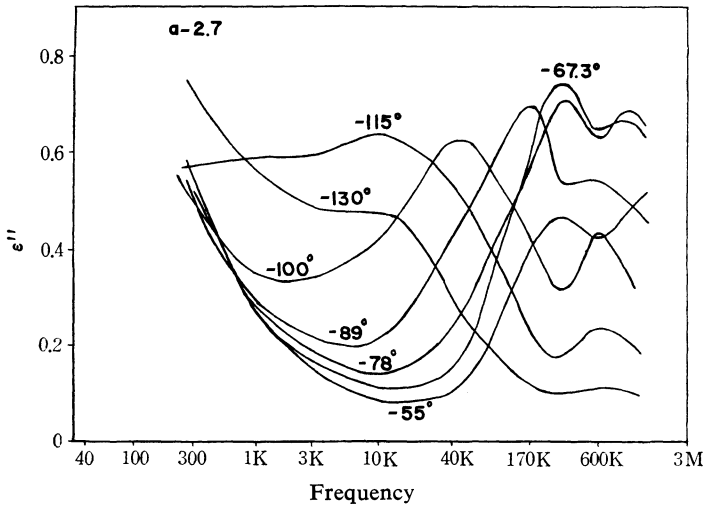


Fig. 4. Dielectric loss of specimen a-2.7.

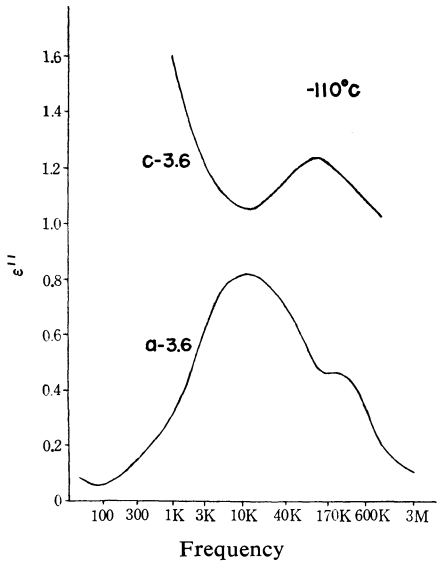


Fig. 5. Comparison of dielectric loss of specimens a and c.

not, however, that of a simple mechanism, as the shapes of the semi-circular Cole-Cole plots show in Figs. 6 and 7. Their asymmetric shape is, of course, partly due to the inclusion of the temperature-independent loss in the plots, but it also suggests a distribution of the relaxation times. The so-called activation plots of the log of the frequency that gives maximum ε'' versus $1/T$ are linear and the activation energies were obtained therefrom (Table I). The location fo the absorption maxima for a-2.7 was determined with difficulty; therefore, its activation energy may be in error by as much as 1 kcal./mol. It would be interesting to note a correlation between the activation energies and the differential heat of hydration or dehydration; either quantity shows a minimum or maximum between $n=2$ and 3. Generally these activation energy values are consistent with a mechanism of the molecular rotation of water accompanying the dissociation of several weak hydrogen bonds.

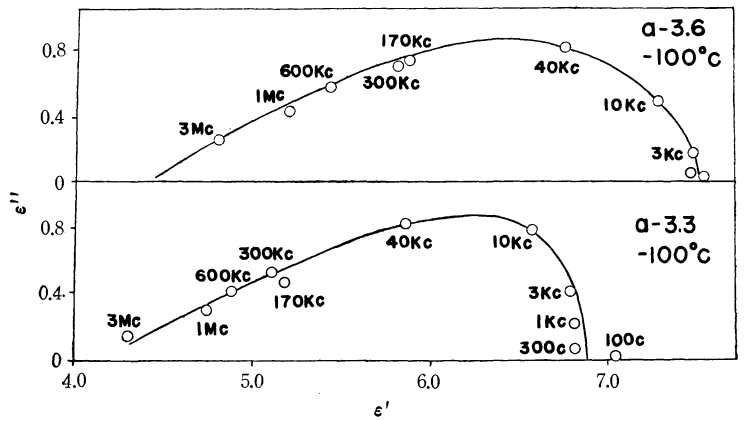


Fig. 6. Cole-Cole diagrams of specimens a.

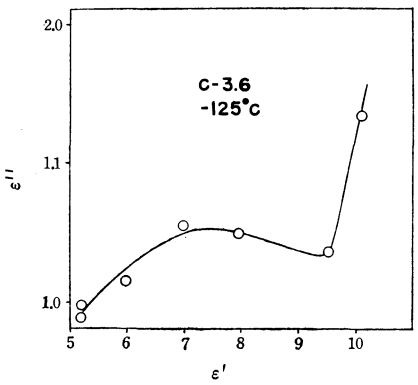


Fig. 7. Cole-Cole diagram of specimen c.

TABLE I. ACTIVATION ENERGIES (kcal./mol.)

a-3.6	7.3	c-3.6	5.6
a-3.3	7.9	c-2.9	4.9
a-2.7	4.7	c-0.43	5.5
a-0.9	6.8	c-0.27	8.3

There is one feature of interest in the temperature dependence of the maximum of ε'', as is most evident in Fig. 3. The maximum of ε'' increases with the temperature as the absorption becomes sharper; its rates of increase are different above and below about $-90°C$. Such differentce in behavior is also seen in the static dielectric constant, ε'_0 and these are compared in Fig. 8. There is a sharp break in ε'_0 at $-90°C$ as well as in ε''_{max} for the specimen a-3.3. In contrast, ε'_0 for the specimen a-3.6 decreases linearly as the temperature is raised with the same slope as does ε'_0 for a-3.3 above $-90°C$. Such a decrease is

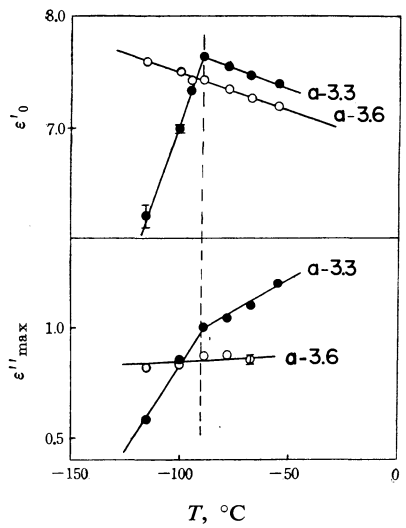


Fig. 8. Static dielectric constants and the loss maxima as a function of temperature.

due to thermal agitation opposing the static polarization. We shall now examine the structural mechanism in which a break point in ε'_0 appears with a-3.3. The two possible sites, α and β, for water molecules should have different potential energies; the β sites become stable only after the surrounding α sites have been occupied by water molecules. There must thus be an equilibrium partition of water molecules for a fixed total number of water molecules between the two types of sites, a partition governed by the Boltzmann distribution. The potential energy at a β site depends on the configuration of the environment and, therefore, has a certain distribution. At the lowest temperatures, the α sites will be almost filled if n is larger than 3, while a fraction of the β sites will remain vacant. Thus, the molecules are more or less fixed rigid, giving a small static polarization. As the temperature is raised, some molecules at the α sites would be vaporized into the β sites, leaving 'defects' behind at the α sites. When this occurs, an average β site molecule will see a potential field which is relaxed to some extent because of the defect formation. Thus the static dielectric constant will tend to increase until a critical temperature ($-90°C$ for $n=3.3$) is reached, at which the maximum possible number of O–H groups can be oriented in the direction of the applied electric field either through the dissociation of O–H··· O hydrogen bonds or through the rotation of water molecules and the reformation of the hydrogen bonds, the number being consistent with the equilibrium partition of molecules between the α and β sites.

Assuming that there are two different states of minimum potential energies, corresponding to different hydrogen bond schemes, we may estimate the difference in the potential energies by a formal application of a plot of $\log \varepsilon'' T$ against $1/T$.[6] Figure 9 shows the results thus obtained; this, however, should not be considered as representing the potential curve of a molecule but be regarded as the total potential energy of the assembly of water molecules. The potential energy difference of a-3.3 drops by about 0.7 kcal./mol. from 1.6 to 0.9 kcal./mol. at $-90°C$, at which kT_c amounts to about 0.4 kcal./mol.

When the water content is larger, say, when $n=3.6$, this critical temperature would be lowered because the number of vacant β sites is much smaller. This may be a reason for the failure to observe a break in ε'_0 for a-3.6. Such a mechanism of defect formation and the aquisition of molecular mobility is also

6) J. S. Dryden and R. J. Meakins, *Rev. Pure Appl. Chem.*, 7, 15 (1957).

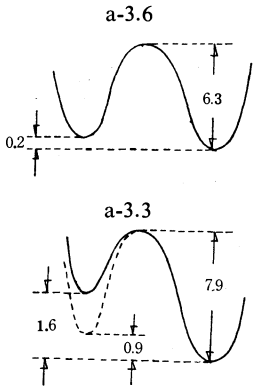


Fig. 9. Schematic potential energy curves for the assembly of water molecules.
—— Below −90°C, - - - Above −90°C

related to the results of thermodynamic investigation, in which an isothermal order-disorder phenomenon was observed in the differential heat and entropy of sorption of water by the anhydrous crystal.[3] It is possible that the transition phenomenon found here by the dielectric measurements may have some consequences on such other properties as the heat capacity of the partly hydrated crystal of this salt.

Summary

The dielectric constant and loss of single crystals of DL-$[Co(en)_3]Cl_3 \cdot nH_2O$ have been measured between −150°C and room temperature in the frequency range 40 c./s. and 3 Mc./s. The water content, n, was varied from 0.27 to 3.6. The anomalous dispersion and relaxation absorption due to the hindered rotation of water have been observed and they are strongly dependent on n. The activation energies for the relaxation absorption have been determined for different n values and for different orientations of the crystals. A molecular mechanism for the absorption has been presented on the basis of the zeolitic nature of the water molecules in the crystal as determined previously from structural[2] and thermodynamic[3] investigation.

The authors' thanks are due to Mr. Nobuo Nakamura for part of the measurements with an "a" specimen.

Department of Chemistry
Faculty of Science
Osaka University
Nakanoshima, Osaka.

Electrical Conductivity of Organic Semiconductors at High Pressure

By Yoshiya HARADA, Yusei MARUYAMA, Ichimin SHIROTANI and Hiroo INOKUCHI

(Received May 22, 1964)

Recently, the effect of high pressure on the electrical conductivity of polycyclic aromatic hydrocarbons and quinones has been studied.[1] In each case, the observed conductivity increases by several orders of magnitude at high pressure. This behaviour seems to be closely associated with the increase in the amount of overlap between adjacent molecules.

In this report, we will attempt to calculate the band structure of the anthracene crystal at atmospheric pressure and also at 160 kilobars in order to see what differences may be expected in the electrical conductivity.

Following LeBlanc,[2] the treatment of the tight-binding approximation was used. In the calculation of the band energy for both electrons and holes, the interaction of the anthracene molecule, sited in the crystal with a monoclinic structure C_{2h}^5,[3] with twelve neighbour molecules was considered:

$$E(\boldsymbol{k}) = \text{const} + 2E_b \cos \boldsymbol{k}\boldsymbol{b} + 2E_c \cos \boldsymbol{k}\boldsymbol{c} \pm | 2E_{a/2\,b/2}[\cos \boldsymbol{k}(\boldsymbol{a}/2+\boldsymbol{b}/2) + \cos \boldsymbol{k}(\boldsymbol{a}/2-\boldsymbol{b}/2)] + 2E_{a/2\,b/2\,c}[\cos \boldsymbol{k}(\boldsymbol{a}/2+\boldsymbol{b}/2+\boldsymbol{c}) + \cos \boldsymbol{k}(\boldsymbol{a}/2-\boldsymbol{b}/2+\boldsymbol{c})] | \quad (1)$$

where $\boldsymbol{a}$, $\boldsymbol{b}$ and $\boldsymbol{c}$ denote the unit-cell vectors,

1) a) G. A. Samara and H. G. Drickamer, *J. Chem. Phys.*, 37, 474 (1962); b) H. Inokuchi, I. Shirotani and S. Minomura, This Bulletin, 37, 1234 (1964).

2) O. H. LeBlanc, Jr., *J. Chem. Phys.*, 35, 1275 (1961); G. D. Thaxton, R. C. Jarnagin and M. Silver, ibid., 66, 2461 (1962).

3) V. C. Sinclair, J. M. Robertson and A. M. Mathieson, *Acta Cryst.*, 3, 251 (1950).

and E_b, E_c, $E_{a/2\,b/2}$ and $E_{a/2\,b/2\,c}$ represent intermolecular resonance integrals. These integrals were calculated*1 by the method used by LeBlanc, except that all of the two-centre interatomic integrals were considered for the evaluation of each intermolecular integral (Eqs. A10 and A11 given by LeBlanc have been corrected by Katz et al.[4]). Since the crystal structure of anthracene under pressure has not yet been determined, the resonance integrals at high pressure were calculated by assuming that the crystal is compressed isotropically without changes in the orientations of lattice vectors and molecules. From the relation between pressure and volume given by Samara and Drickamer,[1a] the lattice distances at 160 kilobars were estimated to be 88% of those at atmospheric pressure. Figure 1 shows the

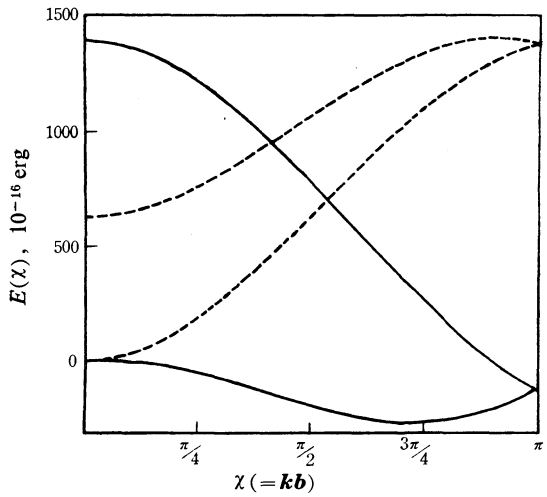


Fig. 1. Energy contours for both electrons (solid line) and holes (dashed line) in the $\boldsymbol{b}^{-1}$ direction at 160 kilobars. The origins of the energy scales have been arbitrarily chosen to make $E(0)$ the same for both bands.

contour of $E(\boldsymbol{k})$ for each band at 160 kilobars in the $\boldsymbol{b}^{-1}$ direction in the Brillouin zone. The total band widths of the electrons and holes at 160 kilobars are 1.65×10^{-13} erg and 1.39×10^{-13} erg, these values being 5.2 and 5.8 times as large as those calculated at atmospheric pressure. If we assume that the carrier-scattering can be described by the constant mean free time, $\tau(\boldsymbol{k})=\tau_0$, the mobility components are given by:

$$\mu_{ij}=e\tau_0<v_iv_j>/\boldsymbol{kT} \qquad (2)$$

where v_i is the i th component of the carrier velocity, $\mathbf{v}$, which is given by:

$$\mathbf{v}=(1/\hbar)\partial E(\boldsymbol{k})/\partial\boldsymbol{k} \qquad (3)$$

The quantity $<v_iv_j>$ is a statistical average over the band. The velocity components and the mean square velocities of both carriers in the a, b and c' directions are given in Table I.*2

Table I shows that the mobilities, on the whole, increase the magnitude by several tens times at 160 kilobars.*3 (The values of the c' components are incredible. In order to obtain reasonable results for this component, a refined treatment such as Katz et al.'s[4] is necessary.) The observed pressure effect on the conductivity of quaterrylene, $C_{40}H_{20}$, and violanthrone, $C_{34}H_{16}O_2$, is given in Table II,[1b] where the ratios of the number of carriers, $n_{160\text{ kb}}/n_{\text{atm}}$, and of the mobilities, $\mu_{160\text{ kb}}/\mu_{\text{atm}}$, are estimated from the $n\propto\exp(-\Delta\varepsilon/2\boldsymbol{kT})$ and $\sigma\propto n\mu$ relations. On the basis of this estimation, the sharp drop in the resistivity at a high pressure is attributed to the great increase in the concentrations of charge carriers, $10^3\sim10^4$ times, and to the increment of the mobilities, $10^1\sim10^2$ times, as is to be expected from the band theory treatment. When the electrical conductitvity of the anthracene crystal is compared with that of a larger aromatic hydrocarbon crystal, a similar behaviour is found. In the case of the circumanthracene ($C_{40}H_{16}$) crystal, it is found theoretically that the mobilities of the carriers are 2~3 times as large as those of the anthracene crystal.[5] On the other hand, the increase in the concentrations of charge carriers is estimated to be 10^7

*1 To faciliate the calculation, a digital computer, Facom 202, was programmed. About 20 sec. are required to compute a intermolecular resonance integral of the anthracene crystal.

4) J. I. Katz, S. A. Rice, S. Choi and J. Jortner, *J. Chem. Phys.*, **39**, 1683 (1963).

*2 Recently, Katz et al. (Ref. 4) refined the band calculation using the SCF carbon atomic orbital represented in the form of a linear combination of four Slater wave functions. The band widths calculated by their method are about five times larger than those found by LeBlanc. Although the present treatment is inadequate for the evaluation of the magnitude of the band widths and the velocity components, it might be useful for the estimation of the ratios of these values at a high pressure to those at atmospheric pressure. This is illustrated by the following table, which shows the mobility change due to the application of a pressure of 3000 atm.

Crystal direction	$\mu_{3000\text{ atm}}/\mu_{\text{atm}}$ Electron			Hole		
	Exp.[a]	Calcd.[b]	Calcd.[c]	Exp.[a]	Calcd.[b]	Calcd.[c]
a	1.4	1.1	1.2	1.4	1.0	1.2
b	1.3	1.2	1.3	1.4	1.1	1.3
c'	1.0	0.9	1.3	1.4	1.3	1.6

a) R. G. Kepler, *Phys. Rev.*, **119**, 1226 (1960).
b) Katz et al.
c) Present work.

*3 For the pressure dependence of the mobility, the change in the mean free time may have a much less important role than the change in the unit-cell dimensions (Ref. 4).

5) Y. Harada, Y. Maruyama, H. Inokuchi and N. Matsubara, to be published.

TABLE I. VELOCITY COMPONENTS AND MEAN SQUARE VELOCITY

	Electron			Hole		
	Atm. pressure (10^{10} cm^2/sec^2)	160 kb. (10^{10} cm^2/sec^2)	Ratio	Atm. pressure (10^{10} cm^2/sec^2)	160 kb. (10^{10} cm^2/sec^2)	Ratio
$<v^2_a>$	10.4	111	11	5.6	34	6
$<v^2_b>$	9.3	262	28	10.2	404	40
$<v^2_{c'}>$	0.04	46	1100	1.3	386	290
$<v^2>$	19.8	419	21	17.1	824	48

TABLE II. THE OBSERVED PRESSURE DEPENDENCE OF THE CONDUCTIVITY

	Atm. pressure		160 kb.			
	σ, $\Omega^{-1}\cdot$cm^{-1}	$\Delta\varepsilon$, eV.	σ, $\Omega^{-1}\cdot$cm^{-1}	$\Delta\varepsilon$, eV.	$n_{160\text{ kb}}/n_{\text{atm}}$ [a]	$\mu_{160\text{ kb}}/\mu_{\text{atm}}$
Quaterrylene	8.3×10^{-9}	0.61	1.4×10^{-4}	0.16	6×10^{3}	3
Violanthrone	4.3×10^{-11}	0.78	1.4×10^{-3}	0.20	8×10^{4}	400

a) $n_{160\text{kb}}$ and n_{atm} mean the concentrations of charge carriers at 160 kilobars and at atmospheric pressure, respectively.

times (anthracene, $\Delta\varepsilon=2.7$ eV.[6]; circumanthracene, $\Delta\varepsilon=1.8$ eV.[7]). Hence, in this case also, the increment of the conductivity may be due mostly to the great increase in charge carriers resulting from the lowering of the energy gap value.

Summary

In order to study the effect of high pressure on the electrical conductivity of organic semiconductors, the band structure of the anthracene crystal has been calculated at atmospheric pressure and also at 160 kilobars, using the treatment of the tight-binding approximation. The total band widths of both electrons and holes at 160 kilobars are 5~6 times as large as those at atmospheric pressure. Although the mobilities of both carriers, on the whole, increase in magnitude by several tens times at 160 kilobars, the sharp drop in the resistivity at high pressure may be due mostly to the great increase in the concentrations of the charge carriers (10^3~10^4 times).

The Institute for Solid State Physics
The University of Tokyo
Azabu, Tokyo

6) H. Inokuchi, This Bulletin, **29**, 131 (1956).
7) N. Matsubara, H. Inokuchi and Y. Maruyama, to be published.

NOTES

The Seebeck Effect in an Electrolytic Thermocouple Involving Ion-permselective Membranes

By Toshio IKEDA and Masao TSUCHIYA*

(Received March 30, 1964)

Several years ago, Tyrrell and his co-workers[1] reported on the Seebeck effect on the purely electrolytic thermocouple of the following system:

$$\underset{T}{\mathrm{Ag/AgX,\ MX}(m)}\ \Big|\ \underset{T}{\text{Ion exchanger in M}^+\text{ form (MR)}}\ \Big|\ \underset{T+\Delta T}{\mathrm{MX}(m)},\ \underset{T}{\mathrm{AgX/Ag}} \qquad (1)$$

Their purpose was to explain the thermal sensation of nerve systems. Recently, we have studied an electrolytic thermocouple of the following type:

$$\underset{T}{\mathrm{Hg/HgCl,\ KCl}(m^\circ)}\ \overset{\mathrm{D}}{\vdots}\ \underset{T}{\mathrm{KCl}(m)}\ \overset{\mathrm{D'}}{\vdots}\ \underset{T+\Delta T}{\mathrm{KCl}(m^\circ)},\ \underset{T}{\mathrm{HgCl/Hg}} \qquad (2)$$

where D and D' are ion-permselective membranes of an identical nature, but kept at different temperatures, T and $T+\Delta T$ respectively; the whole system is symmetrical in its construction, except for the temperature gradient applied to it.

As can easily be seen from the structure, the EMF of the cell 2 consists of two parts: one is the difference between the two isothermal membrane potentials arising at two membranes kept at different temperatures, T and $T+\Delta T$ respectively; the other is the difference between the two thermal diffusion potentials[2] which are revealed in opposite directions in two solution phases of different concentrations, m° and m. By taking the sign convention of EMF, ΔE, of the cell 2 to follow the sign of the calomel electrode on the hot side, we have, then, for the first approximation:

$$\boldsymbol{F}\Delta E=\frac{\partial}{\partial T}\left[\sum_k \frac{t_k'}{z_k}\boldsymbol{R}T\ln\frac{m_k\gamma_k}{m_k^\circ\gamma_k^\circ}\right]\Delta T - \frac{\partial}{\partial m}\left[\sum_k \frac{t_k Q_k^*}{z_k T}\Delta T\right](m-m^\circ) \qquad (3)$$

where $\boldsymbol{F}$ and $\boldsymbol{R}$ have their usual meanings; T is the absolute temperature; t_k and t_k' are the transport numbers of k-th ion species of z_k valency in the solution and membrane phases respectively; m_k and γ_k are the molality and the activity coefficient of k-th ion species on the molality scale, and the symbols with the superfix o refer to those in the outer electrolytic solution. Q_k^* is the ionic heat of transfer of k-th ion species. As judged from the Q_k^* values,[3,4] the second term on the right side of Eq. 3 can be ignored as compared with the first. Moreover, if a single 1, 1 valent electrolyte is used and if the membranes are perfectly permselective exclusively to one ion species (for example, to K^+), (i.e., in the case of $t'_{K^+}=1$, $t'_{Cl^-}=0$; accordingly, $\partial t'_{K^+}/\partial T=0$, $\partial t'_{Cl^-}/\partial T=0$), Eq. 3 can practically be approximated to $\boldsymbol{F}\mathrm{d}E/\mathrm{d}T = 2.303\boldsymbol{R}\log_{10}(m_{K^+}\gamma_{K^+}/m^\circ_{K^+}\gamma^\circ_{K^+})$, since the contribution from $\partial\ln\gamma_{K^+}/\partial T$ is very small, not exceeding 3% of the total in most cases.

Oxidized collodion membranes[5,6] prepared in a bag form, of nearly equivalent nature, were pasted with collodion to the nozzles of both terminal calomel electrodes. The membranes used were nearly completely permselective to cations, as judged from their apparent cation transport number being found to be about 0.97. Anion permselective membranes

* Present address: Tokyo Metropolitan Isotope Centre, Setagaya, Tokyo

1) H. J. V. Tyrrell, D. A. Taylor and C. M. Williams, *Nature*, **177**, 668 (1956).

2) E.g., H. J. V. Tyrrell, "Diffusion and Heat Flow in Liquids," Butterworths, London (1961), p. 59.

3) T. Ikeda, *Rep. Liberal Arts Sci. Fac., Shizuoka Univ., Nat. Sci.*, **2**, 153 (1959).

4) P. N. Snowdon, and J. C. R. Turner, *Trans. Faraday Soc.*, **56**, 1409 (1960).

5) H. P. Gregor and K. Sollner, *J. Phys. Chem.*, **50**, 53 (1946).

6) T. Ikeda and K. Tarumoto, *Rep. Liberal Arts Sci. Fac., Shizuoka Univ., Nat. Sci.*, **3**, 109 (1961); ibid., **3**, 165 (1962).

were prepared by forming a resin in the cellophane matrix by diffusing formaldehyde and aniline hydrochloride in aqueous media from either side of a cellophane that was tied with cotton thread to the endings of the nozzeles of two terminal calomel electrodes. The apparent anion transport numbers of these membranes were found to be about 0.91. The electrode nozzles so prepared were inserted into the appropriate compartments of an H-shaped cell filled with an m molal potassium chloride sulution. The temperature of two legs of the H-cell was controlled by thermostated water in Dewar vessels, fixed on one side, while it was varied around the mean temperature of 25°C on the other side. The EMF of the cell 2 was measured by varying, for the sake of experimental convenience, the concentration, m, of the inner pottasium chloride solution, while that of the outer was fixed at a convenient value. The EMF was found, for all values of m, to be proportional to the temperature difference, ΔT, in the temperature range studied. In Fig. 1 the temperature coefficient, dE/dT, was plotted against $\log m\gamma_{\pm}$, where $\gamma_{\pm}$ is the mean ionic activity coefficient. A nearly linear relation with a slope of about 197 μV./deg. (which was very close to the theoretical value, $2.3\boldsymbol{R/F}$) was found there, well agreeing with the present theory and with Tyrrell's results for the system 1. Reverse phenomena were found when anion-selective membranes were used in place of cation-selective membranes. The slope was somewhat higher than the theoretical expectation; however, this might be due to some change in the chemical nature of the anion-selective membranes used here, because these membranes were found to exhibit a faster fading of the isothermal membrane potential at higher temperatures.

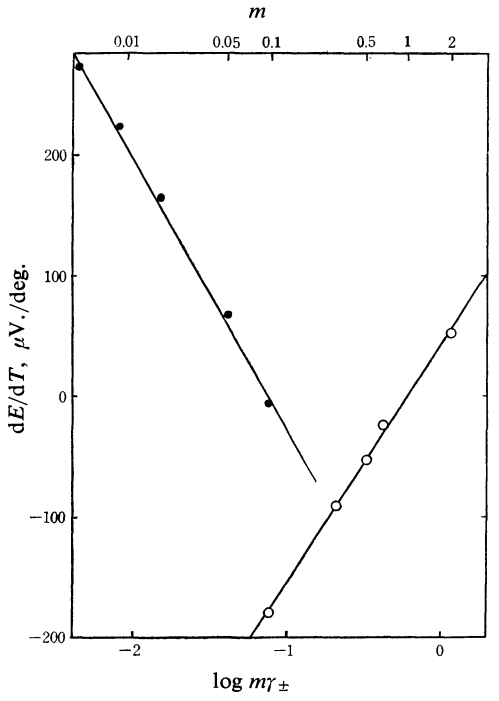


Fig. 1. Initial thermoelectric power dE/dT of the system 2.
○, for the system, oxidized collodion membranes being used, where m^o was fixed at 1 M.
●, for the system, aniline-formaldehyde resin membranes being used, where m^o was fixed at 0.1 M.

These facts indicate that the mechanism for the generation of EMF is perhaps the same in both systems, 1 and 2. The magnitude of dE/dT here obtained is in itself probably insufficient to explain why it is a stimulant in producing the thermal sensation, but several tens of nerve fibers would serve, if the cooperative function of the nerve fiber systems is taken into consideration.

Department of Chemistry
Shizuoka University
Oiwa, Shizuoka

The Direct Resolution of DL-*Aspartic Acid by the Use of an Optically Active Amine*[1]

By Kaoru HARADA

(Received April 9, 1964)

N-Acyl DL-amino acids have been used in most cases for the chemical and enzymatic resolution of DL-α-amino acids. However, for acidic amino acids, various other methods of resolution have been employed. DL-Glutamic acid was resolved by seeding,[2] by an optically-active amine[3] and by lysine[4] without using its *N*-acyl derivative. DL-Aspartic acid was resolved from its supersaturated copper complex solution by seeding it with L- or D-aspartic acid copper complexes.[5] DL-Aspartic acid was resolved by preferential crystallization with optically-active glutamic acid[6] and by the direct salt formation of optically-active lysine.[4] DL-Aspartic acid was also partially resolved on a starch column.[7]

In this report, the direct resolution of DL-aspartic acid by the use of optically-active α-methylbenzylamine[8] will be described. The optically-active amine has been used in several stereospecific syntheses of α-amino acids.[9-12] The use of D(−)α-methylbenzylamine ($[\alpha]_D^{27}=-40.6°$) resulted in the crystallization of L-aspartic acid D-amine salt ($[\alpha]_D^{27}=-9.7°$) from the reaction mixture. L(+)Amine ($[\alpha]_D^{27}=+39.3°$) resulted in D-aspartic acid L-amine salt ($[\alpha]_D^{27}=+10.9$). These salts were dissolved in water, and the pH was adjusted to about 2.8 to precipitate L- or D-aspartic acid. Optically-pure L-aspartic acid ($[\alpha]_D^{27}=+25.0°$) and almost pure D-aspartic acid ($[\alpha]_D^{27}=-23.0°$) were obtained. Optically-impure D- and L-aspartic acid (optical purity 50~60%) were isolated from the mother liquors of crystallization. D-Aspartic acid D-amine salt was prepared in order to compare it with its diastereomer. The solubility of the salt in the resolution solvent was much higher than that of its diatereomer. The optically-active amine could not be applied for the resolution of free DL-glutamic acid.

Experimental

Standard Aspartic Acid Amine Salts. — *(L-Aspartic Acid D-Amine) Salt.* — L-Aspartic acid (0.67 g., 0.005 mol.) was dissolved in a mixture of 2.0 ml. of water and 0.66 g. (0.005 mol.) of D(−)-methylbenzylamine ($[\alpha]_D^{27}=-40.6°$ in benzene). To this, 10 ml. of methanol and 5 ml. of acetone were added, and the mixture was kept in a refrigerator overnight. The (L-aspartic acid D-amine) salt crystallized; m. p. 260~263°C (decomp.), $[\alpha]_D^{27}=-9.9°$ (*c* 2.04, water). Found: C, 56.48; H, 7.34; N, 11.23. Calcd. for $C_{12}H_{18}N_2O_4$: C, 56.68; H, 7.13; N, 11.02%.

(D-Aspartic Acid L-Amine) Salt. — The salt was obtained from D-aspartic acid ($[\alpha]_D^{27}=-24.3°$) and L(+) amine, $[\alpha]_D^{27}=+10.5°$ (*c* 2.13 water). Found: C, 56.43; H, 7.14; N, 11.18%.

(D-Aspartic Acid D-Amine) Salt.—The salt did not crystallize under the above conditions, but it did crystallize upon the addition of an extra 10 ml. of acetone to the salt solution; m. p. 258~263°C (decomp.), $[\alpha]_D^{27}=+9.2°$ (*c* 1.04, water). Found: C, 56.66; H, 7.17; N, 10.92%.

The Resolution of DL-Aspartic Acid. — DL-Aspartic acid (6.65 g., 0.05 mol.) was dissolved in a mixture of 200 ml. of water and 6.10 g. (0.05 mol.) of D(−)α-methylbenzylamine ($[\alpha]_D^{27}=-40.6°$ in benzene) and filtered. To this, 50 ml. of methanol and 60 ml. of acetone were added, and the flask was rubbed with a glass rod (or preferably seeded with L-aspartic acid D-amine salt) and kept overnight in a refrigerator. The product, 4.70 g. (71%) of (L-aspartic acid D-amine) salt, was recrystallized by dissolving it in 12 ml. of water and precipitated with 15 ml. of methanol and 35 ml. of acetone. Pure salt (3.60 g.) was obtained; m. p. 260~263°C (decomp.), $[\alpha]_D^{27}=-9.7°$ (*c* 2.18, water). Found: C, 56.68; H, 6.97; N, 11.01. Calcd. for $C_{12}H_{18}N_2O_4$: C, 56.68; H, 7.13; N, 11.02%.

In the same way, (D-aspartic acid L-amine) salt was isolated by the use of L(+)-α-methylbenzylamine ($[\alpha]_D^{27}=+39.3°$ in benzene); 4.50 g. of salt was thereby isolated. After recrystallization, 3.48 g. of pure salt was obtained; m. p. 260~263°C

1) Contribution number 31 of the Institute for Space Biosciences, Florida State University.
2) Japanese Pat. 2972 (1956), *Chem. Abstr.*, **51**, 2135 (1957).
3) F. H. Radke, R. B. Fearing and S. W. Fox, *J. Am. Chem. Soc.*, **76**, 2801 (1954).
4) British Pat. 773653, *Chem. Abstr.*, **51**, 14, 794.
5) K. Harada and S. W. Fox, *Nature*, **194**, 768 (1962).
6) British Pat. 773660, *Chem. Abstr.*, **51**, 17984; U. S. Pat. 2790001, *Chem. Abstr.*, **51**, 13910.
7) German Pat. 1016713, *Chem. Abstr.*, 541344.
8) W. Theilacker and H. Winkler, *Chem. Ber.*, **87**, 690 (1954); B. Helberich and W. Portz, ibid., **86**, 1034 (1953); A. W. Ingersoll, "Organic Syntheses," Coll. Vol. II, 506 (1943).
9) J. C. Sheehan and R. E. Chandler, *J. Am. Chem. Soc.*, **83**, 4791 (1961).
10) R. G. Hiskey and R. C. Northrop, ibid., **83**, 4798 (1961).
11) K. Harada, *Nature*, **200**, 1201 (1963).
12) K. Harada and S. W. Fox, *Naturwissenschaften*, **51**, 106 (1964).

(decomp.), $[\alpha]_D^{27} = +10.9°$ (*c* 2.08, water). Found: C, 56.63; H, 7.03; N, 11.13%.

Optically-Active Aspartic Acid. — *L-Aspartic Acid.*—Three grams of (L-aspartic acid D-amine) salt was dissolved in 15 ml. of water, and the pH was adjusted to about 2.8 by the addition of 3 N hydrochloric acid. Then 15 ml. of ethanol was added, and the mixture was kept in a refrigerator overnight. The crystallized L-aspartic acid was filtered and washed with cold water and absolute alcohol. L-Aspartic acid (1.35 g.) was obtained; $[\alpha]_D^{27} = +25.0°$ (*c* 1.97, 6 N HCl). Found: C, 36.25; H, 5.39; N, 10.48. Calcd. for $C_4H_7NO_4$: C, 36.09; H, 5.30; N, 10.52%. From the mother liquor, optically-impure D-aspartic acid (1.50 g.) was obtained, $[\alpha]_D^{27} = -12.3°$ (*c* 1.07, 6 N HCl). Found: C, 36.21; H, 5.43; N, 10.34%.

D-Aspartic Acid. — D-Aspartic acid L-amine salt (1.20 g.) was treated in the way described above. D-Aspartic acid (0.53 g.) was isolated; $[\alpha]_D^{27} = -23.0°$ (*c* 2.30, 6 N HCl). Found: C, 35.88; H, 5.45; N, 10.37%.

The author is indebted to Professor Sidney W. Fox of this Institute for his helpful discussions. This work was supported by National Aeronautics and Space Administration Grant Number NsG-173-62.

Institute for Space Biosciences
and Department of Chemistry
Florida State University
Tallahassee, Florida, U. S. A.

A Tracer Study on the Source of Carbon Dioxide in the Chromic Acid Oxidation of Toluene and Fluorene

By Yoshiro OGATA and Hiroyoshi TABUCHI

(Received April 11, 1964)

In our previous reports[1,2] it has been found that the chromic acid oxidation of toluenes or fluorene in acetic acid gave carbon dioxide, together with benzoic acids or fluorenone respectively. The following mechanism was suggested to explain the second-order rate with chromium trioxide and the evolution of carbon dioxide:

$$C_6H_5CH_3 + 2CrO_3 \rightarrow$$

$$C_6H_5CH\left(\begin{matrix}O\\ \|\\ O\text{-}Cr\text{-}OH\\ \\ O\text{-}Cr\text{-}OH\\ \|\\ O\end{matrix}\right) \xrightarrow{2CrO_3} C_6H_5COOH$$

$$+ 2Cr_2O_3 + H_2O + 3O \quad (1)$$

In order to get more information on the source of carbon dioxide, the oxidations to toluene and fluorene were carried out under conditions similar to those described in the previous reports, using labeled acetic acid as the solvent. The liberated carbon dioxide was taken out as barium carbonate, and the radioactivity estimated. The radioactivity of only 18 cpm in barium carbonate obtained from the oxidation of toluene (No. 1 in Table I) shows that the carbon dioxide derived from the oxidation of acetic acid is only 2.5% ($18\times100/716$) of the total carbon dioxide evolved, where 716 cpm is the radioactivity of the solvent acetic acid. The values for fluorene (Nos. 4 and 5 in Table I) show that 1.7~2.8% of carbon dioxide is derived from acetic acid. Benzoic acid was found to be stable under the experimental conditions (No. 3 in Table I).

If the side chain of toluene is attacked, the reaction products should contain benzene, phenols, quinones and/or biphenyl. Only *p*-benzoquinone was detected by gas chromatography, however. It was found by visible spectrophotometry that the amount of quinone was very small. It was observed that quinone was easily oxidized to carbon dioxide and water by an acetic acid solution of chromic acid (No. 8 in Table I).

In conclusion, the benzene ring of toluene is probably completely broken by active oxygen to carbon dioxide; i.e., the side chain of toluene and/or benzoic acid is oxidized by the active oxygen produced from Eq. 1 to quinone, and then the quinone is further oxidized by chromic acid to carbon dioxide and water. However, the consumption of the starting material, toluene, by this attack of active oxygen is so small compared with that of chromium trioxide that there is no appreciable influence on the rate equation.

1) Y. Ogata, A. Fukui and S. Yuguchi, *J. Am. Chem. Soc.*, **74**, 2707 (1952).
2) Y. Ogata and H. Akimoto, *J. Org. Chem.*, **27**, 294 (1962).

Table I. Chromic acid oxidations in acetic acid

Solvent, CH_3CO_2H : 15 ml. for Nos. 1—3 and 8 and 30 ml. for Nos. 4—7; CrO_3 : 4.15×10^{-3} mol. for Nos. 1—3 and 7.29×10^{-3} mol. for Nos. 4—7

No.	Substrate (10^{-3} mol.)	Temp. °C	Time hr.	Obtained $BaCO_3$ g.	Radioactivity CH_3CO_2H c.p.m.	Radioactivity $BaCO_3$ c.p.m.
1	Toluene (0.833)	70	3	0.211	716	18
2	None	70	3	0.065	0	0
3	Benzoic acid (0.833)	70	3	0.080	0	0
4	Fluorene (2.43)	40	2	0.218	358	10
5	Fluprene (2.43)	40	2	0.201	358	6
6	None	40	2	0.008	0	0
7	Fluorenone (2.43)	40	2	0.276	0	0
8	*p*-Benzoquinone (0.833)	70	3	0.682	0	0

Similar results were obtained in the tracer study of the chromic acid oxidation of fluorene in acetic acid-1-^{14}C (Nos. 4 and 5 in Table I); this indicates that the aromatic ring is completely broken by active oxygen to produce carbon dioxide.

Experimental

Materials.—All the materials were purified as in the previous papers.[1,2] Acetic acid-1-^{14}C was synthesized from labeled barium carbonate via the reaction with methyl magnesium iodide.[3] The radioactivity of all the radioactive materials were measured by a Geiger-Müller counter after their conversion to barium carbonate. The radioactivities of barium carbonate were measured by using layers of infinite thickness and corrected for their background.

Oxidation. — The carbon dioxide evolved was swept out by passing oxygen-free dry nitrogen gas through and then absorbed by aqueous barium hydroxide after passing it through aniline to eliminate the acetic acid.

The Gas Chromatography of the Oxidation Products.—The solution of the reaction product was added to sodium bicarbonate to neutralize acetic acid and benzoic acid and then extracted with ethyl ether. The extract was dried and analyzed by gas chromatography on a 1.5 m. copper column packed with Silicon DC 703 at a helium pressure of 21 p. s. i. at 70°C (for benzene), at 100°C (for quinone), at 170°C (for phenol) or at 190°C (for biphenyl). No indication of the presence of benzene, phenol or biphenyl was observed. *p*-Benzoquinone was identified by having the same peak as the authentic sample and also by color tests with sulfuric acid or sodium hydroxide.[4]

The Estimation of the Concentration of Quinone.—The reaction products was extracted with ether, the extract being analyzed spectrophotometrically at the wavelength of the absorption maximum, 430 mμ with 1 cm. cells. The reaction mixture was found to contain ca. 7×10^{-3} M benzoquinone, which was to be less 1/30 of the calculated concentration (240×10^{-3} M) on the assumption that one mole of toluene gave one mole each of carbon dioxide and quinone.

The authors wish to thank Dr. E. Nakano and Dr. Y. Izawa for their aid in performing these experiments.

Department of Applied Chemistry
Faculty of Engineering
Nagoya University
Chikusa-ku, Nagoya

3) M. Calvin, C. Heidelberger, J. C. Reid, B. M. Tolbert and P. F. Yankwich, "Isotopic Carbon," John Wiley & Sons, Inc., New York (1949), p. 175.

4) R. E. Kirk and D. F. Othmer, "Encyclopedia of Chemical Technology," Vol. XI, Interscience Encyclopaedia Inc., New York (1950), p. 410.

*The Electrical Properties of the Poly(N-vinyl Carbazole)-Tetracyanoquinodimethane Charge Transfer Complex**

By Akimasa TANIGUCHI, Seiichi KANDA, Takeshi NOGAITO, Shigekazu KUSABAYASHI, Hiroshi MIKAWA and Kazuo ITO

(Received April 21, 1964)

Tetracyanoquinodimethane (abbreviated as TCNQ) forms a charge transfer complexes with various amines.[1] The electrical resistivity of these compounds is fairly low, and some of them show an ESR signal.[1,2]

It is to be expected that vinyl polymers with π-electron systems of aromatic amines will form charge transfer complexes with TCNQ and also that the complexes have conductive characteristics. Plasticity may also be expected to be retained in the product complex.

Charge transfer complexes derived from polyvinylanthracene,[3] polyethinylnaphthalene,[4] polyvinylpyridine,[5] polyvinylnaphthalene[6] and polyvinylmesitylene[6] have been reported.

In the present work, the electrical and optical properties of the charge transfer complex between poly(*N*-vinyl carbazole) and TCNQ have been investigated. The photoconductive properties of poly(*N*-vinyl carbazole) and its sensitization with TCNQ and other compounds acting as acceptors have already been described.[7]

Preparation. — The poly(*N*-vinyl carbazole) used is Luvican M170 (Badische Anilin u. Soda Fabrik A. G.). TCNQ was prepared by the method described in the literature.[8]

Poly(N-vinyl Carbazole)-TCNQ Charge Transfer Complexes.—These complexes were prepared easily by dissolving both components in chloroform at room temperature. The dark green material thus obtained was fairly stable thermally, with a softening point between 210 ~270°C. It was possible to make a film of the complex by evaporating the solution containing the material.

In preparing the complex, the ratio between the amounts of the two components were changed as shown in Table I. The mole ratio between the carbazole monomer unit of poly(*N*-vinyl carbazole) and TCNQ in the various complexes obtained are shown in the table. The mole ratios of the components were estimated spectroscopically from the intensities of the absorption peaks at 330 and 400 mμ.

As reference substances, an *N*-ethyl carbazole-TCNQ complex and a carbazole-TCNQ complex were also prepaped.

N-Ethyl Carbazole-TCNQ Charge Transfer Complex.—One hundred ninty-five milligrams (10^{-3} mol.) of *N*-ethyl carbazole and 204 mg. (10^{-3} mol.) of TCNQ were mixed as a chloroform solution (100 ml.). The solution immediately turned dark green, and a crystalline solid separated. The solution was evaporated to half of its volume after one hour, and the precipitated crystalline complex was filtered. Dark green needles; sublimation temperature above 160°C; yield 270 mg.

Found: C, 77.10; H, 4.59; N, 17.73. Calcd. for a one-to-one complex $C_{26}H_{17}N_5$: C, 78.19; H, 4.26; N, 17.53%.

Carbazole-TCNQ Charge Transfer Complex.—One hundred sixty-seven milligrams (10^{-3} mol.) of carbazole and 204 mg. (10^{-3} mol.) of TCNQ were mixed as in the case of ethyl carbazole. Sublimations temperature, 210~250°C; yield, 310 mg.

Found: C, 76.70; H, 4.41; N, 19.54. Calcd. for a one-to-one complex $C_{24}H_{13}N_5$: C, 78.00; H, 3.24; N, 18.55%.

Spectroscopic Properties. — The absorption spectra of the charge transfer complex between poly(*N*-vinyl carbazole) and TCNQ are shown in Fig. 1. In chloroform the main bands are at 330, 400 and 620 mμ, of these, 330 mμ is the absorption due to poly(*N*-vinyl carbazole) itself and 400 mμ, that due to TCNQ. The 620 mμ band is, consequently, the so-called charge transfer band between the two components. The absorption spectra of the glassy solid film

* Presented at the 16th Annual Meeting of the Chemical Society of Japan, Tokyo, April, 1963.

1) L. R. Melby, R. J. Harder, W. R. Hertler, W. Mahler, R. E. Benson and W. E. Mochel, *J. Am. Chem. Soc.*, **84**, 3374 (1962).

2) D. B. Chesnut, H. Foster and W. D. Phillips, *J. Chem. Phys.*, **34**, 684 (1961).

3) H. Inoue, K. Noda, S. Takiuchi and E. Imoto, *J. Chem. Soc. Japan, Ind. Chem. Sec.* (*Kogyo Kagaku Zasshi*), **65**, 1286 (1962).

4) S. Kambara and M. Hatano, Presented at the 10th Annual Meeting of the Society of Polymer Science, Japan, June, 1962.

5) A. Mizoguchi, H. Moriga, T. Shimizu and Y. Amano, *National Technical Report*, **9**, 407 (1963).

6) W. Slough, *Trans. Faraday Soc.*, **58**, 2360 (1962).

7) S. Oka, T. Mori, S. Kusabayashi, A. Taniguchi, Y. Yamamoto, M. Ishiguro and H. Mikawa, *Electrophotography* (*Japan*), 5 (No. 3) 19 (1964).

8) D. S. Acker, R. J. Harder, W. R. Hertler, W. Mahler, L. R. Melby, R. E. Benson and W. E. Mochel, *J. Am. Chem. Soc.*, **82**, 6408 (1960).

of the complex are very similar to those of the chloroform solution, having maxima at 330, 400 and 600 mμ.

As a reference, the absorption spectrum of the *N*-ethyl carbazole - TCNQ complex was also measured. In the chloroform solution, a charge transfer band was observed around 560 mμ, as is shown in Fig. 1.

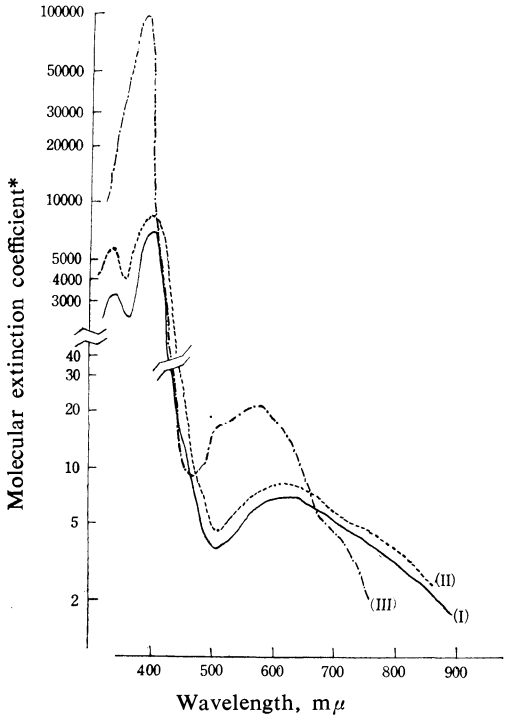


Fig. 1. Absorption spectra of some complexes.

(I) Poly(*N*-vinyl carbazole) and TCNQ were dissolved in chloroform in the ratio 10 : 1.
(II) Poly(*N*-vinyl carbazole) - TCNQ complex film (arbitrary unit).
(III) *N*-Ethyl carbazole - TCNQ complex in chloroform.
* This value is calculated by dividing the optical density of the solution as observed with the mol./l. concentration of the carbazole monomer units present in the solution.

Electrical Properties.—The electrical conductivity of the material was measured with a pellet made under 5000 kg./cm^2 pressure with a silver-paste electrode by the DC method, the applied voltage being 20~2000 V./cm. The relation between the current and the applied voltage obeyed Ohm's law in this range. The relationship between the logarithm of the resistivity and the reciprocal of the temperature is shown for the complexes in Fig. 2. The specific resistivity at room temperature and the band gap, ε, as calculated from the temperature dependence of the resistivity by the equation $\rho = \rho_0 \exp(\varepsilon/2kT)$ are tabulated in Table I. The specific resistivity of poly(*N*-vinyl carbazole) itself was above 10^{17} Ωcm. The conductivities of the *N*-ethyl carbazole - TCNQ complex and the carbazole-TCNQ complex are also listed in this table.

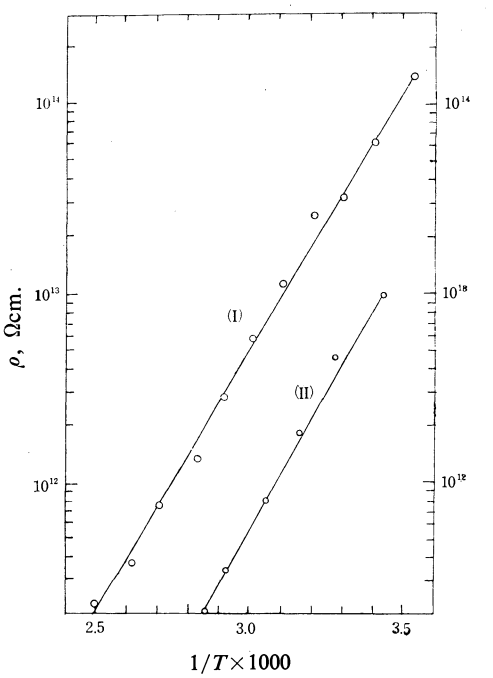


Fig. 2. Temperature dependence of the resistivity.
(I) Poly(*N*-vinyl carbazole) - TCNQ complex (sample No. 5).
(II) *N*-Ethyl carbazole - TCNQ complex

TABLE I. PROPERTIES OF VARIOUS COMPLEXES

No.	Weight ratio between both components used in preparation	Mole ratio between carbazole monomer unit and TCNQ in the complex	Specific resistivity at room temperature Ωcm.	ε eV.
Poly(*N*-vinyl carbazole) - TCNQ				
1	1 : 1	34 : 1	5.0×10^{15}	1.4
2	2 : 1	38 : 1	1.2×10^{14}	1.4
3	5 : 1	31 : 1	1.1×10^{16}	1.5
4	10 : 1	35 : 1	2.4×10^{14}	1.3
5	20 : 1	57 : 1	1.4×10^{14}	1.1
N-Ethyl carbazole - TCNQ				
6	1 : 1	1 : 1	1.8×10^{13}	1.1
Carbazole-TCNQ				
7	1 : 1	1 : 1	7.0×10^{10}	1.1

Summary

Poly(*N*-vinyl carbazole) (specific resistivity, above 10^{17} Ωcm.) gives a dark-green charge transfer complex with tetracyanoquinodimethane.

The specific resistivity of the complexes at room temperature is $10^{14}\sim10^{16}$ Ωcm. and the band-gap energy is 1.1∼1.5 eV. The film-forming property of poly(*N*-vinyl carbazole) is retained in the complex. The charge transfer band is observed at about 620 mμ.

The authors wish to thank Mr. Takuzo Fujino and Mr. Tsuneyo Shishido for their elementary analyses.

Institute of Scientific and Industrial Research
Osaka University
Sakai, Osaka

SHORT COMMUNICATIONS

An Improved Fusion Method for the Synthesis of Purine Nucleosides. The Acid-catalyzed Reactions of $N_{(7)}$- or $N_{(9)}$-Acylpurines with Acylated Sugars

By Yoshiharu ISHIDO, Akira HOSONO, Sadanori ISOME, Akira MARUYAMA and Tetsuo SATO

(Received May 25, 1964)

In previous papers[1] from our laboratory, the acid-catalyzed fusion reaction of purines with acylated sugars has been reported. Recently, the method has been applied to the synthesis of nucleosides of D-xylose,[2a] 2-deoxy-D-ribose,[2b,3] and deoxyaminosugars.[3]

The extensive experiments on the acidic catalysts for this reaction made it clear that the compounds formulated as R-SO_3H, picric acid, and many inorganic acidic compounds were effective. It is of great interest that amphoteric acids, such as sulfanilic and sulfamic acids, showed fairly good catalytic effects.[4]

On the other hand, perspective observation of the reactivity of purine derivatives in the fusion reaction made us aware of the fact that there is no rational correlation between the reactivity of purines and the polar effect of their substituent groups on the reaction centers, though such correlation was confirmed in the fusion reaction of phenols with acylated sugars.[3] Accordingly, it was deduced that this fact was probably due to the fusibility of purine derivatives.[4b,c]

In fact, the reactions of purines with a high fusibility, such as 2, 6-dichloropurine (I) [m. p. 181°C (decomp.)[5]], halogenopurines, and theophylline, proceeded in a homogeneous state to yield the corresponding purine nucleosides, 2, 6-dichloro-9-(2', 3', 5'-tri-*O*-acetyl-β-D-ribofuranosyl)purine (II)[4b,c] {m. p. 158~159°C, $[\alpha]_D^{21.5}$ −5.7° (*c* 1.05, chloroform), λ_{max}^{EtOH} 253 mμ (ε, 6100) and 274.5 mμ (ε, 9800), λ_{min}^{EtOH} 258 mμ (ε, 5800)}, and others, generally in a good yield (40~80% yield of the theoretical yileds)[4]. On the other hand, amino- or hydroxypurines with extremely high melting points were usually hard to fuse on the reaction and were not practically reactive.[4] These results have led to the suggestion that easily-fusible purine derivatives might be favorable for the fusion reaction.

Thereupon, purines which are acylated at a nitrogen atom of the imidazole nucleus and have much lower melting points than those of the parent purines have been applied to the reaction.

Birkofer[6] prepared diacyladenines by refiuxing adenine with excess acid anhydrides. Montgomery[7] also obtained monoacethlyalogenopurines by refluxing diaminohalogenopyrimidines with ethyl orthoformate in acetic anhydride. He deduced from the infrared spectra that the acetyl group should be linked to a nitrogen atom of the imidazole moiety of the purine nucleus. The melting points of these acyl purines are much lower (30~200°C) than those of the parent purine.

We have newly obtained acyl derivatives of theophylline ($N_{(7)}$-acetyl, m. p. 156~157°C;

1) T. Sato, T. Simadate and Y. Ishido *J. Chem. Soc. Japan, Pure Chem. Sec.* (*Nippon Kagaku Zasshi*), **81**, 1440, 1442 (1960); T. Simadate, Y. Ishido, and T. Sato, ibid., **82**, 938 (1961); T. Simadate, ibid., **82**, 1261 (1961); Y. Ishido and T. Sato, This Bulletin, **34**, 1347 (1961).

2) a) W. W. Lee, A. P. Martinez, G. L. Tong and L. Goodman, *Chem. Ind.* (*London*), **1963**, 2007; b) M. J. Robins, W. A. Bowles and R. K. Robins, *J. Am. Chem. Soc.*, **86**, 1251 (1964).

3) Y. Ishido, T. Matsuba, A. Hosono and T. Sato, International Symposium on the Chemistry of Natural Products, Kyoto, Japan, April, 1964.

4) a) Y. Ishido and T. Sato, 15th Annual Meeting of Chemical Society of Japan, Kyoto, April, 1962; b) Y. Ishido, Doctoral Thesis, Tokyo Institute of Technology, Japan, March, 1963; c) Y. Ishido, A. Hosono, Y. Kikuchi and T. Sato; Y. Ishido, A. Hosono, Y. Kikuchi and T. Sato; Y. Ishido, A. Hosono, Y. Kikuchi, S. Isome, A. Maruyama, and T. Sato, 17th Annual Meeting of the Chmical Society of Japan, Tokyo, Japan, March, April, 1964.

5) G. B. Elion and G. H. Hitchings, *J. Am. Chem. Soc.*, **78**, 3508 (1956).

6) L. Birkofer, *Ber.*, **76**, 769 (1943).

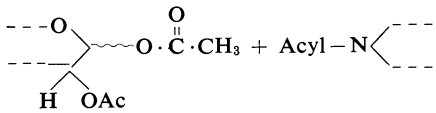
7) J. A. Montgomery, *J. Am. Chem. Soc.*, **78**, 1928 (1956).

$N_{(7)}$-propionyl, m. p. 129~130°C; $N_{(7)}$-*n*-butyryl, m. p. 88~90°C), I ($N_{(9)}$-propionyl, m. p. 169~171°C; $N_{(9)}$-*n*-butyryl, m. p. 104~106°C), guanine (2-*NH*-, $N_{(9)}$-diacetyl, m. p. 261~263°C), and 5,6-dimethyl-benzimidazole (*N*-acetyl, m. p. 136~139°C), etc. The yields of these derivatives range from 70 to 90% of the theoretical yields.

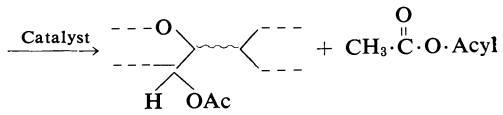
Among these derivatives, the acetyl derivatives gave the best results on the reaction with 1,2,3,5-tetra-*O*-acetyl-β-D-ribofuranose in the presence of sulfamic acid as the catalyst at a suitable temperature. Thus, 7-β-D-ribofuranosyltheophylline, II, 2-methylthioadenosine, adenosine, and guanosine were obtained in 82, 82, 57, 14, and 28% yield of the theoretical yields respectively. It was found that the yields of these nucleosides were raised by 10 to 30% compared with those reported previously.[1-4a,b]

The concomitant production of acid anhydrides in this modified fusion reaction was confirmed by infrared spectra, while acetic acid was formed in the reaction of free purines with acetylated sugars. This fact provides a further chemical proof of the interpretation[7] based on the infrared spectra of monoacetylhalogenopurines.

In view of the above facts, the most reasonable scheme of the modified reaction may be written as follows:



Acetylated sugars Acylpurines



Purine nucleoside acetates Acid anhydrides

A detailed investigation of the improved method and related matters will be reported in the near future.

Department of Chemistry
Tokyo Institute of Technology
Meguro-ku, Tokyo (*Y. I., A. H. & T. S.*)

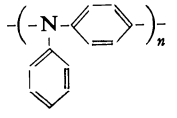
Research Division
Tokyo Tanabe Co., Ltd.
Adachi-ku, Tokyo (*S. I. & A. M.*)

Electric Conductivity and Electron Spin Resonance of Semiconductive Complexes of Polymer Species of Diphenylamine

By Keiji KUWATA, Yuzuru SATO and Kozo HIROTA

(Received July 14, 1964)

In a previous communication,[1] the formation of a stable polymer species from diphenylamine under an oxidative atmosphere with a vanadium pentoxide catalyst was reported, and the polymer structure composed of a structural unit was proposed as follows:



$n=3\sim17$

TABLE I. SPECIFIC RESISTANCE AND CONCENTRATION OF THE UNPAIRED ELECTRON FOR THE COMPLEXES AT ROOM TEMPERATURE (30°C)

Acceptor for one structural unit* mol.	Specific resistance Ω cm.	Concn. of unpaired electron spin/g.	Line width** ΔH_{msl} gauss
Complexes of iodine			
None	1.9×10^{11}	1.6×10^{18}	8
0.05	4.5×10^{8}	3.9×10^{19}	10
0.12	2.6×10^{6}	4.9×10^{19}	10
0.15	5.3×10^{5}	5.1×10^{19}	12
0.25	4.1×10^{5}	5.2×10^{19}	13
0.33	2.1×10^{5}	6.9×10^{19}	12
1.00	3.4×10^{4}	5.3×10^{19}	12
1.50	3.0×10^{4}	1.7×10^{19}	12
Complexes of chloranil			
0.25	2.4×10^{8}	2.4×10^{19}	13
0.33	2.5×10^{8}	5.5×10^{19}	13
Complexes of TCNE			
0.25	1.7×10^{6}	5.0×10^{19}	11
0.33	8.1×10^{5}	2.1×10^{20}	12
1.00	1.7×10^{6}	4.8×10^{19}	12

* Mol. wt. (Rast) of the polymer, 1.3×10^{3}.
** Broad singlets for solids, but hf structures of five lines were observed for the benzene solutions of the complexes.

Molecular complexes of the polymer species of DPA, a good electron donor because of the structure shown above, with some electron acceptors were prepared, and their semiconductive properties and concentrations of the unpaired electron were measured.

For both measurements, a benzene solution of iodine, chloranil or tetracyanoethylene (TCNE) was mixed with a benzene solution of the polymer, because of its low solubility with other solvents, and the solvent was removed, finally under a vacuum.

A sample with a high specific resistance was measured by the use of a vibrating-reed-type millivoltmeter.*

The specific resistance and concentration of each complex are shown in Table I.

The relative amount of iodine strongly bound to the polymer was determined to be about one-fifth mole to a structural unit of the polymer by the elementary analysis of a complex, which was washed repeatedly with an aqueous potassium iodide solution until no more iodine was liberated into the solution.

This relative amount of iodine is somewhat lower than that obtained for the most conductive complex, i. e., one-and-a-half mole to a structural unit, and the excess amount of iodine, more than one-fifth, obviously increases the conductivity.

The highest concentration of the unpaired electron, however, is obtained for a complex with the different composition of one mole of iodine to three structural units (cf. Table I).

This complicated phenomenon seems to be caused by the excess amount of iodine bound weakly to the complex.

Department of Chemistry
Faculty of Science
Osaka University
Nakanoshima, Osaka

1) H. Hirota and Y. Kageyama, This Bulletin, **37**, 593 (1964).

* Measurement was made at the Institute for Industry and Science of Osaka University.

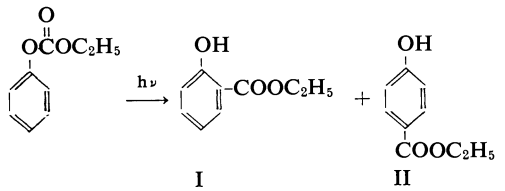
The Photochemical Rearrangement of Ethyl Phenyl Carbonate

By Chyongjin PAC and Shigeru TSUTSUMI

(Received July 31, 1964)

It has been reported that the migration of the acyl group in phenyl acetate occurs under the influence of ultraviolet light[1] in a manner similar to that of the Fries-reaction.[2] Such photochemical reactions of catechol acetate,[1] anilides,[3] phenyl benzoates[4] and *p-t*-butylphenyl benzoates[5] have been investigated and have supplied a convenient method for the preparation of a number of hydroxy or amino aromatic ketones.

The migration of the alkoxycarbonyl group, however, has been scarcely observed at all. In the course of the investigation of the reaction of ethoxycarbonyl radical in hydrocarbons,[6] it was found that the migration of the ethoxycarbonyl group took place in the photochemical reaction of ethyl phenyl carbonate (EPC), thus affording ethyl salicylate and ethyl *p*-oxybenzoate in fairly good yields.



I II

After the irradiation of EPC (13 g.) in 150 ml. of acetic acid for 120 hr. with a low pressure mercury arc (100 W.), the irradiated mixture was worked up as usual and gave ethyl salicylate, I (a 16% yield based on the EPC used), ethyl *p*-oxybenzoate, II (25%), and phenol (7~8%), while 26% of the EPC was recovered.

These products were identified by infrared spectroscopic and gas chromatographic measurements, mixed melting point tests with authentic samples, and elementary analyses.

In a similar way, the photochemical reaction of EPC in ethanol afforded I (17%), II (18%) and phenol (13%), while 23% of the EPC was recovered.

When ether was used as a solvent, a decrease in the yield was observed in I (8~10%) and II (10%), while phenol (13%) and EPC (39%) were also detected.

In non-polar solvents such as benzene or *n*-heptane, the wall of the light source was covered with polymeric products during the course of irradiation, and only trace amounts of the products or none at all were detected. However, it is not clear whether or not there were any solvent effects on the photochemical rearrangement of EPC.

On the basis of the results of mixed irradiation experiments,[7] it has been suggested that the migration of the acyl group is intramolecular, and Kobsa[5] showed that, upon the absorption of a light quantum, the ester decomposed into a pair of radicals in a solvent cage, which then underwent subsequent reactions.

Considering the above facts on the migration of the acyl group, the photochemical rearrangement of EPC may be expected to be intramolecular. The details of this reaction are now being investigated.

Department of Chemical Technology
Faculty of Engineering
Osaka University
Miyakojima-ku, Osaka

1) J. C. Anderson and C. B. Reese, *Proc. Chem. Soc.*, **1960**, 217.
2) A. H. Blatt, "Organic Reactions," Vol. 1, John Wiley & Sons, Inc., New York (1942), p. 342.
3) Dov Elad, *Tetrahedron Letters*, **1963**, 873.
4) C. H. Kuo, R. D. Hoffsommer, H. L. Slates, D. Taub and N. L. Wendler, *Chem. & Ind.*, **1960**, 1627.
5) H. Kobsa, *J. Org. Chem.*, **27**, 2293 (1962).
6) A preliminary report, This Bulletin, **36**, 234 (1963).
7) J. C. Anderson and C. B. Reese, *J. Chem. Soc.*, **1963**, 1781.

The Transfer Coefficient of a Redox Process at Varying pH Values as Determined by the Faradaic Rectification Method

By H. P. Agarwal

(Received September 21, 1961)

The periodic variation of an electrode potential about a mean potential when the electrode is polarized by a sinusoidal current is known as rectification by electrode reaction. This phenomenon, when first observed in a solution containing a redox couple, was named the "redoxokinetic effect,"[1] but it is now generally known as the Faradaic rectification.[2,3] The recent development of the Faradaic rectification allows us to study the kinetics of fast electrode processes conveniently.[4] The study can be divided into two parts. The first of them relates to the study at the mercury-aqueous solution interface by the method followed by Barker and his co-authors,[3] but corrections for the double-layer structure in the solution of the boundary-value problem and for the alternating voltage control across the Faradaic impedance at high frequencies are necessary, as has been pointed out by Matsuda and Delahay.[5] The second method previously adopted by the present author,[6] consists of studying the reaction at the platinum-aqueous solution interface, where the solution contains an equimolecular concentration of oxidant and reductant. The latter has the advantage that no correction for kinetic parameters, as suggested by Matsuda and Delahay, is necessary.

The hydrogen ion concentration of the medium used as the supporting electrolyte for the reactants has a tremendous influence on the electrode kinetics and the shift in mean potential, i. e., the redoxokinetic potential,[7] ψ; hence, the effect of pH on the transfer coefficient has been studied in the present work.

Experimental

The method for measuring a. c. voltage incident and the shift in mean potential was the same as has been described earlier.[6] The cell contained an 0.001 M solution of quinhydrone (A. R.) in a buffer solution of known pH. The pH of the buffer used varied from pH 1.4 to pH 8.1. For buffers of pH 1.4 to 4.62, sodium acetate (A. R.) and hydrochloric acid (A. R.) solutions were used; on the other hand, for buffers having pH 6.1 to pH. 8.1 solutions of disodium hydrogen phosphate (E. Merck) and potassium dihydrogen phosphate (E, Merck), the concentration of each being 1/15 M were mixed in suitable proportions to obtain a buffer of the desired pH. The exact pH of each solution was confirmed using a Leeds and Northrup pH-meter. The results obtained are given in Table I, which does not, however, include the results obtained with the buffer with pH 8.1 for want of reproducibility. For the sake of brevity, the readings of ψ obtained at 8 mV. of a. c. have not been included, as they were found to be exactly four

Table I. Shift in mean potential, ψ, at 4 mV. of A. C. of the buffer solutions of quinhydrone 0.001 M in relation to the frequency of A. C. and pH of the solutions*,**(29±0.05°C)

Frequency c./sec.	ψ, μV. pH				
	1.40	2.10	4.62	6.10	7.10
100	34	24	18	−36	−104
200	38	34	12	−24	−53
500	38	34	4	−10	−24
1000	38	34	−1	−2	−8
2000	38	34	−1	−2	−4

* Dimensions of bright, polished platinum-foil electrodes used:

A. C. electrodes	Length cm.	Breadth cm.
1	1.6	1.0
2 (connected to the earth)	1.6	0.95
Reference electrode	1.6	1.0

** With the increase in pH, the values of ψ decrease in magnitude at the corresponding frequency. In the range of pH up to 6.1, ψ becomes constant at higher frequencies, but beyond it no such constancy is observed and the system tends to be more unstable.

1) K. S. G. Doss and H. P. Agarwal, *J. Sci. Ind. Res.*, **9 B**, 280 (1950).
2) K. B. Oldham, *Trans. Faraday Soc.*, **53**, 80 (1957).
3) G. C. Barker, R. L. Faircloth and A. W. Gardner, *Nature*, **181**, 247 (1958); G. C. Barker, *Anal. Chim. Acta*, **18**, 118 (1958).
4) H. Matsuda and P. Delahay, *J. Phys. Chem.*, **64**, 332 (1960).
5) H. Matsuda and P. Delahay, *J. Am. Chem. Soc.*, **82**, 1547 (1960).
6) H. P. Agarwal, *J. Electroanal. Chem.*, **5**, 236 (1963); *J. Electrochem. Soc.*, **110**, 237 (1963).
7) H. P. Agarwal and Y. K. Gupta, *J. Sci. Soc. India*, **2**, 52 (1953).

times those shown at 4 mV. of a. c. in Table I at the corresponding frequency.

Results and Discussion

It can be seen from Table I that ψ, the shift in the mean potential, is constant at a frequency of 200 c./sec. or above when the pH of the solution is 1.4 or 2.1. Below a frequency of 200 c./sec., ψ decreases, but to confirm whether it decreases with the square root of frequency, further work at frequencies below 100 c./sec. is necessary. With the increase in the pH of the solution, ψ becomes negative; it becomes constant at a frequency of 1000 c./sec. or above (columms of pH 4.62 and pH 6.1 in Table I). With a lowering of the frequency, ψ increases in magnitude and is not proportional to the square root of frequency; therefore, the determination of the standard rate constant in such solutions is not possible. If the pH of the supporting electrolyte increases beyond 6.1, no constancy in the value of ψ is attained, even at frequency of 2000 c./sec. (column of pH 7.1 in Table I). When the pH of the medium is increased further, say, up to 8.1, the entire system becomes unstable and no reproducible observations are possible. At pH 8.1 the quinhydrone system is unstable, and so the entire solution in the cell looks black or brownish. As the constancy in the mean potential is reached at higher frequencies in the pH range of the solution from 1.4 to 6.1, the values of the transfer coefficient α, at different pH values have been calculated from the theoretical equation[8] applicable at high frequencies:

$$\alpha = 0.5 - \frac{2\psi RT}{V^2 nF}$$

where R is the gas constant, T is the absolute temperature, n is the valency, F is the Faraday constant, and V is the a. c. voltage incident. The transfer coefficients of the quinhydrone system determined from the above equation at pH 1.4, 2.1, 4.62 and 6.1 are, respectively, 0.376, 0.389, 0.503 and 0.506 at 29°C. These results show that the transfer coefficient decreases rapidly with the lowering in the pH of the medium, but with the pH values above 4.62, the variation in the transfer coefficient is low. Further, the values of transfer coefficients lower than 0.5 indicate that, at higher hydrogen ion concentrations, the depolarising action of hydroquinone during the anodic half wave increases. When the transfer coefficient exceeds 0.5, which usually takes place at higher pH values, the conversion of quinone into hydroquinone during the cathodic half wave is favoured. Thus, the knowledge of the transfer coefficient of an electrode reaction at varying pH values helps us to understand the mechanism of electrode processes. It is interesting to note that, in buffers of higher pH values, ψ is tremendously affected in the lower frequency range.

8) K. S. G. Doss and H. P. Agarwal, *Proc. Indian Acad. Sci.*, **34**, 263 (1951); ibid., **35**, 45 (1952).

Summary

The transfer coefficient of 0.001 M quinhydrone in buffer solutions of various pH values has been determined by Faradaic rectification studies. The value of α at 29°C has been found to be 0.376 at pH 1.4, 0.389 at pH 2.1, 0.503 at pH 4.62, and 0.506 at pH 6.1. The transfer coefficients determined at various pH values, help us to understand the mechanism of electrode processes.

Department of Chemistry
Motilal Vigyan Mahavidyalaya
Bhopal, India

A Mass Spectrometric Investigation of Petroleum. III.[1] *The Determination of the Alkyl Side Chain Number on Aromatics in the High Boiling Range Fraction of Petroleum*

By Shozo Oshima

(Received October 1, 1963)

Hitherto, the alkyl side chain number on alkyl aromatics in the high boiling range fraction of petroleum has been determined by the infrared spectrometric assigment of the ratios of CH_2 and CH_3. However, the accuracy of this method is not satisfactory, and only a mean value is obtained when there are more than two types of co-existing compounds.

The present author has reported the total carbon number of the alkyl side chain as one of a series of studies of the petroleum fraction.[1,2] In this series of studies, the alkyl side chain number must be determined in order to ascertain the carbon number of each alkyl side chain.

For this purpose, the cleavage mechanism of alkyl aromatics under electron impact was studied, and a method was devised by which the alkyl side chain number could be determined from the finding of the α and β cleavage characteristic of the aromatic ring. Thus mass spectrometry can determine the alkyl side chain numbers for different types of coexisting compounds.

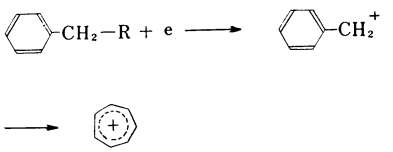
Experimental

Several authentic aromatics were measured by a Hitachi-RMU 5B type mass spectrometer. Mass spectral data of other unavailable compounds were obtained from the literature.[3]

Theoretical

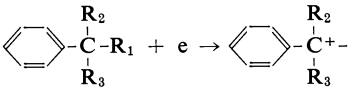
The Mass Spectra of Alkylbenzene.—Under electron impact *n*-alkylbenzene is stabilized as the tropylium ion according to the β bond cleavage.[4] Therefore, *m/e* 91 is a very intense peak in the spectrum.

However, branched alkylbenzene at the α-position cleaves itself to yield the *m/e* $(89+R_2+R_3)$ ion, and some of these ions decompose

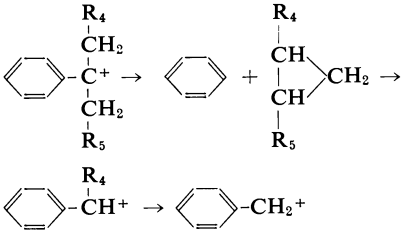


m/e 91

into the *m/e* $(91+R_4)$ or the *m/e* $(91+R_5)$ ion, the *m/e* 91 ion are produced by further rearrangement.[5-7]



(R_2, R_3=hydrogen or alkyl chain)



Alkylbenzene with more than two alkyl substituents takes an α cleavage in addition to the β cleavage described above. When the substituent is longer than the propyl group, the cleavage of the β bond is observed, while the α cleavage is observed when it is the methyl or ethyl group.

Thus, monosubstituted alkylbenzenes give their most intense peak according to the β cleavage, while polysubstituted alkylbenzenes give intense peaks according to the β and α cleavages as well.

The following equation indicates the carbon number of the alkyl side chain on the ion produced according to the β cleavage:

$$b=a(n-1)/n+1 \qquad (1)$$

where

b: the total carbon number of the alkyl side chain on the ion produced;

1) Part II. S. Oshima, A. Katsumata and K. Fujii, *Mass Spectroscopy*, **11**, 46 (1963).
2) S. Oshima, T. Nishishita and K. Fujii, *J. Chem. Soc. Japan, Pure Chem. Sec.* (*Nippon Kagaku Zasshi*), **84**, 646 (1963).
3) Catalog of Mass Spectral Data, A. P. I. Research Project 44.
4) S. Meyerson and P. N. Rylander, *J. Chem. Phys.*, **27**, 901 (1957).
5) W. H. McFadden and A. L. Wahrhaftig, *J. Am. Chem. Soc.*, **78**, 1572 (1956).
6) P. N. Rylander and S. Meyerson, ibid., **78**, 5799 (1956).
7) F. W. McLafferty, *Appl. Spectroscopy*, **11**, 148 (1957).

a: the total carbon number of the alkyl side chain on the original molecule, and
n: the alkyl side chain number.

If the ion is formed according to the α cleavage, on the other hand, the equation will be;

$$b=a(n-1)/n \qquad (2)$$

Since the total carbon number of the alkyl side chain on the ion (b) is obtained from the most intense peak in the spectrum, the alkyl side chain number (n) can be obtained by determining the a value from the most intense peak in the spectrum.

The alkyl side chain number (n) was calculated from Eqs. 1 and 2 for 89 kinds of mass spectral data of authentic alkylbenzenes possessing from 3 to 12 carbons in the alkyl side chain and involving from 1 to 6 alkyl side chain numbers. Figure 1 indicates the relationship between the real side chain number and n from Eqs. 1 and 2. The n values which were derived from the β cleavage process agree with the real value when the chain number is small, but they differ when the chain number becomes more than three. On the other hand, the n from the α cleavage process shows good agreement with the real value when the chain number is large, but they differ greatly when the chain number is less than 4.

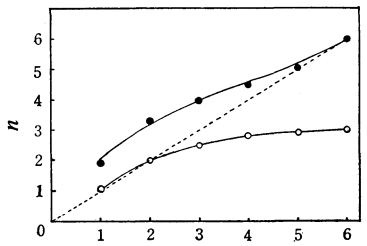


Fig. 1. Number of alkyl radical at ring (real value) and n at alkylbenzene.
● α-cleavage ○ β-cleavage

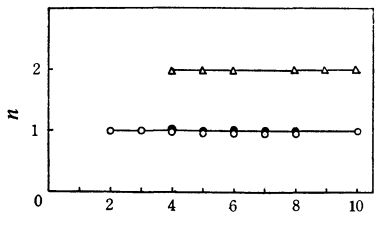
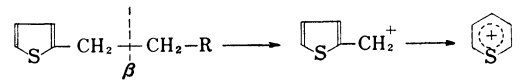


Fig. 2. Carbon number of alkyl radical and n at alkylthiophene.
○ n-alkylthiophene
● iso-(2)-alkylthiophene
△ di-n-alkylthiophene

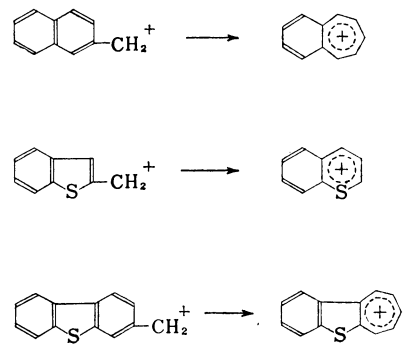
Alkylthiophene.—The most intense peak in the spectrum of alkylthiophene is generally due to the β cleavage of the alkyl side chain. This results from the hypothetical formation of the thiacyclohexatrienium ion, which is similar to the tropylium ion observed in alkylbenzene.



The n values calculated from Eq. 1 for 27 authentic alkylthiophenes showed good agreement with the real values. Figure 2 indicates the relationship between n and the carbon number of the alkyl side chain.

Miscellaneous Compounds.—The most intense peaks in the mass spectra of naphthalene, benzothiophene and dibenzothiophene also result from the β cleavage of alkyl side chains.

These ions are thought to be stabilized by the following process:



The Determination of *a*.—The a value of the high boiling range aromatic fraction in petroleum is determined by the following procedure. An aromatic mixture of petroleum is separated into small fractions by liquid chromatography in order to separate the coexisting compound types which overlap on the same mass numbers in the case of the low voltage ionization method. However, if the mass difference between the two aromatic rings is larger than b, overlapping compound types are permitted to coexist in the same fraction. When these isolated aromatic mixture are measured by the low voltage ionization method, the alkyl carbon number of the most abundant molecule is obtained according to the author's method.[2] Thus, the a value is determined.

The Determination of *b*.—When the isolated sample mentioned above is then measured under 50~100 eV. to obtain fragment ions, the most intense peak in the spectrum is b. On the other hand, in the presence of more than two types of compounds, the most intense

peak among the objective compounds has to be taken as b.

The Determination of n. — There are two procedures for determining n for alkylbenzenes. The first method is to multiply a correction value by n as calculated from Eq. 1, assuming β cleavage. Table I indicates the correction value. The other method is as follows; Eq. 1 is used where $n=1$ or 2, Eq. 2 is used where $n=5$ or 6, and the mean value between Eqs. 1 and 2 is used where $n=3$ or 4. Equation 1 is used for alkylthiophene, and it is also adopted for naphthalene, benzothiophene and dibenzothiophene in spite of the scarce calibration data about them.

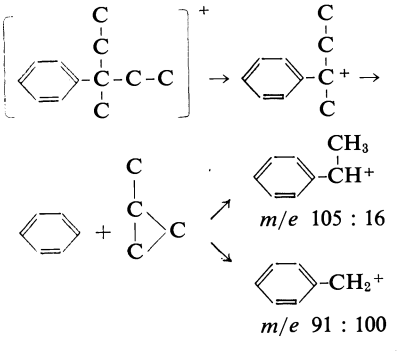
TABLE I. CORRECTION VALUES OF n

Chain number	1	2	3	4	5	6
Correction value	1	1	1.2	1.4	1.7	2.0

Discussion

If the most intense fragment peak in the spectrum is a factor determining the alkyl side chain number, the cleavage mechanism should not be influenced by the alkyl side chain number or by other structure requirements.

Monoalkylbenzenes should give the most intense peak on the same mass number. If α carbon has no side chain, monoalkylbenzenes actually give the most intense peak at m/e 91 without exception. Methylated (α) monoalkylbenzenes give the most intense peak at m/e 105 according to the β cleavage, and the ratio of m/e 105 to m/e 91 is about 10%. This value is unchanged even if the chain length is changed. Moreover, α-dimethyl monoalkylbenzenes give the most intense peak at m/e 119 and the ratio of m/e 119 to m/e 91 is about 40~60%, which is also independent of the length of the alkyl side chain. However, when ethyl or a longer alkyl group ($>C_3$) is attached to the α carbon, m/e 91 becomes a intense peak. For example, 3-ethyl-3-pentylbenzene is cleaved as follows:



Therefore, normal alkylbenzenes and branched alkylbenzenes having ethyl or a longer alkyl group ($>C_3$) on α carbon are cleaved to form the most intense peak at the same mass number. However, α-methyl monoalkylbenzenes cause an error, as is indicated in Fig. 3. Polysubstituted methyl or ethyl benzene produces α-cleavage rather than β-cleavage ions. Figure 4 shows the ratio of the α cleavage to the β cleavage in the case of dialkylbenzene. When the carbon number of the alkyl chain is C_1 or C_2, a large amount of α cleavage is observed; it would be expected

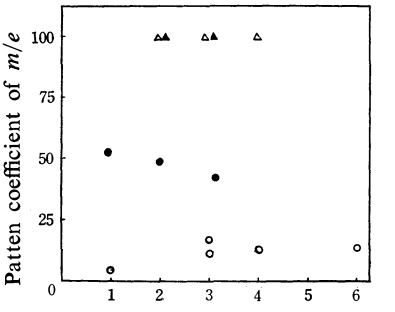
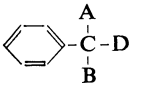


Fig. 3. Peak intensity of m/e 91 at monoalkylbenzene.



○ A=CH_3, B=H, ● A=CH_3, B=CH_3
△ A≥C_2H_5, B=H, ▲ A≥C_2H_5, B≥CH_3

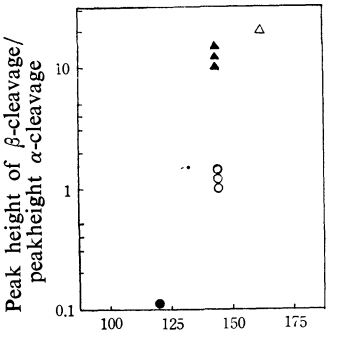


Fig. 4. Ratio of α-cleavage ion to β-cleavage ion at alkylbenzene.
● methylethylbenzene
○ diethylbenzene
▲ methylpropylbenzene
△ dipropylbenzene

that this inclination would become more marked as the benzene ring is substituted more. This means that an increase in the alkyl side chain number disturbs the determination of the alkyl side chain number from the β-cleaved ion. Accordingly, a correction value is required.

Figure 5 shows the effect of the carbon number of the alkyl chain. The n value from the α cleavage tends to decrease as the carbon number increases in n-alkylbenzene. Other alkylbenzenes, however, do not show this inclination. Therefore, the effect of the carbon number should not be considered excessive.

The following facts have been established about the sensitivity of β-cleaved ions. Monoalkylbenzenes are cleaved to form the hydrogen-rearranged m/e 92 ion as well as the m/e 91 ion, and there is a certain relationship between

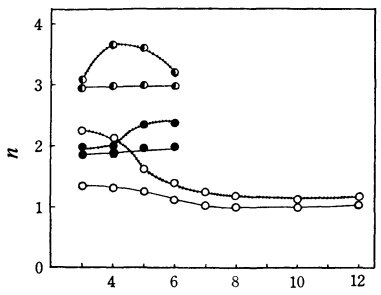


Fig. 5. Carbon number of alkyl radical and n at alkylbenzene.
○ radical number : 1
● radical number : 2
◐ radical number : 3
⫲ α-cleavage — β-cleavage

the molecular ion peak height and the summed peak height of m/e 91 and 92. The ratio of the molecular ion and the summed peak height (m/e 91+92) tends to decrease when the number of carbon which are lost as a neutral radical after β cleavage increases. On the other hand, when the number of carbons is within C_3 to C_5, this ratio becames constant.[8] This means that the number of β-cleaved ions is about the same within a certain size range of the alkyl chain. This makes it desirable to use the β cleavage process for the determination of the alkyl side chain number.

According to Fig. 1, the choice of Eq. 2 for the determination of the alkyl side chain number is preferable to the C_5 and C_6 of the side chain. However, considering the cleavage mechanism, the chance of error elsewhere is increased.

Alkylbenzenes in the high-boiling-range petroleum fraction are considered to include all kinds of alkylbenzenes. Because of the above reason, the calculated alkyl side chain number is, after all, the average value. Charlet reported that in almost all cases the alkyl side chain number is about 3 to 4 in the high boiling fraction of petroleum.[9] Alkyl side chain numbers (n) calculated from Eq. 1 and corrected according to Table I for alkylbenzene and naphthalene in the aromatic fraction isolated from light gas oil were 3 or 4, which agreed well with the findings of infrared spectrometry. It was clear that a and b could be determined by examining the same sample for which the n was determined.

According to a number of spectral data, it may be considered that the alkyl side chain number of alkylthiophene can be determined by Eq. 1, but much more data are required for naphthalenes, benzothiophenes, dibenzothiophenes and other aromatics.

Summary

The cleavage mechanism of alkylbenzene and other compounds under electron impact has been studied. The following facts are evident. If the ion from the aromatic compound is formed according to β cleavage under electron impact, the carbon number of the alkyl side chain on the compound may be indicated by the following equation;

$$b=a(n-1)/n+1 \quad (1)$$

where

b: the total carbon number of the alkyl side chain in the ion produced;
a: the total carbon number of the alkyl side chain in the original molecule, and
n: the alkyl side chain number.

If the ion is formed according to α cleavage, the equation will be:

$$b=a(n-1)/n \quad (2)$$

The effects of the alkyl side chain number and the structure upon n values from Eqs. 1 and 2 have also been studied. From the study, a method has been devised by which the alkyl side chain number of aromatics in the high-boiling-range fraction of petroleum can be determined from the total carbon number of the alkyl side chain in the molecule ion and the carbon number of the alkyl side chain in the peak showing the most intense peak in the spectrum.

The author wishes to express his hearty thans to Mr. Tsunehiko Kozuma for his kind guidance and to Mr. Kinya Fujii for his assistance.

Research Center
Maruzen Oil Co.
Kaiso-gun, Wakayama

8) H. M. Grubb and S. Meyerson, "Mass Spectrometry of Organic Ions," Academic Press, New York (1963), p. 457.

9) E. M. Charlet, K. P. Lanneau and F. B. Johnson, Cleveland Meeting, Am. Chem. Soc., Petr. Div., 105, April, 1951.

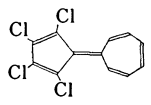
Reaction of Tropone with 1,2,3,4-Tetrachlorocyclopentadiene. A Novel Rearrangement Reaction to Fulvenes[1]

By Yoshio KITAHARA,* Ichiro MURATA,* Makoto FUNAMIZU* and Takashi ASANO**

(Received December 20, 1963)

Sesquifulvalene (cycloheptatrienylidenecyclopentadiene),[2] one of the non-alternant hydrocarbons, is an interesting substance, both theoretically and chemically, which has been recently synthesized by Prinzbach and Rosswog;[3] some of its derivatives are also known, such as tetrabenzo-,[4] 1, 2, 3, 4-tetraphenyl-,[5] 1, 2-benzo-3-benzyl-,[6] 1-benzyl-,[3] and 1-(*p*-methoxybenzyl)-sesquifulvalene.[3] Attempts have been also made in this laboratory to synthesize sesquifulvalene, while syntheses of the quinone compounds, sesquifulvalene-1, 4-quinone and 2, 3-benzosesquifulvalene-1, 4-quinone,[7,8] have already been reported.

McBee[9] found that 1, 2, 3, 4-tetrachlorocyclopentadiene[9,10] (I) undergoes condensation with various aromatic aldehydes to form the corresponding fulvene derivatives, while Kitahara and Doi[11] found that tropone (II) undergoes condensation with malononitrile and the cyanoacetic ester to form 8, 8-dicyanoheptafulvene[11,12] and 8-cyano-8-ethoxycarbonylheptafulvene[11,12] respectively.



(III)

Considering these facts, it seemed possible to synthesize 1, 2, 3, 4-tetrachlorosesquifulvalene (III) by the reaction of I and II; examinations were therefore made on this point. A solution of I and II in a large volume of ethanol was allowed to stand at room temperature, and the ultraviolet absorption spectrum[13] of the solution, which gradually turned red, was measured in order to follow the progress of the reaction. The intensity of the absorption maximum of II, near 300 mμ, gradually decreased, and a new maximum appeared at 374 mμ. The ratio of the absorbances at 374 and 300 mμ, taken at definite intervals, gradually increased until the value remained constant at around 1.9 after 40 hr. From this reaction mixture, red prisms (IV), m. p. 116~117°C, were obtained. The analytical values of IV failed to agree with $C_{12}H_6Cl_4$ (III) but unexpectedly agreed with the formula, $C_{14}H_{11}OCl_3$. The infrared spectrum[14] of IV showed absorption bands at 1255 and 1043 cm^{-1} due to aromatic ether bonds, and the NMR spectrum[15] had a triplet at 8.55 τ and a quartet at 5.90 τ corresponding to the protons of an ethoxyl group. Elementary analysis and these spectra suggested that one of the chlorine atoms had been replaced by an ethoxyl group.

When the reaction of I and II in methanol was carried out in a thermostatic bath at 20°C, the absorbancy ratio at 374 and 300 mμ reached a constant value of 3.4 after about 40 hr. From this reaction mixture, two kinds of product were obtained: red prisms (V), m. p. 117~118°C, and reddish orange needles (VI), m. p. 77~78°C. Elementary analyses indicated that both V and VI had the molecular formula $C_{13}H_9OCl_3$. Since the infrared spectrum of V exhibited absorption bands at 1257 and 1026 cm^{-1}, due to aromatic ether bonds, and those of VI exhibited such bands at 1263 and 1025

* Present address: Department of Chemistry, Faculty of Science, Tohoku University, Sendai.
** Present address: Santoku Chemical Co., Ltd., Sendai.

1) Paper read at the Tohoku Local Meeting of the Chemical Society of Japan, Sendai, June 1961.
2) W. von E. Doering, "Theoretical Organic Chemistry" (Kekule Symposium), Butterworth Publishers, London (1959), p. 35.
3) H. Prinzbach and W. Rosswog, *Angew. Chem.*, 73, 543 (1961).
4) B. Pullman, A. Pullman, E. D. Bergman, H. Berthod, E. Fisher, Y. Hirshberg, D. Lavie and M. Mayot, *Bull. soc. chim. France*, 19, 73 (1952).
5) H. Prinzbach, *Angew. Chem.*, 73, 169 (1961).
6) H. Prinzbach and D. Seip, ibid., 73, 169 (1961).
7) Y. Kitahara, I. Murata and T. Asano, This Bulletin, 34, 589 (1961).
8) Y. Kitahara, I. Murata and T. Asano, ibid., 37, 924 (1964).
9) E. T. McBee, R. K. Meyers and C. F. Baranauckas, *J. Am. Chem. Soc.*, 77, 86 (1955).
10) A. Roedig and L. Horning, *Chem. Ber.*, 88, 2003 (1955).
11) Y. Kitahara and K. Doi, Paper presented at the Tohoku Local Meeting of the Chemical Society of Japan, Akita, October, 1961,
12) T. Nozoe, T. Mukai, K. Osaka and N. Shishido, This Bulletin, 34, 1384 (1961).
13) Ultraviolet spectra were measured with a Hitachi photoelectric spectrometer, model EPU-2.
14) The infrared spectra were measured with a Perkin-Elmer model 21 spectrophotometer, provided with a NaCl prism.
15) The NMR spectra were run by the Research Institute of Mitsubishi Chemical Industry Co. on a Varian A-60 instrument in a CS_2 solution. Tetramethylsilane was used as the internal standard.

cm^{-1}, and since the NMR spectrum showed absorptions at 6.13 τ (singlet) for V and 6.19 τ (singlet) for VI, corresponding to the methoxyl protons, it appeared that a methoxyl group had been introduced by this reaction.

The reaction between II and 1, 2, 3, 4-tetrabromocyclopentadiene[16] (VII) followed an entirely analogous course; red plates (VIII), m. p. 128~129°C, and red prisms (IX), m. p. 90~91°C, were obtaind.

From the foregoing experimental evidence and the presence of an absorption maximum in the comparatively long wavelength region at 374 mμ in the ultraviolet spectra of the products (V, VI, VIII, IX), V and VI were assumed to be isomers formed by the replacement of one of the four chlorine atoms in III by a methoxyl group.

The examination of the infrared spectrum in the C–H out-of-plane region indicated the presence of an absorption corresponding to an *o*-disubstituted benzene at 749 cm^{-1} in V and that of a *p*-disubstituted benzene at 818 cm^{-1} in VI. The sharp absorption at 852 cm^{-1} in V and at 861 cm^{-1} in VI is considered to be due to the C–H of a tri-substituted double bond.

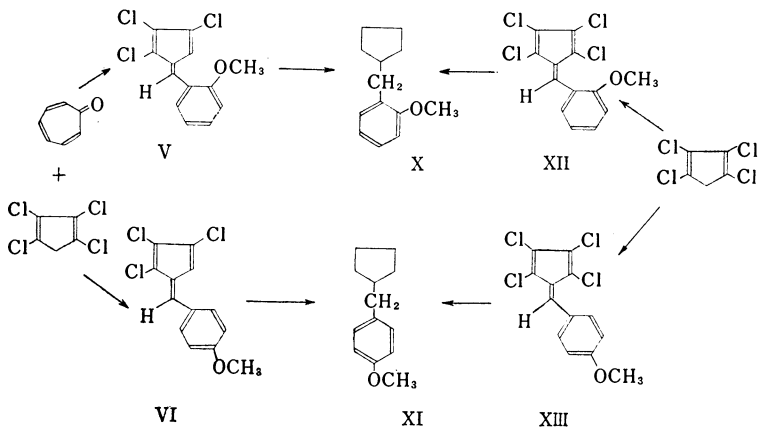
The catalytic reduction of V in methanol, in the presence of sodium acetate and using palladium-carbon as a catalyst, resulted in the absoption of 6 molar equivalents of hydrogen, and a colorless oil (X) was obtained. A similar reduction of VI also afforded a colorless oil (XI).

The infrared spectra of the reduction products, X and XI, indicated the absorption of an aromatic ether bond at 1247 and 1034 cm^{-1} in X and at 1253 and 1039 cm^{-1} in XI, absorptions which are practically unchanged from those of V and VI. If the methoxyl group had been present in the five-membered ring, the absorption of the ether bond in the reduction products (X and XI) would have shifted to about 1150~1060 cm^{-1}.[17] The absorption of the C–H out-of-plane vibration in the *o*-disubstituted benzene still apears at 752 cm^{-1} in X, and that of the *p*-disubstituted benzene, at 833 cm^{-1} in XI.

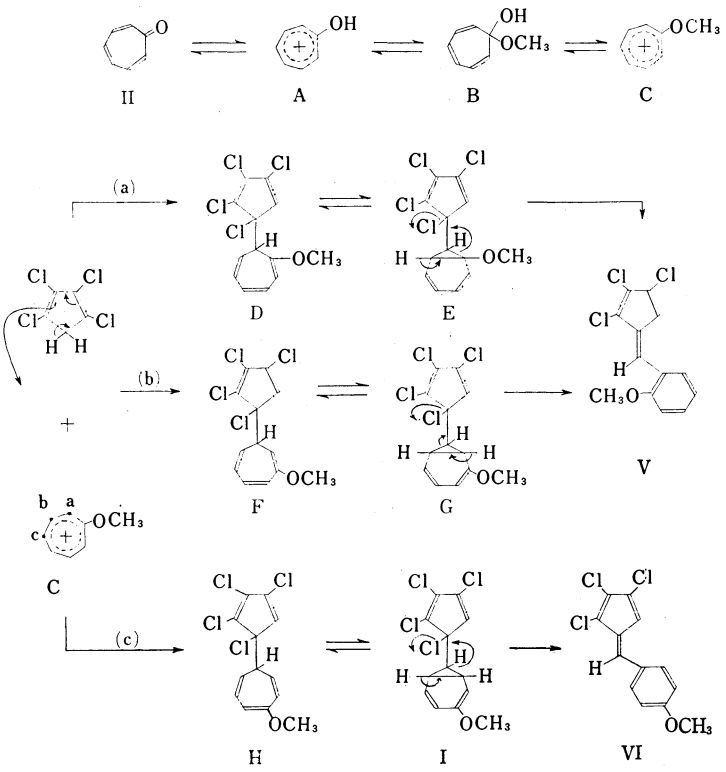
The ultraviolet absorption spectra of X and XI are very similar to that of anisole.[18]

From these considerations, it may be concluded that the structure of V and VI is not the anticipated sesquifulvalene skeleton, like III, but that the products are probably trichloro-6-(*o*-methoxyphenyl)fulvene and trichloro-6-(*p*-methoxyphenyl)fulvene for V and VI respectively.

In order to prove these structures, the condensation of I with *o*- and *p*-anisaldehyde respectively was carried out in ethanol. When the products thus obtained, 1, 2, 3, 4-tetrachloro-6-(*o*-methoxyphenyl)fulvene (XII), m. p. 166°C, and 1, 2, 3, 4-tetrachloro-6-(*p*-methoxyphenyl)-fulvene[9] (XIII), m. p. 123°C, were submitted to catalytic reduction over palladium-carbon in methanol, in the presence of sodium acetate; 7 molar equivalents of hydrogen were absorbed in each case to give two colorless oils (X′ and XI′). The ultraviolet and infrared spectra of X′ and XI′ were identical in all respects with those of X and XI.



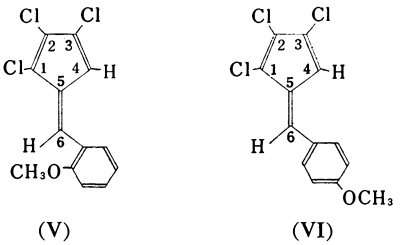
16) R. Riemschneider, G. Englemenn and K. Rosswitz, *Z. Naturforsch.*, **116**, 172 (1956).
17) L. F. Bellamy, "The Infra-red Spectra of Complex Molecules," Methuen Co., London (1958), p. 114.
18) R. A. Friedel and M. Orchin, "Ultraviolet Spectra of Aromatic Compounds", John Wiley and Sons Inc., New York (1951), Nos. 55, 56.



The results have afforded evidence of the structures assigned to V and VI, with the exception of the positions of three chlorine atoms. From the mechanism of this rearrangement reaction, it may be expected that the three chlorine atoms will be located at the 1-, 2- and 3-positions.

An examination of the physicochemical properties of tropone (II) has let us to consider it to have an ionic structure because of the contribution of six π electrons resulting from the polarization of the carbonyl group.[19,20] Consequently, an equilibrium exists, in methanolic solution of tropone, among the hydroxytropylium cation (A), hemiketal (B), and the methoxytropylium cation (C), as is indicated below, and the reaction may be considered to proceed via C. The attack of I on C may be possible at any of the three positions, a, b and c. If the attack occurs at a *o*-methoxy derivatives (V) will form from a norcaradiene type intermediate (E), and then be rearranged. If the reaction takes the b course, the rearrangement of the norcaradiene intermediate (G) will form V by the liberation of the proton adjacent to the methoxyl group. If the reaction follows the c course, the rearrangement of the intermediate (I) may be considered to form the VI by the liberation of the γ-proton of the methoxyl group. From such a rearrangement mechanism, the three chlorine atoms should be in the 1-, 2- and 3-positions in both V and VI.

The structures of V and VI were further confirmed from their NMR spectra. V had signals at 6.13 τ (singlet, OCH_3), 3.52 τ (doublet, J=1 c. p. s., 4-H), 2.37τ (partially resolved doublet, 6-H), and 3.3~2.5 τ (multiplet, four protons of the benzene ring). VI had signals



19) H. J. Dauben and H. J. Ringold, *J. Am. Chem. Soc.*, 73, 876 (1951).

20) W. von E. Doering and F. L. Detert, ibid., 73, 876 (1951).

21) The 4- and 6-protons was assigned by means of a comparison of their spectra with that of 1, 2, 3, 4-tetrachloro-6-(*p*-methoxyphenyl)fulvene (XIII). XIII lacked a signal in the 3.5 τ region, but the peaks due to the methoxyl- (6.18 τ, singlet) and A_2B_2-type absorptions (3.14 τ, doublet, J=9 c. p. s., 2.44 τ, doublet, J=9 c. p. s.) and the 6-proton (2.52 τ, singlet) were present. Therefore, the more shielded signals in V and VI (3.52 τ, 3.43 τ) can be assigned to a 4-proton, while the more deshielded signals (2.37 τ, 2.78 τ) can be assigned to a 6-proton.

at 6.19 τ (singlet, OCH_3), 3.43 τ (doublet, J=1 c. p. s., 4-H), 2.78 τ (partially resolved doublet, 6-H)[21], and at 3.14 τ and 2.55 τ (J=9 c. p. s.).

The doublet splitting pattern of the 4- and 6-protons (J=1 c. p. s.) can be interpreted only in the case of structures V and VI.[22]

The reaction of 1, 2, 3, 4, 5-pentabromocyclopentadiene (XIV) and tropylium bromide (XV) produced red needles, m. p. 79°C, which were identical with 1, 2, 3, 4-tetrabromo-6-phenylfulvene (XVI), which was obtained by the reaction, under McBee's conditions,[9] of 1, 2, 3, 4-tetrabromocylopentadiene (VII) and benzaldehyde. Since the reaction of XIV and XV, neither of which contains a methoxyl group, results in rearrangement, it seems certain that the liberation of a proton acts as the driving force of this rearrangement reaction.

The foregoing experimental facts have shown that the reaction of I and II in methanol results in an entirely new type of rearrangement reaction in which the methoxyl group enters the seven-membered ring (a six-membered ring after the rearrangement) and in which a chlorine atom in the five-membered ring is liberated.

Experimental

The Reaction of Tropone (II) 1, 2, 3, 4-Tetrachlorocyclopentadiene (I).—*Reaction in Ethanol.*— A solution of tropone (2.12 g.) and 1, 2, 3, 4-tetrachlorocyclopentadiene (4.08 g.) in ethanol (250 ml.) was allowed to stand at room temperature; the ultraviolet absorption spectrum of the reaction mixture was measured at definite intervals. The ratio of absorbances at 374 and 300 mμ became almost constant at 1.9 after about 40 hr.

The reaction mixture was then poured into ice water, and the red oil which separated was washed with water and dried over phosphorus pentoxide. This oil when treated with cyclohexane formed red crystals (0.6 g.), m. p. 110~115°C. Recrystallization from methanol gave IV as red prisms, m. p. 116~117°C.

Found: C, 55.42, 56.00; H, 3.65, 3.80. Calcd. for $C_{14}H_{11}OCl_3$: C, 55.74; H, 3.68%.

UV λ_{max}^{MeOH} mμ (log ε): 248 (3.80), 323 (4.11), 374 (4.27).

Reaction in Methanol.— A solution of tropone (10.0 g.) and 1, 2, 3, 4-tetrachlorocyclopentadiene (19.2 g.) in methanol (1200 ml.) was allowed to stand in a thermostatic bath at 20°C; the ultraviolet spectrum of the reaction mixture was measured at definite intervals. The ratio of absorbances at 374 and 300 mμ became constant at ca. 3.4 after about 45 hr. The methanol solution was evaporated under reduced pressure to one-half the original volume, and then poured into 1000 ml. of ice water and extracted thoroughly with petroleum ether (b. p. 36°C). The petroleum ether layer was washed with water, dried over magnesium sulfate, and evaporated. The oily residue crytasllized on the addition of a small amount of methanol; recrystallization from methanol gave 3.0 g. of crude V, melting at 116~118°C.

The recrystallization mother liquor of V was chromatographed over an alumina column (45×300 mm.). Elution with petroleum ether (600 ml.) gave 2.3 g. of crude V, m. p. 114~116°C, further elution with the same solvent (450 ml.) afforded 2.95 g. of crude VI, m. p. 72~75°C.

The recrystallization of crude V from methanol gave red prisms with a m. p. of 117~118°C.

Found: C, 54.41; H, 2.95. Calcd. for $C_{13}H_9OCl_3$: C, 54.29; H, 3.16%.

UV λ_{max}^{MeOH} mμ (log ε): 248 (3.84), 320 (4.11), 373 (4.27).

The Recrystallization of crude VI from ethanol afforded reddish orange needles, m. p. 77~78°C.

Found: C, 54.33; H, 3.16. Calcd. for $C_{13}H_9OCl_3$: C, 54.29; H, 3.16%.

UV λ_{max}^{MeOH} mμ (log ε): 250 (4.02), 374 (4.55).

The Reduction of 1, 2, 3-Trichloro-6-(*o*-methoxyphenyl)fulvene (V).—A solution of V (2.9 g.) in 100 ml. of methanol, with 5% palladium-carbon (0.1 g.) and anhydrous sodium acetate (2.5 g.), was shaken with hydrogen at an ordinary temperature and pressure; 6 molar equivalents of hydrogen were absorbed in about 1 hr. The solution was then filtered and evaporated. After the addition of water, the residue was extracted with petroleum ether, and the extract was dried over magnesium sulfate and then evaporated. The residual oil was submitted to distillation under reduced pressure gave 1.1 g. of a colorless oil, X.

Found: C, 81.49; H, 9.36. Calcd. for $C_{13}H_{18}O$: C, 82.06; H, 9.54%.

UV λ_{max}^{MeOH} mμ (log ε): 220 (3.86), 272 (3.32).

IR: 1609, 1592, 1247, 1034, 752 cm^{-1}.

The Reduction of 1, 2, 3-Trichloro-6-(*p*-methoxyphenyl)fulvene (VI).—The catalytic reduction of VI (2.9 g.) in methanol, under the same conditions as for V, afforded 1.2 g. of a colorless oil, XI.

Found: C, 82.09; H, 9.34. Calcd. for $C_{13}H_{15}O$: C, 82.06; H, 9.54%.

UV λ_{max}^{MeOH} mμ (log ε): 225 (4.08), 278 (3.16).

IR: 1618, 1590, 1520, 1523, 1039, 833 cm^{-1}.

1, 2, 3, 4-Tetrachloro-6-(*p*-methoxyphenyl)fulvene (XIII).— Synthesis according to the method of McBee yielded XIII as reddish orange needles, m. p. 122~123°C.

UV λ_{max}^{MeOH} mμ (log ε): 255 (3.98), 385 (4.38).

1, 2, 3, 4-Tetrachloro-6-(*o*-methoxyphenyl)fulvene (XII).—A solution of 1, 2, 3, 4-tetrachlorocyclopentadiene (4.1 g.) and *o*-anisaldehyde (2.72 g.) in ethanol (10 ml.) was refluxed on a water bath for 2~3 hr., and then cooled. The crystals which separated were collected by filtration. Recrystallization from ethanol gave red needles m. p. 165~166°C.

22) The long range 1, 3-spin-spin coupling of a vinylic proton with an allylic proton is a well-recognized phenomenon. S. Alexander, *J. Chem. Phys.*, **28**, 355 (1958); **32**, 1700 (1960); R. R. Fraser and D. E. McGreer, *Can. J. Chem.*, **39**, 505 (1961); E. B. Whipple, J. H. Goldstein and G. R. McClure, *J. Am. Chem. Soc.*, **82**, 3811 (1960); E. B. Whipple, *J. Chem. Phys.*, **35**, 1039 (1961); A. A. Bothner-By and C. Naar-Colin, *J. Am. Chem. Soc.*, **83**, 231 (1961); A. A. Bothner-By, C. Naar-Colin and H. Gunther, ibid., **84**, 2748 (1962).

Found: C, 58.55; H, 4.00. Calcd. for $C_{13}H_5OCl_4$: C, 58.08; H, 3.73%.

UV λ_{max}^{MeOH} mμ (log ε): 255 (3.84), 330 (4.06), 374 (4.19).

The Reduction of XII and XIII.—The catalytic reduction of XII and XIII under the same conditions as in the reduction of V and VI yielded two colorless oils, X′ and XI′. The ultraviolet and the infrared absorption spectra of X′ and XI′ were identical with those of X and XI respectively, indicating the identity of X and X′, and XI and XI′, respectively (*o*- and *p*-methoxybenzylcyclopentanes).

1, 2, 3, 4, 5-Pentabromocyclopentadiene (XIV).—A mixture of 1, 2, 3, 4, 5, 5-hexabromocyclopentadiene (21.5 g.) in ethanol was hydrogenated. One molar equivalent (900 ml.) of hydrogen was absorbed. Ether was added to the reaction mixture to dissolve the crystal which had separated, and the solution was then filtered and evaporated. The crystalline residue (14.9 g.) after recrystallization from petroleum ether afforded XIV as colorless needles (8.55 g.), m. p. 104°C.

Found: C, 13.17; H, 0.36. Calcd. for C_5HBr_5: C, 13.04; H, 0.22%.

1,2,3,4-Tetrabromo-6-phenylfulvene (XVI).—a) A suspension of tropylium bromide (0.34 g.) and 1, 2, 3, 4, 5-pentabromocyclopentadiene (0.92 g.) in carbon tetrachloride (3 ml.) was refluxed on a water bath for 2 hr.; a vigorous evolution of hydrogen bromide gas was observed during the reaction. The carbon tetrachloride was removed under reduced pressure, and the residual oil was heated for 4 hr. at 80°C to complete the evolution of hydrogen bromide. The oil was dissolved in a small amount of benzene, treated with activated charcoal, and then purified by alumina chromatography, using petroleum ether as an eluant. The crystals so obtained were recrystallized from ethanol to afford reddish-brown, silky needles XVI, m. p. 78~79°C.

Found: C, 30.73; H, 1.44. Calcd. for $C_{12}H_{16}Br_4$: C, 30.67; H, 1.29%.

UV λ_{max}^{MeOH} mμ (log ε): 280 (3.75), 343 (4.24).

b) A solution of 1,2,3,4-tetrabromocyclopentadiene (0.765 g.) and benzaldehyde (0.215 g.) in ethanol (2 ml.) was refluxed on a water bath for 10 hr. The solvent was then evaporated, and the residue was recrystallized from ethanol to give 0.42 g. of XVI, m. p. 78~79°C, which showed no depression on admixture with XVI obtained as in a).

Reaction of Tropone (II) and 1, 2, 3, 4-Tetrabromocyclopentadiene (IV).—A solution of tropone (0.65 g.) and 1, 2, 3, 4-tetrabromocyclopentadiene (2.30 g.) in methanol (150 ml.) was allowed to stand at room temperature for 6 hr. The solution was then concentrated under reduced pressure, and the crystals which formed were filtered off. Recrystallization from ethanol afforded VIII as red plates (0.75 g.), m. p. 128~129°C.

Found: C, 37.57; H, 2.34. Calcd. for $C_{13}H_9OBr_3$: C, 37.09; H, 2.13%.

UV λ_{max}^{MeOH} mμ (log ε): 250 (3.79), 330 (sh.), 375 (4.30).

The evaporation of the mother liquor from VIII, and the chromatography over alumina of the residue in petroleum ether, gave 0.83 g. of crude IX m. p. 85~87°C. Recrystallization from methanol afforded red prisms, m. p. 90~91°C.

Found: C, 37.51; H, 2.34. Calcd. for $C_{13}H_9OBr_3$: C, 37.09; H, 2.13%.

UV λ_{max}^{MeOH} mμ (log ε): 250 (3.94), 380 (4.54).

The authors are indebted to the Research Institute of the Mitsubishi Chemical Co., Ltd., for the measurement of NMR spectra, and to Miss Yoko Endo and Miss Yukiko Endo of this Institute for their elementary analyses. The authors are also grateful to the Sankyo Co., Ltd., for its financial support of the present research.

The Chemical Research Institute of Non-Aqueous Solutions
Tohoku University
Katahira-cho, Sendai

The Oxidation of Fe^{2+} by Ultrasound

By Satya PRAKASH, Jata Dhari PANDEY and Rajendra SINGH

(Received January 10, 1964)

Among the various unusual chemical effects produced by high frequency intense sound waves, much interest has been shown recently in the oxidation reactions of aqueous solutions of inorganic salts, e.g., the oxidation of iodide ions,[1-8] the oxidation of ferrous ions,[9-14] the oxidation of cerous ions,[13,14] and the reduction of acidified potassium permanganate[15] and neutral ferrocyanide.[14,15]

The present paper will report on a study of the oxidation of acidic ferrous ammonium sulphate by the intense ultrasonics of 1 Mc.

Experimental

In the present investigation, the source of ultrasonic power was a commercially-available ultrasonic generator, Mullard Type E-7562, which is meant for all purposes requiring high power ultrasonic waves at high frequencies. In addition to the generator, the other accessories were a suitable ultrasonic bath, a proper reaction vessel, and an easy procedure for the coupling of the reaction vessel with the transducer. The basic circuit of the oscillator is shown in Fig. 1. It consists of mainly a number of condensers (C), a tuning coil (L) which is of a variable type and which can be detached from the instrument and replaced by another coil designed for another frequency, and Mullard's silica envelop, triode-type TYS_4-500, which is used to generate radiofrequency power. The oscillator was self-biased, and meters were provided to read the cathode current up to 1 amp., high tension up to 3.500 V., and radiofrequency output voltage up to 10 kV. The transducer used was made of barium titanate ceramics with a frequency of 1 Mc. The

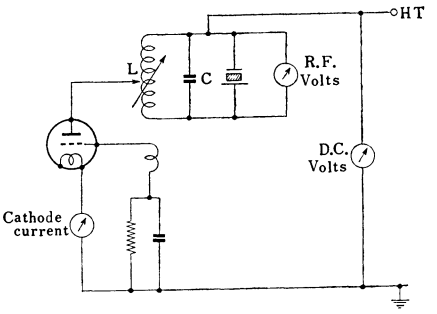


Fig. 1. Simplified oscillator circuit of ultrasonic generator.

major portion of the work was done at a fixed electrical output to the transducer, except when the effect of sonic intensity was to be studied. The reaction vessel was a 250-ml. flat bottomed jena glass battle with ground glass stopper. This reaction bottle was held vertically above the transducer in a water bath and the position so adjusted as to produce a maximum fountain inside the vessel when the ultrasound passed through. The other details of the experimental technique have already been described in previous communications.[16,17] The temperature was kept at 31.5 ± 0.1°C.

Materials. — A stock solution of 0.1 N ferrous ammonium sulphate (A. R., B. D. H.), acidified with A. R. sulphuric acid, was prepared in doubly-distilled water. A ceric sulphate solution of about 0.1 N was prepared from B. D. H.-quality salt by dissolving 34 g. of the salt in 50 ml. of 1 : 1 sulphuric acid (A. R. quality) and making it up to 500 ml. with doubly-distilled water. This solution was then standardised by titrating it against a standard ferrous ammonium sulphate solution, using N phenylanthranilic acid in alcohol as an indicator.

Results and Discussion

In a series of experiments, 25 ml. portions of ferrous ammonium sulphate solutions of known concentrations were placed in the reaction bottle and subjected to ultrasonic waves for different periods of time. The radiofrequency output voltage was kept constant, equal to 2.0 kV. (approx.). As a result of the ultrasonic exposure, the ferrous content of the solution changed to ferric; this was estimated

1) H. Liu and S. Wu, *J. Am. Chem. Soc.*, **56**, 1005 (1934).
2) W. T. Richards and A. L. Loomis, ibid., **49**, 3086 (1927).
3) J. Bhar, *J. Sci. Ind. Res. (India)*, **1**, 106 (1943).
4) N. Sata and K. Nakashima, This Bulletin, **18**, 220 (1943).
5) A Weissler and H. W. Cooper, *Mfg. Chemist.*, **19**, 505 (1948).
6) R. O. Prudhomme and P. Grabar *J. chim. phys.*, **43**, 323 (1949).
7) A. Weissler, H. W. Cooper and S. Snyder, *J. Am. Chem. Soc.*, **72**, 1769 (1950).
8) A. Weissler, *J. Acoust. Soc. Am.*, **25**, 651 (1953).
9) N. Miller, *Trans. Faraday Soc.*, **46**, 546 (1950).
10) N. Miller, *J. chim. phys.*, **48**, 242 (1951).
11) I. E. El'Piner and A. V. Sokol'skaya, *Dok. Akad. Nauk. S. S. S. R.*, **129**, 202 (1960).
12) M. Haissinsky and R. Julien, *J. chim. phys.*, **57**, 664 (1960).
13) A. Weissler, *J. Acoust. Soc. Am.*, **32**, 283 (1960).
14) M. Haissinsky and R. Rivayrand, *J. chim. phys.*, **59**, 623 (1962).
15) S. Witekowa, *Roczniki Chem.*, **36**, 693 (1962).
16) S. Prakash and S. C. Srivastava, *J. Ind. Chem. Soc.*, **35**, 797 (1958).
17) S. Prakash and S. Prakash, *Z. phys. Chem.*, **221**, 145 (1962).

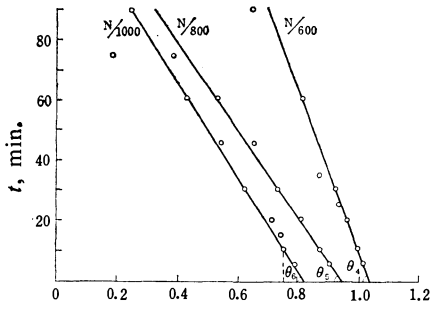


Fig. 2. Plot of $\log_{10}(a-x)$ vs. t.

a is the initial concentration of ferrous ammonium sulphate and x, the change in concentration after t min.

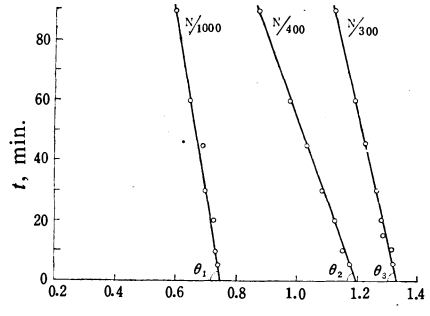


Fig. 3. Plot of $\log_{10}(a-x)$ vs. t.

TABLE I. KINETICS OF OXIDATION OF Fe^{2+} BY ULTRASOUND AT DIFFERENT CONCENTRATIONS OF $FeSO_4(NH_4)_2SO_4 \cdot 6HO_2$

Initial concn. of $FeSO_4(NH_4)_2SO_4 \cdot 6H_2O$	$k_1 \times 10^3$ min^{-1}	
	$k_1 = (2.303/t) \cdot \log_{10}(a/(a-x))$*	Graphically from slopes (Figs. 2 and 3)
N/100	3.779	4.145
N/300	5.411	5.200
N/400	8.407	8.171
N/600	8.925	8.348
N/800	16.885	15.545
N/1000	18.520	19.969

* a Initial concentration
x Concentration at time t

volumetrically from time to time. The results are shown in Figs. 2 and 3. A study of the kinetics showed that the reaction is of the first order. The rate constant obtained is shown in Table I.

A perusal of the table will show that the order of the reaction does not change with the concentration and that the rate increases considerably at higher dilutions of ferrous ammonium sulphate. The values of k_1 as calculated from the equation and from the graph (Figs. 2 and 3) are approximately the same, with a maximum error of about 7 per cent. It can also be predicted that, when the concentration is decreased ten times, the values of k_1 increase by about five times, when the concentration of the solution is halved, k_1 is almost doubled, and so on.

We also investigated the effect of the intensity of ultrasound on the rate of reaction. The results are shown in Fig. 4, where the variation in the constants with acoustic power is given. At a fixed concentration (N/500) of ferrous ammonium sulphate, the kinetics of the reaction was studied by varying the R.F. output. The order velocity constants, as calculated both theoretically and graphically, are given in Table II.

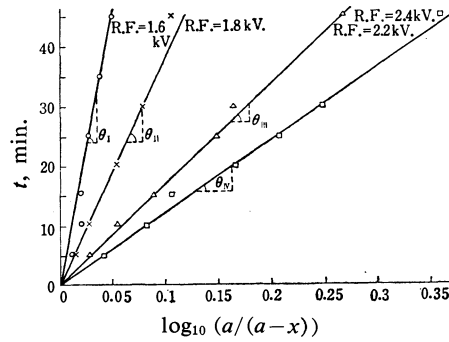


Fig. 4. The effect of ultrasonic intensity.

TABLE II. KINETICS OF REACTION AT DIFFERENT INTENSITIES OF ULTRASOUND

R. F. output kV.	$k_1 \times 10^3$ min^{-1}	
	$k_1 = (2.303/t) \cdot \log_{10}(a/(a-x))$	From graph (Fig. 4)
1.6	3.048	2.530
1.8	6.266	6.073
2.2	13.685	13.160
2.4	18.684	18.679

It is clear from the above data, as well as from Fig. 4, that the sonic intensity has a pronounced effect on the rate of reaction. The values of k_1 continuously increase with an increase in the R. F. output voltage. Further, it may also be concluded that the increase in k_1 values is slower at lower powers than at higher ones.

It is well known that chemical reactions do not occur at very low intensities. Nearly all the observed chemical effects of ultrasonic irradiation in liquid systems occur only at intensities sufficient to induce cavitation within the system. Cavitation is only initiated when and where the pressure amplitude is

greater than the cavitation threshold amplitude. Above this threshold value the reaction rate increases continuously. The increase in intensity will result in an increase in the cavitational intensity, which may be defined as the capability of cavities to bring about chemical reactions. It is evident that, as the number of cavitational holes increases, more and more cavities will form and collapse, resulting in an increase in the rate of the reaction. In the experimental procedure, it was found in most cases that the initial rate (k_1) was slightly higher than the rates during the progress of the reaction. The higher initial rate is most probably connected with the absence of scattering gas bubbles in the very beginning of the reaction.

The formation of hydrogen peroxide from water, when it is exposed to ultrasonic waves, is a complex process, involving many interrelated reactions. The most probable mechanism of the sonolysis of water is the free radical mechanism proposed recently by Weissler,[18] Lindström et al.,[19] Prudhomme et al.[20], and others.[14,21] They have all suggested the formation of H_2O_2 and some freee radicals, such as H, OH and HO_2. According to Weissler, the various steps involved may be written as:

$$H\cdot OH \rightarrow H + OH$$
$$H + H \rightarrow H_2$$
$$OH + OH \rightarrow H_2O_2$$
$$H + H_2O_2 \rightarrow H_2O + OH$$
$$OH + H_2 \rightarrow H_2O + H$$

In oxygenated solutions, additional hydrogen peroxide may be formed by a route involving, perhydroxyl (HO_2) radical:

$$H + O_2 \rightarrow HO_2$$
$$HO_2 + HO_2 \rightarrow H_2O_2 + O_2$$

When a solution of ferrous ammonium sulphate in water is exposed to ultrasonic waves, the formation of H, OH, HO_2 and H_2O_2, as has been described above, is the primary step. Since the cavitation bubbles collapse and those formed at the solid nuclei are weak, the direct decomposition of ferrous ammonium sulphate is doubtful. The presence of a gas[21-25] is always a necessary condition for the occurrence of cavitational chemical reactions. Most probably, the primary decompositions due to the cavitation take place in the gas phase inside the cavitation bubbles.[26,27] Therefore, the oxidation of potassium iodide or of ferrous ammonium sulphfate may be regarded as a secondary reaction brought about by the products of the primary reactions.

The major pioneering work introducing the concept of inorganic free radicals in the field of reaction kinetics was that of Haber and Weiss.[28-29] We have made use as follows of the steps suggested to explain the oxidation mechanism:

	Heat, kcal.
$Fe^{2+} + H_2O_2 \rightarrow Fe^{3+} + OH^- + OH$	
$\rightarrow Fe^{3+}\cdot OH^- + OH$	$-(5 \text{ to } 7)$
$Fe^{2+} + OH \rightarrow Fe^{3+} + OH^-$	$+42$
$Fe^{2+} + HO_2 \rightleftarrows Fe^{3+} + HO_2^-$	$+29$

The $Fe^{3+}\cdot OH^-$ radical may further combine as:

$$Fe^{3+}\cdot OH^- + OH \rightarrow Fe^{2+} + H_2O_2 \quad +(5 \text{ to } 7)$$

The heats of reaction are taken from Uri's review.[30]

The auto-oxidation of Fe^{2+} may also take place due to activated oxygen:

$$Fe^{2+} + O_2 \rightarrow Fe^{3+} + O_2^-$$

At a lower concentration the formation of chain carriers (H_2O_2, HO_2 and OH) is enhanced, resulting in an increase in the reaction rate.

Summary

With the help of Mullard's high frequency ultrasonic generator, type E-7562, with a barium titanate transducer with a frequency of 1 Mc, the oxidation of an acidic ferrous ammonium sulphate solution has been studied. The kinetics of the reaction, at six different concentrations of a ferrous ammonium sulphate solution and at four different ultrasonic intensities has been investigated. The reaction has been found to obey the first order kinetics. A probable mechanism based on the Haber-Weiss work has also been proposed.

The authors wish to express their deep sense of gratitude to the Council of Scientific and Industrial Research, India, for supporting

18) A. Weissler, *J. Am. Chem. Soc.*, **81**, 1077 (1959).
19) O. Lindström and O. Lamm, *J. Phys. & Colloid Chem.*, **55**, 1139 (1951).
20) R. O. Prudhomme and P. Grabar, *J. chim. phys.*, **46**, 323 (1949).
21) B. H. Jennings and S. N. Townsend, *J. Phys. Chem.*, **65**, 1574 (1961).
22) K. Littlewood, *J. Roy. Inst. Chem.*, **86**, 78 (1962).
23) S. C. Srivastava and N. Berkowitz, *Can. J. Chem.*, **41**, 1787 (1963).
24) V. Griffing, *J. Chem. Phys.*, **18**, 997 (1950).
25) A. Weissler, ibid., **18**, 1513 (1950).
26) S. C. Srivastava and N. Berkoweitz, *Can. J. Chem.*, in press.
27) O. Lindström, *J. Acoust. Soc. Am.*, **27**, 654 (1955).
28) F. Haber and J. Weiss, *Naturwiss.*, **20**, 948 (1932).
29) F. Haber and J. Weiss, *Proc. Roy. Soc.*, **A147**, 332 (1934).
30) N. Uri, *Chem. Revs.*, **50**, 375 (1952).

their work, and for the award of a Senior Research Fellowship to one of them (Dr. Jata Dhari Pandey).

Department of Chemistry
University of Allahabad
Allahabad, India

Analysis of the Volatile Constituents of Hamanasu Absolute Oil

By Kiichi NISHIMURA, Tsutomu SAKAI, Mieko OGAWA and Yoshio HIROSE

(Received January 18, 1964)

Previously[1] three of the present authors presented detailed analytical data on the volatile constituents of commercial Hamanasu flower absolute oil and predicted the presence of a minute quantity of a component which is thought to be essential for the floral note of the Hamanasu flower. This report will present some additional data and observations which have been obtained in preliminary attempts to separate this characteristic ingredient.

Experimental

Preliminary Separation of the Materials. — To remove unnecessary non-volatile fractions, 100 g. of commercial Hamanasu absolute oil was steam-distilled; 65 g. of volatile oil was thereby obtained. Then, by treating this volatile oil three times with 5 g. of the Girard T reagent, 30 mg. of the carbonyl fraction was separated. As has been reported, the volatile fraction of Hamanasu absolute oil is composed mainly of phenylethyl alcohol, and it was desirable to separate the gross part of it in order to facilitate the further fractionation of minute components. For this purpose, a mixture of 62 g. of the volatile oil, 100 g. of phthalic anhydride, and 100 cc. of benzene was refluxed for 3 hr. on a water-bath. Acid phthalate and the excess phthalic anhydride were removed from the reaction mixture in the usual way, leaving 7.4 g. of unchanged oil. The same procedure was repeated to give 1.9 g. of an oil which was shown to contain only a few alcoholic compound by measuring its infrared spectrum. Alcoholic compounds regenerated from the acid phthalate by alkaline hydrolysis had a rather simple oder of phenylethyl alcohol and seemed to contain no characteristic ingredients.

Gas Chromatography.—Gas chromatography was carried out using a Shimadzu GC-2B type gas chromatograph: column; polyethylene glycol (25%) on celite, 3 m.; temp., 170°C; carrier gas, N_2.

Liquid Chromatography.—Mallinickrodt's silicic acid was used as the adsorbent, and a hexane solution of ether (3%, 5%, 10%, 30%), as the elute solvent.

Paper Chromatography. — 2,4-Dinitrophenylhydrazones were chromatographed, on a filter paper impregnated with *N,N*-dimethylformamide as the stationary phase, by developing it with cyclohexane saturated with *N,N*-dimethylformamide.

Results and Discussion

The final non-alcoholic oil was subjected to adsorption chromatography and separated into 18 fractions. Each fraction was analyzed by means of gas chromatography and infrared spectroscopy. The compounds identified are shown in Table I.

For illustration, the full composition of the volatile fraction of Hamanasu absolute oil is presented in Table II (in which the dotted items are newly added as a result of this study), together with the composition of Bulgarian rose oil, in which the content of every component was estimated in the authors' laboratory. Carbonyl compounds that could be identified only by paper chromatography are omitted from this table, as they will be discussed in a later part of this report.

It may safely be predicted that the effect of the combination of the constituents of Hamanasu oil is essentially the same as that of Bulgarian rose oil, although the proportions of some ingredients are quite different in these two species of rose. It is curious that there seems to be no organoleptic evaluation of rose oxide in the litrature. The authors reconstituted Hamanasu oil according to their complete analytical data and observed that rose oxide has a marked effect in adding freshness to the floral note. However, some other component is still missing, the floral tone itself; for the time being, this missing component is insufficiently substituted for by ionone or irone.

The carbonyl fraction, separated by the Girard T reagent, was treated with an acidic solution of 2,4-dinitrophenylhydrazine. The products were extracted with chloroform, concentrated to a small volume, and subjected to

1) K. Nishimura, T. Sakai and Y. Hirose, *J. Chem. Soc. Japan, Pure Chem. Sec.* (*Nippon Kagaku Zasshi*), **83**, 745 (1962).

TABLE I. THE COMPOUNDS NEWLY IDENTIFIED FROM HAMANASU ABSOLUTE OIL

Compound	Note	Fr. No.
Hydrocarbon	IR, solid paraffin	1, 2
Citronellyl acetate	RT,* 9.3 min IR, 8.1 μ (acetate) span.—citronellol	3, 4
Neryl acetate	RT, 10.5 min. IR, 8.1 μ (acetate) sapn.—nerol	3
Geranyl acetate	RT, 11.5 min. IR, 8.1 μ (acetate) sapn.—geraniol	3, 4
Rose oxide	RT, 5.2 min. IR, 7.9, 8.4, 8.5, 9.1, 11.3, 11.9 μ	4, 5
Benzyl formate	RT, 14.2 min. IR, 8.6 μ (formate) sapn.—benzyl alcohol	5, 6
Phenylethyl acetate	RT, 13.0 min. IR, 8.1 μ (acetate) sapn.—phenylethyl alcohol	7,8,9, 10, 11
Eugenol	RT, 33.5 min. IR, 3.0, 6.1, 7.3, 8.7, 8.9, 9.6, 10.9, 12.1, 12.5 μ	10, 11, 12
Methyleugenol	RT, 20.6 min. IR, 6.6, 7.9, 8.1, 8.7, 9.7, 10.9, 11.7, 12.3, 13.0 μ	12**

* Gas chromatography, stationary phase: polyethylene glycol on celite; temp.: 180°C; carrier gas: N_2.

** Fractions 13 to 18, were mainly phthalic acid diester.

paper chromatography. When the same procedure was followed as with Bulgarian rose oil, it was found that the chromatogram of the carbonyl fraction of Hamanasu oil is very simillar to that of Bulgarian rose oil. These results are shown in Table III.

Every spot of each chromatogram was cut into pieces and extracted with chloroform, and the ultraviolet adsorption of each extract was measured in neutral and basic solutions (Table IV).

When the deterioration of the peak at the end of one hour was observed, all spots except spot No. 2 from Bulgarian rose oil and spots No. 1 to 4 from Hamanasu oil developed an aliphatic aldehyde character. This would account for the well-known fact that lower homologs of aliphatic aldehyde occur frequently

TABLE II. FULL COMPOSITION OF THE VOLATILE FRACTION OF HAMANASU ABSOLUTE OIL AND BULGARIAN ROSE OIL

Compound	Hamanasu %	Bulgarian rose, %
Aliphatic hydrocarbon	+	3.9
p-Menth-1-ene	0.1	—
Myrcene	—	0.5
Rose oxide	0.2	0.6
Linalool	2.9	3.5
Citronellol	2.5	38.5
Geraniol	1.5	9.6
Nerol	1.0	4.5
Phenylethyl alcohol	86.3	2.3
Benzyl alcohol	1.1	?
Nonyl alcohol	+	?
Heptyl alcohol	+	?
Hexyl alcohol	—	+
Phenylethyl acetate	0.3	?
Benzyl formate	0.1	—
Citronellyl acetate	0.2	4.2
Geranyl acetate	0.3	0.6
Neryl acetate	0.1	+
Nonyl aldehyde	+	?
Benzaldehyde	+	?
Citral	—	0.3
γ-Nonalactone	+	?
Eugenol	0.5	1.5
Methyleugenol	0.3	4.7

TABLE III. THE SPOTS OF PAPER CHROMATOGRAMS

Hamanasu oil

Spot No.	R_f	Reference compound (R_f)
1	0.18	Formaldehyde (0.18)
2	0.26	Acetaldehyde (0.26)
3	0.29	Benzaldehyde (0.28)
4	0.37	Phenylacetaldehyde (0.35) Propionaldehyde (0.38) Acetone (0.36)
5	0.50	Ethyl methyl ketone (0.50)
6	0.54	Butyraldehyde (0.54)
7	0.62	Methyl propyl ketone (0.61)
8	0.74	Citral (0.74)
9	0.91	Methyl nonyl ketone (0.92)

Bulgarian rose oil

Spot No.	R_f	Reference compound (R_f)
1	0.18	Formaldehyde (0.18)
2	0.26	Acetaldehyde (0.26)
3	0.37	Phenyacetaldehyde (0.35) Propionaldehyde (0.38) Acetone (0.36)
4	0.54	Butyraldehyde (0.54)
5	0.64	Valeraldehyde (0.63) Methyl propyl ketone (0.61)
6	0.70	Methyl heptenone (0.71) Octyl aldehyde (0.70)
7	0.74	Citral (0.73)

TABLE IV. UV ABSORPTION SPECTRA OF EACH SPOT OF PAPER CHROMATOGRAM

Hamanasu oil

Spot No.	Neutral solution λ_{max}	Alkaline solution (0.25 N NaOH in EtOH) λ_{max}	Optical density (E) $t=$ 0 min.	$t=$ 60 min.	$E_{t=60}/E_{t=0}$
	mμ	mμ			%
1	367	440	0.40	0.20	50.0
		530	0.26	0.14	54.0
2	366	444	0.65	0.59	90.8
		535	0.30	0.25	83.3
3	368	437	0.80	0.70	87.5
		540	0.48	0.30	62.5
4	368	440	0.70	0.48	68.6
		535	0.48	0.30	62.5
5	367	438	0.65	0.64	98.4
		545	0.40	0.40	100
6	368	440	0.20	0.20	100
		540	0.11	0.11	100
7	368	440	0.20	0.19	95.0
		—	—	—	—
8	368	442	0.29	0.29	100
		530	0.17	0.17	100
9	367	438	0.57	0.56	98.2
		540	0.26	0.26	100

Bulgarian rose oil

Spot No.	Neutral solution λ_{max}	Alkaline solution (0.25 N NaOH in EtOH) λ_{max}	Optical density (E) $t=$ 0 min.	$t=$ 60 min.	$E_{t=60}/E_{t=0}$
	mμ	mμ			%
1	356	435	0.25	0.16	64.2
		525	0.10	0.03	30.0
2	364	435	0.19	0.19	100
		525	0.08	0.08	100
3	365	435	0.49	0.47	96.3
		520	0.29	0.28	98.1
4	365	440	0.13	0.09	68.4
		530	0.05	0.03	60.0
5	364	437	0.38	0.25	66.8
		530	0.21	0.11	52.8
6	360	437	0.80	0.53	65.8
		530	0.48	0.25	52.6
7	360	437	0.63	0.42	67.7
		540	0.35	0.19	53.3

in natural products as common ingredients and/or as degradation products in the course of processing.

The aliphatic aldehyde character was not shown by spot No. 2 from Bulgarian rose oil and spot No. 6 from Hamanasu oil, however, in spite of the fact that the R_f values of these spots correspond to those of acetaldehyde and butyraldehyde respectively. Neither spot corresponds to any simple ketones or aromatic aldehydes. After all, these rose oils probably contain some unknown compounds of an α,β-unsaturated aldehyde or polyfunctional ketone character.

In 1958, Panayotov and Ivanov[2] applied the paper chromatographic technique to the carbonyl fraction isolated by the extraction of Bulgarian rose oil with a sodium bisulfite solution; they thus identified eight components, including cinnamaldehyde, salicylic aldehyde and carvone, by merely referring to the R_f value of each spot. However, it was difficult for the authors of this paper to derive any positive evidence of the presence of those carbonyl compounds in either Bulgarian rose oil or Hamanasu oil, even by taking both liquid and paper chromatographic data into account.

Summary

The separation of the carbonyl fraction and the non-alcoholic fraction, by the Girard T reagent and phthalic anhydride respectively, from the principal constituent, phenylethyl alcohol, of Hamanasu flower absolute oil, and the successive analyses of each fraction have been carried out in order to elucidate the essential olfactory ingredient of the rose oil. The attempt resulted in adding some new components to those listed in the previous report: rose oxide, citronellyl acetate, geranyl acetate and methyleugenol.

The variety of the components has been proven to be essentially the same as in Bulgarian rose oil, although the proportion differs in some components.

The Institute of Food Chemistry
Kita-ku, Osaka

2) I. Panayotov and D. Ivanov, *Perf. Essent. Oil Record*, **49**, 231 (1958).

Synthesis of Benzocyclobutene by Photochemical Desulfonylation

By Yoshinobu ODAIRA, Kenzo YAMAJI and Shigeru TSUTSUMI

(Received March 9, 1964)

As part of the investigation of the synthesis of cyclic compounds, studies of the decarbonylation of cycloalkanones[1,2] and the denitrogenation of diazo-cycloalkanones[3-8] by photochemical reaction have been extensively carried out by several groups of workers in recent years. Little attention has, however, been paid to the synthesis of cyclic compounds by the photo-desulfonylation of the cyclic sulfone; up to the present, no reports along this line have been made.

On the other hand, concerning the desulfonylation of cyclic sulfone, it has been shown in earlier papers[9,10] that a few cyclic compounds were produced by pyrolyses of the corresponding cyclic sulfones. On the whole, however, not only were the pyrolytic conditions employed in the above experiments very drastic, but also the yields of the resulting cyclic compounds were rather insignificant. For example, the pyrolysis of 1, 3-dihydroisothianaphthene-2, 2-dioxide in the molten state at temperatures between 280°C and 300°C[7] gave a mixture of *o*-xylene, benzocyclobutene and 1, 2, 5, 6-dibenzocycloöctadiene in yields as low as 3.2, 12.8 and 4.0% respectively.

It was well known that the aromatic compounds containing a sulfonyl group exhibit intense absorption in the ultraviolet region. Therefore, it might be expected that the desulfonylation of aromatic sulfone would be photochemically accelerated by the collisional transfer of vibrational energy from excited molecules to foreign molecules.

The present investigation was undertaken to confirm the feasibility of the synthesis of the benzocyclobutene ring system by the photolysis of 1, 3-dihydroisothianaphtene-2, 2-dioxide.

1) R. Srinivasan, *J. Am. Chem. Soc.*, **81**, 1546, 5891 (1959); **83**, 2591, 4344, 4348 (1961).
2) C. Trumbore, ibid., **84**, 4025 (1962).
3) L. Hornor, W. Kirmse and K. Muth, *Chem. Ber.*, **88**, 934 (1955); **91**, 430 (1958).
4) P. Yates and E. Rabb, *J. Am. Chem. Soc.*, **79**, 5760 (1957).
5) V. Franzen, *Ann.*, **602**, 199 (1957).
6) W. Kirmes, *Angew. Chem.*, **71**, 537 (1959).
7) M. Cava, M. Mitchell and A. Deana, *J. Am. Chem. Soc.*, **80**, 2260 (1958); *J. Org. Chem.*, **27**, 1908 (1962).
8) O. Süs and K. Möller, *Ann.*, **593**, 91, 99 (1955).
9) H. Kloosterziel and H. Bacher, *Rec. trav. chim.*, **71**, 1235 (1952).
10) M. Cava and A. Deana, *J. Am. Chem. Soc.*, **81**, 4266 (1959); *J. Org. Chem.*, **25**, 1481 (1960).

Results and Discussion

The results of the formation of benzocyclobutene by the decomposition of the sulfone are listed in Table I.

TABLE I. DECOMPOSITION OF 1, 3-DIHYDROISOTHIANAPHTHENE-2, 2-DIOXIDE[a]

Expt. No.	Temp. °C	Irradiation	Benzocyclobutene yield,[b] %
1	200	−	2.6
2	200	+	4.0
3	250	−	17.5
4	250	+	24.9
5	300	−	30.7
6	300	+	39.2
7	350	−	42.0
8	350	+	53.2

a) Each experiment was carried out in the reduced pressure system.
b) Based on total amount of the sulfone used.

In each case, benzocyclobutene was obtained as the major product, together with small amounts of 1, 2, 5, 6-dibenzocycloöctadiene; in addition, the molar ratios of benzocyclobutene and 1, 2, 5, 6-dibenzocycloöctadiene were approximately between 3.9 and 4.1. In some cases, however, with irradiation (Expt. 4 and 6), the products were contaminated by a trace amount of *o*-xylene. From the above results, it may be concluded that the temperature change, within the range of 200~350°C, has an obvious effect on the conversion of the sulfone and that the irradiation considerably accelerates the desulfonylation of the sulfone. As has been described earlier, in every reaction under reduced pressure it has been observed that the ultraviolet-light has no remarkable effect on the molar ratio of benzocyclobutene and 1, 2, 5, 6-dibenzocycloöctadiene. On the other hand, in the reaction under the atmospheric pressure (Expt. 9), the formation of 1, 2, 5, 6-dibenzocycloöctadiene increases, while the formation of benzocyclobutene, on the contrary, decreases, the formation of a small amount of *o*-xylene being clearly observed, as is shown in Table II.

Although one would expect that, from the stand point of chemical equilibrium, reducing

TABLE II. EFFECT OF REACTION PRESSURE ON THE COMPOSITION OF PRODUCT

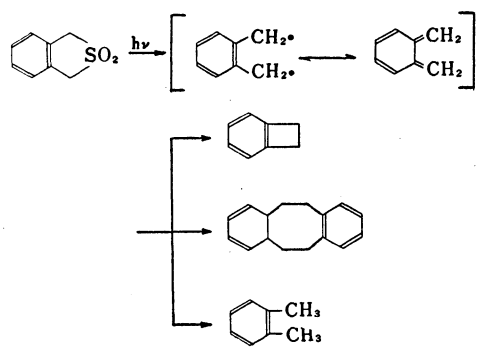
Expt. No.	Temp. °C	Press. mmHg	Yield,[a] %		
			Benzocyclobutene	Dibenzocyclooctadiene	*o*-Xylene
5	300	12~15	30.7	8.1	—
9[b]	300	760	7.8	28.3	2.0

a) Based on total amount of the sulfone.
b) In the absence of ultraviolet-light.

the pressure would accelerates the desulfonylation considerably, the total amount of the decomposition product was nearly equal to the amount of the reaction product under the reduced pressure. Moreover, in order to ascertain the thermal behavior of benzocyclobutene, a further experiment was carried out. When benzocyclobutene was heated under atmospheric pressure at 300°C for 2 hr., 1, 2, 5, 6-dibenzocycloöctadiene was formed in a 57.1% yield, along with a trace amount of *o*-xylene.

In view of the above facts, the most reasonable conclusions to be drawn are that the rate of desulfonylation is independent of the reaction pressure, and that the reaction pressure plays a very important role in the further reaction of the intermediate *o*-xylylene biradical generated by the desulfonylation of the sulfone. Namely, as soon as benzocyclobutene is formed by desulfonylation under reduced pressure, it is immediately removed from the reaction vessel without collision with the other. Consequently, the dimerization of benzocyclobutene was considerably suppressed.

It seems to be more reasonable to consider that the decomposition of 1, 3-dihydroisothianaphthene-2, 2-dioxide may proceed through the intermediate *o*-xylylene biradical, which may be a mesomeric species, and be generated by the desulfonylation of the above sulfone. The intramolecular cyclization of the biradical will lead to benzocyclobutene and the dimerization to 1, 2, 5, 6-dibenzocycloöctadine. Furthermore, it may perhaps be presumed that *o*-xylene is formed by the hydrogen abstraction of the intermediate biradical from the sulfone or the above cyclic products.



Further investigations into the photochemical desulfonylation of various cyclic sulfones are being carried out in this laboratory.

Experimental

Materials. — Forty grams of 1, 3-dihydroisothianaphthene, prepared according to the directions of Cava et al.,[10] were added drop by drop, over a period of 3.5 hr., into 11.3% peracetic acid (930 ml.) with stirring. The temperature was maintatined at 5~10°C during the addition of the sulfide, and after the addition was complete, the mixture was allowed to stand at room temperature for 1 day. After cold water (1000 ml.) had then been stirred into the above mixture, the crude sulfone was precipitated, collected by filtration, and dried. The concentration of the mother liquors in vacuo gave an additional sulfone. Three recrystallizations from benzene-petroleum ether gave 44.6 g. (90.3%) of 1, 3-dihydroisothianaphthene-2, 2-dioxide, m. p. 148.5 ~149.0°C.

Found: C, 57.08; H, 4.81. Calcd. for $C_8H_8O_2S$: C, 57.14; H, 4.80%.

Apparatus and Procedure.—The photolyses were conducted in a reaction vessel connected by a stopcock to a manometer, two traps and a vacuum pump. The reaction vessel, containing a thermometer and the low pressure mercury resonance lamp (100 W.), was a cylindrical glass cell, with an internal diameter of 8.0 cm. and a length of 25 cm.; it was coiled with the flexible heater and placed on the shaking machine. Pulverized 1, 3-dihydroisothianaphthene-2, 2-dioxide (5.0 g.) was placed in the reaction tube, and a considerable volume of glass-wool was stuffed into the output-part of the reaction vessel to avoid trouble due to the sublimation of the starting material. Before the reaction began, the system was swept by nitrogen gas and evacuated to 12~15 mmHg. The reactions, regardless of the presence or absence of the ultraviolet-light, were carried out at 200~350°C with shaking at the reduced pressure of 12~15 mmHg for 5 hr.

After the reaction was complete, the volatile product, which had been collected in traps cooled at −78°C by a dry-ice-acetone bath was, analyzed by gas chromatography, using a 3 m. tricresyl phosphate column at 110°C; it was thus confirmed to be usually composed of only one component, except for the rare case when that component is accompanied by a trace of *o*-xylene. The volatile product

was distilled under reduced pressure, giving a colorless benzocyclobutene, b. p. 52.0~52.5°C/22 mmHg, n_D^{21} 1.5405 (Lit.[11] b. p. 50.5~51.0°C/20 mmHg; n_D^{20} 1.5421). It showed infrared absorption bands at 1580, 1545, 1475, 778 and 717 cm^{-1} (*o*-disubstituted benzene); the ultraviolet spectrum of this compound was in full accordance with that described in the literature.

A mixture of 0.5 g. of benzocyclobutene and 0.6 g. of maleic anhydride in 1.5 ml. of benzene was heated in a sealed tube at 130°C for 30 hr. After the reaction mixture had been distilled under reduced pressure to remove any unchanged substances, the residual solid was sublimed at 150~165°C/3 mmHg. Recrystallization of the sublimate from benzene gave 0.55 g. of 1,2,3,4-tetrahydronaphthalene-*cis*-2,3-dicarboxylic anhydride as white needles, m. p. 188.0~188.5°C (Lit.[12] m. p. 189°C).

The brownish residue in the reaction vessel was extracted with a large amount of petroleum ether as completely as possible. The ethereal extract was then dried over anhydrous sodium sulfate, and the solvent was evaporated. The residue was dissolved in benzene - light-petroleum ether (1 : 10) and chromatographed over alumina. The evaporation of the solvent from the effluent left colorles crystals. Recrystallization from ethyl alcohol afforded 1,2,5,6-dibenzocycloöctadiene as white needles, m. p. 108°C (Lit.[10] m. p. 109~110°C).

Found: C, 92.38; H, 7.41. Calcd. for $C_{16}H_{16}$: C, 92.26; H, 7.74%.

It showed infrared absorption bands at 1595, 1585, 1485, 755 and 733 cm^{-1} (*o*-disubstituted benzene); and at 3000 cm^{-1} (=C-H). Moreover, in its ultraviolet spctrum, the maximum absorptions were present in 264.0 mμ ($\log \varepsilon$ 2.965) and 272.0 mμ ($\log \varepsilon$ 2.667) in 95% ethyl alcohol.

Summary

The synthesis of benzocyclobutene by the photochemical desulfonylation of 1,3-dihydroisothianaphthene-2,2-dioxide has been studied and the following results obtained; 1) The irradiation considerably accelerates the desulfonylation of the sulfone, while the ultraviolet-light has no remarkable effect on the molar ratio of the formed benzocyclobutene and 1,2,5,6-dibenzocycloöctadiene. 2) The rate of desulfonylation is independent of pressure, and the reaction pressure plays a very important role in the further reaction of the intermediate *o*-xylylene biradical produced by the desulfonylation.

Department of Chemical Technology
Faculty of Engineering
Osaka University
Miyakojima-ku Osaka

11) M. Cava and D. Napier, *J. Am. Chem. Soc.*, **78**, 500 (1956).
12) K. Alder and M. Fremery, *Tetrahedron*, **1961**, 197.

The Complexometric Estimation of Ferric Iron

By Balwant SINGH, M. S. MANKOTIA and H. S. LAMBA

(Received March 17, 1964)

1, 2-Diaminocyclohexane-*N*, *N*, *N'*, *N'*-tetraacetic acid (CyDTA) forms a very stable 1 : 1 complex with ferric iron, and the complex serves as a basis for the complexometric determination of this metal. Přibil[1] used salicylic acid as an indicator for the complexometric determination of iron(III) with CyDTA (disodium salt). Martinez and Mendoza[2] suggested the use of sulphosalicylic acid, tiron and potassium thiocyanate as indicators for the determination of ferric iron with CyDTA at pH values from 2 to 5 and at a temperature of 50°C, but they found that the results were 1 to 5 per cent too high. Přibil and Sir[3] determined iron(III) in the presence of aluminium and titanium in a weakly alkaline pyridine solution by masking aluminium and titanium with a two per cent solution of ammonium fluoride. An excess of CyDTA was added and back titrated with zinc chloride or zinc sulphate, using Eriochrome Black T as an indicator. Martinez and Mendoza[4] have also determined ferric iron photometrically with CyDTA at pH 4. Koroz and Poczoc[5] estimated iron(III) in the presence of calcium and magnesium, with sulphosalicylic acid as an indicator, at pH values from 2 to 3 at 60°C.

No more evidence is available in the literature for the determination of ferric iron with

1) R. Přibil, *Chem. Listy*, **49**, 179 (1955).
2) F. B. Martinez and R. Rey Mendoza, *Quim. e. Ind., Bilbao*, **6** (1), 3 (1959).
3) R. Přibil and Z. Sir, *Coll. Czechslov. Chem. Communs.*, **20**, 871 (1955).
4) F. B. Martinez and R. R. Mendoza, *Chemist-Analyst*, **47**, 94 (1958).
5) E. Koros and I. Poczoc, *Magyar Kem. Foly*, **64**, 7, 250 (1958).

CyDTA. In the present work, an attempt has been made to determine ferric iron alone as well as in the presence of various metal ions by titration with CyDTA (disodium salt), using pyrocatechol violet at pH 3.09 or *p*-anisidine-thiocyanate at pH 4.2 as an indicator. The end point of the complexometric titration in both cases is very sharp, and there is no dragging of indicator colour near the end point. The titrations can be successfully made at room temperature.

Experimental

The Preparation of Standard CyDTA (Disodium Salt). — 0.05 M CyDTA (disodium salt) was prepared by dissolving 35.45 g. of CyDTA in 400 ml. of boiling 0.5 N sodium hydroxide and diluting it to two litres in metal-free distilled water. This was further diluted ten times to prepare 0.005 M CyDTA (disodium salt).

The Preparation of a *p*-Anisidine-thiocyanate Indicator Solution.[6]—9.7175 g. of potassium thiocyanate were dissolved in water, and the volume made to 50 ml. In ethyl alcohol 1.2315 g. of *p*-anisidine were dissolved and the total volume of the solution was made to 50 ml. The two solutions were then mixed together, and the mixture used as *p*-anisidine-thiocyanate indicator.

The Preparation of a Pyrocatechol Violet Indicator Solution.—0.1 g. of pyrocatechol violet was dissolved in distilled water, and its volume made to 100 ml.

Results

The Estimation of Ferric Iron in Presence of Other Metal Ions.—An aliquot of a ferric nitrate solution was taken in a conical flask containing 50 ml. of water, and then 2 to 3 drops of pyrocatechol violet or *p*-anisidine-thiocyanate were added to it. A sodium acetate and hydrochloric acid buffer was added to adjust the pH of the solution to 3.09 or 1.42 respectively. The mixture was titrated with 0.005 M CyDTA (disodium salt). The end

TABLE I. THE TITRATION OF FERRIC IRON WITH 0.005 M 1,2-DIAMINOCYCLOHEXANE-TETRAACETIC ACID (DISODIUM SALT)

Metal salts added		Weight of $Fe(NO_3)_3 \cdot 9H_2O$		
		Taken	Found	
			Pyrocatechol violet indicator	*p*-Anisidine-thiocyanate indicator
	g.	g.	g.	g.
		0.0040	0.0040	0.0040
		0.0202	0.0202	0.0202
$BaCl_2 \cdot 2H_2O$	0.0048	0.0081	0.0081	0.0081
	0.0073	0.0121	0.0121	0.0121
$CaCl_2 \cdot 2H_2O$	0.0058	0.0162	0.0162	0.0162
	0.0073	0.0202	0.0203	0.0203
$Sr(NO_3)_2$	0.0021	0.0040	0.0040	0.0040
	0.0042	0.0081	0.0081	0.0081
$Cr(NO_3)_3 \cdot 9H_2O$	0.0120	0.0121	0.0122	0.0121
	0.0160	0.0162	0.0162	0.0162
$Hg(NO_3)_2 \cdot H_2O$	0.0035	0.0040	0.0041	0.0040
	0.0173	0.0202	0.0202	0.0202
$Th(NO_3)_4 \cdot 4H_2O$	0.0220	0.0162	0.0324	0.0324
	0.0275	0.0202	0.0404	0.0404
NaF	0.0012	0.0121	No end point	No end point
	0.0021	0·0202		
$(NH_4)_2C_2O_4 \cdot H_2O$	0.0056	0.0162	No end point	No end point
	0.0071	0.0202		
$CuSO_4 \cdot 5H_2O$	0.0050	0.0081	No end point	No end point
	0.0125	0.0202		
$Ni(CH_3COO)_2 \cdot 4H_2O$	0.0075	0.0124	No end point	No end point
	0.0099	0.0162		
$CoCl_2 \cdot 6H_2O$	0.0042	0.0081	No end point	No end point
	0.0119	0.0202		
$MnCl_2 \cdot 4H_2O$	0.0054	0.0121	No end point	No end point
	0.0099	0.0201		

6) B. Singh, S. S. Sahota and M. S. Mankotia, *Z. anal. Chem.*, **173**, 275 (1960).

point was marked by a sharp colour change from blue to yellow in the case of pyrocatechol violet and from violet to yellow when *p*-anisidine-thiocyanate was used as the indicator. The titration was then performed in the presence of barium chloride, calcium chloride, strontium nitrate, chromium nitrate, mercuric nitrate, magnesium sulphate, thorium nitrate, sodium fluoride, ammonium oxalate, copper sulphate, nickel acetate, cobalt chloride and manganese chloride respectively. Some typical results are given in Table I.

From the data given in Table I it is evident that ferric iron, alone or in the presence of Ba^{2+}, Ca^{2+}, Sr^{2+}, Cr^{3+}, or Hg^{2+}, can be determined volumetrically by titrating it with a CyDTA (disodium salt) solution, using pyrocatechol violet or *p*-anisidine-thiocyanate as an indicator.

Thorium nitrate interferes in this titration, because CyDTA forms a 1 : 1 complex with thorium as well as with iron(III) ; the amount of CyDTA used is, therefore, double that required for the estimation of iron(III). In the presence of sodium fluoride and ammonium oxalate, there is no end point in the complexometric determination of ferric iron with CyDTA (disodium salt) because of the formation of stable complexes of iron fiuoride and iron oxalate respectively. Because of the presence of coloured compounds (copper sulphate, cobalt chloride and manganese chloride), no end point was detected in these titrations.

Summary

Ferric iron has been determined, alone or in the presence of Ba^{2+}, Ca^{2+}, Sr^{2+}, Cr^{3+} or Hg^{2+}, by titrating it with CyDTA (disodium salt), using pyrocatechol violet and *p*-anisidine-thiocyanate as indicators at pH 3.09 and 1.42 respectively. Th^{4+}, F^-, $C_2O_4^{2-}$, Cu^{2+}, Ni^{2+}, Co^{2+} and Mn^{2+} have been found to interfere in the complexometric estimation of ferric iron with CyDTA (disodium salt).

The authors wish to take this opportunity to thank the Council of Scientific and Industrial Research (India) for the award of Junior Fellowship to one of them (M. S. M.), thus enabling him to pursue the study of complexometric titrations.

Chemistry Department
Punjabi University
Patiala, India

The Kinetics of the Reaction of Aromatic Ketones with Nitrous Acid in Sulfuric Acid

By Yoshiro OGATA, Yoshiaki FURUYA and Masahiro ITO

(Received March 17, 1964)

The present authors have previously reported that the rate-determining step for the nitrosation of cyclohexyl aryl ketones in sulfuric acid (SNIA process) is the enolization of the ketone.[1] The present paper will describe the effect of the structure of alkyl phenyl ketones on the rate, where the alkyl groups are methyl, isopropyl and isobutyl. The rates were measured by means of ultraviolet spectrophotometry. The rate data, together with the observed reaction products, including gaseous products, were analyzed to get some information on the reaction mechanism.

Experimental

Materials.—Commercial acetophenone was purified by distillation; b. p. 195~196.5°C. *p*-Methylacetophenone (b. p. 117.5~118.1C/31 mmHg), *p*-chloroacetophenone[2] (b. p. 126~127.5°C/27 mmHg), propiophenone[3] (b. p. 108~109°C/23.5 mmHg) and isobutyrophenone[4] (b. p. 106~107°C/21.0 mmHg) were prepared by Friedel-Crafts reactions of the corresponding aromatics with the corresponding acid anhydrides or acyl chlorides. *m*-Nitroacetophenone[5] was prepared by the nitration of acetophenone and recrystallized from ethanol; m. p. 78.8~79.2°C.

Isonitrosoacetophenone[6] was obtained by the reaction of acetophenone with methyl nitrite in ethyl ether and was recrystallized from toluene, m. p. 127~128.5°C. Phenylglyoxal[7] was prepared

1) Y. Ogata, Y. Furuya and M. Ito, *J. Am. Chem. Soc.*, **85**, 3649 (1963).

2) "Organic Syntheses," Coll. Vol. I, 109 (1941).
3) W. T. Read, *J. Am. Chem. Soc.*, **44**, 1751 (1922).
4) C. Schmidt, *Ber.*, **22**, 3250, Anm. 2 (1891).
5) "Organic Syntheses," Coll. Vol. II, 434 (1943).
6) W. K. Slater, *J. Chem. Soc.*, **117**, 589 (1920); "Organic Syntheses," Coll. Vol. II, 363 (1943).
7) "Organic Syntheses" Coll. Vol. II, 509 (1943).

by the oxidation of acetophenone with selenium dioxide in dioxane; b. p. 94~96°C/24.8 mmHg.

The Reaction Products.—*From Acetophenone.*—A solution of 20 ml. of 2.0 M acetophenone in 98.0% sulfuric acid and a solution of 40 ml. of 1.5 M sodium nitrite in 98.0% sulfuric acid were mixed; the mixture was then kept standing at 70°C for 7 hr. The resulting solution was diluted with water and extracted with ether. The ethereal extract was treated with aqueous alkali, and the aqueous layer was then acidified with hydrochloric acid and filtered. Benzoic acid was obtained; 4.6 g. (93.0%); λ_{max}=228 mμ; m. p. and mixture m. p. 123~124.8°C.

From Propiophenone.—A mixture of propiophenone (4.0 g.) and sodium nitrite (2.8 g.) in 98% sulfuric acid was allowed to stand at 70°C for 6 hr. Benzoic acid was obtained; 3.6 g. (97%); m. p. and mixture m. p. 120.5~122°C.

From Isobutyrophenone.—A mixture of isobutyrophenone (7.2 g.) and sodium nitrite (4.2 g.) in 95% sulfuric acid was heated at 60°C for 4.5 hr. The obtained product contained benzoic acid (5.6 g. (94%); m. p. and mixture m. p. 123~124°C) and acetoxime (0.7 g. (20%); m. p. and mixture m. p. 60~61°C (lit.[8] m. p. 60°C)).

From Isonitrosoacetophenone.—Isonitrosoacetophenone (1 g.) in 98% sulfuric acid was heated for 4 hr. at 70°C, yielding benzoic acid (0.8 g. (97%); m. p. and mixture m. p. 122~123.5°C).

Ultraviolet Spectrophotometry and Chemical Analysis.—The conversion curves were prepared as has been previously described.[1] The following different extinctions were employed: acetophenone, (E_{228}—E_{241}) vs. (E_{241}—E_{280}); *p*-methylacetophenone (E_{237}—E_{252}) vs. (E_{252}—E_{280}); *p*-chloroacetophenone, (E_{237}—E_{250}) vs. (E_{250}—E_{280}); *m*-nitroacetophenone, (E_{217}—E_{256}) vs. (E_{217}—E_{300}); propiophenone, (E_{228}—E_{240}) vs. (E_{240}—E_{270}), and isobutyrophenone, (E_{228}—E_{241}) vs. (E_{241}—E_{270}).

A Typical Run for the Rate Measurements.—A solution of 5 ml. of 0.4 M acetophenone in 98.6% sulfuric acid in a stoppered flask was brought to temperature equilibrium at 70°C. Then the reaction was started by the addition of 0.5 M sodium nitrite (5 ml.) in 98.6% sulfuric acid at 70°C. Aliquots (0.5 ml. each) were taken out at appropriate time intervals, and each aliquot was diluted with methanol to a 10^{-4} M total concentration of aryl ketone plus aryl carboxylic acid. The conversion percentage was determined graphically.

Results and Discussion

Acetophenone.—The rate of the reaction of acetophenone in 98.6% sulfuric acid with an initial concentration of 0.2 M ketone and in 0.097~0.388 M nitrous acid at 70°C satisfied the second-order rate law (Table I):

$$v = k\,[\text{ketone}]\,[HNO_2]$$

Lowering the concentration of sulfuric acid resulted in an increase in the amount of by-products, including gas, and, hence, a deviation from the second-order rate law; e. g., with 86% sulfuric acid the yield of benzoic acid was poor (30%).

It has been known that isonitrosoacetophenone PhCOCH=NOH is isolable as an intermediate in the reaction of acetophenone with nitrosyl chloride in ethanolic pyridine.[9] The authors observed that isonitrosoacetophenone converted rapidly to benzoic acid in sulfuric acid at 70°C, the conversion slowing down with a decrease in the sulfuric acid concentration as measured spectrophotometrically. When the conversion was made in dilute sulfuric acid in the presence of nitrous acid, nitrous oxide was detected by gas chromatography (Table II), as reported in the reaction of isonitrosoacetophenone with nitrosyl chloride.[9] Phenyl glyoxal, which has been known as one of the other products in the reaction using nitrosyl chloride,[9] was converted to a tarry material in sulfuric acid.

TABLE I. THE RATE DATA OF NITROSATION OF ALKYL PHENYL KETONES IN 98.6% SULFURIC ACID

Ketone	Temp. °C	Initial concn. of ketone M	Initial concn. of HNO_2 M	First-order rate constant k sec^{-1}	Second-order rate constant k' $l.\,mol^{-1}\,sec^{-1}$
Acetophenone	70	0.200	0.097		2.45×10^{-4}
		0.200	0.194		2.02×10^{-4}
		0.200	0.291		2.58×10^{-4}
		0.200	0.388		2.52×10^{-4}
Propiophenone	60	0.0200	0.0198		2.40×10^{-3}
		0.0200	0.0395		2.49×10^{-3}
		0.0400	0.0198		2.28×10^{-3}
		0.0400	0.0395		2.91×10^{-3}
		0.0400	0.0792		2.54×10^{-3}
Isobutyrophenone	60	0.0100	0.0198	2.38×10^{-4}	1.49×10^{-2}
		0.0200	0.0198	1.96×10^{-4}	1.45×10^{-2}
		0.0200	0.0397	2.43×10^{-4}	0.73×10^{-2}
		0.0400	0.0198	1.97×10^{-4}	0.84×10^{-2}
		0.0200	0.0099	1.51×10^{-4}	3.68×10^{-2}

8) "The Merck Index," Merck & Co., Rahway, New Jersey (1960), p. 9.

9) C. T. Manning and H. A. Stansbury, Jr., *J. Am. Chem. Soc.*, **81**, 3885 (1959).

Propiophenone.—The reaction in 98.6% sulfuric acid at 60°C was first-order with both ketone and nitrous acid, as in the case of acetophenone (Table I). The product contained a quantitative amount of benzoic acid. Lowering the acidity of the solution resulted in the evolution of a gas which contained nitrous oxide and carbon monoxide (Table II).

Isobutyrophenone.—The rate law was different from those of acetophenone and propiophenone in that it obeyed the following first order equation (Table I):

$$v = k\,[\text{ketone}]$$

TABLE II. GAS CHROMATOGRAPHIC ANALYSIS OF EVOLUTION GASES FROM NITOSATION MIXTURES OF ACETOPHENONE, PROPIOPHENONE AND ISONITROSOACETOPHENONE IN 86.0% SULFURIC ACID AT 70°C

Column: Activated charcoal (30~60 mesh), 3 m.
Carrier Gas: Hydrogen with a flow rate of 88 ml./min.
Temp.: 80°C

Ketone or authentic sample	Molar ratio [ketone]/[HNO_2]	Retention volume ml.	
Acetophenone	1 : 2	1500	9150
Isonitrosoacetophenone	1 : 1	1500	9150
Isonitrosoacetophenone	1 : 0	1500	—
Propiophenone	1 : 1	1500	9150
CO*	—	1500	—
N_2O**	—	—	9150

* The authentic sample was obtained by the reaction of formic acid with sulfuric acid.
** The sample was prepared by the pyrolysis of ammonium nitrate.

TABLE III. SUBSTITUENT EFFECT ON THE NITROSATION OF ACETOPHENONE

Substituent	σ	k l. mol^{-1} sec.$^{-1}$
p-CH_3	−0.170	4.84×10^{-4}
H	0	2.39×10^{-4}
p-Cl	+0.227	3.83×10^{-4}
m-NO_2	+0.710	1.72×10^{-2}

Substituent Effect. — The effect of substituents (p-CH_3, p-Cl and m-NO_2) in acetophenone is shown in Table III and Fig. 1. Electron-attracting groups accelerate the reaction with Hammett's ρ value of +2.6.

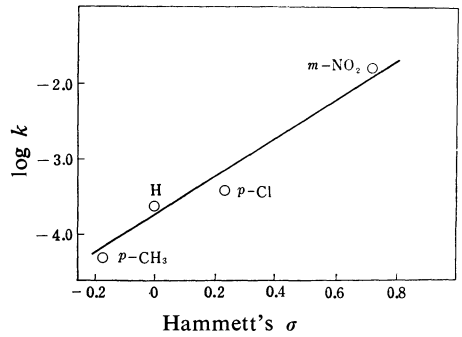


Fig. 1. Substituent effect on nitrosation of acetophenone in 98.6% sulfuric acid at 70°C.

Energies and Entropies of Activation. — The rate constants, energies and entropies of activation in 98.6% sulfuric acid at various temperatures are shown in Table IV.

Reaction Mechanism. — The above findings suggest that the rate-determining step for isobutyrophenone is the enolization of the ketone, as has been observerd in cyclohexyl phenyl

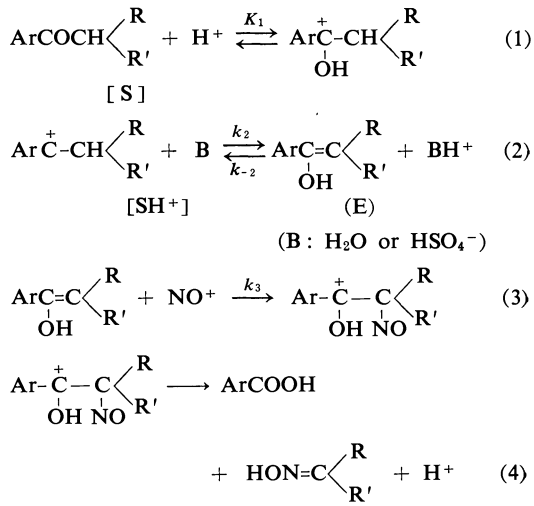


TABLE IV. THE RATE CONSTANTS AT VARIOUS TEMPERATURES, ENERGY OF ACTIVATION E_a AND ENTROPY OF ACTIVATION $\Delta S^{\neq}$ FOR THE NITROSATION OF THREE KETONES

Reaction temp. °C	Acetophenone $k\times10^4$ l. mol^{-1} sec^{-1}	Propiophenone $k\times10^3$ l. mol^{-1} sec^{-1}	Isobutyrophenone $k\times10^4$ sec^{-1}
50	0.18	—	0.52
60	0.63	2.52	1.62
70	2.39	5.58	3.71
80	5.16	12.7	—
E_a, kcal./mol.	24.4	20.4	21.8
$\Delta S^{\neq}$, e. u.	−4.3	−9.1	−10.5

ketone,[1] while the rate-determining step for acetophenone or propiophenone is an attack of nitrosonium ions.

$$HON{=}C\begin{matrix}R\\ \diagup\\ \diagdown\\ R'\end{matrix} \longrightarrow RCONHR' \text{ (or } R'CONHR) \quad (5)$$

Defining k and K as the rate and equilibrium constants for the subscripted steps, and S and E as ketone and enol respectively, the following equations are derived by means of the stationary-state method:

$$k_2[SH^+][B] = k_{-2}[E][BH^+] + k_3[E][NO^+] \quad (6)$$

The introduction of the relation:

$$[SH^+] = K_1[H^+](a-x)/(1+K_1[H^+]) \quad (7)$$

into Eq. 6 gives Eq. 8, where $(a-x)$ is the stoichiometric concentration of ketone.

$$[E] = \frac{K_1k_2[B][H^+](a-x)}{(k_{-2}[BH^+]+k_3[NO^+])(1+K_1[H^+])} \quad (8)$$

Therefore, assuming that step 4 is very fast, the rate of the formation of benzoic acid may be expressed as:

$$v = k[NO^+][E] = \frac{K_1k_2[NO^+][B][H^+](a-x)}{(k_{-2}[BH^+]+k_3[NO^+])(1+K_1[H^+])} \quad (9)$$

The observed results imply that $k_{-2}[BH^+] \gg k_3[NO^+]$ with acetophnone and propiophenone, while $k_{-2}[BH^+] \ll k_3[NO^+]$ with isobutyrophenone and cyclohexyl aryl ketone; i.e., the rate is determined by step 2. The deprotonation of the conjugate acid of isobutyrophenone is more difficult because of the steric hindrance, electron-releasing effect of the methyl group and also the decrease in the number of α-hydrogen atoms: therefore, step 2 may be slowed down to a rate-determining step. A slight increase in the first-order rate constant with an increase in the initial concentration of nitrous acid was observed with isobutyrophenone; this may be explained by a small tendency of the rate to be rather second-order.

Electron-attracting groups in acetophenone accelerate the reaction, probably because of their favorable effect on deprotonation step 2. The substituent effect was reversed for the bromination of acetophenone in 75% aqueous acetic acid.[10] The facts may be explained by the lower acidity of the latter reaction, by which protonation step 1 is affected by substituents, while ketones in sulfuric acid are completely protonated.

A direct attack of nitrosonium ions on the α-position of ketone may lead to the second-order rate law, but this electrophilc attack is less probable because of the strong electron-withdrawal of the carbonyl group. Moreover, the rate-determining decomposition of nitrosoketone (Eq. 4) is unconceivable, since it was observed that nitrosoketone in sulfuric acid decomposes much faster than the nitrosation of the ketone. The rate of step 4 increases with an increase in the acidity of the sulfuric acid solution; hence, the amount of by-product decreases.

Summary

The rates of the reaction of acetophenone, ring-substituted acetophenones, propiophenone and isobutyrophenone with nitrous acid in 98.6% sulfuric acid have been measured by means of spectrophotometry. The rates have been expressed as $v=k$[ketone][NO^+] with acetophenones and propiophenone, while they are $v=k$[ketone] with isobutyrophenone. The electron-attracting groups in acetophenone accelerate the reaction with Hammett's ρ value of +2.6. A probable mechanism has been suggested which involves a rate-determining nitrosation of enolized ketone for acetophenone and propiophenone, and a rate-determining enolization of ketone for isbutyrophenone.

Department of Applied Chemistry
Faculty of Engineering
Nagoya University
Chikusa-ku, Nagoya

10) D. P. Evans, V. G. Morgan and H. B. Watson, *J. Chem. Soc.*, **1935**, 1167.

Metal Complexes of Mononitrosochromotropic Acid. A Study of the Copper Complex and Its Chelometric Titrations

By Sachindra Kumar DATTA and Sachindra Nath SAHA

(Received March 17, 1964)

It appears that chromotropic acid forms two nitroso derivatives; mononitroso and dinitroso.[1] The dinitrosochromotropic acid has been used by Steigmann[2] for the detection of copper, nickel and palladium. Datta[3] used this compound for the complexometric and spectrophotometric determination of thorium. The mononitroso derivative has been utilised by various workers for the detection and determination of copper, cobalt and nickel. Since the two nitroso compounds of chromotropic acid give colour reactions with many metals, a thorough investigation of the colour complexes and their probable analytical applications has been undertaken by the present authors.[5] The following elements were found to give coloured products with mononitrosochromotropic acid: copper, palladium, cobalt, nickel, magnesium, manganese, vanadium, uranium, beryllium, iron(III), chromium, cerium(III), lanthanum, gold, thorium, zirconium, etc. Lead and cobalt(III) form a coloured precipitate. Methods for the detection of most of these and of fluoride ion on the spot plate and filter paper have already been developed.[6]

The present paper will deal with the copper complex of mononitrosochromotropic acid (abbreviated as MNCA) and will make a thorough study of its application in the complexometric determination of copper. This reagent has been used recently by Pande and Srivastava,[7] and later by Sen and Srivastava,[8] as an indicator in the titration of copper with EDTA. However, they carried out such titrations only in a pure solution, and the interference in the titration has not been studied in detail. The direct titration of copper with nitrosochromotropic acid carried out by Ansbacher and his co-workers[9] proved very unsatisfactory to the present authors. The method was also rejected as unsuitable by Conn et al.[10] in their determination of copper in milk. However, in all the works carried out by various workers, nitrosochromotropic acid was present in the solution in which it was prepared and that solution was employed as such, without isolating the pure product. The present authors prepared and isolated the compound in its pure form and used it for the experiments reported on here and earlier. The study of the copper complex by various physico-chemical methods and the spectrophotometric determination of copper with this reagent will be reported on shortly.

Experimental

Reagents and Chemicals.—*Copper Solution.*—A stock solution of A. R. copper sulphate pentahydrate was prepared in water containing a little sulphuric acid and was estimated with EDTA, using PAN as an indicator. The other copper salts were made from reagent-grade salts.

Reagent Solution.—Mononitrosochromotropic acid (MNCA) was prepared as has been reported earlier.[6] A 0.05% solution in water was used. Other indicator solutions: PAN, a 0.05% solution in ethanol; murexide, a saturated solution in water; pyrocatechol violet, a 0.1% solution in water, and Chrome Azurol S, a 0.4% solution in water.

EDTA. — Disodium dihydrogen ethylenediaminetetraacetate dihydrate (A. R.) was dissolved in water to make 0.05, 0.01 and 0.001 M solutions; it was estimated as usual by means of a standard calcium solution. The other reagents and chemicals used were also of reagent grade.

Apparatus. — A Beckman Model H-2 pH meter was used for the adjustment of the pH of the solutions.

Results

The Reaction of Copper with Mononitrosochromotropic Acid.—MNCA reacts with copper in a weakly acidic or weakly alkaline medium

1) F. J. Welcher, "Organic Analytical Reageant," Vol. III, D. Van Nostrand Co., N. Y. (1947).
2) A. Steigmann, *J. Soc. Chem. Ind.* (*London*), **62**, 42 (1943).
3) S. K. Datta, *Anal. Chim. Acta*, **15**, 415 (1956); **16**, 115 (1957).
4) C. Brenner, *Helv. Chim. Acta*, **3**, 90 (1920); O. Sheets and M. Gieger, *Ind. Eng. Chem., Anal. Ed.*, **7**, 109 (1935).
5) S. K. Datta and P. N. Ghose, *Naturwiss.*, **45**, 515 (1958).
6) S. K. Datta and S. N. Saha, *Mikrochim. Acta*, **3**, 24, (1961).
7) C. S. Pandey and T. S. Srivastava, *Z. anal. Chem.*, **184**, 248 (1961).
8) A. B. Sen and T. S. Srivastava, ibid., **187**, 401 (1962).
9) S. Ansbacher, R. E. Remington and F. B. Cupl, *Ind. Eng. Chem.*, **3**, 312 (1931).
10) L. W. Conn, A. W. Johnson, H. A. Trebler and V. Karpenko, ibid., **7**, 15 (1935).

to form a violet- or permanganate-coloured soluble complex. The formation of the copper complex with various copper salts has been studied. A few drops of an MNCA solution were added to 0.05 M solutions of different copper salts, which had previously been rendered almost neutral, and then the pH was raised by adding a 0.1 M ammonium hydroxide solution. The colour changes are noted in Table I. It appears that the same complex is formed with various copper salts and that the colour deepens only when the pH is raised.

TABLE I. REACTIONS OF MNCA WITH DIFFERENT COPPER SALTS

Copper salt	pH	Colour reactions
Copper sulphate	3.4	Pale pink
	8.0	Permanganate colour
Copper chloride	4.0	Pink
	7.8	Violet
Copper nitrate	4.2	Pink
	8.0	Violet
Copper acetate	5.5	Bluish violet
	7.8	Violet
Copper ammonium sulphate	5.2	Pale permanganate colour
	8.4	Violet
Copper ammonium chloride	3.5	Pink
	6.8	Violet
Copper oxalate	5.4	Violet colour on boiling
Copper citrate	3.4	Reddish pink
	7.3	Violet
Copper tartrate	3.2	Pale pink
	7.8	Pale violet
Copper perchlorate	3.8	Pink
	7.2	Violet
Copper glycinate	—	No colour formation at any pH
Copper iodate	4.4	Pink colour, intensifies on heating

Preliminary Studies of the Stability of the Copper Complex.—To 100 ml. of a 0.1 M copper sulphate solution, a solution of 1 M sodium acetate was added slowly until the pH became 5.6 to 6 and the volume had been diluted to 200 ml. To this mixture 50 ml. of 0.4 M MNCA was added, and the mixture was kept in a water bath at 40°C for 5 min. to complete the reaction. A deep-red-violet copper complex formed in the solution. The complex could not be isolated in the solid state or extracted by any organic solvent.

To 5 ml. of this complex solution, various substances (acids, alkalis, oxidizing agents, reducing agents, protective colloids, alcohols, ketones, amines, amino acids, polyhydroxy alcohols and other organic substances) were added in order to study the stability or instability of the copper complex in their presence. The results indicated are: The copper complex appears to be stable as such for about a week, and it remains stable in the presence of protective colloids, starch, gelatine, etc., for about a fortnight. The mineral acid decomposes it, and it breaks below pH 5. The colour intensifies with ammonium hydroxide, sodium hydroxide and potassium hydroxide, up to a pH of 9. No change is observed with ammonium carbonate. Among the oxidizing agents, a 0.1 M solution of potassium permanganate or dichromate at pH 5.6 to 5.8 discharges the colour of the complex slowly, but in the presence of acid, the decomposition is immediate. Hydrogen peroxide discharges the colour at once. Persulphates and periodates also decompose the complex. The reducing agents (ascorbic acid, hydroxylamine hydrochloride, hydroquinone in an alcoholic solution, sodium sulphite, etc.) break the complex, and the colour changes to yellow. With hydrogen sulphide, a black precipitate of copper sulphide forms. The complex is decomposed by thiosulphate, potassium iodide, ferro- and ferricyanides, and ammonium sulfocyanide, but it does not change with fluorides, molybdates, selenates, ammoniacal potassium iodide, or thiosulphate. The organic solvents, such as alcohols, ketones, esters, chloroform, carbon tetrachloride, and polyhydroxy alcohols, do not change the colour, nor can the complex be extracted in the organic phase. With acetylacetone, the complex breaks and the lower layer becomes blue because of the formation of copper acetylacetonate, while the upper layer becomes orange because of the liberation of the free reagent. Glycine and EDTA displaced copper from its complex.

The Titrimetric Determination of Copper with EDTA Using MNCA as an Indicator.—As the copper complex of MNCA is less stable than the copper-EDTA complex, the direct titration of copper with EDTA, using MNCA as an indicator, is possible. The end-point colour change is from a permanganate or violet colour to a greenish yellow or to an almost colourless state in a dilute solution. The optimum conditions for such titration have been developed from the study of various factors, such as pH, buffer solutions, the temperature, the dilution of the volume and the concentration and age of the indicator solution.

The Effect of pH and Buffer Solutions.—The titration of copper with EDTA has been carried out at various pH values in order to study the effect of hydrogen ion concentration in the titration employing this indicator. The effect of using different buffer solutions in fixing the pH has also been examined. One millilitre of a copper solution was mixed with 2 ml. of buffer solution, and the volume was diluted to about 30 ml. and 4 drops of an indicator solution (0.02%) were added. The

TABLE II. EFFECT OF pH AND BUFFER IN THE EDTA TITRATION OF COPPER
1 ml. of 0.1 M $CuSO_4$, taken 10 ml. of 0.01 M EDTA

Buffer used	pH	EDTA, reqd. ml.	Remarks on end point
Sodium acetate-hydrochloric acid	3.4	4.2	Pink colour changes to pale yellow end point not sharp
	4.5	6.3	
	5.0	7.2	
Sodium acetate	5.2	8.0	Red-violet to light green, fairly sharp
	5.56	9.1	
	5.86	9.95	Sharp end point
	6.30	9.96	Sharp end point
	6.51	10.02	Sharp end point
	6.60	10.05	Sharp end point
Ammonium acetate - acetic acid	5.2	8.60	Reddish pink to pale yellow, not sharp
	5.4	8.85	
Pyridine	5.6	8.82	Pink to greenish yellow, sharp end point
	6.1	9.20	
	6.8	9.95	Violet to greenish yellow, sharp end point
	7.0	10.10	Violet to greenish yellow, sharp end point
Ammonium chloride - ammonia	6.6	9.85	Pink to pale yellow, sharp end point
	7.0	9.90	
	7.2	10.01	Permanganate to pale yellow, sharp end point
	7.6	10.05	
	7.8	9.98	
	8.1	10.10	
	8.6	10.20	End point not sharp
	9.4	10.32	End point not sharp
Triethanolamine	7.4	10.12	Bluish violet to almost colourless, fairly sharp end point
	8.0	10.15	
	8.6	10.18	End point not sharp
	9.0	10.25	
	10.2	10.55	

mixture was then titrated with 0.01 M EDTA in the cold. Some of the results of this titration have been recorded in Table II and represented in Fig. 1.

The results indicate that pH range from 6.8 to 7 with a pyridine - hydrochloric acid buffer was suitable for the titration of copper. A sharp colour transition was obtained. Triethanolamine gave a little higher result, and the colour change at the end point was also not very sharp. An ammonium chloride - ammonia buffer gave good results from pH 7 to 8. A very sharp end point from a permanganate colour to pale yellow was obtained with this buffer. The titration at lower pH values, from 5.8 to 6.5, may also be carried out with a sodium acetate buffer, the end point colour transition is then sharp but not as good as that obtained with an ammonium chloride - ammonia buffer. Other buffers were not found suitable.

The Effect of Temperature.—Titration at different temperatures from 10 to 66°C showed that the complex is stable up to 40°C and that the titrations may be made at room temperature without any loss of accuracy.

The Effect of the Concentration of the Indicator.—In order to examine whether the concentration of the indicator solution has any effect on the titre value and on the sharpness of end point, titrations were carried out with different amounts of the indicator in 50 ml. of the titrant. It was seen that, in an ammonium chloride - ammonia buffer, when a few drops of a 0.05% indicator solution were gradually added to the pale blue copper solution, the blue colour gradually faded, the solution became almost colourless and then turned a pale permanganate colour, and, at the end point with EDTA, the colour changed to pale yellow or became nearly colourless. However, with a large ammount of indicator, the colour is deep yellow or orange, and with a larger amount of copper, the end point colour is a greenish-yellow. Too great an excess of the indicator obscures the end point. Good results are obtained with 0.2 to 0.5 ml. of a 0.05% indicator solution for a solution containing about 6 mg. of copper. The same results were

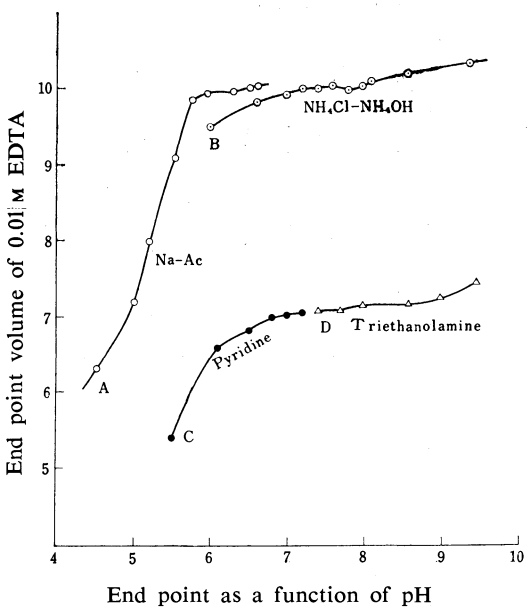


Fig. 1. The end point as a function of pH in the EDTA titration of copper. EDTA, 0.01 M
Curve A : 0.1 M $CuSO_4$ 1 ml., using sodium acetate buffer
Curve B : 0.1 M $CuSO_4$ 1 ml., using ammonium chloride-ammonia buffer
Curve C : 0.1 M $CuSO_4$ 0.7 ml., using pyridine buffer
Curve D : 0.1 M $CuSO_4$ 0.7 ml., using triethanolamine buffer

obtained with a sodium acetate or pyridine buffer.

The Effect of the Dilution of Volume.—Titration was carried out by varying the volume of the titrant without changing the amount of indicator or copper. A 50 ml. volume gave good results. With a larger amount of copper, for instance, more than 10 mg., the volume should be about 100 ml. or larger.

The Age of the Indicator Solution.—The solution of the indicator is not very stable. A solution, once prepared, may be used for only a week with little loss of accuracy. It is desirable that the titrations always be carried out with solutions which are not older than two or three days, and such solutions should always be kept in amber-coloured bottles.

The Effect of Ketonic Solvents in the Titrant.—The sharpness of the end point of the titration has been found to improve slightly in the presence of some ketones, like acetone, diacetone alcohol or ethyl methyl ketone. The addition of about 10 ml. acetone per 50 ml. of volume was found to give good results.

Procedures Recommended for Pure Copper Solution.—a) Take 10 ml. of a nearly copper solution containing about 6~10 mg. copper in a 250 ml. conical flask, and add 2 ml. of 1 M ammonium chloride solution and 5 drops of 2 M ammonium hydroxide, 10 ml. of acetone and 4 drops of 0.05% indicator solution. Dilute the mixture to 50 ml. Adjust the pH to 7.2 to 7.4 with one or two more drops of ammonia. The solution then assumes a permanganate colour. Titrate in the cold with 0.01 M EDTA until the colour sharply changes to pale yellow. This method may be used for the determination of 2 to 30 mg. of copper in a solution.

b) To the above copper solution, add 1 ml. of pyridine and 4 drops of the indicator. Dilute to 50 ml. with water. The pH should be 7; if it is below, add 1 or 2 drops of a dilute pyridine solution (0.2%) in order to raise it to 7. The colour of the solution is violet. Titrate with EDTA. At the end point the colour changes from bluish-violet to greenish yellow or becomes almost colourless. This method is useful for the estimation of 2 mg. to 20 mg. of copper.

c) To an almost neutral copper solution, add 2 ml. of a sodium acetate solution, 10 ml. of acetone and 4 drops of the indicator. Dilute to 50 ml. with water. Adjust the pH to 6.2~6.6 with a few drops more of a sodium acetate solution and titrate it as before with EDTA until the colour changes from red-violet to light green. From 2 to about 60 mg. of copper may be determined by this method with accuracy. With more than 60 mg. of copper, the end point passes through a series of colour changes, from red-violet to blue-violet, bluish grey, grey, and, finally, yellowish green. Here the end point is a bit long-drawn and not sharp.

Some typical results of titrations in the lower range are recorded in Table III. The titration of copper was also carried out side by side by following the prescribed procedures but using other indicators (viz. PAN,[11] murexide,[12] pyrocatechol violet[13] and Chrome Azurol S[14]) for the sake of comparison. The results indicate that the new indicator, mononitrosochromotropic acid, is satisfactory, being as effective as the standard indicators mentioned above.

The Micro Titration of Copper.—Microgram quantities of copper may be determined with EDTA, using MNCA, with a fair degree of accuracy. The minimum quantity of copper that may be titrated by this procedure is about 7 μg.; with a lesser amount, a sharp

11) K. L. Cheng and R. H. Bray, *Anal. Chem.*, **27**, 782 (1955).
12) H. Flaschka, "EDTA Titrations," Pergamon Press, London (1959), p. 78.
13) V. Suk and M. Malat, *Chemist-Analyst*, **45**, 30 (1956).
14) M. Theis, *Z. anal. Chem.*, **144**, 275 (1955).

TABLE III. EDTA TITRATION OF COPPER IN PURE SOLUTION

Indicator used	Cu taken mg.	pH adjusted with	pH	EDTA, 0.01 M Reqd. ml.	EDTA, 0.01 M Theo. ml.	End point colour
MNCA	8.472	NH_4Cl-NH_4OH	7.4	13.30	13.33	Permanganate to pale yellow
	2.118	NH_4Cl-NH_4OH	7.2	3.34	3.33	
	4.236	Pyridine	7.0	6.67	6.67	Bluish-violet to greenish-yellow
	2.118	Pyridine	6.8	3.35	3.33	
	8.472	Na-acetate	6.4	13.35	13.33	Red-violet to light green
	2.118	Na-acetate	6.2	3.32	3.33	
PAN	4.236	Acetate buffer	5.0	6.65	6.67	Red-violet to yellow
	2.118	Acetate buffer	5.0	3.30	3.33	
Murexide	8.472	NH_4Cl-NH_4OH	10.0	13.36	13.33	Yellowish-green to violet
	2.118	NH_4Cl-NH_4OH	10.0	3.32	3.33	
Pyrocatechol violet	8.118	Acetate buffer	5.6	3.30	3.33	Blue to yellow
	4.236	Acetate buffer	5.6	6.62	6.67	
Chrome Azurol S	8.472	Na-acetate	6.5	13.29	13.33	Blue to light-green
	2.118	Na-acetate	6.5	3.30	3.33	

TABLE IV. MICRO TITRATION OF COPPER

Cu taken μg.	Cu found μg.	Diff. μg.	Cu taken μg.	Cu found μg.	Diff. μg.
41.31	41.33	0.02	12.71	12.76	0.05
31.78	31.75	0.03	9.54	9.59	0.05
25.42	25.40	0.02	6.36	6.43	0.07
15.89	15.84	0.05	3.18	3.38	0.20

TABLE V. TITRATION OF COPPER IN THE PRESENCE OF ORGANIC SUBSTANCES

0.1 M $CuSO_4$ solution, taken 0.5~5 ml. of 0.01 M EDTA

Substances added	Amount ml.	Buffer used	pH	EDTA, 0.01 M reqd.	Remark
Pyridine	1	—	7.0	5.0	Sharp end point
Quinoline	0.5	NH_4Cl-NH_4OH	7.6	4.88	End point not sharp
Pyperidine	0.5	—	7.8	5.0	Sharp end point, violet to greenish yellow
Urea (5%)	2	Na-acetate	6.4	4.92	Sharp end point
Glycine (1%)	2	NH_4Cl-NH_4OH	7.2	—	Complex does not form
Monoethanolamine	0.5	—	7.6	4.7	Not sharp
Diethanolamine	0.5	—	8.0	4.87	Not sharp
Triethanolamine	0.5	—	8.0	4.98	Sharp end point
Ethylene glycol	1	Na-acetate	6.4	4.98	Sharp end doint
Propylene glycol	1	Na-acetate	6.2	4.92	Sharp
Glycerol	1	Na-acetate	6.4	4.95	Sharp
Diacetone	2	Na-acetate	6.4	5.0	Sharp
Ethyl methyl ketone	2	Na-acetate	6.1	5.1	Sharp
Tricresylphosphate in acetone (1%)	2	Na-acetate	5.8	4.8	Fairly sharp
Tri-*n*-butylphosphate in acetone (1%)	2	Na-acetate	6.4	5.1	Fairly sharp
Dibutylphthalate in acetone (1%)	2	Na-acetate	6.2	4.95	Fairly sharp

end point is not obtained. Some of the results of this titration carried out by following the procedure given below are recorded in Table IV.

Procedure.—To a solution containing about 10 to 100 μg. of copper, add 0.5 ml. of 0.5 M ammonium chloride, 2 drops of 0.5 M ammonium hydroxide, and 1 drop of a 0.02% indicator. Dilute to 10 ml. with warm water (40°C). The pH is now between 7 to 7.4. Now titrate with 0.001 M EDTA until it changes from a pink to a colourless state. The end point is

TABLE VI. TITRATION OF COPPER IN PRESENCE OF MASKING AGENTS
0.1 M Copper solution, taken 0.5~5 ml. of 0.01 M EDTA

Masking agent	Amount ml.	pH	EDTA, 0.01 M ml.	Remark
Citric acid (10%)	4	7.4	4.94	Blackish end point in excess
Tartaric acid (10%)	5	7.4	4.97	Permanganate to yellow, sharp
Oxalic acid (10%)	2	7.6	4.96	Pale greenish yellow end point
Ascorbic acid (2%)	2	—	—	Complex does not form
Glycollic acid (2%)	2	—	—	Complex does not form
Sulfosalicylic acid (5%)	2	7.2	—	Complex does not form
Hexamine (20%)	2	6.6	5.0	Yellowish green, sharp
Triethanolamine	0.5	8	4.98	Almost colorless
Hydroxylamine hydrochloride (2%)	2	—	—	Complex does not form
Thiourea in NH_4OH (1%)	2	7.4	4.95	Not sharp
Sodium fluoride (10%)	2	7.2	5.05	Sharp end point
Ammonium fluoride (10%)	3	7.4	4.98	Sharp end point
Ammonium bifluoride (10%)	3	7.4	4.97	Sharp end point
Disodium hydrogen phosphate (10%)	5	7.6	5.10	Fairly sharp
Potassium cyanide (2%)	3	7.2	—	Copper is masked
Potassium iodide in ammonia (5%)	3	7.4	4.98	Fairly sharp
Sodium thiosulfate in ammonia (2.5%)	5	7.8	4.94	Fairly sharp
Potassium fluoride and potassium tartrate (1 : 1) in ammonia (2%)	5	7.8	5.15	Fairly sharp

The p. c. in the above solutions indicate the amount in gram dissolved in 100 ml. of water or ammonia (5 M).

sharp. The titration may also be made by using a sodium acetate buffer, the pH is adjusted to 6.4 by adding a 0.2 M sodium acetate solution drop by drop, and the titration is carried out as before.

Titration in the Presence of Various Organic Substances.—It was observed that the copper complex of MNCA was stable in the presence of many organic compounds. The titration of copper with EDTA has been carried out in mixtures containing various organic amines and other complexing agents in order to examine whether the copper present in the solution becomes available to MNCA and, subsequently, to EDTA for its complexometric titration. The results of such titrations, under the conditions stated, are given in Table V. In the case of quinoline, 0.5 ml. of it was dissolved in a mixture of 15 ml. acetone and 10 ml. ethanol, the copper solution added, and the pH of the mixture raised to 7.4 with 2 ml. ammonium chloride and a few drops of 1 M ammonium hydroxide the mixture was then diluted to 50 ml. and titrated as before with EDTA.

The Effect of Masking Agents.—In order to examine the effect of masking agents on the indicator-copper complex and the possibility of using them as masking agents for the elimination of the interference of various metal ions, titrations of copper in the presence of some well-known masking substances have been carried out. The results are recorded in Table VI. It may be seen that a number of such complexing agents do not interfere with the titration, but that those which form strong complexes with copper itself, such as potassium cyanide and glycine, cannot be used. The copper-indicator complex does not form in the presence of those reducing agents which may also be used as masking agents, such as ascorbic acid, hydroquinone and hydroxylamine.

The Study of Interference by Diverse Ions in the Titration. — As the EDTA titration of copper is best carried out in a weakly alkaline medium, many cations (e. g., zinc, nickel, cobalt, calcium, magnesium, barium, lead, cadmium and the rare earths) interfere in the process. When the titration is done in an acetate buffer at pH 5.8 to 6.4, small amounts of calcium, barium and magnesium may be tolerated, and the addition of a little ammonium fluoride improves results. The interference of iron(II) and aluminium may be removed by using triethanolamine, sodium or ammonium fluoride in both ammoniacal and sodium acetate solutions. Mercury(II) may be masked by an ammoniacal potassium iodide solution. The addition of oxalic acid removes the interference of zirconium. The method is effective when copper is separated from the mixture of cations containing tartaric acid with thioacetamide or hydrogen sulphide and the EDTA titration is applied. Silver and alkali metals do not interfere. Table VII shows some of the results.

TABLE VII. EFFECT OF FOREIGN IONS ON TITRATION OF COPPER
Copper taken (0.1 M solution), 1~10 ml. of 0.01 M EDTA

Ions present	Quantity mg.	Buffer used	Masking agent	EDTA, reqd.
Na	28.42	NH_4Cl-NH_4OH	—	10.04
K	20.16	NH_4Cl-NH_4OH	—	10.02
Ag	7.2	NH_4Cl-NH_4OH	—	9.93
Hg(II)	6.51	NH_4Cl-NH_4OH	KI in NH_4OH	9.95
Fe(III)	6.60	—	Triethanolamine	10.11
		Na-acetate	NaF	10.05
Al	4.33	Na-acetate	Triethanolamine	10.14
		Na-acetate	NaF	9.98
		Na-acetate	Ammonium fluoride	10.06
		NH_4Cl-NH_4OH	Tartaric acid	10.13
Mg	5.82	Na-acetate	—	9.97
Ca	7.56	Na-acetate	—	10.09
Sr	10.06	Na-acetate	—	10.06
Zr	4.32	Na-acetate	Oxalic acid	10.10

Discussion and Summary

The copper complex of mononitrosochromotropic acid (MNCA) forms in a weakly acidic or a weakly basic solution, and the colour of the complex in solution deepens as the pH is raised (from pH 5 to 5.4 it is pink, from 5.4 to 6.6 it is red-violet, from 6.6 to 7.2 the colour is permanganate-violet, and at higher values pH up to 8.5, it is blue-violet). The complex decomposes at higher pH values. The same copper complex appears to form in all the above pH ranges. The complex is stable in the presence of many inorganic substances, but it is decomposed by oxidising and reducing agents and also by substances that form stronger complexes with copper. The copper complex, however, could not be extracted with any of the organic solvents commonly employed in solvent extraction methods. MNCA may be successfully used as an indicator in the complexometric titration of copper with EDTA.

The titrations carried out with this indicator, side by side with other indicators for copper, indicated that the new indicator may be placed in the same group as murexide, PAN, pyrocatechol violet or Chrome Azurol S with regard to the sharpness of the end point, colour contrast, accuracy, and precision in the titration of copper. The titration may be performed at different pH ranges using different buffer solutions: with sodium acetate at pH 5.8 to 6.5, with pyridine at pH 6.8 to 7, and with ammonium chloride and ammonia at pH 7 to 8. The change in the end point colour is from reddish-violet, bluish-violet or permanganate-violet to pale greenish yellow. Copper may be titrated in the macro range from 2 to 60 mg. of copper and in the micro-range down to 7 μg. by using this indicator.

The effect of various complexing agents, polyhydroxy alcohols, amines, amino acids and other masking agents, etc., on the EDTA titration of copper has also been studied; a number of them do not appear to interfere. The cations that form EDTA complexes in the same pH range as copper interfere in the titration, however. Iron and aluminium may be masked by triethanolamine or sodium fluoride, mercury(II), by ammoniacal potassium iodide, and zirconium, by oxalate. The alkali and alkaline earth metals do not interfere.

The authors express their thanks to M/S Dojindo & Co., Japan, for kindly supplying samples of pyrocatechol violet and Chrome Azurol S used in this work.

Department of Chemistry
Victoria (Government) College
Coochbehar, India

Structural Studies of the Gum Jeol Polysaccharide

By A. K. BHATTACHARYYA and A. K. MUKHERJEE*

(Received March 24, 1964)

Gum Jeol (Odina Wodier, Roxb) has been reported[1] to contain galactose, arabinose and galacturonic acid as constituent units. An aldobiuronic acid has also been reported. The constitution of the degraded gum obtained by the removal of the labile arabinose units has also been described.[2] This paper will report on the structural studies of the whole gum obtained by its repeated purification (equivalent weight 1150).

The supernatant liquid obtained during autohydrolysis was found by paper chromatography to contain a large proportion of L-arabinose, a trace of D-galactose, and an oligosaccharide having R_{gal} 1.36 in solvent G. The mixture was resolved on a cellulose column using solvent A, and the pure oligosaccharide obtained from fraction III was converted to a sirup. The molecular weight as determined by the alkaline hypoiodite method was 274, showing it to be a disaccharide of two pentose units. This was characterised as 3-*O*-L-arabofuranosyl-L-arabinose from hydrolysis and periodate oxidation studies (vide Experimental Section).

The purified gum was methylated[3-5] to a fully methylated polysaccharide showing no hydroxyl band in the infrared spectrum in the region of 3500~3600 cm^{-1}. It was soluble in chloroform and had $[\alpha]_D^{32}$ −37° (in chloroform). A portion of the methylated gum was subjected to methanolysis under conditions known to cause no cleavage of aldobiuronic acid. The methyl ester was hydrolysed with barium hydroxide,[6] and the acid fraction was separated by adsorbing it on Dowex 1-X4 (acetate-form) anion-exchange resin. The neutral glycosides were converted to a mixture of methyl sugars, which were separated on a cellulose column and identified through their crystalline derivatives (vide Experimental Section). These are shown in Table I.

The acid fraction was displaced from the resin column with 1 N sulphuric acid. Neutralisation, deionisation with Amberite IR-120(H) cation-exchange resin, and the evaporation of the resulting solution yielded a thick sirup with $[\alpha]_D^{32}$ +64° (in chloroform). This has been shown[2] to be 3-*O*-(2,3,4-tri-*O*-methyl-D-galactopyranosyluronic acid)-2,4-di-*O*-methyl-D-galactose, since, on reduction of the methyl ester methyl glycoside and subsequent hydrolysis, it afforded two methyl sugars, viz., 2,3,4-tri-*O*-methyl-D-galactose and 2,4-di-*O*-methyl-D-galactose in equimolecular proportions.

The mole proportions of these components were determined by weighing the different pure fractions obtained by column chromatography and by calculating the amounts of the pure components from the mixtures with the aid of specific rotations (vide Experimental Section). The hypoiodite method[6a] could not

TABLE I. ANALYSIS OF THE HYDROLYSATE OF THE METHYLATED GUM (NEUTRAL PART)

	Methyl sugar	R_g*	$[\alpha]_D$	Crystalline derivative	Mole proportion
1	2,3,5-Tri-*O*-methyl-L-arabinose	0.96	−40°	Amide	2.03
2	2,3,4,6-Tetra-*O*-methyl-D-galactose	0.89	+108°	Anilide	3.1
3	2,3,4-Tri-*O*-methyl-D-galactose	0.70	+114°	Anilide	1.0
4	2,4-Di-*O*-methyl-D-galactose	0.46	+86°	Anilide	1.94
5	2-*O*-Methyl-L-arabinose	0.40	+98°	Ph·hydrazone	1.05
6	2-*O*-Methyl-D-galactose	0.28	+79°	Anilide	1.1

* R_g values are with reference to 2,3,4,6-tetra-*O*-methyl-D-glucose in solvent C.

* Present address: Department of Organic Chemistry, Jadavpur University, Calcutta-32, India.

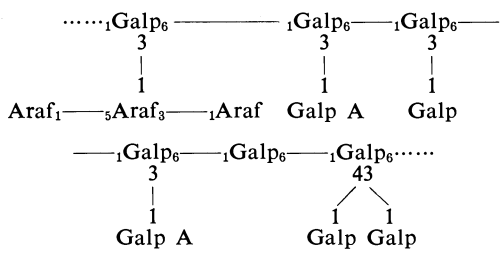
1) S. M. Mukherjee and P. K. Dhar, *J. Sci. & Industr. Res.*, **18B**, 219 (1959).
2) A. K. Bhattacharyya and C. V. N. Rao, *Can. J. Chem.*, **42**, 107 (1964).
3) W. N. Haworth, *J. Chem. Soc.*, **108**, 8 (1915).
4) T. Purdie and J. C. Irvine, ibid., **83**, 1021 (1903).
5) E. L. Falconer and G. A. Adams, *Can. J. Chem.*, **34**, 338 (1956).
6) G. G. S. Dutton and F. Smith, *J. Am. Chem. Soc.*, **78**, 2505, 3744 (1956).
6a) E. L. Hirst, L. Hough and J. K. N. Jones, *J. Chem. Soc.*, **1949**, 928.

be used since it was found difficult to separate the different components quantitatively on paper chromatogram.

From the above results, the following conclusions can be drawn. The characterisation of 2, 3, 5-tri-*O*-methyl-L-arabinose and 2, 3, 4, 6-tetra-*O*-methyl-D-galactose shows that both arabofuranose and galactopyranose residues are present as non-reducing end groups. The presence of 2, 3, 4-tri-*O*-methyl-D-galactose in the trimethyl fraction of the hexose units indicates that the main chain is 1→6 linked. The absence of a dimethyl arabinose indicates that arabinose is not present in the backbone chain of the molecule. The fact that the molecule is highly branched is supported by the characterisation of 2, 4-di- and 2-*O*-methyl-D-galactose and 2-*O*-methyl-L-arabinose. It is also clear that the galactose units which are singly-branched are linked through C_1, C_3 and C_6, while those which are doubly-branched are linked through C_1, C_3, C_4, C_6. The branched arabinose units are, however, linked through C_1, C_3, C_5.

The isolation and characterisation of 2, 4-di-*O*-methyl and 2, 3, 4-tri-*O*-methyl-D-galactose from the aldobiuronic acid fraction of the methylated gum, after reduction and subsequent hydrolysis, indicate clearly that the reducing galactose moiety of the aldobiuronic acid is a part of the main chain and that the uronic acid is present as a single-unit side chain.

From these results and from our knowledge of the structure of the repeating unit of the degraded gum,[2] a possible structure of the repeating unit of the whole gum polysaccharide may be as in Fig. 1.



where Galp = a D-galactopyranosyl unit, Galp A = a D-galactopyranosyluronic acid unit, and Araf = a L-arabofuranosyl unit.

It should be pointed out here that, from the results obtained above, it is not possible to assign the exact sequence of the different groups shown. This repeating unit, however, explains the products obtained from the hydrolysate of the whole gum. It also explains the change in the molar ratio of the compounds of the hydrolysates of the methylated whole gum and of methylated degraded gum shown in Table II.

TABLE II. CHANGE IN THE MOLAR RATIO OF THE METHYL SUGARS IN METHYLATED DEGRADED GUM AND METHYLATED WHOLE GUM

Methyl sugar	Methylated degraded gum	Methylated whole gum
2, 3, 5-Tri-*O*-methyl-L-arabinose	—	2
2, 3, 4, 6-Tetra-*O*-methyl-D-galactose	3	3
2, 3, 4-Tri-*O*-methyl-D-galactose	2	1
2, 4-Di-*O*-methyl-D-galactose	1	2
2-*O*-Methyl-L-arabinose	—	1
2-*O*-Methyl-D-galactose	1	1
Methylated aldobiuronic acid	2	2

During autohydrolysis, the labile arabofuranose units are cleaved out and the degraded gum shows the above behaviour.

The above structure, however, does not explain why the supernatant liquid from autohydrolysis should give only one kind of disaccharide, 3-*O*-L-arabofuranosyl-L-arabinose, and not the other, 5-*O*-L-arabofuranosyl-L-arabinose, which could not be obtained. This may, however, be due to the preferential cleavage of the 1→5 glycosidic bond to the 1→3 bond.

The results of the methylation studies were supported by the data obtained from the periodate oxidation of the gum using periodic acid.[7-9] It was found that the gum consumed 7.58 mol. of the oxidant in 30 hr. (constant), liberating 3.40 mol. of formic acid in 25 hr. (constant) per equivalent of the gum. Considering the facts that (1) a non-reducing galactopyranose unit or galactopyranosyluronic acid unit and a 1→6 linked galactopyranose unit of the backbone chain consume 2 mol. of periodic acid, liberating one mole of formic acid, that (2) galactopyranose units linked through C_1, C_3 and C_6 or C_1, C_3, C_4 and C_6 cannot react with periodic acid, that (3) each non-reducing arabofuranose unit should consume one mole of periodic acid without liberating any formic acid, and, that (4) the arabinose units linked through C_1, C_3, and C_5 do not react at all with periodic acid, the consumption of periodic acid and the liberation of formic acid per equivalent of the gum (assuming the above structure) works out as 7.30 and 3.13 mol. respectively.

The periodate oxidised gum, after reduction with sodium borohydride[10] and the usual

7) F. Smith, *J. Chem. Soc.*, **1951**, 2646.
8) E. L. Hirst, J. K. N. Jones and W. O. Jones, ibid., **1939**, 1880.
9) P. A. Levene and L. C. Kreider, *J. Biol. Chem.*, **120**, 591 (1937).
10) M. Abdel-Akber, J. K. Hamilton, R. Montgomery and F. Smith, *J. Am. Chem. Soc.*, **74**, 4970 (1952).

subsequent treatment, was precipitated with ethanol. The product on hydrolysis gave D-galactose 38.45% and L-arabinose 5.33% (as anhydrosugars). These values are good agreement with the values (36.7% anhydro galactose and 5.98% anhydro arabinose) calculated from the above structure.

The molecular weight of the methylated gum as determined by the light-scattering method was found to be 1.68×10^5. The molecular weight of one repeating unit of the methylated gum, on the basis of the proposed structure, is 2724. Hence, the D.P. of the gum-polysaccharide works out to be 62.

Experimental

Chromatographic separations were carried out using a descending technique with Whatman No. 1 filter papers. The solvent systems employed were: (A) ethyl acetate : pyridine : water (8 : 2 : 1); (B) *n*-butanol : acetic acid : water (4 : 1 : 5) upper layer; (C) *n*-butanol : ethanol : water (40 : 11 : 19); (D) *n*-butanol : ethanol : water (5 : 1 : 4) upper layer; (E) ethyl methyl ketone - water azeotrope; (F) ethyl acetate : acetic acid : water (9 : 2 : 2), and (G) ethyl acetate : acetic acid : water (3 : 1 : 3) upper layer. Aniline oxalate and ammoniacal silver nitrate spray reagents were used in developing the paper chromatograms.

Evaporations were carried out under reduced pressure at bath temperatures of 35~40°C. All the values of specific rotations are at equilibrium.

The isolation and purification of the gum have already been described in details.[2] The purified gum had 8.8% moisture; 0.79% ash; $[\alpha]_D^{30}$ −44° (*c* 0.5, 4% sodium hydroxide solution); equivalent wt., 1150 (acidimetry); 14.5% anhydro uronic acid;[11] 21.7% pentosan;[12] no nitrogen; and 0.51% methoxyl.[13] The gum on hydrolysis gave D-galactose (63.7%) and L-arabinose (19.5%) as estimated by the periodate method.[14]

The Examination of the Supernatant Liquid Obtained during the Autohydrolysis of the gum.—The procedure for the autohydrolysis of gum Jeol has been discussed before.[2] After the precipitation of the degraded gum, the supernatant liquid was collected and concentrated to a small volume. This, on paper chromatographic separation, indicated the presence of arabinose, a trace of galactose and an oligosaccharide (R_{gal} 1.36 in solvent G). The mixture (ca. 500 mg.) was fractionated on a cellulose column (60×3.5 cm.), using solvent A and cutting 20 ml. portions in each tube. The eluate, after paper chromatographic examination, was separated into three fractions.

Fraction I (380 ml.) containing only L-arabinose, was evaporated (410 mg.) and then crystallized from methanol; m. p. and mixed m. p. 152~154°C (with L-arabinose), $[\alpha]_D^{30}$ +108° (*c* 0.8, water). Fraction II (60 ml.) contained a mixture of galactose (trace) and the oligosaccharide (fraction III) (12 mg.) and was not examined further. Fraction III (160 ml.), containing chromatographically-pure oligosaccharide and with $[\alpha]_D^{32}$ +90° (*c* 0.5, water), was evaporated to a sirup (52.6 mg.). The oligosaccharide, on hydrolysis with 1 N sulphuric acid followed by the usual treatment, gave spot of only arabinose on a paper chromatogram. The molecular weight, as determined by the alkaline hypoiodite method, was 274 (calculated for a disaccharide of two pentose units, 282). The sirup (ca. 31.5 mg.) was oxidised with a sodium metaperiodate solution (3 M, 1 ml.) in an acetate buffer (pH 3.7, 49 ml.) in the dark at 0°C. The consumption of periodate became constant in two-and-a-half hours, amounting to 2.08 mol. per mole of the disaccharide.

The Methylation of the Gum.—The purified gum (10 g.) was methylated with dimethylsulphate and sodium hydroxide[3] (four times) and then by Purdie's method[4] (four times), following the method of Falconer and Adams.[5] The fully-methylated gum was a light yellow solid (7.5 g.) with $[\alpha]_D^{32}$ −37° (*c* 0.9, chloroform) and 42.2% methoxyl; it showed no hydroxyl band in the infrared spectrum.

The Methanolysis and Hydrolysis of the Methylated Gum. An Examination of the Neutral Part.—A portion of the methylated gum (2 g.) was refluxed with 2.5% dry methanolic hydrogen chloride (50 ml.) for 16 hr. (constant rotation). The solution was then neutralised (silver carbonate), filtered, and evaporated to a sirup. The sirup was heated with an aqueous barium hydroxide[6] solution (2%, 30 ml.) on a boiling water bath for 4 hr. at 80°C. The solution was neutralised (carbon dioxide gas) and then centrifuged. The resulting solution was deionised with Amberlite IR-120(H), and the acidic component was quantitatively adsorbed on Dowex 1-X4 (acetate) resin. The column was thoroughly washed with water to collect the neutral fraction, which was concentrated to a sirup (5 ml.) and then hydrolysed with 1 N sulphuric acid (50 ml.) at the temperature of a boiling-water bath for 14 hr. (constant rotation). The solution was neutralised (barium carbonate), filtered, deionised, and concentrated to a sirup. The paper chromatographic examination of the sirup using solvents C and D indicated the presence of 2,3,5-tri-*O*-methyl-L-arabinose, 2,3,4,6-tetra-, 2,3,4-tri-, 2,4-di-*O*-methyl-D-galactose 2-*O*-methyl-L-arabinose, and 2-*O*-methyl-D-galactose.

The mixture of methyl sugars (1.0 g.) was resolved on a cellulose column (80×3.5 cm.) using solvent E and collecting 10 ml. in each tube in an automatic fraction-collector. The eluates after chromatographic examination were separated into ten fractions and separately evaporated to sirups. Table III shows the various fractions so obtained.

The Examination of the Fractions and Characterisation of the Methyl Sugars.—*Fraction 1.*—The sirup, $[\alpha]_D^{30}$ −40° (*c* 1, water), was chromatographically pure. The sugar was converted to 2,3,5-tri-*O*-methyl-L-arabonamide through its lactone

11) C. Doree, "The Methods of Cellulose Chemistry," 2nd Ed., Chapman & Hall, London (1947), p. 391.
12) C. Doree, ibid., p. 381.
13) E. P. Clark, "Semi-micro Quantitative Organic Analysis," Academic Press, New York (1943), p. 68.
14) E. L. Hirst and J. K. N. Jones, *J. Chem. Soc.*, **1949**, 1659.

TABLE III. THE NEUTRAL FRACTIONS OBTAINED AFTER METHANOLYSIS AND HYDROLYSIS OF THE METHYLATED GUM

Fraction	Tube No.	Sugars detectable by paper chromatography	Sugar given on demethyltion[15]	R_g*	-OCH_3 %	$[\alpha]_D$	Yield mg.
1	34—40	2,3,5-Tri-*O*-methyl-L-arabinose	Arabinose	0.96	48.24	−40°	138.2
2	41—44	2,3,5-Tri-*O*-methyl-L-arabinose and 2,3,4,6-Tetra-*O*-methyl-D-galactose	Arabinose and Galactose	—	—	+39°	67.0
3	45—54	2,3,4,6-Tetra-*O*-methyl-D-galactose	Galactose	0.89	51.8	+108°	265.1
4	55—58	2,3,4,6-Tetra-*O*-methyl-D-galactose, 2,3,4-Tri-*O*-methyl-D-galactose and probably Di-*O*-methyl-arabinose (trace)	Galactose and Arabinose	—	—	+111°	51.0
5	59—66	2,3,4-Tri-*O*-methyl-D-galactose	Galactose	0.70	41.9	+114°	81.0
6	74—89	2,4-Di-*O*-methyl-D-galactose	Galactose	0.46	29.0	+86°	145.3
7	90—99	2,4-Di-*O*-methyl-D-galactose and 2-*O*-methyl-L-arabinose	Galactose and Arabinose	—	—	+90°	54.2
8	100—109	2-*O*-Methyl-L-arabinose	Arabinose	0.40	18.3	+98°	50.2
9	110—117	2-*O*-Methyl-L-arabinose and 2-*O*-methyl-D-galactose	Galactose and Arabinose	—	—	+86°	13.5
10	118—136	2-*O*-Methyl-D-galactose	Galactose	0.28	15.8	+79°	80.5

* R_g values are with reference to 2,3,4,6-tetra-*O*-methyl-D-glucose in solvent C.

m. p. and mixed m. p. 134~136°C (lit. 136~138°C), $[\alpha]_D^{31}$ +18° (*c* 0.5, water), lit. +20°.[16]

Fraction 2.—The sirup (67 mg.) had $[\alpha]_D^{30}$ +39° (*c* 1, water) and was found by paper chromatography to be a mixture of 2,3,6-tri-*O*-methyl-L-arabinose and 2,3,4,6-tetra-*O*-methyl-D-galactose. On demethylation, the sirup gave galactose and arabinose. From the specific rotation value of the mixture, the amounts of the trimethyl arabinose and tetramethyl galactose were found to be 31.2 mg. and 35.8 mg. respectively.

Fraction 3.—This fraction, with $[\alpha]_D^{30}$ +108° (*c* 1.05, water), was chromatographically pure. The 2,3,4,6-tetra-*O*-methyl-D-galactose was characterised through the crystalline *N*-phenyl-2,3,4,6-tetra-*O*-methyl-D-galactosylamine, m. p. and mixed m. p. 187~189°C,[17] $[\alpha]_D^{30}$ +36° (*c* 0.5, acetone), lit. +39°.[18]

Fraction 4.—The sirup, with $[\alpha]_D^{30}$ +111° (*c* 0.8, water), was found by paper chromatography to be a mixture of 2,3,4,6-tetra- and 2,3,4-tri-*O*-methyl-D-galactose and a trace of methyl arabinose. On demethylation, it gave spots of galactose and arabinose (faint). Disregarding the trace amount of methyl arabinose, the amounts of the tetra- and trimethyl galactose were calculated to be 32.1 and 18.9 mg. respectively from the specific rotation value.

Fraction 5.—The chromatographically-pure fraction had $[\alpha]_D^{30}$ +114°C (*c* 1, water) and was proved to be 2,3,4-tri-*O*-methyl-D-galactose by preparing its aniline derivative, m. p. and mixed m. p. 163~164°C.[19] The melting point depressed on admixture with the aniline derivative of 2,4,6-tri-*O*-methyl-D-galactose.

Fraction 6.—The sirup, with $[\alpha]_D^{30}$ +86° (*c* 1.2, water), was chromatographically pure. On trituration with ether, followed by drying in vacuo, the sirup was converted into a crystalline solid which, on crystallisation from a small volume of ethanol, yielded crystals with an m. p. and mixed m. p. of 98~100°C (with 2,4-di-*O*-methyl-D-galactose monohydrate), lit. 98~99°C.[20] It was further characterised through the crystalline *N*-phenyl-2,4-di-*O*-methyl-D-galactosylamine; m. p. and mixed m. p. 214~215°C, lit. 216°C.[20]

Fraction 7.—The sirup (54.2 mg.), with $[\alpha]_D^{29}$ +90° (*c* 0.6, water), gave galactose and arabinose on demethylation. The mixture, on paper chromatographic examination, indicated the presence of 2,4-di-*O*-methyl-D-galactose and 2-*O*-methyl-L-arabinose. By comparing the specific rotation values of the mixture and of its components, the amounts of dimethyl galactose and monomethyl arabinose were found to be 36.1 and 18.1 mg. respectively.

Fraction 8.—The chromatographically-pure fraction had $[\alpha]_D^{31}$ +98° (*c* 0.9, water) and was identified as 2-*O*-methyl-L-arabinose by conversion to the crystalline phenyl hydrazone; m. p. and mixed m. p. 111~112°C, lit 114°C.[21]

Fraction 9.—The fraction (13.5 mg.) had $[\alpha]_D^{28}$ +86° (*c* 0.5, water) and gave, on demethylation, spots of galactose and arabinose, along with other partially-methylated sugars on a paper chromatogram. The mixture had components which had

15) L. Hough, J. K. N. Jones and W. H. Wadman, *J. Chem. Soc.*, **1950**, 1702.
16) R. A. Laidlaw and E. G. V. Pereival, ibid., **1949**, 1600.
17) A. K. Mukherjee, D. Chowdhuri and P. Bagchi, *Can. J. Chem.*, **39**, 1408 (1961).
18) P. Andrew, L. Hough and J. K. N. Jones, *J. Am. Chem. Soc.*, **74**, 4029 (1952).
19) M. Abdel-Akher, F. Smith and D. Spriestersbach, *J. Chem. Soc.*, **1952**, 3637.
20) P. Andrews, L. Hough and J. K. N. Jones, ibid., **1954**, 806.
21) J. K. N. Jones, P. W. Kent and M. Stacey, ibid., **1947**, 1341.

the same R_g values as those of 2-*O*-methyl-L-arabinose and 2-*O*-methyl-D-galactose; from the specific rotation value, their amounts were found to be 5.0 and 8.0 mg. respectively.

Fraction 10. — This pure fraction, with $[\alpha]_D^{26}$ +77° (*c* 1.02, water), was proved to be 2-*O*-methyl-D-galactose by converting it to crystalline *N*-phenyl--2-*O*-methyl-D-galactosylamine; m. p. and mixed m. p. 158~159°C, lit. 165°C.[22]

The Examination of the Acid Fraction. — The acid fraction was displaced from the column of Dowex 1-X4 (acetate) resin with 1N sulphuric acid. The neutralisation, deionisation and evaporation of the resulting solution yielded a thick sirup (495 mg.) which had $[\alpha]_D^{32}$ +64° (*c* 1.05, chloroform). A portion of the sirup (ca. 340 mg.) was converted to the methyl ester methyl glycoside by Fischer's method, reduced with lithium aluminium hydride in dry ether,[23,24] and then hydrolysed with 1N sulphuric acid. The hydrolysate, after the usual treatment, was converted to a sirup (264 mg.) which, on paper chromatographic examination using solvents C and D, revealed the presence of 2,3,4-tri-*O*-methyl-D-galactose and 2,4-di-*O*-methyl-D-galactose, with a trace amount of tetramethyl galactose. The mixture (125 mg.) was separated on Whatman No. 3MM filter paper using solvent D. The first fraction (56 mg.) had $[\alpha]_D^{32}$ +107° (*c* 1.1, water) and was identified[2] as 2,3,4-tri-*O*-methyl-D-galactose by preparing the crystalline *N*-phenyl-2,3,4-tri-*O*-D-galactosylamine, m. p. and mixed m. p. 164~166°C, $[\alpha]_D^{31}$ +38° (*c* 0.5, acetone). The second fraction (52 mg.) had $[\alpha]_D^{31}$ +84° (*c* 1.05, water) and was characterised[2] as 2,4-di-*O*-methyl-D-galactose by preparing its aniline derivative, m. p. and mixed m. p. 218~219°C. The amounts of the two components obtained after separation indicate that they are in an equimolecular proportion.

Periodate Oxidation Studies of the Gum.—The gum (110.9 mg.) was dispersed in water (50 ml.) and was treated with a 0.2 M periodic acid solution in water (50 ml.). The oxidation was conducted by shaking the reaction mixture in the dark at 15°C. The liberated formic acid and the periodic acid consumption during the reaction were estimated in the usual way[25] at regular intervals of time. The liberation of formic acid became constant after 25 hr., corresponding to 3.40 mol. (after correction for the titratable acidity of the gum and periodic acid), while the periodate uptake became constant after 30 hr., corresponding to 7.58 mol. per equivalent of the gum.

The periodate-oxidised gum (102.5 mg.) was neutralised (barium hydroxide) and filtered, and to the clear solution sodium borohydride (150 mg.) was added. The reduction was then allowed to proceed for 4 hr. at room temperature. After the usual treatment, the resulting solution was poured into ethanol to precipitate the periodate-oxidised reduced gum, which was triturated with ethanol and then by dry ether and finally dried in vacuo at 40°C. Yield, 62.2 mg. The precipitated polysaccharide (ca. 40 mg.) was hydrolysed with 2N sulphuric acid at the temperature of a boiling-water bath for 24 hr. The amounts of galactose and arabinose left unattacked by periodic acid, as estimated by using D-ribose as a reference sugar, were found (as anhydro sugars) to be 38.45% each.

The Determination of the Molecular Weight of the Methylated Gum.—All measurements of the intensity of scattered light for the molecular weight determination of the methylated gum were carried out with a Brice-Phoenix light-scattering photometer (Model OM 1000 A), using a semi-octagonal cell. The concentrations used were over a range of $(1\sim7)\times10^{-3}$ g./ml., and the working standard method was used to calculate the turbidity, τ. The molecular weight was found to be 1.68×10^5, as calculated by the dissymmetry method[26] assuming the particle-scattering factor of P 90°[27,28] for the random coil.

Summary

The polysaccharide obtained from gum jeol has been shown to be composed of D-galactose, L-arabinose, and D-galacturonic acid. The hydrolysis of the fully-methylated gum yielded 2, 3, 5-tri-*O*-methyl-L-arabinose (2.03 mol.), 2,3, 4, 5-tetra-*O*-methyl-D-galactose (3.1 mol.), 2, 3, 4-tri-*O*-methyl-D-galactose (1 mol.), 2,4-di-*O*-methyl-D-galactose (1.94 mol.), 2-*O*-methyl-L-arabinoses (1.05 mol.) and 2-*O*-methyl-D-galactose (1.1 mol.) in the neutral fraction of the hydrolysate. The reduced acidic fraction gave 2, 3, 4-tri-*O*-methyl-D-galactose (2 mol.) and 2, 4-di-*O*-methyl-D-galactose (2 mol.). The structural significance has been discussed from the above results and from the results of periodate oxidation studies of the gum. The molecular weight of the methylated gum has also been determined by the light-scattering method.

The authors wish to thank Dr. P. Bagchi, Director of Research, East India Pharmaceutical Works, Ltd., Calcutta, and Dr. C. V. N. Rao, Research Officer, Department of Macromolecules, Indian Association for the Cultivation of Science, Calcutta, for their interest in and advice about this paper.

Department of Macromolecules
Indian Association for the
Cultivation of Science
Calcutta-32, India

22) E. L. Hirst and J. K. N. Jones, ibid., **1946**, 506.
23) M. Abdel-Akher and F. Smith, *Nature*, **166**, 1037 (1950).
24) F. Smith, *J. Chem. Soc.*, **1951**, 2646.
25) P. Fleury and J. Lange, *J. Pharm. Chem.*, **17(8)** 107 (1933).
26) P. Debye, *J. Phys. Chem.*, **51**, 18 (1943).
27) G. Oster, *Chem. Revs.*, **43**, 352 (1948).
28) P. Doty and R. F. Steiner, *J. Chem. Phys.*, **28**, 1211 (1950).

The Reduction of Isothiocyanato-ammine Complexes of Chromium(III) at the Dropping Mercury Electrode

By Nobuyuki TANAKA, Tasuku ITO and Reita TAMAMUSHI

(Received March 24, 1964)

The polarographic behavior of some isothiocyanato complexes of chromium(III) has been reported. Maki, Shimura and Tsuchida[1] investigated the polarographic behavior of several isothiocyanato chromium(III) complexes in neutral unbuffered solutions. The electrode process of hexaisothiocyanatochromate(III) was studied by Fischerová and Fischer,[2] and the polarographic behavior of some isothiocyanato-ammine chromium(III) complexes in Divers' liquid was reported by Ichniowski and Clifford.[3] Meanwhile, an extremely high adsorbability of isothiocyanato complexes on the mercury electrode has been demonstrated.[4] A systematic study of the electrode processes of a series of isothiocyanato chromium(III) complexes seems, therefore, to be worthwhile and desirable.

In this paper, the reduction of isothiocyanato-ammine chromium(III) complex ions, $[Cr(NCS)_p(NH_3)_{6-p}]^{(3-p)+}$ ($p=0, 1, 2, 4$ and 6), at the dropping mercury electrode has been studied by the measurement of the direct current, the alternating current and the Kalousek polarograms. The electrode processes of these complexes have been discussed on the basis of other chromium(III) complexes which were previously studied.[5-8]

Experimental

Materials.—$[Cr(NH_3)_6]Cl_3$,[9] $[Cr(NCS)_2(NH_3)_4]Cl$,[10] $NH_4[Cr(NCS)_4(NH_3)_2]\cdot 2/3H_2O$[11] and $K_3[Cr(NCS)_6]\cdot 4H_2O$[12] were prepared according to the procedures described in the literature. $[Cr(NCS)(NH_3)_5]Cl_2$ was prepared by a modification of the procedure of Werner and Halben.[13] The complexes were identified by the measurement of the absorption spectra and by the determination of the nitrogen and chromium contents. The nitrogen content was determined by the usual method, and the chromium content by a method which has previously been reported.[7] The analysis gave the following results:

$[Cr(NH_3)_6]Cl_3$
Calcd.: Cr, 19.9; N, 32.2%
Found: Cr, 19.0; N, 31.3%
$[Cr(NCS)(NH_3)_5]Cl_2$
Calcd.: Cr, 19.5; N, 31.6%
Found: Cr, 19.4; N, 31.8%
$[Cr(NCS)_2(NH_3)_4]Cl$
Calcd.: Cr, 19.1; N, 30.9%
Found: Cr, 18.5; N, 30.1%
$NH_4[Cr(NCS)_4(NH_3)_2]\cdot 2/3H_2O$
Calcd.: Cr, 14.9; N, 28.2%
Found: Cr, 14.6; N, 27.6%
$K_3[Cr(NCS)_6]\cdot 4H_2O$
Calcd.: Cr, 8.82; N, 14.2%
Found: Cr, 8.55; N, 14.2%

All the chemicals used were of a guaranteed reagent grade.

Apparatus and Procedure.—Direct-current (d. c.) and alternating-current (a. c.) polarograms were recorded with a Yanagimoto Model PR-2 pen-recording polarograph and a Yanagimoto Galvarecorder Y-GR 2 respectively. The Kalousek circuit and the cell equipments used were the same as have been reported previously.[7] The dropping mercury electrode (DME) employed had an m value of 1.62_5 mg./sec. and a drop-time, t_d, of 5.21 sec. when measured in an air-free solution containing 0.9 M potassium chloride, 0.1 M acetate buffer and 0.005% gelatin at -0.5 V. vs. SCE and at 50 cm. of height of the mercury reservoir. The potential of DME was referred to the saturated calomel electrode (SCE). The cell temperature was maintained at 25°C by means of a water thermostat. The dissolved oxygen in the electrolytic solution was removed by bubbling pure nitrogen gas through the solution.

All the measurements were carried out in the solution of ionic strength 1.0 containing 0.1 M acetate buffer (pH 4.7) and 0.005% gelatin or 2×10^{-5} M LEO (polyoxyethylene lauryl ether) unless otherwise stated. As the complexes are not stable in an aqueous solution, each solution for the electrolysis

1) N. Maki, Y. Shimura and R. Tsuchida, This Bulletin, **31**, 413 (1958).
2) E. Fischerová and O. Fischer, *Collection Czechoslov. Chem. Commun.*, **26**, 2570 (1961).
3) T. C. Ichniowski and A. F. Clifford, *J. Inorg. Nucl. Chem.*, **22**, 133 (1961).
4) N. Tanaka, E. Kyuno, G. Satô and R. Tamamushi, *J. Phys. Chem.*, **66**, 2706 (1962).
5) N. Tanaka and G. Satô *Nature*, **197**, 176 (1963).
6) N. Tanaka, K. Ebata and G. Satô, This Bulletin, **36**, 912 (1963).
7) N. Tanaka, Y. Sato, R, Tamamushi and G. Satô ibid., **36**, 1059 (1963).
8) N. Tanaka, E. Itabashi and E. Kyuno, ibid., **36**, 917 (1963).
9) M. Mori, *J. Chem. Soc. Japan, Pure Chem. Sec.* (*Nippon kagaku Zassi*), **74**, 253 (1953).
10) P. Pfeiffer and M. Tilgner, *Z. anorg. Chem.*, **55**, 361 (1907).
11) H. D. Dakin, "Organic Syntheses," Vol. 15, John Wiley & Sons, New York (1935), p. 74.
12) J. Rösler, *Ann.*, **141**, 185 (1867).
13) A. Werner and J. von Halben, *Ber.*, **39**, 2668 (1906).

was made freshly from the dry crystalline chromium-(III) complexes, and polarographic measurements were made as soon as possible after the removal of the dissolved oxygen.

Results

It has been shown in a previous study[6] that isothiocyanato-ammine complex ions of chromium(III), $[Cr(NCS)_p(NH_3)_{6-p}]^{(3-p)+}$, give no well-defined polarographic reduction wave in unbuffered neutral solutions, but do in acetate buffer or acid solutions. As typical examples of the current-potential curve, the polarograms of isothiocyanatopentamminechromium(III) ion, $[Cr(NCS)(NH_3)_5]^{2+}$, are given in Figs. 1 and 2. The maximum appears when the solution does not contain a sufficient amount of maximum suppressor and this can be attributed to the high adsorbability of the complex ions which have thiocyanate coordinated.[4] The addition of 0.005% gelatin or 2×10^{-5} M LEO suppresses this maximum.

The current-potential curves were obtained at various concentrations of the complex ions and at various heights of the mercury reservoir. The limiting current, $\bar{i}_l$, is proportional to the concentration of the complex ion in the range from 0.2 mM to 2.5 mM. Table I presents the linear relationship between the limiting current and the square root of the effective height of the mercury reservoir. These two relationships hold in every case and this indicates clearly that the limiting currents are diffusion-controlled.

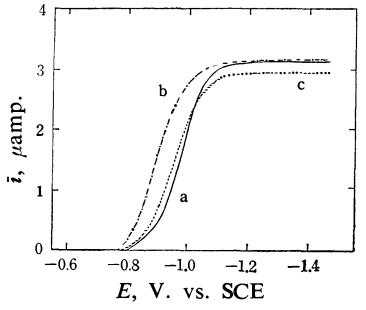


Fig. 1. Polarograms of 1.0 mM $[Cr(NCS)(NH_3)_5]Cl_2$ in 0.9 M KCl (a), 0.9 M KSCN (b) and 0.3 M Na_2SO_4 (c) solutions containing 0.1 M acetate buffer and 0.005% gelatin.

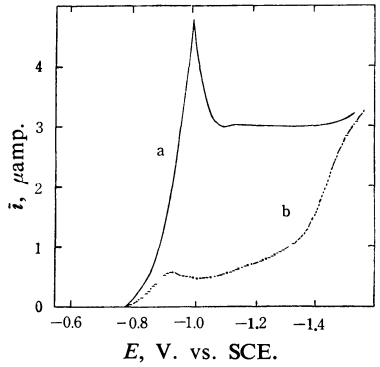


Fig. 2. Polarograms of 1.0 mM $[Cr(NCS)(NH_3)_5](NCS)_2$ in 0.9 M KCl + 0.1 M acetate buffer without maximum suppressor (a) and in 1 M KCl + 0.005% gelatin (b).

TABLE I. EFFECT OF THE HEIGHT OF MERCURY RESERVOIR ON THE LIMITING CURRENT OF 1.0 mM $[Cr(NCS)(NH_3)_5](NCS)_2$ IN THE SOLUTION CONTAINING 0.9 M KSCN, 0.1 M ACETATE BUFFER AND 0.005% GELATIN

$h_{corr.}$, cm.*	$\bar{i}_l/\sqrt{h_{corr.}}$, μamp. $cm^{-1/2}$
58.5	0.59_4
53.5	0.59_4
48.5	0.59_8
43.5	0.59_6
38.5	0.59_7

* Effective height of the mercury reservoir, corrected for the back pressure.

The half-wave potentials and the diffusion current constants, which were obtained in the solutions of ionic strength 1.0 containing various kinds of supporting electrolytes, are given in Table II. The reduction potentials of these complexes have been found to be affected to a great extent by the kind of supporting electrolyte.

Kalousek and a. c. polarograms were recorded to examine the polarographic reversibility of the electrode processes of the complexes. Typical Kalousek polarograms are reproduced in Fig. 3. The effect of the supporting electrolyte on Kalousek and a. c. polarograms is significant.. Nevertheless, all the

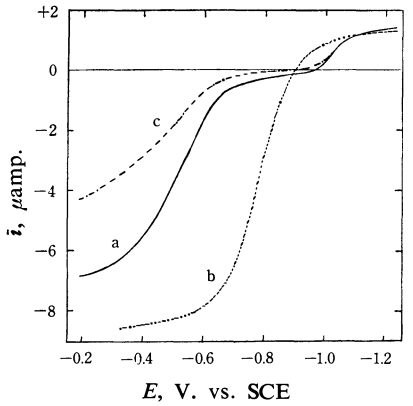


Fig. 3. Kalousek polarograms of 1.0 mM $[Cr(NH_3)_6]Cl_3$ in 0.9 M KCl(a), 0.9 M KSCN (b) and 0.3 M Na_2SO_4(c) solutions containing 0.1 M acetate buffer and 0.005% gelatin. The reduction potential is set up at −1.2 V. vs. SCE.

TABLE II. HALF-WAVE POTENTIALS (V. vs. SCE) AND DIFFUSION CURRENT CONSTANTS (μamp./mM mg$^{2/3}$ sec$^{-1/2}$) OF $[Cr(NCS)_p(NH_3)_{6-p}]^{(3-p)+}$

	In 0.9 M KCl, 0.1 M acetate buffer and 2×10^{-5} M LEO	In 0.3 M Na_2SO_4, 0.1 M acetate buffer and 0.005% gelatin	In 0.9 M KSCN, 0.1 M acetate buffer and 0.005% gelatin	In 0.9 M KI, 0.1 M acetate buffer and 0.005% gelatin
$[Cr(NH_3)_6]^{3+}$	$E_{1/2}=-1.01$	$E_{1/2}=-0.99$	$E_{1/2}=-0.85$	$E_{1/2}=-0.89$
	$I=1.7_3$	$I=1.5_2$	$I=1.7_3$	$I=1.6_6$
$[Cr(NCS)(NH_3)_5]^{2+}$	$E_{1/2}=-0.98$	$E_{1/2}=-0.95$	$E_{1/2}=-0.89$	—
	$I=1.6_1$	$I=1.5_2$	$I=1.6_4$	—
$[Cr(NCS)_2(NH_3)_4]^{+}$	$E_{1/2}=-0.91$	$E_{1/2}=-0.88$	$E_{1/2}=-0.90$	$E_{1/2}=-0.90$
	$I=1.5_9$	$I=1.5_1$	$I=1.6_3$	$I=1.6_6$
$[Cr(NCS)_4(NH_3)_2]^{-}$	$E_{1/2}=-0.80$	$E_{1/2}=-0.78$	$E_{1/2}=-0.83$	$E_{1/2}=-0.81$
	$I=1.5_0$	—	$I=1.5_7$	$I=1.6_1$
$[Cr(NCS)_6]^{3-}$	$E_{1/2}=-0.62$	—	$E_{1/2}=-0.80$	$E_{1/2}=-0.68$
	$I=1.5_0$	—	$I=1.5_3$	$I=1.5_5$

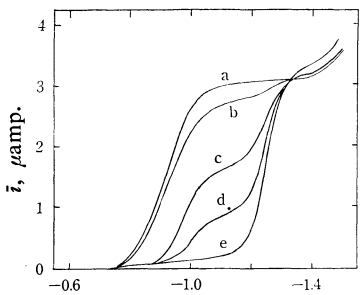


Fig. 4. D. c. polarograms of 1.0 mM $[Cr(NCS)_2(NH_3)_4]Cl_2$ in 0.9 M KSCN, 0.1 M acetate buffer and 0.005% gelatin without (a) and with 0.1 mM (b), 0.5 mM (c), 0.75 mM (d) and 5.0 mM (e) of EDTA.

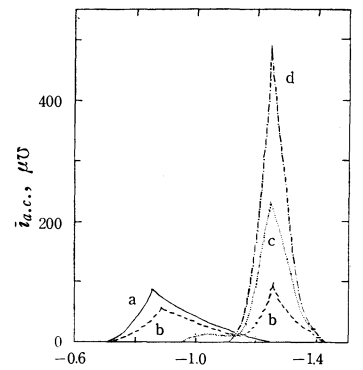


Fig. 5. A. c. polarograms of 1.0 mM $[Cr(NCS)_2(NH_3)_4]Cl_2$ in 0.9 M KSCN, 0.1 M acetate buffer and 0.005% gelatin without (a) and with 0.2 mM (b), 0.5 mM (c) and 5.0 mM (d) of EDTA.

complexes investigated gave similar Kalousek polarograms in a given supporting electrolyte solution.

The measurements of d. c. and a. c. polarograms of $[Cr(NCS)_2(NH_3)_4]^{+}$ were also made in the presence of EDTA (Figs. 4 and 5). The addition of EDTA causes a decrease in the limiting current over some potential range, as seen in Fig. 4. On a. c. polarograms, upon the addition of EDTA, the original wave decreases in height and a new wave appears at −1.25 V.; this wave increases in height with an increasing concentration of EDTA.[14] These phenomena were observed with all of the complexes investigated.

Discussion

One of the distinctive characteristics of the isothiocyanato-ammine complex ions, $[Cr(NCS)_p(NH_3)_{6-p}]^{(3-p)+}$, is their specific adsorption on the mercury electrode,[4] and this is well reflected in their polarographic behavior. The maximum wave shown in Fig. 2 seems to be due to the high adsorbability of the isothiocyanato complexes. The ligand NCS^- is coordinated with the central chromium atom through the nitrogen atom[4,15,16], and consequently the sulfur atom turns to the surface of the electrode.

As is shown in Table II, the supporting electrolyte has an important effect on the half-wave potential. The difference in the ease with which one electron enters in the reacting chromium(III) seems to be changed by some factors determined by the supporting electrolyte used. In potassium chloride or sodium sulfate solutions, the half-wave potential shifts to less negative potentials with an

14) N. Tanaka and H. Ogino, *J. Electroanal. Chem.*, **7**, 332 (1964).
15) Y. Takeuchi and Y. Saito, This Bulletin, **30**, 319 (1957).
16) J. Fujita, K. Nakamoto and M. Kobayashi, *J. Am. Chem. Soc.*, **78**, 3295 (1956).

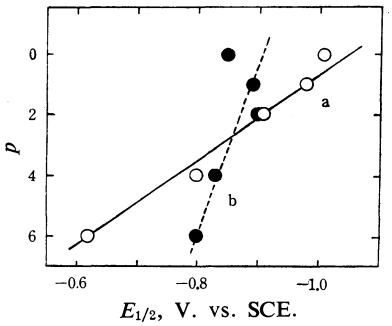


Fig. 6. Relation between p of $[Cr(NCS)_p(NH_3)_{6-p}]^{(3-p)+}$ and the half-wave potential: Half-wave potentials were observed in 0.1 M acetate buffer solutions containing 0.9 M KCl and 2×10^{-5} M LEO (a), and those containing 0.9 M KSCN and 0.005% gelatin (b).

increase in the number of the thiocyanate group coordinated in $[Cr(NCS)_p(NH_3)_{6-p}]^{(3-p)+}$. On the other hand, no such tendency holds in potassium thiocyanate or potassium iodide solutions. Fig. 6 gives the relations between the p value of $[Cr(NCS)_p(NH_3)_{6-p}]^{(3-p)+}$ and the half-wave potential in potassium chloride and potassium thiocyanate solutions. The linear relation in the potassium chloride solution (curve a in Fig. 6) may indicate that the number of the coordinating thiocyanate is one of the important factors in determining the reduction potential. In the potassium thiocyanate solution, the half-wave potentials of the complex cations are at less negative potentials than in the potassium chloride solution, whereas those of the complex anions are at more negative potentials (curve b in Fig. 6). Similar shifts of the half-wave potentials were also observed in potassium iodide solutions.

It seems that the above-mentioned observations can be explained by considering the specific adsorption of thiocyanate ions (or iodide ions) and that of the complex ions, and the electrostatic interaction between the electrode surface and the complex ions. At the concentration of the experimental conditions, a large amount of thiocyanate ions (or iodide ions) is specifically adsorbed at the surface of the DME at the potentials where the complex ions are reduced. The negative charge on the surface of the DME, therefore, is so large that $[Cr(NH_3)_6]^{3+}$, a tervalent cation, is attracted to the electrode surface, whereas $[Cr(NCS)_6]^{3-}$, a tervalent anion, is repelled. This causes the shifts of the reduction potential toward the opposite directions.

However, there is an alternative explanation of this potential shift. Isothiocyanato complexes are very adsorptive at the mercury electrode and seem to be reduced in the adsorbed state. The specific adsorption of the complexes with more NCS^- coordinated are partially disturbed when the adsorptive electrolyte is used. This results in the shift of the half-wave potential to more negative potentials. On the other hand, the reduction of the complex ions with less NCS^- coordinated, e.g., $[Cr(NH_3)_6]^{3+}$, is accelerated by the effect of the adsorbed supporting electrolyte SCN^-, as is the case in the polarographic reduction of Ni^{2+},[17] Zn^{2+} [18] and In^{3+}.[19] The acceleration effect caused by adsorbed SCN^- is seen in the Kalousek and the a. c. polarograms.

In most cases, the log-plot gave no straight line but two straight-line segments or curved lines, except in the case of $[Cr(NH_3)_6]^{3+}$ in a potassium chloride solution. Fig. 7 shows the plots of $\log i/(i_d-i)$ vs. E for the reduction waves of $[Cr(NCS)(NH_3)_5]^{2+}$ in the supporting electrolyte solutions indicated. It should be noted that the steeper portion of the slope comes at less negative potentials in a potassium thiocyanate solution, but at more negative potentials in a potassium chloride solution. This was observed with all of the complexes investigated.

As is seen in Fig. 3, the reversibility of the reduction of chromium(III) to chromium(II) at the dropping mercury electrode varies to some extent with the supporting

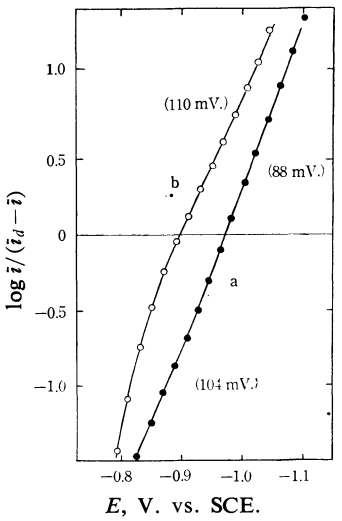


Fig. 7. Log-plots for the reduction waves of 1.0 mM $[Cr(NCS)(NH_3)_5]Cl_2$ in 0.9 M KCl (a) and 0.9 M KSCN (b) solutions containing 0.1 M acetate buffer and 0.005% gelatin.

17) J. J. Lingane and H. Kerlinger, *Ind. Eng. Chem., Anal. Ed.*, **13**, 77 (1941).
18) R. Tamamushi, K. Ishibashi and N. Tanaka, *Z. physik. Chem., N.F.*, **35**, 209 (1962); **39**, 117 (1963).
19) R. Tamamushi, T. Takeuchi and N. Tanaka, 18th International Congress of Pure and Applied Chemistry, Montreal, Canada (August, 1961), No. B3-39.

electrolyte used. The Kalousek polarograms of $[Cr(NH_3)_6]^{3+}$ obtained in potassium chloride and sodium sulfate solutions (curves a and c in Fig. 3), where the anodic waves are clearly separated from the cathodic ones, indicates that the reduction proceeds irreversibly. The corresponding a.c. peaks are as small as that for Ni^{2+} ion, which is known to be of a typical irreversible nature.[7] In a potassium thiocyanate solution (curve b in Fig. 3), however, the polarographic reversibility increases.

The value of $i_p/(n\bar{i}_d\sqrt{t_d})$ represents the degree of the polarographic reversibility of the electrode reaction, where i_p is the peak current of the a.c. wave (in μU), $\bar{i}_d$, the average diffusion current of the corresponding d.c. polarograms (in μamp.), and n, the number of electrons involved in the electrode process[20]. Table III shows the $i_p/(n\bar{i}_d\sqrt{t_d})$ values for the reduction of the complex ions.

TABLE III. VALUES OF $i_p/(n\bar{i}_d\sqrt{t_d})$ (U amp^{-1} sec$^{-1/2}$)

	In 0.9 M KSCN, 0.1 M acetate buffer and 0.005% gelatin	In 0.9 M KCl, 0.1 M acetate buffer and 2×10^{-5} M LEO
$[Cr(NH_3)_6]^{3+}$	16.7	8.1
$[Cr(NCS)(NH_3)_5]^{2+}$	9.9	4.4
$[Cr(NCS)_2(NH_3)_4]^{+}$	14.1	2.6
$[Cr(NCS)_4(NH_3)_2]^{-}$	27.8	10.8
$[Cr(NCS)_6]^{3-}$	44.3	9.3

The a.c. wave height became higher with an increasing p value of $[Cr(NCS)_p(NH_3)_{6-p}]^{(3-p)+}$ in a potassium thiocyanate solution. The reversibility revealed by the a.c. polarography accords well with that revealed by the measurement of the Kalousek polarograms.

All experimental results indicate that no preceding chemical reaction takes place prior to the electron transfer process, which is always followed by a rapid aquation of the divalent species, and that the aquation reaction may contribute to the polarographic reversibility.

From their detailed investigation of the polarographic reduction of $[Cr(NCS)_6]^{3-}$ in a potassium thiocyanate solution, Fischerová and Fischer concluded that the reversibility increased at higher concentrations of potassium thiocyanate.[2] Furthermore, Ichniowski and Clifford, who recently investigated the polarographic behavior of isothiocyanato-ammine complexes of chromium(III) in Divers' liquid, reported that the reduction proceeds reversibly.[3] These facts may suggest that the polarographic reduction proceeds reversibly under conditions where the following chemical reaction does not or hardly occurs.

The effect of EDTA on the reduction waves of $[Cr(NCS)_p(NH_3)_{6-p}]^{(3-p)+}$ is interpreted in the same way as the effect of ethylenediammine on the polarograms of $[Co(NH_3)_6]^{3+}$ which was reported by Laitinen and Kivalo.[21]

The complex ion $[Cr(NCS)_p(NH_3)_{6-p}]^{(3-p)+}$ is reduced at the electrode to form $[Cr(NCS)_p(NH_3)_{6-p}]^{(2-p)+}$, which in turn reacts with EDTA:

$$[Cr(NCS)_p(NH_3)_{6-p}]^{(2-p)+} + EDTA = Cr(II)\text{-}EDTA + pNCS^- + (6-p)NH_3$$

Because of the lability and the relative stability of these divalent chromium complexes, the reaction proceeds rapidly to the right. The Cr(II)-EDTA thus formed may or may not be oxidized at the electrode to the Cr(III)-EDTA complex, depending on the electrode potential. If the oxidation takes place, the oxidation current cancels the reduction current of $[Cr(NCS)_p(NH_3)_{6-p}]^{(3-p)+}$ and the limiting current of the $[Cr(NCS)_p(NH_3)_{6-p}]^{(3-p)+}$ wave decreases. The wave which appears at more negative potentials corresponds to the oxidation-reduction wave of the Cr(II)-EDTA and $[Cr(H_2O)(edta)]^-$ system. The effect of EDTA on the a.c. polarographic wave can be explained in the same way. A detailed study of the d.c. and the a.c. polarography of $[Cr(NCS)_p(NH_3)_{6-p}]^{(3-p)+}$ in the presence of EDTA will be reported elsewhere.

Summary

The reduction of a series of isothiocyanatoammine chromium(III) complexes $[Cr(NCS)_p(NH_3)_{6-p}]^{(3-p)+}$ at the dropping mercury electrode has been studied. The direct current, the alternating current and the Kalousek polarograms of these complexes have been measured in various supporting electrolyte solutions. The nature of the reduction waves, corresponding to the one-electron reduction of chromium(III) to chromium(II), has been discussed.

The authors wish to thank the Ministry of Education for the financial support granted for this research.

Department of Chemistry
Faculty of Science
Tohoku University
Katahira-cho, Sendai

20) M. Senda, M. Senda and I. Tachi, *J. Electrochem. Soc.* Japan (*Denki Kagaku*), 27, 83 (1959).

21) H. A. Laitinen and P. Kivalo, *J. Am. Chem. Soc.*, 75, 2198 (1953).

*The Reduction of Indium(III) in Thiocyanate Solutions at the Dropping Mercury Electrode**

By Nobuyuki TANAKA, Takashi TAKEUCHI and Reita TAMAMUSHI**

(Received June 4, 1964)

The effects of adsorbed ions or molecules on the rate of electrode processes have recently received considerable attention from many investigators. Frumkin was the first to point out the effect of adsorbed cations on the reduction wave of persulfate ions at the dropping mercury electrode. He discussed the dependence of the kinetics of the electrode processes on the surface layer structure.[1] Tamamushi et al. reported the apparent reversibility of the reduction of zinc(II), which increased with the increasing concentration of halide ions in the solution.[2,3]

The reduction wave of indium(III) at the dropping mercury electrode is irreversible and very much drawn-out in sodium nitrate or sodium perchlorate solutions. In potassium thiocyanate or potassium iodide solutions, on the other hand, indium(III) produces a reversible three-electron reduction wave in the potential region between -0.5 and -0.9 V. vs. saturated calomel electrode. Shirai[4,5] found that the polarographic behavior of an indium(III)-thiocyanate system was very peculiar; on the direct current (d.c.) polarogram of the system a minimum appeared at relatively negative potentials, and on the alternating current (a.c.) polarogram a negative admittance was observed in the potential region where the minimum appeared on the d.c. polarogram. However, she gave no explanation of the effect of thiocyanate ions on the reduction process of indium(III) at the electrode.

In the present paper, the acceleration effect of thiocyanate ions on the reduction of indium(III) at the dropping mercury electrode is presented, and the most plausible mechanism to explain the effect is proposed.

Experimental

D.c. and a.c. polarograms were obtained with a pen-recording polarograph, Yanagimoto Galvarecorder Y-GR 2 equipped with an automatic potential scanner. In the more accurate measurement of d.c. polarograms, a manual apparatus similar to that of Kolthoff and Lingane[6] was used. Current-time curves during the life of a mercury drop were recorded with a mechanical oscillograph, Yokogawa type N-6.[7] The faradaic impedance was determined by an impedance bridge used in the previous study.[8] The attachment of the bridge and the electrolysis cell were the same as described previously.[8] The impedance of the cell circuit was measured at the moment immediately before the detachment of the mercury drop. The electrode potential of the dropping mercury electrode (DME) was measured against a saturated calomel electrode (SCE), which was connected to the electrolytic solution through an agar-agar bridge containing 1 M potassium nitrate. In the impedance measurement, a Pt-spiral electrode of a large surface area was used as an auxiliary electrode. The rate of flow of mercury and the drop time of the DME used were 1.14 mg./sec. and 6.71 sec. respectively, being measured in an air-free 0.5 M sodium perchlorate solution containing 1×10^{-6} M polyoxyethylene lauryl ether (LEO) under an applied pressure of 50 cm. of mercury at open circuit. The dissolved oxygen in the electrolytic solution was removed by passing pure nitrogen gas through the solution for about 30 min. All measurements were carried out at 25.0 ± 0.1°C.

A standard solution of indium(III) was prepared by dissolving a known amount of pure indium metal (Kanto Chemical Co. purity 99.99%) in a concentrated nitric acid. All the other chemicals were of an analytical reagent grade. Redistilled water was used for the preparation of solutions. Proper amounts of nitric acid were added to the electrolytic solutions (pH 2.7 to 3.7) to prevent indium(III) ions from the hydrolysis.

* This was partly presented at the 18th International Congress of Pure and Applied Chemistry, Montreal (1961), under the title of "Minimum on the Current-potential Curve in Polarography," and also at the First Australian Conference on Electrochemistry, Sydney and Hobart (1963), under the title of "Effect of Adsorbed Ions and Molecules on the Rates of Electrode Processes at the Dropping Mercury Electrode."

** Present address: The Institute of Physical and Chemical Research, Komagome, Bunkyo-ku, Tokyo.

1) A. Kalish and A. Frumkin, *J. Phys. Chem.* (*U. S. S. R.*), **28**, 1473 (1954).

2) R. Tamamushi, K. Ishibashi and N. Tanaka, *Z. physik. Chem. N. F.*, 35, 209 (1962).

3) R. Tamamushi and N. Tanaka, ibid., **39**, 117 (1963).

4) H. Shirai, *J. Chem. Soc. Japan, Pure Chem. Sec.* (*Nippon Kagaku Zasshi*), **81**, 1248 (1960).

5) T. Takahashi and H. Shirai, *Rev. Polarog.* (*Kyoto*), **11**, 155 (1963).

6) I. M. Kolthoff and J. J. Lingane. "Polarography," Interscience Publishers, New York (1952), p. 297.

7) R. Tamamushi, S. Momiyama and N. Tanaka, *Anal. Chim. Acta*, **23**, 585 (1960).

8) R. Tamamushi and N. Tanaka, *Z. physik. Chem. N. F.*, **28**, 158 (1961).

Results

D. c. polarograms of 1 mM of indium(III) which were obtained in the solutions containing various amounts of thiocyanate ions are given in Fig. 1, where $\bar{i}$ means the average current

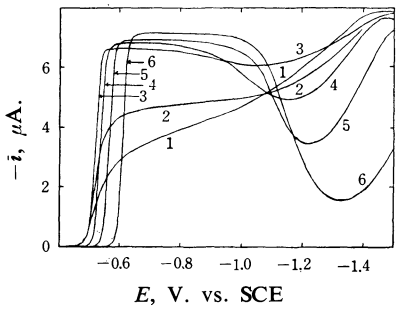


Fig. 1. Direct current polarograms of 1.0 mM $In(NO_3)_3$ in the solutions of ionic strength 1.0 (with $NaNO_3$) containing various concentrations of KSCN and 1×10^{-5} M LEO. The concentrations of KSCN are: (1) 0, (2) 0.0001, (3) 0.002, (4) 0.04, (5) 0.20, (6) 1.00 M.

during the life of a mercury drop.* The ionic strength of the solution was adjusted to be 1.0 with sodium nitrate. In a sodium nitrate solution, the reduction wave of indium(III) was very much drawn-out, and a relatively small cathodic current was observed in the potential region of −0.5 to −0.9 V. vs. SCE (curve 1 in Fig. 1). The cathodic current in this potential region, however, was greatly increased by the addition of a minute amount of thiocyanate ions (curves 2 and 3 in Fig. 1).

The ionic species of indium(III) in the bulk of the solution do not change appreciably by the addition of such a small amount of thiocyanate ions.[9] Therefore, it is suggested that the effect of thiocyanate ions on the reduction of indium(III) at the dropping mercury electrode is mainly due to the change in the state of the electrode surface by the adsorption of thiocyanate ions. When the concentration of thiocyanate ions was larger than 0.02 M, a reversible three-electron reduction wave of indium-(III) was completely developed in the potential region mentioned above. The half-wave potential $E_{1/2}$ of the reduction wave of indium(III) shifted to negative potentials with the increase in the concentration of potassium thiocyanate. Fig. 2 shows the relation between the $E_{1/2}$ and the logarithm of the concentration of potassium thiocyanate. The number of thiocyanate ions coordinated with an indium(III) ion was determined from the slope of this relation, with the result that two thiocyanate ions were coordinated in a 0.3 M potassium thiocyanate solution and four in a 0.8 M potassium thiocyanate solution.

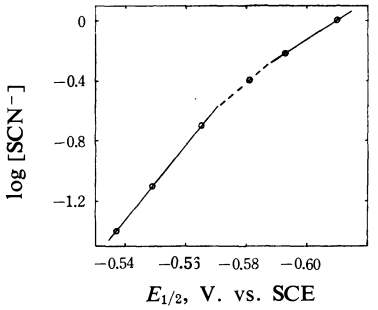


Fig. 2. Half-wave potentials of In(III)-SCN complexes as a function of the logarithm of the thiocyanate concentration.

At more negative potentials, a remarkable minimum appeared on the d. c. polarogram. It should be noticed that, in the In(III)-KSCN system, the minimum was observed in solutions of relatively high ionic strength. Therefore, the appearance of the minimum was unable to be explained on the basis of a simple electrostatic repulsion between the electrode surface and the depolarizing species.[10,11]

The current-time curves during the life of a mercury drop given in Fig. 3 were recorded

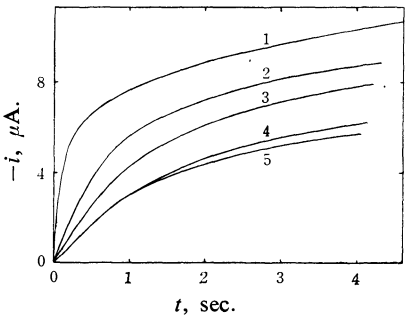


Fig. 3. Current-time curves of 1.0 mM $In(NO_3)_3$ in 0.4 M KSCN obtained at (1) −0.80, (2) −1.10, (3) −1.15, (4) −1.23, (5) −1.29 V. vs. SCE.

with 1.0 mM indium(III) at 0.4 M potassium thiocyanate at various potentials in the region where the minimum appeared on the d. c. polarogram. These current-time curves were approximately represented by the relation:

$$\log|i| = k + \beta \log t$$

* In this study, the sign of the cathodic current is taken as negative.

9) T. P. Radhakrishnan and A. K. Sundaram, *J. Electroanal. Chem.*, 5, 124 (1963).

10) A. Frumkin, *Z. Electrochem.*, 59, 807 (1955); *Trans. Faraday Soc.*, 55, 156 (1959).

11) A. Frumkin and N. Fedorovich, "Progress in Polarography," Vol. 1, Interscience Publishers, New York (1962), p. 223.

where i is the instantaneous current and k, the constant. The values of β were found to be beween 1/6 and 2/3. This suggests that the current in this potential region is partly controlled by some process of a kinetic nature.

An example of a. c. polarograms of 1.0 mM of indium(III) obtained in a 0.4 M potassium thiocyanate solution is shown in Fig. 4 (curve 1). A remarkable negative admittance was observed in the potential region where the d. c. current began to decrease. Such anomalies on the a. c. polarogram were also reported by Shirai for the In(III)-KSCN, Ni(II)-KSCN and Cu(II)-NH_4NO_3 systems.[3] The negative admittance suggested the unique mechanism

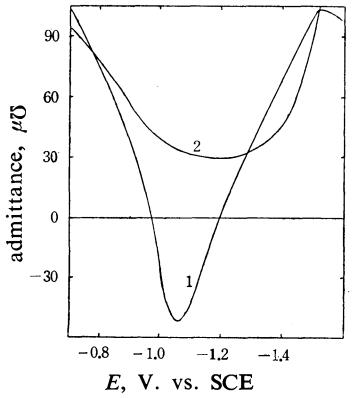


Fig. 4. Alternating current polarograms of (1) 1.0 mM $In(NO_3)_3$ in 0.4 M KSCN and (2) 0.4 M KSCN.

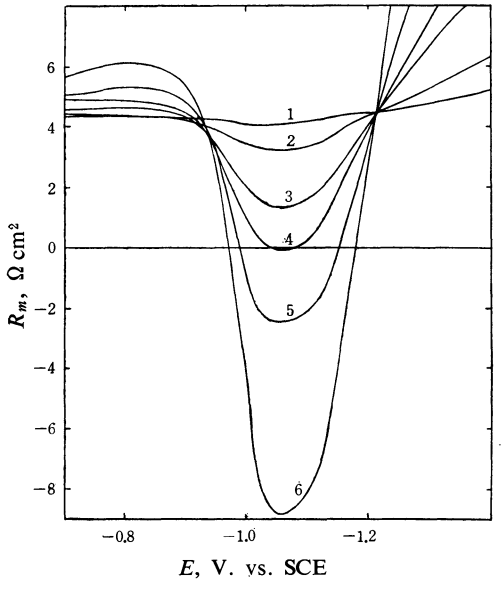


Fig. 5. The resistance component R_m of DME/ 1.0 mM $In(NO_3)_3$−0.4 M KSCN as a function of the electrode potential obtained at frequencies of (1) 1000, (2) 500, (3) 300, (4) 250, (5) 200 and (6) 150 cycles/sec.

of the electroreduction of indium(III) at the electrode surface.

The accurate measurement of the impedance of the electrode-solution interface, which was assumed to be represented with a series combination of the resistance, R_m, and the capacitance, C_m, was carried out by means of an impedance bridge. Fig. 5 shows the relation between the resistance component R_m of the impedance and the electrode potential. At relatively low frequencies, negative values of the resistance component were obtained in the potential region where the negative admittance was observed on the a. c. polarogram. The capacitance component C_m of the impedance was found to be almost the same as that of the supporting electrolyte solution in the whole potential region measured. From those measurements, it can be said that the anomalous negative admittance on the a. c. polarogram results from the negative value of the resistance component of the impedance.

Discussion

The electrical equivalent circuit of a polarizable electrode-solution interface can be represented with the circuit as shown in Fig. 6. If the

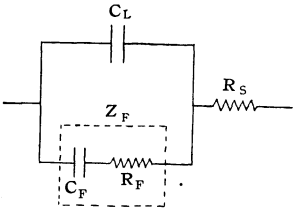


Fig. 6. Equivalent circuit of electrolytic system: C_L, double layer capacity; R_S, resistance of the cell; Z_F faradaic impedance; R_F, polarization resistance; C_F, electrolytic capacitance.

impedance of the electrolytic cell is measured by an impedance bridge with the corresponding arm composed of the resistance R_m and the capacitance C_m in series, R_m is represented as follows:

$$R_m - R_s = \frac{C_F^2 R_F}{\omega^2 C_L^2 C_F^2 R_F^2 + (C_F + C_L)^2} \qquad (1)$$

where ω is the angular frequency of the superimposed alternating current. In order to explain the experimental result that R_m is smaller than the resistance of the solution R_s, the polarization resistance R_F should be negative. The expression of R_F has been presented by Grahame[12,13], and the simplest

12) D. C. Grahame, *J. Electrochem. Soc.*, **99**. C 370 (1952).
13) P. Delahay, "New Instrumental Methods in Electrochemistry," Interscience Publishers, New York (1954), p. 146.

expression is given as follows:

$$R_F = \left(\frac{\partial E}{\partial i}\right)(1+\kappa) \tag{2}$$

$$\kappa = \frac{1}{\sqrt{2}\, nFA\omega^{1/2}D^{1/2}}\left(\frac{\partial i}{\partial C_R} - \frac{\partial i}{\partial C_O}\right) \tag{3}$$

where D is the common diffusion coefficient of the oxidant and the reductant; A, the surface area of the electrode; C_O and C_R, the concentrations of the oxidant and the reductant at the electrode surface respectively; n, the number of electrons involved in the eletron-transfer process, and F, the faraday. Generally, the term $(1+\kappa)$ is positive because the sign of the cathodic current is taken as negative, and consequently the sign of R_F is the same as that of $(\partial E/\partial i)$.

The faradaic current, i, is represented as,

$$i = -nFA(k_c C_O - k_a C_R) \tag{4}$$

where k_c and k_a are the cathodic and the anodic rate constants, respectively. At sufficiently negative potentials compared to the standard potential of the system, the cathodic rate constant k_c is much larger than the anodic one k_a of the electrode reaction. At such potentials the current is given by the equation,

$$i = -nFAk_c C_O \tag{5}$$

Differentiating with respect to the electrode potential E,

$$\left(\frac{\partial i}{\partial E}\right)_{C_O} = -nFA\left(\frac{\partial k_c}{\partial E}\right)C_O \tag{6}$$

is obtained. Eq. 6 indicates that the sign of R_F depends on that of $(\partial k_c/\partial E)$.

As has been described above, it is considered that adsorbed thiocyanate ions on the electrode surface accelerate the reduction of indium(III) at the DME. This may be justified by the fact that the acceleration effect of the thiocyanate ion decreases and the minimum appears on the d.c. polarogram at potentials more negative than about -1.0 V. vs. SCE where thiocyanate ions desorb from the mercury electrode surface.* Therefore, the overall eletrode reaction under the influence of the adsorbed thiocyanate ions may be assumed to consist of two simultaneous processes in parallel:

$$O + ne + Hg(n) \underset{k_{-1}}{\overset{k_1}{\rightleftharpoons}} R \tag{I}$$

$$O + ne + Hg(c) \underset{k_{-2}}{\overset{k_2}{\rightleftharpoons}} R \tag{II}$$

The reaction through path I proceeds at the naked part of the electrode surface, Hg(n), while the reaction through path II proceeds at the electrode surface which is covered with the adsorbed thiocyanate ions, Hg(c); k_1 (or k_{-1}) and k_2 (or k_{-2}) are the reduction (or the oxidation) rate constants of reactions through paths I and II respectively.

If it can be assumed that the reduction of indium(III) through one path proceeds independently of the other, the overall reduction rate constant k_c can be given by a linear combination of k_1 and k_2:

$$k_c = (1-\theta)k_1 + \theta k_2 \tag{7}$$

where θ is the degree of coverage of the electrode surface by thiocyanate ions. Thiocyanate ions are electrocapillary active and are adsorbed on the mercury surface, particularly at the potentials in the positive branch of the electrocapillary curve, whereas, at relatively negative potentials in the negative branch of the electrocapillary curve, they markedly decrease in the degree of adsorption, and the electrode surface is gradually covered with some other species, such as water molecules or the hydrated cations present in the solution. In the region where thiocyanate ions are specifically adsorbed on the electrode surface, the contribution of the reaction at the covered surface to the overall process is so large that the electrode reaction of indium(III) virtually proceeds at the covered surface only. This explains the experimental result that, when the concentration of thiocyanate ions is greater than approximately 0.02 M, a reversible reduction wave is developed.

The contribution of the reaction at the naked electrode, however, is expected to increase as the potential becomes more negative. This results in the gradual decrease in the overall cathodic rate constant k_c with the increase in the negative potential; k_c might be comparable to, or smaller than, the rate of diffusion of the oxidant in a certain negative potential region. It is expected that, in this potential region, the actual d.c. current becomes smaller than that which would be expected for the diffusion-controlled current. When the potential is extremely negative, the electrode reaction of indium(III) proceeds only through path I. The decrease in the d.c. current at potentials more negative than -1.0 V. vs. SCE is considerable; the larger the decrease, the greater the concentration of thiocyanate ions in the solution is. This is probably due to the fact that the species of indium(III) in the bulk of the solution depends on the concentration of thiocyanate ions.

The shape of the current-time curve during the life of a mercury drop shown in Fig. 5

* Detailed studies of the adsorption of thiocyanate ions on the mercury electrode will be reported elsewhere.

suggests that the cathodic current of indium(III) in a potassium thiocyanate solution at the negative potentials where the minimum appears on the d. c. polarogram is partly controlled by some processes of a kinetic nature. This is understandable if the rate of change in the state of the electrode surface during the life of a mercury drop is considered. The adsorption equilibrium of simple ions such as thiocyanate ions at the mercury surface is established almost instantaneously. The coverage θ of the electrode surface with the adsorbed ions is constant over the whole period of the life of a mercury drop, i. e.,

$$\left(\frac{\partial\theta}{\partial \ln t}\right)_E = 0 \quad \text{and} \quad \left(\frac{\partial k_c}{\partial \ln t}\right)_E = 0$$

At the potentials where k_c is smaller than the rate of diffusion, the characteristics of the current-time curve would be similar to those of the usual irreversible process, as is shown in Fig. 5.

The experimental result that the a. c. polarogram of the In(III)-KSCN system gives a negative admittance in a certain potential region can be explained as follows. As has been discussed earlier, this negative admittance results from the negative value of the polarization resistance R_F, the sign of which is opposite to that of $\partial k_c/\partial E$ in the potential region where the anomaly is observed. At such negative potentials, $\partial k_c/\partial E$ can be expressed from Eq. 7 as follows:

$$\frac{\partial k_c}{\partial E} = (k_2 - k_1)\frac{\partial\theta}{\partial E} + (1-\theta)\frac{\partial k_1}{\partial E} + \theta\frac{\partial k_2}{\partial E} \quad (8)$$

In Eq. 8, both the second and the third term of the right-hand side have generally negative values, whereas the first term is considered to be positive because the condition,

$$k_2 - k_1 > 0 \quad \text{and} \quad \frac{\partial\theta}{\partial E} > 0 \quad (9)$$

may be satisfied in the present case. Therefore, the negative value of R_F and, in consequence, the negative admittance are expected when the relation:

$$\left|(k_2-k_1)\frac{\partial\theta}{\partial E}\right| > \left|(1-\theta)\frac{\partial k_1}{\partial E} + \theta\frac{\partial k_2}{\partial E}\right| \quad (10)$$

is statisfied. In the In(III)-KSCN system, it is plausible to assume that both k_2-k_1 and $\partial\theta/\partial E$ are so large that the relation of Eq. 10 holds in the potential region where the anomaly is observed on the a. c. polarogram.

Summary

The reduction process of indium(III) at the dropping mercury electrode in thiocyanate solutions has been investigated by direct current polarography, alternating current polarography and faradaic impedance measurements. The reduction current in the potential region between −0.5 to −0.9 V. vs. saturated calomel electrode is greatly increased by the addition of minute amounts of thiocyanate ions, when a remarkable minimum is observed on the diffusion current plateau at relatively negative potentials. On the alternating current polarogram, indium(III) in a potassium thiocyanate solution gives a negative admittance in the potential region where the minimum appears on the direct current polorogram. The analysis of impedance measurements has shown that the resistance component has a negative value in that potential region. The experimental results have been explained by assuming that the overall electrode process is composed of two simultaneous reactions, one of which proceeds at the naked electrode surface, and the other at the electrode surface covered with adsorbed thiocyanate ions, and by assuming that thiocyanate ions accelerate the reduction of indium(III) at the surface of the electrode.

The authors wish to thank the Ministry of Education for the financial support granted for this research.

Department of Chemistry
Faculty of Science
Tohoku University
Katahira-cho, Sendai

Magneto-chemical Studies of Some Organo-Silicon Compounds Containing Si–O Bonds

By R. L. MITAL

(Received March 23, 1964)

The environmental role of the diamagnetic susceptibilities has been recently studied in detail in the case of some aliphatics,[1-5] and it has been established beyond doubt that the environments do affect the magnetic values. A similar phenomenon appears in silicon chemistry, where there is a much controversy over the atomic susceptibility value of silicon; values ranging from 20.7 to −3.01 have been reported.[6-7]

In two different homologous series of organo-silicon compounds, Pascal's law holds good only if different values are assigned to χ_{Si} in each series.[6] This opens a new era in the magneto-chemical studies of organo-silicon compounds. With this in view, the present paper will deal with the magnetic susceptibilities of a few silicon compounds with different numbers of Si–O bonds, and the results will be discussed from the structural point of view.

Experimental

The substances used were of A. R. quality. Before the magnetic measurements were taken, the purity of the samples was checked by standard methods. The diamagnetic susceptibility of the compounds was measured with the help of a very sensitive microbalance devised by Neogy and Lal.[8] This balance has the capacity of correctly measuring the total susceptibility of the order of 0.5×10^{-12} c.g.s. e.m.u.

This balance essentially consists of a quartz fibre stretched between two pins, one attached to a torsion head and the other to the chuck. The ends of the quartz fibre are fused to two thin quartz rods which are fitted to the brass pins. This system ensures a perfect returning to the zero position of the balance beam for every set of readings. A mirror is attached at the centre of the beam, and a small circular coil of thin copper wire is clamped to the beam at the centre, with its horizontal plane. The two leads of the coils are taken out of the box along the quartz fibre to ensure minimum resistance to the rotation of the beam. In order to reduce the oscillations of the beam, a damping vane is also provided. The coil is connected to a voltage source, lead accumulators in series with a number of rheostats, in order to control the current, and with a standard one ohm resistance, the terminals of which are connected to the test terminals of a potentiometer. The balance is mounted on a sturdy wooden bench above the pole pieces. The constant field gradient is secured by attaching the pole shoes on the pole faces, making an angle of 6° with the pole surface.

The organo-silicon compound is placed in a capsule. This capsule is then suspended from one end of the beam. When the field is switched on, the whole capsule experiences a force, which is measured by sending a current through the copper coil and by measuring the potential drop across the standard one ohm resistance with the help of a high-precision portable pye potentiometer capable of measuring 0.05 mV. For determining the susceptibility of silicon compounds, the push on the capsule filled with the sample is compared with that on the same capsule filled with pure benzene, the mass susceptibility[9] of which was taken to be -0.7081×10^{-6} c.g.s. e.m. units. The results are shown in Table I.

Discussion

From Table I we see that the mean value of χ_{Si} in this series of the compounds is 17.0, while in individual members it varies from 14.4 to 19.1. χ_{Si} has been calculated from the molecular susceptibilities of the compounds and by subtracting from χ_M the atomic susceptibilities of hydrogen (2.0)[10,11] and of oxygen (5.3)[10] and the group susceptibilities of methyl (13.45)[12] and of χ_{CH_2} (11.68[12] units). It is interesting to note that as the number of Si–O bonds increases, the value of χ_{Si} decreases. The observed force constants[13] for the Si–O bond in a number of molecules are all higher than the value calculated by using Siebert's formula, while the Si–O bond is shorter than the sum of the relevant atomic radii.[14] All these observations are consistent with a significant contribution by $p\pi$-$d\pi$ interactions to

1) R. L. Mital, *J. Phys. Soc. Japan*, **18**, 1612 (1963).
2) R. L. Mital, *Z. physik. Chem. Frankfurt*, **36**, 22 (1963).
3) A. Mookherji, R. L. Mital and D. Neogy, *Bull. Nat. Inst. Sci. India*, No. 14, 54 (1959).
4) K. Venkateswarlu and S. Sriraman, *Trans. Faraday Soc.*, **53**, 433 (1957).
5) R. L. Mital, *Bull. De L'Academie Des Sciences, Poland*, **12**, 1 47 (1964).
6) E. W. Abel and R. P. Bush, *Trans. Faraday Soc.*, **59**, 630 (1963).
7) R. M. Mathur, ibid., **54**, 1477 (1958).
8) D. Neogy and R. B. Lal, *J. Counc. Sci. Indust. Res. India*, **21B**, 103 (1962).
9) B. C. Eggleston, D. F. Evans and R. E. Richards, *J. Chem. Soc.*, **1954**, 941.

TABLE I. MOLECULAR DIAMAGNETIC SUSCEPTIBILITIES OF CERTAIN ORGANO-SILICON COMPOUNDS (-10^6 c.g.s. units)

Compound	χ_M (Observed)	χ_{Si}	χ_{Si} (Mean value)	Previously recorded value of χ_{Si} in these compounds
Trimethyl-silanol	66.3	18.6		
Trimethyl-methoxy-silane	78.2	19.1		
Ethoxytri-methylsilane	89.5	19.1		
Dimethyl-dimethoxy-silane	81.6	17.2		
Dimethyldi-ethoxysilane	104.7	17.0	17.0	12.50[7]
Methyldi-ethoxysilane	92.8	17.3		12.75[7]
Di-*n*-propyldi-ethoxysilane	150.8	16.4		
Dimethyl-silanediol	58.4	16.9		
Diethylsilane diol	81.0	16.1		
Methyl-trimethoxy-silane	85.6	15.9		
Methyltri-ethoxysilane	120.3	16.8		12.03[7]
Tetraethoxy-silane	134.5	14.4		12.06[7]

the Si–O bond in organo-silicon compounds. Such interactions decrease the Pauli's diamagnetic term in the well-known van Vleck's quantum mechanical equation:

$$\chi_M = \frac{-Ne^2}{6mc^2}\sum\bar{r}^2 + \frac{2}{3}N\sum_{n'\neq n}\frac{|m_0(n,n')|^2}{h\nu(n',n)}$$

The symbols have the usual significance. This decrease lowers the value of χ_{Si} in the compounds containing Si–O bonds. Thus, the magnetic studies add to the evidence that silicon is capable of forming π bonds with ligands by the use of d-type orbitals involving $p\pi$-$d\pi$ transactions. Such transactions have been beautifully discussed in some detail by Eaborn.[15]

In tetraalkyl silanes, $p\pi$-$d\pi$ bonding is not so specious as in alkoxy silanes, so the value of χ_{Si} in tetraalkyl substituted silanes will be conclusively higher than that in the alkoxy silicon derivatives.

Summary

The diamagnetic susceptibilities of a few organo-silicon compounds have been measured with the help of a very sensitive and accurate microbalance, with an accuracy of the order of 0.5×10^{-12} c.g.s. e.m.u. The mean value of χ_{Si} in these compounds containing Si–O bond is 17.0. The environmental role of Si–O liaisons on the value of χ_{Si} has been discussed from the structural point of view.

The author wishes to express his sincere thanks to Dr. S. Dayal for the gift of organo-silicon compounds; to Professor A. Mookherji, University Professor and Head of the Physics Department, Burdwan University, for allowing him to use laboratory facilities and for giving valuable suggestions, and to Professor R. C. Mehrotra for his encouragement.

University Department of Chemistry
Maharaja's College of Science
Jaipur, India

10) A. Pacault, J. Hoarau and A. Marchand, Adv. Chem. Physics (ed. I. Prigogine), 3, 171 (1961).
11) H. Haberditzl, *Z. Chem.*, 1, 225 (1961).
12) W. R. Angus, Llewelyn and G. Stott, *Trans. Faraday Soc.*, 55, 887 (1959).
13) H. Kriegsmann, *Z. anorg. u. allgem. Chem.*, 299, 138 (1959).
14) K. Yamasaki, A. Kotera, M. Yokoi and Y. Ueda, *J. Chem. Phys.*, 18, 1414 (1950).
15) C. Eaborn, "Organosilicon Compounds," Butterworths, London (1960).

Preferential Ion Transport in Electrodialysis through Ion-exchange Resin Membranes

By W. G. B. MANDERSLOOT

(Received March 24, 1964)

In electrodialysis through ion-exchange resin membranes, different ionic species of the same charge sign are usually transported at different rates.[1-4] Even early in the development of practical permselective membranes, suggestions were made for ion separations by means of electrodialysis.[5] In electrodialytic water treatment, the preferential ion transport has implications with respect to meeting the product specifications (the desired product being either the partially-desalted water or the simultaneously-produced concentrated brine), e. g., with respect to the maximum allowable concentration of precipitate-forming ions in the brine.

Preferential ion transport through permselective membranes can be described from first principles,[6-10] but, as will be shown, the inherent difficulties allow only qualitative conclusions and predictions to be made, particularly in practical systems.

Theoretical Considerations

The migrating counterions are transported consecutively (Fig. 1) through the bulk solution being electrodialysed by electric and convective transport, through the diffusion layer on the respective membrane by electric and diffusional transport, across the solution/membrane interface, through the membrane and across a second membrane/solution interface, and through a second diffusion layer into the bulk of the brine.

Transport through the Membrane.—The electrical transport ratio of two counterions, i and j, in an ion-exchange resin membrane is given by:

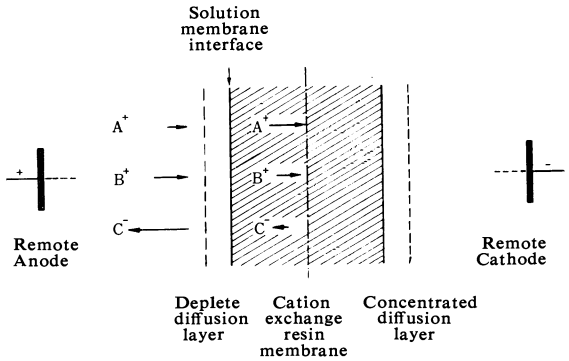


Fig. 1. Preferential ion transport through a single (cation) exchange membrane.

$$\frac{\bar{t}_i}{\bar{t}_j} = \frac{\bar{u}_i \bar{X}_i}{\bar{u}_j \bar{X}_j} \qquad (1)$$

in which t is the transport number, u, the electrical mobility, and X, the fractional contribution of one counterion to the total counterion content; the barred symbols refer to the resin phase.

The mobility of each counterion in the membrane phase is determined by the restricting forces acting on that (hydrated) counterion, by the electrostatic and other binding forces exerted by the fixed ionic groups in the resin, and by the frictional forces encountered. Equation 1 holds for local values; however, ion-exchange resins are known to have some heterogeneity in their crosslinking or pore structure,[11-14] and only average values for $\bar{u}$ and $\bar{X}$ can be measured.

Furthermore, the mobilities of the counterions in the resin are not independent,[15] there occurs some interaction, which can be detected from the non-linearity of a plot of the resin conductance versus the equivalent counterion

1) Y. Onoue, Y. Mizutani and R. Yamane, *J. Electrochem. Soc. Japan (Denki Kagaku)*, **27**, 482, E182 (1959).
2) R. McClintock, R. Neihof and K. Sollner, *J. Electrochem. Soc.*, **107**, 315 (1960).
3) T. Yamabe and T. Tanaka, *J. Chem. Soc. Japan, Ind. Chem. Sec. (Kogyo Kagaku Zasshi)*, **63**, 1342 (1960).
4) T. Yamabe, T. Tanaka and M. Senō, ibid., **63**, 1907 (1960).
5) D. A. Dewey and E. R. Gilliland, U. S. Pat. 2741591; *Fortune*, **44**, 909 (1951).
6) A. M. Peers, *J. Appl. Chem.*, **8**, 59 (1958).
7) A. T. Dibenedetto and E. N. Lightfoot, *Ind. Eng. Chem.*, **50**, 691 (1958).
8) B. A. Cooke and W. G. B. Mandersloot, *Trans. Inst. Chem. Eng.*, **37**, 14 (1959).
9) A. T. Dibenedetto, Thesis 1960 [*Diss. Abstr.*, **21**, 567 (1960)].
10) A. T. Dibenedetto and E. N. Lightfoot, *J. Am. Inst. Chem. Eng.*, **8**, 79 (1963).
11) K. Uberreiter and G. Kanig, *J. Chem. Phys.*, **18**, 399 (1950).
12) D. Reichenberg and D. J. McCauley, *J. Chem. Soc.*, **1955**, 2741.
13) E. Högfeldt, *Ark. Kemi*, **13**, 491 (1959).
14) E. Glueckauf and R. E. Watts, *Nature*, **191**, 904 (1961); *Proc. Roy. Soc.*, **A268**, 339 (1962).
15) K. S. Spiegler and C. D. Coryell, *J. Phys. Chem.*, **56**, 106 (1952).

composition in the resin.[16-19] The deviation from linearity is sometimes negligible;[1,20] it can be expected, that the interaction will be strong in highly-crosslinked ion-exchange resins with a high concentration of fixed ions.

From published data,[21-26] it is apparent that the electrical mobilities of the counterions are governed by much the same factors as those which play an important part in ion-exchange equilibria, namely, the charge and size of the hydrated counterion and the nature and concentration of the fixed ions. Consequently, when a pressure-volume effect is not determining, the preferentially-absorbed counterion often has a relatively low mobility in the resin. It is, therefore, not surprising that some ion-exchange resin membranes specially prepared to have a specific affinity for a certain counterion[27,28] show little specific transport of that ion *across* that membrane. The effect of the preferential absorption of the counterion is then counteracted by the strong binding of that ion. This counteraction can be so strong that, for example, very little Ba^{2+} is transported across a sulphonic acid resin membrane placed in a mixed sodium chloride/barium chloride solution.[29]

When the preferential absoption of one counterion in the resin is caused by the specific exclusion of the other counterion, then the preferentially-absorbed ion may have a relatively high mobility in the resin which enhances the preferential transport of that ion across the membrane.

Transport Across the Solution/Membrane Interface. — The concentration ratio, $\bar{X}_i/\bar{X}_j$, inside the membrane depends on the uptake of the ions from the solution on the membrane surface, which has a different composition from the bulk solution because of polarisation, which is caused by the fact that the transport number in the membrane of the joint counterions is close to 1. It has been pointed out by Dibenedetto[9] that the ion-exchange equilibrium on the interface is hardly affected at all by the current density because the (electrical) transport velocities of the ions are small in comparison with their velocities because of Brownian motion.

If we define the relative affinity coefficient, K_j^i, by:

$$K_j^i \equiv \left(\frac{X^*_j}{\bar{X}_j}\right)^{z_i}\left(\frac{\bar{X}_i}{X^*_i}\right)^{z_j} \qquad (2)$$

in which z is the electrovalency of each counterion and * refers to the solution on the membrane surface, then:

$$\frac{\bar{X}_i}{\bar{X}_j} = \bar{X}_j^{(z_i/z_j-1)} \cdot (K_j^i)^{1/z_j} \cdot \frac{X^*_i}{(X^*_j)^{z_i/z_j}} \qquad (3)$$

It has been shown[19] that K_j^i is the sum of a number of terms and is far from constant when i and j are of unequal valency; K_j^i is, then, dependent on the total external electrolyte concentration and on $\bar{X}_j$ (or X_j). In electrodialytic processes, both the total electrolyte concentration and X_j change with either time or place.

An interesting development is the layered membranes in which a highly conductive ion-exchange resin membrane has been covered on both sides with a thin layer of a less conductive but very highly crosslinked ion-exchange resin,[30] the special properties of this thin layer of resin determining the uptake of counterions from the adjacent solution. The thin layer on the other side of these membranes has been applied for mechanical reasons, but it may simultaneously serve to eliminate the effect of possible polarisation at the first resin/resin interface.

Transport Across the Depleted Diffusion Layer. —If only one electrolyte is present, the system can be described in terms of a diffusion layer with a linear concentration gradient.[8,31,32] In systems with two electrolytes sharing the ion which has the same sign as the fixed ions in the resin membrane, it has been assumed[6-8] that two systems, each with one electrolyte and a linear concentration gradient, can be superimposed (Fig. 2) to arrive at a relation between X^*_i/X^*_j and X_i/X_j. This leads, however, to an inconsistency. With two superimposed linear gradients, t_i/t_j varies in

16) H. P. Gregor and D. M. Wetstone, *Discussions Faraday Soc.*, No. 21, 162 (1956).
17) D. Mackay and P. Meares, *Trans. Faraday Soc.*, **55**, 1221 (1959).
18) E. Jenckel and H. Jacobs, *Chem. Techn. (Berlin)*, **10**, 464 (1958).
19) W. G. B. Mandersloot, This Bulletin, **36**, 1444 (1963).
20) J. B. Andelman, Thesis, 1960 [*Diss. Abstr.*, **21**, 1388 (1960)].
21) E. Jenckel and H. von Lillin, *Koll. Zeit.*, **146**, 159 (1956).
22) G. Manecke and E. Otto-Laupenmühlen, *Z. phys. Chem. N. F.*, **2**, 336 (1954).
23) N. W. Rosenberg, J. H. B. George and W. D. Potter, *J. Electrochem. Soc.*, **104**, 111 (1957).
24) R. P. Puri, F. R. Duke and J. Lomnes, *Iowa State College J. Sci.*, **31**, 25 (1956).
25) E. Heyman and I. J. O'Donell, *J. Coll. Sci.*, **4**, 405 (1959).
26) A. O. Jakubovic, G. J. Hills and J. A. Kitchener, *Trans. Faraday Soc.*, **55**, 1570 (1959).
27) D. Woermann, K. F. Bonhoeffer and F. Helfferich, *Z. phys. Chem. N. F.*, **8**, 265 (1956).
28) H. P. Gregor and R. Kramer, U. S. Dept. Interior, Office of Saline Water, Final report contract 14-01-001-62 (1958).
29) T. Yamabe, M. Senō, T. Tanaka and I. Kamii, This Bulletin, **33**, 1740 (1960).
30) T. Yawataya, H. Hani, Y. Oda and A. Nishihari, *Dechema Monogr.*, **47**, 501 (1962).
31) S. M. Partridge and A. M. Peers, *J. Appl. Chem.*, **8**, 49 (1958).
32) "Demineralisation by Electrodialysis," Ed. by J. R. Wilson, Butterworths, London (1960), p. 12.

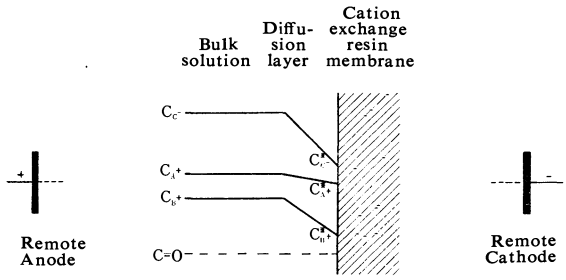


Fig. 2. Concentration gradients across a diffusion layer in a dialysate compartment.

the diffusion layer with the distance from the membrane, because the ratio of the concentrations of the two ions varies (anywhere: $t_i/t_j = u_iC_i/u_jC_j$). Therefore the diffusion fluxes of i and j should also vary across the diffusion layer, but this requires non-linear concentration gradients.

In practical electrodialysis, the effect of polarisation is counteracted by the forced convection of the electrolyte solution towards the membrane surface through the use of convection-inducing devices placed in the path of the solution.[33-36] This makes it virtually impossible to relate X and X^*. The limit to preferential transport for the zero current density may, however, be estimated from

$$\frac{\bar{t}_i}{\bar{t}_j} = \bar{X}_j^{(z_i/z_j-1)} \cdot (K^i_j)^{1/z_j} \cdot \frac{\bar{u}_i X_i}{\bar{u}_j (X_j)^{z_i/z_j}} \qquad (4)$$

while at high current density $\bar{t}_i/\bar{t}_j$ approaches t_i/t_j.

Overall Transport. — More complicating factors are introduced in practical electrodialysis because a number of processes occur simultaneously (Fig. 3). The membranes are not ideally (charge-) selective, and co-ion transport takes place, together with a certain amount of salt diffusion and also osmosis in the opposite direction. The preferential ion transport measured by the analysis of the desalting or the concentrating stream is the total effect of all the processes taking place.

From the considerations given above, it will be clear that a description of the preferential ion transport from first principles is very unattractive and that an empirical approach is to be preferred. Fortunately, the process can be described, under certain conditions, as a separation process with a constant separation factor[6,37] denoted s:

$$\frac{dC_i}{dC_j} = s\frac{C_i}{C_j} \qquad (5)$$

When an amount of saline water is demineralised from concentrations C_i' and C_j' to concentrations C_i'' and C_j'', the integration of Eq. 5 gives:

$$\ln \frac{C_i''}{C_i'} = s \ln \frac{C_j''}{C_j'} \qquad (6)$$

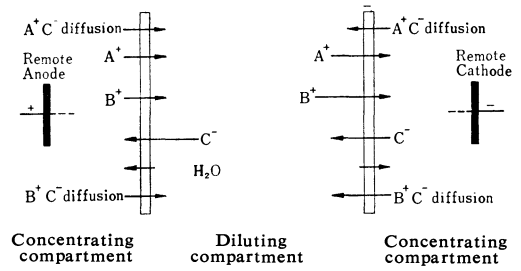


Fig. 3. Transport processes occurring simultaneously in a dialysate compartment.

Experimental

A batch of 10 l. mixed electrolyte solution, contained in an aspirator with a calibrated-level glass for volume measurements, was circulated by a pump through the parallel desalting (or "dialysate") compartments of a membrane pack containing ten such compartments alternating with eleven concentrating (or "brine") compartments (Fig. 4). Samples

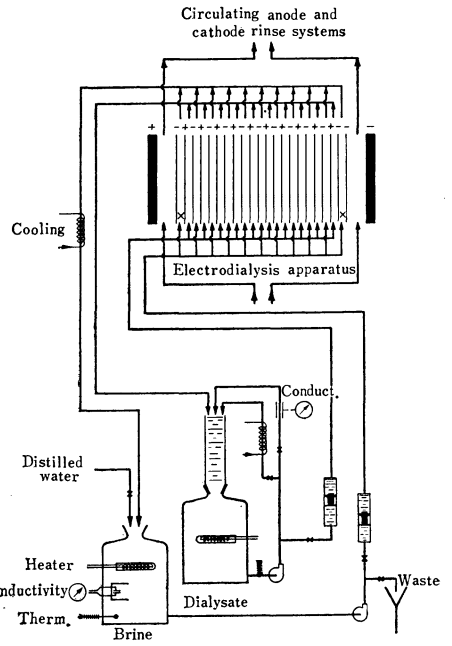


Fig. 4. Experimental set-up; the compartments marked X are connected to calomel electrodes.

33) H. J. Cohan, *Chem. Eng. Progr.*, **57**, No. 12, 72 (1961).
34) J. R. Wilson, *Trans. Inst. Chem. Eng.*, **41**, 3 (1963).
35) M. Seko, *Dechema Monogr.*, **47**, 575 (1962).
36) Ref. 32, p. 216.
37) J. P. Dankese, T. A. Kirkham, G. Maheras, M. S. Mintz, J. H. Powell, N. W. Rosenberg, E. H. Sieveka and J. J. Strobel, U. S. Dept. Interior, Office of Saline Water, R. and D. Progr. Rep. No. 11 (1956).

of the batch, which was thoroughly mixed by a fast flow through a by-pass of the membrane pack, were analyzed at regular intervals, while the total electrolyte content was indicated by a conductivity meter. The vertical compartments with upward flow were formed by the cut-away rectangular centre section of asbestos " steam-jointing " gaskets, 1/32 inch thick, which were filled with perforated corrugated spacers, each compartment having a surface area of 128 cm^2. The first and last brine compartments were connected to calomel electrodes, so that the voltage drop across the membrane pack could be measured by a vacuum-tube voltmeter with a high input resistance. The voltage on these electrodes was kept constant in each experiment. The current-carrying electrodes, having the same surface area as the compartments in the pack, were placed in electrode compartments adjacent to the end brine compartments. A separate electrode rinse solution was circulated through the electrode compartments.

A batch of brine, with the same initial composition as the initial dialysate, though usually double the concentration, was circulated through the brine compartments in parallel. The total electrolyte concentration of the brine, measured with a conductivity cell, was kept approximately constant during each experiment by continuous dilution with distilled water. The flow velocities in the brine and dialysate compartments were 10 cm./sec. All the solutions were thermostatically controlled. Further details on the experimental set-up are given elsewhere.[38]

The following membrane pairs were used:

C. S. I. R. parchment-base-type PS (cation exchange) and G (anion exchange)
Permaplex[39]—C20 and A20
T. N. O.[40]—C60 and A60
A. M. F.[41]—3129 B56 and 96

Results and Discussion

The reasonably general validity of Eq. 6 is illustrated for cation transfer and anion transfer in Figs. 5 and 6 respectively, in which results obtained with a variety of membrane combinations and on different initial water compositions have been brought together. The results of the investigation of the effect of compartmental voltage with T. N. O. membranes and Permaplex membranes are shown in Figs. 7 and 9 respectively.

The results obtained with parchment-base membranes (lines A and in Fig. 5 and line K

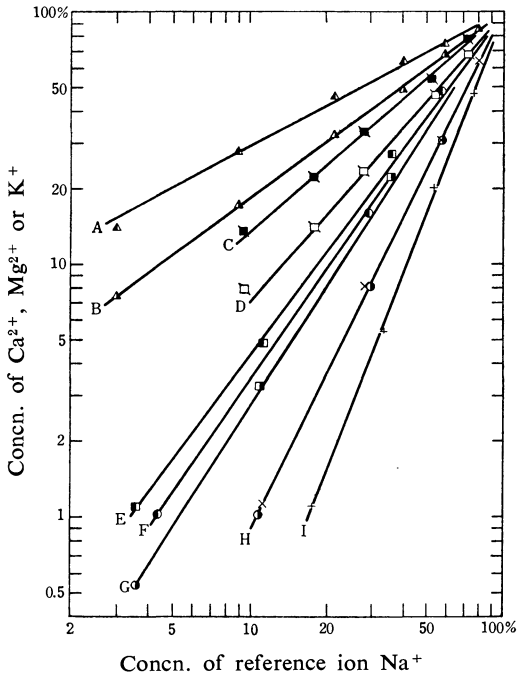
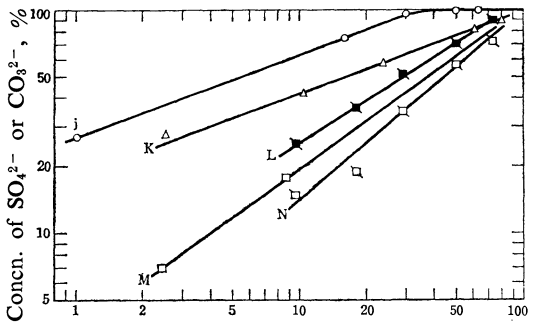


Fig. 5. Preferential cation transport according to Eq. 6, expressed in terms of the % residual concentration of an ion in the dialysate; details in Table I.

Table I. Details of data in Figs. 5 and 6

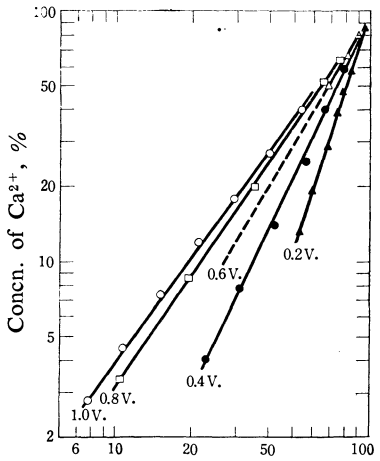
Line	Symbol	Counter ion	Membranes	Initial dialysate
A	◭	Mg^{2+}	C. S. I. R. parchment base membranes	Synthetic sea water
B	◭	Ca^{2+}		
K	△	SO_4^{2-}		
C	■	$Ca^{2+}+Mg^{2+}$	T. N. O. A22 and C21 heterogeneous membranes	Brackish well water[43]
D	□	K^+		
L	■	CO_3^{2-}		
N	□	SO_4^{2-}		
E	◧	Mg^{2+}	Mainly T. N. O. A22 and C21 heterogeneous membranes	Sea water[42]
G	◧	Ca^{2+}		
M	□	SO_4^{2-}		
J	○	SO_4^{2-}	A. M. F. 3129 B56 and 96 homogeneous membranes	Synthetic sea water
F	◐	Mg^{2+}		
H	◑	Ca^{2+}		
H	×	Ca^{2+}		0.25 N $CaCl_2$/0.25 N NaCl
I	+	Ca^{2+}		

38) W. G. B. M nders loot, *J. Electrochem. Soc.*, 111, 838 (1964).
39) The Permutit Comp. Ltd., England.
40) Central Technical Institute, T. N. O., Netherlands.
41) American Machine and Foundry Comp., U. S. A.



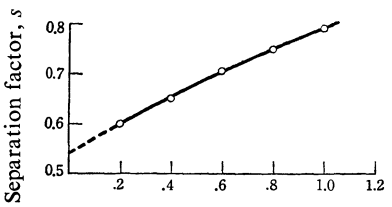
Concn. of reference ion Cl^-, %

Fig. 6. Preferential anion transport according to Eq. 6, expressed in terms of the % residual concentration of an ion in the dialysate; details in Table I.



Concn. of reference ion Na^+, %

Fig. 7. Preferential cation transport through T.N.O. A 60 and C 60 membranes at various compartmental voltages.



Volt per compartment pair

Fig. 8. The separation factors (from Fig. 7) versus compartmental voltage.

in Fig. 6), which were of an early type not highly efficient in sea water, indicate that Eq. 6 holds well even if the detrimental transfer processes indicated in Fig. 3 constitute a considerable portion of total ion transfer.

That the separation factor is independent of the initial composition is indicated by line H in Fig. 5, which represents two experiments with the same membrane pair, the same electric potential drop per compartment pair, and the same flow velocity in the compartments, but on water with a completely different composition, namely, synthetic sea water with a sodium : calcium equivalent ratio of 45 : 2, and a total electrolyte concentration 0.6 N, and a mixed sodium chloride/calcium chloride solution, 0.5 N in Cl^-, with a sodium : calcium equivalent ratio of 1 : 1.

That Eq. 6 holds even when a very small amount of one ion is present is demonstrated by line D in Fig. 5, which represents the removal of a small amount of K^+ from a natural brackish well water. A strong deviation from linearity was found for the separation of Cl^- and SO_4^{2-}, as is indicated in line J in Fig. 6. This will be discussed separately.

The Effect of Compartmental Voltage (Current Density).—This effect is illustrated by the different slopes of lines H and I in Fig. 5, representing identical experiments but run at 1.0 V. and 0.75 V. per compartment pair respectively. It should be noted that during the runs the current density, i, decreases with the electrolyte concentration in the dialysate C, approximately according to[38] $i=\frac{E}{a+b/C}$, in which E is the compartmental voltage and a and b are constants.

The effect of the compartmental voltage drop, which is a measure of the degree of polarisation at a constant flow velocity, was investigated in more detail, using T. N. O. C60 and A60 membranes at 30°C with initial electrolyte concentrations in the dialysate of 0.25 N Cl^- (0.125 N Na^+ and 0.125 N Ca^{2+}), a constant total brine concentration of 0.5 N, and compartmental voltage drops, constant in each run, from 0.2 to 1.0 V. The separation factors derived from the slopes of the lines in Fig. 7 are plotted in Fig. 8 versus the voltage.

Similar experiments have been carried out with Permaplex membranes, but the range of voltages used was higher (0.2 to 1.5 V. per compartment pair) because the higher resistance of these membranes caused the current densities to be 10~20% lower at equal voltages. The non-linearity of the preferential ion transport data, as given in Fig. 9, can be attributed to polarisation, which increases with a decrease in the electrolyte concentration in the dialysate. It is interesting that the lines in Fig. 9 tend to approach the same slope at low concentrations. It was not possible to measure the polarisation in terms of an increase in the electric resistance of the membrane pack. Preferential ion transfer could thus be used as a very sensitive, though rather impractical, measure of the degree of polarisation. Because of the curved lines in Fig. 9, only the separation factors corresponding to the *initial* slopes

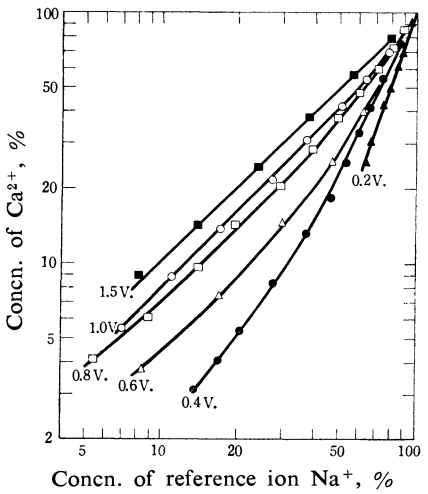


Fig. 9. Preferential cation transport through Permaplex A 20 and C 20 membranes at various compartmental voltages.

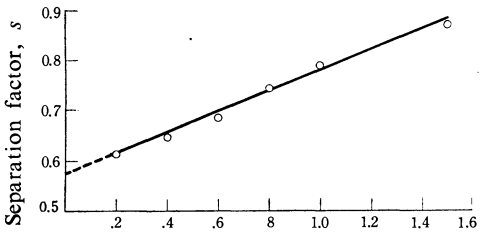


Fig. 10. The separation factors (from initial slopes in Fig. 9) versus compartmental voltage.

have been plotted versus the voltage in Fig. 10. The separation factors in Fig. 10 are approximately the same as in Fig. 9. The values for K_{Ca}^{Na} were also reasonably close for the two types of membranes.[19]

The Effect of the Nature of the Membrane. —Heterogeneous membranes (ground ion-exchange resin embedded in a sheet-forming binder) appear to cause less separation than homogeneous membranes when used under comparable conditions, as is evident from the results shown in Figs. 5 and 6 and in Figs. 7 and 9. This can be explained by the fact that a portion of the ion transport through the heterogeneous membranes is through a liquid path;[44,45] moreover, as has been mentioned in the previous section, the polarisation on these membranes is stronger.[46]

A comparison of the data in Fig. 7 with lines H (1.0 V.) and I (0.75 V.) in Fig. 5 shows that the preferential transport of Ca^{2+} through the homogeneous AMF membranes, which have a high internal concentration of fixed ions, is much more marked than through the T. N. O. membranes, which have a relatively low internal concentration.[19] This can be attributed to the higher affinity of the AMF membranes for calcium ions at intermediate loadings.[19]

The Cl^-/SO_4^{2-} Separation. — In Fig. 6 a strong deviation from linearity is found for the Cl/SO_4 separation using AMF membranes (line J). At high concentrations there is hardly any SO_4^{2-} transport. It increases considerably, however, below a total electrolyte concentration of 0.15 N. This is a reflection of the strong increase in affinity for SO_4^{2-} relative to Cl^- at concentrations below 0.15N;[19] later experiments have shown that this phenomenon is quite general with membranes which are efficient at concentrations above 0.15 N, particularly if the membranes are highly crosslinked.

The Order of Preference.—The order of the preferential transport of common ions at total electrolyte concentrations below 1 N, using highly efficient ion-exchange resin membranes and preventing serious polarisation, as found by us agrees well with most data reported by other workers.[2,16,29,37,41,42,47-54] For cations the general order is $Ca^{2+}>Mg^{2+}>K^+>Na^+>Li^+$, and for anions, $Cl^->SO_4^{2-}>CO_3^{2-}\cdot(HCO_3^-)$ and $NO_3^->Cl^->F^-$. These orders compare very well with those observed in ion exchange equilibria; the relative affinity coefficient, K_j^i, appears to be the determining factor unless the mobility in the membrane of one counterion is greatly reduced by very strong binding forces (e. g., ionpair formation).

Summary

Because of the great difficulties encountered when describing preferential ion transport in

42) Unpublished data taken, with permission, out of a confidential sponsored research report by the Central Technical Institute, T. N. O., Netherlands (1958).
43) G. Drouhin and C. Gomella, Sci. Council for Africa South of the Sahara, publ. 64, 101 (1960).
44) D. K. Hale and D. J. McCauley, *Discussions Faraday Soc.*, No. 21, 208 (1956).
45) H. P. Gregor, Nat. Acad. Sci., Nat. Res. Council, publ. 568, 240 (1958).
46) B. A. Cooke and S. J. v. d. Walt, *Electrochim. Acta*, 5, 216 (1961).
47) E. O. Seipold, Sci. Council for Africa South of the Sahara, publ. 64, 119 (1960).
48) N. Krishnaswamy, *J. Sci. Ind. Res.* (India), 18A, 218 (1959).
49) N. Ishibashi, *J. Chem. Soc. Japan, Ind. Chem. Sec.* (*Kogyo Kagaku Zassi*), 61, 798 (1958).
50) W. E. Katz, *Chem. Eng. Progr.*, 53, 190 (1957).
51) K. Oda, M. Murakoshi, T. Saito and S. Matsuda, *J. Electrochem. Soc. Japan* (*Denki Kagaku*), 25, 328 (1957).
52) N. W. Rosenberg, T. A. Kirkham, C. E. Tirrell and N. E. Saliba, U. S. Dept. Interior, Office of Saline Water, R. and D. Progr. Rep. No. 1 (1954).
53) M. Nagamatsu, *J. Electrochem. Soc. Japan* (*Denki Kagaku*), 25, 565, E117 (1957).
54) T. S. Brun, E. Meisingseth and K. Palmoek, *Årbok Univ. Bergen, Mat.-Naturv. Serie*, 1962, No. 3.

electrodialytic demineralisation from first principles, an empirical approach is more attractive. Preferential ion transport can be described as a simple separation process with a separation factor which is constant for a certain membrane pair under certain conditions, namely, a constant voltage drop per compartment pair at a constant flow velocity in the compartments, high enough to avoid any serious polarisation. Exceptions occur when one counterion is immobilised to a great extent in the resin, when specific strong binding forces are operative (e.g., ionpair formation), and also when the preferential absorption of a counterion is based on the preferential exclusion of the other counterion. The latter appears to be the case in the separation of Cl^- and SO_4^{2-} at high total electrolyte concentrations.

The order and magnitude of preference are, in the first instance, governed by the same factors which govern ion-exchange equilibrium. The separation of ions has been shown to decrease with an increase in the applied electric potential (current density). It has been demonstrated that heterogeneous membranes cause a concentration polarisation at lower current densities than homogeneous membranes and that this early polarisation can be detected from the preferential ion transport data before it can be measured in terms of the resistance of the membrane pack.

The author is indebted to Mr. J. Venlet for his assistance in the experimental work and in the evaluation of the results.

Chemical Engineering Group
Council for Scientific and Industrial Research
Pretoria, South Africa

*The Addition Reactions of Propanol-2 to Ethylene Induced by Gamma-ray Irradiation in the Gaseous Phase**

By Tadashi KURIHARA and Hiroshi HOTTA

(Received March 26, 1964)

It is known that the α-*C*-alkylation of primary and secondary alcohols results from their peroxide- and light-induced reactions with olefins.[1] Similar reactions are also induced by gamma-ray irradiation. The addition reactions of propanol-2 to ethylene in the liquid phase have been studied with gamma-rays by Hirota and Hatada.[2] It would be interesting to study if some differences are found between the liquid and gaseous phases. Therefore, in the present study, the samples were prepared with care so as to prevent them from condensing at the reaction temperatures.

Experimental

Materials.—Propanol-2 was purified by column distillation after refluxing it over calcium oxide. Ethylene (99.8%) was purified repeatedly by vacuum distillation at −196°C. No impurities were found by gas chromatography after these purifications. The samples were collected by vacuum distillation in a hard-glass tube (about 40 ml.).

Irradiation. — The samples were irradiated at 2.2×10^4 r./hr. of cobalt-60 gamma-rays while being kept within ±1°C of the given temperature in a controlled electric heater. The absorbed energy, *E*, is estimated by the equation:

$$E=87.7\times tD(\sum\rho_i m_i) \quad \text{(erg.)} \qquad (1)$$

where t=irradiation time (hr.)
D=dose rate measured by the Fricke dosimeter (r./hr.)
ρ=relative electron density to air
m=mass of the reactant (g.)

The relative electron densities, ρ, are 1.11 and 1.13 for ethylene and propanol-2 respectively.

The experiments were carried out under the conditions listed in Table I.

Analytical.—After irradiation, the total amounts of the gases in the tube and of the non-condensable gases at −196°C were measured. The latter compositions were analyzed by the mass-spectrum method in order to determine the amounts of hydrogen and methane produced. Then the condensed liquids were analyzed immediately by gas chromatography, using a column of PEG 6000 at 70 and 150°C.

* The Radiation Chemistry of Gaseous Alcohols at Elevated Temperatures. I.

1) W. H. Urry, F. W. Stacey, E. S. Huyser and O. O. Juveland, *J. Am. Chem. Soc.*, **76**, 450 (1954).

2) K. Hirota and M. Hatada, This Bulletin, **34**, 1644 (1961).

Results

Non-condensable Gases.—The results of experiments 1—5 (Table I) are shown in Fig. 1 against the irradiation time for the decrement of ethylene (△) and the amount of the non-condensable gases produced (⊙). The *G*-values of hydrogen and methane, based on the total absorbed energy in the mixture, were found to be 4.2 and 3.8 from mass-spectrometric analysis. The corresponding values are 2.77 and 1.65 for the gamma-ray radiolysis of pure propanol-2 at room temperature,[3] and 1.28 and 0.21 for the 2 MeV. electron-radiolysis of ethylene of 150 mmHg at 25°C.[4] These facts suggest that the hydrogen abstraction reactions by hydrogen atoms and methyl radicals are of minor importance in the present chain process.

Table I. Experimental conditions

No.	Composition, 10^{-3} mol.		Temp. °C	Time hr.
	Propanol-2	Ethylene		
1	3.5	2.1	175	4
2	3.5	2.1	175	8
3	3.5	2.1	175	20
4	3.5	2.1	175	40
5	3.5	2.1	175	65
6	3.5	2.1	100	20
7	3.5	2.1	125	20
8	3.5	2.1	150	20
9	3.5	2.1	200	20
10	3.5	0.0	175	20
11	3.5	0.42	175	20
12	3.5	0.80	175	20
13	3.5	1.1	175	20
14	3.5	1.5	175	20
15	3.5	1.8	175	20

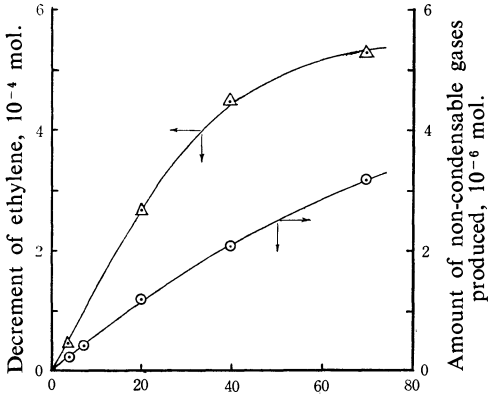


Fig. 1. The decrements of ethylene (△) and the amounts of the non-condensable gases produced (⊙) as a function of irradiation time (experiments 1—5).

Condensable Products.—Compared with the retention time of propanol-2, the gas chromatography gave the twenty-one peaks of the shorter retention time at 70°C and the sixteen peaks of the longer one at 150°C. Among these the identified products are listed in the order of their retention times in Table II. Some results of experiments 1—5 (Table I) are shown in Fig. 2 against the irradiation time for the amounts of acetone (●), 2-methylbutanol-2 (⊙), 2-methylhexanol-2 (△) and 2-methyloctanol-2 (⊡).

Table II. *G*-Value of products*

Isopentane	26
Ethyl isopropyl ether	31
Acetaldehyde	35
Acetone	131
2-Methylbutanol-2 (1 : 1 telomer)	103
Pentanol-2	25
2-Methylhexanol-2 (1 : 2 telomer)	41
Hexanol-2	11
2-Methyloctanol-2 (1 : 3 telomer)	25.5

* From the results of the Experiment 3 (Table I).

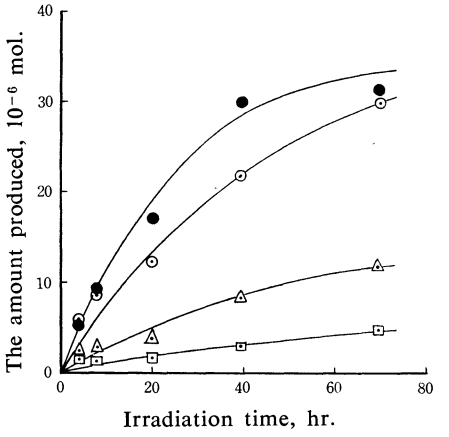


Fig. 2. The amounts of products as a function of irradiation time (experiments 1—5); acetone (●), 2-methylbutanol-2 (1 : 1 telomer) (⊙), 2-methylhexanol-2 (1 : 2 telomer) (△), and 2-methyloctanol-2 (1 : 3 telomer) (⊡).

Although a large number of the products could not be identified, the peak area, A_i, is proportional to the mole concentration, M_i, independent of the materials of the related compounds, as is shown in Fig. 3. Therefore, even if there are some unknown products, the

3) J. D. Strong and J. G. Burr, *J. Am. Chem. Soc.*, **81**, 776 (1959).
4) F. W. Lampe, *Radiation Research*, **10**, 619 (1959).

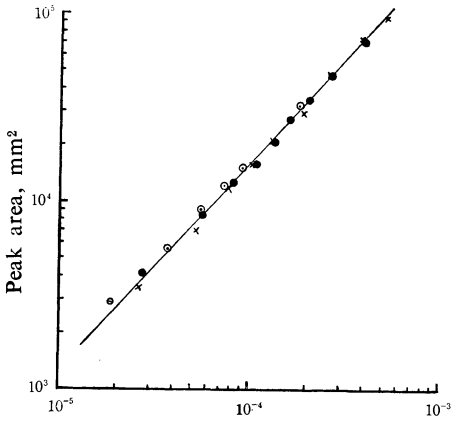


Fig. 3. Peak areas of various materials for gas chromatography at 100°C as a function of their mole concentration; acetone (●), propanol-2 (×) and 2-methylbutanol-2 (⊙).

mole concentration of the respective products, M_i, can be estimated from the gas chromatograph chart by the equation:

$$M_i = M_p \times \frac{A_i}{\sum A_i} \qquad (2)$$

where M_p is the mole concentration of the parent reactant, propanol-2. The $\sum A_i$ is the sum of all the peak areas, including that of propanol-2. Therefore, the G-value is obtained by the equation:

$$G_i = 1.1 \times 10^{12} \times \frac{M_p A_i}{tD(\sum \rho_i)(\sum A_i)} \qquad (3)$$

The G-values, estimated by Eq. 3 from the results of experiment 3 (Table I), are shown in Table II. For this case, the G-value of all the products is 815, judging from the sum of the peak areas, including those for the unidentified products. On the other hand, the G-value of the consumed ethylene is 1800 (cf. Fig. 1). This means that 2.2 ethylene molecules are apparently combined with a propanol-2 molecule.

Discussion

The Overall Reaction Scheme.—A part of the reaction scheme can be assumed to be as shown in Table III from the identified products in Table II, where PH is propanol-2, and, E, ethylene. This indicates that all the radicals which can be expected from propanol-2 are present as precursors. These precursor radicals, I—V (Table III), are formed not only by the reactions shown in Table III, but also by various reactions between propanol-2 and various radicals.

The API's mass-spectral data[5] show that almost all the propanol-2 molecules lose not a hydrogen atom but a methyl radical by ionization. On the other hand, the present findings indicate that the major precursor radical is 1-hydroxyisopropyl, as is to be expected from the radical mechanism. This indicates that the present processes are radical and not ionic, even if initiated by irradiation, namely, ionization and excitation.

The present finding in the gaseous phase is in contrast with the finding in the liquid phase, reported by Hirota and Hatada,[2] that almost all the products were from the 1-hydroxyisopropyl radical, although the mole fraction of ethylene in that experiment was different from that in the present experiments. This may show that the addition reaction is predominant in the liquid phase; it will be shown later that the chain transfer constant is smaller than that in the gaseous phase. In other words, the products produced only in the gaseous phase may perhaps be attributed to the radical transfer reaction of radicals with propanol-2 molecules.

Acetone and Acetaldehyde.—The G-values of acetone and acetaldehyde are nearly equal to those from the radiolysis of gaseous propanol-2 (experiment 10, Table I) and are independent of the mole fraction of ethylene (experiments 3, 11—15, Table I). Therefore, they are assumed to be formed independently of ethylene.

1-Hydroxyisopropyl Radical.—The 1-Hydroxyisopropyl radical (radical I, Table III) is the most important precursor radical formed from propanol-2, as is indicated by the G-value of the telomers in Table III. This radical might react variously with propanol-2 by means of radical transfer reactions as well as by the hydrogen transfer reaction.

It may not necessarily be concluded that acetone is formed through this radical, for the yield of acetone is independent of the ethylene content, which is indispensable for the formation of this radical. Although the molecular detachment of hydrogen from propanol-2 is sometimes assumed for the excited molecule of radiolysis or photolysis and for the thermal formation on the special solid catalysts, this may be supposed not to be the present case.

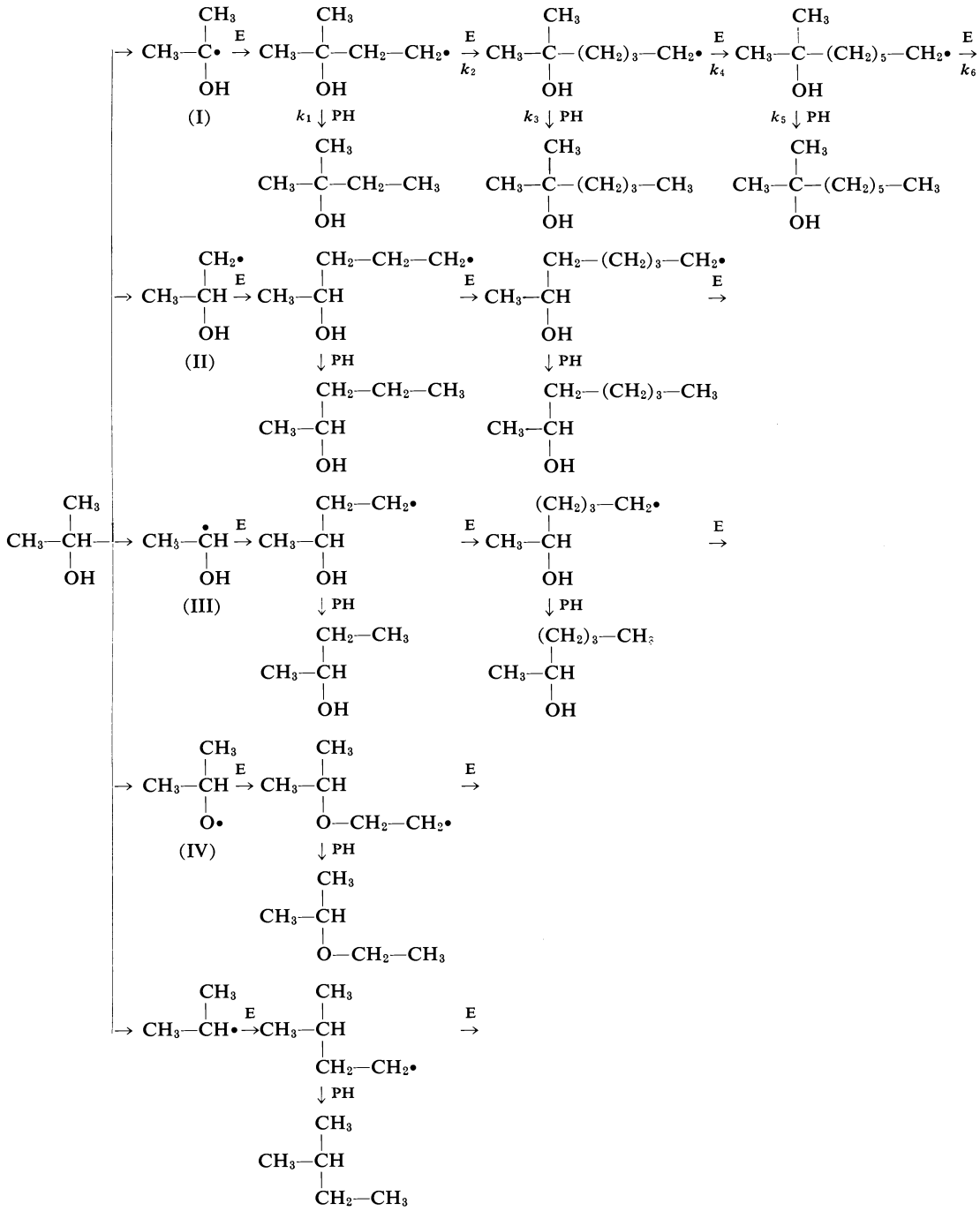
According to Mellow and Burton,[6] the addition reactions, started from this precursor radical, P, shown in Table III, are expressed by the following rate relations:

$$\frac{(\text{P–E–H})}{(\text{P–E–E–H})} = \frac{k_1(\text{PH})}{k_2(\text{E})} + \frac{k_1 k_4}{k_2 k_3} \qquad (4)$$

5) Mass Spectral Data of American Petroleum Institute Research Project 44, Carnegie Inst. Techn., Pittsburgh (1957).

6) F. W. Mellow and M. Burton, *J. Phys. Chem.*, **66**, 2164 (1962).

TABLE III. REACTION SCHEME



and

$$\frac{(\text{P-E-E-H})}{(\text{P-E-E-E-H})}=\frac{k_3(\text{PH})}{k_4(\text{E})}+\frac{k_3k_6}{k_4k_5} \qquad (5)$$

where the symbols are as represented in Table III. The yields of these telomers depend on the ethylene content in the results of experiments 11—15 (Table I). The chain transfer constants, $c_1=k_1/k_2$, $c_2=k_3/k_4$, and $c_3=k_5/k_6$, are estimated by the use of Eqs. 4 and 5 to be 0.62, 0.55±0.05 and 0.50±0.05 from these results.

On the other hand, according to Walling,[7] the chain transfer constants, c_i, can be expressed by the equation:

7) C. Walling, "Free Radicals in Solution," John Wiley and Sons, New York (1957), p. 246.

$$F_i=\frac{c_iR}{\Pi(c_iR+1)} \qquad (6)$$

where F_i is the mole fraction of the i'th telomer to the whole telomers, and R, the mole ratio of the reactants, (PH)/(E). The mole fraction of the respective telomers, F, is plotted against the R in Fig. 4 on the basis of the results of experiments 11—15.

The chain transfer constants, obtained from the curves in Fig. 4 using Eq. 6, are plotted as the function of the R in Fig. 5. On the other hand, the constants in the liquid phase obtained by this method are $c_1=0.062$, $c_2=0.056$, and $c_3=0.073$ at $R=18$;[2] these values are smaller than the present values in the gaseous phase.

The 1-Hydroxyethyl Radical.—The 1-Hydroxyethyl radical, (radical III, Table III) is considered to be one of the precursor on the basis of the presence of hexanol-2, as is shown in Table III. However, butanol-2 could not be identified by gas chromatography, for this peak

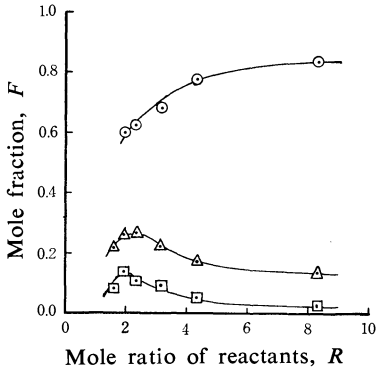


Fig. 4. The mole fractions of the telomers produced, F, as a function of the mole ratio, (propanol-2)/(ethylene), R (experiments 11—15). Marks are the same as in Fig. 2.

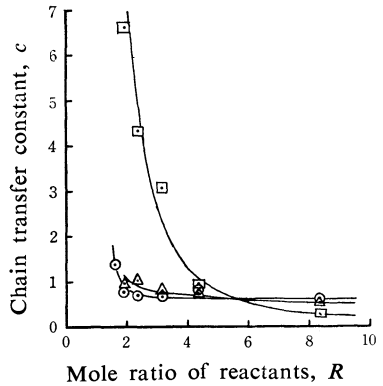


Fig. 5. The chain transfer constants, c, estimated by Eq. 6 as a function of mole ratio, (propanol-2)/(ethylene), R (experiments 11—15); c_1 (⊙), c_2 (△) and c_3 (⊡).

was covered by the tail of 2-methylbutanol-2. Ethanol might be formed by the reaction with propanol-2, but this product could also not be identified because of the large peak of propanol-2. Therefore, the G-value of this precursor radical cannot be estimated quantitatively. However, this is not so important as in the mass-spectrum.

Other Precursor Radicals. — As Table III shows, the 2-hydroxypropyl, isopropoxyl and isopropyl radicals are also assumed to be precursors on the basis of the presence of the identified products. The G-value of heptanol-2, expected from the 2-hydroxypropyl radical, seems to be small.

The Temperature Dependence of the Yields.—The results of experiments 3, 6—9 (Table I) showed that the yields of the products, including the unidentified ones, decreased with a decrease in the temperature, except for the telomers of radical I in Table III, and that the twenty-two products could not be found by gas chromatography from the samples at 100 and 125°C. The amounts of some of the products produced are plotted in Fig. 6 against the reciprocal of the absolute reaction temperature. As is shown by the dotted lines in Fig. 6, the yield of telomers increased also at lower temperatures. This is either due to the condensation of some part of the propanol-2 on the wall of the tube, thus suppressing the radical transfer reactions or disproportionation reactions and promoting the addition reactions in the liquid phase, as has been discussed already, or to such conditions at a lower temperature, even if it is not condensed. This seems to support the latter assumption that a large number of the products are not

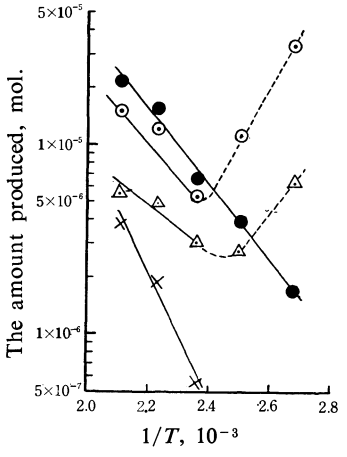


Fig. 6. The amounts of products as a function of the reciprocal of absolute reaction temperature (experiments 3, 6—9); acetone (●), 2-methylbutanol-2 (⊙), 2-methylhexanol-2 (△), and ethyl isopropyl ether (×).

formed at lower temperatures, as has been pointed out above.

The apparent activation energies of the formation of 2-methylbutanol-2, 2-methylhexanol-2, acetone and ethyl isopropyl ether are 8.40, 5.75, 9.19 and 15.7 kcal./mol. respectively, judging from the slope of the curves at higher temperatures in Fig. 6. The value of 2-methylbutanol-2 in the liquid phase is 6.3 kcal./mol. according to Hirota and Hatada.[2] On the other hand, the activation energy of the hydrogen abstraction reaction from propanol-2 by the methyl radical is 7.3 kcal./mol. according to Trotman-Dickenson and Steacie.[8]

Summary

When a mixture of propanol-2 and ethylene was irradiated in the gaseous phase by cobalt-60 gamma-rays at 100°C to 200°C, thirty-seven products were found by gas chromatography from the samples above 150°C in addition to the telomers already reported, while fifteen products were found at 100°C. While the yield of these products increased with an increase in the temperature, the yield of the telomers increased not only with an increase in the temperature but also with a decrease in the temperature below 125°C. The identified products show that all the kinds of radicals, which were expected from propanol-2 are present as the precursors of these products. It has been concluded from these facts that the various radical transfer reactions and disproportionation reactions occur in the gaseous phase, especially above 150°C, although the addition reactions are predominant in the liquid phase at lower temperatures. On the other hand, although 1-hydroxyethyl radical ions are predominant in the electron impact of propanol-2, the 1-hydroxyisopropyl radical is predominant among the precursor radicals. This shows that the present processes are radical and not ionic.

The authors wish to express their thanks to Dr. Hideo Kon, NAIG, for his kind advice.

NAIG Nuclear Research Laboratory
Kawasaki, Kanagawa (T. K.)
Japan Atomic Energy Reasearch Intsitute
Tokai, Ibaraki (H. H.)

8) A. F. Trotman-Dickenson and E. W. R. Steacie, *J. Chem. Phys.*, **19**, 329 (1951).

The Solvent Extraction of Ruthenium with 8-Hydroxyquinoline

By Toyoaki KATO

(Received March 30, 1964)

Because of the difficulty of separating it, ruthenium has prompted studies of a simple and effective method for separation; various isolation schemes for radioactive ruthenium from a fission product mixture have already been reported.[1-5]

The solvent extraction of radioruthenium was accomplished; ruthenium was transferred as its tetroxide into carbon tetrachloride,[4] as perruthenate into pyridine[5] or as its thiocyanate complex into various organic solvents.[6]

On the other hand, numerous organic reagents which can react with ruthenium have been employed for the colorimetric determination, but heating is generally required to develop the color.[7-15]

It has also been stated that in an acetate medium 8-hydroxyquinoline forms a green complex with ruthenium(III) which is extractable

1) C. D. Coryell and N. Sugarman, "Radiochemical Studies," "The Fission Products 2," New York (1951), p. 3.
2) D. N. Hume, ibid., "3" New York (1951), p. 1557.
3) D. L. Love and A. E. Greendale, *Anal. Chem.*, **32**, 780 (1960).
4) J. W. T. Meadows and G. M. Matlack, ibid., **34** 89 (1962).
5) T. Kiba, A. Miura and Y. Sugioka, This Bulletin, **36**, 663 (1963).
6) Y. Oka and T. Kato, *J. Chem. Soc. Japan, Pure Chem. Sec.* (*Nippon Kagaku Zasshi*), **84**, 249 (1963).
7) G. H. Ayres and F. Young, *Anal. Chem.*, **22**, 1277 (1950); **22**, 1281 (1950).
8) R. P. Yaffe and A. F. Voigt, *J. Am. Chem. Soc.*, **74**, 1503 (1952); **74**, 5043 (1952); **74**, 3163 (1952).
9) A. Musil and R. Pietsch, *Z. anal. Chem.*, **137**, 259 (1952).
10) J. E. Currah, A. Fischel, W. A. E. McBryde and F. E. Beamish, *Anal. Chem.*, **24**, 1980 (1952).
11) W. Geilman and R. Neeb, *Z. anal. Chem.*, **152**, 96 (1956).
12) S. B. Knight, R. L. Parks, S. C. Leidt and K. L. Parks, *Anal. Chem.*, **29**, 571 (1957).
13) C. V. Banks and J. W. O'Laughlin, ibid., **29**, 1412 (1957).
14) D. L. Manning and O. Menis, ibid., **34**, 94 (1962).
15) Y. Oka and T. Kato, *J. Chem. Soc. Japan, Pure Chem. Sec.* (*Nippon Kagaku Zasshi*), **84**, 254 (1963).

with chloroform,[16] but the experimental conditions of the complex formation, as well as its extraction behavior, are not known in detail.

In the present work, the investigation of the solvent extraction hehavior of ruthenium with 8-hydroxyquinoline was carried out using radioactive ruthenium, ruthenium-106, as a tracer.

Extraction can also be applied for the removal of the tracer amounts of ruthenium that are ordinarilly met with in the radiochemical separation.

Experimental

Ruthenium Stock Solutions.—A hydrochloric acid solution of ruthenium(IV) was prepared by dissolving "ruthenium trichloride" obtained from the Yokosawa Chem. Co. in 6 M hydrochloric acid.[17] The ruthenium content of this solution was determined as 1.93 mg. Ru/ml. by the method of Taimni.[18]

A nitric acid solution of ruthenium(IV) of a known ruthenium content (1.6 mg. Ru/ml.) was prepared by absorbing gaseous ruthenium tetroxide into 1 N nitric acid containing 3% hydrogen peroxide followed by heating it at 40°C for 30 min. The ruthenium tetroxide was prepared according to Kambara's method,[19] in which "ruthenium trichloride" was oxidized with lead peroxide in a sulfuric acid medium.

A more dilute solution containing 10 μg. Ru/0.1 ml. was prepared by diluting the stock solutions just before use; in every extraction experiment, a 0.1 ml. aliquot of this solution was used.

Radioactive Ruthenium. — Ruthenium-106 as "trichloride" in 8 M hydrochloric acid, with a radiochemical purity of about 99%, was imported from the Radiochemical Centre, Amersham, England. A part of this was diluted with 0.1 M hydrochloric acid to make its radioactivity about 5×10^4 c. p. m./0.1 ml.; this was used as a tracer of ruthenium(IV) in hydrochloric acid. Another part of this was converted into a nitrate solution in the same manner as was described for inactive ruthenium nitrate. This was used as a tracer of the corresponding ruthenium(IV) nitrate after proper dilution with 0.1 M nitric acid, also with a radioactivity of about 5×10^4 c. p. m./0.1 ml.

8-Hydroxyquinoline and Other Chemical Reagnts. — Commercial 8-hydroxyquinoline of guaranteed grade, with the observed melting point of 72.5~74.5°C, was used.

The organic solvents and other reagents were all guaranteed grade reagents. Redistilled water was used.

Apparatus.—For the measurement of the radioactivity, a well-type scintillation counter, Model RSP-1, made by the Kōbe Kôgyô Co., Japan, was employed. For measuring the pH of the aqueous phase, a glass electrode pH meter, Model EHM-1, made by the Hitachi Co., Japan, was employed.

Experimental Procedure.—The procedure for the extraction experiment was, unless otherwise stated, as follows: To an aliquot of 8-hydroxyquinoline dissolved in *n*-propanol or in 10 M acetic acid in a test tube, an aqueous buffer and, if needed, another reagent solution were added to adjust the pH value of the solution, and the total volume was made up to 6 ml. with water. A 0.1 ml. portion of each ruthenium-106 and ruthenium solution (Ru : 10 μg.) was added, and the mixture was kept at an elevated temperature (60°C in most cases) in a constant temperature bath for a time.

After having been cooled in running water, the contents were transferred into a separatory funnel, and the 8-hydroxyquinolate formed was extracted with a suitable aliquot of an organic solvent (2 or 5 ml.) like *n*-butanol or benzene by shaking it for 1 min. An excess quantity of 8-hydroxyquinoline was employed in every extraction system; viz., 2 ml. of 0.05 M 8-hydroxyquinoline (100 μeq.) in *n*-propanol or 1 ml. of 1 M 8-hydroxyquinoline (1 meq.) in a 10 M acetic acid solution was used.

In all extractions, both the organic and aqueous phases, after having been disengaged in a separatory funnel, were drained into two test tubes. The respective ruthenium contents were then estimated by gamma counting, and the percentage extraction was computed as a ratio of the counting rate of the organic extract to the sum of the counting rates of the two phases. The pH of the aqueous phase after extraction was also measured.

Results and Discussion

The Formation of 8-Hydroxyquinolate. — In the preliminary study of the extraction of ruthenium as 8-hydroxyquinolate, it was found that the rate of the formation of 8-hydroxyquinolate, as well as of the extraction, was quite slow at room temperature when an aqueous solution containing ruthenium was shaken with 8-hydroxyquinoline in chloroform, even at relatively high pH values (pH 4~6) and at a high concentration of the reagent (1 M). The formation of the 8-hydroxyquinolate, however, was accelerated when an aqueous solution was kept at an elevated temperature in the presence of an excess reagent as its *n*-propanol solution, so the following equilibrium extraction might be achieved rapidly by shaking it with an additional organic solvent such as chloroform.

As is shown in Fig. 1, the extraction of 8-hydroxyquinolate with 2 ml. of chloroform or *n*-butanol from an aqueous phase under various conditions was accomplished after the aqueous system had been kept at 60°C for 1 hr.

Ruthenium(IV) nitrate was used in this experiment; it will also be used hereafter unless otherwise indicated.

16) E. B. Sandell, "Colorimetric Determination of Traces of Metals," 3rd Ed., Interscience Publisher, New York (1959), p. 791.

17) The predominant species in this solution was $Ru(OH)_2Cl_4^{2-}$, as will be described in a later part of this paper.

18) I. K. Taimni and G. B. S. Salaria, *Anal. Chim. Acta*, **11**, 329 (1954).

19) T. Kambara, *Japan Analyst*, **7**, 439 (1958).

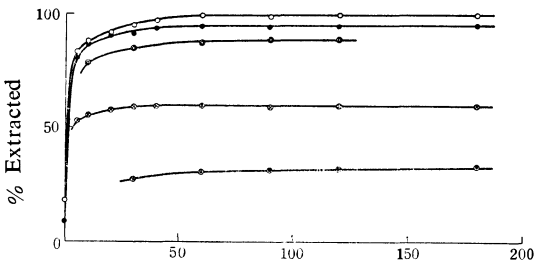


Fig. 1. Effect of heating time on the extraction.
○ pH 6.0 (HOAc - 0.33 M NaOAc), *n*-Butanol
● pH 6.0 (HOAc - 0.33 M NaOAc), Chloroform
◎ pH 3.9 (HOAc - 0.33 M NaOAc), Chloroform
⊗ pH 8.5 (NH_4OH - 0.33 M NH_4Cl), Chloroform
⊙ pH 1.2 (HNO_3 - 0.33 M NaOAc), Chloroform

Extraction Solvent. — The ruthenium 8-hydroxyquinolate formed in an aqueous acetate medium of pH 6 in the manner described above was extracted with each 2 ml. portion of various organic solvents. As is shown in Table I, more than 99% of the original ruthenium is transferred into various organic solvents, except isopropyl ether. *n*-Butanol is especially efficient in retaining 8-hydroxyquinolate.

TABLE I. EXTRACTION BY VARIOUS SOLVENTS

Solvent	% Extracted
n-Butanol	99.3
Isoamyl alcohol	96.4
Cyclohexanone	97.0
Methyl isobutyl ketone	94.5
Isopropyl ether	84.0
Isoamyl acetate	92.1
Benzen	93.0
Carbon tetrachloride	90.1
Chloroform	94.8

Extraction Curves. — The determination of the pH range where the extraction of ruthenium has to be successful was carried out.

The shape of the extraction curve is generally affected by the buffer component employed to adjust the pH of an aqueous phase, thereby emphasizing the importance of the proper selection of the buffer component and its concentration in a system.[20-22]

First, extraction with 2 ml. of *n*-butanol from an aqueous acetate system composed of 0.33 M sodium acetate or ammonium acetate was carried out, varying the pH values with additional dilute nitric acid, acetic acid, or aqueous ammonia. The extraction curve thus obtained is illustrated in Fig. 2, from which the extraction of ruthenium of either tracer (ruthenium-106, carrier-free) or ordinary micro amounts (Ru : 10 μg.) may be found to be almost complete by using 2 ml. of *n*-butanol at the pH value of 4~6.

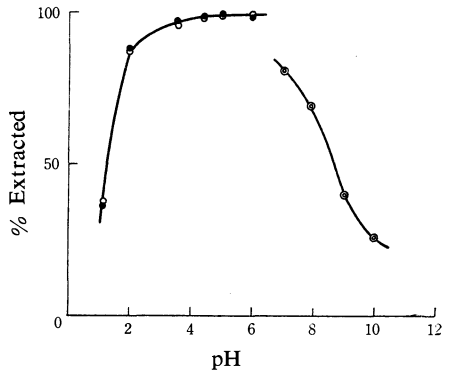


Fig. 2. Effect of pH on the extraction from acetate buffers.
● Ru : carrier-free
○, ◎ Ru : 10 μg.

In an aqueous ammonia - ammonium acetate system, extractability is reduced by an interfering action of the ammonium ion, as will be described later on. Hence, the discontinuity of the extraction curve appeared at about pH 6.

Next, the relation between the percentage extraction of ruthenium and the pH of the aqueous solution containing various buffer components, viz., 0.03 M phthalate, 0.1 M citrate, 0.03 M or 0.1 M phosphate, or an aqueous ammonia - ammonium chloride mixture was investigated. An aqueous solution of sodium hydroxide was used to give the aqueous solution higher pH values. Extraction was also carried out with 2 ml. of *n*-butanol.

The results are illustrated in Fig. 3. In the phthalate system, as well as in the case of acetate, an almost complete extraction was achieved at the pH range of 4~6, but in this pH region extraction is considerably reduced in the presence of citrate. Phosphate and ammonium salts were also unfavorable as buffer components.

Coexisting Substances. — The effects of the coexistence of inorganic salts and organic acids or their salts are given in Table II. With large amouts of chloride, nitrate, sulfate and borate, no significant interferences were observed, but with oxalate and other organic substances, severe interferences resulted.

The Amount of Ruthenium.—The concentration dependence of ruthenium on the extractability was determined in an extremely low

20) H. Irving, C. F. Bell and R. J. P. Williams, *J. Chem. Soc.*, **1952**, 356.
21) N. Suzuki, *Japan Analyst*, **8**, 283 (1959).
22) F. P. Peppard, J. P. Faris, P. R. Gray and G. W. Mason, *J. Phys. Chem.*, **57**, 294 (1953).

TABLE II. EFFECTS OF COEXISTING SUBSTANCES

Coexisting substance	Added as	Concn., M	% Extracted*	pH
Chloride	NaCl	0.4	99.2	5.2
Nitrate	$NaNO_3$	1.3	99.2	5.1
Sulfate	Na_2SO_4	0.2	98.9	5.4
Ammonium salt	NH_4Cl	0.3	91.7	5.3
Borate	H_3BO_3	0.02	97.2	5.5
Phosphate	KH_2PO_4	0.05	81.5	5.7
Citrate	$Na_2HC_6H_5O_7$	0.05	71.1	5.6
Tartrate	$Na_2C_4H_4O_6$	0.05	83.1	5.6
Oxalate	$H_2C_2O_4$	0.05	25.4	5.4
EDTA	EDTA-2Na	0.01	27.3	5.5
Hydroxylamine	$NH_2OH \cdot HCl$	0.02	31.0	5.5
None	—	—	99.3	5.6

* With 2 ml. of *n*-butanol.

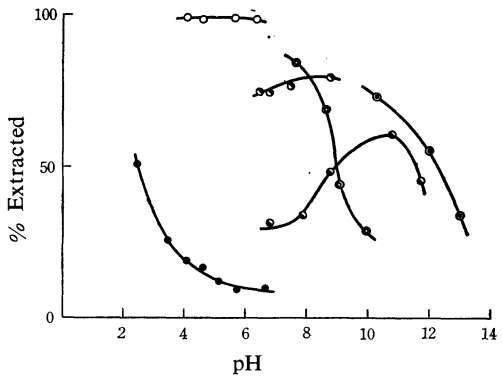


Fig. 3. Effect of pH on the extraction from phthalate, citrate, phosphate and ammonium buffers.
- ○ 0.03 M phthalate
- ● 0.1 M citrate
- ◔ 0.03 M phosphate
- ◕ 0.1 M phosphate
- ◎ 0.3 M ammonium chloride - ammonia
- ⊙ aqueous sodium hydroxide

concentration, from a tracer amount to 2.5×10^{-3} M, in an original aqueous solution. In this experiment, a definite amount of ruthenium(IV) was added to an aqueous solution containing a carrier-free ruthenium-106 tracer, and extraction with 2 ml. of *n*-butanol was carried out at pH 5.6 after heating the solution with an excess reagent, as has been described above.

As is shown in Table III, as much as 99% of the original ruthenium(IV) could be transferred into *n*-butanol as its 8-hydroxyquinolate.

TABLE III. EFFECT OF AMOUNT OF RUTHENIUM

Amount of Ru added, mg.	% Extracted
Carrier-free	99.3
0.01	99.3
0.15	99.1
1.5	99.5

The Extraction of Ruthenium Added as "Trichloride." — As the course of the extraction seemed to consist of the formation of 8-hydroxyquinolate in aqueous - *n*-propanol - acetate systems and its distribution into the organic solvent, the effect of the heating time, the concentration dependence of ruthenium and the pH range for complete extraction were also investigated when both of ruthenium and ruthenium-106 solutions were added as "trichloride" in hydrochloric acid. The results presented in Figs. 4, 5 and 6 show that the percentage extraction reaches a limiting value upon one hour's heating at 60°C and that the value is held constant over a wide concentration range of ruthenium; almost complete extraction can be achieved in the pH range of 4~6 by 2 ml. of *n*-butanol. This behavior is closely similar to that observed in the case of nitrate, in which the oxidation state of ruthenium is quadrivalent.[23] As is shown in Table II. extraction was, however, reduced to an appreciable extent in the presence

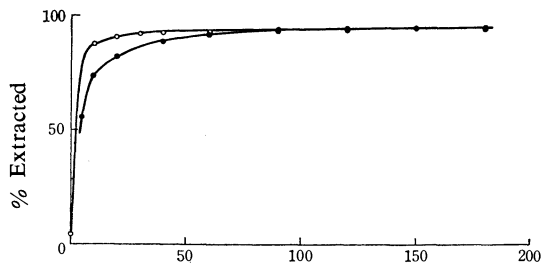


Fig 4. Effect of heating time on the extraction (Ruthenium was added as "trichloride").
- ○ pH 5.6, Chloroform
- ● pH 4.4, Chldroform

23) J. S. Anderson and J. D. M. McConnell, *J. Inorg. Nucl. Chem.*, **1**, 371 (1955).

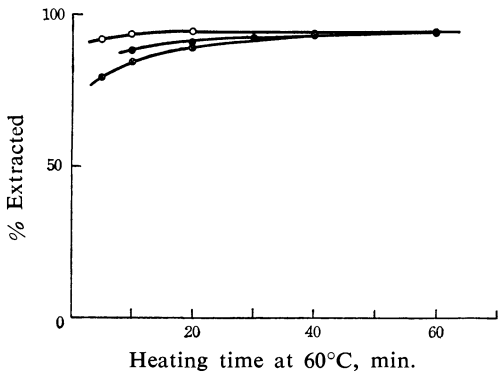


Fig. 5. Effect of heating time on the extraction in different amount of ruthenium (added as "trichloride").
pH 5.6 acetate buffer, chloroform
⊗ Ru : carrier-free
● Ru : 10 μg.
○ Ru : 100 μg.

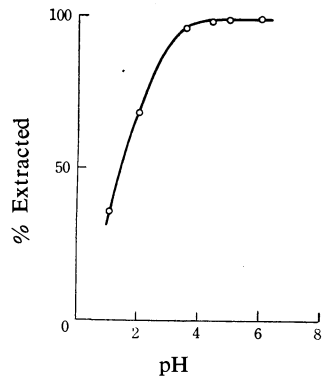


Fig. 6. Effect of pH on the extraction from acetate buffers (Ruthenium was added as "trichloride").
Solvent : 2 ml. of *n*-Butanol

of hydroxylamine hydrochloride, which reduces ruthenium(IV) to tervalent.[24] It has been mentioned that ruthenium(III) in hydrochloric acid is fairly air-oxidized to the ruthenium(IV) state; hence, a commercial water-soluble ruthenium trichloride is usually composed, at least in part, of ruthenium(III) salt.[25]

Indeed, when "ruthenium trichloride" was dissolved in 6 M hydrochloric acid, its absorption spectrum was characterized by intense peaks at 385 and 254 mμ, together with a minor peak at 476 mμ corresponding to that of the chloro-ruthenium(IV) species; according to Wehner's paper,[26] this was defined as $Ru(OH)_2Cl_4^{2-}$. Air-oxidation occurred to both inactive and radioactive ruthenium; therefore, the extraction behavior of 8-hydroxyquinolate has to be identical with that of ruthenium(IV).

The Improvement of the Extraction System. — Thus the extraction of ruthenium in *n*-butanol as 8-hydroxyquinolate is completed from an aqueous *n*-propanolic solution, but the back extraction of ruthenium from an organic extract composed of a *n*-propanol - *n*-butanol mixture can not be performed because of the water-miscible property of this solvent mixture. Therefore, it is desirable to modify an extraction system so as to produce a favorable separation of ruthenium from the organic extactants. On the other hand, it is also desirable to make the rate of approach to the extraction equilibrium higher than has been observed in previous parts. Consequently, the behavior was further examined in a system involving the formation of 8-hydroxyquinolate with a still larger amount of the reagent and subsequent extraction with an almost water-immiscible solvent such as benzene.

Hereafter, ruthenium(IV) nitrate was again used, and the aqueous phase was prepared by adding an acetic acid solution of 8-hydroxyquinoline (up to 1 meq.) and adjusting the pH of the resulting solution to 4 with an additional 1 ml. portion of 2 M sodium acetate, as has been described in the Experimental section.

The effect of heating time on the extractability is shown in Fig. 7, where the percentage extraction in an equilibrium extraction with 2 ml. of *n*-butanol reaches a constant value of 99.3% with 1 meq. of the reagent after being heated for 30 min. at 60°C or for 10 min. at 80°C. In these cases, 99.0% of the ruthenium

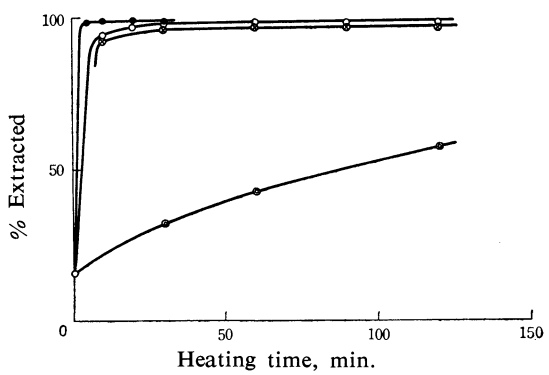


Fig. 7. Factors affecting the rate of approach to extraction equilibrium.
● 80°C, 8-Hydroxyquinoline : 1 meq.
○ 60°C, 8-Hydroxyquinoline : 1 meq.
⊗ 60°C, 8-Hydroxyquinoline : 0.1 meq.
◎ 20°C, 8-Hydroxyquinoline : 1 meq.

24) F. P. Treadwell and W. T. Hall, "Analytical Chemistry I," John Wiley & Sons., New York (1930), p. 563.
25) G. Brauer, "Hanbduch der Präparativen Anorganischen Chemie," Ferdinand Enke Verlag, Stuttgart (1953), p. 1195.
26) P. Wehner and J. C. Hindman, *J. Phys. Chem.*, **56**, 10 (1952).

is extracted with 5 ml. of benzene. It may also be seen that the formation of 8-hydroxyquinolate at room temperature is unfavorably slow. The percentage extraction reached 78% after the aqueous phase had stood for about 40 hr. In the presence of 100 μeq. of the reagent, the extraction by 2 ml. of *n*-butanol was somewhat reduced to 97%.

Shaking Time.—With a large amount of the reagent, it is to be expected from the extraction rate that the equilibrium can be readily achieved by directly agitating both phases without heating. Therefore, an aqueous acetate system containing 1 meq. of the reagent was mixed with each 5 ml. portion of *n*-butanol or benzene. The effect of the shaking time on the extractability is given in Fig. 8, where the equilibrium extraction can not be attained even by a shaking of up to 2 hr. Because it requires a longer time for equilibration, the formation of the extractable 8-hydoxyquinolate in an aqueous system by heatnig should be followed by the extraction.

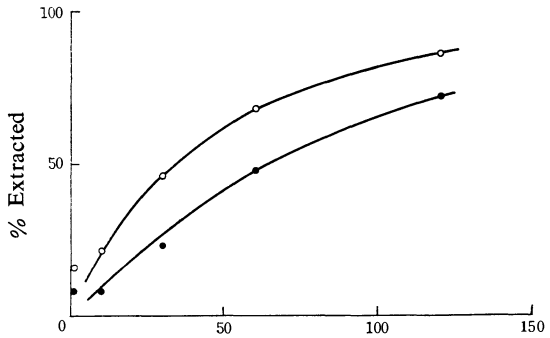


Fig. 8. Effect of shaking time on the extraction
○ *n*-Butanol
● Benzene

It may also be concluded that the complex formation in the aqueous phase is the limiting step in this separation method.

The Presence of a Water-Miscible Solvent.—Although the benzene extraction was sufficient for the extraction of ruthenim, the enhancement of extractability was recognized with *n*-butanol as the extracting solvent and, morever, with *n*-propanol present in an aqueous system.

The fairly water-miscible solvents seemed to be efficient for the formation and subsequent extraction of 8-hydroxyquinolate. It has been discussed now, in a chelate extraction system, a good extraction can be attained by the effect of a mixed solvent.[27,28] On the basis of these considerations, further investigation was carried out with such solvents to produce some different media for the formation of 8-hydroxyquinolate. First, the 8-hydroxyquinolate was formed in 6.2 ml. of the aqueous solution containing 1 ml. of a water-miscible solvent, such as *n*-propanol, methyl cellosolve, ethylene glycol, dioxane and pyridine, and then the extraction was carried ont with 2 ml. of benzene. As is shown in Table IV, the percentage extraction is greater to a minor, but appreciable, extent in the presence of any of the solvents excepting pyridine, than in their absence. No simple relation can be found between the solvent character and the extractability, as the extractability does not reach its highest point even with dioxane, which has the lowest dielectric constant among the solvents. In the presence of *n*-butanol, the highest result was attained, and by the later *n*-butanol extraction, the extractability might be enhanced remarkably: a combination of 2 ml. of *n*-propanol and 5 ml. of *n*-butanol resulted in the 99.9% extraction of ruthenium.

TABLE IV. EFFECT OF THE PRESENCE OF WATER MISCIBLE SOLVENT

Solvent	% Extracted in 2 ml. of benzene
n-Propanol	98.5, 99.5*
Methyl cellosolve	97.0
Ethylene glycol	97.9
Dioxane	98.0
Pyridine	49.3
None	96.9, 99.0**

* With 2 ml. of *n*-propanol.
** With 5 ml. of benzene.

Back Extration.—To examine the conditions for the back extraction of ruthenium, a 5 ml. aliquot of the benzene containing 8-hydroxyquinolate was shaken with an equal volume of aqueous mineral acids or an aqueous solution of some organic reagents. The results are given in Table V and Fig. 9. The back

TABLE V. BACK EXTRACTION OF RUTHENIUM

Back Extractant	Shaking time, min.	% Back Extracted
pH 4.5 acetate buffer	1	1.2
1 M HCl	1	1.5
11.6 M HCl	10	95.0
1 M HNO_3	1	1.5
0.5 M H_2SO_4	1	1.4
9 M H_2SO_4	10	97.0
0.1 M EDTA	10	4.3
0.3 M Oxalic acid	10	2.8
0.3 M Sodium citrate	10	1.3
0.1 M Hydroxylamine	10	1.5

27) N. Suzuki and T. Kato, *J. Chem. Soc. Japan, Pure Chem. Sec.* (*Nippon Kagaku Zasshi*), **80**, 1148 (1959); *Sci. Rept. Tohoku. Univ., Ser. I*, **43**, 152 (1959).
28) C. L. Luke and M. E. Campbell, *Anal. Chem.*, **26**, 1778 (1954).

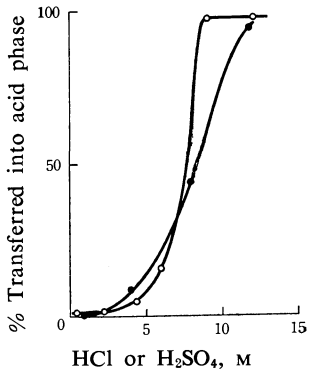


Fig. 9. Stripping of ruthenium by hydrochloric and sulfuric acid.
Shaking time: 10 min.
● HCl
○ H_2SO_4

extraction of ruthenium was not attained appreciably with the various back extractants listed in Table V except for concentrated mineral acid.

8-Hydroxyquinolate, once formed, retains its extractable property, even in a range of extremely low pH values where the excess reagent is transferred into the aqueous phase as a protonated form of 8-hydroxyquinoline, H_2Ox^+.[29] Washing a benzene extract with 1 N mineral acid, almost all the excess reagent can be removed with as little a loss of ruthenium as 1.5%. 8-Hydroxyquinolate is released by contact with more concentrated hydrochloric or sulfuric acid, and 95% of the ruthenium is found in concentrated hydrochloric acid after 10 minutes' agitation.

The Application of Solvent Extraction. — Ruthenium(IV) 8-hydroxyquinolate is greenish-yellow in color. The absorption spectrum of the benzene solution, shown in Fig. 10, is characterized by an intense peak at 437 mμ and a broad maximum at about 700 mμ in the visible range.[30] The colorimetric determination of a minute amount of ruthenium can be attained directly in the organic extract; the experimental conditions for this purpose will be described in detail elsewhere.

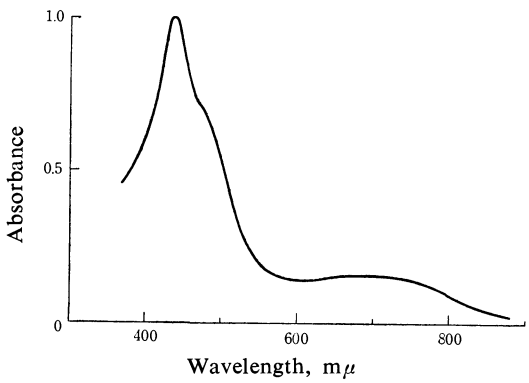


Fig. 10. Absorption spectrum of ruthenium(IV)-8-hydroxyquinolate in benzene extract.
Ru: 32 μg.
Solvent: 10 ml. of benzene

Next, the elements in mixed fission products were tested for their extractable properties by this method. Each pure nuclide in a carrier-free state[31] was subjected individualy to the experimental procedure; extraction with 5 ml. of benzene from an aqueous acetate solution of pH 4 containing 1 meq. of the reagent, and back extraction with an equal volume of 1 N nitric acid. Table VI shows 86.6% of the original zirconium-niobium-95 is accompanied by ruthenium-106 in the benzene extract but is completely separated by the following acid washings. The decontamination from the nuclides tested is complete. Ruthenium-103, 106 of a high radiochemical purity can be obtained from the mixed fission products by this extraction method.

Table VI. Behavior of some fission product nuclides

Nuclide	% Found in benzene extract	% Found in 1 N nitric acid*
Cs-137	1.0	94.3
Ce-144	1.8	95.5
Zr-Nb-95	86.6	98.9
Sr-90	0	—
Y-90	0.7	—
Ru-106	99.0	1.5

* Expressed as a percentage of c. p. m. found in acid phase to that contained in orginal benezene extract.

Summary

The solvent extraction behavior of ruthenium(IV) with 8-hydroxyquinoline has been investigated in detail using ruthenium-106 as a tracer.

The complex formation in the aqueous phase is fairly slow and is the limiting step in the procedure, but it can be enhanced by heating. Complete extraction is attainable with *n*-butanol, benzene and other organic solvents after 8-hydroxyquinolate has been formed by one hour's heating at 60°C with the excess reagent in an aqueous acetate medium of pH 4~6. *n*-Propanol, especially when combined with *n*-butanol, is an efficient extraction solvent. The presence of ammonium salts, organic

29) S. Lacroix, *Anal. Chim. Acta*, **1**, 260 (1947).

30) For measurement, an auto-recording spectrophotometer, Model EPS-2, made by the Hitachi Co., Japan, was employed.

31) Imported from the Radioisotopes Division of Oak Ridge National Laboratory, U. S. A.

acids or their salts causes interference. 8-Hydroxyquinolate, once formed, remains extractable even at very low pH values. The stripping of ruthenium from the benzene extract is accomplished by contact with concentrated hydrochloric acid.

This solvent extraction is applicable to the colorimetric determination of minute amounts of ruthenium and to the isolation of ruthenium activities in mixed fission products.

The author wishes to express his hearty thanks to Professor Yoshinaga Oka for his kind suggestions and fruitful discussions in the course of this work.

Department of Chemistry
Faculty of Science
Tohoku University
Katahira-cho, Sendai

The Synthesis of 8-Hydroxy-1-oxaazulan-2-one and Its Derivatives by the Condensation of 3-Bromotropolones with Diethyl Malonate and Ethyl Acetoacetate

By Kahei TAKASE

(Received April 11, 1964)

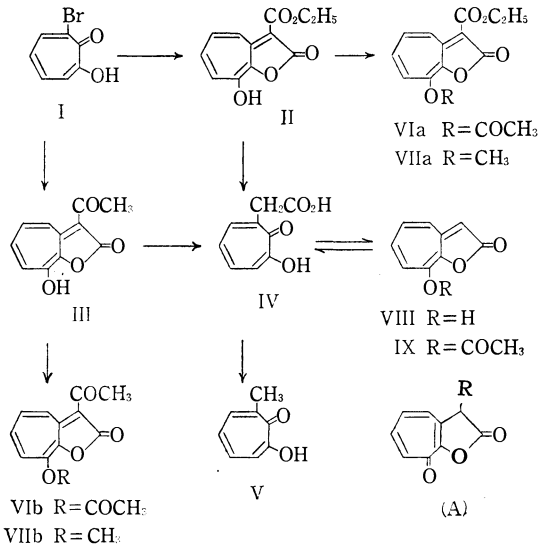
During studies of the C-alkylation of tropolones by anionoid substitution reaction, it has been found that the reaction of 3-bromotropolones and diethyl malonate or ethyl acetoacetate afforded as condensation products 8-hydroxy-1-oxaazulan-2-one (8-hydroxy-2H-cyclohepta[b]furan-2-one) derivatives. The alkyl derivatives of these condensation products have also been obtained by the extension of this reaction to alkyl derivatives of 3-bromotropolone. Moreover, 8-hydroxy-1-oxaazulan-2-one itself and 3-carboxymethyltropolones have been derived from these condensation products. In this paper, the synthesis and some reactions of 8-hydroxy-1-oxaazulan-2-ones will be described.

Hartley[1] reported that *o*-bromobenzoic acid reacted with diethyl malonate or ethyl acetoacetate, in the presence of a copper catalyst, to give condensation products. This reaction has now been extended to 3-bromotropolone (I). The heating of I with diethyl sodiomalonate, in the presence of copper acetate, gave an acidic compound (II), $C_{12}H_{10}O_5$ (one OC_2H_5), in a good yield. Under the same conditions, ethyl sodioacetoacetate also gave an acidic compound (III), $C_{11}H_8O_4$ (no OC_2H_5). These condensation products were soluble in alkalis, but they did not show any coloration with a ferric chloride solution. When heated in concentrated hydrobromic acid, II afforded an acidic compound IV while evolving carbon dioxide. The heating of II in a sodium hydroxide solution also gave IV. Acid IV is a dibasic acid with pK_a, 4.52 and 8.77,[2] and showed a green color with a ferric chloride solution. The heating of IV in pyridine gave 3-methyltropolone (V)[3] while carbon dioxide was evolved.

These results indicate that the acid IV is 3-carboxymethyltropolone and that, consequently, II is a condensation product possessing the malonic ester group at the 3-position of the tropolone nucleus. The lactone structure (A) may also be assumed for II from the analytical values and the negative ferric chloride test, which suggests that the hydroxyl group of tropolone is masked. However, II is a monobasic acid with pK_a, 3.57,[4] which value would be due to the enolic hydroxyl, not to the opening of the lactone ring. Furthermore, the acetylation of II with acetic anhydride gave a neutral monoacetate (VIa), and the methylation of II with diazomethane gave a neutral monomethyl derivative (VIIa). The ultraviolet absorption spectra of both VIa and VIIa are similar to those of 1-oxaazulan-2-ones,[5] as Fig. 2 shows. The ultraviolet absorption spectrum of II, as is shown in Fig. 1, is also similar to those of 1-oxaazulan-2-ones, although its maxima show a slight hypsochromic shift.

1) W. R. H. Hartley, *J. Chem. Soc.*, **1929**, 1870.
2) N. Tanaka, I. T. Oiwa, T. Kurosawa and T. Nozoe, This Bulletin, **32**, 92 (1959).
3) T. Nozoe, T. Mukai and K. Takase, *Proc. Japan Acad.*, **27**, 561 (1951); *Sci. Repts. Tohoku Univ.*, I, **36**, 40 (1952); T. Nozoe, T. Mukai and K. Matsui, *Proc. Japan Acad.*, **27**, 646 (1951); T. Nozoe, T. Mukai, M. Kunori, T. Muroi and K. Matsui, *Sci. Repts. Tohoku Univ.*, I, **35**, 242 (1952).
4) The dissociation constants were measured by Mrs. Toshiko Kurosawa of the Chemical Laboratory, Faculty of Science, Tohoku University; to her the author's thanks are due.
5) S. Seto, *Sci. Repts. Tohoku Univ.*, I, **37**, 367 (1953).

From this evidence, II is assumed to be 3-ethoxycarbonyl-8-hydroxy-1-oxaazulan-2-one, and VIa and VIIa, to be 3-ethoxycarbonyl-8-acetoxy- and 3-ethoxycarbonyl-8-methoxy-1-oxaazulan-2-one respectively.



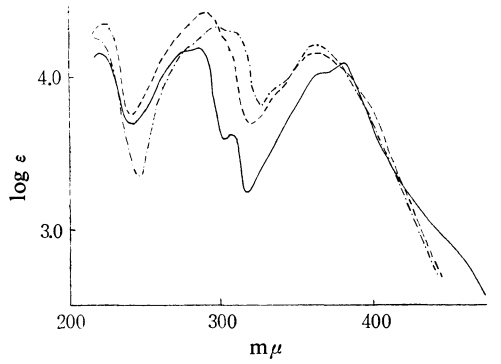


Fig. 1. UV spectra of II (------), III (-·-·-) and VIII (——) in methanol.

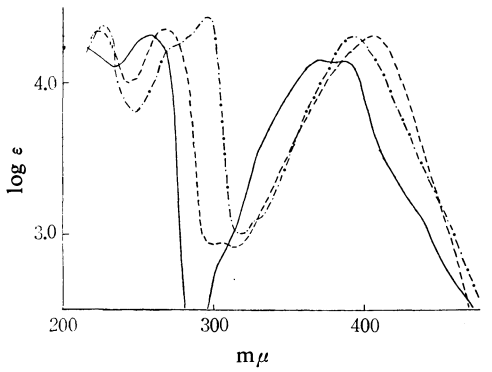


Fig. 2. UV spectra of VIa (------), VIIa (-·-·-) and IX (——) in methanol.

The condensation product (III) is assumed to be 3-acetyl-8-hydroxy-1-oxaazulan-2-one, similar to II, from the following evidence. This compound III is a monobasic acid with pK_a, 3.44,[4] and gave a neutral monoacetate VIb and a neutral monomethyl ether VIIb. The ultraviolet absorption spectra of III and of its acetate VIb and methyl ether VIIb are similar to those of II and of its derivatives, VIa and VIIa, respectively. The heating of III in concentrated hydrobromic acid afforded IV as well as liberated acetic acid.

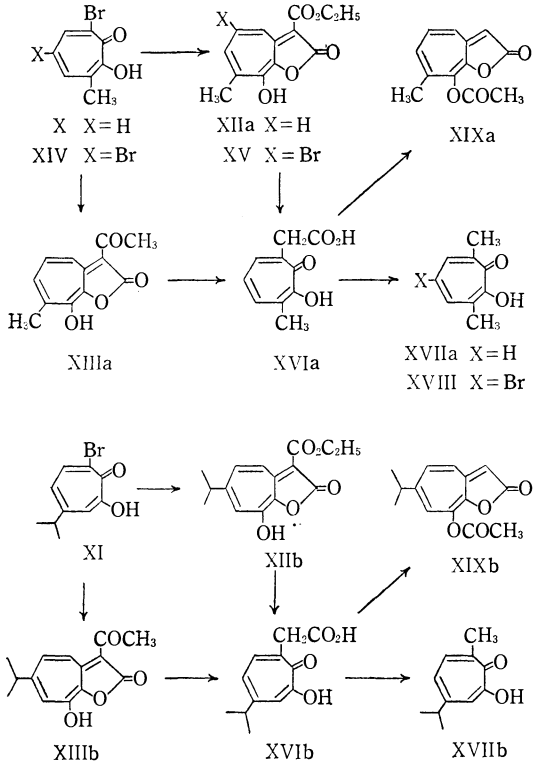
The parent compound, 8-hydroxy-1-oxaazulan-2-one (VIII) was obtained as orange crystals by dissolving IV in concentrated sulfuric acid and then pouring the mixture into ice-water. Its ultraviolet absorption curve is similar to those of 1-oxaazulan-2-ones, as Fig. 1 shows. When heated in an aqueous solvent, VIII was easily hydrolized to IV. The acetylation of VIII gave an acetate IX, which was also obtained from IV by heating it with acetic anhydride. The ultraviolet absorption spectrum, as shown in Fig. 2, indicates that IX is 8-acetoxy-1-oxaazulan-2-one. The hydrolysis of IX by heating with acids gave IV.

Alkyl derivatives of 8-hydroxy-1-oxaazulan-2-ones were obtained by the extension of this condensation reaction to alkyl derivatives of 3-bromotropolone. When heated with diethyl sodiomalonate or ethyl sodioacetoacetate, both 3-bromo-7-methyltropolone (X)[6] and 3-bromo-6-isopropyltropolone (XI)[7] gave corresponding condensation products, XIIa, b and XIIIa, b, respectively. All of these compounds are acidic and gave neutral monoacetate. The ultraviolet absorption spectra of these compounds and their acetates are closely similar to those of 8-hydroxy-1-oxaazulan-2-ones (II and III) and their acetates respectively. From this evidence, the condensation products, XIIa, b and XIIIa, b, are assumed to be 3-ethoxycarbonyl-7-methyl-, 3-ethoxycarbonyl-6-isopropyl-, 3-acetyl-7-methyl- and 3-acetyl-6-isopropyl-8-hydroxy-1-oxaazulan-2-one respectively. 3, 5-Dibromo-7-methyltropolone (XIV)[6] also reacted with diethyl sodiomalonate to give a condensation product XV. The structure of XV was established from the facts that its ultraviolet absorption spectrum is similar to those of 8-hydroxy-1-oxaazulan-2-ones and that its catalytic debromination gave XIIa.

When heated in concentrated hydrobromic acid, both XIIa and XIIIa afforded 3-carboxymethyl-7-methyltropolone (XVIa) and both

6) K. Takase, *Bull. Chem. Research Inst. Non-Aqueous Solns. Tohoku Univ.*, **13**, 169 (1964).

7) T. Nozoe, T. Mukai and K. Takase, *Proc. Japan Acad.*, **26** (8), 19 (1950); T. Nozoe, E. Sebe, S. Mayama and S. Iwamoto, *Sci. Repts. Tohoku Univ.*, I, **36**, 184 (1952).



XIIb and XIIIb afforded 3-carboxymethyl-6-isopropyltropolone (XVIb). The decarboxylation of XVIa and XVIb by heating in pyridine afforded 3, 7-dimethyltropolone (XVIIa)[3] and 6-isopropyl-3-methyltropolone (XVIIb)[3] respectively. The bromination of XVIIa gave 5-bromo-3, 7-dimethyltropolone (XVIII). When XVIa and XVIb were treated with acetic anhydride, they gave 7-methyl-8-acetoxy- (XIXa) and 6-isopropyl-8-acetoxy-1-oxaazulan-2-one (XIXb) respectively. The ultraviolet absorption spectra of XIXa and XIXb are similar to those of 1-oxaazulan-2-ones. Acetoxy derivatives XIXa, b were easily hydrolized by heating them in concentrated acid or dilute alkalis, affording carboxymethyltropolones (XVIa, b).

These condensation reactions did not proceed without the use of copper acetate. 5-Bromotropolone did not react with diethyl malonate and ethyl acetoacetate under these conditions, while 3, 7-dibromotropolone afforded resinous substances.

Experimental[8]

3-Ethoxycarbonyl-8-hydroxy-1-oxaazulan-2-one (II).—To a solution of diethyl sodiomalonate prepared by dissolving sodium (12.0 g.) in a mixture of diethyl malonate (100 ml.) and dry dioxane (200 ml.), 3-bromotropolone (I) (20.0 g.) and copper acetate (200 mg.) were added; the mixture was then refluxed for 6 hr. After the addition of water (200 ml.), the mixture was shaken with ether (200 ml.) and the aqueous layer was acidified with 6 N hydrochloric acid and allowed to stand overnight. The crystals thereby formed were collected and washed with chloroform to give II (17.6 g.), m. p. 208°C (decomp.). Recrystallization from acetone afforded yellow needles, m. p. 225°C (decomp.).

λ_{max}^{MeOH} mμ (log ε); 222 (4.35), 290 (4.43), 357 (4.15).

Found: C, 61.60; H, 4.52; OC_2H_5, 19.22. Calcd. for $C_{12}H_{10}O_5$: C, 61.54; H, 4.30; OC_2H_5, 19.20%.

3-Acetyl-8-hydroxy-1-oxaazulan-2-one (III).—To a solution of ethyl sodioacetoacetate prepared by dissolving sodium (12.0 g.) in a mixture of ethyl acetoacetate (90 g.) and dry dioxane (160 ml.), I (20.0 g.) and copper acetate (400 mg.) were added; the mixture was then refluxed for 18 hr. The reaction mixture was treated as described in the above experiment to give III (19.0 g.), m. p. 278°C (decomp.). Recrystallization from a large amount of acetone gave yellow silky needles, m. p. 285°C (decomp.).

λ_{max}^{MeOH} mμ (log ε); 294 (4.32), 361 (4.19).

Found: C, 64.82; H, 4.26. Calcd. for $C_{11}H_8O_4$: C, 64.70; H, 3.95%.

3-Carboxymethyltropolone (IV).—*a) From II.*—A mixture of II (3.95 g.) and concentrated hydrobromic acid (30 ml.) was heated at 130~140°C for 2 hr. The mixture was poured into ice-water (50 g.) and adjusted to pH 3 with a potassium hydroxide solution, the crystals thereby obtained were collected by filtration, affording IV (1.14 g.), m. p. 170°C (decomp.). From the mother liquor, further crops of IV (1.38 g.), m. p. 171°C (decomp.), were obtained by continuous extraction with ether for 20 hr. Recrystallization from dimethylformamide afforded pale yellow needles, m. p. 174°C (decomp.).

λ_{max}^{MeOH} mμ (log ε); 243 (4.26), 329 (3.94), 391 (3.91).

Found: C, 59.67; H, 4.66. Calcd. for $C_9H_8O_4$: C, 60.00; H, 4.48%.

b) From III.—A mixture of III (4.0 g.) and concentrated hydrobromic acid (30 ml.) was treated as in a), affording IV (2.70 g.) as yellow needles, m. p. 170°C (decomp.).

c) The Heating of II in Alkali.—A solution of II (200 mg.) in a 2 N sodium hydroxide solution (3 ml.) was heated for 5 hr. The mixture was then acidified with 6 N hydrochloric acid and continuously extracted with ether for 5 hr., affording IV (100 mg.) as pale yellow needles, m. p. 170°C (decomp.).

3-Methyltropolone (V).—A mixture of IV (5.00 g.) and pyridine (15 ml.) was heated under reflux for 3 hr. After the addition of water, the mixture was acidified with 6 N hydrochloric acid and extracted with chloroform. The solvent was evaporated, the residue was sublimed at 110~120°C under reduced pressure, and the sublimate was recrystallized from cyclohexane to give V (3.32 g.) as colorless plates, m. p. 49~50°C, which showed

8) All melting points are uncorrected.

no depression of melting point on admixture with an authentic specimen.[8]

3-Ethoxycarbonyl-8-acetoxy-1-oxaazulan-2-one (VIa).—A mixture of II (1.00 g.) and acetic anhydride (2.5 ml.) was heated at 140°C for 1 hr. Water was added, and the crystals thereby formed were collected and recrystallized from ethanol to give VIa (1.00 g.) as yellow needles, m. p. 135~136°C.

λ_{max}^{MeOH} mμ (log ε); 223 (4.33), 265 (4.34), 402 (4.29).

Found: C, 60.91; H, 4.71. Calcd. for $C_{14}H_{12}O_6$: C, 60.87; H, 4.38%.

The heating of VIa in concentrated hydrobromic acid at 140°C for 1 hr. gave IV.

3-Acetyl-8-acetoxy-1-oxaazulan-2-one (VIb).—A mixture of III (1.00 g.) and acetic anhydride (1 ml.) was treated as described in the above experiment, affording VIb (1.00 g.) as orangish yellow needles, m. p. 168~169°C, after recrystallization from ethanol.

λ_{max}^{MeOH} mμ (log ε); 225 (4.47), 277 (4.41), 416 (4.38).

Found: C, 63.67; H, 4.05. Calcd. for $C_{13}H_{10}O_5$: C, 63.41; H, 4.09%.

3-Ethoxycarbonyl-8-methoxy-1-oxaazulan-2-one (VIIa).—Into a suspension of II (460 mg.) in ethyl acetate (10 ml.), an ethereal solution of diazomethane (3.5 ml.) was stirred while it was being cooled. The mixture was then stirred for 10 hr., and the crystals thereby formed were collected and recrystallized from ethanol to give VIIa (310 mg.) as yellow needles, m. p. 142~143°C.

λ_{max}^{MeOH} mμ (log ε); 225 (4.38), 295 (4.43), 392 (4.31).

Found: C, 62.83; H, 4.87. Calcd. for $C_{13}H_{12}O_5$: C, 62.90; H, 4.87%.

The heating of VIIa in concentrated hydrobromic acid at 140°C for 1 hr. gave V.

3-Acetyl-8-methoxy-1-oxaazulan-2-one (VIIb).—III (410 mg.) was treated with diazomethane as described in the above experiment, affording VIIb (320 mg.) as orangish yellow needles, m. p. 231~232°C (decomp.) after recrystallization from ethanol.

λ_{max}^{MeOH} mμ (log ε); 228 (4.39), 258 (4.08), 300 (4.47), 404 (4.35).

Found: C, 66.02; H, 4.68; OCH_3, 14.21. Calcd. for $C_{12}H_{10}O_4$: C, 66.05; H, 4.62; OCH_3, 14.05%.

8-Hydroxy-1-oxaazulan-2-one (VIII).—A solution of IV (400 mg.) in concentrated sulfuric acid (1 ml.) was poured into ice-water to give VIII (220 mg.), m. p. 220°C (decomp.). Recrystallization from a mixture of dioxane and dimethylformamide gave orangish yellow prisms, m. p. 223°C (decomp.).

λ_{max}^{MeOH} mμ (log ε); 220 (4.16), 275 (4.17), 285 (4.18), 305 (3.62), 380 (4.09).

Found: C, 66.41; H, 3.87. Calcd. for $C_9H_6O_3$: C, 66.67; H, 3.73%.

8-Acetoxy-1-oxaazulan-2-one (IX).—*a) From IV.*—A mixture of IV (1.00 g.) and acetic anhydride (2 ml.) was heated at 140°C for 2 hr. After the addition of water (30 ml.), the mixture was extracted with benzene and the benzene solution was passed through a short column of silica gel, affording IX (930 mg.), m. p. 140~150°C. Recrystallization from methanol gave orange prisms or needles, m. p. 151~152°C.

λ_{max}^{MeOH} mμ (log ε); 257 (4.30), 369 (4.14), 387 (4.14).

Found: C, 64.63; H, 4.00. Calcd. for $C_{11}H_8O_4$: C, 64.70; H, 3.95%.

The heating of IX in concentrated hydrobromic acid at 140°C for 1 hr. gave IV.

b) From VIII.—A mixture of VIII (100 mg.) and acetic anhydride (0.5 ml.) was treated as in a), affording IX (100 mg.), m. p. 151~152°C.

3-Ethoxycarbonyl-7-methyl-8-hydroxy-1-oxaazulan-2-one (XIIa).—To a solution of diethyl sodiomalonate prepared by dissolving sodium (600 mg.) in a mixture of dioxane (10 ml.) and diethyl malonate (6 ml.), 3-bromo-7-methyltropolone (X) (1.07 g.) and copper acetate (50 mg.) were added; the mixture was then heated under refluxing for 15 hr. The reaction mixture was diluted with water and acidified with 6 N hydrochloric acid. The crystals thereby formed were collected and recrystallized from acetone to give XIIa (1.02 g.) as yellow silky needles, m. p. 201°C (decomp.).

λ_{max}^{MeOH} mμ (log ε); 227 (4.29), 295 (4.46), 355 (4.13).

Found: C, 63.08; H, 4.88. Calcd. for $C_{13}H_{12}O_5$: C, 62.90; H, 4.87%.

Acetate: m. p. 146~147°C, yellow needles (from methanol).

λ_{max}^{MeOH} mμ (log ε); 230 (4.43), 267 (4.40), 408 (4.40).

Found: C, 62.12; H, 4.83. Calcd. for $C_{15}H_{14}O_6$: C, 62.06; H, 4.86%.

3-Ethoxycarbonyl-6-isopropyl-8-hydroxy-1-oxaazulan-2-one (XIIb).—To a solution of diethyl sodiomalonate prepared by dissolving sodium (3.0 g.) in a mixture of dioxane (40 ml.) and diethyl malonate (25 ml.), 3-bromo-6-isopropyltropolone (XI) (6.0 g.) and copper acetate (100 mg.) were added; the mixture was then heated under refluxing for 15 hr. The reaction mixture was treated as described in the above experiment to give XIIb (5.28 g.) as yellow needles, m. p. 214~215°C, after recrystallization from acetone.

λ_{max}^{MeOH} mμ (log ε); 230 (4.46), 290 (4.50), 355 (4.26).

Found: C, 65.47; H, 5.72. Calcd. for $C_{15}H_{16}O_5$: C, 65.21; H, 5.84%.

Acetate: m. p. 116~117°C, yellow needles (from methanol).

λ_{max}^{MeOH} mμ (log ε); 230 (4.43), 270 (4.34), 410 (4.38).

Found: C, 64.26; H, 5.61. Calcd. for $C_{17}H_{18}O_6$: C, 64.14; H, 5.70%.

3-Acetyl-7-methyl-8-hydroxy-1-oxaazulan-2-one (XIIIa).—To a solution of ethyl sodioacetoacetate prepared by dissolving sodium (600 mg.) in a mixture of dioxane (10 ml.) and ethyl acetoacetate (5 ml.), X (1.07 g.) and copper acetate (50 mg.) were added; the mixture was then heated under refluxing for 20 hr. The reaction mixture was treated as described in the above experiment to give XIIIa (980 mg.) as yellow silky needles, m. p.

265°C (decomp.), after recrystallization from acetone.

λ_{max}^{MeOH} mμ (log ε); 225 (4.25), 295 (4.41), 362 (4.12).

Found: C, 66.19; H, 5.12. Calcd. for $C_{12}H_{10}O_4$: C, 66.05; H, 4.62%.

Acetate: m. p. 200~201°C, orange prisms (from methanol).

λ_{max}^{MeOH} mμ (log ε); 230 (4.37), 275 (4.25), 421 (4.30).

Found: C, 64.74; H, 4.56. Calcd. for $C_{14}H_{12}O_5$: C, 64.61; H, 4.65%.

3-Acetyl-6-isopropyl-8-hydroxy-1-oxaazulan-2-one (XIIIb).—To a solution of ethyl sodioacetoacetate prepared by dissolving sodium (3.0 g.) in a mixture of dioxane (40 ml.) and ethyl acetoacetate (22 ml.), XI (6.0 g.) and copper acetate (100 mg.) were added; the mixture was then heated under refluxing for 15 hr. The reaction mixture was treated as described in the above experiment to give XIIIb (5.60 g.) as yellow needles, m. p. 253°C (decomp.), after recrystallization from acetone.

λ_{max}^{MeOH} mμ (log ε); 230 (4.30), 293 (4.38), 367 (4.16).

Found: C, 68.31; H, 5.72. Calcd. for $C_{14}H_{14}O_4$: C, 68.20; H, 5.73%.

Acetate: m. p. 105~106°C, yellow needles (from methanol).

λ_{max}^{MeOH} mμ (log ε); 230 (4.43), 278 (4.33), 420 (4.39).

Found: C, 66.85; H, 5.39. Calcd. for $C_{16}H_{16}O_5$: C, 66.66; H, 5.59%.

5-Bromo-3-ethoxycarbonyl-7-methyl-8-hydroxy-1-oxaazulan-2-one (XV).—To a solution of diethyl sodiomalonate prepared from sodium (100 mg.), dioxane (4 ml.) and diethyl malonate (0.9 ml.), 5,7-dibromo-3-methyltropolone (XIV) (400 mg.) and copper acetate (50 mg.) were added; the mixture was then heated under refluxing for 20 hr. After the addition of water (5 ml.), the sodium salt thereby formed was collected, dissolved in hot water and acidified with 6 N hydrochloric acid to give XV (310 mg.) as yellow needles, m. p. 275°C (decomp.), after recrystallization from dioxane.

λ_{max}^{MeOH} mμ (log ε); 240 (4.36), 300 (4.49), 363 (4.14).

Found: C, 48.05; H, 3.54. Calcd. for $C_{13}H_{11}O_5Br$: C, 47.73; H, 3.39%.

The Debromination of XV.—When a solution of XV (160 mg.) and sodium acetate (100 mg.) in water (5 ml.), in the presence of palladium-carbon (10 mg.), was shaken with hydrogen, 13.3 ml. of hydrogen was absorbed during a 3.5 hr. period. The catalyst was then filtered off and the filtrate acidified with 6 N hydrochloric acid to give XIIa as yellow needles, m. p. 201°C (decomp.), after recrystallization from acetone.

3-Carboxymethyl-7-methyltropolone (XVIa).—*a) From XIIa.*—A mixture of XIIa (490 mg.) and concentrated hydrobromic acid (3 ml.) was heated at 130~140°C for 45 min. The reaction mixture was then diluted with water and adjusted to pH 3 with a potassium hydroxide solution, and the crystals thereby formed were collected and recrystallized from glacial acetic acid to give XVIa (360 mg.) as pale yellow needles, m. p. 177°C (decomp.).

λ_{max}^{MeOH} mμ (log ε); 242 (4.49), 320 (3.81), 355 (3.78), 370 (3.81).

Found: C, 61.97; H, 5.20. Calcd. for $C_{10}H_{10}O_4$: C, 61.85; H, 5.19%.

b) From XIIIa.—A mixture of XIIIa (320 mg.) and concentrated hydrobromic acid (3 ml.) was heated at 130~140°C for 2 hr.; the crystals thereby formed were collected by filtration to give dark green needles, m. p. over 300°C (110 mg.).

λ_{max}^{MeOH} mμ; 227, 312, 355, 450.

Found: C, 57.91; H, 3.76%.

The filtrate was adjusted to pH 3 with a potassium hydroxide solution, affording XVIa (160 mg.) as yellow needles, m. p. 177°C (decomp.), after recrystallization from glacial acetic acid.

3-Carboxymethyl-6-isopropyltropolone (XVIb).—*a) From XIIb.*—A mixture of XIIb (500 mg.) and concentrated hydrobromic acid (6 ml.) was heated at 130~140°C for 2 hr. After it had cooled, the mixture was poured into water (20 ml,) to give XVIb (360 mg.), m. p. 158°C (decomp.). Recrystallization from chloroform afforded colorless needles, m. p. 160°C (decomp.).

λ_{max}^{MeOH} mμ (log ε); 245 (4.47), 335 (3.84), 368 (3.81).

Found: C, 64.50; H, 6.23. Calcd. for $C_{12}H_{14}O_4$: C, 64.85; H, 6.35%.

b) From XIIIb.—A mixture of XIIIb (500 mg.) and concentrated hydrobromic acid (6 ml.) was treated as in a), affording XVIb (340 mg.) as colorless needles, m. p. 160°C (decomp.), after recrystallization from chloroform.

3,7-Dimethyltropolone (XVIIa).—A mixture of XVIa (200 mg.) and pyridine (2 ml.) was heated under refluxing for 6 hr. After the addition of water (5 ml.), the mixture was acidified with 6 N hydrochloric acid and extracted with chloroform. The solvent was evaporated, the residue was sublimed at about 100°C under reduced pressure, and the sublimate was recrystallized from petroleum ether to give XVIIa (80 mg.) as colorless plates, m. p. 68~70°C, which was undepressed on admixture with an authentic specimen.[3]

λ_{max}^{MeOH} mμ (log ε); 243 (4.53), 320 (3.79), 355 (3.77), 370 (3.81).

6-Isopropyl-3-methyltropolone (XVIIb).—A mixture of XVIb (500 mg.) and pyridine (1 ml.) was heated under refluxing for 5 hr. After the addition of water (5 ml.), the mixture was acidified with 6 N hydrochloric acid and extracted with chloroform. The removal of the solvent left an oil, which was then distilled under reduced pressure to give XVIIb (330 mg.) as a pale yellow oil. The *p*-tolylazo derivative of this oil showed no depression of melting point on admixture with the known 5-(*p*-tolylazo)-6-isopropyl-3-methyltropolone.[3]

5-Bromo-3,7-dimethyltropolone (XVIII).—To a solution of XVIIa (30 mg.) in methanol (2 ml.), bromine (30 mg.) was added; the mixture was then stirred for 2 hr. Water was added, and the crystals thereby formed were recrystallized from methanol to give XVIII (40 mg.) as colorless plates, m. p. 136~137°C.

λ_{max}^{MeOH} mμ (log ε) ; 245 (4.48), 330 (3.97), 368 (3.64), 387 (3.64).

Found : C, 47.51 ; H, 4.14. Calcd. for $C_9H_9O_2Br$: C, 47.19 ; H, 3.96%.

7-Methyl-8-acetoxy-1-oxaazulan-2-one (XIXa).—A mixture of XVIa (120 mg.) and acetic anhydride (0.4 ml.) was heated at 140°C for 2 hr. Water was added, and the crystals thereby formed were recrystallized from methanol to give XIXa (120 mg.) as orange prisms, m. p. 127~128°C.

λ_{max}^{MeOH} mμ (log ε) ; 228 (4.31), 257 (4.35), 392 (4.22).

Found : C, 66.00 ; H, 5.08. Calcd. for $C_{12}H_{10}O_4$: C, 66.05 ; H, 4.62%.

6-Isopropyl-8-acetoxy-1-oxaazulan-2-one (XIXb).—A mixture of XVIb (1.00 g.) and acetic anhydride (2 ml.) was treated as described in the above experiment to give XIXb (880 mg.) as orange prisms, m. p. 101~102°C, after recrystallization from methanol.

λ_{max}^{MeHO} mμ (log ε) ; 228 (4.23), 255 (4.29), 373 (4.22), 388 (4.23).

Found : C, 68.47 ; H, 5.56. Calcd. for $C_{14}H_{14}O_4$: C, 68.27 ; H, 5.73%.

The author wishes to express his gratitude to Professor Tetsuo Nozoe for his kind and unfailing guidance throughout the course of this work. He is also indebted to Messrs. Masaru Ogata and Hiromoto Ishiyama for their technical cooperation, and to Miss Ayako Iwanaga for her elementary analyses.

Department of Chemistry
Faculty of Science
Tohoku University
Katahira-cho, Sendai

*Syntheses of Peptides Related to the N-Terminal Structure of Corticotropin. III. The Synthesis of L-Histidyl-L-phenylalanyl-L-arginyl-L-tryptophan, the Smallest Peptide Exhibiting the Melanocyte-stimulating and the Lipolytic Activities**

By Hideo OTSUKA and Ken INOUYE

(Received April 13, 1964)

This investigation was undertaken to find out the minimum structure required for the two extra-adrenal activities of corticotropin as a melanocyte-stimulating hormone (MSH) and a lipolytic agent.

There have been reports on the relationship between these hormonal activities and the chemical structure. Hofmann and Yajima,[1] for instance, concluded from their synthetic studies that two things were essential for the MSH activity, the sequence His-Phe-Arg-Try-Gly (positions 6 to 10) in the corticotropin and in the α-MSH molecules and the presence of the histidine and the tryptophan residues at their respective positions. Pickering and Li[2] reached the same conclusion from their studies of synthetic peptides.

Concerning the activity as lipolytic or adipokinetic agents, Raben et al.[3] first reported that a peptide, H-Ser-Tyr-Ser-Met-Glu(NH_2)-His-Phe-Arg-OH, which corresponded to the γ-amide derivative of the *N*-terminal octapeptide sequence of the corticotropin and α-MSH molecules, was inactive, when it was lengthened at the carboxyl end to a decapeptide, H-Ser-Tyr-Ser-Met-Glu-His-Phe-Arg-Try-Gly-OH, the activity was encountered. Tanaka, Pickering and Li[4] also reported that the smallest peptide which was active in rat adipose tissue was the *N*-terminal decapeptide, whereas a pentapeptide, H-His-Phe-Arg-Try-Gly-OH, was still active in the rabbit.

It has not yet been examined whether or not the glycine next to the tryptophan (position 9) is essential to these activities. Therefore, we synthesized a tetrapeptide, L-histidyl-L-phenylalanyl-L-arginyl-L-tryptophan, and assayed it for MSH activity by the in vitro frog skin method.[5] It was found that the peptide exhibited the same level of potency

* A part of this work has been briefly communicated: H. Otsuka and K. Inouye, This Bulletin, **37**, 289 (1964).

1) K. Hofmann and H. Yajima, "Recent Progress in Hormone Research," Vol. 18, Academic Press Inc., New York (1962), p. 41.

2) B. T. Pickering and C. H. Li, *Biochim. Biophys. Acta*, **62**, 475 (1962).

3) M. S. Raben, Ruth Landolt, F. A. Smith, K. Hofmann and H. Yajima, *Nature*, **189**, 681 (1961).

4) A. Tanaka, B. T. Pickering and C. H. Li, *Arch. Biochem. Biophys.*, **99**, 294 (1962).

5) K. Shizume, A. B. Lerner and T. B. Fitzpatrick, *Endocrinology*, **54**, 553 (1954); A. B. Lerner and M. R. Wright, "Methods of Biochemical Analysis," Vol. 8, Interscience Publishers, New York (1960), p. 295.

(3.6×10^4 units per gram) as pentapeptides, L-histidyl-L-phenylalanyl-L-arginyl-L-tryptophyl-glycine[6,7] and its D-phenylalanine analog.[8] This may show that the glycine is not only not essential for the activity, but that it is not so stimulating, as is the case with a hexapeptide, H-Gly-His-Phe-Arg-Try-Gly-OH,[9] in which the *N*-terminal glycine shows a tenfold increase in potency as compared with the pentapeptide without the *N*-terminal glycine. The tetrapeptide was also active as a lipolytic agent at a dose of 1000 μg. in rabbit perirenal adipose tissue. This potency is comparable to that reported for the pentapeptide.[4] From this finding, it may be concluded that the glycine is not essential also for the lipolytic activity.

One of the difficulties in the synthesis of the tetrapeptide is that the tryptophan resides at the carboxyl end of the molecule. The saponification of the tryptophan ester was accompanied by the fission of the peptide bonds. We have failed also in an attempt to prepare the *t*-butyl ester of tryptophan which may be removed by a mild acid solvolysis. Therefore, it appeared most promising to employ the benzyl ester, which could be removed by means of catalytic or chemical reduction. In order to minimize the racemization which occurs during peptide synthesis, a step-by-step procedure, by which a peptide chain is extended from the carboxyl end, may be recommended. However, all the intermediate products that we have tried so far, namely, the various derivatives of N^G-tosyl(or nitro)-L-arginyl-L-tryptophan and L-phenylalanyl-N^G-tosyl(or nitro)-L-arginyl-L-tryptophan, failed to crystallize. Because of this disadvantage, it was very difficult to remove the impurities[10] which were produced during the repeated treatment of the tryptophan peptide in order to remove its amino-protecting group with such an acid reagent as hydrogen bromide-acetic acid or trifluoroacetic acid. Fortunately, we could obtain the hydrazide of *t*-butyloxycarbonyl-L-phenylalanyl-N^G-tosyl-L-arginine in a crystalline state. As is well known, the azide coupling procedure is free from racemization.[11] Therefore, the procedure for the synthesis of the tetrapeptide was designed as follows:

The crystalline N^G-tosyl-L-arginine methyl ester (III, free base) was coupled with *t*-butyloxycarbonyl-L-phenylalanine by the *N*, *N'*-dicyclohexylcarbodiimide (DCCI) method.[12] The resultant protected dipeptide (VII) was converted into the crystalline hydrazide (IX). The coupling of the azide (derived from compound IX) with L-tryptophan benzyl ester gave the protected tripeptide, *t*-butyloxycarbonyl-L-phenylalanyl-N^G-tosyl-L-arginyl-L-tryptophan benzyl ester (XI). The amino-protecting group of compound XI was removed by treatment with trifluoroacetic acid,[13] affording the tripeptide ester, L-phenylalanyl-N^G-tosyl-L-arginyl-L-tryptophan benzyl ester. This tripeptide ester was next condensed with N^α, N^{Im}-dicarbobenzoxy-L-histidine[14] by the DCCI procedure to obtain the protected tetrapeptide, N^α, N^{Im}-dicarbobenzoxy-L-histidyl-L-phenylalanyl-N^G-tosyl-L-arginyl-L-tryptophan benzyl ester (XII). Then, the reduction of compound XII in sodium in liquid ammonia was performed in order to remove all the protecting groups, namely, the two carbobenzoxy, one tosyl and one benzyl ester, groups. The resultant free tetrapeptide (XIII) was purified on a carboxymethyl cellulose column. The purified product was then submitted to paper chromatography in a solvent system consisting of *n*-butanol - acetic acid - water (4 : 1 : 2), and to electrophoresis on paper at pH 3.8, 6.6 and 11.1; these tests indicated that it behaves as a homogeneous substance. Moreover, the tetrapeptide obtained was found to be completely digestible by leucine aminopeptidase to give an amino acid composition in molar ratios which are consistent with the theoretical values.

The azide-coupling procedure has never before been employed when the nitroarginine residue has been included in the carboxyl moiety to be activated, because the nitroguanidino function may be decomposed by the action of hydrazine.[15] As is shown above, it is a valuable advantage that the N^G-tosyl-arginine is entirely free from this trouble. In the step of coupling Phe-Arg with Try for the preparation of compound XI, the DCCI method was also tried in place of the azide procedure, but the product had a low optical rotation ($[\alpha]_D^{25}$ $-4.4°$ (methanol)). This means that some racemization occurred in the arginine residue.

6) K. Hofmann, M. E. Woolner, H. Yajima, G. Spühler, T. A. Thompson and E. T. Schwartz, *J. Am. Chem. Soc.*, **80**, 6458 (1958).
7) R. Schwyzer and C. H. Li, *Nature*, **182**, 1669 (1958).
8) E. Schnabel and C. H. Li, *J. Am. Chem. Soc.*, **82**, 4576 (1960).
9) E. Schnabel and C. H. Li, *J. Biol. Chem.*, **235**, 2010 (1960).
10) D. M. Theodoropoulos and J. S. Fruton, *Biochemistry*, **1**, 933 (1962).
11) M. B. North and G. T. Young, *Chem. & Ind.*, **1955**, 1597; N. A. Smart, G. T. Young and M. W. Williams, *J. Chem. Soc.*, **1960**, 3902.
12) J. C. Sheehan and G. P. Hess, *J. Am. Chem. Soc.*, **77**, 1067 (1955).
13) H. Kappeler and R. Schwyzer, *Helv. Chim. Acta*, **43**, 1453 (1960).
14) K. Inouye and H. Otsuka, *J. Org. Chem.*, **27**, 4236 (1962).
15) J. S. Fruton, "Advances in Protein Chemistry," Vol. 5, Academic Press Inc., New York (1949), p. 1.

In connection with these studies, we have next achieved an improved synthesis of the tetrapeptide; this synthesis consists of the catalytic hydrogenation of a derivative with low solubility, N^{α}, N^{Im}-dicarbobenzoxy-L-histidyl-L-phenylalanyl-nitro-L-arginyl-L-tryptophan benzyl ester (m. p. 167~168°C decomp., $[\alpha]_D^{24.5}$ −12.3° (dimethylformamide)). This compound was obtained from crystalline N^{α}, N^{Im}-dicarbobenzoxy-L-histidine *p*-nitrophenyl ester (m. p. 112~113°C, $[\alpha]_D^{24.5}$ −15.0° (ethyl acetate))[16] and L-phenylalanyl-nitro-L-arginyl-L-tryptophan benzyl ester, which was synthesized in a step-by-step manner from the carboxyl end by the use of the *t*-butyloxycarbonyl group[19,20] as an amino-protecting element in conjugation with the DCCI procedure. This improved procedure for the synthesis of the protected tetrapeptide gave an over-all yield, based on L-tryptophan benzyl ester, of approximately 50%. The details of these experiments will be published elsewhere.

Experimental

All melting points are uncorrected.

N^{G}-Tosyl-L-arginine Monohydrate (I).—To 15 g. of crystalline N^{α}-carbobenzoxy-N^{G}-tosyl-L-arginine (m. p. 102~106°C),[21] 130 g. of 25% (w/w) hydrogen bromide in acetic acid was added; the mixture then stood at room temperature for 30 min., after which time the solvent was removed at 40~45°C in vacuo. The oily residue was dissolved in 60 ml. of water and shaken with 60 ml. of ethyl acetate. The aqueous layer was washed further with ethyl acetate, cooled in an ice-bath, and neutralized to pH 8.6~8.8 by the addition of 28% aqueous ammonia to separate colorless crystals. After refrigeration overnight, the crystals were collected, washed with cold water, and dried; yield, 10.33 g. (92.1%); m. p. 142~147°C. Recrystallization from water gave lustrous crystals; recovery 94%, m. p. 145~149°C, $[\alpha]_D^{23.5}$ −3.9±1° (*c* 2.435, methanol), $[\alpha]_D^{24}$ +18.1±0.8° (*c* 2.518, N HCl); lit.[21]: m. p. 146~150°C, $[\alpha]_D^{25}$ −5.5° (*c* 1.3, methanol).

Found: C, 45.36; H, 6.41; N, 16.46; S. 9.11; H_2O, 5.18. Calcd. for $C_{13}H_{20}O_4N_4S \cdot H_2O$: C, 45.07; H, 6.40; N, 16.17; S. 9.26; H_2O, 5.20%.

N^{α}-Carbobenzoxy-N^{G}-tosyl-L-arginine Methyl Ester (II).—To 50 ml. of anhydrous methanol which had previously been cooled below −10°C, 1.20 ml. (0.0165 mol.) of thionyl chloride and 6.93 g. (0.015 mol.) of N^{α}-carbobenzoxy-N^{G}-tosyl-L-arginine were added. The solution was stirred for 4 hr. and then let stand overnight at 0°C. After the removal of the solvent in vacuo the resulting sirup was dissolved in 50 ml. of ethyl acetate, washed with water, 5% sodium bicarbonate and with water, and dried over sodium sulfate. The evaporation of the solvent gave a foamy residue, which was then dried over phosphorus pentoxide in vacuo; yield, 6.59 g. (92.2%), colorless amorphous powder, $[\alpha]_D^{25.5}$ −8.7±0.4° (*c* 4.972, methanol). A single spot was visible in thin-layer chromatography on silica gel in ethyl acetate (R_f =0.43).

Found: C, 55.39; H, 6.36; N, 11.15; S, 6.28. Calcd. for $C_{22}H_{28}O_6N_4S$: C, 55.45; H, 5.92; N, 11.76; S. 6.73%.

N^{G}-Tosyl-L-arginine Methyl Ester (Free Base) (III).—Compound II (15.00 g.) was dissolved in 97 g. of 38% (w/w) hydrogen bromide in acetic acid, and the reaction mixture was allowed to stand at room temperature for 60 min. and evaporated in vacuo at 40~45°C. The residue was dissolved in 40 ml. of water and washed three times with 50 ml. portions of ethyl acetate to afford an aqueous solution of the ester hydrobromide, which gave a single ninhydrin reactive spot (R_f=0.63) on paper in the *n*-butanol-acetic acid-water (4:1:2) system.

To the aqueous solution of the hydrobromide obtained above, 60 ml. of methylene chloride was added, the mixture was then shaken with 30 ml. of ice-cold 50% (w/v) potassium carbonate at 0°C. The aqueous phase was extracted again with methylene chloride, and the combined extract was dried over anhydrous sodium sulfate and evaporated in vacuo at 30°C to afford a gummy residue, which crystallized upon being dissolved in a small volume of methylene chloride. After the addition of ether, the mixture was refrigerated overnight and the crystals were filtered off, washed with ether and dried; yield, 9.71 g. (94.6% based on compound II used); m.p. 97°C (soften over 93°C). Recrystallization from the same solvent gave a sample for analyses; m. p. 98.5°C (soften over 95°C), $[\alpha]_D^{25}$ +14.8±1° (*c* 2.424, methanol).

Found: C, 48.78; H, 6.48; N, 15.92; S, 9.66. Calcd. for $C_{14}H_{22}O_4N_4S$: C, 49.11; H, 6.48; N, 16.36; S, 9.36%.

***t*-Butyloxycarbonyl-L-phenylalanine Dicyclohexylamine Salt (VI).**—*By t-Butyl p-Nitrophenyl Carbonate.*[19]—The free acid was synthesized by almost the same procedure as that described by Anderson and McGregor.[19] The product was ultimately crystallized from ethyl acetate and a large volume of petroleum ether as colorless fine needles. Since the isolation of the crystals was rather troublesome, the product was isolated and estimated as dicyclohexylamine salt.[22]

To an ethereal solution of the sirupy product (4.72 g.), which was obtained from 3.30 g. (0.02 mol.) of L-phenylalanine and 7.18 g. (0.03 mol.) of *t*-butyl *p*-nitrophenyl carbonate, a solution of 3.23 g. (0.018 mol.) of dicyclohexylamine (DCHA) in ether was added at 0°C. The DCHA salt which

16) Lit.: m. p. 86~90°C,[17] 109~110°C;[18] the optical rotation was not given.
17) F. Sakiyama, This Bulletin, **35**, 1943 (1962).
18) J. Meienhofer, *Chimia*, **16**, 385 (1962).
19) G. W. Anderson and A. C. McGregor, *J. Am. Chem. Soc.*, **79**, 6180 (1957).
20) L. A. Carpino, ibid., **79**, 98 (1957); L. A. Carpino, C. A. Giza and B. A. Carpino, ibid., **81**, 955 (1959).
21) J. Ramachandran and C. H. Li, *J. Org. Chem.*, **27**, 4006 (1962).
22) E. Klieger, E. Schröder and H. Gibian, *Liebigs Ann. Chem.*, **640**, 157 (1961); F. Weygand and K. Hunger, *Z. Naturforsch.*, **13b**, 50 (1958); *Chem. Abstr.*, **52**, 10880 (1958).

separated soon was filtered off, washed with ether, and dried; yield, 7.86 g. (88.0% based on L-phenylalanine used); m. p. 209~214°C decomp., $[\alpha]_D^{27}$ +29.2±2° (*c* 1.025, methanol).

Found: C, 70.13; H, 9.67; N, 6.36. Calcd. for $C_{26}H_{42}O_4N_2$: C, 69.92; H, 9.48; N, 6.27%.

By t-Butyl Azidoformate.[20]—The amorphous free acid, which was obtained by the method of Schwyzer et al.[23] from 8.3 g. (0.05 mol.) of L-phenylalanine and 14.3 g. (0.10 mol.) of *t*-butyl azidoformate,[24] was converted into the DCHA salt as described above; yield, 17.43 g. (78.2% based on L-phenylalanine used); m. p. 210~212°C decomp., $[\alpha]_D^{25.5}$ +28.9±0.5° (*c* 1.048, methanol).

Found: C, 71.09; H, 9.70; N, 6.37. Calcd. for $C_{26}H_{42}O_4N_2$: C, 69.92; H, 9.48; N, 6.27%.

L-Tryptophan Methyl Ester (V).—*L-Tryptophan Methyl Ester Acetate.*—A crude sample of L-tryptophan methyl ester hydrochloride[25] was converted into the acetate for purification. A mixture of the hydrochloride dissolved in a small volume of water and ether was shaken with 50% (w/v) potassium carbonate at 0°C. The ether phase was dried over sodium sulfate, to which an appropriate amount of glacial acetic acid was added to separate L-tryptophan methyl ester acetate as colorless thin needles; m. p. 106~108°C, $[\alpha]_D^{24.5}$ +15.3±1° (*c* 2.615, water).

Found: C, 60.50; H, 6.67; N, 10.09: Calcd. for $C_{12}H_{14}O_2N_2 \cdot CH_3COOH$: C, 60.42; H, 6.52; N, 10.07%.

Free Ester (V).—A suspension of 1.67 g. (6.0 mmol.) of the ester acetate obtained above in 20 ml. of methylene chloride was shaken with 5 ml. of ice-cold 50% (w/v) potassium carbonate in an ice-salt bath. The aqueous phase was then extracted again with methylene chloride. The combined organic extract was, after having been dried over sodium sulfate, evaporated at 25°C in vacuo to afford a sirupy residue, which crystallized easily from ether-petroleum ether; yield, 1.28 g. (97.8%); m. p. 90~91°C, $[\alpha]_D^{23.5}$ +36.3±1° (*c* 2.577, methanol).

Found: C, 66.12; H, 6.54; N, 12.92. Calcd. for $C_{12}H_{14}O_2N_2$: C, 66.04; H, 6.47; N, 12.84%.

L-Tryptophan Benzyl Ester (VI).—*L-Tryptophan Benzyl Ester p-Toluenesulfonate.*—A mixture of 20.42 g. (0.1 mol.) of L-tryptophan and 20.9 g. (0.11 mol.) of *p*-toluenesulfonic acid monohydrate in 150 ml. of benzyl alcohol was stirred at 90~100°C under a slow stream of nitrogen. After 6 hr. anhydrous ether (750 ml.) was introduced, and the precipitates (the salt of unesterified tryptophan) was filtered off (14.94 g.). From the filtrate the crystalline *p*-toluenesulfonate of the benzyl ester separated slowly in the form of needles; yield, 25.15 g.; m. p. 171~173°C.

Found: C, 64.59; H, 5.73; N, 6.22. Calcd. for $C_{25}H_{26}O_5N_2S$: C, 64.36; H, 5.62; N, 6.00%.

Free Ester (VI).—To 3.50 g. (7.5 mmol.) of the *p*-toluenesulfonate obtained above, 10 ml. of water and 30 ml. of ether were added. The mixture was then shaken with 10 ml. of 50% (w/v) potassium carbonate. The aqueous phase was extracted again with ether. The combined extract was dried over sodium sulfate and evaporated in vacuo to give a solid residue, which was then recrystallized from ether-petroleum ether; yield, 1.97 g. (89.4%); m. p. 71°C, $[\alpha]_D^{26.5}$ +12.8±1° (*c* 2.067, methanol); lit.[26] m. p. 71~72°C.

Found: C, 73.47; H, 6.22; N, 9.63. Calcd. for $C_{18}H_{18}O_2N_2$: C, 73.45; H, 6.16; N, 9.52%.

***t*-Butyloxycarbonyl-L-phenylalanyl-N^G-tosyl-L-arginine Methyl Ester (VII).**—To a suspension of 3.125 g. (7.0 mmol.) of compound IV in 70 ml. of 50% ethanol, 7 ml. (wet volume) of Dowex-50W×8 (H^+-form) was added; the mixture was then shaken at room temperature for 30 min. After the removal of the resin, the filtrate was evaporated in vacuo at 40~45°C. The resulting sirup was dissolved in ether, and the solution was, after having been dried over anhydrous sodium sulfate, evaporated again to obtain *t*-butyloxycarbonyl-L-phenylalanine in an essentially quantitative yield.

The acyl amino acid obtained above was dissolved in methylene chloride; to the mixture 2.40 g. (7.0 mmol.) of compound V and a methylene chloride solution of 1.45 g. (7.0 mmol.) of *N*, *N'*-dicyclohexylcarbodiimide (DCCI) were then added at 0°. The reaction mixture (total volume 25 ml.) was let stand at 0°C overnight and then filtered to remove the separated urea (1.49 g., 95.2%). The filtrate was evaporated to afford a sirupy residue, which was redissolved in 40 ml. of ethyl acetate, washed successively with ice-cold N hydrochloric acid, water, 5% sodium bicarbonate, water and finally with saturated sodium chloride, and dried over anhydrous sodium sulfate. After the removal of the solvent, the residue was dissolved in 7 to 8 ml. of acetonitrile, cooled at 0°C for 30 min., and then filtered to remove a slight amount of the urea. The evaporation of the solvent gave a foamy residue which was dried over phosphorous pentoxide; yield, 4.13 g. (100%); m. p. 93~98°C, $[\alpha]_D^{25}$ −5.9±0.5° (*c* 4.647, methanol). Thin-layer chromatography on silica gel in ethyl acetate gave a single spot reactive to ninhydrin when previously treated with concentrated hydrochloric acid.

Found: C, 56.78; H, 7.01; N, 11.82; S. 5.55. Calcd. for $C_{28}H_{39}O_7N_5S$: C, 57.03; H, 6.67; N, 11.88; S, 5.44%.

***t*-Butyloxycarbonyl-L-phenylalanyl-N^G-tosyl-L-arginine (VIII).**—To a solution of 3.245 g. (5.5 mmol.) of compound VII in 16 ml. of methanol, 5.5 ml. of 2 N sodium hydroxide was added. The mixture was shaken at room temperature for 30 min. and then neutralized at 0°C by the addition of 11.0 ml. of ice-cold N hydrochloric acid and 20 ml. of water. The product thus precipitated was extracted three times with ethyl acetate. The combined organic phase was washed twice with

23) R. Schwyzer, P. Sieber and H. Kappeler, *Helv. Chim. Acta*, **42**, 2662 (1959).

24) *t*-Butyl carbazate, the key intermediate to the azide, was also easily obtained from *t*-butyl *p*-nitrophenyl carbonate[19] in a 90% yield.

25) R. A. Boissonnas, St. Guttmann, R. L. Huguenin, P.-A. Jaquenoud and Ed. Sandrin, *Helv. Chim. Acta*, **41**, 1867 (1958).

26) M. Brenner and W. Huber, ibid., **36**, 1109 (1953).

water and shaken with 15 ml. of M sodium bicarbonate and twice with water. The aqueous extracts were combined, washed three times with ethyl acetate, and then acidified at 0°C with ice-cold 4 N hydrochloric acid in the presence of 30 ml. of ethyl acetate. The aqueous phase was extracted twice with ethyl acetate. The combined ethyl acetate solution was washed once with ice-cold N hydrochloric acid and once with water until the washing became almost neutral; it was then dried over sodium sulfate and evaporated in vacuo at 30°C to afford a colorless, foamy residue which was dried over phosphorus pentoxide; yield, 3.05 g. (96.4%); m. p. 100~110°C, $[\alpha]_D^{24}$ +1.0±0.5° (*c* 4.226, methanol). A sample was treated with an-anhydrous trifluoroacetic acid at room temperature for 60 min. and then chromatographed on paper in the *n*-butanol - acetic acid - water (4 : 1 : 2) system to give a single ninhydrin reactive spot with R_f =0.80.

Found: C, 56.04; H, 6.78; N, 11.43; S. 5.81. Calcd. for $C_{27}H_{37}O_7N_5S$: C, 56.33; H, 6.48; N, 12.17; S, 5.57%.

***t*-Butyloxycarbonyl-L-phenylalanyl-N^G-tosyl-L-arginine Hydrazide (IX).**—Compound VII (4.86 g., 8.25 mmol.) was dissolved in 48 ml. of anhydrous ethanol, and then 4.05 ml. of hydrazine hydrate was added at 0°C. The mixture was allowed to stand at 0°C for 3 days and then, after the addition of 50 ml. of water, concentrated to about 40 ml. in vacuo at 40°C. The sirupy precipitate was extracted three times with ethyl acetate, and the organic extracts were combined, washed twice, with water and with saturated sodium chloride, and dried over sodium sulfate. The crystalline hydrazide, which separated during the concentration of the ethyl acetate solution, was collected, washed twice with ice-cold ethyl acetate, and dried; yield, 4.58 g. (94.1%); m. p. 110~114°C. Recrystallization from methanol - ethyl acetate did not alter the melting point; $[\alpha]_D^{24}$ −6.3±1° (*c* 2.440, methanol).

Found: C, 55.22; H, 7.19; N, 16.61; S, 5.50. Calcd. for $C_{27}H_{39}O_6N_7S$: C, 54.99; H, 6.67; N, 16.63; S, 5.44%.

***t*-Butyloxycarbonyl-L-phenylalanyl-N^G-tosyl-L-arginyl-L-tryptophan Methyl Ester (X).**—*A) By the Carbodiimide Method.*—Compound VIII (2.88 g., 5.0 mmol.) and 1.09 g. (5.0 mmol.) of L-tryptophan methyl ester (V) were dissolved in 15 ml. of acetonitrile; to this solution was added under ice-cooling 1.03 g. (5.0 mmol.) of DCCI dissolved in a small volume of acetonitrile. The reaction mixture was then allowed to stand at 0°C overnight. After the removal of the separated urea (1.04 g., 92.5%), the filtrate was evaporated in vacuo at 35°C. The resulting sirupy residue was dissolved in 30 ml. of ethyl acetate, and the solution was washed with ice-cold N hydrochloric acid, water, 5% sodium bicarbonate, and water, and dried over anhydrous sodium sulfate. The evaporation of the solvent gave a foamy residue which was dried over phosphorus pentoxide in vacuo; yield, 3.68 g. (94.8%). The crude acyltripeptide ester (1.20 g.) obtained above was dissolved in 10 ml. of ethyl acetate, and the solution was passed through a column of dry silica gel (about 200 g.) with more ethyl acetate. The 3 ml.-fractions were collected, and those of tube Nos. 41—146, which contained the desired compound, were pooled and evaporated to dryness in vacuo to give an amorphous solid; wt. 0.86 g. (recovery 71.5%), m. p. 110~120°C, $[\alpha]_D^{25}$ −3.4±0.5° (*c* 4.546, methanol). Thin-layer chromatography on silica gel in ethyl acetate gave a single Ehrlich reactive spot. The single spot was also visible when the plate was heated after having been treated with sulfuric acid.

Found: C, 60.13; H, 6.66; N, 12.03; S, 4.33. Calcd. for $C_{39}H_{49}O_8N_7S$: C, 60.37; H, 6.37; N, 12.64; S, 4.13%.

B) By the Azide Method.—To a solution of 2.95 g. (5.0 mmol.) of compound IX in dimethylformamide (12 ml.), which had previously been cooled below −10°C, 25 ml. of ice-cold N hydrochloric acid and 2.75 ml. of ice-cold 2M sodium nitrite were added; the mixture was then stirred at −10°C for three min., after which time 20 ml. of ice-cold saturated sodium chloride was introduced. The separated azide was then extracted three times with 20 ml.-portions of cold ethyl acetate. The organic extract was washed with 20 ml. of ice-cold M sodium carbonate and 20 ml. of ice-cold saturated sodium chloride, and dried over anhydrous sodium sulfate. To this ethyl acetate solution 1.07 g. (4.85 mmol.) of L-tryptophan methyl ester (V) was then added, and the mixture was allowed to stand at 0°C. After 47 hr. the reaction mixture was washed with ice-cold N hydrochloric acid, water, 5% sodium bicarbonate, water and, finally, saturated sodium chloride, and dried over sodium sulfate. The evaporation of the solvent gave a foamy residue which was dried over phosphorus pentoxide in vacuo; yield, 3.41 g. (90.8%). The crude product obtained above was purified on a silica gel column in almost the same way as has been described in A) to afford 2.80 g. (recovery 82.2%) of the pure tripeptide derivative, which was homogeneous in thin-layer chromatography; m. p. 110~120°C $[\alpha]_D^{26}$ −3.2±0.5° (*c* 4.417, methanol).

Found: C, 59.31; H, 6.60; N, 12.08; S, 4.10. Calcd. for $C_{39}H_{49}O_8N_7S$: C, 60.37; H, 6.37; N, 12.64; S, 4.13%.

***t*-Butyloxycarbonyl-L-phenylalanyl-N^G-tosyl-L-arginyl-L-tryptophan Benzyl Ester (XI).**—*t*-Butyloxycarbonyl-L-phenylalanyl-N^G-tosyl-L-arginine azide (prepared from 2.95 g. (5.0 mmol.) of the hydrazide (IX) as described above) and 1.47 g. (5.0 mmol.) of L-tryptophan benzyl ester (VI) were coupled in a ethyl acetate solution, almost as in case of the corresponding methyl ester (X), to give 3.24 g. (76.2%) of the crude peptide. A 3.14 g.-sample of the crude product was purified on silica gel (150 g.) as in the case of compound X; wt., 2.70 g. (recovery 86%), $[\alpha]_D^{24.5}$ −6.6±0.5° (*c* 4.095, methanol).

Found: C, 63.31; H, 6.42; N, 11.12; S, 3.68. Calcd. for $C_{45}H_{53}O_8N_7S$: C, 63.44; H, 6.27; N, 11.51; S, 3.76%.

The carbodiimide procedure was also employed in coupling compound VIII with L-tryptophan

benzyl ester (VI), as in the case of compound X, to obtain the same tripeptide derivative. The product was homogeneous in chromatography, but it had a low optical rotation; $[\alpha]_D^{25}$ $-4.4\pm0.6°$ (*c* 2.428, methanol).

N^{α}, N^{Im}-Dicarbobenzoxy-L-histidyl-L-phenylalanyl-N^{G}-tosyl-L-arginyl-L-tryptophan Benzyl Ester (XII).—Compound XI (2.45 g., 2.88 mmol.) was dissolved in 7.0 ml. of anhydrous trifluoroacetic acid at 0°C, and the solution was let stand at room temperature for 1 hr. under nitrogen. To this solution was then introduced about 100 ml. of anhydrous ether under ice-cooling. The resulting precipitates were collected, washed thoroughly with anhydrous ether, and dried to give 2.34 g. (94.0%) of L-phenylalanyl-N^{G}-tosyl-L-arginyl-L-tryptophan benzyl ester trifluoroacetate.

The ester trifluoroacetate (0.866 g., 1.0 mmol.), which had been dissolved in 15 ml. of ethyl acetate, was shaken with 10 ml. of ice-cold 50% (w/v) potassium carbonate at 0°C. The organic phase was then washed with saturated sodium chloride, dried over sodium sulfate, and evaporated in vacuo at 30°C under nitrogen to afford a foamy residue (0.86 g.) The free tripeptide ester thus obtained was then dissolved in 10 ml. of acetonitrile, along with 0.423 g. (1.0 mmol.) of N^{α}, N^{Im}-dicarbobenzoxy-L-histidine.[14] To this solution was added 0.206 g. (1.0 mmol.) of DCCI dissolved in a small volume of acetonitrile; the mixture was allowed to stand at 0°C for 20 hr. After the separated urea had been removed by filtration, the filtrate was evaporated in vacuo at 35°C. The sirupy residue was redissolved in ethyl acetate, washed with ice-cold N hydrochloric acid, water, 5% sodium bicarbonate and water, and dried over sodium sulfate. The evaporation of the solvent gave an amorphous solid residue; yield, 1.15 g. (99.3%). The crude product (1.15 g.), which was dissolved in 10 ml. of ethyl acetate, was applied onto a column of silica gel (60 g.) which had been previously stabilized with ethyl acetate; it was then eluted with the same solvent. The fractions containing the desired compound were pooled and evaporated to afford an amorphous solid residue; wt. 0.81 g. (recovery 70%); m. p. 97~105°C, $[\alpha]_D^{24.5}$ $-10.9\pm1°$ (*c* 1.825, methanol). Thin-layer chromatography on silica gel in ethyl acetate gave a single spot, which was reactive to the Ehrlich but not to the Pauly reagent.

Found: C, 64.26; H, 5.85; N, 11.94; S, 2.97. Calcd. for $C_{62}H_{64}O_{11}N_{10}S$: C, 64.34; H, 5.57; N, 12.10; S, 2.77%.

L-Histidyl-L-phenylalanyl-L-arginyl-L-tryptophan Monoacetate Dihydrate (XIII).—The protected tetrapeptide XII (500 mg.) was dissolved in 170 ml. of liquid ammonia which had been distilled from sodium; small pieces of sodium were then added over an interval of 20~25 min. until a blue color persisted. After the addition of 0.18 ml. of acetic acid, most of the ammonia was allowed to evaporate spontaneously; the rest was removed in vacuo to dryness over an ice-bath. The residue was dissolved in 40 ml. of 0.1 N acetic acid, and the solution was filtered through a Celite pad to remove any insoluble precipitates. The filtrate was passed through an Amberlite CG-50 column (wet vol. 14 cc.) in order to desalt it.[27] The column was washed with 700 ml. of 0.25% acetic acid and 50 ml. of water, and the peptide was then eluted with a solution consisting of pyridine-acetic acid-water (30 : 4 : 66 by volume). The eluate was evaporated in vacuo at 45°C, and the residue was dissolved in about 10 ml. of 0.1 N acetic acid. The lyophilization of this solution gave the crude tetrapeptide; yield, 306 mg. (95.8%). The crude product (230 mg.) was dissolved in about 20 ml. of a 0.025 M ammonium acetate buffer (pH 6.45), and this solution was added to a column (1.33×43 cm.) of carboxymethyl cellulose (Serva, 0.6 meq./g.) which had been equilibrated with the same buffer. The column was then eluted successively with the following ammonium acetate buffers (pH 6.45): 0.025 M (250 ml.), 0.0375 M (700 ml.), 0.05 M (350 ml.), and 0.075 M (1050 ml.). Individual fractions (7.5 ml. each) were collected at a flow rate of approximately 2 ml. per min. Absorbancy measurements at 280 mμ revealed the presence of one major and at least four minor components in the chromatogram. The fractions corresponding to the major peak, which was eluted with the 0.075 M buffer at the end, were pooled, the bulk of water was removed in vacuo, and the rest was lyophilized repeatedly to a constant weight; wt., 122 mg. (50.8% based on the protected peptide). The purified sample behaved as a single ninhydrin, Pauly, Ehrlich and Sakaguchi reactive spot in paper chromatography in the *n*-butanol-acetic acid-water (4 : 1 : 2) system (R_f = 0.52~0.55), and in paper electrophoresis at pH 3.8, 6.6 and 11.1. λ_{max}^{HCl} 280.5 mμ (ε 5100), 288 mμ (ε 4250); $[\alpha]_D^{24.5}$ $-5.4\pm2°$ (*c* 0.947, N HCl). Amino acid ratios[28] in acid hydrolysate: His 1.00, Phe 1.00, Arg 1.03, (Try 0.79, decomposed partially with acid) (recovery 92.2%); amino acid ratios[28] in leucine aminopeptidase digest[29]: His 1.00, Phe 1.03, Arg 0.97, Try 0.98 (recovery 92.5%).

Found: C, 55.32; H, 6.71; N, 18.02. Calcd. for $C_{32}H_{40}O_5N_{10}\cdot CH_3COOH\cdot 2H_2O$: C, 55.12; H, 6.53; N, 18.91%.

Summary

1) A tetrapeptide, L-histidyl-L-phenylalanyl-L-arginyl-L-tryptophan, corresponding to the amino-acid sequence of positions 6 to 9 in the corticotropin and α-MSH molecules has been synthesized.

2) This synthetic tetrapeptide has been found to exhibit an MSH potency of 3.6×10^4 units per gram in the in vitro frog skin assay, and it is also active on lipolysis in rabbit perirenal adipose tissue. These results may confirm that the glycine at position 10

27) C. H. Li, J. Meienhofer, E. Schnabel, D. Chung, T-b. Lo and J. Ramachandran, *J. Am. Chem. Soc.*, **83**, 4449 (1961).

28) D. H. Spackman, W. H. Stein and S. Moore, *Anal. Chem.*, **30**, 1191 (1958).

29) LAP Lot No. 5930, Worthington Biochemical Corporation, Freehold, New Jersey, U. S. A.

in the molecules of corticotropin and α-MSH is not essential for these biological activities.

3) It has been shown that the azide-couling procedure can be employed successfully for the synthesis of arginyl peptides provided it is used in combination with the N^G-tosyl-arginine.

4) The preparation of N^G-tosyl-L-arginine and some of the relevant compounds has been described.

The authors wish to express their sincere thanks to Professor Choh Hao Li, Hormone Research Laboratory, University of California, for his courtesy in supplying a standard preparation of α-MSH. The authors are also indebted to Dr. Akira Tanaka for his assay of the lipolytic activity, Dr. Mitsuo Ebata for his amino acid analyses, Dr. Kaoru Kuriyama for his optical rotation measurements, Dr. Satoshi Mizukami for his elementary microanalyses, and Miss Yoshiko Jono and Mr. Makoto Kanayama for their able technical assistance.

Biochemistry Division
Shionogi Research Laboratory
Shionogi & Co., Ltd.
Fukushima-ku, Osaka

Syntheses of Peptides Related to the N-Terminal Structure of Corticotropin. IV. The Synthesis of the Amino Acid Sequences, Lys-Pro-Val-Gly and Lys-Pro-Val-Gly-Lys

By Hideo OTSUKA, Ken INOUYE and Yoshiko JONO

(Received May 29, 1964)

In the course of our synthetic studies of corticotropin peptides, the tetra- and penta-peptide derivatives, which have amino acid sequences corresponding to positions 11 to 14 and 11 to 15 respectively of the corticotropin molecule, have been obtained. The ε-amino function of the lysine residues, which were incorporated in these peptides, was protected by the introduction of the *t*-butyloxycarbonyl group after the procedure described by Schwyzer and Rittel.[1] In the coupling steps throughout the synthesis, the *N*,*N'*-dicyclohexylcarbodiimide (DCCI) method[2] was used in combination with the carbobenzoxy-protecting group for α-amino functions. Both of these peptides were built up in a step-by-step procedure from their carboxyl terminals, and at the same time alternative routes of preparing the tripeptide intermediates were also tried. The details of these syntheses will be described in this paper. Synthetic procedures were summarized in Figs. 1 and 2.

The Synthesis of the Lys-Pro-Val-Gly-Lys Sequence.—N^{ε}-*t*-Butyloxycarbonyl-L-lysine[1] was converted as usual into N^{α}-carbobenzoxy-N^{ε}-*t*-butyloxycarbonyl-L-lysine, which was isolated in the form of the crystalline dicyclohexylamine salt (I). The free acid from compound I was then treated with diazomethane to prepare the diacyl-L-lysine methyl ester (II), which was obtained in a crystalline state (m. p. 62~63°C). The catalytic hydrogenation of compound II in methanol containing acetic acid gave crystalline N^{ε}-*t*-butyloxycarbonyl-L-lysine methyl ester acetate (III). The free ester derived from compound III was coupled with carbobenzoxyglycine to obtain carbobenzoxyglycyl-N^{ε}-*t*-butyloxycarbonyl-L-lysine methyl ester (IV). Compound IV was hydrogenated, and the resultant dipeptide ester was condensed with carbobenzoxy-L-valine, thus affording carbobenzoxy-L-valylglycyl-N^{ε}-*t*-butyloxycarbonyl-L-lysine methyl ester (VII). The prolonged hydrogenation of compound IV yielded a large amount of a diketopiperazine like side product, even in the presence of excess acetic acid. The coupling of carbobenzoxy-L-proline with the hydrogenation product of compound VII gave a tetrapeptide derivative, carbobenzoxy-L-prolyl-L-valylglycyl-N^{ε}-*t*-butyloxycarbonyl-L-lysine methyl ester (VIII). The crystalline tetrapeptide ester (free base) (IX) was yielded by the catalytic hydrogenation of compound VIII. The hydrogenation was accelerated considerably by the addition of acetic acid; otherwise it proceeded very slowly. Compound VIII was then united with the free acid from compound I to obtain the crystalline

1) R. Schwyzer and W. Rittel, *Helv. Chim. Acta*, **44**, 159 (1961).
2) J. C. Sheehan and G. P. Hess, *J. Am. Chem. Soc.*, **77**, 1067 (1955).

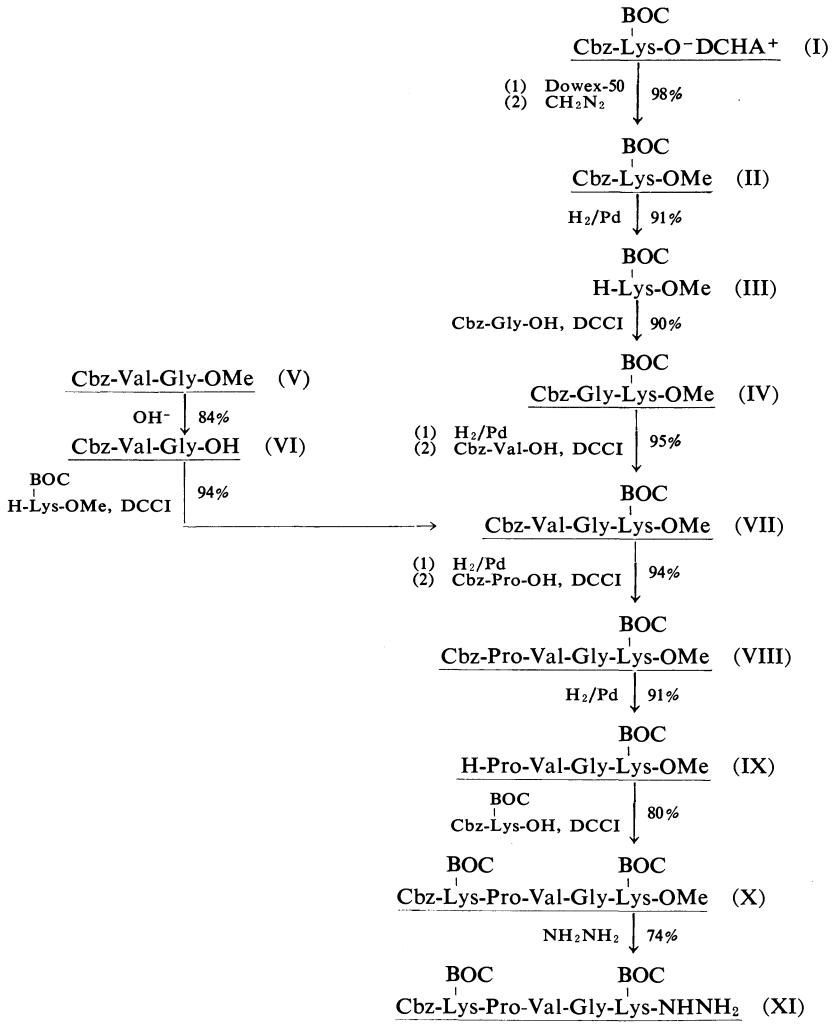
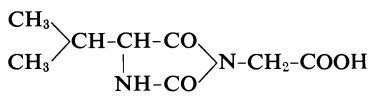


Fig. 1. Procedures for synthesis of the Lys-Pro-Val-Gly-Lys sequence. Cbz, carbobenzoxy; BOC, *t*-butyloxycarbonyl; Me, methyl; DCCI, *N*,*N*'-dicyclohexylcarbodiimide; DCHA, dicyclohexylamine.
Underline indicates that the compound was obtained in a crystalline form.

pentapeptide derivative, N^{α}-carbobenzoxy-N^{ε}-*t*-butyloxycarbonyl-L-lysyl-L-prolyl-L-valylglycyl-N^{ε}-*t*-butyloxycarbonyl-L-lysine methyl ester (X), which could be converted into the corresponding crystalline hydrazide (XI).

The tripeptide intermediate, compound VII, was prepared also by the condensation of the free ester of compound III with carbobenzoxy-L-valylglycine (VI), which was derived from the preceding methyl ester (V) by saponification. Maclaren[3] has described how the saponification of carbobenzoxy-L-leucylglycine ethyl ester is accompanied by a side reaction, producing a cyclic compound with a hydantoin structure, when excess alkali is used. We have observed that the crystalline product, which was obtained by the saponification of compound V, had a little higher nitrogen content and a little lower carbon content than the theoretical values calculated for compound VI. This fact may suggest that the crude sample of compound VI was contaminated, even when an exactly equivalent amount of alkali was used on the saponification, by a small amount of such a side product as is shown below. The pure sample could, however, be isolated after recrystallization from ethanol-water in a moderately high yield.



The Synthesis of the Lys-Pro-Val-Gly Sequence. — Carbobenzoxy-L-valylglycine methyl

3) J. A. Maclaren, *Australian J. Chem.*, **11**, 360 (1958).

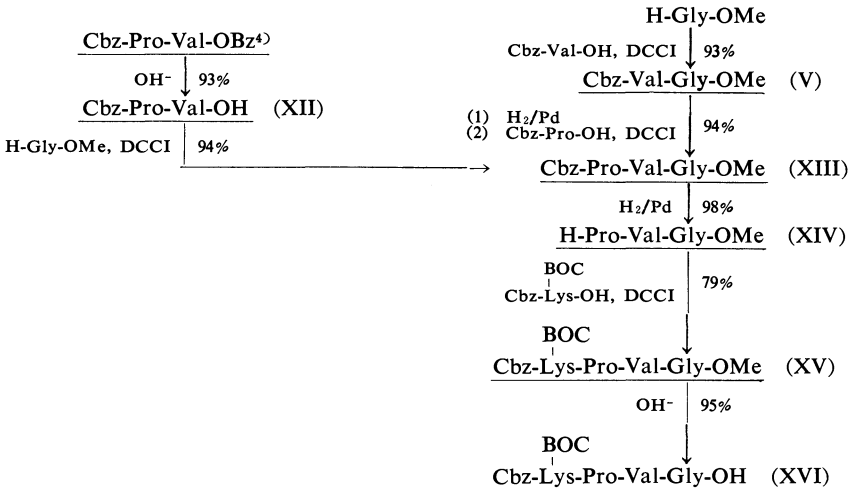


Fig. 2. Procedures for synthesis of the Lys-Pro-Val-Gly sequence. Cbz, carbobenzoxy; BOC, *t*-butyloxycarbonyl; Me, methyl; Bz, benzyl; DCCI, *N,N'*-dicyclohexycarbodiimide. Underline indicates that the compound was obtained in a crystalline form.

ester (V) was hydrogenated, and the resultant dipeptide ester was coupled with carbobenzoxy-L-proline to obtain a tripeptide intermediate, carbobenzoxy-L-prolyl-L-valylglycine methyl ester (XIII). This compound was also prepared through another procedure, consisting of the condensation of glycine methyl ester with carbobenzoxy-L-prolyl-L-valine (XII), which was derived from the crystalline benzyl ester[4] in a 90% yield by saponification. The corresponding methyl ester was, however, saponified to obtain compound XII in only a 50% yield.[5,6] This fact may indicate that the steric effect of the isopropyl side group in the valine methyl ester is more remarkable than that in the case of the benzyl ester.

The catalytic hydrogenation of compound XIII gave a crystalline tripeptide ester (XIV); this was next coupled with the free acid from compound I affording the crystalline tetrapeptide, N^{α}-carbobenzoxy-N^{ε}-*t*-butyloxycarbonyl-L-lysyl-L-prolyl-L-valylglycine methyl ester (XV), from which the corresponding acid XVI was derived by saponification.

Experimental

All melting points are uncorrected. The catalytic hydrogenation was carried out in a closed vessel connected with another small one, filled with soda lime, in which the evolved carbon dioxide was to be absorbed.

N^{α}-Carbobenzoxy-N^{ε}-*t*-butyloxycarbonyl-L-lysine Dicyclohexylamine Salt (I). — An 8.62 g.-sample (0.035 mol.) of N^{ε}-*t*-butyloxycarbonyl-L-lysine[1] (m. p. 226~227°C (decomp.), $[\alpha]_D^{25}$ +6.5±2° (*c* 1.085, 2 N ammonia)) and 6.0 g. of sodium bicarbonate were dissolved in 70 ml. of N sodium hydroxide and 30 ml. of water. The mixture was covered with 20 ml. of ether, and to this was added drop by drop 6.58 g. (0.0385 mol.) of benzyl chloroformate while it was being vigorously stirred at 0°C. The reaction mixture was stirred at 0°C for 30 min. and then at room temperature for 2 hr. After the ether phase had been removed, the aqueous solution was washed with ether and acidified to pH 2 at 0°C with ice-cold 4 N hydrochloric acid. The ensuing sirupy precipitates were taken up into cold ethyl acetate, and the organic solution was washed twice with water, dried over anhydrous sodium sulfate, and evaporated to dryness in vacuo. The resultant foamy residue was dissolved in ether, and the solution was mixed with an ethereal solution of 7.0 ml. (0.035 mol.) dicyclohexylamine (DCHA) and kept in a refrigerator overnight. The separated crystals were then collected, washed with ether, and dried; yield, 18.59 g. (94.8%); m. p. 148~149°C (sintering over 135°C). Recrystallization from methanol-ether gave 14.95 g. of colorless needles (recovery 80.5%); m. p. 153~155°C, $[\alpha]_D^{26}$ +5.5± 0.5° (*c* 4.564, methanol).

Found: C, 66.28; H, 9.43; N, 7.39. Calcd. for $C_{19}H_{28}O_6N_2 \cdot C_{12}H_{23}N$: C, 66.28; H, 9.15; N, 7.48%.

N^{α}-Carbobenzoxy-N^{ε}-*t*-butyloxycarbonyl-L-lysine Methyl Ester (II).—A suspension of 11.23 g. (0.02 mol.) of compound I in 160 ml. of 60% ethanol was shaken at room temperature for 30 min. in the presence of 20 ml. (wet volume) of Dowex-50W ×8 (H^+ form). After the resin had been removed by filtration, the filtrate was evaporated in vacuo at 40°C. The resultant oil was dissolved in ether and dried over anhydrous sodium sulfate. To this solution was added an ethereal solution of diazomethane at 0°C until the yellow color persisted; the mixture was then kept at 0°C for 10 min., after which time a few drops of acetic acid were

4) K. Inouye and H. Otsuka, This Bulletin, **34**, 4 (1961).
5) R. L. M. Synge, *Biochem. J.*, **42**, 99 (1948).
6) J. Meienhofer, *Chimia*, **16**, 385 (1962).

added to decompose the excess diazomethane. The solution was next washed successively with water, 5% sodium bicarbonate and water, dried over anhydrous sodium sulfate, and evaporated in vacuo, affording a dense oil which crystallized from ethyl acetate - petroleum ether; yield, 7.70 g. (97.7%); m. p. 60~61.5°C. Recrystallization from the same solvent system gave a sample for analyses; m. p. 62~63°C, $[\alpha]_D^{26}$ −9.3±1° (*c* 2.045, acetone). Lit. oil, $[\alpha]_D^{26}$ −10.6±0.5° (*c* 1.90, acetone);[1] m. p. 57°C, $[\alpha]_D$ not given.[7]

Found: C, 61.22; H, 7.59; N, 7.10. Calcd. for $C_{20}H_{30}O_6N_2$: C, 60.90; H, 7.67; N, 7.10%.

N^{ε}-*t*-Butyloxycarbonyl-L-lysine Methyl Ester Acetate (III).—Compound II (1.972 g., 5.0 mmol.), which was dissolved in 20 ml. of methanol and 0.5 ml. of acetic acid, was hydrogenated over a palladium black catalyst for 2 hr. After the catalyst had been filtered off, the solvent was removed in vacuo. The sirupy residue was dissolved in ether, and the solution was kept in a refrigerator overnight to afford the ester acetate in the form of needles; yield, 1.465 g. (91.4%); m. p. 78~79°C, $[\alpha]_D^{26}$ +17.0±1° (*c* 2.134, methanol).[8]

Found: C, 52.46; H, 8.86; N, 8.77. Calcd. for $C_{12}H_{24}O_4N_2 \cdot CH_3COOH$: C, 52.48; H, 8.81; N, 8.74%.

Carbobenzoxyglycyl-N^{ε}-*t*-butyloxycarbonyl-L-lysine Methyl Ester (IV).—To a solution of 0.802 g. (2.5 mmol.) of compound III in 1 ml. of water were added 15 ml. of methylene chloride and 5 ml. of ice-cold 50% (w/v) potassium carbonate, and the mixture was shaken vigorously at 0°C. The aqueous phase was extracted again with cold methylene chloride. The organic extracts were pooled, dried over anhydrous sodium sulfate, and evaporated in vacuo at a both temperature of 25°C. The resultant oily residue was dissolved in methylene chloride together with 0.523 g. (2.5 mmol.) of carbobenzoxyglycine, and to this was added a methylene chloride solution of 0.517 g. (2.5 mmol.) of *N,N'*-dicyclohexylcarbodiimide (DCCI) at 0°C. The reaction mixture (total volume ca. 20 ml.) was then kept in a refrigerator overnight. After the separated *N,N'*-dicyclohexylurea had been removed by filtration (0.545 g., 97.2%), the filtrate was evaporated in vacuo. The sirupy residue was dissolved in ethyl acetate, and this solution was washed successively with ice-cold N hydrochloric acid, water, 5% sodium bicarbonate and water, dried over anhydrous sodium sulfate, and evaporated in vacuo to give a sirup, which crystallized during storage in a refrigerator; yield, 1.013 g. (90.0%); m. p. 71~73°C. These crystals were recrystallized from ethyl acetate-petroleum ether, affording lustrous thin needles in a recovery of 92.5%, m. p. 74~75°C, $[\alpha]_D^{24.5}$ −8.04±0.5° (*c* 3.136, methanol).

Found: C, 58.58; H, 7.44; N, 9.60. Calcd. for $C_{22}H_{33}O_7N_3$: C, 58.52; H, 7.37; N, 9.31%.

Carbobenzoxy-L-valylglycine Methyl Ester (V).—Carbobenzoxy-L-valine (10.05 g., 0.04 mol.) and 3.56 g. (0.04 mol.) of freshly-distilled glycine methyl ester were coupled in the presence of 8.26 g. (0.04 mol.) of DCCI in a methylene chloride solution, almost as in case of compound IV. After the removal of the urea, the crystalline product was isolated from the filtrate during concentration; yield, 11.99 g. (93.2%); m. p. 159~161°C. Recrystallization from 40 ml. of chloroform and 160 ml. of ether gave 11.45 g. of needles (recovery 95.7%); m. p. 161~161.5°C, $[\alpha]_D^{23}$ −28.6±1° (*c* 2.205, methanol).

Found: C, 59.45; H, 6.83; N, 8.70. Calcd. for $C_{16}H_{22}O_5N_2$: C, 59.61; H, 6.88; N, 8.69%.

Carbobenzoxy-L-valylglycine (VI).—To a suspension of 3.224 g. (0.01 mol.) of compound V in 25 ml. of methanol was added 10.0 ml. of N sodium hydroxide; the mixture was then shaken at room temperature for 60 min. The resultant solution was diluted by the addition of 20 ml. of water and then acidified with N hydrochloric acid at 0°C. The precipitates were taken into ethyl acetate, and the organic solution was evaporated in vacuo affording a crystalline residue, which was redissolved in 40 ml. of ethyl acetate and extracted three times with 5% sodium bicarbonate. The aqueous extracts were combined and acidified again with 4 N hydrochloric acid at 0°C. The resultant precipitates were extracted with ethyl acetate and crystallized from ethyl acetate - ether; yield, 3.04 g. (98.5%); m. p. (130~132°C) 147~148°C, $[\alpha]_D^{24}$ −23.5±1° (*c* 2.032, methanol).

Found: C, 56.47; H, 6.36; N, 9.66. Calcd. for $C_{15}H_{20}O_5N_2$: C, 58.43; H, 6.54; N, 9.09%.

A 2.37 g.-sample of the crude product obtained above was recrystallized from ethanol-water (1 : 7) to give 2.03 g. of needles with a m. p. of 141~142°C. Recrystallization from the same solvent system gave a sample for analyses; m. p. 141~142°C, $[\alpha]_D^{25}$ −24.9±1° (*c* 2.474, methanol); lit.[9] m. p. 146°C, $[\alpha]_D^{22}$ −24.2±0.2° (*c* 5, methanol).

Found: C, 58.14; H, 6.52; N, 9.03. Calcd. for $C_{15}H_{20}O_5N_2$: C, 58.43; H, 6.54; N, 9.09%.

Carbobenzoxy-L-valylglycyl-N^{ε}-*t*-butyloxycarbonyl-L-lysine Methyl Ester (VII).—*A) By Val plus Gly-Lys.*—A 3.05 g.-sample (6.75 mmol.) of compound IV dissolved in 30 ml. of methanol and 1.5 ml. of acetic acid was hydrogenated over palladium for 2.25 hr. After the catalyst had been removed, the filtrate was evaporated in vacuo at 30°C. The ensuing oily residue was dissolved in 25 ml. of water, and the solution was washed twice with ethyl acetate and concentrated to about 10 ml. at 35~40°C in vacuo. To this concentrate was introduced 40 ml. of methylene chloride; the mixture was then shaken with 20 ml. of ice-cold 50% (w/v) potassium carbonate in an ice-bath. After the aqueous phase had been extracted twice more with cold methylene chloride, the organic extracts were combined, dried over anhydrous sodium sulfate, and evaporated in vacuo to give the dipeptide ester as a sirup in a quantitative yield.

The dipeptide ester obtained above and 1.70 g. (6.75 mmol.) of carbobenzoxy-L-valine were coupled, using 1.395 g. (6.75 mmol.) of DCCI in a methylene chloride solution in the same manner as has been

7) K. Sturm, R. Geiger and W. Siedel, *Chem. Ber.*, **96**, 609 (1963).

8) The value of $[\alpha]_D^{25}$ +19.0±1.0° (*c* 1.09, methanol) was given for the corresponding hydrochloride.[1]

9) W. Grassmann and E. Wünsch, *Chem. Ber.*, **91**, 449 (1958).

described above. After the separated urea had been filtered off, the solvent was removed in vacuo to give a crystalline solid mass, which was redissolved in 10 ml. of hot ethyl acetate; then, after the addition of 20 ml. of ether, the solution was kept in a refrigerator overnight. Crystalline precipitates were collected, washed with ether and dried; yield, 3.51 g. (94.5%); m. p. 128.5~129°C. Recrystallization from acetonitrile gave colorless needles with a m. p. of 130~131°C, $[\alpha]_D^{24.5}$ −12.2 ±1° (*c* 2.483, methanol).

Found: C, 59.22; H, 7.83; N, 10.17. Calcd. for $C_{27}H_{42}O_8N_4$: C, 58.89; H, 7.69; N, 10.18%.

B) By Val-Gly plus Lys.—Compound VI (0.772 g., 2.5 mmol.) and N^{ε}-*t*-butyloxycarbonyl-L-lysine methyl ester (prepared from 0.802 g. (2.5 mmol.) of compound III as described in case of compound IV) were coupled in the presence of 0.517 g. (2.5 mmol.) of DCCI in a methylene chloride solution. The reaction mixture was treated as described in A) to obtain the tripeptide; yield, 1.29 g. (93.7%), m. p. 130~131°C. These crystals were recrystallized from ethyl acetate-ether in a recovery of 94.8%, m. p. 131~132°C, $[\alpha]_D^{25.5}$ −12.1±0.5° (*c* 3.151, methanol).

Found: C, 59.16; H, 7.87; N, 10.19. Calcd. for $C_{27}H_{42}O_8N_4$: C, 58.89; H, 7.69; N, 10.18%.

Carbobenzoxy-L-prolyl-L-valylglycyl-N^{ε}-*t*-butyloxycarbonyl-L-lysine Methyl Ester (VIII).—Compound VII (6.61 g., 0.012 mol.) was dissolved in 60 ml. of methanol and hydrogenated over palladium black for 2.5 hr. After the catalyst had been removed, the filtrate was evaporated in vacuo at a bath temperature of 30°C to afford the tripeptide ester as a colorless foam. The tripeptide ester obtained above and 2.99 g. (0.012 mol.) of carbobenzoxy-L-proline were coupled by the use of 2.48 g. (0.012 mol.) of DCCI in methylene chloride in the same manner as above. After the urea had been removed (2.57 g., 95.5%), the evaporation of the solution gave a foamy residue, which crystallized from ethyl acetate-ether; yield, 7.31 g. (94.1%), m. p. 142~143°C. Recrystallization from ethyl acetate gave a sample for analyses, m. p. 143~144°C, $[\alpha]_D^{23}$ −50.6±1° (*c* 2.558, methanol).

Found: C, 59.47; H, 7.79; N, 10.64. Calcd. for $C_{32}H_{49}O_9N_5$: C, 59.33; H, 7.62; N, 10.81%.

L-Prolyl-L-valylglycyl-N^{ε}-*t*-butyloxycarbonyl-L-lysine Methyl Ester (IX).—Compound VIII (0.972 g.), which was dissolved in 15 ml. of methanol containing 0.5 ml. of acetic acid, was hydrogenated in the presence of a palladium black catalyst for 2 hr. The catalyst was removed by filtration, and the filtrate was evaporated in vacuo to give a colorless and clear oil. The oily residue was dissolved in 5 ml. of water, and the aqueous solution was, after being washed with ethyl acetate, mixed with 10 ml. of methylene chloride. The mixture was then shaken vigorously with 5 ml. of 50% (w/v) potassium carbonate at 0°C and the aqueous phase was extracted again with methylene chloride. The organic extracts were combined, dried over anhydrous sodium sulfate, and evaporated in vacuo to give a crystalline solid mass, which was washed with ether and dried; yield, 0.700 g. (90.9%), m. p. 98~102°C. Recrystallization from methanol-ether gave needles with a m. p. of 104~106°C, $[\alpha]_D^{24.5}$ −34.4±1.5° (*c* 1.762, methanol).

Found: C, 56.13; H, 8.49; N, 13.71. Calcd. for $C_{24}H_{43}O_7N_5$: C, 56.12; H, 8.44; N, 13.64%.

N^{α}-Carbobenzoxy-N^{ε}-*t*-butyloxycarbonyl-L-lysyl-L-prolyl-L-valylglycyl-N^{ε}-*t*-butyloxycarbonyl-L-lysine Methyl Ester (X).—N^{α}-Carbobenzoxy-N^{ε}-*t*-butyloxycarbonyl-L-lysine (prepared from 0.528 g. (0.94 mmol.) of the DCHA salt (I) as described in the preparation of compound II) and 0.483 g. (0.94 mmol.) of the crystalline tetrapeptide ester (IX) were condensed by the use of 0.194 g. (0.94 mmol.) of DCCI in methylene chloride in the same manner as has been described above. After the urea (0.190 g., 90.4%) had been removed, the methylene chloride solution was washed successively with ice-cold N hydrochloric acid, water, 5% sodium bicarbonate and finally with water, dried over anhydrous sodium sulfate, and concentrated in vacuo. Gelatinous precipitates separated upon the addition of ether; yield, 0.728 g. (88.5%), m. p. 98~103°C. The amorphous solid crystallized in needles with a 90.0% recovery during the slow evaporation of the acetone solution in a cold room; m. p. 105~107°C, $[\alpha]_D^{25}$ −55.2±1° (*c* 2.126, methanol).

Found: C, 58.92; H, 7.98; N, 11.14. Calcd. for $C_{43}H_{69}O_{12}N_7$: C, 58.95; H, 7.94; N, 11.19%.

N^{α}-Carbobenzoxy-N^{ε}-*t*-butyloxycarbonyl-L-lysyl-L-prolyl-L-valylglycyl-N^{ε}-*t*-butyloxycarbonyl-L-lysine Hydrazide (XI).—A mixture of 0.876 g. (1.0 mmol.) of compound X and 0.5 ml. of hydrazine hydrate in 10 ml. of methanol was heated under reflux at a bath temperature of 90~95°C. The crystalline hydrazide started to separate in about one hour. After 2 hr. the bath was removed; the reaction mixture was allowed to stand at room temperature overnight and then refrigerated. The crystals were filtered off, washed with ice-cold methanol-ether (1 : 2) and with ether, and dried to give 0.615 g.; m. p. 194~195°C. The concentration of the mother liquor afforded an additional quantity of crystals; 0.084 g., m. p. 190~191.5°C. The total yield amounted to 0.699 g. (79.9%). The recrystallization of these crystals from methanol gave fine needles with a m. p. of 194~195°C in a recovery of 92.5%; $[\alpha]_D^{24.5}$ −31.3±1° (*c* 1.949, dimethylformamide).

Found: C, 57.58; H, 7.87; N, 14.28. Calcd. for $C_{42}H_{69}O_{11}N_9$: C, 57.58; H, 7.94; N, 14.39%.

Carbobenzoxy-L-prolyl-L-valine (XII).—To a solution of 8.77 g. (0.02 mol.) of carbobenzoxy-L-prolyl-L-valine benzyl ester (m. p. 91~92°C), which had been prepared as described previously,[4] in 50 ml. of methanol, 20 ml. of 2 N sodium hydroxide was added, and the mixture was shaken at room temperature for 60 min. The resultant solution was neutralized at 0°C with 40 ml. of ice-cold N hydrochloric acid, concentrated to about 50 ml. at 35°C in vacuo, and extracted three times with ethyl acetate. The organic extracts were combined and then shaken three times with M sodium bicarbonate. The pooled aqueous solution was, after being washed twice with ethyl acetate, acidified with 4 N hydrochloric acid. The oily precipitate was then taken into ethyl acetate. The ethyl acetate extracts were combined, washed twice with water, dried over anhydrous sodium sulfate, and evaporated at 35°C in

vacuo to afford a crystalline mass, which was dissolved in hot ethyl acetate and precipitated by the addition of petroleum ether; yield, 6.48 g. (93.0%), m. p. 136~137°C. A sample for analyses was obtained by recrystallization from ethyl acetate - ether (2 : 5) in the form of needles; m. p. 136.5~137.5°C, $[\alpha]_D^{22.5}$ $-56.1\pm1°$ (*c* 2.140, methanol.). Lit. m. p. 134~135°C, $[\alpha]_D^{18}$ $-58°$ (*c* 2.8, methanol);[5] m. p. 136°C, $[\alpha]_D^{25}$ $-57.8°$ (*c* 1.2, methanol).[6]

Found: C, 62.34; H, 7.15; N, 7.95. Calcd. for $C_{18}H_{24}O_5N_2$: C, 62.05; H, 6.94; N, 8.04%.

Carbobenzoxy-L-prolyl-L-valylglycine Methyl Ester (XIII). — *A) By Pro plus Val-Gly.* — Carbobenzoxy-L-valylglycine methyl ester (V) (3.22 g., 0.01 mol.), which was suspended in 30 ml. of methanol containing 2 ml. of 20% hydrogen chloride in methanol, was hydrogenated in the presence of palladium black for 2.5 hr. After the catalyst had been removed, the filtrate was evaporated in vacuo at 30°C. The resultant foamy residue was dissolved in 10 ml. of water, and the solution was washed twice with ethyl acetate. To this aqueous solution was added 20 ml. of methylene chloride and solid sodium chloride to the point of saturation. The mixture was then shaken with 10 ml. of ice-cold 50% (w/v) potassium carbonate at 0°C. The aqueous phase was then extracted twice more with cold methylene chloride. The organic extracts were combined, dried over anhydrous sodium sulfate, and evaporated at 25°C in vacuo to give the dipeptide ester as an oil. The obtained dipeptide ester and 2.49 g. (0.01 mol.) of carbobenzoxy-L-proline were coupled using 2.06 g. (0.01 mol.) of DCCI in a methylene chloride solution in the same manner as has been described above. After the removal of the separated urea, the filtrate was washed successively with N hydrochloric acid, water, 5% sodium bicarbonate and water, dried over anhydrous sodium sulfate, and evaporated in vacuo to give a foamy residue which crystallized from acetone-ether; yield, 3.92 g. (93.6%), m. p. 131~132°C (sintering over 127°C). The recrystallization from the same solvent system gave a sample for analyses; m. p. 131~132°C, $[\alpha]_D^{23.5}$ $-91.6\pm1°$ (*c* 2.130, methanol).

Found: C, 60.13; H, 6.89; N, 10.13. Calcd. for $C_{21}H_{29}O_6N_3$: C, 60.13; H, 6.97; N, 10.02%.

B) By Pro-Val plus Gly.—Compound XII (6.10 g., 0.0175 mol.) and 1.56 g. (0.0175 mol.) of freshly-distilled glycine methyl ester were coupled in the presence of 3.62 g. (0.0175 mol.) of DCCI in methylene chloride as above. The reaction mixture was then treated in the manner described in A) to obtain the tripeptide; yield, 6.85 g. (93.5%); m. p. 132~133°C. Recrystallization from acetone-ether did not alter the m. p.; $[\alpha]_D^{25}$ $-91.0\pm1°$ (*c* 2.158, methanol). Lit. m. p. 111~112°C, $[\alpha]_D^{25}$ $-90.4°$ (*c* 1.6, methanol);[10] amorph., m. p. 125~127°C, $[\alpha]_D^{24}$ $-89.7°$ (*c* 1.05, methanol).[11]

Found: C, 60.23; H, 7.03; N, 10.36. Calcd. for $C_{21}H_{29}O_6N_3$: C, 60.13; H, 6.97; N, 10.02%.

L-Prolyl-L-valylglycine Methyl Ester (XIV). — Compound XIII (5.25 g., 0.0125 mol.) was dissolved in 80 ml. of methanol and then hydrogenated over a palladium black catalyst for 1.5 hr. After the catalyst had been removed, the solvent was evaporated at 30°C in vacuo. The crystalline solid residue was recrystallized from methanol - ether - petroleum ether to give fine needles; yield, 3.475 g. (97.6%), m. p. 150°C, $[\alpha]_D^{25}$ $-76.8\pm1°$ (*c* 1.987, methanol); lit.[10] m. p. 140~142°C, $[\alpha]_D$ not given.

Found: C, 54.86; H, 8.17; N, 14.69. Calcd. for $C_{13}H_{23}O_4N_3$: C, 54.72; H, 8.12; N, 14.73%.

N^{α}-Carbobenzoxy-N^{ε}-*t*-butyloxycarbonyl-L-lysyl-L-prolyl-L-valylglycine Methyl Ester (XV).—Compound XIV (2.85 g., 0.01 mol.) and N^{α}-carbobenzoxy-N^{ε}-*t*-butyloxycarbonyl-L-lysine (derived from 5.62 g. (0.01 mol.) of the DCHA salt (I)) were united by the use of 2.06 g. (0.01 mol.) of DCCI in a methylene chloride solution in the same manner as has been described above. The urea was then filtered off (1.99 g., 89.0%), and the filtrate was evaporated in vacuo to afford a foamy residue. The residue was dissolved in ethyl acetate, and the solution was washed successively with ice-cold N hydrochloric acid, water, 5% sodium bicarbonate and water, and dried over anhydrous sodium sulfate. Gelatinous precipitates (5.70 g., 88.1%), which separated during the concentration of the ethyl acetate solution, crystallized from acetone in needles; yield, 5.13 g. (79.2%); m. p. 125~127°C. Recrystallization from acetone afforded thin lustrous needles as a sample for analyses; m. p. 128~129°C, $[\alpha]_D^{24.5}$ $-80.4\pm1°$ (*c* 2.035, methanol).

Found: C, 59.65; H, 7.70; N, 10.70. Calcd. for $C_{32}H_{49}O_9N_5$: C, 59.33; H, 7.62; N, 10.81%.

N^{α}-Carbobenzoxy-N^{ε}-*t*-butyloxycarbonyl-L-lysyl-L-prolyl-L-valylglycine (XVI). — To a solution of 3.24 g. (0.005 mol.) of compound XV in 12 ml. of methanol, 5.0 ml. of 2 N sodium hydroxide was added at 0°C; the mixture was then shaken at room temperature for 60 min., after which time the solution was cooled in an ice-bath, diluted with 25 ml. of water, and then neutralized with 10.0 ml. of N hydrochloric acid. The resultant sirupy precipitates were taken into ethyl acetate and the organic solution was evaporated in vacuo to remove the methanol. The residue, which was dissolved again in ethyl acetate, was washed with cold water containing a few drops of N hydrochloric acid and with saturated sodium chloride, dried over anhydrous sodium sulfate, and concentrated in vacuo. The addition of twice as much ether gave gelatinous precipitates slowly. These precipitates were washed with ether and dried; yield, 2.87 g. (95.3%), m. p. 107~117°C, $[\alpha]_D^{24.5}$ $-79.6\pm1°$ (*c* 2.593, methanol); lit.[7] m. p. 116~118°C, $[\alpha]_D^{20}$ $-81.4\pm2°$ (*c* 1, methanol).

Found: C, 58.34; H, 7.55; N, 11.02. Calcd. for $C_{31}H_{47}O_9N_5$: C, 58.75; H, 7.48; N, 11.05%.

Summary

The amino acid sequence Lys-Pro-Val-Gly-Lys, which corresponds to positions 11 to 15 of the corticotropin molecule, has been synthesized in the form of a crystalline derivative,

10) C. H. Li, J. Meienhofer, E. Schnabel, D. Chung, T-b. Lo and J. Ramachandran, *J. Am. Chem. Soc.*, **83**, 4449 (1961).

11) K. Hofmann, E. Stutz, G. Spühler, H. Yajima and E. T. Schwartz, ibid., **82**, 3727 (1961).

N^{α}-carbobenzoxy-N^{ε}-*t*-butyloxycarbonyl-L-lysyl-L-prolyl-L-valyl-glycyl-N^{ε}-*t*-butyloxycarbonyl-L-lysine methyl ester, from which the crystalline hydrazide has then been obtained. The synthesis of the Lys-Pro-Val-Gly sequence corresponding to positions 11 to 14 of corticotropin has also been described.

Grateful aknowledgment is made to Dr. Kaoru Kuriyama and his staff for their optical rotation measurements, to Dr. Satoshi Mizukami and his staff for their elementary microanalyses, and to Mr. Makoto Kanayama for his technical assistance.

Biochemistry Division
Shionogi Research Laboratory
Shionogi & Co., Ltd.
Fukushima-ku, Osaka

The Behavior of Silicon, Aluminum, Iron, Magnesium, Calcium, Sodium and Potassium in Fumarolic Gas at the Mihara Volcano, Japan

By Hiroshi KAMIYA

(Received April 13, 1964)

The studies by Day and Shepherd[1,2] of gases evolved from the lava lake at Kilauea and by Allen and Zies[3,4] from the fumaroles at Valley of Ten Thousand Smokes are well known among the many investigations of volcanic gases. Recently Ellis[5] and Matsuo[6-8] also discussed the chemical equilibria in highly volatile components.

Krauskopf[9] has reviewed the possibility of vapor transport in the course of ore deposition. Observation of materials deposited in fumaroles shows that low volatile elements have been deposited directly from gases. In volcanic gases, water is the most abundant component, although the water content is variable. Morey[10,11] believes that water vapor would be able to dissolve and transport many elements of a low volatility at a high temperature and a high pressure. In some cases the vapor transport of relatively low volatile components, either as dissolved or gaseous compounds, is considered to account for the compositional differences in minerals and rocks of volcanic origin.[12,13]

According to White,[14] the vapor transport plays an important part in feeding various kinds of chemical species into hot spring water which has brought a great amount of the elements to the earth's surface. It is evident that water in either a gas or a liquid state would be an efficient transporting agent of many elements.

The principal purpose of this paper is to investigate the behavior of low volatile components in fumarolic gas at relatively high temperatures.

A Description of the Mihara Volcano

The Mihara Volcano on Izu-Oshima Island, situated 120 km. south of Tokyo, is one of the most active volcanoes in Japan. Geological, mineralogical and chemical studies on Mt. Mihara have been made in detail by Tsuboi,[15] Iwasaki,[16] Tsuya,[17] Kuno[18] and many other investigators.[19-21]

Since the eruption in 1957, however, the volcano has been dormant; recently only a small amount of ashes is sometimes ejected from the crater. There are many fumaroles along the cracks on the scoria cone in the southwestern part of the crater. The highest

* Present address: Department of Chemistry, Nagoya Institute of Technology, Chikusa-ku, Nagoya.

1) A. L. Day and E. S. Shepherd, *Geol. Soc. Am. Bull.*, **24**, 573 (1913).
2) E. S. Shepherd, *Am. J. Sci.*, **35A**, 311 (1938).
3) E. T. Allen and E. G. Zies, *Nat. Geog. Soc., Contributed Tech. Papers, 1, Katmai Ser.*, No. 2, 75 (1923).
4) E. G. Zies, *Am. J. Sci.*, **35A**, 385 (1938).
5) A. J. Ellis, ibid., **255**, 416 (1957).
6) S. Matsuo, *J. Earth Sci., Nagoya Univ.*, **8**, 222 (1960).
7) S. Matsuo, ibid., **9**, 80 (1961).
8) S. Matsuo, ibid., **9**, 101 (1961).
9) K. B. Krauskopf, *Econ, Geol.*, **52**, 786 (1957).
10) G. W. Morey and J. M. Hesselgesser, ibid., **46**, 821 (1951).
11) G. W. Morey, ibid., **52**, 225 (1957).
12) C. H. Smyth, *Am. J. Sci.*, **36**, 33 (1913).
13) H. Kuno and S. Taneda, *J. Geol. Soc. Japan*, **47**, 62 (1940).
14) D. E. White, *Geol. Soc. Am. Bull.*, **68**, 1637 (1957).
15) S. Tsuboi, *J. Coll. Sci., Tokyo Imp. Univ.*, **43**, pt. 6,1 (1920).
16) I. Iwasaki, *J. Chem. Soc. Japan (Nippon Kwagaku Kwaishi)*, **56**, 1511 (1935).
17) H. Tsuya, *Bull. Earthq. Res. Inst.*, **15**, 215 (1937).
18) H. Kuno, *Tr. Am. Geoph. Union*, **34**, 267 (1953).
19) H. Tsuya, R. Morimoto and J. Ossaka, *Bull. Earthq. Res. Inst.*, **32**, 35 (1954).
20) H. Tsuya, R. Morimoto and J. Ossaka, ibid., **32**, 289 (1954).
21) H. Tsuya, R. Morimoto and J. Ossaka, ibid., **33**, 79 (1955).

temperature of the fumaroles was over 400°C in 1959. The temperature of these fumaroles, however, gradually decreased, until in 1961 the highest fell to 350°C.

Unlike the fumarolic gases in many other volcanoes, the gases at this volcano are admixture, with a great amount of air.[22] Excluding the air, the major constituents of the gas are carbon dioxide, hydrogen halides and sulfur compounds, water being extremely dominant. The fact that sulfur dioxide and free sulfuric acid, but no hydrogen sulfide, are detected in those fumarolic gases would account for a lack of free sulfur deposits at the orifice of the fumaroles. Deposits from gases and such decomposition products of ash and scoria as anhydrite, opal and clay minerals have been found at the orifices.[23-25] A map of the crater is shown in Fig. 1.

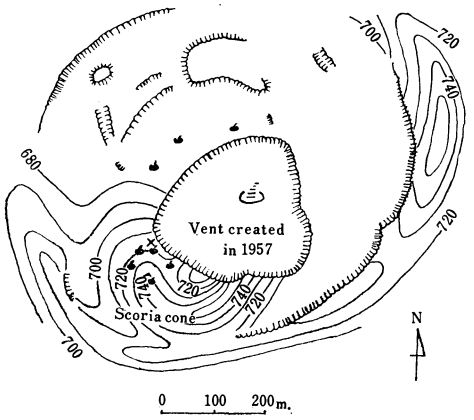


Fig. 1. Crater of Mihara Volcano.

Numerals in map represent meter above the sea-level.
× Position where condensed water was collected.
(≡) Fumarole
This was published by Oshima observatory of the Japan Meteorological Agency, on 20th in June, 1961.

Experimental

The Sampling of Condensed Water.—One end of a hard glass tube 2.5 cm. in diameter, bent at a right angle, was inserted into a fumarole, and the other end was connected with a 5 m. glass tube to which a 5 m. polyvinyl-chloride tube was attached. A 1 l. polyethylene bottle was fitted with the end of the polyvinyl-chloride tube in order to collect any water condensed by air cooling (Fig. 2). By this means, the elements transported in gases for the most part come to dissolve in the condensed water.

From one of the many fumaroles, thirty-eight samples of condensed water were collected during the period from April to September, 1959, and fifty samples, from May to July, 1961.

The orifice temperature of the fumarole was measured by an alomel-chromel thermocouple and an electric-resistance thermometer with an attached recorder.

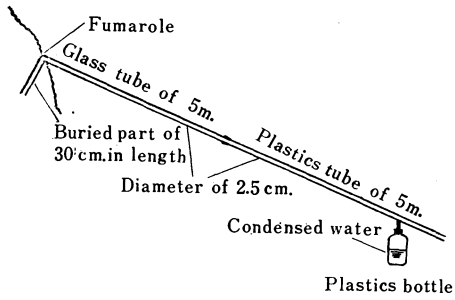


Fig. 2. Equipment for collecting condensed water from a fumarole.

The Analytical Method.—The condensed water was analyzed for acidity and for sulfate, chloride, silicon, aluminum, iron, calcium, magnesium, sodium and potassium.

1) Acidity.—The determination of acidity was carried out by titration with a sodium hydroxide solution using methyl orange as an indicator.

2) SO_4^{2-}.*—The sulfate was measured by means of the barium sulfate turbidity developed with a barium chloride gelatin solution.

3) Cl^-.—The chloride was determined by Mohr's method.

4) Silicon.—The silicon was determined colorimetrically by a molybdenum blue method.**

5) Aluminum.—The determination of aluminum was made by measuring the optical density of the red color of the complex formed with aluminon after extraction of iron with cupferron into chloroform.

6) Iron.—The determination of iron was carried out by reducing with hydroxylamine all the iron to a ferrous state, and then by making a colorimetric measurement of the absorbance of the red color developed with α,α'-bipyridyl or *o*-phenanthroline.

7) Calcium and Magnesium.—The sum of calcium and magnesium was determined by titrating them with an EDTA solution in the presence of Eriochrome Black T at pH 10. The calcium was independently determined by titration with an EDTA solution in strong alkaline media using Dotite NN as an indicator. The amount of magnesium was

22) I. Iwasaki, T. Ozawa, M. Yoshida, T. Katsura, B. Iwasaki, M. Kamada and M. Hirayama, *Bull. Tokyo Inst. Tech.*, No. 47, 1 (1962).
23) R. Morimoto and J. Ossaka, *J. Geog.*, **60**, 136 (1951).
24) I. Iwasaki, ibid., **60**, 140 (1951).
25) K. Noguchi, H. Kamiya and H. Kawase, *J. Chem. Soc. Japan, Pure Chem. Sec.* (*Nippon Kagaku Zasshi*), **84**, 121 (1963).

* In the condensed water samples which were transferred to the laboratory, neither sulfur dioxide nor hydrogen sulfide was detected.
** By this method only the dissolved or less coagulated silica can be determined. However, no difference was found between the results of the above direct determination and those of the total silica determination.

calculated by subtracting the amount of calcium from the sum.

8) Sodium and Potassium. — The sodium and potassium were determined by means of flame photometry.

Results and Discussion

The Variation in the Concentration of the Components in Condensed Water. — Figure 3 shows the variations in the orifice temperature of the fumarole, the acidity of the condensed waters and the concentrations of the nine components (i.e., sulfate, chloride, silicon, aluminum, iron, calcium, magnesium, sodium and potassium), in the period from April to September, 1959, and from May to July, 1961.

In 1959 the measurement of the orifice temperature was discontinued because the thermometer was damaged. However, the continued gradual decrease in the temperature was assured by interpolation.

As may be seen in Fig. 3, the concentrations of the components in the condensed waters changed markedly, even in a short

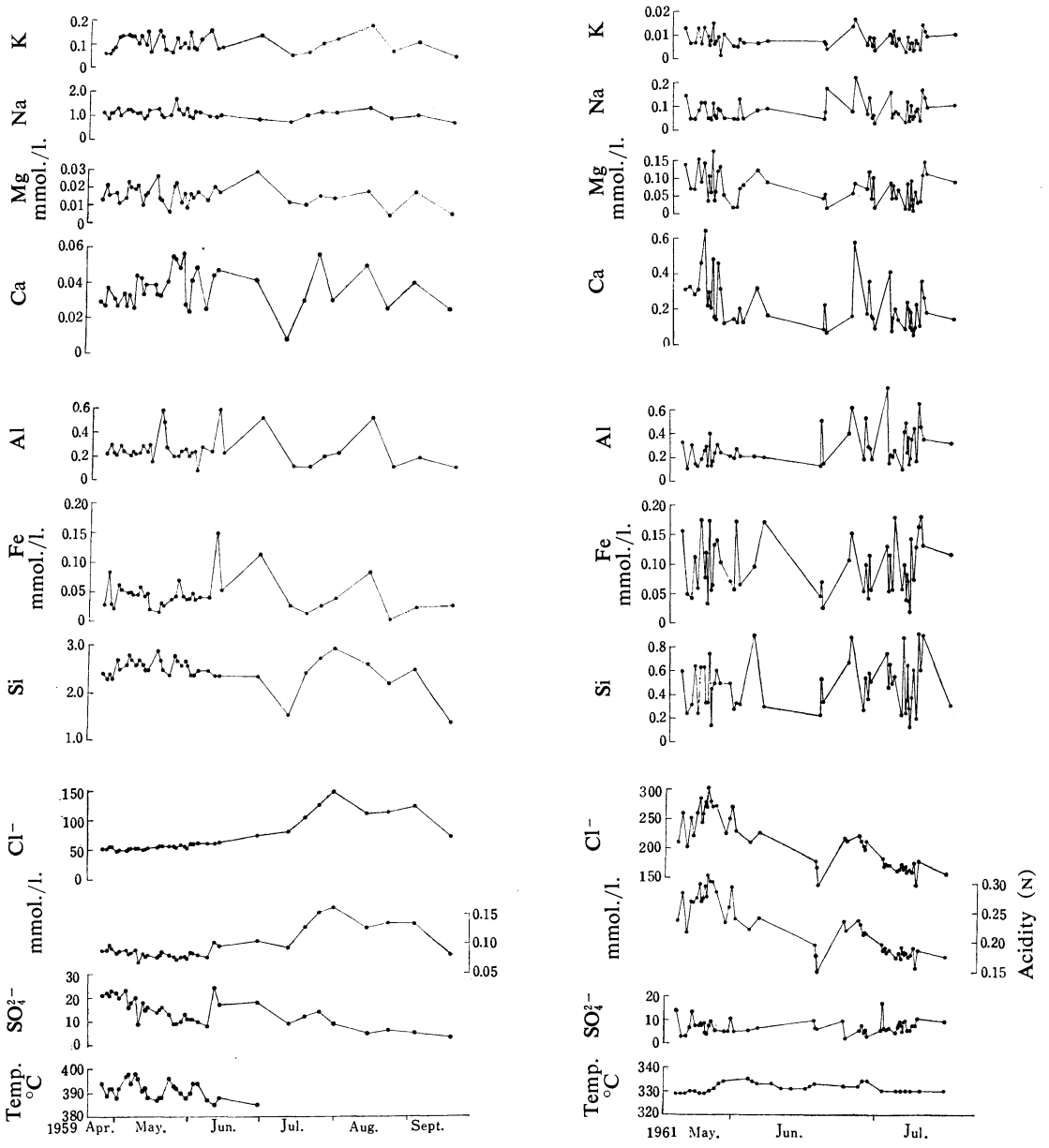


Fig. 3. Variation of orifice temperature of fumarole, acidity of condensed water and concentrations of components in condensed water in 1959 and 1961.

TABLE I. AVERAGE CONCENTRATION, ITS STANDARD DEVIATION AND VARIATION COEFFICIENT OF NINE COMPONENTS IN CONDENSED WATER, AND RATIO OF AVERAGE CONCENTRATION IN 1961 TO THAT IN 1959

	In 1959			In 1961			
	Average concn. mmol./l.	Standard deviation	Std. Dev. / Av. Concn. (ratio)	Average concn. mmol./l.	Standard deviation	Std. Dev. / Av. Concn. (ratio)	Av. Concn. ('61) / Av. Concn. ('59) (ratio)
Si	2.5	0.29	0.12	0.47	0.21	0.45	0.19
Al	0.27	0.12	0.46	0.28	0.15	0.53	1.0
Fe	0.047	0.027	0.57	0.094	0.047	0.50	2.0
Mg	0.016	0.005	0.32	0.072	0.042	0.59	4.5
Ca	0.037	0.011	0.29	0.22	0.14	0.62	5.9
Na	1.1	0.20	0.18	0.081	0.042	0.51	0.074
K	0.11	0.03	0.31	0.008	0.003	0.44	0.07
SO_4	14	5.7	0.41	7.0	2.8	0.40	0.5
Cl	67	25	0.38	208	44.7	0.21	3.1
Temp.	about 390°C			about 330°C			

interval. Mizutani and Matsuo[26] have observed similar variations in calcium and magnesium concentrations in condensed waters drawn from a fumarole at the Showa-shinzan Volcano.

On the basis of thermodynamic calculations, Ellis[5] and Matsuo[6-8] have shown that the chemical composition of volcanic gases should change in accordance with the temperature, the pressure and the type of magma. Some volcanologists even anticipate that eruptions can be predicted by measuring such a compositional change of gases.[26-29]

Table I gives the average concentrations, the standard deviations of the concentrations and the ratios of the standard deviations to the average concentrations denoting the variation coefficient, in both 1959 and 1961.

As given by the variation coefficients in Table I, the low volatile components differ considerably in their modes of variation in 1959; for example, the variation of silicon is the smallest, and that of iron the largest. In 1961, however, no marked differences exist among variation coefficients, which are generally larger than those in 1959. As for the highly volatile components, the variation of sulfate was much the same in both 1959 and 1961, while that of chloride in 1961 was much smaller than in 1959.

A Comparison between the Average Concentrations in 1959 and 1961.—The ratios of the average concentrations in 1961 to those in 1959 are shown in the final column of Table I.

The decrease in the orifice temperature, 390°C in 1959 to 330°C in 1961, resulted in the threefold increase in the chloride concentration; on the other hand, it also reduced the sulfate concentration by half.

The titrated acidity almost corresponds to the total gram-equivalent of the determined chloride and sulfate ions, as may be seen in Fig. 4. This means that chloride and sulfate ions are present in condensed water for the most part as free acid; in other words, the condensed water is practically a mixture of hydrochloric and sulfuric acids because of the small contribution of cations other than hydrogen ions (Table I).

The much stronger acidity in 1961 than in 1959 may be attributed to the increase in chloride (Fig. 4).

As for the low volatile components, in 1961 the average concentrations of sodium, potassium and silicon became lower; on the other hand, those of calcium, magnesium and iron became higher, while that of aluminum remained constant, as compared with those in 1959. This cannot be explained as a results of a simple vaporization of such a compound as metal chloride with a relatively high vapor pressure. As has been pointed out by Krauskopf,[9] coexistent water vapor and sulfur compounds should also be taken into consideration.

It will be evident that the amount of heat supplied by gas determines the orifice temperature of a fumarole.[30] Unfortunately, since neither the flow rate of the fumarolic gas nor the condensation rate of the water vapor was measured, it is uncertain whether the decrease

26) Y. Mizutani and S. Matsuo, *Volcanolog. Soc. Japan Bull.*, Ser. 2, 3, 119 (1959).
27) J. H. Payne and S. S. Ballard, *Science*, **92**, 218 (1940).
28) K. Noguchi, *J. Chem. Soc. Japan (Nippon Kwagaku Kwaishi)*, **56**, 1495 (1935).
29) K. Noguchi and H. Kamiya, *Bull. Volcanol.*, **26**, 368 (1963).
30) K. Takahashi and S. Oana, *Repts. Geol. Survey Japan*, No. 170, 115 (1957).

TABLE II. MOLE PERCENTAGE OF SEVEN COMPONENTS IN LAVA AND CONDENSED WATER AND RATIO OF MOLE PERCENTAGE IN CONDENSED WATER TO THAT IN LAVA

Component	Lava (R)	In 1959		In 1961	
		Condensed water (G)	G/R	Condensed water (G')	G'/R
	%	%	(ratio)	%	(ratio)
Si	51.1	61	1.2	38	0.75
Al	17.7	6.5	0.37	23	1.3
Fe	10.5	1.1	0.10	7.7	0.73
Mg	6.8	0.4	0.06	5.9	0.87
Ca	10.2	0.9	0.09	18	1.8
Na	3.2	28	8.8	6.6	2.1
K	0.4	2.7	6.8	0.63	1.6

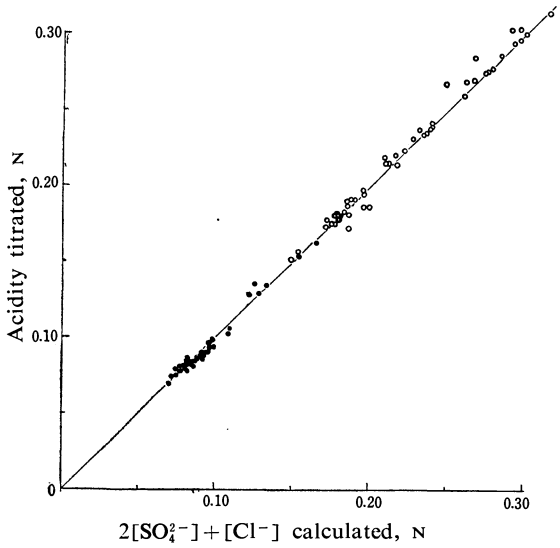


Fig. 4. Comparison between acidity titrated and acidity calculated by regarding all of the sulfate and chloride ions as free acids. A straight line, which meets with the axes at angles of 45 degree, represents the identity of both acidities.
• Sample in 1959 ○ Sample in 1961

in the orifice temperature can be attributed to the decrease in the gas temperature itself or to the decrease in the flow rate.

Assuming that the water vapor content in the fumarolic gas changes according to the environmental conditions, it seems likely that the variation in the ratio of the content of a certain component to that of water vapor in gas, i. e., the variation in the concentration of a chemical component in condensed water, differs by chance. Therefore, a simple comparison of two average concentrations of a component for the two periods (1959 and 1961) would not decisively indicate the increase or decrease in the content of a chemical component in gas.

The Transport of the Low Volatile Components in the Fumarolic Gas.—While the gas is ascending from magma to the earth's surface through conduits with a decreasing temperature and a decreasing pressure gradient, the low volatile components in the gas might be partly deposited and so removed from the gas in the course of its ascending. The chemical composition of the condensed water should, therefore, be considered to be the result of various reactions during the ascending process.

Table II gives the mole percentages of the seven components, i. e., silicon, aluminum, iron, magnesium, calcium, sodium and potassium, in the lava of this volcano[19] and in the condensed water, and the ratio of the mole percentage of each component in the condensed water to that in the lava. The ratio may be considered to be a measure of the ease with which a chemical component is transported in gas. The ratio for the seven components may be concluded to be in the following order:

Na>K>Si>Al>Fe and Ca>Mg in 1959

and

Na>Ca>K>Al>Mg, Si and Fe in 1961.

Sodium was the most mobile component in both 1959 and 1961. Silicon was relatively mobile in 1959, but it turned out to be one of the least mobile components in 1961. On the contrary, calcium was one of the least mobile components in 1959, but the most mobile one after sodium in 1961.

The great mobility of sodium, potassium and silicon in 1959 corresponds to the conclusions by Kennedy,[31,32] Moery[10] and White.[14] According to them, many alkali chlorides and silica are transported in water at sufficiently high temperatures and pressures.

As may be noticed in Table II, the mole percentages of the seven components in condensed waters, i. e., in gases, are considerably different from those in lava. If such gases

31) S. Sourirajan and G. C. Kennedy, *Am. J. Sci.*, **260**, 115 (1962).
32) G. C. Kennedy, *Econ. Geol.*, **45**, 629 (1950).

are formed and separated out of a magma, compositional changes in the residual magma may be expected.

The writer wishes to express his indebtedness to Professor Kimio Noguchi for having been good enough to read the manuscript and for his helpful advice, and also to Mr. Minoru Yamamoto for his help in analyzing samples.

Department of Chemistry
Faculty of Science
Tokyo Metropolitan University
Setagaya-ku, Tokyo

The Thermal Membrane Potential as a Function of the Apparent Ionic Transport Number of Membranes

By Toshio IKEDA, Masao TSUCHIYA* and Masaru NAKANO**

(Received April 20, 1964)

Some aspects of the "thermal membrane potential" (TMP) have previously been reported by one of us[1,2] in relation to its general properties and the theoretical basis for it. TMP is an EMF that appears at an ion-selective membrane, M, placed between two identical electrolytic solutions of the same concentration, m, in contact with one another, the two solutions are, however, kept at different temperatures, T and $T + \Delta T$. TMP can be measured by the the following cell system:

$$\underset{T}{\mathrm{Hg/HgCl}},\ \underset{T}{\mathrm{RX}(m)}\ \vdots\ \underset{T+\Delta T}{\mathrm{RX}(m)},\ \underset{T}{\mathrm{HgCl/Hg}} \quad (1)$$
$$\qquad\qquad\qquad\qquad\quad \mathrm{M}$$

where R represents the cation species, and X, the anion species, reversible to the electrodes of insoluble mercurous salt, HgX. On the other hand, the EMF of cell 1, and consequently the TMP, is very sensitive to the ionic permeability of the membrane used. The purpose of the present work is to find experimentally the relation between the EMF or its temperature coefficient (i. e., the thermoelectric power) and the ionic permeability of the membrane used in the cells of type 1, where the apparent ionic transport number of the membrane was adopted to represent the degree of the ionic permselectivity of the membrane.

Experimental

Materials. — GR chemicals were used without further purification in most cases. Ordinary distilled water was used in preparing the solutions. The mercury used for the calomel electrodes was purified by vacuum distillation after making the usual chemical refinements. Mercurous chloride, which was washed in advance by repeated decantation with the same solution of potassium chloride as that used for the meaurements, was used for the preparation of calomel electrodes. A pair of calomel electrodes was prepared after the usual manner in an identical way by the use of the same solution of potassium chloride as that used for the measurements of the TMP. Prior to the use of these calomel electrodes, they were let stand at least for five days in order to age them.

The Preparation of Membranes.—*Cation Permeable Membranes.* — An "oxidized" collodion membrane, according to Gregor and Sollner,[3] is advantageous because of its high cationic selectivity even with low electric resistance. The "oxidized" collodion membranes used in the present work were prepared according to the method found by one of us for getting membranes of graded cationic permeability.[4]

Anion Permeable Membranes. — A weak base-type cellophane matrix membrane of aniline-formaldehyde resin was prepared in the following way. A piece of cellophane membrane was cleaned by washing it with ether and water and was then tied with cotton thread at the end of a beaker cut off at its bottom. The beaker thus provided with a cellophane bottom was immersed in aqueous 1 M aniline hydrochloride, and a 5% aqueous formaldehyde solution acidified with a small amount of hydrochloric acid was placed on the cellophane membrane to let aniline-formaldehyde resin form in the membrane phase by means of diffusion. The most convenient temperature for the practical control of the resin-forming process was about 30°C. After about half an hour the membrane became yellowish orange as the result of the formation of the aniline-formaldehyde polymer. This cellophane

* Present address: Tokyo Metropolitan Isotope Centre, Tokyo.
** Present address: Japan Balqua Ind. Co., Tokyo.

1) T. Ikeda, *J. Chem. Phys.*, **28**, 166 (1958); **31**, 267 (1959).
2) T. Ikeda, *Rep. Liberal Arts Sci. Fac., Shizuoka Univ., Nat. Sci.*, **2**, 237 (1960).
3) H. P. Gregor and K. Sollner, *J. Phys. Chem.*, **50**, 53 (1946).
4) T. Ikeda and K. Tarumoto, *Rep. Liberal Arts Sci. Fac., Shizuoka Univ., Nat. Sci.*, **3**, 109 (1961); **3**, 165 (1962).

polymer matrix was washed with water overnight and stored for ready use in the electrolytic solution to be used for the experiment. Membranes prepared in such a way were found to be permselective to anions, exhibiting an anionic transport number of about 0.9 or less for the chloride ions. On the other hand, the anionic transport number of membranes of this type gradually diminishes down to about 0.6 in about two months when they are stored in aqueous media, presumably because of hydrolysis, but the rate of its change is so slow that this change will not practically disturb measurements that can be performed within a short time (about half an hour). This characteristic is, in a reverse sense, rather convenient for getting a serial run of measurements for different values of transport numbers; the same membrane can even be used if an appropriate interval is allowed for.

Cell System.—The cell system used in the present work was nearly the same as that reported on in a previous paper,[2] but some improvements were made in it. The cell is divided into two symmetrical compartments by a water-tight membrane which was placed between the brims of these two cell parts, sandwiched between two rubber sheets. This cell is suited also for measuring the isothermal membrane potential with the same membrane as was used for measuring the TMP. The cell used in the present work is sketched in Fig. 1. Here,

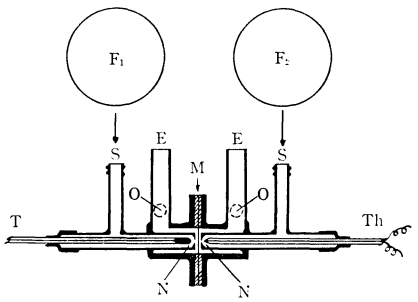


Fig. 1. Cell system.

M is the membrane, N is a fixed nozzle about 1 mm. in diameter at its orifice, S is the inlet for the solution by means of a siphon, and O is the outlet for the solution if it overflows. E is the connection for the terminal calomel electrode. F_1 and F_2 are flasks of about 3 l. which contain identical solutions. F_1 was kept at room temperature, while F_2 was kept in a bath whose temperature was controlled by a weak electric heater. F_2 was provided with an effective reflux condenser. These two solutions, identical but controlled at different temperatures, were let flow from F_1 and F_2 into the respective cell compartments through the respective nozzle, N, by means of polyvinyl chloride tube siphons at a rate above 50 cc./min. (This rate was the lowest limit for producing a stationary value of the EMF of the cell used; the flow rate employed by us was between 50 and 120 cc./min.). The solutions were then let spout against the respective sides of the membrane, M, to produce a clear-cut temperature gradient at the membrane. T is a mercury thermometer with 0.1°C divisions to be used for reading the temperature of the solution of F_1 at the instant immediately before it runs out of the orifice of the left-side nozzle to strike the left side of the membrane. On the other hand, Th is a thermister of the pencil type, which is convenient for reading the instantaneous variation in temperature of the solution of F_2 immediately before it runs out of the orifice of the right-side nozzle to strike the right side of the membrane.

To eliminate the heterogeneous thermocell effect, two calomel electrodes were kept at the same, constant temperature by placing them together in moderately running service water, whose temperature fluctuation did not exceed even ± 0.1°C per hour. TMP is substantially so small that every care must be taken not to introduce stray EMF's such as that coming from the drift of the electrode potentials due to a mechanical shock imposed accidentally upon the calomel electrodes, and such as those due to some thermoelectric effects of any sort which happen to occur in the system.

TMP was measured to a precision down to 0.1 μV. with a Yokogawa P-7-type potentiometer for low-voltage use by the aid of a highly sensitive galvanometer as a zero indicator. Here, we have adopted the convention for marking the EMF of this cell positive when the sign of the hot-side electrode is more positive. The apparent transport number of the membrane was detrermined from the isothermal membrane potentials observed at a concentration ratio of 0.05 M potassium chloride/0.1 M potassium chloride immediately before or after the TMP measurements.

Results and Discussion

The plots of EMF against T are shown in Figs. 2 and 3 for membranes with different degrees of ionic permselectivity. The EMF of cell 1 under the isothermal conditions is not always zero; it differs from run to run, presumably because of the asymmetry of the conditions of the two terminal electrodes. However, as long as such an asymmetric potential maintains itself at a constant value during the measuring run, it will not interfere with the present purpose of determining the thermoelectric power, dE/dT. The EMF, E, of cell 1 was found to be practically linear with the temperature difference, ΔT, and to respond well to the change in temperature of the solutions on either side of the membrane, irrespective of the degree of ionic permselectivity of the membrane used. When the flows of the solution on either side of the membrane were stopped, TMP returned immediately to the original isothermal value, but it promptly recovered its proper value when the flow of the solution was resumed. If these conditions could not be satisfied, the attempt to observe EMF was abandoned as not possible. The other properties were entirely the same

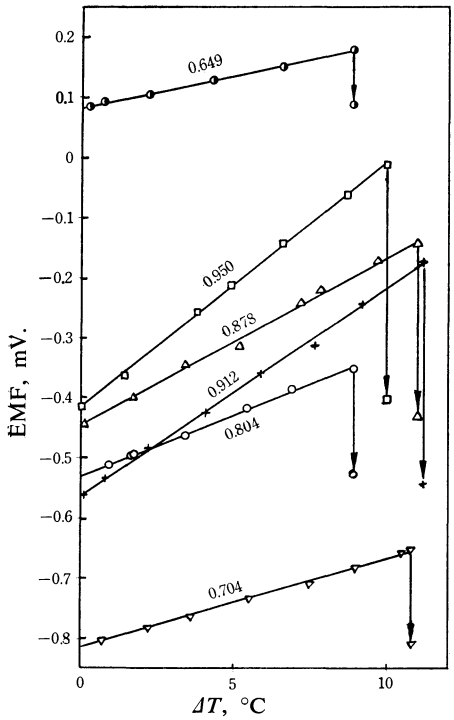


Fig. 2. EMF for oxidized collodion membranes in 0.1 M KCl. Figure attached to each line represents the apparent cationic transport number, t'_+, of the membrane applied. Vertical arrows show the return of potential to the isothermal value on stopping the flow.

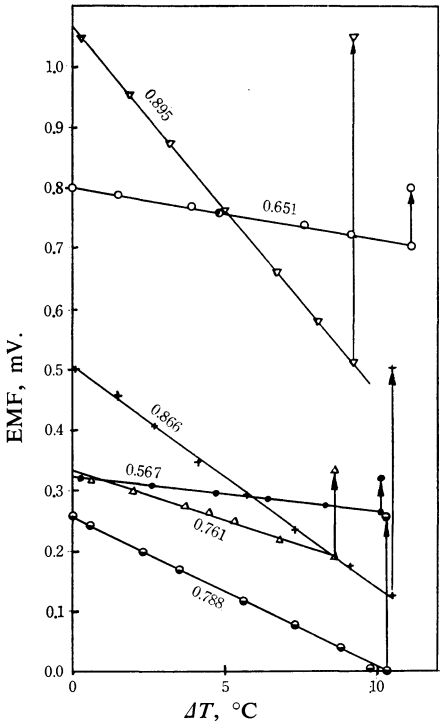


Fig. 3. EMF for aniline-formaldehyde resin-cellophane matrix membranes in 0.1 M KCl. Figure attached to each line represents the apparent anionic transport number, t'_-, of the membrane applied. Vertical arrows show the return of the potential to the isothermal value on stopping the flow.

as those found in previous works,[1,2] so the details are omitted here.

In Figs. 4 and 5 the values of dE/dT were plotted against the apparent ionic transport number, t'_+ or t'_- of the membranes. Here we found that the dE/dT values were characteristic of the nature of the membrane used, with negative signs for positive membranes ($t'_- > 0.5$), and positive signs for negative membranes ($t'_+ > 0.5$). In either negative or positive membranes, the absolute value of dE/dT is reduced practically to zero by the extrapolation at $t'_- = 0.5$ (or at $t'_+ = 0.5$) ; it gradually increases when the degree of the ionic permselectivity of the membrane is increased, and it precipitously reaches the highest limit characteristic of the nature of the membane at the extreme transport numbers of $t'_- = 1$ (or $t'_+ = 1$). In general, the absolute value of dE/dT for positive membranes was found always to be much higher than that for negative membranes at the equivalent values of the degree of the ion permselectivies of these two membranes.

According to our theory on the TMP,[2] dE/dT should be linear with the apparent transport number, t'_K, of the membrane used,

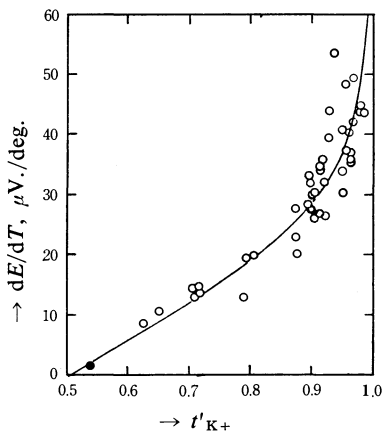


Fig. 4. Relation between thermoelectric power and apparent cationic transport number of oxidized collodion membranes in 0.1 M KCl. Black circle indicates the value for cellophane.

provided that the heats of the transfer of ions in the membrane phase are constant. However, as is clear in Figs. 4 and 5, this is not the case. This fact might indicate that the heats of the transfer of ions in the membrane phase

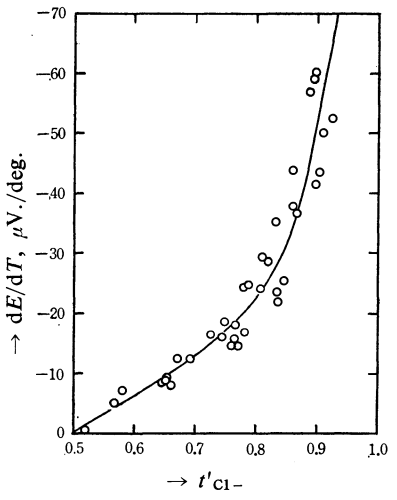


Fig. 5. Relation between thermoelectric power and apparent anionic transport number of aniline-formaldehyde resin-cellophane matrix membranes in 0.1 M KCl.

should be a function of the apparent ionic transport number of that membrane. This conclusion is very plausible; since the heats of the transfer of ions are substantially of a kinetic nature, accordingly the value of ionic heats of transfer in the membrane phase should depend on the membrane structure or on its measure, such as the apparent ionic transport number of the membrane. The relation between the ionic heat of transfer in the membrane phase and the apparent ionic transport number of the membrane has not yet been clarified, but it should be studied.

Summary

The thermal membrane potential (TMP) has been studied as a function of the apparent ionic transport number of ionselective membranes. The temperature coefficient of TMP, the thermoelectric power, has been found to be a continuously increasing function of the apparent ionic transport number of the membranes used, starting from zero at the neutral point, where the membrane exhibits no selectivity for ions, and approaching with acceleration when the ionic transport number of the membrane is increased until it reaches its highest limit at the perfect ion permselectivity. The sign of the thermoelectric power has been found to be positive for negative membranes, and negative for positive membranes. The absolute value of the thermoelectric power is higher for positive membranes than for negative membranes at equivalent degrees of ion permselectivity.

Department of Chemistry
Shizuoka University
Oiwa, Shizuoka

Transported Entropies and Conventional Eastman Entropies of the Transfer of Some Univalent Ions in Aqueous Solutions at 25°C

By Toshio IKEDA

(Received April 25, 1964)

An absolute estimation of the transported entropies* of individual ions was carried out previously by the present writer.[1,2] However, recently Turner and his co-workers[3] have reported reliable, and perhaps final, values of the Soret coefficient for a number of 1 : 1-electrolytes by using a conductivity method, and since the data of the Soret coefficients used in our previous calculations were less reliable than Turner's values, and since much the same thing can be said of the data on initial thermoelectric powers used previously, it is worthwhile to recalculate the transported entropies of single ions by using the most accurate data now available.

General. — The transported entropy for a single ion can be calculated exclusively from the experimental data on the initial thermoelectric power of the thermocell and the Soret coefficient without making any conventional

* The term "entropy of transfer" as defined by De Groot was used in the previous work and indicated with the symbol S^*, which is quite identical with the "transported entropy" used here with the symbol $\bar{\bar{S}}$. However, the usage of the former is undesirable, because such use causes confusion with the Eastman entropy of transfer, S^*, defined by Q^*/T, where Q^* is the heat of transfer at the absolute temperature, T.

1) T. Ikeda, This Bulletin, **32**, 97 (1959).

2) T. Ikeda, *Rep. Liberal Arts Sci. Fac., Shizuoka Univ., Nat. Sci.*, **2**, 153 (1959).

3) P. N. Snowdon and J. C. R. Turner, *Trans. Faraday Soc.*, **56**, 1409 (1960).

TABLE I. ELECTROCHEMICAL DATA AT 25°C AND 0.01 M

t_+=cationic transport number; $\gamma_\pm$=mean activity coefficient; $\gamma'=-\boldsymbol{R}T\mathrm{d}\ln\gamma_\pm/\mathrm{d}T$ (in cal./deg.); $B=1+\mathrm{d}\ln\gamma_\pm/\mathrm{d}\ln m$; σ=Soret coefficient (in deg^{-1})

Electrolyte	t_+[a]	$\gamma_\pm$[b]	γ'	B	$-\sigma\times10^3$[c]
HCl	0.8251	0.904	0.04	0.958	9.01
LiCl	0.3289	0.906	0.10	0.969	−0.01
NaCl	0.3918	0.903	0.09	0.958	2.02
KCl	0.4902	0.902	0.10	0.956	1.43
RbCl	0.497	0.903	0.10	0.945	2.33
CsCl	0.504	0.896	0.11	0.942	2.44
LiBr	0.3226	0.909	0.05	0.962	0.05
NaBr	0.3853	0.9137	0.05	0.963	2.12
KBr	0.4833	0.9033	0.02	0.957	1.46
LiI	(0.235)	(0.908)	0.03	0.961	−1.47
NaI	(0.395)	0.917	0.02	0.958	0.54
KI	0.4884	0.905	0.02	0.960	−0.11
NaOH	0.1952	0.903	0.10	0.951	13.76
KOH	0.2658	0.901	0.07	0.954	13.31

a) B. E. Conway, "Electrochemical Data," Elsevier Publishing Co., Amsterdam, Netherlands (1952).
b) Ref. 7.
c) Ref. 3.

assumption other than postulating the additivity for the partial molar ion entropies as well as for the ionic entropies (or heats) of transfer, though this property is now commonly acceptable, particularly in dilute solutions. The basic relations for calculating the transported entropies of individual ions are just the same as those used in the previous works.[1,2] In the simpler case, where the electrolyte contains a single salt giving two kinds of univalent ions, they are:[1,2,4]

$$\overline{\overline{S}}_+=-\boldsymbol{F}\varepsilon_0-\overline{\overline{S}}_{el}+\Delta S^\circ{}_M-2t_-\boldsymbol{RT}B\sigma \quad (1)$$

and

$$\overline{\overline{S}}_-=\boldsymbol{F}\varepsilon_0+\overline{\overline{S}}_{el}-\Delta S^\circ{}_M-2t_+\boldsymbol{RT}B\sigma+(S_++S_-) \quad (2)$$

when the initial thermoelectric power for thermocells with cation-reversible electrodes is available, and

$$\overline{\overline{S}}_+=-\boldsymbol{F}\varepsilon_0-\overline{\overline{S}}_{el}+\Delta S^\circ{}_R-2t_-\boldsymbol{RT}B\sigma+(S_++S_-) \quad (3)$$

and

$$\overline{\overline{S}}_-=\boldsymbol{F}\varepsilon_0+\overline{\overline{S}}_{el}-\Delta S^\circ{}_R-2t_+\boldsymbol{RT}B\sigma \quad (4)$$

when the ε_0 for thermocells with anion-reversible electrodes is available. Here, $\boldsymbol{F}$ is the Faraday constant. $\overline{\overline{S}}_k$ represents the transported entropy of k ion species in an m molar solution; it is defined by $\overline{\overline{S}}_k=S_k+S_k{}^*$, where S_k and $S_k{}^*$ are the absolute partial molar entropy and the absolute molar Eastman entropy of the transfer of k ion species respectively. The latter $S_k{}^*$, the Eastman entropy of the transfer of k ion species, is related to the Soret coefficient, σ, as follows: for a 1 : 1- electrolyte it is

$$\sigma=-\frac{\mathrm{d}\ln m}{\mathrm{d}T}=-\frac{S_+{}^*+S_-{}^*}{2\boldsymbol{RT}B},\quad B=\left(1+\frac{\mathrm{d}\ln\gamma_\pm}{\mathrm{d}\ln m}\right)_T \quad (5)$$

where $\boldsymbol{R}$ is the gas constant; T is the absolute temperature and $\gamma_\pm$ is the mean ion activity coefficient on the molality scale at the molality of m. $\overline{\overline{S}}_{el}$ denotes the transported entropy of electrons in the metallic leads of the thermocell concerned. t_+ and t_- are, respectively, the transport numbers of cations and anions. Finally, $\Delta S^\circ{}_M$ and $\Delta S^\circ{}_R$ refer to the contributions from the changes in the standard molar entropies of the electrode materials of the thermocells for the electrode reactions per Faraday. They differ with the electrode system; their practical forms are: $\Delta S^\circ{}_M=1/2\,S^\circ{}_{H_2}$ for a hydrogen electrode; $\Delta S^\circ{}_R=S^\circ{}_{Ag}-S^\circ{}_{AgX}$ for electrodes of silver/silver halide; $S^\circ{}_{Hg}-S^\circ{}_{HgCl}$ for mercury/calomel electrodes and $1/2(S^\circ{}_{Hg}-S^\circ{}_{HgO}-S^\circ{}_{H_2O})$ for mercury/mercuric oxide electrodes when alkali hydroxide is used as an electrolyte.

Calculations. — The salt entropy, (S_++S_-), was calculated in a formal manner by:

$$S_++S_-=S^\circ{}_++S^\circ{}_--2\boldsymbol{R}\ln m\gamma_\pm-2\boldsymbol{RT}\,\mathrm{d}\ln\gamma_\pm/\mathrm{d}T$$

where $S^\circ{}_+$ and $S^\circ{}_-$ are, respectively, the

4) For example, H. J. V. Tyrrell, "Diffusion and Heat Flow in Liquids," Butterworths, London (1961).

TABLE II. TRANSPORTED ENTROPIES, $\overline{\overline{S}}_+$ AND $\overline{\overline{S}}_-$, AND "REDUCED" TRANSPORTED ENTROPIES, $\overline{\overline{S}}^\circ_+$ AND $\overline{\overline{S}}^\circ_-$, FOR CATION AND ANION SPECIES, RESPECTIVELY, AT 25°C AND 0.01 M

ε_0=initial thermoelectric power

Electrolyte	Thermocell electrodes	ε_0 μV./deg.	$\overline{\overline{S}}_+$ e. u.	$\overline{\overline{S}}_-$ e. u.	$\overline{\overline{S}}^\circ_+$ e. u.	$\overline{\overline{S}}^\circ_-$ e. u.
HCl	Pt/H_2	142[a]	14.07	28.45	4.67	19.05
	Ag/AgCl	288[b]	14.67	27.90	5.23	18.50
	Hg/HgCl	636[c]	14.51	28.06	5.07	18.61
	Hg/HgCl	639[d]	14.44	28.12	5.00	18.72
LiCl	Ag/AgCl	669[b]	8.85	28.24	−0.60	18.79
	Hg/HgCl	1006[d]	8.94	28.15	−0.51	18.70
NaCl	Ag/AgCl	631[b]	20.44	28.27	10.98	18.81
	Hg/HgCl	963[d]	20.65	28.06	11.19	18.60
KCl	Ag/AgCl	640[b]	29.88	28.37	20.42	18.90
	Hg/HgCl	972[d]	30.09	28.16	20.63	18.69
RbCl	Ag/AgCl	614[a]	35.47	28.27	26.00	18.81
CsCl	Ag/AgCl	607[a]	38.82	28.19	29.33	18.70
LiBr	Ag/AgBr	831.3[c]	8.65	34.63	−0.75	25.20
NaBr	Ag/AgBr	788.8[c]	20.36	34.56	10.98	25.14
KBr	Ag/AgBr	794.6[c]	29.78	34.35	20.41	25.14
LiI	Ag/AgI	946[e]	8.50	38.57	−0.87	29.19
NaI	Ag/AgI	902[e]	20.44	38.19	11.08	28.83
KI	Ag/AgI	918[e]	29.87	38.25	20.50	28.88
NaOH	Hg/HgO	661.0[c]	19.92	26.03	10.46	16.56
KOH	Hg/HgO	617.0[c]	29.64	25.99	20.21	16.55

a) F. M. Goyan, Thesis, Univ. of California (1937).
b) J. C. Goodrich, Thesis, Univ. of California (1941).
c) J. C. Goodrich, F. M. Goyan, E. E. Morse, R. G. Preston and M. B. Young, *J. Am. Chem. Soc.*, **72**, 4411 (1950).
d) M. B. Young, Thesis, Univ. of California (1935).
e) R. G. Preston, Thesis, Univ. of California (1941).

standard partial molar entropies of cations and anions; their conventional values are given by Latimer and his co-workers.[5] The salt entropy is independent of the convention adopted in assigning its ion constituents; its absolute value is given on the basis of the third law. The other values of the standard entropies may be available in NBS service.[6] The values of B in 5 were obtained graphically from the mean ion activity coefficients.[7] The temperature coefficients of the mean ion activity coefficients can rarely be obtained by direct observation, so in most cases they were estimated by differentiating the Debye-Hückel equation. The transported entropy of electrons, $\overline{\overline{S}}_{el}$, in the metallic leads of thermocelles was approximated by the entropy of electrons; e. g., 0.04 e. u. for copper, and 0.05 e. u. for silver.[2] The other numerical data necessary for the calculations are listed in Table I, except for the ε_0 values, which are listed in Table II. All the data cited in the tables were taken at 25°C and 0.01 M. The σ values listed in Table I are those of Snowdon-Turner, but they have been corrected to 25°C at a rate[8] of $0.01\times10^{-3}\cdot deg^{-1}$ per degree of deviation in the mean temperature, at which the Soret coefficients were measured, from 25°C, since their original values were determined at mean temperatures slightly different from 25°C, ranging from 24.8°C to 25.4°C.

Upon applying these new data regarding σ and ε_0 as listed in Tables I and II to Eqs. 1—4, we get the transported entropies of individual ion species, i. e., $\overline{\overline{S}}_+$ and $\overline{\overline{S}}_-$. The results are listed in Table II. The single-ion transported entropies, $\overline{\overline{S}}_+$ and $\overline{\overline{S}}_-$, here obtained have been found to have their proper values characteristic of the nature of ions; they are nearly independent of the other ions present in the solution and of the type of the thermocells participating. This consequence is very important in yielding the transported entropies

5) W. M. Latimer, K. S. Pitzer and W. V. Smith, *J. Am. Chem. Soc.*, **60**, 1829 (1938).
6) "Selected Values of Chemical Thermodynamic Properties," National Bureau of Standards, U. S. Government Printing Office, Washington, D. C. (1952).
7) Landolt-Börnstein, "Physik. Chem. Tabellen," Erg. Bd. II (1931), III (1936).
8) J. N. Agar and J. C. R. Turner, *Proc. Roy. Soc.*, **A255**, 307 (1960).

TABLE III. MEAN AND SELF-CONSISTENT VALUES OF "REDUCED" TRANPORTED ENTROPIES, $\bar{\bar{S}}^{\circ}_{k}$, AND CONVENTIONAL EASTMAN ENTROPIES OF TRANSFER, S_k^*, (IN cal./deg./mol.), AND HEATS OF TRANSFER, Q_k^*, (IN cal./mol.) FOR INDIVIDUAL IONS AT 25°C AND 0.01 M

The value in parentheses was adopted as the standard for estimating the self-consistent values of $\bar{\bar{S}}^{\circ}_{k}$.

Ion	$\bar{\bar{S}}^{\circ}_{k}$ mean	$\bar{\bar{S}}^{\circ}_{k}$ selfcon.	S°_{k}(con) Ref. 5	S_k^*(con) Eq. 8	Q_k^*(con)
H^+	4.99±0.15	5.00	0	5.00	1490
Li^+	−0.68±0.11	−0.54	4.7	−5.24	−1562
Na^+	10.98±0.18	11.06	14.0	−2.94	− 878
K^+	20.43±0.10	20.59	24.2	−3.61	−1077
Rb^+	26.00	26.08	28.7	−2.62	− 782
Cs^+	29.33	29.30	31.8	−2.50	− 745
OH^-	16.56±0.01	16.06	−2.49	18.55	5530
Cl^-	18.73±0.10	(18.73)	13.5	5.23	1560
Br^-	25.16±0.02	25.01	19.7	5.31	1584
I^-	28.97±0.13	28.83	25.3	3.53	1052

as an absolute (not conventional) partial molar quantity without making any conventional assumptions. It would be desirable, if possible, to split $\bar{\bar{S}}_k$ into its two constituents, the absolute partial molar entropy, S_k, and the absolute molar Eastman entropy of transfer, S_k^*; however, we have no basis for doing so as yet.

On the other hand, it would be convenient to use a "reduced" quantity defined by ($\bar{\bar{S}}^{\circ}_{k} \equiv S^{\circ}_{k} + S_k^*$), which is equivalent to ($\bar{\bar{S}}_k - \boldsymbol{R} \ln m\gamma_k - \boldsymbol{RT} \mathrm{d} \ln \gamma_k / \mathrm{d}T$), in comparing $\bar{\bar{S}}_k$ values given at different concentrations, since $\bar{\bar{S}}_k$ depends greatly upon the concentration. To do this, $\gamma_+ = \gamma_- = \gamma_\pm$ was assumed for uni-univalent electrolytes. Calculated values of $\bar{\bar{S}}^{\circ}_{k}$ for cation and anion species are listed on the last two columns in Table II.

By using the calculated values of $\bar{\bar{S}}^{\circ}_{k}$ in Table II we have determined self-consistent values of $\bar{\bar{S}}^{\circ}_{k}$ for individual ion species by the following process: the most probable value of the "reduced" transported entropy of one ion species, for example, of the chloride ion (because so much data on it is available in the present case), was used as the standard for the estimation of the "reduced" transported entropies of its conjugate cations by subtracting it from $\bar{\bar{S}}^{\circ}_{MCl}$, the "reduced" transported entropy of any chloride MCl, which is calculable as the sum of the standard entropy and the Eastman entropy of transfer for one mole of the chloride MCl. Then the value of $\bar{\bar{S}}^{\circ}_{M^+}$, the "reduced" transported entropy of the cation, M^+, here determined was subtracted from $\bar{\bar{S}}^{\circ}_{MX}$, the "reduced" transported entropy of the other electrolyte, MX, with a common cation, M^+, to yield a self-consistent value of $\bar{\bar{S}}^{\circ}_{X^-}$ for any anion species, X^-. The process may then be extended.

The agreements between the self-consistent values thus determined and the simple average of $\bar{\bar{S}}^{\circ}_{k}$ for individual ion species from Table II are found in Table III to be fairly good, except for the hydroxide ion; the lack of agreement here may be due to the fact that the Soret coefficients of the hydroxides observed by Snowdon and Turner were somewhat lower. At any rate, the fact that such a good harmony was found might indicate, in other words, that the values of the Soret coefficient measured by Snowdon and Turner were quite proper.

Entropies of Transfer Based on the Convention of $\bar{\bar{S}}^{\circ}_{H^+}$(con)≡0. — The relation between the absolute (abs) and the conventional (con) standard molar entropies for k ion species of the ionic valency z_k can be written as follows:

$$\left.\begin{aligned} S^{\circ}_{H^+}(\mathrm{con}) &\equiv 0 \\ S^{\circ}_{k}(\mathrm{con}) &= S^{\circ}_{k}(\mathrm{abs}) - z_k S^{\circ}_{H^+}(\mathrm{abs}) \end{aligned}\right\} \quad (6)$$

We may define further the absolute and the conventional molar Eastman entropies of transfer respectively by the following equations:

$$S_k^*(\mathrm{abs}) = \bar{\bar{S}}^{\circ}_{k} - S^{\circ}_{k}(\mathrm{abs}) \quad (7)$$

and

$$S_k^*(\mathrm{con}) = \bar{\bar{S}}^{\circ}_{k} - S^{\circ}_{k}(\mathrm{con}) \quad (8)$$

By taking 6 into account, we have the alternative expression for S_k^*(con) as follows:

$$S_k^*(\mathrm{con}) = S_k^*(\mathrm{abs}) + z_k S^{\circ}_{H^+}(\mathrm{abs}) \quad (9)$$

or

$$Q_k^*(\text{con}) = Q_k^*(\text{abs}) + z_k T S^\circ_{H^+}(\text{abs}) \quad (10)$$

Equation 9 gives a definite basis for the conventional Eastman entropy of transfer as defined by 8 to be based on the same convention as that adopted in assigning the ion entropy: the convention of $S^\circ_{H^+}(\text{con}) \equiv 0$ for an aqueous hydrogen ion of one molal activity at 25°C and 1 atm.

Now, if only $S^\circ_{H^+}(\text{abs})$ were known, all the absolute values of S_k^* could be known from Eq. 9; however, the absolute values of $S^\circ_{H^+}$ estimated so far by some authors[9-12] are not sufficient as yet to realize such a purpose. Consequently, only the conventional values of S_k^* and Q_k^* (as based on the convention of zero for the hydrogen ion, not for the chloride ion as adopted by most authors) were calculated; they are listed in the last two columns in Table III. These conventional values may be converted easily into absolute ones by the aid of Eq. 9 or 10, when $S^\circ_{H^+}(\text{abs})$ is available. The values of $S_k^*(\text{con})$ or $Q_k^*(\text{con})$ in Table III may be used conveniently for predicting unknown Soret coefficients by means of a combination of the ions indicated in the table.

9) J. C. Goodrich, F. M. Goyan, E. E. Morse, R. G. Preston and M. B. Young, *J. Am. Chem. Soc.*, **72**, 4411 (1950).
10) D. D. Eley and M. G. Evans, *Trans. Faraday Soc.*, **34**, 1093 (1938).
11) W. M. Latimer, K. S. Pitzer and C. M. Slansky, *J. Chem. Phys.*, **7**, 108 (1939).
12) R. M. Noyes, *J. Am. Chem. Soc.*, **84**, 513 (1962).

Summary

Absolute ionic transported entropies, conventional ionic Eastman entropies of transfer, and conventional ionic heats of transfer, using the same convention ($S^\circ_{H^+} \equiv 0$) as that adopted in assigning conventional standard ionic entropies, have been recalculated for ten univalent ions from the most accurate data now available on the initial thermoelectric powers and the Soret coefficients.

Department of Chemistry
Shizuoka University
Oiwa, Shizuoka

The Potential Constants of Phosphorus Trihalide and Phosphoryl Halides

By Yasuo NAKAI and Kumiko MORI

(Received May 2, 1964)

The Raman and infrared spectra of phosphorus trihalides and phosphoryl halides in the solid, liquid and vapor phases have previously been obtained.[1a,1b] The normal vibrations of PCl_3 and PBr_3 have been calculated on the basis of the general quadratic potential function derived by Howard and Wilson.[2] Using the mean square amplitudes of vibration obtained from gaseous electron diffraction experiments, together with the normal vibration frequencies, Iwasaki and Hedberg attempted to get a reasonable set of potential constants of the general quadratic function where the interaction terms between bond stretching and angle deformation are included.[3] On the other hand, no detailed studies of the potential constants of phosphoryl halides have yet been tried.

It is necessary to undertake a theoretical treatment of the experimental data on the vibrational spectra of phosphorus compounds in order to obtain reasonable potential constants which are transferable among phosphorus compounds.

At first the normal vibrations of pyramidal-type molecules, such as PCl_3 and PBr_3, were calculated by means of a modified Urey-Bradley force field (UBFF), and then phosphoryl halides, $OPCl_3$ and $OPBr_3$ were calculated by

1) a) PF_3: H. S. Gutowsky and A. D. Liehr, *J. Chem. Phys.*, **20**, 1652 (1952); M. L. Delwaulle and F. François, ibid., **46**, 87 (1949).
PCl_3: M. L. Delwaulle, *Compt. rend.*, **224**, 389 (1947); M. L. Lorenzell and K. D. Moler, ibid., **248**, 1980 (1959); M. L. Lorenzell, ibid., **252**, 3219 (1961).
PBr_3: M. L. Delwaulle and F. François, *J. Phys. Radium*, **7**, 15, 53 (1946).
b) OPF_3: M. L. Delwaulle and F. François, *Compt. rend.*, **226**, 895 (1948); **222**, 550, 1173 (1946); *J. Chim. Phys.*, **46**, 87 (1949); H. S. Gutowsky and A. D. Liehr, *J. Chem. Phys.*, **20**, 1652 (1952).
$OPCl_3$: M. L. Delwaulle and F. François, *Compt. rend.*, **220**, 817 (1945); *J. Phys. Radium*, **7**, 15, 53 (1946).
$OPBr_3$: M. L. Delwaulle and F. François, *Bull. soc. chim. France*, **13**, 206 (1946); *J. Chim. Phys.*, **45**, 50 (1948).

2) J. B. Howard and E. B. Wilson, ibid., **2**, 630 (1934); H. S. Gutowsky and A. D. Liehr, ibid., **20**, 1652 (1952); V. Lorenzell and K. D. Moler, *Compt. rend.*, **248**, 1980 (1959); V. Lorenzell, ibid., **252**, 3219 (1961); P. W. Davis and R. A. Oetjen, *J. Mol. Spectry.*, **2**, 253 (1958).

3) M. Iwasaki and K. Hedberg, *J. Chem. Phys.*, **36**, 594 (1962).

means of a Urey-Bradley-Shimanouchi force field (UBSFF). It was found that there exists a relationship between the potential constants of the PCl_3, PBr_3, $OPCl_3$ and $OPBr_3$ compounds and the constants for the mixed halogen phosphorus compounds, PCl_2Br, $PClBr_2$, $OPCl_2 \cdot Br$ and $OPClBr_2$.

Normal Coordinate Treatment and Results

The Calculation of the Potential Constants of PCl_3 and PBr_3.—The Raman spectra of PCl_3 and PBr_3 reported by Delwaulle were used for the calculation of the potential constants in the present study. PCl_3 and PBr_3 have the pyramidal-type structure with C_{3v} symmetry.

As a potential function, the following modified UBFF was used:

$$V=\sum K'_{t0}\Delta r_{t0}+1/2\sum K_{t0}(\Delta r_{t0})^2 + \sum H'_{t0f}(r_{t0}r_{f0})^{1/2}\Delta\phi_{t0f}+1/2\sum H_{t0f}r_{t0}r_{f0}\cdot (\Delta\phi_{t0f})^2+\sum F'_{tf}\Delta q_{tf}+1/2\sum F_{tf}(\Delta q_{tf})^2 + \sum k_{tf}(\Delta r_{t0})(\Delta r_{f0}) + \sum h_{ijk}(r_{i0}r_{j0})^{1/2}(r_{j0}r_{k0})^{1/2}(\Delta\phi_{t0f})(\Delta\phi_{j0k}) \quad (1)$$

where K, H and F are the potential constants for bond stretching, angle deformation and interaction between non-bonded atoms respectively; k and h are the interaction terms between two bond-stretching coordinates and between two angle-deformation coordinates respectively. The following symmetry coordinates were used:

$$S_1(A_1)=3^{-1/2}(\Delta r_{01}+\Delta r_{02}+\Delta r_{03})$$
$$S_2(A_1)=3^{-1/2}(\Delta\phi_{102}+\Delta\phi_{203}+\Delta\phi_{301})$$
$$S_3(E)=2^{-1/2}(\Delta r_{02}-\Delta r_{03})$$
$$S_4(E)=2^{-1/2}(\Delta\phi_{301}-\Delta\phi_{102})$$
$$S_3^*(E)=6^{-1/2}(2\Delta r_{01}-\Delta r_{02}-\Delta r_{03})$$
$$S_4^*(E)=6^{-1/2}(2\Delta\phi_{203}-\Delta\phi_{301}-\Delta\phi_{102})$$

The secular equation, $|GF-E\lambda|=0$, is set up according to Wilson's method.[4]

An IBM model 7090 digital computer was used for the numerical computations involved in the normal coordinate treatment.

In the calculations using the simple UBFF, where k and h are assumed to be zero and F' is $-F/10$, the stretching, K_{AS}, and deformation, H_{AS}, potential constants of PCl_3 (and PBr_3) against F were determined from the two frequencies observed at 510 cm^{-1} and 257 cm^{-1} (380 cm^{-1} and 162 cm^{-1}) belonging to the A_1 species; also K_{ES} and H_{ES} were determined from the 480 cm^{-1} and 190 cm^{-1} (400 cm^{-1} and 116 cm^{-1}) belonging to the E species. A convenient representation of the relationship among the potential constants is obtained by plotting K and H against F in Figs. 1 and 2.

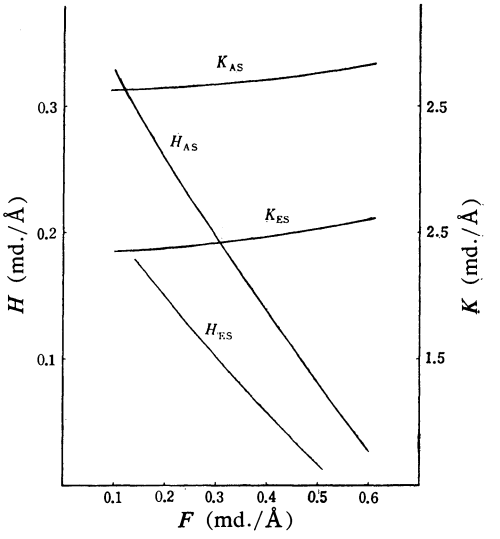


Fig. 1. The correlation of potential constants for PCl_3.

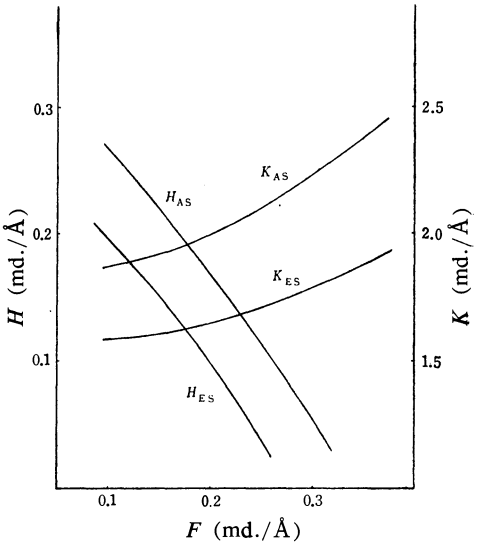


Fig. 2. The correlation of potential constants for PBr_3.

All the combinations of the K and H potential constants for the A_1 species are incompatible with those of the E species. We could not find any common values for the potential constants of the two symmetry species.

Therefore, we used a modified UBFF in our calculations. The relationship between the potential constants, K and H, of the simple UBFF and those of the modified UBFF may be expressed as follows:

4) E. B. Wilson, Jr., ibid., 7, 1047 (1939); 9, 76 (1941).

Table I. Potential constants (md./Å) and molecular parameters of phosphorus chloride

	K	H	k	h	F_{calcd}	r, Å	ϕ(degree)
PCl_3	2.182	0.168	0.217	0.036	0.244	2.039	100° 27′
PBr_3	1.870	0.106	0.110	0.021	0.231	2.18	101° 5′
$AsCl_3$*	2.021	0.148	0.182	0.025	0.127	2.16	98° 4′
$SbCl_3$*	1.774	0.164	0.199	0.030	0.032	2.33	99° 5′
$BiCl_3$*	1.186	0.100	0.172	0.025	0.010	2.48	100° 0′

* The potential constants of the Vth group elements were calculated by the same method.

Table II. Molecular parameters of phosphoryl chloride and bromide

	r_{01}	r_{02}	ϕ_{102}	ϕ_{203}
$OPCl_3$	1.45 Å	1.99 Å	115° 16′	103° 6′
$OPBr_3$	1.45 Å	2.18 Å	117°	101°

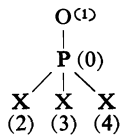


Table III. Potential constants of phosphoryl chloride and bromide (md./Å)

	$OPCl_3$			$OPBr_3$	
	Set 1	Set 2		Set 1	Set 2
$K_{P=O}$	9	9.85	$K_{P=O}$	9	9.50
K_{P-Cl}	2.2	2.54	K_{P-Br}	1.9	1.9
$F_{O\cdot\cdot(P)\cdot\cdot Cl}$	0.13	0.25	$F_{O\cdot\cdot(P)\cdot\cdot Cl}$	0.10	0.10
$F_{Cl\cdot\cdot(P)\cdot\cdot Cl}$	0.27	0.27	$F_{Br\cdot\cdot(P)\cdot\cdot Br}$	0.25	0.25
H_{OPCl}	0.2	0.286	H_{OPBr}	0.15	0.28
H_{ClPCl}	0.2	0.12	H_{BrPBr}	0.1	0.1
χ(md. Å)	0.06	0.06	χ(md. Å)	0.04	0.04

$$K=1/3(K_{AS}+2K_{ES}) \qquad k=1/3(K_{AS}-K_{ES})$$
$$H=1/3(H_{AS}+2K_{ES}) \qquad h=1/3(H_{AS}-H_{ES})$$

where K_{AS} and H_{AS}, and K_{ES} and H_{ES} are the stretching and deformation constants obtained from the A_1 and E species respectively, using the simple UBFF. The repulsive potential constants, $F_{Cl\cdot\cdot(P)\cdot\cdot Cl}$ and $F_{Br\cdot\cdot(P)\cdot\cdot Br}$, are estimated from the interatomic forces between Ar··Ar atoms and also from those between Kr··Kr atoms on the basis of the Lennard-Jones potential.[5] The potential constants, K, H, k and h, can be calculated from the observed frequencies by using the modified UBFF.

The potential constants and molecular parameters[6] are shown in Table I.

The Calculation of the Potential Constants of $OPCl_3$ and $OPBr_3$.—In order to investigate the relationship between the potential constants of phosphoryl halides and phosphorus trihalides, the normal vibrations of $OPCl_3$ and $OPBr_3$ were also calculated on the basis of the UBSFF. For this type of molecule, the internal tension, due to the redundancy among six angles is introduced.[7]

The following set of linear combinations of internal coordinates was chosen as the symmetry coordinates:

For the A_1 type:

$$S_1=\Delta r_{01}$$
$$S_2=3^{-1/2}(\Delta r_{02}+\Delta r_{03}+\Delta r_{04})$$
$$S_3=(3A^2+3B^2)^{-1/2}[B(\Delta\phi_{102}+\Delta\phi_{103}+\Delta\phi_{104}) - A(\Delta\phi_{304}+\Delta\phi_{402}+\Delta\phi_{203})]$$
$$S_4=(3A^2+3B^2)^{-1/2}[A(\Delta\phi_{102}+\Delta\phi_{103}+\Delta\phi_{104}) + B(\Delta\phi_{304}+\Delta\phi_{402}+\Delta\phi_{203})]$$

(S_4 is redundant.)

$$A=2ab(c-1)^2 \qquad B=2d(c-1)(a^2-c)$$
$$a=\cos\phi_{102}, \quad b=\sin\phi_{102}, \quad c=\cos\phi_{203}, \quad d=\sin\phi_{203}$$

For the E type:

$$S_5=6^{-1/2}(2\Delta r_{02}-\Delta r_{03}-\Delta r_{04})$$
$$S_6=6^{-1/2}(2\Delta\phi_{102}-\Delta\phi_{103}-\Delta\phi_{104})$$
$$S_7=6^{-1/2}(2\Delta\phi_{304}-\Delta\phi_{402}-\Delta\phi_{203})$$
$$S_5^*=2^{-1/2}(\Delta r_{03}-\Delta r_{04})$$
$$S_6^*=2^{-1/2}(\Delta\phi_{103}-\Delta\phi_{104})$$
$$S_7^*=2^{-1/2}(\Delta\phi_{402}-\Delta\phi_{203})$$

5) T. Shimanouchi, *Pure Appl. Chem.*, 7, 131 (1963).
6) P. W. Allen and L. E. Sutton, *Acta Cryst.*, 3, 46 (1950).
7) T. Shimanouchi, *Bull. Inst. Phys. Chem. Research (Tokyo)*, 21, 825 (1942).

TABLE IV. OBSERVED AND CALCULATED FREQUENCIES (IN cm^{-1})

a) $OPCl_3$

	ν_{obs}	ν^1_{calcd}	Δ^1	ν^2_{calcd}	Δ^2
A_1 species	1292	1231	− 4.7	1292	0
	486	444	− 8.6	480	−1.2
	268	265	− 1.1	256	−4.5
E species	582	542	− 7.0	587	+0.9
	337	269	−20.0	339	+0.6
	191	218	+14.1	191	0

b) $OPBr_3$

	ν_{obs}	ν^1_{calcd}	Δ^1	ν^2_{calcd}	Δ^2
A_1 species	1260	1225	− 2.8	1259	−0.1
	340	336	− 1.2	342	+0.6
	173	166	− 4.0	176	+1.7
E species	488	446	− 8.6	486	+0.2
	267	217	−18.7	266	−0.4
	118	122	+ 3.4	122	+3.4

Δ: Percent deviation $100(\nu_{calcd}-\nu_{obs})/\nu_{obs}$

The molecular parameters[8] used in the calculations are given in Table II.

The potential constants of set 1 (Table III) were estimated from those of PX_3. Then the potential constants of set 2 (Table III) were selected to yield a better agreement between the observed and calculated frequencies for $OPCl_3$ and $OPBr_3$, except for $F_{Cl\cdot\cdot(P)\cdot\cdot Cl}$ and $F_{Br\cdot\cdot(P)\cdot\cdot Br}$, which were estimated from the Lennard-Jones potential as in the case of PX_3-type molecules. The calculated frequencies are compared with the observed frequencies in Table IV.

The Potential Constants of Mixed Halides of Phosphorus Compounds: PCl_2Br, $PClBr_2$, $OPCl_2Br$ and $OPClBr_2$.—Delwaulle and others[9] have shown that the mixing of PCl_3 and PBr_3 yields PCl_2Br and $PClBr_2$.

The normal vibrations of PCl_2Br and $PClBr_2$ were calculated. The values of the stretching-potential constants, K_{PCl} and K_{PBr}, were transferred from those of PCl_3 and PBr_3, while those of the deformation constant, H_{ClPBr}, and the repulsive constant, $F_{Cl\cdot\cdot(P)\cdot\cdot Br}$, for PCl_2Br and $PClBr_2$ were assumed to be the harmonic mean of those for PCl_3 and PBr_3 as follows:

$$k_{ij}=2\,[k_{ii}k_{jj}/(k_{ii}+k_{jj})]$$

The derivation of the values of the $[h]$ constants, for example, $h_{ClPBr\cdot BrPBr}$ may be shown as follows:

$$h_{ClPBr\cdot BrPBr}=2\,[h_{ClPBr}\cdot h_{BrPBr}/(k_{ClPBr}+h_{BrPBr})]$$

where

$$h_{ClPBr}=2\,[h_{ClPCl}\cdot h_{BrPBr}/(h_{ClPCl}+h_{BrPBr})].$$

Those potential constants of PCl_2Br and $PClBr_2$ are shown in Table V. The arithmetic mean was taken for the value of molecular parameters. Table VI compares the observed and calculated frequencies for PCl_2Br and $PClBr_2$.

The normal vibrations of $OPCl_2Br$ and $OPClBr_2$ were calculated by the same method as was used for PCl_2Br and $PClBr_2$.

TABLE V. POTENTIAL CONSTANTS OF MIXED HALOGEN COMPOUNDS (md./Å)

PCl_2Br		$PClBr_2$	
K_{P-Cl}	2.182	K_{P-Cl}	2.182
K_{P-Br}	1.870	K_{P-Br}	1.870
H_{ClPBr}	0.130	H_{ClPBr}	0.130
H_{ClPCl}	0.168	H_{BrPBr}	0.106
$F_{Cl\cdot\cdot(P)\cdot\cdot Cl}$	0.244	$F_{Br\cdot\cdot(P)\cdot\cdot Br}$	0.231
$F_{Cl\cdot\cdot(P)\cdot\cdot Br}$	0.237	$F_{Cl\cdot\cdot(P)\cdot\cdot Br}$	0.237
$k_{PCl\cdot PBr}$	0.146	$k_{PCl\cdot PBr}$	0.146
$k_{PCl\cdot PCl}$	0.217	$k_{PBr\cdot PBr}$	0.110
$h_{ClPBr\cdot BrPBr}$	0.023	$h_{ClPBr\cdot BrPBr}$	0.023
$h_{ClPCl\cdot ClPBr}$	0.031	$h_{ClPCl\cdot ClPBr}$	0.031
$h_{ClPBr\cdot ClPBr}$	0.026	$h_{ClPBr\cdot ClPBr}$	0.026
$OPCl_2Br$		$OPClBr_2$	
$K_{P=O}$	9.72	$K_{P=O}$	9.77
K_{P-Cl}	2.54	K_{P-Cl}	2.54
K_{P-Br}	1.90	K_{P-Br}	1.90
$F_{O\cdot\cdot(P)\cdot\cdot Cl}$	0.25	$F_{O\cdot\cdot(P)\cdot\cdot Cl}$	0.25
$F_{O\cdot\cdot(P)\cdot\cdot Br}$	0.10	$F_{O\cdot\cdot(P)\cdot\cdot Br}$	0.10
$F_{Cl\cdot\cdot(P)\cdot\cdot Cl}$	0.27	$F_{Br\cdot\cdot(P)\cdot\cdot Br}$	0.25
$F_{Cl\cdot\cdot(P)\cdot\cdot Br}$	0.26	$F_{Cl\cdot\cdot(P)\cdot\cdot Br}$	0.26
H_{OPCl}	0.286	H_{OPCl}	0.286
H_{OPBr}	0.28	H_{OPBr}	0.28
H_{ClPCl}	0.12	H_{BrPBr}	0.10
H_{ClPBr}	0.11	H_{ClPBr}	0.11
χ(md. Å)	0.06	χ(md. Å)	0.04

8) Q. Williams, J. Sheridan and W. Gordy, *J. Chem. Phys.*, **20**, 164 (1952).

9) M. L. Delwaulle and M. Bridoux, *Compt. rend.*, **248**, 1342 (1959); M. L. Delwaulle and G. Schilling, ibid., **244**, 70 (1957); M. L. Delwaulle and F. François, ibid., **223**, 796 (1946).

TABLE VI. OBSERVED AND CALCULATED FREQUENCIES (IN cm^{-1}) OF PHOSPHORUS HALIDES

	PCl_2Br			$PClBr_2$		
	Obs.	Calcd.	Δ	Obs.	Calcd.	Δ
A′ species	510	499	− 2.2	480	488	+ 1.7
	361	398	+10.2	386	396	+ 2.6
	230	231	+ 0.4	197	207	+ 5.1
	166	166	0	153	160	+ 4.6
A″ species	479	409	−14.6	400	404	+ 1.0
	149	156	+ 4.7	123	145	+17.9

TABLE VII. OBSERVED AND CALCULATED FREQUENCIES OF $OPCl_2Br$ AND $OPClBr_2$ (IN $cm.^{-1}$)

	$OPCl_2Br$			$OPClBr_2$		
	Obs.	Calcd.	Δ	Obs.	Calcd.	Δ
A′ species	1285	1285	0	1275	1275	0
	546	543	−0.4	552	567	+2.7
	432	424	−1.9	391	398	+1.8
	285	278	−2.5	291	294	+1.0
	242	235	−2.9	209	210	+0.5
	172	173	+0.5	130	131	+0.8
A″ species	580	587	+1.2	492	489	−0.6
	327	338	+3.3	271	266	−1.8
	161	162	+0.6	157	156	−0.6

The calculated frequencies are compared with those obtained by Delwaulle et al.[10] in Table VII.

The agreement between the observed and calculated frequencies is satisfactory. Therefore, it is reasonable to assume the transferability of the potential constants among the compounds.

Discussion

The modified UBFF shown in Eq. 1 may be applied to such pyramidal molecules as PCl_3 and PBr_3, and the UBSFF, to such unsymmetric tetrahedral molecules as $OPCl_3$ and $OPBr_3$. Different force fields were used for the PX_3-type and OPX_3-type molecules in the present paper. However, the potential constants may involve physically significant common values among them.

The repulsion terms between the nonbonded halogen atoms for PCl_3 and PBr_3 are estimated from the interaction forces between atoms, on the basis of the Lennard-Jones potential. The K, H, k and h potential constants are the functions of the repulsion constant, F. On the other hand, the potential constants for $OPCl_3$ and $OPBr_3$ have been selected to produce the best agreement between the observed and calculated frequencies.

It was found that the values of K and H of OPX_3 are nearly the same as those of pyramidal molecules, PX_3. This result shows that there is a correlation between the potential constants of phosphoryl and phosphorus halogenides.

In the case of fluorine compounds, the potential constants are not transferable. A further investigation will be necessary in order to estimate the potential constant of $F\cdots F$ nonbonded repulsion.

The k and h potential constants may rise from the resonance energy because of the interaction between the unpaired electron of the P atom and the electrons existing in the PX bond and on the ẌPX plane.

In the calculation of the normal vibrations of mixed trihalogen phosphorus and phosphoryl compounds as well as of dihalogenide carbonyl, better results were obtained by the use of a harmonic mean than by the use of an arithmetical or geometric mean in the estimation of the potential constants. When the values calculated using the harmonic mean are compared with the values which are selected to produce the best agreement between the observed and calculated frequencies, the difference between the observed and calculated frequencies are of nearly the same order for both cases of phosphoryl halides.

Bell et al.[11] have shown that there is a linear correlation between the phosphoryl-absorption wavelength in phosphoryl halides

10) V. W. Kuchen, H. Ecke and H. G. Beckers, *Z. anorg. u. allgem. Chem.*, **313**, 138 (1961); M. L. Delwaulle and F. François, *J. Chim. Phys.*, **46**, 87 (1949); M. L. Delwaulle and F. François, *Compt. rend.*, **220**, 817 (1945); **222**, 550, 1173, 1391 (1946); **224**, 389 (1947); **226**, 895 (1948).

11) J. V. Bell, J. Heisler, H. Tannenbaum and T. Goldensen, *J. Am. Chem. Soc.*, **76**, 5185 (1954).

and the sum of the Pauling electronegativity constants of the halogens. In our present investigation, it was found that a linear correlation is obtained by plotting the phosphoryl potential constants in phosphoryl halides against the sum of the Pauling electronegativity, as is shown in Fig. 3. The value of the

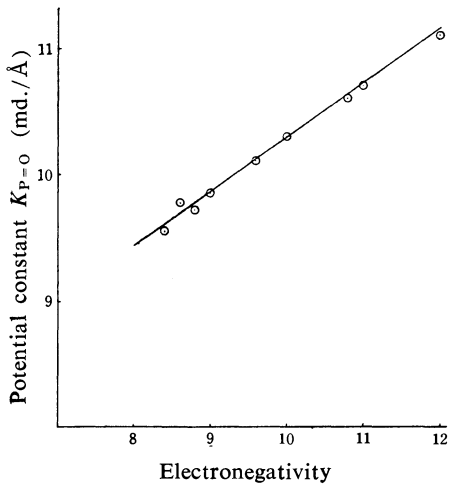


Fig. 3. The correlation between the P=O stretching constant and the sum of electronegativity.

	Sum of electronegativity	Potential constant
$OPBr_3$	8.4	9.5
$OPClBr_2$	8.6	9.77
$OPCl_2Br$	8.8	9.72
$OPCl_3$	9.0	9.85
$OPFBr_2$	9.6	10.10
$OPFCl_2$	10.0	10.30
OPF_2Br	10.8	10.60
OPF_2Cl	11.0	10.70
OPF_3	12.0	11.10

phosphoryl-stretching constant rises higher as the sum of the Pauling electronegativity increases. The effects of various substituents upon the P=O-stretching constant in many types of phosphoryl compounds may be due to an induced polarization. It may be interpreted that in the P-oxide the electronic structure can be represented as resonance hybrids: $R_3P^+-O^- \leftrightarrow R_3P=O$.

Summary

It is important to calculate the potential constants of phosphorus compounds systematically in order to determine physically meaningful potential constants.

First the normal vibrations of such pyramidal-type molecules as PCl_3 and PBr_3 have been calculated by the use of a Urey-Bradley force field as supplemented by the interaction terms between two bond-stretching coordinates and between two angle-deformation coordinates, and then such phosphoryl halogenides as $OPCl_3$ and $OPBr_3$ have been calculated by the use of a Urey-Bradley-Shimanouchi force field.

The repulsion terms between nonbonded halogen atoms have been estimated from the interaction forces between inert atoms based on the Lennard-Jones formula.

The force fields used for the PX_3-type and OPX_3-type molecules in the present paper are different. However, it has been found that a relationship exists between the potential constants of such compounds as PCl_3, PBr_3, $OPCl_3$ and $OPBr_3$, and those for mixed halogen phosphorus compounds, such as PCl_2Br, $PClBr_2$, $OPCl_2Br$ and $OPClBr_2$.

The additional potential terms used for the PX_3 type may arise from the resonance energy because of the interaction between the unpaired electrons of the P atom and the electrons existing in the PX bond and on the XPX plane.

In our present investigation, a linear correlation has been found to exist between the phosphoryl potential constants in phosphoryl halides and the sum of the Pauling electronegativity constants of the halogens.

The authors wish to express their thanks to Professor Takehiko Shimanouchi and Assistant Professor Ichiro Nakagawa of the University of Tokyo for their helpful discussion and advice.

Central Research Laboratory
Tokyo Shibaura Electric Co., Ltd.
Kawasaki-shi, Kanagawa

Radiation-Induced Selective Main-chain Scission in Polyvinyl Alcohol

By Yutaka HIRANO*

(Received May 2, 1964)

The overall effect of high energy radiation on organic substance is generally accepted to be the production of main-chain scission, with a corresponding decrease in the molecular weight and/or a crosslinking which finally forms an insoluble three-dimensional network structure.[1-4] This behavior on irradiation has been correlated with the chemical structure of a repeating monomer unit in polymers and/or with their physicochemical properties just under irradiation.[5-7] As a general rule, those polymers which have at least one hydrogen atom on every carbon atom become crosslinked, while those which have one quarternary carbon atom in a monomer unit are degraded.[6]

Several papers[8-10] have already been presented on the radiation-induced changes in polyvinyl alcohol. It is generally accepted that the irradiation of the polymer produces the main-chain scission and carbonyl group at the end of the chain fractured and/or in the main-chain.

This paper is concerned with the effect of such structural variations as head-to-head linkage on the radiation-induced main-chain scission of polyvinyl alcohol.

There are two types of chemical structures in the main-chain of polyvinyl alcohol.[11] One is the regular, predominant head-to-tail structure, in which the monomer substituent OH occurs on alternate carbon atoms of the chain. Another is the anomalous structure in which a pair of substituents is situated on consecutive carbon atoms. The latter arises from the head-to-head addition of vinyl acetate, which gives a mother polymer for polyvinyl alcohol. This anomalous structure occurs on the average in every several tens of monomer units in the "usual" polymer.

Another paper[12] has briefly suggested that the main-chain scission of polyvinyl alcohol on irradiation might occur at one part of this anomalous structure, i.e., the 1,2-glycol structure. In the present investigation, polyvinyl alcohols which are different in the proportion of the 1,2-glycol structure to the main-chain have been irradiated. A more complete picture of the experimental evidence for the selective main-chain scission at the special chemical structure in the polymer will be given here. The mechanism of the selective main-chain scission will also be discussed.

Experimental

The Preparation of Polyvinyl Alcohols for Irradiation Studies. — Vinyl acetate monomers, freshly distilled in a stream of nitrogen, were polymerized under various conditions, as is indicated in Table I. The resulting mixture of polymers and unreacted monomers was dissolved in benzene, from which the polymer was precipitated by the addition of an excess of petroleum ether. The polymers were then converted to polyvinyl alcohol by stirring, for 1 hr. at room temperature, a 3% solution of the polymer in methanol containing

TABLE I. PREPARATION AND PROPERTIES OF POLYVINYL ALCOHOLS STUDIED

Sample	Polymerization				P	δ*2
	AIBN %*1	Temp. °C	Time hr.	Conv. %		mol. %
A	—	—	—	—	149	0.0
B*3	3×10^{-2}	60	25	91	148	1.11
C	—	30	—	—	1460	1.17
D*4	—	60	—	50	1580	1.54
E	6×10^{-3}	140	2	23	1200	2.61
F	5×10^{-3}	170	2.5	26	890	2.81
G	2×10^{-3}	200	0.5	28	760	3.00
H	6.7% water-containing D-polymer					

*1 α-α' azobisisobutyronitrile
*2 1,2-glycol structure content
*3 75% ethanol solution polymerization
*4 "usual" polymer, 20% methanol solution polymerization

* Present address: Research Laboratory, Kurashiki Rayon Co., Ltd., Kurashiki, Okayama.

1) P. Alexander, R. M. Black and A. Charlesby, *Proc. Roy. Soc.*, **A232**, 31 (1955).
2) P. Alexander, A. Charlesby and M. Ross, ibid., **A223**, 392 (1954).
3) A. Charlesby, ibid., **A222**, 60 (1954).
4) A. Charlesby, *J. Polymer Sci.*, **11**, 513 (1953).
5) L. A. Wall, ibid., **17**, 141 (1955).
6) A. A. Miller, E. J. Lawton and J. S. Balwit, *J. Phys. Chem.*, **60**, 599 (1956).
7) A. Chapiro, *J. Chim. Phys.*, **53**, 295 (1956).
8) A. Danno, *J. Phys. Soc. Japan*, **13**, 609, 614 (1958).
9) I. Sakurada, A. Nakajima and H. Aoki, *Isotopes and Radiation (in Japanese)*, **1**, 185 (1958).
10) M. Matsumoto and A. Danno, "Large Radiation Source in Industry," Vol. 1, p. 331, IAEA (1960).
11) P. J. Flory and F. S. Leutner, *J. Polymer Sci.*, **3**, 880 (1948); ibid., **5**, 267 (1950).
12) Y. Hirano and A. Amemiya, This Bulletin, **34**, 292 (1961).

0.05 mol. sodium hydroxide per liter. The precipitated product was dissolved in water containing a small amount of alkali in order to make the conversion more complete. After the solution had been left standing for 1 hr., polyvinyl alcohol was precipitated by pouring it into an excess of methanol. The product was purified by extraction with methanol, using a Soxhelt extractor. Then it was dried in a vacuum to a constant weight and stored in a desiccator over calcium chloride.

Polyvinyl alcohol containing no 1,2-glycol structure in the main-chain was obtained by the oxidation of "usual" polyvinyl alcohol with sodium periodate, which selectively attacks the 1,2-glycol structure.[13] "Usual" polyvinyl alcohol was dissolved in water in a 4% solution, and five times as much reagent as was consumed was added as an aqueous solution. The oxidation reaction was conducted at 30°C for 1 hr. with a constant stirring. It was thus established that all the 1,2-glycol structures in polymer are severed under these experimental conditions. The reaction mixture was then poured into an excess of cooled methanol. It was necessary to use cooled methanol for carrying out the precipitation without a substantial loss of the oxidized polymer, because the degree of polymerization of the oxidized polymer was very low. The precipitated polymer was filtered off and then washed well with cooled methanol until the filtrate did not show the presence of IO_3^- and IO_4^- ions any more. Most of the end groups of this oxidized polyvinyl alcohol are supposed to be of a chemical structure such as $-CH_2CHO$ judging from the analogous reaction between monomeric glycols and $NaIO_4$. For the reduction of this aldehyde-type end group to the alcohol-type, the oxidized polymer was treated with $NaBH_4$. A reagent (0.8 g.) was mixed with 100 cc. of the oxidized polymer solution containing 4 g. of polymer. After the solution had stood for 48 hr. while being occasionally stirred at room temperature, the reduced polymer was precipitated into methanol, cooled, and acidified with acetic acid. It was then filtered off and washed with methanol until no borate ions could be detected in the filtrate by flame reaction. Finally it was dried in a vacuum at room temperature.

The water-containing polyvinyl alcohol sample was prepared from the 30% aqueous solution of the polymer by moulding it into a rod-like shape, 3~4 m./m. in diameter and 7~8 cm. long. This water-containing sample was dried at room temperature over a long period of time to the desired extent of water concentration. The mole percent of the 1,2-glycol structure in various polymer samples was computed from the degree of degradation with sodium periodate by the use of Flory's method.[11] Table I lists the preparation and characterization data for the polymers.

The Irradiation of Samples. — Polymer samples (1.5~2.0 g.) were weighed in hard glass tubes for the irradiation in a Co-60 γ-ray source at the Japan Atomic Energy Research Institute. An ambient temperature of about 20°C was maintained during the irradiation.

Each tube containing a dry powder sample for the irradiation was evacuated to the pressure of 10^{-4} mmHg. In all casses, the vacuum was retained overnight, indicating that there was no significant amount of precipitant or solvent left in the polymer; then each tube was sealed under a vacuum. Each tube containing the water containing polymer was then sealed in the presence of air and irradiated.

Molecular Weight Measurement.— The solution viscosities of the irradiated polymer samples were measured in water at 30°C using an Ostwald-type viscometer. Three or four concentrations of each of the irradiated polymers were run, and the plots of both the viscosity number, η_{sp}/c, and the logarithmic viscosity number, $\ln(\eta_r/c)$, versus the concentration were extrapolated to zero concentration in order to determine their limiting viscosity number, $[\eta]$. The limiting viscosity numbers of polymers which are irradiated and subsequently oxidized with sodium periodate were obtained from the single-concentration viscosity data at a concentration sufficiently low to obviate the extrapolation of $\ln(\eta_r/c)$ to infinite dilution. Five times as much reagent as was consumed was added to a 10 cc. portion of the irradiated polymer solution containing around 0.13 g. of the polymer. After this mixture had stood for 30 min. at 30°C, the viscosities were measured. Polymer concentrations were computed from the known concentration of the initial aqueous solution and the total volume after the reagent was added. Molecular weights were computed from the following relationship;[14]

$$[\eta] = 6.66 \times 10^{-4} M^{0.64}$$

where $[\eta]$ is expressed in deciliters/gram.

Results and Discussion

The Irradiation of Water-containing Polyvinyl Alcohol. — The viscosity changes in the irradiated water-containing polyvinyl alcohol before and after oxidation with $NaIO_4$ are shown in Fig. 1. It is found that a sudden gel formation occurs in the irradiated polymer, although the molecular weight of the polymer decreases gradually during the initial period of irradiation. This behavior on irradiation is very similar to that of the irradiated polypropylene.[15] The minimum radiation dose necessary to produce a gel is estimated to be about 23 Mr.

On the other hand, the limiting viscosity number of the polymer which is irradiated and subsequently oxidized with $NaIO_4$ steadily increases with the radiation dose.

Figure 2 illustrates schematically the main-chain scission and/or crosslinking of polyvinyl

13) E. L. Jackson in R. Adams, "Organic Reaction," Vol. 2, Wiley, New York (1944), p. 341.

14) A. Nakajima et al., *Chem. High Polymer (Kobunshi Kagaku)*, **6**, 460 (1948).

15) R. M. Black and B. J. Lyons, *Proc. Roy. Soc.*, **A234**, 322 (1959).

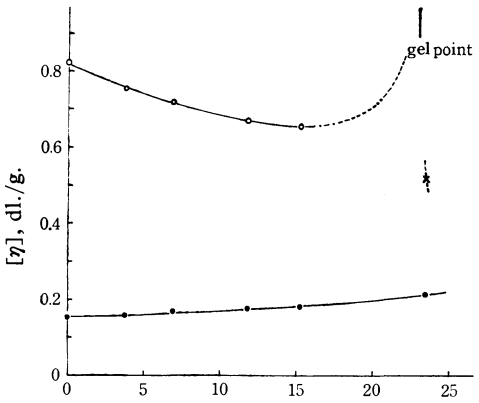


Fig. 1. Viscosity changes of irradiated water-containing polyvinyl alcohol (δ=1.54 mol.%) before and after oxidation with sodium periodate: Water content 6.7% (w/w). Intensity 4×10^4 r./hr. (○) before oxidation, (●) after oxidation, (×) viscosity of the soluble fraction (99.2%) of irradiated sample.

alcohol subjected to irradiation and/or chemical degradation with $NaIO_4$.

According to the theory of radiation-induced simultaneous degradation and crosslinking as developed by Saito,[16] the changes in the limiting viscosity number of the irradiated polymer are expressed as follows:

$$\eta(R)/\eta(0)=1+\{\alpha(\alpha+2)(\alpha+7)/6-\alpha\lambda\}(cuR)+[\alpha(\alpha+1)\{(\alpha+2)(\alpha+3)(\alpha+7)(\alpha+14)/90-(\alpha+2)(\alpha+7)\lambda/3+\lambda^2\}](cuR)^2+\cdots\cdots \quad (1)$$

where λ is ratio of the probability of the main-chain scission, r, and crosslinking, c, of monomer unit per unit of radiation dose; $\eta(0)$ and $\eta(R)$ are the limiting viscosity numbers of the polymer at zero dose and at radiation dose, R, respectively; u is a measure of the initial number average molecular weight, and α is the exponent of the relation between the viscosity and the molecular weight. This formula predicts that, if λ and α are the same in polymers, plots of $\eta(R)/\eta(0)$ versus uR of each of polymers can be superposed one upon the other by translation along the abscissa.

Provided that there are no differences in λ between the 1,3-glycol structure and the 1,2-glycol structure, the λ of *o*-PVA in Fig. 2 is equal to that of the "usual" PVA. Thus, *o-i*-PVA should decrease in viscosity with the radiation dose, since *i*-PVA decreases in viscosity during the initial period of irradiation. The treatment of this *o-i*-PVA with $NaIO_4$ might produce a further decrease in viscosity, if there exist 1,2-glycol structures formed by radiation-induced crosslinking. Furthermore, the degree of main-chain scission and crosslinking produced in this *o-i-o*-PVA is just the same as that in *i-o*-PVA, as is shown in Fig. 2.

The above-mentioned discussion leads us to the consideration that the viscosity of the "usual" PVA which is irradiated and subsequently oxidized with $NaIO_4$ should decrease with the radiation dose. This is inconsistent with the results shown in Fig. 1. The steady increase in the viscosity of irradiated and subsequently oxidized "usual" PVA would suggest that λ in a polymer which contains no 1,2-glycol structure is lower than that in a polymer which contains a 1,2-glycol structure in the main-chain. This discrepancy is considered to be partly due to the selective main-chain scission at a chemical structure such as a 1,2-glycol type on irradiation.

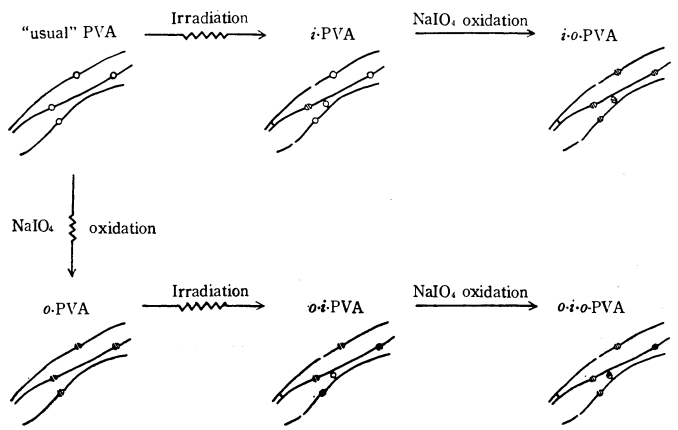


Fig. 2. Schematic main-chain scission and crosslinking of polyvinyl alcohol: —— 1,3-glycol structure, ○ 1,2-glycol structure.

16) O. Saito, *J. Phys. Soc. Japan*, **13**, 1465 (1958).

The Irradiation of Polyvinyl Alcohols Which are Different in the Proportion of the 1, 2-Glycol Structure. — Figure 3 illustrates the results of the irradiation of "usual" polyvinyl alcohol as the reciprocal degree of the polymerization versus the radiation dose, R. A monotonous decrease in the molecular weight, but no gel formation, was observed for this dry specimen up to 130 Mr., which is in contrast with water-containing specimen. The main-chain scission process is predominant and does not depend on the radiation intensity in the range covered. No color has been detected in any irradiated specimens in a vacuum in contrast with the yellow coloration which appears upon irradiation in air.

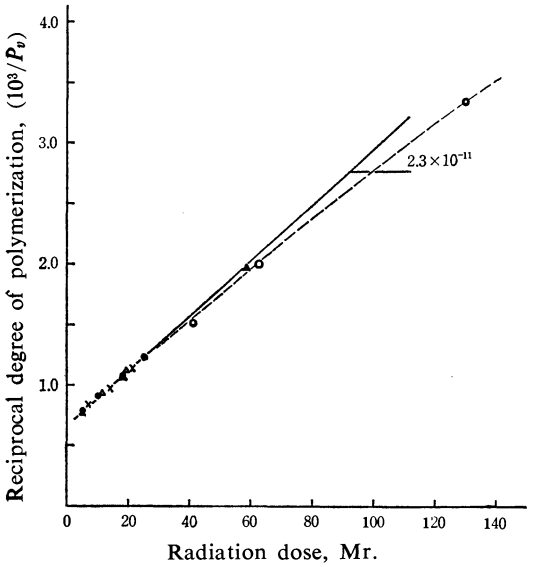


Fig. 3. Changes in the reciprocal degree of polymerization of irradiated polyvinyl alcohol ($\delta=1.54$ mol.%) with radiation dose: (×) 10^6 r./hr., (●) 6.4×10^5 r./hr., (△) 5.8×10^5 r./hr., (○) 2.8×10^4 r./hr.

Similar plots for the various polyvinyl alcohols which are different in the proportion of the 1, 2-glycol structure in the main-chain are shown in Figs. 4 and 5. The linearity of the curves obtained shows that the number of the main-chain scission produced is proportional to the radiation dose.

Pure random radiation-induced main-chain scission of the polymer reduces the initial molecular weight distribution to the most probable one and, then, predicts linear plots between $1/P_v$ and R. The relation is:[1]

$$(1/P_v)=(1/P_{v_1})+w(KNE_d)^{-1}(R_2-R_1) \quad (2)$$

where P_{v_1} and P_{v_2} are the viscosity average degree of polymerization of the polymer at radiation doses R_1 and R_2 ($R_1<R_2$) respectively, N is Avogadro's number, E_d is the average energy absorbed in eV. per main-chain scission produced, 1 r.$=5.81\times10^{13}$ eV./g., w is the molecular weight of structural unit, and K is the ratio of the viscosity average degree of polymerization to the number average one, which is given by $K=\{\Gamma(\alpha+2)\}^{1/\alpha}$.

For polyvinyl alcohol with $w=44$ and $\alpha=0.64$, we may, therefore, calculate $E_d=2.32\times10^{-9}$ eV./slope for various specimens from Figs. 4

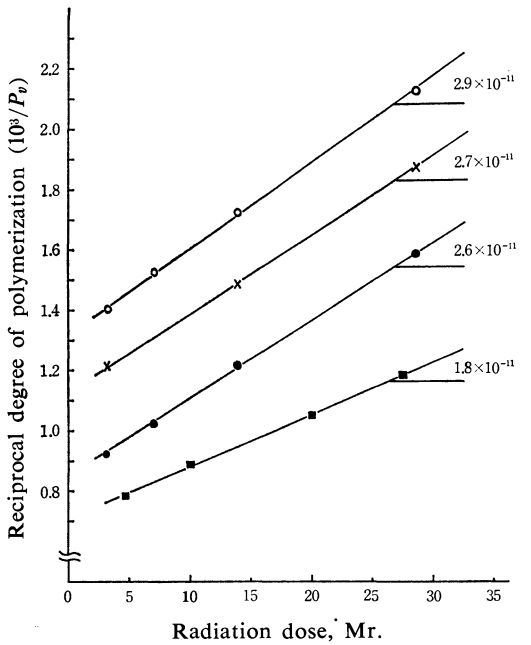


Fig. 4. Changes in the reciprocal degree of polymerization of polyvinyl alcohol samples with radiation dose: 1,2-glycol structure content, (○) 3.00, (×) 2.81, (●) 2.61, (■) 1.17 mol.%. Intensity 6.4×10^5 r./hr.

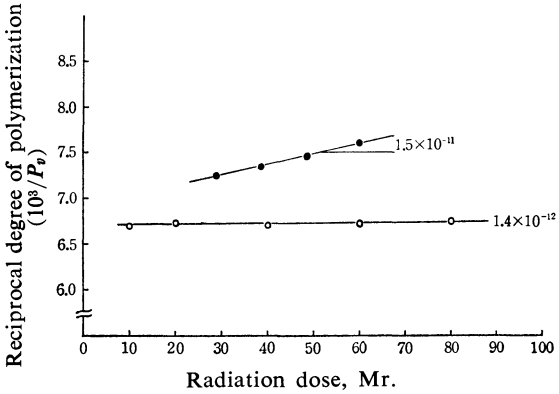


Fig. 5. Changes in the reciprocal degree of polymerization of polyvinyl alcohol samples with radiation dose: 1,2-glycol structure content, (○) 0.00, (●) 1.11 mol.%. Intensity 6.4×10^5 r./hr.

TABLE II. VARIATION IN E_d AND G_d WITH 1,2-GLYCOL STRUCTURE CONTENT

δ, mol. %	E_d, eV.	G_d
0.0	1670	0.06
1.11	154	0.65
1.17	128	0.78
1.54	100	1.00
2.61	88	1.13
2.81	85	1.17
3.00	79	1.26

and 5. In Table II the results are given as a function of the 1,2-glycol structure content, δ, in the polymer chain. The difference in G value for main-chain scission between $\delta=0$ mol.% specimen and $\delta=1.11$ mol.% one, which have nearly identical original degrees of polymerization, is beyond the range of experimental error. This fact definitely shows the predominant radiation-induced main-chain scission at a special part, such as the 1,2-glycol structure in the polymer chain.

Since it is not unreasonable to assume that the 1,2-glycol structures are distributed at random throughout the polymer, the molecular weight distribution of the irradiated polymer will approximate the most probable distribution, even if only these anomalous structures are selectively fractured on irradiation. This selectivity will, however, reduce the number of these structures on irradiation. Consequently, the average absorbed energy needed to produce a main-chain fracture varies as a function of the radiation dose and must increase gradually with an increase in the radiation dose. The departure from the linear relation between $1/P_v$ and R at high radiation doses in Fig. 3 may be ascribed to this specificity.

The Mechanism of Radiation-Induced Main-chain Scission.—A rapid approach to a certain value of G_d was observed with the increase in the 1,2-glycol content in the polymer chain (Table II and Fig. 6). It may, therefore, be suggested that a transfer of energy occurs from the 1,3-glycol structure to the 1,2-glycol structure along the polymer chain and that the latter part suffers a sacrificial damage. On the basis of the random distribution of the 1,2-glycol structure in the polymer chain, it is possible to deduce, from the G_d dependence on δ, the range of energy transfer offered by the 1,2-glycol structure. For this purpose let M represent the 1,3-glycol structure, I, the 1,2-glycol structure, and n, the number of units as a measure of the maximum range of energy transfer from M to I.

The relative probability of some configurations about a given M will be considered to be a function of the mole fraction of the 1,2-glycol structure, δ in the polymer chain. The

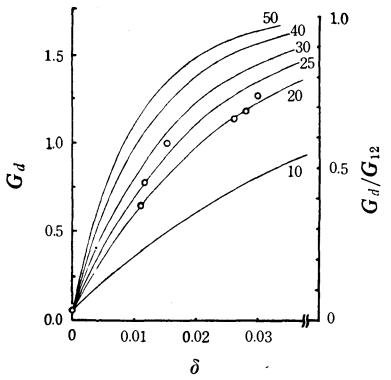


Fig. 6. G value for the main-chain scission plotted against the mole fraction of 1,2-glycol structure. Figures on the curve are the numbers of the monomer units in which the transfer of absorbed energy occurs.

probability of such a configuration when none of I is present within its n nearest neighbors on either side of M will be given as $(1-\delta)^{2n}$. In this configuration M can not lose its energy by transferring it to I and consequently, will be fractured with the probability of bond rupture per unit radiation dose, r_{13}. On the other hand, the probability of such a configuration when one or more I's are in existence within its n nearest neighbors on either side is equal to $1-(1-\delta)^{2n}$. In this case the energy transfer will occur from a given M to I. M will be protected against the bond ruputure by I. The released energy from M, however, will migrate and be "trapped" in one of the nearest neighboring I's. Therefore, this will give rise to a bond rupture of I, the probability of which is r_{12}. In other words, the 1,2-glycol structure may serve as an "energy sink" and draw off energy from the 1,3-glycol structure and dissipate it with the subsequent, sacrificial bond rupture. Thus, the total number of main-chain scissions, dS, produced with the radiation dose, dR, will be given by the equation:

$$dS=N(1-\delta)(1-\delta)^{2n}r_{13}dR+N(1-\delta)\times\{1-(1-\delta)^{2n}\}r_{12}dR+N\delta r_{12}dR \qquad (3)$$

where N is the total number of units in the irradiated system.

By rewriting Eq. 3, we obtain:

$$(1/N)(dS/dR)=r=r_{12}-(r_{12}-r_{13})(1-\delta)^{2n+1} \qquad (4)$$

The term on the left-hand side of Eq. 4 indicates the average probability for the main-chain scission of the polymer during irradiation. Thus, we obtain, by the use of the G_d value:

$$(G_d/G_{12})=1-\{1-(G_{13}/G_{12})\}(1-\delta)^{2n+1} \qquad (5)$$

As $G_{13}=0.06$, G_{12} was evaluated as about 1.7 from Fig. 5 by the extrapolation of experimental results to $\delta=100$ mol.%.

A plot of (G_d/G_{12}) versus δ is shown in Fig. 6, along with the calculated curves for several values of n. It may be seen in the figure that the experimental points, although scattered, lie between two curves for which n is 20 and 25. For $n=20$, it is estimated that the range of energy transfer is about 60 Å along the zigzag chain of the polymer.

The phenyl group is known to have a protecting effect against radiation-induced changes in various co-polymer systems.[17-20] The energy transfer process is also postulated, and a value of $n=1\sim6$ for its range is estimated. The evaluated value, $n=20$, for polyvinyl alcohol is quite large. However, a transfer of energy over distances of 50 Å or more is estimated in scintilater systems.[21,22]

Summary

Polyvinyl alcohols which are different in the mole fraction of the head-to-head structure, in which two of -OH substituents are situated on consecutive carbon atoms, have been irradiated with Co-60 gamma rays in a vacuum at room temperature in order to investigate the effect of this anomalous structure on the radiation-induced main-chain scission of the polymer. The selective main-chain scission in polyvinyl alcohol has been observed at such positions as the head-to-head structure. The average absorbed energy necessary to produce a main-chain scission, i.e., E_d, is about 1700 eV. for polyvinyl alcohol containing no head-to-head structure, while E_d is 100 eV. for polyvinyl alcohol containing a 1.54 mol.% head-to-head structure. A rapid increase up to a certain value in G_d, the number of chain scissions produced per 100 eV. of energy absorbed by the polymer, has been observed with the increase in the head-to-head structure content in the polymer chain. Thus, it has been postulated that there is a transfer of radiation energy from the head-to-tail structure to the head-to-head structure. An estimation has been made on the range of energy transfer from the G_d dependency on the concentration of the head-to-head structure.

The author is much indebted to Professor Ayao Amemiya of The University of Tokyo for his invaluable advice and encouragement throughout this work.

Department of Applied Physics
Faculty of Engineering
The University of Tokyo
Hongo, Tokyo

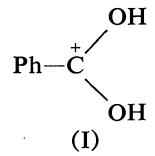
17) P. Alexander and A. Charlesby, *Proc. Roy. Soc.*, **A230**, 136 (1955).
18) S. Okamura and Y. Oishi, *Isotopes and Radiation (in Japanese)*, **2**, 400 (1959).
19) M. Koike and A. Danno, *J. Phys. Soc. Japan*, **15**, 150 (1960).
20) E. Witt, *J. Polymer Sci.*, **41**, 507 (1959).
21) O. Simpson, *Proc. Roy. Soc.*, **A238**, 402 (1957).
22) F. A. Bovey, "The Effects of Ionizing Radiation on Natural and Synthetic High Polymers," Interscience, New York (1958), p. 57.

The Electronic Structures of the Protonated Benzoic Acid and the Related Ions

By Haruo HOSOYA and Saburo NAGAKURA

(Received May 8, 1964)

There are two possible positions of the protonation of the carboxyl group: one of them, the oxygen atom of the carbonyl group, and the other, the oxygen atom of the hydroxyl group. In a previous paper[1] we studied the structures of protonated benzoic acid and mesitoic acid by the aid of various spectroscopic methods, such as ultraviolet, infrared and Raman spectra. Consequently, we succeeded in obtaining direct evidence that, in strongly acidic media, a proton attacks the carbonyl oxygen atom of benzoic acid, giving the (ion benzoic acidium ion):



(I)

Stewart and Yates[2] indirectly induced the

1) H. Hosoya and S. Nagakura, *Spectrochim. Acta*, **17**, 324 (1961).

2) R. Stewart and K. Yates, *J. Am. Chem. Soc.*, **82**, 4059 (1960).

same conclusion from ultraviolet absorption measurements showing that the relative magnitudes of the basicities of the benzoic acid derivatives are well correlated with those of the corresponding benzaldehyde and acetophenone derivatives.

Furthermore, it was shown in the previous paper that the ultraviolet absorption spectrum of benzoic acid changes considerably upon the protonation. This reveals that the distribution and energy of the π-electrons of benzoic acid are greatly affected by the protonation. In order to obtain deeper knowledge on this point, we have undertaken to calculate the electronic structures of the benzoic acidium ion (I) and of such related ions as α-hydroxylbenzyl cations.

Method of Calculation

Only π-electrons were explicitly taken into account in the present calculations. Furthermore, the ion was considered to be composed of an electron donor and an acceptor: for example, the benzoic acidium ion (I) was considered to be composed of the two hydroxyl groups serving as an electron donor and the benzyl cation, as an electron acceptor. The ground and the lower excited states of I can be expressed as a linear combination of the ground, locally excited and charge-transfer configurations.[3] The locally excited configurations can be caused by the local excitation within the benzyl cation, and the charge-transfer configurations, by the electron transfer from the hydroxyl groups to the benzyl cation. Calculations of this kind have already been shown to give reliable results for the interpretation of electronic spectra of various unsaturated compounds.[4]

Component MO's. — Roothaan's LCAO-SCF molecular orbitals (φ_1, φ_2,……, φ_7) of the benzyl cation were calculated by Hanazaki et al.[5] on the assumptions that all the C–C bond lengths are 1.39 Å and that all the bond angles are 120°. These MO's are expressed as linear combinations of the Slater-type atomic orbitals with different effective nuclear charges (Z's), the magnitudes of which are, considering the assumed relation between Z's and the net charge densities, q's, self-consistent with the calculated q's on the respective carbon atoms. Symmetric (φ_s) and antisymmetric (φ_a) group orbitals were constructed from the two $2p\pi$ atomic orbitals, (χ^1_{OH} and χ^2_{OH}) of the hydroxyl oxygen atoms. The nine above-mentioned component molecular orbitals are given in Table I.

The Configurations and Their Energies. — In addition to the ground configuration, singlet and singly excited configurations with energies lower than 7 eV. were taken. In Table II they are grouped into symmetric (S) and antisymmetric (A) configurations with respect to the σ_V plane shown in Fig. 1. ψ_P and ψ_Q are, respectively, symmetric and antisymmetric charge-transfer configurations, in which an electron migrates from the oxygen atoms to the benzyl cation. ψ_β, ψ_γ and ψ_δ, and ψ_α, ψ_ε and ψ_ζ are symmetric and antimagnetric locally excited configurations respectively. The energies of ψ_α (2.75 eV.) and ψ_β (3.74 eV.) were taken to be equal to the lowest two transition energies of the benzyl cation observed by Hanazaki et al.[5]

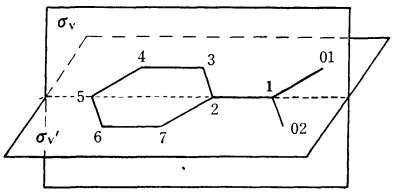


Fig. 1. Geometry and numbering of the atoms of the benzoic acidium ion I.

TABLE I. COMPONENT MOLECULAR ORBITALS

$\psi_k=\sum_p C_{kp}\chi_p \quad k,p=1,2,\cdots\cdots,7$[a] $\quad \varphi_{s,a}=1/\sqrt{2}\,(\chi_{01}\pm\chi_{02})$

$k \diagdown p$	1	2	3	4	5	6	7
1	0.3413	0.5360	0.3940	0.3116	0.3027	0.3116	0.3940
2	0.4481	0.4463	0.0163	−0.3777	−0.5600	−0.3777	0.0163
3	0	0	0.5279	0.4705	0	−0.4705	−0.5279
4	0.6987	−0.1120	−0.4041	0.0235	0.4142	0.0235	−0.4041
5	0	0	0.4705	−0.5279	0	0.5279	−0.4705
6	0.4073	−0.5785	0.1859	0.2888	−0.5134	0.2888	0.1859
7	0.1694	−0.4078	0.3829	−0.4199	0.3989	−0.4199	0.3829

a) The numbering of the carbon atomic orbitals is given in Fig. 1.

3) H. C. Longuet-Higgins and J. N. Murrell, *Proc. Phys. Soc.*, A68, 601 (1955); J. N. Murrell, ibid., A68, 969 (1955).
4) S. Nagakura, *Mol. Phys.*, 3, 105 (1960); H. Hosoya, J. Tanaka and S. Nagakura, This Bulletin, 33, 850 (1960); *Tetrahedron*, 18, 859 (1962), etc.
5) I. Hanazaki and S. Nagakura, unpublished.

Table II. Configurations and their energies

Configuration	Character	Energy, eV.
(Symmetric)		
$\phi_G=\lvert 1\bar{1}2\bar{2}3\bar{3}s\bar{s}a\bar{a}\rvert$ [a]	Ground	0
$\phi_P=1/\sqrt{2}\{\lvert 1\bar{1}2\bar{2}3\bar{3}s4a\bar{a}\rvert+\lvert 1\bar{1}2\bar{2}3\bar{3}4sa\bar{a}\rvert\}$	CT[b]	3.12[d]
$\phi_\beta=1/\sqrt{2}\{\lvert 1\bar{1}2\bar{4}3\bar{3}s\bar{s}a\bar{a}\rvert+\lvert 1\bar{1}4\bar{2}3\bar{3}s\bar{s}a\bar{a}\rvert\}$	LE[c]	3.74[e]
$\phi_\gamma=1/\sqrt{2}\{\lvert 1\bar{4}2\bar{2}33s\bar{s}a\bar{a}\rvert+\lvert 4\bar{1}2\bar{2}3\bar{3}s\bar{s}4\bar{a}\rvert\}$	LE	5.97[d]
$\phi_\delta=1/\sqrt{2}\{\lvert 1\bar{1}2\bar{2}3\bar{5}s\bar{s}a\bar{a}\rvert+\lvert 1\bar{1}2\bar{2}5\bar{3}s\bar{s}a\bar{a}\rvert\}$	LE	6.39[d]
(Antisymmetric)		
$\phi_\alpha=1/\sqrt{2}\{\lvert 1\bar{1}2\bar{2}34\bar{s}s\bar{a}\rvert+\lvert 1\bar{1}2\bar{2}43\bar{s}s\bar{a}\rvert\}$	LE	2.75[e]
$\phi_Q=1/\sqrt{2}\{\lvert 1\bar{1}2\bar{2}33\bar{s}s\bar{a}4\rvert+\lvert 1\bar{1}2\bar{2}33\bar{s}s4\bar{a}\rvert\}$	CT	3.12[d]
$\phi_\varepsilon=1/\sqrt{2}\{\lvert 1\bar{1}2\bar{2}36\bar{s}s\bar{a}\rvert+\lvert 1\bar{1}2\bar{2}63\bar{s}s\bar{a}\rvert\}$	LE	6.52[d]
$\phi_\zeta=1/\sqrt{2}\{\lvert 1\bar{1}2\bar{5}33\bar{s}s\bar{a}\rvert+\lvert 1\bar{1}5\bar{2}33\bar{s}s\bar{a}\rvert\}$	LE	6.90[d]

a) $\phi_G=1/\sqrt{10}!\sum_p(-1)^p P\begin{Bmatrix}\varphi_1(1)&\varphi_1(2)&\varphi_2(3)&\varphi_2(4)&\varphi_3(5)&\varphi_3(6)&\varphi_s(7)&\varphi_s(8)&\varphi_a(9)&\varphi_a(10)\\ \alpha(1)&\beta(2)&\alpha(3)&\beta(4)&\alpha(5)&\beta(6)&\alpha(7)&\beta(8)&\alpha(9)&\beta(10)\end{Bmatrix}$
$=\lvert\varphi_1(1)\ \varphi_1(\bar{2})\ \varphi_2(3)\ \varphi_2(\bar{4})\ \varphi_3(5)\ \varphi_3(\bar{6})\ \varphi_s(7)\ \varphi_s(\bar{8})\ \varphi_a(9)\ \varphi_a(\bar{10})\rvert$

b) Charge-transfer

c) Local excitation

d) Calculated values (Ref. 5)

e) Observed values (Ref. 5)

The energies of the other locally excited configurations were those calculated by them. The energies of the two charge-transfer configurations were estimated to be the difference between the ionization potentials of methanol (10.85 eV., observed[6]) and the benzyl radical (7.73., calculated[7]).[8]

Configuration Interaction. — The above-mentioned configurations interact with one another through the core and electronic repulsion parts in the total electronic Hamiltonian H:

$$H=\sum_i H^{\text{core}}(i)+\sum_{i>j}e^2/r_{ij}$$

$$H^{\text{core}}(i)=H^{\text{core}}_{\text{benzyl}}(i)+H^{\text{core}}_{\text{OH}}(i)$$

The antisymmetrized product wave functions, $\lvert k\bar{l}m\bar{n}\cdots\cdots\rvert$ and $\lvert k'\bar{l}'m'\bar{n}'\cdots\cdots\rvert$, interact with each other through the above Hamiltonian. The interaction energies can be degraded under the zero-differential overlap approximation[9,10] into the atomic integrals as follows:

(i) $\langle\varphi^*_k(i)\lvert H^{\text{core}}(i)\rvert\varphi_{k'}(i)\rangle=H^{\text{core}}_{kk'}$

if $k\neq k'$, $l=l'$, $m=m'$, $n=n'$, ……,

where

$H^{\text{core}}_{kk'}=0$, if k and k' are pertinent to the same composite,

$H^{\text{core}}_{kk'}=C_{kp}C_{k'q}\beta_{pq}$, if k and k' are pertinent to the two different composites which are jointed together through the bond between the p and q atoms,

C_{kp}: the LCAO coefficient for the p-th atom in the k-th MO, and

β_{pq}: the core resonance integral for the p—q bond.

(ii) $\langle\varphi^*_k(i)\varphi^*_l(j)\lvert e^2/r_{ij}\rvert\varphi_{k'}(i)\varphi_{l'}(j)\rangle$
$=(kk'\lvert ll')_{\text{MO}}$
$=\sum_{p,q}C^*_{kp}C_{k'p}C^*_{lq}C_{l'o}(pp\lvert qq)_{\text{AO}}$

if $k\neq k'$, $l\neq l'$, $m=m'$, $n=n'$,……

(iii) $\langle\varphi^*_k(i)\varphi^*_m(j)\lvert e^2/r_{ij}\rvert\varphi_{k'}(i)\varphi_{m'}(j)\rangle$
$=(kk'\lvert mm')_{\text{MO}}-(km'\lvert mk')_{\text{MO}}$
$=\sum_{p,q}(C^*_{kp}C_{k'p}C^*_{mq}C_{m'q}$
$-C^*_{kp}C_{m'p}C^*_{mq}C_{k'q})(pp\lvert qq)_{\text{AO}}$

if $k\neq k'$, $l=l'$, $m\neq m'$, $n=n'$,……

(iv) 0 otherwise.

Consequently, the non-zero off-diagonal matrix elements were obtained as follows:

$$H_{GP}=\sqrt{2}\langle\varphi_4H\varphi_s\rangle=2C_{41}\beta_{CO}=1.3974\beta_{CO}$$

$$H_{\beta P}=-\langle\varphi_2H\varphi_s\rangle=-\sqrt{2}C_{21}\beta_{CO}=-0.6337\beta_{CO}$$

$$H_{\beta\delta}=2(24\lvert 35)_{\text{MO}}-(23\lvert 45)_{\text{MO}}$$
$$=2\times0.4438-0.1736=0.7140\text{ eV.}$$

$$H_{p\gamma}=-\langle\varphi_1H\varphi_s\rangle=-\sqrt{2}C_{11}\beta_{CO}=-0.4827\beta_{CO}$$

$$H_{\gamma\delta}=2(14\lvert 35)_{\text{MO}}-(13\lvert 45)_{\text{MO}}$$
$$=-2\times0.3134+0.6004=-0.0264\text{ eV.}$$

$$H_{\alpha\zeta}=2(25\lvert 34)_{\text{MO}}-(23\lvert 45)_{\text{MO}}$$
$$=-2\times0.3954-0.1674=-0.9582\text{ eV.}$$

6) K. Watanabe, *J. Chem. phys.*, **26**, 542 (1957).

7) N. S. Hush and J. A. Pople, *Trans. Faraday Soc.*, **51**, 600 (1955).

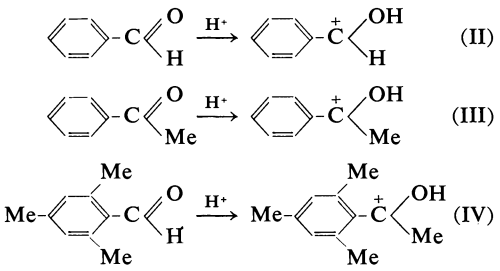
8) In this calculation, the interaction between the two lone-pair π-electrons on the different oxygen atoms of the $-\overset{+}{C}\overset{OH}{\underset{OH}{<}}$ group is not taken into account. Furthermore, the difference in the electrostatic interaction energies before and after the electron transfer was estimated to be small and was, therefore, disregarded.

9) R. Pariser and R. G. Parr, *J. Chem. Phys.*, **21**, 466, 767 (1953).

10) J. A. Pople, *Trans. Faraday Soc.*, **49**, 1375 (1953); *Proc. Phys. Soc.*, **A68**, 81 (1955).

The LCAO MO coefficients C's and the Coulomb repulsion integrals of the type $(pp|qq)_{AO}$ were calculated by Hanazaki et al.[5] using Pariser and Parr's approximation.[9]

Matrix Elements for the Related Ions. — Similar calculations were performed for the benzaldehydium ion (II), the acetophenonium ion (III) and the 2, 4, 6-trimethylbenzaldehydium ion (IV), which are, respectively, the monohydroxyl derivatives of the benzyl, α-methylbenzyl and 2, 4, 6-trimethylbenzyl cations. These ions are known to be produced, presumably from benzaldehyde, acetophenone and mesitaldehyde respectively, in strongly acidic media.



Each of these ions is separated into an electron donor (the hydroxyl group) and an electron accepter (the benzyl, α-methylbenzyl and 2, 4, 6-trimethylbenzyl cations for II, III and IV respectively). The interaction between the components is taken into account by means of the configurational interaction among the ground, locally excited and charge-transfer configurations. These three cations have only one hydroxyl group and, accordingly, one charge-transfer configuration,

$$\psi_O = 1/\sqrt{2}\{|1\bar{1}2\bar{2}3\bar{3}0\bar{4}| + |1\bar{1}2\bar{2}3\bar{3}4\bar{0}|\}$$

where 0 is the abbreviated representation of the $2p\pi$ atomic orbital, χ_O, of oxygen. The off-diagonal elements, H_{GO}, $H_{\beta O}$ and $H_{O\delta}$, with which the ψ_O configuration is related, are equal to $1/\sqrt{2}H_{GP}$, $1/\sqrt{2}H_{\beta P}$ and $1/\sqrt{2}H_{P\delta}$ respectively. The E_α (the energy of the α-locally excited configuration and E_β (the energy of the β-locally excited configuration) of III and IV were taken from the observed transition energies of the α-methylbenzyl (2.88 and 4.07 eV.) and 2, 4, 6-trimethylbenzyl (2.64 and 3.65 eV.) cations respectively.[5] The electron affinities of these parent ions were taken to be 7.43 eV. and 6.88 eV. respectively, by referring to the observed ionization potentials of the benzyl radical derivative[11] and methylbenzenes.[6,12,13]

Results and Discussion

Calculated Energy Levels and Wave Functions. —Calculations were performed, using the core resonance integral β as a parameter for each ion, by the aid of an electronic computer FACOM-202 in our institute. The calculated energy levels and wave functions are given in Fig. 2 and Table III, the cation I being taken as an example and the value of β_{CO} being taken to be equal to -2.0 eV., the optimal value for the energy level calculations.

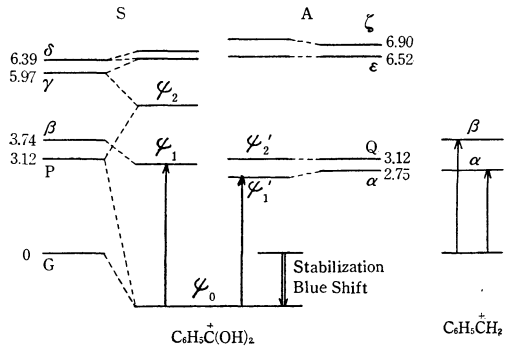


Fig. 2. Energy level diagram showing configuration interaction for the ion I.

In order to obtain accurate experimental results on the absorption intensities, the ultraviolet absorption spectra of the ions I—IV in concentrated sulfuric acid were remeasured by the present authors, since most of the published data[14] for these ions have been concerned only with the location and peak intensity of the second longest wavelength band. Table IV summarizes the calculated and observed transition energies, ΔW, the calculated and observed oscillator strengths, f, the predicted directions of their transition moments, the half-widths of the second longest wavelength bands, $\nu_{1/2}$, the π-electronic stabilization energies due to the configuration interaction, ΔE, and the optimal β_{CO} values. The difficulty of the intensity calculation being kept in mind, it may be said that agreements between the calculated and observed values are good except for the oscillator strength of the $W_0 \rightarrow W_2$ transition of I.

11) A. G. Harrison, P. Kebarle and F. P. Lossing, *J. Am. Chem. Soc.*, **83**, 777 (1961).

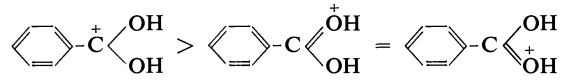
12) It was assumed that the ionization potential of the α-methylbenzyl radical is nearly equal to that of the p-methylbenzyl radical (7.46 eV.).[11] Also, the difference between the ionization potentials of the 2, 4, 6-trimethylbenzyl radical and the benzyl radical was assumed to be equal to the difference between mesitylene (8.39 eV.)[6] and benzene (9.24 eV.)[6]. One methyl group substituted at these hydrocarbon species seems to be lower the ionization potential by about 0.3 eV.

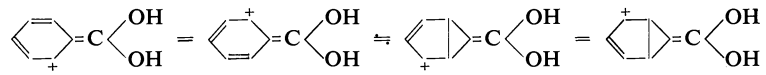
13) Although the cations II, III and IV do not possess the C_{2v} symmetry properties, the secular equations for them were factorized into groups in the same manner as for the case of the cation I because of the nil value of the coefficient C_{31}. Therefore, the matrix elements other than the above-mentioned ones are equal to the corresponding elements for the case of I.

14) W. M. Schubert and R. E. Zahler, *J. Am. Chem. Soc.*, **76**, 1 (1954); R. Stewart and K. Yates, ibid., **80**, 6355 (1958); K. Yates and R. Stewart, *Can. J. Chem.*, **37**, 664 (1959).

Charge Densities and Stabilization Energies. —From the wave functions given in Table III, the π-electronic charge densities for the ground and two excited states of I were calculated as shown in Fig. 3, which also shows those of the ground state of the benzyl cation for purposes of comparison. The result on the protonated benzoic acid may be translated roughly into the valence bond method description as follows:

State — The degree of contribution of each resonance structure

Ground state (W_0) 

Excited state (W_1') 

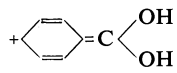
Excited state (W_1) 

TABLE III. ENERGY LEVELS AND WAVE FUNCTIONS OF THE BENZOIC ACIDIUM ION

Energy, eV.	Wave function
Symmetric	
$W_0=-1.753$	$\Psi_0=0.8389\phi_G-0.1227\phi_\beta+0.5261\phi_P-0.0657\phi_\gamma+0.0106\phi_\delta$
$W_1=2.953$	$\Psi_1=0.3839\phi_G+0.8027\phi_\beta-0.4055\phi_P+0.1282\phi_\gamma-0.1658\phi_\delta$
$W_2=4.898$	$\Psi_2=-0.3279\phi_G+0.4812\phi_\beta+0.5746\phi_P-0.5230\phi_\gamma-0.2394\phi_\delta$
$W_3=6.430$	$\Psi_3=-0.1408\phi_G-0.0079\phi_\beta+0.3240\phi_P+0.7138\phi_\gamma-0.6047\phi_\delta$
$W_4=6.693$	$\Psi_4=-0.1469\phi_G+0.3302\phi_\beta+0.3517\phi_P+0.4430\phi_\gamma+0.7412\phi_\delta$
Antisymmetric	
$W_1'=2.540$	$\Psi_1'=0.9767\phi_\alpha+0.2146\phi_\zeta$
$W_2'=3.120$	$\Psi_2'=\phi_Q$
$W_3'=6.520$	$\Psi_3'=\phi_\varepsilon$
$W_4'=7.110$	$\Psi_4'=0.2146\phi_\alpha-0.9767\phi_\zeta$

TABLE IV. THEORETICAL AND OBSERVED RESULTS ON THE BENZOIC ACIDIUM CATION AND ITS RELATED CATIONS

		ΔW, eV.		f [a]		b)	$\nu_{1/2}$ cm^{-1}	ΔE eV.	β_{CO} eV.
		Calcd.	Obs.[c]	Calcd.	Obs.[c]				
I	$PhC^{+}(OH)_2$	4.29	4.16	0.067	0.032	$\perp$	3900	1.75	−2.0
		4.71, 4.87	4.73	0.693, 0.171	0.297	∥, $\perp$			
		6.65	6.20	0.058	0.4	∥			
II	$PhC^{+}H(OH)$	3.72	3.64	0.065	0.028	$\sim\perp$	3300	1.00	−2.2
		4.15	4.20	0.702	0.308	$\sim$∥			
		5.77	5.99	0.079	0.2	$\sim$∥			
III	$PhC^{+}CH_3(OH)$	3.61	3.70	0.065	0.024	$\sim\perp$	3000	0.94	−2.0
		4.19	4.22	0.720	0.268	$\sim$∥			
		5.66	6.14	0.053	0.15	$\sim$∥			
IV	$MesC^{+}H(OH)$	3.29	3.21	0.065	0.037	$\sim\perp$	2900	0.71	−2.0
		3.95	3.91	0.660	0.276	$\sim$∥			
		5.72	5.6	0.099	0.1	$\sim$∥			

a) The oscillator strengths were calculated by the following equations:

$f_{calcd}=4.704\times10^{-7}\tilde{\nu}Q^2$ ($\tilde{\nu}$ in cm^{-1}, Q in Debye)

$f_{obs}=4.32\times10^{-9}\int\varepsilon d\tilde{\nu}$ ($\tilde{\nu}$ in cm^{-1}, ε in $l.\cdot cm^{-1}\cdot mol^{-1}$)

b) Directions of the calculated transition moments (with respect to the long axis of the molecule).

c) All the observed values were obtained by the present authors.

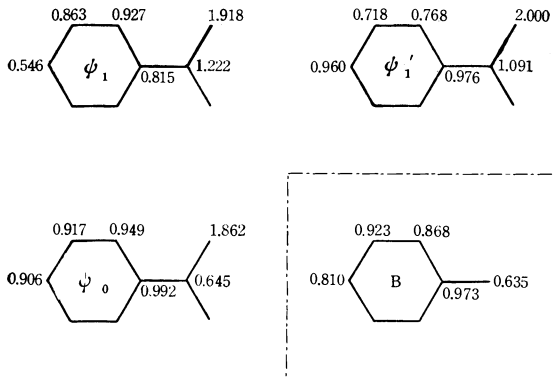


Fig. 3. π-Electronic charge-densities of the various states of the benzoic acidium ion (ψ_0, ψ_1', ψ_1) and of the ground state of the benzyl cation (**B**).

The π-electronic densities of the ground and excited states of the other ions are not very different from the corresponding values of I.

The stabilization energy, ΔE, due to delocalization of π-electrons amounts to 1.75 eV. for I, as is shown in Table IV. Most of this stabilization energy is brought about by the contribution of the charge-transfer configuration, ψ_P. Of the four ions concerned here, I is the most stable. According to our experiments, the ultraviolet absorption spectrum of benzoic acid in concentrated sulfuric acid does not change appreciably for more than ten days, while a gradual change is observed for the other ions. It may be expected that the hydroxyl groups stabilize the benzyl cation to some extent by their conjugation and steric hindrance effects. A similar stabilization effect is also found with the methyl group; the benzyl cation can not be stably produced under the usual conditions, while α- and/or ortho-methyl-substituted benzyl cations are stable enough for spectroscopic detection[15] because of the hyperconjugative and steric potencies of the methyl group.

The Shift of Bands of the Benzyl Cation by the Substitution.—The benzyl cation is characterized by its reddish color, while II is yellow and I is colorless, and their stabilities increase in just this order. These inclinations through less prominent, are also found for the α-methylated benzyl cations, which may be regarded as one of the most typical examples predictable of the unequivocal effect of hyperconjugation in ionic species.[5,15] The energy level diagram in Fig. 2 shows that the substitution of an electron donating group at the α-carbon atom of the benzyl cation, through the charge-transfer configuration, ψ_P, not only stabilizes the ion but also shifts the β-band ($\psi_G \rightarrow \psi_\beta$ transition) of the benzyl cation to blue. This is because the mixing of the charge-transfer configuration with the ground configuration, ψ_G, considerably lowers its energy, while the energy of the lowest excited configuration, ψ_β or ψ_P which had the same symmetry property as ψ_G, is little affected. Furthermore, because of the nil value of the coefficient C_{31}, α-substitution has no effect on the ψ_α configuration but makes the α-band ($\psi_G \rightarrow \psi_\alpha$ transition band) of the benzyl cation also shift to blue. On the other hand, as may be seen from the results of II and IV, the substitution of an electron-donating group at the benzene ring carbon atom (especially at the *o*- or *p*-position) is found to shift these characteristic bands to red. This phenomenon can be explained as resulting from the lowering of the ψ_α and ψ_β levels by the charge delocalization.

For the other ions the substitution effects on the absorption spectra are almost the same as those for I except for the second longest wavelength band. Because they have only one hydroxyl group, those ions have no ψ_Q configuration; therefore, unlike I, their second longest wavelength bands are not doubly degenerated. The observed half-widths of the second lowest bands seem to support this interpretation (see Table IV).

The Institute for Solid State Physics
The University of Tokyo
Azabu, Tokyo (S. N.)

The Institute for Physical and Chemical Research
Kamifujimae, Tokyo (H. H. & S. N.)

15) M. C. R. Symons, *J. Chem. Soc.*, **1959**, 958.

Charge-Transfer Complexes of Trinitrobenzene with Tetramethyl-p-phenylenediamine and p-Dimethoxybenzene

By Suehiro IWATA, Hiroshi TSUBOMURA* and Saburo NAGAKURA

(Received May 19, 1964)

Charge-transfer molecular complexes[1] between 1, 3, 5-trinitrobenzene (abbreviated hereafter to TNB) and some donor molecules have been studied very extensively.[2] For example, Foster and Thomson reported that the tetramethyl-*p*-phenylenediamine - TNB complex shows the charge-transfer absorption at 614 mμ in acetonitrile and at 583 mμ in cyclohexane, and that this complex is dissociated into ions in water and methanol.[3] Thus far, however, no quantitative consideration of the equilibrium constants and the heats of formation of this complex has been made.

In the present paper spectroscopic studies have been carried out with tetramethyl-*p*-phenylenediamine - TNB and *p*-dimethoxybenzene - TNB complexes, and the equilibrium constant and the heat of formation have been determined. Consequently, it has been found that the tetramethyl-*p*-phenylenediamine complex has the largest heat of formation and the longest wavelength charge-transfer absorption band among the TNB complexs studied so far.

Experimental

Materials. — TNB and *p*-dimethoxybenzene were purified by recrystallizing them from ethanol; their melting points were 120°C and 54.5°C, respectively. Tetramethyl-*p*-phenylenediamine (abbreviated hereafter to TMPD) was obtained by neutralizing its hydrochloride, and it was purified by vacuum sublimation.

n-Heptane was shaken with concentrated sulfuric acid, then washed with water, dried with calcium chloride and thereafter with sodium, and finally fractionally distilled.

Measurements.—A Cary recording spectrophotometer, model 14, was used for the measurements of the ultraviolet and visible absorption spectra. These spectra were measured by using cylindrical cells of 10 cm. light path length made of fused silica. The donor and the acceptor solutions, which were separately prepared, were mixed with each other just before the absorption measurements. For the experiments of the temperature dependence of the absorption intensity, we used a cell box with a heater, controlling the temperature with a thermister.

Results and Discussion

TMPD-TNB Complex.—The mixed solution of TMPD with TNB was violet. The absorption spectrum of this colored solution is shown in Fig. 1. The absorption maximum appears at 620 mμ (2.0 eV.). This absorption band may be thought to be Mulliken's charge-transfer band characteristic of the 1 : 1 molecular complex between TMPD as an electron donor and TNB as an electron acceptor. In order to make sure of this point and to evaluate the equilibrium constant for this system, Benesi-Hidebrand's equation[4] was applied.

Since, in the present experiments, the concentration of TMPD was much larger than that of TNB,[5] Benesi-Hildebrand's equation is applicable:

$$\frac{1}{\varepsilon^*}=\frac{C_a l}{D}=\frac{1}{K\varepsilon}\frac{1}{C_d}+\frac{1}{\varepsilon} \qquad (1)$$

where C_a and C_d are the initial concentrations

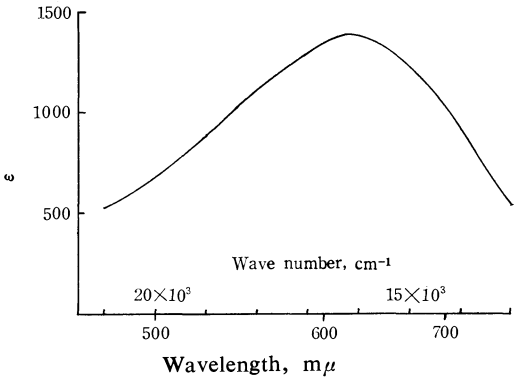


Fig. 1. The visible absorption spectrum of the molecular complex between TMPD and TNB in *n*-heptane (at 30°C).

* Present address: Faculty of Engineering Science, Osaka University, Toyonaka, Osaka.

1) R. S. Mulliken, *J. Am. Chem. Soc.*, **74**, 811 (1952).

2) G. Briegleb, "Elektronen-Donator-Acceptor-Komplexe," Springer - Verlag, Berlin - Göttingen - Heidelberg (1961).

3) R. Foster and T. J. Thomson, *Trans. Faraday Soc.*, **58**, 860 (1962).

4) H. A. Benesi and J. H. Hildebrand, *J. Am. Chem. Soc.*, **71**, 2703 (1949).

5) The initial concentrations of TNB and TMPD actually taken in the present experiment are $2.81\sim2.99\times10^{-4}$ mol./l. and $5\sim20\times10^{-3}$ mol./l. respectively.

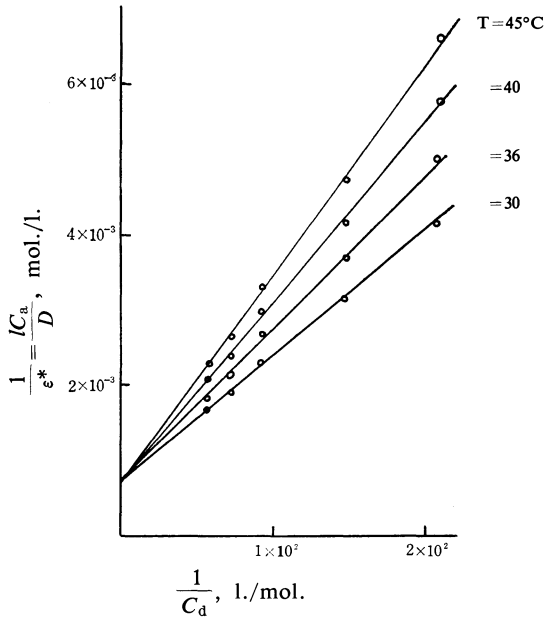


Fig. 2. Benesi-Hildebrand's plots for the TMPD-TNB system in *n*-heptane at various temperatures. Optical densities are measured at 620 mμ.

of the electron donor and acceptor respectively; K, the equilibrium constant for the 1 : 1 complex formation; D, the absorbancy; ε, the molar extinction coefficient, and l, the light path length of the cell. As may be seen in Fig. 2, a straight-line relationship is completely satisfied between $1/\varepsilon^*$ and $1/C_d$. This means that the 1 : 1 charge-transfer complex is formed between TMPD and TNB and that the charge-transfer band characteristic of the complex appears at 620 mμ. From the straight line obtained by the least-squares method, the equilibrium constant for the complex formation and the molar extinction coefficient of the charge-transfer band were determined by following the usual method.[4] The results obtained at 600, 620 and 640 mμ are given in Table I.[6]

Using the equilibrium constants at various temperatures given in Table I, we evaluated the heat of formation (ΔH) and the entropy change (ΔS) by the usual method.[7] The evaluated values are as follows:

$$\Delta H = -7.9 \text{ kcal./mol.} \qquad \Delta S = -18 \text{ e. u.}$$

These ΔH and ΔS values were the greatest of

Table I. The equilibrium constant (K in l./mol.) and the molar extinction coefficient (ε) of the TMPD-TNB complex evaluated at 600, 620 and 640 mμ

Temp. °C	K_{620}	K_{600}	K_{600}	Averaged	ε_{620}
30	44.4	42.8	44.4	43.9	1370
36	37.1	36.8	36.7	36.9	1340
40	29.3	30.0	29.2	29.5	1440
45	23.7	23.8	23.9	23.8	1520

the known TNB molecular complexes. This seems to be closely related with the fact that the TMPD-TNB complex has a smaller transition energy of the charge-transfer band ($h\nu_{CT}$ =2.0 eV.) than do the other TNB complexes.

Briegleb et al.[8] obtained the empirical formula of the relation between the ionization potentials (I) of the donor molecules and the transition energies of the charge-transfer bands ($h\nu_{CT}$) of TNB complexes:

$$h\nu_{CT} = I - 5.00 + \frac{0.70}{I - 5.00} \qquad (3)$$

From this relation and the observed $h\nu_{CT}$ value, the ionization potential of TMPD (I_{TMPD}) is evaluated to be 6.55 eV. A similar formula concerning chloranil complexes[8] leads to the I_{TMPD} value of 6.62 eV. It should be noticed that these two I_{TMPD} values are consistent with each other. Thus, it is concluded that TMPD has a small ionization potential and that in these two TMPD complexes the dative structure contributes largely to the ground state. This is related with the fact that TMPD complexes have a tendency to dissociate into ions in such polar solvents as methanol and acetonitrile.[3,9]

p-Dimethoxybenzene - TNB Complex. — The color of the mixed solution of *p*-dimethoxybenzene with TNB was yellow. The absorption spectrum ot this solution is given in

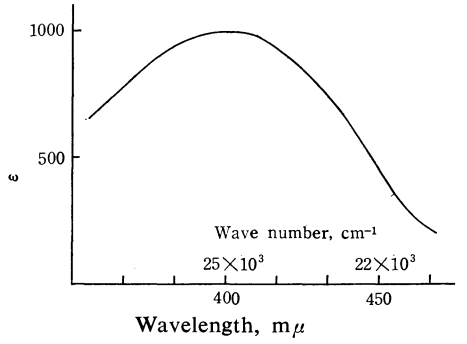


Fig. 3. The visible absorption spectrum of the molecular complex between *p*-dimethoxybenzene and TNB in *n*-heptane (at 22°C).

6) When, in the place of Eq. 1, the more precise Eq. 2 was used:

$$\frac{C_d}{\varepsilon^*} = \frac{lC_aC_d}{D} = \frac{1}{\varepsilon K} + \frac{1}{\varepsilon}(C_d + C_a) \qquad (2)$$

K=43.9 l./mol. and ε=1370 (at 620 mμ and 30°C) were obtained. These values are consistent with the corresponding values obtained by Eq. 1.

7) S. Nagakura, *J. Am. Chem. Soc.*, **80**, 520 (1958).

8) Chapter VI of Ref. 2.

9) W. Liptay, G. Briegleb and K. Schidler, *Z. Elektrochem.*, **66**, 331 (1962).

Fig. 3. The absorption band characteristic of the charge-transfer interaction between *p*-dimethoxybenzene and TNB appears at 400 mμ. By applying Eq. 1 to the absorbancy values measured at 420 mμ,[10] the equilibrium constant and the molar extinction coefficient were evaluated. The results are given in Table II.

From the temperature dependence of the equilibrium constants given in Table II, the heat of formation (ΔH) and the entropy change (ΔS) for the complex formation can be determined as follows:

$$\Delta H = -3.2 \text{ kcal./mol.}$$

$$\Delta S = -4.2 \text{ e. u.}$$

Furthermore, the molar extinction coefficient at the peak wavelength of the charge-transfer band could be evaluated as ~1000 by the aid of the equilibrium constant value obtained at 22°C.

TABLE II. THE EQUILIBRIUM CONSTANT (K) OF THE *p*-DIMETHOXYBENZENE-TEB COMPLEX EVALUATED AT 420 mμ

Temp., °C	19	22	25	28	31	36	40
K, l./mol.	3.5	3.3	3.1	2.9	2.8	2.5	2.3

By applying Eq. 3 to the peak wavelength of the charge-transfer band for the complex between *p*-dimethoxybenzene and TNB, the ionization potential of *p*-dimethoxybenzene could be obtained as 7.9 eV. This value is reasonable in view of the fact that the ionization potential of anisole has been determined as 8.2 eV. from the photoionization experiment of Watanabe.[11]

The Institute for Solid State Physics
The University of Tokyo
Azabu, Tokyo

10) The absorption maximum of the charge-transfer band is 400 mμ. In this wavelength region, however, there is a superposition of absorption due to TNB itself, so equilibrium constants are calculated by using the optical density at 420 mμ.

11) K. Watanabe, *J. Chem. Phys.*, **26**, 542 (1957).

Ammonia-Synthesis Iron Catalysts Containing Magnesia as Their Principal Promoter. II. The Texture and Structure of the Catalysts[1]

By Hiroshi UCHIDA, Iwao TERAO,[2] Kiyoshi OGAWA and Masaaki OBA

(Received May 11, 1964)

The preceding paper[3] discussed the performances of the catalysts which were promoted singly by magnesia and doubly or triply by other oxides besides magnesia. The roles played by the individual promoters were discussed in terms of their effects on the specific activity per unit of specific surface area and on the extent of the specific surface area. The present investigation has been made to obtain a comprehensive picture of the texture and structure of these catalysts and to attain a further understanding of the effects of individual promoters on the catalyst performances from the structural point of view.

Experimental

The catalysts investigated were an unpromoted catalyst (cat. M-O), a couple of singly-promoted catalysts with different magnesia contents (cats. M-1 and -2), three doubly-promoted catalysts containing potash, lime, and silica as the respective second promoters (cats. M-3, -4 and -5, respectively), and two triply-promoted catalysts containing different amounts of magnesia but with fixed amounts of potash and silica (cats. M-7 and -8). For the sake of comparison, one of the catalysts of the alumina-promoted type (cat. A-102) was also investigated. Their promoter-compositions are illustrated in Table I.

The preceding paper[3] presented data on the bed density and the specific surface area of the samples after their use in the synthesis run. In the present study, the total pore volume, the average diameters of pores and particles, the fraction of the surface occupied by free iron, and so forth, all concerning the samples drawn from the same sources, have been determined. The total pore volume, V_{po} (cc./g.), was calculated from the difference between the volumes by the mercury and helium displacement methods, i. e., $V_{po}=V_{Hg}-V_{He}$. The bulk density of the catalyst granule, ρ_b(g./cc.), was given by a reciprocal of V_{Hg}, while the true density of the catalyst material, ρ_t(g./cc.), was given by a reciprocal of V_{He}. The catalyst porosity, or the void

1) This paper is the 16th in a series of articles of dealing with the ammonia synthesis iron catalysts.
2) Present address: Japan Gas-Chemical Co., Enokicho, Niigata.
3) H. Uchida, I. Terao and K. Ogawa, This Bulletin, 37, 653 (1964).

TABLE I. PHYSICAL PROPERTIES OF SAMPLES

Catalyst	Promoter-composition wt. %	Hg volume cc./g.	Densities Hg g./cc.	Densities He g./cc.	Surface area $m^2/g.$	Pore volume cc./g.	Porosity	Average pore diameter Å	V_{CO}/V_m
M-O	Unpromoted	0.202	4.95	7.69	1.15	0.072	0.36	2500	—
M-1	2MgO	9.238	4.20	7.52	3.02	0.105	0.44	1390	—
M-2	5MgO	0.253	3.95	7.04	5.57	0.111	0.44	780	0.23
M-3	5MgO, $1K_2O$	0.276	3.69	7.19	1.05	0.137	0.50	5220	0.14
M-4	4MgO, 1CaO	0.251	3.98	7.35	4.63	0.115	0.46	990	—
M-5	4MgO, $1SiO_2$	0.254	3.94	6.90	12.00	0.109	0.43	360	0.23
M-7	2MgO, $1SiO_2$, $1K_2O$	0.256	3.91	7.19	4.67	0.117	0.46	1000	0.14
M-8	4MgO, $1SiO_2$, $1K_2O$	0.267	3.75	6.99	9.37	0.124	0.46	530	0.36
A-102	$2Al_2O_3$, 1CaO, $1K_2O$	0.276	3.62	7.30	6.67	0.139	0.50	820	0.10

fraction of a catalyst granule, was available from V_{po}/V_{Hg}. On the assumption of open-end cylindrical pores, the average pore diameter, $\bar{d}_{po}$ (cm.), was computed from the equation $\bar{d}_{po}=4V_{po}/S$, while, on the assumption that the catalyst granule consists of a loose packing of spherical or cubic particles, the average particle diameter, d_{pa}, was computed from the equation $\bar{d}_{pa}=6/(S\rho_t)$. In the above equations, S ($cm^2/g.$) stands for the specific surface area. Following the method of Emmett and Brunauer,[4] the fraction of surface occupied by free iron was expressed by the ratio of the carbon monoxide volume which was chemisorbed at −78°C, V_{CO}, to the nitrogen volume which formed a monolayer over the entire surface, V_m. The adsorption measurements were conducted by a conventional volumetric method. V_{CO} was determined from the difference between the total carbon monoxide adsorption at −196°C and the subsequent adsorption at this temperature after evaculation at −78°C, while V_m was determined by means of the BET equation applied to the nitrogen adsorption isotherm at −196°C.

In order to obtain additional information on the catalyst texture, the catalysts were examined by optical and electron microscopy. The oxide catalyst samples were polished on one surface by ordinary methods, finishing with a final buffing of soft cloth with wet alumina; they were then observed under an optical microscope before and after etching with hydrochloric acid. In some particular cases, the etched samples were reduced with hydrogn at temperatures between 380 and 500°C in a cell attached to a high-temperature microscope, and the structural changes in the surface with time of reduction were observed under a microscope. The hydrogen flow rate was approximately 5 l./hr. Electron microscopic observations were made by a JEM-6A electron microscope on replicas of the etched surfaces shadowed with chromium-carbon and also on finely ground powders of the catalyst samples before and after their use in the synthesis run. The samples were ground in castor oil.

X-Ray diffraction patterns were taken on powdered samples less than 200 mesh in size as well as on the samples after their use in the synthesis run, by means of a Geigerflex D-3F X-ray diffractometer. Fe $K\alpha$ radiation from a sealed-off X-ray tube equipped with berylium windows and with a manganese dioxide filter was used at 30 kV. and 7.5 mamp.

Results and Discussion

The Texture of Catalysts after Use in the Synthesis Run. — Table I summarizes the data on the mercury volume, mercury and helium densities, pore volume, porosity, average pore diameter, the fraction of the surface occupied by free iron, and the specific surface area. The comparison between the mercury volumes of cat. M-O and cat. M-1 shows that magnesia alone is already effective in preventing the catalyst granules from shrinking during the reduction process and subsequent synthesis run. The porosity values of the promoted catalysts fall in a narrow range from 0.43 to 0.50, all values being higher than the 0.36 of cat. M-O. In view of the fact cat. M-3 gives a higher porosity than cat. M-O, it is likely that the individual granule of the former catalyst consists of particles more loosely packed than those of the latter in spite of nearly the same extent of the specific surface area. In fact the average pore diameter is twice as large as that of cat. M-O. With regards to other catalysts, the average pore size depends mainly on the extent of the specific surface area, since their pore volumes are within the narrow range. The effects on the particle size of the addition of promoters will be described later in connection with the effects on the crystallite dimension.

The fraction of the surface occupied by the free iron of catalysts of the magnesia-promoted type, including the catalyst singly promoted by magnesia, is always small; this result is similar to that with catalysts of the alumina-promoted type. The result is, however, opposite to that of Kobosev et al.,[5] who stated that magnesia was entirely surface-inactive in the

4) P. H. Emmett and S. Brunauer, *J. Am. Chem. Soc.*, 62, 1732 (1940).

5) N. I. Kobosev, B. V. Erofeev, I. B. Kaverin and A. N. Bogoyavlenskaya, *Acta Physicochim, U. S. S. R.*, 1, 483 (1943).

TABLE II. LATTICE CONSTANT OF OXIDE CATALYST (a), CRYSTALLITE WIDTH OF REDUCED CATALYST (D), AND AVERAGE PARTICLE DIAMETER ($\bar{d}$)

Catalyst	M-O	M-1	M-2	M-3	M-4	M-5	M-7	M-8	A-102
a, Å	8.396	8.395	8.395	8.393	8.402	8.393	8.396	8.393	8.391
D, Å	560	300	310	640	280	250	300	290	390
$\bar{d}$, Å	6760	2640	1530	7950	1760	730	1790	920	1220

course of the reduction of an iron oxide. One explanation of these apparently different results may be that magnesia is surface-inactive in the earlier reduction stage, where the iron particles poduced by reduction remain extremely small in size, but that magnesia is apt to accumulate on the surface with the particle growth. This explanation is not contradictory to the facts that the reduction of cat. M-1 in the earlier stage takes place at a rate nearly as fast as the reduction of a pure magnetite, but that the last traces of oxygen can be removed only with difficulty.[3] The other promoters besides magnesia play scarcely any significant role in the change in the fraction; e. g., the fraction of cat. M-4 is of almost the same extent as that of cat. M-2.[6]

The Crystal Structure of the Catalysts before and after Use in the Synthesis Run.—The lattice constants of oxide catalysts were calculated on the basis of the α_1-line from the (553) or (731) plane of Fe_3O_4, the Bragg angle of which could be measured with a reasonable accuracy. The results are summarized in Table II. The addition of magnesia does not cause any changes in the lattice constant of a pure magnetite. This is quite different from the finding with the alumina addition by Westrik,[8] who pointed out that the lattice constant appears to decrease linearly with the ratio $Al^{3+}/(Fe^{3+}+Al^{3+})$ and who concluded that alumina is dissolved in the magnetite lattice. The linear relationship just referred to, on the other hand, can be interpreted in terms of the Vegard equation of $a=a_1M_1+a_2M_2$, where a is the lattice constant of the promoted catalyst, a_1 and a_2 are the lattice constants of Fe_3O_4 and Al_2FeO_4 spinel respectively, and M_1 and M_2 are the respective contents in mole fraction. Accordingly, Al_2O_3 and FeO in Fe_3O_4 combine to form the Al_2FeO_4 spinel, and the resulting spinel is in a solid solution with Fe_3O_4. If an identical mechanism is applied to the addition of magnesia, the lattice constant of cat. M-1 or cat. M-2 is expected to decrease with the magnesia content because the lattice constant of the $MgFe_2O_4$ spinel ($a=8.36$ Å) is smaller than that of pure magnetite. It is more likely, according to Goldschmidt,[9] that the Mg^{2+} ions cannot enter the lattice as substituents of the Fe^{2+} ions but that they can occupy the empty interstices in the magnetite lattice. Cat. M-4 gives the larger lattice constant, as can be expected from the larger size of Ca^{2+} ions.

From the broadening of the X-ray diffraction lines, which can be almost entirely accounted for by the occurrence of small crystallites,[10] the crystallite width of the samples after the synthesis run was calculated by means of the Scherrer formula: $D=C\lambda/B\cos\theta$. In this formula, D is the crystallite width, λ is the wave length of an X-ray radiation (1.937 Å for the Fe-K line), B is the true half-breadth (angular) of the diffraction line, θ is the Bragg angle, and C is 0.9. The graphs given by Jones[11] were used to make correction for the $\alpha_1\alpha_2$-doublet and to evaluate the true diffraction breadth on the basis of the experimental data. The calculations were made on the basis of the line from the (110) plane. The results are compared in Table II with those on the average particle diameter.

Apart from the results concerning cat. M-3, the crystallite widths of the catalysts of the magnesia-promoted type fall in a narrow range between 250 and 310 Å, whereas the average particle sizes of these catalysts fall in a far wider range from 700 to 2600 Å (cf. Table II). These facts indicate that the individual particles of these catalysts consist of from about 10 to several hundred crystallites and that the particle size is more strongly dependent on the promoter-composition than is the crystallite width. It is worthwhile to notice that not only the individual particles of cat. M-O but also those of cat. M-3 consist of more than 1000 crystallites. The comparison of the crystallite width and the particle size of cat. M-O with the respective values of cat. M-1 clearly

6) In connection with this finding, we want to call attention to the results of Hall et al.[7] who measured on this kind of catalyst the changes in the specific surface area and in the carbon monoxide chemisorption with the reduction progress in a hydrogen flow at atmospheric pressure and found a much higher value of the fraction after the complete reduction. The disagreement may perhaps be due to the different treatments to which the catalyst samples have been submitted.

7) W. K. Hall, H. Tarn and R. B. Anderson, *J. Am. Chem. Soc.*, **72**, 5436 (1950).

8) R. Westrik, *J. Chem. Phys.*, **21**, 2094 (1953).

9) H. J. Goldschmidt, *Nature*, **137**, 478 (1946).

10) A. Nielsen, "An Investigation on Promoted Iron Catalysts for the Synthesis of Ammonia," Jul. Gjellerups Forlag, Copenhagen (1956), p. 165.

11) F. W. Jones, *Proc. Roy. Soc.*, **A160**, 16 (1963).

shows that the addition of magnesia largely contributes to a retardation of the growth of crystallites and particles, though not so much as does alumina (as for the particle growth, cf. Ref. 12), during the periods of reduction and synthesis. The effect is considerably pronounced when silica is added as the second promoter, but it is cancelled out in the presence of potash. Lime added as the second promoter scarcely affects the growth.

It is generally accepted[13] that the iron crystallites and particles probably unite quite easily to grow in size whenever they come in contact wihthout a barrier of promoter oxides. Marked growth, however, does not always take place because there is an interfacial layer of promoter oxides, as in the case of cat. M-3. Accordingly, the interfacial oxide layer capable of retarding the particle growth requires certain characteristics as regards the melting point of the oxide material; the crystallites are apt to combine more easily when the interfacial layer contains potash, which has a lower melting point than magnesia. The relatively small particle sizes of the triply-promoted catalysts, cats. M-6 and -8, are probably due to the fact (cf. Ref. 14) that silica acts to keep potash within the particles; as a consequence, the small fraction of potash coverage is established.

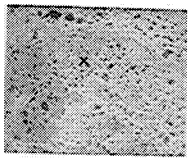
In view of the above picture of the catalysts, one might expect, at first glance, a lower specific activity per unit of the surface area, k' (atm.$^{0.5}$ ml./hr. m^2), with a larger size of the particles, for the particle growth is accompanied by the formation of crystallographic planes more closely packed than the (111) α-iron plane, whose specific activity is higher than that of any other planes. However, the situation is sometimes reversed; e. g., k' at 400°C of cat. M-3 (2.10×10^2), with a large particle size, is higher than that (2.4×10) of cat. M-5, with a much smaller particle size[3].

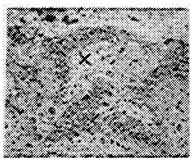
Microscopic and Electron Microscopic Structures of the Oxide Catalysts. — One can make easily finish the polishing of the catalysts of the magnesia-promoted type than those of the alumina-promoted type.[15] Photographs 1, 4 and 7 show the respective optical micrographs of the polished surfaces of cats. M-1, A-102 and M-7, while Phots. 2 and 5 show those after the etching of M-1 and A-102 catalysts. As is evident from the microphotographs, cats. M-1 and -7 of the magnesia-promoted type possess a larger number of holes and cavities than cat. A-102 of the alumina-promoted type, being more porous in structure. A close examination of Phots. 1 and 2 of cat. M-1 reveals that the etched figures are apt to appear in the region which is light gray on the polished surface. The etched figure appears to be a hill-and-valley structure on an electron micrograph (Phot. 8). Magnesia may be more concentrated in the light gray region, and it may give rise to the etching or the faster dissolution of the oxide material. In contrast, cat. A-102 gives an etched figure characterized by a mosaic structure of well-developed grains, across which a number of clear-cuts run in parallel (Phot. 5), and the individual grains consist btoh of a great many plate-shaped subgrains and a few single crystallites of the octahedral type (Phots. 9 and 10). Additional information on the shape of subgrains can be obtained from the respective electron micrographs (Phots. 11 and 12) taken of the finely ground powders of cats. M-1 and A-102. The powders from cat. M-1 are massive and irregular in shape, whereas the great majority of powders from cat. A-102 are plate-shaped. Cat. M-7 gives a polished surface which includes more pores and after the etching, shows grains of an irregular shape surrounded by narrow cracks. This catalyst gives both the plate-shaped and massive powders.[16]

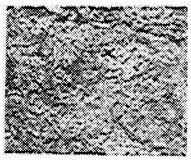
The Change in the Structure of the Catalysts with the Progress of the Reduction.—In connection with our previous finding[3] that the reduction of the catalysts of the magnesia-promoted type in a current of synthesis gas at a high pressure proceeds more rapidly than that of cat. A-102 of the alumina-promoted type, the change in the surface of the etched samples with the progress of reduction was pursued for each catalyst under a high-temperature microscope. The rusults are exemplified in Phots. 3 and 6 for cats. M-1 and A-102 respectively.

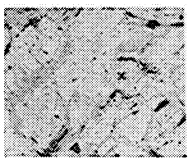
As for cat. A-102, reduction takes place along the grain boundaries and sub-boundaries to result in the deeper grooves; hence, the reduction on the individual grains with only a few sub-boundaries proceeds at a very slow rate, probably because of the rapid accumulation of alumina on these surfaces. In contrast to this, the reduction of cat. M-1 starts at a great many domains scattered rather homogeneously over the whole surface, and a large number of small pores and narrow cracks appear before the reduction penetrates through the wall surfaces of the pores as well as of

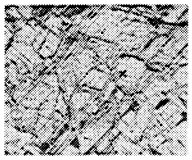
12) H. Uchida and N. Todo, *J. Chem. Soc. Japan, Ind. Chem. Sec.* (*Kogyo Kagaku Zassi*), **60**, 1235 (1957).
13) A. Nielsen, Ref. 10, p. 175.
14) H. Uchida and N. Todo, This Bulletin, **29**, 20 (1956).
15) The hardness on the Vicker's scale was 345 kg./mm^2 for cat. M-1 in contrast to 390 kg./mm^2 for cat. A-102.
16) The microphotographs taken after the etching and electron micrographs of cat. M-7 will be illustrated elsewhere.

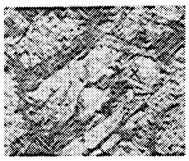

Phot. 1. 100×

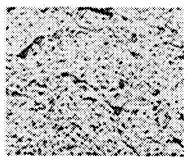

Phot. 2.


Phot. 3.

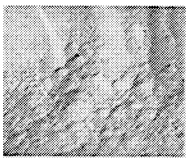

Phot. 4.

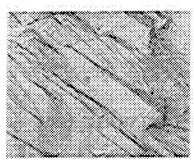

Phot. 5.

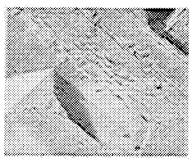

Phot. 6.

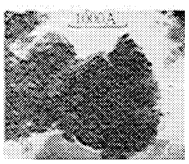

Phot. 7.

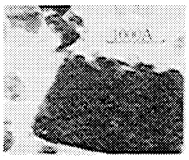
Phots. 1—7: Microphotographs of oxide catalysts. Phots. 1—3: Cat. M-1. Phots. 4—6: Cat. A-102. Phot. 7: Cat. M-7. Phots. 1, 4, and 7: Polished surface. Phots. 2 and 5: Polished and etched surface. Phot. 3: After reduction for 5 hr. at 380°C and 4 hr. at 500°C. Phot. 6: After reduction for 2 hr. at 400°C and 4 hr. at 510°C.

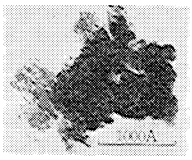

Phot. 8. 10000×


Phot. 9. 10000×


Phot. 10. 1000×


Phot. 11.


Phot. 12.


Phot. 13.


Phot. 14.

Phots. 8—10. Electron micrographs of replicas of polished and etched surface of oxide catalyst. Phot. 8: Cat. M-1. Phots. 9—10: Cat. A-102. Phots. 11—14: Electron micrographs of catalyst powders before and after use in the synthesis run. Phot. 11: Cat. M-1 before the use. Phot. 12: Cat. A-102 before the use. Phot. 13: Cat. M-1 after the use. Phot. 14: Cat. A-102 after the use.

the cracks into the interior. In this way, the reduction of cat. M-1 in the earlier stage proceeds more rapidly than that of cat. A-102. This finding gives additional support to Kobosev's view that magnesia is ineffective in retarding the reduction rate. Nevertheless, one must keep in mind the fact that magnesia acts as an effective stabilizer for the catalysts.

The Electon-microscopic Structure of the Catalysts after the Synthesis Run. — Electron microscopic investigations of the ammonia synthesis iron catalysts have been made by McCarty and Anderson[17] and more recently by Schaefer[18]. Their results are of much interest, because they gave us a direct concept of the catalyst structure. However, their results refer mainly to the pore structure of the catalysts after reduction under rather mild conditions at atmospheric pressure; they do not permit a detailed consideration of the particle structure of the catalysts in use at a high pressure. The present observations, therefore, have been made on finely ground powders from the catalyst samples after ammonia synthesis.[19]

The results are exemplified in Phots. 13 and 14 for cats. M-1 and A-102 respectively, revealing that the powders from cat. M-1 are massive and irregular in shape, whereas the powders from cat. A-102 are mainly thin-plated. The photographs, when compare with the corresponding photographs of the oxide catalysts (Phots. 11 and 12), indicate that the subparticles after the synthesis run can still retain their original shape. This finding seems to support the view of Westrik and

17) J. T. McCarty and R. B. Anderson, *J. Appl. Phys.*, **22**, 1441 (1957).
18) K. Schaefer, *Z. Electrochem.*, **64**, 1190 (1960).
19) The catalyst samples subjected to ammonia synthesis at a high pressure differ considerably in texture from the samples reduced at atmospheric pressure (cf. Ref. 12).

Zwietering[20] that both the habit and the orientation of the iron formed are very strongly affected by the oxide from which it has originated. For the plate-shaped subparticles, a thickness of 410 Å is calculated by means of the $\bar{d}_{pa}=2/\rho_t S$[21] formula, a value which is in good agreement with the crystallite width of 390 Å computed from the X-ray line broadening.

A highly active catalyst is usually furnished with both a moderately large specific surface area and a high specific activity per unit of the surface area.[22] However, the high specific activity is sometimes accompanied by a small extent of the specific surface area, and vice versa. In this connection, the above-mentioned finding suggests that a structure of the raw catalyst such as that revealed by the photographs of highly active cat. A-102 is favorable for establishing a large extent of the specific surface area of the high specific activity. The optical and electron microscopy of the catalysts may thus provide a convenient means for us to search for promoter-compositions which would be able to produce high-activity of catalysts.

Summary

This paper has presented data on such textures as the specific surface area, the pore volume, the average diameter of particles and pores, the fraction of the surface occupied by free iron and so forth, and on such structures as the lattice constant in the oxidic state and the crystallite width after the synthesis run of individual catalysts of the magnesia-promoted type, together with data on both a pure magnetite and a catalyst of the alumina-promoted type. It has also included the results of the examination of the catalysts by means of optical and electron microscopy.

Although the magnesia used as a promoter may be surface-inactive at the earlier stage of reduction, it tends at the later stage to cover the major portion of the particle surface and acts to retard the particle growth as well as the crystallite growth. The retarding effect on the growth is cancelled out when potash is added as the second promoter, but it is considerably pronounced in the presence of silica. Apart from the catalyst doubly promoted by magnesia and potash, the particle size of the promoted catalysts ranges from 700 to 2600 Å, but the crystallite widths lie in a far narrower range, between 250 to 390 Å. The specific activity per unit of the surface area is not always higher for the catalysts of the smaller particle sizes.

The lattice constant of a pure magnetite is not changed by the addition of magnesia, indicating that the Mg^{2+} ions occupy the empty interstices in the magnetite lattice.

The microscopic and electron-microscopic structures of the polished and etched surfaces of oxide catalysts of the magnesia-promoted type are very different from those of the alumina-promoted type. In view of the change in the microscopic structure of the surface with the reduction progress, an explanation in terms of the different reduction rates between the two types of catalysts is probable.

On the basis of the fact that the subparticles of the catalyst after the synthesis run still retain the original shape of the corresponding oxide catalyst, either plate-shaped or massive, the electron-microscopic as well as the microscopic observation of the polished and etched surface of the oxide catalyst can afford a means for predicting the promoter-composition which will produce a highly active catalyst.

Government Chemical Industrial Research Institute, Tokyo
Shibuya-ku, Tokyo

20) R. W. Westrik and Z. Zwietering, *Proc. Kon. Ned. Akad. v. Wetenschappen*, **B56**, 492 (1953).
21) On the assumption of plate-shaped subparticles, the thickness, $\bar{d}_{pa}$, is calculated from this formula.
22) Strictly speaking, the bed density should be taken into account, but it varies only a little among the catalysts under investigation.

On the Melting Temperature of Nucleic Acid in Solution

By Masamichi TSUBOI

(Received May 12, 1964)

Many natural and synthetic nucleic acids take doubly-stranded helical conformations in aqueous solutions at room temperature.[1] On raising the temperature of such a solution, a strand separation takes place, and the helical molecule turns to two single-stranded random coils. The process can be followed by the viscosity, the optical density (at 260 mμ), or the optical rotation measurement of the solution.[2] It is found that the transition occurs within a narrow temperature range. This transition is considered to be the "melting" of a one-dimensional "crystal." The temperature at the midpoint of the transition is denoted by T_m and may be called "the melting temperature." The melting temperature, T_m, of a nucleic acid in a solution varies according to the base composition of the nucleic acid, the salt concentration of the solution, and the pH of the solution. Some chemicals, such as caffeine,[3] spermine,[4] and actinomycin D,[5] when they are added to the solution, also affect the T_m value. This paper will present some discussion of these variations of T_m on the basis of a simple application of the mass action law to the strand-separation reaction.

Let us assume that, in a solution of a nucleic acid at a temperature in the vicinity of the melting temperature, there are only three kinds of molecules (see Fig. 1): the double-helix molecule (AB), and the two complementary single-stranded molecules (A and B), and that there is no molecule (such as C in Fig. 1) in which a half-way strand-separation takes place. This assumption is somewhat justified by the fact that in the CsCl density-gradient spectrum of partially heat-denatured deoxyribonucleic acid, no bands are observed corresponding to the molecules in which a half-way strand-separation takes place.[6]

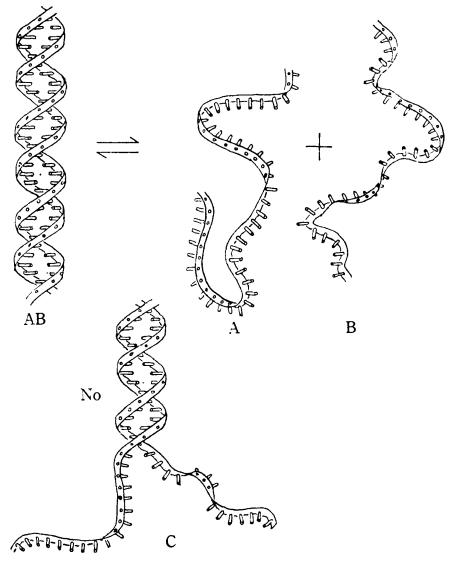


Fig. 1. A schematic representation of a transition of a doubly-stranded helix (AB) of a nucleic acid to two single-stranded random coils (A and B). The form C, where a half-way strand separation takes place, is not considered to exist.

Let us assume also that the melting of nucleic adid is essentially a reversible process, and that the irreversibility observed of deoxyribonucleic acid (DNA) is only an apparent one, an extremely long time being required for the complete "crystallization" (reformation of the perfect double-helix structure). This extremely low reaction rate is probably due to an extremely high activation entropy in the reformation reaction of DNA. As one can easily imagine, the chance is extremely low of any two complementary DNA chains to approach each other in such a way that the original proper base pairings can be reformed. The rate of double-helix reformation is quite high in a system where no such activation entropy is required. Thus, the melting of the double-helix molecule composed of 1:1 polydeoxyribothymidylic acid and polydeoxyriboadenylic acid, poly(dT+dA), was found to be completely reversible.[7] We have also observed

1) See, for example, R. F. Steiner and R. F. Beers, Jr., "Polynucleotides," Elsevier Publishing Company, New York (1961).

2) P. Doty, J. Marmur and N. Sueoka, Brookhaven Symposia in Biology, "Structure and Function of Genetic Elements," No. 12, 1 (1959).

3) P. O. P. Ts'o, G. K. Helmkamp and C. Sander, *Proc. Nat. Acad. Sci. (U. S. A.)*, **48**, 686 (1962).

4) M. Mandel, *J. Mol. Biol.*, **5**, 435 (1962).

5) M. Tsuboi, S. Higuchi, Y. Kyogoku, K. Matsuo and A. Wada, *Chem. Pharm. Bull.*, **12**, 501 (1964).

6) J. Marmur, C. L. Schildkraut and P. Doty, Fifteenth Annual Symposium on Fundamental Cancer Research, "The Molecular Basis of Neoplasia," Univ. of Texas, Austin, U. S. A. (1961), p. 9.

7) P. Doty, Discussion in Brookhaven Symposium in Biology, No. 12, "Structure and Function of Genetic Elements," 24 (1959).

that, for the 1 : 1 complex of polyriboinosinic acid and polyribocytidylic acid, poly(I+C), the same optical density profile is obtained on heating and cooling.[8]

We can now consider that the "melting" problem is simply the problem of the dissociation equilibrium of the type:

$$AB \rightleftarrows A + B \qquad (1)$$

The equilibrium constant may be expressed as:

$$K=\frac{[A]\,[B]}{[AB]}=\frac{(1-f)^2}{f}a \qquad (2)$$

Here, f is the fraction of the double-helix molecules, and a is the total concentration of the nucleic acid in question. At the melting temperature, T_m, f equals[9] 1/2, and the equilibrium constant is given by:

$$K_m=\frac{1}{2}a \qquad (3)$$

The K_m is related to the enthalpy (ΔE) and the entropy (ΔS) of melting as:

$$-RT_m \ln K_m=\Delta E-T_m\Delta S \qquad (4)$$

1. The Guanine-Cytosine Content and Melting Temperature of DNA

The enthalpy of the melting of a deoxyribonucleic acid (DNA) may be given as:

$$\Delta E=n[\Delta\varepsilon_1 g+\Delta\varepsilon_2(1-g)] \qquad (5)$$

where $\Delta\varepsilon_1$ is the enthalpy of melting assigned to one cytosine-guanine bridge; $\Delta\varepsilon_2$, that assigned to one adenine-thymine bridge; g, the guanine plus cytosine content (GC content) of the DNA in question, and n, the mean number of bridges in the double-helix structure of the DNA in question. From Eqs. 3, 4 and 5, we obtain the relation:

$$g=\frac{\Delta S-R\ln 0.5a}{n(\Delta\varepsilon_1-\Delta\varepsilon_2)}T_m-\frac{\Delta\varepsilon_2}{\Delta\varepsilon_1-\Delta\varepsilon_2} \qquad (6)$$

If ΔS, $\Delta\varepsilon_1$, and $\Delta\varepsilon_2$ are assumed to be constants independent of T_m, then Eq. 6 shows that the melting temperature, T_m, should be a linear function of the GC content, g, of the DNA in question. This linear relation is just what was observed by Marmur and Doty.[10]* The straight lines obtained by them are reproduced in Fig. 2. The slope and intercept

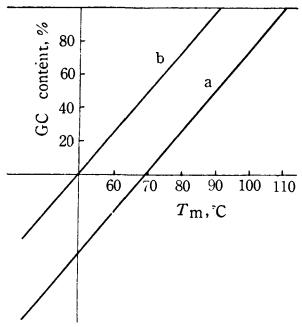


Fig. 2. Dependence of T_m on the guanine plus cytosine content of DNA.[10] The straight line a was obtained from the examination of the solution with 0.15 mol./l. NaCl plus 0.015 mol./l. Na-citrate, and the line b of the solution with 0.01 mol./l. PO_4 plus 0.001 mol./l. EDTA.

of the line for the solutions with 0.15 mol./l. sodium chloride are found to be respectively 1/42 and −8.1. Therefore, from Eq. 6, we obtain

$$\frac{\Delta S-R\ln 0.5\,a}{n(\Delta\varepsilon_1-\Delta\varepsilon_2)}=\frac{1}{42} \qquad (7)$$

and

$$\frac{\Delta\varepsilon_2}{\Delta\varepsilon_1-\Delta\varepsilon_2}=8.1 \qquad (8)$$

The 7 and 8 relations are given graphically in Figs. 3 and 4 respectively. At present the values of $\Delta\varepsilon_1$, $\Delta\varepsilon_2$, $\Delta\varepsilon_1-\Delta\varepsilon_2$, and $(\Delta S-R\times\ln 0.5\,a)/n$ are all unknown. However, if one

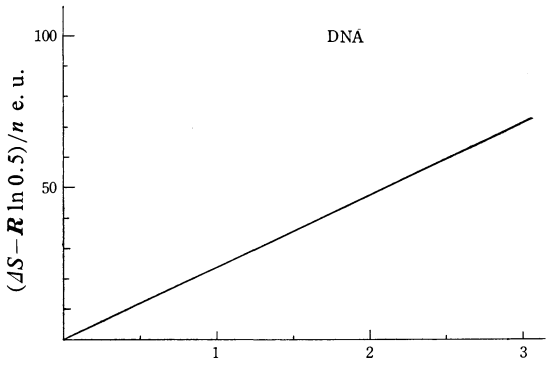


Fig. 3. Relation of $(\Delta S-R\ln 0.5\,a)/n$ and $\Delta\varepsilon_1-\Delta\varepsilon_2$ for DNA in the solution with 0.15 mol./l. NaCl plus 0.015 mol./l. Na-citrate.

8) K. Matsuo and M. Tsuboi, *Chem. Pharm. Bull.*, to be published.

9) It was pointed by J. Applequist (*J. Am. Chem. Soc.*, **83**, 3158 (1961)) that the hypochromism of nucleic acid at 260 mμ is not always proportional to f. Therefore, if the transition is followed by the measurement of the optical density at 260 mμ, the apparent midpoint of the transition does not always give the point where f=0.5. However, this does not seriously affect the present discussion, where T_m is required only as an operational quantity.

10) J. Marmur and P. Doty, *J. Mol. Biol.*, **5**, 109 (1961).

* Here it should be mentioned that M. Ozawa, M. Tanaka and E. Teramoto (*J. Phys. Soc. Japan*, **18**, 551 (1963)) explained the linear relation between the T_m and the GC content of DNA on the basis of essentially the same idea as above but with a somewhat different expression—an experssion of statistical mechanics. The present writer's thermodynamic expression was first described at the 10th Nucleic Acid Symposium, Kanazawa, May, 1962.

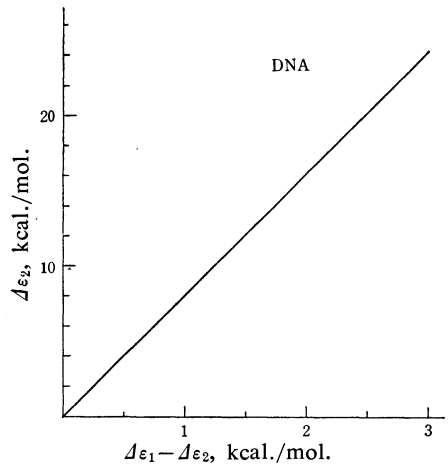


Fig. 4. Relation of $\Delta\varepsilon_2$ and $\Delta\varepsilon_1-\Delta\varepsilon_2$ for DNA in the solution with .0.15 mol./l. NaCl plus 0.015 mol./l. Na-citrate.

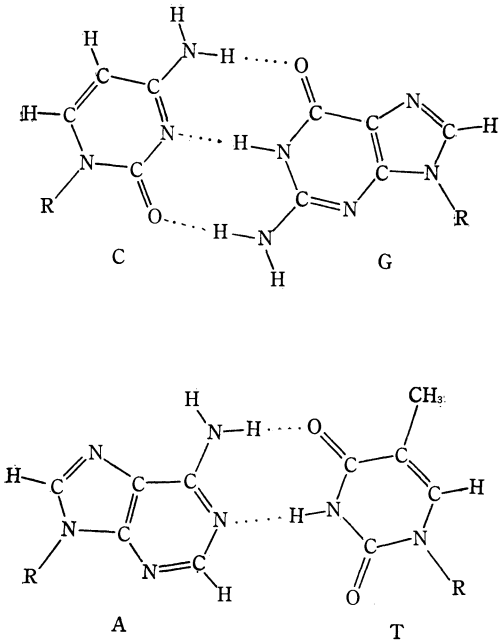


Fig. 5. Hydrogen bonds between cytosine (C) and guanine (G) residues and between adenine (A) and thymine (T) residues.[11]

of these values is fixed, all of these values can be determined by these relations. It has been pointed out[11] that, as is shown in Fig. 5, cytosine and guanine can form three hydrogen bonds, while adenine and thymine can form only two hydrogen bonds. If the stability of the helical conformation came solely from these hydrogen bonds, and if each of these hydrogen bonds made an equal contribution to the stability, $\Delta\varepsilon_2/(\Delta\varepsilon_1-\Delta\varepsilon_2)$ should be equal to 2. The actual value of 8.1 indicates that the third hydrogen bond in the cytosine-guanine bridge makes a relatively small contribution to the stability of the helix.

2. The Degree of Protonation and the Melting Temperature of Polyriboadenylic Acid

Polyriboadenylic acid (poly A) is known to form a two-stranded helical complex in its acidic solution.[12] It has been found that the melting temperature of this complex depends upon the degree of the protonation of the adenine residue. According to the experimental results obtained by Fresco and Klemperer,[12] the melting temperature is 90°C for a 0.88 degree of protonation (at pH 4.25) and 68°C for a 0.76 degree of protonation (at pH 4.86). At pH 4.25, the fraction (g_1) of the AH^+—AH^+ pair is about $0.88\times0.88=0.78$, the fraction (g_2) of the AH^+-A pair is about $0.88\times0.12=0.11$, and the fraction (g_3) of the A—A pair is about $0.12\times0.12=0.01$, where A and AH^+ indicate the adenine residue and protonated adenine residue respectively. At pH 4.86, the fraction (g_1) of the AH^+-AH^+ pair is about $0.76\times0.76=0.58$, the fraction (g_2) of the AH^+-A pair is about $0.76\times0.24=0.18$, and the fraction (g_3) of the A—A pair is about $0.24\times0.24=0.06$. Let the contribution of the AH^+-AH^+ pair to the helix stability be $\Delta\varepsilon_1$, that of the AH^+-A pair, $\Delta\varepsilon_2$, and that of the A—A pair, $\Delta\varepsilon_3$. Now we obtain the relation:

$$\Delta E=n(\Delta\varepsilon_1 g_1+\Delta\varepsilon_2 g_2+\Delta\varepsilon_3 g_3) \tag{9}$$

instead of Eq. 5, and the relation

$$g_1=\frac{\Delta S-\boldsymbol{R}\ln 0.5\,a}{n(\Delta\varepsilon_1-\Delta\varepsilon_2)}T_m-\frac{\Delta\varepsilon_2-(\Delta\varepsilon_2-\Delta\varepsilon_3)g_3}{\Delta\varepsilon_1-\Delta\varepsilon_2} \tag{10}$$

instead of Eq. 6. It is assumed that

$$\Delta\varepsilon_2-\Delta\varepsilon_3=\Delta\varepsilon_1-\Delta\varepsilon_2 \tag{11}$$

then Eq. 10 becomes

$$g_1-g_3=\frac{\Delta S-\boldsymbol{R}\ln 0.5\,a}{n(\Delta\varepsilon_1-\Delta\varepsilon_2)}T_m=\frac{\Delta\varepsilon_2}{\Delta\varepsilon_1-\Delta\varepsilon_2} \tag{12}$$

Thus we obtain

$$\frac{\Delta S-\boldsymbol{R}\ln 0.5\,a}{n(\Delta\varepsilon_1-\Delta\varepsilon_2)}=0.0114\ \text{deg}^{-1} \tag{13}$$

and

$$\Delta\varepsilon_2/(\Delta\varepsilon_1-\Delta\varepsilon_2)=3.4 \tag{14}$$

from the observed relation of g_1-g_3 and T_m (see Fig. 6). Therefore, it may be concluded that, very roughly, the AH^+-AH^+ pair gives $(3.4+1.0)/3.4=1.3$ times the contribution to

11) L. Pauling and R. Corey, *Arch. Biochem. Biophys.*, **65**, 164 (1956).

12) J. R. Fresco and E. Klamperer, *Ann. New York Acad. Sci.*, **81**, 730 (1959).

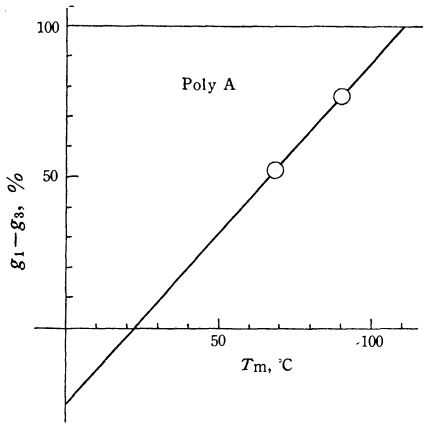


Fig. 6. T_m plotted against g_1-g_3 of poly A in the solution with 0.15 mol./l. NaCl.

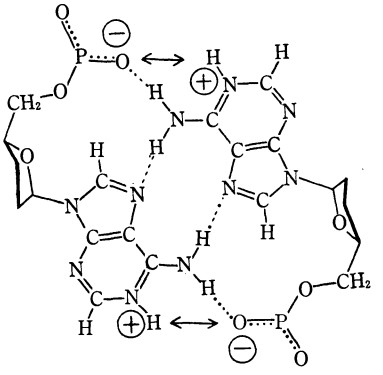


Fig. 7. Hydrogen bonds between two adenine residues.[13]

the helix stability given by the AH^+-A pair.

It has been pointed out[13] that two adenylic acid residues can form the four hydrogen bonds shown in Fig. 7, and that the additional stability of the protonated poly A may be attributed to an electrostatic force between the positively-charged $(N_1H)^+$ group of the protonated adenine residue in one of the two intertwined helices and the negatively-charged phosphate group in the other helix. The amount of this stability may be estimated from the difference between the pK values of poly A and adenosine. From the titration curve (at 25°C) of the poly A solution with 0.15 molal sodium chloride,[12] the pK of poly A may be estimated as about 5.5. On the other hand, Levene and Simms[14] reported the pK for adenosine to be 3.5. This means that protonated poly A needs more free energy for deprotonation than does protonated adenosine. The difference is:

$$(\boldsymbol{RT}/\log_{10} e)(5.5-3.5)=2.8 \text{ kcal./mol.}$$

where T is the absolute temperature of the solution and e is the base of the natural logarithm. This difference may be attributed mostly to the additional stability of the protonated poly A because of the above-mentioned electrostatic force. If we assume, on this basis, that

$$\Delta\varepsilon_1-\Delta\varepsilon_2=2.8 \text{ kcal./mol.}$$

then the values of $\Delta\varepsilon_1$, $\Delta\varepsilon_2$, $\Delta\varepsilon_3$, and $(\Delta S-\boldsymbol{R}\ln 0.5\,a)/n$ are calculated by Eqs. 11, 13, and 14 as follows:

$$\Delta\varepsilon_1=12.2 \text{ kcal./mol.}$$

$$\Delta\varepsilon_2=9.4 \text{ kcal./mol.}$$

$$\Delta\varepsilon_3=6.6 \text{ kcal./mol.}$$

$$(\Delta S-\boldsymbol{R}\ln 0.5\,a)/n=32 \text{ e.u.}$$

3. The Effect of Salt Concentration

The melting temperature of nucleic acid is greatly influenced by the ionic strength of the solution. Marmur and Doty[10] showed this to be the case for E. coli K-12 DNA heated in various concentrations of potassium chloride. It was found that, when the salt concentration is raised, the T_m goes up in the manner shown in Fig. 8.

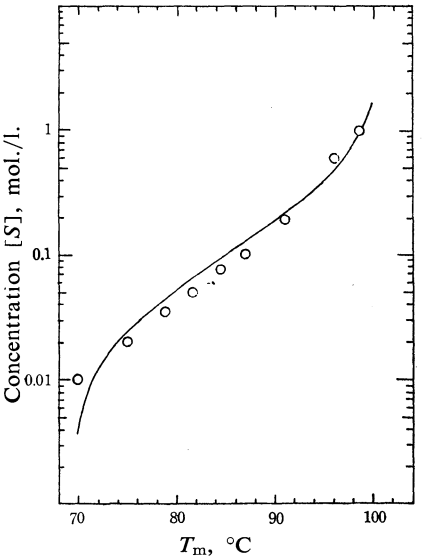


Fig. 8. T_m of E. coli K12 DNA plotted against the KCl concentration (in logarithmic scale) in the solution.

○: From the data given by Marmur and Doty.[10]

—: Theoretical curve on the assumption that $K'=10(\text{mol./l.})^{-1}$, $(\Delta S-\boldsymbol{R}\ln 0.5\,a)/\alpha N=0.0304 \text{ deg}^{-1}$, and $E_0/\alpha N=10.4$.

It would be expected that raising the salt concentration of the suspending medium would

13) A. Rich, D. R. Davies, F. H. C. Crick and J. D. Watson, *J. Mol. Biol.*, 3, 71 (1961).

14) P. A. Levene and H. S. Simms, *J. Biol. Chem.*, 65, 519 (1925).

produce a shielding of the repulsive forces of the charged phosphate groups of the DNA molecule, and that this would produce an additional stability of the helical form and, thus, a higher melting temperature. Let us assume that the shielding occurs through an adsorption of the cations by the DNA molecules at the PO_2^- groups, and that, for this adsorption, Klolz's equation,[15]

$$\frac{1}{r}=\frac{1}{K'N}\frac{1}{[S]}+\frac{1}{N} \qquad (15)$$

is valid. In Eq. 15, r is the average number of the cations in question adsorbed by one double-helical DNA molecule AB; N, the maximum number of the cations that can be adsorbed by one double-helical DNA molecule; $[S]$, the concentration of the cations free from the adsorption, and K', the equilibrium constant (at T_m) of each of the reactions:

$$\begin{aligned}&AB+S=AB\cdot S\\&AB\cdot S+S=AB\cdot S_2\\&AB\cdot S_2+S=AB\cdot S_3 \qquad (16)\end{aligned}$$

and

$$AB\cdot S_{N-1}+S=AB\cdot S_N$$

In the present case, ΔE in Eq. 4 may be given as

$$\Delta E=\Delta E_0+\alpha r \qquad (17)$$

where ΔE_0 is the enthalpy of the melting of DNA without cations, and α, the increase of ΔE caused by the adsorption of one cation. From Eqs. 4, 15 and 17, we obtain the relation,

$$(\Delta S-\boldsymbol{R}\ln 0.5a)T_m=\Delta E_0+\alpha NK'[S]/(1+K'[S]) \qquad (18)$$

The melting temperature of DNA is usually examined at a concentration of 20 μg./ml., i.e., about 6×10^{-5} mol. nucleotide per liter. In a solution with such a low concentration of DNA, the free cation concentration $[S]$ is practically equal to its total concentration ($10^{-2}\sim1$ mol./l.). Therefore, Eq. 18 is considered to give the T_m value as a function of the salt concentration ($\fallingdotseq[S]$). The equilibrium constant K' is a function of T_m, as

$$K'=\exp(\Delta S'/\boldsymbol{R})\exp(-\Delta E'/\boldsymbol{R}T_m) \qquad (19)$$

where $\Delta E'$ and $\Delta S'$ are, respectively, the enthalpy and the entropy of each of the reactions 16. If $\Delta E'$ is small, however, K' is practically constant over a small range of T_m (see Fig. 9). As will be mentioned below, this is actually the case for the adsorption of cations by the DNA molecules. It would be convenient to draw curves representing the relations between $[S]$ and $K'[S]/(1+K'[S])$ for various K' values, as in Fig. 10. The abscissa $K'[S]/(1+K'[S])$ should have a linear relation with the T_m in question, since, from Eq. 18,

$$K'[S]/(1+K'[S])=[(\Delta S-\boldsymbol{R}\ln 0.5a)/\alpha N]T_m-\Delta E_0/\alpha N \qquad (19)$$

A comparison of Fig. 8 and Fig. 10 shows that the observed effect of the KCl concentration of the T_m of DNA can be well explained by what has been presented and by assuming that

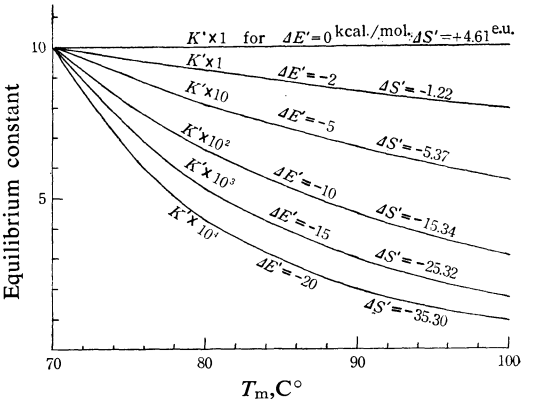


Fig. 9. Equilibrium constant K' plotted against the temperature in question (T_m). $\Delta E'$ and $\Delta S'$ are the enthalpy and entropy of the reaction in question (see Eq. 19 in the text).

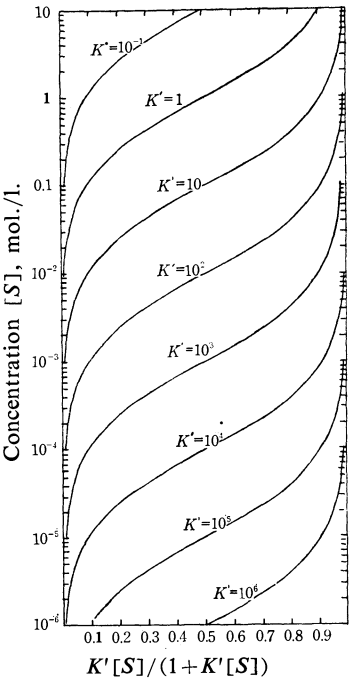


Fig. 10. Relations between $[S]$ (in logalithmic scale) and $K'[S]/(1+K'[S])$ for various K' values.

15) I. M. Klotz, "Protein Interactions" in H. Neurath and K. Bailey (ed.), "The Proteins," Academic Press, New York (1953).

$K'=10$ (mol./l.)$^{-1}$

$(\Delta S-\boldsymbol{R}\ln 0.5\,a)/\alpha N=0.0304$ deg^{-1}

and

$\Delta E_0/\alpha N=10.4$

It may be pointed out here that straight lines of T_m vs. GC-content observed by Marmur and Doty[10] at different salt concentrations are almost parallel to each other (see Fig. 2). The lines have the same slope but different intercepts. On the basis of Eq. 6, this means that, at different salt concentrations, the values of $(\Delta S-\boldsymbol{R}\ln 0.5\,a)/n(\Delta\varepsilon_1-\Delta\varepsilon_2)$ are equal to each other, but that the values of $\Delta\varepsilon_2/(\Delta\varepsilon_1-\Delta\varepsilon_2)$ are different from each other. This suggests that the stability of the helical form of DNA due to the base pairing is not affected (and that thus the $\Delta\varepsilon_1-\Delta\varepsilon_2$ value is not affected) by the salt concentration.

From the fact that the two straight lines, in question are parallel,[10] another interesting conculsion may be drawn: The $\Delta E'$ is very small for the adsorption of cations by the DNA molecules. The increase in T_m (denoted as ΔT_m) when the salt concentration is raised from "0.01 M PO_4+0.001 M versene" to "0.15 M NaCl+0.015 M Na citrate" should be proportional to the K' value on the basis of Eq. 18. If the $\Delta E'$ in question is -2 kcal./mol. or so, the K' (and therefore ΔT_m) should decrease appreciably when the T_m is raised from 70 to 90°C (see Fig. 9). The experimental results of Marmur and Doty[10] (given in Fig. 2) indicate that this is not actually the case, and that ΔT_m (and therefore K') remains constant at any T_m in the 70~90°C range. Thus, the absolute value of $\Delta E'$ is considered to be much smaller than 2 kcal./mol. If the absolute value of $\Delta E'$ is smaller than 1.6 kcal./mol. ($\Delta E>-1.6$ kcal./mol.) and if $K'=10$ (mol./l.)$^{-1}$, as has been given above, then $\Delta S'$ should be positive. The positive $\Delta S'$ obtained here may be interpreted as indicating that the adsorption of cations by the DNA molecules takes place through a hydrophobic bond.[16]

4. The Effect of Spermine

Spermine $NH_3^+(CH_2)_3NH_2^+(CH_2)_4NH_2^+\cdot(CH_2)_3NH_3^+$ is known to cause, when it is added to a DNA solution, an increase in the T_m of DNA.[4,17] This is considered to be due to the formation of complex molecules of spermine plus double-helical DNA, which are more stable than the double-helical DNA molecules free from spermine.

The binding reaction of spermine molecules, S, with double-helical DNA molecules, AB, may be expressed by Eqs. 15 and 16 of the preceding section. The enthalpy of melting the ΔE of such a spermine-DNA complex may be expressed by Eq. 17, and the melting temperature, T_m, may be given by Eq. 18. When T_m is plotted against $\log_{10}[S]$, a curve similar to those given in Fig. 9 is obtained. From a comparison of such a curve and those in Fig. 9, the K' value is estimated to be about 10^5 (mol./l.)$^{-1}$ in solutions with 0.03 mol./l. sodium chloride at 80°C, and about 10^3 (mol./l.)$^{-1}$ in solutions with 0.15 mol./l. sodium chloride at 90°C. Thus, it may be seen that the equilibrium constant, K', for spermine is much higher than that for potassium cation and that it depends greatly upon the salt concentration in the solution.

Mandel[4] examined the effects of spermine on the T_m values of solutions of DNA's obtained from a number of different sources and with different guanine-cytosine contents (GC-content). He observed that the extent of the increase in T_m (ΔT_m) becomes smaller with the increase in GC-content. Thus, $\Delta T_m=3.1$°C for a DNA with a GC-content of 26% ($T_m=81.3$°C), while $\Delta T_m=1$°C for a DNA with a GC-content of 58% ($T_m=95.8$°C). He concluded that ΔT_m is a function of the adenine-thymine content of the DNA sample. In the present writer's view, however, what he observed is mostly to be attributed to the effect of the temperature on the K' value; it is not to be directly correlated with the base composition of DNA.

As has been mentioned above, the interaction of the spermine molecule with the DNA molecule is very strong, and $\Delta E'$ for the present case may be as high as $-10\sim-20$ kcal./mol. or so. If it is -20 kcal./mol., for instance, the K' value at 95°C can be only one-third of that at 80°C (see Fig. 9). It is quite possible that such a lowering in K' value causes the lowering in ΔT_m value mentioned above. In addition, we have recently obtained[8] a bit of evidence which shows that the existence of the adenine-thymine base pairing in a nucleic acid is not a necessary condition for the interaction with spermine; the addition of only 0.0005 mol./l. of spermine produces a marked elevation of the T_m (from 58 to 90°C) of 1:1 complex polyriboinosinic acid plus polyribocytidylic acid, poly(I+C), which contains no adenine-thymine base pair.

There it remains much to be done before we can discuss the molecular structure of the spermine-DNA complex in the molecular structure of the spermine-DNA complex in detail. On the basis of what we have so far obtained,

16) See, for example, G. Némethy and H. A. Scheraga, *J. Phys. Chem.*, **66**, 1773 (1962).
17) H. Tabor, *Biochemistry*, **1**, 496 (1962).

however, the writer would like to present a possible model of that structure here.

Quite recently, Iitaka and Huse[18] have determined the crystal structure of spermine phosphate hexahydrate. The results suggest in a very interesting way how the spermine molecule may combine with the DNA molecule in the double-helix form.

In the crystal structure of spermin phosphate hexahydrate, there is a sheet which consists of HPO_4^{2-} ions and water molecules formed by the O-H···H hydrogen bonds. The sheet contains parallel chains of phosphate ions running along the a axis. The phosphate-phosphate distance along the a axis is 7.96 Å, while the chain-chain distance along the b axis (in the sheet) is 11.6 Å. As Iitaka and Huse[18] pointed out, there is a certain similarity between the arrangement of phosphate groups found in spermine phosphate and that found in crystalline DNA. Langridge et al.[19] have shown the arrangement of phosphate groups along the polynucleotide helices in the B-form of LiDNA. In this structure, two oxygen atoms of the phosphate group, which share one negative formal charge, are turned outwards and so are readily available for interaction with proteins, water, etc. (see Fig. 11).

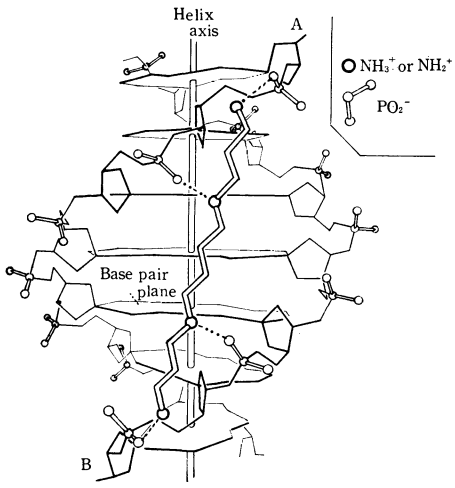


Fig. 11. A proposed model of spermine plus double-helical DNA.

The distance between successive phosphate groups along the helix is about 7.3 Å, which may be compared with the phosphate-phosphate distance, 7.96 Å, along the a axis in the phosphate chain in the spermine phosphate crystal. The perpendicular distance between two polynucleotide chains (chain A and B of the double-helix) across the shallow groove in LiDNA is about 13 Å, while in the spermine phosphate crystal the separation of the phosphate chains within the same sheet is found to be 11.6 Å, as has been given above. The spermine molecule in the spermine phosphate crystal is in the form of the fully-extended zigzag chain, and it is placed parallel to the phosphate-water sheet, forming an oblique bridge across the adjacent two phosphates chains in the same sheet. One of the two NH_3^+ groups makes a strong hydrogen bond with a phosphate group in the one chain, and the other NH_3^+ group makes a similar hydrogen bond with a phosphate group in the other chain. One of the two NH_2^+ groups makes a strong hydrogen bond with another phosphate group in the former chain, and the other NH_2^+ group makes a similar hydrogen bond with another phosphate group in the latter chain.

On the basis of what has been described above, it may be proposed that the spermine molecule combines with the double-helical NDA molecule, so that it forms an oblique bridge across the shallow groove between the two polynucleotide helices, A and B, as is shown in Fig. 11. A molecular model building shows that each of the NH_3^+ and the NH_2^+ groups on one end of a spermine molecule can form a strong hydrogen bond with one of the two adjacent phosphate groups in the DNA chain A, and that at the same time both the NH_3^+ and the NH_2^+ groups on the other end of the spermine molecule can form a similar hydrogen bond with one of the two adjacent phosphate groups in the DNA chain B. In this way, the spermine molecule may function as a clamp for binding two chains (A and B) together, and thus for stabilizing the double-helical structure of DNA.[20]

5. The Effect of Actinomycin D

The effect of actinomycin D on the T_m of DNA has recently been examined by Tsuboi et al.[5] Of what has been observed, the following two facts are to be pointed out here: First, only a very small amount (2.5×10^{-5}

18) Y. Iitaka and Y. Huse, This Bulletin, 37, 437 (1964); *Acta Cryst.*, in press.

19) R. Langridge, D. A. Marvin, W. E. Seeds, H. R. Wilson, C. W. Hooper, M. H. F. Wilkins and L. D. Hamilton, *J. Mol. Biol.*, 2, 38 (1960).

20) Iitaka and Huse (Ref. 18) showed that, in tne spermine phosphate hexahydrate crystal, the phosphate chains of the adjoining sheets as well as of the same sheet are bound together strongly by the spermine molecules. Likewise, a spermine molecule may function not only as a clamp for binding two polynucleotide helices together but also as an "adhesive" for binding two double-helical DNA molecules. It was found (Ref. 4) that, at concentrations of spermine in excess of 0.005 mol./l., visible aggregation of the DNA strands occurs. This fact may be interpreted as due to the above-mentioned "adhesive" function of the spermine molecule.

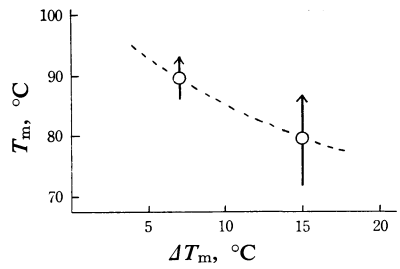


Fig. 12. Amount of elevation of T_m(ΔT_m) of calf-thymus DNA caused by addition of actinomycin D, plotted against the T_m of the solution.

mol./l.) is necessary to cause a marked elevation of T_m (72°C to 87°C). Secondly, the amount of elevation, ΔT_m, depends upon the original T_m value; ΔT_m is lower in a DNA solution with high a T_m (see Fig. 12).

On the basis of what has been discussed in this paper, the first fact may be interpreted as indicating that actinomycine D molecules are bound by the helical DNA molecule with a very high K' value and/or a very high α value. The second fact may be interpreted as indicating that the K' value depends greatly upon the temperature of the solution, because there is a high $\Delta E'$ value in each of the binding reactions, Eqs. 16.

6. The Effect of Caffeine, etc.

Ts'o, Helmkamp, and Sander[3] observed that the T_m's of polyriboadenylic acid (poly A) and DNA are lowered when caffeine, nucleosides, and related compounds are added to the solutions. Ts'o and Lu[21] found, on the other hand, that caffeine, for example, is bound by the random coil poly A with $K'=5.8$ (mol./l.)$^{-1}$ at 5°C, while it is much less strongly bound by the helical poly A ($K'<(1$ mol./l.)$^{-1}$ at 5°C). As they mentioned, the lowering of T_m may be related to the fact that caffeine (for example) interacts more strongly with the coil form of nucleic acids than with the helical form.

Also, for the present problem, Eqs. 17 and 18 are considered to be valid provided that the meanings are somewhat different of α, r, N, K' and $[S]$. α is now a negative value and represents the decrease in ΔE caused by the binding of caffeine to the coil form poly A. K' is the equilibrium constant (at T_m) of each of the reactions:

$$\begin{aligned} &A+S=AS \\ &AS+S=AS_2 \\ &AS_2+S=AS_2 \end{aligned} \qquad (20)$$

and

$$AS_{N-1}+S=AS_N$$

r is the average number of caffeine molecules bound by one random-coil poly A molecule (A); N, the maximum number of caffeine molecules that can be bound by one random-coil poly A molecule (A), and $[S]$, the concentration of the caffeine molecules free from poly A (which is practically equal to the total concentration of caffeine in the present case). From Eq. 18, the amount of the lowering of T_m ($-\Delta T_m$) due to the addition of $[S]$ of caffeine, etc., to the solution is expressed as:

$$\Delta T_m=\frac{\alpha K'[S]/(1+K'[S])}{(\Delta S-\boldsymbol{R}\ln 0.5\,a)/N} \qquad (21)$$

By the use of this expression, and by the use of the data obtained by Ts'o et al.[3,21] (plotted in Fig. 13 by circles) an attempt has

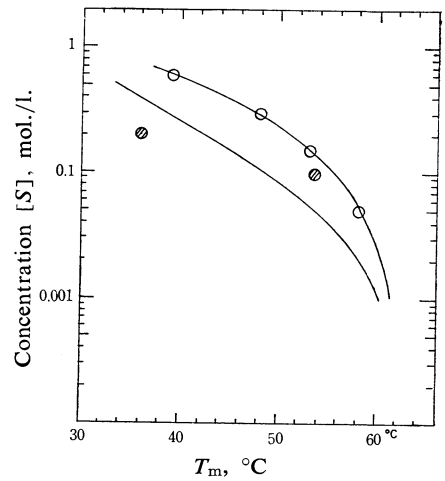


Fig. 13. T_m of poly A at pH 4.85 plotted against the concentration of caffeine (black circles) and purine (white circles) added to the solution.[3] Curves were obtained by a calculation based upon Eq. 21, and by assuming that $\alpha=1.2$ kcal./mol. and $K'=5.8$ (mol./l.)$^{-1}$ for purine and that $\alpha=1.3$ kcal./mol. and $K'=2$ (mol./l.)$^{-1}$ for caffeine. $(\Delta S-\boldsymbol{R}\ln 0.5\,a)/N$ was assumed to be 32 e.u. for both cases.

been made to estimate the α value for the case of caffeine plus poly A and also for the case of purine plus poly A. In both of these cases, $(\Delta S-\boldsymbol{R}\ln 0.5\,a)/N$ for poly A is assumed to be 32 e.u., which is equal to the value of $(\Delta S-\boldsymbol{R}\ln 0.5\,a)/n$ of poly A given in the last paragraph of section 2. Because the hydrophobic forces are considered to play a predominant role in the interaction of caffeine (or purine) with random-coil poly A,[3] the enthalpy of binding $\Delta E'$ for the present cases would be small. Therefore, K' value for caffeine plus

21) P. O. P. Ts'o and P. Lu, *Proc. Nat. Acad. Sci. (U. S. A.)*, **51**, 17 (1964). Their nK corresponds to K' in this paper.

poly A is assumed to be 5.8 $(\text{mol./l.})^{-1}$ not only at 5°C but also in the vicinity of T_m (40～60°C). The data given in Fig. 13 suggest that the K' value is slightly lower for the case of purine plus poly A than that for the case of caffeine plus poly A; it is assumed to be 2 $(\text{mol./l.})^{-1}$ for the former case. Therefore, the α value is calculated to be −1.2 kcal./mol. for the case of caffeine plus poly A and −1.3 kcal./mol. for the case of purine plus poly A. By these values of α, the date given in Fig. 13 can be well explained (see the theoretical curves in the figure). Thus, it may be concluded that the binding of one caffeine or purine molecule to the random-coil poly A casuses a lowering of the ΔE (enthalpy of melting) by 1.2～1.3 kcal./mol.

Summary

The mass action law has been applied to the "melting" process of nucleic acids and also to the binding process of small ions or molecules. On the basis of previously-obtained data on the variation of the melting temperature of nucleic acids caused by interaction with small ions and molecules, some of the enthalpy, entropy, and free energy changes involved in the processes have been estimated. A model has been proposed of how the spermine molecule may interact with the deoxyribonucleic acid molecule to stabilize the double-helical conformation of the latter molecule.

This work was supported by a grant from the United States Public Health Service, No. GM-10024-01, and also by a grant from the Ministry of Education of Japan.

Faculty of Pharmaceutical Science
University of Tokyo
Hongo, Tokyo

The Stability of Calcium Complexes of Purely-separated Polyphosphate

By Masaji MIURA and Yoshiki MORIGUCHI

(Received May 12, 1964)

The complex formation of linear-chain polyphosphates with various metals has been studied by several authors.[1-5] Their studies, however, have dealt with polyphosphates with molecular weight distributions. The investigation of complexes of purely-separated polyphosphates, except pyrophosphate and triphosphate, has not yet been undertaken. This is probably in part due to the difficulty of separating individual polyphosphates from their mixture in sufficient quantities and in part to their low stability for a hydrolytic degradation.[6] As their stability decreases with decrease in the pH of the solution, the measurements of the stability constants of polyphosphate complexes must be carried out at as high a pH as possible, and so it is difficult to apply such an usual method as pH titration.

The purpose of this study is twofold, namely, 1) to investigate the effect of the thain length of purely-separated polyphosphates on the stability of their calcium complexes, and to compare the present results with those given by Irani et al. and others[1,2] and 2) to investigate the effect of the ionic strength on the structure of calcium complexes of polyphosphates with various chain lengths from the point of view that polyphosphate is a kind of polyelectrolyte.

Experimental

The Synthesis and Separation of Polyphosphates.[6,7] — A polyphosphate glass was prepared by the pyrolysis of a mixture of sodium dihydrogen phosphate and disodium hydrogen phosphate containing ^{32}P at 800°C for 5 hr. Each linear-chain polyphosphate with a chain length of 4—8 phosphorus atoms was separated from the mixture of polyphosphates by anion-exchange chromatography using the H-form of Dowex 1X4 (100~200 mesh).

1) R. R. Irani and C. F. Callis, *J. Phys. Chem.*, **64**, 1398 (1960).
2) J. I. Watters and S. M. Lambert, *J. Am. Chem. Soc.*, **81**, 3201 (1959).
3) J. R. Van Wazer and D. A. Campanella, ibid., **72**, 655 (1950).
4) U. P. Strauss and P. D. Ross, ibid., **81**, 5295 (1959).
5) W. Wieker, A. Grossmann and E. Thilo, *Z. anorg. u. allgem. Chem.*, **307**, 42 (1960).
6) S. Otani, M. Miura and T. Doi, *J. Chem. Soc. Japan, Ind. Chem. Sec.* (*Kogyo Kagaku Zasshi*), **66**, 593 (1963).
7) W. Wieker, *Z. Elektrochem.*, **64**, 1047 (1960).

An aqueous solution of sodium chloride was used as an eluent. Each polyphosphate was precipitated from the effluent by adding benzidin, and the precipitate was repeatedly washed with distilled water until the filtrate was free from chloride ions.

The benzidin polyphosphates thus obtained were transformed into tetramethylammonium polyphosphates by adding an aqueous solution of tetramethylammonium hydroxide. The isolated benzidin was separated from the polyphosphate solution by extraction with chloroform.

The pH of tetramethylammonium polyphosphate solutions was kept over 10 by adding tetramethylammonium hydroxide, and the solutions were stocked in a refrigerator to avoid hydrolytic degradation.

The G. R.-grade pyrophosphate and triphosphate were repeatedly crystallized from water and an ethanol-water mixture respectively.[8] Both of them were transformed into free acids by the use of cation-exchange resin.[1]

The concentration of each polyphosphate was determined by a radio tracer technique, while those of pyrophosphate and triphosphate were determined by means of pH titration.

Reagents.—The tetramethylammonium hydroxide and bromide were both G. R.-grade reagents and were used without further purification. The calcium solutions used as titrants were $5.01_2\times10^{-2}$, $1.02_9\times10^{-1}$ and $2.05_8\times10^{-1}$ M calcium nitrate standardized with disodium ethylenediaminetetraacetate at a pH of 13 in the presence of a calcon indicator.[9]

Apparatus and Procedure. — The nephelometer used in the present work was an A. K. A. spectrophotometer, which was reconstructed so we could keep the temperature in a cell-room constant and could stir a sample solution in a cell by means of a micromotor.

The solutions of polyphosphate and of oxalic acid as a precipitating agent were pipetted into a cell. The total ionic strength of the solution was adjusted to either 0.1 or 1.0 by adding a 3 M solution or crystals of tetramethylammonium bromide. Distilled water was added to the solution until its volume was 30~33 ml., and then the pH of the solution was kept at 10~12 by adding an aqueous solution of tetramethylammonium hydroxide.

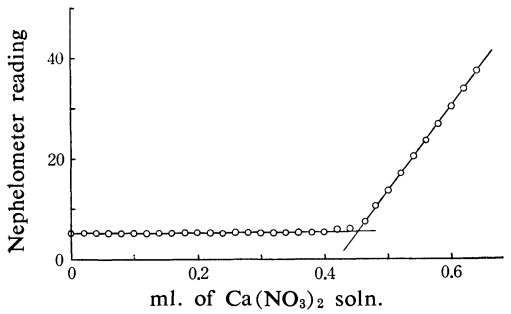


Fig. 1. An example of nephelometric titrations for the calcium-oxalate-polyphosphate system.

8) R. N. Bell, *Anal. Chem.*, **24**, 1997 (1952).

9) C. A. Goetz and R. C. Smith, *Iowa State J. Sci.*, **34**, No. 1, 81 (1959).

The nephelometric titration was carried out at 25±0.5°C under a nitrogen atmosphere by adding a standard solution of calcium nitrate through a calibrated microburet. The solution was vigorously stirred during the titration. At five-minute intervals titrant shots were taken. This procedure was proved by a preliminary test to avoid supersaturation and to give equilibrium values. An example of the results of the titration is shown in Fig. 1.

It was verified by ion-exchange chromatography and paper chromatography that the degradation of polyphosphate did not occur during the titration.[6,10]

The Treatment of Date

The evaluation of the stability constants of the calcium polyphosphate complexes was performed by a method similar to that reported by Irani et al.[1] Assuming that a polyphosphate chain consists of some sites, $L(\theta)$, which can bind a calcium ion to θ phosphorus atoms,* that these sites are mutually independent, and that the concentration of free calcium ions is negligibly small at the end-point compared with that of the calcium complex, the stability of the calcium complex at pH over 10 can be evaluated by means of the following equation:

$$\beta=\left(\frac{L_tA}{\theta yz}-1\right)\frac{K_{sp}}{[C_2O_4]_t} \qquad (1)$$

where β is the dissociation constant of the complex given by Eq. 2; L_t, the total concentration of the polyphosphate expressed by moles of phosphorus per liter; A, the total volume of the sample solution at the end-point; y, the number or ml. of z M calcium solution added until the end-point; $[C_2O_4]_t$, the concentration of oxalic acid, and K_{sp}, the solubility product of calcium oxalate expressed by Eq. 3. The literature values of K_{sp} are 1.32×10^{-8} and 7.80×10^{-8} at the ionic strengths of 0.1 and 1.0 respectively.[1]

$$\beta=\frac{[Ca]\,[L(\theta)]}{[CaL(\theta)]} \qquad (2)$$

$$K_{sp}=[Ca]\,[C_2O_4] \qquad (3)$$

Thus, β can be calculated from Eq. 1 if θ is known. θ can be evaluated by the measurements at two different concentrations of oxalic acid, if the temperature, ionic strength and pH are kept constant. Namely, if y_1 and y_2 are obtained at two different concentrations of oxalic acid, $[C_2O_4]_{t_1}$ and $[C_2O_4]_{t_2}$, the elimination of β from Eq. 1 gives Eq. 4:

10) H. Grunze and E. Thilo, *Sitz. ber. deut. Akad. Wiss. Berlin Kl. Math. u. allgem. Naturw.*, **1953**, No. 5.

* The θ does not always indicate a so-called "co-ordination number," since it has not yet been clarified whether or not the bond between polyphosphate and calcium ions is a definite co-ordination one.

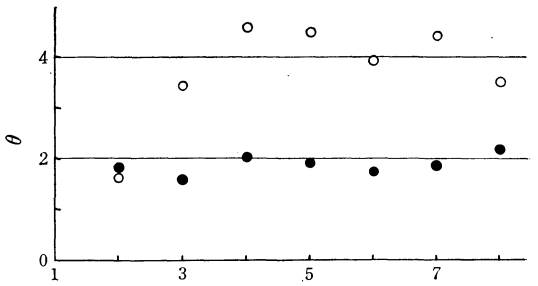
$$\theta=\frac{(L_{t_1}A_1/y_1z_1)\,[C_2O_4]_t-(L_t\,A_2/y_2z_2)\,[C_2O_4]_{t_1}}{[C_2O_4]_t-[C_2O_4]_{t_1}} \quad (4)$$

Charges on the ions in Eqs. 1—4 were omitted for purposes of simplification.

Results and Discussion

The nephelometric titration data are summarized in Table I. The θ values are plotted against the chain lengths of polyphosphate in Fig. 2. From this figure, the values of θ at an ionic strength of 0.1 are found to be about 2 regardless of the chain length, while the corresponding values at an ionic strength of 1.0 vary between 2 and 4 with the number of phosphorus atoms per chain. This may be due to an effect on the configuration of the polyphosphate chain of the supporting electrolyte added in order to adjust the ionic strength. As the polyphosphate is a kind of polyelectrolyte, the presence of the supporting electrolyte may cause the polyphosphate chain to coil up as a result of the decrease in electrostatic repulsion on the chain.[11] The coiled chain with an appropriate configuration may easily assume a value of θ higher than two.

The negative logarithms of the dissociation constants, β, of calcium polyphosphate complexes are summarized in Table II, along with the results of Irani et al., and they are plotted against the chain length in Fig. 3. As for the value of θ used to evaluate β from Eq. 1,



Number of phosphorus atoms per chain

Fig. 2. Relation between the number of phosphorus atoms bound by a calcium ion and the chain length of the polyphosphate. Ionic strength; ●: 0.1, ○: 1.0.

an 2, 3 or 4 integer, near the value shown in Fig. 2, was used. The values of θ reported by Irani et al. are independent of the ionic strengths and take the same values at the ionic strengths of both 0.1 and 1.0 (θ; 2, 3 and 4 for the chain lengths of 2, 3 and 6 phosphorus atoms respectively), whereas in this paper, the values of θ at an ionic strength of 0.1 are different from those at 1.0, except for pyrophosphate. Therefore, the stability constants given by Irani et al. were recalculated using the same values of θ as those used in the present study; the results are shown in Table II.

As may be seen in Fig. 3, the stability of calcium polyphosphate complexes increases with the chain length at the ionic strengths

TABLE I. SUMMARY OF DATA FOR NEPHELOMETRIC TITRATION OF CALCIUM-OXALATE-POLYPHOSPHATE SYSTEM AT 25°C

Polyphosphate	Number of phosphorus atoms per chain	Ionic strength	Moles of phosphorus per liter $L_{t_1}\times10^3$	Moles of phosphorus per liter $L_{t_2}\times10^3$	Concn. of Ca. soln. $z\times10^2$ mol./l.	ml. of Ca soln. (y) added to end-point for the following ml. of 0.2 M $H_2C_2O_4$ soln. 1.0 (y_1)	ml. of Ca soln. (y) added to end-point for the following ml. of 0.2 M $H_2C_2O_4$ soln. 2.0 (y_2)	Total vol. at end-point ml. A_1	Total vol. at end-point ml. A_2
Pyro-phosphate	2	0.1	21.5_0	21.5_0	20.5_8	0.557	0.334	30.557	30.668
		1.0	64.8_7	64.8_7	10.2_9	0.304	0.172	33.447	33.378
Tri-	3	0.1	10.8_9	18.1_5	20.5_8	0.498	0.548	30.498	30.548
		1.0	9.85_7	9.77_9	10.2_9	0.684	0.534	33.826	33.941
Tetra-	4	0.1	3.02_2	3.25_8	5.01_2	0.582	0.453	30.582	30.453
		1.0	2.94_9	2.94_4	10.2_9	0.199	0.193	33.341	33.401
Penta-	5	0.1	2.88_1	2.88_1	5.01_2	0.518	0.356	30.518	30.356
		1.0	2.60_8	2.60_3	10.2_9	0.175	0.165	33.317	33.373
Hexa-	6	0.1	2.72_6	2.90_0	5.01_2	0.569	0.419	30.569	30.419
		1.0	2.62_5	2.62_0	10.2_9	0.189	0.168	33.330	33.376
Hepta-	7	0.1	2.70_3	2.70_3	5.01_2	0.559	0.401	30.559	30.401
		1.0	2.40_2	2.44_2	10.2_9	0.179	0.176	33.942	33.384
Octa-	8	0.1	2.24_6	2.24_6	10.2_9	0.218	0.169	30.218	30.169
		1.0	2.11_7	2.11_4	10.2_9	0.163	0.163	33.306	33.345

11) R. M. Fuoss, *Discussions Faraday Soc.*, **11**, 125 (1951).

TABLE II. STABILITY OF CALCIUM POLYPHOSPHATES AT 25°C

Polyphosphate	Ionic strength	θ	Neg. log. of dissociation constant $[C_2O_4]_{t_1}$	$[C_2O_4]_{t_2}$	Av.	Ref.
Ortho-phosphate	0.2					1.63[14]
Pyro-	0.1	2	5.43	5.42	5.42	5.39[1]
	1.0	2	4.49	4.48	4.49	4.89[1]
Tri-	0.1	2	5.90	5.83	5.87	5.90[1]
	1.0	3	5.12	5.17	5.15	5.36[1]
Tetra-	0.1	2	5.93	5.92	5.93	
	1.0	4	5.58	5.81	5.69	
Penta-	0.1	2	5.86	5.84	5.85	
	1.0	4	5.57	5.74	5.65	
Hexa-	0.1	2	6.03	5.96	6.00	5.92[1]
	1.0	4	5.79	5.76	5.77	5.78[1]
Hepta-	0.1	2	6.02	5.98	6.00	
	1.0	4	5.86	6.07	5.96	
Octa-	0.1	2	5.99	6.03	6.01	
	1.0	4	6.16	5.79	5.98	

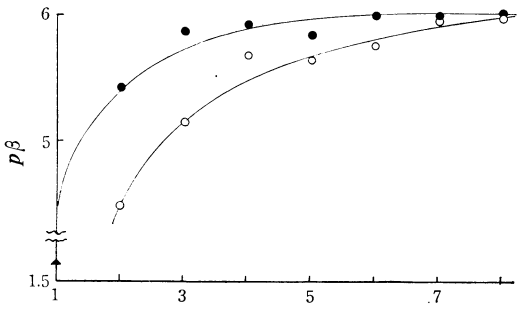


Fig. 3. Relation between stability constants of calcium polyphosphate complexes and chain lengths of the polyphosphates at 25°C. Ionic strength; ●: 0.1, ○: 1.0, ▲: 0.2.[14]

of both 0.1 and 1.0 and levels off at the chain length of 6—7 phosphorus atoms when the ionic strength is 0.1, though not yet when it is 1.0. The increase in the stability with the chain length was also reported by Irani et al. and by Van Wazer et al.[12] This phenomenon is probably in part due to an increase in the charge density on a polyphosphate chain and in part to an effect of the chain configuration on the complex formation.

A comparison of the present results with those of Irani et al. shows that the stability constant of unfractionated polyphosphate with an average chain length of 6 phosphorus atoms agrees with that of purely-separated hexaphosphate in this work within the range of experimental error. From this result, it seems reasonable to conclude that the stability constant of the calcium complex of any polyphosphate is equivalent to that of a mixture of polyphosphates with the same average chain length, if the mixture does not contain ortho- or pyrophosphate. It has been verified by means of ion-exchange chromatography that ortho- and pyrophosphate are not present in the polyphosphate mixture prepared by the method described above.

It raises some questions that Irani et al. carried out the nephelometric titration using the precipitating agent not only at the same concentrations as ours, but at higher concentrations up to about eight times that of polyphosphate. As the stability constant of the calcium oxalate complex is considerably large, i. e., 10^3,[13] the dissolution of the complex can not be disregarded when the concentration of oxalic acid is too high compared with that of polyphosphate. This is supported by the fact that the dissociation constant of the triphosphate complex tends to decrease with an increase in the concentration of oxalic acid (e. g., β; 3.84, 1.22 and 1.06×10^{-6} for the 1.33, 2.00 and 2.67×10^{-2} M concentrations of oxalic acid respectively, at the ionic strength of 0.1).

The assumptions for the site in the derivation of Eq. 1 still remain to be discussed in more detail with regard to the structure of such polyelectrolyte complexes as calcium polyphosphate; these questions will be clarified in due course.

Summary

The formation of calcium complexes of purely-separated linear chain polyphosphates

12) J. R. Van Wazer and C. F. Callis, *Chem. Revs.*, **58**, 1011 (1958).

13) R. W. Money and C. W. Davies, *Trans. Faraday Soc.*, **28**, 609 (1932).

14) R. M. Smith and R. A. Alberty, *J. Am. Chem. Soc.*, **78**, 2376 (1956).

with chain lengths of 2～8 phosphorus atoms has been studied by means of nephelometric titration at 25°C, pH values of 10～12, and ionic strengths of 0.1 and 1.0. The following results have been obtained: 1) The number of phosphorus atoms bound to a calcium ion is about 2, regardless of the chain length at an ionic strength of 0.1, while it varies from 2 to 4 according to the chain length at an ionic strength of 1.0; 2) The stability of calcium polyphosphates increases with the chain length at both ionic strengths and levels off at a chain length of 6～7 when the ionic strength is 0.1, though not yet when it is 1.0; and 3) The stability constant of a calcium complex of any long-chain polyphosphate is almost equal to that of a mixture of polyphosphates with the same average chain length.

The authors wish to thank Dr. Sadaichi Otani for his helpful advice relating to the synthesis and separation of polyphosphates.

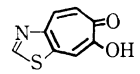
Department of Chemistry
Faculty of Science
Hiroshima University
Hiroshima

Cycloheptathiazole Derivatives. III. The Synthesis of Cycloheptathiazol-8-one and Its Derivatives

By Shuichi SETO and Kyozo OGURA

(Received May 15, 1964)

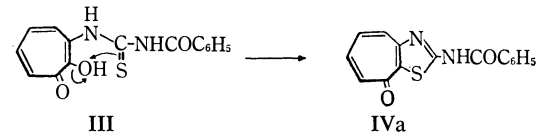
In the preceding papers of this series,[1,2] the syntheses of 7-hydroxycycloheptathiazol-6-one (I) and its 2-substituted derivatives were reported.



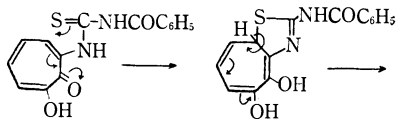
I

These series of compounds are interesting from the point of view of biological action and pharmacology, so the present authors have made a further investigation of the syntheses of another type of cycloheptathiazoles. This paper will describe the synthesis of cycloheptathiazol-8-one and its allied compounds.

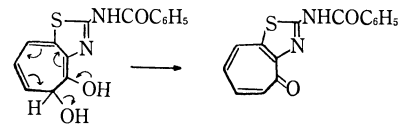
The reaction of 3-aminotropolone (II) with benzoylisothiocyanate gave *N*-tropolon-3-yl-*N'*-benzoylthiourea (III), which was easily dehydrated by the action of acid or alkali, or merely by heating, to afford a cyclization product (IV). The ultraviolet and infrared absorption spectra suggested that IV might be a tropone derivative with a fused ring. The fact that the oxidation of IV with potassium permanganate gave 2-benzamidothiazole-4, 5-dicarboxylic acid (V), which had been previously synthesized in an authentic route,[1] showed that IV should have a thiazole ring. Therefore, the product is likely to be 2-benzamidocycloheptathiazol-8-one (IVa). However, another type of cyclization product, cycloheptathiazol-4-one derivative (IVb) could not be excluded, since abnormalities have often been found in the cyclization reaction of troponoid compounds.[1,3]



III IVa



III



IVb

The following facts, however, exclude the structure IVb. 3-Aminotropolone (II) reacted smoothly with thiobenzoylthioacetic acid in the presence of alkali to give directly a cyclization product VI whose ultraviolet spectrum was similar to that of IV but quite different

1) S. Seto, Y. Nishiyama and K. Ogura, This Bulletin, 35, 1998 (1962).

2) S. Seto, K. Ogura and Y. Nishiyama, ibid., 36, 173 (1963).

3) T. Nozoe, S. Seto, S. Matsumura and T. Asano, *Proc. Japan Acad.*, 32, 339 (1956); T. Nozoe et al., "Daiyukikagaku," Asakurashoten, Tokyo (1960), p. 182, etc.

from that of the 2-phenylcycloheptathiazol-4-one (VII) synthesized by Nozoe et al.[4] (Fig. 1). When VI was treated with alkali, 3-benzamidotropolone (VIII) was obtained. These facts show that VI must be 2-phenylcycloheptathiazol-8-one; consequently, IV probably has the structure IVa.

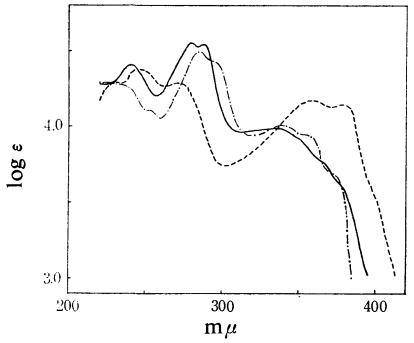
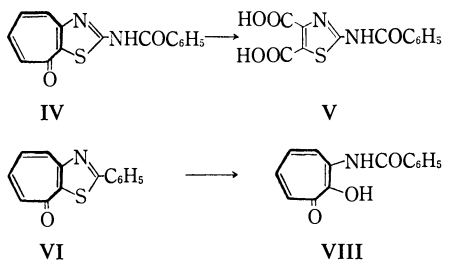


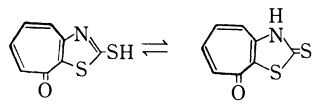
Fig. 1. Ultraviolet absorption spectra of IV (——), VI (·—·—·—·) and 2-phenylcycloheptathiazol-4-one[4] (------) in methanol.



IV V

VI VIII

The 2-benzamido derivative IV is stable to alkali, and the fission of the thiazole ring does not occur, even when it is heated in an alkaline solution, but a stable salt is formed. The warming of IV in concentrated sulfuric acid gave 2-aminocycloheptathiazol-8-one (IX). When 3-aminotropolone (II) was treated with carbon disulfide in the presence of alkali, yellow crystals of $C_8H_5ONS_2$ (X), were obtained in a good yield. This substance is sparingly soluble in organic solvents and is fairly acidic. The infrared absorption spectrum exhibits multiplet absorption bands in the 2700~3100 cm^{-1} region due to its associated NH group, and the strongest absorption band corresponding to the carbonyl group shifted to a longer wave length region (1540 cm^{-1}) compared with those of IV and VI. The ultraviolet absorption spectrum of X is also markedly different from those of IV and VI. These facts indicate that X is probably 2-mercaptocycloheptathiazol-8-one, which exists as the thiazoline form Xb predominantly. This situation



Xa Xb

is quite similar to that of 2-mercaptobenzothiazole, which was tentatively investigated by Bellamy and Rogasch.[5] The ultraviolet absorption curve of X in methanol seems to correspond mainly to a stable anion formed by dissociation in the diluted solution, since the addition of acid causes a large hypsochromic shift, while the addition of alkali changes the spectrum only a few millimicrons.

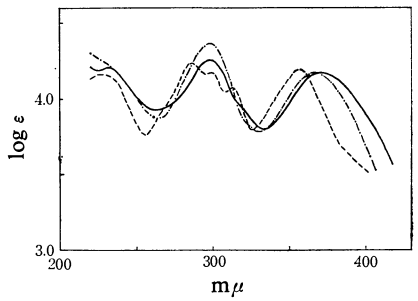
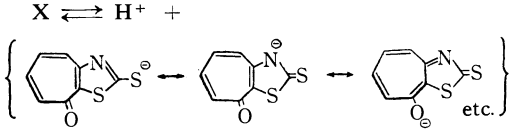


Fig. 2. Ultraviolet absorption spectra of X in methanol (——), in 0.1 N NaOH (·—·—·) and in 0.24 N HCl-MeOH (------).



The reaction of X with methyl iodide, benzyl chloride and monochloroacetic acid in the presence of alkali afforded *S*-methyl (XI), *S*-benzyl (XII) and *S*-carboxymethyl (XIII) derivatives respectively. All these compounds show ultraviolet absorptions of the same type as in the case of IV and VI. The treatment of X with thionyl chloride gave 2-chlorocycloheptathiazol-8-one (XIV), which was converted to 2-amino derivative (IX) by reaction with liquid ammonia. By this fact the relation between these compounds was established as is summarized in scheme 1. Finally, cycloheptathiazol-8-one (XV) was obtained by the treatment of X with hydrogen peroxide in *t*-butanol. The infrared absorption spectrum is shown in Fig. 4. Bis(cycloheptathiazol-8-on-2-yl)-disulfide (XVI) was also obtained by the reaction of X with hydrogen peroxide under rather mild conditions.

It is interesting to note that the ultraviolet absorption spectra of both XIV and XV are

4) T. Nozoe, T. Aso and K. Takahashi, This Bulletin, 35, 2003 (1962).

5) L. J. Bellamy and P. E. Rogasch, *Proc. Roy. Soc.*, 254, 103 (1960).

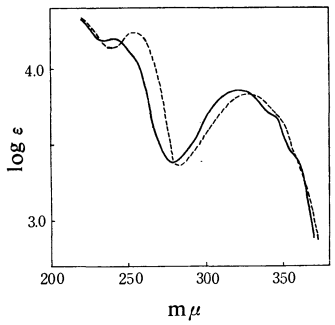
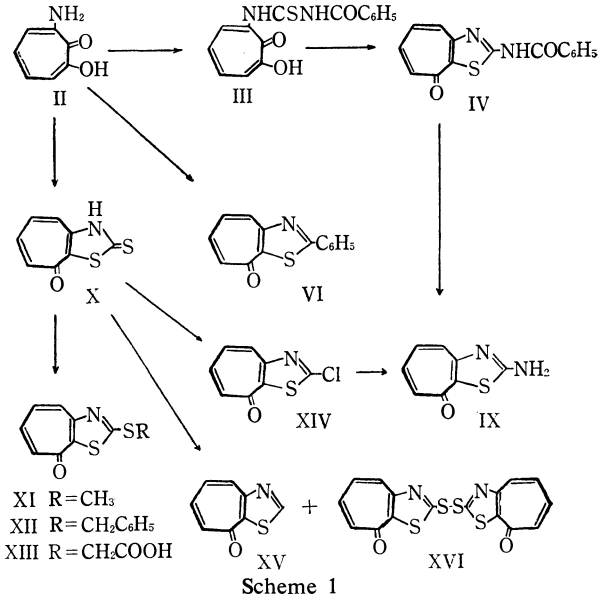


Fig. 3. Ultraviolet absorption spectra of XIV (------) and XV (——) in methanol.

of the tropone type and quite different from those of cycloheptathiazol-8-one derivatives replaced at the 2-position by an electron-releasing group. This seems to imply that the contribution of the conjugation between the



Scheme 1

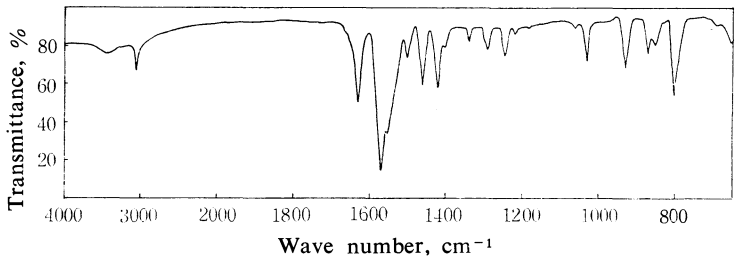
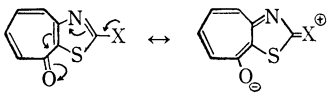
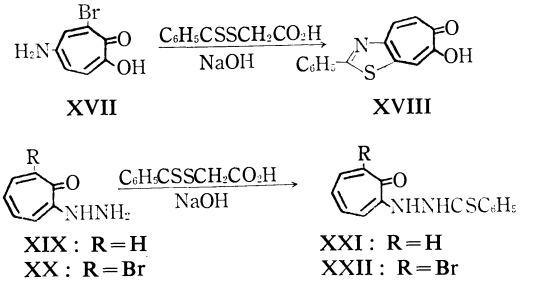


Fig. 4. Infrared absorption spectrum of XV in KBr disk.

electron-releasing group and the carbonyl group is very significant.



The reaction of thiobenzoylthioacetic acid with 3-bromo-5-aminotropolone (XVII) was also examined; it was found that the reaction proceeded easily in the presence of alkali at room temperature, furnishing 2-phenyl-7-hydroxycycloheptathiazol-6-one (XVIII) in the same manner as has been described in the preceding paper.[1] The elucidation of the structure was made by a comparison of its spectral data with those of the corresponding 7-hydroxycycloheptathiazol-6-one derivatives studied previously.[1] 2-Aminotropone did not react with thiobenzoylthioacetic acid, while 2-hydrazinotropone and its 7-bromo derivative reacted with the reagent to give *N*-thiobenzoyl derivatives, XXI and XXII respectively, which failed to be converted into any cyclization product.



Scheme 2

Experimental*

***N*-Tropolon-3-yl-*N'*-benzoylthiourea (III).**—A solution of II (100 mg.) and benzoylisothiocyanate (160 mg.) in ethanol (2 ml.) was stirred at 50~60°C for 1 hr. The yellow crystals that precipitated were collected and washed with methanol. This substance showed double melting point, 145~150°C and 260°C. Yield, 130 mg.

* All melting points are uncorrected. The microanalyses were carried out by Misses Yōko Endo and Yukiko Endo of this Institute, to whom the authors are indebted.

λ_{max}^{MeOH} mμ (log ε) : 268 (4.62), 380 (4.07).

Found : C, 60.30 ; H, 3.81 ; N, 9.08. Calcd. for $C_{15}H_{12}O_3N_2S$: C, 60.00 ; H, 4.03 ; N, 9.33%.

2-Benzamidocycloheptathiazol-8-one (IV). — a) When III (450 mg.) was stirred in a 50% aqueous sodium hydroxide solution (10 ml.), an orange precipitate was formed immediately. When this precipitate was gradually dissolved while being stirred at room temperature, yellow crystals soon separated out. After it had been stirred for 1 hr., the mixture was acidified with diluted hydrochloric acid, and the crystals were collected and recrystallized from ethanol to afford colorless crystals, m. p. 285~287°C (decomp.). Yield, 400 mg.

λ_{max}^{MeOH} mμ (log ε) : 240 (4.41), 279 (4.55), 289 (4.54), 340 (3.99).

Found : C, 63.10 ; H, 3.37 ; N, 9.81. Calcd. for $C_{15}H_{10}O_2N_2S$: C, 63.83 ; H, 3.57 ; N, 9.93%.

b) A solution of III (40 mg.) in concentrated sulfuric acid (0.5 ml.) was allowed to stand at room temperature overnight. The colorless precipitate that separated upon the addition of cracked ice to the solution was collected and recrystallized from ethanol. Yield, 30 mg.

c) A suspension of III (40 mg.) in ethanol (10 ml.) was refluxed for 30 min. ; the yellow prisms that separated out when it was cooled to room temperature were collected. Yield, 20 mg.

The Oxidation of IV with Potassium Permanganate.—To a solution of IV (40 mg.) in a 10% aqueous sodium hydroxide solution (1 ml.), a potassium permanganate solution (potassium permanganate, 100 mg. ; water, 2 ml.) was added ; this mixture was stirred at room temperature for 3 hr. After the decomposition of the excess permanganate by the addition of formalin, manganese dioxide was removed by filtration. The acidification of the filtrate with diluted hydrochloric acid, adjusted to pH 1, caused the precipitation of colorless crystals, which were identified with an authentic specimen of 2-benzamidothiazole-4, 5-dicarboxylic acid by a comparison of their infrared and ultraviolet spectra.[6]

2-Phenylcycloheptathiazol-8-one (VI).—A solution of II (100 mg.) and thiobenzoylthioacetic acid (180 mg.) in a 10% aqueous sodium hydroxide solution (1 ml.) was allowed to stand overnight ; the colorless needles which separated were then collected and recrystallized from ethanol to give colorless prisms, m. p. 138~139°C. Yield, 25 mg.

λ_{max}^{MeOH} mμ (log ε) : 240 (4.25 sh.), 285 (4.50), 295 (4.43 sh.), 340 (4.00).

Found : C, 70.60 ; H, 3.45 ; N, 5.70. Calcd. for $C_{14}H_9ONS$: C, 70.29 ; H, 3.79 ; N, 5.86%.

The Reaction of VI with Alkali. — When a mixture of VI (20 mg.) in a 30% aqueous potassium hydroxide solution (1 ml.) was heated on a water bath for a few minutes, a yellow precipitate appeared. After it had been cooled, the mixture was acidified with diluted hydrochloric acid, and the precipitate was collected. Recrystallization from ethanol gave pale yellow needles of m. p. 142~144°C, undepressed on admixture with 3-benzamidotropolone.

2-Aminocycloheptathiazol-8-one (IX). — A solution of IV (400 mg.) in concentrated sulfuric acid (4 ml.) was heated at 110°C for 4 hr. The brownish-yellow solution thereby obtained was poured into cracked ice and neutralized with a saturated sodium bicarbonate solution, and the precipitate was collected. The acidification of the filtrate gave colorless crystals of benzoic acid. The precipitate collected was recrystallized from methanol to afford yellow prisms, m. p. 225~245°C (decomp.). Yield. 100 mg.

λ_{max}^{MeOH} mμ (log ε) : 244 (4.10), 280 (4.38), 290 (4.32 sh.), 322 (3.91), 335 (3.91).

Found : C, 53.56 ; H, 3.68 ; N, 14.53. Calcd. for $C_8H_6ON_2S$: C, 53.93 ; H, 3.40 ; N, 15.73%.

2-Mercaptocycloheptathiazol-8-one (X).—A mixture of II (400 mg.), carbon disulfide (2 ml.) and ethanol (2.4 ml.) in a 10% aqueous sodium hydroxide solution (3 ml.) was stirred at room temperature for 2 hr. After the removal of the ethanol and the excess carbon disulfide under reduced pressure, the residual solution was acidified with diluted hydrochloric acid and adjusted to pH 3 ; the yellow precipitate thereby formed was collected and recrystallized from ethanol to give yellow scales, m. p. 255~300°C (decomp.). Yield, 550 mg.

λ_{max}^{MeOH} mμ (log ε) : 231 (4.21), 299 (4.25), 372 (4.16).

Found : C, 49.42 ; H, 3.17 ; N, 7.49. Calcd. for $C_8H_5ONS_2$: C, 49.24 ; H, 2.58 ; N, 7.18%.

2-Methylthiocycloheptathiazol-8-one (XI).—When a mixture of X (50 mg.), potassium carbonate (80 mg.) and methyl iodide (40 mg.) in water (1.5 ml.) was stirred at room temperature for 1.5 hr., a colorless precipitate appeared. This precipitate was collected and recrystallized from ethanol to give pale yellow prisms, m. p. 112~113°C. Yield, 40 mg.

λ_{max}^{MeOH} mμ (log ε) : 230 (4.20), 284 (4.36 sh.), 293 (4.38), 330 (3.96).

Found : C, 51.16 ; H, 3.15 ; N, 6.19. Calcd. for $C_9H_7ONS_2$: C, 51.68 ; H, 3.37 ; N, 6.76%.

2-Benzylthiocycloheptathiazol-8-one (XII).—A mixture of X (50 mg.), potassium carbonate (80 mg.) and benzyl chloride (40 mg.) in water (1.5 ml.) was stirred at 40°C for 2 hr. The precipitate thereby formed was collected and recrystallized from methanol to give pale yellow needles, m. p. 138~140°C. Yield, 40 mg.

λ_{max}^{MeOH} mμ (log ε) : 230 (4.26), 285 (4.33 sh.), 294 (4.37), 336 (4.00).

Found : C, 63.18 ; H, 3.88 ; N, 4.79. Calcd. for $C_{15}H_{11}ONS_2$: C, 63.16 ; H, 3.89 ; N, 4.91%.

2-Carboxymethylthiocycloheptathiazol-8-one (XIII).—A mixture of X (20 mg.), sodium carbonate (80 mg.) and monochloroacetic acid (30 mg.) in water (0.5 ml.) was stirred at room temperature for 1.5 hr. The solution thereby obtained was acidified with diluted hydrochloric acid and adjusted to pH ca. 2, and the precipitate was collected by filtration. Recrystallization from ethanol afforded pale yellow crystals, m. p. 233~235°C. Yield, 10 mg.

6) Y. Nishiyama and Y. Ikegami, *Bull. Chem. Res. Inst. Non-Aqu. Solns., Tohoku Univ.*, **12**, 43 (1963).

λ_{max}^{MeOH} mμ (log ε) : 235 (4.34), 285 (4.36 sh.), 295 (4.38), 338 (4.01).

Found : C, 47.93 ; H, 3.48 ; N, 5.73. Calcd. for $C_{10}H_7O_3NS_2$: C, 47.44 ; H, 2.79 ; N, 5.53%.

2-Chlorocycloheptathiazol-8-one (XIV). — To a solution of X (40 mg.) in dry benzene (0.5 ml.), thionyl chloride (0.3 ml.) was added, and the mixture was allowed to stand at room temperature for 1.5 hr. After the evaporation of benzene and the excess thionyl chloride, the residue was neutralized with an aqueous sodium bicarbonate solution and extracted with benzene. The combined benzene solution was evaporated and the residue was sublimed at 110°C under reduced pressure (3 mmHg). Recrystallization of the sublimate from benzene-petroleum ether gave colorless needles, m. p. 125~128°C. Yield, ca. 5 mg.

λ_{max}^{MeOH} mμ (log ε) : 255 (4.24), 332 (3.82).

Found : C, 48.58 ; H, 2.59 ; N, 7.19. Calcd. for C_8H_4ONSCl : C, 48.16 ; H, 2.02 ; N, 7.09%.

The Reaction of XIV with Liquid Ammonia.—A solution of XIV (10 mg.) in liquid ammonia (15 ml.) was allowed to stand at room temperature for 2 days. After the evaporation of the liquid ammonia, water (2 ml.) was added to the residue and the precipitate was collected and recrystallized from methanol to give yellow prisms, which were identified with 2-aminocycloheptathiazol-8-one (IX) by a comparison of their infrared absorption spectra.

Cycloheptathiazol-8-one (XV).—A mixture of X (50 mg.) and 30% hydrogen peroxide (0.2 ml.) in *t*-butanol (2 ml.) was heated at 90°C for 2 hr. Then the color of the precipitate gradually faded, and finally all the precipitate was dissolved. After the evaporation of the solvent under reduced pressure, the residue was neutralized with sodium carbonate and extracted with ether. The combined ether solution, after being dried over sodium sulfate, was passed through a column of alumina. The evaporation of the eluate left colorless needles, which were collected and recrystallized from benzene-petroleum ether to give colorless needles, m. p. 134~138°C. Yield, 10 mg.

λ_{max}^{MeOH} mμ (log ε) : 240 (4.20), 320 (3.85).

Found : C, 58.26 ; H, 3.29 ; N, 8.18. Calcd. for C_8H_5ONS : C, 58.90 ; H, 3.09 ; N, 8.59%.

Bis(cycloheptathiazol-8-on-2-yl) disulfide (XVI).—A mixture of X (50 mg.) and 30% hydrogen peroxide (0.2 ml.) in *t*-butanol (2 ml.) was warmed while being stirred at 80°C for 10 min. The colorless crystals thereby formed were collected and washed with hot methanol, m. p. 200~203°C. Yield, 20 mg.

Found : C, 49.22 ; H, 2.40 ; N, 7.10. Calcd. for $C_{16}H_8O_2N_2S_4$: C, 49.46 ; H, 2.08 ; N, 7.21%.

2-Phenyl-7-hydroxycycloheptathiazol-6-one (XVIII).—A solution of XVII (100 mg.) and thiobenzoylthioacetic acid (100 mg.) in a 2 N sodium hydroxide solution (0.8 ml.) and water (2 ml.) was allowed to stand at room temperature for 30 min. A yellow precipitate began to separate out after about 10 min. After the mixture had been neutralized with diluted sulfuric acid and adjusted to pH 2, the precipitate was collected and recrystallized from acetone-methanol to give pale yellow crystals, m. p. 220~222°C. Yield, 120 mg. The filtrate contained one atom equivalent of bromide ions.

λ_{max}^{MeOH} mμ (log ε) : 268 (4.54), 380 (4.35).

Found : C, 65.70 ; H, 3.34 ; N, 5.40. Calcd. for $C_{14}H_9O_2NS$: C, 65.88 ; H, 3.55 ; N, 5.49%.

***N*-(Tropon-2-yl)-*N'*-thiobenzoylhydrazide (XXI).**—When a mixture of 2-hydrazinotropone (50 mg.) and thiobenzoylthioacetic acid (50 mg.) in a 5% sodium hydroxide solution (2 ml.) was stirred for 1 hr., orange crystals appeared. After the neutralization of the mixture with diluted hydrochloric acid, the crystals were collected and recrystallized from ethanol to give yellow needles, m. p. 169~170°C. Yield, 50 mg.

λ_{max}^{MeOH} mμ (log ε) : 234 (4.46), 457 (4.38).

Found : C, 65.27 ; H, 4.73 ; N, 10.70. Calcd. for $C_{14}H_{12}ON_2S$: C, 65.62 ; H, 4.72 ; N, 10.93%.

***N*-(7-Bromotropon-2-yl)-*N'*-thiobenzoylhydrazide (XXII).**—When a mixture of 2-hydrazino-7-bromotropone (50 mg.) and thiobenzoylthioacetic acid (50 mg.) in a 5% sodium hydroxide solution (2 ml.) was stirred at room temperature for 1 hr., orange scales appeared. The crystals were collected and acidified with diluted hydrochloric acid to yield a yellow powder, which was collected by filtration and recrystallized from methanol to afford orange scales, m. p. 272~273°C. Yield, 50 mg.

Found : C, 50.06 ; H, 3.33 ; N, 7.85. Calcd. for $C_{14}H_{11}ON_2SBr$: C, 50,15 ; H, 3.31 ; N, 8.36%.

The authors wish to express their sincere gratitude to the Sankyo Co., Ltd., which defrayed a part of the expenses for the present research.

The Chemical Research Institute of Non-Aqueous Solutions
Tohoku University
Katahira-cho, Sendai

An Electron Spin Resonance Study of Irradiated Polymethylacrylate

By Hiroshi YOSHIDA*, Toshiyuki KODAIRA, Kozo TSUJI, Koichiro HAYASHI and Seizo OKAMURA

(Received May 20, 1964)

The decaying behavior of free radicals in irradiated polymers has been studied by the electron spin resonance (ESR) method with polymethylmethacrylate,[1,2] polyvinylchloride,[3,4] polyvinylalcohol,[5] polyoxymethylene[6] and polypropylene.[7] In most cases, free radicals follow a first-order or a second-order decay reaction, depending on the polymer and temperature range studied. It has been reported, in addition, that free radicals in many irradiated polymers, such as polyethylene,[8] polyvinylalcohol,[5,9] polytrifluorochloroethylene[8] and polycarbonate,[10] decay readily near the glass transition temperature. In order to study the decaying behavior of free radicals, the glass transition temperature should thus be taken into account.

For the convenience of experimental procedures, polymethylacrylate (PMA), with the glass transition temperature of +3°C, was used in the present investigation. First, ESR spectra of irratiated PMA were recorded at various temperatures and then interpreted. Irradiated methacrylate and polyethylacrylate were also studied for the sake of comparison. Quantitative studies of the decaying behavior of the free radicals in PMA were made below and above the glass transition temperature. The results obtained were then discussed in terms of molecular motion in the polymer and in terms of the structure of the free radicals.

Experimental

The PMA samples were prepared by the bulk polymerization of commercial methylacrylate after the usual purification. The polymer obtained was precipitated twice from an acetone solution with water and dried in vacuo.

The irradiations were carried out with 1.5 MeV. electrons from a Van de Graaff accelerator (dose rate: 1.5×10^5 rad./sec.) at −196°C. The PMA samples were irradiated in glass tubes which were sealed under a vacuum better than 10^{-4} mmHg.

ESR spectra were observed with a reflection-type x-band spectrometer using low-frequency field modulation (80 c. p. s.). Most observations were made at −196°C or at 12°C, using a TE_{011} cylindrical and a TE_{102} rectangular sample cavity respectively.

Results and Discussion

Observed Spectra and Their Interpretation.— PMA, irradiated and measured at −196°C, gave ESR spectra of the shape shown in Fig. 1 (a), with the irradiation dose of 3×10^7 rad. The spectra had no distinct hyperfine structure. With successive warming of the samples to −78°C, −45°C, −10°C and +18°C, the spectra changed from a singlet with the half-height width of 36 oerst. into a triplet, as Fig. 1 shows. Irradiated PMA gave the triplet spectrum at 12°C shown in Fig. 2 (a) immediately after warming to that temperature. This spectrum is the same as that reported by Ormerod and Charlesby.[2] The separation of the triplet

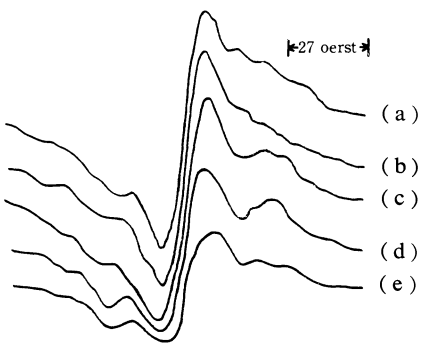


Fig. 1. ESR spectra of PMA irradiated and observed at −196°C (irradiation with 3×10^7 rad.): (a) without warming, (b) after warming to −78°C for 82 min., (c) after warming to −45°C for 87 min., (d) after warming to −10°C for 57 min., (e) after warming to +18°C for 8 min.

* Present address: Division of Polymer Technology, Royal Institute of Technology, Stockholm, Sweden.

1) S. Ohnishi and I. Nitta, *J. Polymer Sci.*, **38**, 451 (1959).
2) M. G. Ormerod and A. Charlesby, *Polymer*, **5**, 67 (1964).
3) Z. Kuri, H. Ueda and S. Shida, *J. Chem. Phys.*, **32**, 371 (1960).
4) D. R. Loy, *J. Polymer Sci.*, **50**, 245 (1961).
5) S. Shida, Z. Kuri and Y. Fujiwara, *Ann. Rept. Japanese Assoc. Rad. Res. Polymers*, **1**, 263 (1958/1959).
6) M. Nieman, T. S. Fedoseeva, G. V. Chubarova, A. L. Buchachenko and Ya. S. Lebedev, *Vysokomolekul. Soedin.*, **5**, 1339 (1963).
7) V. K. Milintshuk, S. Ya. Pshezhetskii, A. G. Kotov, V. I. Tupikov and V. I. Tsivenko, ibid., **5**, 71 (1963).
8) N. Tamura, H. Kashiwabara and S. Ogawa, *Ann. Rept. Japanese Assoc. Rad. Res. Polymers*, **1**, 237 (1958/1959).
9) N. Tamura, ibid., **2**, 369 (1960).
10) H. Kashiwabara and K. Shinohara, ibid., **2**, 373 (1960).

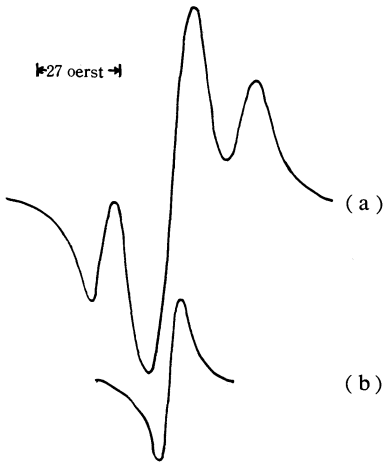


Fig. 2. ESR spectra of PMA irradiated at −196°C with the dose of 3×10^7 rad. and observed at 12°C: (a) immediately after warming to 12°C, (b) after 20 hr. at 12°C.

hyperfine components was 22 oerst. The central peak was a little more intense than the expected intensity distribution of 1 : 2 : 1. This may be due to an overlapping with a singlet spectrum, which showed ΔH_{mse} of 22 oerst. and was still observed after standing 20 hours at room temperature. The change of the spectra from a singlet at a low temperature to a triplet at room temperature was irreversible.

For comparison with the triplet spectra of irradiated PMA mentioned above, the ESR spectra of irradiated methylacrylate and irradiated polyethylacrylate were also studied.

Methylacrylate (MA) was solidified at −196°C and was irradiated at the same temperature under a vacuum. Irradiated MA gave a triplet spectrum with a separation of 22 oerst. at −196°C, as Fig. 3 shows. With an increase in the temperature, the spectrum became weaker, without changing its shape, until it disappeared completely below −78°C. On the other hand, MA which had been irradiated at −196°C with 5×10^7 rad. and warmed to −78°C gave white precipitates when dissolved at −78°C in petroleum ether. Apparently

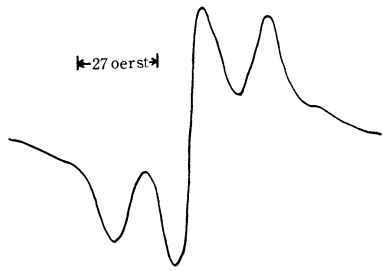


Fig. 3. ESR spectrum of methylacrylate irradiated and observed at −196°C, with the dose of 5×10^7 rad.

polymerization occurs in MA irradiated at −196°C and warmed to −78°C. It is probable that the free radicals giving a triplet spectrum are propagating end groups which disappear with the termination of the propagating chains.

Polyethylacrylate (PEA) was prepared, and its spectra were examined in the same way as those of PMA. PEA irradiated at −196°C gave the quintet spectrum shown in Fig. 4 (a), as has been reported previously.[2] With an increase in the temperature the spectrum changed irreversibly, to a triplet with the separation of 22 oerst. The triplet spectrum of irradiated PEA was much less stable than that of PMA.

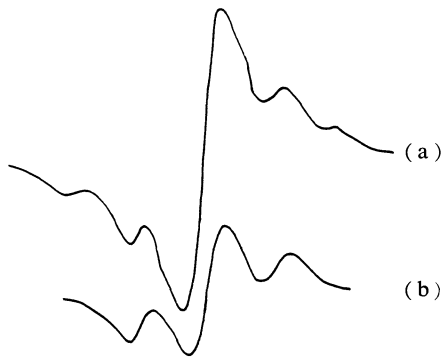


Fig. 4. ESR spectra of PEA irradiated at −196°C with the dose of 3×10^7 rad.: (a) observed at −196°C without warming, (b) observed at about −26°C immediately after warming to this temperature.

It has been reported that propagating radicals in vinyl polymerizations give triplet spectra.[11-15] It is not unreasonable to interpret the triplet spectrum of irradiated PMA as being due to propagating radicals, ~~~~$-CH_2-\dot{C}H(COOCH_3)$, as in the case of irradiated MA. With both PMA and MA, the separation between triplet hyperfine components was the same.

An alternative interpretation would be that the triplet spectrum of PMA is due to the radical structure, $-CH_2-CH(COO\dot{C}H_2)-CH_2-$, but this is not probable because irradiated PEA gave the same triplet.

The Formation and Decay of Free Radicals in PMA.—The concentration of free radicals in PMA increased with the irradiation dose, as

11) G. Adler, D. Ballantine and B. Baysel, *J. Polymer Sci.*, **48**, 195 (1960).
12) S. E. Blesler, E. N. Kazbekov and E. M. Saminskii, *Polymer Sci. U. S. S. R.*, **1**, 540 (1960).
13) R. Bensasson and R. Marx, *J. Polymer Sci.*, **48**, 53 (1960).
14) I. Nitta, S. Ohnishi and Y. Shioji, *Ann. Rept. Japanese Assoc. Rad., Res. Polymers*, **3**, 319 (1961).
15) Y. Shioji, S. Ohnishi and I. Nitta, *J. Polymer Sci.*, **A1**, 3373 (1963).

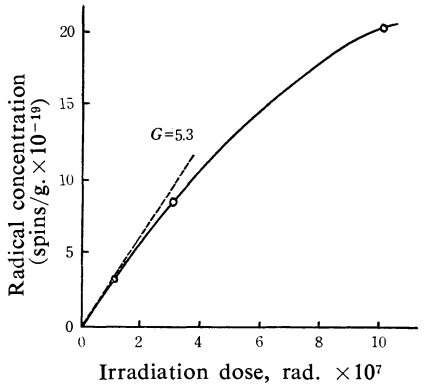


Fig. 5. Formation of free radicals in PMA irradiated at −196°C with the dose rate of 1.5×10^5 rad./sec. and observed at the same temperature.

is shown in Fig. 5. Irradiations and measurements were carried out at −196°C. From the initial slope of the curve in Fig. 5, the G value is calculated to be 5.3, with reference to the formation of free radicals which are stable at −196°C. The absolute value is correct within a 50% range of experimental error, and it is in accordance with that reported by Ormerod and Charlesby.[2]

Figure 6 shows the decaying behavior of free radicals in irradiated PMA when warmed

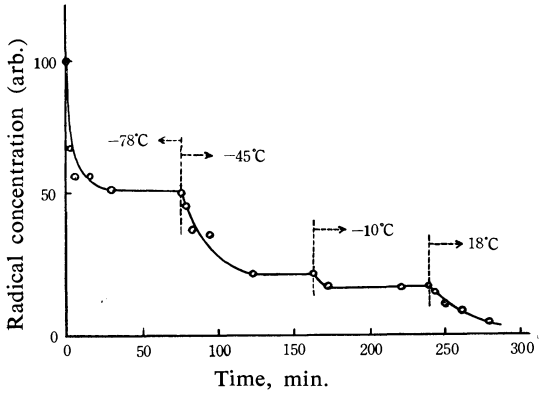


Fig. 6. Decay of free radicals in PMA irradiated at −196°C with the dose of 3×10^7 rad. with successive warming at several temperatures.

successively to a series of temperatures. At temperatures below the glass transition point of PMA, the radical concentration decreased rapidly at the beginning of warming, but it readily attained a final value at each temperature. At temperatures of transition point, the free radicals disappeared following a 2nd order decay process.

The same decaying behavior as that observed for PMA below the glass transition temperature was also reported for polymethylmethacrylate.[2] A possible interpretation for the behavior—in rigid PMA below its glass transition point—is that the thermal activation process which causes the disappearance of free radicals has a wide distribution of activation energies. A similar interpretation was applied by Semenov to the decaying behavior of free radicals in a mixture of *n*-octylalcohol, water and hydroperoxide which was solidified and irradiated at −196°C.[16]

The decay of free radicals in PMA was examined at different temperatures above the glass transition point. As Fig. 7 shows, the observed results fitted well to a 2nd-order decay process, $-d[R\cdot]/dt=k[R\cdot]^2$, except at the beginning of warming. Free radicals which disappeared in this range of warming temperature gave a triplet spectrum. The deviation from the 2nd-order decay at the beginning may be caused by free radicals which disappeared at the transient temperature from −196°C to each warming temperature. The rate constant, k, was obtained from the diagram

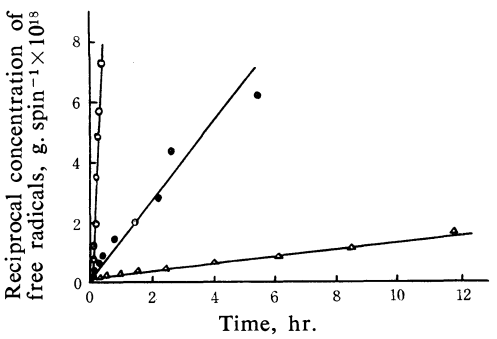


Fig. 7. Decay of free radicals in PMA, irradiated at −196°C with the dose of 3×10^7 rad. and measured at different temperatures.
○ 30°C ● 20°C △ 12°C

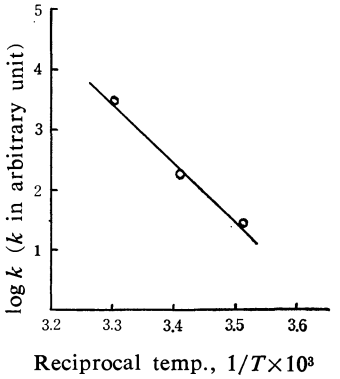


Fig. 8. Rate constants for radical recombination vs. reciprocal temperatures.

16) N. Semenov, Private communication (1962).

in Fig. 7; it is plotted as a function of the reciprocal temperatures in Fig. 8. The activation energy for k was 44 kcal./mol.

The activation energy for segmental motion in PMA has been reported to be 40 kcal./mol. from mechanical dispersion measurements.[17] The good agreement between the activation energies obtained from the mechanical measurements and from the decay of free radicals suggests that the free radicals in PMA giving a triplet spectrum disappear through recombination caused by segmental motion in the polymer. The assignment of the triplet spectrum as being due to the radical structure ~~~~$-CH_2-\dot{C}H(COOCH_3)$ is not in contradiction to the previously-discussed decaying mechanism of the free radicals.

17) Y. Wada, "Physics of Polymers" (in Japanese), Ed. by Phys. Soc. Japan, Asakura-shoten, Tokyo (1963), p. 169.

The authors wish to express their thanks to Professor Bengt Rånby for his kind reading of this manuscript. They are also grateful to Dr. Yōta Nakai for providing facilities for irradiation with a Van de Graaff accelerator and to Dr. Shun-ichi Ohnishi for his valuable discussions.

Department of Polymer Chemistry
Faculty of Engineering
Kyoto University
Sakyo-ku, Kyoto

The Structure of Glassy Carbon

By Tokiti NODA and Michio INAGAKI

(Received May 22, 1964)

It has already been reported that the properties of glassy carbon are remarkably different from those of usual electrographitized carbons.[1,2]

In this work, the structure of glassy carbon will be investigated by determining the interlayer spacing, the crystallite size, the disorganized carbon content and the radial distribution function of glassy carbon by means of X-ray diffraction techniques, and a structural model of glassy carbon will be proposed.

Experimental and Results

Two groups of glassy carbon, A and B, were used as the samples in this work. The samples of both groups were heat-treated at temperatures ranging from 500° to 3000°C.

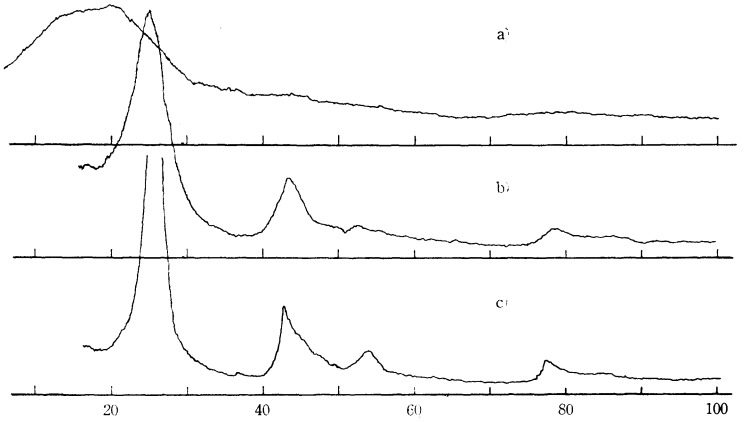


Fig. 1. X-Ray diffraction patterns of glassy carbon treated at a) 500°C, b) 1500°C, and c) 3000°C.

1) S. Yamada and H. Sato, *Nature*, **193**, 261 (1962).

2) S. Yamada, H. Sato and T. Ishii, presented at the Sixth Biennial Conference on Carbon, Pittsburgh, 1963.

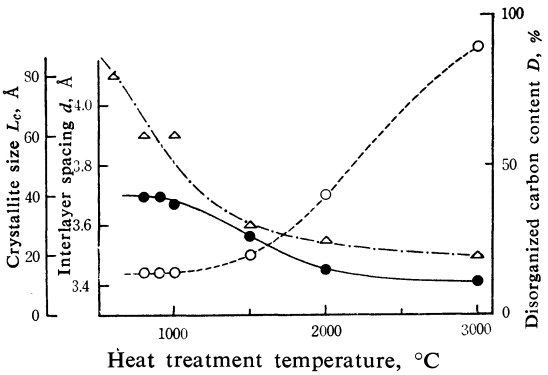


Fig. 2. Variations in the interlayer spacing d, the crystallite size L_c and the disorganized carbon content D with the heat-treatment temperature.
●: Interlayer spacing d
○: Crystallite size L_c
△: Disorganized carbon content D

The X-ray diffraction patterns are shown for the samples in the A group in Fig. 1. In Fig. 2, the variations of the interlayer spacing, d, the crystallite size, L_c, and the disorganized carbon content, D, are shown as functions of the heat-treatment temperature. The interlayer spacing and the crystallite size were measured from the observed (002) diffraction profile. With the sample heat-treated at 3000°C, the lattice constants, c_0 and a_0, and the crystallite sizes, L_c and L_a, were measured from (002) and (10) diffractions using an extra-pure silicon powder as an inner standard. It was found that $c_0=6.810$Å, $a_0=2.418$Å, $L_c=82$Å and $L_a=39$Å. The content of disorganized carbon, which did not participate in the graphite-like layer structure, was determined using the same method as Franklin.[3] The method consists of the determination of the most pertinent D value which makes the I'-profile symmetrical. For the glassy carbon heat-treated at 1500°C, the original I-profile and the symmetrical I'-profile, which corresponds to the D value of 30%, are shown in Fig. 3. The value of I' is calculated from Eq. 1:

$$I'=\frac{s^2}{0.0606}\cdot\frac{I-D}{1-D} \qquad (1)$$

where $s=2\sin\theta/\lambda$

$$I=\frac{I_{obs}-I_{Inc}}{I_{co}}$$

In the above equation, I_{co} and I_{Inc} are the intensities of the coherent and incoherent scattering of carbon respectively. The observed intensity, I_{obs}, of (002) diffraction had

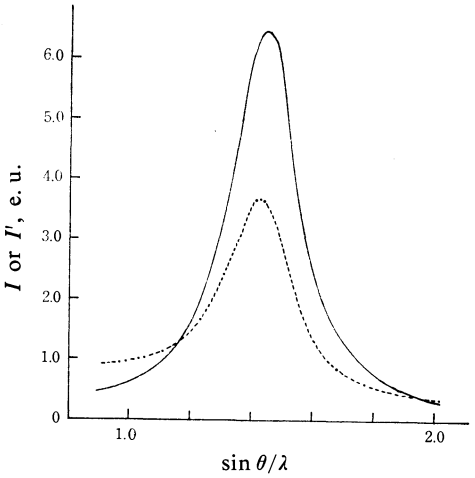


Fig. 3. Determination of the disorganized carbon content D.
……: I-profile, ——: I'-profile which corresponds to the D value of 30%.

been corrected for the various intensity factors, such as absorption and Lorentz-polarization factors, and then normalized to electron units by fitting the theoretical and experimental intensities in the range of s from 1.00 to 1.20Å^{-1}. The measurement of the diffraction intensity was made by means of point-by-point fixed counting at an angular interval of 0.5° and using CuK_α radiation.

In the variations of the interlayer spacing, the crystallite size and the disorganized carbon content with heat treatment, no remarkable difference was found between the samples in the A and B groups.

For each sample, the radial distribution

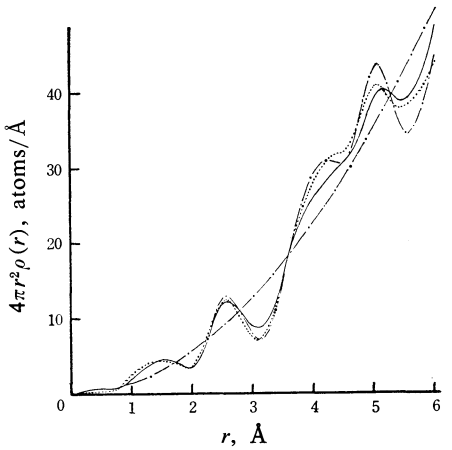


Fig. 4. Radial distribution curve of glassy carbon.
——: Treated at 900°C
……: Treated at 1500°C
-·-·-: Treated at 2000°C
—·—: Mean electron density $4\pi r^2\rho_0$

3) R. E. Franklin, *Acta Cryst.*, 3, 107 (1950).

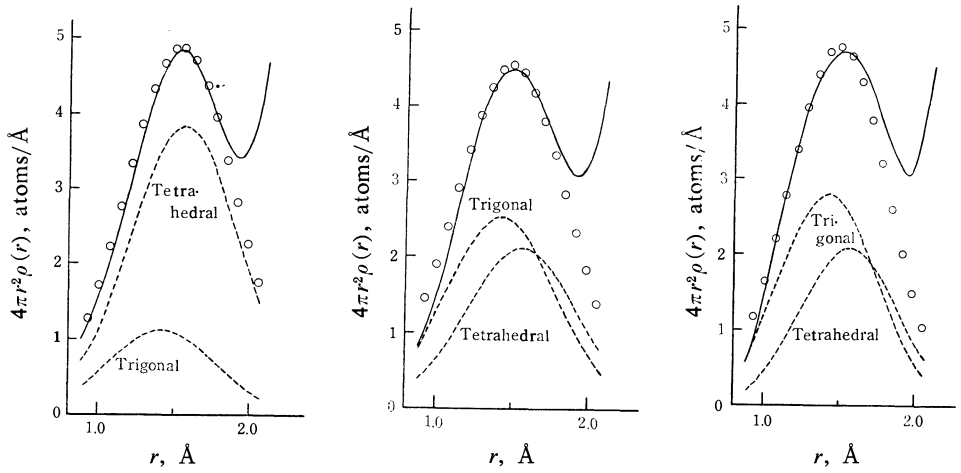
function, $4\pi r^2\rho(r)$, was calculated by means of the summation of Eq. 2:

$$4\pi r^2\rho(r) = 4\pi r^2\rho_0 + 8\pi r \sum_{s=0.08}^{1.60} s\cdot i(s)\cdot e^{as^2}\cdot \sin(2\pi rs)\Delta s \quad (2)$$

where $s = 2\sin\theta/\lambda$

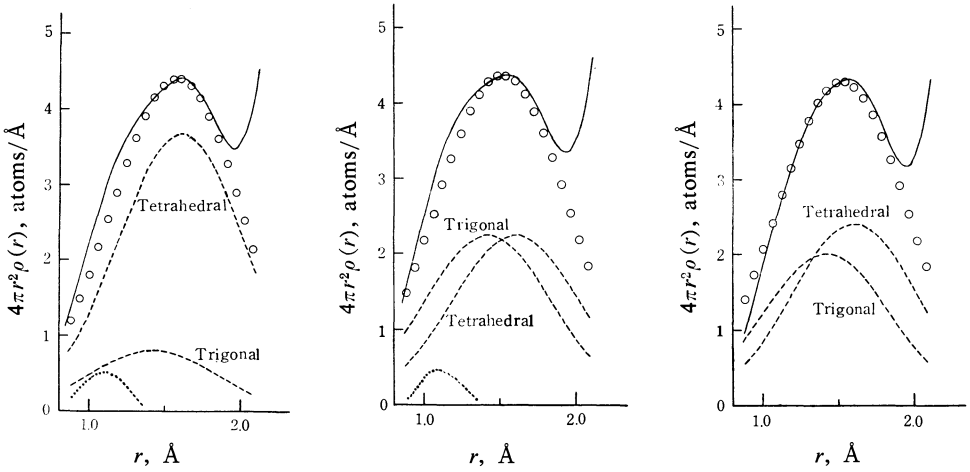
$$i(s) = \frac{I_{obs} - (I_{co} + I_{inc})}{I_{co}}$$

In the above equation, the value of ρ_0 was calculated as 0.113 atoms/Å^3 using the theoretical density of graphite of 2.25 g./cm^3. The interval, Δs, of the above summation was 0.02 Å^{-1}. The factor e^{-as^2} was the artificial temperature factor, and the value of a in this factor was determined as 0.90 so that the value of this factor would be equal to 0.10 at the upper limit of s. The observed intensity, I_{obs}, had been corrected for the various intensity factors and then normalized to electron units on the basis of the range of s from 1.50 to 1.60 Å^{-1}. The measurement of the diffraction intensity was made by means of point-by-point fixed counting and using CuK_α radiation in the range of s from 0.08 to 1.20 Å^{-1} and by using MoK_α radiation in the range of s from 1.20 to 1.60 Å^{-1}. The radial distribution curves for three samples of the B group are shown in Fig. 4.



a) 850°C-treated b) 1500°C-treated c) 2000°C-treated

Fig. 5. Separation of the first peak of the radial distribution curve into component curves with the glassy carbons in the A group.
——: Observed curve ------: Component curve ○○○○: Composite curve



a) 800°C-treated b) 1500°C-treated c) 2000°C-treated

Fig. 6. Separation of the first peak of the radial distribution curve into the component curves with the glassy carbons in the B group.
——: Observed curve ------: Component curve
○○○○: Composite curve ·····: Remainder curve

The first peak of the radial distribution curve, whose position corresponds to the distance to the nearest neighbour atoms, is represented by the solid line in Figs. 5 and 6. Since the mean co-ordination number obtained from the area under the observed curve was in the range of 3~4 and since the first peak was located at around 1.5~1.6Å, it was assumed that glassy carbon is mainly composed of two types of carbon atoms, one having a tetrahedral relation to its neighbours, like diamond, and the other having a trigonal relation to its neighbours, like graphite. In this paper, these two types of carbon atoms are called tetrahedral and trigonal carbon atoms respectively. Therefore, the first observed peak was separated into two component curves corresponding to trigonal and tetrahedral carbon atoms on the assumption that the curve for each carbon atom had the Gaussian form. For example, the first observed peak for the glassy carbon heat-treated at 850°C could be separated with a negligible remainder when the two component curves were expressed as follows:

For tetrahedral carbon atom

$$\frac{9.6}{\sqrt{2\pi}} \cdot \exp\left\{-\frac{1}{2} \cdot \left(\frac{r-1.56}{0.36}\right)^2\right\}$$

For trigonal carbon atom

$$\frac{2.8}{\sqrt{2\pi}} \cdot \exp\left\{-\frac{1}{2} \cdot \left(\frac{r-1.42}{0.36}\right)^2\right\}$$

The separated curves are shown by the broken lines in the figures. With several samples of the B group, particularly with samples heat-treated at low temperatures, the remainder between the observed curve and the composite curve was not negligible, as is shown by the dotted line in Fig. 6.

Discussion

The X-ray diffraction pattern for glassy carbon is very similar to that for a carbon black. The interlayer spacing decreases and the crystallite size increases with an increase in the heat treatment temperature. These variations are also similar to the variations with heat treatment for usual carbon materials. It can be said that graphitization, that is to say, the developments of a graphite-like layer structure, proceeds in glassy carbon. The deduction that the graphite-like layer structure is developed in glassy carbon with heat treatment could be drawn from the variations in other properties,[2,4] such as electrical resistivity and the Hall coefficient, with heat treatment. However, glassy carbon is a typical non-graphitizing carbon because the progress of its graphitization is very little in comparison with that of graphitizing carbons, as can be seen in Fig. 2. The degree of graphitization for the glassy carbon heat-treated at 3000°C was almost the same as that for the petroleum coke heat-treated at about 1900°C. With the glassy carbon heat-treated at low temperatures such as 500~600°C, the (002) diffraction was not well-defined, and the disorganized carbon content was as large as 80%. The glassy carbon heat-treated at a low temperature should be called an organic solid. The radial distribution curve for the glassy carbon heat-treated at 500°C converged to the mean electron density, $4\pi r^2\rho_0$, beyond $r=4$Å. With an increase in the heat treatment temperature, the values of r at the maxima on the observed radial distribution curves approach those for graphite; that is to say, $r=1.4$, 2.6, 4.0 and 5.0 Å. This result is consistent with the variations in the interlayer spacing, the crystallite size and the disorganized carbon content with the heat treatment temperature.

With the samples of the A group, the curve which is composed of two component curves, corresponding to trigonal and tetrahedral carbon atoms, coincides quite well with the observed curve. The content of the tetrahedral carbon atom was calculated from the mean co-ordination numbers of the component curves, taking into consideration the fact that the theoretical co-ordination numbers for tetrahedral and trigonal carbon atoms are 4 and 3 respectively. It was found that the calculated content of the tetrahedral carbon atom is in good coincidence with the disorganized carbon content. With the samples of the B group, particularly with the samples heat-treated at low temperatures, the coincidence between the observed curve and the composite curve was not as complete as with the samples of the A group. A small number of carbon atoms with another relation to their neighbours may also exist in glassy carbon. From the remainder curve, which is located at around 1.1Å, the carbon-hydrogen bond can be expected. However, the carbon-carbon triple bond and the carbon-oxygen double bond might be assumed because such a separation procedure of the first peak is not very accurate.

As has been described above, the graphite-like layer structure was developed in glassy carbon with heat treatment, and no diffraction line which corresponds to that of the other structures was detected in the X-ray diffraction pattern of glassy carbon. Therefore, it can

4) T. Yamaguchi, *Carbon*, **1**, 47 (1963).

be assumed that the trigonal carbon atoms form the graphite-like layer structure and that the tetrahedral carbon atoms form no regular structure. From these results, a structural model of glassy carbon can be proposed, in which tetrahedral carbon atoms form the main part of the criss-cross linkages which link the graphits-like layers in a random way. Furukawa[5] has proposed a somewhat different structural model of glassy carbon, a three-dimensional irregular network configuration of carbon atoms without assuming a significant graphite-like layer structure.

The reason why the structure of glassy carbon is somewhat different in the A and B groups has not yet been made clear. However, it can be said that the conditions of the production of glassy carbon may have a certain effect on its structure. Yamaguchi[4] also used two types of glassy carbon, one impermeable to gas and the other rather porous.

Summary

The structure of glassy carbon has been investigated by determining the interlayer spacing, crystallite size and disorganized carbon content, and by an analysis of the radial distribution function.

Glassy carbon has been found to be a typical non-graphitizing carbon. From the analysis of the first peak of the radial distribution curve, it has been assumed that not only trigonal but also tetrahedral carbon atoms exist in glassy carbon. A structural model of glassy carbon has been proposed; in this model tetrahedral carbon atoms form the main part of the criss-cross linkages which link graphite-like layers in a random way.

The authors wish to thank Dr. Yoshihiro Sumiyoshi, Miss Yukiko Matsunaga and Mr. Motohiro Yamamoto for their assistance in the calculation of the radial distribution function. Thanks are also due to the Tokai Electrode Mfg. Co. for supplying the samples.

Department of Applied Chemistry
Faculty of Engineering
Nagoya University
Chikusa-ku, Nagoya

5) K. Furukawa, Private communication.

Studies on Antibiotics and Related Substances. XIX. The Synthesis of cis-2-Aminocyclohexyl D-Glucosaminide

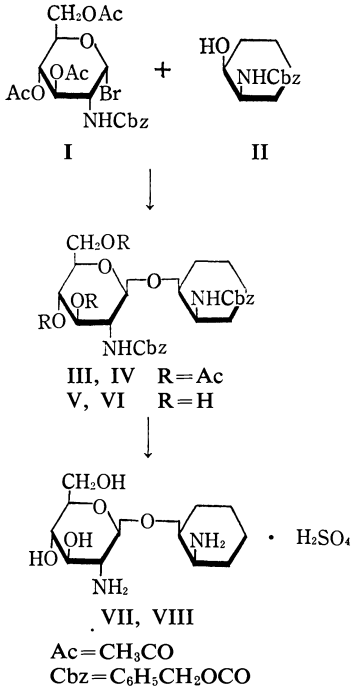
By Tetsuo SUAMI, Seiichiro OGAWA, Teruo YOSHIZAWA and Sumio UMEZAWA

(Received May 30, 1964)

Previous studies of the synthesis of *trans*-2-aminocyclohexyl D-glucosaminide[1] have stimulated our interest in the synthesis of *cis*-2-aminocyclohexyl D-glucosaminide. In the present paper, the synthesis of two diastereomers of *cis*-2-aminocyclohexyl D-glucosaminide will be described.

The starting compound, *dl-cis*-2-aminocyclohexanol, was prepared by the following two method: the hydrogenation of *o*-acetamidophenol,[2] and the inversion reaction of *dl-trans*-2-aminocyclohexanol.[3] An attempt to resolve the racemic *cis*-2-aminocyclohexanol with tartaric acid or di-*O*-benzoyl tartaric acid did not yield a satisfactory result. Therefore, *dl-cis*-2-aminocyclohexanol was treated with carbobenzyloxy chloride to yield *N*-carbobenzyloxy-*dl-cis*-2-aminocyclohexanol (II) in 86% yield. The condensation of II with α-1-bromo-3, 4, 6-tri-*O*-acetyl-*N*-carbobenzyloxy-D-glucosamine (I)[4] in the presence of mercuric cyanide gave a mixture of glucosaminides (III and IV), which was then separated by fractional recrystallization to III, m. p. 155°C, $[\alpha]_D^{12}$ +25.2° and IV, m. p. 138°C, $[\alpha]_D^{28}$ −36.5°. Considering their optical rotations and elemental analyses, III and IV might be identified as *N*-carbobenzyloxy-*d-cis*-2-aminocyclohexyl 3, 4, 6-tri-*O*-acetyl-*N*-carbobenzyloxy-β-D-glucosaminide and *N*-carbobenzyloxy-*l-cis*-2-aminocyclohexyl 3, 4, 6-tri-*O*-acetyl-*N*-carbobenzyloxy-β-D-glucosaminide respectively. The deacetylation of

1) T. Suami, S. Ogawa and S. Umezawa, This Bulletin, **36**, 459 (1963).
2) G. E. McCasland, R. K. Clark, Jr., and H. E. Carter, *J. Am. Chem. Soc.*, **71**, 637 (1949).
3) A. C. Cope, E. Ciganek and J. Lazar, ibid., **82**, 2591 (1962).
4) J. C. Jruine, D. McNicoll and A. Hynd, *J. Chem. Soc.*, **1911**, 250; L. Zervas and S. Konstas, *Chem. Ber.*, **93**, 435 (1960).



III and IV with methanol saturated with ammonia gave V, $[\alpha]_D^{20}$ +20.6° and VI, $[\alpha]_D^{25}$ −59.2° respectively. The catalytic hydrogenolysis of V and VI, followed by neutralization with sulfuric acid, yielded crystalline sulfate, VII $[\alpha]_D^{15}$ +10.2° and VIII, $[\alpha]_D^{15}$ −50.8° respectively. The designation of VII and VIII as β-anomers is based on their optical rotations, which are less dextrorotatory than those of α-anomers in an analogous compound,[5] and on their infrared spectra.[6]

Experimental

All melting points are corrected. The infrared spectra were recorded in potassium bromide pellets.

***dl-cis*-2-Aminocyclohexanol Hydrochloride.**—a) *dl-cis*-2-Aminocyclohexanol hydrochloride was prepared from *o*-acetamidophenol by the method of Carter et al.[2] in 14% yield.

b) *dl-cis*-Isomer was obtained from *dl-trans*-2-aminocyclohexanol by the method of Cope et al.[3] in 50% yield.

***dl-cis*-2-Acetamidocyclohexanol Acetate.**—A two gram portion of *dl-cis*-2-aminocyclohexanol was treated with a large excess of acetic anhydride for 48 hr. at room temperature. The mixture was then evaporated under reduced pressure, and the residue was distilled in vacuo to yield 2.5 g. (72%) of a viscous oil, b. p. 140~155°C/4 mmHg. After it had stood for three months at room temperature, it crystallized completely. The product was recrystallized twice from benzene and petroleum ether to give the melting point of 71~73°C.

Found: C, 60.58; H, 8.76; N, 7.11. Calcd. for $C_{10}H_{17}NO_3$: C, 60.28; H, 8.66; N, 7.03%.

The Kunz hydrolysis[7] of the product indicated that one acetyl group (1.05) was bound in an ester and another one in an amide form.

***N*-Carbobenzyloxy-*dl-cis*-2-aminocyclohexanol (II).**—*dl-cis*-2-Aminocyclohexanol hydrochloride was treated with carbobenzyloxy chloride in the presence of an excess of sodium bicarbonate to give II, m. p. 72~73°C in 85.5% yield (lit.[8] m. p. 72~73°C).

***N*-Carbobenzyloxy-*cis*-2-aminocyclohexyl 3, 4, 6-Tri-*O*-acetyl-*N*-carbobenzyloxy-β-D-glucosaminide (III and IV).**—A mixture of 8.0 g. of I and 8.0 g. of II in 100 ml. of anhydrous benzene was heated under reflux while being mechanically stirred for 7 hr. with 8.0 g. of mercuric cyanide. The mixture was then filtered to remove any insoluble substance. The filtrate was diluted with 230 ml. of chloroform and washed with a 10% sodium chloride solution and cold water. The solvent was removed under reduced pressure to give a semicrystalline residue. The residue was dissolved in 23 ml. of absolute ethanol and kept in a refrigerator to yield 1.4 g. of the product, m. p. 150~165°C. The crude product was repeatedly recrystallized from methanol-water (2 : 1) to yield 0.87 g. of needles (III), m. p. 154~155°C. $[\alpha]_D^{12}$ +25.2° (*c* 1.63, chloroform).

Found: C, 61.04; H, 6.25; N, 4.11. Calcd. for $C_{34}H_{42}N_2O_{16}$: C, 60.88; H, 6.31; N, 4.18%.

The alcoholic mother liquor was added to ether to give 3.0 g. of the product, m. p. 66~68°C. The crude product was fractionally recrystallized from methanol-water (2 : 1) to yield 1.2 g. of needles (IV), m. p. 136~138°C. $[\alpha]_D^{28}$ −36.5° (*c* 1.07, chloroform).

Found: C, 61.07; H, 6.48; N, 4.25. Calcd. for $C_{34}H_{42}N_2O_{16}$: C, 60.88; H, 6.31; N, 4.18%.

Further recrystallizations of III and IV did not raise their melting points or optical rotations.

***N*-Carbobenzyloxy-*d*-*cis*-2-aminocyclohexyl *N*-Carbobenzyloxy-β-D-glucosaminide (V).**—III (0.7 g.) was suspended in 30 ml. of methanol saturated with ammonia at 5°C. After it had been kept overnight in a refrigerator, the solution was evaporated under reduced pressure to yield a colorless syrup. The product was washed with a small amount of water and then repeatedly recrystallized from acetone-ether to yield 0.35 g. of the amorphous product (61.6%), m. p. 114~116.5°C, $[\alpha]_D^{20}$ +20.6° (*c* 1.92, methanol).

Found: C, 61.60; H, 6.59; N, 5.07. Calcd. for $C_{28}H_{36}N_2O_9$: C, 61.75; H, 6.66; N, 5.14%.

***N*-Carbobenzyloxy-*l*-*cis*-2-aminocyclohexyl *N*-Carbobenzyloxy-β-D-glucosaminide (VI).**—IV (0.6 g.) was treated by being placed in a refrigerator overnight with 30 ml. of methanol saturated with ammonia. The solution was treated similarly with III to yield 0.4 g. of crystals (89%), m. p. 160.5~162°C, $[\alpha]_D^{25}$ −59.2° (*c* 0.92, methanol).

5) S. Umezawa and T. Tsuchiya, *J. Antibiotics, Ser. A*, **15**, 51 (1962); T. H. Haskell, T. C. French and Q. R. Bartz, *J. Am. Chem. Soc.*, **81**, 3481 (1959).

6) S. A. Barker, E. J. Bourne, M. Stacey and D. H. Whiffen, *Chem. & Ind.*, **1953**, 196; *J. Chem. Soc.*, **1954**, 171.

7) A. Kunz and C. S. Hudson, *J. Am. Chem. Soc.*, **48** 1982 (1926).

8) D. Ben-Ishai, ibid., **78**, 4962 (1956).

Found: C, 61.91; H, 6.46; N, 5.05. Calcd. for $C_{28}H_{36}N_2O_9$: C, 61.75; H, 6.66; N, 5.14%.

***d-cis*-2-Aminocyclohexyl β-D-Glucosaminide Sulfate (VII).**—A solution of V (1.09 g.) in 25 ml. of absolute methanol was hydrogenated for 40 hr. at room temperature in a hydrogen stream over palladium black (400 mg.). The mixture was then filtered to remove the catalyst, and the filtrate was evaporated under reduced pressure to dryness. The crude product (0.57 g.) was obtained after drying it over phosphorus pentoxide. $[\alpha]_D^{20}$ −12.6° (*c* 2.85, methanol). The crude free base (0.55 g.) was neutralized with 0.1 N sulfuric acid to pH 7, and the solution was filtered to remove a small amount of insoluble substance. Then the filtrate was evaporated under reduced pressure to yield 1 ml. of a residual solution. The addition of absolute ethanol to the solution gave 253 mg. of colorless needles (34%) melting at 275°C (decomp.). $[\alpha]_D^{15}$ +10.2° (*c* 2.64, water).

Found: C, 38.76; H, 6.82; N, 7.56; S, 8.23. Calcd. for $C_{12}H_{24}N_2O_5 \cdot H_2SO_4$: C, 38.49; H, 7.00; N, 7.48; S, 8.56%.

IR: 883 cm^{-1} (type 2b of β-D-glucopyranoside).

***l-cis*-2-Aminocyclohexyl β-D-glucosaminide Sulfate (VIII).**—A 0.33 g. portion of VI was treated in a manner similar to that described above for V to give 140 mg. of crystals (31.4%) melting at 270°C (decomp.). $[\alpha]_D^{15}$ −50.8° (*c* 3.27, water).

Found: C, 38.34; H, 7.11; N, 7.37; S, 8.27. Calcd. for $C_{12}H_{24}N_2O_5 \cdot H_2SO_4$: C, 38.49; H, 7.00; N, 7.48; S, 8.56%.

IR: 887 cm^{-1} (type 2b of β-D-glucopyranoside).

Paper Chromatography.—VII and VIII showed a single spot of R_f 0.38 and 0.26 respectively, in an ascending development at 22.5°C in an ethyl acetate-pyridine-acetic acid-water (5 : 5 : 1 : 3) system[9] (R_f of D-glucosamine hydrochloride: 0.29) on Toyo filter paper No. 50. The spots were detected by means of a spray of ninhydrin in pyridine.

Bioassays. — VII and VIII showed almost no antimicrobial activity against E. coli when examined with a paper-disk method.

The authors are indebted to Mr. Saburo Nakada for his microanalysis, to Mrs. Setsuko Iriyama for her bioassays, to Miss Sunao Ohata for her infrared spectra, and to Mr. Kenji Yabe, Mr. Kiyoshi Imoto and Miss Sumiko Uchida for their assistance in analytical experiments. This research has been in part supported by the Asahi Glass Foundation for Contributions to Industrial Technology.

Department of Applied Chemistry
Faculty of Engineering
Keio University
Koganei-shi, Tokyo

9) F. G. Fischer and H. Dorfel,, *Hoppe-Seyler's Z. physiol. Chem.*, **301**, 224 (1955).

*Electronic Spectrum of Fluorenone**

By Akira KUBOYAMA

(Received June 2, 1964)

Heretofore the electronic spectra of fluorenone and its derivatives have been reported on by many authors. Though fluorenone is a fundamental substance in organic chemistry, there have been few papers in which these spectra have been studied in detail either theoretically or experimentally. In this work, the electronic spectrum of fluorenone in various solvents will be measured, and from these results and from the results calculated with the simple MO[1] method for the π-electronic system of fluorenone the nature of each absorption band of fluorenone will be studied. It will be shown that the weak absorption band near 380 mμ, which has been heretofore regarded as an $n\rightarrow\pi^*$ band,[2-5] is really a $\pi\rightarrow\pi^*$ band.

Experimental and Results

Materials. — Commercially-available fluorenone was purified by means of vacuum sublimation (m. p. 83~84°C). All the solvents used in the present study were of special grade. Ethanol (99.5 vol.%) was distilled. Chloroform was washed several times with water, dried with calcium chloride, and distilled. Carbon tetrachloride was dried with calcium chloride and distilled. Dioxane and

* The major part of this paper was presented at the Symposium on the Electronic Structure of Molecules, Sendai, October, 1963.

1) In this paper the term "molecular orbital" is abbreviated as "MO."

2) E. D. Bergmann, G. Berthier, Y. Hirshberg, E. Loewenthal, B. Pullman and A. Pullman, *Bull. soc. chim. France*, **17**, 669 (1951).

3) J. R. Platt, *J. Chem. Phys.*, **19**, 101 (1951).

4) F. Dörr, *Z. Elektrochem.*, **61**, 950 (1957).

5) E. Lippert and H. Walter, *Angew. Chem.*, **71**, 429 (1959).

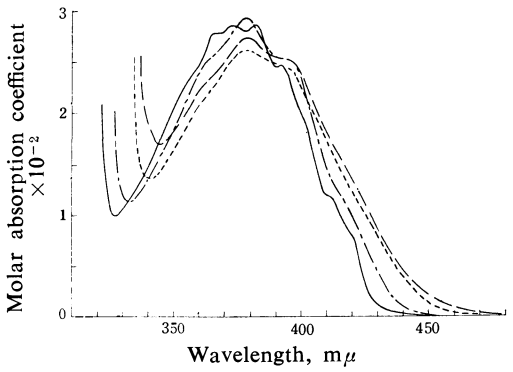


Fig. 1. Fluorenone. Solvent; —— *n*-heptane, —— ethanol, ---- chloroform, —·— carbon tetrachloride.

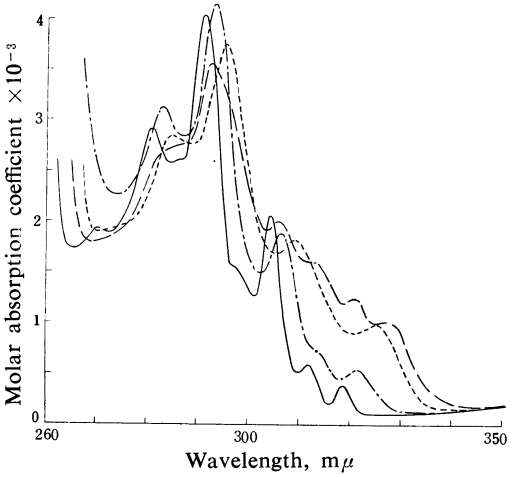


Fig. 2. Fluorenone. Solvent; —— *n*-heptane, —— ethanol, ---- chloroform, —·— carbon tetrachloride.

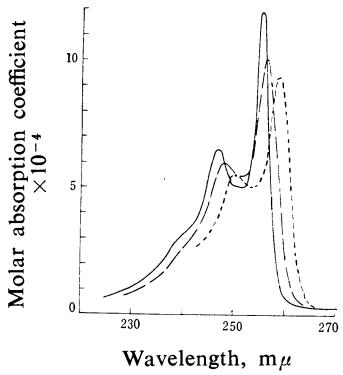


Fig. 3. Fluorenone. Solvent; —— *n*-heptane, —— ethanol, ---- chloroform.

n-heptane were purified according to the methods described in a previous paper.[6]

6) A. Kuboyama, This Bulletin, **33**, 1027 (1960); *J. Chem. Soc. Japan, Pure Chem. Sec.* (*Nippon Kagaku Zasshi*), **81**, 558 (1960).

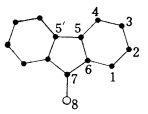
Measurements. — The absorption spectra were measured with a Cary 14M recording spectrophotometer with the fused quartz cells of 1 and 5 cm. path.

Results.—The absorption spectra obtained are given in Figs. 1—3.

Method of Calculation

It is thought that, in the calculations with the MO method for the π-electronic system of unsaturated carbonyl compounds such as fluorenone, the effect of the configuration interaction in explaining the low energy electronic spectra qualitatively is not indispensable as in quinones,[7,8] and so, that the results obtained with the simple MO method are useful to some extent in this case. Therefore, in this work we used results obtained with the simple MO method.

Though the molecular dimensions of fluorenone have never been established, considering the molecular dimensions of fluorene studied by X-ray analysis[9] it is thought that fluorenone is planar or almost so, and that in the calculations with the simple MO method the Coulomb and the exchange integrals used in quinones can reasonably be applied to fluorenone. In *o*- and *p*-benzoquinones,[8] in order to make the MO's in the simple MO method simulate those obtained with the SCF MO method, including electronic interaction, the Coulomb integral (α_i) of the oxygen atom should be far smaller (in β units) than those generally used; the exchange integral (β_{ij}) of the conventional single bond also should be smaller (in β units) than those generally used. These new integral values are thought to be better than those generally used. The integral values used with this in mind are shown in Chart 1(a). The dependence of the orbital energy levels upon the Coulomb integral of



(a)

$\alpha_1=\alpha_2=\cdots=\alpha_6=\alpha_7=\alpha$
$\alpha_8=\alpha+0.3\beta$
$\beta_{12}=\beta_{23}=\cdots=\beta_{56}=0.9\beta$
$\beta_{55'}=\beta_{67}=0.5\beta$
$\beta_{78}=1.2\beta$

(b)

$\alpha_1=\alpha_2=\cdots=\alpha_6=\alpha$
$\alpha_7=\alpha+0.2\beta$
$\alpha_8=\alpha+1.3\beta$
$\beta_{12}=\beta_{23}=\cdots=\beta_{56}=\beta_{78}=\beta$
$\beta_{55'}=\beta_{67}=0.9\beta$

Chart I. Values of Coulomb and exchange integrals

7) J. W. Sidman, *J. Chem. Phys.*, **27**, 429 (1957).

8) A. Kuboyama and K. Wada, Published in the Annual Meeting of the Chemical Society of Japan (1964).

9) G. M. Brown and M. H. Bortner, *Acta Cryst.*, **7**, 139 (1954); D. M. Burns and J. I'ball, *Nature*, **173**, 635 (1954); *Proc. Roy. Soc.*, **A227**, 200 (1955).

the oxygen atom of fluorenone was also calculated. Furthermore, the calculations with the integral values used in our previous studies[10] of quinones were also carried out for the sake of comparison. These integral values are shown in Chart I(b).

Calculated Results and Discussion

As may be seen in Figs. 1—3, it appears that fluorenone has three absorption bands (near 380 mμ, 300 mμ, and 250 mμ, respectively) in the near-ultraviolet region. Unfortunately, the vibrational structure of the 380 mμ band is not clear. The 380 mμ band shifts considerably toward longer wavelengths from *n*-heptane to carbon tetrachloride, chloroform, and ethanol. In chloroform and ethanol the 380 mμ band is at almost the same position and seems to be at a little longer wavelengths than in carbon tetrachloride. The shift of the center of the 380 mμ band from *n*-heptane to chloroform and ethanol is estimated at ca. 8 mμ. As for the 300 mμ band, in *n*-heptane, the intervals (ca. 770 cm^{-1}) in the three peaks on the longer wavelength side (at 319 mμ, 311.5 mμ and 304 mμ, respectively) are far smaller than that (1470 cm^{-1}) between the two peaks on the shorter wavelength side (at 291 mμ and 281 mμ). The former peak group shifs ca. 10 mμ toward longer wavelengths from *n*-heptane to ethanol, while the latter one shifts only ca. 1.5 mμ toward longer wavelengths. The orders of the magnitude of the red-shift[11] of the former and the latter peak groups in various solvents are ethanol>chloroform>carbon tetrachloride and chloroform>carbon tetrachloride>ethanol respectively.

These differences in vibrational structure and solvent effect between the two peak groups show that the two peak groups originate in different eletronic transitions. The 250 mμ band shifts only ca. 1 mμ toward longer wavelengths from *n*-heptane to ethanol, and the order of the magnitude of the red-shift is chloroform>ethanol, as in the 290 mμ band. The interval (1235 cm^{-1}) between the two peaks (at 255 mμ and 247 mμ) of the 250 mμ band in *n*-heptane also almost agrees with that of the 290 mμ band in *n*-heptane. From the facts mentioned above it may be concluded that fluorenone has four absorption bands in the near-ultraviolet region (near 380 mμ, 310 mμ, 290 mμ, and 250 mμ respectively). The facts about the vibrational structure and solvent effect mentioned above may show that the excited electronic states of the 290 mμ and 250 mμ bands are substantially similar and different from that of the 310 mμ band.

Considering that, as a proton-donor in the hydrogen-bond formation, ethanol is stronger than chloroform and that *n*-heptane and carbon tetrachloride are not proton donors, the large red-shift of the 310 mμ band in ethanol and chloroform is thought to be mainly due to hydrogen-bond formation between the carbonyl oxygen atom of fluorenone and these solvents. On the other hand, the polarizability of solvents is generally thought to be almost equally effective for the red-shifts of all absorption bands of solutes. The order of the magnitudes of the polarizability of various solvents, as a bulk effect, agrees with that of the refractive indices of the solvents. The refractive indices[12] (for the sodium D line at 20°C) of chloroform and carbon tetrachloride (1.445 and 1.463 respectively) are considerably larger than those[12] of ethanol and *n*-heptane (1.361 and 1.388 respectively). Therefore, from the facts mentioned above, it may reasonably be concluded that, for the red-shift of the 310 mμ band, the hydrogen-bond formation mentioned above is far more effective than the polarizability of the solvents and that, for the red-shifts of the 290 mμ and 250 mμ bands, the hydrogen-bond formation mentioned above is less effective than the polarizability of the solvents. As for the 380 mμ band, for its red-shift the hydrogen-bond formation mentioned above is thought to be effective.

The 310 mμ, 290 mμ, and 250 mμ bands may be safely regarded as $\pi\rightarrow\pi^*$ bands. The 380 mμ band has, heretofore, been described as an $n\rightarrow\pi^*$ band. As has been pointed out by Blealey and Kasha,[13] however, $n\rightarrow\pi^*$ bands shift toward longer wavelengths with hydrogen-bond formation between hetero-atoms in solutes, participating in the $n\rightarrow\pi^*$ transition, and solvents. Therefore, the solvent effect for the 380 mμ band shows that this band should be a $\pi\rightarrow\pi^*$ band. The maximum molar absorption coefficient of the 380 mμ band (ca. 250) seems too large for $n\rightarrow\pi^*$ bands of planar unsaturated carbonyl compounds. It is well known that $n\rightarrow\pi^*$ bands shift toward shorter wavelengths with the substitution of electron-donating groups, such

10) A. Kuboyama, This Bulletin, **31**, 752 (1958); **32**, 1226 (1959).

11) In this paper the terms "shifts of absorption bands toward longer wavelengths and toward shorter wavelengths" are abbreviated as a "red-shift" and "blue-shift", respectively.

12) A. Weissberger et al., "Organic Solvent," Interscience Publishers, Inc., New York, N. Y. (1955), pp. 59, 91, 193 and 194.

13) G. J. Blealey and M. Kasha, *J. Am. Chem. Soc.*, **77**, 4462 (1955).

TABLE I. POSITIONS OF THE CENTER OF THE 380 mμ BAND

	Solvent	λ(mμ)	Lit.
Fluorenone	*n*-Heptane	~377	
Fluorenone	Ethanol	~385	
2-Methylfluorenone	Isooctane	~395	Ref. 2
3-Methylfluorenone	Isooctane	~375	Ref. 2
2-Dimethylaminofluorenone	Heptane	~485	Ref. 18
2-Dimethylaminofluorenone	Ethanol	~520	Ref. 18
2-Hydroxyfluorenone	Dioxane	~425	Ref. 18
3-Methoxyfluorenone	Isooctane	~365	Ref. 19

as alkyl, hydroxyl, and amino groups.[14-17] In Table I, the center positions of the 380 mμ bands of several, electron-donating-group substituted fluorenones in various solvents are shown. The solvent effects by *n*-heptane and isooctane are thought to be nearly the same. From this table it may be seen that the 380 mμ band shifts toward longer wavelengths with "2"-substitution and more or less toward shorter wavelengths with "3"-substitution respectively. This "2"-substitution effect also shows that the 380 mμ band should be a $\pi\rightarrow\pi^*$ band. All the experimental facts mentioned above show that the 380 mμ band should be a $\pi\rightarrow\pi^*$ band. Therefore, the 380 mμ band will henceforth be so regarded. Since the position of the $n\rightarrow\pi^*$ band of fluorenone is thought to be not far from that of the 380 mμ band, the former band is probably hidden in the latter one because of its low intensity. The blue-shift of the 380 mμ band with the "3"-substitution of electron-donating groups will be explained later on the basis of the π-electronic structure of fluorenone.

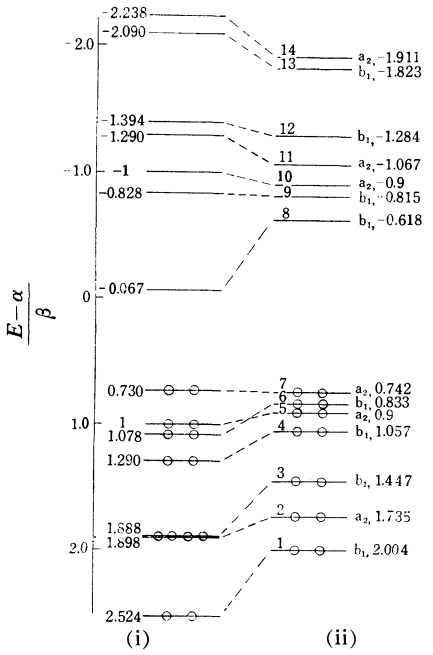


Fig. 4a. Orbital energy levels of fluorenone.

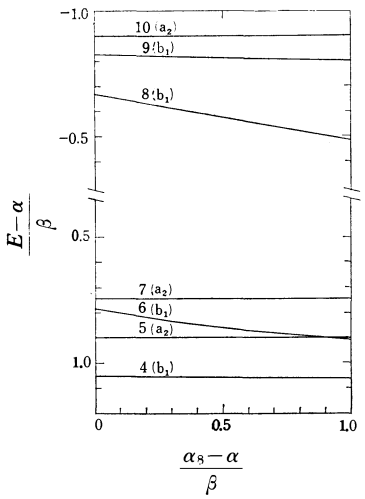


Fig. 4b. Dependence of orbital energies upon Coulomb integral of oxygen atom.

The calculated orbital energy levels of fluorenone and the dependence of energy upon the Coulomb integral of the oxygen atom of fluorenone are shown in Figs. 4a and 4b, respectively. The energy levels in Fig. 4a(i) were obtained with the integral values in Chart I(b). The MO's are classified according to their symmetry properties in the symmetry group C_{2v}. Considering Figs. 4a and 4b together, the transitions which may reasonably be assigned to the 380 mμ band are thought to be safely limited to the three transitions (7→8, 6→8, and 5→8) on the basis of the magnitude of transition energy. It is reasonable to expect that, with the hydrogen-bond formation between fluorenone and solvents, the Coulomb integral of the oxygen atom of fluorenone becomes larger (in β unit). In Fig. 4b it may be seen that, with the increase in the Coulomb integral of the oxygen

14) H. Bada, *J. Chem. Soc. Japan, Pure Chem. Sec.* (*Nippon Kagaku Zassi*), **72**, 341 (1951).
15) S. Nagakura, This Bulletin, **25**, 164 (1952).
16) L. E. Orgel, *J. Chem. Soc.*, **1955**, 121.
17) A. Kuboyama, *J. Chem. Soc. Japan, Pure Chem. Sec.* (*Nippon Kagaku Zassi*), **77**, 1062 (1956).

atom, the energies of the transitions (7→8 and 5→8) become smaller to a larger extent than that of the transition (6→8). Therefore, from the solvent effect the 380 mμ band may favorably be assigned to either of the two transitions (7→8 or 5→8), both ($A_1 \rightarrow B_2$). Similarly, from the solvent effect, the 310 mμ band also may be assigned to either of these two transitions.

The blue-shift of the 380 mμ band with the "3"-substitution of electron-donating groups is explained as follows. Generally, in a transition ($m \rightarrow n$) in a π-electronic system, where m and n denote orbital energy levels in the simple MO method, the change in the transition energy with the substitution of electron-donating groups in the j-th atom position of the π-electronic system depends upon C^2_{mj} and C^2_{nj} in the approximation of the perturbation method,[17] where C_{ij} denotes the coefficient of the j-th atomic orbital of the LCAO MO of the i-th orbital energy level. If $C^2_{mj} \gtrsim C^2_{nj}$, the transition energy decreases with the substitution, and if C^2_{mj} is considerably smaller than C^2_{nj}, we may expect that the transition energy will rather increase with the substitution. In Table II, the C^2_{ij} values of fluorenone ($i=5, 6, 7, 8$; $j=2, 3$) are shown. In Table II, in all the cases ((a), (b), and (c)), the relative magnitudes of C^2_{ij} are similar; on the basis of them, only the transition (7→8) ($A_1 \rightarrow B_2$) can reasonably be assigned to the 380 mμ band in consideration of the substitution effect mentioned before; therefore, the transition (5→8) ($A_1 \rightarrow B_2$) may be assigned to the 310 mμ band. According to this assignment, from Table II the blue-shift of the 310 mμ band with the "2"-substitution of electron-donating groups may be expected, but, unfortunately, we have no available data about this point. In fluorenone only two kinds of electronic transition ($A_1 \rightarrow B_2$ and $A_1 \rightarrow A_1$) are possible. Therefore, the assignment of the 290 mμ and 250 mμ bands to the transition ($A_1 \rightarrow A_1$) is thus favorable.[20] The directions of the polarization of the transitions ($A_1 \rightarrow B_2$ and $A_1 \rightarrow A_1$) are perpendicular to and along the C–O bond axis of fluorenone respectively.

TABLE II. VALUES OF C^2_{ij}

(1)

	C^2_{52}	C^2_{62}	C^2_{72}	C^2_{82}
(a)	0	0.001	0.160	0.066
(b)	0	0	0.160	0.031
(c)	0	0	0.159	0.017

(2)

	C^2_{53}	C^2_{63}	C^2_{73}	C^2_{83}
(a)	0.125	0.116	0.027	0.070
(b)	0.125	0.114	0.027	0.065
(c)	0.125	0.084	0.021	0.068

Note: In (a) and (c) integral values in Charts I(a) and I(b) respectively were used. In (b) the integral values in Chart I(a) were used except that $\alpha_8=\alpha+\beta$.

Summary

The electronic spectrum of fluorenone in various solvents has been measured; from these results and from the results obtained with the simple MO method for the π-electronic system of fluorenone, the nature of each absorption band of fluorenone has been studied. It has been concluded that fluorenone has four $\pi \rightarrow \pi^*$ absorption bands (near 380 mμ, 310 mμ, 290 mμ, and 250 mμ respectively) in the near-ultraviolet region. The assignments of the 380 mμ and 310 mμ bands to the transition ($A_1 \rightarrow B_2$) and the 290 mμ and 250 mμ bands to the transition ($A_1 \rightarrow A_1$) are favorable in view of the obtained results.

The author wishes to express his thanks to Mr. Kōichi Wada of the Yokohama Customs House for his kind assistance.

Government Chemical Industrial Research Institute, Tokyo
Shibuya-ku, Tokyo

18) E. D. Bergmann et al., *Bull. soc. chim. France*, **18**, 70 (1952).
19) S. Cohen, *J. Am. Chem. Soc.*, **79**, 1500 (1957).
20) From the solvent effect the 290 mμ band seems to be reasonably assigned to the transition (6→8) in Fig. 4b.

*Semiconductivity of Phenanthrene Single Crystals**

By Shoichi MATSUMOTO and Tomomichi TSUKADA

(Received June 6, 1964)

Extensive studies have been made of the electrical properties of the anthracene single crystal,[1-4] which is now regarded as a model substance for the investigation of the semiconductive properties of aromatic hydrocarbons.

In order to elucidate the mechanism of electronic conduction in organic solids, it is also important to accumulate reliable data on the electrical properties of other relatively simple hydrocarbons. However, on phenanthrene, a structural isomer of anthracene, the available experimental results are quite limited.[5]

In the present work, the electrical conductivity and its anisotropy will be studied in detail on phenanthrene single crystals, and the results will be compared with the related behavior of anthracene.

Experimental

Material.—Powdered phenanthrene of a chemical-purpose grade obtained from the Eastman Kodak Company was purified by recrystallization from an ethanol solution, followed by vacuum sublimation. Each purification process was carefully repeated more than four times.

In the fluorescence spectrum of the resultant flaky and colorless sample, there was no peak other than those of phenanthrene reported in the literature,[6] except for a slight variation in the intensity. This variation may be due to the difference in the crystalline state.

Crystal Growth.—Crystals of purified phenanthrene with a melting point of 103°C were grown by means of a modified Bridgeman method.

In the electrical furnace applied here, the upper part was maintained at a temperature a little higher than the melting point of the sample, and the bottom part, at a temperature lower; there was a large temperature gradient, about 10°C/cm., in the middle part.

The powdered sample was sealed under a 10^{-3}~10^{-4} mmHg vacuum into a cylindrical glass tube, the bottom of which was sharpened like a pencil. The tube was lowered at the rate of 1~2 mm. per hour through the center of the furnace.

In this process, the crystal grew its ab plane perpendicular to the isothermal plane in the furnace.

Crystals of about 8×8×15 mm. could thus be made, but in most cases, cracks developed along the ab plane soon after the preparation. Therefore, only uncracked portions were cut out from them to use for the electrical measurement.

Specimen Cell.—An electrical conductivity cell of the sandwich type was prepared on a Teflon block, as is schematically shown in Fig. 1.

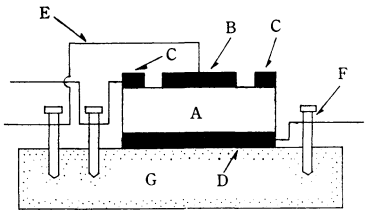


Fig. 1. The conductivity cell of sandwich type.
A: Crystal, B: Front electrode
C: Guard-ring electrode
D: Back electrode, E: Lead wire
F: Terminal, G: Teflon block

The cell had a guard-ring electrode which was grounded in order to prevent an effect of the surface current.

Silver paste (Ecco Bond), which was found to make ohmic contact with this sample, as will be described in the following paragraph, was applied as electrodes. The following two kinds of cells were used to measure the electrical resistivity in two crystallographic directions: the ⊥ab plane and the // ab plane.

(1) The ⊥ab cell, the electrodes of which were painted on both sides of the ab plane of a crystal in order to evaluate the electrical resistivity perpendicular to this plane ($\rho_{\perp ab}$).

(2) The //ab cell, the electrodes of which were attached on both sides of the plane perpendicular to the ab plane in order to observe the electrical resistivity parallel to the ab plane ($\rho_{/\!/ ab}$).

Measurements.—The measuring apparatus consisted of a vibrating reed electrometer (Takeda TR-88).

The current-voltage characteristics were examined in an atmosphere of air and nitrogen gas in order to find the effect of an ambient atmosphere on the electrical conductivity of the sample. The measurement of the temperature dependence of the electrical resistivity was made over the temperature range

* This paper was presented at the 17th Annual Meeting of the Chemical Society of Japan, April, 1964, Tokyo.

1) H. Mette and H. Pick, *Z. Physik*, **134**, 566 (1953).
2) H. Inokuchi, This Bulletin, **29**, 131 (1956).
3) R. G. Kepler, *Phys. Rev.*, **119**, 1226 (1960).
4) O. H. LeBlanc, Jr., *J. Chem. Phys.*, **35**, 1275 (1961).
5) J. B. Rust, F. A. Haak and J. P. Nolta, "Wadd Technical Report," 60-111 (1960).
6) R. C. Sangster and J. W. Irvine, Jr., *J. Chem. Phys.*, **24**, 670 (1956).

from 24 to 75°C for both increasing and decreasing temperatures.

Results and Discussion

The current-voltage characteristics of the specimen //ab cell in air and in nitrogen gas at room temperature are shown in Fig. 2.

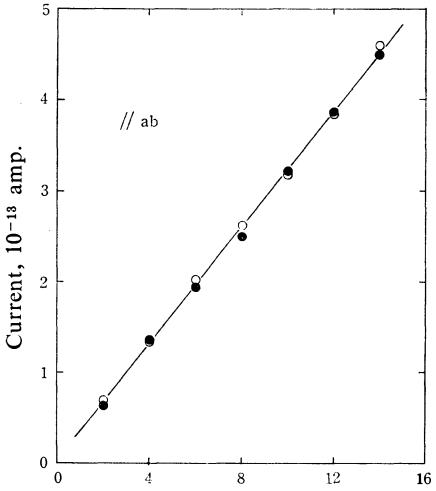


Fig. 2. The current-voltage characteristics of phenanthrene.
○ in air
● in nitrogen gas

There was no difference between the current in air and that in nitrogen gas within the range of experimental error. Therefore, the observation of the temperature dependence of the electrical resistivity was made in air.

As is exemplified by the same figure, the current-voltage relation was linear up to 1600 V. per cm. A similar result was obtained for the specimen ⊥ ab cell.

As has been reported in many papers on the semiconductive property of organic compounds, the observed temperature dependence of the electrical resistivity of phenanthrene is, for both increasing and decreasing temperatures, in good agreement with the following expression, as is shown in Fig. 3.

$$\rho = \rho_0 \exp(\Delta\varepsilon/2kT)$$

where ρ is the electrical resistivity, $\Delta\varepsilon$ is the thermal activation energy, k is the Boltzmann constant, and T is the abolute temperature. The values of $\Delta\varepsilon$, ρ_0, and the resistivity at 15°C, ρ_{15}, are given in Table I. The last value was estimated by extrapolation from the observed temperature dependence.

There is no anisotropy in the value of the activation energy. An anisotropy can be found, however, in the value of the electrical

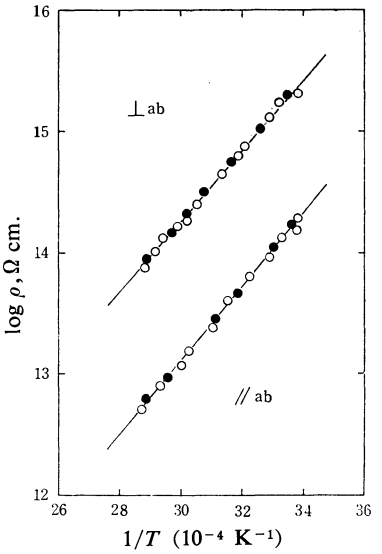


Fig. 3. The temperature dependance of the resistivity of phenanthrene.
○ for increasing temperature
● for decreasing temperature

TABLE I. THE ELECTRICAL RESISTIVITY OF PHENANTHRENE OBSERVED FROM ⊥ab CELL AND //ab CELL

	ρ_{15}, Ω cm.	$\Delta\varepsilon$, eV.	ρ_0, Ω cm.
Phenanthrene			
⊥ab	4.8×10^{15}	1.14	5.5×10^{5}
//ab	1.9×10^{14}	1.15	1.8×10^{4}
powder*	1.4×10^{16}	1.3	6×10^{4}
Anthracene			
⊥ab**	10^{22}	2.7	1×10^{-2}
powder*	1.7×10^{20}	2.47	4×10^{-2}

* From J. B. Rust et al.
** From H. Inokuchi et al.

resistivity; the electrical resistivity measured on the ab plane ($\rho_{//ab}$) is lower by a factor of about twenty-five than that perpendicular to this plane ($\sigma_{\perp ab}$).

The electrical conductivity (σ) can be expressed as $\rho = |e|n\mu$, where n is the concentration of the charge carrier and μ, the mobility of the carrier.

Since no anisotropy is found in the activation energy, it is not likely that the concentration of the charge carrier varies according to the direction of the electric field. Therefore, it seems that the observed anisotropy in the electrical conductivity results from the difference in the mobility of the charge carrier. This assumption has been affirmed by the mobility anisotropy in anthracene obtained through a pulsed photoconductivity technique[3] and tight-binding band calculations.[4]

The conductivity anisotropy observed with a

phenanthrene crystal is, however, larger than that of anthracene reported by Mette and Pick,[1] who have found that in the anthracene crystal, the conductivity on the ab plane is a few times higher than that in the direction perpendicular to the plane. Such a difference might be due to the difference in the band structures between phenanthrene and anthracene.

As the molecules in a phenanthrene crystal are arranged so that the molecular planes are nearly perpendicular to the ab plane,[7,8] the overlapping of π-orbitals are largest in the direction parallel to the ab plane. The resistivity is lowest in this direction, as has been found to be true in anthracene[1] and other substances.[9]

There is an appreciable difference between phenanthrene and anthracence in the absolute values of $\Delta\varepsilon$ and ρ_{15}, as is shown in Table I. A similar result has been reported also by Rust et al. as a result of their experiment with powder specimens.[5]

Therefore, we must conclude that while phenanthrene and antheacene are structural isomers and have similar crystallographic characters,[7,8,10] the electrical properties of the two substances are markedly different.

7) B. S. Basak, *Acta Cryst.*, **1**, 224 (1948).
8) J. Trotter, ibid., **16**, 605 (1963).
9) H. Inokuchi, H. Kuroda and H. Akamatu, This Bulletin, **34**, 749 (1961).
10) A. McL. Mathieson, J. M. Robertson and V. C. Sinclair, *Acta Cryst.*, **3**, 245 (1950); V. C. Sinclair, J. M. Robertson and A. McL. Mathieson, ibid., **3**, 251 (1950).

Summary

Phenanthrene single crystals have been grown by means of a modified Bridgeman method. The electrical conductivity has been measured for two crystallographic directions, $\perp$ ab and $/\!/$ab.

The electrical resistivity is not affected appreciably by ambient oxygen. The temperature dependence of electrical resistivity can be described as $\rho=\rho_0\exp(\Delta\varepsilon/2kT)$, where the activation energy ($\Delta\varepsilon$) is 1.14 eV. for $\perp$ab and 1.15 eV. for $/\!/$ ab; the two values agree well. A large anisotropy has been found in the resistivity at 15°C. The resistivity is 4.8×10^{15} Ω cm. and 1.9×10^{14} Ω cm. for $\perp$ ab and $/\!/$ab respectively.

It has been concluded that, although phenanthrene is an isomer of anthracene, the electrical properties of phenanthrene differ considerably from those of anthracene.

The authors wish to thank Dr. Haruo Kuroda for many valuable discussions and suggestions, Dr. Toru Matsushita for his helpful advice on the growth of crystals, and Dr. Yoshiro Fukao for his X-ray analysis.

Department of Chemistry
Central Research Laboratory
Tokyo Shibaura Electric Co., Ltd.
Kawasaki-shi Kanagawa

Studies of the Synthetic Inorganic Ion Exchanger. IV.[1] *The Separation of the Fission Product and Uranium by Means of a Stannic Phosphate Cation Exchanger*

By Yasushi INOUE, Shin SUZUKI and Hidehiro GOTO

(Received May 6, 1964)

The separation of uranium and fission products is one of the main parts of the reprocessing of irradiated nuclear fuels. In such a process it is better to use the unit processes which can be applied to the remote handling operations and which are not interfered with by the irradiation of the high dose of ionized radiation. In this respect, the ion exchange method employing the stannic phosphate cation exchanger which has been developed in this laboratory is considered to be one of the most promising methods.

Stannic phosphate, besides its resistivity against ionized radiation, has various other excellent characteristics and was applied to the separation of fission products in the preceding study of this series.[2] Using various concentrations of nitric acid and ammonium chloride

1) Y. Inoue, This Bulletin, **36**, 1324 (1963).

2) Y. Inoue, ibid., **36**, 1316 (1963).

solutions as the eluants, the separation was achieved on small columns in a relatively simple operation. It had, however, a shortcoming in that some of the rare earths was eluted with cesium.

The purpose of this study is to modify the method for the mutual separation of fission products in order to prevent the contamination of cesium and to establish a method for the separation of uranium from the fission products.

Experiment

Reagents.—*Ion Exchanger.*—The stannic phosphate used was prepared by the method described previously.[2]

Radioactive Isotopes.—They were the same as those of the last paper of this series.[1]

All the other reagents, such as uranyl nitrate, nitric acid, phosphoric acid, acetic acid, sodium carbonate and ammonium chloride, were of the highest grade of purity.

Apparatus.—All the absorption measurements were made with a Hitachi spectrophotometer, model EPU-2, with 1 cm. silica transmission cells. The pH meter, radiation measurement instruments and fraction collector were those described in the foregoing report.

Procedure.—*The Determination of Uranium.*—In the presence of phosphate, the thiocyanate-spectrophotometric method[3] cannot be used because of the strong interference from phosphate. In this case, the sodium carbonate-hydrogen peroxide-sodium hydroxide method[4] was employed. The calibration curves were made in the presence of the same amount of phosphoric acid as in the sample solution in order to eliminate the interference from phosphate. The procedure was as follows: After less than 10 ml. of the sample solution had been placed in a 100 ml. beaker, the volume was brought to about 10 ml. with distilled water. The pH of the solution was adjusted with sodium hydroxide, and then it was transfered into a 25 ml. volumetric flask. Five milliliters of 5% sodium carbonate, 1 ml. of 10% sodium hydroxide and 2 ml. of 3% hydrogen peroxide solutions were added succesively. After this new solution had been diluted to the 25 ml. mark, the absorbance of the solution was measured against a corresponding blank at the wavelength of 370 or 400 mμ. The concentration of uranium was calculated from the relationship between the absorbance and the concentration represented in Table I.

TABLE I. RELATIONSHIP BETWEEN ABSORBANCE AND CONCENTRATION OF URANIUM IN THE PRESENCE OF PHOSPHORIC ACID

Concn. of H_3PO_4, M	(μg./ml.)/unit absorbance	
	370 mμ	400 mμ
0.0	159.8	238.0
10^{-3}	160.9	239.3
10^{-2}	164.2	238.1
10^{-1}	185.2	238.6
2×10^{-1}	196.5	244.8
4×10^{-1}	232.5	276.6
1.0	281.8	333.2

3) E. B. Sandell, "Colorimetric Determination of Traces of Metals," Interscience Publishers, New York (1959), p. 916.
4) Ibid., p. 915.

The Determination of the Distribution Coefficients.—The distribution coefficients were determined by equilibrating 500 mg. of the ion exchanger in a thermostat at 25°C with 50 ml. of suitable solutions for two or three days. This was followed by the filtration of the mixture and by the analysis of the filtrate. If necessary, the pH of the filtrate was measured. The metallic ion content of the exchanger after equilibrium was estimated from the difference between the total initial and final concentrations of metal present in the solution.

The distribution coefficients were calculated by means of the usual relationship:

$$K_d=\frac{\left(\begin{array}{c}\text{Amount of cation in exchanger/}\\ \text{Wt. of exchanger in g.}\end{array}\right)}{\left(\begin{array}{c}\text{Amount of cation in solution/}\\ \text{Vol. of solution in ml.}\end{array}\right)}$$

Cerium was carrier-free ^{144}Ce, and the concentration of uranium was 10^{-3} M. They were determined radiochemically and spectrophotometrically respectively.

Column Operation.—The column was prepared as follows. To 2 g. of a dried exchanger in the hydrogen form (100~200 mesh), sufficient distilled water was added to allow a mixing thorough enough to expel any adhering air bubbles. After this mixing, the slurry was poured into a glass column, 7 mm. in internal diameter, using glass wool as a column support. The column thus prepared had a height of 40 mm. The flow rate of the influent was controlled according to the rate of exchange for each experiment and is described in figures of the elution curve. For making elution curves, effluents were received in polyethylene test tubes in suitable amounts; their radioactivities were measured with a well-type scintillation counter, and their uranium contents were determined by the method described above. When beta-rays were used for the measurement of the radioactivity, one drop of solution from every 2 g. of the effluents was placed on an aluminum dish, and their radioactivities were measured by a G. M. counter in the usual manner.

Results

The Modification of the Separation Method of a Fission Product Solution.—In the mutual separation of fission products, cesium was not obtained in a radiochemically pure state when it was eluted by a 3 M ammonium chloride solution as has been described previously. When this eluant was applied to the fission product solution containing uranium, rare earths and also uranium were eluted by this eluant, as will be shown later. This is perhaps

because of the partial elution of rare earths and uranium by the hydrogen ions which are replaced from the column by the action of concentrated ammonium ions. This is supported by the fact that this objectionable phenomenon is less pronounced when the exchanger is treated with a sufficient amount of 3 M ammonium chloride beforehand. Even with this pretreatment, however, the exchanger was not completely converted to the ammonium form. (This was clearly indicated by the fact that when an ammonium carbonate solution came in contact with the exchanger, bubbles of carbon dioxide were generated.) Moreover, even if the exchanger were completely converted to the ammonium form, the contamination of cesium would not be eliminated, as the presence of some acid in the eluant is needed for the complete elution of strontium, which is completed before the elution of cesium. Therefore, at all events, it is essential to devise a procedure by which cesium can be eluted in a radiochemically pure state.

It is conceivable that the interfering effect of the remaining hydrogen ions can be eliminated by the treatment of the column with a neutral solution before the elution of cesium. As one such reagent, ammonium acetate was chosen, and, as is shown in Fig. 1, a clear-cut elution curve was obtained. It was confirmed by the radiochemical analyses of several representative aliquots of the effluents that no contamination of cerium occurred in the cesium fraction.

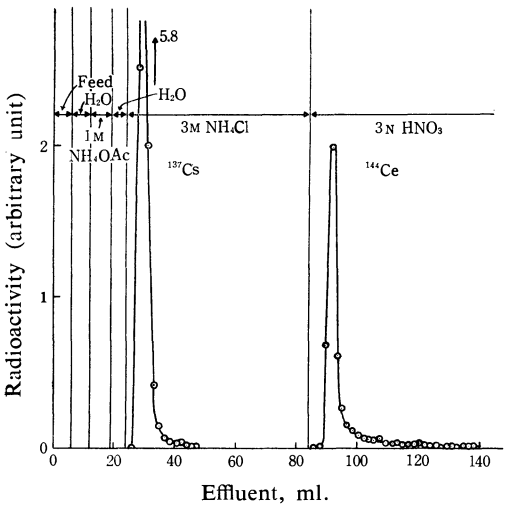


Fig. 1. Separation of ^{144}Ce and ^{137}Cs. Flow rate: 0.5~0.6 ml./min.

Furthermore, this procedure did not affect at all the elution processes after that of 3 M ammonium chloride.

The Distribution Coefficients of Uranium in a Nitric Acid Solution.—To contribute to the establishment of the method of separation, the distribution coefficients of uranium were determined in a nitric acid medium, as is shown in Table II. For the purpose of comparison, the values for nuclides present in fission products are cited in the table quoted from the preceding report. The distribution coefficients of uranium decrease with an increase in the acidity and resemble those of rare earths. From these results, it is expected that the separation of uranium from rare earths by nitric acid is very difficult, while that from other nuclides is easy. First the conditions for the mutual separation of uranium and individual nuclides in fission products were determined; then the separation of uranium and gross fission products was carried out.

TABLE II. DISTRIBUTION COEFFICIENTS IN NITRIC ACID SOLUTION (ml./g.)

Acidity N	Nuclides				
	UO_2(II)	^{95}Zr	^{95}Nb	^{137}Cs	^{89}Sr
0.0	2.9×10^3	—	—	—	—
0.1	3.5×10^2	2.7×10^3	2.2×10^3	3.8×10^3	6.7×10
0.5	4.1×10	3.5×10^3	2.6×10^3	1.3×10^3	~7
1.0	2.0×10	3.5×10^3	2.7×10^3	1.8×10^2	~2
3.0	6.1	3.6×10^3	2.5×10^3	1.0×10^2	~2
10.0	1.2	3.7×10^3	4.0×10^3	~3.7	~0

Acidity N	Nuclides			
	^{90}Y	^{144}Ce(III)	^{144}Ce(IV)	^{106}Ru
0.0	—	—	—	—
0.1	1.4×10^3	9.3×10^2	6.5×10^2	~0
0.5	1.6×10	1.2×10	1.1×10	~0
1.0	~3.6	~4	~1	~0
3.0	~2	~2	~1	~3
10.0	~0	~0	~0	~8

The Separation of ^{89}Sr and Uranium.—The separation of ^{89}Sr and uranium was carried

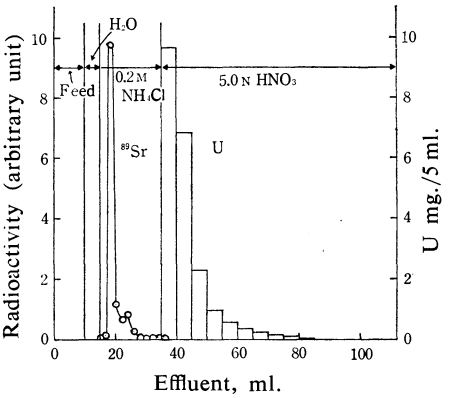


Fig. 2. Separation of ^{89}Sr and uranium. Flow rate: 0.5~0.6 ml./min.

out by the hydrogen-form exchanger. Ten milliliters of a sample solution containing a 10^{-2} M uranyl nitrate and carrier-free ^{89}Sr were passed through the column, and then 0.2~0.5 M ammonium chloride and 5 N nitric acid solutions were passed through in order to elute strontium and uranium successively. The separation went well, as is shown in Fig. 2. When an ammonium-form exchanger was used, it was necessary to use an eluant containing some acid in order to make a complete elution of strontium. A part of the uranium was also eluted by this reagent; therefore, an ammonium-form exchanger cannot be used in the separation of these elements.

The Separation of ^{137}Cs and Uranium.—When the hydrogen-form exchanger was used, uranium was eluted partly in 3 M ammonium chloride, as in the case of rare earths, as is shown in Fig. 3. The treatment of the column with a 1 M ammonium acetate solution before the elution of cesium made it possible to prevent the contamination of uranium, and separation was satisfactory, as is shown in Fig. 4.

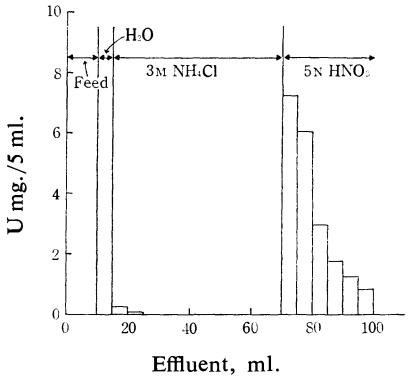


Fig. 3. Elution of uranium from hydrogen form exchanger.
Flow rate: 0.5~0.6 ml./min.

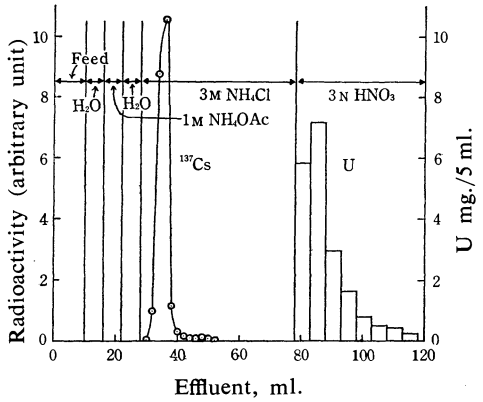


Fig. 4. Separation of ^{137}Cs and uranium.
Flow rate: 0.5~0.6 ml./min.

The Separation of ^{144}Ce and Uranium.—These two elements cannot be eluted by ammonium chloride, and separation by nitric acid seems to be very difficult, as is indicated by the results of Table II. This was also confirmed experimentally by the detailed investigation of the elution curves of uranium using various concentrations of nitric acid as eluants. Therefore, it is necessary to search for the other eluants. For this purpose, various concentrations of ammonium carbonate, ammonium carbonate-ammonium acetate, ammonium carbonate-ammonium chloride, ammonium carbonate-acetic acid-ammonium acetate, sulfuric acid, potassium sulfate, acetic acid-sodium acetate and phosphoric acid were investigated. Among these, ammonium carbonate-ammonium chloride and phosphoric acid looked promising and were investigated in detail.

The Ammonium Carbonate-Ammonium Chloride System.—The distribution coefficients of uranium and cerium measured in this system are presented in Table III. The distribution coefficients of uranium decreased with a decreasing pH, while those of cerium increased. As was described in the foregoing report, this exchanger is unstable at high pH values, so that possibly a low pH is preferable. With 5×10^{-2} M ammonium carbonate-3 M ammonium chloride, the differences between their distribution coefficients were very large, and the pH of the solution was low enough. Consequently, this condition seems to be quite suitable for the separation of these elements. According to this principle, the elution of uranium and cerium was conducted by using 5×10^{-2} M ammonium carbonate-3 M ammonium chloride and 1 N nitric acid as the eluants respectively. Uranium exhibited a sharp elution peak, but it showed considerable tailing and the yield was only 40% with an initial 150 ml. of eluants (Figs. 5 a and b). In other words, although it was possible to remove cerium from uranium

TABLE III. DISTRIBUTION COEFFICIENTS OF URANIUM AND CERIUM IN AMMONIUM CARBONATE-AMMONIUM CHLORIDE SYSTEM

Concn. of $(NH_4)_2CO_3$ M	Concn. of NH_4Cl M	pH	K_d (ml./g.) U	Ce
10^{-1}	10^{-1}	8.9	1.65×10^{2}	4.20×10
10^{-1}	5×10^{-1}	8.6	8.88×10	9.12×10
10^{-1}	1	8.4	6.18×10	4.20×10^{2}
10^{-1}	3	8.0	2.70×10	8.09×10^{2}
5×10^{-2}	10^{-1}	8.6	4.13×10	1.62×10^{2}
5×10^{-2}	5×10^{-1}	8.2	3.61×10	3.00×10^{2}
5×10^{-2}	1	8.0	3.02×10	5.42×10^{2}
5×10^{-2}	3	7.5	1.88×10	8.80×10^{2}

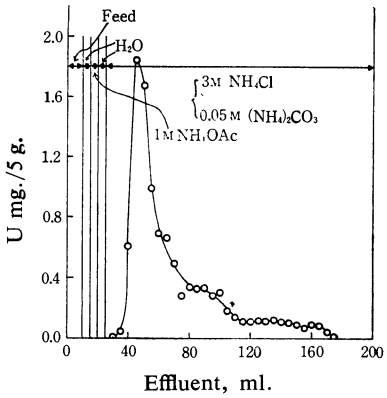


Fig. 5a. Elution of uranium by carbonate solution.
Flow rate: 0.3~0.4 ml./min.

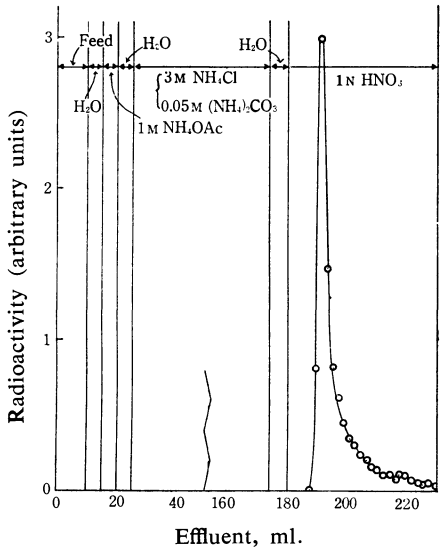


Fig. 5b. Elution of cerium.
Flow rate: 0.3~0.4 ml./min.

completely, the yield was very low, so this method of separation was by no means suitable.

The Phosphoric Acid System.—The distribution coefficients of uranium and cerium in various concentrations of phosphoric acid solutions are shown in Table IV. The distribution coefficients of uranium decreased monotonously with an increase in the acid concentration, and scarcely any uranium was adsorbed from phosphoric acid solutions above 1 M. On the contrary, although the distribution coefficients of cerium showed a maximum value between 0.1 and 0.5 M acidity and then rather decreased with an increase in the acidity, still it showed a fairly high value of about 3600 in 1 M phosphoric acid; it thus differed considerably from the uranium, and so it may be

Table IV. Distribution coefficients of uranium and ^{144}Ce(III) in phosphoric acid solution

Concn. of H_3PO_4 M	K_d (ml./g.) Ce	U
0.021	—	447
0.050	2.73×10^3	159
0.100	6.62×10^3	73.1
0.205	—	39.2
0.500	6.62×10^3	5.05
1.000	3.56×10^3	0.79
5.000	5.84×10	0.00

presumed that the condition is suitable for use. Ten milliliters of a sample solution containing 10^{-3} M uranium and carrier-free ^{144}Ce were poured into a hydrogen-form exchanger bed; when the level of the solution reached the top of the exchanger bed, 5 ml. of water, 60 ml. of 1 M phosphoric acid, 6 ml. of water and 50 ml. of 3 N nitric acid were passed through the column succesively. One of the examples is shown in Fig. 6. The elution curve showed

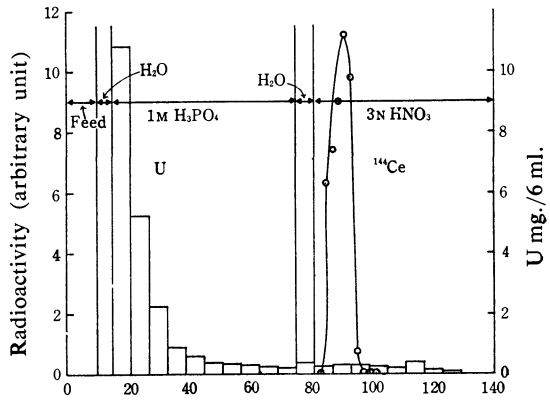


Fig. 6. Separation of uranium and ^{144}Ce.
Flow rate: 1 M H_3PO_4, 0.2 ml./min.; 3 N HNO_3 0.5~0.6 ml./min.

tailing to some extent, and the yield of uranium was about 92%. The use of a larger volume of phosphoric acid improves the yield, but it is not practical, as can be predicted from the shape of the elution curve. In any case, it is easy to recover over 90% of uranium without any contamination of cerium. The unfavorable tailing results from the slow rate of exchange.

The Behavior of Zirconium and Niobium.—The behavior of ^{95}Zr and ^{95}Nb in equilibrium was also investigated. As these nuclides were eluted partly by 1 M phosphoric acid, there was fear of contaminating uranium. As has been described previously, uranium was quantitatively eluted by nitric acid above 1 N but

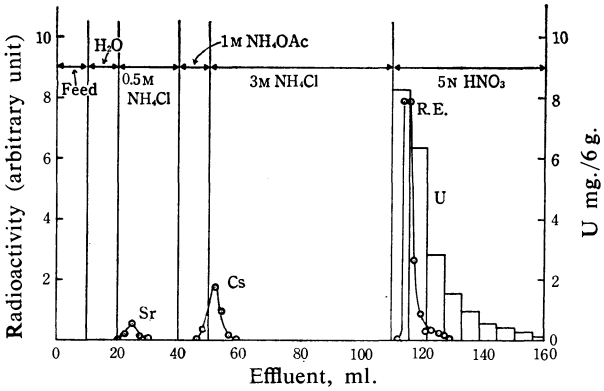


Fig. 7a. Separation of uranium and fission product.
Flow rate: 0.5~0.6 ml./min.

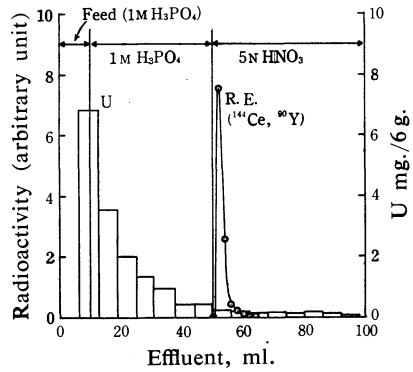


Fig. 7b. Separation of uranium and rare earths.
Flow rate: 1 M H_3PO_4, 0.2 ml./min.; 5 N HNO_3; 0.5~0.6 ml./min.

zirconium and niobium were not eluted at all. Therefore, the separation of uranium and a zirconium-niobium mixture was achieved by means of 3 N nitric acid.

The Separation of Uranium and the Fission Product.—Putting the above results together, the best conditions for the separation of uranium and the fission product were decided upon. To the sample solution, 5 ml. of concentrated perchloric acid were added; this was boiled until a yellow color had appeared once and then diminished. (It is advisable to lead the distillate into water in order to prevent any health hazard.) Then the residual solution was evaporated almost to dryness on a hot plate. After it had cooled, 1 ml. of 1 N nitric acid was added; the mixture was heated to dissolve the residue and then diluted to 10 ml. with water. This was poured into an exchanger bed; when the level of the solution reached the top of the exchanger bed, 10 ml. of water (by which no adsorbable form of zirconium and niobium could be washed out), 20 ml. of 0.5 M ammonium chloride (the elution of strontium), 10 ml. of 1 M ammonium acetate, 100 ml. of 3 M ammonium chloride (the elution of cesium), and 100 ml. of 5 N nitric acid (the elution of uranium and rare earths) were passed through the column successively. The 5 N nitric acid effluent was heated on a hot plate until the metastannic acid had coagulated completely. After the effluent had been cooled and diluted enough to prevent any destruction of filter paper, it was filtered to remove the metastannic acid (no uranium is lost by this procedure), and then the filtrate was evaporated almost to dryness. After it had cooled again, 10 ml. of 1 M phosphoric acid was added, and heated to dissolve the residue. This was poured into another exchanger bed, and, after the level of the solution had reached the top of the exchanger bed, 1 M phosphoric acid was percolated in until the yellow color of the column faded. A 5 N nitric acid solution was also passed through to elute rare earths. The elution curves are shown in Figs. 7a and b. The yields of uranium and beta and gamma decontamination factors are summarized in Table V. It goes without saying that if the fission product is cooled long enough to provide the decay of zirconium-95, radiochemically pure uranium can be collected in the 1 M phosphoric acid effluant which is inserted between 3 M ammonium chloride and 5 N nitric acid in the above procedure. This is shown in Fig. 8.

TABLE V. YIELD AND DECONTAMINATION FACTOR OF URANIUM
(uranium added; 23.81 mg.)

Uranium recovery		Decontamination factor	
Found (mg.)	%	β	γ
22.22	93.3	2.4×10^3	2.0×10^3
22.22	93.3	1.1×10^3	7.0×10^2
21.46	90.0	2.3×10^3	1.7×10^3

The Enhancement of the Yield of Uranium.—As can be seen from Table V, the yield of uranium was 90% or so; for the improvement of the recovery of uranium it is necessary to use a larger volume of eluant; the large volume of the eluant and the time needed make it impractical in all respects. If the saturation of a column by uranium does not affect the adsorption of rare earths, the column can be used for the uptake of rare earths until the break-through capacity for them is saturated. If a uranium solution contains only a low concentration of rare earths, such as a

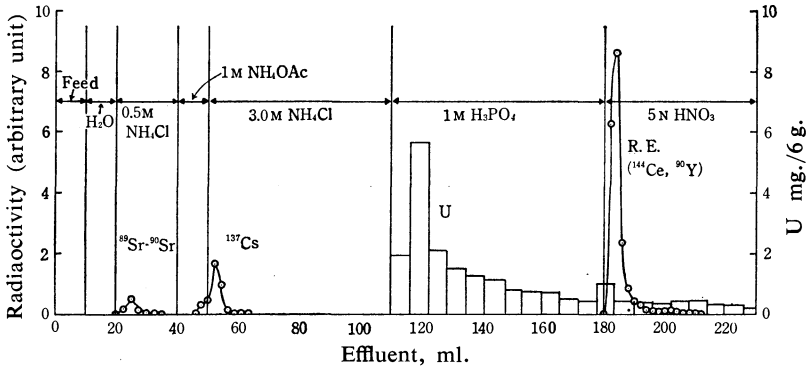


Fig. 8 Separation of uranium and fission product (in the absence of ^{95}Zr-^{95}Nb). Flow rate : 0.5~0.6 ml./min. except with 1 M H_3PO_4 (0.2 ml./min.)

carrier-free concentration, the perfect recovery of rare earth-free uranium can be accomplished by such a simple method as passing the solution through a column previously treated with a uranium solution, and this column could be used to an almost unlimited extent. When a 1 M phosphoric acid solution saturated with cerium ions was used, the column quantitatively adsorbed cerium from 26 ml. of the solution and then started to break through. This corresponded to about 0.2 meq. of cerium(III).

Summary

The separation of fission products and uranium has been carried out by means of a stannic phosphate cation exchanger. By using various concentrations of nitric acid and ammonium chloride solutions as eluants, the separation of uranium-strontium and uranium-cesium has been easily performed, but that of uranium-rare earths is very difficult. Among the various reagents investigated, a 1 M phosphoric acid solution is most suitable for the separation of uranium from rare earths. In view of the above results, the separation of uranium and gross fission products has been carried out; the resultant yield of uranium is more than 90%, and the decontamination factor is $(2\sim3)\times10^3$.

Part of the expenses for this investigation have been defrayed by a grant-in-aid by the ministry of education.

The Research Institute for Iron Steel and Other Metals
Tohoku University
Katahira-cho, Sendai

NOTES

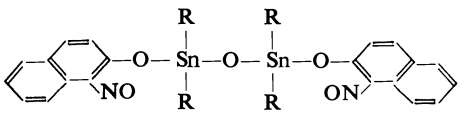
The Reaction of Dialkyltin Dichlorides with α-Nitroso-β-naphthol

By Toshio TANAKA, Ryuhei UE-EDA, Masanori WADA and Rokuro OKAWARA

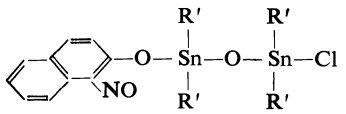
(Received March 4, 1964)

Dialkyltin dichlorides react with 8-hydroxyquinoline at the mole ratio of 1:2 to give dialkyltin bis(8-hydroxyquinolinates),[1,2] and with 2,2'-bipyridyl and 1,10-phenanthroline at the mole ratio of 1:1 to give dialkyltin(2,2'-bipyridyl) dichlorides and dialkyltin(1,10-phenanthroline) dichlorides[2,3] respectively. From these facts, bidentate ligand molecules, KeH, with protonating hydrogen had been expected to react with dialkyltin dichlorides to give the compounds of the R_2SnKe_2 type, compounds which might have the chelate structure containing a hexa-coordinated tin atom.

Such an expectation does not, however, seem to be true in the case of α-nitroso-β-naphthol, which reacted with dimethyltin dichloride under similar conditions to give tetramethyl-1,3-bis(α-nitroso-β-naphthoxy)distannoxane, $[(C_{10}H_6NO_2)(CH_3)_2Sn]_2O$ (Ia), but not dimethyltin bis(α-nitroso-β-naphtholate), $(CH_3)_2Sn(C_{10}H_6NO_2)_2$. Diethyltin dichloride also gave the corresponding distannoxane (Ib). On the other hand, under similar conditions, di-*n*-propyltin and di-*n*-butyltin dichlorides gave tetraalkyl-1-(α-nitroso-β-naphthoxy)-3-chlorodistannoxanes, $(C_{10}H_6NO_2)R'_2SnOSnR'_2Cl$ (II).



(Ia) $R=CH_3$
(Ib) $R=C_2H_5$



(IIa) $R'=n\text{-}C_3H_7$
(IIb) $R'=n\text{-}C_4H_9$

The infrared spectra of these distannoxanes I and II in the potassium bromide region are shown in Fig. 1, together with that of α-nitroso-β-naphthol. It was previously found by the present authors and by others that a

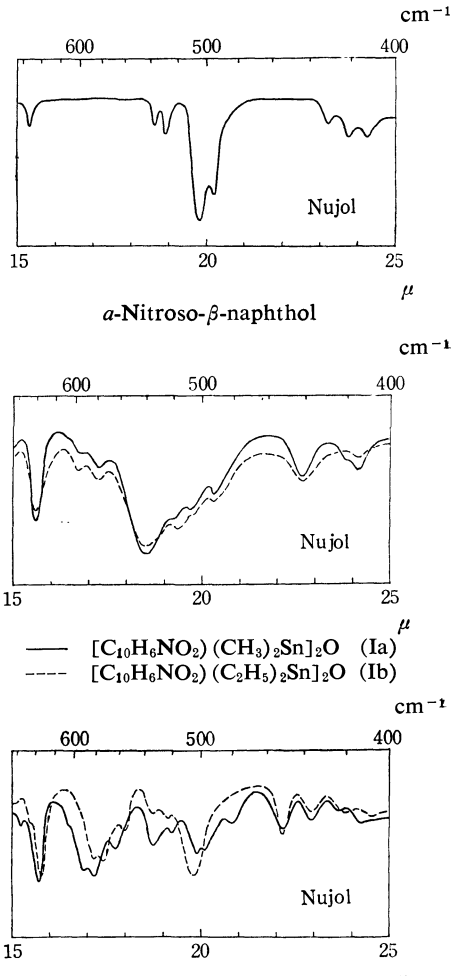
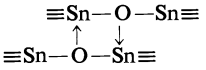


Fig. 1. Infrared spectra of α-nitroso-β-naphthol and its distannoxane derivatives.

1) D. Blake, G. E. Coates and J. M. Tate, *J. Chem. Soc.*, **1961**, 756.
2) T. Tanaka, M. Komura, Y. Kawasaki and R. Okawara, *J. Organometal. Chem.*, **1**, 484 (1964).
3) D. L. Alleston and A. G. Davies, *J. Chem. Soc.*, **1962**, 2050.

broad band near 600 cm^{-1} would be associated with the Sn–O–Sn stretching vibration in dimeric distannoxanes (III).[4,5] Although this



(III)

characteristic band has here been observed in the two compounds shown in I, the Sn–O–Sn stretching vibration in the compounds of II was observed at a lower frequency and with a different shape. Considering these spectra, the association of the latter two compounds in the solid state may be different from that of the former. The presence of the chelate structure in these compounds is, however, not yet obvious from the results of the present investigation.

Experimental

Materials.—Dialkyltin dichlorides supplied by the Nitto Kasei Company were purified either by sublimation or by recrystallization from ligroin or petroleum ether. α-Nitroso-β-naphthol was obtained commercially and checked with the melting point.

The Reaction of Dialkyltin Dichlorides with α-Nitroso-β-naphthol.—Into a solution of 1.0 g. (0.006 mol.) of α-nitroso-β-naphthol and 0.66 g. (0.003 mol.) of dimethyltin dichloride in 25 ml. of methanol, 6 ml. of 1 N ammonium hydroxide in methanol was slowly stirred in over a period of about one hour. During an additional three hours of stirring, a yellow precipitate gradually appeared, and the solution changed from dark green to brown. The precipitate was then filtered off, repeatedly washed with benzene, and dried under reduced pressure. Yield, 90%. M. p.>230°C. Found: C, 44.09; H, 3.73; Sn, 35.84. Calcd. for $[(C_{10}H_6NO_2)(CH_3)_2Sn]_2O$: C, 43.82; H, 3.68; Sn, 36.08%. This compound Ia was also obtained in almost the same yield by the reaction of dimethyltin dichloride with α-nitroso-β-naphthol at the mole ratio of 1 : 1. Similarly, diethyltin dichloride reacted with α-nitroso-β-naphthol to give a yellowish green precipitate. Recrystallization from a methanol-chloroform mixture (volume ratio 2 : 1) gave a dark brown crystalline compound (Ib). Yield, 70%. M. p. 163°C. Found: C, 47.04; H, 4.47; Sn, 32.92. Calcd. for $[(C_{10}H_6NO_2)(C_2H_5)_2Sn]_2O$: C, 47.11; H, 4.52; Sn, 33.25%. By a similar procedure with di-*n*-propyltin dichloride, a yellowish brown precipitate was obtained. Recrystallization from a dichloromethane-ligroin mixture gave a dark brown crystalline material (IIa). Yield, 40%. M. p. 159~160°C. Found: C, 41.60; H, 5.41; Sn, 37.61. Calcd. for $(C_{10}H_6NO_2)(C_3H_7)_2SnOSn(C_3H_7)_2Cl$: C, 41.72; H, 5.41; Sn, 37.48%. Di-*n*-butyltin dichloride gave a yellowish precipitate, which was recrystallized from methanol (IIb). Yield, 50%. M. p. 140~141°C. Found: C, 45.22; H, 6.04; Sn, 34.39. Calcd. for $(C_{10}H_6NO_2)(C_4H_9)_2SnOSn(C_4H_9)_2Cl$: C, 45.29; H, 6.14; Sn, 34.43%. The same compound was also prepared by the neutralization of the mixture of tetra-*n*-butyl-1,3-dichlorodistannoxane, $[(C_4H_9)_2ClSn]_2O$, and α-nitroso-β-naphthol at the mole ratio of 1 : 2 in methanol with 1 N ammonium hydroxide. This compound was identified by mixed melting point determination with the compound derived from di-*n*-butyltin dichloride.

Even when di-*n*-propyl and di-*n*-butyltin dichlorides were treated with a large excess of α-nitroso-β-naphthol and then neutralized, only the corresponding compounds of type II were obtained, not the compounds of type I.

Infrared Spectra.—The infrared spectra were taken in mulls in Nujol by a Hitachi EPI-2G grating infrared spectrophotometer.

Department of Applied Chemistry
Osaka University
Miyakojima-ku, Osaka

4) R. Okawara and M. Wada, *J. Organometal. Chem.*, **1**, 81 (1963); M. P. Brown, R. Okawara and E. G. Rochow, *Spectrochim. Acta*, **16**, 595 (1960).
5) R. C. Poller, *J. Inorg. Nucl. Chem.*, **24**, 593 (1962).

The Crystal Structure of Tohdite

By Goro YAMAGUCHI, Hiroaki YANAGIDA and Shuitiro ONO

(Received March 12, 1964)

The synthetic procedure and some crystallographic data of a new alumina hydrate, Tohdite $5Al_2O_3 \cdot H_2O$, were reported in a previous paper.[1] The crystallographic data are summarized in Table I. In the present work we will attempt to determine the crystal structure of Tohdite from the X-ray powder diffraction data.

Experimental

Crystals of Tohdite can be prepared by the hydrothermal treatment of boehmite with a small amount of some mineralizer. They occur in a variety of forms, such as hexagonal plates and needles. They are not, however, suitable for the

1) G. Yamaguchi, H. Yanagida and S. Ono, This Bulletin, 37, 752 (1964).

TABLE I.

Crystal system	hexagonal (or trigonal)
Unit cell dimensions	$a=5.576$ Å, $c=8.768$ Å
Formula unit per unit cell.	$5Al_2O_3 \cdot H_2O$
Measured density	3.72 ± 0.02 g./cm^3
Calculated density	3.71 g./cm^3
Refractive index	$\omega=1.738 \sim 1.748$, $\omega-\varepsilon<0.01$
Systematic extinctions in powder diagram	(hhl) for $l=2n+1$

TABLE II. X-RAY DATA FOR TOHDITE

hkl	d_o	d_c	I_o	I_c
100	4.85	4.8286	10	9
002	4.38	4.3840	23	19
101	4.23	4.2296	11	17
102	3.246	3.2458	60	59
110	2.788	2.7878	12	10
103	2.500	2.5003	54	42
200	2.416	2.4143	12	18
112	2.352	2.3524	77	96
201	2.329	2.3277	38	47
004	2.192	2.1920	4	2
202	2.1146	2.1148	100	84
104		1.9960	*	2
203	1.8614	1.8614	48	73
120		1.8250	*	1
121		1.7867	*	2
114		1.7237	*	1
122	1.6854	1.6849	13	16
105	1.6482	1.6482	4	4
204	1.6232	1.6229	26	33
300		1.6095	*	2
301		1.5831	*	0
123	1.5479	1.5480	34	19
302	1.5105	1.5105	20	22
006	1.4609	1.4613	4	3
205	1.4190	1.4188	68	54
303		1.4099	*	0
124		1.4026	*	1
106		1.3987	*	1
220	1.3939	1.3939	85	74
130		1.3392	*	0
222	1.3283	1.3278	5	5
131		1.3239		
304		1.2974	*	2
116		1.2943	*	4
132	1.2809	1.2808	6	6
125		1.2645	3	3
206	1.2499	1.2502	7	13
133	1.2173	1.2175		
107		1.2124	21	15
400		1.2072		
401	1.1966	1.1959	5	5
305		1.1858	*	0
402	1.1639	1.1638	6	9
134		1.1455	*	0
126		1.1407	*	1
403	1.1158	1.1158	9	11
207	1.1121	1.1118		
230		1.1078	*	0
231		1.0990	4	5
008	1.0960	1.0960		

(Values marked * were not observed.)

measurement of the relative X-ray diffraction intensities, since the specimens always show preferred orientations. A new method for preparation has been found as follows. Eta-alumina was obtained from a dehydration, at 800°C in air, of bayerite $Al(OH)_3$ which had been prepared by neutralizing an aluminum chloride aqueous solution with ammonia. The eta-alumina was inverted to a microcrystalline tohdite when treated hydrothermally under a water vapor pressure of about 200 atm. at 460°C. Tohdite prepared by this method was used for the intensity measurement, since it showed no preferred orientation.

The X-ray diffraction data for Tohdite in Table II were recorded on a diffractometer using Cu$K\alpha$-radiation. A set of I_o experimental intensities relative to 202 was obtained by measuring the areas under the diffraction peaks.

Structure Analysis

In the following discussion, we will disregard the contribution of the two hydrogen atoms of the formula $5Al_2O_3 \cdot H_2O$ to the diffraction intensities and will instead pay attention to the arrangement of the 10 aluminum atoms and 16 oxygen atoms in the unit cell.

The unit cell of Tohdite is clearly related to those of kappa- and beta-alumina. (Kappa-alumina is the dehydrated product of Tohdite.) The lattice constants of Tohdite and these aluminas based on orthohexagonal lattices[2] are compared in Table III.

TABLE III. ORTHOHEXAGONAL LATTICE CONSTANTS OF TOHDITE AND KAPPA- AND BETA-ALUMINA (IN Å)

Kappa-alumina	$a=16.80$	$b=9.71$	$c=17.85$
Beta-alumina	$a=5.56$	$b=9.65$	$c=22.55$
	$3a=16.70$		
Tohdite	$a=5.58$	$b=9.66$	$c=8.77$
	$3a=16.73$		$2c=17.54$

The crystal structures of kappa- and beta-alumina were studied by Saalfeld[2] and Beevers[3] respectively. The similarity between the unit cell of Tohdite and those of the above-mentioned aluminas indicates that in the Tohdite structure the layers of oxygen and aluminum atoms lie alternatively in sheets perpendicular to the c-axis and that the unit cell of Tohdite is formed by the close stacking of 4 oxygen layers, each layer containing 4 oxygen atoms. The high density and refractive index of Tohdite also imply a close-packed arrangement of oxygen atoms.

For the arrangement of aluminum atoms, it is well known that there are two types of aluminum positions, that is, octahedral sites

2) H. Saalfeld, *N. Jb. Abh.*, **95**, 1 (1960).
3) C. A. Beevers and M. A. S. Ross, *Z. Krist.*, **97**, 59 (1937).

and tetrahedral sites. In this case, since the 10 aluminum atoms in the unit cell are distributed over 4 aluminum layers, it can easily be assumed that two aluminum layers contain 2 aluminum atoms each, while the other two layers contain 3 atoms each.

With the above-mentioned extinctions the following space groups are possible; P31c, $P\bar{3}1c$, $P6_3mc$, $P\bar{6}2c$ and $P6_3/mmc$. The latter two of them, however, must be rejected, because the arrangement of the reflection planes and axial glide planes characteristic of these groups causes an unreasonable arrangement of aluminum atoms. $P\bar{3}1c$ characterized by centers of symmetry and axial glide planes is also improbable for a similar reason. Therefore, Tohdite must belong to the P31c or $P6_3mc$ group. Since there is no evidence of trigonal symmetry, the more highly symmetrical space group, $P6_3mc$, may be assumed for Tohdite.

First the sequence of the oxygen layers can be determined as:

$$\dot{A}BAC\dot{A}BA\dot{C}A, \text{ etc.}$$

(following theusual nomenclature),

since the unit cell contains a screw hexads, 6_3, in the [001]-direction. The vertical dashes denote the boundaries of the unit cells in the [001]-direction. Second, the arrangement of aluminum atoms must be taken into consideration. Since there are two types of aluminum positions, as has been mentioned above, we were able to assume several trial arrangements. These arrangements were examined and rejected bacause of the poor agreement of the calculated with the observed intensities. The best result was obtained by placing aluminum atoms at (1/6 1/3 3/8), (2/3 1/3 1/8) (octahedral sites) and (1/3 2/3 μ) (tetrahedral sites). μ is approximately 0.068.

Results

The atomic parameters are given in Table IV. A set of relative intensities for these atomic positions, I_c, was calculated by means of the following equation:

$$I_c = KnD\frac{1+\cos^2 2\theta}{\sin^2\theta\cdot\cos\theta}|F|^2$$

where θ is the Bragg angle; F, a structure factor; n, the multiplicity; D, a temperature factor for $B=1.62$ Å^2, and K, a scale factor. They give the agreement factor

$$\frac{\sum_{hkl}(I_o\sim I_c)}{\sum_{hkl}I_o}$$

of 0.26, where the unobserved reflections marked * were excluded.

Futher refinements on the basis of the data of the powder diagram are hardly possible. It, therefore, remains conceivable that the atoms may be slightly displaced from these special positions of $P6_3mc$ and that a less symmetrical space group should be taken for this crystal. However, it is sure that the structure given covers the principal features of the Tohdite lattice.

Table IV. Position parameters

Atom	x/a	y/a	z/c	Number of equivalent positions
O(1)	0	0	0	2
O(2)	1/2	0	0	6
O(3)	1/3	1/6	1/4	6
O(4)	1/3	2/3	1/4	2
Al(1)	1/6	1/3	3/8	6
Al(2)	2/3	1/3	1/8	2
Al(3)	1/3	2/3	0.068	2

Figure 1 shows a unit cell of Tohdite. In this structure four-fifths of the aluminum atoms are in octahedral sites, and the rest, in tetrahedral sites. Interatomic distances calculated from the atomic positions in Table IV are given in Table V. There are two different atomic distances for tetrahedral bonds, since the aluminum atoms in tetrahedral sites are not placed at the centers of the tetrahedra.

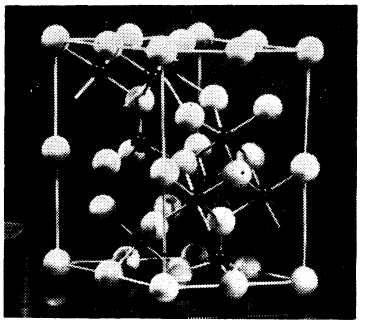


Fig. 1. The unit cell of the Tohdite structure. Oxygen atoms are shown as large and aluminum atoms as small spheres.

Table V. Interatomic distances (in Å)

O-O (I)	within a layer	2.79
O-O (II)	between layers	2.72
Al-O (I)	octahedral bond	1.95
Al-O (II)	tetrahedral bond	1.72 1.60

The authors wish to express their thanks to Mr. Tadao Shimizu and Mrs. Katsue Saito for their valuable assistance.

Department of Industrial Chemistry
Faculty of Engineering
The University of Tokyo
Hongo, Tokyo

*Harze aus Formaldehyd. LXXXI. Anlagerungen von mono- und difunktionellen Thiolen, Thiolsäuren und Dioxim an Methylenbisacrylamid**

Von Minoru IMOTO, Koichi KONDO und Kiichi TAKEMOTO

(Eingegangen am 22. April, 1964)

Die Umsetzung von Acrylonitril mit Formaldehyd ist bisher schon von einigen Forschern untersucht worden. Bei der Umsetzung in Anwesenheit von Schwefelsäure gewinnt man als Hauptprodukt Hexahydro-1, 3, 5-*s*-triazin[1] oder Methylenbisacrylamid[2] je nach ihrer Menge und Konzentration. Im Laufe von unseren Untersuchungen über die Polymersynthese durch Polyaddition hat es uns interessiert, die Reaktionsfähigkeit dieser an beiden Enden vinylgruppenhaltigen Verbindung, Methylenbisacrylamid (abgekürzt MBAA), weiter zu erforschen, über die bisher noch keine Angaben vorliegen. Wir haben gefunden, dass Thiolen und Thiolsäuren an die Vinylgruppen des MBAAs sehr anlagerungsfähig sind, und ausserdem, dass die zweifunktionellen Verbindungen wie Dithiolen und Dithiolsäuren auf dieselbe Weise durch Wasserstoffübertragung zu polymeren Substanzen führen.

Experimentelle Ergebnisse

Anlagerung von Thiolen oder Thiolsäuren an MBAA.—Über die Anlagerungen von Thiolen an Olefinen ist schon viel berichtet worden. Es ist bekannt, dass Thiolen unter alkalischer Bedingung leicht an α,β-ungesättigten Carbonylverbindungen, Acrylnitril und auch an Acrylamid anlagern.[3] Dass die Anlagerung von Thiolen und Thiolsäuren an C=C Bindungen glatt verläuft, ist wohl auch bei den Umsetzungen an dehydrochloriertes Polyvinylchlorid bestätigt worden.[4]

Die Anlagerung von Thiolen und Thiolsäuren an MBAA wurde in Dioxanlösung bei Raumtemperatur durchgeführt. Äthylmercaptan und Thiophenol wurden als Thiolen, und Thiobenzoesäure und Thioessigsäure wurden als Thiolsäuren benutzt. Als Katalysator wurden bei der Umsetzung von Thiobenzoesäure Schwefelsäure, und in allen anderen Fällen Natriumalkoxyd benutzt. Die Umsetzungen verlaufen bei allen Fällen schon bei Raumtemperatur exothermisch sehr glatt, und die Anlagerungsprodukte waren als farblose Substanzen ausgeschieden. Bei erhöhter Temperatur war vorwiegend nur die thermische Polymerisation von MBAA verlaufen, und es gab keine Addukten.

Die Tabelle I zeigt die Ergebnisse der Umsetzungen.

TABELLE I. ANLAGERUNGEN VON THIOLEN UND THIOLSÄUREN AN MBAA (bei Raumtemperatur, in Dioxan)

RSH	Katalysator	Schmp. des Produktes °C	Ausbeute %
CH_3CH_2SH	C_2H_5ONa	183～184	46
C_6H_5SH	t-C_4H_9ONa	186～187	82
CH_3COSH	C_2H_5ONa	171～172.5	40
C_6H_5COSH	H_2SO_4	205～206	90

$$2RSH + CH_2=CHCNHCH_2NHCCH=CH_2 \longrightarrow RSCH_2CH_2CNHCH_2NHCCH_2CH_2SR$$

Bei der Umsetzung mit Thiophenol unter Zugabe von Natriumäthylat war die Ausbeute sehr klein, und das gewonnene Produkt zeigte keinen scharfen Schmelzpunkt. Bei der Umsetzung mit Thioessigsäure wurde eine unschmelzbare, durchaus unlösliche Substanz gewonnen, wenn Schwefelsäure als Katalysator gebraucht wurde.

Ausser Thiolsäuren und Thiolen wurden die Anlagerungen von Benzoesäure und Anilin an MBAA auch versucht, was uns aber nicht gelungen ist.

Polyaddition von Dithiolen und Dithiolsäuren an MBAA.—Die Umsetzung von MBAA mit Dithiolen und Dithiolsäuren wurde in der gleichen Weise in Dioxanlösung bei Raumtemperatur durchgeführt. Dithioglykol wurde als Dithiol, und Dithioterephthalsäure wurde als

* LXXX Mitt.: M. Imoto, N. Nakajima, S. Tajima und K. Takemoto, *J. Chem. Soc. Japan, Ind. Chem. Sec.* (*Kogyo Kagaku Zasshi*), **67**, 1090 (1964).

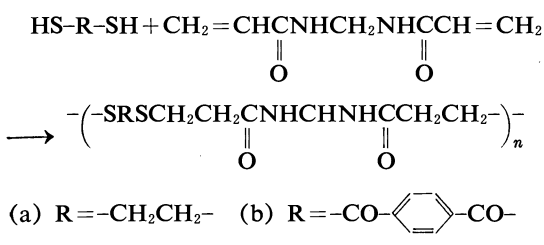
1) T. L. Gresham und T. R. Steadman, *J. Am. Chem. Soc.*, **71**, 1872 (1949).

2) E. E. Magat und B. F. Farie, ibid., **73**, 1028 (1951).

3) F. W. Stacey und J. F. Harris, Org. Reactions, **13**, 150 (1963).

4) K. Takemoto, *J. Chem. Soc. Japan, Ind. Chem. Sec.* (*Kogyo Kagaku Zassi*), **62**, 1934 (1959); **63**, 183 (1960).

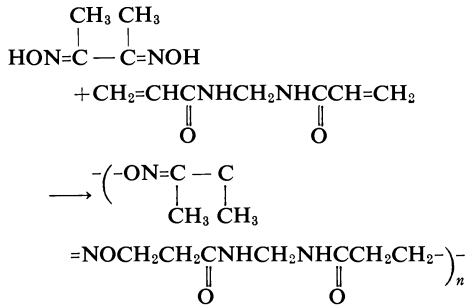
Dithiolsäure gewählt. Als Katalysator waren bei diesem Fall Salzsäure oder Schwefelsäure, und bei jenem Fall Natriumäthoxyd gewählt. In beiden Fällen wurden polymere Substanzen gewonnen. Die Umsetzung kann wie folgt angenommen werden.



Das bei der Umsetzung mit Dithioglykol gewonnene Produkt ist unschmelzbar und auch unlöslich, verkohlt aber bei ungefähr 240°C. Das bei der mit Dithioterephthalsäure gewonnene Produkt ist auch unschmelzbar und in fast allen gewöhnlichen organischen Lösungsmitteln unlöslich,. ausser in Ameisensäure, Eisessig und in Dimethylsulfoxyd, wo es jedoch nur schwer löslich ist. Es verkohlt bei ungefähr 230°C.

Zum Unterschied von der Umsetzung mit Dithioglykol wurde bei der Umsetzung mit Äthylenglykol kein polymeres Anlagerungsprodukt erhalten.

Polyaddition von Dioxim an MBAA. — Die Polyaddition von MBAA mit Diäthylglyoxim wurde in Anwesenheit von Triton B als Katalysator in Dimethylformamid bei Raumtemperatur durchgeführt. Die Umfällung von gewonnenen Produckt aus Essigsäure/Äther wurde wiederholt, und eine farblose, amorphe polymere Substanz erhalten. Die Umsetzung kann wie folgt formuliert werden.



Dieses Produkt ist in gewöhnlichen polaren Lösungsmitteln wie Wasser, Alkohol und Eisessig löslich. Es schmelzt bei 217~235°C, und die Grenzviskosität war 0.036 in Eisessig bei 25°C. Aus diesem Wert kann man vermuten, dass das unter oben erwähnten Bedingungen gewonnene Produkt nicht sehr hochmolekular ist.

Experimenteller Teil

Ausgangsmaterialien. — Thiobenzoesäure wurde aus Benzoylchlorid,[5] und Dithioterephthalsäure wurde aus Terephthalsäurechlorid[6] hergestellt. Ausser diesen wurden nur handelsübliche Produkte benutzt. Dioxan, Eisessig und Dimethylsulfoxyd wurden nach der gewöhnlichen Vorschrift gereinigt. Die Grenzviskosität wurde mit einem Ubbelohde'schen Viskometer gemessen.

MBAA wurde nach der Vorschrift von Magat et al.[2] durch die Umsetzung von Acrylnitril mit 37%igen Formaldehydlösung in Anwesenheit von Hydrochinon bei 40°C dargestellt. Die Ausbeute war 80%. Farblose Nadeln, Schmp. 178~180°C (Lit., 185°C), Molekulargewicht, 159 (kryoskopisch) (Ber., 154%).

Anlagerung von Äthylmercaptan an MBAA.— Zu 4.1 g (0.066 mol.) Äthylmercaptan, die sich mit 12 ccm Dioxan und Natriumäthylat (C_2H_5OH 46 g, Na 0.1 g) in einem vierhalsigen Rundkolben (200 ccm.) befand, wurde bei 20°C 70 ccm Dioxanlösung von 5.1 g. (0.033 mol.) MBAA in 10 Min zugetropft. Die Temperatur stieg schnell bis auf 28°C und das Produkt wurde als farblose Substanz ausgeschieden. Nach weiterem dreistündigen Umrühren wurde es abfiltriert. Rohausbeute 4.2 g (46% d. T.). Die Kristalle wurden aus Äthanol-Wasser und Äthanol je zweimal umkristallisiert. Das so erhaltene Blättchen zeigte den Schmelzpunkt 183~184°C.

Gef.: C, 47.66; H, 7.96; N, 10.14; S, 22.21. Ber. für $C_{11}H_{22}N_2O_2S_2$: C, 47.45; H, 7.96; N, 10.06; S, 23.03.

Anlagerung von anderen Thiolverbindungen an MBAA. — Die Umsetzungen von MBAA mit Thiophenol unter Zugabe von Natrium-*t*-butylat, mit Thioessigsäure unter Zugabe von Natriumäthylat, und mit Thiobenzoesäure unter Zugabe von Schwefelsäure wurden in der gleichen Weise durchgeführt, und die erhaltenen farblosen Produkte wurden umkristallisiert.

Reaktionsprodukt mit Thiophenol;

Gef.: C, 61.01; H, 6.19; N, 7.30; S, 16.52. Ber. für $C_{19}H_{22}N_2O_2S_2$: C, 60.93; H, 5.92; N, 7.48; S, 17.12%.

Reaktionsprodukt mit Thioessigsäure;

Gef.: C, 43.47; H, 6.01; N, 9.34; S, 19.79. Ber. für $C_{11}H_{18}N_2O_4S_2$: C, 43.12; H, 5.92; N, 9.14; S, 20.93%.

Reaktionsprodukt mit Thiobenzoesäure;

Gef.: C, 58.68; H, 5.27; N, 6.78; S, 15.89. Ber. für $C_{21}H_{22}N_2O_4S_2$: C, 58.58; H, 5.15; N, 6.50; S, 14.89%.

Die IR-Banden von -CONHR- (bei 3300, 3070, 1655 und 1550 cm^{-1}) sind an jeden Reaktionsprodukten noch vorhanden, während die Banden von CH_2=CH- (bei 2975, 1620, 990 und 910 cm^{-1}) nicht mehr aufgetreten sind. Bei den Reaktionsprodukten mit Äthylmercaptan traten die neuen Banden von C-S-Bindung (bei 790 und 770 cm^{-1}) ausser den Banden von CH_3- und -CH_2- Bindungen,

5) P. Noble und D. S. Tarbell, "Org. Syntheses," Coll. Vol., 4, 924 (1962).
6) S. Sunner und T. Nilson, *Svensk. Kem. Tid.*, **54**, 163 (1942); *Chem. Abstr.*, **38**, 3249 (1944).

bei dem mit Thioessigsäure weiter die Bande von >C=O (bei 1690 cm^{-1}), und bei dem mit Thiophenol und Thiobenzoesäure die Banden der Phenylgruppe (bei 1580, 1120, 735 und 690 cm^{-1}) auf.

Polyaddition von Dithiol und Dithiolsäure an MBAA.—*Umsetzung von MBAA mit Dithioglykol.* —Zu 2.4 g (0.025 mol.) Dithioglykol, die sich mit 20 ccm Dioxan und Natriumäthylat (C_2H_5OH 92 g, Na 0.1 g) in einem vierhalsigen Rundkolben (200 ccm) befindet, wurde bei Raumtemperatur 70 ccm Dioxanlösung von 3.9 g (0.025 mol.) MBAA in 15 Min zugetropft, wobei das Produkt sogleich ausgeschieden wurde. Nach weiterem fünfstündigem Umrühren wurde es abfiltriert. Rohausbeute 2.3 g. Das erhaltene Produkt wurde wegen der Unlöslichkeit in allen Lösungsmitteln mit Wasser und Äthanol gewaschen und dann mit Wasser-Äthanol unter Rückfluss ausgekocht.

Umsetzung von MBAA mit Dithioterephthalsäure. —Zu 70 ccm Dioxanlösung von 2.6 g (0.016 mol.) MBAA wurde in Anwesenheit von 1.0 g konz. Salzsäure 3.1 g (0.016 mol.) Dithioterephthalsäure, das in 50 ccm Dioxan suspendiert worden ist, in 40 Min zugetropft, wobei die Mischung unter Bildung von Niederschlägen sogleich trüb wurde. Nach fünfstündigem Umrühren wurde sie abfiltriert. Farbloses Pulver mit der Ausbeute von 5.7 g. Es wurde aus Eisessig-Methanol zweimal umgefällt. Das Produkt färbt sich beim Stehenlassen.

Die IR-Banden dieser zwei Produkte traten auch bei 2900 cm^{-1} (-CH_2- Bindung) ausser der Bande von -CONHR- Bindung auf, während beim Reaktionsprodukt mit Dithioterephthalsäure noch weitere Banden der Phenylgruppe (bei 1150, 850 und 780 cm^{-1}) aufgetreten sind.

Anlagerung von Dioxim an MBAA.—Zu 40 ccm Dimethylformamidlösung von 2.0 g (0.013 mol.) MBAA wurde bei Raumtemperatur 10 ccm Dimethylformamidlösung von 1.5 g (0.013 mol.) Dimethylglyoxim in 15 Min zugetropft und nach einer halben Stunde wurde 3 ccm Triton B weiter zugesetzt. Das Reaktionsgegemisch wurde bei Raumtemperatur noch 2 Std umgerührt. Nach vierundzwanzigstündigem Stehenlassen wurde weiter eine kleine Menge Wasser zugesetzt, und der ganze Inhalt in überschüssigen Äther gegossen. Der Niederschlag wurde abgesaugt und wurde nach dreimaligen Umfällungen aus Eisessig-Äther getrocknet. Ausbeute 0.2 g.

Das gewonnene Produkt zeigte die IR-Banden von CH_3- (bei 1370 cm^{-1}) und CH_2=CH- (bei 900 und 990 cm^{-1}) ausser der Bande von -CONHR- Bindung.

Zusammenfassung

Thiolen und Thiolsäuren lagern sich leicht an Methylenbisacrylamid in Dioxanlösung unter Zugabe von katalytischer Menge Alkoxyde oder Mineralsäuren bei Raumtemperatur an. Bei den Umsetzungen von Dithiolen und Dithiolsäuren mit Methylenbisacrylamid wurden unschmelzbare und in allen gewöhnlichen organischen Lösungsmitteln unlösliche polymere Substanzen gewonnen, die bei ungefähr 230~240°C verkohlen. Aus der Umsetzung von Dimethylglyoxim mit Methylenbisacrylamid wurde eine in polaren Lösungsmitteln lösliche Substanz erhalten, deren Grenzviskositätswert aber nicht sehr gross ist.

Abteilung der Angewandte Chemie
Technische Fakultät der
Städtischen Universität Osaka
Sumiyoshi-ku, Osaka

Studies of the Behaviors of Carrier-free Radioisotopes. I. The Coprecipitation of Cadmium-115 with Ferric Hydroxide

By Fujio ICHIKAWA

(Received April 25, 1964)

It is well-known that some carrier-free radioisotopes are coprecipitated with ferric hydroxide. The mechanism of the coprecipitation is not always identical, however. There are four groups of elements which are coprecipitated with ferric hydroxide; the first, the cations which are precipitated as insoluble hydroxides when a macro quantity of the cation exists in the solution (rare earths, etc.); the second, the cations which are not precipitated as hydroxides (strontium, etc.); the third, the anions which form insoluble compounds with ferric ions in the solution of a macro concentration (phosphate, etc.); the last, the anions which do not form insoluble compounds with ferric ions (sulfate, etc.).

In the present paper, the coprecipitation behavior of carrier-free cadmium with ferric hydroxide will be studied.

Experimental

A mixture of cadmium-115g (53 h) and cadmium-115m (43 d) was used as a carrier-free tracer of cadmium. These radioisotopes were separated from the uranium target, which was bombarded with 50 MeV. protons by the synchrocycrorton at the

Institute for Nuclear Study, the University of Tokyo. The target was dissolved into a few milliliters of 8 N nitric acid, and the cadmium was separated from uranium and other fission products by means of ion-exchange and coprecipitation techniques. According to the γ-ray spectrum and the decay curve of the cadmium fraction, only cadmium-115m, cadmium-115g and its daughter, indium-115m, could be detected.

The cadmium-115 solution, the ferric chloride solution, and the carrier or hold-back carrier solution were mixed in a 10~15 ml. centrifugal tube; then a freshly-prepared ammonium hydroxide or sodium hydroxide solution was added to this tube, and the contents were centrifuged. The radioactivities of the initial and supernatant solutions were measured by a scintillation counter after the two days which were required to obtain radioequilibrium between cadmium-115g and indium-115m. The coprecipitation ratio was calculated from these data.

Results and Discussion

The coprecipitation ratio of cadimium was measured as a function of the ferric, cadmium, ammonium and other ion concentrations.

It is to be expected that cadmium will form stable ammine complex ions in the presence of ammonium ions and will not be coprecipitated with ferric hydroxide. However, when ammonium hydroxide was used as a precipitant, about half the amount of carrier-free cadmium was coprecipitated with 10 mg. ferric hydroxide. This ratio increased logarithmically with the amount of precipitate (cf. Fig. 1). The ratio depended also on the concentration of ammonium ions at a constant pH value. Figure 2 shows this relation and proves that the formation of an ammine complex causes a decrease in the coprecipitation ratio. The cadmium concentration varied from a carrier-free concentration (10^{-12} M) to 1 M. The coprecipitation ratio did not change in concentrations less than 10^{-7} M, whereas in higher concentrations it decreased rapidly, as is shown in Fig. 3.

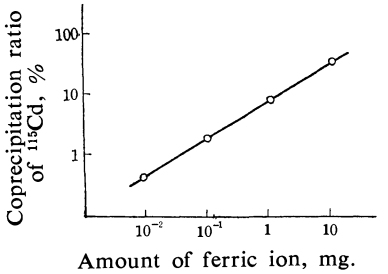


Fig. 1. Coprecipitation ratio of carrier-free cadmium with $Fe(OH)_3$ as a function of the amount of precipitate.

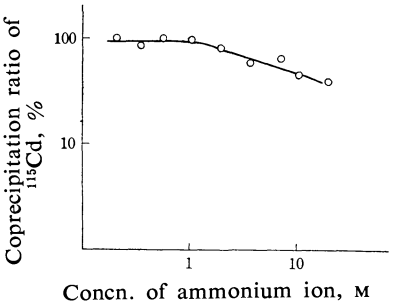


Fig. 2. Coprecipitation ratio of carrier-free cadmium with $Fe(OH)_3$ as a function of ammonium ion concentration.

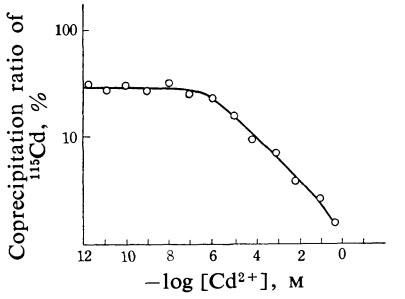


Fig. 3. Coprecipitation ratio of cadmium with $Fe(OH)_3$ as a function of cadmium ion concentration.

The existence of such ions as zinc, cobalt and copper, which form soluble ammine complexes, decreased the coprecipitation ratio of carrier-free cadmium. The addition of barium ions also depressed the coprecipitation.

When sodium hydroxide was used as a precipitant, the carrier-free cadmium was coprecipitated entirely with ferric hydroxide. These facts suggest that: 1) the coprecipitation of carrier-free cadmium is based upon the adsorption of cadmium ions and its ammine complex ions on the negatively-charged surface of ferric hydroxide, 2) the adsorption of ammine complex ions is less than that of simple ions, and 3) the cations which exist in the ammoniacal solution behave as hold-back carriers for carrier-free cadmium because of their occupation of the adsorption surface.

The author wishes to express his thanks to Dr. Haruo Natsume for his encouragement of this work and also to Mr. Tadashi Sato for experimental assistance.

Department of Chemistry
Japan Atomic Energy Research Institute
Tokai, Ibaraki

Stability Order in Metal Chelate Compounds. III.[1] *4-Nitro- and 4-Chlorocatechol Complexes**

By Yukito MURAKAMI and Masasuke TOKUNAGA

(Received May 25, 1964)

In view of the relatively high stabilities of the zinc(II) chelates of the catechol derivatives,[2] it was decided to investigate the interaction of bivalent transition metal ions with other catechol derivatives. The ligands employed in the present work are 4-nitro- and 4-chlorocatechol. Since both the nitro and the chloro group, as well as the sulfonate and carboxylate groups, are known to act as electron-withdrawing substituents, the extent of the effects of these substituents on the chelate stability and on the dissociation of catechol protons is estimated.

Experimental

The preparation of metal solutions, and the apparatus and procedures for potentiometric titration, have been mentioned elsewhere.[2,3]

4-Nitrocatechol.[4] — Into a mixture of catechol and sodium nitrite dissolved in water was added 2.5 M sulfuric acid at 0°C with stirring. After the addition of sulfuric acid had been completed, the reaction mixture was treated with ether; the product was recovered from the ether extract. The yellow needle-like crystals were recrystallized from benzene and purified further by vacuum sublimation at 1 mmHg and 130~140°C; m. p.: found, 176~177°C; reported,[4] 172~174°C.

Found: C, 46.40; H, 3.15; N, 9.20. Calcd. for $C_6H_5O_4N$: C, 46.46; H, 3.25; N, 9.03%.

4-Chlorocatechol.[5]—Sulfuryl chloride was added gradually to an ether solution of catechol at nearly 0°C. The reaction mixture was stirred for approximately one hour at 0°C, and then the crude material was recovered as ether was removed from the solution under reduced pressure. This material was recrystallized from benzene as white crystals; m. p.: found, 87.2~88.2°C; reported,[6] 88°C.

Found: C, 50.03; H, 3.47. Calcd. for $C_6H_5O_2Cl$: C, 49.85; H, 3.49%.

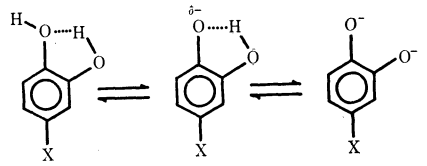
Results and Discussion

Acid Dissociation Constants.—The dissociating catechol protons of both 4-nitro- and 4-chlorocatechol were found to behave in a manner similar to those of catechol derivatives reported previously.[2] The acid dissociation constants of the present catechols are summarized in Table I. It is obvious that the

TABLE I. ACID DISSOCIATION CONSTANTS OF THE CATECHOLS
30±0.1°C, μ=0.10 M (KNO_3)

Ligand	pK_{H_2L}	pK_{HL}
4-Nitrocatechol	6.59	10.75
4-Chlorocatechol	8.43	11.54

nitro group situated at the 4-position has a profound electron-withdrawing effect on the dissociation of catechol protons, thus lowering both pK_{H_2L} and pK_{HL} values. Therefore, the dissociation of the protons of 4-nitrocatechol must take an alternative process to that assumed for the 4-sulfo and 4-carboxy derivatives,[2] as is shown in Chart 1. Meanwhile, since the chloro group exerts a greater electron-withdrawing effect at its meta position than at the para, 4-chlorocatechol must undergo the same dissociation as the nitro derivative.



X=NO_2, Cl

Chart 1. Dissociation process of catechol-protons.

Chelate Stability Constants. — The stability constants for the bivalent metal chelate compounds with the two catechol derivatives of the present study are summarized in Table II. Among the metal chelates of catechol derivatives studied in these laboratories, the following stability order with respect to a ligand was established:

* Contribution No. 66 from the Department of Organic Synthesis, Faculty of Engineering, Kyushu University.

1) Part II: Y. Murakami and M. Takagi, This Bulletin, **37**, 268 (1964).

2) Y. Murakami, K. Nakamura and M. Tokunaga, ibid., **36**, 669 (1963).

3) Y. Murakami, ibid., **35**, 52 (1962).

4) D. H. Rosenblatt, J. Epstein and M. Levitch, *J. Am. Chem. Soc.*, **75**, 3277 (1953).

5) R. Willstätter and H. E. Müller, *Ber.*, **44**, 2182 (1911).

6) J. Frejka, B. Šefránek and J. Zika, *Collection Czechoslov. Chem. Commun.*, **9**, 238 (1937).

Table II. Stability constants of the bivalent metal chelates of catechol derivatives

$30\pm0.1°C$, $\mu=0.10$ M (KNO_3)

Ligand	4-Nitrocatechol			4-Chlorocatechol		
	$\log K_1$	$\log K_2$	$\log K_3$	$\log K_1$	$\log K_2$	$\log K_3$
Zn(II)	8.20	6.80		8.63	6.82	
Cu(II)	11.65	9.28		12.56	9.83	
Ni(II)	7.82	5.27	3.81	7.90	5.00	4.16
Co(II)	7.48	5.31	3.14	7.64	6.37	4.23
Mn(II)	6.51	4.74		6.82	4.66	

4-nitrocatechol<catechol<4-chlorocatechol~4-carboxycatechol<4-sulfocatechol<Tiron.

There has been found no systematic relationship between the ligand basicity and the chelate stability, partly because of the difference between the dissociation process of the present ligands and that previously reported.[2] It is interesting to note that the 4-nitrocatechol chelates show relatively large stability constants for the lower basicity of the ligand. This is presumably due in part to the resonance contribution of the nitro group to the stabilization of the chelate ring.

The stability order among the transition metals treated in this work was found to be the same as that previously reported;[2] it follows the sequence:

manganese(II)<cobalt(II)~nickel(II)<zinc(II)<copper(II).

Department of Organic Synthesis
Faculty of Engineering
Kyushu University
Hakozaki, Fukuoka

SHORT COMMUNICATION

*The Mechanism of the Photochromism and Thermochromism of 2, 2', 4, 4', 5, 5'-Hexaphenyl-1, 1'-biimidazolyl**

By Taro HAYASHI, Koko MAEDA and Midori MORINAGA

(Received August 4, 1964)

We previously found[1,2] that 2, 2', 4, 4', 5, 5'-hexaphenyl-1, 1'-biimidazolyl (I) ($C_{42}H_{30}N_4$, fine pale yellow prisms, m. p. 199~201°C (decomp.)) and its various substitution compounds exhibited photochromism and thermochromism in both a solution and a solid state. A pale yellow benzene solution of I showed an absorption maximum at 280 mμ (ε=28500) at 15°C, while the solution which turned reddish purple upon irradiation with sunlight at 15°C or upon heating on a water bath in the dark showed new absorption maxima at 347 mμ (ε=1100), 520 mμ (shoulder) and 554 mμ (ε=190) with a decrease in the absorbance of 280 mμ and was found to exhibit an electron spin resonance (g value: 2.003). When the solution irradiated was immediately placed in a dark room, the absorbance of 347 mμ and 554 mμ gradually decreased with the recovery of the absorbance of 280 mμ, an isosbestic point being shown at 309 mμ, and a decrease in the electron spin resonance was also found.

In a benzene solution of I (C=1.49×10^{-5} mol./l.) the absorbance of 347 mμ was measured in the dark at 19.0, 36.1, 45.5 and 50.5°C in order to measure the absorbance due only to thermochromism, A_1. In the same solution when irradiated for 3 min. with a mercury vapor lamp at the temperatures mentioned above, a decrease in the absorbance of 347 mμ, A_2, due both to photochromism and thermochromism with time, was measured beginning immediately after irradiation at the temperatures mentioned above. When the difference between A_2 and A_1 of the same temperature, which was the decrease in the absorbance due

* Presented at the 16th Annual Meeting of the Chemical Society of Japan, Tokyo, April, 1963.

1) T. Hayashi and K. Maeda, This Bulletin, 33, 566 (1960).

2) T. Hayashi, K. Maeda, S. Shida and K. Nakada, *J. Chem. Phys.*, 32, 1568 (1960); T. Hayashi and K. Maeda, This Bulletin, 35, 2057 (1962).

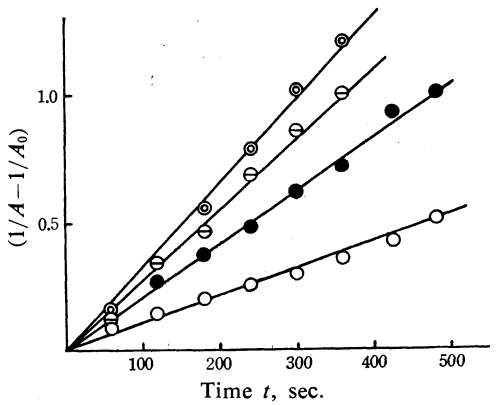
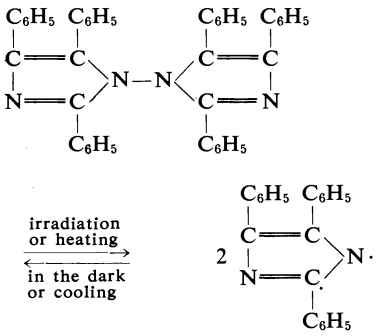


Fig. 1. The rate of the decrease of the absorbance A of 347 mμ in a solution ($C=1.49\times10^{-5}$ mol./l.) of hexaphenylbiimidazolyl.
$A_0 : A$ at $t=0$
—◎— 50.5°C —⊖— 45.5°C
—●— 36.1°C —○— 19.0°C

only to photochromism, A, was calculated, the reciprocal of A was found to decrease linearly with time, as is shown in Fig. 1. The linearity shows that the reaction which causes absorbance A to decrease obeys the rate law for a second-order reaction, since the absorbance of 347 mμ was confirmed to obey Beer's law in a benzene solution of a concentration lower than about 10^{-5} mol./l. at 15°C. This finding suggests that this reaction is a recombination of 2, 4, 5-triphenylimidazolyl radicals formed by the homolytic dissociation of I and that the mechanisms of the photochromism and thermochromism of hexaphenyl-biimidazolyl (I) may be represented by the following equation:



This mechanism was supported by the determination of the molecular weight in a benzene solution ($C=0.0124$ mol./l.) with a macro-cryoscopic method carried out in a dark room, which showed a decrease in molecular weight from 600 to 440 with irradiation. From the rate constants which were obtained from the measurements shown in Fig. 1, the activation energy for the recombination of 2, 4, 5-triphenylimidazolyl radicals was determined to be 7.3 kcal./mol. The equilibrium constants for the thermal homolytic dissociation of I were estimated to be approximately 3.1×10^{-4} (49.0°C), 4.7×10^{-4} (53.8°C) and 1.1×10^{-3} (60.4°C) from the absorbance of 554 mμ due to thermochromism by the mass action law and Beer's law and from the equilibrium constants, ΔH for this reaction was estimated to be about 23 kcal./mol.

Department of Chemistry
Faculty of Science
Ochanomizu University
Bunkyo-ku, Tokyo

Infinite Circular Gas Chromatographic Columns[1]

By Samuel SIDEMAN

(Received February 1, 1964)

The use of infinite circular columns in gas chromatography has been proposed by Martin[2] in his address, "Past, Present and Future of Gas Chromatography," before the first International Symposium on Gas Chromatography (ISA). He suggested that "if you have two columns and two substances that are very difficult to separate, you can arrange to drive the pair of substances into the first column and then, when it gets near one end, you connect it to the other column and you continue blowing until it's gone right into the second column, monitoring its passage with an extremely small detector, probably a katharometer in this case. When it is safely in the second column, you disconnect the first column and start blowing in the end of the second column and carry on until it's started into the first one again. And so you go on, round and round and round."

Porter and Johnson[3,4] utilized a circular column to obtain data for extractive distillation. Using a pump to circulate the gas into the column, they were thus able to use volatile liquids as partitioning solvents.

The search for a chromatographic column suitable for the separation of components with very small separation factors, such as nitrogen isotopes, has been going on in these laboratories for the last few years. Some of the very long columns used exhibited extremely high retention times (up to nine hours in some cases). Appreciable pressure drops were required, and a rapid decrease in the efficiency of the column occurred because of the evaporation of the liquid phase.

As these difficulties are obviously absent in circular infinite columns, it was of interest to study other characteristics of such systems. The effect of column length, i.e., the number of cycles, on the width of the peaks was examined, both by theory and experiment, and the feasibility of utilizing this technique for the separation of components was investigated.

1) Part of this work was presented at the 29th Meeting of the Israel Chemical Society: S. Sideman, *Bull. Res. Coun. Israel*, **10A**, No. 3, 20 (1961).
2) A. J. P. Martin, "Gas Ghromatography," 1957, Coates et al. Eds., Acad. Press, New York (1959), p. 243.
3) R. S. Porter and J. F. Johnson, *Nature*, **183**, 391 (1959).
4) R. S. Porter and J. F. Johnson, *Ind. Eng. Chem.*, **52**, 691 (1950).

Apparatus

Two mechanisms for circulating the sample gas in the column were compared.

A) An Infinite Column with Externally-supplied Carrier Gas.—Figure 1 illustrates the system used. Two short columns, with a thermal conductivity cell (T. C. C.) at each end, were connected head to tail. Two pairs of electrically-operated valves were used to direct the flow in a closed circuit. One of the valves of each pair was connected to the carrier gas cylinder, while the other vented to the atmosphere. Once the sample reached the end of one column, a signal from the T. C. C. energized one pair of valves and simultaneously de-energized the other pair. The sample was thus directed into the second half of the circuit, and vice versa. A delay-relay unit (Fig. 2) was incorporated in the system to ensure the delayed operation of the valves. This was achieved by deactivating a triggering micro-switch set in the recorder for the time

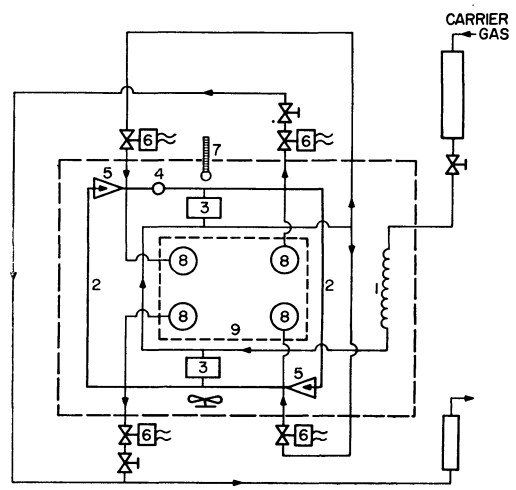


Fig. 1. Schematic diagram of an infinite circular gas chromatographic column of the "two half cycles" type.
1 : Preheating coil 2 : Chromatographic column 3 : T. C. C. 4 : Sample injection block 5 : Check valve 6 : Solenoid valve 7 : Thermometer 8 : Pressure gauge 9 : Pressure gauge panel

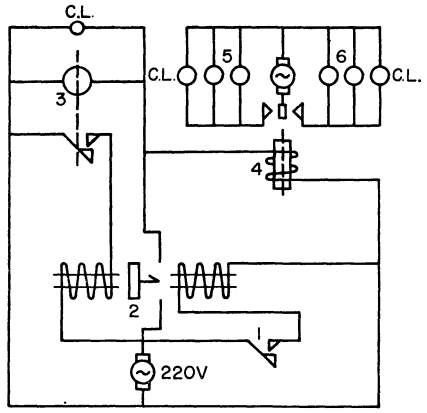


Fig. 2. Wiring diagram of delay-relay unit and operating valves.
1 : Triggering microswitch (in recorder) 2 : Mechanical latch-relay 3 : Electric timer (motor) 4 : Electromagnet affecting the changing of the solenoid valves 5 : Solenoid valves of first half cycle 6 : Solenoid valves of second half cycle C. L.: Control lamp

needed for the sample to pass through the T. C. C. By this arrangement the leading peak in each half-cycle entering the T. C. C. triggered the micro-switch, which in turn alternated the electric valves.

Some experiments were conducted with one T. C. C. only. In this arrangement the two half-columns were so connected that the reference and sample sides of the T. C. C. alternated for each half cycle. The base line drift

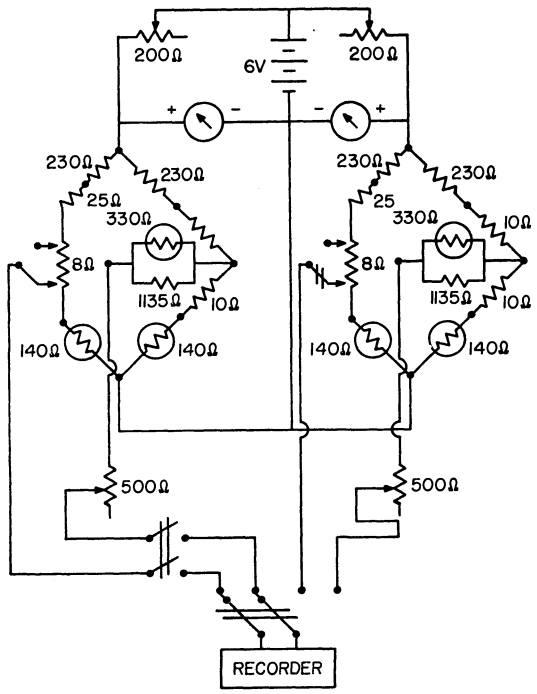


Fig. 3. Wiring diagram of the two T. C. C.s.

caused by peak broadening discouraged further work with this arrangement; therefore, two T. C. C.s were connected, one at the end of each half-circuit. Figure 3 illustrates the wiring of the two T. C. C.s.

B) An Infinite Column with Gas Circulation Pump.—The arrangement of the apparatus is illustrated in Fig. 4. Except for a short length of unpacked tubing which passed through the squeeze pump (a Sigmamotor type), the column and the T. C. C. were housed in an air-thermostat. The plastic tubing used was coated with polyvinyl alcohol to prevent losses of the compound tested by diffusion through the wall. A rotameter was used to calibrate the gas flow

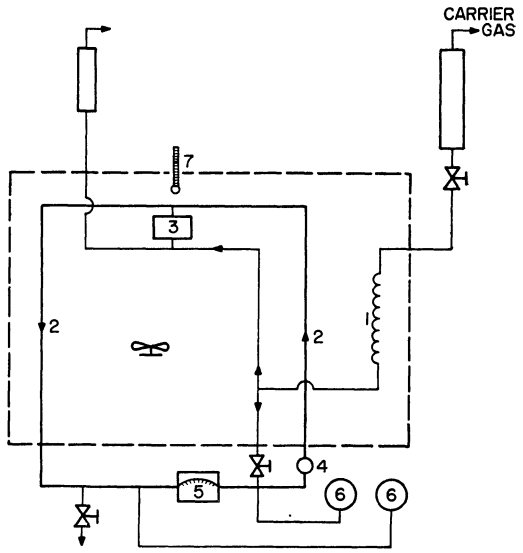


Fig. 4. Schematic diagram of an infinite circular gas chromatographic column of the "pump" type.
1 : Preheater coil 2 : Chromatographic column 3 : Thermal conductivity cell 4 : Sample injection block 5 : Squeeze pump 6 : Pressure gauge 7 : Thermometer

through the column. Pressure gauges across the pump provided pressure drop measurements. These were connected to the column through copper capillaries, thus ensuring a minimum voidage in the column. The rotameter was taken out of the system after the desired flow rate had been fixed. Variations in the flow caused by the removal of the rotameter were sufficiently small to be disregarded. By opening two needle valves (at the inlet and outlet of the pump), the apparatus could be used as a standard gas chromatograph.

Advantages and Disadvantages of the Above Mechanisms

The obvious advantage of the "half-cycle," method A, over the "pump" method, B, is

that there is no risk of mixing the sample, since it does not require an external pump and since it can be constructed with a minimum dead volume. The disadvantages, however, are discouraging. An elaborate apparatus is needed, and the control mechanism is rather complicated. A base line shift occurs when the valves are alternated at each half-cycle, and this has to be corrected for either manually or automatically. Moreover, pressure waves due to sudden pressure variation at each half-cycle cause the sample to contract in the gas-phase only, thus disturbing the equilibrium and broadening the peak. Under these conditions, no efficient separation seems feasible.

The main advantage of the pump technique is its simplicity. It is easy to operate at various absolute pressures. The main disadvantage is, of course, the mixing of the sample as it passes through the pump, which may result in undesired peak broadening.

The Effect of the Number of Cycles on Peak Width

Theoretical. — Under ideal conditions gas chromatographic peaks closely approach the normal distribution curve; i. e., the curve approaches the base-line (or zero concentration line) asymptotically. Thus, theoretically, the width of the peak is infinite. In practice, the width is measured at some convenient place. The common procedure is to measure the width between the intercepts of the tangents to the peak passing through the inflection points at the base-line. The width thus obtained is equal to 4σ, where σ is the standard deviation.

For the usual case where the volume of the sample S is negligible ($0.5 > S/v\sqrt{n}$), the width of the peak, W, has been shown (Van Deemter et al.[5]) to be:

$$W = 4v\sqrt{n} \qquad (1)$$

where v is the volume of one theoretical stage and n is the number of theoretical plates in the column. The retention volume, V_r, has also been shown to be:

$$V_r = vn \qquad (2)$$

The combination of these two equations enables us to determine the theoretical number of stages by the well-known relation:

$$n = 16(V_r/W)^2$$

where both W and V_r are measured in the same units (volume, time or length).

Assuming that the number of stages in the column is directly proportional to the length of the column, Eq. 1 can be written:

$$W = K'\sqrt{NL + L'} \quad \text{or:} \quad W^2 = K(NL + L') \qquad (3)$$

where K is a proportionality constant, N is the number of cycles (starting from the T. C. C.), L is the length of the column, and L' is the length of the fragment of the column from the injection block to the T. C. C. When the apparatus is so constructed that $L' = 0$

$$W^2 = KNL \qquad (3a)$$

or, when $L' = 1/2L$

$$W^2 = KL(N + 1/2) \qquad (3b)$$

Equation 3 indicates that the higher the number of cycles, the wider the peak becomes.

The assumption of the linear proportionality of n and L can be experimentally verified for non-overlapping peaks. Let subscript i represent the number of the consecutive peaks. Then, from Eq. 1, the ratio of the widths of two consecutive peaks is:

$$\frac{W_{i+1}}{W_i} = \frac{\sqrt{n_{i+1}}}{\sqrt{n_i}} = \frac{\sqrt{L_{i+1}}}{\sqrt{L_i}} \qquad (4)$$

Now, if L is expressed in half-cycles, i. e., $L_1 = (1/2)L(=L')$, $L_2 = (3/2)L$, $L_3 = (5/2)L$, etc., substitution in Eq. 4 gives:

$$\frac{W_{i+1}}{W_i} = \sqrt{\frac{2i+1}{2i-1}} \qquad (4a)$$

which is the theoretical value of the ratio of the widths of two consecutive peaks.

Experimental.—An example of the chromatograms obtained using the first mechanism is given in Fig. 5. No attempt was made to draw quantitative conclusions from these experiments.

Figure 6 shows a chromatogram obtained using the pump technique with a sample of ethyl methyl ketone. The column was 8 m. long, was packed with polyethylene powder, 50~70 mesh, which was coated with 15% glycerol. A polyethylene packing was chosen for this work because of its low pressure-drop characteristics. The column was flushed for about two hours with carrier gas before each

Table I. The relationship between consecutive peaks

Peak No.	Width W, mm.	Retention volume V_r, mm.	W_{i+1}/W_i Exp.	W_{i+1}/W_i Theor.
1	27	56	1	1
2	47.6	150	1.76	1.73
3	58.6	243.5	1.23	1.29
(4)	69*	337	1.18	1.18
(5)	84*	431		1.13

* Uncertain values due to a base-line shift upwards.

5) Van Deemter et al., *Chem. Eng. Sci.*, 5, 271 (1956).

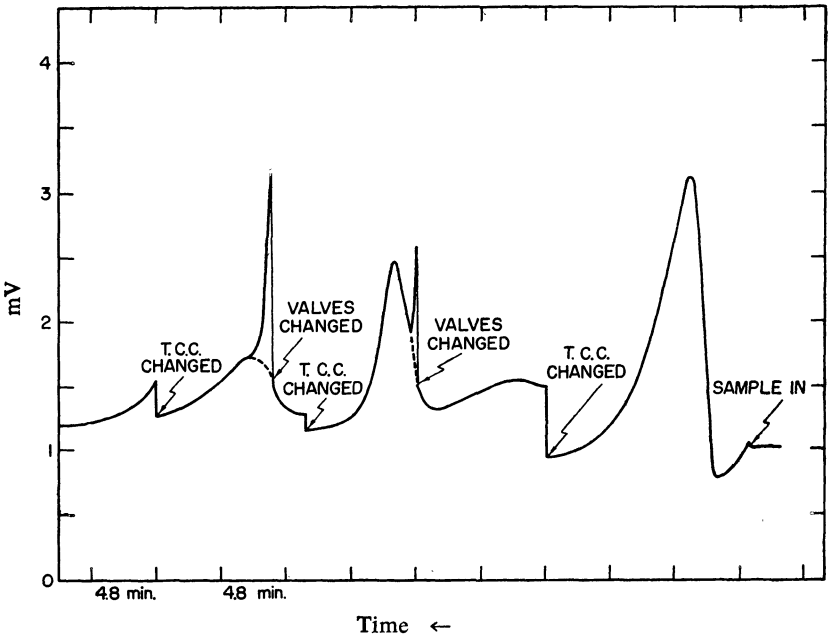


Fig. 5. Chromatograms obtained with the "two half cycles" type of column. Ether, 41°C, nitrogen gas, 55 cc./min.

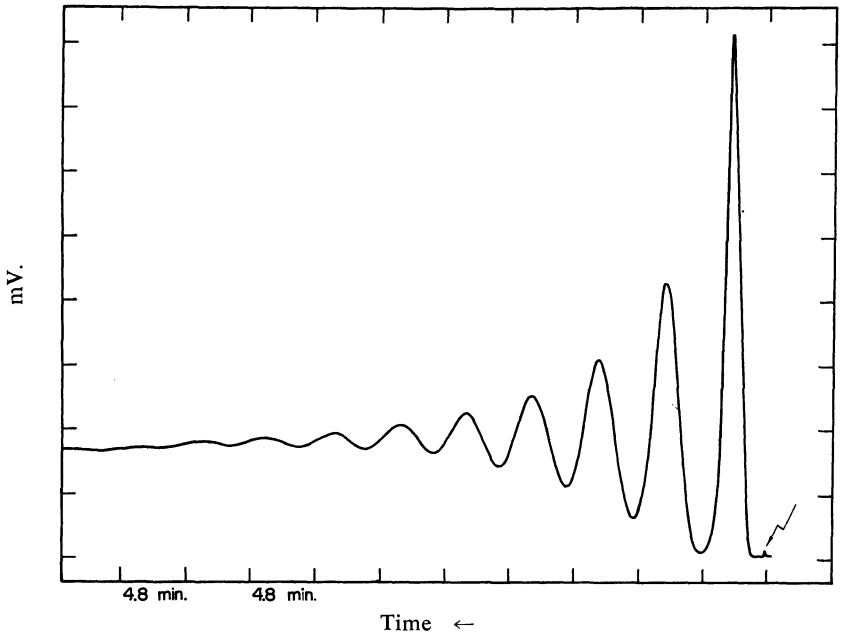


Fig. 6. Chromatograms obtained in a circular column of the "pump" type. Sample: M.E.K. Column: Polyethylene powder 50~70 mesh, 15% glycerol, 45°C

run to remove traces of material left over from previous experiments.

A set of measurements from an experimental run with a sample of *n*-heptane is given in Table I. Only the first three peaks could be measured with a fair degree of reliability. Once the peaks met head to tail, the base-line shifted upwards; consequently, accurate measurement was not possible.

Figure 7 was drawn according to Eq. 3b and shows good agreement between experiment and theory. Agreement is also evident in Fig. 8,

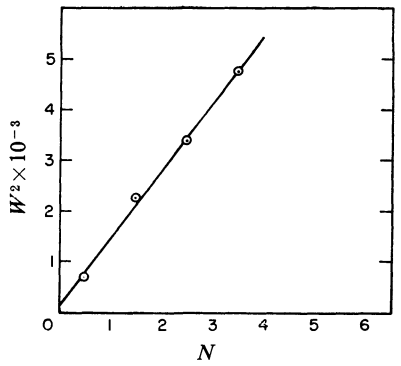


Fig. 7. Relationship between peak width (measured at zero base line) and number of cycles.

$$W^2=KL(N+1/2)$$

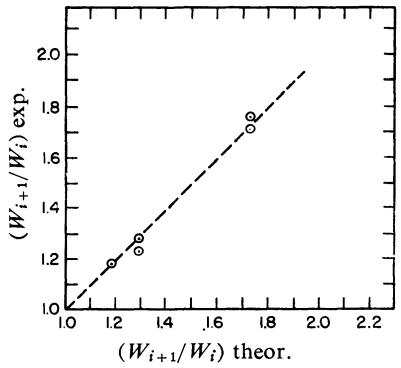


Fig. 8. Theoretical vs. experimental peak width ratio of consecutive peaks.
Sample gas : *n*-Heptane, 45°C

which shows the experimental versus theoretical width ratio of the consecutive peaks given in Table I.

Discussion and Conclusions

The characteristics and performance of infinite circular columns in gas chromatography have been studied. Two mechanisms for gas circulation in the column have been experimentally compared. The half-cycle-type mechanism proved to be rather unsuccessful because of intermittent pressure drops inherent in this mode of operation. The pump mechanism was found easy to operate and was used for most of the experimental work conducted. The separate effect of mixing due to pump action is yet to be studied. The theoretical relationship of the width to the number of cycles has been experimentally verified.

The results obtained in this study discourage the use of low-efficiency columns, with about 100 theoretical plates, for separation purposes. This is in agreement with our previous report[6] that separation is feasible only with high-efficiency columns, where the width of the peak is less than a half, and preferably a quarter, of the retention volume of the first peak. With the low-pressure, low-efficiency polyethylene column used in this work, head and tail mixing of the consecutive peaks occurred and no separation was feasible. Other packed columns with a higher number of theoretical plates could not be used with the given pump mechanism because of the higher pressure drops required. Nevertheless, the reported pump mechanism, though presently limited only to low-pressure, low-efficiency columns, may be used for some particular applications, where the following advantages may be utilized:

(1) The use of short circular columns instead of the usual long columns eliminates the high pressure differential between inlet and outlet.

(2) Absolute retention times can be read directly, with no need for dead volume corrections, sometimes even without pressure corrections.

(3) Volatile solvents can be used as column coating with practically no aging of the column.

(4) Uniform coating can be made in situ.

(5) The behaviour of ternary systems can be easily studied, and separation factors applicable to extractive distillation can be evaluated.

Thanks are due to Mr. B. Gal-Or for his co-operation in this work and to Messrs. Z. Chouri, J. Margalit, M. Marton, E. Kutzinsky and G. Hirsh, senior students in the Department of Chemical Engineering, Technion-Israel Institute of Technology, for carrying out part of the experimental work.

Department of Chemical Engineering
Technion-Israel Institute of Technology
Haifa, Israel

6) S. Sideman, *Chem. Eng. Sci.*, 18, 95 (1963).

A Study of the Hydration of Calcium Orthoplumbate. III. The Behavior of Dehydration

By Masumi KOISHI

(Received March 7, 1964)

The following facts have been observed regarding the process and products of the hydration of calcium orthoplumbate at various temperatures in an atmosphere of nitrogen-water vapor:[1] i) In the hydration process, the mole ratio of CaO/PbO_2 in calcium orthoplumbate decreased linearly, while that of H_2O/CaO decreased step-by-step, with the increase in temperature. ii) The powder which appeared in the hydration process changed color parallel with the inversion rate of the anhydrous compound. iii) The composition and nature of completely-hydrated products at various temperatures were examined by X-ray diffraction analysis, thermobalance analysis, chemical analysis, differential thermal analysis, infrared absorption spectrum and electron microscopy. The results of all the methods showed good agreement.

In this paper, the dehydration of calcium orthoplumbate hydrates will be examined by a differential thermal analysis pattern, and the information thus obtained will be used for analyzing the dehydration behavior of the crystalline water and negative catalytic effects of calcium hydroxide. The results of present experiment will support the conclusion of the previous paper. The reaction order (n) and the frequency factor (A) of the dehydration stage will also be discussed.

Theoretical

The Determination of the Activation Energy (E) and the Frequency Factor (A). — The activation energy (E) was obtained from the variation in the peak temperature with the rate of heating.[2] Kissinger derived the following equation from the theoretical consideration:

$$\frac{d(\ln \phi/T_m^2)}{d(1/T_m)} = -\frac{E}{R} \qquad (1)$$

where ϕ(°C/min.) denotes the rate of heating; T_m (°K), the temperature of maximum deflection; R, the gas constant, and E, the activation energy. The variation in the peak temperature with the rate of heating is governed only by the activation energy. The plot of $-R\cdot\ln \phi/T_m^2$ vs. $1/T_m$ should give a straight line; the slope of this line will be E according to Eq. 1.

The reaction order (n) and the frequency factor (A) are calculated from Eqs. 2 and 3:

$$n(1-x)_m^{n-1} = 1 + (n-1)\cdot 2RT_m/E \qquad (2)$$

$$E\phi/RT_m^2 = A\cdot n(1-x)_m^{n-1}\cdot e^{-E/RT_m} \qquad (3)$$

where $(1-x)_m$ denotes the amount of material left unreacted and n, the empirical order of reaction.

The Estimation of the Reaction Order from the Peak Shape.—Kissinger proposed a "shape index (S)" to obtain the reaction order. When S is plotted against n^2, the points fall roughly on a straight line defined by

$$S = 0.63\cdot n^2 \qquad (4)$$

This expression was used to estimate the reaction order of the dehydration reaction from the differential thermal analysis data.

Experimental Procedure

Material.—*Calcium Orthoplumbate Hydrate-Calcium Hydroxide Mixtures.*—The mixture applied in this experiment was prepared by hydrating calcium orthoplumbate. The process of hydration was carried out at 30, 50, 80 and 100°C in an atmosphere of nitrogen-water vapor. The ratio of H_2O/Ca_2PbO_4 was 10 in the process. Hydration finished after 390 min. Hydrated mixtures were identified by X-ray diffraction patterns, differential thermal analysis curves, thermobalance, and chemical measurements.

Calcium Orthoplumbate Hydrate. — The Franke method[3] was applied in order to remove calcium hydroxide from hydrated mixtures. The Franke method (or the acetoacetic ester method) for the extraction of free calcium hydroxide in calcium orthoplumbate hydrate-calcium hydroxide mixtures gave good results.

The general formula $(2-N)CaO\cdot PbO_2\cdot mH_2O + N\cdot Ca(OH)_2$ was assigned to the completely-hydrated mixture in the preceding paper.[1]

The samples employed for thermal analysis are

1) This paper was presented at the Autumn Meeting of the Japan Society of Color Material, Tokyo, 1960; *J. Chem. Soc. Japan, Ind. Chem. Sec.* (*Kogyo Kagaku Zasshi*), **67**, (1964), in press.

2) H. E. Kissinger, *J. Research Natl. Bur. Standards*, **57**, 217 (1956); *Anal. Chem.*, **29**, 1702 (1957).

3) E. E. Pressler, S. Brunauer and D. L. Kantro, *Anal. Chem.*, **28**, 897 (1956).

TABLE I. MATERIALS USED FOR DIFFERENTIAL THERMAL ANALYSIS

Material	Composition: Hydrate $(2-N)$	Composition: Hydrate m	Composition: Free $Ca(OH)_2$ N	Condition of reaction: Temp. °C	Condition of reaction: Time min.
A	1.5	3.0	0.5	50	390
B	1.2	1.8	0.8	80	390
C	1.0	1.0	1.0	100	390
D	1.5	3.0	—	50	390
E	1.2	1.8	—	80	390
F	1.0	1.0	—	100	390
G	$Ca(OH)_2$: Extra pure reagent				
H	$Mg(OH)_2$: Extra pure reagent				

Formula: $(2-N)CaO \cdot PbO_2 \cdot mH_2O + NCa(OH)_2$

listed in Table I. Samples A, B and C were calcium orthoplumbate hydrate - calcium hydroxide mixtures. D, E and F were calcium orthoplumbate hydrate. Two chemical reagents, calcium hydroxide, and magnesium hydroxide, were employed as reference samples.

Apparatus and Procedure. — The apparatus of differential thermal analysis employed in this work consists of an analytical furnace, a transformer, and recording equipment. Specimen holders made of pure nickel have a diameter of 1/4 inch and a length of 1/2 inch.

A chromel-alumel thermocouple was used. The reference material was α-aluminum oxide. Each of the eight samples was run in differential thermal analysis at the rate of 3, 4, 5, 7, 9, 10 and 13°C per min. to determine the variation in the peak temperature with the rate of heating. The samples were ground to pass through a 250-mesh sieve. Specimen holders were filled loosely with 500 mg. of the sample, and a gentle tapping was carried out. The standard deviation of a single measurement was within 2.5°C. The thermobalance apparatus employed in this work was the same as that described in the preceding paper.[1] The loss in weight was recorded continuously as the furnace temperature increased. About 1 g. of the sample was used for each determination.

Results and Discussion

The loss in weight accompanying the heat treatment of calcium orthoplumbate hydrate and calcium orthoplumbate hydrate - calcium hydroxide mixtures in the thermobalance measurement is given in Figs. 1 and 2 respectively.

It is apparent from Figs. 1 and 2 that the dehydration of samples D, E and F proceeds in one stage, and that of A, B and C, in three

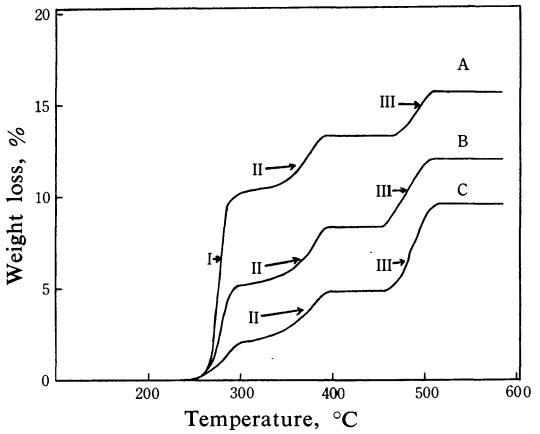


Fig. 1. Thermobalance results for calcium orthoplumbate hydrate - calcium hydroxide mixtures.

TABLE II. DATA OF DIFFERENTIAL THERMAL ANALYSIS MEASUREMENTS

Heating rate ϕ	Peak temp. (T_m, °C): A I	A II	A III	B I	B II	B III	C I	C II	C III	D	E	F	G	H	Ia
3	322	—	534	316	402	—	318	405	—	303	306	306	540	411	461
4	333	—	—	324	—	543	—	410	—	317	320	—	553	—	469
5	—	—	—	336	414	—	337	416	552	—	—	332	—	431	484
7	353	—	565	—	421	—	346	422	—	348	350	352	578	443	494
9	365	—	—	—	447	578	—	427	—	361	363	362	587	454	505
10	368	—	—	360	429	—	359	—	580	—	370	370	—	—	—
13	—	—	—	370	—	—	370	—	590	382	—	—	602	465	—
ϕ	Shape index (S)														
3	0.73	—	0.27	0.71	0.59	—	0.80	0.54	—	0.48	0.58	0.67	0.28	0.67	0.12
4	0.76	—	—	0.80	—	0.28	—	0.59	—	0.49	0.57	—	0.22	—	0.11
5	—	—	—	0.74	0.51	—	0.73	0.53	0.26	—	—	0.66	—	0.61	0.13
7	0.76	—	0.28	—	0.54	—	0.75	0.50	—	0.49	0.60	0.74	0.28	0.65	0.16
9	0.71	—	—	—	0.50	0.28	—	0.54	—	0.58	0.58	0.75	0.29	0.63	0.19
10	0.81	—	—	0.77	0.54	—	0.76	—	0.27	—	0.60	0.71	—	—	—
13	—	—	—	0.76	—	—	0.74	—	0.28	0.48	—	—	0.28	0.63	—

Ia; ϕ=3, 4, 5, 6, 10, 12.5

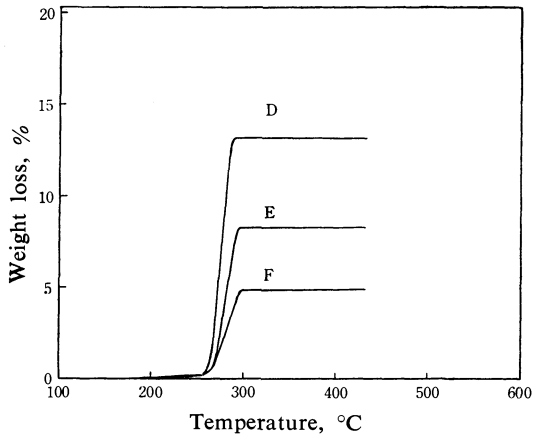


Fig. 2. Thermobalance results for calcium orthoplumbate hydrate.

stages. Stages I and II in Fig. 1 seem to show the first and second stage of the dehydration respectively; III may show the decomposition of calcium hydroxide.

The results of the differential thermal analysis experiments with samples A—H are listed in Table II. In the case of samples A, B and C the dehydration proceeded in two steps in the range of 316～370°C and 402～430°C when the rate of heating was varied from 3°C per min. to 13°C per min. On the other hand, in the case of the extracted hydrate (D, E and F), the dehydration proceeded in one step. The dehydration temperature was 303～382°C.

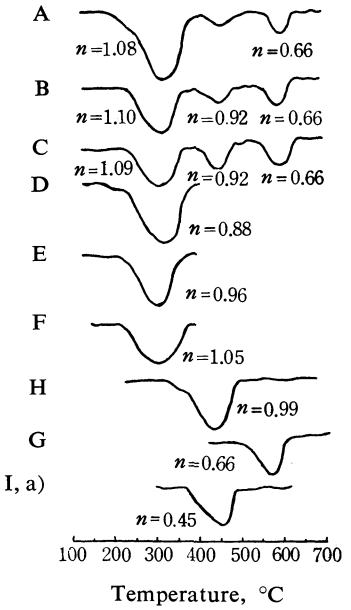


Fig. 3. Typical differential thermal analysis curves for the samples used in the present study.

It may be concluded from the comparison of the results of the thermobalance with those of the differential thermal analysis that the dehydration of the two-stage mechanism starts at a slightly higher temperature and proceeds over a wider range than does the one-stage dehydration.

This conclusion seems to show that the dehydration of the hydrated mixture is partially retarded by the presence of liberated calcium hydroxide. This negative catalytic

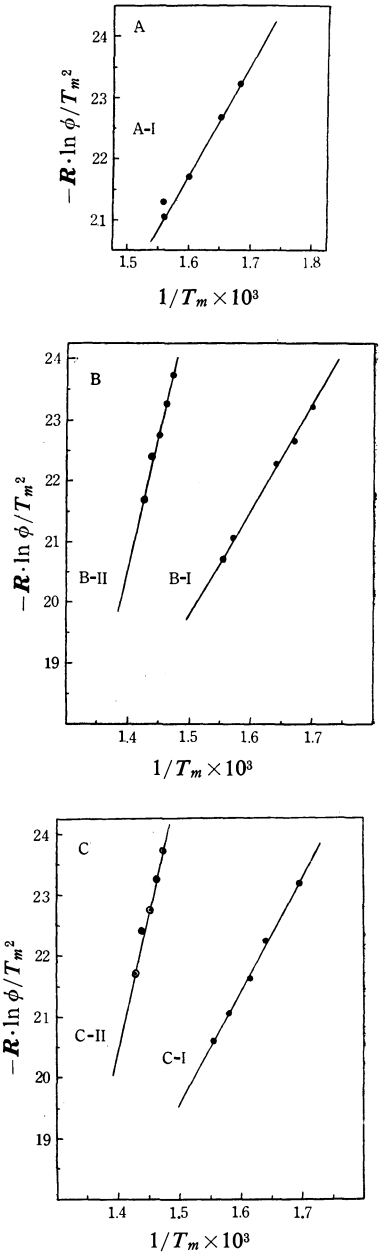


Fig. 4. Differential thermal analysis data obtained for samples A, B and C.

action of calcium hydroxide can reasonably be explained by the results of the reaction order (n) and the activation energy (E).

The shape of the endothermic peak associated with the thermal decomposition of these samples is depicted in Fig. 3. The corresponding values of n obtained from Eq. 4 are also given there. Each differential thermal analysis datum in Table II gives a straight line of $-R\cdot\ln\phi/T_m^2$ vs. $1/T_m$, thus enabling us to calculate the activation energy (E). The case of A is shown in Fig. 4 as an example. The values of n, A and E obtained are given in Table III.

TABLE III. KINETIC RESULTS BY DIFFERENTIAL THERMAL ANALYSIS METHODS

Material		n	ln A	E, kcal./mol.
A	I*	1.08	12.85	18.2
	II**	—	—	—
	III***	0.66	18.05	33.0
B	I	1.10	12.86	18.0
	II	0.92	27.62	41.0
	III	0.66	18.05	33.0
C	I	1.09	12.82	18.0
	II	0.92	29.94	43.0
	III	0.66	18.05	33.0
D		0.88	7.15	11.5
E		0.96	7.11	11.5
F		1.05	7.57	12.1
G		0.66	16.02	30.7
H		0.99	15.84	25.0
I	a)	0.55 to 0.44	15.18	31.4
	b)	0.69	13.26	27.2

* First dehydration step.
** Second dehydration step.
*** Liberated calcium hydroxide.
a) Kissinger's data by DTA method for Brucite.
b) Kissinger's data by isothermal weight-loss measurements for Brucite.

Gregg and Razouk reported that the reaction order of Brucite $Mg(OH)_2$ was 0.66 and the activation energy, 27.6 kcal. per mole. Kissinger[2] obtained the reaction order of 0.55~0.44 and the activation energy of 31.4 kcal. per mole from his differential thermal analysis, and the reaction order of 0.69 and the activation energy of 27.2 kcal. per mole, from the results of the isothermal reaction rate for the same compound. The value of the reaction order of magnesium hydroxide (0.99) reported in this paper (Table III) differs from those reported by Kissinger and by Gregg and Razouk, but the activation energy of 25.0 kcal. per mole is similar to their values in order of magnitude.

The values of the reaction order derived from the differential thermal analysis are nearly equal to unity in the cases of samples A, B and C. While the activation energies of the first dehydration were found to be 18.2, 18.0, and 18.0 kcal. per mole, those of the second dehydration were from 41.0 to 43 kcal. per mole. The second dehydration of sample A was not obtained exactly. The activation energies for D, E and F were

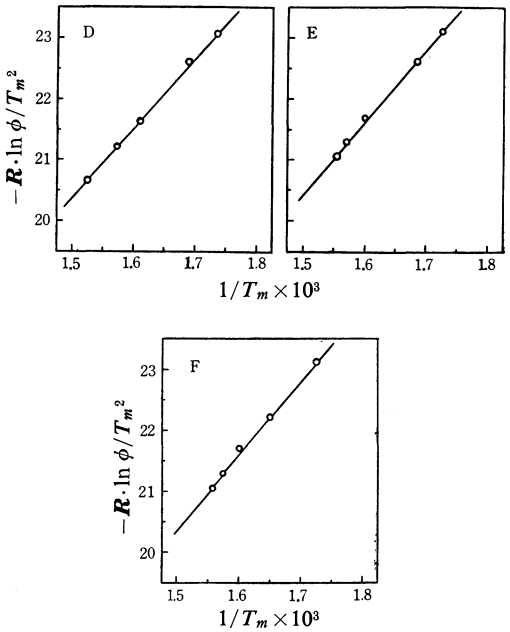


Fig. 5. Differential thermal analysis data obtained for samples D, E and F.

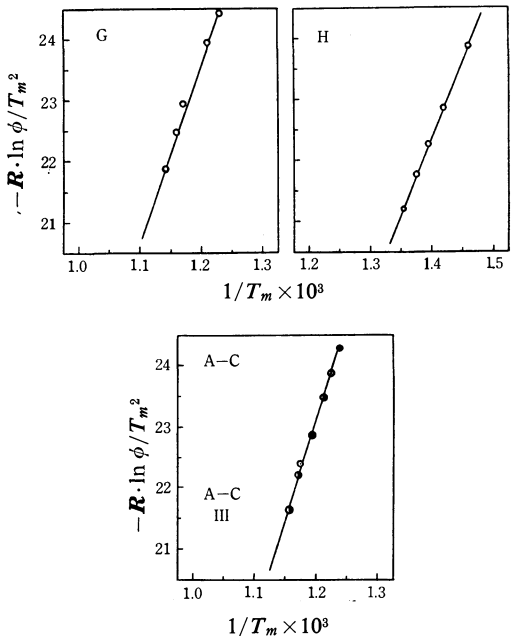


Fig. 6. Differential thermal analysis data obtained for samples A, B and C.
● 50°C; ○, 80°C; ◑, 100°C (temperature of hydration)

found to be 11.5, 11.5 and 12.1 kcal. per mole; the reaction orders of E and F were nearly equal to unity, while that of D was apart from unity, that is, 0.88. The lack of agreement in the case of the dehydration of sample D can not be explained. The difference in activation energy between the first and second dehydration processes indicates that the dehydration is influenced by the inhibitive action of the calcium hydroxide liberated; that is, the elevation of the activation energy of the second dehydration seems to arise from the fact that small particles of calcium hydroxide liberated in hydrate mixtures are firmly bound to the hydrate.

The behavior of the binding of calcium hydroxide to hydrate is considered to be as follows: a comparison of the electron micrograph reported in the preceding paper[1] with the above-mentioned results suggests that the crystals of calcium hydroxide produced by the hydration link together to form a three-dimensional network and that hydrated calcium orthoplumbate fills up the space existing in the calcium hydroxide network. The three-dimensional network of calcium hydroxide may be a linkage consisting of crystals of a spherical form, as suggested by the results of Sato,[4] because the values of the reaction order in this study agree with those of Sato.

4) N. Sato, *J. Chem. Soc. Japan, Pure Chem. Sec.* (*Nippon Kagaku Zassi*), **76**, 862 (1955).

Summary

The behavior of the dehydration of a hydrate mixture of calcium orthoplumbate and calcium hydroxide and of the hydrate of calcium orthoplumbate has been studied with a thermobalance and by differential thermal analysis.

It has been shown that the dehydration of crystalline water in the hydrate mixture was retarded by the presence of the calcium hydroxide liberated; this conclusion has been based on both the activation energy of the hydrate and its loss of weight.

It seems that calcium orthoplumbate fills the space in a network consisting of calcium hydroxide particles.

The author wishes to express his gratitude to Professor Ayao Kitahara of Tokyo College of Science for his continuous encouragement and helpful discussions throughout this work.

Department of Applied Chemistry
Faculty of Science
Tokyo College of Science
Kagurazaka, Shinjuku-ku, Tokyo

A Semi-empirical MO Theory of σ Electron Systems. I. General Theory*

By Hidekazu HAMANO**

(Received March 10, 1964)

Most of the theoretical work on organic molecules that has been reported so far is connected with π electron systems; relatively little is known about the electronic states of the σ electrons. However, recent progress in experimental techniques such as nuclear magnetic resonance, nuclear quadrupole resonance, and electron spin resonance has made it desirable to obtain some more theoretical information about the electronic states of the σ electrons in organic molecules. The present paper constitutes an attempt in this direction.

* This work was supported by a grant from the U. S. Army Research Office (Durham) and the National Science Foundation to the University of Pennsylvania.

** On leave of absence from Tokyo Gakugei University, Tokyo, Japan.

It is obvious that any theoretical description of the σ electrons in organic molecules will be of an approximate nature. We plan to base our discussion on the SCF LCAO MO method as developed by Roothaan,[1] a method which has been successfully applied to small molecules. However, we will be forced to introduce some additional approximations, since a straightforward application of Roothaan's theory is not feasible for large organic molecules.

Let us consider a molecule with a closed-shell ground state. It is assumed that each doubly-occupied SCF LCAO MO may, in principle, be associated with either a lone pair or a localized σ bond, though in Roothaan's complete treatment each SCF LCAO

MO should, in principle, be represented as a linear combination of all available atomic orbitals in the molecule. In a first approximation we represent the SCF LCAO MO's that are associated with lone pairs or σ bonds as linear combinations of the corresponding atomic orbitals on the atoms. If we substitute the MO into the analogue of the Roothaan equations[1] and then solve them, we may anticipate one solution for each lone pair and two solutions for each bond; the solution with the lower energy will be called the bonding orbital, and the other solution, the anti-bonding orbital. In the following pages the expression "*to a first approximation*" refers to the above calculation. The first-order treatment is considerably less accurate than a complete SCF LCAO MO calculation would have been, but we may use its results as a starting point for a second-order treatment which will give results that are of an accuracy comparable with that of the solutions of the complete SCF LCAO MO calculations.

It is possible to construct molecular orbitals as linear combinations of the lone-pair, bonding and anti-bonding orbitals obtained above. This approach might be called the LCBO MO method (with molecular orbitals represented as linear combinations of bond or lone-pair orbitals). The coefficients in these linear combinations are unknown, but it may be assumed that in each case there is a major contribution from a lone-pair or a bonding orbital and that the coefficients of the anti-bonding orbitals are significantly smaller. Therefore, they may be determined by means of a perturbation method. In the following remarks we will use the expression "*to a second approximation*" as referring to the results of this perturbation treatment.

We will be forced to introduce some semi-empirical features into the theory, especially in connection with estimating the non-diagonal elements of the matrix that represent the interaction between different bonds or lone pairs, since a non-empirical evaluation of these quantities would be very tedious. This semi-empirical procedure supplies a convenient tool for dealing with large organic molecules.

The general theory will be developed in this paper; applications and some further details will be discussed in subsequent papers.

I. First Order Theory.—*General Considerations.*—In developing our theory we will basically follow Roothaan's method.[1] However, we will replace Roothaan's LCAO approximation by the LCBO approach. We will also consider a molecule with a closed-shell ground state. The inner electrons may be taken as being adequately represented by means of the inner-shell atomic orbitals; hence, only the valence electrons need to be taken into account.

The molecular $2N$-electron ground state wave function is represented as an antisymmetrized product of molecular spin orbitals:

$$\Phi=\{(2N!)\}^{-1/2}\sum_{\mathbf{P}}P\delta_{\mathbf{P}} \times\{\prod_{i}\phi_i(2i-1)\phi_i(2i)\alpha(2i-1)\beta(2i)\} \quad (1)$$

where the ϕ_i are suitable molecular orbitals, which are represented as LCAO in Roothaan's theory.[1] We may also write the MO as linear combinations of orbitals that are localized in specific bonds or lone pairs such as those proposed by Edmiston and Ruedenberg[2] or Lennard-Jones,[3] which are obtained by means of a unitary transformation. We will go one step further and take the orbitals as bond or lone-pair orbitals themselves. The validity of this procedure is not immediately obvious, however, and so it may be useful to clarify its theoretical basis and the relation between the LCAO and LCBO approximations.

We may represent the bond orbitals as linear combinations of valence atomic orbitals (LCVAO):

$$\varphi_p=a_p(A,p)+b_p(B,p) \quad (2)$$

where A, p and B, p are the valence AO of both atoms respectively, and each φ_p is normalized. The valence AO (A, p), (B, p) and lone-pair orbitals φ_f may be represented as linear combinations of the AO on the corresponding atoms:

$$A,p=\sum_{\lambda}d_{\lambda}^{p}\chi_{\lambda}^{A}, \qquad .\ \varphi_f=\sum_{\mu}d_{\mu}^{f}\chi_{\mu}^{A} \quad (3)$$

where χ_{λ}^{A} is the λth AO of atom A and d_{λ}^{p} is its coefficient in the pth bond orbital. This set of hybridized AO's belonging to the same atom may be taken as orthonormal and equivalent. Each bond orbital, φ_p, may be supposed to be obtained by solving an equation for bond p. Usually two different solutions are obtained, a bonding orbital, φ_p^+ and an anti-bonding orbital, φ_p^-; they are orthogonal to one another. In this way, we may replace a set of atomic orbitals by an equivalent set of valence orbitals and also replace the paired valence AO (A, p) and (B, p) by the bonding φ_p^+ and anti-bonding

1) C. C. J. Roothaan, *Revs. Mod. Phys.*, **23**, 69 (1951).

2) C. Edmiston and K. Ruedenberg, ibid., **35**, 457 (1963); see also, S. F. Boys, ibid., **32**, 296 (1960).

3) J. Lennard-Jones, *Proc. Roy. Soc.*, **A198**, 1, 14 (1949). He called these orbitals "*equivalent orbitals.*"

φ_p^- orbitals. We may thus represent the MO's as linear combinations of bond or lone-pair orbitals instead of the LCAO approximation:

$$\psi_i = \sum_p c_{ip}\varphi_p \tag{4}$$

The variational procedure for minimizing the total energy of the molecule then leads to the following equation:

$$\boldsymbol{L}\boldsymbol{c}_i = \varepsilon_i \boldsymbol{S}\boldsymbol{c}_i \tag{5}$$

where $\boldsymbol{L}$ is the set of LCBO SCF Hamiltonian matrix elements which are given by:

$$\begin{aligned}\boldsymbol{L}_{pq}^{+-} &= \langle\varphi_p^+|\boldsymbol{H}|\varphi_q^-\rangle \\ &+ \sum_i [2\langle\psi_i(1)\varphi_p^+(2)|r_{12}^{-1}|\psi_i(1)\varphi_q^-(2)\rangle \\ &- \langle\psi_i(1)\varphi_p^+(2)|r_{12}^{-1}|\varphi_q^-(1)\psi_i(2)\rangle], \text{ etc.}\end{aligned} \tag{6}$$

The $\boldsymbol{H}$ is the Hamiltonian for the electrons in the combined potential field of the nuclei and inner-shell electrons. The column vectors, $\boldsymbol{c}_i$ represent the coefficients of the BO in the ith MO, ε_i is the eigenvalue of the MO, and $\boldsymbol{S}$ is an overlap matrix with elements $S_{pq}^{+-} = \langle\varphi_p^+|\varphi_q^-\rangle$, etc. Equation 5 is the secular equation for the SCF LCBO MO.

It would, however, be as difficult as in the LCAO approach to obtain a reliable solution of Eq. 5 from *ab initio* calculations; we therefore wish to solve the equation by introducing the following approach. The matrix elements, S_{pq}^{+-}, are usually smaller than the S_{pq}^{++} or S_{pq}^{--} since the signs of the coefficients, a_p or b_p, of the valence AO in the bond orbital defined by Eq. 2 are different for the bonding and anti-bonding orbitals, and since the overlap integrals between unpaired valence AO's are generally small (they are zero for the AO on the same atom). Since the delocalization of the σ electrons is considered to be small, we may also assume that the $\boldsymbol{L}_{pq}^{+-}$ are relatively small. They may be considered as small perturbations. We will discuss this in greater detail in the second order theory described in Section II. In the first order treatment these smaller terms may, therefore, be neglected. Equations 4 and 5 are then reduced to:

$$\psi_i^+ = \sum_p c_{ip}^+\varphi_p^+, \qquad \psi_i^- = \sum_p c_{ip}^-\varphi_p^- \tag{7}$$

$$\boldsymbol{L}^+\boldsymbol{c}_i^+ = \varepsilon_i^+\boldsymbol{S}^+\boldsymbol{c}_i^+, \qquad \boldsymbol{L}^-\boldsymbol{c}_i^- = \varepsilon_i^-\boldsymbol{S}^-\boldsymbol{c}_i^- \tag{8}$$

where the plus and minus signs refer to quantities connected with the φ_p^+ and φ_p^- respectively. In this approximation, the ψ_i^+ and ψ_k^- are determined from two independent sets of equations, representing the occupied and unoccupied MO respectively in the molecular ground state. We will only discuss the equations for the occupied orbitals, since the other equations are in every way equivalent. For the sake of brevity, we will omit the plus sign in the following remarks.

The non-orthogonality between the different BO's will cause some complications in the subsequent discussion; it is, therefore, convenient to introduce, according to Löwdin,[4] the following orthogonalized BO (OBO):

$$\varphi^\circ = \varphi(\boldsymbol{1}+\boldsymbol{S}^\circ)^{-1/2} \tag{9}$$

where $\boldsymbol{1}$ is a unit matrix and $\boldsymbol{S}^\circ$ is an overlap matrix with the elements:

$$S_{pq}^\circ = S_{pq} - \delta_{pq}, \quad \delta_{pq} = \begin{cases}1 & (p=q)\\ 0 & (p\neq q)\end{cases} \tag{10}$$

Equations 7 and 8 may, then, be written as:

$$\psi_i = \sum_p c_{ip}^\circ\varphi_p^\circ \tag{11}$$

$$\boldsymbol{L}\boldsymbol{c}_i^\circ = \varepsilon_i\boldsymbol{c}_i^\circ \tag{12}$$

where

$$\boldsymbol{c}^\circ = (\boldsymbol{1}+\boldsymbol{S}^\circ)^{1/2}\boldsymbol{c}$$

Since the matrix $\boldsymbol{c}^\circ$ is unitary, the molecular wave function, Φ°, and the electronic energy, W_e°, of the ground state may be written as:

$$\begin{aligned}\Phi^\circ = \{(2N)!\}^{-1/2}\sum_{\mathbf{P}}\boldsymbol{P}\delta_{\mathbf{P}} \\ \times\{\Pi_p\varphi_p^\circ(2p-1)\varphi_p^\circ(2p)\alpha(2p-1)\beta(2p)\}\end{aligned} \tag{13}$$

$$W_e^\circ = \sum_p \overline{W}_p = \sum_p [2\overline{H}_p + \sum_q (2\overline{J}_{pq} - \overline{K}_{pq})] \tag{14}$$

where the summation is to be performed over all the OBO's. The $\overline{H}_p$, $\overline{J}_{pq}$ and $\overline{K}_{pq}$ are core, Coulomb, and exchange integrals respectively with regard to OBO.

It would be a tedious procedure to use the OBO to perform calculations on large molecules. Fortunately, the overlap integrals between different BO's are usually much smaller than those between directly-bonded AO's. The possible consequences of the non-orthogonality of these orbitals have been discussed by Löwdin,[4] by means of OBO instead of non-orthogonal BO. They may, therefore, be neglected. In this approximation, the

4) P. O. Löwdin, *J. Chem. Phys.*, **18**, 365 (1950).

OBO's are reduced to the corresponding BO's. Equations 12, 13 and 14 may be rewritten as:

$$\boldsymbol{L}\boldsymbol{c}_i=\varepsilon_i\boldsymbol{c}_i \tag{15}$$

$$\Phi^\circ=\{(2N)!\}^{-1/2}\sum_{\mathbf{P}}\boldsymbol{P}\delta_{\mathbf{P}}\times\{\Pi_{\mathrm{p}}\varphi_{\mathrm{p}}(2p-1)\varphi_{\mathrm{p}}(2p)\alpha(2p-1)\beta(2p)\} \tag{16}$$

$$W_{\mathrm{e}}^\circ=2\sum_{\mathrm{p}}H_{\mathrm{p}}+\sum_{\mathrm{pq}}(2J_{\mathrm{pq}}-K_{\mathrm{pq}}) \tag{17}$$

Equations 16 and 17 show that the quantities in terms of the MO's may, instead, be expressed in terms of BO's in the first order treatment. Therefore, we may use the BO's instead of the MO's as a basis for the discussion of the first order theory. The method for determining the BO's will be discussed in the next subsection.

SCF Bond Orbital Approach. — Let us now proceed to determine the explicit form of the BO's which are represented by the variational function of Eqs. 2 and 3. Since we wish to make use of the SCF procedure, our method may be called the "*SCF BO approach.*"

Most σ electron systems of organic molecules contain some heteropolar bonds. It may be convenient to introduce the bond polarity parameter proposed by Mulliken:[5]

$$Q_{\mathrm{p}}=Q_{\mathrm{p}}^{\mathrm{A}}=b_{\mathrm{p}}^2-a_{\mathrm{p}}^2=(b_{\mathrm{p}}^2+a_{\mathrm{p}}b_{\mathrm{p}}S_{\mathrm{p}})-(a_{\mathrm{p}}^2+a_{\mathrm{p}}b_{\mathrm{p}}S_{\mathrm{p}})=-Q_{\mathrm{p}}^{\mathrm{B}} \tag{18}$$

where

$$S_{\mathrm{p}}=\langle\mathrm{A,p}|\mathrm{B,p}\rangle$$

The numerical evaluation of the various integrals involving atomic orbitals would be quite tedious. If we neglect the differential overlap between valence AO's in different BO's, we may simplify matters by making use of Mulliken's approximation:[5]

$$(\mathrm{A,p:B,p})\sim 1/2S_{\mathrm{p}}[(\mathrm{A,p:A,p})+(\mathrm{B,p:B,p})] \tag{19}$$

Nevertheless, the exchange integrals between the valence AO's on the same atom belonging to adjacent bonds or lone pairs need not necessarily be negligible; they have to be explicitly taken into account. Equation 17 may then be rewritten as:

$$\begin{aligned}W_{\mathrm{e}}^\circ=&\sum_{\mathrm{R,p}}(1-Q_{\mathrm{p}}^{\mathrm{R}})H_{\mathrm{R,p}}+2\sum_{\mathrm{p}}F_{\mathrm{p}}\gamma_{\mathrm{p}}\\&+1/4\sum_{\mathrm{R,pU,p}}(1-Q_{\mathrm{p}}^{\mathrm{R}})(1-Q_{\mathrm{p}}^{\mathrm{U}})J_{\mathrm{R,pU,p}}\\&+1/2\sum_{\mathrm{R,pT,q}}(1-Q_{\mathrm{p}}^{\mathrm{R}})(1-Q_{\mathrm{q}}^{\mathrm{T}})(J_{\mathrm{R,pT,q}}\\&-1/2\delta_{\mathrm{R,pT,q}}K_{\mathrm{R,pT,q}})+2\sum_{\mathrm{f}}H_{\mathrm{f}}\\&+2\sum_{\mathrm{fg}}(J_{\mathrm{fg}}-1/2\delta_{\mathrm{fg}}K_{\mathrm{fg}})\\&+\sum_{\mathrm{fR,p}}(1-Q_{\mathrm{p}}^{\mathrm{R}})(J_{\mathrm{fR,p}}-1/2\delta_{\mathrm{fR,p}}K_{\mathrm{fR,p}})\end{aligned} \tag{20}$$

where

$$F_{\mathrm{p}}=2a_{\mathrm{p}}b_{\mathrm{p}}=[-S_{\mathrm{p}}+\{1-(1-S_{\mathrm{p}}^2)Q_{\mathrm{p}}^2\}^{1/2}]/(1-S_{\mathrm{p}}^2) \tag{21}$$

$$\gamma_{\mathrm{p}}=H_{\mathrm{A,pB,p}}-1/2S_{\mathrm{p}}(H_{\mathrm{A,p}}+H_{\mathrm{B,p}}) \tag{22}$$

and where the R, p, U, p, etc., stand for the valence AO (A, p), (B, p), etc.; f and g refer to lone pair orbitals; $\delta_{\mathrm{R,pT,q}}$, etc., are taken as unity if the R, p and T, q are the valence AO's of the same atom in different bonds, otherwise they are zero.

The variational procedure leads to the following simultaneous equation:

$$\partial W_{\mathrm{e}}^\circ/\partial Q_{\mathrm{p}}=0 \tag{23}$$

$$\partial W_{\mathrm{e}}^\circ/\partial d_\lambda=0,\ \text{etc.} \tag{24}$$

In general, the explicit solutions of Eq. 24 may complicate the discussion; they correspond to the information on the atomic valence state. We may assume that the solutions of Eq. 24 have already been obtained implicitly and that they may then be inserted into Eq. 23. This does not mean that a calculation of the valence states of atoms in molecules is not important—their significance has already been emphasized by Moffitt[6-8]—, but only that it would be beyond the scope of this paper to discuss them here. Equation 23 may now be written as:

$$\begin{aligned}&(H_{\mathrm{B,p}}-H_{\mathrm{A,p}})-2Q_{\mathrm{p}}M_{\mathrm{p}}\gamma_{\mathrm{p}}+1/2(J_{\mathrm{B,pB,p}}\\&-J_{\mathrm{A,pA,p}})+Q_{\mathrm{p}}[1/2(J_{\mathrm{A,pA,p}}+J_{\mathrm{B,pB,p}})\\&-J_{\mathrm{A,pB,p}}]+\sum_{\mathrm{T,q}\neq\mathrm{p}}(1-Q_{\mathrm{q}}^{\mathrm{T}})[(J_{\mathrm{B,pT,q}}\\&-1/2\delta_{\mathrm{B,pT,q}}K_{\mathrm{B,pT,q}})-(J_{\mathrm{A,pT,q}}-1/2\delta_{\mathrm{A,pT,q}}\cdot\\&K_{\mathrm{A,pT,q}})]+2\sum_{\mathrm{f}}[(J_{\mathrm{B,pf}}-1/2\delta_{\mathrm{B,pf}}K_{\mathrm{B,pf}})\\&-(J_{\mathrm{A,pf}}-1/2\delta_{\mathrm{A,pf}}K_{\mathrm{A,pf}})]=0\end{aligned} \tag{25}$$

where;

$$M_{\mathrm{p}}=[1-(1-S_{\mathrm{p}}^2)Q_{\mathrm{p}}^2]^{-1/2}=1+1/2(1-S_{\mathrm{p}}^2)Q_{\mathrm{p}}^2+3/8(1-S_{\mathrm{p}}^2)^2Q_{\mathrm{p}}^4+\cdots\cdots \tag{26}$$

Since we are now considering electron pair bonds, even the small values of the polarity parameters may be of interest. By expanding M_{p} as above and by taking only the zeroth and first powers of Q_{p}, we obtain for Eq. 25:

5) R. S. Mulliken, ibid., **46**, 497, 675 (1949).

6) W. Moffitt, *Proc. Roy. Soc.*, **A202**, 534 (1950).
7) W. Moffitt, ibid., **A210**, 245 (1951).
8) W. Moffitt, *Reports Prog. Phys.*, **17**, 173 (1954).

$$Q_p = K_p [(\chi_{B,p} - \chi_{A,p}) + \sum_{\substack{T,q \\ (q \neq p)}} Q_p^T \{(J_{B,pT,q} - 1/2\delta_{B,pT,q} K_{B,pT,q}) - (J_{A,pT,q} - 1/2\delta_{A,pT,q} K_{A,pT,q})\}] \quad (27)$$

where;

$$K_p = [1/2(J_{A,pA,p} + J_{B,pB,p}) - J_{A,pB,p} - 2\gamma_p]^{-1} \quad (28)$$

$$\chi_{U,p} = \chi^\circ_{U,p} + \chi'_{U,p} \quad (29)$$

$$\chi^\circ_{U,p} = -\varepsilon^\circ_{U,pU,p} - 1/2 J^\circ_{U,pU,p} \quad (30)$$

$$\chi'_{U,p} = -H'_{U,p} - \sum_{\substack{T,q \\ (q \neq p)}} J'_{U,pT,q} - 2\sum_f J'_{U,pf} \quad (31)$$

$$\varepsilon^\circ_{U,pU,p} = H^\circ_{U,p} + \sum_{\substack{T,q \\ (q \neq p)}} (J^\circ_{U,pT,q} - 1/2 K^\circ_{U,pT,q}) + 2\sum_f (J^\circ_{U,pf} - 1/2 K^\circ_{U,pf}) \quad (32)$$

The superscripts small circle and prime refer to the corresponding one-center and two-center integrals respectively under the conditions $H^\circ_{U,p} + H'_{U,p} = H_{U,p}$, etc. $\varepsilon^\circ_{U,pU,p}$ is the Hartree-Fock energy parameter associated with U, p in the valence state of the atom U and generally not an eigenvalue of the hybridized AO. The $\chi_{U,p}$, $\chi^\circ_{U,p}$, and $\chi'_{U,p}$ may be defined as the "*intramolecular electronegativity of the atom U for the bond p*," "*the electronegativity of the atom U for the bond p*," *and* "*the induced electronegativity of the atom U for the bond p*," respectively; the second quantity is specific for the atom and is equivalent to the electronegativity scale defined by Moffitt;[9] the third quantity consequently also the first, depend on the interaction energy with the other atoms. We may approximate the $\chi^\circ_{U,p}$ as:

$$\chi^\circ_{U,p} \sim 1/2(I_{U,p} + E_{U,p}) \quad (33)$$

where the approximations $-\varepsilon^\circ_{U,pU,p} \sim I_{U,p}$, $J^\circ_{U,pU,p} \sim I_{U,p} - E_{U,p}$ are used; the $I_{U,p}$ and $E_{U,p}$ are the corresponding ionization potential and electron affinity respectively. This definition of electronegativity agrees with the one given by Mulliken.[10]

We may also give a different definition of the electronegativity scale without changing our conclusions. If we add the quantity $J_{A,pB,p}$ to the $-\chi'_{A,p}$ and $-\chi'_{B,p}$ respectively, we obtain the quantities $\varepsilon'_{A,pA,p} = -\chi'_{A,p} + J_{A,pB,p}$, etc., which are the neutral penetration energies and which are usually small. From these quantities, a different electronegativity scale may be defined:

$$\chi_{U,p} = -\varepsilon_{U,pU,p} - 1/2 J_{U,pU,p} \quad (34)$$

where

$$\varepsilon_{U,pU,p} = \varepsilon^\circ_{U,pU,p} + \varepsilon'_{U,pU,p} \quad (35)$$

Equation 34 corresponds to the generalized definition of Moffitt's electronegativity scale.[9] This procedure causes no changes in the results of Eq. 27, because we have $\chi'_{B,p} - \chi'_{A,p} = \varepsilon'_{A,pA,p} - \varepsilon'_{B,pB,p}$. These quantities are generally very small; they become important only if the quantity $(\chi^\circ_{B,p} - \chi^\circ_{A,p})$ is zero or very small, because the order of the magnitude of $(\chi'_{B,p} - \chi'_{A,p})$ may then become compatible with $(\chi^\circ_{B,p} - \chi^\circ_{A,p})$. This effect may, therefore be called the "*homopolar inductive effect or the quantum-mechanical inductive effect;*" it depends on the position of the bond in the molecule, but not on the polarities of the other bonds.

The K_p's are considered to be specific for the bond p, because the γ_p's are not supposed to depend on the adjacent atoms or bonds, as follows from their definition. They are also defined as:

$$K_p = \partial Q_p / \partial(\chi_{B,p} - \chi_{A,p}) \quad (36)$$

This suggests that the K_p may be called the "*auto-polarizability of the bond p*"; that is, the K_p measures the change of Q_p when the electronegativity difference is changed. The K_p may be approximated by:

$$K_p \sim [1/2\{I_{A,p} - E_{B,p}) + (I_{B,p} - E_{A,p})\} - J_{A,pB,p} - 2\gamma_p]^{-1} \quad (37)$$

The first term is the average energy of the ion pairs A^+B^- and A^-B^+ at infinite distances, and the second and third terms correspond to the average values of the Coulomb attraction and exchange repulsion energies of these ion pairs respectively. To a good approximation, therefore, K_p is regarded as an inverse of the average energy of the ion pairs A^+B^- and A^-B^+ at the equilibrium distance of bond p. We may conclude that the mobilities of the electrons in the bond decrease with an increase in the average energy of these two ion pairs. The sign of K_p is always positive, because the second and third terms of Eq. 28 have opposite signs and their sum—which corresponds to the interaction energy between atoms A and B—is small compared with the first term, which is always

9) W. Moffitt, *Proc. Roy. Soc.*, **A202**, 548 (1950).
10) R. S. Mulliken, *J. Chem. Phys.*, **2**, 782 (1934).

positive. This is important for the interpretation of the empirical rules, as will be shown later.

Now we wish to introduce the following inductive parameter:

$$\begin{aligned}\Pi_{pq} = K_p[&(J_{B,pA,q} - 1/2\delta_{B,pA,q}K_{B,pA,q}) \\ &- (J_{A,pA,q} - 1/2\delta_{A,pA,q}K_{A,pA,q}) \\ &- (J_{B,pB,q} - 1/2\delta_{B,pB,q}K_{B,pB,q}) \\ &+ (J_{A,pB,q} - 1/2\delta_{A,pB,q}K_{A,pB,q})] \\ \equiv &\delta_{\mathbf{P}+\mathbf{P}'}\Pi_{\mathbf{P}(B,pA,p)\mathbf{P}'(A,qB,q)} \\ &(q \neq p) \end{aligned} \tag{38}$$

where $\mathbf{P}$ and $\mathbf{P}'$ are the operators which represent the permutations of the orders of B, p, A, p, etc., and where $\delta_{\mathbf{P}+\mathbf{P}'}$ is unity when $(\mathbf{P}+\mathbf{P}')$ is even, and otherwise minus unity. Equation 27 may now be simplified as:

$$Q_p = Q_p^\circ + Q_p' \tag{39}$$

where

$$Q_p^\circ = K_p(\chi_{B,p} - \chi_{A,p}) \tag{40}$$

$$Q_p' = \sum_{q \neq p} \Pi_{pq}Q_q \tag{41}$$

It follows from these equations that the bond polarity, Q_p, consists of the following two parts: 1) Q_p°, the specific bond polarity of the bond p, which is determined by the electronegativity difference if we neglect the small homopolar inductive effect, and 2) Q_p', the induced bond polarity, which is induced by the polarity of the other bonds. These equations also give another definition of Π_{pq}:

$$\Pi_{pq} = \partial Q_p/\partial Q_q \tag{42}$$

This means that Π_{pq} is a measure of the change in Q_p when Q_q is changed; it may be defined as the "*mutual polarizability of the bond p to the bond q*" for $p \neq q$. For $p = q$, the quantity Π_{pp} is always unity and may be defined as the "*self-polarizability of the bond p.*" The Π_{pq}'s have the following additional properties:

$$\Pi_{pq}/\Pi_{qp} = K_p/K_q, \quad 0 < |\Pi_{pq}| < 1 \quad (q \neq p) \tag{43}$$

So far we have considered one specified bond p only. Equations 27 and 39, however, are in principle simultaneous equation. We will proceed to derive their explicit solutions. we obtain the explicit solution of Eq. 27 as:

$$\overline{Q}_p = \Delta_p/\Delta_n, \quad (p = 1, 2, 3, \ldots\ldots, n) \tag{44}$$

where;

$$\Delta_n = \det\{2\delta_{pq} - \Pi_{pq}\} \tag{45}$$

which is a determinant of n rows and columns; Δ_p is obtained from Δ_n by replacing the pth column of Δ_n by the column $(Q_1^\circ, Q_2^\circ, Q_3^\circ, \ldots\ldots, Q_n^\circ)$; n and p denote the total number of bonds in the molecule and the pth bond respectively and $\overline{Q}_p$ stands for the corresponding SCF value of Q_p.

Let us now define the following quantity:

$$\overline{\Pi}_{pq} = (-1)^{p+q}\Delta_n^{pq}/\Delta_n = \partial\overline{Q}_p/\partial Q_q^\circ \tag{46}$$

where Δ_n^{pq} is the determinant obtained by striking out from Δ_n the pth column and qth row. $\overline{\Pi}_{pq}(p \neq q)$ may be called the "*SCF mutual polarizability of the bond p to the bond q*" corresponding to Π_{pq}, and $\overline{\Pi}_{pp}$, "*SCF self-polarizability of the bond p*" corresponding to Π_{pp}. These definitions allow us to rewrite:

$$\overline{\boldsymbol{Q}} = \overline{\boldsymbol{\Pi}}\boldsymbol{Q}^\circ \tag{47}$$

where $\overline{\boldsymbol{Q}}$ and $\boldsymbol{Q}^\circ$ are column vectors whose components are given by Eqs. 44 and 40 respectively, and where $\overline{\boldsymbol{\Pi}}$ is a matrix with components that are given by Eq. 46. That is, these components are combined by the relation $Q_p = \sum_q \overline{\Pi}_{pq}Q_q^\circ$.

We have so far considered only the case where the bond polarities are small. In general, the quantity K_p may formally be written as:

$$\begin{aligned}K_p = [&1/2(J_{A,pA,p} + J_{B,pB,p}) \\ &- J_{A,pB,p} - 2M_p\gamma_p]^{-1}\end{aligned} \tag{48}$$

Apparently we obtain the general theory if we replace γ_p by $M_p\gamma_p$, as is indicated by Eq. 28. The extreme values for M_p are reached for $|Q_p| = 0$ (pure homopolar bond) as $M_p = 1$ and for $|Q_p| = 1$ (pure ionic bond) as $M_p = |S_p|^{-1}$. Since, in the interval $0 \leqq |Q_p| \leqq 1$, M_p is a monotonous and single-value function of Q_p, it will have all the values between 1 and $|S_p|^{-1}$. If Q_p is no longer small with respect to unity, it is necessary to solve Eq. 47 by means of an SCF procedure and by considering the explicit dependence of M_p on Q_p. This may become a very cumbersome problem. Since, in general, $\overline{Q}_p$ will not be very different from Q_p°, we may take to a first approximation the M_p value which corresponds to Q_p°. This will not affect the values of K_p very much.[11] The K_p may then be defined specifically for the bond p, and we may follow the the preceding argument just as it is.

11) Since the S_p values for σ bonds are usually around 0.5, M_p can only take values from 1 to 2. Therefore this may be a satisfactory approximation.

The SCF bond polarities, $\overline{Q}_p$, thus obtained enable us to determine the coefficients, a_p and b_p, of the valence AO as:

$$a_p^2=1/2(1-\overline{Q}_p-F_pS_p), \text{ and}$$

$$b_p^2=1/2(1+\overline{Q}_p-F_pS_p) \quad (49)$$

The corresponding values, $\overline{Q}_p^-$, for the anti-bonding orbital of the bond p may similarly be derived if it is borne in mind that $\overline{Q}_p^-=-\overline{Q}_p^+$ as a result of the orthogonality between the bonding and anti-bonding orbitals of the bond p.

We are now in a position to solve the secular equation 15 by taking the SCF BO as a basis. We will then be able to determine the first order SCF LCBO MO's and their eigenvalues. The method will be described in Section III in connection with the semi-empirical approach.

II. Second Order Theory.—In the first order treatment we neglected the interactions between bonding and anti-bonding orbitals. We will now proceed to a more accurate treatment in which these interactions are explicitly considered. Since they are usually small, they may be treated as perturbations. We may then take the above sets of the SCF LCBO MO's and their eigenvalues as a basis for developing the second order theory.

The overlap integrals between the bonding and anti-bonding orbitals may be neglected even in this higher approximation, as has been discussed above. By making use of first and second order perturbation theories, we easily obtain the following perturbed MO's ψ_i, their eigenvalues, ε_i, and also the molecular electronic energy, W_e:

$$\psi_i=\psi_i^+-\sum_k[\beta_{ik}^{+-}/(\varepsilon_k^- -\varepsilon_i^+)]\psi_k^- \quad (50)$$

$$\varepsilon_i=\varepsilon_i^+-\sum_k(\beta_{ik}^{+-})^2/(\varepsilon_k^- -\varepsilon_i^+) \quad (51)$$

$$W_e=W_e^\circ-\sum_{ik}(\beta_{ik}^{+-})^2/(\varepsilon_k^- -\varepsilon_i^+) \quad (52)$$

where β_{ik}^{+-} is the component of the Hamiltonian matrix that represents the interactions between occupied and unoccupied MO's in a first order theory. The occupied MO's and their eigenvalues in the ground state only are described here. The corresponding quantities for unoccupied MO's are obtained in a similar fashion.

Since all the BO's are represented as linear combinations of the AO's, the LCBO MO's may finally be reduced to the LCAO's. These LCAO MO's may then be considered to be good approximations of Roothaan's SCF LCAO MO's. The localized MO's obtained from these MO's by means of a unitary transformation are now not strictly localized in the specific bonds or lone pairs, whereas in the first order theory the orbitals have been the BO's themselves. Therefore, the second order theory includes a consideration of the delocalization of bond or lone pair electrons, which is generally taken to be small for σ-electron systems. In our theory the delocalization is described in terms of the electron transfer from bonding to antibonding orbitals on different bonds.

III. Semi-empirical Approach.—Le us now set out to solve Eq. 15, which is the secular equation in the first order theory. By making use of the results obtained in Section I, we can easily estimate the values of the diagonal elements, L_{pp}, of the SCF LCBO Hamiltonian matrix. Since within the present approximation the matrix $\boldsymbol{c}$ is unitary, the L_{pp}^{++} may be rewritten as:

$$\begin{aligned}L_{pp}^{++}&=H_p+\sum_q(2J_{pq}-K_{pq})\\&=-1/2(\chi_{A,p}+\chi_{B,p})+1/2J_{A,pB,p}\\&\quad+1/4\overline{Q}_p(J_{B,pB,p}+J_{A,pA,p})-1/2\sum_{\substack{T,q\\(q\neq p)}}\overline{Q}_q^T\cdot\\&\quad[(J_{A,pT,q}-1/2\delta_{A,pT,q}K_{A,pT,q})\\&\quad+(J_{B,pT,q}-1/2\delta_{B,pT,q}K_{B,pT,q})]\\&\quad+(F_p+M_p\overline{Q}_p^2)\gamma_p \quad (53)\end{aligned}$$

and, for lone pairs:

$$L_{ff}^{++}=-\chi_{ff}-\sum_{R,p}\overline{Q}_p^R(J_{fR,p}-1/2\delta_{fR,p}K_{fR,p}) \quad (54)$$

where:

$$\begin{aligned}\chi_{ff}&=-H_f-2\sum_g(J_{fg}-1/2\delta_{fg}K_{fg})\\&\quad-\sum_{R,p}(J_{fR,p}-1/2\delta_{fR,p}K_{fR,p}) \quad (55)\end{aligned}$$

$\chi_{A,p}$, etc. are defined by Eq. 29. The corresponding L_{pp}^{--} values for the anti-bonding orbital of the bond p are similarly derived. However, we do not obtain the values for the non-diagonal elements, $L_{pq}(p\neq q)$, in this way because these quantities are not considered in the treatment described in Section I. Non-empirical calculations of these quantities are usually very tedious, especially for the large organic molecules that we wish to consider. Furthermore, even if Eq. 15 were solved, we would find the same difficulty in estimating the β_{pq}^{+-}, which will appear in the calculation of β_{ik}^{+-} in the second order theory. There-

fore, we wish to propose the following semi-empirical method:

1) The values of $\alpha_{pp}(\equiv L_{pp}$ including $L_{pp}^{--})$, etc. are determined non-empirically from Eq. 53 or 54.

2) The values of $\beta_{pq}^{++}(\equiv L_{pq}^{++})$, etc. are taken as empirical parameters, and Eq. 15 is then solved.

3) The values of β_{pq}^{+-} are also taken as empirical parameters. These assumptions enable us to perform perturbation calculations.

4) The results of the calculations are used to estimate the values of β_{pq}^{++}, β_{pq}^{+-}, etc., from the observed ionization potentials, spectroscopic data, etc.

The present semi-empirical method for σ-electron systems is very similar to the method developed by Pariser and Parr[12] for π-electron systems, as may be seen from our procedure for determining the α and β values. Since it is a relatively simple method, we expect it to be applicable to calculations of many properties of complex molecules.

IV. Inductive and Resonance Effects.—The concepts of "*inductive effect*" and "*resonance effect*," both of which are related to electron migration, have proved to be useful in organic chemistry. The inductive effect was originally defined as a classical electrostatic effect.[12,13] Even though several theoretical studies[13-18] of the inductive effect have been reported, we feel that its theoretical foundation has not yet been properly established. Therefore, we will try to discuss it on the basis of our theory.

In general, the inductive parameters, Π_{pq}, which were defined by Eq. 38 will be especially large if p and q are two adjacent bonds. If the adjacent bonds, p and q, are chosen in such a way that the A, p and A, q are AO's of the same atom, A, the sign of Π_{pq} should be negative and, therefore, Q_p and Q_q should have opposite signs, because the second term in the brackets of Eq. 38 is then dominant and K_p is positive. The intra-bond charge transfer in bonds p and q should, therefore, follow the direction of the arrows in Fig. 1. When this theorem is applied to

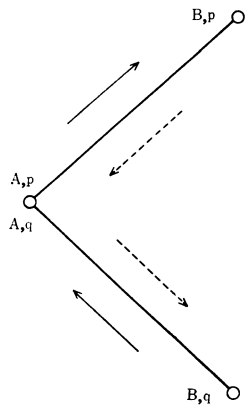


Fig. 1. Intra-bond charge transfers in the adjacent bonds p and q caused by the inductive effect.

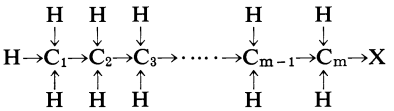


Fig. 2. Intra-bond charge transfers in the $C_mH_{2m+1}X$ molecule caused by the inductive effect.

the adjacent bonds of large molecules, for example, to the mono-substituted *n*-hydrocarbons, $C_mH_{2m+1}X$, the intra-bond electron transfers should follow the arrows in Fig. 2, since we take X to be more electronegative than the carbon. This conclusion agrees with that of the classical treatment[13] of the inductive effect. Equation 41 may thus be regarded as a quantum-mechanical representation of the inductive effect. The similarity between classical and quantum-mechanical results is confirmed by an inspection of the brackets of Eq. 38, which correspond to Coulomb interactions between the (A, p), (B, p), (A, q) and (B, q) if we take the (A, p) and (B, q) to be positive point charges and the (A, q) and (B, p) to be negative point charges or vice versa. It has thus been shown that the procedure for determining the bond polarity in the first order theory corresponds to a consideration of the inductive effect. Hereafter we will use the term "*inductive effect*" in this sense. The application of the inductive effect will be described in the second paper of this series.

The significance of the resonance effect for conjugated systems is well established; it is accompanied by a stabilization energy of the molecule which has been called "*resonance energy*" or "*conjugation energy*." On the other hand, for σ-electron systems, this effect is generally taken to be small. In our theory

12) R. Pariser and R. G. Parr, *J. Chem. Phys.*, **21**, 466, 767 (1953).
13) K. Higashi, *J. Chem. Soc. Japan (Nippon Kwagaku Kwaishi)*, **57**, 1006 (1936).
14) L. G. Groves and S. Sugden, *J. Chem. Soc.*, **1937**, 158.
15) R. P. Smith, T. Ree, J. L. Magee and H. Eyring, *J. Am. Chem. Soc.*, **73**, 2263 (1951).
16) J. M. Cahill and C. R. Mueller, *J. Chem. Phys.*, **24**, 513 (1956).
17) C. D. Re, *J. Chem. Soc.*, **1958**, 4031.
18) S. Maeda, This Bulletin, **31**, 260 (1958).

it has been defined as the delocalization of σ-bond electrons in the second order theory. The resonance energy of molecules is then represented by the second term of Eq. 52. We will use the term "*resonance effect*" in the above sense.

We have thus defined the two effects separately on the basis of reasonable approximations; previous theories did not even distinguish between the two effects. The differences will become more obvious in the following considerations. In the first order theory, the electron density in each BO is equal to two, and the bond order[19] between different BO's is zero in our approximation. The inductive effect may then be defined as an intra-bond charge transfer; even then the electron density in each bond or lone pair is still two and the inter-bond orders are zero. On the other hand, the resonance effect corresponds to an inter-bond charge transfer from bonding to anti-bonding orbitals on different bonds.

Discussion

The present semi-empirical MO theory may not be as rigorous as the non-empirical SCF LCAO MO method but at least it makes it possible to deal satisfactorily with large molecules. Essentially based on the Hartree-Fock method, it is obtained by introducing some additional assumptions and approximations. However, it is impossible to avoid the deficiencies inherent in all one-electron methods; this causes the K_p to predict equal probabilities for the two possible ionic structures, A^+B^- and A^-B^+. This defect may be removed by considering the correlation between the paired electrons with opposite spins. This correlation problem has already been discussed by several authors.[20-25]

It may be valuable to compare our approach with previous theoretical work on the subject. Lennard-Jones[13] and his collaborators[26-28] have shown that the usual delocalized MO for saturated molecules may be replaced by a set of equivalent orbitals. However, their determination requires a knowledge of molecular symmetry. Recently Edmiston and Ruedenberg[2] proposed a method for determining more general localized MO's that do not follow from the molecular symmetry. The authors suggest that in a more precise theory each MO may be represented as a linear combination of the above localized orbitals. Although the localized orbitals are sometimes hard to determine, especially for large organic molecules, it is possible to overcome this difficulty by replacing the orbitals by the ordinary bond orbitals; this was done in the LCBO MO theory of Brown.[29] In this treatment the MO's are represented as linear combinations of bonding orbitals only, and the contributions of the anti-bonding orbitals are neglected. It was subsequently pointed out by Dewar and Pettit[30] that the contributions from the anti-bonding orbitals to the molecular energy, though small, are not negligible and that they ought to be taken into account. This delocalization effect of σ-electrons was also accounted for by Mulliken et al.[31] in terms of hyperconjugation.

The practical advantage of our theory is that it is closely connected with familiar chemical concepts such as inductive effect and electronegativity. This makes it possible to explain some previously proposed empirical rules. The details will be described in subsequent papers.

It is worth noting that the definitions of the absolute scale of electronegativity are independent of the different approaches. Our definition agrees with those obtained by Parks and Parr[20] or Oohata,[23] who used different approaches in which the correlation is taken into account; that is, all the results lead to the Moffitt scale.[9] This seems to support the validity of the absolute electronegativity scale. A detailed discussion of the electronegativity will be presented in a subsequent paper.

Summary

A semi-empirical MO theory is proposed for complex saturated molecules. In a first-order treatment, each MO is represented as a localized function that contains only the AO connected with one bond or atom. This enables us to define a set of bonding, anti-bonding and lone-pair orbitals. The molecular wave function is obtained as an anti-symmetrized product of the bonding and lone-pair orbitals.

19) The bond orders between BO are defined in the same way as for AO, the term "*inter-bond bond order*" is sometimes used in this paper.
20) J. M. Parks and R. G. Parr, *J. Chem. Phys.*, **28**, 335 (1958).
21) A. C. Hurley, J. Lennard-Jones and J. A. Pople, *Proc. Roy. Soc.*, **A220**, 446 (1953).
22) K. Oohata, *J. Phys. Soc. Japan*, **15**, 1048 (1960).
23) K. Oohata, *Prog. Theor. Phys.*, **25**, 215 (1961).
24) O. Sinanoglu, *J. Chem. Phys.*, **33**, 1212 (1960).
25) J. M. Foster and S. F. Boys, *Revs. Modern Phys.*, **32**, 300 (1960).
26) G. G. Hall and J. Lennard-Jones, *Proc. Roy. Soc.*, **A202**, 155 (1950).
27) J. Lennard-Jones and J. A. Pople, ibid., **A202**, 166 (1950).
28) J. Lennard-Jones and G. G. Hall, *Discussions Faraday Soc.*, **10**, 18 (1951).
29) R. D. Brown, *J. Chem. Soc.*, **1953**, 2615.
30) M. J. S. Dewar and R. Pettit, ibid., **1954**, 1625.
31) R. S. Mulliken, C. A. Rieke and W. G. Brown, *J. Am. Chem. Soc.*, **63**, 41 (1941).

In this approximate theory we discuss the definitions of the electronegativity scale and of the inductive effect; the electronegativity scales proposed by Moffitt and Mulliken are obtained as special cases. In a subsequent, more accurate second-order theory each MO is represented as a linear combination of all bonding, anti-bonding and lone-pair orbitals; this treatment is made by means of the perturbation theory. A semi-empirical approach is developed by taking the interactions between different bonds as empirical parameters. No applications of the general theory are presented here; they will be discussed in subsequent papers.

The author wishes to thank Dr. H. F. Hameka for his stimulating interest and encouragement and Professor R. G. Parr for his reading of the manuscript.

Department of Chemistry
University of Pennsylvania
Philadelphia 4, Pennsylvania, U.S.A.

A Semi-empirical MO Theory of σ Electron Systems. II. Bond Polarity and Electronegativity*

By Hidekazu HAMANO**

(Received March 10, 1964)

In a previous paper,[1] we outlined a first and second order semi-empirical MO theory for σ electron systems. In the first order theory each σ bond is represented by a bonding orbital, and the wave function of a saturated molecule is obtained as an anti-symmetrized product of doubly-occupied bonding or lone-pair orbitals. We then discussed the polarity of the bond orbitals by introducing the bond polarity parameters, Q_p. It was shown that the bond polarity parameter is determined not only by the electronegativity difference but also by the inductive effect. This enables us to make theoretical predictions of experimental properties on the basis of bond polarity parameters. Many experimental quantities, such as dipole moments, nuclear quadrupole coupling constants,[2,3] and fluorine chemical shifts,[4,5] may be approximately calculated from the bond polarity parameters. In this paper we wish to apply our previous first order theory to a calculation of these properties for several organic molecules.

It has been shown that our definition of electronegativity includes the Moffitt[6] or Mulliken[7] scales as special cases. In addition, several other methods[3,8-11] have been proposed for obtaining the electronegativity constants from either experimental or theoretical atomic quantities. However the important question, why such a crude model based on atomic electronegativity constants can so successfully describe bond properties, has never been properly investigated theoretically. In this paper, we will attempt to answer this question by means of our first order theory. In connection with this problem, we will also investigate how the electronegativity scale of Pauling,[8] which was obtained empirically, fits into our theory.

I. The Electronegativity Scale and the Ionic Character of Bonds. — In this section we wish to discuss the connection between the various electronegativity scales and the ionic character of the bonds. We will take Eq. 39 of reference 1, $Q_p = Q_p^\circ + Q_p'$, as a starting point for this discussion. The Q_p° and Q_p' are the specific and induced bond polarities respectively

* This work was supported by grants from the U. S. Army Research Office (Durbam) and the National Science Foundation to the University of Pennsylvania.

** On leave of absence from Tokyo Gakugei University, Tokyo, Japan.

1) Part I of this series, This Bulletin, **37**, 1574 (1964).

2) C. H. Townes and B. P. Dailey, *J. Chem. Phys.*, **17**, 782 (1949).

3) W. Gordy, W. V. Smith and R. F. Trambarulo, "Microwave Spectroscopy," John Wiley & Sons, Inc., N. Y. (1953).

4) A. Saika and C. P. Slichter, *J. Chem. Phys.*, **22**, 26 (1954).

5) For the hydrogen chemical shifts, this is not true often; the contribution of the excited states are then important.

6) W. Moffitt, *Proc. Roy. Soc.*, **A202**, 548 (1950).

7) R. S. Mulliken, *J. Chem. Phys.*, **2**, 782 (1934).

8) L. Pauling, "The Nature of Chemical Bond," Cornell Univ. Press, N. Y. (1945).

9) H. O. Pritchard and H. A. Skinner, *Chem. Revs.*, **55**, 745 (1955).

10) J. M. Parks and R. G. Parr, *J. Chem. Phys.*, **28**, 335 (1958).

11) K. Oohata, *Prog. Theor. Phys. Japan*, **25**, 215 (1961).

defined by Eqs. 40 and 41 of Ref 1. If we considered the bond polarities on the basis only of the atomic electronegativity differences, we could construct a crude model in which bond polarity is regarded as specific for the bond, independent of the surroundings. Fortunately, the contribution of the induced polarity, Q'_p, based on the inductive effect to total bond polarity, Q_p, will not change our conclusions significantly.[12] It has already been recognized empirically that such a seemingly crude approximation may lead to useful conclusions. Therefore, only each specific bond is discussed here; the inclusion of the inductive effect will be presented in the following section. In addition, since we will consider atomic electronegativities only, we may neglect the homopolar inductive effect,[1] which is generally small. We thus obtain the following simple relation:

$$Q_p = K_p(\chi^\circ_{B,p} - \chi^\circ_{A,p}) \qquad (1)$$

where $\chi^\circ_{B,p}$ and $\chi^\circ_{A,p}$ are defined as the Moffitt scale[6] of the electronegativity of atoms B and A respectively.

Let us now consider the bond polarity on the basis of of the atomic properties. Moffitt[6,13,14] has shown that this is roughly equivalent with the situation where the two atoms, A and B, are an infinite distance apart, but still in the same valence states as they would be at their equilibrium distance. If we adopt the approximation[15], $-\varepsilon^\circ_{A,pA,p} \sim I_{A,p}$, $J^\circ_{A,pA,p} \sim I_{A,p} - E_{A,p}$, etc., where the I and E are the corresponding ionization potential and electron affinity respectively, the Moffitt scale[6] of the electronegativity may then be reduced to the Mulliken scale[7] and the Q_p at the infinite distance may be written as:

$$Q^\infty_p = K^\infty_p(\chi^\circ_{B,p} - \chi^\circ_{A,p}) = K^\infty_p\,[1/2(I_{B,p} + E_{B,p}) - 1/2(I_{A,p} + E_{A,p})] \qquad (2)$$

where

$$K^\infty_p = 2\,[(I_{B,p} - E_{A,p}) + (I_{A,p} - E_{B,p})]^{-1} \qquad (3)$$

The Q^∞_p and K^∞_p refer to infinite internuclear separation. The values of Q^∞_p, K^∞_p and $|\chi^\circ_{B,p} - \chi^\circ_{A,p}|$ for various bonds are tabulated in Table I, and the relation between Q^∞_p and $|\chi^\circ_{B,p} - \chi^\circ_{A,p}|$ is illustrated in Fig. 1. The values of I and E used are taken from the tables of Pritchard and Skinner.[9] Equation 2 is similar to the definition of ionicity proposed by Wilmshurst[16] or by Hinze et al.[17] The curve in Fig. 1 is similar to the results obtained by

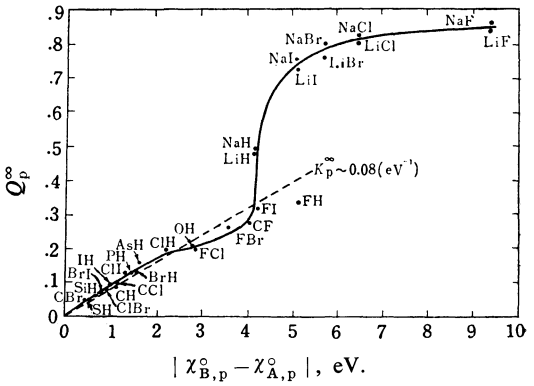


Fig. 1. Relalion between Q^∞_p and $|\chi^\circ_{B,p} - \chi^\circ_{A,p}|$.

TABLE I. VALUES OF BOND PARAMETERS

Bond[a]	$\lvert\chi^\circ_{B,p} - \chi^\circ_{A,p}\rvert$, eV.	K^∞_p, eV^{-1}	Q^∞_p
Li(s)-H(s)	4.21	0.113	0.48
Na(s)-H(s)	4.23	0.116	0.49
C(sp^3)-H(s)	1.13	0.084	0.09
Si(sp^3)-H(s)	0.51	0.100	0.05
O(p)-H(s)	2.82	0.073	0.21
F(p)-H(s)	5.15	0.066	0.34
Cl(p)-H(s)	2.28	0.083	0.19
Br(p)-H(s)	1.53	0.087	0.13
I(p)-H(s)	0.91	0.091	0.08
S(p)-H(s)	0.43	0.088	0.04
P(p)-H(s)	1.45	0.092	0.13
As(p)-H(s)	1.67	0.095	0.16
C(sp^3)-F(p)	4.02	0.071	0.28
C(sp^3)-Cl(p)	1.15	0.090	0.10
C(sp^3)-Br(p)	0.40	0.095	0.04
F(p)-Cl(p)	2.87	0.070	0.20
F(p)-Br(p)	3.62	0.073	0.26
F(p)-I(p)	4.24	0.076	0.32
Cl(p)-Br(p)	0.75	0.094	0.07
Cl(p)-I(p)	1.37	0.098	0.13
Br(p)-I(p)	0.62	0.105	0.06
Li(s)-F(p)	9.36	0.090	0.84
Na(s)-F(p)	9.38	0.092	0.86
Li(s)-Cl(p)	6.49	0.124	0.81
Na(s)-Cl(p)	6.51	0.128	0.83
Li(s)-Br(p)	5.74	0.134	0.77
Na(s)-Br(p)	5.76	0.139	0.80
Li(s)-I(p)	5.12	0.144	0.74
Na(s)-I(p)	5.14	0.149	0.76

a) The parentheses indicate the corresponding valence state.

12) In fact the values of Π_{pq} are much smaller than unity as will be shown in the following section.
13) W. Moffitt, *Proc. Roy. Soc.*, **A202**, 534 (1950); **A210**, 245 (1951).
14) W. Moffitt, *Reports Prog. Phys.*, **17**, 173 (1954).
15) See Ref. 1 also.
16) J. K. Wilmshurst, *J. Chem. Phys.*, **30**, 561 (1959).
17) J. Hinze, M. A. Whitehead and H. H. Jaffe, *J. Am. Chem. Soc.*, **85**, 148 (1963).

Pauling[8] or by Dailey and Townes[18] except for the FH bond.

It may be seen from Table I and Fig. 1 that, for $|\chi^{\circ}_{B,p}-\chi^{\circ}_{A,p}|<4$ eV. or for $Q^{\infty}_{p}<0.3$, the K^{∞}_{p} are nearly constant. In this range, therefore, the Q^{∞}_{p} may be regarded as proportional to the electronegativity differences. The dotted line in Fig. 1 ($K^{\infty}_{p}\sim 0.08\,eV^{-1}$) seems to confirm this inference. We may say, therefore, that for all covalent bonds $K_{p}\sim 0.08\,eV^{-1}$. The fact that the point for the FH bond in Fig. 1 lies very closely to the dotted line seems to indicate that this bond is also essentially covalent. On the other hand, the bonds involving the alkali metals have to be regarded as strongly polar bonds. It follows from Table I that these great polarities are due not only to the large electronegativity difference but also to the large values of K_{p} which result from the small values of the ionization potentials and the electron affinities of the alkali metals. In general, however, the K_{p} seem to be insensitive to electronegativity differences. The reasons for this will now be discussed.

At first sight, it appears from Eq. 3 that the values of K_{p} depend on electronegativity differences. The K_{p} values, however, depend on the average sum of the energies of the ion pairs $A^{-}B^{+}$ and $A^{+}B^{-}$, and the electronegativity differences, on the difference between them. An inspection of the periodic table will reveal that most polar bonds are formed between metallic elements which have small electronegativities and non-metallic elements which have large electronegativities. Consequently, the average value of the energies of the ion pairs $A^{-}B^{+}$ and $A^{+}B^{-}$ is practically independent of the variations in electronegativity between the different metallic elements or between the non-metallic elements. We believe that the general validity and usefulness of the concept of electronegativity may be explained by the above considerations, and also by the fact that the homopolar inductive effect is usually small,[1] so that the differences in electronegativity depend on atomic quantities only.

We will now proceed to discuss the relation between our electronegativity scale and Pauling's scale.[8] Pauling's electronegativity scale has been defined as:

$$|X_{B}-X_{A}|=\sqrt{\Delta} \qquad (4)$$

where Δ is the "*ionic-covalent resonance energy*" in terms of eV. On the other hand, anticipating some results of the following paper,[19] we plan to show that, for bonds with small polarities, the ionic-covalent resonance energy, Δ_{p}, in our theory is given by:

$$\Delta_{p}=1/2K_{p}|\chi^{\circ}_{B,p}-\chi^{\circ}_{A,p}|^{2} \qquad (5)$$

If the two quantities, Δ and Δ_{p}, are equivalent, we obtain:

$$|X_{B}-X_{A}|=(1/2K_{p})^{1/2}|\chi^{\circ}_{B,p}-\chi^{\circ}_{A,p}| \qquad (6)$$

This leads to the following relation:

$$X_{P}=(1/2K_{p})^{1/2}\chi^{\circ}_{M} \qquad (7)$$

where X_{P} and χ°_{M} stand for Pauling[8] and Mulliken[7] scales of electronegativity in terms of eV. We then have

$$X_{P}/\chi^{\circ}_{M}=(1/2K_{p})^{-1/2}\sim 0.22\,(eV^{-1/2}) \qquad (8)$$

where the value $K_{p}\sim 0.08\,eV^{-1}$ has been substituted. This value is empirically known to be 0.32 or 0.36 ($eV^{-1/2}$).[9] The discrepancy between these values may partially be due to our definitions and approximations, especially to the crude evaluation of K_{p}. This difficulty has been discussed by Mulliken.[20] We will also try to explain it.

Differences in electronegativity are important, not the values themselves; we may thus add an arbitrary constant value to all electronegativities. Pauling's scale[21] has been arbitrarily determined by adjusting it to Eq. 4 under the arithmetic mean assumption, which may often be replaced by the geometrical mean.[22,23] On the other hand, the Mulliken scale may be regarded as an absolute scale of electronegativity. Consequently, the Pauling scale may not be adequately given by Eq. 7. The ionic-covalent resonance energy, Δ_{p}, in our theory may be defined adequately only for small bond polarities.[19] Therefore, it is not surprising that the value evaluated from Eq. 8 does not agree with the empirical value.

II. Some Applications of the Inductive Effect. —We will now proceed to discuss the case of polyatomic molecules by starting from the complete first order theory. Since this includes a consideration of the inductive effect, we may call it "*an application of the inductive effect.*" In this section, we wish to apply the inductive effect to two types of molecules, namely, MX_{n} and *n*-alkyl halide molecules (n-$C_{m}H_{2m+1}X$). We will take Eq. 47 of Ref. 1 as the basic equation for the discussion of this section:

18) B. P. Dailey and C. H. Townes, *J. Chem. Phys.*, **23**, 118 (1955).

19) Part III of this series, This Bulletin, **37**, 1592 (1964).
20) R. S. Mulliken, ibid., **3**, 573 (1935).
21) Pauling arbitrarily adopted $X_{H}=2.1$ and $X_{F}=4.0$.
22) T. L. Cottrell and L. E. Sutton, *Proc. Roy. Soc.*, **A207**, 49 (1951).
23) A. C. Hurley, ibid., **A218**, 333 (1953).

$$\overline{Q}_p = \sum_q \overline{\Pi}_{pq} Q_p^\circ \qquad (9)$$

where $\overline{Q}_p$ is the SCF bond polarity of the bond p and the $\overline{\Pi}_{pq}$ values are the SCF polarizabilities which are defined by Eq. 46 of Ref. 1.

A) MX_n-type Molecules.—Let us consider a molecule with n equivalent bonds MX. From Eq. 9, we obtain for the bond MX;

$$\overline{Q}_{MX} = Q_{MX}^\circ / [1-(n-1)\overline{\Pi}_{(MX,p)(MX,q)}] \qquad (10)$$
$$(p \neq q)$$

Since $\overline{\Pi}_{(MX,p)(MX,q)}$ is taken as negative here, it may be concluded that the bond polarities of the MX bonds in the MX_n-type molecules generally decrease with an increase in the number of MX bonds. We are led to believe, therefore, that the small CH bond polarity of methane is due not only to the original small polarity of the CH bond itself, but also to the inductive effect. This conclusion may also be extended to the CH_3 and CH_2 radicals of saturated hydrocarbons. Consequently, it follows that the CH bonds in saturated hydrocarbons may be almost homopolar, which is in agreement with the general opinion and all available experimental information. Another example we wish to consider is the series of the halomethanes, CH_3X, CH_2X_2, CHX_3 and CX_4 (X= halogen). It has been empirically shown that, in the above order, the dipole moments decrease, the magnitudes of halogen nuclear quadrupole coupling constants $|eQq_X|$ increase (as Table II shows), and the fluorine chemical shifts, δ_F,[24] increase as −21.00, −8.09, −1.82 and 0. By making use of the above conclusion together with the gradual decreasing s characters of the halogen bonding orbitals in the above order, which will be shown in the next subsection, apart from the induced polarity of the CH bonds,[25,26] the dipole moments may be explained by the decreasing CX bond moments,[27] and the eQq_X and δ_F values, by means of the Townes-Dailey[2] and Saika-Slichter[4,28] formulas respectively. These formulas are shown in Appendices A and B respectively.

The chlorine nuclear quadrupole coupling constants of some chloro-compounds which are listed in Table III may also be interpreted on this basis. The present conclusion agrees with previous findings.[29,30]

TABLE II. MOLECULAR DIPOLE MOMENTS μ AND HALOGEN NUCLEAR QUADRUPOLE COUPLING CONSTANTS $|eQq_X|$ OF HALOMETHANES

Molecule	μ, D[a]	$\lvert eQq_X\rvert$, Mc.[a,b]
CH_3Cl	1.87[c,d]	68.4
CH_2Cl_2	1.62[c]	72.47
$CHCl_3$	1.06[c]	76.98
CCl_4	—	81.85
CH_3Br	1.80[d]	529
CH_2Br_2	1.43[e]	563
$CHBr_3$	1.3;[f] 0.99[g]	601
CH_3I	1.65[d]	1766
CH_2I_2	(1.10)[h]	1897
CHI_3	(0.99)[h]	2047
CI_4	—	2130

a) The values of μ are for the gaseous phase except for the values between parentheses. The values of $|eQq_X|$ are for the solid state.
b) H. Robinson, H. G. Dehmelt and W. Gordy, *J. Chem. Phys.*, **22**, 511 (1954).
c) G. A. Barlay and R. J. W. LeFevre, *J. Chem. Soc.*, **1950**, 556.
d) Ref. 3.
e) H. A. Stuart, "Die Struktur des Freien Moleküls," Springer (1952), p. 290.
f) *Trans. Faraday Soc.*, **30**, Appendix (1934).
g) Y. K. Syrkin and M. E. Dyatkina, "Structure of Molecules and the Chemical Bond," Intersci. Publ., New York (1950).
h) A. E. van Arkel and J. L. Snoek. *Rec. trav. chim.*, **52**, 719 (1933).

TABLE III. CHLORINE NUCLEAR QUADRUPOLE COUPLING CONSTANTS OF SOME CHLORO-COMPOUNDS

Molecule	$\lvert eQq_{Cl}\rvert$, Mc.[a]	
$CCl_3 \cdot CHCl_2$	79.9	($-CCl_3$)
	77.7	($-CHCl_2$)
$CH_2Cl \cdot COOH$	73.15	
$CHCl_2 \cdot COOH$	76.79	
$CCl_3 \cdot COOH$	80.25	

a) Ref. 3

B) n-Alkyl Halide Molecules. — The n-alkyl halide molecules (n-$C_mH_{2m+1}X$) may be re-

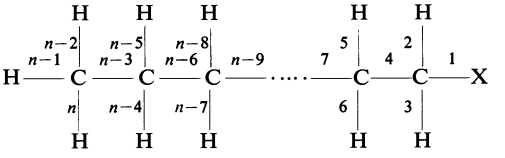


Fig. 2. Numbers of each bond in the $C_mH_{2m+1}X$ molecules.

24) L. H. Meyer and H. S. Gutowsky, *J. Phys. Chem.*, **57**, 481 (1953). The reported values have been multiplied by 10^5.
25) S. Maeda, This Bulletin, **31**, 260 (1958).
26) The experimental data cannot be explained by considering the induced polarity of the CH bonds only. Fortunately, however, this effect seems to be small from a theoretical viewpoint also.[25]
27) The bond moment here includes the lone pair moments of the corresponding atoms. See Ref. 19 also.
28) This argument is based on the assumption that the excitation energies ΔE, as will be given in Eq. B-2, would be of the same order of the magnitudes in this series. The validity of this is not obvious, but it would not be too bad an approximation.[4]
29) E. Warhurst, *Trans. Faraday Soc.*, **45**, 461 (1949).
30) H. Hamano, *J. Chem. Soc. Japan, Pure Chem. Sec.* (*Nippon Kagaku Zassi*), **77**, 746 (1956); **79**, 362 (1958).

garded as typical examples of the inductive effect. The numbers of each bond are defined as shown in Fig. 2: For the CX and CH bonds, the AO of the carbon atoms are taken as valence AO A_{CX} and A_{CH}, and those of the halogen and hydrogen atoms, as valence AO B_{CX} and B_{CH} respectively; for the CC bonds, the AO of the carbon atoms closer to the CX bond are taken as A_{CC}. For the sake of simplicity, the following assumptions are made:

1) It is assumed that $Q_2^\circ = Q_3^\circ = Q_4^\circ = \cdots\cdots = Q_n^\circ = 0$, which means that we take all bonds originally homopolar except for the CX bond.

2) Only the values of Π_{pq} between adjacent bonds are considered; the others are taken to be zero.

From Eq. 9 we then obtain:

$$ {}^m\overline{Q}_j = {}^m\overline{\Pi}_{j1} Q_1^\circ, \quad (j = 1, 2, 3, \cdots\cdots, n) \tag{11} $$

where the superscript m indicates the number of carbon atoms in each molecule, and ${}^m\overline{\Pi}_{j1}$ is given by:

$$ {}^m\overline{\Pi}_{j1} = (-1)^{j+1}\, {}^m\Delta_n^{j1} / {}^m\Delta_n \tag{12} $$

where ${}^m\Delta_n$ is the determinant of n rows and columns given by:

${}^m\Delta_n =$

$$
\begin{vmatrix}
1 & \Pi_{XH} & \Pi_{XH} & \Pi_{XC} & & & & & & & & \\
\Pi_{HX} & 1 & \Pi_{HH} & \Pi_{HC} & & & & & & & & \\
\Pi_{HX} & \Pi_{HH} & 1 & \Pi_{HC} & & & & & & & & \\
\Pi_{CX} & \Pi_{CH} & \Pi_{CH} & 1 & -\Pi_{CH} & -\Pi_{CH} & -\Pi_{CC} & & & & & \\
 & & & -\Pi_{HC} & 1 & \Pi_{HH} & \Pi_{HC} & & & & & \\
 & & & -\Pi_{HC} & \Pi_{HH} & 1 & \Pi_{HC} & & & & & \\
 & & & -\Pi_{CC} & \Pi_{CH} & \Pi_{CH} & 1 & -\Pi_{CH} & -\Pi_{CH} & -\Pi_{CC} & & \\
 & & & & & & -\Pi_{HC} & 1 & \Pi_{HH} & \Pi_{HC} & & \\
 & & & & & & -\Pi_{HC} & \Pi_{HH} & 1 & \Pi_{HC} & & \\
 & & & & & & -\Pi_{CC} & \Pi_{CH} & \Pi_{CH} & 1 & -\Pi_{CH} & \\
 & & & & & & & & & -\Pi_{HC} & & \\
 & & & & & & & & & & & \\
 & & & & & & & & & & & \\
 & & & & & & & & &

we consider that the first derivatives $d^m\overline{\Pi}_{11}/dm=(\partial^m\overline{\Pi}_{11}/\partial\rho_{m-1})(d\rho_{m-1}/dm)$, etc. Since $\Pi\ll1$,[31] we may limit ourselves to a consideration of the terms quadratic in Π. We then obtain :[32]

$$\partial^m\overline{\Pi}_{11}/\partial\rho_{m-1}\sim(-\Pi_{XC}\Pi_{CX})(e\rho_{m-1}+f)^{-2}<0 \quad (18)$$

$$\partial^m\overline{\Pi}_{21}/\partial\rho_{m-1}\sim(-\Pi_{CX}\Pi_{HC})(e\rho_{m-1}+f)^{-2}<0 \quad (19)$$

$$\partial^m\overline{\Pi}_{41}/\partial\rho_{m-1}\sim(\Pi_{CX})(e\rho_{m-1}+f)^{-2}>0 \quad (20)$$

Next let us examine the properties of the series ρ_m. From Eq. 17 we obtain the recurrent formula

$$d\rho_{m-1}/dm=(ad-bc)(c\rho_{m-2}+d)^{-2}d\rho_{m-2}/dm \quad (21)$$

We know, by considering Eq. 21 and the numerical values[31] of Π_{CC}, Π_{CH} and Π_{HC}, that the ρ_m and $(d\rho_{m-1}/dm)$ are monotonously decreasing and increasing functions of m respectively and that $\lim_{m\to\infty}(d\rho_{m-1}/dm)=0$. From the above results, we obtain the following:

$$d^m\overline{\Pi}_{11}/dm>0, \qquad d^m\overline{\Pi}_{21}/dm>0$$
$$d^m\overline{\Pi}_{41}/dm<0 \quad (22)$$

$$d^{2m}\overline{\Pi}_{11}/dm^2<0, \qquad d^{2m}\overline{\Pi}_{21}/dm^2<0$$
$$d^{2m}\overline{\Pi}_{41}/dm^2>0 \quad (23)$$

$$\lim_{m\to\infty}(d^m\overline{\Pi}_{11}/dm)=\lim_{m\to\infty}(d^m\overline{\Pi}_{21}/dm)$$
$$=\lim_{m\to\infty}(d^m\overline{\Pi}_{41}/dm)=0 \quad (24)$$

Since the signs of ${}^m\overline{Q}_1$, ${}^m\overline{Q}_2={}^m\overline{Q}_3$ and ${}^m\overline{Q}_4$ are positive, negative and negative respectively, it may be concluded that the polarity of the CX bonds increases with an increase in the number of carbon atoms and that the induced polarities of the CC and CH bonds increase and decrease with an increase in the number of carbon atoms respectively. If the number of carbon atoms becomes very large, all these quantities reach a saturation value asymptotically. It follows from Eqs. 18—20 that, in the present approximation, the ratios of the variations of the CX, CH and CC bond polarities are given by:

$$|d^m\overline{Q}_1/dm|:|d^m\overline{Q}_2/dm|:|d^m\overline{Q}_4/dm|$$
$$=\Pi_{XC}:\Pi_{HC}:1 \quad (25)$$

Equation 25 indicates that the variation in the induced polarity of the CC bond is most significant of all. Our conclusions may also be extended to the more distant CC and CH bonds, but they are not valid for the case of CH_3X molecules.

For CH_3X molecules, we have:

$${}^1\overline{\Pi}_{11}=[1-(3\Pi_{XH}\Pi_{HX})(1+2\Pi_{HH})^{-1}]^{-1} \quad (26)$$

$${}^1\overline{\Pi}_{21}=(-\Pi_{HX})(1+2\Pi_{HH}-3\Pi_{XH}\Pi_{HX})^{-1} \quad (27)$$

We will now attempt to compare the ${}^1\overline{\Pi}_{11}$ for CH_3X with the ${}^2\overline{\Pi}_{11}$ for C_2H_5X. The ${}^2\overline{\Pi}_{11}$ may be approximated by

$${}^2\overline{\Pi}_{11}\sim[1-(2\Pi_{XH}\Pi_{HX}+\Pi_{XC}\Pi_{CX})$$
$$\times(1+\Pi_{HH}-5\Pi_{CH}\Pi_{HC})^{-1}]^{-1} \quad (28)$$

By comparing the second terms of Eqs. 26 and 28, it may be concluded that ${}^2\overline{\Pi}_{11}>{}^1\overline{\Pi}_{11}$. Therefore, the previous argument is valid for all molecules of the series $C_mH_{2m+1}X$ except for the ${}^1\overline{\Pi}_{21}$.

So far we have disregarded changes in the valence states of the stoms, especially for the halogenes. In principle, a variation in the bond polarity is accompanied by a change in the hybridization of the corresponding AO. However, a complete calculation would be difficult, so we will discuss the problem qualitatively on the following assumptions:

1) All the valence AO of carbon atoms are assumed to be the usual sp^3 hybrids; only the hybridization of the valence AO of the halogens will be considered explicitly.

2) The s character in the halogen bonding orbitals is assumed to be small. The empirical data[2,3,18] on the nuclear quadrupole coupling constants of the halogens support this assumption.

3) The interaction between the halogen atom and the non-adjacent alkyl group may be accounted for by means of the CX bond polarity, $\overline{Q}_1$, only.

If the valence AO of the halogens are represented by Eqs. A-4 and A-5 in Appendix A, the electronic energy, W_e°, of these molecules may be written as:

$$W_e^\circ=a^2\Delta W(1-\overline{Q}_1)-\overline{Q}_1E_X+W_X(a=0)$$
$$+1/4(1-\overline{Q}_1)^2(J_{CC}+J_{X(b\sigma)X(b\sigma)})$$
$$+(1-\overline{Q}_1)H_C+2F_1\gamma_1+1/2(1-\overline{Q}_1^2)J_{CX(b\sigma)}$$
$$+4(1-\overline{Q}_1)J_{C\Pi}+(1+\overline{Q}_1)H'_{X(b\sigma)}$$
$$+4H'_\Pi+2H'_{X(b\sigma)}+R_r \quad (29)$$

where

$$W_X(a=0)=2I(s)+5I(p)+F^\circ(ss)+10F^\circ(pp)$$
$$-10/25F^2(pp)+10F^\circ(sp)-5/3G^1(sp) \quad (30)$$

31) The values calculated from simple Slater AO are $\Pi_{CC}=0.16$, $\Pi_{CH}=0.10$, $\Pi_{HC}=0.12$ and $\Pi_{HH}=0.08$, respectively so that this approximation seems to be reasonable.

32) In Eq. 20, we have also neglected the small term $2(\Pi_{CX}\Pi_{HH}-\Pi_{HX}\Pi_{CH})$.

$$\Delta W = I(\mathrm{p}) - I(\mathrm{s}) - F^{\circ}(\mathrm{ss}) - 4F^{\circ}(\mathrm{sp}) + 2/3G^{1}(\mathrm{sp}) + 5F^{\circ}(\mathrm{pp}) - 10/25F^{2}(\mathrm{pp}) \quad (31)$$

$$E_{\mathrm{X}} = -I(\mathrm{p}) - 2F^{\circ}(\mathrm{sp}) + 1/3G^{1}(\mathrm{sp}) - 5F^{\circ}(\mathrm{pp}) + 10/25F^{2}(\mathrm{pp}) \quad (32)$$

and where the subscripts 1, C and Π stand for the CX bond, the carbon AO associated with it, and the halogen Π orbitals respectively. The a^2 values describe the amount of s character in the halogen bonding orbitals. R_{r} is the energy of the alkyl group (except for the CX bond), including the interaction energy with the CX bond. $W_{\mathrm{X}}(a=0)$, ΔW and E_{X} are the valence state energy of the halogens for the configuration $(ns)^2(np\sigma)(np\Pi)^4V_1$, its promotion energy to the $(ns)(np\sigma)^2(np\Pi)^4 \cdot V_1$, and the electron affinity of halogens for the p orbital respectively. I, F and G are Slater parameters,[33] where s and p stand for the ns and np orbitals of the halogen respectively. The variational procedure for Eq. 29, neglecting small terms, yields:

$$\begin{aligned} a \sim & [(1+S_1)^{-2}S_{\mathrm{Cs}}\gamma_1 - F_1\{H_{\mathrm{Cs}} - 1/2S_{\mathrm{Cs}}(H_{\mathrm{X(b}\sigma)} + H_{\mathrm{C}})\}] - 1/2(1-\overline{Q}_1^2)(\mathrm{CC}\,|\,\mathrm{sp}) + (1-\overline{Q}_1 \\ & + F_1S_1)(\mathrm{C}:\mathrm{sp})/[[\Delta W(1-\overline{Q}_1) \\ & + 1/2(1-\overline{Q}_1)^2\{-F^{\circ}(\mathrm{pp}) - 4/25F^{2}(\mathrm{pp}) \\ & + F^{\circ}(\mathrm{sp}) + 2/3G^{1}(\mathrm{sp})\} + [(1+S_1)^{-2}S_{\mathrm{Cp}}\gamma_1 \\ & - F_1\{H_{\mathrm{Cp}} - 1/2S_{\mathrm{Cp}}(H_{\mathrm{X(b}\sigma)} + H_{\mathrm{C}})\}] \\ & - F_1S_1\{I(\mathrm{s}) - I(\mathrm{p})\}]] \end{aligned} \quad (33)$$

where

$$S_{\mathrm{Cs}} = \langle \mathrm{C}\,|\,\mathrm{s}\rangle, \qquad S_{\mathrm{Cp}} = \langle \mathrm{C}\,|\,\mathrm{p}\rangle$$

$$(\mathrm{CC}\,|\,\mathrm{sp}) = \langle \mathrm{C(1)s(2)}\,|\,r_{12}^{-1}\,|\,\mathrm{C(1)p(2)}\rangle$$

$$(\mathrm{C};\ \mathrm{sp}) = \langle \mathrm{s}\,|\,-1/r_{\mathrm{C}}\,|\,\mathrm{p}\rangle$$

The first terms of the numerator and denominator are both positive and greater than the following terms. From Eq. 33, neglecting small terms, we have

$$da^2/d\overline{Q}_1 \sim 2a^2/(1-\overline{Q}_1) \quad (34)$$

This shows that the variation of a^2 is less than that of $\overline{Q}_1$ and the corresponding derivative is positive.

Now we will consider the same relation from a different point of view. Clearly we hope that the results thus obtained agrees with Eq. 34. The variation in the electronegativity, $\chi_{\mathrm{X}}^{\circ}$, of the halogen as a function of a^2 is given by:

$$d\chi_{\mathrm{X}}^{\circ}/da^2 = \Delta W + Y \quad (35)$$

where

$$\begin{aligned} Y = & F^{\circ}(\mathrm{sp}) + 2/3G^{1}(\mathrm{sp}) - F^{\circ}(\mathrm{pp}) - 4/25F^{2}(\mathrm{pp}) \\ & + a^2[F^{\circ}(\mathrm{ss}) + F^{\circ}(\mathrm{pp}) + 4/25F^{2}(\mathrm{pp}) \\ & - 2F^{\circ}(\mathrm{sp}) - 4/3G^{1}(\mathrm{sp})] \end{aligned}$$

Since, for $a^2 \ll 1$, the Y value will generally be positive, Eq. 35 shows that $\chi_{\mathrm{X}}^{\circ}$ increases with an increase in the amount of s character. The ${}^{\mathrm{m}}\Pi_{11}$ are insensitive to variations in a^2 and are closed to unity, as may be seen from the definition. We have then

$$d\overline{Q}_1/da^2 \sim (dK_{\mathrm{CX}}/da^2)(\chi_{\mathrm{X}}^{\circ} - \chi_{\mathrm{C}}^{\circ}) + K_{\mathrm{CX}}(d\chi_{\mathrm{X}}^{\circ}/da^2) \quad (36)$$

where

$$dK_{\mathrm{CX}}/da^2 = K_{\mathrm{CX}}{}^2[-Y + d(J_{\mathrm{CX(b}\sigma)} + 2\gamma_1)/da^2] \sim -0.01Y(\mathrm{eV}^{-1}) \quad (37)$$

The second term of Eq. 37, which is connected with the strength of the bond, is much smaller than the first term, so it may be neglected and the approximate value, $K_{\mathrm{CX}} \sim 0.1$ $(\mathrm{eV}.^{-1})$, substituted. The substitution of Eqs. 35 and 37 into Eq. 36 yields

$$d\overline{Q}_1/da^2 \sim 0.1\Delta W + (0.06 \sim 0.1)Y \quad (38)$$

where the fact that $|\chi_{\mathrm{X}}^{\circ} - \chi_{\mathrm{C}}^{\circ}|$ is 4 eV. or less for all the halogens is used. Experimental data on ΔW are, unfortunately, not available, but the estimated values of Pritchard and Skinner[9] are F: 21 eV.; Cl: ~11 eV.; Br: ~11 eV.; I: ~8 eV. The exact values of Y are not known, but they are probably compatible with or less than ΔW. It follows, therefore, that the derivative of $\overline{Q}_1$ with respect to a^2 is always larger than unity. This agrees qualitatively with Eq. 34.

It may be concluded that both the polarity of the CX bond and the amount of s character in the bonding orbital of the halogen increase with an increase in the number of carbon atoms, but that the first effect is more important than the second. (For the CI bond, however, they are probably equally important.) The previous conclusion should, therefore, be modified as follows: The increasing polarities in the CX bonds are caused not only by the increasing polarizability, ${}^{\mathrm{m}}\overline{\Pi}_{11}$, but also by the increasing electronegativity, $\chi_{\mathrm{X}}^{\circ}$, in connection with the increasing amount of s character. Both the amount of s character and the polarities of the CX bonds reach saturation values if the carbon atoms become very numerous.

33) J. C. Slater, *Phys. Rev.*, **34**, 1293 (1929).

34) H. Yoshizumi, *Trans. Faraday Soc.*, **53**, 125 (1957).

TABLE IV. DIPOLE MOMENTS OF ALKYL HALIDES (IN DEBYE UNITS)

Chloride	μ	Bromide	μ	Iodide	μ
CH_3Cl	1.87[a]	CH_3Br	1.80[a]	CH_3I	1.65[a]
C_2H_5Cl	1.98[b]	C_2H_5Br	1.99[c]	C_2H_5I	1.93[c]
	2.00[c]		2.01[d]		1.87[d]
n-C_3H_7Cl	2.04[c]	n-C_3H_7Br	2.01[e]	n-C_3H_7I	1.97[e]
			2.15[d]		2.01[d]
n-C_4H_9Cl	2.11[d]	n-C_4H_9Br	2.15[d]	n-C_4H_9I	2.08[d]
	2.04[f]				

a) Ref. 3.
b) J. C. Jelatis, *Tech. Rep.*, 7, O. N. R. Contract N5 ori-78 T. O. I. Lab. Ins. Res. Mass. Inst. Tech. (1947).
c) P. C. Mahanti, *Phil. Mag.*, (7) **20**, 274 (1935).
d) L. G. Groves and S. Sugden, *J. Chem. Soc.*, **1937**, 158.
e) R. Sanger, O. Steiger and K. Gachter, *Helv. Phys. Acta*, **5**, 200 (1932).
f) C. P. Smyth and K. B. McAlpine, *J. Chem. Phys.*, **3**, 347 (1935).
g) R. H. Wiswall and C. P. Smyth, ibid., **9**, 356 (1941).

TABLE V. NUCLEAR QUADRUPOLE COUPLING CONSTANTS OF ALKYL HALIDES $|eQq_X|$ (IN Mc. UNITS)

Chloride	$\lvert eQq_{Cl}\rvert$[a]	Bromide	$\lvert eQq_{Br}\rvert$[b]	Iodide	$\lvert eQq_I\rvert$[b]
CH_3Cl	68.1	CH_3Br	528.9	CH_3I	1753
C_2H_5Cl	65.4	C_2H_5Br	497.0	C_2H_5I	1647
n-C_3H_7Cl	65.9	n-C_3H_7Br	503.0	n-C_3H_7I	1672
n-C_4H_9Cl	66.5	n-C_4H_9Br	499.9	n-C_4H_9I	1660

a) H. O. Hooper and P. J. Bray, *J. Chem. Phys.*, **33**, 334 (1960).
b) S. Kojima, K. Tsukada, S. Ogawa and A. Shimauchi, ibid., **21**, 1415 (1953).

These conclusions may be extended to similar halogen compounds, for example, the halomethanes, because the behavior of molecules is accounted for only by the CX bond polarity here. This has already been shown in Subsection II-A).

It has been shown that the dipole moments of alkyl halides increase with an increase in the number of carbon atoms and that they also tend to a saturation value,[35] as Table IV shows. This fact may be interpreted as follows: Both the induced dipole moments of the CC bonds and the moments of the CX bonds increase with an increase in the number of carbon atoms, while the lone pair moment of the halogens behaves similarly. The CH bond moments decrease, and they oppose the increase in molecular dipole moments, but this effect is small.[25] The saturation of the dipole moment may be explained by the saturation of all the quantities involved.

Information on the CX bonds may also be obtained from a consideration of the molecular quadrupole coupling constants, eQq_X of the halogens. They show an oscillating decrease with an increase in the number of carbon atoms, as is listed in Table V. This behavior is caused by crystal fields; it may be explained by considering the different unit cells[35] for compounds with even and odd numbers of carbon atoms. The saturation effect may be obscured, especially by this influence. In this connection, it may be of interest to observe that the boiling points[36] of these molecules or paraffins increase monotonously with an increase in the carbon numbers, whereas the melting points[36] increase in an oscillatory fashion. We may expect, therefore, the eQq_X values for free molecules to decrease monotonously. This inference seems to be confirmed if they are interpreted by the Townes-Dailey formula in Appendix A.

Discussion

We have shown that the first order theory, which contains the electronegativity and the inductive effect, is particularly valuable for a discussion of the bond polarity; it makes it possible to give a qualitative interpretation of the experimental dipole moments, nuclear quadrupole coupling constants, etc. It may then be noticed that the SCF procedure is indispensable to the interpretation of the above experimental data. The physical meaning of the SCF procedure may be explained in connection with the inductive effect as follows: The polarities induced in the other bonds by a certain polar bond may also polarize the

35) A. Mueller, *Proc. Roy. Soc.*, **A120**, 437 (1928).

36) N. A. Lange, "Handbook of Chemistry," Handbook Publ. Inc., Ohio (1956).

original bond.[37] We can then determine the accurate charge distribution in the molecule by considering all the correlations among the intra-molecular bonds. This corresponds to the exact solution of the many-body problem on the assembly of charged particles; it corresponds to our SCF procedure also. In fact, the correspondence between the quantum-mechanical and classical inductive effects has been pointed out. A close inspection of the examples shown in Section II will confirm the above explanation. Furthermore, the theory may be extended even to infinite polymers, as has been shown in Subsection II-B). This suggests that the present theory may be applicable to very large molecules. Although in the present treatment, the second order theory has been omitted, it ought to be taken into account in the quantitative discussion; the delocalization of the lone pair electrons on the halogen atoms—they attribute to the highest occupied orbitals in saturated molecules—may be especially important.

In Section I, the validity of the electronegativity scale has been discussed on the assumption that the polarity of bonds may be inferred from the valence state of the atoms in the infinite separation. This seems to confirm the idea of "*atoms in molecules*" developed by Moffitt.[13,14] It is not true for the inductive effect; however, the valence state of atoms is important even then.

Summary

A previously proposed theory is applied to a study of the electronegativity scale and the ionic character of bonds. The general validity of the electronegativity scale and also the relation between the Mulliken and Pauling scales are discussed. The previously defined inductive effect is used as a basis for calculations on MX_n-type molecules and on *n*-alkyl halide molecule. The results are then used for the qualitative interpretation of the experimental dipole moments, nuclear quadrupole coupling constants and fluorine chemical shifts.

The author wishes to thank Dr. H. F. Hameka for his stimulating interest and encouragement, and Professor R. G. Parr for reading the manuscript.

Department of Chemistry
University of Pennsylvania
Philadelphia 4, Pennsylvania, U. S. A.

Appendix A. The Derivation of the Townes-Dailey Formula.—The electronic contributions to the nuclear quadrupole coupling constants, eQq, for axially symmetric molecules are represented by:

$$eQq=eQ\langle\Phi^{o}|r^{-3}(3\cos^2\theta-1)|\Phi^{o}\rangle \qquad \text{(A-1)}$$

where e and Q are the electronic charge and the nuclear quadrupole moment of the coupled atom respectively; Φ^{o} is the molecular wave function which is given by Eq. 16 of Ref. 1. The contribution of the inner-shell electrons of the coupled atom may be neglected.[2,3,18] Because of the rapid decrease of the function r^{-3}, we will consider only the contribution of the coupled atom. In this approximation, we obtain

$$eQq=2eQ\sum_{p}\langle\varphi_p|r^{-3}(3\cos^2\theta-1)|\varphi_p\rangle \qquad \text{(A-2)}$$

where φ_p refers to the bonds connected with the coupled atom or its lone pairs.

Now let us consider the case of a halogen atom. For the MX bond (X=halogen), we have

$$\varphi_{MX}=c_M M+c_X X(b\sigma) \qquad \text{(A-3)}$$

where

$$X(b\sigma)=a(ns)+(1-a^2)^{1/2}(np\sigma) \qquad \text{(A-4)}$$

$$X(l\sigma)=(1-a^2)^{1/2}(ns)-a(np\sigma) \qquad \text{(A-5)}$$

The M refers to the AO of the atom M, and $X(b\sigma)$ and $X(l\sigma)$ are the bonding and lone pair orbitals respectively of the halogen with σ symmetry, together with the lone pair orbitals, $n\Pi$ and $n\overline{\Pi}$, with Π symmetry. The parameter a is the hybridization factor, and n can take the values 3, 4 and 5 for Cl, Br and I. The substitution of Eqs. A-3, A-4 and A-5 into Eq. A-2 yields:

$$eQq_X=(1-a^2)(-1+Q_{MX}-F_{MX}S_{MX})eQq_{np\sigma} \qquad \text{(A-6)}$$

If we neglect the overlap S_{MX}, we have the following simple formula:

$$eQq_X=-(1-a^2)(1-Q_{MX})eQq_{np\sigma} \qquad \text{(A-7)}$$

This is equivalent to the Townes-Dailey formula,[2] which was derived from a valence bond treatment. It may be rewritten:

$$eQq_X=-2/5eQ(1-a^2)(1-Q_{MX})\langle np|r^{-3}|np\rangle \qquad \text{(A-8)}$$

where the integral is the mean value of r^{-3} for the np orbital of the free halogen atom.

Appendix B. The Derivation of the Saika-Slichter Formula. — On the assupmtion that the second (paramagnetic) term in Ramsey's equation[38] is mainly responsible for the chemical shifts in fluorine, the chemical shift may be approximated by

$$\Delta\sigma=-(4/3\Delta E)(0|\sum_{jk}\boldsymbol{m}_j\boldsymbol{m}_k\boldsymbol{r}_k^{-3}|0) \qquad \text{(B-1)}$$

The various quantities in this formula are defined in Ramsey's paper.[38] In the same way as in Appendix A, we obtain

$$\Delta\sigma=-(2/3\Delta E)(e^2\hbar^2/m^2c^2)(1-a^2)(1-Q_{MF})\times\langle 2p|r^{-3}|2p\rangle \qquad \text{(B-2)}$$

This corresponds to the Saika-Slichter formula.[4] It resembles the Townes-Dailey formula given by Eq. A-8, as has already been predicted by Saika and Slichter.[4]

37) It is called "*reaction field*" in classical theory.
38) N. F. Ramsey, *Phys. Rev.*, **78**, 699 (1950).

A Semi-empirical MO Theory of σ Electron Systems. III. The Bond Additivity Rule*

By Hidekazu HAMANO**

(Received March 10, 1964)

We have already established[1,2] that σ electron systems may usually be regarded as consisting of localized electron pairs, and that our first order theory corresponds to the localized bond model. This idea seems to be supported by the fact that many molecular quantities, such as heats of formation, dipole moments, and polarizabilities,[3] may be derived by means of bond additivity rules. At first sight, therefore, the empirical additivity rules seem to be based essentially on the localization of σ electrons. However, we have shown[2] in the first order theory how same bonds may vary in different molecules because of changes in the bond polarity which are due to the inductive effect. This suggests that the different bond quantities may be assigned to the bonds in different molecules and that the additivity rules do not necessarily hold.

On the other hand, some deviations from the additivity of bond properties due to the delocalization effects have been found. This has been accounted for in our theory as the second order approximation.[1] In spite of these facts, it appears that the empirical rules reveal a much more exact additivity of all the bond properties than should be expected. This problem for the additivity of bond energies has been discussed by several authors[4-7] using different approaches, but the additivity of bond moments in only a few molecules has been discussed.[8,9] We wish to discuss the additivity of bond energies and bond moments in general in this paper, including our second order theory, especially by taking the influence of the inductive effect into consideration.

I. The Bond Additivity of the Heat of Formation.—By making use of previous results[1] of the first and second order theory, we obtain the heats of the formation of molecules:

$$W=\sum_{\mathrm{p}}\overline{W}_{\mathrm{p}}^{-2}\sum_{\mathrm{ik}}(\beta_{\mathrm{ik}}^{+-})^2/(\varepsilon_{\mathrm{k}}^{-}-\varepsilon_{\mathrm{i}}^{+}) +1/2\sum_{\mathrm{lm}}Z_{\mathrm{l}}'Z_{\mathrm{m}}'/R_{\mathrm{lm}}-\sum_{\mathrm{a}}W_{\mathrm{a}}^{\circ} \quad (1)$$

where $\overline{W}_{\mathrm{p}}$ is the bond energy for each orthogonalized BO defined by Eq. 14 of Ref. 1; the second term is a resonance energy in terms of our second order theory; Z_{l}' and Z_{m}' denote the effective nuclear charges of the atoms l and m including the inner shell electrons, respectively; R_{lm} is the internuclear distance, and W_{a}° is the energy of the atom a at infinite separation, excluding the energy of the inner-shell electrons. The third term, which corresponds to the internuclear repulsion energy including inner-shell electrons, may be rewritten as:

$$\sum_{\mathrm{lm}}Z_{\mathrm{l}}'Z_{\mathrm{m}}'/R_{\mathrm{lm}}=\sum_{\mathrm{ab}}Z_{\mathrm{a}}'Z_{\mathrm{b}}'/R_{\mathrm{ab}}+\sum_{\mathrm{cd}}Z_{\mathrm{c}}'Z_{\mathrm{d}}'/R_{\mathrm{cd}} \quad (2)$$

where the a and b denote the directly-bonded atoms, and the c and d, the other pairs. The $\sum\overline{W}_{\mathrm{p}}$ may be expanded as a power series in S_{pq}:[10]

$$\sum_{\mathrm{p}}\overline{W}_{\mathrm{p}}=\sum_{\mathrm{p}}W_{\mathrm{pp}}-\sum_{\substack{\mathrm{pq}\\(\mathrm{q}\neq\mathrm{p})}}S_{\mathrm{pq}}W_{\mathrm{pq}}+\cdots\cdots \quad (3)$$

where

$$W_{\mathrm{pq}}=2H_{\mathrm{pq}}+(2-\delta_{\mathrm{pq}})\sum_{\mathrm{r}}[2\langle\varphi_{\mathrm{r}}(1)\varphi_{\mathrm{p}}(2)\cdot|r_{12}^{-1}|\varphi_{\mathrm{r}}(1)\varphi_{\mathrm{q}}(2)\rangle-\langle\varphi_{\mathrm{r}}(1)\varphi_{\mathrm{p}}(2)\cdot|r_{12}^{-1}|\varphi_{\mathrm{q}}(1)\varphi_{\mathrm{r}}(2)\rangle] \text{ etc.}$$

Since, in general, the overlap integrals, S_{pq}, between different BO are much smaller than the integrals, S_{p}, between directly-bonded

* This work was supported by a grant from the U. S. Army Research Office (Durham) and the National Science Foundation to the University of Pennsylvania.

** On leave of absence from Tokyo Gakugei University, Tokyo, Japan.

1) The first paper of this series. This Bulletin, **37**. 1574 (1964).
2) The second paper of this series. ibid., **37**, 1583 (1964).
3) K. G. Denbigh, *Trans. Faraday Soc.*, **36**, 936 (1940).
4) R. D. Brown, *J. Chem. Soc.*, **1953**, 2615.
5) G. G. Hall, *Proc. Roy. Soc.*, **A213**, 113 (1952).
6) J. M. Parks and R. G. Parr, *J. Chem. Phys.*, **28**, 335 (1958).
7) T. L. Allen and H. Shull, ibid., **35**, 1644 (1961).
8) C. A. Coulson, *Trans. Faraday Soc.*, **38**, 433 (1942); **33**, 388 (1937).
9) W. C. Hamilton, *J. Chem. Phys.*, **26**, 345 (1957).
10) Here the expansion $(1+S^{\circ})_{\mathrm{pq}}^{-1/2}=\delta_{\mathrm{pp}}-1/2S_{\mathrm{pq}}+3/8\sum_{\mathrm{r}}S_{\mathrm{pr}}S_{\mathrm{rq}}\cdots$ is used. See also Eqs. 9 and 10 of Ref. 1.

orbitals, only terms containing zeroth and first powers of S_{pq} in Eq. 3 may be considered. The first term, W_{pp}, may be regarded as the energy of the pth bond or lone pair; the sum is equivalent to the W_e° given by Eq. 17 or 20 of Ref. 1, whereas the second term, W_{pq}, is connected with the interaction energy between different bonds or lone pairs.

First let us examine the quantity W_e°. Since the discussion of the bond additivity may be restricted to the case of bonds with small polarities, we may use the approximation $F_p \sim (1+S_p)^{-1} - 1/2Q_p^2$.[1] Thus we obtain for W_e°:

$$W_e^\circ = \sum_a (W_a + W_a') + \sum_p{}' (E_p + \Delta_p) \tag{4}$$

where

$$\begin{aligned} W_a = {} & \sum_{R,\,p(a)} H^\circ_{R,p(a)} + 2 \sum_{f(a)} H^\circ_{f(a)} + \\ & 1/2 \sum_{\substack{R,\,p(a)\\ (q\neq p)}} \sum_{T,\,q(a)} (J^\circ_{R,p(a)T,q(a)} - 1/2K^\circ_{R,p(a)T,q(a)}) \\ & + 2 \sum_{f(a)R,p(a)} (J^\circ_{f(a)R,p(a)} - 1/2K^\circ_{f(a)R,p(a)}) \\ & + 2 \sum_{f(a)g(a)} (J^\circ_{f(a)g(a)} - 1/2K^\circ_{f(a)g(a)}) \end{aligned} \tag{5}$$

$$\begin{aligned} W_a' = {} & \sum_{R,p(a)} H'_{R,p(a)} + 2 \sum_{f(a)} H'_{f(a)} + 1/2 \\ & \sum_{\substack{R,p(a)T,q\\ (q\neq p)}} J'_{R,p(a)T,q} + \sum_{f(a)R,p} J''_{f,(a)R,p} \\ & + \sum_{R,p(a)f} J''_{R,p(a)f} + 2 \sum_{f(a)g} J''_{f(a)g} \end{aligned} \tag{6}$$

$$\begin{aligned} E_p = {} & (H^*_{A,p} + H^*_{B,p}) + 2(\sum_{f(A)} H^*_{f(A)} + \sum_{f(B)} H^*_{f(B)}) \\ & + 1/4(J^\circ_{A,pA,p} + J^\circ_{B,pB,p}) + 1/2(\sum_{\substack{B,q\\ (q\neq p)}} J^*_{A,pB,q} \\ & + \sum_{A,q} J^*_{B,pA,q}) + 2(\sum_{f(B)} J^*_{A,pf(B)} + \sum_{f(A)} J^*_{B,pf(A)}) \\ & + 4 \sum_{f(A)g(B)} J^*_{f(A)g(B)} + 1/2J^*_{A,pB,p} + 2\gamma_p(1+S_p)^{-1} \end{aligned} \tag{7}$$

$$\begin{aligned} \Delta_p = {} & \overline{Q}_p^2 \, [1/4(J_{A,pA,p} + J_{B,pB,p}) - 1/2J^*_{A,pB,p} \\ & - \gamma_p] + \overline{Q}_p [(H_{B,p} - H_{A,p}) + 1/2(J_{B,pB,p} \\ & - J_{A,pA,p}) + \sum_{\substack{T,\,q\\ (q\neq p)}} (1 - \overline{Q}_q^T)\{(J_{B,pT,q} \\ & - 1/2\delta_{B,pT,q}K_{B,pT,q}) - (J_{A,pT,q} - \\ & 1/2\delta_{A,pT,q}K_{A,pT,q})\} + 2\sum_f \{(J_{fB,p} - \\ & 1/2\delta_{fB,p}K_{fB,p}) - (J_{fA,p} - 1/2\delta_{fA,p}K_{fA,p})\}] \end{aligned} \tag{8}$$

and where $\sum_a$ and $\sum_p{}'$ denote summations over all atoms and over all bonds except lone pairs respectively; the parenthesis, (a), etc., of the AO refer to the atom, a etc., and the R, p, etc., stand for the valence AO A, p, B, p etc. The superscripts, small circle, asterisk and double prime of H, J, etc., denote the one-center integrals, two-center integrals between directly-bonded atoms and two-center integrals between the other paired atoms respectively under the conditions $H = H^\circ + H^* + H''$, etc. The symbol W_a represents the valence state energy of the atom a: the E_p and Δ_p correspond to the covalent bond energy and the ionic-covalent resonance energy of the bond p respectively. By using Eqs. 2, 3 and 4, Eq. 1 may be reduced to

$$\begin{aligned} W = {} & \sum_a \Delta W_a + [\sum_p{}' (E_p + \Delta_p) + 1/2\sum_{ab} Z'_a Z'_b / R_{ab}] \\ & + (\sum_a W'_a + 1/2\sum_{cd} Z'_c Z'_d / R_{cd}) - \sum_{\substack{pq\\ (q\neq p)}} S_{pq} W_{pq} \\ & - 2\sum_{ik} (\beta^{+-}_{ik})^2 / (\varepsilon^-_k - \varepsilon^+_i) \end{aligned} \tag{9}$$

where $\Delta W_a (= W_a - W_a^\circ)$ is the promotion energy of the atom a. If there are n_a bonds connected with the atom a, then its contribution to the bond energy for each bond separately may be estimated as $\Delta W_a / n_a$, because the empirical bond energy contains implicitly the energy of lone pairs and all hybridized AO are here considered to be equivalent to each other. As can be seen from Eq. 6, the third term of Eq. 9 may be approximated as

$$\sum_a W'_a + 1/2\sum_{cd} Z'_c Z'_d / R_{cd} \sim 0 \tag{10}$$

The fourth and fifth terms of Eq. 9 are related to interaction energies between different bonds or lone pairs; although actually they may not be assigned to specific bonds or lone pairs, nevertheless it is possible[11] to do this in a strictly formal sense. Since usually $S_{pq} > 0$ and $W_{pq} < 0$, the fourth and fifth terms may be taken to be positive and negative respectively. It follows that the two terms tend to cancel each other and that the contribution of these terms to the bond energies is small.

Let us now consider the influence of the inductive effect on the heats of formation.

11) The fourth term may be assigned to specific bonds or lone pairs as follows from Eq. 3. It was shown by Dewar and Pettit (M. J. S. Dewar and R. Pettit, *J. Chem. Soc.*, **1954**, 1625) that if all bond orbitals are degenerated or almost degenerated the fifth term may be approximated by

$$\sum_{ik} (\beta_{ik}{}^{+-})^2 / (\varepsilon_k{}^- - \varepsilon_i{}^+) \sim \sum_{\substack{pq\\ (p\neq q)}} (\beta_{pq}{}^{+-})^2 / (\varepsilon_q{}^- - \varepsilon_p{}^+)$$

where the p and q stand for bonding and antibonding orbitals respectively.

By using the results of Ref. 1, the Δ_p may be rewritten as:

$$\Delta_p = -1/2\, K_p^{-1}\, \overline{Q}_p^2$$
$$= -1/2K_p^{-1}\,[\overline{\Pi}_{pp}Q_p^{\circ 2} + 2\overline{\Pi}_{pp}Q_p^{\circ}\sum_{q\neq p}\overline{\Pi}_{pq}Q_q^{\circ} + (\sum_{q\neq p}\overline{\Pi}_{pq}Q_q^{\circ})^2] \quad (11)$$

The second and third terms correspond to the induced energy at the bond p, they are generally small compared with the first term, because the quantities Q° and $\overline{\Pi}_{pq}$ $(p\neq q)$ are smaller than unity and $\overline{\Pi}_{pp}$ is nearly equal to unity here.[1,2] For an essentially covalent bond ($Q_p^\circ = 0$), the third term is important, but it is still small. It follows that the influence of the inductive effect on resonance energies is insignificant. Equation 11 also shows that the Δ_p values are negative and that their absolute values increase with an increase in the bond polarity; this has already been included in Pauling's theory.[12]

It may be difficult to predict the influence of the inductive effect on the fourth and fifth terms of Eq. 9; however, it can be inferred as follows: Electron transfer by the inductive effect occurs, as in Fig. 1 of Ref. 1, so that the induced energy in the term $S_{pq}W_{pq}$ tends to be cancelled and the induced energies in the paired quantities, $(\beta_{pq}^{+-})^2$ and $(\beta_{qp}^{+-})^2$, which appear in the quantities $(\beta_{Ik}^{+-})^2$ also tend to cancel each other.[13] It seems, therefore, that the influence of the inductive effect on the heat of formation is very small. For example, in the series CH_3X, CH_2X_2, CHX_3 and CX_4 (X=Cl, Br, I), by taking the CH bond energies to be 90.4 kcal./mol.,[14] the C–Cl bond energies are empirically obtained as 71, 70, 70 and 69.6 kcal./mol.,[14] the C–Br bond energies, as 57, 57, 58 and 58 kcal./mol.,[14] and the C–I bond energies, as 43, 43 and 43 kcal./mol.[14] respectively. As has been shown in Ref. 2, however, the polarities of the CX bonds in these series are all changed by the inductive effect. Nevertheless, these bond energies and also the CH bond energies appear to be almost constant. This seems to confirm our inference. The bond energy, D_p, of the bond p, therefore, may be obtained as:

$$D_p = |\Delta W_A/n_A + \Delta W_B/n_B + E_p + Z'_A Z'_B/R_{AB} - 1/2K_p^{-1}\, Q_p^{\circ 2} + \lambda_p| \quad (12)$$

Since the variation in the promotion energy, ΔW, from molecule to molecule is generally small, at least for similar molecules, as has been discussed in Ref. 2, each term of Eq. 12 except the last term may be regarded as specific for the bond p. The λ_p is a small correction term which is mainly due to the interaction energy between the bond p and its adjacent bonds or lone pairs. However, this term is implicitly included in the empirical bond energy. Actually, for the branched isomers of hydrocarbons, small deviations in the empirical bond energies have been reported.[15] For a series of similar molecules such as hydrocarbons, however, this relative variation may be expected to be quite small, because the λ_p values are nearly constant. The D_p may thus be regarded as the empirical bond energy. To an even cruder approximation, the D_p may be rewritten as

$$D_p \sim |\Delta W_A/n_A + \Delta W_B/n_B + 1/4(J_{A,pA,p} + J_{B,pB,p}) + (B:A,\ pA,\ p) + (A:B,\ pB,\ p) + 1/2J_{A,pB,p} + 2\gamma_p(1+S_p)^{-1} - 1/2K_pQ_p^{\circ 2} + \lambda_p| \quad (13)$$

In this approximation, it is shown that the lone pairs on both the atoms A and B make no contributions to the bond energy except indirectly. The bond energy is then regarded as specific for the bond only.

Another necessary condition for bond additivity is that the length of one particular bond be the same in different positions or molecules. This condition is satisfied for saturated compounds, but it is well known that the bond lengths in nonsaturated compounds may vary considerably. It may thus be concluded that bond energies are not only additive but also remain constant for different molecules in saturated compounds.

II. The Bond Additivity of the Dipole Moment.—If nuclei and inner-shell electrons are regarded as point charges, the molecular dipole moment, μ, may be given by:

$$\mu = e\,[\langle \boldsymbol{r}_e\rangle - \sum_a Z'_a \boldsymbol{R}_a] \quad (14)$$

where

$$\langle \boldsymbol{r}_e\rangle = \langle \Phi^* |\ \boldsymbol{r}_e\ | \Phi\rangle$$

The $\boldsymbol{R}_a$ and $\boldsymbol{r}_e$ are the radius vectors which represent the position of the nucleus of the atom a and the electrons respectively, and Φ is the molecular wave function given by Eq. 1 of Ref. 1. By using the previous results,[1] we obtain

$$\langle \boldsymbol{r}_e\rangle = 2\sum_I [\boldsymbol{r}_I^+ - 2\sum_k \boldsymbol{r}_{Ik}^{+-}\ \beta_{Ik}^{+-}/(\varepsilon_k^- - \varepsilon_I^+)$$

12) L. Pauling, "The Nature of the Chemical Bond," Cornell Univ. Press, N. Y. (1945).
13) See also Ref. 11.
14) M. L. Huggins, *J. Am. Chem. Soc.*, **75**, 4123 (1953).
15) J. R. Platt, *J. Chem. Phys.*, **15**, 419 (1947).

$$+\sum_{kl} \boldsymbol{r}^{-}_{kl}\ \beta^{+}_{ik}{}^{-}\beta^{+}_{il}{}^{-}/(\varepsilon^{-}_{k}-\varepsilon^{+}_{i})\ (\varepsilon^{-}_{l}-\varepsilon^{+}_{i})] \tag{15}$$

where

$$\boldsymbol{r}^{+}_{ik}{}^{-}=\langle\psi^{+}_{i}\,|\boldsymbol{r}_{e}|\,\psi^{-}_{k}\rangle, \qquad \boldsymbol{r}^{+}_{i}\equiv\boldsymbol{r}^{+}_{ii}{}^{+}, \text{ etc.}$$

The subscript i refers to the unperturbed filled MO, and the subscripts k and 1, to the unperturbed empty MO respectively. The last term is relatively small; it will, therefore, be neglected. According to a discussion similar to that of the previous section, we obtain[10]

$$\sum_{i}\boldsymbol{r}^{+}_{i}=\sum_{p}\overline{\boldsymbol{r}}_{p}=\sum_{p}\boldsymbol{r}_{p}-\sum_{\substack{pq\\(p\neq q)}}S_{pq}\boldsymbol{r}_{pq} \tag{16}$$

where the $\overline{\boldsymbol{r}}_{p}$ and $\boldsymbol{r}_{p}$ are the corresponding quantities for OBO p and BO p respectively. Equation 15 may now be reduced to:

$$\langle\boldsymbol{r}_{e}\rangle=2\sum_{p}\boldsymbol{r}_{p}-2\sum_{\substack{pq\\(p\neq q)}}S_{pq}\boldsymbol{r}_{pq} -4\sum_{ik}\boldsymbol{p}^{+}_{ik}{}^{-}\ \beta^{+}_{ik}{}^{-}/(\varepsilon^{-}_{k}-\varepsilon^{+}_{i}) \tag{17}$$

The first term may be assigned to a specific bond or a lone pair, but this is not necessarily true for the other terms. By using Eqs. 18 and 21 of Ref. 1, $\boldsymbol{r}_{p}$ may be represented as:

$$\begin{aligned}\boldsymbol{r}_{p}&=1/2\,[(1-\overline{Q}_{p}-F_{p}S_{p})\boldsymbol{r}_{A,p}+(1+\overline{Q}_{p}\\&\quad-F_{p}S_{p})\boldsymbol{r}_{B,p}+2F_{p}\boldsymbol{r}_{A,pB,p}=1/2\,[(\boldsymbol{R}_{A}+\boldsymbol{R}_{B})\\&\quad+(\boldsymbol{r}^{x}_{A,p}+\boldsymbol{r}^{x}_{B,p})+\overline{Q}_{p}(\boldsymbol{R}_{p}+\boldsymbol{r}^{x}_{B,p}-\boldsymbol{r}^{x}_{A,p})\\&\quad-F_{p}\boldsymbol{V}_{p}]\end{aligned} \tag{18}$$

where

$$\boldsymbol{V}_{p}=S_{p}(\boldsymbol{r}_{A,p}+\boldsymbol{r}_{B,p})-2\boldsymbol{r}_{A,pB,p}$$

$$\boldsymbol{r}_{U,p}=\boldsymbol{R}_{U}+\boldsymbol{r}^{x}_{U,p} \qquad (U=A, B)$$

The $\boldsymbol{R}_{U}$ and $\boldsymbol{r}^{x}_{U,p}$ stand for the radius vector for the nucleus of the atom U and the atomic dipole vector of AO U, p respectively. $\boldsymbol{R}_{p}$ is the vector pointing from nucleus A to nucleus B along the bond p with the distance R_{AB} as its magnitude. In a similar way, we have for lone pairs:

$$\boldsymbol{r}_{f(a)}=\boldsymbol{R}_{a}+\boldsymbol{r}^{x}_{f(a)} \tag{19}$$

We thus obtain:

$$\begin{aligned}2\sum_{p}\boldsymbol{r}_{p}&\equiv2(\textstyle\sum'_{p}\boldsymbol{r}_{p}+\sum'_{f}\boldsymbol{r}_{f})=\sum_{a}Z'_{a}\boldsymbol{R}_{a}+\sum_{a}\boldsymbol{r}^{x}_{a}\\&\quad+\textstyle\sum'_{p}\overline{Q}_{p}(\overline{\boldsymbol{R}}_{p}+\boldsymbol{r}^{x}_{B,p}-\boldsymbol{r}^{x}_{A,p})-\sum'_{p}F_{p}\boldsymbol{V}_{p}\end{aligned} \tag{20}$$

where

$$\boldsymbol{r}^{x}_{a}=\sum_{U,p(a)}{}'\boldsymbol{r}^{x}_{U,p(a)}+2\sum_{f(a)}{}'\boldsymbol{r}^{x}_{f(a)} \tag{21}$$

$\sum'_{p}$ and $\sum'_{f}$ denote summations over bonds and lone pairs exclusively, and U, p(a) stands for the AO belonging to the atom a and the bond p. Since the valence AO of the atom a may be an equivalent set in the present treatment, the total atomic dipole of the atom a given by Eq. 21 may be rewritten as

$$\boldsymbol{r}^{x}_{a}=\sum_{f(a)}{}'\boldsymbol{r}^{x}_{f(a)} \tag{22}$$

This shows that the total atomic dipole vanishes except for the lone pair dipole. By using Eqs. 17, 20 and 22, the molecular dipole moment, μ, may now be written as

$$\begin{aligned}\mu=e\,[&\textstyle\sum'_{f}\boldsymbol{r}_{f}+\sum'_{p}\overline{Q}_{p}(\boldsymbol{R}_{p}+\boldsymbol{r}^{x}_{B,p}-\boldsymbol{r}^{x}_{A,p})-\sum'_{p}F_{p}\boldsymbol{r}_{p}\\&-2\sum_{\substack{pq\\(p\neq q)}}S_{pq}\boldsymbol{r}_{pq}-4\sum_{ik}\boldsymbol{r}^{+}_{ik}{}^{-}\beta^{+}_{ik}{}^{-}/(\varepsilon^{-}_{k}-\varepsilon^{+}_{i})]\end{aligned} \tag{23}$$

If we restrict ourselves to the case of small bond polarity, apart from the last two terms of Eq. 23, which may not be specific for localized bonds or lone pairs, the bond moment, μ_{p}, may be defined by:

$$\begin{aligned}\mu_{p}=e\,[\{&(\textstyle\sum_{f(A)}{}'\boldsymbol{r}^{x}_{f(A)})_{p}+(\sum_{f(B)}{}'\boldsymbol{r}^{x}_{f(B)})_{p}\}-\boldsymbol{V}_{p}/(1+S_{p})\\&+\overline{Q}_{p}(\boldsymbol{R}_{p}+\boldsymbol{r}^{x}_{B,p}-\boldsymbol{r}^{x}_{A,p})+1/2\overline{Q}_{p}\boldsymbol{V}_{p}\}]\end{aligned} \tag{24}$$

where $e(\sum_{f(A)}{}'\boldsymbol{r}^{x}_{f(A)})_{p}$ and $e(\sum_{f(B)}{}'\boldsymbol{r}^{x}_{f(B)})_{p}$ are the components of the lone pair moments of the atoms A and B respectively in the direction of the bond p. The first term, therefore, is the part of the atomic dipole due to the lone pairs; it vanishes for atoms such as tetrahedral carbon. It follows that in the atomic dipoles only the lone pairs contribute to the bond moments if we neglect the indirect contributions from the other terms of Eq. 24. This conclusion agrees with previous works,[9,16,17] and the significance of the lone pair dipole has been emphasized by several authors.[9,16-19] The second term is the homopolar dipole moment which is especially significant for homopolar bonds, and the third term is the heteropolar dipole, which is due to the bond polarity. In Mulliken's approximation[20] the homopolar dipole term vanishes; in addition, if the atomic dipole is neglected, we obtain

$$\mu_{p}=e\overline{Q}_{p}\boldsymbol{R}_{p} \tag{25}$$

The bond moment, μ_{p}, then coincides with the

16) J. A. Pople, *Proc. Roy.* Soc., **A202**, 323 (1950).
17) H. F. Hameka and A. M. Liquori, *Mol. Phys.*, **1**, 9 (1958).
18) D. Z. Robinson, *J. Chem. Phys.*, **17**, 1022 (1949).
19) H. Hamano and H. F. Hameka, *Tetrahedron*, **18**, 985 (1962).
20) R. S. Mulliken, *J. Chem. Phys.*, **46**, 497, 675 (1949).

corresponding empirical quantity.[6] This approximation, however, is generally not correct. The significance of the homopolar dipole has also been stressed by several authors.[8,18,19,21-23] For instance, the actual calculation[8,17,23] of the bond moment of the CH bond, which is regarded as nearly homopolar, yields a large value for this term, even if the atomic dipole is neglected. In spite of these facts, the concept of bond moments as given by Eq. 25 has proved to be a useful tool in the interpretation of experimental dipole moments.

The quantum mechanical theory does not seem to be in agreement with this. However, the discrepancy may be interpreted as follows: A vector summation over the whole molecule of the atomic dipoles and homopolar dipoles of Eq. 24 may tend to cancel some of the terms that cause the discrepancies. This statement may not have a general validity, but it seems to be correct for many organic compounds where all the bonds connected to one central atom usually point in opposite directions. The same inference may be true for the last two terms of Eq. 23; they also tend to cancel each other. In fact, the empirical bond moments are usually much smaller than those given by Eq. 24; sometimes their directions are even opposite to the theoretical ones.[23] In addition, if it is borne in mind that the empirical bond moments are not uniquely defined and that it is permissible to omit the quantities which are cancelled in summing over the whole molecule as long as this sum reproduces the total molecular dipole moment, it is not surprising that the theoretical and empirical bond moments are not in agreement with one another.

We will now consider the influence of the inductive effect on the bond moment. Since the Q_p consists of the specific Q_p° and induced Q_p' polarities,[1] if follows from Eq. 24 that the induced bond moment is nearly proportional to the induced polarity, Q_p'. The intra-bond electron transfers caused by the inductive effect occur as in Figs. 1 or 2 of Ref. 1, so the vector sum of the induced bond moment throughout the molecule may be additive. Besides, each bond moment is sensitive to variations in the hybridization. The bond moment, μ_p, may thus be defined as different in different molecules, and the molecular dipole moments may depend greatly on the inductive effect. The dipole moments of the series of CH_3X, CH_2X_2 and CHX_3 (X=halogens), which are tabulated in Table II of Ref. 2, seem to support this argument; if the CX and CH bond moments in these series were constant, the CH_2X_2 molecules would have the larger dipole moments and the CH_3X and CHX_3 molecules would have the same smaller moments. The experimental data, however, show that the dipole moments of these series decrease in the above order. This discrepancy has already been discussed in the preceding paper.[2] Another example has also been shown in Ref. 2. The assumption of a uniform bond moment, therefore, may be a poor approximation when the inductive effect is taken into consideration. Bond moments do not remain constant for different molecules, whereas for bond energies they do.

The previous argument assumes again that all bond lengths are constant; the validity of this assumption has already been discussed in the previous section.

Discussion

In the present treatment, it has been shown that the bond additivity is valid only if the delocalization of the bond electrons in σ electron systems is small. At first sight, therefore, it appears that the bond additivity is based only on the localization of the electrons in their bonds. The justification of the bond additivity, however, is essentially due to the following: If the BO are taken as a basis, such physical quantities as heats of formation and dipole moments may be represented by the matrices of the corresponding operators with respect to the BO. By means of a unitary transformation these matrices may be diagonalized; the heat of formation or the dipole moment of the molecule is then obtained as the trace of the matrix. After the transformation, each diagonal element may formally be assigned to one specific bond. However, since the trace of the matrix remains invariant,[24] we may also take the diagonal elements of the original matrix as each describing a separate bond. Their sum will then correctly represent either the total heat of formation or the dipole moment of the molecucle, even though the diagonal elements bofore and after the unitary transformation are not necessarily the same.[25] For bond

21) R. S. Mulliken, *J. Chem. Phys.*, 3, 573 (1935).
22) C. A. Coulson and M. T. Rogers, ibid., 35, 593 (1961).
23) H. Hamano, ibid., 34, 1678 (1961).

24) Actually this is true only for the localized MO, but since the orbitals are sufficiently localized in each specific bond or lone pair, it is a reasonably good approximation for the BO also.

25) This is equivalent with the principle of spectroscopic stability as introduced by Born et al. (M. Born, W. Heisenberg and P. Jordan, *Zeits. f. Physik*, 35, 557 (1926)). In fact, the theoretical background for many semi-empirical models in physical and chemical problems, especially for sum rules, is due to this principle; the details and some examples appear in Van Vleck's book (J. H. Van Vleck, "Electric and Magnetic Susceptibilities," Oxford Univ. Press, London (1932)), in connection with the principle of spectroscopic stability.

energies this was discussed in Ref. 1; for bond moments it is shown in Eq. 16.

The validity of the concept of bond additivity is due not only to the facts above, but also to the accidental cancellations when summing over the whole molecule. These cancellations occur in different ways for different quantities and then determine whether the bond quantities are constant or not from molecule to molecule, the former case for bond energies and the latter for bond moments. These facts often make the empirical bond quantities appear to be different quantities from those obtained quatum-mechanically.[26] This is especially true for bond moments. In practice, if the bond quatities are constant for different molecules, we say that the bond additivity rule holds. In this sense, dipole moments do not follow the additivity rule.

Chemists have often discussed the physical quantities of molecules by using the "*chemical bond*" concept. At first sight it seems to follow from our considerations that this concept is not meaningful theoretically because the bond orbitals are not eigenfunctions and molecular-observable quantities should be derived as expectation values of the molecular wave function. The present argument, however, shows that the chemical bond is a reasonable concept as long as it is used to discuss properties belonging to the total molecule. The situation is the same for the valence AO's of atoms; they are also equivalent orbitals which are not eigenfunction. The concept of these localized orbitals is thus very useful for chemists, even though it does not have physical significance. It is also worth noting that the concept of bond is not directly connected with the empirical bond additivity rules, as has been discussed above.

26) The contribution of lone pairs then vanishes in the approximation of Eq. 13 for heats of formation and does not vanish for dipole moments, its influence is implicitly accounted for by adjusting the empirical value for the bond quantity.

Summary

The aditivity rules for bond energies and bond moments are discussed on the basis of a previously-proposed theory. The results show that the apparent additivities are partially caused by accidental cancellations when summing over the molecule and essentially by the invariance of the trace of the matrix representing the molecular quantity. Bond energies are then constant in different molecules, whereas bond moments are not, mainly because of the inductive effect.

The author wishes to thank Dr. H. F. Hameka for his stimulating interest and encouragement, and Professor R. G. Parr for his reading the manuscript.

Department of Chemistry
University of Pennsylvania
Philadelphia 4, Pennsylvania, U. S. A.

*The Homolytic Methoxylation of Aromatic Compounds by the Anodic Oxidation of Methanol**

By Tadao INOUE, Kikuhiko KOYAMA and Shigeru TSUTSUMI

(Received April 11, 1964)

In a previous paper,[1] we have described how the anodic oxidation of methanol in the presence of alkylated aromatic hydrocarbons produces α-methoxy derivatives, which might be formed by the reaction of a methoxyl radical generated by the electrolysis of methanol as an intermediate.

The present study was undertaken to provide additional information about the anodic methoxylation of aromatic compounds. Thus, diphenylmethane, indan and tetralin, which are known as compounds with hydrogen atoms reactive towards autoxidation[2] or other free-radical reactions,[3] were chosen as the aromatic compounds.

* Reported at the 16th Annual Meeting of the Chemical Society of Japan, Tokyo, April, 1963.

1) T. Inoue, K. Matsuoka, T. Matsuoka, K. Koyama and S. Tsutsumi, *J. Chem. Soc. Japan, Ind. Chem. Sec. (Kogyo Kagaku Zasshi)*, **66**, 1659 (1963).

2) H. Hartmann and M. Seiberth, *Helv. Chim. Acta*, **15**, 1390 (1932); H. Hock and W. Svemihl, *Ber.*, **66**, 61 (1933).

3) G. Sosnovsky and N. C. Yang, *J. Org. Chem.*, **25**, 899 (1960); K. Sima, Y. Shigemitsu and S. Tsutsumi, This Bulletin, **35**, 1728 (1962).

TABLE I. ANODIC METHOXYLATION OF TETRALIN

Expt. No.	CH_3OH g. (mol.)	Metallic sodium g.	Tetralin g. (mol.)	Current density amp./dm²	Amp. hr.	Product I, α-methoxytetralin g.	% c)	Current yield, % d)
1 a)	75(2.34)	0.5	40(0.30)	8.3	30.0	9.0	22	10
2 b)	75(2.34)	0.5	40(0.30)	6.5	18.8	5.6	14	10
3 a)	75(2.34)	0.5	45(0.34)	8.3	35.0	13.1	29.1	13

a) The electrolysis was carried out under following initial electrolytic conditions: current, 0.5 amp.; volt, 15 V.; temp., 12°C.
b) The electrodes, 2.3×3.3 cm², were used.
c) Based on tetralin used.
d) The current yields are based on the calculation that two moles of methanol should be oxidized to give a one-mole of the product I.

TABLE II. ANODIC METHOXYLATION OF INDAN

Expt. No.	CH_3OH g. (mol.)	Metallic sodium g.	Indan g. (mol.)	Current density amp./dm²	Amp. hr.	Product II, α-methoxyindan g.	%	Current yield, %
1 a)	75(2.34)	0:5	40(0.34)	8.3	30.0	6.4	15.1	8

TABLE III. ANODIC METHOXYLATION OF DIPHENYLMETHANE

Expt. No.	CH_3OH g. (mol.)	Metallic sodium g.	Diphenyl-methane g. (mol.)	Current density amp./dm²	Amp. hr.	Product III, α-methoxydiphenylmethane g.	Current yield, %
1 e)	75(2.34)	0.2	26.5(0.15)	1.6~4.2	6.7	0.9	3.6
2 f)	100(3.1)	0.5	50 (0.27)	3.3	17.6	1.8	2.9

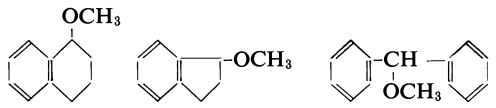
e) Initial electrolytic conditions: current, 0.1~0.25 amp.; volt, 7~12 V.; temp., 33°C.
f) Initial electrolytic conditions: current, 0.2 amp.; volt, 25 V.; temp., 33 °C.

Results and Discussion

The electrolyses were carried out using two platinum foil electrodes at 15~20°C, and the current density was kept approximately 8.3 amp./dm², according to the procedure described earlier.[1] The anodic oxidation of methanol containing sodium methoxide in the presence of tetralin afforded α-methoxytetralin (I) as a main product (current yield: 10~13%) and a small amount of formaldehyde, which was identified as its 2,4-dinitrophenylhydrazone, but the formation of the other isomeric methoxytetralin or of the dimeric product was not observed. When indan or diphenylmethane was used instead of tetralin, α-methoxyindan (II) (current yield: 8%) or α-methoxydiphenylmethane (III) (current yield: 2.9~3.6%) was obtained as the main product in each case. The experimental results obtained are summarized in Tables I, II and III. These products were analyzed by gas chromatography and infrared spectroscopy.

From these results, it can be considered that the methoxylated products are produced through a mechanism involving the attack of methoxy radicals upon the hydrocarbons; this hypothesis is based on the following reasons:

(A) The Position of Substitution: The reaction products clearly indicated that the methoxyl group was introduced in the α-position of the hydrocarbons, at which the hydrogen abstraction took place by ordinary free-radical reactions.[3-5]



(I) (II) (III)

(B) The Reactivity of the Aromatic Compounds: The relative reactivities were obtained by the following calculations: A/BC, where A: the yield (mol.) of α-methoxylated products; B: amp. hr. and C: the number of active hydrogen atoms.

TABLE IV. THE RELATIVE REACTIVITY OF THE AROMATIC HYDROCARBONS

Hydrocarbon	Product	A/B	A/BC
Diphenylmethane	III	6.7×10^{-4}	3.3×10^{-4}
Indan	II	14.4×10^{-4}	3.6×10^{-4}
Tetralin	I	23.1×10^{-4}	11.6×10^{-4}

The data given in Table IV indicate that the reactivity of these compounds in these electrolyses increases in the following order:

4) J. A. Meyer, V. Stannett and M. Szwarc, *J. Am. Chem. Soc.*, **83**, 25 (1961).
5) G. A. Russell, ibid., **78**, 1047 (1956); A. L. Williams, F. A. Oberright and J. W. Brooks, ibid., **78**, 1190 (1956).

diphenylmethane < indan < tetralin

This increasing order of the reactivities of these hydrocarbons is also observed in other free-radical reactions involving ROO·, *t*-BuO· and CH_3· radicals.[4,5]

The results obtained here, however, show a remarkable contrast to the observations that a methoxyl radical formed by the decomposition of peroxides reacts with the aromatic hydrocarbons to give high yields of methanol and benzylic dimers, but no methoxylated products.[6,7] Such an anomalous reaction in these electrolyses can be explained as follows:

(a) Since the environment around the electrode might have a particularly high concentration of the methoxyl radical, the benzylic radicals resulting from the hydrogen abstraction by the methoxyl radical would be expected to react preferentially with the methoxyl radical and, consequently, not to give the dimeric products.

(b) As another possible rationalization, the following reaction path may be considered:

$$R\cdot \xrightarrow[\text{anode}]{-e} R^+ \xrightarrow{CH_3O^-} ROCH_3$$

Recently, Bonner and Mango[8] reported that electrolytically-generated benzyl radicals in the Kolbe electrolysis were oxidized with greater ease. Thus, the possibility that the free radical might be oxidized to carbonium ions to give solvolysis product can not be excluded in the present case.

Therefore, it may be assumed that the α-methoxylated products would be produced by the following course:

$$CH_3ONa \longrightarrow CH_3O^- + Na^+$$

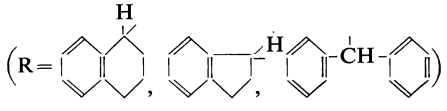
$$CH_3O^- \xrightarrow[\text{anode}]{-e} CH_3O\cdot$$

$$CH_3O\cdot + RH \longrightarrow CH_3OH + R\cdot$$

$$CH_3O\cdot + R\cdot \longrightarrow ROCH_3$$

or

$$R\cdot \xrightarrow[\text{anode}]{-e} R^+ \xrightarrow{CH_3O^-} ROCH_3$$



Experimental

All melting points and boiling points illustrated in the report are uncorrected. Electrolyses were carried out with the apparatus previously described.[1]

Materials.—When commercial tetralin was treated with solid sodium hydroxide and distilled from sodium, a fraction (b. p. 81.5~83°C/14 mmHg, $n_D^{20}=1.5380$) was collected. Indan was prepared by the reduction of α-chloroindan[9] with lithium aluminum hydride in a dry ethereal solution; b. p. 176~177°C (lit.,[10] b. p. 177°C), $n_D^{20}=1.5382$. Diphenylmethane was obtained commercially and was carefully distilled from sodium; b. p. 122~123°C/10 mmHg, $n_D^{20}=1.5767$. Methanol was purified in the manner described earlier.[1] These materials were confirmed to be pure by gas chromatography.

The Anodic Oxidation of Methanol in the Presence of Tetralin.—The reaction conditions and the yields of the product I are summarized in Table I.

R-3 is exemplified as follows: Metallic sodium (0.5 g., 0.022 mol.) was dissolved in 75 g. of absolute methanol, and then 45 g. of tetralin (0.34 mol.) was added to the mixture. After dry nitrogen had been bubbled through the mixture for about 1 hr., the mixture was electrolyzed at 12°C for 78 hr. and a current was maintained at nearly 0.5 amp. During the course of the electrolysis, tetralin was gradually dissolved and the electrolyzed solution turned brown in color. The reaction mixture was worked up in a manner similar to that used in an experiment described earlier.[1] After the ether had been removed, the oily residue (44.5 g.) was distilled under diminished pressure to give the following fractions:

Fraction	B. p., °C/mmHg	Weight, g.
1	40~62/1~2	29.3
2	62~83/1~2	8.3
3	83~120/1~2	1.6
4	Residue	2.0

By gas chromatographic analysis (conditions: column, P. E. G. 6000 and P. E. DA, 3 m.; column temperature, 160°C; carrier gas, H_2), it was shown that every fraction except fraction 4 was a mixture of unreacted tetralin and α-methoxytetralin, and that the total amount of this product was 13.1 g. Fraction 2 was chromatographed over silica gel (2.5×58 cm.). Elusion with benzene led to the isolation of unreacted tetralin, and α-methoxytetralin; b. p. 80~82°C/2 mmHg, $n_D^{15}=1.5363$.

Found: C, 81.22; H, 8.60. Calcd. for $C_{11}H_{14}O$: C, 81.44; H, 8.70%.

The infrared spectrum of the latter compound showed the characteristic absorption band at 1092 cm^{-1} (C-O-C of aliphatic ether) and was identical with that of an authentic sample prepared as described below.

The Synthesis of α-Methoxytetralin.—α-Methoxy-β-bromotetralin was prepared by the reaction of α, β-dibromotetralin with methanol according to the procedure of Braun;[11] b. p. 118~120°C/2~3 mmHg (lit., b. p. 151~152°C/13 mmHg). α-Methoxytetralin was prepared by the reduction of α-methoxy-β-bromotetralin with lithium aluminum hydride in dry ether and was purified by the column chromotography (column; silica gel, 2.5×58 cm.; eluted with

6) P. Gray and A. Williams, *Chem. Revs.*, **55**, 268 (1959).
7) H. C. McBay and O. Tucker, *J. Org. Chem.*, **19**, 869 (1954).
8) W. A. Bonner and F. D. Mango, ibid., **29**, 430 (1964).
9) R. Weissgerber, *Ber.*, **44**, II, 1444 (1911).
10) A. V. Gross, J. M. Mavity and J. Mattox, *Ind. Eng. Chem.*, **38**, 1041 (1946).
11) J. V. Braun and G. Kirschbaum, *Ber.*, **54**, 612 (1921).

benzene). B. p. 80~81.5°C/1~2 mmHg, $n_D^{15}=1.5371$.

The Anodic Oxidation of Methanol in the Presence of Indan. — To a solution of sodium methoxide (0.5 g., 0.022 mol.) in 75 g. of absolute methanol, 45 g. (0.38 mol.) of indan was added. This new solution, after dry nitrogen had been bubbled through, was electrolyzed for 93 hr. under the following initial conditions: current, 0.5 amp.; volt, 15 V.; temperature, 12°C; current density, 8.3 amp./dm². During the course of the reaction, both electrodes were mutually exchanged at intervals to avoid the deposition of resinous materials. When the electrolyzed solution was treated in a manner similar to the experiment described earlier,[1] it gave the following fractions:

Fraction	B. p., °C/mmHg	Weight, g.
1	~50/1~2	24.5
2	50~82/1~2	7.9
3	82~100/1~2	3.0
4	Residue	3.5

Gas chromatographic analysis (column, P. E. G. 6000 and P. E. DA, 3 m.; column temperature, 159°C; carrier gas, H_2) showed that fractions 1, 2 and 3 were mixtures of unreacted indan and α-methoxyindan, and that the total amount of this product was 6.8 g.

Fraction 2 was chromatographed over silica gel and eluted with benzene to give following fractions:

Fraction	B. p., °C/mmHg	Weight, g.
a	55~57/10	1.5 $n_D^{20}=1.5380$
b	65~66/1~2	6.1 $n_D^{17}=1.5312$

Fraction a was identified as unreacted indan by gas chromatographic and infrared spectroscopic analysis.

Fraction b was identified as α-methoxylated indan, since the infrared spectrum of fraction b was identical with that of an authentic sample prepared by the following method and since it exhibited a characteristic absorption band at 1087 cm^{-1} (assigned to aliphatic ether C-O-C).

Found: C, 80.83; H, 8.39. Calcd. for $C_{10}H_{12}O$: C, 81.04; H, 8.16%.

The Synthesis of α-Methoxyindan.—α-Chloroindan was prepared by the reaction of indene with dry hydrochloric acid at 0~−10°C according to the procedure of Weissgerber.[9] B. p. 104~105°C/21~22 mmHg. α-Methoxyindan was prepared by the reaction of α-chloroindan with sodium methoxide in a methanol solution; b. p. 65~66°C/1~2 mmHg, $n_D^{17}=1.5312$.

The Anodic Oxidation of Methanol in the Presence of Diphenylmethane. —Metallic sodium (0.5 g.) was dissolved in 100 g. (3.1 mol.) of methanol, and then 50 g. (0.27 mol.) of diphenylmethane was added. The mixture was electrolyzed for 88 hr. under the following electrolytic conditions: current, 0.2 amp.; volt, 25 V.; temperature, 33°C; current density, 3.3 amp./dm². The reaction mixture was worked up in a manner similar to that used in an experiment described earlier.[1] From the ethereal layer, the following fractions were obtained:

Fraction	B. p., °C/mmHg	Weight, g.
1	102~111/2~3	39.3
2	111~126/2~3	2.5
3	126~152/2~3	1.1
4	Residue	4.5

By gas chromatographic analysis (conditions: column, P. E. G. 6000, 3 m.; column temperature, 192°C; carrier gas, H_2), it was also shown that every fraction except fraction 4 was a mixture of unreacted diphenylmethane and α-methoxydiphenylmethane, and that the total amount of this product was 1.8 g.

Fractions 2 and 3 were submitted to preparative gas chromatography (column, P. E. G. 6000, 6 m.; column temperature, 190°C; carrier gas, N_2), and the pure α-methoxydiphenylmethane was isolated; b. p. 120~121°C/2~3 mmHg, $n_D^{20}=1.5658$.

Found: C, 84.79; H, 7.19. Calcd. for $C_{14}H_{14}O$: C, 84.81; H, 7.12%.

The infrared spectrum of this product showed a strong C-O-C band at 1092 cm^{-1} and was identical with that of a sample prepared by the methylation of benzhydrol (0.015 mol.) with methyl iodide (0.09 mol.) and silver oxide (0.035 mol.); b. p. 120~121°C/2~3 mmHg, $n_D^{20}=1.5653$.

The authors wish to thank Dr. Yoshinobu Odaira and Dr. Noboru Sonoda for their helpful suggestions and encouragement.

Department of Chemical Technology
Faculty of Engineering
Osaka University
Miyakojima-ku, Osaka

*The Synthesis of Methacrylic Esters by Carboxylation Reaction of Methylacetylene. I. Methyl Methacrylate; Reaction Conditions and Products**

By Yasumasa SAKAKIBARA

(Received May 7, 1964)

In previous papers[1,2] the present author has reported the synthesis of methylacetylene by the pyrolysis of propylene. In this connection, it is of great interest to synthesize methacrylic esters, especially methyl methacrylate, by the carboxylation reaction of methylacetylene.

Numerous investigations have been made of the synthesis of acrylic esters by the carboxylation of acetylene;[3] the following three processes are known:

The stoichiometric process

$$4CH{\equiv}CH + Ni(CO)_4 + 4ROH + 2HCl \rightarrow 4CH_2{=}CHCO_2R + NiCl_2 + H_2$$

The catalytic process

$$CH{\equiv}CH + CO + ROH \xrightarrow{\text{Catalyst}} CH_2{=}CHCO_2R$$

Catalyst: Nickel halides, triphenylphosphine nickel complexes, etc.

The semicatalytic process**

The stoichiometric process plus

$$CH{\equiv}CH + CO + ROH \xrightarrow{Ni(CO)_4} CH_2{=}CHCO_2R$$

Concerning the carboxylation of methylacetylene, however, very little has been published. One article by Yakubovich and Volkova[4] and one patent[5] have described the synthesis of methacrylic acid and its lower alkyl esters by the stoichiometric process (low yields). Recently, it has been reported by another patent[6] that aminoalkyl methacrylates were synthesized in fairly good yields from methylacetylene by the semicatalytic process. Jones et al.,[7] investigating the carboxylation of various monosubstituted acetylenes by the stoichiometric process, obtained ethyl α-butylacrylate in a 50% yield from butylacetylene. This paper will describe the synthesis of methyl methacrylate by the carboxylation reaction of methylacetylene. In this investigation the reaction will be examined by both the stoichiometric and catalytic, including the semicatalytic, processes.

Experimental

Materials. — Methylacetylene was prepared by the dehydrobromination of propylene bromide with potassium hydroxide.[8] The crude methylacetylene was purified by fractional distillation through a Podbielniak-type low-temperature column (80 cm. × 1.5 cm.); b. p. −23∼−22°C. The purity was higher than 98.5 mol.%; allene was shown to be the principal impurity by gas chromatographic analysis.

Carbon monoxide (99.7 mol.% pure) was purchased from the Takachiho Chemical Co.

Metal Carbonyls. — Nickel tetracarbonyl,[9] chromium hexacarbonyl,[10] and dicobalt octacarbonyl[11] were prepared by the usual methods.

Nickel tetracarbonyl: a colorless, transparent liquid; b. p. 42∼43°C (lit. 43°C).

Chromium hexacarbonyl: colorless crystals; m. p. 153∼155°C (lit. 152∼155°C).

Dicobalt octacarbonyl: dark-brown crystals; m. p. 51°C (lit. 51°C).

Nickel Halides and Triphenylphosphine Nickel Bromide Complexes.—Anhydrous nickel bromide and

* Presented at the 16th Annual Meeting of the Chemical Society of Japan, Tokyo, April, 1963.

1) Y. Sakakibara, This Bulletin, **37**, 1262 (1964).

2) Y. Sakakibara, ibid., **37**, 1268 (1964).

3) a) J. W. Copenhaver and M. H. Bigelow, "Acetylene and Carbon Monoxide Chemistry," Reinhold Publishing Corp., New York (1949), p. 246; b) W. Reppe, *Ann.*, **582**, 1 (1953); c) K. Ohashi, S. Suzuki, H. Ito, M. Yonezawa and K.Ueno, *J. Chem. Soc. Japan, Ind. Chem. Sec.* (*Kogyo Kagaku Zassi*), **55**, 120, 607, 718 (1952); d) M. Maki, *J. Fuel Soc. Japan*, **32**, 410, 414 (1953); e) K. Yamamoto, K. Sato and M. Oku, This Bulletin, **27**, 491 (I-VI) (1954); f) M. Salkind, E. H. Riddle and R. W. Keefer, *Ind. Eng. Chem.*, **51**, 1328 (1959); Numerous patents.

** This process is a modification of Reppe's stoichiometric reaction: a catalytic reaction of carbon monoxide, acetylene, and alcohol by nickel carbonyl is superimposed upon the stoichiometric reaction (See Ref. 3f). In this paper, this process is classified as a catalytic process.

4) A. Ya. Yakubovich and E. V. Volkova, *Doklady Akad. Nauk S.S.S.R.*, **84**, 1183 (1952); (*Chem. Abstr.*, **47**, 3278 (1953)).

5) National Lead Co., Brit. Pat. 887433 (1962); (*Chem. Abstr.*, **57**, 11027 (1962)).

6) N. T. Gehshan and E. H. Specht, U. S. Pat. 2990403 (1961); (*Chem. Abstr.*, **56**, 9933 (1962)).

7) a) E. R. H. Jones, T. Y. Shen and M. C. Whiting, *J. Chem. Soc.*, **1950**, 230; b) **1951**, 766.

8) G. B. Heisig and H. M. Davis, *J. Am. Chem. Soc.*, **57**, 339 (1935).

9) W. Reppe and coworkers, *Ann.*, **582**, 116 (1953).

10) G. Brauer, "Handbuch der Präparativen Anorganischen Chemie," Ferdinand Enke Verlag, Stuttgart (1954), p. 1340; B. B. Owen, J. English, Jr., H. G. Cassidy and C. V. Dundon, *J. Am. Chem. Soc.*, **69**, 1723 (1947).

11) A. A. Blanchard and P. Gilmont, ibid., **62**, 1192 (1940).

nickel iodide were prepared by drying their hydrates at 140°C.[12]

Bis(triphenylphosphine)nickel dibromide, $(Ph_3P)_2NiBr_2$, was prepared by Yamamoto's procedure.[3e] It was a deep green solid; m. p. 218~220°C (lit. 221~222°C) (Found: C, 58.57; H, 4.31%).

Bis(triphenylphosphine)nickel dibromide *n*-butyl bromide, $(Ph_3P_2)_2NiBr_2BuBr$, was prepared by Reppe's procedure.[13] It was a bluish green solid; m. p. 178°C (lit. 178°C) (Found: C, 54.62; H, 4.71%).

Carboxylation. — *Stoichiometric Process.* — Two methods were employed. A) In a 200 ml., four-necked flask equipped with a mercury-sealed stirrer, a gas inlet, a dropping funnel, a thermometer, and a reflux condenser, methanol, concentrated hydrochloric acid, and hydroquinone were placed. The condenser was the same one as that of Jones et al.[14] and contained a mixture of dry ice-ethanol kept at about −20°C. The air in the flask was replaced completely by nitrogen while the flask was heated on a water bath. About 1 ml. of nickel carbonyl was added, and methylacetylene or a gas mixture of methylacetylene and acetylene was bubbled continuously through the solution while it was vigorously stirred. When the reaction began, as shown by a rise in the temperature and, in some cases, by a transient brown coloration, the remainder of the nickel carbonyl was added drop by drop at such a rate that the temperature remained constant. After dropping all amounts of nickel carbonyl, gas was introduced until the absorption stopped practically.

B) A 100 ml. electromagnetic stirring-type autoclave was charged with methanol, concentrated hydrochloric acid, nickel carbonyl, and hydroquinone. The vessel was then cooled to about −40°C and the air was replaced completely by nitrogen. After evacuation, methylacetylene was added by distillation. The vessel was heated slowly to about 80°C, at which temperature a vigorous reaction began; when a marked rise in the temperature was observed, the heating was stopped or weakened. After the mixture had cooled to room temperature, the remaining gas was discharged and collected in a gas holder for the analysis.

Catalytic Process. — A 100 ml. electromagnetic stirring-type autoclave was charged with methanol, a catalyst, hydroquinone, and methylacetylene in the same manner as in the above Process-B. Carbon monoxide was added to give a pressure of 15~25 atm. in most cases. The vessel was then heated to 150~290°C. During the period of reaction, when the partial pressure of carbon monoxide fell to about 10 atm. (at 170°C, about a 30 atm. pressure resulted from a mixture of methanol (20 ml.) and methylacetylene (8 g.)), carbon monoxide was added repeatedly to maintain a partial pressure of 10~40 atm. at the reaction temperature. In most cases, the reaction was continued until the absorption of carbon monoxide stopped practically. After the mixture had cooled to room temperature, the remaining gas was discharged through two traps cooled with ice-water (trap 1) and with dry ice-ethanol (−60°C, trap 2). The condensate in trap 2 was composed mainly of methyl ether and unreacted methylacetylene.

The Separation and Identification of Reaction Products.—*Waste Gases.* — These were analyzed by gas chromatography using the following three different columns: (1) a molecular sieve 5A column (2.4 m.) for hydrogen, nitrogen, methane, and carbon monoxide at 60°C, (2) a 30% (by weight) dioctyl phthalate column (4.7 m.) at room temperature, and (3) an 8.0% β, β'-oxydipropionitrile on silica gel column (2.5 m.) at 70°C for other gaseous substances.

Nickel Carbonyl.—In several cases, the nickel carbonyl, unchanged or formed from nickel-containing catalysts, was determined by a slight modification of the method of Jones et al.[7b]

Liquid Products.—The reaction mixture was poured into dilute sulfuric acid and extracted with methylene chloride. Acetone and esters were determined by gas chromatographic analysis of the extract. Two columns, a 2.4 m. column of 23% β, β'-oxydipropionitrile and a 2.4 m. column of 25% squalane, were used at 70°C, with a flow rate of 50 ml./min. of hydrogen as a carrier gas; *p*-xylene and toluene were selected as the internal standard substances respectively. The retention times measured under these conditions are shown in Table I.

TABLE I. RETENTION TIMES

Compound	Retention time, min.	
	β, β'-Oxydipropionitrile	Squalane
Methylene chloride	4.9	2.5
Methanol	7.3	1.0
Acetone	8.5	1.8
Methyl isobutyrate	8.7	8.9
Methyl propionate	9.1	5.5
Methyl acrylate	10.4	4.9
Methyl *n*-butyrate	14.6	12.6
Toluene	14.7	26.3
Methyl methacrylate	14.9	11.5
Water	17.2	2.0
p-Xylene	24.0	64.8
Methyl *trans*-crotonate	33.8	18.2

The above extract was washed thoroughly with a 7% sodium hydrogen carbonate solution, and the neutral and acidic fractions were separated. The alkaline solution was acidified with dilute sulfuric acid and extracted with methylene chloride. This extract was then condensed and flash-distilled at reduced pressure. The distillate was analyzed by gas chromatography to determine the carboxylic acids. The analysis was performed by a 2.4 m. column of 21% dioctyl sebacate +4% sebacic acid[15]

12) G. Brauer, "Handbuch der Präparativen Anorganischen Chemie," Ferdinand Enke Verlag, Stuttgart (1954), pp. 1155-1157.
13) W. Reppe, French Pat. 961010; (*Chem. Abstr.*, **46**, 5617 (1952)).
14) E. H. Jones, T. Y. Shen and M. C. Whiting, *J. Chem. Soc.*, **1951**, 48.
15) G. Raupp, *Angew. Chem.*, **71**, 284 (1959).

at 140°C, using chlorobenzene as an internal standard substance. On the other hand, the neutral fraction was condensed and flash-distilled at reduced pressure to give an ester fraction (~80°C/150 mmHg), a high-boiling fraction (60~100°C/50 mmHg), and a residue. In most cases of experiments which were carried out by the catalytic process, the extract, without separating the neutral and acidic fractions, was worked up like the above neutral fraction. The high-boiling fraction was analyzed by gas chromatography to determine the carboxylic acids.

By fractionating low-boiling fractions collected from several runs, the following compounds were isolated and identified:

Acetone; b. p. 56~57°C: 2,4-dinitrophenylhydrazone; m. p. 125°C (Found: N, 23.62%).

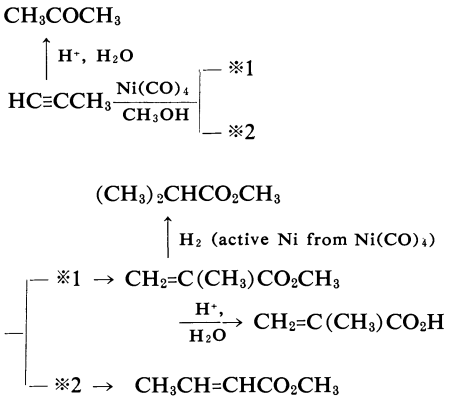
Methyl methacrylate; b. p. 47~48°C/112 mmHg, n_D^{20} 1.4149, d_4^{20} 0.947 (Found: C, 60.04; H, 8.25%).

Methyl *trans*-crotonate; b. p. 57~58°C/84 mmHg, n_D^{20} 1.4248, d_4^{20} 0.944 (Found: C, 59.85; H, 8.36%).

Results and Discussion

Stoichiometric Process.—*Carboxylation under Atmospheric Pressure.*—The carboxylation reaction was performed by introducing methylacetylene into a solution of methanol and concentrated hydrochloric acid with nickel carbonyl. The results are shown in Table II. By this method methylacetylene was not carboxylated so rapidly as acetylene. Even at a temperature of 73~76°C, no obvious reaction occurred, and methyl methacrylate was obtained in only a slight yield (3.6%, based on the methylacetylene consumed); about one half of the methylacetylene was recovered (Run 61). In this run, although the greater part (70%) of the nickel carbonyl used was consumed, most of carbon monoxide resulting from its decomposition was found in the waste gas as free carbon monoxide without having reacted with methylacetylene. When *n*-butanol was used instead of methanol, the reaction appeared to proceed slowly at 72~76°C after an induction period of several minutes, but the yield of butyl methacrylate was low (16%, Run 59). The addition of acetylene accelerated the reaction considerably. When a gas mixture of methylacetylene and acetylene in a 1 to 2:1 volume ratio was employed, a vigorous exothermic reaction occurred after a short induction period. The rate of the reaction became slower when the ratio of methylacetylene to acetylene is increased, and in the case of the 3:1 ratio, the reaction proceeded slowly under continuous heating (Run 57). In the case of the 2:1 ratio, the total yield of methyl methacrylate and methacrylic acid was 45%, the best yield in these three runs (Runs 56–58), while the total yield of methyl acrylate and acrylic acid produced from acetylene was 66%. The total yield of the carboxylation products (monomeric) of methylacetylene was always much lower than that of acetylene, and the residue (expressed as Rd in Table II) increased with an increase in the ratio of methylacetylene in the gas mixture. In view of these results, it is likely that, compared with acetylene, methylacetylene is difficult to carboxylate, but it can be polymerized and/or added to olefinic compounds such as methyl methacrylate, methyl acrylate, etc., under the conditions of the carboxylation reaction.

In addition to methyl methacrylate and methacrylic acid, methyl *trans*-crotonate, methyl isobutyrate, and acetone were obtained from methylacetylene as by-products in small amounts. The routes of formation of these substances are presumed to be as follows:



It should be noted that methyl isobutyrate, formed by the hydrogenation of methyl methacrylate, was obtained in much lower yields than was the methyl propionate formed by the hydrogenation of methyl acrylate, especially in Run 57, where the methylacetylene/acetylene ratio is 3:1.

Carboxylation under Pressure.—As the carboxylation reaction of methylacetylene did not proceed smoothly under atmospheric pressure, the reaction was examined by heating the reactants in an autoclave. By this method the carboxylation was achieved readily. The results are shown in Table III. In all cases, when the reaction temperature attained about 80°C a vigorous reaction took place, as was evidenced by a sudden marked rise in the temperature and a fall in the pressure. For example, in Run 16, the reaction temperature rose rapidly from 80 to 105°C, and a maximum pressure, at 14 atm., was reached at 82°C. In Run 63, where an excess of methylacetylene was used, 1.23 times the theoretical amount of methylacetylene (based on the nickel carbonyl used) was absorbed, and methyl

TABLE II. STOICHIOMETRIC PROCESS UNDER ATMOSPHERIC PRESSURE

Methanol, 32 ml.; concd. hydrochloric acid, 20 ml.; hydroquinone, 0.1 g.

Run No.	Acetylene and nickel carbonyl	Reaction temp. °C	Reaction time hr.-min.	Recovered acetylene C_3H_4 l.	Recovered acetylene C_2H_2 l.	Product[a] From C_3H_4 MMA %	MAA %	Other product %	From C_2H_2 %	HBM g.	Rd g.
61	C_3H_4 3.55 l. (6.0 g.) $Ni(CO)_4$ 4.8 g.	73~76	4.00	1.61 (2.7 g.)		3.6 (2.7)	Trace	MC Trace MIB 1.2 A 2.1		—	0.8
58	C_3H_4-C_2H_2 1 : 1 12.0 l. (17°C) $Ni(CO)_4$ 17.0 g.	38~48	2.08	0.20	0.24	35.6 (43.6)	3.8 (4.7)	MC 0.4 MIB 0.4 A 0.7	MA 66.8 (80.9) AA 2.3 MP 2.3	4.1	3.7
56	C_3H_4-C_2H_2 2 : 1 11.9 l. $Ni(CO)_4$ 17.6 g.	50~57	3.50	0.99	0.55	40.7 (43.2)	4.0 (4.2)	MC 0.3 MIB 0.7 A 1.8	MA 64.5 (67.3) AA 1.9 MP 8.7	2.8	5.6
57	C_3H_4-C_2H_2 3 : 1 12.3 l. $Ni(CO)_4$ 17.1 g.	54~58	4.30	0.35	0.12	30.0 (37.2)	1.9 (2.4)	MC 0.8 MIB 0.8 A 1.9	MA 45.2 (56.0) AA 1.0 MP 16.8	2.0	7.9
59[b]	C_3H_4 4.57 l. $Ni(CO)_4$ 7.7 g.	72~76	3.00	0.2		BMA 16.1 (17.1)	1.2 (1.3)	A 4.5			

a) MMA=methyl methacrylate, MAA=methacrylic acid, MC=methyl crotonate (*trans*), MIB=methyl isobutyrate, A=acetone, MA=methyl acrylate, AA=acrylic acid, MP=methyl propionate, HBM=high-boiling materials, Rd=residue. The yields were calculated on the basis of the acetylenes consumed. The values shown in parentheses are the yields based on the nickel carbonyl used, but, in the case of the mixed gas, those based on the amount of the nickel carbonyl divided into two parts in the ratio of methylacetylene to acetylene.

b) Butanol (46 ml.) and concentrated hydrochloric acid (10 ml.) were used. BMA=butyl methacrylate.

TABLE III. STOICHIOMETRIC PROCESS UNDER PRESSURE

Methanol, 30 ml.; concd. hydrochloric acid, 12 ml.; nickel carbonyl, 10.7 g.; hydroquinone, 0.1 g.

Run No.	C_3H_4 g.	C_3H_4/$Ni(CO)_4$ equivalent ratio	Reaction temp. °C	Reaction time min.	Recovered C_3H_4 g.	Product[a] MMA %	MAA %	MC %	MIB %	A %	HBM g.	Rd g.
16	10.4	1.03	16~ 80 80~105	55 30	Trace	36.8 (38.0)	4.9 (5.1)	0.8 (0.8)	1.2 (1.2)	—	2.9	2.7
63	13.5	1.34 (1.23)[b]	80~116	40	1.1	44.5 (55.0)	4.9 (6.1)	2.3 (2.8)	0.3 (0.3)	1.7	4.0	1.8
15	14.7	1.46	90~120	90	—	(58.8)	(7.4)	(2.0)	(1.2)	—	3.7	1.3

a) The values shown in parentheses are the yields based on the nickel carbonyl used.

b) This value is the ratio of the amount of methylacetylene absorbed to the theoretical amount based on the nickel carbonyl used.

methacrylate was obtained in a 45% yield, together with methacrylic acid in a 5% yield. On the other hand, the best total yield of methyl methacrylate and methacrylic acid, based on nickel carbonyl, was 66% (Run 15).

In all runs, considerable amounts of high-boiling materials (b. p. 87~92°C/47 mmHg, n_D^{20} 1.4760 in Run 15), in addition to small amounts of methyl crotonate, methyl isobutyrate, and acetone, were obtained as by-products. Although the high-boiling materials appeared to be C_7 olefinic esters formed by the dimerization of methylacetylene and the subsequent carboxylation and/or by the addition of methylacetylene to methyl methacrylate, no further study was made. In the stoichiometric reaction, one mole of hydrogen per mole of nickel carbonyl must be formed, if the reaction formula is correct. In reality, however, most of the hydrogen formed appeared to react with unsaturated substances. For example, in Run 63, only 16% of the theoretical amount of hydrogen was found in the waste gas (1920 ml.) as free (4 ml.) or combined hydrogen, that is, as hydrogen which added to methylacetylene to give propylene (227 ml.), as is shown in Table IV. Furthermore,

Table IV. Composition of waste gas

Run No.	63	57
Total amount, ml.	1920	1600
Composition, vol.%		
Nitrogen	7.6	19.5
Hydrogen	0.2	0.1
Carbon monoxide	25.9	26.7
Ethylene	0.1	1.7
Acetylene	—	7.3
Propylene	11.8	8.2
Allene	0.2	0.2
Methylacetylene	33.5	21.6
Methyl chloride	13.2	8.1
Nickel carbonyl	0.9	3.1
Others	6.6	3.5

in view of the fact that the yield of methyl isobutyrate was also small, it may be concluded that most of the hydrogen must be added to unsaturated high-molecular substances. This was observed similarly in Run 57, carried out under atmospheric pressure. In this case, only 7% of the theoretical amount of hydrogen was accounted for by the presence of free or combined hydrogen in the waste gas (Table IV), while 21% and 3% were accounted for by the formation of methyl propionate and methyl isobutyrate respectively.

Catalytic Process.—*Nickel Halide and Triphenylphosphine Nickel Bromide Complex Catalysts.*—The results are shown in Table V. Generally, in the presence of these catalysts

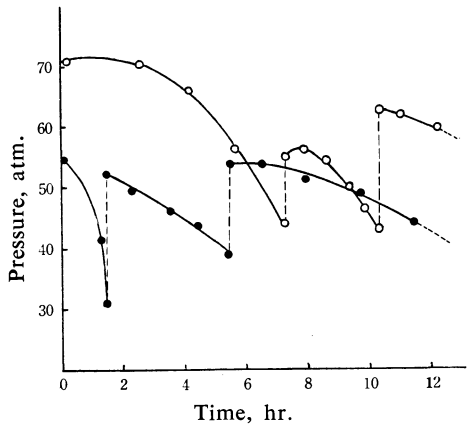


Fig. 1. Variation in total pressure with the reaction time-I*: ●, Run 41; ○, Run 44.
* The vertical broken lines show the added pressure of carbon monoxide.

the reaction proceeded fairly smoothly at a temperature of 170~180°C and under about a 10 atm. partial pressure of carbon monoxide, as is illustrated by the variation in total pressure shown in Fig. 1. A high pressure of carbon monoxide gave a slow rate of reaction. For example, in the case of about a 75 atm. partial pressure of carbon monoxide (total pressure, 105 atm.), the decrease in pressure during a reaction time of 10 hr. was only two atms. The induction period appeared to be reduced with the decrease in the partial pressure of carbon monoxide when other conditions were the same.

Triphenylphosphine nickel bromide and triphenylphosphine nickel bromide butyl bromide complexes gave better results than those obtained by nickel bromide and iodide, though these complexes have been reported to decompose with the separation of triphenylphosphine in methanol.[3a,3e] The total yield of methyl methacrylate and methacrylic acid was, however, unsatisfactory (best yield: 47% in Run 44), and a fairly long reaction time was required for the completion of the reaction.

The low yield appeared to be due chiefly to the loss of methylacetylene by polymerization leading to the formation of high-molecular substances (expressed as HBM and Rd in Table V). Particularly, large quantities of high-molecular substances were formed in cases where a vigorous exothermic reaction occurred in the early stages of the reaction, as shown by a marked fall in pressure (Run 41 in Table V and Fig. 1). Such a vigorous reaction was often encountered when the reaction was carried out at a low pressure of carbon monoxide (partial pressure below about 10 atm.) in the presence of the complex catalysts; it was observed that, at that time,

TABLE V. CATALYTIC PROCESS USING NICKEL HALIDES AND TRIPHENYLPHOSPHINE NICKEL BROMIDE COMPLEXES

Hydroquinone, 0.05 g.

Run No.	C_3H_4 g.	CH_3OH ml.	Catalyst	g.	CO Pressure[a] atm.	CO Absorption amount[b] %	Reaction temp. °C	Reaction time hr.	Recoverd C_3H_4 g.	Product[c] MMA %	MAA %	MC %	A %	HBM g.	Rd g.
20	8.2	20	$NiBr_2$	1.5	64～39	37	170～175	16.0	0.7	18.0	0.7	2.3	23.5	1.1	3.5
19	6.3	15	$NiBr_2$ CH_3J	1.5 0.13	75～38	71	(150～153 168～173	4.0) 36	0	29.3	(unreacted) —	5.1	18.6	1.5	2.4
18	5.0	15	NiJ_2	2.0	58～31	93	168～174	9.8	—	24.8	2.8	4.8	6.9	1.5	2.8
41	8.4	20	$(Ph_3P)_2NiBr_2$	1.4	57～31	40	170～175	19.6	0.2	18.0	1.1	3.4	2.6	0.8	6.5
36	7.6	20	$(Ph_3P)_2NiBr_2$	1.4	63～36	60	170～175	16.4	0.3	38.9	1.9	7.2	2.8	1.1	3.6
44	8.0	20	$(Ph_3P)_2NiBr_2$	1.4	71～40	58	170～175	21.5	0.3	44.2	2.4	8.3	3.6	0.7	3.8
42	7.1	20	$(Ph_3P)_2NiBr_2$- C_4H_9Br	1.7	57～38	53	170～175	19.7	0.1	36.0	2.0	6.5	6.9	0.7	4.5
35	8.4	20	Ph_3P $NiBr_2$ C_4H_9Br	1.0 0.4 0.5	59～43	45	170～175	28.0	0.3	26.3	4.0	4.5	14.4	0.8	4.3
32	8.6	20	Ph_3P $NiBr_2$ CH_3J	1.0 0.4 0.3	56～34	54	170～175	18.2	0.4	28.8	1.2	5.3	4.2	0.8	5.2

a) The range of total pressure during the reaction period is shown.
b) Expressed as percentage of the theoretical amount based on methylacetylene.
c) The yield of crotonic acid (*trans*) was below 1%.

TABLE VI. CATALYTIC PROCESS USING METAL CARBONYLS

Hydroquinone, 0.1 g.

Run No.	C_3H_4 g.	CH_3OH ml.	Metal carbonyl g.	Additive ml.	CO[a] Pressure atm.	CO[a] Absorption amount %	Reaction temp. °C	Reaction time hr.	Recovered C_3H_4 g.	Product[b] MMA %	MAA %	MC %	A %	HBM g.	Rd g.
25	6.3	20	$Ni(CO)_4$ 1.9	Concd. HCl 1.6	54～ 33(15)	34	160～170 190～200	2.0 9.7	0.1	31.7	1.4	3.2	15.5	1.0	1.7
23	7.7	20	2.0	1.7	77～ 30(26)	40	180～185	4.8	1.0	32.8	1.4	5.4	4.1	0.8	1.7
24	7.5	20	2.0	1.7	132～ 75(58)	48	198～202	11.5	0	33.2	1.9	5.9	18.4	0.3	1.3
22	8.4	20	$Ni(CO)_4$ 4.6	H_2O 0	88～ 82(29)	4	180～195	13.0	6.6	2.3	—	—	—	—	—
27	7.7	20	2.0	0	91～ 43(25)	33	200～205	6.0	Trace	12.0	0	3.1	Trace	0.3	7.5
28	7.4	20	2.0	0	150～128(59)	27	220～230	56	1.4	2.7	0	0.6	8.1	1.0	3.7
26	7.4	20	2.0	1.3	84～ 40(25)	54	200～205	6.6	Trace	37.8	1.3	8.1	1.9	0.8	3.1
31	11.7	18	2.0	2	82～ 36(25)	49	180～186	19.5	1.0	33.0	3.5	7.0	0.7	1.3	4.9
30	8.1	15	2.0	5	70～ 45(25)	56	165～170	15.7	0.2	32.0	13.5	6.6	0.9	1.0	2.4
67	8.0	50	$Co_2(CO)_8$ 0.5	H_2O 0	123～ 85(82)	44	150～155	7.5	2.5	Trace	0	—	Trace	0.9	5.1
65	9.6	20	1.8	5	140～116(30)	20	270～280	17.8	0	Trace	—	Trace	14.4	1.8	5.0
68	8.8	40	$Cr(CO)_6$ 0.6	H_2O 0	303～245(73)	16	280～293	16.0	0.4	Trace	0	Trace	3.2	1.1	5.6
66	8.8	20	1.5	5	141～137(29)	—	250～255	9.2	6.3	1.8	Trace	Trace	5.6	—	1.9
69	8.2	30	0.6	10	302～223(74)	41	280～290	13.3	0.2	5.5	—	2.0	6.0	2.1	7.4

a) See footnotes a) and b) in Table V. The values in parentheses show initial pressure (in first addition) of carbon monoxide at room temperature.
b) The maximum yields of methyl isobutyrate and crotonic acid were 1.0% (Run 24) and 1.7% (Run 30), respectively.

most of the methylacetylene was consumed in reacting with much smaller amounts of carbon monoxide. This implies that methylacetylene is liable to polymerize under the conditions, as might be supposed from the reports of Reppe and Schweckendiek,[16] and Meriwether et al.,[17] who have investigated the polymerization of acetylenes by triphenylphosphine nickel bromide and triphenylphosphine nickel carbonyl complexes. Thus, the yield of the carboxylation products would be improved by adopting a continuous method, because the addition of methylacetylene suppresses the polymerization of methylacetylene. Furthermore, a continuous addition of carbon monoxide at optimum partial pressure (about 10 atm.) would reduce the reaction time.

Acetone was formed in considerable yields (3~24%) by the reaction of methylacetylene with water, which is formed by the formation of methyl ether from methanol. The ratio of methyl crotonate to methyl methacrylate was about 1 to 5; this ratio was much higher than that of the stoichiometric process where the reaction proceeded at lower temperatures (Table III). In all cases, methyl ether was formed in considerable quantities (10~50%, based on the methanol used).

The nickel halides and triphenylphosphine nickel bromide complexes used as catalysts changed considerably in the reaction. In all cases nickel carbonyl was formed, probably by the following reaction: $NiBr_2+2CH_3OH+5CO \rightarrow Ni(CO)_4+2CH_3Br+H_2O+CO_2$. In Run 42 nickel carbonyl was obtained in a 20% yield (based on the nickel complex used). The nickel carbonyl formed may be supposed to participate in the carboxylation reaction, in view of the catalytic action of nickel carbonyl which will be mentioned below. In certain cases the formation of nickel hydroxide as fine precipitates was observed.

Metal Carbonyl Catalysts.—The results are shown in Table VI. In the case of the nickel carbonyl catalyst, all experiments, except Runs 22 and 31, were carried out in the presence of one-fourth of the theoretical amount of nickel carbonyl (based on methylacetylene). Runs 23–25 are examples of experiments which were carried out semi-catalytically. The total yield of methyl methacrylate and methacrylic acid was low (35%) under these conditions. The results, however, suggest the possibility that this process, especially in a continuous method, may be so developed as to become a good process for the synthesis of methyl methacrylate from methylacetylene, as in the case of the carboxylation of acetylene. Concerning the occurrence of the reaction, it was observed that the reaction required a high temperature when a high initial pressure of carbon monoxide was applied. The relation between the reaction temperature (lowest) and the pressure of carbon monoxide is shown in Fig. 2. However, in this figure the reaction temperature (80°C) in the case of the stoichiometric process was taken as that for zero atm. pressure of carbon monoxide.

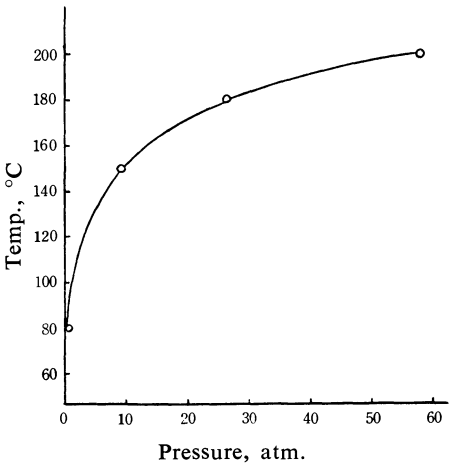


Fig. 2. Relation between the reaction temperature and the pressure (at room temp.) of carbon monoxide.

The reaction was similarly examined in the absence of hydrochloric acid. In cases where the acid was not added, scarcely any methyl methacrylate was formed at 180~195°C (Run 22), and it was obtained in a low yield (12%) at 200~205°C (Run 27). When water was present, the carboxylation reaction proceeded without the addition of any acid. This is an interesting fact, since it is generally known that nickel carbonyl without the addition of acid is not capable of forming acrylic esters from acetylene. The temperature at which the reaction occurred became lower as the amount of water was increased (Runs 26, 31, and 30). The reaction proceeded more readily in Run 30 (15 ml. methanol+5 ml. water) than in Run 23 (20 ml. methanol+1.7 ml. concentrated hydrochloric acid). The total yield of methyl methacrylate and methacrylic acid was better in the presence of water than in the presence of hydrochloric acid, and the best total yield was 46% (Run 30). Fortunately, by the use of water instead of hydrochloric acid, the formation of acetone (below 2%) and of methyl ether was suppressed.

In most cases, the greater part of the nickel

16) W. Reppe and W. J. Schweckendiek, *Ann.*, **506**, 104 (1948).
17) L. S. Meriwether, E. C. Colthup, G. W. Kennerly and R. N. Reusch, *J. Org. Chem.*, **26**, 5155 (1961).

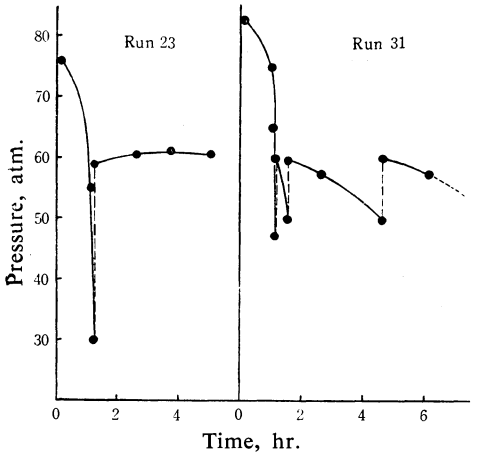


Fig. 3. Variation in total pressure with the reaction time-II.*
* The vertical broken lines show the added pressure of carbon monoxide.

carbonyl used as a catalyst was decomposed to give nickel chloride (in the presence of hydrochloric acid) or nickel hyroxide as fine precipitates. The decomposition was especially marked in cases where such a vigorous reaction as consumed, in a moment, all the carbon monoxide in the reaction vessel, occurred in the early stages of the reaction. Run 23 is given as an example of such cases in Fig. 3, which shows the variation in the total pressure of the reactants with the reaction time. In this run, the reaction stopped after the pressure fell rapidly, probably because of the decomposition of all the amounts of nickel carbonyl (compare with Run 31 in Fig. 3). Furthermore, it is noteworthy that such a vigorous reaction as has been described above appeared to result from two reactions of the carboxylation reaction and of the polymerization (inclusive of addition) reaction of methylacetylene, and that the latter reaction was probably a main cause of the poor yield of the carboxylation products. Thus, it may be supposed to be necessary, for keeping a long life of nickel carbonyl as a catalyst and for obtaining a better yield of methyl methacrylate, to add methylacetylene under controls. The performance of the carboxylation reaction by a semicontinuous method will be reported on in a subsequent publication.

Dicobalt octacarbonyl and chromium hexacarbonyl were not effective as catalysts for the carboxylation of methylacetylene (Runs 65—69). In the case of chromium hexacarbonyl, methyl methacrylate was obtained in only a slight yield (5%) in the presence of water and at the high temperature of 280～290°C (Run 69).

Summary

The synthesis of methyl methacrylate (MMA) by the carboxylation reaction of methylacetylene has been investigated.

Stoichiometric process: The carboxylation reaction was carried out under atmospheric pressure by premixing a 25～50 vol.% of acetylene in methylacetylene and under pressure (heating to 80°C). The total yields of MMA and MAA (methacrylic acid) were 45% (based on the methylacetylene consumed) under atmospheric pressure and 49% (66% (based on the nickel carbonyl used)) under pressure. Small amounts of methyl *trans*-crotonate, methyl isobutyrate, acetone, etc., were obtained as by-products, together with considerable amounts of high-boiling materials (not investigated).

Catalytic process: The reaction proceeded comparatively smoothly at 170～180°C and under about a 10 atm. partial pressure of carbon monoxide when triphenylphosphine nickel bromide complexes and nickel carbonyl-concentrated hydrochloric acid were used as catalysts. A triphenylphosphine nickel bromide catalyst, $(Ph_3P)_2NiBr_2$, gave the best total yield, 47%. It was found that, without the addition of acid, nickel carbonyl exhibits a catalytic action in the presence of water at 170～180°C. The total yield of MMA and MAA by this method was 46%. Fortunately, scarcely any acetone or methyl ether were formed. In view of this series of experimental results, it may be supposed that the poor total yield of MMA and MAA is chiefly due to the loss of methylacetylene by polymerization.

The author wishes to express his thanks to Professor Sango Kunichika of Kyoto University for his helpful advice and kind encouragement throughout this work. Also, the author wishes to thank Mrs. Toshiko Ikegami of Kyoto University for her microanalysis.

Institute for Chemical Research
Kyoto University
Daigaku-cho, Takatsuki

The Coprecipitation of Yttrium with Calcium Oxalate

By Tsunenobu SHIGEMATSU, Masayuki TABUSHI and Masakazu MATSUI

(Received May 7, 1964)

The coprecipitation method has been widely used for the chemical concentration or enrichment of trace elements from such extremely dilute solutions as natural water and for the chemical separation of radioisotopes.

There are two typical distribution laws in the coprecipitation mechanism. One, called the homogeneous distribution law, has been employed by Chlopin[1] and Henderson and Kracek[2]; it is expressed as follows:

$$\left(\frac{\text{tracer}}{\text{carrier}}\right)_{\text{crystal}} = D\left(\frac{\text{tracer}}{\text{carrier}}\right)_{\text{solution}} \quad (1)$$

where D is the homogeneous distribution coefficient and is constant for a given system. It represents a state of true thermodynamic equilibrium, in which the crystal phase has been digested enough for it to reach a homogeneous concentration.

The other law, offered by Doerner and Hoskins,[3] is called the logarithmic distribution law; it is expressed as follows:

$$\log\left(\frac{\text{initial quantity}}{\text{quantity left in soln.}}\right)_{\text{tracer}} = \lambda \log\left(\frac{\text{initial quantity}}{\text{quantity left in soln.}}\right)_{\text{carrier}} \quad (2)$$

where λ is the logalithmic distribution coefficient, which is constant for a given system. This law is obeyed when the rate of precipitation is slow enough to establish a replacement equilibrium on each layer of the crystal. A crystal formed in such circumstances retains a radial concentration gradient in which the tracer component is distributed throughout in a logalithmic manner. If λ is larger than unity, the tracer component is enriched in the crystal and the concentration of the tracer component is at a maximum at the center of each crystal and decreases gradually toward the outer part of the crystal; when λ is smaller than unity, the reverse is true.

It is of interest to study the coprecipitation from a homogeneous solution, because the crystals formed are large and more perfect, and because the precipitation process is more reproducible. Feibuch, Rowly and Gordon[4] reported that the coprecipitation of pairs of rare earth oxalates from homogeneous systems obeyed the logarithmic distribution law.

Calcium oxalate is often used as a coprecipitant,[5] and Purkayastha and Bhattacharyya[6] showed that the coprecipitation of yttrium and europium with calcium oxalate also followed the logarithmic distribution law. In our previous research,[7] it was observed that the coprecipitation of scandium with calcium oxalate was influenced by the conditions of the reacting solutions; in the pH range between 2.0 and 3.5, the system followed the logarithmic distribution law, whereas with a rise in pH value, it deviated gradually from the law until it began to obey the homogeneous distribution law near pH 4. The limiting distribution coefficient,[8] the value of distribution coefficients extrapolated to zero per cent of the calcium precipitated, changed with the pH value of the reacting solutions from 1.10 at an initial pH of 4.67 to about 18 at an initial pH of 2.43.

In this research the coprecipitation of yttrium with calcium oxalate was investigated. The effects of the pH value, the tracer component to the carrier ratio, the concentration of the buffer solution and several other variables on the distribution coefficient were investigated, using yttrium-91 as a tracer.

Experimental

Apparatus and Reagents. — Radioactivity countings were made with a Phillips halogen-quenched G-M tube connected to a Metro dekatron scaler, Model D-5. A Hitachi-Horiba glass electrode pH meter, Model M-3, was used for the pH measurements.

Yttrium-91 was supplied as chloride in hydrochloric acid by The Radiochemical Centre, Amersham, England, and was diluted to make a solution of 1 μc./ml. Reagent-grade dimethyl oxalate was

1) W. Chlopin, *Z. anorg. u. allgemg. Chem.*, **143**, 97 (1925).
2) L. M. Henderson and F. C. Kracek, *J. Am. Chem. Soc.*, **49**, 738 (1927).
3) H. A. Doerner and W. M. Hoskins, ibid., **47**, 662 (1925).
4) A. M. Feibuch, K. Rowley and L. Gordon, *Anal. Chem.*, **30**, 1605 (1958).
5) T. Shigematsu, M. Tabushi, Y. Nishikawa, K. Hiraki, S. Goda and R. Inoue, *J. Chem. Soc. Japan, Pure Chem. Sec. (Nippon Kagaku Zasshi)*, **84**, 336 (1963).
6) B. C. Purkayastha and S. N. Bhattacharyya *J. Inorg. Nucl. Chem.*, **10**, 103 (1959).
7) T. Shigematsu, M. Tabushi and M. Matsui, *Bull. Inst. Chem. Res., Kyoto Univ.*, **40**, 381 (1962).
8) M. L. Salutsky, J. G. Stites, Jr., and A. W. Martin, *Anal. Chem.*, **25**, 1677 (1953).

purified by recrystallizing it from dry methanol and was stored in a dry atmosphere to prevent the hydrolysis upon contact with moisture. The yttrium solution was prepared by dissolving reagent-grade yttrium oxide in hydrochloric acid. Calcium solution (2 M) was prepared by dissolving dry calcium carbonate in hydrochloric acid and diluting it with water. The EDTA solution (0.01 M) containing a EDTA-Mg complex was standardized by means of a calcium standard solution.

The other chemicals were chemically pure or reagent-grade materials.

Procedure. — An aliquot of a calcium chloride stock solution and a yttrium-91 solution with an appropriate amount of inactive yttrium is placed in a 250-ml. Erlenmeyer flask. A suitable volume of 10 N acetic acid or formic acid (as a buffer solution), a 10 N sodium hydroxide solution and a known weight of dry dimethyl oxalate in distilled water are added, the resulting solution is diluted to 200 ml., and then the pH value is measured. The flask with a reflux condenser is placed in a thermostat, and the solution is stirred continuously with a mechanical stirrer to prevent supersaturation.

When the temperature of the solution rises to a certain value, 2 ml. of the solution is pipetted out into a glass-counting dish 25 mm. in diameter. After calcium begins to precipitate with the oxalate ions released from dimethyl oxalate, 2.0 ml. of the solution is pipetted out from the reacting solution through a sintered glass filter into a counting dish at appropriate intervals of time.

The yttrium-91 activity of the liquid sample in the dish is measured in order to determine the amount of yttrium in the filtrate. The solution is then washed with hydrochloric acid into a beaker, dried slowly, and ashed by fuming it with concentrated perchloric acid on a hot plate. After adding water and a buffer solution, the calcium ions are titrated with a 0.01 M EDTA standard solution containing its magnesium chelate, using Eriochrome Black T as an indicator. The homogeneous and logarithmic distribution coefficients, D and λ, are calculated from Eqs. 1 and 2.

Results and Discussion

The Effect of the pH Value on the Coprecipitation.—The percentages of yttrium coprecipitated and of calcium precipitated in the fraction of calcium oxalate at several pH values are plotted in Figs. 1 and 2.

Figures 1 and 2 show that yttrium is enriched in the precipitate in the pH range investigated, and that the extent of enrichment increases as the pH decreases. The distribution coefficients were also calculated; a few typical examples are shown in Table I. The distribution of yttrium on the calcium oxalate obeys the logarithmic distribution law; this agrees with Purkayastha and Bhattacharyya's results,[6] which were obtained in a 3 N acetate medium. As has been previously reported,[7] the pH value of the reacting solution influenced

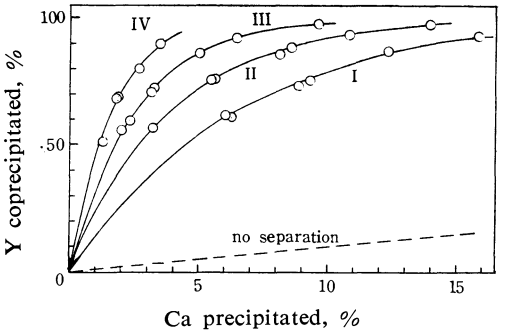


Fig. 1. Coprecipitation of yttrium with calcium oxalate in an acetate buffer solution. pH: I, 4.62; II, 4.20; III, 3.97; IV, 3.67; Y: 1.12×10^{-6} M, Ca: 0.2 M, dimethyl oxalate: 0.1 M, acetate: 1 M, temp.: 60°C. vol.: 200 ml.

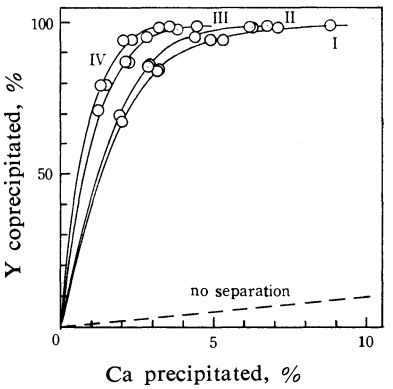


Fig. 2. Coprecipitation of yttrium on calcium oxalate in formic buffer solution. pH: I, 4.08; II, 3.42; III, 3.01; IV, 2.62; formic acid: 1 M. Others are same to in Fig. 1.

not only the distribution coefficient, but also the type of the distribution in a scandium-calcium system. In this yttrium system, however, the logalithmic distribution law is obeyed regardless of the pH value in the given range, although the coefficient increases with a decreases in the pH value.

The logarithmic distribution coefficient, λ, is plotted against the initial pH of the solution in Fig. 3. The limiting distribution coefficient of the scandium-calcium system is also shown for the sake of comparison.

There is a difference between the distribution curves obtained in acetate and in formate buffer solutions; this may be due to the property of the complex compounds of yttrium and calcium ions with acetate or formate.

The Effect of the Yttrium Concentration on the Distribution Coefficient.—The calcium oxalate was precipitated in the solutions, containing 3.37×10^{-6} M to 1.12×10^{-4} M yttrium;

TABLE I. COPRECIPITATION OF YTTRIUM WITH CALCIUM OXALATE

Ca: 0.2 M, Y: 1.12×10^{-6} M, dimethyl oxalate: 0.1 M, temp.: 60°C

Reaction time min.	Ca pptd. %	λ
[(A) initial pH: 4.62, 1 M acetate solution]		
105	6.02	15.1
106	5.96	15.4
157	8.85	14.3
158	9.27	14.6
250	12.83	15.0
340	15.79	15.5
410	18.67	15.5
	Average	15.1
[(B) initial pH: 3.97, 1 M acetate solution]		
102	1.96	40.8
107	2.26	39.4
150	3.14	38.4
155	3.27	38.4
180	5.00	38.6
225	6.39	38.6
300	9.58	36.9
	Average	38.7
[(C) initial pH: 3.01, 1 M formate solution]		
93	1.22	102.4
120	2.11	95.4
120	2.21	92.5
152	2.79	107.9
182	3.80	100.7
195	4.45	93.4
	Average	98.7

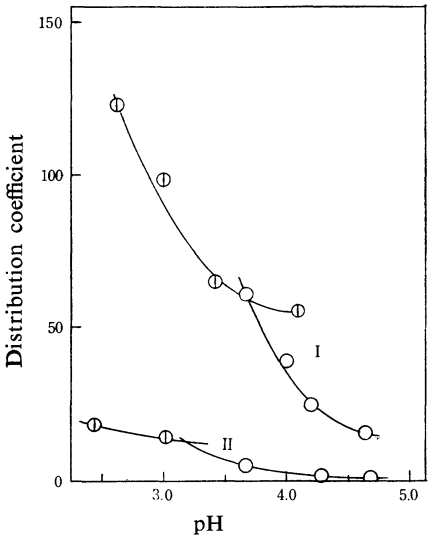


Fig. 3. The effect of pH on the distribution coefficient.
I: Y-Ca system, II: Sc-Ca system. -ⓘ-: 1 M formate solution, -○-: 1 M acetate solution.

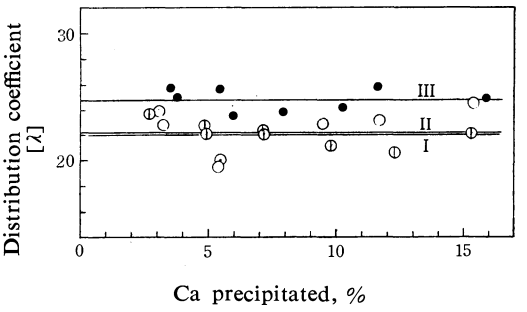


Fig. 4. The effect of yttrium concentration on distribution coefficient. pH: 4.24, I -ⓘ-: $Y=3.37\times10^{-6}$ M, $\lambda=22.0$; II -○-: $Y=3.37\times10^{-5}$ M, $\lambda=22.1$; III -●-: $Y=1.12\times10^{-4}$ M, $\lambda=24.9$.

the effect of the yttrium concentration is indicated in Fig. 4. No significant change in the logarithmic distribution coefficient is observed, and the mean value of λ is also in good agreement with the value ($\lambda=23$) as estimated from the curve in Fig. 3 (yttrium concentration: 1.12×10^{-6} M), at pH 4.23. This is in contrast with the scandium system, where the limiting distribution coefficient decreases as the concentration of the tracer component increases.

The Effect of the Rate of Precipitation.— Because the rate of precipitation depends upon the concentration of the dimethyl oxalate at a given pH, the effect of the latter was studied in order to examine the effect of the former.

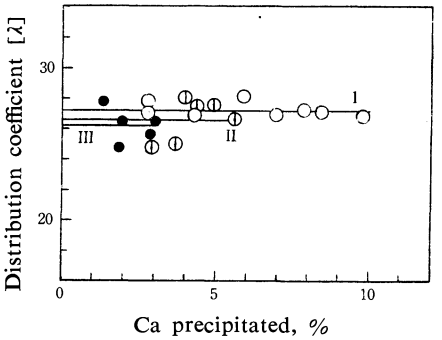


Fig. 5. The effect of the concentration of dimethyl oxalate. pH: 4.16, I -○-: 0.05 M ester, $\lambda=27.2$; II -ⓘ-: 0.02 M ester, $\lambda=26.5$; III -●-: 0.01 M ester, $\lambda=26.5$.

Figure 5 shows that the logarithmic distribution coefficient (measured at pH 4.16) is almost constant, even when the concentration of the ester changes from 0.01 M to 0.05 M, values which correspond to 1/20 and 1/4 of the stoichiometric quantity necessary to complete the precipitation of calcium ions. The value of λ obtained at pH 4.16 in Fig. 3 (ester

concentration: 0.1 M) is 26.5, which is approximately the same as the value in Fig. 5. The time required to precipitate 3 per cent of the calcium ion was about 1540, 450, 200 and 90 min. when the concentration of the dimethyl oxalate was 0.01, 0.02, 0.05 and 0.1 M respectively.

The Effect of Acetate Ion Concentration on the Coefficient.—The effect of the acetate concentration was examined with solutions containing 1.0 M, 0.5 M and 0.25 M of acetate; the results obtained at pH 4.10 are represented in Table II. The logarithmic distribution law is obeyed, but the value of the distribution coefficient is remarkably influenced by the acetate concentration. The mean values of λ were 30 at 1.0 M, 70 at 0.5 M and 186 at 0.25 M of acetate.

TABLE II. EFFECT OF THE ACETATE ION ON DISTRIBUTION COEFFICIENT

Ca: 0.1 M, Y: 1.12×10^{-6} M, dimethyl oxalate: 0.1 M, initial pH: 4.0, temp.: 60°C

Ca pptd. %	Y copptd. %		λ
(A) 1 M acetate			
3.01	60.14		29.9
5.36	81.87		31.0
5.39	81.23		30.2
8.43	92.89		30.0
8.40	92.46		29.5
10.02	95.85		30.0
12.52	98.11		29.7
		Average	30.0
(B) 0.5 M acetate			
1.63	66.15		66.2
3.03	88.30		69.6
5.01	97.40		71.1
5.03	97.39		70.6
5.94	98.86		73.2
		Average	70.1
(C) 0.25 M acetate			
0.63	69.95		190
1.34	91.18		180
2.17	98.53		192
2.91	99.658		193
2.91	99.488		179
3.75	99.935		180
		Average	186

When the acetate concentration decreases and, consequently, the buffer action weakens, the pH-drift during the precipitation process is not negligible. However, the fact that the differences in the distribution coefficients of Experiments A, B and C are much larger than the fluctuation of data in each experiment can not be explained by such a pH-drift. It is reasonable to assume that acetate ions affect the enrichment of yttrium into the solid phase because of their complex formation.

As has been mentioned above, the distribution coefficient increases monotonically with a decrease in the pH value (see Fig. 3). One of the reasons, perhaps the major, might be also the complex formation of metal ions with acetate or formate, which dissociate more as the pH rises, although such complicated questions as the formation of a hydroxocomplex should also be taken into consideration.

It is interesting to compare the yttrium-calcium system with the scandium-calcium system. There are distinct differences between them. Firstly, in the yttrium-calcium system, the logarithmic distribution law is followed regardless of the pH in the given range, while the distribution of scandium changes gradually from logarithmic to homogeneous with an increase in the pH. Secondly, the molar ratio of the tracer component to the carrier affects the distribution coefficient in the scandium system, but not in the yttrium system. Lastly, under similar conditions yttrium gives larger distribution coefficients than does scandium.

A strict discussion is difficult, because a tervalent element coprecipitates with bivalent calcium as an oxalate and because the properties of the crystal are not clear. However, the results described above seem to show that yttrium is more stable than scandium in the calcium oxalate crystal. This may be caused by the fact that the ionic radius of bivalent calcium is nearer to that of tervalent yttrium than to that of tervalent scandium.

Institute for Chemical Research
Kyoto University
Sakyo-ku, Kyoto

*Nuclear Magnetic Resonance Spectra of Polymethyl Methacrylate in Solution. I. An Attempt to make Stereoregularity Measurements**

By Yoshinori KATO and Atsuo NISHIOKA

(Received May 12, 1964)

Recent studies by Bovey et al.[1-3] of polymethyl methacrylate have demonstrated that high resolution nuclear magnetic resonance methods are applicable to the determination of the stereochemical configurations of polymer chains. The stereoregular polymerizations of methacrylic acid esters have been investigated[4,5] since 1958. The crystal structure of isotactic polymethyl methacrylate was proposed by Stroupe et al.[6] on the basis of the X-ray fiber pattern, and in order to measure the degree of stereoregularity of the polymer, an infrared spectrometer was employed by several workers.[7-10] The latter method gave a rather qualitative description of the chain structure. By the use of this method, however, we can not find out the difference between the syndiotactic and the atactic polymers. For this purpose, the nuclear magnetic resonance method would be the most powerful one, because new information about the stereochemical configuration of the polymer chains can be obtained from the spectra.

An attempt is made in this paper not only to estimate the tacticity of the polymer but also to find out the relation between the polymer and the polymerization mechanism by means of an analysis of the spectra.

Experimental

Since a detailed description of the polymerization was given by Watanabe et al.,[4,11] only a brief summary of the methods will be given here.

Free Radical Polymerization.—Each polymerization from −35°C to 0°C was carried out in a flask containing 8.0 ml. of methyl methacrylate in 20 ml. of toluene and 2.0 g. of benzoin by means of photosensitization by ultraviolet light. Dry nitrogen was introduced into the flask during the polymerization. Benzoyl peroxide (B.P.O.) was used as the initiator between 20°C and 70°C. Together with amounts of methyl methacrylate and toluene the same as those mentioned above, 0.1 g. of B.P.O. was sealed in a reaction vessel which had previously been flushed with nitrogen. Then the vessel was kept turning round in a constant temperature bath. At temperatures higher than 100°C, thermal polymerizations were employed. After an appropriate reaction time, the polymerization was stopped and the polymer products were poured into methanol. Then the precipitates were reprecipitated from an acetone solution and was dried in vacuo at about 50°C.

Polymerization Using Grignard's Reagent Catalysts.—*n*-Butylmagnesiumbromide and isobutylmagnesiumbromide were prepared as solutions in

TABLE I. POLYMERIZATION CONDITIONS OF METHYL METHACRYLATE POLYMERS

Sample No.	Catalyst	Solvent for polymerization	Polymerization temp., °C.
1			−35
2	Benzoin+UV	Toluene	−25
3			−15
4			0
5			20
6	B.P.O.	Toluene	40
7			70
8			100
9	—	Toluene	150
10	Di-*n*-butylmagnesium		−50
11	Isobutylmagnesiumbromide	Toluene	−50
12	*n*-Butylmagnesiumbromide		−50

* Part of this paper was presented at the Annual Meeting of the Physical Society of Japan, Sapporo, September, 1960.

1) F. A. Bovey and G. V. D. Tiers, *J. Polymer Sci.*, **44**, 173 (1960).
2) A. Nishioka, H. Watanabe, I. Yamaguchi and H. Shimizu, ibid., **45**, 232 (1960).
3) U. Johnsen and K. Tessmar, *Kolloid Zeits.*, **168**, 160 (1960).
4) H. Watanabe and Y. Sono, paper presented at the Local Meeting of the Chemical Society of Japan, Nagoya, November, 1958.
5) T. G. Fox, W. E. Goode, S. Gratch, C. M. Huggett, J. F. Kincaid, A. Spell and J. D. Stroupe, *J. Polymer Sci.*, **31**, 173 (1958).
6) J. D. Stroupe and R. E. Hughes, *J. Am. Chem. Soc.*, **80**, 2341 (1958).
7) T. G. Fox, B. S. Garrett, W. E. Woode, S. Gratch, T. F. Kincaid, A. Spell and J. D. Stroupe, ibid., **80**, 1768 (1958).
8) U. Baumann, H. Schreiber and K. Tessmar, *Makromol. Chem.*, **36**, 81 (1960).
9) H. Watanabe, K. Abe, Y. Sono and A. Nishioka, paper presented at the International Symposium on Macromolecular Chemistry, Moscow, June, 1960. A. Nishioka, H. Watanabe, K. Abe and Y. Sono, *J. Polymer Sci.*, **48**, 241 (1960).
10) W. E. Goode, F. H. Owens, R. P. Fellman, W. H. Snyder and J. E. Moore, ibid., **46**, 317 (1960).
11) H. Watanabe, Y. Kato and A. Nishioka, *J. Chem. Soc. Japan, Ind. Chem. Sec.* (*Kogyo Kagaku Zasshi*), **65**, 270 (1962)

toluene. For the former, for instance, polymerization was carried out by adding it (along with 2.54×10^{-3} mol. of bromine) to a mixture of 40 ml. of toluene and 20 ml. of methyl methacrylate at $-50°C$. A similar polymerization was made using di-*n*-butylmagnesium as a catalyst to examine the effect of the chemical components of the catalyst on the structure of the polymer. The polymerization conditions of methyl methacrylate are shown in Table I.

NMR Spectra.—The instrument employed for these measurements was a Varian Model V-4300-C spectrometer operating at 56.4 Mc./s. Spectra were taken at 20°C, using about 0.5 ml. of the solution of the polymer in ethanol-free chloroform (3% W/V). Since tetramethylsilane as an internal standard was not available, the scale of the abscissa of Fig. 1 is expressed in parts per million, with reference to the peak due to the methoxy group ($-OCH_3$). Three characteristic peaks at the right of the spectrum are assigned to α-methyl groups of the polymer. Since their relative intensities play an important role in our discussion, the spectra were exactly traced on section paper and were decomposed into three symmetrical peaks one by one, while the total area of the three peaks was kept unchanged. These trials should be repeated until a satisfactory similarity among the corresponding isolated peaks of all spectra is attained. Once a reasonable decomposition is accomplished for one spectrum, the results may be applied to another. It seems that for our spectra the values of the relative area thus obtained are more accurate than those measured with a planimeter.

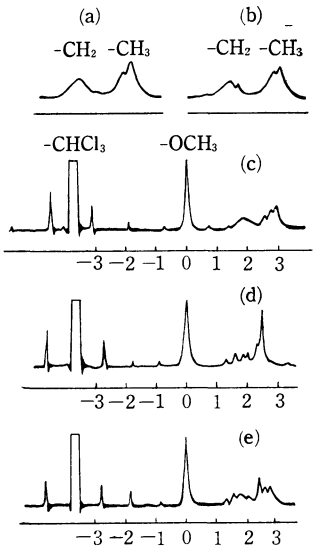


Fig. 1. NMR spectra of 3 per cent chloroform solutions of polymethyl methacrylates, obtained at 56.4 Mc./sec. and 20°C.

(a) sample 6 (b) sample 8
(c) sample 10 (d) sample 11
(e) sample 12

Results and Representation

Some examples of the results are shown in Fig. 1. There are remarkable changes in both the $-CH_2$ and α-CH_3 regions. Especially, the relative intensities of the three peaks at the right vary with the conditions of polymerization, while their peak positions remain unchanged. As one of the authors[2,4] and other workers[1,3] have already mentioned, these changes in spectra are caused by an magnetic anisotropy effect of the ester carbonyl groups in combination with the conformation and stereochemical configuration of these polymer chains. Every monomer unit in a polymer chain of methyl methacrylate has an asymmetric carbon atom, and its placement may be designated as *d* or *l*. For the sake of convenience, they will be replaced in this paper by 0 and 1 respectively. It doesn't matter whether an arbitrary monomer unit in the polymer chain is represented by 0 (or 1). Assuming that any one of these monomer units corresponds to 0 (or 1), all the other monomer units may be classified without ambiguity. Assume two operators "$\oplus$" and "$\ominus$", similar to logical symbols, as follows:

a	b	$\oplus\{ab\}$,	$\ominus\{ab\}$
0	0	0	I
0	1	1	D_1
1	0	1	D_2
1	1	0	S

where the letters *a* and *b* represent either 0 or 1, and *ab* represents two consecutive digits formed in a binary sequence of 0's and 1's. The bottom row of this table, for instance, means that every pair of 1's (.... 1 1 ....) in the binary sequence must be replaced by 0 after the operation "$\oplus$." Therefore, a binary sequence of ten digits long (for example,

$$A=1\,1\,0\,0\,0\,1\,0\,1\,0\,0),$$

is transformed into:

$$B=\oplus\{A\}=0\,1\,0\,0\,1\,1\,1\,1\,0,$$

where A denotes the sequence A, the length of which is always reduced by one digit after the operation. In a like manner, every pair of 1's in the binary sequence must be changed to S by the operation "$\ominus$." When the above-mentioned meaning of 0 and 1 is taken into account, the binary sequence A may be recognized as a partial model of the polymer chains we are concerned with, and sequence B represents the states of the bonds of the monomer units which together construct the polymer chain. Applying operation "$\ominus$" to the sequence B yields a sequence

$$C=\ominus\{B\}=\ominus\oplus\{A\}=D_1D_2ID_1SSSD_2,$$

where D's are the units which break I- or S-sequences. We have called them "ditactic" (or di-syndiotactic) units in the meaning of the sequence A, because they themselves alone are constructed to the sequence as follows:

..... 1 1 0 0 1 1 0 0 1 1 0 0 .....

D-units as defined here are exactly the same as Bovey's h-units,[1] which were called "heterotactic configurations" (i.e., *ldd*, *dll*, *ddl*, or *lld*). It is apparent that in the sequence $\ominus \oplus \{A\}$, D_1's and D_2's appear in couples, sometimes by turns, and sometimes at both ends of I- or S-subsequences. Therefore, in an infinite sequence, both D_1 and D_2 should have the same probability of occurrence. In addition to this, it may be pointed out that even D's appear between two I- or S-subsequences, while odd D's are allowed to exist between I- and S-subsequences.

The facts that the α-methyl peak in general splits into three peaks and that the relative intensitites vary noticeably, suggest that every successive three-monomer unit in the polymer chains contributes to their peak intensities. From the viewpoint of nuclear magnetic resonance phenomena, the α-methyl group of any monomer unit is not affected very much by the other monomer units, except by the nearest neighbors on both sides. From the same point of view, we may explain that D_1- and D_2-units are essentially the same and that the α-methyl groups of polymethyl methacrylate are now classified into three species symbolized by I, D and S. It is conceivable that there exists a close relationship between these three species of α-methyl groups and the three α-methyl peaks in Fig. 1. The much useful information[4,5,12] so far obtained about the polymerization of methyl methacrylate leads to the following conclusion: The three α-methyl peaks are due to I-, D- and S-units, from left to right, respectively. The relative area of each peak is proportional to the ratio of the corresponding units to the whole polymer chain. Figure 1 shows that the left peak, ascribed to I-units, is very high in the spectrum of polymers using isobuthylmagnesiumbromide as a catalyst. On the contrary, for samples prepared with free radical initiators, the other two peaks are moderately high, and a tendency towards decreasing S-units can be observed as the polymerization temperature increases. The spectrum of the sample polymerized with di-*n*-butylmagnesium is a typical one; in it these three peaks are competitively high. It should be noticed that the D-unit of the polymer chains has been detected for the first time; no method except high resolution NMR is available at present for the direct measurement of the unit.

In order to facilitate the representation of the fractions of three units which appear in a sequence $\ominus \oplus \{A\}$, a ternary diagram as shown in Fig. 2 was employed. Any point plotted in

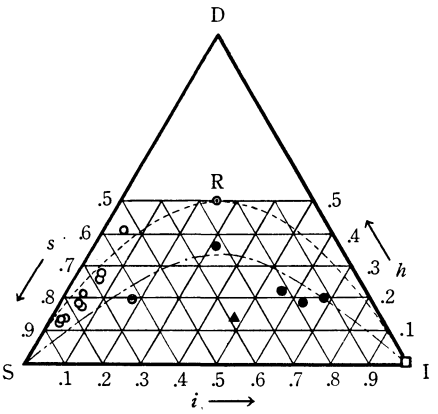


Fig. 2. Ternary diagram illustrating the stereochemical configuration of molecular chains of polymethyl methacrylate.

the ternary diagram represents only one type of stereochemical configuration of the polymer chain, because the corresponding I-, D- and S-units are always unique in their proportions. The apex at the top of the diagram is assumed to correspond to the configuration of polymer chains including only D-units; the others give, respectively, the configurations of pure isotactic and syndiotactic polymer chains in the meaning of Natta.[13] Making use of a geometrical theorem, the relation:

$$i+h+s=1 \qquad (1)$$

is valid for any point in the ternary diagram, where i, h and s represent the probabilities of finding I-, D- and S-units respectively in a sequence $\ominus \oplus \{A\}$. The dotted curve, SRI, and the point, R, will be discussed in the following section. Table II presents the results of quantitative measurements of the relative contributions due to three α-methyl peaks of the polymers prepared in various polymerization conditions. They correspond to the plots shown in Fig. 2.

For the methylene peaks of polymethyl methacrylate, a striking difference is found between the spectra of isotactic and syndiotactic polymethyl methacrylates. A quartet

12) R. G. J. Miller, B. Mills, P. A. Small, A. Turner-Jones and D. G. M. Wood, *J. Chem. Ind.* (*London*), **1958**, 1323.

13) G. Natta, *J. Polymer Sci.*, **34**, 3 (1959).

due to the methylene protons of the polymer can be observed in the former, while there is only a single, though rather broad peak in the latter. This point may be explained on the basis of the NMR spectrum of AB system.[14] Two protons of a methylene group are thought to be non-equivalent when they are just on the "0" bond in an infinite sequence, $\oplus\{A\}$. They, therefore, give rise to absorption lines which consist of a pair of doublets. In case they are on the "1" bond, they are equivalent and yield a single absorption peak. The values of the chemical shift, $(\delta_A-\delta_B)$, and the coupling constant, J_{AB}, as estimated from the spectrum of sample 11 in Fig. 1, are 37.0 c/s and 15.5 c/s respectively. These values are well in accordance with those obtained by Bovey et al.[1,3] In view of the above discussion, it is apparent that the configuration of the polymer chains can be determined in this case, not in the meaning of the sequence $\ominus\oplus\{A\}$, but in that of the sequence $\oplus\{A\}$. That is, the information about *D*-units can not be obtained, at least explicitly, by the analysis of the methylene peaks in the NMR spectrum of polymethyl methacrylate.

Polymer Characterization

In the preceding section, a short description was given of how the *D*-units behave in the sequence $\ominus\oplus\{A\}$. The sequence without a *D*-unit represents an isotactic or syndiotactic polymer chain, which is essentially the same as defined by Natta. In this case, the number of isotactic or syndiotactic sequences is only one, and its length is two units shorter than that of the original sequence, *A*; in other words, the number of the units in the sequence is less by two than that of the monomer units in the polymer chain. When any *D* is contained in the sequence, the situation is quite different. Some of the units belonging, in a sense, to the isotactic or syndiotactic part are counted this time in the sequence of *D*-units. This apparently indicates that a molecular chain in which isotactic and syndiotactic parts both exist contains one *D*-unit or more. A stereoblock polymer may be defined as one for which *h*, the proportion of *D*'s in the sequence $\ominus\oplus\{A\}$, is properly small in contrast with the large proportion of both *I*'s and *S*'s. As a general rule, the larger the proportion of *D*'s, the shorter the average length of *I*- and *S*-sequences becomes. Each average length of sequences is a characteristic measure of the polymer chain. On some assumptions in the polymerization steps, let us consider two cases:

Case 1. A Polymer with a Probability of a Specified Bond.—As was explained in the previous section, the states of bonds may be specified by two digits, "0" and "1", in the meaning of the sequence $\oplus\{A\}$. Let us assume that the probability of the occurrence of 0-digits in the sequence $\oplus\{A\}$ is designated by *p*. In terms of polymerization, it may be defined as the probability that the monomer unit at the end of a growing chain will add another monomer of the same designation, that is, of the same placement. The expected number of times that a sequence $\ominus\oplus\{A\}$ of the length *N* will contain the subsequence of *I*-units of the length *k* is given by:

$$\overline{X}_{I,k}=(N-k-1)p^{k+1}(1-p)^2+2p^{k+1}(1-p) \tag{2}$$

for $k\leqq N-1$, and

$$\overline{X}_{I,N}=p^{N+1} \tag{3}$$

which are easily derived from the calculation of the number of times that a binary sequence $\oplus\{A\}$ of the length $(N+1)$ includes consecutive 0-digits of the length $(k+1)$. Hence, the number of *I*-units in the sequence $\ominus\oplus\{A\}$ is:

$$\begin{aligned}[I] &= \sum_{k=1}^{(N+1)p-1} k\{(N-k-1)p^{k+1}(1-p)^2 \\ &\quad +2p^{k+1}(1-p)\}=p(1-p)\{(N-1)(1-p) \\ &\quad +2\}\sum_{k=1}^{(N+1)p-1} kp^k-p(1-p)^2\sum_{k=1}^{(N+1)p-1} k^2p^k\end{aligned} \tag{4}$$

The number of successive *I*-units of the length *k* included in the sequence $\ominus\oplus\{A\}$ is also given by:

$$\begin{aligned}[\{I\}] &= \sum_{k=1}^{(N+1)p-1} \{(N-k-1)p^{k+1}(1-p)^2 \\ &\quad +2p^{k+1}(1-p)\}=p(1-p)\{(N-1)(1-p) \\ &\quad +2\}\sum_{k=1}^{(N+1)p-1} p^k-p(1-p)^2\sum_{k=1}^{(N+1)p-1} kp^k\end{aligned} \tag{5}$$

When *N* is very large, Eqs. 4 and 5 are approximated as follows:

$$[I]\approx p(1-p)^2N\sum_{k=1}^{\infty} kp^k=p^2N \tag{6}$$

$$[\{I\}]\approx p(1-p)^2N\sum_{k=1}^{\infty} p^k=p^2(1-p)N \tag{7}$$

For an infinite sequence, it is necessary to take the limit of Eqs. 4 and 5. Thefore, the average length of successive *I*-units in the sequence $\ominus\oplus\{A\}$ is given by

$$\langle I\rangle=\lim_{N\to\infty}\frac{[I]}{[\{I\}]}=\frac{1}{1-p} \tag{8}$$

14) H. J. Bernstein, J. A. Pople and W. G. Schneider, *Can. J. Chem.*, 35, 65 (1957).

In like manner, results are obtained for *S*-units:

$$[S] = (1-p)^2 N \tag{9}$$

$$\langle S \rangle = 1/p \tag{10}$$

The summations, however, of even and odd *D*'s must be taken separately, since even *D*'s come into existence only between two *I*- or *S*-subsequences, while odd *D*'s come into existence between *I*- and *S*-subsequences. Thus, the number of *D*-units can be obtained straightforwardly:

$$\begin{aligned}[D] = {} & \{p^3+(1-p)^3\}\sum_{k=1}^{(N+1)p-1}\{2k(N-2k-1)p^k(1-p)^k\} \\ & +2\{p^2+(1-p)^2\}\sum_{k=1}^{(N+1)p-1}2kp^k(1-p)^k \\ & +2p(1-p)\sum_{k=1}^{(N+1)p-1}\{(2k-1)(N-2k)p^k(1-p)^k\} \\ & +2\sum_{k=1}^{(N+1)p-1}(2k-1)p^k(1-p)^k \end{aligned} \tag{11}$$

and

$$\begin{aligned}[\{D\}] = {} & \{p^3+(1-p)^3\}\sum_{k=1}^{(N+1)p-1}(N-2k-1)p^k(1-p)^k \\ & +2\{p^2+(1-p)^2\}\sum_{k=1}^{(N+1)p-1}p^k(1-p)^k \\ & +2p(1-p)\sum_{k=1}^{(N+1)p-1}\{(N-2k)p^k(1-p)^k\} \\ & +2\sum_{k=1}^{(N+1)p-1}p^k(1-p)^k \end{aligned} \tag{12}$$

where it is assumed that $p \leqq 1/2$. For $p > 1/2$, the results do not differ from Eqs. 11 and 12 except that p and $(1-p)$ replace each other. Taking the limit of the summations in Eqs. 11 and 12 gives the final results:

$$[D] \approx 2p(1-p)N \tag{13}$$

$$[\{D\}] \approx p(1-p)N \tag{14}$$

It is very interesting that the average length of successive *D*-units becomes equal to two units; that is,

$$\langle D \rangle = 2 \tag{15}$$

If we divide the number of units of each species by the total number of units in the sequence, we get the probability of the occurrence of the unit in the sequence; therefore, for this case Eqs. 6, 9 and 13 give:

$$i = p^2 \tag{16}$$

$$s = (1-p)^2 \tag{17}$$

$$h = 2p(1-p) \tag{18}$$

where i, s and h are the same probabilities that appeared in Eq. 1. Eliminating the parameter, p, from Eqs. 16 to 18, we find that

$$h/2 = \sqrt{i \cdot s} \tag{19}$$

This relationship can be seen in Fig. 2 as a dotted locus *S R I*. When the probability of making a 0-digit in a sequence $\oplus\{A\}$ is given, the structure of the sequence $\ominus \oplus \{A\}$ is always represented by one of the points just on the locus *S R I*. In terms of our experiments, this may be explained as follows. If the manner of the monomer addition, that is, the state of the bond, is specified by a single probability, p, the α-methyl groups of the polymethyl methacrylate so obtained give a spectrum which can be represented by a point on the curve *S R I*. The point "*R*" in the ternary diagram is of great interest because the value of p just equals one-half. This means that it exactly corresponds to the so-called random polymerization, and that, if the above mentioned probability is applicable, it may be considered as a special case of this model.

Case 2. The Stereoblock Polymer.—It is very difficult to put bounds to "stereoblock" polymers. According to the designation of the placements, they are composed of two kinds of blocks, such as 00000 and 111, which are formed alternately in the polymerization steps. When the lengths of these subsequences are rather too short, the polymer is no longer a stereoblock one. In all cases, however, the sequence lengths of *D*-units in the sequence $\ominus \oplus \{A\}$ should remain short. For the sake of simplicity, it is assumed that any *D*-unit appears "solo" throughout this section; two special cases, corresponding to two different mechanisms of polymerization, will be treated below.

First, we assume an infinitely long polymer chain in which isotactic and syndiotactic blocks appear "alternately" and in which the number of monomer units in the blocks varies from three to infinity. As an example, all sequences of "specified bonds" including any single 0-digit, such as

..... 1 1 1 1 0 1 1 1 .....

are excluded, since it is transformed by the operator "$\ominus$" into:

..... *I I I D D I I* .....

Then, for the *I*- and *S*-parts of the stereoblock polymer chain, it is found that

$$[\{I\}] = [\{S\}] = (i+s)N\sum_{k=1}^{\infty}\left(\frac{i}{i+s}\right)^{k}\left(\frac{s}{i+s}\right)^{2} = \frac{is}{i+s}N \tag{20}$$

for the very large integer, N, which equals the number of monomer units contained in the polymer chain. The other notations in Eq. 20 are exactly the same as those mentioned in the preceding section. By using the relation:

$$[\{I\}] + [\{S\}] = [\{D\}] \tag{21}$$

which holds for infinite sequences, the number of subsequences of D-units is given by:

$$[\{D\}] = \frac{2}{1/i + 1/s}N \tag{22}$$

which leads to:

$$h = \frac{2}{1/i+1/s} \tag{23}$$

since it is assumed that $[D] = [\{D\}] = hN$. $\langle I\rangle$ and $\langle S\rangle$ in this case can be represented by i, h and s:

$$\langle I\rangle = 2i/h \tag{24}$$

$$\langle S\rangle = 2s/h \tag{25}$$

The chain curve plotted in Fig. 2 exhibits the relation among i, h and s given by Eq. 23. If we accept the above model, this curve represents the spectra of the α-methyl groups of the methyl methacrylate polymer chains which would be formed in a manner that alternations from an isotactic chain growth to a syndiotactic one and vice versa occur quite at random.

In the second place, let us discuss the polymer chain designated by the following sequence:

$$\overbrace{\text{..... } D\,I\,I \text{ ..... } I\,I}^{\langle I\rangle}\ D\ \overbrace{S\,S \text{ ..... } S}^{\langle S\rangle}\,D \text{ .....}$$

in which isotactic blocks of length $\langle I\rangle$ and syndiotactic blocks of length $\langle S\rangle$ are formed alternately, leaving single D-units at every change. Then, we have

$$i = \langle I\rangle/(\langle I\rangle + \langle S\rangle + 2) \tag{26}$$

$$s = \langle S\rangle/(\langle I\rangle + \langle S\rangle + 2) \tag{27}$$

$$h = 2/(\langle I\rangle + \langle S\rangle + 2) \tag{28}$$

and Eqs. 24 and 25 again hold. In this case, if the values of $\langle I\rangle$ and $\langle S\rangle$ are given, Eqs. 26 to 28 correspond to the definite plot in the ternary diagram.

Discussion

We have now reached the point where we can discuss the relation between our models and the experimental results.

If a polymerization of methyl methacrylate occurs quite at random in the meaning of stereochemical placements of the monomer units, the polymers so obtained give the spectrum of α-methyl groups which may be represented by the point R in Fig. 2. All the experimental results, however, are scattered far from the point. This apparently indicates that the random polymerization in the strict sense can not be achieved, even if a free radical polymerization at a high temperature is employed. We may also conclude from Fig. 2 that essentially different mechanisms of polymerization give polymers of different structures. For polymers prepared with free radical initiators, the model described in the previous section (see Case 1) seems to be applicable. The probability, p, can be calculated by Eq. 17; the results are shown in Table II. It is conceivable that p depends almost entirely upon the polymerization temperature of the sample.

Table II. Characteristic parameters of free radical polymethyl methacrylate as a function of the polymerization temperature

Sample No.	Proportion of α-methyl peak area			p	$\langle I\rangle$	$\langle S\rangle$*
	i	h	s			
1	0.02	0.13	0.85	0.08	1.1	14.1
2	0.02	0.14	0.84	0.08	1.1	13.0
3	0.03	0.14	0.83	0.09	1.1	12.9
4	0.05	0.18	0.77	0.12	1.1	9.6
5	0.04	0.19	0.77	0.12	1.1	9.1
6	0.04	0.21	0.75	0.13	1.1	8.1
7	0.06	0.26	0.68	0.18	1.2	6.2
8	0.05	0.28	0.67	0.18	1.2	5.8
9	0.05	0.41	0.54	0.27	1.4	3.6

* Calculated from Eq. 34.

According to the procedure of Fordham,[15] the probability, p, may be written in the form:

$$p = \frac{k_i}{k_i + k_s} \tag{29}$$

where k_i and k_s are the rate constants for the addition of monomer units to the chain to form isotactic and syndiotactic placements respectively. We have, then,

$$\frac{k_i}{k_s} = \frac{p}{1-p} = \exp\{\Delta(\Delta S)/R\}\exp\{-\Delta(\Delta H)/RT\} \tag{30}$$

where $\Delta(\Delta S) = \Delta S_i - \Delta S_s$ and where $\Delta(\Delta H) = \Delta H_i - \Delta H_s$, which are the differences in activation entropies and in activation enthalpies

15) J. W. L. Fordham, *J. Polymer Sci.*, **39**, 321 (1959).

respectively between an isotactic placement and a syndiotactic one. Equation 30 shows that the logarithm of $p/(1-p)$ is linear in reciprocal temperature and that the values of $\Delta(\Delta H)$ and $\Delta(\Delta S)$ can be found from the slope and the intercept at $1/T=0$ respectively. In Fig. 3 are plotted the results from which we obtain:[11]

$$\Delta(\Delta H) = (1.58\pm0.07)\,\text{kcal.}$$

and $\Delta(\Delta S) = (0.67\pm0.24)$ e. u.

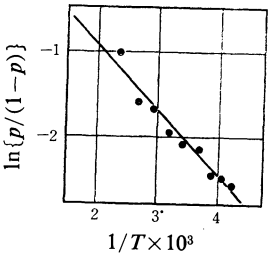


Fig. 3. $\ln\{p/(1-p)\}$ vs. $1/T$ for polymethyl methacrylate prepared in free radical polymerization.

These results are considerably larger than those obtained by other workers.[16,17] Substituting these values into Eq. 30, we find

$$\frac{k_i}{k_s} = 1.95\exp(-1580/\boldsymbol{RT}) \tag{31}$$

so that from Eqs. 17 and 29, the proportion of S-units will be:

$$s = \left\{\frac{1}{1+1.95\exp(-1580/\boldsymbol{RT})}\right\}^2 \tag{32}$$

Since the melting point of toluene is −95°C, Eq. 32 shows that the proportion of S-units attainable in practice in the polymer chain is less than 95 per cent. On the other hand, the random polymerization could be obtained, if it were possible, at about 1000°C. As a matter of fact, however, the polymerization would occur only below the ceiling-temperature[18] of the system.

Even the polymer made at room temperature contains fairly long sequences of S-units. The average sequence lengths of I- and S-units can be calculated from the equations given below:

$$\langle I\rangle = 1+h/2s \tag{33}$$

$$\langle S\rangle = 1+2s/h \tag{34}$$

The results are shown in Table II.

As we have seen in Fig. 2, the mechanism of anionic polymerization can not be explained by the model used for free radical polymerization. Let us now consider the applicability of the two models developed in the previous section for the stereoblock polymer. Of course, there are a few points to be clarified beforehand. First, it is very difficult to define the term "stereoblock" exactly, but no further discussion is needed here. Secondly, the polymer prepared with an anionic initiator might consist of molecular chains formed in several polymerization mechanisms, which could each perhaps be described in the same manner as the free radical polymers. The observations, however, on the difference in activation energies between isotactic and syndiotactic placements of a monomer-unit would not seem to support this assumption. The distribution range in the ternary diagram is too narrow to cover the cases of anionic polymerization. In case a sample is a mixture of polymer chains of different tacticities, its apparent i, h and s values can be calculated from these values of the componenents. In terms of the ternary diagram, this may be explained as follows. Just on each point of the ternary diagram we assume a material particle of the same mass as the corresponding component. Then, the overall structure of the sample can be represented by the center of gravity for the system of these material particles. It seems, therefore, impossible to deduce the plots for anionic polymerization products from the experimental results for free radical polymers.

As has been mentioned earlier, two models developed in the previous section for stereoblock polymers are special ones, because of their assumption that $\langle D\rangle=1$. One is a random-sequence-length model for its I- and S-parts, while the other is a constant-sequence-length model. The former is represented by the chain curve in Fig. 4. Some of the experimental results seem to satisfy Eq. 23 approximately when Bovey's data[1] are taken into account. One of our plots, however, deviates considerably from the curve. This may be partly due to the separation of three

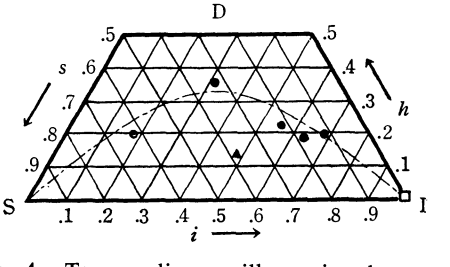


Fig. 4. Ternary diagram illustrating the stereochemical configuration of methyl methacrylate polymers prepared with anionic initiators: sample 10 ◓, sample 11 □, and sample 12 ▲, Bovey's data ●.

16) F. A. Bovey, *J. Polymer Sci.*, **46**, 95 (1960).
17) T. G. Fox and H. W. Schnecko, *Polymer*, **3**, 575 (1962).
18) R. D. Snow and F. E. Frey, *Ind. Eng. Chem. (Industr.)*, **30**, 176 (1938).

rather poorly resolved α-methyl peaks, since it is attended with a little difficulty. Mainly, however, it seems to arise from the fact that the mechanism of polymerization is more complicated.

For the latter model, the avrerage sequence lenghths $\langle I \rangle$ and $\langle S \rangle$ are introduced as the parameters, but as yet we have not sufficient information to evaluate them. Using the values of samples 10 and 12, we obtain $\langle I \rangle = 1.8$ and $\langle S \rangle = 6.2$ for the former and $\langle I \rangle = 7.5$ and $\langle S \rangle = 5.8$ for the latter. We might say that the steric hindrance for each stereochemical configuration of molecular chains would be one of the origins that make blocks of a constant length. It seems, however, rather improbable that such a long and constant sequence length as calculated above could be ascribed to this origin. On the contrary, it seems possible that in anionic polymerizations the behavior of metallic counterions brings us stereoblock polymers.[1] One example is that a metallic counterion contributes to the isotactic chain growth for a certain period, and then leaves from the chain end for the following period, allowing the syndiotactic chain growth. Alternation between these two states yields a stereoblock polymer chain, but this case would preferably be included in our former model. In actual fact, the mechanism of anionic polymerization is beyond our depth because of its complexity.

In the course of the decomposition of spectra, we found that, at room temperature, the *I* part of methyl methacrylate polymer chains gives a somewhat narrower resonance peak of α-methyl groups than that ascribed to the *S* part. Recently, at a higher temperature, we have observed the inversion of apparent peak heights between *I*- and *S*-peaks in some of the stereoblock polymers. This probably corresponds to the remarkable difference in glass temperature between isotactic and syndiotactic polymethyl methacrylates.[7] The detailed investigation of these problems must be the subject of future research.

Summary

The NMR spectra of polymethyl methacrylates prepared with various initiators have been examined. Three resonance peaks of α-methyl protons observed with an increasing magnetic field correspond to three species of the monomer units, i. e., *I*-, *D*- and *S*-units respectively. The proportion of each peak area may be used to characterize the stereoregularity of the polymer chain. A ternary diagram has been proposed to represent the stereochemical configuration of the polymers. Together with the average sequence lengths of the units, the possible polymerization mechanisms are considered. Free radical polymers of methyl methacrylate seem to be describable with a single parameter which depends only on the polymerization temperature. Some polymers prepared with anionic initiators show a stereoblock character. The polymerization mechanism has also been discussed in some idealized cases.

We are grateful to Dr. Haruaki Watanabe for materials used in this work and for many helpful suggestions. We are also much indebted to Dr. Akibumi Danno of the Japan Atomic Energy Research Institute for permitting us to use the NMR spectrometer.

The Electrical Communication Laboratory
Musashino, Tokyo

Proton Magnetic Resonance Spectra of Polypropylene in Solution

By Yoshinori KATO and Atsuo NISHIOKA

(Received June 1, 1964)

During recent years, high resolution nuclear magnetic resonance spectroscopy has been applied to the study of polymers. In some cases, however, the polymer is not fully soluble to the required concentration, so that a well-resolved spectrum can not be obtained. When we use this method, there are a few restrictions on both the polymer and the solvent. First of all, a polymer solution of an appropriate concentration, say at least five per cent or so, is necessary for a detailed analysis of the NMR spectrum. On the other hand, the resonance peaks due to the solvent itself should not disturb those of the polymer.

In the case of ordinary polypropylene, the molecular weight is so high that we can scarcely obtain a well-resolved spectrum even at elevated temperatures. We have applied, therefore, a "weak" controlled thermal degradation to polypropylene in order to reduce the molecular weight and increase the solubility. The thermal degradation employed was so weak that it did not give rise to any significant change in the infrared absorption spectrum of the sample. By making use of this technique, an attempt is made in this paper to measure the degree of stereoregularity of polypropylene. A further object of the work is to study a saturated polymer with small difference in chemical shift.

So far as we know, few investigations[1-3] using high resolution NMR spectrometers have been made of polypropylene. This probably arises from the complexity of the spectrum because of the small difference in chemical shift. Very recently, a spin decoupling technique has been successfully employed to observe the stereochemical configurations of the molecular chains of some polymers.[4,5] This technique, as well as the use of partially-deuterated polymers, will be an effective means to overcome the complexity of the spectrum.

1) S. Sato, R. Chûjô, T. Ozeki and E. Nagai, *J. Polymer Sci.*, **62**, S 101 (1962).
2) F. C. Stehling, paper presented at the Washington Meeting of the American Chemical Society, Washington, March, 1962.
3) K. Nukada and S. Ônishi, paper presented at the Symposium on High Polymers, Nagoya, October, 1963.
4) S. Satoh, R. Chûjô and E. Nagai, paper presented at the Meeting of the Physical Society of Japan, Fukuoka, October, 1963.
5) F. A. Bovey, E. W. Anderson and D. C. Douglass, *J. Chem. Phys.*, **39**, 1199 (1963).

Experimental

Several kinds of commercial polypropylene were used in this work. The limiting viscosity numbers of the original samples, $[\eta]$, are shown in Table I.

TABLE I. LIMITING VISCOSITY NUMBER AND DENSITY OF ORIGINAL SAMPLE

Original sample	$[\eta]$*	Density
A	1.28	0.9126
B	1.71	0.9095
C-1	1.35	0.9080
C-2	1.52	

* Obtained at 135°C in tetraline.

For the sample, C-2 NMR measurements were carried out without any preliminary treatment. The other samples were first extracted with boiling *n*-heptane. The solvent had been renewed every three hours until no precipitate could be seen when it was poured into methanol. Then, the residue was separated by filtration and dried at 60°C in a vacuum. This was used as the sample termed "*n*-heptane-insoluble" in Table II. On the other hand, the extracted polymers were precipitated in a large amount of methanol; after filtration, they were dried in vacuo at 40°C. Then they were extracted with ether to give the *n*-heptane-extracted and the ether-soluble samples in the table. The acetone-extracted sample (sample 10) was obtained from an atactic polypropylene (C-3) by extraction with boiling acetone; again the residue was extracted with ether to prepare the ether-extracted sample (sample 2). The thermal degradation of the samples was carried out in vacuo. The conditions are shown in Table II. For samples 3, 5, 7 and 9 the processes of extraction were omitted and the thermal degradation technique immediately employed, while for samples 1, 2 and 10 only the former processes were employed. Finally, the other samples were obtained by thermal degradation of the residues remaining after the extraction with *n*-heptane.

All spectra were obtained with a Varian DP-60 spectrometer at about 140°C, except for the spectrum of the polypropene-1,1-d_2 sample. For this sample a nuclear magnetic resonance spectrometer, Mullard SL44 Mk. II, operating at 40 Mc/s was employed. Each 10% sample in *o*-dichlorobenzene was sealed in a glass tube together with a 0.2% antioxidant and 0.4% tetramethylsilane as internal standards. The peak positions were determined by using the sideband technique and were expressed by "the τ-scale."[6]

6) G. V. D. Tiers, *J. Phys. Chem.*, **62**, 1151 (1958); *J. Chem. Phys.*, **29**, 963 (1958).

TABLE II. PREPARATION AND PROPERTY OF EACH SAMPLE

Sample No.	Original sample	Preliminary treatment		Property	
		Extraction	Thermal degradation	$[\eta]$	Density
1	C-1	*n*-Heptane-extracted	—	0.85	0.9102
2	C-3*	Ether-extracted	—	0.82	0.9114
3	C-1	—	290°C, 3hr.	0.85	0.9102
4	C-1	*n*-Heptane-insoluble	280°C, 5hr.	0.82	0.9114
5	A	—	270°C, 0.5hr.	0.82	0.9125
6	A	*n*-Heptane-insoluble	290°C, 3hr.	0.87	0.9126
7	B	—	270°C, 3hr.	0.85	0.9132
8	B	*n*-Heptane-insoluble	300°C, 5hr.	0.81	0.9122
9	C-2	—	—	(1.52)	
10	C-3*	Acetone-extracted			

* An atactic polypropylene.

Results and Discussion

The Study of Each Spectrum.—Typical spectra are shown in Fig. 1, except for that of sample 1, from which we could not obtain well-resolved spectrum by any means.

Several points of interest have come to light during the course of the measurements. First, the spectrum of sample 10 is somewhat different from those of the others, and it doesn't change in the temperature range 23~140°C. Contrary to our result, the corresponding spectrum given by Satoh et al.[1] (their sample 2) exhibits a prominent peak at 8.75 τ. This is probably due to the fact that their sample was polymerized by a Ziegler-type catalyst, while ours were not. That is, the peak at 8.75 τ may be ascribed to some *n*-paraffins or polyethylenes. This fact may be of interest, but it will not be gone into further here. Secondly, the difference between the spectrum of sample 2 and that of sample 8 has attracted our great interest. Especially, the remarkable change in the middle region of the spectra seems to suggest the possibility of the stereoregularity measurement of the polymer chains. According to Natta, the ether soluble sample consists of molecular chains with an atactic configuration. Therefore, the spectrum of sample 2 shown in Fig. 1 may be decomposed into two parts, one isotactic and one syndiotactic. On the other hand, the *n*-heptane-insoluble fraction contains mainly isotactic molecular chains. Therefore, the spectrum of sample 8 must be very similar to that of a purely isotactic polymer. This point will be discussed in detail later.

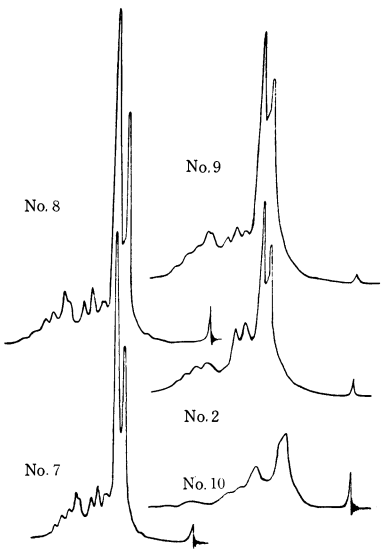


Fig. 1. NMR spectra of the samples shown in Table II.

The physical properties of each sample after the preliminary treatments are also given in Table II. A comparison of the spectra in Fig. 1 leads to the conclusion that the solubility of polypropylene roughly depends on the value of $[\eta]$. However, in the case of sample 9, a rather well-resolved spectrum was obtained regardless of the large value of $[\eta]$. This result is probably due to the fact that the sample consists of molecular chains with less isotactic configurations. As was mentioned in the previous section, the extraction procedure always preceded the thermal degradation when both were needed. In contrast, when the thermal degradation was carried out before the extraction, all the *n*-heptane-insoluble samples gave poorly-resolved spectra, though their final values of $[\eta]$ were much the same as those of the samples shown in Table II. This implies that the extraction procedure depends on both the stereoregularity of the polymer chains and the molecular weight distribution. At the present stage, it seems difficult to foretell which thermal degradation

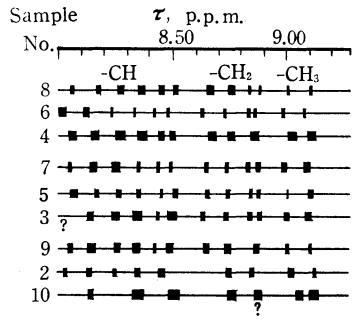


Fig. 2. Values of chemical shift for the samples given in Table II.

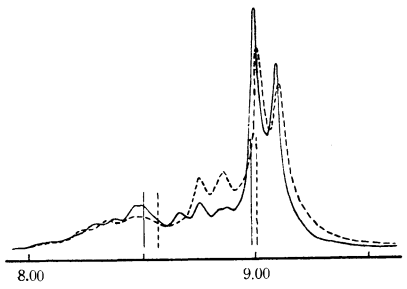


Fig. 3. Normalized spectra of isotactic and atactic polypropylenes. Vertical lines devide the whole area into three parts in the ratio of 1 : 2 : 3 from left to right.

—— Isotactic P. Pr.
--- Atactic P. Pr.

condition is adequate to a certain polypropylene. In any case, however, the thermal degradation must be carried out as mildly as possible.

Figure 2 shows the values of the chemical shift for each sample. We can not find out any difference among the samples separated from various brands of polypropylene except for that between samples 2 and 10. The resonance peaks between 8.95 τ and 9.15 τ are ascribed to the methyl groups. It is found that the methyl resonance of atactic polypropylene shows a slight shift towards a higher magnetic field than that of isotactic polypropylene. Unfortunately, however, the shift is not large enough to be employed for the stereoregularity measurements. Very recently, this small shift has been independently confirmed more accurately by Nukada et al.[3]

Normalized spectra of atactic and isotactic polypropylenes, i. e., samples 2 and 8, are shown in Fig. 3. Vertical solid and broken lines separate the whole area of each spectrum into three parts in the ratio of 1 : 2 : 3 from left to right. These three parts roughly correspond to the α-proton, methylene and methyl resonances respectively. As we have already pointed out, the central parts corresponding to the methylene resonance are markedly different from each other. Especially, the resonance region of the methylene groups in the isotactic part of the polymer chains seems to be much broader than that in the syndiotactic part. We can not observe any noticeable change in any α-proton resonance region.

Now, let us assume that the ideal spectrum of either isotactic or syndiotactic polypropylene is available, and that the stereochemical configuration of the polymer chain is homogeneous; all the observed spectra can then be separated straightforwardly into isotactic and syndiotactic components, so that the degree of stereoregularity of each sample may be determined. The homogeneity of the configuration will be realized to a considerable extent by the extraction of the sample with a suitable solvent. Thus, not only the preparation of an absolutely isotactic polymer but also a theoretical approach to the ideal spectrum is a matter of importance for the measurement of stereoregularity. It is known that isotactic polypropylene can be easily obtained as the residue of extraction with *n*-heptane from the commercial sample, whereas it is rather difficult to obtain syndiotactic polypropylene. However, even the former will not give the ideal spectrum in the strict sense. We believe that the analysis of spectra is the shortest way at present to obtain the ideal spectrum.

For the sake of convenience, we have introduced the following value, X, as a measure of the stereoregularity of the polymer chain:[7]

$$X=\frac{\left(\begin{array}{c}\text{Relative intensity of}\\ \text{the peak at } 8.87\,\tau\end{array}\right)}{\left(\begin{array}{c}\text{Average relative intensity of}\\ \text{the peaks at } 9.0\,\tau \text{ and } 9.1\,\tau\end{array}\right)}$$

At first, we used apparent peak heights instead of the peak areas to evaluate the X-value; we found that the X-value varies from 0.15 to 0.50 in accordance with the stereochemical configuration of the polymer chain. On such occasions, however, not the peak height but the peak area should be used if possible. Therefore, our next problem was to separate each peak in order to measure the relative area. In case the spectrum is not so well resolved, it is very important to have some knowledge concerning the relative intensities of the peaks as well as the peak positions of the ideal spectrum. Therefore, we shall try to calculate the theoretical spectra due to the methylene groups of polypropylene.

7) Y. Kato and A. Nishioka, paper presented at the 3rd Symposium on Nuclear Magnetic Resonance Spectroscopy, Osaka, November, 1963.

ABC_2 and A_2B_2 Spectra. — In some vinyl polymers, the "backbone" methylene protons will approximately give rise to the NMR spectra of the ABC_2 (or A_2B_2) system in the notation of Bernstein et al.[8] Let us assume that the electron-coupled spin-spin nuclear magnetic interaction between any two hydrogen nuclei can be disregarded if more than two carbon-carbon bonds separate the nuclei. For the sake of simplicity, we will consider first a molecular chain with a planar zigzag conformation. Then, together with the neighboring α-protons, the metylene protons in the isotactic part can be regarded as an ABC_2 spin system, where the α-protons refer to C_2, while in the syndiotactic part they all together constitute a A_2B_2 spin system, where the methylene protons refer to A_2. This is the case with polypropylene if the spin-spin coupling constants between the methylene and the methyl protons are very small. For isotactic polypropylene the individual polymer molecules assume "gauche" rather than "trans" configurations and are, therefore, frozen in helical conformations, that is, the three-monomers one-turn helix. If the helical conformation is preserved even in the solution, the methylene resonance would be expected to give an A_2B_2 spectrum, contrary to the case of a planar zigzag conformation.

The basic functions and the complete matrix for the A_2B_2 spin system have been given by Pople et al.[9] In this system there are two electronic screening constants, σ_A and σ_B, together with four different spin coupling constants, J_{AA}, J_{AB}, J'_{AB}, J_{BB}. The chemical shift difference, δ_{AB}, is given by $\sigma_A-\sigma_B$.

By evaluation of the matrix elements one finds that the secular determinant factors into one 4×4, five 2×2, and two 1×1 submatrices. A total of twenty-eight transitions have to be considered in this case.

Next, the complete set of wave functions and all the elements of the matrix of the spin Hamiltonian for the ABC_2 system have been written by Cohen et al.[10] However, their analysis has been applied only to the ABX_2 case, where the resonance of the nucleus C is well removed from those of the A and B nuclei. In general, the ABC_2 spin system involves seven different constants, σ_A, σ_B and σ_C, and J_1, J_2, J_3 and J_4. However, because of disregarding all the spin-spin coupling constants between any two α-protons, the parameter J_4 vanishes in the present case, as is shown in Fig. 4.

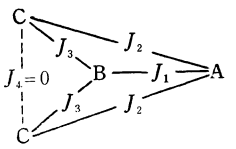


Fig. 4. Spin-spin coupling constants for the ABC_2 case, where $J_4=0$.

For this case the Hamiltonian operator is:

$$\mathscr{H} = \mathscr{H}^{(0)} + \mathscr{H}^{(1)} \quad (1)$$

Where:

$$\mathscr{H}^{(0)} = -\nu_A I_Z(A) - \nu_B I_Z(B) - \nu_C\{I_Z(C_1) + I_Z(C_2)\} \quad (2)$$

$$\mathscr{H}^{(1)} = J_1\boldsymbol{I}(A)\cdot\boldsymbol{I}(B) + J_2\boldsymbol{I}(A)\cdot\boldsymbol{I}(C_1) + J_2\boldsymbol{I}(A)\cdot\boldsymbol{I}(C_2) + J_3\boldsymbol{I}(B)\cdot\boldsymbol{I}(C_1) + J_3\boldsymbol{I}(B)\cdot\boldsymbol{I}(C_2) \quad (3)$$

where:

$\nu_1=\eta H_0(1-\sigma_1)$

H_0 is the external magnetic field,

η is a constant which converts magnetic units to energy units in cycles per second (c/s),

$\boldsymbol{I}$ is the nuclear spin vector, and

I_z is the Z component of the vector $\boldsymbol{I}$.

Adopting the notation of Pople et al.,[9] the complete set of basic functions and the matrix elements of the spin Hamiltonian is given in Table III. The diagonalization of the Hamiltonian involves the solution of one 4×4 matrix and two 3×3 matrices. In such a case, the numerical method must be used. In addition, the trial-and-error fitting procedure is so tedious that all the calculations were carried out with a digital computer, Musashino-1-β. Therefore, Tables III, IV and V are arranged so as to draw up a program for the electronic digital computer immediately. Table V lists both the resonance frequencies and the relative peak intensities; transitions are allowed only between the eigenfunctions of the same symmetry and with total spins differing by 1 from each other. Accordingly, thirty-four transitions in all are allowed in the ABC_2 case. Following Bernstein et al.,[8] each transition may be labeled as an A, B or C transition according to the change in spin, giving rise to the resonance line when the chemical shifts are much greater than the spin-spin coupling constants. When all the species of nuclei change their spin simultaneously, the line is labeled as a combination line.

Calculated Spectra.—The spectrum of syndiotactic polypropylene has been calculated by

8) H. J. Bernstein, J. A. Pople and W. G. Schneider, *Can. J. Chem.*, **35**, 65 (1957).

9) J. A. Pople, W. G. Schneider and H. J. Bernstein, "High Resolution Nuclear Magnetic Resonance," McGraw-Hill Book Co., Inc., New York, N. Y. (1959), p. 138.

10) A. D. Cohen and N. Sheppard, *Proc. Roy. Soc.*, **A252**, 488 (1959).

TABLE III. BASIC FUNCTIONS AND COMPLETE MATRIX ELEMENTS OF THE HAMILTONIAN FOR ABC_2 SPIN SYSTEM*

i	Function Ψ_i	Diagonal element						Off-diagonal element
		$\nu_1/2$	$\nu_2/2$	ν_3	$J_1/4$	$J_2/2$	$J_3/2$	
0	$\alpha\alpha\alpha\alpha$	+	+	+	+	+	+	
1	$(1/\sqrt{2})\alpha\alpha(\alpha\beta+\beta\alpha)$	+	+		+			$H_{1,2}$, $H_{4,6}$, $H_{5,7}$, $H_{8,10}$ $=J_2/\sqrt{2}$
2	$\beta\alpha\alpha\alpha$	−	+	+	−	−	+	
3	$\alpha\beta\alpha\alpha$	+	−	+	−	+	−	
4	$\alpha\alpha\beta\beta$	+	+	−	+	−	−	
5	$(1/\sqrt{2})\alpha\beta(\alpha\beta+\beta\alpha)$	+	−		−			$H_{1,3}$, $H_{4,5}$, $H_{6,7}$, $H_{9,10}$ $=J_3/\sqrt{2}$
6	$(1/\sqrt{2})\beta\alpha(\alpha\beta+\beta\alpha)$	−	+		−			
7	$\beta\beta\alpha\alpha$	−	−	+	+	−	−	
8	$\alpha\beta\beta\beta$	+	−	−	−	−	+	
9	$\beta\alpha\beta\beta$	−	+	−	−	+	−	
10	$(1/\sqrt{2})\beta\beta(\alpha\beta+\beta\alpha)$	−	−		+			$H_{2,3}$, $H_{5,6}$, $H_{13,14}$, $H_{8,9}$ $=J_1/2$
11	$\beta\beta\beta\beta$	−	−	−	+	+	+	
12	$(1/\sqrt{2})\alpha\alpha(\alpha\beta-\beta\alpha)$	+	+		+			
13	$(1/\sqrt{2})\alpha\beta(\alpha\beta-\beta\alpha)$	+	−		−			
14	$(1/\sqrt{2})\beta\alpha(\alpha\beta-\beta\alpha)$	−	+		−			$H_{4,7}=0$,
15	$(1/\sqrt{2})\beta\beta(\alpha\beta-\beta\alpha)$	−	−		+			$(\Psi_m\|H\|\Psi_n)\equiv H_{m,n}$.

* Spin-spin coupling constant J_4 has been omitted (see text).

TABLE IV. EIGENVALUES AND EIGENFUNCTIONS FOR THE ABC_2 SPIN SYSTEM

Eigenvalue	Symmetry of wave function and total spin	Eigenfunction
E_0	S_2	$a_{0,0}\Psi_0$
E_1	S_1	$a_{1,1}\Psi_1+a_{1,2}\Psi_2+a_{1,3}\Psi_3$
E_2		$a_{2,1}\Psi_1+a_{2,2}\Psi_2+a_{2,3}\Psi_3$
E_3		$a_{3,1}\Psi_1+a_{3,2}\Psi_2+a_{3,3}\Psi_3$
E_4	S_0	$a_{4,4}\Psi_4+a_{4,5}\Psi_5+a_{4,6}\Psi_6+a_{4,7}\Psi_7$
E_5		$a_{5,4}\Psi_4+a_{5,5}\Psi_5+a_{5,6}\Psi_6+a_{5,7}\Psi_7$
E_6		$a_{6,4}\Psi_4+a_{6,5}\Psi_5+a_{6,6}\Psi_6+a_{6,7}\Psi_7$
E_7		$a_{7,4}\Psi_4+a_{7,5}\Psi_5+a_{7,6}\Psi_6+a_{7,7}\Psi_7$
E_8	S_{-1}	$a_{8,8}\Psi_8+a_{8,9}\Psi_9+a_{8,10}\Psi_{10}$
E_9		$a_{9,8}\Psi_8+a_{9,9}\Psi_9+a_{9,10}\Psi_{10}$
E_{10}		$a_{10,8}\Psi_8+a_{10,9}\Psi_9+a_{10,10}\Psi_{10}$
E_{11}	S_{-2}	$a_{11,11}\Psi_{11}$
E_{12}	a_1	$a_{12,12}\Psi_{12}$
E_{13}	a_0	$a_{13,13}\Psi_{13}+a_{13,14}\Psi_{14}$
E_{14}		$a_{14,13}\Psi_{13}+a_{14,14}\Psi_{14}$
E_{15}	a_{-1}	$a_{15,15}\Psi_{15}$

Satoh et al.[1] In this work we will calculate the spectrum due to methylene protons present mainly in the isotactic part of the polymer chains. However, it is assumed that the spectra can be analyzed in terms of the ABC_2 spin system.

Fortunately, while this calculation was being carried out, it was kindly pointed out to the authors by Mr. Yoshihito Komatsu that the NMR spectra of polypropene-2-d_1 and polypropene-2, 3, 3, 3,-d_4 had been examined by Stehling.[2] According to the results, the spectra of polypropene-2-d_1 samples are quite analogous to those of polypropene-2, 3, 3, 3-d_4 samples, except that an additional peak due to the methyl protons can be observed. Though the methyl groups in the isotactic part of the polymer chains are not equivalent to those in the syndiotactic part, both of them give rise to the same unresolved resonance peak. This probably proves that the spin-spin coupling constant between methylene and methyl protons of polypropylene is fairly small. Therefore, we can neglect it as an approximation to reduce the complicated spectrum due to the methylene protons to the ABC_2 or A_2B_2 case.

By means of an electronic computer, attempts were made to find some sets of the chemical shifts and the spin-spin coupling constants which fit the frequencies of the observed lines. In practice, three resonance peaks at 8.65 τ, 8.75 τ and 8.87 τ were used in order to judge whether or not the set of δ and J parameters fits the resonance frequencies of the observed

TABLE V. ALLOWED TRANSITIONS FOR THE ABC_2 SPIN SYSTEM

Transition	Frequency $\nu=\Delta E/h$.	Relative intensity	Nucleus
1	E_1-E_0	$[(\sqrt{2}a_{1,1}+a_{2,1}+a_{3,1})a_{0,0}]^2$	A
2	E_2	etc.	B
3	E_3		C
4	E_4-E_1	$[a_{1,1}(\sqrt{2}a_{4,4}+a_{5,4}+a_{6,4})$	C
5	E_5	$+a_{2,1}(\sqrt{2}a_{6,4}+a_{7,4})$	B
6	E_6	$+a_{3,1}(\sqrt{2}a_{5,4}+a_{7,4})]_2$	A
7	E_7	etc.	comb.
8	E_4-E_2		comb.
9	E_5		comb.
10	E_6		C
11	E_7		B
12	E_4-E_3		comb.
13	E_5		C
14	E_6		comb.
15	E_7		A
16	E_8-E_4	$[a_{4,4}(a_{8,8}+a_{9,8})$	B
17	E_9	$+a_{5,4}(\sqrt{2}a_{8,8}+a_{10,8})$	A
18	E_{10}	$+a_{6,4}(\sqrt{2}a_{9,8}+a_{10,8})$	comb.
19	E_8-E_5	$+\sqrt{2}a_{7,4}\cdot a_{10,8}]^2$	C
20	E_9	etc.	comb.
21	E_{10}		A
22	E_8-E_6		comb.
23	E_9		C
24	E_{10}		B
25	E_8-E_7		comb.
26	E_9		comb.
27	E_{10}		C
28	$E_{11}-E_8$	$[a_{11,11}(a_{8,8}+a_{9,8}+\sqrt{2}a_{10,8})]^2$	A
29	$E_{11}-E_9$	etc.	B
30	$E_{11}-E_{10}$		C
31	$E_{13}-E_{12}$	$[a_{12,12}(a_{13,13}+a_{14,13})]^2$	B
32	E_{14}	etc.	A
33	$E_{15}-E_{13}$	$[a_{15,15}(a_{13,13}+a_{14,13})]^2$	A
34	$E_{15}-E_{14}$	etc.	B

peaks. In the judgment a tolerence of ± 2 c/s was taken into account. We assumed in the first place that $\nu_A-\nu_C=40.5$ c/s, and that $\nu_B-\nu_C=13.5$ c/s, and we tried to obtain some sets of the other parameters which approximately fit the resonance positions. From the study of a series of acetylated sugars, it has been established by Lemieux et al.[11] that the spin-spin coupling constant for a pair of axial hydrogens on adjacent carbon atoms is in the 5~8 c/s range, that that for pairs of equatorial hydrogens is 3~4 c/s, and that that for axial and equatorial hydrogens is 2~3 c/s. Therefore, the parameters J_2 and J_3 were chosen within the range from -10 to $+10$ c/s. Since the simultaneous change of all signs of the spin-spin coupling constants does not affect the spectrum, the sign of J_1 was arbitrarily chosen as positive in each case. The absolute value of J_1 was varied progressively by 0.5 c/s within the 12~14 c/s.

The parameter J_1 was taken to be $+13.5$ c/s. The applicability of this value has also been confirmed by the spectra of polypropene-

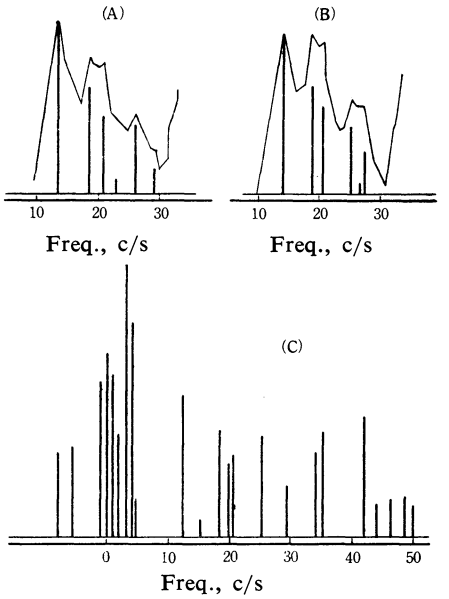


Fig. 5. ABC_2 spectra calculated with the sets of parameters; $\nu_A-\nu_C=40.5$ c/s, $\nu_B-\nu_C=13.5$ c/s, $J_1=13.5$ c/s and (A) $J_2=2.0$ c/s, $J_3=-7.0$ c/s; (B) $J_2=-3.0$ c/s, $J_3=-6.0$ c/s and (C) $J_2=-7.0$ c/s, $J_3=8.0$ c/s.

11) R. V. Lemieux, R. K. Kullnig, H. J. Bernstein and W. G. Schneider, *J. Am. Chem. Soc.*, **80**, 2237 (1958).

2, 3, 3, 3-d_4 obtained by Stehling. The two non-equivalent methylene protons give a typical spectrum of the AB system, and the value of J observed from the spectrum has been reported to be about 13.2 c/s.[2)]

For all the sets of parameters which fit the observed line positions, we calculated the peak intensities in order to compare them with the observed resonance peaks. It was found that only three sets fit the observed peaks moderately well. They are shown in Fig. 5. From the appearance of the above-mentioned three resonance peaks, especially that of the central one, we may conclude that the best fit at this stage is this set of parameters:

$$\nu_A-\nu_C=40.5 \text{ c/s}$$
$$\nu_B-\nu_C=13.5 \text{ c/s}$$
$$J_1=13.5 \text{ c/s}$$
$$J_2=-7.0 \text{ c/s}$$
$$J_3=8.0 \text{ c/s}$$

Furthermore, the electronic computer was used to revise the set of parameters so as to find a best fit. The revised parameters were:

$$\nu_A-\nu_C=39.0 \text{ c/s}$$
$$\nu_B-\nu_C=14.0 \text{ c/s}$$
$$J_1=13.5 \text{ c/s}$$
$$J_2=-6.0 \text{ c/s}$$
$$J_3=7.5 \text{ c/s}$$

From these values it may be concluded that the conformation of isotactic polypropylene in solution is somewhat different from that of the solid, that is, the helical conformation.

Further revision seems to be of little avail so long as we consider only the above-mentioned three peaks, because they are rather poorly resolved. Therefore, the information concerning the positions and intensities involves a slight ambiguity. The calculated spectrum for this set of parameters is illustrated in Fig. 6, where each resonance line in the central part has been replaced by an isosceles triangle with the same height as the line and a 4 c/s half-height peak width. By synthesizing the triangles, the theoretical spectrum for the methylene protons can be obtained. It should be noticed that resonance region of the methylene protons contained in isotactic polypropylene is very wide. Accordingly, great care must be taken in the analysis of the spectrum.

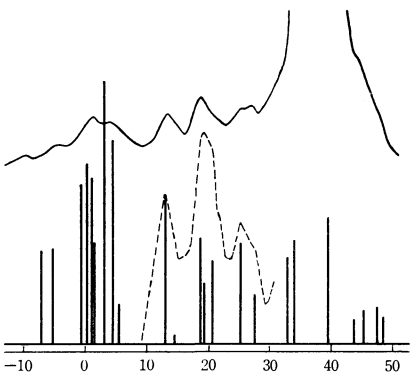


Fig. 6. Comparison between the experimental and the theoretical spectra of polypropylene. The parameters of the calculated spectrum are $\nu_A-\nu_C=39.0$ c/s, $\nu_B-\nu_C=14.0$ c/s, $J_1=13.5$ c/s, $J_2=-6.0$ c/s and $J_3=7.5$ c/s.

The Analysis of Observed Spectra. — In the preceding section, the theoretical spectrum of methylene protons in isotactic polypropylene was obtained. When the total intensity (or area) of the spectrum is normalized to unity, the relative intensities of the three resonance peaks at 8.65 τ, 8.75 τ and 8.87 τ are 0.0426, 0.0733 and 0.0437 respectively. For the sake of convenience, let us denote these three resonance peaks as A-, B- and C-peaks respectively. Both the B- and C-peaks contain more than two calculated resonance lines, whereas the A-peak has only one effective peak. Each one of the resonance lines contained in B- and C-peaks can be assigned as a combination line. This information is very important for decomposing each peak in the observed spectra as a means of measuring the degree of stereoregularity of the polymer chain.

As has already been explained, syndiotactic polypropylene gives rise to the resonance peaks due to the methylene groups, which can be interpreted in terms of a A_2B_2 spin system. Therefore, with the following constants:

$$\delta_{AB}=27.0 \text{ c/s}$$
$$J_{AA}=13.5 \text{ c/s}$$
$$J_{AB}=8.0 \text{ c/s}$$
$$J'_{AB}=6.0 \text{ c/s}$$
$$J_{BB}=0 \text{ c/s}$$

the spectrum of the methylene protons has been calculated. The result is shown in Fig. 7. In this case, however, the observed spectrum is very simple, as one can easily imagine from the spectrum of atactic polypropylene (sample 2). Hence, only two very similar resonance peaks due to the methylene protons will be available for revising the set of parameters. Therefore, there remain some ambiguities in the theoretical spectrum of syndiotactic polypropylene. However, it is a striking feature of the spectrum that no resonance peak can be observed in the vicinity of 8.65 τ. On this basis the degree

TABLE VI. ANALYSIS OF OBSERVED SPECTRA[a)]

Sample No.	Obsered peak intensity		Isotactic component			Estimated syndiotactic fraction at B and C peaks
	A	B+C	x[b)]	x'[c)]	x''[d)]	
2	0.020_9	0.22_0	0.49	0.46	0.38	0.31
5	0.036_4	0.13_4	0.85	0.91	0.90	0.21
7	0.038_0	0.12_6	0.89	0.96	0.95	0.18
8	0.040_2	0.12_4	0.94	0.97	0.96	0.19

a) The whole area is normalized.
b) Calculated from the fraction of A-peak.
c) Based on the assumption that the (B+C) fraction of the ideal spectrum of syndiotactic polypropylene equals 0.30_7.
d) Based on the spectrum shown in Fig. 7.

of stereoregularity of any given sample can be estimated if an well-resolved NMR spectrum is available. From the fraction of the A-peak in each spectrum, we calculated the proportion of the isotactic component, x, for the several samples given in Table II. Then, by using the sum of the fractions of the B- and C-peaks, the proportion of the syndiotactic component at the peak positions was estimated. The results are given in Table VI. The resolution of the spectrum of sample 9 was so poor that the estimation was not made. The values of x calculated above probably include some errors because it is difficult to separate a small A-peak. Therefore, we assumed that the fraction of the syndiotactic component at the B- and C-peak positions equals 0.30_7, which can be obtained from the results concerning sample 2 in Table VI. Then we calculated again the proportion of the isotactic component, x'. The results are listed in the next column of x in Table VI.

Finally, the spectrum of polypropene-1, 1-d_2 was obtained at 40 Mc/s. The results shown in Fig. 8 show a poorly-resolved spectrum because of the high molecular weight of the sample. However, a set of parameters:

$$\delta_{AB}=27.0\ \text{c/s}$$
$$J_{AB}=6.0\ \text{c/s}$$

for the AB_3 spin system fits the contour of the observed spectrum very well. Converting these parameters to the case of 60 Mc/s, it seems obvious that no overlap will be observed between the α-proton resonances of polypropylene and the methylene proton ones, except for the 8.40~8.55 τ region.

From Figs. 5, 6 and 7 the theoretical X-value for isotactic polypropylene has been found to be $X_I=0.13_7$, and that for syndiotactic polypropylene, $X_S=0.55$.

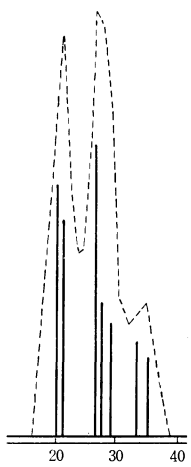


Fig. 7. The A_2 part of A_2B_2 type spectra with the parameters: $\delta_{AB}=27.0$ c/s, $J_{AB}=6.0$ c/s and $J'_{AB}=8.0$ c/s.

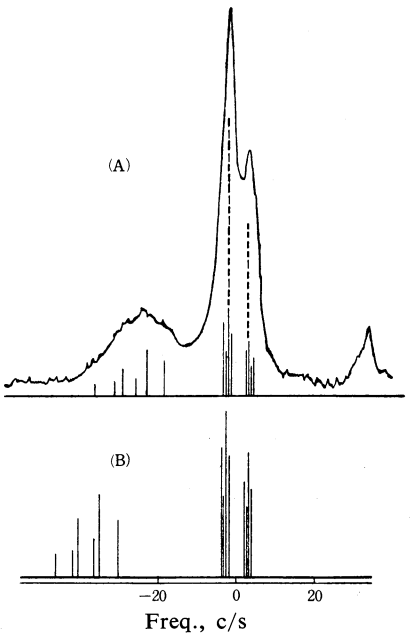


Fig. 8. NMR spectrum of polypropene-1,1-d_2 obtained at 40 Mc/s (A), together with the theoretical analysis at 60 Mc/s (B). The dotted line means the sum of each group of resonance lines.

As a conclusion, if an well-resolved NMR spectrum of a given polypropylene sample is available, the proportion of the isotactic part (x') can be evaluated by measuring only the fraction of the area of the B- and C-peaks (F_1). The formula for the evaluation is:

$$x' = \frac{0.307 - F_1}{0.190}$$

If the value of x' is close to unity, the following formula:

$$x' = \frac{F_0}{0.0426}$$

which is based entirely upon the theoretical spectrum of isotactic polypropylene, may be used, where F_0 means the fraction of the area of the A-peak.

In the near future the better resolution of individual resonance peaks will permit a more precise analysis of the stereoregularity of polypropylene.

Summary

The application of the NMR method to the study of commercial polypropylene seems to be restricted by some difficulties. A weak thermal degradation technique has therefore been employed to reduce the molecular weight of the polypropylene sample. However, the correspondence between the resultant molecular weight and the resolution of the spectrum is not always unique.

A remarkable difference between the NMR spectrum of isotactic polypropylene and that of atactic polypropylene can be found in the methylene resonance region. As an approximation, one may assume that the methylene groups of isotactic polypropylene give rise to the partial spectrum of an ABC_2 spin system, whereas those of syndiotactic polypropylene give rise to the partial spectrum of an A_2B_2 spin system. By means of an electronic computer, the best set of the δ and J parameters for the methylene resonance of isotactic polypropylene has been obtained. The results fit the observed spectrum fairly well. Using this information, the degree of stereoregularity (isotaxy) of a given polypropylene can be calculated. This method is applicable if an well-resolved NMR spectrum is available.

We are much indebted to Mr. Yoshihito Komatsu of the Daiwa Spinning Co., Ltd., for his sample preparation and preliminary treatment, and to Dr. Kô Abe for supplying a deuterated polymer sample. We are also indebted to Dr. Osamu Yamamoto and Mr. Teruo Suzuki of the Government Chemical Industrial Research Institute, Tokyo, for their measurements of NMR spectra. Thanks are due to Mr. Kôichi Mizuta of the Musashi Institute of Technology for his generous assistance in carrying out the numerical calculations.

The Electrical Communication Laboratory
Musashino, Tokyo

*A High Resolution Nuclear Magnetic Resonance Study of the Styrene-Methylmethacrylate Copolymer**

By Yoshinori KATO, Nobuyuki ASHIKARI and Atsuo NISHIOKA

(Received June 9, 1964)

Since Bovey et al.[1] drew attention to the fact that new information about the configuration of polymer chains can be obtained from the high resolution nuclear magnetic resonance spectra, it has been a matter of great concern to us to find some direct evidence for the "copolymer structure" by means of the NMR method. In a preceding paper[2] it was shown that the microstructure of the methyl methacrylate polymer chains can be analyzed to a great extent by the aid of the NMR spectra. In that case the discovery of the *D*-unit (or the heterotactic unit) remarkably improved our knowledge about the stereo regularity of polymer chains. Especially by making use of the concept of the *D*-unit, the difference between

* This paper was read at the 14th Annual Meeting of the Chemical Society of Japan, Tokyo, April, 1961.

1) F. A. Bovey, G. V. D. Tiers and G. Filipovich, *J. Polymer Sci.*, **38**, 73 (1959).

2) Y. Kato and A. Nishioka, This Bulletin, **37**, 1614 (1964).

random and stereoblock polymers can be difined more distinctly. Stereoreglar polymers may be regarded as a kind of copolymer in the sense that they consist of two different species of monomer placements, isotactic and syndiotactic. Therefore, some of the problems we considered in our previous study of polymethyl methacrylate may be applicable to the case of the copolymer.

On the other hand, it is well-known that a benzene ring placed in a magnetic field exhibits a long-range shielding effect which arises from the diamagnetic circulation of the π-electrons.[1,3] Therefore, in polymers such as polystyrene, which contains aromatic rings, some anomalies may be observed in the NMR resonance peaks of the α-protons, methylene protons, and the like. In such cases we may consider the aromatic ring as "a probe" to obtain some valuable information concerning the microstructure of the polymer. For these reasons we have studied the styrene-methyl methacrylate copolymer in solution by means of the NMR method.

At first we expected that the resonance peak due to α-methyl groups of methyl methacrylate would be separated into three peaks, as is the case with polymethyl methacrylate. If so, the dependence of the stereoregularity on the mole per cent of methyl methacrylate in the copolymer could have been obtained. Contrary to our expectations, however, the α-methyl peak does not separate explicitly, but quite a new anomaly can be found in the resonance region due to the methoxy groups.[4] A similar result could be obtained from the NMR spectra of the paraxylylene-methylmethacrylate copolymer.[5]

It is the purpose of this paper to interpret the NMR spectra of the styrene-methylmethacrylate copolymer in order to obtain some information concerning the copolymer structures Using this information it will be possible to study the kinetics of the radical copolymerization.

Experimental

Each sample was prepared in free radical polymerization at 40°C with triisopropylboron as a catalyst. Details of the polymerization conditions are listed in Table I. Proton magnetic resonance measurements were made at 20°C using a Varian V-4300-C spectrometer operating at 56.4 Mc/s. The concentration of the sample in carbon tetrachloride was varied within the range of 6~11% so as to make easy the observation of the minor component of each copolymer sample. The side band technique was employed to estimate the chemical shifts. However, since tetramethylsilane as an internal reference was not available, we could not express the peak positions in the τ-scale.

Table I. Preparation of styrene-methylmethacrylate copolymers

Sample No.	Mol. % of MMA charged	% conv.
1	81.2	11.21
2	61.9	8.35
3	51.9	7.93
4	41.9	7.08
4'	41.9	7.66
5	20.8	7.56

Results and Discussion

Figure 1 shows the NMR spectra of a polystyrene sample, a polymethyl methacrylate smple and of a mixture of these two polymers. The significance of these spectra is that we can not find any particular change in the NMR spectrum when these two polymers are mixed in the solution. The observed spectra of the copolymer samples are shown in Fig. 2. The sharp peaks at the extreme left may be due to a small quantity of an impurity such as benzene or chloroform. We examined this point and confirmed that the peak appears at the same position as the resonance peak of chloroform within the range of experimental error. Therefore, chemical shifts are expressed in parts per millon referred to this peak. The nearest peak to this is the aromatic proton resonance. In the spectra of samples 1 to 3 the phenyl resonance gives rise to a

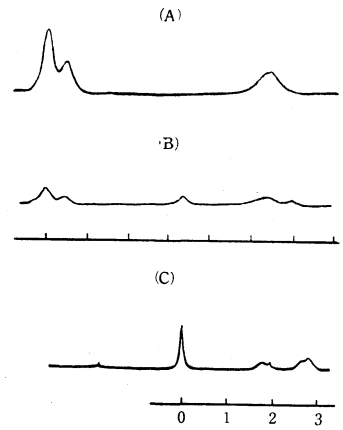


Fig. 1. NMR spectra of (A) polystyrene, (C) polymethyl methacrylate, and (B) the mixture of these two polymers in the ratio of 1 : 1.

3) L. M. Jackman, "Applications of Nuclear Magnetic Resonance Spectroscopy in Organic Chemistry," Pergamon Press, London (1959).
4) A. Nishioka, Y. Kato and N. Ashikari, *J. Polymer Sci.*, **62**, S10 (1962).
5) A. Nishioka, Y. Kato and H. Mitsuoka, ibid., **62**, S9 (1962).

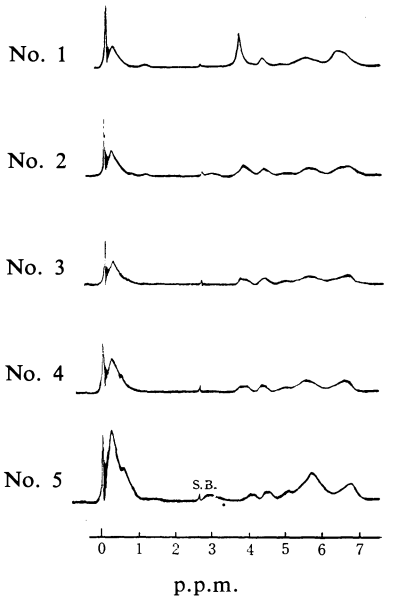


Fig. 2. NMR spectra of styrene-methylmethacrylate copolymers.

broad but single peak, whereas in the rest two separate peaks can be observed. A similar change of spectra has already been found by Bovey et al.[1] in their study of the styrene-butadiene copolymer. They attributed this change to the steric restriction of the phenyl groups. In the copolymer the average sequence length of styrene blocks may base short as several styrene monomer units. According to Bovey's criterion, these short styrene blocks give rise to a single resonance peak at 3.0 τ. However, if the average sequence length is longer than ten styrene units, the phenyl resonance always splits into two peaks. It was also confirmed by Bovey et al. that the smaller phenyl peak is due to the ortho-protons.

The comparison of the spectrum of sample 1 with that given in Fig. 1 (C) clearly shows that some remarkable changes have taken place in the resonance region of the methoxy groups contained in methyl methacrylate. For the sake of convenience, let us denote the three peaks at (3.8±0.2), (4.4±0.1) and 5.0 p.p.m. in our scale of the chemical shift as A-, B- and C-peaks respectively. It is then evident that the A-peak is due to the methoxy groups of methyl methacrylate, but that the relative peak area is considerably smaller than the corresponding peak of Fig. 1 (C). Here, we shall leave the B and C peaks untouched for the moment.

Next, the peak at about 5.6 p.p.m. can be assigned to the methylene protons. Since these protons are equally contained in styrene and methyl methacrylate, the relative area of this peak remains constant independently of the mole per cent of methyl methacrylate in the copolymer. Therefore, the normalization factor of the spectrum may be obtained as the reciprocal peak area of the methlene resonace. The peak at about 6.6 p.p.m. may be the α-methyl resonance. If so, the methyl peak area must be equal to that due to the methoxy groups of methyl methacrylate. The α-proton resonance of styrene is perhaps embedded on the left side of the methylene peak. In addition, the unknown peak C defined above overlaps with the methylene resonance. In order to settle these problems we measured the relative area of each peak. The results are shown in Fig. 3. In the measurement the α-proton peaks could not be separated from the methylene peaks explicitly. We separated them by remembering that the fraction

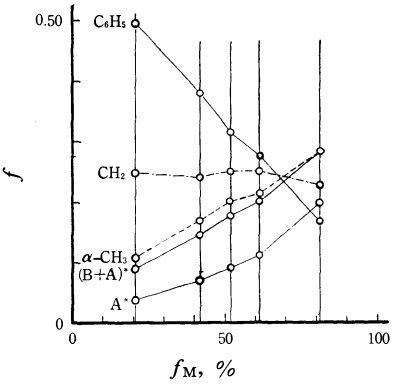


Fig. 3. Fraction of peak area (f_M) obtained from the NMR spectrum of styrene-methylmethacrylate copolymer plotted against mole per cent of methyl methacrylate charged (f).
* See text.

of the peak area of the methylene resonance is invariable. Therefore, the results may include small errors. However, it may safely be concluded from Fig. 3, that both the A- and B-peaks can be ascribed to the methoxy groups of methyl methacrylate. The sum of the A- and B-peak areas seems to be less than the peak area of the α-methyl resonance. This implies that there exist some other resonance peaks due to the methoxy groups. Judging from the possible configurations of the copolymer in connection with the long-range shielding effect of aromatic rings,[6,7] these unknown peaks may be found in the vicinity of the C-peak. Recently Bovey[8] has reported on this copolymer. Since his interpretations were based

6) J. A. Pople, *J. Chem. Phys.*, **24**, 1111 (1956).
7) J. S. Waugh and R. W. Fessenden, *J. Am. Chem. Soc.*, **79**, 846 (1957).
8) F. A. Bovey, *J. Polymer Sci.*, **62**, 197 (1962).

TABLE II. CHEMICAL SHIFTS FOR STYRENE-METHYLMETHACRYLATE COPOLYMERS AND HOMOPOLYMERS IN CARBON TETRACHLORIDE

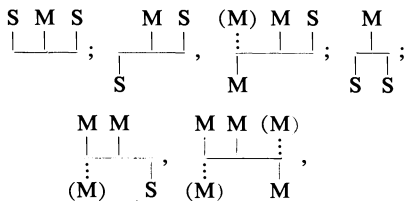
Sample No.	Aromatic	Chemical shift (p.p.m.)* $-OCH_3$*			$-CH_2$	α-CH_3
		A*	B*	C*		
1	0.22	3.72	4.34	5.05	5.60	6.42
2	0.23	3.81	4.37	5.13	5.58	6.64
3	0.23, 0.49	3.84	4.45	5.02	5.62	6.67
4	0.27, 0.48	3.93	4.44	5.03	5.64	6.72
5	0.28, 0.62	4.06	4.51	5.04	5.64	6.73
6**	0.28, 0.74		—	?	5.64	—
7***	—	(3.83)	—	—	(5.63)	(6.34~6.73)

* See text.
** Styrene homopolymer.
*** Three per cent stereoblock PMMA in chloroform.

on the well-resolved NMR spectra observed at 90°C, many interesting results have been obtained. Especially the change in the resonance region of methoxy groups with the mole per cent of methyl methacrylate in the monomer feed seems to offer a key to the analysis of the microstructure of the polymer chains. Introducing some assumptions, we may treat this problem in a way analogous to that used in the case of polymethyl methacrylate.[2]

In the case of this copolymer it is evident that not the stereoregular placement, but the placement of the styrene monomer unit referred to that of the neighboring methyl methacrylate unit is very important. On the assumption that any methyl methacrylate monomer unit in the copolymer chain can be classified only by its relative placement to the neighboring styrene monomer units on one or both sides, it may readily be seen that there are six configurations of three consecutive monomer units. In principle they may be expected to give rise to six different resonances of methoxy groups in the central methyl methacrylate units.

The configurations may be symbolically illustrated thus:



where S and M stand for styrene and methyl methacrylate monomer units respectively. A vertical line above (or below) the horizontal one represents a so-called *d*- or *l*-unit, and a broken line stands for one equivalent alternate. Perhaps the first configuration will give rise to a resonance at a higher magnetic field than the others. The resonance due to the second configuration will appear close to that due to the third. Though the fourth contains a styrene units at the each end, its resonance magnetic field may be very little different from those of the last two. The spectra of samples 3 to 5 shown in Fig. 1 seem to be in accordance with our interpretation, especially in the methoxy resonance region. However, because of the poor resolution, we can not discuss the problem further at present.

Another evidence of copolymer structure is provided by the interpretation of the chemical shifts. As is shown in Table II, the peak position of the α-methyl resonance shifts towards a higher magnetic field as the styrene component of the polymer chain increases. This is also in accordance with the results obtained by Bovey et al.[1,8] from the styrene-butadiene and methylmethacrylate-styrene copolymers. However, the exact stereochemical information which was available in the case of polymethyl methacrylate can no longer be obtained from this copolymer. In fact, only a slight change in the line shape of the α-methyl resonance can be observed. The same is true for the resonance line shapes of the styrene component.[9] In short, the methoxy resonance plays an important role in the NMR spectra of this copolymer.

As an example of a quantitative analysis of NMR spectra, the monomer reactivity ratio[10-13] was estimated from the measurements of the peak areas of both phenyl and α-methyl resonances. The copolymer composition curve is shown in Fig. 4.

9) R. J. Kern and J. V. Pustinger, *Nature*, **185**, 236 (1960).
10) T. Alfrey, Jr. and G. Goldfinger, *J. Chem. Phys.*, **12**, 205 (1944).
11) F. R. Mayo and F. M. Lewis, *J. Am. Chem. Soc.*, **66**, 1594 (1944).
12) F. T. Wall, ibid., **66**, 2050 (1944).
13) C. H. Bamford, W. G. Barb, A. D. Jenkins and P. F. Onyon, "The Kinetics of Vinyl Polymerization by Radical Mechanisms," Butterworths Publications Ltd., London (1958).

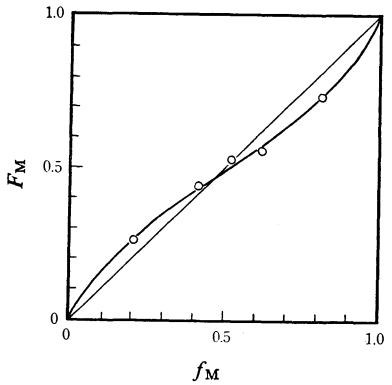


Fig. 4. Copolymer composition curve for the styrene-methylmethacrylate system. F_M, f_M are the mole fractions of MMA in copolymer and in monomer mixture. The heavy line is the theoretical curve for $r_1=0.56$, $r_2=0.50$; ○: experimental results.

The results,

$$r_1 \text{ (styrene)} = 0.56 \pm 0.01$$

$$r_2 \text{ (MMA)} = 0.50 \pm 0.03$$

are in good agreement with the values given by Lewis et al.:[14]

Monomer reactivity ratio	Polymerization temp. 60°C	131°C
r_1 (styrene)	0.52±0.026	0.590±0.026
r_2 (MMA)	0.46±0.026	0.536±0.026

Summary

The information concerning *D*-units in methyl methacrylate polymer chains has inproved our knowledge about the stereoregularity of the polymer.[2] As an extension of the study, we have examined styrene-methylmethacrylate copolymers prepared under various polymerization conditions. In these cases, the α-methyl resonance of methyl methacrylate does not change, except that the peak position shifts towards a higher magnetic field as the styrene component of the polymer chain increases. A direct evidence of the copolymer structure has been obtained by the analysis of the methoxy resonance. A total of six methoxy resonance lines can be observed if any methyl methacrylate monomer unit in the copolymer chain can be classified only in terms of its placement relative to the neighboring styrene monomer units.

Monomer reactivity ratios have been estimated from the NMR spectra. The results are r_1 (styrene) $=0.56\pm0.01$ and r_2 (MMA) $=0.50\pm0.03$.

The authors are indebted to Dr. Naohiro Hayakawa for his kind help in the NMR measurement.

The Electrical Communication Laboratory
Musashino, Tokyo

14) F. M. Lewis, C. Walling, W. Cummings, E. R. Briggs and F. R. Mayo, *J. Am. Chem. Soc.*, **70**, 1519 (1948).

Theoretical Studies of Light Scattering by Polydispersed Colloidal Systems of Spherical Particles[1)]

By Masayuki NAKAGAKI and Tsugiyo SHIMOYAMA

(Received May 13, 1964)

Recently light scattering has been widely used as a useful method to determine the size of colloidal particles. The method has become available as a result of the extensive improvement of experimental techniques and the development of theoretical information, at least, for monodispersed systems. Actual colloidal systems are, however, polydispersed, and their particle-size distribution is yet to be determined. For this purpose, it is, of course, desirable to determine the entire shape of the distribution curve experimentally, but that would require a great deal of experimental data of a very high precision. Therefore, one must often be satisfied with the determination of the values of a few parameters in an approximate presupposed equation and with the determination of a kind of average particle size. This approximate method is not unsatisfactory if the actual distribution curve has one maximum only. Heller et al. assumed a special shape of the distribution

1) Presented before the 14th Discussion of Colloid Chemistry, Ueda, October, 1961, and the 15th Annual Meeting of the Chemical Society of Japan, Kyoto, April, 1962.

function containing two parameters and studied the polarization ratio[2] and the turbidity.[3] Dettmar et al.[4] calculated the specific turbidity for the log-normal distribution of two parameters.

In the experiments of light scattering, however, the specific scattering intensity and the dissymmetry factor are frequently measured. Therefore, the effect of polydispersity on these quantities is of interest. The results obtained by using a three-parameter distribution function will be reported here.

Theoretical

Presupposed Distribution Curve.—If the distribution curve of the particle size has one maximum point, the distribution maximum, the width of the distribution and the dissymmetry of the distribution curve will be of main interest. A modified Gaussian curve containing the above-mentioned three parameters was used in the present experiment.

In the study of light scattering by colloidal spheres, the relative particle size:

$$\alpha=2\pi r/\lambda \tag{1}$$

is used, where r is the particle radius and λ is the wavelength of light in the dispersion medium. The particle-size distribution in weight, $W(\alpha)$, is assumed to have its maximum point at α_m, and for $\alpha<\alpha_m$ the function $W(\alpha)=W_1(\alpha)$ is a Gaussian function with the standard deviation of $\Delta\alpha_1$, and for $\alpha<\alpha_m$ the function $W(\alpha)=W_2(\alpha)$ is that with $\Delta\alpha_2$. Therefore, by using the average width of the distribution,

$$\langle\Delta\alpha\rangle=(\Delta\alpha_1+\Delta\alpha_2)/2 \tag{2}$$

and the dissymmetry of the distribution,

$$\Delta=\Delta\alpha_1-\Delta\alpha_2 \tag{3}$$

the distribution in weight will be;

$$\left.\begin{aligned} W_1(\alpha)&=(1/\langle\Delta\alpha\rangle)\phi(x_1)\\ x_1&=(\alpha-\alpha_m)/\Delta\alpha_1\end{aligned}\right\}\ \text{for}\ \alpha>\alpha_m \tag{4}$$

and

$$\left.\begin{aligned} W_2(\alpha)&=(1/\langle\Delta\alpha\rangle)\phi(x_2)\\ x_2&=(\alpha_m-\alpha)/\Delta\alpha_2\end{aligned}\right\}\ \text{for}\ \alpha<\alpha_m \tag{5}$$

where the function ϕ is the normalized Gaussian function;

$$\phi(x)=(1/\sqrt{2\pi})\exp(-x^2/2) \tag{6}$$

Mathematically, the function $W_2(\alpha)$ extends to the negative of α, and the $W(\alpha)$ given above by the combination of Eqs. 4 and 5 is normalized over the range from $-\infty$ to $+\infty$. Actually, however, the size distribution function should tend to zero when the α value approaches zero and should be meaningless for a negative value of α. Therefore, Eq. 5 is to be used only for $0<\alpha<\alpha_m$, and the functions of Eqs. 4 and 5 are to be re-normalized by dividing them with a factor $(\Delta\alpha_1/2\langle\Delta\alpha\rangle+f\Delta\alpha_2/2\langle\Delta\alpha\rangle)$, where

$$f=2\int_{-\alpha_m/\Delta\alpha_2}^{0}\phi(x)\mathrm{d}x \tag{7}$$

In this method, the value of $W_2(0)$ is not equal to zero. This discrepancy, is, however not serious in practice because the scattered light intensity rapidly decreases to zero when α decreases to zero.

Calculation of Mean Values. — The mean value, $\langle G\rangle$, of a quantity, G, for the presupposed distribution of the particle size can be calculated by the equation:

$$\langle G\rangle=(g_1+g_2)/(\Delta\alpha_1+f\Delta\alpha_2) \tag{8}$$

where

$$\left.\begin{aligned} g_1&=2\langle\Delta\alpha\rangle\int_{\alpha_m}^{\infty}GW_1(\alpha)\mathrm{d}\alpha\\ g_2&=2\langle\Delta\alpha\rangle\int_{0}^{\alpha_m}GW_2(\alpha)\mathrm{d}\alpha\end{aligned}\right\} \tag{9}$$

For the numerical calculation of g_1 and g_2 in this paper, the entire range of α is divided into equal intervals of $(\delta\alpha)=0.2$ and approximate summations instead of integrations were made because the numerical values of the scattered light intensity were available only at this interval of α. Therefore

$$\left.\begin{aligned} g_1&=2(\delta\alpha)\sum_{x_1=0}^{\infty}{}'G\phi(x_1)\\ g_2&=2(\delta\alpha)\sum_{x_2=0}^{\alpha_m/\Delta\alpha_2}{}'G\phi(x_2)\end{aligned}\right\} \tag{10}$$

In these summations, the terms for $x_1=0$ and $x_2=0$ were multiplied by 1/2 because the same term is included in both summations, g_1 and g_2.

The Specific Scattering Intensity and Dissymmetry Factor. — The quantities measured most often in the study of colloidal systems are the specific scattering intensity,[5] J_θ/I_0c, and the dissymmetry factor, z, where J_θ is the intensity per unit solid angle of the light scattered at the angle,[6] θ; I_0 is the intensity of the incident beam, and c is the concentration of the dispersed phase in g./100 ml. The

2) A. F. Stevenson, W. Heller and M. L. Wallach, *J. Chem. Phys.*, **34**, 1789 (1961); W. Heller and M. L. Wallach, *J. Phys. Chem.*, **67**, 2577 (1963).

3) M. L. Wallach, W. Heller and A. F. Stevenson, *J. Chem. Phys.*, **34**, 1796 (1961).

4) H.-K. Dettmar, W. Lode and E. Marre, *Kolloid-Z.*, **188**, 28 (1963).

5) The value extrapolated to the infinite dilution should be compared with the theoretical value.

6) The scattering angle, γ, usually used in the case of a colloidal system according to Mie is related to the angle, θ, used here by the equation: $\gamma=180°-\theta$.

specific scattering intensity can be expressed theoretically by

$$J_\theta/I_0c=(N/c)(\lambda^2/4\pi^2)i_\theta \tag{11}$$

where N is the number of particles per unit of volume and i_θ is the function defined elsewhere.[7] If the system is polydispersed, the observed specific scattering intensity should be an average value defined by:

$$\langle J_\theta\rangle/I_0c=(\lambda^2/4\pi^2c)\langle Ni_\theta\rangle \tag{12}$$

or, by using Eq. 1;

$$\langle J_\theta\rangle/I_0c=(3/200\lambda\rho_2)\langle i_\theta/\alpha^3\rangle \tag{13}$$

where ρ_2 is the density of the dispersed phase. For the sake of the simplicity of numerical computation, a quantity, Y_θ, is used, which is to be determined experimentally by:

$$Y_\theta=(200/3)\lambda\rho_2\langle J_\theta\rangle/I_0c \tag{14a}$$

and computed theoretically by;

$$Y_\theta=\langle i_\theta/\alpha^3\rangle \tag{14b}$$

The dissymmetry factor, z, is:

$$z=Y_{45}/Y_{135}=\langle i_{45}/\alpha^3\rangle/\langle i_{135}/\alpha^3\rangle \tag{15}$$

Results and Discussion

Numerical Values of Y_θ and z.—Numerical values of Y_{45}, Y_{90}, Y_{135} and z for unpolarized light have been calculated according to Eqs. 8, 10, 14b and 15 for $m=1.20$ and $\alpha_m=0$ (0.2) 3.0, and for $\Delta\alpha_1=0$ (0.2) 1.0 and $\Delta\alpha_2=0$ (0.2) 1.0. For the calculations, the values of i_θ/α^3 were taken from the table published by Pangonis and Heller[8] for $\alpha=0$ (0.2) 7.0 for monodispersed systems. Some of the results of the computation are shown in the following figures.

Figure 1 shows the relation between Y_{90} and α_m when $\Delta=0$ and $\langle\Delta\alpha\rangle=0$ (0.2) 1.0. Each curve of Y_{90} vs. α_m has a maximum point at about $\alpha_m=1.6\sim1.7$; this curve becomes less steep as the $\langle\Delta\alpha\rangle$ value increases. The value of Y_{90} is mostly independent of $\langle\Delta\alpha\rangle$ at about $\alpha_m=0\sim1.0$ and $\alpha_m=2.3$. According to a figure (not shown here) designed to illustrate the relation between Y_{45} and α_m for $\Delta=0$ and $\langle\Delta\alpha\rangle=0$ (0.2) 1.0, it is concluded that the Y_{45} increases monotonously in the range of $\alpha_m=3.0$. The curves become less steep as the

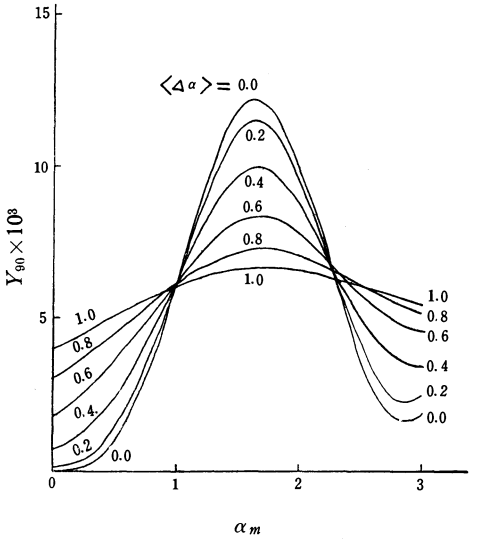


Fig. 1. Relation between Y_{90} vs. α_m for $m=1.20$, $\Delta=0$ and for various $\langle\Delta\alpha\rangle$ values.

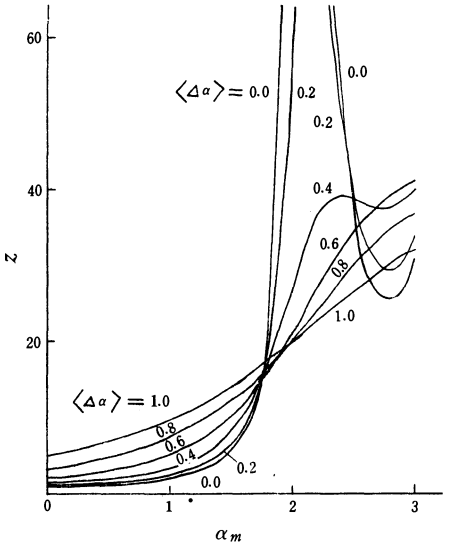


Fig. 2. Relation between z and α_m for $m=1.20$, $\Delta=0$ and for various $\langle\Delta\alpha\rangle$ values.

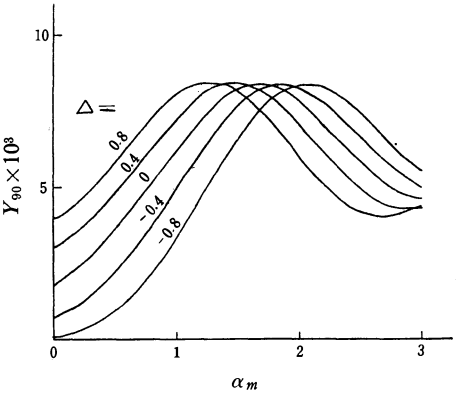


Fig. 3. Relation between Y_{90} and α_m for $m=1.20$, $\langle\Delta\alpha\rangle=0.6$ and for various Δ values.

7) E. g., W. Heller, M. Nakagaki and M. L. Wallach, *J. Chem. Phys.*, 30, 444 (1959).

8) W. J. Pangonis, W. Helleer. "Angular Scattering Functions for Spherical Particles," Wayne State University Press, Detroit, U. S. A. (1960).

$\langle \Delta\alpha \rangle$ values increase. The value of Y_{45} is mostly independent of $\langle \Delta\alpha \rangle$ at about $\alpha_m = 1.85$. According to a figure (not shown here) designed to illustrate the relation between Y_{135} and α_m for $\Delta = 0$ and $\langle \Delta\alpha \rangle = 0$ (0.2) 1.0, it is concluded that each curve of Y_{135} vs. α_m has a maximum point at about $\alpha_m = 1.3$, a minimum point at about $\alpha_m = 2.15$, and another maximum point at about $\alpha_m = 2.8$, when $\langle \Delta\alpha \rangle$ is not too large. The curves become less steep as the $\langle \Delta\alpha \rangle$ values increase. The values of Y_{135} at about $\alpha_m = 0.75$, 1.75, and 2.5 are mostly independent of $\langle \Delta\alpha \rangle$.

The dissymmetry factor, z, for $m = 1.20$ is shown in Fig. 2 for $\Delta = 0$ and $\langle \Delta\alpha \rangle = 0$ (0.2) 3.0. In the range of $\alpha_m = 0 \sim 3.0$, the z value has a maximum point at about $\alpha_m = 2.2$ and a minimum point at about $\alpha_m = 2.8$. The greater the $\langle \Delta\alpha \rangle$, the lower the maximum point becomes; at last the curve comes to increase monotonously with α_m when $\langle \Delta\alpha \rangle \geq 0.6$. The variation of z with $\langle \Delta\alpha \rangle$ is small at about $\alpha_m = 1.75$.

The change in the quantities due to the variation of $\Delta = -0.8(0.4) + 0.8$ were then studied. As is shown in Fig. 3, the curve of Y_{90} vs. α_m for $m = 1.20$ and $\langle \Delta\alpha \rangle = 0.6$ has one maximum in the range $\alpha_m = 0 \sim 3.0$; the curve is shifted to the left when $\Delta > 0$, and to the right when $\Delta < 0$, with the increase in $|\Delta|$. Similar shifts of curves were also observed in the cases of Y_{45} vs. α_m, Y_{135} vs. α_m and z vs. α_m (not shown here).

A Method to Determine the Parameter Values of the Distribution Functions. — The distribution function of the particle size presupposed previously had three parameters, α_m, $\langle \Delta\alpha \rangle$ and Δ. The three parameters can, in principle, be determined experimentally if three independent quantities, for example, Y_{90}, Y_{45}

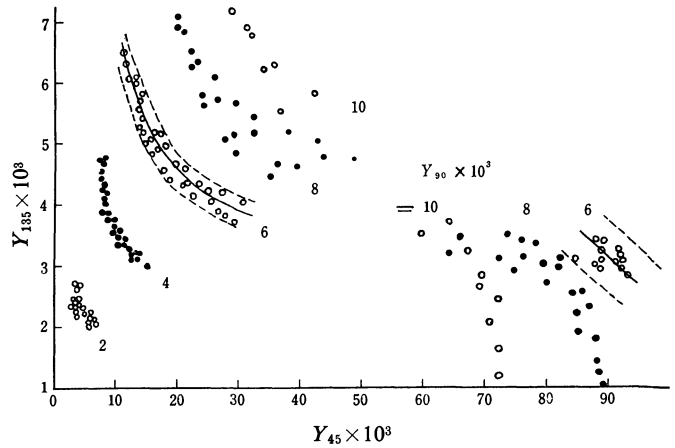


Fig. 4. Relation between Y_{45} and Y_{135} for various Y_{90} values of $m = 1.20$.

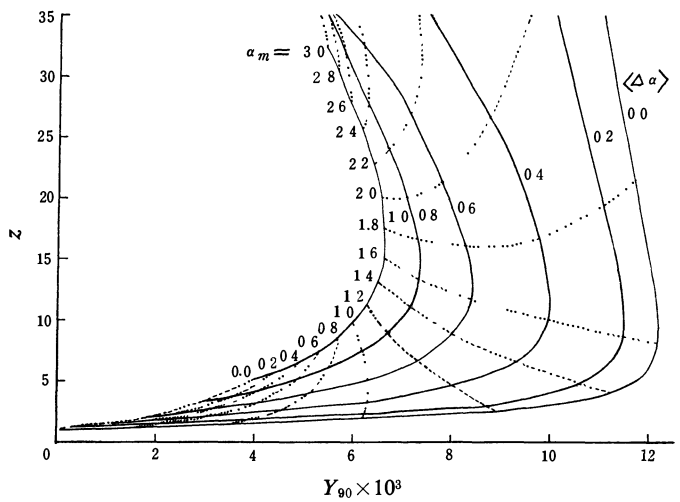


Fig. 5. Relation between z and Y_{90} for $m = 1.20$.

and Y_{135}, are measured with sufficient accuracy. In practice, however, the extent of the accuracy required for the procedure should be examined. In this connection, the values of Y_{45} and Y_{135} corresponding to several fixed values of Y_{90} are plotted[9] in Fig. 4 on the basis of the previously-computed values of Y_{90}, Y_{45} and Y_{135} for various α_m, $\langle\Delta\alpha\rangle$ and Δ values. The points for a given Y_{90} value are located in two separate regions, because the Y_{90} vs. α_m relation has a maximum. If the three quantities Y_{90}, Y_{45} and Y_{135} are entirely independent of each other and if all of three parameters α_m, $\langle\Delta\alpha\rangle$ and Δ can be determined experimentally, the points for a given Y_{90} value should be distributed over a sufficiently wide region on the $Y_{45}-Y_{135}$ plane. The actual distribution of the points, however, is not extended over a region, but is collapsed mostly on either one of two lines, as is shown in Fig. 4. If one assumes lines as drawn arbitrarily for the sake of illustration in Fig. 4, for example, for $Y_{90}=6\times10^{-3}$, one should be able to determine accurately the distance of points from these lines in order to be able to estimate the three parameter values experimentally. If the experimental errors of both Y_{45} and Y_{135} are as much as $\pm5\%$, the experimental values would be scatterd between the dotted lines in Fig. 4. This makes the experimental determination of the distance from the lines impossible when $\langle\Delta\alpha\rangle$ is smaller than 1.0 and $|\Delta|$ is smaller than 0.8. The accuracy of the experiment should be better than $\pm0.2\%$ in order to be able to determine three parameters with an accuracy of about $\pm4\%$.

If the accuracy of the experiment is not very good, as is described above, one must be satisfied with a distribution function of two parameters. The parameters to be adopted would be α_m and $\langle\Delta\alpha\rangle$ by assuming $\Delta=0$. This means that the distributsion of the particle radius is approximated by the usual Gaussian function. The two parameters, α_m and $\langle\Delta\alpha\rangle$, can be determined by measuring two independent quantities, for example, Y_{90} and z as in the usual light-scattering studies, on the basis of a chart such as Fig. 5 for $m=1.20$, constructed by using the results of the theoretical computation. The multivaluedness of α_m for a given Y_{90} value or the existence of a maximum point in the Y_{90} vs. α_m relation as shown in Fig. 1 or 3 does not make the analysis ambiguous if the maximum is only one or if the α_m value is less than 3.0, because the z values corresponding to the ascending and descending branches of the $Y_{90}-\alpha_m$ curve are different each other. In Fig. 5, the line for $\alpha_m=1.0$ is almost vertical because the dependence of Y_{90} on $\langle\Delta\alpha\rangle$ is small for this α_m value, and the line for $\alpha_m=1.8$ is almost horizontal because the dependence of z on $\langle\Delta\alpha\rangle$ is small for this α_m value, as has been described above.

Weight-averaged Particle Radius. — As a measure of the particle size, the α_m value corresponding to the most probable particle radius has been used so far. In light-scattering studies, however, the weight-average molecular weight is usually determined, especially for high polymer solutions. In the case of

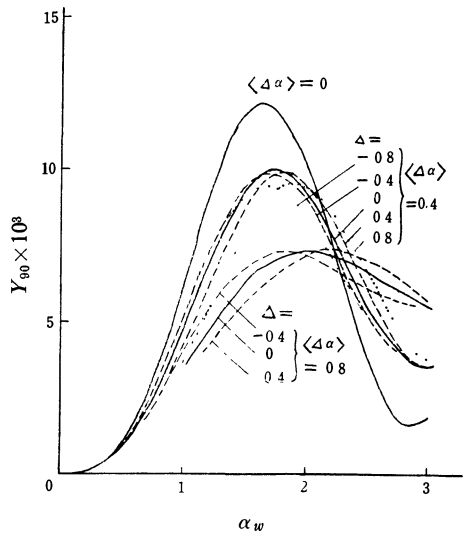


Fig. 6. Relation between Y_{90} and α_w for $m=1.20$.

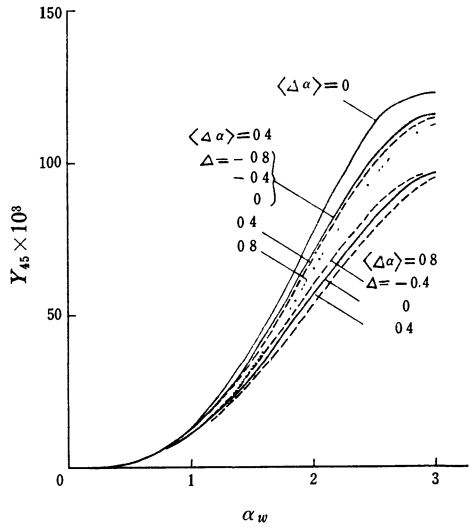


Fig. 7. Relation between Y_{45} and α_w for $m=1.20$.

9) A given value of Y_{90} corresponds to one or two (since Y_{90}-α_m relation has a maximum) values of α_m for each set of ($\langle\Delta\alpha\rangle$, Δ), and each set of (α_m, $\langle\Delta\alpha\rangle$, Δ) gives the corresponding Y_{45} and Y_{135} values.

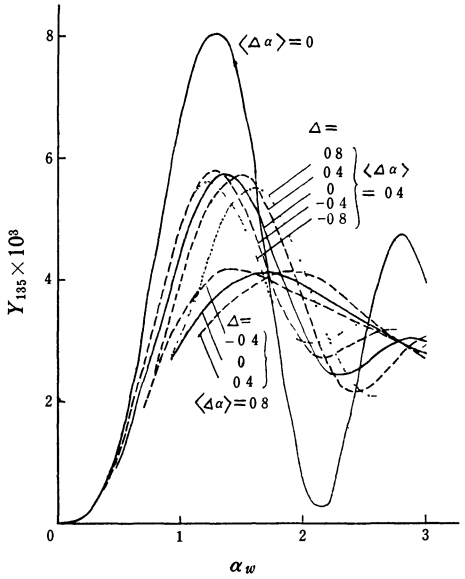


Fig. 8. Relation between Y_{135} and α_w for $m=1.20$.

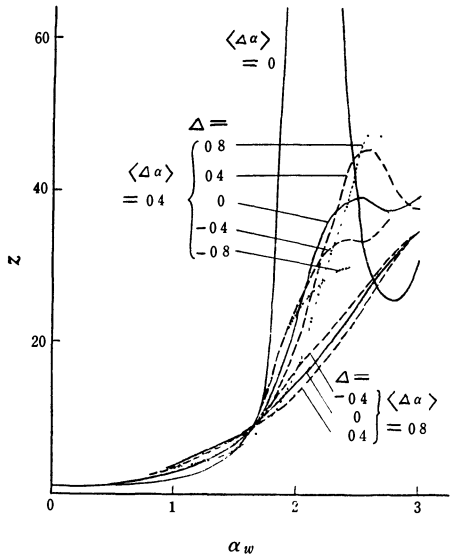


Fig. 9. Relation between z and α_w for $m=1.20$.

colloidal systems, too, the weight-averaged α^3 value may be preferable. Therefore, the cubic root of the weight-averaged α^3 value:

$$\alpha_w=\sqrt[3]{\langle\alpha^3\rangle} \tag{16}$$

may be used as a measure of the particle size of a polydispersed system. The theoretical value of $\langle\alpha^3\rangle$ for the presupposed distribution function was calculated according to Eqs. 8 and 10 for various α_m, $\langle\Delta\alpha\rangle$ and Δ values, and the previously discussed Y_θ and z vs. α_m relations were redrawn to Y_θ and z vs. α_w relations. The results of Y_{90} vs. α_w are shown in Fig. 6, those for Y_{45} vs. α_w in Fig. 7 those for Y_{135} vs. α_w in Fig. 8, and those for z vs. α_w in Fig. 9 for $m=1.20$ and for several combinations of $\langle\Delta\alpha\rangle$ and Δ. From these figures, it may be concluded: (1) the curves are mostly dependent on neither $\langle\Delta\alpha\rangle$ nor Δ if α_w is small. They coincide with the curve of $\langle\Delta\alpha\rangle=0$, although the deviation from the latter becomes the greater, the larger the α_w value; (2) the shape of the curves is determined mainly by the value of $\langle\Delta\alpha\rangle$; (3) the curves are shifted to either side when the Δ value comes to be different from zero, but the effect of Δ is not as great as that of $\langle\Delta\alpha\rangle$.

The fact that the curves coincide with each other when α_w is small is a natural consequence of Rayleigh's theory. Therefore, the value of α_{obs} obtained experimentally from the observed Y_θ values on the basis of the theoretical Y_θ vs. α relation of a monodispersed system is equal to α_w for a polydispersed system when the α_{obs} is smaller than about 0.6. When the value of α_{obs} is greater than about 0.6, however, another method is required to obtain the α_w value from the experimental Y_θ and z values.

An Empirical Method to Determine α_w.— When the Y_{90} value of a polydispersed system is measured, the values of α_{90} and z_{90} are determined where α_{90} and z_{90} are the α and z values of a monodispersed system having the same Y_{90} value as the polydispersed system.

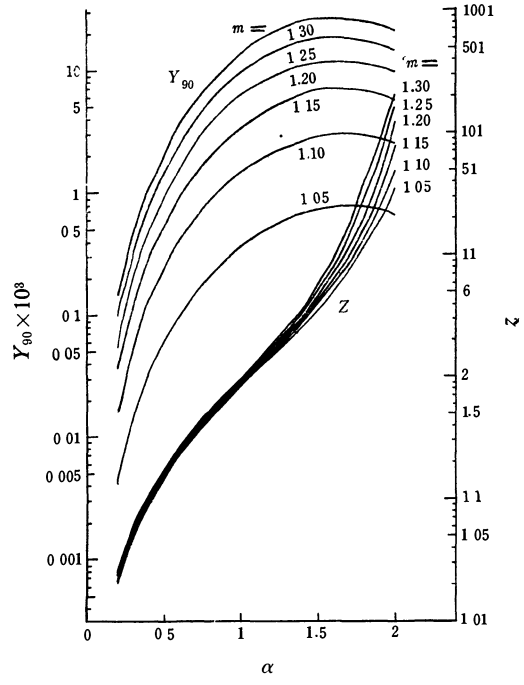


Fig. 10. Relations between Y_{90} and Z vs. α.

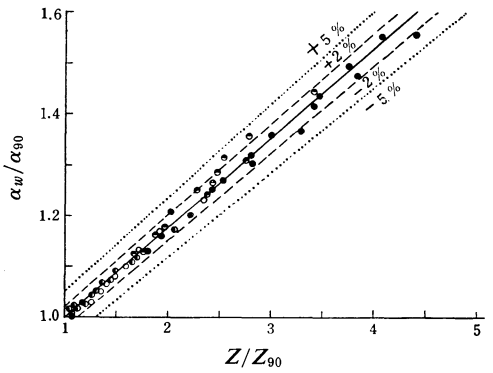


Fig. 11. Relation between α_w/α_{90} and Z/Z_{90} for $m=1.20$ and for $\langle\Delta\alpha\rangle=0.4$, $\Delta<0$ (◐), $=0$ (○), <0 (◓) and for $\langle\Delta\alpha\rangle=0.8$ (●).

For this purpose Fig. 10 may be used. In it the theoretical Y_{90} value is plotted on the left-side ordinate in a log scale, while the theoretical z value is plotted on the right-side ordinate in a $\log(z-1)$ scale, for various m-values of the monodispersed system. From Fig. 10, the values of α_{90} and z_{90} corresponding to the Y_{90}(obs) can be read off by using the curve for the m value of the system.

The Y_{90} and z values supposed to be measured for various polydispersed systems of $m=1.20$ can be obtained from the theoretical results described in the preceding paragraphs of this paper. By using these values and Fig. 10, it may be empirically concluded, as is shown in Fig. 11, that a linear relation holds approximately between α_w/α_{90} and z/z_{90}, at least within the range of $\langle\Delta\alpha\rangle$ and Δ values examined in this paper. Therefore, the following empirical equation:

$$\alpha_w/\alpha_{90}=1+k(z/z_{90}-1) \qquad (17)$$

is obtained with $k=0.176$ for $m=1.20$. This relation can then be used in order to determine the α_w value from the experimentally-determined Y_{90} and z values. In order to see the extent of the error arising in this method, the curves corresponding to errors of $\pm2\%$ and $\pm5\%$ are drawn on Fig. 11. Almost all points are located within the range of $\pm2\%$ precision. It was estimated, further, that the error was within 2% for $\alpha_w<1.2$ if $\langle\Delta\alpha\rangle=0.4$ and $\Delta=\pm0.8$ or if $\langle\Delta\alpha\rangle=0.8$ and $\Delta=\pm0.4$, and within 5% for $\alpha_w<1.5$ for the same $\langle\Delta\alpha\rangle$ and Δ values.

Similar studies have been made for other m values; the values of k thus obtained are shown in Table I. The error was not very dependent on the m values and was within 2% for $\alpha_w<1.5$ and within 5% for $\alpha_w<1.6$ if $\langle\Delta\alpha\rangle=0.4$ and $\Delta=0$.

Table I. Coefficients k for various m-values

m	k	m	k
1.05	0.207	1.20	0.176
1.10	0.192	1.25	0.172
1.15	0.182	1.30	0.169

Summary

In order to study the light scattering of polydispersed colloidal systems of spherical particles, a weight distribution function, $W(\alpha)$, of the relative particle radius α has been assumed to be a modified Gaussian function with three parameters: the most probable α-value, α_m; the width of the distribution, $\langle\Delta\alpha\rangle$, and the dissymmetry of the distribution, Δ. The values of Y_θ, which is proportional to the specific scattering intensity, for $\theta=45°$, 90° and 135°, and the dissymmetry factor, $z=Y_{45}/Y_{135}$, have then been computed.

In principle, it should be possible to determine three parameters of the particle size distribution, α_m, $\langle\Delta\alpha\rangle$ and Δ, from the observed values of three independent quantities, Y_{45}, Y_{90} and Y_{135}. It has, however, been concluded that practically the method requires very precise experiments. If one is satisfied with a distribution function of two parameters, α_m and $\langle\Delta\alpha\rangle$, the values of these parameters can be determined from the experimentally-obtained Y_{90} and z values on the basis of a chart constructed theoretically.

The value of α_w, which is the cubic root of weight-averaged $\langle\alpha^3\rangle$, is equal to the α value obtained from the measured specific scattering intensity by assuming that the system is monodispersed when α is small. If α is not small, the value of α_w can be obtained according to the empirical equation:

$$\alpha_w/\alpha_{90}=1+k(z/z_{90}-1)$$

The error will be within about 5% if $\alpha_w<1.5$.

Faculty of Pharmaceutical Sciences
Kyoto University
Sakyo-ku, Kyoto

The Synthesis and Reactions of 4-(5-Phenyl-3-pyrazolyl)tropolones

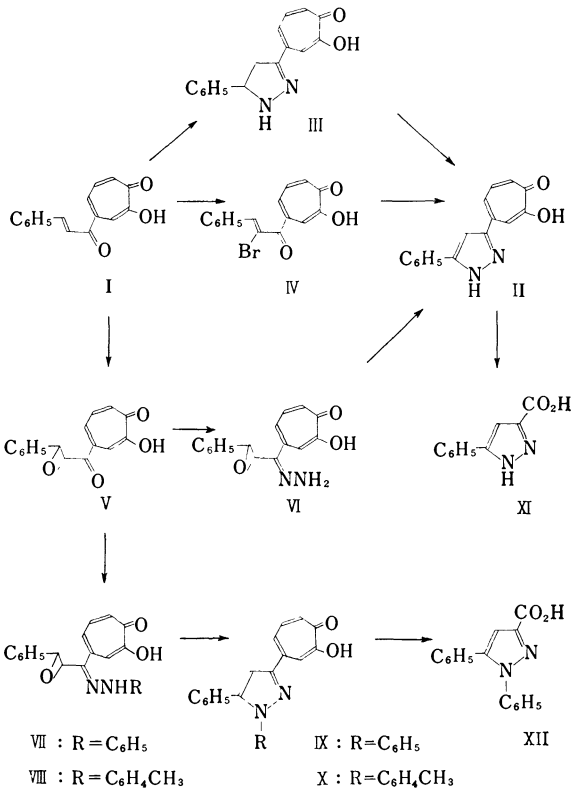
By Tetsuo NOZOE, Kahei TAKASE and Yasuhiro MOCHIZUKI

(Received May 13, 1964)

Troponoid compounds containing a non-condensed heteroaromatic ring are expected to be interesting not only because of their chemical properties but also because of their potential biological properties. Because such compounds had never been synthesized, the present authors synthesized some pyrazolyltropolones, starting from 4-cinnamoyltropolone (I) obtained by the condensation of 4-acetyltropolone and benzaldehyde,[1] and investigated their chemical natures.

4-(5-Phenyl-3-pyrazolyl)tropolone (II), the structure of which was established as mentioned below, was synthesized by the following three routes: i) The dehydrogenation of 4-(4, 5-dihydro-5-phenyl-3-pyrazolyl)tropolone (III) obtained by a reaction of I with hydrazine (a 24% over-all yield from I). ii) The reaction of 4-(α-bromocinnamoyl)tropolone (IV),[2] obtained by the bromination of I, with hydrazine (a 22% yield from I). iii) The ring formation of the hydrazone (VI) of 4-(2, 3-epoxy-3-phenylpropionyl)tropolone (V),[2] obtained by the oxidation of I with alkaline hydrogen peroxide (a 40% yield from I). The third method seemed to be the best. In the same way, 4-(1, 5-diphenyl-3-pyrazolyl)-tropolone (IX) and 4-[5-phenyl-1-(*p*-tolyl)-3-pyrozolyl]tropolone (X) were also obtained from phenylhydrazone (VII) and *p*-tolylhydrazone (VIII) of epoxide (V) in 98% and 87% yields respectively. Compounds II, III, IX and X were all proved to be tropolone derivatives by the facts that they were soluble in alkali, reacted positively to the ferric chloride test and formed a greenish-yellow copper chelate. The alkaline permanganate oxidation of II and IX gave 5-phenylpyrazole-3-carboxylic acid (XI)[3] and 1, 5-diphenylpyrazole-3-carboxylic acid (XII)[4] in good yields. The compound, III, was presumed to be a pyrazoline rather than a hydrazone derivative because of its stability to acid. The structures of II, III, IX and X were established by these facts, as is shown in the scheme.

The azo-coupling of II with *p*-toluenediazonium chloride gave an orange-colored 5-(*p*-tolylazo) derivative, the position of the azo group being inferred from analogy with the azo-coupling reaction of the other tropolones.[5] The methylation of II and IX with diazomethane afforded two kinds of methyl ethers, XIIIa and XIIIb, and XIVa and XIVb respectively. The structures of these ethers were inferred from their infrared spectra, in which a strong absorption appeared at 819 for XIIIa, 815 for XIVa, 797 for XIIIb and 795 cm^{-1} for XIVb in Nujol mull. These data suggest that these ethers possess the structures shown.[6] Furthermore, it was interesting to note that the ultraviolet absorption spectra of 4-substituted 2-methoxytropones (XIIIa and XIVa)



1) T. Nozoe, K. Takase and M. Ogata, *Chem. & Ind.*, 1957, 1070.
2) T. Nozoe, K. Takase, K. Suzuki and K. Sasaki, to be published.
3) C. Beyer and L. Claisen, *Ber.*, 20, 2185 (1887); A. Bschler, ibid., 25, 3144 (1892).
4) C. Bulow, ibid., 37, 2200 (1904).
5) T. Nozoe, *Fortschr. Chem. org. Naturst.*, 13, 233 (1956).
6) 2, 4-Disubstituted tropones show the characteristic absorption in the range 810~840 cm^{-1}, and 2, 6-disubstituted tropones show it in the range 770~800 cm^{-1}; T. Nozoe, K. Takase and M. Yasunami, to be published.

and 6-substituted isomers (XIIIb and XIVb) differed from each other remarkably in the long-wave region, as is shown in Fig. 1. Such was also the case in isomeric methyl ethers of styryltropolone[7] and in 3- and 4-phenyltropones,[8] this is probably due to the difference in the cross-conjugation system between the aromatic-ring and the unsaturated-ketone systems in a seven-membered ring.

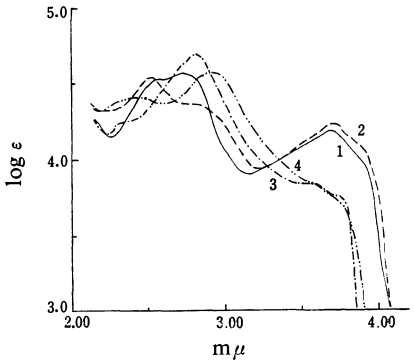
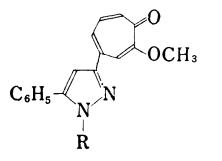
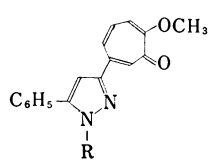


Fig. 1. Ultraviolet absorption spectra of
1: 2-Methoxy-4-(5-phenyl-3-pyrazolyl)tropone (XIIa),
2: 2-Methoxy-4-(1,5-diphenylpyrazolyl)tropone (XIVa),
3: 2-Methoxy-6-(5-phenylpyrazolyl)tropone (XIIIb) and
4: 2-Methoxy-6-(1,5-diphenylpyrazolyl)tropone (XIVb)
in methanol.

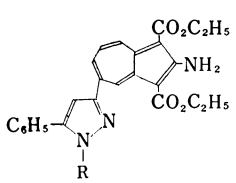
Methyl ethers (XIIIa, b and XIVa, b) were easily hydrolyzed to the original tropolones with alkali. They also gave, by the action of ethyl cyanoacetate in the presence of sodium ethoxide, pyrazolylazulene derivatives (XV, XVI and XVIIa),[9] the structures of which were inferred from their analytical data and their ultraviolet and infrared absorption spectra. These properties of pyrazolyltropolones, e.g., the formation of two kinds of reactive methyl ethers, were quite similar to those of usual monocyclic tropolones rather than those of tropolones fused with aromatic nuclei, e.g., benzotropolone[10a] or pyridotropolones.[10b]



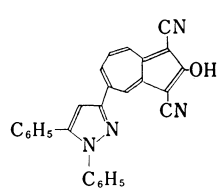
XIIIa: R=H
XIVa: R=C_6H_5



XIIIb: R=H
XIVb: R=C_6H_5



XV: R=H
XVI: R=C_6H_5



XVII

Experimental[11]

4-(4,5-Dihydro-5-phenyl-3-pyrazolyl)tropolone (III).—A mixture of 4-cinnamoyltropolone (I) (500 mg.), ethanol (4 ml.), 80% hydrazine hydrate (0.2 ml.) and glacial acetic acid (5 drops) was heated under reflux for 5 min. The crystals thereby formed were collected and recrystallized from ethanol to give III (430 mg.) as yellow prisms, m.p. 132~133°C.

Found: C, 71.82; H, 4.91; N, 10.64. Calcd. for $C_{16}H_{14}O_2N_2$: C, 72.16; H, 5.30; N, 10.52%.

λ_{max}^{MeOH} mμ (log ε); 235 (4.29), 320 (4.31), 365~390 (4.15).

N-Acetate.—M.p. 181°C, pale yellow micro-needles (from ethanol).

Found: C, 69.32; H, 5.05; N, 8.96. Calcd. for $C_{18}H_{16}O_3N_2$: C, 70.11; H, 5.23; N, 9.09%.

4-(5-Phenyl-3-pyrazolyl)tropolone (II).—*a) From III.*—A mixture of III (270 mg.), chloranil (370 mg.), and glacial acetic acid (2 ml.) was heated under reflux for 3 hr. After the crystals (dihydrochloranil) which separated out on cooling had been filtered off, the solvent was removed from the filtrate and the residue was recrystallized from ethanol, affording II (80 mg.), m.p. 186~187°C. Further recrystallization from ethanol gave cream yellow silky needles, m.p. 190~191°C.

Found: C, 72.45; H, 4.65; N, 10.63. Calcd. for $C_{16}H_{12}O_2N_2$: C, 72.71; H, 4.58; N, 10.60%.

λ_{max}^{MeOH} mμ (log ε); 280 (4.61), 390 (3.93).

b) From 4-(α-Bromocinnamoyl)tropolone (IV).—To a suspension of IV (1.36 g.) in methanol (10 ml.), 80% hydrazine hydrate (0.4 ml.) was added, and the mixture was heated under reflux for 20 min. The crystals thereby formed were collected and recrystallized from ethanol to give II (655 mg.) as cream-yellow silky needles, m.p. 190~191°C.

c) From 4-(2,3-Epoxy-3-phenylpropionoyl)tropolone (V).—A mixture of V (1.54 g.), ethanol (50 ml.) and 80% hydrazine hydrate (0.5 ml.) was heated under reflux for 1 hr. and then cooled to give the hydrazone (VI) (820 mg.), m.p. 194°C (decomp.). Recrystallization from ethanol afforded yellow plates, m.p. 204°C (decomp.).

Found: C, 67.84; H, 5.07; N, 9.83. Calcd. for $C_{16}H_{14}O_3N_2$: C, 68.07; H, 5.00; N, 9.92%.

7) H. Matsumura, *J. Chem. Soc. Japan, Pure Chem. Sec. (Nippon Kagaku Zassi)*, **77**, 330 (1956); **78**, 669 (1957).
8) T. Ikemi, T. Nozoe and H. Sugiyama, *Chem. & Ind.*, **1960**, 932.
9) Cf. T. Nozoe, S. Seto, S. Matsumura and Y. Murase, This Bulletin, **35**, 1179 (1962).
10) a) T. Nozoe et al., "Dai Yuki Kagaku (Comprehensive Organic Chemistry)," Vol. **13**, Asakura-Shoten, Tokyo (1960), Chapter 14.
b) T. Nozoe et al., ibid., Chapter 26.
11) All melting points are uncorrected.

λ_{max}^{MeOH} mμ (log ε); 237 (4.23), 320 (4.33), 370 (4.12).

A mixture of the hydrazone (VI) (640 mg.), ethanol (50 ml.) and 6 N hydrochloric acid (3 drops) was heated under reflux for 1 hr. and then cooled to give II (470 mg.) as cream-yellow silky needles m. p. 190~191°C.

4-(1, 5-Diphenyl-3-pyrazolyl)tropolone (IX). — A mixture of epoxide (V) (1.35 g.), ethanol (40 ml.) and phenylhydrazine (0.8 ml.) was heated under reflux for 1 hr. and then concentrated to a small volume and allowed to cool to give the phenylhydrazone (VII) (1.69 g.), m. p. 199~201°C. Recrystallization from ethanol-dioxane afforded orange-yellow micro-needles, m. p. 207~209°C.

Found: C, 73.69; H, 4.94; N, 7.45. Calcd. for $C_{22}H_{18}O_3N_2$: C, 73.73; H, 5.06; N, 7.82%.

A mixture of the phenylhydrazone (VII) (1.69 g.), ethanol (70 ml.) and 6 N hydrochloric acid (10 drops) was heated under reflux for 40 min. and then concentrated to a small volume and allowed to cool to give IX (1.36 g.), m. p. 170~172°C. Recrystallization from ethanol afforded cream-yellow prisms, m. p. 171~172°C.

Found: C, 77.74; H, 4.56; N, 8.08. Calcd. for $C_{22}H_{16}O_2N_2$: C, 77.63; H, 4.74; N, 8.23%.

λ_{max}^{MeOH} mμ (log ε); 252 (4.45), 292 (4.50), 393 (3.91).

4-[5-Phenyl-1-(*p*-tolyl)-3-pyrazolyl]tropolone (X). — A mixture of epoxide (V) (270 mg.), ethanol (7 ml.) and *p*-tolylhydrazine (180 mg.) was heated under reflux for 40 min. and allowed to cool to give the *p*-tolylhydrazone (VIII) (350 mg.), m. p. 188~189°C. Recrystallization from ethanol-dioxane formed reddish orange prisms, m. p. 192~193°C.

Found: C, 73.74; H, 5.33; N, 7.36. Calcd. for $C_{23}H_{20}O_3N_2$: C, 74.17; H, 5.41; N, 7.52%.

A mixture of this *p*-tolylhydrazone (90 mg.), ethanol (5 ml.) and 6 N hydrochloric acid (1 drop) was heated under reflux for 1 hr. and then allowed to cool to give X (80 mg.), m. p. 166~168°C. Recrystallization from ethanol afforded cream-yellow needles, m. p. 169.5~170°C.

Found: C, 77.72; H, 4.97; N, 7.30. Calcd. for $C_{23}H_{18}O_2N_2$: C, 77.95; H, 5.12; N, 7.91%.

λ_{max}^{MeOH} mμ (log ε); 252 (4.45), 292 (4.46), 393 (3.90).

The Oxidation of II.—Into a solution of II (530 mg.) in a mixture of 6 N potassium hydroxide solution (2.5 ml.) and water (60 ml.), powdered potassium permanganate (2.80 g.) was stirred in small portions at room temperature; 2.56 g. of potassium permanganate were consumed rapidly. After stirring was continued for a further 3 hr., the excess permanganate was decomposed by the addition of methanol, the manganese dioxide which separated out was filtered off, and the filtrate was acidified to pH 2 with 6 N hydrochloric acid and extracted with ether. After the solution had been dried over anhydrous sodium sulfate, the solvent was removed from the extract to leave colorless crystals (330 mg.), m. p. 230~234°C. Recrystallization from aqueous methanol afforded 5-phenylpyrazole-3-carboxylic acid (XI) as colorless needles, m. p. 234~235°C (decomp.); it was identified by admixture with an authentic specimen[3] and also by a comparison of their infrared spectra.

Found: C, 63.42; H, 3.96; N, 14.47. Calcd. for $C_{10}H_8O_2N_2$: C, 63.82; H, 4.29; N, 14.89%.

The Oxidation of IX.—To a solution of IX (680 mg.) in a mixture of 6 N potassium hydroxide solution (5.5 ml.) and water (180 ml.), powdered potassium permanganate (2.95 g.) was added in small portions; the reaction mixture was treated in a manner similar to that above to give colorless crystals (430 mg.), m. p. 175~182°C. Recrystallization from aqueous methanol afforded 1,5-diphenylpyrazole-3-carboxylic acid (XII) as colorless needles, m. p. 183~184°C; it was identified by admixture with an authentic specimen[4] and by a comparison of their infrared spectra.

Found: C, 73.29; H, 4.96; N, 10.47. Calcd. for $C_{16}H_{12}O_2N_2$: C, 72.71; H, 4.58; N, 10.60%.

The *p*-Tolylazo Compound of II. — Into a solution of II (260 mg.) in pyridine (1.7 ml.), a solution of *p*-toluenediazonium chloride prepared from *p*-toluidine (120 mg.) by the usual method, was stirred under cooling. The mixture was then stirred for an additional 2 hr. and allowed to stand overnight. The crystals so obtained were collected by filtration and washed with a small amount of benzene to give 4-(5-phenyl-3-pyrazolyl)-5-(*p*-tolylazo)tropolone (250 mg.) as orange crystals, m. p. 220.5~221°C.

Found: C, 72.02; H, 4.47; N, 14.78. Calcd. or $C_{23}H_{18}O_2N_4$: C, 72.23; H, 4.74; N, 14.65%.

λ_{max}^{MeOH} mμ (log ε); 255 (4.57), 422 (4.50).

Methyl Ethers of II: 2-Methoxy-4-(5-phenyl-3-pyrazolyl)tropone (XIIIa) and 2-Methoxy-6-(5-phenyl-3-pyrozolyl)tropone (XIIIb).—To a solution of II (800 mg.) in ethyl acetate (150 ml.), an ethereal solution of diazomethane (13 ml.) was added. After additional stirring for 3 hr., the mixture was concentrated to a small volume to give crystals (690 mg.); m. p. 207~213°C. Recrystallization from methanol gave XIIIb (330 mg.) as cream-yellow needles, m. p. 252~253°C.

Found: C, 73.27; H,. 4.92; N, 9.71. Calcd. for $C_{17}H_{14}O_2N_2$: C, 73.36; H, 5.07; N, 10.07%.

λ_{max}^{MeOH} mμ (log ε); 280 (4.67).

The crystals, obtained from the mother liquor by the removal of the solvent, were fractionally recrystallized from methanol to give XIIIa (180 mg.) as cream-yellow plates, m. p. 235°C.

Found: C, 73.05; H, 4.99; N, 9.71. Calcd. for $C_{17}H_{14}O_2N_2$: C, 73.36; H, 5.07; N, 10.07%.

λ_{max}^{MeOH} mμ (log ε); 273 (4.55), 368 (4.17).

The heating of XIIIa or XIIIb with a dilute potassium hydroxide solution in aqueous ethanol gave II in a 60% yield.

Methyl Ethers of IX: 2-Methoxy-4-(1, 5-diphenyl-3-pyrazolyl)tropone (XIVa) and 2-Methoxy-6-(1, 5-diphenyl-3-pyrozolyl)tropone (XIVb).—Into a solution of IX (1.00 g.) in ethyl acetate (70 ml.), an ethereal solution of diazomethane (15 ml.) was stirred under cooling. After additional stirring for 4 hr., the mixture was allowed to stand overnight to give XIVb (440 mg.), m. p. 220~221°C, which was recrystallized from methanol as cream-colored needles, m. p. 223~224°C.

Found: C, 77.81; H, 4.88; N, 7.87. Calcd. for $C_{23}H_{18}O_2N_2$: C, 77.95; H, 5.12; N, 7.91%.

λ_{max}^{MeOH} mμ (log ε); 247 (4.40), 292 (4.56).

Removing the solvent from the mother liquor afforded crystals, from which XIVa (260 mg.) was obtained as pale yellow micro-needles, m. p. 168~169°C, after recrystallization from methanol.

Found: C, 77.71; H, 4.89; N, 7.94. Calcd. for $C_{23}H_{18}O_2N_2$: C, 77.95; H, 5.12; N, 7.91%.

λ_{max}^{MeOH} mμ (log ε); 252 (4.54), 370 (4.22).

The heating of XIVa or XIVb with a 2 N potassium hydroxide solution in aqueous ethanol afforded IX in a 60% yield.

Diethyl 2-Amino-5-(5-phenyl-3-pyrozolyl)azulene-1, 3-dicarboxylate (XV). — To a sodium ethoxide solution, prepared by dissolving sodium (300 mg.) in anhydrous ethanol (2 ml.), ethyl cyanoacetate (300 mg.) and then a solution of XIIIa (300 mg.) in anhydrous ethanol (50 ml.) were added. After having been allowed to stand for one day, the mixture was diluted with water (150 ml.) and extracted with benzene. The removal of the solvent from the extract left an oily substance, which was crystallized by the addition of a small amount of methanol, giving XV (170 mg.) as orange micro-crystals, m. p. 237~238°C.

Found: C, 69.92; H, 5.19; N, 9.36. Calcd. for $C_{25}H_{23}O_4N_3$: C, 69.91; H, 5.40; N, 9.76%.

λ_{max}^{MeOH} mμ (log ε); 259 (4.61), 343 (4.91), 462 (3.45). IR (KBr); 3420, 3290 (NH_2); 3200 (NH); 1667 (C=O) cm^{-1}.

Diethyl 2-Amino-5-(1, 5-diphenyl-3-pyrazolyl)azulene-1, 3-dicarboxylate (XVI) and 1, 3-Dicyano-2-hydroxy-5-(1,5-diphenyl-3-pyrozolyl)azulene (XVII). —Into a suspension of ethyl sodiocyanoacetate in ethanol, prepared from sodium (30 mg.), anhydrous ethanol (2 ml.) and ethyl cyanoacetate (250 mg.), a solution of methyl ether (a mixture of XIVa and XIVb) (250 mg.) in a mixture of anhydrous ethanol (15 ml.) and dry dioxane (10 ml.) was stirred. After having been allowed to stand for one day, the mixture was diluted with water and extracted with benzene. The removal of the solvent from the extract afforded XVI (190 mg.) as orange prisms, m. p. 179°C, after recrystallization from methanol.

Found: C, 73.89; H, 5.16; N, 8.18. Calcd. for $C_{31}H_{27}O_4N_3$: C, 73.64; H, 5.39; N, 8.31%.

λ_{max}^{MeOH} mμ (log ε); 253 (4.58), 346 (4.96), 462 (3.50). IR (KBr); 3440, 3310 (NH_2); 1658 (C=O) cm^{-1}.

An aqueous layer was acidified with 6 N hydrochloric acid and extracted with benzene. The solvent was removed from the extract and the residue was recrystallized from ethanol to give XVII (50 mg.) as orange micro-crystals, m. p. over 280°C.

Found: C, 78.64; H, 3.68; N, 13.22. Calcd. for $C_{27}H_{16}ON_4$: C, 78.60; H, 3.88; N, 13.59%.

λ_{max}^{MeOH} mμ (log ε); 233 (4.64), 345 (4.96), 393 (4.00), 470 (3.54). IR (KBr); 3010 (broad) (OH); 2210 (C≡N) cm^{-1}.

A part of the expenses for the present series of experiments were defrayed by a grant-in-aid from the Sankyo Co., Ltd., to which the authors' thanks are due.

Department of Chemistry
Faculty of Science
Tohoku University
Katahira-cho, Sendai

*The Synthesis of Diethyl 2-Hydroxyazulene-1, 3-dicarboxylate from Troponoids and Some Reactions of 2-Hydroxyazulene Derivatives**

By Tetsuo NOZOE, Kahei TAKASE and Noboru SHIMAZAKI

(Received June 15, 1964)

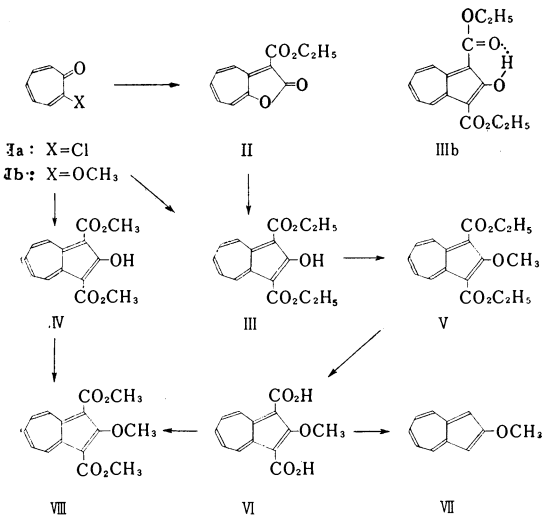
It has been reported that 2-chlorotropone and 2-methoxytropone react with ethyl cyanoacetate or malononitrile, in the presence of sodium ethoxide, to give azulene derivatives.[1] On the other hand, 1-oxaazulan-2-one (2*H*-cyclohepta[b]furan-2-one) derivatives have been obtained by the reaction of these tropone derivatives and diethyl malonate or ethyl acetoacetate.[2] We have reexamined these reactions with an interest in the azulene synthesis from troponoids and found that the reaction of 2-chlorotropone or 2-methoxytropone and malonic ester affords a new azulene derivative, 2-hydroxyazulene-1, 3-dicarboxylic ester. Some reactions of this azulene will be described here.

The reaction of 2-chlorotropone (Ia) and diethyl sodiomalonate in dry benzene gave 3-ethoxycarbonyl-1-oxaazulane-2-one (II), as has already been reported.[2] Furthermore, the reaction of 2-chlorotropone (Ia) or 2-methoxy

* Presented at the 15th Annual Meeting of the Chemical Society of Japan, Kyoto, April, 1962.

1) T. Nozoe, S. Matsumura, Y. Murase and S. Seto, *Chem. & Ind.*, **1955**, 1257; T. Nozoe, S. Seto, S. Matsumura and Y. Murase, This Bulletin, **35**, 1179 (1962).

2) S. Seto, *Sci. Repts. Tohoku Univ.*, I, **37**, 367 (1953).



tropone (Ib) diethyl malonate, in the presence of one or two molar equivalents of sodium ethoxide, in ethanol also gave II. However, when this reaction was carried out in ethanol by the use of an excess of sodium ethoxide, a yellowish-orange compound (III), $C_{16}H_{16}O_5$, was obtained in place of II. Further, the reaction of 2-methoxytropone with dimethyl malonate by the use of an excess of sodium methoxide in methanol afforded an orange compound (IV), $C_{14}H_{12}O_5$. These products are acidic and gave sparingly soluble sodium salts, red acetates and red *p*-nitrobenzoates. The ultraviolet absorption spectra of III and IV were similar to that of diethyl 2-aminoazulene-1,3-dicarboxylate,[1] as Fig. 1 shows. These findings suggest that III and IV are the diethyl and dimethyl esters of 2-hydroxyazulene-1,3-dicarboxylic acid respectively. The structures of III and IV were confirmed by the following

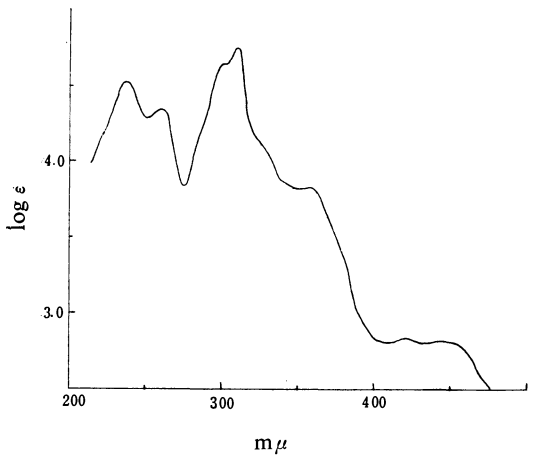


Fig. 1. The ultraviolet absorption spectrum of diethl 2-hydroxyazulene-1,3-dicarboxylate (III) in methanol.

evidence. The methylation of III with diazomethane gave diethyl 2-methoxyazulene-1,3-dicarboxylate (V). The alkaline hydroysis of V, followed by the decarboxylation of the dicarboxylic acid (VI) thereby obtained, gave 2-methoxyazulene (VII).[3] On the other hand, the methylation of IV with diazomethane gave dimethyl 2-methoxy-azulene-1,3-dicarboxylate (VIII), which was identical with the dimethyl ester of dicarboxylic acid (VI).

The above mentioned experiments show without ambiguity that the reaction of 2-chloro- (Ia) or 2-methoxytropone (Ib) and the malonic ester affords the 1-oxaazulan-2-one derivative (II) or 2-hydroxyazulene derivatives (III) according to the amount of the ethoxide used. This evidence indicates that II is a reaction intermediate in the formation of azulene (III) from troponoids (I). This was confirmed by the finding that II easily reacted which diethyl malonate, in the presence of an excess of sodium ethoxide, to give III in a good yield.

It is known[3] that the chlorine atom of diethyl 2-chloroazulene-1,3-dicarboxylate (IX) is easily replaced by various anionoid reagents. In comparison with IX, the behavior of the methoxyl group of diethyl 2-methoxyazulene-1,3-dicarboxylate (V) towards some anionoid reagents was examined. The methoxy group of V was replaced by the ethoxyl group when heated with sodium ethoxide, affording diethyl 2-ethoxyazulene-1,3-dicarboxylate (X). The alkaline hydrolysis of X, followed by the decarboxylation of the dicarboxylic acid thereby obtained, gave 2-ethoxyazulene (XI).[4] When V was heated with alcoholic potassium hydroxide, the methoxy group was replaced by the ethoxyl group, along with the elimination of the ethoxycarbonyl group, to give XI directly. The methoxyl group of V was also replaced by methylamine and by hydrazine to give diethyl-2-methylaminoazulene-1,3-dicarboxylate (XII)[4] and diethyl 2-hydrazinoazulene-1,3-dicarboxylate (XIII)[4] respectively. Contrary to the case of IX,[3] V did not react with alcoholic ammonia, dimethylamine and aniline.

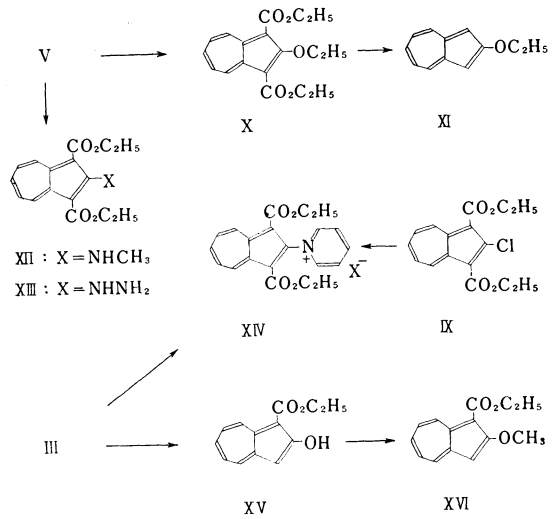
The efforts to replace the hydroxyl group of III with chlorine were unsuccessful; that is, III was recovered on treatment with thionyl chloride or phosphorous oxychloride. The tosylation of III with *p*-toluenesulfonyl chloride in pyridine gave pyridinium salt (XIV) in place of the *p*-tolylsulfonyloxy derivative. The picrate of XIV was identical with that of

3) T. Nozoe, S. Seto and S. Matsumura, This Bulletin, 35, 1990 (1962).

4) The compounds which have been derived from diethyl 2-chloroazulene-1,3-dicarboxylate (IX) have been reported[3] as oil.

the compound obtained by the treatment of IX with pyridine.[5] This is because the initially formed tosylate reacted with pyridine to give XIV.

Diethyl 2-aminoazulene-1, 3-dicarboxylate was brominated easily to give the 6-bromo derivative,[1] but the bromination of III ended only in its recovery. Nitrosation and azo-coupling reaction on III also recovered the starting material.



For the synthesis of 2-hydroxyazulene, the hydrolysis of III was examined. The alkaline hydrolysis of III gave ethyl 2-hydroxyazulene-1-carboxylate (XV), which afforded an acetate and a *p*-nitrobenzoate, along with an oily substance which changed to a black substance which was insoluble organic solvents. The methylation of XV gave ethyl 2-methoxyazulene-1-carboxylate (XVI). The acid hydrolysis of III gave only an insoluble black substance. The formation of these insoluble matters is assumed to be due to the polymerization of the unstable 2-hydroxyazulene which is formed. In the infrared spectra, III shows two absorptions (1675 and 1639 cm^{-1}) and due to an ester carbonyl, while its methyl ether (IV), shows only one absorption (1984 cm^{-1}). This evidence indicates that III exists as an intramolecular hydrogen-bonded structure (IIIa), which enhances the stability of this compound.

Experimental[6]

Diethyl 2-Hydroxyazulene-1, 3-dicarboxylate (III).—*a) From 2-Chlorotropone (Ia).*—To a sodium ethoxide solution prepared from sodium (700 mg.) and absolute ethanol (50 ml.), diethyl malonate (2.4 g.) and Ia (700 mg.) were added, and the mixture was allowed to stand for 40 hr. at room temerature; the reaction mixture then turned into a gelatinous orange mass. Water was added, and the sodium salts thereby separated out were collected and dissolved in glacial acetic acid. This solution was diluted with water and extracted with chloroform. The solvent was evaporated and the residue was recrystallized from ethanol to give III (700 mg.) as orangish yellow needles, m. p. 95~96°C.

Found: C, 66.60; H, 5.42. Calcd. for $C_{16}H_{16}O_5$: C, 66.67; H, 5.55%.

λ_{max}^{MeOH} mμ (log ε); 237 (4.53), 260 (4.34), 310 (4.75), 360 (3.83), 420 (2.84).

Acetate.—m. p. 129.5~130°C, red needles (from ethanol).

Found: C, 65.55; H, 5.67. Calcd. for $C_{18}H_{18}O_5$: C, 65.44; H, 5.49%.

λ_{max}^{MeOH} mμ (log ε); 235 (4.53), 270 (4.40), 300 (4.69), 335 (3.80), 365 (3.89), 480 (2.83).

p-Nitrobenzoate.—m. p. 180~181°C, red needles (from ethanol).

Found: C, 63.18; H, 4.59; N, 3.34. Calcd. for $C_{23}H_{19}O_8N$: C, 63.15; H, 4.38; N, 3.20%.

λ_{max}^{MeOH} mμ (log ε); 233 (4.59), 267 (4.53), 300 (4.81), 333 (3.91), 365 (3.93), 460 (2.88), 480 (2.91).

b) From 2-Methoxytropone (Ib).—To a sodium ethoxide solution prepared from sodium (11.6 g.) and absolute ethanol (300 ml.), diethyl malonate (48 g.) and Ib (13.6 g.) were added, and the mixture was allowed to stand for 40 hr. at room temperature. When the reaction mixture was then treated as in a), III (15.8 g.) was obtained as orangish yellow needles, m.p. 95~96°C.

c) From 2-Ethoxycarbonyl-1-oxaazulan-2-one (II).—To a sodium ethoxide solution prepared from sodium (230 mg.) and absolute ethanol (20 ml.), diethylmalonate (800 mg.) and II (500 mg.) were added. The mixture was treated as in a), and III (430 mg.) was obtained as organish yellow needles, m. p. (95~96°C).

Dimethyl 2-Hydroxyazulene-1, 3-dicarboxylate (IV).—To a sodium methoxide solution prepared from sodium (3.95 g.) and absolute methanol (85 ml.), dimethyl malonate (12 g.) and 2-methoxytropone (4.23 g.) were added, and the mixture was allowed to stand for 40 hr. at room temperature. The reaction mixture was treated as described in the above experiment, and IV (4.90 g.) was obtained as reddish orange needles or yellowish orange needles, m. p. 144~145°C, after recrystallization from ethyl acetate.

Found: C, 64.87; H, 4.49. Calcd. for $C_{14}H_{12}O_5$: C, 64.61; H, 4.65%.

λ_{max}^{MeOH} mμ (log ε); 238 (4.49), 260 (4.31), 310 (4.74), 356 (3.82), 450 (2.86).

Acetate.—m. p. 151~153°C, red needles (from ethyl acetate).

Found: C, 63.71; H, 4.75. Calcd. for $C_{16}H_{14}O_6$: C, 63.57; H, 4.67%.

λ_{max}^{MeOH} mμ (log ε); [233 (4.52), [268 (4.40), 300 (4.70), 335 (3.81), 350 (3.78), 363 (3.89), 410 (2.55), 475 (2.85).

p-Nitrobenzoate.—m. p. 221~222°C, red needles (from dimethylformamide).

5) T. Nozoe and M. Oyama, to be published.
6) All melting points are uncorrected.

Found: C, 62.14; H, 3.60; N, 3.59. Calcd. for $C_{21}H_{15}O_8N$: C, 61.61; H, 3.69; N, 3.42%.

λ_{max}^{MeOH} mμ; 233, 266, 300, 363, 410, 470.

Diethyl 2-Methoxyazulene-1, 3-dicarboxylate (V).—To a suspension of III (1.50 g.), in ether (5 ml.), an ethereal solution of diazomethane (20 ml.) was added, and the mixture was stirred for 3 hr. while being cooled with ice-water. The solvent was evaporated and the oily residue was passed through a short column of amlumina with ether to give V (1.50 g.) as a red oil.

Found: C, 67.08; H, 5.98. Calcd. for $C_{17}H_{18}O_5$: C, 67.54; H, 6.00%.

λ_{max}^{MeOH} mμ (log ε); 235 (4.50), 265 (4.27), 305 (4.66), 345 (3.77), 480 (2.50).

2-Methoxyazulene-1, 3-dicarboxylic Acid (VI).—To a solution of V (600 mg.) in ethanol (8 ml.), a 2 N potassium hydroxide solution (6 ml.) was added, the mixture was then heated under reflux for 4 hr. The reaction mixture was acidified with 6 N hydrochloric acid to give VI (440 mg.) as orange micro crystals, m. p. 205~208°C.

Found: C, 63.50; H, 4.04. Calcd. for $C_{13}H_{10}O_5$: C, 63.41; H, 4.09%.

2-Methoxyazulene (VII).—The heating of VI (400 mg.) at about 200°C to effect decarboxylation, followed by sublimation under reduced pressure, gave a violet sublimate. This was recrystallized from methanol to give VII (80 mg.) as violet plates, m. p. 79~80°C; VII was identified with an authentic specimen[3] by admixture and by a comparison of the infrared spectrum.

Dimethyl 2-Methoxyazulene-1, 3-dicarboxylate (VIII).—*a) From Dimethyl 2-Hydroxyazulene-1,3-dicarboxylate (IV).*—To a suspension of IV (300 mg.) in ether (2 ml.), an ethereal solution of diazomethane (10 ml.) was added; the mixture was then stirred for 3 hr. while being cooled with ice-water. The residual oil obtained by the evaporation of the solvent was passed through a short column of alumina with ether and recrystallized from methanol to give VIII (280 mg.) as red needles, m. p. 69~70°C, reported[3] m. p. 61~62°C.

Found: C, 65.86; H, 4.91. Calcd. for $C_{15}H_{14}O_5$: C, 65.69; H, 5.15%.

λ_{max}^{MeOH} mμ (log ε); 235 (4.45), 267 (4.29), 305 (4.71), 340 (3.83), 410 (2.39), 470 (2.69).

b) From 2-Methoxyazulene-1,3-dicarboxylic Acid (VI).—To a suspension of VI (200 mg.) in ether (2 ml.), an ethereal solution of diazomethane (10 ml.) was added, and the mixture was stirred for 3 hr. while being cooled with ice-water. When the reaction mixture was treated as in a), VIII (150 mg.) was obtained as red needles, m. p. 69~70°C.

Diethyl 2-Ethoxyazulene-1, 3-dicarboxylate (X).—A mixture of V (400 mg.) and a 1 M sodium ethoxide solution (3 ml.) was heated under reflux for 3 hr. The reaction mixture was diluted with water and extracted with chloroform. The solvent was removed, and residue was passed through a short column of alumina with ether to give X (150 mg.) as red plates, m. p. 47~49°C.[4]

Found: C, 69.72; H, 6.51. Calcd. for $C_{18}H_{20}O_5$: C, 68.34; H, 6.37%.

2-Ethoxyazulene (XI).—*a) From Diethyl 2-Ethoxyazulene-1, 3-dicarboxylate (X).*—To a solution of X (200 mg.) in ethanol (4 ml.), a 2 N potassium hydroxide solution (2 ml.) was added, and the mixture was heated under reflux for 4 hr. The reaction mixture was acidified with 6 N hydrochloric acid to give 2-ethoxyazulene-1,3-dicarboxylic acid (150 mg.) as orange micro crystals, m. p. 200~205°C. This acid (130 mg.) was heated to effect decarboxylation and then sublimed at reduced pressure. The sublimate was passed through a short column of alumina with ether and recrystallized from ethanol to give XI (50 mg.) as violet plates, m. p. 76~77°C.[4]

Found: C, 83.61; H, 6.81. Calcd. for $C_{12}H_{12}O$: C, 83.69; H, 7.02%.

λ_{max}^{MeOH} mμ (log ε); 238 (4.08), 276 (4.78), 284 (4.85), 315 (3.77), 340 (3.58), 355 (3.75), 370 (3.69), 395 (2.67), 410 (2.64), 440 (2.44).

b) From Diethyl 2-Methoxyazulene-1,3-dicarboxylate (V).—To a solution of potassium hydroxide (400 ml.) in ethanol (10 ml.), V (600 mg.) was added, and the mixture was heated under reflux for 8 hr. The reaction mixture was diluted with water, neutralized with 6 N hydrochloric acid, and extracted with ether. The ether extract was chromatographed through an alumina column, and the evaporated of the solvent from the effluent left crystals, which were recrystallized from ethanol to give XI (100 mg.) as violet plates, m. p. 76~77°C.

Diethyl 2-(Methylamino)azulene-1, 3-dicarboxylate (XII).—A mixture of V (300 mg.), a 40% aqueous methylamine solution (2 ml.) and ethanol (2 ml.) was heated under reflux for 2 hr. The reaction mixture was diluted with water, neutrallized with 6 N hydrochloric acid, and extracted with chloroform. The solvent was evaporated and the residual oil was passed through a short column of alumina with ether to give XII (210 mg.) as orange plates, m. p. 48~50°C.[4]

Found: C, 68.16; H, 5.97; N, 4.29. Calcd. for $C_{17}H_{19}O_4N$: C, 67.76; H, 6.36; N, 4.65%.

λ_{max}^{MeOH} mμ (log ε); 230 (4.15), 255 (4.30), 280 (4.28), 324 (4.67), 410 (3.87), 460 (3.35).

Picrate.—m. p. 113~114°C, orange micro prisms (from ethanol).

Found: C, 52.32; H, 3.83; N, 10.38. Calcd. for $C_{23}H_{22}O_{11}N_4$: C, 52.07; H, 4.15; N, 10.56%.

Diethyl 2-(Hydrazino)azulene-1, 3-dicarboxylate (XIII).—To a solution of V (600 ml.) in ethanal (2 ml.), 80% hydrazine hydrate (2 ml.) was added, and the mixture was heated at 100°C for 3 min. The crystals thereby formed were collected and recrystallized from ethanol to give XIII (500 mg.) as yellow needles m. p. 108~109°C.[4]

Found: C, 63.67; H, 5.86; N, 9.29. Calcd. for $C_{16}H_{18}O_4N_2$: C, 63.56; H, 6.00; N, 9.27%.

λ_{max}^{MeOH} mμ (log ε); 246 (4.35), 273 (4.41), 316 (4.73), 363 (3.88).

Acetate.—m. p. 129~130°C (reported[3] m. p. 132°C), yellow needles (from methanol).

Found: C, 62.85; H, 5.58; N, 7.90. Calcd. for $C_{18}H_{20}O_5N_2$: C, 62.78; H, 5.85; N, 8.14%.

***N*-(1, 3-Diethoxycarbonylazulen-2-yl)pyridinium *p*-Toluenesulfonate (XIV).**—To a solution of III (600 mg.) in pyridine (3 ml.), *p*-toluenesulfonyl chloride (600 mg.) was added, and the mixture was stirred

for 3 hr. while being cooled with ice-water. The mixture diluted with water and extacted with chloroform. The solvent was evaporated, and the residue was recrystallized from ethanol to give XIV (680 mg.) as red needles, m. p. 184~185°C.

Found: C, 64.46; H, 4.81; N, 2.64. Calcd. for $C_{28}H_{27}O_7NS$: C, 64.48; H, 5.22; N, 2.69%.

λ_{max}^{MeOH} mμ (log ε); 228 (4.57), 269 (4.45), 296 (4.67), 320 (3.90), 356 (4.04), 470 (3.02).

***N*-(1, 3-Diethoxycarbonylazulen-2-yl)pyridinium Picrate.**—To a solution of XIV (50 mg.) in ethanol (2 ml.), a saturated alcoholic picric acid solution (1 ml.) was added to give picrate (60 mg.) as orange micro-prisms, m. p. 212~213°C.

Found: C, 55.75; H, 3.69; N, 9.59. Calcd. for $C_{27}H_{22}O_{11}N_4$: C, 56.05; H, 3.81; N, 9.68%.

Ethyl 2-Hydroxyazulene-1-carboxylate (XV).—A mixture of III (300 mg.) and a 2 N potassium hydroxide solution (2 ml.) in ethanol (8 ml.) was heated under reflux for 3 hr. The reaction mixture was then diluted with water, acidified with 6 N hydrochloric acid, and extracted with ether. The oily material obtained by the evaporation of the solvent was dissolved in benzene and chromatographed through a silica gel column. The evaporation of the solvent from the effluent left crystals, which were recrystallized from ethanol gave XV (150 mg.) as red needles, m. p. 75~76°C.

Found: C, 72.15; H, 5.64. Calcd. for $C_{13}H_{12}O_3$: C, 72.21; H, 5.59%.

λ_{max}^{MeOH} mμ (log ε); 293 (4.72), 304 (4.80), 350 (3.75), 450 (2.56), 490 (2.42).

p-Nitrobenzoate.—m. p. 191~193°C, reddish violet needles (from benzene).

Found: C, 66.06; H, 4.01; N, 3.74. Calcd. for $C_{20}H_{15}O_6N$: C, 65.75; H, 4.14; N, 3.83%.

Ethyl 2-Methoxyazulene-1-carboxylate (XVI).—To a suspension of XV (50 mg.) in ether, an ethereal solution of diazomethane (1 ml.) was added, and the mixture was stirred for 3 hr. while being cooled with ice-water. The solvent was evaporated, and the residue was passed through a short column of alumina with benzene to give XVI (50 mg.) as red needles, m. p. 64~65°C.

Found: C, 72.97; H, 5.66. Calcd. for $C_{14}H_{14}O_3$: C, 73.02; H, 6.13%.

A part of the expenses for the present series of experiments were defrayed by a grant-in-aid for Scientific Research from the Sankyo Co., Ltd., and from the Upjohn Co., Ltd. The infrared spectra were measured by using a Shimadzu infrared spectrophotometer IR-27 purchased by a grant-in-aid for Scientific Research from the Toyo Rayon Co., Ltd. The authors wish to express their deep gratitude for these contributions.

Department of Chemistry
Faculty of Science
Tohoku University
Katahira-cho, Sendai

*The Mechanism of the Formation of Terephthalic Acid from Benzonitrile**

By Yoshiro OGATA, Yoshiaki FURUYA, Tadashi NOSHIRO and Tadahiro Go

(Received May 13, 1964)

It has been claimed by Henkel and Cie[1] that terephthalic acid can be obtained by the reaction of benzonitrile and potassium carbonate in either the presence or absence of a cadmium catalyst.

Although the reaction seems to proceed by way of benzoic acid, it is curious that the reaction proceeds even in the absence of a catalyst, since it has been known that benzoic acid cannot give an appreciable amount of terephthalic acid under the same conditions.

Moreover, the stoichiometry of the reaction and the cleaving bond in C_6H_5–C≡N are still not clear. The present paper will describe the results of our mechanistic study by means of a tracer study with radioactive carbonate and also the results of a study of reaction products together with the effect of conditions on the composition of the products.

Experimental

Typical Procedure for the Preparation of Terephthalic Acid from Benzonitrile. — An intimate mixture of benzonitrile (1.0 g., 0.01 mol.), finely powdered dry potassium carbonate (2.76 g., 0.02 mol.) and cadmium iodide (0.50 g., 0.00137 mol.) was placed in a sealed tube. The tube was enveloped with glass wool and placed in an autoclave together with toluene (ca. 30 ml.) in ordor to balance the internal pressure of the tube. The reaction was carried out at 360~500°C for 2.5~7 hr. The product was extracted with petroleum

* Contribution No. 56.

1) a) Henkel and Cie, DAS 1027656 (1958); Brit. Pat. 808894 (1959). b) Henkel and Cie, DAS 1051841 (1959); U. S. Pat. 2913488 (1959). c) Henkel and Cie, DAS 1053491 (1959); U. S. Pat. 2866815 (1958).

TABLE I. YIELDS OF TEREPHTHALIC ACID FROM BENZONITRILE, POTASSIUM BENZOATE OR BENZAMIDE
Reaction time, 2.5 hr. except a)

Reactant				Reaction temp.	Product Yield of terephthalic acid	
C_6H_5CN g.	K_2CO_3 g.	CdI_2 g.	KOCN g.	°C	mg.	%
1.0	2.76	0.50	—	490	267.0	33.1
1.0	2.76	0.50	—	490[a)]	265.6	33.0
1.0	2.76	0.50	0.81	490	173.6	21.5
1.0	1.38	—	0.81	460	63.8	8.0
$C_6H_5CO_2K$ g.						
1.6	2.76	0.50	—	490	276.4	34.3
1.6	1.38	—	0.81	490	63.5	7.9
1.6	—	—	0.81	470	83.5	10.4
$C_6H_5CONH_2$ g.						
1.21	2.76	0.50	—	490	69.6	8.6
1.21	2.76	0.50	—	490[a)]	85.8	10.7

a) Reaction time, 7.0 hr.

ether (20 ml.), and the extract was analyzed to determine the benzonitrile and benzoic acid contents. The benzonitrile was identified by ultraviolet spectrography and by hydrolysis to benzoic acid; m. p. and mixture m. p. 122.5°C. Benzene was identified by ultraviolet spectrography and by nitration to *m*-dinitrobenzene; m. p. and mixture m. p. 88°C. The residual solid of the extraction was dissolved in hot water (100 ml.), filtered, acidified with hydrochloric acid, and again filtered while hot. The precipitate after drying gave terephthalic acid, which on esterification gave dimethyl terephthalate, m. p. and mixture m. p. 140°C. The filtrate was extracted with ether, the extract after the evaporation of the ether being washed with chloroform to extract benzoic acid alone, separating it from the residual isophthalic and terephthalic acids. The results are shown in Table I, together with the results of terephthalic acid formation from benzoic acid and benzamide.

The Estimation of Isophthalic and Terephthalic Acids in the Products.—Ultraviolet spectrophotometry was used. The reaction mixture was dissolved in hot water (100 ml.). The filtered solution was acidified and filtered after cooling. The precipitate after drying was analyzed for isophthalic and terephthalic acids contents by means of ultraviolet spectrophotometry by measuring the extinction at the wavelength of 284.7 mμ (for terephthalic acid) or of 280.5 mμ and 288.4 mμ (for isophthalic acid).[2] These data, shown in Table III, are of special interest in connection with the effect of potassium cyanate on the ratio of isophthalic acid to terephthalic acid in the product.

The Formation of Benzonitrile from Benzoic Acid and Potassium Cyanate. — A mixture of potassium benzoate (1.6 g., 0.01 mol.) and potassium cyanate (0.81 g., 0.01 mol.) was heated in a sealed tube at 470°C for 2.5 hr. Terephthalic acid (83.5 mg.) was obtained. The other products were analyzed by gas chromatography employing a Yanagimoto Model GCG-220 operated with a 1.3 m. column packed with Silicone D. C. 703 using helium with a flow rate of 28.4 ml./min. at 80°C for benzene (367 mg.) and of 31.25 ml./min. at 150°C for benzonitrile (13.8 mg., 1.4%). The retention times were 3.66 min. for benzene and 7.4 min. for benzonitrile. Quantitative determinations were made using the corresponding authentic sample as an internal standard.

The Formation of Terephthalic Acid from Benzamide.—A mixture of benzamide (1.21 g., 0.01 mol.), cadmium iodide and potassium carbonate was heated under the same conditions as above and worked up similarly. The results are shown in Table I.

Tracer Experiments.—Labeled carbon dioxide-^{14}C was evolved by hydrochloric acid from labeled barium carbonate obtained from the Isotope Center of Japan and absorbed in an aqueous solution of a calculated amount of potassium hydroxide. The solution was then evaporated to dryness in a vacuum, yielding labeled potassium carbonate. The method for the isolation of the product was the same as that given as a typical procedure above. The radioactivities of samples were expressed as those of the corresponding barium carbonates. All the data in Table II are averages of duplicate experiments; they have been calibrated for their background against standard barium carbonate.

Results and Discussion

The product from the cadmium salt-catalyzed reaction of benzonitrile with potassium carbonate was found to contain benzoic, isophthalic and terephthalic acids, together with benzene and potassium cyanate. Potassium was identified by converting it with aniline hydrochloride to phenylurea; m. p. and mixture m. p. 147°C.

2) N. Berman, C. H. Ruof and H. C. Howard, *Anal. Chem.*, 23, 1882 (1951).

It was confirmed by gas chromatography that potassium cyanate and benzoic acid can form a small quantity of benzonitrile. Therefore, the stoichiometric equation may be:

$$C_6H_5CN + K_2CO_3 \rightleftharpoons C_6H_5COOK + KOCN$$

$$2\,C_6H_5COOK \rightarrow p\text{- and } m\text{-}KOOC\text{-}C_6H_4\text{-}COOK + C_6H_6$$

Here, the first step is reversible, and the second step is a disproportionation of the benzoic acid formed which has been confirmed by a tracer study previously reported.[3]

However, it is still strange that the conversion of bonzonitrile to potassium terephthalate is possible without a cadmium catalyst. It is probable that the potassium cyanate formed behaves as a catalyst for the terephthalate synthesis, since it was observed that the added potassium cyanate possessed a slight catalytic ability to convert potassium benzoate to terephthalate (Table I).

It is apparent that potassium cyanate has the effect of increasing the ratio of isophthalic to terephthalic acid in the product (Table III). The meta : para ratio becomes exceptionally small in the presence of a cadmium catalyst (Table III).

The tracer experiments with cadmium iodide and $K_2{}^{14}CO_3$ indicated that only 1/10.72 of the original activity was incorporated in the terephthalate produced from normal benzonitrile. The extent of the incorporation was very close to the value (1/10.63) obtained in conversion of potassium benzoate to terephthalate with $K_2{}^{14}CO_3$ and CdI_2 in a sealed tube under the same conditions. Since radioactivities were

Table II. Tracer experiments for the conversion of benzonitrile or potassium benzoate to benzoic acid and/or terephthalic acid

Reaction time, 2.5 hr.

Reactant[a]	(g.)	Temp. °C	Product counted	Radioactivity c.p.m.
C_6H_5CN	(0.5)[b]	490	Benzoic acid	24
$C_6H_5CO_2K$	(0.8)[b]	490		5
C_6H_5CN	(0.5)	360		4
C_6H_5CN	(0.5)	425		3
$C_6H_5CO_2K$	(0.8)	425		3
$C_6H_5CO_2K$	(0.8)	490		100
C_6H_5CN	(0.5)	490		211
$C_6H_5CO_2K$	(0.8)	490	Terephthalic acid	244
$C_6H_5CO_2K$	(0.8)	490		246

a) 1.38 g. of $K_2{}^{14}CO_3$ (2616 c.p.m. as $Ba^{14}CO_3$) and 0.25 g. of CdI_2 were added to the reactants.
b) Without cadmium iodide.

Table III. The effect of potassium cyanate on the ratio of isophthalic acid to terephthalic acid

Reaction time, 2.5 hr.
Starting material $C_6H_5CO_2K$ 1.60 g.

KOCN g.	m-C_6H_4-$(CO_2K)_2$ mg.	p-C_6H_4-$(CO_2K)_2$ mg.	m/p ratio	Temp. °C
0.41	166	134	1.24	475
0.81	212	123	1.72	475
1.62	217	119	1.82	475
4.05[a]	48	183	0.26	480

a) 0.30 g. of CdI_2 was added.

detected in the recovered benzoate in the cadmium-catalyzed conversion of benzonitrile or potassium benzoate to potassium terephthalate, the labeled carbon is introduced by the exchange of the carboxylate group in the benzoate.

In spite of the description of the pertinent Patent,[1] the yield of potassium terephthalate from benzamide at 490°C in a sealed tube under the same conditions was low; this implies that the reaction of benzonitrile to the terephtalate may not proceed via benzamide. The formation of terephthalic acid from benzamide, claimed in the patent,[1] may be the result of the formation of benzonitrile from benzamide by dehydration.

These facts suggest that the reaction of benzonitrile with potassium carbonate to form terephthalate is a conversion to potassium benzoate, followed by disproportionation. Here, the carboxylate group of benzoate may be exchanged with carbonate in the presence of a cadmium catalyst:

$$C_6H_5COOK \underset{(Cd^{2+})}{\overset{{}^{14}CO_3{}^{2-}}{\rightleftharpoons}} C_6H_5{}^{14}COOK$$

There seems to be no chance for the introduction of a carboxyl group from outside carbonate or carbon dioxide except at the exchange in benzoate. The extent of the exchange of carboxylate groups increases with an increase in the reaction temperature, and the exchange is catalyzed by cadmium salts. It is of interest to note that the exchange is impossible without a cadmium catalyst and that this situation is different from that of phthalate, where the exchange is possible without cadmium salt.[3a]

Summary

A mixture of benzonitrile, cadmium iodide and potassium carbonate has given, when heated in a sealed tube at 360~500°C, terephthalic acid (21~33%), together with a considerable amount of isophthalic acid. The

3) a) Y. Ogata, M. Tsuchida and A. Muramoto, *J. Am. Chem. Soc.*, **79**, 6005 (1957); b) Y. Ogata. *Chem. & Chem. Ind. (Japan)*, **11**, 148 (1958); c) Y. Ogata, M. Hojo and M. Morikawa, *J. Org. Chem.*, **25**, 2082 (1960).

reaction was possible without a cadmium catalyst, but the yield of terephthalic acid was poorer (8.0%). The tracer study with $K_2{}^{14}CO_3$, as well as the identification of cyanate in the products, showed that the reaction proceeds by way of the conversion of benzonitrile to potassium benzoate and potassium cyanate, followed by the disproportionation of potassium benzoate to potassium terephthalate and isophthalate. Potassium cyanate seems to be a weak catalyst for the disproportionation.

Department of Applied Chemistry
Faculty of Engineering
Nagoya University
Chikusa-ku, Nagoya

Electron Spin Resonance of the Acenaphthylene Anion Radical

By Masamoto IWAIZUMI and Taro ISOBE

(Received May 16, 1964)

The electron spin resonance spectra of the anion radicals of an aromatic system provide much interesting information about these molecules. In particular, the approximate proportionality between the proton hyperfine constant and the π-electron spin density has yielded valuable information about the distribution of the unpaired electron, enabling one to test theoretical predictions.[1-11] However, some radicals produced by alkali metal reduction have been shown to exhibit some anomalous hyperfine structures, which can be attributed to the interaction of the radicals with the metal ions.[12-14]

The present investigation was undertaken to obtain more refined hyperfine coupling constants of the acenaphthylene anion radical than those previously reported and to examine the effects of the presence of metal ions on the hyperfine structure of this radical.

Experimental

To prepare the anion radical, both alkali metal reduction and electrolytic reduction methods were applied. In the former, the entire series of alkali metals, i.e., lithium, sodium, potassium, rubidium and cesium were used as reducing agents, with dioxane, tetrahydrofuran (THF), dimethoxyethane (DME), and dimethylformamide (DMF) as the respective solvents. In the latter, DMF, acetonitrile and a mixture of DMF and dioxane were used as solvents, tetra-*n*-propylammonium perchlorate as the supporting electrolyte, and the reduction was carried out in the electrolysis cell with a platinum anode and a mercury pool cathode, which was so designed that the electrolysis was possible within the microwave cavity. The ESR spectra were measured with a Hitachi X-band ESR spectrometer, model MPU-3B, employing field modulation at 100 kc./s. The preparation of the radicals and the measurement of the ESR spectra were carried out at room temperature (22.0~24.0°C).

Results and Discussion

The ESR Spectra and the Effect of Metal Ion Association on the Hyperfine Structures.— Figure 1 shows the ESR spectrum of the radical prepared with sodium in THF, together with the reconstruction based on the hyperfine coupling constants listed in Table I. As may be seen from this figure, the spectrum may be completely interpreted as arising from the coupling with four sets of two equivalent protons of the acenaphthylene anion radical. In the cases of the radicals other than those derived from the reduction with rubidium or cesium in DME, THF or dioxane, with lithium sodium or potassium in dioxane, and with potassium in THF respectively, the spectra show hyperfine splittings, similar to, though not strictly identical with, that given in Fig. 1. Figure 2, for example, shows the spectrum obtained from the radical prepared with sodium in DME: it should be compared with the spectrum given in Fig. 1.

1) E. de Boer and S. I. Weissman, *J. Am. Chem. Soc.*, **80**, 4549 (1958).
2) G. J. Hoijtink, *Mol. Phys.*, **1**, 159 (1958).
3) A. D. McLachlan, ibid., **3**, 233 (1960).
4) I. Bernal, P. H. Rieger and G. K. Fraenkel, *J. Chem. Phys.*, **37**, 1489 (1962).
5) P. H. Rieger and G. K. Fraenkel, ibid., **37**, 2795 (1962).
6) P. H. Rieger and G. K. Fraenkel, ibid., **37**, 2811 (1962).
7) A. Carrington and J. dos Santos-Veiga, *Mol. Phys.*, **5**, 21 (1962).
8) J. R. Bolton, A. Carrington and J. dos Santos-Veiga, ibid., **5**, 465 (1962).
9) A. Carrington and P. F. Todd, ibid., **6**, 161 (1963).
10) P. H. Rieger and G. K. Fraenkel, *J. Chem. Phys.*, **39**, 609 (1963).
11) K. Ishizu, This Bulletin, **36**, 938 (1963).
12) R. L. Ward, *J. Chem. Phys.*, **32**, 410 (1960).
13) R. L. Ward, *J. Am. Chem. Soc.*, **83**, 1296 (1961).
14) N. M. Atherton and S. I. Weissman, ibid., **83**, 1330 (1961).

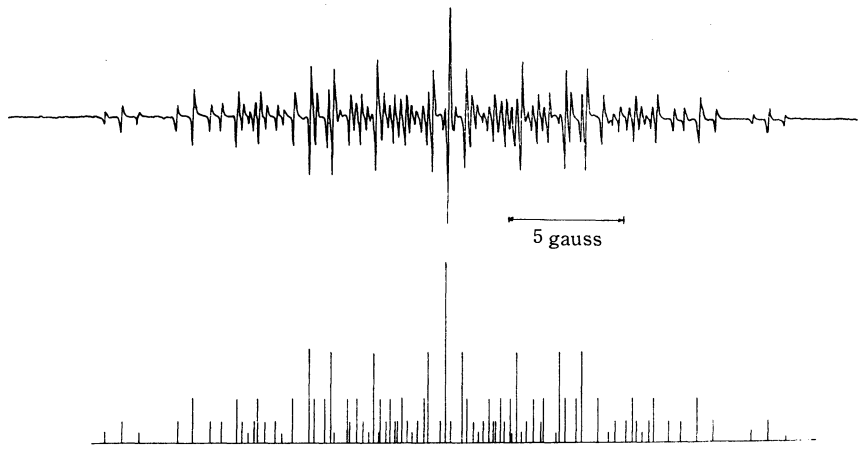


Fig. 1. The ESR spectrum of acenaphthylene anion radical prepared by the reduction with sodium in THF and the reconstruction based on the assumed coupling constants.

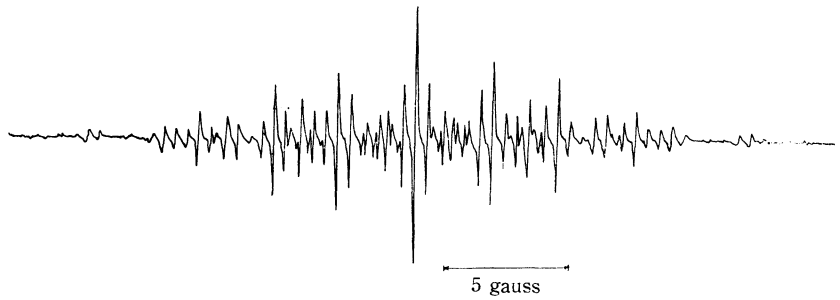


Fig. 2. The ESR spectrum of acenaphthylene anion radical prepared by the reduction with sodium in DME.

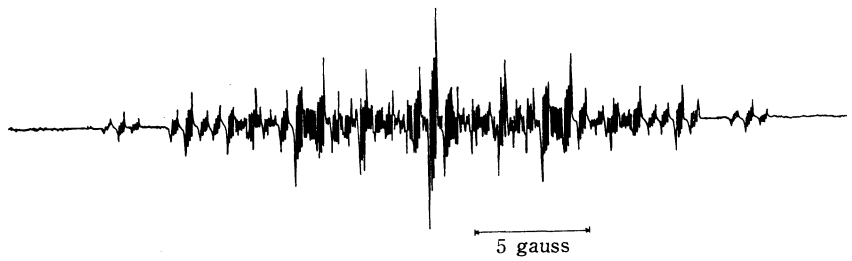


Fig. 3. The ESR spectrum of acenaphthylene anion radical prepared by the reduction with potassium in dioxane.

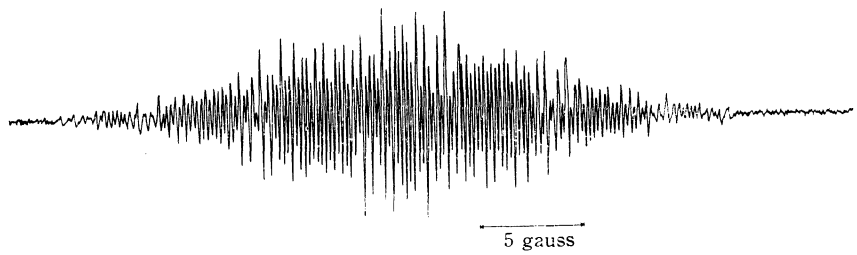


Fig. 4. The ESR spectrum of acenaphthylene anion radical prepared by the reduction with rubidium in dioxane.

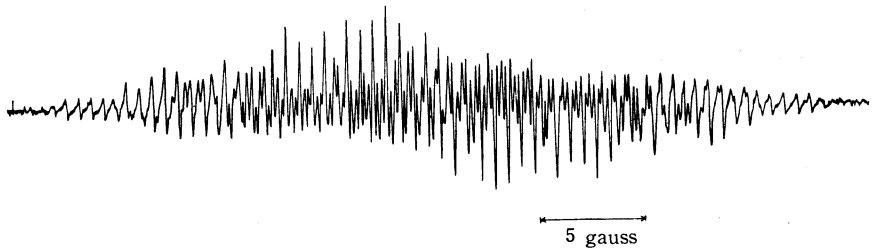


Fig. 5. The ESR spectrum of acenaphthylene anion radical prepared by the reduction with cesium in dioxane.

TABLE I. EXPERIMENTAL HYPERFINE COUPLING CONSTANTS (in gauss)

a) Li-acenaphthylene anion radical

Position	DMF	DME	THF	Dioxane
1, 2	3.06	3.10	3.20	3.19
3, 8	4.51	4.58	4.75	5.23
4, 7	0.46	0.48	0.62	0.94
5, 6	5.60	5.72	5.80	6.01
Metal	—	—	—	0.14

b) Na-acenaphthylene anion radical

Position	DMF	DME	THF	Dioxane
1, 2	3.06	3.09	3.09	3.10
3, 8	4.51	4.63	4.95	5.17
4, 7	0.46	0.55	0.71	0.79
5, 6	5.60	5.71	5.87	6.03
Metal	—	—	—	0.06

c) K-acenaphthylene anion radical

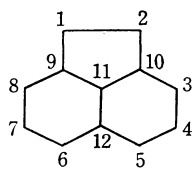
Position	DMF	DME	THF	Dioxane
1, 2	3.06	3.06	3.08	3.03
3, 8	4.51	4.75	4.87	4.94
4, 7	0.46	0.59	0·62	0.65
5, 6	5.60	5.78	5.89	5.90
Metal	—	—	0.07	0.09

d) Cs-acenaphthylene anion radical

Position	DMF	DME	THF	Dioxane
1, 2	3.06	2.99	2.93	2.93
3, 8	4.51	4.73	4.69	4.77
4, 7	0.46	0.58	0.59	0.61
5, 6	5.60	5.79	5.87	5.76
Metal	—	1.07	1.17	1.22

e) Electrolytic reduction

Position	In DMF, acetonitrile and a 1 : 1 mixture of DMF and dioxane
1, 2	3.06
3, 8	4.51
4, 7	0.46
5, 6	5.60



In contrast, the spectra from the radicals prepared with rubidium or cesium in DME, THF or dioxane, with lithium, sodium or potassium in dioxane and with potassium in THF show more complicated hyperfine structures than those expected from the couplings with only the protons of the acenaphthylene anion radical. For examples, Figs. 3—5 show the spectra from the radicals prepared in dioxane with potassium, rubidium and cesium respectively. In the cases of the reduction with lithium, sodium or potassium in dioxane, and with potassium in THF, each line of the normal hyperfine pattern of the acenaphthylene radical is further split into four lines with equal intensities, while in the cases with cesium in DME, THF or dioxane, each line is further split into eight lines with equal intensities. These additional splittings can be explained by the interaction of the odd electron with each metal nucleus, viz., lithium, sodium or potassium of spin 3/2, and cesium of spin 7/2 respectively. In the cases of reduction with rubidium, too, we believe that the anomalous feature in the hyperfine structures is due to the interaction of the odd electron with two kinds of rubidium nuclei of spin 5/2 and 3/2, although the analysis of the spectra has not yet been completed.

The hyperfine coupling constants of the protons and the metal nuclei obtained from these spectra are listed in Table I. The assignment of the splittings to the respective proton positions was made on the basis of theoretical calculations for the odd-electron distribution. In a previous work,[1] the lack of resolution made it impossible to obtain a proton coupling at position 4 or to show a difference between positions 3 and 5.

All the spectra observed from the chemically- and electrolytically-produced radicals in the DMF solution agree with each other quite well and yield essentially the same coupling constants. However, in the other solvents, there is some small change in the proton hyperfine splittings as one goes from one metal to another. In the cases of electrolytically-produced radicals,

no appreciable variation of hyperfine structures with the solvents was observed. It may be considered, therefore, that the variation of the hyperfine splittings with the solvents or with alkali metals is caused by the association between the anion radical and metal ions.

As may be seen from Table I, the magnitude of the coupling of the cesium nucleus increases in the series of DMF-DME-THF-dioxane. In dioxane, which is nonpolar in nature, the splittings of all the alkali metals were observed. On the contrary, in the DMF solution no splittings due to any metal nuclei were observed. It may be concluded, therefore, that the association between the anion radical and metal ions increases in the series of DMF-DME-THF-dioxane solutions, and that the difference in the proton hyperfine coupling constants from those in the DMF solution is due to metal ion association.

In the dioxane solutions, the difference in proton hyperfine splittings from those in the DMF solutions is largest for the lithium-acenaphthylene anion radical; in going to the cesium-acenaphthylene anion radical it decreases. In view of studies by Mathius and others[15-17] on the optical absorption and reactivities of some radicals, it seems reasonable to consider that the lithium ion affects most strongly the proton hyperfine couplings of the anion radicals and that as the cationic radius increases the effect decreases. However, in the DME solutions, the difference in the proton hyperfine splitting from those in a DMF solutions is largest for the cesium-acenaphthylene radical and smallest for the lithium-acenaphthylene radical. We are not able to offer any explanation of this. However, leaving aside this question, it can be seen from Table I that the hyperfine coupling constants of the protons belonging to the six-membered ring increase by metal ion association, especially at position 3. However, the splitting constant at position 1 is not so affected; rather, it decreases in the case of the cesium-acenaphthylene anion radical.

Since the isotropic proton hyperfine splitting in the π-electron radicals has been shown to be linearly related to the π-lectron spin density,[18] the variation in the proton coupling constants observed here may be attributed to the redistribution of the π-electron spin densities caused by the cationic field of metal ions. According to the spin distribution predicted by McLachlan's method, the increase in the coupling constants at positions 2, 3 and 5 corresponds to the increase in the positive spin densities, and that at position 4, to the increase in the negative spin density.

The change in hyperfine coupling constants caused by metal ion association can be observed in some other aromatic anion radicals, but the magnitudes are not as large as those observed here. Furthermore, it is of interest to note that in the acenaphtylene anion radical the hyperfine coupling of the sodium nucleus is smaller than that of the lithium or potassium nucleus. In many cases reported previously larger couplings have been observed for the sodium nucleus than for the lithium or potassium nuclei.[7,14,19-22] Further work is in progress on the effect of metal ion association on the hyperfine coupling constants of the other aromatic anion radicals; a detailed discussion will be reported at a later date.

Calculated Hyperfine Coupling Constants and Spin Densities.—Table II shows the spin densities and hyperfine coupling constants calculated on the basis of the Hückel and McLachlan[3] methods. When these values are compared with the experimental values obtained in the DMF solution, the agreement seems rather good in spite of the neglect of the variation in the σ-π interaction parameter Q in McConnell's equation with bond angles. However, the total width of the spectrum is much larger than the usual values of 23~27 gauss. It may be considered, therefore, that negative spin densities possibly exist in the acenaphthylene anion radical, as may be expected from the calculations based on the McLachlan method.

TABLE II. CALCULATED HYPERFINE COUPLING CONSTANTS AND SPIN DENSITIES

Position	Hückel method*1		McLachlan method*2	
	Hyperfine constant gauss	Spin densitity	Hyperfine constant gauss	Spin density
1,2	3.28	0.104	2.90	0.101
2,8	4.76	0.151	4.74	0.196
4,7	0.04	0.014	0.99	−0.041
5,6	5.61	0.178	5.92	0.245
9,10	—	0.053	—	0.027
11	—	0	—	−0.012
12	—	0	—	−0.045

*1 Proportionality constant Q in McConnell's equation is assumed to be −31.5 gauss.
*2 Based on McLachlan's procedure.[3]

15) A. Mathias and E. Warhurst, *Trans. Faraday Soc.*, **58**, 948 (1962).
16) D. G. Powell and E. Warhurst, ibid., **58**, 953 (1962).
17) N. S. Hush and J. R. Rowlands, *Mol. Phys.*, **6**, 201 (1963).
18) H. M. McConnell, *J. Chem. Phys.*, **24**, 632 (1956).
19) F. C. Adam and S. I. Weissman, *J. Am. Chem. Soc.*, **80**, 1518 (1958).
20) R. L. Ward and M. P. Klein, *J. Chem. Phys.*, **28**, 518 (1958).
21) P. B. Ayscough and R. Wilson, *J. Chem. Soc.*, **1963**, 5412.
22) K. Nakamura and Y. Deguchi, This Bulletin, **36**, 359 (1963).

This work was partially supported by a grant-in-aid for fundamental scientific research from the Ministry of Education, to which the authors' thanks are due.

Chemical Research Institute of Non-aqueous Solutions
Tohoku University
Katahira-cho, Sendai

Studies of Chemical Kinetics by Means of the Velocity of Sound. I. The Hydrolysis of Acetic Esters

By Tatsuya YASUNAGA, Nobuhide TATSUMOTO and Masaji MIURA

(Received May 22, 1964)

The velocity of sound is a function of the density and compressibility of fluids, and it is an important quantity in studying their physical properties. On the other hand, a chemical reaction in a solution causes a change in its compressibility because of the appearance and disappearance of molecular and ionic species. Therefore, the rate of chemical reactions can be determined by sound velocity measurements.

The ultrasonic velocity is one of a few physical quantities which can be determined with a very high degree of accuracy. One of the present authors[1] has determined the amount of ionic hydration and the critical micelle concentration of surfactants by means of a variable-path ultrasonic interferometer, the most accurate apparatus hitherto known for measuring the ultrasonic velocity. One disadvantage of this apparatus is, however, that it takes about one hour for one run of experiments in the velocity measurement. It is difficult, therefore, to trace thereby a rapid change in the sound velocity.

The sing-around method is a newly-develped technique in which the velocity is determined by the frequency measurement. Since the frequency can be determined quickly and precisely by means of the frequency counter, this method has the advantage over that of the interferometer when the velocity of sound varies with time.

In the present study, such chemical changes of a moderate rate as the hydrolysis of esters will be traced by means of the sing-around method.

1) T. Yasunaga, *J. Chem. Soc. Japan, Pure Chem. Sec. (Nippon Kagaku Zassi)*, **72**, 87 (1951); T. Yasunaga and T. Sasaki, ibid., **72**, 89 (1951); T. Sasaki, T. Yasunaga and H. Fujiwara, ibid., **73**, 181 (1952).

2) F. Shepard, Jr., U. S. Pat. 2333688 (1943); W. E. Knock, U. S. Pat. 2400309 (1946).

3) M. Greenspan and C. E. Tschiegg, *J. Research Natl. Bur. Standards*, **59**, 249 (1957); *Rev. Sci. Instr.*, **28**, 897 (1957).

Apparatus

The sing-around method, originally invented by Shepard and Knock,[2] has been developed recently by Greenspan and Tschieff.[3] The apparatus used in the present study was similar to that reported by the latter workers.

A schematic diagram of the circuit is given in Fig. 1. The principle of the operation of the circuit is as follows: The apparatus consists essentially of a pair of piezoelectric transducers, made of quartz crystals, mounted on both ends of a tube to form a sound path of a fixed length. An unmodulated pulse for starting the operation is generated by a pulse generator and fed to a sending transducer. The pulse received by a receiving transducer is then led to a high-gain pulse-shaping amplifier, and the amplified pulse retriggers the same pulse generator to emit the second pulse. By the repetition of this process, a train of repeated pulses is generated. When the path length is fixed, the frequency of the repeated pulses depends on the propagation velocity of the sound in the sample liquid and also on the circuit delays. The total time delay for a single cycle, τ, is given as:

$$\tau = 1/f = t_e + l/u \qquad (1)$$

where f is the frequency of the pulse repetition; t_e, the sum of electrical delays: u, the velocity of sound, and l, the path length.

The frequency was measured with a frequency counter. The time intervals of the gate for the frequency measurement were made as follows. First 5 Mc. continuous wave was generated by a temperature-controlled crystal oscillator, and then the frequency was lowered to 1 kc. by a multiplier circuit. The frequency of the 5 Mc. oscillator was monitored by the standard frequency of JJY. After it had been modified to the square wave, the 1 kc. wave

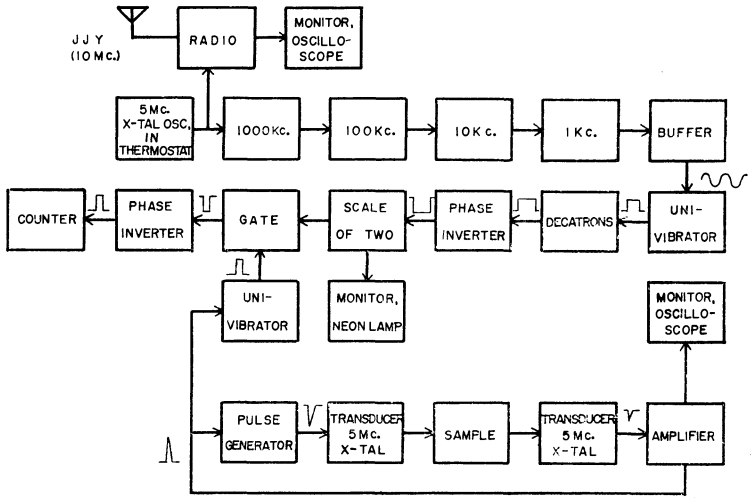


Fig. 1. Block diagram of sing-around velocimeter.

was fed to the decatron circuit to generate the 10 sec. intervals for the gate opening.

The repetition frequency was counted by the counter with six decatrons. The initiating pulse was generated by a blocking oscillator, using a pulse transformer with a ferrite core. The rise time of the pulse was less than 50 mμ sec., while the pulse width was about 200 mμ sec.

The cell shown in Fig. 2 was made of a pyrex tube, 16 mm. and 100 mm. in diameter and length respectively. The transducers, which had the 5 Mc. resonance frequency, were gold-plated x-cut crystals 20 mm. in diameter and 0.8 mm. thick. The grounding was made by thrusting the peripheries of the inner surfaces of transducers against brass rings on the ends of the glass tube. An epoxy resin was used to attach the transducers to the tube and also to protect the rings from the chemical attack.

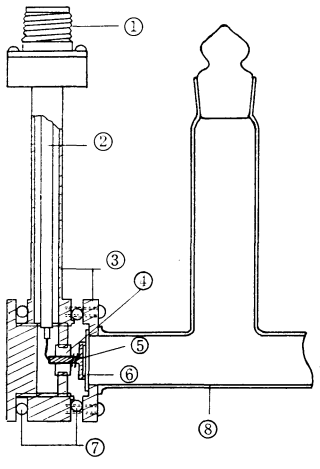


Fig. 2. Sectional diagram of one end of the cell, (1) connector, (2) coaxial cable, (3) brass, (4) polystyrene, (5) spring, (6) 5 Mc. quartz crystal, (7) neoprene O-ring, (8) pyrex tube.

The stability of the apparatus was examined by using water at 30±0.002°C for about thirty hours. The results given in Table I show that the sing-around velocimeter works steadily for a prolonged period with a high degree of accuracy. Since it requires only ten seconds to measure the sound velocity each time, slight and rapid changes in velocity in the solutions with respect to the reaction time can be traced continuously with a high degree of accuracy.

Table I. Change in the repetition frequency in water with time at 30±0.002°C

Time, hr.	2	3	5	7	24	27	31
f, cycl./sec.	15766.5	15766.4	15766.6	15766.6	15766.6	15766.4	15766.6

Experimental

Both methyl and ethyl acetates were used in this study. In one flask, an aqueous solution of a reactant was prepared and in the other a hydrochloric acid solution was placed, separately. After thermal equilibrium was reached, the two solutions were mixed together in one of the flasks, and then the counting of the reaction time was started. Then the mixture was transferred into a measuring cell immersed in advance in the same thermostat, and the change in the repetition frequency with the reaction time was traced by the frequency counter. The concentration of acetic acid in the

equilibrium mixture was determined by titration with dilute sodium hydroxide.

Chemically pure grade reagents were used without further purification.

Results and Discussion

In Figs. 3a and 3b, the pulse repetition frequencies during the reaction period are plotted against the reaction time. As may be seen from the figures, the frequency increases with time for ethyl acetate, while it decreases with time for methyl acetate.

These reactions can be expressed as follows:

$$CH_3COOR + H_2O \underset{k_2}{\overset{k_1}{\rightleftharpoons}} CH_3COOH + ROH \qquad (2)$$

and they are obviously bimolecular and reversible, although they can be treated as monomolecular in a dilute aqueous solution. The differential equation follows:

$$dx/dt = k_1(b-x)(w-x) - k_2x^2 \qquad (3)$$

where b is the initial concentration of an ester; x, the decrease in concentration after time t; w, the concentration of water, and k_1 and k_2, the velocity constants of hydrolysis and esterification respectively. Writing $k_2/k_1 = K$, the equilibrium constant, where:

$$K = (b-x)(w-x)/x^2 \qquad (4)$$

we can integrate Eq. 3 as:

$$\ln[\{A+(w+b)+2(K-1)x\}/\{A-(w+b)-2(K-1)x\}] = Ak_1t + \ln[\{A+(w+b)\}/\{A-(w+b)\}] \qquad (5)$$

where

$$A = \sqrt{(w+b)^2+4(K-1)wb}$$

If it is assumed that the change in the sound velocity is proportional to that in the concentration, the following expression results for ethyl acetate:

$$X \propto (u-u_0) \qquad (6)$$

where u_0 is the sound velocity at $t=0$. From Eq. 1, the difference in the sound velocities may be given as:

$$u-u_0 = l(f-f_0)/\{1-t_e(f+f_0)+ff_0t_e^2\} \qquad (7)$$

where f_0 is the repetition frequency at $t=0$. For the present apparatus, t_e, f and l are 4×10^{-8} sec^{-1}, 1.5×10^4 cycl./sec. and 10 cm. respectively, and the terms $t_e(f+f_0)$ and $ff_0t_e^2$ in Eq. 7 are both negligible in comparison with unity. The term $(u-u_0)$ is, therefore, proportional to $(f-f_0)$. Thus,

$$x = \alpha(f-f_0) \qquad (8)$$

where α is a constant. Consequently, Eq. 5 reduces to:

$$\ln[\{A+(w+b)+2\alpha(K-1)(f-f_0)\}/\{A-(w+b)-2\alpha(K-1)(f-f_0)\}] = Ak_1t + \ln[\{A+(w+b)\}/\{A-(w+b)\}] \qquad (9)$$

The left hand side of Eq. 9 is plotted against the reaction time in Fig. 4, and the value of

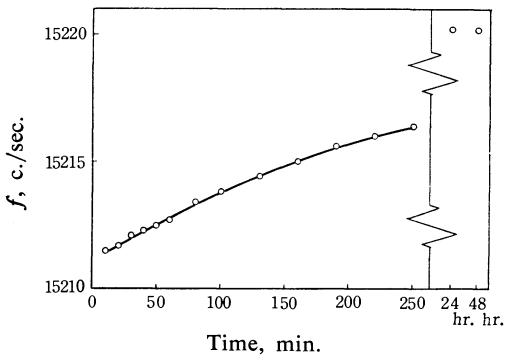


Fig. 3a. Change in velocity of sound with reaction time for ethyl acetate (25°C).

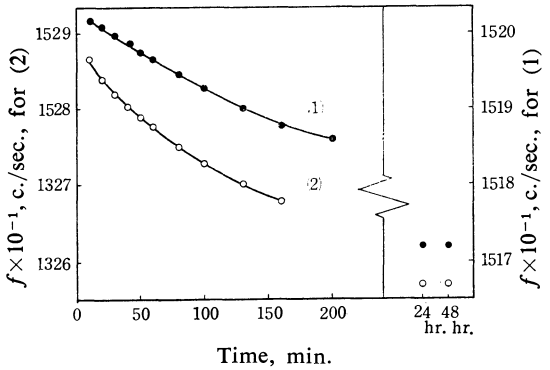


Fig. 3b. Change in velocity of sound with reaction time for methyl acetate, (1) 25°C, (2) 30°C.

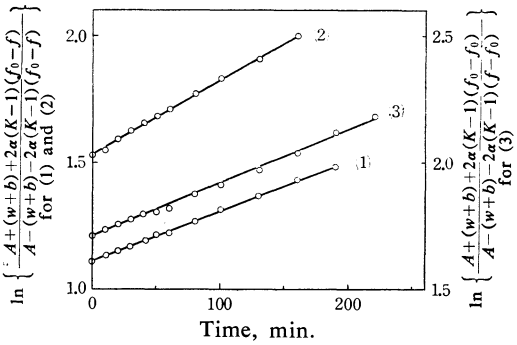


Fig. 4. The diagram of the hydrolysis of esters, (1) methyl acetate (25°C), (2) methyl acetate (30°C), (3) ethyl acetate (25°C).

f_0 is estimated by extrapolating f to $t=0$ in Figs. 3a and 3b. For methyl acetate the following equation holds instead of Eq. 8:

$$x=\alpha(f_0-f) \tag{10}$$

The value of α can be obtained from Eq. 11:

$$x_\infty=\alpha(f_\infty-f_0) \text{ or } x_\infty=\alpha(f_0-f_\infty) \tag{11}$$

where x_∞ and f_∞ are the concentration of products and the repetition frequency in the equilibrium state respectively. The measured points fall on a straight line for each one of the hydrolysis reactions studied in the present paper, as is shown in Fig. 4. The values of k_1 and k_2 obtained from the data given in Fig. 4 are listed in Table II, where those values reported by others are also included. As may be seen in the table, the values of the rate constant obtained in this study are in good agreement with those determined by other methods. The present results confirm that the sound velocity measurement by the sing-around method is applicable to the study of the chemical kinetics of such simple reactions as the hydrolysis of acetic esters. Further, it may also be expected that the present method can be extended to the study of faster reactions.

TABLE II. THE RATE CONSTANTS

Temp. °C	Initial concn. M	Concn. of HCl N	k_1 (M min.)$^{-1}$	k_2 (M min.)$^{-1}$
Methyl acetate				
25	0.595	0.547	6.23×10^{-5}	5.67×10^{-4}
30	0.595	0.547	12.2×10^{-5}	4.66×10^{-4}
24.3[4]	0.6857	0.5	6.23×10^{-5}	2.84×10^{-4}
Ethyl acetate				
25	0.490	0.565	8.84×10^{-5}	3.25×10^{-4}
25[5]	0.47	0.473	6.005×10^{-5}	2.25×10^{-4}
25[5]	0.47	0.660	8.603×10^{-5}	3.22×10^{-4}

Department of Chemistry
Faculty of Science
Hiroshima University
Higashisenda-machi, Hiroshima

4) B. O. Griffith, W. Cudmore and M. Lewis, *J. Chem. Soc.*, **109**, 67 (1916).
5) H. S. Harned and R. Pfanstiel, *J. Am. Chem. Soc.*, **44**, 2193 (1922).

Ultrasonic Studies of the Hydration of Various Compounds in an Ethanol-Water Mixed Solvent. II. The Hydration of Organic Compounds

By Tatsuya YASUNAGA, Isamu USUI, Koichi IWATA and Masaji MIURA

(Received May 22, 1964)

In a previous paper,[1] it was reported that the degree of the hydration of inorganic electrolytes in a mixed solvent of ethanol and water can be determined by measuring the lowering of the ethanol concentration corresponding to the maximum point caused by the addition of the electrolytes in the plot of the sound velocity against the composition of the mixed solvent. A number of methods have been reported for the determination of the degree of hydration. Some of these methods are, however, applicable only to hydration of an electrostatic nature, and others, only to that of hydrogen bonding.

In the present study an attempt is made to determine, by the previous method, the degree of the hydration of such organic compounds as glucose, sucrose, glycine and gelatine.

1) T. Yasunaga, Y. Hirata, Y. Kawano and M. Miura, This Bulletin, 37, 867 (1964).

Experimental

Method. — The technique of measurement was similar to that reported in detail in the previous paper.[1]

Materials.—The materials described in Table I have been selected as examples of organic compounds. The solubilities of these compounds in

TABLE I. THE SOLUBILITIES OF ORGANIC COMPOUNDS IN ETHANOL

Compound	Solubility
Glucose	0.22 g./100 g. satd. solution (25°C)[2]
Sucrose	0.0 g./100 cc. ethanol (14°C)[3]
Glycine	0.029 g./100 cc. satd. solution (25°C)[2]
Gelatine	0.024 g./100 g. 99.69% ethanol (25°C)

2) A. Seidell, "Solubilities of Inorganic Compounds," 3rd ed., D. van Nostrand Company, New York (1941).

3) Landolt-Börnstein, Physikalisch-Chemische Tabellen, III (1923), p. 723.

ethanol are given in the table, together with the results measured for gelatine in our laboratory. They show that the mutual interaction between these compounds and ethanol is very small and may be disregarded without causing a serious error in the estimation of the hydration. Glucose, sucrose and glycine were guaranteed pure grade reagents and were used without further purification. Gelatine was purified by precipitation, with the addition of ethanol from its aqueous solution.

Results

The change in the velocity of sound when ethanol is added to the aqueous solutions of the compounds at various concentrations is presented graphically in Figs. 1—4. The amount of ethanol in the solution needed to give a maximum in the sound velocity decreases with the increasing concentration of the solute. The amount of hydration calculated from Eq. 1 in the previous paper[1] is shown in Fig. 5;

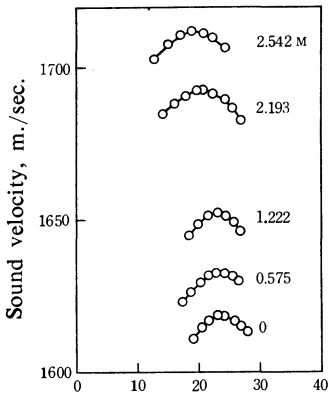


Fig. 1. Sound velocity in ethanol-water solution of glucose.

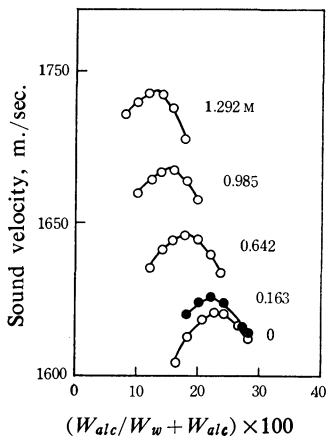


Fig. 2. Sound velocity in ethanol-water solution of sucrose.

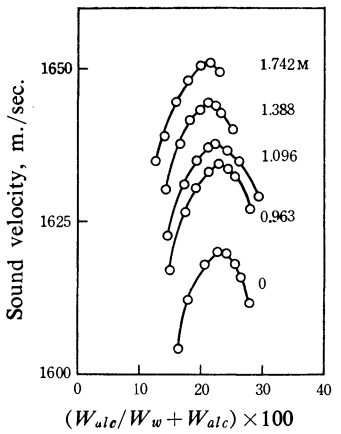


Fig. 3. Sound velocity in ethanol-water solution of glycine.

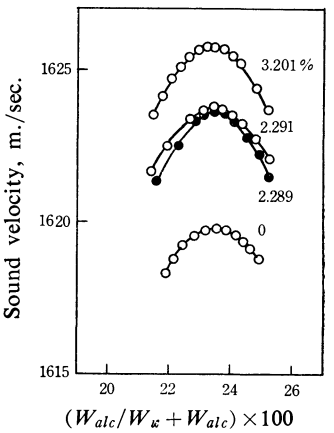


Fig. 4. Sound velocity in ethanol-water solution of gelatine.

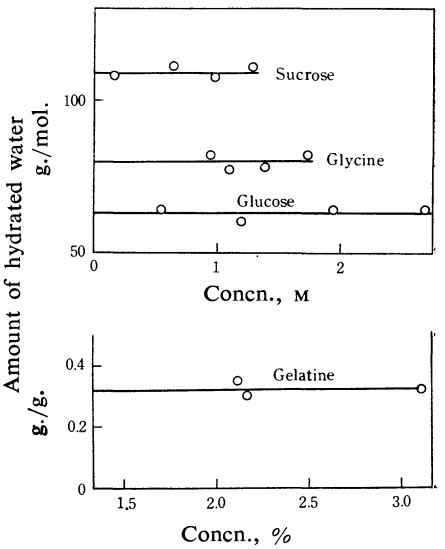


Fig. 5. Amount of hydration.

it is constant with respect to the concentration. The values for the degree of hydration at an infinite dilution, as calculated from Fig. 5, are given in Table II, together with those obtained by other experimental methods.

Table II. Comparison of the degree of hydration

Compound	This method mol./mol.	Activity method[4] mol./mol.	Sound velocity[5] mol./mol.
Glucose	3.5	2.0	3.5
Sucrose	6.1	4.8	3.8
Glycine	4.4		2.9[6]
Gelatine	0.32 g./g.		0.27 g./g.[7]

Discussion

The degree of the hydration obtained in the present study is constant and is independent of the concentration for all the compounds. This result is in good accord with the expectation from the principle of the calculation of the degree of hydration proposed in this paper. The numerical value of the degree of hydration also agrees well with those obtained by other workers, as is shown in Table II. These facts indicate that the findings concerning the degree of hydration given in the table are quite reasonable, as has been discussed in the previous paper, and that an acoustical structure of the solution of ethanol and water at the maximum velocity of sound is not affected by the presence of inorganic electrolytes or organic compounds.

As can be seen in Table II in this paper and from Table III in the previous paper, various methods have been used to determine different types of the degree of hydration. As has been shown in the previous report, the hydration for inorganic compounds is caused by the electro-static interaction between ions and water molecules, whereas the hydration for organic compounds, as reported in this paper, is mainly caused by hydrogen bonding.

The results in these two papers lead us to the conclusion that the present experimental method can be used to determine the degree of hydration of both types, electrostatic and hydrogen-bonded. Therefore, further developement of this method will facilitate the study of the hydration of polymers which are soluble in water and insoluble in ethanol.

4) Y. Miyahara, *Kagaku*, **29**, 365 (1959).
5) H. Shiio, *J. Am. Chem. Soc.*, **80**, 70 (1958).
6) Y. Miyahara, This Bulletin, **26**, 390 (1953).
7) H. Shiio, *J. Chem. Soc. Japan, Pure Chem. Sec.* (*Nippon Kagaku Zassi*), **74**, 203 (1953).

Department of Chemistry
Faculty of Science
Hiroshima University
Higashisenda-machi, Hiroshima

Nature of the π-Electronic Spectra of Aromatic Compounds.[1] *I. Aromatic Hydrocarbons and Their Hydroxyl Derivatives*

By Kichisuke NISHIMOTO* and Ryoichi FUJISHIRO

(Received May 12, 1964)

It is very interesting, for several reasons, to carry out the systematic theoretical analysis of the π-electronic spectra of aromatic compounds in the visible and near-ultraviolet regions. First, the spectra of aromatic hydrocarbons show some remarkable regularities.[2,3] There is, for instance, a noticeable empirical relation, pointed out by Clar,[2] between the wavelengths of the weakest band and the strongest band in the spectrum of an aromatic hydrocarbon. Second, the effect of the substitution on the spectrum of the parent hydrocarbon depends largely upon the position at which the substituent is attached to the molecule.[4] Thirdly, the π-electronic spectrum of a *N*-heterocycle bears a noteworthy resemblance to that of the corresponding hydrocarbon,[4,5] although the replacement of –CH=

1) Presented in part at the International Symposium on Molecular Structure and Spectroscopy, Tokyo, Japan, September, 1962.

* Present address: Mellon Institute, 4400 Fifth Avenue, Pittsburgh, Pennsylvania, 15213, U. S. A.

2) E. Clar, "Aromatische Kohlenwasserstoffe," Springer-Verlag, Berlin (1952).

3) H. B. Klevens and J. R. Platt, *J. Chem. Phys.*, **17**, 470 (1949).

4) R. A. Friedel and M. Qrchin, "Ultraviolet Spectra of Aromatic Compounds," John Wiley and Sons, New York (1951).

5) V. Zanker, *Z. physik. Chem.* (*Frankfurt*), **2**, 52 (1954).

with -N= brings little change in the intensity and frequency of the spectrum of the parent hydrocarbon.

Recently, many excellent theoretical works on the π-electronic spectra of aromatic hydrocarbons have been published.[6-13] However, very few systematic theoretical studies of the nature of the π-electronic spectra of aromatic derivatives have been made, except for benzene derivatives.[14-20] In previous papers[21,22] we have studied the electronic spectra of phenol, α- and β-naphthols by the ASMO-CI method. Our theory expected that all the ^1L_b absorptions would be polarized in the direction perpendicular to their C–O bond axes. Our next interest has been to study the electronic spectra of more complicated derivatives, such as anthrols and nitroanthracenes. However, it is hard to study them by the ordinary ASMO-CI method.

The primary purpose of the present study is, therefore, to propose a theoretical procedure for the systematic study of the nature of π-electronic spectra of aromatic derivatives with a minimum of theoretical effort. The method is based on a limited LCMO approximation. It has been generally recognized that the Pariser-Parr's theory[11] is the best semi-empirical ASMO theory at present. However, the theory gives a rather unsatisfactory result for the transition energy of the benzene B_{2U} spectrum. This result is attributable to the estimation of two center-electron repulsion integrals, $\gamma_{\mu\nu}$. Recently, we have proposed an approximation[23] for the estimation of $\gamma_{\mu\nu}$ within the framework of zero differential overlap approximation, and we have successfully applied it to the SCF calculation of benzene *N*-heterocycles[23,24] and to the ASMO calculation of the electronic structure of some aromatic hydroxyl derivatives.[21,22,25]

In this paper, we will, first, study and elucidate the π-electronic spectra of several catacondensed hydrocarbons, whose general formula is $C_{4n+2}H_{2n+4}$, and will examine the existence of the Clar relation, by means of the ASMO-CI method. Next, we will study the effect of the substitution of a hydroxyl group on the nature of the π-electronic spectrum of the parent hydrocarbon. In subsequent papers, we will apply the present method to the aromatic nitro derivatives and the aromatic *N*-heterocycles.

Theoretical Procedure

The procedure of calculation may be summarized as follows: First, we calculate the eight lowest excited states, four of which are singlets and the others, triplets, of the parent hydrocarbon by means of the ASMO-CI method. The configurational wave function associated with a given electron configuration is represented by an antisymmetrized product of the Hückel molecular orbitals (HMO), which are obtainable in Ref. 26. The ground state wave function and the energy are described by the symbols Ψ_0 and H_0 respectively. The excited configurational function associated with the transition of one electron from an occupied orbital, ϕ_i, to a vacant orbital, $\phi_{k'}$, and the corresponding configurational energy are represented by $^1\chi_{ik'}$ and $^1H_{ik',ik'}$ or by $^3\chi_{ik'}$ and $^3H_{ik',ik'}$ respectively. (Here, the superscripts 1 and 3 indicate singlet and triplet respectively.)

It is interesting to note that the number of nodal planes, perpendicular to the molecular plane, of a given HMO is closely related to the orbital ring quantum number in the free electron theory.[6] It may, therefore, be closely connected with the selection rule for the transition. To a first approximation, it is, therefore, reasonable to assume that the "optical electrons" are those in the higher occupied orbitals, which have n nodal planes perpendicular to the molecular plane, and that the transitions from these orbitals to the lower vacant orbitals, which have $(n+1)$ nodal planes, are primarily responsible for the absorption spectrum in the longest wavelength regions.

For an aromatic hydrocarbon, there are two such higher occupied orbitals and two lower vacant orbitals, so that we can have four kinds of transitions from their combinations. In

6) J. R. Platt, *J. Chem. Phys.*, **17**, 484 (1949); **18**, 1168 (1950).
7) R. G. Parr and R. Pariser, ibid., **21**, 466, 767 (1953); **23**, 711 (1955).
8) M. J. S. Dewar and H. C. Longuet-Higgins, *Proc. Phys. Soc., (London)*, **A67**, 795 (1954).
9) W. Moffitt, *J. Chem. Phys.*, **22**, 320 (1954).
10) J. A. Pople, *Proc. Phys. Soc. (London)*, **A68**, 81 (1955).
11) N. S. Ham and K. Ruedenberg, *J. Chem. Phys.*, **25**, 13 (1956).
12) R. Pariser, ibid.. **24**, 250 (1956); **25**, 1112 (1956).
13) R. L. Hummel and K. Ruedenberg, *J. Phys. Chem.*, **66**, 2334 (1962).
14) S. Nagakura and J. Tanaka, *J. Chem. Phys.*, **22**, 236 (1954).
15) S. Nagakura, ibid., **23**, 1441 (1955).
16) H. C. Longuet-Higgins and J. N. Murrell, *Proc. Phys. Soc. (London)*, **A68**, 601 (1955).
17) J. N. Murrell, ibid., **A68**, 969 (1955).
18) J. Tanaka and S. Nagakura, *J. Chem. Phys.*, **24**, 1274 (1956).
19) L. Goodman and H. Shull, ibid., **27**, 1388 (1957).
20) I. Fischer-Hjalmer, *Ark. für Fys.*, **21**, 123 (1962).
21) K. Nishimoto and R. Fujishiro, This Bulletin, **31**, 1036 (1958).
22) K. Nishimoto, *J. Phys. Chem.*, **67**, 1443 (1963).
23) K. Nishimoto and N. Mataga, *Z. physik. Chem. (Frankfurt)*, **12**, 335 (1957).
24) N. Mataga and K. Nishimoto, ibid., **13**, 140 (1957).
25) K. Nishimoto and R. Fujishiro, This Bulletin **35**, 905 (1962).
26) C. A. Coulson and R. Daudel, "Dictionary of Values of Molecular Constants," C. N. R. S. and I. C. I., Ltd., Paris (1955).

order to discuss the spectra of aromatic compounds systematically, it will be convenient to use the following notation: 1) The higher one of the two higher occupied orbitals in a hydrocarbon is designated as ψ°_1, and the other as ψ°_2. 2) The lower one of the two lower vacant orbitals is designated as $\psi^\circ_{1'}$ and the other as $\psi^\circ_{2'}$. As Coulson-Rushbrook[27] and Longuet-Higgins[28] have pointed out, in an alternant hydrocarbon the molecular orbitals appear in pairs. Because of this peculiar property, the configurations $\chi_{12'}$ and $\chi_{21'}$ are degenerate. Therefore, we have the following relation:

$$H_{12',12'} = H_{21',21'} \tag{1}$$

In addition, because of the molecular symmetry, the configurations $\chi_{11'}$ and $\chi_{22'}$ combine together, as do as $\chi_{12'}$ and $\chi_{21'}$. As a result, the excited state should be divided into two classes, which may be expressed as follows:

$$\left.\begin{aligned} \Psi(\mathrm{L_a}) &= A\chi_{11'} + B\chi_{22'} \\ \Psi(\mathrm{B_a}) &= B\chi_{11'} - A\chi_{22'} \\ \Psi(\mathrm{L_b}) &= \frac{1}{\sqrt{2}}(\chi_{12'} - \chi_{21'}) \\ \Psi(\mathrm{B_b}) &= \frac{1}{\sqrt{2}}(\chi_{12'} + \chi_{21'}) \end{aligned}\right\} \tag{2}$$

where the letter in parenthesis is Platt's notation characterizing the nature of the excited state.

The interconfigurational energy, $H_{ik',jl'}$ which is given by

$$H_{ik',jl'} = \int \chi_{ik'} H \chi_{jl'} \mathrm{d}\tau \tag{3}$$

where H is the total Hamiltonian, is calculated by the method described in our previous paper.[25] The present calculations concern the interaction between only a few configurations, so it is not necessary to use a constant value of the semi-empirical parameter β_{CC}, which is a core integral over the neighboring carbon $2p\pi$AO's from molecule to molecule, since the β_{CC} value should depend more or less upon how many configurations are taken into account. As a matter of convenience, the value of β_{CC} is chosen here for each hydrocarbon to fit the observed absorption maxima of either the ^1B_b or ^1L_b species.

When the HMO's of the parent hydrocarbon are written as $\psi^\circ_{2n+1}, \cdots, \psi^\circ_1, \psi^\circ_{1'}, \cdots, \psi^\circ_{(2n+1)'}$ and those of the substituent, as $\theta_1, \cdots, \theta_m$, the HMO of an aromatic derivative, ψ_i, is exactly represented by the linear combinations of these unperturbed MO's:

$$\psi_i = \sum_k b_{ik}\psi^\circ_k + \sum_j b_{ij}\theta_j \tag{4}$$

However, since we are concerned with the electronic spectra of aromatic derivatives in the longest wavelength regions, we will be able satisfactorily to explain them by considering only the higher occupied and the lower vacant unperturbed MO's, which make the most important contribution to the lowest excited states of the molecule. From this point of view, we introduce a limited LCMO approximation and express ψ_i as:

$$\psi_i = C_{i2}\psi^\circ_2 + C_{i1}\psi^\circ_1 + C_{i1'}\psi^\circ_{1'} + C_{i2'}\psi^\circ_{2'} + C_{is}\theta_s + C_{is'}\theta_{s'} \tag{5}$$

where θ_s and $\theta_{s'}$ are the highest occupied and the lowest vacant HMO of a substituent respectively. C_{ij} is a coefficient to be determined by the variation principle, using appropriate parameters.

When the substituent is an auxochromic group, such as OH, NH_2, or $N(CH_3)_2$, there is no $\theta_{s'}$ (if we neglect the hyperconjugation effect). Therefore, in this case, ψ_i should be necessarily expressed by the linear combination of five unperturbed MO's:

$$\psi_i = C_{i2}\psi^\circ_2 + C_{i1}\psi^\circ_1 + C_{i1'}\psi^\circ_{1'} + C_{i2'}\psi^\circ_{2'} + C_{is}\theta_s \tag{6}$$

where θ_s is the lone pair orbital centered at the substituent. In the case of hydroxyl derivatives, we assume the conventional Coulomb integral, α_O, for the hydroxyl group to be:

$$\alpha_O = \alpha + 1.5\beta$$

and the conventional resonance integral to be:

$$\beta_{CO} = 0.7\beta$$

These are the values reported in our previous paper.[21]

The Hartree-Fock-like orbital energy associated with ψ_i is given by:

$$\bar{\varepsilon}_i = \int \psi_i F \psi_i \mathrm{d}\tau \tag{7}$$

where F is the Hartree-Fock operator, whose general expression has been given in Roothaan's article,[29] for the system. For the sake of simplicity, $\bar{\varepsilon}_i$ is estimated by the following approximation:

$$\begin{aligned} \bar{\varepsilon} = {} & (C^2_{i2} - C^2_{i2'})\bar{\varepsilon}^\circ_2 + (C^2_{i1} - C^2_{i1'})\bar{\varepsilon}^\circ_1 \\ & + C^2_{is}\bar{\varepsilon}^\circ_s + C^2_{is'}\bar{\varepsilon}^\circ_{s'} \\ & + 2C_{is}[(C_{i2} \pm c_{i2'})H_{2s} + (C_{i1} \pm C_{i1'})H_{1s}] \\ & + 2C_{is'}[(C_{i2} \pm C_{is'})H_{2s'} + (C_{i1} \pm C_{i1'})H_{1s'}] \end{aligned}$$

where the upper and lower signs are associated with the α- and β-substitution respectively.

27) C. A. Coulson and G. S. Rushbrook, *Proc. Camb. Phil. Soc.*, **36**, 193 (1940).
28) H. C. Longuet-Higgins, *J. Chem. Phys.*, **18**, 265 (1950).
29) C. C. J. Roothaan, *Revs. Modern Phys.*, **23**, 69 (1951).

Interaction energies, H_{2s}, H_{1s}, $H_{2s'}$ and $H_{1s'}$, are approximated by:

$$H_{2s}=\int \psi^{\circ}{}_2(1)H_{\mathrm{core}}(1)\theta_s(1)\mathrm{d}\tau$$

$$H_{1s}=\int \psi^{\circ}{}_1(1)H_{\mathrm{core}}(1)\theta_s(1)\mathrm{d}\tau$$

$$H_{2s'}=\int \psi^{\circ}{}_2(1)H_{\mathrm{cere}}(1)\theta_{s'}(1)\mathrm{d}\tau$$

$$H_{1s'}=\int \psi^{\circ}{}_1(1)H_{\mathrm{core}}(1)\theta_{s'}(1)\mathrm{d}\tau$$

$\bar{\varepsilon}^{\circ}{}_2$, $\bar{\varepsilon}^{\circ}{}_1$, $\bar{\varepsilon}^{\circ}{}_s$ and $\bar{\varepsilon}^{\circ}{}_{s'}$ are the Hartree-Fock-like orbital energies associated with $\psi^{\circ}{}_2$, $\psi^{\circ}{}_1$, θ_s and $\theta_{s'}$ respectively. Therefore, the configurational energy is given by;

$$^{1,3}H_{ik',ik'}=\bar{\varepsilon}_{k'}-\bar{\varepsilon}_i-[ii\mid k'k']+[ik'\mid ik'] \pm [ik'\mid ik'] \quad (9)$$

where

$$[ik\mid jl]=\int \phi_i(1)\phi_k(1)\frac{e^2}{r_{12}}\phi_j(2)\phi_l(2)\mathrm{d}\tau$$

The plus and minus signs are combined with the singlet and triplet configurations respectively. The interconfigurational energy is simply approximated by:

$$^{1,3}H_{ik',jl'}=-[ij\mid k'l']+[ik'\mid jl'] \pm [ik'\mid jl'] \quad (10)$$

This approximation means that a given configuration interacts with other configurations through only the electron repulsion term in the total Hamiltonian.

In the calculation of the molecular integrals of a hydroxyl derivative, we use the following approximation:

1) $\bar{\varepsilon}^{\circ}{}_s$ has a constant value of -11.649 eV., the value of the integral over the oxygen $2p\pi$ atomic orbital (AO) with respect to the Hartree-Fock Hamiltonian of phenol.[21]

2) The core integral over the neighboring carbon and oxygen $2p\pi$AO's is assigned a constant value of -1.664 eV., which is estimated as $0.7\times(\beta_{CC}$ of benzene).

3) The electron repulsion integrals over AO's are calculated by the method described in our previous papers.[21,25]

For convenience, we lay down the following rule for the numbering of the MO's of a derivative. We name the orbital which contains θ_s to the extent of more than 50%, ϕ_s, and the orbital which contains $\psi^{\circ}{}_2$ to the extent of more than 50%, ϕ_2, and so on. Using this rule, the excited state wave function for an aromatic derivative can be adequately given by the linear combination of six configurations:

$$\Psi_a=d_{a1}\chi_{11'}+d_{a2}\chi_{22'}+d_{a3}\chi_{12'}+d_{a4}\chi_{21'}+d_{a5}\chi_{s1'}+d_{a6}\chi_{1s'} \quad (11)$$

The coefficient d_{at} is to be determined by the variation principle.

In order to study the π-electronic spectra of aromatic compounds systematically, we use Platt's nomenclature[6] and set up the following somewhat artificial criterion for the assignment of the electronic transitions: we describe the excited state which is characterized by $d_{a1}>0$, $d_{a2}>0$ and $d^2{}_{a1}+d^2{}_{a2}>0.5$ as the L_a species. Here, d_{a1} is a coefficient which appeared in Eq. 11. The state which is characterized by $d_{a3}>0$, $d_{a4}>0$ and $d^2{}_{a3}+d^2{}_{a4}>0.5$, we designate as the B_b species. The criteria are arranged in Table I. In the table, C-T indicates an intramolecular charge transfer state. When we use these criteria, we will be able to assign theoretically the π-electronic excited states of a conjugated system without any trouble.

Table I. Assignment of the electronic transition in aromatic compounds

State	Characterization		
L_a	$d_{a1}>0$	$d_{a2}>0$	$d^2{}_{a1}+d^2{}_{a2}>0.5$
L_b	$d_{a3}>0$ or $d_{a3}<0$	$d_{a4}<0$ or $d_{a4}>0$	$d^2{}_{a3}+d^2{}_{a4}>0.5$
B_b	$d_{a3}>0$	$d_{a4}>0$	$d^2{}_{a3}+d^2{}_{a4}>0.5$
B_a	$d_{a1}>0$	$d_{a2}<0$	$d^2{}_{a1}+d^2{}_{a2}>0.5$
$(C\text{-}T)_1$		$d^2{}_{a5}>0.5$	
$(C\text{-}T)_2$		$d^2{}_{a6}>0.5$	

In the present calculations, the excited state wave function of a hydroxyl derivative is approximated by the linear combination of only four configurations, $\chi_{11'}$, $\chi_{22'}$, $\chi_{12'}$ and $\chi_{21'}$, for two reasons. First, ϕ_s is located deep

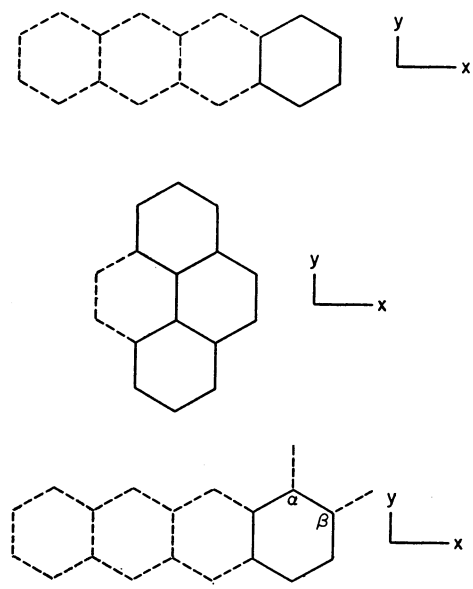


Fig. 1. Structures of aromatic hydrocarbons and their hydroxyl derivatives.

TABLE II. CALCULATED EXCITATION ENERGIES, OSCILLATOR STRENGTHS AND POLARIZATIONS

Excited state	Excitation energy, eV.		Oscillator strength		Polarization
	Calcd.	Exptl.	Calcd.	Exptl.	
		Benzene			
$\Psi(^1L_b)$	4.880	4.88[a]	0	0.0014[a]	x
$\Psi(^1L_a)$	6.119	6.14[a]	0	0.10 [a]	y
$\Psi(^1B_b)$	6.941	6.74[a]	1.186	—	x
$\Psi(^1B_a)$	6.941	6.74[a]	1.186	—	y
$\Psi(^3L_a)$	3.143	3.65[b]	0	—	
$\Psi(^3B_b)$	4.880	—	0	—	
$\Psi(^3L_b)$	4.012	—	0	—	
$\Psi(^3B_a)$	4.012	—	0	—	
		Naphthalene			
$\Psi(^1L_b)$	3.990	3.99[c]	0	0.002[c]	x
$\Psi(^1L_a)$	4.236	4.51[c]	0.273	0.10 [c]	y
$\Psi(^1B_b)$	5.608	5.62[c]	2.119	1.70 [c]	x
$\Psi(^1B_a)$	6.185	—	0.854	—	y
$\Psi(^3L_a)$	2.279	2.64[d]	0	—	
$\Psi(^3B_b)$	3.990	—	0	—	
$\Psi(^3L_b)$	3.485	—	0	—	
$\Psi(^3B_a)$	4.065	—	0	—	
		Anthracene			
$\Psi(^1L_a)$	3.300	3.31 [e]	0.363	0.10 [f]	y
$\Psi(^1L_b)$	3.649	—	0	—	x
$\Psi(^1B_b)$	4.930	4.930[e]	2.848	2.28 [f]	x
$\Psi(^1B_a)$	6.098	6.66 [f]	0.756	0.65 [f]	y
$\Psi(^3L_a)$	1.510	1.85 [g]	0	—	
$\Psi(^3B_b)$	3.649	—	0	—	
$\Psi(^3L_b)$	3.328	—	0	—	
$\Psi(^3B_a)$	4.482	—	0	—	
		Tetracene			
$\Psi(^1L_a)$	2.786	2.63[e]	0.400	0.98[f]	y
$\Psi(^1L_b)$	3.507	—	0	—	x
$\Psi(^1B_b)$	4.520	4.52[e]	3.411	1.85[f]	x
$\Psi(^1B_a)$	6.070	5.88[f]	0.728	0.45[f]	y
$\Psi(^3L_a)$	1.125	1.27[h]	0	—	
$\Psi(^3B_b)$	3.507	—	0	—	
$\Psi(^3L_b)$	3.292	—	0	—	
$\Psi(^3B_a)$	4.768	—	0	—	
		Phenanthrene			
$\Psi(^1L_b)$	3.797	3.59[e]	0	0.003[f]	x
$\Psi(^1L_a)$	4.119	4.24[e]	0.566	0.18 [f]	y
$\Psi(^1B_b)$	4.874	4.94[e]	1.072	1.09 [f]	x
$\Psi(^1B_a)$	4.934	6.62[f]	1.174	0.59 [f]	y
$\Psi(^3L_a)$	2.451	2.68[i]	0	—	
$\Psi(^3L_b)$	3.174	—	0	—	
$\Psi(^3B_b)$	3.797	—	0	—	
$\Psi(^3B_a)$	3.457	—	0	—	
		Pyrene			
$\Psi(^1L_b)$	3.276	3.34[e]	0	—	x
$\Psi(^1L_a)$	3.490	3.72[e]	0.673	—	y
$\Psi(^1B_b)$	4.560	4.56[e]	1.263	—	x
$\Psi(^1B_a)$	5.171	5.14[e]	1.449	—	y
$\Psi(^3L_a)$	1.722	—	0	—	
$\Psi(^3L_b)$	2.926	—	0	—	
$\Psi(^3B_b)$	3.276	—	0	—	
$\Psi(^3B_a)$	3.674	—	0	—	

a) H. Baba, This Bulletin, **34**, 76 (1961).
b) H. Shull, *J. Chem. Phys.*, **17**, 295 (1949).
c) H. Baba and S. Suzuki, This Bulletin, **34**, 82 (1961).
d) J. Ferguson, T. Iredale and J. A. Taylor, *J. Chem. Soc.*, **1954**, 3160.
e) Reference 2.
f) Reference 3.
g) M. R. Padhye, S. P. McGlynn and M. Kasha, *J. Chem. Phys.*, **24**, 588 (1956).
h) S. P. McGlynn M. R. Padhye and M. Kasha, ibid., **23**, 593 (1955).
i) K. Kanda and B. Shimada, *Spectrochim. Acta*, **13**, 211 (1959).

TABLE III. CALCULATED INTERCONFIGURATIONAL ENERGIES FOR HYDROCARBONS (in eV.)

	Benzene	Naphthalene	Anthracene	Tetracene	Phenanthrene	Pyrene
$^1H_{11',11'}-H_0$	6.5301	4.3695	3.3768	2.8454	4.2380	3.6639
$^1H_{22',22'}-H_0$	6.5301	6.0517	6.0213	6.0104	4.8150	4.9968
$^1H_{11',22'}$	−0.4113	−0.4916	−0.4578	−0.4372	−0.2882	−0.5120
$^1H_{12',12'}-H_0$	5.9107	4.7991	4.2895	4.0136	4.3354	3.9180
$^1H_{12',21'}$	1.0307	0.8092	0.6404	0.5064	0.5386	0.6420
$^3H_{11',11'}-H_0$	3.5775	2.3155	1.5188	1.1286	2.5590	1.7373
$^3H_{22',22'}-H_0$	3.5775	4.0285	4.4733	4.7652	3.3494	3.6584
$^3H_{11',22'}$	−0.4341	−0.2526	−0.1608	−0.1078	−0.3114	−0.1748
$^3H_{12',12'}-H_0$	4.4459	3.7373	3.4883	3.3994	3.4854	3.1012
$^3H_{12',21'}$	−0.4341	−0.2526	−0.1608	−0.1078	−0.3114	−0.1748

and apart from the others. Secondly, the interconfigurational energies between $\chi_{s1'}$ and the other configurations are relatively small.

The core structures and the molecular axes of hydrocarbons and their hydroxyl derivatives are shown in Fig. 1. Here, we assume that each molecular framework is made of the appropriate regular hexagon systems, with the constant bond length of 1.397 Å, the experimental carbon-carbon bond distance for benzene.[30]

The intensity of the absorption associated with the one-electron transition from Ψ_o to Ψ_a is calculated by:[31]

$$f=1.085\times10^{11}\tilde{\nu}_{oa}(D_{oa})^2 \qquad (12)$$

where $\tilde{\nu}_{oa}$ is the frequency of the transition in cm^{-1}. $\vec{D}_{oa}$ is the transition moment defined by:

$$\vec{D}_{oa}=\int \Psi_o \sum e_i r_i \Psi_a d\tau \qquad (13)$$

where e_i and r_i are the charge and the position vector of the i-th charged particle respectively. $\vec{D}_{oa}$ gives the direction of the polarization of the absorption band. Therefore, we usually use $\vec{D}_{oa}$ in assigning and classifying the electronic spectrum of a molecule.

Results and Discussion

The spectrum of a hydrocarbon in the visible and near ultraviolet regions usually contains four main absorptions. On the basis of a free electron model (perimeter model), Platt[6] classified these bands as ^1L_b, ^1L_a, ^1B_b and ^1B_a respectively. There is the following remarkable empirical relation, pointed out by Clar,[2] between the wavelength maxima of the weak ^1L_b band and the very strong ^1B_b band:

$$\lambda(^1L_b)/\lambda(^1B_b)=1.35 \qquad (14)$$

The calculated results of hydrocarbons are summarized in Table II, where they are also compared with the experimental data. The calculated interconfigurational energies are collected in Table III. The results are in satisfactory agreement with the experimental findings. The calculated $\lambda(^1L_b)/\lambda(^1B_b)$ values are given in Table IV. The results lead to this correlation equation:

$$\lambda(^1L_b)/\lambda(^1B_b)=1.36\pm0.06 \qquad (15)$$

That is, the present theory suggests approximately the existence of the Clar relation.

TABLE IV. CALCULATED RATIO OF THE WAVELENGTH OF ^1L_b SPECIES, $\lambda(^1L_b)$, TO THE WAVELENGTH OF ^1B_b, $\lambda(^1B_b)$

Molecule	$\lambda(^1L_b)/\lambda(^1B_b)$
Benzene	1.42
Naphthalene	1.41
Anthracene	1.35
Tetracene	1.29
Phenanthrene	1.28
Pyrene	1.39

Semi-empirically estimated β_{CC} values are collected in Table V. A plot of β_{CC} against n, the number of carbon atoms included in a given hydrocarbon, gives a good correlation, as is shown in Fig. 2. The correlation line is given by:

$$\beta_{CC}(n)=0.571\times10^{-0.0522n}+2.100\ \text{eV}. \qquad (16)$$

Alternant aromatic hydrocarbons can be broadly divided into two isomeric series: One is the linear series in which the rings are arranged linearly, as in anthracene. The other

TABLE V. SEMI-EMPIRICALLY ESTIMATED β_{CC} VALUES FOR HYDROCARBONS

Molecule	β_{CC} (in eV.)
Benzene	−2.3777
Naphthalene	−2.2310
Anthracene	−2.2062
Tetracene	−2.1673
Phenanthrene	(−2.2062)
Pyrene	−2.1863

30) B. P. Stoicheff, *Can. J. Phys.*, **32**, 339 (1954).
31) R. S. Mulliken and C. A. Rieke, *Rep. Progr. Phys.*, **8**, 231 (1941).

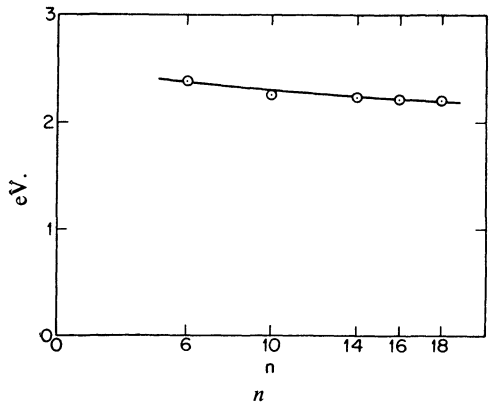


Fig. 2. A plot of β_{CC} against the number of carbon atom, n, contained in the hydrocarbon.

is the angular series, of which phenanthrene is the first member. As is shown in Fig. 4, in the linear series there is a steady displacement of the group of the maxima towards longer wavelengths with the increasing length of the conjugated system.

The molecules of the linear series have symmetry planes along both their short and long axes. The transition moments for allowed transitions can, then, be either perpendicular or parallel to the long axis of the molecule (x-axis in Fig. 1) or, alternatively, allowed transitions have either transverse or longitudinal polarization. The present calculation expects that the transitions from the ground state to $\Psi(^1L_a)$ or to $\Psi(^1B_a)$ will be polarized in the direction of the molecular y-axis, whereas the transitions from the ground state to $\Psi(^1L_b)$ or to $\Psi(^1B_b)$ will have the polarizations in the direction of the molecular x-axis. In assigning the spectrum of phenanthrene, there

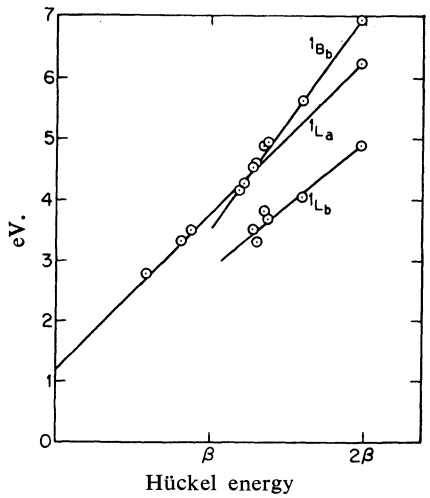


Fig. 3. A plot of the calculated singlet frequency against the corresponding Hückel energy.

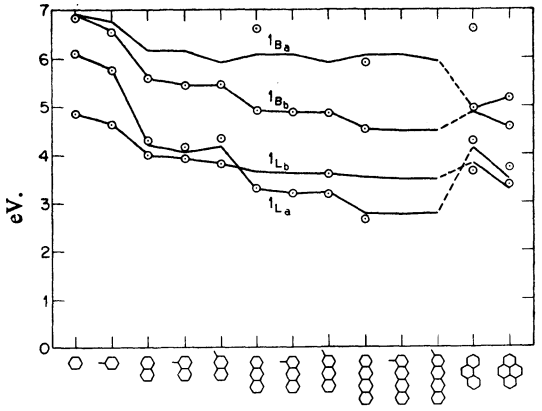


Fig. 4. Comparison of calculated and experimental singlet states. The experimental values are represented by circles.

is a puzzling question. We can treat it as a modified naphthalene spectrum. However, in the light of our theoretical results, it seems better to regard the spectra of phenanthrene and pyrene as modified biphenyl spectra. Their molecular axis should, therefore, be fixed as in Fig. 1 for the study of the electronic spectra. Unfortunately, with a few exceptions, the experimental polarizations are unknown.

The present calculation anticipates that the transition from the ground state to the $\Psi(^1L_b)$ will be forbidden if the molecule rests at the equilibrium configuration. However, the molecule continuously vibrates around the equilibrium positions with rather small amplitudes, and some of the vibrations may instantaneously break down the molecular symmetry. As a result, the forbidden ^1L_b absorption would barely appear through the coupling with such vibrations, accompanied by the vibrational fine structure as in the benzene 260 mμ absorption.

Our results show that the intensity of the ^1L_a absorption should increase with the length of the conjugated system. However, the observed oscillator strengths have practically the same value from molecule to molecule. Moreover, the calculated oscillator strength associated with the ^1B_b absorption seems somewhat larger than the observed values. The reason for this is probably to be found partly in the limited configuration interaction treatment and partly in the point charge approximation.

It is interesting to examine whether or not any interrelationships exist between the calculated frequency and the corresponding orbital energy difference in the Hückel theory. A plot of the calculated frequency against the corresponding Hückel energy gives a rather good correlation, as Fig. 3 shows.

Our approximation for two center electron

TABLE VI. CALCULATED EXCITATION ENERGIES, OSCILLATOR STRENGTHS OF AROMATIC HYDROXYL DERIVATIVES

The theoretical results are compared with experimental data.

Excited state	Excitation energy eV. Calcd.	Exptl.	Oscillator strength Calcd.	Exptl.
		Phenol		
$\Psi(^1L_b)$	4.672	4.55[a]	0.0146	0.0213[a]
$\Psi(^1L_a)$	5.792	5.83[a]	0.113	0.103[a]
$\Psi(^1B_b)$	6.626	6.53[a]	0.976	—
$\Psi(^1B_a)$	6.799	—	1.231	—
$\Psi(^3L_a)$	3.088	—	0	—
$\Psi(^3L_b)$	3.905	—	0	—
$\Psi(^3B_b)$	4.804	—	0	—
$\Psi(^3B_a)$	3.869	—	0	—
		α-Naphthol		
$\Psi(^1L_b)$	3.906	3.86[c]	0.0059	0.016[c]
$\Psi(^1L_a)$	4.065	4.29[c]	0.335	0.102[c]
$\Psi(^1B_b)$	5.462	{5.40[c] {5.80	1.952	{0.328[c] {0.892
$\Psi(^1B_a)$	6.178	—	0.863	—
$\Psi(^3L_a)$	2.152	—	0	—
$\Psi(^3L_b)$	3.418	—	0	—
$\Psi(^3B_b)$	3.931	—	0	—
$\Psi(^3B_a)$	4.059	—	0	—
		β-Naphthol		
$\Psi(^1L_b)$	3.834	3.78[c]	0.0412	0.0211[c]
$\Psi(^1L_a)$	4.187	4.54[c]	0.199	0.0811[c]
$\Psi(^1B_b)$	5.490	5.53[c]	2.191	1.06 [c]
$\Psi(^1B_a)$	5.912	—	0.863	—
$\Psi(^3L_a)$	2.248	—	0	—
$\Psi(^3L_b)$	3.371	—	0	—
$\Psi(^3B_b)$	3.809	—	0	—
$\Psi(^3B_a)$	4.062	—	0	—
		α-Anthrol		
$\Psi(^1L_a)$	3.216	3.19[j]	0.391	—
$\Psi(^1L_b)$	3.613	—	0.0027	—
$\Psi(^1B_b)$	4.867	4.90[j]	2.740	—
$\Psi(^1B_a)$	6.097	—	0.761	—
$\Psi(^3L_a)$	1.458	—	0	—
$\Psi(^3L_b)$	3.295	—	0	—
$\Psi(^3B_b)$	3.620	—	0	—
$\Psi(^3B_a)$	4.481	—	0	—
		β-Anthrol		
$\Psi(^1L_a)$	3.230	3.56[j]	0.321	—
$\Psi(^1L_b)$	3.612	3.16[j]	0.0255	—
$\Psi(^1B_b)$	4.873	4.88[j]	2.988	—
$\Psi(^1B_a)$	5.906	—	0.756	—
$\Psi(^3L_a)$	1.496	—	0	—
$\Psi(^3L_b)$	3.258	—	0	—
$\Psi(^3B_b)$	3.589	—	0	—
$\Psi(^3B_a)$	4.424	—	0	—
		1-OH Tetracene		
$\Psi(^1L_a)$	2.738	—	0.413	—
$\Psi(^1L_b)$	3.487	—	0.0014	—
$\Psi(^1B_b)$	4.488	—	3.339	—
$\Psi(^1B_a)$	6.069	—	0.730	—
$\Psi(^3L_a)$	1.101	—	0	—
$\Psi(^3L_b)$	3.273	—	0	—
$\Psi(^3B_b)$	3.490	—	0	—
$\Psi(^3B_a)$	4.768	—	0	—
		2-OH Tetracene		
$\Psi(^1L_a)$	2.754	—	0.282	—
$\Psi(^1L_b)$	3.478	—	0.0082	—
$\Psi(^1B_b)$	4.492	—	3.592	—
$\Psi(^1B_a)$	5.936	—	0.724	—
$\Psi(^3L_a)$	1.118	—	0	—
$\Psi(^3L_b)$	3.246	—	0	—
$\Psi(^3B_b)$	3.474	—	0	—
$\Psi(^3B_a)$	4.726	—	0	—

a) Reference a in Table II.
c) Reference c in Table II.
j) Reference 34.

repulsion integrals seems to be adequate for the calculation of singlet states, but not for triplet states. There is a reason for this. Our approximation has been found from the benzene singlet spectrum by a trial and error procedure. As Linnett indicated in his book,[32] the electron correlation in the singlet state differs entirely from that in the triplet state. It is probable that our approximation implicitly includes the electron correlation in the singlet state, therefore, it perhaps does not explain the electron correlation in the triplet state.

In the present calculations, we have introduced the following two somewhat drastic approximations: for a molecule, the core integral, β_{CC}, has been fixed at a constant value, and only the four lowest excited configurations have been taken into account. The observed distances in a polyacene are usually not the same.[33] It is natural that the value of β_{CC} should vary with the variation in the bond distances. However, in this paper, we have used HMO's in which the bond dependence of the resonance integral has been neglected. Therefore, so far as we use HMO's in the theory, a constant β approximation may be reasonable. In order to improve the theory, we have to apply the SCF-MO theory with reference to the bond distance dependence of core integrals.

Next, we will consider the excited states of

32) J. W. Linnett, "Wave Mechanics and Valency," Methuen and Co., London (1960).
33) F. Ahmad and D. J. W. Cruickshank, *Acta Cryst.*, 5, 852 (1952).

TABLE VII. CALCULATED INTERCONFIGURATIONAL ENERGIES FOR AROMATIC HYDROXYL DERIVATIVES (in eV.)

	Phenol	α-Naphthol	β-Naphthol	α-Anthrol	β-Anthrol	1-OH Tetracene	2-OH Tetracene
$^1H_{11',11'}-H_0$	6.0608	4.1911	4.2159	3.2916	3.3109	2.7967	2.8081
$^1H_{22',22'}-H_0$	6.5301	6.0517	5.7708	6.0213	5.8312	6.0104	5.8812
$^1H_{12',12'}-H_0$	5.2722	4.5599	4.7915	4.1873	4.2952	3.9619	4.0241
$^1H_{21',21'}-H_0$	6.0255	4.8086	4.6442	4.2922	4.1838	4.0136	3.9454
$^1H_{11',22'}$	−0.4452	−0.5011	−0.4641	−0.4609	−0.4258	−0.4378	−0.4091
$^1H_{11',12'}$	0	0	0.0884	0	0.0377	0	0.0211
$^1H_{11',21'}$	0	0	−0.1123	0	−0.0470	0	−0.0157
$^1H_{22',12'}$	0	0	0.1063	0	0.0666	0	0.0250
$^1H_{22',21'}$	0	0	−0.0099	0	0.0272	0	0.0324
$^1H_{12',21'}$	0.9016	0.7681	0.7809	0.6249	0.6358	0.4996	0.5063
$^3H_{11',11'}-H_0$	3.3794	2.1819	2.3121	1.4664	1.5099	1.1045	1.1231
$^3H_{22',22'}-H_0$	3.5775	4.0285	3.9746	4.4733	4.4148	4.7652	4.7226
$^3H_{12',12'}-H_0$	4.1106	3.5803	3.6629	3.4133	3.4700	3.3585	3.3953
$^3H_{21',21'}-H_0$	4.5989	3.7684	3.5410	3.5020	3.3734	3.4050	3.3228
$^3H_{11',22'}$	−0.3776	−0.2385	−0.2285	−0.1563	−0.1590	−0.1060	−0.1079
$^3H_{11',12'}$	0	0	−0.1000	0	−0.0275	0	−0.0107
$^3H_{11',21'}$	0	0	0.1803	0	0.0954	0	0.0651
$^3H_{22',12'}$	0	0	−0.0841	0	−0.0142	0	0.0002
$^3H_{22',21'}$	0	0	0.1073	0	0.0168	0	−0.0002
$^3H_{12',21'}$	−0.3776	−0.2385	−0.2285	−0.1563	−0.1590	−0.1060	−0.1079

the hydroxyl derivatives. Generally speaking, the absorption spectra of aromatic hydroxyl derivatives in the near ultraviolet regions closely resemble those of the parent hydrocarbons,[4,34] except that the absorption bands are usually shifted to somewhat longer wavelengths. However, in the polycyclic hydroxyl derivatives, not all the possible positions of substitution are identical, so the various groups of absorption bands (^1L_b, ^1L_a, ^1B_b and ^1B_a) are not always shifted to the same extent. For example, there is a noticeable difference between the spectral changes caused by the substitutions at the α- and β-positions. In this paper, the effect on the electronic spectrum of the substitution of a hydroxyl group at the α- or β-position of the parent hydrocarbon has been studied.

The calculated results of the hydroxyl derivatives are summarized in Table VI, where they are also compared with the experimental data. The calculated interconfigurational energies are collected in Table VII. The theoretical singlet frequencies are in satisfactory agreement with the experimental findings. It is suprising that the interconfigurational energies for α-hydroxyl derivatives are practically the same as those for the parent hydrocarbons. Their calculation is, however, an elaborate task, so it is convenient, for a first approximation, to use the latter in place of the former.

The substitution of a hydroxyl group on the parent hydrocarbon has the following effects: first, it breaks out the molecular symmetry of D_{2h} or D_{6h} and removes the peculiar degeneracy of the two configurations, $\chi_{12'}$ and $\chi_{21'}$. As a result, the theoretical oscillator strength of the ^1L_b absorption is not zero, but has a definite value. Furthermore, all the excited configurations will interact with each other. Secondly, a lone-pair orbital of the substituent conjugates with the π-electron system of the parent hydrocarbon. This usually results in something of a spectral red shift. Figure 4 shows the interrelation between the lower singlet states. The present theory suggests that the ^1L_a bands of the parent hydrocarbons are most sensitive for the α-substitution, whereas the β-substitution has no significant effect on them. On the other hand, the ^1L_b bands are

TABLE VIII. POLARIZATIONS OF THE ELECTRONIC TRANSITIONS IN AROMATIC DERIVATIVES

Molecule	Polarization $\Psi_0 \rightarrow \Psi(^1L_a)$	$\Psi_0 \rightarrow \Psi(^1L_b)$	$\Psi_0 \rightarrow \Psi(^1B_b)$	$\Psi_0 \rightarrow \Psi(^1B_a)$
Phenol	90°	180°	180°	90°
α-Naphthol	86°	180°	180°	89°
α-Anthrol	85°	180°	180°	89°
1-OH Tetracene	86°	180°	180°	89°
β-Naphthol	99°	115°	181°	78°
β-Anthrol	97°	72°	181°	79°
2-OH Tetracene	94°	41°	181°	80°

Note: Numerical value gives an angle between the transition moment vector and x-axis of the molecule.

34) H. Baba and S. Suzuki, This Bulletin, 34. 82 (1961); 35. 683 (1962).

remarkably affected by the β-substitution, while they are only slightly influenced by the α-substitution. It is interesting to note that the effect of substitution gradually decreases with the length of the parent conjugated systems.

We have a special interest in the effect of substitution on the direction of the polarization of the electronic transition of the parent hydrocarbon, because the nature of the electronic excited states of the molecule is frequently discussed on the basis of the polarization of the electronic transition.

The calculated results are summarized in Table VIII. Our calculations show that, in α-derivatives, in spite of the absence of D_{2h} or D_{6h} symmetry each absorption band should be polarized in the direction of the short or long molecular axis of the parent hydrocarbon systems. That is, the characteristics of the spectrum of the parent hydrocarbon are not changed in this case. On the other hand, in β-derivatives, the nature of the spectrum of parent hydrocarbons is considerably lost, because all the excited configurations interact strongly with each other. In β-naphthol, for example, the ^1L_b species contains a configuration $\chi_{11'}$ to the extent of about 26% and is polarized approximately in the direction perpendicular to the carbonoxygen bond. Moreover, the present theory expects that, if we try to assign the excited states of β-anthrol on the basis of the experimental polarization, it will be impossible to distinguish the ^1L_a and ^1L_b bands. Unfortunately, no experiments connected with the polarization of the electronic transition in the aromatic hydroxyl derivative have yet given us any results. In β-derivatives the direction of polarization moves gradually towards that of the parent hydrocarbon with an increase in the length of the conjugated system.

The calculated oscillator strength of the α-derivative exhibits a striking contrast to that of the β-derivative. Namely, by α-substitution, the ^1L_a absorption is intensified, whereas the ^1B_b absorption is slightly weakened. On the contrary, the β-substitution has the effects of intensifying the latter absorption and weakening the former absorption. Moreover, the ^1L_b absorption is considerably intensified by the β-substitution, while it is only slightly increased in intensity by the α-substitution. These results are in accord with the experimental data.[4]

The theoretical results for phenol, α- and β-naphthols in the present theory are in satisfactory agreement with those based on the ASMO-CI method.[21,22] This fact suggests that the present theory is reasonable and adequate for the purpose of making a systematic study of the electronic spectra of aromatic derivatives with a minimum of theoretical effort.

Summary

The π-electronic spectra of a number of aromatic hydrocarbons and their hydroxyl derivatives have been theoretically studied by the ASMO-CI method within the framework of a limited LCMO approximation. The calculated singlet frequencies are in satisfactory agreement with the experimental findings. The experimental Clar relation is obtained theoretically. The present theory suggests that the substitution of a hydroxyl group at the α-position of the parent hydrocarbon has effects of a substantial red shift in the ^1L_a band and a rather small shift in the ^1L_b band, but the band characteristics are practically the same as those of the parent hydrocarbon. On the other hand, the substitution at the β-position has the effect of mixing the ^1L_a species with the ^1L_b species to a considerable extent, so that the band characteristics of the parent hydrocarbon should be considerably modified by this type of substitution. In the light of the present theory, it is better to regard the spectra of phenanthrene and pyrene as modified biphenyl spectra. A plot of the calculated frequency against the corresponding Hückel energy gives a rather good correlation.

The authors wish to express their gratitude to Dr. Andrew D. Liehr, of the Mellon Institute, for his help with the manuscript.

Department of Chemistry
Faculty of Science
Osaka City University
Sumiyoshi-ku, Osaka

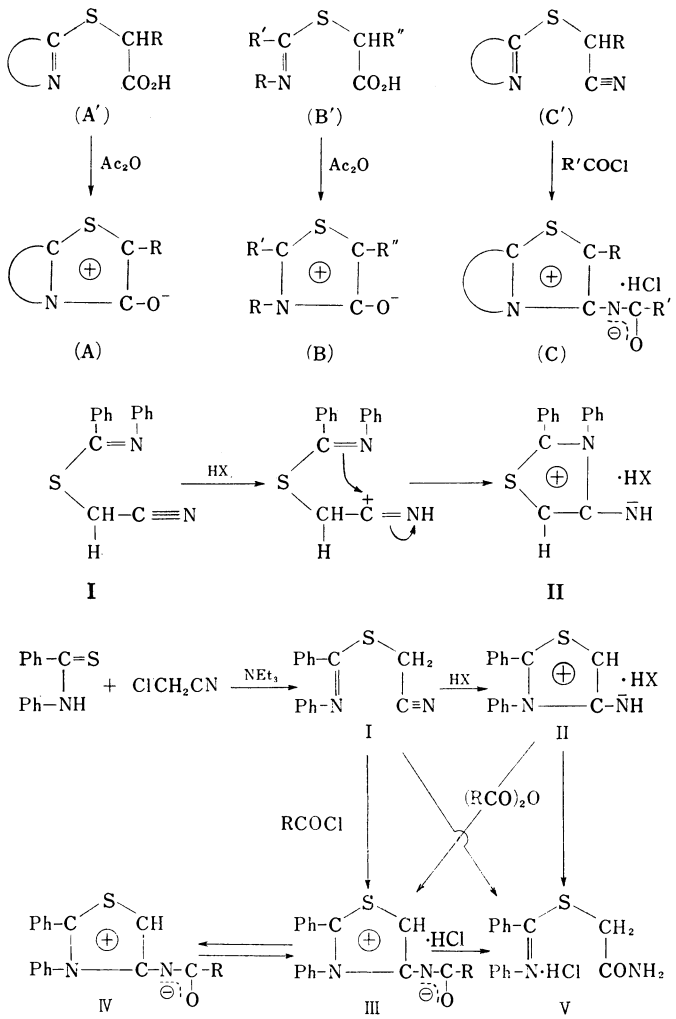
*The Reactions of N-Substituted Thioamides with α-Halonitriles**[,1)]

By Hirohide CHOSHO, Kunihiro ICHIMURA and Masaki OHTA

(Received May 25, 1964)

In the previous papers of this series, it has been described how the meso-ionic compounds A and B are obtained by the treatment of carboxymethylmercapto derivatives (A′ and B′) with acetic anhydride,[2,3)] and how the treatment of cyanomethylmercapto derivatives of heterocyclic nitrogen compounds (C′) with acyl chloride gives compounds of the type C.[2)] The present paper will report the synthesis of non-condensed compounds of the type C by the reaction of *N*-substituted thioamides with α-halonitriles, since it is interesting to investigate the properties and the reactivities of this ring system.

As a preliminary stage in the formation of this ring system, thiobenzanilide was condensed



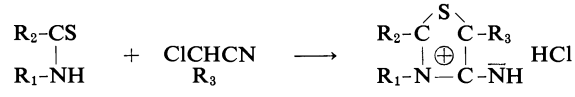
* Presented at the 17th Annual Meeting of the Chemical Society of Japan, Tokyo, March, 1964.

1) Studies of Meso-ionic Compounds. Part XIX.

2) H. Kato, K. Tanaka and M. Ohta, This Bulletin, 35, 1901 (1962).

3) Part XVIII: M. Ohta, H. Chosho, C. Shin and K. Ichimura, *J. Chem. Soc. Japan, Pure Chem. Sec.* (*Nippon Kagaku Zasshi*), 85, 440 (1964).

TABLE I. THIAZONE IMINE HYDROCHLORIDES PREPARED FROM *N*-SUBSTITUTED THIOAMIDES WITH α-HALONITRILES



Substituent			Color of crystal	Yield %	M. p. (decomp.) °C	Analysis					
						Found, %			Calcd., %		
						C	H	N	C	H	N
R_1	R_2	R_3									
Ph	Ph	H	Yellow	96	207	61.88	4.74	9.78	62.38	4.50	9.71
CH_3	Ph	H	Pale yellow	67	201	53.16	5.03	12.49	52.98	4.86	12.36
Ph	CH_3	H	Colorless	80	173	52.92	5.10	12.60	52.98	4.86	12.36
$PhCH_2$	Ph	H	Yellow	50	192	63.18	5.00	9.49	63.47	4.96	9.26
Ph	$PhCH_2$	H	Yellow	86	190	—	—	9.05	—	—	9.26
$PhCH_2$	Ph	Ph	Orange	60	176	69.90	5.01	7.39	69.70	5.05	7.39
Ph	Ph	Ph	Yellow*	14	155	58.33	3.62	12.66	58.17	3.41	12.57

* This was identified as picrate.

with chloroacetonitrile in the presence of triethylamine to afford *S*-cyanomethylisothiobenzanilide (I). The treatment of this intermediate with hydrogen chloride in benzene or 2-propanol gave the expected product, "thiazone imine hydrochloride"[4] (II; X=Cl), the structure of which was deduced by an elementary analysis, by the absence of absorption due to the nitrile group in its infrared spectrum, and by the appearance of a band at 3250 cm^{-1} which may be due to the nitrogen-hydrogen stretching frequency. In addition, the hydrochloride (II; X=Cl) showed a characteristic band at 360 mμ ($\varepsilon=6.55\times10^3$) in its ultraviolet spectrum suggestive of the heterocyclic system. This ring formation seems to proceed as a result of the interaction of two polar groups, by a mechanism similar to that of sydnone imine salts.[5] The hydrochloride (II; X=Cl) was converted into the nitrate (II; $X=NO_3$) by the treatment with silver nitrate. On the treatment of I with a strong organic acid such as picric acid and *p*-toluenesulfonic acid, the ring formation took place to produce the thiazone imine salts of corresponding acid. The structure was confirmed by infrared spectra and by the fact that this picrate was identical with that obtained by the treatment of the thiazone imine hydrochloride (II; X=Cl) with picric acid.

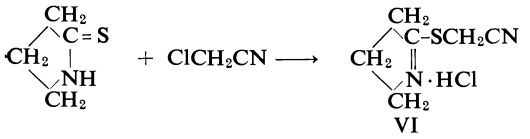
Thiazone imine hydrochloride was converted into *N*-acyl derivatives III by the treatment with acid anhydride. The hydrochlorides of these *N*-acyl derivatives were also yielded by the treatment of I with the corresponding acyl chloride, as in the case of the compound C. The neutralization of the hydrochlorides of *N*-acyl compounds III gave free bases with high melting points, which could then be readily reconverted into the original hydrogen chlorides by the action of hydrogen chloride.

We attempted to prepare *S*-(α-cyanobenzyl)-isothiobenzanilide from thiobenzanilide and α-chlorophenylacetonitrile in the presence of triethylamine, which would be expected to form a 2, 3, 5-triphenylthiazone imine derivative, but only α, α'-dicyanostilbene resulted; this must be a condensation product of two moles of α-chlorophenylacetonitrile. It was, however, found that the hydrochloride (II; X=Cl) was also obtained by heating thiobenzanilide and chloroacetonitrile without a solvent or in biphenyl. This fact suggested that the other thiazone imine derivatives could also be obtained from the corresponding *N*-substituted thioamides and α-chloronitriles without isolating the intermediates. Actually, in a similar manner, some thiazone imine hydrochlorides were prepared from both components, as is shown in Table I. On the other hand, the reaction of thiopyrrolidone with chloroacetonitrile did not afford the expected heterocyclic compound, but alternatively formed *S*-cyanomethylisothiopyrrolidone hydrochloride (VI), the structural evidence for which is based on the elementary analysis and on its infrared spectrum.

The hydrochlorides of thiazone imines (II; X=Cl) decomposed in alkaline conditions, showing themselves incapable of existence as

4) This heterocyclic compound can be named "Ψ-4-imino-2, 3-diphenyl-3, 4-dihydrothiazole hydrochloride," according to Baker's proposal (*J. Chem. Soc.*, **1949**, 311), the symbol Ψ indicating the hybrid ionic structure. In the preceding paper the meso-ionic compound B was provisionally named "thiazone"; in the present paper the authors will refer to II derived from "thiazone" as salts of "thiazone imine" for the sake of simplification in naming.

5) P. Brookes and J. Walker, *J. Chem. Soc.*, **1957**, 4409.



a free base in contrast with the *N*-acylated free base IV. An acidic hydrolysis of the thiazone imine hydrochloride afforded an amide V, which was also produced by the acidic hydrolysis of the *N*-acetyl salt (III; R=CH_3) and *S*-cyanomethylisothiobenzanilide (I).

The reactivities of the compounds obtained above and the related derivatives containing other functional groups will be reported shortly.

Experimental

***S*-Cyanomethylisothiobenzanilide (I).** — Triethylamine (5 cc.) was added to a solution of thiobenzanilide (5 g.) and chloroacetonitrile (1.8 g.) in benzene (25 cc.), and the mixture was heated at 50°C for nine hours. After the mixture had stood overnight, the separated triethylamine hydrochloride was filtered off. The filtrate was evaporated to dryness under reduced pressure, and the residual crystals were collected. Recrystallization from ether-petroleum ether gave 3 g. of *S*-cyanomethylisothiobenzanilide as colorless needles; m. p. 68~69°C.

Found: C, 71.05; H, 4.83; N, 11.24. Calcd. for $C_{15}H_{12}N_2S$: C, 71.42; H, 4.76; N, 11.11%.

The Action of Hydrogen Chloride on I.—a) A 2-propanol solution of I (1 g.) was treated with 2-propanol saturated with hydrogen chloride. After the solution had stood, 2, 3-diphenylthiazone imine hydrochloride (II; X=Cl) precipitated; this was collected and washed with acetone. The yield was 0.8 g. It was purified by reprecipitation from an ethanolic solution with ether (see Table I).

b) The same hydrochloride was also obtained by passing dry hydrogen chloride into a benzene solution of I.

The Action of Picric Acid on I.—An ethanolic solution of I was treated with a solution of picric acid in ethanol to yield picrate (II; HX=picric acid) as yellow needles, which were recrystallized from 2-propanol, m. p. 177°C (decomp.).

Found: C, 52.23; H, 2.81; N, 14.47. Calcd. for $C_{21}H_{15}N_5O_7S$: C, 52.40; H, 3.21; N, 14.55%.

The Action of *p*-Toluenesulfonic Acid on I.—*p*-Toluenesulfonic acid (0.2 g.) in benzene was added to a benzene solution of I (0.1 g.). A yellow oil separated out. After the removal of the solvent, it was dissolved in methanol, and *p*-toluenesulfonate (II; HX=*p*-toluenesulfonic acid) was precipitated by adding ether drop by drop. This yellow needles (0.15 g.) melted at 197°C with decomposition.

Found: C, 62.28; H, 4.99; N, 6.60. Calcd. for $C_{22}H_{20}N_2O_3S_2$: C, 62.27; H, 4.75; N, 6.60%.

The Conversion of 2, 3-Diphenylthiazone Imine Hydrochloride (II; X=Cl) to Other Salts.—*Nitrate.*—Ten per cent aqueous silver nitrate was added to an aqueous solution of the hydrochloride (II; X=Cl) (1 g.). After the silver chloride had been filtered off, the filtrate was evaporated under reduced pressure and the residual crystals were collected by filtration. The yield was 0.9 g. Recrystallization from 2-propanol gave pure nitrate (II; X=NO_3) as yellow needles; m. p. 173.5°C (decomp.).

Found: C, 56.89; H, 4.19; N, 13.49. Calcd., for $C_{15}H_{13}N_3O_3S$: C, 57.14; H, 4.16; N, 13.33%.

Picrate.—The hydrochloride (II; X=Cl) in ethanol was treated with ethanol saturated with picric acid. Yellow needles; m. p. 177°C (unchanged by admixture with the picrate obtained above).

The Conversion of 2, 3-Diphenylthiazone Imine Hydrochloride (II; X=Cl) into *N*-Acetyl Derivatives (III and IV; R=CH_3).—When suspension of the hydrochloride (II; X=Cl) (2 g.) in acetic anhydride (10 cc.) was heated at 90°C for six hours, the reaction mixture turned into a clear solution. In about half an hour crystals precipitated, and the mixture was heated for a further two hours. The crystals were then filtered and washed with acetone. Yield, 2 g. Reprecipitation from an ethanolic solution with ether gave pure hydrochloride of *N*-acetyl-2, 3-diphenylthiazone imine (III; R=CH_3) as colorless needles; m. p. 290°C.

Found: C, 61.84; H, 4.76; N, 8.48. Calcd. for $C_{17}H_{15}N_2OSCl$: C, 61.50; H, 4.52; N, 8.47%.

This hydrochloride of the *N*-acetyl compound was treated with aqueous sodium hydrogen carbonate to yield 0.8 g. of its free base (IV; R=CH_3). Recrystallization from ethanol gave yellow needles; m. p. 198°C (decomp.).

Found: C, 69.55; H, 4.86; N, 9.59. Calcd. for $C_{17}H_{14}N_2OS$: C, 69.39; H, 4.76; N, 9.53%.

The Conversion of 2, 3-Diphenylthiazone Imine Hydrochloride (II; X=Cl) into an *N*-Benzoyl Derivative (IV; R=Ph).—A mixture of the hydrochloride (II; X=Cl) (2 g.) and the excess benzoic anhydride (4.9 g.) was heated at 150~160°C for one hour. The reaction mixture was then washed with hot benzene, and the crystals were collected. They were then suspended in water, treated with aqueous sodium hydrogen carbonate, filtered again, and washed with 2-propanol. Yield, 1.0 g. Recrystallization from ethanol gave a pure free base of an *N*-benzoyl compound (IV; R=Ph) as yellow needles; m. p. 211~212°C (decomp.).

Found: C, 73.95; H, 4.63; N, 7.87. Calcd. for $C_{22}H_{16}N_2OS$: C, 74.14; H, 4.53; N, 8.27%.

The Reaction of *S*-Cyanomethylisothiobenzanilide (I) with Acetyl Chloride.—*S*-Cyanomethylisothiobenzanilide (I) (1.0 g.) and acetyl chloride (0.32 g.) were heated in benzene at 60°C for three hours, and the precipitate was collected. An aqueous solution of the precipitate was treated with aqueous sodium hydrogen carbonate to yield yellow crystals. Recrystallization from ethanol gave the free base of an *N*-acetyl compound (IV; R=CH_3) as yellow needles; m. p. 198°C (decomp.), undepressed on admixture with a sample prepared from II with acetic anhydride.

The Reaction of *S*-Cyanomethylisothiobenzanilide (I) with Benzoyl Chloride.—The mixture of *S*-cyanomethylisothiobenzanilide (I) (1.0 g.) and the excess of benzoyl chloride was heated at 90°C for

one hour, and crystals were precipitated. The precipitate was then filtered and washed with benzene. The treatment of this precipitate with aqueous sodium hydrogen carbonate gave yellow crystals, which were filtered, washed with 2-propanol, and recrystallized from ethanol. The yield of the free base of an *N*-benzoyl compound (IV; R=Ph), m. p. 211~212°C (undepressed on admixture with a sample prepared from II with benzoic anhydride), was 1.0 g.

The Hydrolysis of *S*-Cyanomethylisothiobenzanilide (I).—A suspension of *S*-cyanomethylisothiobenzanilide (I) (0.5 g.) in 10% aqueous hydrochloric acid (5 cc.) was heated gently on a water bath for twenty minutes, and then the hydrolysate was crystallized by being left standing. The yield of hydrochloride of *S*-carbamoylisothiobenzanilide (V), m. p. 65~70°C, was 0.4 g. Recrystallization from chloroform raised the melting point to 85~88°C. Colorless crystals.

Found: C, 55.20; H, 5.38; N, 8.51. Calcd. for $C_{15}H_{15}N_2SOCl \cdot H_2O$: C, 55.46; H, 5.23; N, 8.62%.

The Hydrolysis of 2, 3-Diphenylthiazone Imine Hydrochloride (II; X=Cl).—The hydrochloride (II; X=Cl) (1 g.) in 10% aqueous hydrochloric acid was heated on a steam bath for a few minutes. Oil separated and solidified when the mixture was left standing. The solid was filtered and recrystallized from acetone. The yield was 1.0 g.; m. p. 85~88°C, undepressed by admixture with the above hydrolysate prepared from I.

The Hydrolysis of *N*-Acetyl-2, 3-Diphenylthiazone Imine Hydrochloride (III; X=CH_3).—The hydrochloride of the *N*-acetyl compound (1 g.) was hydrolysed with 10% aqueous hydrochloric acid in a manner similar to that above. The yield was 0.8 g.; m. p. 85~88°C, not depressed by admixture with the hydrolysate obtained above.

An Attempt to Prepare *S*-(α-Cyanobenzyl)-isothiobenzanilide. — Thiobenzanilide (5 g.) and α-chlorophenylacetonitrile (4 g.) were dissolved in benzene (40 cc.), triethylamine (10 cc.) was added, and the mixture was refluxed for two hours. After the mixture had stood overnight, triethylamine hydrochloride (3.5 g.) was filtered off, and the solvent was removed under reduced pressure from the filtrate. The residue crystallized by scratching. The crystals were collected and washed with methanol. Recrystallization from methanol gave *cis*-α, α-dicyanostilbene as colorless needles; m. p. 158°C (reported m. p. 160°C).[6]

Found: C, 83.46; H, 4.43; N, 11.87. Calcd. for $C_{16}H_{10}N_2$: C, 83.51; H, 4.35; N, 12.17%.

A General Procedure for Preparing Thiazone Imine Hydrochlorides.—a) *N*-Substituted thioamide and α-chloronitrile (a small excess) were heated on a steam bath, until the fused reaction mixture got more viscous with a rapid rise in the temperature. The cooled viscous product was then crystallized by rubbing it with acetone, filtered, and washed with acetone. Reprecipitation from an ethanolic solution with ether gave pure thiazone imine hydrochloride.

b) *N*-Substituted thioamide, α-chloronitrile, and biphenyl as a solvent were heated at about 120°C while being stirred. The reaction mixture was then cooled as soon as the temperature began to rise, and acetone was added in order to remove the biphenyl. The acetone-insoluble hydrochloride of the heterocyclic compound was then collected, washed with acetone, and purified by reprecipitation from an ethanolic solution with ether.

The Reaction of Thiopyrrolidone with Chloroacetonitrile.—A mixture of thiopyrrolidone (1 g.) and the excess chloroacetonitrile was heated. The reaction started suddenly in about fifteen minutes with the evolution of heat, but it was at once interrupted by cooling. The solid was washed with ethanol. Yield, 1.35 g. This *S*-cyanomethylisothiopyrrolidone hydrochloride (VI) was thoroughly washed with methanol in order to analyze it.

Found: C, 40.54; H, 5.23; N, 15.89. Calcd. for $C_6H_9N_2SCl$: C, 40.79; H, 5.10; N, 15.86%.

IR: 2250 (-C≡N), 1610 (⟩C=N⟨+) cm^{-1}.

The authors are grateful to the Kyorin Pharmaceutical Co., Ltd., for recording the ultraviolet spectra.

Laboratory of Organic Chemistry
Tokyo Institute of Technology
Meguro-ku, Tokyo

6) J. v. Braun, *Ber.*, **36**, 2652 (1903).

*Color Reactions of 3-Methyl-2-benzothiazolone Hydrazone with Phenol Derivatives. I. The Spectrophotometric Microdetermination of Catechol, Hydroquinone and Resorcinol**

By Eijiro KAMATA

(Received May 27, 1964)

Since Hünig and Fritsch[1] described the oxidative coupling of 3-methyl-2-benzothiazolone hydrazone (MBTH) with various organic compounds, MBTH has been used to detect and determine trace amounts of various types of organic compounds.[2-5]

In the present paper new spectrophotometric procedures for the determination of catechol, hydroquinone and resorcinol with MBTH will be reported.**

Experimental

Reagents.—*Standard Solutions of Catechol, Hydroquinone and Resorcinol (5 μg./ml.).*—Prepared freshly daily.

3-Methyl-2-benzothiazolone Hydrazone Hydrochloride.—The reagent is commercially available. A 0.4% aqueous solution and a 0.5% methanol solution of the salt were prepared.

Oxidants.—a) 1%(w/v) Ferric Chloride Solution. b) 2%(w/v) Potassium Ferricyanide Solution. — Prepared freshly daily.

Other Reagents.—Methanol. Acetone. Concentrated ammonia. (0.7+100) Ammonia. 8N Hydrochloric Acid. 10 %Mohr's Salt Solution.—Prepared within 10 min. before use.

Apparatus. — Beckman Model DK-II and DU spectrophotometers. Hitachi ESP-2 spectrophotometer. Coleman Model 14 spectrophotometer.

Results and Discussion

Preliminary Experiments. — The sensitivities and selectivities of the color reactions of catechol, hydroquinone and resorcinol with MBTH are largely dependent on the hydrogen ion concentration and on the conditions of oxidation.

In an ammoniacal medium (pH ~11.5) catechol gives a pink color with MBTH, dissolved oxygen acting as an oxidant for the oxidative coupling. In the same medium, hydroquinone gives a blue color, which fades into brown within 2 min. However, this blue color can be stabilized a further 3 min. by acetone. Resorcinol gives only a weak yellow color under these conditions, and its absorbance is negligibly low at the λ max. of the blue color obtained from hydroquinone.

In a weakly alkaline medium (pH 8~9), catechol, hydroquinone and resorcinol give a red or orange color with MBTH in the presence of ferricyanide. In this condition reproducible results are obtained only for resorcinol.

In the acidic ferric-ferrous redox buffer, catechol gives a violet color with MBTH. Under the same conditions hydroquinone and resorcinol give a weak red or orange color. Thus the medium is more selective for catechol than the ammoniacal medium.

In a higher hydrochloric acid solution (~1.2 N), catechol, hydroquinone and resorcinol give a red or orange color with MBTH in the presence of ferric chloride. These conditions are favorable for the determination of hydroquinone and resorcinol in a mixture of the two.

Taking these results and others into consideration, the following procedures have been elaborated:

TABLE I. SPECTROPHOTOMETRIC DETERMINATION OF DIHYDROXYBENZENE

Dihydroxybenzene	λ_{max} mμ	$\varepsilon \times 10^{-4}$	Color	Procedure
Catechol	510	2.8	Pink	1a
Catechol	550	2.4	Vioelt	1b
Hydroquinone	610	1.5	Blue	2
Resorcinol	495	5.2	Orange	4
Resorcinol	515	2.9	Orange	3

Recommended Procedures and The Effect of Various Factors

1) The Determination of Catechol.—a) In an Ammoniacal Medium. — To 2 ml. of a test

* A part of this paper was presented at the 14th Annual Meeting of the Chemical Society of Japan, Kyoto, 1961.

1) S. Hünig and K. H. Fritsch, *Ann.*, **609**, 143 (1957).

2) E. Sawicki, T. R. Hauser, T. W. Stanley and W. Elbert, *Anal. Chem.*, **33**, 93 (1961).

3) E. Sawicki, T. W. Stanley, T. R. Hauser, W. Elbert and J. L. Noe, ibid., **22**, 722 (1961).

4) E. Sawicki, T. R. Hauser, T. W. Stanley, W. Elbert and F. T. Fox, ibid., **33**, 1574 (1961).

5) E. Sawicki, T. W. Stanley, T. R. Hauser and S. McPherson, *Chemist-Analyst*, **50**, 68 (1961).

** Studies of the reaction mechanism of catechol, hydroquinone and resorcinol with MBTH are in progress. Applications of MBTH to the analysis of phenol derivatives will be published elsewhere.

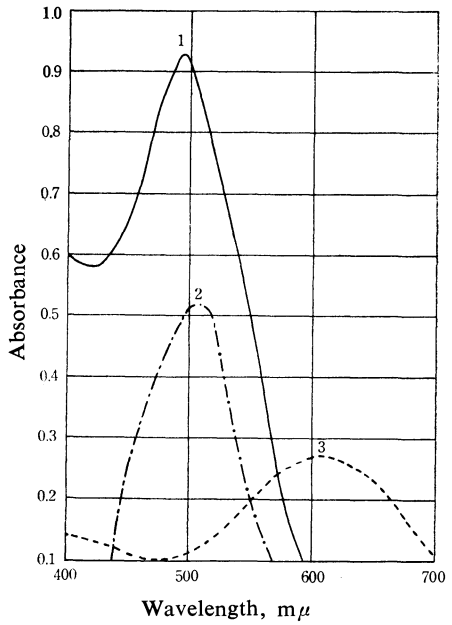


Fig. 1. Visible absorption spectra obtained in determination of catechol, hydroquinone and resorcinol in alkaline solution. 1. Resorcinol, 20 μg. (Procedure 4). 2. Catechol, 20 μg. (Procedure 1a). 3. Hydroquinone, 20 μg. (Procedure 2).

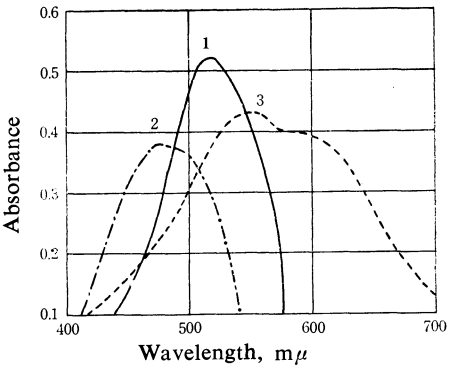


Fig. 2. Visible absorption spectra obtained in determination of catechol, hydroquinone and resorcinol in acid solution. 1. Resorcinol, 20 μg. (Procedure 3). 2. Hydroquinone, 20 μg. (Procedure 3). 3. Catechol, 20 μg. (Procedure 1b).

solution 4 ml. of a 0.5% MBTH methanol solution is added, and then 2 ml. of methanol and 2 ml. of concentrated ammonia. After the mixture has stood for 15 min., the absorbance is read at the wavelength of 510 mμ.

The Effect of Various Factors. — The absorbance reaches a maximum from 10 to 12 min. after the addition of ammonia. Very little change in the absorbance is noticed for a further 30 min. upon the addition of 2~3 ml. of concentrated ammonia. A lesser amount of concentrated ammonia is not sufficient to stabilize the product, and a decrease in the absorbance is observed after 25 min. upon the addition of 1 ml. of concentrated ammonia. The best results are obtainable with an MBTH hydrochloride concentration more than 0.2%. Beer's law is obeyed from 0 to 10 μg. of catechol. The molar absorptivity is 2.8×10^4 (Table I). The absorption spectrum is given in Fig. 1.

Derivatives of catechol give rise to a pink color. Hydroquinone and its derivatives and *p*-benzoquinone give rise to a brown color. The presence of less resorcinol than the equivalent amount of catechol does not interfere with the determination of catechol.

b) In the Medium of a Ferric-ferrous Salts Solution.—To 4 ml. of a test solution 2 ml. of a 0.4% MBTH aqueous solution is added, and then 1.6 ml. of a 10% Mohr's salt solution and 0.4 ml. of a 1% ferric chloride solution. After the mixture has stood for 5 min., 2 ml. of a acetone is added. The absorbance is read at the wavelength of 550 mμ within 30 min.

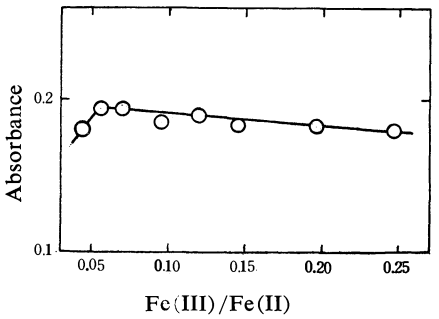


Fig. 3. Effect of Fe(III)/Fe(II) ratio on absorbance in procedure 1b. Catechol, 5 μg.

The Effect of Various Factors.—The absorbance reaches a maximum 4min. after the addition of the ferric chloride solution, and very little change in the absorbance is noticed for the next 6 min. The color is further stabilized for more than 30 min. by acetone. Best results are obtainable with a ratio Fe(III)/Fe(II) of about 0.06 (Fig. 3). The concentration of MBTH hydrochloride must be controlled below 0.1%; otherwise a turbid solution is obtained. The pH of the solution after the addition of all reagents is 3.0. At higher pH values the absorbance decreases and ferric hydroxide precipitates.

At lower pH values (pH 1~2) the violet color turns pink. In a solution containing ferric ions but not ferrous ions, catechol instantaneously gives a violet color with MBTH, and this color rapidly turns dark brown. In these two cases the reaction is no

TABLE II. DETERMINATION OF HYDROQUINONE AND RESORCINOL IN THE PRESENCE OF EACH OTHER

Hydroquinone, added μg.	Resorcinol, added μg.	Absorbance at 510 mμ	Net absorbance for resorcinol*	Calculated absorbance for resorcinol**	Recovery of resorcinol %
2.5	2.5	0.175	0.115	0.110	105
5.0	2.5	0.235	0.115	0.110	105
10	2.5	0.350	0.110	0.110	100
2.5	5.0	0.285	0.225	0.220	102
5.0	5.0	0.345	0.225	0.220	102
10	5.0	0.455	0.215	0.220	98

* Calculated from the following equation: Absorbance at 510 mμ − 0.024 × μg. of hydroquinone.
** Calculated from the calibration curve for resorcinol constructed by procedure 3.

longer selective for catechol, the sensitivities of the reaction of hydroquinone and resorcinol being comparable with that of catechol.

Beer's law is obeyed from 0 to 15 μg. of catechol. The molar absorptivity is 2.4×10^4 (Table I). The absorption spectrum is given in Fig. 2.

The presence of 2 μg. of hydroquinone or 5 μg. of resorcinol does not interfere with the determination of catechol. Derivatives of catechol give rise to a violet or blue color.

2) The Determination of Hydroquinone.—To 3 ml. of a test solution 3 ml. of a 0.5% MBTH methanol solution is added, and then 1 ml. of concentrated ammonia. After 1 min. 3 ml. of acetone is added to the solution. The absorbance is read at the wavelength of 610 mμ within 3 min.

The Effect of Various Factors. — The maximum absorbance is reached 40 sec. after the addition of ammonia, and very little change in the absorbance is noticed for the next 50 sec. The color is further stabilized for 3 min. by acetone. Acetone takes part also in making the solution clear. The absorbance is depressed in a methanol concentration more than 30%(v/v). Best results are obtainable with a 0.15% MBTH hydrochloride concentration and the addition of 1 or 2 ml. of ammonia. An increase or decrease in the concentration of MBTH or ammonia results in a decrease in the absorbance. Beer's law is obeyed from 0 to 10 μg. of hydroquinone. The molar absorptivity is 1.5×10^4 (Table I). The absorption spectrum is given in Fig. 1.

Catechol interferes with the reaction between hydroquinone and MBTH. Derivatives of hydroquinone and *p*-benzoquinone give rise to a blue color. The presence of resorcinol up to 100 μg. does not interfere with the determination of hydroquinone.

3) The Determination of Hydroquinone and Resorcinol in a Mixture of the Two. — To 4.5 ml. of a test solution 3 ml. of a 0.4% MBTH aqueous solution is added, and then 1.5 ml. of 8 N hydrochloric acid and 1 ml. of a 1% ferric chloride solution. Then the solution is heated for 2 min. in a water bath at 80°C. The solution is cooled in running tap water. Using a reagent blank as reference, the absorbance is read within 30 min. at the wavelength of 510 mμ, which corresponds to the sum of hydroquinone and resorcinol.

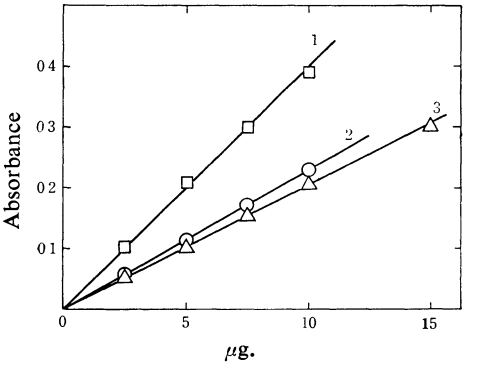


Fig. 4. Calibration curves for hydroquinone and resorcinol. 1. Resorcinol at 510 mμ (Procedure 3). 2. Hydroquinone at 510 mμ (Procedure 3). 3. Hydroquinone at 610 mμ (Procedure 2).

Refering to the content of hydroquinone previously determined by procedure 2 and to standard curves for resorcinol and hydroquinone constructed by this procedure (Fig. 4), the amount of resorcinol in mixtures with hydrquinone can be calculated by the following equation:

$$\mu g.\ \text{of resorcinol} = (\text{absorbance at } 510\ m\mu - 0.024\times \mu g.\ \text{of hydroquinone})\times 22.7$$

The Effect of Various Factors. — At room temperature the absorbance increases gradually, reaches a maximum, and decreases. After two minutes' heating in a water bath at 80°C, the reaction proceeds to completion, and no further change in absorbance is observed, even after the solution has stood for 30 min. at room temperature. The optimum range of the hydrochloric acid concentration is from 1.0 to 1.6 N for resorcinol and about 1.2 N for hydroquinone

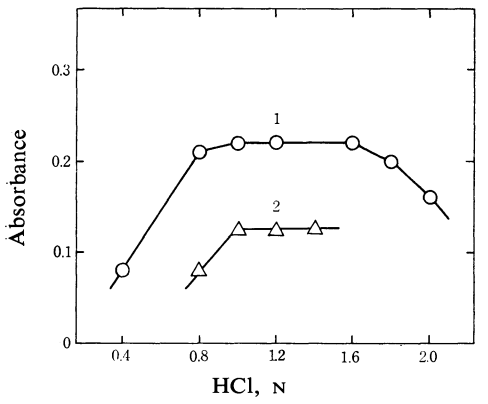


Fig. 5. Effect of acidity on absorbance in procedure 3. 1. Resorcinol, 5 μg. 2. Hydroquinone, 5 μg.

hydroquinone (Fig. 5). The optimum concentration of ferric chloride is from 0.10 to 0.14%. Best results are obtainable with an MBTH hydrochloride concentration more than 0.10%. Beer's law is obeyed from 0 to 7.5 μg. for resorcinol and from 0 to 10 μg. for hydroquinone. The molar absorptivity for resorcinol is 2.9×10^4 (Table I). Absorption spectra are given in Fig. 2.

Derivatives of dihydroxybenzene such as catechol give rise to an orange or red color.

Results of the recovery test for resorcinol in mixtures with hydroquinone are given in Table II. As is shown in the last column of the same table, the recoveries of resorcinol are from 98 to 105%.

4) The Determination of Resorcinol. — To 3 ml. of a test solution 0.5 ml. of a 0.5% MBTH methanol solution is added, and then 4.5 ml. of methanol, 1 ml. of (0.7+100) ammonia and 1 ml. of a 2% ferricyanide solution. The pH of the solution must be 8~9. The absorbance is read at the wavelength of 490 mμ within 30 min.

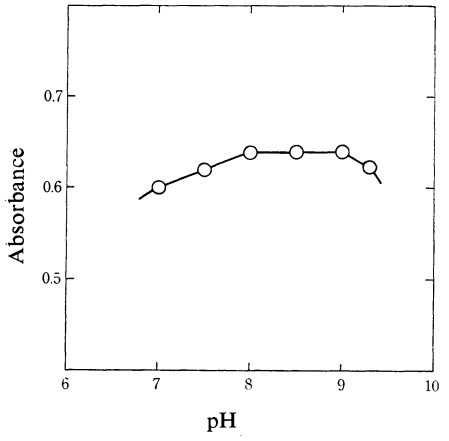


Fig. 6. Effect of pH on absorbance in procedure 4. Resorcinol, 10 μg.

The Effect of Various Factors.—The absorbance reaches a maximum a few minutes after the addition of the ferricyanide solution. Very little change in the absorbance is noticed for the next 30 min. The optimum range of the MBTH hydrochloride concentration is from 0.02 to 0.03% in the methanol concentration of about 50%(v/v). A turbid solution is obtained with a higher MBTH concentration. The optimum pH range is from 8 to 9 (Fig. 6). The use of an ammonia - ammonium chloride buffer is not recommended, the absorbance being depressed in the buffer. The concentration of potassium ferricyanide should be kept very close to 0.02%; otherwise precipitation occurs. Beer's law is obeyed from 0 to 10 μg. of resorcinol. The molar absorptivity is 5.2×10^4 (Table I). The absorption spectrum is given in Fig. 1.

Phenol derivatives give reddish colors.

Summary

New spectrophotometric procedures for determining microgram amounts of catechol, hydroquinone and resorcinol with MBTH have been described. The sensitivities and selectivities of the reactions are largely dependent on the pH and on the conditions of oxidation: 1) In an ammoniacal medium MBTH gives a stable pink color with catechol and, with hydroquinone, a blue color which is stabilized by acetone. Resorcinol gives only a faint color under these conditions. 2) When ferricyanide is used as an oxidant in a weakly alkaline solution, MBTH gives a sensitive orange color with resorcinol. 3) In an acidic ferric-ferrous redox buffer, MBTH gives a violet color with catechol. At pH 3 the reaction is selective for catechol. 4) Ferric chloride in 1.2N hydrochloric acid is favorable for the determination of hydroquinone and resorcinol in a mixture of the two.

We are grateful to Professor Motoharu Tanaka for his invaluable advice and criticism.

Laboratory of Analytical Chemistry
Faculty of Science
Nagoya University
Chikusa-ku, Nagoya

The Base-catalyzed Condensation of o-Nitroacetophenone. I. Some Properties of the Condensation Products

By Takeo SAKAN, Kousuke KUSUDA[1] and Toshio MIWA

(Received May 28, 1964)

The reaction of nitrobenzene with phenylmagnesium bromide is known to yield diphenylamine.[2] However, Newman and Smith[3] have found that *m*-nitrobenzaldehyde reacts smoothly with phenylmagnesium bromide at the low temperature of $-70°C$ to give *m*-nitrobenzhydrol, while the reaction gives only a tarry product at room temperature. This technique has been applied also to *o*-nitrobenzaldehyde.[4]

It seemed interesting to see what the reactions would be to the action of sodium acetylide upon *o*-nitroacetophenone at such a low temperature.

The treatment of *o*-nitroacetophenone with sodium acetylide in liquid ammonia at $-70°C$ yielded an orange-red crystalline compound, m. p. 171~172°C of a weak acidity (pK_a ca. 5.9) in a moderate yield, along with *o*-nitrobenzoic acid. A series of following papers will report on the elucidation of the structure and the reactions of this product, which will be referred to as compound A throughout this series.

The elementary analysis of compound A did not afford a constant result; rather, the results depended upon the kind of solvents from which it was recrystallized (see Experimental section). The analytical results agreed approximately with the $C_{17}H_{14}O_5N_2$ composition, which was supported by analyses of some of its derivatives (see below). The measrement of the *C*-methyl number gave a value of 0.72. The absence of a distinct absorption in the carbonyl region of the infrared spectrum of compound A suggests that the weak acidity of this compound may be due to an enolic group, to which a band near 3300 cm^{-1} can be assigned (Fig. 1). The absorption bands at 1535 and 1355 cm^{-1} correspond to the nitro group.

When compound A was treated with diazomethane or dimethyl sulfate and potassium carbonate, a yellow methyl ether, $C_{18}H_{16}O_5N_2$, was obtained. Similarly, the treatment of compound A with diethyl sulfate and potassium carbonate produced an ethyl ether, $C_{19}H_{18}O_5N_2$. These derivatives had lost the acidity as well as the absorption band near 3300 cm^{-1} of the original compound; these facts seem to support the speculation that the acidity of compound A may be attributed to an enolic function. The methyl ether has a weak absorption band at 3000 cm^{-1} which is shifted to 3250 cm^{-1} with an increase in its intensity in the carbon tetrachloride solution. Another conspicuous difference in the infrared spectrum of the methyl ether from that of compound A is the appearance of a new band, of a medium intensity, at 1616 cm^{-1}.

The ultraviolet spectra of compound A and its alkyl ethers possess a characteristic intense band near 380 mμ. The position of the band of compound A is shifted to ca. 400 mμ and the intensity of the band is increased when the compound is dissolved in aqueous alkali. On the other hand, such behavior is not observed in the case of its alkyl ethers.

The molecular formula of compound A, $C_{17}H_{14}O_5N_2$, was confirmed by elementary analyses of its alkyl ethers and by the determination of the molecular weight of the methyl ether by the Barger method. With this composition, compound A was assumed to be formed by the dehydrogenative condensation of three moles of *o*-nitroacetophenone with the simultaneous cleavage of one mole of *o*-nitrobenzoic acid.[5]

$$3\,C_8H_7O_3N \rightarrow C_{17}H_{14}O_5O_2+C_7H_6O_4N+H_2$$

If this condensation proceeds according to the stoichiometry of the equation and is terminated by the formation of the stable salts of both the products, the best yield compound A can be expected on the use of two gram atoms of sodium per three moles of *o*-nitroacetophenone;[6] this is indeed the case, as Table I

1) Present address: Research Institute of Atomic Energy, Osaka City University, Kita-ku, Osaka.

2) H. Gilman and R. McCracken, *J. Am. Chem. Soc.*, **51**, 821 (1929).

3) M. S. Newman and A. S. Smith, *J. Org. Chem.*, **13**, 592 (1948).

4) D. H. Hey and R. D. Mulley, *J. Chem. Soc.*, **1952**, 2276.

5) Although a pair of reagents, liquid ammonia and sodium, sounds like the conditions of the Birch reduction, the coexistence of a nitro compound and a strong base, sodium amide or acetylide, may produce oxidizing circumstances similar to those of the nitrobenzene and alkali pair.

6) Strictly speaking, the consumption of the nitro compound by reduction during the reaction is neglected.

TABLE I. BASE-CATALYZED CONDENSATION OF *o*-NITROACETOPHENONE

Per mole of *o*-nitroacetophenone		Compd. A	Compd. B	*o*-Nitrobenzoic acid	Recovered
Liq. NH_3 l.	Sodium g. atom	%[a]	%[b]	%[a,b]	%
1.3	0.57	37	—	121	49
2.1	0.63	54	—	31	30
1.0	0.67	50	—	70	c)
1.0	0.67	62	—	50	c)
3.2	1.04	34	—	53	45
6.6	3.45	—	26	71	58
1.0[d]	0.67	46	—	c)	c)
0.8[e]	0.67	45	—	c)	c)

a) The yield was calculated using the Eq. 1. The recovered ketone, if weighed, was reduced from the starting material on the calculation.
b) The yield of compound B was calculated by postulating that the compound had been formed according to the following equation:

$$2\ C_8H_7O_3N + NH_3 \rightarrow C_9H_{10}O_2N_2 + C_7H_5O_4N + H_2$$

c) The amount was not recorded.
d) Sodium amide was used in stead of sodium acetylide.
e) The reaction was carried out under an atmosphere of nitrogen.

shows. Without the introduction of acetylene, which might be unnecessary for the reaction, a comparative yield of compound A was obtained, and the reaction was rather violent. The fact that a similar result was obtained under an atmosphere of nitrogen excluded the possibility of the dehydrogenation by atmospheric oxygen.

When the condensation was carried out with a large excess of sodium, compound A was not formed, but a colorless product, $C_9H_{10}O_2N_2$, named compound B was obtained in a low yield.

The oxidation of compound A with alkaline hydrogen peroxide gave a weakly acidic substance, $C_{17}H_{12}O_5N_2$, m. p. 226~227°C. This compound was also obtained when the reaction mixture of the condensation had been allowed to stand in air for a long time before acidification. This substance is named dehydro-compound A.

Dehydro-compound A was methylated with dimethyl sulfate and potassium carbonate in a way similar to that used in the methylation of compound A to give a neutral methyl ether, $C_{18}H_{14}O_5N_2$. The methyl ether was obtained also by the oxidation of compound A

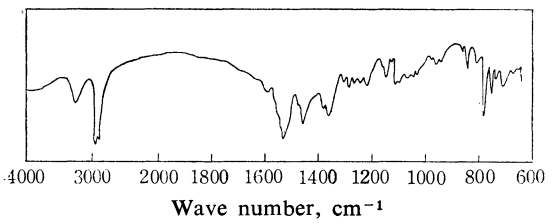


Fig. 1. Infrared spectrum of compound A (Nujol mull).

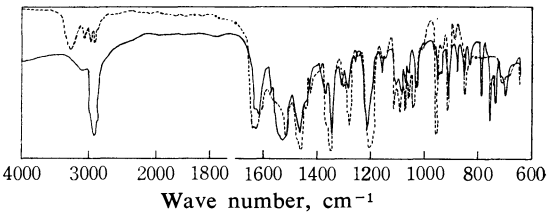


Fig. 2. Infrared spectrum of compound A methyl ether. (—— Nujol mull; ---- 0.06 M CCl_4 solution).

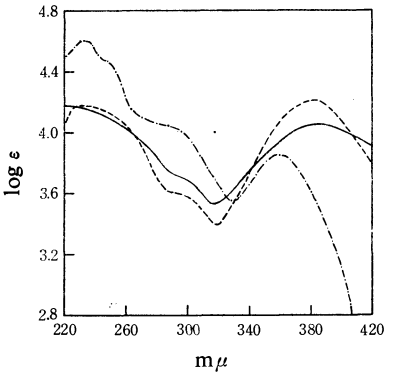


Fig. 3. Ultraviolet spectra (in ethanol) of compound A (——), compound A methyl ether (----) and dehydro-compound A (-·-·-).

methyl ether with periodic acid in dioxane. The ozonization of compound A ethyl ether produced a small amount of dehydro-compound A ethyl ether.[7] It should be pointed out that the dehydrogenation of compound A or its

7) See Part II: T. Sakan, K. Kusuda and T. Miwa, This Bulletin, 37, 1681 (1964).

alkyl ethers took place very readily with a variety of oxidizing agents.

In the ultraviolet spectra of dehydro-compound A and its methyl ether, the characteristic band near 380 mμ of the compound A series disappeared and a new band showed up near 350 m. This striking change in the spectrum suggests that a major reaction had occurred during the dehydrogenation.

Experimental[8]

The Condensation of *o*-Nitroacetophenone by Sodium Acetylide. *a) Compound A.*—Into 100 cc. of liquid ammonia saturated with acetylene, 1.5 g. (0.065 g. atom) of sodium was added in small pieces. After all the sodium had been added, 16.5 g. (0.1 mol.) of *o*-nitroacetophenone in 20 cc. of dry ether was stirred in one portion at −70°C. A violent exothermic reaction (the temperature of the reaction mixture reached −50°C) took place, giving a dark red mixture. The mixture was then kept at −50∼−60°C for one hour, 4.0 g. (0.075 mol.) of ammonium chloride was added, and the liquid ammonia was allowed to evaporate while about 50 cc. of ether was added. When the reaction mixture had reached the room temperature, a further amount of ether and some water were added. The separated ethereal solution was extracted with several portions of a 10% sodium hydroxide solution, and the aqueous extracts were added to the original aqueous layer. (From the ethereal solution, after concentration followed by distillation in vacuo, *o*-nitroacetophenone was recovered.) The combined aqueous solution, dark red in color, was washed with ether, acidified with hydrochloric acid, and extracted with ether. The ethereal solution was washed with a sodium bicarbonate solution until the washing became reddish.[9] The concentration of the ethereal solution gave orange-red needles, which, after recrystallization from ethanol, melted at 170∼171°C. Recrystallization from non-polar solvents gave somewhat yellowish crystals of the same melting point. The pK_a value (ca. 5.9) in an aqueous solution was not accurate because of the poor solubility of this compound in water. λ_{max} 382∼384 (4.05). ν_{max} 3286 (OH), 1535, 1355, 844 (NO_2).

Found: (a) From benzene-ligroin: C, 63.10; H, 4.46; N, 7.52. (b) From chloroform: C, 62.52; H, 4.22; N, 8.08. (c) From ethanol: C, 62.68; H, 4.17; N, 8.48. *C*-Methyl group[10]: 0.72. Calcd. for $C_{17}H_{14}O_5N_2$: C, 62.57; H, 4.32; N, 8.59%. The results of the condensation under various conditions, are listed in Table I.

b) Compound B.—*o*-Nitroacetophenone (10.0 g., 0.061 mol.) was subjected to condensation with sodium acetylide prepared from acetylene 5.0 g. (0.22 g. atom) of sodium in 400 cc. of liquid ammonia, and the reaction mixture was worked up in a way similar to that described in a). There was obtained 0.4 g. of a crystalline substance insoluble both in the ethereal and alkaline aqueous layers. From the neutral fraction, 5.8 g. of an oil boiling at 146°C/2.5 mmHg was obtained. The 2,4-dinitrophenylhydrazone of the oil, m. p. 166∼167°C, was identified as that of *o*-nitroacetophenone. The acid fraction gave 1.0 g. of crude *o*-nitrobenzoic acid. The insoluble material was dissolved in N hydrochloric acid, and the solution was treated with active carbon and then made alkaline with aqueous ammonia to give faintly brown plates decomposing at 236°C. λ_{max} 230 (4.18), 291 (3.92). ν_{max} 3280 (OH), 2860∼2500 (NH or OH[6]), 1672 (C=O).

Found: C, 60.82; H, 5.78; N, 15.69. Calcd. for $C_9H_{10}O_2N_2$: C, 60.66; H, 5.66; N, 15.72%.

Compound A Methyl Ether. — *a) With Diazomethane.*—A solution of 400 mg. (1.22 mmol.) of crude compound A in a little methanol was treated with an ethereal solution of diazomethane prepared from 4.0 g. (40 mmol.) of nitrosomethylurea. A benzene solution of the crude product was adsorbed on a small amount of active alumina. Benzene eluted 342 mg. (82%) of yellow crystals, which, after recrystallization from petroleum benzine, melted at 114∼115.5°C. λ_{max} 230 (4.17), 383 (4.21). ν_{max} 1533, 1347, 851 (NO_2).

Found: C, 63.58; H, 4.77; N, 8.36. Mol. wt. (Barger) 325±25. Calcd. for $C_{18}H_{16}O_5N_2$: C, 63.52; H, 4.74; N, 8.23%. Mol. wt. 340.

Elution with 50 cc. of benzene containing one drop of ethanol gave 44 mg. of dehydro-compound A methyl ether m. p. 127°C (see below).

b) With Dimethyl Sulfate and Potassium Carbonate.—A mixture of 1.6 g. (4.7 mmol.) of crude compound A, 1.0 g. (7.9 mmol.) of dimethyl sulfate, and 1.1 g. (8.0 mmol.) of potassium carbonate in 20 cc. of acetone was refluxed for 20 min. The insoluble substances were then removed by filtration, and the acetone was evaporated under reduced pressure to give a viscous oil.[11] The oil was purified in the way described in a) to give a quantitative yield of the methyl ether m. p. 113∼115°C and a trace of dehydro-compound A methyl ether, m. p. 127°C.

Compound A Ethyl Ether.—A mixture of 3.3 g. (10 mmol.) of crude compound A, 1.6 g. (10 mmol.) of diethyl sulfate, and 1.4 g. (11 mmol.) of potassium carbonate in 50 cc. of acetone was refluxed for one hour. The reaction mixture was worked out in a way similar to that described in methylation b). Chromatographic purification gave 3.4 g. (94%) of the ethyl ether, which was recrystallized from ether m. p. 117∼118°C.

8) All melting points are uncorrected. Unless otherwise noted, ultraviolet spectra were taken in ethanol and infrared spectra, in Nujol mull; Peak positions and intensities are expressed in λ_{max} mμ (log ε) and in ν_{max} cm^{-1}, respectively. The authors are much indebted to Mr. Jun'ichi Gōda and his associates for their elementary analyses and to Mrs. Michino Butsugan and Miss Hiromi Tokuda for their infrared determinations for this series of papers.

9) A considerable amount of compound A was extracted by aqueous sodium bicarbonate because of its acidity.

10) E. J. Eisenbraun, S. M. McElvain and B. F. Aycock, *J. Am. Chem. Soc.*, **76**, 607 (1954). The measurement was carried out by Dr. Akira Fujino, to whom the authors are indebted.

11) Superheating during the evaporation caused a severe resinification that made it impossible to obtain the methyl ether.

Found: C, 64.13; H, 4.89; N, 8.16. Calcd. for $C_{19}H_{18}O_5N_2$: C, 64.40; H, 5.12; N, 7.91%.

Dehydro-compound A.—To a warm solution of 4.0 g. (12 mmol.) of crude compound A in 150 cc. of a 2% sodium hydroxide solution was added 20 cc. of 30% hydrogen peroxide. The mixture was then stirred well and allowed to stand overnight to from a yellowish gel. The crystal-cake formed on acidification with 20% hydrochloric acid was crushed, collected by filtration, washed successively with water and ethanol, and then dried. Dehydro-compound A (3.5 g.) was recrystallized from chloroform and ligroin to give faintly grayish prisms melting at 226~227°C. This compound is rather unstable to light. λ_{max} 234 (4.60), 358 (3.85). ν_{max} 3145 (OH), 1675, 1600 (C=O), 1517, 1340 (NO_2).

Found: C, 63.44; H, 3.78; N, 8.79. Calcd. for $C_{17}H_{12}O_5N_2$: C, 62.96; H, 3.73; N, 8.64%.

Dehydro-compound A Methyl Ether.—A mixture of 470 mg. (1.44 mmol.) of dehydro-compound A, 0.2 g. (1.5 mmol.) of dimethyl sulfate, and 0.22 g. (1.6 mmol.) of potassium carbonate in acetone was refluxed for one hour. The removal of the insoluble material by filtration, followed by the evaporation of the solvent in vacuo, left crystals, which were then chromatographed on a short column of active alumina in benzene to give a quantitative yield of the methyl ether. After recrystallization from benzene-ligroin, it melted at 129.5~130°C. λ_{max} 230~231 (4.58), 285~287 (4.05), 350~352 (3.78). ν_{max} 1684, 1647 (C=O), 1534, 1355 (NO_2).

Found: C, 63.94; H, 4.25; N, 8.34. Calcd. for $C_{18}H_{14}O_5N_2$: C, 63.90; H, 4.17; N, 8.28%.

The Periodic Acid Oxidation of Compound A Methyl Ether.—A mixture of 500 mg. (1.47 mmol.) of compound A methyl ether, 380 mg. (1.42 mmol.) of sodium periodate, and 1.44 mg. of sulfuric acid in 9 cc. of dioxane was left to stand at room temperature for six days. The addition of water, followed by the evaporation of the solvent under reduced pressure, was repeated to remove the dioxane. The resulting aqueous solution was then extracted with ether-benzene, and the extract was washed with aqueous sodium bicarbonate and dried. The evaporation of the solvent under reduced pressure and the chromatography of the residue on active alumina gave 188 mg. of dehydro-compound A methyl ether, which, after recrystallization from benzene-ligroin, metled at 129.5~130°C. A mixed melting point determination with an authentic samle of the methyl ether showed no depression.

Faculty of Science
Osaka City University
Sumiyoshi-ku, Osaka

The Base-catalyzed Condensation of o-Nitroacetophenone. II. The Ozonolysis of Methyl Ether of Compound A, a Condensation Product, and the Structure of Compound B, Another Product

By Takeo SAKAN, Kousuke KUSUDA[1] and Toshio MIWA

(Received May 28, 1964)

The base-catalyzed condensation of *o*-nitroacetophenone has been reported to give an orange-red product, $C_{17}H_{14}O_5N_2$, named compound A.[2] In order to elucidate the structure of this compound, its methyl ether was ozonolyzed. The ozonolysis of compound A methyl ether yielded a colorless neutral compound, $C_{10}H_{11}O_3N$, along with *o*-nitrobenzoic acid, *o*-nitroacetophenone and formaldehyde.

The measurement of the *C*-methyl number of the C_{10}-compound gave a value of 0.64; a positive alkoxyl group test[3] showed the presence of an alkoxyl group. This compound gave negative reactions both with a ferric hydroxamate test[4] and with various carbonyl reagents, indicating the absence of either an ester or a keto function. On the other hand, it gave positive results with the Millon and Folin-Dennis reactions.[5] After hydrolysis,

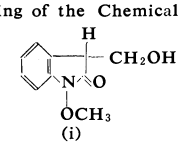
1) Present address: Research Institute of Atomic Energy, Osaka City University, Kita-ku, Osaka.

2) T. Sakan, K. Kusuda and T. Miwa, This Bulletin, 37, 1678 (1964).

3) N. D. Cheronis, "Micro and Semimicro Methods," Interscience Publisher, New York (1954), p. 454.

4) Ibid., p. 460.

5) Since the oxindoles with no hydrogen atom at their β-position had generally given a negative Folin-Dennis reaction, formula i was assigned to this compound (The 11th Annual Meeting of the Chemical Society of Japan,



(i)

Tokyo, April, 1958). Later this formula was found to be false by the confirmation of the presence of a *C*-methyl group. A color test with ammonium phosphomolybdate is more specific to the presence of the β-hydrogen of oxindole derivatives (T. Tokuyama, The 12th Annual Meeting of the Chemical Society of Japan, Kyoto, April, 1959); the C_{10}-compound gave a negative reaction with this reagent.

followed by diazotization and coupling with β-naphthol, it developed an orange color. The vapor of the zinc-dust distillation gave a violet spin-splinter reaction. These color reactions,[6] associated with the features of the ultraviolet spectrum[7] (Fig. 1), suggested the presence of an oxindole system in this compound. The carbonyl bond (1715 cm^{-1}) of the infrared spectrum of the compound can be assigned to the oxindole carbonyl. The *N*-unsubstituted oxindoles usually exhibit a broad band near 3200 cm^{-1}.[8] The absence of any bands above 3000 cm^{-1} of the infrared spectrum of the compound, except for a sharp band at 3410 cm^{-1}, indicated that the postulated oxindole nucleus can be substituted at the nitogen atom.

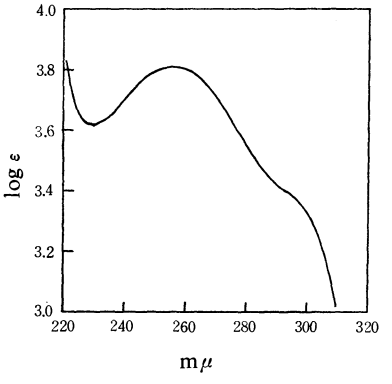


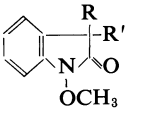
Fig. 1. Ultraviolet spectrum of the C_{10}-compound (I) in ethanol.

The acylation of the C_{10}-compound by acetic anhydride or *p*-nitrobenzoyl chloride in the presence of pyridine gave the corresponding *O*-acyl derivatives, as is indicated by their infrared spectra (see Experimental section). The disappearance of the 3410 cm^{-1} band in these spectra demonstrated that the band of the original compound should be attributed to a hydroxyl group.

On the basis of these results, the C_{10}-compound may be considered to be an *N*-substituted oxindole derivative with a hydroxyl, a methoxyl and a methyl group as substituents. The neutral property of the compound excluded the possibility that it might be a hydroxamic acid. Therefore, this compound was assumed to be 1-methoxy-3-methyldioxindole (I).

The treatment of the C_{10}-compound with thionyl chloride and pyridine produced a chloride II, which was hydrogenated in the presence of palladium-on-carbon and sodium acetate to a chlorine-free oil considered to be 1-methoxy-3-methyloxindole (III).

On the other hand, 1-methoxyoxindole (IV)[9] was formylated with ethyl formate in the presence of sodium ethoxide.[10] The formylation product, V, was hydrogenated over palladium-on-carbon to compound III. Both the compound from the ozonolysis and that from the synthetic path showed quite identical infrared spectra. The oily oxindole, III, was characterized by bromination to a crystalline monobromine atom of which was tentatively located at the position 5 of the oxindole system.



I, R=CH_3, R'=OH
II, R=CH_3, R'=Cl
III, R=CH_3, R'=H
IV, R=R'=H
V, R, R'=CHOH

Interestingly, the hydrogenation of V over Raney nickel caused a further reduction to 3-methyloxindole.

In order to confirm whether the *O*-methyl group of the C_{10}-compound had been introduced by the methylation of compound A, the ethyl ether of the latter was ozonolyzed. From ethyl ether of latter was ozonolyzed. From the neutral fraction two unknown compounds besides *o*-nitroacetophenone were isolated. One of the unkonwn compounds, $C_{19}H_{11}O_5N_2$, was supposed to be dehydro-compound A[2] ethyl ether on the basis of its ultraviolet spectrum.

The other unknown product, $C_{11}H_{13}O_3N$, was assigned the 1-ethoxyoxindole structure I (OEt for OMe) by analogy with the above-mentioned C_{10}-compound; this assignment was confirmed by its ultraviolet and infrared spectra, which were similar to those of the latter. Consequently, it is apparent that the hydroxyl group of weak acidity in compound A is not an enolic one, but one attached to a nitrogen atom, as in an oxime or in a hydroxamic acid. Hence, compound A contains an *N*-hydroxyindoline and an *o*-nitrophenyl moiety in its molecule.

The base-catalyzed condensation of *o*-nitroacetophenone using a large excess of sodium acetylide yielded no compound A, but formed a faintly yellow product, compound B.[2]

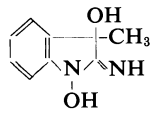
Contrary to the weakly acid compound A, this compound was basic and soluble in dilute hydrochloric and. It was recovered as precipitates from the acid solution when it was made alkaline with aqueous ammonia. It was insoluble in aqueous sodium bicarbonate. Hot aqueous alkali dissolved it gradually, with the

6) H. Wieland and B. Witkop, *Ann.*, **543**, 171 (1940).
7) For the ultraviolet spectra of oxindoles see, e. g., J. W. Cornforth, C. E. Dargliesh and A. Neuberger, *Biochem. J.*, **48**, 598 (1951).
8) J. M. Bruce and F. K. Sutcliffe, *J. Chem. Soc.*, **1957**, 4789.
9) W. B. Wright, Jr., and K. H. Collins, *J. Am. Chem. Soc.*, **78**, 221 (1956).
10) P. L. Julian, J. Pikel and F. E. Wentz, ibid., **57**, 2026 (1935).

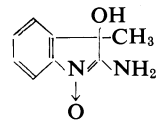
evolution of ammonia. The vapor of zinc-dust distillation gave a violet pine-splinter reaction, indicating the formation of the indole derivative. The green color developed with alcoholic ferric chloride quickly turned yellow. Aqueous ferric chloride gave the pale blue color characteristic of α-aminopyridine *N*-oxides.[11]

The attempted methylation of compound B by treatment with dimethyl sulfate and potassium carbonate afforded a compound melting at 134~135°C and with the evolution of ammonia. This compound was shown to be identical with the C_{10}-compound I obtained above by the ozonolysis of the compound A methyl ether.

On the basis of these results compound B may be represented by either of the following tautomeric structures, VIa or VIb:



VIa



VIb

Experimental[12]

The Ozonolysis of Compound A Methyl Ether. 1-Methoxy-3-methyldioxindole (I). — *a) Oxidative Decomposition.*—A solution of 1.31 g. (3.88 mmol.) of compound A methyl ether[2] in 40 cc. of ethyl acetate, which had been chilled in an ice-bath, was saturated with ozone and allowed to stand in an ice-bath overnight. The solvent was then removed by distillation under reduced pressure in the cold, and the remaining red oil was added to a mixture of 0.4 g. of sodium dichromate in 40 cc. of acetic acid to cause a violent reaction, with foaming. The mixture, diluted with water, was extracted continuously with ether, and the extract washed with aqueous sodium bicarbonate. The acid fraction (469 mg., 72%) was recrystallized from benzene-petroleum benzine to give crystal melting at 145~147°C. No depression was observed in a mixed melting point determination with *o*-nitrobenzoic acid.

The removal of the solvent in vacuo from the ethereal solution left a viscous oil, which deposited a small amount of crystals when left standing. The residue in benzene was adsorbed on active alumina. Four fractions taken with benzene gave a yellow oil weighing 61 mg., 60 mg., 63 mg. and 37 mg. respectively. The first three of them (184 mg. in total, 30%) showed identical infrared (ν_{max} 1695 (C=O), 1522, 1348 (NO_2)) and ultraviolet (λ_{max} 259) spectra. The combined oil was then converted to a 2,4-dinitrophenylhydrazone melting at 164~165°C, which was identified with that of *o*-nitroacetophenone by a mixed melting point determination.

Elution with benzene containing some ethanol yielded 38 mg. (5.1%) of crystals, which, after recrystallization from benzene-ligroin, melted at 134~136°C. λ_{max} 257 (3.81). ν_{max} 3410 (OH), 1715 (C=O).

Found: C, 62.37; H, 6.06; N, 7.47; *C*-methyl, 0.62. Calcd. for $C_{10}H_{11}O_3N$: C, 62.16; H, 5.74; N, 7.25%.

A solution of 5 mg. of the C_{10}-compound in one drop of pyridine was treated with about 5 mg. of *p*-nitrobenzoyl chloride under ice-cooling, and the mixture was allowed to stand overnight. The removal of the pyridine under reduced pressure, followed by washing successively with two portions of water, 5% aqueous sodium carbonate and water, gave a *p*-nitrobenzoate, which melted at 107~109°C after recrystallization from ethanol. ν_{max} 1745, 1730 (C=O).

A solution of 51 mg. of the C_{10}-compound in 15 drops of pyridine, cooled with ice, was treated with 4 drops of acetic anhydride. After being kept for 6 hr. at room temperature, the mixture was decomposed by the addition of water. The resulting oil was washed with N hydrochloric acid, water and aqueous sodium carbonate, and then taken into benzene. The benzene solution, after drying, was filtered through a short column of active alumina. The removal of the solvent left an oily acetate. ν_{max} 1745 (shoulder), 1739 (C=O).

b) Decompsition with Water. — Compound A methyl ether (623 mg., 1.83 mmol.), dissolved in ethyl acetate, was saturated with ozone. The resulting ozonide, as a solution, was decomposed by the addition of water. The organic layer was separated from the aqueous layer, which was extracted with ether. The extract, combined with the original organic layer, was worked out as described in a). The acid fraction gave 279 mg. (91%) of crude *o*-nitrobenzoic acid. The neutral fraction was adsorbed on alumina. A yellow oil (100 mg.) was eluted by benzene. Elution with benzene containing a small amount of ethanol gave 98 mg. (28%) of a crude C_{10}-compound.

c) Reductive Decomposition.—After a solution of 308 mg. (0.91 mmol.) of compound A methyl ether in 20 cc. of ethyl acetate had been saturated with ozone, the solution was shaken saturated sulfurous acid and worked out as described in a). From the acid fraction, 96.5 mg. (63.9%) of crude *o*-nitrobenzoic acid was obtained. The removal of the solvent from the neutral fraction immediately gave 124 mg. (71.1%) of crystals, which after, recrystallization from benzene-ligroin, melted at 136°C. The chromatography of the mother liquor of recrystallization gave a small amount of oil. It was assumed to be *o*-nitroacetophenone because of a positive reaction with 2,4-dinitrophenylhydrazine.

d) In Carbon Tetrachroride. — A solution of 429 mg. of compound A methyl ether in 80 cc. of carbon tetrachloride, chilled with ice, was saturated with ozone. After it had been allowed to stand overnight, the solution deposited a resinous material on the wall of the flask. The resinous material

11) G. T. Newbold and F. S. Spring, *J. Chem. Soc.*, **1949**, S133; W. Sharp and F. S. Spring, ibid., **1951**, 932; J. D. Loudon and G. Tennant, ibid., **1960**, 3466.

12) All melting points are not corrected. Unless otherwise noted, ultraviolet spectra were taken in ethanol and infrared spectra in Nujol mull; they are expressed in λ_{max} mμ (log ε) and in ν_{max} cm^{-1}, respectively.

was dissolved by the addition of ethyl acetate, and the ozonide was decomposed by the addition of 70 cc. of water. The aqueous solution gave a positive reaction with 2,4-dinitrophenylhydrazine and chromotropic acid (formaldehyde).[13] The aqueous solution was then distilled, and 35 cc. of the distillate was treated with 12 cc. of a saturated aqueous methone solution and allowed to stand, thus depositing small needles melting at 183~185°C, which did not depress the melting point of the methone derivative of formaldehyde.

3-Formyl-1-methoxyoxindole (V). — Into a hot sodium ethoxide solution prepared from 1.0 g. (44 mmol.) of sodium and 13 cc. of dry ethanol was added a mixture of 4.4 g. (27 mmol.) of 1-methoxyoxindole[9] and 3.0 g. (40 mmol.) of ethyl formate, the reaction mixture solidifying into a pink cake with heat evolution. The cake was dissolved with 120 cc. of water, and the solution was acidified with hydrochloric acid to separate yellowish brown precipitates, which were collected by filtration, washed with 50% aqueous ethanol and recrystallized from ethanol to give 2.9 g. (56%) of V decomposing at 190°C. ν_{max} 2650 (OH), 1658 (C=O).

Found: C, 62.84; H, 4.75; N, 7.51. Calcd. for $C_{10}H_9O_3N$: C, 62.82; H, 4.75; N, 7.33%.

1-Methoxy-3-methyloxindole (III).—*a) From 1-Methoxy-3-methyldioxindole (I).*—A solution of 62 mg. (0.32 mmol.) of the C_{10}-compound in 1 cc. of pyridine was treated with 35 mg. (0.42 mmol.) of thionyl chloride. After being kept at room temperature for 18 hr., the mixture was diluted with ether and washed with water. The removal of the ether by distillation left 47 mg. of crystals, m. p. 78~102°C, which showed positive in a Beilstein test. The filtration of a benzene solution of the crystals through a short column of alumina gave 16 mg. of the chloride II. ν_{max} 1739 (C=O).

A solution of 45 mg. (0.21 mmol.) of the chloride II in ethanol was hydrogenated in the presence of 17.5 mg. (0.21 mmol.) of sodium acetate and 20 mg. of 5% palladium-on-carbon. Within 40 min. 7.9 cc. (14°C) of hydrogen was absorbed. After the removal of the catalyst by filtration, followed by the evaporation of the solvent in vacuo, the residue, as a benzene solution, was filtered through a short column of alumina to give 35 mg. of an oil. The oil showed an infrared spectrum (ν_{max} 1736~1721 (C=O)) quite identical with that of 1-methoxy-3-methyloxindole synthesized below.

b) From 3-Formyl-1-methoxyoxindole (V). — A solution of 170 mg. (0.89 mmol.) of the formylation product V in 10 cc. 95% ethanol was hydrogenated in the presence of 80 mg. of 5% palladium-on-carbon. Within 2 hr. 5.6 cc. (13°C) of hydrogen was absorbed. Work-up in a way similar to that described in a) gave III as an oil, which was characterized as a bromide. The elution of the alumina with benzene containing a little ethanol yielded crystals melting at little ethanol yielded crystals melting at 110~125°C. The hydrogenation of V over Raney nickel in ethanol also gave crystals, m. p. 118~120°C, as a sole product. They were assumed to be 3-methyloxindole (reported m. p. 123°C[14]).

5(?)-Bromo-1-methoxy-3-methyloxindole. — Into seven-tenths of a solution of 120 mg. (0.77 mmol.) of bromine and 140 mg. (1.54 mmol.) of potassium bromide in 5 cc. of water, 95 mg. (0.54 mmol.) of oily oxindole III was added, and the mixture was left to stand overnight. The mixture was then extracted with ether. The evaporation of the ether produced 94 mg. (48%) of pale yellow crystals, which, after filtration, as a benzene solution, through alumina, followed by recrystallization from benzene-ligroin, melted at 90~92°C.

Found: C, 46.91; H, 4.18; N, 6.21. Calcd. for $C_{10}H_{10}O_2NBr$: C, 46.89; H, 3.94; N, 5.47%.

The Ozonolysis of Compound A Ethyl Ether.—A solution of 492 mg. (1.39 mmol.) of the ethyl ether[2] in 36 cc. ethyl acetate was saturated with ozone, and the ozonide was decomposed with saturated aqueous sulfurous acid. Work-up in a way similar to that described in the ozonolysis of the methyl ether c) gave 125 mg. (54%) of *o*-nitrobenzoic acid and 260 mg. of the neutral fraction. The latter, dissolved in benzene, was adsorbed on alumina. The first crop eluted with benzene gave 27 mg. of an oil, which was identified with *o*-nitroacetophenone by derivation to its 2,4-dinitrophenylhydrazone. The second crop eluted with the same solvent gave 27.5 mg. of crystals, which, after recrystallization from benzene-ligroin, melted at 130~131°C. On the basis of the elementary analysis, the compound was assumed to be dehydro-compound A ethyl ether.

Found: C, 64.58; H, 4.56. Calcd. for $C_{19}H_{16}O_5N_2$: C, 64.77; H, 4.58%.

Elution with benzene containing a little ethanol yielded 79 mg. of crystals, which were recrystallized from benzene-ligroin; m. p. 80~81°C. λ_{max} 259 (3.59). ν_{max} 3344 (OH), 1704 (C=O).

Found: C, 63.51; H, 6:45; N, 6.97. Calcd. for $C_{11}H_{13}O_3N$: C, 63.75; H, 6.32; N, 6.76%.

The Attempted Methylation Compound B.—A mixture of 104 mg. of compound B, 5 cc. of acetone, 183 mg. of dimethyl sulfate and 200 mg. of potassium carbonate was heated under reflux for 5 hr. During the heating, the evolution of ammonia was observed (detected by the Nessler reaction and with litmus paper). After the removal of inorganic substances and of recovered compound B by filtration, followed by the evaporation of the solvent in vacuo, the remaining residue was dissolved in 100 cc. of benzene containing 3 drops of ethanol and the solution was filtered through a short column of alumina. The evaporation of the solvent left 37 mg. of crystals, which, after recrysallization from benzene-ligroin, melted at 134~135°C. This compound was identified with the 1-methoxy-3-methyldioxindole (I) obtained above by the ozonolysis of compound A methyl ether by a mixed melting point determination. By treating the insoluble material of the reaction mixture with water, 57 mg. of compound B remained undissolved.

Faculty of Science
Osaka City University
Sumiyoshi-ku, Osaka

13) F. Feigl, "Spot Tests," Vol. II, Elsevier Publ., New York (1954), p. 240.

14) K. Brunner, *Monatsh.*, 18, 533 (1897).

Studies of the Hydration and the Structure of Water and Their Roles in Protein Structure. I. The Effective Volumes of 1-1 Electrolytes in Aqueous Solutions and the Electrostriction of Water[1)]

By Sachio Goto*

(Received May 29, 1964)

Recently several reports[2-8)] on the conformation of proteins have drawn attention to the properties and structure of water from the viewpoint of the stabilization of hydrophobic bonds. However, although there is a considerable literature on the properties and structure of water, there are still many problems to be solved.[7-15)]

In a series of studies, of which this is the first report, we propose to give information on the hydration and the structure of water and to elucidate the role of water in maintaining the conformation of proteins. As a basis for a consideration of these problems, the present paper is devoted primarily to the hydration of electrolytes.

There have been numerous investigations[16-25)] in different ways of the hydration of electrolytes in aqueous solutions. However, in all cases the results have been obtained in terms of various differing assumptions and there are large discrepancies between the results obtained.[17,18,26,27)] In addition, the state of the water of hydration is unknown. If the effective volumes of ions in aqueous solutions were known, various questions concerning the state and number of molecules of the water of hydration could be resolved. This problem is especially important in the case of uni-univalent (1-1) electrolytes.[23,28)] This paper will report on the effective volumes of ions and the magnitudes of the electrostriction of the solvent as analyzed from a measurement of their density at various concentrations in aqueous salt solutions. The state of the water around the ions will also be discussed.

The volumes of inorganic salts in aqueous solutions are apparently smaller than the volumes in their respective crystals, due to the contraction of the solvent by electrostatic attraction between ions and water dipoles. However, the volume of lithium iodide in solution is greater than that of its crystals.[29)] To obtain details on the magnitude of electrostriction, it is necessary to know the effective volumes of salts in solution rather than in crystals.

Calculation

The values for densities in aqueous salt solutions used in the calculations are quoted from the International Critical Table.

The reciprocal of the density (d_m) of a solution which contains m g. of the solute in 100 g. of the solution corresponds to the volume (V_m) of 1 g. of the solution. Therefore, the volume (V_c) of a solution containing 100 g. of water and c g. of solute can be written as follows:

$$V_c = \frac{100}{d_m} \times \frac{100}{100-m} \qquad (1)$$

1) Presented at the 16th Annual Meeting of the Chemical Society of Japan, Tokyo, April, 1963.

* Present address: Institute for Infectious Diseases, The University of Tokyo, Shiba Shirokane-Daimachi, Minato-ku, Tokyo.

2) I. M. Klotz, *Science*, **128**, 815 (1958).
3) W. Kauzmann, *Advances in Protein Chem.*, **14**, 1 (1959).
4) A. Szent-Gyorgyi, "Bioenergetics," Academic Press, N. Y. (1957).
5) R. E. Weber and C. Tanford, *J. Am. Chem. Soc.*, **81**, 3255 (1959).
9) I. M. Klotz and S. W. Luborsky, ibid., **81**, 5119 (1959)
7) G. Nemethy and H. A. Scheraga, *J. Chem. Phys.*, **36**, 3382, 3401 (1962).
8) G. Nemethy and H. A. Scheraga, *J. Phys. Chem.*, **66**, 1773 (1962).
9) J. D. Bernal and R. H. Fowler, *J. Chem. Phys.*, **1**, 515 (1933).
10) J. A. Pople, *Proc. Roy. Soc.*, **A205**, 163 (1951).
11) G. H. Haggis, J. B. Hasted and T. J. Buchanan, *J. Chem. Phys.*, **20**, 1452 (1952).
12) H. S. Frank, *Proc. Roy. Soc.*, **A247**, 481 (1958).
13) L. Pauling, "The Nature of the Chemical Bond," 3rd ed., Cornell University Press, Ithaca, N. Y. (1960).
14) G. Wada, This Bulletin, **34**, 955 (1961).
15) H. S. Frank and A. S., Quist, *J. Chem. Phys.*, **34**, 604 (1961).
16) A. Passinski, *Acta Physicochim. U. R. S. S.*, **8**, 385 (1938).
17) A. M. Azzam, *Z. Elektrochem.*, **58**, 889 (1954).
18) A. M. Azzam, *Z. physik. Chem.*, **33**, 320 (1962).
19) E. R. Nightingale, Jr., *J. Phys. Chem.*, **63**, 1381 (1959).
20) H. S. Frank and W. Y. Wen, *Discussions Faraday Soc.*, **24**, 133 (1957).
21) K. Tamura and T. Sasaki, This Bulletin, **36**, 975 (1963).
22) M. Kaminsky, *Discussions Faraday Soc.*, **24**, 171 (1957).
23) P. Mukerjee, *J. Phys. Chem.*, **65**, 740, 744 (1961).
24) J. H. Wang, ibid., **58**, 686 (1954).
25) F. S. Feates and D. J. G. Ives., *J. Chem. Soc.*, **1956**, 2798.
26) J. O'M. Bockris, *Quart. Rev.*, **3**, 173 (1949).
27) R. P. Bell, *Endeavour*, **17**, 31 (1958).
28) R. Gopal and R. K. Srivastava, *J. Phys. Chem.*, **66**, 2704 (1962).
29) R. W. Gurney, "Ionic Processes in Solution," McGraw-Hill Book Co., N. Y. (1953).

$$=c\bar{v}+\frac{100}{d_o}-V^e{}_c \tag{2}$$

where $\bar{v}$ is the effective specific volume of salt in the solution; $V^e{}_c$, the volume of water decreased by electrostriction, and d_o, the density of pure water. c is given by:

$$c=\frac{100m}{100-m} \tag{3}$$

On changing the concentration, c, from c_i to c_j, we find:

$$\bar{v}_{i,j}=\frac{V_{ci}-V_{cj}}{c_i-c_j}=\frac{dV}{dc} \tag{4}$$

$$=\bar{v}-\frac{V^e{}_{ci}-V^e{}_{cj}}{c_i-c_j}=\bar{v}-\frac{dV^e}{dc} \tag{5}$$

where $\bar{v}_{i,j}$ corresponds to the apparent specific volume of the salt at a given concentration range. If $V^e{}_{ci}$ becomes equivalent to $V^e{}_{cj}$ with an increase in the concentration or if $dV^e/dc=0$, $\bar{v}_{i,j}$ will correspond to the effective specific volume of the salt in solution, because all the solvent water will be attracted by ions at a high concentration. In consequence, the volume of water (100 g.) may approach a constant ($100/d_o-V^e{}_{max}$) with an increase in the concentration of the solute, as is shown by curve B in Fig. 1.

Next, with regard to the correlation between V_c and the concentration of salt, the relation given in Eqs. 6 holds true empirically.

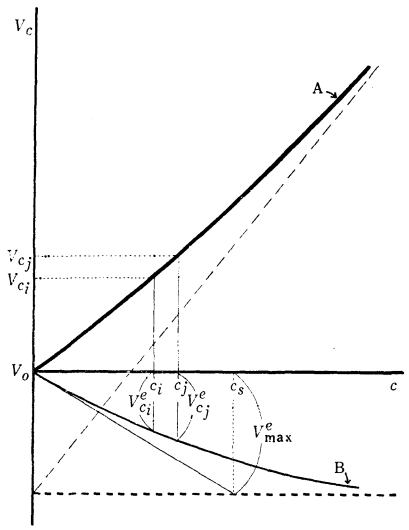


Fig. 1. Schematic representation of the volumes of the solution and the solvent plotted against the concentration of salt.
Curve A: volumes of solutions containing 100 g. of water.
Curve B: volumes of the solvent.
$V^e{}_{ci}$ and $V^e{}_{cj}$ represent the volumes of water decreased by electrostriction.

$$V_c=c\bar{v}+\frac{100}{d_o}-(1-e^{-kc})V^e{}_{max} \tag{6-a}$$

$$=c\bar{v}+\frac{100}{d_o}-(1-r^c)V^e{}_{max} \tag{6-b}$$

$$V_M=M\bar{v}_{mol}+\frac{1000}{d_o}-10(1-e^{-k'M})V^e{}_{max} \tag{6-c}$$

where M in Eq. 6-c indicates the molal concentration of salt and $\bar{v}_{mol}$ is the effective molar volume of salt in the solution. V_M is the volume of a solution containing 1000 g. of water and M moles of solute. The three parameters, $\bar{v}$, r and $V^e{}_{max}$, in Eq. 6-b were determined by the method of least squares on an electronic computer.

Further, from Eq. 5, the difference between $\bar{v}_{i,j}$ at an infinite dilution or the apparent specific volume, $\bar{v}_o$, of a salt, and its effective specific volume, $\bar{v}$, corresponds to the magnitude of electrostriction, v^e, per 1 g. of salt at an infinite dilution, which can be obtained from Eq. 8:

$$v^e=\bar{v}-\bar{v}_o \tag{7}$$

$$=kV^e{}_{max} \tag{8}$$

Results and Discussion

Figure 1 gives a schematic representation of the volumes of the solution and the solvent in the aqueous solution of a strong 1-1 electrolyte. The volume of the solution does not increase linearly with the concentration on account of the electrostriction of the solvent. This phenomenon may be due to the extremely rapid exchange reaction between hydrated and unhydrated water or to the overlap of hydrated water layers. In consequence, two curves, for the volumes of the solution (V_c) and of the solvent (V_s) respectively, are drawn under the following conditions;

$$\frac{dV_c}{dc}>0 \quad \text{and} \quad \frac{d^2V_c}{dc^2}>0$$

and

$$\frac{dV_s}{dc}<0 \quad \text{and} \quad \frac{d^2V_s}{dc^2}>0$$

Using Eq. 6-b, we analyzed these curves for the solutions of 1-1 electrolytes and determined the effective specific volumes, $\bar{v}$, of salt in an aqueous solution and the maximum volumes, $V^e{}_{max}$, of water decreased by the electrostriction; then, from Eqs. 7 and 8, the apparent specific volumes, $\bar{v}_o$, and the magnitudes of electrostriction, v^e, were calculated. The values obtained are listed in Table I.

For the least square calculation, we used the densities, d_m(*obeserved*), quoted from the

TABLE I. VARIOUS CALCULATED SPECIFIC VALUES FOR AQUEOUS 1-1 ELECTROLYTE SOLUTIONS AT 20°C

Salt	m_c	r (in Eq. 6-b)	v	V^e_{max} ml.	v^e	v_o
LiCl	14	0.881023	0.5046	0.740	0.0936	0.4110
LiBr	18	0.900352	0.3076	0.280	0.0294	0.2782
LiI	30	0.915110	0.2751	0.118	0.0105	0.2646
NaCl	16	0.935300	0.4036	1.688	0.1129	0.2907
NaBr	18	0.937087	0.2714	0.669	0.0435	0.2279
NaI	18	0.950911	0.2541	0.447	0.0225	0.2316
KCl	16	0.920720	0.4390	0.934	0.0771	0.3619
KBr	18	0.933030	0.3200	0.515	0.0357	0.2843
KI	18	0.950652	0.2936	0.432	0.0218	0.2718
RbCl	18	0.929748	0.3029	0.512	0.0373	0.2656
RbBr	24	0.956536	0.2635	0.642	0.0285	0.2350
RbI	24	0.967556	0.2545	0.533	0.0176	0.2370
CsCl	18	0.953201	0.2606	0.548	0.0263	0.2343
CsBr	18	0.929158	0.2309	0.204	0.0150	0.2159
CsI	30	0.938835	0.2311	0.155	0.0098	0.2213

TABLE II. COMPARISON OF THE OBSERVED AND CALCULATED RESULTS THE EXAMPLE SHOWS THE VALUES FOR A SOLUTION OF SODIUM CHLORIDE AT 20°C

m	c	M	Observed		Calculated		Δd_m
			d_m	V_c, ml.	d_m	V_c, ml.	
0	0	0	0.99823	100.177_3			0
2	2.041	0.349	1.01246	100.785_0	1.01246	100.785_3	0
4	4.167	0.713	1.02680	101.447_9	1.02680	101.448_0	0
6	6.383	1.082	1.04127	102.166_6	1.04127	102.166_5	0
8	8.696	1.488	1.05589	102.942_2	1.05589	102.942_0	0
10	11.111	1.901	1.07068	103.776_2	1.07068	103.776_0	0
12	13.636	2.332	1.08566	104.670_3	1.08566	104.670_4	0
14	16.278	2.786	1.10085	105.626_6	1.10085	105.627_1	0
16	19.048	3.259	1.11626	106.648_6	1.11627	106.648_4	0.00001
18	21.951	3.757	1.13190	107.740_3	1.13193	107.736_9	0.00003
20	25	4.279	1.14779	108.904_9	1.14788	108.895_6	0.00009
22	28.205	4.825	1.16395	110.146_6	1.16415	110.128_0	0.00020
24	31.579	5.402	1.18040	111.469_8	1.18074	111.437_9	0.00034
26	35.135	6.015	1.19717	112.878_8	1.19768	112.830_0	0.00051

International Critical Table, of the solutions at the concentration, m, of salt from zero to that, m_c, described in Table I at intervals of 2 g. Within this concentration range, all the data, $d_m(observed)$, agree completely with the results, $d_m(calculated)$, calculated from Eqs. 6-b and 1 using the parameters obtained. As an example, the results calculated for a solution of sodium chloride are shown in Table II.

As may be seen from Table II, however, at very high concentrations $d_m(calculated)$ values deviate slightly from $d_m(observed)$ values. This phenomenon may be interpreted as follows.

Instead of Eq. 2, as a function of the molal concentration of salt Eq. 9 is obtained:

$$V_M = M\bar{v}_{mol} + \frac{1000}{d_o} - V^e{}_M \qquad (9)$$

The volume of water decreased by the electrostriction, $V^e{}_M(observed)$, at any given concentration of salt is obtained from Eq. 9; also, $V^e{}_M(calculated)$ can be calculated from Eq. 6-c as:

$$V^e{}_M = 10(1-e^{-k'M})V^e{}_{max} \qquad (10)$$

In Fig. 2, $V^e{}_M(observed)$ and $V^e{}_M(calculated)$ are plotted against the molal concentration of some 1-1 electrolytes in solutions taken as typical examples. As may be seen from this figure, $V^e{}_M(observed)$ deviates from $V^e{}_M(calculated)$ at high concentrations; this may be caused by the change in the effective volume of salt in a solution as a result of the formation of ion pairs. In consequence, $\bar{v}_{i,j}$ in Eq. 5 at high concentrations may approach the specific volume of salt in the crystal state. In fact, for most

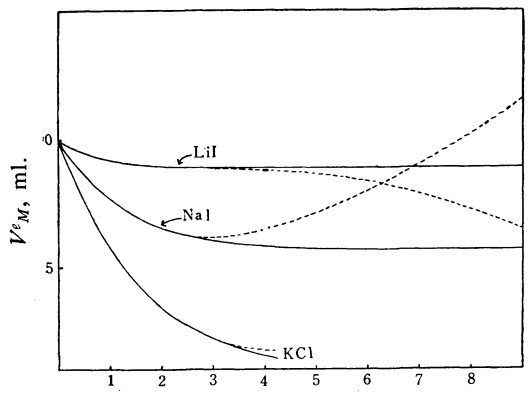


Fig. 2. Volume of water decreased by the electrostriction, V^e_M, plotted against the molal concentration of a few 1-1 electrolytes at 20°C as examples.
—— V^e_M(calculated)
- - - V^e_M(observed)

of the electrolytes calculated this expectation is realized.

On the other hand, if the hydration is related only to the shrinkage of the solvent due to electrostatic attraction, the lithium ion, which has the smallest ionic radius of all univalent cations, should have the largest electrostriction effect. However, in contrast, as may be seen from Fig. 3, which shows the curves for V^e_M(calculated) obtained from Eq. 10 plotted against the molal concentration of salt, and v^e_{mol} in Table III, which represents the magnitude of the molal electrostriction, the order of the molal electrostriction of univalent cations was found to be as follows:

$$Na^+ > K^+ > Rb^+ > Cs^+ > Li^+$$

Therefore, the behavior of the lithium ion in an aqueous solution seems to be unusual. It is well known that the lithium ion in an aqueous solution has an abnormal viscosity[19,22] and compressibility[16] compared with other univalent ions. Frank and Wen[20] and Kaminsky[22], therefore, suggested that there is a clathrate around the lithium ion; our results support this conception. One of these results is described in the present paper; the other will be reported in subsequent papers.

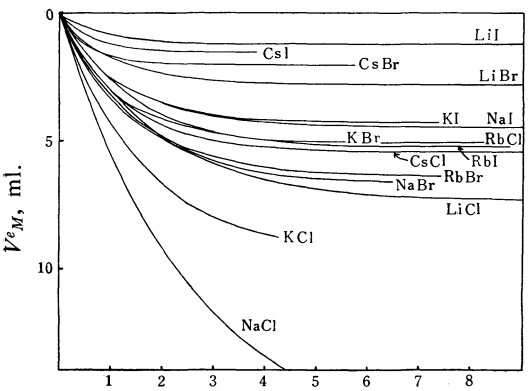


Fig. 3. Volume of water decreased by the electrostriction, V^e_M(calculated) obtained from Eq. 10, plotted against the molal concentration of the salt at 20°C.

There have been several reports on the clathrate structures of water around inert gases,[30,31] hydrocarbons[3,7,32,33] and ions[20,25,34-36]. A clathrate consists of water molecules bound mutually with hydrogen bonds and has a lower density than pure water.[7,8] If these conceptions are valid, then it becomes much easier to understand why v^e_{mol} and V^e_{max} are small for lithium salts. Hydration water seems to exist partly as a clathrate around the lithium ion, the density of which is low.

As may be seen from Table III, the effective molar volumes for various 1-1 electrolytes in aqueous solutions are stoichiometrically additive. The existence of this stoichiometric relation suggests that the results are accurate.

On the other hand, as may be seen from Fig. 3, the volume of the water of solutions

TABLE. III. VARIOUS CALCULATED MOLAR VALUES FOR 1-1 ELECTROLYTE SOLUTIONS AND THE NUMBER OF MOLECULES OF WATER OF HYDRATION, N, AT 20°C

Salt	k' (in Eq. 6-c)	$\bar{v}_{mol}$ ml.	v^e_{mol} ml.	$\bar{v}_{o(mol)}$ ml.	N mol. H_2O/ mol. solute
LiCl	0.536	21.4	3.97	17.4	30
LiBr	0.912	26.7	2.55	24.2	51
LiI	1.187	36.8	1.40	35.4	66
NaCl	0.391	23.6	6.60	17.0	22
NaBr	0.669	27.9	4.48	23.4	37
NaI	0.754	38.1	3.37	34.7	42
KCl	0.616	32.7	5.75	27.0	34
KBr	0.825	38.1	4.25	33.9	46
KI	0.841	48.8	3.63	45.2	47
RbCl	0.880	36.6	4.51	32.1	49
RbBr	0.734	43.6	4.72	38.9	38
RbI	0.701	54.1	3.73	50.4	28
CsCl	0.806	43.9	4.42	39.5	45
CsBr	1.565	49.1	3.18	46.0	87
CsI	1.640	60.0	2.54	57.5	96

30) W. F. Claussen, *J. Chem. Phys.*, **19**, 259, 662, 1425 (1951).
31) W. F. Claussen and M. F. Polglase, *J. Am. Chem. Soc.*, **74**, 4817 (1952).
32) H. S. Frank, *J. Chem. Phys.*, **13**, 478, 493 (1945).
33) H. S. Frank and M. W. Evans, ibid., **13**, 507 (1945).
34) D. Feil and G. A. Jeffrey, ibid., **35**, 1863 (1961).
35) M. Bonamico, G. A. Jeffrey and R. K. McMullan, ibid., **37**, 2219 (1962).
36) G. A. Jeffrey and R. K. McMullan, ibid., **37**, 2231 (1962).

of lithium bromide and iodide decreases very little as a result of electrostriction. Thus, the difference in density between pure and hydrated water is apparently small. Therefore, the results support the theory that the hydration water around the lithium ion, perhaps in the secondary hydration shell, exists as a clathrate of a lower density.

Another point of interest shown in Fig. 3 is that the curves for V^e_M in rubidium salt and cesium salt solutions decreased very little, as in lithium salt solutions. This suggests very strongly that there is a clathrate around the rubidium and cesium ions, too. Further evidence for this conception will be given in subsequent papers in this series. Furthermore, Fig. 3 indicates the presence of a clathrate around the bromide and iodide ions, too.

Studies were made of the number of the molecules of the water of hydration of ions. The curve shown in Fig. 3 converges to the constant, V^e_{max}, which corresponds to the decrease in the volume of water when it is completely hydrated to the ions. Values for V^e_{max} for various electrolytes obtained from Eq. 6 are listed in Table I. As may be seen from Fig. 1, the tangent of curve B at an infinite dilution intersects the constant, V^e_{max}, at the concentration c_s. The relation between these is represented as follows:

$$\frac{V^e_{max}}{v^e} = c_s \tag{11}$$

$$\frac{100}{c_s} = H_s \tag{12}$$

where H_s is the weight (g.) of water hydrated to 1 g. of the solute. The value of c_s agrees with the reciprocal of k in Eq. 6-a. The number of the molecules of the water of hydration of ions, N, is obtained by the following equation:

$$N = \frac{H_s}{18} \times (\textit{molecular weight of solute}) \tag{13}$$

The values of N are listed in Table III. As may be seen from this table, the hydration numbers of ions are quite large, even though this estimation cause something of an error. The hydration number includes the primary hydration water molecules which are orientated towards the ions and affected by the electrostriction effect. However, the number is so great that it is not possible to explain the properties of 1-1 electrolytes by this effect alone. Therefore, there are probably clathrates around the ions.

In addition, it is of interest to draw attention to the significance of Pauling's model of the structure of water with regard to clathrate compounds.[13,15,37] In this model the number of water molecules per unit is about the same as the number of hydration of ions and the diameter acting as a cavity is the same as in a primary hydration shell.

The character of the clathrate formation of ions will be supported by experiments by means of nuclear magnetic resonance spectrometry and ultrasonic interferometry to be described in subsequent papers. The other strong evidence for the existence of a clathrate around ions is that of various reports[20,33-35] on the clathrate around tetraalkylammonium ions.

Summary

The effective volumes, the apparent volumes and the magnitudes of electrostriction for various 1-1 electrolytes in aqueous solutions have been determined from an analysis of the densities of solutions at various concentrations. The molar values thus obtained are stoichiometrically additive. The state of water molecules around ions and particularly the existence of clathrates around various univalent ions, such as lithium, rubidium, cesium, bromide and iodide, and the numbers of hydration water have also been discussed.

The author wishes to express his hearty thanks to Professor Toshizo Isemura for his kind guidance and encouragement, and to Dr. Yoshihiko Takada for his help in the electronic computer calculations.

Division of Physical Chemistry
Institute for Protein Research
Osaka University
Kita-ku, Osaka

37) L. Pauling "Hydrogen Bonding," Papers Symposium, Ljubljana, 1957, 1-5 (pub. 1959).

Studies of the Hydration and the Structure of Water and Their Roles in Protein Structure. II. The Hydration of Electrolytes by Ultrasonic Interferometry and Its Temperature Dependence

By Toshizo ISEMURA and Sachio GOTO*

(Received May 29, 1964)

In a previous paper[1] of this series, we studied the effective volumes of ions, the magnitudes of electrostriction and the numbers of the hydration water of the ions of various 1-1 electrolytes. From the results we establisehd the existence of clathrates not only around the lithium ion, but also around the ions of rubidium, cesium, bromide and iodide, perhaps as a secondary hydration shell.

The present paper will primarily report on the numbers of hydration for various strong electrolytes as measured by the method of ultrasonic interferometry.

There are several methods to determine numbers of hydration, for example, by compressibility,[2] diffusion,[3] viscosity[4] or the dielectric constant[5]. Each is based on a different characteristic, and the significance of each character in relation to hydration is specific. Consequently, the numbers of hydration water calculated by these different methods are very different.

In the present work the method of compressibility was used. In this method there are mainly two ways to estimate the numbers of hydration water: (1), the compressibility of hydration water is assumed to be zero[2,6-13] and (2), it is assumed to be equal to that of ice.[14,15]

It is uncertain whether or not the compressibility of the solute is nearly zero. In reports on macromolecules, such as proteins, the compressibility of the solute has sometimes been disregarded[12,13] and sometimes not.[16,17] However, for small ions it may always be possible to neglect the compressibility of the solute.[2,6]

The Significance of the Compressibility of the Solution

If a part of the solvent (expressed in volume fraction), v_0, changes to v_2 as a result of hydration, the compressibility of the solution, β, may be derived as follows:

$$\beta = V_1\beta_1 + V_0\beta_0 - v_0\beta_0 + v_2\beta_2 \qquad (1)$$

where v_1, V_0 and V_2 are the volume fractions of the solute, solvent and hydrated water respectively, and β_1, β_0 and β_2 are the compressibilities of the solute, solvent and hydrated water respectively. The partial specific volume of the solute, $\bar{v}$, is given as $V_1/c=\bar{v}$, where c is the weight concentration of the solute. If it can be assumed that $v_0=v_2$, the following equation is obtained from Eq. 1 and is valid under the experimental conditions:

$$\frac{\beta_0-\beta}{c} - \bar{v}\beta_0 = \bar{v} - \beta_1 + \frac{v_2}{c}(\beta_0-\beta_2) \equiv K \qquad (2)$$

The adiabatic compressibility is determined experimentally by measuring the sound velocity, u, and the density, d, from the relation:

$$\beta = \frac{1}{u^2 d} \qquad (3)$$

Therefore, the left side of Eq. 2 can be determined experimentally.

Experimental

The sound velocity in the solution was measured with an ultrasonic interferometer at a frequency of 5 Mc./sec. Details of the method for measuring the wavelength have been given by Passynski.[2]

* Present address: Institute for infectious Diseases, The University of Tokyo, Shiba Shirokane-Daimachi, Minato-ku, Tokyo.

1) S. Goto, This Bulletin, **37**, 1685 (1964).
2) A. Passinski, *Acta Physicochim. U. R. S. S.*, **8**, 385 (1938).
3) J. H. Wang, *J. Phys. Chem.*, **58**, 686 (1954).
4) E. R. Nightingale, Jr., ibid., **63**, 1381 (1959).
5) G. H. Haggis, J. B. Hasted and T. J. Buchanan, *J. Chem. Phys.*, **20**, 1452 (1952).
6) T. Sasaki and T. Yasunaga, This Bulletin, **28**, 269 (1955).
7) T. Sasaki and T. Yasunaga, ibid., **26**, 175 (1953).
8) Y. Miyahara, ibid., **25**, 326 (1952).
9) Y. Miyahara, ibid., **26**, 390 (1953).
10) A. Passynsky, *Acta Physicochim. U. R. S. S.*, **22**, 137 (1947).
11) A. Passynsky, ibid., **22**, 263 (1947).
12) A. G. Pasynskli and I. E. Elpiner, *Doklady Akad. Nauk S. S. S. R.*, **105**, 1296 (1955).
13) I. E. Elpiner and N. I. Pishkina, *Biofizika*, **4**, 129 (1959).
14) H. Shiio, *J. Am. Chem. Soc.*, **80**, 70 (1958).
15) H. Shiio, T. Ogawa and H. Yoshihashi, ibid., **77**, 4980 (1955).
16) Y. Miyahara, This Bulletin, **29**, 741 (1956).
17) B. Jacobson, *Arkiv För Kemi*, **2**, 177 (1950).

The values for the density of solutions were obtained by the pycnometer method developed by Lipkin et al.[18] The concentrations of the solutions were determined by measuring their densities. Measurements were made from 15 to 50°C at intervals of 5°C.

Results and Discussion

As may be seen from Eq. 2, to estimate the number of hydration it is necessary to assume the compressibilities of both the solute, β_1 and hydrated water, β_2. However, in aqueous solutions of strong electrolytes the compressibility of the solute is probably zero, as has been assumed by many authors.[2,6] Therefore, only the compressibility of hydrated water is uncertain in the calculation of the number of hydration from Eq. 2.

In an aqueous electrolyte solution, the strong electric field produced by the ion orientates the water molecules and causes the volume of the water to decrease. This is called the electrostriction effect.[19] This effect is probably exhibited mainly in the primary hydration shell of most 1-1 electrolytes. However, as has been described in the previous paper[1] of this series, there is a clathrate around the ions, perhaps as a secondary hydration shell. It is probably unreasonable to disregard the compressibilities of these water molecules in the secondary hydration shell or of those in the clathrate, which consists of water molecules bound mutually with hydrogen bonds. Shiio[14,15] considered the compressibility of all the hydrated water molecules in aqueous solutions of amino acids, proteins and saccharides to be the same as that of ice (18×10^{-12} cm^2/dyn.) in connection with a term, the iceberg of hydration.[20]

As has been described above, there are still some unsolved problems with regard to the compressibility of hydrated water. However, for the purpose of comparing different electrolytes, we temporarily assumed that the compressibilities of both solute and hydrated water were zero and determined the numbers of hydration on the basis of this assumption.

Figure 1 shows the numbers of hydration for various strong electrolytes in aqueous solutions and their dependence on the temperature. These numbers were obtained using Eq. 2, while the values for the partial specific volume, v, of 1-1 electrolytes are from the previous paper. In the case of 1-2 electrolytes, the apparent partial specific volumes were used. Figure 1 shows that in all these electrolyte solutions the numbers of hydration decrease with an increase in the temperature. In solutions of 1-1 electrolytes, the numbers

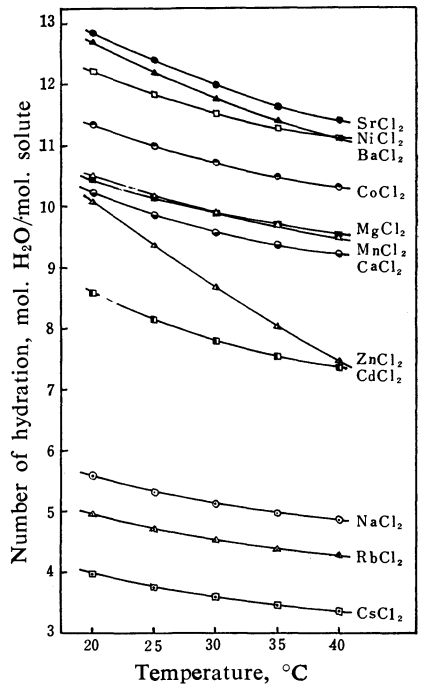


Fig. 1. Numbers of hydration for various 1-1 and 1-2 electrolytes and their dependence on the temperature (assuming that the compressibilities of both solute and hydrated water are zero).

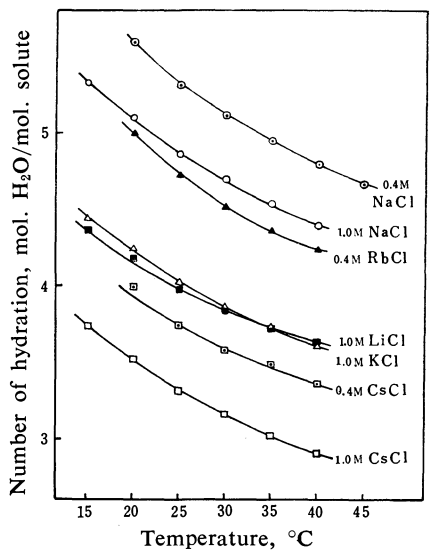


Fig. 2. Numbers of hydration for various 1-1 electrolytes and their dependences on the temperature and concentration.

18) M. R. Lipkin, J. A. Davison, W. T. Harvey and S. S. Kurtz, Jr., *Ind. Enz. Chem. Anal. Edt.*, **16**, 55 (1944).
19) R. W. Gurney, "Ionic Processes in Solution," McGraw-Hill Book Co., New York (1953).
20) H. S. Frank and M. W. Evans, *J. Chem. Phys.*, **13**, 507 (1945).

of hydration are different from each other at the same temperature, but they decrease in parallel with each other with an increase in the temperature. The same is true for solutions of 1-2 electrolytes also. This phenomenon is significant in contrast to the results obtained for the amino acids to be described in a subsequent paper. As may be seen from Fig. 2, the hydration numbers are also dependent on the concentration. Therefore, the number of hydration should be determined at an infinite dilution. However, since many authors[2,6,21-23] have determined these numbers for various concentrations and since the measurement of these numbers is not the main purpose of this paper, their concentration dependence was not studied.

Table I summarizes the numbers of hydration of various electrolytes at 20 and 40°C. As may be seen from this table, for most electrolytes the change in the number of hydration with the temperature for 1-1 electrolytes is about two-thirds of that for 1-2 electrolytes. That is to say, the change with the temperature is proportional to the number of ions in the solution. This can be explained as follows: the states of hydrated water which are built up in a strong electric field are not affected simply by the change in the temperature but also by the exchange reaction velocity between the unhydrated and hydrated water molecules.

The numbers of hydration of various electrolytes at 20°C (when their compressibilities are assumed to be zero) decrease in the following order:

$$Sr^{2+}>Ba^{2+}>Ni^{2+}>Co^{2+}>Mn^{2+}>Mg^{2+}>$$
$$Ca^{2+}>Cd^{2+}>Na^{+}>Rb^{+}>K^{+}>Li^{+}>Cs^{+}$$

This finding contradicts the results obtained from the dielectric constants,[5] entropy,[19] viscosity,[4] and so on. The disagreement may be due to differences between the definitions of hydration.

TABLE I. HYDRATION NUMBERS OF VARIOUS ELECTROLYTES IN AQUEOUS SOLUTIONS AT 20 AND 40°C (ASSUMING THAT THE COMPRESSIBILITIES OF BOTH SOLUTE AND HYDRATED WATER ARE ZERO)

Salt	Concn. mol./l.	Number of hydration mol. H_2O/mol.		
		20°C	40°C	Δv_2
LiCl	0.99	4.20	3.65	0.55
NaCl	0.99	5.15	4.45	0.70
KCl	1.00	4.25	3.60	0.65
RbCl	0.42	4.95	4.25	0.70
CsCl	1.00	3.50	2.90	0.60
$MgCl_2$	0.50	10.45	9.50	0.95
$CaCl_2$	0.45	10.25	9.20	1.05
$SrCl_2$	0.30	12.85	11.40	1.45
$BaCl_2$	0.22	12.70	11.10	1.60
$CdCl_2$	0.33	8.60	7.35	1.25
$MnCl_2$	0.31	10.50	9.45	1.05
$CoCl_2$	0.42	11.35	10.30	1.05
$NiCl_2$	0.38	12.25	11.10	1.15

TABLE II. COMPARISON OF β_c, THE COMPRESSIBILITY CHANGE OF THE SOLVENT, WITH V^e_c, THE VOLUME OF WATER DECREASED BY ELECTROSTRICTION (GIVEN IN THE PREVIOUS PAPER) AT 20°C

Salt	Concn. mol./l.	β_c	V^e_c	β_c/V^e_c
LiCl	0.989	0.340	0.305	1.11
NaCl	0.992	0.415	0.538	0.77
KCl	0.997	0.347	0.426	0.81
RbCl	0.415	0.171	0.156	1.10
CsCl	1.001	0.289	0.303	0.95

The values for K in Eq. 2 were compared with the V^e_c, the volume of water decreased by the electrostriction, given in the previous paper.[1] The results for 1-1 electrolytes at 20°C are summarized in Table II, where c is the molal concentration of the electrolyte. β_c, the compressibility change of the solvent, is given as

$$\beta_c = K \times c$$

As may be seen from this table, the β_c/V^e_c value for sodium and potassium chloride is about 0.8, but the values for lithium, rubidium and cesium chloride are larger (0.95~1.1) than for sodium and potassium chloride. This suggests that the compressibility of hydration water varies with the states of the hydration water, as for instance, in the primary and secondary hydration shells. In the previous paper of this series, we suggested that there are hydration water molecules around such ions as lithium, rubidium and cesium, as clathrates with nearly the same density as pure water. Though this hydration water probably does not affect the volume change, it may affect the compressibility of the solvent to some extent (causing a change from zero, for example, to that of ice.) In consequence, the compressibility of an electrolyte solution is not in proportion to the electrostriction effect.

Summary

The numbers of hydration of various 1-1 and 1-2 electrolytes in aqueous solutions and their

21) B. B. Owen and H. L. Simons, *J. Phys. Chem.*, **61**, 479 (1957).
22) B. B. Owen and P. L. Kronick, ibid., **65**, 84 (1961).
23) R. Barthel, *J. Acous. Soc. Amer.*, **26**, 227 (1954).

dependence on the temperature have been determined by the method of ultrasonic interferometry. The relation between the hydration and the compressibility of aqueous electrolyte solutions has been discussed and further evidence obtained for the existence of the clathrates as hydration shells, as was suggested in the previous paper.

Division of Physicai Chemistry
Institute for Protein Research
Osaka University
Kita-ku, Osaka

Studies of the Hydration and the Structure of Water and Their Roles in Protein Structure. III. Proton Magnetic Resonance Shifts of Water in Aqueous Solutions of Electrolytes and Their Relation to the Structure of Water

By Sachio GOTO* and Toshizo ISEMURA

(Received May 29, 1964)

In the preceding papers[1,2] of this series we reported on the states of water in aqueous electrolyte solutions and proposed that there are clathrates around various ions, perhaps forming an secondary hydration shell. In the present paper the effect of electrolytes and organic compounds on the structure of water, as estimated by measuring the chemical shift of the nuclear magnetic resonance frequency of water protons, will be described. It has been assumed that the number of hydrogen bond between water molecules decreases with an increase in the temperature and also that the structure of water is affected by such variables as the pressure and composition of the solution. A proton magnetic resonance spectrometer is one of the most useful instruments for studying weak molecular interactions, particularly those of hydrogen bonds.[3]

Experimental

A JNM-3 high-resolution nuclear magnetic resonance spectrometer operating at 40 Mc./sec. in conjunction with an 12-in. magnet (Japan Electron Optics Laboratory Co.) was used. Proton magnetic resonance shifts relative to pure water were measured for the various salt solutions using the side-band method. The shifts observed for aqueous salt solutions were corrected for bulk diamagnetic susceptibilities. Acetone was found to be a suitable internal reference substance when corrections were made for the diamagnetic susceptibilities of salts, since the methyl protons of acetone are chemically unreactive and their resonance shifts are independent of the temperature. The procedure used was as follows: The same amount of acetone was added to the test salt solution and to the solvent used as an external reference. The relative shift of the methyl protons of acetone thus measured depends on the difference between the bulk diamagnetic susceptibility of the solution and that of the solvent. Therefore, it can be used to correct the observed proton magnetic resonance shifts of water protons.

All the solutions studied were prepared in a 0.01 M sodium ethylenediaminetetraacetate (EDTA) buffer and were adjusted to pH 7.0.

Measurements were made at 20°C.

Results

The relative shifts of the proton resonances of aqueous solutions containing various electrolytes or organic compounds are presented in Figs. 1, 2 and 3, where the shift, δ, is expressed in c. p. s. (at 40 Mc./sec.). A positive value indicates a shift to a higher resonance field than that of the external reference. Figure 1 shows the observed relative shifts of water protons (uncorrected for bulk diamagnetic susceptibilities) at various concentrations of salts. Figure 2 shows the corrected relative shifts for the bulk diamagnetic susceptibilities obtained by the measurement of the relative shift of the methyl protons of acetone. This correction is very important since the bulk diamagnetic susceptibilities of salt solutions are of the same order of magnitude or often even larger than the proton resonance shifts.

* Present address: Institute for Infectious Diseases, The University of Tokyo, Shiba Shirokane-Daimachi, Minato-ku, Tokyo.

1) S. Goto, This Bulletin, 37, 1685 (1964).

2) T. Isemura and S. Goto, ibid., 37, 1690 (1964).

3) J. A. Pople, W. G. Schneider and H. J. Bernstein, "High-Resolution Nuclear Magnetic Resonance," McGraw-Hill Book Co., N. Y. (1959).

4) H. G. Hertz and W. Spalthoff, *Z. Elektrochem.*, 63, 1096 (1959).

These relative shifts were additive in all the salt solutions studied. Thus, as assumed by Hertz and Spalthoff,[4] if the relative shifts caused by potassium and by chloride ions in an aqueous potassium chloride solution are arbitrarily assumed to be equal, the relative shifts for each ion can be estimated. Figure 3 shows the dependence of the relative shifts for various ions on the concentration of the solution.

Discussion

The present paper will report on the effect of 1-1 electrolytes and organic compounds on the structures of water. Measurements were made of the shift of the nuclear magnetic resonance frequency of the protons of water molecules. At present a few reports[4-6] are available on the shift of water protons in aqueous solutions of various diamagnetic salts. However, in these reports the corrections of

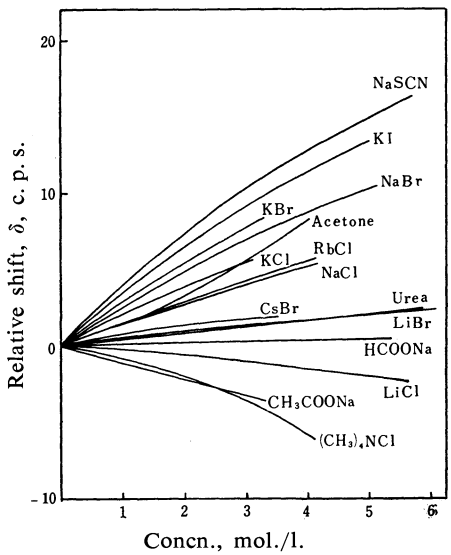


Fig. 1. Relative shifts of water protons (uncorrected) in aqueous solutions of electrolytes and organic compounds as a function of the concentration.

the diamagnetic susceptibilities of salts do not seem to be satisfactory. Shoolery and Alder,[5] for instance, did not make this correction.

From Figs. 1 and 2 it can be seen that the relative shifts are in some cases as great as several cycles per second, which may be comparable with the correction values for ionic diamagnetic susceptibilities. Therefore, the shifts of water protons without correction for

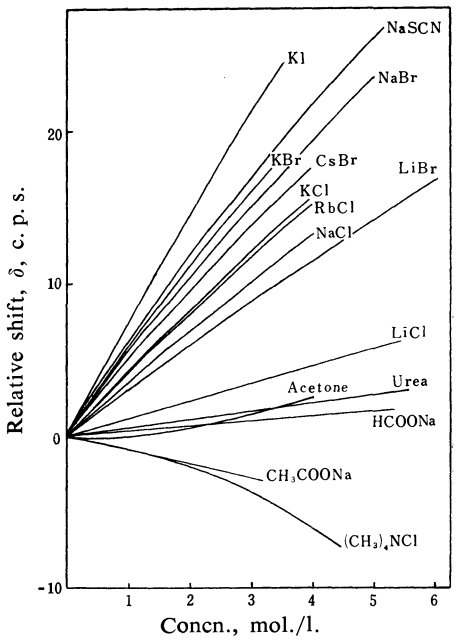


Fig. 2. Relative shifts of water protons (corrected for the bulk diamagnetic susceptibilities) in aqueous solutions of electrolytes and organic compounds as a function of the concentration.

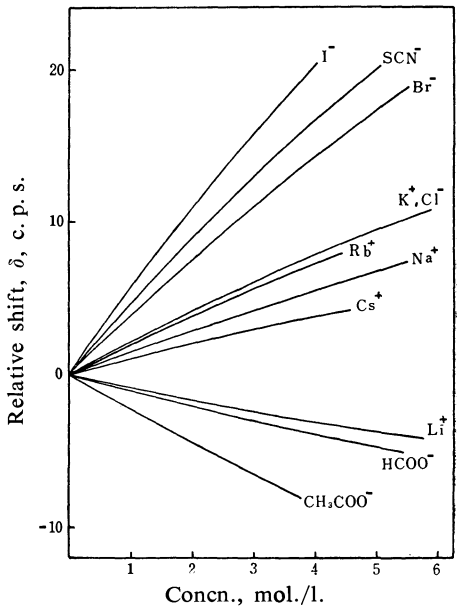


Fig. 3. Relative shifts of water protons for various ions as a function of the concentration (assuming that the relative shifts for potassium and chloride ions are equal).

the bulk diamagnetic susceptibility do not show any real shift in aqueous salt solutions. Fabricand and Goldberg[6] have recommended the use of Pauling's values for the theoretical

5) J. N. Shoolery and B. J. Alder, *J. Chem. Phys.*, **23**, 805 (1955).
6) B. P. Fabricand and S. Goldberg, ibid., **34**, 1624 (1961).

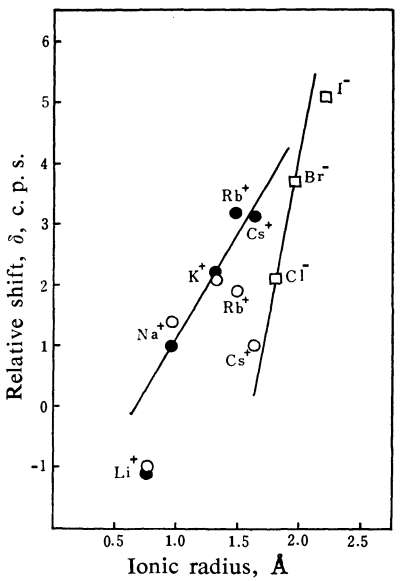


Fig. 4. Relative shifts of water protons for each ion at a concentration of 1 mol./l. as a function of the ionic crystal radius.
-●- Corrected from Pauling's theoretical diamagnetic susceptibilities.
-○,□- Obtained in this paper.

diamagnetic susceptibilities of crystals for this correction, because the relationship between the relative shifts, thus corrected, and the ionic crystal radius are linear. However, such a linear relation does not always hold true, since the behavior of water molecules in the presence of electrolytes is very complex, as has been described in the preceding papers.[1,2]

As has been mentioned above, acetone is a suitable homogeneous internal reference for studying the proton magnetic resonance of water. If corrections for the observed relative shifts of water protons are made using this method, no linear relation, such as that of Fabricand and Goldberg, holds any longer. This is shown in Fig. 4, which illustrates the relation between the ionic crystal radius and the relative shift of 1 M salts obtained from Fig. 3 and from calculations using Pauling's theoretical ionic diamagnetic susceptibilities for corrections. The straight lines are drawn in accordance with the values of Fabricand and Goldberg. The deviation from this linear relation is striking in the case of lithium and cesium ions. This will be discussed below.

Shoolery and Alder[5] interpreted the relative shifts of water protons in terms of the following two factors; (1) the ionic electric field distorts the polarization effect; and (2) the ion disrupts the structure of water and breaks the hydrogen bonds between water molecules. In the former case, the water molecule is polarized so that fewer electrons are found on the proton, which is therefore less shielded from the external magnetic field. On the other hand, in the latter case, the hydrogen bonds are generally broken by the ions. When a solute particle is pushed into a space between water molecules, the hydrogen bonds between water molecules are broken. Therefore, the proton is more shielded from the external magnetic field. This effect eventually counteracts the polarization effect on the proton.

As is shown in Figs. 2 and 3, in general, the resonance frequency of water protons in an inorganic salt solution is higher than that in pure water, and there is a tendency for a shift to a higher field to occur with an increase in the ionic radius. The direction of this shift agrees with that of the breakage of the hydrogen bonds. The results obtained in this experiment clearly demonstrate that the relative shift is more sensitive to the hydrogen bonds of water than the polarization effect.

Figure 3 shows the results obtained using the shift of the methyl protons of acetone for the correction of the diamagnetic susceptibility. It can be seen that the cesium ion is not so effective as the potassium ion in producing a water proton shift, although it has a larger ionic radius. This result agrees with those obtained by Hertz and Spalthoff[4] and Sato.*

It is generally believed that the number of the water hydrogen bonds decreases with an increase in the ionic radius.[7] In addition, the water molecules are thought to be less polarized when the ionic size is great. As a result of these effects, the proton is more shielded, and thus the relative shift to a high field becomes larger. In this respect, the behavior of the cesium ion is unusual. However, in the preceding papers of this series we proposed that around such ions as the cesium ion there is a clathrate which consists of water molecules mutually bound with hydrogen bonds. This conclusion is strongly supported by the present results, obtained by the method of nuclear magnetic resonance. This method is very sensitive to the state of hydrogen bonding, as will be described below.

In aqueous electrolyte solutions, the degree of hydration increases with a decrease in the ionic radius, as has been shown previously by studies of the ionic mobilities,[7] diffusion coefficients,[8] viscosity,[9] etc. However, the previous results were all based on various assumptions. Around ions there are not only water molecules of primary hydration but also

* Personal communication.

7) R. W. Gurney, "Ionic Processes in Solution," McGraw-Hill Book Co., New York (1953).

8) J. H. Wang, *J. Phys. Chem.*, **58**, 686 (1954).

9) E. R. Nightingale, Jr., ibid., **63**, 1381 (1959).

of secondary hydration, the structures of which are different from that of pure water. The ions with strong electric fields, such as lithium, beryllium and magnesium, cause not only the contact of water molecules with the ions but also exert an orienting influence on more remote water molecules, resulting in a secondary hydration shell.[10,11]

Furthermore, in most electrolytes the water molecules in the first hydration shell probably exert an ordering effect upon the outer molecules by means of hydrogen bonding. This may also be inferred from a comparison of the behavior of anions and cations. As is shown in Fig. 4, the relative shifts of anions in relation to the ionic radius varies linearly. On the basis of viscosity studies,[9,10] anions such as chloride, bromide and iodide are thought to have little hydration, but to break the water structure. On the other hand, in the case of cations the relative shifts do not vary linearly with the ionic radius. The viscosity of an electrolyte solution referred to a cation is also complicated. These findings perhaps result from differences in the orientation of the water molecules to the ions.

Frank and Evans[12] suggested that an iceberg is formed around non-polar groups. Icebergs have also been demonstrated in gas hydrates,[13] proteins,[14-16] and molecular ions.[11,17,18] From studies of the partial molal heat capacities[11] and X-ray diffraction,[18] it has been suggested that the clathrates are formed around the tetraalkylammonium ions. Similarly, as is shown in Fig. 2, the resonance frequency of water protons affected by the tetramethylammonium ion shifts to a lower field than that in pure water. Compared with other ions, the number of hydrogen bondings of water molecules around the tetramethylammonium ion is probably large. That is to say, the shift is in agreement with the direction of the formation of hydrogen bonding, in spite of its larger size, which has a small polarization effect on water molecules. This result also supports the consideration that the shifts of water protons as a result of the presence of ions are mainly due to a change in the number of hydrogen bonds.

From these facts, it is likely that clathrates are formed around the cesium as well as the tetramethylammonium ion. This may be the reason why the increase in the relative shifts to higher fields is reduced in an aqueous cesium salt solution. In the case of the cesium ion, however, the increase in the number of hydrogen bonds is not greater than the decrease in the number of hydrogen bonds broken, since the relative shift is still positive.

On the other hand, another mechanism must be considered for the lithium ion, which has a smaller ionic radius and exerts a negative shift on the proton resonance. The lithium ion has a larger polarization intensity and exerts an orientating influence not only on the neighboring water molecules but also on remote water molecules. It is known that the lithium ion has a larger effective radius in viscosity.[9] The fact that the relative shift of the lithium ion is found at a lower resonance frequency than that deduced from the linear relation with the ionic crystal radius may be explained as follows: the many water molecules orientated to the ion change the relative shift to a lower field, and water molecules outside the orientated water molecule may induce the formation of hydrogen bondings between water molecules.

Thus, each of these ions, as has been mentioned above, would contribute to the denaturation of proteins and nucleic acids. For example, as there are two kinds of hydration, one of which is orientated to the polar groups of proteins and the other orientated as an iceberg or a clathrate around the non-polar groups of the protein, both these hydrations may be important in maintaining the secondary and tertiary structures of protein. Thus we must consider the actions of ions as protein-denaturing agents in connection with breakers and inducers of the water structure. Details of this will be discussed in the following paper.

Similarly, as may be seen from Fig. 3, formate and acetate ions also form a water structure with increased hydrogen bonds. The acetate ion has more ability to form hydrogen bondings than the formate ion. The methyl group of acetate may cause the formation of clathrates.

Furthermore, as is shown in Fig. 2, urea caused a slight breakage of the water structure. However, as urea has hydrophilic groups, water molecules are attracted to the urea molecule. There may be two kinds of water molecules around the urea molecule: water molecules with broken hydrogen bonds, and those with more than normal hydrogen bonding. This mechanism may resemble that of the large ions, such as cesium or formate. The number of these broken and formed hydrogen bonds may

10) M. Kaminsky, *Discussions Faraday Soc.*, **24**, 171 (1957).
11) H. S. Frank and W. Y. Wen, ibid., **24**, 133 (1957).
12) H. S. Frank and M. W. Evans, *J. Chem. Phys.*, **13**, 507 (1945).
13) W. F. Claussen, ibid., **19**, 259, 1425 (1951).
14) I. M. Klotz, *Science*, **128**, 815 (1958).
15) W. Kauzmann, *Advances in Protein Chem.*, **14**, 1 (1959).
16) G. Nemethy and H. A. Scheraga, *J. Phys. Chem.*, **66**, 1773 (1962).
17) F. S. Feates and D. J. G. Ives, *J. Chem. Soc.*, **1956**, 2798.
18) D. Feil and G. A. Jeffrey, *J. Chem. Phys.*, **35**, 1863 (1961).

be nearly the same. Therefore, it appears from these properties of urea that the phenomenon of the urea denaturation of proteins is complicated by such variables as the concentration of urea, the temperature and the kinds of substance.[19-21]

Summary

The effects of various electrolytes and organic compounds on the structure of water, and particularly on hydrogen bonding, have been investigated by measuring the chemical shift of water protons in the nuclear magnetic resonance frequency. The chemical shift observed for salt solutions has been corrected for the bulk diamagnetic susceptibility, using methyl protons of acetone as a reference. The chemical shifts of water protons in aqueous solutions of various solutes have been considered.

Division of Physical Chemistry
Institute for Protein Research
Osaka University
Kita-ku, Osaka

19) K. Hamaguchi, K. Rokkaku, M. Funatsu and K. Hayashi, *J. Biochem.*, **48**, 351 (1960).
20) M. Levy and J. P. Magoulas, *Fed. Proc.*, **20**, 381 (1961); **21**, 405 (1962).
21) W. Bruning and A. Holtzer, *J. Am. Chem. Soc.*, **83**, 4865 (1961).

Studies of the Hydration and the Structure of Water and Their Roles in Protein Structure. IV. The Hydration of Amino Acids and Oligopeptides[1]

By Sachio GOTO* and Toshizo ISEMURA

(Received May 29, 1964)

To what degree is hydration formed around the molecules of proteins and nucleic acids? How does the hydration contribute to the maintenance of their native structure? What structure may be considered for the hydration?

It seems that solutions to these problems are essential for an understanding of the behavior of biological macromolecules in aqueous solutions. Nevertheless, we have as yet little information about such problems. However, since the molecules of proteins or nucleic acids are hydrated, it is natural to consider that the structure of the solvent water affects the state of the hydration around the macromolecules and, correspondingly, affects the configurations to a great extent. The possibility that the structure of the solvent water and the structure and degree of hydration around protein molecules play important roles in maintaining the native structure can be inferred from a study of the denaturation processes. Facts which suggest the dependence of the configuration of proteins or nucleic acids on the structure of the solvent water have been accumulated recently.[2-4]

In the preceding papers of this series[6-7] we reported on the states of water in aqueous electrolyte solutions and proposed that there are clathrates around various ions. The present paper will report on the numbers of hydration for various amino acids, oligopeptides and saccharides, as measured by the method of ultrasonic interferometry.

Experimental

The methods used in this study have been described in a previous paper.[6] The amino acids and oligopeptides used were supplied by the Peptide Center of the Institute for Protein Research, Osaka University.

Results and Discussion

The following equation, described in a preceding paper[6] as Eq. 2, was used for the determination of the number of hydration:

$$\frac{\beta_0-\beta}{c}-\bar{v}\beta_0=-\bar{v}\beta_1+\frac{v_2}{c}(\beta_0-\beta_2)\equiv K$$

1) Presented at the 15th Annual Meeting of the Chemical Society of Japan, Kyoto, April, 1962.

* Present address: Institute for Infectious Diseases, The University of Tokyo, Shiba Shirokane-Daimachi, Minato-ku, Tokyo.

2) I. M. Klotz, *Science*, **128**, 815 (1958).
3) G. Nemethy and H. A. Scheraga, *J. Phys. Chem.*, **66**, 1773 (1962).
4) K. Hamaguchi and E. P. Geiduschek, *J. Am. Chem. Soc.*, **84**, 1329 (1962).
5) S. Goto, This Bulletin, **37**, (1964).
6) T. Isemura and S. Goto, ibid., **37**, 1690 (1964).
7) S. Goto and T. Isemura, ibid., **37**, 1693 (1964).

where β, β_1, β_0 and β_2 are the compressibilities of the solution, solute, solvent and hydrated water respectively; v, the partial specific volume of the solute; c, the weight concentration of the solute, and v_2, the volume fraction of the hydrated water. From the results reported by Shiio,[8,9] it can be assumed that the compressibilities of the solutes, amino acids and saccharides are zero. Therefore, as in the previous study, for the purpose of comparing various amino acids, oligopeptides and saccharides we temporarily assumed that the compressibilities of both solute and hydrated water were zero and determined the numbers of hydration on the basis of this assumption.

As has been described in the preceding paper, in aqueous 1-1 electrolyte solutions the numbers of hydration of the electrolytes differ from each other at any given temperature, but decrease in parallel with an increase in the temperature. As may be seen from Fig. 1, the number of hydration of glycine decreases in parallel with those of 1-1 electrolytes with an increase in the temperature. This suggests that both the cation and the anion of the amino acid resemble those of strong electrolytes in the mechanism of hydration and that the hydration of the ions is strong and depends only slightly on the temperature.

From Fig. 2 it is clear, from a comparison of the numbers of hydration of aspartic acid and asparagine or glutamic acid and glutamine, that the dependence on the temperature of the acid type is greater than that of the amide

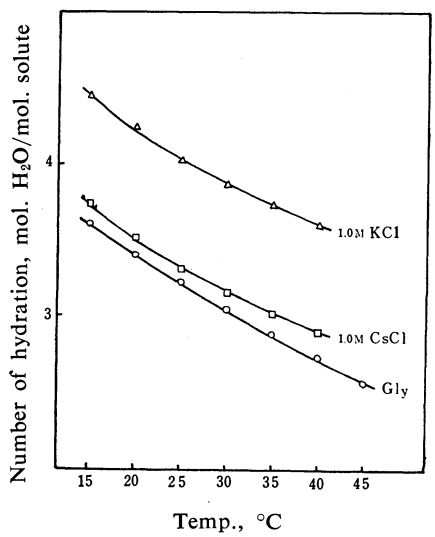


Fig. 1. Numbers of hydration and their temperature dependence.

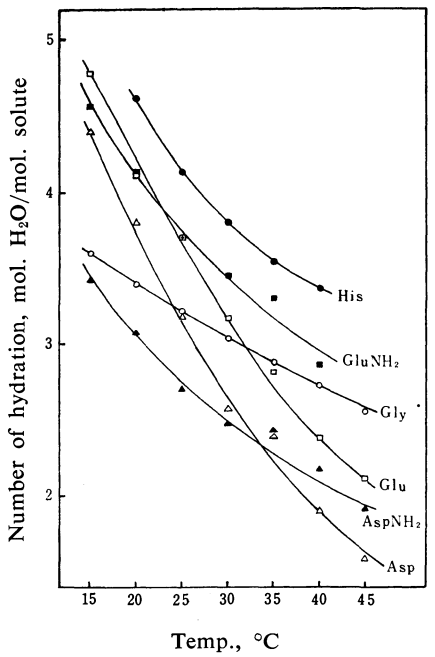


Fig. 2. Numbers of hydration and their temperature dependence.

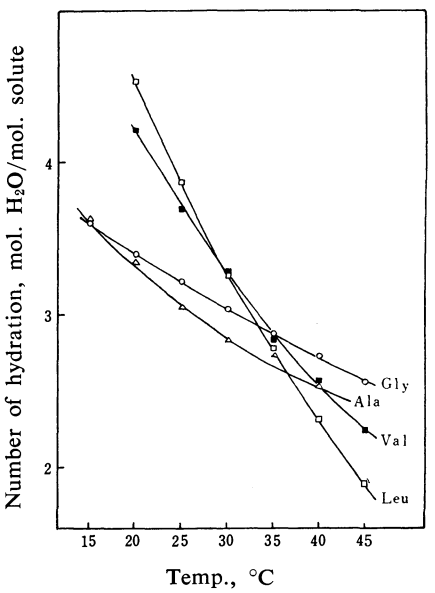


Fig. 3. Numbers of hydration and their temperature dependence.

type. This finding is similar to that seen in the comparison of 1-1 and 1-2 electrolytes described in a preceding paper. This also suggests that the state of hydration of the amide group is different from that of ionic groups. On the other hand, histidine, a basic amino acid, in an aqueous solution has a number of hydration which is larger, but its dependence

8) H. Shiio, *J. Am. Chem. Soc.*, **80**, 70 (1958).
9) K. Ito and H. Shiio, This Bulletin, **30**, 745 (1957).

on the temperature is less than those of acidic amino acids.

Figure 3 shows the numbers of hydration of some aliphatic amino acids and their temperature dependence. At lower temperatures the numbers of hydration increase with an increase in the hydrophobic side chains, as may be seen by a comparison of the numbers of hydration for alanine, valine and leucine. This apparently indicates that there is hydration around the non-polar side chain. Frank and Evans[10] suggested the existence of icebergs around non-polar substances judging from the thermodynamic properties of their solutions. Also, from the results of X-ray studies, Jeffrey et al.[11-13] proposed that the structure of water around tetraalkylammonium salts consists of molecules of water mutually bound by hydrogen bonds and forming clathrates. From the data given in Table I, it will be seen that at 20°C the difference in the numbers of the hydration water of alanine and valine is about 1 mol. H_2O/mol. solute. Their numbers were determined assuming that the compressibility of the hydrated water was zero. However, as was mentioned in the preceding paper, compressibility of the water of this hydration clathrate may not be negligible. Therefore, it may be that the number of molecules of the water of hydration around non-polar side chains is quite large.

Another point of interest is that the hydration of the hydrophobic side chains of amino acids depends greatly on the temperature, although the hydration of strong electrolytes and the ionic sites of amino acids depends only slightly on the temperature, as has been mentioned above. As may be seen from Table I, the difference in the number of hydration water at 20°C and at 40°C increases in the following order: glycine, alanine, valine and leucine. This phenomenon is to be regarded as additional evidence for the hypotheses that the icebergs melt with an increase in the temperature or that the structure of the clathrates is broken down at higher temperatures.[10,14,15]

Similarly, as may be seen from Fig. 4, the hydration of the side chain of methionine, containing a sulfur atom, is similar to that of the aliphatic hydrocarbon chain in such an amino acid as valine.

Table I. Numbers of hydration of various compounds and their temperature dependence

The numbers were determined assuming the compressibilities of both the solute and the hydrated water to be zero

Solute (2%)	Number of hydration (mol. H_2O/mol. solute) 20°C	40°C	Difference in numbers at 20 and 40°C
Gly	3.40	2.73	0.67
Ala	3.35	2.53	0.82
Val	4.22	2.56	1.66
Leu	4.53	2.31	2.22
Ser	4.04	3.14	0.90
Thr	4.06	2.93	1.13
Met	4.53	2.60	1.93
Asp[a]	3.80	1.90	1.90
$AspNH_2$	3.07	2.17	0.90
Glu[b]	4.11	2.38	1.73
$GluNH_2$	4.13	2.86	1.27
His	4.62	3.37	1.25
Phe	4.48	2.10	2.38
Pro	3.26	1.85	1.41
$(Gly)_2$	4.70	3.70	1.00
$(Gly)_3$	5.66	4.22	1.44
$(Gly)_4$[c]	6.38	4.79	1.59
Sucrose	3.42	1.60	1.82
Mannite	2.39	1.33	1.06

a) 0.50%
b) 0.76%
c) 0.95%

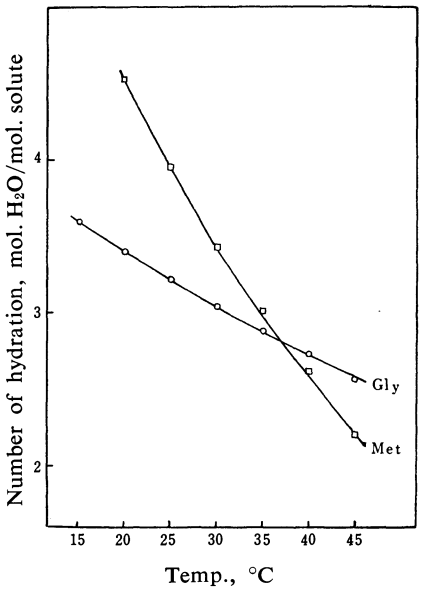


Fig. 4. Numbers of hydration and their temperature dependence.

10) H. S. Frank and M. W. Evans, *J. Chem. Phys.*, **13**, 507 (1945).
11) D. Feil and G. A. Jeffrey, ibid., **35**, 1863 (1961).
12) M. Bonamico, G. A. Jeffrey and R. K. McMullan, ibid., **37**, 2219 (1962).
13) G. A. Jeffrey and R. K. McMullan, ibid., **37**, 2231 (1962).
14) H. S. Frank and W. Y. Wen, *Discussions Faraday Soc.*, **24**, 133 (1957).
15) F. S. Feates and D. J. G. Ives, *J. Chem. Soc.*, **1956**, 2798.

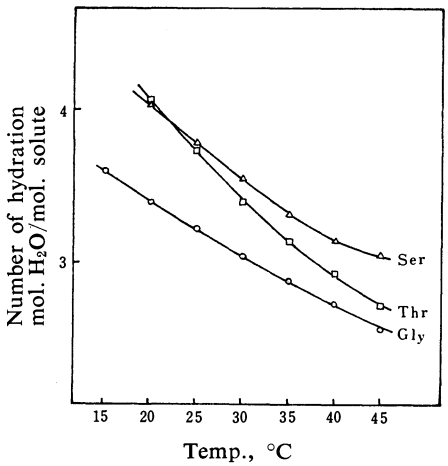


Fig. 5. Numbers of hydration and their temperature dependence.

On the other hand, as may be seen from Fig. 5 and Table I, the side chains of serine and threonine, in which there is a hydroxyl group, cause a slight increase in the numbers of hydration, but the numbers for serine and threonine decrease in parallel with that of glycine with an increase in the temperature. This suggests that the hydration of hydrophilic groups, such as the hydroxyl group, is comparatively small and acts competitively with that of hydrophobic groups, and that the former is stronger. The evidence for these conclusions is given in Fig. 6. The hydration of the hydroxyl group is suggested more strongly from the results for sucrose and mannite.

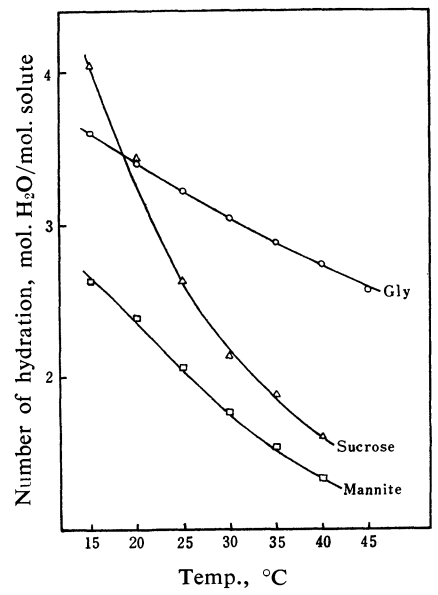


Fig. 6. Numbers of hydration and their temperature dependence.

These saccharides have several hydroxyl radicals, but their numbers of hydration are comparatively small. Also, Table I indicates that the number of hydration of sucrose decreases greatly with an increase in the temperature.

The numbers of the hydration of proline, a cyclic imino acid, and phenylalanine, containing a benzene ring, are shown in Fig. 7. As may be seen from this figure, the hydration of phenylalanine is very similar to that of leucine. This indicates that the phenyl radical is also hydrated. On the other hand, the hydration of proline is nearly the same as that of glycine, but at a higher temperature it is nearly the same as that of leucine and phenylalanine. From the results for proline and sucrose, it seems that the hydration of cyclic compounds is very dependent on the temperature.

As may be seen from Fig. 7, the numbers of the hydration of leucine and phenylalanine at higher temperatures are much smaller than that of glycine. It can be supposed that the hydration of hydrophobic regions is not only broken at higher temperatures, but that it also affects the hydration of ionic sites, giving mutual compensation.

The hydration of peptide bonds was also investigated. Pauling[16] reported that there is no adsorption of water on the peptide bond.

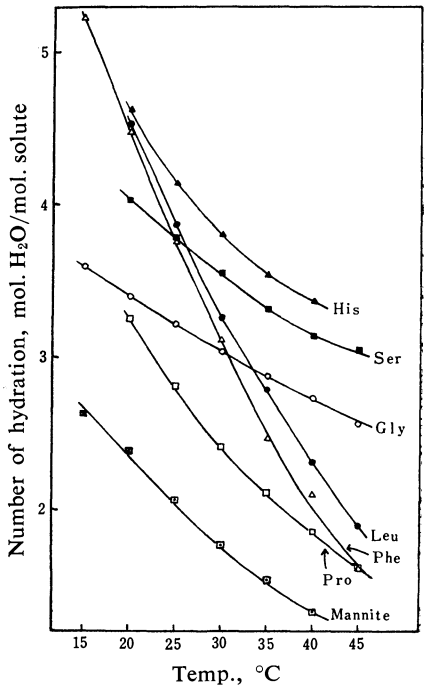


Fig. 7. Numbers of hydration and their temperature dependence.

16) L. Pauling, *J. Am. Chem. Soc.*, **67**, 555 (1945).

On the other hand, Mellon et al.[17] reported the hydration of peptide bonds. As may be seen from Fig. 8, the results for glycine, diglycine, triglycine and tetraglycine indicate that the peptide bond is hydrated. The stoichiometry of their numbers of hydration and their temperature dependence are good. Therefore the hydration of the peptide bond is probably like that of hydrophilic groups.

In conclusion, the hydration of various amino acids and the effect of various conditions on these hydrations differ. However, the hydration of amino acids can be classified roughly into the following three types: the hydration of (1) ionic sites, (2) hydrophilic sites, and (3) hydrophobic sites. Further, the hydrations of the hydrophobic sites of various amino acids differ in number and in temperature dependence. These properties may effect various physicochemical properties of proteins, such as their secondary and tertiary structures, the stability of their hydrophobic bonds, and the processes of their denaturation. Further studies of these problems will be reported in a following paper.

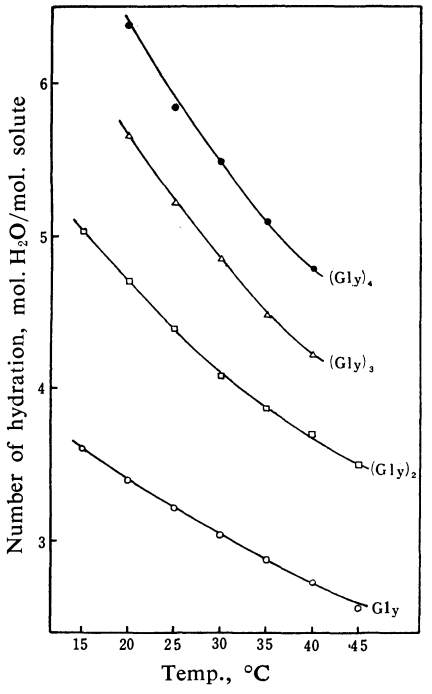


Fig. 8. Numbers of hydration and their temperature dependence.

It is very interesting that the results obtained by Whitney and Tanford[18] on the solubilities of amino acids in aqueous urea solutions agree with our results on the temperature dependence of the hydrations of amino acids. Therefore, the solubility of various compound must depend on their states and numbers of hydration.

Summary

The numbers of hydration of various amino acids, oligopeptides and saccharides in aqueous solutions and their dependence on the temperature have been determined by the method of ultrasonic interferometry. The hydration on ionic, hydrophilic and hydrophobic sites has been discussed. Particularly, evidence for the hydration around hydrophobic groups has been obtained. Also, we have established the hydration of the peptide bond.

The authors wish to express their hearty thanks to Dr. Kozo Hamaguchi for his valuable advice and discussion. Thanks are also due to Mrs. Reiko Kiyoi for preparing peptides for this work.

Division of Physical Chemistry
Institute for Protein Research
Osaka University
Kita-ku, Osaka

17) E. F. Mellon, A. H. Korn, E. L. Kokes and S. R. Hoover, ibid., 73, 1870 (1951).

18) P. L. Whitney and C. Tanford, *J. Biol. Chem.*, 237, PC1735 (1962).

On the Mechanism of Dehydrogenation of the 2, 4, 5-Triphenyl-4, 5-dihydroimidazole over Solid Catalysts

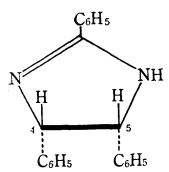
By Taro HAYASHI, Mineko KUYAMA, Emiko TAKIZAWA and Masako HATA

(Received June 1, 1964)

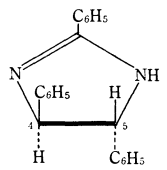
There have been a number of stereochemical studies of the hydrogenation of olefinic double bonds and aromatic rings over metal catalysts.[1,2] The results suggest that, at least in the cases of platinum catalysts used at room temperature, cis-addition predominates both in the hydrogenation of olefinic double bonds[1] and in the hydrogenation of aromatic rings.[2,3]

In contrast with the case of hydrogenation, however, little is known about the mechanism of dehydrogenation over metal catalysts. In order to obtain some information about the mechanism of the dehydrogenation of ring compounds over metal catalysts, the catalytic dehydrogenations of a dihydroimidazole ring over a Raney nickel catalyst and other metal catalysts have been studied. The present paper will report on the results of an investigation with stereoisomers of 2, 4, 5-triphenyl-4, 5-dihydroimidazole.

2, 4, 5 - Triphenyl - 4, 5 - dihydroimidazole is known to give three stereoisomers because of the differences in the conformations of the 4- and 5-hydrogen atoms; the cis isomer, amarine, which is not resolvable into optical antipodes, and the trans isomer, isoamarine, which is resolvable into optical antipodes, *d*- and *l*-isoamarine.



isoamarine



amarine

The dehydrogenations of amarine and *dl*-isoamarine in solutions over such solid catalysts as Raney nickel, platinum black, palladium black and active carbon have been investigated to ascertain the steric course of the dehydrogenation at the adjacent carbon atoms of a planar ring.

Experimental

Amarine and *dl*-isoamarine were prepared by the method of Japp and Moir;[4] amarine, m. p. 130~131°C, and *dl*-isoamarine, m. p. 200~201°C.

Raney nickel, platinum black and palladium black were prepared by the ordinary methods. The active carbon used was Norite-A. The reagents and solvents used were special-grade chemicals of Wako Pure Chemical Industries, Ltd.

The investigations of dehydrogenation with solid catalysts were carried out by the following procedure. A solution of 0.1~0.6 g. of amarine or isoamarine in 5~25 ml. of a solvent was refluxed with 0.1~0.5 g. of a catalyst for 3 hr. Then the catalyst was filtered off and washed. The filtrate was evaporated under reduced pressure, and the residue was warmed with 2 N hydrochloric acid. The amarine and isoamarine were dissolved, whereas the 2, 4, 5-triphenylimidazole (lophine) formed by the dehydrogenation was scarcely dissolved at all. The lophine was filtered off, and the weight of the lophine was determined to ascertain the extent of dehydrogenation carried out in the solution with a catalyst.

Results and Discussion

When amarine was heated in a hard glass tube at about 140°C[5] in a boiling xylene bath for 3 hr., amarine[6] was completely dehydrogenated in a molten state, giving lophine (m. p. 271~272°C), which was identified by no depression of its melting point on mixture with an authentic sample. However, when amarine was heated at 110°C in a boiling toluene bath in which amarine did not melt, dehydrogenation did not take place. The dehydrogenation of isoamarine did not occur at all when it was heated in a hard glass tube at 140°C in a boiling xylene bath in which isoamrine was not in a molten state. The dehydrogenation of isoamarine occurred

1) K. N. Campbell and B. K. Campbell, *Chem. Revs.*, **31**, 138 (1942); A. Farkas and L. Farkas, *Trans. Faraday Soc.*, **33**, 837 (1937).

2) R. P. Linstead, W. E. Doering, S. B. Davis, P. Levine and R. R. Whetstone, *J. Am. Chem. Soc.*, **64**, 1985 (1942). In this report a number of references about hydrogenation over platinum, palladium and nickel catalysts are cited.

3) R. B. Woodward and W. E. Doering, ibid., **67**, 864 (1945).

4) F. R. Japp and J. Moir, *J. Chem. Soc.*, **77**, 781 (1900).

5) A catalytic action of hard glass in the dehydrogenation of molten amarine was recognized, since the dehydrogenation of amarine did not occur in a quartz tube at 140°C.

6) H. L. Snape and A. Brook, *J. Chem. Soc.*, **75**, 211 (1881).

in a molten state at 240°C. These facts showed that amarine, the cis isomer, tended to be subjected to dehydrogenation in itself much more easily than *dl*-isoamarine, the trans isomer.[7] When amarine was heated in a solution in xylene, toluene or benzene under reflux for 3 hr., lophine, the product of the dehydrogenaton, was not isolated. As expected, the dehydrogenation of isoamarine did not take place in solutions under the same experimental conditions. Hence, it was confirmed that neither amarine nor isoamarine was subjected to dehydrogenation by refluxing solutions without the addition of a catalyst, at least below 140°C.

Raney nickel was found to exhibit a catalytic action in dehydrogenation of the *cis*-4, 5-dihydroimidazole ring, since the hydrogenation of amarine with Raney nickel in ethanol at room temperature yielded 2, 4, 5-tricyclohexylimidazole, from which the 4- and 5-hydrogen atoms of amarine had been removed, along with *cis*-2, 4, 5-tricyclohexyl-4, 5-dihydroimidazole.[8] The dehydrogenation of amarine and isoamarine over Raney nickel in solutions was first investigated.

A solution of 0.5 g. of amarine in 20 ml. of xylene was refluxed at 140°C in an oil bath for 3 hr. with Raney nickel, prepared from 0.7 g. of Raney nickel alloy powder. The xylene was then evaporated in vacuo, the residue being extracted with ethanol. The ethanolic solution was poured into water to yield a precipitate. The filtered precipitate was treated with 2 N hydrochloric acid to separate lophine. An almost theoretical amount of lophine was obtained. This result showed that amarine was completely dehydrogenated at 140°C in xylene with Raney nickel. Under the same conditions, no dehydrogenation of isoamarine occurred. Without the presence of oxygen, amarine was dehydrogenated with Raney nickel by refluxing a solution in xylene in an atmosphere of hydrogen or nitrogen. Hence, the dehydrogenation of amarine with Raney nickel in xylene was not due to oxidation, but was directly concerned with the catalyst. The dehydrogenation of amarine with Raney nickel was also completely effected by refluxing solutions in toluene, benzene, ethyl methyl ketone or acetone and partly occurred in cyclohexane, carbon tetrachloride or ethanol[9]. No dehydrogenation of amarine was effected by refluxing solutions in ethyl acetate, hexane, chloroform, acetic acid or pyridine with Raney nickel. In each of these solvents, no dehydrogenation of isoamarine took place either. These results indicate that, in the presence of solid catalysts, amarine in solutions is dehydrogenated in the absence of oxygen, even at rather low temperatures, such as the boiling points of benzene and acetone, and that the nature of solvents, as well as the temperature of reflux, is a strongly effective factor in dehydrogenation, although the polar nature of the solvents appears to play no part in the dehydrogenation, its mechanism being consequently considered to be non-ionic.

As in the experiments with Raney nickel, platinum black and palladium black, the dehydrogenation of amarine was carried out by refluxing solutions in xylene, toluene or benzene respectively. No dehydrogenation of isoamarine took place with these catalysts either.

With active carbon, which usually shows no catalytic action in hydrogenation, amarine was dehydrogenated by refluxing solutions in xylene, toluene, benzene or acetone without the presence of oxygen, whereas no dehydrogenation of isoamarine was effected under the same conditions.

Since the dehydrogenation of amarine over active carbon suggested that adsorption on solid catalysts might be strongly effective in the dehydrogenation of amarine, adsorptions of amarine and isoamarine on active carbon from solution in benzene were measured at room temperature. Amarine 0.14 g. was adsorbed on 0.58 g. of active carbon from a solution of 0.30 g. of amarine in 35.0 ml. of benzene at 22.5°C, whereas hardly any isoamarine was adsorbed on active carbon under the same conditions. As was expected from the conformational structures of these stereoisomers, the difference in the adsorptions was very marked of these isomers.

From the experimental results mentioned above, the steric course of the dehydrogenation of amarine was considered to be as follows; an amarine molecule is adsorbed on a solid catalyst with the side of plane of the imidazole ring, from which two cis hydrogen atoms at the 4- and 5-carbon atoms project. These two hydrogen atoms lie very close to the surface of the solid catalyst in such an adsorbed state. (Isoamarine is not adsorbed, since there exists no molecular side such as

7) When amarine and isoamarine were each heated at 300°C in a hard glass tube, both compounds, which were in molten states at this temperature, were dehydrogenated to yield lophine with a small amount of *trans*-stilbene.

8) T. Hayashi and M. Kuyama, *Natural Science Reports of Ochanomizu University*, 6, 99 (1955).

9) Although no dehydrogenation of amarine occurred when solutions were refluxed in ethanol or methanol without solid catalysts, the dehydrogenation of amarine did take place in butanol or pentanol without solid catalysts. In the latter cases oxygen was found to be necessary. This fact shows that the mechanism of dehydrogenation by reflusing solutions in alcohols is different from that in the other solvents mentioned above.

that of amarine mentioned above.) Both hydrogen atoms, which originally tend to move from the imidazole ring, as has been mentioned above, are eliminated from the 4- and 5-carbon atoms under the effect of the solid catalyst. Isoamarine is not dehydrogenated with a solid catalyst, since isoamarine is not be adsorbed on a solid catalyst.

This mechanism was supported by the following experiment with sulfur. When a solution of amarine in xylene was refluxed with fine powders of sulfur, amarine was dehydrogenated and hydrogen sulfide was evolve. The dehydrogenation of amarine is likely to follow the reverse couse to the *cis*-hydrogenation of aromatic rings over a platinum catalyst.[5]

Summary

1) Amarine has been completely dehydrogenated, without the presence of oxygen, by refluxing solutions in xylene, toluene, benzene or acetone with Raney nickel, whereas no dehydrogenation of isoamarine occurred at all under the same conditions. Amarine was also dehydrogenated without the presence of oxygen by refluxing solutions with platinum black, palladium black or active carbon. The dehydrogenation of amarine, carried out by refluxing a solution in benzene with sulfur powder, was accompanied by the evolution of hydrogen sulfide.

2) Amarine was adsorbed with active carbon from a solution in benzene at room temperature, whereas hardly any isoamarine was adsorbed under the same conditions, the difference in the dehydrogenation behavior of these cis- and trans-isomers being very marked.

3) Considering the results obtained, the dehydrogenation of amarine by refluxing solutions with solid catalysts may reasonably be considered *cis*-dehydrogenation, the mechanism being as follows; an amarine molecule is adsorbed on solid catalysts with the side of the plane of an imidazole ring, to which cis 4- and 5-hydrogen atoms are attached, and these hydrogen atoms, which tend to move from the imidazole ring, are eliminated under the effect of solid catalysts. Isoamarine, which has a trans-conformation unfavorable to adsorption, is not subjected to dehydrogenation with solid catalysts.

The authors wish to express their hearty thanks to Dr. Hiroshi Midorikawa of the Institute of Physical and Chemical Research for his kind help, and to the Ministry of Education for its grant-in-aid for scientific research.

Department of Chemistry
Faculty of Science
Ochanomizu University
Bunkyo-ku, Tokyo

The Reaction of Carbon Monoxide with Organometallic Compounds. IX. The Syntheses of Cyclic Ketones and Polyketones by the Reaction of Carbon Monoxide with Polymethylene Dilithiums*[1]

By Membo RYANG, Yoshihiko SAWA, Terukuni HASIMOTO and Shigeru TSUTSUMI

(Received June 10, 1964)

In the preceding paper[2] of this series, it was reported that carbon monoxide reacted with organolithium compounds in an ether solution at $-70°C$, producing corresponding symmetrical ketones in good yields. In these reactions, it was assumed that carbon monoxide attacked organolithium compounds nucleophilically and abstracted the lithium as lithium carbonyl, producing symmetrical ketones (Eq. 1):

$$2\,\text{R-Li} + 3\,\text{CO} \rightarrow \text{R-}\underset{\underset{\text{O}}{\|}}{\text{C}}\text{-R} + 2\,\text{LiCO} \qquad (1)$$

As this new method is simple and can be extended to similar reactions in good yields, the present authors carried out the reaction of carbon monoxide with polymethylenedilithiums by applying this reaction to a

* Part VIII: This Bulletin, 37, 341 (1964).

1) This work was presented at the 16th Annual Meeting of the Chemical Society of Japan, Tokyo, April, 1963.

2) M. Ryang and S. Tsutsumi, This Bulletin, 35, 1121 (1962).

TABLE I.

	$Li(CH_2)_4Li$			$Li(CH_2)_5Li$			$Li(CH_2)_6Li$	
	1	2	3	1	2	3	1	2
$Br(CH_2)_nBr$ (mol.)	0.1	0.025	0.025	0.1	0.1	0.1	0.1	0.1
Li (g. atom)	0.5	0.13	0.13	0.5	0.5	0.5	0.5	0.5
Ethyl ether (ml.)	200	200	400	150	180	250	200	300
Product (g.)								
a) Polymer	5.0	0.5	0.4	5.8	7.8	6.6	7.5	5.7
b) Cyclic ketone	0.2	0.2	0.8	0	0.1	0.2	0.3	0.6
c) Dialdehyde	0.6	0.1	0.2	0.8	0.1	0.2	0.2	0.3
d) Trimer	1.6	0.1	0.1	0.7	0.5	0.3	0.3	1.2
e) Tetramer	0.1	0.1	0.2	0	0	0	0.2	0.4
f) Acid	0.6	0	0	0.5	0.4	0.3	0.6	0.4

synthetic method of cyclic ketones (by intramolecular ketonization) and poly-ketones (by intermolecular ketonization).

The polymethylenedilithiums (tetramethylenedilithium, pentamethylenedilithium and hexamethylenedilithium) were prepared by the reaction of the corresponding polymethylenedibromide with methallic lithium in an ether solution at $-10\sim-5°C$.[3] Then pure, dry carbon monoxide was bubbled into the solution at $-70°C$. Thus cyclic ketones (Eq. 2) (cyclopentanone, cyclohexanone and cycloheptanone) and several poly-ketones (Eq.3) were synthesized :

$$Li(CH_2)_nLi + 3CO \longrightarrow (CH_2)_n\overset{\frown}{C}{=}O + 2LiCO \qquad (2)$$

$$m\,Li(CH_2)_nLi + 3m\,CO \longrightarrow H\text{-}\left[\text{-}\underset{\underset{O}{\|}}{C}\text{-}(CH_2)_n\text{-}\right]_m\text{-}\underset{\underset{O}{\|}}{CH} + 2m\,LiCO \qquad (3)$$

n=4, 5 and 6.

The synthesis of poly-ketones by the reaction of ethylene and carbon monoxide under high carbon monoxide pressure was exclusively studied by Hanford, Brubaker and Coffman.[4] Brubaker, Coffman and Hoehn[5] have reported detailed studies of the formation condition and structure of the poly-ketone. These reactions were carried out under high carbon monoxide pressure and the carbonyl groups were irregularly inserted, while the authors' method can be used at low temperatures under atmospheric pressure and the carbonyl groups in poly-ketones are regularly inserted.

Also, we have undertaken a study of the effect of dilution with a solvent (diethyl ether) on the yields of cyclic ketones; it has been found that the yields of cyclic ketones are considerably increased by the high dilution of polymethylenedilithium with a solvent.

Results and Discussion

The results of the reactions of carbon monoxide with polymethylenedilithiums are summarized in Table I.

Poly-ketones. — The poly-ketones (products a) were obtained as an ether-insoluble precipitate after the hydrolysis of the reaction mixtures with dilute hydrochloric acid and purification by the ordinary method.[5]

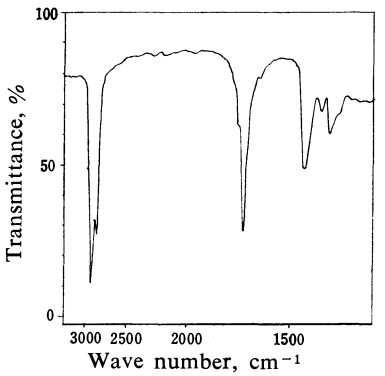


Fig. 1. Infrared spectrum of poly-ketone, $-[-\underset{\underset{O}{\|}}{C}-(-CH_2)_5-]_n-$

TABLE II. THE EFFECT OF DILUTION WITH A SOLVENT

	1	2	3
$Br\text{-}(CH_2)_4\text{-}Br$ (mol.)	0.1	0.025	0.025
Diethyl ether (ml.)	200	200	400
The degree of dilution	1	4	8
Cyclopentanone, yield* (%)	2.5	10	40
Poly-ketone, yield* (%)	56	24	19

* The calculations of yields are based on the amount of tetramethylenedibromide used.

3) R. West and E. Rochow, *J. Org. Chem.*, **18**, 1739 (1953).
4) H. Gilman, *Organic Chemistry: An Advanced Treatise*, Vol. IV, 1025—1042.
5) M. M. Brubaker, D. D. Coffman and H. H. Hoehn, *J. Am. Chem. Soc.*, **74**, 1509 (1952).

TABLE III.

Fraction		$Li(CH_2)_4Li$	$Li(CH_2)_5Li$	$Li(CH_2)_6Li$
(1)	b. p.	60～ 90°C/70 mmHg	60～ 80°C/30 mmHg	65～ 85°C/12 mmHg
(2)	b. p.	110～150°C/17 mmHg	140～160°C/25 mmHg	100～125°C/17 mmHg
(3)	b. p.	155～160°C/ 3 mmHg	150～170°C/ 3 mmHg	155～164°C/17 mmHg
(3)	b. p.	～180°C/ 3 mmHg		～160°C/ 3 mmHg

The infrared spectra of the poly-ketones showed the presence of methylene and a carbonyl group (1690～1700 cm^{-1}); the elementary analysis of these poly-ketones are correct for $C_{n+1}H_{2n}O$ (n=4, 5, 6,), which indicates that these poly-ketones have a $-[-(CH_2)_n-\overset{\overset{O}{\|}}{C}-]-$ unit as a monomer unit. Typical infrared spectra of poly-ketone are reproduced in Fig. 1.

Cyclic Ketones. — Cyclic ketones (products b) were obtained by the distillation of the neutral part under reduced pressure, and their structures were determined by ordinary methods, such as elementary analysis, mixed-melting-point measurements of their 2, 4-dinitrophenylhydrazones, and infrared spectra measurements. It was found that dilutions of polymethylenedilithiums with diethyl ether lead to increasing yields of cyclic ketones and decreasing yields of poly-ketones. (Cf., for example, Table II.) This method of synthesizing cyclic ketones under high dilution with a solvent seemed to be the simplest way to prepare cyclic ketones from aliphatic compounds. (Earlier methods may be seen in the literature cited in Ref. 6.)

Other Products. — Various by-products were produced by these reactions. Among these by-products, the following compuuds (I—III) were isolated; their structures were assumed on the basis of the results of elementary analyses, infrared spectra measurements and molecular weight measurements.

$$Br(CH_2)_n-\overset{\overset{O}{\|}}{C}H, \qquad HC-\overset{\overset{O}{\|}}{C}-(CH_2)_n-\overset{\overset{O}{\|}}{C}H,$$

I II

$$HC(CH_2)_4\overset{\overset{O}{\|}}{C}(CH_2)_4\overset{\overset{O}{\|}}{C}(CH_2)_4\overset{\overset{O}{\|}}{C}H$$

III

These products are thought to be the precursors to the poly-ketones.

Experimental

Materials.—Commercial polymethylenedibromides were purified by fractional distillation: tetramethylenedibromide (b. p. 113～115°C/60 mmHg), pentamethylenedibromide (b. p. 118～119°C/34 mmHg, n_D^{15} 1.5146), and hexamethylenedibromide (b. p. 138～139°C/34 mmHg, n_D^{15} 1.5111).

The Preparation of Polymethylenedilithiums.— Into a 500 ml. four-necked flask equipped with a mechanical stirrer, a low temperature thermemoter, a reflux condenser protected from moisture, a gas bubbler and a dropping funnel, 50 ml. of anhydrous diethyl ether (dried over sodium) were placed; after the apparatus had been swept with dry oxygen-free nitrogen, 3.5 g. (0.5 g. atom.) of lithium in the form of small pieces of thin coil was added. A solution of polymethylenedibromide (0.1 mol.) in 100 ml. of anhydrous diethyl ether was stirred in via the dropping funnel over a period of 1 hr., while the internal temperature was maintained at −10～−5°C.

The Reaction of Carbon Monoxide with Polymethylenedilithium.—After the addition had been completed, the stirring was continued for another hour, after which the reaction mixture was cooled to −70°C with a dry ice-methanol bath kept at −78°C. Dry pure carbon monoxide was then introduced from the gas bubbler at a rate of 0.5 l./min. for 1 hr. The reaction mixture was then decomposed with 50 ml. of 95% ethanol and, further, with 100 ml. of 6 N hydrochloric acid. Then poly-ketone was precipitated as an ether-insoluble solid and was filtered off under reduced pressure. The organic layer separated from the filtrate was treated with three succesive 50-ml. portions of saturated aqueous potassium carbonate and divided into (1) the organic layer and (2) the potassium carbonate solution.

Poly-ketones. — The precipitate was dissolved in hot benzene, and then this solution was added to methanol by means of a vigorous agitation. The polymer, separated as a powder, was filtered; this procedure was repeated three times, and then the polymer was dried to a constant weight. The elementary analysis of these poly-ketones are:

$-[-(CH_2)_4-\overset{\overset{O}{\|}}{C}-]-$ polymer. Found: C, 70.99; H, 8.93. Calcd. for C_5H_8O: C, 71.39; H. 9.53%

$-[-(CH_2)_5-\overset{\overset{O}{\|}}{C}-]-$ polymer. Found; C, 74.40; H, 10.80. Calcd. for $C_6H_{10}O$: C, 73.43; H, 10.27%.

$-[-(CH_2)_6-\overset{\overset{O}{\|}}{C}-]-$ polymer. Found: C, 76.59; H, 10.83. Calcd. for $C_7H_{12}O$: C, 75.00; H, 10.78%.

The organic layers containing neutral compounds were washed with water and dried over anhydrous sodium sulfate. The brownish residual oils obtained after the removal of the solvent were distilled under reduced pressure to give the following fractions (Table III).

6) L. Ruzicka et al., *Helv. Chim. Acta*, **9**, 249, 499 (1926); J. C. Sauer, *J. Am. Chem. Soc.*, **69**, 2448 (1947); J. Heer and K. Miescher, *Helv. Chim. Acta*, **31**, 1289 (1948); Monsanto Chemical Co., *Chem. & Eng. News*, **1957**, 85; K. Ziegler et al., *Ann.*, **504**, 94 (1933).

Cyclic Ketones.—Fraction 1 was assumed to be mainly cyclic ketones, which were identified by mixed-melting-point measurements of their 2, 4-dinitrophenylhydrazones and by elementary analysis. The yields of cyclic ketones were calculated from the results of gas chromatographic analysis (Column-SiDC 550, 2 m.; or P. E. G. 6000, 2 m.; carrier gas, H_2).

Cyclopentanone. — 2, 4 - Dinitrophenylhydrazone (m. p. 144°C, recrystallized from ethanol).

Found: C, 49.62; H, 4.25. Calcd. for $C_{11}H_{12}O_4N_4$: C, 49.80; H, 4.53%.

Cyclohexanone. — 2, 4 - Dinitrophenylhydrazone (m. p. 157.5~158°C, recrystallized from ethanol).

Found: C, 52.16; H, 5.09. Calcd. for $C_{12}H_{14}O_4N_4$: C, 51.80; H, 5.07%.

Cycloheptanone. — 2, 4 - Dinitrophenylhydrazone (m. p. 146.5~147°C, recystallized from ethanol).

Found: C, 53.13; H, 5.32. Calcd. for $C_{13}H_{16}O_4N_4$: C, 53. 42; H, 5.52%.

From fraction 1 (from hexamethylenedilithium), 6-bromohexamethylenealdehyde was also isolated. 2, 4-Dinitrophenylhydrazone (m. p. 227~228°C, recrystallized from ethylacetate).

Found: C, 42.20; H, 4.83. Calcd. for $C_{13}H_{17}O_4N_4Br$: C, 41.83; H, 4.60%.

Dialdehyde. — Fraction 2 was assumed to be dialdehyde, $HCO(CH_2)_nCHO$; n=4, 5, 6. Pimeloaldehyde (II) was identified from the results of the mixed-melting-point measurement of its 2, 4-dinitrophenylhydrazone (m. p. 183~184°C, recrystallized from ethanol-ethylacetate).

Found: C, 46.32; H, 3.98, Calcd. for $C_{19}H_{20}O_8N_8$: C, 46.74; H, 4.09%.

Ketoaldehyde (trimer).—Fraction 3 was assumed to be ketoaldehyde (trimer) from the results of its infrared spectra and molecular weight measurements. For example, tetradeca-5, 10-dione-1, 14-dialdehyde (III);

Found: C, 70.21; H, 9.74. Mol. wt. (in benzene). 285. Calcd. for $C_{16}H_{24}O_4$: C, 68.05; H; 9.28%. Mol. wt. 282.

IR Spectrum.—1680 cm^{-1} and 1700 cm^{-1}.

Other Products.—The sublimable brownish crystals obtained from fraction 3 (in tetramethylenedilithium) were recrystallized from benzene to give yellowish crystals, m. p. 202°C; mol. wt. 145; elementary analysis: C, 72.98; H, 7.56%; IR spectrum 1670 cm^{-1}). However, the structure of these crystals has not yet been determined. The acidic parts were not examined.

Summary

The reactions of carbon monoxide with tetramethylenedilithium, hexamethylenedilithium and pentamethylenedilithium at −70°C have yielded the corresponding poly-ketones (monomer unit: $-CO(CH_2)_n-$, n=4, 5 and 6) and cyclic ketones (cyclopentanone, cyclohexanone and cycloheptanone). In these reactions, high dilutions of polymethylenedilithiums with a solvent (diethyl ether) lead to the formation of cyclic ketones in good yields. For example, cyclopentanone has been obtained in a 40% theoretical yield.

Department of Chemical Technology
Faculty of Engineering
Osaka University
Miyakojima-ku, Osaka

NOTES

Benzyl Esters of α-Amino Acids

By Yoshio IWAKURA, Katsumi HAYASHI, Sanam KANG and Kunio NAKAOJI

(Received May 14, 1964)

It has well been known that benzyl esters of α-amino acids provide versatile intermediates for the polypeptide synthesis.[1-3] Various methods have been reported for the preparation of hydrochlorides or other salts of α-amino acid benzyl esters; the treatment of α-amino acid with benzyl alcohol saturated with dry hydrogen chloride,[4-6] the reaction of α-amino acid chloride hydrochloride and benzyl alcohol,[7-9] the treatment of *p*-toluenesulfonic

1) B. F. Erlanger and E. Brand, *J. Am. Chem. Soc.*, **73**, 3508 (1951).
2) B. F. Erlanger and R. H. Hall, ibid., **76**, 5781 (1954).
3) K. Miller and H. Waelsch, ibid., **74**, 1092 (1952).
4) E. Abderhalden and S. Suzuki, *Z. physiol. chem.*, **176**, 101 (1928).
5) R. E. Neuman and E. L. Smith, *J. Biol. Chem.*, **193**, 97 (1951).
6) H. Sachs and E. Brand, *J. Am. Chem. Soc.*, **75**, 4608 (1953).
7) E. Fischer, *Ber.*, **38**, 2914 (1905).
8) R. Ruggli, R. Ratti and E. Henzi, *Helv. Chim. Acta*, **12**, 361 (1929).
9) C. R. Harrinton and T. H. Mead, *Biochem. J.*, **30**, 1958 (1936).

TABLE I. BENZYL ESTER HYDROCHLORIDES OF α-AMINO ACIDS

Amino acid	Benzyl ester hydrochlorides of α-amino acids				
	M. p., °C.	Yield, %	Formula	Nitrogen, %	
				Calcd.	Found
Glycine	129	28	$C_9H_{12}O_2NCl$	6.97	6.99
L-Valine	138	78	$C_{12}H_{18}O_2NCl$	5.85	5.91
DL-Valine	91	95	$C_{12}H_{18}O_2NCl$	5.75	5.91
L-Leucine	145	62	$C_{13}H_{20}O_2NCl$	5.45	5.72
L-Phenylalanine	202	96	$C_{16}H_{18}O_2NCl$	4.80	4.82

acid or the benzenesulfonic acid salt of α-amino acid with benzyl alcohol,[3,10-13] and the reaction of α-amino acid and benzyl alcohol in polyphosphoric acid.[14]

Erlanger and Brand have synthesized benzyl ester hydrochlorides of glycine, D- and L-alanines by causing the corresponding *N*-carboanhydrides (NCAs) to react with benzyl alcohol in the presence of dry hydrogen chloride in ether.[1] In this preparation, the NCAs have been made by the reaction of *N*-carbobenzoxy α-amino acid with phosphorus pentachloride.

During the course of our investigation of poly-α-amino acid synthesis, we have found that the preparation from NCAs makes a convenient method for benzyl ester hydrochlorides of α-amino acids when it is combined with the phosgenation process of α-amino acids, which is now recognized as the most useful route to NCAs. The synthesis of L-alanine benzyl ester hydrochloride by this process has been briefly reported by Rudinger and Pravda.[15]

The phosgenation was carried out in an inert solvent, such as tetrahydrofuran, dioxane, benzene and toluene, at a temperature between 40 and 80°C. When the solvent was removed after the phosgenation was completed, a curde NCA was obtained; this was further treated with a solution of benzyl alcohol in dry ether containing dry hydrogen chloride. The reaction proceeded smoothly at room temperature; carbon dioxide was evolved, and the benzyl ester hydrochloride was precipitated out of the solution. The ether-soluble benzyl ester hydrochloride of L-leucine was isolated by removing the solvent and then recrystallizing it from chloroform/cyclohexane.

In the phosgenation, a prolonged reaction time and a large excess of phosgene decreased the yield of product, mainly because of the formation of *N*-carbonyl α-amino acid chloride.[16] In order to shorten the reaction time, it was necessary to use a finely powdered α-amino acid and to create an efficient agitation through the introduction of phosgene. The preparation is summarized in Table I.

Experimental

L-Phenylalanine Benzyl Ester Hydrochloride. — Into a mixture of 20.0 g (0.12 mol.) of finely powdered L-phenylalanine suspended in 200 ml. of dry tetrahydrofuran, phosgene was stirred efficiently in a thin stream at a temperature between 50 and 60°C. The mixture gave a clear solution after about forty minutes. The solution was then evaporated under reduced pressure, and the residue (crude NCA of L-phenylalanine) was dissolved in 200 ml. of ether containing 7 g. (0.19 mol.) of dry hydrogen chloride. To the solution 20 g. (0.19 mol.) of benzyl alcohol was immediately added. The evolution of carbon dioxide began approximately ten to fifteen minutes after the mixing. The mixture was then allowed to stand at room temperature overnight protected from moisture. The whole mixture became a solid mass because of the precipitation of L-phenylalanine benzyl ester hydrochloride, which was collected on a sintered glass filter and washed repeatedly with dry ether. The product weighed 33.2 g. (96%) and melted at 200~201°C. It was recrystallized from benzene. M. p. 202°C.

L-Valine Benzyl Ester Hydrochloride.—Thirty-five grams (0.30 mol.) of L-valine was phosgenated in 400 ml. of tetrahydrofuran at 50°C. The crude NCA of L-valine was treated with 65 g. (0.6 mol.) of benzyl alcohol in 500 ml. of ether containing 22 g. (0.6 mol.) of dry hydrogen chloride. The product, L-valine benzyl ester hydrochloride, weighed 57 g. (78%). It was recrystallized from ethyl acetate. M. p. 137~138°C.

L-Leucine Benzyl Ester Hydrochloride.—Twenty grams (0.153 mol.) of L-leucine was phosgenated in 200 ml. of tetrahydrofuran at 50°C. A clear solution was obtained within one hour. The crude NCA of L-leucine was treated with 25 g. (0.23 mol.) of benzyl alcohol in 200 ml. of ether containing

10) P. C. Crofts, J. H. H. Markes and H. N. Rydon, *J. Chem. Soc.*, **1959**, 3610.
11) N. Izumiya and S. Makisumi, *J. Chem. Soc. Japan, Pure Chem. Sec.* (*Nippon Kagaku Zassi*), **78**, 662 (1957).
12) L. Zervas, M. Winitz and J. P. Greenstein, *J. Org. Chem.*, **22**, 1515 (1957).
13) J. P. Cipera and R. V. V. Nicholls, *Chem. & Ind.*, **1955**, 16.
14) B. F. Erlanger and R. H. Hall, *J. Am. Chem. Soc.*, **76**, 5781 (1954).
15) J. Rudinger and Z. Pravda, *Chem. Listy*, **52**, 120 (1958).
16) Y. Iwakura and S. Kang, presented at the 16th Annual Meeting of the Chemical Society of Japan, Tokyo, March, 1963.

10 g. (0.27 mol.) of dry hydrogen chloride. After the solution had been allowed to stand overnight the solvent was removed by distillation. The product was dissolved in a small amount of chloroform and reprecipitated with cyclohexane. The yield was 24.5 g. (62%). M. p. 144~145°C.

Glycine and D,L-Valine Benzyl Ester Hydrochlorides. — They were prepared by the same procedure as has been described above. The results are listed in Table I.

The authors wish to thank the Ajinomoto Co. for supplying various α-amino acids.

Department of Synthetic Chemistry
Faculty of Engineering
The University of Tokyo
Hongo, Tokyo

The Melting of Glassy Carbon

By Tokiti NODA and Michio INAGAKI

(Received May 22, 1964)

It has previously been reported[1] that carbon was melted at 4000°K under a pressure of 110 atm. and that the molten carbon had the same lattice constants as natural graphite, i. e., $c_0=6.707_8$ Å and $a_0=2.461_4$ Å. However, Bundy[2] has reported that the carbon which was melted under very high pressure and using the flash heating technique had a large lattice constant, 6.748 Å for c_0. In the present work, glassy carbon, which has been found to be a typical non-graphitizing carbon,[3,4] was melted in the same pressure vessel as has been reported on previously.[1]

Glassy carbon rods 4 mm. in diameter, which had previously been heat-treated at 2000°C, were melted by the passage of electrical current directly through them in argon under a pressure above 110 atm. The melting of carbon usually occurred in the middle part of the rod. With a coke-based carbon, the molten carbon formed a ball attached to a crater-type cavity.[1] With glassy carbon, the melting started in the inner part of the rod and made a molten mass of a thin spindle form along the central axis of the rod. Frequently, the molten carbon spouted out from the break of the cavity wall, and a narrow but long cavity of a spindle form was formed inside the rod. The spouted molten carbon was scattered in balls smaller than 0.5 mm. in diameter. When a glassy carbon rod 5 mm. in diameter was used, the spouted molten carbon had a cochleate appearance. Minute fragments of the molten carbon were also found on the inside wall of the cavity.

The molten carbon was soft and of a metallic luster. Its lattice constant, c_0, was 6.708 Å. The X-ray powder pattern for a rod specimen cut out from the molten carbon had only diffraction lines of the hexagonal modification of graphite, and none of the rhombohedral modification. By grinding the same carbon in a mortar, however, traces of the rhombohedral modification were detected from the X-ray pattern.

In one case, where no change in the appearance of the rod specimen was observed after the passage through of an electrical current, a cavity about 10 mm. long and about 1.5 mm. in diameter at the maximum was found in the central part of the rod. The wall of the cavity was composed of three layers, which

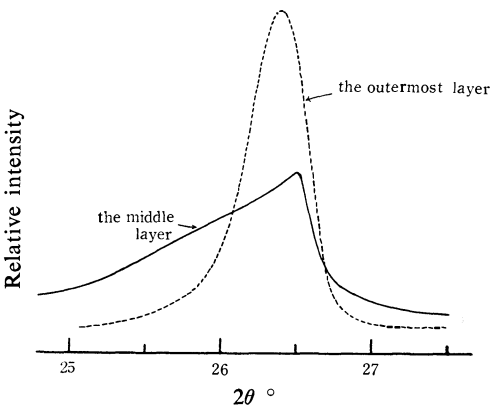


Fig. 1. Profiles of (002) diffraction for the outermost and the middle layers of the cavity wall.

1) T. Noda, "Proceeding of the International Symposium on High Temperature Technology," MacGraw-Hill, New York (1959), p. 286.
2) F. P. Bundy, *J. Chem. Phys.*, 35, 618 (1963).
3) S. Yamada, H. Sato and T. Ishii, presented at the Sixth Biennial Conference on Carbon, Pittsburgh, 1963.
4) T. Noda and M. Inagaki, This Bulletin, to be published

were clearly distinguished from each other in hardness and appearance. The innermost layer was the molten carbon, judging from its properties and its lattice constant, c_0. The outermost layer, which was about 0.05 mm. thick, was so soft that it could be whittled by a razor blade, but it had no metallic luster. Its lattice constant, c_0, was measured as 6.748 Å. It seemed that the graphitization of this part was promoted by the presence of a minute amount of oxygen mixed in the ambient gas phase of argon.[5] The carbon of the middle layer was very hard and showed a conchoidal fracture, which was one of the characteristics of glassy carbon. As is shown in Fig. 1, the profile of (002) diffraction for the middle layer was unsymmetrical, while the profiles for the other layers were symmetrical. This unsymmetrical profile shows that the non-graphitized part remained in the glassy carbon at the middle layer, even after heating at temperatures very near to the melting point of carbon. This phenomenon is somewhat similar to the finding that the crater part of the rod of a coke-based carbon had the lattice constant, c_0, of 6.714 Å.[1] It must be noticed that glassy carbon did not lose its characteristics, even at temperatures very near to its melting point.

Department of Applied Chemistry
Faculty of Engineering
Nagoya University
Chikusa-ku, Nagoya

5) T. Noda and M. Inagaki, *Carbon*, to be published.

The Electronic Structures of NO_2, NO_2^+ and NO_2^-

By Hiroshi KATO, Teijiro YONEZAWA, Keiji MOROKUMA and Kenichi FUKUI

(Received may 25, 1964)

Several quantum-mechanical investigations have been carried out on the electronic structures of NO_2,[1,2,3] NO_2^+,[1,4,5] and NO_2^-.[1] That is, Walsh[1] discussed the electronic structure of these molecules by qualitative considerations. Tanaka[2] and McEwen[3] treated the π electronic structure of NO_2 by the LCAO SCF method, and, further, McEwen investigated the σ non-bonding electrons by the semi-emprical method.

On the other hand, the present authors and others have developed the Hückel molecular orbital treatment of saturated compounds and also the σ electronic structure of unsaturated compounds.[6] Hoffmann has recently proposed an extended Hückel molecular orbital method in which σ and π electronic structures of saturated and unsaturated hydrocarbons are treated simultaneously.[7]

In the present paper, the electronic structures of NO_2, NO_2^+ and NO_2^- will be calculated by Hoffmann's method, and some physico-chemical properties of these compounds will be discussed.

Method of Calculation

By Hoffmann's method the molecular orbitals (MO) of these compounds are represented by the linear combination of valency atomic orbitals (AO), that is, the 2s, $2p_x$, $2p_y$ and $2p_z$ orbitals of the nitrogen and oxygen atoms. Therefore, the secular determinant is given by

$$\det |H_{ij}-ES_{ij}| = 0$$

whers H_{ij} is the off-diagonal element and S_{ij} is the overlap integral between the ith and jth atomic orbitals. The values of the diagonal elements, H_{ii}, are given with reference to those given by Skinner and Pritchard[8]:

$H(2s, N) = -27.5$ eV. $H(2p, N) = -14.5$ eV.

$H(2s, O) = -35.3$ eV. $H(2p, O) = -17.8$ eV.

and the off-diagonal element, H_{ij}, is expressed as:

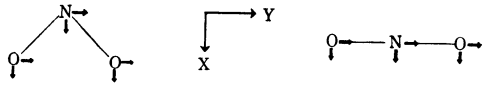
$$H_{ij} = 0.5K(H_{ij}+H_{ji})S_{ij}$$

where the value of K is taken as 1.75, as in Hoffmann's paper,[7] and the values of S_{ij} are

1) A. D. Walsh, *J. Chem. Soc.*, **1953**, 2266.
2) J. Tanaka, *J. Chem. Soc. Japan, Pure Chem. Sec. (Nippon Kagaku Zassi)*, **78**, 1643 (1957).
3) K. L. McEwen, *J. Chem. Phys.*, **32**, 1801 (1961).
4) S. Nagakura and J. Tanaka, *J. Chem. Soc. Japan, Pure Chem. Sec. (Nippon Kagaku Zassi)*, **75**, 993 (1954).
5) E. Clementi and A. D. McLean, *J. Chem. Phys.*, **39**, 323 (1963).
6) K. Fukui, H. Kato and T. Yonezawa, This Bulletin, **34**, 442, 1111, 1814 (1961); K. Fukui, H. Kato, T. Yonezawa, K. Morokuma, A. Imamura and C. Nagata, ibid., **35**, 38 (1962); K. Morokuma, K. Fukui, T. Yonezawa and H. Kato, ibid., **36**, 47 (1963).
7) R. Hoffmann, *J. Chem. Phys.*, **39**, 1397 (1963); ibid., **40**, 2474, 2480, 2745 (1964).
8) H. A. Skinner and H. O. Pritchard, *Chem. Revs.*, **55**, 745 (1955).

obtained by Mulliken's Table.[9]

The shapes of these molecules are given as follows:[10] The N–O distance is 1.15 Å for NO_2^+, 1.20 Å for NO_2, and 1.235 Å for NO_2^-, and the angle of ONO is 180° for NO_2^+, 132° for NO_2, and 115° for NO_2^-. Thus, NO_2 and NO_2^- belong to the point group C_{2v}, and NO_2^+ belong to the group $D_{\infty h}$. The coordinate is taken as shown in Fig. 1, where the p_z orbitals are perpendicular to the XY plane.



NO_2, NO_2^- NO_2^+

Fig. 1. The coordinates and the directions of p_x, p_y orbitals.

Results and Discussion

Electronic Levels and Distributions.—The calculated MO energies (in eV.) and the values of the coefficients of AO's in some MOs are listed in Table I (a), (b) and (c), together with the irreducible representations of each MO. From the results listed in Table I, the following facts can be deduced: In NO_2^+, the highest occupied orbital (HO) consists of the π orbitals of the oxygen atoms, the odd electron in NO_2 is mainly localized on the lone-pair orbital of the nitrogen atom, and a

TABLE I. (a) MOLECULAR ORBITALS OF NO_2^+

Irreducible representation	Orbital energy, eV.	Molecular orbital***
e_{1u}*	−10.88	$0.953Z_N-0.484(Z_O+Z_O')$
e_{1u}*	−10.88	$0.953X_N-0.484(X_O+X_O')$
e_{1g}**	−17.72	$0.710(X_O-X_O')$
e_{1g}**	−17.72	$0.710(Z_O-Z_O')$
a_{2u}	−18.75	$-0.251Y_N-0.135(S_O-S_O')+0.621(Y_O+Y_O')$
e_{1u}	−19.28	$0.428Z_N+0.556(Z_O+Z_O')$
e_{1u}	−19.28	$0.428X_N+0.556(X_O+X_O')$

* The lowest vacant orbitals (degenerated)
** The highest occupied orbitals (degenerated)
*** The notations S_N, X_N, Y_N and Z_N denote the 2s, $2p_x$, $2p_y$ and $2p_z$ orbitals of the nitrogen atom and the prime is used to represent the orbitals of the second oxygen atom.

TABLE I. (b) MOLECULAR ORBITALS OF NO_2

Irreducible representation	Orbital energy, eV.	Molecular orbital***
b_1*	−11.58	$0.949Z_N-0.454(Z_O+Z_O')$
a_1**	−13.19	$0.319S_N-0.802X_N-0.022(S_O+S_O')-0.037(Y_O-Y_O')+0.487(X_O+X_O')$
b_2	−17.46	$-0.061Y_N-0.005(S_O-S_O')+0.472(Y_O+Y_O')+0.537(X_O-X_O')$
a_2	−17.69	$0.710(Z_O-Z_O')$
b_2	−18.85	$0.275Y_N+0.131(S_O-S_O')-0.426(Y_O+Y_O')+0.416(X_O-X_O')$
a_1	−18.98	$-0.060S_N+0.368X_N-0.061(S_O+S_O')+0.366(Y_O-Y_O')+0.461(X_O+X_O')$
b_1	−19.11	$0.414Z_N+0.570(Z_O+Z_O')$

* The lowest vacant orbital. ** The odd electron orbital.

TABLE I. (c) MOLECULAR ORBITALS OF NO_2^-

Irreducible representation	Orbital energy, eV.	Molecular orbital***
b_1*	−11.91	$0.948Z_N-0.437(Z_O+Z_O')$
a_1**	−14.24	$0.355S_N-0.736X_N-0.011(S_O+S_O')-0.016(Y_O-Y_O')+0.491(X_O+X_O')$
b_2	−17.18	$-0.082Y_N+0.006(S_O-S_O')+0.576(Y_O-Y_O')+0.491(X_O+X_O')$
a_2	−17.65	$0.711(Z_O-Z_O')$
b_2	−18.88	$0.294Y_N+0.124(S_O-S_O')-0.345(Y_O+Y_O')+0.501(X_O-X_O')$
a_1	−18.89	$-0.080S_N+0.327X_N-0.072(S_O+S_O')+0.426(Y_O-Y_O')+0.390(X_O+X_O')$
b_1	−19.04	$0.404Z_N+0.578(Z_O+Z_O')$

* The lowest vacant orbital. ** The highest occupied orbital.

9) R. S. Mulliken, C. A. Rieke, D. Orloff and H. Orloff, *J. Chem. Phys.*, **17**, 1248 (1949).

10) A. D. Mitchell, L. C. Cross et al., "Table of Interatomic Distances and Configuration in Molecules and Ions," The Chemical Society, London (1958).

TABLE II. THE TYPES OF TRANSITION AND THE CALCULATED AND OBSERVED TRANSITION ENERGIES OF NO_2 (eV.)

	Type of transition by Walsh	Calcd. eV.	Obs. eV.
from	$-(b_1)^2(a_1)^2(b_2)^2(a_2)^2(b_2)^2(a_1)$		
to	$-(b_1)^2(a_1)^2(b_2)^2(a_2)^2(b_2)^2(b_1)$	1.61	1.36~3.87
	$-(b_1)^2(a_1)^2(b_2)^2(a_2)^2(b_2)(a_1)^2$	4.27	
	$-(b_1)^2(a_1)^2(b_2)^2(a_2)(b_2)^2(a_1)^2$	4.50 *	
	$-(b_1)^2(a_1)^2(b_2)^2(a_2)^2(b_2)(a_1)(b_1)$	5.88 *	
	$-(b_1)^2(a_1)^2(b_2)^2(a_2)(b_2)^2(a_1)(b_1)$	6.11	4.77~5.46
	$-(b_1)^2(a_1)^2(b_2)(a_2)^2(b_2)^2(a_1)^2$	5.66	
	$-(b_1)^2(a_1)(b_2)^2(a_2)^2(b_2)^2(a_1)^2$	5.80	7.75~9.18
	$-(b_1)(a_1)^2(b_2)^2(a_2)^2(b_2)^2(a_1)^2$	5.92	

* Forbidden transitions

similar tendency is observed in the HO of NO_2^-. The lowest orbitals (LV) of these compounds are all π anti-bonding orbitals, largely localized on the nitrogen atom. The order of our calculated orbitals of NO_2 and NO_2^- are consistent with the results estimated by Walsh[1],* and that of NO_2^+, with the results of Clementi and McLean.[5]

The energy of LV of NO_2^+ was estimated as -11 eV. by Nagakura and Tanaka[4]; the present result is -10.88 eV. The energy of the HO of NO_2 is calculated as -13.19 eV., while the value obtained by McEwen was -13.21 eV. The observed ionization energy is 13.98[11] or 11.7 eV[12],**. The π orbital energies of NO_2 obtained by the present calculations are -19.11, -17.69 and -11.58 eV., while by the LCAO SCF method, Tanaka[2] computed -18.86, -15.63 and $+0.40$ eV. and McEwen obtained -19.18, -15.85 and -2.23 eV..

The electronic distributions of the above-mentioned results, however, are considerably different. That is, the magnitudes of the π electron densities obtained by Tanaka are 1.018 on the nitrogen atom and 1.491 on the oxygen atom, whereas the values obtained by McEwen are 0.728 on the nitrogen atom and 1.637 on the oxygen atom in NO_2. In our calculations, the values of the atomic populations[13] of π electrons are 0.516 on the nitrogen atom and 1.742 on the oxygen atom in this molecule. For the odd electron distributions, the values by McEwen are 0.364 on the nitrogen atom and 0.318 on the oxygen atom, while our calculated atomic populations are 0.630 on the nitrogen atom and 0.158 on the oxygen atom. The net charges by our calculations are $+1.68$ on the nitrogen atom and -0.84 on the oxyen atom (considering all valence electrons), whereas Tanaka estimated the net charges to be $+0.88$ on the nitrogen atom and -0.44 on the oxygen atom (including σ and π electrons). Our calculated negative charge of the oxygen atom, however, seems to be too large. Although this might partly arise from the oozing of nitrogen lone-pairs, the difference in electronegativity between nitrogen and oxygen atoms might be overestimated to a certain extent in the present treatment.

Reactivity.—As has been described in the section on electronic levels, the highest occupied orbitals of NO_2 and NO_2^- are the lone-pair orbitals, in which the bonding electrons are largely localized on the nitrogen atom.*** Accordingly, by our frontier electron theory, the radical reaction of NO_2 will more likely take place at the nitrogen atom than at the oxygen atom. This theory may be supported by the following experimental facts: The hydrogen atom abstraction reaction by NO_2 produces $H:NO_2$,[1] and the structure of N_2O_4, produced by the association of NO_2, is regarded as $O_2N:NO_2$ rather than $ONO:NO_2$.[14] The structure of N_2O_3 produced from NO and NO_2 is represented by $ON:NO_2$.[14] Also, the NO_2^- ion mostly reacts with alkyl ions to form a nitro-compounds.[1] Considering the values of the coefficients of the AO's of the HO orbital in NO_2 and NO_2^-, the reaction described above may occur partly at the oxygen atoms, corresponding to the experience in the reaction of alkyl compounds with NO_2 producing the nitrous esters as by-products.[15]

Similarly, for the NO_2^+ cation, the "nucleophilic" reaction will take place on the nitrogen atom (for instance, as in the "electrophilic" nitration of aromatic hydrocarbons), and it may be predicted that the electrophilic reaction

* McEwen assumed a different order in NO_2, that is, $-(b_1)^2(a_2)^2(a_1)^2(b_2)^2(a_1)$. (cf. Table II.)

** The calculated energy of the HO of NO_2^- seems to be too low. This discrepancy might be partly attributed to the disregard of the change in Coulomb integrals in the ionized state.

*** The Lone-pair orbital of the nitrogen atom is directed towards $(-X)$. This may have some relation with its orientation as a nitrating reagent.

11) J. Collin and F. P. Lossing, *J. Chem. Phys.*, **28**, 900 (1958).

12) K. Watanabe, ibid., **26**, 542 (1957).

13) R. S. Mulliken, ibid., **23**, 1833 (1955).

14) See, e.g., R. B. Heslop and P. L. Robinson, "Inorganic Chemistry," Elsevier Pub. Co., London (1960).

15) See, e.g., B. T. Brooks, C. E. Boord et al., "The Chemistry of Petroleum Hydrocarbons," Reinhold Pub., N. Y. (1954).

will occur on the oxygen atoms.

Transition Energy. — Walsh discussed in detail the ultraviolet spectroscopic data of NO_2 in connection with the type of transition.[1] The types of transition estimated by Walsh and the calculated energy differences are summarized in Table II, together with the observed absorptions. Except for the transition to the highest vacant a_1 orbital,* the calculated values agree well with the observed values. On the other hand, the π-π transition energies computed by Tanaka[2] are 8.30 and 7.53 eV, while our calculated values are 7.36 and 6.11 eV.

As has been mentioned above, the calculated results have a good correlation with the experimental values and other calculations, though there are a few discrepancies. The discrepancy of the electron distribution can be modified by the ω-technique[16] or by using larger values of the parameter K (in particular for π-π bonding). This point will be published in the near future.

A part of the calculations have been carried out on the digital computer, KDC-I, of Kyoto University.

Faculty of Engineering
Kyoto University
Sakyo-ku, Kyoto

* The calculated energy of the highest vacant a_1 orbital is +18.19 eV.

16) G. W. Wheland and D. E. Mann, *J. Chem., Phys.*, **17**, 264 (1949).

SHORT COMMUNICATIONS

The Effect of Magnetic Field on the Radiation-induced Polymerization of Formaldehyde in the Solid State at a Low Temperature

By Yoneho TABATA, Harutaka KIMURA, Hiroshi SOBUE and Keichi OSHIMA

(Received April 11, 1964)

The radiation-induced solid state polymerization of formaldehyde has been reported by several workers.[1,2] In this paper, the effect of magnetic field on this radiation-induced polymerization of formaldehyde in the solid state will be reported.

The experimental apparatus is shown in Fig. 1. The apparatus consists of a pair of electromagnets, a ^{137}Cs γ-irradiation source, and shieldings, as is shown in the figure. The irradiation space is covered by a thick lead wall on the top, while a pair of electromagnets serve as side walls, the maximum magnetic field of which is 6×10^3 gauss. A Dewar vessel is inserted from the upper side into a hole in this lead shield, as is shown in Fig. 1-a. The radiation source is ^{137}Cs of 40 curies, and the structure of the capsule of the source is as shown in Fig. 1-c. The source is located inside the lead container which is installed at the bottom of the electromagnet. The source can be moved from the safe position (inside the container) up to the irradiation space by remote control.

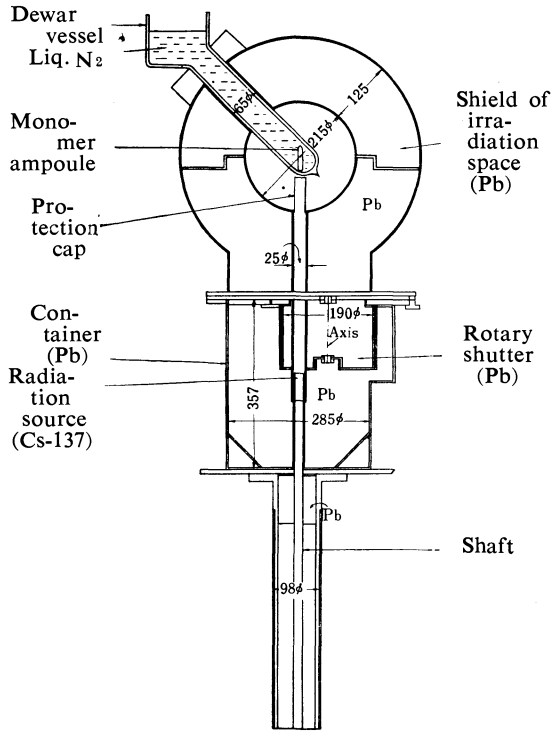


Fig. 1-a. Apparatus of the irradiation.

1) C. Chachaty, M. Magat and L. Terminassan, *J. Polymer Sci.*, **48**, 139 (1960).
2) Y. Tsuda, ibid., **49**, 369 (1960).

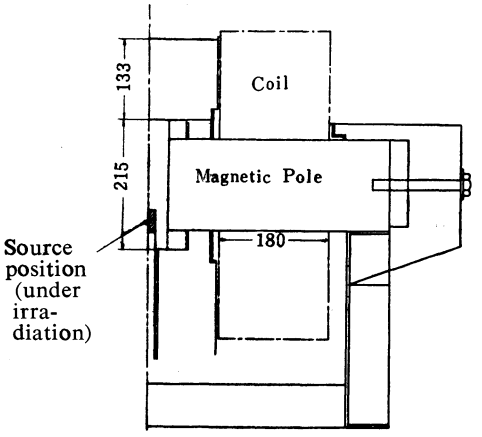


Fig. 1-b. A side view of the electromagnet and shielidings.

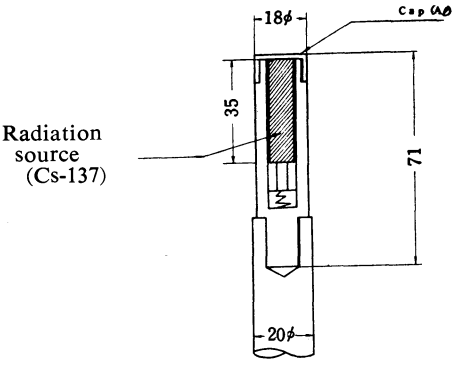


Fig. 1-c. Datails of the ^{137}Cs source.

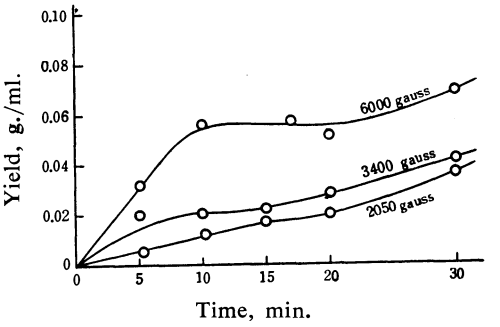


Fig. 2. The relation between the polymerization yield and the irradiation time in various magnitudes of magnetic field. Dose rate was 4.3×10^2 r./hr.

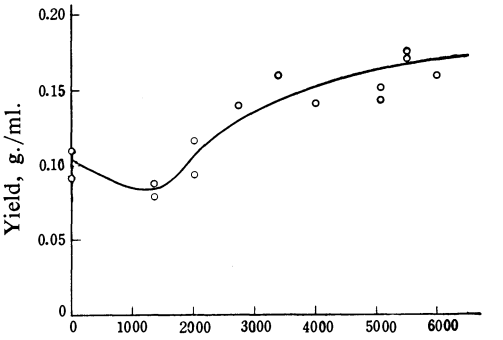


Fig. 3. The relation between the polymerization yield and the magnitudes of magnetic field at −196°C. Dose rate was 1.6×10^3 r./hr.

Formaldehyde was prepared by the heat-decomposition of para-formaldehyde at 160～170°C; it was then refined by distillation in vacuo at −78°C. The monomer was prepared and purified, just prior to use. The monomer in a glass tube was sufficiently degassed and sealed in vacuo. Irradiation was carried out by γ-rays in the solid state of the monomer at −130°C and −196°C, under the influence of the magnetic field. The yield of the polymerization was determined gravimetrically.

The relation between the polymerization yield and the irradiation time for various magnitudes of the magnetic fields at −196°C is shown in Fig. 2. It is obvious from the figure that the rate of polymerization increases with the magnitude of the magnetic field and that the saturation value of the yield also increases.

The relation between the polymerization yield and the magnitude of the magnetic field in the solid state polymerization at −196°C is shown in Fig. 3. The dose rate was 1600 r./hr. and the irradiation time was 10 min.; hence, the total dose was 270 r. To prevent an explosive polymerization, the dosage was appreciably lower than the 400 r. above which Chachaty and Magat[1] have observed that an explosive polymerization takes place.

From the experimental results, it is evident that the polymerization yield increases with the magnitude of the magnetic field in the region of 1500～6000 gauss.

The polymerization was also carried out at −130°C under the same irradiation conditions. It was found from the experiments that the polymerization yield was not affected by the magnetic field at −130°C; on the contrary, however, the polymerization was affected profoundly by the magnetic field at −196°C.

It is difficult to explain this interesting phenomena at the present stage of investigation. However, there are three possible explanation; the first is the interaction of the δ-ray (electrons ejected by an incident γ-ray) with the magnetic field, the second is the effect of the magnetic field on the termination reaction, and the third is the effect of the magnetic field on

a collective excited state of the monomer crystal.

The details of the results will be reported in the near future.

Faculty of Engineering
The University of Tokyo
Hongo, Tokyo

The Electron Spin Resonance of Sodium Polyphosphate Labeled with ^{32}P

By Masaji MIURA and Akinori HASEGAWA

(Received August 13, 1964)

Many substances, such as alkali halides, glasses and so on, become colored upon irradiation with X-, γ- or β-rays. In the literature no reports have been found, however, on the coloration of a substance by the internal irradiation from its radioactive constituent. We have recently found that sodium polyphosphate labeled with ^{32}P (SPP*) becomes red on standing but that the color fades away when it is heated to 200°C. We also studied this substance by means of a ESR technique and found that the absorption bands of ESR are closely related with the red color of SPP.*

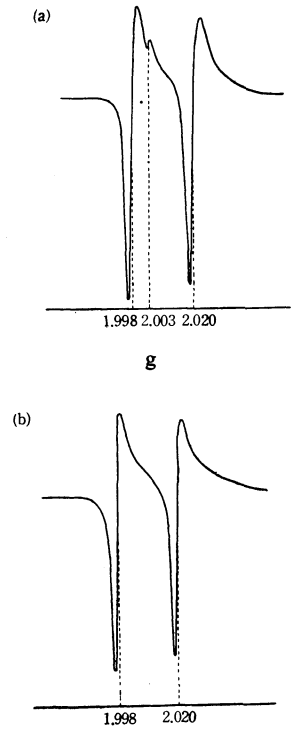


Fig. 1. ESR spectra at 77°K:
(a) SPP*, (b) SPP irradiated with X-rays.

Sodium polyphosphate (SPP), the so-called Graham salt, was prepared by heating sodium dihydrogen phosphate at 800°C for 6 hr. and then cooling rapidly on dry ice.

SPP irradiated with X-rays from a copper target gave two absorption bands of ESR, at $g=1.998$ and 2.020 (Fig. 1b), while SPP itself showed no absorption bands. On the other hand, SPP* exhibited one weak shoulder, at $g=2.003$ (Fig. 1a), in addition to two strong absorption bands, as in the case of SPP irradiated with X-rays. When SPP* was heated at 150°C for 20 min., its color became faint and the shoulder in ESR sbsorption band disappeared; the remaining two bands are of the same shapes as those of irradiated SPP. The intensity of each of two bands was similarly reduced by the heat treatment. It seems, therefore, that these two bands have the same origin. On the other hand only one absorption band was obtained from SPP* which had been prepared by using ^{32}P, a large part of which had already decayed to ^{32}S. This band corresponds to the shoulder in Fig. 1. a.

This conclusion follows from these results: SPP* as well as irradiatd SPP has two absorption bands, at $g=1.998$ and 2.020, which may be the hyperfine structure arising from the interaction of a trapped electron with a phosphorus nucleus (^{31}P, $I=1/2$), as has already been pointed out.[1] Further, SPP* has a shoulder, at $g=2.003$, which may result from a free electron near the sulfur atom (^{32}S, $I=0$) which is the decay product of ^{32}P. This is supported by the fact that the radical of sulfur is easily produced by the irradiation.

Full details will be published later.

Department of Chemistry
Faculty of Science
Hiroshima University
Hiroshima

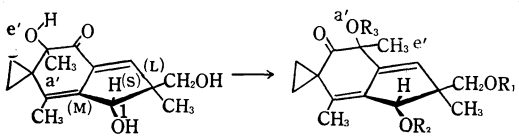
1) G. O. Karapetyan and D. M. Yudin, *Fiz. Tverd. Tela*, 3, 2827 (1961); Y. Nakai, This Bulletin, 37, 1089 (1964).

The Stereochemistry of Illudin S (Lampterol)[1,2a]

By Takeshi MATSUMOTO, Yohei FUKUOKA, Akitami ICHIHARA, Yoshihiro MORI, Haruhisa SHIRAHAMA, Yutaro TAKAHASHI and Masahiko WATANABE

(Received August 14, 1964)

Recently the structure of illudin S,[3] an antitumor substance obtained from a culture liquid of *Clitocybe illudens*, has been proposed. We now wish to propose stereochemical formula I for illudin S on the basis of the following evidence.



I

II : $R_1, R_2, R_3 = H$

III : $R_1, R_2 =$  , $R_3 = H$

IV : $R_1, R_2 =$  , $R_3 = COCH_3$

V : $R_1, R_2 = H$, $R_3 = COCH_3$

The infrared spectrum[4] of illudin S in carbon tetrachloride (7.84×10^{-4} mol.) showed absorption bands at 3631 cm^{-1} (ε, 58.4, free primary OH), 3601 cm^{-1} (ε, 68.4 free secondary allylic OH) and 3485 cm^{-1} (ε, 67.1 bonded tertiary OH), while illudin M,[3] in which the hydroxymethyl group is replaced by a methyl group, showed bands with almost identical intensities at 3601 cm^{-1} (ε, 61.6, free secondary OH) and 3485 cm^{-1} (ε, 71.7, bonded tertiary OH) in carbon tetrachloride (7.72×10^{-4} mol.).

These observations clearly indicate the trans orientation of the hydroxymethyl group and the secondary hydroxyl group.

Isoilludin S[2a,b] (II), formed by the acyloin rearrangement of illudin S with alumina, has infrared absorption bands at 3632 cm^{-1} (ε, 41.4, free primary OH), 3601 cm^{-1} (ε, 56.5, free secondary OH) and 3503 cm^{-1} (ε, 65.2, bonded tertiary OH) in carbon tetrachloride (1.03×10^{-3} mol.). These data show that the tertiary hydroxyl group has a pseudoequatorial conformation in illudin S (the stronger hydrogen bond) and a pseudoaxial conformation in isoilludin S.

The treatment of isoilludin S (II) with dihydropyran and the subsequent acetylation of the dipyranyl compound III, gave IV, which was then hydrolyzed with methanolic hydrogen chloride to monoacetylisoilludin S (V) : τ, 8.90, 8.42, 8.31 (methyl groups), 7.89 ($2\times CH_3CO_2-$), 6.58 ($-CH_2OH$), 5.31 (proton α to hydroxyl group), 4.62 (olefinic proton), and 7.95~9.15 (two methylene groups of cyclopropane), whose infrared spectrum in carbon tetrachloride (1.00×10^{-3} mol.) showed, in addition to an absorption band at 3603 cm^{-1} resulting from a secondary hydroxyl group, an absorption band at 2632 cm^{-1} (free primary OH) with a rather decreased intensity and a newly-appeared band at 3532 cm^{-1} (bonded primary OH).

These results provide evidence of the cis orientaion of the hydroxymethyl group and of the tertiary hydroxyl groups in isoilludin S (II).

The stereochemistry of illudin S should, therefore, be represented by formula I in view of the known steric course of acyloin migration.[6]

The absolute configuration of illudin S was determined by applying Horeau's procedure.[7]

When I (0.2×10^{-3} mol.) was treated with ($\pm$) α-phenylbutyric anhydride (0.1×10^{-2} mol.),

1) Presented at the IUPAC Symposium on the Chemistry of Natural products, Kyoto, Japan, April, 1964.

2) a) Lampterol, which was isolated from *Lampteromyces Japonicus*, has been proven identical with illudin S on the basis of direct comparison of their nuclear magnetic resonance and infrared spectra as well as mixing melting point.

Cf., H. Shirahama, Y. Fukuoka and T. Matsumoto, *J. Chem. Soc. Japan, Pure Chem. Sec.* (*Nippon Kagaku Zasshi*), **83**, 1289 (1962); H. Shirahama, Y. Fukuoka and T. Matsumoto, This Bulletin, **35**, 1047 (1962); K. Nakanishi, M. Ohashi, N. Suzuki, M. Tada, Y. Yamada and S. Inagaki, *Yakugaku Zasshi*, **83**, 377 (1963):

b) $C_{15}H_{20}O_4$, m. p. 179~180°C; λ_{max}^{EtoH} 252 mμ (log ε, 4.3)

ν_{max}^{KBr} 3420, 1960, 1645, 1365, 1018 cm^{-1}; τ, 8.84, 8.49, 8.32 (three methyl groups), 7.7~8.9 (two methylene groups of cyclopropane), 7.55 (OH), 6.61 (CH_2OH), 5.40 (proton α to hydroxyl group), 4.30 (olefinic proton). Details about the structure of isoilludin S will be reported in the near future.

3) T. C. McMorris and M. Anchel, *J. Am. Chem. Soc.*, **85**, 831 (1963).

4) The infrared spectra were measured on a Nippon Bunko grating infrared spectrometer, Model DS-401G, using 50 mm. KRS cell under high resolution condition.

5) Nuclear magnetic resonance spectra were measured on JNM-3H-60 high resolution NMR spectrometer.

6) W. A. Jacobs and W. S. Pelletier, *J. Org. Chem.*, **22**, 1428 (1957).

7) A. Horeau, *Tetrahedron Letters*, 506 (1961); 965 (1962).

the resultant α-phenylbutyric acid showed a rotation of $\alpha_D^{20}+8.75°$ (optical yield, 9.01%). Since the steric requirement of substituents around C_1 can be regarded to be as indicated in formula I, it may be concluded that illudin S should have the absolute configuration of I.

Department of Chemistry
Faculty of Science
Hokkaido University
Sapporo

A Kinetic Study of the Photochromism of 2,2',4,4',5,5'-Hexaphenyl-1,1'-biimidazolyl with Electron Spin Resonance

By Taro HAYASHI, Koko MAEDA and Makoto TAKEUCHI

(Received August 19, 1964)

The mechanism the of photochromism[1] of 2, 2', 4, 4', 5, 5'- hexaphenyl - 1, 1' - biimidazolyl, m. p. 199~201°C, in a solution has been studied with electron spin resonance. In a benzene solution ($C=1.48\times10^{-4}$ mol./l.) which turned from pale yellow to reddish purple when irradiated with a mercury vapor lamp for 3 min., the ESR was measured.[2] The line width (peak to peak) of the ESR signal (w in Fig. 1) was 9.1 gauss, and its g value was measured as 2.003. The intensity of the ESR signal, h in Fig. 1, gradually decreased with time in the dark, while its line width scarcely changed in 20 min. When the recording of the first signal had been almost finished, the sweep direction of the magnetic field was reversed and an ESR signal was immediately recorded. When this was followed by a similar procedure, the chart shown in Fig. 1 was obtained. The signal intensity, h, and the time, t, at which a signal curve intersected the base line was measured for every ESR signal on the chart. A graph of the reciprocal of h versus the time, t, gave a straight line, as is shown in Fig. 2.

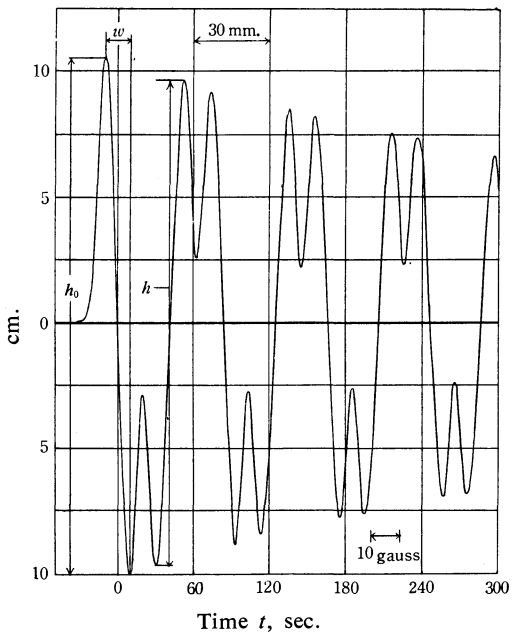


Fig. 1. Intensity change of an ESR signal of a benzene solution of hexaphenyl-biimidazolyl ($C=1.48\times10^{-4}$ mol./l.) with time in the dark at 23°C.
Gain, −34 db; modulation width, 3 gauss

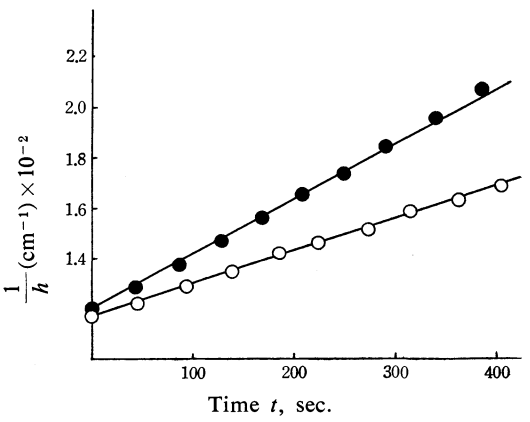


Fig. 2. A graph of $1/h$ vs. time t.
h: the intensity (cm.) of an ESR signal in Fig. 1.
-●- hexaphenyl-biimidazolyl
-○- hexa-*p*-tolyl-biimidazolyl

1) T. Hayashi and K. Maeda, This Bulletin, 33, 566 (1960); T. Hayashi, K. Maeda, S. Shida and K. Nakada, *J. Chem. Phys.*, 32, 1568 (1960); T. Hayashi and K. Maeda, This Bulletin, 35, 2057 (1962); T. Hayashi, K. Maeda and K. Morinaga, ibid., in press.

2) An electron spin resonance instrument of the Japan Electron Optics Laboratory Co., type JES-3BX (standard frequency 9400 Mc; modulation frequency 100 kc).

The linearity shows that the reaction which diminishes an ESR signal is a second-order radical reaction, since the signal intensity, h, is assumed to be approximately proportional to the concentration of free radicals, provided that the line width does not change, as in the present case. The radical reaction is considered to be a recombination of triphenylimidazolyl radicals. This conclusion agrees with the mechanism of photochromism, which has been confirmed[1] to be the homolytic dissociation of an N–N bond of hexaphenyl-biimidazolyl to triphenyl-imidazolyl.

A similar kinetic study of the photochromism of 2, 2', 4, 4', 5, 5'-hexa-*p*-tolyl-1, 1'-biimidazolyl, m. p. 194~195°C, with an ESR signal gave a similar conclusion, showing that the substitution of methyl groups diminished the rate of the recombination of free radicals.

Department of Chemistry
Faculty of Science
Ochanomizu University
Bunkyo-ku, Tokyo (T. H. & K. M.)

Japan Electron Optics Laboratory Co.
Akishima-shi, Tokyo (M. T.)

A New Colorimetric Determination of Nitrate Ions by Solvent Extraction with Crystal Violet

By Yuroku YAMAMOTO, Sumio UCHIKAWA and Kozo AKABORI

(Received September 2, 1964)

In the course of our study[1] of the solvent extraction of anions, it was found that nitrate ions can be extracted into chlorobenzene when the aqueous solution contains an excess of crystal violet and that there is a linear relationship between the color intensity of the organic phase and the concentration of the nitrate ions.

Figure 1 shows the absorption spectra of crystal violet; curve 1 is a spectrum of the extract when nitrate ions are absent, while curve 2 is that of the extract with nitrate ions. The crystal violet was extracted with chlorobenzene from the aqueous solution at pH 6.0 buffered with phosphate. It was thus shown that, when a small amount of nitrate ions is present, the cation of crystal violet is quite extractable into the organic layer. The maximum of absorbance is found at 595 mμ in the organic phase, but in the aqueous phase the maximum is slightly shifted to 591 mμ (curve 3). A maximum extraction is obtained in the range of pH 5.0~7.0, when the molar concentration of the dyestuff is held at the concentration of 10^{-4} M. The recommended procedure for the calibration curve is as follows.

Mix 5 ml. of the crystal violet chloride solution (1×10^{-3} M), 2 ml. of a phosphate buffer solution (1 M, pH 6.0) and various volumes of the standard nitrate solution (5×10^{-5} M). Dilute to 25 ml. with distilled water. Take the aliquot (10.0 ml.) into a separatory funnel. Shake the solution with 10.0 ml. of chlorobenzene for 5 min. Transfer the organic layer

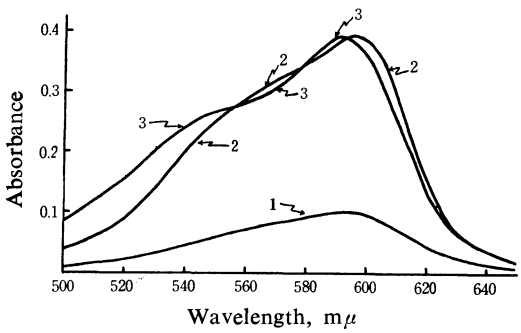


Fig. 1. Absorption spectra.
Reference: Curves 1 and 2, chlorobenzene
Curve 3, water
Curve 1: Spectrum of organic phase extracted from the aqueous solution (10 ml.), containing crystal violet (2×10^{-4} M), KH_2PO_4 (0.08 M), but nitrate ions are absent. pH 6.0
Curve 2: Spectrum of organic phase extracted from the aqueous solution (10 ml.), containing the same component as that of curve 1 and nitrate ions (2×10^{-5} M). pH 6.0
Curve 3: Spectrum of the aqueous solution of crystal violet (4×10^{-6} M). pH 6.0 (KH_2PO_4: 0.08 M)

1) Y. Yamamoto et al., This Bulletin, 37, 434, 594, 785 (1964).

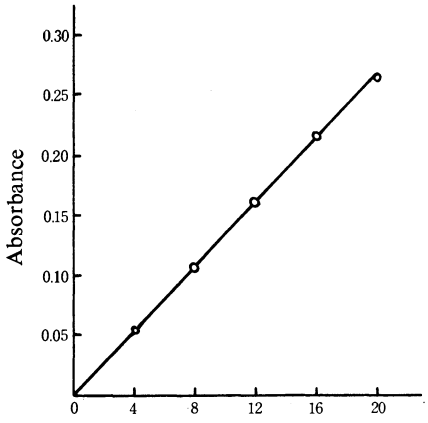


Fig. 2. Calibration curve at 595 mμ.
Reference: Reagent blank
Water phase { Crystal violet 2×10^{-4} M; KH_2PO_4 0.08 M; NO_3^- $x\times10^{-6}$ M; pH 6.0

into the cell, and measure the absorbance at 595 mμ using a reagent blank as a reference. Beer's law is followed in the range of 4×10^{-6} $\sim2\times10^{-5}$ M. The presence of diverse ions, such as phosphate and sulfate, does not interfere with the determination, even when they are present in amounts 1000 times that of the nitrate. Chloride give rise to a slight positive error when it exists in an amount more than ten times that of the nitrate.

Although various colorimetric methods for nitrate are known,[2] the method presently proposed is based on a different mechanism of color development and has a higher sensitivity.

Department of Chemistry
Faculty of Science
Hiroshima University
Higashisenda, Hiroshima

2) D. F. Boltz, "Colorimetric Determination of Nonmetals," Interscience Publisher, New York (1958), p, 135.

The Direct Formation of Biferrocenyl and Polyferrocenyls from Ferrocenyllithium

By Kazuo HATA, Izumi MOTOYAMA and Hamao WATANABE

(Received September 10, 1964)

Although many synthetic methods of biferrocenyl have been proposed, all of these routes are circuitous and troublesome. Moreover, the formation of polyferrocenyls other than biferrocenyl has never been reported. The present authors wish to report on the direct formation of biferrocenyl and polyferrocenyls from ferrocenyllithium.

In a previous paper[1] the synthesis of glycidylferrocenes was reported. In the course of this synthesis, when chlorohydrin derivatives of ferrocene were derived from the products of the reaction between ferrocenyllithium and epichlorohydrin, a small amount of biferrocenyl was obtained as orange crystals. The yield was ca. 0.3% based on ferrocene. In order to determine the step of the formation of biferrocenyl, a mixture containing lithiated ferrocene was hydrolyzed by pouring it into ice water immediately after the reaction of ferrocene and *n*-butyllithium in ether. An organic solid mixture, obtained from the ethereal layer, was submitted to vacuum sublimation in order to collect the recovered ferrocene. Even in this reaction biferrocenyl was isolated from the sublimation residue in a 0.4% yield. On the other hand, the reaction between *n*-butyl bromide and ferrocene in an ethereal solution did not occur, and the formation of biferrocenyl could not be observed. From these facts, it is obvious that biferrocenyl was directly derived from ferrocenyllithium, and that the formation of biferrocenyl is attributable to the Wurtz-type reaction as follows:[2]

$$\mathrm{FcLi} \xrightarrow{n\text{-BuBr}^*} \mathrm{FcBr} \xrightarrow{\mathrm{FcLi}} \mathrm{Fc\text{-}Fc}$$

$$\mathrm{FcLi} \xrightarrow{\mathrm{FcBr}} 2\mathrm{Fc}\cdot \longrightarrow \mathrm{Fc\text{-}Fc}$$

$$\mathrm{FcLi} \longrightarrow \mathrm{Fc}\cdot \longrightarrow 1/2\ \mathrm{Fc\text{-}Fc}$$

(Fc = ferrocenyl)

Among these reactions, the radical species are considered on the basis of the results mentioned below to be mainly participated in the formation of biferrocenyl. The radical

1) K. Hata, I. Motoyama and H. Watanabe, This Bulletin, **36**, 1698 (1963).

2) D. Bryce-Smith, *J. Chem. Soc.*, **1956**, 1603.

* *n*-Butyl bromide may remain after the reaction with lithium metal in the preparation of *n*-butyllithium.

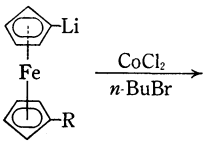
TABLE I. THE ANALYTICAL RESULTS OF THE PRODUCTS

Compound	Yield based on FcH %	Elemental analysis	Found %	Calcd. %	M. p. in sealed capillary °C	Mol. weight Found	Mol. weight Calcd.	Solubility in benzene
I	ca. 11	C	64.78	64.91	233.8~234.5	370*	370	Soluble
		H	5.05	4.90		330**		
II	ca. 5	C	64.89	65.03	226.5~227.2	554*	554	Sparingly soluble
		H	4.81	4.73				
III	ca. 6.5	C	67.61	67.64	68.2~ 70.2	446*	426	Very soluble
		H	5.95	6.19		400**		

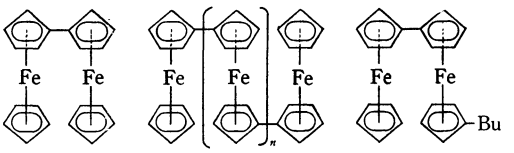
* Determined by the Rast method.
** Determined with a vapor pressure osmometer.

mechanism is also suitable for the explanation of the experimental results which Goldberg et al. have observed previously.[3]

With a view to finding a possibility of the formation of any polyferrocenyls and one of the increase in the yield of biferrocenyl, a reaction of ferrocenyllithium and cobaltous chloride was carried out according to the method reported by Kharasch and his co-workers,[4] and Wittig and Lehmann.[5] A small amount of anhydrous cobaltous chloride was added to an anhydrous ethereal solution of lithiated ferrocene, in the presence of an equimolar amount of *n*-butyl bromide to the ferrocence used as the starting material. A considerably vigorous reaction occurred, with an evolution of gas as had been expected. After the reaction was over, the mixture was poured into ice water in order to hydrolyze the remained lithium compounds, and many solid products were separated from the organic mixture by means of an appropriate procedure. The products were found to be biferrocenyl, butylated biferrocenyl, terferrocenyl, many polyferrocenyls and butylated polyferrocenyls, some of which were not yet identified. The analytical results of the identified products are shown in Table I. The identification was also supported by their infrared spectra. Other polyferrocenyls and butylated polyferrocenyls were found to have a larger molecular weight than 600, and they are scarcely soluble in common organic solvents. As a whole, about 36% of the ferrocene used was converted into these reaction products. A detailed investigation of all these products is in progress and will be reported on later.



R=H and/or Li



(I) (II) $n=1$ $n \geqq 1$ (III)

Department of Chemistry
Faculty of Science
Tokyo Metropolitan University
Setagaya-ku, Tokyo

3) S. I. Goldberg and D. W. Mayo, *Chem. & Ind.*, **1959**, 671; S. I. Goldberg, D. W. Mayo and J. A. Alford, *J. Org. Chem.*, **28**, 1708 (1963).
4) M. S. Kharasch, D. W. Lewis and W. B. Reynolds, *J. Am. Chem. Soc.*, **65**, 498 (1943).
5) G. Wittig and G. Lehmann, *Chem. Ber.*, **90**, 875 (1957).

Iron(III) Chloride-Triphenyl Phosphite as a New Catalyst for the Polymerization of Tetrahydrofuran

By Iwo YAMASHITA and Minoru SERIZAWA

(Received September 15, 1964)

The polymerization of tetrahydrofuran by the use of Friedel-Crafts catalysts with co-catalysts, such as alkylene oxides, active halogen compounds and so on, was first examined by Meerwein.[1] Subsequently Muetterties[2] reported the use of phosphorus pentafluoride to give a polymer. Recently Saegusa et al.,[3] Weissermel and Nölken[4] and the present authors[5] have reported that triethyl aluminum is a effective catalyst when used with co-catalysts. In this communication, it will be reported that iron(III) chloride-triphenyl phosphite is an interesting new catalyst system for the polymerization of tetrahydrofuran.

Bulk polymerization was carried out in a nitrogen atmosphere in a sealed glass ampoule. The polymerization mixture was allowed to stand at a desired temperature. The polymeric product was isolated by pouring the reaction mixture into a large amount of diluted hydro chloric acid (0.001~0.005 N). The crude polymer was washed with methanol and then dissolved in tetrahydrofuran. The purified polymer was recovered by again pouring the solution into a large excess of water and then dried in vacuo at room temperature.

The effects of the amount of iron(III) chloride and the polymerization temperature on the yield and the reduced viscosity of the polymer are shown in Figs. 1, 2A and 2B.

When the other Lewis-acid (aluminum

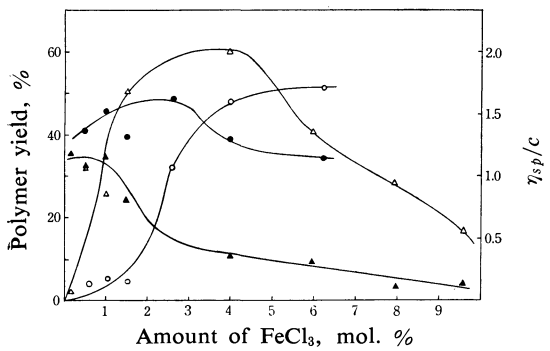


Fig. 1. The yield and the reduced viscosity of polymer vs. the amount of $FeCl_3$.
THF 0.05 mol., $(PhO)_3P$ 0.05 mol. % to monomer
Polymerization time 24 hr.
-△- Yield of polymer at 30°C
-○- Yield of polymer at 0°C
-▲- η_{sp}/c of polymer at 30°C
-●- η_{sp}/c of polymer at 0°C
(η_{sp}/c was measured on a solution of 0.2 g. polymer in 100 ml, of benzene at 30°C)

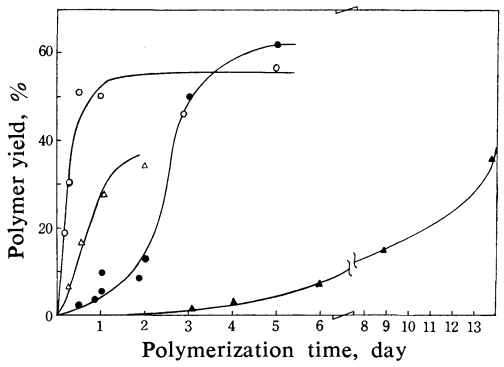


Fig. 2-A. The yield of polymer vs. polymerization time.
THF: 0.05 mol., $FeCl_3$: 1.5 mol. %, $(PhO)_3P$: 0.5 mol. %
-○- at 30°C
-△- at 15°C
-●- at 0°C
-▲- at −20°C

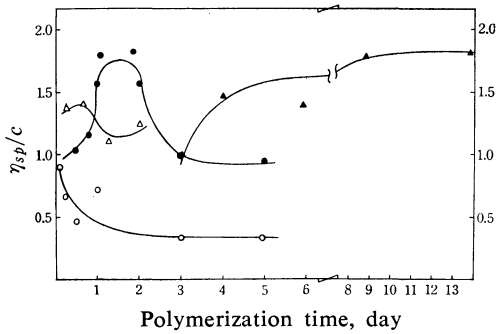


Fig. 2-B. The reduced viscosity of polymer vs. polymerization time.

1) H. Meerwein, *Angew. Chem.*, **72**, 927 (1960).
2) E. L. Muetterties, U. S. Pat. 2856370 (1958).
3) T. Saegusa, H. Imai and J. Furukawa, *Makromol. Chem.*, **65**, 60 (1963).
4) K. Weissermel and E. Nölken, ibid., **68**, 140 (1963).
5) I. Yamashita, M. Serizawa and T. Miyakawa, This Bulletin, **36**, 1368 (1963).

chloride, boron fluoride etherate, titanium chloride and zinc chloride) was used in place of iron(III) chloride, together with triphenyl phosphite, these catalyst systems gave no polymer under the polymerization conditions examined. Moreover, none of the polymerizations occurred when triphenyl phosphite was used alone or when iron(III) chloride itself was used as a catalyst.

The infrared spectra, the solubilities and the thermal properties of the polymer were very similar to those of the polytetrahydrofuran prepared by the use of the other catalysts (phosphorous pentafluoride[2] and triethyl aluminum-epichlorohydrin[3]).

Further details on such polymerization results and on the role of triphenyl phosphite in such a catalyst system will soon be published.

Government Industrial Research Institute, Osaka
Oyodo-ku, Osaka

The Solvent Effects of Esterification: The Reaction of l-Menthol with Acetyl Chloride in Liquid Sulfur Dioxide[*1]

By Niichiro TOKURA[*2] and Fuminori AKIYAMA[*2]

(Received January 6, 1964)

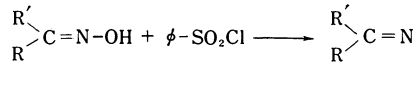
It has been reported in a previous paper[1] that, in the rearrangement of cyclohexanone oxime *p*-toluenesulfonate in various solvents, there are no clearcut correlations between the log. of the rate constants versus the dielectric constants, the dipole moments or the *Z*-values of the solvents. Among the solvents used, liquid sulfur dioxide gave the largest rate constant for the rearrangement. It has been suggested that liquid sulfur dioxide, as an electrophilic solvent, favors the formation of a *bare* cation, without interfering with the formation of the aza-cyclopropenyl cation which is a requisite intermediate to carrying out the Beckmann rearrangement.

It has also been indicated in previous paper[2-4] that the rate of the cationic polymerization of styrene in liquid sulfur dioxide is the fastest among the solvents used for the polymerization, giving a polymer of the highest degree of polymerization with a narrow molecular weight distribution.

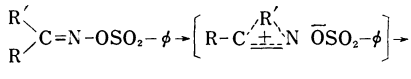
On the other hand, it has already been shown that the reaction rate of the Wagner-Meerwein rearrangement[5] is very fast in liquid sulfur dioxide and that the decomposition of an allylsulfinate is the fastest in liquid sulfur dioxide.[6]

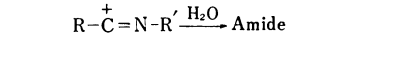
On the contrary, the rate of the Menschutkin reaction[7] in liquid sulfur dioxide is the slowest among the solvents used. All of these results naturally lead to the conclusion that in liquid sulfur dioxide those reactions are advantageous in which cations or carbonium ions play the principal role, while the reactions of anions or carbanions are retarded or inhibited by strong interaction with liquid sulfur dioxide. In general, the reaction of $\rho<0$, (ρ is a constant in Hammett's relation, $\log k/k_0=\rho\sigma$[8]), is very much favored in liquid sulfur dioxide, as is seen in the Beckmann rearrangement and in cationic polymerization.[2,3,9]

The purpose of the present article on the esterification of *l*-menthol is to study the solvent effects on the esterification in connection with the elucidation of the solvent effects of the Beckmann rearrangement,[10] since the latter rearrangement consists of two, consecutive steps, viz., the esterification of the oxime and the rearrangement of the oxime ester, as may be illustrated as follows:



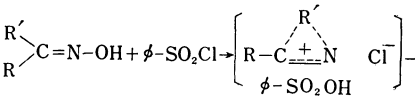
(1)





(2)

Alternately, a concerted one-step mechanism may also be considered:



(3)

When the rearrangement follows the consecutive processes 1 and 2, the solvent effects of the esterification may have an important bearing and influence if the rate-determining step is the esterification of the oxime. The solvent effects of the rearrangement step have already been discussed.[1] It has been believed that, in liquid sulfur dioxide, an acyl halide such as acetyl chloride is partly ionized, such as:

*1 Substitution in Liquid Sulfur Dioxide, Part IV. Part III; N. Tokura and Y. Kondo, This Bulletin, **36**, 200 (1963).

*2 Present address: Department of Applied Chemistry, Faculty of Engineering, Osaka University, Higashinoda, Osaka.

1) N. Tokura, T. Kawahara and S. Ikeda, This Bulletin, **37**, 138 (1964).
2) R. Asami and N. Tokura, *J. Polymer Sci.*, **42**, 545 (1960).
3) N. Tokura, M. Matsuda and M. Iino, This Bulletin, **36**, 278 (1963).
4) M. Matsuda, *Kobunshi*, **13**, 88 (1964).
5) L. P. Hammett, "Physical Organic Chemistry," McGraw-Hill, New York (1940), p. 318.
6) S. H. Sharman, F. F. Caserio, R. F. Nystron, J. C. Leak and W. G. Young, *J. Am. Chem. Soc.*, **80**, 5965 (1958).
7) N. Tokura and Y. Kondo, This Bulletin, **36**, 200 (1963).
8) Cf. Ref. 5, p. 186.
9) N. Tokura, T. Kawahara and T. Watanabe, This Bulletin, **36**, 760 (1963).
10) N. Tokura, K. Shiina and T. Terashima, ibid., **35**, 1986 (1962).

$$CH_3COCl = CH_3CO^+ + Cl^- \quad (4)$$

as has been evidenced by the cationic polymerization of styrene with acetyl chloride as an initiator in liquid sulfur dioxide. Thus the esterification of an alcohol in liquid sulfur dioxide by acyl halide is expected to proceed with an unusual rapidity.

l-Menthol was chosen as the alcohol because of the convenience of its kinetic rate measurement by polarimetry. Acetyl chloride was used as the acylating agent. As was expected, the esterification rate in liquid sulfur dioxide was the largest among the solvents used.

Experimental

Materials. — The commercial *l*-menthol was used without further purification, m. p. 41.5~43°C, $[\alpha]_D^{25}$ in benzene=47.6°. Acetyl chloride was distilled, and a fraction with a b. p. of 52.0~53.0°C was used. Liquid sulfur dioxide was dried with phosphorus pentoxide and distilled. The other solvents were purified by the authorized methods as indicated in a previous paper.[1]

Polarimetry.—A Shimadzu Lippich II-type polarimeter with a sodium lamp (D-line, 589.2 mμ) in a thermostat was used. A pressure cell about 2.2 dm. long and 10 mm. in diameter and equipped with a needle valve on its center was used for the measurement of the rate in liquid sulfur dioxide (Fig. 1). An ordinary polarimetry cell was used for the measurement in other solvents. As the initial concentration, 0.45 mole per liter each of *l*-menthol and acetyl chloride was used.

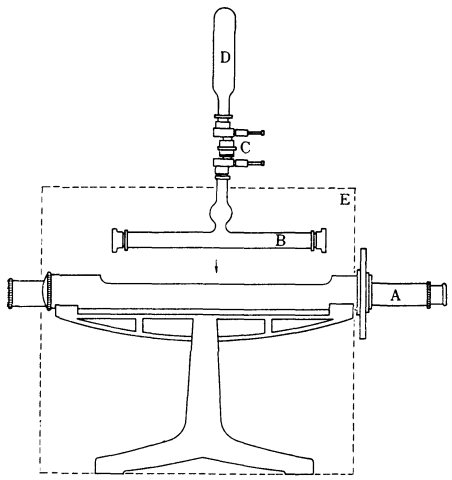


Fig. 1. A polarimeter equipped with a pressure cell.

A: Polarimeter
B: Measuring pressure cell
C: A joint-coupling with two kneedle valves
D: A pressure cell
E: A thermostat

Kinetic Procedure.—The rate of the esterification was followed conveniently by polarimetry. However, the specific rotations of *l*-menthol slightly differed from solvent to solvent.

The esterification is a reversible reaction and generally might be acid-catalyzed, so the reaction rate should be expressed as:

Rate = (Rate of the forward reaction)
− (Rate of the reverse reaction)
+ (Acid catalysis by HCl formed by the reaction)

However, since the over-all yield of the ester after the reaction was over 80~90 per cent and since the catalytic effect of HCl in such non-aqueous solvents was found to be negligibly small (Fig. 2), the rate expression may be simplified to the following equation, especially when the rate is estimated in the initial stage of the reaction. Then the rate is:

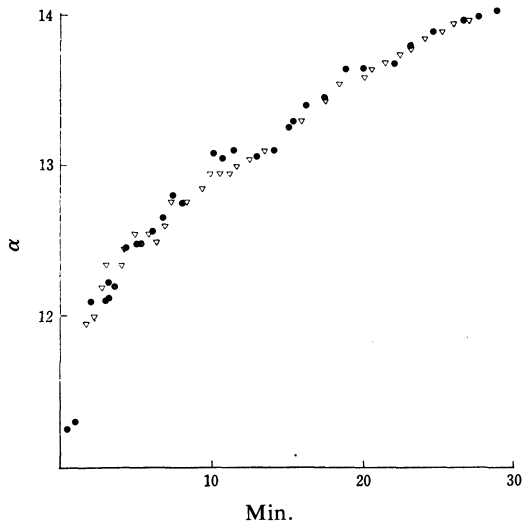


Fig. 2. Effect of HCl concentrations on the reaction rate.
● HCl 0.926 mol./l. ▽ HCl 0.501 mol./l.
liq. SO_2 38.38 mol. % SO_2-CCl_4 system

$$\text{Rate} = dx/dt = k(a-x)^2 \quad (5)$$

where equimolar initial concentrations, a, of *l*-menthol and acetyl chloride were used, k is the second order rate constant, and x is the concentration of the ester at time t. Equation 5 is integrated to Eq. 6:

$$1/(a-x) - 1/a = k \cdot t \quad (6)$$

We can assume, at $t=0$, $\alpha_0 = a \cdot [R]_A^\circ \cdot l$, and $t=t$, that $\alpha_t = (a-x) \cdot [R]_A^\circ \cdot l + x \cdot [R]_E^\circ \cdot l$, where l is the length of the cell of the polarimeter in dm., α_0 and α_t are rotations at the times 0 and t, $[R]_A^\circ$ is the molar rotation of *l*-menthol (degree·dm^{-1}·mol^{-1}·l.), and $[R]_E^\circ$ is that of the ester formed. After the completion of the reaction, α_t at the end or α_∞ may be written approximately as:

$$\alpha_\infty = a \cdot [R]_E^\circ \cdot l \quad (7)$$

$$\alpha_\infty - \alpha_t = (a-x) \cdot l \cdot ([R]_E^\circ - [R]_A^\circ)$$

Then:

$$\alpha - x = (\alpha_\infty - \alpha_t)/l \cdot ([R]^\circ_E - [R]^\circ_A) \quad (8)$$

$$a = (\alpha_\infty - \alpha_0)/l \cdot ([R]^\circ_E - [R]^\circ_A) \quad (9)$$

Substituting 8 and 9 in 6, we get:

$$1/(\alpha_\infty - \alpha_t) - 1/(\alpha_\infty - \alpha_0) = k \cdot t/l \cdot ([R]^\circ_E - [R]^\circ_A) \quad (10)$$

The second-order rate constant, k, may be obtained from the slope of a linear plot, $1/(\alpha_\infty - \alpha_t)$ vs. t. An example is shown in Fig. 3. The specific rotations of the alcohol and the ester, $[\alpha_A]^{25}_D$ and $[\alpha_E]^{25}_D$, are listed in Table I.

Table I. Specific rotations in various solvents at 25°C

Solvent	$[\alpha_A]^{25}_D$	$[\alpha_E]^{25}_D$
Dimethylformamide	46.1	72.3
Nitromethane	42.0	76.4
Chloroform	45.1	80.2
Ethylenedichloride	45.5	72.7
Benzene	47.6	73.7
Toluene	46.3	70.2
Acetonitrile	50.7	74.3
Ethyl methyl ketone	44.5	71.8
Tetrahydrofuran	48.4	77.6
Liq. SO_2	53.5	84.8

$[\alpha_A]^{25}_D$: Specific rotation of *l*-menthol
$[\alpha_E]^{25}_D$: Specific rotation of *l*-menthyl acetate

Since the rate of the esterification in liquid sulfur dioxide was fast enough to allow the estimation of

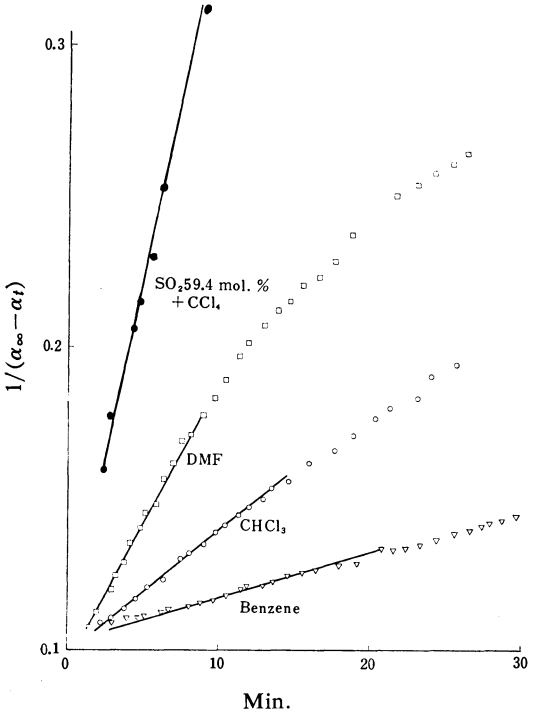


Fig. 3. Typical runs in various solvents.
DMF: Dimethylformamide

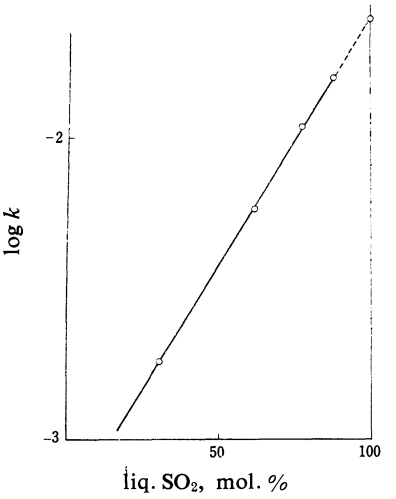


Fig. 4. Log k vs. liq. SO_2 mol. % in liq. SO_2-CCl_4 mixtures.
liq. SO_2 100 mol. % $k = 6.95 \times 10^{-2}$ l./mol. sec.

the rate constant by this procedure, the rate constant in liquid sulfur dioxide was obtained by the following extraporation. A variety of mixtures of liquid sulfur dioxide in carbon tetrachloride were prepared, and the rates in these mixtures were estimated. The log·k's vs. the molar per cents of sulfur dioxide concentrations-plots were strictly linear, and the line was extrapolated to the 100 per cent sulfur dioxide to obtain the rate constant, k, in liquid sulfur dioxide. The rates of the esterification in other solvents were directly measured by the above procedure; the results are listed in Table II, together with the values of liquid sulfur dioxide.

Table II. The second-order rate constants of the esterification at 25°C *l*-Menthol and acetyl chloride

Solvent	k, l. mol^{-1} sec^{-1}
Dimethylformamide	2.66×10^{-3}
Nitromethane	2.17×10^{-3}
Chloroform	1.26×10^{-3}
Ethylenedichloride	8.61×10^{-4}
Benzene	3.56×10^{-4}
Toluene	3.47×10^{-4}
Acetonitrile	2.85×10^{-4}
Ethyl methyl ketone	6.27×10^{-5}
Tetrahydrofuran	5.05×10^{-5}
Liq. SO_2	6.95×10^{-2}
Carbon tetrachloride	0

Results and Discussion

The solvent effects of the esterification of *l*-menthol with acetyl chloride have been shown in Table II. The rate was the largest in liquid sulfur dioxide. Moreover, the order of the specific rates in the respective solvents

is similar to that in the case of the Beckmann rearrangement. The orders are:
Esterification:

Liq. SO_2 > Dimethylformamide> Nitromethane> $CHCl_3$> Ethylenedichloride> Benzene> Toluene> Ethyl methyl ketone> Tetrahydrofuran> CCl_4

Rearrangement:[9]

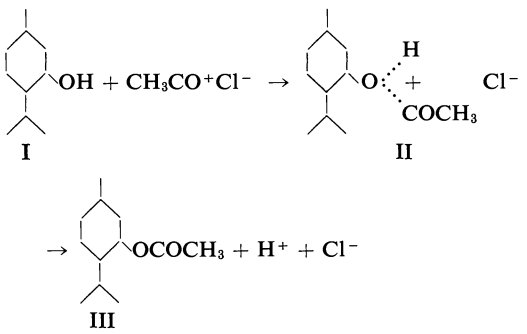
Liq. SO_2 > CH_3OH > CH_3COOH> Nitromethane> Ethanol> CH_3CN> Pyridine> $CHCl_3$> Acetone> Ethylenedichloride> Ethyl methyl ketone> CCl_4

As a control experiment, the optical stabilities of *l*-menthol and *l*-menthyl acetate in each solvent have also been examined. These materials were both optically stable in any solvent used for the experiment at 25°C.

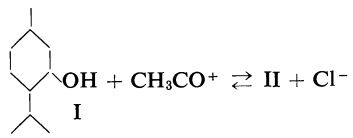
No catalytic effect of hydrochloric acid on the reaction rate was observed (Fig. 2). The lack of acid catalysis may be accounted for by the observation that the dissociation of hydrochloric acid in liquid sulfur dioxide and in a non-aqueous solvent is very small as compared to that in water and may be presumed to result in triplet- or multiplet-ion formation.[10] Although the esterifications obey a strictly second-order rate law within the experimental limitations, the mechanism of the reaction may differ somewhat according to the nature of the solvent.

In a solvent such as liquid sulfur dioxide, acetyl chloride may ionize to acetylium cation and chloride anion as in Eq. 4, though the degree of the dissociation may not be very large. A *bare* (unsolvated) acetylium ion is to be expected in this case, while chloride anion may be strongly solvated by liquid sulfur dioxide. Thus, the rate-determining attack of the acylium ion on the oxygen atom of the alcohol is facile and effective. In Scheme 1, if the rate-determining step is the formation of intermediate II, the step of expelling a proton from II being very fast, the reaction rate must be determined by the effective concentration of the acylium cations. In liquid sulfur dioxide, the reaction rate is very large since a *bare* cation, viz., a free cation not solvated by the solvent, is thought to be available and the effective concentration of the cations is assumed to be the largest.

On the other hand, ethyl methyl ketone and tetrahydrofuran are solvents in which the cations or the carbonium ions are strongly solvated by the solvents; thus the effective concentration of the cations is rather depressed. Nitromethane, chloroform, ethylenedichloride, benzene and toluene rank midway between these two kinds of solvents. It is interesting that, in dimethylformamide, the reaction is also rapid in spite of the nucleophilicity of this solvent. A different reaction mechanism may be considered, though a second-order rate law still holds. One possibility is that a rate-determining proton abstraction, preceded by an equilibrium of the formation of II (Scheme 2), is very easy in dimethylformamide.



Scheme 1



Scheme 2

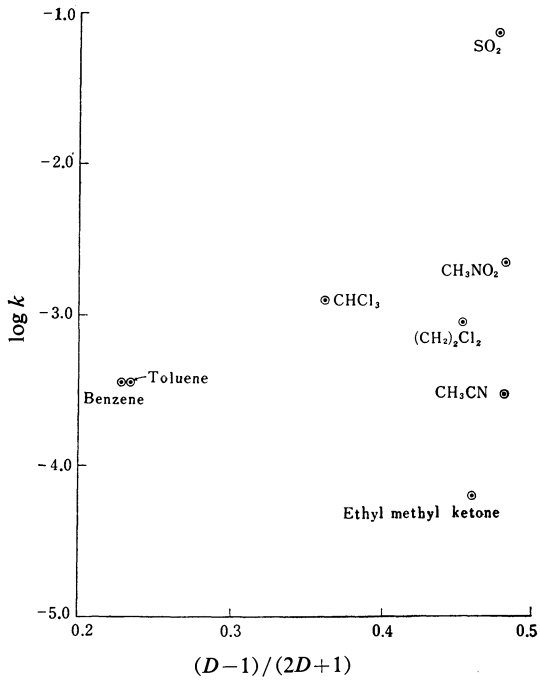


Fig. 5. Log k vs. $(D-1)/(2D+1)$ plots.

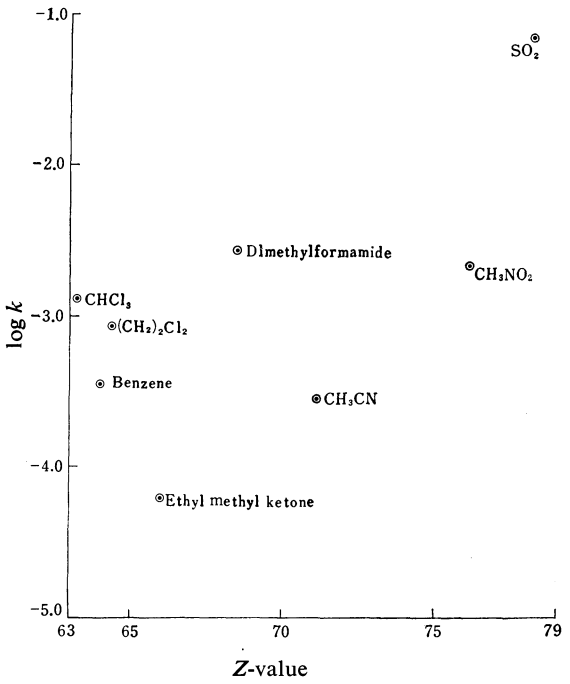


Fig. 6. Relationship between log k and Z-value.

The rate constants in various solvents vs. the ionizing powers (such as the dielectric constants and Z-values) of the solvents-relations, were further examined, as is illustrated in Figs. 5 and 6. The plots of log·k vs. $(D-1)/(2D+1)$ or Z-value[11] resulted in complete randomness, without any linear correlation.

Summary

The solvent effects of the esterification of *l*-menthol with acetyl chloride in various solvents have been examined polarimetrically. In liquid sulfur dioxide, the rate of the esterification was the fastest among the solvents used. A *bare* carbonium ion formation in liquid sulfur dioxide may be the reason for this. The comparably large rate in dimethylformamide has also been discussed, along with the solvent effects in various other solvents.

The authors are indebted to the Seitetsu Kagaku K. K. for the gift of liquid sulfur dioxide.

The Chemical Research Institute of Non-Aqueous Solutions
Tohoku University
Katahira-cho, Sendai

11) E. M. Kosower, *J. Am. Chem. Soc.*, **80**, 3235 (1958).

The Stability Constants of the Palladium, Copper, Nickel, Zinc and Manganese Chelates of 3-Hydroxy-3-phenyl-1-o-tolyltriazene and -1-p-tolyltriazene

By D. N. PUROHIT and N. C. SOGANI

(Received February 14, 1964)

In a previous communication,[1] the stabilities of the palladium, copper, nickel, zinc and manganese chelates of 3-hydroxy-3-phenyl-1-*p*-chlorophenyltriazene have been reported. The present investigation will deal with the influence of methyl groups at ortho and para positions of the parent compounds upon the stabilities of the metal chelates formed by them.

Experimental

Solutions of the Chelating Agents.—3-Hydroxy-3-phenyl-1-*o*-tolyltriazene and 3-hydroxy-3-phenyl-1-*p*-tolyltriazene were prepared by employing the method of Sogani et al.[2,3] Weighed amounts of these compounds were dissolved in a 70% v/v dioxane-water mixture, and the solution was diluted to give a 0.04 M solution. Solutions of 0.002 M palladium, copper, nickel, zinc and manganese ions and 0.02 M sodium hydroxide were prepared by usual, classical methods.

Potentiometric Titration. — Ten milliliters of a 0.04 M chelating agent solution in a 70% v/v dioxane-water mixture were pipetted in a titration vessel. A sufficient amount of 0.02 M nitric acid was added to it to lower the pH to about 2. The final ionic concentration was maintained at 0.1 M

1) D. N. Purohit and N. C. Sogani, This Bulletin, 37, 476 (1964).

2) T. C. Jain, H. K. L. Gupta and N. C. Sogani, *J. Indian Chem. Soc.*, 37, 531 (1960).

3) D. N. Purohit, Ph. D. Thesis, University of Rajasthan, Jaipur, India, 1963.

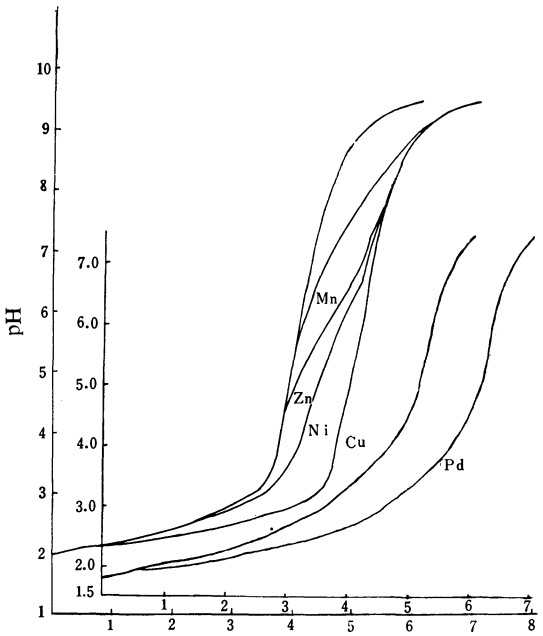
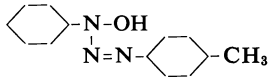


Fig. 1. Titration curves for



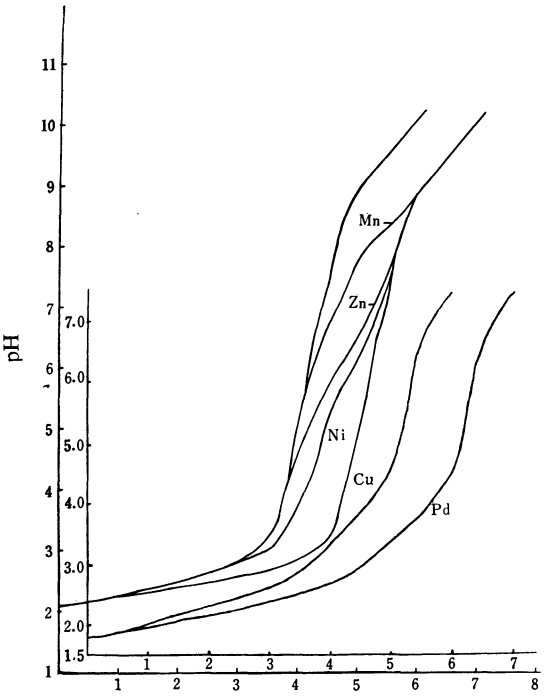
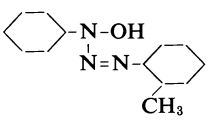


Fig. 2. Titration curves for



by adding 2.5 ml. of 2 M potassium chloride. When titrating in the presence of metal ions, 5 ml. of a 0.002 M metal solution were added at this stage. The total volume of the contents was increased to 50 ml. by adding varying amounts of dioxane and distilled water in such proportions that it finally became a 70% v/v dioxane-water mixture. It was then titrated against 0.02 M sodium hydroxide. The temperature of the solution throughout the titration was maintained at 25±0.5°C. The titration curves are given in Figs. 1 and 2.

Calculations. — The pK_a values of 3-hydroxy-3-phenyl-1-*o*-tolyltriazene and 3-hydroxy-3-phenyl-1-*p*-tolyltriazene have been determined spectrophotometrically as 11.55 and 11.78 respectively. These values were used for calculating free chelating ion concentrations at different pH values. The values of $\bar{n}$ were calculated as has been described earlier.[1] The formation curves for metal chelates are given in Figs. 3 and 4. The values of log k_1 and log k_2

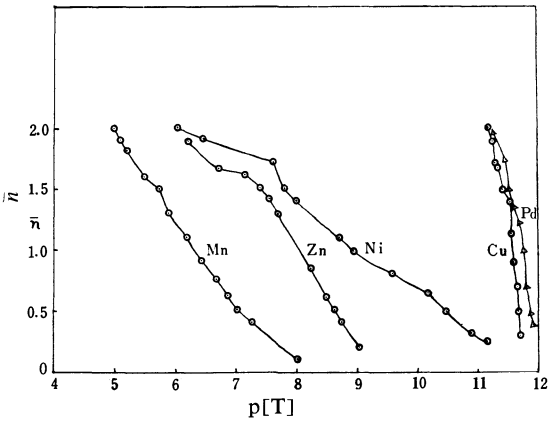
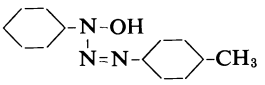


Fig. 3. Formation curves for metal chelates of



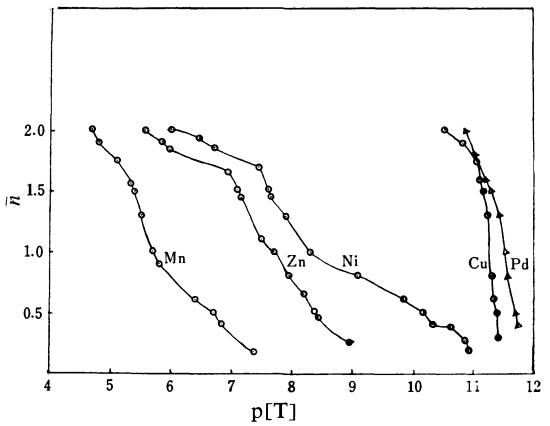


Fig. 4. Formation curves for metal chelates of

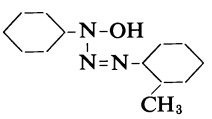


TABLE I. THE STABILITY CONSTANTS OF THE METAL CHELATES OF 3-HYDROXY-3-PHENYL-1-*o*-TOLYLTRIAZENE AND 3-HYDROXY-3-PHENYL-1-*p*-TOLYLTRIAZENE

Metal	3-Hydroxy-3-phenyl-1-*o*-tolyltriazene		3-Hydroxy-3-phenyl-1-*p*-tolyltriazene	
	$\log\beta_1$ ($\log k_1$) (first stability const.)	$\log\beta_2$ ($\log k_1k_2$) (over all stability const.)	$\log\beta_1$	$\log\beta_2$
Palladium	11.70	22.97	11.89	23.35
Copper	11.35	22.47	11.69	23.09
Nickel	10.17	17.76	10.46	81.23
Zinc	8.38	15.46	8.62	15.99
Manganese	6.68	12.07	7.02	12.74

for different metal chelates were read directly from the formation curves; they are given in Table I.

Discussion

An examination of the titration curves will show that curves for hydroxytriazenes in the presence of metal ions lie considerably below the simple chelating agent curves. This is due to the liberation of hydroxytriazene protons during complex formation. The chelate formation of palladium starts at pH 1.9; that of copper, at pH 2.0; that of nickel, at pH 2.6; that of zinc, at pH 4.5, and that of manganese, at pH 5.7. This corresponds to the order of stabilities of the hydroxytriazene chelates of these metals.

For the sake of simplicity, only the stabilities of palladium chelates with different hydroxytriazenes are discussed. A comparison of the values of the overall stability constants of the palladium chelates of para-chloro-substituted (reported earlier, $\log\beta_2=20.95$), ortho- and para-methyl-substituted ($\log\beta_2=22.97$ and 23.35 respectively) with the parent hydroxytriazene[3] ($\log\beta_2=22.66$) reveals that, while the chloro substitution lowers the stability of the resulting chelate, the methyl substitution increases it. The $-$I effect of the halogen lowers the pK_a value of the chloro-substituted hydroxytriazene (pK_a of parent compound $=11.41$, and chloro-substituted, $=10.72$) and hence the stability of its metal chelates.

The stabilities of the chelates given by methyl-substituted compounds are higher than those of the parent hydroxytriazene. This is due to the +I effect (electron pushing) of the methyl group. A hyperconjugation effect for the methyl group would have a similar effect. The hydroxytriazene with a methyl group at the ortho position should have been a weaker acid and formed more stable complexes than its para isomer because of the nearness of the +I effect of the group on –OH-bearing nitrogen atoms. However, the contrary is true. The greater acidity and lesser stability of the chelates of the ortho isomer compared to the para isomer are due to the ortho effect of the methyl group.

Summary

The stabilities of the palladium, copper, nickel, zinc and manganese chelates of 3-hydroxy-3-phenyl-1-*o*-tolyltriazene and 3-hydroxy-3-phenyl-1-*p*-tolyltriazene have been determined in a 70% v/v dioxane-water mixture and at an ionic strength of 0.1 M potassium chloride, by employing the Bjerrum-Calvin pH titration technique.

The authors wish to express their gratitude to Professor R. C. Mehrotra for providing facilities in the department. They are also grateful to the University Grants Commission for granting a research scholarship to one of them (D. N. Purohit).

Chemistry Department
University of Rajasthan
Jaipur, India

*The Preparation of Phosphorus-32 in a High Specific Activity Using the Szilard-Chalmers Effect**

By Kichizo TANAKA

(Received February 17, 1964)

It is desirable that reference sources of radioactive isotope be of a high purity and also of a high specific activity, particularly in the case of β-ray emitters. In the case of phosphorus-32, the carrier-free source has usually been prepared by the (n, p) reaction on a sulfur target. However, this source is often contaminated with a considerable amount of phosphorus-33, which is produced by the (n, p) reaction on the sulfur-33 in the target. It is possible to prepare phosphorus-32 free from phosphorus-33 by the use of the (n, γ) reaction of phosphorus-31; however, its specific activity is considerably less than the product of the (n, p) reaction.

The Szilard-Chalmers process is considered to be an effective method for preparing phosphorus-32 of a high specific activity, which then furnishes a stock solution for the preparation of the reference sources. In this paper the process for the preparation of phosphorus-32 in a high specific activity using the Szilard-Chalmers effect will be studied with several inorganic phosphorus compounds.

Experimental

Target Materials. — The sodium dihydrogen phosphate, disodium hydrogen phosphite and sodium hypophosphite used were guaranteed reagents from the Wako Chemicals Co. The disodium hydrogen phosphate, potassium dihydrogen phosphate, dipotassium hydrogen phosphate and tripotassium phosphate were guaranteed reagents from the Kanto Chemicals Co. Each of these hydrated salts was dehydrated, dried, and analyzed as has been previously reported.[1]

Neutron Irradiation.—The salts were irradiated in the JRR-1 reactor (a water-boiler type, operated at 40 kW.). The salts, sealed in a polyethylene tube in the presence of air, were irradiated at an ambient reactor temperature. After irradiation, the samples were stored in a Dewar vessel cooled with dry ice for about one week.

The Preparation of the Ion Exchange Resin Column. — Strongly basic anion exchange resin (Diaion SA 100, 100~200 meshes) was washed with a large excess of concentrated hydrochloric acid and redistilled water and was then made into a column 0.8 cm. in diameter and 10 cm. long. The column was washed with 50 ml. of a chloride solution (eluting agent I in Fig. 1) before use.

Separation Procedure. — The irradiated sample was dissolved in an equimolar mixture of a 0.025 M potassium chloride solution and 0.025 M hydrochloric acid, and the concentration of the sample was made 0.1 M. In order to find the best conditions for separating orthophosphate and pyrophosphate ions, the following items were studied: the concentrations andmixing the ratio of the chlorides, the concentration of the irradiated salt in the sample solution, and the composition of the eluting agent. The separation of complex phosphate mixtures by the ion exchange method has been studied by several other workers,[2-7] and several different procedures have been proposed. However, in the present experiment, some improvement of the separation process was necessary because trace amounts of complex polyphosphate ion had to be separated from a large amount of orthophosphate, orthophosphite or hypophosphite ions. From the orthophosphate containing a trace amount of pyrophosphate ions, e. g., 1 μM of pyrophosphate in 0.1 M of orthophosphate, the pyrophosphate was

TABLE I. VOLUME OF THE ELUTING AGENT I REQUIRED FOR COMPLETE ELUTION OF ORTHOPHOSPHATE IONS

Orthophosphate concentration	Volume of sample solution	Required volume of eluting agent I*
M	ml.	ml.
0.1	10	55
0.1	50	135
0.1	100	220
0.5	10	120
1	10	210
1	50	230
1	100	420

* Pyrophosphate was eluted from 80 ml. to 250 ml.

* This work was partly presented at the 15th Annual Meeting of the Chemical Society of Japan, Tokyo, April, 1962,

1) H. Baba, K. Tanaka and K. Yoshihara, This Bulletin, **36**, 928 (1963).

2) J. Beukenkamp, W. Rieman and S. Lindenbaum, *Anal. Chem.*, **26**, 505 (1954).

3) S. Lindenbaum, T. V. Peters and W. Rieman, *Anal. Chim. Acta.*, **11**, 530 (1954).

4) J. A. Grande and J. Beukenkamp, *Anal. Chem.*, **28**, 1497 (1956).

5) J. P. Ebel and N. Busch, *Compt. rend.*, **242**, 647 (1956).

6) M. Matsuhashi, *J. Biochem.*, **44**, 65 (1957).

7) H. J. Weiser, Jr., *J. Am. Oil Chemists' Soc.*, **34**, 124 (1957).

cleanly separated by eluting it with 0.025 M of an equimolar chloride mixture solution. To avoid the incomplete separation between orthophosphate and pyrophosphate ions caused by the tailing of the former, the total aliquot of the sample solution was made 10 ml. per column for each run. The tailing of orthophosphate ions was influenced by the concentration of irradiated salt in the sample solution and the volume of the sample solution, as is shown in Table I. The overall separation procedure is shown in Fig. 1. It was

Irradiated target
↓ Dissolve in 0.025 M KCl+0.025 M HCl mixed solution (prepare 0.1 M of sample solution)
↓ Each 10 ml. of sample solution to each column
Anion exchange resin column (0.8 cm. in diameter×10 cm. long of Diaion SA 100, 100~200 meshes, flow rate 0.8 ml./min.)
↓ Eluting agent I, 60 ml. of 0.025 M KCl +0.025 M HCl mixed solution
↓ Eluting agent II, 50 ml. of 8 M HCl solution
8 M HCl fraction
↓ Boiled and concentrated
↓ Adjusted acidity, total activity and assayed
Product

Fig. 1. Separation procedure with ion exchange resin.

found that when orthophosphate, orthophosphite or hypophosphite containing trace amounts of pyrophosphate and higher polyphosphate ions in a chloride solution was passed through the column, the pyrophosphate and higher polyphosphates were adsorbed on the resin column, while the orthophosphate, orthophosphite and hypophosphite ions were completely eluted with 60 ml. of the chloride solution. The adsorded polyphosphate ions were eluted with an 8 M hydrochloric acid solution.

The Chemical Analysis of Phosphorus.—For the analysis of phosphorus, the sample solution was evaporated to fuming with sulfuric acid after the addition of 5 ml. of concentrated nitric acid, 1 ml. of 40% perchloric acid, and 0.5 ml. of concentrated sulfuric acid. The residual sulfuric acid solution was then diluted to a 1 N acid solution. The trace amounts of phosphorus were analyzed by the colorimetry reported by Gaitanis.[8] The ammonium phosphomolybdate, formed by the addition of ammonium molybdate to the pretreated sample solution in 1 N sulfuric acid, was extracted with benzene. The solvent phase extracted was shaken with a stannous chloride solution, and the absorbancy of the solvent phase was measured at 735 mμ. The macroamounts of phosphorus, on the other hand, were analyzed by gravimetry with an ammonium phosphomolybdate precipitate.

8) M. J. Gaitanis, "Master Analytical Manual," Section 1-12, TID-7015 (1957).

Radioactivity Measurements.—The sample solution was evaporated in a glass planchet 2.5 cm. in diameter and was counted with a thin-end window-type G. M. gas flow counter. The decay rate was measured by the G. M. counter in its constant geometry. The 2π-β counter, whose efficiency was corrected by a 4π-β counter for phosphorus-32 activity, was used for the absolute measurement of phosphorus-32 activity. In this absolute measurement, small portions of the sample solution were dropped on a stainless steel disk covered with a thin Ducocement film, weighed, evaporated to dryness, and counted.

Results and Discussion

The distribution of the chemical species containing phosphorus-32 in neutron-irradiated phosphorus compounds has been studied by many workers,[9-23] and also the fragmentation of chemical species induced by the thermal neutron capture of phosphorus-31 in phosphates has been discussed. However, many questions still remain. In the present experiment, it was found that phosphorus-32 could be recovered in the polyphosphate fraction with specific activities considerably higher than those of the original irradiated salts, such as orthophosphates, orthophosphite, or hypophosphite.

The recoveries and enrichment factors obtained by the ion exchange method for several irrradiated samples are shown in Table II. All the samples were irradiated for 2 hr. in the same capsule in the pneumatic tube (the nominal neutron flux, 0.64×10^{12} n./cm^2·sec.) of the JRR-1. Each value shown in the table is the average of three separate experiments. It may be seen in the table that the recovery is higher for the orthophosphates, except tripotassium phosphate, than those for sodium orthophosphite and sodium hypophosphite. The residual activity in the resin

9) W. F. Libby, *J. Am. Chem. Soc.*, **62**, 1930 (1940).
10) A. H. W. Aten, Jr., *Rec. trav. chim.*, **61**, 467 (1942).
11) A. G. Maddock, *Research*, **2**, 556 (1949).
12) W. D. E. Thomas and D. J. D. Nicholas, *Nature*, **163**, 719 (1949).
13) J. G. A. Fiskell, W. A. Delong and W. F. Oliver, *Can. J. Chem.*, **30**, 9 (1952).
14) A. H. W. Aten, Jr., H. van der Straaten and P. C. Riesebos, *Science*, **115**, 267 (1952).
15) P. A. Sellers, T. R. Sato and H. H. Strain, *J. Inorg. Nucl. Chem.*, **5**, 31 (1957).
16) T. R. Sato, P. A. Sellers and H. H. Strain, ibid., **11**, 84 (1959).
17) R. F. C. Claridge and A. G. Maddock, "Proceedings of the Chemical Effects of Nuclear Transformations," Vol. 1, IAEA, Prague (1961), p. 475.
18) L. Lindner and G. Harbottle, ibid. (1961), p. 485.
19) T. R. Sato and H. H. Strain, ibid. (1961), p. 503.
20) M. Shima and S. Utsumi, *J. Inorg. Nucl. Chem.*, **20**, 177 (1961).
21) K. Yoshihara and T. Yokoshima, This Bulletin, **34**, 123 (1961).
22) R. F. C. Claridge and A. G. Maddock, *Trans. Faraday Soc.*, **57**, 1392 (1961); **59**, 935 (1963).
23) H. Baba, *Nippon Genshiryoku Gakkaishi*, **5**, 917 (1963).

TABLE II. RECOVERY AND ENRICHMENT FACTOR

Target material	Recovery %	Enrichment factor
NaH_2PO_4	57.6±0.6	$(2.1\pm0.7)\times10^3$
Na_2HPO_4	62.2±1.6	$(2.3\pm0.5)\times10^3$
Na_3PO_4	54.3±1.3	$(4.2\pm0.8)\times10^3$
KH_2PO_4	52.4±1.0	$(8.7\pm1.4)\times10^3$
K_2HPO_4	49.6±2.6	$(1.8\pm0.3)\times10^2$
K_3PO_4	40.7±1.9	$(8.0\pm2.5)\times10^2$
Na_2HPO_3	42.4±1.4	$(4.8\pm0.1)\times10^2$
NaH_2PO_2	25.4±1.6	$(4.4\pm0.6)\times10^2$

column after elution with 8 M hydrochloric acid was found to be less than 0.1% of the total activity.

Experiments were than carried out in order to observe the fluctuations in the preparation of phosphorus-32 with a high specific activity when several samples of the same salt were separately irradiated. The results obtained in the case of potassium dihydrogen phosphate are shown in Table III. The recoveries are within a range of deviation of less than 2 per cent, whereas the enrichment factors show considerable fluctuations. The polyphosphate

TABLE III. RECOVERY AND ENRICHMENT FACTOR OBTAINED BY THE TREATMENT OF IRRADIATED KH_2PO_4

Irradiation condition	Recovery %	Enrichment factor
2 hr. No. 16 hole of JRR-1	50.0	7.6×10^3
	54.4	9.7×10^3
	52.9	1.1×10^4
	56.8	4.6×10^3
	57.2	1.8×10^3
	av. 54.2±1.2	$(6.6\pm1.5)\times10^3$
15 hr. No. 12 hole of JRR-1	38.1	4.4×10^3
	41.9	4.1×10^3
	42.2	4.4×10^3
	41.4	5.4×10^3
	43.0	8.6×10^3
	43.5	1.1×10^4
	av. 41.6±0.8	$(6.3\pm1.0)\times10^3$

in unirradiated samples was also separated by the ion exchange method, and the phosphorus amounts in the polyphosphate fraction were determined by colorimetry. The amount of phosphorus per gram of sample adsorbed on the resin column, which was detected as the polyphosphate fraction, is shown in Table IV for the unirradiated samples. There was not much difference between the amounts adsorbed on the resin column for the unirradiated and irradiated samples. However, the amount of the polyphosphate formed by neutron irradiation in a reactor seemed to be of the order of the values to be expected from the results

TABLE IV. AMOUNTS OF PHOSPHORUS IN THE FRACTION OF POLYPHOSPHATE (MAINLY PYROPHOSPHATE) CONTAINED IN TARGET MATERIALTS

Target material	μg. as P in 1 g. of target materials
NaH_2PO_4	53
Na_2HPO_4	35
Na_3PO_4	18
KH_2PO_4	15
K_2HPO_4	250*
K_3PO_4	120
Na_2HPO_3	40
NaH_2PO_2	10

* approximate value.

of the polyphosphate formation by gamma irradiation.[24]

The recoveries obtained under different irradiation conditions are shown in Table V, where the irradiation time dependence of the recovery is specifically shown. The neutron flux and other irradiation conditions, for example, the intensity of gamma rays, vary with their position in a reactor. However, the

TABLE V. EFFECT OF IRRADIATION TIME IN A REACTOR

Target material	Irradiation time	Irradiation hole of JRR-1*	Percentage recovery	Enrichment factor
NaH_2PO_4	30 min.	16	50.0	1.8×10^3
	60 min.	16	50.8	1.8×10^3
	120 min.	16	57.6	2.2×10^3
	300 min.	2**	53.8	2.0×10^3
	15 hr.	12	54.7	2.4×10^3
Na_2HPO_4	30 min.	16	61.9	3.1×10^3
	60 min.	16	60.2	2.4×10^3
	120 min.	16	62.2	2.3×10^3
	300 min.	2	67.4	2.2×10^3
	15 hr.	12	63.5	3.4×10^3
KH_2PO_4	30 min.	16	53.8	1.9×10^4
	60 min.	16	50.0	1.0×10^4
	120 min.	16	54.2	6.6×10^3
	300 min.	2	42.4	5.7×10^3
	15 hr.	12	43.5	1.1×10^4
K_2HPO_4	30 min.	16	46.6	4.7×10^2
	60 min.	16	41.4	2.4×10^2
	120 min.	16	49.6	1.8×10^2
	300 min.	2	43.9	2.2×10^2
	15 hr.	12	42.9	3.0×10^2

* No. 16- a pneumatic tube, No. 2- a horizontal hole, No. 12- a vertical hole.

** No. 2 and No. 16 holes are placed in symmetrical position of JRR-1 reactor.

24) K. Tanaka, This Bulletin, 37, 1032 (1964).

recovery was not much affected by the irradiation time for several orthophosphates in the time range of 30 min. to 15 hr.

The product obtained by treating the potassium dihydrogen phosphate was evaporated to dryness, and an analysis of the radiochemical purity was made. The gross decay curve was measured for the time more than ten times the half life of phosphorus-32. The decay rate for the curve was constant and was exactly the same as for phosphorus-32 (14.3 day). The absorption curves of radiation with an aluminum disk were also obtained for this product. The curves obtained 150 days after irradiation were compared with those 20 days after irradiation. The two curves were the same. No weak β-ray emitters could be detected for the product.

The products thus prepared were radiochemically pure, no gamma ray peaks were observed by scintillation spectrometry with a NaI crystal, and the total solids which were detected after the evaporation of the product solution were less than 0.1 mg./ml. The specific activity higher than 1 mc./mg. could be prepared, even in irradiations of total neutrons of approximately 2×10^{15}.

Summary

A process has been developed for obtaining phosphorus-32 free from phosphorus-33 and with a high specific activity. Phosphorus-32 has been prepared by an anion exchange method, in which a chloride solution containing 0.025 M of potassium chloride and 0.025 M of hydrochloric acid of neutron irradiated phosphate was passed through the column of a strongly basic anion exchanger, and the adsorbed phosphorus-32 has been eluted with 8 M hydrochloric acid. The anhydrous orthophosphate shows a good recovery compared with several orthophosphates, sodium orthophosphite and sodium hypophosphite. The recovery is not much affected by the irradiation time. Enrichment factors higher than 10^3 have been obtained.

The author wishes to express his appreciation to Dr. Kenjiro Kimura, Director of this Institute, to Dr. Nagao Shibata, and to Professor Shizuo Fujiwara of the University of Tokyo for their interest and encouragement. The author also wishes to express his thanks to Dr. Kenji Yoshihara for his discussions.

Radioisotope Production Laboratory
Japan Atomic Energy Research Institute
Tokai-mura, Ibaraki

The Polarographic Determination of Divalent Tin in Sodium Formate

By G. S. DESHMUKH and S. V. S. S. MURTY*

(Received April 8, 1964)

Heyrovsky,[1] Kalousek[2] and Lingane[3] have recommended 1 molar sodium hydroxide as a supporting electrolyte for the polarographic determination of stannous tin. In this medium, Sn^{2+} gives both anodic and cathodic waves. Well-defined cathodic and anodic polarograms of stannous tin in an acetic acid - ammonium acetate buffer have been adopted for the determination of the element by Pribil[4] and Desesa[5]. The use of sodium citrate, sodium hydroxide and alkali tartrate solutions as supporting electrolytes has been indicated by Kalousek,[2] Shakhov[6] and Lingane[7]. In the latter case the half-wave potential of the anodic polarogram was found to be dependent on the pH of the solution, on the concentration of sodium tartrate, and on that of stannous tin. The symmetry of the wave was also affected by the above parameters. However, the half-wave potential of the cathodic polarogram was constant under these conditions.

A similar type of polarographic behaviour of stannous tin in sodium formate has now been observed. It has already been mentioned that

* Junior Research Fellow, C. S. I. R.

1) J. Heyrovsky and D. Ilkovic, *Collection Czechoslov. Chem. Communs.*, **7**, 198 (1935).

2) M. Kalousek, ibid., **11**, 592 (1939).

3) J. J. Lingane, *Ind. Eng. Chem. Anal. Ed.*, **15**, 583 (1943).

4) R. Pribil; Z. Roubal and E. Svatek, *Collection Czechoslov. Chem. Communs.*, **18**, 43 (1953).

5) M. A. Desesa, D. N. Hume, A. G. Glamm and D. Deford, *Anal. Chem.*, **25**, 983 (1953).

6) A. S. Shakhov, *J. Appl. Chem. U. S. S. R.*, **12**, 1555 (1939).

7) J. J. Lingane, *J. Am. Chem. Soc.*, **65**, 866 (1943).

stannous tin yields well-defined anodic and cathodic polarograms in sodium formate.[8] The behaviour of the anodic polarogram of tin is of considerable importance for its determination in the presence of other metallic elements with which it is commonly associated. The present investigation was, therefore, undertaken to obtain detailed information about the polarographic characteristics of stannous and stannic complexes in sodium formate media.

Experimental

The polarograms were recorded at 25±0.1°C with a Leeds and Northrup Electrochemograph, type E; the capillary characteristics with the open circuit were $m=3.09$ mg./sec. and $t=3$ sec. The pH of the solution was measured with a line-operated Beckmann Zeromatic pH meter.

Sodium formate of a pure-reagent-grade quality was used to prepare solutions of the desired strength. Stannous chloride solution was prepared by dissolving pure metallic tin in the requisite quantity of concentrated hydrochloric acid and storing the solution in an inert atmosphere. Nitrogen was bubbled through the solutions in order to deaerate them and the inert atmosphere was maintained to prevent the oxidation of stannous tin while the polarograms were being recorded. Freshly-prepared gelatin was used as the maximum suppressor. The pH of the solution was adjusted by means of pure formic acid.

Results and Discussion

Effect of pH.—Table I shows that the pH exerts profound effect on the half-wave potentials of the anodic polarogram. The anodic half-wave potential became more positive as the pH was decreased from 3.7 to 3.1. As the pH increased from 3.1, however, the anodic polarogram was characterized by a drawn-out wave which finally merged with the initial plateau of the cathodic polarogram at pH 5.2. The half-wave potential of the cathodic polarogram was not altered with the change in pH.

TABLE I. EFFECT OF pH ON DIVALENT TIN POLAROGRAMS

Formate concn., 1 M Gelatin, 0.005%
Concn. of Sn^{2+}, 1.584 mg.

Sample No.	pH	$E_{1/2}$, V. vs. SCE	
		Anodic	Cathodic
1	3.1	−0.17	−0.56
2	3.3	−0.185	−0.56
3	3.5	−0.195	−0.56
4	3.7	−0.23	−0.56
5	5.2	Anodic wave merged with cathodic wave	

Effect of Formate Concentration.—Variation in the formate concentration has an appreciable effect on the half-wave potential of the anodic and cathodic polarograms of stannous tin. The half-wave potential of the anodic polarogram shifted to negative potentials with the increase in the formate concentration, thus showing the formation of a more stabilized complex. The $E_{1/2}$ of the cathodic polarogram was, however, shifted to negative potentials, this shift being comparatively much less pronounced than that observed with the anodic polarogram. The diffusion current of both the polarograms was suppressed with the increase in formate concentration, especially above 1.5 M; this might be due to the increased viscosity of the medium. The results are reported in Table II.

TABLE II. EFFECT OF FORMATE CONCENTRATION ON Sn^{2+} POLAROGRAMS

pH ~3.5 Gelatin, 0.005%
Concn. of Sn^{2+}, 1.584 mg.

Sample No.	Concn. of formate M	$E_{1/2}$, V. vs. SCE	
		Anodic	Cathodic
1	0.3	−0.13	−0.525
2	0.5	−0.155	−0.54
3	1.0	−0.185	−0.555
4	1.5	−0.19	−0.575
5	2.0	−0.215	−0.59
6	2.5	−0.23	−0.605

Effect of Stannous Tin Concentration.—The anodic half-wave potential shifted to positive potentials with the increase in stannous tin concentration. For example, with 1 molar sodium formate and at pH 3.0 with 0.005% gelatin, the anodic half-wave potentials of 0.514, 1.028, 2.056, 3.084 and 4.112 mM were, respectively, −0.185, −0.175, −0.15, −0.09 and −0.035 V. vs. SCE. On the other hand, the cathodic half-wave potential in the above experiments remained constant at −0.57 V. (cf. Fig. 1).

These results indicate that the oxidation of the stannous formate complex was thermodynamically irreversible at the dropping electrode. The irreversibility was confirmed by investigating polarograms of stannic tin in formate media. In formate solutions stannic tin does not show a reduction wave, whereas, if the stannic-stannous system is reversible, a reduction wave would be observed with stannic formate solutions at the same potential at which the anodic wave occurs with the stannous formate solutions. The irreversibility of the

8) G. S. Deshmukh and Y. D. Kane, *J. Sci. Ind. Research*, **21B**, 135 (1962).

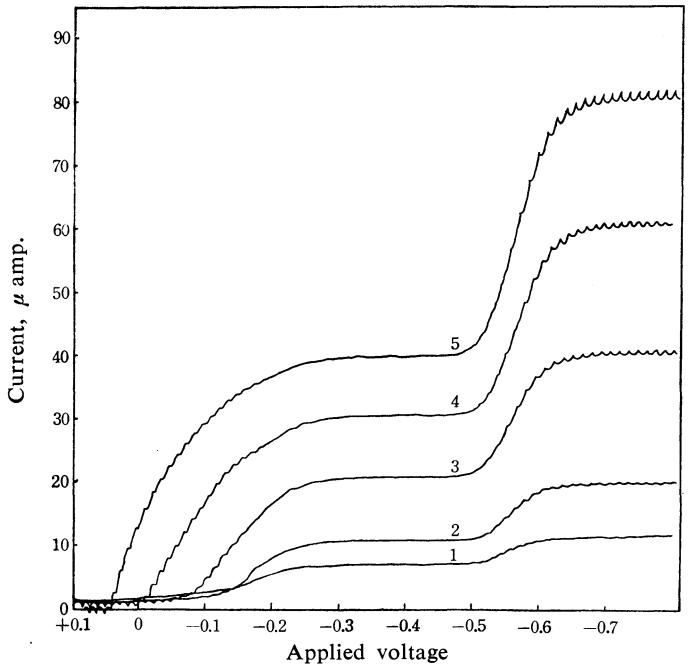


Fig. 1. The polarograms of (1) 0.514 (2) 1.028 (3) 2.056 (4) 3.084 and (5) 4.112 mM Sn^{2+} in 1 M sodium formate. pH=3.0 Gelatin=0.005%

anodic polarogram was also increased with the concentration of Sn^{2+}, as is evidenced by the increase in the difference between $E_{3/4}$ and $E_{1/4}$. Thus, with 1 molar formate at pH 3.0 with 0.005% gelatin, the difference between $E_{3/4}$ and $E_{1/4}$ of the anodic polarogram of 1.028, 2.056, 3.084 and 4.112 mM was 60, 80, 100 and 120 mV. vs. SCE respectively, but for the cathodic polarogram it was constant, the values always being 50 mV. For a thermodynamically-reversible wave, the expected value should be 28 mV. This shows that the cathodic wave was also irreversible.

Calibration curves were drawn with 1 molar sodium formate at pH 3.0±0.1. It was observed that the diffusion current was directly proportional to the concentration of tin for both the anodic and cathodic polarograms between 10^{-5} to 10^{-4} M.

Summary

Well-defined cathodic and anodic polarograms of stannous tin in sodium formate have been reported. The diffusion current is directly proportional to the concentration of stannous tin between 10^{-5} to 10^{-4} M. The anodic half-wave potential of tin is shifted to positive values with the increase in the concentration of Sn^{2+}, whereas the cathodic half-wave potential is constant. The anodic polarogram is highly irreversible. The cathodic polarogram is also irreversible. The irreversibility of the anodic polarogram is increased with the concentration of stannous formate. This is evidenced by a corresponding increase in the difference between $E_{3/4}$ and $E_{1/4}$. Above pH 5.0 the anodic polarogram merges with the cathodic polarogram, thereby limiting the polarographic determination of Sn^{2+} to the pH value 3～5. The $E_{1/2}$ of the anodic polarogram shifts to negative potentials when the pH was increased, whereas that of the cathodic wave is constant. The polarogram with equal wave heights obtained in 1 molar sodium formate at pH 3.0 with 0.005% gelatin has been taken for the determination of tin.

Sincere thanks of the authors are due to Professor G. B. Singh for providing the necessary facilities.

Department of Chemistry
Banaras Hindu University
Varanasi-5, India

Studies of Ammonium Dioxovanadium(V) Bisoxalate Dihydrate

By D. N. SATHYANARAYANA and C. C. PATEL

(Received April 7, 1964)

Complexes of vanadium containing VO_2^+ are rare. Ammonium dioxovanadium(V) bis-(oxalate) tetrahydrate was prepared by Rosenheim[1] by treating an ammonium oxalate solution with vanadium pentoxide; his compound was said to be remarkably stable. Although this oxalato complex has been known since 1893, its physico-chemical properties, except the conductivity of its aqueous solution,[2] have not been investigated. During the course of our investigations of oxovanadium(IV) complexes, it was thought desirable to study some properties of the ammonium dioxovanadium-(V) bis(oxalate) complex and to assign it a structure.

Experimental

Materials Employed.—The oxalic acid dihydrate, ammonium oxalate monohydrate and ammonium meta-vanadate were of reagent grade. Vanadium pentoxide was prepared by heating ammonium meta-vanadate (A. R.) at 450°C for about 2 hr.

Preparation.—When a solution of ammonium oxalate is boiled with vanadium pentoxide,[1] ammonium dioxovanadium(V) bis(oxalate) is not easily obtained. Hence, an easy method was developed to prepare the complex from ammonium meta-vanadate on the basis of the following possible reaction:

$$NH_4VO_3 + H_2C_2O_4 + (NH_4)_2C_2O_4 \rightarrow (NH_4)_3[VO_2(C_2O_4)_2] + H_2O$$

When calculated amounts of oxalic acid and ammonium oxalate were added to an aqueous solution of the metavanadate so that the molar ratio of $NH_4VO_3 : H_2C_2O_4 : (NH_4)_2C_2O_4$ was 1 : 1 : 1, a quick reaction occurred, giving a deep yellow solution. An excess of oxalic acid has to be avoided to prevent the reduction of pentavalent vanadium. A drop or two of dilute hydrogen peroxide was added to prevent any reduction of vanadium(V). The solution was warmed on a water bath to decompose the hydrogen peroxide and filtered through a sintered glass funnel. The filtrate was concentrated by passing a current of dry air at room temperature; when yellow crystals were obtained in about two days. The crystals were separated from the mother liquor and recrystallized from water. The crystals were then air-dried and analysed.[3]

Vanadium was estimated by igniting a known amount of the complex (about 200 mg.) to vanadium pentoxide, the oxalate by oxidation with potassium permanganate and ammonia by its liberation with aqueous alkali. The water was determined by the weight loss of the complex over anhydrous phosphorus pentoxide in a vacuum The V_2O_5, $C_2O_4^{2-}$, NH_4^+ and H_2O found were 26.1, 50.0, 15.1 and 10.2% respectively, while the corresponding calculated values for $(NH_4)_3[VO_2 \cdot (C_2O_4)_2] \cdot 2H_2O$ are 26.07, 50.42, 15.51 and 10.32% respectively. Thus, the complex obtained is a dihydrate and not the tetrahydrate.[1]

The complex is highly soluble in water, but insoluble in most of the organic solvents. When the complex was kept over fused calcium chloride, it lost both the molecules of water, giving a pale yellow powder. The complex is highly susceptible to reduction by oxalic acid and acid vapours. Ion-migration experiments in an aqueous solution indicated that vanadium was present wholly in the anion. The molecular weight determination in aqueous solutions by Beckmann's cryoscopic method showed that the complex dissociated into four ions.

Apparatus.—*Magnetic Susceptibility.*—The magnetic susceptibilities of the powdered samples were determined by the Gouy method[4] at room temperature, using $Hg[Co(NCS)_4]$ as the calibrant.

Thermal Studies.—The thermal behaviour of the complex was studied by both the differential thermal (DTA) and thermogravimetric (TGA) analyses. The DTA studies were carried out by a standard manual apparatus[5] using chromel-alumel thermocouples. The powdered samples (200 mg.) were pyrolysed at a heating rate of 8±1°C per minute in atmospheric air. The TGA studies were carried out with a quartz spring balance using 150~160 mg. of the substance, the rate of heating being maintained at 3°C per minute.

Absorption Spectral Studies.—The electronic spectrum of an aqueous solution of the complex was studied with a Hilger-Uvispek spectrophotometer, model H 700, using a pair of 1 cm. matched quartz cells. The infrared spectrum of the complex in Nujol mull was taken with a double-beam Perkin-Elmer Infracord spectrophotometer, model 137, employing sodium chloride optics.

1) A. Rosenheim, *Z. anorg. Chem.*, **4**, 352 (1893).
2) A. Rosenheim, ibid., **4**, 368 (1893).
3) A. I. Vogel, "A Text Book of Quantitative Inorganic Analysis," Longmans, Green and Co., London (1951), pp. 273, 319.
4) P. W. Selwood, "Magnetochemistry," Interscience, New York (1956).
5) N. S. K. Prasad and C. C. Patel, *J. Indian Inst. Sci.*, **36**, 23 (1954).

Results and Discussion

The magnetic susceptibility measurements indicated the compound to be diamagnetic, showing the pentavalent oxidation state of vanadium. The diamagnetic susceptibility found was $\chi = -0.51 \times 10^{-6}$ c. g. s. units.

The Thermal Behaviour of the Complex.—The differential thermogram of the complex is given in Fig 1. The small endothermic peak at 75°C is due to the loss of absorbed moisture. The medium endothermic peak at 125°C in the range from 85 to 145°C is due to the complete loss of two water molecules. The big endothermic peak at 225°C in the 170~270°C range was identified by heating the complex at 200°C for about 15 min. and by then analysing[3] the solid product, which corresponded to ammonium di-oxovanadium-(IV) trisoxalate, $(NH_4)_2[(VO)_2(C_2O_4)_3]$. (Analysis found in %: V_2O_5, 41.3 and $C_2O_4^{2-}$, 61.4, while the calculated % were V_2O_5, 41.94 and $C_2O_4^{2-}$, 60.83). The reaction taking place at 200°C can be represented as follows:

$$2(NH_4)_3[VO_2(C_2O_4)_2] \rightarrow (NH_4)_2[(VO)_2(C_2O_4)_3] + 2CO_2 + 4NH_3 + 2H_2O \quad (1)$$

The complex formed at 200°C is bluish-grey in colour and is paramagnetic, indicating the quadrivalency of vanadium. The complex is soluble in water, giving a bluish-green solution. Recently, it has been shown that europic(III) oxalate gives rise to europous(II) oxalate during the thermal decomposition of the former.[6] A number of other metal oxalato complexes, for example, those of nickel,[7] ferric[8] and plutonium[9], are also known to behave in a similar fashion.

The exothermic peak at 300°C is due to the decomposition of the dioxovanadium(IV) oxalato complex formed, giving rise to vanadium dioxide. This peak is followed by a big exothermic peak, with a maximum at 350°C. This peak was identified as due to the oxidation of vanadium dioxide to vanadium pentoxide.

The percentage-weight-loss vs. temperature curve is given in Fig. 2. The break in the curve corresponding to 170°C shows the completion of the loss of two water molecules from the complex, giving rise to the anhydrous oxalato complex. The anhydrous complex is found to be stable below 200°C. The formation of the intermediate compound $(NH_4)_2 \cdot [(VO)_2(C_2O_4)_3]$ starts from 200°C and is complete near 260°C (loss: 38%). The intermediate compound then starts decomposing, yielding vanadium(IV) oxide. The oxidation of vanadium(IV) oxide to vandium(V) oxide is not clearly shown by the TGA curve, probably because of the small gain in weight and the small contraction of the quartz spring with the increase in temperature.[10]

The Electronic Spectrum of the Complex.—In the ultraviolet region, there is a band below 220 mμ ($\log \varepsilon > 4.5$) and a shoulder at 265 mμ ($\log \varepsilon = 3.9$). These strong absorption

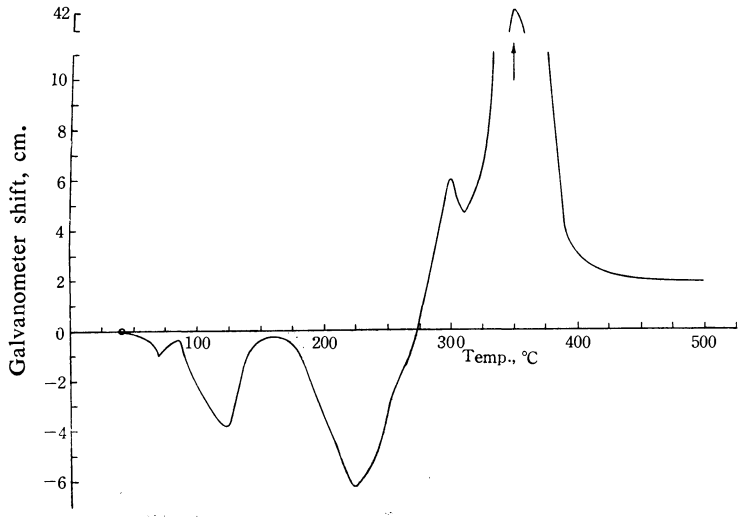


Fig. 1. DTA curve of $(NH_4)_3[VO_2(C_2O_4)_2] \cdot 2H_2O$.

6) A. Glasner, E. Levy and M. Steinberg, *J. Inorg. Nucl. Chem.*, 25, 1415 (1963).
7) P. W. M. Jacobs and A. R. Tariq Tureishy, *Trans. Faraday Soc.*, 58, 551 (1962).
8) J. B. Holden, Jr., *Diss. Abstr.*, 23, 62 (1962).
9) G. S. Rao, M. S. Subramanian and G. A. Welch, *J. Inorg. Nucl. Chem.*, 25, 1293 (1963).
10) R. M. Dell and V. J. Wheeler, AERE-R3424 Report of U. K. Atomic Energy Establishment, Harwell (1960).

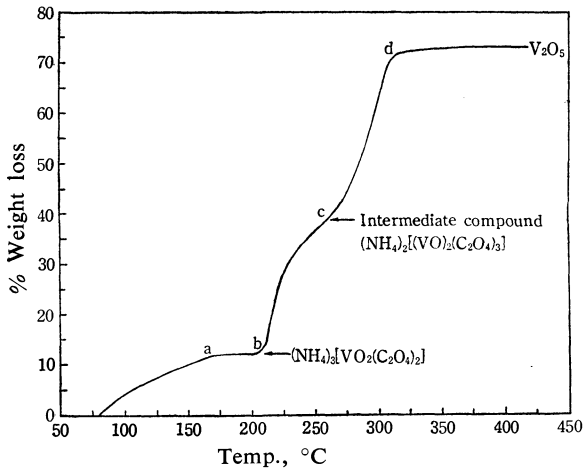


Fig. 2. TGA curve of $(NH_4)_3[VO_2(C_2O_4)_2]\cdot 2H_2O$.

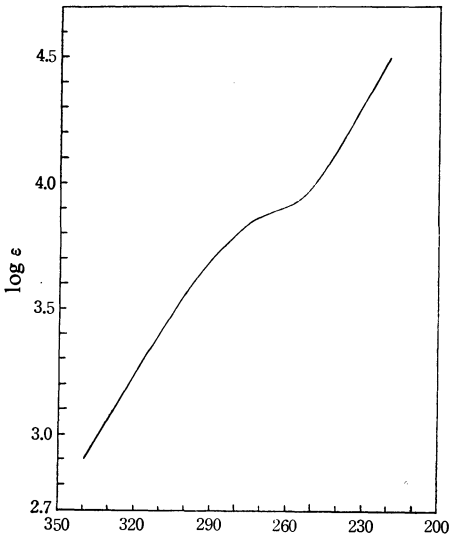


Fig. 3. Electronic absorption spectrum of $(NH_4)_3[VO_2(C_2O_4)_2]\cdot 2H_2O$ in water. Concn., 1×10^{-4} M.

bands can be assigned to the charge transfer arising from the promotion of an electron from the π-orbital of oxygen to the vacant 3d orbitals of the vanadium of the VO_2^+ group. In the oxovanadium complex containing the VO^{2+} ion, there is a band below 220 mμ ($\log\varepsilon=4.0$) and a shoulder at 245 mμ ($\log\varepsilon=3.2$); these are assigned as electron-transfer bands arising from the promotion of an electron from the oxygen π-orbital to the 3d levels of the vanadium of the VO^{2+} ion.[11] In the present complex containing the VO_2^+ ion, the absorption bands have shifted to higher wavelengths with an increase in the intensity. This effect may be due to the presence of another oxygen atom, with a certain amount of π-bonding to vanadium, along the V-O axis and a higher valence state of vanadium in the VO_2^+ ion.

The ultraviolet absorption spectra of a large number of oxalato complexes resemble those of dimethyl oxalate and molecular oxalic acid, with a low intensity band in the 250~270 mμ[12] region. This carboxylate band in the present compound has obviously merged with the intense electron-transfer band occurring in the ultraviolet region. No absorption peak was observed in the visible region, but the ultraviolet absorption band extends up to nearly 400 mμ. The light yellow colour of the compound, therefore, appears to be due to the charge transfer.

The infrared band assignments of the complex are given in Table I. The presence of a strong band around 3550 cm^{-1} indicates crystal lattice water. The strong band at 3080 cm^{-1} is due to the NH stretching of NH_4 groups.[13] The band at 1629 cm^{-1} may be due to the bending of water. The bands arising due to the oxalate group are assigned after Fujita, Martell and Nakamoto.[14] The spectrum shows a very strong absorption at 1720 cm^{-1}, indicating a highly covalent character of the bonds between the metal and the oxalate group.[15]

Table I. The assignment of the observed frequencies* in cm^{-1} of the infrared spectrum of $(NH_4)_3[VO_2(C_2O_4)_2]\cdot 2H_2O$

Frequency	Assignment
3550 s	$\nu_a(H_2O)$
3080 vs	$\nu(NH)$
1720 s	$\nu_a(C{=}O)$ (ν_7)
1669 s	$\nu_a(C{=}O)$ (ν_1)
1629 s	$\delta(H_2O)$ and $\delta(NH_4)$ (asy)
1381 vs	$\nu_s(C\text{-}O)+\nu(C\text{-}C)$ (ν_2) [overlapped by Nujol band]
1270 s	$\nu_s(C\text{-}O)+\delta(O\text{-}C{=}O)$ (ν_8)
924 s	$\nu_a(O\text{-}V\text{-}O)$
876 s	$\nu_s(C\text{-}O)+\delta(O\text{-}C{=}O)$ (ν_3)
866 s	$\nu_s(O\text{-}V\text{-}O)$
800 m	$\delta(O\text{-}C{=}O)+\nu(M\text{-}O)$ (ν_9)

* s=strong, vs=very strong, m=medium ν=stretching, ν_s=symmetrical stretching, ν_a=antisymmetric stretching, and δ=in-plane deformation vibrations

11) C. J. Ballhausen and H. B. Gray, *Inorg. Chem.*, **1**, 111 (1962).
12) K. V. Krishnamurthy and G. M. Harris, *Chem. Revs.*, **61**, 213 (1961).
13) H. W. Morgan, P. A. Staats and J. H. Goldstein, *J. Chem. Phys.*, **27**, 1212 (1957).
14) J. Fujita, A. E. Martell and K. Nakamoto, ibid., **36**, 324 (1962).
15) M. J. Schmelz, T. Miyazawa, S. Mizushima, T. J. Lane and J. V. Quagliano, *Spectrochim. Acta*, **9**, 51 (1957).

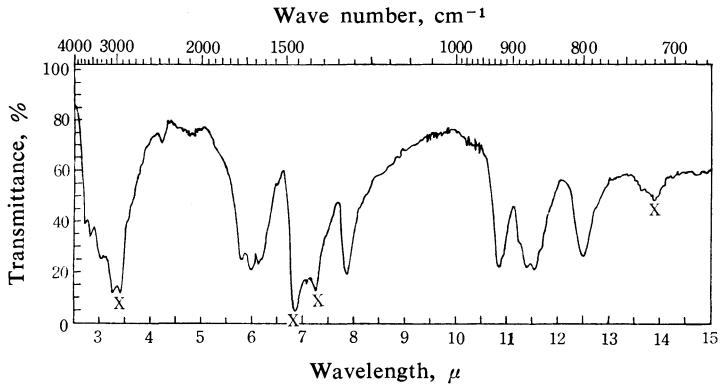


Fig. 4. Infrared spectrum of $(NH_4)_3[VO_2(C_2O_4)_2]\cdot 2H_2O$.

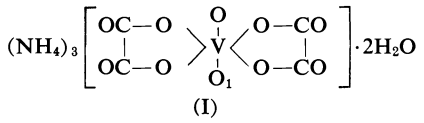
The infrared spectrum of the complex is given in Fig. 4

The band at 924 cm^{-1} is assigned to O–V–O asymmetrical stretching frequency, although it is predominantly a V–O mutiple-bond stretching frequency. Selbin et al.[16] assigned the strong band around 980 cm^{-1} to the V–O stretching in the oxovanadium compounds. It is interesting to note that the V–O stretching in the present complex occurs at a frequency much lower than that of the V–O stretching in hydrated oxovanadium(IV) oxalates (985 cm^{-1}) and in ammonium oxovanadium(IV) bisoxalates (978 cm^{-1}).[16] The lowering of the V–O frequency in the present case is due to the oxygen atom in the sixth position (of an octahedral structure) along the V–O axis, which is vacant in the above oxalates.[16] Such a position of oxygen will have the effect of slightly weakening the V–O bond, with also some reduction in its π-bond character. Nakamoto et al.[17] reported the lowering of the V–O stretching from 995 to 964 cm^{-1} in the solid complexes the addition of one pyridine molecule to oxovanadium(IV) bisacetylacetonate, $VO(acac)_2$.

Another band at 866 cm^{-1}, occurring as a doublet, may be due to the symmetrical stretching of O–V–O. The appearance of this second band may be due to the absence of the centre of symmetry of the O–V–O linear group, as has been suggested in the literature.[18,19]

The Structure of the Complex

Since the two water molecules in the complex are easily lost and since the infrared spectrum does not give any evidence of their being coordinated to the metal atom, they are considered to be lattice-held. Further, the infrared spectrum shows that the oxalate groups are covalently bonded. Hence, a six-coordinated octahedral structure with d^2sp^3 bonding can be assigned to the complex anion (I):



(I)

As there are no d electrons in vanadium(V), no distortion from the linear arrangement of the oxygen atom is expected in the VO_2^+ group of the complex.[18,19] Since the complex easily undergoes reduction to the oxovanadium-(IV) state at about 200°C, as given by Eq. 1, it is likely that one of the oxygen atoms (say, O_1) in the VO_2 group of the complex is more weakly bonded than the other. This is supported by the similar instances of V_2O_5[20](V), $KVO_3\cdot H_2O$[21](V) and VO_2[22](IV), in which it has been found by X-ray diffraction studies that one of the V–O bonds is much shorter than the rest. A sulphate oxygen along the V–O axis, completing the octahedral structure in $VOSO_4\cdot 5H_2O$,[23] is held at a much longer distance than the four water molecules in the tetragonal plane, and the V–O bond of VO^{2+} complexes is much shorter than the other bonds.[23,24] This characteristic feature of the oxovanadium compounds can be attributed to the strong V–O bond with a predominantly high π character. The appearance of the two

16) J. Selbin, L. H. Holmes, Jr., and S. P. McGlynn, *J. Inorg. Nucl. Chem.*, **25**, 1359 (1963).
17) K. Nakamoto, Y. Marimoto and A. E. Martell, *J. Am. Chem. Soc.*, **83**, 4533 (1961).
18) W. E. Addison, "Structural Principles in Inorganic Compounds," Longmans, London (1961), p. 119.
19) E. Cartmell and G. W. A. Fowles, "Valency and Molecular Structure," Butterworths, London (1961), p. 210.
20) A. Byström, K. A. Wilhelmi and O. Brotzen, *Acta Chem. Scand.*, **4**, 1119 (1950).
21) B. Anderson, ibid., **10**, 623 (1956).
22) C. L. Christ, J. R. Clark and H. T. Evans, Jr., *Acta Cryst.*, **7**, 801 (1954).
23) M. B. Palma-Vittorelli, M. U. Palma and F. Sgarlata, *Nuovo Cimento (Series 10)*, **3**, 718 (1956); G. Lundgren, *Rec. trav. chim.*, **75**, 585 (1956).
24) R. P. Dodge, D. H. Templeton and A. Zalkin, *J. Chem. Phys.*, **35**, 55 (1961).

vibrational stretching frequencies of the O–V–O may thus be due to the differently bonded oxygen atoms.

Summary

A simple method for the preparation of the yellow diamagnetic complex, $(NH_4)_3[VO_2 \cdot (C_2O_4)_2] \cdot 2H_2O$, is described. Around 200°C, the complex suffers decomposition, giving a bluish-grey paramagnetic compound $(NH_4)_2 \cdot [(VO)_2(C_2O_4)_3]$. The infrared spectrum of the yellow complex shows a covalent bonding between vanadium and the oxalate groups. The absorption in the ultraviolet region is due to the electron transfer within the VO_2 group. An octahedral structure, with the two linearly-arranged oxide oxygens at unequal lengths from vanadium(V), is suggested for the complex anion.

The authors wish to thank Professor M. R. A. Rao for his keen interest in this work.

Department of Inorganic and Physical Chemistry
Indian Institute of Science
Bangalore 12, India

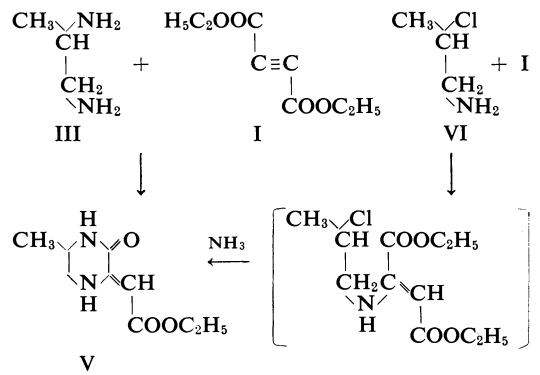
The Reaction of Acetylenecarboxylic Acid with Amines. XII.[1] *On the Hydrolysis of the Products Obtained by the Reactions of Diethyl Acetylenedicarboxylate with Amines*[*1]

By Yasuo IWANAMI, Yoshihisa KENJO,[*2] Koji NISHIBE,[*3] Makoto KAJIURA[*3] and Seiko ISOYAMA

(Received April 11, 1964)

In the preceding papers of this series, the products of the reactions of diethyl acetylenedicarboxylate (I) with amines, diethyl *N*-substituted-aminofumarates (type A),[2-4] 2-oxo-3-ethoxycarbonylmethylene-3,4,5,6-tetrahydro-2*H*-1, 4-oxazines (type B),[4,5] 2-oxo-3-ethoxycarbonylmethylene-3, 4-dihydro-2*H*-1, 4-benzoxazines (type C),[4,5] and 2-oxo-3-ethoxycarbonylmethylene-1, 2, 3, 4-tetrahydroquinoxalines (type E)[6-9] have been reported. It has been shown[3-9] that the compounds of types A, B and C are hydrolyzed into pyruvic acid (VII), carbon dioxide, and amines by the cleavage of the heterocyclic rings of types B and C, while the quinoxaline rings of the copomunds of type E remain unchanged, with only a decarboxylation of the side chain.

The present paper deals with the synthesis 2-oxo-3-ethoxycarbonylmethylenepiperazines (type D), and with the different behaviors of types D and E in hydrolysis. When ethylenediamine (II) and propylenediamine (III) were added to I, exothermic reactions occurred, and 2-oxo-3-ethoxycarbonylmethylenepiperazine (IV) and its 6-methyl derivative V were obtained respectively. While the 5-methyl derivative also seemed to have been produced in the reaction of I with III, only the 6-methyl derivative V could be isolated from the reaction mixture. The structural assignment of V was



1) Part XI: Iwanami, *J. Chem. Soc. Japan, Pure Chem. Sec.* (*Nippon Kagaku Zasshi*), **83**, 600 (1962).

*1 Presented in part at the 16th Annual Meeting of the Chemical Society of Japan, Tokyo, April, 1963.

*2 Present address: Research Laboratory of Resource Utilization, Tokyo Institute of Technology, Meguro-ku, Tokyo.

*3 Present address: Research Laboratory, Yokohama Rubber Co., Ltd., Hiratsuka City.

2) Y. Iwanami, *J. Chem. Soc. Japan, Pure Chem. Sec.* (*Nippon Kagaku Zasshi*), **82**, 632 (1961).

3) Y. Iwanami, ibid., **82**, 634 (1961).

4) Y. Iwanami, ibid., **83**, 593 (1962).

5) Y. Iwanami, ibid., **82**, 780 (1961).

6) Y. Iwanami, ibid., **82**, 778 (1961).

7) Y. Iwanami, ibid., **83**, 161 (1962).

8) Y. Iwanami, ibid., **83**, 316 (1962).

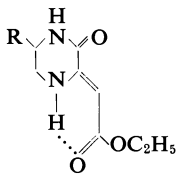
9) Y. Iwanami, ibid., **83**, 590 (1962).

supported by a successful conversion of the reaction product from I and 1-amino-2-chloropropane (VI) into a substance which was identical with V.

The chelate structure[4] of IV and V is suggested by their infrared spectra, the main absorption maxima of which are shown in Table I.

TABLE I. MAIN INFRARED ABSORPTION BANDS (KBr disk) (cm^{-1})

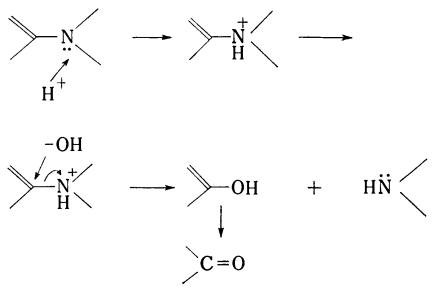
Product	Amine ν_{NH}	Chelated ester $\nu_{C=O}$	Amide $\nu_{C=O}$	Double bond $\nu_{C=C}$
IV	3350	1692	1660	1615
V	3365	1694	1650	1623



IV: R=H
V: R=CH_3

By hydrolysis with hydrochloric acid, both IV and V gave puruvic acid (VII), carbon dioxide, and the amines (II and III), as is shown in Chart 1. The formation of VII and carbon dioxide can be explained by assuming the intermediate formation of oxalacetic acid. Thus, the hydrolysis, followed by the decarboxylation, of the newly-synthesized compounds of type D is quite similar to that of the compounds of types A, B and C reported on in the preceding papers. Diethyl *N*-(*n*-butyl)-aminofumarate (VIII), 4-methyl-2-oxo-3-ethoxycarbonylmethylene-3, 4, 5, 6-tetrahydro-2*H*-1, 4-oxazine (X), 6-chloro-2-oxo-3-ethoxycarbonylmethylene-3, 4-dihydro-2*H*-1, 4-benzoxazine (XII) and 2-oxo-3-ethoxycarbonylmethylene-1,2,3,4-tetrahydroquinoxaline (XIV) were newly hydrolyzed. Their decarboxylation caused by hydrolysis is also similar to that in the above cases, except for that of XIV.

On the other hand, the decarboxylation of XIV through its hydrolysis gave 2-oxo-3-methyl-1, 2-dihydrobenzoquinoxaline (XV), although its structure resembles that of the compounds of type D. In any discussion of the above discrepancy, the breaking of the carbon-nitrogen bond which occurs by hydrolysis in all these compounds except in the compounds of type E seems to be important. The splitting mechanism in the compounds of types A, B, C and D, which have an enamine structure, is probably as follows:



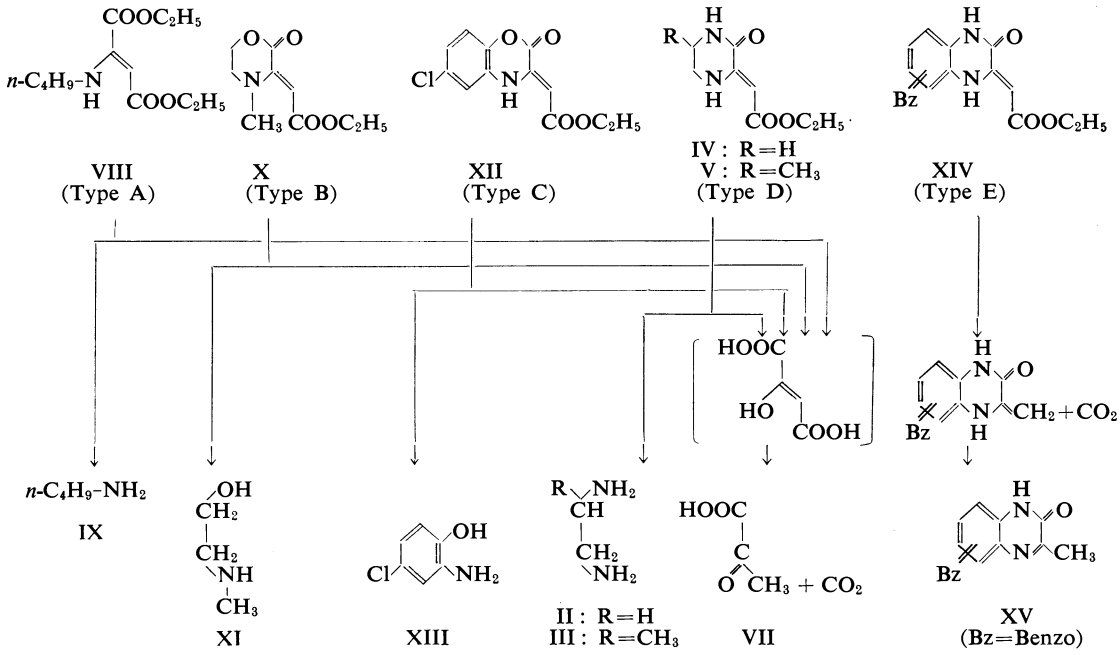
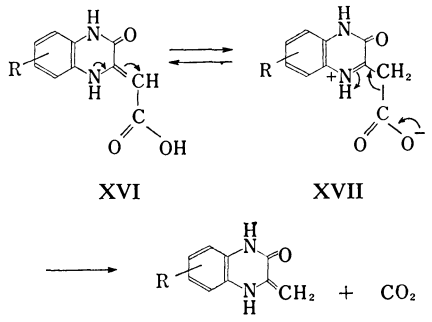


Chart 1

Hünig, Lücke and Benzing[10] have shown that ordinary simple enamine was easily hydrolyzed into a carbonyl compound and an amine even when such an enamine was titrated with dilute hydrochloric acid.[11]

An independent type of hydrolysis observed in the compounds of type E can be analogously explained by Doering and Pasternak's hypothesis[12] regarding the decarboxylation hydrolysis of ethyl α-pyridylacetates. That is to say, the tautomerization of enamine (XVI) to ketimine (XVII) appears to take place when the compounds of type E are hydrolyzed to the corresponding acid (XVI). Then the spontaneous decarboxylation may be supposed to proceed as follows:

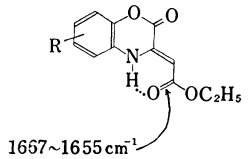


XVI XVII

At least in the case of the compounds of type E, assuming the formation of the intermediate acid (XVI) is fairly satisfactory as a means of interpreting the decarboxylation mechanism, although it is not known whether the corresponding acids of A—E are intermediately formed or not. Probably an insufficient tautomerization of the compounds of types A, B, C and D to their ketimine forms causes them to be hydrolyzed as enamines.

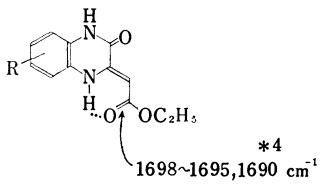
The carbon-carbon double bond of the enamine form conjugates with two carbonyl groups. Furthermore, the chelate ring[4] needs the double bond of the enamine form. The two carbonyl groups and the chelate ring will, therefore, facilitate the adoption of the enamine form shown in Chart 1. In the case of the compounds of type E, however, it is tempting to tautomerize them into the ketimine form, because they have a condensed aromatic ring and the ketimine double bond is stabilized by taking a quinoxaline structure. Thus, the different decarboxylation mechanisms of the compounds of type D and E appears to depend on whether or not they have an aromatic ring.

However, the compounds of type C, which have a condensed aromatic ring, are hydrolyzed to result in the cleavage of a oxazine ring, as in the case of the compounds of type B. This discrepancy may be explained on grounds that the quinoxaline ring of the compounds of type E is more stabilized by an easier mesomerism through its whole ring than through the benzoxazine ring of the compounds of type C. The chelate bond in the compounds of type E is, therefore, weakened for the reason already described. Evidence of such a tendency is given by the shift of the infrared absorption[4,13] of chelated ester-carbonyl groups.



1667~1655 cm^{-1}

Type C
R=H, 6-NO_2 and 6-Cl



*4
1698~1695,1690 cm^{-1}

Type E
R=H, 6-CH_3, 7-CH_3, 7-Cl, 6-NO_2 and 6, 7-Benzo

The larger shift towads a lower frequency in the compounds of type C than that in type E is observed. The presence of the more stabilized chelate ring in the compounds of type C appears to support the above hypothetical interpretation.

Experimental

2-Oxo-3-ethoxycarbonylmethylenepiperazine (IV). —Into a solution of I (1.7 g., 0.01 mol.) in ethanol (25 ml.), a solution of II (0.6 g., 0.01 mol.) in ethanol (25 ml.) was dropped with stirring. The mixture became brown, and its temperature rose

10) S. Hünig, E. Lücke and E. Benzing, *Chem. Ber.*, **91**, 129 (1958).
11) S. Hünig, E. Benzing and E. Lücke, ibid., **90**, 2833 (1957).
12) E. Doering and V. Z. Pasternak, *J. Am. Chem. Soc.*, **72**, 143 (1950).

*4 In most of the compounds of type E, carbonyl groups give rise to absorption bands in regions which do not overlap with those of type D (1694~1692 cm^{-1}), A (1673~1665 cm^{-1}), B (1672 cm^{-1}) and C (1667~1655 cm^{-1}). In the case of R=H, however, the region (1690 cm^{-1}) overlaps with that of type D; this result is not satisfactory for the above interpretation. Nevertheless, there is experimental evidence of a dissimilarity in decomposition between the compounds of types E and D, which may thus come to show clearly different absorption bands in their excited state. At least it should be noted that the absorption band of type E is in the region nearest to that of the normal ester-carbonyl group.
13) Y. Iwanami, *J. Chem. Soc. Japan, Pure Chem. Sec.* (*Nippon Kagaku Zasshi*), **83**, 597 (1962).

to 35°C from the room temperature (28°C). After the mixture had been stirred for a further 35 min., the solvent was removed in vacuo, and the residue was allowed to stand overnight in an ice box. The crystals formed (1.0 g., 56%) were then filtered off and recrystallized from ethanol to afford IV as colorless flakes; m. p. 164~165°C (corr.).

Found: C, 51.87; H, 6.68; N, 15.01. Calcd. for $C_8H_{12}O_3N_2$: C, 52.16; H, 6.57; N, 15.21%.

6-Methyl-2-oxo-3-ethoxycarbonylmethylenepiperazine (V).—Into a solution of I (1.7 g., 0.01 mol.) in ethanol (100 ml.), a solution of III (0.7 g., 0.01 mol.) in ethanol (100 ml.) was added dropwise with stirring. The mixture gradually became yellow, and its temperature reached 23°C from the room temperature (17°C). The crystals deposited (1.8 g., 89%) were recrystallized from ethanol to give V as colorless prisms; m. p. 166~167°C (corr.).

Found: C, 54.52; H, 6.99; N, 13.86. Calcd. for $C_9H_{14}O_3N_2$: C, 54.53; H, 7.12; N, 14.13%.

The Formation of V by the Amination of the Reaction Product from I and 1-Amino-2-chloropropane (VI).—VI hydrochloride was prepared according to Schaefer's[14] and Ulrich's[15] methods; colorless crystals melting at 179~181°C (lit.[15] m. p. 180~181°C) were obtained. The free amine VI was obtained by treating the hydrochloride with aqueous sodium hydroxide and by distilling the resulting oil under diminished pressure; colorless liquid boiling at 59~61°C/378 mmHg (lit.[14] b. p. about 70°C under slightly reduced pressure) was obtained.

Into a solution of I (5.0 g., 0.03 mol.) in ethanol (100 ml.), a solution of VI (2.5 g., 0.03 mol.) in ethanol (100 ml.) was dropped with stirring. A yellow color developed in the mixture, and the temperature of the mixture rose to 24°C from the room temperature (19°C). After the mixture had been stirred for a further 30 min., the solvent was removed in vacuo. To a solution of residual oil in ethanol (20 ml.), a saturated solution of ammonia in ethanol (30 ml.) was added, and the mixture was heated at 100°C for 4 hr. in a sealed tube. The mixture was then evaporated to dryness, and water was added to the remaining dark red oil. The suspension was extracted with benzene, and the solvent was removed in vacuo. The residue was allowed to stand for two weeks in an ice box, and then a vacuum desiccator. The crystals thereby formed were collected by filtration and repeatedly washed with ether. The recrystallization of the crystals (20 mg., 0.3%) from ethanol gave colorless prisms; m. p. 166~167°C (corr.) (Found: N, 13.82%). No depression of the melting point was observed on admixture with V.

6-Chloro-2-oxo-3-ethoxycarbonylmethylene-3, 4-dihydro-2*H*-1, 4-benzoxazine (XII).—To a solution of I (1.7 g., 0.01 mol.) in ethanol (20 ml.), a solution of 4-chloro-2-aminophenol (XIII) (1.5 g., 0.01 mol.) in ethanol (30 ml.) was added. The temperature of the mixture reached 24°C from the room temperature (21°C). After the mixture had stood overnight, the precipitated crystals (2.5 g., 94%) were collected by filtration and recrystallized from ethanol to afford XII as pale yellow needles; m. p. 122~123°C (corr.).

Found: C, 53.73; H, 4.08; N, 5.49. Calcd. for $C_{12}H_{10}O_4NCl$: C, 53.85; H, 3.77; N, 5.23%.

IR (KBr disk): 3260, 1765, 1655, 1625 cm^{-1}.

2-Oxo-3-ethoxycarbonylmethylene-1, 2, 3, 4-tetrahydro-5, 6(or 7, 8)-benzoquinoxaline (XIV).[*5]—Into a solution of I (1.7 g., 0.01 mol.) in ethanol (50 ml.), a solution of 1, 2-diaminonaphthalene (1.6 g., 0.01 mol.) in ethanol (500 ml.) was added with stirring. After the mixture had been stirred for 1 hr., the precipitated crystals (1.7 g., 60%) were collected by filtration and recrystallized from a large amount of ethanol to give XIV as orange needles; m. p. 227~228°C (corr.).

Found: C, 67.85; H, 5.36; N, 10.06. Calcd. for $C_{16}H_{14}O_3N_2$: C, 68.07; H, 5.00; N, 9.92%.

The Hydrolysis of IV.—One neck of a two necked flask was equipped with a reflux condenser. Into the other neck an inlet tube for bubbling the reaction mixture with a stream of air was fitted. The end of the inlet tube was connected to the outlet of two, in-series-connected scrubbing bottles containing aqueous sodium hydroxide for eliminating carbon dioxide from the air stream. A glass tube joined the top of the condenser to a wash bottle containing water. This was in turn connected to an empty bottle, which served as a trap, and to an absorption bottle containing an aqueous barium hydroxide solution. IV (0.80 g.) was placed in the flask, and 6 N hydrochloric acid (60 ml.) was added. By applying gentle suction (about 750 mmHg) to the outlet of the absorption bottle, a slow stream of air was continuously introduced into the mixture. The mixture bubbled with air was refluxed for 3 hr. During the reflux, IV was gradually dissolved and carbon dioxide was evolved. The precipitated barium carbonate in the absorption bottle was collected by filtration and dried after it had been washed with water (0.65 g., 76%).

A half of the solution containing the hydrolysates was partially concentrated in vacuo, and the crystals thereby formed were recrystallized from water to give the hydrochloride of II as colorless prisms; m. p. 240°C (subl.) (microscopically observed) (the description on its melting point in the literature: sublimes;[16] does not melt at 270°C[17]) (Found: C, 18.30; H, 7.75. Calcd. for $C_2H_{10}N_2Cl_2$: C, 18.05; H, 7.58%).

The remaining half of the solution was diluted with water until the concentration of hydrochloric acid became 2 N, and to the resulting solution the saturated solution of 2, 4-dinitrophenylhydrazine in 2 N hydrochloric acid was added. The precipitated crystals (0.36 g., 62%) were collected and recrystallized from ethanol to give 2, 4-dinitrophenylhydrazone of VII as yellow plates; m. p. 222°C (lit. m. p. 221~222°C) (Found: C, 40.46; H, 3.08. Calcd. for $C_9H_9O_6N_4$: C, 40.30; H, 3.01%).

The Hydrolysis of V.—6 N Hydrochloric acid (80 ml.) was added to V (1.0 g.). In a manner similar

14) F. C. Schaefer, *J. Am. Chem. Soc.*, 77, 5929 (1955).
15) H. Ulrich, U. S. Pat. 2163181 (1939).

*5 The infrared absorption of this compound will be reported on in a following paper, together with the structural assignment and the location of its benzo group.
16) A. W. Ipatow, *J. Russ. Phys. Chem. Soc.*, 49, 302 (1917).
17) T. Curtius and H. Hechtenberg, *J. prakt. Chem.*, 105, 215 (1920)

to that described above, the mixture was refluxed for 1 hr., and the evolved carbon dioxide was collected as barium carbonate (0.73 g., 73%). Although a half of the hydrolyzed solution was evaporated to dryness, the resulting hygroscopic hydrochloride of III failed to crystallize. The residue was dissolved in alkali, and the presence of III was confirmed by paper chromatography (ascending); solvent: 1-butanol saturated with a 25% aqueous solution of acetic acid; paper: Tōyō Roshi No. 50; location reagent: 0.2% bromophenol blue in ethanol. The same R_f value (0.36) with an authentic specimen was observed. The alkaline solution was then evaporated under diminished pressure, and the vapor was introduced into a solution of picric acid in ethanol. The deposited crystals (0.22 g., 21%) were collected and recrystallized from water to afford the picrate of III as yellow prisms; m. p. 273°C (lit.[18] m. p. 273°C) (Found: N, 21.30. Calcd. for $C_{15}H_{16}O_{14}N_8$: N, 21.05%).

From the other half of the solution, VII was isolated as its 2, 4-dinitrophenylhydrazone, which was recrystallized from ethanol to give yellow plates; m. p. 221~222°C (Found: N, 20.95. Calcd. for $C_9H_8O_6N_4$: N, 20.89%).

The Hydrolysis of VIII, X and XII.—The syntheses of VIII and X have been reported in the preceding paper.[4]

6 N Hydrochloric acid (100, 100 and 50 ml.) was added to VIII (2.4 g.), X (2.0 g.) and XII (0.50 g.) respectively in the flask of an apparatus similar to that described above, but nitrogen instead of carbon dioxide-free air was bubbled into the mixture under a slightly elevated pressure. In every case, VIII, X and XII, barium carbonate (1.2, 1.7 and 0.32 g. respectively; 61, 72 and 89% respectively) was precipitated in an absorption bottle. From a very small portion of the reaction mixtures, IX, XI and XIII were detected by paper chromatography, and the same R_f values (0.60, 0.26 and 0.18 respectively) with authentic specimens were observed. The separately-formed VII was isolated from the remaining mixtures as its 2, 4-dinitrophenylhydrazone (1.9, 1.5 and 0.46 g.; 75, 56 and 94%), which was recrystallized from ethanol to give yellow plates; m. p. 221~222°C (Found: C, 40.30; H, 3.28, C, 40.61; H, 3.13, and C, 40.17; H, 3.32%).

The Hydrolysis of XIV.—XIV (1.0 g.) was placed in the flask of the above-described apparatus, to which 6 N hydrochloric acid (100 ml.) was then added. The mixture was refluxed 3 hr., and the evolved gas was led into an absorption bottle with a stream of nitrogen. The precipitated barium carbonate (0.54 g., 79%) was separated. After the mixture had stood overnight, dark brown crystals were deposited; they became brown after being washed with water. The dried crystals (0.53 g., 71%) were recrystallized from ethanol with decolorizing carbon to give XV as colorless needles; m. p. 295~296°C (corr.).

Found: C, 74.45; H, 4.99; N, 13.33. Calcd. for $C_{13}H_{10}ON_2$: C, 74.27; H, 5.33; N, 13.54%.

18) A. Windaus et al., *Ber.*, **54**, 2750 (1921).

Summary

2-Oxo-3-ethoxycarbonylmethylenepiperazine (IV) and its 6-methyl derivative (V) have been synthesized by the reactions of diethyl acetylenedicarboxylate with ethylenediamine and propylenediamine. These compounds (IV and V), the previously-reported diethyl *N*-(*n*-butyl)aminofumarate (VIII), 4-methyl-2-oxo-3-ethoxycarbonylmethylene-3, 4, 5, 6-tetrahydro-2*H*-1, 4-oxazine (X), the newly-synthesized 6-chloro-2-oxo-3-ethoxycarbonylmethylene-3, 4-dihydro-2*H*-1, 4-benzoxazine (XII), and 2-oxo-3-ethoxycarbonylmethylene-1, 2, 3, 4-tetrahydrobenzoquinoxaline (XIV) have been hydrolyzed with 6 N hydrochloric acid. The compound XIV has been hydrolyzed, with decarboxylation, to give 2-oxo-3-methyl-1, 2-dihydrobenzoquinoxaline, while all the other compounds have been hydrolyzed into pyruvic acid, carbon dioxide, and the amines by the splitting of the carbon-nitrogen bond.

These two types of hydrolyses shown by the compounds have been discussed in connection with their tautomerism between enamine and ketimine forms.

The authors wish to express their deep gratitude to The late Professor Shin-ichiro Fujise for his valuable instruction and advice.

Department of Chemistry
The Medical Institute of Sasaki Foundation
Kanda-Surugadai, Tokyo

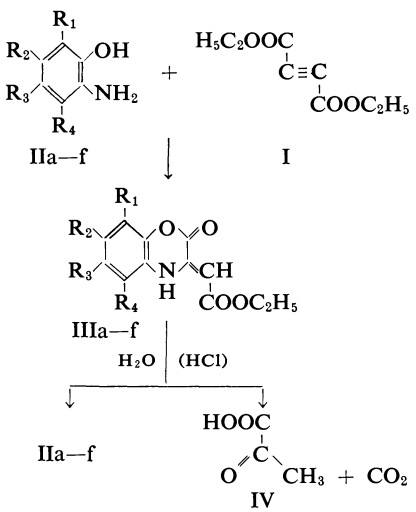
Die Reaktion von Acetylencarbonsäure mit Aminen. XIII.[1] *Substituierte 2-Oxo-3-äthoxycarbonylmethylen-3, 4-dihydro-2H-1, 4-benzoxazine*

Von Yasuo IWANAMI, Seiko ISOYAMA und Yoshihisa KENJO

(Eingegangen am 30. Mai, 1964)

Durch Einwirkung von Acetylen-dicarbonsäure-diäthylester (I) auf Aminophenole (II) in analoger Weise wie früher bereits kurz beschrieben[2] konnten substituierte 2-Oxo-3-äthoxycarbonylmethylen-3, 4-dihydro-2*H*-1, 4-benzoxazine (III) dargestellt werden.

Wenn man Rücksicht auf diese Reaktion nimmt, kann man leicht verstehen, dass sich die spontane Cyclisation des als Zwischenprodukt entstehenden substituierten *N*-(2-Hydroxy-phenyl)-amino-fumarsäure-diäthyl-esters ohne Erhitzen vollzieht.

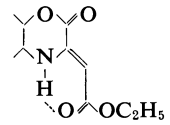


IIa—f und IIIa—f

a: $R_1=R_2=R_4=H$, $R_3=CH_3$
b: $R_1=R_2=R_4=H$, $R_3=NH_2$
c: $R_2=R_4=H$, $R_1=CH_3$, $R_3=NO_2$
d: $R_1=R_2=H$, R_3, R_4 = Benzo
e: $R_1=H$, $R_2=SO_3H$, R_3, R_4 = Benzo
f*: $R_1=R_2=R_4=H$, $R_3=Cl$

Alle diese Produkte (IIIa—f) fluoreszieren wie die Übersicht in Tabelle I.

Die Infrarot-Spektren von IIIa—f zeigen im Bereich zwischen 1670 und 1644 cm^{-1} deutlich erkennbare Estercarbonylbanden, die nach niedrigeren Frequenzen auss erordentlich verschoben sind. Im Vergleich mit den entsprechenden Banden der analogen Substanzen[2,3] wird die Existenz von einer ähnlichen Chelatbindung[3] zwischen einer Estercarbonyl- und einer Aminogruppe gezeigt.



Durch saure Hydrolyse wurden IIIa—f zu Brenztraubensäure (IV) und Kohlendioxyd unter Wiederbildung der entsprechenden Amine (IIa—f) abgespalten.

TABELLE I. FLUORESZENZ DER PRODUKTE BEIM BESTRAHLEN MIT UV-LICHT DER WELLENLÄNGE 365 mμ

Verbindung	Lösung in EtOH: Fluoreszenz-Maximum*2 mμ	Lösung in EtOH: Relative Intensität*3/ Mol (%)	Fluoreszenzfarbe der Kristalle
IIIa	492	52	hellgelb
IIIb			zinnoberrot
IIIc	ca. 480	ca. 0.57	dunkelgelb
IIId	494	100	gelb
IIIe	469		orange
IIIf	458	32	grünlich gelb

Beschreibung der Versuche

6-Methyl-2-oxo-3-äthoxycarbonylmethylen-3, 4-dihydro-2*H*-1, 4-benzoxazin (IIIa).—Eine Lösung von 1.3 g (0.01 Mol) 4-Methyl-2-aminophenol (IIa) in 30 ccm Äthanol liess man unter Rühren zu einer Lösung von 1.7 g (0.01 Mol) I in 20 ccm Äthanol tropfen. Bald begann sich die Temperatur der Mischung zu erhöhen, die von Raumtemperatur (21°C) bis 25°C anstieg, und ein gelbbrauner kristalliner Niederschlag begann auszufallen. Nach der Zugabe wurde die Mischung noch 1.5 Stunden weiter gerührt, und über Nacht bei Raumtemperatur

1) Mitteil. XII: Y. Iwanami u. a., Dieses Bulletin, **37**, 1740 (1964).
2) Y. Iwanami, *J. Chem. Soc. Japan, Pure Chem. Sec.* (*Nippon Kagaku Zasshi*), **82**, 780 (1961).
* Die Synthese von IIIf ist schon in der vorstehenden Arbeit[1] beschrieben worden.
3) Y. Iwanami, ebenda., **83**, 593 (1962).
*2 Die Fluoreszenz-Spektren wurden mit einem Spektrophotometer Hitachi Typ UPI-2 und seinem Nebenstückapparat für Fluoreszenz aufgenommen.
*3 Wegen der Ungleichheit von jedem Fluoreszenz-Maximum kann der Wert nicht so genau sein, der für dem von IIId=100% berechnet wird.

stehen gelassen. Am anderen Tage wurde der ausgeschiedene Niederschlag abfiltriert. Das Filtrat wurde unter vermindertem Druck eingedampft, wobei noch ein wenig Niederschlag zurückblieb. Ausb. 2.4 g (97% d. Th.). Diese gesamten Niederschläge wurden dreimal aus Äthanol umkristallisiert: faserartige glänzendgelbe Nadeln vom Schmp. 98~99°C.

Gef.: C, 63.00; H, 5.45; N, 5.98. Ber. für $C_{13}H_{13}O_4N$: C, 63.15; H, 5.30: N, 5.67%.

UV-Spektrum: λ_{max}^{EtOH} mμ (log ε) 255 (4.10), 370 (4.20). IR-Spektrum (KBr): 3295, 1772, 1669, 1620 cm^{-1}.

6-Amino-2-oxo-3-äthoxycarbonylmethylen-3, 4-dihydro-2*H*-1, 4-benzoxazine (IIIb).—Zu einer Lösung von 3.4 g (0.02 Mol) I in 30 ccm Äthanol/Wasser (1 : 1) wurden eine Lösung von 3.95 g (0.02 Mol) 2,4-Diaminophenol (IIb)-Hydrochloride (Amidol) in 80 ccm Äthanol/Wasser (1 : 1) und dann eine Lösung von 1.6 g (0.04 Mol) Natriumhydroxyd im 20 ccm des gleichen Lösungsmittels unter Rühren getropft. Bald begannen rotbraune Kristalle langsam sich auszuscheiden, die nach 2 stdg. Stehenlassen bei Raumtemperatur abfiltriert wurden. Ausb. 2.9 g (59% d. Th.) Dreimalige Umkristallisation aus Äthanol ergab rotbraune Nadeln vom Schmp. 180~181°C (korr.).

Gef.: C, 57.71; H, 4.95; N, 11.48. Ber. für $C_{12}H_{12}O_4N_2$: C, 58.06; H, 4.87; N, 11.29%.

UV-Spektrum: λ_{max}^{EtOH} mμ (log ε) 255 (3.99), 370 (4.03). IR-Spektrum (KBr): 3272, 1754, 1644, 1619 cm^{-1}.

6-Nitro-8-methyl-2-oxo-3-äthoxycarbonylmethylen-3, 4-dihydro-2*H*-1, 4-benzoxazin (IIIc).—Das Hydrochlorid von 4-Nitro-6-methyl-2-aminophenol (IIc) wurde nach Cazeneuve[4] dargestellt.

Zu einer Lösung von 1.7 g (0.01 Mol) I in 70 ccm Äthanol/Wasser (25 : 1) wurden eine Lösung von 2.3 g (0.01 Mol) IIc-Hydrochlorid in 35 ccm Äthanol/Wasser (25 : 1) und dann eine Lösung von 0.4 g Natriumhydroxyd im 5 ccm gleichen Lösungsmittel unter Rühren getropft. Während der Zugabe färbte sich die Lösung orange. Nach ungefähr 10 Minuten bildete sich ein gelber kristalliner Niederschlag, der abfiltriert und aus Äthanol umkristallisiert wurde: faserartige gelbe Nadeln vom Schmp. 148.5~149°C (korr.). Ausb. 0.4 g (14% d. Th.).

Gef.: C, 53.28; H, 4.18; N, 9.77. Ber. für $C_{13}H_{12}O_6N_2$: C, 53.43; H, 4.14; N, 9.59%.

UV-Spektrum: λ_{max}^{EtOH} mμ (log ε) 260 (4.15), 340 (4.03). IR-Spektrum (KBr): 3250, 1771, 1670, 1625 cm^{-1}.

3-Oxo-2-äthoxycarbonylmethylen-1, 2-dihydro-3*H*-naphth[2, 1-b]-1, 4-oxazin (IIId).—Zu einer Lösung von 3.4 g (0.02 Mol) I in 80 ccm Äthanol/Wasser (3 : 1) wurde eine Lösung von 1-Amino-2-naphthol (IId), dargestellt aus 3.5 g (0.02 Mol) 1-Nitroso-2-naphthol (in 135 ccm Äthanol und 135 ccm Wasser) und 11 g Natriumhydrosulfit, zugegeben. Während der Zugabe färbte sich die Lösung rotbraun. Nach wenigen Minuten schieden sich gelbe Kristalle aus, die mit Äther gewaschen wurden. Ausb. 1.9 g (34% d. Th.). Nach Umkristallisieren aus Äthanol/Benzol gelbe Nadeln vom Schmp. 155.5~156.5°C (korr.).

Gef.: C, 67.51; H, 4.81; N, 4.92. Ber. für $C_{16}H_{13}O_4N$: C, 67.84; H, 4.63; N, 4.95%.

UV-Spektrum: λ_{max}^{EtOH} mμ (log ε) 245 (4.39), 320 (3.91) 390 (4.02). IR-Spektrum (KBr): 3224, 1770, 1653 1622 cm^{-1}.

3-Oxo-2-äthoxycarbonylmethylen-1, 2-dihydro-3*H*-naphth[2, 1-b]-1, 4-oxazin-6-sulfonsäure (IIIe).—4.8 g (0.02 Mol) 1-Amino-2-naphthol-4-sulfonsäure (IIe) wurde in einer Lösung von 0.8 g Natriumhydroxyd in 30 ccm Wasser gelöst und unter Rühren 90 ccm Äthanol hinzugefügt. Diese Lösung wurde zu einer Lösung von 3.4 g (0.02 Mol) I in 120 ccm Äthanol/Wasser (3 : 1) unter kräftigem Rühren tropfenweise gegeben. Die Reaktion war etwas exotherm und die Temperatur der Mischung erhöhte sich von Raumtemperatur (ca. 20°C) bis 23°C. Während der Zugabe bildete sin brauner kristalliner Niederschlag, der abfiltriert und mit Wasser gewaschen wurde. Das zurückbleibende gelbbraune Rohprodukt des IIIe-Natriumsalzes wurde über konz. Schwefelsäure getrocknet, Schmp. 248~250°C. Ausb. 6.5 g (84.5% d. Th.).

Man versetzte 3.85 g (0.01 Mol) Natriumsalz unter Rühren mit 1.7 ccm 6 N Salzsäure und 10 ccm Wasser. Die Mischung wurde 30 Minuten bei Raumtemperatur gerührt. Die freie Sulfonsäure (IIIe) (mit 2 Mol Kristallwasser) wurde abfiltriert und fünfmal mit Wasser gewaschen. Durch verlustreiches Umkristallisieren aus viel Äthanol erhielt man IIIe rein in zitronengelben Nadeln vom Schmp. 284.5°C (korr.) (Zers.).

Gef.: C, 48.02; H, 4.40; N, 3.72; H_2O, 9.06. Ber. für $C_{16}H_{13}O_7NS \cdot 2H_2O$: C, 48.12; H, 4.29; N, 3.51; H_2O, 9.02%.

UV-Spektrum: λ_{max}^{EtOH} mμ (log ε) 248 (4.41), 380 (4.10). IR-Spektrum (KBr): 3541, 1753, 1647, 1623 cm^{-1}.

Hydrolyse von IIIa—f.—Eine Suspension von 0.5 g IIIe (kristallwasserhaltige) in 50 ccm 6 N Salzsäure wurde 2.5 Stunden unter Rückfluss gekocht, wobei die suspendierten Kristalle sich allmählich lösten und die Lösung sich rotbraun färbte. Während des Erhitzens bildete sich langsam ein grauweisser mikrokristalliner Niederschlag, der abfiltriert und mit Wasser gewaschen wurde. Ausb. 0.3 g (97% d. Th. als $^1/_2H_2O$-haltige Kristalle von IIe).

Gef.: C, 48.67; H, 4.48; N, 5.69. Ber. für $C_{10}H_9O_4NS \cdot {}^1/_2H_2O$: C, 48.78; H, 4.06; N, 5.64%.

Das Filtrat versetzte man mit der doppelten Menge Wasser und zu dieser verdünnten Lösung wurde eine überschüssige gesättigte Lösung von 2,4-Dinitro-phenylhydrazin in 2 N Salzsäure zugegeben. Nach dem Stehenlassen über Nacht wurde der gelbe Niederschlag abfiltriert. Ausb. 0.3 g (79% d. Th.). Durch Umkristallisieren aus Äthanol erhielt man Brenztraubensäure (IV) rein als deren 2,4-Dinitrophenylhydrazon vom Schmp. 221~222°C (Lit.[5]: 221~222°C). Die Substanz war identish mit einem authentischen Präparat durch Vergleich auf papierchromatographischem Wege. R_f-Wert: 0.86 nach aufsteigender Methode auf Tōyō Roshi Nr. 50 mit

4) M. P. Cazeneuve, *Bull. soc. chim.*, **17**, 206 (1897).

5) V. Subramaniam, B. Stent und U. K. Walker, *J. Chem. Soc.*, **1929**, 2490.

dem Gemisch von *n*-Butanol/25% wässriger Essigsäure-Lösung (1 : 1).

Die anderen Oxazine IIIa—d und IIIf konnten unter gleicher Bedingung wie bei IIIe hydrolysiert werden. Die entstehenden Aminophenole (IIa—d und IIf) und IV wurden als deren Hydrochloride und deren 2,4-Dinitro-phenylhydrazon chromatographiert und respektive mit den authentischen Präparaten identifiziert. Das Hydrazon wurden in der oben beschriebenen Weise und die Hydrochloride nach aufsteigender Methode auf ein gleiches Papier mit Methanol/Isoamylalkohol/Benzol/Wasser (40 : 20 : 20 : 20) isoliert. Die Aminophenole auf Chromatogramm wurden durch Besprühen mit 0.2% Natriumnitrit-Lösung in 0.1 N Salzsäure bzw. 0.2% *N*-Äthyl-α-naphthylamin-hydrochlorid-Lösung in Äthanol angefärbt.[6]

R_f-Werte: IIa, 0.72; IIb, 0.59; IIc, 0.84; IId, 0.76 und IIf, 0.82.

Laboratorium für Organische Chemie und Biochemie
Das Medizinische Institut der Sasaki Stiftung
Kanda-Surugadai, Tokyo

6) B. Ekman, *Acta Chem. Scand.*, 2, 383 (1948).

Heptafulvenes. I. The Synthesis of 8,8-Dicyano-2,3-dihydroxyheptafulvene[1]

By Yoshio KITAHARA, Kozo DOI and Tadahiro KATO

(Received April 21, 1964)

A number of studies of the substitution reactions accompanying rearrangement, which are explainable by an elimination-addition mechanism involving benzyne or its related intermediates, have been made, and a detailed review of this problem has been published.[2] In the field of tropolone chemistry, several reactions deduced to involve analogous intermediate tropolonyne[2] or dehydrotropolone (I, exactly its anion) have also been found: the formations of 3-hydroxy- (III) and 4-hydroxytropolones (IV) from 3-bromotropolone (II) by high-temperature alkaline hydrolysis,[3,4] of 4-cyanotropolone (V) from II reaction with potassium cyanide,[5] and of 4-aminotropolone (VII) from 3-iodotropolone (VI) by treatment with potassium amide in liquid ammonia.[6]



I



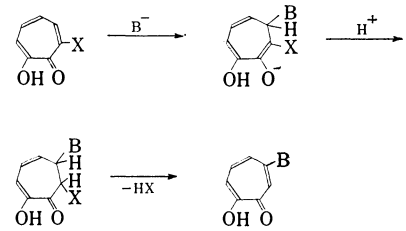
II: X=Br
III: X=OH
VI: X=I



IV: X=OH
V: X=CN
VII: X=NH_2

Very recently, novel examples of synthesizing bicyclic tropolones by intramolecular cyclization involving dehydrobromination have also been reported.[7]

In these reactions of halotropolones, however, the following process is also a possible mechanism to explain the above abnormal substitutions:[8]



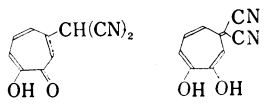
The Michael-type addition of an anion (B^-) to halotropolone, which is an unsaturated conjugated carbonyl compound, would occur, and then hydrogen halide would be eliminated, giving an abnormal substitution product.

No experimental proofs of these possible mechanisms have yet been obtained, so further detailed investigations of these abnormal substitution reactions are desirable. Some compounds containing an active methylene were found to be phenylated in a reaction with benzyne in liquid ammonia.[9] Accordingly,

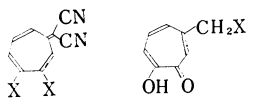
1) This work was presented at the General Meeting of the Hokkaido district of the Chemical Society of Japan, July, 1960.
2) H. Heaney, *Chem. Revs.*, **62**, 81 (1962).
3) T. Nozoe and Y. Kitahara, *Proc. Japan Acad.*, **30**, 204 (1954).
4) Y. Kitahara, *Sci. Repts. Tohoku Univ., Ser. I*, **39**, 258 (1956).
5) Y. Kitahara, ibid., **40**, 74 (1956).
6) K. Doi, This Bulletin, **34**, 497 (1961).
7) K. Ogura, ibid., **35**, 808 (1962).
8) Y. Kitahara, *Sci. Repts. Tohoku Univ., Ser. I*, **39**, 250 (1956).
9) W. W. Leake and R. Levine, *J. Am. Chem. Soc.*, **81**, 1169, 1627 (1959); J. F. Bunnett and T. K. Brotherton, *J. Org. Chem.*, **23**, 904 (1958).

the authors expected to obtain 4-dicyanomethyltropolone (VIII) from the reaction of 3-iodotropolone (VI) with malononitrile under similar conditions. The product actually obtaind, however, was confirmed to be a heptafulvene derivative (IX), and an enolic isomer of VIII, the details of which will be described in this paper.

3-Iodotropolone (VI) reacted with sodiomalononitrile in liquid ammonia to give a yellow product with the composition of $C_{10}H_6O_2N_2$ in about a 30 per cent yield. Its ultraviolet absorption maxima (Fig. 1) are at a longer wavelength region than those anticipated for the structure VIII, and its infrared spectrum indicates the presence of the conjugated nitrile grouping (Table I). Therefore,



VIII IX



X: X=OCH_3 XII: X=CO_2H
XI: X=OAc XIII: X=H
XVI: X=H

this product is deduced not to be the expected tropolone derivative (VIII) but its enolic isomer, 8, 8-dicyano-2, 3-dihydroxyheptafulvene (IX). This deduction is strongly supported by the fact that IX reacted with diazomethane and acetic anhydride to yield the dimethoxy (X) and diacetoxy (XI) derivatives respectively. On being heated in concentrated sulfuric acid, IX was hydrolyzed and partially decarboxylated to give 4-carboxymethyltropolone (XII), which led to 4-methyltropolone (XIII). From the above facts, the position of the dicyanomethylene grouping of IX can also be elucidated. In the course of the formation of the carboxymethyl derivative (XII) from IX, the corresponding dicarboxymethyltropolone or its isomeric heptafulvene derivative was assumed as an intermediate, but it has not yet been actually isolated.

On being treated with dilute alkali under mild conditions, both X and XI were readily hydrolyzed to give IX, maintaining the dicyanoheptafulvene skeleton. It is possible that the reactivities of the methoxyl and acetoxyl groups of the above heptafulvenes, X and XI, depend on their positions, but in alkaline hydrolyses of X and XI no partially hydrolyzed products other than IX have been isolated.

The methylation of IX with dimethyl sulfate give a yellow monomethylated product (XIV), which led to the dimethoxy derivative (X) upon reaction with diazomethane and to the acetoxy derivative (XV) upon heating with acetic anhydride. These facts indicate that the reactivities of the two hydroxyl groups of IX depend on their positions in the heptafulvene nucleus. A study attempting to determine the position of methoxyl group of the partially-methylated product, XIV, will be reported elsewhere.



XIVa: X=OH XIVb: X=OH
XVa: X=OAc XVb: X=OAc

Figure 1 indicates the ultraviolet absorption spectra of three heptafulvene derivatives, the features of which resemble those of 8, 8-dicyanoheptafulvene[10] (XVI).

Table I indicates some principal absorption maxima of the infrared spectra of the heptafulvenes compared with those[10] of XVI. The details of these spectroscopic analyses will be described in the near future.

As has been described hitherto, it has been clarified that 3-iodotropolone (VI) reacts with sodiomalononitrile in liquid ammonia to yield an abnormally-substituted product, 8, 8-dicyano-2, 3-dihydroxyheptafulvene (IX), which is an enol form of 4-dicyanomethyltropolone (VIII). For the following reasons, this reaction presumably proceeds by way of an intermediate dehydrotropolone or tropolonyne (I), as has been stated by other authors.[2,6] First, this

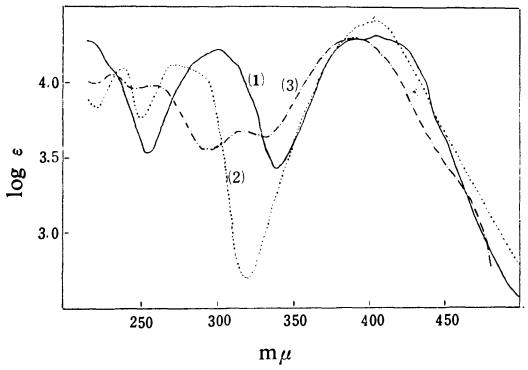


Fig. 1. The ultraviolet absorption spectra of 8, 8-dicyanoheptafulvene derivatives.

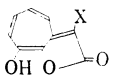
(1) 2, 3-Dihydroxy-(IX)
(2) 2, 3-Dimethoxy-(X)
(3) 2, 3-Diacetoxy-(XI)

10) T. Nozoe, T. Mukai, K. Osaka and N. Shishido, This Bulletin, 34, 1384 (1961).

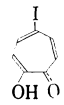
Table I. The infrared absorption maxima of 8,8-dicyanoheptafulvenes (cm^{-1})

XVI	2205	1633	1585	1520	1490	1406	1269	885
IX	2190 2215	1626	1570	1550	1485	1410	1260	874
X	2205	1630	1564	1550	1487	1412	1284	862
XI	2220	1645	1597	1560	1490	1405	1265	870

reaction proceeds under as mild conditions as in the amination of halobenzenes.[2] Second, the addition of a carbanion to the intermediate (I) would be expected to occur at the 4-position rather than the 3-position because of the polar effect of the carbonyl group. Third, under forced conditions, 3-halotropolones were found to react with carbanions to give normal substitution products: for example, when 3-bromotropolone (II) was heated with a sodium compound of acetoacetate or malonate in dioxane, a normally-substituted product (XVII: X=$COCH_3$ or $CO_2C_2H_5$) was obtained, although ring closure was followed.[11]



XVII



XVIII

Under conditions similar to those in the case of VI, however, 5-iodotropolone (XVIII) has been found not to react with sodio- or potassiomalononitrile. Taking this fact into account, we can say that the above abnormal substitution reaction, which led to an enolic form (IX) of VIII from a reaction of 3-iodotropolone (VI) and malononitrile, presumably proceeds by way of the above-mentioned addition-elimination mechanism, involving the Michael-type reaction rather than elimiation-addition-involving tropolonyne (I). Some efforts to resolve this problem are now being made.

Heptafulvene itself was first synthesized in 1954 and found to be an extremely unstable liquid,[12] in spite of having 13.2 kcal./mol. of stabilization energy based on the heat of hydrogenation.[13] Nozoe and his collaborators indicated, however, that some heptafulvenes having two electronegative groups at the 8-position are fairly stable, and that especially 8,8-dicyanoheptafulvene (XVI) resists bromination, Diels-Alder addition, and catalytic hydrogenation over palladium carbon.[10] The present authors have been able to synthesize many heptafulvenes by the new synthetic method described above and have studied their properties as a new system of non-benzenoid aromatic compounds. Details will be reported in the following papers.

11) K. Takase, ibid., to be published.
12) W. von E. Doering and D. W. Wiley, *Tetrahedron*, **11**, 183 (1960).
13) R. B. Turner, W. R. Meador, W. von E. Doering, J. R. Mayer and D. W. Wiley, *J. Am. Chem. Soc.*, **79**, 4127 (1957).

Experimental

The ultraviolet absorption spectra were measured in a methanol solution with a Hitachi model EPU-2A spectrophotometer. The infrared absorption spectra were measured on potassium bromide disks with a Hitachi model EPI-2 infrared spectrometer, using rock salt prisms. All melting points are uncorrected.

8,8-Dicyano-2,3-dihydroxyheptafulvene (IX). — The addition of malononitrile (4 g.) to a sodium amide solution prepared from liquid ammonia (300 ml.), sodium (5.6 g.) and a catalytic amount of ferric nitrate gave sodiomalononitrile as silver-white crystals. Into this mixture 3-iodotropolone (VI, 15 g.) was stirred at −50°C over a period of a few minutes, and then the mixture was gently refluxed at −33°C for 2 hr. After ammonium chloride (4.8 g.) had been added, the ammonia was allowed to evaporate. The solid residue was washed out with water (300 ml.) and some insoluble solid (6 g.), which consisted mainly of ammonium salt of VI, was removed by filtration. When this filtrate was acidified with dilute hydrochloric acid, yellow solids separated out; these solids, after filtration and recrystallization from acetone, gave IX (3.6 g.) as yellow prisms; m. p. 222°C (decomp.)

Found: C, 64.58; H, 3.56; N, 15.22. Calcd. for $C_{10}H_6O_2N_2$: C, 64.51; H, 3.25; N, 15.05%.

λ_{max} mμ (log ε): 300 (4.19), 390 (4.25), 405 (4.26).

8,8-Dicyano-2,3-dimethoxyheptafulvene (X). — To a stirred suspension of IX (1.2 g.) in ethanol (50 ml.) an excess of diazomethane in ether was added with ice cooling. The evaporated residue in vacuo was dissolved in ethyl acetate, the solution was chromatographed over alumina using ethyl acetate, and the reddish effluents were collected; these effluents, after evaporation in vacuo and recrystallization from the same solvent, yielded X (0.6 g.) as orange needles; m. p. 227~228°C.

Found: C, 67.44; H, 4.42; N, 13.32. Calcd. for $C_{12}H_{10}O_2N_2$: C, 67.28; H, 4.71; N, 13.08%.

λ_{max} mμ (log ε): 238 (4.09), 273 (4.11), 405 (4.38).

2,3-Diacetoxy-8,8-dicyanoheptafulvene (XI). — IX (0.1 g.) and acetic anhydride (4 ml.) were heated under reflux for 1 hr. The excess acetic anhydride was then removed under reduced pressure, and the residue was crystallized from ethyl acetate to give XI as red needles; m. p. 166~167°C.

Found: C, 62.36; H, 3.76; N, 10.36. Calcd. for $C_{14}H_{10}O_4N_2$: C, 62.22; H, 3.73; N, 10.37%.

λ_{max} mμ (log ε): 230 (4.03), 260 (3.96), 315 (3.67), 390 (4.28).

The Acid Hydrolysis of 8,8-Dicyano-2,3-dihydroxyheptafulvene (IX).—A mixture of IX (0.56 g.) and 75% sulfuric acid (4 ml.) was heated at 100°C for 1 hr., diluted with water (10 ml.), and then cooled. 4-Carboxymethyltropolone (XII, 0.25 g.)

precipitated out as colorless needles; m. p. 154~155°C (decomp.). When heated at its decomposition point, XII gave 4-methyltropolone (XIII), m. p. 76~77°C. The melting points of XII and XIII did not show any depression on admixture with respective authentic samples.[14]

The Alkaline Hydrolysis of 8, 8-Dicyano-2, 3-dimethoxyheptafulvene (X).—A mixture of X (0.1 g.) and 2 N methanolic sodium hydroxide (10 ml.) was heated under reflux for 5 min., and then the solvent was removed under reduced pressure. The acidification of the residue with dilute sulfuric acid afforded IX (0.08 g.) m. p., alone and mixed, 222°C (decomp.).

The Alkaline Hydrolysis of 2, 3-Diacetoxy-8, 8-dicyanoheptafulvene (XI).—A mixture of XI (0.1 g.) and 2 N sodium hydroxide (5 ml.) was heated on a water bath for 1 hr.; neutralization with dilute sulfuric acid then yielded IX, m. p., alone and mixed, 222°C (decomp.).

The Methylation of 8, 8-Dicyano-2, 3-dihydroxyheptafulvene (IX) with Dimethyl Sulfate.—Dimethyl sulfate (1 g.) was added to the solution of IX (0.2 g.) in 2 N sodium hydroxide (2 ml.) under ice cooling, and then the mixture was stirred for 4 hr. The precipitated solid, after collection by filtration and subsequent recrystallization from acetone, gave a monomethylated product (XIV, 0.2 g.) as yellow prisms; m. p. 164~165°C.

Found: C, 65.73; H, 4.23; N, 13.86. Calcd. for $C_{11}H_8O_2N_2$: C, 65.99; H, 4.03; N, 13.99%.

14) T. Nozoe, Y. Kitahara, K. Doi, M. Funamizu and T. Terasawa, *Bull. Chem. Res. Inst. Non-Aqueous Solutions, Tohoku Univ.*, 10, 199 (1961).

XIV reacted with an excess of diazomethane in ether to give the dimethoxyl derivative (X), m. p., alone and mixed, 227~228°C.

3 (2)-Acetoxy-8, 8-dicyano-2 (3)-methoxyheptafulvene (XV).—A mixture of XIV (0.08 g.) and acetic anhydride (1 ml.) was heated under reflux for 1 hr.; the residue obtained after the removal of acetic anhydride under reduced pressure was crystallized from ethyl acetate, giving XV as red needles; m. p. 141~142°C.

Found: N, 11.57. Calcd. for $C_{13}H_{10}O_3N_2$: N, 11.33%.

The Reaction of 5-Iodotropolone (XVIII) and Sodiomalononitrile.—To a mixture of sodium amide or potassium amide and malononitrile in liquid ammonia, XVIII was added; the following procedure was essentially that used in the case of VI. No reaction product other than the starting material was isolated.

The authors wish to take this opportunity to express their gratitude to the Ministry of Education and to the Sankyo Co., Ltd., for their financial support. The authors wish also to thank the Misses Yoko Endo and Yukiko Endo of this Institute for carrying out the microanalyses.

The Chemical Research Institute of Non-Aqueous Solutions
Tohoku University
Katahira-cho, Sendai

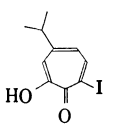
Heptafulvenes. II. The Synthesis of 8, 8-Dicyano-2, 3-dihydroxy-isopropylheptafulvenes[1]

By Yoshio KITAHARA, Kozo DOI and Tadahiro KATO

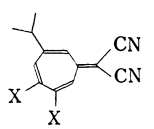
(Received April 21, 1964)

Our recently reported[2] method of synthesizing heptafulvenes has now been applied to two isopropyl derivatives of 3-iodotropolone; the experimental results will be described in this paper.

From the reaction of 3-iodo-6-isopropyltropolone (I) with sodiomalononitrile in liquid ammonia, a yellow product with a poor solubility in common organic solvents was obtained in a 48 per cent yield. Its ultraviolet absorption spectrum (Table I) is similar to that of 8, 8-dicyano-2, 3-dihydroxyheptafulvene,[2] while its infrared spectrum (Table II) indicates the presence of conjugated nitrile groups. This product II gave dimethyl III and diacetyl IV derivatives when treated with diazomethane and acetic anhydride respectively; when treated with dimethylsulfate, II afforded the monomethyl ether X.



I



II: X=OH
III: X=OCH_3
IV: X=OAc

1) This work was presented in part at Tohoku Local Meetings of the Chemical Society of Japan held in June, 1959, and October, 1961.

2) Y. Kitahara, K. Doi and T. Kato, This Bulletin, 37, 1747 (1964).

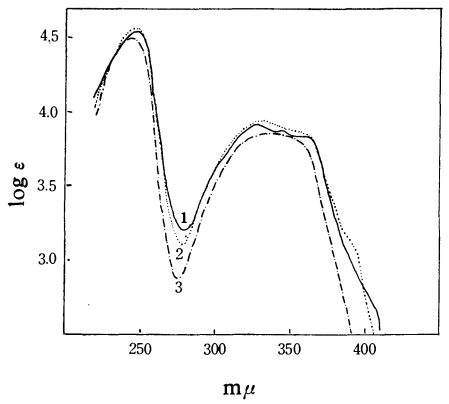
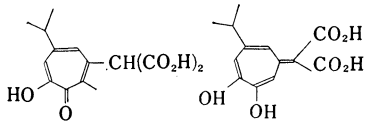
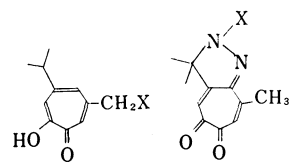


Fig. 1. Ultraviolet absorption spectra of
1: 4-dicarboxymethyl-(V),
2: 4-carboxymethyl-(VII), and
3: 4-methyl-(VIII)-6-isopropyltropolone.

In the preceding paper,[2] it was shown that when 8, 8-dicyano-2, 3-dihydroxyheptafulvene was heated with sulfuric acid, 4-carboxylmethyltropolone was formed as a hydrolysis product. When the heptafulvene (II) was carefully heated with sulfuric acid following the directions previously described,[2] the 4-dicarboxymethyltropolone derivative V was obtained as a hydrolysis product. From the fact that its ultraviolet spectrum (Fig. 1) resembles the spectrum of an alkyltropolone more closely than that of the heptafulvene (II), this hydrolysis product appears to be a tropolone (V) rather than a heptafulvene (VI) derivative. When V was heated to its decomposition point, it gave the 4-carboxymethyltropolone derivative VII, which showed a depression of its melting point on admixture with authentic 3-carboxymethyl-6-isopropyltropolone.[3] The further decarboxylation of VII yielded the 4-methyltropolone derivative VIII, which was not identical with authentic 6-isopropyl-3-methyltropolone.[3]



V VI

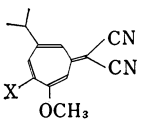


VII: X=CO_2H IX: X=*p*-Tolyl
VIII: X=H

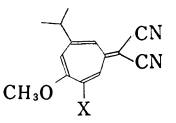
3) K. Takase, This Bulletin, to be published.

The methyltropolone VIII reacted with diazotized *p*-toluidine to yield 4', 6-dimethylhinopurpurin (IX) rather than the expected *p*-tolyazotropolone. On the basis of a comparison of its ultraviolet spectrum with that of hinopurpurin itself,[4] structure IX was assigned to the compound.

In the preceding paper[2] it was also reported that mild hydrolyses of 2, 3-dimethoxy- and 2, 3-diacetoxy-8, 8-dicyanoheptafulvenes gave 8, 8-dicyano-2,3-dihydroxyheptafulvene. On the other hand, the isopropyl-dimethoxy derivative (III) was found to be partially demethylated to X under the same conditions. III was regenerated when X was treated with diazomethane;



Xa: X=OH
XIa: X=OAc

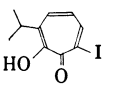


Xb: X=OH
XIb: X=OAc

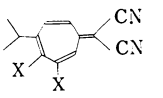
X afforded a monoacetate XI. The further heating of the monomethoxyheptafulvene (X) in dilute alkali gave the dihydroxy derivative II. The careful hydrolysis of the diacetoxy compound IV yielded only II.

The fact that the dimethoxyheptafulvene (III) is easily hydrolyzed to II and then to V suggests that the replacement of the methoxyl groups of the heptafulvene may be possible with other nucleophilic reagents, but no experiments have been undertaken to verify this.

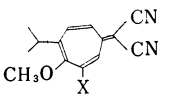
Analogous results were obtained from another isopropyltropolone derivative XII. Dihydroxyheptafulvene (XIII) easily formed a dimethoxy XIV derivative with diazomethane and diacetate XV when reacted with acetic anhydride. It also gave a monomethoxy compound XVI by reaction with dimethyl sulfate; this could be acetylated to XVII.

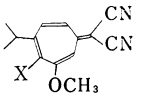


XII



XIII: X=OH
XIV: X=OCH_3
XV: X=OAc





XVIa: X=OH
XVIIa: X=OAc

XVIb: X=OH
XVIIb: X=OAc

The ultraviolet and infrared absorption maxima for these heptafulvenes are summarized

4) T. Nozoe, T. Ikemi and T. Ozeki, *Proc. Japan Acad.*, **31**, 455 (1955).

TABLE I. THE ULTRAVIOLET ABSORPTION MAXIMA

Compound	mμ	log ε	mμ	log ε	mμ	log ε	mμ	log ε
VII	220	4.41	307	4.32			392	4.36
XVIII	220	4.33	300	4.21			390	4.32
VIII	242	4.33	275	4.21	290	4.20	405	4.45
XIX	243	4.20	275	4.18			405	4.40
IX	235	4.17	265	4.12			390	4.37
XX	233	4.20	260	4.15			395	4.42
XV	222	4.39	310	4.40	322	4.41	383	4.45
XXI	223	4.30	240	4.21	293	4.02	433	4.56
XVI	240	4.29	265	4.01			415	4.42
XXII	235	4.15	260	4.10			393	4.40

TABLE II. PRINCIPAL MAXIMA OF THE INFRARED SPECTRA (cm^{-1})

VII	2180 2202	1632	1583	1532	1467	—	1260	875
XVIII	2190 2220	1620	1565	1535	1496	1416	1275	882
VIII	2190 2205	1640	1575	1545	1465	1415	1260	875
XIX	2220	1632	1576	1523	1495	1405	1290	856
XX	2220	1635	1593	1526	1500	1404	1296	868
XV	2185 2202	1632	1595	1545	1485	1418	1275	873
XXI	2210	1632	1576	1540	1502	1402	1285	865
XXII	2218	1632	1588	1525	1495	1400	1295	870

in Tables I and II; these data will be discussed elsewhere.

Experimental

The ultraviolet absorption spectra were measured for methanol solutions on a Hitachi model EPU-2 recording spectrophotometer. The infrared absorption spectra were measured on a Hitachi model EPU-510 infrared spectrometer (rock salt prism, potassium bromide pellet). All melting points are uncorrected.

8, 8-Dicyano-2, 3-dihydroxy-5-isopropylheptafulvene (II).—The addition of malononitrile (3.3 g.) to a sodium amide solution prepared from sodium (3.4 g.) and liquid ammonia (300 ml.) gave sodiomalononitrile as silver white crystals. I (14.5 g.) was stirred into this mixture at −50°C over a period of 10 min., and the resulting deep red solution was refluxed for 2 hr. under atmospheric pressure. After the addition of ammonium chloride (8 g.), the ammonia was allowed to evaporate. The residue was then washed with water (300 ml.), and the insoluble substance was filtered off. The acidification of the filtrate precipitated a yellow solid which, after recrystallization from methanol, gave II as yellow needles, m. p. 227°C (decomp.), 5.5 g. (48%).

Found: C, 68.85; H, 5.26: N, 12.34. Calcd. for $C_{13}H_{12}O_2N_2$: C, 68.41; H, 5.30; N, 12.27%.

8, 8-Dicyano-2, 3-dimethoxy-5-isopropylheptafulvene (III).—To a cooled, stirred solution of II (0.23 g.) in methanol (10 ml.) an ether solution of diazomethane was added until no more gas was evolved. After 1 hr., the solvent was removed, and a solution of the residue in ethyl acetate was chromatographed over alumina (1.5×10 cm.). The yellowish orange eluate was collected and evaporated under reduced pressure. The recrystallization of the residue from ethyl acetate afforded II as yellowish orange prisms, m. p. 176~177°C, 0.2 g.

Found: C, 70.19; H, 6.32; N, 10.90; mol. wt. (Rast), 263. Calcd. for $C_{15}H_{16}O_2N_2$: C, 70.29; H, 6.29; N, 10.93%; mol. wt. 256.

2, 3-Diacetoxy-8, 8-dicyano-5-isopropylheptafulvene (IV).—II (0.2 g.) in acetic anhydride (5 ml.) was heated under reflux for 2 hr. The removal of the solvent under reduced pressure and the recrystallization of the residue from benzene gave reddish needles, m. p. 138~140°C, 0.1 g.

Found: C, 65.36; H, 4.77; N, 9.03. Calcd. for $C_{17}H_{16}O_4N_2$: C, 65.37; H, 5.16; N, 8.97%.

4-Dicarboxymethyl-6-isopropyltropolone (V).—A mixture of II (0.46 g.) and 75% sulfuric acid (3 ml.) was heated at 80~90°C for 1 hr., and then diluted with water to 10 ml. and cooled. The colorless crystals which separated were filtered and recrystallized from methanol to afford V as colorless prisms, m. p. 135~136°C (decomp.), 0.36 g. A methanol solution of V showed a red coloration with ferric chloride.

Found: C, 51.86; H, 6.29. Calcd. for $C_{13}H_{14}O_6 \cdot H_2O$: C, 51.65; H, 6.00%.

4-Carboxymethyl-6-isopropyltropolone (VII).—V (0.13 g.) was heated at its decomposition point until no more carbon dioxide was evolved. The product formed colorless crystals when allowed to cool under reduced pressure. Recrystallization from a mixture of benzene and methanol gave VII as colorless prisms, m. p. 153~154°C (decomp.), 0.07 g.

Found: C, 64.59; H, 6.49. Calcd. for $C_{12}H_{14}O_4$: C, 64.85; H, 6.35%.

VII decomposes sodium hydrogencarbonate, and its alcoholic solution showed a red coloration with ferric chloride. A mixture of VII and 3-carboxymethyl-6-isopropyltropolone (m. p. 153~154°C (decomp.))[3] had an m. p. of 120~125°C.

6-Isopropyl-4-methyltropolone (VIII).—VII (0.11 g.) was heated at its decomposition point in a sublimation apparatus until the evolution of carbon dioxide ceased; then it was submitted to sublimation in vacuo. The recrystallization of the sublimate from petroleum ether (b. p. 40~60°C) gave VIII as white prisms, m. p. 52~53°C, 0.05 g.

Found: C, 74.16; H, 7.80; mol. wt. (Rast), 192. Calcd. for $C_{11}H_{14}O_2$: C, 74.13; H, 7.92%; mol. wt., 188.

VIII did not afford a picrate or an *o*-phenylenediamine compound, thus differing from 6-isopropyl-3-methyltropolone (liquid).[3]

The Azo-coupling of 6-Isopropyl-4-methyltropolone (VIII).—A diazonium chloride solution prepared from *p*-toluidine (30 mg.) was stirred into a cooled solution of VIII (45 mg.) in pyridine (2 ml.) over a period of 10 min. After 30 min., the reddish solution was acidified with dilute hydrochloric acid, and the resulting reddish violet solution was extracted with ethyl acetate (30 ml.). The extract was chromatographed over alumina (1×5 cm.), and the reddish violet eluate was collected. After the removal of the solvent under reduced pressure, the residue was recrystallized from cyclohexane, giving the dimethylhinopurpurin compound IX as reddish violet needles, m. p. 130~132°C.

λ_{max}^{MeOH} mμ (log ε): 257 (4.49), 320 (4.09), 360 (3.98), 500 (4.09).

Found: C, 37.67; H, 5.73; N, 9.42. Calcd. for $C_{18}H_{18}O_2N_2$: C, 73.45; H, 6.16; N, 9.52%.

The Alkaline Hydrolysis of 8, 8-Dicyano-2, 3-dimethoxy-5-isopropylheptafulvene (III).—III (0.1 g.) in 2 N methanolic sodium hydroxide (5 ml.) was heated under reflux for 5 min. The neutralization with dilute hydrochloric acid caused the separation of crystals which, after recrystallization from acetic acid, gave 8,8-dicyano-3(or 2)-hydroxy-5-isopropyl-2(or 3)-methoxyheptafulvene (X) as yellow leaflets, m. p. 278°C (decomp.).

Found: C, 69.55; H, 5.74; N, 11.60. Calcd. for $C_{14}H_{14}O_2N_2$: C, 69.40; H, 5.83; N, 11.56%.

Upon treatment with diazomethane in ether, X gave a product which showed no depression of its melting point on admixture with an authentic sample of III. X was soluble in aqueous caustic alkali, and its alcoholic solution did not show any coloration with ferric chloride. When it is heated under reflux in 2 N methanolic sodium hydroxide for 2 hr., III and II are afforded.

3(or 2)-Acetoxy-8, 8-dicyano-5-isopropyl-2(or 3)-methoxyheptafulvene (XI).—A solution of X (0.1 g.) in acetic anhydride (2 ml.) was heated under reflux for 1 hr. The solvent was then evaporated under reduced pressure; the residue after recrytallization from benzene afforded XI as reddish orange needles, m. p. 185~186°C.

Found: C, 67.83; H, 5.18; N, 9.99. Calcd. for $C_{16}H_{16}O_3N_2$: C, 67.59; H, 5.67; N, 9.85%.

The Alkaline Hydrolysis of 2, 3-Diacetoxy-8, 8-dicyano-5-isopropylheptafulvene (IV).—A solution of IV (0.1 g.) in 2 N methanolic sodium hydroxide (5 ml.) was heated under reflux for 10 min. Neutralization with dilute hydrochloric acid afforded II, m. p. and mixed m. p. 227°C (decomp.) with an authentic sample.

The Methylation of 8, 8-Dicyano-2, 3-dihydroxy-5-isopropylheptafulvene (II) with Dimethyl Sulfate.—A mixture of II (0.46 g.), sodium hydroxide (0.2 g.), water (5 ml.), and dimethyl sulfate (0.63 g.) was stirred at room temperature for 2 hr. The crystals which separated out were filtered off and recrystallized from acetic acid to give X (0.42 g.), m. p. and mixed m. p. with an authentic sample, 278°C (decomp.).

3-Iodo-7-isopropyltropolone (XII).—To a refluxing mixture of 3-isopropyltropolone (41 g.), anhydrous potassium carbonate (72 g.) and methanol (300 ml.), a solution of iodine (64 g.) and potassium iodide (42 g.) in methanol (300 ml.) was added drop by drop; refluxing was then continued for an additional 4 hr. After most of the methanol had been removed under reduced pressure, the residue was diluted with dilute sulfuric acid and then extracted with chloroform. The extract was washed with sodium hydrogen sulfite and then dried. The removal of the solvent gave crude XII as a dark red oil, 58 g.

Into a cooled solution of the oil (0.2 g.) in pyridine (3 ml.) a solution of *p*-toluenediazonium chloride prepared from *p*-toluidine (0.11 g.) was stirred. After 1 hr. the mixture was diluted with dilute hydrochloric acid, and the crystals which separated out were recrystallized from acetone to give 3-iodo-7-isopropyl-5-*p*-tolylazotropolone as orange needles, m. p. 167~168°C; 90% yield.

Found: C, 50.35; H, 4.29; N, 6.88. Calcd. for $C_{17}H_{17}O_2N_2I$: C, 50.01; H, 4.19; N, 6.86%.

8, 8-Dicyano-2, 3-dihydroxy-4-isopropylheptafulvene (XIII).—XII (41 g.) was added to a mixture of malononitrile (14 g.), liquid ammonia (500 ml.) and sodium amide prepared from sodium (16 g.). The subsequent procedure is the same as that used in the case of I. After recrystallization from a mixture of methanol and acetone, XIII was obtained as yellowish orange needles, m. p. 242°C (decomp.), 13 g.

Found: C, 68.75; H, 5.19; N, 12.28. Calcd. for $C_{13}H_{12}O_2N_2$: C, 68.41; H, 5.30; N, 12.27%.

8, 8-Dicyano-2, 3-dimethoxy-4-isopropylheptafulvene (XIV).—A solution of diazomethane in ether was added to a mixture of XIII (0.7 g.) and ethanol (3 ml.) with stirring and cooling. After the removal of the solvent under reduced pressure, the product was dissolved in ethyl acetate and chromatographed over alumina. The reddish orange eluates were evaporated to afford XIV as reddish prisms, m. p. 124~125°C, 0.25 g.

Found: C, 70.08; H, 5.89; N, 10.59. Calcd. for $C_{15}H_{16}O_2N_2$: C, 70.29; H, 6.29; N, 10.93%.

2, 3-Diacetoxy-8, 8-dicyano-4-isopropylheptafulvene (XV).—A mixture of XIII (0.2 g.) and acetic anhydride (5 ml.) was heated under reflux for 3 hr., and then the solvent was removed under reduced pressure. The residue was recrystallized from ethyl acetate to give XV (0.1 g.) as reddish prisms, m. p.

183～184°C, 0.1 g.

Found: C, 65.46; H, 5.06; N, 8.93. Calcd. for $C_{17}H_{16}O_4N_2$: C, 65.37; H, 5.16; N, 8.97%.

The Methylation of 8, 8-Dicyano-2, 3-dihydroxy-4-isopropylheptafulvene (XIII) with Dimethyl Sulfate.—To a solution of XIII (0.45 g.) in 2 N sodium hydroxide (6 ml.) dimethyl sulfate (1.6 g.) was added, and then the mixture was stirred at room temperature for 6 hr. The crystals which separated out were filtered and recrystallized from methanol to give XVI as yellow prisms, m. p. 254～255°C (decomp.), 0.4 g.

Found: C, 69.34; H, 5.86; N, 11.79. Calcd. for $C_{14}H_{14}O_2N_2$: C, 69.40; H, 5.83; N, 11.56%.

The treatment of XVI with diazomethane in ether afforded XIV. When XVI was heated in acetic anhydride, the acetyl derivative XVII was yielded as reddish orange needles, m. p. 176～178°C.

Found: C, 67.75; H, 5.47; N, 9.55. Calcd. for $C_{16}H_{16}O_3N_2$: C, 67.59; H, 5.67; N, 9.85%.

The authors wish to take this opportunity to express their sincere gratitude to the Ministry of Education and to the Sankyo Co., Ltd., for their financial support. They also wish to thank the Misses Yoko Endo and Yukiko Endo of this Institute for carrying out the microanalyses.

The Chemical Research Institute of Non-Aqueous Solutions
Tohoku University
Katahira-cho, Sendai

Heptafulvenes. III.[1] *The Synthesis of 8-Cyanoheptafulvenes*[2]

By Yoshio KITAHARA, Kozo DOI and Yoshio SATO

(Received April 24, 1964)

Heptafulvene (I), which is a theoretically-interesting non-benzenoid aromatic hydrocarbon, was synthesized and found to be an extremely unstable liquid.[3] It was discovered,[1,4] however, that its derivatives substituted by two electronegative groups at the 8-position, i. e., 8, 8-dicyano- (II: X=CN) and 8-cyano-8-ethoxycarbonylheptafulvene (II: X=CO_2Et), are fairly stable.

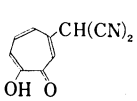
In a previous paper,[5] we have reported that the reaction product of 3-iodotropolone (III) with sodiomalononitrile in liquid ammonia is not a tropolone (IV) but its enolic isomer, 8, 8-dicyano-2, 3-dihydroxyheptafulvene (V). Similar results were also found in the case of two isopropyl derivatives of III.[1]

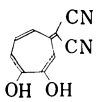


I

II

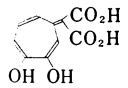


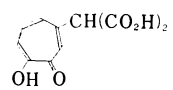




III: X=H IV V
IX: X=CH_3
X: X=i-C_3H_7

On the other hand, an acid hydrolysis product of V was also found not to be a heptafulvene (VI) but a tropolone derivative (VII).[1] Therefore, it seemed interesting to study keto-enol tautomerisms between tropolone derivatives possessing a side-chain with active hydrogen at the α-position and the corresponding heptafulvenes. We have found that cyanomethyltropolones gave diacetyl derivatives of the heptafulvene-type on acetylation:





VI VII

Details will be described in this paper.

When 3-iodotropolone (III) reacted with sodioacetonitrile in liquid ammonia, 4-cyanomethyltropolone (VIII) was obtained in a 26 per cent yield. Its structure was confirmed by direct comparison with the dehydration product of 4-carbamoylmethyltropolone.[6] It has been reported that a similar reaction of

1) Part II of this series: Y. Kitahara, K. Doi and T. Kato, This Bulletin, **37**, 1750 (1964).

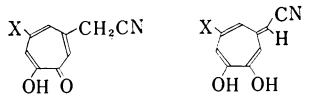
2) This work was presented at the 14th Annual Meeting of the Chemical Society of Japan, Tokyo, April, 1961.

3) W. von E. Doering and D. W. Wiley, *Tetrahedron*, **11**, 183 (1960).

4) T. Nozoe, T. Mukai, K. Osaka and N. Shishido, This Bulletin, **34**, 1384 (1961).

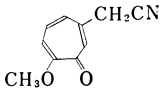
5) Y. Kitahara, K. Doi and T. Kato, This Bulletin, **37**, 1747 (1964).

6) T. Nozoe, Y. Kitahara, K. Doi, M. Funamizu and T. Terasawa, *Bull. Chem. Research Inst. Non-Aqueous Solutions, Tohoku Univ.*, **10**, 199 (1961).

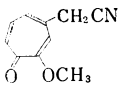


VIII: X=H
XI: X=CH_3
XII: X=*i*-C_3H_7

XIII



XIV



XV

chlorobenzene and acetonitrile afforded diphenylacetonitrile other than phenylacetonitrile,[7] but in this case no by-products other than VIII were isolated. In a similar manner, alkyl derivatives (IX and X) of 3-iodotropolone also gave corresponding cyanomethyltropolones (XI and XII).

Figure 1 indicates the ultraviolet absorption curves which are characteristic of other alkyltropolones, while Table I shows several principal maxima of the infrared absorption spectra of the cyanomethyltropolones.

This spectral evidence suggests that the above reaction products of iodotropolones and sodioacetonitrile are tropolone derivatives and that they cannot be their enolic forms (XIII). 4-Cyanomethyltropolone (VIII) afforded only

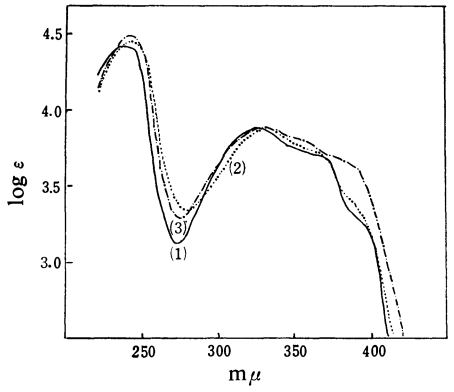


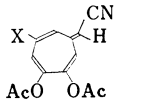
Fig. 1. Ultraviolet absorption spectra of
(1) 4-cyanomethyl-(VIII),
(2) 4-cyanomethyl-6-methyl-(XI), and
(3) 4-cyanomethyl-6-isopropyl-(XII) tropolone.

TABLE I. INFRARED ABSORPTION MAXIMA OF 4-CYANOMETHYLTROPOLONES (cm^{-1})

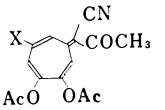
	ν_{OH}	$\nu_{C\equiv N}$	$\nu_{C=O}$	$\nu_{C=C}$	δ_{CH_2}
VIII	3200	2255	1613	1553	1410
IX	3200	2260	1613	1546	1413
XII	3150	2255	1608	1535	1420

two kinds of crystalline monomethoxytropone derivatives on treatment with diazomethane. The structures of these products, 6-cyanomethyl-2-methoxy- (XIV) and 4-cyanomethyl-2-methoxytropone (XV), were determined by a comparison of their absorption peaks based on the CH out-of-plane vibration of the infrared spectra with those of other known substituted tropones[8]: the peaks at 778 (XIV) and 828 (XV) correspond to those at 776 of 2-methoxy-6-methyltropone and 822 cm^{-1} of 2-methoxytropone respectively.

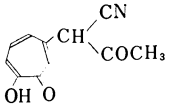
On the other hand, we have found that cyanomethyltropolones yielded products of the heptafulvene-type on acetylation. When 4-cyanomethyltropolone (VIII) was treated in pyridine with acetic anhydride at room temperature, 8-cyano-2, 3-diacetoxyheptafulvene (XVI) and 8-acetyl-8-cyano-2, 3-diacetoxyheptafulvene (XVII) were obtained. The structures of these products were easily drawn out from their analytical values, ultraviolet (Figs. 2 and 3) and infrared spectra (Table II), and hydrolyzed to the starting material VIII under mild conditions.



XVI: X=H
XIX: X=CH_3
XXI: X=*i*-C_3H_7



XVII: X=H
XX: X=CH_3



XVIII

An attempted further acetylation of the diacetyl compound XVI to the triacetyl derivative (XVII) was found to result in only the recovery of the starting material. In the course of the formation of XVII from VIII, there may exist an intermediate, such as XVIII or its enol isomer, which has not yet been isolated.

The similar acetylation of two other alkyl-4-cyanomethyltropolones afforded also similar results: XI yielded both diacetyl (XIX) and triacetyl (XX) derivatives, but XII only a diacetyl compound (XXI). The ultraviolet absorption spectra of these heptafulvenes are shown in Figs. 2 and 3.

Table II indicates some principal maxima of

7) F. W. Bergstrom and R. Agostinho, *J. Am. Chem. Soc.*, 67, 2152 (1945).

8) K. Takase, M. Yasunami and T. Nozoe, to be published.

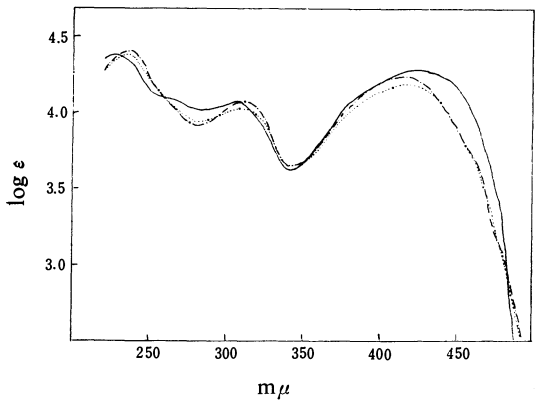


Fig. 2. Ultraviolet absorption spectra of 8-cyanoheptafulvenes (XVI, ——; XIX, ------; XXI, —·—·—).

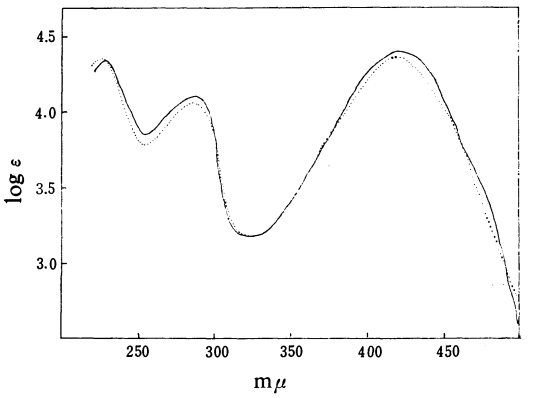


Fig. 3. Ultraviolet absorption spectra of 8-acetylheptafulvenes (XVII, ——; XX, ------).

TABLE II. PRINCIPAL MAXIMA OF THE INFRARED SPECTRA OF 8-CYANOHEPTAFULVENES (cm^{-1})

	$\nu_{C\equiv N}$	$\nu_{C=O}$	$\nu_{C=O}$	$\nu_{C=C}$	ν_{C-O}
XVI	2210	1760		1640	1210
XIX	2200	1762		1635	1188
XXI	2200	1766		1635	1195
XVII	2200	1775	1650	1615	1215
XX	2195	1770	1650	1640	1200

the infrared absorption spectra of these heptafulvenes. The bands based on the stretching vibration of nitrile groups correspond to the conjugated cyano groups and satisfy their presumed structures. The maxima in the second and fifth columns have strong intensities and can be assigned to acetate groups. The bands at 1650 cm^{-1} of XVII and XX, which are sharp and moderately strong, probably indicate the conjugated ketones. The maxima in the fourth column, based on carbon-carbon double bonds, are medium or weak and are distinguishable from those at 1650 cm^{-1}. Bands corresponding to these have also been discussed in 8, 8-dicyanoheptafulvenes,[1,5] fulvene[9] and 6, 6-dialkylfulvenes.[10] The band of heptafulvene itself has been reported to appear at 1585 cm^{-1} (strong).[3]

Experimental

The ultraviolet absorption spectra in methanol were measured with a Hitachi model EPU-2 recording spectrometer. The infrared spectra were measured with a Perkin-Elmer model 21 infrared spectrometer (rock salt prism and potassium bromide pellets). All melting points are uncorrected.

4-Cyanomethyltropolone (VIII).—Into a sodium amide solution prepared from liquid ammonia (400 ml.) and sodium (9.2 g.) acetonitrile (7 g.) at −50°C was stirred. After 10 min., iodotropolone (III, 25 g.) was added to the above mixture, and then it was stirred while the ammonia was refluxed at atmospheric pressure for 2 hr. After ammonium chloride was added, ammonia was evaporated. The residue was dissolved in water (500 ml.), and the insoluble matter was filtered off. The filtrate was acidified and extracted with ethyl acetate (500 ml.). After the solvent had been removed, the residue was recrystallized from a mixture of benzene and methanol, giving VIII as colorless scales; m. p. and mixed m. p.[6] 134~135°C; 4.2 g. (26% yield).

4-Cyanomethyl-6-methyltropolone (XI). — This was prepared from IX (26.2 g.) under the same conditions as those used for III. Recrystallization from ethyl acetate gave XI (2.6 g., 15%) as colorless prisms; m. p. 154~155°C.

Found: C, 68.72; H, 5.07; N, 8.01. Calcd. for $C_{10}H_9O_2N$: C, 68.56; H, 5.18; N, 8.00%.

4-Cyanomethyl-6-isopropyltropolone (XII).—This was prepared from X (29 g.) under the conditions used for III. Recrystallization from benzene gave XII as colorless needles; m. p. 83~84°C; 8.2 g. (40%).

Found: C, 70.67; H, 5.78; N, 6.66. Calcd. for $C_{12}H_{13}O_2N$: C, 70.91; H, 6.45; N, 6.89%.

XII (0.19 g.) in 75% sulfuric acid (2 ml.) was heated at 150°C for 1 hr., diluted with water, and extracted with ethyl acetate. After the solvent had been removed, the residue was recrystallized from petroleum ether, giving 6-isopropyl-4-methyltropolone; m. p. and mixed[1] m. p. 42~43°C.

The Methylation of 4-Cyanomethyltropolone (VIII). — The addition of an ethereal solution of diazomethane to a cooled suspension of VIII (2 g.) in methanol (5 ml.) caused a violent evolution of gas, and the mixture became a clear solution. When the colorless crystals which separated out soon were filtered, a crude mixture of methoxytropones, m. p. 105~115°C, was obtained (1.9 g.). Fractional crystallization from ethyl acetate gave 6-cyanomethyl-2-methoxytropone (XIV) as colorless prisms from the less soluble portion, m. p. 130~131°C; 0.7 g.; Found: C, 68.66; H, 4.85; N, 8.07. Calcd. for $C_{10}H_9O_2N$: C, 68.56; H, 5.18;

9) J. Theic and J. Wiemann, *Bull. soc. chim. France*, **1956**, 177.
10) J. H. Day and R. Jennkins, *J. Org. Chem.*, **23**, 2039 (1958).

N, 8.00%. λ_{max} mμ (log ε) : 237 (4.42), 320 (3.93). ν_{max} cm^{-1} : 2250, 1630, 1410, 778 ; and 4-cyanomethyl-2-methoxytropone (XV) as colorless needles from the more soluble portion, m. p. 139~140°C ; 0.9 g.; Found : C, 68.64 ; H, 4.83 ; N, 7.98%. λ_{max} mμ (log ε) : 240 (4.43), 320 (3.89). ν_{max} cm^{-1} : 2258, 1630, 1425, 828.

The Acetylation of 4-Cyanomethyltropolone (VIII).—To a solution of VIII (0.2 g.) in pyridine (3 ml.), acetic anhydride (0.5 g.) was added. The mixture was stirred at room temperature for 3 hr., and then acidified with cold dilute hydrochloric acid and extracted with ethyl acetate. The addition of benzene to the residue of the evaporation of the solvent separated out a yellowish solid. Filtration and recrystallization from acetone gave 2,3-diacetoxy-8-cyanoheptafulvene (XVI) as yellow needles ; m. p. 172°C ; 0.05 g.

Found : C, 63.95 ; H, 4.20 ; N, 5.64. Calcd. for $C_{13}H_{11}O_4N$: C, 63.67 ; H, 4.52 ; N, 5.71%.

The benzene filtrate, from which XVI had been removed, was chromatographed on alumina using benzene, and red effluents were collected. The benzene was removed from the effluent, and the residue was recrystallized from a mixture of benzene and cyclohexane to give 8-acetyl-8-cyano-2,3-diacetoxyheptafulvene (XVII) as reddish orange needles ; m. p. 154°C ; 0.1 g.

Found : C, 62.41 ; H, 4.40 ; N, 4.99. Calcd. for $C_{15}H_{13}O_5N$: C, 62.71 ; H, 4.56 ; N, 4.88%.

Further reaction of XVI with acetic anhydride in pyridine resulted in the recovery of only the starting material.

The Alkaline Hydrolysis of XVI and XVII.—XVI (0.12 g.) in 2 N sodium hydroxide (5 ml.) was heated at 50°C for 20 min., and then the solution was acidified with dilute hydrochloric acid, giving 4-cyanomethyltropolone (VIII). The hydrolysis of XVII under the same conditions resulted in the formation of VIII.

The Acetylation of 4-Cyanomethyl-6-methyltropolone (XI).—A solution of XI (0.35 g.), pyridine (4 ml.) and acetic anhydride (0.6 g.) was stirred at room temperature for 3 hr., neutralized by dilute hydrochloric acid, and then extracted with ethyl acetate. The evaporation of the solvent and fractional recrystallization from ethyl acetate gave the following products, which are arranged in the order of increasing solubility to the solvent :

i) 8-Acetyl-8-cyano-2,3-diacetoxy-5-methylheptafulvene (XX) ; m. p. 151~152°C ; reddish orange needles ; 0.2 g.

Found : C, 63.80 ; H, 4.56 ; N, 4.93. Calcd. for $C_{16}H_{15}O_5N$: C, 63.78 ; H, 5.02 ; N, 4.65%.

ii) 8-Cyano-2,3-diacetoxy-5-methylheptafulvene (XIX) ; m. p. 150~151°C ; yellow prisms ; 0.08 g.

Found : C, 65.17 ; H, 5.03 ; N, 5.54. Calcd. for $C_{14}H_{13}O_4N$: C, 64.86 ; H, 5.05 ; N, 5.40%.

iii) 4-Cyanomethyl-6-methyltropolone acetate ; m. p. 118~119°C ; colorless needles ; 0.03 g.

Found : C, 66.20 ; H, 5.09 ; N, 6.69. Calcd. for $C_{12}H_{11}O_3N$: C, 66.35 ; H, 5.10 ; N, 6.45%. λ_{max} mμ (log ε) : 235 (4.43), 318 (3.90). ν_{max} cm^{-1} : 2255, 1755, 1615, 1406.

The Acetylation of 4-Cyanomethyl-6-isopropyltropolone (XII).—A solution of XII (0.38 g.), pyridine (4 ml.) and acetic anhydride (0.6 g.) was stirred at room temperature for 3 hr. and then treated in the same manner as was used in the case of VIII. After recrystallization from ethyl acetate, 8-cyano-2,3-diacetoxy-5-isopropylheptafulvene (XXI) was obtained as yellow needles ; m. p. 154~155°C ; 0.16 g.

Found : C, 67.10 ; H, 5.74 ; N, 5.05. Calcd. for $C_{16}H_{17}O_4N$: C, 66.88 ; H, 5.96 ; N, 4.88%.

The authors wish to take this opportunity to express their gratitude to the Ministry of Education and to the Sankyo Co., Ltd., for their financial support. They wish also to thank to the Misses Yoko Endo and Yukiko Endo of this Institute for carrying out the microanalyses.

The Chemical Research Institute of Non-Aqueous Solutions
Tohoku University
Katahira-cho, Sendai

*Studies of the Configuration and Conformation of Vinyl-type Polymers. III. The Temperature Dependence of the Infrared Spectra of 2,4-Dichloropentane as a Model Compound of Polyvinyl Chloride**

By Kazuyoshi IIMURA, Takatsugu HAMA, Teruo SHIBUYA and Masatami TAKEDA

(Received April 27, 1964)

In a previous study[1] of the temperature dependence of the infrared spectra of polyvinyl chloride (PVC) in cyclohexanone solution, we found that the intensity ratio of the 696 cm^{-1} band to the 616 cm^{-1} band depends on the temperature, and that this temperature dependence increases with an increase in the syndiotactic configuration of the PVC chain. The temperature dependence has been interpreted as being due to the energy differences among the conformational isomers in the syndiotactic sequences of the PVC chain. Recently, Germar et al. have made a similar study of PVC using the CH_2 bending bands[2] at 1428 and 1432 cm^{-1} and the C–Cl stretching bands[3] near 600~700 cm^{-1}, and have determined its syndiotacticity.

Shimanouchi and Tasumi,[4] however, have studied the infrared spectra of *meso*- and *dl*-2, 4-dichloropentanes as a model compound of PVC and have suggested that the *dl*-compound, which has the same configuration as the syndiotactic PVC, exists only in one stable conformation in which the C–C chain takes the extended T-T form. This suggests that the syndiotactic sequence in PVC might have the only stable conformation in solution; if so, our previons explanation would be invalid, as well as the explanation by Germar et al.

In order to obtain further information on this problem, we have studied the infrared spectra of the *moso*- and *dl*-compounds in various physical states.

Experimental

2, 4-Dichloropentane was prepared from acetylacetone; 2, 4-pentanediol was prepared[5] by the catalytic hydrogenation of acetylacetone with Raney nickel in an autoclave (H_2 pressure: 125 atm.; reaction temperature: 115~125°C; reaction time: 150 min.), and it was converted to 2, 4-dichloropentane by reaction with thionylcloride.[6] The boiling point range of the product was 142~144°C. For the separation of the *meso*- and *dl*-compounds, a Beckman Megachrom preparative gas chromatograph has been used. The purity of the separated compound was certified by infrared inspection.

A Hitachi EPI-2-type double-beam spectrophotometer equipped with a KBr prism was used for the measurement of the infrared spectra. The observation of the solution spectra and their temperature dependence was carried out by using a closed-type cell mounted in a heating device. In order to aid the compensation of absorptions caused by the solvent, a variable-thickness-type cell was inserted in the path of the reference beam. The absorption spectra in a gaseous state were observed with a gas cell 7 cm. in optical path length and with a heating device.

The absorption spectrum in the region of the C–Cl stretching vibrations, which is sensitive to the conformational changes, was also examined.

Results and Discussion

The infrared spectra of the *meso*- and *dl*-compounds in the cyclohexanone solutions at room temperatures are shown in Fig. 1. The results are very similar to the infrared spectra of the pure liquids observed by Shimanouchi and Tasumi;[4] the *meso*-compound has two absorption bands at 683 and 616 cm^{-1}, and the *dl*-compound also has two absorption bands at 629 and 607 cm^{-1}. On the basis of the empirical rules concerning the relation between the frequencies of the C–Cl stretching bands of some chlorohydrocarbons and their geometrical conformations, Shimanouchi and Tasumi[4] have concluded that the *dl*-compound has only one stable conformation in which the C–C chain takes the T-T conformation, and that the *meso*-compound is stable in the conformation of the T-G or G'-T with respect to the C–C

* A part of this work was presented on the 16th Annual Meeting of the Chemical Society of Japan, Tokyo, April, 1963, and at the 12th Symposium on Macromolecular Chemistry, Nagoya, 1963.

1) M. Takeda and K. Iimura, *J. Polymer Sci.*, **57**, 383 (1962).

2) H. Germar, K. H. Hellwege and U. Johnsen, *Makromol. Chem.*, **60**, 106 (1963).

3) H. Germer, *Kolloid-Z.*, **193**, 25 (1963).

4) T. Shimanouchi and M. Tasumi, *Spectrochim. Acta*, **17**, 755 (1961).

5) M. Shiraki and H. Nagai, *J. Chem. Soc. Japan, Pure Chem. Sec. (Nippon Kagaku Zasshi)*, **81**, 976 (1960).

6) S. Okumura, "Jikken Yuki Kagaku" (Experiment in Organic Chemistry), I, Kyōritsu-Shuppan, Tokyo (1953), p. 158.

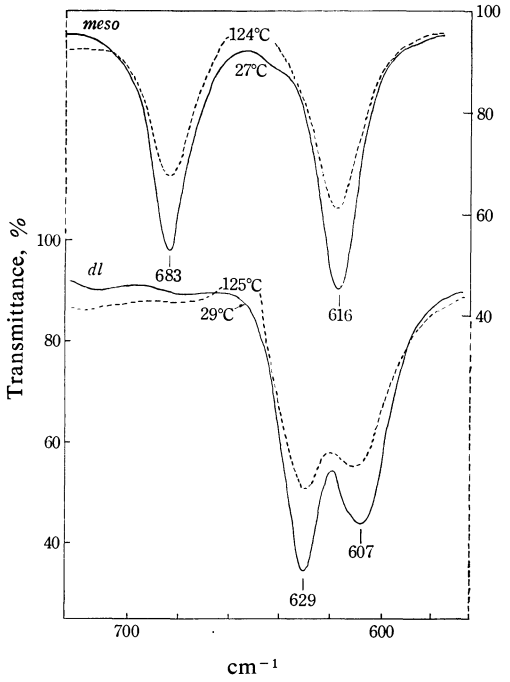


Fig. 1. The infrared spectra of the *meso*- and the *dl*-compounds in a cyclohexanone solution at the various temperatures.

main chain, as Fig. 2 shows. Since the T-G conformation is a mirror-image of the G'-T conformation, both conformations should give the same spectra. The observed infrared spectra of the *dl*- and the *meso*-compounds in the cyclohexanone solutions are caused by the structures of the T-T and the T-G or G'-T conformations respectively.

The purpose of this investigation is to investigate the possible existence of the other species of the rotational isomer of both compounds in a cyclohexanone solution at higher temperatures. Especially, the G'-G' conformation for the *dl*-compound may be expected to appear in the solution at higher temperatures, because the potential energy of the G'-G' conformation would be the next lowest after that of the T-T conformation.[3,8]

However, the infrared spectra of both the *dl*- and the *meso*-compounds in solution at a temperature near 120°C are identical with the respective spectra at room temperature, as is shown in Fig. 1. In the gaseous state, none of the new bands which could be expected from the new conformational isomers other than the T-T conformation in the *dl*-compound can be observed, even in the higher temperatures near 170°C. For the *meso*-compound, in the

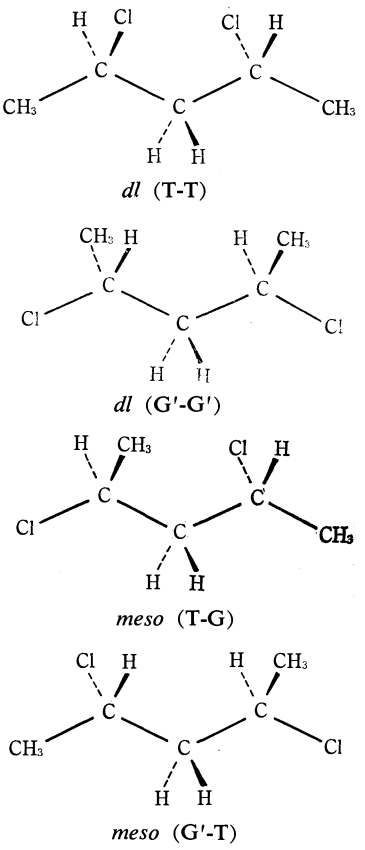


Fig. 2. The probable conformations in the *meso*- and the *dl*-compounds.

gaseous state the infrared spectrum at 164°C does not differ from that at room temperature. These results are shown in Fig. 3.

These facts show that the G'-G' conformation in the *dl*-compound may be rejected because the band centered near 690 cm^{-1}, which is expected from the stretching vibration of the C–Cl bond trans to the adjacent C–C bond in the G'-G' conformation, does not appear in the spectra of the *dl*-compound. Thus, it may be concluded that the sole structure which is stable in the *dl*-compound in the cyclohexanone solution is the structure of the T-T extended conformation in the temperature range of this investigation, as in the previous examination of the solution spectra of PVC. For the *meso*-compound, no stable structures other than the T-G or G'-T conformation could be found in the same temperature range. Consequently, it is impossible to explain the temperature dependence of the intensities of the C–Cl stretching bands of the solution spectra of PVC as being due to the rotational isomerism of the polymer chain so long as 2,4-dichloropentanes are applied as model compounds of PVC.

7) T. Shimanouchi, S. Tsuchiya and S. Mizushima, *Kōbunshi*, **8**, 202 (1959).
8) J. W. L. Fordham, *J. Polymer Sci.*, **39**, 321 (1959).

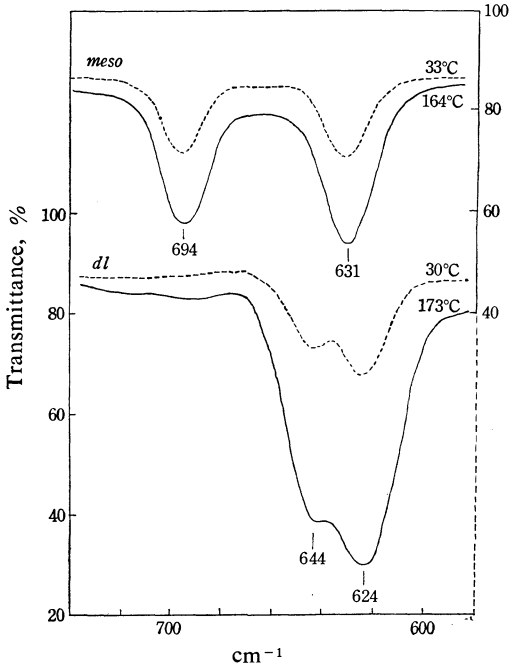


Fig. 3. The infrared spectra of the *meso*- and the *dl*-compounds in the gaseous state at the various temperatures.

In order to obtain further information on the temperature dependence of the intensities of the C–Cl stretching bands of PVC, the infrared spectra of a mixture of 1 cc. of the *meso*-compound and 2.4 cc. of the *dl*-compound (a model of 70% syndiotactic PVC) was investigated in the cyclohexanone solution. In the spectrum of the mixture, the highest frequency and the second highest frequency are caused by the *meso*- and *dl*-compounds respectively. The band at 616 cm^{-1} of the *meso*-compound and the band at 607 cm^{-1} of the *dl*-compound are superposed on the band centered to 612 cm^{-1}. As is shown in Fig. 4, the intensity ratio, D_{612}/D_{683}, of the mixture depends only slightly on the temperature, while the corresponding intensity ratio, D_{616}/D_{696}, of PVC depends strongly on the temperature. In the case of the isolated compound, the relative intensity of the two C–Cl stretching bands of the *meso*-compound only slighty depends on the temperature. However, that of the *dl*-compound shows a remarkable dependence on temperature, as Fig. 5 shows. The change in the intensity ratio D_{612}/D_{683} in the solution spectra of the mixture with heating is dut to the contribution from the temperature effect on the intensities of the absorption bands of the *dl*-component. However, the reason why the greater temperature effect can be found in the *dl*-compound can not be determined.

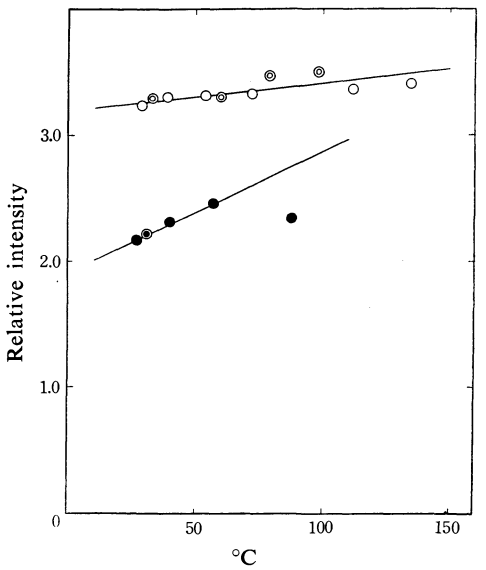


Fig. 4. The temperature dependence of the relative intensities of the C–Cl stretching bands of the *dl-meso* mixture and of the syndiotactic PVC (polymerized at −60°C) in cyclohexanone solutions. The double circles denote the observed points obtained on cooling.

-○- D_{612}/D_{683}, *dl-meso* mixture (*dl* 70%)
-●- D_{616}/D_{696}, PVC polymerized at −60°C

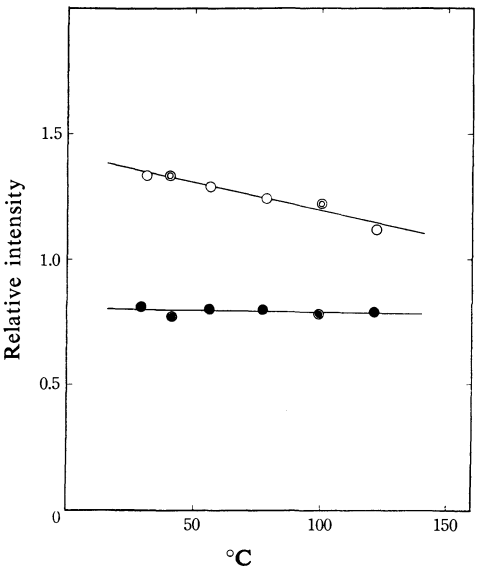


Fig. 5. The temperature dependence of the relative intensities of the two C–Cl stretching bands in the *dl*- and the *meso*-compounds in cyclohexanone solutions. The double circles; as for Fig. 4.

-○- *dl*, D_{629}/D_{607}
-●- *meso*, D_{683}/D_{616}

The remarkable temperature dependence of the solution spectra of PVC may probably be ascribed to the effect of the interchain interaction among the polymers. This speculation is consistent with the result reported by Asahina and Enomoto;[9] in a cyclohexanone solution, the intensity of the 648 cm^{-1} band of PVC has a tendency to decrease with the concentration decrease of the syndiotacticity. In a rather concentrated solution, it seems likely that the longer syndiotactic sequences of the polymer chain lie in a quasi-crystalline state, in which the conformation of the polymer chain may be in the extended T-T form. As Fig. 6 shows, this is confirmed by the fact that, in the solution spectra, the intensity of the 648 cm^{-1} band to which the crystalline syndiotactic parts contribute[10] becomes stronger as the polymerization temperature of the polymer is lowered. Figure 7 gives the intensity change with the heating of the C–Cl stretching bands of the syndiotactic PVC (polymerized at −60°C) in the cyclohexanone solution. With an increase in the temperature, the desolvation of the quasi-crystalline parts in the solution occurs and leads to a decrease in the relative intensity ratio, D_{648}/D_{696}, accompanied by an increase in the relative intensity ratio, D_{616}/D_{696}. In the later intensity ratio, the 616 cm^{-1} band has been assigned to the amorphous syndiotactic part.[10]

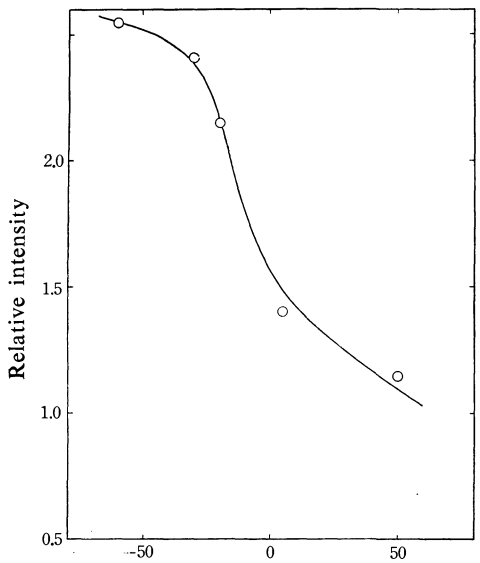


Fig. 6. The relation between the relative intensities of the C-Cl stretching bands of PVCs in cyclohexanone solutions at 30~35°C, against the polymerization temperature of the polymers. -○- D_{648}/D_{696}

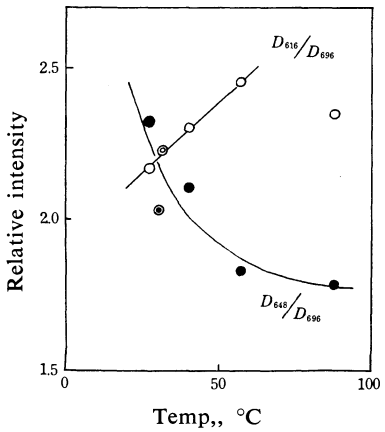


Fig. 7. The temperature dependence of the relative intensities of the C-Cl stretching bands of the syndiotactic PVC (polymerized at −60°C) in a cyclohexanone solution. The double circles; as for Fig. 4.

In the light of the above experimental results, we have come to the following conclusions. Firstly, if the C–Cl stretching bands fall in different frequency regions depending on the two substituents which are trans to the Cl atom across the two adjacent C–C bonds, as has been pointed out by Krimm,[11] a compound which at least consists of the three monomeric units of PVC must be employed as a model compound of PVC. Secondly, the temperature dependence of the absorption intensity in the spectra of PVC cannot be directly related to the rotational isomerism of the polymer chain. Moreover, the intensity of the C–Cl stretching bands of the syndiotactic and the isotactic sequences of PVC may be differently affected by the temperature.

In addition to the results given by us[1] and Germar[3], such a temperature effect on the intensity of the C–Cl stretching band and the effect of the interchain interactions among the polymers must be taken into account in the interpretation of the temperature dependence on the infrared spectra of PVC.

We are indebted to Dr. Yōichirō Mashiko and Mr. Hiroshi Tomita of the Government Industrial Research Institute of Tokyo for letting us use the Beckman Megachrom of that Institute.

Department of Chemistry
Faculty of Science
Tokyo College of Science
Kagurazaka, Shinjuku-ku, Tokyo

9) M. Asahina and S. Enomoto, *J. Chem. Soc. Japan, Pure Chem. Sec. (Nippon Kagaku Zasshi)*, **81**, 1011 (1960).
10) M. Tasumi and T. Shimanouchi, *Spectrochim. Acta*, **17**, 731 (1961).
11) S. Krimm, International Symposium on Molecular Structure and Spectroscopy, Tokyo, Sept., 1962.

*Nuclear Magnetic Resonance Spectra of Polymethyl Methacrylate in Solution. II. The Calibration of the Infrared Absorption Method and Some Applications to the Study of the Polymerization Mechanism**

By Yoshinori KATO, Haruaki WATANABE and Atsuo NISHIOKA

(Received May 12, 1964)

In the preceding paper,[1] it was shown that the degree of the stereoregularity of polymethyl methacrylate could be determined from the NMR spectrum by analyzing three peaks due to α-methyl protons. The proportions of their areas were represented in the ternary diagram with a single point. For free radical polymers, the plots were found to be in good accordance with a relationship that was represented by a unique curve in the diagram. It was also found that the manner of the growth of the molecular chains in free radical polymerization could be described by a single parameter, p, which depends only upon the polymerization temperature. On the other hand, polymers prepared in anionic polymerization exhibited quite different stereochemical configurations from those obtained in free radical polymerization, depending on the initiators employed.

It is the purpose of this paper to extend our method further and to apply it, as far as possible, to the investigation of the anionic polymerization mechanisms. As a matter of convenience, the infrared method[2] calibrated by our NMR method has been frequently employed for the measurement of the stereoregularity. The same notations as have been discussed in the previous paper will be used here.

Experimental

The preparation of samples and the NMR spectra have already been described in the preceding paper.[1] The infrared spectra were observed with a Hitachi EPI-2 infrared spectrometer. In order to improve the reproducibility of the results, the sample films were made on glass plates from a benzene solution by evaporating the solvent. So far as we know, benzene is the best solvent to use to obtain sample films uniform in thickness. Two pairs of bands of the infrared spectra, i. e., the 1063 cm^{-1} and 1393 cm^{-1} and the 749 cm^{-1} and 757 cm^{-1} bands, were used to estimate the fractions of the *S*- and *I*-parts of the sample respectively.[2,3] The rest was taken to be the *D*-part. The estimations were based on a quantitative curve which had been obtained through the analysis of mixtures of two samples. The infrared spectrum of a "stereoblock polymer" is exactly the same as that of a mixture of isotactic and syndiotactic polymers if the proportions of their quantities are appropriately chosen. Therefore, two standard samples were employed to fix the quantitative curve; one was a polymethyl methacrylate prepared with benzoyl peroxide at −35°C, and the other was a sample obtained with phenylmagnesium bromide at 20°C. The stereochemical configurations of these samples were determined by the NMR method. For the former, $s=0.85$ and $h=0.13$, while for the latter almost all of the monomer placements in the molecular chains were recognized as isotactic. Taking account of these findings, the samples were mixed in various proportions to

TABLE I. COMPARISON OF THE TACTICITY MEASUREMENTS OF POLYMETHYL METHACRYLATE BY TWO METHODS

Polymerization temp., °C	NMR method		IR method	
	h	*s*	*h*	*s*
−35*	0.13	0.85	0.13	0.85
−25	0.14	0.84	0.15	0.83
−15	0.14	0.83	0.17	0.81
0	0.18	0.77	0.19	0.78
20	0.19	0.77	0.23	0.74
40	0.21	0.75	0.26	0.70
70	0.26	0.68	0.29	0.65
100	0.28	0.67	0.30	0.62
150	0.41	0.54	0.37	0.55
—**	0.14	0.40	0.14	0.38

* One of the two standard samples employed to calibrate the IR method.

** Polymer prepared with Grignard's reagent as a catalyst; other samples were made in a free radical polymerization.

* Part of this paper was presented at the Annual Meeting of the Physical Society of Japan, Matsumoto, May, 1961. This paper was also read at the 1st Symposium on "The Application of High Resolution Nuclear Magnetic Resonance Spectroscopy to Chemistry," Tokyo, November, 1961.

1) Y. Kato and A. Nishioka, This Bulletin, 37, 1614 (1964).

2) H. Watanabe, Y. Kato and A. Nishioka, *J. Chem. Soc. Japan, Ind. Chem. Sec.* (*Kogyo Kagaku Zasshi*), 65, 270 (1962).

3) U. Baumann, H. Schreiber and K. Tessmar, *Makromol. Chem.*, 36, 81 (1960).

obtain the infrared spectra. Once the quantitative curve is fixed, the estimation of the degree of stereoregularity for any polymethyl methacrylate becomes possible. Part of the results, together with those obtained by the NMR method, are given for ready comparison in Table I. There is practical agreement between these two sets of results. Therefore, they will be used without distinction throughout the rest of this paper.

The extraction of the sample with acetone was carried out at room temperature in order to measure the stereoregularities of both the extract and the residue. If any difference is found between them, the process of polymerization will consist of more than one mechanism.

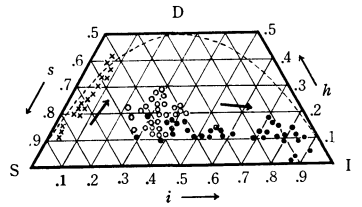


Fig. 1. Ternary diagram representing the stereoregularities of polymethyl methacrylates prepared with free radical initiators (×), and anionic initiators: R_2Mg (○), and RMgBr (●). Two bold arrows indicate how the stereoregularities vary as the polymerization temperature increases.

Results

To examine the habit of distribution in the ternary diagram, many samples, prepared with different catalysts at various polymerization temperatures, were used. The results are shown in Fig. 1. Most of them were obtained by the infrared method described above. The types of catalyst for our anionic polymerization of methyl methacrylate may be represented as RMgBr and R_2Mg, where R indicates an alkyl group, and so on. For our experiments, ethyl, *n*-butyl, *n*-propyl, *n*-amyl, *n*-heptyl and phenyl groups have been taken as R in RMgBr, and, again, ethyl, *n*-butyl, isobutyl, phenyl and cyclohexyl groups as R in R_2Mg.

From Fig. 1 it may be seen that the polymer prepared with an R_2Mg-type catalyst, especially at 0°C and below, seems to have a rather constant stereochemical configuration regardless of the polymerization temperature and the species of R. As compared with the above polymer, the stereochemical configuration of the polymer with RMgBr as a catalyst is more isotactic and varies to a considerable degree with the polymerization temperature. The bold horizontal arrow in Fig. 1 indicates how the configuration changes as the polymerization temperature increases from −78°C to 20°C.

It is not correct to base discussions of the mechanism of polymerization upon the apparent stereochemical configuration of the polymer chains if the apparent configuration is not homogeneous. In fact, the extraction of the samples with acetone frequently resulted in two components with different stereoregularities. For polymers made with R_2Mg as the catalyst, the extracted components include more *D*-units than the residues. On the other hand, samples with RMgBr as the catalyst seem to contain both isotactic (the extracts) and stereoblock (the residues) components. In Fig. 2 are collected the results of the extraction with acetone. As has been mentioned previously, a mixture of two components of different stereoregularities exhibits an average stereochemical configuration. This configuration can be represented, in terms of our ternary diagram, by the point which divides the distance between the two plots corresponding to the two components in the inverse ratio of each weight. Therefore, in order to discuss the mechanism of the polymerization, it is necessary to weigh both the extract and the residue separately. Otherwise we can not say which mechanism is more important in the course of polymerization. These average configurations are also shown in Fig. 2.

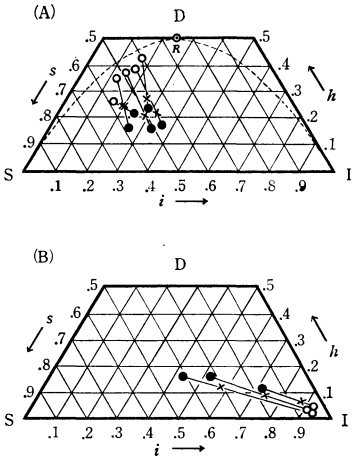


Fig. 2. Ternary representation of the stereoregularities of the acetone-extract (○) and the residue (●) of the samples: (A) with R_2Mg, at −50°C; (B) with ethylmagnesium-bromide; at −40, −20 and −10°C. The average configurations of unseparated samples are represented by the crosses, ×.

Statistical Treatment. — In the preceding paper, a simple statistical method was applied to some cases.

Here we will initially consider the concept of the Ising model, which has been used in formulating the statistical mechanics of the

linear chain.[4] In has also been applied in an extended way to a problem of the polymer chain by Chûjô and Miyake.[5] Since the proportions of *I*-, *D*- and *S*-units in the polymer chains are given through the analysis of the NMR spectrum, the statistical method can be applied to interpret any locus in the ternary diagram which corresponds to the change in stereoregularity of polymers with the polymerization temperature under the conditions of a definite type of catalyst. For free radical polymers, however, the situation is so simple that, on the basis of the statistics, we can discuss the mechanism of the polymerization itself.[1]

In order to cover all the distributions of the plots in the ternary diagram, two parameters must be introduced, because the degree of freedom of our data obtained from NMR measurements is two by nature; that is the proportions of stereoregularity of the three components, *i*, *h* and *s*, always satisfy the relationship;

$$i+h+s=1 \tag{1}$$

and, therefore, only two of them are independent.

We define a transition matrix as:

$$\boldsymbol{A}=\begin{array}{c} \\ 0 \\ 1 \end{array}\begin{array}{c} \begin{array}{cc} 0 & 1 \end{array} \\ \begin{pmatrix} BC & B^{1/2} \\ B^{1/2} & 1 \end{pmatrix} \end{array} \tag{2}$$

where B and C are the parameters whose physical meanings are to be clarified in connection with the polymerization reaction. The notations of rows and columns are the same as those defined with the sequence $\oplus\{A\}$, which represents the states of bonds. Let us denote the product of the matrix as:

$$\boldsymbol{A}^n=\overbrace{\boldsymbol{A}\times\boldsymbol{A}\times\cdots\cdots\times\boldsymbol{A}}^{n} \tag{3}$$

Then it can easily be shown that the element of $\boldsymbol{A}^n$, for example, in the upper row and the right column represents the possible transitions which begin with the state "0" and end in the state "1". The number of ways of transition equals 2^{n-1}, the same as the number of terms contained in the matrix element. The correspondence between the element expressed by B and C and the binary sequence of 0's and 1's, that is, the sequence $\oplus\{A\}$, is illustrated (for $n=10$) in the following example:

$$\begin{array}{cccccccc} 0 & 0 & 1 & 0 & 0 & 1 & 0 & \\ BC\times & B^{1/2}\times & B^{1/2}\times & BC\times & B^{1/2}\times & B^{1/2}\times & B^{1/2}\times & \\ 1 & 0 & 1 & 1 & : \oplus\{A\} & & & \\ \times B^{1/2}\times & B^{1/2}\times 1 & = & B^{11/2}C^2 & & & & \end{array}$$

From this, we may say that the matrix element increases by the factor of B when any 0 occurs in the sequence $\oplus\{A\}$, and by the factor of C only when a 0-0 pair is formed in it. The square root of B in Eq. 2 was taken so as to prevent the double counting of 0's. Since the above-mentioned 0-0 pair represents two isotactic placements among three consecutive monomer units, we may say that C in Eq. 2 has been introduced to denote a kind of longer-range effect which will occur within the three consecutive monomer units. As is always the case with very long chains,[6] we can close the sequence $\oplus\{A\}$ on the assumption that the first digit is equal to the last one. On this assumption, the off-diagonal elements of the matrix $\boldsymbol{A}^n$ vanish for the large integer, N. Our next problem is to calculate only the sum of the diagonal elements which will contain, on our assumption, all the possible sequences of $\oplus\{A\}$. In practice, however, the sequences are represented by two parameters, B and C, in the sum instead of by 0 and 1. We designate the sum by Z. Then, for instance, the number of 0's in a possible sequence of $\oplus\{A\}$ equals the weighted mean of all the terms in Z, each weighted by the power of B. Therefore, it can be obtained as the partial derivative of $\ln Z$ with respect to $\ln B$.

It is clear that:

$$Z=\text{Trace}\,(\boldsymbol{A}^n) \tag{4}$$

If we transform $\boldsymbol{A}$ into a diagonal matrix:

$$\boldsymbol{S}^{-1}\boldsymbol{A}\boldsymbol{S}=\begin{pmatrix}\lambda_1 & 0\\ 0 & \lambda_2\end{pmatrix} \tag{5}$$

then from Eq. 4 we get:

$$\begin{aligned} Z&=\text{Trace}\,((\boldsymbol{S}^{-1}\boldsymbol{A}\boldsymbol{S})^n)\\ &=\text{Trace}\begin{pmatrix}\lambda_1{}^n & 0\\ 0 & \lambda_2{}^n\end{pmatrix}=\lambda_1{}^n+\lambda_2{}^n \end{aligned} \tag{6}$$

Without the loss of generality, we may assume here that $\lambda_1 > \lambda_2$.

Finally, if the length, n, of the sequence $\oplus\{A\}$ tends to infinity, the smaller root, λ_2, may be neglected. That is:

$$Z\cong\lambda_1{}^n \tag{7}$$

The larger eigenvalue, λ_1, can be given from the secular equation:

$$\begin{vmatrix} BC-\lambda & B^{1/2} \\ B^{1/2} & 1-\lambda \end{vmatrix}=0 \tag{8}$$

4) H. A. Kramers and G. H. Wannier, *Phys. Rev.*, **60**, 252 (1941).

5) R. Chûjô and A. Miyake, *Busseiron-Kenkyu*, [2], **3**, 754 (1958), (in Japanese); A. Miyake, ibid., [2], **4**, 671 (1958); A. Miyake and R. Chûjô, *J. Polymer Sci.*, **46**, 163 (1960).

6) E. W. Montroll, *J. Chem. Phys.*, **9**, 26 (1941).

and the results is:

$$\lambda_1=\frac{BC+1+\sqrt{(BC-1)^2+4B}}{2} \tag{9}$$

From this equation, the probability of the occurrence of 0's in a possible sequences of $\oplus\{A\}$ is given by:

$$P_0=\frac{1}{n}\cdot\frac{\partial \ln Z}{\partial \ln B}=\frac{\partial \ln \lambda_1}{\partial \ln B}$$

$$=\frac{BC\sqrt{(BC-1)^2+4B}+BC(BC-1)+2B}{(BC+1)\sqrt{(BC-1)^2+4B}+(BC-1)^2+4B} \tag{10}$$

and that of 1's is found to be:

$$P_1=1-P_0$$

$$=\frac{\sqrt{(BC-1)^2+4B}-(BC-1)+2B}{(BC+1)\sqrt{(BC-1)^2+4B}+(BC-1)^2+4B} \tag{11}$$

In the sequence $\ominus\oplus\{A\}$, the relationships:

$$P_0=i+h/2 \tag{12}$$

and

$$P_1=s+h/2 \tag{13}$$

must hold, where i, h and s represent the probabilities of the occurrence of I-, D- and S-units respectively in the sequence $\ominus\oplus\{A\}$. Since

$$i=\frac{\partial \ln \lambda_1}{\partial \ln C}$$

$$=\frac{BC\sqrt{(BC-1)^2+4B}+BC(BC-1)}{(BC+1)\sqrt{(BC-1)^2+4B}+(BC-1)^2+4B} \tag{14}$$

therefore, from Eq. 10 to Eq. 13, it is found that:

$$s=\frac{\sqrt{(BC-1)^2+4B}-(BC-1)}{(BC+1)\sqrt{(BC-1)^2+4B}+(BC-1)^2+4B} \tag{15}$$

$$h=\frac{4B}{(BC+1)\sqrt{(BC-1)^2+4B}+(BC-1)^2+4B} \tag{16}$$

Here we notice that when the parameter C tends to unity, these results must become as follows:[7]

$$i=B^2/(B+1)^2 \tag{14'}$$

$$s=1/(B+1)^2 \tag{15'}$$

$$h=2B/(B+1)^2 \tag{16'}$$

Equations 14' to 16' correspond to Eqs. 16 to 18 in the previous paper,[1] where only the single parameter p was introduced into our discussion. The equivalent to Eq. 19 in the paper may be obtained from Eqs. 14 to 16 as:

$$4i\cdot s/h^2=C \tag{17}$$

This means that the parameter C is a measure of the deviation from the single parameter case. When C is given, the locus in the ternary diagram will be fixed by using Eqs. 1 and 17.

Using h and s, BC and B may be represented as:

$$BC=1+\left(\frac{h}{s}\right)\left(\frac{1-2s-h}{2-2s-h}\right) \tag{18}$$

$$B=\frac{1}{4}\left(\frac{h}{s}\right)^2\left\{\frac{1}{2-2s-h}\right\} \tag{19}$$

Further, we define the following matrix to calculate the average sequence lengths in the sequence $\ominus\oplus\{A\}$:

$$\boldsymbol{G}=\begin{array}{c} \\ 0\,0 \\ 0\,1 \\ 1\,0 \\ 1\,1 \end{array}\begin{array}{c} \begin{array}{cccc} 0\,0 & 0\,1 & 1\,0 & 1\,1 \end{array} \\ \begin{pmatrix} BC & B^{2/3}C^{1/2}E & 0 & 0 \\ 0 & 0 & B^{2/3} & B^{1/3}F \\ B^{2/3}C^{1/2}E & B^{1/3} & 0 & 0 \\ 0 & 0 & B^{1/3}F & 1 \end{pmatrix} \end{array} \tag{20}$$

The derivation of the matrix element in the 00th row and the 01th column, which corresponds to an ID pair, is illustrated in the following sequence of $\oplus\{A\}$:

$$\cdots\cdots\ 1\quad 0\quad 0\quad 0\quad 1\ \cdots\cdots$$

$$1\quad B^{1/3}\quad \underbrace{B^{1/3}\ B^{1/3}}\quad 1$$

$$1\quad C\quad \underbrace{C\quad 1}$$

$$E\quad 1\quad E$$

Two temporary parameters, E and F, have been introduced into Eq. 20 to specify the pairs, ID (or DI) and SD (or DS) respectively. The secular equation of this problem is:

$$\begin{vmatrix} BC-\lambda & B^{2/3}C^{1/2}E & 0 & 0 \\ 0 & -\lambda & B^{2/3} & B^{1/3}F \\ B^{2/3}C^{1/2}E & B^{1/3} & -\lambda & 0 \\ 0 & 0 & B^{1/3}F & 1-\lambda \end{vmatrix}=0 \tag{21}$$

which is equivalent to the equation:

$$\lambda^4-(1+BC)\lambda^3+B(C-1)\lambda^2$$
$$+B(1+BC-F-BCE^2)\lambda$$
$$+B^2C(E^2+F^2-1-E^2F^2)=0 \tag{22}$$

Let us denote the largest eigenvalue by λ_2. If we replace both E and F by unity, λ_2 becomes equal to λ_1. Therefore, in our previous notation[1] we obtain:

$$[\{I\}]=\frac{n}{2}\lim_{E,F\to 1}\frac{\partial \ln \lambda_2}{\partial \ln E}$$

$$=\frac{nB^2C}{4\lambda_1^3-3(1+BC)\lambda_1^2+2B(C-1)\lambda_1} \tag{23}$$

7) A. Miyake, Private communication.

Finally, from Eqs. 9 and 23 we get:

$$\langle I\rangle = [I]/[\{I\}] = \lambda_1(\lambda_1-1)/B$$
$$= \frac{BC^2-C+2+C\sqrt{(BC-1)^2+4B}}{2} \quad (24)$$

Similarly,

$$\langle S\rangle = \frac{\lambda_1-B(C-1)}{B}$$
$$= \frac{1-BC+2B+\sqrt{(BC-1)^2+4B}}{2B} \quad (25)$$

and

$$\langle D\rangle = \frac{2\lambda_1}{BC+1} = \frac{BC+1+\sqrt{(BC-1)^2+4B}}{BC+1} \quad (26)$$

are obtained by noticing that

$$[\{I\}] + [\{S\}] = [\{D\}] \quad (27)$$

Using measurable values, these average lengths may be written in this form;

$$\langle I\rangle = 1+2i/h \quad (28)$$
$$\langle S\rangle = 1+2s/h \quad (29)$$
$$\langle D\rangle = 1+h/\{1-h-(i-s)^2\} \quad (30)$$

The same procedure has been independently developed by Miyake and Sakakibara.[8] In spite of our different interpretation of the parameters, the two sets of obtained results are easily interchangeable by replacing our BC and B parameters with their B and C^2 parameters respectively.

Discussion

Table II lists the observed results of the samples prepared in anionic polymerization. They are also shown in Fig. 2.

Since the product of the parameters B and C corresponds to the probability of forming a 0-0 pair in the sequence $\oplus\{A\}$, the polymer characterized by $BC=1$ has the same values of i and s. It is easily shown that when $BC>1$, the value of i is larger than that of s, while when $BC<1$, that of i is smaller. The average sequence lengths can be calculated from Eqs. 28 to 30; they are given in Table III.

The extraction with acetone has been made in expectation of separating the contributions from several different mechanisms which coexist in our anionic polymerization.

As for the sample prepared with an R_2Mg-type catalyst, the stereochemical configuration depends little upon the polymerization temperature, especially between $-30°C$ and $-60°C$. Therefore, the extraction was carried out only with the samples obtained at $-50°C$. It must be noticed that, in the ternary diagram, the plots for the soluble parts are located comparatively near the point, R, which corresponds to the random polymer. This implies that the configuration of these parts resembles that of the polymer made in free radical polymerization. Unfortunately, because of the narrow range of the polymerization temperature, we can not conclude at present whether or not the mechanism yielding these soluble parts may be interpreted by the single parameter p.

Assuming, however, the uniformity of stereochemical configuration in each polymer chain, it is certain that two mechanisms of polymerization take place with an R_2Mg-type catalyst. They may be ascribed to two states of the catalyst, such as the monomer state and the associated state.[9] If this is the case probably the catalyst in the former state would produce polymer chains with a configuration similar to those obtained in free radical polymerization. On the other hand, the catalyst in the latter state would have a strong influence on the addition of the monomer and yield more stereoregular polymer chains. In

TABLE II. STEREOCHEMICAL CONFIGURATIONS OF SEPARATED COMPONENTS OF THE SAMPLES PREPARED WITH ANIONIC INITIATORS

Sample No.	Polymerization temp., °C	Catalyst	Extraction with acetone	Configuration h	Configuration s
1	−40			0.04	0.06
2	−20		Soluble	0.04	0.03
3	−10	Ethyl-magnesium-bromide		0.04	0.04
4	−40			0.18	0.41
5	−20		Insoluble	0.15	0.33
6	−10			0.11	0.18
7	−50			0.08	0.09
8	−40			0.04	0.07
9	−30		Soluble	0.04	0.05
10	−20			0.03	0.05
11	−10	Phenyl-magnesium-bromide		0	0
12	−50			0.19	0.35
13	−40			0.15	0.35
14	−30		Insoluble	0.15	0.34
15	−20			0.16	0.22
16	−10			0.10	0.15
17	−50	Diethyl-magnesium	Soluble	0.26	0.58
18			Insoluble	0.21	0.53
19	−50	Di-*n*-butyl-magnesium	Soluble	0.39	0.45
20			Insoluble	0.16	0.46
21	−50	Diisobutyl-magnesium	Soluble	0.36	0.53
22			Insoluble	0.16	0.59
23	−50	Diphenyl-magnesium	Soluble	0.44	0.40
24			Insoluble	0.21	0.50
25	−50	Dicyclo-hexyl-magnesium	Soluble	0.38	0.49
26			Insoluble	0.15	0.51

8) A. Miyake, and M. Sakakibara, *Rep. Progress Polymer Phys. Japan*, **5**, 257 (1962).

9) J. Furukawa, *Kagaku-no-ryoiki*, **12**, 85 (1958), (in Japanese).

TABLE III. CALCULATED PARAMETERS AND AVERAGE SEQUENCE LENGTHS

Sample No.	Parameter			Average sequence length		
	BC	$B^{1/2}$	C	I	S	D
1	1.31	0.10	13.7	47.6	3.95	1.16
2	1.63	0.15	71.0	47.9	2.49	1.27
3	1.47	0.13	91.8	47.5	2.99	1.22
4	1.00	0.22	20.7	5.55	5.55	1.22
5	1.07	0.19	30.4	7.93	5.39	1.18
6	1.21	0.17	42.0	13.8	4.27	1.18
7	1.38	0.17	46.7	21.8	3.25	1.22
8	1.26	0.09	160	45.5	4.50	1.14
9	1.37	0.11	114	46.5	3.50	1.18
10	1.28	0.08	203	62.3	4.33	1.14
11	~1	—	—	—	—	—
12	1.05	0.24	17.9	5.85	4.68	1.24
13	1.06	0.18	31.0	7.66	5.66	1.18
14	1.06	0.19	30.8	7.80	5.53	1.18
15	1.21	0.24	21.4	8.75	3.75	1.24
16	1.25	0.17	45.1	16.0	4.00	1.19
17	0.68	0.35	5.50	2.23	5.45	1.46
18	0.85	0.26	12.5	3.48	6.06	1.29
19	0.65	0.59	1.89	1.82	3.30	1.74
20	0.97	0.19	27.3	5.76	6.76	1.19
21	0.51	0.53	1.80	1.61	3.94	1.77
22	0.86	0.19	23.1	4.13	8.37	1.22
23	0.65	0.70	1.32	1.73	2.82	1.88
24	0.89	0.26	13.2	3.76	5.76	1.28
25	0.56	0.57	1.76	1.68	3.58	1.78
26	0.94	0.18	30.8	5.53	7.82	1.18

fact, the results shown in Fig. 2 demonstrate that the insoluble part of the sample made with an R_2Mg catalyst has nearly the same stereochemical configuration as that of the polymer prepared with RMgBr as a catalyst. These facts may be also found from the values of the parameters $B^{1/2}$ and C collected in Table II. For each sample prepared with various R_2Mg-type catalysts, a comparison of the parameters of the insoluble part with those of the soluble one clearly shows that the value of B decreases, while that of C conspicuously increases. For the sake of simplicity, let us assume here that no essential change will occur in the S-blocks of both parts. Then, following the notations defined with the sequence $\ominus \oplus\{A\}$, the above-mentioned change of parameters indicates the possibility of forming subsequences which contain even D's between I-blocks, such as:

$$\cdots\cdots SIIIDDIIDDDDIS\cdots\cdots$$

Of course, we have no evidence to support the assumption concerning the S-blocks, so it is impossible to discuss the formation of such polymer chains. However, as has been mentioned already, from the unique locus of the plots in the ternary diagram, it seems quite reasonable to conclude that two mechanisms take place in the course of the polymerization using an R_2Mg catalyst and that they yield both atactic and stereoblock polymer chains separately.

Next, let us consider the polymers made with an RMgBr catalyst. In this case, the results of the viscosity measurement strongly suggest that the apparent difference in the configuration parameters between the soluble and the insoluble parts can not be attributed to the polymerization mechanisms alone. This point has been examined in detail using the polymer prepared at $-78°C$. The typical value of η_{sp}/C ($C=0.20$ g./100 cc.) for the soluble part in acetone is about 0.2, while that for the insoluble part is about 0.6. In spite of these broad molecular weight distributions, the average stereochemical configurations did not change with the values of conversion. On this basis, we may conclude that a single mechanism takes place in the polymerization catalyzed by RMgBr.

It has been shown that the statistical treatment of the polymer chain is a convenient method for the analysis of the polymerization mechanism. However, there is a limitation in this treatment. Since the NMR spectra of polymethyl methacrylate can only give the proportions of I-, D- and S-units in the polymer chains, any longer-range effect needs another parameter whose interpretation is not always unique. Recently several workers[8,10-12] have dealt with the data obtained from the NMR spectra, and very recently the applicability of the statistics based on these data has been discussed in detail from the viewpoint of statistical stationarity.[13]

Summary

In the preceding paper[1] it was reported that the degree of the stereoregularity of polymethyl methacrylate could be determined from the NMR spectrum through the analysis of three peaks due to the α-methyl groups. It has been found that the infrared spectrum can also give an equivalent result if it is once calibrated by the NMR method.

We have considered a statistical method to interpret any locus in the ternary diagram which corresponds to the change in the stereoregularity of polymers with the polymerization temperature and with the type of catalyst. By

10) U. Johnsen, *Kolloid Z.*, **178**, 161 (1961).
11) R. L. Miller, *J. Polymer Sci.*, **56**, 375 (1962).
12) F. P. Price, *J. Chem. Phys.*, **36**, 209 (1962).
13) B. D. Coleman and T. G. Fox, *J. Polymer Sci.*, **A1**, 3183 (1963).

introducing two parameters, the average sequence lengths of *I*-, *D*- and *S*-blocks have been calculated.

On the other hand, the acetone-extraction of the samples prepared in anionic polymerization has been carried out in order to determine the degree of stereoregularity of both the extract and the residue. From the plots in the ternary diagram, we have discussed some mechanisms of the anionic polymerization. We may conclude that two different mechanisms take place in the course of the polymerization using an R_2Mg catalyst in contrast with the polymerization catalyzed by RMgBr.

We wish to thank Professor Akira Miyake of the Department of Physics, International Christian University, for his valuable advice and criticism.

The Electrical Communication Laboratory
Musashino, Tokyo

A Possibility for Determining the Entropies of Electrolytes from the Initial Thermoelectric Powers of Thermocells

By Toshio IKEDA

(Received May 13, 1964)

The partial molar entropy of a uni-univalent electrolyte (MX) in an aqueous m molal solution, can usually be calculated by the formal formula:

$$\left.\begin{aligned} S_{MX} &= S_+ + S_- = S^\circ_{MX} - 2\boldsymbol{R} \ln m\gamma_\pm \\ &\quad - 2\boldsymbol{R}\boldsymbol{T} \mathrm{d} \ln \gamma_\pm / \mathrm{d}\boldsymbol{T} \\ S^\circ_{MX} &= S^\circ_+ + S^\circ_- \end{aligned}\right\} \quad (1)$$

where S_+ and S_- are the partial molar entropies of cations and anions respectively, and S°_+ and S°_- refer to those at the standard state; $\gamma_\pm$ denotes the mean ion activity coefficient; $\boldsymbol{R}$ is the gas constant and $\boldsymbol{T}$ is the absolute temperature. The conventional values of the standard partial molar entropies of ions are available in Latimer's work[1] and also in NBS services.[2] Slight differences can be seen between them, however, and they are always worked up to yield the third-law molecular entropies (S°_{MX}) so as to be independent of the choice of the convention for the ion entropies. At any rate, it must be noted that most of these values have been determined from thermodynamic data on isothermal systems. The present writer will report a rather different basis for determining the partial molar entropies of electrolytes in aqueous solutions at the third-law convention from the thermoelectric data on non-isothermal systems without making any conventional assumptions.

1) W. M. Latimer, K. S. Pitzer and W. V. Smith, *J. Am. Chem. Soc.*, **60**, 1829 (1938).

2) F. D. Rossini, D. D. Wagman, W. H. Evans, S. Levine and I. Jaffe, "Selected Values of Chemical Thermodynamic Properties," National Bureau of Standards, U. S. Government Printing Office, Washington, D. C. (1952).

Thermodynamic Relations. — In the case of thermocells with a single uni-univalent electrolyte, MX, which yields M^+ and X^- on dissociation, the initial thermoelectric power, ε_0, can be written as follows:[3]

$$\boldsymbol{F}\varepsilon_0^{\mathrm{C}} = -t_+ S^*_+ + t_- S^*_- + \Delta S^{\circ\mathrm{C}} - (S^{\mathrm{C}}_{\mathrm{el}} + S^{*\mathrm{C}}_{\mathrm{el}}) - S_+ \quad (2)$$

for thermocells with cation-reversible electrodes, whose characteristics are indicated by the superscript C, and

$$\boldsymbol{F}\varepsilon_0^{\mathrm{A}} = -t_+ S^*_+ + t_- S^*_- + \Delta S^{\circ\mathrm{A}} - (S^{\mathrm{A}}_{\mathrm{el}} + S^{*\mathrm{A}}_{\mathrm{el}}) + S_- \quad (3)$$

for thermocells with anion-reversible electrodes, whose characteristics are indicated by the superscript A. Here, $\boldsymbol{F}$ is the Faraday constant; t_+ and t_- are the transport numbers of cations and anions respectively, related in $t_+ + t_- = 1$ by difinition; S^*_+ and S^*_- are the partial molar Eastman entropies of the transfer of cations and anions respectively, the quantities defined by the ionic heats of transfer divided by the absolute temperature; S_{el} and S^*_{el} are the partial molar entropy and the entropy of the transfer of electrons in the metallic leads of the thermocell respectively; S_+ and S_- are the partial molar entropies of cations and anions respectively; ΔS°'s refer to the contributions from the changes in the standard molar entropies of the electrode materials of the thermocells for the electrode reactions per Faraday, differing according to the electrode

3) E. g., H. J. V. Tyrrell, "Diffusion and Heat Flows in Liquids," Butterworths, London (1961).

TABLE I. PARTIAL MOLAR ENTROPIES OF HYDROCHLORIC, HYDROBROMIC, AND HYDROIODIC ACIDS AT 25°C AND 0.01 M, AND AT THE STANDARD STATE

Case	a	b	c	d
HX	HCl	HCl	HBr	HI
Electrode system, A	Hg/HgCl	Ag/AgCl	Ag/AgBr	Ag/AgI
Leads for A	Pt	Ag	Ag	Ag
ε_0^A (μV./deg.)[a]	639	288*	435*	570
ε_0^C (μV./deg.)[a,b]	142	142	146	135
$\gamma_\pm$ (m=0.01)	0.904	0.904	0.906	0.908
$d\ln\gamma_\pm/dT$ (deg^{-1})	-7×10^{-5}	-7×10^{-5}	-7×10^{-5}	-7×10^{-5}
S_{HX}(e. u.) (m=0.01)[c]	32.2_9	31.5_9	37.5_3	42.8_7
S°_{HX}(e. u.),[d] this work	13.4_9	12.7_9	18.6_6	24.1_1
S°_{HX}(e. u.) Latimer[e]	13.5	13.5	19.7	25.3
S°_{HX}(e. u.) NBS[f]	13.17	13.17	19.29	26.14

a) Refs. 3 and 4.
b) Platinum leads are used for the electrodes C, Pt/H_2.
c) Eq. 4.
d) S_{HX} (in Eq. 4) $+2\boldsymbol{R}\ln m\gamma_\pm+2\boldsymbol{R}T d\ln\gamma_\pm/dT$
e) Ref. 1.
f) Ref. 2.
* If an alternative value of $\varepsilon_0^A=296$ μV./deg., which is given by interpolation of Sasaki's recent data on thermocell [Ag/AgCl, HCl (0.01 M)] at 25°C, is used, we get $S_{HCl}=31.7_6$ e. u. or $S^\circ_{HCl}=12.9_6$ e. u. (K. Sasaki, *J. Chem. Soc. Japan, Pure Chem. Sec. (Nippon Kagaku Zasshi)*, **82**, 654 (1961); Haase and his co-worker gave 290 μV./deg. for [Ag/AgCl, HCl (0.01 M)] and 437.7 μV./deg. for [Ag/AgBr, HBr (0.01 M)] at 25°C (R. Haase and H. Schönert, *Z. physik. Chem. N. F.*, **25**, 193 (1960)).

systems (their practical forms are, for example, $\Delta S^{\circ C}=(1/2)S^\circ_{H_2}$ for a hydrogen electrode; $\Delta S^{\circ A}=S^\circ_{Ag}-S^\circ_{AgX}$ for silver/silver halide electrodes, $S^\circ_{Hg}-S^\circ_{HgCl}$ for mercury/mercurous chloride electrodes, and so on). From Eqs. 2 and 3, the partial molar entropy of a uni-univalent electrolyte, MX, is derived as follows:

$$S_{MX}=S_+ +S_- =\boldsymbol{F}(\varepsilon_0^A-\varepsilon_0^C)+\Delta S^{\circ C}-\Delta S^{\circ A} -(S_{el}^C+S_{el}^{*C}-S_{el}^A-S_{el}^{*A}) \quad (4)$$

Since the quantities on the right-hand-side of 4 are all measurable experimentally, the left-hand-side quantity can be determined.

Calculations. — In the literature, however, there are unexpectedly few examples to which the present method is applicable.[4,5] The only examples now available are the following combinations of thermocell systems;* (a) [Pt, H_2/HCl] with [Hg/HgCl, HCl]; (b) [Pt, H_2/HCl] with [Ag/AgCl, HCl]; (c) [Pt, H_2/HBr] with [Ag/AgBr, HBr], and (d) [Pt, H_2/HI] with [Ag/AgI, HI], all at 25°C and 0.01 M. The values of the initial thermoelectric powers which were used in our calculations are accurate to within 1.8 μV./deg. at worst, judging from the accuracy of other experiments we have performed along similar lines. Finally, the entropy terms regarding electrons in the metallic leads of two thermocells can be estimated from the thermoelectric power of a thermocouple composed of two metals of the same kinds as those used as the leads in these thermocells. The thermoelectric power, ε(C/A), of a metal C with respect to A can be defined as follows:[3]

$$\boldsymbol{F}\varepsilon(C/A)=-(S_{el}^C+S_{el}^{*C}-S_{el}^A-S_{el}^{*A}) \quad (5)$$

Here the sign of ε(C/A) was taken, in accordance with the convention adopted by most authors, to be positive if the current so produced in the thermocouple flows at the cold junction from C to A. According to Temkin and Khoroshin,[6] we have ε(Pt/Cu) = -6.39 μV./deg. at 25°C, while ε(Ag/Cu) = $+0.08\pm0.01$ μV./deg. was observed by the present writer. Therefore, we have ε(Pt/Ag) = -6.47 μV./deg., or equivalent to -0.15 e.u.; it is ready to use in the cases of b, c and d. In the case of a, on the other hand, such an electronic contribution vanishes, because the electrode leads of these two thermocells are both made of the same platinum. By using the authorized values of the standard partial molar entropies ($S^\circ_{H_2}$ = 31.211 ($\pm$0.01) e. u.,[2] $S^\circ_{Hg(liq.)}=18.187$ ($\pm$0.02) e. u.,[7] $S^\circ_{HgCl}=23.4$ e. u.[2], $S^\circ_{Ag}=10.206$ ($\pm$0.01)

4) Ref. 3, p. 285.
5) T. Ikeda, *Rep. Liberal Arts Sci. Fac., Shizuoka Univ., Nat. Sci.*, 2, 159 (1959).
* For example, [Ag/AgCl, HCl] represents a thermocell system, Ag/AgCl (T), HCl, AgCl/Ag ($T+\Delta T$).
6) M. I. Temkin and A. V. Khoroshin, *Zhur. Flz. Khim.*, 26, 500 (1952).
7) R. H. Busey and W. F. Giauque, *J. Am. Chem. Soc.*, 75, 806 (1953).

e. u.,[2,8] $S^{\circ}_{AgCl}=22.97\pm0.10$ e. u.[2,9] $S^{\circ}_{AgBr}=25.62\pm0.10$ e. u.[9] and $S^{\circ}_{AgI}=27.59$ (±0.4) e. u.[10]), all at the third-law convention, the errors indicated in the brackets being estimated by us, taking into consideration the accuracy of the data given in the original papers), we can get from 4 the third-law partial molar entropies of three halide acids at 25°C and 0.01 M, as well as their standard values by the aid of 1. The results are listed in Table I. Here the calculated values of entropies are found to be lower than the accepted values[1,2] except for the case of a. Consequently, if the thermoelectric data on thermocells and the entropy data on the electrode materials are correct in our calculations, the current standard partial molar entropies of halide acids, particularly those of hydrobromic acid and hydroiodic acid, might have to be corrected considerably; our values may be accurate to within 0.2 e. u. in the cases of b and c, and may be within 0.5 e. u. in the case of d (the accuracy of the case of a can not be estimated because we do not know the probable error of S°_{HgCl}). The disagreement between the calculated values of S_{HCl} in the cases of a and b might be due to the use of an incorrect value of S°_{HgCl} in the calculations.

8) P. F. Meads, W. C. Forsythe and W. F. Giauque, ibid., 63, 1902 (1941).
9) E. D. Eastman and R. T. Milner, *J. Chem. Phys.*, **1**, 444 (1933).
10) K. S. Pitzer, *J. Am. Chem. Soc.*, 63, 516 (1941).

Summary

An alternative method for determining the third-law partial molar entropies of electrolytes in aqueous solutions from the data on non-isothermal systems has been presented. They can be obtained from the difference between the initial thermoelectric powers of two different thermocells, the one being formed by cation-reversible electrodes and the other being formed by anion-reversible electrodes, both with common electrolytes of the same concentration. The partial molar entropies have been calculated to be 31.59, 37.53 and 42.87 e. u. for hydrochloric acid, hydrobromic acid, and hydroiodic acid respectively at 25°C and 0.01 M.

Department of Chemistry
Shizuoka University
Oiwa, Shizuoka

*Infrared Spectra and Rotational Isomerism of Some Long-chain n-Alkoxy Ethanols**

By T. K. K. SRINIVASAN, C. I. JOSE and A. B. BISWAS

(Received May 14, 1964)

In connection with a program on water evaporation control, the infrared spectra of a series of alkoxy ethanols, $CH_3(CH_2)_nO-CH_2-CH_2-OH$, where $n=13$, 15, 17, 19 and 21, have been investigated in various physical states. These studies show that the ethanols exhibit rotational isomerism and that the changes in the spectra can be related to definite geometrical arrangements of the molecule.

The alkoxy ethanols have a long chain of CH_2 groups as well as an OCH_2CH_2OH group. As a liquid or in solution, molecules containing long CH_2 chains give a large number of absorption bands because of the various conformations possible by rotation around the single bonds.[1] These sometimes show up as broad bands on account of overlapping. In the crystalline state, on the other hand, only a single rotational species is usually accommodated, and the absorption pattern is considerably simplified.[2] In polyethylene[3] and certain other long-chain compounds[4,5] additional bands appear as a result of the specific molecular arrangement of the CH_2 chain (orthorhombic) in the crystal favorable for intermolecular coupling. The ($O-CH_2-CH_2-O$) group can be considered to take up independently a gauche or trans configuration by rotation around the single bonds. However, the presence of a hydroxyl group suitably

* Communication No. 591 from the National Chemical Laboratory, Poona-8, India.

1) S. Mizushima, "Structure of Molecules and Internal Rotation," Academic Press, New York (1954).

2) N. Sheppard, *Advances Spectroscopy*, **1**, 288 (1959).

3) S. Krimm, C. Y. Liang and G. B. B. M. Sutherland, *J. Chem. Phys.*, **25**, 549 (1956).

4) D. Chapman, *J. Chem. Soc.*, **1957**, 4489.

5) R. G. Snyder, *J. Mol. Spectroscopy*, **4**, 411 (1960); **7**, 116 (1961).

located for intramolecular hydrogen bonding[6] with ether oxygen can be expected to influence the type of configuration taken by the molecule.

It is known that the compounds of the type $X-CH_2-CH_2-X$ give four rocking modes, two each corresponding to the gauche (A and B) and trans (A_u and B_g) configurations with C_2 and C_{2h} symmetries respectively, in the 1000 cm^{-1}~700 cm^{-1} region. While both the gauche modes are active, only the A_u trans mode is active in the infrared region. Though these modes are sensitive to changes in the remaining part of the molecule, they have been found useful in identifying rotational isomers of a large number of compounds.[7,8] Indirect evidence can also be obtained regarding the configuration of the $(O-CH_2-CH_2-O)$ group by studies of the hydroxyl group attached to one of its CH_2 groups.

In the present study, the infrared spectra of alkoxy ethanols have been discussed and the configurations of the $(O-CH_2-CH_2-O)$ group investigated in solution as well as in the liquid and solid states by analysis of the CH_2 rocking modes in the 1000 cm^{-1}~700 cm^{-1} region and of the hydroxyl stretching bands.

Experimental

The spectra were obtained either with a Perkin-Elmer model 221 instrument, equipped with an NaCl prism, or a Grubb Parsons model S3, with an LiF prism.

The preparation and purity of the alkoxy ethanols have been reported elsewhere.[9] A heating cell was constructed to obtain the spectra of solid and liquid films (Fig. 1) between sodium chloride plates at a few relevant temperatures. The reproducibility of the spectra upon repeated heatings or coolings of the substances was checked in situ; little variation in position and intensity was observed. The temperature during a run, as measured with a calibrated copper-constantan thermocouple, was maintained within $\pm 1°C$.

The spectra of solutions of octa-decoxy-ethanol (ODE) in carbon tetrachloride and carbon disulfide are also given (Fig. 1) to show their similarity with that of the liquid. The spectra of these compounds in carbon tetrachloride were studied particularly, using a variable path cell, in the hydroxyl-stretching region in order to elucidate the nature of the internal hydrogen bonding and of the rotational isomerism of these molecules.

Results and Discussion

Since the absorption characteristics of the different alkoxy ethanols are alike, the discussion will center upon ODE.

In the CH stretching region strong bands at 2925 cm^{-1} and 2850 cm^{-1} are observed in both the solid and liquid states; they are ascribed to the CH stretching modes of the CH_2 and CH_3 groups.[10] The additional band at 2958 cm^{-1} observed in the solid state is grouped with a similar sharpening and doubling of the bands near 1110 cm^{-1} and 1060 cm^{-1} observed on liquid-solid transformation.

The absorption bands at 1466 (S) and 1376~1379 (W) observed in the solid and liquid states are assigned to the CH deformation of the CH_2 and CH_3 groups.[10] The band at 1471 cm^{-1}, which appears as a shoulder in the solid state and which is observed as a separate band in the compound $CH_3(CH_2)_{17}(O-CH_2-CH_2)_2OH$ is assigned to the CH deformation mode of the CH_2 groups adjacent to oxygen. The absorption bands in the 1416~1403 cm^{-1} region are similar to those observed for normal higher alcohols at 1412 cm^{-1}; they are ascribed to the C–O stretching or O–H deformation modes.[10]

The 1360 cm^{-1}~1150 cm^{-1} region in the spectra of the solid alkoxy ethanols features a band progression of irregular intensity, varying from medium to weak. In the liquid state, they broaden out completely, as is observed in other long-chain compounds; they are ascribed to the CH_2 wagging modes. Below 1150 cm^{-1} strong broad bands at 1117 cm^{-1} and 1056 cm^{-1} are observed in the liquid state. The band near 1050 cm^{-1} is characteristic of a primary alcohol[10] and is considered to arise either from an OH deformation or C–O stretching mode. However, normal vibration calculations and the analysis of *n*-paraffin spectra indicate skeletal modes of hydrocarbon chains (C-C stretching) in the 1050 cm^{-1}~950 cm^{-1} region.[11] The observed enhanced intensity of the band at 1058 cm^{-1} is, therefore, due to the overlapping of both the C–O stretching or O–H deformation and the skeletal modes. The band progression from 1050 cm^{-1} to 950 cm^{-1} would correspond to the various C–C skeletal modes.[12]

In a large number of ethers, a band at about 1120 cm^{-1} is noticed; in dimethyl ether this has been ascribed to an antisymmetric C–O–C stretching vibration. Hence, the band at 1117 cm^{-1} may be assigned to a C–O–C stretching mode. In the solid state, the two

6) S. Mizushima, T. Shimanouchi, T. Miyazawa, K. Abe and M. Yasumi, *J. Chem. Phys.*, **19**, 1477 (1951).
7) A. Miyake, *J. Am. Chem. Soc.*, **82**, 3040 (1960).
8) J. K. Brown, N. Sheppard and D. M. Simpson, *Phil. Trans.*, **A247**, 35 (1954).
9) A. V. Deo, N. R. Sanjana, S. B. Kulkarni, M. K. Gharpurey and A. B. Biswas, *Nature*, **187**, 870 (1960).
10) L. J. Bellamy, "The Infrared Spectra of Complex Molecules," John Wiley & Sons., New York (1958).
11) R. G. Snyder and J. H. Schachtschneider, *Spectrochim. Acta*, **19**, 85, 117 (1963).
12) M. Tasumi, T. Shimanouchi, A. Watanabe and R. Goto, ibid., **20**, 629 (1964).

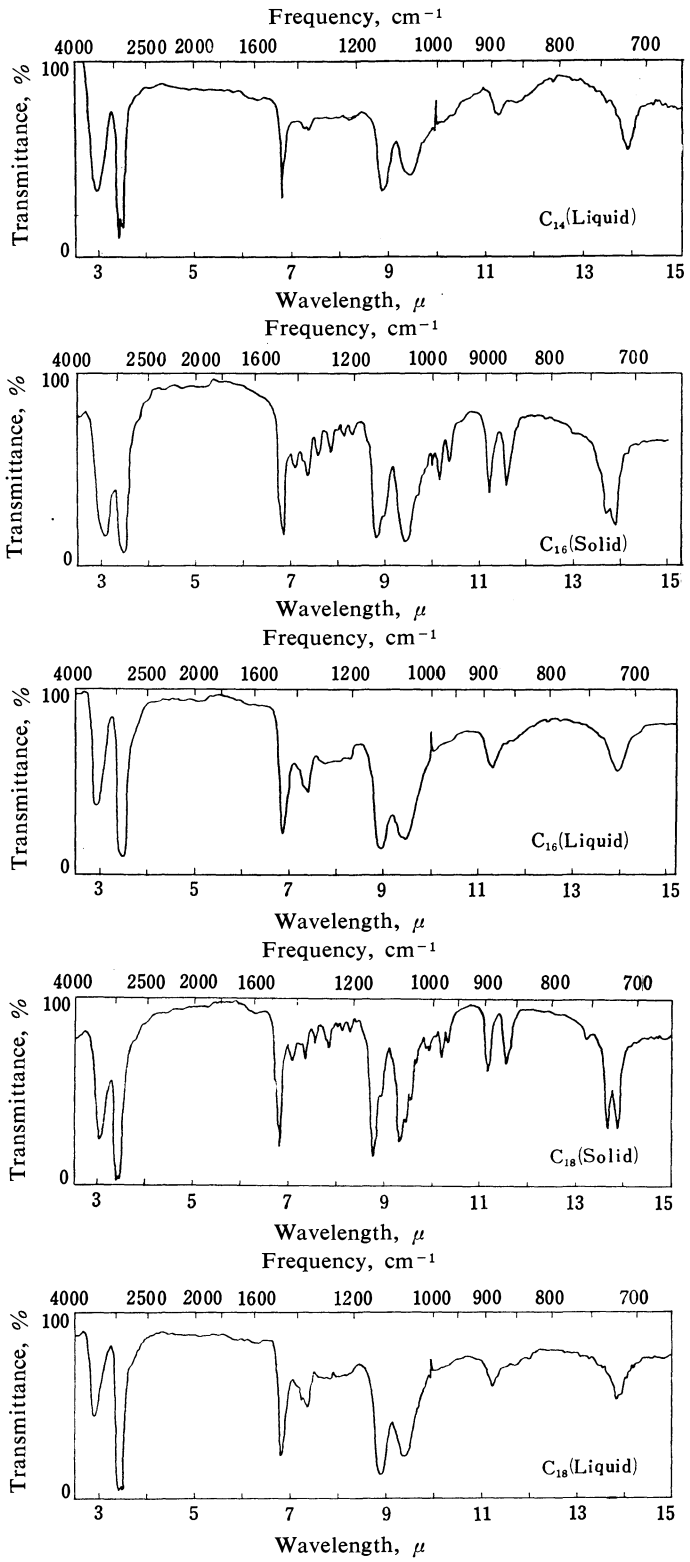
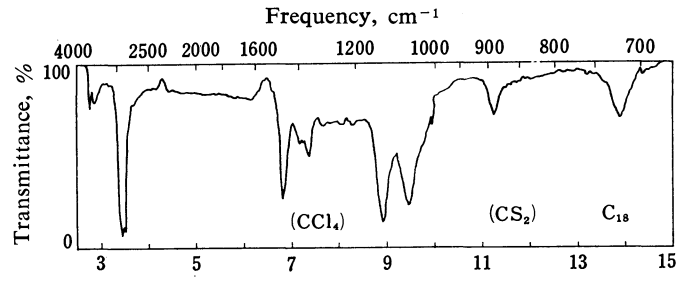
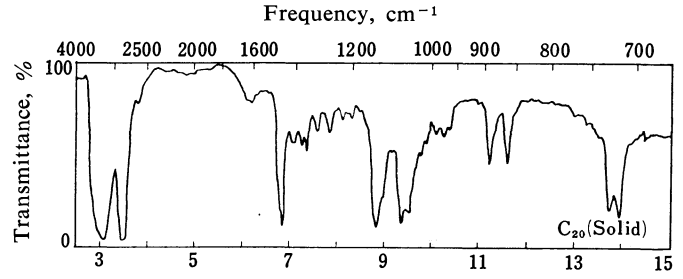
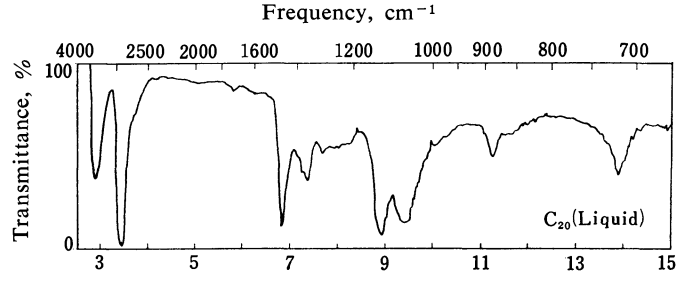


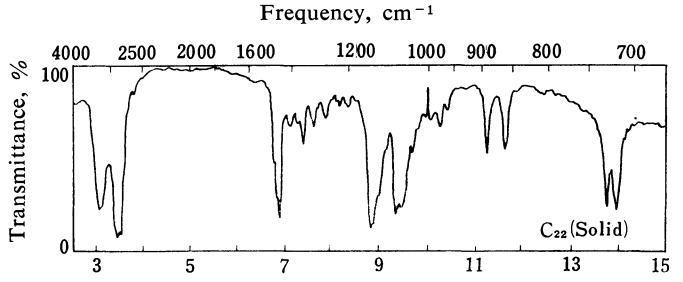
Fig. 1. Infrared spectra of

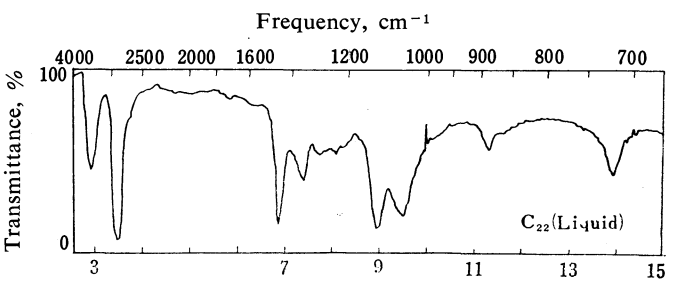
$CH_3(CH_2)_{13}$-O-CH_2-CH_2-OH : C_{14} (liquid)
$CH_3(CH_2)_{15}$-O-CH_2-CH_2-OH : C_{16} (solid) ; C_{16} (liquid)
$CH_3(CH_2)_{17}$-O-CH_2-CH_2-OH : C_{18} (solid) ; C_{18} (liquid)











$CH_3(CH_2)_{17}$-O-CH_2-CH_2-OH : C_{18} (solution)
$CH_3(CH_2)_{19}$-O-CH_2-CH_2-OH : C_{20} (solid) ; C_{20} (liquid)
$CH_3(CH_2)_{21}$-O-CH_2-CH_2-OH : C_{22} (solid) ; C_{22} (liquid)

bands in the liquid are found doubled and sharpend at 1117 cm^{-1} and 1137 cm^{-1} and at 1058 cm^{-1} and 1071 cm^{-1} respectively. The sharpening and doubling of bands on liquid-solid transformation observed in this region and also in the CH stretching region (see above) appears to be due to an imposed symmetry in the crystalline state or to changes due to hydrogen bonding rather than to rotational isomerism. The splitting of bands due to intermolecular effects[5] has so far been established only for CH_2 chains among long-chain compounds. However, a similar doubling and sharpening of bands observed in the case of $CH_3(CH_2)_{17}(O\text{-}CH_2\text{-}CH_2)_2OH$, in which the splitting of the CH_2 rocking at 720 cm^{-1} is absent (see below), indicates that they are not connected with the intermolecular interaction of the long sequence of CH_2 groups.

The 950 cm^{-1}~800 cm^{-1} Region. — In this region considerable changes are observed in the spectra of alkoxy ethanols. In the liquid state or in solution, only a band of medium intensity is observed at 889 cm^{-1}. This is in good agreement with that observed by Chalkowsky[13] for the lower liquid homologues at 892 cm^{-1}. In the solid state, on the other hand, two sharp bands of almost equal intensity (medium) at 864 cm^{-1} and 892 cm^{-1} are observed, in addition to a weak band at 962 cm^{-1}. From the measurement of the areas under the bands during the liquid-solid transformation, it was found that the band at 864 cm^{-1} developed at the expense of that at 889 cm^{-1}. The development of the band at 864 cm^{-1} at the expense of that at 889 cm^{-1} during crystallization may be explained as the conversion of one of the rotational isomer into another. The assignment of the bands to the two rotational isomers was made by comparison with disubstituted ethanes, particularly ethylene glycol, its derivatives and polymers. It has been shown by theoretical calculations[14] that in disubstituted ethanes the CH_2 rocking frequencies increase in the order A_u(trans)< B(gauche)<A(gauche)<B_g(trans), so that the gauche mode frequencies lie between those of the trans modes. This has been well established in the case of the simple disubstituted ethanes $X\text{-}CH_2\text{-}CH_2\text{-}Y$, where X and Y are CH_3, Cl, Br, SCN, etc. Miyake[7] recently assigned CH_2 rocking modes of the $(O\text{-}CH_2\text{-}CH_2\text{-}O)$ group in ethylene glycol, its derivatives and polymers on the above basis. He found that the A_u type mode of the $(O\text{-}CH_2\text{-}CH_2\text{-}O)$ group occurs near 850 cm^{-1}, which is about 100 cm^{-1} higher than in compounds where the two oxygens are replaced by other atoms, and that the spacing between the two A and B gauche forms is approximately 20 cm^{-1}. In the present case, therefore, the bands 864 cm^{-1} and 964 cm^{-1} are assigned to the CH_2 trans modes A_u and B_g of the $(O\text{-}CH_2\text{-}CH_2\text{-}O)$ group respectively and the band at 889 cm^{-1}, to the two gauche modes coalesced into one. A single band for a gauche mode has also been observed at 895 cm^{-1} for polyethylene terephthalate.[15] The formation of the cis species with a higher symmetry, C_{2v}, may be a possible explanation for a single CH_2 rocking mode for the gauche form.[16]

The above assignment indicates that the $(O\text{-}CH_2\text{-}CH_2\text{-}O)$ group in alkoxy ethanols has a predominantly gauche configuration in a liquid or in solution, while in the crystalline state both the gauche and trans forms are present in approximately equal numbers. The presence of the gauche configuration in solution is supported by observations in the hydroxyl-stretching region. In the case of polyethylene glycol, it has been concluded by Miyake[7] that a gauche configuration is predominant in the melt, while both the gauche and trans forms exist in the solid state. In contrast, Davison,[17] and Kuroda and Kubo,[18] on the basis of a different assignment of the CH_2 rocking modes, have arrived at a complete gauche configuration in the solid state. Recently Miyazawa[19] has made calculations for the infrared frequencies and molecular conformations of various polymers by a normal coordinate treatment and compared the results with the observed results. In the case of polyethylene glycol these studies have shown that the most likely structural model consists of trans-gauche-trans (TGT) conformations of the $(O\text{-}CH_2\text{-}CH_2\text{-}O)$ group. Further recent X-Ray diffraction studies[20] of the long-chain alcohols with an odd number of carbon atoms have shown that both trans and gauche configurations of the OH group are present in the crystalline state.

The 730 cm^{-1}~720 cm^{-1} Region.—The bands in this region are attributed to the methylene rocking modes of the long hydrocarbon chain. The band at 719 cm^{-1} in the liquid state splits into two bands, at 729 cm^{-1} and 719 cm^{-1}, of almost equal intensity in the solid state, as observed in the case of polyethylene[3] and certain long-chain compounds. Chapman[4] has shown that the presence of two bands of the

13) N. Chalkowsky, R. H. Martin and R. Van Nechal, *Bull. Soc. Chem. Belges.*, **65**, 458 (1956).
14) L. Nakagawa and S. Mizushima, This Bulletin, **28**, 589 (1955).
15) A. Miyake, *J. Polymer Sci.*, **38**, 486 (1959).
16) Y. Kuroda and M. Kubo, ibid., **26**, 323 (1957).
17) W. H. T. Davison, *J. Chem. Soc.*, **1955**, 3270.
18) Y. Kuroda and M. Kubo, *J. Polymer Sci.*, **36**, 453 (1959).
19) T. Miyazawa, K. Fukushima and Y. Ideguchi, *J. Chem. Phys.*, **37**, 2764 (1962).
20) A. Watanabe, This Bulletin, **36**, 336 (1963).

same intensity indicates an orthorhombic packing of the CH_2 chains, while both the hexagonal and triclinic packing give rise to a single band in this region. Using this criterion, the long CH_2 chain in alkoxy ethanols would be expected to have an orthorhombic packing (orthorhombic sub-cell). It is interesting to note that the compound $CH_3(CH_2)_{17}(O-CH_2-CH_2)_2OH$ shows only a single band[21] at 729 cm^{-1} in the solid state, while the absorption pattern in the 950~800 cm^{-1} regions remains similar to that of the alkoxy ethanols.

Solution Spectra.—ODE (Fig. 2) in a dilute

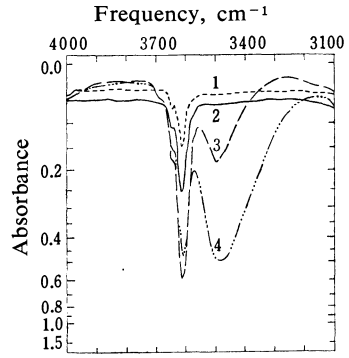


Fig. 2. Octadecoxy ethanol (ODE) in carbon tetrachloride.

1 ------ 0.005 M (3 mm. path length)
2 —— 0.01 M (3 mm. path length)
3 - - - 0.1 M (1 mm. path length)
4 ·····- 0.5 M (0.2 mm. path length)

carbon tetrachloride solution (0.005 M~0.01 M) shows a strong band at 3600 cm^{-1} and a weak band at 3636 cm^{-1}. These, as in the methoxy ethanol reported on by Flett[22] and by Kuhn[23], would correspond to monomer units of the intramolecularly bonded gauche, and trans or nonbonded gauche, forms respectively. At higher concentrations until the solubility limit at about 0.5 M is reached, a dimer band at 3480±10 cm^{-1} is observed which increases in intensity with the concentration at the expense of the band at 3600 cm^{-1}.* at 0.1 M, in addition to the dimer and monomer bands at 3484 cm^{-1} and 3636 cm^{-1} respectively. In the liquid state ODE shows only the broad dimer band at 3465 cm^{-1}. The ODA (octadecanol) shows, on the other hand, a broad polymer band at 3350 cm^{-1} in the liquid and bands at 3270 cm^{-1} and 3230 cm^{-1} in the solid state.[24]

During solidification the band at 3465 cm^{-1} in ODE is slowly shifted to lower frequencies; in the crystalline solid, it is located as a strong broad band at 3260 cm^{-1}. The dimer formation of alkoxy ethanols in the liquid state, in contrast to higher polymers by normal long chain alcohols in the liquid state and even in solution, supports the earlier conclusion that, in the liquid state, the alkoxy ethanols exist predominantly in gauche configuration.

Summary

The infrared spectra of *n*-alkoxy ethanols $CH_3(CH_2)_nO-CH_2-CH_2-OH$ with $n=13$, 15, 17, 19 and 21 have been obtained in the solid and liquid states as well as in solution. From a study of the CH_2 rocking modes of the ($O-CH_2-CH_2-O$) group at 893 cm^{-1} and 864 cm^{-1} during liquid-solid transformation and from the solution spectra in the hydroxyl-stretching region, it has been shown that this group exists predominantly in a gauche configuration in liquids or in solution, while both gauche and trans configurations are present in the solid state.

The authors are grateful to Professor Sanichiro Mizushima and Drs. Ichiro Nakagawa and Mitsuo Tasumi of the University of Tokyo, Japan, for their valuable comments and for communicating results on the infrared spectra of normal higher alcohols prior to publication.

We are also grateful to Dr. (Miss) S. B. Kulkarni for supplying the purified compounds used in the present studies.

National Chemical Laboratory
Poona-8, India

21) Unpublished work.
22) M. ST. C. Flett, *Spectrochim. Acta*, **10**, 21 (1957).
23) M. Kuhn, W. Lüttke and R. Mecke, *Z. Anal. Chem.*, **170**, 106 (1959).

* The octadecanol (ODA) on the other hand shows a polymer band 3363 cm^{-1}.
24) M. M. Davies, *J. Chem. Phys.*, **8**, 577 (1940).

Heats of Mixing for Binary Mixtures. The Energy of Hydrogen Bonding between Alcohol and Ketone Molecules

By Sachio MURAKAMI, Kazuo AMAYA* and Ryoichi FUJISHIRO

(Received May 29, 1964)

It is well known that the measurement of the heats of mixing of associated solutions is significant in investigating the interaction energy in a single component and between the different components. In a particular case such as the alcohol-nonpolar solvent system, such thermochemical treatments have already been extensively carried out and have revealed the energy of the intermolecular hydrogen bonding between alcohol molecules.[1] In cases where the associated solutions consist of alcohol and acceptor components, such as ketone, thermochemical data are not ample and detailed enough to allow us to estimate the energy of the intermolecular hydrogen bonding between these pair molecules.

In this paper we shall report the heats of mixing for such alcohol - ketone systems as isopropanol - acetone and *s*-butanol - ethyl methyl ketone systems, as well as those for alcohol - hexane and ketone - hexane systems, and shall estimate the energy of the hydrogen bonding of the O–H···O= type by means of the thermochemical cycle.

Experimental

Materials.—All the samples were purified from commercial products according to the usual method described in the literature,[2] and then they were finally distilled with a Stedman-type column. Considerable attention was devoted to removing the small amount of remaining water; as a result, these fractionated samples did not show a peak for water on a gas chromatogram. Therefore, the water content in these samples was estimated to be 1/100 weight percent or less.

Apparatus and Procedure.—A block diagram of the entire apparatus for measuring heats of mixing is shown in Fig. 1. The calorimeter is of the twin type, shown in Fig. 2, consisting of a mixing vessel and a reference vessel, each held with a vessel holder and fixed in a submarine vessel, installed in a water thermostat at 25°C kept constant to 1/1000°C. The mixing vessel is similar to that described in a previous paper[3] but was modified in some points, as is shown in Fig. 3. For the measurement of dilute solutions, another mixing vessel was used, one which was larger than that one used in the moderate concentration range and which could accomodate about 4 ml. of the liquid sample.

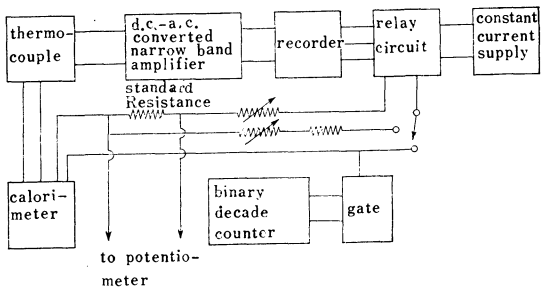


Fig. 1. Block diagram of the apparatus.

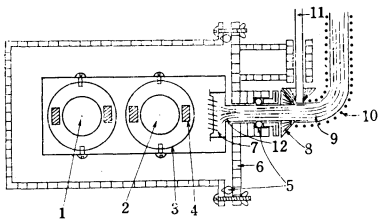


Fig. 2. Calorimeter

1: Reference vessel holder
2: Mixing vessel holder
3: Brass ring
4: Teflon spacer
5: "O" ring rubber packing
6: Submarine vessel
7: Hermetic seal
8: Bebel gear
9: Rubber tube
10: Spring wire
11: Handle
12: Pivot

Before mixing, two components are separated by mercury in the mixing vessel; during mixing, the holder is turned upside down by rotating it around the pivot through the manipulation of the handle from the outside of the submarine vessel.

The temperature change on mixing is detected as the difference in the thermal electromotive force of the thermocouple between the mixing vessel and the reference vessel, which acts as a reference bath for the thermocouple and which contains only mercury. Even a small difference in the electric

* Goverment Chemical Industrial Research Institute, Tokyo, Shibuya-Ku, Tokyo.

1) L. Sarolea-Mathot, *Trans. Faraday Soc.*, **49**, 8 (1953); J. A. Barker, *J. Chem. Phys.*, **20**, 1526 (1952).

2) A. Weissberger and E. S. Proskauer, "Organic Solvents," Interscience Publishers, New York (1955).

3) K. Amaya, This Bulletin, **34**, 1271 (1961).

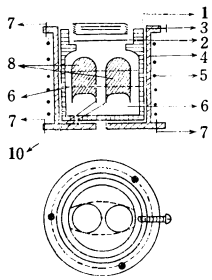


Fig. 3. Cross section and upper side view of vessel holder and mixing vessel.

1: Stainless steel vessel
2: Teflon packing
3: Male screw
4: Vessel holder
5: Heater
6: Mercury
7: Thermocouple
8: Sample liquids
9: Spring steel plates
10: Glass bells

potential is amplified by the d.c.—a.c. converted narrow band amplifier, the output signal of which is fed to an automatic pen recorder (YEW type E-30). With this amplifier a $\pm 1\times10^{-8}$ V. change can be detected; the temperature coefficient of one junction of a copper-constantan thermocouple is about 40 μV./°C, so that the sensitivity of our thermometer made of 7 junctions corresponds to about $\pm 3\times10^{-5}$ deg.

The main construction of the electrical circuit for the automatic thermal compensation is almost the same as that described previously, except that the meter relay is replaced with a microswitch connected to the recorder. The period during which the electric current from the constant current supply passes through the calorimeter heater is automatically registered on the binary decade counter operated with a standard 100 kc. oscillator.

Results and Discussion

The results obtained are given in Tables I, II, III, IV, V and VI and in Figs. 4 and 5, where x_1 is the mole fraction of component 1, and where ΔH^M and $\Delta H^M_{x_1}$ are the heats of mixing expressed as cal./mol. of the mixture and those expressed as kcal./mol. of component 1 at mole fraction x_1 respectively.

Plotting $\Delta H^M_{x_1}$ against x_1 and then extrapolating the curve to the infinite dilution ($x_1 \rightarrow 0$) for each system, as is shown in Figs. 4 and 5, we can obtain the heat of mixing per mole of component 1 at the infinite dilution as: 1.76 kcal. for the isopropanol (1) - acetone (2) system, 2.15 kcal. for the acetone (1) - *n*-hexane (2) system, 1.82 kcal. for the *s*-butanol (1) - ethyl methyl ketone (2) system and 1.90 kcal. for the ethyl methyl ketone (1) - *n*-hexane (2) system.

Table I. Heat of mixing of isopropanol (1) and acetone (2)

Mole fraction of the component 1, x_1	ΔH^M, cal./mol. of mixture	$\Delta H^M_{x_1}$, kcal./mol. of the component 1
0.00515	8.97	1.74
0.0143	24.2	1.69
0.0573	91.7	1.60
0.0607	94.0	1.55
0.0803	121.1	1.37
0.128	175.0	1.37
0.134	183.0	1.37
0.225	267.4	1.19
0.398	362.5	0.910
0.438	360.9	0.824
0.451	378.1	0.839
0.489	390.6	0.800
0.613	351.6	0.573
0.724	313.1	0.432
0.800	254.5	0.318
0.879	179.6	0.204

Table II. Heat of mixing of *s*-butanol (1) and ethyl methyl ketone (2)

x_1	ΔH^M cal./mol.	$\Delta H^M_{x_1}$ kcal./mol.
0.1470	225.2	1.532
0.3136	373.0	1.189
0.5073	404.8	0.7980
0.5492	409.1	0.7449
0.6250	387.8	0.6204
0.7606	317.9	0.4178

Table III. Heat of mixing of acetone (1) and *n*-hexane (2)

x_1	ΔH^M cal./mol.	$\Delta H^M_{x_1}$ kcal./mol.
0.0513	97.9	1.91
0.0671	119.0	1.77
0.0771	136.8	1.78
0.1466	219.1	1.49
0.1748	250.2	1.44
0.3587	362.5	1.01
0.5561	376.6	0.677
0.7357	288.8	0.393
0.8988	131.7	0.147

Table IV. Heat of mixing of ethyl methyl ketone (1) and *n*-hexane (2)

x_1	ΔH^M cal./mol.	$\Delta H^M_{x_1}$ kcal./mol.
0.0563	84.7	1.51
0.0819	118.3	1.44
0.1424	164.2	1.15
0.2398	235.2	0.982
0.3305	277.6	0.840
0.4342	302.7	0.697
0.5547	297.4	0.536
0.7525	226.1	0.301

TABLE V. HEAT OF MIXING OF ISOPROPANOL (1) AMD *n*-HEXANE (2)

x_1	ΔH^M cal./mol.	$\Delta H^M_{x_1}$ kcal./mol.
0.1332	133.5	1.00
0.2270	180.1	0.794
0.3052	195.3	0.640
0.4085	191.0	0.468
0.5453	185.8	0.341
0.8005	96.5	0.121
0.8758	50.5	0.058

TABLE VI. HEAT OF MIXING OF *s*-BUTANOL (1) AND *n*-HEXANE (2)

x_1	ΔH^M cal./mol.	$\Delta H^M_{x_1}$ kcal./mol.
0.1655	174.5	1.06
0.2959	216.8	0.733
0.4319	222.2	0.515
0.5823	198.4	0.341
0.7337	158.8	0.216
0.8279	101.2	0.122

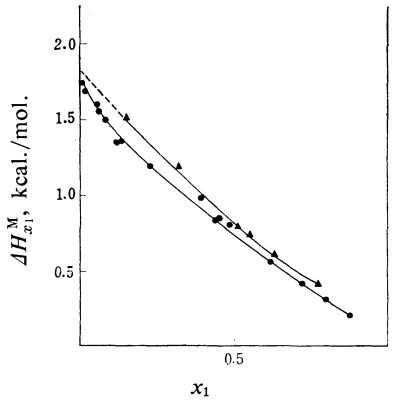


Fig. 4. Heats of mixing, alcohol - ketone systems.

● Isopropanol + Acetone
▲ *s*-Butanol + Ethyl methyl ketone

We also measured the heats of mixing $\Delta H^M_{x_1}$ for the isopropanol - *n*-hexane (2) and the *s*-butanol (1) - *n*-hexane (2) systems; the results obtained are plotted in Fig. 6 against x_1, together with the dotted curves for other kinds of alcohol - *n*-hexane systems taken from the literature.[4] As this figure shows, the curves are very steep at small x_1 values, and the extrapolation to $x_1=0$ is apt to produce some errors. The value of $\lim_{x_1\to 0} \Delta H^M_{x_1}$ obtained by Pahlk[4] for the isopropanol-hexane system is 5.90 kcal., and his $\Delta H^M_{x_1}$-x_1 curve coincides with ours in the concentrated range, as is

4) Landolt-Börnstein, "Physikalishe-Chemischen Tabellen," Springer, Berlin (1936); G. von Elbe, *J. Chem. Phys.*, 2, 73 (934).

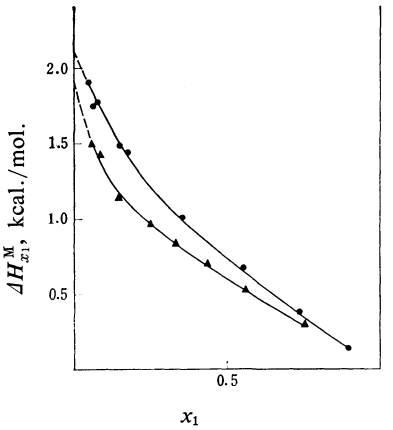


Fig. 5. Heats of mixing, ketone - *n*-hexane systems.

● Acetone + *n*-Hexane
▲ Ethyl methyl ketone + *n*-Hexane

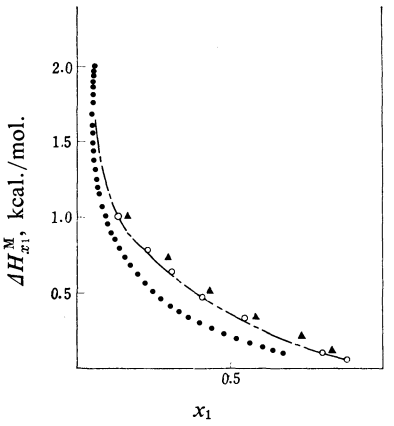


Fig. 6. Heat of mixing, alcohol - *n*-hexane systems.

··· *n*-Alcohol + *n*-Hexane (from Pahlk)
-·- Isopropanol + *n*-Hexane (from Pahlk)
○ Isopropanol + *n*-Hexane
▲ *s*-Butanol + *n*-Hexane
$\lim_{x\to 0} \Delta H^M_{x_1}$=5.8 kcal. for the dotted curve
$\lim_{x\to 0} \Delta H^M_{x_1}$=5.9 kcal. for the broken curve

shown in Fig. 6. Therefore, we have adopted 5.90 kcal. for the $\lim_{x_1\to 0} \Delta H^M_{x_1}$ of this system. For the *s*-butanol - hexane system, however, we could not find a $\lim_{x_1\to 0} \Delta H^M_{x_1}$ in the literature. In order to estimate the value for this system, we compared $\Delta H^M_{x_1}$ for the normal alcohol - hexane systems with those for the secondary alcohol - hexane systems. In the former cases, the $\lim_{x_1\to 0} \Delta H^M_{x_1}$ values were reported to be 5.8 kcal.,[4] and for the isopropanol system this value is 5.9 kcal., as has been mentioned above. On the basis of the comparison of these three curves

TABLE VII. PHYSICAL CONSTANTS OE ALCOHOL-KETONE COMPLEXES NECESSARY FOR THE CALCULATION OF Eq. 2, AND CALCULATED VALUES OF ΔG_i AND ΔH_i^d

	μ D	t °C	α $\times 10^{-23}$	a^3 $\times 10^{-23}$ cc.	$-\Delta G_K$ kcal./mol.	$-\Delta H_K^d$ kcal./mol.	$-\Delta G_H$ kcal./mol.	$-\Delta H_H^d$ kcal./mol.
Isopropanol-Acetone complex	4.20	15	1.3339	5.9062	2.5428		0.8800	
						4.00		1.495
		20	1.3342	5.9434	2.5176		0.8694	
						3.98		1.481
		25	1.3345	5.9806	2.4924	—	0.8588	—
					Average	3.99	Average	1.49
s-Butanol-Ethyl methyl ketone complex	4.08	15	1.6957	7.1489	1.9838		0.6895	
						3.08		1.15
		20	1.6977	7.1908	1.9648		0.6815	
						3.08		1.14
		25	1.6997	7.2328	1.9457	—	0.6735	—
					Average	3.08	Average	1.15

Dielectric constant;

t°C	15	20	25
n-Hexane	1.897	1.890	1.883
acetone	(21.7)	21.2	20.7
Ethyl methyl ketone	18.98	18.51	18.07

in Fig. 6, we may estimate $\lim_{x_1 \to 0} \Delta H_{x_1}^M$ to be 6.0 kcal. or a little less for the *s*-butanol - hexane system.

In pure alcohol, all the molecules form hydrogen bondings with each other, while each alcohol molecule in the infinite dilution of alcohol in hexane is surrounded by hexane molecules and the hydrogen bonds are broken. Therefore, the values of about 6 kcal. represent energy sufficient to break the hydrogen bonds of pure alcohol. Similarly, the $\lim_{x_1 \to 0} \Delta H_{x_1}^M$ value for each alcohol - ketone system corresponds to the energy of transfer from the pure alcohol state to one in which each alcohol molecule makes a hydrogen bond with a ketone molecule and in which such complexes are surrounded with a large amount of the ketone medium. Roughly speaking, the difference between the $\lim_{x_1 \to 0} \Delta H_{x_1}^M$ value for the alcohol - ketone system and that for the same alcohol - hexane system, that is about 4 kcal., may correspond to the energy of alcohol - ketone hydrogen bonding.

In order to estimate these hydrogen bond energies in some detail, we have considered the thermochemical cycle shown in Fig. 7, where A, K, H and A-K represent molecules of alcohol, ketone, hexane and alcohol - ketone complexes respectively, and where the hypothetical state IV is assumed. Further, we assume that the whole system contains one mole of A, x mol. of K, and y mol. of H, and that $1 \ll x \ll y$.

Judging from this figure, it is reasonable to consider that the true hydrogen bond energy of the A-K complex is equal to the energy change, ΔH_5, for process 5 from state III to state IV. This energy change is easily given by the thermochemical cycle as:

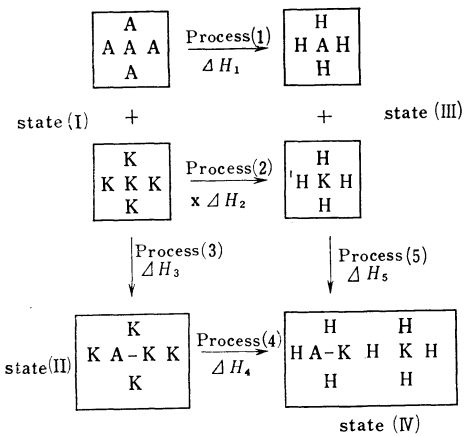


Fig. 7. Thermochemical cycle.

State (I) : One mole of alcohol and x mol. of ketone, both being separated.
State (II) : One mole of A-K complex in the ketone medium, each complex being separated each other.
State (III) : One mole of alcohol, x mol. of ketone in the hexane medium.
State (IV) : One mole of A-K complex and $x-1$ mol. of ketone in the hexane medium.
Process (1) : One mole of alcohol is diluted by a large amount of hexane.
Process (2) : x mol. of ketone are diluted by a large quantities of hexane.
Process (3) : Mixing of alcohol and ketone.
Process (4) : The state (II) is diluted by a large quantities of hexane without breaking A-K complex.

$$\Delta H_5 = -\Delta H_1 - x\Delta H_2 + \Delta H_3 + \Delta H_4 \qquad (1)$$

Since ΔH_1, ΔH_2 and ΔH_3 were measured, it is necessary to estimate the ΔH_4 in process 4 in order to determine ΔH_5.

Two energy changes will contribute to ΔH_4.

The first one, ΔH_4^{KH}, is the heat of the dilution of $(x-1)$ mol. of ketone by large quantities of hexane, which is equal to $(x-1)\ \Delta H_2$. The second one, ΔH_4^d, is due to the difference in the dipolar stabilization enegy of an A-K complex dipole arising from the reaction field by different media, though the van der Waals energy contributes in the latter case to some extent, though this extent is very difficult to estimate and so is disregarded here.

To estimate the energy change for the latter case, we have followed the usual treatment of polar liquids by Onsager,[5] according to which the dipolar stabilization free energy, ΔG_i, is expressed as:

$$\Delta G_i = -(1/2)\mu^2 R/(1-R\alpha)$$
$$R = 2(\varepsilon_i - 1)/(2\varepsilon_i + 1)a^3 \qquad (2)$$

where μ, a and α are the dipole moment, the molecular radius, and the polarizability of the A-K complex, respectively, and where ε_i is the dielectric constant of the medium, i, that is, K or H. Further, the dipolar stabilization energy, ΔH_4^d (i=H or K), is obtained from ΔG_i as:

$$\Delta H_i^d = \frac{\partial(\Delta G_i/T)}{\partial(1/T)}$$

Therefore, the dipolar part of the energy change in process 4 may be given as:

$$\Delta H_4^d = \Delta H_H^d - \Delta H_K^d$$

The data necessary for this calculation and the results obtained are summarized in Table VII. The values of the dipole moment of A-K complexes were determined by the vector addition of those of two component molecules, and the α and a of a complex molecule were assumed to be the sum of those of the two component molecules.

The ΔH_4^d values thus obtained are 2.50 kcal. for the isopropanol - acetone and 1.93 kcal. for the *s*-butanol - ethyl methyl ketone systems. To check the magnitude of these energies, we obtained the difference between the dipolar energy of one mole of ketone in the hexane medium and that of one mole of pure ketone by calculations similar to those described above. The results are as follows: 2.48 kcal. for acetone - hexane and 1.88 kcal. for ethyl methyl ketone - hexane. These values should correspond to the dipolar part of the heats of the dilution of ketone in hexane. Since the measured heats of dilution are 2.15 kcal. and 1.90 kcal. for acetone and ethyl methyl ketone respectively, the calculated dipolar energies are more than or nearly equal to the heats of dilution, indicating that the dipolar energies have been overestimated, particularly in the system containing such small molecules as acetone. Therefore, the ΔH_4^d value of 2.50 kcal. for isopropanol - acetone seems to be overestimated and some correction (at least 0.4 kcal.) may be necessary.

Using ΔH_4^d and other measured values, ΔH_5 is calculated by Eq. 1 as:

for isopropanol - acetone:

$$\Delta H_5 = -5.90 - 2.15\,x + 1.76 + 2.50 + 2.15(x-1)$$
$$= -3.79 \text{ kcal.}$$

for *s*-butanol - ethyl methyl ketone:

$$\Delta H_5 = -6.0 - 1.90\,x + 1.82 + 1.93 + 1.90(x-1)$$
$$= -4.15 \text{ kcal.}$$

Taking account of the overestimation of dipolar energy, the hydrogen bond energy of alcohol - ketone complexes may be estimated to be about 4 kcal. or a little more for the two systems.

Summary

A microcalorimeter of the twin type has been constructed, one which is operated semi-automatically. Using this apparatus, the heats of mixing for alcohol - ketone, alcohol - hexane, and ketone - hexane solutions have been measured. From these heats of mixing, the hydrogen bond energy of the O–H···O= type has been estimated to be about 4 kcal. by means of the thermochemical cycle.

The authors wish to thank Dr. Ko Kimura for his kind advice. The expenses of this work have been partly defrayed by a Grant from the Ministry of Education.

Department of Chemistry
Faculty of Science
Osaka City University
Sumiyoshi-ku, Osaka

5) C. G. Böttcher, "Theory of Electric Polarisation," Elsevier Publishing Co., Houston (1952).

Studies of Methionine Sulfoxide. I. The Acidic Degradation of Methionine Sulfoxide

By Kensaku MORIHARA

(Received June 4, 1964)

Although biochemical attention[1-3] has recently been focussed on methionine sulfoxide (MSO), the chemical properties of this amino acid have not been sufficiently investigated. It is well-known that MSO is converted to methionine by the action of hydrochloric acid under the usual conditions for the acidic hydrolysis of proteins with hydrochloric acid, and it is also known that on storage of a hydrochloric acid solution of methionine (Met), the formation of MSO by oxidation occurs in air.

This action of hydrochloric acid upon sulfoxide is unusual and has been reported in only a few cases. In the case of MSO, the reaction does not seem to be a simple reduction, as Reiner et al. observed in the course of their studies of the agene factor of wheat flour. They observed that MSO yielded two additional ninhydrin positive spots besides Met on a paper chromatogram after acidic hydrolysis.[4]

In the present work, in order to investigate the mechanism of the degradation and chemical properties of this amino acid through the action of hydrochloric acid upon it, the degradation products will be isolated.

On treating MSO with 12 N hydrochloric acid at 105°C in a sealed tube for 20 hr., seven ninhydrin positive spots were observed on two-dimensional chromatograms. The hydrolyzate was submitted to column chromatography, and four of the seven products were isolated and identified as methionine, homoserine, homocystine and homolanthionine.

Results and Discussion

Two-Dimensional Paper Chromatography.— The reaction mixture obtained by the hydrolysis of 31.7 mg. of DL-MSO with 2 ml. of 12 N hydrochloric acid in a sealed tube was treated with the cation exchange resin, Amberlite IR-120 (H^+) in the usual manner in order to remove hydrogen chloride. The resulting mixture of reaction products was submitted to two dimensional paper chromatography. As may be seen in Figs. 1 and 2, seven ninhydrin-positive spots were observed on the chromatograms and the main product, spot A, appeared to be Met judging from its R_f values. Spot B seemed rather unstable, and its location and size varied according to the reaction condition. The size of this spot B decreased with the reaction period, whereas the sizes of spots C, D and E increased with the reaction time. This must indicate that the compound giving spot B was a precursor of the substances in spots C, D and E. Spot B seemed to be too unstable and spots F and G were too small to attempt their identification. Therefore, the isolation of only the substances corresponding to spots C, D and E was carried out.

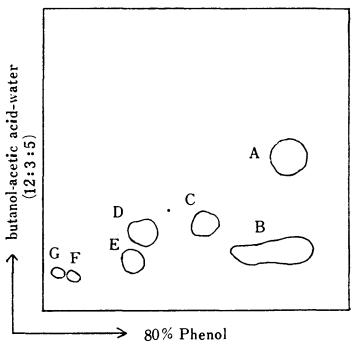


Fig. 1. Two-dimensional chromatogram I.

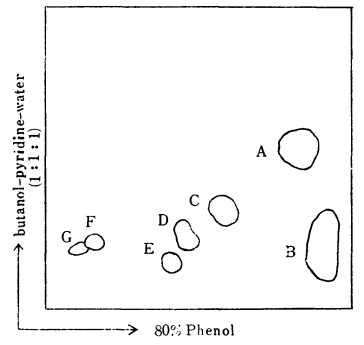


Fig. 2. Two-dimensional chromatogram II.

1) S. Black, E. M. Harte, B. Hudson and L. Wartofsky, *J. Biol. Chem.*, **235**, 2910 (1960).
2) J. F. Thompson, C. J. Morris and R. M. Zacharius, *Nature*, **178**, 593 (1956).
3) T. Sugawa, H. Akedo and M. Suda, *J. Biochem. (Japan)*, **47**, 131 (1960).
4) L. Reiner, F. Misani, T. W. Fair, P. Weiss and M. G. Cordasco, *J. Am. Chem. Soc.*, **72**, 2297 (1950).

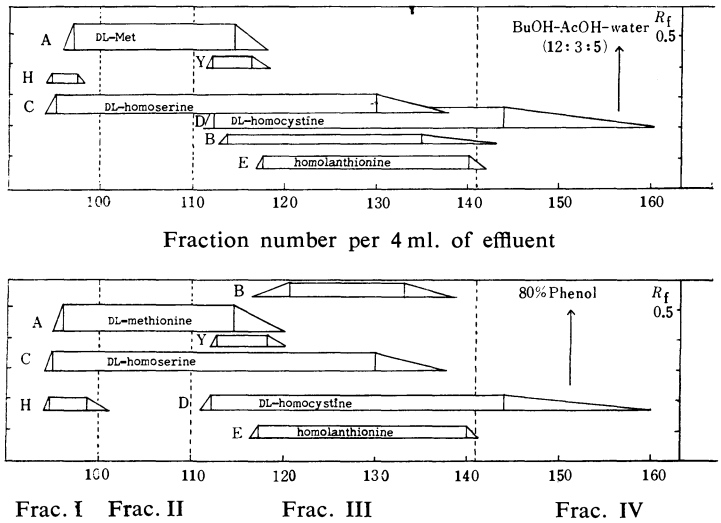


Fig. 3. Displacement chromatography of the hydrolyzate.

Elution Chromatographic Separation. — To isolate the reaction products from the hydrolyzate of 5 g. of DL-MSO, fractionation was carried out by displacement chromatography on a column of the Amberlite CG-120 type II with 0.5 N ammonia and then by gradient chromatography with 4 N hydrochloric acid, following the procedure of Hirs et al.[5] with some modifications. Aliquots of each fraction were analyzed by one dimensional paper chlomatography. The results are summarized in Figs. 3, 4 and 5. The five spots of Fig. 1, spots A, B, C, D and E, correspond to five zones of Fig. 3, zones A, B, C, D and E respectively. However, the zones corresponding to spots F and G were not obtained, and, on the other hand, a new zone H appeared which did not correspond to any spot in Fig. 1. These products were too small in quantity to be identified. Moreover, unknown ninhydrin-negative yellow zone was observed, as is shown in Fig. 3.

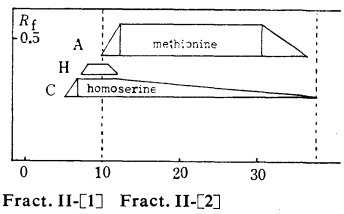


Fig. 4. Rechromatography of fraction II.

Products Isolated and Identified. — DL-Met, corresponding to spot A, was isolated as crystals from fractions II-[2] and III-[4]; DL-homoserine, corresponding to spot C, from fraction III-[2]; DL-homocystine, corresponding to spot D, from fraction IV, and homolanthionine, corresponding to spot E, from fraction III-[6].

From the other fractions, though they contained ninhydrin-positive materials, no pure product was isolated.

The Mechanism of Degradation.—From the results obtained, the route of the degradation of MSO seems to be complex; the most plausible one is drawn in Fig. 6. Route A is the ordinary route of the reduction of MSO to Met.

The initial products in route B may be supposed to be methane sulfinic and α-amino-β,γ-dehydro butyric acid if an elimination reaction takes place, or methane sulfinic acid and homoserine, if hydrolytic splitting occurs.

However, according to Ostemayer et al.[6], *S*-methylcysteine sulfoxide is split into methane sulfinic acid and dehydroalanine, the latter being further decomposed to ammonia and pyruvic acid in hot dilute sulfuric acid. Therefore, we suggest that an analogous reaction series occurs in the case of MSO and that it is reasonable to assume that α-amino-β,γ-dehydro butyric acid is an intermediate. Route C is the rearrangement of the sulfoxide to yield homocysteine and formaldehyde, and the resulting homocysteine can be easily converted to homocystine by air oxidation.

The formation of homolanthionine is explained by the addition of homocysteine to α-amino-β,γ-dehydro butyric acid.

When MSO was treated with 6 N hydrochloric acid for 12 hr., only one ninhydrin-positive

5) H. W. Hirs, S. Moore and M. W. Stein, *J. Am. Chem. Soc.*, **76**, 6063 (1954).

6) F. Ostermayer and D. S. Tarbell, *J. Am. Chem. Soc.*, **82**, 3752 (1960).

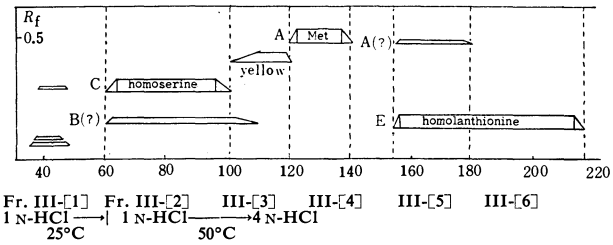


Fig. 5. Gradient chromatography of fraction III.

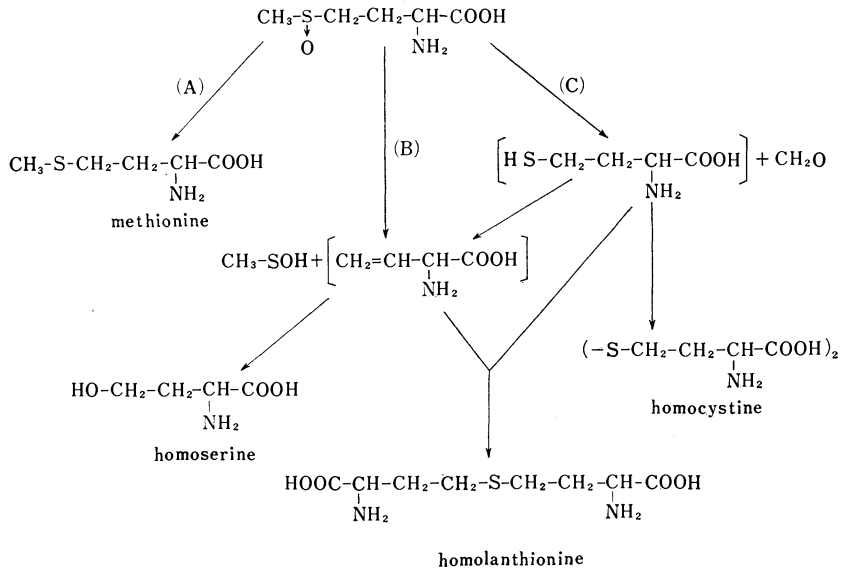


Fig. 6

spot of Met was detected on the paper chromatogram, showing that only the reduction of route A took place, and that only when it is treated with 12 N hydrochloric acid the complex reactions of routes B and C take place, thus giving rise to the above-mentioned products. Therefore, the fact that these products have not been detected in the usual hydrolyzate of protein with 6 N hydrochloric acid does not completely exclude the possibility of the presence of a MSO residue in protein molecules.

Experimental

Materials.—DL-Methionine sulfoxide was prepared by the method of Toenis et al.[7] with the slight modification of using more methanol and less water. M. p. 186°C (decomp.).

Found: C, 36.35; H, 6.89; N, 8.56. Calcd. for $C_5H_{11}O_3NS$: C, 36.35; H, 6.71; N, 8.48%.

Concentrated hydrochloric acid prepared by the saturation of distilled water with hydrogen chloride gas was used first, but later concentrated hydrochloric acid, special grade, purchased from Wakō Pure Chemical Industries, Ltd., was used, as it was proved to give the same result.

Hydrolysis and Chromatographic Separation.—Five grams of DL-methionine sulfoxide were dissolved in 30 ml. of concentrated hydrochloric acid, and the mixture was heated in a sealed tube at 105°C for 20 hr. The hydrolyzate was then brought to dryness and transferred to a column of the Amberlite CG-120 type II (H^+ form), 1.5 cm.×25 cm. Distilled water was passed through the column until the effluent became neutral. Then the absorbed hydrolytic products were eluted with 0.15 N ammonium hydroxide at 60°C, and the effluent was collected in 4 ml. fractions. An aliquot of each fraction was submitted to one dimensional chromatography (BuOH : AcOH : Water—12 : 3 : 5) in order to analyze the components. Fraction II was rechromatographed in the same way.

For the further fractionation of fraction III, the chromatographic system described by Hirs et al.[5] was employed with some modifications. A shorter column than that described by Hirs et al. (40 cm. ×2 cm.) was used, and Amberlite CG-120 type II was employed instead of Dowex 50×4. The column was pretreated with 10 volumes of 1 N hydrochloric acid.

7) G. Toenis and J. J. Kolb, *J. Biol. Chem.*, **128**, 399 (1939).

Fraction III was brought to dryness and dissolved in a few milliliters of 1 N hydrochloric acid, and the solution was transferred to the column. The chromatography was carried out by elution with 1 N hydrochloric acid at a room temperature of 25°C, and the effluent was collected in 4 ml. fractions. When 324 ml. of effluent had been eluted, the concentration of hydrochloric acid was gradually increased from 1 to 4 N using a mixing chamber of 200 ml., and the temperature of the column was raised and kept at 50°C. Each fraction was dried, and the components were analyzed by one-dimensional paper chromatography. As may be seen in Fig. 5, homocystine was not eluted under these conditions.

DL-Methionine.—Fraction II-[2] was decolorized with active charcoal and concentrated under reduced pressure until it was almost dry. The ethanol was added, and the resulted solution was allowed to stand. The precipitate formed was collected by filtration and recrystallized from water and ethanol. The recrystallization was repeated until the contaminating homoserine and another ninhydrin-positive material had been removed. The crystals formed were identical in their infrared spectrum with authentic methionine. From fraction III-[4], pure methionine was also isolated without decolorization after the fraction had been treated with ion exchange resin to remove the hydrogen chloride.

DL-Homoserine. — Fraction III-[2] was concentrated under reduced pressure and treated with cation exchange resin to remove the hydrogen chloride in the usual manner. The ammoniacal effluent was concentrated, ethanol was added to this solution until the cloudy point was obtained, and then the solution was allowed to stand. The resulting precipitate was collected and recrystallized from water and ethanol.

Found: C, 39.68; H, 7.53; N, 11.04. Calcd. for $C_4H_9O_3N$: C, 40.33; H, 7.62; N, 11.76%.

The infrared spectrum of this material and its R_f values in two solvent systems, *n*-butanol - acetic acid - water (12 : 3 : 5) and 80% aqueous phenol, were identical with those of authentic L-homoserine obtained from the Kyowa Hakko Kogyo Co., Ltd.

DL-Homocystine. — Fraction IV was treated in virtually the same way as methionine, and an amino acid was isolated. M. p. 258°C.

Found: C, 35.43; H, 6.60; N, 9.50. Calcd. for $C_8H_{16}O_4N_2S_2$: C, 35.82; H, 6.01; N, 10.45%.

Though the value of the nitrogen content was less for homocystine, the chromatographic behavior and infrared spectrum of this material were identical with those of authentic DL-homocystine perchased from Wakō Pure Chemical Industries Co., Ltd.

Homolanthionine. — An amino acid was isolated from fraction III-[6] in virtually the same way as homoserine. In this case, decolorization was necessary as the ammoniacal effluent was acompanied with an unknown red violet material. M. p. 270°C (decomp.).

Found: C, 40.25; H, 6.97; N, 11.92. Calcd. for $C_8H_{16}O_6N_2S$: C, 40.67; H, 6.83; N, 11.86%.

The authentic homolanthionine prepared from DL-menthionine and DL-homoserine according to the procedure described by Stekol[8] was found to contain three components on paper chromatograms, DL-homolanthionine, meso-homolanthionine and a trace of unchanged DL-methionine. However, the infrared spectrum of the isolated amino acid was identical with that of a mixture of DL and meso-homolanthionine, and its R_f values in two solvent systems, *n*-butanol - acetic acid - water (12 : 3 : 5) and 80% aqueous phenol, were identical with those of one component of the mixture. Therefore, the amino acid isolated must be an isomer of homolanthionine.

The author is indebted to Professor Shiro Akabori and Dr. Yoshiharu Izumi for their constant interest and encouragement in this work, and to the Misses Kiku Koike and Masako Kawakita of this Institute for their elemental analysis.

Division of Organic Chemistry
Institute for Protein Research
Osaka University
Kita-ku, Osaka

8) J. A. Stekol, *J. Biol. Chem.*, **173**, 153 (1948).

Studies of Methionine Sulfoxide. II. The Transformation of Methionine Hydantoin Sulfoxide

By Kensaku MORIHARA

(Received June 4, 1964)

During our study[1] of the acidic degradation of methionine sulfoxide (MSO), the products homocystine, homolanthionine, homoserine and methionine (Met) were isolated. The formation of homocystine and homolanthionine indicated that the demethylation of MSO occurs much more easily than that of Met, for Met does not give the above-mentioned products under these conditions. Moreover, it may be assumed that this demethylation is due to the conversion of the sulfoxide group to give *S*-hydroxymethyl-homocysteine.

Smythe studied the action of some kinds of hydrogen chloride on dibenzyl sulfoxide in detail and suggested that there was a dynamic tautomerism between the sulfoxide and the corresponding α-oxy-sulfide during the reaction.[2] Later, Horner et al. demonstrated that several sulfoxides were converted to the corresponding α-acyloxy-sulfoxides in a good yield by the action of acid anhydride.[3] Therefore, it is reasonable to assume that such a rearrangement occurs to yield *S*-hydroxymethyl-homocysteine derivatives from MSO prior to demethylation, as has already been reported in the previous paper.[1] This transformation of sulfoxide to α-hydroxy-sulfide radicals is very interesting with regard to the biochemical role of sulfoxides, especially that of MSO.[4]

In this paper, it will be demonstrated that the quantitative transformation of methionine hydantoin sulfoxide (MHSO) occurs through the action of acetic anhydride, yielding the corresponding α-acetoxy-sulfide, the structure of which will be determined mainly from the fact that formaldehyde is quantitatively released from the product when it is hydrolyzed with acid or alkali.

Results and Discussion

The Transformation of MHSO. — The substrate of this reaction, MHSO, was prepared as white crystals by the oxidation of DL-methionine hydantoin (MH) with hydrogen peroxide. MHSO is a strongly polar substance, as it is freely soluble in water, slightly soluble in alcohol, and insoluble in other non-polar solvents, while MH is freely soluble in non-polar solvents but insoluble in water. MHSO was used instead of MSO in this study because when MSO was treated just as MHSO with acetic anhydride, the color of the reaction mixture turned red-brown, showing that an undesirable side reaction, mainly due to the formation of azlactone, took place. On the other hand, when a suspension of MHSO (1.74 g.) in acetic anhydride (3 ml.) was heated under reflux on an oil-bath, it was resolved in a few minutes, and the color of the reaction mixture turned only slightly yellow, showing that no side reaction occurred. The reaction was allowed to proceed for about an hour, and then excess water was added to decompose the unchanged acetic anhydride. The resulting mixture was concentrated under reduced pressure to remove the acetic acid and water. The residue was then extracted with ethyl acetate, an the extract washed with water and dried on sodium sulfate. When the ethyl acetate was removed under reduced pressure, a yellow syrup was obtained (about 2.0 g.). This material was quite different from MHSO; it was insoluble in water and easily soluble in ethyl acetate, showing, as expected, that the strong polarity of MHSO had been lost by the action of acetic anhydride to give the corresponding α-acetoxy-sulfides, as is shown in Fig. 1. Only when the reaction was stopped within a few minutes was the starting MHSO recovered from the aqueous layer.

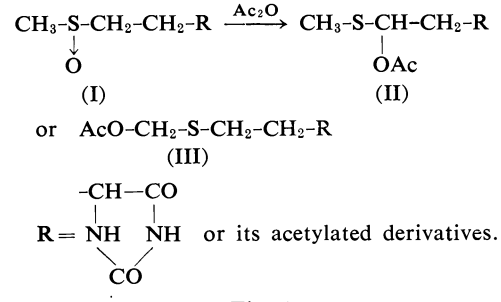


Fig. 1

1) K. Morihara, This Bulletin, 37, 1781 (1964).
2) J. A. Smythe, *J. Chem. Soc.*, 95, 349 (1909).
3) L. Horner and P. Kaiser, *Annal. D. Chem.*, 626, 19 (1959).
4) S. Oae, T. Kitao, S. Kawamura and Y. Kitaoka, 35th General Meeting of the Japanese Biochemical Society, September, 1962.

The Structure of the Product.—Attempts to purify and crystallize the product in order to determine its structure were unsuccessful. However, from the results of Horner et al. it seems that the structure is either II or III.

Desulfurization with Raney nickel[5] was carried out to see whether the structure was II or III. If it was II, homoserine derivatives should be formed, while if it is III, α-amino-butyric acid derivatives may be expected by this treatment. A small portion of the syrup was treated with Raney nickel for about 3 hr. The catalyst was then filtered off, and the filtrate was hydrolyzed with 6 N hydrochloric acid. The hydrolyzate was evaporated to dryness and submitted to paper chromatography.

Only one ninhydrin-positive spot was detected, and this had the same R_f value as an authentic sample of α-amino-butyric acid, showing that only III was formed when MHSO was treated with acetic anhydride. Furthermore, it was expected that formaldehyde should be formed from III or methyl mercaptan from II when the syrup was hydrolyzed with acid or alkali. Small portions of the syrup was transferred to Kjehldahl distilling tubes, together with 6 N sulfuric acid, or to 3 N sodium hydroxide, and the samples were submitted to steam-distillation for 15 min. The distillate was neutralized with sodium bicarbonate when it had been treated with sulfuric acid. To the distillates was added a 0.4% aqueous solution of dimedone, and the mixtures were allowed to stand overnight. White needle-shaped crystals were obtained; they melted at 189°C and were identified as formaldimedone[6] by infrared spectroscopy. This also showed that III was the product, and, though a slight mercaptan-like odor was detected in the distillate, no aldehyde was detected with Schiff's reagent in the residual mixture. In the same way, when the reaction mixture of MHSO, treated with acetic anhydride and then by hydrolysis with sulfuric acid or sodium hydroxide, was submitted to steam distillation, formaldehyde was also caught directly as the dimedone derivative.

The Recovery of Formaldehyde.—To confirm the above results, the formaldehyde released from MHSO was determined quantitatively. Five samples of MHSO, each about 100 mg., were boiled with 2 ml. of acetic anhydride for 3, 10, 30, 60 and 180 min. respectively, while another sample of about 100 mg. of methionine hydantoin (MH), was treated in the same way, for 180 min., as a control. The reaction was stopped by then addition of 1 ml. of water to each reaction mixture. Then to each was added 5 ml. of 6 N sulfuric acid, and the solutions were distilled for 15 min. with steam as has been described above. The distillates were received in ice-cooled Erlenmeyer flasks containing sodium bicarbonate roughly equivalent to 2 ml. of acetic anhydride suspended in 10 ml. of water. The distillate was neutralized with sodium bicarbonate or acetic acid, and then the distilled formaldehyde was determined by iodometry by the direct bisulfite method.[7] The results are shown in Table I. The quantitative liberation of formaldehyde from MHSO was observed during the first 30 min. of the reaction period. This confirms that the product of the rearrangement is not II but III, and it also suggests that this rearrangement is essentially useful for the determination of MSO and its derivatives. When MSO was treated by the same procedure as MHSO, the reaction mixture turned red-brown; formaldehyde was also distilled off and trapped as the dimedone derivative, but its recovery was low and not quantitative, and, furthermore, this results was so reproducible as that with MHSO.

Table I. Quantitative liberation of formaldehyde from MHSO

Substrate mg. (μ mol.)	Reaction period	Formaldehyde found μ mol.	Recovery %
MHSO 99.5 (523)	3	112	21.2
100.2 (527)	10	417	92.2
101.7 (534)	30	533	100
101.2 (532)	60	525	99
100.8 (531)	180	539	101
MH 99.6 (573)	180	0	0

In conclusion, although this procedure is not suitable for the determination of MSO for the above-mentioned reason, it may be practically useful for the determination of MHSO itself, even if the iodometric titration by the direct bisulfite method is somewhat troublesome and time-consuming.

Experimental

The Preparation of DL-Methionine Hydantoin (MH) and Its Sulfoxide (MHSO).—DL-Methionine hydantoin (MH) was prepared by boiling DL-methionine with an aqueous urea solution in the usual manner.[8] M. p. 94°C.

Found: C, 41.43; H, 5.63; N, 16.25. Calcd. for $C_6H_{10}O_2N_2S$: C, 41.38; H, 5.79; N, 16.09%.

Seventeen and a half grams (0.1 mol.) of DL-methionine-hydantoin was dissolved in 200 ml. of methanol while being gently warmed. This solution was then cooled, and 15 ml. of a (30%) hydrogen

5) K. Vogler, *Helv. Chim. Acta*, **30**, 1766 (1947).
6) D. Vorländer, *Ber.*, **58B**, 2656 (1925).
7) L. H. Dounally, *Ind. Eng. Chem. Anal. Ed.*, **25**, 91 (1933).
8) F. Lippich, *Ber.*, **41**, 2974 (1908).

peroxide solution was added drop by drop over about a 30 min. period. The reaction temperature was kept below 20°C by cooling, and the solution was allowed to stand for a further 3 hr. Then the mixture was concentrated to 20~30 ml. under reduced pressure at below 40°C. One hundred milliliters of benzene was added, and the resulting azeotropic mixture was distilled off to remove any traces of water. This procedure was repeated twice, and on concentration the mixture became cloudy and the crystalline product precipitated. About 40 ml. of acetone was added in small portions to precipitate the crystalline product completely. White crystals were collected by filtration and washed first with acetone and then with a small amount of ether. The yield of the crude product was 19 g. Nineteen grams of the product was suspended in 19 ml of water, resolved by warming, and filtered. Then 250 ml. of acetone was added in small portions while the solution was being cooled, and the mixture was stored in a refrigerator overnight. The fine white crystals obtained were washed with a small amount of acetone and then with ether. The yield was 15.75 g.; M. p. 156~157°C (corr.)

Found: C, 37.46; H, 5.27; N, 14.42. Calcd. for $C_6H_{10}O_3N_2S$: C, 37.90; H, 5.30; N, 14.73%.

This substance is soluble in water and hot methanol. It is slightly soluble in hot ethanol but insoluble in methanol, ethanol, acetone, ethyl acetate and ether.

The author is indebted to the Misses Kiku Koike and Masako Kawakita of this Institute for their elemental analysis.

Division of Organic Chemistry
Institute for Protein Research
Osaka University
Kita-ku, Osaka

Studies of Methionine Sulfoxide. III. A New Colorimetric Method for the Determination of Methionine Sulfoxide and Its Derivatives

By Kensaku MORIHARA

(Received June 9, 1964)

In a previous paper of this series,[1] the author reported that a rearrangement reaction occurred when methionine hydantoin sulfoxide (MHSO) was treated with acetic anhydride giving the corresponding α-acetoxy-thio-ether quantitatively. In the present work, a new photometrical method for the determination of methionine sulfoxide (MSO) and its derivatives based on this rearrangement reaction will be established. The method is based on the facts that formaldehyde is easily released from the products of the rearrangement reaction by hydrolysis and that it can be determined photochemically by using chromotropic acid.[2]

Though one is needed for biochemical studies, no direct method for the determination of MSO in the presence of methionine (Met) has yet been reported except that of polarography.[3] Recently, Neumann et al. developed an indirect procedure for the chromatographic determination of MSO residues in ribonuclease,[4] but their method cannot be applied to the routine analysis of MSO as it is very complicated. On the other hand, the present method is very simple and suitable for routine determinations of MSO, although it is impossible to use it to analyze the MSO residues in proteins accurately.

1) K. Morihara, This Bulletin, **37**, 1785 (1964).
2) D. A. MacFadyen, *J. Biol. Chem.*, **158**, 107 (1945).
3) K. Morihara, 13th Annual Meeting of the Chemical Society of Japan, Tokyo, April, 1960.
4) N. P. Neumann, S. Moore and W. H. Stein, *Biochem.*, **1**, 68 (1960).

Results and Discussion

The Colorimetric Determination of the Formaldehyde Released from MSO and MHSO.— The formaldehyde released from the products of the above-mentioned rearrangement reaction can be effectively determined by the photometrical method of MacFadyen using chromotropic acid.[2] As the chromotropic acid reagent is strongly acidic, its use could eliminate the necessity of treating the reaction mixture with acid or alkali to release the formaldehyde. The procedure for the determination is given below (see "Recommended Procedure"). The experiments reported in this paper were carried out essentially by means of this procedure.

Reaction Conditions. — As is summarized in Table I, various conditions for the rearrangement were investigated. Thirty minutes boiling with acetic anhydride was found to be the most practical condition.

The Reaction Period of the Rearrangement. —To find the time taken for the rearrangement reaction, the formaldehydes released from

TABLE I. REACTION CONDITIONS

Condition	O. D. (observed)
Reflux for 30 min. (bath temp. 140°C)	0.391
Reflux for 30 min. (bath temp. 170~180°C)	0.382
97°C for 30 min.	0.057
97°C for 120 min.	0.357
97°C for 150 min. and then room temp. for 17 hr.	0.344
97°C for 20 hr.	0.332

MHSO and from MSO were successively analyzed by the colorimetric method. The results obtained are shown in Fig. 1; they confirm the results previously reported. The liberation of formaldehyde from MHSO began more rapidly than that from MSO without any lag in time, and the optical density became constant after the first 10 min. On the other hand, the liberation of formaldehyde from MSO was rather slow for the first 5 min. In this period, an azlactone ring may be formed prior to the rearrangement. The optical density became a little less after about 20 min., as the reaction period became longer, indicating that some unkown decomposition reaction took place. Twenty to 30 min. was a suitable reaction period for either reaction. In all the experiments described below, therefore, the reaction period was 30 min.

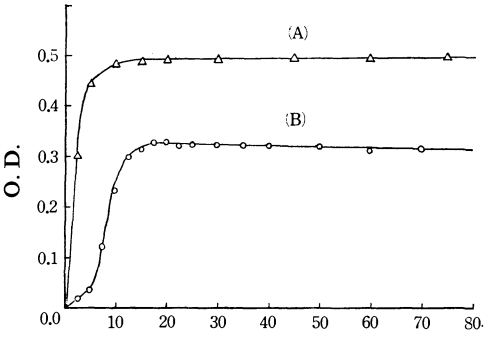


Fig. 1. Reaction period.
(A) MHSO 31.2 μ mol. in 1 ml. of acetic acid
(B) MSO 29.3 μ mol. in 1 ml. of acetic acid

The Optimal Ratio of Acetic Anhydride to Acetic Acid.—It was observed experimentally that the recovery of formaldehyde was affected by the amount of acetic anhydride relative to that of the sample solution, though the acetic anhydride used was stoichiometrically sufficient for the reaction. The results are shown in Fig. 2.

Thus, in standard determinations 2 ml. of acetic anhydride and 1 ml. of an acetic acid solution of the sample were used.

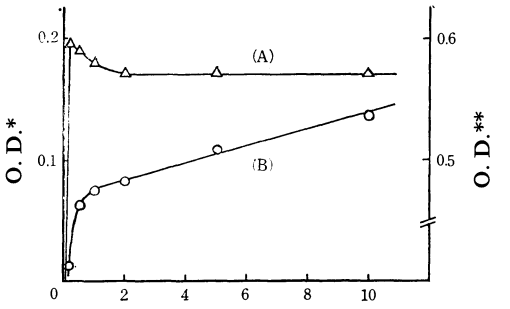


Fig. 2. Ratio (volume of acetic anhydride/volume of acetic acid solution of substrate).
(A) MSO (B) MHSO
* For curve A ** For curve B

The Period of Heating with a Chromotropic Acid Reagent.—In the usual procedure for the determination of formaldehyde with a chromotropic acid reagent, full color development was obtained by heating the solution at 100°C for 30 min. In this case, however, the chromotropic acid reagent acted in two ways: as a hydrolytic reagent to liberate formaldehyde on the one hand, and as a color reagent for the resulting formaldehyde on the other. Thus the optimal heating period had to be tested experimentally. As is shown in Table II, the optical density of the color increased with the heating period, but that of an authentic formaldehyde solution also increased at almost the same rate. Therefore, heating at 100°C for 30 min. was adopted as the standard procedure. However, in the presence of a large amount of an interfering substance, heating for 30 min. was not always sufficient, as will be mentioned below. In such cases, the period had to be prolonged until the optical density became the maximum value.

TABLE II. PERIOD OF HEATING WITH CHROMOTROPIC ACID REAGENT

Substrate	Heating period min.	O. D. (observed)
Diluted reaction mixture*	30	0.592
	60	0.612
	120	0.635
	180	0.641
	240	0.655
	300	0.670
Standard formaldehyde solution**	30	0.962
	60	0.981
	120	0.988
	180	1.009
	240	1.021
	300	1.043

1 ml. of sample solution was mixed with 10 ml. of chromotropic reagent.
* 6.06×10^{-1} μ mol. per ml.
** 6.55×10^{-1} μ mol. per ml.

Standard Curves of MHSO and MSO.—As is shown in Fig. 3, good linear standard curves of MHSO and MSO were obtained in the range between 1.0×10^{-1} μ mol. per ml. and at least 8.0×10^{-1} μ mol. per ml. It was found that, as the standard curve of MHSO was more constant and was reproducible in different determinations than that of MSO, the standard curve in Fig. 3 (C) could be used with a good accuracy. However, the standard curve of MSO shown in Fig. 3 (B) was more variable in different determinations, though it was always linear, so a parallel solution of MSO of a known concentration must be treated under the same conditions in order to determine the exact amount of MSO in a given sample. However, the variation in the standard curve of MSO was so slight that in practice MSO could be determined with a maximal error of only 5 per cent even when curve B in Fig. 3 was used. Moreover, when a ratio of 1 ml. of acetic anhydride to 1 ml. of MSO acetic acid solution was used, almost the same linear standard curve was obtained (curve A in Fig. 3.) However, this standard curve was more variable in different determinations than that obtained with 2 ml. of acetic anhydride (curve B in Fig. 3).

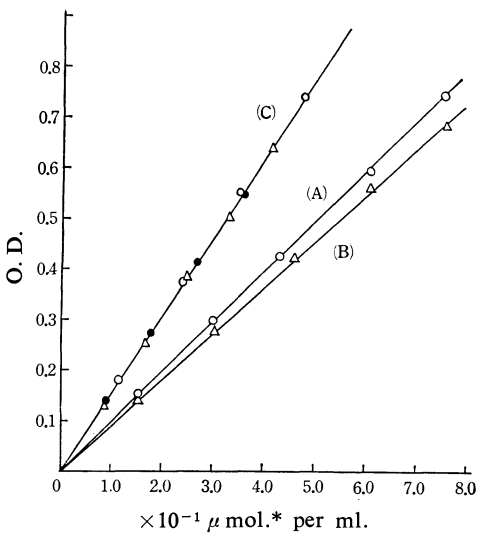


Fig. 3. Standard curves of MSO and MHSO.
(A) MSO 1 ml. of acetic anhydride and 1 ml. of an acetic acid sample solution were used.
(B) MHSO 2 ml. of acetic anhydride and 1 ml. of the sample solution were used.
(C) MHSO -○- and -●- 1 ml. of acetic anhydride and 1 ml. of the sample solution were used. The determinations were independently carried out.
-△- 2 ml. of acetic anhydride and 1 ml. of the sample solution were used.
* Final concentration of substrate when the reaction mixture was diluted to 100 ml.
The procedure used is described in "Recommended Procedure."

The Recovery of the Formaldehyde Released from MHSO and MSO. — It has previously been reported that the quantitative liberation of formaldehyde may be confirmed by iodometric titration.[5] This result was confirmed by the photometrical method. An exact, known weight of hexamethylene tetramine which had been twice purified by sublimation was dissolved in 100 ml. of 3 N sulfuric acid. To hydrolyze the hexamethylenetetramine to formaldehyde, this solution was incubated at 80°C until the aliquots gave a constant value for optical density when treated with a chromotropic reagent. Using this hydrolyzate as the standard formaldehyde solution, an optical density of 0.498 was obtained for 31.2 μ mol. of formaldehyde and an optical density of 0.648, for 41.1 μ mol. of MHSO. Thus the optical density per 1 μ mol. of the two was identical; the recovery was quantitative. The recovery of formaldehyde from MSO was determind indirectly by a comparison with that from MHSO, which was reacted in parallel; it was always found to be about 60 per cent of that of MHSO.

The Recovery of Formaldehyde from Other Derivatives of MSO and Their Standard Curves. —To ascertain why the recovery of formaldehyde from MSO was considerably lower than that from MHSO, the relationship between the structure of the sulfoxide and the recovery of formaldehyde was investigated by studying the

Table III. Recoveries of MSO derivatives

Substrate*	Recovery** %
Acetyl methionine sulfoxide (AcMSO)	57.0
Benzoyl methionine sulfoxide (BzMSO)	66.5
Carbobenzoxy methionine sulfoxide (CbzMSO)	87.5
Carbobenzoxy methionine sulfoxide ethyl ester (CbzMSO-OEt)	59.5
Carbobenzoxy *S*-oxo-methionyl methionine sulfoxide ethyl ester (CbzMSO-MSO-OEt)	90.5
2,4-Dinitrophenyl methionine sulfoxide (DNP-MSO)	43.0

* Substrates in 1 ml. of acetic acid were mixed with 2 ml. of acetic anhydride in the standard manner.
** Recoveries were measured by comparison of their O. D. with the O. D. of a sample of MHSO treated in parallel.

5) L. H. Donnally, *Ind. Eng. Chem. Anal. Ed.*, **25**, 91 (1933).

TABLE IV. INTERFERENCE BY ACYL AMINO ACID AND PREVIOUSLY TREATED AMINO ACID

Substrate (S)	Interfering substance* (I)	(I)/(S) (by mol.)	O. D. (corrected)	Recovery %
20.05 μ mol. MHSO	45 mg. glycine	30	299	96.8
20.05 μ mol. MHSO	75 mg. acetyl glycine	30	299	96.8
20.05 μ mol. MHSO	90 mg. methionine	30	288	90.3
20.05 μ mol. MHSO	114 mg. acetyl methionine	30	287	90.0
20.05 μ mol. MHSO	(Previously treated)**			
20.05 μ mol. MHSO	60 mg. methionine	20	309	97.5
20.05 μ mol. MHSO	90 mg. methionine	30	305	96.3
20.05 μ mol. MHSO	120 mg. methionine	40	292	92.1

* Interfering substances were added to the sample solution which were then treated in the standard manner.

** Methionine suspended in 1 ml. of acetic acid was treated with 2 ml. of acetic anhydride for 30 min. The resulting reaction mixture was added to that of MHSO and diluted to 100 ml. with water, and the resulting solution was measured as usual. O. D. was corrected by drawing 2 times of "blank."

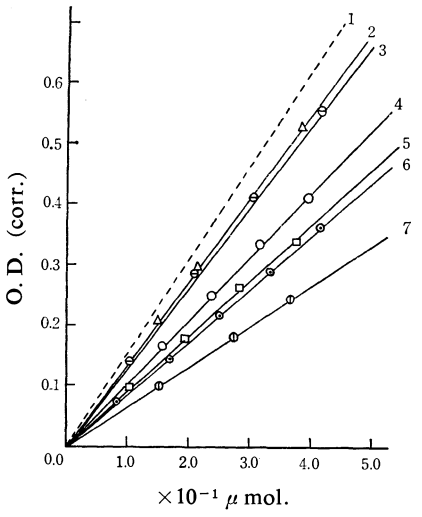


Fig. 4. Standard curves of derivatives of MSO.
1 MHSO 2 Cbz-MSO-MSO-OEt
3 Cbz-MSO 4 Bz-MSO
5 Cbz-MSO-OEt 6 AcMSO
7 DNP-MSO

standard curves of their recoveries. The results are shown in Table III and Fig. 4, but no clear conclusion can be deduced from them. The recovery from AcMSO* was almost identical with that from MSO, indicating that azlactone formation occurred prior to the rearrangement reaction. This conclusion was also supported by the curve in Fig. 1 mentioned above. Thus, it seems unlikely that steric hinderance due to the hydantoin ring decides the direction of the rearrangement to give a quantitative liberation of formaldehyde, because the steric effect due to the azlactone ring seems similar to that due to the hydantoin ring. This is also supported by the fact that the recovery of formaldehyde from Cbz-MSO,* Cbz-MSO-OEt* and Cbz-MSO-MSO-OEt* was not quantitative, though there is more steric hinderance in these compounds. Moreover, it is impossible to ascribe the lower recovery of formaldehyde from MSO than from MHSO to the consumption of sulfoxide by the oxidation of the amino group, because the recovery of formaldehyde from AcMSO, which had no amino group to be oxidized, was identical with that from MSO. Another possibility is that the azlactone formed from MSO strongly inhibited the color reaction of chromotropic acid. Although this possibility was indirectly disproved by the fact that an equivalent molarity of Met scarcely interfered at all with the determination of MSO and MHSO, this possibility was examined directly. If interference occurred, the addition of acyl amino acids, which easily form azlactones, to the substrate solution, or the addition of the acyl

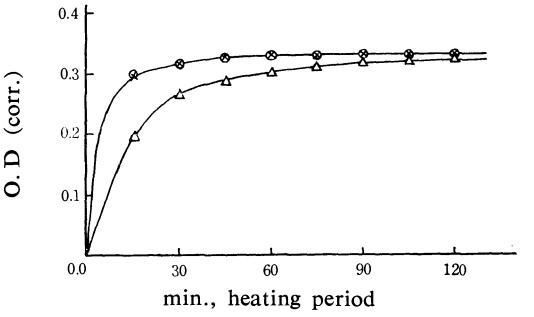


Fig. 5. Development of the color under copresence of interfering substances.
-○- 20.05 μ mol. MHSO
-×- 20.05 μ mol. MHSO plus 800 μ mol. glycine
-△- 20.05 μ mol. MHSO plus 800 μ mol. methionine

* Each abbreviation is explained in the "Experimental" Section.

amino acid to the reaction mixture of MHSO after they have been treated with acetic anhydride should markedly inhibit the color developed with a chromotropic acid reagent.

As is shown in Table IV, this did not hold true. Furthermore, when large amounts of Met were present, the inhibition observed could be overcome by prolonging the heating period with a chromotropic acid reagent, as may be seen in Fig. 5. Thus, the cause of the relatively lower recovery of formaldehyde from MSO than from MHSO is uncertain. Perhaps the hydantoin stabilizes the sulfoxide group in the molecule, since it acts on hydrogen peroxide as a stabilizer.

TABLE V. INTERFERENCE BY OTHER SUBSTANCES

Substrate (S) μ mol.	Interfering subsance (I) mg.	Approximate molar ratio, I/S	Recovery %
MSO 39.9	30 methionine	5	96
	60 methionine	10	100
	120 methionine	20	92
	180 methionine	30	81
MSO 39.9	35 glycine	10	98
	52 glycine	15	99
	44 threonine	10	95
	59 glutamic acid	10	102
	44 cystine	5	96
	97 cystine	10	86
	23 serine	5	79
	39 serine	10	76
MSO 39.9	32 histidine	5	67
	59 histidine	10	61
	48 cysteine hydrochloride	10	17
	66 ascorbic acid	10	56
	42 trimethylamine oxide	10	530
	45 dimethyl sulfoxide	10	805
	39 tryptophane	5	34 (?)
	78 tryptophane	10	45
	36 tyrosine	5	64 (?)
	72 tyrosine	10	79
	31 dimethyl formamide	10	100
MHSO 21.3	17 glycine	10	100
	34 glycine	20	92
	10 serine	5	99
	22 serine	10	104 (?)
	24 threonine	5	96
	35 glutamic acid	10	96
	26 cystine	5	94
	48 cystine	10	94
	48 leucine	10	98
	19 histidine	5	89
	39 histidine	10	84
	15 cysteine	5	5
	20 tyrosine	5	75
	36 tyrosine	10	66

Interference by Other Substances. — For the practical application of the method it is necessary to know what kinds of substances interfere with the present determination. As may be seen in Table V, MSO and MHSO were each determined in the presence of various substances. In the case of the inhibition of methionine, which is required in biochemical studies, the presence of 10 times the molarity of MSO scarcely affected the results at all, but more than 20 times the molarity reduced the value to some extent. However, even this does not decrease the usefulness of the present method much.

Substances that interfere markedly can mainly be divided into four groups. The first group are reducing substances, e.g., cysteine hydrochloride and ascorbic acid. These substances are thought to reduce the sulfoxide prior to the rearrangement. The second group (e.g., trimethylamine oxide and dimethyl sulfoxide) are substances that release formaldehyde when treated with acetic anhydride and subsequent hydrolysis. Here, it should be noted that trimethylamine oxide also released formaldehyde under these conditions. It seems possible that methyl-*N*-oxide might be determined by this method.

The third group (e.g., tryptophan) are substances that are decomposed so as to cause complications when treated with a strong acid.

The forth group (e.g., tyrosine) are substances that compete with chromotropic acid in combination with formaldehyde.

The last case was studied as follows. The substance to be tested, tyrosine in the present case, was added to a reaction mixture containing MHSO treated with acetic anhydride; the mixture was then boiled with a chromotropic

TABLE VI. INHIBITION OF CHROMOTROPIC ACID DEVELOPMENT WITH TYROSINE

Substrate	Tyrosine added, mg.	O. D. (corrected)
Diluted reaction mixture* (1 ml.)	0	0.300**
Diluted reaction mixture* (1 ml.)	5	0.232
Diluted reaction mixture* (1 ml.)	10	0.207
Diluted reaction mixture* (1 ml.)	20	0.194

* Containing 2.13×10^{-1} μ mol. of MHSO per ml.

** Average of five measurements. Tyrosine was added to the diluted reaction mixture and the resulting suspension was depeloped with chromotropic acid in the standard way.

TABLE VII. DETERMINATION OF MIXTURES OF MHSO AND MSO

Substrate	O. D. observed (corrected)	O. D.* calcd.	O. D. observed/ O. D. calcd., %
MSO plus MHSO			
0 μ mol. +21.3 μ mol.	0.335	0.330	98.5
10.1 +15.9	0.332	0.338	98.2
20.2 +10.6	0.342	0.347	98.5
30.3 + 5.3	0.359	0.356	100.5
40.4 + 0	0.365	0.365	100.0

* The O. D. calculated is O. D. (MSO) plus O. D. (MHSO), here O. D. (MSO) and O. D. (MHSO) are obtained independently from calibration curves obtained in parallel.

reagent in the standard way. As may be seen in Table VI, tyrosine inhibited the color developed with the chromotropic acid reagent.

Determinations were made on a mixture of MHSO and MSO. No mutual interference was observed, and the recoveries were additive in the range of concentrations studied, as may be seen in Table VII. As is shown in Table VIII, the protein ovoalbumine does not seem to interfere with the determination of MSO or MHSO.

TABLE VIII. INTERFERENCE BY PROTEIN

Substrate	Ovoalbmin added, mg.	O. D. (corrected)	Recovery %
40.4 μ mol. MSO	10	0.370	103.6
40.4 μ mol. MSO	20	0.360	100.2
21.3 μ mol. MHSO	10	0.315	97.3
21.3 μ mol. MHSO	20	0.322	99.3

The Determination of MSO and MHSO in an Aqueous Solution. — As the method was to be applied to biochemical measurements of samples of MSO or its derivatives, the present method had to be used on aqueous mixtures of the substrates. When acetic anhydride was present in more than five times the molarity of water, the water in the aqueous solution was completely converted to acetic acid. Subsequent boiling resulted in the rearrangement, and satisfactory results were obtained, as is shown in Fig. 6. In these experiments, the ratio of 7.5 ml. of acetic anhydride was used to 0.5 ml. of MSO and MHSO aqueous solutions.

Recommended Procedure.—When the sample to be analyzed is in the solid state, dilute it exactly with purified acetic acid (see "Experimental" section) in a measuring flask to about 10 to 60 μ mol. of the substrate per ml. Pipette 1 ml. of this sample solution into a test tube attached to a suitable reflux condenser, and then add 2 ml. of purified acetic anhydride (see "Experimental" section). After stirring, heat the mixture under reflux for 30 min. on an oil bath.

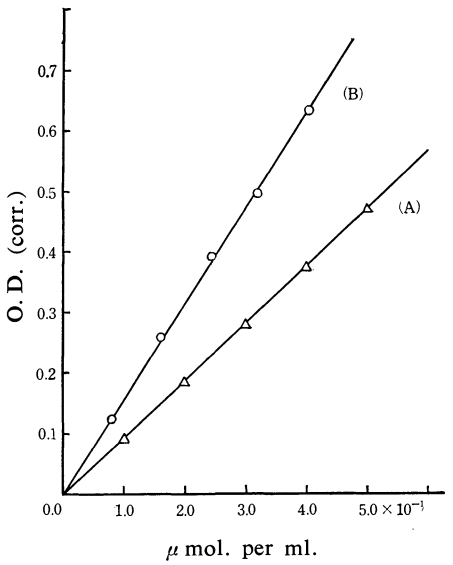


Fig. 6. Standard curves of MSO and MHSO in aqueous solution.
(A) MSO (B) MHSO

A standard solution of the sulfoxide which contains a known amount of the substrate (10 to 60 μ mol. per ml.), as a control, and 1 ml. of the purified acetic acid, as a blank, should be treated in the same way. When the sample to be analyzed is in an aqueous solution, dilute it with purified acetic acid to about 10 to 60 μ mol. per ml. Add 7.5 ml. of purified acetic anhydride to 0.5 ml. of the sample solution, and heat the mixture as described above. The standard aqueous solution of the sulfoxide and 0.5 ml. of water, as a blank, should be treated in parallel. Cool the reaction mixtures with water, and dilute them to 100 ml. with distilled water. Transfer 1 ml. of the resulting solution to a test tube, and then add 10 ml. of a chromotropic acid reagent; after stirring, heat the mixture in a boiling water bath for 30 min. When many other substances are present, it is desirable to prolong the heating period until a constant optical density is observed, since a heating period of 30 min. is

not always sufficient, as has been described above. After the mixture has been cooled to room temperature, measure the color developed with a photometer at 580 mμ. The optical density of the blank should then be subtracted from that of the sample. The optical density obtained here is O. D. (corrected).

As Beer's law holds exactly in the present concentration range, the sulfoxide can be determined by comparison with the optical density of the standard solution. For methionine sulfoxide the accuracy is within a range of error of 3 per cent.

Experimental

The Preparation of Acetyl Methionine Sulfoxide (AcMSO). — This material was obtained by the oxidation of acetyl-L-methionine, m. p. 101~103°C, prepared by the Schotten-Baumann reaction in the standard way. To 1.9 g. of acetyl-L-methionine dissolved in a mixture of 2 ml. of methanol and 2 ml. of water, 2 ml. of a 30% hydrogen peroxide solution was added while the mixture was cooled on ice; the solution was then allowed to stand for 1.5 hr. at room temperature. The reaction mixture was concentrated to a syrup under reduced pressure at below 40°C, and the syrup was dehydrated three times with benzene by the azeotropic procedure. The residual syrup was dissolved in a small amount of acetone and stored in a refrigerator for a long time, with occasional scratching until crystallization occurred. Crystals were collected, washed thoroughly with cold ethanol, and recrystallized from hot acetone. Yield, 500 mg.; m. p. 181~183°C.

Found: C, 40.60; H, 6.28; N, 6.72. Calcd. for $C_7H_{13}O_4NS$: C, 40.50; H, 6.36; N, 6.82%.

The Preparation of Benzoyl-L-methionine Sulfoxide (BzMSO). — Benzoyl-L-methionine (0.6 g.) (m. p. 85~90°C), prepared by the stndard Schotten-Baumann reaction was dissolved in 5 ml. of acetone, and 0.3 ml. of 30% hydrogen peroxide was added to the solution while the mixture was cooled with water. Then the mixture was allowed to stand for an hour at room temperature. When the solution was concentrated under reduced pressure at 40°C, a powder was obtained. The crystalline powder was collected by filtration and recrystallized with acetic acid containing 30 per cent water. The yield was 0.1 g.; m. p. 184~185°C.

Found: C, 53.72; H, 5.58; N, 5.21; S, 11.90. Calcd. for $C_{12}H_{15}O_4NS$: C, 54.09; H, 5.31; N, 5.60; S, 11.98%.

The Preparation of Carbobenzoxy-L-methionine Sulfoxide (Cbz-MSO).—To 5.67 g. (0.02 mol. of Cbz-Met in 50 ml. of methanol was added 2.2 ml. of a (30%) hydrogen peroxide solution with mechanically stirring in for 20 min. at 0~5°C. The solution was then allowed to stand for a further 2 hr. at room temperature. Fifteen milliliters of water was added to the mixture, which was then concentrated to about 20 ml. under reduced pressure at 35°C to remove the methanol. The resulting aqueous mixture was extracted four times with 25 ml. of ethyl acetate. The ethyl acetate extracts were combined and washed with a small amount of a saturated aqueous sodium chloride solution, and then dried over sodium sulfate overniglt. The dried ethyl acetate solution was concentrated under reduced pressure at below 40°C until the residue became slightly viscous. When seeded with Cbz-MSO (see below), the solution became cloudy, and on storage in a refrigerator crystallization occurred. The crystalline product was collected, washed with a mixture of ether and petroleum benzine, and dried in vacuo. The yield was 4.8 g., or 80%. The material was then recrystallized from methanol-water. M. p. 134°C.

Found: C, 52.44; H, 5.64; N, 4.61. Calcd. for $C_{13}H_{17}O_5NS$: C, 52.16; H, 5.72; N, 4.68%.

The Cbz-MSO used for seeding was obtained as follows: The ethyl acetate extract mentioned above was concentrated to a syrup and dissolved in a minimum amount of 1 N sodium hydroxide. The alkaline solution was titrated drop by drop with 6 N sulfuric acid until it became cloudy. One drop of 1 N sodium hydroxide was added to make the solution clear, and then the mixture was stored in a refrigerator for a few days. Fine needle-like crystals were obtained. Yield, 38%.

The Preparation of the Carbobenzoxy Methionine Sulfoxide Ethyl Ester (Cbz-MSO-OEt).— This compound was obtained by the esterification of Cbz-MSO in ethanol containing thionylchloride. To 10 ml. of ethanol at below −10°C was added, drop by drop, 0.65 ml. (9 mmol.) of thionylchloride. After 15 min. 2.14 g. of Cbz-MSO (7.15 mmol.) was added with strring and then the mixture was allowed to stand for about 24 hr. at room temperature. The ethanol was distilled off under reduced pressure, and the residual syrup was washed thoroughly with ether by decantation. The syrup, covered with ether, was kept in deep-freeze for about two weeks. Aggregated white crystals were deposited. The crystals were filtered off, washed thoroughly with ether, and dried in vacuo. The yield was 1.37 g. (58%). On the addition of petroleum benzine to the combined ether extracts, a second crop of crystals was obtained. These were recrystallized from ethyl acetate-petroleum benzine. M. p. 53.5°C.

Found: C, 55.21; H, 6.46; N, 4.96. Calcd. for $C_{15}H_{21}O_5NS$: C, 55.04; H, 6.47; N, 4.28%.

The Preparation of the Carbobenzoxy-*S*-oxomethionyl Methionine Sulfoxide Ethyl Ester (Cbz-MSO-MSO-OEt). — Cbz-Met-Met-OEt, prepared by the mixed anhydride method, was easily oxidized to Cbz-MSO-MSO-OEt with a hydrogen peroxide solution. To Cbz-Met-Met-OEt (2.21 g.; 5 mmol.) in a mixture of 30 ml. of water and 300 ml. of methanol, 1.2 ml. of (30%) hydrogen peroxide solution was added; the mixture was then allowed to stand overnight. The mixture was concentrated under reduced pressure to obtain a solid white product. The yield was 0.6 g., and the crystals melted at 185~186°C.

From the mother liquor 0.7 g. of the product was obtained. The second crop of crystals melted at 165~171°C, and from the mother liquor of the second crop, 0.8 g. of the product was obtained (m. p. 110~112°C). 0.6 g. of the first crop was

recrystallized from a methanol-ether mixture. Yield, 0.45 g.; m. p. 189~190°C.

Found: C, 50.52; H, 6.40; N, 5.75. Calcd. for $C_{20}H_{30}O_7N_2S_2$: C, 50.61; H, 6.37; N, 5.90%.

The Preparation of 2, 4-Dinitrophenyl-L-methionine Sulfoxide (DNP-MSO).—This compound was prepared according to the directions of Levy et al.; [6] m. p. 195°C (Ref. 184.5°C).

Found: C, 39.91; H, 4.15; N, 12.47. Calcd. for $C_{11}H_{13}O_7N_3S$: C, 39.88; H, 3.96; N, 12.68%.

The Purification of Acetic Acid and Acetic Anhydride.—The usual methods for the purification of acetic acid, and acetic anhydride, were not satisfactory for the present photometrical method. Acetic acid was, however, purified effectively as follows. A solution of 5 per cent phenylhydrazine (by weight) in 10 per cent (by volume) of acetic anhydride and 800 ml. of acetic acid was boiled under reflux for several hours. The acid was then distilled, and the fraction boiling at 115~117°C was collected. Distillation was repeated two or three times. The purified acid was kept in a brown bottle. When it was diluted 10 times (by volume) with distilled water, 1 ml. of the resulting solution showed an optical density of 0.005~0.008 when treated with 10 ml. of a chromotropic acid reagent.

Acetic anhydride was purified as follows: 800 ml. of acetic anhydride was mixed with a few drops of concentrated sulfuric acid, and the mixture was boiled under reflux for several hours. The mixture, which turned dark, was distilled, and the fraction boiling at 137~139°C was collected. One milliliter of the anhydride had an optical density of about 0.025 when treated with 10 ml. of a chromotropic reagent.

6) A. L. Levy and D. Chung, *J. Am. Chem. Soc.*, **77**, 2899 (1955).

Chromotropic Acid Reagent. — A chromotropic acid, disodium 1,8-dihydroxynaphthalene-3,6-disulfonate, commercially available, was recrystallized from a mixture of water and ethanol. One gram of the purified salt was dissolved in 100 ml. of distilled water, and 400 ml. of 24 N sulfuric acid was added to this solution.

Summary

1) A new colorimetric method for the determination of methionine sulfoxide and its derivatives on the basis of the rearrangement of sulfoxide by the action of acetic anhydride has been established.

2) From about 10 μ to 80 μ mol. of methionine sulfoxide can be determined with an experimental error of 3 per cent.

3) The interference with the reaction by various amino acids and related substances has been investigated.

4) Several compounds related to methionine sulfoxide have been prepared and analyzed by the present method.

The author is indebted to Professor Shiro Akabori and Dr. Yoshiharu Izumi for their constant interest and encouragement in this work, and to the Misses Kiku Koike and Masako Kawakita of this Institute for their elemental analyses.

Division of Organic Chemistry
Institute for Protein Research
Osaka University
Kita-ku, Osaka

The Anodic Oxidation of Esters

By Toshihiko OKUBO and Shigeru TSUTSUMI

(Received June 4, 1964)

A previous work[1] in this series dealt with the electrochemical coupling reaction of diethyl malonate and ethyl acetoacetate in absolute alcohol. Although the desired products were obtained in a small yield, they were contaminated with many by-products which were formed by the electrolysis of the alcohol itself. It has also been concluded that the solvent might play an important role in this reaction.

Therefore, as a new attempt, the present work was carried out for the purposes of obtaining a better yield of the dimer of esters in the electrolysis and of controlling the side reaction by using acetonitrile as a solvent, with no active hydrogen, and, as a supporting electrolyte, a potassium iodide which gave a better conductivity than the sodium salt of esters in the same solvent.[2]

The dimerization of esters is a novel method not only because of the electrolysis but also because of the chemical synthetic method.

In order to make a comparison with the case of an absolute alcohol, a malonic ester,

1) T. Okubo and S. Tsutsumi, *Tec. Rep. Osaka Univ.* **13**, 495 (1963).

2) E. White, *J. Chem. Soc.*, **1928**, 1414. (Although the data are for conductivities in an alcohol solution, this statement is also true for an acetonitrile solution in our blank test.)

an acetoacetic ester and a phenylacetic ester were used in this experiment.

Results and Discussion

The yield of a coupling product was calculated on the basis of the amount of product per unit qantity of electricity.

The experimental results are summarized in Table I.

As is shown in the table, the modified method in which acetonitrile was used as a solvent afforded more satisfactory results in all cases.

The Electrochemical Coupling of Esters in an Alcoholic Solution.—According to the explanation proposed by Allen,[3] the electrolytic coupling of these esters in an alcoholic solution proceeds in a manner similar to that of the Kolbe reaction, with the exception that no carbon dioxide is eliminated, as is shown below.

Step 1) The metallation of the ester (The formation of the anion of the ester)

$$Na + H\text{-}\underset{\diagup}{\overset{\diagdown}{C}}COOR \longrightarrow Na\text{-}\underset{\diagup}{\overset{\diagdown}{C}}\,COOR$$

Step 2) The dissociation of the alkali salt of the ester

$$Na\text{-}\underset{\diagup}{\overset{\diagdown}{C}}COOR \rightleftarrows Na^+ + -\underset{\diagup}{\overset{\ominus}{C}}COOR$$

Step 3) The anodic oxidation of the anion

$$\ominus\!\!\diagdown\!CCOOHR \xrightarrow{-e} \cdot\!\diagdown\!CCOOR \longrightarrow$$

$$ROOCC\text{-}\underset{\diagup\ \diagdown}{\overset{\diagup\ \diagdown}{C}}COOR$$

For the electrolysis in an alcoholic solution, it was observed that the reactivity of the ester toward the electrolytic coupling was dependent on the electron-attracting force of the substituents on the methyl group (CH_3) of ethyl acetate ($CH_3COOC_2H_5$). The decrease in the reactivity of the ester caused by the substituent was in the order; carbethoxy $COOC_2H_5$, acetyl CH_3CO and phenyl C_6H_5. The order was just the same as Taft's substituent constants[4] for CH_2X–, as is shown below.

$$C_6H_5, +0.215 < CH_3CO, +0.60 < COOC_2H_5, +0.7$$

On the reaction of ethyl acetoacetate and ethyl phenylacetate in alcohol, because their releasing force of hydrogen is lower than that of ethyl malonate, the yield of coupling products was very poor (ethyl acetoacetate, 0.2 g./amp. hr.; ethyl phenylacetate, a trace, and by the following reaction, acetoaldehyde and its polymeric material were the main products;

$$C_2H_5O\overset{\ominus}{:} \longrightarrow C_2H_5O\cdot + e$$

$$C_2H_5O\cdot \longrightarrow CH_3CHO + 1/2\ H_2$$

The Electrochemical Coupling of Esters in an Acetonitrile Solution.—When these esters were submitted to electrolysis in a potassium iodide-acetonitrile medium, the dimer of esters was yielded, especially in the cases of both ethyl acetoacetate and ethyl phenylacetate. The dimer which could not hitherto be isolated as a crystal in the case of an alcoholic solution was obtained as a fine crystal and in a good yield.

The reasons for this may be as follows:

1) An acetonitrile was scarcely oxidized in

Table I. Summary of the results

Ester	Product: In absolute alcohol	Product: In acetonitrile
Diethyl malonate	$HC(COOC_2H_5)_2$ | $HC(COOC_2H_5)_2$ (1.4 g./amp. hr.)	$HC(COOC_2H_5)_2$ | $HC(COOC_2H_5)_2$ (2.1 g./amp. hr.) (0.013 mol./amp. hr.)
Ethyl acetoacetate	(1) $CH_3COCH(COOC_2H_5)$ | $CH_3COCH(COOC_2H_5)$ (identified as acetonylacetone) (0.2 g./amp. hr.) (2) CH_3CHO and polymeric materials	$CH_3COCH(COOC_2H_5)$ | $CH_3COCH(COOC_2H_5)$ (1.5 g./amp. hr.) (0.0115 mol./amp. hr.)
Ethyl phenylacetate	(1) $C_6H_5CH(COOC_2H_5)$ | $C_6H_5CH(COOC_2H_5)$ (trace) (2) CH_3CHO and polymeric meterials	(1) $C_6H_5CH(COOC_2H_5)$ | $C_6H_5CH(COOC_2H_5)$ (2.3 g./amp. hr.) (0.014 mol./amp. hr.) (2) a small amount of a tarry product

3) M. J. Allen, "Organic Electrode Processes," Reinhold Pub. Corp., New York (1958), p. 111.

4) M. S. Newman, "Steric Effects in Organic Chemistry," John Wiley and Sons, New York (1956), p. 595.

the anodic oxidation as compared with an alcohol, and the amounts of by-products are small.

2) The dissociation of the potassium salt of the ester is easier than that of sodium salt.

3) The velocity of the reaction was accelerated by the action of the iodide formed, as is shown in the reaction path.

The yield of coupling products indicated in (mol./amp. hr.) was nearly constant in each case. It is noticeable that the difference in the acidity between esters is not very important in the reactions in acetonitrile because the acidities of the esters used are much stronger than that of acetonitrile.[5]

The following reaction path may be inferred.

$$KI \longrightarrow K^+ + I^- \quad (1)$$

$$K^+ \xrightarrow{+e} K\cdot \quad (2)$$

$$I^- \xrightarrow{-e} I\cdot \quad (3)$$

$$K\cdot + RCH_2COOC_2H_5 \longrightarrow RC(K)HCOOC_2H_5 + 1/2\ H_2 \quad (4)$$

$$RCH(K)COOC_2H_5 \longrightarrow R\bar{C}HCOOC_2H_5 + K^+ \quad (5)$$

$$R\bar{C}HCOOC_2H_5 \xrightarrow{-e} R\dot{C}HCOOC_2H_5 \quad (6)$$

$$2R\dot{C}HCOOC_2H_5 \longrightarrow \begin{matrix} RCHCOOC_2H_5 \\ | \\ R\dot{C}HCOOC_2H_5 \end{matrix} \quad (7)$$

$$I\cdot + RC(K)HCOOC_2H_5 \longrightarrow KI + R\dot{C}HCOOC_2H_5 \quad (8)$$

$R = C_6H_5,\ COOC_2H_5,\ CH_3CO$

Experimental*

Materials.—*Acetonitrile.*—Commercial grade acetonitrile was carefully purified in the usual manner. (B. p. 81.0°C, n_D^{20} 1.3440).

Ethyl Malonate and Ethyl Acetoacetate (commercial grade) were fractionated. (Ethyl malonate: b. p. 197~198°C, n_D^{18} 1.4120; Ethyl acetoacetate: b. p. 89~90°C/30 mmHg, n_D^{20} 1.4190) Ethyl phenylacetate was prepared by the method given in the literature[6] (115~117°C/20 mmHg, n_D^{23} 1.4959).

Apparatus.—Electrolyses were carried out in a cylindrical glass vessel fitted with a reflux condenser and two platinum foil electrodes with an area of 20×30 mm^2 and spaced 5 mm. apart. During the coures of the electrolysis, the contents were stirred magnetically and the temperature was controlled by a water bath.

The Electrolysis of Ethyl Malonate in Acetonitril Containing Potassium Iodide.—A solution of 30 g. of ethyl malonate and 0.5 g. of potassium iodide in 100 ml. of acetonitrile was electrolyzed at 10°C for 36 hr. A current was maintained at 0.2 amp. After the removal of the acetonitrile, the electrolyte solution was poured into cold water and extracted with ether. The ethereal layer was then washed with water and dried over anhydrous magnesium sulfate, and the ether was removed. The remaining oil was distilled under reduced pressure. The fraction with a b. p. of 180~187°C/12 mmHg was 15 g. After recrystallization from alcohol, they afforded tetraethyl ethanetetracarboxylate (m. p. 74~75°C), and the melting point was undepressed on admixture with an authentic sample.[7] Moreover the infrared spectrum of this compound was identical with that of an authentic sample.

The Electrolysis of Ethyl Acetoacetate in Acetonitrile Containing Potassium Iodide.—A mixture of 30 g. of ethyl acetoacetate, 0.5 g. of potassium iodide, and 100 ml. of acetonitrile was electrolyzed at 10°C for 27 hr. During the electrolysis, a current was maintained at 0.3 amp. After the removal of the acetonitrile, the residue was vigorously shaken with cold water and a solid was separated by filtration. When the solid was then washed with water and dried in vacuo, the yield was 12 g. It was then recrystallized from alcohol (m. p. 81~83°C). The recrystallization of this crystal from aqueous alcohol gave the β-form of diethyl diacetosuccinate* (m. p. 86.5~88°C). The melting point of this compound was not depressed on admixture with an authentic sample prepared according to the directions of Knorr and Haber.[8] The infrared spectra of the compound were identical with those of an authentic sample.

Found: C, 55.72; H, 6.83. Calcd. for $C_{12}H_{18}O_6$: C, 55.81; H, 6.97%.

The Electrolysis of Ethyl Phenylacetate in Acetonitrile Containing Potassium Iodide.—The experiment was conducted in a manner essentially similar to that of the experiment described above. The solid (m. p. 128~135°C) (3.5 g.) was suspended between aqueous and ethereal layers, and the residue (14 g.) was obtained from an ethereal layer. The solids were combined and submitted to sublimation. The sublimated crystals were extracted with hot petroleum ether (b. p. 40~55°C) to remove low melting parts. The remaining crystals were recrystallized from alcohol, melted at 138.5~140°C and identified as ethyl β-diphenyl-succinate[9] by mixed melting point measurement.

Found: C, 73.27; H, 6.62. Calcd. for $C_{20}H_{22}O_4$: C, 73.61; H, 6.74%.

A trace of unidentified crystals (m. p. 77~81°C) was obtained from the hot petroleum ether-soluble part.

The Electrolysis of the Sodium Salt of Ethyl Phenylacetate in Absolute Alcohol.—To a solution of 25 g. of ethyl phenylacetate in 100 ml. of absolute alcohol, 0.5 g. of sodium was added, and then the

5) D. J. Cram, "Organic Chemistry," McGraw-Hill Book Co., New York (1959), pp. 172, 176.

* Melting points and boiling points are uncorrected.

6) "Organic Syntheses," Coll. Vol. I (1948), p. 270.

7) C. A. Bischoff, *Ber.*, **17**, 2781 (1884).

* Diethyl diacetosuccinate has many tautomers. Among them are the β-form (diketo form) and the γ-form (diketo form). Their melting points are 89~90°C (plate form) and 74°C (needle form) respectively. In the presence of water, the γ-form is transformed into the β-form.

8) L. Knorr and F. Haber, ibid., **27**, 1155 (1894).

9) H. Wren and C. J. Still, *J. Chem. Soc.*, **1915**, 444.

solution was subjected to electrolysis. The electrolysis was carried out at an average current of 0.2 amp. at 20°C for 30 hr. The precipitate (2 g.) was separated by filtration. This precipitate was dissolved in water, acidified with dilute hydrochloric acid, and then extracted with ether. After the removal of the ether, a trace of crude crystals was obtained; when sublimated, it yielded ethyl β-diphenylsuccinate (m. p. 120~135°C). An attempt to purify this compound was unsuccessful. After the evaporation of the alcohol, the filtrate was distilled under reduced pressure to give the following fractions.:

Fraction 1: 100~118°C/20 mmHg 17.8 g. (unchanged ester)
Fraction 2: 40~80°C/3 mmHg
Fraction 3: 80~85°C/3 mmHg 1 g. n_D^{24} 1.496
Fraction 4: 100~110°C/3 mmHg 0.9 g. n_D^{24} 1.500
Fraction 5: 115~130°C/3 mmHg 0.9 g. n_D^{24} 1.558

Fraction 2 was converted into its 2,4-dinitrophenylhydrazone (m. p. 230~233°C (recrystallized from a mixture of alcohol and nitrobenzene)). As the I. R. of this hydrazone showed no C=O band, the fraction seems not to be an ester and aldehyde polymer resulting from the electolysis of alcohol. Fractions 3, 4, and 5 were soluble in both ether and alcohol, and the I. R. of these fractions showed the characteristic absorption bands of the ester.

We wish to express our thanks to Mr. Yoshinobu Odaira and Mr. Kikuhiko Koyama for their advice during the course of this work, and also to Miss Junko Maenaka for her elemental analysis.

Department of Chemical Technology
Faculty of Engineering
Osaka University
Miyakojima-ku, Osaka

*Characterization of the Alumina-Boria Catalyst**

By Yūsuke Izumi and Tadao Shiba

(Received June 5, 1964)

Alumina-boria is a well-known type of acidic cracking catalyst.[1,2] However, the details of its characterization still remain unsettled, in contrast to the case of silica-alumina, which has been the subject of numerous investigations. It has been previously suggested[3-6] that active alumina may react with boric acid to form strongly acidic centers, but more experimental evidence is necessary for an understanding of the reaction and of a probable mechanism of the development of activity. Although Ikebe[4] showed the remarkable effect of the chemical composition of alumina-boria upon its cracking activity, little is known so far about the best method of preparing the catalyst. This study was undertaken in order to obtain such information.

The present investigation started from the observation that the activity of alumina-boria was considerably affected by the chemical and the physical nature of the alumina used as the catalyst-base, the effect of the conditions of catalyst preparation upon the activity of the toluene disproportionation was examined. In the second step, the chemical interaction of active alumina with boric acid was studied by thermographic analysis, and the mechanism of developement of activity was discussed on the basis of the results, together with those of X-ray diffraction, infrared absorption and the colorination of adsorbed indicators. Kinetic studies of some specific reactions over alumina-boria were made in order to establish the applicability of the catalyst.[7-11]

Experimental

Alumina as a Catalyst Base.—A hydrous alumina gel was prepared at a given pH by adding an aqueous solution of ammonia (4 N) to a solution of aluminum nitrate (10%). The precipitate was washed to remove nitrate ion and dried in an electric oven for several hours at 130°C to form an alumina hydrate. The greater part of the alumina

* This paper is an abridgment of a series of studies of the alumina-boria catalyst previously published.[7-11])

1) W. A. Bailey, U. S. Pat 2377744 (1945.)
2) N. V. de B. P. M., Dutch, Pat. 65287 and 62287.
3) C. L. Thomas, *End. Ing. Chem.*, **41**, 2564 (1949).
4) K. Ikebe, *J. Chem. Soc. Japan, Ind. Chem. Sec.* (*Kogyo Kagaku Zassi*), **61**, 437 (1958).
5) K. Ikebe, ibid., **61**, 575 (1958).
6) K. Ikebe, N. Hara, K. Mita and K. Shimizu, *J. Fuel Soc. Japan* (*Nenryo Kyokai Shi*), **37**, 257 (1958).
7) Y. Izumi and T. Shiba, *J. Chem. Soc. Japan, Pure Chem. Sec.* (*Nippon Kagaku Zasshi*), **84**, 699 (1963).
8) Y. Izumi and T. Shiba, *J. Chem. Soc. Japan, Ind. Chem. Sec.* (*Kogyo Kagaku Zasshi*), **66**, 1817 (1963).
9) Y. Izumi and T. Shiba, ibid., **67**, 559 (1964).
10) Y. Izumi and T. Shiba, ibid., **67**, 564 (1964).
11) Y. Izumi N. Idemoto and T. Shiba, Catalysis Club of Japan, *Shokubai* (*Catalyst*), **5**, 277 (1963).

hydrate, which was obtained at pH 10 with or without the aging of the precipitate, was found to consist of bayerite, while the alumina hydrate prepared at pH 7 to 8.2 showed a clear diffraction pattern assigned to gibbsite. It was suggested that the particle sizes of these two kinds of aluminum trihydroxide might be supposed to be very fine,[12,13] since only one endothermic peak was observed, at about 330 to 370°C, in the course of the thermal transformation.[7] Gibbsite and bayerite were dehydrated by calcination at 300 to 600°C in a muffle furnace for several hours, and transformed into χ-alumina and η-alumina respectively, as is shown in Table I.

Table I. X-Ray analysis of alumina for a catalyst base

Condition of precipitation pH, aging	Calcination temp. °C	Structure of alumina	Relative intensity of maximum diffraction peak*
10, none	130	Bayerite	>100
		Gibbsite	20
	300	η-Alumina	7
	400	η-Alumina	10
	500	η-Alumina	15
	600	η-Alumina	18
10, 30 days	130	Bayerite	>100
		Gibbsite	20
	300	η-Alumina	8
	400	η-Alumina	10
	600	η-Alumina	20
8.2, 30 days	130	Gibbsite	>100
8.0, none	400	χ-Alumina	7
8.0, 30 days	400	χ-Alumina	8
7.0, none	400	χ-Alumina	3
7.0, 30 days	400	χ-Alumina	7

* Angular position of the maximum diffraction peak (2θ); gibbsite 18.3°, bayerite 18.8°, η-alumina 66.8°, χ-alumina 67.2°.

The Preparation of Alumina-Boria. — Both hydrous and anhydrous alumina were used as catalyst bases. Powdered alumina was impregnated with the required amount of an aqueous solution of boric acid, and the mixture was heated in a kneader by an infrared lamp in order to evaporate the excess water. The resulting wet composite was pelleted into cylindrical form (4 mm.ϕ×4 mm.); then the pellets were calcined at 400 to 500°C for 4 hr. in a muffle furnace.

The Determination of Boria Content.—Boron in silicate ores is generally determined by a fusion method, but in the present case it was found that boric acid was so easily extracted from the catalyst with hot water that an almost complete determination was possible by means of titration with a sodium hydroxide solution in the presence of mannitol. The boria content thus determined agreed well with that determined by the fusion method,[14] as well as with that calculated from the amount of boric acid which was impregnated into the alumina. Such easy extraction of boric acid suggests that the structure of alumina-boria may be very different from that of aluminum borate. All the boria contents shown in the experimental results were calculated from the amount of boric acid used in the catalyst preparation (B_2O_3/cat., wt.%).

Reaction Apparatus and Product Analysis.—Some specific reactions over an alumina-boria catalyst were carried out with a fixed-bed flow reactor under atmospheric pressure. The reactor consisted of a Pyrex double tube (24 mm.ϕ×600 mm.—10 mm.ϕ× 600 mm.) and a feeder which was a syringe driven by a clock sinker. The reactor was placed vertically in a fluidized bed of powdered alumina with automatic temperature regulation.

The reaction products were analyzed by gas chromatography at 80°C using a column packed with 30% D. O. P. on celite. For the separation of xylene isomers, a 5 m. column of 30% 7,8-benzoquinoline[15] was used.

Acidity and Acid Strength Measurements.—The acidity of alumina-boria was determined following Benesi's[16] and Leftin-Hall's[17] methods as modified by Shiba and his co-workers.[18] The total acidity was determined by *n*-butylamine titration, using benzeneazodiphenylamine as an indicator, and the Lewis acidity, by the chemisorption of triphenylmethyl chloride on alumina-boria. The difference between the total and the Lewis acidity was attributed to the Brönsted acidity.

Color tests were made[16] by transferring roughly 0.1 g. of a dried, powdered sample into a test tube which contained 5 ml. of dry cyclohexane, adding a few drops of a solution of indicator in cyclohexane, and, after leaving it overnight, observing the color of the adsorbed indicator. The indicators used were benzeneazodiphenylamine, dicinnamalacetone and benzalacetophenone. Their acidic colors are purple, red and yellow, and the values of pK_a are +1.5, −3.0 and −5.6 respectively.

Other Measurements. — The differential thermal analysis for the examination of chemical interaction between alumina and boric acid was carried out under atmospheric pressure. The sample holder was a quartz vessel 5 mm. in diameter and 20 mm. deep.

X-Ray diffractions were recorded by a Phillips X-ray diffractometer with Ni-filtered Cu-K_α radiation.

Infrared absorption measurement was made on samples in potassium bromide discs in the region between 2 and 16 microns, using a Shimadzu AR-275 spectrophotometer.

12) K. Funaki and Y. Shimizu, *J. Electrochem. Soc. Japan (Denki Kagaku)*, **28**, 302, 358 (1960).
13) K. Sakamoto, *J. Ceram. Assoc. Japan (Yogyo Kyokai Shi)*, **67**, C 114 (1959).
14) K. Kimura, "Muki Teiryo Bunseki" (Inorganic Quantitative Analysis), Kyoritsu Shuppan, Tokyo (1954), p. 345.
15) D. H. Desty, A. Goldup and W. T. Swanton, *Nature*, **183**, 107 (1959).
16) H. A. Benesi, *J. Am. Chem. Soc.*, **78**, 5490 (1956); *J. Phys. Chem.*, **61**, 970 (1957).
17) H. P. Leftin and W. K. Hall, Proc. Intern. Congr. on Catalysis, 2nd., Paris, No. 65 (1960).
18) T. Shiba, M. Sato, H. Nishimura, A. Hattori and K. Yoshida, 16th Annual Meeting of the Chemical Society of Japan, Tokyo, 1963.

The Structural Effect of Alumina Used for a Catalyst Base

The relationship of the structure of alumina used for a catalyst base with both the activity and the acidity of alumina-boria is shown in Figs. 1 and 2. The conversion of toluene* is taken for the activity since the selectivity of the disproportionation of toluene is almost identical with the different catalyst compositions (the mole ratio of produced xylene to benzene was 0.9±0.05). Both the η-alumina and χ-alumina used for catalyst bases were calcined at 400°C so as to give maximum activities of the catalysts.

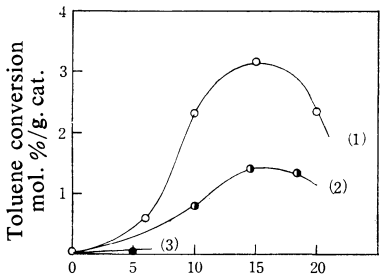


Fig. 1. Activity of toluene disproportionation over alumina-boria at 480°C.
Catalyst; 5.0 g. Feed rate: 0.030 mol./hr.
(1) η-Alumina base (2) χ-Alumina base
(3) α-Alumina base

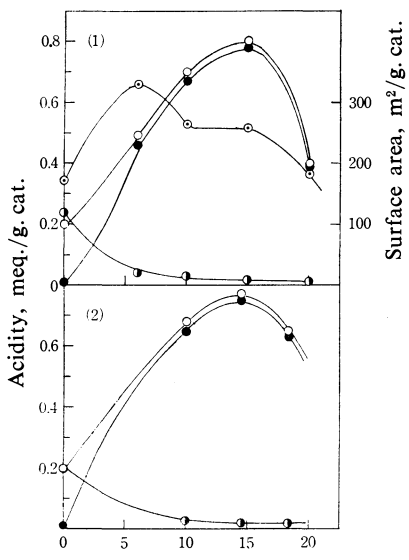


Fig. 2. Acidity of alumina-boria prepared from η-alumina (1) and χ-alumina (2).
○ Total acidity ◑ Lewis acidity
● Brönsted acidity ⊙ Surface area

* The conversion represents the value which was obtained with an "equilibrated" catalyst. The decrease in activity with the length of run will be discussed later.

The catalyst prepared from η-alumina gave a higher activity than that from χ-alumina, while α-alumina was an ineffective base. The maximum activity was obtained at 15 wt.% of boria** in both of the active catalysts. It is suggested that the excessive boria might have been deposited on active sites, so lowering the activity, since boria by itself showed little activity. The aging treatment of the alumina used for a catalyst base was found to have little effect on the activity.[7]

The greater part of the acidic centers of alumina-boria are of the Brönsted type, as is shown in Fig. 2. By comparing Fig. 1 with Fig. 2, it may also be seen that the catalytic activity has a correlation with the Brönsted acidity. This information fits in well with the reliable conception that the reaction may proceed via a carbonium ion mechanism. The surface area of the catalyst did not have any definite relationship with the activity. The activity per unit of Brönsted acidity of the catalyst derived from η-alumina was much higher than of that derived from χ-alumina.[7] This may be due to the difference in acid strength or in the distribution of acid sites among the effective catalyst surfaces, because the structural deviation of η-alumina from χ-alumina is generally recognized as the difference in the distribution of aluminum ions among oxygen ions.[12]

As for the synthetic silica-alumina, the catalyst of 50 wt. % of silica showed a best activity of toluene conversion (1.6 mol. %/g. cat. at the

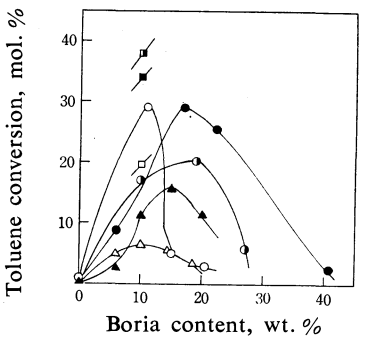


Fig. 3. Effect of the calcination temperature of η-alumina for a catalyst base upon the activity of toluene disproportionation at 480°C.
Calcined at 300°C ■, 400°C ◧, 500°C ○, and 600°C □. Dried at 130°C ◑ (bayerite). Hydrous gel ●.
Catalyst: 20.1 g., feed rate: 0.0285 mol./hr.
Calcined at 400°C ▲, and 550°C △.
Catalyst: 5.0 g., feed rate: 0.0300 mol./hr.

** Ikebe[4] has shown that the maximum cracking activity of alumina-boria is obtained at about 12~15 wt.% boria, and that the alumina used for his catalyst base contains hydrous alumina.

same condition as shown in Fig. 1) and the maximum Brönsted acidity (0.164 meq./g. cat.); the total acidity was 0.300 meq./g. cat. The result indicates that the activity per unit mass of the silica-alumina is much lower than that of the alumina-boria prepared from η-alumina. This is probably due to the lower concentration of acid sites in the former in spite of its higher activity per unit of Brönsted acidity.

The effect of the calcination temperature of the alumina used for the catalyst base upon the activity is shown in Fig. 3. The maximum activity was given by the catalyst which was derived from η-alumina calcined at 400°C. In view of the higher crystallinity of the alumina with the higher calcination temperature, it may be concluded that an alumina calcined at a higher temperature may be less reactive upon boric acid, resulting in a less effective base for the catalyst.

The Development of Active Centers

The Chemical Interaction of Alumina with Boric Acid. — Ikebe and his co-workers[6] have shown that the thermogram of a hydrous alumina alone and that of an alumina impregnated with boric acid were almost identical. This result may be explained as an overlapping of the endothermic transformation of the hydrous alumina with the thermographic behavior of chemical interaction between alumina and boric acid. They concluded from an X-ray study that boric acid reacts with alumina at about 300 to 400°C on the basis of their observation of the disappearance of some sharp diffraction peaks of a mixture of hydrous alumina and boric acid at that temperature. However, a careful examination of their data shows that the interaction might have occurred at a lower temperature, since some angular locations of the diffraction peaks of the hydrous alumina* are almost identical with those of boric acid or of boron oxide.**

In the procedure of the differential thermal analysis in the present study, the probable thermal effects of alumina and the remaining water were eliminated, in order to obtain clear information about the interaction, by the use of a powdered anhydrous η-alumina as the reference and a dry mixture of the same weight of the alumina and various amounts of powdered boric acid as the sample. It is not unsuitable to test the chemical interaction by the use of the dry mixture because the activity of alumina-boria prepared from the dry mixture was almost identical with that of the catalyst derived by impregnation in an aqueous solution so long as the boria content was the same. The results of the differential thermal analysis are shown in Fig. 4. In the case of the η-alumina-boric acid system, the *a* or *b* composite (corresponding to 15 or 20% boria) gives only one broad endothermic peak, at about 130°C. On the other hand, the thermogram of the *c* or *d* composite (corresponding to 25 or 30% boria respectively) shows two sharp peaks, at approximately 170 and 185°C, besides a broad shoulder at 130°C. These peaks apparently accord with the two sharp peaks given in the transformation of boric acid alone (curve *h*) or of the α-alumina-boric acid system (curve *g*). Since two peaks of the *g* or *h* curve give no shoulder at 130°C, they clearly and even quantitatively correspond to

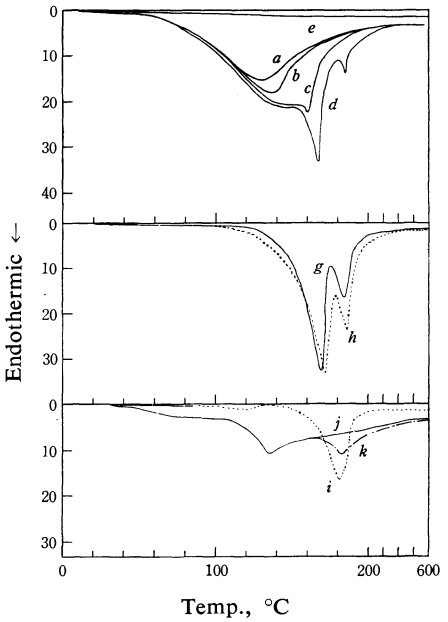


Fig. 4. Differential thermal analysis of the systems of alumina-boric acid (*a*, *b*, *c*, *d*, *g*) and alumina-metaboric acid (*i*, *j*, *k*).
Rate of heating: 4.4°C/min.
Standard side: η-alumina (0.1385 g.) for *a*, *b*, *c*, *d*, *e*, *j* and *k*. α-alumina (0.1385 g.) for *g*, *h* and *i*.
Sample side: η-alumina (0.1385 g.) with boric acid corresponding to boria content (%), *a* 15, *b* 20, *c* 25, *d* 30 and *e* 0. η-Alumina (0.1385 g.) with metaboric acid corresponding to boria content (%), *j* 15, *k* 30. α-Alumina (0.1385 g.) with boric acid corresponding to boria content (%), *g* 15. α-Alumina (0.1385 g.) with metaboric acid corresponding to boria content (%), *i* 30. *h* consists of boric acid alone (the same weight of boric acid as in the *a* sample).

* $2\theta = 28.1°$ and 14.4° for boehmite with a strong intensity.
** $2\theta = 27.9°$ (for H_3BO_3 and B_2O_3), and 14.6° for B_2O_3 with a medium intensity.

the transformations of boric acid into metaboric acid, and of metaboric acid into boria, respectively.[19] As for the η-alumina-metaboric acid system, a peak at 183°C in the thermogram of the *k* composite (corresponding to 30% boria), as well as a peak at 181°C of the *i* curve (metaboric acid), indicates the formation of isolated boria from metaboric acid, while the *j* composite (corresponding to 15% boria) gives only one endothermic peak, at 135°C. Judging from the results, it is probable that boric acid is dehydrated to form metaboric acid as an intermediate and that it reacts with an active anhydrous alumina at about 130°C to yield active centers, while boric acid does not react with α-alumina. It is also shown that excessive boric acid is transformed into isolated boria which might be deposited on the active centers and so lower the activity. The reactivity of χ-alumina with boric acid was found to be almost identical to that of η-alumina.[7]

The X-Ray Study of Alumina-Boria.—Table II gives the results of the X-ray diffraction of some catalysts with different compositions prepared from various forms of alumina. The relative diffraction intensity of the η-alumina which remains in the catalyst derived from anhydrous alumina is not very much reduced with the increase in boria content, whereas the intensity of the alumina in the catalyst made from hydrous alumina were remarkably reduced. This fact indicates that the reaction between anhydrous alumina and boric acid is probably localized on the surface of the alumina and that the crystal structure of alumina is not very much disturbed, whereas boric acid reacts more uniformly with hydrous alumina. In comparison with Fig. 3, it is supposed that excessive boria reduces the activity of alumina-boria because of the deposition of isolated boria. It is also shown that the reactivity of α-alumina with boric acid is very poor, since the diffraction of isolated boria appeared even in the composite of 5% boria. Attention must also be paid to the fact that alumina-boria did not give any definite diffraction pattern characteristic of aluminum borates such as $9Al_2O_3 \cdot B_2O_3$, $2Al_2O_3 \cdot B_2O_3$ and $Al_2O_3 \cdot B_2O_3$.

TABLE II. X-RAY ANALYSIS OF THE ALUMINA-BORIA CATALYST CALCINED AT 500°C

Alumina for catalyst base	Boria content*	Structure of catalyst	Relative intensity of maximum diffraction peak**
Alumina gel	0.0	η-Alumina	15
without aging	6.2	η-Alumina	12
	16.8	η-Alumina	6
	21.9	η-Alumina	5
		Boria	4
	40.7	η-Alumina	5
		Boria	15
Bayerite	10.2	η-Alumina	11
	19.0	η-Alumina	4
		Boria	2
	27.1	η-Alumina	4
		Boria	4
η-Alumina	11.2	η-Alumina	14
	14.9	η-Alumina	12
	20.3	η-Alumina	12
		Boria	6
α-Alumina	5.0	α-Alumina	>100
		Boria	3
	15.0	α-Alumina	>100
		Boria	5

* Boria content (B_2O_3/cat., wt.%) represents the value determined by an extraction analysis except with the catalyst derived from α-alumina.

** Angular position of the maximum diffraction peak (2θ); η-alumina 66.8°, α-alumina 43.3°, boria 27.9°.

The Infrared Spectra of Alumina-Boria.—Among the spectra shown in Fig. 5, the spectrum of boria is quoted from Brame's publication.[20] The strong intensity band at 7 μ in the spectra of boric acid and boria is

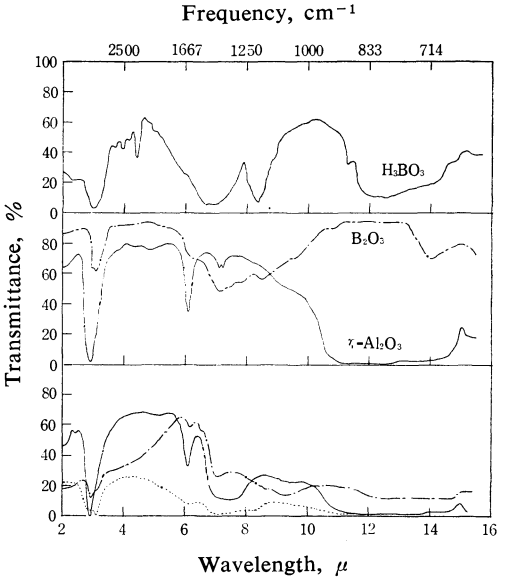


Fig. 5. Infrared spectra of boric acid, boria and alumina-boria.
———: η-Alumina-boria (10% boria)
------: η-Alumina-boria (30% boria)
—·—·: α-Alumina-boria (10% boria)

19) J. Haladjian and G. Carpéni, *Bull. soc. chim. France*, [9], **1956**, 1679.

20) E. G. Brame, Jr., J. L. Margrave and V. W. Moloche, *J. Inorg. & Nuclear Chem.*, 5, 48 (1957).

Table III. Coloration of Hammett indicators on catalysts

Sample	Calcination temp. °C	Hammett indicators (pK_a) Benzeneazodiphenylamine (+1.5)	Dicinnamalacetone (−3.0)	Benzalacetophenone (−5.6)
η or χ-alumina alone	400	No change	—*	—
η or χ-alumina-boric acid (corresponding to 15 wt. % boria)	Without heating	Red	No change	—
	100～200	Purple	Orange	No change
	300～400	Purple	Orange	Yellow
Boric acid	Without heating	No change	—	—
Metaboric acid	100	No change	—	—
Evacuated boria	450	No change	—	—

* — Denotes that no further examinations were required.

assigned to the B–O vibration.[21-23] A slight shift in the position of the B–O vibration-band center towards longer wavelengths, as well as a considerable change in the band shape, was observed in the spectrum of the alumina-boria catalyst with 10% boria. In view of the mass effect[20] of the aluminum atom upon the B–O vibration, it is suggested that alumina may react with boric acid and that a B–O–Al bond is formed in the catalyst. On the other hand, the band position of the B–O vibration of the catalyst prepared from α-alumina (10% boria) accorded with that of boria. This shows that α-alumina is inactive for the interaction with boric acid. The disappearance of the B–O–H bending band in the case of the catalyst (10% boria) which appears at 8.3 μ with strong intensity in the spectrum of boric acid may suggest that such a bond as Al–O–B–O–Al is formed in the course of the fore-treatment of the catalyst.

The Effect of the Calcination Temperature of the Catalyst upon the Activity.—The activities and acid strengths of some alumina-boria catalysts calcined at different temperatures are shown in Fig. 6 and Table III. It was observed that the heating of the mixture of active alumina and boric acid at a temperature as low as 100°C brought about an acid color with benzeneazodiphenylamine (pK_a +1.5), while the alumina alone and evacuated boria did not give the acid color by calcination, even at 400°C. This is consistent with the conclusion of the thermographic analysis. The data in Fig. 6, however, indicate that an effective catalyst for toluene disproportionation or for xylene isomerization could be obtained by calcination above 400°C. Since the catalyst gave an acid color with benzalacetophenone

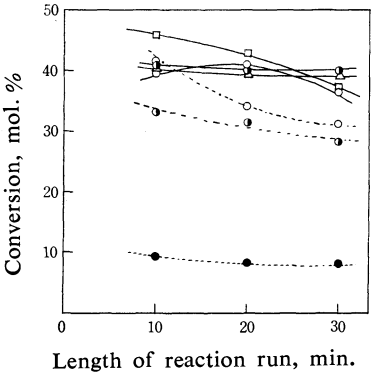


Fig. 6. Effect of the calcination temperature of catalysts upon activity.
Catalyst: η-Alumina-boria (10 wt. % boria) calcined at 300°C ●, 400°C ◑, 500°C ○, 600°C △, 700°C □.
——: Toluene disproportionation at 480°C, catalyst 20.1 g., feed rate 0.0285 mol./hr.
----: *o*-Xylene isomerization at 300°C, catalyst 6.0 g., feed rate 0.0520 mol./hr.

(pK_a −5.6) only when it was heated above 300°C, it may be concluded that the catalyst should be activated at a higher temperature than 400°C in order to develop the activity for these reactions. This is analogous to the finding of Topchiev's study of the alumina-chromia catalyst.[23] It is suggested, consequently, that the large amount of water which is produced in the course of chemical interaction between alumina and boric acid, and which still remains adsorbed on the resulting catalyst, hinders the development of activity.

Kinetic Studies of Some Specific Reactions over an Alumina-Boria Catalyst

The Disproportionation of Toluene.—A number of kinetic studies of the transalkylation

21) R. R. Servoss and H. M. Clark, *J. Chem. Phys.*, **26**, 1175 (1957).
22) D. E. Bethell and N. Sheppard, *Trans. Faraday Soc.*, **51**, 9 (1954).
23) A. V. Topchiev, B. A. Krentsel, A. I. Perelman and K. G. Miesserov, *Polymer Sci.*, **34**, 129 (1959).

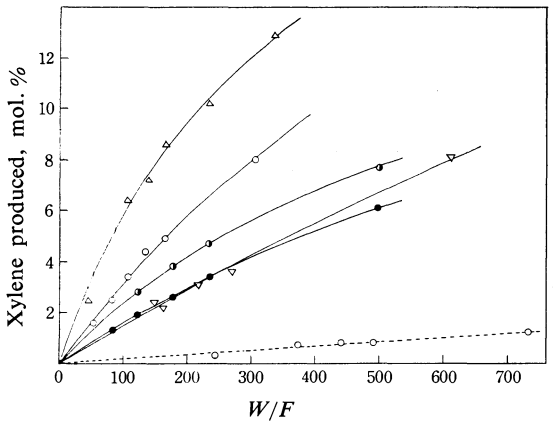


Fig. 7. Formation of xylene in toluene disproportionation
Reaction temperature (°C): 510 △, 480 ○◑ ●, 450 ▽.
Partial pressure (atm.): 1.0 △○▽, 0.8 ◑, 0.6 ●.
——: Fresh alumina-boria catalyst (10 wt.% boria, η-alumina for base). Stationary-state activity was almost identical with fresh and four times regenerated catalysts.
----: Commercial silica-alumina catalyst which was regenerated five times in order to obtain constant activity.

of aromatic compounds with solid acidic catalysts have been made by several workers.[24-28] However, few studies of these reactions with an alumina-boria catalyst have been kinetically forwarded. In the present paper, the role of the catalyst and the reaction kinetics are discussed. The results of the disproportionation of toluene at 450 to 510°C, with or without the dilution of the reactants with nitrogen, are shown in Fig. 7. Among the products, the quantity of benzene was larger than that of xylene in every run, and some cracking reactions (the demethylation of toluene and xylene) were found to occur simultaneously. A small amount of a gaseous substance was produced; it consisted of hydrogen and methane (in a 9 : 1 mol. ratio). These side reactions caused a decrease in the activity of the catalyst as a result of the coke formation. For this reason, the samples were taken when the activity became constant about an hour after the start of the run. The reaction scheme is expressed as follows:

Disproportionation:

$$2C_6H_5CH_3 = C_6H_6 + C_6H_4(CH_3)_2$$

Cracking:

$$\begin{cases} C_6H_5CH_3 \rightarrow C_6H_6 + CH_2\cdot \\ C_6H_4(CH_3)_2 \rightarrow C_6H_5CH_3 + CH_2\cdot \end{cases}$$

Johnson and Watson[24] studied the formation of toluene from benzene and xylene over a silica-alumina catalyst and showed that the rate was controlled by the surface reaction between the adjacent centers occupied by adsorbed reactants. In the present study, the disproportionation of toluene was likewise well interpreted kinetically by assuming that the rate was controlled by the surface reaction. The rate is described by an expression following the Langmuir-Hinshelwood mechanism;

Rate of disproportionation:

$$r_d = \frac{C_d(p^2_t - p_b p_x/K_d)}{(1+K_b p_b + K_t p_t + K_x p_x)^2} \qquad (1)$$

where C_d is the rate constant; K_d, the equilibrium constant of the disproportionation and p_b, p_t and p_x and K_b, K_t and K_x, partial pressures (atm.) and adsorption equilibrium constants for benzene, toluene and xylene respectively. Other expressions for the rate derived from the Rideal mechanism and the adsorption or desorption-controlling mechanisms were found to be unsuccessful in explaining the results of an examination of the relationship between the initial rate of the formation of xylene and the partial pressure of the feed. The overall rate of the reaction is given by the following expression, by assuming that the retardation term of the denominator of Eq. 1 is constant so long as the partial pressure of the feed is fixed;

$$\left.\begin{aligned} &\text{The rate of the formation of xylene:} \\ &\quad r_x = dx/d(W/F) = k_d(p^2_t - p_b p_x/K_d)/2 - k_x p_x \\ &\text{The rate of the formation of benzene:} \\ &\quad r_b = db/d(W/F) = k_d(p^2_t - p_b p_x/K_d)/2 + k_t p_t \\ &\text{The rate of subsequent cracking:} \\ &\quad r_c = r_b - r_x \end{aligned}\right\} \qquad (2)$$

where k_d, k_x and k_t denote rate constants of toluene disproportionation, xylene cracking and toluene cracking at a constant partial pressure of the feed; W the mass of the catalyst (g.); F the feed rate (mol./hr.) and x and b, mole fractions of xylene and benzene in the product. The above assumption is found to hold true because there is a good linear relationship between r_x/p_x and $(p^2_t - p_b p_x/K_d)/p_x$, as is shown in Fig. 8. The k_d values at 1 atm. of partial pressure of the feed are listed in

24) L. N. Johnson and K. N. Watson, *Natl. Petrol. News, Tech. Sec.*, (8) 9 (1946).
25) E. Echigoya, T. Watanabe and K. Morikawa, 16th Annual Meeting of Chemical Society of Japan, Tokyo, 1963.
26) K. Tarama, S. Teranishi, K. Hattori and T. Hosoi, ibid.
27) T. Amemiya, E. Tsunetomi, E. Nakamura and T. Nakazawa, *J. Japan Petrol. Inc.* (*Sekiyu Gakkai Shi*), 3, 813 (1960).
28) T. Amemiya, E. Tsunetomi, E. Nakamura, T. Nakazawa, M. Shimizu and H. Chiba, ibid., 3, 988 (1960).

Table IV. Apparent rate constants and selectivity

Partial pressure of the feed: 1 atm. E_a: apparent activation energy (kcal./mol.)
P: Pre-exponential factor

Catalyst	Reaction temp. °C	Apparent rate constants: Toluene disproportionation, $k_d \times 10^4$ (mol./hr. cat. g. atm^2) from Fig. 8, from Fig. 10		Toluene cracking $k_t \times 10^5$ (mol./hr. cat. g. atm.)	Xylene cracking $k_x \times 10^4$ (mol./hr. cat. g. atm.)	Selectivity S_t	Selectivity S_x
Alumina-boria (10 wt. % boria)	450	2.9	3.1	1.0	4.2	29	0.69
	480	6.6	6.7	3.5	8.3	19	0.80
	510	13.7	13.9	8.6	14.7	16	0.93
	E_a	29.3		39.7	23.6		
	P	2.0×10^5		1.1×10^7	3.6×10^3		
		$k_d \times 10^5$, from Fig. 10		$k_t \times 10^6$	$k_x \times 10^5$		
Silica-alumina* (commercial)	480	3.4		8.8	3.7	3.9	0.92
	510	6.2					
	540	10.9					
	E_a	24.0					
	P	2.8×10^2					

* k_d of fresh silica-alumina at 480°C: 1.75×10^{-4}
k_d of once regenerated silica-alumina at 480°C: 0.80×10^{-4}

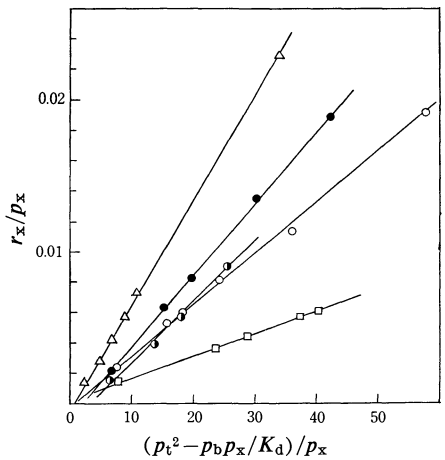


Fig. 8. Constancy of the retardation term of Eq. 1.
Reaction temperature (°C): △ 510, ○◑● 480, □ 450
Partial pressure (atm.): △○□ 1.0, ◑ 0.8, ● 0.6

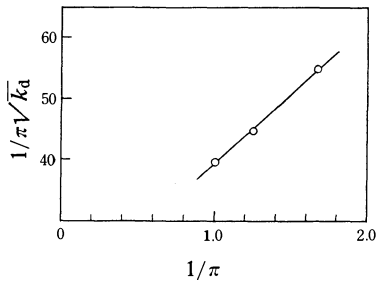


Fig. 9. Consistence of the rate expression derived from the Langmuir-Hinshelwood mechanism.

Table IV. From an examination of Eq. 1 for the reaction in the presence of benzene in the feed,[8] the following relation is found:

$$2K_t \fallingdotseq K_b + K_x$$
$$(K_t=0.48,\ K_b=0.42,\ K_x=0.63)$$

Accordingly, the rate constant, k_d, is expressed by the equation:

$$k_d = C_d/(1+\sum K_i p_i)^2 = C_d/(1+K_t\pi)^2$$
or $$1/\pi = (\sqrt{C_d}/\pi\sqrt{k_d}) - K_t \quad (3)$$

where π represents the partial pressure of the feed. The consistence of the above mechanism was verified by a linear relationship between $1/\pi$ and $1/\pi\sqrt{k_d}$ for the reaction at 480°C, as is illustrated in Fig. 9, and the mean value of K_t was obtained. The numerical expression of the disproportionation of toluene is as follows:

$$r_d = \frac{34.9\exp(-7400/T)}{\{1+4.12\times10^{-6}\pi\exp(9060/T)\}^2} \times (p^2_t - p_b p_x/K_d)$$

(mol./hr. g. cat.), $T=723$ up to 783°K.

The mean value of the heat of the adsorption of reactants, 18 kcal./mol.

The apparent activation energy, 14.7 kcal./mol.

The relation between the time factor (W/F) and the mole fraction of xylene in the product (x) is described approximately by an integrated expression:

$$W/F = -\{\ln(1-mx)\}/n \quad (4)$$

when m and n denote constants when the

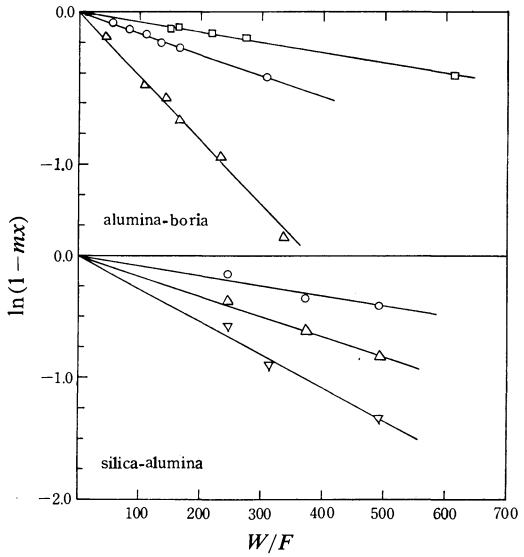


Fig. 10. Consistence of the integrated expression of Eq. 4 with experimental results at 1 atm. of partial pressure of the feed.

Alumina-boria				Silica-alumina			
	°C	m	$n\times10^3$		°C	m	$n\times10^4$
-□-	450	4.2	0.66	-○-	480	5.0	0.84
-○-	480	4.2	1.41	-△-	510	5.0	1.54
-△-	510	6.0	4.16	-▽-	540	5.0	2.72

reaction temperature is fixed. The consistency of Eq. 4 with the results of the reactions over alumina-boria and a commercial silica-alumina is shown in Fig. 10, where the optimum values of the constant, m, are also given. Equations 2 and 4 give the following relation:

$$\{dx/d(W/F)\}_{WF\to0}=n/m=k_d/2 \qquad (5)$$

Table IV demonstrates the good accordance of k_d values calculated from Eq. 5 with those calculated from Eq. 2.

In the next place, the selectivity of the disproportionation is to be discussed. The following expression is derived from Eq. 2:

$$\{(1-dx/db)/2\}(p^2_t-p_bp_x/k_d)/p_x = (1/S_x)+(1/S_t)(dx/db)(p_t/p_x) \qquad (6)$$

where $S_t(=k_d/k_t)$ and $S_x(=k_d/k_x)$ are defined as the selectivities of the disproportionation to toluene cracking and to xylene cracking respectively. Since dx/db can be calculated graphically, the numercal values of S_t and S_x are obtained by plotting the left term of Eq. 6 against $(dx/db)(p_t/p_x)$. The linear relationship of Eq. 6 is shown in Fig. 11. The values of S_t and S_x are calculated and listed in Table IV. It may be concluded that both the selectivity and the activity of alumina-boria are much higher than those of the commercial silica-alumina. The lower activity of the latter may be due principally to a higher tendency

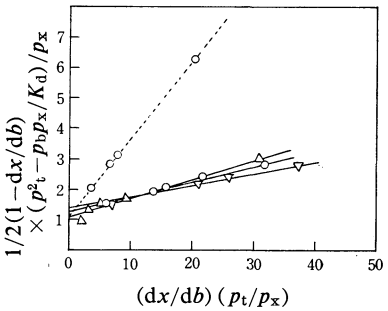


Fig. 11. Linear relationship between the left term of Eq. 6 with $(dx/db)(p_t/p_x)$.
Reaction temp. (°C): △ 510, ○ 480, ▽ 450.
——: Alumina-boria
----: Silica-alumina

of coke fomation as well as to a lower concentration of active centers. The difference between the apparent activation energy of toluene cracking and that of xylene cracking, which are given in Table IV, suggests that the cracking reactivity is affected by the basicity of the aromatic nucleus.

The Decrease in Activity upon Coke Formation.—The toluene conversion of the disproportionation decreased with the length of the run and approached a constant value asymptotically, as is shown in Fig. 12. A carbon deposit on alumina-boria caused by the subsequent cracking reactions was observed, but regeneration could be easily accomplished by burning off the coke with air, giving the original activity. It may probably be concluded that a carbonaceous material covers the active

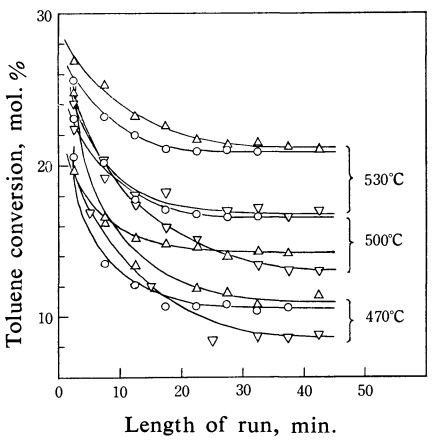


Fig. 12. Decrease in the activity of toluene disproportionation over the alumina-boria catalyst (15 wt. % boria).
Mass of catalyst: 5.0 g., ○ fresh, △ regenerated once, ▽ twice.
Feed rate: ○, △ 0.0568 mol./hr., ▽ 0.0660 mol./hr.

centers of the catalyst and lowers the activity.[29-31] Assuming that the concentration of active sites decreases in proportion to the amount of coke produced by the cracking of toluene and xylene, the following expression is given, taking into account the facts that the cracking of benzene is negligible and that the concentration of active centers is approximately proportional to the toluene conversion:

$$q=q_0\left\{1-\phi F\int_0^{\theta}(b-x)\,\mathrm{d}\theta\right\} \qquad (7)$$

where q_0 is the initial toluene conversion; q, the toluene conversion at a given time of run (θ); ϕ, the deactivation coefficient; b and x, the mole fractions of benzene and xylene of the product at θ, and F, the feed rate of toluene. The term of the integration denotes the cumulative quantity of cracking up to θ. When it is replaced by the average mole fraction of benzene ($\bar{b}$) and xylene ($\bar{x}$) instead of b and x during each successive fraction of time ($\Delta\theta$), the integration in Eq. 7 is expressed as a summation of the fractional terms. Assuming further that a stationary-state conversion, q_s, is reached at a certain length of run when the covering effect of the coke on the active sites approaches equilibrium, a relative activity, q/q_s, is given by the following equation:

$$\left.\begin{aligned} q/q_s&=R\{1-\phi F\textstyle\sum(\bar{b}-\bar{x})\,\Delta\theta\}\\ R&=q_0/q_s\end{aligned}\right\} \qquad (8)$$

The linear relationship between q/q_s and $F\sum(\bar{b}-\bar{x})\Delta\theta$ is shown in Fig. 13. Since the deactivation coefficient and the relative activity, R, were approximately constant at a given reaction temperature, irrespective of either the regeneration of the catalyst or the change in the feed rate, the above interpretation of the decrease in activity seems to be analytically proved. If the ϕ coefficient is proportional to the adsorption equilibrium constant of the contaminant, a 4.2 kcal./mol. value is obtained for the apparent heat of its adsorption. The change in the ϕ values with the reaction temperature may be caused by the difference in the mechanism of the coke formation.[31] From a similar analysis of decrease in the activity of alumina-boria catalysts of different compositions, the relationship between the acidity and the initial activity, which is given as the product of q_s and R, is confirmed to be almost analogous to the correlation between the activity of the "equilibrated" catalyst and its acidity.[11]

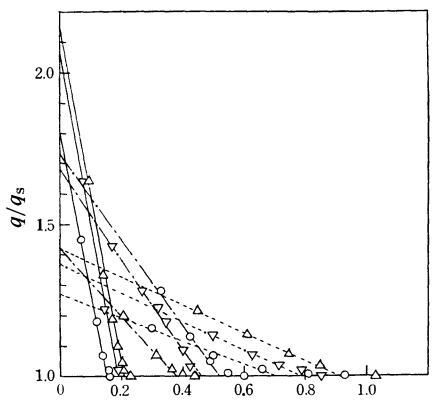


Fig. 13. Relation between the relative activity (q/q_s) and the cumulative amount of cracking ($F\sum(\bar{b}-\bar{x})\Delta\theta$). See Fig. 12 for symbols. Reaction temp. (°C): —— 470, —·—· 500, ---- 530

		○	△	▽
470°C	R	1.8	2.2	2.1
	ϕ	2.9	2.6	2.8
500°C	R	1.7	1.4	1.7
	ϕ	0.82	0.76	0.90
530°C	R	1.3	1.4	1.4
	ϕ	0.30	0.33	0.33

The Isomerization of Xylene.—In the course of the isomerization of xylene, toluene and trimethylbenzene were produced simultaneously. Since the amount of benzene produced was negligible under the conditions of this study, only the disproportionation of xylene was taken into consideration as a side reaction.

Table V. Rate constants of xylene isomerization over the alumina-boria catalyst (15% boria, η-alumina for base) at 420 to 480°C

Rate constant of xylene isomerization, $k_{1j}=k'_{1j}/(1+\pi K_x)$, (mol./hr. cat. g. atm.)
Rate constant of xylene disproportionation, $k_d=k'_d/(1+\pi K_x)^2$, (mol./hr. cat. g. atm^2)

	Rate constant (T: °K)	Activation energy kcal./mol.
k'_{om}	$28.4\exp(-4758/T)$	9.46
k'_{op}	$0.204\exp(-2258/T)$	4.49
k'_{mo}	$22.6\exp(-4954/T)$	9.84
k'_{mp}	$0.499\exp(-2218/T)$	4.41
k'_{po}	$2.05\exp(-3736/T)$	7.42
k'_{pm}	$7.95\exp(-3671/T)$	7.29
k'_d	$87.3\exp(-6302/T)$	12.52
K_x*	$0.0426\exp(1585/T)$	3.15**

* K_x denotes the average adsorption equilibrium constant of the reactants.
** The value represents the average heat of adsorption of the reactants.

29) W. G. Appleby, J. W. Gibson and G. M. Good, Div. Petrol. Chem., Am. Chem. Soc., New York (Sept. 1960), 5, No. 4, B.
30) E. M. Gladrow and C. N. Kimberlin, Jr., ibid., B-79.
31) D. J. Wynnermen, ibid.

Assuming that both the rate of the isomerization and that of the disproportionation are controlled by surface reactions between adsorbed xylene molecules, the overall rate of the isomerization for the xylene isomers may be described by following expressions:

$$\left.\begin{aligned}
&\text{The rate of conversion of } o\text{-xylene:}\\
&r_o=-\mathrm{d}o/\mathrm{d}(W/F)=\pi\{(k_{om}+k_{op})o-k_{mo}m-k_{po}p\}+\pi^2k_d ox\\
&\text{The rate of conversion of } m\text{-xylene:}\\
&r_m=-\mathrm{d}m/\mathrm{d}(W/F)=\pi\{(k_{mo}+k_{mp})m-k_{om}o-k_{pm}p\}+\pi^2k_d mx\\
&\text{The rate of conversion of } p\text{-xylene:}\\
&r_p=-\mathrm{d}p/\mathrm{d}(W/F)=\pi\{(k_{po}+p_{pm})p-k_{op}o-k_{mp}m\}+\pi^2k_d px\\
&\text{The rate of disproportionation of xylene:}\\
&r_d=-\mathrm{d}x/\mathrm{d}(W/F)=\pi^2k_d x^2\\
&\text{or}\qquad (1/x)-1=\pi^2k_d(W/F)\\
&k_{ij}=k'_{ij}/(1+\pi K_x)\\
&k_d=k'_d/(1+\pi K_x)^2\\
&x=o+m+p
\end{aligned}\right\}\quad(9)$$

where o, m, p denote mole fractions of o-, m-, p-xylene in the product; k'_{ij}, the rate constant of the isomerization of the i-isomer to the j-isomer; k'_d, the average rate constant of the disproportionation of xylene isomers; π, the partial pressure of the total reactants, which is almost identical to that of the feed; K_x, the average adsorption equilibrium constant of the reactants; W, the mass of the catalyst, and F, the feed rate. The sum of k_{om} and k_{op} was obtained numerically from the initial rate of o-xylene conversion. The linear relationship between $1/\pi$ and $1/\pi(k_{om}+k_{op})$ gave the numerical values of $(k'_{om}+k'_{op})$ and K_x. All the constants in Eq. 9 were determined by a similar analysis searching for the initial rates of conversion of other isomers and by using the integrated formula of the disproportionation.[9] Table V represents the numerical expressions of the rates of isomerization and disproportionation. A comparison between the equilibrium constants of isomerization calculated from thermodynamic data[32] and those

Table VI. Equilibrium constants of xylene isomerization calculated from thermodynamic data

Reaction temp., °C	K_{pm}*	K_{om}	K_{op}
420	2.22(1.96)**	2.15(1.73)	0.965(0.886)
450	2.22(2.13)	2.10(1.50)	0.946(0.706)
480	2.22(2.32)	2.06(1.71)	0.928(0.737)

* K_{ij} denotes the equilibrium constant of isomerization of the i-isomer to the j-isomer.
** The value in parentheses was calculated from experimental data.

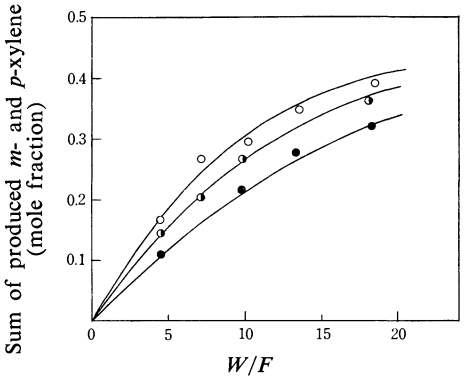


Fig. 14. Isomerization of o-xylene at 480°C over the alumina-boria catalyst (15 wt. %, η-alumina for base).
Partial pressure of the feed (atm.): ○ 1.00, ◑ 0.75, ● 0.50
——: Calculated from Eq. 10

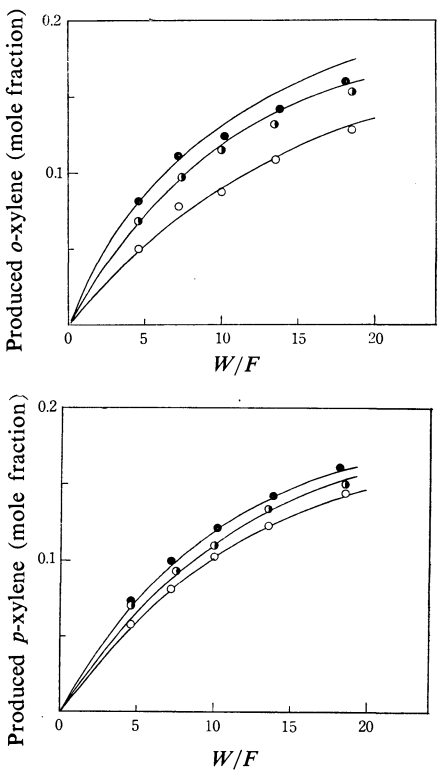


Fig. 15. Isomerization of m-xylene at 1 atm. of partial pressure of the feed.
Reaction temp. (°C): ○ 420, ◑ 450, ● 480
——: Calculated from Eq. 10

32) W. J. Taylor, D. D. Wagman, M. G. Williams, K. S. Pitzer and F. D. Rossini, *J. Research Nat. Bur. Standards.* **37**, 95 (1946).

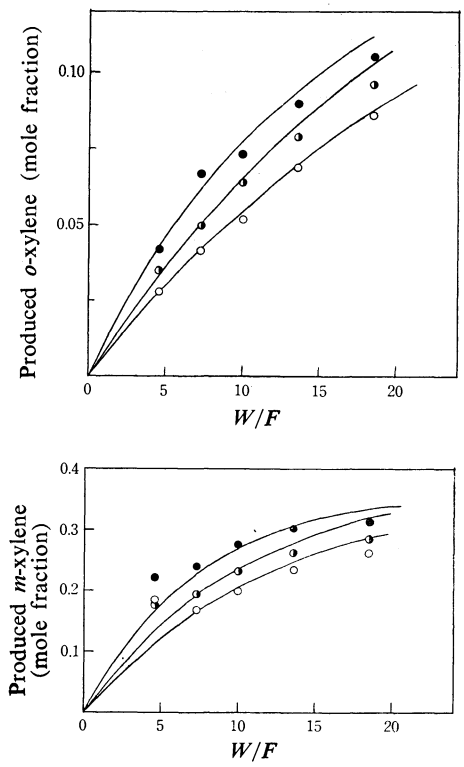


Fig. 16. Isomerization of *p*-xylene at 1 atm. of partial pressure of the feed.
Reaction temp. (°C): ○ 420, ◑ 450, ● 480
——: Calculated from Eq. 10

obtained by the experiment is shown in Table VI.

Amemiya and his co-workes[27,28] reported that the rate of xylene isomerization over a silica-alumina catalyst may be described by expressions similar to those in Eq. 9 except for the terms of the subsequent disproportionation. The integrated formula derived by them, however, was applicable only to such isomeric compositions as were not far from equilibrium. In the present study, the following integrated expressions are proposed for a wide range of the isomeric composition, (they include the subsequent disproportionation) :

$$\left.\begin{aligned} \ln\{(o_0-o_e x)/(o-o_e x)\} &= \alpha(W/F) \\ \ln\{(m_0-m_e x)/(m-m_e x)\} &= \beta(W/F) \\ \ln\{(p_0-p_e x)/(p-p_e x)\} &= \gamma(W/F) \end{aligned}\right\} \quad (10)$$

where o_0, m_0, p_0 are initial mole fractions of xylene isomers in the feed; o_e, m_e, p_e, equilibrium mole fractions of the isomers, and α, β, γ, the constants which are determined by a comparison of Eq. 9 with the differentiated forms of Eq. 10. The experimental data are very consistent with the expression of Eq. 10, as is shown in Figs. 14, 15 and 16.

Transethylation between Benzene and Diethylbenzene. — The reaction was carried out at 450°C, and ethylbenzene was produced with a negligible amount of toluene and gaseous products. The results are kinetically described by the following numerical rate expression, which is derived from the Langmuir-Hinshelwood mechanism:[10] the rate of formation of ethylbenzene at 450°C (mol./hr. cat. g.):

$$r = dx/d(W/F) = \frac{0.281(p_b p_d - p^2_e/K)}{(1+2.76p_b+11.85p_e+1.58p_d)^2} \quad (11)$$

where x denotes the mole fraction of ethylbenzene in the product; p_b, p_e, p_d, the partial pressures (atm.) of benzene, ethylbenzene and diethylbenzene; W, the mass of the catalyst (g.), and F, the feed rate (mol./hr.). Since any side reactions can be neglected, Eq. 11 is easily integrated. The results are very consistent with the observed data, as is shown in Fig. 17, where the experimental finding of the reaction over a synthetic silica-alumina is also given for the sake of comparison. The acitivity of the silica-alumina was less than that of the alumina-boria. This is probably due to the lower concentration of active sites in the former.

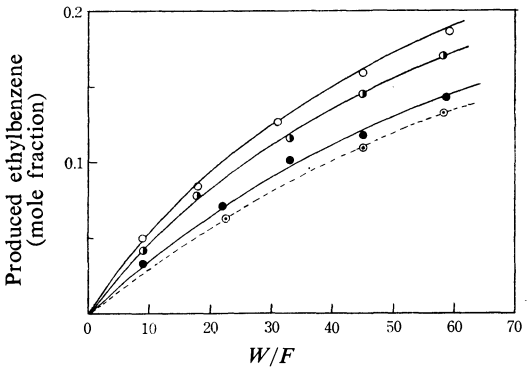


Fig. 17. Transethylation between benzene and diethylbenzene over the alumina-boria catalyst (15 wt. % boria, η-alumina for base) at 450°C using an equimolecular mixture as the feed.
Partial pressure of the feed (atm.): ○⊙ 1.00, ◑ 0.75, ● 0.50
——: Calculated from integrated expression of Eq. 11
----: Activity of a synthetic silica-alumina catalyst (50 wt. % SiO_2)

Summary

This study has aimed to secure an optimum means for the preparation of an alumina-boria catalyst by a systematic examination of the relationship between the physical characteristics of the catalyst and its activity, and to clarify

the mechanism of the development of activity on the basis of the experimental evidence about the chemical interaction of alumina with boric acid and about the chemical structure of the catalyst. The applicability of the catalyst has been studied kinetically for some specific reactions relating to the transalkylation of aromatic compounds. It has been found that alumina-boria shows a higher activity for these reactions than does silica-alumina.

The results and conclusion may be summarized as follows:

I) Boric acid is dehydrated to produce metaboric acid as a probable intermediate and reacts with an active alumina at about 130°C with little disturbance of the crystal structure of alumina, and effective acidic centers are produced. Most of the acid centers are of the Brönsted type. Alumina-boria does not show any definite chemical structure characteristic of aluminum borates, such as $9Al_2O_3 \cdot B_2O_3$, $2Al_2O_3 \cdot B_2O_3$ or $Al_2O_3 \cdot B_2O_3$. It is suggested that such a bond as Al–O–B–O–Al may be formed between surfaces of the crystal structure of alumina and may result in acidic centers.

II) The catalytic activity of toluene disproportionation shows a good correlation with the Brönsted acidity. This is well compatible with the likely theory that the reaction proceeds via a carbonium ion mechanism.

III) The activity of the disproportionation is considerably affected by the structure of the alumina used as the catalyst base as well as by the boria content of the catalyst. The catalyst prepared from η-alumina shows a higher activity than that from χ-alumina, while α-alumina does not give an active catalyst because of its poor reactivity with boric acid. A rise in the crystallinity of alumina lowers the reactivity. Excessive boria reduces the catalytic activity. An effective catalyst for the transalkylation of aromatic compounds can be obtained when alumina-boria is calcined above 400°C.

IV) The results of such reactions as the disproportionation of toluene, the isomerization of xylene and the transethylation between benzene and diethylbenzene can be well interpreted kinetically by assuming that the rates of these reactions are controlled by surface reactions between adsorbed molecules of the reactants.

V) In the disproportionation of toluene, a decrease in the activity of the catalyst with the length of the run was observed. This phenomenon can be explained analytically by taking into account the fact that some contaminant such as the carbonaceous material, which is produced by side reactions (cracking of toluene and xylene), covers effective sites of the catalyst.

VI) It seems to be due essentially to the higher concentration of active sites in alumina-boria that its activity of the transalkylation of aromatic compounds is higher than that of silica-alumina.

Tokuyama Soda Co., Ltd.
Tokuyama-shi, Yamaguchi (Y. I.)

Tokyo Institute of Technology
Meguro-ku, Tokyo (T. S.)

Studies of Peptide Antibiotics. I. Dipeptide Anhydrides as Models of Cyclic Peptide Antibiotics

By Nobuo IZUMIYA, Tetsuo KATO, Yoshimasa FUJITA, Motonori OHNO and Michio KONDO

(Received June 9, 1964)

Some peptide antibiotics,[1] such as gramicidin S, tyrocidin A and polymixin B, possess several structural features in common. These include a cyclic structure, a basic character due to the presence of one or more diamino acid residues, and the possession of at least one D-amino acid residue. The effectiveness of a cyclic structure for an antibiotic activity is indicated by the finding that a synthetic open-chain decapeptide, with the same sequence of amino acid residues as is found in gramicidin S, shows a weaker antibacterial activity than that of gramicidin S.[2]

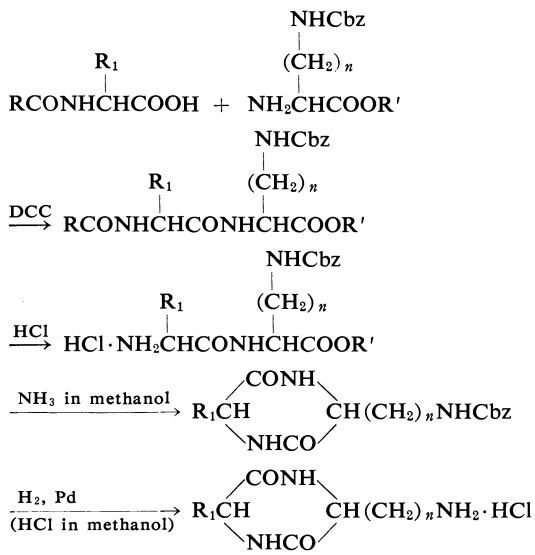
Since dipeptide anhydrides, wherein one (or

1) R. O. Studer and K. Vogler, *Helv. Chim. Acta*, **45**, 819 (1962).

2) B. F. Erlanger and L. Goode, *Nature*, **174**, 840 (1954); *Science*, **131**, 669 (1960).

both) of the component amino acid residues possesses a D-configuration and a basic character, reveal the characteristics mentioned above, it became of interest to ascertain whether these relatively simple compounds would exhibit the antibacterial properties. For that purpose, the L-L, D-D, D-L and L-D stereomers of both valyllysine anhydride and phenylalanyllysine anhydride, and the L-L and D-L stereomers of both valylornithine anhydride and phenylalanylornithine anhydride were selected as model compounds. Lysine was used as one of the diamino acids because Schwyzer and Sieber[3] had reported that no loss in activity occured upon the replacement of an ornithine residue in gramicidin S with a lysine residue. Ornithine, valine and phenylalanine were chosen because of their relatively high frequency of occurrence in cyclic peptide antibiotics of natural origin.[1]

The sequence of reaction employed for the synthesis of the anhydrides is indicated in the following equations. All final dipeptide anhydride hydrochlorides were crystalline materials which showed satisfactory elemental analyses. The L-L and D-D antipodes of the final products exhibited specific rotation values that were equal in absolute value within the limits of experimental error, as did the D-L and L-D antipodes. The products revealed no contamination with other ninhydrin-positive materials when subjected to paper chromatography.



R-: H- or $C(CH_3)_3O$-, R_1: $(CH_3)_2CH$- or $C_6H_5CH_2$-, n: 3 or 4, R'-: $-CH_3$ or $-C_2H_5$, Cbz-: $C_6H_5CH_2OCO$-, DCC: dicyclohexylcarbodiimide.

3) R. Schwyzer and P. Sieber, *Helv. Chim. Acta*, **41**, 1582 (1958).

Since in this laboratory it has been reported that L-valyl-L-lysine amide and L-phenylalanyl-L-lysine amide are susceptible to the hydrolytic action of trypsin at the lysine carbonyl linkage,[4] it became relevant to determine whether this same enzyme would similarly cleave L-valyl-L-lysine anhydride and L-phenylalanyl-L-lysine anhydride at the same linkage with the formation of valyllysine and phenylalanyllysine respectively as the hydrolytic products. In addition, the known susceptibility of phenylalanine-containing peptides to the hydrolytic action of chymotrypsin[5] indicated that the possible conversion of L-phenylalanyl-L-lysine anhydride to lysylphenylalanine by this enzyme should also be studied. For the purpose of chromatographic comparison, valyllysines, phenylalanyllysines and lysylphenylalanine were synthesized via the mixed anhydride method, and their R_f values ascertained. Finally, paper chromatography of the enzymic digests showed only a single ninhydrin-positive spot, which possessed the same R_f values as the unhydrolyzed dipeptide anhydride substrate.

In order to ascertain whether or not the dipeptide anhydrides described herein possessed antibacterial activity, the effect of various levels of the anhydrides on the growth response of *B. subtilis*, *St. aureus*, *E. coli* and *Pr. vulgaris* was examined. No retardation of growth was noted with any one of these microorganisms, at levels for each compound at 100 μg. per ml. of the assay medium. In this connection, it should be noted that Fruton has shown no influence by D-leucyl-L-tryptophan anhydride[6] on the growth of several microorganisms. From these findings, it appears that other structural characteristics in addition to those described previously are necessary, such as a certain minimum ring size, before a peptide molecule can exhibit antibacterial properties. Further experiments on the preparation and properties of larger cyclic peptides are thus in progress in this laboratory.

Experimental

Melting points are uncorrected. Samples are prepared for analysis by drying them at 100°C in vacuo for 2 hr.

Formyl-D-valine (I) and Formyl-D-phenylalanine (II).—Each of these compounds was prepared, according to the procedure of Sheehan and Yang,[7] by the treatment of D-valine or D-phenylalanine

4) N. Izumiya, T. Yamashita, H. Uchio and K. Kitagawa, *Arch. Biochem. Biophys.*, **90**, 170 (1960).

5) H. Neurath and G. W. Schwert, *Chem. Revs.*, **46**, 69 (1950); T. Yamashita and N. Izumiya, *J. Biochem.*, **46**, 991 (1959).

6) J. S. Fruton, *J. Am. Chem. Soc.*, **70**, 1280 (1946).

7) J. C. Sheehan and D-D. H. Yang, ibid., **80**, 1154 (1958).

with 98% formic acid and acetic anhydride; yield, 84% and 80%, m. p. 152~153°C and 167°C, $[\alpha]_D^{20}$ −13.1° and −75.2° (*c* 2, ethanol), for I and II respectively. Each of these compounds had been obtained previously by the resolution of formyl-DL-valine or -phenylalanine with brucine;[8-10] m. p. 153°C[8] and 148~149°C[9], $[\alpha]_D^{20}$ −12.8°[8] and −13°[9] for I, and m. p. 167°C,[10] $[\alpha]_D$ −75.2°[10] for II.

ε-Carbobenzoxy-D-lysine Methyl Ester Hydrochloride.—This compound was prepared as was the L-antipode;[11] m. p. 114~116°C; $[\alpha]_D^{25}$ −16.9° (*c* 2, water). The reported values for the L-antipode[11] are m. p. 117°C and $[\alpha]_D^{25}$ +17.2°.

δ-Carbobenzoxy-L-ornithine Ethyl Ester *p*-Toluene-sulfonate (III).—This compound was prepared according to the general procedure of Kato et al.[12] Thus, a suspension of δ-carbobenzoxy-L-ornithine[13] (53.3 g.) and *p*-toluenesulfonic acid monohydrate (42 g.) in a mixture of ethanol (80 ml.) and carbon tetrachloride (400 ml.) was refluxed, and the water liberated was removed as an azeotropic mixture. The reaction mixture was then concentrated in vacuo, and the residual material treated with ether. The precipitate filtered off was recrystallized from hot acetone (170 ml.)-ether (650 ml.); 87 g. (95%); m. p. 111~112°C; $[\alpha]_D^{20}$ +8.9° (*c* 2, dimethylformamide).

Found: C, 56.19; H, 6.56; N, 6.17. Calcd. for $C_{22}H_{30}O_7N_2S$: C, 56.63; H, 6.48; N, 6.01%.

***t*-Butyloxycarbonyl-D-phenylalanine (IV).**—This compound was prepared as an oily product in the same manner as was the L-antipode;[14] yield, 88%. As a minor modification, sodium bicarbonate was used instead of magnesium oxide.[14] The reported yield of the oily L-antipode is 79%.[14]

Formylvalyl-ε-carbobenzoxylysine Methyl Esters (V—VIII).—The coupling reaction was achieved according to the general procedure of Sheehan et al.[15] To a stirred solution of formyl-L-valine[7] or I (7.26 g., 0.05 mol.), ε-carbobenzoxy-L(or D)-lysine methyl ester hydrochloride (16.55 g., 0.05 mol.), and triethyl amine (7.0 ml.) in a mixture of tetrahydrofuran (150 ml.) and chloroform (150 ml.), at 0°C, was added DCC (10.3 g.) The mixture was stored in the cold overnight, after which time the L-L and D-D stereomers were recovered as described under a), and the D-L and L-D stereomers, as described under b). a) The precipitated dicyclohexylurea was removed, and the filtrate was concentrated in vacuo to an oil. After the latter had been dissolved in chloroform (300 ml.), the solution was washed successively with 4% sodium bicarbonate, 2% hydrochloric acid, and water. The organic layer was dried over sodium sulfate and concentrated in vacuo, and the residual material was treated with ether and petroleum ether. The precipitate filtered off was recrystallized from ethyl acetate (30 ml.) - ether (60 ml.) - petroleum ether (60 ml.). b) The dicyclohexylurea, admixed with a small amount of the desired product, precipitated. After the crystals of the latter had been taken into a solution by warming them at 50°C, the reaction mixture was cooled to room temperature under tap water and the urea filtered off. The remainder of the procedure was identical with that described under a) above. Recrystallization was effected from ethyl acetate (90 ml.) - ether (50 ml.) - petroleum ether (50 ml.). The elemental analyses, yields, and physical constants of the compounds so procured are given in Table I.

Formylphenylalanyl-ε-carbobenzoxylysine Methyl Esters (IX—XII).—These compounds were prepared on a 0.05 mol. scale following the procedure described above. The recrystallization of the crude products was achieved from ethyl acetate - petroleum ether (70 ml.: 50 ml. for IX and X, and 110 ml.: 30 ml. for XI and XII).

Formyl-L-phenylalanyl-ε-carbobenzoxy-L-lysine Ethyl Ester (XIII).—This compound was prepared from formyl-L-phenylalanine and ε-carbobenzoxy-L-lysine ethyl ester *p*-toluenesulfonate[12] in the same manner as that used for V and was recrystallized from ethyl acetate - ether - petroleum ether.

Formylvalyl-δ-carbobenzoxyornithine Ethyl Esters (XIV—XV).—These compounds were prepared following the procedure described for the preparation of V. The L-L stereomer (XIV) was more soluble in ethyl acetate than the D-L stereomer (XV), as was observed in the cases of V and VII.

***t*-Butyloxycarbonyl-L-valyl-δ-carbobenzoxy-L-ornithine Ethyl Ester (XVI).**—This compound was prepared by the treatment of a solution of *t*-butyloxycarbonyl-L-valine[14] (2.18 g.), III (4.66 g.) and triethyl amine (1.4 ml.) in tetrahydrofuran-chloroform with DCC (2.06 g.), following essentially the same procedure as that employed for the preparation of V. As a minor alteration, however, 0.5 M citric acid was used instead of 2% hydrochloric acid to wash the reaction mixture.

Formylphenylalanyl-δ-carbobenzoxyornithine Ethyl Esters.—The L-L stereomer (XVII) was prepared following the procedure described for the preparation of V. The D-L stereomer was obtained as crystals with a m. p. of 145~149°C in a yield of 63%; however, the elemental analyses were not satisfactory.

***t*-Butyloxycarbonyl-D-phenylalanyl-δ-carbobenzoxy-L-ornithine Ethyl Ester (XVIII).**—This compound was obtained from IV and III by the procedure described in the case of XVI. The recrystallization of the crude product was achieved from ethyl acetate - ether - petroleum ether.

Valyl-ε-carbobenzoxylysine Methyl Ester Hydrochlorides (XIX—XXII).—A suspension of 8.43 g. each of V—VIII in 0.5 N methanolic hydrogen chloride (60 ml.) was stored at room temperature for 2 days. The resulting clear solution was then concentrated in vacuo. The treatment of the residual material with acetone and ether led to a

8) E. Fischer, *Ber.*, **39**, 2320 (1906).
9) M. A. Nyman and R. M. Herbst, *J. Org. Chem.*, **15**, 108 (1950).
10) E. Fischer and W. Schoeller, *Ann.*, **375**, 1 (1907).
11) M. Bergmann, L. Zervas and W. F. Ross, *J. Biol. Chem.*, **111**, 245 (1935).
12) T. Kato, S. Makisumi, M. Ohno and N. Izumiya, *J. Chem. Soc. Japan, Pure Chem. Sec.* (*Nippon Kagaku Zasshi*), **83**, 1151 (1962).
13) J. I. Harris and T. S. Work, *Biochem. J.*, **46**, 582 (1950).
14) R. Schwyzer, P. Sieber and H. Kappeler, *Helv. Chim. Acta*, **42**, 2622 (1959).
15) J. C. Sheehan and G. P. Hess, *J. Am. Chem. Soc.*, **77**, 1067 (1955); J. C. Sheehan, M. Goodman and G. P. Hess, ibid., **78**, 1367 (1956).

TABLE I. YIELDS, PHYSICAL CONSTANTS AND ANALYSES OF COMPOUNDS

Compound[a]		Yield %	M. p. °C	$[\alpha]_D^{20}$ [b]	Molecular formula	Calcd., %			Found, %		
						C	H	N	C	H	N
For-Val-LysCbz-OMe	L-L (V)	56	140~143	−11.9	$C_{21}H_{31}O_6N_3$	59.84	7.41	9.97	60.26	7.43	9.84
	D-D (VI)	59	140~143	+12.0	$C_{21}H_{31}O_6N_3$	59.84	7.41	9.97	60.07	7.34	9.82
	D-L (VII)	55	149	−16.0	$C_{21}H_{31}O_6N_3$	59.84	7.41	9.97	60.15	7.41	9.92
	L-D (VIII)	58	148	+14.9	$C_{21}H_{31}O_6N_3$	59.84	7.41	9.97	59.98	7.47	9.83
For-Phe-LysCbz-OMe	L-L (IX)	75	125	− 4.5	$C_{25}H_{31}O_6N_3$	63.94	6.66	8.95	63.84	6.78	9.02
	D-D (X)	78	125	+ 3.9	$C_{25}H_{31}O_6N_3$	63.94	6.66	8.95	64.02	6.77	9.25
	D-L (XI)	68	134~136	−11.8	$C_{25}H_{31}O_6N_3$	63.94	6.66	8.95	64.20	7.01	9.21
	L-D (XII)	67	133~135	+11.0	$C_{25}H_{31}O_6N_3$	63.94	6.66	8.95	64.25	6.73	9.16
For-Phe-LysCbz-OEt	L-L (XIII)	74	118~120	− 7.1	$C_{26}H_{33}O_6N_3$	64.58	6.88	8.69	64.24	6.89	8.72
For-Val-OrnCbz-OEt	L-L (XIV)	54	117~120	−12.1	$C_{21}H_{31}O_6N_3$	59.84	7.41	9.97	59.59	7.53	9.94
	D-L (XV)	55	140~142	−15.8	$C_{21}H_{31}O_6N_3$	59.84	7.41	9.97	59.79	7.83	9.67
BOC-Val-OrnCbz-OEt	L-L (XVI)	57	107~109	−6.5	$C_{25}H_{39}O_7N_3$	60.83	7.96	8.51	60.82	7.71	8.68
For-Phe-OrnCbz-OEt	L-L (XVII)	73	124~126	− 9.0	$C_{25}H_{31}O_6N_3$	63.94	6.66	8.95	64.18	6.79	9.20
BOC-Phe-OrnCbz-OEt	D-L (XVIII)	78	117	− 3.7	$C_{29}H_{39}O_7N_3$	64.30	7.26	7.76	64.41	7.33	7.71
H-Val-LysCbz-OMe·HCl	L-L (XIX)	77	154	0	$C_{20}H_{32}O_5N_3Cl$	55.87	7.50	9.77	55.81	7.52	9.72
	D-D (XX)	73	153~154	0	$C_{20}H_{32}O_5N_3Cl$	55.87	7.50	9.77	55.54	7.61	9.74
	D-L (XXI)	80	161	−43.0	$C_{20}H_{32}O_5N_3Cl$	55.87	7.50	9.77	55.63	7.68	9.69
	L-D (XXII)	75	161	+43.8	$C_{20}H_{32}O_5N_3Cl$	55.87	7.50	9.77	55.82	7.57	9.79
H-Phe-LysCbz-OMe·HCl	L-L (XXIII)	72	153~154	− 9.3	$C_{24}H_{32}O_5N_3Cl$	60.32	6.75	8.79	60.31	6.95	8.83
	D-D (XXIV)	75	154~155	+10.1	$C_{24}H_{32}O_5N_3Cl$	60.32	6.75	8.79	60.14	6.99	8.64
H-Val-OrnCbz-OEt·HCl	L-L (XXVII)	83	175~177	+19.9	$C_{20}H_{32}O_5N_3Cl$	55.87	7.50	9.77	55.66	7.59	9.58
H-Phe-OrnCbz-OEt·HCl	L-L (XXIX)	85	120~125	− 7.7	$C_{24}H_{32}O_5N_3Cl$	60.32	6.75	8.79	59.74	6.92	8.69
Val◇LysCbz	L-L (XXXI)	88	162~164	−46.1	$C_{19}H_{27}O_4N_3$	63.14	7.53	11.63	63.04	7.53	11.62
	D-D (XXXII)	86	161~164	+45.0	$C_{19}H_{27}O_4N_3$	63.14	7.53	11.63	63.11	7.34	11.44
	D-L (XXXIII)	90	198~200	− 4.3	$C_{19}H_{27}O_4N_3$	63.14	7.53	11.63	63.16	7.44	11.64
	L-D (XXXIV)	91	199~201	+ 3.2	$C_{19}H_{27}O_4N_3$	63.14	7.53	11.63	63.12	7.44	11.71
Phe◇LysCbz	L-L (XXXV)	83	206~208	−26.1	$C_{23}H_{27}O_4N_3$	67.46	6.65	10.26	67.51	6.76	10.22
	D-D (XXXVI)	87	205~207	+25.5	$C_{23}H_{27}O_4N_3$	67.46	6.65	10.26	67.34	6.76	10.23
	D-L (XXXVII)	85[c]	171	−10.0	$C_{23}H_{27}O_4N_3$	67.46	6.65	10.26	67.85	6.95	10.31
	L-D (XXXVIII)	75[c]	171	+10.5	$C_{23}H_{27}O_4N_3$	67.46	6.65	10.26	67.87	7.05	10.25
Val◇OrnCbz	L-L (XXXIX)	80	206~208	−47.4	$C_{18}H_{25}O_4N_3$	62.23	7.25	12.10	62.25	7.28	12.24
	D-L (XL)	68[c]	208~210	− 6.8	$C_{18}H_{25}O_4N_3$	62.23	7.25	12.10	62.74	7.54	12.08
Phe◇OrnCbz	L-L (XLI)	72	210~212	−12.9	$C_{22}H_{25}O_4N_3$	66.82	6.37	10.63	66.74	6.41	10.59
	D-L (XLII)	66[c]	175~178	− 3.4	$C_{22}H_{25}O_4N_3$	66.82	6.37	10.63	66.30	6.67	10.40
Val◇Lys·HCl	L-L (XLIII)	77	254~256	−54.1	$C_{11}H_{22}O_2N_3Cl$	50.07	8.41	15.92	50.02	8.24	15.82
	D-D (XLIV)	84	253~255	+53.6	$C_{11}H_{22}O_2N_3Cl$	50.07	8.41	15.92	49.84	8.48	15.73

TABLE I. (Continued)

Compound[a]		Yield %	M. p. °C	$[\alpha]_D^{20}$ [b]	Molecular formula	Calcd., %			Found, %		
						C	H	N	C	H	N
	D-L (XLV)	90	282	− 5.4	$C_{11}H_{22}O_2N_3Cl$	50.07	8.41	15.92	50.26	8.47	15.73
	L-D (XIVI)	90	282～283	+ 5.8	$C_{11}H_{22}O_2O_3Cl$	50.07	8.41	15.92	50.04	8.41	15.71
Phe◇Lys·HCl	L-L (XLVII)	94	>270	+ 2.5	$C_{15}H_{22}O_2N_3Cl$	57.80	7.12	13.48	57.72	7.26	13.53
	D-D (XLVIII)	91	>270	− 2.0	$C_{15}H_{22}O_2N_3Cl$	57.80	7.12	13.48	57.64	7.10	13.51
	D-L (XLIX)	88	>255	−46	$C_{15}H_{22}O_2N_3Cl$	57.80	7.12	13.48	58.14	7.24	13.66
	L-D (L)	90	>255	+48	$C_{15}H_{22}O_2N_3Cl$	57.80	7.12	13.48	57.83	7.26	13.42
Val◇Orn·HCl	L-L (LI)	90	255～257	−54.7	$C_{10}H_{20}O_2N_3Cl$	48.10	8.07	16.83	48.07	8.08	16.32
	D-L (LII)	66	265～268	− 4.0	$C_{10}H_{20}O_2N_3Cl$	48.10	8.07	16.83	48.11	8.28	16.80
Phe◇Orn·HCl	L-L (LIII)	68	245～246	+ 8.7	$C_{14}H_{20}O_2N_3Cl$	56.46	6.77	14.38	56.65	6.86	14.16
	D-L (LIV)	75	249～250	−50.4	$C_{14}H_{20}O_2N_3Cl$	56.46	6.77	14.38	56.57	6.82	14.52
Cbz-Val-LysCbz-OMe	L-L (LV)	76	124～126	0	$C_{28}H_{37}O_7N_3$	63.74	7.07	7.97	63.71	7.10	7.98
	D-D (LVI)	74	124～126	0	$C_{28}H_{37}O_7N_3$	63.74	7.07	7.97	63.34	7.28	7.93
	D-L (LVII)	71	163	−15.4	$C_{28}H_{37}O_7N_3$	63.74	7.07	7.97	63.62	7.18	7.84
	L-D (LVIII)	77	164	+16.1	$C_{28}H_{37}O_7N_3$	63.74	7.07	7.97	63.33	7.08	7.97
Cbz-Phe-LysCbz-OEt	L-L (LIX)	85	150	− 8.7	$C_{33}H_{39}O_7N_3$	67.21	6.67	7.13	66.74	6.53	6.84
	D-L (LX)	82	148	+ 4.0	$C_{33}H_{39}O_7N_3$	67.21	6.67	7.13	67.17	6.72	7.04
Cbz-Val-LysCbz-OH	L-L (LXI)	90	139～140	+ 5.0	$C_{27}H_{35}O_7N_3$	63.14	6.87	8.18	62.84	6.90	8.14
	D-D (LXII)	94	139～140	− 5.9	$C_{27}H_{35}O_7N_3$	63.14	6.87	8.18	62.74	6.73	8.20
	D-L (LXIII)	96	123～125	+13.7	$C_{27}H_{35}O_7N_3$	63.14	6.87	8.18	62.91	6.99	8.17
	L-D (LXIV)	97	124～126	−14.5	$C_{27}H_{35}O_7N_3$	63.14	6.87	8.18	63.08	6.82	8.12
Cbz-Phe-LysCbz-OH	L-L (LXV)	95	108～111	− 3.3	$C_{31}H_{35}O_7N_3$	66.29	6.28	7.48	66.23	6.31	7.48
	D-L (LXVI)	93	147	+ 4.3	$C_{31}H_{35}O_7N_3$	66.29	6.28	7.48	66.31	6.29	7.43
H-Val-Lys-OH·HCl	L-L (LXVII)	85	241～243	+25.4	$C_{11}H_{24}O_3N_3Cl$	46.89	8.59	14.91	46.83	8.86	14.89
	D-D (LXVIII)	84	242～243	−25.3	$C_{11}H_{24}O_3N_3Cl$	46.89	8.59	14.91	46.64	8.76	14.99
	D-L (LXIX)[d]	81	—	−50	$C_{11}H_{24}O_3N_3Cl$	46.89	8.59	14.91	46.42	8.81	14.53
	L-D (LXX)[d]	78	—	+48	$C_{11}H_{24}O_3N_3Cl$	46.89	8.59	14.91	46.71	8.83	14.49
H-Phe-Lys-OH·HCl	L-L (LXXI)[d]	79	—	+24	$C_{15}H_{24}O_3N_3Cl$	57.42	7.70	13.39	56.87	7.91	13.31
	D-L (LXXII)[d]	74	—	−80	$C_{15}H_{24}O_3N_3Cl$	57.42	7.70	13.39	57.21	8.03	13.11
Cbz-LysCbz-Phe-OBz	L-L (LXXIII)	67	141	−10.4	$C_{38}H_{41}O_7N_3$	70.03	6.34	6.45	70.01	6.28	6.48
H-Lys-Phe-OH·HCl	L-L (LXXIV)	76	143～145	+35.0	$C_{15}H_{24}O_3N_3Cl$	54.64	7.33	12.75	54.55	7.42	12.63

a) Abbreviations are as follows; For: formyl, BOC: *t*-butyloxycarbonyl, LysCbz: ε-carbobenzoxylysine residue, OrnCbz: δ-carbobenzoxyornithine residue, Val◇Lys·HCl L-L: L-valyl-L-lysine anhydride monohydrochloride.

b) Optical rotations were determined using a 20 cm. tube. All concentrations were 1% except the compounds, XLIX and L. Concentrations of XLIX and L were 0.3%.

c) Yield was based on the parent formyl or *t*-butyloxycarbonyl carbobenzoxy-substituted dipeptide ester.

d) This was hydroscopic crystal; optical rotation was approximate.

crystalline product which was recrystallized from acetone-ether. Although the crystallization of the L-D and D-L stereomers occurred more readily than that of the L-L and D-D stereomers, the latter nevertheless crystallized within an hour by the procedure described above.

Phenylalanyl-ε-carbobenzoxylysine Methyl Ester Hydrochlorides (XXIII—XXVI). — These compounds were prepared following the procedure described above. Although the L-L and D-D stereomers (XXIII, XXIV) could be recrystallized from methanol-acetone-ether, attempts to solidify the D-L and L-D forms (XXV, XXVI) were unsuccessful.

Valyl-δ-carbobenzoxyornithine Ethyl Ester Hydrochlorides (XXVII,XXVIII).—The L-L stereomer (XXVII) was prepared as follows: To a solution of XVI (4.94 g.) in ethyl acetate (15 ml.), 4 N hydrogen chloride in ethyl acetate (50 ml.) was added. The reaction mixture was stored at room temperature for 3 hr. and then evaporated in vacuo. The residual crystals were filtered off with the aid of ether and recrystallized from methanol-ether. The melting point was 175~177°C, as is shown in Table I. The crystalline product was also obtained from the formyl dipeptide ester (XIV) with methanolic hydrogen chloride. This compound, however, showed the low melting point of 108~115°C and did not give the analytically-pure valyl-δ-carbobenzoxyornithine anhydride.

The oily D-L stereomer (XXVIII) was obtained from the formyl dipeptide ester (XV). Attempts to solidify the oil were unsuccessful, although this oily product gave the analytically-pure dipeptide anhydride (XL).

Phenylalanyl-δ-carbobenzoxyornithine Ethyl Ester Hydrochlorides (XXIX, XXX).—The crystalline L-L stereomer (XXIX) was obtained from the formyl dipeptide ester (XVII) by the procedure described in the case of XIX, while the oily D-L stereomer (XXX) was obtained from the *t*-butyloxycarbonyl dipeptide ester (XVIII) as in the case of XXVII.

Valyl-ε-carbobenzoxylysine Anhydrides (XXXI—XXXIV).—A solution of 4.3 g. each of XIX—XXII in 100 ml. of methanol, which had been previously saturated with dry ammonia at 0°C, was stored in a glass-stoppered bottle at room temperature for 2 days.[16] In the case of the L-D and D-L stereomers (XXXIII and XXXIV), a mass of crystals appeared within about 1 hr. whereas a complete solution was maintained with the L-L and D-D stereomers (XXXI and XXXII) over the entire reaction period. The reaction mixture was then concentrated to dryness with a rotary evaporator, and the crystalline residue was filtered off with the aid of a little water. The recrystallization of XXXI and XXXII was achieved from 30% methanol (85 ml.), whereas 50% ethanol (100 ml.) was used with XXXIII and XXXIV.

Phenylalanyl-ε-carbobenzoxylysine Anhydrides (XXXV—XXXVIII). — The conversion of XXIII—XXVI to XXXV—XXXVIII followed the same procedure as was employed in the preparation of XXXI—XXXIII. Recrystallization was effected from 70% ethanol.

Valyl-δ-carbobenzoxyornithine Anhydrides (XXXIX, XL) and Phenylalanyl-δ-carbobenzoxyornithine Anhydrides (XLI, XLII).—These compounds were obtained from the dipeptide ester hydrochlorides, XXVII, XXVIII, XXIX and XXX, as described in the cases of XXXI and XXXIII. Recrystallization was effected from 40% ethanol for XXXIX and XL, and from 70% ethanol for XLI and XLII.

Valyllysine Anhydride Hydrochlorides (XLIII—XLVI).—A suspension of 3.61 g. (0.01 mol.) each of XXXI—XXXIV in 0.1 N methanolic hydrogen chloride (105 ml.) was subjected to hydrogenolysis with dry hydrogen in the presence of palladium black which had previously been washed with methanol. Upon the completion of the reaction, the catalyst was removed by filtration, with prior warming if necessary to dissolve any product which may have precipitated, and the filtrate was concentrated to dryness in vacuo. The crystalline product was then filtered off, with the aid of a mixture of acetone and ether, and recrystallized from methanol-acetone.

Phenylalanyllysine Anhydride Hydrochlorides (XLVII—L). — A suspension of 2.05 g. each of XXXV—XXXVIII in acetic acid (50 ml.) was subjected to hydrogenolysis as has been described above. The filtrate was then concentrated to dryness, the residual material was dissolved in water, and the solution was treated with 1 N hydrochloric acid (5.3 ml.). After the concentration of the solution, the residual product was recovered by filtration with the aid of acetone. Recrystallization was effected from methanol-acetone.

Valylornithine Anhydride Hydrochlorides (LI, LII).—These compounds were obtained from XXXIX and XL as has been described in the case of XLIII. The D-L stereomer (LII) was less soluble in methanol than the L-L stereomer (LI).

Phenylalanylornithine Anhydride Hydrochlorides (LIII, LIV). — These compounds were obtained from XLI and XLII as has been described in the case of XLIII. The air-dried crystals contained half moles of crystal waters; they lost 3.0% (LIII) and 3.2% (LIV) of their weight upon being dried for 3 hr. in vacuo at 100°C. Calcd. for $C_{14}H_{20}O_3N_3Cl \cdot 1/2H_2O$: H_2O, 2.94%.

Carbobenzoxyvalyl-ε-carbobenzoxylysine Methyl Esters (LV—LVIII).—To a stirred solution of carbobenzoxy-L(or D)-valine[17] (5.03 g.) and triethyl amine (2.8 ml.) in toluene (40 ml.) at 0°C, isobutylchlorocarbonate (2.7 ml.) was added.[18] After 15 min., a mixture of ε-carbobenzoxy-L(or D)-lysine methyl ester hydrochloride (6.61 g.) and triethyl amine (2.8 ml.) in chloroform (40 ml.) was also added. The reaction mixture was then left at room temperature overnight, after which time LV and LVI were recovered as has been described under a), and LVII and LVIII, as has been described under b). a) After being washed successively with 4% sodium bicarbonate, 2% hydrochloric acid, and water, the organic layer was dried over sodium

16) E. Fischer and K. Raske, *Ber.*, 39, 3981 (1906).

17) R. L. M. Synge, *Biochem. J.*, 42, 99 (1948).

18) J. R. Vaughan, Jr., and R. L. Osato, *J. Am. Chem. Soc.*, 73, 5553 (1951).

sulfate and concentrated to dryness. The crystalline residue was recrystallized from ethyl acetate-petroleum ether. b) The mass of crystals which precipitated was filtered off after the addition of 80 ml. of petroleum ether and some water. Recrystallization was achieved from acetone-ether-petroleum ether.

Carbobenzoxyphenylalanyl-ε-carbobenzoxylysine Ethyl Esters (LIX, LX).—These compounds were prepared from carbobenzoxy-L-phenylalanine[19] and ε-carbobenzoxy-L-lysine ethyl ester *p*-toluenesulfonate[12] in the manner described above.

Carbobenzoxyvalyl-ε-carbobenzoxylysines (LXI—LXIV).—To a solution of 5.28 g. each of LV—LVIII in dioxane (100 ml.), 1 N sodium hydroxide (11 ml.) was added. The reaction mixture was then stored at room temperature for 6 hr., after which time it was neutralized with 1 N hydrochloric acid (12 ml.) and concentrated to dryness in vacuo. The residual material was filtered off with the aid of water, dried well, and recrystallized from ethyl acetate-petroleum ether.

Carbobenzoxyphenylalanyl-ε-carbobenzoxylysines (LXV, LXVI).—These compounds were prepared from LIX and LX following the procedure described above.

Valyllysine Hydrochlorides (LXVII—LXX).—A solution of 2.57 g. (0.005 mol.) each of LXI—LXIV in a mixture of methanol (60 ml.) and 0.5 N hydrochloric acid (10.3 g.) was subjected to hydrogenolysis in the presence of palladium black. The filtrate was then evaporated to dryness in vacuo, and the residual product was filtered off with the aid of ethanol or a mixture of ethanol and acetone. The L-L and D-D stereomers (LXVII, LXVIII) were recrystallized from water (5 ml.)-ethanol (30 ml.). The L-D and D-L stereomers (LXIX, LXX) were obtained as hygroscopic crystalline products. However, their paper chromatographic behavior in a number of solvent systems indicated that they gave only a single ninhydrin-positive spot and, hence, were suitable as chromatographic reference compounds for the present purposes.

Phenylalanyllysine Hydrochlorides (LXXI, LXXII).—The hydrogenolysis of LXV and LXVI was carried out in the manner described above. The free dipeptide hydrochlorides were obtained as hygroscopic crystals. However, each of them yielded only a single ninhydrin-positive spot when subjected to paper chromatographic criteria.

α,ε-Dicarbobenzoxy-L-lysyl-L-phenylalanine Benzyl Ester (LXXIII).—This compound was prepared from α, ε-dicarbobenzoxy-L-lysine[11] and, L-phenylalanine benzyl ester[20] in the same manner as was used for LV.

L-Lysyl-L-phenylalanine Hydrochloride (LXXIV). This compound was obtained from LXXIII by hydrogenolysis, and was recrystallized from water-ethanol.

***Rf* Values.**—The R_f values of the compounds on ascending paper chromatography, employing *n*-butanol-acetic acid-pyridine-water (15 : 3 : 10 : 12, v/v) and No. 50 paper of the Toyo Roshi Co., are given in Table II. The R_f values of the L-L and D-D antipodes were the same within the limits of experimental error, as were those of the D-L and L-D antipodes. The R_f value for a L-L stereomer, however, differed appreciably from that of the diastereomeric L-D stereomer. In this connection, it should be noted that, recently, some results on the paper chromatographic separation of diastereomeric dipeptides have been published.[21]

Table II. R_f values of dipeptide anhydrides and dipeptides

Compound	Configuration	R_f volue
Val◇Lys·HCl	L-L or D-D	0.50
	D-L or L-D	0.52
Phe◇Lys·HCl	L-L or D-D	0.54
	D-L or L-D	0.60
Val◇Orn·HCl	L-L	0.47
	D-L	0.51
Phe◇Orn·HCl	L-L	0.53
	D-L	0.58
H-Val-Lys-OH·HCl	L-L or D-D	0.25
	D-L or L-D	0.20
H-Phe-Lys-OH·HCl	L-L	0.32
	D-L	0.27
H-Lys-Phe-OH·HCl	L-L	0.34

The Action of Enzymes on Dipeptide Anhydrides.—To a 1 ml. flask were added 0.01 mmol. each of XLIII—XLVI and XLVII—L, crystalline trypsin (3.0 mg.) and a 0.2 M phosphate buffer (0.5 ml.) at pH 7.5 The solution was made up to 1 ml. by water and incubated at 37°C for 24 hr. Similar experiments with each of XLVII—L and crystalline α-chymotrypsin (3.0 mg.) were also carried out. Paper chromatographic analysis of an aliquot sample of the enzymic digests yielded only a single ninhydrin-positive spot, which, in each instance, possessed the same R_f values as the unhydrolyzed dipeptide anhydride substrates.

Biological Assays.* — The microorganisms employed were *B. subtilis* (*Bacillus subtilis* PCI 219), *St. aureus* (*Staphylococcus aureus* FDA 2099), *E. coli* (*Escherichia coli* IFO 3044), and *Pr. vulgaris* (*Proteus vulgaris* IFO 3045). The minimum amounts of the compounds necessary for the complete inhibition of growth were determined by a dilution method with a bouillon agar medium at pH 7.0. As is shown in Table III, no antibacterial activity by the dipeptide anhydrides was observed against any of the microorganisms used even at a high concentration of each compound. In contrast with the lack of activity of each dipeptide anhydride, gramicidin S, a cyclic decapeptide, exhibited considerable activity against some of the microorganisms.

Erlanger and Goode have reported that, in a synthetic medium, the minimum amount of gramicidin S for the complete inhibition of the growth of *E. coli* was 5 μg. per ml.[2] As is indicated in

19) W. Grassmann and E. Wünsch, *Chem. Ber.*, **91**, 449, 462 (1958).

20) N. Izumiya and S. Makisumi, *J. Chem. Soc. Japan, Pure Chem. Sec.* (*Nippon Kagaku Zasst*), **78**, 662, 1768 (1957).

21) T. Sokolowska and J. F. Biernat, *J. Chromatogr.*, **13**, 269 (1964).

* The authors are indebted to the Research Laboratories, Takeda Chemical Industries, Ltd., Osaka, for the biological assays.

TABLE III. INHIBITORY ACTIVITY OF PEPTIDE ANHYDRIDES ON MICROORGANISMS

Compound	Amount of compound necessary for complete inhibition of growth, μg./ml.			
	B. subtilis	*St. aureus*	*E. coli*	*Pr. vulgaris*
Gramicidin S·H_2SO_4[a)]	12.5	12.5	>100	50
Val◇Lys·HCl (XLIII—XLVI)	>100	>100	>100	>100
Phe◇Lys·HCl (XLVII—L)	>100	>100	>100	>100
Val◇Orn·HCl (LI, LII)	>100	>100	>100	>100
Phe◇Orn·HCl (LIII, LIV)	>100	>100	>100	>100

a) A product of Astra Co., U.S.A.

Table III, in a bouillon medium, gramicidin S exhibited no activity at the 100 μg. per ml. level. In this connection, experiments concerning the growth inhibition of *E. coli* in a synthetic medium by the dipeptide anhydrides, XLIII—LIV, are in progress in this laboratory.

Summary

The D-D, L-L, D-L and L-D stereomers of both valyllysine anhydride and phenylalanyllysine anhydride, and the D-L and L-L stereomers of both valylornithine anhydride and phenylalanylornithine anhydride, have been synthesized in order to compare them with the cyclic peptide antibiotics, with which they possess several structural features in common.

Synthesis has been achiveved by the dicyclohexylcarbodiimide-induced condensation of formyl, (or *t*-butyloxycarbonyl) valine (or phenylalanine) with the ω-carbobenzoxylysine (or ornithine) ester, followed by the treatment of the resulting acyl dipeptide ester with hydrogen chloride in methanol or ethyl acetate to remove the formyl- or *t*-butyloxycarbonyl-blocking group. The dipeptide ester hydrochlorides so derived have been converted by the action of ammonia to the corresponding carbobenzoxy-substituted dipeptide anhydrides and these, in turn, transformed to the desired unacylated dipeptide anhydride hydrochlorides by palladium-catalyzed hydrogenolysis.

Enzymic experiments have been carried out to determine whether the dipeptide anhydride hydrochlorides are attacked by trypsin or chymotrypsin. The results indicate that no hydrolysis of any of the anhydrides occurs. In this connection, valyllysines, phenylalanyllysines and lysylphenylalanine have been synthesized for the purposes of chromatographic comparison.

The effects of the dipeptide anhydride hydrochlorides on bacterial growth have been examined. The results indicate that no antibacterial activities are observed against microorganisms in a bouillon agar medium.

The authors are grateful to Dr. Milton Winitz, of the National Institutes of Health, U.S.A., for his valuable suggestions and generous assistance in the preparation of this manuscript.

Laboratory of Biochemistry
Faculty of Science
Kyushu University
Fukuoka

Kinetics and Isotope Effect in Methanol Synthesis at Low Pressures

By Toyoyasu SAIDA and Atsumu OZAKI

(Received June 11, 1964)

The methanol synthesis has been the object of many investigations, among which a few works have been devoted to the kinetics of the reaction. The kinetic equations thus obtained are different from each other in form:

by Temkin et al. at low pressures:[1]

$$r=kC_{H_2}C_{CO}^{0.6}/C_{CH_3OH} \quad (1)$$

by Natta et al. at high pressures:[2]

$$r=kP_{H_2}^{2}\cdot P_{CO}/(A+BP_{CO}+CP_{H_2}+DP_{CH_3OH})^3 \quad (2)$$

by Ogino et al. at high pressures[3]:

$$r=k(P_{H_2}^{2}\cdot P_{CO})^{0.7} \quad (3)$$

although they may all be approximated to (3) or (1) in nature. In consequence, different fundamental postulates of the rate-determining step in the synthesis of methanol have been suggested, that is, the adsorption of carbon monoxide or hydrogen for (1), the surface reaction for (2), and the desorption of the product methanol for (3).

Such disagreement in interpreting the kinetics of the same reaction is suspicious, since the equations are all similar in nature. In this connection, the isotope effect on the reaction rate has been useful in identifying the rate-determining step of many reactions. The effect in methanol synthesis, however, has not been reported. Corval and Viallard[4] studied the synthesis of heavy methanol CD_3OD, but they didn't compare the rate with that of light methanol. It was, therefore, decided to undertake an investigation of the isotope effect in methanol synthesis. The work was done in the vicinity of atmospheric pressure with a reactant mixture of varying compositions.

Experimental

Reagents.—Cylinder hydrogen was passed over a platinum catalyst to remove any oxygen and then dried with liquid nitrogen. Deuterium gas was prepared by the reaction of heavy water of 99.7% D, which had been supplied by the Showa Denko Co., with a magnesium ribbon at 400 to 450°C. Carbon monoxide was prepared by the decomposition of sodium formate with concentrated sulfuric acid and was passed over sodalime and dried with liquid nitrogen. The catalyst was supplied in a partially-reduced state by the Government Chemical Industrial Research Institute, Tokyo, and contained zinc, chromium, and copper in the atomic ratio of 1 : 0.49 : 0.16.[5] The catalyst was used as particles of 1 to 2 mm. The reduction of the catalyst was carried out with the reactant gas of excess hydrogen in situ at 250°C for 12 hr.

Experimental Procedures. — The experiments were carried out at a constant pressure in a closed flowing system, which is shown schematically in Fig. 1. The synthesis mixtures were circulated on the catalyst at various velocities by means of an all-glass electromagnetic pump. In order to preheat the gas mixture, the reaction tube was packed 5 cm. thick with glass beads over the catalyst bed (10 mm. thick), through which the gas stream flowed downwards. The catalyst was placed on a fritted glass plate of a coarse grade. A thermocouple well was inserted through the glass beads bed and the catalyst bed. The reaction tube was

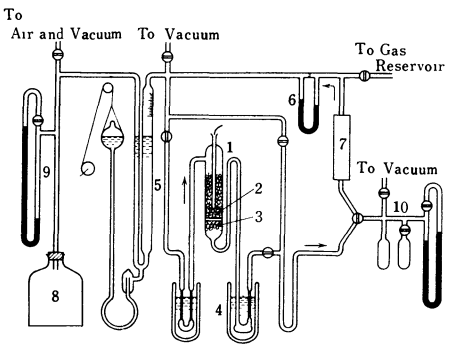


Fig. 1. Apparatus.

1 Reactor
2 Catalyst bed
3 Inert packing as a bed support
4 Traps
5 Buret
6 Flow meter
7 Circulating pump
8 A tank of 50 l. as a buffer
9 Manometer
10 Manometer for vapor pressure measurement

1) V. M. Cherednichenko and M. I. Temkin, *Zhur. Fiz. Khim.*, **31**, 1072 (1957).
2) G. Natta, P. Pino, G. Mazzanti and I. Pasquon, *LaChimica e L'Industria*, **35**, 705 (1953).
3) H. Uchida and Y. Ogino, This Bulletin, **31**, 45 (1958).
4) M. M. Corval and M. R. Viallard, *Bull. soc. chim. France*, **50**, 484 (1954); *J. chim. phys.*, **51**, 619 (1954).
5) Y. Ogino, M. Oba and H. Uchida, This Bulletin, **33**, 358 (1960).

placed in an aluminum block furnace, and the temperature was controlled within ±0.5°C by means of a thermoelectric temperature controller. The temperature difference between the two ends of the catalyst bed was within 0.2°C during the measurement. The two traps, which were placed before and after the reaction tube, were put into the same liquid-nitrogen bath, and the liquid level of the bath was adjusted to a certain position during the measurement. According to Temkin et al., the satisfactory trapping of methanol vapor with liquid nitrogen is difficult because the vapor tends to form aerosol. In order to avoid this difficulty, the trap next to the reaction tube shown in Fig. 1 was designed so as to give a low linear gas velocity; that is, the trap was made from a tube 18 mm. in inner diameter at the bottom corresponding to the liner velocity of 0.1 cm./sec. at the liquid nitrogen temperature for the gas velocity of 3 l. N. T. P/hr. It was confirmed by the absence of deposition in the other trap that the trap was satisfactory for condensing the methanol vapor.

The reaction rates were measured by following the volume decrease with the gas burette. The volume of the closed system was about 300 ml. besides the burette volume of 70 ml. The reaction products, a mixture of methanol and carbon dioxide collected in the trap during the rate measurements, were subjected to vapor pressure measurements at 0°C and −78°C; cf. the right section of the diagram Fig. 1. The amounts of both products were estimated from these quantities. The respective rates of the formation of both products were calculated as the rates of the volume decrease of the reaction system multiplied by a conversion factor which will be shown later.

Results

In the preliminary experiments on the synthesis at 160 to 230°C, it was shown that the carbon dioxide formation was remarkable at higher temperatures, while the reaction rate was too slow to observe at temperatures lower than 180°C. Accordingly, the measurement of the temperature coefficient of the reaction rate was abandoned and the reaction temperature was fixed at 180°C throughout the experiments.

Since the carbon dioxide formation was not negligible even at 180°C, the reaction path of the formation ought to be assigned in order to give a correction to the reaction rate of methanol synthesis. There can be considered to be three possible ways of carbon dioxide formation:

i) $2CO = CO_2 + C$

ii) $2CO + 2H_2 = CO_2 + CH_4$

iii) The oxidation of CO by the catalyst

In the present analysis, reaction ii was excluded because of the absence of methane in the circulating gas after several hours of reaction. The detection of methane was carried out by gas chromatography. Reaction iii was improbable because the catalyst was, prior to use, thoroughly reduced at a higher temperature, 250°C, than the reaction temperature, 180°C, using the reactant gas, and because no degradation of catalytic activity to form carbon dioxide was observed. Consequently, it was postulated that the carbon dioxide was formed via reaction i. Thus, the rate of the volume decrease due to the formation of methanol and of carbon dioxide, r_M and r_C (N ml./hr.) respectively, was estimated by the equation:

$$r_M = 3N_M r_A/(3N_M + 2N_C) \quad (1)$$

$$r_C = 2N_C r_A/(3N_M + 2N_C) \quad (2)$$

where r_A is the measured rate of volume decrease, N ml./hr., and N_M and N_C are the amounts of methanol and carbon dioxide (mole) formed in each run, each of which was continued for four hours. Since the per-pass conversions were very low and within 5% of the equilibrium conversions, the estimated rate, r_M or r_C, is the initial rate.

The effects of total pressure, P, on r_M and r_C are shown in Fig. 2 for a constant molar

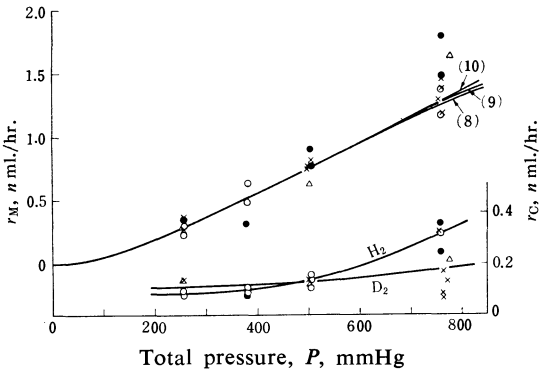


Fig. 2. Total pressure dependence of the rates with stoichiometric mixture.
○ H_2 s. v. 900 ● H_2 s. v. 1800
× D_2 s. v. 900 △ D_2 s. v. 1800

ratio n(=H_2/CO or D_2/CO). Figure 3 shows the variations of r_M and r_C with n at atmospheric pressure. All the experimental data are the time averages, in each run carried out at a fixed condition for four hours. The optimum methanol formation appears at a n value of around 2.

As may be seen in Fig. 2, no marked influence was observed on r_M by changing the space velocity from 900 to 1800. Since the variation in space velocity should give rise to a different value of methanol vapor pressure in the catalyst bed, it seems that methanol has no effect on r_M under the present experimental conditions.

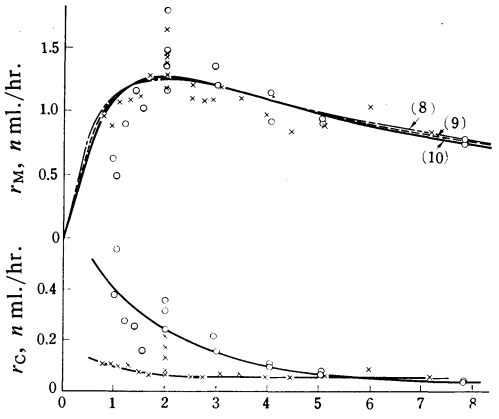


Fig. 3. Variation of the rates with gas composition under 1 atm.
180°C 1 atm s. v.: 900 hr^{-1}

The deuterium isotope effect in methanol synthesis was not observed, as can be seen in Fig. 2, and Fig. 3; that is, both plots for protium and deuterium are distributed along the same line and show no systematical deviation from each other. This result was confirmed by changing the reactant gases in the order; H-D-H-D-D.

On the other hand, the isotope effect was found in the carbon dioxide formation at higher concentrations of carbon monoxide. The amount of carbon dioxide formed was near 20% (mole) of methanol in most runs, the highest value being 30%.

A Kinetic Analysis of the Results

A kinetic equation which incorporates the experimental results shown in Fig. 2 was selected in the following way. A general form, expressed with the total pressure, P,

$$r_M = kP^l/(1+aP^m)^s \quad (3)$$

was considered, and the possible combinations of l, m and s were tested one by one, assigning every half interger from 0.5 to 3 for l and m, and every integer from 1 to 3 for s. Equation 3 was transformed into:

$$1/k^{1/s} + aP^m/k^{1/s} = (P^l/r_M)^{1/s} \quad (4)$$

and the linearity of P^m against $(P^l/r_M)^{1/s}$ was examined.

Table I. Suitable combinations of l, m, and s

No.	1	2	3	4	5	6
l	2	2.5	3	2.5	3	3
m	1	1	1	1.5	1.5	2
s	2	2	2	1	1	1

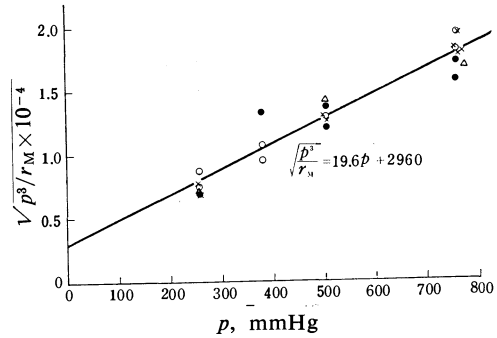


Fig. 4

The suitable combinations thus found were as shown in Table I.
However, the best fit was obtained in Nos. 2 and 3. The plots in No. 3 are exemplified in Fig. 4.

Equation 3 rewritten in terms of the partial pressures, p_{H_2} and p_{CO}, and of n, assuming a first-order dependence on p_{CO}, i.e. the kinetic term of the $k' p_{H_2}{}^{l-1} p_{CO}$ form. For example, with $m=1$, the rewritten equation is:

$$r_M = k' {}_{H_2}{}^{l-1} p_{CO}/(1+a_1 p_{H_2}+a_2 p_{CO})^s \quad (5)$$

$$= \frac{k' n^{l-1} P^l/(n+1)^l}{[1+(na_1+a_2)P/(n+1)]^s} \quad (6)$$

where $k' = k(n+1)^l/n^{l-1}$.

Equation 6 was transformed to:

$$(1+a_2P)+(1+a_1P)n = [k' n^{l-1} P^l (n+1)^{l/s} r_M]^{1/s} \quad (7)$$

The linear relation of the right side of Eq. 7 against n was examined for the l-m-s combinations shown in Table 1, using a k' value obtained by the linear relation of Eq. 4. Any combination which gave a negative value for a_1 or a_2 was discarded. Thus, the suitable combinations in these plots were Nos. 1, 2 and 3 of Table I, in all of which $m=1$ and $s=2$. In other words, these equations are as follows:

$$r_M = k' p_H p_{CO}/(1+a_1 p_{H_2}+a_2 p_{CO})^2 \quad (8)$$

$$r_M = k' p_{H_2}{}^{1.5} p_{CO}/(1+a_1 p_{H_2}+a_1 p_{CO})^2 \quad (9)$$

$$r_M = k' p_{H_2}{}^2 p_{CO}/(1+a_1 p_{H_2}+a_2 p_{CO})^2 \quad (10)$$

The plots in No. 3 are exemplified in Fig. 5, where some systematic deviation is observed in the lower range of n for only the protium series. This deviation was also observed for the other l-m-s combinations.

The k', a_1 and a_2 constants were recalculated by the least squares method with all the data shown in Figs. 2 and 3, excepting those obtained with n values lower than 2 in the case of protium. The best values thus obtained are given in Table II.

TABLE II. BEST VALUES OF k', a_1 AND a_2

Equation	k' $(2H_2+CO)N$ ml.*/ hr. 2.493 g. cat.	k' mol.*/ hr. g. cat.	a_1 $mmHg^{-1}$	a_1 atm^{-1}	a_2 $mmHg^{-1}$	a_2 atm^{-1}
(8)	$(3.09\pm0.28)\times10^{-5}$	$(1.06\pm0.09)\times10^{-4}$	$(4.93\pm0.97)\times10^{-4}$	0.375 ± 0.073	$(2.11\pm0.21)\times10^{-3}$	1.60 ± 0.16
(9)	$(4.35\pm0.64)\times10^{-6}$	$(4.13\pm0.61)\times10^{-4}$	$(2.40\pm0.29)\times10^{-3}$	$1.83\ \pm0.22$	$(3.70\pm0.45)\times10^{-3}$	2.82 ± 0.34
(10)	$(1.36\pm0.50)\times10^{-6}$	$(3.56\pm1.30)\times10^{-3}$	$(0.99\pm0.21)\times10^{-2}$	$7.51\ \pm1.57$	$(0.91\pm0.21)\times10^{-2}$	6.95 ± 1.57

* These dimensions are consistent with those of r_M.

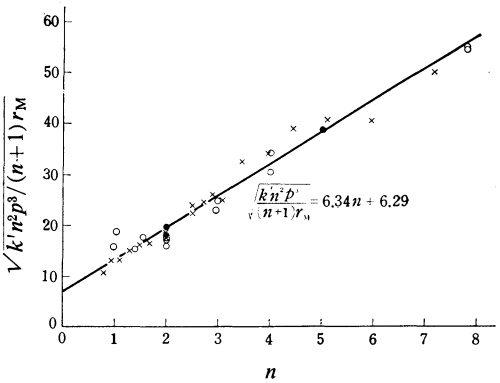


Fig. 5

The rate of methanol formation was calculated using Eqs. 8, 9 and 10 and are shown in Figs. 2 and 3 with lines. These lines overlap each other, and the experimental points are located along them, although some deviations are clearly seen in the lower range of n values.

Discussion

Kinetic Equation.—The range of experimental conditions was not wide enough to discriminate a single rate equation. The three equations finally reached all have the adsorption terms of both hydrogen and carbon monoxide in accordance with the equation of Natta et al., although the exponent to the adsorption term, s, is different. The adsorption term of methanol may disappear because of the low conversion in the present experiment.

The rates of methanol formation under elevated pressures were estimated using the above three equations. The estimated rate with Eq. 8 was independent of the pressure above 20 atm., but not with Eqs. 9 and 10. This independence of the reaction pressure is contradictory with the established fact of pressure dependency in the methanol synthesis. Hence, Eq. 8 may be abandoned.

The kinetic terms $p_{H_2}{}^{1.5}p_{CO}$ and $p_{H_2}{}^2p_{CO}$ of Eqs. 9 and 10 respectively resemble with those of Natta et al. and of Ogino et al.

If the following elementary reactions are assumed to constitute the methanol synthesis:

$$CO + H_2 \rightarrow HCHO \quad (I)$$

$$HCHO + H_2 \rightarrow CH_3OH \quad (II)$$

then Eq. 10 conforms to the postulate that reaction II is rate-determing, because the partial pressure of HCHO, the reactant of reaction II, is expressed as $K_I p_H p_{CO}$, where K_I is the equilibrium constant of reaction II.

For Eq. 9, the reaction scheme may be as follows:

$$H_2 \rightleftarrows 2H(a) \quad (III)$$

$$CO + 2H(a) \rightarrow CH_2O(a) \quad (IV)$$

$$CH_2O(a) + H(a) \rightarrow CH_3O(a) \quad (V)$$

$$CH_3O(a) + H(a) \rightarrow CH_3OH \quad (VI)$$

with reaction V being rate-determining.

The discrimination of the above two schemes must auait further investigation.

Isotope Effect.—The fact that no isotope effect is found in the methanol formation may give rise to the view that the adsorption of carbon monoxide is rate-determining. However, the rate equations obtained here and by other investigators suggest that this view is by no means valid, because the kinetic term of the rate equations clearly depends on the hydrogen pressure. In other words, the rate equations suggest a rate-determining step in which hydrogen or a hydrogen-containing species is involved. A complete interpretation of the above discrepancy can follow only further investigation.

The hydrogen isotope effect was observed in the carbon dioxide formation, particularly in the higher concentrations of carbon monoxide, where the deviation from the rate equation for methanol formation was also observed. These observations may suggest that the carbon dioxide formation takes place on an active site different from that of the methanol formation. Since hydrogen is not involved in the reaction path assumed for the carbon dioxide formation, the observed isotope effect must be ascribed to the higher surface coverage with deuterium, which suppresses the carbon dioxide formation. However, such an interpretation of the results should be subjected to further investigation.

The authors are grateful to Dr. Hiroshi Uchida and Dr. Yoshisada Ogino of the Goverment Chemical Industrial Reseach Institute for providing the catalyst.

Research Laboratory of Resources Utilization
Tokyo Institute of Technology
Meguro-ku, Tokyo (A. O.)

Toyo Gas Chemical Co.
Muromachi, Chuo-ku, Tokyo (T. S.)

Chronopotentiometry of Hexamminechromium(III) Ions in Acetate Buffer Solutions

By Nobuyuki TANAKA, Akifumi YAMADA and Reita TAMAMUSHI*

(Received June 12, 1964)

The reduction of hexamminechromium(III) ions at the dropping mercury electrode has been studied by several investigators under a fairly wide range of conditions.[1-6] Its characteristics in aqueous solutions, both neutral and acid, have been extensively discussed in two recent papers from this Laboratory.[2,6] The first paper demonstrated the role of hydrogen ions on the polarographic reduction of hexamminechromium(III), while the second was concerned with the study of the nature of the one-electron reduction wave of the complex in neutral and acid aqueous solutions.

The present chronopotentiometric investigation was undertaken to support the validity of some of the conclusions reported previously,[6] and to obtain a further insight into the mechanism of the electroreduction of hexamminechromium(III) ions.

Experimental

Hexamminechromium(III) chloride was prepared according to the method of Mori ;[7] the chromium and nitrogen contents were determined by the usual methods.

Found: Cr, 19.79; N, 31.6. Calcd. for $[Cr(NH_3)_6]Cl_3$: Cr, 19.96; N, 32.2%.

As the complex is sensitive to light and not very stable in an aqueous solution,[8] precautions were taken when it was used. All other chemicals were of analytical reagent grade. Redistilled water was used to prepare the solutions of desired concentrations. The contamination of the solutions with surface-active substances was carefully avoided.

A modified apparatus of the constant current supply described in the literature[9] was used for all measurements. A dropping mercury electrode of a long drop time (about 60 sec.) was used for a cathode. A mercury pool electrode with a large surface area served as an anode, which was connected to the cathode compartment of the cell through a salt bridge of low resistance. The characteristics of the dropping mercury electrode used in this study are given in Table I. A potential-time curve was obtained in a small fraction of a drop life, so that the surface area of the mercury drop did not change appreciably during the measurement.[10,11] Potentials of the dropping mercury electrode (working electrode) were measured against a saturated calomel electrode (SCE). The potential difference between the reference and the working electrode was fed through a direct-current preamplifier to a Toshiba oscilloscope, Model ST-1747A. The alternating voltage of audiofrequency from an oscillator, Yokogawa OV-21A, was supplied for the beam modulation. The transition time was

TABLE I. CHARACTERISTICS OF THE DROPPING MERCURY ELECTRODE

Mercury height h cm.	Rate of flow of mercury, m mg. sec.$^{-1}$	Drop time t_d sec.
25	0.116_4	61
70	0.341_6	22

Measured in a deaerated solution containing 0.1 M acetate buffer and 0.9 M NH_4Cl at open circuit.

* Present address: The Institute of Physical and Chemical Research, Komagome, Bunkyo-ku, Tokyo.

1) N. Maki, Y. Shimura and R. Tsuchida, This Bulletin, 31, 413 (1958).
2) N. Tanaka and G. Satô, *Nature*, 197, 176 (1963).
3) J. A. Friend and P. W. Smith, *J. Phys. Chem.*, 63, 314 (1959).
4) T. C. Ichniowski and A. F. Clifford, *J. Inorg. Nucl. Chem.*, 22, 133 (1961).
5) A. A. Vlček, "Progress in Inorganic Chemistry," Vol. 5, Interscience Publishers, Inc., New York, N. Y. (1963), p. 362.
6) N. Tanaka, K. Ebata and G. Satô, This Bulletin, 36, 912 (1963).
7) M. Mori, *J. Chem. Soc. Japan, Pure Chem. Sec. (Nippon Kagaku Zassi)*, 74, 253 (1953).
8) D. Jørgensen and J. Bjerrum, *Acta Chem. Scand.*, 12, 1047 (1958).
9) T. Murayama, *Sci. Repts. Tohoku Univ., Ser. I*, 45, 84 (1961).
10) L. Gierst and A. Juliard, Int. Comm. Electrochem. Therm. Kin., Proceedings of the 2nd Meeting, Tamburini, Milan, 1950, pp. 117 and 229.
11) L. Gierst and A. Juliard, *J. Phys. Chem.*, 57, 701 (1953).

determined by the method of Kuwana.[12] Dissolved oxygen in the electrolytic solution was removed by bubbling purified nitrogen gas through the solution. All measurements were made at 25±0.1°C.

Results

When a hanging mercury drop electrode was used for a working electrode, no reproducible chronopotentiogram was observed. At a dropping mercury electrode, however, reproducible chronopotentiograms were obtained. Figure 1 shows a typical example of a cathodic chronopotentiogram of hexamminechromium-(III) ions obtained in an acetate buffer solution.

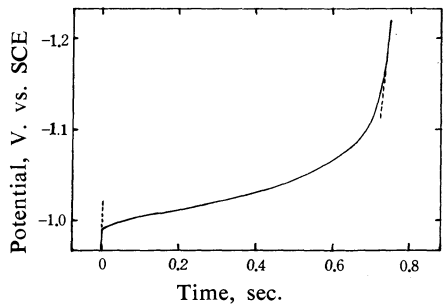


Fig. 1. Chronopotentiogram of 5 mM $[Cr(NH_3)_6]Cl_3$ in 0.1 M acetate buffer + 0.9 M NH_4Cl (pH 4.6) at 25°C. Current density, 1.44_8 mamp. cm^{-2}; surface area of the electrode, 2.93 mm^2. The measurement was started at 55 sec. after the beginning of the growth of a mercury drop.

The effect of the aging of the electrode has been reported by several authors.[9,11,13] Therefore, some preliminary measurements were made with hexamminechromium(III) ions at the slowly dropping mercury electrode. The results given in Table II clearly indicate that no appreciable effect of the aging was observed under the present experimental conditions.

TABLE II. EFFECTS OF THE AGING OF THE SLOWLY DROPPING MFRCURY ELECTRODE ON THE CHRONOPOTENTIOGRAM OF 1 mM $[Cr(NH_3)_6]Cl_3$ OBTAINED IN 0.9 M NH_4Cl + 0.1 M ACETATE BUFFER

θ* sec.	$E_{\tau/4}$ V. vs. SCE	τ sec.	i, mamp.·cm^{-2}	$i\tau^{1/2}$ mamp.·$sec^{1/2}cm^{-2}$
15	-1.03_3	0.140	0.693	0.259
30	-1.03_4	0.139	0.696	0.259
55	-1.03_4	0.140	0.693	0.259

* Time elapsed since the beginning of the growth of a mercury drop.

12) C. D. Russell and J. M. Peterson, *J. Electroanal. Chem.*, **5**, 467 (1963).
13) T. Nagai, *J. Chem. Soc. Japan, Pure Chem. Sec. (Nippon Kagaku Zasshi)* **81**, 93 (1960).

The values of $i\tau^{1/2}$, where i is the current density at the polarizable electrode and τ the transition time, were determined at various current densities for the reduction of hexamminechromium(III) ions at a dropping mercury electrode, with the results given in Table III, which shows that the product $i\tau^{1/2}$ is independent of the current density. This clearly indicates that hexamminechromium(III) ions are directly reduced at the electrode without any preceding chemical reactions prior to the electron-transfer process, being in a satisfactory agreement with the previous conclusion obtained in the polarographic study of the same complex.[6]

Measurements were also made at various concentrations of the complex. The results are presented in Table IV. The average value of $i\sqrt{\tau}/C_O^\circ$ obtained from some hundred runs, where C_O° represents the bulk concentration of the complex, was 0.256 mamp. $sec^{1/2}$ cm^{-2}· mM^{-1}. It may be assumed that a theoretical equation derived for a linear diffusion process is applied to the present system without introducing any significant error. According

TABLE III. TRANSITION TIMES FOR THE REDUCTION OF 2 mM $[Cr(NH_3)_6]Cl_3$ AT VARIOUS CURRENT DENSITIES

i mamp.cm^{-2}	τ sec.	$i\tau^{1/2}$, mamp.$sec^{1/2}cm^{-2}$
In 0.1 M acetate buffer + 0.9 M NH_4Cl		
0.443	1.37_0	0.518
0.574	0.801	0.514
0.745	0.475	0.513
0.972	0.282	0.515
1.25_9	0.169	0.518
1.63_9	0.100_2	0.519
2.28_4	0.0515	0.518
2.96_1	0.0302	0.515
4.16_8	0.0153	0.516
In 0.1 M acetate buffer + 0.9 M KCl		
0.476_2	1.15_7	0.512
1.39_0	0.133_2	0.507

TABLE IV. $i\tau^{1/2}/C_O^\circ$ FOR THE REDUCTION OF $[Cr(NH_3)_6]Cl_3$

C_O° mM	i mamp.cm^{-2}	τ sec.	$i\tau^{1/2}/C_O^\circ$ mamp.·$sec^{1/2}cm^{-2}mM^{-1}$
In 0.1 M acetate buffer + 0.9 M NH_4Cl (pH 4.6)			
5.00	1.44_8	0.736	0.249
2.85	1.08_2	0.441	0.252
2.15	1.44_4	0.146_3	0.257
2.00	2.28_4	0.0515	0.259
1.60	0.892	0.211_7	0.256
1.00	0.696	0.139	0.259
0.89	0.499	0.215_6	0.260
In 0.1 M acetate buffer + 0.9 M KCl (pH 4.6)			
2.00	0.476_2	1.15_7	0.256
2.00	1.39_0	0.133_2	0.254

to Sand[14] the value of $i\sqrt{\tau}/C_O^\circ$ for a linear diffusion is given by:

$$\frac{i\sqrt{\tau}}{C_O^\circ}=\frac{\sqrt{\pi}}{2}\ nF\sqrt{D_O}=85.51\ n\sqrt{D_O} \qquad (1)$$

where F is the Faraday; C_O°, the bulk concentration expressed in mM; D_O, the diffusion coefficient expressed in $cm^2\ sec^{-1}$ and n the number of electrons involved in the electroreduction. Introducing one for n and $0.85\times10^{-5}\ cm^2\ sec^{-1}$ for D_O, which was determined polarographically, the theoretical value of $i\sqrt{\tau}/C_O^\circ$ is calculated to be 0.250 mamp.$\cdot sec^{1/2}\ cm^{-2}\ mM^{-1}$. This value is in a good agreement with the experimental one.

The potential at $t=\tau/4$ ($E_{\tau/4}$) and the potential at $t=0$ ($E_{t=0}$) were dependent on the current density and the concentration of the complex; these potentials change linearly with log i and log C_O° as are shown in Figs. 2 and 3.

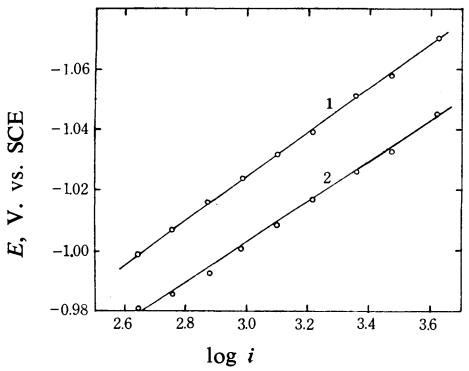


Fig. 2. Relations of (1) $E_{\tau/4}$ with log i and (2) $E_{t=0}$ with log i of 2 mM $[Cr(NH_3)_6]Cl_3$ obtained in 0.1 M acetate buffer + 0.9 M NH_4Cl (pH 4.6). Ohmic drop is corrected.

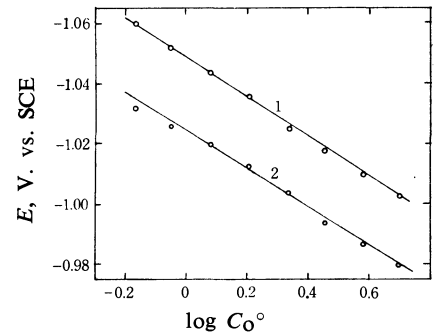


Fig. 3. Relations of (1) $E_{\tau/4}$ with log C_O° and (2) $E_{t=0}$ with log C_O° obtained at various concentrations of $[Cr(NH_3)_6]Cl_3$ in 0.1 M acetate buffer + 0.9 M NH_4Cl (pH4.6) at current density of 1.08_2 mamp. cm^{-2}.

Figure 4 shows the plots of the logarithmic functions of time against the electrode potential.[15] A plot of log $\{(\sqrt{\tau}-\sqrt{t})/\sqrt{t}\}$ versus E yields no straight line, but that of log $(\sqrt{\tau}-\sqrt{t})$ versus E yields a straight line with a reciprocal slope of 76 mV.

An example of the potential-time curves obtained by the electrolysis at a constant cathodic current followed by the anodic oxidation at the constant anodic current of

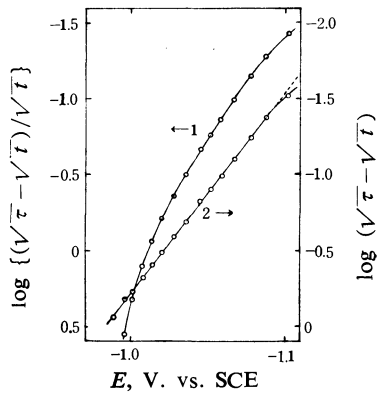


Fig. 4. Relations of (1) log $\{(\sqrt{\tau}-\sqrt{t})/\sqrt{t}\}$ vs. E and (2) log $(\sqrt{\tau}-\sqrt{t})$ vs. E obtained with 5 mM $[Cr(NH_3)_6]Cl_3$ in 0.1 M acetate buffer + 0.9 M NH_4Cl (pH 4.6).

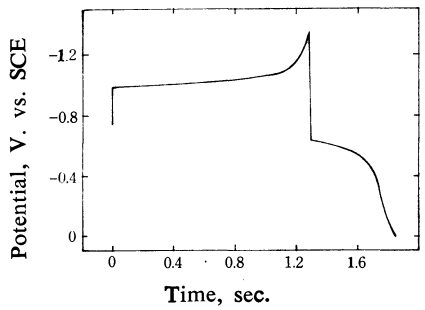


Fig. 5. Chronopotentiogram for the reduction and subsequent reoxidation of 2 mM $[Cr(NH_3)_6]Cl_3$ in 0.1 M acetate buffer + 0.9 M NH_4Cl (pH 4.6) at current density of 0.470_6 mamp. cm^{-2}.

TABLE V. TRANSITION TIMES FOR THE REOXIDATION PROCESS OF 2 mM $[Cr(NH_3)_6]Cl_3$ RECORDED IN 0.1 M ACETATE BUFFER + 0.9 M KCl AT CURRENT DENSITY OF 0.461_0 mamp. cm^{-2}

τ_c sec.	τ_a sec.	τ_c/τ_a	$E^c_{t=0}$* V. vs. SCE	$E^a_{t=0}$** V. vs. SCE
1.10	0.36_7	3.0_0	−0.98	−0.63
0.99_3	0.33_3	2.9_5		
0.86_6	0.28_3	3.0_6		

* Potential of the cathodic wave at time zero.
** Potential of the anodic wave at time zero.

14) H. J. S. Sand, *Phil. Mag.*, 1, 45 (1901).

15) W. H. Reinmuth, *Anal. Chem.*, 32, 1514 (1960).

the same magnitude with the opposite sign is given in Fig. 5. The cathodic and the anodic potential-time curves are separated by approximately 0.35 V. The ratio τ_c/τ_a determined with 2 mM hexamminechromium(III) ions in an acetate buffer solution is presented in Table V, where τ_c is the transition time for the cathodic process and τ_a, that for the following anodic process. The ratio of τ_c/τ_a fluctuates around 3, the theoretical value that is expected when the reduced species is soluble and the current densities at the forward and the reverse process are equal in magnitude.[16]

Discussion

The mechanism of electroreduction of the heamminechromium(III) ions in acid buffer solutions has been reported as follows;[6]

$$[Cr(NH_3)_6]^{3+} + e \rightleftharpoons [Cr(NH_3)_6]^{2+} \quad (2)$$

$$[Cr(NH_3)_6]^{2+} + n\,H_3O^+ \rightarrow [Cr(H_2O)_n(NH_3)_{6-n}]^{2+} + n\,NH_4^+ \quad (3)$$

It may be concluded from the d. c. polarographic and the chronopotentiometric investigations that hexamminechromium(III) ions are directly reduced at the dropping mercury electrode without any preceding chemical reaction prior to the electron-transfer process. The Kalousek polarograms[6] and the current-reversal chronopotentiograms indicate that the overall process of the reduction of hexamminechromium(III) to chromium(II) proceeds irreversibly at the dropping mercury electrode:

$$[Cr(NH_3)_6]^{3+} + e + n\,H_3O^+ \rightarrow [Cr(H_2O)_n(NH_3)_{6-n}]^{2+} + n\,NH_4^+ \quad (4)$$

Two mechanisms may be considered. One is that, although the electron-transfer process given by Eq. 2 proceeds reversibly, the net electrode process appears to be irreversible on account of the extreme rapidity of the following chemical reactions, while the other is that the electron-transfer process itself proceeds irreversibly.

The characteristics of the chronopotentiogram for the first[17-19] and the second[20,21] mechanism have already been analyzed theoretically, which are given in Table VI.[15]

In the reduction of hexamminechromium(III), the plot of log $(\sqrt{\tau}-\sqrt{t})$ vs. E yields a straight line, whose slope is somewhat greater than 59 mV., a theoretical value expected for a reversible one-electron reduction at 25°C. This suggests the possibility of the electron-transfer process itself being irreversible. According to the results of theoretical analysis given in Table VI, the slope of the plot should be equal to the constant $RT/\alpha nF$ independently of the concentration of the hexamminechromium(III) and the current density i. However, as is seen in Table VII, the slopes of the plots obtained experimentally vary with the transition time, and increase with increasing current density at the same concentration of the complex. This fact can not be explained satisfactorily by the mechanism which assumes the totally irreversible electron-transfer process.

Recently, Gellings[22] studied the characteristics of the current-potential curves for the electrode process of kinetic nature, where he proposed a method by which the potential can be expressed as a function of the current by the application of Lagrange's theorem. This method was applied in this study to a general treatment for the chronopotentiometric potential-time curve for the process represented by the following scheme:

TABLE VI. DIAGNOSTIC CRITERIA FOR KINETIC SCHEMES

No.	Kinetic schem	Linear ln-plot	Slope of ln-plot	$\frac{\partial E_{\tau/4}}{\partial \ln i}$	$\frac{\partial E_{\tau/4}}{\partial \ln C_O^\circ}$	$\frac{\tau_a}{\tau_c}$
1	$O \rightleftharpoons R \rightarrow Y$	$\sqrt{\tau}-\sqrt{t}$	RT/nF	$-RT/nF$	RT/nF	0 or 1/3
2	$O \rightarrow R$	$\sqrt{\tau}-\sqrt{t}$	$RT/\alpha nF$	$-RT/\alpha nF$	$RT/\alpha nF$	1/3 or 0

Potential relations for kinetic schemes

1 $$E = E_e^\circ + \frac{RT}{nF}\ln(\sqrt{\tau}-\sqrt{t}) + \frac{RT}{2nF}\ln\frac{\sigma_f^*}{\pi}$$

2 $$E = E_e^\circ + \frac{RT}{\alpha nF}\ln(\sqrt{\tau}-\sqrt{t}) + \frac{RT}{\alpha nF}\ln\frac{2k_s^{**}}{\sqrt{\pi D}}$$

* σ_f: Rate constant for a following chemical reaction.
** k_s: Rate constant for electron-transfer at $E=E_e^\circ$.

16) A. C. Testa and W. H. Reinmuth, *Anal. Chem.*, 32, 1512 (1960).
17) P. Delahay, C. C. Mattax and T. Berzins, *J. Am. Chem. Soc.*, 76, 5319 (1954).
18) W. K. Snead and A. E. Remick, ibid., 79, 6121 (1957).
19) W. H. Reinmuth and A. C. Testa, *Anal. Chem.*, 32, 1518 (1960).
20) P. Delahay and T. Berzins, *J. Am. Chem. Soc.*, 75, 2486 (1953).
21) P. Delahay and G. Mamantov, *Anal. Chem.*, 27, 478 (1955).
22) P. J. Gellings, *Z. Elektrochem.*, 66, 477, 481 (1962).

TABLE VII. KINETIC PARAMETERS OF HEXAMMINECHROMIUM(III) OBTAINED FROM THE CHRONOPOTENTIOMETRIC MEASUREMENTS

C_O° mM	i, mamp.$\cdot$ cm^{-2}	τ sec.	$E_{t=0}$* V. vs. SCE	log-plot slope, mV.
2.00	1.63_9	0.100_0	-1.01_7	85
2.85	1.08_2	0.439	-0.99_1	80
5.00	1.44_8	0.736	-0.98_4	76
2.00	0.44_3	1.36_9	-0.98_0	73

* Corrected for ohmic drop across the electrolytic cell.

$$O+ne \rightleftharpoons R \tag{5}$$

$$R \underset{\sigma_b}{\overset{\sigma_f}{\rightleftharpoons}} Y \quad (\sigma_f/\sigma_b \gg 1) \tag{6}$$

where O is a reducible substance, R its reduction product, Y a substance which is neither reduced nor oxidized at the potentials where the reduction of O occurs and σ_f and σ_b are the rate constants of the following chemical reaction.

When $|i/i_0|$ is less than 2, where i_0 means the exchange current density for the electrochemical reaction given by Eq. 5, i. e., in the case of a reversible electron-transfer, Eq. 7 holds:

$$\psi=\ln\frac{g}{h}+\sum_{n=1}^{\infty}B_n\frac{f^n}{g^{n\beta}h^{n\alpha}} \tag{7}$$

with $\psi=\dfrac{nF}{RT}(E-E_e^\circ)$, $f=i/i_0$, $g=C_O/C_O^\circ$, $h=C_R/C_O^\circ$ and $B_n=\dfrac{(-1)^n\Gamma(n\alpha)}{n!\Gamma(n\alpha-n+1)}$

for which the condition for convergence is:

$$|f\alpha^\alpha\beta^\beta/(g^\beta h^\alpha)|<1$$

In the case of a large current density ($|i/i_0|>2$), i. e., in the case of an irreversible electron-transfer, Eq. 8 is satisfied:

$$-\alpha\psi=\ln\frac{f}{g}+\sum_{n=1}^{\infty}A_n\frac{h^n g^{n\beta/\alpha}}{f^{n(1+\beta/\alpha)}} \tag{8}$$

with $A_n=\dfrac{\Gamma\left(n-\dfrac{n}{\alpha}\right)}{n!\Gamma\left(1-\dfrac{n}{\alpha}\right)}$

for which the condition for convergence is:

$$|h^\alpha g^\beta/(\alpha^\alpha\beta^\beta f)|<1$$

In Eqs. 7 and 8, α and β represent the transfer coefficients for the cathodic and the anodic process respectively ($\alpha+\beta=1$), C_O and C_R the concentrations of O and R at the electrode surface respectively, C_O° represents the concentration of O in the bulk of the solution, E the potential of cathode at time t, E_e the formal standard potential of the electroactive couple, A_n and B_n are the coefficients in power series[22] and Γ is the gamma function. According to Delahay et al.[17] the concentrations of O and R at the electrode surface are given as:

$$C_O(0,t)=C_O^\circ-\frac{2i\sqrt{t}}{nF\sqrt{\pi}\sqrt{D_O}} \tag{9}$$

$$C_R(0,t)=\frac{i}{nF\sqrt{D}}\left(\frac{2\sqrt{t}}{\sqrt{\pi}K}+\frac{\mathrm{erf}\sqrt{\sigma_f t}}{\sqrt{\sigma_f}}\right)$$

where K is the equilibrium constant for the reaction given by Eq. 6 ($K\gg1$), D the common value of D_R and D_Y which are assumed to be the same, and erf means the error function. Introducing Eq. 9 into Eqs. 7 and 8, Eqs. 10 and 11 are obtained for a reversible and an irreversible electron-transfer process respectively. In Eqs. 10 and 11, k_s represents the rate constant for the electron-transfer process at $E=E_e^\circ$.

In Eq. 10 the potential at $t=0$ ($E_{t=0}$) becomes definite only when $\sqrt{\sigma_f t}>2$, otherwise

$$E=E_e^\circ+\frac{RT}{nF}\ln\frac{1-\sqrt{t/\tau}}{\dfrac{i}{nFC_O^\circ\sqrt{D}}\left(\dfrac{2\sqrt{t}}{\sqrt{\pi}K}+\dfrac{\mathrm{erf}\sqrt{\sigma_f t}}{\sqrt{\sigma_f}}\right)}+\frac{RT}{nF}\sum_{n=1}^{\infty}B_n\frac{(i/i_0)^n}{(1-\sqrt{t/\tau})^{n\beta}\left[\sqrt{D_O/D}\left(\dfrac{1}{K}\sqrt{t/\tau}+\dfrac{\sqrt{\pi}}{2}\dfrac{\mathrm{erf}\sqrt{\sigma_f t}}{\sqrt{\sigma_f\tau}}\right)\right]^{n\alpha}} \tag{10}$$

(for a reveversible electron-transfer)

$$E=E_e^\circ+\frac{\alpha nF}{RT}\ln\frac{1-\sqrt{t/\tau}}{\dfrac{i}{nFk_sC_O^\circ}}-\frac{RT}{\alpha nF}\sum_{n=1}^{\infty}A_n\frac{(1-\sqrt{t/\tau})^{n\beta/\alpha}\left[\sqrt{D_O/D}\left(\dfrac{1}{K}\sqrt{t/\tau}+\dfrac{\sqrt{\pi}}{2}\dfrac{\mathrm{erf}\sqrt{\sigma_f t}}{\sqrt{\sigma_f\tau}}\right)\right]^n}{(i/i_0)^{n(1+\beta/\alpha)}} \tag{11}$$

(for an irreversible electron-transfer)

becomes infinite, since the value of the error function virtually is equal to unity for an argument larger than 2. When $\sqrt{\sigma_f t} > 2$, the plot of E vs. log $(\sqrt{\tau} - \sqrt{t})$ should yield a straig lhtine whose slope is equal to $2.3RT/nF$. In Eq. 11, on the other hand, $E_{t=0}$ is independent of σ_f, because the additional term (the third term) of the equation becomes zero when t equals zero. Hence, $E_{t=0}$ vs. log i and $E_{t=0}$ vs. log C_O° should yield straight lines whose slopes equal $-2.3\,RT/\alpha nF$ and $2.3\,RT/\alpha nF$ respectively. Finally, in both Eqs. 10 and 11, it is expected that the logarithmic term, log $(\sqrt{\tau} - \sqrt{t})$, varies with potential linearly or curvilinearly depending on the magnitude of the additional term of the equations. This explains the experimental results that the slope of the apparently linear log-plot varied with the transition time. (See Table VII).

The value of $E_{t=0}$ was found to change linearly with log i and with log C_O°. If Eq. 11 can be applied, the absolute value of the reciprocal slopes of $E_{t=0}$ vs. log i and $E_{t=0}$ vs. log C_O° should be equal to the constant $2.3RT/\alpha nF$, because the additional term of Eq. 11 approaches zero at $t=0$. In the experiments, the reciprocal slopes of $E_{t=0}$ vs. log i and $E_{t=0}$ vs. log C_O° were found to be -66 mV. and 65 mV. respectively at 25°C, as are seen in Figs. 2 and 3. Thus, every slope of log-plot was somewhat greater than 59 mV., a theoretical value expected for a reversible one-electron reduction at 25°C. As for the potential at $t=0$ ($E_{t=0}$), definite values were obtained, which also support the mechanism given by Eq. 11. Consequently, the irreversibility of the electron-transfer process itself is favorably inferred.

In view of the above-mentioned facts a reasonable conclusion that may be drawn from the available data is that hexamminechromium-(III) ions are irreversibly reduced at the dropping mercury electrode without any preceding chemical reactions prior to the more or less irreversible electron-transfer process, followed by the rapid aquation of the reduced species.

Summary

The reduction of hexamminechromium(III) ions at the dropping mercury electrode has been studied chronopotentiometrically in acetate buffer solutions. The electrolysis at constant cathodic current gives a well-defined chronopotentiogram which corresponds to the one-electron reduction of chromium(III) to chromium(II), but the anodic chronopotentiogram which is obtained by the electrolysis at constant anodic current is clearly separated from the cathodic one.

A general treatment for a chronopotentiometric potential-time curve for the electrode process with the following chemical reaction has been developed by the application of Lagrange's theorem. The results indicate that hexamminechromium(III) ions are irreversibly reduced at the dropping mercury electrode without any preceding chemical reactions prior to the more or less irreversible electron-transfer process, followed by the rapid aquation of the reduced species.

The authors wish to thank the Ministry of Education for the financial support granted for this research.

Department of Chemistry
Faculty of Science
Tohoku University
Katahira-cho, Sendai

The Chlorine Content of Hawaiian Lavas

By Bunji IWASAKI and Takashi KATSURA

(Received June 13, 1964)

Studies of the chlorine content of Hawaiian lavas have been published by Shepherd,[1] Iwasaki et al.,[2] and Yoshida et al.[3] Nevertheless, the rock samples used in their studies were small in number and collected from only a few localities. Recently, 141 new chemical analyses of Hawaiian lavas systematically collected have been reported by Macdonald and Katsura.[4]

In the present paper, the distribution of chlorine in the Hawaiian lavas will be investigated in order to answer the following principal questions: Is there any change in the chlorine content of rocks which were extruded at different times in volcanic history? Is it clear that chlorine tends to be enriched in rock of an alkalic type? Does the frequency distribution of chlorine show a lognormality? Is there any regional change in the chlorine content of the rocks?

Experimental

Rock Specimens.—The rock specimens used for the present study cover all of the rock types found in the Hawaiian Islands, e. g., tholeiitic basalt, tholeiitic olivine basalt, alkalic basalt, alkalic olivine basalt, basanite, basanitoid, ankaramite, hawaiite, mugearite, and trachyte, as defined by Macdonald and Katsura.[4] Most of them were collected by Macdonald during the 1960~1961 period, during which time one of the authors of this paper joined him under a National Science Foundation grant.[5,6]

Method of Analysis. — The total chlorine was determined by the method of Iwasaki et al.[7] with some improvements. About 200 mg. of a fine powdered rock sample was fused with anhydrous sodium carbonate in a platinum crucible. After cooling, the chlorine was completely extracted with hot redistilled water and was determined photometrically by the thiocyanate method.[8]

The water-soluble chlorine in rocks was determined as follows: About 1.00 g. of a fine powdered (100 to 150 mesh) rock sample was put into a centrifugal vessel containing 15 ml. of redistilled water. The vessel was then vigorously shaken about 1 min. After the mixture had stood overnight at room temperature, the solution in the vessel was separated from the rock sample by centrifuge. Almost all of the soluble chlorine was extracted by this procedure. About 0.1 ml. of concentrated perchloric acid was then added to the solution. The total soluble chlorine thus extracted was determined by the method shown above.

The total chlorine in approximately 160 Hawaiian volcanic rocks was duplicatedly determined two or more times, but the water-soluble chlorine was determined only one or two times. It may safely be said that the precision for the present determination of chlorine is within ±5% over the whole range of chlorine contents obtained here.

In addition to the reproducibility of the results of the analyses, a cross-check analysis of one sample was made by Dorothy Powers, with the aid of Dr. H. A. Powers and under the supervision of L. C. Peck, in the laboratory of the Geological Survey in Denver, Colorado, U. S. A. The value of 0.018% chlorine in a rock specimen, G-2907 in Table I-b obtained by the present authors is in good agreement with that obtained by Mrs. Powers, (0.02% chlorine).

According to Shepherd,[1] the chlorine content in the 1926 Mauna Loan volcanic rocks was 0.01% chlorine; as may be seen in Table I-b, the corresponding value for the same rock obtained by the present authors was 0.008% chlorine (C-133). Taking account of the difference in rock specimens, it may be said that these values are in good accordance.

Results

Tables I-a, I-b give both the insoluble and total chlorine contents in the Hawaiian lavas. The insoluble chlorine content was calculated by subtracting the water-soluble chlorine from the total chlorine.

Discussion

Water-soluble Chlorine in Rocks.—It has been found by Kuroda and Sandell[9] and by Iwasaki

1) E. S. Shepherd, *Am. J. Sci.*, **238**, 117 (1940).
2) I. Iwasaki, T. Katsura, N. Sakato and M. Hirayama, *J. Chem. Soc. Japan, Pure Chem. Sec.* (*Nippon Kagaku Zassi*), **78**, 164 (1957).
3) M. Yoshida, T. Ozawa and T. Katsura, Read at the Meeting of the Volcanological Society of Japan, March, 1963.
4) G. A. Macdonald and T. Katsura, *J. Petrology*, **5**, 82 (1964).
5) C. A. Macdonald and T. Katsura, *Pacific Science*, **15**, 358 (1961).
6) G. A. Macdonald and T. Katsura, *Am. Geophys. Union, Monograph*, No. 6, 187 (1962).
7) I. Iwasaki, T. Katsura and N. Sakato, *J. Chem. Soc. Japan, Pure Chem. Sec.* (*Nippon Kagaku Zassi*), **76**, 1116 (1955).
8) A. Tomonari, ibid., **83**, 693 (1962).
9) P. K. Kuroda and E. B. Sandell, *Bull. Geol. Soc. Am.*, **64**, 879 (1953).

TABLE I-a. CHLORINE CONTENT OF THE VOLCANIC ROCKS IN THE ISLANDS OF HAWAII

Specimen	Volcano	Type of rock	Total Cl %	Insoluble Cl, %	Specimen	Volcano	Type of rock	Total Cl %	Insoluble Cl, %
C-1	Waianae	Tb	0.010	0.009	C-57	Kohala	Tb	0.008	0.006
C-2		Tb	0.008	0.007	C-58		Tb	0.007	0.006
C-3		Tb	0.015	0.014	C-59		Tb	0.007	0.006
C-4		Tb	0.009	0.007	C-60		Tb	0.006	0.005
C-5		Tb	0.019	0.007	C-61		Tb	0.010	0.004
C-6		Tb	0.010	0.006	C-62		Tb	0.006	0.005
C-7		Tb	0.010	0.006	C-63		Tb	0.012	0.003
C-8		Tb	0.007	0.006	C-64		Tb	0.007	0.006
C-9		Tb	0.011	0.010	C-65		Fpb	0.006	0.004
C-10		Tb	0.010	0.009	C-66		Tb	0.007	0.007
C-11		Tb	0.008	0.006	C-70		Aob	0.008	0.007
C-12		Tb	0.019	0.006	C-69		Aob	0.007	0.005
C-13		Tb	0.009	0.007	C-68		Ha	0.037	0.034
C-14		Tb	0.008	0.007	C-134		Mu	0.008	0.006
C-15		Tb	0.008	0.006	C-77	Mauna Kea	Aob	0.050	0.010
C-16		Tb	0.012	0.010	C-78		Aob	0.062	0.007
C-17		Tb	0.012	0.008	C-76		Ak	0.010	0.008
C-18		Tb	0.017	0.008	C-75		Tob	0.007	0.006
C-19		Tb	0.008	0.007	C-74		Tb	0.007	0.005
C-20		Tb	0.012	0.007	C-71		Ak	0.011	0.009
C-21		Tb	0.008	0.006	C-67		Ak	0.010	0.009
C-22		Tb	0.026	0.006	C-72		Ha	0.024	0.021
C-23		Tb	0.011	0.008	C-73		Ha	0.008	0.006
C-24		Tb	0.019	0.011	C-79		Ha	0.009	0.007
C-25		Tb	0.029	0.007	1902		Ha	0.013	0.012
C-26		Tb	0.012	0.008	TK8200		Aob	0.009	0.007
C-27		Tb	0.012	0.007	C-80	Kauai	Tb	0.006	0.005
C-28		Tb	0.021	0.007	C-81		Tb	0.007	0.006
C-29		Tb	0.020	0.008	C-82		Tb	0.006	0.005
C-33		Tb	0.158	0.020	C-83		Tb	0.007	0.006
C-34		Tb	0.041	0.006	C-84		Oc	0.007	0.004
C-35		Tb	0.015	0.011	C-85		Tb	0.012	0.010
C-36		Tb	0.015	0.008	C-86		Tb	0.008	0.007
C-37		Tb	0.015	0.008	C-87		Tob	0.007	0.005
C-38		Tb	0.009	0.007	C-88		Tb	0.008	0.007
C-39		Tb	0.016	0.010	C-89		Tb	0.006	0.005
C-40		Tb	0.016	0.007	C-90		Bs	0.008	0.006
C-41		Tb	0.051	0.013	C-91		Aob	0.013	0.011
C-46		Tb	0.012	0.010	C-93	West Maui	Tb	0.008	0.007
C-47		Tb	0.009	0.006	C-94		Tb	0.010	0.007
C-48		Tb	0.011	0.010	C-95		Tb	0.007	0.006
C-49		Tob	0.023	0.013	C-96		Tb	0.007	0.006
C-50		Tob	0.013	0.010	C-97		Tb	0.020	0.006
C-51		Tb	0.010	0.009	C-98		Tb	0.007	0.006
C-52		Ha	0.008	0.006	C-99		Tb	0.008	0.007
C-30		Aob	0.007	0.006	C-100		Tb	0.218	0.012
C-31		Fpb	0.006	0.005	C-101		Tb	0.007	0.005
C-31′		G	0.008	n.d.	C-102		Tb	0.006	0.005
C-42		Ha	0.024	0.023	C-103		Tb	0.008	0.007
C-44	Molokai	Aob	0.014	0.010	C-104		Tb	0.011	0.006
C-45		Ha	0.023	0.020	C-105		Tob	0.009	0.007
C-53	Kohala	Tb	0.098	0.006	C-106		Tb	0.006	0.005
C-54		Tb	0.065	0.010	C-107		Tb	0.012	0.009
C-55		Tob	0.006	0.005	C-108		Tob	0.006	0.004
C-56		Tb	0.007	0.006	C-109		Tb	0.017	0.014

TABLE I-a. (Continued)

Specimen	Volcano	Type of rock	Total Cl %	Insoluble Cl, %	Specimen	Volcano	Type of rock	Total Cl %	Insoluble Cl, %
C-110	West Maui	Tb	0.030	0.025	C-128	West Maui	Tr	0.021	0.001
C-111		Tb	0.013	0.012	C-115		Bs	0.067	0.066
C-112		Tob	0.025	0.012	C-130		Bs	0.042	0.017
C-113		Tob	0.041	0.010	C-123	Haleakala	Oc	0.006	0.006
C-114		Aob	0.017	0.013	C-122		Tob	0.006	0.006
C-117		Tob	0.072	0.019	C-124		Ab	0.009	0.008
C-118		Aob	0.007	0.005	C-125		Aob	0.008	0.007
C-119		Tob	0.017	0.013	C-126		Aob	0.007	0.007
C-120		Tob	0.009	0.006	C-121		Tob	0.008	0.007
C-92		Mu	0.038	0.019	C-127		Ha	0.033	0.031
C-116		Tr	0.009	0.003	C-129		Bt	0.032	0.027

Abbreviation used in Table I has the following meaning: Tb, tholeiite basalt. Tob, tholeiite olivine basalt. Ab, alkalic basalt. Aob, alkalic olivine basalt. Fpb, feldspar phyric basalt. Ha, hawaiite. G, groundmass. Mu, mugearite. Ak, ankaramite. Oc, oceanite. Bs, basanite. Bt, basanitoid. Tr, trachyte.

TABLE I-b. CHLORINE CONTENT OF THF DATED HAWAIIAN VOLCANIC ROCKS

Specimen	Volcano	Date (year)	Type of rock	Total Cl, %	Insoluble Cl, %
2005	Hualalai	1801	Aob	0.015	0.012
2204	Mauna Loa	1843	Tb	0.008	0.006
2202		1855	Tb	0.007	0.006
2003		1859	Tb	0.008	0.007
2015		1868	Tb	0.006	0.005
2201		1881	Tb	0.008	0.007
2014		1887	Tb	0.007	0.005
2203		1899	Tb	0.006	0.005
2013		1907	Tb	0.007	0.006
2012		1907	Tb	0.007	0.006
2010		1919	Tb	0.009	0.009
C-133		1926	Tb	0.008	0.007
2205		1935	Tb	0.008	0.006
2206-a		1935	Tb	0.008	0.007
2206-b		1935	Tb	0.007	0.005
2007		1950	Tb	0.007	0.007
1803	Kilauea	1750	Tb	0.010	0.009
2103		1921	Tb	0.013	0.011
2104		1954	Tb	0.014	0.012
C-131		1955	Tb	0.017	0.017
C-132		1955	Tb	0.017	0.016
1802		1955	Tb	0.017	0.016
G-2907		1955	Tb	0.018	n.d.
2101-a		1959	Tb	0.011	0.009
2101-b		1959	Tb	0.012	n.d.
Tachylite		1959		0.018	n.d.
Melt		1959		0.016	0.014
1805		1960	Tb	0.016	0.014
1806		1960	Tb	0.018	0.014
1808		1960	Tb	0.015	0.014
Pele's hair		1959		0.016	n.d.

et al.[2] that volcanic rocks generally contain a very small amount of water-soluble chlorine compared with amount of total chlorine when the specimens are fresh. Table II shows the amounts of both the total and the water-soluble chlorines of the historic fresh lavas from Mauna Loa and Kilauea. The amount of water-soluble chlorine varies from 0.000 to 0.004% chlorine, as may be seen in Table II,

TABLE II. VARIATION OF CHLORINE CONTENT IN ROCK SAMPLES AT DIFFERENT PERIODS OF AN ERUPTION

	Total Cl %	Insoluble Cl %
The 1955 Kilauea Eruption (Puna)		
C-131	0.017	0.016
C-132	0.017	0.016
G-2907	0.018	n.d.
1802	0.017	0.016
The 1960 Kilauea Eruption (Kapoho)		
1805	0.016	0.014
1806	0.018	0.014
1808	0.015	0.014
The 1935 Mauna Loa Eruption		
2205	0.008	0.006
2206	0.008	0.007
The 1959 Kilauea Iki Eruption		
2101	0.011	0.009
2101-a	0.012	n.d.

while the total chlorine content has a slightly wider range, from 0.006 to 0.018% chlorine. The amount of water-soluble chlorine is presumably independent of the total chlorine content, and it seems to be almost constant. On the other hand, a rock sample such as C-33 has a high amount of water-soluble chlorine (0.16% chlorine). The specimen was collected about 2 feet above sea level at the end of a spur; as has been pointed out by Macdonald the specimen has without doubt been washed with sea-water, but it appeared very fresh. Considering this, a rock specimen with a high amount of water-soluble chlorine has possibly been contaminated by sea-water, etc. Indeed, there was only a very small amount of water-soluble chlorine even in a fresh a rock specimen, and we can hardly distinguish the chlorine which was primarily present in a rock sample just after the extrusion from the chlorine due to contamination; however, we may presume that the contaminated chlorine could be completely extracted with water. In the following discussion we will employ the amount of insoluble chlorine, though it is tedious work to determine the soluble chlorine as well as the total chlorine.

The Manner of Occurence of Chlorine in Rocks.—Based on the studies by Shepherd,[1] Behne,[10] and Kuroda and Sandell,[9] Correns[11] summarized the manner of occurence of chlorine in igneous rocks, and pointed out that in all probability the chlorine content of igneous rocks does depend either upon their mineralogical composition or upon their modes of crystallization. Iwasaki et al.[2] determined the chlorine content of about 190 volcanic rocks from Japan, Korea, Manchuria (China), and Hawaii, and of pebbles dredged near Jimmu Seamount,[12] and made it clear that there seems to be no distinct relationship between the chlorine content and the major chemical constituents, especially with respect to the phosphorous and water contents on which Kuroda and Sandell[9] focussed their attention. Iwasaki et al.,[2] therefore, concluded that the chlorine distribution may largely be attributed to the quenching condition at high temperature, at which a magma is equilibrated with the gaseous phase.

The chlorine content of apatite in igneous rocks other than volcanic rocks was determined by Kind,[13] Behne,[10] and Vasilieva,[14] and the average chlorine content of apatite in igneous rocks was estimated by Behne[10] as 0.30% chlorine. Assuming that the Hawaiian volcanic rocks contain apatite in which 0.3% chlorine is contained as an essential constituent on the average, the calculations will lead to the result that the contribution of chlorine due to the appatite present in rocks is limited only to the magnitude of 0.002% chlorine provided the average phosphorus content in Hawaiian tholeiitic basalts is 0.26% P_2O_5.[4] In fact, no close relationship existed between the chlorine content and the phosphorus content. For instance, specimen C-73 in Table I-a is low in chlorine in spite of a high phosphorus content. It is, therefore, clear that apatite in Hawaiian volcanic rocks is of little importance in the distribution of chlorine.

Mica is rarely found in Hawaiian volcanic rocks; as may be seen in Table I-a, the rock specimens, C-73, and C-79, which contain abundant dark mica are low in chlorine (0.006 and 0.007% respectively). Therefore, mica is also of little importance as a chlorine-carrier. The chlorine content of olivine separated from the 1959 lava of Kilauea Iki was very low (0.003% chlorine, as determined by T. Ozawa)

10) W. Behne, *Geochim. et Cosmochim. Acta*, 3, 186 (1953).
11) C. W. Correns, "Physics and Chemistry of the Earth," Vol. I, Ed. by L. H. Ahrens, K. Rankama and S. K. Runcon, McGraw-Hill, New York (1956), p. 180.
12) H. Kuno, R. L. Fisher and N. Nasu, *Deep-Sea Research*, 3, 126 (1956).
13) A. Kind, *Chemie der Erde*, **12**, 50 (1938).
14) Z. V. Vasilieva, *Geokhimiya*, 704 (1957.)

in comparison with that of the original rock (0.012% chlorine).

In contrast to the facts mentioned above, the chlorine content of a ground mass in specimen C-31 (0.008% chlorine), which is a feldspar-phyric basalt and 50% occupied by feldspar phenocryst, is higher than that of the original rocks (0.005% chlorine). It is clear that almost all the chlorine in the bulk is provided by the ground mass, which represents the liquid part of the rock when it was extruded at high temperature. According to Yoshida,[15] the chlorine compounds are evolved at 600°C, and the amount of evolved chlorine compounds increases gradually with an elevation of temperature. It may be considered that the rock samples studied by Yoshida contain an appreciable amount of groundmass, that the glassy parts begin crystallizing at 600°C at a significant speed, and that the chlorine dissolved in the glassy parts is forced to escape to the atmosphere. In addition, it has been found by Iwasaki[16] that the enrichment of chlorine in a rock sample collected from the middle part of one thick basaltic lava flow resulted from the larger amount of glassy parts solidified at the latest stage of the cooling process.

The Variation in the Chlorine Content of the Rock Samples of One Eruption.—Table II shows some examples of the variation in chlorine content of rock samples representing different periods of the time during each dated eruption of Kilauea and Mauna Loa. These samples all belong to aphyric-type basalt, and the amount of phenocrysts is less than 5% (tholeiitic basalt). It may, therefore, be assumed that the chlorine content of a lava flow extruded at a definite period of year will be almost constant when we take rocks with the same texture. In addition, Iwasaki and Ozawa[17] made it clear that the chlorine contents of approximately 120 rock samples of the 1950~1951 lava flow of O-sima Volcano, Japan, were quite homogeneous and ranged from 0.029 to 0.036% chlorine, irrespective of their appearance.

The Variation in the Chlorine Content of Rocks in Stratigraphical Sequences.—From the preceding discussion, we could expect that the chlorine content of a rock will depend mainly on the chlorine dissolved in an original silicate melt which came in contact with a gaseous phase containing a small amount of chlorine compounds. It would be valuable, in studying the descent of magmas, to see whether or not there is any variation in the chlorine content of rocks of each volcano in stratigraphical sequence. In Table I-a, the rock samples are presented in order of stratigraphical sequences; for instance, C-1 represents the lower parts in the stratigraphy of the Waianae Range, and C-52, the uppermost part.

As may be seen in Table I-a, there is a small variation in the insoluble chlorine content of rocks in most of volcanoes with the exception of the West Maui Volcano. Roughly speaking, these variations range from 0.005 to 0.01% chlorine, and there seems no distinct variation scheme with respect to the stratigraphical sequences. In contrast, it may be seen in Table I-b that the rock specimens of Kilauea are higher in chlorine content than those of Mauna Loa. This may be explained, in one way, by the two different magma batches proposed by Powers[18] which are different in chemical composition. Another explanation rests on the difference in volatile-escaping tendency during the movement of a melt from a magma chamber to the surface of the earth; the path in Mauna Loa is longer than in Kilauea.

In the case of West Maui, there seems to be an increase in the chlorine content of rocks toward the end of the period of volcanic eruption.

The Relationship between the Rock Types and the Chlorine Content.—A study by Macdonald[19] has elucidated many detail of the relationships of the tholeiitic rocks of the main shield volcano, which make up about 99 per cent of the volume as an over-all average in Hawaii; only a small percentage of Hawaiian rocks consist of the alkalic rocks which covered the late-stage cap of the volcanic mountains. The numbers of analyzed rock specimens in this study are not proportional to the volumes of each rock type, but the frequency diagrams of insoluble chlorine content in both tholeiitic and non-tholeiitic rocks are given in Figs. 1-a, 1-b. As may be seen in Figs. 1-a, 1b- the chlorine content of both tholeiitic and alkalic basalts range from 0.005 to 0.014%, with a few exceptions in tholeiitic basalt. On the other hand, the chlorine contents of hawaiite are scattered over a wide range from 0.006 to 0.034%. The same distribution will be seen in basanite and basanitoid group, ranging from 0.006 to 0.066%, though there are only four samples. The highest chlorine content was found in trachyte obsidian of Hualalai (0.12%). The other trachytes contain very small amounts of chlorine

15) M. Yoshida, This Bulletin, **36**, 773 (1963).
16) B. Iwasaki, Read at the Meeting of the Volcanological Society of Japan, October, 1963.
17) I. Iwasaki and T. Ozawa, Read at the Meeting of the Volcanological Society of Japan, May, 1959.
18) H. A. Powers, *Geochim. et. Cosmochim. Acta*, 7, 77 (1955).
19) G. A. Macdonald, *J. Geophys. Res.*, **68**, 5100 (1963).

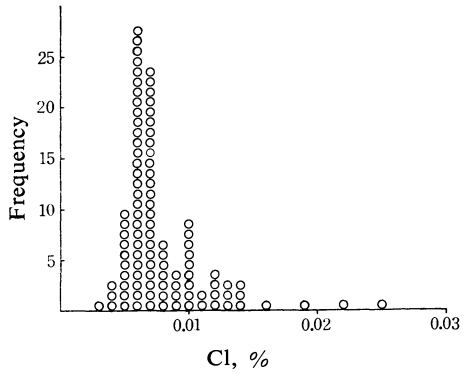


Fig. 1-a. Frequency diagram of insoluble chlorine content in tholeiitic basalts.
○ Tholeiitic basalt

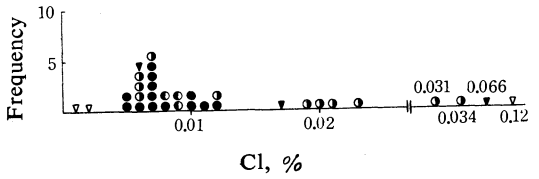


Fig. 1-b. Frequency diagram of insoluble chlorine content in non-tholeiitic basalts.
● Alkalic basalt
◑ Hawaiite and mugearite
◐ Ankaramite
△ Trachyte
▲ Basanite and basanitoid

(0.001 and 0.003%); thus the range of chlorine content here is larger than in the basanite group.

In general, it is difficult to say that alkali-rich rocks have more chlorine than tholeiitic rocks. We can, however, safely say that the rocks containing much chlorine are without exception of alkali-rich types.

The Frequency Distribution of the Chlorine Contents in Hawaiian Lavas.—Figure 2 gives three cumulative frequency distributions of insoluble chlorine contents of rocks from Waianae, from West Maui, and from all Hawaian volconoes. They show approximately lognormalities, rather than normalities. Strictly speaking, a bi-log-normality is appropriate for Waianae and for all Hawaiian volcanoes. This is in striking contrast to the finding of Iwasaki[16] that the frequency diagram of the chlorine content of the 1950~1951 lava flow of O-sima, Izu, shows a normality. Provided that the frequency diagram of the insoluble chlorine contents in Hawaiian lavas is log-normal, and that the water-soluble chlorine content of a rock is 0.001% chlorine, we obtain the mean chlorine content of Hawaiian lavas as, 0.008% chlorine.

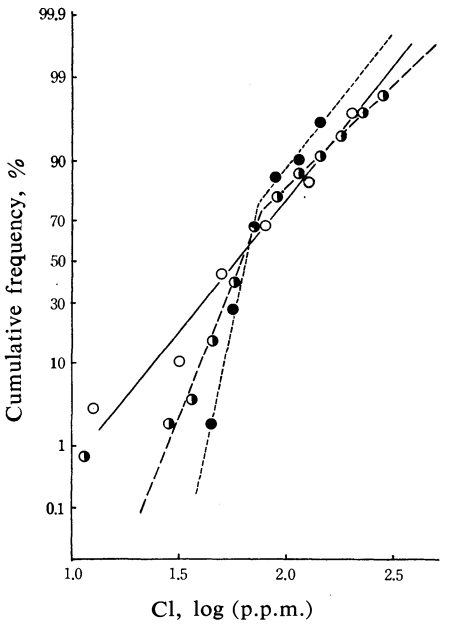


Fig. 2. Cumulative frequency distribution of insoluble chlorine content of rocks.
○ West Maui Volcano
● Waianae Volcano
◑ All Hawaiian lavas

It is valuable to know whether or not the chlorine content of rocks of one region differs from that of others. With respect to this regional variation, Kuroda and Sandell[9] mentioned that Japanese lavas are lower in chlorine content than those of the U. S. A. On the other hand, Iwasaki et al.[2] mentioned that Japanese volcanic rocks do not significantly differ in chlorine content from igneous rocks elsewhere in the world. Here we will compare the chlorine contents of Hawaiian and Japanese basalts. The total chlorine content, that is, 0.001% plus insoluble chlorine, is used in Hawaiian basalts. For the present purpose, we will adopt the available data of the volcanic rocks in Japan studied by Iwasaki et al.[2] Figure 3 shows two cumulative frequency distributions of the chlorine contents of Hawaiian and Japanese basalts. They show approximately lognormal distributions. Japanese basalts are clearly higher in chlorine than are Hawaiian basalts. As may be seen in the slope of straight lines in Fig. 3, the former is greater in the dispersion of chlorine content than is the latter. The mean chlorine contents of two basalts are 0.015% in Japan and 0.008% in Hawaii. The former is, therefore, about twice as high as the latter. Judging from the results obtained, it can be confidently stated that a regional difference in chlorine content exists between Hawaiian and Japanese basalts.

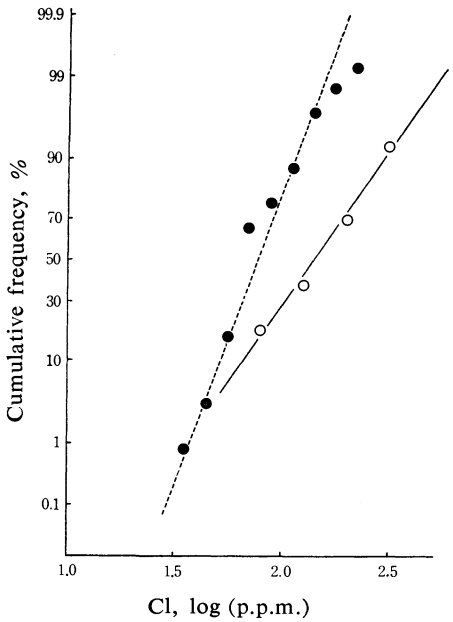


Fig. 3. Cumulative frequency distribution of chlorine content in Hawaiian and Japanese basalts.
○ Japanese basalt
● Hawaiian basalt

Conclusion

The foregoing evidence: (1) makes it clear that a narrow variation in the insoluble chlorine contents of rocks is common in the history of most Hawaiian volcanoes, especially in the tholeiitic rock series; (2) confirms that the alkali-rich rocks containing much insoluble chlorine are erupted at nearly the end of the volcanic history, although the alkali-rich rocks are not always higher in chlorine content than the tholeiitic rocks; (3) shows, however, that the high chlorine contents are selectively found in the alkali-rich rocks without exception; (4) indicates that the frequency diagram of the insoluble chlorine in Hawaiian lavas is bi-lognormally distributed, while the mean value of chlorine content is 0.008%; (5) shows that a regional difference in chlorine content may be seen in basalts between the islands of Hawaii and Japan, and (6) suggests that the chlorine in rocks is concentrated in the glassy parts, irrespective of their mineral assemblages.

The authors wish to express their hearty thanks to Professor Gordon A. Macdonald, Hawaii Institute of Geophysics of the University of Hawaii, for his valuable advice and criticism in field observations. Their thanks are also due to Professor Iwaji Iwasaki, Tokyo Institute of Technology, who encouraged them throughout the study. Mr. Takejiro Ozawa kindly analyzed the chlorine content of olivine.

Department of Chemistry
Tokyo Institute of Technology
Meguro-ku, Tokyo

Studies on Fluorene Derivatives. XXIII. The Synthesis of 2'-Bromotribiphenylenepropane and Some Related Observations*

By Kazuo SUZUKI and Minoru FUJIMOTO

(Received June 15, 1964)

2'-Bromotribiphenylenepropane (I) was first obtained by the Michael condensation of dibiphenyleneethylene (II) with 2-bromofluorene. The thermal decomposition of such tribiphenylenepropane hydrocarbons is invariably accompanied by the formation of the 9-fluorenyl free radical species. Thus two tribiphenylenepropane isomers (m. p. 291~293°C (decomp.), m. p. 257°C (decomp.)), 2,2'-dibromodibiphenyleneethane, II and dibiphenyleneethane can be obtained by the decomposition of I, as has previously been reported in this series.[1)]

The present investigation will deal with the synthesis of I by the use of 9-fluorenyllithiums, and will reexamine the side reaction in the Michael condensation of II with 2-bromofluorene. The origin of the by-products can be understood on the basis of a sequence of condensation and disproportionation steps.

By refluxing II and 2-bromofluorene in pyridine in the presence of one percent of potassium hydroxide or sodium carbonate, I, a small

* XXII of this series: K. Suzuki and M. Momoi, This Bulletin, 36, 1693 (1963).

1) K. Suzuki, *J. Chem. Soc. Japan, Pure Chem. Sec.* (*Nippon Kagaku Zassi*), 75, 711 (1954).

Table I. Reaction products of dibiphenyleneethylene (II) and 2-bromofluorene

Starting material g.		Solvent		Reaction time	Reaction product, g.					Recvd. g.
II	2-Br-fluorene	Pyridine ml.	Aqeous alkali ml.	hr.	I	Tri-biphenyl-enepropane	Fluore-none	2-Br-fluore-none	2, 7-diBr-fluore-none IV	II
3.3	2.5	20	10% KOH 2	40	1.6	m. p. 289～291°C 0.2	0.02	0.2	0.05 —	0.3
3.3	2.5	20	10% Na_2CO_3 2	35	3.9	—	0.02	0.2	— Trace	0.2

Table II. Alkaline cleavage of 2'-bromotribiphenylenepropane (I) in pyridine solution

Material g.	Solvent		Reaction time	Reaction product, g.						Recvd. g.
2'-Br-tribi-phenylene-propane	Pyridine ml.	10% Aq. KOH ml.	hr.	Fluo-rene	Fluore-none	2-Br-fluore-none	2, 7-diBr-fluore-none	II	IV	I
1.0	20	2	40	0.03	0.01	0.15	—	0.01	—	0.52
3.0	30	3	40	0.095	0.04	0.2	—	0.05	Trace	1.65
2-Br-fluorene 1.0	20	2	20	—	—	0.2	0.15	—	—	2-Br-fluorene 0.5

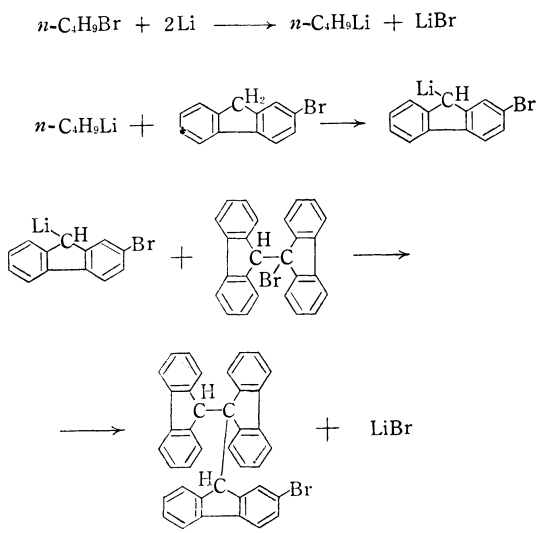
amount of tribiphenylenepropane (m. p. 289～291°C),[2] fluorenone, 2-bromofluorenone and 2'-bromodibiphenyleneethylene (IV)[3] were obtained; they were then characterized by a combination of column chromatography, sublimation and recrystallization. I was obtained in a good yield (79%) by the use of one percent sodium carbonate. These results are summarized in Table I.

Moreover, a highly substituted I might lead to II and 2-bromo-9-fluorenyl anions or IV and 9-fluorenyl anions by the elimination of the protons in the 9'- or 9''-positions of I in the pyridine-base solution. On the other hand, a minor portion of III, by means of a proton transfer, could form IV and fluorenyl ions. Then, tribiphenylenepropane (m. p. 289～291°C) could be formed by the addition of fluorenyl ions to II. This compound is identical with that of Suzuki,[2] as is shown by the fact that they have the same infrared absorption spectra and by mixed melting point determination. Figure 1. illustrates these reaction sequences.

I was then refluxed in pyridine with one percent potassium hydroxide under the same conditions for forty hours. Small amounts of fluorene, fluorenone, 2-bromofluorenone and dibiphenyleneethylenes were isolated from the reaction mixture. These results are summarized in Table II. Fluorenone and 2-bromofluorenone might be formed by the oxidation of fluorene and 2-bromofluorene respectively. 2, 7-Dibromofluorenone was obtained when 2-bromofluorene was treated similarly (see Table II), but it seems difficult to explain the formation of this compound.

These compounds were identified by mixed melting points, elementary analyses and infrared absorption spectra.

Aromatic hydrocarbons like fluorene and 9-phenylfluorene[4] have been successfully metalated by organo-lithium compounds. I was



I

2) K. Suzuki, *J. Chem. Soc. Japan, Pure Chem. Sec.* (*Nippon Kagaku Zassi*) **70**, 189 (1949); K. Suzuki, *Technol. Repts. Tôhoku Univ.*, **XIX**, 63 (1955).

3) S. Kajigaeshi, *J. Chem. Soc. Japan, Pure Chem. Sec.* (*Nippon Kagaku Zasshi*), **83**, 102 (1962)

4) H. Gilman and R. D. Gorsich, *J. Org. Chem.*, 33, 550 (1958).

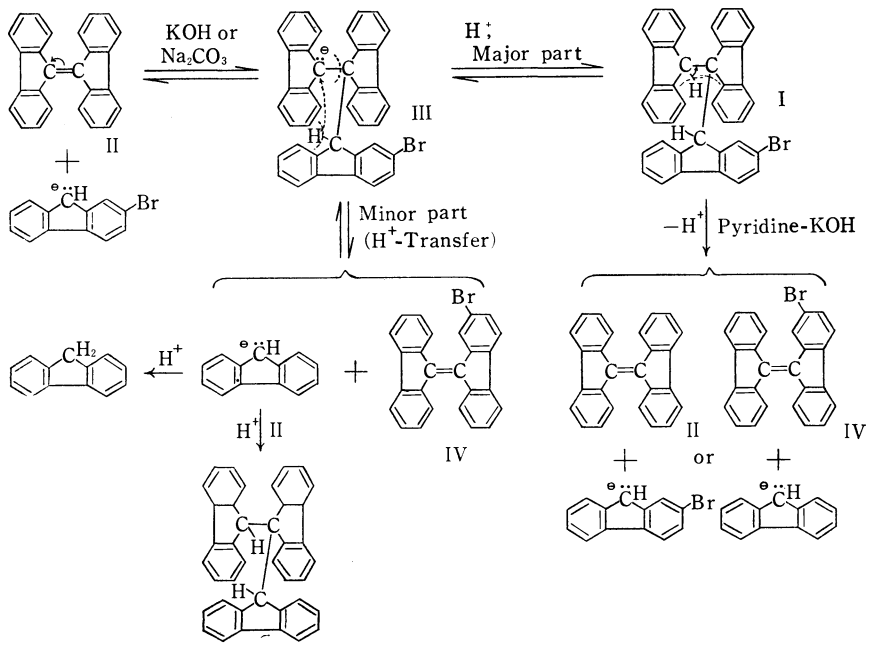


Fig. 1.

prepared by the following combinations of 9-fluorenyllithiums under similar conditions: 9-bromodibiphenyleneethane and 2-bromo-9-fluorenyllithium, 9-lithiodibiphenyleneethane and 2,9-dibromofluorene, 2',9-dibromodibiphenyleneethane and 9-fluorenyllithium and 2'-bromo-9-lithiodibiphenyleneethane and 9-bromofluorene; the yields were 41.3%, 26.1%, 42.6% and 4.0% respectively. The identity of these compounds was confirmed by a comparison of their infrared absorption spectra with those of authentic compounds.

Dibiphenyleneethanes did not react so satisfactorily with metallic lithium to form 9-lithiodibiphenyleneethanes.

The generalized reaction scheme is shown in Fig. 2.

Experimental*

The Michael Condensation of Dibiphenyleneethylene (II) with 2-Bromofluorene.—A solution of 3.3 g. of II, 2.5 g. of 2-bromofluorene and 2 ml. of a 10% aqueous solution of potassium hydroxide in 20 ml. of pyridine was refluxed for 40 hr., during which time the red color turned dark. After cooling, the reaction mixture was poured into water, and the orange-red precipitate was filtered. The crude product was extracted with hot benzene. The benzene solution was washed with water, dried over anhydrous calcium chloride, and then chromatographed on alumina.

Fluorenone (m. p. 83°C, 0.02 g.) and 2-bromofluorenone (m. p. 143~144°C, 0.2 g.) were isolated from the yellow band in the column and fractionally recrystallized from alcohol. Their identity was confirmed by mixed melting points with authentic samples.

Upon the evaporation of the first two fractions, a red solution, a crystalline material, was deposited. This was separated into yellow crystals and a red benzene solution by filtration. The yellow crystals were digested several times with ethyl acetate; this solution, upon evaporation, gave a small amount of an unknown colorless compound, which melted with bubbling at 120°C, and then gradually solidified and melted again at 255°C (decomp.). The mixed melting point with I was not depressed (254°C (decomp.)). The infrared absorption spectrum was partly different from that of I and did show absorptions at 1730, 1368, 1250 and 1050 cm^{-1} not as did I.

UV: $\lambda_{max}^{CHCl_3}$ $m\mu$ (log ε): 304 (4.22) and 272 (4.73).

The residue was extracted with hot ethyl acetate, and I was obtained from the extracts (m. p. 255°C (decomp.); 1.6 g.).

UV: $\lambda_{max}^{CHCl_3}$ $m\mu$ (log ε): 304 (4.06) and 272 (4.60).

The last insoluble part was recrystallized from benzene and gave tribiphenylenepropane, m. p. 289~291°C (0.2 g.), which did not react to a Beilstein test.

The red benzene mother solution was chromatographed again on alumina. II (0.3 g.) was recovered from the first fraction. The second and third fractions, upon evaporation, left a yellow solid which was recrystallized from ethanol to yield 0.05 g. of 2,7-dibromofluorenone, m. p. 200~202°C;

* All melting points are uncorrected.

(reported[5] m. p. 202~203°C). (Found : Br, 47.33. Calcd. for $C_{13}H_6OBr_2$: Br, 47.28%; IR ; 1714 cm^{-1} (ν C=O) (KBr-disk). This compound was identified by the melting point and the mixed melting point determination and by comparing its infrared absorption spectrum with that of an authentic sample of 2, 7-dibromofluorenone.

The Reaction of 2'-Bromotribiphenylenepropane (I) in a Pyridine-Potassium Hydroxide Solution.—A mixture of 3.0 g. of I and 3 ml. of a 10% aqueous solution of potassium hydroxide in 30 ml. of pyridine was refluxed for 40 hr., giving a dark red solution. The reaction mixture was then poured into water to yield an orange-red precipitate. The work-up of the products by column chromatography (benzene), sublimation and recrystallization gave fluorene (m. p. 114°C, 0.095 g.), fluorenone (m. p. 83°C, 0.04 g.), 2-bromofluorenone (m. p. 143~145°C, 0.2 g.), II (m. p. 187°C, 0.05 g.), IV (m. p. 150~152°C, trace) and the recovered starting material (1.65 g.). All compounds were identified by mixed melting point. These results are presented in Table II.

The Synthesis of 2'-Bromotribiphenylenepropane (I).—1) *n*-Butyl lithium was prepared from 2.0 g. (0.015 mol.) of *n*-butyl bromide in 20 ml. of anhydrous ether and 0.2 g. (0.03 g. atom) of lithium in 20 ml. of anhydrous ether. Then, 2-bromo-9-fluorenyl lithium was prepared by adding 2.9 g. (0.012 mol.) of 2-bromofluorene in 30 ml. of anhydrous xylene to the *n*-butyl lithium solution. Into this mixture there was added slowly with stirring a solution of anhydrous xylene containing 4.9 g. of 9-bromodipiphenyleneethane. After the reaction mixture had stood at room temperature overnight, the precipitate was filtered and then hydrolyzed with dilute ammonium chloride and recrystallized from benzene to give 2.4 g. of I (m. p. 257°C, decomp.; 41.3% (Balance yield); identical by mixed melting point and infrared absorption spectra with the authentic sample).

In addition, 0.6 g. of 9-hydroxydibiphenyleneethane[6] (m. p. 191~193°C) and 0.2 g. of dibiphenyleneethylene (m. p. 187°C) were isolated by chromatography in benzene on alumina.

2) I was obtained by the reaction of 9-fluorenyl lithium with 2', 9-dibromodibiphenyleneethane in a 42.6% yield.

3) A solution of 0.015 mol. of *n*-butyl lithium in 20 ml. of ether was added to a solution of 4.1 g. (0.01 mol.) of 9-bromodibiphenyleneethane in 30 ml. of xylene under the same conditions as in the first method. The wine-red color turned to brown-red, and a yellowish brown precipitate was formed. To this resulting solution there was added 10 ml. of anhydrous xylene containing 3.2 g. (0.01 mol.) of 2, 9-dibromofluorene.

The product was filtered off, hydrolyzed, and then recrystallized from benzene to give I (m. p. 257°C, decomp.; 0.6 g., 26.1%). This propane was identical with the authentic sample of I as shown by mixed melting point determination and infrared absorption spectrum. The xylene mother solution was evaporated to dryness under reduced pressure, and 2, 9-dibromofluorene (1.2 g.) was recovered by chromatography in benzene on alumina.

4) I was also obtained in a 4.0% yield by the reaction between 2'-bromo-9-lithiodibiphenyleneethane and 9-bromofluorene.

The authors wish to express their gratitude to Drs. John and Elizabeth Weisburger of the National Institute of Health, U.S.A., for valuable information, and to Dr. Shôji Kajigaeshi of Kyushu University, Mr. Shigeto Nakagawa and Mr. Masanori Shigehara for their assistance.

Department of Industrial Chemistry
Faculty of Engineeing
Utsunomiya University
Ishii-cho, Utsunomiya (K. S.)

Department of Industrial Chemistry
Faculty of Engineering
Yamaguchi University
Tokiwadai, Ube (M. F.)

5) J. Schmidt and K. Bauer, *Ber.*, **38**, 3737 (1905).

6) This compound might arise from the hydrolysis of 9-bromodibiphenyleneethane as a result of the effect of alumina.

Some Properties of Polyoxyethylene Dodecyl Ether over a Wide Range of Polyoxyethylene Chain-lengths

By Fumikatsu TOKIWA

(Received June 16, 1964)

There have been a number of studies of the properties of polyoxyethylated non-ionic surfactants in relation to their polyoxyethylene chain-lengths. Most of these studies have, however, been limited to the non-ionic surfactants with relatively short polyoxyethylene chains; little attention has been paid to the surfactants with considerably long polyoxyethylene chains. Their properties depend to a large extent on the average number of oxyethylene units present. It is, therefore, desirable to have data for non-ionic surfactants over a wide range of the chain-lengths of polyoxyethylene in order better to understand the effect of chain-length on their properties.

The author[1,2] has previously shown the relationship between the properties of polyoxyethylene dodecyl ether, such as its micellar molecular weight, its solubilization and its viscosity, and its polyoxyethylene chain-lengths above the critical micelle concentration.

The present paper will deal with the purification of a non-ionic surfactant, including the determination of its molecular weight, and chromatographic and infrared spectral studies, from short up to quite long polyoxyethylene chains. It is always of importance, when one studies the properties of a polyoxyethylated non-ionic surfactant, to purify the sample, i. e., to remove polyethylene glycol, a by-product of the addition reaction, from the sample. In addition, this paper will deal with the surface tension of aqueous solutions and with the solubilization of oil-soluble dye, on the basis of which the variation in critical micelle concentration with polyoxyethylene chain-length will be discussed.

Experimental

Materials.—Polyoxyethylene dodecyl ethers (abbreviated to PODE), $C_{12}H_{25}O(CH_2CH_2O)_pH$, were prepared from dodecyl alcohol of a high purity. The average degrees of the polymerization of ethylene oxide, p, in these samples are listed in Table I. The purification of the samples and the determination of their molecular weights were carried out as will be described below. Polyethylene glycol (abbreviated to PEG), the molecular weight of which was approximately 4000, was obtained from the Carbide and Carbon Chemicals Co.

The Purification of PODE.—The purification of the samples was carried out by the extraction method by countercurrent partition,[3] using water-saturated *n*-butanol and *n*-butanol-saturated water, in order to remove PEG, a by-product of the reaction.

The purification by liquid chromatography was also attempted for this purpose by using alumina (200 mesh powder for chromatographic analysis) as an adsorbent. Two different solvent systems were used, one a mixture of *n*-butanol and water, the other acetone alone. However, the former was somewhat disadvantageous in the sense that it affords only a small amount of purified sample at one time, and the latter was not satisfactory. Thus, the attempt at purification by liquid chromatography was abandoned.

It was confirmed, by testing through paper chromatography, that the samples purified by the extraction method contained no detectable free PEG. The development was carried out by applying a mixture of *n*-butanol, acetone and water (4 : 1 : 5 by volume[4]). The evaporation of the developer was followed by visualization in the Dragendorff reagent.

The Determination of Molecular Weights.—The molecular weights of PODE were determined by the freezing point depression of their benzene solutions by means of the Beckman method with the usual precautions. The molecular weights were also determined by the anhydrous acetic acid-pyridine method, which is commonly used for measuring hydroxyl values.

Infrared Absorption Spectra.—Infrared measurements were performed on a Shimadzu Type IR-27 spectrometer using a sodium chloride prism. The infrared spectra of PODE were recorded in a liquid or solid state, the PODE with a longer polyoxyethylene chain being solid.

Surface Tension.—Surface tensions were measured by the drop weight method with a tip 5.03 mm. in diameter in a thermostat of 30 ± 0.1°C. The observed values were corrected by using the correction factor of Harkins and Brown. The duration time after the formation of a drop was 0.5～5.0 min., depending on the concentration of the solutions. Under these conditions there was no appreciable change in the surface tension.

Solubilization. — Yellow-OB, an oil-soluble dye used as a solubilizate, was purified by repeated

1) F. Tokiwa, This Bulletin, **35**, 1737 (1962).
2) F. Tokiwa, ibid., **36**, 222 (1963).
3) K. Nagase and K. Sakaguchi, *J. Chem. Soc. Japan, Ind. Chem. Sec.* (*Kogyo Kagaku Zasshi*), **64**, 635 (1961).
4) K. Hattori and K. Konishi, ibid., **64**, 1195 (1961).

recrystallization from an ethanol-water mixture. Solubilizations were run in a water bath at a constant temperature of 30±0.1°C for 24 hr. to attain equilibrium, the method described in a previous paper[2] being employed. The amounts of solubilized dyes were determined by optical density measurements using a spectrophotometer, Shimadzu model B-60.

Results and Discussion

Molecular Weights and R_f-Values.—In Table I the molecular weights of the original PODE, obtained from the gain in weight by the addition of ethyhlene oxide, are compared with those of the purified PODE estimated from the freezing-point depressions and the terminal hydroxyl values.* Essentially, the molecular weights obtained from the freezing-point depressions should be equal to those obtained from the hydroxyl values, since both of these molecular weights are number-average molecular weights. The values shown in Table I indicate that they are nearly in agreement with each other and, at the same time, verify that PODE molecules do not form micelles in benzene over a considerably wide range of polyoxyethylene chain-lengths.

The variation in R_f-value with the polyoxyethylene chain-length, i. e., the value of p, is show in Fig. 1-a for the purified PODE and the original PODE containing a small amount of PEG (approximately 5%). Figure 1-b also illustrates the variation in R_f-value with the HLB-value for these samples. The R_f-values decrease with increasing values values of p or HLB. The values of purified PODE are slightly higher than those of the original PODE. On the other hand, the R_f-value of the PEG contained in original PODE seems

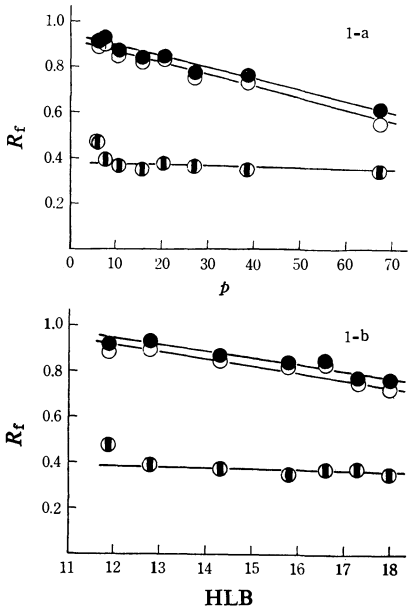


Fig. 1. Relationship between the R_f-value and the p-value (1-a) or the HLB-value (1-b) for purified (●) and original PODE (○), and PEG (◐).

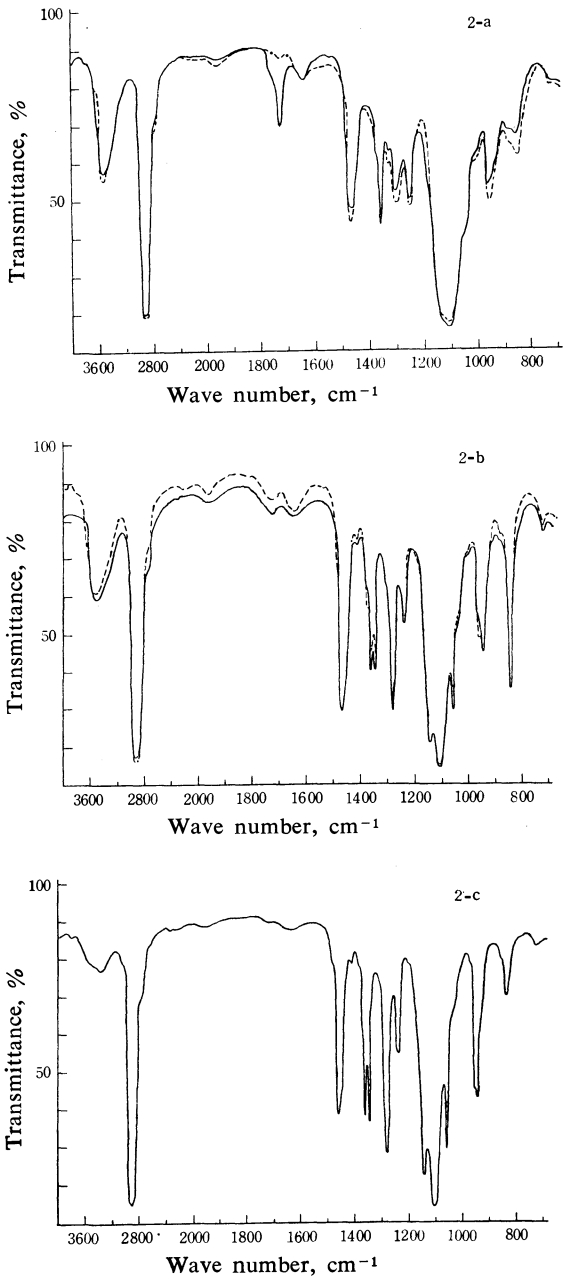


Fig. 2. Infrared spectra of purified (solid curve) and original PODE (dashed curve) for p=10.6 (2-a) and p=20.4 (2-b), and PEG (2-c).

* The hydroxyl value is the number of milligrams of potassium hydroxide equivalent to the hydroxyl content of a one gram sample.

TABLE I. MOLECULAR WEIGHTS AND CRITICAL MICELLE CONCENTRATION OF PODE AS A FUNCTION OF POLYOXYETHYLENE CHAIN-LENGTH

Sample[a)]	Molecular weight		CMC (mol./l. $\times 10^4$)	
	from freezing pt. depresion	from hydroxyl value	from surface tension	from solubilization
PODE- 6.2	640 ($\bar{p}$= 6.2)	468 ($\bar{p}$= 6.4)	—	0.8
PODE- 7.6	501 (= 7.2)	510 (= 7.4)	2.0~3.2	0.9
PODE-10.6	645 (=10.4)	625 (=10.0)	—	1.2
PODE-15.8	870 (=15.5)	857 (=15.2)	2.0~3.5	1.8
PODE-20.4	1070 (=20.0)	1110 (=21.0)	—	2.1
PODE-27.1	1330 (=26.0)	1380 (=27.1)	3.0~4.5	2.5
PODE-38.6	1810 (=37.0)	1790 (=36.5)	4.0~6.0	3.6
PODE-67.3	—	—	—	5.7

a) The numbers listed after PODE represent the average numbers of oxyethylene units per molecule, which were obtained from the gain in weight by the addition of ethylene oxide.

to be nearly independent of the value of p or HLB.

Infrared Spectra and Surface Tension. — The infrared spectra of purified PODE are compared with those of original PODE. Some of these spectra are shown in Fig. 2, together with the spectrum of PEG. The spectra of the purified samples are identical with those of the original samples except for one absorption band. With purified PODE, a relatively strong absorption appeared at 1725 cm^{-1} up to the PODE value of p=15.8, as may be seen in Fig. 2-a. However, the original PODE and the purified PODE with p-values larger than 20.4 either showed no appreciable absorption at all or had a very weak absorption at 1725 cm^{-1}.

All the absorptions in the region of the frequencies lower than 1500 cm^{-1} have already been assigned by Davison.[5)] The absorption at 1725 cm^{-1} suggests the presence of carbonyl groups in the molecule of purified PODE, since carbonyl absorption is commonly observed around this frequency.[6,7)] The ether bonding in polyoxyalkylene compounds is known to be not very stable in the presence of heating, light, oxidizing agents, and so on.[8-11)] It is possible, therefore, to assume that a certain change occurs through autoxidation[9,10,12,13)] at the ether bonding in the PODE molecule during the course of purification, thus forming carbonyl group in the molecule, whatever the detailed mechanism is. Nemoto[13)] has suggested that the ether bonding of polyoxyethylated non-ionic surfactants is attacked by autoxidation.

Carbonyl absorptions will arise from the -COOH, -COOR, -CHO and >CO groups. If the above assumption is right, there is a possibility of finding one or more of these groups in the purified PODE. In fact, the acid values and the ester values** of all the PODE showing carbonyl absorptions were found to have a range of 10~14 and 11~16 respectively; these values are considered to be rather smaller than those expected from the intensity of the absorption observed. Qualitative tests with 2, 4-dinitrophenyl hydrazine[14)] and benzidine showed the presence of a trace of carbonyl groups, suggesting that the samples contain aldehyde and/or ketone groups. Thus, the reason why such a remarkable absorption appeared at 1725 cm^{-1} with purified PODE could be explained partially by the above data. However, the reason why this absorption was observed exclusively in the case of the PODE with p values smaller than 15.8 is not explainable clearly. Research is continuing to learn more about this problem.

The surface tensions of aqueous solutions of (a) original and (b) purified PODE and (c) the purified PODE to which 5% of PEG had been added to make the sample original were measured for the purpose of learning the effect of the carbonyl group, which was found in purified PODE, on the surface activity. Typical surface tension vs. concentration curves are shown in Fig. 3. The surface tension of PODE solutions is characterized by a sharp initial decrease, followed by a gradual flattening. The inflection of the curve corresponds

5) W. H. T. Davison, *J. Chem. Soc.*, **1955**, 3270.
6) L. J. Bellamy, "The Infra-Red Spectra of Complex Molecules," Methuen, London (1958), p. 132.
7) G. Delzenne and G. Smets, *Makromol. Chem.*, **18/19**, 82 (1956).
8) C. E. Schweitzer, R. N. MacDonald and J. O. Punderson, *J. Applied Polymer Sci.*, **1**, 158 (1959).
9) S. L. Madolsky and S. Strauss, *J. Polymer Sci.*, **36**, 183 (1959).
10) C. W. McGray, Jr., ibid., **46**, 51 (1960).
11) L. E. St. Pierre and C. C. Price, *J. Am. Chem. Soc.*, **78**, 3432 (1956).
12) W. G. Lloyd, ibid., **78**, 72 (1956).
13) Y. Nemoto and T. Imai, *J. Chem. Soc. Japan, Ind. Chem. Sec.* (*Kogyo Kagaku Zassi*), **62**, 483 (1959).

** The definition of these values is similar to that of the hydroxyl value described already.
14) O. L. Brady, *J. Chem. Soc.*, **1931**, 756.

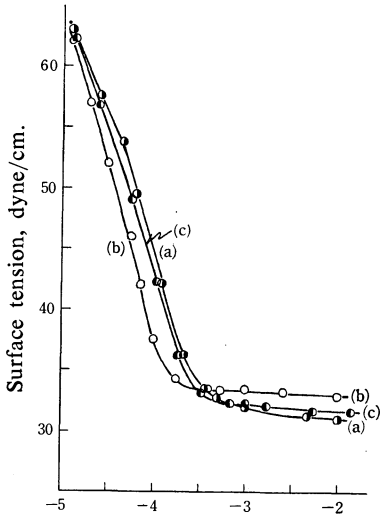


Fig. 3. Surface tension vs. concentration curves of aqueous solutions of PODE with $p=7.6$ at 30°C; (a) original PODE, (b) purified PODE and (c) the purified PODE to which 5% PEG was added.

to the critical micelle concentration (CMC); it is not so sharp as that of the ionic surfactant because of the distribution of the molecular weights of PODE.

With the PODE with a p value of 7.6, curve c is more similar to curve a than to curve b, as may be seen in Fig. 3. This indicates that PEG has a tendency to make the surface tension higher below the CMC. However, no significant difference in surface tension among the curves of a, b and c could be observed. It could be considered, therefore, that the carbonyl group found in the purified sample by infrared absorption influences the surface activity not very strongly.

The Critical Micelle Concentration.—Figure 4 illustrates the solubilization curves, in which the amounts of solubilized dye are plotted against the concentrations of PODE. The solubilization behavior of PODE is somewhat different from that commonly observed for ionic surfactants. With ionic surfactants, scarcely any solubilization takes place until the concentration of surfactant reaches the CMC,[16] while in the case of PODE the amounts of dye solubilized increase gradually with the increasing concentration, even below the CMC. This may be explained by the following. The sample of PODE has a certain distribution of molecular weights, and some

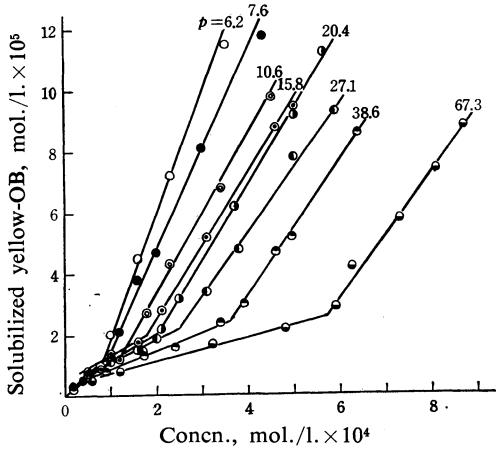


Fig. 4. Solubilization of yellow-OB vs. concentration of PODE curves at 30°C.

solubilization can take place in the region of the surfactant concentration which is lower than the CMC. A much more complicated micellar equilibrium, but which is fundamentally of the same type, appears to occur in non-ionic surfactant solutions.

Solubilization is generally regarded as an effect which begins to be noticeable at the CMC. The break point in the solubilization vs. concentration curve corresponds to the CMC. Table I shows the CMC values of PODE in relation to the chain-length of polyoxyethylene; they increase with the increase in the values of p. The CMC's obtained from the solubilization were relatively sharp as compared with those obtained from the surface tension. The CMC values of PODE are of an order of 10^{-4} mol., in agreement with the results of other investigations of polyoxyethylated surfactants.[17,18]

Concerning the relationship between the CMC value and the polyoxyethylene chain-length, Nakagawa and Kuriyama have already proposed a theory,[19] which is satisfactorily comparable with experimental results over a relatively limited range of chain-lengths, using methoxy polyoxyethylene decyl and dodecyl ethers.[17] Hsiao et al.[18] have also reported that, with aqueous solutions of Igepals (condensate products of alkyl phenol with ethylene oxide), the rate of increase in CMC values is given by the expression:

$$\ln (\mathrm{CMC}) = k + aR$$

where a and k are constants, and where R

15) E. Funakubo, "Identification of Organic Compounds," Yoken-do, Tokyo (1954), p. 326.
16) M. E. L. McBain and E. Hutchinson, "Solubilization," Academic Press, New York (1955), p. 45.
17) T. Nakagawa, K. Kuriyama and K. Tori, *J. Chem. Soc. Japan, Pure Chem. Sec. (Nippon Kagaku Zassi)*, **78**, 1573 (1957).
18) L. Hsiao, H. N. Dunning and P. B. Lorenz, *J. Phys. Chem.*, **60**, 657 (1956).
19) T. Nakagawa and K. Kuriyama, *J. Chem. Soc. Japan, Pure Chem. Sec. (Nippon Kagaku Zassi)*, **78**, 1568 (1957).

represents the mole ratio of oxyethylene to phenol.

According to Hsiao et al., the logarithm of the CMC value given in Table I was plotted as a function of the polyoxyethylene chain-length, as is shown in Fig. 5-a. Such a straight line as he obtained was not obtained in the present experiment. However, if the ordinate is expressed on an ordinary scale, as is illustrated in Fig. 5-b, the relation between the CMC and p value seems to be rather linear; it can be written by:

$$\mathrm{CMC} = (0.30 + 0.083p) \times 10^{-4}$$

This equation indicates that the effect of the oxyethylene unit in the hydrophilic chain on the CMC value is not so marked as that of the methylene unit in the hydrophobic chain. It was reported that the CMC value is approximately doubled by decreasing the number of methylene groups in the hydrophobic chain by one.[15] This is in interesting contrast to the solubility phenomena, where an oxyethylene unit is equivalent to one methylene unit.[20]

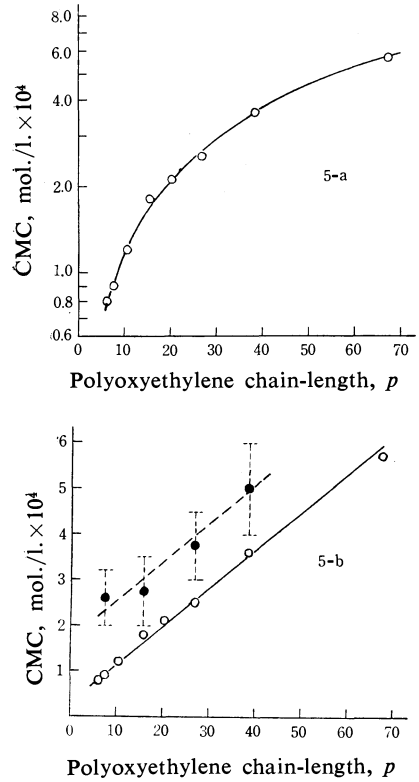


Fig. 5. The relationship between critical micelle concentration and polyoxyethylene chain-length; the ordinate is expressed in a logarithmic scale (5-a) and in decimal scale (5-b) (the dotted line represents the data from surface-tension measurements).

Summary

The fundamental properties of polyoxyethylene dodecyl ether (PODE) with different polyoxyethylene chain-lengths (p) have been studied over a wide range of p values. The molecular weights of the PODE, purified by the extraction method using water-saturated *n*-butanol and *n*-butanol-saturated water, have been determined by both the freezing point depressions of benzene solutions and the hydroxyl values of PODE; the molecular weights as determined by the different methods are in nearly complete agreement with each other. The R_f-values of the original samples containing small amounts of PEG are slightly lower than those of the purified samples, and the PEG contained in original samples show an almost constant R_f-value, irrespective of the p value.

The infrared spectra of purified PODE have been compared with those of the original ones. The spectra of the purified PODE with p-values smaller than about 16 exhibited a carbonyl absorption at 1725 cm^{-1}. However, the reason for this could be established only partially. The effect of the carbonyl group found in the above PODE on the surface tension of aqueous solutions was not observed distinctly.

The solubilization behavior of PODE differs somewhat from the behavior of ordinary ionic surfactants, and some solubilization can take place in the region of the surfactant concentration which is lower than the CMC. There appears to be a simple relationship between the CMC values, obtained from solubilization vs. concentration curves, and the p values of PODE over a wide range of p values.

The author wishes to express his hearty thanks to Professor Toshizo Isemura of Osaka University for his kind advice. He also wishes to express his appreciation to Mr. Zen'ichi Miyagawa, Director of this Laboratory, for the permission to publish this paper, and to Dr. Iwao Maruta for his encouragement.

Kao-Atlas Labortory
Kao Soap Co., Ltd.
Wakayama

20) M. N. Fineman, G. L. Brown and R. J. Myers, *J. Phys. Chem.*, **56**, 963 (1952).

The Conversion of (−)-α-Santonin into (−)-β-Santonin

By Masao NAKAZAKI and Koichiro NAEMURA

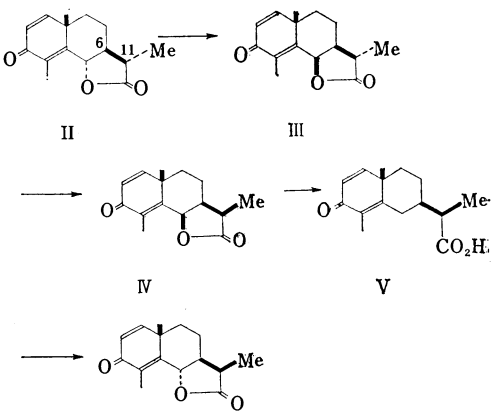
(Received June 16, 1964)

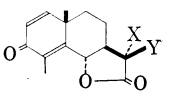
(−)-β-Santonin (I), together with (−)-α-santonin (II), was isolated by Clemo from samples of *Artemisia* obtained from the North-West Frontier of India[1] and was shown to be the C_{11} epimer of (−)-α-santonin by various chemical correlations.[2] Recently, Cocker and McMurry[3] converted (−)-β-santonin into (−)-α-santonin by boiling it with potassium carbonate in a xylene solution, but the reverse transformation has not yet been accomplished.

Since we happened to need a quantity of (−)-β-santonin for a stereochemical study of eudesmane-type sesquiterpene, we have tried to convert (−)-α-santonin into difficult-to-obtain (−)-β-santonin. In this communication we will report a successful attempt to effect this transformation.

Thermodynamical stability of the C_{11} methyl group is affected very subtly by the modes of the lactone-ring junctures of the santonin series of compounds. When both the C_{10} angular methyl group and the C_7 side chain have β-configurations,[4,5] the α-configuration is the choice for the stable configuration of the C_{11} methyl group in the *trans*-lactone, as can be seen from the above-mentioned work of Cocker and McMurry.[6] However, in the *cis*-lactone the situation is completely reversed; β-configuration is now favored by the C_{11} methyl group. These stereochemical relations were dramatically demonstrated by the stereospecific decarboxylations[7,8] of the epimeric pair of the lactone-acids, VIa and VIb, with *trans*-lactone junctures and the epimeric pair of the *cis*-lactone acids, VIIa and VIIb, with *cis*-lactone junctures; the former gave racemic α-santonin (II) exclusively, and the latter yielded racemic 6-epi-β-santonin (IV). Barton and his co-workers[9] made use of these experimental facts when they treated (−)-6-epi-α-santonin (III) derived from (−)-α-santonin following Ishikawa's procedure,[10] with potassium *t*-butoxide to obtain (−)-6-epi-β-santonin (IV), which is eventually our starting material.

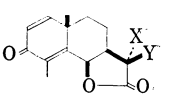
The reductive cleavage of the *cis*-lactone





VIa X=CO_2H, Y=Me

b X=Me, Y=CO_2H



VIIa X=CO_2H, Y=Me

b X=Me, Y=CO_2H

1) G. R. Clemo, *J. Chem. Soc.*, **1934**, 1343. Kawatani also isolated (−)-β-santonin from various samples of *Artemisia* indigenous to Manchuria. T. Kawatani, *J. Pharm. Soc. Japan*, **73**, 783 (1953); T. Kawatani and T. Takeuchi, ibid., **74**, 793 (1954).

2) Summerized in J. Simonsen and D. H. R. Barton, "The Terpenes," Vol. III, Cambridge Univ. Press (1952), p. 320.

3) W. Cocker and T. B. H. McMurry, *J. Chem. Soc.*, **1955**, 4430.

4) All configurations in this paper are depicted in absolute sense. Cf. M. Nakazaki and H. Arakawa, *Proc. Chem. Soc.*, **1962**, 151; This Bulletin, **37**, 464 (1964); M. Nakazaki and K. Ikematsu, ibid., **35**, 1904 (1962); **37**, 459 (1964).

5) According to the steroid convention, L. F. Fieser and M. Fieser, "Steroids," Reinhold Pub. Corp., New York (1959).

6) Unfortunately Cocker and co-workers interpreted this fact wrongly and assumed that (−)-α-santonin has β-configuration at the asymmetric center. (W. Cocker and T. B. H. McMurry, *Tetrahedron*, **8**, 181 (1960)). Assuming that this *trans*-lactones of santonin series are isosteric with the C/D rings of steroids, Miki (T. Miki, *J. Pharm. Soc. Japan*, **75**, 416 (1955)) correctly deduced the α-configuration at this center, which was eventually proved by the Prelog's method. (Y. Abe, T. Miki, M. Sumi and T. Toga, *Chem. & Ind.*, **1956**, 953. Cf. Ref. 4.).

7) H. Ishikawa, *J. Pharm. Soc. Japan*, **76**, 500 (1956). He used the racemic compounds, but the ones with natural configurations are shown in VI and VII.

8) For these stereospecific reactions, the presence of the dienone structure is not necessarily requisite. M. Nishikawa, H. Hagiwara and K. Morita, ibid., **78**, 134 (1958).

9) D. H. R. Barton, J. E. D. Levisalles and J. T. Pinhey, *J. Chem. Soc.*, **1962**, 3472. To confirm the structure IV, IV was converted to (−)-β-desmotroposantonin. See Experimental section.

10) H. Ishikawa, *J. Pharm. Soc. Japan*, **76**, 504 (1956).

ring of IV with zinc powder afforded (−)-3-oxo-11-epi-eusantona-1,4-dienic acid (V),[11,12] b. p. 160～180°C/10^{-3} mmHg, $[\alpha]_D$ −107°.

The last of the synthetic sequence was achieved by selenium dioxide oxidation,[13] which has been shown to provide *trans*-lactone stereospecifically and which was successfully applied to the elegant total synthesis of (−)-α-santonin by the Takeda group.[14] This last operation afforded a 10% yield of (−)-β-santonin (I), m. p. 211～212°C, $[\alpha]_D$ −133° (in chloroform), the identity of which was established by mixed melting point determination and by a comparison of the infrared spectrum with an authentic sample of natural (−)-β-santonin,[15] as well as by the conversion into (−)-β-desmotroposantonin.

Experimental

(−)-6-Epi-α-santonin (III).—(−)-α-Santonin (II) was epimerized at C_6 according to the procedure of Ishikawa,[10] affording (−)-6-epi-α-santonin, m. p. 102～105°C, $[\alpha]_D^{10}$ −311° (*c* 1.5, ethanol); yield, 60%.

(−)-6-Epi-β-santonin (IV).—The epimerization of (−)-6-epi-α-santonin (III) at C_{11} was achieved following Barton's procedure.[9] Since the purification of III was accompanied by a considerable loss, the intermediate III was not purified but was directly converted into IV, m. p. 185～186°C, $[\alpha]_D^{10}$ −309° (*c* 0.56, ethanol), yield, 42% from (−)-α-santonin.

The Isomerization to (−)-β-Desmotroposantonin.—A solution of 0.1 g. of (−)-6-epi-β-santonin (IV) in 10 cc. of 55% sulfuric acid was kept at 55°C for 15 hr. Dilution with water precipitated crystals which were recrystallized from methanol to give needles, m. p. 250～252°C, $[\alpha]_D^{18}$ −115° (*c* 0.42, ethanol). A mixture of an equal amount of this (−)-β-desmotroposantonin with (+)-β-desmotroposantonin[2] was recrystallized from ethanol to yield racemic β-desmotroposantonin, m. p. 225～231°C.[2]

(−)-3-Oxo-11-epi-eusantona-1,4-dienic Acid (V).—To a solution of 3.6 g. of (−)-6-epi-β-santonin (IV) in 80 cc. of methanol, 8 g. of zinc powder was added. After 4 cc. of acetic acid had then been added, the reaction mixture was refluxed on a water bath for 8 min., cooled, and filtered. The solution was concentrated in vacuo to half volume and extracted with ether. After being washed with water, the ether solution was extracted with 10% aqueous sodium carbonate. The aqueous layer was made acidic with 2 N hydrochloric acid and extracted with benzene. The benzene extracts were combined, washed with water and a saturated sodium chlorine solution, and then dried over anhydrous magnesium sulfate. When the solvent was removed in vacuo, the residue ($[\alpha]_D^{13}$ −102° (*c* 3.0, ethanol)) was obtained; this was purified by chromatography on 80 g. of silica gel to yield 3.0 g. of a viscous oil. Distillation afforded a pale yellow liquid, b. p. 160～180°C (bath temperature)/10^{-3} mmHg, $[\alpha]_D^{24}$ −107° (*c* 3.8, ethanol). An ultraviolet spectrum in ethanol indicated a peak at 240 mμ (log ε 4.03).

Found: C, 71.25; H, 8.30. Calcd. for $C_{15}H_{20}O_3$: C, 72.55; H, 8.12%.

Cyclohexylamine Salt.—The salt was recrystallized from ethyl acetate to yield needles, m. p. 173～174°C, $[\alpha]_D^{24}$ −54.7° (*c* 0.7, ethanol).

Found: C, 72.30; H, 9.44; N, 4.01. Calcd. for $C_{21}H_{33}O_3N$: C, 72.58; H, 9.57; N, 4.03%.

2,4-Dinitrophenylhydrazone.—The 2,4-dinitrophenylhydrazone was prepared by the usual procedure and recrystallized from ethanol to give red needles, m. p. 216～218°C.

Found: N, 13.26. Calcd. for $C_{21}H_{24}O_6N_4$: N, 13.08%.

(−)-β-Santonin (I).—A mixture of 1.1 g. of the acid V, 1.1 g. of selenium dioxide, 22 cc. of acetic acid and 0.4 cc. of water was refluxed for 6 hr. The solution, freed from the selenium which precipitated, was then concentrated in vacuo, and the residue was extracted with benzene. The benzene extract was washed with water, 5% aqueous sodium carbonate, and water successively, and dried over anhydrous sodium sulfate. When the solution was concentrated, a crystalline solid separated. The product was filtered and recrystallized from methanol to give 0.1 g. of crystals, m. p. 211～212°C, $[\alpha]_D^{24}$ −133° (*c* 0.46, chloroform). A mixed melting point determination with an authentic (−)-β-santonin gave no depression. The identity was further confirmed by the infrared spectra of the synthetic and natural product, which were indistinguishable.

Found: C, 73.04; H, 7.44. Calcd. for $C_{15}H_{18}O_3$: C, 73.14; H, 7.37%.

The Isomerization to (−)-β-Desmotroposantonin.—A solution of 50 mg. of the synthetic (−)-β-santonin (I) in 2 cc. of 55% sulfuric acid was kept at 55°C for 15 hr. The crystals, which were deposited upon the addition of water were recrystallized from methanol to give needles, m. p. 251～253°C. The mixed melting point with (−)-β-desmotroposantonin obtained from (−)-6-epi-β-santonin (vide supra) was 250～252°C.

Found: C, 72.66; H, 7.52. Calcd. for $C_{15}H_{18}O_3$: C, 73.14; H, 7.37%.

We are much indebted to the Nitto Kasei Co. for its financial support and to Dr. Toyohiko Kawatani, The National Hygienic Laboratory, Tokyo, for his generous gift of natural (−)-β-santonin. This work was partially supported by a grant-in-aid for fundamental scientific research from the Ministry of Education, to which the authors' thanks are due.

Department of Chemistry
Faculty of Engineering Science
Osaka University
Kita-Toneyama, Toyonaka

11) For the nomenclature, see Ref. 14.
12) The racemic compound, m. p. 147°C was prepared from racemic 6-epi-β-santonin "santonin D". T. Miki, *J. Pharm. Soc. Japan*, **75**, 412 (1955).
13) T. Miki, ibid., **75**, 407 (1955).
14) Y. Abe, T. Harukawa, H. Ishikawa, T. Miki, M. Sumi and T. Toga, *J. Am. Chem. Soc.*, **78**, 1422 (1956).
15) Generously supplied by Dr. Toyohiko Kawatani, National Hygienic Laboratory, Tokyo.

*Carbonyl Absorption Bands in the Infrared Spectra of Some Cyclic Imides with a Five-membered Ring**

By Taku MATSUO

(Received June 18, 1964)

Organic acid anhydrides always show two characteristic absorption bands in the 1750~1850 cm^{-1} region of their infrared spectra. It was originally suggested that these two bands come from a mechanical coupling of the two carbonyl groups in acid anhydrides.[1] Bellamy and his coworkers observed a parallel correlation between the variations in the frequencies of the two absorption bands of acid anhydrides in many solvents with widely different polarities, and concluded that both bands could be assigned to carbonyl absorptions.[2] Since the relative intensity of the higher frequency absorption band decreases as the acid anhydride forms a closed ring, Dauben and Epstein,[3] as well as Bellamy et al.,[2] considered the higher and the lower frequency absorptions to be due to the in-phase and out-of-phase vibrations respectively of the two carbonyl groups.

Many cyclic imides[4] are also known to have two characteristic absorption bands similar to the split carbonyl absorption bands of acid anhydrides described above. The carbonyl groups of both acid anhydride and cyclic imide are characterized by a structure, O=C–X–C=O where X is an atom carrying lone-pair electrons. Mirone and Chiorboli suggested, in their study of the vibrational spectra of maleic anhydride,[5] that the splitting of the carbonyl absorption is mainly due to the electronic stabilization of the out-of-phase vibration through a contribution of the ionic structures, $O^-–C=O^+–C=O$ and $O=C–O^+=C–O^-$. A quite analogous situation would be expected for derivatives of cyclic imide where two carbonyl groups are connected by a nitrogen atom. The nature of one substituent, R, on the imide group would determine the relative importance of the ionic structures, $O^-–C=\underset{\displaystyle R}{N^+}–C=O$ and $O=C–\underset{\displaystyle R}{N^+}=C–O^-$. Therefore, the extent of the splitting of the carbonyl absorptions is expected to be different when the infrared spectra of a series of *N*-substituted cyclic imides are compared. The infrared spectra of *N*-substituted derivatives of maleimide, phthalimide and succinimide will be examined and their carbonyl absorption bands compared in this paper.

Experimental

Phthalimide was purchased from Wako Pure Chemical Industries, Ltd., and was used after repeated recrystallizations from ethanol. *N*-Methylphthalimide was prepared from potassium phthalimide and methyliodide by a conventional method. Smith and Emerson's method[6] was used to synthesize *N*-*t*-butylphthalimide. *N*-Cyclohexyl-, *N*-benzyl- and *N*-(substituted phenyl)-phthalimides were prepared by the dehydration of the corresponding phthalamic acids by heating them above 200°C. The products were treated with activated charcoal in acetic acid and were purified by repeated recrystallizations from either methanol or benzene.

Maleimide was prepared from furan-maleic-anhydride adducts according to the procedure of Berson and Swidler.[7] *N*-Ethyl- and *N*-arylmaleimides were made from the corresponding maleamic acids through dehydration by the use of sodium acetate and acetic anhydride at 100°C. *N*-Cyclohexyl- and *N*-benzylmaleimides were prepared from (±)-malic acid and cyclohexlamine and benzylamine respectively.[8]

Succinimide was prepared by heating succinic anhydride with aqueous ammonia. All of the *N*-substituted succinimides were prepared by dehydrating the corresponding succinamic acids in a bath maintained between 200°C and 220°C.

The substituents on the nitrogen atom of the imides investigated and their melting points as measured on a Kofler micro-hot stage are listed below:

Phthalimides: hydrogen, 241; methyl, 136; *t*-butyl, 60; cyclohexyl, 174; benzyl, 118; phenyl, 212; *o*-tolyl, 185; *m*-tolyl, 174; *p*-tolyl, 209; *o*-methoxyphenyl, 158; *m*-methoxyphenyl, 126; *p*-methoxyphenyl, 164°C.

* Contribution No. 54 from the Department of Organic Synthesis, Faculty of Engineering, Kyushu University.

1) W. H. T. Davison, *J. Chem. Soc.*, **1951**, 2456.

2) L. J. Bellamy, B. R. Connelly, A. R. Philpotts and R. L. Williams, *Z. Elektrochem.*, **64**, 563 (1960).

3) W. G. Dauben and W. E. Epstein, *J. Org. Chem.*, **24**, 1595 (1959).

4) a) A. E. Kellie, D. G. O'Sullivan and P. W. Sadler, *J. Chem. Soc.*, **1956**, 3809;
b) R. A. Abramovitch, ibid., **1957**, 1413;
c) W. R. Roderick, *J. Am. Chem. Soc.*, **79**, 1710 (1957);
d) P. Bassignana, C. Cogrossi, G. P. Mattiot and M. Gillio-Tos, *Spectrochim. Acta*, **18**, 809 (1962).

5) P. Mirone and P. Chiorboli, ibid., **18**, 1425 (1962).

6) L. I. Smith and O. H. Emerson, "Organic Syntheses," Col. Vol. III, 152 (1955).

7) J. A. Berson and R. Swidler, *J. Am. Chem. Soc.*, **76**, 4066 (1954).

8) R. Lukes and M. Pergal, *Collection Czech. Chem. Commun.*, **27**, 1387 (1962); *Chem. Abstr.*, **57**, 7082f (1962).

Maleimides: hydrogen, 93; ethyl, 44; cyclohexyl, 89; benzyl, 70; phenyl, 90; *p*-tolyl, 155; *p*-methoxyphenyl, 155°C.

Succinimides: hydrogen, 125; benzyl, 104; phenyl, 158; *p*-tolyl, 157; *p*-methoxyphenyl, 166°C.

The infrared spectra were measured with a Nihon Bunko model DS 301 double-beam infrared spectrophotometer with sodium chloride optics. Benzene and acetonitrile were used as solvents. The spectra were obtained with the solution (of the order of $\sim 10^{-2}$ M) in closed cells 0.05, 0.1 or 1 mm. thick.

Experimental Results and Discussion

In general, the two carbonyl absorption bands can be easily identified in the infrared spectra of *N*-substituted phthalimides and succinimides. Typical examples are shown in Fig. 1 and Fig. 2 for *N*-methylphthalimide and *N*-benzylsuccinimide respectively. The higher frequency band with a low intensity is indicated by H, and the counterpart with a low intensity on the lower frequency side is denoted as the L band. *N*-Substituted maleimides, however, do

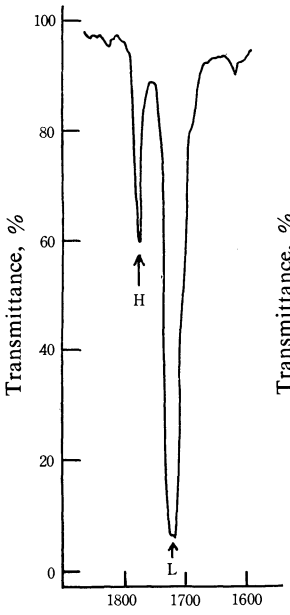


Fig. 1. Carbonyl absorption bands of *N*-methylphthalimide.

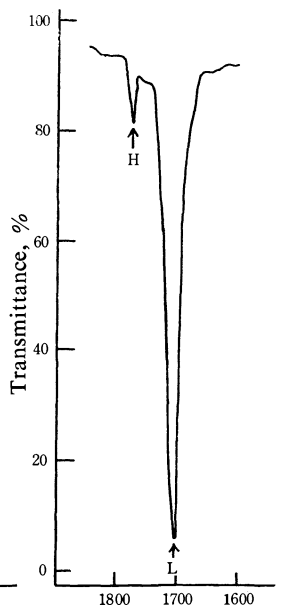


Fig. 2. Carbonyl absorption bands of *N*-benzylsuccinimide.

not show well-defined peaks to be assigned to the H bands in their spectra obtained in the solution. The higher frequency bands appear a little more clearly if the spectra are measured in solid states. Examples can be seen in the spectra of *N*-phenylmaleimide as shown in Fig. 3.

The carbonyl absorption bands, ν_H and ν_L, of the compounds investigated are summarized in Tables I, II and III.

For all types of imides studied, ν_L varies more sensitively than ν_H does upon the substitution on the nitrogen atom. The quotient,

Table I. Carbonyl absorption bands of *N*-substituted phthalimides

Substituent	Solvent[a]	ν_H[b] cm^{-1}	ν_L[c] cm^{-1}	Q[d] 10^{-4}
Hydrogen	B	1781	1747	0.96
Methyl	B	1778	1721	1.63
Methyl	A	1778	1722	1.60
t-Butyl	B	1780	1721	1.69
Cyclohexyl	A	1774	1715	1.69
Benzyl	A	1779	1725	1.54
Phenyl	A	1788	1721 1741	1.62[e]
Phenyl	B	1788	1721 1741	1.62[e]
p-Tolyl	A	1790	1727	1.79
p-Tolyl	B	1789	1727	1.76
m-Tolyl	A	1782	1732	1.42
m-Tolyl	B	1780	1731	1.40
o-Tolyl	A	1788	1731	1.62
o-Tolyl	B	1787	1729	1.65
p-Methoxyphenyl	A	1788	1722	1.88
p-Methoxyphenyl	B	1787	1722	1.85
m-Methoxyphenyl	A	1780	1729	1.45
m-Methoxyphenyl	B	1781	1730	1.45
o-Methoxyphenyl	A	1788	1728	1.71
o-Methoxyphenyl	B	1784	1724	1.71
Potassium	Nujol	1708	1619 1600 1585	3.2

a) A and B stand for acetonitrile and benzene respectively.
b) Frequency of the low-intensity band.
c) Frequency of the high-intensity band. The center of the band was taken as ν_L when the shape was rather broad.
d) $Q=(\nu_H-\nu_L)/(\nu_H+\nu_L)$.
e) Two strong bands were observed at the location of the L band. The intensity ratio of the two bands varies with the solvent. Therefore, the two bands were considered to be a doublet due to the Fermi resonance between the true L band and another band of unknown nature. The central position of the doublet was then used to calculate the value given here.

Table II. Carbonyl absorption bands of *N*-substituted succinimides

Substituent	Solvent	ν_H cm^{-1}	ν_L cm^{-1}	Q 10^{-4}
Hydrogen	A	1769	1728	1.17
Ethyl	A	1779	1708	2.04
Benzyl	A	1774	1705	1.99
Phenyl	A	1780	1715	1.86
p-Tolyl	A	1779	1715	1.83
p-Methoxyphenyl	A	1780	1715	1.86

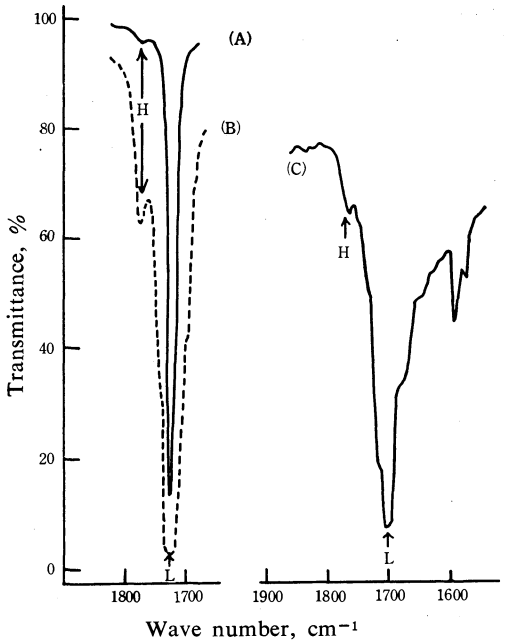


Fig. 3. Carbonyl absorption bands of *N*-phenylmaleimide.
(A) Acetonitrile solution (0.1 mm. thick).
(B) Acetonitrile solution (1 mm. thick).
(C) Solid (Nujol).

TABLE III. CARBONYL ABSORPTION BANDS OF *N*-SUBSTITUTED MALEIMIDES

Substituent	Solvent	ν_H cm^{-1}	ν_L cm^{-1}	Q 10^{-4}
Hydrogen	A	1770	1737	0.94
Ethyl	A	1772	1718	1.55
Cyclohexyl	A	1773	1711	1.78
Benzyl	A	1778	1718	1.73
Phenyl	A	1777	1727	1.43
p-Tolyl	A	1778	1725	1.51
p-Methoxyphenyl	A	1778	1727	1.45

$(\nu_H-\nu_L)/(\nu_H+\nu_L)$, or Q as given in the tables, was calculated from the data as a measure of the coupling of the carbonyl groups. The Q-values shown in the fifth columns of Tables I, II and III also appear to be dependent on the type of substituent on the nitrogen atom.

The effect of substitution on the nitrogen atom can be seen most clearly in the series of phthalimide derivatives. The substituents here can be classified into three groups depending on the type of atom directly attached to the imide group. Phthalimide, with a hydrogen atom at the nitrogen atom instead of the substituent, makes up the first group by itself. The values of ν_L and Q are the largest and the least respectively among the phthalimide series. The second group consists of compounds where substituents are attached to the imide group through the carbon atom of sp^3 hybridization. *N*-Alkyl- and *N*-benzylphthalimides belong to this group. Considerably lower ν_L-values are observed for the compounds of this group in comparison with that of phthalimide. The Q-values become larger in turn. In the third group, where the substituents are aromatic, ν_L and Q are close to those of the second group. A minor variation is observed when the phenyl group attached to the nitrogen atom has substituents of a different electronic nature.

Three factors are considered to be important in analyzing the effects of a substituent on the splitting of carbonyl absorptions summarized above;

(1) the effect of the mass of a substituent, R, on the vibrational mode of the absorption in question,
(2) the electronic factors which affect the π-electron system of imide the group, and
(3) the steric strain in the five-membered ring of the imide group.

The large difference between phthalimide and its *N*-substituted derivatives might be due to the first factor. Considering the little difference observed between the carbonyl absorption bands of *N*-methyl- and *N*-*t*-butylphthalimides, however, it seems reasonable to conclude that the effect of mass is almost negligible and that the vibrational mode is fairly well localized on carbonyl groups. Hydrogen bonding in phthalimide can not give the answer either, since the effect should be in the reverse direction.[9] The electronic factor, to be considered next, determines the extent of the contribution of the ionic structures, O^-–C=N^+(R)–C=O and O=C–N^+(R)=C–O^-, in the imide system. Other things being equal, an electron-donating substituent is preferred in stabilizing the ionic structures under discussion. The effect of this type could be best measured by the Hammet's sigma-values or other similar parameters representing the electronic character of a substituent. Then the extent of the stabilization of the ionic structures by a substituent, R, is expected to be in the following order;

alkyl group > hydrogen ≅ aromatic group.

The observed values of ν_L and Q indicate an order far from the prediction. Thus it is clear that some factors other than the simple electronic effect are also important. One of the factors is the steric requirement for the lone-pair electrons to be used in conjugation with the carbonyl groups. Lumbroso and

9) C. M. Lee and W. D. Kumler, *J. Am. Chem. Soc.*, 83, 4586 (1961).

Dabard[10] measured the dipole-moments of phthalimide and *N*-methylphthalimide and estimated that the N–R bonds make angles between fifty and sixty degrees in relation to the planes of the imide groups. The angles correspond to the case where the nitrogen atom uses orbitals close to sp^3-hybridization. Lumbroso et al.[11] also suggested that *N*-phenylphthalimide takes an axial and planar conformation, implying sp^2-hybrid orbitals for the nitrogen atom. The change of hybridization from the sp^3 to the sp^2 type facilitates the electron release from the nitrogen atom to carbonyl groups and stabilizes the ionic structures discussed above. The investigation of the longest wavelength absorptions in the electronic spectra of phthalimide series[12] also indicates that the extent of electron donation from the nitrogen atom to the carbonyl groups increases as the substituent is changed in the order of hydrogen, alkyl- and aryl groups. Therefore, it is quite reasonable that the ν_L-values of *N*-arylphthalimides are much less than that of phthalimide itself, contrary to the prediction based on their sigma-values. Reasoning along this line can not account for the fact that the ν_L-values of *N*-alkylphthalimides are close to (or rather less than) those of *N*-arylphthalimides. The only factor left to be considered at this point is the steric strain of the imide ring. The carbonyl absorptions of glutaric anhydride, for example, are observed at considerably lower frequencies (1812 and 1764 cm^{-1}) than those (1863 and 1790 cm^{-1}) of succinic anhydride. The existence of steric strain in the five-membered ring of succinic anhydride is certainly responsible for the shift of its carbonyl absorptions to higher frequencies. A similar strain should be expected for the five-membered rings of phthalimide and its derivatives. The size of the cyclic imide ring, however, may be somewhat different for various types of the hybridization of the nitrogen atom in an imide group. Thus, the ring strain is expected to be dependent on the particular substituent on the nitrogen atom. According to the ν_L-values, the alkyl groups apparently relieve the ring strain to a better extent than do aryl groups. Similar trends were observed also for alkyl- and aryl groups as the *N*-substituents of maleimide and succinimide, as will be discussed later.

The behavior of *N*-arylphthalimide is strongly correlated to the electronic effect of the substituent on the phenyl group. If the steric arrangements are taken as the same among the compounds of this group, the stabilization of the ionic structures of the imide system should be directly affected by the electronic nature of a substituent on the phenyl group. Arranged in the order of decreasing ν_L or increasing *Q*-values, the substituents on the para position give the series;

hydrogen < methyl group < methoxyl group;

and the effects of substituting positions for a given substituent (CH_3 or OCH_3) are;

meta < ortho < para.

These orders agree, qualitatively, with the prediction based on the linear free energy relationships, such as Hammet's sigma-values, of the substituents.

Potassium phthalimide presents a case where the substituent, R, is formed of the paired electrons responsible for the negative charge on the nitrogen atom. Therefore, the extent of the contribution of the ionic structures is expected to be the greatest among the phthalimide series. The carbonyl absorptions in the infrared spectra of potassium phthalimide in the solid state are shown in Fig. 4. The lower frequency absorption is split into a triplet for some unknown reasons, so the center of the triplet is taken tentatively to be ν_L. Both carbonyl absorptions, ν_H and ν_L, are shifted to a considerably lower frequency region, and the *Q*-value is the largest among the phthalimide series, just as expected.

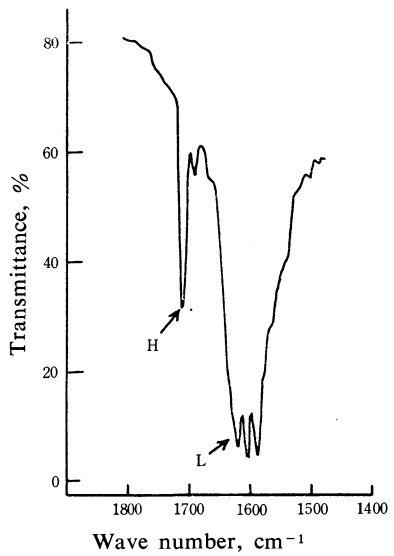


Fig. 4. Carbonyl absorption bands of potassium phthalimide (Nujol).

The carbonyl absorptions of both the succinimide and the maleimide series show a

10) H. Lumbroso and R. Dabard, *Bull. soc. chim. France*, 1959, 749.
11) A. Arcoria, H. Lumbroso and R. Passerini, ibid., 1959, 754.
12) T. Matsuo, presented in part at the 17th Annual Meeting of the Chemical Society of Japan, Tokyo, April, 1964. Manuscript for the details is under preparation for publication.

dependence on their substituents similar to that observed in the phthalimide series. The frequencies of the high intensity absorptions increase in the following order for both series;

N-alkylimides < *N*-arylimides < imide itself.

The minor variation observed in the carbonyl absorptions of *N*-(substituted phenyl)-phthalimides can hardly be noticed in the cases of the corresponding derivatives of succinimide and maleimide. On the other hand, the investigation of the electronic spectra[12] of *N*-substituted maleimides, as shown in Fig. 5,

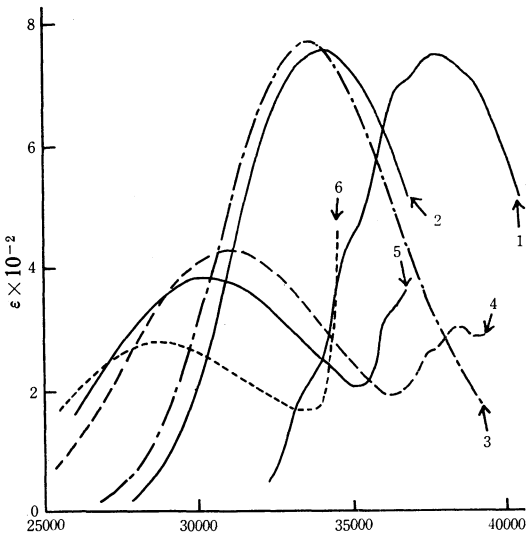


Fig. 5. The absorption spectra of maleimide and its *N*-substituted derivatives in *n*-hexane: 1, maleimide; 2, *N*-ethylmaleimide; 3, *N*-cyclohexylmaleimide; 4, *N*-phenylmaleimide; 5, *N*-(*p*-tolyl)-maleimide; *N*-(*p*-methoxyphenyl)-maleimide.

indicates a trend in the effects of the substituents similar to that mentioned in the phthalimide series. When the substituent is changed in the order of hydrogen, methyl, phenyl, *p*-tolyl and *p*-methoxyphenyl, the longest wavelength absorption band shows a steady red shift as the result of the increase in electron donation from the nitrogen atom to the carbonyl groups. Therefore, the electronic factors apparently have much less effect on the frequencies of carbonyl absorptions in the infrared spectra of maleimide and succinimide derivatives than in the cases of *N*-substituted phthalimides. Because the five-membered ring is fused to the phenyl group in phthalimide derivatives, the framework of the imide system is expected to be fairly tight in this series. On the other hand the corresponding derivaties of succinimide and maleimide have a rather flexible ring system since only hydrogen atoms are attached to the C–C bond joining the carbonyl groups. Thus, the electronic effect of a substituent on the carbonyl frequencies seems to be reduced when the rigidity of the imide ring decreases.

Another problem raised in the infrared spectra of the maleimide series is the extremely low intensity of its higher frequency carbonyl absorption. Judging from the high intensity of the corresponding band in the Raman spectra[13] of maleimide, there seems to be little doubt that the band is due to a symmetrical vibration of the carbonyl groups. The absorption band of the same nature is relatively strong in the infrared spectra of maleic anhydride, the π-electron system of which is isoelectronic to that of maleimide. Thus, the exact answer to this intensity problem is not known at present; the question must be left for future study.

In summary, the lower frequency carbonyl absorption bands of cyclic imides have been found to be strongly affected by the substituent on the nitrogen atom. The effects can be explained in terms of the following factors;

(1) the extent of electron donation from the nitrogen atom, and
(2) the steric strain in the five-membered ring.

The higher frequency carbonyl bands, however, are much less sensitive to these factors. Further study of the problem by means of the normal coordinate treatment, in correlation with the above observations, is expected to reveal the true nature of the two carbonyl absorption bands in the infrared spectra of acid anhydrides and cyclic imides.

The author wishes to thank Miss Yuko Tomita for her help in the measurement of the infrared spectra reported in this paper.

Department of Organic Synthesis
Faculty of Engineering
Kyushu University
Hakozaki, Fukuoka

13) P. Chiorboli and P. Mirone, *Ann. chim. (Rome)*, **42**, 681 (1952).

*Physical Properties and Structure of Polyacetonitrile**

By Eizo OIKAWA** and Shu KAMBARA

(Received June 18, 1964)

Although many kinds of polymeric semiconductors have been synthesized, most of them have consisted of carbon-carbon conjugated systems. When nitrogen, which has a free pair of electrons, is involved in a linear conjugated system, it may be expected that polymer will have different properties than when involved in a carbon-carbon conjugated system. Thus, the polymer of a linear alternate carbon-nitrogen conjugated sequence seems to be an interesting object for studies of physical and chemical properties.

As a polymer that has carbon-nitrogen conjugated double bonds, the polymer of cyanic acid is well known. This, however, is not a pure linear polymer of carbon-nitrogen conjugated double bonds; rather, it appears to have a ladder-like structure.[1] The same type of polymer was recently produced from cyanic acid under irradiation.[2] These polymers of cyanic acid have a low degree of polymerization, and their electric conductivity has not been measured. Other examples of polymerization by irradiation are the solid phase polymerization of nitriles at low temperatures[3] and the ring-opening polymerization of cyanuric chloride,[4] but the yield and the molecular weight of both polymers appear to be small.

Thermally-degraded polyacrylonitrile[5,6] and polycopperphthalocyanine[7] are of this type as well. The former has a considerably high electric conductivity when it is heated at a high temperature (e. g., 500°C); the latter also has good electric conductivity.

Recently Kargin et al. synthesized a linear polymer of carbon-nitrogen conjugated double bonds by heating the complex of acetonitrile with zinc chloride; they then examined the electrical properties of the polymer.[8] The same type of polymer has also been synthesized by high voltage discharge, although it has a low molecular weight.[9]

We have studied the polymerization of acetonitrile complexes with several kinds of metal chlorides and have reported the correlations of the infrared shifts of the nitrile-stretching frequency in the Lewis acid complexes with the polymerizability.[10] Moreover, we have obtained some information concerning the properties and structure of the polymer.

Experimental

Materials.—The metal chlorides used are titanium tetrachloride, zirconium tetrachloride, stannic chloride, aluminum chloride, gallium chloride, ferric chloride, and zinc chloride. Commercial reagents were used, including acetonitrile, but gallium chloride was prepared from gallium metal and hydrogen chloride[11] and was purified by sublimation.

Acetonitrile was used after distillation and drying over calcium hydride.

Titanium tetrachloride and stannic chloride were distilled just before the preparation of the complex.

Ferric chloride, zirconium tetrachloride and aluminum chloride were purified by sublimation.

For zinc chloride, a guaranteed reagent was used after drying it at an elevated temperature under reduced pressure.

The Preparation of Complexes.—The distillate or the solid mass of metal chloride was cooled with dry ice-methanol or liquid nitrogen in a flask, into which a little more than the calculated amount (molar ratio $RCN/MX_n=2/1$) of the acetonitrile was added drop by drop in an atmosphere of nitrogen. The excess nitrile was then distilled off under reduced pressure. The complexes were purified by sublimation. Since ferric chloride, zinc chloride and gallium chloride complexes could not be sublimed, these three chlorides were carefully purified before preparation. The complexes were handled afterwards in a dry box because they are easily decomposed, even by moisture in the air.

* Presented in part at the 15th (Kyoto, April, 1962) and 16th (Tokyo, April, 1963) Annual Meetings of the Chemical Society of Japan.

** Present address: Faculty of Engineering, Niigata University, Nagaoka, Niigata.

1) T. Völker, *Angew. Chem.*, **72**, 379 (1960).
2) D. Hummel and O. Janssen, *Z. physik. Chem. (N. F.)*, **31**, 111 (1962).
3) Y. Tabata, E. Oda and H. Sobue, *J. Polymer Sci.*, **45**, 469 (1960).
4) S. Okamura, K. Hayashi, M. Nishii and Y. Nakamura, *Isotopes and Radiations*, **4**, 69 (1961).
5) A. V. Topchiev and B. A. Kargin, *Doklady Akad. Nauk. SSSR*, **128**, 312 (1959).
6) N. Grassie and J. N. Hay, *J. Polymer Sci.*, **56**, 189 (1962).
7) A. Epstein and B. S. Wildi, *J. Chem. Phys.*, **32**, 342 (1960).
8) B. A. Kargin, B. A. Kabanov, B. P. Zubov and A. B. Zezin, *Doklady Akad. Nauk. SSSR*, **139**, 605 (1961).
9) W. G. Deichert and M. C. Tobin, *J. Polymer Sci.*, **54**, 39 (1961).
10) E. Oikawa and S. Kambara, ibid., **B2**, 649 (1964).
11) W. C. Johnson and C. A. Haskew, "Inorganic Syntheses," **1**, 26 (1939).

The properties and analyses of the complexes have been given in a previous publication.[10]

Polymerization.—After having been rinsed with nitrogen, a definite amount of complex was sealed into a thick-wall ampoule under the reduced pressure of 10^{-2} mmHg. The ampoule was then heated in a controlled electric furnace for the required time. The product prepared from the complex was powdered, and water was added. The product was filtered and washed repeatedly with distilled water or diluted hydrochloric acid, since water readily decomposes the complex and dissolves metal chlorides. When the heating time was shorter or the temperature was lower, the filtration was often difficult. Then a centrifuge was used. The infrared spectrum of the filtrate did not show the absorption due to the C=N conjugated double bond at about 1600 cm^{-1}. This suggests that the polymer is scarcely dissolved at all in the filtrate.

Most of the polymers obtained were dark brown to black and were insoluble in common organic solvents, although they were soluble in mineral acids.

The Addition of Silver Nitrate.—About 0.1 g. of a polymer was dispersed in an aqueous 1/10 N silver nitrate solution for 24 hr. at an ordinary temperature. The dispersed liquid was then filtered, and the residue was washed repeatedly with distilled water.

The Measurements of Physical Properties. — 1) The X-ray diffraction measurements were carried out using Cu$K\alpha$ of 30 kV., 20 mamp., and a scanning speed of $2\theta=2°$/min.

2) The infrared absorption spectra were obtained by the usual KBr-pellet method.

3) The intrinsic viscosities of the polymers in sulfuric acid were measured at 40 ± 0.03°C using a modified Ubbelohde viscometer. Since the value of the intrinsic viscosily and the linear gradient of η_{sp}/c versus c did not vary when the same solution was measured again after a week, the polymer in sulfuric acid does not seem to be degraded.

4) The electric conductivity, σ, was measured under the pressure of 90 kg./cm^2. The current was measured with a vibration-reed electrometer. The temperature was raised by 0.5°C/min. from room temperature to about 100°C. The energy gap, ΔE_g, can be determined from the gradient of log σ versus $1/T$:

$$\sigma=\sigma_0\exp(-\Delta E_g/2\boldsymbol{k}T) \quad (1)$$

5) Stable unpaired electrons included in the polymers were observed with an ESR spectrometer at the Nissei Industry Co. Ltd.

Results and Discussion

Electric Conductivity.—The electric conductivity values of 10^{-10} to 10^{-5} $\Omega^{-1}cm^{-1}$ summarized in Table I indicate that the polymer is a semiconductor. The electric conductivity increases and the activation energy decreases when the heat treatment of the complex is increased at a given temperature or at a given

TABLE I. ELECTRICAL PROPERTIES OF POLYACETONITRILE

No.	Temp. °C	Heating time, hr.	Elec. cond. σ $\Omega^{-1}cm^{-1}$ (20~22°C)	Energy gap ΔE_g, eV.	σ_0 $\Omega^{-1}cm^{-1}$
T234	230	4	1.2×10^{-8}	0.73	2.5×10^{-2}
T238		8	1.8×10^{-8}	0.70	1.9×10^{-2}
T254	250	4	2.5×10^{-8}	0.66	1.9×10^{-2}
T258		8	3.5×10^{-8}	0.68	2.2×10^{-2}
T304	300	4	1.4×10^{-7}	0.64	3.0×10^{-2}
T308		8	3.2×10^{-7}	0.6	4.1×10^{-2}
T354	350	4	3.5×10^{-7}	0.57	2.6×10^{-2}
T358		8	5.1×10^{-7}	0.53	1.7×10^{-2}
F254	250	4	2.9×10^{-10}	—	—
F258		8	3.6×10^{-10}	0.97	6.7×10^{-2}
F304	300	4	1.2×10^{-8}	—	—
F308		8	1.4×10^{-7}	—	—
F354	350	4	5.1×10^{-6}	0.40	1.6×10^{-2}
A354	350	4	1.3×10^{-9}	1.03	1.1
A356		6	2.5×10^{-9}	—	—
A358		8	2.8×10^{-9}	—	—
Z254	250	4	4.2×10^{-10}	1.22	21
Z304	300	4	3.9×10^{-10}	—	—
Z308		8	1.1×10^{-9}	—	—
Z354	350	4	3.0×10^{-9}	1.08	5.7
Z358		8	6.6×10^{-8}	—	—
S234	230	4	3.1×10^{-10}	—	—
S254	250	4	1.4×10^{-9}	—	—
S258		8	1.7×10^{-9}	0.86	5.6×10^{-2}

T : Product from titanium tetrachloride complex
F : Product from ferric chloride complex
A : Product from aluminum chloride complex
Z : Product from zinc chloride complex
S : Product from stannic chloride complex

heating time. This suggests that the formation of conjugated double bonds becomes more extensive in the polymer at a higher temperature and a longer heating time, while Eley et al. have shown that ΔE_g decreases to a limiting value as the number of conjugated double bonds increases.[12]

TABLE II. ADDITION OF SILVER NITRATE TO THE POLYMERS

No.	Wt. increase g./g. polymer
T234	0.487
T238	0.516
T254	0.311
T258	0.417
T304	0.419
T308	0.177
T354	0.288
T358	0.590

The number of conjugated π electrons in a polymer chain can be estimated from ΔE_g in Table I if Eley's calculation for a carbon-carbon conjugated system may be applied to a carbon-nitrogen conjugated system. The numbers obtained in this way were 17 for Z254 (ΔE_g= 1.22) to 50 for F354 (ΔE_g=0.40). One-half of this value is the mean number of conjugated double bonds if the polymer is regarded as a completely linear carbon-nitrogen conjugated chain.

The products from the ferric chloride complex show the greatest change in σ at a given change in the heating temperature.

The Addition of Silver Nitrate.—The weight increases in polymers upon the addition of silver nitrate are shown in Table II. They are sizable and seem to be due to chemisorption rather than to mere adsorption. Since the C=N bonds characteristically take up noble metal ions, these considerable weight increases support the idea that the polymer contains C=N bonds.[1] However, the values are not strictly reproducible because they depend on the surface area of the powdered samples.

X-Ray Diffraction. — In X-ray diffraction patterns no sharp peak could be seen, but the 2θ=25° peak (d=3.56 Å) is comparable with that of phthalocyanine (2θ=26°, d=3.38 Å),[13] consisting of a big circular carbon-nitrogen conjugated system. If parts of the resulting polymer are considered to form a band-like structure, the value of 3.56 Å would correspond to the distance between the bands.

It was found that polymers produced in a shorter heating time and at a lower temperature had a higher intensity of diffraction, probably indicating that these polymers have a relatively high regularity.

Electron Spin Resonance.—All the samples showed singlet spectra, as are seen in polyacetylene,[14] under the measuring conditions (Fig. 1). The g-factors were estimated to be from 2.0046 to 2.0003, but most of them have the value of nearly 2.0023, which is the value of a free electron. Hence, the unpaired electrons in polyacetonitrile are believed to be stabilized by resonance energy in a highly conjugated system and to be in a state similar to that of free electrons.

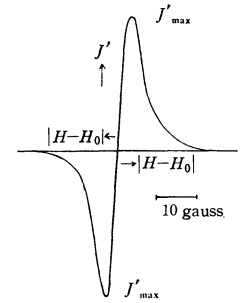


Fig. 1. ESR derivative curve of A352.

The relative spin concentrations in each group of metal chloride decreased with the temperature except for the Z-group and the G-group (products of the gallium chloride complex), in which the concentrations increased with the temperature; this has not yet been explained reasonably.

According to the method of analysis of the line shape proposed by Tikhomirova and Voevodskii,[15] the Gaussian (2) and Lorentzian (3) equations may be described, as respectively:

$$\log(y/J') = a^2y^2/2.3 + \log(0.427/J'_{max}\ a) \quad (2)$$

$$\sqrt{y/J'} = 0.57/\sqrt{bJ'_{max}} + (0.57b\sqrt{b}/\sqrt{J'_{max}})y^2 \quad (3)$$

where $a^2=1/1.45\ \Delta H_G{}^2$, $b^2=1/\Delta H_L{}^2$, $y=H-H_o$, and J' represents the ordinate (arbitrary unit) in a differential spectrum (Fig. 1).

ΔH_G and ΔH_L are obtained from the slope of the linear part in Eqs. 2 and 3 respectively. The value of ΔH corresponding to the transition region between 2 and 3 is ΔH_e. An example is illustrated for A352 in Figs. 1 and 2. Figure 2 suggests that the ESR line investigated is Lorentzian in the center, but Gaussian beyond ΔH=7.6 gauss.

12) D. D. Eley and G. D. Parfitt, *Trans. Faraday Soc.*, **51**, 1529 (1955).
13) H. Akamatu and H. Inokuchi, "Solid State Physics," Ist ed., Academic Press Inc., New York (1961), Vol. 12, p. 102.
14) M. Hatano, S. Kambara and S. Okamoto, *J. Polymer Sci.*, **51**, s26 (1961); S. Kambara and M. Hatano, *Bull. Tokyo Institute Technology*, No. 52, 109 (1963).
15) N. N. Tikhomirova and V. V. Voevodskii, *Optics and Spectroscopy*, **7**, 486 (1959).

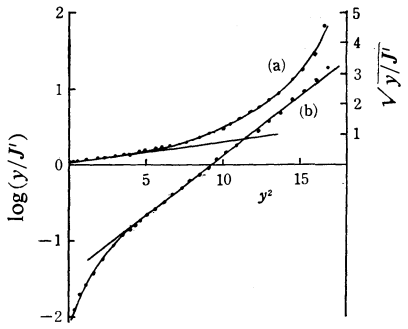


Fig. 2. Linearized form of A352 ESR curve.
Curve a: in coordinates corresponding to a Lorentzian relation
Curve b: in coordinates corresponding to a Gaussian relation
Abssissa: y^2 in arbitrary units ($y^2=10=1.46$ gauss)

The results of the analyses of line shape are summarized in Table III. The relatively small deviations of $\Delta H_G^2/\Delta H_L \Delta H_e$ from unity indicate that the analysis is valid. Table III shows

TABLE III. ANALYSES OF THE ESR LINE SHAPE

No.	ΔH_e	ΔH_G	ΔH_L	$\Delta H_G^2/\Delta H_e \Delta H_L$
T234	13	7.1	3.9	1.0
T254	11	7.3	4.1	1.15
T258	13	7.6	3.6	1.2
Z304	9.0	5.8	4.1	0.91
Z308	7.6	5.0	3.7	0.91
Z354	8.0	5.4	4.5	0.81
F252	12	7.8	5.0	1.01
F256	11	6.8	4.6	0.91
A352	7.6	5.4	4.0	0.96
A353	7.6	5.1	4.1	0.84
A372	6.6	4.5	4.9	0.80
G303	9.4	6.5	5.3	0.85
G322	9.4	6.4	4.8	0.91
G323	8.9	6.1	5.2	0.81

a tendency for ΔH_G and ΔH_e to decrease simultaneously with the increase in the heating temperature. This is more clearly illustrated in Fig. 3. This decrease may not be clear between different complex groups at the same temperature, or at the difference of about fifty degrees, but when the temperature is raised from 230°C to 370°C, distinct decreases in ΔH_G and ΔH_e appear.

The outstanding decreases of ΔH_G and ΔH_e in the pyrolysis of polyvinyl chloride have been explained as resulting from the increase of C=C conjugated double bonds in the process of dehydrochlorination, together with the formation of aromatic rings between polymer chains.[15] The extension of the conjugated system will bring about a delocalization of electrons and an exchange interaction between

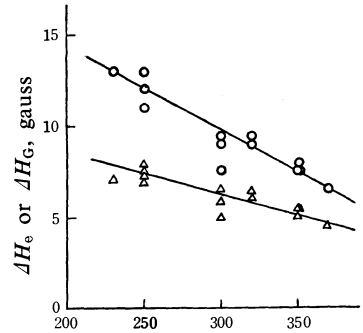


Fig. 3. Correlation of ΔH_e and ΔH_G with heating temperature.
○: ΔH_e, △: ΔH_G

unpaired electrons, resulting in a gradual decrease of ΔH_G and ΔH_e. A similar explanation could be applied to polyacetonitrile. A higher heating temperature will bring about not only the extension of the C=N conjugated system, but also a cross-linking between polymer chains, which may decrease ΔH_G and ΔH_e. The cross-linking is expected from the experimental fact that ammonia was detected after polymerization, and from the results of a noncrystalline pattern of X-ray diffraction, infrared spectra, viscometric measurements (Fig. 5), and elementary analyses (Table IV).

Infrared Absorption. — An infrared spectrum of polyacetonitrile is shown in Fig. 4, where

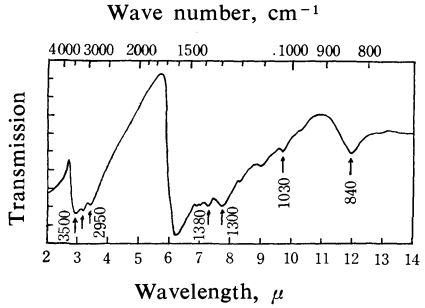


Fig. 4. Infrared spectrum of A304.

the absorption at 2247 cm^{-1} due to the nitrile groups completely disappears and a new strong absorption at 1600 cm^{-1} appears, one which is due to the sequence of C=N bonds, presumably also contributed by C=C double bonds resulting from the separation of ammonia. The existence of C=C double bonds is also supported by the decoloration of a neutral dilute potassium permanganate solution at an ordinary temperature. The oxidation of CH_3 and C=N groups needs more severe conditions. Moreover, a second new absorption, at 840 cm^{-1}, appears; this does not appear in the spectrum of acetonitrile. This absorpition may be due

TABLE IV. ANALYSES OF THE POLYMERS

No.	C	H	N	Cl	O	Ash	Total	C/H	C/N
T234	58.3	4.2	21.5	—	10.1	0.3	94.4	14.0	2.7
T238	55.8	4.0	20.2	—	9.4	0.5	89.9	13.9	2.8
T254[a)]	56.9	4.6	22.1	0.7	16.9	0.9	102.1	12.5	2.6
T258	58.4	4.4	20.2	—	10.2	1.0	94.2	13.4	2.9
T304[b)]	57.3	4.2	18.7	—	10.3	4.2	94.7	13.8	3.1
T308	57.9	4.0	17.1	0.8	—	4.7	84.5	14.3	3.4
Calcd.[c)]	58.6	7.3	34.1	0	0	0	100	8.0	1.7

a) Experimental formula: $C_9H_9N_3O_2$
b) Experimental formula: $C_{15}H_{13}N_4O_2$
c) Calculated value for CH_3CN

to the C–H in $>C=\underset{\underset{H}{|}}{C}-$, and probably >N–H. The absorptions at 2950, 1380, 1300 and 1030 cm^{-1} are weak, but they may be assigned to CH_3 groups. The absorptions at 3200 and 3500 cm^{-1} may be due to imine, amine or hydroxyl groups.

It may be reasonable to consider that the metal halide behaves as a cationic reagent with a trace of water and gives rise to cationic polymerization, nearly as in the case of the heating of polyacrylonitrile,[16] as follows:

$$n\,N\equiv\underset{\underset{R}{|}}{C} + H^+[MX_n(OH)]^- \rightarrow$$

$$HN=\underset{\underset{R}{|}}{C}-(-N=\underset{\underset{R}{|}}{C})_{n-1}{}^+[MX_n(OH)]^- \rightarrow$$

$$HN=\underset{\underset{R}{|}}{C}-(-N=\underset{\underset{R}{|}}{C}-)_{n-1}-OH + MX_n \qquad (4)$$

The experimental fact of separation of ammonia may be brought about by pyrolysis when the complex is heated for a longer time; it gives, for example, the following change in the structure of the polymer:

$$\begin{array}{l} CH_3 \\ NH=C-N=C- \\ \qquad\quad | \\ \qquad CH_3 \\ H_2CH \\ -N=C-N= \end{array} \xrightarrow[-NH_3]{} \begin{array}{l} CH_3 \\ C-N=C- \\ \| \quad\quad | \\ HC \quad CH_3 \\ -N=C-N= \end{array} \qquad (5)$$

This change is supported to some extent by the obscure absorptions due to CH_3 groups, and by the electric conductivities, the oxidation test and ESR analyses. It is also supported by the elementary analyses of the polymers given in Table IV.

It should be noted that the polymers of a highly conjugated system find it difficult to combust completely.

The simultaneous decreases in H and N contents corresponding to increases in the C/H and C/N ratios are attributed to the evolution of ammonia. These changes and the considerable oxygen content indicate that polyacetonitrile may consist of not completely conjugated double bonds of carbon-nitrogen, together with other groups containing oxygen. The followings will be most probable means of the introduction of oxygen into the polymer;

(a) The oxidation of the C=C bond which may be formed in the separation of ammonia. This oxidation is predominant in polyacetylenes.[14]

(b) Hydroxyl groups of polymer end as given in Eq. 4. This contribution to the introduction of oxygen will be small.

It can not be concluded from the infrared spectrum whether or not the polymers have carbonyl groups, because the band due to the carbonyl groups will overlap the band due to the C=N bonds.

Viscometric Measurements. — The intrinsic viscosities $[\eta]$ of the polymers from the titanium terachloride complex versus polymer yields and t^2 (t=heating time, hr.) are shown in Fig. 5. If the polymer consists of a linear chain, then $[\eta]$ versus t^2, as Kargin et at. indicated,[8] should be linear through the origin. However, the linear line greatly deviates from the origin. This fact and an unusual increase in $[\eta]$ with the increase in yields support the structual change illustrated in Eq. 5.

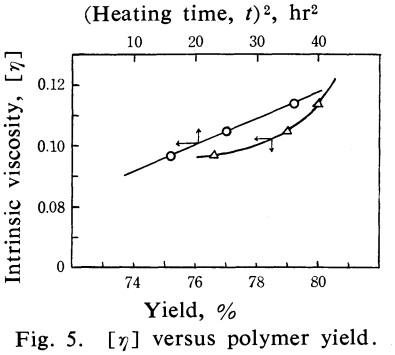


Fig. 5. $[\eta]$ versus polymer yield.

Summary

The fact that a polymer containing C=N double bonds is formed from saturated nitrile

16) W. J. Burlant and J. L. Parsons, *J. Polymer Sci.*, **22**, 249 (1956).

complexes with metal chlorides is supported by the infrared absorption at about 1600 cm^{-1} and the characteristic addition of silver nitrate. The polyacetonitrile has an electric conductivity from 10^{-10} to 10^{-5} $\Omega^{-1}cm^{-1}$ and an energy gap from 0.4 to 1.2 eV., indicating that the polymer is an organic semiconductor.

The electric conductivity increases and the energy gap decreases with increases in the heating time and temperature, suggesting a more extensive formation of a conjugated system, including also C=C double bonds among polymer chains at a higher temperature. This theory is supported by the evolution of ammonia, resulting in simultaneous decreases of the H and N contents of the polymer, the appearance of the absorption at 840 cm^{-1}, by oxidation by potassium permanganate, by analyses of ESR line shapes, and by viscometric measurements. This structual change may bring about a noncrystalline pattern in X-ray diffraction. Therefore, it is indicated that polyacetonitrile does not have a complete C=N conjugated sequence because of some pyrolysis, accompanied by the extension of a conjugated sustem such as cross-linking at a higher temperature and a longer heating.

The authors are very grateful to Professor Kiichiro Kubo and Mr. Seiki Kato for their X-ray data, to Mr. Toyoji Saito for his elementary analyses, to the Nissei Industry Co., Ltd., for its ESR measurements, and to the Dainihon Ink Co., Ltd., for its oxygen analyses. They also wish to express their thanks to Dr. Masahiro Hatano for his helpful suggestions.

Research Laboratoy of Natural Resources Utilization
Tokyo Institute of Technology
Meguro-ku, Tokyo

The Radiolysis of Liquid cis-2-Butene

By Yoshihiko HATANO, Shoji SHIDA and Shin SATO

(Received June 18, 1964)

Previous investigations of the radiation chemistry of unsaturated hydrocarbons have dealt almost exclusively with radiation-induced polymerization; little attention has been paid to the minor low-molecular-weight products. It therefore appeared of interest to investigate the low-molecular-weight products in the expectation that they might be produced through the non-free radical mechanism. This was of interest because it has been known that olefins (e.g., *cis*-2-butene in this investigation) and other unsaturated compounds behave as effective scavengers for hydrogen and free radicals.[1] Thus, almost all free radicals from the radiolysis of unsaturated compounds may easily react to form dimers and higher polymers, and may not contribute to the formation of the low-molecular-weight products (e.g., hydrogen and $C_1 \sim C_4$ products from C_4 hydrocarbons). Detailed studies of such systems might assist the understanding of the essential features of the molecular mechanism in the radiation chemistry. With these prospects, the radiolysis of liquid *cis*-2-butene at room temperature was undertaken in this investigation. *cis*-2-Butene is simple in chemical structure, although it is readily liquefied.

There has been, to the authors' knowledge, only one paper[2] dealing with the radiolysis of *cis*-2-butene. Kaufman[2] carried out the irradiation of butenes in gas and liquid phases and suggested that the ion-molecule processes are applicable to the dimer formation. On the other hand, Cundall[3,4] carried out radiolysis on particular systems (butenes in hydrocarbon solvents) and explained the cis-trans isomerization of 2-butene by means of the energy transfer mechanism from solvents. In this case the isomerization of 2-butene is not due to the direct effect of radiation.

Experimental

Materials.—Matheson pure-grade *cis*-2-butene was used after the usual degassing and bulb-to-bulb distillations. It was found by gas chromatography to contain less than 0.4% *trans*-2-butene. Commercial reagents of chemically-pure-grade benzene,

1) K. Kikuchi, S. Sato and S. Shida, *J. Chem. Soc. Japan, Pure Chem. Sec.* (*Nippon Kagaku Zasshi*), **84**, 561 (1963).

2) P. C. Kaufman, *J. Phys. Chem.*, **67**, 1671 (1963).

3) R. B. Cundall and P. A. Griffiths, *J. Am. Chem. Soc.*, **85**, 1211 (1963).

4) R. B. Cundall and P. A. Griffiths, *Discussions Faraday Soc.*, **36**, 111 (1963).

naphthalene, anthracene, iodine, and *p*-benzoquinone were used as additives without further purification.

Irradiation.—The radiation employed in the radiolysis of liquid *cis*-2-butene was γ-rays from 16000 c. ^{60}Co. Measured amounts of *cis*-2-butene were sealed in vacuo at −196°C in glass ampoules 10 mm. in diameter and of a 10 ml. capacity fitted with breaker seals. Irradiations were made at room temperature. The total doses were 0.30×10^{21} to 3.59×10^{21} eV./g. for examining the dose dependence of products and 2.90×10^{21} eV./g. throughout the experiments to which additive materials were applied. The dose rate was 2.21×10^{19} eV./g. hr.

Analysis. — After irradiations the sample tubes were attached to the vacuum line and the seals were broken. The gases non-condensable at −196°C (hydrogen and methane) were collected and measured by an analysis device composed of a Toepler pump, a McLeod gauge, and a copper oxide furnace. Products condensable at −196°C were expanded into a reservior of a sufficiently large volume to maintain hydrocarbons up to C_8 in the gas phase. Aliquots of the gaseous mixture were then analyzed by a home-made reduced-pressure-type gas chromatograph. For the separation of $C_1\sim C_4$ hydrocarbons, a benzyl ether column was mainly used at room temperature, but a squalane-alumina column and a dimethylsulfolane column were also used. For the separation of $C_5\sim C_8$ hydrocarbons, a dioctylphthalate column was used at 80°C. After distillation of the volatile products in vacuo at room temperature, a viscous residue was found on the wall of the glass ampoules. This substance was readily soluble in acetone and was determined gravimetrically as a polymer of the butene.

Results and Dicussion

The major products in the radiolysis of liquid *cis*-2-butene at room temperature are hydrogen, *n*-butane, 1-butene, *trans*-2-butene, C_8 hydrocarbons, and higher polymers. Small amounts of $C_1\sim C_3$ and $C_5\sim C_7$ hydrocarbons are also formed. The formation of each product was estimated as a function of the energy absorbed in the liquid *cis*-2-butene (Fig. 1). The data in Fig. 1 show that each product formation is directly proportional to the energy absorbed; that is, the radiation chemical yield, *G*, the number of molecules formed per 100 eV. of energy absorbed in the system, is independent of the total energy absorbed. In view of the fact that *cis*-2-butene itself is an effective radical scavenger,*1 this result can be readily understood.

The *G*-values of products in the radiolysis of liquid *cis*-2-butene at room temperature have been determined from Fig. 1 and are shown in Table I. The sum of *G*-values for hydrogen and $C_1\sim C_4$ hydrocarbons in Table I is 5.20, whereas it is 9.41 in the radiolysis of liquid *n*-butane at room temperature;[7] these results indicate that a smaller amount of gaseous products (55% of the latter) is formed from an unsaturated hydrocarbon than from a saturated one. Further, the ratio $\{G(C_1\sim C_3)+G(C_5\sim C_7)\}/\{G(C_4)+G(C_8)\}$ is 0.098 for *cis*-2-butene and 1.53 for *n*-butane[7] respectively, where $\{G(C_1\sim C_3)+G(C_5\sim C_7)\}$ represents the yield for the C–C bond rupture. These results indicate that in the butene radiolysis the reactive species formed by the C–C bond rupture (e. g., C_1, C_2, and C_3 radicals) do not make an important contribution to the formation of

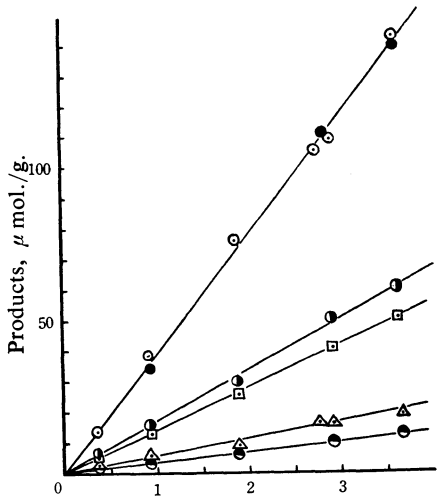


Fig. 1. Variation of products formation as a function of the energy absorbed, in the radiolysis of liquid *cis*-2-butene at room temperature. Dose rate: 2.21×10^{19} eV./g. hr.

Table I. The *G*-value of the products in the radiolysis of liquid *cis*-2-butene

Irradiation was made at room temperature. Dose rate was 2.21×10^{19} eV./g. hr.

H_2	1.02	1-C_4H_8	0.40
CH_4	0.21	*trans*-2-C_4H_8	2.29
C_2H_6	0.03	1,3-C_4H_6	0.10
C_2H_4	0.08	C_5	<0.01
C_2H_2	0.11	C_6	trace
C_3H_6	0.13	C_7	<0.01
n-C_4H_{10}	0.83	C_8	2.30

*1 The gradual decrease in the *G*-values at higher doses has often been observed in the radiolysis of saturated hydrocarbons and explained by the scavenging effect of olefin products.[5,6]

5) H. A. Dewhurst, *J. Phys. Chem.*, **62**, 15 (1958).

6) S. Sato and S. Shida, *J. Chem. Soc. Japan, Pure Chem. Sec. (Nippon Kagaku Zasshi)*, **82**, 435 (1961).

7) T. Miyazaki, S. Arai and S. Shida, This Bulletin, **37**, 1352 (1964).

low-molecular-weight products, but that the greater part of these reactive species may be converted to dimers or higher polymers.

Iodine and *p*-benzoquinone (BQ) were used as radical scavengers more effective than olefins. Table II lists several molecular and radical yields obtained with a *cis*-2-butene/BQ solution. The concentration range of BQ used here is 40 to 180 mM. With a *cis*-2-butene/I_2 solution (although we shall omit detailed information here), the same additive effect on the products formation except for the isomerization were observed as in the *cis*-2-butene/BQ system. The marked increase in the rate of cis-trans isomerization observed with the *cis*-2-butene/I_2 solution ($G=5.5$ at 10 mM) might be due to the catalytic action of iodine atoms and/or the electron-capture effect of iodine molecules. It seems that the effect of added iodine on the reaction mechanism is complicated and presents some difficulty.[8] As is shown in Table II, the free radical mechanism is not important for the formation of any low-molecular-weight products except methane and *n*-butane. Since 95% of *n*-butane is produced through the free radical mechanism, it is proposed that *n*-butane formation occurs by the disproportionation of *s*-butyl radicals: $2C_4H_9 \rightarrow C_4H_8 + C_4H_{10}$. Assuming that *cis*- and *trans*-2-butene are produced simultaneously with *n*-butane in the ratio of 1:1 in the disproportionation reaction, then one obtains the expected radical yield of *trans*-2-butene as 0.32, $\{G_R(n\text{-}C_4H_{10}) - G_R(1\text{-}C_4H_8)\}/2$, which is in good agreement with the observed value, i. e., 0.29.*2 Thus, at least 80% of the *trans*-2-butene is formed through the molecular mechanism.

Since the greater part of the low-molecular-weight products are formed through the molecular mechanism described above, such aromatic hydrocarbons as benzene, naphthalene, and anthracene were used as additives; they were expected to exert remarkable effects on the molecular mechanism. The variation in product yields with the concentration of the additives is given in Fig. 2. The rate of cis-trans isomerization is markedly affected by the sort of additives and their concentrations, whereas the rate of the formation of other products is not so much affected as in the case of isomerization. The increase in G(*trans*-2-butene) at lower concentrations and the decrease at higher concentrations are obvious. On the other hand, the dependence of G(*n*-butane) on additive concentrations is much less than that of G(*trans*-2-butene). Therefore, the decrease in G(*trans*-2-butene) at higher concentrations is not due to the radical-scavenging effect by additives.

The rate of cis-trans isomerization in pure liquid *cis*-2-butene is independent of the total doses, as is shown in Fig. 1. Therefore, the

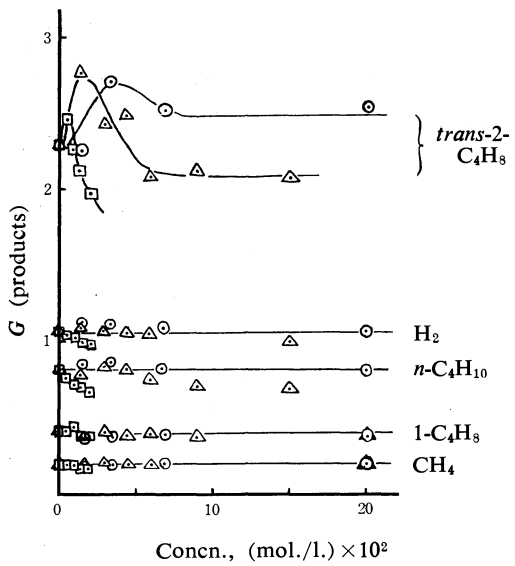


Fig. 2. Additive effects of benzene, nahthalene and anthracene on products formation in the radiolysis of liquid *cis*-2-butene at room temperature. Total dose: 2.90×10^{21} eV./g., Dose rate: 2.21×10^{19} eV./g. hr.
⊙ Benzene △ Naphthalene ⊡ Anthracene

TABLE II. THE MOLECULAR AND RADICAL YIELD OF THE PRODUCTS IN THE RADIOLYSIS OF LIQUID *cis*-2-BUTENE

Irradiation was made at room temperature.
p-Benzoquinone was used as a radical scavenger.
Total dose: 2.90×10^{21} eV./g.
Dose rate: 2.21×10^{19} eV./g. hr.

Product	Radical yield		Molecular yield	
	G_R	$(\%)_R$	G_M	$(\%)_M$
H_2	0.00	0	1.02	100
CH_4	0.12	57	0.09	43
C_2H_2	0.00	0	0.11	100
C_3H_6	0.00	0	0.13	100
n-C_4H_{10}	0.79	95	0.04	5
1-C_4H_8	0.16	40	0.24	60
trans-2-C_4H_8	0.29	13	2.00	87

8) T. Kudo and S. Shida, to be published.

*2 On the other hand, if an assumption is made that in the disproportionation reaction of *s*-butyl radicals 1-butene, *trans*-2-butene, and *cis*-2-butene are produced with the ratio of 2:1:1, respectively,[9] as found in the corresponding gas-phase reaction, then the radical yield of *trans*-2-butene might be $0.79\times1/4=0.2$ and that of 1-butene $0.79\times1/2=0.4$. The former is again in agreement with the observed value, but not the latter. It is probable that the ratio of 1-butene to *cis*- or *trans*-2-butene is not the same as the ratio in the gas phase.

9) B. S. Radinovitch and R. W. Diesen, *J. Chem. Phys.*, **30**, 735 (1959).

increase in G(*trans*-2-butene) at a lower concentration of additives is not due to the protection by aromatics of the initially-formed *trans*-2-butene from radical attack, a protection which was observed with olefin formation in the radiolysis of a cyclohexane/benzene mixture.[10]

The ionization potentials of benzene, naphthalene, and anthracene have been offered as 9.52, 8.12 and 7.23 eV., and their electron affinities as 2.19, 2.59, and 3.11 eV. respectively.[11] For *cis*-2-butene, the ionization potential is 9.34 eV.,[12] and the electron affinity is less than the values for the aromatics.[13] On the other hand, it may be considered that in the lower concentration of additives the interaction between additives and electrons prevails over the interaction between additives and positive butene ions in a spur, and that with an increasing concentration of additives the latter interaction cannot be set aside. Thus, comparing the results in Fig. 2 with the values listed above one may conclude that the increase in G(*trans*-2-butene) at a lower concentration of additives corresponds to the electron affinities of additives and the decrease at higher concentrations, to the ionization potentials of additives.

In view of the above discussion, the most reasonable conclusion to be drawn from the available data is as follows: The increase in G(*trans*-2-butene) at a lower concentration of additives may be due to the electron-capture effect of additives, which prolongs the lifetime of positive butene ions. As a result, the recombination process of electrons will be altered:

a) $\mathrm{Cis} \rightarrow \mathrm{Cis}^+ + \mathrm{e}$ (Cis; *cis*-2-butene)

b) $\mathrm{e} + \mathrm{M} \rightarrow \mathrm{M}^-$ (M; additives)

c) $\mathrm{Cis}^+ \rightarrow \mathrm{Trans}^+$ (Trans; *trans*-2-butene)

d) $\mathrm{Cis}^+ + \mathrm{e} \rightarrow \mathrm{Cis}^* \rightarrow 1/4$; Cis (singlet)
$\searrow$ 3/4; Cis (triplet) $\rightarrow$ 3/8; Trans
$\searrow$ 3/8; Cis

e) $\mathrm{Trans}^+ + \mathrm{e} \rightarrow \mathrm{Trans}^* \rightarrow 1/4$; Trans (singlet)
$\searrow$ 3/4; Trans (triplet) $\rightarrow$ 3/8; Trans
$\searrow$ 3/8; Cis

where asterisks indicate excited states involving high levels of the different state manifolds, and "singlet" and "triplet" indicate the ground state and the first excited triplet state respectively. The additional processes b, c and e may occur beside the processes a and d if the additives are used. From the processes d and e, the net value, 1/4 of the primary ionization of *cis*-2-butene, additionally contributes to the cis-trans isomerization in the presence of sufficient amounts of the additives, since it might be considered that singlet and triplet states are formed by the recombination of electrons and positive butene ions in the ratio of 1 : 3. When the concentration of additives is increased however, the isomerization due to the process $\mathrm{Cis}^+ + \mathrm{M}^-$ cannot be set aside in comparison with the processes d and e. When the concentration is increased further, $\mathrm{Cis}^+ + \mathrm{M}^-$ prevails over $\mathrm{Trans}^+ + \mathrm{M}^-$, and finally the contribution, the above "1/4," may be ignored. Since butene has a lower ionization potential than benzene, the charge transfer from butene to benzene will be impossible. Although the electronic energy levels of 2-butene are not known with any accuracy, the electronic excitation transfer from butene to benzene may also be impossible. This is supported by theoretical considerations[14-16] and by experimental results from the studies of the benzene-photosensitzed isomerization of 2-butene.[17],*3 When benzene is used as an additive, therefore, no further decrease in G(*trans*-2-butene) is observed with an increase in the concentration. Since butene has a higher triplet energy and a higher ionization potential than naphthalene and anthracene, both electronic excitation transfer and charge transfer are possible as follows:

$$\mathrm{Cis}^* \text{ (triplet)} + \mathrm{M} \text{ (singlet)} \rightarrow \mathrm{Cis} \text{ (singlet)} + \mathrm{M}^* \text{ (triplet)}$$

$$\mathrm{Cis}^+ + \mathrm{M} \rightarrow \mathrm{Cis} + \mathrm{M}^+$$

When naphthalene and anthracene are used as additives, therefore, a steeper decrease in G(*trans*-2-butene) at higher concentrations is observed. From investigations of the sensitized fluorescence,[19] however, an electronic excitation transfer is possible only when two atoms or molecules have energy levels lying near enough together to raise a quantum mechanical resonance effect between them.

10) K. Kikuchi, S. Sato and S. Shida, The 17th Annual Meeting of the Chemical Society of Japan, Tokyo (1964).
11) F. A. Matsen, *J. Chem. Phys.*, **24**, 602 (1956).
12) J. Collins and F. P. Lossing, *J. Am. Chem. Soc.*, **81**, 2064 (1959).
13) P. C. Chang, N. C. Yang and C. D. Wagner, ibid., **81**, 2060 (1959).
14) D. F. Evans, *J. Chem. Soc.*, **1960**, 1735.
15) V. A. Crawford, *Quart. Rev.*, **3**, 226 (1949).
16) J. R. Platt, *J. Chem. Phys.*, **18**, 1168 (1950).
17) S. Sato, K. Kikuchi and M. Tanaka, ibid., **39**, 239 (1963).
*3 Furthermore, the experiment on the naphthalene-photosensitized reaction of 2-butene was undertaken in this Institute. However, the reaction products were scarcely observed.[18]
18) T. Terao and S. Sato, private communications (1964).
19) A. C. G. Mitchell and M. W. Zemansky, "Resonance Radiation and Excited Atoms," Cambridge University Press, London (1934), p. 62.

Consequently, it may be considered that only the charge transfer process plays a leading role in this case, since the difference between the lowest triplet energy levels of 2-butene and that of naphthalene (2.6 eV.)[20] or that of anthracene (1.9 eV.)[20] is too large compared with that of benzene (3.6 eV).[20,21]

Summary

The radiolysis of *cis*-2-butene has been studied in the liquid phase at room temperature.

(1) The major products (and their *G*-values) were hydrogen (1.02), *n*-butane (0.83), 1-butene (0.40), *trans*-2-butene (2.29), C_8 hydrocarbons (2.30), and higher polymers, the *G*-values being independent of the total dose. Small amounts of $C_1 \sim C_3$ and $C_5 \sim C_7$ hydrocarbons were also formed. The hydrogen and the lower hydrocarbons except for *n*-butane were found, by using *p*-benzoquinone as a radical scavenger, to be produced for the most part through the molecular mechanism.

(2) The addition of benzene, naphthalene, and anthracene to liquid *cis*-butene have remarkable effects on the formation of *trans*-2-butene; thus, the cis-trans isomerization increases at a lower concentration of additives, while it decreases at a higher concentration of additives. The radical scavenging effect cannot explain these results. From a comparison of the experimental results with the ionization potentials and electron affinities of aromatics, it has been concluded that the increase in the isomerization at lower concentrations is due to the electron capture effect of additives, while the decrease at higher concentrations is due to the charge transfer from the butene to the additives.

This research was supported, in part, by the Watanabe Memorial Foundation for Scientific Research Promotion, to which the authors are grateful. This experiment owes much to Dr. Hirofumi Danno, who offered us a ^{60}Co-γ source at the Japan Atomic Energy Research Institute.

Laboratory of Physical Chemistry
Tokyo Institute of Technology
Meguro-ku, Tokyo (Y. H. & S. Sh.)

Department of Applied Physics
Tokyo Institute of Technology
Meguro-ku, Tokyo (S. Sa.)

20) R. Pariser, *J. Chem. Phys.*, **24**, 250 (1956).
21) H. B. Klevans and J. R. Platt, ibid., **17**, 470 (1949).

The Direct Iodination of Polyalkylbenzenes by the Crossed Jacobsen Reaction[1]

By Hitomi SUZUKI,* Takashi SUGIYAMA and Ryozo GOTO

(Received June 19, 1964)

The direct iodination of aromatic compounds may be effected satisfactorily when these compounds contain such activating groups as hydroxyl or amino groups. If we wish to introduce an iodine atom directly into a nucleus not activated by such powerful activating groups, however, the reaction must be carried out in the presence of an effective oxidizing agent. The reagents commonly employed are iodic acid,[2] common or fuming sulfuric acid,[3] nitric acid,[4] heavy metal oxides,[5] sodium persulfate or perchlorate,[6] silver salts,[7] ferric chloride,[8] and organic peroxides.[9] In the literature, however, few of these reagents have been employed with the

1) Part V on the Jacobsen Reaction; Part IV: This Bulletin, **36**, 1642 (1963).

* Present address: Department of Chemistry, Faculty of Science, Kyoto University, Kyoto.

2) A. Kekulé, *Ann.*, **137**, 162 (1866); A. Klages and W. Storp, *J. prakt. Chem.*, (2), **65**, 568 (1902); F. Boedtker, *Bull. soc. chim. France*, (4), **45**, 649 (1929); H. O. Wirth, O. Königstein and W. Kern, *Ann.*, **634**, 84 (1960).

3) A. Neumann, *Ann.*, **241**, 84 (1887); E. Rupp, *Ber.*, **29**, 1625 (1896); J. F. Durand and M. Mancet, *Bull., soc. chim. France*, (5), **2**, 665 (1935); "Organic Syntheses," Vol. 27, 78 (1947); Vol. 30, 55 (1950).

4) R. L. Datta and N. R. Chatterjee, *J. Am. Chem. Soc.*, **39**, 435 (1917); ibid., **41**, 292 (1919); A. Edinger and P. Goldberg, *Ber.*, **33**, 2875 (1900); "Organic Syntheses," Coll., Vol. I, 323 (1956).

5) A. Töhl, *Ber.*, **25**, 1521 (1892); Th. Curtius and H. Thyssen, *J. prakt. Chem.*, (2), **65**, 1, (1902); "Organic Sytheses," Coll., Vol. II., 375 (1943).

6) K. Elbs and A. Jaroslawzew, *J. prakt. Chem.*, (2), **88**, 92 (1913).

7) L. Birckenbach and J. Goubeau *Ber.*, **65**, 395 (1932); D. H. Derbyshire and W. A. Waters, *J. Chem. Soc.*, **1950**, 3694; I. R. L. Barker and W. A. Waters, ibid., **1952**, 150; "Organic Syntheses," Vol. 36, **46** (1956).

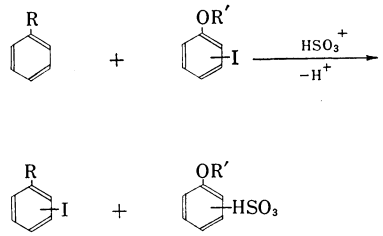
8) L. Meyer, *Ann.*, **231**, 195 (1885); *J. prakt. Chem.*, (2), **34**, 502 (1886).

9) H. Erlenmeyer, *Helv.*, **9**, 819 (1926); ibid., **10**, 620 (1927); Y. Ogata and H. Nakasima, *Tetrahedron*, **20**, 43 (1964).

highly alkylated benzenes. As the reaction proceeds through an electrophilic attack of an iodine atom on the nucleus, an increase in the number of alkyl groups attached to the ring enhances the reactivity of the compound. This increase, however, brings about an enhanced susceptibility of the compound to the undesired action of an oxidizing agent, and also to an increased steric repulsion to the entry of a bulky iodine atom into the nucleus. Both these effects reduce the yield of the product so markedly that most of the above reagents cannot be used successfully for the purpose of synthesizing iodo polyalkylbenzenes. Thus, from the synthetic point of view, the direct iodination of highly alkylated compounds is not necessarily a simple matter to effect. For example, if we use sulfuric acid or nitric acid as an oxidizing agent, the sulfonation or the nitration of the compound often proceeds in preference to iodination. Ferric chloride gives a complex mixture in which the desired iodinated product is a minor component, whereas iodic acid or organic peroxides afford the products, in most cases, in unsatisfactorily low yields.

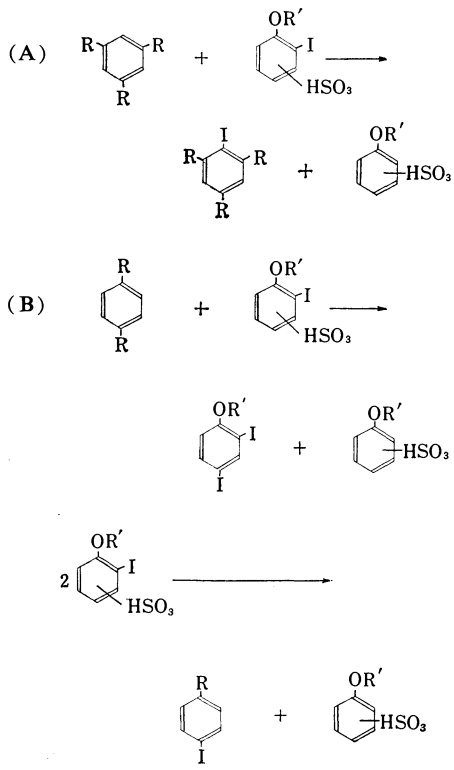
In earlier papers of this series,[10] we have shown that iodophenols and iodoanisoles, in the presence of sulfuric acid, readily undergo the disproportionation at room temperatures and afford polyiodo compounds in fairly high yields. This fact suggested to us that iodophenols or iodoanisoles might be used in conjunction with sulfuric acid as iodinating agents. The present work will present the results of an attempt to use these compounds as iodinating agents for polyalkylbenzenes.

This reaction may be represented by the following general equation:



In the present work, we used *o*-iodoanisole as an iodinating agent. In this reaction (the crossed Jacobsen reaction), the iodination of polyalkylbenzene competes with the disproportionation of *o*-iodoanisole. Since the iodine cation reacts more readily with iodoanisole to form polyiodo anisoles, care must be taken to select conditions which do not favor their formation. This was done by carrying out the reaction in an excess of hydrocarbon, thus avoiding the presence of excess iodoanisole in the system. Under these conditions, iodoanisole cannot successfully compete with the hydrocarbon, and the iodine cation, once formed, goes on to react with the excess hydrocarbon to give the iodinated product. On the other hand, the presence of a large excess of sulfuric acid causes such undesirable side reactions as sulfonation, the migration of the alkyl group, and the further decomposition of the iodinated products (iodo polyalkylbenzenes are generally unstable towards sulfuric acid and are readily decomposed to the resinous materials and free iodine). In order to prevent these side reactions, the hydrocarbon was brought to the simultaneous action of *o*-iodoanisole and sulfuric acid; that is, to the polyalkylbenzene to be iodinated, sulfuric acid and *o*-iodoanisole were simultaneously added drop by drop, while their proportion was maintained slightly in excess of the sulfuric acid.

Nine polyalkylbenzenes were subjected to the crossed Jacobsen reaction: pseudocumene, durene, pentamethylbenzene, *sym*-triethylbenzene, *sym*-tetraethylbenzene, *p*-diisopropylbenzene, *sym*-triisopropylbenzene, *sym*-tetraisopropylbenzene, and *p*-di-*t*-butylbenzene. Only polymethyl- and polyethylbenzenes underwent



10) H. Suzuki and R. Goto, *J. Chem. Soc. Japan, Pure Chem. Sec.* (*Nippon Kagaku Zasshi*), **84**, 167 (1963); ibid., **84**, 284 (1963); This Bulletin, **36**, 389 (1963).

this reaction smoothly at room temperature and gave acceptable yields of the products. Polyisopropyl- and poly-*t*-butylbenzenes, as would be expected from our previous works,[10] gave the iodinated products in poor yields. With some compounds, one of the isopropyl or *t*-butyl groups which occupied a position favorable, with respect to the directing effect of other groups present, to the entry of the iodine cation, is in part replaced. Thus, depending upon the structure of the polyalkylbenzenes, the reaction may occur by two different routes, A and B.

With polymethyl- and polyethylbenzenes which are activated by alkyl groups but not so overcrowded with them, the reaction proceeds through the route A. With polyisopropyl and poly-*t*-butylbenzenes, the aversion to the entry of a bulky iodine atom into the nucleus suppresses the formation of normal products so markedly that the reaction proceeds chiefly through the route B and results in either the replacement of an alkyl group or the disproportionation of *o*-iodoanisole.

The direct iodination of polyalkylbenzenes by the crossed Jacobsen reaction is characterized by the absence of a powerful oxidizing reagent, mild reaction conditions, and the easy separation of the products. This reaction, the use of which as a practical means of synthesis seems to be somewhat limited, affords a simple one-step preparation of iodinated polyalkylbenzenes from readily-available starting materials.

Experimental

1) General Procedure.—*a) Liquid Hydrocarbon.*—In a 100 ml. four-necked flask, fitted with a thermometer, a reflux condenser, and two dropping funnels, each a containing sulfuric acid and *o*-iodoanisole, the hydrocarbon was placed and magnetically stirred. The flask was then immersed in a water-bath and heated to the desired temperature. Sulfuric acid and *o*-iodoanisole were added drop by drop at such a rate that a slight excess of sulfuric acid was maintained in the system. Under these conditions, no alkyl migration occured. After completion of dropping, the mixture was stirred for some additional hours and then poured into water. The resulting organic layer was extracted with a small amount of ether, and the extract was washed with a diluted sodium bisulfite solution to remove free iodine and then dried over anhydrous calcium chloride. After this drying, the ether was removed by distillation. The fractionation of the residual oil gave some amounts of unchanged hydrocarbon, followed by the expected iodinated polyalkylbenzene.

b) Solid Hydrocarbon.—Solid hydrocarbon was dissolved in a small amount of cyclohexane and then subjected to iodination in the manner described above. After the completion of the reaction, the mixture was poured into water; the organic layer was separated, washed with a diluted solution of sodium bisulfite, and freed from the solvent. The crystalline residue was chromatographed on an alumina column. The elution of the column with petroleum ether gave unchanged hydrocarbon, followed by the desired iodinated product, which was then recrystallized from an appropriate solvent to yield the pure product. 2, 4-Diiodoanisole, a disproportionation product, was held on a column and readily removed from the iodinated polyalkylbenzene.

2) Dialkylbenzenes. — *p-Diisopropylbenzene.* — *p*-Diisopropylbenzene (24.3 g., 0.15 mol.) was stirred and warmed to 35～40°C. *o*-Iodoanisole (23.4 g., 0.10 mol.) and sulfuric acid (15 g., 0.15 mol.) were added over a 1.5-hr. period. The reddish-violet mixture was, after 4 hours' agitation, poured into water and worked up as described in 1a). The distillation of the oil gave unchanged *p*-diisopropylbenzene (13.8 g., b. p. 91～93°C/19 mmHg), a mixture of *o*-iodoanisole and a lower-boiling iodo compound (7.1 g., b. p. 105～120°C/19 mmHg), a higher-boiling iodo compound (6.4 g., b. p. 140～160°C/19 mmHg), and a residue (ca. 2.0 g.). The mixture fraction, on oxidation, gave a small amount of *p*-iodobenzoic acid, m. p. 262～265°C. Thus, the iodination of *p*-diisopropylbenzene was accompanied by the partial replacement of one of the isopropyl groups. The redistillation of the higher-boiling fraction gave 6.0 g. of monoiodo-*p*-diisopropylbenzene, b. p. 143～146°C/22 mmHg.

Found: C, 49.71; H, 5.81. Calcd. for $C_{12}H_{17}I$: C, 50.00; H, 5.95%.

p-Di-t-butylbenzene.—To the stirred solution of *p*-di-*t*-butylbenzene (3.7 g., 0.02 mol.) in cyclohexane (25 ml.) *o*-iodoanisole (5.9 g., 0.025 mol.) and sulfuric acid (3.0 g., 0.03 mol.) were added at 30～33°C. The reaction mixture turned immediately dark-violet, and a remarkable liberation of free iodine was observed. After 3 hours' agitation, the mixture was worked up as described in 1b). The crystalline residue (6.4 g.), chromatographed on an alumina column, gave unchanged *p*-di-*t*-butylbenzene (3.1 g., m. p. 75～76°C), a pink-colored oil (ca. 0.5 g.), and 2, 4-diiodoanisole (2.5 g., m. p. 65～67°C). After the mixture had stood in the refrigerator, some feather-like crystals were separated out from the oil fraction, which, on recrystallization several times from petroleum ether, gave white soft needles, m. p. 49～50°C. The elemental analysis of this material indicated that it was diiodinated di-*t*-butylbenzene, whose structure, inferred by analogy, might be 2, 5-diiodo-1, 4-di-*t*-butylbenzene.[11]

Found: C, 37.65; H, 4.27. Calcd. for $C_{14}H_{20}I_2$: C, 38.04; H, 4.56%.

The oily part was supposed to be a mixture of *p*-iodo-*t*-butylbenzene, a monoiodinated product, and unchanged *o*-iodoanisole, but none of them could be identified because of its small quantity.

3) Trialkylbenzenes.—*Pseudocumene (1, 2, 4-Trimethylbenzene).*—Pseudocumene (12.0 g., 0.1 mol.)

11) The Jacobsen reaction of halogenobenzenes usually proceeds like the progressive halogenation of the parent compound. Cf. H. Suzuki, This Bulletin, **36**, 1642 (1963).

was iodinated by using *o*-iodoanisole (15.6 g., 0.15 mol.) and sulfuric acid (10 g., 0.1 mol.), and 14.5 g. of a monoiodinated product, b. p. 121~125°C/17~18 mmHg, was obtained. This might be a mixture of several isomers, because it could not be completely solidified on standing in ice bath. The comparatively low yield (69% based on the unrecovered hydrocarbon) is attributed in part to the easy sulfonation of pseudocumene, and in part to the instability of the product towards the action of sulfuric acid. 5-Iodopseudocumene, m. p. 34~36°C.

Found: C, 43.77; H, 4.48. Calcd. for $C_9H_{11}I$: C, 43.92; H, 4.51%.

sym-Triethylbenzene.—To *sym*-triethylbenzene (24.3 g., 0.15 mol.), *o*-iodoanisole (23.4 g., 0.1 mol.) and sulfuric acid (15 g., 0.15 mol.) were added at 30~32°C over a 1.5 hr. period. Little iodine was liberated. After standing overnight, the mixture was worked up as usual. The fractionation of the oil gave unchanged triethylbenzene (12.7 g., b. p. 115~117°C/29 mmHg), *o*-iodoanisole (4.5 g., b. p. 112~115°C/18 mmHg), a monoiodinated fraction (17.9 g., b. p. 150~153°C/16 mmHg), and a residue (ca. 0.5 g.). The redistillation of the monoiodinated fraction gave 17.1 g. of monoiodo-*sym*-triethylbenzene (b. p. 169~170°C/31 mmHg).

Found: C, 49.74; H, 6.00. Calcd. for $C_{12}H_{11}I$: C, 50.01; H, 5.95%.

sym-Triisopropylbenzene.—*sym*-Triisopropylbenzene (20.4 g., 0.1 mol.) was iodinated with *o*-iodoanisole (15.6 g., 0.07 mol.) and sulfuric acid (10 g., 0.1 mol.) at 35~38°C by the same method used above. After 3 hours agitation, the mixture was left to stand overnight. Working up as usual and the distillation of the residual oil gave the starting materials unchanged (20.0 g., b. p. 114~120°C/18 mmHg), iodine containing a higher boiling fraction (6.5 g., b. p. 130~180°C/18 mmHg), and a residue (ca. 2.0 g.). This high boiling fraction was chromatographed on a short column to remove 2,4-diiodoanisole. It yielded 5.9 g. of monoiodo-*sym*-triisopropylbenzene, b. p. 173~175°C/28 mmHg.

Found: C, 54.06; H, 7.02. Calcd. for $C_{15}H_{23}I$: C, 54.56; H, 7.02%.

4) Tetraalkylbenzenes.—*Durene* (*sym-Tetramethylbenzene*).—Durene (4.0 g., 0.03 mol.) was dissolved in cyclohexane (5 ml.) and then iodinated with *o*-iodoanisole (11.7 g., 0.05 mol.) and sulfuric acid (7 g., 0.07 mol.) at 30~35°C. Little iodine was liberated. After 4 hr., the mixture was, diluted with water and extracted with cyclohexane. The evaporation of the solvent, followed by the chromatography of the residual oil on an alumina column, gave unchanged durene (ca. 0.5 g.) and monoiododurene (5.2 g., m. p. 80~81°C). A mixed melting point determination with an authentic specimen showed no depression.

Found: C, 46.29; H, 5.10. Calcd. for $C_{10}H_{13}I$: C, 46.16; H, 5.04%.

sym - Tetraethylbenzene. — *sym* - Tetraethylbenzene (28.5 g., 0.15 mol.) was iodinated by using *o*-iodoanisole (23.4 g., 0.1 mol.) and sulfuric acid (15 g., 0.15 mol.) at 30~33°C. After 4 hr., the mixture was treated as usual. The distillation of the oily product gave the starting materials unchanged (23.5 g., b. p. 105~135°C/19 mmHg), an iodinated products fraction (15.5 g., b. p. 155~175°C/19 mmHg), and a residue (ca. 2.0 g). To remove 2, 4-diiodoanisole, the iodinated products fraction was chromatographed on an alumina column with petroleum ether. The redistillation of the resulting oily material yielded 13.5 g. of modoiodo-*sym*-tetraethylbenzene, b. p. 186~188°C/26 mmHg.

Found: C, 52.60; H, 6.57. Calcd. for $C_{14}H_{21}I$: C, 53.17; H, 6.70%.

sym-Tetraisopropylbenzene.—Attempts to iodinate this compound gave only the starting material unchanged and 2, 4-diiodoanisole. A large amount of free iodine was liberated, and the disproportion of *o*-iodoanisole was the only reaction that proceeded.

5) Pentamethylbenzene.—To the stirred solution of pentamethylbenzene (7.4 g., 0.05 mol.) in cyclohexane (10 ml.), *o*-iodoanisole (15.2 g., 0.07 mol.) and sulfuric acid (10 g., 0.1 mol.) were added at 34~36°C over a 1.5 hr. period. After 4 hr., the mixture was worked up as usual. The chromatography of the crystalline residue on an alumina column gave unchanged pentamethylbenzene (ca. 1.0 g., m. p. 51~53°C), iodopentamethylbenzene (7.9 g., m. p. 141~142°C), and a small amount of 2, 4-diiodoanisole. The melting point of our iodopentamethylbenzene differs from that of Töhl (m. p. 129°C)[5] by 12°C.

Found: C, 48.22; H, 5.59. Calcd. for $C_{11}H_{15}I$: C, 48.18; H, 5.52%.

Summary

A method has been developed for the direct iodination of certain polyalkylbenzenes by the transfer of an iodine atom of iodoanisole. It consists of the simultaneous addition of iodoanisole and sulfuric acid to the polyalkylbenzene to which the transfer is to be made. In this way, iodo compounds have been prepared from eight polyalkylbenzenes.

The authors wish to acknowledge the valuable suggestions of Professor Sango Kunichika.

Institute for Chemical Research
Kyoto University
Takatsuki, Osaka

Acid-base Concept and Catalytic Activity of Oxides

By Ken-ichi TANAKA* and Kenzi TAMARU**

(Received July 1, 1964)

In heterogeneous catalysis by metal oxide, many close correlations between the catalytic activity, including its selectivity, and the acidity of the oxide have been indicated. Most commonly the correlations have been discussed in connection with such typical acidic solid catalysts as silica-alumina. However, a more general treatment has been undertaken in this report to study the general trend of the catalytic activity of metal oxides.

Generally speaking, the strength of an acid is determined by the equilibrium constant between the acid and a base, such as water, for instance, in the following manner:

$$HA + H_2O = H_3O^+ + A^-$$

The more the equilibrium shifts to the right, the stronger the acid HA. It simultaneously depends upon the strength of the conjugate base, A^-; the weaker the conjugate base, thus with less of a tendency to combine with the proton, the stronger, the acid HA. Consequently, the strength of the acid depends upon the relative strength of the acid and its conjugate base.[1]

As is generally accepted, strong acids, such as sulfuric and nitride acids, are neuteralized with water molecules in an aqueous solution to show a "leveling effect," and their acidity practically drops to that of H_3O^+. Consequently, the stronger acids can stay comparatively strong in a medium, the protonated forms of which are stronger acids than the original acids.

Accordingly, it is considered that the proton on an oxide surface can behave as a strong acid if the oxide surface is more acidic, or less basic. The less basic the oxide surface is, and thus with less of a tendency to hold protons, the stronger the "protonated" surface of the oxide behaves as an acid, as the conjugate base is weak. When an acid comes into contact with an oxide surface, it can stay acidic if the protonated surface of the oxide is more acidic, while it is neutralized to form a salt if the oxide is more basic, showing a "leveling effect."

In the case of oxy-acids, it has been shown that the strength of the acid is closely correlated with the partial charge on the oxygen in the acid, or in the conjugate base, as shown in Fig. 1.[2] A high degree of deficiency of electrons on the oxygen is associated with a high acidity of the acid. For instance, as a more electronegative atom is added to an oxy-acid, the electronegativity of the acid increases, with a low partial charge on the oxygen, and the strength of the acid increases. The electronegative atom attracts electrons to itself until the electronegativity of each atom in the acid molecule is equalized. The acidities of hypochlorous, chlorous, chloric and perchloric acids are examples.

The acidity of the oxide surface can be treated in a similar manner, and the partial charge on the oxygen in the oxide can be correlated with the acidity of the oxide surface. The data on the partial charge on the

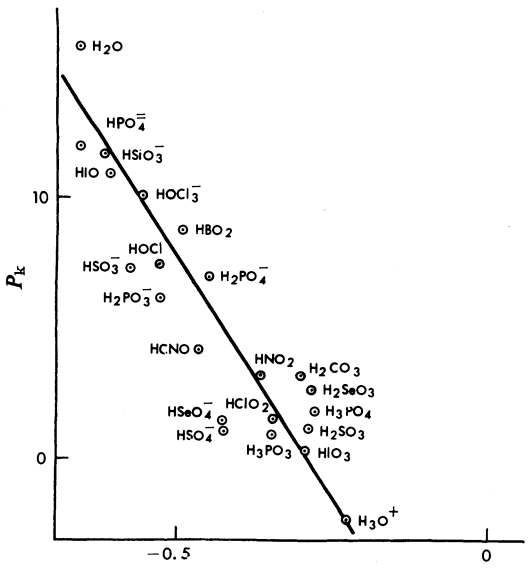


Fig. 1. The dependence of acidity upon relative partial charge on oxygen in oxy-acids. (by Sanderson[2])

* Present address: Research Laboratory of Resources Utilization, Tokyo Institute of Technology, Meguro-ku, Tokyo.

** Present address: Department of Chemistry, Faculty of Science, The University of Tokyo, Hongo, Tokyo.

1) E.g. C. A. Vander Werf, "Acids, Bases, and the Chemistry of the Covalent Bond," Reinhold Pub. Corp., N. Y. (1961).

2) R. T. Sanderson, "Chemical Periodicity," Reinhold Pub, Corp., N. Y. (1960).

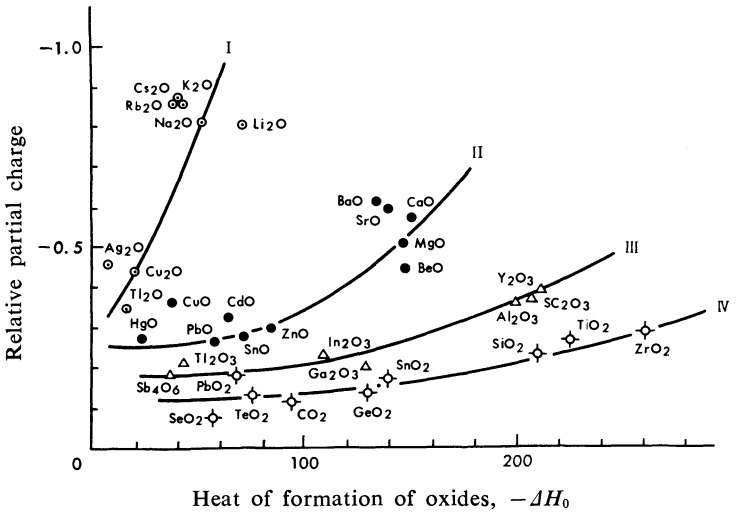


Fig. 2. The relation between the partial charge on oxygen and the heat of formation of oxides (kcal./metal atom).

oxygen in the oxides, which are given by Sanderson,[2] are not available in many oxides. However, as far as all the available data are concerned, a reasonably good correlation can be established between the partial charge and the heat of the formation of the oxides, as is shown in Fig. 2. In the figure, it may be seen that the partial negative charge on oxygen in the oxide becomes lower as the oxidation number of metals increases, and also as the heat of formation of the oxides decreases.

The metals which have lower heats of formation of the oxides have a comparatively higher electronegativities, and the difference between their electronegativities and that of oxygen is small, and they have a more covalent nature in the bond, which results in a low partial charge of oxygen and a high acidity. In these ways, the acid-base concept is applicable to the surface catalysis, especially those by oxide catalysts.

An example where the acidity of the oxide surface seemingly plays a role in the catalysis is the decomposition of alcohol and formic acid.[3-8] In the decomposition of alcohol and formic acid, a common trend has been observed in their selectivity, as is shown in Fig. 3,[3]

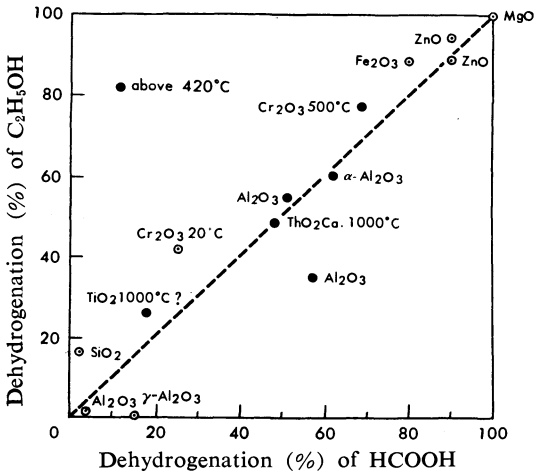


Fig. 3. The selectivity in the decomposition of formic acid and ethyl alcohol on metal oxides. (by Mars[3])

and the dehydration reaction is promoted by the acid, while the dehydrogenation reaction is promoted by the base, phenomena which are analogous to the homogeneous catalytic decomposition of alcohol and formic acid. If we plot the data by Mars[3] against the heat of formation, $(-\Delta H_0)$, Fig. 4 is obtained. Though the number of the oxide in the figure is not large enough, it may be concluded that the selectivity to dehydrogenation increases as the valency of the metal decreases (that is, as the oxide becomes more basic).

As to the effect of the heat treatment of the catalyst on the selectivity, Schwab[4] has revealed that it reduces the dehydration rate, while, in many cases, it increases the dehydrogenation rate. When the catalyst is treated

3) P. Mars, "The Mechanism of Heterogeneous Catalysis," Ed. by J. H. de Boer, Elsevier Pub. Co., Amsterdam (1960), p. 49.
4) G. M. Schwab and E. Schwab-Agallides, *J. Am. Chem. Soc.*, **71**, 1806 (1949).
5) A. Frachon de Pradel and B. Imelik, *J. chim. phys.*, **56**, 1 (1959).
6) J. H. de Boer and J. M. Vleeskens, *Koninkl. Ned. Akad. Wetenschap., Proc. Ser. B.*, **60**, 234 (1957); **61**, 2, 85 (1958).
7) F. Wolf and H. Beyer, *Z. anorg. u. allgem. Chem.*, **300**, 33 (1959).
8) J. J. F. Scholten, P. Mars, P. G. Menon and R. van Hardeveld, Third International Congress on Catalysis, Amsterdam, 1964.

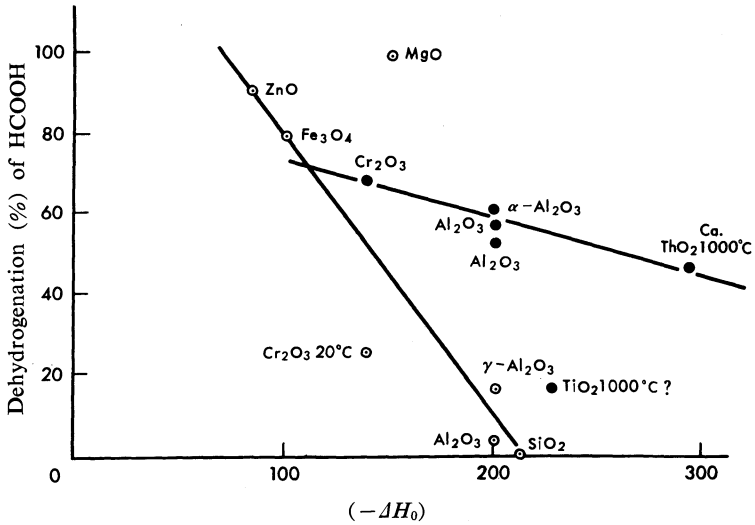


Fig. 4. The selectivity to dehydrogenation of formic acid on metal oxides and their heats of formation (kcal./metal atom).

at higher temperatures, with less oxygen on the surface, the surface behaves in a more basic manner, having a higher partial charge of oxygen, much like such general Brönsted oxy-acids as hypochlorous acid.

The general correlation of the catalytic activity with its acidity is also shown by the retardation of the dehydration reaction by basic substances: The addition of potassium hydroxide or calcium hydroxide reduces the catalytic activity of alumina and silica in the dehydration markedly.[5]

The kinetics of the overall reaction can also be interpreted on the same basis. The dehydration of formic acid is zero-order in formic acid and is not slowed down by the reaction products, while the decomposition of alcohol is retarded by water and is between zero- and first-order in alcohol. The strength of the acidity is in the decreasing order; formic acid>water>alcohol, which is the same order as with the strength of the adsorption on oxide surface. Accordingly, the kinetic behavior of the overall reaction may also reasonably be explained on the common basis.

Eucken attempted to correlate the selectivity of the decomposition with the quantity:

$$\eta=\frac{(\text{cation radius})^3}{(\text{mol. volume per cation})\,(\text{charge of cation})}$$

while Mars[3] worked with;

$$\left(\frac{\text{cation radius}}{\text{anion radius}}\right)^3\frac{1}{(\text{cation charge})^2}$$

The dehydration proceeds when the cation radius is small, that of the anion is large, and the charge of the cation is high. From the electrostatic point of view, a smaller cation radius implies more of a tendency to attract electrons (a stronger acid), while the higher cation charge and the larger anion radius are associated with the acidic property of the oxide. Accordingly, $1/\eta$ is a parameter of the electronegativities or the acidity of metal oxides. Mars suggested the possibility that formic acid donates a proton to the catalyst to result in dehydrogenation, as in the case of a metal catalyst.[3] The basicity of the catalyst surface would be associated with the dehydrogenation selectivity in a similar way.

In the hydration of propylene, the catalytic activities of metal sulfates are as follows, in

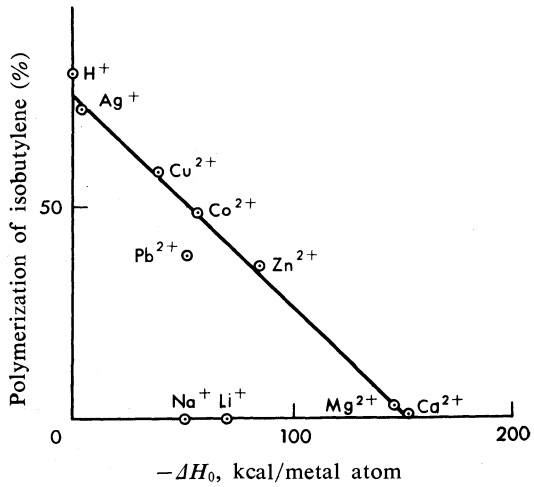


Fig. 5. The catalytic activity of metal phosphates for the polymerization of isobutylene and the heats of formation of the corresponding oxides.

decreasing order:[9] $Fe^{3+} > Al^{3+} > Cr^{3+} > Cu^{2+} > Zn^{2+} > Co^{2+} > Cd^{2+} > Ni^{2+} > Mn^{2+} > Mg^{2+} > K^{+}$, Na^{+}. They obey the general acidity rule—the more acidic ion has a higher activity, much as in the dehydration of alcohol. The sulfates which contain acidic, or less basic, metal ions, have much catalytic activity and, if the charge of metal ions is the same, the activity is high when $-\Delta H_0$ is low. The catalytic activity of phosphates for the polymerization of isobutylene[10] is shown in Fig. 5, where acidic salts are active in the reaction.

The interpretation of the selectivity of the oxide catalyst on the basis of the semi-conductor does not seem likely, for magnesium oxide and silicon dioxide are both insulators and also both the dehydrogenating zinc oxide and the dehydrating titanium(IV) oxide are seemingly *n*-type semi-conductors, as Mars pointed out previously.[3] Thus the acid-base concept of oxide seems to be really useful in interpreting their catalytic behavior.

The chemisorption of gases on the metal surface has been successfully correlated with the heat of the formation of the highest oxide of the metal, and this heat of formation and the electronegativities of gases approximately determine the initial heat of chemisorption of any gases on many metals, according to the available data.[11] The catalytic activity of metals, accordingly, has also been correlated with the heat of the formation of the metal oxide,[12] and, in a similar manner, that for metal oxide has been treated in connection with the heat of the oxide, or with its acidity.

9) Y. Ogino, *Catalyst* (*Shokubai*), 3, 191 (1961).
10) G. Shima and N. Ohta, *Shokubai* (*Res. Inst. Catalysis, Hokkaido Univ.*), 3, 112 (1948).
11) K. Tanaka and K. Tamaru, *J. Catalysis*, 2, 366 (1963).
12) K. Tanaka and K. Tamaru, Presented at the 16th Annual Meeting of the Chemical Society of Japan, Tokyo, April, 1963; to be published.

Summary

The catalytic activity of metal oxide has been correlated with the acidity of the oxide surface. The acidity depends upon the partial charge on the oxygen in the oxide and also upon the heat of the formation of the oxide. Consequently, the catalytic behavior may be correlated with the heat of the formation of the oxide, as in the cases of the chemisorption of gases and catalytic activity by metals.

The decomposition of formic acid and alcohol and the polymerization of isobutylene have been treated on the basis of this concept, and the selectivity, or activity, of these reactions, their reaction kinetics, and also the effect of heat treatment have been discussed.

Department of Chemistry
Yokohama National University
Minami-ku, Yokohama

NMR Studies of the Rates of Inversion of o, o'-Bridged Biphenyls[1]

By Michinori Ōki, Hiizu Iwamura and Naohiro Hayakawa

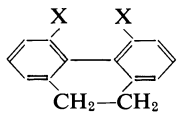
(Received July 9, 1964)

Since the success in the optical resolution of 6, 6'-dinitrodiphenic acid achieved by Christie and Kenner,[2] there have been accumulated many examples of the enantiomers of biphenyls in which the rotation around the pivot bond in the biphenyl skeleton is restricted either by the bulky groups on the ortho-positions or by bridging the two ortho-positions on either ring with a suitable ring number. As early as 1927[3] the kinetic examination of the restricted rotation was performed by measuring the rate of the racemization of the optically labile biphenyls with a polarimeter. The collected data were analyzed by Adams and Yan[4] in order to correlate the optical stability with the steric bulkiness of the ortho-substituents; that study contributed much to modern structural organic chemistry inasmuch as it introduced a measure of steric effects.

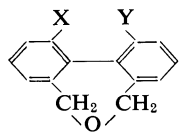
Although it is convenient, however, the polarimetric method expects inevitably the prior optical resolution of the samples, and so it can not be applied to those with a short life-time (with a $t_{1/2}$ less than a few minutes at room temperature). Lately the demand for

1) Preliminary communication; M. Ōki, H. Iwamura and N. Hayakawa, This Bulletin, **36**, 1542 (1963).
2) G. H. Christie and J. Kenner, *J. Chem. Soc.*, **1922**, 614.
3) R. Kuhn and O. Albrecht, *Ann*, **455**. 272 (1927).
4) R. Adams and H. C. Yan, *Chem. Revs.*, **12**, 261 (1932).

means of measuring the faster rate of rotation and inversion has been met, by the NMR technique[1,5,6] which, when properly applied,[7,8] should explore the rate processes with the first order rate constant of 1 to 10^3 sec^{-1}. The present paper constitutes a full description of a study of the rates of inversion of 9, 10-dihydrophenanthrenes (I, III, V) and 5, 7-dihydrodibenz [c, e] oxepins (II, IV, VI, VII, VIII).[1]



I: X=H
III: X=CH_3
V: X+X=CH_2CH_2



II: X=Y=H
IV: X=Y=CH_3
VI: X+Y=CH_2OCH_2
VII: X+Y=CH_2CH_2
VIII: X=H, Y=NO_2

When these biphenyls are fixed as non-planar or when the half-lives of their inversion are relatively long, the spectra of the bridging methylene groups will be composed of the A_2B_2 multiplets in I, III and V and AB quartets in II, IV, VI, VII and VIII. On the occasion of the other extreme, e. g., when the rate of the inversion is large relative to the chemical shift, δ_{AB}, in c. p. s. units, the spectra of the bridging methylene groups are expected to be composed of a singlet (A_4 and A_2 respectively). In the intermediate rate of the inversion, the spectra will change with the temperature, and the shape can be related to the life-time of the inversion. Therefore, the measurement of the NMR spectra was performed over a wide range of temperature.

Experimental

Spectral Measurements.—The NMR spectra were preliminarily obtained on a Varian V-4300 spectrometer operating at 56.4 Mc./sec., with a variable temperature probe accessory and a Dewar probe insert attached. The temperature was read from the microvoltage in the copper-constantan thermocouple mounted on the inside wall of the probe insert according to the calibration curve; the temperature can be regarded as accurate to ±1.0°C. Later all the measurements above −60°C were reexamined on a Varian A-60 spectrometer equipped with a variable temperature accessory at 60 Mc./sec.; the spectral data to be reported are based on the latter measurement unless otherwise stated.

The samples for the low- and high-temperature measurement were dissolved in carbon disulfide and in tetrachloroethylene respectively, to make ca. 10% solutions.

Within the measurement of a given sample, the strength of H_1 was held constant at around 0.04 mG. of the dial setting of the r. f. field, and the spectra were established as being far below the saturation condition by observing no lowering in the peak intensity on a slight raising of the r. f. field. The apparent amplitude of the normal signals decreases as the temperature ascends, mainly because of the thermal expansion of the solvent and the consequent apparent dilution. Accordingly, only the recorder level was changed, if necessary, from temperature to temperature, to determine the desired amplitude of the signals. Frequencies were read with respect to tetramethylsilane as an internal standard, and the usual sweep rate was 1 c.p.s./sec.

Since T_2 is practically determined by the inhomogeneity of the magnetic field, T_2 was regarded as independent of the kind of proton and so was measured directly from the width of the signal of tetramethylsilane by the wiggle-decay measurement.[7,9,10]

Materials.—The samples used for the measurement were known compounds, unless otherwise stated, and their physical constants agreed well with those in the literature.

1, 11-Ethano-5, 7-dihydrodibenz[c, e]oxepin (VII).—Ozone was passed from the generator into a solution of 5 g. of 4, 5-dihydropyrene in 100 ml. of chloroform for five hours at the nominal rate of 2 g./hr. at 0°C. Chloroform was distilled under diminished pressure, and the residue was dissolved in 50 ml. of ether. The solution was then added, drop by drop, into a solution of 5 g. of lithium aluminum hydride in 100 ml. of ether. This mixture was heated under reflux for an hour. The excess lithium aluminum hydride was destroyed by the addition of ethyl acetate, and then 100 ml. of 5% sulfuric acid was added to decompose the alkoxides. The organic layer was separated, and the aqueous layer was extracted with three 50 ml. portions of ether. The combined ether solution was washed with a 5% sodium bicarbonate solution and dried over potassium carbonate. The residue, obtained after the removal of the ether, was freed from the unoxidized starting material by chromatography on an alumina column; 4, 5-dihydropyrene was eluted with petroleum ether, and 4, 5-bishydroxymethyl-9, 10-dihydrophenanthrene, with ether.

The bishydroxymethyl compound was, without identification, dissolved in 100 ml. of toluene and heated under reflux with 0.5 g. of *p*-toluenesulfonic acid for eight hours. The solution was washed twice with 5% sodium bicarbonate, and the toluene was distilled off. The residue was recrystallized from petroleum ether to give 2 g. of VII, m. p. 92 ~93°C.

Found: C, 86.51; H, 6.39. Calcd. for $C_{16}H_{14}O$: C, 86.45; H, 6.35%.

1-Nitro-5, 7-dihydrodibenz[c, e]oxepin (VIII).—To

5) W. L. Meyer and R. B. Meyer, *J. Am. Chem. Soc.*, **85**, 2170 (1963).
6) R. J. Kurland, M. B. Rubin and W. B. Wise, *J. Chem. Phys.*, **40**, 2426 (1964).
7) H. Strehlow, in A. Weissberger, "Technique of Organic Chemistry," Vol. VIII, Interscience, New York, N. Y. (1963), Chap. 17, p. 865.
8) H. Iwamura, *Kagaku no Ryoiki*, **17**, 266 (1963).
9) B. A. Jacobsohn and R. K. Wangsness, *Phys. Rev.*, **73**, 942 (1948).
10) G. V. D. Tiers, *J. Phys. Chem.*, **65**, 1916 (1961).

a stirred mixture of 300 ml. of a sodium borohydride solution (1 M in diethylene glycol diethyl ether) and 50 ml. of an anhydrous aluminum chloride solution (2 M in the same solvent),[11] 20 g. of dimethyl 6-nitrodiphenate[12] was added; the resulting solution was warmed on a water bath to 75°C. After five hours' heating, the mixture was cooled to room temperature and poured onto ice-water containing 1 N hydrochloric acid to decompose the remaining reagent; the solution was then evaporated on a water bath, and the higher boiling solvent was distilled under reduced pressure by the application of a water pump. The remaining solid was recrystallized from benzene to afford 13 g. of 2,2'-bishydroxymethyl-6-nitrobiphenyl, m. p. 93°C.

Found: C, 64.95; H, 5.37; N, 5.46. Calcd. for $C_{14}H_{13}O_4N$: C, 64.86; H, 5.05; N, 5.40%.

The bishydroxymethyl compound (7.8 g.) was heated with 200 ml. of 50% sulfuric acid at 100°C for an hour.[13] On cooling, the oily mass solidified and was recrystallized from ethanol to give 5.0 g. of the desired oxepin, m. p. 115°C.

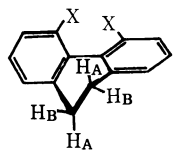
Found: C, 69.84; H, 4.68; N, 5.79. Calcd. for $C_{14}H_{11}O_3N$: C, 69.90; H, 4.59; N, 5.80%.

Results and Discussion

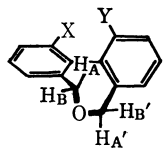
The *o,o'*-bridged biphenyls can be classified into three groups according to the characteristic dependence of their NMR spectra on the change in temperature.

i) Rigid Biphenyls and Biphenyls of a Slow Inversion Rate.—III,[13] IV[14] and VI[15] have been separated into optical antipodes and shown not to racemize easily at room temperature. In these rigid structures, two protons on a methylene group are situated in different magnetic environments and, consequently, are not equivalent (IX and X). As expected, the signals assigned to the methylene protons are of a multiplet structure, although, in the spectrum of III, the separation is not clear and the broadness of the signal relative to those of methyl and TMS is the sole indication at 60 Mc./sec.[16] Table I shows the observed chemical shifts and coupling constants of the methylene protons, together with the half-life of racemization at room temperature.

In order to see the origin of the difference in the chemical shift between the two methylene protons, δ_{AB}, molecular models were



IX



X

Table I. Rigid biphenyls and biphenyls of a slow inversion rate

Compound	Spectrum pattern	τ-value (center)	δ_{AB} c.p.s.	J_{AB} c.p.s.	$t_{1/2}^{23°}$ min.
III	(A_2B_2)	7.38	(6)	—	162[14]
IV	AB	6.00	19.6	11.0	
VI	AB	5.65	22.8	11.5	11

Table II. Long-range shielding of methylene protons by the benzene rings

		ρ_1*	z_1	ρ_2	z_2	$\Delta\sigma$ p.p.m.	δ_{AB} p.p.m.
III	H_A	2.27	0.65	2.14	1.50	−0.62	0.22
	H_B	2.47	0.25	3.27	0.91	−0.84	
IV	H_A	2.28	0.40	1.43	1.63	+0.05	0.74
	H_B	2.35	0.19	2.60	2.10	−0.69	

* ρ and z are cylindrical coordinates expressed in units of the radius of the benzene ring (1.39Å) with the z axis normal to the plane of the ring at its center and with the origin at the center. 1 and 2 refer to the contiguous and the remote benzene rings respectively.

set up using conventional structural dimensions,[17] and the difference in the effect of the long-range shielding of the two benzene rings on the two protons in a methylene group was calculated according to the numerical table of Johnson and Bovey.[18] As regards the length of the pivot bond, R, and the interplanar angle, θ, made by the two benzene rings, of III and IV, it is not proper to adopt those of I and II[19] respectively, because the conjugation bands in the ultraviolet spectra of III and IV have been shown[20] to exhibit a hypsochromic shift of 4~5 mμ from those of I and II respectively. Therefore, these parameters were calculated according to the method of Suzuki[19,21] from the absorption maxima of the conjugation band; $R=1.49$Å and $\theta=29°$

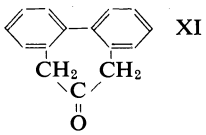
11) H. C. Brown and B. C. S. Rao, *J. Am. Chem. Soc.*, **78**, 2582 (1956).
12) J. W. Brooks, M. M. Harris and K. E. Howlett, *J. Chem. Soc.*, **1957**, 1934.
13) G. Wittig and H. Zimmermann, *Chem. Ber.*, **86**, 629 (1953).
14) K. Mislow and H. B. Hopps, *J. Am. Chem. Soc.*, **84**, 3018 (1962).
15) K. Mislow and M. A. W. Glass, ibid., **83**, 2780 (1961).
16) In the "High Resolution NMR Spectra Catalog," Vol. II, issued by Varian Associates, Palo Alto, California, U. S. A., the methylene proton signal measured at 100 Mc./sec. is listed as spectrum No. 654, δ_{AB} being 0.1 p. p. m.
17) Ar-C_{sp^3} distance, 1.51 Å; C-H distance, 1.09 Å; C-O distance, 1.42 Å; CH_2-CH_2 distance, 1.54 Å.
18) C. E. Johnson, Jr., and F. A. Bovey, *J. Chem. Phys.*, **29**, 1012 (1958).
19) H. Suzuki, This Bulletin, **32**, 1340, 1350, 1357 (1959).
20) E. A. Braude and W. F. Forbes, *J. Chem. Soc.*, **1955**, 3776.
21) ν_A's are 38314 cm^{-1} (261.0 mμ) and 41152 cm^{-1} (243 mμ) for III and IV respectively. As the longer-wavelength-side reference, ν_L=37735 cm^{-1} (265 mμ) of 9, 10-dihydrophenanthrene was adopted, for which $\theta=20°$ (G. H. Beavan, D. M. Hall, M. S. Lesslie and E. E. Turner, *J. Chem. Soc.*, **1952**, 854).

for III, and $R=1.51$ Å and $\theta=57°$ for IV.[22]

Table II summarizes the results of the calculation. Agreement in δ_{AB} is fairly good in III, considering the approximation used in the calculation. In IV, however, the calculation leads to a δ_{AB} value higher by 0.4 p. p. m.; this discrepancy should be ascribed to the anisotropy of the neighboring oxygen atom.

The spectra of this class of biphenyls can thus be characterized by the split methylene signals and by no temperature dependence of the spectra in the conventional temperature range of the commercial NMR spectrometer. The rate of inversion can be estimated to be not more than δ_{AB} sec^{-1} at the highest temperature attained by the measurement. Thus, the upper limit of the rate and the lower limit of the energy of activation for racemization can be drawn.

ii) Biphenyls of a Fast Inversion Rate.—I, V and XI show a singlet methylene signal at room temperature and retain the singlet as low as −90°C. Table III shows the chemical



XI

shifts of the methylene protons at room temperature. They are quite independent of the temperature, and only the displacement within 10 c. p. s. towards the higher applied magnetic field is usually observed as the temperature is lowered to −60°C.

TABLE III. THE CHEMICAL SHIFTS OF THE METHYLENE PROTONS
(in carbon disulfide at room temperature)

	I	V	XI
τ-value	7.18	7.15	6.68

There are three possibilities for the temperature-independent singlet methylene signals: 1) The inherent identity of the chemical shifts of the two methylene protons by the genuine or virtual coplanarity of the skeleton. Fluorene, which has a singlet methylene signal at τ, 6.19, is a typical example. 2) The coincidence of the chemical shifts, which in this case are determined by the anisotropy of the neighboring groups, mainly of the two benzene rings, and by the solvent effect, as exemplified by the methylene protons in 1, 11-dimethyl-5, 7-dihydrodibenz [c, e] thiepin in deuteriochloroform.[23,24] 3) rapid inversion and consequent averaging of the magnetic environment.

Case 2 can possibly be explored by the study of the solvent effect.[24] Cases 1 and 3 can be discriminated by the inspection of the ultraviolet spectra, since the ultraviolet spectroscopy conforms to the Franck-Condon principle and, even in case 3, information on the structure at the ground state can be obtained and the non-coplanarity is accompanied by a hypsochromic shift of the conjugation band at ca. 250 mμ.

As far as I, V and XI are concerned, it is likely[20] that they belong to case 3. In these circumstances, the rates of inversion can be estimated to be not less than δ_{AB} sec^{-1} at the lowest temperature measured, and so the higher limit of the energy of activation can be deduced. Since log A of the inversion in o,o'-bridged biphenyls is, on the average, 12,[25] the activation energy of the inversion is obtained as less than 9 kcal./mol. in I, V and XI.

iii) Biphenyls of an Intermediate Inversion Rate. — Although VII shows, at room temperature, two singlet signals at τ 7.20 and τ 5.75 due to the protons on the CH_2CH_2 and CH_2OCH_2 groups respectively, the latter signal begins to decrease and gradually broaden as the temperature goes down to −50°C. At −58°C, the separation into a vague multiplet sets in. At −60°C, a resonance pattern of a characteristic AB-quartet can be clearly recognized, as is shown in Fig. 1. Below −80°C, the signal is rigorously determined as $\delta_{AB}=25.9$ c. p. s. and $J_{AB}=11.4$ c. p. s. at 56.4 Mc./sec. Even at this temperature, the signal at the higher applied magnetic field does not separate into an apparent multiplet, but is only broadened a little. Since the δ_{AB} of the methylene protons on the CH_2CH_2 group is smaller, the averaging of the resonance signals is still occurring in the rate process through which the signal due to CH_2OCH_2 with a larger δ_{AB} does not coalesce. Since the exchange broadening of the two interacting nuclear spin resonance signals has been treated theoretically by Alexander,[26] the analysis of the variation in this behavior of spectra with the temperature can be performed. The height of the coalesced singlet relative to that at zero life-time, $(v/v_0)_{max}$, can be related to the

22) In order to accomodate the molecular models with these structural parameters, a slight distortion of the bond angles in the cyclohexadiene and the dihydrooxepin rings in III and IV respectively is necessary. They are within 2° and do not affect the result materially.

23) "High Resolution NMR spectra Catalog," Vol. II, No. 657, Varian Associates, Palo Alto, California, U. S. A.

24) While this manuscript was being prepared, K. Mislow and his coworkers published a lengthy NMR study of the bridged biphenyls and showed a remarkable solvent effect (*J. Am. Chem. Soc.*, **86**, 1710 (1964)).

25) D. M. Hall and M. M. Harris, *J. Chem. Soc.*, **1960**, 490.

26) S. Alexander, *J. Chem. Phys.*, **37**, 967 (1962).

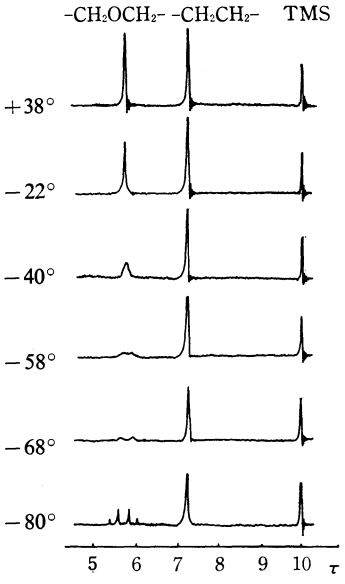


Fig. 1. Temperature dependence of the methylene proton signals of VII (at 56.4 Mc./sec.).

mean life-time, τ, through the observed parameters, δ_{AB}, J_{AB}, and T_2, according to Eq. 1.

$$(v/v_0)_{max} = 1 - \frac{2T_2\delta_{AB}^2\tau + (T_2^2\delta_{AB}^4 + \delta_{AB}^2)\tau^2}{4 + 4\left(\frac{1}{T_2} + T_2\delta_{AB}^2\right)\tau + \left\{\left(\frac{1}{T_2} + T_2\delta_{AB}^2\right)^2 + J_{AB}^2\right\}\tau^2} \quad (1)^{27)}$$

Furthermore, at the very time of coalescence, Eq. 2 is obtained, provided $1/T_2$ is zero:

$$\tau_c = \frac{\sqrt{2}}{\pi(\delta_{AB}^2 + 6J_{AB}^2)^{1/2}} \quad (2)^{28)}$$

Figure 2 corresponds to Eq. 1 applied to VII, and τ at a given temperature can now be obtained graphically from the $(v/v_0)_{max}$ observed in Table IV. $\log(1/\tau)$'s make a straight line against $1/T$, and from the slope, the energy of activation of the inversion can be determined (Table VI).

Since the two methylene groups in VIII are no longer equivalent, VIII exhibits double AB-quartets at room temperature: CH_2 attached to the benzene ring without a nitro-group, τ, 5.77 (center), $\delta_{AB}=28.7$, $J_{AB}=11.80$ c. p. s.; and attached to the benzene ring with a nitro-group, τ, 5.61 (center), $\delta_{AB}=16.05$, $J_{AB}=11.4$ c. p. s.

27) Obtained from the imaginary part of Eq. 57 in reference 26 by putting $\Delta=0$. v_0 can be obtained by extrapolating the peak height, v, vs. the $1/T$ curve to an infinite temperature.

28) Equation 2 is derived by putting the second derivative at $\Delta=0$ of the imaginary part of Eq. 57[26] equal to zero. τ_c stands for the life-time just when the quartet signal coalesces to a singlet signal.

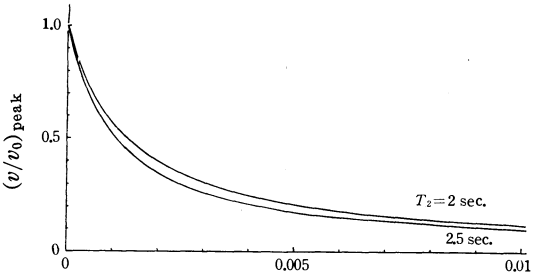


Fig. 2. Relation between the relative peak heights and the mean life-time for VII; $\delta_{AB}=27.5$, $J_{AB}=11.4$ c. p. s., in Eq. 1.[29)]

Table IV. Variation in the peak heights of the methylene signals in VII with the temperature

t, °C	$(v/v_0)_{max}$**	$\log(1/\tau)$
40	0.999	—
22	0.986	4.80
0	0.965	4.37
−10	0.909	3.92
−20	0.804	3.50
−30	0.678	3.18
−40	0.538	2.95
−50	0.241	2.38
−58	—	1.94*

* $\log(1/\tau_c)$

** The v at each temperature is relative to the height of the TMS signal on the same chart.

Contrary to the optically rather stable biphenyls (group i), the quartet signals deform easily as the temperature rises. The quartet at the lower applied magnetic field begins to broaden earlier and coalesces at 56°C, while that at the higher field has the coalescence temperature of 65°C. In the preliminary communication,[1)] the kinetic parameters of the rate process were determined from the two coalescence temperatures of the resonance signals with different chemical shifts. Since it is difficult to determine the temperature of coalescence as accurately as ±2°C, however, there is a danger that the data will contain undesirable errors. Therefore, VIII was subjected to the same analysis as was VII.

Figure 3 shows the dependence of the apparent spectra on the temperature. In Table V are recorded the data on the peak heights.

$\log(1/\tau)$'s from two pairs of CH_2 protons lie on the same line against $1/T$ (Fig. 4);

29) T_2 values ranged between 2.0 and 2.5 sec. in the present measurements. The Arrhenius parameters are rather insensitive to T_2, and the error of ± 0.5 sec. in T_2 corresponds to the 5% inaccuracy of the results.

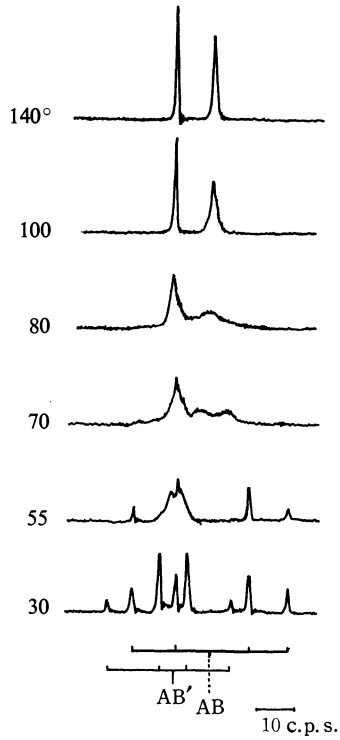
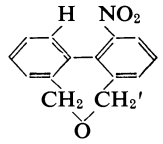


Fig. 3. Temperature dependence of the methylene proton signals of VIII.

TABLE V. VARIATION IN THE PEAK HEIGHTS OF THE METHYLENE SIGNALS IN VIII WITH THE TEMPERATURE



t, °C	$(v/v_0)_{max}$	τ, sec.	$(v/v_0)'_{max}$	τ', sec.
60	—	—	0.303	0.0089
70	0.171	0.0057	0.459	0.0046
80	0.267	0.0034	0.642	0.0022
90	0.476	0.0014	0.798	0.0010
100	0.648	0.00066	0.908	0.00039
110	0.824	0.00026	0.936	0.00028
120	0.835	0.00024	0.963	0.00016
140	0.905	0.00013	0.982	0.000075

from the slope, the energy of activation was determined (Table VI).

Although the authors could not find the broadening of the singlet signal in II in a preliminary study, later measurements revealed a coalescence temperature of as low as ca. −85°C, as has been pointed out by Kurland.[6] II, therefore, belongs to this class of biphenyls and will be dealt with in relation to the effect of the internal interaction of the substituents on the rate of inversion, together

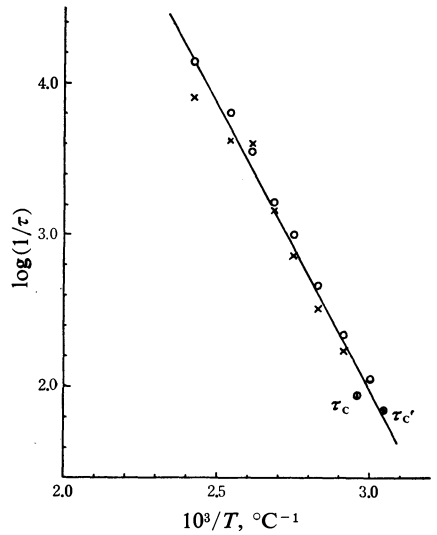
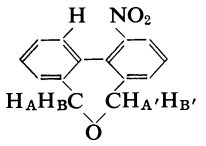


Fig. 4. Temperature dependence of the inversion rate for VIII.



× ; AB pair
○ ; A′B′ pair

TABLE VI. ARRHENIUS PARAMETERS OF THE INVERSION OF *o*, *o*′-BRIDGED BIPHENYLS

	E, kcal./mol.	log A
I	<9	12*
II	9.6±0.7[6]	
III	23.1[14]	12.8
IV	20	
V	<9	12*
VI	20.2[15]	11.7
VII**	10.5±0.5	12.6±0.4
VIII**	16.5±0.7	12.8±0.4

* Assumed value
** Present work

with 5, 7-dihydrodibenz [c, e] thiepin and 1-methyl-3,4 : 5,6-dibenzocyclohepta-3, 5-dien-1-ol.

In conclusion, the NMR technique is unique in determining the rate of inversion of those biphenyl derivatives which can not be submitted to the conventional polarimetric method because of their too great optical lability. The technique will undoubtedly find more applications in related fields.

Department of Chemistry
Faculty of Science
The University of Tokyo
Hongo, Tokyo (M. O. & H. I.)

Japan Atomic Energy
Research Institute
Tokai-mura, Ibaraki (N. H.)

Crystal Structures of Two Isomers of Bromo-methoxy Tropone

By Kozo FURUKAWA*1 Yoshio SASADA,*2 Akira SHIMADA*3 and Tokunosuké WATANABÉ*4

(Received July 11, 1964)

Hitherto we have reported on the crystal structures of several compounds with a seven-membered carbon ring[1-9] in order to elucidate the structures of molecules, accurate molecular dimensions, and the types of molecular packing as a measure of the forces exerted between molecules. As a part of this series, this paper will deal with the crystal structures of two isomers of bromo-methoxy tropone. Remarkable differences in dipole moment and chemical behavior between these isomers have already been reported and discussed in relation to their conformations.[10,11] It is hoped that this paper's determination of their molecular structures will throw light on these problems.

Experimental

Crystals of two isomers of bromo-methoxy tropone, $C_8H_7O_2Br$, were kindly supplied by Professor Tetsuo Nozoe, Tohoku University. Both of these crystallize out in the form of needle-like prisms; the melting point is 91°C for the 7-bromo isomer (7-bromo-2-methoxy tropone) and 76°C for the 3-bromo isomer (3-bromo-2-methoxy tropone).

Oscillation and Weissenberg photographs were taken around two principal axes for each by means of the Cu$K\alpha$ radiation, and the multiple-film technique was used to correlate the strong and weak reflections. The intensities were estimated by visual comparison with a calibrated scale, and the corrections for polarization, Lorentz and absorption factors were made in the usual way.

The crystal data thus obtained, the dimensions of the crystals used, and the range of intensity observed are given below.

7-Bromo Isomer.—Four molecules in an orthorhombic unit cell with $a=26.56$, $b=6.09$, and $c=4.97$ Å. Absent spectra: ($hk0$) when h is odd, ($0k0$) when k is odd, and ($00l$) when l is odd. Space group: $Pn2_1a$. Volume of the unit cell: 803.7 Å^3. Linear absorption coefficient for Cu$K\alpha$ radiation: $\mu=67.5\,cm^{-1}$. Total number of electrons per unit cell: $F(000)=424$. Rectangular dimensions of a cross section of crystals: 0.02×0.03 cm. for the c and b axis rotations. The relative intensities ranged from 1800 to 1 for ($hk0$) reflections and from 1200 to 1 for ($h0l$) reflections. Reflections from 92 planes were observed out of 108 possible ($hk0$)'s, and those from 129 planes out of 162 possible ($h0l$)'s.

3-Bromo Isomer.—Four molecules in a monoclinic unit cell with $a=7.64$, $b=26.57$, $c=3.99$ Å, and $\beta=101.5°$. Absent spectra: ($h0l$) when h is odd, and ($0k0$) when k is odd. Space group: $P2_1/a$. Volume of the unit cell: 793.7 Å.^{3} Linear absorption coefficient for CuK_α radiation: $\mu=68.2\,cm^{-1}$. Total number of electrons per unit cell: $F(000)=424$. Rectangular dimensions of a cross-section of crystals: 0.02×0.02 cm. and 0.03×0.04 cm. for the c and a axis rotations respectively. The relative intensities ranged from 510 to 1 for ($hk0$) reflections and from 2210 to 1 for ($0kl$) reflections. Reflections from 100 planes were observed out of 167 possible ($hk0$)'s, and those from 100 planes out of 121 possible ($h0l$)'s.

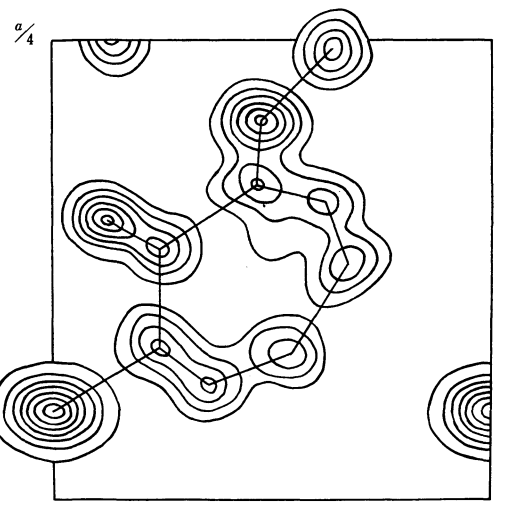
Structure Determination

7-Bromo Isomer.—A modified Patterson projection $P(UV)$ was synthesized, the modification factors being of the form of $(1/f)\cdot \exp B'(\sin\theta/\lambda)^2$, where f is the atomic scattering factor and an appropriate B' value is chosen to get a good resolution. This Patterson map showed not only the position of the bromine atom, but also clearly showed the shape of the molecule projected on the (001) plane, with an ambiguity for the methyl group. Two peaks were observed, both of which could be assigned to the methyl group. Thus, two sets of initial atomic coordinates were obtained, where the y coordinate of the bromine atom is taken arbitrarily to be zero because the b axis is polar in this space group. Atomic coordinates for each model structure

*1 Present address: Faculty of Technology, Kyoto University, Sakyo-ku, Kyoto.
*2 Present address: Institute for Protein Research, Osaka University, Kita-ku, Osaka.
*3 Present address: Faculty of Science, Osaka City University, Sumiyoshi-ku, Osaka.
*4 Present address: Department of Physics, College of General Education, Osaka University, Toyonaka, Osaka.

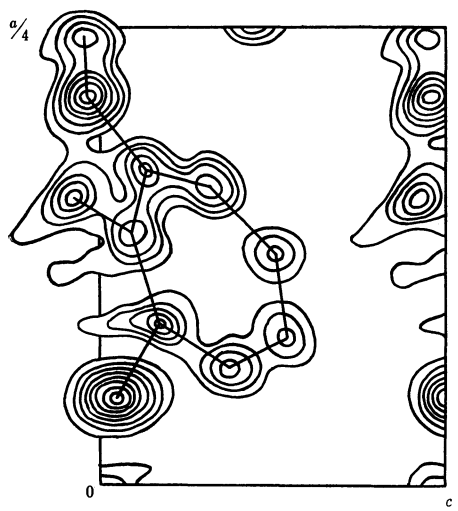
1) Y. Sasada, K. Osaki and I. Nitta, *Acta Cryst.*, **7**, 113 (1954).
2) Y. Sasada and I. Nitta, ibid., **9**, 205 (1956).
3) Y. Sasada and I. Nitta, This Bulletin, **30**, 62 (1956).
4) R. Shiono, *Acta Cryst.*, **14**, 42 (1961).
5) Y. Sasada, This Bulletin, **32**, 165 (1959).
6) Y. Sasada, ibid., **32**, 171 (1959).
7) C. Tamura, Y. Sasada and I. Nitta, ibid., **32**, 458 (1959).
8) Y. Takaki, Y. Sasada and I. Nitta, *J. Phys. Soc. Japan*, **14**, 771 (1959).
9) K. Osaki, unpublished.
10) Y. Kurita, S. Seto, T. Nozoe and M. Kubo, This Bulletin, **26**, 272 (1953).
11) T. Nozoe, Y. Kitahara and S. Masamune, *Proc. Japan Acad.*, **27**, 649 (1951).

were refined by successive Fourier and partial difference syntheses. The rate of convergence was rather low because of the presence of the heavy atom and the lack of a center of symmetry. The Fourier projection derived from the first model structure contained, in addition to the peaks expected from the initial structure, an unnegligible peak at the position where the methyl group was assumed in the second model structure. Since successive Fourier refinements did not make this ghost peak disappear, the first model structure was abandoned. The second model structure gave a fairly reasonable electron density distribution and a better agreement between observed and calculated structure factors than did the first model. The final electron density projection on the (001) plane is shown in Fig. 1 (a). The discrepancy index, $\Sigma||F_o|-|F_c||/\Sigma|F_o|$, reduced to 0.150 for ($hk0$) reflections if non-observed reflections were omitted. The best over-all temperature factor, B, was 4.4 Å^2.



the c axis downward

Fig. 1 (a)



the b axis upward

Fig. 1 (b)

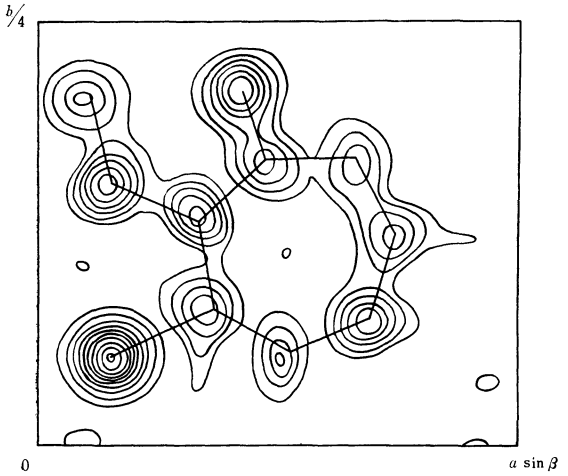
Fig. 1. Electron density of 7-bromo-2-methoxy tropone projected along (a) the c and (b) the b axes. Contours at equi-intervals in an arbitrary scale. One for every five countour lines are drawn around the bromine atom.

The coordinates of the bromine atom in the (010) projection were deduced easily from the Patterson function, $P(UW)$. The first Fourier projection of the electron density in this plane, calculated with $F(h0l)$'s of signs which result from the bromine atom alone, definitely showed the positions of all the atoms in the molecule. The atomic coordinates were refined by the successive Fourier method. The final electron density projection on the (010) plane is shown in Fig. 1(b) ; the discrepancy index was 0.181 for the ($h0l$) zone if non-observed reflections were omitted. The best over-all B factor was 3.0 Å^2.

Although a significant anisotropic thermal motion of the bromine atom was observed from the two projections of the electron density distribution, no correction was made for anisotropic temperature factors. The final atomic coordinates are listed in Table I(a),

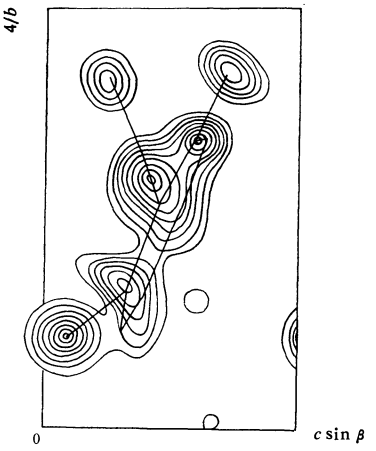
TABLE I. ATOMIC COORDINATES

	Atom	x/a	y/b	z/c
(a)	7-Bromo-2-methoxy tropone			
	Br	0.047_6	0.000	0.047
	O_1	0.154	0.122	−0.069
	O_2	0.208	0.472	−0.031
	C_1	0.138	0.258	0.100
	C_2	0.170	0.450	0.133
	C_3	0.163	0.626	0.327
	C_4	0.126	0.675	0.515
	C_5	0.082	0.543	0.542
	C_6	0.065	0.357	0.393
	C_7	0.087	0.248	0.180
	CH_3	0.245	0.637	−0.037
(b)	3-Bromo-2-methoxy tropone			
	Br	0.149_9	0.054_2	0.092_9
	O_1	0.423	0.209	0.711
	O_2	0.154	0.157	0.390
	C_1	0.467	0.169	0.590
	C_2	0.330	0.133	0.450
	C_3	0.364	0.082	0.330
	C_4	0.525	0.056	0.300
	C_5	0.690	0.078	0.390
	C_6	0.738	0.126	0.530
	C_7	0.653	0.171	0.640
	CH_3	0.110	0.209	0.240



the c axis upward

Fig. 2(a)



the a axis downward

Fig. 2(b)

Fig. 2. Electron density of 3-bromo-2-methoxy tropone projected along (a) the c and (b) the a axes. Contours at equi-intervals on an arbitrary scale. One for every five contour lines are drawn around the bromine atom.

where the x coordinates are the weighted mean of those obtained from the two projections.

3-Bromo Isomer. — The first clue to an approximate structure was obtained, much as in the case of the 7-bromo isomer, by the modified Patterson function, $P(UV)$, along the short c axis. The refinement of each atomic coordinate thus obtained was also done by successive Fourier and partial difference syntheses.

With reference to the x and y coordinates of atoms, the z parameter of each atom was estimated by the trial-and-error method and was refined by the ordinary Fourier method. The final electron density projections along the c and a axes are shown in Figs. 2 (a) and (b) respectively. The final atomic coordinates are listed in Table I(b); the best over-all B factor was found to be 4.0 Å^2. At this stage, the discrepancy indices reduced to 0.152 for ($hk0$) and 0.172 for ($0kl$) if non-observed reflections were omitted.

Discussion

The position of the substituted bromine atom in each isomer was established without any ambiguity from the Fourier projections of the electron density, thus confirming the structural formulae assigned to the two isomers by organo-chemical research.[11]

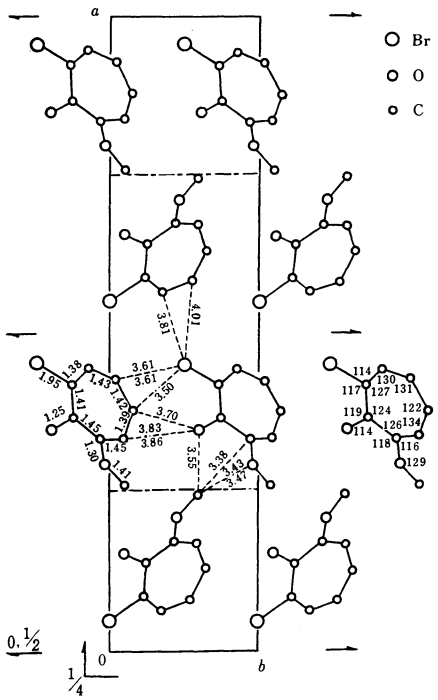
As a result of the disturbance of the heavy atom, the atomic coordinates are not very accurate, the accuracies of bond lengths being estimated to be about 0.1 Å or more. Within the limits of errors, all the bond lengths and angles shown in Figs. 3 (a) and (b) are considered to be normal. Although the seven-membered carbon ring is found to be approximately planar, the methoxy oxygen, the carbonyl oxygen and the bromine atoms deviate significantly from the ring plane, alternately in opposite directions, so as to keep away from each other.

Another point to be discussed is the conformation of the methoxy group. Let us call three typical conformations the perpendicular, cis and trans forms. In the perpendicular form the methyl group lies on a plane perpendicular to the ring through O_2 and C_2, while in the cis and trans forms the methyl group is located on the ring plane nearest to and furthest from the carbonyl oxygen atom respectively. The methoxy group of the 3-bromo isomer takes a conformation between the cis and perpendicular forms, while that of the 7-bromo isomer has a conformation between the perpendicular and trans forms. These conformations might be caused by a great steric repulsion from the bromine atom and are in agreement with the chemical fact that the 3-bromo isomer is more liable to aromatization than is the 7-bromo isomer.[11]

The dipole moments of these isomers have been measured and compared with the theoretical values for various conformations by Kurita, Seto, Nozoe and Kubo.[10] According to these authors, the observed moments of the 3-bromo and the 7-bromo isomers (3.31 D for the former and 5.51 D for the latter) are closest to the theoretical values for the cis and perpendicular form respectively. Although the

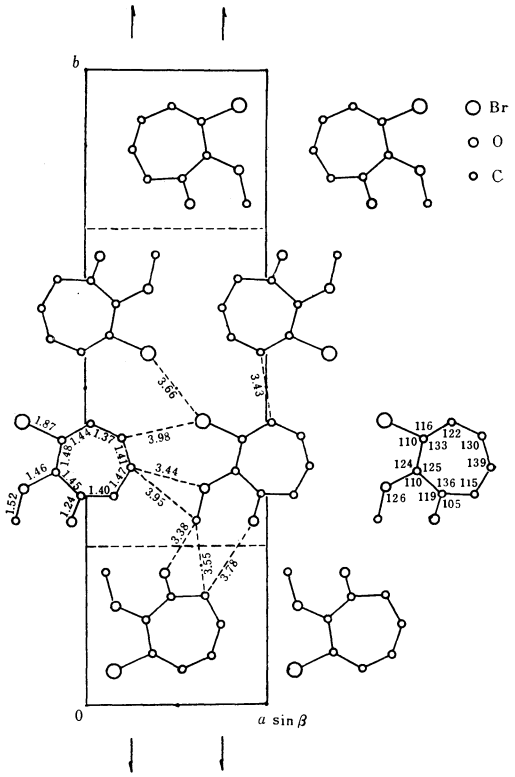
structure of the molecule in crystalline states is not necessarily the same as that in solutions, the molecular structure of the two isomers described in this paper are compatible with the conclusion derived from the dipole moment measurements.

The crystal structure projected along the c axis of the 7-bromo isomer and that projected along the c axis of the 3-bromo isomer are shown in Figs. 3(a) and (b) respectively. It should be noted that the features of molecular arrangement in the crystals of the two isomers are very similar, as can be seen in the lower-half cells shown in Figs. 3(a) and (b), in spite of a considerable difference in the dipole moments of the two isomers. However, while the upper-half cell of the 3-bromo isomer is antiparallel to the lower with respect to the direction of the C–Br bond, so that the crystal is centro-symmetric, the upper-half cell of the 7-bromo isomer is parallel to the lower, so that the crystal is polar. The difference in the melting points of the two compounds is probably connected with this difference in their molecular arrangement.



the c axis downward

Fig. 3(a)



the c axis upward

Fig. 3(b)

Fig. 3. Crystal structure of (a) 7-bromo- and (b) 3-bromo-2-methoxy tropone, with interatomic distances (Å) and bond angles (°).

The authors wish to express their deep thanks to Professor Tetsuo Nozoe and his collaborators for their continued encouragement and for supplying the materials. They are also grateful to Professor Ray Pepinsky for his interest in this work and acknowledge the support of Contract N60nr-26916 for X-RAC computations in the early stage of the research. They are also indebted to Mr. Taichi Tagawa and Mr. Chiaki Kawamura for their assistance in the numerical calculations.

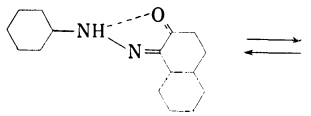
Faculty of Science
Osaka University
Kita-ku, Osaka

*Studies of Absorption Spectra of Azo Dyes and Their Metal-complexes. VI. The Tautomerism of Phenolazo-β-naphthols and of Phenolazo-α-naphthols**

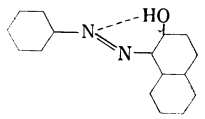
By Yoshiharu YAGI

(Received July 15, 1963)

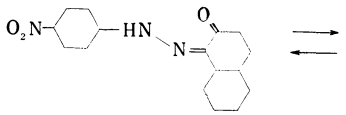
It had long been recognized[1] that phenylazo-β-naphthol (I) and phenylazo-α-naphthol (XI) are in a tautomeric equilibrium between the azo and the quinonehydrazone forms. This study was undertaken in order to obtain more information about this tautomerism.



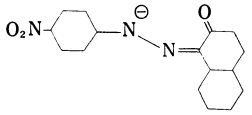
(I)



(II)



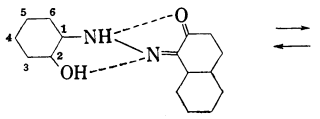
(III)



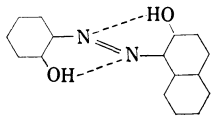
(IV)

In an aqueous methanol containing sodium hydroxide, the hydrazone band[2] of I near 500 mμ markedly decreases in intensity, while the absorption intensity of the azo band increases near 445 mμ. If I turns into a sodium salt by an addition of alkali metal hydroxide, thus forming an anionic species, there should be an appreciable bathochromic displacement of the bands according to the polarity increase of the absorbing system. Compound I, therefore, is not considered to from a salt under such conditions. However, azo compound III, known as pigment Para Red, is an exceptional case. This exists almost exclusively in the phenylhydrazone form (488.6 mμ in 95% methanol) as a result of the strong electron-withdrawing property of a nitro group. The addition of sodium hydroxide to this system, however, causes the appearance of a new band near 550 mμ, and the hydrazone band disappears with an increase in the concentration of alkali metal hydroxide. It is evident that III forms an anion IV in such circumstances, since no band corresponding to the azo form has been observed.

In the equilibrium of phenolazo-β-naphthol (V) in various organic solvents, the hydrazone form is generally more dominant than azo compound I. The phenolic hydroxyl group of V or XII is, in any solvent, in an undissociated state, whereas those of phenolazoacetoacetamides in Part II[3] have been found to be strongly acidic, and thus their dissociation occured in aqueous alcohol.



(V)



(VI)

It had previously[4] been known that such *o,o'*-dihydroxyazo compounds as V undergo marked color changes according to the pH ranges of the media, neutral (weakly acidic), weakly alkaline or strongly alkaline. However, no exact explanation of this has yet been made. Compound V in aqueous 50% methanol shows the hydrazone and the azo bands at 508 mμ

* Parts I—V, This Bulletin, **36**, 487, 492, 500, 506, 512 (1963).

1) K. Auwers et. al. *Ann.*, **378**, 210 (1911); **487**, 79 (1931); A. Burawoy et al. ibid., **503**, 180 (1933); **504**, 71 (1933); **509**, 60 (1934); R. Kuhn and F. Bär, ibid., **516**, 143.

2) A. Burawoy, *J. Chem. Soc.*, **1952**, 4793.

3) Y. Yagi, This Bulletin, **36**, 492 (1963).

4) H. Shingu et al., *J. Chem. Soc. Japan (Nippon Kwagaku Kwaishi)*, **60**, 542, 595 (1939); J. B. Müller et al., *Helv. Chim. Acta*, **35**, 2579 (1952).

TABLE I. ELECTRONIC ABSORPTION SPECTRA OF PHENOLAZO-β-NAPHTHOLS

Compound	Solvent	Absorption band λ_{max}, mμ ($\varepsilon_{max}\times10^{-4}$)				
V	50% MeOH	538.5*(1.81) 508.0 (2.12) 422.1 (0.72)		314.8(0.65)	261.5 (1.08)	230.8(2.99)
V	Same as above but containing 0.01 N NaOH	576.1 (2.06)	387.0(0.52)	327.8(0.50)	283.0*(0.84) 267.0*(1.20)	222.3(3.10)
V	Same as above but containing 0.1 N NaOH	573.8 (1.86)	389.8(0.51)	328.3(0.48)	283.3*(0.85) 266.5*(1.24)	227.7(2.82)
V	Same as above but containing 0.5 N KOH	608.5*(0.60) 526.7 (1.23) 446.1*(0.84)		336.0(0.48)	268.0*(1.57)	235.8(2.61)
5-NO_2 Derivative	95% MeOH	590.0*(0.73) 517.5 (1.82) 392.0*(0.92)		309.5(1.16)	261.0*(1.38)	228.9(3.33)
5-NO_2 Derivative	Same as above but containing 0.01 N NaOH	561.5 (2.27) 401.9 (1.16)		329.0(1.00)	268.1*(1.28)	230.6(2.89)
5-NO_2 Derivative	Same as above but containing 0.5 N KOH	550.3 (1.70) 440.0 (1.23)		363.0(1.12)	275.4*(1.34)	235.2(2.72)
4-NO_2 Derivative	95% MeOH	612.4*(0.89) 529.7 (2.32) 405.0*(0.69)		325.0(0.70) 306.*5(0.62)	263.5*(0.97)	227.4(3.35)
4-NO_2 Derivative	Same as above but containing 0.01 N NaOH	584.5 (2.64) 395.3 (0.73)		323.2(0.80)	269.3*(1.33)	231.5(3.31)
4-NO_2 Derivative	Same as above but containing 0.5 N KOH	588.7 (2.28) 400.6 (0.67)		323.3(0.77)	268.3*(1.48)	233.2(3.19)

A group of bands is shown in the same column. Visible absorption bands are shown in the same column.

* Inflection.

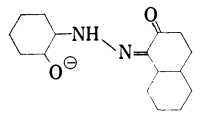
TABLE II. ELECTRONIC ABSORPTION SPECTRA OF PHENYL- AND PHENOLAZO-α-NAPHTHOL

Compound	Solvent	Absorption band λ_{max}, mμ ($\varepsilon_{max}\times10^{-4}$)				
I	*n*-Hexane	492.5 (1.48) 424.0*(0.70)	352.5 (1.05)	297.7 (1.64) 289.8 (1.65) 265.9*(0.84)	240.7*(1.24) 224.2 (1.77)	
II	*n*-Hexane	559.2*(0.08)	467.8 (1.53)	346.8 (1.16)	302.3 (1.49) 292.3*(1.38)	266.8*(0.65) 258.0*(0.76) 225.9 (2.14)
	Chloroform	562.9*(0.26)	477.2 (1.54)	349.9 (1.19)	303.8 (1.58) 295.3*(1.48)	—
	Acetic acid	552.5*(0.81)	486.3 (1.41)	349.0 (0.95)	300.8 (1.52) 292.0*(1.42)	—
	Methanol**-chloroform		560.5*(1.05) 512.3 (1.49) 486.0*(1.40)	349.0 (0.80)	303.5 (1.41) 294.3*(1.30)	—

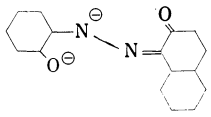
** A chloroformic solution containing 30 g. of methanol per 100 ml.

and 422.1 mμ respectively. When measured in the medium roughly the same but containing sodium hydroxide, the hydrazone band undergoes a remarkable shift toward a longer wavelength in the alkali concentration near about 0.01～0.1 N. The molecular structure at this state corresponds to structure VII.

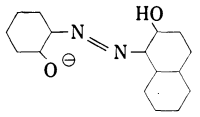
In the neighborhood of the concentration about 0.5～1.0 N, it is noteworthy that the relative intensity of the azo band markedly increases at about 450 mμ. If a two-step dissociation, VII→VIII or IX→X, occurs upon the concentration increase of sodium hydroxide, the increased polarity of the absorbing system



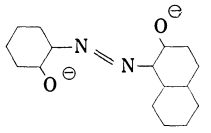
(VII)



(VIII)



(IX)

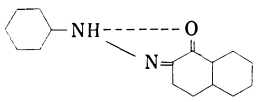


(X)

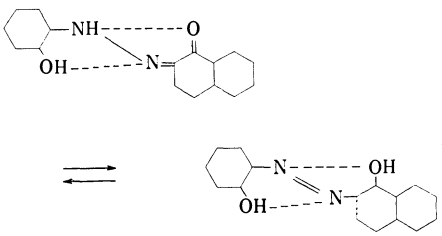
would cause a displacement of the spectrum toward a longer wavelength as compared with the absorption maximum of the ionized hydrazone form corresponding to VII. Such spectral change, therefore, may be attributed to the fact that the tautomeric equilibrium is inclined to the azo form, presumably because of (i) an increase in the basic nature of the solvent system, and (ii) an elevation of the electron-donating power of the hydroxyl upon dissociation.

The spectra of the derivatives of V supported the above explanation: the 5-NO_2 derivative in neutral 95% methanol has an absorption corresponding to structure VII as a shoulder (560 mμ) of the main hydrazone band (517 mμ). By the addition of alkali metal hydroxide, the main hydrazone band is turned into this new band. In spite of the concentration increase of alkali metal hydroxide, the location of this band does not change. The azo band, however, undergoes a slight bathochromic and hyperchromic displacement. In the case of the 4-NO_2 derivative, however, the hydrazone structure is exclusively dominant because the electronegative nitro group is para to the hydrazone group. The weak azo band shows no change in location and in intensity in spite of the concentration increase of alkali metal hydroxide. It follows that it is harder for a dissociation VI→IX to proceed than for a dissociation V→VII.

The tautomerism of phenylazo-α-naphthol (XI) is somewhat different from that of I. In *n*-hexane, the weak inflection at 424 mμ proves the slight existence of the azo form of XI, as is shown in Table II. However, the hydrazone band of XI (λ_{max} 507.5 mμ; ε_{max} 1.68×10^4) in 50% aqueous methanol undergoes almost no change in intensity and in location, in spite of the basicity increase of the solvent upon the addition of sodium hydroxide to this system. These facts show that the azo $\rightleftarrows$ quinonehydrazone tautomeric equilibria of the compounds of type XI are biased toward the hydrazone tautomer in any solvent.



(XI)



(XII)

With regard to phenolazo-α-naphthol (XII) the tautomeric eqilibrium is biased to the azo form as a result of the electropositive character of the phenolic hydroxyl group.[5] In the visible absorption region, there is a weak inflection at a longer wavelength side (about 500 mμ) of the main aborption band. This absorption has a relatively high intensity in an acetic acid medium whereas the intensity of the main absorption band at 486.3 mμ is relatively low. In a polar solvent such as methanol, XII also shows a sharply absorbing band at 528.5 mμ, and there is no absorption on a longer wavelength side. Moreover, the visible absorption maximum of XII in *n*-hexane is located at a shorter wavelength position than that of XI, notwithstanding the introduction of the hydroxyl group, with its effectively auxochromic nature.

The azo $\rightleftarrows$ quinonehydrazone tautomerism of XII, therefore, is concluded to be as follows; XII in non-polar solvents exists exclusively as the azo form, resulting in the merely slight appearance of the hydrazone form as the inflection. This equilibrium, however, is susceptible to any increase in the polarity in the solvent system.

The spectral behavior in a mixed solvent system, as is shown in the table, confirms the above view; the addition of methanol to the chloroformic solution of XII converts the visible bands into what appears to be a single absorption band. Such spectra suggest nearly equal contributions of the azo and the hydrazone forms to the tautomeric equilibrium; i. e., the former appears as an inflection at 486.0 mμ, and the latter, at 560.5 mμ.

The author wishes to express his deep gratitude to the late Professor Ryutaro Tsuchida for his kindness in participating in discussions

5) A. Burawoy and A. R. Thompson, *J. Chem. Soc.*, **1953**, 1443.

throughout this work. The author is also indebted to the Sumitomo Chemical Co., Ltd., for its permission to publish this work and to Mr. Kikuo Kimura for his assistance in this study.

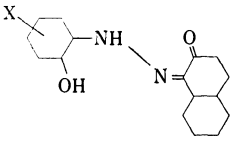
Osaka Works
Sumitomo Chemical Co., Ltd.
Konohana-ku, Osaka

Studies of the Absorption Spectra of Azo Dyes and Their Metal-complexes. VII. The Absorption Spectra of the Metal-complexes Derived from Phenolazo-α- and Phenolazo-β-naphthols[*1]

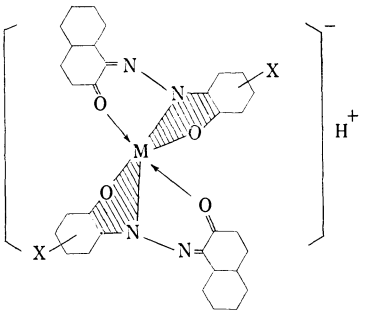
By Yoshiharu YAGI

(Received July 15, 1963)

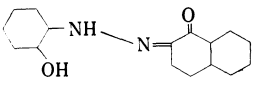
The relations between the spectral variation caused by the 2 : 1-metal-complex formation and the nature of the metal-ligand linkages have been investigated with respect to phenolazo-β-naphthols and phenolazo-α-naphthols.



(I)



(II)



(III)

(X : Substituent)

The derivatives of I and III in 95% methanol containing 0.1 g. of acetic acid per liter[*2] exist almost exclusively in the hydrazone form, and their phenolic hydroxyls are fixed in an undissociated state.[1] Most of these derivatives have weak shoulders near 400~420 mμ, shoulders which are due to the small quantity of the azo tautomer in the azo-quinonehydrazone equilibrium.[2]

The 2 : 1-chromium(III)- and cobalt(III)-complexes of the derivatives of I and III, which have an octahedral conformation around the central metal atom,[3] are considered to have the bond type as in II, as was pointed out in Parts III and IV of this study. All the complexes in this study have been purified by column chromatographic separation and by successive reprecipitation.

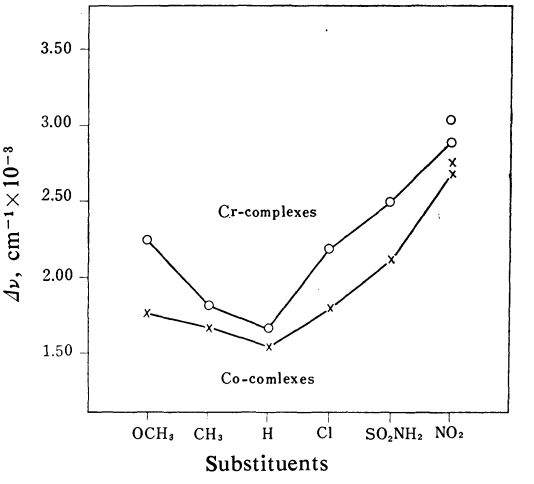


Fig. 1. Relation between the substituents and the shifts of the visible absorption bands with complex-formation ($\Delta\nu$) ; Single marks, 4-NO_2 substituted derivatives. Full lines, 5-substituted derivatives

*1 Parts I-V, This Bulletin, **36**, 487, 492, 500, 506, 512 (1963).

*2 Such a medium-containing acid has been used to prevent the dissociation of the phenolic hydroxyl.

1) Y. Yagi, Part VI of this study This Bulletin, **37**, 1875 (1964).

2) K. Auwers et. al. *Ann.*, **378**, 210 (1911) ; **487**, 79 (1931) ; A. Burawoy et. al. ibid., **503**, 180 (1933) ; **504**, 71 (1933) ; **509**, 60 (1934) ; A. Burawoy et. al., *J. Chem. Soc.*, **1953**, 1443 ; **1952**, 3734.

3) P. Pfeiffer and S. Saure, *Ber.*, **74**, 935 (1941).

TABLE I. VISIBLE ABSORPTION SPECTRA OF THE DERIVATIVES OF I AND THEIR METAL-COMPLEXES

Derivative	Absorption bands, λ_{max}, mμ ($\varepsilon_{max}\times10^{-4}$) Ligand dyes	Chromium-complexes	Cobalt-complexes
5-OCH_3	521.4 (1.88), 389.8*(0.50)	654.6*(1.51), 590.8 (2.49), 476.3*(1.11)	574.3, 535.6*
5-CH_3	506.8 (2.15)	618.5*(1.51), 558.0 (2.63), 464.4 (1.36)	553.7 (2.79), 515.0*(2.44), 481.0*(1.76)
H	533.2*(1.75), 503.2 (2.06), 397.8*(0.72)	610.5*(1.49), 548.9 (2.52), 461.5*(1.45)	545.5 (2.74), 514.9 (2.48), 474.5*(1.80)
5-Cl	516.3 (2.08), 403.5*(0.66)	624.0*(1.35), 582.0 (2.18), 473.7*(1.13)	569.0 (2.58), 528.9*(2.24)
5-SO_2NH_2	531.0*(1.74), 501.9 (2.05), 405.0*(0.68)	618.0*(1.56), 573.8 (2.19), 456.5*(1.35)	561.4 (2.64), 522.9*(2.26), 484.6*(1.80)
5-NO_2	496.1 (2.14), 380.6*(0.72)	633.5*(1.64), 579.2 (2.04), 481.4*(1.49)	572.5 (2.61), 532.9*(2.19), 488.5*(1.78)
4-NO_2	512.9 (2.86)	662.3*(2.29), 606.8 (2.88), 500.9*(1.69)	596.0 (3.51), 555.6*(2.98)

The solvent used is 95% methanol containing 0.1 g. of acetic acid per liter.
* Inflection.
Owing to the slight solubility of the cobalt-complex of 5-OCH_3 derivative, the measurement has been made qualitatively.

TABLE II. ELECTRONIC ABSORPTION SPECTRA OF DERIVATIVES OF III AND THEIR METAL-COMPLEXES

Derivative	Metal	Absorption bands, λ_{max}, mμ ($\varepsilon_{max}\times10^{-4}$)					
5-CH_3	None	510.8*(1.70)	523.9 (2.04)	386.0 (0.67)	303.6 (1.50)	245.6*(1.56)	
	Cr		566.1 (2.79)	324.3 (3.33)	273.0*(2.67)	233.5 (5.71)	
	Co		559.8 (—)	519.1*(—)	313.0 (—)	244.8 (—)	
H	None	550.7*(1.67)	515.5 (2.05)	380.0 (0.80)	301.9 (1.52)	244.2*(1.58)	
	Cr	614.0*(1.55)	557.2 (2.44)	322.0 (2.88)	269.0*(2.51)	232.3 (4.94)	
	Co		552.3 (—)	515.0*(—)	310.7 (—)	241.7 (—)	
5-NO_2	None		506.1 (2.29)	368.5 (1.19)	291.9 (2.45)	241.*0(1.63)	
	Cr	639.2*(1.51)	565.5 (2.38)	410.0*(1.93)	330.5 (3.91)	265.5*(2.55)	233.3 (4.03)
	Co		551.1 (2.89)	475.0*(2.19)	395.5*(2.14)	311.5 (4.86)	251.7*(4.35)

The main bands in the visible region are shown in the second column.

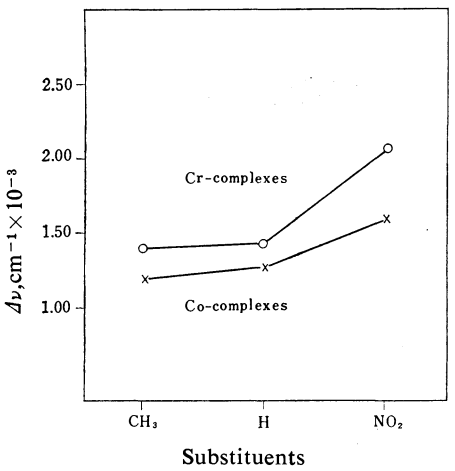


Fig. 2. Relation between the substituents and the shifts of the visible absorption bands with complex-formation; the substituents are on the 5-position of the phenolic nuclei.

As to the chromium(III)- and the cobalt(III)-complexes in the same solvent system as above, the visible absorption bands of the ligands undergo marked bathochromic displacements, resulting in very broad and depressed bands. Generally, the molar extinction coefficients of the complexes alter in the Cr<Co manner, and the half-value widths, in the Co<Cr manner. For instance, the visible absorption band of the chromium(III)-complex (the cobalt(III)-complexes in parenthesis) of (II, X=H) is: λ_{max} =548.9(545.5) mμ, ε=2.52(2.74)$\times10^4$, and the half-value width, l=6.08(4.49)$\times10^3$ cm^{-1}. It is of further interest that there is an inflection at a longer or shorter wavelength side of the main visible band in the spectra of the chromium(III)- or the cobalt(III)-complexes respectively. These are not due to the polarization of the M–O (M, tervalent metal; O, phenolic oxygen) bond by a negative substituent, as was pointed out in Part V, because they show no change in relative

intensity and/or in location as a result of the polarity change of the solvent, and because they also exist in the spectra of the complexes with no nitro group. Their origin is, at present, not known.

The bathochromic shifts of the visible absorption bands of the derivatives of I and III with the complex-formation ($\Delta\nu$, cm^{-1}: differences of absorption maxima between the ligand and the corresponding complex) are shown in Figs. 1 and 2. The substituents at abscissa are conveniently arranged in the generally accepted order[4] of electronegativity at regular intervals.

The bathochromic shifts of the bands with the complex-formation may be ascribed mainly to two factors;[5] (i) the polarity of the M–O (O, phenolic oxygen) bond; i. e., any alteration of the electronic configuration, which polarizes the bond, causes a red-shift[6] of the visible absorption band, and (ii) the perturbation of the π-electron system by the $d\pi$-$p\pi$ interaction between the hydrazone group and the central metal, i. e., the appearance of the resonance stabilized system involving the aromatic nuclei and the chelate ring system.

In the series of complexes II if factor i is markedly dominant, as was shown in the series of complexes in Parts III–V, the 5-OCH_3 derivatives do not have such bathochromic shifts as those of the 5-Cl derivative, as is shown in Fig. 1. It is reasonable to consider that factor ii contributes much to these shifts of bands, since the ligand molecule of II has two powerful aromatic nuclei connected with the hydrazone bridge. Therefore, in the case of the complex the phenolic nucleus of which is substituted by a group of powerful resonance effects, the resonating system involving the d-electrons of the central metal is stabilized, resulting in an increase in the polarizability of the π-electron system and, hence, the bathochromic displacement of the visible absorption band. The visible absorption bands of the complexes, substituted by a nitro group in the 4-position, i. e., in the position para to the hydrazone group, are located at longer wavelength positions than those of the corresponding 5-substituted derivatives. This is presumably because of an intensified effect of factor ii.

With regard to the complexes of III in Fig. 2, however, factors i and ii are considered to be almost equally operative. The relationship between the $\Delta\nu$ and the electronegativities of the substituents if factor i should dominate will be shown in a forthcoming paper.[7]

It has previously been concluded in the series of phenolazoacetoacetamides that the chromium(III)-complex has the ionic M–O (O, phenolic oxygen) bond, whereas the cobalt(III)-complex has the covalent bond. In the II and III series, however, such a peculiarity would be relatively small, since the difference in $\Delta\nu$ between the chromium(III)- and the cobalt(III)-complex is relatively small (that is, the visible absorption positions of both complexes are close together).

The author is grateful to the late Professor Ryutaro Tsuchida of Osaka University for his encouragement and kindness in participating in discussions throughout this work. The author also wishes to express his gratitude to the Sumitomo Chemical Co., Ltd., for its permission to publish this work, and to Mr. Kikuo Kimura and Mr. Masao Kitajima for their assistance in this study.

Osaka Works
Sumitomo Chemical Co., Ltd.
Konohana-Ku, Osaka

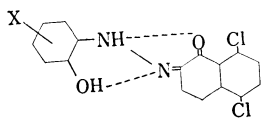
4) L. P. Hammett, *Chem. Revs.*, **17**, 125 (1935); H. H. Jaffé, ibid., **53**, 191 (1953); H. C. Brown and Y. Okamoto, *J. Am. Chem. Soc.*, **80**, 4979 (1958).
5) Y. Yagi, This Bulletin, **36**, 506 (1963).
6) A. Burawoy and E. Spinner, *J. Chem. Soc.*, **1955**, 2557.
7) Y. Yagi, This Bulletin, **37**, 1881 (1964).

Studies of the Absorption Spectra of Azo Dyes and Their Metal-complexes. VIII. The Absorption Spectra of Azo Compounds Derived from 5,8-Dichloro-1-naphthol and Their Metal-complexes

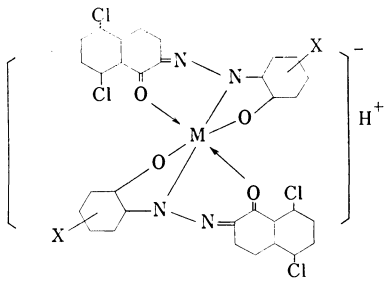
By Yoshiharu YAGI

(Received August 5, 1963)

In the field of dye chemistry, the 2 : 1-metal complex dyes (II) derived from 2-(2'-hydroxyarylazo) - 5, 8 - dichloro-1-naphthols (I) have been of much interest[1] because of their deeper and relatively clear dyeing shades on the proteinic fibers as compared with the series of complexes studied previously.[2,3] This paper has been undertaken to obtain fundamental information on these azo compounds and their metal complexes.



(I)



(II)
(X: Substituent)

Table I shows the electronic absorption spectra of compound I (X=H) and its methoxy analogue. The characteristic shape of each absorption band exhibits almost no change in spite of the polarity variation of the media. It is noteworthy that both compounds in Table I show splittings of the visible absorption bands and that such absorption maxima are located at markedly longer wavelengths than those of phenolazo-β-naphthols and phenolazo-α-naphthols.[3] If the azo and the quinonehydrazone form coexist[1,3,4] the azo band should appear at about 450 mμ or at a longer wavelength than 450 mμ. No such absorption can, however, be observed at all in a variety of solvents. Compound I and/or its derivatives, therefore, are considered to have the hydrazone structure exclusively.

Table II shows the electronic absorption spectra of the 2 : 1-chromium(III)- and cobalt-(III)- complexes (II) of ligands I, the phenolic nuclei of which are substituted by various kinds of groups in the 4- or 5-position. Marked band-shifts with the complex formation are observed over all the spectra, particularly in the visible region, resulting in appreciably bathochromic displacements and the broad deformation of the bands.

As to the spectra of ligands I, the λ_{max} values of the visible absorptions are in the region of 513~570 mμ and shift towards shorter wavelengths with the introduction of the electronegative substituent at the 5-position of the phenolic ring. There are characteristic inflections close to the main visible bands of the ligands and of their metal-complexes in Table II. In some ligands I (when X=H and

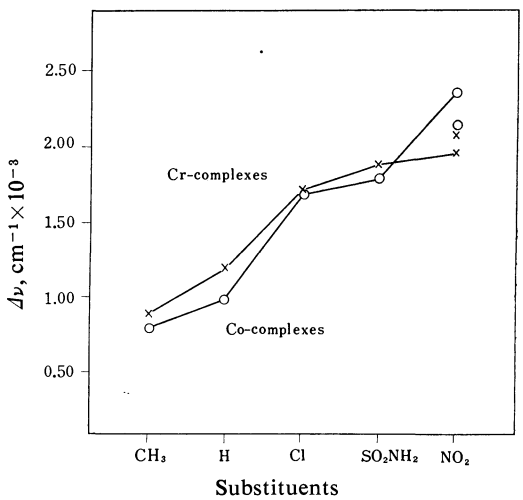


Fig. 1. Relation between the substituents and the shifts of the visible absorption bands with complex-formation.
Full lines, 5-substituted derivatives, single marks, 4-substituted derivatives

1) CIBA Ltd., Brit. Pat. 724157; U. S. Pat. 2495244; Swiss Pat. 305634-5.
2) Y. Yagi, Part I-V of this study, This Bulletin, **36**, 487, 492, 500, 506, 512 (1963).
3) Y. Yagi, Part VI of this study, This Bulletin, **37**, 1875 (1964).
4) K. Auwers et al., *Ann.*, **378**, 210 (1911); **487**, 79 (1931); A. Burawoy et al., ibid., **503**, 180 (1933); **504**, 71 (1933); **509**, 60 (1934).

TABLE I. ELECTRONIC ABSORPTION SPECTRA OF DERIVATIVES OF 2-PHENYLAZO-5,8-DICHLORO-1-NAPHTHOL IN VARIOUS SOLVENT

Compound	Solvent	Absorption bands, λ_{max}, mμ ($\varepsilon_{max}\times10^{-4}$)						
2-(2'-Methoxy-phenylazo)-5,8-dichlor-1-naphthol	St. Solv.	550.0 (1.42)	525.0 (1.44)	(383.0*) (0.60)	(358.3*) (0.70)	319.0 (0.99)	305.7 (1.03)	246.5 (1.60)
	n-Hexane	543.8 (1.30)	512.6 (1.28)	(383.0*) (0.51)	(357.3*) (0.64)	319.2 (0.84)	302.5 (0.89)	247.0 (1.36)
2-(2'-Hydroxy-phenylazo)-5,8-dichlor-1-naphthol (I)	50% MeOH	558.4 (2.30)	531.4 (2.34)	(394.0*) (0.50)	355.0*) (0.82)	320.6 (1.50)	305.3* (1.34)	247.9 (1.57)
	Pyridine	569.7 (2.69)	535.3 (2.54)	(399.0*) (0.50)	362.0* (0.83)	325.7 (1.33)	309.7* (1.21)	—

St. Solv.: A standard solvent which denotes 95% aqueous methanol containing 0.1 g. of acetic acid per liter.
* Inflection.
Absorption bands in parentheses are indistinct bands.

TABLE II. VISIBLE ABSORPTION SPECTRA OF THE DERIVATIVES OF (I) AND THEIR METAL-COMPLEXES

Substituent	Absorption bands; λ_{max}, mμ ($\varepsilon_{max}\times10^{-4}$)											
	Ligand Dyes				Chromium-complexes				Cobalt-complexes			
5-CH_3	570.0	(2.48)	536.9	(2.48)	(610.2*)	(1.90)	561.4	(2.77)	564.2	(2.94)	522.9*	(2.43)
H	554.4	(2.43)	524.2	(2.47)	(611.2*)	(1.58)	553.1	(2.96)	558.9	(2.92)	516.7*	(2.39)
5-Cl	558.4*	(2.29)	521.2	(2.64)	(614.4*)	(2.25)	571.7	(2.91)	571.9	(2.94)	530.0*	(2.33)
5-SO_2NH_2	553.0*	(2.18)	516.0	(2.64)	642.9*	(1.58)	568.8	(2.53)	571.4	(3.00)	528.5*	(2.39)
5-NO_2	549.0*	(2.05)	513.5	(2.59)	644.0*	(1.95)	584.2	(2.38)	570.6	(3.01)	527.3*	(2.43) 486.8*(1.96)
4-NO_2	573.1*	(2.66)	535.0	(3.21)	672.2*	(2.45)	603.4	(2.94)	601.7	(3.51)	556.7*	(2.75)

The solvent used is 95% aqueous methanol containing 0.1 g. of acetic acid per liter (the standard solvent).

CH_3), the inflection forms an absorption band, and its intensity is just that, or almost equal to that, of the main band. Regarding the complex bands, the inflection is located on the shorter or the longer wavelength side of the main absorption band of the cobalt(III) or the chromium(III) complex respectively; generally the more electronegative the substituent in the phenolic nucleus, the more intensive the inflection.

The degree of the bathochromic shifts of the visible absorption bands of I and its derivatives with the complex formation, i.e., $\Delta\nu$ (in cm^{-1}) [(ν_{max} of a ligand-band) − (ν_{max} of the corresponding complex-band)] is shown in Fig. 1. Substituents at the abscissa are conveniently arranged in the order of the electronegativity at regular intervals.[5] In this graph, the absorption maxima of the shorter wavelength-side band have been taken as the location of the visible absorptions of the ligands (I, when X=CH_3 and H).

The magnitudes of $\Delta\nu$ in these systems are smaller than those of the phenolazo-β-naphthol series but nearly equal to those of the phenolazo-α-naphthol series discussed in the preceding paper.[6]

As was described in part III of this study, such bathochromic displacements of the bands with the complex formation may be ascribed mainly to two factors; (i) the polarity of the M–O (M, tervalent central metal; O, phenolic oxygen) bond, and (ii) the formation of the resonance-stabilized system involving the aromatic nuclei and the chelate rings. It would be reasonable to apply the above consideration to the system of this study.

If factor ii predominates, the perturbation of the π-electron system by the dπ-pπ interaction between the hydrazone group and the central metal will be emphasized in a system that has a group with a resonance effect as the substituent X. For example, a CH_3 group would cause a larger $\Delta\nu$ value than that in the case of X=H.[6] However, Fig. 1 shows a tendency toward a linear increase in the $\Delta\nu$ value with the increase in the negativity of the substituent. This suggests the dominant character of factor i. Moreover, the actual gradient of the graph becomes markedly steeper, taking into account the fact that the ν_{max} of the ligands (X=H and CH_3) have been taken from the shorter wavelength side bands. Although various factors are conceivable in accounting for such band shifts, the following explanation is considered to be the most reasonable: in the 2:1-metal complexes of formula II, there is a steric repulsion between

5) L. P. Hammett, *Chem. Revs.*, **17**, 125 (1935); H. H. Jaffé, ibid., **53**, 191 (1953); H. C. Brown et al., *J. Am. Chem. Soc.*, **80**, 4979 (1958).
6) Y. Yagi, Part. VII of this study, This Bulletin, **37**, 1878 (1964).

the chlorine atom and the quinone oxygen atom, so that the coplanarity of the chelate ring involving the metal atom and the quinone oxygen is much reduced (i. e., factor ii is not effectively operative). Thus, an electron-withdrawing group such as an $-NO_2$ polarizes the M–O bond and increases the polarizability of the absorbing system, resulting in the bathochromic displacements of the visible absorption bands. Such polarization can probably be attributed to both the resonance and the inductive effects, since the $\Delta\nu$ values of the 4-NO_2 derivatives are also appreciably large.

In the metal-complex systems of the previous papers, the wavelength locations of the visible absorption bands have been in the order, Cr> Co. However, this order is reversed in the greater part of Fig. 1. This is presumably because the M–O bond is more ionic in the cobalt(III)-complexes than in the chromium-(III)-complexes.

The author wishes to express hearty thanks to the late Professor Ryutaro Tsuchida of Osaka University for his valuable discussions and encouragement. Thanks are also to be accorded to the Sumitomo Chemical Co., Ltd., for permission to publish this work and to Mr. Kikuo Kimura and Mr. Masao Kitajima for their assistance throughout this study.

Osaka Works
Sumitomo Chemical Co., Ltd.
Konohana-ku, Osaka

NOTES

Note on the Association of 3,6-Bis-dimethylaminoacridine in Some Organic Solvents

By Andrzej OLSZOWSKI and Zdzisław RUZIEWICZ

(Received June 12, 1964)

The electronic spectra of 3,6-bis-dimethylaminoacridine (BDAA), i. e., of the acridine orange base, have been subjected to numerous investigations. Mataga[1] has examined the absorption spectra of this compound* in various non-aqueous solvents and reached the conclusion that BDAA dissolved in acetone, buthanol, ethanol and methanol is in a marked degree associated forming the dimers. At concentrations of BDAA of the order of 10^{-6} mol. per liter, this author has obtained only one absorption band, with a maximum at about 500 mμ. With an increasing concentration of BDAA, this band diminished and simultaneously a new band with a maximum at 425~430 mμ, was gradually formed.

In connection with our investigations of the mutual interaction between BDAA and some organic acids in non-aqueous solvents,[3] we have examined anew the dimerization of BDAA in some solvents and have obtained results differing from those cited above.

BDAA was obtained from acridine orange (G. T. Gurr Ltd., London), and was purified chromatographically by a method given by Zanker,[4] the melting point (181~182°C) was in keeping with the literature data.[4] By using proper purification methods[5] the solvents were obtained free from any traces of acids, bases and moisture.

We have found that the absorption spectrum of BDAA in acetone, dioxane, pyridine, benzene and styrene has only one band visible in all the concentrations between 10^{-6} and 10^{-2} mol./1. The maximum of this band lies in range between 23400 and 23600 cm^{-1} (between 427 and 424 mμ) in the dependence of the used

1) N. Mataga, This Bulletin, **30**, 375 (1957).

* In the cited work[1] BDAA was described as 2,8-bis-dimethylaminoacridine probably as a result of the use of another sequence of the numeration of atoms in the rings. However, the description of the preparation method of this compound leaves no doubt that in the work of Mataga[1] an acridine orange base was examined. Cf. also.[2]

2) N. Mataga and S. Tsuno, This Bulletin, **30**, 711 (1957).

3) A. Olszowski and Z. Ruziewicz, *Bull. Acad. Polon. Sci., sér. sci. math. astr. phys.*, in press.

4) V. Zanker, *Z. physik. Chem.*, **199**, 225 (1952).

5) A. Weissberger (Editor), "Technique of Organic Chemistry," Vol. VII, "Organic Solvents," 2nd ed., Interscience Publ., New York (1955).

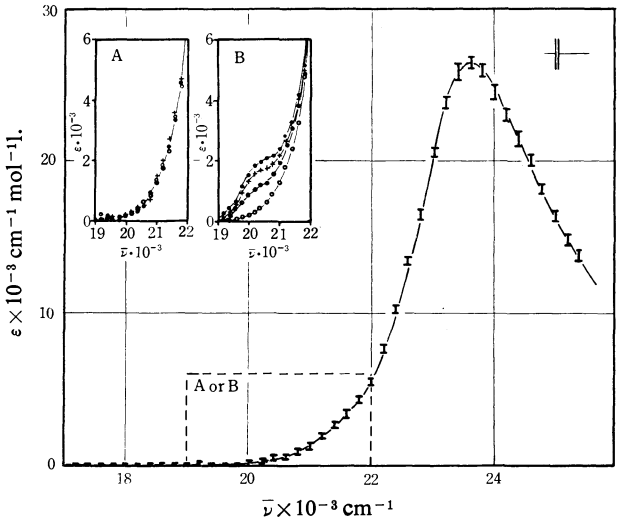


Fig. 1. Absorption spectrum of BDAA solution in acetone.
"A" Part of spectrum in the range of 19000~22000 cm^{-1}; solvent—absolute acetone.
"B" The same part of spectrum, solvent—acetone containing traces of water (<0.1%).
Experimental points correspond to the following BDAA concentrations: ●—● 4.0×10^{-6}, +—+ 4.0×10^{-5}, ◐—◐ 1.6×10^{-4}, ○—○ 6.0×10^{-3} mole per liter.

solvent, and its molar absorptivity at a maximum is equal to 25000~29000 $mol^{-1}\,cm^{-1}\,l$. The corresponding results obtained for the acetone solutions are shown in Figs. 1 and 1A. According to the data of Mataga[1] the above band should appear as a result of the BDAA dimers; however, because of the lack of any relation between the molar absorptivity and the concentration, and because of the presence of this band even at low BDAA concentration, we hold that this band is characteristic of the BDAA monomers. We have not found any changes indicating the association of BDAA molecules in the cases mentioned. It should be emphasized that in pyridine, in which, according to Mataga,[1] no association occurs, we have also observed the same band with a maximum at 23400 cm^{-1}.

The band with a maximum at about 20200 cm^{-1} (495 mμ), which according to Mataga should belong to the BDAA monomer, appears when some compounds of strong proton-donor properties are introduced to the solutions of BDAA in non-aqueous solvents. (Cf. Fig. 2, curves 5 and 6). The mutual interaction of BDAA with week proton donors such as methanol (Fig. 2, curve 3) or phenol[2] through the hydrogen bond brings about only a weak shift of the 23400 cm^{-1} band towards longer wavelengths. However, under the action of carboxylic acids probably some proton transfer from the acid molecule towards nitrogen in the acridine ring of the BDAA molecule takes place, bringing about the formation of an ionic pair. In our opinion this effect seems to be responsible for the appearance of the 20200 cm^{-1} band. This conclusion is to some extent

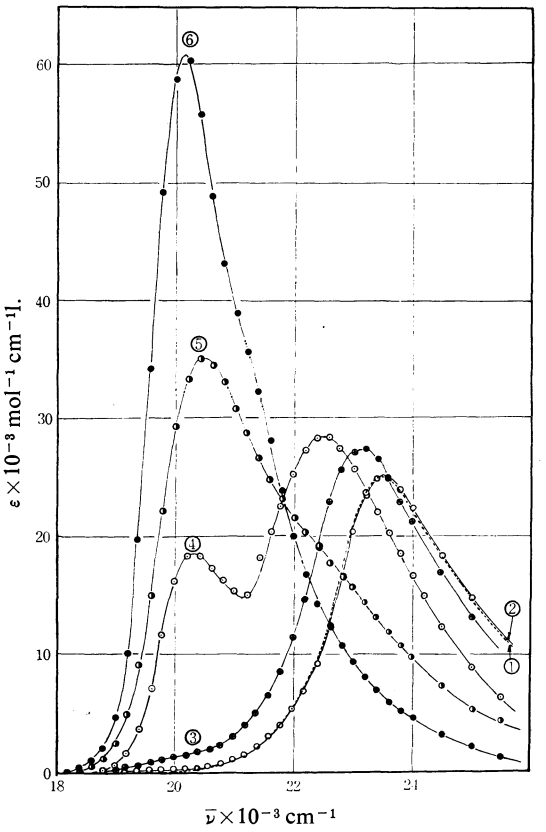


Fig. 2. Absorption spectra of BDAA ($c=4.0\times10^{-5}$) in solutions of benzene.
1: without addition of third component
2: with acetone ($c=2.2\times10^{-1}$)
3: with methanol ($c=2.0\times10^{-1}$)
4: with *p*-hydroxybenzonitrile ($c=1.33\times10^{-3}$)
5: with benzoic acid ($c=1.22\times10^{-3}$)
6: with trichloroacetic acid ($c=1.20\times10^{-4}$)
All concentrations in mole per liter.

confirmed by the fact that an analogous band appears in aqueous and alcohol solutions containing the acridine orange cations, i. e., monocations of BDAA.[4,6] We have also observed an intermediate state by adding *p*-hydroxybenzonitrile to the BDAA solution, thus producing both the shift of the 23400 cm^{-1} band towards red and the appearance of the 20200 cm^{-1} band (Fig. 2, curve 4).

In solvents not sufficiently dried or containing some acidic contaminations besides the 23400 cm^{-1} band, the band at 20200 cm^{-1} appears too. This kind of spectrum was obtained when we used not sufficiently dehydrated acetone (Fig. 1B) or acrylonitrile which we had not succeeded in purifying to a sufficient degree. However, the intensity of the 20200 cm^{-1} band in acrylonitrile does not exceed 15% of the intensity of the 23400 cm^{-1} band, even at very low concentrations of BDAA, and essentially depends on the mode of purifying the solvent. Hence, even in this case we cannot ascertain any association of BDAA.

A more detailed discussion of acidic-basic interaction in BDAA solutions will be published shortly.[3]

Department of Physical Chemistry
Technical University
Wroctaw, Poland

6) V. Zanker, *Z. physik. Chem.*, **200**, 250 (1952).

The Temperature Dependence of the Limiting Conductances of the Aqueous Solutions of Some Aromatic Sulfonates

By Hatsuho UEDAIRA and Hisashi UEDAIRA

(Received June 23, 1964)

In a previous paper[1], it was reported that hydrophobic bonding plays an important role in the association of the dye ion. It is thought that the transport properties of such organic ions as the dye ion will be influenced by the ice-like structure of water around the non-polar group. These transport properties will also be affected by the interaction between water and the ionized group of organic ions. In this investigation, the limiting equivalent conductances will be obtained for sodium salts of benzenesulfonic (to be abbreviated BSNa), α-naphthalenesulfonic (NSNa), *m*-benzenedisulfonic (BDSNa), and 1,5-naphthalenedisulfonic (NDSNa) acids at 35, 45, and 55°C (and at 25°C for NSNa), and the activation energies of the limiting mobilities for these sulfonate ions, U, will be calculated.

Experimental

Sodium sulfonates were decolorised with active carbon and recrystallized four times for BSNa, NSNa, and NDSNa (G. R. Tokyo Kasei Co.) or six times BDSNa (technical grade) from a water-ethanol solution and dried at 110°C over phosphorus pentoxide.

The experimental method of conductance has been reported elsewhere.[1]

1) H. Uedaira and H. Uedaira, *Kolloid-Z. Z. für Polym.*, **194**, 148 (1964).

Results and Discussion

The limiting equivalent conductances, λ°, of sulfonates were obtained by the Fuoss-Onsager extended equation:

$$\lambda=\lambda^\circ-SC^{1/2}+EC\ \log\ C+JC$$

The symbols are as defined by Fuoss and Accascina.[2] The limiting mobilities, λ_-°, of sulfonate ions were obtained from these limiting conductances.[3] The activation energies, U, of sulfonate ions were calculated from the temperature dependence of their limiting mobilities. The plots of $\log\lambda^\circ$ against $1/T$ are linear for all sulfonate ions in the range of experimental temperatures; thus the activation energies are independent of the temperature. The results are given in Table I. In Table I the radii, r, of the equivalent spheres obtained from models based on Pauling[4] are given also.

As may be seen from Table I, the relation between the activation energy of the limiting mobility and the ionic radius is not linear. Though the ionic radius of BDS^{-2} is nearly

2) R. M. Fuoss and F. Accascina, "Electrolytic Conductance," Academic Press, N. Y. (1960).

3) The values of λ_+° (Na^+) were taken from R. A. Robinson and R. H. Stokes, "Electrolyte Solutions," 2nd ed., Butterworth, London (1959), p. 465.

4) L. Pauling, "The Nature of the Chemical Bond," Cornell University Press, Ithaca, N. Y. (1960), Chapters 5 and 10.

Table I. The limiting mobilities at various temperatures and activation energies of sulfonate ions

Ion	Temp. °C	λ° $cm^2\Omega^{-1}$ $equiv^{-1}$	r Å	U kcal.·mol^{-1}
BS^-	25	34.9[5a]		
	35	41.8	3.50	3.36
	45	50.0		
	55	58.7		
NS^-	25	29.3		
	35	36.6	3.71	3.75
	45	43.6		
	55	52.4		
BDS^{2-}	25	59.9[5b]		
	35	70.0	3.70	3.32
	45	85.9		
	55	99.8		
NDS^{2-}	35	57.8		
	45	70.0	3.89	3.54
	55	82.6		

equal to that of NS^-, the value of U for the former is smaller than that for the latter. Consequently, the activation energy depends not only on the size of the ion, but also on the ion-solvent interaction.

An aromatic sulfonate ion differs from an inorganic ion in having both a hydrophobic part (aromatic ring) and a hydrophilic part (sulfonic group). Each of the two parts has a different interaction with water. The aromatic part increases the ice-like structure of the watar in its neighborhood.[6,7] Therefore, the local viscosity of the water in this region should be higher than that of bulk water. According to Samoilov,[8] the activation energy of the ion transport depends upon the exchange of water molecules in the immediate neighborhood of the ion. As the frequency of the exchange of water molecules around the aromatic ring should be smaller than that of bulk water, the sulfonate ion with the larger aromatic ring has the larger activation energy, and the smaller mobility.

The sulfonic group is considered to be a mono-valent ion with a large radius, and the nearest neighbor water molecules around such ions become more mobile than in pure water because of the destruction of the structure of water by the ionic field.[8]

It is interesting to compare the limiting mobility of the BS^- ion with that of the benzoate ion. The limiting mobility at 25°C and the activation energy of the benzoate ion are 32.5 $cm^2\Omega^{-1}equiv^{-1}$ and 4.21 kcal. mol^{-1} respectively,[9] and its ion radius is 3.35 Å. Though the benzoate ion is smaller than the BS^- ion, the former has the smaller mobility and the larger activation energy. Gurney[10] suggested that the water structure close to the carboxyl group is in order. Consequently, the frequency of the exchange of the water around the carboxyl group is smaller than that of bulk water. The difference between the limiting mobilities of the BS^- ion and the benzoate ion is explained by the structure-breaking effect of the sulfonic group. The sulfonic group will also partially break out the ice-like structure around the aromatic ring.

Thus, it is clear that the activation energy of the NS^- ion is the largest and that of the BDS^{2-} ion is the smallest, and that the mobility of the NS^- ion is the smallest and that of the BDS^{2-} ion is the largest. The interactions between the water and hydrophobic part and the ionized group of organic ions play important roles in the transport properties.

The Textile Research Institute
of Japanese Government
Kanagawa, Yokohama

5) a) M. Yokoi and G. Atkinson, *J. Am. Chem. Soc.*, **83**, 4367 (1961); b) G. Atkinson, M. Yokoi and C. J. Hallada, ibid., **83**, 1570 (1961).
6) H. S. Frank and M. W. Evans, *J. Chem. Phys.*, **13**, 507 (1945).
7) G. Neméthy and H. A. Scherage, ibid., **36**, 3401 (1962).
8) O. Ya. Samoilov, *Discussions Faraday Soc.*, **24**, 141 (1957). "Struktura Vodn'kh Rastvorov Elektrolitov i Gidrataziya Ionov," Moskva (1957), Glava 3.
9) Landolt-Börnstein Tabellen, 6 Auflage, 2 Band, 7 Teil II, Spriger Verlag, Berlin, 1960, p. 267.
10) R. W. Gurney, "Ionic Processes in Solution," McGraw-Hill, N. Y. (1953), Chap. 9.

The Synthesis of 7-Methoxy-5′,6′-methylenedioxybenzofurano(3′,2′; 3,4)coumarin

By Kenji FUKUI, Mitsuru NAKAYAMA and Haruo SESITA

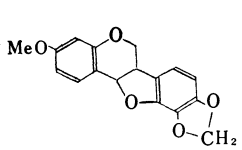
(Received July 10, 1964)

The structure of pterocarpin was proposed by McGookin et al. as 7-methoxy-6′,7′-methylenedioxy-2′,3′-dihydrobenzofurano(3′,2′; 3,4)-chroman (I).[1] Recently, on the basis of nuclear magnetic resonance spectral analysis, Bredenberg and Shoolery proposed the revised structure of 7-methoxy-5′,6′-methylenedioxy-2′,3′-dihydrobenzofurano(3′,2′; 3,4)chroman (II).[2] 7-Methoxy-5′,6′-methylenedioxybenzofurano(3′,2′; 3,4)coumarin (III) has an oxygen pattern similar to that of II in the aromatic rings.

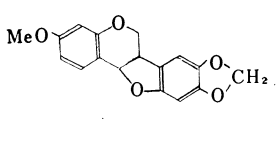
The synthesis of the coumarin (III) by the methylenation reaction of 7,5′,6′-trihydroxy compound (IV)[3] has, however, so far been unsuccessful. On the other hand, 7,5′,6′-trimethoxy compound (V)[3] has already been obtained by the methylation of IV.

In the present paper, we will describe the synthesis of III from 7-methoxy-4-hydroxycoumarin (VI)[4] by the Wanzlick method.[5]

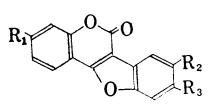
The dehydrogenatic condensation of catechol and VI in the presence of potassium ferricyanide gave a 40% yield of 7-methoxy-5′,6′-dihydroxybenzofurano(3′,2′; 3,4)coumarin (VII) (m. p. > 300°C). VII gave a strong fluorescence in ethanol or acetone and a dark violet color reaction with alcoholic ferric chloride. A dimethyl ether (V) (m. p. 247~248°C) and a diacetate (VIII) (m. p. 225~226°C) of VII were prepared. The former showed no depression of the melting point on admixture with an authentic sample.[3] The methylenation of VII with methylene iodide afforded III (m. p. 269~270°C). III gave a green color reaction with gallic acid, and its infrared spectrum showed the absorption peaks at 1038 and 920 cm^{-1}, indicating the presence of a methylenedioxy group.[6] Moreover, the ultraviolet spectra of III and V are essentially identical (Fig. 1), and III gave a strong fluorescence in ethanol or acetone.



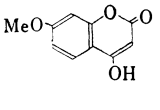
I



II



III



VI

R_1=OMe,
R_2-R_3=O−CH_2−O

IV R_1, R_2, R_3=OH
V R_1, R_2, R_3=OMe
VII R_1=OMe, R_2, R_3=OH
VIII R_1=OMe, R_2, R_3=OAc

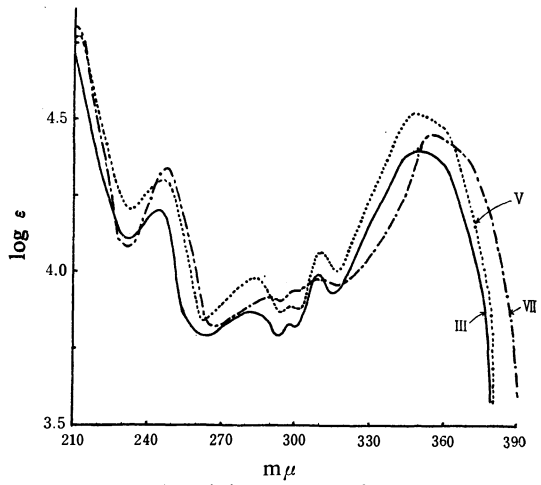


Fig. 1. Ultraviolet spectra of III, V, and VII (ethanol).

Experimental*

7-Methoxy-5′,6′-dihydroxybenzofurano(3′,2′; 3,4)coumarin (VII).—To a solution of VI[4] (m. p. 255~256°C) (1.0 g.) and catechol (0.3 g.) in a mixture of acetone (90 ml.) and water (15 ml.), a solution of potassium ferricyanide (3.5 g.) and sodium acetate (18 g.) in water (30 ml.) was added.

1) A. McGookin, A. Robertson and W. B. Whalley, *J. Chem. Soc.*, **1940**, 787.
2) J. B-Son Bredenberg and J. N. Shoolery, *Tetrahedron Letters*, No. 9, 285 (1961).
3) K. Fukui and M. Nakayama, *J. Chem. Soc. Japan, Pure Chem. Sec.* (*Nippon Kagaku Zasshi*), to be published.
4) J. Boyd and A. Robertson, *J. Chem. Soc.*, **1948**, 174.
5) H. W. Wanzlick, R. Gritzky and H. Heidepriem, *Chem. Ber.*, **96**, 305 (1963).
6) L. H. Briggs, L. D. Colebrook, H. M. Fales and W. C. Wieldmann, *Anal. Chem.*, **29**, 904 (1957).

* All melting points are uncorrected; the infrared spectra were measured in Nujol, while the ultraviolet spectra were measured in an ethanol solution.

After 1.5 hr., the resulting mixture was filtered from the precipitates (inorganic salts). The residue was washed with a solution (acetone : water = 3 : 1). The combined filtrate was then treated with 46% formic acid (10 ml.), concentrated to ca. 80 ml. in vacuo, and then left overnight. The precipitates were collected and recrystallized from acetone to given VII in the form of pale yellow needles; m. p. > 300°C; yield 0.65 g. (40%). This gave a blue fluorescence in ethanol or acetone and a dark violet color with an alcoholic ferric chloride solution. IR: 3310 (broad) (OH); 1725 (α-pyrone) cm^{-1}. UV: λ_{max} mμ (log ε); 210 (4.80), 250 (4.34), 288 (3.92), 301_1 (3.94), 310 (3.97), 355 (4.45).

Found: C, 64.69; H, 3.11. Calcd. for $C_{16}H_{10}O_6$: C, 64.43; H, 3.38%.

The diacetate (VIII): acetic anhydride-pyridine method; m. p. 225~226°C (colorless needles from acetone). IR: 1776, 1759, 1730 (acetate, α-pyrone) cm^{-1}. UV: λ_{max} mμ (log ε); 240 (4.34), 266 (3.90), 288.5_1 (3.90), 299 (4.12), 335 (4.54), 342_1 (4.44), 351 (4.45).

Found: C, 62.58; H, 3.54. Calcd. for $C_{20}H_{14}O_8$: C, 62.83; H, 3.69%.

7, 5', 6'-Trimethoxybenzofurano (3', 2'; 3, 4) coumarin (V).—A mixture of VII (0.5 g.) methyl iodide (1.0 g.) and anhydrous potassium carbonate (3.0 g.) in anhydrous acetone (300 ml.) was refluxed for 5 hr. on a steam bath. The reaction mixture was then filtered from the precipitates. The filtrate was distilled and the residue was recrystallized from acetone to give V in the form of colorless needles; m. p. 247~248°C; yield 0.5 g. (88%). This was identical with an authentic sample[3] (m. p. 248~249°C) and gave a blue fluorescence in ethanol or acetone. IR: 1730 (α-pyrone) cm^{-1}. UV: λ_{max} mμ (log ε); 211 (4.77), 246 (4.30), 283.5 (3.98), 297 (3.89), 310 (4.06), 348 (4.52).

Found: C, 66.21, H, 4.42. Calcd. for $C_{18}H_{14}O_6$: C, 66.25; H, 4.32%.

7-Methoxy-5', 6'-methylenedioxybenzofurano (3', 2'; 3, 4) coumarin (III).—A mixture of VII (0.5 g.), methylene iodide (1.0 g.) and anhydrous potassium carbonate (3.0 g.) in acetone (300 ml.) was refluxed for 30 hr. on a steam bath; then the solvent was evaporated. The water was added to the residue. The resulting precipitates were collected and recrystallized from acetone to give III in the form of colorless microcrystals; m. p. 269~270°C; yield 0.25 g. (47%). This gave a green color reaction with gallic acid and a blue fluorescence in ethanol or acetone. IR: 1746 (α-pyrone); 1038, 943 (O-CH_2-O). UV: λ_{max} mμ (log ε); 245 (4.25), 283 (3.87), 297 (3.83), 309 (3.99), 347 (4.40).

Found: C, 65.52; H, 3.14. Calcd. for $C_{17}H_{10}O_6$: C, 65.81; H, 3.25%.

The authors are grateful to the members of the Faculty of Pharmacology of Toyama University for their microanalyses. This work was supported in part by a grant-in-aid from the Ministry of Education.

Department of Chemistry
Faculty of Science
Hiroshima University
Higashi-Sendamachi, Hiroshima

SHORT COMMUNICATIONS

Iridodiols, the Effective Components of Actinidia Polygama for Chrysopidae

By Takeo SAKAN, Sachihiko ISOE, Suong Be HYEON, Teiichi ONO and Ichirō TAKAGI

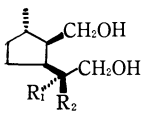
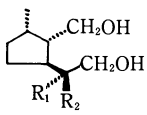
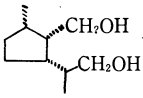
(Received July 17, 1964; in revised form November 4, 1964)

In previous papers[1] we reported the structures of matatabilactone and actinidine, the effective components of *Actinidia Polygama* Miq. for Felidae animals. It has been privately communicated[2] that the male of a sort of lacewing (*Chrysopa septempunctata* Wesmael)[3] is also attracted by the same plant. Attempts have now been made to isolate the effective component from the gall of *Actinidia Polygama* Miq. The elaborate column chromatography on alumina and silicic acid of the neutral fraction extracted from the ground gall with

1) T. Sakan, A. Fujino, F. Murai, Y. Butsugan and A. Suzui, This Bulletin, **32**, 315, 1155 (1959).

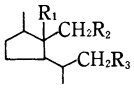
2) Private communications from Dr. E. Kezuka of Tōyō University, Dr. S. Ishii of Kyoto University, and Dr. H. Furukawa of Tokyo Gakugei University; G. Takagi, *Nōgyō* (*J. Agr. Soc. Japan*), No. 802, 33 (1950). Dr. S. Ishii, presented at The Annual Meeting of The Society of The Japanese Applied Entomology and Zoology, Tokyo, April, 1964.

3) We have observed that *Chrysopa japana* Okamoto also is attracted by *Actinidai Polygama*.

I II III

α : R_1=Me, R_2=H β : R_1=H, R_2=Me
δ : R_1=H, R_2=Me γ : R_1=Me, R_2=H



IV : R_1=R_2=H, R_3=OH
V : R_1=R_3=H, R_2=OH
VI : R_1=R_3=OH, R_2=H

methanol yielded an oil which had a potent activity. Although the vapor phase chromatography of this oil revealed three close peaks and the thin layer chromatography of this oil gave two spots, the mass spectrum and the infrared spectrum of this oil were in close agreement with those of α-iridodiol (I),[4] m. p. 80°C, derived from isoiridomyrmecin by lithium aluminum hydride reduction. Therefore, this seemed to be a mixture of α-iridodiol and its stereoisomers. In fact, the α-iridodiol derived from isoiridomyrmecin showed activity of almost the same order for *Chrysopa* as for the oil obtained above.

Fortunately we could assign all peaks in the vapor-phase chromatography of the oil as α or δ-iridodiol (I),[4] β or γ-iridodiol (II)[5] and all *cis*-iridodiol (III)[6] by a comparison of the retention times. The isolation of each effective component is in progress. In addition to iridodiols, the synthetic alcohols IV, V, and VI[6] also showed activity of a much lower order.

Faculty of Science
Osaka City University
Sumiyoshi-ku, Osaka

4) Greek prefixes in the designation of skytanthine series were used for the nomenclature of iridodiols. E. J. Eisenbraun, T. George, B. Riniker and C. Djerassi, *J. Am. Chem. Soc.*, **82**, 3648 (1960); E. J. Eisenbraun, A. Bright and H. H. Appel, *Chem. & Ind.*, **1962**, 1242.

5) Prepared by the lithium aluminum hydride reduction of the corresponding nepetalinic acids kindly supplied by Dr. E. J. Eisenbraun of Oklahoma State University.

6) Unpublished work.

7) Unpublished work.

The Polymerization of Acetylenes with Dicyclopentadienyl-vanadium

By Ryuichiro TSUMURA and Nobue HAGIHARA

(Received August 18, 1964)

Although a large number of organometallic complexes have been reported in which aromatic rings such as cyclopentadienyl and benzene are coordinated to the transition metals, their possible catalyses have not yet been extensively studied. It has previously been shown in our laboratory that the oxygenated product of dibenzene-chromium has a catalytic activity of the polymerization of ethylene.[1] We will now report that paramagnetic dicyclopentadienyl-vanadium[2] (I) catalytically polymerizes various acetylenes. This seems to be the first example of the polymerization of acetylenes with metallocene only.

As a typical experiment, in a 100 ml. stainless steel autoclave 0.375 g. (2.07 mmol.) of I was dissolved in 50 ml. of benzene under nitrogen. Acetylene was introduced to about 15 kg./cm^2. The reaction system was then continuously shaken and maintained under the pressure of 15~22 kg./cm^2, by means of the occasional addition of acetylene, at 80°C for 6 hr. When the reaction muds were treated with a solution of methanol and hydrochloric acid (1 : 1 by volume) under nitrogen, they gave 2.85 g. of a black solid (Found : C, 87.94 ; H, 7.34 ; Ash, 0.00%). In a similar reaction in toluene, no liquid products such as benzene and linear oligomers were found.

The black solid was thermally stable at 200°C and insoluble in all organic solvents. The infrared spectrum was essentially identical to that of the conjugated *trans*-polyacetylene obtained by Natta et al.[3] and by Hatano[4]. The polymer was gradually oxidized when left standing in air, in a few months changing into an orange solid whose infrared spectrum showed

1) H. Yamazaki, M. Yamaguchi and N. Hagihara, *J. Chem. Soc. Japan, Pure Chem. Sec.* (*Nippon Kagaku Zasshi*), **83**, 959 (1962) ; *Annual Reports of the Institute for Fibre Research*, **16**, 495 (1963).

2) E. O. Fischer and S. Vigoureux, *Chem. Ber.*, **91**, 2205 (1958).

3) G. Natta, G. Mazzanti and P. Corradini, *Atti. Accad. naz. Lincei, Rend. Classe Sci. fis. mat. nat.*, **25**, 3 (1958).

4) M. Hatano, *J. Chem. Soc. Japan, Ind. Chem. Sec.* (*Kogyo Kagaku Zasshi*), **65**, 723 (1962).

TABLE I. THE POLYMERIZATION OF ALKYNES WITH I[a]

Alkyne g.	Catalyst g.	Conversion %	Product[b] Cyclic trimer g.	Product[b] Oligomer g.	Mixture of trimers Ratio[c] 1, 3, 5-/1, 2, 4-	Mixture of trimers B. p. °C	Mixture of trimers n_D^{20}
$CH_3C{\equiv}CH$ 7.0	0.445	34.6	2.32	0.10	42/58	165~70	1.5057
n-$C_3H_7C{\equiv}CH$ 11.04	0.464	74.8	8.02	0.25	36/64	101/3 mmHg	1.4930
n-$C_4H_9C{\equiv}CH$ 10.45	0.453	67.4	6.85	0.20	35/65	134/3 mmHg	1.4902
$C_6H_5C{\equiv}CH$ 8.60	0.385	98.8	Dimer 0.3	8.2	M. p.	Oligomer 123~125°C,	M. w. 493[d]

a) The alkyne and catalyst I were dissolved in 30 ml. of benzene under nitrogen, and the solution was heated at 100°C in an ampule for 5 hr. (1-alkynes) or for 4 hr. (phenylacetylene).
b) The liquid products were separated by distillation, and the solid products were isolated by reprecipitation.
c) The proportion of 1, 3, 5- to 1, 2, 4-trisubstitution was determined by gas chromatographic analyses.
d) By the cryoscopic benzene method.

the presence of carbonyl and hydroxyl groups. A suspension of the black polymer in carbon tetrachloride added chlorine to give a white solid, which was then soluble in dimethyl formamide. These facts indicate that the black solid obtained may be a linear, high-molecular-weight polymer, containing quite long sequences of conjugated double bonds in the trans configuration.

1-Alkynes have been polymerized by catalyst I, too. The experimental results are summarized in Table I. The infrared spectra of the products showed that they are composed of mixtures containing 1, 3, 5- and 1, 2, 4-trialkylbenzene as the major products and a small quantity of higher oligomers. *t*-Butylacetylene was inert in the catalytic reaction; a bulky *t*-butyl radical is presumed to hinder cyclotrimerization by the catalyst.

Phenylacetylene gave an orange-yellow solid, whose infrared spectrum and molecular weight indicate that it may be a linear oligomer in the trans configuration. No cyclization to benzene derivatives was observed in this reaction. Attempts to polymerize propargyl alcohol and disubstituted acetylenes, such as 3-heptyne, 2-butyne-1, 4-diol, and tolane, were unsuccessful.

It is of great interest that the catalysis of dicyclopentadienyl-vanadium is remarkably selective, as has been mentioned above, and different from that[5] of bis(triphenylphosphine)-dicarbonyl-nickel in the catalytic polymerization of acetylenes. In relation to this problem, we have prepared some new, highly air-sensitive acetylene complexes such as π-$C_5H_5(C_2H_2)$-$V(CO)_2$. The investigation of the acetylene complexes of vanadium will be published elesewhere.

The Institute of Scientific and Industrial Research
Osaka University
Sakai, Osaka

5) L. S. Meriwether, M. F. Leto, E. C. Colthup and G. W. Kennerly, *J. Org. Chem.*, 27, 3930 (1962).

The Radioactivation Analysis of Graphite for Nitrogen by the $^{14}N(p, \alpha)^{11}C$ Reaction

By Tadashi NOZAKI and Kazuhiko YAZAWA

(Received August 22, 1964)

A successful method for analyzing graphite for an ultra-trace quantity of nitrogen will be presented. All the methods ever previously reported for determing trace nitrogen (the vacuum-fusion technique, the Kjeldahl method, emission and mass spectroscopy, radioactivation analysis by $^{14}N(n, 2n)^{13}N$ or $^{14}N(\gamma, n)^{13}N$,[1] etc.) are either inapplicable to graphite or are of limited sensitivity. Further, any surface once exposed to air is contaminated with nitrogen. Making use of radioactivation analysis by means of a $^{14}N(p, \alpha)^{11}C$ reaction, we succeeded in determining as small an amount as several tens p. p. b. of nitrogen in pyro-graphite. Recently, pyro-graphite prepared by the thermal decomposition of pyridine was found to have very interesting semiconductor characteristics, which would be due to the presence of a trace of nitrogen.

The excitation function for $^{14}N(p, \alpha)^{11}C$ up to 15 MeV. was measured by the stacked-foil method, each foil being a nylon film about 22 mg./cm^2 thick. The results showed that 1 p. p. m. of nitrogen in carbon gave 5.3×10^3 d. p. s. ^{11}C as the thick-target saturation-activity for 15 MeV.-1 μamp. protons. The mean recoil range of the ^{11}C for the 14.2 MeV. proton was also measured by inserting a recoil-catcher in the stack; it was found to be 0.36 mg./cm^2. With a $^{16}O(\alpha, pn)^{18}F$ reaction, we previously showed that the surface layer, of a thickness about five times the recoil range of ^{18}F, should be removed in order to eliminate the effect of surface oxygen.[3] Therefore, the surface layer about 1.8 mg./cm^2 thick is removed in the present case. Since the irradiated graphite also contained ^{13}N (formed by $^{13}C(p, n)^{13}N$)[4] and longer-lived nuclides (from impurities), chemical treatment was necessary for a reliable measurement of the ^{11}C. Oxidation in strong phosphoric acid developed by Kiba et al.[5] proved useful in decomposing the sample. The graphite itself was the carrier of ^{11}C.

A plate of pyro-graphite ($30 \times 10 \times 2$ mm.) was placed on a water-cooled target-holder and irradiate with protons (15 MeV., 5 μamp., 10 min.). After the surface layer had been uniformly removed by mechanical grinding, the sample was finely pulverized. It was then added into a flask containing strong phosphoric acid (50 ml.), sulfuric acid (30 ml.) and potassium iodate (25 g.) heated to 160~170°C. Gentle heating was continued, and the carbon dioxide formed was introduced into another flask containing sodium hydroxide (2 N, 200 ml.). To make the absorption of carbon dioxide in a closed system smooth and easy, the air in both the flasks had been replaced with nitrogen oxides (from sodium nitrite and sulfuric acid), and the contents of the absorption flask were separated from atmospheric air by a movable layer of carbon tetrachloride. The nitrogen oxides worked also as a hold-back carrier of ^{13}N. When the oxidation became less vigorous, even at 240°C, perchloric acid (65%, a few milliliters) was carefully dripped in to complete the reaction. When all the graphite had been oxidized, nitrogen oxides were passed through to carry all the carbon dioxide into the sodium hydroxide solution. After. the solution had been treated with hydrazine hydrate (1 g.), barium carbonate was precipitated and filtered off. The process after the irradiation required 40 to 50 min. The recovery was almost quantitative, but so large a quantity of barium carbonate was formed that only a part of it was taken for the activity measurement. The annihilation radiation was measured by a scintillation counter of a known efficiency. The decay curve and the γ-ray spectrum were satisfying for a reliable determination of ^{11}C. The nitrogen content was calculated from the disintegration-rate by the absolute method, the only possible source of interference being $^{11}B(p, n)^{11}C$ under our conditions.

Pyro-graphites made from pyridine contained 1 to several p. p. m. of nitrogen, while those made from propane had less than a few hundred p. p. b. This method appears to be

1) E. g. R. C. Koch, "Activation Analysis Handbook," Academic Rress, New York and London (1960), p. 38.
2) K. Takeya and K. Yazawa, Symposium on Carbon, Tokyo 1964.
3) K. Saitô et al., *Intern. J. Appl. Rad. & Isotopes*, **14**, 358 (1963).
4) A. B. Whitehead, *Can. J. Phys.* **36**, 1283 (1958).
5) T. Kiba, *Chem. and. Chem. Ind. (Chem. Soc. Japan)*, **11**, 730 (1958).
6) M. Furukawa et al., *J. Phys. Soc. Japan*, **15**, 2168 (1960).

by far the most sensitive method for nitrogen, the detection limit being several p. p. b. A detailed paper will be submitted for publication in the near future.

Institute of Physical and Chemical Research
Bunkyo-ku, Tokyo (T. N.)

University of Electro-Communications
Chôfu, Tokyo (K. Y.)

*The Partial Structure of Pederin**

By Takeshi MATSUMOTO, Satoshi TSUTSUI, Mitsutoshi YANAGIYA, Seiichi YASUDA, Sawae MAENO, Junji KAWASHIMA, Akira UETA and Masuo MURAKAMI

(Received September 7, 1964)

In 1949, one of the present authors (A. U.)[1] reported the isolation of a toxic principle, m. p. 114°C, from *Paederus fuscipes*. Reinvestigation of this material has now revealed that it is identical with pederin, $C_{25}H_{45}O_6N$, isolated from the same insect by Pavan and Bo[2] in 1953 and recently studied chemically by Quilico et al. and Cardani.[3,4] The infrared spectrum of pederin exhibits bands at 3480, 3380 (OH, NH), 1665, 1510 (NHCO), 3060 and 900 cm^{-1} ($\rangle C{=}CH_2$). Contrary to the opinion of the Italian workers, however, the latter two bands indicate the presence of at least one double bond in pederin. Since no other band is observable in the olefinic C–H stretching vibration region,[5] the only additional double bond that could possibly be present would be tetrasubstituted. The double bond is not conjugated ($\varepsilon_{200\,m\mu}$ 1400). On being treated with acetic anhydride and pyridine, pederin affords a diacetate, $C_{29}H_{49}O_{11}N$[6], m. p. 106°C, which shows bands at 3500 (broad, OH), 3360 (NHCO), 1740, 1720 (CH_3CO_2), 1700, 1520 (CONH), 3060 and 1650 cm^{-1} ($\rangle C{=}CH_2$). The NMR spectrum of pederin[7] exhibits its main peaks at the following positions (these peaks are assignable to the following groups by comparison with the spectrum of its diacetate): τ 9.11, 9.04 (each s, CH_3–$\overset{|}{C}$–), 8.98, 8.82 (each d, J 7 c. p. s., $\underline{CH_3}$–$\overset{|}{C}$–H), 7.55 (s, –$\overset{|}{C}$–CH_2–CO), 6.67 (s, 2 OCH_3), 6.61 (s, 2 OCH_3 and –O–CH_2–$\overset{|}{C}$–)[8], 6.20 (broad, 2 $\underline{H}$–$\overset{|}{C}$–OCH_3), 5.65 (s, $\underline{H}$–$\overset{|}{C}$–OH), 5.26, 5.18 (each broad s, $\rangle C{=}CH_2$) and 4.66 (m, $\overset{C}{H}\rangle C\langle\overset{OR}{OR}$). Since the peak due to the –$\overset{|}{C}$–CH_2–O– group in pederin does not shift appreciably to a lower field in the spectrum of diacetate, the oxygen atom in this group must be ethereal. Thus, out of the nine oxygen atoms of pederin, four are present as methoxyl groups, one as an amide, one as a C–O–CH_2–$\overset{|}{C}$– group and three as hydroxyl groups, two of which are acylable. A dimethyl acetal group is absent, since the *m/e* 75 peak is negligibly weak in the mass spectrum of both pederin and its diacetate. The spectroscopic evidence described above, coupled with the chemical findings[3] that preudopederin yields oxamic acid upon oxidation and that pederin

* Read before the 17th Annual Meeting of the Chemical Society of Japan, March, 1964.

1) A. Ueta, *Kyushu Igaku Zasshi (Journal of Kurume Medical College, Kyushu)*, **1949**, 249.

2) M. Pavan and G. Bo, *Phys. Com. et Oecol.*, **3**, 307 (1953); M. Pavan, "Richerche biologiche e mediche su pederina e su estratti purifficatti di *Paederus fuscipes* Curt.," M. Ponzio, Pavia (1963).

3) A. Quilico, C. Cardani, D. Chiringhelli and M. Pavan, *La Chim. e l'Ind.*, **43**, 1434 (1961); C. Cardani, D. Chiringhelli and A. Quilico, "Abstracts of Papers, International Symposium on the Chemistry of Natural Products," Kyoto (1964), p. 139.

4) The identity of the two substances was confirmed by a direct comparison of m. p.'s and infrared spectra. We wish to express our sincere thanks to Professor Cardani for his generous gift of a sample of pederin.

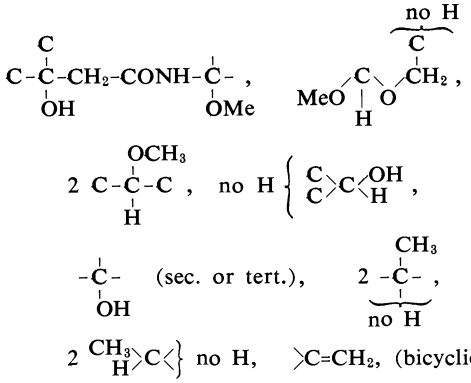
5) The infrared spectrum was obtained by means of a JASCO 401G grating spectrometer.

6) The molecular formulas of diacetate and pederin itself were confirmed by elemental analysis and mass spectrometry. The mass spectra were measured by Mr. Hiroshi Sato of the Hitachi Naka works, to whom our sincere thanks are due.

7) Measured in a $CDCl_3$ solution containing a small amount of pyridine as a stabilizer for pederin; pederin is very sensitive to acids.

8) In the spectrum of diacetate, the peak due to the -OCH_2-$\overset{|}{C}$- group appears at 6.52 as a broad singlet while the peaks due to methoxyl groups appear at 6.60 (3H), 6.64 (6H) and 6.83 (3H); the singlet line at 5.65 ($\underline{H}$-$\overset{|}{C}$-OH) in the spectrum of pederin is shifted to 4.70. The intensity of the broad absorption centered at 6.20 indicates the presence of two -$\overset{|}{C}$H-OCH_3 groups in acetate.

readily splits off ammonia upon treatment with acid, suggest the presence of the following moieties in pederin:



The molecular formula indicates that pederin is bicyclic if the tetrasubstituted double bond is absent.

Chemistry Department
Faculty of Science
Hokkaido University
Sapporo (T. M., S. T., M. Y., S. Y., S. M. & J. K.)

School of Medecine
Kurume University
Kurume (A. U.)

Research Institute
Yamanouchi Pharmaceutical Co.
Itabashi-ku, Tokyo (M. M.)

The Appearance of Free Radicals during the Photo-decomposition of Nitrosobenzenes

By Kazuhiro MARUYAMA, Rikuhei TANIKAGA and Ryozo GOTO

(Received October 3, 1964)

It has been reported that azoxybenzene, *p*- and *o*-hydroxyazobenzene, nitrobenzene, aniline and other minor amounts of hydroxyazoxybenzenes were formed by the photochemical decomposition of nitrosobenzene.[1] The present authors examined the process of the photochemical decomposition of several nitrosobenzene derivatives by using the ESR technique.

The subject of this investigation is the decomposition of nitrosobenzene, *o*-, *m*-, and *p*-methylnitrosobenzene, and *o*-, *m*-, and *p*-chloronitrosobenzene. Pure nitrosobenzene derivatives were dissolved in dry pure tetrahydrofuran and completely degased and illuminated by a 400-W. high pressure mercury-arc lamp at room temperature. These nitrosobenzene derivatives without exception produce free radicals from the beginning of decomposition. As the decomposition proceeds, the

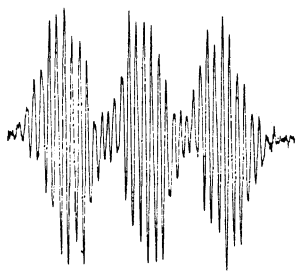


Fig. 1(a) ESR spectrum of free radicals produced by the photo-decomposition of nitrosobenzene.

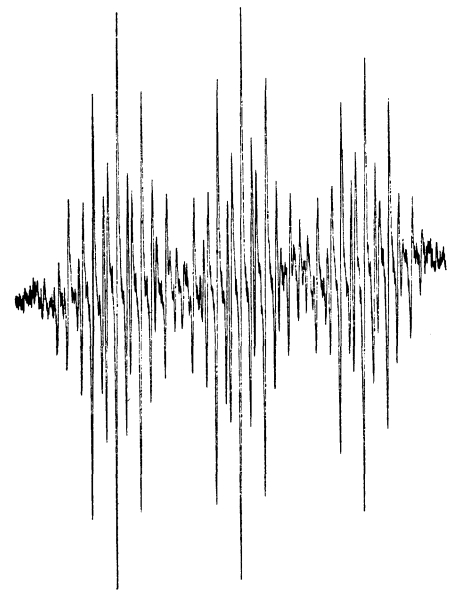


Fig. 1(b) ESR spectrum of free radicals produced by the photo-decomposition of *m*-chloronitrosobenzene.

1) E. Bamberger, *Ber.*, 35, 1606 (1902).

color of the solutions changed from green to brown. The free radicals produced were identified as the derivatives of diphenylnitroxide by the hyperfine structures of their ESR spectra; some of them are reproduced in Fig. 1.

It is noteworthy that the radicals produced from *o*-, *m*-, and *p*-substituted derivatives of nitrosobenzene were highly position-specific; *o*-methylnitrosobenzene decomposed to *o*,*o*'-dimethyldiphenylnitroxide, *m*-nitrosobenzene to *m*,*m*'-dimethyldiphenylnitroxide, *p*-methylnitrosobenzene to *p*,*p*'-dimethyldiphenylnitroxide, *o*-chloronitrosobenzene to *o*,*o*'-dichlorodiphenylnitroxide, *m*-chloronitrosobenzene to *m*,*m*'-dichlorodiphenylnitroxide, *p*-chloronitrosobenzene to *p*,*p*'-dichlorodiphenylnitroxide, and so on. Their ESR spectra show well-resolved hyperfine structures. Diphenylnitroxide, *m*,*m*'-dimethylnitroxide, and *p*,*p*'-dimethyldiphenylnitroxide were identified by a comparison of their ESR spectra with those of known samples. *p*,*p*'-Dichlorodiphenylnitroxide, *m*,*m*'-dichlorodiphenylnitroxide and *o*,*o*'-dichlorodiphenylnitroxide were clearly identified from the analysis of the ESR spectra obtained. Only *o*,*o*'-dimethyldiphenylnitroxide remains to be clarified completely; its spectrum shows a rather broad hyperfine structure.

Experimental.—*Derivatives of Nitrosobenzene.*—All the nitosobenzenes described above were synthesised from the corresponding nitro-derivatives. Nitro-derivatives were reduced to the corresponding hydroxylamine derivatives and oxidized to the nitroso-derivatives by a ferric chloride solution. The nitroso-derivatives obtained were carefully recrystallized from ethanol until their solutions in tetrahydrofuran became free from any ESR signal. Their physical constants were: nitrosobenzene, m. p. 68°C; *o*-methylnitrosobenzene, m. p. 72.5°C; *m*-methylnitrosobenzene, m. p. 53.5°C: *p*-methylnitrosobenzene, m. p. 49.0°C; *o*-chloronitrosobenzene, m. p. 56.5°C; *m*-chloronitrosobenzene, m. p. 72.0°C; *p*-chloronitrosobenzene, m. p. 89.5~90.0°C.

The ESR measurements were carried out by using a JEOL-3X spectrometer manufactured by the Japan Electron Optics Laboratory.

We are now performing the chemical analysis of the photo-decomposition products of nitrosobenzene derivatives, along with an ESR study to find the precise mechanism of the photochemical decomposition of nitrosobenzene derivatives.

Department of Chemistry
Faculty of Science
Kyoto University
Sakyo-ku, Kyoto

The Ultraviolet Spectra of Some Polysilanes[1]

By Hideki SAKURAI and Makoto KUMADA

(Received October 9, 1964)

A recent article[2] prompts us to report some results of our own studies on p_π-d_π bonding in polysilanes. Although the literature contains several references to the participation of 3d orbitals fo silicon to effect enhanced bonding in phenyl[3] or vinyl-substituted silanes,[4] the investigation of this kind of participation has not been extended to the spectral study.

Ultraviolet spectroscopic investigations, however, afford an obvious source of information concerning the electronic levels of these molecules, and will serve to provide an important criterion for the existence of dative p_π-d_π bonding.

During the course of our study of the properties of silicon-silicon bonding, it has been found that polysilanes with a phenyl or vinyl group have a very intense absorption in the ultraviolet region, unlike phenyltrimethylsilane[5] and vinyltrimethylsilane.[6]

The absorption spectra of some phenyl or vinyl substituted disilanes and trisilanes in *n*-hexane were studied in the ultraviolet region, 210~260 mμ; the experimental results are presented in Table I. Hexamethyldisilane, the

1) Presented in part at the Symposium of Organometallic Chemistry, Nagoya, October 13, 1963.

2) H. Gilman, W. H. Atwell and G. L. Schwebke, *Chem. & Ind.*, **1964**, 1063.

3) C. Eaborn, "Organosilicon Compounds," Butterworths Scientific Publications, London (1960), Chap. 3.

4) J. J. Eisch and J. T. Trainor, *J. Org. Chem.*, **28**, 487, 2870 (1963); J. J. Eisch and R. T. Beuhler, ibid., **28**, 2876 (1963).

5) K. Bowden and E. A. Braude, *J. Chem. Soc.*, **1952**, 1068.

6) C. E. Scott and C. C. Price, *J. Am. Chem. Soc.*, **81**, 2670 (1959).

parent compound, was found to have no absorption in this region.

Recently, Hague and Prince[7] have reported an intense absorption at 246.5 mμ for hexaphenyldisilane. They described this absorption as an interaction between phenyl groups through the silicon-silicon bond. However, judging from the table, apparently the most striking red shift in the absorption maxima is observed for phenylpentamethyldisilane; namely, the introduction of a pentamethyldisilyl group into benzene causes a red shift to the extent of 28 mμ in the 200 mμ-band.[8]

TABLE I. UV SPECTRA OF SOME POLYSILANES

Polysilane	λ_{max} mμ	ε_{max}
$PhSiMe_2SiMe_3$	231.0	10900
$PhSiMe_2SiMe_2Ph$	238.0	18500
$Ph_2SiMeSiMePh_2$	240.0	25900
$CH_2=CH-SiMe_2SiMe_3$	223.2	5200
$CH_2=CH-SiMe_2SiMe_2-CH=CH_2$	227.0	9790
$PhSiMe_2SiMe_2SiMe_3$	240.0	15400
	221.3	13000
$Me_3SiSiMePhSiMe_3$	243.0	13000

Therefore, the evidence thus obtained suggests that the pentamethyldisilyl group can interact directly with the phenyl group, possibly by p_π-d_π conjugation. A rather small shift in the absorption maxima can be found when a second phenyl group is introduced into phenylpentamethyldisilane at the vicinal position, while the absorption intensity increases. Almost the same trends are observed for vinylpentamethyldisilane and divinyltetramethyldisilane.

Since the trimethylsilyl group has only a small bathochromic effect on benzene[5] or ethylene,[6] it seems reasonable to assume that the silicon-silicon bond is essential as a chromophore to make an enhanced conjugation with benzene or ethylene.

Further details will be published later.

Department of Synthetic Chemistry
Faculty of Engineering
Kyoto University
Sakyo-ku, Kyoto

7) D. N. Hague and R. H. Prince, *Proc. Chem. Soc.*, 300 (1962).

8) Fine structures in the 260 mμ-band are almost masked by the strong absorption near 235 mμ in phenyl-substituted polysilanes.

*Preparation of δ-Cyanovaleric Acid Ester by Cathodic Crossed Coupling**,***

By Kiichiro SUGINO, Kozo SHIRAI and Tsutomu NONAKA

(Received October 12, 1964)

An electrolytic method for preparing adipodinitrile by the cathodic hydrodimerisation of acrylonitrile has recently been described.[1] We have now attempted to extend this to the preparation of the δ-cyanovaleric acid ester by the cathodic crossed coupling of acrylonitrile and the acrylic acid ester.

After many trials, it has now been found that the desired product can be obtained in a good yield when a mixture of a large amount of acrylonitrile (1 mol.) and a small amount of methyl acrylate (1/5 mol.) is reduced at the mercury cathode at as low a potential as possible (about −1.80 V. vs. SCE) in an electrolyte containing quaternary ammonium salt and with a slight excess of the theoretical amount of current. The yield and the current efficiency were both as high as 60% as calculated on the basis of the methyl acrylate used. A small amount of adipodinitrile was produced as a by-product, but neither dimethyl adipate nor propionitrile was produced. The product can be easily separated from the mixture of reaction products and unreacted starting materials by fractional distillation.

* Organic Electrode Process, Part 28; Part 27; *J. Electrochem. Soc.*, **110**, 918 (1963).

** Just before we read this paper at the Symposium on Organic Synthesis using Free Radical Reaction held at Osaka on September 1964[2], M. M. Baiser had also reported the same process in the July issue of the *Journal of Organic Chemistry*.[3] However, his conditions were somewhat different from the ours, and the yield was lower than that in the present paper. Our patent application to the Japanese patent office is dated July 15, 1964.

1) M. M. Baiser, Extended Abstract of Electro-Organic Division, Fall Meeting of The Electrochemical Society, Sept.-Oct. 1963, p. 14; *J. Electrochem. Soc.*, **111**, 215 (1964).

2) K. Sugino, K. Shirai and T. Nonaka, Extended Abstract of the Symposium on Organic Synthesis using Free Radical Reaction, sponsored by the Chemical Society of Japan, September 1964, p. 31.

3) M. M. Baiser, *J. Org. Chem.*, **29**, 1670 (1964).

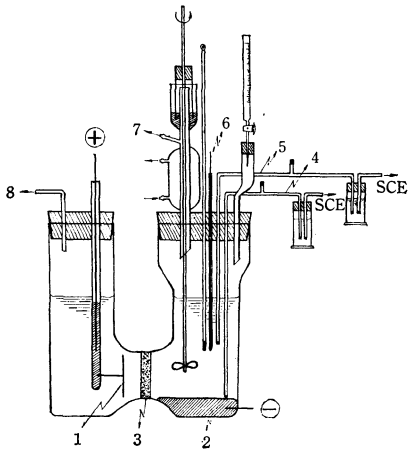


Fig. 1

1. Pt anode
2. Hg cathode
3. Diaphragm
4. Salt bridge for electrolyser use
5. Salt bridge for pH-meter use
6. Antimony electrode
7, 8. Gas outlets

This may be a new and simple route for preparing this compound from raw materials easily obtainable.

Experimental.—The cell used is an H-type cell; it is shown in Fig. 1. A fine-sintered glass diaphragm separated the cathode chamber from the anode chamber. The cathode chamber was closed with a rubber stopper equipped with a burette, a thermometer, a stirrer through the reflux condenser, two salt bridges connected with reference electrodes, and an antimony electrode connected with the pH meter. A mercury pool at the bottom of the cathode chamber served as the cathode. A platinum disk anode was placed vertically near the diaphragm. A controlled potential electrolyser, constructed by the Yanagimoto Co. in Kyoto, was used for the direct current power supply. The temperature was maintained at 30°C by cooling the cell with water.

A mixture of acrylonitrile (17.3 g., 1/3 mol.) and methyl acrylate (5.7 g., 1/15 mol.) was added to a concentrated aqueous solution of tetraethylammonium *p*-toluenesulfonate (consisting of 25 g. of salt and 25 g. of water), which served as the catholyte. The anolyte was the same electrolyte solution. The electrolysis was carried out by controlling the cathode potential at −1.80 V. A current of 0.70 amp. (cathodic current density: 6 amp./dm^2) flowed at the beggining (cell voltage: 17 V.), but it decreased to 0.50 amp. (cell voltage: 13 V.) at the end. The total amount of current passed was 3.57 amp. hr. (the theoretical amount for methyl acrylate). During the electrolysis, the catholyte was vigorously agitated by a stirrer. The pH of the catholyte was controlled at 5∼8 by adding *p*-toluenesulfonic acid.

After the reduction, the catholyte was thoroughly extracted with benzene. The distillation* of the dried (calcium chloride) benzene solution at temperatures up to 100°C left a light-yellow viscous liquid. After the absence of dimethyl adipate had been confirmed by a distillation test, the liquid was analyzed by vapor phase chromatography.** It consisted of 5.8 g. of methyl δ-cyanovalerate and 1.8 g. of adipodinitrile. Then the liquid was distilled under reduced pressure, to give 5.3 g. of methyl δ-cyanovalerate, b. p. 110°C at 7 mmHg and 1.7 g. of adipodinitrile, b. p. 126∼130°C at 7 mmHg.

For further confirmation, a portion of methyl δ-cyanovalerate fraction was hydrogenated in the presence of a nickel catalyst in an ethereal solution at 100∼120°C and 130 atm. to methyl ε-aminocaproate, which, in turn, was converted to ε-caprolactam by heating it in methanol at 220°C under a 60 atmospheric hydrogen pressure.[4] The methyl ε-aminocaproate and ε-caprolactam thus obtained had b. p. of 88∼89°C at 7 mmHg and 126°C at 8 mmHg respectively, and the latter solidified on standing.

Laboratory of Organic Electrochemistry
Department of Applied Electrochemistry
Tokyo Institute of Technology
Meguro-ku, Tokyo

* The distillate was analyzed by vapor phase chromatography. The results showed that propionitrile was not formed and that the unchanged starting materials could be recovered almost quantitatively. As for methyl propionate, it could not be analysed by this method. However, if it existed the amount would be very small.

** Silicone (DC 550): Stationary phase, 2 m.; carrier gas, H_2; flow rate, 40 cc./min., 203°C.

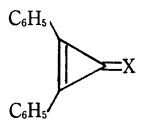
4) Japanese Pat. 218607.

Some Derivatives of 2, 3-Diphenylcyclopropenone[1]

By Yoshio KITAHARA and Makoto FUNAMIZU

(Received October 19, 1964)

Recently, the aromaticity of the cyclopropenyl system has been investigated theoretically as well as experimentally in several countries.[3] In connection with our studies of the cycloheptatrienyl system, we compared these two systems. This paper will describe the preparation of 2, 3-diphenylcyclopropenethione (I), 3-dicyanomethylene-1, 2-diphenyl-1-cyclopropene (II), 2, 3-diphenylcyclopropenone oxime (III) and 3, 3-dichloro-1, 2-diphenyl-1-cyclopropene (IV) from 2, 3-diphenylcyclopropenone (V).



I: X=S
II: X=C(CN)$_2$
III: X=NOH
IV: X=Cl$_2$
V: X=O

2, 3-Diphenylcyclopropenethione (I). — The reaction of 2, 3-diphenylcyclopropenone[4] (V) with phosphorus pentasulfide in dry benzene at 50~60°C gave 68% of I; m. p. 125~126°C (decomp.), yellow prisms from methanol. Found: C, 81.16; H, 4.70. Calcd. for $C_{15}H_{10}S$: C, 81.06; H, 4.54%. IR (KBr disk):[5] 1780(m), 1597(m), 1438(m), 1350(vs), 1310(s), 1298(s), 1170(m), 1015(m), 760(s), 682(s), 658(m) cm^{-1}; (in CCl_4): 3050(m), 1780(m), 1597(m), 1450(m), 1358(vs), 1311(s), 1298(s), 1172(m), 1020(m) cm^{-1}. The bands at 1780 and 1350~1358 cm^{-1} may be due to the C=C stretching in a three-membered ring and to C=S stretching[6] respectively. UV λ_{max} mμ (log ε) (in cyclohexane): 236(4.32), 245(4.52), 268(4.40), 284(4.28), 298(4.06), 360(3.98); (in methanol): 227(4.17), 234(4.11), 265(4.39), 277(4.36), 336(4.14). The dipole moment of I in benzene at 30°C is 5.8 D. The hydrolysis of I with 75% sulfuric acid regenerated V.

3-Dicyanomethylene-1, 2-diphenyl-1-cyclopropene (II).—The refluxing of V with malononitrile in freshly-distilled acetic anhydride in the presence of a minute amount of boron trifluoride afforded 23% of II; m. p. 299°C (decomp.), pale yellow prisms from tetrahydrofuran. Found: C, 84.64; H, 3.93; N, 10.88. Calcd. for $C_{18}H_{10}N_2$: C, 85.02; H, 3.96; N, 11.02%. IR (KBr disk):[5] 2210(s), 2190(s), 1865(m), 1600(m), 1507(s), 1477(s), 1444(s), 1393(s), 1375(s), 769(s), 687(s) cm^{-1}. UV λ_{max} mμ (log ε) (in dioxane): 244(4.28), 274(4.43), 293(4.45), 306(4.40), 362(4.06). The dipole moment II in dioxane at 30°C is 9.3 D.

2, 3-Diphenylcyclopropenone Oxime (III). — The reaction of V with hydroxylamine hydrochloride in methanol and the neutralization of the resulting mixture with sodium hydrogencarbonate yielded 24% of III, m. p. 99~101°C, colorless prisms. Found: C, 81.35; H, 4.92; N, 6.16. Calcd. for $C_{15}H_{11}ON$: C, 81.43; H, 5.01; N, 6.33%. IR (KBr disk):[5] 3420 (s), 3250(s), 1875(m), 1850(m), 1593(s), 1450(s), 1360(s), 866(s), 764(vs), 690(vs) cm^{-1}.

3, 3-Dichloro-1, 2-Diphenyl-1-cyclopropene (IV).—When V was allowed to react with phosphorus pentachloride in chloroform, it gave IV,[7] m. p. 123~126°C. IR[5] (in CCl_4): 1810(w), 1630(m), 1600(w), 1450(s); (in CS_2): 1342(s), 1145(s), 1120(s), 1013(m), 911(m), 760(s), 725(m), 701(s), 680(s) cm^{-1}. The structure of IV was suggested by a comparison of its infrared spectrum with that of tetrachlorocyclopropene,[8] by the quantitative regeneration of V by hydrolysis with water, and by the neutralization equivalent of the hydrogen chloride yielded in the hydrolysis reaction. Details of this report, a comparison with the corresponding cycloheptatrienyl

1) A part of this paper was presented as a special lecture at the Symposium on Molecular Structure, Sendai, October 3, 1963. Two other communications[2] prompted us to report in the preliminary form. This investigation was supported in part by a donation from the Sankyo Co., Tokyo.

2) E. D. Bergmann and I. Agranat, *J. Am. Chem. Soc.*, **86**, 3587 (1964); A. S. Kende and P. T. Izzo, ibid., **86**, 3587 (1964).

3) J. D. Roberts, A. Streitwieser, Jr. and C. M. Regan, ibid., **74**, 106 (1956); S. L. Manatt and J. D. Roberts, *J. Org. Chem.*, **24**, 1336 (1959); R. Breslow and P. Dowd, *J. Am. Chem. Soc.*, **85**, 2729 (1963) and ref. cited therein; A. S. Kende, ibid., **85**, 1882 (1963); M. A. Battiste, ibid., **86**, 944 (1964); M. E. Volpin et al., *Izvest. Akad, Nauk SSSR, otdel, Kim Nauk*, **1959**, 560; *Doklady Akad Nauk SSSR*, **139**, 1107 (1961).

4) Prepared by the method of R. Breslow (*J. Am. Chem. Soc.*, **85**, 234 (1963)).

5) Only significant bands are shown.

6) The ratio between the $\nu_{c=o}$ of cyclopropenone and the $\nu_{c=s}$ of the corresponding thioketone is 1.33~1.37. This obeys Mecke's rule. Cf. R. Mecke, R. Mecke and A. Lüffringhans, *Chem. Ber.*, **90**, 975 (1957).

7) Microanalysis could not be carried out because of this substance's high hygroscopic property.

8) S. W. Tobey and R. West, *Tetrahedron Letters*, 1179 (1963).

system, and the dipole moment[9] of the compounds will be reported on in the near future.

The Chemical Research Institute of Non-Aqueous Solutions
Tohoku University
Katahira-cho, Sendai

9) S. Katagiri, M. Saga, H. Azumi, M. Funamizu and Kitahara, to be published.